Can. J. Chem. Downloaded from www.nrcresearchpress.com by 210.87.254.5 on 09/05/12
For personal use only.

Canadian Journal of Chemistry

Issued by THE NATIONAL RESEARCH COUNCIL OF CANADA

VOLUME 43 JANUARY 1965 NUMBER 1

THE SYNTHESIS OF GLUCOSINALBIN AND GLUCOAUBRIETIN[1]

M. H. BENN

Department of Chemistry, University of Alberta, Calgary, Alberta

Received August 10, 1964

ABSTRACT

The first synthesis of the glucosinalbin and glucoaubrietin anions has been achieved by sulfonation and deacetylation of the thiohydroximates obtained by addition of tetraacetylglucopyranosyl mercaptan to *p*-acetoxyphenylacetonitrile oxide and *p*-methoxyphenylacetonitrile oxide.

The mustard oil glucosides form a group of natural compounds widely distributed through the plant kingdom and particularly common in the order Rhoeadales, especially within the families Cruciferae and Capparidaceae of this order (1). Eminent amongst these compounds is sinalbin, the glucosidic precursor of the mustard oil responsible for the well known flavor of white mustard, *Sinapis alba* L., a plant which has been used for medicinal and condimental purposes for some 25 centuries (2).

Sinalbin was first isolated from *Sinapis alba* in 1831 by Robiquet and Boutron (3). In 1897 Gadamer (4) proposed the general structure (I) for the mustard oil glucosides, sinalbin being (I)(R = *p*-$HOC_6H_4CH_2$, X = sinapinium cation).[2]

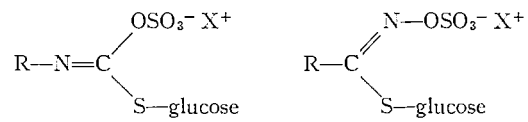

(I) (II)

In spite of the failure of this structure to account for several of the observed reactions of the mustard oil glucosides,[3] it was accepted until 1956, when Ettlinger and Lundeen (6) pointed out that all the observed properties and reactions were consistent with the structure (II).[4] New degradative evidence supported this structure, the correctness of which was conclusively established (7) by the synthesis of a compound with the structure (II)(R = $C_6H_5CH_2$, X = $(CH_3)_4N$) which proved to be identical with the tetramethylammonium salt[5] of the naturally occurring mustard oil glucoside, glucotropaeolin.

[1]*Presented in part at the 47th Canadian Chemical Conference, Kingston, Ontario, June 2, 1964.*

[2]*As isolated from plant material, the cation commonly associated with the mustard oil glucoside anion is potassium. Sinalbin is unique in that it is the cation of the choline ester of 3,5-dimethoxy-4-hydroxycinnamic acid (the sinapinium ion) which is associated with the anion (glucosinalbin). Occasionally, it is convenient to isolate the mustard oil glucosides as tetramethylammonium salts (see footnote 5).*

[3]*In particular, the formation under certain circumstances of nitriles, sulfur, and carbon disulfide. See ref. 5 for a discussion of these reactions.*

[4]*Glucose = β-D-glucopyranosyl residue.*

[5]*Ettlinger and Lundeen (6) found the tetramethylammonium salts to have superior crystallizing properties to the potassium salts.*

Can. J. Chem. Downloaded from www.nrcresearchpress.com by 210.87.254.5 on 09/05/12
For personal use only.

Recently, in connection with certain biosynthetic and biochemical studies, we developed a new synthesis of the mustard oil glucosides, the key feature of which was the construction of the thiohydroximate skeleton by the addition of a thiol to a nitrile oxide (8). This synthesis has been used to prepare several of the simple mustard oil glucosides[6] and we now describe its successful application in the synthesis of glucosinalbin and the related mustard oil glucoside, glucoaubrietin[7] (II)(R = p-$CH_3OC_6H_4CH_2$, X = K).

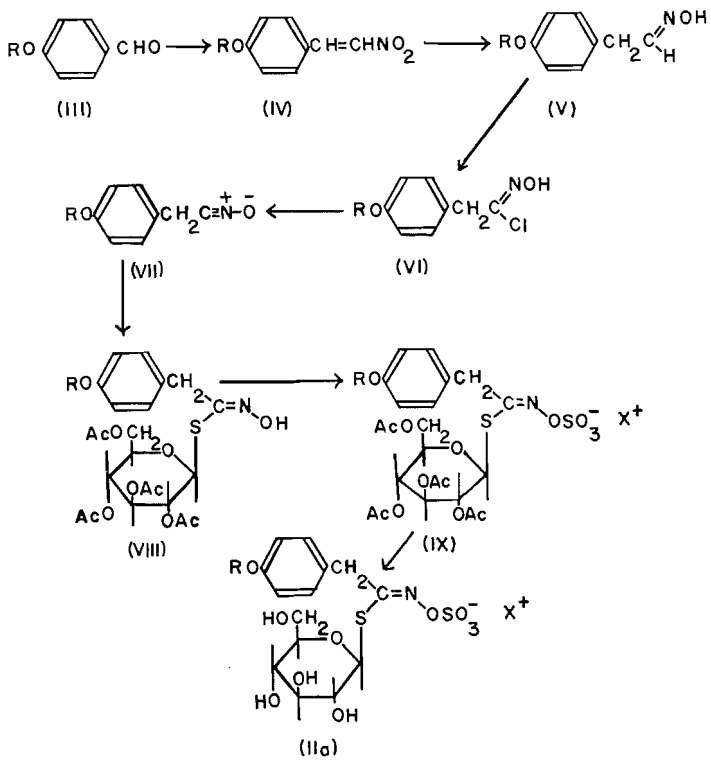

p-Hydroxy-ω-nitrostyrene (IV, R = H), produced by the ammonium acetate catalyzed condensation of p-hydroxybenzaldehyde (III, R = H) and nitromethane (12), was acetylated and then hydrogenated, in pyridine solution, over palladium–charcoal,[8] to produce p-acetoxyphenylacetaldoxime (V, R = CH_3CO). However, in contrast to the hydrogenation of p-methoxy-ω-nitrostyrene, the yield of oxime was poor and this step was the worst in the entire synthesis of glucosinalbin. The oxime was converted to the crystalline hydroxamoyl chloride (VI, R = CH_3CO) upon treatment with chlorine. Reaction of 2,3,4,6-tetra-O-acetyl-β-D-glucopyranosyl mercaptan with the nitrile oxide

[6]*Glucotropaeolin (9a), glucocapparin (II) (R = CH_3, X = K) (9b), glucolepidiin (R = CH_3CH_2, X = K) (9c), glucoputranjivin (II)(R = $(CH_3)_2CH$, X = K) (9c), and gluconasturtiin (II, R = $C_6H_5CH_2CH_2$, X = K)(9d). A very similar synthesis has been developed by Dr. Ettlinger and used to synthesize glucocapparin and glucotropaeolin. This work is described in "Final Report on Contract DA-19-129-QM-1059, Project 7-84-06-032, Simplified Food Logistics" by G. Dateo and M. G. Ettlinger.*

[7]*Glucoaubrietin occurs in plants of the genus Aubrieta (10). It may be recognized as glucosinalbin in which the phenolic hydroxyl has been methylated and it will be interesting to see whether or not glucosinalbin is the biogenetic precursor of glucoaubrietin. A recent study by Kindl (11) has shown that glucosinalbin is biosynthesized, in Sinapis alba, from phenylalanine more efficiently than from tyrosine. The biosynthesis apparently proceeds via the degradation of these α-amino acids to p-coumaric acid.*

[8]*Conditions established by Reichert and Koch (13) for the preparation of substituted phenylacetaldoximes from ω-nitro styrenes.*

(VIII, R = CH_3CO), produced *in situ*, in ether solution, by the action of triethylamine upon the hydroxamoyl chloride, afforded S-(2,3,4,6-tetra-O-acetyl-β-D-glucopyranosyl)-*p*-acetoxyphenylacetothiohydroximate ("pentaacetylproglucosinalbin") (VIII, R = CH_3CO). Sulfonation of this compound with pyridine – sulfur trioxide, followed by treatment with potassium bicarbonate, gave potassium pentaacetylglucosinalbate (IX, R = CH_3CO, X = K).

Deacetylation with methanolic ammonia gave potassium glucosinalbate which was converted by cation exchange chromatography to the tetramethylammonium salt (II*a*, R = H, X = $(CH_3)_4N$). This crystallized well and proved to be identical with a sample of natural origin.[9]

Glucoaubrietin was synthesized by an analogous set of reactions, starting with anisaldehyde (III, R = CH_3), and isolated as the well crystalline tetramethylammonium salt.

These are the first reported syntheses of the glucosinalbin and glucoaubrietin anions.

EXPERIMENTAL

p-Acetoxy-ω-nitrostyrene (IV) (R = CH_3CO)

p-Hydroxy-ω-nitrostyrene (12)(10 g) was dissolved in acetic anhydride (100 ml) containing fused anhydrous sodium acetate (3 g), the solution refluxed gently for 4 h, then poured into crushed ice (1 kg). The fine, light-yellow precipitate was filtered off and recrystallized from acetone – petroleum ether to give the acetate as long, silky, pale-yellow needles, m.p. 161–162° (11.2 g, 88%). Lit. (14) m.p. 158–159°.

p-Acetoxyphenylacetaldoxime (V)(R = CH_3CO)

p-Acetoxy-ω-nitrostyrene (10 g) was dissolved in pyridine (100 ml), palladium–charcoal catalyst (0.5 g) added, the reaction mixture warmed to 50°, and then hydrogenated in a Parr apparatus at 30 p.s.i. Uptake of hydrogen was complete in 15 min and was slightly less than the theoretical amount. The reaction mixture was filtered through Celite, the pale-yellow filtrate poured into ice-cold, dilute sulfuric acid (4 *N*, 750 ml) and extracted with ether (4 × 150 ml).

The ether extracts were combined, dried ($MgSO_4$), and filtered. Fine colorless crystals separated, m.p. 183–184°, apparently dimeric[10] material. The ether extracts were concentrated under reduced pressure to a thin slurry of crystals in a light-brown oil. Addition of benzene, followed by filtration, gave a further yield of the dimer (total 0.58 g). The benzene solution was concentrated somewhat and petroleum ether added to the warm solution until a permanent opalescence was produced. Upon standing, an oil separated, accompanied by pale-yellow, needle-shaped crystals. The crystals were separated and the oil redissolved in benzene and the solution again treated with petroleum ether. In this way, a total of three crops of crystals was obtained (1.7 g). These were combined and twice recrystallized from benezene – petroleum ether to give pale, straw-colored needles of the oxime, m.p. 92–94° (1.35 g, 14%).

Anal. Calcd. for $C_{10}H_{11}NO_3$: C, 62.16; H, 5.74; N, 7.25. Found: C, 62.62; H, 5.75; N, 7.05.

p-Acetoxyphenylacetohydroxamoyl Chloride (VI)(R = CH_3CO)

p-Acetoxyphenylacetaldoxime (250 mg) was dissolved in ether (30 ml), the solution cooled to 0° in an ice–salt bath, and a slow stream of chlorine was bubbled through the solution. Careful removal of solvent (bath < 10°) from the azure-colored solution left a white crystalline residue which was twice recrystallized from ether to give fine needles with a blue–green tint, sintering at 90°, m.p. 116° (206 mg, 70%).

Anal. Calcd. for $C_{10}H_{10}ClNO_3$: C, 52.76; H, 4.45; Cl, 15.58. Found: C, 53.03; H, 4.70; Cl, 15.56.

S-(2,3,4,6-tetra-O-acetyl-β-D-glucopyranosyl)p-acetoxyphenylacetothiohydroximate (pentaacetylproglucosinalbin) (VIII)(R = CH_3CO)

p-Acetoxyphenylacetaldoxime (0.80 g) was converted to the hydroxamoyl chloride as above, the entire product was dissolved in dry ether (250 ml) and added to a stirred solution of 2,3,4,6-tetra-O-acetyl-β-D-glucopyranosyl mercaptan (1.6 g) in dry ether (100 ml), followed by triethylamine (2 ml) in ether (10 ml). There was immediate separation of triethylamine hydrochloride and the pale-blue color of the solution was discharged. After 30 min at room temperature, the reaction mixture was poured into ice-cold, dilute aqueous sulfuric acid (500 ml, 1 *N*) and shaken. The ether layer was separated, dried ($MgSO_4$), and evaporated to yield a colorless oil which crystallized and recrystallized from ether – petroleum ether in small colorless prisms, m.p. 157–158° (1.30 g, 60%). $[\alpha]_D^{25}$ −9.5° (*c*, 2 in $CHCl_3$).

Anal. Calcd. for $C_{24}H_{29}NO_{12}S$: C, 51.88; H, 5.26; N, 2.52. Found: C, 51.82; H, 5.36; N, 2.50.

[9]*Obtained from Calbiochem, 3625 Medford St., Los Angeles 63.*

[10]*Sonn and Schellenburg (15) previously reported that catalytic hydrogenation of ω-nitrostyrenes in alcoholic or acetic acid solution results in extensive dimer formation.*

Can. J. Chem. Downloaded from www.nrcresearchpress.com by 210.87.254.5 on 09/05/12
For personal use only.

Can. J. Chem. Downloaded from www.nrcresearchpress.com by 210.87.254.5 on 09/05/12
For personal use only.

Tetramethylammonium Glucosinalbate (IIa) (R = H, X = $(CH_3)_4N$)

Pentaacetylproglucosinalbin (300 mg) and freshly prepared pyridine – sulfur trioxide complex (200 mg) were stirred together in dry pyridine (3 ml) at room temperature for 24 h. The reaction mixture was poured into water (50 ml) containing potassium hydrogen carbonate (500 mg). The homogeneous, deep-orange-colored solution was freeze dried, the residue extracted with boiling 95% (v/v) aqueous ethanol (3 × 20 ml), and the extracts filtered hot. The combined orange-colored extracts deposited discolored and rather amorphous solids on cooling, the infrared spectrum of which (in KBr disc) suggested that they were the desired potassium pentaacetylglucosinalbate accompanied by partially deacetylated material. Accordingly, the combined ethanol filtrates were evaporated to dryness and the residue combined with the solids which had separated from solution. The total solids were dissolved in methanol (40 ml) previously saturated with ammonia and the solution kept at room temperature over night. Removal of solvent under reduced pressure left a brown glass which was taken up in water (5 ml) and applied to the top of a column (1 × 15 cm) of Dowex-50 cation exchange resin in the tetramethylammonium form. The column was eluted with water (30 ml) and the brown eluates were adjusted to pH 8 by addition of a drop of glacial acetic acid and freeze dried. The residual glassy solids were taken up in a little methanol and the solution filtered and diluted with absolute ethanol until a rather dirty and gummy precipitate separated. This was filtered off and the filtrate treated with 2 drops of water and absolute ethanol until turbid. On standing, first at room temperature and then at 0°, small off-white prisms separated from the solution. These were collected and recrystallized from aqueous ethanol to give almost colorless prisms of tetramethylammonium glucosinalbate, m.p. 192–195° (decomp.) (open capillary) (96 mg, 36%). The infrared spectrum (KBr disc) was identical with that of an authentic specimen of tetramethylammonium glucosinalbate of natural origin and the melting point was undepressed on admixture with this salt. $[\alpha]_D^{24}$ −20° (*c*, 2 in H_2O). Lit. (6) m.p. 191–192° (decomp.), $[\alpha]_D^{35}$ −19° (in H_2O). The product was also homogeneous when examined by paper chromatography (16).

p-Methoxyphenylacetaldoxime (V)(R = CH_3)

p-Methoxy-ω-nitrostyrene (12) (5.0 g) in pyridine (100 ml) was hydrogenated over 10% palladium–charcoal at room temperature and 30 p.s.i. Hydrogen uptake was rapid and ceased after 15 min. The reaction mixture was worked up as described above for *p*-acetoxyphenylacetaldoxime to yield a yellow oil containing suspended crystals. The oil was taken up in ether, in which the crystals were insoluble, and filtered. The residual crystals of *dimer* were recrystallized from ethanol–benzene in colorless, felted plates, m.p. 232–234°.

Anal. Calcd. for $C_{18}H_{20}N_2O_4$: C, 65.83; H, 6.11; N, 8.53. Found: C, 65.77; H, 6.33; N, 8.51.

Evaporation of the ether extract gave a yellow oil which crystallized from benzene-petroleum ether. Recrystallization with a single treatment with animal charcoal from ethanol gave colorless plates, m.p. 120° (3.5 g, 77%). Lit. (13) m.p. 120°.

S-(2,3,4,6-tetra-O-acetyl-β-D-glucopyranosyl)p-methoxyphenylacetothiohydroximate (tetraacetylproglucoaubrietin) (VIII)(R = CH_3)

p-Methoxyphenylacetaldoxime (1.0 g) was dissolved in dry chloroform (25 ml), the solution cooled to 0°, and a slow stream of dry chlorine bubbled through the solution for 20 min. The initially blue, now green solution was worked up in the usual manner (bath < 40°). The product was an off-white mass of crystals of *p*-methoxyphenylacetohydroxamoyl chloride, which readily decomposed on standing at room temperature. The hydroxamoyl chloride was taken up in ether (10 ml) and added to a gently stirred solution of 2,3,4,6-tetra-O-acetyl-β-D-glucosyl mercaptan (2.0 g) in ether (200 ml), followed by a solution of triethylamine (2.5 ml) in ether (10 ml). After 30 min at room temperature, the reaction mixture was worked up in the usual fashion to yield a pale-brown oil. The oil was taken up in ethanol, treated with animal charcoal, and the hot, filtered solution diluted with petroleum ether until just turbid. On cooling, long, colorless, felted needles separated, m.p. 160–163°, raised to 164–166° after two further recrystallizations from ethanol. (1.9 g, 54%). $[\alpha]_D^{25}$ −12° (*c*, 2 in $CHCl_3$).

Anal. Calcd. for $C_{23}H_{29}NO_{11}S$: C, 52.36; H, 5.54; N, 2.66; S, 6.08. Found: C, 52.76; H, 5.86; N, 2.60; S, 6.15.

Tetraacetylglucoaubrietin (IX) (R = CH_3)

Tetraacetylproglucoaubrietin (410 mg) was dissolved in dry pyridine (5 ml), pyridine – sulfur trioxide (180 mg) added, and the reaction mixture stirred at room temperature for 18 h. (A homogeneous solution was obtained after 3 h.) The reaction mixture was poured into water (30 ml) containing potassium hydrogen carbonate (250 mg) and the homogeneous solution was then freeze dried. The residue was extracted with boiling 95% (v/v) aqueous ethanol (5 × 15 ml), and the extracts filtered hot. Colorless, fine, needle-shaped crystals separated, m.p. 185–190°, and recrystallized from 95% ethanol as colorless needles, m.p. 187–190° (277 mg, 55%). $[\alpha]_D^{27}$ −14° (*c*, 2 in 1:1 (v/v) aqueous ethanol).

Anal. Calcd. for $C_{23}H_{28}NO_{14}S_2K.2H_2O$: C, 40.52; H, 4.73; N, 2.05; S, 9.41; K, 5.74. Found: C, 39.96; H, 4.31; N, 1.99; S, 9.37; K, 5.74.

Glucoaubrietin (IIa) ($R = CH_3$, $X = (CH_3)_4N$)

Tetraacetylglucoaubrietin (220 mg) was dissolved in anhydrous methanol (10 ml) saturated with ammonia and the solution kept at room temperature overnight. Removal of solvent under reduced pressure left an ethanol-insoluble gum. The gum was taken up in a little methanol and 1 drop of water added, followed by absolute ethanol. The white, hygroscopic, amorphous precipitate was taken up in a few drops of water and absolute ethanol added to the warm solution until a permanent turbidity was produced. After storing at 0° overnight, the fine, colorless, granular precipitate was filtered off. It again proved to be hygroscopic, setting to a hard, powderable glass, m.p. 148–155° (decomp.). Paper chromatography revealed that the product was homogeneous with R_F 0.33.

Anal. Calcd. for $C_{15}H_{20}NO_{10}S_2K$: C, 37.22; H, 4.22; S, 13.43. Found on an undried sample: C, 37.73; H, 4.99; S, 13.80.

Evaporation of the mother liquors yielded more solid which was combined with the crystallized material and converted to the tetramethylammonium salt as described for glucosinalbin. In this case, the freeze-dried eluates yielded a residue which crystallized directly from aqueous ethanol in small colorless prisms, m.p. 187–189° (88 mg, 41%). $[\alpha]_D^{27}$ −21° (*c*, 2 in H_2O). The product was homogeneous when examined by paper chromatography (16).

Anal. Calcd. for $C_{19}H_{32}N_2O_{10}S_2$: C, 44.52; H, 6.29; N, 5.47; S, 12.51. Found: C, 44.45; H, 6.36; N, 5.19; S, 12.50.

ACKNOWLEDGMENTS

We are grateful to the National Research Council for financial support of this work and to Miss Patricia Wales who prepared the *p*-methoxy-ω-nitrostyrene.

REFERENCES

1. A. KJAER. Fortschr. Chem. Org. Naturstoffe, **18**, 122 (1960).
2. THE GREEK HERBAL OF DIOSCORIDES. *Transl. by* J. Goodyer. *Edited by* R. T. Gunther. Hafner Co., New York. 1959.
3. ROBIQUET and F. BOUTRON-CHARLARD. J. Pharm. Chim. **17**, 279 (1831).
4. J. GADAMER. Ber. **30**, 2327 (1897).
5. F. CHALLENGER. *In* Aspects of the organic chemistry of sulphur. Butterworths, London. 1959.
6. M. G. ETTLINGER and A. J. LUNDEEN. J. Am. Chem. Soc. **78**, 4172 (1956).
7. M. G. ETTLINGER and A. J. LUNDEEN. J. Am. Chem. Soc. **79**, 1764 (1957).
8. M. H. BENN. Can. J. Chem. In press.
9. (*a*) M. H. BENN, Can. J. Chem. **41**, 2836 (1963); (*b*) Can. J. Chem. **42**, 163 (1964); (*c*) M. H. BENN and D. MEAKIN. In preparation; (*d*) J. Chem. Soc. In press.
10. A. KJAER, R. GMELIN, and R. B. JENSEN. Acta Chem. Scand. **10**, 26 (1956).
11. H. KINDL. Monatsh. **95**, 339 (1964).
12. C. B. GAIRAUD and G. R. LAPPIN. J. Org. Chem. **18**, 1 (1953).
13. B. REICHERT and W. KOCH. Arch. Pharm. **273**, 265 (1935).
14. G. HAHN and K. STIEHL. Ber. **71**, 2154 (1938).
15. A. SONN and A. SCHELLENBURG. Ber. **50**, 1513 (1917).
16. O. E. SCHULTZ and R. GMELIN. Z. Naturforsch. **8b**, 151 (1953).

Can. J. Chem. Downloaded from www.nrcresearchpress.com by 210.87.254.5 on 09/05/12
For personal use only.

Can. J. Chem. Downloaded from www.nrcresearchpress.com by 210.87.254.5 on 09/05/12
For personal use only.

SUPERSONIC MOLECULAR BEAMS

II. THEORY OF THE FORMATION OF SUPERSONIC MOLECULAR BEAMS

J. P. VALLEAU AND J. M. DECKERS
Lash Miller Chemical Laboratories, University of Toronto, Toronto, Ontario

Received June 19, 1964

ABSTRACT

Supersonic molecular beams may be isolated from gas which has been allowed to expand through a nozzle. This paper concerns the kinetic theory of the isolation of such beams, taking into account the effect of collisions in the region between the skimmer and the collimator. These collisions turn out to be important. In particular, they offer an explanation of two interesting phenomena: (*a*) the existence of a *maximum* beam intensity as the distance is varied between the nozzle and the collimating system and (*b*), in a mixed beam, large increases in the intensity of the heavy gas as its initial concentration is reduced by replacement with a much lighter gas. The theory is compared with various experimental results. Although severe approximations have been introduced into the theory, it appears to predict the above phenomena in a way that is better than qualitative.

1. INTRODUCTION

A considerable amount of data is accumulating on the behavior of supersonic molecular beams formed by expansion through a nozzle. The experimental setup for such a beam is shown schematically in Fig. 1. Gases, initially at a pressure p_0 (number density n_0), are allowed to expand through a nozzle into a region of much lower pressure. The gas in the core of the nozzle exhaust is thereby accelerated to supersonic velocities. A beam is isolated from this core by two small apertures known as the skimmer and the collimator.

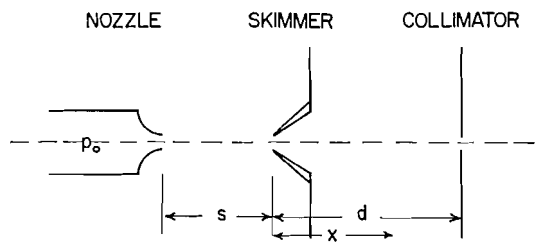

FIG. 1. Schematic diagram of beam-forming apparatus.

Two results of these experiments appear very surprising at first sight. As the distance s between the nozzle and the skimmer is increased from small values, one might expect a monotonic decrease in beam intensity. One might also expect a beam intensity roughly proportional to p_0. This is the behavior, in both respects, predicted by the original analysis of the beam problem, according to Kantrowitz and Grey (1). In practice it is found (2) that with increasing s the intensity *increases* in a certain range, then passes through a maximum, and finally decreases. Furthermore, at s-values below the maximum the intensity depends very little on p_0.

The other observation concerns mixed beams. If a beam is made from a mixture of a heavy gas and a light gas, it is usually found that the beam is very much enriched in the heavier gas. This is easy to explain (cf. Section 3), but it is more surprising that at fixed

p_0 a *dilution* of heavy gas with light gas leads to a large *increase* in beam intensity, although the beam consists almost entirely of the heavy gas.

We believe that these effects are due largely to the effect of collisions, occurring in the region between the skimmer and the collimator, between the beam molecules. The theoretical problem of taking account of these collisions is not a simple one, so that we have had to be satisfied for the moment with a theory involving several approximations. Nonetheless, the above effects are described in a way that is better than qualitative (cf. Section 4).

In an earlier paper (3) we examined the effects of collisions in the isolated beam (i.e. downstream from the collimator). We showed that in a mixed beam collisional depletion of light molecules would be more rapid than that of heavy molecules. One can expect this collisional enrichment of heavy molecules to be far more effective in the higher density region between the skimmer and collimator.

The only suggestion previously put forward to account for these effects involved the consequences of a postulated shock wave set up before the skimmer aperture. We discuss later (Section 5) some recent experimental work of Reis and Fenn (4) on this matter. Evidently, mass separation effects due to such shock waves can occur in molecular beams under some conditions, though those are not yet established. At the same time it appears certain that the collisional effect discussed in this paper is large and generally important and may well explain many of the observations on beams.

2. THEORY

The theoretical development is based on the approximation that the flow of the gas forming the beam remains "hydrodynamic" up to the skimmer, where it becomes "molecular". This approximation is implicit in the analysis of Kantrowitz and Grey (1) and others (5, 6) and allows one to estimate the Mach number $\mathscr{M}$ of the beam from the distance between the nozzle and the skimmer. It is obvious that the flow does not in practice change instantly from one regime to the other; the present picture is that, because the skimmer suddenly removes the outer envelope of flowing gas, the transition takes place rather rapidly. The approximation appears to be a useful one.

There are evidently cases where this approximation will not be suitable. If the gas at the skimmer is sufficiently dense, the expansion region will penetrate into the region between the skimmer and the collimator; the present theory cannot describe this situation. At the other extreme, for very low densities, the expansion may quit before the gases reach the skimmer; it should be possible to adapt the theory to describe this situation (cf. Section 5).

According to the above basic approximation, the Mach number at the skimmer is determined by the distance s, between the nozzle and the skimmer, measured in nozzle diameters. In the limit of low background pressure, $\mathscr{M}$ is given by Woolf's (7) generalizations of the calculations of Owen and Thornhill (8). The temperature T and the mean velocity $\bar{v}$ in the beam are then given by the laws of isentropic expansion:

$$T_0/T = 1 + (\gamma - 1)\mathscr{M}^2/2, \qquad [2.1]$$

$$\bar{v} = (2C_p(T_0 - T)/M)^{1/2} = \mathscr{M}(\gamma RT/M)^{1/2}, \qquad [2.2]$$

where T_0 is the stagnation temperature, C_p the molar heat capacity, γ the specific heat ratio C_p/C_v, M the molecular weight of the gas, and R the gas constant per mole. We have shown previously (3) that as a result of collisions in the beam there is a small decrease in

Can. J. Chem. Downloaded from www.nrcresearchpress.com by 210.87.254.5 on 09/05/12
For personal use only.

T and increase in $\bar{v}$ in moving down the beam; we take no account here of this second-order effect.

We wish to calculate the number density n_c of the gas at the collimator and hence the beam intensity $n_c\bar{v}$. To do this it is only necessary to consider a cylindrical region based on the skimmer aperture and stretching a distance d to the collimator. Molecules enter this region at the skimmer with a density n_s. The density n_c at the collimator is much less than n_s for two reasons:

(*a*) the natural trajectories of most of the molecules at the skimmer carry them across the boundary of the cylinder before they reach the collimator; this may be called the convective or diffusive loss of molecules;

(*b*) most collisions between pairs of molecules throw the colliding molecules out of the cylindrical region rather quickly; this may be called the collisional loss.

If there were no collisions the density could be calculated from purely geometrical considerations; let us call this "collision free" density, at a distance x from the skimmer, $n'(x)$. Due to collisions the density $n(x)$ will be less than $n'(x)$ and this will reduce the convective loss by a factor of roughly n/n'. We may therefore write an approximate equation for the attenuation of the density $n(x)$, taking account of collisions, as follows;

$$\frac{dn}{dx} = \frac{n}{n'}\frac{dn'}{dx} - \frac{\lambda n^2}{\bar{v}}, \qquad [2.3]$$

where $\lambda n^2/2$ is the collision frequency per unit volume at a density n. This equation implicitly assumes that the density is uniform across the cylinder, which is not strictly the case. It also ignores the effect of collisions on the flow pattern of the gases and the fact that some collisions will in fact knock molecules *into* the beam.

We can easily solve [2.3] to obtain

$$n(X) = n'(X) \Big/ \left[1 + (1/\bar{v}) \int_0^X \lambda n'(x)\, dx\right], \qquad [2.4]$$

where X is some particular value of x. It is therefore necessary to estimate n', the density in the collision-free case.

To do this we require the Maxwellian probability distribution,

$$p(w) = \frac{mw}{kT} \exp\left\{-\frac{mw^2}{2kT}\right\}, \qquad [2.5]$$

for a molecule of mass m, in the skimmer, to have a transverse speed w. If we disregard the thermal spread of the velocities parallel to the axis (by comparison with the mean velocity $\bar{v}$), we can show that

$$n'(X) = \frac{2n_s}{\pi}\int_0^{a\bar{v}/X}\left[\arccos\frac{wX}{a\bar{v}} - \frac{wX}{a\bar{v}}\left(1 - \frac{w^2X^2}{a^2\bar{v}^2}\right)^{1/2}\right]\frac{mw}{kT}\exp\left\{-\frac{mw^2}{2kT}\right\}dw, \qquad [2.6]$$

where a is the diameter of the skimmer. Unfortunately, this cannot be integrated analytically, so we have turned to a rougher approximation. We treat the diffusive problem as though all the molecules entered at the center of the skimmer. Then all molecules with a transverse speed less than $a\bar{v}/2X$ will remain in the beam at X. Thus

$$\begin{aligned} n'(X) &\approx n_s\int_0^{a\bar{v}/2X}\frac{mw}{kT}\exp\left\{-\frac{mw^2}{2kT}\right\}dw \\ &= n_s\left[1 - \exp\left\{-\frac{ma^2\bar{v}^2}{8kTX^2}\right\}\right]. \end{aligned} \qquad [2.7]$$

Can. J. Chem. Downloaded from www.nrcresearchpress.com by 210.87.254.5 on 09/05/12
For personal use only.

This approximation is rather drastic for small values of X, where it will somewhat overestimate the density; it becomes a very good approximation for large X, of course. It may be noted that [2.7] becomes an inverse square law for large X. It is convenient to introduce a quantity α, having the dimensions of length, as follows;

$$[2.8] \qquad \alpha = \left(\frac{m\bar{v}^2}{8kT}\right)^{1/2} a = \left(\frac{\gamma}{2}\right)^{1/2} \frac{\mathscr{M}}{2} a,$$

where the second form comes from [2.2].

We now wish to use the result [2.7],

$$n'(x) = n_s[1 - \exp(-\alpha^2/x^2)],$$

to evaluate the density $n(X)$, [2.4], and in particular the density $n_c \equiv n(d)$, at the collimator. There is some difficulty concerning the collision coefficient λ. Strictly speaking this should be regarded as a function of x; it will change with position because the transverse velocity distributions are constantly truncated as a result of the convective effect discussed earlier. Thus the molecules very near the skimmer may have considerable transverse velocities, and a three-dimensional collision problem arises. This is, however, rapidly converted into an approximately one-dimensional problem on moving away from the skimmer orifice, since only those molecules having small transverse velocities will remain in the core of the beam. In this conversion, λ will decrease by a factor of two. For the present approximate development we ignore this variation. The integration may then be carried out (cf. Appendix) to give

$$[2.9] \qquad n(X) = \frac{n_s[1 - \exp(-\alpha^2/X^2)]}{1 + (\lambda n_s/\bar{v})\{\pi^{1/2}\alpha[1 - \operatorname{erf}(\alpha/X)] + X[1 - \exp(-\alpha^2/X^2)]\}},$$

which is the desired result. The density in the skimmer n_s, is related to the stagnation density n_0 by the isentropic expansion law

$$[2.10] \qquad \frac{n_0}{n_s} = \left(1 + \frac{\gamma - 1}{2}\mathscr{M}^2\right)^{\frac{1}{\gamma-1}}.$$

For a typcial molecular beam experiment, (a/d) is usually 10^{-2} or less, and (cf. 2.8) α/d is small compared to unity. In estimating the density n_c at the collimator, one will thus usually, to a good approximation, be in the inverse square region of [2.7]:

$$[2.11] \qquad n_c \approx \frac{n_s\alpha^2/d^2}{1 + (\lambda n_s/\bar{v})\{\pi^{1/2}\alpha - \pi^{1/2}\alpha \operatorname{erf}(\alpha/d) + \alpha^2/d\}}.$$

Some further simplification is possible in practical cases. The second and third terms in the bracket of the denominator are small compared to the first, and furthermore they partially cancel. For $(\alpha/d) \lesssim 0.1$, $\pi^{1/2}\operatorname{erf}(\alpha/d) \approx 2\alpha/d$ very closely, so that

$$[2.12] \qquad n_c \approx \frac{n_s\alpha^2/d^2}{1 + (\lambda n_s/\bar{v})\{\pi^{1/2}\alpha - \alpha^2/d\}},$$

where the final term of the bracket is small compared to the first.

To estimate the magnitude of the collisional effect, one requires the ratio $\lambda/\bar{v}$, and we use here the value $\lambda = 2\sigma^2(\pi RT/M)^{1/2}$ calculated previously (3) for collisions in the beam; σ is the collision diameter of the molecules. With [2.2] this gives

$$[2.13] \qquad \lambda/\bar{v} = (2\sigma^2/\mathscr{M})(\pi/\gamma)^{1/2}.$$

Can. J. Chem. Downloaded from www.nrcresearchpress.com by 210.87.254.5 on 09/05/12
For personal use only.

Inserting [2.10] and [2.13] into [2.12] and recalling the definition [2.8], we obtain

$$[2.14] \qquad n_c \approx \frac{n_0 \mathscr{M}^2 a^2 \gamma / 8d^2}{[1 + (\gamma - 1)\mathscr{M}^2/2]^{1/(\gamma-1)} + [\pi\sigma^2 a n_0/(2)^{1/2}][1 - (\gamma/2\pi)^{1/2}(\mathscr{M} a/2d)]}.$$

It is evident from this expression that the collisional effect, described by the second half of the denominator, should be important. For typical beam experiments ($a \sim 10^{-1}$ cm, $n_0 \sim 10^{17}$ molecules/cc, $\sigma \sim 10$ Å), this term will be $\sim 10^2$ to 10^4 and certainly not negligible compared to the other term. At low Mach numbers the collisional term will in fact dominate the denominator, so that the intensity, $n_c\bar{v}$, of the beam will *increase* with $\mathscr{M}$. At high Mach numbers the other term will dominate, and the intensity will fall off with $\mathscr{M}$ as expected according to the Kantrowitz and Grey analysis. The existence of the maximum in the intensity curve is thus explained qualitatively. Evidently, at low Mach numbers the intensity will depend very little on the nozzle density n_0, as observed experimentally. In Section 4 the above expression is compared with some experimental data.

3. ENRICHMENT AND INTENSITY IN MIXED BEAMS

If a beam is formed from a mixture of a light and a heavy gas, a large concentration enrichment of the heavy gas is to be expected. Suppose only that the mean velocities and temperatures of the two gases remain the same up to the skimmer. The light gas will accordingly have a higher transverse velocity than the heavy gas and will therefore diffuse out of the core of the beam, between the skimmer and the collimator, more rapidly than the heavy gas. We shall see that this convective effect is sufficient to give the separation ratios observed by Greene, Brewer, and Milne (9). Waterman and Stern (10) invoked somewhat similar ideas in attempting to explain the mass separation effects they have observed.

What is more surprising is that, for a fixed nozzle pressure p_0, a reduction of the mole fraction of the heavy gas leads to a very much *increased* intensity in the beam of heavy gas produced. This cannot be explained by the convective effect mentioned above, so we turn again to studying the effects of collisions. Suppose the two gases are labelled 1, 2. Then by analogy with [2.3] we can write

$$[3.1] \qquad \frac{dn_1}{dx} = \left(\frac{n_1}{n_1'}\right)\frac{dn_1'}{dx} + \frac{\lambda_{11} n_1^2}{\bar{v}} + \frac{\lambda_{12} n_1 n_2}{\bar{v}},$$

$$[3.2] \qquad \frac{dn_2}{dx} = \left(\frac{n_2}{n_2'}\right)\frac{dn_2'}{dx} + \frac{\lambda_{21} n_1 n_2}{\bar{v}} + \frac{\lambda_{22} n_2^2}{\bar{v}}.$$

Since not all collisions will be effective in removing molecules from the beam, we now think of the λ's as describing only "effective" collisions. In particular, collisions between light and heavy molecules will affect the paths of the heavy molecules much less than those of the light, as discussed elsewhere (3); thus we may expect $\lambda_{12} \ll \lambda_{21}$, where 1 is the heavy gas.

Equations [3.1,2] are not easy to solve. If, however, we make the approximation $\lambda_{12} = 0$, eq. [3.1] for the heavy gas takes the form [2.3] found for a pure beam. In doing this we ignore the effect of collisions with light molecules in removing heavy ones from the beam. The argument can then proceed exactly as for a pure heavy gas, except that the density of the heavy gas in the nozzle is only $X_1 n_0$, where X_1 is the mole fraction of the heavy gas in the stagnation gas mixture, while $\bar{v}$ in the mixed beam will be given by

$$[3.3] \qquad \bar{v} = \mathscr{M}(\bar{\gamma} RT/\bar{M})^{1/2},$$

Can. J. Chem. Downloaded from www.nrcresearchpress.com by 210.87.254.5 on 09/05/12
For personal use only.

where

$$\bar{M} = X_1 M_1 + X_2 M_2, \tag{3.4}$$

and

$$\bar{\gamma} = \frac{X_1 C_{p_1} + X_2 C_{p_2}}{X_1 C_{v_1} + X_2 C_{v_2}}. \tag{3.5}$$

By making the appropriate modifications to the argument of the preceding section (Section 2) we can write an approximate expression for the intensity of the heavy gas in a beam formed from a mixture of gases of very different masses. If we drop, from the denominator (cf. [2.14]), the small term containing a/d, we obtain

$$n_{1c}\bar{v} = \frac{X_1 n_0 \mathscr{M}^3 \bar{\gamma}^{3/2} a^2 M_1 (RT)^{1/2}/8\bar{M}^{3/2} d^2}{[1 + (\gamma - 1)\mathscr{M}^2/2]^{1/\gamma-1} + \pi\sigma_1^2 a X_1 n_0/(2)^{1/2}}, \tag{3.6}$$

where σ_1 is the collision diameter of the heavy gas. This is the result we shall compare with experiment. It has some interesting features. For low Mach numbers the collisional term again dominates the denominator. As a result the explicit dependence of the intensity on X_1 practically disappears, and the intensity will be roughly proportional, at fixed $\mathscr{M}$ and n_0, to $(\bar{\gamma}/\bar{M})^{3/2}$. However, $\bar{M}$ will decrease rapidly as X_1 is reduced. This explains the very high intensities of heavy gas obtained with mixed beams for low Mach numbers. For *high* Mach numbers the beam temperature T becomes small so that the collision rate is reduced. Under these conditions the collisional term no longer dominates the denominator and the intensity behaves more like $X_1(\bar{\gamma}/\bar{M})^{3/2}$; less dramatic intensity increases on dilution are to be expected in this case.

4. COMPARISON WITH EXPERIMENTS

The above predictions are here compared with some measurements already reported in the literature or obtained in this laboratory.

Deckers and Fenn (2) have measured the absolute intensity of some nitrogen beams for various stagnation pressures and over a wide range of nozzle–skimmer distances; the results show the typical maxima of intensity as this distance is varied. For the conditions of these beams (cf. [2.14]), $(\gamma/2)^{1/2}(\mathscr{M}a/2d) \ll 1$, and we may, as before, drop the final term of the denominator:

$$n_c \simeq \frac{n_0 \mathscr{M}^2 \gamma a^2/8d^2}{[1 + (\gamma - 1)\mathscr{M}^2/2]^{1/\gamma-1} + can_0}. \tag{4.1}$$

The factor c as given by the above approximate theory is $\pi\sigma^2/(2)^{1/2}$. It therefore depends rather strongly on the collision diameter σ, which is not easy to estimate closely for the beam collisions, since these take place at a very low temperature and therefore at low relative velocities. The numerical factor $\pi/(2)^{1/2}$ is also rather suspect in view of the approximations we have introduced into the theory. For these reasons we have regarded c as an adjustable parameter in fitting experimental results, but we shall check that the value obtained leads to a reasonable value for σ. We have determined c from the position of the maximum intensity, as follows. By differentiating [4.1] with respect to the Mach number $\mathscr{M}$ we obtain a relation between c and the Mach number at which the *maximum* beam intensity occurs, for a fixed stagnation density. Woolf's relation (7) was used to obtain this Mach number from the measured nozzle–skimmer distance s. When this was done for nitrogen, at a stagnation pressure of 10 torr, it was found that $can_0 = 1\,050$; this corresponds to a collision diameter σ of 8.8 Å, which is of the expected magnitude.

Can. J. Chem. Downloaded from www.nrcresearchpress.com by 210.87.254.5 on 09/05/12
For personal use only.

Using this single value of c, we can predict the dependence of the beam intensities $n_c\bar{v}$ on both s and p_0. The predictions are compared with experiment (2) in Fig. 2. It is apparent that the pressure dependence of the peak position has been explained semiquantitatively (cf. Table I); we regard this as a strong argument for the correctness of the theoretical explanation. In Fig. 2 the theoretical curves have been plotted on one scale, the experimental curves on a different scale; this was done to allow a better comparison of the shapes of these curves. It is possible, however, to predict the *absolute* intensities on the basis of the theory, and these are compared with experiment for the three peak heights in Table I. No new parameters are introduced in making this comparison, and it is worth recalling that the one parameter c was determined without using the value of any intensity. The predicted intensities are too high by a factor of about three, possibly as a result of further attenuation due to scattering by background molecules and by those reflected from the skimmer, as was suggested by Anderson and Fenn (11).

A completely independent determination of the parameter c for nitrogen was obtained using the molecular beam apparatus in this department (12). Not only was a different pressure (20 torr) used, but the geometry of the beam was rather different. The two estimates differed by less than 5%. It might be mentioned that one may expect the mean collision diameters to be temperature-dependent, and we have taken no account of this in making these experimental comparisons.

TABLE I

	Peak position s (nozzle diameters)		10^{-16} peak height (molecules/cm^2 s)	
p_0	Experimental	Theoretical	Experimental	Theoretical
10	9	9	2.7	6.3
50	18	19	4.3	12.7
100	24.5	26	4.9	17.1

The increasing intensity at very low s-values for the higher pressures is presumably due to a continuation of the hydrodynamic expansion into the region downstream from the skimmer. It was mentioned earlier that the model cannot cope with this situation. At high s-values, for the high pressures, the intensity appears to fall off more rapidly than predicted, leading to sharper peaks than the theoretical ones. This behavior seems to be typical and is not yet explained. It may arise from a breakdown of the isentropic expansion law [2.10] and perhaps from the higher background pressures that must be tolerated with higher stagnation pressures p_0.

In Fig. 3 is shown the result of similar calculations for some results on argon reported by Greene, Brewer, and Milne (9); only the shapes of the curves may be compared, since the results for each stagnation pressure have been reported on their own arbitrary scale. In drawing the theoretical curves the parameter c was chosen to roughly match the position of the peak which occurs for $p_0 = 760$ torr; this value of c corresponds to $can_0 = 25 \times 10^3$ at that pressure. The authors have not made clear the precise size of the skimmer used in these experiments, and this makes it impossible* to determine the value of the collision diameter σ implied by the derived value of can_0; a similar determination for argon based on results taken in this laboratory led, however, to $\sigma = 5.6$ Å. Because of the larger value of γ for argon, as compared with nitrogen, much higher Mach numbers must be reached before

**It also makes it impossible to apply the more accurate expressions [2.12] or [2.9], which would be preferable where such high Mach numbers are involved.*

Can. J. Chem. Downloaded from www.nrcresearchpress.com by 210.87.254.5 on 09/05/12
For personal use only.

Can. J. Chem. Downloaded from www.nrcresearchpress.com by 210.87.254.5 on 09/05/12
For personal use only.

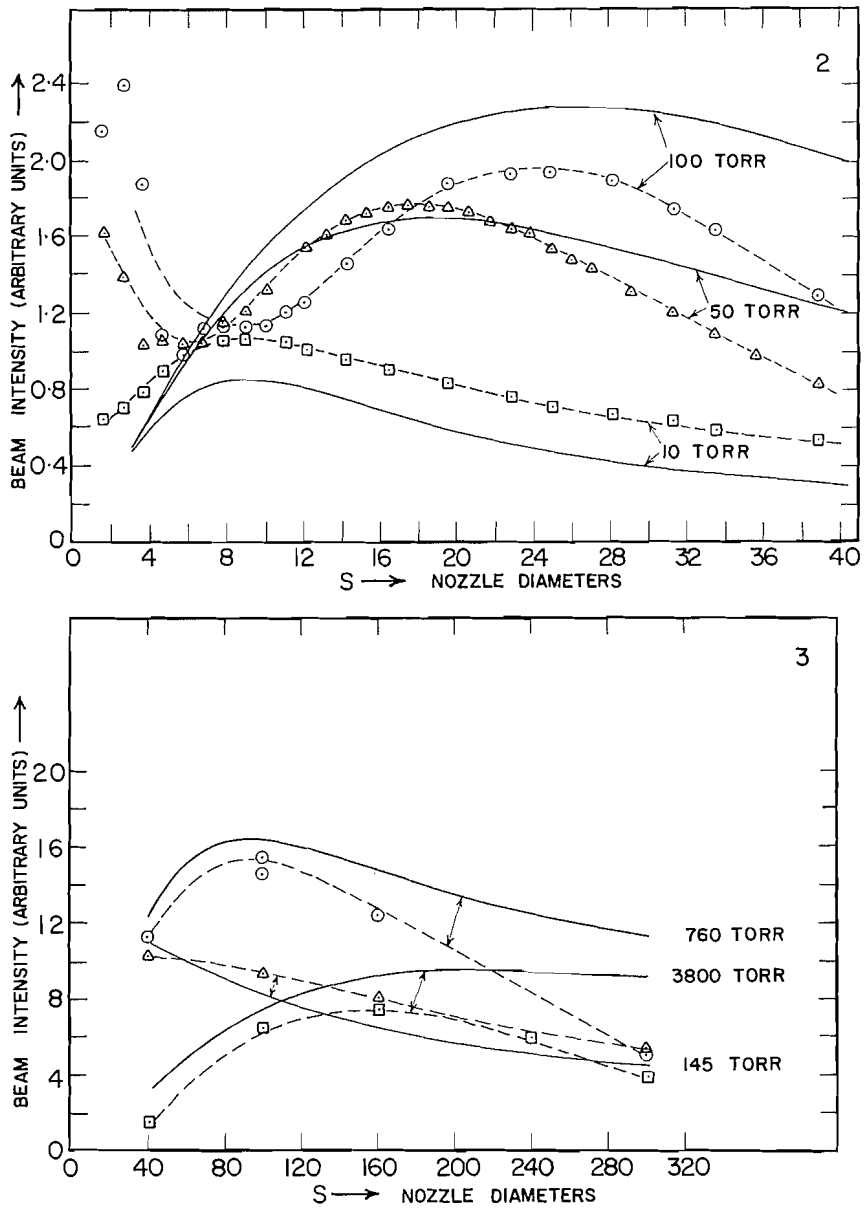

FIG. 2. Dependence of beam intensity on the distance s between the nozzle and the skimmer. The experimental points (2) are for nitrogen, and the solid lines show the intensity variations predicted by [4.1].

FIG. 3. Dependence of beam intensity on the distance s between the nozzle and the skimmer for argon beams (9). The solid curves show the variations predicted by [4.1].

the domination of the collisional term in [4.1] is overcome. This explains why the peaks occur at much larger nozzle-to-skimmer distances for argon than for diatomic gases. One can see again the characteristic fall-off of intensity with large s-values, which probably accounts for the shift of the peak position from that predicted for $p_0 = 5$ atm. It is very likely that this is connected here with a "quitting" of the expansion before it reaches the very high ratios implied by the large s-values.

Can. J. Chem. Downloaded from www.nrcresearchpress.com by 210.87.254.5 on 09/05/12
For personal use only.

However, a more interesting test of the theory may be made using the results reported by Greene, Brewer, and Milne (9). The authors have published curves of beam intensity as a function of p_0, for fixed beam geometry, with two different nozzle sizes (cf. Fig. 4). The nozzle-to-skimmer distance was 3 mm. The intensity is proportional to p_0 over a wide range, but gradually becomes less dependent on p_0 at high pressures. It is easy to understand this behavior by reference to our result [4.1]. The Mach number is now fixed by the unvarying geometry of the beam. When p_0 and hence n_0 are small the collisional term is small, and the density and intensity will be proportional to n_0. At high pressures, on the other hand, the collisional term will dominate the denominator, so that the intensity will become independent of n_0. The only effect of changing to a larger nozzle diameter is, in this view, that of reducing the ratio of nozzle–skimmer distance s to the nozzle diameter, and thus reducing the Mach number of the beam. In Fig. 4 we have plotted the predictions of our theory, using the value of c derived above, along with the experimental points. It can be seen that the behavior is qualitatively correct, and that the two curves cross at about the pressure for which this crossing is observed experimentally.

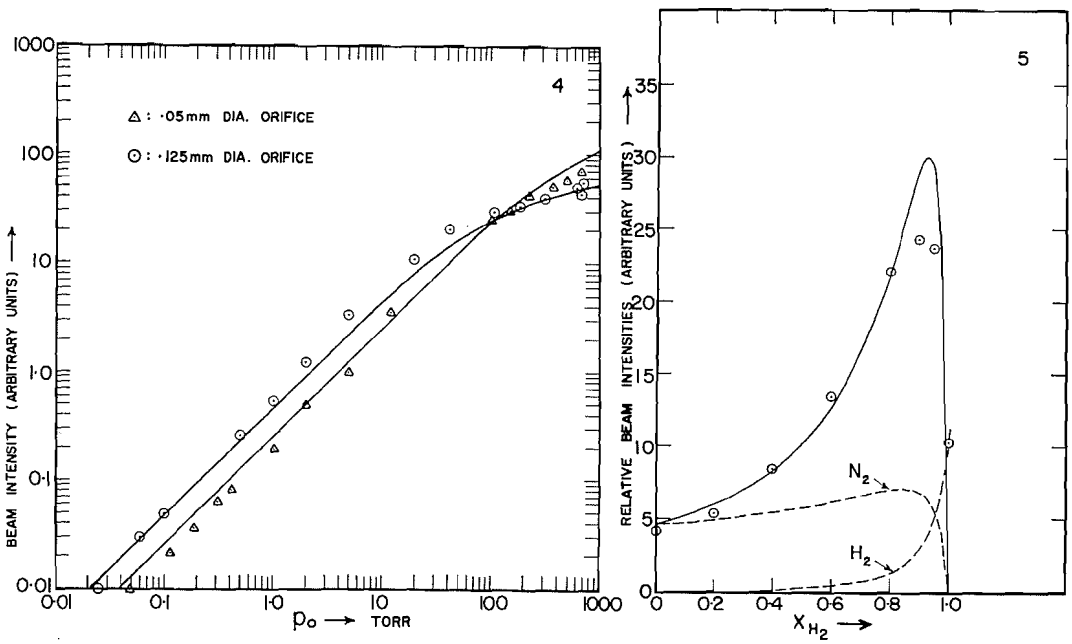

FIG. 4. Experimental (9) and predicted [4.1] pressure dependences of argon beam intensities for two different nozzle diameters.

FIG. 5. Predicted concentration dependence [3.6] of nitrogen intensity in beams formed by expanding mixtures of nitrogen and hydrogen (p_0 = 20 torr, s = 5.5 nozzle diameters), along with some experimental beam intensity values (12). The dashed lines show the intensity variations to be expected for the two gases if no collisions occurred.

Turning to mixed beams, we show in Fig. 5 the nitrogen intensity predicted by [3.6] in nitrogen–hydrogen beams of various compositions, for a stagnation pressure p_0 of 20 torr and with a fixed nozzle–skimmer distance s of 5.5 nozzle diameters. No account has been taken of the temperature dependence of the specific heat of hydrogen. The only parameter involved is the value of the nitrogen collision diameter σ, obtained from experiments on pure nitrogen beams. The figure also shows some experimental results obtained in this

laboratory (12); the agreement is very heartening. It is not surprising to find the experimental peak intensity lower than the theoretical, since the effect of mixed collisions on the intensity of the heavy gas, which we have ignored, is bound to become important for beams rich in the light gas; i.e. λ_{12} in [3.1] is not really zero.

The dashed curves show the concentration variations of the intensities of the nitrogen and hydrogen, predicted in the *absence* of any collisions. It is evident that the purely convective effect mentioned earlier leads by itself to a large enrichment of the heavy gas, but that the high intensities obtained cannot be so explained. When collisions are taken into account, the curve for the *light* gas will lie near to or below the collision-free curve shown. The relative inefficiency of mixed collisions in removing heavy molecules has therefore, according to the present argument, led to a substantial extra enrichment of the heavy gas.

These collisional effects are, of course, important only for beams with Mach numbers sufficiently low that the collisional term in the denominator of our expression [3.6] is not negligible. For beams of high Mach numbers one would therefore expect a less marked peak in the observed intensities, and this has been found to be the case (12).

Greene, Brewer, and Milne carried out many experiments on mixtures of gases, and measured the separation ratio α,

$$\alpha = \frac{(I)_1/(I)_2}{X_1/X_2}$$

where $(I)_i$ is the intensity of i molecules in the beam. It was found that α was very closely proportional to M_1/M_2, the ratio of the molecular weights. This is easy to explain in terms of our theoretical development. One can see from [3.6] that, providing the Mach number of the beam is high enough that the collisional term does not dominate the denominator, the intensity of a particular component i will be proportional to X_iM_i. This conclusion will not be affected by taking account of the mixed collisions. It leads to $\alpha = M_1/M_2$, the result obtained by Greene, Brewer, and Milne.

5. DISCUSSION

It is evident from the above that the effects of post-skimmer collisions on beam intensity and composition cannot be ignored. The theoretical development of this paper offers, in spite of the approximations involved, a description of beam intensities and composition which is better than qualitative.

There is evidently room for improvement in the theoretical development. In particular the "point source" approximation used in deriving the collision free density $n'(x)$ should be removed, and the position dependence of the collision parameter λ should be taken into account. These two approximations are only serious for small values of x, and as it happens they tend to cancel each other out in this region. This is because the former approximation overestimates the density, while the other underestimates the number of collisions which result from this density.

The theory is in an even less satisfactory position for mixtures. An effort should evidently be made to take some account of collisions between unlike molecules by solving equations like [3.1,2].

For very large values of s it is, of course, likely that the expansion will "quit" before the gases reach the skimmer, the gases going over to virtually molecular flow. This could be treated in a rough way by supposing a definite distance s_q at which the flow (suddenly) goes over from a hydrodynamic expansion regime to molecular flow. For values of s

Can. J. Chem. Downloaded from www.nrcresearchpress.com by 210.87.254.5 on 09/05/12
For personal use only.

greater than this it would be supposed that the Mach number is that corresponding to s_q. This is not simply equivalent to moving the skimmer back to s_q, however, since the collimator can now scavenge molecules from an area at s_q larger than the area of the skimmer. It should, however, prove possible to extend the theory to cover such cases.

Some most interesting work was reported recently by Reis and Fenn (4). They have measured mass separation effects in supersonic expansions sampled with impact probes. It was found (cf. Waterman and Stern (10, 13)) that the heavier gas was enriched in the probe. Reis and Fenn ascribe this separation to the existence of a detached shock wave ahead of the probe; the greater directional persistence of the heavier molecules leads to their enrichment in the probe. It should be emphasized that the experimental arrangement here is quite different from that involved in the beam experiments described earlier. In particular, the existence of substantial pressures in the "stagnation" probes will encourage the formation of shock waves; in the beam experiments the region behind the skimmer is not geometrically confined and is strongly pumped, so that the background pressure is normally in the region of 10^{-5} torr. The formation of shock waves is therefore much less likely. The mass separations we predict in beams are, for most conditions, much larger than those observed with impact probes and behave rather differently with the parameter s. It is clear that under certain conditions of dense beams, shocks may occur in front of the skimmer with accompanying mass separation; no evidence of this behavior has been identified under usual beam conditions.

A second interesting observation of Reis and Fenn was made with a "static" probe. With this, the composition of the beam was sampled by withdrawing gas *laterally* into a needle-shaped probe. No mass separation was observed. This confirms the contention of Reis and Fenn (cf. also Chow (14)) that the separation effects they observed are due to the probe, rather than intrinsic to the gas expansion. It also confirms the similar assumption made in our theoretical development: we explain separation effects in beams as due to the collimating system, not to the expansion.

ACKNOWLEDGMENTS

Acknowledgment for support of this research is made to the donors of "The Petroleum Research Fund", administered by the American Chemical Society, and to the National Research Council of Canada for a major equipment grant and for a grant in support of the molecular beam research. We are also grateful to the University of Toronto for special financial assistance with the molecular beam program.

REFERENCES

1. A. KANTROWITZ and J. GREY. Rev. Sci. Instr. **22**, 328 (1951).
2. J. M. DECKERS and J. B. FENN. Rev. Sci. Instr. **34**, 96 (1963).
3. J. P. VALLEAU and J. M. DECKERS. Can. J. Chem. **42**, 225 (1964).
4. V. H. REIS and J. B. FENN. J. Chem. Phys. **39**, 3240 (1963).
5. R. N. ZAPATA, H. M. PARKER, and J. H. BODINE. Proc. Second Intern. Symp. Rarefied Gas Dynamics, Berkeley, Calif., 1960. p. 67. (Publ. 1961).
6. J. B. FENN and J. M. DECKERS. Proc. Third Intern. Symp. Rarefied Gas Dynamics, Paris, 1962. p. 497. (Publ. 1963).
7. W. S. WOOLFF. Private communication from B. French. (These curves appeared in report 6-90-63-61 of the Lockheed Missile and Space Company, Sunnyvale, California, entitled Self-similar Development of Inviscid Hypersonic Free Jet Flow, by F. S. Sherman.)
8. P. L. OWEN and C. K. THORNHILL. Aero. Res. Council (U.K.) R and M No. 2616. (1948).
9. F. T. GREENE, J. BREWER, and TH. A. MILNE. J. Chem. Phys. **40**, 1488 (1964).
10. P. C. WATERMAN and S. A. STERN. J. Chem. Phys. **31**, 405 (1959).
11. J. B. ANDERSON and J. B. FENN. Proc. Fourth Intern. Symp. Rarefied Gas Dynamics, Toronto, July, 1964. To be published.
12. M. BOURGUIGNON, R. G. ALBRIGHT, R. L. LE ROY, J. M. DECKERS, and J. P. VALLEAU. To be published.
13. S. A. STERN, P. C. WATERMAN, and T. F. SINCLAIR. J. Chem. Phys. **33**, 805 (1960).
14. R. R. CHOW. IER Tech. Rept. HE-150-175, University of California.

Can. J. Chem. Downloaded from www.nrcresearchpress.com by 210.87.254.5 on 09/05/12
For personal use only.

APPENDIX

According to the approximation whereby the variation of λ with x is ignored (Section 2), we may write [2.4] in the form

$$[A.1] \qquad n(X) = n'(X) \Big/ \left\{1 + (\lambda n_s/\bar{v}) \int_0^X [1 - \exp(-\alpha^2/x^2)]\, dx\right\}.$$

The integral in the denominator is easily evaluated. It can be written

$$X - \int_0^X \exp(-\alpha^2/x^2)\, dx,$$

and integrating once by parts we obtain

$$X - X \exp(-\alpha^2/X^2) + 2\alpha^2 \int_0^X [\exp(-\alpha^2/x^2)/x^2]\, dx.$$

Making the substitution $y = \alpha/x$ in the final integral we obtain

$$[A.2] \qquad X[1 - \exp(-\alpha^2/X^2)] + (\pi)^{1/2}\alpha[\operatorname{erf}(\infty) - \operatorname{erf}(\alpha/X)],$$

where

$$[A.3] \qquad \operatorname{erf}(t) = \frac{2}{(\pi)^{1/2}} \int_0^t e^{-y^2}\, dy$$

and accordingly erf $(\infty) = 1$. When [A.2] is combined with [A.1] we arrive at the result [2.9].

Can. J. Chem. Downloaded from www.nrcresearchpress.com by 210.87.254.5 on 09/05/12
For personal use only.

Can. J. Chem. Downloaded from www.nrcresearchpress.com by 210.87.254.42 on 09/05/12
For personal use only.

SYNTHÈSES DE LA *TERT*-BUTYL-4 DIMÉTHYL-2,2 CYCLOHEXANONE ET DE SES DÉRIVÉS[1]

JEAN-CLAUDE RICHER ET GUY PERRAULT[2]
Département de Chimie, Université de Montréal, Montréal, Québec

Reçu le 25 mai 1964

RÉSUMÉ

Deux méthodes sont proposées pour la synthèse de la *tert*-butyl-4 diméthyl-2,2 cyclohexanone. Les configurations des alcools isomères qui dérivent de cette cétone ont été déterminées. La différence d'énergie libre entre ces deux alcools s'établit à 0.28 kcal/mole. La stéréochimie des réductions de cette cétone est examinée.

INTRODUCTION

De nombreuses études sur l'équilibre conformationel du cyclohexanol (I) ont été rapportées (voir ref. 1). Ces travaux faisant appel à des techniques directes comme l'équilibration des *tert*-butyl-4 cyclohexanols (2) ou indirectes telles que la mesure de vitesses de réaction de dérivés (3, 4), la position de bandes dans les spectres de résonance magnétique nucléaire (r.m.n.) (5) et l'examen des spectres infrarouges (6) ont permis d'établir que la différence d'énergie libre entre le cyclohexanol axial et le cyclohexanol équatorial s'établit entre 0.33 et 0.96 kcal/mole. La valeur la plus probable serait d'environ 0.8 kcal/mole (7).

I II

Aucune étude de ce genre n'a toutefois été rapportée au sujet du diméthyl-2,2 cyclohexanol (II). La synthèse des *tert*-butyl-4 diméthyl-2,2 cyclohexanols *cis* (III*a*) et *trans* (IV*a*), modèles conformationnellement fixés des triterpènes et des stéroïdes-4,4 diméthylés, a donc été réalisée et l'équilibre conformationel du diméthyl-2,2 cyclohexanol (II) a été examiné.

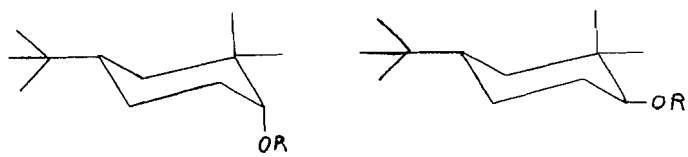

III IV

a, R = H.
b, R = *p*—NO_2—C_6H_4—COO—.
c, R = *o*—COOH—C_6H_4—COO—.

[1]*Ce travail, extrait du mémoire de maîtrise soumis par Guy Perrault à la Faculté des sciences de l'Université de Montréal, a été présenté en partie lors du 46ème congrès annuel de l'institut de Chimie du Canada, Toronto, Juin 1963.*

[2]*Boursier du Conseil National de Recherches 1962–1963.*

RÉSULTATS ET DISCUSSION

Synthèses de la tert-butyl-4 diméthyl-2,2 cyclohexanone (VIII)

Le *tert*-butyl-4 diméthyl-2,2 cyclohexanone (VIII) est préparée suivant les deux séquences de réactions résumées dans le schéma I.

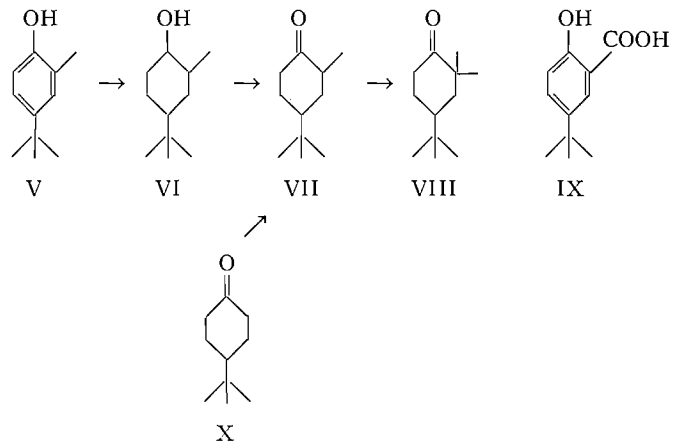

SCHÉMA I

L'hydrogénation du *tert*-butyl-4 méthyl-2 phénol (V) selon le procédé de Adams (8) conduit, après saponification du produit brut, aux divers isomères du *tert*-butyl-4 méthyl-2 cyclohexanol (VI). La stéréochimie des alcools obtenus est établie grâce aux temps de rétention rapportés par Sicher et ses collaborateurs (7), pour chacun des alcools VI. Les pourcentages relatifs de chacun des isomères sont résumés au Tableau I. Il est à noter que la stéréochimie des produits isolés par Sicher *et al.* (9) lors de l'hydrogénation de l'acide *tert*-butyl-4 salicylique (IX) est identique à celle des produits formés en prépondérance dans le présent travail.

TABLEAU I

Stéréochimie de l'hydrogénation catalytique du *tert*-butyl-4 méthyl-2 phénol (V)

Produit	Temps relatif de rétention		% formé
	Sicher	Présent travail	
cis-cis (a,e,e)*	0.630	0.680	62
trans-trans (e,e,e)*	0.775	0.800	30
trans-cis (a,a,e)*	0.833		
cis-trans (e,a,e)*	1.000	1.000	8

*Les substituants ( ) sont dans l'ordre (alcool, méthyle, *tert*-butyle).

L'oxydation du mélange des alcools épimères (VI) selon la technique de Brown et Garg (10) fournit la *tert*-butyl-4 méthyl-2 cyclohexanone (VII) n_D^{25} 1.4580, qui est caractérisée par sa semicarbazone;[3] Darzens et Rost (11) avaient rapporté que cette semicarbazone ne se forme pas. La méthylation de la *tert*-butyl-4 méthyl-2 cyclohexanone (VII) par l'iodure de méthyle en présence d'amidure de sodium selon la méthode de

Can. J. Chem. Downloaded from www.nrcresearchpress.com by 210.87.254.42 on 09/05/12
For personal use only.

Haller (12) conduit à la *tert*-butyl-4 diméthyl-2,2 cyclohexanone (VIII),[3] p.é. 61–63° à 1.5 mm Hg et n_D^{25} 1.4558.

Des expériences ayant pour but d'introduire directement deux groupements méthyles sur la molécule de *tert*-butyl-4 cyclohexanone (X) ont été tentées sans succès: la méthylation par un excès d'iodure de méthyle en présence d'amidure de sodium dans l'éther ou le benzène a toujours conduit à des mélanges réactionnels où la *tert*-butyl-4 méthyl-2 cyclohexanone (VII) est présente en prépondérance. La *tert*-butyl-4 diméthyl-2,2 cyclohexanone (VIII) peut toutefois être obtenue en procédant à deux méthylations successives de la *tert*-butyl-4 cyclohexanone (X); la cétone désirée (VIII) est obtenue aux côtés de la *tert*-butyl-4 méthyl-2 cyclohexanone (VII) dans le rapport de 72:28.

Le spectre infrarouge de la cétone *gem*-diméthylée (VIII) montre une bande cétonique à 1 708 cm^{-1} alors que pour la cétone monométhylée (VII) la bande carbonyle apparaît à 1 715 cm^{-1}; Mazur et Sondheimer (13) ont déjà noté un déplacement bathochrome semblable dans les spectres de cétones terpéniques. Dans le spectre de résonance magnétique nucléaire (r.m.n.) des cétones (VII et VIII), le groupe méthyle de la cétone (VII) se présente sous forme de doublet ($J = 4.5$) centré à 0.94 p.p.m. alors que les deux méthyles de la cétone (VIII) apparaissent respectivement à 0.97 et 1.10 p.p.m.

La réduction de la *tert*-butyl-4 diméthyl-2,2 cyclohexanone (VIII) par le sodium et l'éthanol (14) conduit au *tert*-butyl-4 diméthyl-2,2 cyclohexanol *trans* (IV*a*);[3] cet alcool de point de fusion 87–88° est purifié par l'intermédiaire de son *p*-nitrobenzoate (IV*b*) de p.f. 116.5–117.5°. L'alcool *cis* (III*a*)[3] p.f. 87–88° est obtenu par chromatographie sur alumine ou en phase gazeuse préparative du produit de réduction de la cétone selon la méthode de Meerwein-Pondorf-Varley (15); le *p*-nitrobenzoate (III*b*) de cet alcool fond à 112–113°. Il est à noter que les phtalates acides (III*c* et IV*c*) de chacun de ces alcools ont été préparés et que leurs points de fusion sont identiques à 155–156°; un mélange de ces deux phtalates acides fond à 120–125° alors qu'un mélange de deux alcools isomères fond à 65–70°.

La configuration *trans* proposée pour l'alcool obtenu par réduction de la cétone VII à l'aide du sodium et de l'éthanol est basée sur son mode de formation (14), sa rétention plus grande lors de la chromatographie sur alumine (14) et en phase gazeuse, la présence d'une bande à 1 035 cm^{-1} dans son spectre infrarouge (16), le déplacement chimique (−187 c.p.s.) de son hydrogène carbinolique (calculé d'après Eliel (17) −180 c.p.s.), la vitesse relative de saponification de son phtalate acide (4, 18, 19) et sa vitesse relative d'oxydation chromique (4, 19–22). Les propriétés respectives des alcools isomères sont résumées dans le Tableau II.

TABLEAU II

Propriétés des alcools III*a* et IV*a*

	Alcool *trans* (IV*a*)	*cis* (III*a*)
Point de fusion	87–88°	87–88°
Temps de rétention (min)*	25	22
Infrarouge†	1 035 cm^{-1}	1 023 cm^{-1}
$-\delta_N$‡	187	198.5
$10^5 \times k_2$ (l $mole^{-1}$ s^{-1})§	27.40	7.64
$10^3 \times k_2$ (l $mole^{-1}$ s^{-1})‖	11.73	19.49

*Temps de rétention lors de la chromatographie en phase gazeuse.
†Vibration de valence C—O.
‡Déplacement chimique de l'hydrogène carbinolique. Les auteurs remercient vivement le Dr. Eliel et ses collaborateurs pour la détermination de ces valeurs.
§Vitesse de saponification du phtalate acide.
‖Vitesse d'oxydation chromique de l'alcool. Les auteurs remercient sincèrement C. Gilardeau pour la détermination de ces valeurs.

[3]*Les points de fusion et les analyses des produits nouveaux sont résumés dans la partie expérimentale (Tableau V).*

Can. J. Chem. Downloaded from www.nrcresearchpress.com by 210.87.254.42 on 09/05/12
For personal use only.

Grâce aux vitesses d'oxydation et utilisant l'équation proposée par Sicher (7),

$$\Delta F = RT \ln k_{ax}/k_{eq},$$

pour relier l'énergie libre entre les alcools isomères et leurs vitesses d'oxydation, il est possible d'établir à 0.30 kcal/mole la différence d'énergie libre entre les alcools; l'équilibration directe (2) dont les résultats sont résumés au Tableau III et la r.m.n. (5) nous permettent d'établir cette valeur à 0.28 et 0.26 kcal/mole respectivement. Pour l'ensemble des méthodes employées la différence d'énergie libre entre l'alcool axial (III*a*) et l'alcool équatorial (IV*a*) est donc estimé à 0.28 ± 0.02 kcal/mole.

TABLEAU III

Équilibration des alcools (2)

Produit de départ	% *cis*	% *trans*
Alcool *cis* (III*a*)	38	62
Alcool *trans* (IV*a*)	43	57
Cétone (VIII)	40	60
Moyenne	40	60

L'examen des modèles moléculaires des alcools isomères nous montre que dans l'alcool *trans* (IV*a*), le groupe —OH équatorial est soumis à deux interactions gauches de groupes CH_3 alors que dans l'alcool *cis*, (III*a*), le groupe hydroxyle axial n'est gauche que par rapport à un seul groupement méthyle. La différence de 0.52 kcal/mole qui existe entre la valeur de 0.8 kcal/mole acceptée (7) pour le ΔF entre un OH axial et équatorial dans un cyclohexane simple et la valeur de 0.28 kcal/mole trouvée ici pour la différence d'énergie dans un cyclohexanol *gem*-diméthylé en position α doit donc être assignée à une interaction gauche entre un OH et un CH_3. Cette valeur de 0.52 kcal/mole se rapproche beaucoup des valeurs 0.5 et 0.4 kcal/mole rapportées respectivement par Sicher (7) et Noyce (23) pour l'interaction entre un groupe —OH équatorial et un groupe CH_3 axial.

Considérant que l'alcool équatorial (IV*a*) dans le système décrit ici est moins stable que le *tert*-butyl-4 cyclohexanol *trans* non substitué, les résultats obtenus (voir Tableau IV) lors de la réduction de la cétone (VIII) par les hydrures complexes peuvent difficilement s'accommoder avec la notion de "product development control" (24) et se comprennent facilement lorsqu'il est réalisé que l'un des groupes méthyles (axial en position 2) "cache" la face équatoriale du groupement carbonyle et favorise une attaque du côté le moins empêché de la molécule, à savoir la face axiale du groupement carbonyle. Le même raisonnement expliquerait la surprenante quantité d'alcool *trans* (IV*a*) (voir Tableau IV) formée au cours de l'hydrogénation catalytique de la cétone (VIII).

TABLEAU IV

Réductions de la *tert*-butyl-4 diméthyl-2,2 cyclohexanone

Agent réducteur	Rendement en alcools, %	% relatifs	
		Alcool *cis*	Alcool *trans*
PtO_2/éthanol (14)	83	25	75
PtO_2/acide acétique (4)	100	25	75
$NaBH_4$/alcool isopropylique (25)	100	8	92
$LiAlH_4$/éther anhydre (23)	99	5	95
LiAl (O-*tert*-butyl)$_3$H/THF (26)	35	0	100
Al (O-*i*-propyl)$_3$/alcool isopropylique (15)	100	55	45

Can. J. Chem. Downloaded from www.nrcresearchpress.com by 210.87.254.42 on 09/05/12
For personal use only.

TABLEAU V

Propriétés et analyses des produits nouveaux

Produit		Points de fusion	Analyse % C		% H		% N	
			Calculé	Trouvé	Calculé	Trouvé	Calculé	Trouvé
Semicarbazone de VII	$C_{12}H_{23}ON_3$	162–163	63.96	63.43	10.29	9.84	18.65	18.74
2,4-DNP de VII	$C_{17}H_{24}O_4N_4$	164–165	58.61	59.46	6.94	6.89	16.08	16.16
VIII	$C_{12}H_{22}O$		79.06	78.72	12.16	12.01		
Semicarbazone de VIII	$C_{13}H_{25}ON_3$	193–194	65.23	65.05	10.53	10.59	17.55	17.65
2,4-DNP VIII	$C_{18}H_{26}O_4N_4$	184–185	59.65	59.78	7.13	6.98	15.46	15.79
Alcool *trans* IV*a*	$C_{12}H_{24}O$	87–88	78.20	78.14	13.12	12.95		
p-Nitrobenzoate IV*b*	$C_{19}H_{27}O_4N$	116.5–117.5	68.44	68.29	8.16	8.33	4.20	4.17
Phtalate acide IV*c*	$C_{20}H_{28}O_4$	155–156	72.26	72.22	8.47	8.52		
Alcool *cis* III*c*	$C_{12}H_{24}O$	87–88	78.20	77.87	13.12	13.20		
p-Nitrobenzoate IIIb	$C_{19}H_{27}O_4N$	112–113	68.44	68.74	8.16	8.33	4.20	4.30
Phtalate acide III*c*	$C_{20}H_{28}O_4$	155–156	72.26	71.86	8.47	8.47		

PARTIE EXPÉRIMENTALE

Les points de fusion ont été déterminés en tubes capillaires ouverts au moyen d'un thermomètre étalonné avec des substances pures de pointe de fusion connus. Les spectres infrarouges ont été mesurés sur un appareil Perkin–Elmer modèle 21, double faisceau avec prisme de NaCl. Les indices de réfraction ont été déterminés à l'aide d'un réfractomètre Abbé 60. Les analyses par chromatographie en phase gazeuse sont effectuées sur un appareil Kromo-Tog, modèle K-2 de la compagnie Burrel; des colonnes de 2.5 m de polyester de Craig sur Kromat-FB 20% p/p ont été utilisées pour ces analyses. Les spectres r.m.n. ont été mesuré à l'aide d'un appareil Varian A-60 pour des solutions dans CCl_4; la position des bandes (échelles δ) en p.p.m. se réfère au tétraméthylsilane utilisé comme standard interne. Les analyses élémentaires sont de C. Daesslé, Organic Microanalysis, Montréal.

La chromatographie en phase gazeuse préparative a été effectuée sur un appareil Fisher Prep Partitioner utilisant 6 colonnes de 50 cm chacune chargées de 20% de polyester de Craig sur Chromosorb P à 160 °C.

Les 2,4-dinitrophenylhydrazones, semicarbazones, phtalates acides et *p*-nitrobenzoates ont été préparés selon les méthodes usuelles (27).

Les vitesses de saponification sont obtenues par mesure de conductivité dans une cellule de type "Freas" branchée à un pont de comparaison de la compagnie Electro-Measurements Inc, modèle 260. La cellule est immergée durant toute l'expérience dans un bain à température constante maintenue à 50 ± 0.1°.

TABLEAU VI

Vitesse de saponification des phtalates acides III*c* et IV*c* à 50 °C

Phtalate acide		Concentration (mmole/l)	10^5k (l mole^{-1} s^{-1})	
trans (IV*c*)		40.0	27.41	
		36.1	27.00	
		36.1	27.78	
	Moyenne			27.40
cis (III*c*)		36.1	7.88	
		40.0	7.40	
	Moyenne			7.64

Les mesures sont effectuées sur des solutions aqueuses équimoléculaires en soude et en sel sodé du phtalate acide à saponifier et les constantes de vitesse sont calculées d'après la méthode du temps infini (28) et les résultats sont résumés dans le Tableau VI.

REMERCIEMENTS

Les auteurs remercient vivement le Conseil National de Recherches du Canada pour l'aide financiaire apportée sous forme d'octroi de recherches (A-1295) et de bourse d'étude; la compagnie Dow Chemicals of Canada, Ltd., pour un généreux échantillon de *tert*-butyl-4 cyclohexanone et la compagnie Pitt-Consol Chemical Company, Library, Pa., pour un généreux échantillon de *tert*-butyl-4 méthyl-2 phénol.

Can. J. Chem. Downloaded from www.nrcresearchpress.com by 210.87.254.42 on 09/05/12
For personal use only.

BIBLIOGRAPHIE

1. E. L. ELIEL. J. Chem. Educ. **37**, 126 (1960).
2. E. L. ELIEL et R. S. RO. J. Am. Chem. Soc. **79**, 5992 (1957).
3. E. L. ELIEL et C. A. LUHKACK. J. Am. Chem. Soc. **79**, 5986 (1957).
4. S. WINSTEIN et N. J. HOLNESS. J. Am. Chem. Soc. **77**, 5562 (1955).
5. E. L. ELIEL et M. H. GIANNI. Tetrahedron Letters, 97 (1962).
6. G. GHIURDOGLU et W. MASSCHELEIN. Bull. Soc. Chim. Belg. **69**, 154 (1960).
7. J. SIPOS, J. KRUPICKA, M. TICHY et J. SICHER. Collection Czech. Chem. Commun. **27**, 2079 (1962).
8. R. ADAMS et J. R. MARSHALL. J. Am. Chem. Soc. **59**, 1970 (1928).
9. J. SICHER, J. SIPOS et M. TICHY. Collection Czech. Chem. Commun. **26**, 847 (1961).
10. H. C. BROWN et C. P. GARG. J. Am. Chem. Soc. **83**, 2952 (1961).
11. G. DARZENS et H. ROST. Compt. Rend. **152**, 609 (1911).
12. A. HALLER et R. CORNUBERT. Compt. Rend. **181**, 81 (1925).
13. Y. MAZUR et F. SONDHEIMER. J. Am. Chem. Soc. **80**, 6296 (1958).
14. D. H. R. BARTON et R. C. COOKSON. Quart. Rev. **10**, 44 (1956).
15. A. L. WILD. *Dans* Organic reactions. Vol. II. P. Adams (*Editor*). Wiley, New York. 1946. p. 178.
16. A. R. H. COLE, R. N. JONES et K. DOBRINER. J. Am. Chem. Soc. **74**, 5571 (1952).
17. E. L. ELIEL, M. H. GIANNI, T. H. WILLIAMS et J. B. STOTHERS. Tetrahedron Letters, 741 (1962).
18. D. CAPON, R. CORNUBERT, Y. FAGNONO et G. IVANOWSKY. Bull. Soc. Chim. France, 240 (1961).
19. G. VAVON. Bull. Soc. Chim. France, 937 (1931).
20. J. C. RICHER, L. A. PILATO et E. L. ELIEL. Chem. Ind. 2007 (1961).
21. H. FAVRE et J. C. RICHER. Can. J. Chem. **37**, 411, 417 (1959).
22. J. SCHREIBER et A. ESCHEMOSER. Helv. Chim. Acta, **38**, 1529 (1955).
23. D. S. NOYCE et L. J. DOLBY. J. Org. Chem. **26**, 3619 (1961).
24. W. G. DAUBEN, G. J. FONKEN et D. S. NOYCE. J. Am. Chem. Soc. **78**, 2579 (1956).
25. D. M. S. WHEELER et J. W. HUFFMAN. Experientia, **16**, 516 (1960).
26. H. C. BROWN et R. F. MCFARLIN. J. Am. Chem. Soc. **72**, 252 (1956).
27. R. L. SHRINER, R. C. FUSON et D. Y. CURTIN (*Editors*). The systematic identification of organic compounds. John Wiley and Sons Inc., New York. 1962.
28. F. DANIELS, J. H. MATHEWS, J. W. WILLIAMS, P. BENDER, G. W. MURPHY et R. A. ALBERTY (*Editors*). Experimental physical chemistry. McGraw-Hill Book Company Inc. 1949. p. 143.

Can. J. Chem. Downloaded from www.nrcresearchpress.com by 210.87.254.42 on 09/05/12
For personal use only.

Can. J. Chem. Downloaded from www.nrcresearchpress.com by 210.87.254.5 on 09/05/12
For personal use only.

THE OXYMERCURATION OF 4-METHYLENECYCLOHEXANEMETHANOL

N. L. WEINBERG AND GEORGE F WRIGHT
Department of Chemistry, University of Toronto, Toronto, Ontario
Received August 24, 1964

ABSTRACT

The oxymercuration of 4-methylenecyclohexanemethanol in *tert*-butyl alcohol yields 1-chloromercurimethylnorcineole which may be converted to 1-methylnorcineole by borohydride reduction or to 4-chloromercurimethyl-4-↑-hydroxycyclohexane-↓-carboxylic acid. This may be deoxymercurated to 4-methylenecyclohexanecarboxylic acid and reduced with borohydride to 4-↓-methyl-4-↑-hydroxycyclohexane-↓-carboxylic acid.

The oxymercuration of alkenols has been accomplished before. Sand and Singer (1, 2), as well as others (3), found that the hydroxyl group in 2,6-dimethylheptene-5-ol and in α-terpineol (1, 2, 4) is involved in the reaction with the consequences that cyclic ethers are formed. The same type of reaction has now been carried out with 4-methylenecyclohexanemethanol to ascertain the effect of a terminal double bond in this reaction.

When mercuric acetate in an excess of 4-methylenecyclohexanemethanol, I, is stirred for 3 days according to the method used for preparation of chloromercuricineole (4), the results are unpleasant. An unworkable gum is formed which is probably a mixture of the geoisomers of 4-acetoxymercurimethyl-4-acetoxycyclohexanemethanol, II. However, the expected product, chloromercurimethylnorcineole (III, 4-chloromercurimethyl [2,2,2,]-bicyclo-8-oxaoctane) can be obtained in 33% yield with difficulty. Dilution of the reaction system with 2,5-dioxahexane does not improve the situation, but the yield of III is doubled when *tert*-butyl alcohol is used to dilute the reaction system.

The reduction of the gum by use of sodium borohydride leads only to 4-methylenecyclohexanemethanol but reduction of III to 1-methylnorcineole, IV, occurs smoothly. The correspondence of the infrared spectrum of IV with that of 1,8-cineole which it resembles in odor leaves little doubt about its [2,2,2] bicyclic structure but it does not designate the position of the chloromercuri group in III.

This group might be linked to C-2 or C-9, depending on whether the double bond does or does not shift during oxymercuration. Two pieces of evidence show that chloromercuri is on C-9. First the substance III is recovered configurationally unchanged when it is subjected to reaction with hydrazine hydrate under conditions (5) to promote epimerization, which would be possible only at C-2. Secondly it undergoes permanganate oxidation, not to give a norcineolic acid V comparable with the cineolic acid from 2-chloromercuricineole, but instead 4-chloromercurimethyl-4-hydroxyhexanecarboxylic acid, VI. This acid can be deoxymercurated to 4-methylenecyclohexanecarboxylic acid VII and the latter may be re-oxymercurated to VI. Since VII has been characterized by ozonization to formaldehyde and the known 4-ketocyclohexanecarboxylic acid, VIII (6), it seems to be highly probable that oxymercuration of I leads to the primary chloromercurial.

Evidently the alkaline permanganate oxidation of III is accompanied by prototropic rearrangement of the carboxyl group in the product VI, probably during saponification of the lactone that is formed initially. This rearrangement is revealed when VI undergoes reduction with sodium borohydride reduction. The reduction product seems to be 4-↑-hydroxy-4-↓-methylcyclohexane-↓-carboxylic acid, IX, which is also the product when

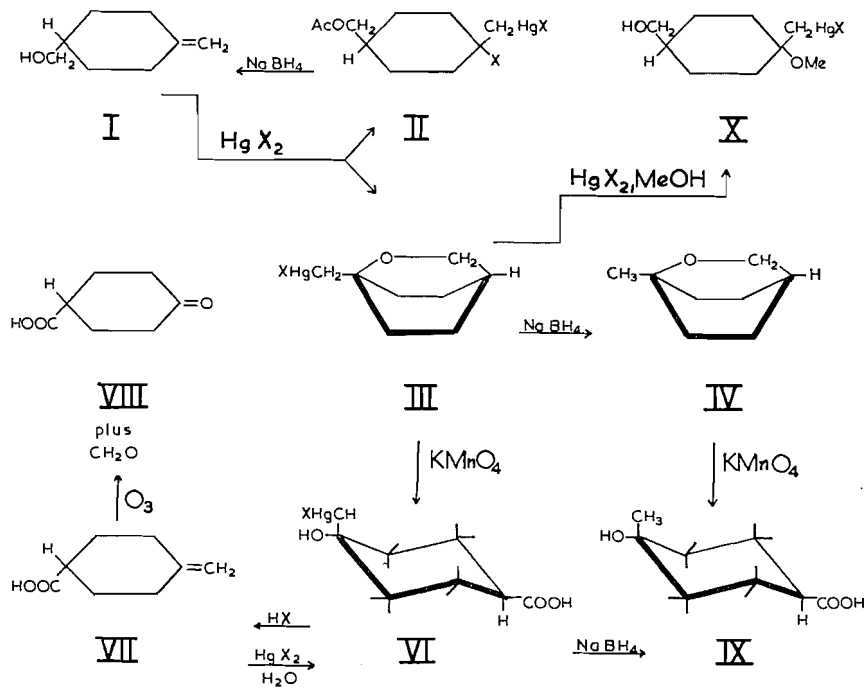

1-methylnorcineole, IV, is oxidized by means of potassium permanganate. This acid corresponds with that defined by Vila and Coll (7) as the *cis*-geoisomer. Like their acid of slightly lower melting point ours will not form a lactone (6, 8) but, instead, is dehydrated to 4-methyl-Δ^3-cyclohexanecarboxylic acid.

Besides the chemical evidence for the structure of III there is confirmation from the proton magnetic resonance spectrum. The simple spectrum of Fig. 1 shows clearly that band 3 is due to the methylene group attached to the 4-chloromercuri group because the spin interaction with ^{199}Hg gives rise to the side bands 2 and 6 spaced equally at 1.5 p.p.m. The chemical shift of the methylene portions represented by band 3 is somewhat greater (5.1 p.p.m. relative to benzene) than the values of 4.3 and 4.5 p.p.m. quoted by Cotton and Leto (9) for the chloromercurimethyl group in β-hydroxyethylmercuric acetate and the analogous anhydride respectively; this upfield shift must be attributed to the greater electrofelicity of the chlorine substituent. The 3.4 p.p.m. shift for oxymethylene (band I) and 5.3 p.p.m. for ring methylene are within the ranges 3.4–3.9 and 5.3–5.8 quoted by Chamberlain (10) for bicylic systems, while the 5.5 p.p.m. shift upfield from benzene for tertiary hydrogen is higher, probably in consequence of the cyclic distortion, than that specified (11) for this linkage in isobutane and 2,3-dimethylbutane.

It is of interest that treatment of the acetate analogue of III (X = OAc) with mercuric acetate in methanol leads to a single geoisomer of the methoxy derivative VIII rather than the expected mixture of two isomers.

EXPERIMENTAL

Physical Constants

Melting points have been corrected against reliable standards. The infrared spectra have been determined by use of a Beckman IR-4 spectrometer using polyethylene wax wafers (12 000 p.s.i.) and in carbon tetrachloride in the 900 – 3 000 cm^{-1} region and absorptions are recorded in cm^{-1} at extinctions (E) calculated from peak heights. Nuclear magnetic resonance (n.m.r.) spectra in carbon tetrachloride were determined by use of a Varian HR-60 spectrometer with the aid and advice of Professor S.S. Danyluk.

Can. J. Chem. Downloaded from www.nrcresearchpress.com by 210.87.254.5 on 09/05/12
For personal use only.

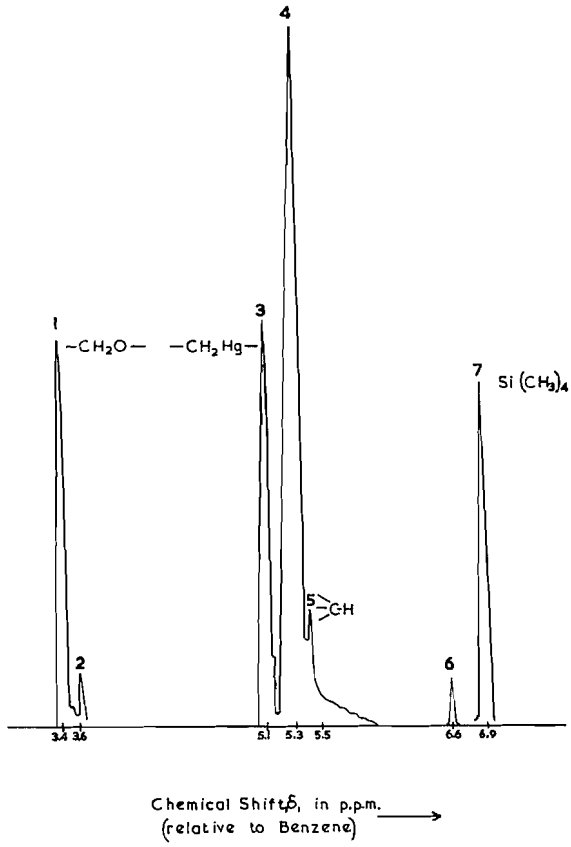

FIG. 1.

Reagents

Tertiary butyl alcohol was twice distilled from sodium wire under nitrogen (40), b.p. 82.8° at 760 mm, m.p. 25.5°. Glycol ether was distilled, after a positive benzophenone test under nitrogen, b.p. 85.5°, n_D^{20} 1.3792. Reagent grade B.D.H. mercuric acetate was recrystallized from glacial acetic acid, washed with 95% ethanol on a suction funnel, and dried at room temperature at 15 mm for 48 h. The alkene, 4-methylenecyclohexanemethanol, I, courtesy of Tennessee Eastman Company, was distilled at 40–41 °C at 0.001 mm. A heart-cut was taken, m.p. 19.5–18.5°, n_D^{20} 1.48275.

1-Chloromercurimethylnorcineole, III

(a) Use of Excess 4-Methylenecyclohexanemethanol I

Following the method of Brook and Wright (4) for the preparation of α-2-chloromercuricineole, a suspension of 82 g (0.65 mole) of 4-methylenecyclohexanemethanol I and 21 g (0.065 mole) of mercuric acetate was shaken at room temperature for 3 days. The system on filtration yielded 0.08 g of mercurous salt. Distillation of the filtrate at 0.001 mm, 28–40°, yielded 66 g (about 0.5 mole) of excess 4-methylenecyclohexanemethanol contaminated with acetic acid. The residue was suspended in 200 ml of petroleum ether (60–70°) in a separatory funnel and, on shaking, a gummy layer separated and was removed. The petroleum ether layer was then extracted with 1 × 200 and 3 × 50 ml portions of 10% aqueous sodium hydroxide, followed by 3 × 50 ml water. To the combined filtered aqueous extracts was added 12.0 g (0.2 mole) of sodium chloride, and carbon dioxide was bubbled into this solution for 12 h at 4°. Filtration by suction gave 9 g (0.25 mole), 38%, of chloromercurimethylnorcineole III, m.p. 95–97°. After three crystallizations from 95° ethanol (6 ml/g) followed by treatment with Darco, a white solid melting at 101.1–102 °C was obtained.

Anal. Calcd. for $C_8H_{13}ClHgO$: C, 26.6; H, 3.63, Found: C, 26.7; H, 3.82.

The infrared spectrum (10% in P.E. wax) is (306) 15.3, (316) 15.9, (394) 9.28, (419) 8.94, (512) 9.37, (531) 9.19, (578) 9.18, (623) 9.33, (749) 10.3, (783) 9.22, (813) 9.48.

The gum produced in this reaction seems to be a mixture. Treatment of its ether solution with an excess of mercuric chloride or with aqueous sodium chloride failed to produce a crystalline product. When 50 g was

Can. J. Chem. Downloaded from www.nrcresearchpress.com by 210.87.254.5 on 09/05/12
For personal use only.

added to 50 ml of concentrated hydrochloric acid this system underwent complete solution within 2 min. After 15 min the system was neutralized by means of 40% aqueous sodium hydroxide and the mercuric oxide was filtered off into a celite bed in a tared Buchner funnel, water washed, and air dried, weight 32 g, 0.148 mole.

The filtrate from the removal of mercuric oxide was steam distilled and the distillate was extracted 4 times with 50 ml portions of chloroform. The combined extract, dried over magnesium sulfate was distilled, finally at 8 mm, to yield 190 g (0.151 mole) b.p. 90–91°. The infrared spectrum showed that this distillate was 4-methylenecyclohexanemethanol, I, in high purity. The same compound was obtained when II was treated with sodium borohydride.

The use of 500 ml of 2,5-dioxahexane as a diluent did not diminish the formation of gum, and 11 g of mercurous salt was formed during the otherwise comparable reaction.

(b) Use of tert-Butyl Alcohol as Reaction Medium

To 19.1 g (0.06 mole) of mercuric acetate in 400 ml (4.4 mole) of tertiary butyl alcohol was added 7.7 g (0.061 mole) of 4-methylenecyclohexanemethanol, I. After stirring for 48 h at room temperature, the milky suspension was filtered giving 1.0 g of mercurous salt. The filtrate was added to 200 ml of 3% (0.1 mole) aqueous sodium chloride solution. After evaporation of the *tert*-butyl alcohol at 30–35° and 20 mm, the mercurial was filtered off by suction and dried at 40° and 15 mm, for 24 h to yield 14.4 g (0.04 mole, 67%) of chloromercurimethylnorcineole III, m.p. 98–99.5°. Two crystallizations from 95% ethanol raised the m.p. to 101–102°. A mixture melting point with a sample from part (*a*) was not depressed.

The mercurial III was deoxymercurated by treatment of 3.69 g (0.01 mole) with 25 ml of 10% hydrochloric acid. When solution was complete after 5 min the system was extracted with three 25 ml portions of petroleum ether (b.p. 60–70°). The combined extract, washed with 30 ml of water, was dried over magnesium sulfate. Evaporation of the solvent left 1.2 g (96%) which was converted to the dinitrobenzoate, m.p. 97–98°, identified by mixture melting point with an authentic sample (12).

When the mercurial III in alkaline solution was heated with an excess of 100% hydrazine hydrate an oil was formed. This oil is evidently a 40% yield of the bis-mercurial because it may be converted quantitatively to III, m.p. 98.5–99°, by treatment with an equivalent of mercuric acetate in diethyl ether and then with aqueous sodium chloride.

4-↓-Chloromercurimethyl-4↑-hydroxycyclohexane-↓-carboxylic Acid, VI

A solution of 7.6 g (0.02 mole) of chloromercurimethylnorcineole, III, in 30 ml of 10% aqueous sodium hydroxide was added to 3.2 g (0.02 mole) of potassium permanganate in 200 ml of water. After 1 day at 20–25° the excess permanganate was destroyed by addition of 5 ml of ethanol. After 1 h the system was filtered. The filtrate was vacuum evaporated to a volume of 140 ml, then treated with 1 g (0.02 mole) of sodium chloride. This solution cooled to 0° was slowly acidified by means of 1.8% hydrochloric acid until precipitation was complete. The product, filtered, water washed, and dried at 35° (15 mm), weighed 3.0 g (38%) m.p. 145° (decomp.) when the sample was inserted at 130°.

Anal. Calcd. for $C_8H_{13}ClHgO_3$: C, 24.4; H, 3.33. Found: C, 24.7; H, 3.59.

The infrared spectrum of a sample 10% in polyethylene wax is 311 (1.6), 390 (2.9), 413 (2.9), 432 (2.0), 498 (1.8), 521 (5.2), 594 (1.6), 628 (0.2), 645 (1.5), 756 (3.4), 181 (1.9), 844 (3.2).

This acid may be obtained also by treatment of 0.5 g (0.0036 mole) of 4-methylenecyclohexanecarboxylic acid, VII, with 1.29 g (0.0036 mole) of mercuric acetate in 50 ml of water for 12 h at 20–25°. Then the milky suspension was treated with 2 ml of saturated aqueous sodium chloride. The product was filtered and crystallized from 50 ml of 1:1 methanol–acetone, 0.8 g, (56%) m.p. 141–143°. The mixture melting point with the oxidation product was not lowered and the infrared spectrum was identical.

4-Methylenecyclohexanecarboxylic Acid, VII

A quantity of 7.86 g (0.02 mole) of 4-chloromercurimethyl-4-hydroxycyclohexanecarboxylic acid was dissolved in 20 ml of 6% hydrochloric acid and then was extracted 5 times with 50 ml portions of chloroform. The combined extract, washed twice with 50 ml portion of water was dried with magnesium sulfate and vacuum evaporated to leave 2.69 g (93%) of vile-smelling 4-methylenecarboxylic acid, VII, m.p. 56°. Crystallization from 16 ml of 1:7 ethanol–water raised this m.p. to 57.5–58°; Neutralization equivalent: calcd. 140; found, 141.

Anal. Calcd. for $C_8H_{12}O_2$: C, 68.6; H, 8.63. Found: C, 68.4; H, 8.65.

The infrared spectrum, 4% in carbon tetrachloride is 890 (41.4), 905 (10.6), 930 (broad, 9.85), 995 (1.24), 1 085 (3.88), 1 180 (9.76), 1 230 (30.2), 1 305 (214), 1 410 (21.1), 1 440 (16.1), 1 635 (11.3), 1 700 (74.8), 1 740 (6.59), 2 650 (broad, 15.1), 2 950 (broad, 46.0).

4-Ketocyclohexanecarboxylic Acid, VIII

Into 20 ml of sodium-dried *tert*-butyl alcohol was dissolved (0.231 g, 0.00165 mole) of 4-methylenecyclohexanecarboxylic acid XIII. Ozone (9%) was passed into this solution for 60 min at room temperature and then the ozonide was reduced with solid sodium borohydride (added pinchwise until no more oxidizing materials were present). The solution was then steam distilled into 20 ml of 95% ethanol containing 0.5 g (0.0036 mole) of dimethyldihydroresorcinol. After standing for 2 h the organic solvents were evaporated off,

Can. J. Chem. Downloaded from www.nrcresearchpress.com by 210.87.254.5 on 09/05/12
For personal use only.

leaving a solid which was filtered by suction, washed with a little methanol, and dried; weight of solid 0.11 g (0.0038 mole, 23% yield), m.p. 190°. A mixed melting point with an authentic sample of formaldehyde–dimedone was not lowered.

The steam distillation residue was examined for the other product of the ozonolysis, 4-ketocyclohexanecarboxylic acid, VIII. The solution was acidified to pH 2 and extracted with 8 × 25 ml diethyl ether. These combined ether extracts were then washed with 2 × 10 ml water and dried over magnesium sulfate. On filtration and subsequent evaporation of the ether, an oil was obtained as residue. An oxime was prepared from it and crystallized from benzene, weight 20 mg (0.00013 mole, 8% yield), m.p. 146–147° (6).

1-Methylnorcineole

A solution of 10.8 g (0.030 mole) of chloromercurimethylnorcineole, III, in 20 ml of 10% aqueous sodium hydroxide was stirred at room temperature. A second solution consisting of 0.3 g (0.006 mole) of sodium borohydride in 50 ml of 10% aqueous sodium hydroxide was added dropwise over 30 min. After 1 h, the aqueous supernatant liquid was extracted with 5 × 25 ml of diethyl ether, and the combined ether extracts washed with 3 × 10 ml water and then dried over calcium chloride for 12 h. Filtration with subsequent evaporation of the diethyl ether at 20° (15 mm) left 3.0 g (0.024 mole, 80%) of a colorless oil having an odor similar to 1,8-cineole but more penetrating. The oil was distilled at 31° (8 mm) or 155° (750 mm); n_D^{20} 1.42685; d_4^{26} 0.962.

Anal. Calcd. for $C_8H_{14}O$: C, 76.2; H, 11.2. Found C, 76.0; H, 11.3.

The infrared spectrum of this 1-methyl-1,8-norcineole is shown in Table I in comparison with the spectrum

TABLE I

Infrared spectra of methylnorcineole and cineole

Methylnorcineole	2 940 (177),	2 860 (123),	2 700 (13)	—	
Cineole	2 890 (167),	2 860 (96),	1 800 (6),	168 (15),	1 450 (75)
Methylnorcineole	1 435 (43),	1 368 (66),	1 345 (33),	1 305 (13),	—
Cineole	1 432 (45),	1 368 (96),	1 348 (72),	1 329 (14),	1 295 (35)
Methylnorcineole	1 240 (27),		1 200 (52),	1 170 (31),	1 110 (32)
Cineole	1 262 (25),	1 223 (49),	1 205 (86),	1 165 (64),	1 110 (30)
Methylnorcineole		1 032 (172),	1 010 (33),	—	935 (94)
Cineole	1 072 (105),	1 045 (69),	1 009 (27),	975 (3),	922 (8)
Methylnorcineole	913 (9),	872 (10),	855 (55),	—	
Cineole	915 (22),	880 (8),	857 (8),	835 (45)	

of 1,8-cineole, both 0.128 *M* in carbon tetrachloride. The parenthetical values are extinction coefficients for the indicated wave numbers.

4-↓-Methyl-4↑-hydroxycyclohexane-↓-carboxylic Acid, IX

(a) From 1-Methylnorcineole, IV

To a solution of 2.5 g (0.016 mole) of potassium permanganate in 150 ml of water was added 0.5 g (0.004 mole) of methylnorcineole, IV. After 1 day at 20–25° the system was treated with 2 ml of ethanol. When the pink color had disappeared the mixture was filtered. The filtrate, concentrated to a volume of 50 ml by evaporation, was chilled to 0° and acidified by means of 16% hydrochloric acid. The precipitated acid weighed 0.4 g (63%), m.p. 156–156.5°. Crystallization from hot water raised this m.p. to 156.2–156.5°.

Anal. Calcd. for $C_8H_{14}O_3$: C, 60.7; H, 8.92. Found: C, 60.6; H, 8.95.

When this acid was heated at 90° for 30 min (8) the lactone, m.p. 60–70°, was not formed. Instead 4-methyl-Δ^3-cyclohexenecarboxylic acid, m.p. 99–100°, was obtained by chloroform extraction. It formed a dibromide, m.p. 104°.

(b) From 4-Chloromercurimethyl-4-hydroxycyclohexanecarboxylic Acid, VI

A solution of 0.8 g (0.002 mole) of VI in 10 ml of 1% aqueous sodium hydroxide was heated with 0.10 g (0.0026 mole) of solid sodium borohydride during 15 min. One hour later 0.35 g (0.0018 atom) of metallic mercury was filtered off. The filtrate was evaporated to a volume of 3 ml and then was acidified by use of 5% aqueous sulfuric acid. With cooling to 0°, the crude acid 0.3 g (94%), m.p. 149–155°, was crystallized from water for mixture melting point (not depressed) with IX from the oxidation procedure.

4-Chloromercurimethyl-4-methoxycyclohexanemethanol, X

To a solution of 4.45 g (0.012 mole) of chloromercurimethylnorcineole, III, in 100 ml of pure, dry, oxygen-free methanol was added 2.0 g (0.012 mole) of silver acetate. After stirring for 0.5 h under nitrogen, the silver chloride was filtered off and 2 ml of glacial acetic acid was added along with 3.8 g (0.0012 mole) of mercuric acetate. The solution was shaken for 95 h at room temperature, but still tested positive for mercuric salt with 10% sodium hydroxide solution. Then the solution was basified with 10% aqueous sodium hydroxide and filtered by suction, using Celite, to remove mercuric oxide. On addition of 5 ml of saturated aqueous sodium chloride solution, carbon dioxide was bubbled into the system. After 1 h, 2.3 g of fluffy white solid was

Can. J. Chem. Downloaded from www.nrcresearchpress.com by 210.87.254.5 on 09/05/12
For personal use only.

filtered off, m.p. 156–158°. The solid was recrystallized from 50 ml of 50% aqueous ethanol and dried over KOH pellets for 24 h at 65°(10 mm), m.p. 157–158°.

This methoxymercurial was soluble but stable in 10% aqueous sodium hydriodide. It was recovered almost completely after 0.30 g was dissolved in 10 ml acetic anhydride although 12 mg of mercurous chloride precipitated during the process.

Anal. Calcd. for $C_9H_{17}ClHgO_2$: C, 27.3; H, 4.36. Found: C, 27.3; 4.45.

The infrared spectrum, 3% in potassium bromide, was 2 925 (220), 2 850 (200), 2 925 (220), 2 850 (200), 1 625 (58.2), 1 450 (77.5), 1 430 (86.4), 1 320 (87.6), 1 265 (76.0), 1 220 (46.8), 1 200 (49.3), 1 170 (77.5), 1 145 (71.8), 1 135 (71.8), 1 097 (80.4), 1 060 (284), 1 045 (250), 997 (48.0), 970 (86.4), 950 (104), 925 (83.3), 877 (134), 798 (29.2), 755 (63.5), 705 (64.8).

The formation of this single methoxymercurial from acetoxymercurimethylnorcineole is in contrast to the pair of methoxymercurials obtained from I and mercuric acetate in methanol. One of the pair melted at 157–158 and the other at 118–119°, after separation by crystallization from methanol.

REFERENCES

1. SAND and SINGER. Ber. **35**, 3170 (1902).
2. SAND and SINGER. Ann. **329**, 166 (1903).
3. A. G. BROOK, A. RODGMAN, and G. F WRIGHT. J. Org. Chem. **17**, 988 (1952).
4. A. G. BROOK and G. F WRIGHT. J. Org. Chem. **22**, 1314 (1957).
5. G. F WRIGHT. Can. J. Chem. **30**, 268 (1952).
6. W. H. PERKIN, JR. J. Chem. Soc. **85**, 416 (1904).
7. J. P. VILA and C. COLL. Anales Real Soc. Espan. Fis. Quim. Madrid, Ser. B, **49**, 547 (1955); Chem. Abstr. **49**, 8143*f* (1955).
8. W. H. PERKIN, JR. J. Chem. Soc. **85**, 660 (1904).
9. F. R. COTTON and J. R. LETO. J. Am. Chem. Soc. **80**, 4823 (1958).
10. N. F. CHAMBERLAIN. Anal. Chem. **31**, 56 (1959).
11. J. A. POPLE, W. G. SCHNEIDER, and H. J BERNSTEIN. High Resolution nuclear magnetic resonance. McGraw-Hill, New York. 1959. p. 78.
12. C. HAGGIS and L. N. OWEN. J. Chem. Soc. 404 (1953).

Can. J. Chem. Downloaded from www.nrcresearchpress.com by 210.87.254.5 on 09/05/12
For personal use only.

Can. J. Chem. Downloaded from www.nrcresearchpress.com by 210.87.254.42 on 09/05/12
For personal use only.

THE WATER-SOLUBLE POLYSACCHARIDES OF DERMATOPHYTES

IV. GALACTOMANNANS I FROM TRICHOPHYTON GRANULOSUM, TRICHOPHYTON INTERDIGITALE, MICROSPORUM QUINCKEANUM, TRICHOPHYTON RUBRUM, AND TRICHOPHYTON SCHÖNLEINII[1]

C. T. BISHOP AND M. B. PERRY
Division of Biosciences, National Research Council, Ottawa, Canada
AND
F. BLANK
The Skin and Cancer Hospital, Temple University School of Medicine, Philadelphia, Pennsylvania
AND
F. P. COOPER
Division of Biosciences, National Research Council, Ottawa, Canada

Received September 18, 1964

ABSTRACT

A group of polysaccharides, called galactomannans I, were precipitated as their insoluble copper complexes from aqueous solutions of the crude polysaccharides obtained from each of the organisms designated in the title. The five galactomannans I were homogeneous under conditions of electrophoresis and ultracentrifugation and had high positive specific rotations. The major constituent monosaccharide was D-mannose; amounts of D-galactose ranged from nil for the polysaccharide from *T. rubrum* to 13% for that from *T. schönleinii*. Methylation and hydrolysis of the five galactomannans I yielded varying amounts of the following: 2,3,5,6-tetra-*O*-methyl-D-galactose (not present in the products from *T. rubrum*), 2,3,4,6-tetra-*O*-methyl-D-mannose, 2,3,4-tri-*O*-methyl-D-mannose, 2,4,6-tri-*O*-methyl-D-mannose, 3,4-di-*O*-methyl-D-mannose, and 3,5-di-*O*-methyl-D-mannose. Periodate oxidation results agreed with the methylation studies. The gross structural features of each galactomannan I appear to be the same, namely, a basic chain of $1 \rightarrow 6$ linked α-D-mannopyranose units for approximately every 22 of which there is a $1 \rightarrow 3$ linked α-D-mannopyranose residue. Branch points occur along the $1 \rightarrow 6$ linked chain at the C_2 positions of the D-mannopyranose units and once in every 45 units at the C_2 position of a $1 \rightarrow 6$ linked D-mannofuranose residue. The D-galactose in the polysaccharides is present exclusively as non-reducing terminal furanose units; non-reducing terminal units of D-mannopyranose are also present. The variations in the identities and relative amounts of the non-reducing terminal units were the only apparent differences in the gross structural features within this group of polysaccharides.

The objective of this continuing program on polysaccharides of dermatophytes is to relate polysaccharide structure to species differences and immunological properties. As reported previously (1), preliminary examination of five dermatophytes showed that each had a similar pattern of water-soluble polysaccharides, specifically, two galactomannans and a glucan. At present the investigations will be limited to comparisons of gross structural features of the polysaccharides in each of the above three groups as revealed by methylation and periodate oxidation studies. The results of immunochemical tests may necessitate more detailed studies of fine structure at a later stage.

The present paper describes the isolation and gross structural features of one group of galactomannans (called galactomannan I) from *Trichophyton granulosum* Sabouraud, 1909, *Trichophyton interdigitale* Priestley, 1917, *Microsporum quinckeanum* (Zopf) Guiart and Grigorakis, 1928, *Trichophyton rubrum* (Castellani) Sabouraud, 1911, and *Trichophyton schönleinii* (Lebert) Langeron and Milochevitch, 1930.

Crude polysaccharides were extracted from powdered cells of the organisms in yields of 5–10% as described previously for *T. granulosum* (2). The products were tan-colored

[1]*Issued as N.R.C. No. 8201.*

powders which contained significant amounts of ash and nitrogen, yielded mannose, glucose, and galactose on hydrolysis, and showed at least three migrating components on moving-boundary electrophoresis in borate buffer. Fehling solution, added to aqueous solutions of the crude polysaccharides from each organism, precipitated the first group of polysaccharides as insoluble copper complexes (3). Recovery of the polysaccharides from their insoluble copper complexes yielded ash-free, nitrogen-free products, each of which showed a single, sharp, symmetrical peak under conditions of electrophoresis and ultracentrifugation. Table I shows some of the properties of this group of polysaccharides,

TABLE I

Properties of galactomannans I from dermatophytes

Organism	$[\alpha]_D$ (in water)	Hydrolysis products, %		$\mu \times 10^{-5}$ ($cm^2\ V^{-1}\ s^{-1}$)
		D-Galactose	D-Mannose	
T. granulosum	+78°	7.5	92.5	8.4
T. interdigitale	+80°	12.0	88.0	8.4
M. quinckeanum	+78°	4.5	95.5	8.4
T. rubrum	+80°	0.	100.	8.4
T. schönleinii	+64°	13.0	87.0	8.4

called galactomannans I. The specific rotations were high and positive and the only one which differed significantly from the others was that of the galactomannan I from *T. schönleinii*. Because the constituent sugars were identified as the D-enantiomorphs, the high, positive specific rotations indicated that the majority of glycosidic linkages in the galactomannans I were in the α-configuration. The major constituent monosaccharide was D-mannose and the amount of D-galactose in the polysaccharides ranged from 13% for the one from *T. schönleinii* to 0 for that from *T. rubrum*. This latter polysaccharide must therefore be classified as a mannan; for comparative purposes and because of its obvious association with the other polysaccharides in this group, it is included in the galactomannans I. The polysaccharides in Table I were indistinguishable by electrophoresis, having identical mobilities in borate buffer.

The galactomannans I were methylated fully and then hydrolyzed to yield mixtures of D-mannose and D-galactose methyl ethers. These mixtures were analyzed by a combination of gas–liquid, paper, and thin-layer chromatography. The gas–liquid chromatogram of one typical mixture is shown in Fig. 1. The two components in peak 1 were resolvable on another liquid phase and also by paper chromatography. Some 3,5-di-*O*-methyl-D-mannose was also present in the hydrolysis products but in amounts too small to be shown in Fig. 1. The relative amounts of *O*-methyl sugars in the mixtures were determined by integration of the peaks on the gas–liquid chromatograms and these results were checked by preparative paper chromatography. The amount of 3,5-di-*O*-methyl-D-mannose was determined, as a percentage of the di-*O*-methyl fraction, by the quantities isolated from thin-layer chromatograms. The quantitative results for each of the galactomannans I are given in Table II; each of the *O*-methyl sugars was characterized by isolation of a crystalline derivative. The molar ratios are based on a degree of polymerization of 45 which was the value found for the methylated galactomannans I by osmometry.

From these results it is clear that the polysaccharides in this group contain the same structural units with some variations in the relative amounts of such units. Thus, branch points occur in each polysaccharide at the C_2 and C_6 positions of D-mannopyranose and to a lesser extent of D-mannofuranose units, giving rise to the 3,4- and 3,5-di-*O*-methyl-D

Can. J. Chem. Downloaded from www.nrcresearchpress.com by 210.87.254.42 on 09/05/12
For personal use only.

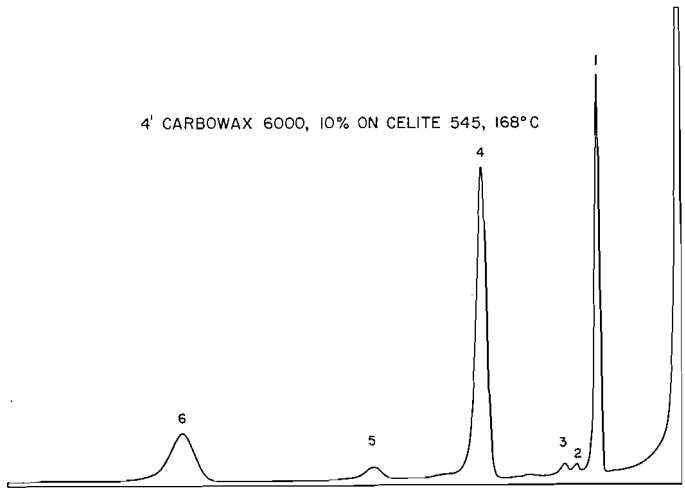

FIG. 1. Gas–liquid chromatograph of methyl glycosides of hydrolysis products from methylated galactomannan I of *T. interdigitale*. (1) Methyl 2,3,4,6-tetra-*O*-methyl-α-D-mannoside and methyl 2,3,5,6-tetra-*O*-methyl-α-D-galactoside, (2) methyl 2,3,5,6-tetra-*O*-methyl-β-D-galactoside, (3) methyl 2,3,4,6-tetra-*O*-methyl-β-D-mannoside, (4) methyl 2,3,4-tri-*O*-methyl-α-D-mannoside (shoulder following peak 4 is methyl 2,4,6-tri-*O*-methyl-α-D-mannoside), (5) methyl 2,3,4-tri-*O*-methyl-β-D-mannoside, (6) methyl 3,4-di-*O*-methyl-α-D-mannoside.

mannoses respectively. The unbranched portions of the galactomannans I are formed predominantly by 1 → 6 linked D-mannopyranose units yielding 2,3,4-tri-*O*-methyl-D-mannose in the methylation study. For every 20–22 of such linkages there is one D-mannopyranose unit which participates in a 1 → 3 linkage as shown by the presence of 2,4,6-tri-*O*-methyl-D-mannose. Some of the non-reducing terminal units are D-mannopyranose giving 2,3,4,6-tetra-*O*-methyl-D-mannose; others are formed by D-galactofuranose residues which give 2,3,5,6-tetra-*O*-methyl-D-galactose. The latter was the only derivative of D-galactose found in the products from methylation and showed that this sugar was present in the polysaccharides exclusively as non-reducing, terminal furanose residues. This conclusion was supported by an earlier, more detailed investigation (4) of one of these galactomannans I where it was shown that all of the D-galactose could be removed by mild acid hydrolysis leaving an undegraded mannan. The amount of 2,3,5,6-tetra-*O*-methyl-D-galactose in the products from two of the galactomannans I, those from *T. granulosum* and *M. quinckeanum*, did not account for all of the D-galactose present in the polysaccharide (cf. Table I). These losses could not have occurred by evaporation of this volatile product after hydrolysis of the methylated polysaccharide because the amount of end-group corresponded to the branch points as required by theory. The D-galactofuranose units must therefore have been lost during the methylation, possibly by oxidative degradation or hydrolysis under alkaline conditions. Similar loss of D-galactofuranose units during methylation has been reported in the investigation of a galactomannan-peptide fraction from *T. mentagrophytes* (5).

The methylation results showed that each of the five polysaccharides in this group contained the structural units I–VI and were very similar indeed. The range of numbers given for each unit indicates the maximum variation in the amounts of that unit within the group of polysaccharides; it does not represent the limits of error in its estimation. Table III shows the results of periodate oxidation of the galactomannans I and the values calculated from structural units I–VI for each polysaccharide. The agreement was good and the results therefore supported the conclusions based on the methylation studies.

Can. J. Chem. Downloaded from www.nrcresearchpress.com by 210.87.254.42 on 09/05/12
For personal use only.

Can. J. Chem. Downloaded from www.nrcresearchpress.com by 210.87.254.42 on 09/05/12
For personal use only.

TABLE II

Hydrolysis products from methylated galactomannans I

O-Methyl sugar	*T. granulosum* (%)	(Moles)*	*T. interdigitale* (4) (%)	(Moles)*	*M. quinckeanum* (%)	(Moles)*	*T. rubrum* (%)	(Moles)*	*T. schönleinii* (%)	(Moles)*
2,3,5,6-Tetra-*O*-methyl-D-galactose	0.6	(0.25)	11.8	(5.0)	2.5	(1.06)	0.0	(0.0)	11.0	(4.6)
2,3,4,6-Tetra-*O*-methyl-D-mannose	26.6	(11.3)	14.9	(6.3)	27.6	(11.7)	28.5	(12.0)	13.8	(5.8)
2,3,4-Tri-*O*-methyl-D-mannose	48.2	(21.7)	46.6	(21.0)	44.8	(20.2)	42.2	(19.0)	46.2	(20.8)
2,4,6-Tri-*O*-methyl-D-mannose	2.0	(0.9)	1.8	(0.8)	1.4	(0.6)	1.8	(0.8)	2.1	(0.9)
3,4-Di-*O*-methyl-D-mannose	21.5	(10.4)	23.7	(11.4)	22.5	(10.8)	25.3	(12.2)	25.6	(12.3)
3,5-Di-*O*-methyl-D-mannose	1.1	(0.5)	1.2	(0.5)	1.2	(0.5)	2.2	(1.0)	1.3	(0.6)

*Per 45 unit polysaccharide.

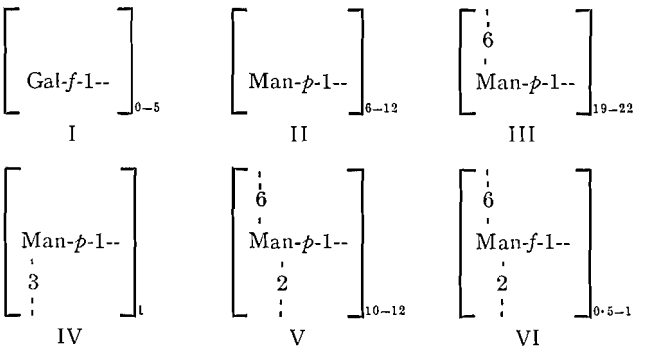

TABLE III

Periodate oxidation of galactomannans I

Organism	Periodate consumed*		Formic acid produced*	
	Calcd.	Found	Calcd.	Found
T. granulosum	1.70	1.60	0.73	0.77
T. interdigitale	1.72	1.73	0.62	0.67
M. quinckeanum	1.72	1.60	0.72	0.73
T. rubrum	1.67	1.60	0.69	0.71
T. schönleinii	1.67	1.60	0.59	0.52

*In moles per mole anhydrohexose.

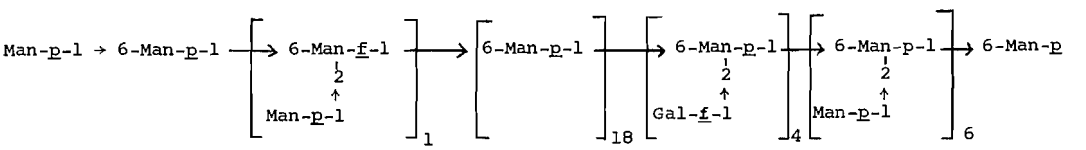

FIG. 2. General structure for galactomannans I.

The simplest general structure that can be proposed for this group of polysaccharides is shown in Fig. 2. This visualizes a basic chain of $1 \rightarrow 6$ linked α-D-mannopyranose units, with approximately one α-D-mannofuranose unit in every 45 residues. Single unit side chains of D-mannopyranose and D-galactofuranose are attached at intervals along the basic chain through the C_2 position of the D-mannose units. The structure in Fig. 2 is based on a polysaccharide of 45 units because that was the degree of polymerization found for the methylated galactomannans I by osmometry. The differences between the individual polysaccharides in this group then arise in the identity and number of non-reducing terminal units which form or terminate the side chains. The present evidence does not permit any conclusions about the length or distribution of side chains but variations in this aspect of the structure cannot be great because infrared spectra of each of the polysaccharides were superimposable.

It is tempting to speculate that polysaccharides with such similar structural features would display the same serological characteristics. However, it has been shown (6, 7) that the nature of non-reducing terminal units, and the structural units adjacent to them, are important factors in determining the specificity of a polysaccharide in serological reactions. The variations in non-reducing terminal units found in the galactomannans I may therefore be sufficient to confer serological specificity. Immunochemical tests presently

Can. J. Chem. Downloaded from www.nrcresearchpress.com by 210.87.254.42 on 09/05/12
For personal use only.

being done in the laboratory of one of the authors (F.B.) should provide definitive evidence on this point. Although it is possible that the structural variations found in this group of polysaccharides were caused by partial degradation to different extents during isolation, this is considered unlikely because exactly the same conditions were used throughout. Fuke (8) reported that polysaccharides from six pathogenic fungi (only one of which, *T. interdigitale*, is included in the present study) gave cross-serological reactions and were therefore not specific for the organism. However, the crude polysaccharide preparations used in that work were not tested for homogeneity and cross reactions of non-specific components could have interfered with the tests. Barker and co-workers (5) have studied the structure of a galactomannan-peptide allergen from *T. mentagrophytes* and have attributed the "immediate" and "delayed" hypersensitivity responses elicited by the molecule to the carbohydrate and protein moieties respectively. The carbohydrate portion was shown to contain D-galactofuranose non-reducing terminal units as in the galactomannans I described in the present paper. However, the D-mannose units in the glycopeptide from *T. mentagrophytes* were joined predominantly by $1 \rightarrow 2$ and $1 \rightarrow 4$ linkages while those in the galactomannans I were linked predominantly $1 \rightarrow 6$ with $1 \rightarrow 2$ glycosidic bonds occurring only at branch points. Since the aim of the present work is to relate structure to serological properties in the *polysaccharides* from dermatophytes the products were freed of protein which would undoubtedly interfere in the serological tests.

Gross structures of the two other groups of polysaccharides, the glucans and the galactomannans II, will be described in subsequent papers; a study of one of the glucans has already been published (1). The galactomannan from *T. granulosum* that was described earlier (2) is now known to have been a mixture. The criteria of homogeneity used in that work were (*a*) a single fraction by chromatography on diethylaminoethyl cellulose (9) and (*b*) a single peak on moving boundary electrophoresis (10). Since that time it has been found that the galactomannans I and II from a single organism are not separable by method (*a*) but can be resolved by precipitation of galactomannan I as its insoluble copper complex. The two galactomannans thus separated had very similar electrophoretic mobilities, 8.4×10^{-5} and 8.1×10^{-5}, requiring prolonged electrophoresis to see even a partial separation.

The structural relation between the polysaccharides described here and those isolated from other sources have been adequately discussed in other papers (2, 4, 5).

EXPERIMENTAL

Paper chromatograms were run by the descending method using the following solvent systems (v/v):
(*a*) pyridine : ethyl acetate : water—1:2.5:2.5 (upper phase).
(*b*) butanone saturated with water.
(*c*) butan-1-ol : ethanol : water—3:1:1.

R_g values represent movement relative to 2,3,4,6-tetra-*O*-methyl-D-glucose. Whatman 3MM paper was used for paper electrophoreses (11) in 0.1 *M* sodium tetraborate at 750 V (potential gradient, 25 V/cm) and 25–40 mA for 1.5 h; M_g values represent movement relative to glucose. A Tiselius-type, Spinco model H apparatus was used for moving boundary electrophoresis in 0.05 *M* borate buffer (10). A Pye Argon Chromatograph and an F and M Model 500 chromatograph were used for gas–liquid chromatography (12); the column packings were (A) 10% carbowax 6 000 on Chromosorb W, 100–120 mesh, 150 °C, (B) 15% polyphenyl ether on Gas Chrom A, 100–120 mesh, 150 °C. Thin-layer chromatograms were on silica gel G using benzene : acetone—1:1 as developing solvent (13). Preparative thin-layer chromatography was done on 0.6 mm layers of silica gel G on 20 × 20 cm glass plates. Zones on the preparative thin-layer chromatograms were detected by a transfer technique: guide strips of thoroughly wet Whatman No. 1 paper were pressed onto the plate which had been sprayed with methanol. The strips were then removed, air dried, and sprayed to provide a template of the chromatogram. The separate zones were then marked, scraped from the plate, and the products were recovered by elution with methanol. Sugars on paper chromatograms, electrophoretograms, and thin-layer templates were detected by the *p*-anisidine hydrochloride spray

Can. J. Chem. Downloaded from www.nrcresearchpress.com by 210.87.254.42 on 09/05/12
For personal use only.

reagent (14). Solvents were evaporated at 35–40 °C under diminished pressure; melting points are corrected; specific rotations are equilibrium values unless otherwise specified.

Isolation of Crude Polysaccharides

T. granulosum was grown in a liquid medium containing 4% maltose (2); *T. interdigitale, M. quinckeanum, T. Rubrum,* and *T. Schönleinii* were grown on a solid medium consisting of 4% cerelose (glucose), 1% neopeptone "Difco", 0.05% yeast extract "Difco", 0.001% thiamine, 0.005% inositol, and 1.5% agar made up in tap water. The polysaccharides were extracted from the dried mycelia as described previously for *T. granulosum* (2). The polysaccharide preparations were light brown powders containing 0.5–0.7% of nitrogen and 5–8% of ash. Yields based on the weight of dried mycelium ranged from 4.7% for *M. quinckeanum* to 10% for *T. granulosum* and the total amounts of crude polysaccharides obtained were between 80 and 100 g. Hydrolysis of samples (5 mg) of each preparation by *N* sulfuric acid (1.5 ml) at 97 °C in a sealed tube for 12 h yielded glucose, galactose, and mannose as shown by paper chromatography of the hydrolysate in solvent A.

Isolation of Galactomannans I

The crude polysaccharides from each organism were fractionated by addition of Fehling solution according to the following typical experiment. Crude polysaccharide (60 g) was suspended in water (250 ml); to the stirred mixture was added Fehling solution B (600 ml) in which the polysaccharides dissolved completely. Addition of Fehling solution A (600 ml) caused formation of a blue, curdy precipitate and the mixture was stirred for a further 1/2 h. The precipitate was removed by centrifugation, washed three times with water (600 ml each time) in a Waring Blendor, and suspended in ice water (300 ml). The copper complex was decomposed by addition of acetic acid at such a rate that the temperature never rose above 10 °C. The clear solution was diluted with methanol until precipitation was complete. The gummy precipitate, which was allowed to settle out overnight, was dissolved in water (200 ml) and the solution was deionized by passage through columns of Amberlite ion-exchange resins IR-120 and IR-45. The deionized solution was concentrated to a thin sirup to which ethanol was then added until precipitation was complete. The precipitate was removed by centrifugation, washed successively with ethanol, ether, and light petroleum (b.p. 30–60 °C), and then dried to yield galactomannan I. Yields based on the crude polysaccharide preparations were as follows: *T. granulosum* (32.2%), *T. interdigitale* (27.0%), *M. quinckeanum* (13.7%), *T. rubrum* (37.2%), and *T. schönleinii* (32.0%). Samples (150 mg) of each of these galactomannans I were dissolved separately in 0.05 *M* sodium tetraborate (15 ml), equilibrated with the same buffer by dialysis, and examined by moving boundary electrophoresis (10). Each sample showed a single, sharp, symmetrical peak throughout the test which ran for 6.5 h (mobilities are given in Table I). The sample solutions were recovered from the electrophoresis experiments and centrifuged in a model E Spinco ultracentrifuge at 20 °C for 80 min at a rotor speed of 59 000 r.p.m.; only a single component was detected in each sample.

Estimation and Identification of Constituent Sugars

Hydrolysis of each of the above polysaccharides, under conditions given for hydrolysis of the crude preparations, yielded mannose as the major constituent sugar with smaller amounts of galactose as shown by paper chromatography in solvent A. Samples (20 mg) of each galactomannan I in *N* hydrochloric acid (1 ml) had the initial specific rotations given in Table I. These rotations changed when the solutions were heated on a boiling water bath and reached the following constant values after 4.5 h: *T. granulosum* (+19.5%), *T. interdigitale* (+22.5°), *M. quinckeanum* (+17.4°), *T. rubrum* (+14.6°), and *T. schönleinii* (+23°). The percentages of D-mannose and D-galactose given in Table I were calculated from the final specific rotations of the hydrolysates. They were confirmed (mean deviation ±1.0 in 100) by the phenol–sulfuric acid method (15) after separation of the sugars by paper chromatography (solvent A) and by gas–liquid chromatography of the acetylated alditols derived from the sugars in the hydrolysate (16).

The sugars in hydrolysates of 100 mg of each polysaccharide were isolated by preparative paper chromatography (solvent A) and characterized as D-galactose and D-mannose by preparation of the phenylosazone (17), m.p. 194–196 °C, and the *p*-nitroanilide (18) m.p. 217–218 °C, respectively. Melting points of mixtures of these two products with their respective authentic samples were not depressed.

Methylation of Galactomannans I

The galactomannans I from *T. granulosum* (4.5 g), *T. interdigitale* (5.0 g), *M. quinckeanum* (5.0 g), *T. rubrum* (4.5 g), and *T. schönleinii* (4.0 g) were each dissolved in water (25 ml) and methylated by the dropwise addition of dimethyl sulfate (25 ml) and 40% aqueous sodium hydroxide (50 ml) (19). Four additions of the same amounts of reagents were made in the first 10 h and then a further five additions were made, one every 24 h. The partially methylated products were recovered in good yield by extraction into chloroform; yields, *T. granulosum* (4.4 g), *T. interdigitale* (5.4 g), *M. quinckeanum* (5.1 g), *T. rubrum* (4.6 g), and *T. schönleinii* (3.8 g). These products contained 37–40% of methoxyl groups and were further methylated by Purdie reagents (20) to yield fully methylated galactomannans I having no hydroxyl absorption in the infrared. Yields and methoxyl contents: *T. granulosum* (3.6 g; OCH_3, 45.6%), *T. interdigitale* (5.0 g; OCH_3, 44.5%), *M. quinckeanum* (4.4 g; OCH_3, 46.2%), *T. rubrum* (3.8 g; OCH_3, 45.0%), *T. schönleinii* (3.5 g; OCH_3, 44.5%); theoretical methoxyl content is 45.6%. Each methylated galactomannan I had a

Can. J. Chem. Downloaded from www.nrcresearchpress.com by 210.87.254.42 on 09/05/12
For personal use only.

degree of polymerization of 45 as determined by osmometry in chloroform solution using a Mechrolab vapor pressure osmometer.

Hydrolysis Products from Methylated Galactomannans I

Quantitative estimation.—The methylated galactomannans I were each hydrolyzed by the following procedure. Methylated galactomannan I (1.0 g) was dissolved in ice-cold 72% sulfuric acid (8.0 ml) and the solution was left at room temperature for 45 min. Water (50 ml) was added and the solution was heated on a steam bath for 4 h (21). The hydrolysate was neutralized with barium carbonate, barium salts were removed by filtration, and water was removed from the filtrate by azeotropic distillation with ethanol at atmospheric pressure. Ethanol was removed by azeotropic distillation with benzene. This procedure avoided the losses of fully methylated sugars that occur during evaporation under diminished pressure.

A small portion (ca. 50 mg) of the mixture of hydrolysis products was heated under reflux overnight with 1% methanolic hydrogen chloride. The solution was neutralized by Duolite A4 ion-exchange resin and then examined by gas–liquid chromatography. The separation of one of the mixtures, that from the methylated galactomannan I from *T. interdigitale*, on column A is shown in Fig. 1 and is typical of the chromatograms given by each of the five mixtures of hydrolysis products. Relative amounts of the separated components were estimated by triangulation of the peaks on the gas–liquid chromatogram. The response of the β-ionization detector was the same for methyl tetra-*O*- and methyl tri-O-methyl hexosides which, however, gave 1.3 times greater response than the methyl di-*O*-methyl hexosides on a molar basis. The values obtained by direct triangulation of peaks for the methyl di-*O*-methyl hexosides were therefore multiplied by 1.3 as a calibration factor.

As a check on the quantitative data from gas–liquid chromatography another portion of each hydrolysate was separated by preparative paper chromatography (solvent B). The comparative results are shown below for one of the mixtures; the others gave very similar results.

Preparative paper chromatography		Gas–liquid chromatography
1.0 (parts)	tetra-*O*-methyl hexose	1.0 (parts)
2.0	tri-*O*-methyl hexose	2.03
1.0	di-*O*-methyl hexose	0.92

The amounts of individual components within the tetra-, tri-, and di-*O*-methyl fractions were not compared because complete resolution of the mixture was not obtainable by paper chromatography. The amounts of 2,3,5,6-tetra-*O*-methyl-D-galactose in the mixtures were estimated by gas–liquid chromatography of the methyl glycosides on column B. Under these conditions the methyl 2,3,4,6-tetra-*O*-methyl-α-D-mannoside had a retention volume of 1.10 relative to that of the methyl 2,3,5,6-tetra-*O*-methyl-α-D-galactoside. This 10% difference in retention volumes was ample for the estimation of the two components. No 2,3,5,6-tetra-*O*-methyl-D-galactose was present in the mixture from *T. rubrum*. All of the quantitative data in Table II, except that for 3,5-di-*O*-methyl-D-mannose, was therefore obtained by gas–liquid chromatography and the ratio of tetra- : tri- : di-*O*-methyl hexoses was checked by preparative paper chromatography. The 3,5-di-*O*-methyl-D-mannose was estimated as a percentage of the di-*O*-methyl fraction after separation by thin-layer chromatography as described below.

Isolation and Identification

To avoid repetition only one description of the isolation and characterization of the *O*-methyl sugars is given. It should be emphasized, however, that each *O*-methyl sugar in each of the five mixtures of hydrolysis products was identified as described here.

The mixtures of *O*-methyl sugars from hydrolysis of the methylated galactomannans I were resolved by preparative thin-layer chromatography using 20 × 20 cm plates loaded with 50–75 mg of the mixture. The fractions obtained are given below in order of greatest mobility; in our experience, relative rates of movement on thin-layer chromatograms are not sufficiently reproducible to warrant citation.

Fraction I.—A sirup which gave a single spot (R_G 1.04) on paper chromatography (solvent B) and a grey color with the spray reagent. Bromine oxidation yielded a sirupy lactone which was converted to a crystalline amide in methanol saturated with ammonia. Recrystallization of the amide from butanone yielded a product whose melting point was 154–155 °C, unchanged when the sample was mixed with authentic 2,3,5,6-tetra-*O*-methyl-D-galactonamide (22).

Fraction II.—The sirupy product showed a single spot (R_G 0.98) on paper chromatography (solvent B) and gave a red color with the spray reagent. The product was refluxed overnight in methanol containing Amberlite IR-120 ion-exchange resin. Evaporation of the solution left a residue which crystallized from light petroleum (b.p. 30–60 °C) and had m.p. 38–39 °C, $[\alpha]_D^{21}$ +69° (*c*, 1.5 in methanol). The melting point of a mixture of this product with an authentic sample of methyl 2,3,4,6-tetra-*O*-methyl-α-D-mannoside (23) was 38–39 °C.

A further portion of this fraction was converted to its anilide which was recrystallized from butanone : ether, m.p. 145–146 °C, $[\alpha]_D^{22}$ −10° (*c*, 1.0 in methanol). The melting point was undepressed when the sample was mixed with authentic *N*-phenyl-2,3,4,6-tetra-*O*-methyl-D-mannosylamine (24).

Fraction III.—This component ran on the thin-layer chromatograms as a very small zone just ahead of

Can. J. Chem. Downloaded from www.nrcresearchpress.com by 210.87.254.42 on 09/05/12
For personal use only.

Fraction IV with which it was usually contaminated after elution of the zones. A pure product was obtained by refractionation on thin-layer chromatograms. It had R_G 0.88 on paper chromatography in solvent B and M_G 0.0 on paper electrophoresis. The derived methyl glycoside had the same retention volume on gas–liquid chromatography (column A) as an authentic sample of methyl 2,4,6-tri-*O*-methyl-α-D-mannoside. Fraction III crystallized when seeded with 2,4,6-tri-*O*-methyl-D-mannose and had m.p. 60–62 °C, unchanged on admixture with 2,4,6-tri-*O*-methyl-D-mannose monohydrate (25).

Fraction IV.—The sirupy product gave a single spot (R_G 0.72) on paper chromatography (solvent B) and on paper electrophoresis (M_G 0.0). Oxidation by bromine yielded a sirupy lactone which was converted to the derived amide in methanol saturated with ammonia. The amide crystallized and recrystallization from butanone yielded 2,3,4-tri-*O*-methyl-D-mannonamide (26), m.p. 142–143°, unchanged by admixture with an authentic sample, $[\alpha]_D^{21}$ +5° (*c*, 1.0 in water).

Fraction V.—This component ran on thin-layer chromatograms as a small zone just ahead of Fraction VI. Refractionation was required to obtain a pure product. Fraction V showed one spot (R_G 0.66) on paper chromatography in solvent C; 3,4-di-*O*-methyl-D-mannose had R_G 0.72 in the same solvent. Paper electrophoresis also showed only one component, M_G 0.56; 3,4-di-*O*-methyl-D-mannose had M_G 0.54. Fraction V crystallized spontaneously and after recrystallization from butanone had m.p. 125–126 °C, undepressed by admixture with an authentic sample of 3,5-di-*O*-methyl-D-mannose (27). Yields of fraction V and the weights of the total di-*O*-methyl sugars (fractions V + VI) respectively in the five mixtures were: *T. rubrum* (11.0 mg and 123 mg), *T. granulosum*, *T. interdigitale*, *M. quinckeanum*, and *T. schönleinii* (4.8–5.1 mg and 97–102 mg). Fraction V therefore constituted 9% of the di-*O*-methyl fraction from the galactomannan I of *T. rubrum* and approximately 5% of the di-*O*-methyl fractions from the others.

Fraction VI.—This fraction crystallized spontaneously. It showed a single spot on paper chromatograms in solvents B and C (R_G 0.40 and 0.72 respectively) and on paper electrophoresis (M_G 0.54). Recrystallization from butanone yielded 3,4-di-*O*-methyl-D-mannose (28), m.p. 71–73 °C undepressed on admixture with an authentic sample, $[\alpha]_D^{21}$ +32° (*c*, 2.0 in methanol). The di-*O*-methyl sugar was converted to its methyl glycoside which crystallized from ether to yield a product with m.p. 86–87 °C, $[\alpha]_D^{21}$ +87° (*c*, 1% in methanol); the melting point was unchanged when the product was mixed with an authentic sample of methyl 3,4-di-*O*-methyl-α-D-mannoside (29).

Periodate Oxidations

Samples (11.35 mg) of each of the galactomannans I were dissolved in 0.015 *M* sodium periodate (10 ml) and stored in the dark at room temperature. At intervals aliquots (0.1 ml) were removed and diluted to 25 ml with water and periodate was determined spectrophotometrically (30). Periodate consumptions reached the constant values given in Table III after 24 h.

To each of the remaining oxidation solutions was added 2 drops of butan-1,3-diol and the solutions were set aside for 1 h. Aliquots (4 ml) were then removed and titrated to phenolphthalein end point to give the values for formic acid produced.

ACKNOWLEDGMENT

These investigations were supported, in part, by a grant from the John A. Hartford Foundation, Inc., New York.

REFERENCES

1. H. Alfes, C. T. Bishop, and F. Blank. Can. J. Chem. **41**, 2621 (1963).
2. C. T. Bishop, F. Blank, and M. Hranisavljevic-Jakovljevic. Can. J. Chem. **40**, 1816 (1962).
3. E. Salkowski. Ber. **27**, 497 (1894).
4. F. Blank and M. B. Perry. Can. J. Chem. **42**, 2862 (1964).
5. S. A. Barker, C. N. D. Cruickshank, and J. H. Holden. Biochim. Biophys. Acta, **74**, 239 (1963).
6. M. Heidelberger. Progr. Chem. Org. Nat. Prod. **18**, 503 (1960).
7. E. A. Kabat and M. M. Mayer. Experimental immunochemistry. Charles C. Thomas, Publisher, Springfield, Ill. 1961.
8. F. Fuke. J. Biochem. Tokyo, **35**, 263 (1942).
9. H. Neukom, H. Deuel, W. J. Heri, and W. Kündig. Helv. Chim. Acta, **43**, 64 (1960).
10. D. H. Northcote. Biochem. J. **58**, 353 (1954).
11. A. B. Foster. Advan. Carbohydrate Chem. **12**, 81 (1957).
12. C. T. Bishop. Methods Biochem. Analy. **10**, 1 (1962).
13. R. Tschesche and G. Balle. Tetrahedron, **19**, 2323 (1963).
14. L. Hough, J. K. N. Jones, and W. H. Wadman. J. Chem. Soc. 1702 (1950).
15. M. Dubois, K. A. Gilles, J. K. Hamilton, P. A. Rebers, and F. Smith. Anal. Chem. **28**, 350 (1956).
16. S. W. Gunner, J. K. N. Jones, and M. B. Perry. Chem. Ind. London, 255 (1961).
17. E. Fischer and J. Tafel. Ber. **20**, 3390 (1887).
18. F. Weygand, W. Perkow, and P. Kuhner. Chem. Ber. **84**, 594 (1951).
19. W. N. Haworth. J. Chem. Soc. **107**, 8 (1915).
20. T. Purdie and J. C. Irvine. J. Chem. Soc. **83**, 1021 (1903).

Can. J. Chem. Downloaded from www.nrcresearchpress.com by 210.87.254.42 on 09/05/12
For personal use only.

21. I. CROON, G. HERRSTRÖM, G. KULL, and B. LINDBERG. Acta Chem. Scand. **14**, 1338 (1960).
22. R. W. HUMPHREYS, J. PRYDE, and E. T. WATERS. J. Chem. Soc. 1298 (1931).
23. J. C. IRVINE and A. M. MOODIE. J. Chem. Soc. **87**, 1462 (1905).
24. J. C. IRVINE and D. MCNICOLL. J. Chem. Soc. **97**, 1449 (1910).
25. N. PRENTICE, L. S. CUENDET, and F. SMITH. J. Am. Chem. Soc. **78**, 4439 (1956).
26. W. N. HAWORTH, E. L. HIRST, F. A. ISHERWOOD, and J. K. N. JONES. J. Chem. Soc. 1878 (1939).
27. B. URBAS, G. A. ADAMS, and C. T. BISHOP. Can. J. Chem. **42**, 2093 (1964).
28. P. A. J. GORIN and A. S. PERLIN. Can. J. Chem. **34**, 1796 (1956).
29. W. N. HAWORTH, R. L. HEATH, and S. PEAT. J. Chem. Soc. 833 (1941).
30. G. O. ASPINALL and R. J. FERRIER. Chem. Ind. London, 1216 (1957).

Can. J. Chem. Downloaded from www.nrcresearchpress.com by 210.87.254.42 on 09/05/12
For personal use only.

Can. J. Chem. Downloaded from www.nrcresearchpress.com by 210.87.254.5 on 09/05/12
For personal use only.

SECONDARY KINETIC ISOTOPE EFFECTS IN BIMOLECULAR NUCLEOPHILIC SUBSTITUTIONS

II. α-DEUTERIUM EFFECTS IN MENSCHUTKIN REACTIONS OF METHYL IODIDE[1]

K. T. LEFFEK AND J. W. MACLEAN
Department of Chemistry, Dalhousie University, Halifax, Nova Scotia
Received July 22, 1964

ABSTRACT

Secondary deuterium isotope effects have been measured for the reactions between methyl and methyl-d_3 iodides and a series of tertiary amines in benzene solvent. Deuterium substitution increased the rate of each reaction but the rate ratios (k_H/k_D) show no systematic change with variation in the structure of the amine. The isotope effect for the reaction with 2-picoline was measured at different temperatures over a range of 40 deg and shows no change. These isotope effects may be rationalized as internal rotational effects of the methyl group or as solvation effects.

Many of the kinetic secondary deuterium isotope effects recorded in the literature have been measured in reaction systems in which solvation of the reaction site is an important, but relatively unknown, factor. For such systems it is very difficult to assess what part of the isotopic rate change is due to solvation phenomena and what part comes about as a result of internal changes in the reacting molecule. Investigations of the dependence of secondary isotope effect on solvent composition give no clear answer to this problem. Shiner and Verbanic (1) found that isotope effects produced by α-deuteration of the alkyl group in *p*-alkyl benzhydryl chlorides solvolyzing in aqueous acetone were markedly dependent on the water content of the solvent, although the isotopic rate ratios were all quite close to unity. For α-deuterated methyl and ethyl *p*-bromobenzenesulfonates, Lewis and co-workers (2) found only very small changes in the isotope effect between the two solvents, methanol and acetic acid, which they interpreted on the basis of a difference in mechanism of reaction rather than a direct solvation difference. Similar changes in isotope effect, presumably due to mechanism changes, were observed by Lewis and Boozer (3) in the solvolysis reactions of 2-pentyl-1,1,1,3,3,d_5-*p*-toluenesulfonate in acetic acid, formic acid, and 80% aqueous ethanol. Similar results were observed by Winstein and Takahashi (4) for 3-methyl-2-butyl-3*d*-*p*-toluenesulfonate solvolyzing in the same solvents.

Thus changing the solvent gives information concerning solvation isotope effects which is not separable from information concerning effects resulting from changes in mechanism. Apart from the deuterated *p*-alkyl benzhydryl chlorides, there is no clear change of isotope effect with solvent for which there is not at least the possibility of a mechanistic change.

Recently, Leffek, Robertson, and Sugamori (5) proposed that the β-deuterium isotope effects in the water solvolyses of isopropyl compounds, which are rate changes brought about by changes in the entropy of activation, were due to differences in the barriers to rotation of the methyl and methyl-d_3 groups and differences in these barriers between the initial and transition states of the reaction. Although a reasonably large part of the observed effect could be accounted for on this theory, the unimportance of solvation as the source of the effect was not proved. Halevi and co-workers have suggested that these

[1]*Presented at the 47th Annual Conference of the Chemical Institute of Canada, Kingston, Ontario, June, 1964.*

results be rationalized in terms of solvation (6) and hold that "it is still reasonable to suppose that most secondary isotope effects, at least in a nonpolar solvent, would arise substantially from zero-point energy differences" (7). This supposition is tested in the present investigation for the reaction-type

$$R_3N + CH_3I \rightarrow R_3{}^+NCH_3 + I^-$$

studied in solvent benzene.

RESULTS AND DISCUSSION

Rate constants and isotopic rate ratios are given in Table I for the reactions of six tertiary amines with methyl and methyl-d_3 iodide in benzene solvent. All rate constants are corrected for expansion of the solvent. The rate constants observed in the present work for the reactions of triethylamine and pyridine with normal methyl iodide substantially agree with the values reported by Winkler and Hinshelwood (8).

TABLE I

Secondary deuterium isotope effects for the reactions between methyl iodide and tertiary amines at 50.03 ± 0.05 °C

Tertiary amine	No. of runs	10^5k_H (l/mole s)	10^5k_D (l/mole s)	k_H/k_D ± std. error
Triethylamine	3	$454._9$	$518._6$	$0.87_7 \pm 0.004$
Tri-*n*-propylamine	2	$116._5$	$130._4$	0.89_3
Tri-*n*-butylamine	3	$127._4$	$142._2$	$0.89_6 \pm 0.001$
Pyridine	4	6.99_8	7.61_4	$0.91_9 \pm 0.002$
2-Picoline	4	3.66_8	4.18_4	$0.87_7 \pm 0.002$
2,6-Lutidine	3	0.416_9	0.475_3	$0.87_6 \pm 0.002$

The deuterated methyl iodide reacts faster than the normal compound with all of the amines studied. The direction of the rate change is thus the same as that observed for similar reactions; for instance, the solvolysis in water of methyl-d_3 iodide (9) yields a rate ratio $k_H/k_D = 0.87$ and the reaction between pyridine and methyl-*t* iodide in benzene (10) gives a tritium isotope effect $k_H/k_T = 0.96$.

The rate ratios in Table I show very little variation with the amine reactant. According to Llewellyn, Robertson, and Scott (9), the isotope effect in the solvolyses of methyl halides depends upon the proximity of the entering group to the carbon atom at which substitution is taking place. Thus they observed greater inverse isotope effects the greater the S_N2 character of the solvolysis. This generalization has been shown to fail for the bimolecular attack of thiosulfate ion on alkyl bromides (11) and therefore may not be applicable to all types of nucleophilic substitutions. If, however, it were true for Menschutkin reactions, it could be concluded that the proximity of the nitrogen atom of the attacking amine to the carbon atom of the methyl iodide was approximately the same in the transition state for all six amines. This is not an unreasonable model for the transition state despite the fact that the amount of steric hindrance to reaction changes by a very large amount in, for instance, going from pyridine to 2,6-lutidine (12). The constancy of the isotope effect for tertiary amines of widely differing steric characteristics does not prove that the isotope effect is unconnected with the steric effect as the k_H/k_D ratio measures only the difference in steric effect between CH_3 and CD_3 for a given reaction. This difference may not change significantly even though the steric hindrance to reaction changes from one amine to another.

Can. J. Chem. Downloaded from www.nrcresearchpress.com by 210.87.254.5 on 09/05/12
For personal use only.

TABLE II

Temperature dependence of α-deuterium isotope effect for the reaction between methyl iodide and 2-picoline

No. of runs	$10^5 k_H$ (l/mole s)	$10^5 k_D$ (l/mole s)	Temp. (°C)	k_H/k_D
1	1.84_0	2.09_8	40.02	0.87_7
1	2.64_1	2.96_4	45.09	0.89_1
4	3.66_8	4.18_4	50.03	0.87_7
1	5.18_1	5.89_2	55.03	0.87_9
1	7.05_8	8.09_0	60.03	0.87_3
1	9.99_7	11.2_4	65.09	0.88_9
1	13.4_0	15.2_7	70.14	0.87_8
1	18.0_9	20.6_4	75.05	0.87_6
1	23.6_4	26.8_1	80.04	0.88_2

The reaction of 2-picoline with methyl iodide was chosen to carry out a study of the dependence of the rate ratio on temperature. The results given in Table II show that the isotope effect is constant over a temperature range of 40 deg. By the method of least squares, the rate ratios were fitted to the equation

$$[1] \qquad \log_{10}(k_H/k_D) = \frac{(\Delta H_D^{\ddagger} - \Delta H_H^{\ddagger})}{2.303RT} - \frac{(\Delta S_D^{\ddagger} - \Delta S_H^{\ddagger})}{2.303R}$$

which is derived from the rate equation of the transition state theory. Calculation of the enthalpy of activation difference and the entropy of activation difference gave

$$(\Delta H_D^{\ddagger} - \Delta H_H^{\ddagger}) = -2 \pm 36 \text{ cal mole}^{-1}$$

and

$$(\Delta S_D^{\ddagger} - \Delta S_H^{\ddagger}) = +0.25 \pm 0.11 \text{ cal mole}^{-1} \text{ deg}^{-1}.$$

The limits quoted in each case are standard deviations.

Thus, the isotope effect in this Menschutkin reaction, in the nonpolar solvent benzene, is an entropy of activation effect.

The 13% inverse α-deuterium isotope effect observed by Robertson and co-workers (9) for the water solvolysis of methyl-d_3 iodide was interpreted in terms of zero-point energy changes of the C—H and C—D bonds between the initial and transition states. The observed isotopic rate ratios for other methyl-d_3 compounds led to the conclusion that the C—H and C—D bending vibrations were inhibited in the transition state relative to the initial state, either by the size of the leaving group or the degree of nucleophilic interaction of the attacking water molecule. The authors examined the possibility of a "thermodynamic" source of the effects but concluded that the zero-point energy changes were probably the origin of the rate changes. This conclusion must be reexamined in the light of the present findings.

The lack of an enthalpy of activation difference between the normal and deuterated methyl iodides for the Menschutkin reaction poses the same problem as the similar result found in the water solvolyses of isopropyl esters (5); i.e., either there are no zero-point energy changes or there is a fortuitous cancellation between opposing changes in the C—H and C—D bonds. The latter alternative seemed to be the more likely (5) because it is very difficult to find a source of entropy of activation which does not simultaneously introduce an enthalpy of activation difference. However, belief in the fortuitous cancellation can only be maintained if the number of systems in which it must be postulated is not too large compared to the total number of systems examined. With the inclusion

Can. J. Chem. Downloaded from www.nrcresearchpress.com by 210.87.254.5 on 09/05/12
For personal use only.

of this investigation, six temperature dependence studies of secondary deuterium isotope effects have been published (1, 5, 13, 14, 15), and three show an entropy of activation difference as the major isotope effect. Therefore, the answer to this problem on a statistical basis must await the accumulation of more data.

Secondary isotope effects may arise if the changes in the partition functions, on going from the initial state to the transition, are not the same for the protium and deuterium compounds. The transition state theory rate expression yields eq. [2],

$$[2] \qquad k_H/k_D = \frac{Q_H^{\ddagger}}{Q_H}\frac{Q_D}{Q_D^{\ddagger}}$$

in which the partition function Q may be factorized into

$$Q_{trans} \times Q_{rot} \times Q_{vib} \times Q_{int\ rot}.$$

Here the vibration partition function is calculated with reference to the minimum of the potential energy curve and therefore contains the zero-point energy component, which may be, and usually is, discussed separately from the remaining partition function contributions. For the translational and rotational contributions, the partition functions are directly proportional to the mass and the product of the moments of inertia, respectively. For a reaction, such as the Menschutkin reaction, in which the transition state is formed by the coalition of two molecules, both the translational and rotational contributions to the rate ratio yield k_H/k_D greater than unity (9), but only of the order of 1 or 2%, if solvation is assumed to be equal for the initial and transition states. An inverse isotope effect of the same order of magnitude can be obtained only if the transition state is assumed to be unsolvated and the initial state solvated, which is an unreasonable postulate for this reaction in which charges are being developed during the activation process on initially neutral molecules.

The contribution from the vibrational partition function (excluding the zero-point energy component) to the isotope effect is probably negligibly small, since Q_{vib} for individual fundamental frequencies greater than 1 000 cm^{-1} is very close to unity (16). These are the vibrations which involve hydrogen in an important way and thus are the ones most affected by deuteration. The fundamental vibrations of the molecule with lower frequencies give values of Q_{vib} greater than one, but are changed much less by deuteration. The only manner in which an inverse vibrational isotope effect can be obtained is to apply some postulate to allow an increase in the vibration frequencies during the activation process, which, as first proposed by Lewis and co-workers (17), gives rise to inverse isotope effects as a result of zero-point energy changes. However, the results of the present investigation remove the grounds on which this explanation was based; i.e., that the observed isotope effects are necessarily zero-point energy effects.

Isotope effects resulting from internal rotation were not considered to be important in the solvolyses of methyl compounds in water (9) but were used later by Leffek, Robertson, and Sugamori to partly explain the entropy of activation isotope effects found in the water solvolyses of isopropyl compounds (5). The same theory applied to the Menschutkin reactions of methyl iodide provides one source of entropy of activation isotope effect which probably contributes to the observed rate ratio.

For an S_N2 reaction involving methyl iodide, the barrier to rotation of the methyl group about the axis of the C—I bond is zero. However, in the transition state of the reaction the carbon–nitrogen bond is partly formed and will have a barrier to internal rotation. For some time it has been thought that the transition state of a Menschutkin

Can. J. Chem. Downloaded from www.nrcresearchpress.com by 210.87.254.5 on 09/05/12
For personal use only.

reaction was very similar to the products (18), and although recent work (19, 20) indicates that this may not be true, the carbon–nitrogen bond must be at least half-formed in the transition state. If the formation of this new barrier to internal rotation is combined with the postulate made by Leffek *et al.* (5) that the barrier to rotation of CH_3 groups is slightly higher than that of CD_3 groups, which, although not predicted by theory, is supported by a limited amount of experimental evidence (21, 22), the entropy of activation for the protium compound will be a larger negative quantity than that for the deuterium compound. Thus, $(\Delta S_D^{\ddagger} - \Delta S_H^{\ddagger})$ will be positive. With assumed reasonable values for the barriers to rotation, a semiquantitative treatment may be made, and the enthalpy and entropy of activation contributions from this source obtained from Pitzer's tables (23). Some examples are given in Table III, from which it may be seen that a significant contribution to the entropy of activation difference is obtained for assumed differences in the barrier to rotation of about 10–20% between the normal and deuterated transition states. The enthalpy of activation contribution from the source is greater for the deuterated molecule than for the protium compound, thus favoring a slower reaction by the former. This effect is in the opposite direction to the enthalpy effect proposed by Lewis *et al.* (17) and Robertson *et al.* (9) and therefore allows the possibility of cancellation of the enthalpy isotope effects.

TABLE III

Contributions to the secondary isotope effects for Menschutkin reactions of methyl iodide from internal rotational effects at 300 °K

Barrier to methyl rotation in transition state (cal mole^{-1})		$(\Delta H_D^{\ddagger} - \Delta H_H^{\ddagger})_{\text{int rot}}$	$(\Delta S_D^{\ddagger} - \Delta S_H^{\ddagger})_{\text{int rot}}$
H compound	D compound	(cal mole^{-1})	(cal mole^{-1} deg^{-1})
1 500	1 500	52	−0.01
1 800	1 500	54	+0.15
2 100	2 100	58	−0.02
2 400	2 100	72	+0.14

From the accumulated experimental data it appears that there is no single source of secondary deuterium isotope effects. Observed rate changes which result from the cancellation of two or more effects will therefore inevitably occur in some, and perhaps many, of the systems studied. Although only two effects are necessary to obtain a cancellation, the real situation may be more complicated. In particular, for all reactions in solution, differences in solvation between the deuterated and normal compounds are an obvious source of isotope effect, but they are very difficult to assess quantitatively. The similarity between the rate ratios for the methyl iodides reacting with tertiary amines in benzene ($k_H/k_D \approx 0.89$), and solvolyzing in water ($k_H/k_D = 0.87$), may be used as an argument against solvation effects as the origin of the rate differences, since quite different solvation effects would be expected for these two reactions. However, this argument is valid only if the isotope effect for the solvolysis reaction is also temperature independent, and even then it is still assailable.

Notwithstanding this argument, solvation may be used to explain the present results in the following manner. Although benzene is a nonpolar solvent, it is polarizable; hence solvation increases during the activation process as the charges on the forming ions are developed. Since carbon–deuterium bonds release electrons inductively slightly better than carbon–hydrogen bonds, the development of the positive charge on the ammonium

Can. J. Chem. Downloaded from www.nrcresearchpress.com by 210.87.254.5 on 09/05/12
For personal use only.

ion should be less for the deuterated compound than for the normal compound, resulting in less strong solvation for the former. Such an effect would yield a rate difference between the two isotopic compounds due to both enthalpy and entropy differences. Since the entropy of activation contributions from this source are negative for both isotopic analogues, with the term for the deuterated compound the smaller one, $(\Delta S_D^{\ddagger} - \Delta S_H^{\ddagger})$ would be positive, but its size is not easily estimated. It may be argued, however, that isotope effects arising directly from isotopic substitution within the substrate molecule should always be more important than those arising from environmental changes of the molecule as a result of the isotopic substitution, the latter being secondary with respect to the former.

In the examples presented in this work and in some other cases, but obviously not in all, changes in the barriers to rotation about single bonds offer a partial explanation of the entropy difference, although other sources of isotope effect are probably operating concurrently.

NOTE ADDED IN PROOF: Recently two important papers by Wolfsberg and Stern have appeared (Pure and Appl. Chem. 8, 255, 325 (1964)), concerning the theory of isotope effects. In particular, it was demonstrated how it is possible to obtain a temperature independent secondary deuterium isotope effect ($k_H/k_D > 1$) as a result of opposing changes in force constants during the activation process. In principle, a similar treatment could be developed for the present results as an alternative to the above interpretation. However, the problem of rationalizing the force constant changes would remain and this problem is no less than that of rationalizing the rate constant isotope effects themselves.

EXPERIMENTAL

Materials

The deuterated methyl iodide, supplied by Merck and Co. Ltd., had a minimum isotopic purity of 99%. Samples from three different batches were analyzed from their mass spectra and each was found to be 99.4% deuterated. The normal methyl iodide and the tertiary amines were reagent grade and each was dried and distilled immediately before use. Reagent grade benzene was refluxed over potassium metal for 4 h, then fractionally distilled.

TABLE IV

Illustrative kinetic runs for the reactions between methyl iodide and methyl-d_3 iodide and tri-*n*-butylamine in benzene at 50.03 ± 0.05 °C

Run 118 at $t = 0$, $[CH_3I] = 0.04258$ *M*, at $t = 0$, $[(C_4H_9)_3N] = 0.09092$ *M*			Run 119 at $t = 0$, $[CD_3I] = 0.04177$ *M*, at $t = 0$, $[(C_4H_9)_3N] = 0.09021$ *M*		
t (min)	$AgNO_3$ titer* (ml)	$10^4 k_2$ (l/mole s)	t (min)	$AgNO_3$ titer* (ml)	$10^4 k_2$ (l/mole s)
20	2.19_5	12.59	20	2.43_5	14.37
40	3.06_5	12.67	40	3.36	14.40
60	3.80_5	12.76	60	4.10	14.24
80	4.41_5	12.72	80	4.71	14.09
100	4.97	12.85	100	5.25	14.11
120	5.40	12.70	120	5.71	14.11
140	5.78	12.60	140	6.09	14.02
Average $k_2 = 12.70 \times 10^{-4}$ l/mole s			Average $k_2 = 14.19 \times 10^{-4}$ l/mole s		

*Volume of 0.0250 *N* $AgNO_3$ equivalent to 4.69 ml sample, corrected for burette errors.

Kinetic Method

Each kinetic run was carried out by immersing sets of sealed tubes, each containing an accurately known volume of reaction mixture (ca. 5 ml), in a constant temperature bath (±0.01° C). After equilibrium had been reached, three tubes were withdrawn and rapidly cooled in dry ice – acetone slush, this time marking

Can. J. Chem. Downloaded from www.nrcresearchpress.com by 210.87.254.5 on 09/05/12
For personal use only.

the kinetic zero. Thereafter tubes were withdrawn singly at regular intervals. The contents of each tube were analyzed by potentiometric titration of the iodide ion with standard silver nitrate solution, using approximately 30 ml of wet acetone as the solvent. Rate constants were calculated from the integrated rate equation for a second-order irreversible reaction. Each isotopic rate ratio was determined by carrying out a pair of runs simultaneously, identical except for the isotopic substitution; an example is given in Table IV. The reactions were generally followed over one to two half-lives. The straight chain tertiary amines have steady second-order rate constants over two half-lives, but the pyridine derivatives gave rate constants which decreased a few per cent ($< 5\%$) during 50% reaction. The constants quoted are nevertheless average values; since the two isotopic reactions were sampled at the same relative times, any parallel errors in the rate constants cancel in the evaluation of the isotopic rate ratio. Several independent pairs of runs were made for each isotope effect determined at 50.03 °C.

ACKNOWLEDGMENTS

The authors are grateful for financial support of this work by the National Research Council and thank Dr. W. D. Jamieson for the determination of the mass spectra.

REFERENCES

1. V. J. Shiner, Jr. and C. J. Verbanic. J. Am. Chem. Soc. **79**, 373 (1957).
2. E. S. Lewis, J. C. Brown, and W. C. Herndon. Can. J. Chem. **39**, 954 (1961).
3. E. S. Lewis and C. E. Boozer. J. Am. Chem. Soc. **76**, 791 (1954).
4. S. Winstein and J. Takahashi. Tetrahedron, **2**, 316 (1958).
5. K. T. Leffek, R. E. Robertson, and S. E. Sugamori. Can. J. Chem. **39**, 1989 (1961).
6. E. A. Halevi, M. Nussim, and A. Ron. J. Chem. Soc. 866 (1963).
7. E. A. Halevi and M. Nussim. J. Chem. Soc. 876 (1963).
8. C. A. Winkler and C. N. Hinshelwood. J. Chem. Soc. 1147 (1935).
9. J. A. Llewellyn, R. E. Robertson, and J. M. W. Scott. Can. J. Chem. **38**, 222 (1960).
10. H. Simon and D. Palm. Chem. Ber. **92**, 2701 (1959).
11. K. T. Leffek. Can. J. Chem. **42**, 851 (1964).
12. H. C. Brown, D. Gintis, and H. Podall. J. Am. Chem. Soc. **78**, 5375 (1956).
13. V. J. Shiner, Jr. J. Am. Chem. Soc. **76**, 1603 (1954).
14. E. S. Lewis and G. M. Coppinger. J. Am. Chem. Soc. **76**, 4495 (1954).
15. K. Mislow, R. Graeve, A. J. Gordon, and G. H. Wahl, Jr. J. Am. Chem. Soc. **85**, 1199 (1963).
16. J. E. Leffler and E. Grunwald. Rates and equilibria of organic reactions. Wiley, New York. 1963. p. 13.
17. R. R. Johnson and E. S. Lewis. Proc. Chem. Soc. 52 (1958).
18. S. Glasstone, K. J. Laidler, and H. Eyring. The theory of rate processes. McGraw-Hill Book Co., New York. 1941. p. 418.
19. J. B. Rossell. J. Chem. Soc. 5183 (1963).
20. A. P. Harris and K. E. Weale. J. Chem. Soc. 146 (1961).
21. J. D. Swalen and C. C. Costain. J. Chem. Phys. **31**, 1562 (1959).
22. E. Tannenbaum, R. J. Myers, and W. D. Gwinn. J. Chem. Phys. **25**, 42 (1956).
23. K. S. Pitzer and W. D. Gwinn. J. Chem. Phys. **10**, 428 (1942).

Can. J. Chem. Downloaded from www.nrcresearchpress.com by 210.87.254.5 on 09/05/12
For personal use only.

Can. J. Chem. Downloaded from www.nrcresearchpress.com by 210.87.254.6 on 09/05/12
For personal use only.

NUCLEAR MAGNETIC RESONANCE INVESTIGATIONS OF SOME GROUP V METAL FLUORIDES AND OXYIONS[1]

J. V. HATTON,[2] Y. SAITO,[3] AND W. G. SCHNEIDER
Division of Pure Chemistry, National Research Council, Ottawa, Canada

Received July 28, 1964

ABSTRACT

The nuclear magnetic resonances of ^{51}V, ^{93}Nb, ^{121}Sb, ^{123}Sb, and ^{181}Ta in solutions of the pentafluorides of these elements were measured. All of these nuclei have large electric quadrupole moments. In most cases the chemical species observed was identified by spin-multiplet splitting of the metal resonance. In aqueous 48% HF solutions the ^{181}Ta resonance could not be observed; the ^{121}Sb and ^{123}Sb resonances consist of a symmetrical septet, corresponding to the hexafluoride ion; the ^{93}Nb resonance consists of a single exchange narrowed line; and the ^{51}V resonance consists of a symmetrical quintet, corresponding to the VOF_4^- ion. In alcohol solution NbF_5 disproportionates to form NbF_6^-, whereas in ether and triethylamine solutions, the complexes $NbF_5 \cdot OEt_2$ and $NbF_5 \cdot NEt_3$ are formed. The latter complexes were confirmed by proton resonance measurements. Resonances of ^{51}V in aqueous solutions of V_2O_5 and of NH_4VO_3 as a function of pH show a parallel behavior and reveal the presence of six different oxyions of vanadium. Five of these resonances are assigned to the species, VO_4^{3-}, VO_3^-, $V_2O_7^{4-}$, $V_3O_{10}^{6-}$ and VO_2^+, on the basis of the resonance line width and the pH range in which the resonance appears.

I. INTRODUCTION

The use of magnetic resonances of heavier nuclei for structural investigations of inorganic compounds has received relatively little attention. The magnetic properties of such nuclei are generally not as favorable for n.m.r. as those of hydrogen and fluorine nuclei. For some nuclei this is primarily a question of low sensitivity due to a low isotopic abundance, but more commonly it is a question of an unfavorable nuclear relaxation time. The majority of heavier nuclei possess relatively large nuclear electric quadrupole moments which strongly couple with surrounding molecular fields and give rise to a short nuclear relaxation time. This results in an enhanced nuclear resonance line width, $\Delta\nu$, given appproximately by the relation (1):

$$\Delta\nu = 1/T_1 = Kh^2(eq)^2(eQ)^2\tau_c. \qquad (1)$$

Here T_1 is the nuclear relaxation time, K is a constant, Q is the nuclear electric quadrupole moment, q is the electric field gradient near the nucleus, and τ_c is the molecular correlation time. When both the nuclear electric quadrupole moment and the field gradient are large, the resonance line may be broadened beyond detection. However, there are many molecular systems in the realm of inorganic chemistry where the field gradient in the vicinity of the nucleus of interest may be expected to be moderately small. Numerous examples of this are to be found in solutions of complex ions where the central atom is surrounded by a number of ligand groups which tend to balance out the fields near the central atom. The complex metal fluorides of the heavier metals provide a specific example of this and, in addition, offer a further advantage. If spin coupling of the fluorine can be observed in the resonance spectrum of the central atom, this immediately identifies the particular chemical species being measured.

[1]*Issued as N.R.C. No. 8174.*
[2]*National Research Council of Canada Postdoctoral Fellow, 1961–1963. Present address: Central Research Laboratory, Dominion Tar and Chemical Company, Senneville, Quebec.*
[3]*National Research Council of Canada Postdoctoral Fellow, 1963–1964.*

The present investigation was undertaken to see to what extent the resonances of nuclei with large electric quadrupole moments could be measured in various chemical species and what kind of information could be derived therefrom. For this purpose several Group V nuclei were selected. Their magnetic properties are summarized in Table I. All of these nuclei have favorable isotopic abundances and all possess large electric quadrupole moments, that for ^{181}Ta being among the largest known.

TABLE I

Magnetic properties of Group V nuclei

Nucleus	Natural abundance (%)	Frequency (Mc/s) (in a field of 14.1 kilogauss)	Magnetic moment (nucl. magnetons)	Spin	Elec. quadr. moment ($e\times10^{-24}$ cm^2)
^{51}V	99.76	15.80	5.145	7/2	0.3
^{93}Nb	100	14.73	6.167	9/2	~0.3
^{121}Sb	57.25	14.37	3.343	5/2	−1.3
^{123}Sb	42.75	7.78	2.534	7/2	−1.7
^{181}Ta	100	7.18	2.1	7/2	6.5

II. NIOBIUM (^{93}Nb)

(a) NbF_5 in Aqueous HF Solution

It has been shown that in the system K_2NbF_7–HF–H_2O, the NbF_6^- ion exists in solution at concentrations of HF in excess of 40.5% (2). Accordingly, dissolution of NbF_5 (m.p. 72 °C) in 48% aqueous HF would be expected to yield the hexafluoride ion. At room temperature the ^{93}Nb resonance of this solution consists of a single, very sharp, intense line. Cooling the solution causes progressive broadening of the resonance line, with no appearance of a multiplet structure at temperatures as low as −70 °C. By analogy with the corresponding behavior of SbF_5 solutions (*vide infra*), it is concluded that in the niobium solution at room temperature the ^{93}Nb resonance is narrowed by rapid fluorine exchange.

(b) NbF_5 in Dry Ethanol

In order to limit fluorine exchange, solutions of NbF_5 in organic solvents were investigated. The ^{93}Nb resonance of a dry ethanol solution at 0 °C, shown in Fig. 1, consists of a symmetrical septet (intensities, 1:6:15:20:15:6:1). As the temperature is increased from 0 to +50 °C, or decreased from 0 to −80 °C, progressive line broadening was observed. The chemical species being observed is undoubtedly NbF_6^-, since to explain the spectrum of Fig. 1 requires that the niobium nucleus "sees" six equivalent F atoms and a small electric field gradient. A similar spectrum has been observed and assigned independently by Packer and Muetterties (3) for NbF_5 in solution in dimethyl formamide. From the multiplet splitting the ^{93}Nb–^{19}F spin coupling constant is found to be 345 ± 5 c/s.

Formation of the hexafluoride ion implies self-dissociation of the dissolved niobium pentafluoride. The ethanol solution has a deep purple color and a high electrical conductivity (10^{-4} Ω^{-1}cm^{-1} for 0.01 *M* solution). Thus it is likely the disproportionation reaction is

$$[1] \qquad NbF_5 \leftrightarrows NbF_6^- + NbF_4^+.$$

This has also been suggested to account for the high conductivity of molten niobium pentafluoride (4). If the species NbF_4^+ had a symmetrical structure it should yield a second ^{93}Nb multiplet resonance considerably displaced from that of the NbF_6^- ion.

Can. J. Chem. Downloaded from www.nrcresearchpress.com by 210.87.254.6 on 09/05/12
For personal use only.

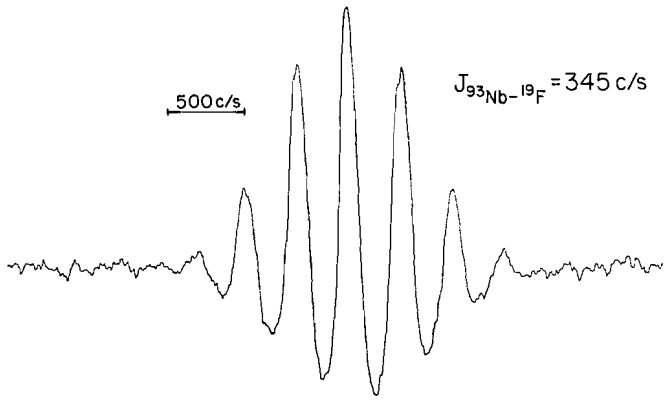

FIG. 1. ^{93}Nb resonance of NbF_5 in dry ethanol; temperature 0 °C.

Since this was not observed, an unsymmetrical structure having a large field gradient at the central atom must be assumed. Such a structure is $NbF_4(EtOH)_2^+$, in which the oxygen of the ethanol solvent takes up two of the octahedral coordination positions. Further ionic dissociation could also yield $NbF_4(OEt)_2^-$. Yet another possibility (5) involves complexing of NbF_5 with an alcohol molecule, followed by elimination of HF to yield $C_2H_5ONbF_4$, and this may proceed in successive steps to:

[2] $$6NbF_5 + 5EtOH \rightarrow 5HNbF_6 + Nb(OEt)_5.$$

The line broadening observed at temperatures above 0 °C is undoubtedly due to fluorine exchange reactions expressed by eq. [1]. The observed line broadening of the NbF_6^- ion at temperatures below 0 °C must then be attributed to possible association effects, either by ion pairing or by additional solvent coordination.

It should be noted also that the ^{93}Nb resonance position of NbF_6^- in ethanol at room temperature is very near that of NbF_6^- in aqueous HF solution (see Table II).

TABLE II

Chemical shifts of niobium and antimony in solutions of the pentafluorides

Compound	Solvent	Nucleus measured	Spectrum	Species in solution	Shift
NbF_5	48% HF	^{93}Nb	Sharp singlet	NbF_6^-	0
NbF_5	Ethanol	^{93}Nb	Sharp septet	NbF_6^- (see text)	−5
NbF_5	Ether	^{93}Nb	Broad singlet	$NbF_5 \cdot OEt_2$	−70
NbF_5	Ethanolic triethylamine	^{93}Nb	Very broad singlet	$NbF_5 \cdot NEt_3$	−155
SbF_5	48% HF	$^{121,123}Sb$	Sharp septet	SbF_6^-	0
SbF_5	Ethanol	^{121}Sb	Broad multiplet*	SbF_6^-	0±2
		^{123}Sb	Very broad multiplet*	SbF_6^-	
SbF_5	Ether	^{121}Sb	Very broad singlet	$SbF_5 \cdot OEt_2$	0±2

*The resonances were temperature dependent (see text).

(c) NbF_5 in Dry Ether

Solutions of NbF_5 in ether exhibit a single very broad resonance line at room temperature, which broadens still further as the temperature is lowered. In this case the resonance is ascribed to the coordination complex $NbF_5 \cdot OEt_2$, which is evidently favored over the

Can. J. Chem. Downloaded from www.nrcresearchpress.com by 210.87.254.6 on 09/05/12
For personal use only.

NbF_6^- ion. The following experiment supports this conclusion. To an alcoholic solution of NbF_5, ether was progressively added until the latter was well in excess. During the course of this dilution, the ^{93}Nb septet resonance becomes progressively weaker, but shows no broadening. In the reverse experiment, i.e. by gradual addition of alcohol to an ethereal solution of NbF_5, the broad niobium resonance gives way almost immediately to the septet resonance characteristic of NbF_6^-. Thus the latter appears to require the presence of ethanol.

(d) NbF_5 in Triethylamine

Freshly prepared solutions of NbF_5 in triethylamine show a very broad resonance signal displaced to lower field with respect to the resonance of alcoholic solutions. The resonance is undoubtedly due to the amine complex, $NbF_5 \cdot NEt_3$, which in time separates from the solution as white crystals.[4] The complex can also be prepared by adding the amine to an ether solution of NbF_5.

The chemical shifts of ^{93}Nb in the NbF_5 solutions examined are summarized in Table II. There is a progressive shift of the resonance to low field in the complexes, $NbF_5 \cdot F^-$, $NbF_5 \cdot OEt_2$, and $NbF_5 \cdot NEt_3$. Because of the dominance of paramagnetic contributions to the Nb nuclear screening in these compounds, the observed order is consistent with increasing covalency in ligand bonding, as appears entirely reasonable.

III. ANTIMONY

Antimony has two magnetic isotopes, ^{121}Sb and ^{123}Sb, with natural abundances of 57% and 43%, respectively. The resonances of both isotopes were examined.

(a) SbF_5 in Aqueous 48% HF

The resonances of both antimony isotopes consist of sharp line septet spectra, confirming SbF_6^- as the stable species in these solutions. The fluorine–antimony spin coupling constants are included in Table III. In contrast to the corresponding niobium solutions, rapid fluorine exchange between SbF_5 and HF does not occur at ordinary temperatures.

TABLE III

Metal–fluorine coupling constants (c/s)

Nucleus X	$J_{M-^{19}F}$	Ion	Solvent
^{51}V	116±5	VOF_4^-	48% HF
^{93}Nb	345±5	NbF_6^-	Ethanol
^{121}Sb	1945±5	SbF_6^-	48% HF
^{121}Sb	1950±50	SbF_6^-	Ethanol
^{123}Sb	1055±5	SbF_6^-	48% HF
^{123}Sb	1050±50	SbF_6^-	Ethanol

(b) SbF_5 in Dry Ethanol

At room temperature the ^{121}Sb resonance consists of a broadened septet, the component lines of which sharpen considerably on heating to +88 °C. At +4 °C the multiplet pattern is obliterated, and only one very broad line is observable. As may be expected, ^{123}Sb, which has the larger nuclear quadrupole moment, exhibits even broader resonances.

As in the case of ethanolic NbF_5 solutions, the stable species is the hexafluoride ion.

[4] *A referee has called our attention to similar complexes formed by* SbF_5 *and* AsF_5 *with organic bases (cf. E. L. Muetterties. Advances in the chemistry of co-ordination compounds. The Macmillan Company, N.Y. 1961. p. 513).*

Can. J. Chem. Downloaded from www.nrcresearchpress.com by 210.87.254.6 on 09/05/12
For personal use only.

However, the broader resonance lines observed for the SbF_6^-, compared with the corresponding Nb resonances at similar temperatures, indicate that some additional complexing interactions must occur.

(c) SbF_5 in Ether

The room temperature ^{121}Sb spectrum consists of one broad line, which sharpens only slightly at higher temperature and broadens still further on cooling to 0 °C.

The chemical shifts of ^{121}Sb for the SbF_5 solutions in 48% aqueous HF, ethanol, and ether are the same to within 2 p.p.m. This again is in sharp contrast to the behavior of niobium solutions and provides further evidence of more complex (possibly polymeric) interactions in the case of the antimony solutions.

IV. TANTALUM

Since the chemistry of tantalum and niobium are generally similar, solutions of TaF_5 in 48% aqueous HF, dry ethanol, and ether were also investigated. Under the present experimental conditions no resonance of ^{181}Ta could be observed in any of these solutions. In spite of the very large electric quadrupole moment of ^{181}Ta, if tantalum were present as the simple TaF_6^- ion, its resonance should have been observed. Thus it is necessary to conclude that less symmetrical coordination complexes are formed, or else that an intermediate rate of fluorine exchange occurs so as to greatly broaden the resonance.

V. PROTON RESONANCES OF METAL FLUORIDE – ETHER COMPLEXES

Confirmatory evidence of complex formation in the metal fluoride – ether systems was obtained from proton resonances of the coordinated ether. Addition of excess metal fluoride to ether results in the formation of an immiscible viscous layer, which separates at the bottom of the solution. These layers are colored: SbF_5, dark brown; NbF_5, mauve; and TaF_5, red-brown. To remove excess ether, these layers were separated and extracted with tetramethylsilane (TMS). Finally, a small amount of the extracted complex was dissolved in TMS and the proton resonance of the ether component was measured relative to the signal of TMS. The results are summarized in Fig. 2. The proton resonance of the CH_3 (triplet) and CH_2 (quartet) groups in pure ether appear at -66.3 c/s and -201.3 c/s respectively from the TMS reference. In the metal fluoride complexes the resonances of both the CH_3 and CH_2 groups are broadened and displaced to lower field, the CH_2 group showing a larger displacement. Also the internal shift, $\Delta\nu$, between the CH_3 and CH_2 groups may be taken as a measure of relative strength of binding in the complex.

If the complex is formulated schematically as:

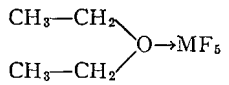

the observed proton resonance shifts are readily understood. Donation of electrons by the ether oxygen atom to the metal effectively makes the oxygen more electronegative. The resulting inductive effects in the bonded ethyl group will then give rise to low-field shifts of the proton resonances. Admittedly the above structure may be oversimplified. For example more complex interactions, schematically indicated by the following,

$$2(MF_5 \cdot OEt_2) \leftrightarrows \overset{-}{M}F_6 \cdot \overset{+}{M}F_4(OEt)_2$$

could also be envisaged and could contribute to line broadening.

Can. J. Chem. Downloaded from www.nrcresearchpress.com by 210.87.254.6 on 09/05/12
For personal use only.

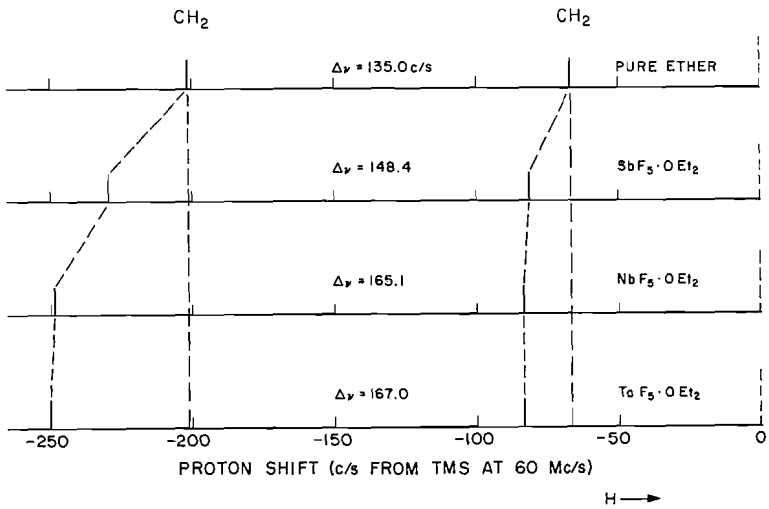

FIG. 2. Proton resonance shifts of ether in $MF_5 \cdot OEt_2$ complexes. The reference is tetramethylsilane (TMS), and $\Delta\nu$ is the internal chemical shift between CH_2 and CH_3 groups.

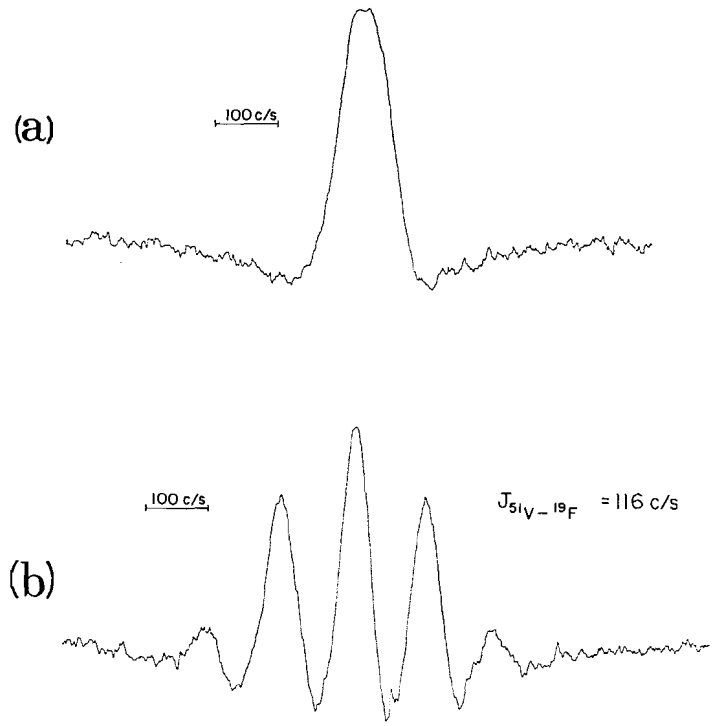

FIG. 3. ^{51}V resonance of V_2O_5 in aqueous 48% HF at a temperature of (*a*) +25 °C and (*b*) −10 °C.

VI. VANADIUM

Vanadium forms a greater variety of compounds than the other Group V metals so far considered, and its magnetic resonances are therefore of particular interest. While vanadium displays several characteristic valence states (not all of which are diamagnetic states), the present measurements are concerned only with the +5 state.

Can. J. Chem. Downloaded from www.nrcresearchpress.com by 210.87.254.6 on 09/05/12
For personal use only.

(a) Vanadium Fluorides

If the vanadium hexafluoride ion is a stable species, it may be expected to occur in solutions of V_2O_5 in 48% aqueous HF. The ^{51}V resonance of this solution at room temperature is reproduced in Fig. 3*a*. The line width is somewhat less than 100 c/s. On cooling the solution, the resonance is observed to broaden and ultimately yields a well resolved symmetrical quintet (Fig. 3*b*). Thus the species being observed is not the hexafluoride ion, but one with four equivalent fluorine atoms. This is undoubtedly the VOF_4^- ion, previously postulated (6, p. 817). This may be expected to have a square pyramid structure with the four equivalent fluorine atoms occupying the base position and the oxygen atom at the apex. Such a structure would not be expected to have a symmetrical field near the central vanadium nucleus.[5] However, as demonstrated by the spectrum of Fig. 3*b*, the resonance lines are fairly narrow. The vanadium–fluorine spin coupling constant is relatively small, 116 c/s (See Table III).

Other oxyfluoro ions of vanadium, for example, $VO_2F_3^{2-}$ and VOF_5^-, have been postulated (7, 8). In an attempt to observe these, solutions of V_2O_5 in 48% aqueous HF containing ammonium fluoride or containing potassium or zinc fluorides in excess were examined. Each gave spectra identical to those shown in Fig. 3, and must accordingly also contain the VOF_4^- ion. However, the presence of other species with very large field gradients at the central vanadium nucleus could conceivably escape detection because of excessive line broadening.

(b) Oxy-ions of Vanadium

Vanadium, like phosphorous, forms a series of oxy-ions in aqueous solutions (6, p. 810). The range of stability of different oxy-ions of vanadium is known to be strongly pH-dependent and to differ markedly from those of phosphorus (9). It was accordingly of some interest to what extent the vanadium resonances of different vanadate and polyvanadate species in solution could be measured. Two separate series of experiments were carried out:

(i) Starting with an aqueous solution of NH_4VO_3, which has a pH of 7.0, the ^{51}V resonance of the solution was measured as the pH was increased by addition of potassium hydroxide or decreased by addition of sulfuric acid.

(ii) A parallel series of measurements were also made starting with an aqueous solution of V_2O_5 in water.

The results are summarized in Table IV and plotted as a function of pH in Fig. 4. The ^{51}V chemical shifts (in p.p.m.) are referred to an aqueous solution of NH_4VO_3 (pH = 7.0). As is evident from Fig. 4, the two series of measurements exhibit very satisfactory agreement and consistency with respect to the chemical shift values of the observed resonances.

The results of Fig. 4 show seven separate vanadium resonances corresponding to at least six different ionic species, and in certain pH ranges two or more of these species coexist in equilibrium. The assignments indicated in Fig. 4 are to be regarded as tentative, although a considerable amount of supporting evidence is available. From pH 7 to pH 9 only one moderately sharp line is observed, and since this must correspond to the starting material, the resonance must be assigned to the metavanadate ion, VO_3^-, (or possibly to hydrated or polymeric forms of this ion). At pH 9.5 to 10, two resonances are observed, an additional rather broad line appearing about 45 p.p.m. to low field from the VO_3^- resonance. This is assigned to the pyrovanadate ion, $V_2O_7^{4-}$, known to exist in alkaline

[5]*The possibility of a trigonal bipyramid structure, with rapid exchange of fluorine atoms, cannot be ruled out.*

Can. J. Chem. Downloaded from www.nrcresearchpress.com by 210.87.254.6 on 09/05/12
For personal use only.

TABLE IV

^{51}V resonance shifts of aqueous NH_4VO_3 (*a*) and aqueous V_2O_5 (*b*) solutions as a function of pH

pH*	Chemical shift with signal intensity†								Color of solution
0.02*a*				−32.4 (vs)					Amber
0.40*b*				−31.1(s)					
0.61*a*				−31.8 (s)					
0.95*b*				−32.3 (m)					
1.37*a*				−34.3 (w)					
1.60*b*				−32.4 (w)					
2.14*a*	Too weak to be observed								Pale orange
2.41*b*	Too weak to be observed								
2.70*b*	−163.3 (vw)	−70.9 (w)	−51.1 (w)						
2.91*a*	−159.5 (w)	−77.6 (m)	−65.5 (s)						
2.94*b*	−166.6 (vw)	−76.4 (vw)	−58.8 (vw)						
3.58*a*	−157.7 (vw)	−78.2 (w)	−65.5 (m)				3.2 (vw)		
3.93*a*	−155.7 (vw)	−75.6 (w)	−61.7 (m)				4.5 (vw)		
4.41*a*	−158.0 (vw)	−78.2 (w)	−62.9 (m)				0.6 (vw)		
5.64*a*	−157.1 (vw)	−76.9 (w)	−61.6 (m)				−2.5 (w)		
6.32*a*	−155.1 (vw)	−74.5 (w)	−64.8 (m)				0.0 (w)		
6.67*b*	−163.3 (vw)	−79.7 (w)	−67.6 (m)				−1.6 (m)		
6.94*b*	−162.2 (vw)	−80.8 (w)	−67.6 (m)				−0.5 (s)		
7.00*a*							0.0 (m)		Yellow
7.17*a*							0.0 (m)		
8.43*a*							−1.3 (m)		
9.14*a*							0.0 (m)		
9.20*a*							−1.3 (m)		
9.25*b*							−0.7 (vw)		
9.53*a*							0.6 (w)		
9.69*b*							−4.9 (s)		
9.79*a*							0.0 (w)		
9.84*b*							−6.0 (s)		
10.06*a*							−12.8 (s)		Colorless
10.25*a*				−40.2 (w)					
10.49*b*				−46.7 (w)			−15.0 (vs)		
10.66*a*							−15.9 (vs)		
11.24*b*				−40.1 (m)			−17.2 (vs)		
11.56*b*				−43.4 (m)			−19.2 (s)		
11.57*a*							−19.7 (s)		
11.60*a*				−40.7 (vw)					
11.80*a*							−19.7 (s)		
13.00*b*				−42.3 (vw)			−20.3 (s)		

*The letter *a* designates aqueous NH_4VO_3 solutions, and *b* designates aqueous V_2O_5 solutions.
†Chemical shifts in p.p.m. were measured relative to aqueous NH_4VO_3 solution (pH = 7.0). Relative intensities, vw, w, m, s, vs, indicate respectively, very weak, weak, medium, strong, and very strong.

solutions (10). The resonance of the latter ion persist also in the range pH 10 to 13, and in this range the resonance of VO_3^- is no longer observable. Instead a new resonance, consisting of a very sharp line, appears at about 15 p.p.m. to lower field. The sharp resonance is indicative of a highly symmetric species and accordingly it is assigned to the orthovanadate ion, VO_4^{3-}, a tetrahedral structure.

Solutions in the acidic pH range are reported (9) to contain more complex (polyvanadate) ions, and V_2O_5 may be precipitated from solution. In the pH range 3.5 to 7.0, four separate vanadium resonances were observed. One of these arises from the VO_3^- ion, the intensity of the resonance becoming progressively weaker as the solution is acidified. Two rather broad and closely spaced lines at 60 to 80 p.p.m. to lower field also appear in the same pH range. The higher field member of this pair has an intensity about twice that of the other. The two lines are accordingly assigned to the $V_3O_{10}^{5-}$ ion. Of the three vanadium nuclei in this ion, two of them (end groups) are equivalent and are in a different environment than the third (middle group). Analagous spectra have been observed for

Can. J. Chem. Downloaded from www.nrcresearchpress.com by 210.87.254.6 on 09/05/12
For personal use only.

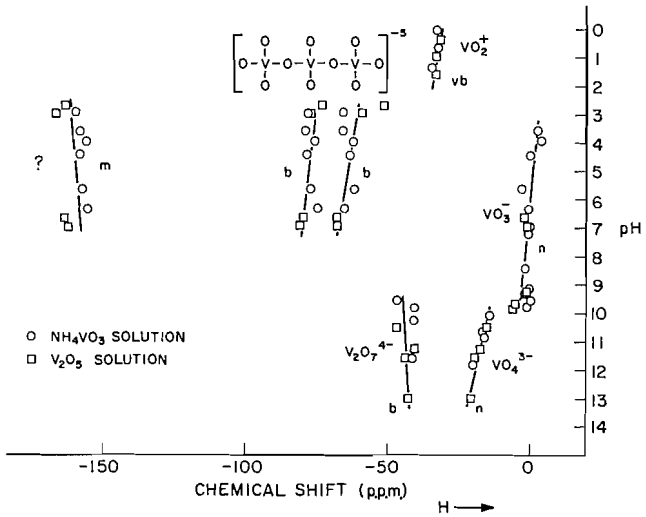

FIG. 4. ^{51}V resonance shifts of aqueous solutions of NH_4VO_3 and of V_2O_5 as a function of pH. Relative line widths of the resonances are indicated as n, m, b, and vb, corresponding to narrow, medium, broad, and very broad, respectively, covering a range of approximately 0.5 to 1.5 kc/s in line width.

^{31}P resonances of polyphosphate ions (11). Finally there is a third and completely separate species coexisting in the same pH range and having a vanadium resonance at much lower field (−160 p.p.m. from VO_3^-). The resonance line is moderately sharp indicating a fairly symmetrical species. This remains to be identified.[6]

At a pH ~ 2.2 a very sharp change in properties occurs, and the color of the solution changes. In solutions having a pH below this value only a single very broad resonance is observed about 30 p.p.m. to the low-field side of the VO_3^- resonance. The broad line is indicative of a large asymmetrical field near the vanadium nucleus. The resonance is accordingly assigned to the vanadyl ion, VO_2^+. Vanadyl sulfates are known stable salts and are obtained from strongly acid solutions (12).

It is evident from these results that a considerable amount of chemical information is derivable from nuclear resonances of complex ions. In some cases these resonances are readily observable, even though the ligand field about the quadrupolar nucleus is not spherically symmetrical. Also, the fact that several separate ionic species can coexist in the solution and their resonances are separately observable implies that exchange reactions between these species are relatively slow. Rapid exchanges (H and OH groups) between individual ions and the aqueous solvent may of course occur. The measured nuclear resonance shift of the ion is then characteristic of its exchange-averaged environment.

VII. EXPERIMENTAL

The metal resonances were measured using a Varian V4210A broad-line spectrometer incorporating a lock-in amplifier with audio phase-sensitive detection. The resonance signals were accordingly recorded as the derivative of the dispersion mode. All spectra were obtained at a magnetic field of 14.1 kilogauss.

Variable temperatures were achieved by means of a Dewar apparatus capable of operating in the range

[6]*The possibility of higher polymeric species in this pH range cannot be ruled out. Thus, for example, the metavanadate ion, VO_3^-, could conceivably be $V_4O_{12}^{4-}$ (see ref. 6, p. 810). However, unless this is a cyclic structure, two vanadium resonances should be observed because of the non-equivalence of the inner and end vanadium atoms, and the two resonances would have a constant relative intensity as the pH is varied. The further question arises whether the species, $V_5O_{14}^{3-}$, which should give three resonance lines, could account for the resonances at −160 p.p.m. and at −60 and −80 p.p.m. In this case the relative intensities of the three lines should be in the ratio of 2:2:1, whereas the observed ratio is 1:1:2.*

Can. J. Chem. Downloaded from www.nrcresearchpress.com by 210.87.254.6 on 09/05/12
For personal use only.

−100 to +200 °C. In this case, the conventional 15 mm i.d. sample tube was replaced by one with i.d. of 10 mm. Accordingly the sample volume is reduced by a factor of 2 and could introduce sensitivity problems for weak resonances. No such problems were encountered here.

Chemical shifts and line separations were measured by keeping H_0 fixed and sweeping the frequency using a Hewlett-Packard frequency counter. Line intensities were measured using low r.f. power in H_1, and the mean of at least five readings was taken.

The samples were prepared by the slow addition of the pentafluoride or oxide to the solvent, which was cooled to moderate the very exothermic reactions. The fluorides of Nb, Ta, and Sb, which are sensitive to moisture, were exposed to the air only during sample preparation. Samples prepared in a dry-box gave identical spectra.

Measurements of pH were carried out using a Beckman model H2 pH meter with a fiber junction calomel reference electrode. The meter was frequently calibrated and the pH values are accurate to ±0.1 pH unit.

Addition of the pentafluorides of Nb, Sb, and Ta to the various solvents employed gave solutions with the properties described below.

Compound	Solvent	Solution properties
NbF_5	48% HF	Colorless
NbF_5	Ethanol	Pale brown if dilute; mauve if concentrated
NbF_5	Ether	Dense mauve oily layer fairly soluble in ether
NbF_5	Ethanolic triethylamine[7]	Pale brown from which white crystals separate in a few hours
SbF_5	48% HF	Pale brown
SbF_5	Ethanol	Olive green
SbF_5	Ether	Dense dark-brown oily layer
TaF_5	48% HF	Colorless
TaF_5	Ethanol	Pale brown
TaF_5	Ether	Dense brown-red oily layer fairly soluble in ether

ACKNOWLEDGMENT

We should like to express our thanks to Mr. G. Ensell for constructing the variable temperature apparatus used in the low-resolution studies.

REFERENCES

1. N. Bloembergen, E. M. Purcell, and R. V. Pound. Phys. Rev. **73**, 679 (1948).
2. G. S. Savchenko and I. V. Tananayev-Zhur. Prikl. Khim. v Mashinostr. Sb. Statei, **19**, 1093 (1946).
3. K. J. Packer and E. L. Muetterties. J. Am. Chem. Soc. **85**, 3035 (1963).
4. F. Fairbrother, W. C. Frith, and A. A. Woolf. J. Chem. Soc. 1031 (1954).
5. J. Chatt. Private communication.
6. N. V. Sidgwick. The chemical elements and their compounds. Vol. I. Clarendon Press, Oxford. 1950. p. 817.
7. P. Melikov and P. Kasanetzky. Z. Anorg. allgem. Chem. **28**, 242 (1901).
8. F. Ephraim. Ber. **36**, 1177 (1903).
9. J. W. Mellor. Treatise on inorganic and theoretical chemistry. Vol. IX. Longmans, Green and Co., London. 1947. p. 758.
10. G. Jander, K. F. Jahr, and H. Witzmann. Z. Anorg. Allgem. Chem. **217**, 65 (1934).
11. C. F. Callis, J. R. Van Wazer, J. N. Shoolery, and W. A. Anderson. J. Am. Chem. Soc. **79**, 2719 (1957).
12. F. J. C. Rossotti and H. Rossotti. Acta. Chem. Scand. **10**, 957 (1956).

[7]$NbF_5 \cdot NEt_3$ *was prepared in this way to moderate the very exothermic reaction which occurs with* $NbF_5 \cdot NEt_3$ *even below 0 °C. When undiluted amine is used, a dark brown tar is immediately formed on contact with* NbF_5*, which is soluble in water. (*NbF_5 *dissolves in water to precipitate white* Nb_2O_5*.)*

Can. J. Chem. Downloaded from www.nrcresearchpress.com by 210.87.254.6 on 09/05/12
For personal use only.

Can. J. Chem. Downloaded from www.nrcresearchpress.com by 210.87.254.105 on 09/05/12
For personal use only.

SULFONIUM SALT SOLVOLYSIS

PART V. MODEL SYSTEMS FOR BIOLOGICAL TRANSMETHYLATION

JAMES B. HYNE AND JAMES H. JENSEN
Department of Chemistry, University of Alberta, Calgary, Alberta

Received June 15, 1964

ABSTRACT

The rates of solvolysis of a series of sulfonium salts which may be considered as models for the biologically important sulfonium salt, S-adenosylmethionine, are discussed in terms of a possible anchimeric role of the carboxyl group of methionine in transmethylation reactions.

INTRODUCTION

In a previous paper in this series (1) the apparent enhancement of the nucleophilicity of the acetate anion in the solvolysis of dimethyl *t*-butyl sulfonium acetate in low-polarity solvents suggested the possibility of a similar role for the carboxylate group in biological transmethylations.

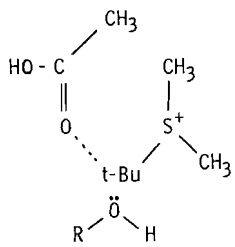

Possible participation in solvolysis

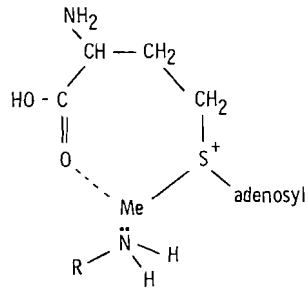

Possible participation in transmethylation

While transmethylation in the biological system normally involves S^+ to N transalkylation, the S^+ to O transalkylation in the solvolysis should be subject to similar assistance from an adjacent participating group, if such an effect is at all operative.

The comparison of the *t*-butyl and methyl group transfers requires explanation. By use of the *t*-butyl group as the transalkylating entity, competition from transfer of the other two groups on the sulfonium sulfur is eliminated. This exclusive transfer of the *t*-butyl entity in preference to either of the other functions was demonstrated by nuclear magnetic resonance (n.m.r.) studies of the products in selected cases. While transmethylation to nitrogen in the biological system cannot take place through a free methyl carbonium ion the possibility does exist for a free *t*-butyl carbonium ion in the solvolysis. However, in the low-polarity medium (0.75 mole fraction ethanol), the carbonium ion will be unstable and participation by such entities as an adjacent carboxyl group will be favored. If a *t*-butyl carbonium ion is envisaged, participation in its transfer by the carboxyl group could be envisaged as a very specific type of solvation if not actual covalent participation. The difference between the *t*-butyl and methyl cases is therefore one of degree of development of the δ^+ charge on the transferring alkyl group and participation might be expected to be operative in both cases.

Can. J. Chem. Downloaded from www.nrcresearchpress.com by 210.87.254.105 on 09/05/12
For personal use only.

To investigate further this type of role for the carboxyl group in transalkylation reactions, we report here a rate study of a series of model compounds of the type:

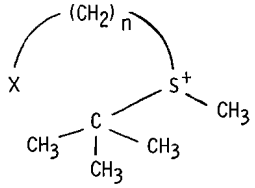

The function $X—(CH_2)_n—$ was varied by changing the value of n and by identifying X as methyl, carboxylic acid, and carboxylic ester groups.

RESULTS

The rate constants for the solvolysis (transalkylation to ROH) of the model sulfonium salts used are presented in Table I. These rate constants were obtained using a conductimetric technique with an initial concentration of the appropriate sulfonium iodide of 2×10^{-3} M in 0.750 mole fraction ethanol in water. The rate constants quoted in Table I are the average values of three determinations reproducible to better than $\pm 2\%$.

TABLE I

Rates of solvolysis of sulphonium iodides in 0.75 mole fraction ethanol-water at 60.00° (s^{-1})

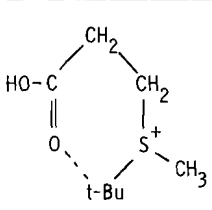

$k = 13.5 \times 10^{-4}$

I

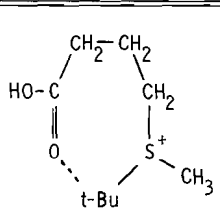

$k = 5.4 \times 10^{-4}$

II

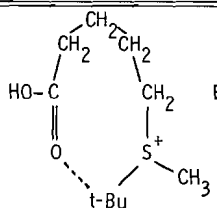

$k = 3.2 \times 10^{-4}$

III

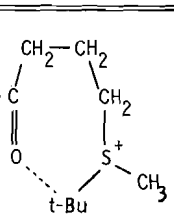

$k = 6.5 \times 10^{-4}$

IV

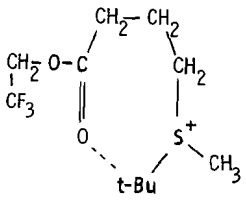

$k = 9.6 \times 10^{-4}$

V

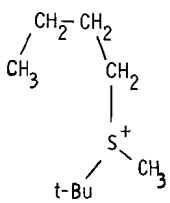

$k = 2.7 \times 10^{-4}$

VI

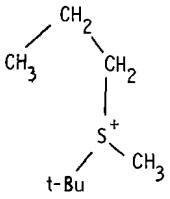

$k = 2.4 \times 10^{-4}$

VII

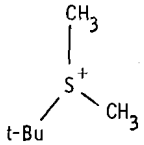

$k = 0.54 \times 10^{-4}$

VIII

DISCUSSION

It would appear from the rate data presented in Table I that the carboxyl group is significantly involved in the solvolysis of the model sulfonium salts. The carboxyl group may interact with the reactive center at the positively charged sulfur or with the developing positive charge at the *t*-butyl carbon atom:

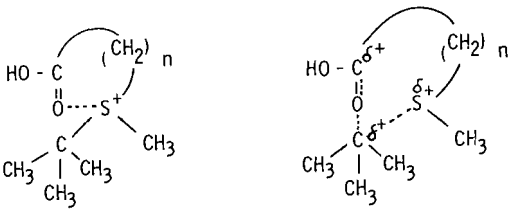

If the predominant interaction of the carboxyl group is with the sulfonium sulfur, the initial state should be stabilized and the reaction rate reduced relative to the case where (X) is an alkyl group. If, on the other hand, the interaction is with the developing center of positive charge at the *t*-butyl carbon atom (i.e. anchimeric assistance) the transition state will be stabilized and the reaction rate should be relatively faster compared to that with an alkyl substituent. As can be seen from Table I the latter interpretation is favored since the apparent rate of solvolysis is increased 5.6 times when (X) is changed from methyl to carboxyl.

Assuming that the interaction of the carboxyl group assists in the delocalization of the developing positive charge on the tertiary carbon atom, it can be seen (Table I) that the rate of solvolysis of the carboxyl sulfonium salts are correlated with the size of the ring formed in the transition state of these sulfonium salts. Thus the solvolysis of the sulfonium salt which involves a six-membered ring, I, is 2.5 times the solvolysis rate of the sulfonium salt which must proceed through a seven-membered ring, II. Since III must form an eight-membered ring for similar participation in the transition state to be operative, the carboxyl group would not be expected to function in this manner to any large extent. In fact III solvolyzes only 20% faster than the alkyl sulfonium salt VI in which no COOH participation is possible.

It should be noted that in the simple hydrocarbon chains, where (X) is methyl, alkyl chain lengthening results in an increase in the rate of solvolysis (VIII < VII < VI). This may be due to a dominant entropy effect in these cases where no participation of the terminal entity of the alkyl chain can take place.

Under the conditions of the reaction the carboxyl group will be predominantly in the protonated form, and the anchimeric role of the carboxyl group is likely to be through the participation of the lone pairs of electrons on the carbonyl oxygen. Thus any factor which would increase the availability of these electrons should increase the amount of anchimeric assistance and therefore the rate of solvolysis of the sulfonium salt. Since the ethyl group would be expected inductively to donate electrons to the carboxyl group more readily than hydrogen, it is not surprising that the sulfonium salt with the ester substituent (IV) solvolyzes more rapidly than the corresponding acid (II).

In this case the substitution of the ethyl group for hydrogen also may give rise to a steric factor similar to the type found for the alkyl substituents. This type of explanation for the increase in rate of solvolysis for the ester group is also suggested in the case of the trifluoro ester, although differences in intramolecular inductive effects will also be important (see later). The salt V solvolyzes more rapidly than the hydrogen analogue, while the prediction based on electronegativity effects on the electron availability at the carboxyl oxygen would be a decrease in rate. Further work will be necessary to separate these various factors in the systems under study.

While the rationalization of the data to this point has been based upon an anchimeric assistance role for the various remote substituents, the possible effect of long range

Can. J. Chem. Downloaded from www.nrcresearchpress.com by 210.87.254.105 on 09/05/12
For personal use only.

Can. J. Chem. Downloaded from www.nrcresearchpress.com by 210.87.254.105 on 09/05/12
For personal use only.

intramolecular inductive influences cannot be unambiguously excluded. The magnitude of such effects, and in particular the manner in which they vary with the remoteness of the substituent from the reaction center, can be estimated using the Hammett-Taft type treatment, i.e. $\log k_X/k_H = \rho^*\sigma^*$ (2) Values for the appropriate ρ^* and σ^* constants are not available for the sulfonium salt systems under study here but values for $\log k_X/k_H$ can be calculated from the observed data as shown in Table II. The value of k_H for the case where two methylene groups are interposed between the COOH substituent and the reaction center is estimated from the rate values for the substituent one and three methylenes removed respectively, i.e., substrates VIII and VII. The highest possible value, namely that for VII is used in Table II. Inductive effects are frequently assumed to decrease by a factor of 1/2 per additional methylene interposed between substituent and reaction center (3). Depending upon the precise value of k_H for the case of two methylenes interposed, the decrease in $\log k_X/k_H$ and hence $\rho^*\sigma^*$ caused by increasing the number of CH_2 groups from two to three is *at least* of this magnitude and is probably larger. Increasing the number of methylenes interposed from three to four, however, results in a five-fold decrease, much larger than is predicted by the Hammett-Taft treatment. It should be noted that lack of knowledge of the appropriate values for ρ^* and σ^* in this argument is not restrictive since ρ^* is assumed constant for the reactions and hence the change in $\log k_X/k_H$ is a true measure of the change in the inductive effect σ^*. Our explanation of this observation is that in the substrates with two and possibly three interposed methylenes anchimeric assistance of the type discussed previously enhances the accelerating role of the substituent through the formation of more or less stable transient ring structures. Such participation is unlikely in the case of four interposed methylenes. The result of such additional anchimeric assistance in the case of two or three interposed methylenes will be to increase k_X and make the k_X/k_H ratios greater than predicted from purely inductive effects. While such an argument cannot be claimed to be conclusive evidence for the dominant role of anchimeric assistance it does indicate that long range inductive effects do not appear to account for all of the observed rate changes.

TABLE II

Rate ratios for COOH and unsubstituted sulfonium salts

Substrates compared	Number of interposed CH_2 groups	Log k_X/k_H	Rate change (decrease)
Estimated from VIII and VII vs. I	2	$\text{Log } \frac{13.5}{>2.4} > 0.75$	1/2
VII vs. II	3	$\text{Log } \frac{5.4}{2.4} = 0.35$	1/5
VI vs. III	4	$\text{Log } \frac{3.2}{2.7} = 0.07$	

This type of anchimeric assistance by a carboxyl function is not unusual; for example Winstein *et al.* (4) have shown that anchimeric assistance is important in the acetolysis of *trans*-2-acetoxycyclohexyl brosylate. It might be argued that in the present study the presence of the bulky *t*-butyl group might prevent participation of the type suggested. We are not, however, insisting that a covalent bond is formed between the carboxyl oxygen and the developing *t*-butyl carbonium ion, but rather that the ester or acid function is a good 'solvent' stabilizing the formation of the incipient carbonium ion. This may be

particularly important in view of the fact that the oxygen is in a preferred configuration for interaction compared with water or ethanol which must be taken from the surrounding solvation shell.

The effect of actually attaching the carboxyl group to the sulfonium salt, as opposed to having it available as a separate molecular entity, may be assessed by comparing the rate of solvolysis of the sulfonium salt I (13.5×10^{-4} s^{-1} at 60°) with the rate constant for the internal ion-pair attack by acetate ion ($1.5\text{–}3.0 \times 10^{-4}$ s^{-1} at 60°) as estimated from the value obtained in the previous paper of this series (1). The favorable entropy effect of actually attaching the participating acetate group to the reacting molecule results in a rate enhancement of some 4 to 8 times.

EXPERIMENTAL

Compounds which could be characterized by literature references were prepared by standard procedures and are listed below with the pertinent physical properties and references. Procedures for preparing new compounds are listed with the physical properties, analyses, and yields. Nuclear magnetic resonance spectra were obtained for all intermediate compounds and sulfonium salts using a Varian A-60 Spectrometer. These spectra (available on request) leave little doubt as to the nature of the products, although the analytical data for some of the sulfonium salts are not in as good agreement with theory as is normally expected. These discrepancies are probably due to the instability of the salts. The salts decomposed readily and were recrystallized immediately before use. All other reagents were "reagent grade" chemicals.

Previously Prepared Compounds

5-Bromopentanoic acid.—Boiling point 110–115° at 2 mm; lit. b.p. 125–131° at 6 mm (5). Yield 50%.

4-Bromobutanoic acid.—Boiling point 92–96° at 2 mm m.p. 31–31.5°, lit. m.p. 32° (6). Yield 90%.

3-Bromopropanoic acid.—Melting point 61–61.5°, lit. m.p. 59.5–61° (7), 62.5° (8). Yield 75%.

Ethyl-(4-bromo)-butanoate.—Boiling point 93–95° at 02 mm; lit. b.p. 96–100° at 20 mm (9), 85–87° at 14 mm (10). Yield 40%.

Dimethyl t-Butyl sulfonium iodide.—Melting point 160–160.5°, lit. m.p. 159–160.2° (11).

Intermediates

2,2,2-Trifluoroethyl-(4-bromo)-butanoate

An ether solution of 4-bromobutanoic acid was dropped into thionyl chloride (100% mole excess) and the mixture refluxed for 1 h, and distilled; b.p. of the acid chloride, 87–89° at 20 mm. The acid chloride was added to 2,2,2-trifluoroethanol (100% mole excess) over a period of 1 h at 0°. The solution was allowed to stand for 1 h at room temperature, then poured into water, extracted with ether, washed with water, sodium carbonate, and water, dried with Drierite, and distilled; b.p. 86–88° at 17 mm. Overall yield 45%.

t-Butyl-n-propyl Sulfide

Sodium hydroxide (0.22 mole) was dissolved in 50 ml of dry ethanol. The *t*-butyl mercaptan (0.11 mole) and then 1-bromopropane (0.1 mole) were added dropwise. The mixture was refluxed for 1 h and then one-half of the ethanol was removed by distillation. Water (50 ml) was added and the layers separated. The water layer was extracted twice with ether, the ether layers being added to the original organic layer. The ether solution was dried with Drierite, the ether removed, and the sulfide distilled; b.p. 133–136° at 660 mm. Yield 50%.

t-Butyl n-Butyl Sulfide

The same procedure as above, using sodium hydroxide (0.22 mole), *t*-butyl mercaptan (0.11 mole), and 1-bromobutane (0.1 mole), was followed; b.p. 159–164° at 660 mm. Yield 55%.

t-Butyl δ-Carboxy-n-butyl Sulfide

Sodium hydroxide (0.375 mole) was dissolved in 50 ml of dry ethanol. The *t*-butyl mercaptan (0.125 mole) and then 5-bromopentanoic acid (0.1 mole) were added dropwise. The mixture was refluxed for 1 h and then one-half of the ethanol was removed by distillation. Water (50 ml) was added and the layers separated. The water layer was extracted with ether twice to remove any ester which formed in the reaction. The water layer was acidified and extracted with ether twice. The ether solution was dried with Drierite, the ether removed, and the sulfide distilled under vacuum; b.p. 110–111° at 0.4 mm. Yield 40%.

t-Butyl γ-Carboxy-n-propyl Sulfide

The same procedure as above, using sodium hydroxide (0.375 mole), *t*-butyl mercaptan (0.125 mole), and 4-bromobutanoic acid (0.1 mole), was followed; b.p. 115–122° at 3 mm. Yield 45%.

Can. J. Chem. Downloaded from www.nrcresearchpress.com by 210.87.254.105 on 09/05/12
For personal use only.

t-Butyl β-Carboxyethyl Sulfide

The same procedure as above, using sodium hydroxide (0.375 mole), *t*-butyl mercaptan (0.125 mole), and 3-bromopropanoic acid (0.1 mole), was followed; b.p. 87–94° at 3 mm. Yield 45%.

t-Butyl γ-Carboethoxy-n-propyl Sulfide

Sodium hydroxide (0.25 mole) was dissolved in 50 ml of dry ethanol. The *t*-butyl mercaptan (0.125 mole) and the ethyl-(4-bromo)-butanoate (0.1 mole) were added dropwise. The mixture was refluxed for 1 h and then one-half of the ethanol was removed by distillation. Water (50 ml) was added and the layers separated. The water layer was extracted with ether. The organic layers were combined and washed with water, dried with Drierite, the ether removed, and the sulfide distilled; b.p. 93–97° at 2 mm. Yield 35%.

t-Butyl Carbo-(β,β,β-trifluoro)-ethoxy-n-propyl Sulfide

The same procedure as above, using sodium hydroxide (0.25 mole), *t*-butyl mercaptan (0.125 mole), and 2,2,2-trifluoroethyl-(4-bromo)-butanoate (0.1 mole), was followed; b.p. 120–122° at 2 mm. Yield 45%.

New Sulfonium Salts

Methyl t-Butyl n-Propyl Sulfonium Iodide (VII)

Methyl iodide (10% mole excess) was added to *t*-butyl *n*-propyl sulfide and allowed to stand for 6 h. The resulting mass was recrystallized three times by dissolving the salt in warm ethanol and then adding sufficient ether to turn the solution cloudy. The solution was then placed in the freezer until precipitation was complete. The solution yielded a white crystalline solid, 60%; m.p. 115.5–116°.

Anal. Calcd. C, 35.04; H, 6.98; S, 11.6. Found: C, 35.28; H, 7.11; S, 11.6.

Methyl t-Butyl n-Butyl Sulfonium Iodide (VI)

Methyl iodide (10% mole excess) was added to *t*-butyl *n*-butyl sulfide and allowed to stand for 6 h. The resulting mass was recrystallized four times from an ethanol–ether mixture as described previously. The mixture yielded a white crystalline solid, 45%; m.p. 96–97°.

Anal. Calcd. C, 37.50; H, 7.34; S, 11.1. Found: C, 37.63; H, 7.47; S, 11.1.

Methyl t-Butyl δ-Carboxy-n-butyl Sulfonium Iodide (III)

Methyl iodide (20% mole excess) was added to *t*-butyl δ-carboxy-*n*-butyl sulfide and allowed to stand for 4 h. The resulting mass was recrystallized three times from an ethanol–ether mixture as described previously. The mixture yielded a white crystalline solid, 35%; m.p. 106.5–107°.

Anal. Calcd. C, 36.15; H, 6.47; S, 9.65. Found: C, 37.37; H, 6.27; S, 9.51.

Methyl t-Butyl γ-Carboxy-n-propyl Sulfonium Iodide (II)

Methyl iodide (20% mole excess) was added to *t*-butyl γ-carboxy-*n*-propyl sulfide and allowed to stand for 4 h. The resulting mass was recrystallized four times from an ethanol–ether mixture as described previously. The mixture yielded a white crystalline solid, 25%; m.p. 116.5–117.5°.

Anal. Calcd. C, 33.97; H, 6.02; S, 10.08. Found: C, 34.19; H, 6.16; S, 9.65.

Methyl t-Butyl β-Carboxyethyl Sulfonium Iodide (I)

Methyl iodide (20% mole excess) was added to *t*-butyl β-carboxyethyl sulfide and allowed to stand for 3 h. The resulting mass was recrystallized three times from an ethanol–ether mixture as previously described. The mixture yielded a white crystalline solid, 25%; m.p. 87.5–89°.

Anal. Calcd. C, 31.59; H, 5.63; S, 10.5. Found: C, 30.11; H, 6.09; S, 9.68.

Methyl t-Butyl γ-carboethoxy-n-propyl Sulfonium Iodide (IV)

Methyl iodide (20% mole excess) was added to *t*-butyl γ-carboethoxy-n-propyl sulfide and allowed to stand for 2 h. The resulting mass was recrystallized three times from an ethanol–ether mixture as previously described. The mixture yielded a slightly yellow crystalline solid, 15%; m.p. 84.5–85°.

Anal. Calcd. C, 38.15; H, 6.70; S, 9.26. Found: C, 38.39; H, 6.65; S, 8.51.

Methyl t-Butyl γ-Carbo-(β,β,β-trifluoro)-ethoxy-n-propyl Sulfonium Iodide (V)

Methyl iodide (20% mole excess) was added to *t*-butyl γ-carbo-(β,β,β-trifluoro)-ethoxy-n-propyl sulfide and allowed to stand for 2 h. The resulting mass was recrystallized four times from an ethanol–ether mixture as previously described. The mixture yielded a slightly yellow crystalline solid, 15%; m.p. 84–84.5°.

Anal. Calcd. C, 33.01; H, 5.04; S, 8.01. Found: C, 33.48; H, 5.22; S, 7.44.

Solvents

Ethanol, Reliance Chemicals "100 per cent" grade was dried with magnesium turnings and distilled; n_{20}^{D} = 1.3606, lit. n_{20}^{D} = 1.3614 (12).

The water used was doubly distilled, with conductance less than 5×10^{-7} mhos.

Rate Determinations

The rate constants were measured conductimetrically using an a-c. bridge at 1 100 c.p.s. as described by Robertson. (13)

ACKNOWLEDGMENT

The authors are grateful for financial assistance from the National Research Council of Canada.

Can. J. Chem. Downloaded from www.nrcresearchpress.com by 210.87.254.105 on 09/05/12
For personal use only.

REFERENCES

1. J. B. HYNE and J. H. JENSEN. Can. J. Chem. **40**, 1394 (1962).
2. J. HINE. Physical organic chemistry. McGraw-Hill. 1962. p. 97.
3. P. E. PETERSON and G. ALLEN. J. Am. Chem. Soc. **85**, 3608 (1963).
4. S. WINSTEIN, H. V. HESS, and R. E. BUCKLES. J. Am. Chem. Soc. **64**, 2796 (1942).
5. R. CHRETEIN. Ann. Chim. Paris, **2**, 682 (1957).
6. G. AKSNES and H. E. PRUE. J. Chem. Soc. 103 (1959).
7. G. S. KOLESNIKOV, T. V. SMIRNOVA, L. I. MIZRAKH, N. N. MIKHAILOVSKAYA, and L. I. SHCHERBO. Zhur. Obshcheĭ Khim. **27**, 3005 (1957).
8 Handbook of chemistry and physics. Chemical Rubber Publishing Co., Cleveland, Ohio. 1959.
9. D. J. CRAM and H. STEINBERG. J. Am. Chem. Soc. **76**, 2753 (1954).
0. J. T. BRAUNKOLTZ and F. G. MANN. J. Chem. Soc. 3368 (1958).
11. J. B. HYNE and R. WOLFGANG. J. Phys. Chem. **64**, 699 (1960).
12. T. E. SMITH and R. F. BONNER. Anal. Chem. **24**, 517 (1952).
13. R. E. ROBERTSON. Can. J. Chem. **33**, 1536 (1955).

Can. J. Chem. Downloaded from www.nrcresearchpress.com by 210.87.254.105 on 09/05/12
For personal use only.

Can. J. Chem. Downloaded from www.nrcresearchpress.com by 210.87.254.40 on 09/05/12
For personal use only.

THE COPPER(II) *SYN*-PHENYL-2-PYRIDYL KETOXIME SYSTEM

PART I[1]

T. L. MEEK AND G. E. CHENEY
Department of Chemistry, Acadia University, Wolfville, Nova Scotia

Received July 13, 1964

ABSTRACT

A survey has been made of the reactions of both geometric isomers of phenyl-2-pyridyl ketoxime with metal ions. The complexes of copper(II) with the *syn*-phenyl isomer have been investigated. Acid dissociation constants of both geometric isomers, and of the 2:1 copper chelate of the *syn*-phenyl oxime have been determined.

INTRODUCTION

Since the initial report on dimethylglyoxime by Tschugaeff (1), the *vic*-dioximes have been studied extensively (2–4) as analytical reagents, and many workers (5–11) have investigated the thermodynamic stability of the chelates of some of these ligands. The abnormally short, strong intramolecular O—H—O bonds known (12, 13) to exist in the copper(II) and nickel(II) chelates of certain *vic*-dioximes are believed to contribute much to the unusual properties of these chelates. Many observers feel that the nature of these hydrogen bonds can be more conveniently studied by employing ligands which coordinate through one oxime nitrogen and one amine-type nitrogen. Reagents of this type which have been studied include 2-methyl-2-amino-3-butanone oxime and some of its N-substituted derivatives (14, 15) and pyridine 2-aldoxime (16–21).

Phenyl-2-pyridyl ketoxime has long been known to act as a chelating agent (22, 23) and has been used as an analytical reagent for various metal ions (24–28). The compound can exist in two isomeric forms, i.e. the phenyl ring may be *syn*- or *anti*- to the oxime group. Vassian and Murmann (29) have reported that the interconversion of the *syn*- and *anti*-isomers is very slow ($t_{\frac{1}{2}} > 4\,000$ min) in 1 *M* acid or alkali at 25 °C and have shown that no appreciable rearrangement occurs in solution at low temperatures. No quantitative work has been reported as yet on the equilibria pertaining to the chelation reactions of this ligand, nor have the structures of its chelates been firmly elucidated. It was thought desirable to conduct such a study, for purposes of comparison with pyridine 2-aldoxime and with the *vic*-dioximes. Therefore, following a qualitative investigation of the reactions of both geometric isomers of the ligand with numerous metal ions, the reaction of copper(II) with the *syn*-phenyl oxime was studied by potentiometric, spectrophotometric, and liquid–liquid extraction techniques.

This report is the first of a series pertaining to the reactions between *syn*-phenyl-2-pyridyl ketoxime and metal ions.

EXPERIMENTAL

Apparatus and Procedures

Potentiometric titrations were conducted on *syn*- and *anti*-phenyl-2-pyridyl ketoxime and on the copper(II) chelates of the former. The apparatus and general procedure employed are identical to those described by Haines (8). The titrant used was 0.1 *N* sodium hydroxide; the solvent system was 50 volume % dioxane–water. All titrations were performed in the presence of a known amount of perchloric acid. Varying mole ratios of ligand to metal were employed.

[1]*This work is taken from the thesis submitted by T. L. Meek to Acadia University in partial fulfillment of the requirements for the M.Sc. degree in Chemistry, April 1964.*

The acid dissociation constants of the *syn*-phenyl oxime were determined spectrophotometrically by the procedure of Flexser *et al.* (30) and by liquid–liquid extraction, using a water-anhydrous chloroform system, after the method of Jankowski and Freiser (31). The buffer solutions used were made up at an initial ionic strength of 2.0 by the addition of sodium chloride; thus after 1:1 dilution, the equilibria studied were occurring in water with an ionic strength of 1.0. All spectrophotometric measurements were taken on a Beckman model DU quartz spectrophotometer equipped with a photomultiplier attachment. Matched 1.00 cm silica cells, calibrated at the wavelengths of interest, were used. The cell compartment was equipped with thermospacers. All pH measurements were taken on a Radiometer pHM4C pH meter equipped with a saturated calomel-Beckman type E2 glass electrode pair. Both absorbance and pH measurements were made at 25.0 ± 0.1 °C.

Analyses

Microanalyses for carbon, hydrogen, and nitrogen were conducted by the Schwarzkopf Microanalytical Laboratories in Woodside, N.Y. The copper analyses were done iodometrically; the chloride analyses were done argentimetrically. In both cases the organic matter was destroyed by mild digestion with warm nitric acid.

Reagents

The two isomers of phenyl-2-pyridyl ketoxime were prepared, separated, and purified after the method of Huntress and Walter (32). The melting point of the *syn*-phenyl isomer was 153.0–153.5 °C; that of the *anti*-phenyl form was 167.0–167.5 °C. (Literature values (32) 150.5–152.5 °C and 165–167 °C respectively.)

The purity of each isomer was determined by potentiometric titration with perchloric acid in glacial acetic acid; in both cases the value obtained was 100.0 ± 0.2%.

Dichloro (syn-Phenyl-2-pyridyl Ketoxime) Copper(II)

Cupric chloride dihydrate (2 g, 0.012 mole) was dissolved in 10 ml of 1:3 hydrochloric acid. To this solution was added 2.5 g (0.0125 mole) of *syn*-phenyl-2-pyridyl ketoxime in 50 ml of 1:3 hydrochloric acid. A bright green precipitate appeared immediately; it was allowed to stand overnight, then filtered off on a glass frit and dried first *in vacuo*, then at 110 °C.

Anal. Calcd. for $Cu(C_{12}H_{10}N_2O)Cl_2$: C, 43.3; H, 3.0; N, 8.4; Cu, 19.1; Cl, 21.3. Found: C, 44.0; H, 3.1; N, 8.4; Cu, 19.2; Cl, 21.2.

Bis (syn-Phenyl-2-pyridyl Ketoxime) Copper(II) Dichloride

Cupric chloride dihydrate (2 g, 0.012 mole) dissolved in 20 ml of 2 *M* sodium chloride was added to a solution of 5 g (0.025 mole) of *syn*-phenyl-2-pyridyl ketoxime in 200 ml of 1:100 hydrochloric acid. The dark green precipitate was allowed to stand overnight, then collected on a glass frit and dried first *in vacuo*, then at 110 °C.

Anal. Calcd. for $[Cu(C_{12}H_{10}N_2O)_2]Cl_2$: C, 54.3; H, 3.8; N, 10.6; Cu, 12.0; Cl, 13.4. Found: C, 54.6; H, 3.7; N, 10.8; Cu, 12.0; Cl, 12.5.

Monohydrogen Bis (syn-Phenyl-2-pyridyl Ketoximato) Copper(II) Chloride

Cupric chloride dihydrate (2 g, 0.012 mole) was dissolved in 100 ml of 1 *M* sodium chloride and placed in a 500 ml extraction flask. A solution of 4.7 g (0.024 mole) of *syn*-phenyl-2-pyridyl ketoxime in 250 ml of chloroform was added. After equilibration, the dark green chloroform phase was drawn off and the aqueous phase was treated with 50 ml aliquots of chloroform until the organic extract was colorless. The combined extracts were boiled to dryness, and the dark green solid was dried first *in vacuo*, then at 110 °C.

Anal. Calcd. for $[Cu(C_{12}H_9N_2O)_2H]Cl$: C, 58.3; H, 3.9; N, 11.3; Cu, 12.9; Cl, 7.2. Found: C, 57.9; H, 4.0; N, 11.0; Cu, 12.4; Cl, 7.0.

Monohydrogen Bis (syn-Phenyl-2-pyridyl Ketoximato) Copper(II) Perchlorate

Cupric perchlorate hexahydrate (2 g, 0.0054 mole) was dissolved in 100 ml of 1 *M* sodium perchlorate. A solution of 2.6 g (0.013 mole) of *syn*-phenyl-2-pyridyl ketoxime in 100 ml of 95% ethanol was added and the dark green precipitate was allowed to stand overnight. The solid was collected on a glass frit and dried first *in vacuo*, then at 110 °C.

Anal. Calcd. for $[Cu(C_{12}H_9N_2O)_2H]ClO_4$: C, 51.6; H, 3.4; N, 10.0; Cu, 11.4. Found: C, 48.7; H, 3.3; N, 9.3; Cu, 11.4.

Di-(μ-hydroxo) Monohydrogen Bis [syn-Phenyl-2-pyridyl Ketoximato Copper(II)] Perchlorate

Cupric perchlorate hexahydrate (2 g, 0.0054 mole) dissolved in 100 ml of 1 *M* sodium perchlorate was treated with a solution of 1.0 g (0.005 mole) of *syn*-phenyl-2-pyridyl ketoxime in 100 ml of 95% ethanol. The dark green precipitate was allowed to stand overnight then collected on a glass frit and dried first *in vacuo*, then at 110 °C.

Anal. Calcd. for $[[Cu(C_{12}H_9N_2O)]_2H(OH)_2]ClO_4$: C, 43.9; H, 3.2; N, 8.5; Cu, 19.3. Found: C, 43.5; H, 3.1; N, 8.9; Cu, 20.3.

Can. J. Chem. Downloaded from www.nrcresearchpress.com by 210.87.254.40 on 09/05/12
For personal use only.

Bis (syn-Phenyl-2-pyridyl Ketoximato) Copper(II)

Cupric perchlorate hexahydrate (5 g, 0.014 mole) was dissolved in 50 ml of water and added to a solution of 6.5 g (0.033 mole) of *syn*-phenyl-2-pyridyl ketoxime in 500 ml of 2 *N* sodium hydroxide. The dark red-brown precipitate was allowed to stand overnight, then collected on a glass frit and dried first *in vacuo*, then at 110 °C.

Anal. Calcd. for $Cu(C_{12}H_9N_2O)_2$: C, 62.9; H, 4.0; N, 12.2; Cu, 13.9. Found: C, 59.5; H, 4.1; N, 11.1; Cu, 14.2.

RESULTS AND DISCUSSION

Preliminary Investigations

The behavior of both geometric isomers of phenyl-2-pyridyl ketoxime toward various metal ions was observed at pH values of 5, 8, and 12 by the procedure of Irving, Butler, and Ring (33). The results indicated that the *syn*-phenyl isomer forms colored complexes, extractable into chloroform, with many transition metal ions; the *anti*-phenyl oxime did not react visibly with any of the metal ions tested.

The stoichiometry of the copper chelate of the *syn*-phenyl isomer was determined by the mole ratio method of Yoe and Jones (34). The results (Fig. 1) indicated that both a 1:1 and a 2:1 chelate are formed.

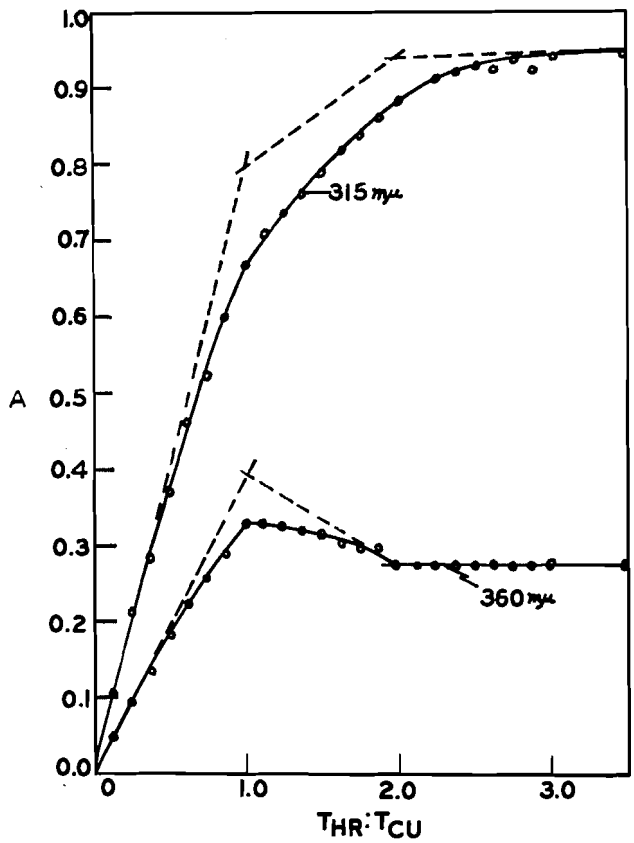

FIG. 1. Mole ratio plots, *syn*-phenyl-2-pyridyl ketoxime and copper(II); aqueous solution, $\mu = 0.1$ — pH = 5.5; A = absorbance; $T_{HR}:T_{Cu}$ = mole ratio of ligand to metal; $T_{Cu} = 8.0 \times 10^{-5}$ *M*; — experimentally obtained curve; – – extrapolated linear segments of experimental curve.

Can. J. Chem. Downloaded from www.nrcresearchpress.com by 210.87.254.40 on 09/05/12
For personal use only.

Acid Dissociation of the Reagents

The dissociation of either isomer of the ketoxime can be represented by the equilibria:

$$H_2R^+ \rightleftharpoons HR + H^+; \quad K_1 = \frac{[H^+][HR]}{[H_2R^+]}$$

$$HR \rightleftharpoons R^- + H^+; \quad K_2 = \frac{[H^+][R^-]}{[HR]},$$

where HR represents the neutral reagent molecule. The first dissociation refers to the protonated pyridine nitrogen atom, the second to the oxime group. The corresponding buffer regions do not overlap, so that K_1 and K_2 may be considered separately. The values obtained for pK_1 and pK_2 for each isomer are listed in Table I, together with values for structurally related compounds included for comparative purposes.

TABLE I

Acid dissociation constants of phenyl-2-pyridyl ketoxime and related compounds

Compound	Method	Medium	pK_{NH}	pK_{NOH}	Ref.
Pyridine	Pot. Spec.	$H_2O(\mu = 0.5)$	5.21		*
2,2′-Bipyridine	Pot.	H_2O	4.33		†
		50% dioxane	3.33		†
Acetoxime	Pot.	Glac. AcOH	1.75[a]		‡
	Pot.	H_2O		10.46[b]	§
anti-Benzaldoxime	Cond.	H_2O		11.33	‖
POX	Pot.	H_2O	3.42	10.04	¶
	Spec.	$H_2O(\mu \rightarrow 0)$	3.56	10.17	**
syn-PPK[c]	Spec.	$H_2O(\mu = 1)$	3.84±0.08	10.71±0.07	
	Extr.	$H_2O(\mu = 1)$	3.90±0.05	10.71±0.09	
	Pot.	50% dioxane	2.86±0.03	12.46±0.06	
anti-PPK[c]	Pot.	50% dioxane	2.30±0.02	12.65±0.07	

Abbreviations: POX = pyridine 2-aldoxime, Pot. = potentiometric, PPK = phenyl-2-pyridyl ketoxime, Spec. = spectrophotometric, Glac. AcOH = glacial acetic acid, Extr. = liquid–liquid extraction, Cond. = conductimetric.

[a]Represents pK in H_2O; converted from calculated value by Hall.‡

[b]Calculated by the author from data in literature.§

[c]Statements of precision are expressed in terms of the standard deviation for a minimum of 12 experimental values in two or more determinations.

*J. Bjerrum and E. J. Nielsen. Acta Chem. Scand. 2, 316 (1948).
†T. R. Harkins and H. Freiser. J. Am. Chem. Soc. 78, 1143 (1956).
‡N. F. Hall. J. Am. Chem. Soc. 52, 5113 (1930).
§A. Gandini and S. Constanza. Gazz. Chim. Ital. 67, 104 (1937).
‖O. L. Brady and R. F. Goldstein. J. Chem. Soc. 1918 (1926).
¶C. H. Liu and C. F. Liu. J. Am. Chem. Soc. 83, 4169 (1961).
**R. Green and I. Freer. J. Phys. Chem. 65, 2211 (1961).

The protonated form of the *anti*-phenyl oxime was found to be somewhat more acidic ($pK_1 = 2.30$ in 50% dioxane–water) than is that of the *syn*-phenyl isomer ($pK_1 = 2.86$ in 50% dioxane–water). Furthermore the neutral form of the *anti*-phenyl isomer is slightly less acidic ($pK_2 = 12.65$) than is that of the *syn*-phenyl isomer ($pK_2 = 12.46$). This can be explained by the existence of a weak N—H hydrogen bond in the uncharged form of the *anti*-phenyl oxime; its structure could be represented by

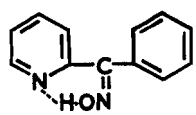

This is analogous to the well-known effect of hydrogen bonding on the acidities of *cis-trans* isomers of α-dicarboxylic acids, first observed by Jones and Soper (35). A similar structure was proposed by Krause, Busch, and Colthup (17) for pyridine 2-aldoxime, on the basis of an infrared spectrophotometric examination.

Can. J. Chem. Downloaded from www.nrcresearchpress.com by 210.87.254.40 on 09/05/12
For personal use only.

The differences between the acid dissociation constants of the *syn*-phenyl oxime in water and in 50% dioxane are in the direction that would be anticipated from consideration of the relative polarities of the two solvents. The values determined by spectrophotometry ($pK_1 = 3.84$; $pK_2 = 10.71$), and by liquid–liquid extraction ($pK_1 = 3.90$; $pK_2 = 10.71$) in the same solvent medium, are in good agreement.

The differences in acidity between *syn*-phenyl-2-pyridyl ketoxime and related compounds can be explained on the basis of structural differences. Consideration of the values listed in Table I reveals that both the pyridine ring and the oxime group are electron-withdrawing and tend to increase the acidity of conjugated functional groups, whereas the phenyl ring is electron-contributing and would cause the opposite effect. Thus the pyridinium nitrogen atom in *syn*-phenyl-2-pyridyl ketoxime would be expected to be considerably more acidic than the corresponding atom in pyridine. The difference in pK_{NH} between the ketoxime and pyridine-2-aldoxime can be attributed in part to the partial satisfaction of the electronegativity of the oxime group by the phenyl ring in the ketoxime and, in part, to the large differences in ionic strengths of the solutions in question. The relatively high pK_{NOH} of the ketoxime may be attributed to the electron-contributing properties of the phenyl ring.

Copper Chelates, Potentiometric Study

The formation constants of the copper(II) – *syn*-phenyl-2-pyridyl ketoxime system could not be evaluated by potentiometric titration because the highest complex was completely formed prior to the addition of alkali under the experimental conditions employed. Further evidence to support the complete formation of the 2:1 *syn*-phenyl-2-pyridyl ketoxime – copper(II) complex at low pH values (pH < 2.5) may be derived from the fact that the complex $Cu(HR)_2Cl_2$ was isolated from 0.1 *M* hydrochloric acid, and an attempt to isolate the corresponding perchlorate complex $Cu(HR)_2(ClO_4)_2$ from 1.0 *M* $HClO_4$ resulted in the precipitation of the species $Cu(RHR)ClO_4$.

In the potentiometric titrations of *syn*-phenyl-2-pyridyl ketoxime in the presence of copper(II) (Fig. 2), two equivalence points corresponding to the neutralization of all the perchloric acid plus one and two protons per molecule of chelate were obtained when the ligand-to-metal mole ratio exceeded 2:1. Therefore, the equilibrium constants K_I and K_{II}, defined by the relations

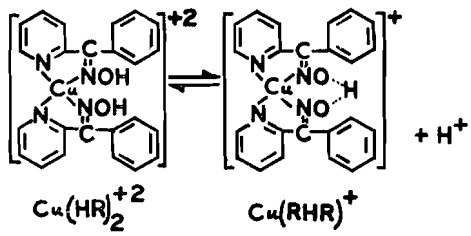

$$K_I = \frac{[Cu(RHR)^+][H^+]}{[Cu(HR)_2^{+2}]},$$

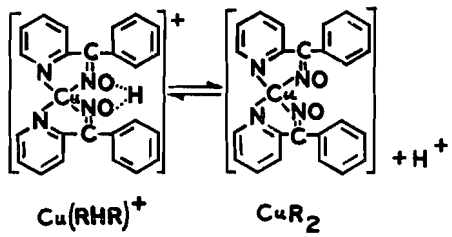

$$K_{II} = \frac{[CuR_2][H^+]}{[Cu(RHR)^+]},$$

Can. J. Chem. Downloaded from www.nrcresearchpress.com by 210.87.254.40 on 09/05/12
For personal use only.

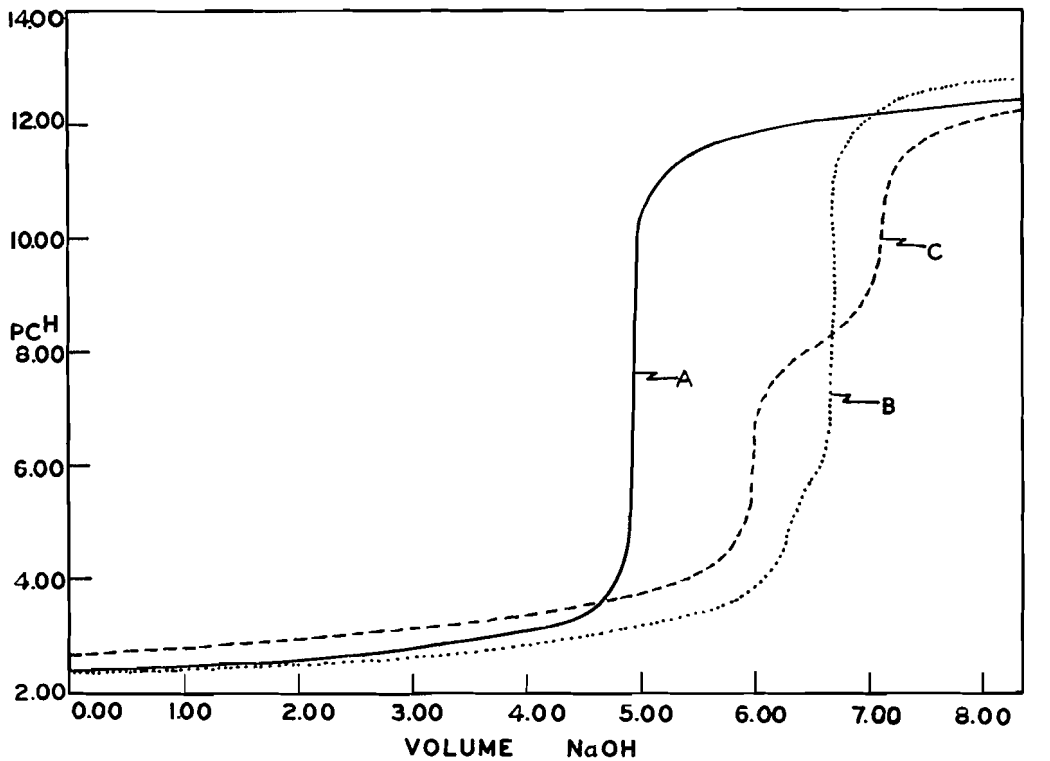

FIG. 2. Titration curves of *syn*-phenyl-2-pyridyl ketoxime and 0.50 mmole $HClO_4$, with 0.10 *N* NaOH in 50% v/v dioxane–water at 25 °C; A = 0.25 mmole HR; B = 0.10 mmole HR, 0.10 mmole copper(II); C = 0.70 mmole HR, 0.10 mmole copper(II).

could be evaluated by separately considering the first and second buffer regions, respectively.

If $\bar{n}_H$ is defined as the number of protons bound per molecule of chelate, it may be shown that, in the first buffer region,

$$[1] \qquad pK_I = p_cH - \log \frac{2 - \bar{n}_H}{\bar{n}_H - 1},$$

while in the second buffer region,

$$[2] \qquad pK_{II} = p_cH - \log \frac{1 - \bar{n}_H}{\bar{n}_H}.$$

The values obtained for pK_I and pK_{II} corresponding to each ligand-to-metal mole ratio employed are listed in Table II, together with other relevant titration data.

The values of pK_I are somewhat questionable, since the dissociation occurs at a very low pH. Thus the number of protons released is very small compared with the total number present, and cannot be measured accurately. Furthermore, the free ligand HR is a stronger base than is $Cu(RHR)^+$, so that when the ligand-to-metal ratio is high, a pseudo-buffer system may be established due to the equilibrium.

$$Cu(HR)_2^{+2} + HR \rightleftharpoons Cu(RHR)^+ + H_2R^+.$$

Can. J. Chem. Downloaded from www.nrcresearchpress.com by 210.87.254.40 on 09/05/12
For personal use only.

TABLE II

Titration data for 2:1 *syn*-phenyl-2-pyridyl ketoxime Copper(II) complex

Mole ratio $T_{HR} : T_{Cu}$	pH at $\bar{n}_H = 1.0$	pH at $\bar{n}_H = 0.5$	pH at start of precipitation	pK_I	pK_{II}
2.02:1	5.12	7.24	7.57	2.2_5	7.2_0
2.99:1	5.79	7.65	8.07	1.7_9	7.7_3
3.04:1	5.98	7.86	—	2.3_8	7.9_2
5.10:1	6.85	8.09	—	2.7_4	8.1_2
7.04:1	6.16	8.06	—	2.7_0	8.0_5
9.92:1	6.25	8.02	—	2.6_4	8.0_0

This is reflected in a virtually constant value of $\bar{n}_H$ over the first 60–80% of the first buffer region when the ligand-to-metal ratio was greater than 5:1.

The values calculated for pK_{II} increased with increasing ligand-to-metal mole ratio until the latter reached 5:1, then remained essentially constant at a value of 8.0–8.1. At ratios of less than 3:1 a green precipitate appeared near the end of the second buffer region, while at ratios greater than 3:1 the solution gradually turned from green to red–brown beyond the first equivalence point. These phenomena are believed due to the polymerization of the sparingly soluble green species CuR_2 to the red–brown polymer $(CuR_2)_n$. As a result of this polymerization reaction, eq. [2] no longer describes the system accurately under conditions which permit the reaction, and cannot be used to evaluate pK_{II}.

Thus it appears that, with respect to both K_I and K_{II}, the values obtained at a ligand-to-metal mole ratio of 2:1 are most reliable.

The very large difference between K_I and K_{II}, both of which may be attributed to the dissociation of a coordinated oxime group, can be accounted for by the existence of a very strong O···H—O bond, analogous to those in the copper(II) and nickel(II) dimethyl glyoxime chelates, in the species $Cu(RHR)^+$. Similar effects have been observed by Murmann (15) with certain aliphatic amine oximes and by other workers (20, 21) with pyridine 2-aldoxime.

The acidity of the oxime group, as measured by the acid dissociation constants, increased markedly on chelation. Such an increase in the acidity of a functional group conjugated with a metal ion in a chelate is a very common effect (20, 21, 36, 37). It would be expected to be very pronounced in this situation inasmuch as the metal ion is directly bonded to the functional group in question.

In the titrations conducted at a ligand-to-metal mole ratio of slightly less than 1:1, the two equivalence points (Fig. 2) correspond to the neutralization of the perchloric acid plus 1.25 and 1.6 protons per ligand molecule. The complex $[(CuRHCuR)(OH)_2]ClO_4$ which could give the structure

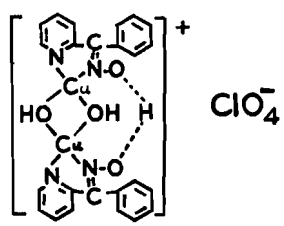

and corresponds to a complex isolated from a similar medium (see Experimental), would necessitate a loss of three protons per molecule of complex overall, or 1.5 per ligand

Can. J. Chem. Downloaded from www.nrcresearchpress.com by 210.87.254.40 on 09/05/12
For personal use only.

molecule. The position of the equivalence points implies that an olation process (which would require the loss of one proton per ligand molecule) occurs first, followed by the formation of the hydrogen bond (which requires the loss of 0.5 proton per ligand molecule); it also indicates that some overlap between these steps occurs. Similar bridged structures have been proposed by Murmann (15) for the species $[(CuAO')_2—H)(OH)_2]^+ClO_4^-$, where AO′ represents an N-substituted aliphatic amine oxime. Krause *et al.* (18) have postulated similar structures for palladium(II) complexes as $(PdPOX)_2Cl_2$ where POX represents the anion of pyridine-2-aldoxime.

The polynuclear structure

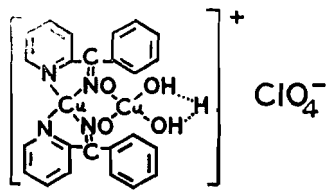

similar to that proposed by Liu and Liu (38) for certain copper(II) chelates of pyridine-2-aldoxime also corresponds to the analytical results. However, if it may be assumed that the stability of the species $Cu(RHR)^+$ is greater than that of the polynuclear complex, the formation of $Cu(RHR)^+$ as an intermediate would be required. This would cause an equivalence point corresponding to the neutralization of perchloric acid plus 0.5 protons per ligand molecule. The absence of such an equivalence point indicates that the species $Cu(RHR)^+$ is not formed, hence that the polynuclear structure need not be considered; it also implies that the 1:1 chelate is formed exclusively, hence that the first formation constant in this system is considerably greater than the second.

Copper Chelates, Liquid–Liquid Extraction Study

An attempt was made to study the extraction of copper(II) into chloroform by *syn*-phenyl-2-pyridyl ketoxime, employing a spectrophotometric analysis of the organic phase after 48 h equilibration at 25.0 °C. However, it proved impossible to determine the formation constant or the acid dissociation constants of the 2:1 copper chelate by this method, since both species $Cu(HR)_2Cl_2$ and $Cu(RHR)Cl$ were extractable into chloroform under the conditions employed; thus the distribution ratios could not be evaluated. Nevertheless, the data given in Table III yield some qualitative information. The increased absorbance of the organic phase with an increase in either pH or $T_{HR}:T_{Cu}$ can be interpreted in both instances as due to the conversion of $Cu(HR)_2^{+2}$ to the more strongly absorbing species $Cu(RHR)^+$. In the former case this would result from simple acidic dissociation, in the latter from the equilibrium

$$Cu(HR)_2^{+2} + HR \rightleftharpoons Cu(RHR)^+ + H_2R^+.$$

At pH values above 5.5, the red–brown polymeric species $(CuR_2)_n$ was extracted.

CONCLUSIONS

If a strongly acidic solution of copper(II) and *syn*-phenyl-2-pyridyl ketoxime at a ligand-to-metal ratio of 1:1 is neutralized, the sequence of equilibria may be represented by

[A1] $$H_2R^+ \rightleftharpoons HR + H^+$$

[A2] $$Cu^{+2} + HR \rightleftharpoons Cu(HR)^{+2}$$

Can. J. Chem. Downloaded from www.nrcresearchpress.com by 210.87.254.40 on 09/05/12
For personal use only.

TABLE III

Extraction of copper(II) by *syn*-phenyl-2-pyridyl ketoxime*

Mole ratio $T_{HR}:T_{Cu} = 2.50:1$		pH = 1.00 ± 0.02	
pH	Absorbance	Mole ratio $T_{HR}:T_{Cu}$	Absorbance
1.00	0.130		
1.04	0.147		
1.06	0.159	2.50	0.130
1.08	0.169	3.00	0.164
1.11	0.189	4.00	0.220
1.17	0.206	5.00	0.265
1.25	0.219	10.00	0.364
1.28	0.240	25.00	0.414
1.34	0.260	100.0	0.426
1.39	0.284		
1.53	0.323		
1.68	0.351		
1.80	0.370		
2.02	0.402		
2.42	0.419		
2.78	0.422		
3.86	0.425		
5.36	0.426		

*In each case, the aqueous phase was prepared by mixing 10.0 ml of 2.132×10^{-3} *M* copper perchlorate and 10.0 ml of 0.2055 *M* sodium chloride. The pH was adjusted with hydrochloric acid. This solution was treated with 20.0 ml of a solution of *syn*-phenyl-2-pyridyl ketoxime in anhydrous chloroform. The absorbance of the organic phase was measured against anhydrous chloroform after 48 h equilibration at 25.0 °C.

[A3] $$2Cu(HR)^{+2} + 2H_2O \rightleftharpoons Cu(HR)_2(OH)_2^{+2} + 2H^+$$

[A4] $$Cu(HR)_2(OH)_2^{+2} \rightleftharpoons CuRHCuR(OH)_2^{+} + H^+,$$

in which the third and fourth steps are proposed to account for the stoichiometry as evidenced by Fig. 2, and it is probable that these equilibria are not completely distinct, or separable.

When the ligand-to-metal ratio is greater than 3:1, the equilibrium sequence may be represented by

[B1] $$H_2R^+ \rightleftharpoons H^+ + HR$$

[B2] $$Cu^{+2} + HR \rightleftharpoons Cu(HR)^{+2}$$

[B3] $$Cu(HR)^{+2} + HR \rightleftharpoons Cu(HR)_2^{+2}$$

[B4] $$Cu(HR)_2^{+2} \rightleftharpoons Cu(RHR)^+ + H^+$$

[B5] $$Cu(RHR)^+ \rightleftharpoons CuR_2 + H^+$$

[B6] $$nCuR_2 \rightleftharpoons (CuR_2)_n,$$

while at ratios between 2:1 and 3:1 the same sequence occurs, with the exception of the last step, [B6].

The formation constants of the chelates $Cu(HR)^{+2}$ and $Cu(HR)_2^{+2}$ could not be evaluated due to the very low pH at which the corresponding equilibria occur. The coexistence of two or more species throughout most of the experimental pH range made it difficult to determine the molar absorptivities of any of the species of interest; thus the evaluation of K_I and K_{II} by spectroscopic methods was precluded. Similarly, the simultaneous extraction of more than one species into chloroform imposed great difficulties on the use of liquid–liquid extraction techniques for this purpose.

The sequence of reactions outlined above raises the question as to whether the reactions between dimethylglyoxime and metal ions could not be more readily represented by

Can. J. Chem. Downloaded from www.nrcresearchpress.com by 210.87.254.40 on 09/05/12
For personal use only.

[C1] $$M^{+2} + HD \rightleftharpoons M(HD)^{+2}$$

[C2] $$M(HD)^{+2} + HD \rightleftharpoons M(HD)_2^{+2}$$

[C3] $$M(HD)_2^{+2} \rightleftharpoons MD_2 + 2H^+,$$

than by the commonly accepted sequence

[D1] $$HD \rightleftharpoons H^+ + D^-$$

[D2] $$M^{+2} + D^- \rightleftharpoons MD^+$$

[D3] $$MD^+ + D^- \rightleftharpoons MD_2,$$

particularly in view of the fact that complexes of the type $Ni(HD)_2Cl_2$ and $Ni(HD)Cl_2$ have been isolated (39, 40). This would invalidate all the previously derived formation constants for MD_2 and the chelates of other *vic*-dioximes, as the presence of charged chelates of the type $M(HD)_{1\rightarrow n}^{+n}$ was not considered in their determination; the reactions [D2] and [D3], to which these constants apply, do not actually represent the formation of the chelates, as do reactions [C1] and [C2]. An investigation of the copper(II)- and nickel(II)-dimethylglyoxime systems is presently in progress.

The structures of the polymer $(CuR_2)_n$, and of the 1:1 bridged complex $[(CuRHCuR)(OH)_2]ClO_4$, are only postulates at this time, but are currently the subject of further study, as is the mechanism of the polymerization reaction. Potentiometric titration data indicates that a 3:1 (or greater) ligand-to-metal mole ratio is a prerequisite for the formation of the polymer, and (Table III) that the reaction occurs at a higher pH than that required to titrate the hydrogen-bonded proton in the species $Cu(RHR)^+$. In addition, an investigation of the infrared and electronic spectra of all the isolated compounds as an aid in structural interpretations is currently under way.

ACKNOWLEDGMENT

The authors gratefully acknowledge the financial support of the National Research Council of Canada, through a departmental research grant and a studentship awarded to T. L. M.

REFERENCES

1. L. TSCHUGAEFF. Z. anorg. Chem. **46**, 144 (1905).
2. H. DIEHL. The applications of the dioximes to analytical chemistry. G. Frederick Smith Chemical Co., Columbus, Ohio. 1940.
3. R. W. VAN DER HAAR and C. V. BANKS. Nickel complexes with some vic-dioximes. Ames Laboratory, Iowa State College. ISC-250.
4. D. T. HOOKER and C. V. BANKS. Preparation, properties, and analytical applications of some substituted alicyclic vic-dioximes. Ames Laboratory, Iowa State College. ISC-597.
5. R. G. CHARLES and H. FREISER. Anal. Chim. Acta, **11**, 101 (1954).
6. D. DYRSSEN, F. KRASOVEC, and L. G. SILLEN. Acta Chem. Scand. **13**, 50 (1959).
7. D. DYRSSEN and M. HENNICHS. Acta Chem. Scand. **15**, 47 (1961).
8. R. A. HAINES, D. E. RYAN, and G. E. CHENEY. Can. J. Chem. **40**, 1149 (1962).
9. C. V. BANKS and J. P. LAPLANTE. Anal. Chim. Acta, **27**, 80 (1962).
10. C. V. BANKS and S. ANDERSON. Inorg. Chem. **2**, 112 (1963).
11. K. BURGER and I. RUFF. Talanta, **10**, 329 (1963).
12. R. C. VOTER, C. V. BANKS, V. A. FASSEL, and P. W. KEHRES. Anal. Chem. **23**, 1730 (1951).
13. A. B. SHARPE and D. B. WAKEFIELD. J. Chem. Soc. 281 (1957).
14. R. K. MURMANN. J. Am. Chem. Soc. **79**, 521 (1957).
15. R. K. MURMANN. J. Am. Chem. Soc. **80**, 4174 (1958).
16. R. A. KRAUSE and D. H. BUSCH. J. Am. Chem. Soc. **82**, 4830 (1960).
17. R. A. KRAUSE, D. H. BUSCH, and N. B. COLTHUP. J. Phys. Chem. **65**, 2216 (1961).
18. R. A. KRAUSE, D. H. BUSCH, and D. JICHA. J. Am. Chem. Soc. **83**, 528 (1961).
19. C. H. LIU and C. F. LIU. J. Am. Chem. Soc. **83**, 2615 (1961).
20. C. H. LIU and C. F. LIU. J. Am. Chem. Soc. **83**, 4169 (1961).
21. G. I. H. HANANIA and D. H. IRVINE. J. Chem. Soc. 2745 (1962).
22. L. TSCHUGAEFF. Ber. **39**, 3382 (1906).
23. L. TSCHUGAEFF. J. Chem. Soc. **105**, 2187 (1914).

Can. J. Chem. Downloaded from www.nrcresearchpress.com by 210.87.254.40 on 09/05/12
For personal use only.

24. B. SEN Anal. Chem. **31**, 881 (1959).
25. B. SEN. Anal. Chim. Acta, **21**, 35 (1959).
26. F. TRUSSEL and H. DIEHL. Anal. Chem. **31**, 1978 (1959).
27. H. HARTKAMP. Z. Anal. Chem. **178**, 19 (1960).
28. J. GUYON and R. K. MURMANN. Anal. Chem. **36**, 1058 (1964).
29. E. G. VASSIAN and R. K. MURMANN. J. Org. Chem. **27**, 4309 (1962).
30. L. A. FLEXSER, L. P. HAMMETT, and A. DINGWALL. J. Am. Chem. Soc. **57**, 2103 (1935).
31. S. J. JANKOWSKI and H. FREISER. Anal. Chem. **33**, 776 (1961).
32. E. H. HUNTRESS and H. C. WALTER. J. Am. Chem. Soc. **70**, 3702 (1948).
33. H. IRVING, E. J. BUTLER, and M. F. RING. J. Chem. Soc. 1489 (1949).
34. J. H. YOE and A. L. JONES. Ind. Eng. Chem. Anal. Ed. **16**, 111 (1944).
35. L. JONES and F. G. SOPER. J. Chem. Soc. 133 (1936).
36. S. BAG, Q. FERNANDO, and H. FREISER. Inorg. Chem. **1**, 887 (1962).
37. A. CORSINI, Q. FERNANDO, and H. FREISER. Inorg. Chem. **2**, 224 (1963).
38. C. H. LIU and C. F. LIU. Inorg. Chem. **3**, 678 (1964).
39. F. PANETH and H. THILO. Z. Anorg. Allgem. Chem. **147**, 196 (1925).
40. A. G. SHARPE and D. B. WAKEFIELD. J. Chem. Soc. 496 (1957).

Can. J. Chem. Downloaded from www.nrcresearchpress.com by 210.87.254.40 on 09/05/12
For personal use only.

Can. J. Chem. Downloaded from www.nrcresearchpress.com by 210.87.254.105 on 09/05/12
For personal use only.

CORRELATIONS OF PROTON COUPLING CONSTANTS IN THE CYCLOPROPANE RING WITH ELECTRONEGATIVITY

CONSIDERATION OF THE PROTON RESONANCE SPECTRUM OF CYCLOPROPYLLITHIUM

T. SCHAEFER, F. HRUSKA,[1] AND G. KOTOWYCZ[2]
Department of Chemistry, University of Manitoba, Winnipeg, Manitoba
Received June 4, 1964

ABSTRACT

The analysis of cyclopropyllithium allows estimates to be made of all proton coupling constants. The exceptionally small couplings across carbon atoms 2 and 3 are examined in the context of correlations of coupling constants with the electronegativities of substituents. It is concluded that, although the couplings involving protons attached to the same carbon as the substituent decrease with increasing electronegativity of the substituent, the opposite is true for couplings involving the protons attached to carbons one bond removed from the substituent. Individual values are suggested for the coupling constants in cyclopropane itself and these agree with the observed ^{13}C side bands in its proton spectrum.

INTRODUCTION

A recent publication (1) gives the proton resonance spectrum of cyclopropyllithium in tetrahydrofuran. This spectrum is an example of an A_2B_2X system (2–4) but it appears to be very nearly a first-order spectrum. In view of the known values of proton coupling constants in the cyclopropane ring (5–10) and in view of our experience with first-order A_2B_2X spectra (3, 4), this is very curious. It can immediately be said that the coupling between the A and B protons in the CH_2CH_2 moiety must be not more than a cycle or two in order to give the observed spectrum (3, 4). This is rather unexpected.

Moreover, from the correlation observed by Williamson between coupling constants and electronegativity in monosubstituted 1,1-dichlorocyclopropanes, quite different values of these couplings would be predicted at first (11). We propose to clarify this situation by showing below that the coupling between A and B protons in cyclopropyllithium is indeed small and that correlations of cyclopropyl coupling constants with electronegativity show a behavior which has not yet been noticed. Furthermore, we deduce values for all the proton coupling constants in cyclopropane itself which should be accurate to about 0.5 c/s.

The Proton Resonance Spectrum of Cyclopropyllithium

1. The Observed Spectrum

The A_2B_2 region* consists of two doublets centered at −0.46 p.p.m. and +0.05 p.p.m. with respect to internal tetramethylsilane (1). The doublet at −0.46 p.p.m. has a splitting of 11.8 c/s while that at +0.05 p.p.m. shows a splitting of 9.5 c/s. Each line of these doublets shows a further splitting of about 1 c/s. The X region at 2.5 p.p.m. consists of nine lines placed symmetrically and the intensities and splitting agree with a first-order interpretation: a triplet of triplets with splittings of 11.8 and 9.5 c/s. A schematic spectrum is shown in I. This amount of information should suffice for our purposes.

[1]*Holder of an N.R.C. Studentship, 1963–1964.*
[2]*Holder of an N.R.C. Bursary, 1963–1964.*
**We take the A proton to be more shielded than the B proton to agree with the formulation of the analysis in ref. 2.*

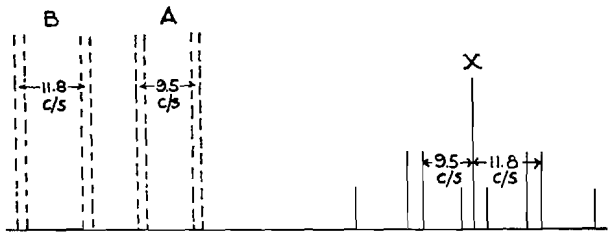

2. The Analysis

The ring proton spectrum can be characterized as in II:

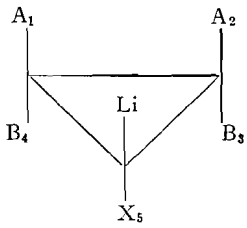

$$\begin{aligned} \upsilon_0(1-\sigma_A) &= 0.05 \text{ p.p.m.}, \\ \upsilon_0(1-\sigma_B) &= -0.46 \text{ p.p.m.}, \\ \upsilon_0(1-\sigma_X) &= 2.5 \text{ p.p.m.} \\ &\text{at 60 Mc/s.} \end{aligned} \qquad \begin{aligned} J_{12} &= J_{34} \\ J_{14} &= J_{23} \\ J_{15} &= J_{25} \\ J_{35} &= J_{45} \\ J_{13} &= J_{24} \end{aligned}$$

II

We shall assume $J_{12} = J_{34}$, which is probably valid to at least 0.5 c/s (6). The matrix elements in the F_z representation were first written down by Richards and Schaefer and can be found in Tables I and II of ref. 2. The Hamiltonian matrix is factored into four 1×1, ten 2×2 and two 4×4 sub-matrices.

From the observed spectrum, however, it is clear that considerably greater factoring must be present in this case. In fact, we must be dealing with an A_2R_2X spectrum, in the notation of Pople and Schaefer (12). It follows from the known matrix elements (2) that the shift between A and B protons, $\upsilon_0(\sigma_A - \sigma_B)$, must be at least 10 times as large as $\frac{1}{2}(J_{23} + J_{13})$, $\frac{1}{2}(J_{23} - J_{13})$, $\frac{1}{\sqrt{2}}J_{23}$, or $\frac{1}{\sqrt{2}}J_{13}$. Normally, $J_{13} = 4$ to 10 c/s, $J_{23} = -4$ to -9 c/s in cyclopropanes and since $\upsilon_0(\sigma_A - \sigma_B) \approx 30$ c/s, this condition is not fulfilled. In the 4×4's of ref. 2, for instance, we have $H_{88} - H_{99} \approx 15$ c/s, while $H_{89} \approx 5$ c/s for normal values of coupling constants (5–10).

We present independent evidence below that both $|J_{23}|$ and $|J_{13}|$ are not much larger than 1 c/s. In that case the problem reduces to an A_2R_2X system with the largest sub-matrices being two 2×2's. Referring to ref. 2 and defining a positive constant A and an angle θ as

[1] $$A \cos 2\theta = \tfrac{1}{2}(J_{13} - J_{23})$$
$$A \sin 2\theta = J_{12},$$

we have

[2] $$\begin{aligned} E_7 &= A - \tfrac{1}{2}J_{12} + \tfrac{1}{2}\upsilon_0(1-\sigma_X) \\ E_8 &= -A - \tfrac{1}{2}J_{12} + \tfrac{1}{2}\upsilon_0(1-\sigma_X) \\ E_{11} &= A - \tfrac{1}{2}J_{12} + \tfrac{1}{2}\upsilon_0(-1+\sigma_X) \\ E_{12} &= -A - \tfrac{1}{2}J_{12} + \tfrac{1}{2}\upsilon_0(-1+\sigma_X) \end{aligned}$$

Can. J. Chem. Downloaded from www.nrcresearchpress.com by 210.87.254.105 on 09/05/12
For personal use only.

for the energies; and for the eigenfunctions we have

[3]
$$\Psi_7^1 = \cos\theta\Psi_7 + \sin\theta\Psi_8$$
$$\Psi_8^1 = -\sin\theta\Psi_7 + \cos\theta\Psi_8$$
$$\Psi_{11}^1 = \cos\theta\Psi_{11} + \sin\theta\Psi_{12}$$
$$\Psi_{12}^1 = -\sin\theta\Psi_{11} + \cos\theta\Psi_{12},$$

where Ψ_7, Ψ_8, Ψ_{11}, and Ψ_{12} are given in ref. 2.

There are 16 transitions for proton X and 24 each for protons A and B (R). They are given in Tables I and II. The 46 combination lines are ignored because their intensity is effectively zero in this case. From Table I and the observed spectrum, it is immediately clear that a first-order spectrum is expected and that $J_{35} = 11.8$ c/s, $J_{15} = 9.5$ c/s. This conclusion affirms the assignment of Seyferth and Cohen (1).

TABLE I

Transitions and intensities of proton X

	Energy, relative to $(1 - \sigma_X)$	Relative intensity		Energy, relative to $(1 - \sigma_X)$	Relative intensity
1.	$+J_{15} + J_{35}$	1	9.	$-J_{35}$	1
2.	$+J_{15}$	1	10.	$-J_{15} - J_{35}$	1
3.	$+J_{35}$	1	11.	$+J_{15}$	1
4.	0	1	12.	$+J_{35}$	1
5.	0	1	13.	0	1
6.	$+J_{35} - J_{15}$	1	14.	0	1
7.	$-J_{35} + J_{15}$	1	15.	$-J_{15}$	1
8.	$-J_{15}$	1	16.	$-J_{35}$	1

TABLE II

Transitions and intensities of A and B protons*

	Energy, relative to $\nu_0(1 - \sigma_A)$	Relative intensity		Energy, relative to $\nu_0(1 - \sigma_A)$	Relative intensity
17.	$+\frac{1}{2}(J_{13} + J_{23} + J_{15})$	2	29.	$\frac{1}{2}(-2J_{12} - J_{15}) + A$	$1 + \sin 2\theta$
18.	$+\frac{1}{2}(2J_{12} + J_{15}) - A$	$1 + \sin 2\theta$	30.	$\frac{1}{2}(-J_{13} - J_{23} - J_{15})$	2
19.	$+\frac{1}{2}(2J_{12} + J_{15}) + A$	$1 - \sin 2\theta$	31.	$\frac{1}{2}(-J_{13} - J_{23} - J_{15})$	2
20.	$+\frac{1}{2}(J_{13} + J_{23} + J_{15})$	2	32.	$\frac{1}{2}(J_{13} + J_{23} - J_{15})$	2
21.	$+\frac{1}{2}(2J_{12} - J_{15}) - A$	$1 + \sin 2\theta$	33.	$\frac{1}{2}(-J_{13} + J_{23} + J_{15})$	1
22.	$+\frac{1}{2}(2J_{12} - J_{15}) + A$	$1 - \sin 2\theta$	34.	$\frac{1}{2}(J_{13} - J_{23} + J_{15})$	1
23.	$\frac{1}{2}(J_{13} + J_{23} - J_{15})$	2	35.	$\frac{1}{2}(-J_{13} + J_{23} - J_{15})$	1
24.	$\frac{1}{2}(-2J_{12} + J_{15}) + A$	$1 + \sin 2\theta$	36.	$\frac{1}{2}(J_{13} - J_{23} - J_{15})$	1
25.	$\frac{1}{2}(-2J_{12} + J_{15}) - A$	$1 - \sin 2\theta$	37.	$\frac{1}{2}(-J_{13} + J_{23} + J_{15})$	1
26.	$\frac{1}{2}(-J_{13} - J_{23} + J_{15})$	2	38.	$\frac{1}{2}(J_{13} - J_{23} + J_{15})$	1
27.	$\frac{1}{2}(-J_{13} - J_{23} + J_{15})$	2	39.	$\frac{1}{2}(J_{13} - J_{23} - J_{15})$	1
28.	$\frac{1}{2}(-2J_{12} - J_{15}) - A$	$1 - \sin 2\theta$	40.	$\frac{1}{2}(-J_{13} + J_{23} - J_{15})$	1

*To obtain the transitions and intensities of the B protons it is only necessary to replace J_{13} by J_{35} and $\nu_0(1-\sigma_A)$ by $\nu_0(1-\sigma_B)$ in the table.

However, from Table II it is clear that conclusions can also be reached about other coupling constants in the ring. From transitions 17 and 23, for instance, $|J_{13} + J_{23}| \approx 1$ c/s since the small splitting in the A spectrum is only about 1 c/s. From a pair of antisymmetrical transitions, i.e. 34 and 38, it follows that $|+J_{13} - J_{23}| \approx 1$ c/s. It appears that $|J_{23}| \approx 0$ or 1 c/s *or* that $|J_{13}| \approx 1$ or 0 c/s, but not both 0 or 1 c/s. In view of the resolution evident in the published spectrum, it is perhaps reasonable to put error limits of 0.5 c/s

Can. J. Chem. Downloaded from www.nrcresearchpress.com by 210.87.254.105 on 09/05/12
For personal use only.

on these values. These small values are consistent with the assumptions made in deducing Table II. Furthermore, from transitions like 18 and 19 and from eq. [1], we have $|J_{12} - A| \approx 0.5$ c/s and $\sin 2\theta \approx 0.9$. Consistency requires $J_{12} \approx 3$ c/s.

We suggest that the following coupling constants in c/s are consistent with the spectrum. For the X proton: $J_{15} = J_{trans} = 9.5$ c/s; $J_{35} = J_{cis} = 11.8$ c/s. For the AB(R) protons: $J_{12} = J_{cis} = 3 \pm 1$ c/s; $J_{13} = J_{trans} = 1.5 \pm 0.5$ c/s; $J_{23} = J_{gem} = -0.5 \pm 0.5$ c/s. We must now see whether these unusual values for the AB(R) protons can be rationalized.

Correlations of Coupling Constants with Electronegativity

1. Trends for J_{gem}

Williamson (11) as well as von R. Schleyer (13) have suggested that coupling constants in the cyclopropane ring are linear functions of the electronegativity (E) of the substituent In Fig. 1 the three types of proton coupling constants for compounds of the type 2-R-1,1-

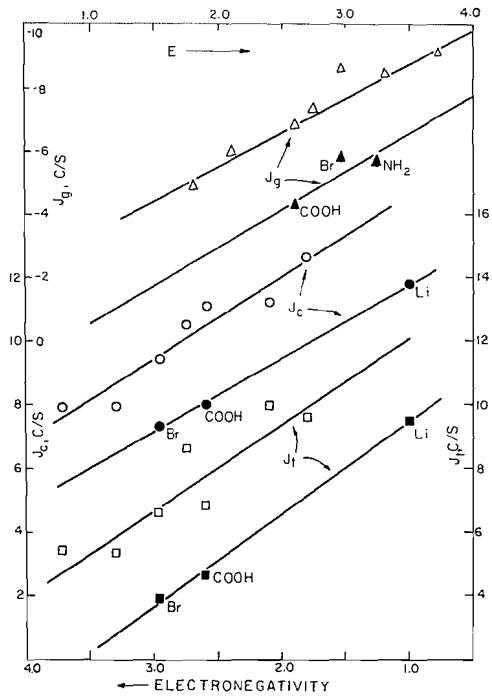

FIG. 1. Plot of proton coupling constants in c/s in 2-R-1,1-dichlorocyclopropanes versus electronegativity of R, open symbols; plot of proton coupling constants in c/s in monosubstituted cyclopropanes versus electronegativity, filled symbols. See text for discussion. Note the three different scales for the coupling constants and that the electronegativity scale decreases from left to right for J_{cis} and J_{trans} and vice versa for J_{gem}.

dichlorocyclopropane are plotted against E. They are represented by the open triangles, circles, and squares for J_{gem}, J_{cis}, and J_{trans}, respectively. The values are those measured and quoted by Williamson (11). We have also included the value for 1,1-dichlorocyclopropane itself ($E_H = 2.1$) which was taken from ref. 8. Representative straight lines have been drawn through the points which show considerable scatter for J_{cis} and J_{trans}. The correlation for J_{cis} is quite satisfactory, although the point for 2-bromo-1,1-dichlorocyclopropane falls off the line.

Can. J. Chem. Downloaded from www.nrcresearchpress.com by 210.87.254.105 on 09/05/12
For personal use only.

In Fig. 1 we have also plotted the coupling constants for a few monosubstituted cyclopropanes, represented by filled symbols. They have been taken from Wiberg and Nist for the bromo and carboxyl compounds (6), from Seyferth and Cohen for the lithium compound (1), and from Hutton and Schaefer for J_{gem} for the amino compound (4). For J_{trans} and J_{cis} the correlation is very good; for J_{gem} it is not as good.* We have taken $E_{NH_2} = 3.25$. Since all the plots are roughly parallel, we have drawn the line through J_{gem} for the monosubstituted compounds as shown. It appears from the plot that J_{gem} for Li is indeed in the vicinity of 0 c/s. We had estimated it to be -0.5 ± 0.5 c/s in the analysis above.

2. Trends for J_{cis} and J_{trans}

Another interesting conclusion from Fig. 1 is that the presence of the two chlorine atoms *increases* the coupling constants numerically by about 2 c/s. This is contrary to what one expects since E dependencies of coupling constants so far published (11, 13–17) demand that J is inversely proportional to E. In the present case, however, the chlorine atoms are situated on a *neighboring* carbon, i.e. on a carbon bonded to the carbons to which the hydrogens are bonded. In the monosubstituted cyclopropanes, as in vinyl compounds (16) or norbornene derivatives (13, 17), one is considering coupling of protons bonded to the carbon to which the substituent is attached.

The important conclusion is that substituents attached to carbon 1 in the cyclopropane ring will decrease the coupling constants between protons attached to carbons 1 and 2 (or 3) as E of the substituent increases, but will *increase* the coupling constants between protons attached to carbons 2 or 3. In cyclopropyllithium, therefore, we expect J_{12}, J_{13}, and J_{23} to be much smaller than in, e.g. bromocyclopropane. This is what we found in the analysis above.

3. Couplings in Cyclopropane

From the ^{13}C side bands in the proton spectrum of cyclopropane, Muller and Pritchard deduced a 7.5 ± 0.5 c/s coupling to adjacent protons (18). From the symmetry of the problem and the observed quintet, it is fairly clear that $J_{cis} + J_{trans} = 15.0 \pm 1.0$ c/s in cyclopropane. We can read off individual values from Fig. 1, assuming $E_H = 2.1$. We obtain $J_{cis} = 9.2$ and $J_{trans} = 6.2$ c/s, in agreement within experimental error with the ^{13}C side band (18). This agreement encourages a prediction for J_{gem} in cyclopropane. From Fig. 1 it is $J_{gem} = -5.6$ c/s. It is suggested that these values will be useful in an eventual analysis of the proton spectra of isotopically substituted cyclopropanes.

ACKNOWLEDGMENTS

We are grateful to the National Research Council for financial assistance.

REFERENCES

1. D. SEYFERTH and H. M. COHEN. J. Organometallic Chem. **1**, 15 (1963).
2. R. E. RICHARDS and T. SCHAEFER. Proc. Roy. Soc. Ser. A, **246**, 429 (1958).
3. T. SCHAEFER and W. G. SCHNEIDER. Can. J. Chem. **37**, 2078 (1959).
4. H. M. HUTTON and T. SCHAEFER. Can. J. Chem. **41**, 2774 (1963).
5. H. M. HUTTON and T. SCHAEFER. Can. J. Chem. **41**, 638 (1963).
6. K. B. WIBERG and B. J. NIST. J. Am. Chem. Soc. **85**, 2788 (1963).
7. J. D. GRAHAM and M. T. ROGERS. J. Am. Chem. Soc. **84**, 2249 (1962).
8. D. J. PATEL, M. E. H. HOWDEN, and J. D. ROBERTS. J. Am. Chem. Soc. **85**, 3218 (1963).
9. D. SEYFERTH, H. YAMAZAKI, and D. L. ALLESTON. J. Org. Chem. **28**, 703 (1963).
10. J. SMIDT and TH. J. DE BOER. Rec. Trav. Chim. **79**, 1235 (1960).
11. K. L. WILLIAMSON, C. A. LANFORD, and C. R. NICHOLSON. J. Am. Chem. Soc. **86**, 762 (1964).

**Perhaps there is some distortion in the trisubstituted rings which leads to a greater scatter for these plots than for the monosubstituted ring.*

Can. J. Chem. Downloaded from www.nrcresearchpress.com by 210.87.254.105 on 09/05/12
For personal use only.

12. J. A. POPLE and T. SCHAEFER. Mol. Phys. **3**, 547 (1960).
13. P. LASZLO and P. VON R. SCHLEYER. J. Am. Chem. Soc. **85**, 2709 (1963).
14. C. N. BANWELL and N. SHEPPARD. Discussions Faraday Soc. **34**, 115 (1962).
15. R. J. ABRAHAM and K. G. R. PACHLER. Mol. Phys. **7**, 167 (1963).
16. T. SCHAEFER. Can. J. Chem. **40**, 1 (1962).
17. K. L. WILLIAMSON. J. Am. Chem. Soc. **85**, 516 (1963).
18. N. MULLER and D. E. PRITCHARD. J. Chem. Phys. **31**, 768 (1959).

Can. J. Chem. Downloaded from www.nrcresearchpress.com by 210.87.254.105 on 09/05/12
For personal use only.

Can. J. Chem. Downloaded from www.nrcresearchpress.com by 210.87.254.105 on 09/05/12
For personal use only.

A SIMPLIFIED PROCEDURE FOR THE ANALYSIS OF COMPLEX NUCLEAR MAGNETIC RESONANCE SPECTRA

I. THE PRINCIPLES OF SUB-SPECTRAL ANALYSIS[1]

P. DIEHL,[2] R. G. JONES,[3] AND H. J. BERNSTEIN
Division of Pure Chemistry, National Research Council, Ottawa, Canada

Received August 25, 1964

ABSTRACT

A general procedure for the analysis of complex n.m.r. spectra has been developed in terms of simpler sub-spectra. The method is applicable to all possible combinations of magnetically equivalent and non-equivalent, strongly and weakly coupled groups of nuclei. It includes the special case of the composite particle model as well as the effective frequency method.

The method is applied, as an example, to the ABB'XX' spectrum of pyridine where the parameters J_{AB}, J_{AX}, the sum of $J_{BX} + J_{BX'}$, δ_{AB}, and δ_{AX} are derived without complete analysis of the spectrum, from the AB_2 sub-spectra of the problem.

INTRODUCTION

The methods which have been devised to analyze the n.m.r. spectra of complex systems have always been dedicated to the simplification of the analysis procedures. These procedures have involved a search for consistencies within the observed spectra.

The matching of observed spacings between lines taken two at a time to theoretical repeated spacings has been used extensively (1).

The composite particle method has been applied to complex systems made up of a number of groups of magnetically equivalent nuclei. The spectra of such complex systems have been attributed to the superposition of simpler spectra associated with the several groups of the system (2).

A more recent and powerful technique, that of "effective frequencies", led to the recognition of distinctive sub-spectra characteristic of the individual subgroups of the system. This method as outlined by the respective authors (3, 4) has been limited to the analysis of spectra of the type AA' . . . BB' . . . R_p . . . X_q where the prime symbol denotes magnetic non-equivalence. In those cases it leads to an impressive simplification of the analysis, and it has been possible to derive all the coupling constants and chemical shift data from the analysis of the sub-spectra of the system.

It is the purpose of this paper to expand the idea of sub-spectral analysis to the analysis of all types of nuclear magnetic resonance spectra, and it will be shown how far one can derive their properties without calculating the matrix elements of the Hamiltonian. The method of analysis to be developed is intended to be applicable to all possible combinations of magnetically equivalent and non-equivalent, strongly and weakly coupled, groups of nuclei. We shall first demonstrate the methods on the almost trivial case of two groups of magnetically equivalent nuclei, the AB_3 case (the A,B notation is that of Pople *et al.* (5)). We shall then proceed to the more complex case of three groups of nuclei partly strongly, partly weakly coupled and magnetically non-equivalent, the ABB'XX' case. We shall finally derive a general formulation of the method, giving rules which accomplish the sub-spectral breakdown.

[1]*Issued as N.R.C. No. 8177.*
[2]*Visiting Scientist, summer 1964. Permanent address: Department of Physics, University of Basel, Basel, Switzerland.*
[3]*N.R.C. Postdoctoral Fellow 1962–1964. Present address: Ministry of Aviation, E.R.D.E., Waltham Abbey, Essex, England.*

Can. J. Chem. Downloaded from www.nrcresearchpress.com by 210.87.254.105 on 09/05/12
For personal use only.

THE METHOD OF SUB-SPECTRAL ANALYSIS

The general spin system is composed of groups of nuclei (homo- or hetero-nuclear), which may or may not be magnetically equivalent, having effective local symmetry (D_3 for $^{12}C^1H_3$) which may be used to construct basic symmetry wave functions for that group. These group wave functions can then be reclassified by their transformation properties under the covering operations of the total molecular point group.

In the following discussion we have considered only systems of spin $\frac{1}{2}$ particles.

The 2^n basic symmetry wave functions of the most general set of nuclei can be constructed by taking appropriate products of basic symmetry wave functions of the interacting groups. The 2^n molecular wave functions are then classified into the various molecular symmetry species.

In the following text the basic symmetry functions for each set of equivalent nuclei and, eventually, the total system will be schematically represented in the tables and figures by horizontal lines characterized by the appropriate quantum numbers which conveniently summarize the relevant data, e.g. $F_z(A_n)$, $F_z(B_m)$, $F_z(X_q)$. We will, for example, use the symbol $\frac{1}{2}$ to denote the single particle function α. The energy level diagram for the total system will be represented by "line patterns" also. Transitions between the various states will be indicated by tie lines. In general we shall proceed from the group basic (local) symmetry wave function diagram to the group basic (molecular) symmetry wave function diagram and then to the molecular basic symmetry wave function diagram. After having allowed mixing of the basic symmetry functions, we shall obtain the stationary state wave function diagram or the "energy level diagram".

Example 1. The AB_3 System

The AB_3 system can belong to either of the isomorphic point groups D_3 or C_{3v}. The basic symmetry functions of the B_3 nuclei can be shown to be divided into four A_1 species functions and two degenerate pairs in the E species (6).

These functions are given in Table I together with the single particle functions of the A nucleus.

TABLE I

Basic symmetry functions of the A and B_3 groups of the AB_3 system, reclassified under the molecular symmetry

Group	F_z	A_1 species functions	E species functions
A	$\frac{1}{2}$	α	
	$-\frac{1}{2}$	β	
B	$\frac{3}{2}$	$\alpha\alpha\alpha$	
	$\frac{1}{2}$	$(\alpha\alpha\beta+\alpha\beta\alpha+\beta\alpha\alpha)3^{-1/2}$	$(2\beta\alpha\alpha-\alpha\beta\alpha-\alpha\alpha\beta)6^{-1/2}$, $(\alpha\beta\alpha-\alpha\alpha\beta)2^{-1/2}$
	$-\frac{1}{2}$	$(\beta\beta\alpha+\beta\alpha\beta+\alpha\beta\beta)3^{-1/2}$	$(2\alpha\beta\beta-\beta\alpha\beta-\beta\beta\alpha)6^{-1/2}$, $(\beta\alpha\beta-\beta\beta\alpha)2^{-1/2}$
	$-\frac{3}{2}$	$\beta\beta\beta$	

The sixteen AB_3 basic symmetry functions are constructed from products of the type $A_1 \times A_1 = A_1$ and $A_1 \times E = E$ and there are therefore eight functions in each symmetry species. The construction of the product functions is schematically represented in Table II.

In this table the function $\underline{\frac{1}{2},\frac{3}{2}}$ in the A_1 species of (AB_3), for example, represents the product of $\alpha(A)$ and $\alpha\alpha\alpha(B_3)$, i.e., $\underline{F_z(A),F_z(B_3)} = \underline{\frac{1}{2},\frac{3}{2}}$. Similarly the $\underline{-\frac{1}{2},\frac{1}{2}}$ function in the E species replaces either of the two functions, $\beta(A)$ $(2\beta\alpha\alpha - \alpha\beta\alpha - \alpha\alpha\beta)6^{-1/2}(B_3)$ or $\beta(A)$ $(\alpha\beta\alpha - \alpha\alpha\beta)2^{-1/2}(B_3)$.

TABLE II

Construction of the basic symmetry product functions of the AB_3 system

F_z	A group, $F_z(A)$		B_3 group, $F_z(B_3)$			AB_3, system $F_z(A)$, $F_z(B_3)$				
	A_1 species		A_1 species	E species		A_1 species		E species		
2						$\frac{1}{2},\frac{3}{2}$				
$\frac{3}{2}$			$\frac{3}{2}$							
1						$\frac{1}{2},\frac{1}{2}$	$-\frac{1}{2},\frac{3}{2}$	$\frac{1}{2},\frac{1}{2}$	$\frac{1}{2},\frac{1}{2}$	
$\frac{1}{2}$	$\frac{1}{2}$		$\frac{1}{2}$	$\frac{1}{2}$ $\frac{1}{2}$						
0		×			→	$\frac{1}{2},-\frac{1}{2}$	$-\frac{1}{2},\frac{1}{2}$	$\frac{1}{2},-\frac{1}{2}$	$-\frac{1}{2},\frac{1}{2}$	$\frac{1}{2},-\frac{1}{2}$ $-\frac{1}{2},\frac{1}{2}$
$-\frac{1}{2}$	$-\frac{1}{2}$		$-\frac{1}{2}$	$-\frac{1}{2}$ $-\frac{1}{2}$						
-1						$\frac{1}{2},-\frac{3}{2}$	$-\frac{1}{2},-\frac{1}{2}$		$-\frac{1}{2},-\frac{1}{2}$	$-\frac{1}{2},-\frac{1}{2}$
$-\frac{3}{2}$			$-\frac{3}{2}$							
-2							$-\frac{1}{2},-\frac{3}{2}$			

The energy level diagram (the stationary state wave function diagram) can be obtained from inspection of Table II. This is because the mixing which would transform the basic molecular symmetry product function diagram into a stationary state wave function diagram does not change the transition pattern. The A and B transitions can now be picked out from the symmetry function diagram (Table II) using the selection rules, $\Delta F_z(B_3) = 0$ and $\Delta F_z(A) = 0$ respectively.

The energy level diagram is given schematically in Fig. 1.

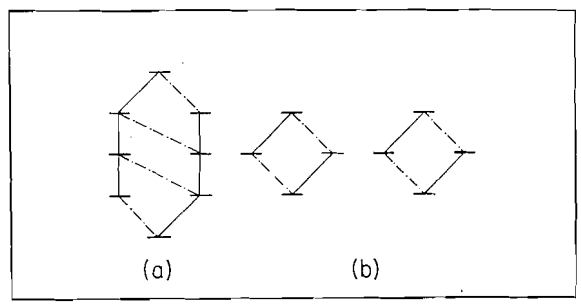

FIG. 1. Schematic energy level diagram of the AB_3 system. The solid tie lines represent B transitions and the broken tie lines represent A transitions; (*a*) A_1 species, (*b*) E species.

The result of these operations is a breakdown of the general AB_3 problem into sub-patterns which can be attributed to simpler problems. The simplicity of these patterns (the maximum determinantal order is two) arises because the molecular symmetry functions belong to the symmetry species A_1 and E are uniquely constructed from $A_1 \times A_1$ and $A_1 \times E$ products (i.e. there are no $E \times A_1 = E$ or $E \times E = A_1 + A_2 + E$ products). Hence the $A_1 \times A_1$ and $A_1 \times E$ product functions form unique groups which do not 'mix' because symmetry forbids it.

The energy level pattern isolated within the A_1 symmetry species is the typical energy level diagram of a system composed of a particle with spin $\frac{1}{2}$ and a particle with spin $\frac{3}{2}$, (composite particle model (2)). The E symmetry species energy level diagram is characteristic of the particle spin $\frac{1}{2}$, particle spin $\frac{1}{2}$ problem denoted *ab*. Lower case italic letters, e.g. *ab*, *abc*, are used to denote nuclei in sub-spectra. This *ab* subproblem can be explicitly solved, provided the correct assignment is made of observed spectral lines, to give all the

Can. J. Chem. Downloaded from www.nrcresearchpress.com by 210.87.254.105 on 09/05/12
For personal use only.

information that can be obtained from the complete AB_3 problem, that is the chemical shift δ_{AB} and the coupling constant J_{AB}. This special case already illustrates the value of sub-spectral analysis.

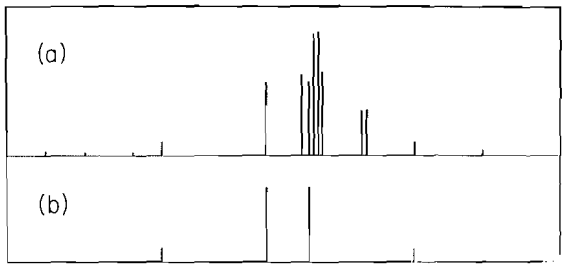

FIG. 2. Calculated spectra of AB_3 system for $J/\delta = 1$: (*a*) superposition of the ($I_A = \frac{1}{2}$, $I_B = \frac{1}{2}$) and the ($I_A = \frac{1}{2}$, $I_B = \frac{3}{2}$) sub-spectra; (*b*) the ($I_A = \frac{1}{2}$, $I_B = \frac{1}{2}$) sub-spectrum.

The spectrum of a typical AB_3 system is given in Fig. 2*a*. The *ab* sub-spectrum is indicated in Fig. 2*b*. Such a sub-spectrum can be easily picked out using previous knowledge such as the repeated spacing properties and typical relative intensity distribution. It is worthwhile pointing out here that in this simple case AB_3, where the nuclei within the groups are magnetically equivalent, the total spin quantum number F (where $F(F+1)$ is the eigenvalue of F^2 (5)) can be used to group the energy levels in a way equivalent to group theory.

Example 2. The ABB′XX′ System

The ABB′XX′ system may be regarded as being composed of three sub-groups, A, BB′, and XX′, where the nuclei within the BB′ and XX′ sub-groups respectively are chemically equivalent. It is possible to construct four basic symmetry wave functions for each of the two sets of equivalent nuclei which may be classified within the local symmetry restrictions as symmetric and antisymmetric with respect to an interchange of the two nuclei. The symmetric functions are $\alpha\alpha$, $(\alpha\beta + \beta\alpha)2^{-1/2}$, and $\beta\beta$ and the single antisymmetric function is $(\alpha\beta - \beta\alpha)2^{-1/2}$.

The overall molecular symmetry when all the nuclei lie in a plane is C_{2v}. This means that the molecule has a two-fold axis of symmetry, C_2, and two mutually perpendicular planes of symmetry σ_v and σ_v' (the plane containing all the nuclei). The possible symmetry species to which the molecular symmetry functions can belong are A_1 and B_2 (7). The functions α and β (A nucleus) as well as $\alpha\alpha$, $(\alpha\beta + \beta\alpha)2^{-1/2}$, and $\beta\beta$ (BB′ and XX′ sub-groups) are symmetric with respect to the C_2 axis, σ_v' and σ_v, and hence can be classified as A_1 functions. The functions $(\beta\alpha - \beta\alpha)2^{-1/2}$ are symmetric with respect to σ_v' but antisymmetric with respect to C_2 and σ_v. These are therefore B_2 symmetry functions. These results are summarized in Table III.

The molecular basic symmetry functions can be constructed by taking the products of all the group functions and classifying them according to their symmetry species as well as their F_z(XX′) and F_z(ABB′XX′), see Table IV.

The four species products are

$$A_1 \times A_1 \times A_1 = A_1, \qquad A_1 \times A_1 \times B_2 = B_2,$$
$$A_1 \times B_2 \times B_2 = A_1, \qquad A_1 \times B_2 \times A_1 = B_2,$$

as, for example,

$$A_1(A) \times A_1(BB') \times A_1(XX') = A_1(ABB'XX').$$

Can. J. Chem. Downloaded from www.nrcresearchpress.com by 210.87.254.105 on 09/05/12
For personal use only.

TABLE III

The basic symmetry functions of the A, BB′, and XX′ subgroups of the planar ABB′XX′ system with C_{2v} symmetry

F_z	Group A	Group BB′		Group XX′	
	A_1 species	A_1 species	B_2 species	A_1 species	B_2 species
1	α	$\alpha\alpha$		$\alpha\alpha$	
$\frac{1}{2}$		$(\alpha\beta+\beta\alpha)2^{-1/2}$	$(\alpha\beta-\beta\alpha)2^{-1/2}$	$(\alpha\beta+\beta\alpha)2^{-1/2}$	$(\alpha\beta-\beta\alpha)2^{-1/2}$
0					
$-\frac{1}{2}$	β				
-1		$\beta\beta$		$\beta\beta$	

An alternative way of arranging the basic molecular symmetry product functions more suitable to the discussion of the X transitions would be according to their F_z(ABB′) (see Fig. 3*b*) instead of F_z(XX′).

Those functions within a given symmetry species with the same F_z(XX′) and F_z(ABB′) can mix. For example, within the ABB′XX′ system A_1 symmetry species of Table IV, the product functions $(A_1 \times A_1 \times A_1)$ $F_z(ABB') = \frac{1}{2}$, $F_z(XX') = 0$ and $(A_1 \times B_2 \times B_2)$ $F_z(ABB') = \frac{1}{2}$, $F_z(XX') = 0$ can mix.

The maximum determinantal order in the A_1 symmetry species will therefore be three. The $(A_1 \times A_1 \times A_1)$, $(A_1 \times B_2 \times B_2)$ $F_z(ABB') = -\frac{1}{2}$ and $F_z(XX') = 0$ functions also can mix. A similar degree of mixing occurs within the B_2 symmetry species. The mixing which transforms the basic molecular symmetry product function diagram into a stationary state wave function diagram does not change the transition pattern. The energy level diagram can therefore be derived from Table IV. It is presented in Fig. 3. Some of the X transitions are indicated in Fig. 3*a* to clarify the relation to Fig. 3*b*.

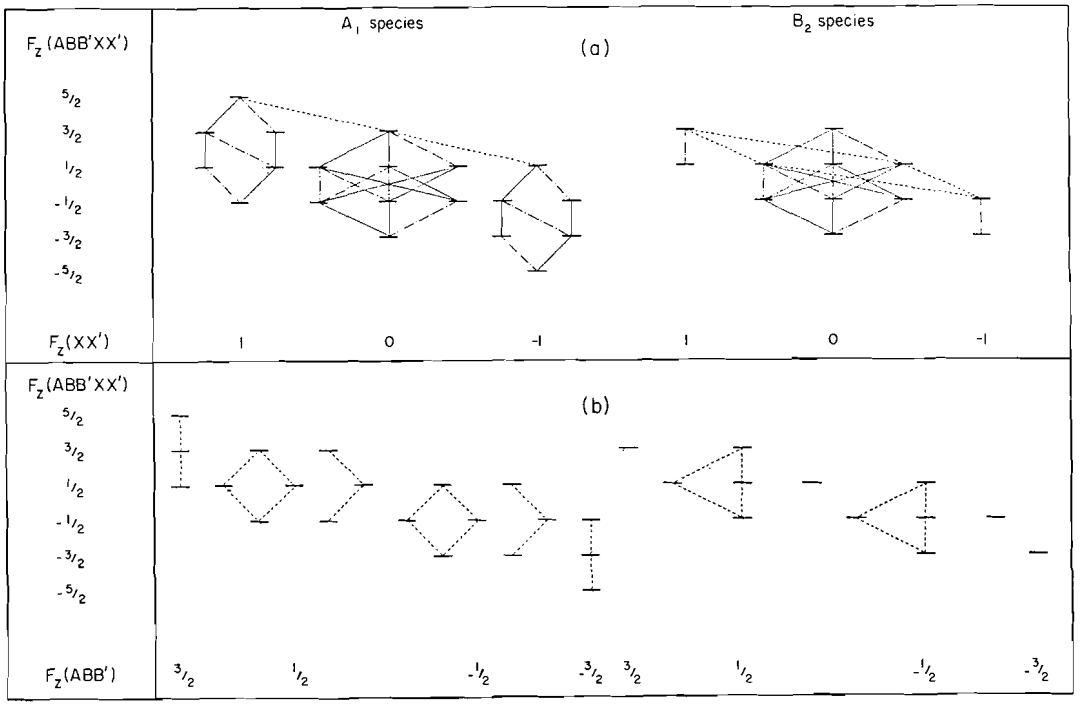

FIG. 3. The energy level diagram and transition pattern for the planar ABB′XX′ system with C_{2v} symmetry: (*a*) B transitions (——) and A transitions (—·—·); (*b*) X transitions (– – –).

Can. J. Chem. Downloaded from www.nrcresearchpress.com by 210.87.254.105 on 09/05/12
For personal use only.

Can. J. Chem. Downloaded from www.nrcresearchpress.com by 210.87.254.105 on 09/05/12
For personal use only.

TABLE IV

The basic symmetry product functions $F_z(A)$, $F_z(BB')$ for the possible values of $F_z(XX')$ in the planar ABB'XX' system with C_{2v} symmetry

F_z(A)	F_z(BB')		F_z(XX')		F_z(ABB'XX')	$A_1\times A_1\times A_1 = A_1$					$A_1\times B_2\times B_2 = A_1$		$A_1\times B_2\times A_1 = B_2$			$A_1\times A_1\times B_2 = B_2$	
A_1 species	A_1 species	B_2 species	A_1 species	B_2 species													
					$\frac{3}{2}$	$\frac{1}{2},\frac{1}{2}$											
	1		1		$\frac{1}{2}$	$\frac{1}{2},0$	$-\frac{1}{2},1$	$\frac{1}{2},1$					$\frac{1}{2},0$			$\frac{1}{2},1$	
$\frac{1}{2}$					$\frac{1}{2}$	$\frac{1}{2},-1$	$-\frac{1}{2},0$	$\frac{1}{2},0$	$-\frac{1}{2},1$	$\frac{1}{2},1$	$\frac{1}{2},0$		$-\frac{1}{2},0$	$\frac{1}{2},0$		$\frac{1}{2},0$	$-\frac{1}{2},1$
$\times$	0	0 $\times$	0	0 $\rightarrow$													
$-\frac{1}{2}$					$-\frac{1}{2}$		$-\frac{1}{2},-1$	$\frac{1}{2},-1$	$-\frac{1}{2},0$	$\frac{1}{2},0$	$-\frac{1}{2},1$	$-\frac{1}{2},0$		$-\frac{1}{2},0$	$\frac{1}{2},0$	$\frac{1}{2},-1$	$-\frac{1}{2},0$
	-1		-1														
					$-\frac{3}{2}$				$-,\frac{1}{2}-1$	$\frac{1}{2},-1$	$-\frac{1}{2},0$				$-\frac{1}{2},0$		$-\frac{1}{2},-1$
					$-\frac{3}{2}$						$-\frac{1}{2},-1$						
					F_z(XX')	1			0		-1	0	1	0	-1	0	

Can. J. Chem. Downloaded from www.nrcresearchpress.com by 210.87.254.105 on 09/05/12
For personal use only.

The character (A, B, or X) of the transitions in Figs. 3*a* and 3*b* has been picked out using the convention of considering the quantum numbers of the basic symmetry functions. It is obvious from Fig. 3*a* that the A and B transitions are contained within three patterns of energy levels in both the A_1 and B_2 symmetry species which are labelled by the $F_z(XX')$ values 1, 0, and -1 respectively. These patterns are characteristic of three particles with spin $\frac{1}{2}$ having certain relations between the coupling constants and the chemical shifts within the system.

The A_1 species $F_z(XX') = 1$ levels together with the B_2 species $F_z(X) = 1$ levels constitute the typical pattern for the AB_2 system. This also is true of the A_1 species, $F_z(X) = -1$ plus the B_2 species $F_z(X) = -1$ levels. The A_1 species, $F_z(X) = 0$ and the B_2 species, $F_z(X) = 0$ independently are characteristic of the ABB′ system which has more than one effective coupling constant between the different types of nuclei. This means that the ABB′ part of an ABB′XX′ spectrum will contain *abb′* as well as simple ab_2 sub-spectra which when sorted out will help the analysis of the problem.

The XX′ transition pattern (of ABB′XX′) breaks down into sub-patterns characterized by $F_z(ABB') = \frac{3}{2}, \frac{1}{2}-\frac{1}{2}$ and $-\frac{3}{2}$ respectively in both the A_1 and B_2 species. It is possible to pick out the $F_z(ABB') = \frac{3}{2},-\frac{3}{2}$ sub-patterns as seemingly non-perturbed patterns characteristic of the two equivalent nuclei (X_2). The symmetric functions appear in the A_1 species and the antisymmetric function in the B_2 species. In Fig. 3*b* the energy levels for $F_z(ABB') = \frac{1}{2}$ and $-\frac{1}{2}$ are grouped 2,3,2 in the A_1 species and 1,3,1 in the B_2 species. On inspection of the possible transitions we find that some of these are combination lines. As a consequence there is a further breakdown possible which converts the 2,3,2 pattern into the known patterns (1,2,1)(XX′) and (1,1,1)(X_2). This breakdown does not necessarily mean that the energies of the transitions are analytical expressions in terms of chemical shifts and coupling constants, since the three wave functions of the 2,3,2 patterns can in general mix strongly.

The ab_2 sub-spectra corresponding to the $F_z(XX')$ values $+1$ and -1 discussed above have been identified as shown in the pyridine spectrum, Fig. 4. A graphical method using a plot of the relative positions of the eight AB_2 transitions as a function of J/δ has been applied. These particular sub-spectra, arising because there is a unique spin configuration where all the spins of the second strongly coupled group (XX′) are either "all up" $(\frac{1}{2},\frac{1}{2})$ or "all down" $(-\frac{1}{2},-\frac{1}{2})$, can be discussed using the effective Larmor frequency method (4). The result is that the two ab_2 patterns are characterized by the same J_{AB} and the two effective shifts,

$$\delta_{ab} = \delta_{AB} \pm \tfrac{1}{2}(J_{BX} + J_{BX} - 2J_{AX}),$$

for $F_z(XX') = +1$ and -1 respectively. Furthermore, the relative intensity of one sub-spectrum is $\frac{1}{4}$ of the total ABB′ intensity.

The identification of all the transitions of the two ab_2 sub-spectra (see Fig. 4*b* and *c*) provides the following parameters: J_{AB}, δ_{AB}, J_{AX}, and the sum of J_{BX} and J_{BX}'. These are obtained, as shown below, from the difference of line positions (δ's) in the ab_2 multiplet pattern.

(1) $J_{AB} = \frac{1}{3}[(\delta_4 - \delta_1) + (\delta_8 - \delta_6)] = \frac{1}{3}[(\delta_{4'} - \delta_{1'}) + (\delta_{8'} - \delta_{6'})]$.

(2) $J_{AX} = \frac{1}{2}(\nu_a - \nu_{a'}) = \frac{1}{2}(\delta_3 - \delta_{3'})$.

(3) $J_{BX} + J_{BX}' = \nu_b - \nu_{b'} = \frac{1}{2}[(\delta_5 + \delta_7) - (\delta_{5'} + \delta_{7'})]$.

(4) $\delta_{AB} = \frac{1}{4}(\delta_5 + \delta_7 + \delta_{5'} + \delta_{7'}) - \frac{1}{2}(\delta_3 + \delta_{3'})$.

Can. J. Chem. Downloaded from www.nrcresearchpress.com by 210.87.254.105 on 09/05/12
For personal use only.

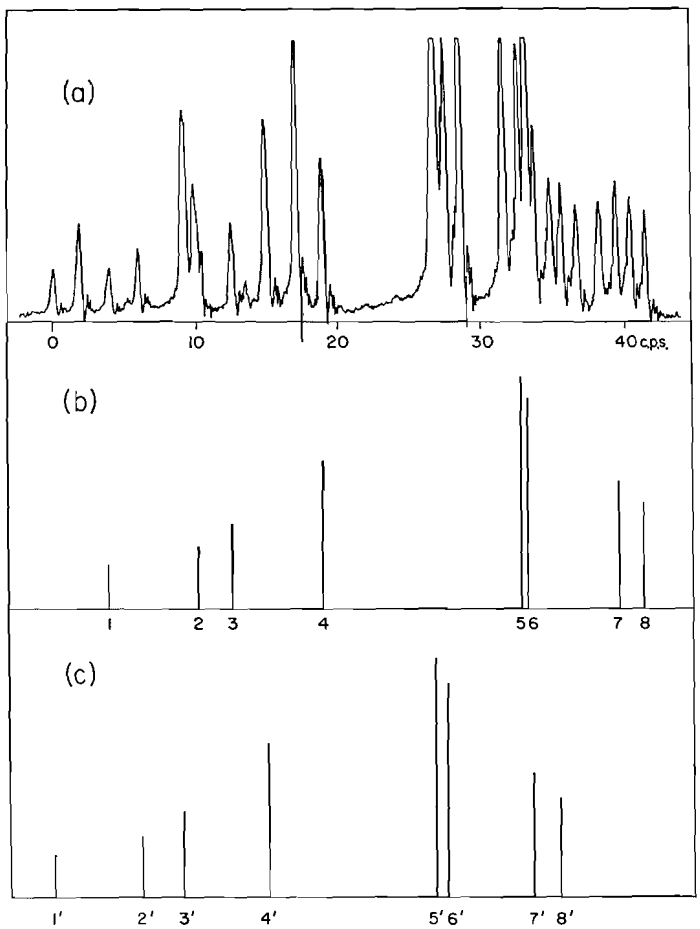

FIG. 4. The proton n.m.r. spectrum of pyridine at 60 Mc/s: (*a*) the ABB′ part of the ABB′XX′ spectrum; (*b*) the ab_2 sub-spectrum corresponding to $F_z(\mathrm{XX}') = +1$,

$$J/\delta = J_{\mathrm{AB}}/\delta_{ab} = J_{\mathrm{AB}}/\delta_{\mathrm{AB}} + \tfrac{1}{2}(J_{\mathrm{BX}} + J_{\mathrm{BX}}' - 2J_{\mathrm{AX}}),$$

(*c*) the ab_2 sub-spectrum corresponding to $F_z(\mathrm{XX}') = -1$,

$$J/\delta = J_{\mathrm{AB}}/\delta_{ab} = J_{\mathrm{AB}}/\delta_{\mathrm{AB}} - \tfrac{1}{2}(J_{\mathrm{BX}} + J_{\mathrm{BX}}' - 2J_{\mathrm{AX}}).$$

(5) The XX′ part of the spectrum will contain transitions corresponding to $F_z(\mathrm{ABB}') = \pm\frac{3}{2}$. These have an energy difference of $J_{\mathrm{AX}} + J_{\mathrm{BX}} + J_{\mathrm{BX}'}$ and their mean gives δ_{X}. The sum of their intensities is equal to $\frac{1}{4}$ of the total (XX′) intensity.

The spectra parameters obtained by the above ab_2 sub-spectral analysis are compared with those obtained in the more conventional way in Table V.

The XX′ part result for the sum $J_{\mathrm{BX}} + J_{\mathrm{BX}}' + J_{\mathrm{AX}}$ is 7.6 ± 0.2 c.p.s., the inaccuracy being due to broadening of lines.

This example shows that it is possible to derive without total analysis of the spectrum all the parameters of the strongly coupled subgroups by picking out the two sub-spectra and analyzing them. In addition, we will obtain the sums of all the intergroup coupling constants from each of the strongly coupled nuclei of one group to all the strongly coupled nuclei of the other group. This method will be of particular interest in, for example,

TABLE V

AB_2 parameters of the ABB'XX' spectrum of pyridine

Parameter	Present work*	Ref. 9
J_{AB}	7.68	7.4–8.2
J_{AX}	1.82	1.3–1.9
$J_{BX}+J_{BX'}$	5.98	5.9–6.4
δ_{AB}	0.37 p.p.m.	0.37 p.p.m.
δ_{AX}	1.13 p.p.m.	1.14 p.p.m.

*Estimated accuracy ±0.05 c.p.s.

solvent effects, where the chemical shift as a function of dilution parameters is desired. It is evident that it is not necessary to do a full analysis of the spectrum for each dilution. The method simply involves picking out the sub-spectra from which the chemical shift can be determined directly.

In the general case where a system is composed of two sets of strongly coupled nuclei separated by a large chemical shift, (AA' . . . BB' . . .)(XX' . . . YY' . . .), we will always find spectra which are of the AA' . . . BB' . . . and XX' . . . YY' . . . type corresponding to the extreme values of F_z(XX' . . . YY' . . .), and F_z(AA' . . . BB' . . .) respectively.

The effective Larmor frequencies of the nuclei A and B, for example, in the relevant sub-spectra are given by the following relations:

$$\nu_a = \nu_A \pm \tfrac{1}{2}\textstyle\sum J_{AX} + J_{AX'} \ldots + J_{AY} + J_{AY'},$$

$$\nu_b = \nu_B \pm \tfrac{1}{2}\textstyle\sum J_{BX} + J_{BX'} \ldots + J_{BY} + J_{BY'}.$$

The effective chemical shift of the respective sub-spectra is given by,

$$\nu_a - \nu_b = \nu_A - \nu_B \pm \tfrac{1}{2}\textstyle\sum (J_{AX} - J_{BX}) + (J_{AX'} - J_{BX'}) \ldots + (J_{AY} - J_{BY}) \ldots .$$

The relative intensity of each of these two sub-spectra compared with the total AA' . . . BB' . . . intensity will be $1/2^n$, where n is the total number of XX' . . . YY' . . . nuclei. For symmetry reasons similar results can be obtained for the XX' . . . YY' . . . part by exchanging XX' . . . and YY' . . . with AA' . . . and BB' . . . .

The total intensity of any sub-spectrum can easily be obtained as the sum of the individual transitions within the sub-spectrum in the limit of magnetic equivalence and no mixing. In this limit, perturbation theory provides the result that the intensity of a transition of nucleus A in a group A_n from the state $(F_{A_n}, m_A - 1)$ to (F_{A_n}, m_A) is equal to

$$(F_{A_n} + m_A)\,(F_{A_n} - m_A + 1),$$

where F_{A_n} is the total spin quantum number which can be added as a second quantum number to the basis local symmetry functions.

As an example, let us consider an AB_3 system. The A wave function characterized by $\underline{F_z(A), F_A} = \underline{\tfrac{1}{2},\tfrac{1}{2}}$, multiplied with the two B_3 wave functions $\underline{\tfrac{1}{2},\tfrac{3}{2}}$ and $\underline{-\tfrac{1}{2},\tfrac{3}{2}}$, will form the product functions

$$\underline{F_z(A),\ F_A F_z(B_3),\ F_{B_3}} = \underline{\tfrac{1}{2},\tfrac{1}{2}\ \tfrac{1}{2},\tfrac{3}{2}} \text{ and } \underline{\tfrac{1}{2},\tfrac{1}{2}\ -\tfrac{1}{2},\tfrac{3}{2}}.$$

The B transition between the two states will, in the limit discussed above, have an intensity of $(\tfrac{3}{2} + \tfrac{1}{2})(\tfrac{3}{2} - \tfrac{1}{2} + 1) = 4$.

These zero order intensities are of additional interest because, together with the coefficients of the mixed wave functions, they determine the actual intensities of the transitions.

Can. J. Chem. Downloaded from www.nrcresearchpress.com by 210.87.254.105 on 09/05/12
For personal use only.

Example 3. The AB_2X_2 System

This example effectively shows the transition from magnetic non-equivalence ABB′XX′ to magnetic equivalence AB_2X_2 from the standpoint of symmetry.

If we choose to twist the XX group through 90° about the C_2 axis of the molecule without disturbing the ABB part, we do not change the overall molecular point group (C_{2v}). We now define σ_v' as the symmetry plane including the ABB group of nuclei and the C_2 axis. The σ_v plane includes the XX group, the A nucleus, and the C_2 axis. It is now necessary to reclassify the XX group basic symmetry functions with respect to the new covering operations. The functions $\alpha\alpha$, $(\alpha\beta + \beta\alpha)2^{-1/2}$, and $\beta\beta$ remain invariant under the covering operations C_2, σ_v, and σ_v' and therefore belong to the A_1 symmetry species. The $(\alpha\beta - \beta\alpha)2^{-1/2}$ function is invariant under the covering operation σ_v and it is transformed into minus itself by the C_2 and σ_v' operations. Hence it belongs to the B_1 symmetry species. Following the procedure outlined by Table III, the molecular symmetry functions may now be classified as indicated below,

ABB′XX′	AB_2X_2
$A_1 \times A_1 \times A_1 = A_1$	$A_1 \times A_1 \times A_1 = A_1$
$A_1 \times B_2 \times B_2 = A_1$	$A_1 \times B_2 \times B_1 = A_2$
$A_1 \times A_1 \times B_2 = B_2$	$A_1 \times A_1 \times B_1 = B_1$
$A_1 \times B_2 \times A_1 = B$	$A_1 \times B_2 \times A_1 = B_2$.

It is now apparent that symmetry forbids the mixing of wave functions observed in example 2, and Table IV represents the complete AB_2X_2 problem with the appropriate relabelling of the molecular symmetry species. The maximum determinantal order is two, and the spectra break down in exactly the way predicted by the effective frequency method (4).

Another way in which the transition from the ABB′XX′ system to the AB_2X_2 system can be made is to allow "free" rotation of the X_2 group relative to the AB_2 group about the C_2 axis of the static system (8).

SUMMARY

The general breakdown of n.m.r. spectra into simpler sub-spectral problems can be summarized as follows.

(1) Construct the basic local symmetry wave functions for the chemically equivalent groups (see Appendix).
(2) Decide on the total molecular symmetry.
(3) Reclassify the basic local symmetry functions according to their transformation properties under the covering operations of the total molecular symmetry and rewrite them in the abbreviated notation as discussed.
(4) Construct the 2^n molecular basic symmetry product wave functions by forming the 2^n possible products of the basic group symmetry functions.
(5) Derive the symmetry species of the products of basic group symmetry functions.
(6) Regroup the molecular wave functions into the molecular symmetry species.
(7) Sort out the transitions of the contributing species (e.g. ABB′ transitions (of ABB′XX′): $\Delta F_z(XX') = 0$; $\Delta F_z(ABB') = \pm 1$.
(8) Isolate the sub-spectral patterns and analyze them.
(9) Using the sub-spectra of maximum $|F_z|$ derive the parameters of the strongly coupled parts.

Can. J. Chem. Downloaded from www.nrcresearchpress.com by 210.87.254.105 on 09/05/12
For personal use only.

(10) In those cases where the Hamiltonian matrix elements of n.m.r. problems are given in the literature in detail (as, for example, Schneider *et al.* (9)), steps 1 to 5 can be deleted and step 7 can be performed on the existing tables.

APPENDIX

The basic local symmetry functions which belong to the various irreducible representations of the local symmetry point group of the n chemically equivalent nuclei A_n are in the literature for two (5), three (6), and four (10) nuclei.

These wave functions are of fundamental importance in the procedures outlined and therefore will be given in this appendix together with additional tables for four and six equivalent nuclei.

The division of the basic local symmetry wave functions for groups of one, two, and three nuclei is simple since there is only one possible point group which describes the local symmetry. The results are given in Table AI using the abbreviated notation described.

TABLE AI

The basic local symmetry wave function diagram for one nucleus (I, identity operation), two nuclei ($D_{\infty h}$ symmetry), and three nuclei (D_3 symmetry)

	$A_2(D_{\infty h})$		$A_3(D_3)$	
A(I)	Symmetric	Antisymmetric	A_1 species	E species
	1		$\frac{3}{2}$	
$\frac{1}{2}$	0	0	$\frac{1}{2}$	$\frac{1}{2}$
$-\frac{1}{2}$	−1		$-\frac{1}{2}$	$-\frac{1}{2}$
			$-\frac{3}{2}$	

Four chemically equivalent nuclei may have a number of space configurations that can be encountered in n.m.r. problems. These are described by the local symmetry as:

(i) C_2, two pairs of protons twisted relative to each other by an angle $\neq 90°$ out of a plane,
(ii) C_{2v}, four protons forming a rectangle (ethylene) or two pairs of adjacent nuclei twisted through 90° relative to one another (allene),
(iii) D_{4h}, four protons forming a square (substituted cyclobutane) for which the proper point group is D_4 since a reflection in the plane of symmetry does not change the configuration as regards the spins, and
(iv) T_d, tetrahedral configuration (methane).

The configuration with T_d symmetry occurs in molecules of the type XA_4 and is a trivial n.m.r. problem. The configuration C_2 is a sub-group (7) of both D_4 and C_{2v}. This means that if the total molecular symmetry of the problem containing the four nuclei A_4 is C_2, then the reclassification of the A_4 wave functions (characterized by either D_4 or C_{2v} local symmetry) can be made direct from tables (7). The basic local symmetry function diagrams are given below in Table AII for four equivalent nuclei with the local symmetries mentioned above.

The most likely configurations which we would expect to find for six chemically

Can. J. Chem. Downloaded from www.nrcresearchpress.com by 210.87.254.105 on 09/05/12
For personal use only.

TABLE AII

Basic local symmetry function diagrams for four chemically equivalent nuclei with the local symmetries C_2, C_{2v}, and D_4*

C_{2v} (planar)	A_1 species	B_2 species
C_2	A species	B species
F_z 2	—	
1	— —	— —
0	— — — —	— —
−1	— —	— —
−2	—	

C_{2v} (not planar)	A_1 species	A_2 species	B_1 species	B_2 species
F_z 2	—			
1	— —		—	—
0	— — —	—	—	—
−1	— —		—	—
−2	—			

D_4	A_1 species	B_1 species	B_2 species	E species†
F_z 2	—			
1	—		—	—
0	— —	—	—	—
−1	—		—	—
−2	—			

*The F_z has been summarized in a column to simplify the diagram. The dashes represent the basic symmetry functions.
†Doubly degenerate.

equivalent nuclei can be described by the three point groups, D_6 (planar hexagon), D_{3h} (fixed, eclipsed ethane protons), and D_{3d} (fixed, staggered ethane protons), which can be shown to be isomorphic (7). As a result of this relation between the point groups it is necessary to write down only one basic symmetry wave function diagram. It is given in Table AIII.

TABLE AIII

The basic local symmetry wave function diagram for six equivalent nuclei with D_6, D_{3h}, and D_{3d} local symmetry

D_6 / D_{3d} / D_{3h}	A_1 / A_{1g} / A_1'	A_2 / A_{2g} / A_2'	B_1 / A_{1u} / A_1''	B_2 / A_{2u} / A_2''	E_1 / E_u / E''	E_2 / E_g / E'
F_z 3	—					
2	—			—	—	—
1	— — —		—	—	— — —	— —
0	— — —	—	—	— — —	— — —	— — —
−1	— — —		—	—	— — —	— —
−2	—			—	—	—
−3	—					

ACKNOWLEDGMENTS

The authors would like to acknowledge helpful discussions with Dr. R. C. Hirst.

One of us (P. D.) gratefully acknowledges support given by the Max Geldner Stiftung, Basel, and by the University of Basel.

Can. J. Chem. Downloaded from www.nrcresearchpress.com by 210.87.254.105 on 09/05/12
For personal use only.

REFERENCES

1. R. J. ABRAHAM and H. J. BERNSTEIN. Can. J. Chem. **39**, 216 (1961).
2. D. R. WHITMAN, L. ONSAGER, M. SAUNDERS, and H. T. DUBBS. J. Chem. Phys. **32**, 67 (1960).
3. J. A. POPLE and T. SCHAEFER. Mol. Phys. **3**, 547 (1961).
4. P. DIEHL and J. A. POPLE. Mol. Phys. **3**, 557 (1961).
5. J. A. POPLE, W. G. SCHNEIDER, and H. J. BERNSTEIN. High-resolution nuclear magnetic resonance. McGraw-Hill Book Co. Inc. 1959.
6. H. M. MCCONNELL, A. D. MCLEAN, and C. A. REILLY. J. Chem. Phys. **23**, 1152 (1955).
7. E. BRIGHT WILSON, JR., J. C. DECIUS, and P. C. CROSS. Molecular vibrations. McGraw-Hill Book Co. Inc. 1955.
8. H. C. LONGUET-HIGGINS. Mol. Phys. **6**, 446 (1963).
9. W. G. SCHNEIDER, H. J. BERNSTEIN, and J. A. POPLE. Can. J. Chem. **35**, 1487 (1957).
10. P. CORIO. Chem. Rev. **60**, 363 (1961).

Can. J. Chem. Downloaded from www.nrcresearchpress.com by 210.87.254.105 on 09/05/12
For personal use only.

Can. J. Chem. Downloaded from www.nrcresearchpress.com by 210.87.254.105 on 09/05/12
For personal use only.

THE MECHANISM OF THE DEHYDROBROMINATION OF TETRA-*O*-ACETYL-α-D-GLUCOPYRANOSYL BROMIDE[1]

R. U. LEMIEUX AND D. R. LINEBACK[2]
Department of Chemistry, University of Alberta, Edmonton, Alberta
Received August 4, 1964

ABSTRACT

The conversion of tetra-*O*-acetyl-α-D-glucopyranosyl bromide (I) to 2-acetoxy-D-glucal triacetate (II) was found to be catalyzed by secondary amines containing *n*-alkyl groups. Substitution at the α-positions of the amine reduced the catalysis. Although triethylamine and tri-*n*-propylamine did not serve as useful catalysts, the less hindered and strongly basic 1,4-diazabicyclo[2,2,2]octane was more effective than diethylamine. The reaction is strongly promoted by polar solvents and added salts—especially tetra-*n*-butylammonium bromide. The course of the reaction involves direct elimination of hydrogen bromide and this reaction is in competition with the formation of acetylated *N*-glucosides. A kinetic study of the reaction using a variety of amines led to the conclusion that the first stage of the reaction is dissociation of I to glycosyloxocarbonium ion strongly solvated by the amine. Depending on the structure of the amine, the second stage of the reaction may involve transfer of the 2-proton to the amine to form II at a faster or slower rate than the formation of the N to C_1 bond of the acetylated *N*-glucoside. Conditions were established for the near quantitative conversion of I to II in about 1/100th the reaction time reported in the literature.

INTRODUCTION

The course of reactions at the anomeric center of *O*-acylated glycosyl halides often depends on a rather delicate balance of the rates of competing reactions. An outstanding example is the formation of 2-acetoxy-D-glucal triacetate (II) in 30–50% yield (1) on reaction of tetra-*O*-acetyl-α-D-glucopyranosyl bromide (I) with diethylamine in benzene. This reaction was discovered in 1927 by Maurer and Mahn (1) in the course of attempts to prepare a variety of *N*-glucosides by reaction of I with amines. It is pertinent to review some of the observations described in the literature concerning the reaction of acetylated glycosyl halides with amines in order to illustrate the strong dependence of the route of reaction on the structure of the amine. Although Micheel and Micheel (2) prepared a variety of quaternary *N*-glycosides through the reaction of trimethylamine with 1,2-*cis*-acetylated glycosyl halides (including I), the products of reactions using other trialkylamines have not been reported although the subject of *N*-glycosides has attracted much interest over several decades. The product of the condensation of I with trimethylamine is well characterized (3), as are the *N*-glucosides resulting from the reaction of I with pyridine (4, 5), with nicotinamide (6, 7), and with other substituted pyridines (8). The reactions of I with a variety of secondary amines including the ethyl ester of sarcosine (9, 10), a variety of *p*-substituted benzylmethylamines (11), and 2,4-disubstituted pyrimidines (12) have been reported to lead to *N*-glucosides in contrast to the dehydrobromination observed in the reaction with diethylamine (1). As will be seen later on, we have found that piperidine, under the conditions studied, catalyzes the elimination more effectively than diethylamine, although Baker (11) reported the preparation of two *different* *N*-(tetra-*O*-acetyl-D-glucosyl)piperidines depending on whether I reacted with piperidine alone or with piperidine in diethyl ether. Chapman and Laird (13) reported a bimolecular mechanism for the reaction of secondary amines with the

[1]*Presented at the 47th Canadian Chemical Conference, Kingston, June 1–3, 1964.*
[2]*Corn Industries Research Foundation Postdoctoral Fellow, 1962–1964. Present address: Department of Biochemistry and Nutrition, University of Nebraska, Lincoln, Nebraska.*

O-acetylglycopyranosyl bromides derived from glucose, galactose, and xylose and noted that substitution at C_1 is usually accompanied by elimination.

The structure of the glycosyl halide can effect the route of reaction as evidenced by formation (14) of the *N*-glucoside on reaction of tetra-*O*-methyl-α-D-glucopyranosyl bromide with diethylamine in benzene under conditions which convert I to II in about 50% yield. Diethylamine was found to cause dehydrobromination of other acetylated (15) and benzoylated (16) glucopyranosyl bromides.

The main purpose of this investigation was to attempt to gain information on the factors which are responsible for the relative rates of the competing reactions and thus help lead to a better understanding and control of reactions at the anomeric center of *O*-acylglycosyl halides.

DISCUSSION OF RESULTS

Except for the data reported in Table I, the reactions of I were followed polarimetrically. As will be seen later on, the rate of reaction is dependent on the concentrations of I, diethylamine, and bromide ion. Thus, it seems likely that the observed polarimetric rates are an expression of a rate process depressed by disappearance of amine and accelerated by the liberation of bromide ion. For these and purely practical reasons, the kinetic studies were performed as much as possible under *pseudo*-first-order conditions using up to tenfold excesses of amine and bromide ion. The rate of change of rotation was very close to a first-order process and the polarimetric data were used to calculate first-order velocity constants from the standard expression, $k = 1/t \ln [(\alpha_0 - \alpha_\infty)/(\alpha_t - \alpha_\infty)]$. In all cases, once the final rotation, α_∞, had been reached, the product was isolated and examined for content by proton magnetic resonance (n.m.r.) spectroscopy.

TABLE I

The powerful catalysis provided by diethylamine*

Concentration of diethylamine, *M*	Concentration of bromide ion, *M*	*T*, °C	*k*, min^{-1}
0	0.4	26	$<10^{-4}$
1.2	0	26	0.01
1.2	0.4	26	0.04
0	0	100	0.006
0	0.4	100	0.03

*The initial concentration of tetra-*O*-acetyl-α-D-glucopyranosyl bromide was in each case 0.4 *M* using a 2:1 *s*-collidine – acetonitrile mixture as solvent. The rates of reaction were estimated by comparing the relative intensities of appropriate signals in the n.m.r. spectra of the products.

The marked catalysis for the elimination provided by diethylamine is evident from the data shown in Table I. An excess of *s*-collidine was used to effectively buffer the reaction medium. It is seen that, in the absence of diethylamine at 26°, no observable reaction occurred. Virtually pure I was present after 24 h. However, on the addition of diethylamine, 3 moles per mole of I, the reaction was half complete in just over 1 h. The further addition of 1 mole of tetra-*n*-butylammonium bromide per mole of I increased the rate by a factor of about 4. In order to achieve reaction at a comparable rate in the absence of diethylamine, the reaction temperature had to be raised from 26° to 100°. As seen in Table VI, the rate of a reaction performed in acetonitrile was increased by a factor of 6.7 on raising the temperature from 25° to 50°. With the assumption of the same temperature coefficient under the reaction conditions given in Table I, the velocity

Can. J. Chem. Downloaded from www.nrcresearchpress.com by 210.87.254.105 on 09/05/12
For personal use only.

constant in the presence of diethylamine and bromide ion at 100° would be about 12 min^{-1}, that is, about 400 times greater than in the absence of diethylamine (k = 0.03 min^{-1}). This amounts to the diethylamine providing a transition state with a free energy about 4.5 kcal/mole less than that which occurs in its absence.

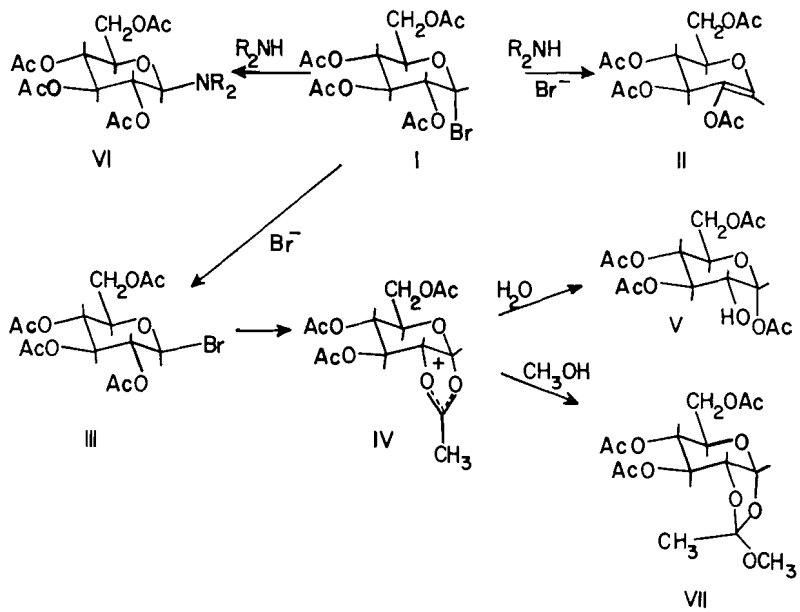

CHART 1

In view of the facts that bromide ion accelerates the formation of II from I and that the reaction of I with bromide ion can be expected to give rise to the β-anomer of I (5), it was necessary to establish whether or not II arose directly from I or from some other derivative of glucose such as the 1,2-acetoxonium ion or α-D-glucopyranose 1,2-(*N*,*N*-diethylorthoacetamide)triacetate. A decision on this matter was reached through the observation that, using diethylamine as catalyst, the 2-acetoxyglucal (II) was formed considerably more rapidly than the β-anomer (III) of I. As seen in Table II, when diethylamine was used, the presence of water in the reaction mixture had little effect on the course of the reaction. Had the elimination proceeded by way of β-acetobromoglucose (III) followed by participation of the 2-acetoxy group to yield the 1,2-acetoxonium ion (IV), in the presence of water, the product of the reaction would be 1,3,4,6-tetra-*O*-acetyl-α-D-glucose (V). The 1,3,4,6-α-tetraacetate (V) is well known to readily isomerize to the 2,3,4,6-α-tetraacetate (17) which can undergo mutarotation. The yields of V reported in Table II *in fact* refer to the total amount of glucose tetraacetate estimated to be in the product. The tetraacetates were the only products when the reaction was carried out in the presence of water but in the absence of diethylamine. That the 1,2-acetoxonium ion is a highly effective scavenger for water is demonstrated by the formation of V in about 30% yield using diisopropylamine as catalyst under conditions which were meant to be anhydrous. The trace of II which formed could only be demonstrated on paper chromatograms. In the presence of an excess of water and using diisopropylamine, as expected, virtually only V was formed. Isomerization of V was extensive in this case. When methanol was present, the methyl orthoacetate (VII) was obtained in 70% yield

Can. J. Chem. Downloaded from www.nrcresearchpress.com by 210.87.254.105 on 09/05/12
For personal use only.

Can. J. Chem. Downloaded from www.nrcresearchpress.com by 210.87.254.105 on 09/05/12
For personal use only.

together with tetraacetate V. Clearly, therefore, under the conditions given in Table II, the rate of the formation of the 2-acetoxyglucal (II) is much greater in the presence of diethylamine than is the rate of the process involving formation of the β-anomer (III) of I. It follows that the formation of II is an elimination process which proceeds directly from I. The inability of diisopropylamine to catalyze the dehydrobromination at rates competitive with either the anomerization of I or the formation of *N*-glucoside shows that the catalysis is highly demanding on the structure of the amine used as catalyst. This facet of the reaction will be considered later.

TABLE II

Effect of the nature of the amine and of the presence of either water or methanol on the course of the reaction*

Amine	Hydroxylic reagent	Composition of product
Diethylamine, 0.4 *M*	Trace of water	95% glucal (II)
Diethylamine, 0.4 *M*	Water, 0.6 *M*	80% glucal (II)
None	Water, 0.6 *M*	90% tetraacetate (V)
Diisopropylamine, 0.4 *M*	Water, 0.6 *M*	90% tetraacetate (V)
Diisopropylamine, 0.4 *M*	Trace of water	Trace of glucal (II) 30% tetraacetate (V) 60% *N*-glucoside (VI)
Diisopropylamine, 0.4 *M*	Methanol, 0.6 *M*	30% tetraacetate (V) 70% orthoacetate (VII)

*The reactions were carried to completion at 25° in acetonitrile 0.05 *M* in tetra-*O*-acetyl-α-D-glucopyranosyl bromide, 0.25 *M* in tetra-*n*-butylammonium bromide, and the amount of water or methanol indicated.

As was seen in Table II, the course of the reaction of I shifted from 2-acetoxyglucal (II) formation to the formation of *N*-glucoside (VI) on changing the amine from diethylamine to diisopropylamine. The formation of *N*-glucoside in these reactions was inferred from the n.m.r. spectra of the products. None of the *N*-glucosides (VI) were isolated in pure state for proper characterization. In view of these results, it was decided to investigate the effect of the structure of the amine on the course of the reaction. The data are listed in Table III.

TABLE III

The effect of the structure of the amine on polarimetric rate and course of reaction*

Amine	k, min^{-1}	Relative rates	2-Acetoxy glucal (II)	*N*-Glucoside (VI)	Tetraacetate (V)
Pyrrolidine	0.3	8.3	90%	—	—
1,4-Diaza[2,2,2]-bicyclooctane	0.17	4.7	90%	—	—
Piperidine	0.14	3.9	90%	—	—
Morpholine	0.041	1.1	40%	50%	—
Diethylamine	0.036	1.0	90%	—	—
Diethylamine-N-D	0.036	1.0	90%	—	—
n-Propylamine	0.036	1.0	—	—	—
R,S-α-Pipecoline	0.035	0.97	80%	—	—
S-α-Pipecoline	0.032	0.89	80%	—	—
Di-*n*-propylamine	0.029	0.80	70%	20%	—
R,S-Coniine	0.025	0.69	60%	30%	—
S-Coniine	0.024	0.67	50%	30%	—
Diisopropylamine	0.014	0.39	Trace	60%	30%
Triethylamine	0.013	0.36	15%	High yield†	—
Tri-*n*-propylamine	0.010	0.28	None	High yield†	—

*The reactions were carried out in acetonitrile at 25° and the initial solution was 0.05 *M* in tetra-*O*-acetyl-α-D-glucosyl bromide, 0.25 *M* in tetra-*n*-butylammonium bromide, and 0.4 *M* in the amine.
†See the Experimental section.

Can. J. Chem. Downloaded from www.nrcresearchpress.com by 210.87.254.105 on 09/05/12
For personal use only.

The largest and smallest polarimetric rates given in Table III differ by a factor of 30 but only a factor of 3 separates the polarimetric rates for the reactions involving diethylamine and triethylamine reactions which follow pronouncedly different courses. With the exception of *n*-propylamine, which led to deacetylation, the yields of 2-acetoxyglucal (II) are greater the higher the polarimetric rate. Perhaps the most striking feature of these data is the excellent correspondence between the polarimetric rate and the steric environment of the nitrogen in the amine, that is, the less hindered the amine to electrophilic attack the greater the rate. Thus, pyrrolidine is a more effective catalyst than piperidine which in turn is more effective than diethylamine. The rates decreased on increasing the lengths of the *n*-alkyl groups of secondary amines. Branching of the alkyl groups at the α-position decreased the rate as evidenced by the relative rates using piperidine, R,S-pipecoline, and R,S-coniine. With diisopropylamine, the rate was as low as that with triethylamine and of the same magnitude as that with tri-*n*-propylamine. It is to be noted that only low yields of the 2-acetoxyglucal (II) were obtained with these hindered amines and except for the reaction with the traces of water, the course of reaction changed to the formation of *N*-glucoside. In fact, the products isolated from the reactions using triethylamine and tri-*n*-propylamine proved to be mixtures of the tetraacetates of glucose. It was judged highly improbable that more than about 30% of these products of hydrolysis were formed during the course of the reaction since great care was taken to exclude water and, if substantial amounts of water had been present, the polarimetric rates should have been higher. It seemed most likely that the reactions produced *N*-glucoside (5) which underwent hydrolysis during the work-up of the reaction mixture. Evidence that this was indeed the case was obtained by observing the reactions at much higher concentrations using n.m.r. spectroscopy. It was found that the presence of the tertiary amines led to the disappearance of I without the formation of appreciable amounts of the 2-acetoxyglucal (II). Instead, products were formed, presumably *N*-glucosides, which were highly sensitive to hydrolysis. Evidence was obtained that α-D-glucopyranose 1,2-(ethyl orthoacetate)triacetate was formed on adding ethanol to the reaction mixture after all the acetobromoglucose (I) had disappeared. These labile *N*-glucosides will be further examined. The reactivities of these compounds is not surprising since it has been shown (2) that treatment of the presumably more stable N-(β-D-glucopyranosyl)-trimethylammonium bromide with base yields 1,6-anhydro-α-D-glucopyranose. Also, an attempt to tritylate the compound led to replacement of the trimethylamine by pyridine (2).

Although the polarimetric rate using *n*-propylamine was the same as that for diethylamine, no 2-acetoxyglucal (II) was detected in the product. The low yield of chloroform-extractable product together with the ready detection of *N*-*n*-propylacetamide in the product indicated that the use of primary amines leads to extensive aminolysis and, therefore, the influence of primary amines on the formation of II could not be profitably studied. It can be noted, however, that although II could not be detected in the product resulting from the use of *n*-propylamine, II was identified by paper chromatography in a reaction using isopropylamine.

In view of the above-mentioned results, it was suspected, at one stage of the investigation, that the formation of II from I resulted from a catalytic ability peculiar to secondary amines. Thus, it could be imagined that the amine not only served as a nucleophile but also engaged the active hydrogen to stabilize the transition state. Evidence that this may not be the case was suggested by the observation that *N*-deuterated diethylamine gave within 5% the same polarimetric rate as the natural diethylamine.

In view of this result, it was anticipated that the catalysis could be provided effectively by a suitably unhindered tertiary amine. In fact, 1,4-diaza[2,2,2]bicyclooctane proved to be an exceptionally good catalyst for the dehydrobromination. It is therefore concluded that the role of the amine is to help delocalize positive charge in the transition state through nucleophilic attack only. On this basis, it would be expected that for the isosteric amines piperidine and morpholine, the stronger amine would be the more effective catalyst. In fact, piperidine, $pk_b = 2.79$, was 3.5 times more effective than morpholine, $pk_b = 5.64$. The high yield of *N*-glucoside from morpholine is noteworthy.

In view of the strong steric demand made on the amine in these reactions, it was anticipated that perhaps quite different rates or routes of reaction would be observed using the enantiomeric forms of such compounds as α-pipecoline and coniine. However, as seen in Table III, the R-forms for these compounds gave polarimetric rates only barely lower than the racemic mixtures and, in each case, the products were essentially the same.

TABLE IV

Dehydrobromination of cyclohexyl bromide*

Tetra-*n*-butyl-ammonium bromide, *M*	Diethylamine	$k \times 10^3$, min^{-1}
0.25	None	1.1
0.50	None	2.2
0.50	0.05 *M*	2.3

*The reaction was carried out at 90° in acetonitrile 0.05 *M* in cyclohexyl bromide, 0.05 *M* in *s*-collidine, and the amounts of the other reagents shown.

The role of the amine in catalyzing the dehydrobromination must be, at least eventually, to accept the departing proton from I. Should this be the only role, then it would be expected that the amines would be effective catalysts under similar reaction conditions for other dehydrobromination reactions. However, as seen in Table IV, diethylamine had no effect on the rate of dehydrobromination of cyclohexyl bromide in acetonitrile containing tetra-*n*-butylammonium bromide. Clearly, the catalysis provided by the diethylamine in this reaction was in no way comparable to that observed in the dehydrobromination of I. It is concluded, therefore, that the catalysis provided by diethylamine (and the other effective amines listed in Table III) is particularly effective for the pyranosyl bromide structures. Under conditions where I was converted to II, using tetra-*n*-butylammonium bromide and diethylamine as catalysts in about 2 h, the dehydrochlorination of tetra-*O*-acetyl-α-D-glucopyranosyl chloride, substituting tetraethylammonium chloride for the tetra-*n*-butylammonium bromide, proceeded to only about 15% after 91 h. About 30% of the starting material remain unchanged. The remainder appeared to be tetraacetates of glucose which presumably arose through the intervention of water.

The ease of the dehydrobromination of I as compared to cyclohexyl bromide is undoubtedly due *mainly* to the ability of the ring-oxygen of I to help delocalize positive charge (13). It seems reasonable therefore to assume that the first stage of the reaction involves change at the anomeric center rather than attack by a nucleophile at the 2-hydrogen as is normally the case for E2 elimination. That the rate of reaction is dependent on the amine concentration is evident from the data contained in Table V. It is seen that doubling the concentration of the amine resulted in about 30% increase in the polarimetric rate. There can be no doubt, in view of the catalysis provided by the amine, that at least a mole of the amine is in the transition state. The observed fractional order

Can. J. Chem. Downloaded from www.nrcresearchpress.com by 210.87.254.105 on 09/05/12
For personal use only.

TABLE V

Effect of the amine concentration on rate*

Time, min	Observed rotation	k, min^{-1}
0.1 *M* in diethylamine		
0	1.698	—
15	1.168	0.0296
20	1.018	0.0307
30	0.788	0.0318
50	0.520	0.0316
70	0.382	0.0313
∞	0.216	—
	Average 0.031 = 0.002	
0.2 *M* in diethylamine		
0	1.708	—
10	1.160	0.0412
15	0.948	0.0423
20	0.788	0.0421
30	0.558	0.0413
50	0.302	0.0407
70	0.185	0.0405
∞	0.090	—
	Average 0.041 = 0.002	
0.4 *M* in diethylamine		
0	1.688	—
10	1.018	0.0535
15	0.778	0.0556
20	0.608	0.0563
30	0.378	0.0565
50	0.178	0.0548
∞	0.076	—
	Average 0.055 = 0.002	

*Polarimetric rates for the conversion of tetra-*O*-acetyl-α-D-glucopyranosyl bromide (I) to 2-acetoxy-D-glucal triacetate (II) at 25° in acetonitrile, 0.05 *M* in I, 0.5 *M* in tetra-*n*-butylammonium bromide, and containing varying amounts of diethylamine.

in diethylamine under conditions which are close to *pseudo*-first-order is perhaps mainly related to association of the nonpolar amine which lowers the effective concentration of monomeric amine. As seen in Table VI, changing the solvent from acetonitrile to benzene decreased the rate by a factor of about 10. This evidence for charge separation in the transition state is supported by the salt effects given in Table VII. Therefore, the fractional order must to some extent also be related to the decrease in the dielectric constant of the solvent with increasing concentration of the amine.

TABLE VI

Effect of solvent polarity and temperature on rate*

Solvent	Tetra-*n*-butyl-ammonium bromide, *M*	k, min^{-1}
At 25°		
Acetonitrile	0.125	0.026
Acetronitrile	0.25	0.036
1:1 Acetonitrile–benzene	0.25	0.024
Benzene	0.125	0.0024
At 50°		
Acetonitrile	0.25	0.24

*Polarimetric rates of reaction of solutions 0.05 *M* in tetra-*O*-acetyl-α-D-glucopyranosyl bromide, 0.4 *M* in diethylamine, and varying concentrations of tetra-*n*-butylammonium bromide.

Can. J. Chem. Downloaded from www.nrcresearchpress.com by 210.87.254.105 on 09/05/12
For personal use only.

TABLE VII

Effect of salt concentration on rate*

Concentration of added salts, M			
$(n\text{-Bu})_4NBr$	$(n\text{-Bu})_4NClO_4$	Et_2NH_2Br	k, min^{-1}
—	—	—	0.013
0.125	—	—	0.026
0.25	—	—	0.036
0.50	—	—	0.058
—	0.50	—	0.022
0.125	0.375	—	0.032
0.25	0.25	—	0.042
—	0.375	0.125	0.021
0.125	0.25	0.125	0.026
0.25	0.125	0.125	0.034

*Polarimetric rates for the formation of 2-acetoxy-D-glucal triacetate from 0.05 M tetra-*O*-acetyl-α-D-glucopyranosyl bromide at 25° in acetonitrile, 0.4 M in diethylamine, and with varying concentrations of salts.

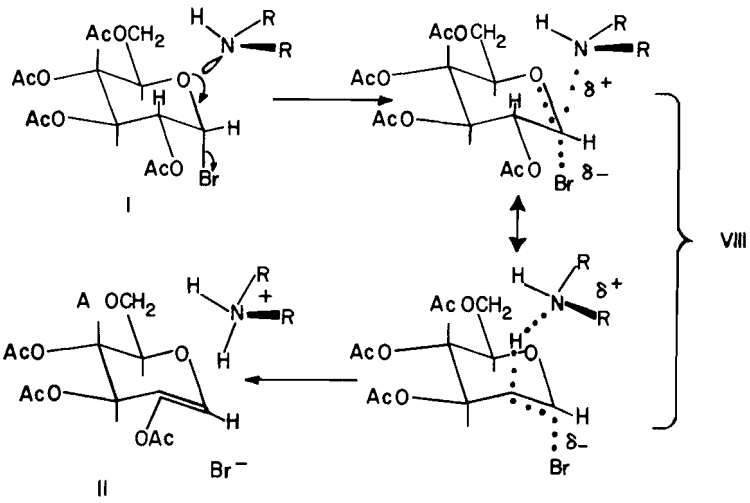

CHART 2

It seems reasonable, on the basis of the above-mentioned experimental data, that the role of the amine in catalyzing the dehydrobromination is to help stabilize the glycosyloxocarbonium bromide which results in dissociation of the glucosyl bromide (I). The positive charge is presumably distributed over the oxygen and carbon atoms and the amine in the intermediate (VIII). In view of the steric effects noted in the data listed in Table III, the bond between the nitrogen and atoms about the anomeric center must be fairly strong. However, the degree of catalysis provided by the amine does not seem large enough for the amine to play a role other than to act as an effective solvating agent for the glucosyloxocarbonium ion. The positive charge would be expected to strongly activate the 2-hydrogen. Therefore, it seems reasonable to expect that such an intermediate (VIII) could collapse to products by two different and competing routes. One route would involve establishment of a covalent N—C bond to form *N*-glucoside. The data in Table III suggest that this is the favorable route for amines with hindered nitrogen. The other route would involve loss of the 2-proton to the amine which necessarily would be well oriented in the intermediate to serve as the proton acceptor. It is conceivable,

Can. J. Chem. Downloaded from www.nrcresearchpress.com by 210.87.254.105 on 09/05/12
For personal use only.

Can. J. Chem. Downloaded from www.nrcresearchpress.com by 210.87.254.105 on 09/05/12
For personal use only.

therefore, that the effectiveness of amines in promoting the dehydrobromination route is directly related to the allowed orientations of the amine relative to the 2-hydrogen in the intermediate. As already mentioned with reference to Table III, it is evident that the less hindered the nitrogen for amines of comparable basic strength the stronger the bonding in the transition state and the greater the yield of the acetoxyglucal (II). Clearly, for example, the non-bonding interactions in the intermediate (VIII) would be less severe for diethylamine than for either diisopropylamine or triethylamine. Furthermore, such steric interactions would tend to prevent the amine from assuming the energetically most favorable orientation coplanar with the O—C—Br atoms and very close to the 2-hydrogen. In view of the charge separation in the transition state, the roles of the solvent effects noted in Table VI and the salt effects seen in Table VII are readily rationalized. The greater effectiveness of bromide ion as compared to perchlorate ion could be assigned to the difference in charge density on these ions. It was surprising to find that the enantiomeric forms for α-pipecoline and coniine possessed almost equal catalytic abilities. It should prove possible to find enantiomers which differ substantially in their abilities to solvate the glucosyloxocarbonium ion and it is planned to examine these possibilities, since the results may help shed light on the stereoselectivity of carbohydrase-enzyme activity.

Following the proposals of Bunnett (18), the mechanism of the amine-catalyzed dehydrobromination of α-acetobromoglucose can be classified as "E2 leaning toward E1" since the breaking of the C—Br bond must be far advanced in the transition state. However, as stated above, the amine likely plays an important role in the breaking of the C—Br bond by solvating the developing cation through non-directive electrostatic bonding. Thus, in a formal sense, the mechanism of the reaction would resemble the merged bimolecular substitution and elimination mechanism proposed by Winstein, Darwish, and Holness (19). The difference would be in the ionic character of the transition state.

In conclusion, the results of this investigation have provided a deepened appreciation of the essential features of the mechanism for the dehydrobromination of tetra-*O*-acetyl-α-D-glucopyranosyl bromide and this knowledge should prove useful in arriving at conditions suitable for the dehydrohalogenation of other *O*-acylglycosyl halides in high, reproducible yields. The results also illustrate how rather small structural changes in a soluble catalyst can modify the route of reaction by changing the relative rates of competing reactions. It can be anticipated that this kind of information will prove useful in future synthetic operations.

EXPERIMENTAL

Tetra-n-butylammonium Bromide (20)

An equimolar mixture of tri-*n*-butylamine and *n*-butyl bromide was heated on the steam bath until homogeneous—about 2 weeks. On cooling, the product solidified and was recrystallized 3 times from ethyl acetate to give a 30% yield of white crystals, m.p. 111–114°, which were dried at room temperature in a high vacuum.

Tetra-n-butylammonium Perchlorate

An aqueous solution of sodium perchlorate, 2.5 *M*, was added, with stirring, to an equivalent amount of aqueous 1.25 *M* tetra-*n*-butylammonium bromide. The precipitate was washed free of bromide ion and treated with ethyl acetate. The organic layer was dried over anhydrous calcium carbonate and pentane was added. The precipitate was collected and the mother liquor was evaporated to dryness. The solids were combined and recrystallized from ethyl acetate to provide an 80% yield of white crystalline product, m.p. 207–210°. The reported melting point is 212–212.5° (21).

Amines

The amines were commercial products purified by fractional distillation through a spinning-band column and stored over potassium hydroxide.

N-Deuterated diethylamine was prepared by exchange of the active hydrogen of diethylamine with deuterium oxide. After five exchanges using equivalent amounts, the amine, which was isolated in each case by distillation through a spinning-band column, no longer produced DOH on mixing with deuterium oxide as evidenced by n.m.r. spectroscopic examination. The compound was dried over sodium metal. The extent of deuteration appeared better than 95% as judged by a comparison of the intensities of the DOH n.m.r. signals for equivalent mixtures of the deuterated and ordinary amines in deuterium oxide.

R,S-α-Pipecoline was resolved following the procedures outlined by Ladenburg (22) and by Marckwald (23). The sticky, solid mass obtained on mixing the amine with D-*dextro*-tartaric acid was triturated with cold water and the crystals twice recrystallized from water. Regeneration of the amine provided S-*dextro*-α-pipecoline, $[\alpha]_D^{25}$ +32.4°; reported (23), $[\alpha]_D$ +31.9°.

R,S-Coniine was prepared as described by Johnson (24) and partially resolved following the directions outlined by Wolffenstein (25). The tartrate, which crystallized on seeding with S-α-pipecoline D-tartrate and isolated by trituration with cold water, was decomposed directly to S-coniine of at least 50% optical purity, $[\alpha]_D^{26}$ +8.7°; reported (25), $[\alpha]_D^{19}$ +15.7°.

Solvents

The acetonitrile was twice refluxed over phosphorous pentoxide for several hours and recovered by distillation under anhydrous conditions. The benzene was dried by distillation and stored over sodium metal

Paper Chromatography

The paper chromatographic examinations of reaction products were made on dimethylsulfoxide impregnated Whatman No. 1 paper using Skellysolve B as the developing phase (26). The zones were located using alkaline silver nitrate (27). 2-Acetoxy-D-glucal triacetate moved faster than other components of the reaction products examined and smaller amounts could be detected in this way than was possible by n.m.r. spectroscopy.

Nuclear Magnetic Resonance Spectra

All spectra were measured with a Varian Associates A-60 spectrometer with chloroform as a solvent and tetramethylsilane as internal standard. The spectrum for pure 2-acetoxy-D-glucal triacetate (II) has a singlet for H-1 at 3.33 τ, a doublet with a spacing of 4 c.p.s. centered at 4.41 τ for H-3, a multiplet centered at 4.75 τ with a half-band width of about 10 c.p.s. for H-4, and a fairly sharp peak at 5.65 τ for H-5, and the two H-6's. The spectrum for tetra-*O*-acetyl-α-D-glucopyranosyl bromide (I) has a doublet with a spacing of 3.8 c.p.s. centered at 3.40 τ for H-1, signals for H-3 and H-4 in the region 4.25 to 4.95 τ and a quartet with spacings of 3.8 and 10 c.p.s. centered at 5.19 τ for H-2. The signals for H-5 and the two H-6's formed a multiplet with the most intense peak at 5.78 τ. The relative amounts of the two compounds in a mixture could be estimated by comparing the signals for the anomeric (H-1) protons. Since the H-1 signal for II overlapped the low-field signal of the doublet for H-1 of I, the composition was estimated by subtracting the intensity of the signal at about 3.42 τ from that at about 3.33 τ and dividing the result by twice the intensity of the 3.42 τ signal. Control experiments showed that the relative amounts of compounds II and I could be estimated in this way to ±10%. The analysis could be confirmed with about the same accuracy by comparing the intensity of the signal for H-2 of I to the total intensity of the H-1 signals. In order to obtain an estimate of the amount of compounds I and II in the product, the total intensity of H-1 signals in the region of 3.3–3.5 τ was compared with the total intensity of signals arising from H-5 and H-6 protons in the region 5.5–6.2 τ, since the latter protons produced their signals in the region indicated for all the acetylated glucose derivatives encountered. The presence of 1,3,4,6-tetra-*O*-acetyl-α-D-glucose in the product was readily detected by the appearance of the signal for H-1 as a doublet with a spacing of 3.5 c.p.s. at 3.77 τ. Also, the signal for the 1-acetoxy group at 7.81 τ was highly characteristic for this compound. The presence of *N*-glucoside (VI) in the product was detected by the appearance of signals characteristic for protons of the aglycon. The amount of the *N*-glucoside (VI) was estimated by comparing the intensities of these signals with the total intensities of the signals for the H-5 and the two H-6 protons. In the reaction using diisopropylamine and in the presence of methanol, see Table II, the presence of the orthoacetate (VII) in the product was established by the characteristic signals at 4.29, 6.72, and 8.30 τ for the anomeric proton, the methoxyl-group protons, and the methyl-group protons of the orthoacetyl group, respectively (5).

Reactions Using Tertiary Amines

In the reactions involving triethylamine and tri-*n*-propylamine, see Table III, the change in specific rotation through the course of the reaction was only about 60% that observed with diethylamine. The product of the reaction using triethylamine was obviously a mixture of 2-acetoxy-D-glucal triacetate (about 15%), 1,3,4,6-tetra-*O*-acetyl-α-D-glucose (about 30%), and the equilibrium mixture of the anomeric 2,3,4,6-tetra-*O*-acetyl-D-glucoses (about 55%). It is known (17) that the 1,3,4,6-tetraacetate isomerizes readily to

Can. J. Chem. Downloaded from www.nrcresearchpress.com by 210.87.254.105 on 09/05/12
For personal use only.

the 2,3,4,6-isomer and the latter compound may have formed in this way. The product of the reaction using tri-*n*-propylamine gave the n.m.r. spectrum for the equilibrium mixture of the anomeric 2,3,4,6-tetra-*O*-acetyl-D-glucoses but no 2-acetoxy-D-glucal triacetate (II). It was therefore apparent that the reaction of I with both triethylamine and tri-*n*-propylamine led to the formation of labile compounds which decomposed during the isolation procedure. This conclusion was substantiated by the following experiments.

Tetra-*O*-acetyl-α-D-glucopyranosyl bromide (I), 0.5 g (1.22 mmoles), and tetra-*n*-butylammonium bromide, 1.96 g (6.1 mmoles), were dissolved in 5 ml of acetonitrile containing 9.8 mmoles of tertiary amine. The n.m.r. spectrum of the solution was measured within a few minutes of dissolution. Spectra were determined at varying intervals of time for the reaction mixture kept at room temperature. When the amine was triethylamine, the solution stayed nearly homogeneous and the n.m.r. spectra showed that the acetobromoglucose (I) had completely reacted within 75 min. The reaction led to the appearance of a doublet with a spacing of about 5 c.p.s. at 3.74 τ. A colorless, crystalline, water-soluble compound, 0.2 g, was deposited in the course of the reaction and identified as triethylamine hydrobromide by n.m.r. spectroscopy. The chemical nature of the carbohydrate product was not established. However, the substance was shown to be highly reactive by an examination of the chemical changes which occurred on the addition of water and dry ethanol. Water was added to one-half of the reaction mixture and, after 1 h, the product was isolated by chloroform–water extraction in the usual manner. The n.m.r. spectrum of the syrupy product in chloroform showed the presence of a compound with a signal at about 4 τ in the form of a doublet with 5.5 c.p.s. spacing. The intensity of the signal relative to the other signals in the 4.5 to 6 τ region required the compound to be the main glucose derivative in the mixture. It was evident that the product contained an appreciable amount of 2,3,4,6-tetra-*O*-acetyl-D-glucose. The syrup was dissolved in 5 ml of dioxane and 0.1 ml of 2 *N* sulfuric acid was added. No appreciable change in rotation occurred over a 10 min period. Dry ethanol was added to the other half of the original reaction solution. After 3 h, the product was isolated by chloroform–water extraction in the usual manner. The n.m.r. spectrum in chloroform showed doublets of about equal intensities at 3.92 and 4.28 τ with spacings of 5.5 and 5 c.p.s., respectively. It seemed probable that the low-field signal arose from the same compound that produced a similarly located doublet of the same spacing in the product resulting from the treatment with water. That the higher-field signal arose from an ethyl 1,2-orthoacetate derivative was clearly apparent from the following observations. α-D-Glucopyranose 1,2-(ethyl orthoacetate) triacetate in chloroform produces a signal at 4.28 τ with a spacing of 5.5 c.p.s. When the syrup was dissolved in 5 ml of dioxane and 0.1 ml of 2 *N* sulfuric acid added, the rotation of the solution changed from 1.75° to 2.63° in 3 min (28). The product was isolated by chloroform–water extraction and its n.m.r. spectrum clearly showed the presence of 1,3,4,6-tetra-*O*-acetyl-α-D-glucose (V) and the 2,3,4,6-tetra-*O*-acetyl-D-glucoses as the main products together with an abaut 5% yield of 2-acetoxy-D-glucal triacetate (II).

When tri-*n*-propylamine was substituted for the triethylamine in the above experiment, the course of the reaction as determined by n.m.r. spectroscopy appeared similar except that the reaction was much slower. The tri-*n*-propylamine was only slightly soluble in the salt solution and this may have been the main reason for the low rate of reaction.

Polarimetric Rates

Tetra-*O*-acetyl-α-D-glucopyranosyl bromide (0.500 g, 1.22 mmoles) and the desired amount of the tetra-*n*-butylammonium salt were weighed into a 25 ml volumetric flask which had been previously rinsed with dry solvent. The flask was stoppered with a serum cap and approximately 10–12 ml of dry solvent added with a syringe. Shaking produced a solution to which was added the desired amount of dry amine. The volume was then rapidly adjusted to 25 ml by the addition of dry solvent. After thorough shaking, a sample was removed with a syringe and introduced into a 0.5 dm polarimetric cell attached to a constant temperature water bath thermostatted at 25°. The remainder of the reaction solution was incubated at 25° during the course of the reaction.

The chart drive (timing mechanism) of a Rudolph Instruments Engineering Co. Automatic Recording Spectropolarimeter (Model 260/655/850/810-614) was turned on at the time the amine was added. The reaction was followed at the sodium D-line until minimum rotation was attained. At this point, the reaction solution was diluted with chloroform (100 ml) and washed successively with water, dilute hydrochloric acid, aqueous sodium bicarbonate, and water. The chloroform solution was dried over anhydrous sodium sulfate and filtered and the solvent removed under reduced pressure. The n.m.r. spectrum of the resulting syrup was determined in chloroform.

Zero-rotation base lines were placed on the chart preceding the polarimetric determination and also following it. The final rotation was verified by visual determination on a Rudolph and Sons precision polarimeter (Model 80). The change in rotation with time could be read directly from the chart record. The kinetic data presented in Table V are typical examples of the results obtained.

Dehydrobromination of Cyclohexyl Bromide

In a typical experiment, a 50 ml acetonitrile solution of cyclohexyl bromide, 0.398 g (2.44 mmoles), 2,4,6-trimethylpyridine (*s*-collidine), 0.298 g (2.44 mmoles), and tetra-*n*-butylammonium bromide, 7.84 g

Can. J. Chem. Downloaded from www.nrcresearchpress.com by 210.87.254.105 on 09/05/12
For personal use only.

(24.4 mmoles), was prepared. Aliquots, 10 ml, were transferred to glass tubes which were sealed and incubated at 90° in an oil bath. An aliquot was kept at room temperature to serve as a control in the following analytical procedures. After varying reaction times, the tubes were cooled and analyzed for hydrogen bromide by titration with standard sodium hydroxide using phenolphthalein as indicator. The relative amounts of cyclohexene and cyclohexyl bromide were determined by gas–liquid partition chromatography using an Apiezon M column and a temperature program of 50–200°. The extents of reaction determined in both ways agreed to within 4%. When a sample of the reaction mixture was analyzed by gas–liquid chromatography, peaks assignable to *n*-butyl bromide and tri-*n*-butylamine were present. These products arose from thermal decomposition of tetra-*n*-butylammonium bromide in the inlet of the F and M Model 500 Gas Chromatograph since these compounds were not present in the volatile fraction of a sample distilled *in vacuo* in a closed system. When diethylamine was present, the amount of hydrogen bromide liberated in the reaction was determined after a fourfold dilution with water by titration to pH 4.5 with 0.05 *N* hydrochloric acid.

*Preparation of 2-Acetoxy-*D*-glucal Triacetate*

Diethylamine, 26.7 g (37.6 ml, 366 mmoles), was added to a suspension of tetra-*O*-acetyl-α-D-glucopyranosyl bromide, 50.0 g (122 mmoles), and tetra-*n*-butylammonium bromide, 39.2 g (122 mmoles), in 25 ml of acetonitrile. An orange hue developed and complete solution was obtained within a few minutes. After 20 min at room temperature, the solution was diluted with 250 ml of chloroform and washed successively with water, dilute hydrochloric acid, aqueous sodium bicarbonate, and water. The chloroform solution was dried over anhydrous sodium sulfate, filtered, and the solvent removed under reduced pressure. The n.m.r. spectrum of the resulting reddish-brown syrup showed the presence of 2-acetoxy-D-glucal triacetate only, and the conversion was therefore virtually quantitative. Crystallization from the minimum amount of ethanol required to dissolve the syrup at room temperature afforded about 80% yields of crystalline material melting at 58–60°. Further crystallizations from ethanol did not increase the uncorrected melting point to above 61° with $[\alpha]_D^{25}$ −20° (*c*, 2 in ethanol). Maurer (29) has reported the compound to melt as high as 65–66°, $[\alpha]_D^{20}$ −20.71° in ethanol.

ACKNOWLEDGMENTS

The research was supported by a Corn Industries Research Foundation grant to R. U. Lemieux. The n.m.r. spectra were measured by R. N. Swindlehurst and Mrs. Gail Conway of this department.

REFERENCES

1. K. MAURER and H. MAHN. Ber. **60**, 1316 (1927).
2. F. MICHEEL and H. MICHEEL. Ber. **63**, 286 (1930); **65**, 258 (1932).
3. P. KARRER and A. P. SMIRNOFF. Helv. Chim. Acta, **4**, 817 (1921).
4. E. FISCHER and H. RASKE. Ber. **43**, 1750 (1910).
5. R. U. LEMIEUX and A. R. MORGAN. J. Am. Chem. Soc. **85**, 1889 (1963).
6. L. J. HAYNES and A. R. TODD. J. Chem. Soc. 303 (1950).
7. R. U. LEMIEUX and J. W. LOWN. Can. J. Chem. **41**, 889 (1963).
8. P. KARRER, B. H. RINGIER, J. BÜCHI, H. FRITZSCHE, and U. SOLMSSEN. Helv. Chim. Acta, **20**, 55 (1937).
9. K. MAURER. Ber. **59**, 287 (1926).
10. K. MAURER and B. SCHIEDT. Z. Physiol. Chem. **206**, 125 (1932); **213**, 110 (1932).
11. J. W. BAKER. J. Chem. Soc. 1205 (1929).
12. G. E. HILBERT and T. B. JOHNSON. J. Am. Chem. Soc. **52**, 4489 (1930). G. E. HILBERT. J. Am. Chem. Soc. **56**, 190 (1934). G. E. HILBERT and E. F. JANSEN. J. Am. Chem. Soc. **58**, 60 (1936).
13. N. B. CHAPMAN and W. E. LAIRD. Chem. Ind. London, 20 (1954).
14. M. L. WOLFROM and D. R. HUSTED. J. Am. Chem. Soc. **59**, 2559 (1937).
15. K. MAURER and A. MÜLLER. Ber. **63**, 2069 (1930). H. G. FLETCHER and C. S. HUDSON. J. Am. Chem. Soc. **69**, 921 (1947).
16. K. MAURER and W. PETSCH. Ber. **66**, 995 (1933). R. T. MAJOR and E. W. COOK. J. Am. Chem. Soc. **58**, 2333 (1936).
17. B. HELFERICH and J. ZIRNER. Chem. Ber. **95**, 2694 (1962).
18. J. F. BUNNETT. Angew. Chem. Intern. Ed. Engl. **1**, 225 (1962).
19. S. WINSTEIN, D. DARWISH, and N. J. HOLNESS. J. Am. Chem. Soc. **78**, 2915 (1956).
20. D. DARWISH. Ph.D. Dissertation, University of California at Los Angeles. 1958.
21. S. WINSTEIN, P. E. KLINEDINST, JR., and G. C. ROBINSON. J. Am. Chem. Soc. **83**, 885 (1961).
22. A. LADENBURG. Ann. **247**, 64 (1888).
23. W. MARCKWALD. Ber. **29**, 43 (1896).
24. A. W. JOHNSON. J. Org. Chem. **25**, 2237 (1960).
25. R. WOLFFENSTEIN. Ber. **27**, 2612 (1894).
26. B. WICKBERG. *In* Methods in carbohydrate chemistry. Vol. 1. *Edited by* R. L. Whistler and M. L. Wolfrom. Academic Press, N.Y. 1962. p. 31.
27. W. E. TREVELYAN, D. P. PROCTER, and J. S. HARRISON. Nature, **166**, 444 (1950).
28. R. U. LEMIEUX and C. BRICE. Can. J. Chem. **33**, 109 (1955).
29. K. MAURER. Ber. **62**, 332 (1929).

Can. J. Chem. Downloaded from www.nrcresearchpress.com by 210.87.254.105 on 09/05/12
For personal use only.

Can. J. Chem. Downloaded from www.nrcresearchpress.com by 210.87.254.40 on 09/05/12
For personal use only.

THE REACTIONS OF METHYLENE RADICALS WITH ACETALDEHYDE AND PROPIONALDEHYDE[1]

M. H. Back
Chemistry Department, The University of Ottawa, Ottawa, Canada

Received August 18, 1964

ABSTRACT

The reactions of methylene radicals with acetaldehyde and propionaldehyde have been studied over the temperature range 48–118 °C and over a range of pressures of aldehyde and carbon dioxide. From acetaldehyde, the main products were carbon monoxide, methane, ethane, and acetone, with small amounts of ethylene at low pressures of acetaldehyde. With carbon dioxide present, small amounts of propylene oxide were formed, but propionaldehyde was not observed. The main products from the reaction with propionaldehyde were carbon monoxide, methane, ethane, and ethylene, with small amounts of methyl ethyl ketone, butene oxide, and isobutyraldehyde. The relation of the results to the relative rates and mode of attack of methylene on the various bonds is discussed.

INTRODUCTION

The reactions of methylene radicals with hydrocarbons have been studied in some detail and a general pattern of reactivity has emerged (1). Methylene appears to be one of the most reactive radicals known and one of the most indiscriminate in its attack upon the various types of hydrocarbon bonds. Less is known about its reactivity with other types of bonds. Reactions with oxygen-containing compounds, for example, have not been extensively studied. In the gas-phase reaction of methylene with isopropyl ether (2) no evidence was found for attack of methylene on the C—O bond. The products appeared to be formed solely by abstraction of hydrogen and insertion into the various C—H bonds. The relative rate of attack on these bonds was similar to that found by Frey (3) and Knox and Trotman-Dickenson (4). This result confirmed the similar conclusion reached by von Franzen and Fikentsher (5) and Doering, Knox, and Jones (6) from a study of the reaction of methylene with aliphatic ethers and tetrahydrofuran in solution. The reaction of methylene with methanol vapor (7) produced, among other products, dimethyl ether, and it was suggested that this was formed by an insertion reaction into the OH bond. However, the possibility of its formation by radical combination reactions could not be ruled out.

The reactivity with carbonyl bonds as compared to C—H bonds is not well known. That methylene does react with carbonyl bonds has been shown by a study of the reaction with carbon monoxide (8) and carbon dioxide (9). With the former, ketene is the product, while with the latter the main product is carbon monoxide, probably initially accompanied by formaldehyde. To obtain more information on the reactivity of methylene towards carbonyl bonds, the aldehydes were chosen as reactants, since they contain three types of bonds: paraffinic C—H bonds, the labile aldehydic C—H bond, and the carbonyl bond. It was hoped that the relative rate and mode of attack of methylene on these various bonds might be measured. The photolysis of ketene was used as a source of methylene radicals.

EXPERIMENTAL

Materials

Acetaldehyde was obtained from Eastman Kodak Company. It was stored as a liquid at 0 °C and was degassed at −78 °C before use. Traces of ethane were thus removed, but a small amount of acetone remained

[1]*Presented at the 47th Canadian Chemical Conference, Kingston, June, 1964.*

as an impurity. Correction for this became large only when very high pressures of acetaldehyde were used. The same treatment was given propionaldehyde, also obtained from Eastman Kodak Company, except that it was stored at room temperature. A trace of acetaldehyde was the main impurity observed in the propionaldehyde.

Ketene was prepared by the method described by Fisher, MacLean, and Schnizer (10) with slight modifications. Nitrogen was used as a carrier gas, and one trap kept at about −40 °C served to separate most of the acetic acid and unreacted acetic anhydride from the ketone. The ketene was then degassed at −196 °C and distilled at −120 °C (*n*-propanol bath). Ethylene could not be detected by gas chromatographic analysis of a sample of the size used in most experiments. It was stored at room temperature and low pressure (< 3 cm) as suggested by Frey (11) and was found to be quite stable for periods of several months.

Carbon dioxide was a Matheson Co. product and was thoroughly degassed before use.

Apparatus

The lamp used for photolysis was a Hanovia S500 medium pressure mercury arc. A filter solution of 2,7-dimethyl-diaza-(3,6)-cycloheptadiene-(1,6)-perchlorate[2] cut off light of wavelength < 3 500 Å. A 500 cc flask, through which water flowed continuously, was placed between the lamp and filter solution and served to collimate the light roughly and to absorb much of the heat generated by the lamp.

Two reaction vessels were used, both of about 250 cc volume. The first was a spherical flask with a central cold-finger for condensing reactants, and without external heating. The second was a cylinder of diameter approximately 5 cm and was fitted inside a steel tube wound with nichrome wire. Reactants were condensed into a small U tube. In some experiments with the cylindrical vessel the reactants were allowed to stand overnight before photolysis and no change in the behavior of the system was observed. These experiments are, however, not sensitive to slight changes in homogeneity of the reactant mixtures.

The pressure in the reaction vessel was measured with a small glass diaphragm gauge used as a null-point indicator. The sensitivity was ±0.5 mm. The volume of the gauge and connecting tubing was not more than 2 or 3 cc.

Analysis

The condensable products of the reaction were fractionated through a series of four traps. The first, at −115 °C, retained most of the acetaldehyde and any higher-boiling products. This was analyzed by gas chromatography on a polypropylene glycol column, 20 ft long, at 25 °C. Acetaldehyde, propionaldehyde, acetone, and propylene oxide were well separated. The same column at 50 °C was found to separate propionaldehyde and the corresponding isomers of butyraldehyde. The second trap was a LeRoy still maintained at −196 °C and the final two traps were held at −210 °C. Except when carbon dioxide was present, the contents of these three traps were analyzed together on a 6 ft silica gel column held at 30 °C. Ethane, carbon dioxide, and ethylene were separated under these conditions. When large amounts of carbon dioxide were present, the C_2 hydrocarbons were distilled from the LeRoy still at about −162 °C.

The noncondensable gases were collected in a Toepler pump – gas burette following the traps and were analyzed by combustion in a copper oxide furnace at about 325 °C.

RESULTS AND DISCUSSION

The complexities and experimental difficulties inherent in the present system did not allow the quantitative determination of rate constants, but only a qualitative interpretation of the modes of attack of methylene on the various bonds in aldehydes. To minimize absorption of light by the aldehyde, light of wavelengths > 3 500 Å was used to dissociate ketene, and in this region the primary quantum yield for dissociation is strongly pressure dependent. Pressure effects on the reaction products were therefore obscured. Furthermore, at high pressures of aldehyde where the quantum yield for dissociation of ketene was very small, direct photolysis of the aldehyde became appreciable, especially at high temperatures where the chain length is long.

Acetaldehyde

Following the general pattern of reactivity of methylene, the possible reactions with acetaldehyde may be outlined as follows

$$[I_0] \qquad CH_2CO + h\nu \rightarrow CH_2 + CO$$

$$[a] \qquad CH_2 + CH_2CO \rightarrow C_2H_4 + CO$$

$$[1] \qquad CH_2 + CH_3CHO \rightarrow [CH_3COCH_3]^*$$

[2]*The author thanks Dr. K. O. Kutschke of the National Research Council for a sample of this compound.*

Can. J. Chem. Downloaded from www.nrcresearchpress.com by 210.87.254.40 on 09/05/12
For personal use only.

$$[S_1] \quad [CH_3COCH_3]^* + M \rightarrow CH_3COCH_3 + M$$

$$[S_2] \quad \rightarrow CH_3CH\text{—}CH_2 + M \quad (\text{O bridging CH and } CH_2)$$

$$[S_3] \quad \rightarrow CH_3CH_2CHO + M$$

$$[D_1] \quad [CH_3COCH_3]^* \rightarrow CH_3 + CH_3CO$$

$$[D_2] \quad \rightarrow CO + 2CH_3$$

$$[D_3] \quad \rightarrow CH_4 + CH_2CO$$

$$[D_4] \quad \rightarrow C_2H_6 + CO$$

$$[2] \quad CH_2 + CH_3CHO \rightarrow CH_3 + CH_3CO$$

$$[3] \quad CH_3 + CH_3CHO \rightarrow CH_4 + CH_3CO$$

$$[4] \quad CH_3 + CH_3 \rightarrow C_2H_6$$

$$[5] \quad CH_3 + CH_3CO \rightarrow CH_3COCH_3$$

$$[6] \quad 2CH_3CO \rightarrow (CH_3CO)_2$$

$$[7] \quad CH_3CO + M \rightarrow CH_3 + CO$$

For simplicity the dissociation of ketene has been represented as a single reaction although, as already mentioned, pressure and temperature effects are important in the efficiency of this step. The designation of the excited molecule formed in reaction [1] is not intended to represent its actual structure, for which several possibilities exist, and which may, indeed, be different for each of the subsequent reactions.

The main products observed were carbon monoxide, methane, ethane, acetone, ethylene, and, under certain conditions, small amounts of propylene oxide. Propionaldehyde was not detected. The yields of products as a function of acetaldehyde pressure at two temperatures are shown in Figs. 1 and 2. At 45 °C the yield of carbon monoxide dropped sharply at first as the primary quantum yield for ketene dissociation decreased, but rose again at higher pressures as the direct photolysis of acetaldehyde became important. The products were similar to those obtained by direct photolysis of acetaldehyde and the main reaction of methylene appeared to be initiation of the chain decomposition of acetaldehyde. The yields of acetone were small and the variation with pressure not pronounced. It is most likely that it was formed mainly by combination of methyl and acetyl radicals rather than by the direct insertion of methylene. The ethylene yield was also small and even at equal pressures of ketene and acetaldehyde was less than the yield of ethane. Reaction of methylene with acetaldehyde thus appears at least as fast as with ketene.

At 118 °C the drop in quantum yield for ketene dissociation with pressure is not as sharp and the rate of decomposition of acetaldehyde much faster. Thus the yields of carbon monoxide and methane rose continuously with pressure. The yield of acetone relative to the yield of ethane has decreased, a result consistent with the suggestion that acetone was formed by combination of methyl and acetyl radicals. Again, no stabilization products were observed.

The decomposition of acetaldehyde may be initiated by reaction with an excited ketene molecule rather than by direct reaction with methylene radicals. However, the maximum energy absorbed by the ketene was 3 660 Å, equivalent to 78 kcal/mole, and this is barely sufficient to cause dissociation of acetaldehyde. Furthermore, the initial drop in carbon monoxide yield as acetaldehyde pressure was increased (Fig. 1) is difficult to explain unless deactivation of ketene occurs without decomposition of acetaldehyde. At 118 °C an energy transfer process may occur to some extent. It will be seen later that the results with propionaldehyde provide additional evidence that methylene radicals are the reactive species.

Can. J. Chem. Downloaded from www.nrcresearchpress.com by 210.87.254.40 on 09/05/12
For personal use only.

Can. J. Chem. Downloaded from www.nrcresearchpress.com by 210.87.254.40 on 09/05/12
For personal use only.

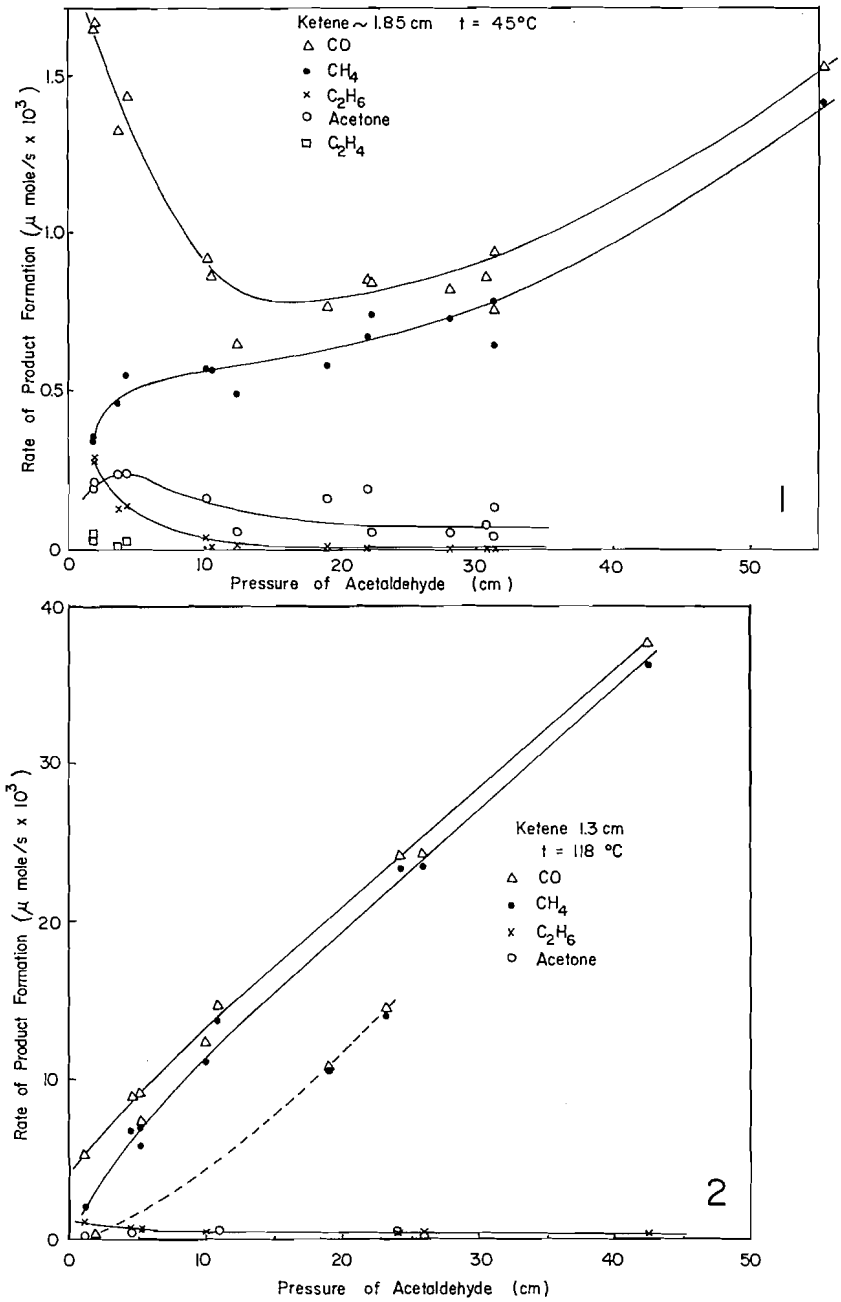

FIGS. 1 and 2. Rate of product formation from the photolysis of ketene in the presence of acetaldehyde. Dotted line shows rate of product formation from photolysis of acetaldehyde by itself.

The yield of methane divided by the square root of the yield of ethane is shown as a function of acetaldehyde pressure at the two temperatures in Figs. 3 and 4. In each case a linear relation was observed down to the lowest pressures used, showing that methane and ethane were formed from methyl radical reactions and not from a molecular decomposition of the excited molecule (reactions $[D_3]$ and $[D_4]$). From the rate constants obtained

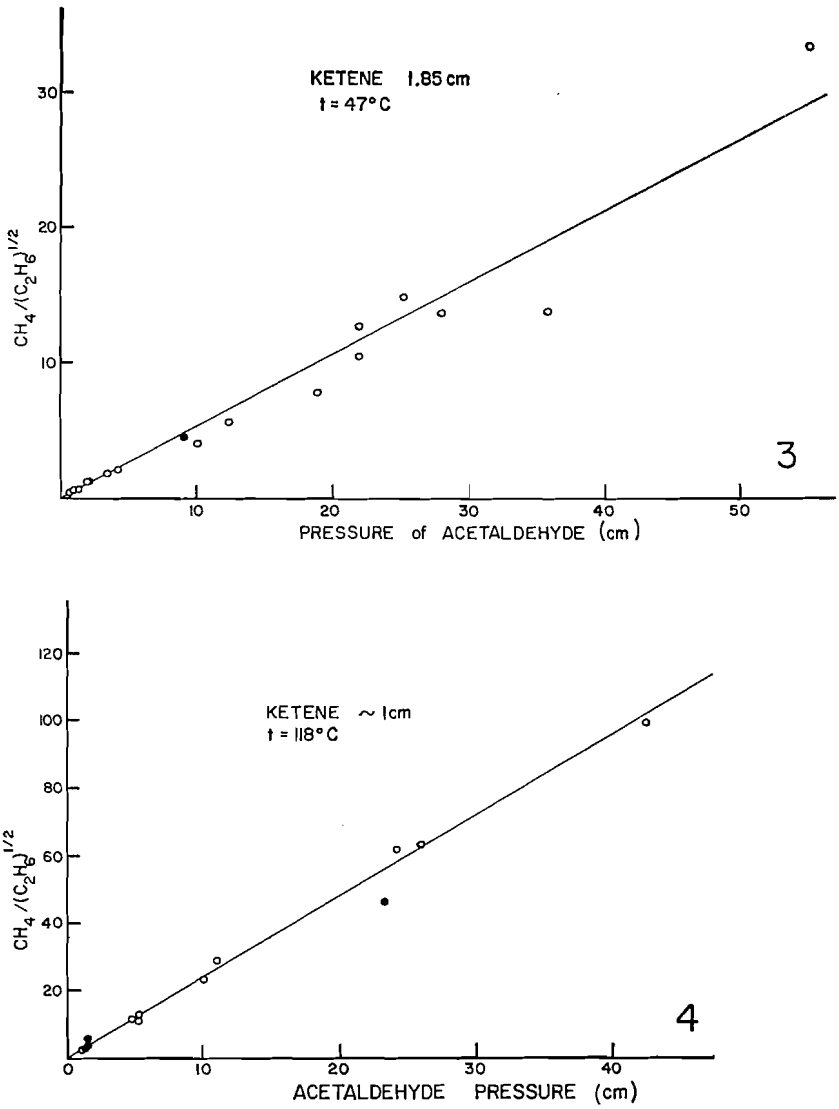

FIGS. 3 and 4. $CH_4/(C_2H_6)^{1/2}$ as a function of acetaldehyde pressure. Filled circles are results from photolysis of acetaldehyde by itself.

from these curves an activation energy of 6.2 kcal/mole was obtained for the abstraction of hydrogen from acetaldehyde. This is in satisfactory agreement with the accepted value of 7.5 kcal/mole (12).

In order to minimize the products from the chain decomposition of acetaldehyde and at the same time increase the pressure, carbon dioxide was added to small, constant amounts of ketene and acetaldehyde. The yields of products at three temperatures are shown in Figs. 5, 6, and 7. The very pronounced increase in yields of all products at 44 °C, before the expected decrease was observed, is not readily explained by any series of reactions and may be a phenomenon associated with the absorption of light in this complex system. Another possibility is that one of the effects of carbon dioxide is to

Can. J. Chem. Downloaded from www.nrcresearchpress.com by 210.87.254.40 on 09/05/12
For personal use only.

Can. J. Chem. Downloaded from www.nrcresearchpress.com by 210.87.254.40 on 09/05/12
For personal use only.

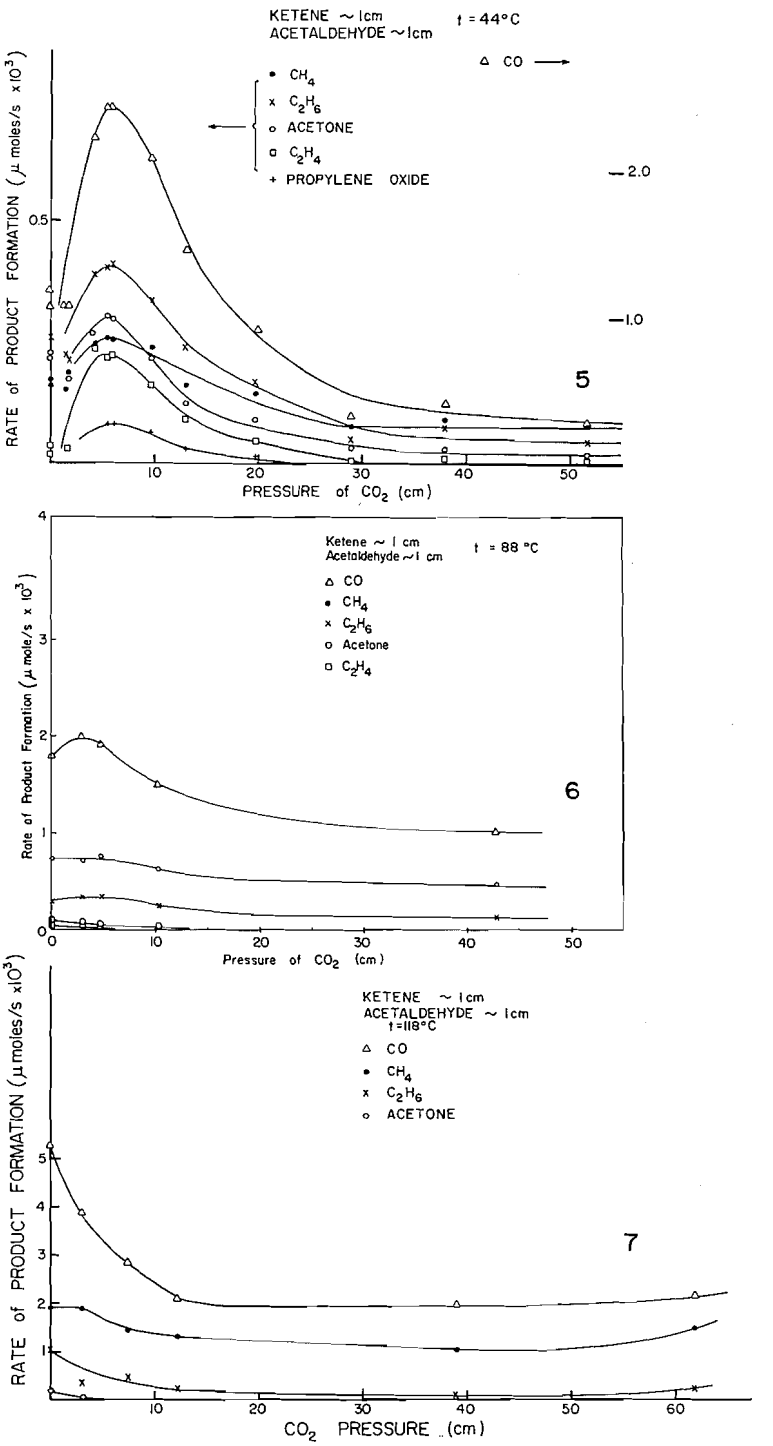

FIGS. 5, 6, and 7. Rate of product formation from the photolysis of ketene in the presence of acetaldehyde and carbon dioxide.

increase the dissociation of ketene into methylene and carbon monoxide relative to the deactivation. The increase in yields of products may thus arise from an increased yield of methylene radicals. At higher pressures deactivation finally becomes faster than dissociation and product yields fall. Since a similar effect was not observed with acetaldehyde by itself, it must be assumed that carbon dioxide is more effective than acetaldehyde in promoting dissociation of ketene rather than deactivation. The effect diminished as the temperature was increased and as the dissociation of ketene was less affected by pressure.

At 44 °C propylene oxide was observed, but in very small yields. A comparison of the variation with pressure of the yield of stabilization product, propylene oxide, and the yield of dissociation product may be made if it is assumed that the yield of radicals from reactions $[D_1]$ and $[D_2]$ may be equated to the yield of termination products from reactions [4], [5], and [6]. Since the yield of biacetyl was not measured, it was estimated by assuming $k_4 = k_5 = k_6$, which gave a total yield of termination product = [ethane + acetone + ((acetone)^2/ethane)]. Plots of these products are shown in Fig. 8. The similar effect of pressure on each type of product is difficult to explain if the yield of propylene oxide is a measure of reaction $[S_2]$ and the termination products are a measure of reactions $[D_1]$ and $[D_2]$. However, if most of the radicals were formed by reaction [2], which is a true abstraction reaction, independent of pressure, and most of the excited propylene oxide was stabilized at fairly low pressures, then the variation in pressure of both types of products will simply reflect the variation in the quantum yield of ketene dissociation. The abstraction reaction may not have been observed in the reactions of methylene radicals with hydrocarbons because in this case its rate may be slower relative to the insertion reaction. With the aldehydes, abstraction of the labile aldehydic hydrogen atom may compete favorably with the insertion.

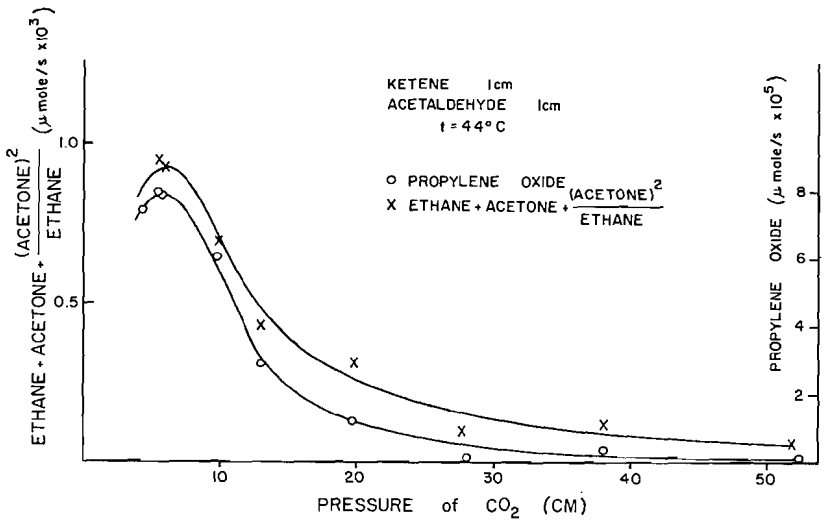

FIG. 8. Propylene oxide and radical yield as a function of carbon dioxide pressure.

An added effect of inert gas is to induce the singlet–triplet transition of the methylene radical, giving an increased concentration of triplet methylene radicals relative to singlet with rising pressure of carbon dioxide. If the triplet state radical were to react more

Can. J. Chem. Downloaded from www.nrcresearchpress.com by 210.87.254.40 on 09/05/12
For personal use only.

readily by reaction [2] than the singlet, then the yield of radicals would not drop as sharply with pressure as expected on the basis of reactions [1], [S], and [D]. This effect may contribute to the similarity of the curves in Fig. 8, but it would be fortuitous if this alone caused the variations with pressure to be almost identical. These results, then, do not provide evidence for a difference in reactivity of singlet and triplet methylene by reaction [2].

Propylene oxide was not observed at 118 °C. From the results of Strachan and Noyes (13) it may be estimated that at this temperature the quantum yield of dissociation of ketene should be 2.5 times that at 45 °C. A yield of propylene oxide equivalent to 2.5 times that observed at 45 °C would have been easily measurable. Its absence again suggests the occurrence of an abstraction reaction which has a higher activation energy than the insertion and hence competes more favorably at the higher temperatures. The small change in temperature would not be expected to affect appreciably the amount of stabilization at any given pressure.

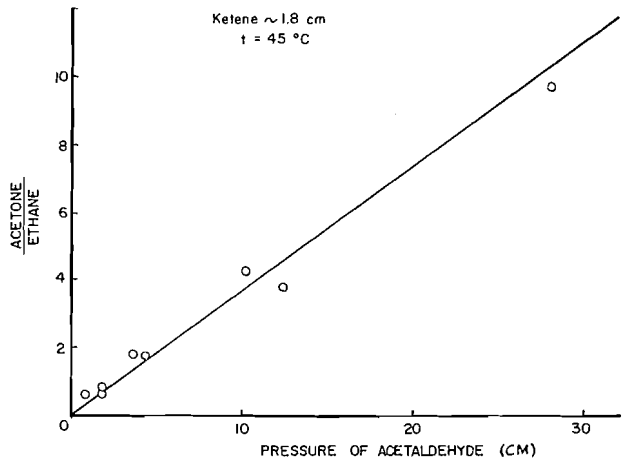

FIG. 9. Ratio of acetyl radical concentration to methyl radical concentration as a function of acetaldehyde pressure.

The ratio of acetone to ethane should be proportional to the ratio of concentration of acetyl radicals to that of methyl radicals. At 45 °C this ratio was found to be a linear function of the acetaldehyde pressure (Fig. 9). Thus for the series of experiments with constant acetaldehyde pressure the ratio would be expected to be unchanged by addition of carbon dioxide. In fact the ratio decreased with increasing total pressure (Fig. 10). This may be an indication of a pressure dependence of the decomposition of the acetyl radical.

Propionaldehyde

A series of reactions similar to those suggested for acetaldehyde would be expected to occur in the reaction of methylene with propionaldehyde. The possible stabilization products are methyl ethyl ketone, *n*-butyraldehyde, isobutyraldehyde, and α-butene oxide. Methyl, ethyl, and possibly propyl radicals may be formed by decomposition of the excited molecule, and these would initiate the chain decomposition of propionaldehyde. In accordance with this the main products observed were carbon monoxide, ethane, methane, ethylene, and small amounts of stabilization products. The results of the

Can. J. Chem. Downloaded from www.nrcresearchpress.com by 210.87.254.40 on 09/05/12
For personal use only.

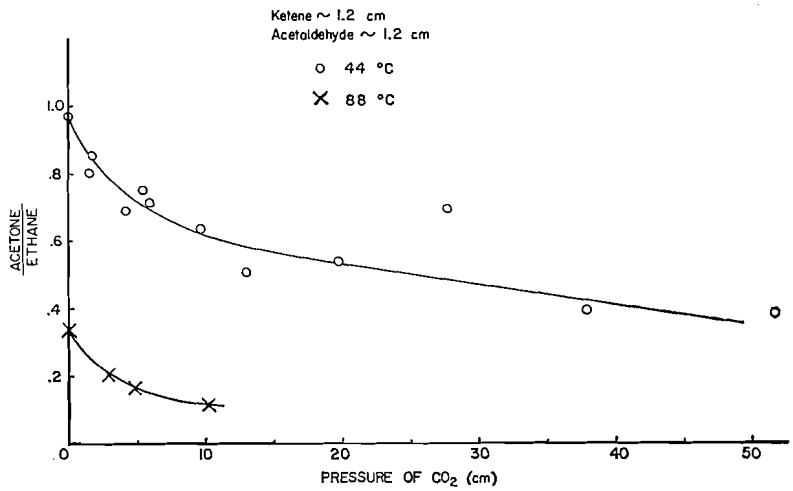

FIG. 10. Ratio of acetyl radical concentration to methyl radical concentration as a function of carbon dioxide pressure for constant acetaldehyde pressure.

photolysis of ketene in the presence of propionaldehyde and carbon dioxide at 85 °C are summarized in Table I. The yields of products at 45 °C as a function of carbon dioxide pressure are shown in Figs. 11 and 12. The yield of ethane was not plotted since it was similar at all pressures to that of methane. There is the suggestion of an inflection point in the variation of yields of the main products with carbon dioxide pressure, but the effect is much less than that observed with acetaldehyde. At 85 °C the yields of all products steadily decreased as the carbon dioxide pressure was increased. The presence of methane is good evidence that initiation of the decomposition of propionaldehyde occurs by reaction of free methylene radicals and not by energy transfer from an excited ketene molecule. Methane was not observed in the photolysis of propionaldehyde by itself.

The yields of stabilization products were still very small compared to those of the main products, carbon monoxide, methane, and ethane. *n*-Butyraldehyde was not observed under any conditions, but isobutyraldehyde was about one-third of the butene oxide. Again, methyl ethyl ketone may have been formed by stabilization or by termination.

The maximum ratio of propylene oxide to carbon monoxide found in the experiments with acetaldehyde was 0.32, but the maximum ratio of [isobutyraldehyde + butene oxide] to carbon monoxide from the reaction with propionaldehyde was 0.014. Stabilization would be expected to occur more readily with propionaldehyde than with acetaldehyde, and the apparently smaller relative yield of stabilization products may be the result of a longer chain length for decomposition of propionaldehyde than for acetaldehyde at the same temperature.

The sharp drop in yield of methyl ethyl ketone with rising pressure probably indicates that at low pressures it was formed largely by combination of radicals and not by stabilization. If the methyl ethyl ketone were formed by stabilization at higher pressures, the reactivity of the aldehydic C—H bond toward insertion of methylene is very similar to that of the secondary C—H bond. The epoxide is still the predominant stabilization product and it would thus appear that addition of methylene across the carbonyl bond is faster than insertion into a primary or secondary C—H bond.

Can. J. Chem. Downloaded from www.nrcresearchpress.com by 210.87.254.40 on 09/05/12
For personal use only.

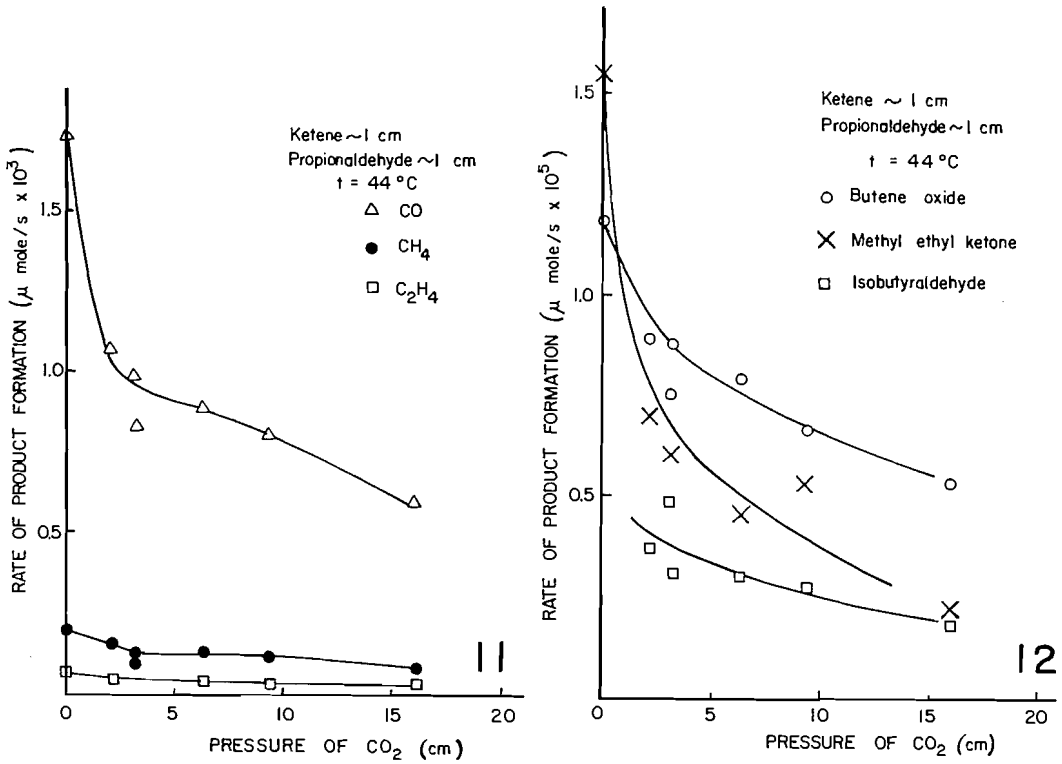

FIGS. 11 and 12. Rate of product formation from the photolysis of ketene in the presence of propionaldehyde and carbon dioxide at 45 °C.

TABLE I

Rate of product formation from the photolysis of ketene in the presence of propionaldehyde and carbon dioxide at 85 °C

	Pressure (cm)				Rate of product formation (μmole/s × 10^3)						
Expt.	Ketene	Propionaldehyde	CO_2	Time (s×10^{-3})	CH_4	CO	C_2H_6	C_2H_4	Isobutyraldehyde	Butene oxide	Methyl ethyl ketone
1	1.02	1.08		10.9	.263	1.42	0.436	0.059	—	—	—
2	1.0	7.5		10.0	.135	1.02	1.13	—	—	—	—
3	1.0	3.8		12.0	.262	1.32	0.711	0.036	—	—	—
4	1.2	9.1		56.9	.147	1.10	0.882	—	—	—	—
5	1.1	1.1	55.5	59.0	.042	0.262	0.0525	0.0086	—	—	—
6	1.25	1.4	27.8	54.7	.0866	0.419	0.140	0.014	—	.0022	.0075
7	1.1	1.3	12.8	54.4	.114	0.570	0.163	0.0198	—	.0028	.0059
8	1.07	1.07	4.95	54.0	.152	0.786		0.031	.002	.056	.0080

It is of interest to compare the present results with those of Cvetanovic (14) on the reaction of oxygen atoms with olefins. In these two reactions the excited molecules formed by the addition of the diradical are isomeric, although the energy content is different in the two cases. The heat of formation of the complex formed by addition of oxygen atoms to propylene is about 64 kcal/mole, while that of the complex formed by the methylene reaction is about 51 kcal/mole[3] assuming no excess energy carried by the radicals. It

[3]$\Delta H_f(CH_2)$ *taken as 90 kcal/mole.*

Can. J. Chem. Downloaded from www.nrcresearchpress.com by 210.87.254.40 on 09/05/12
For personal use only.

might be expected, therefore, that relatively more stabilization of the excited molecule would be observed in the methylene reaction than in the oxygen atom reaction at a given pressure. The converse appears to be true. With propionaldehyde, taking methane as a measure of the dissociation and butene oxide and isobutyraldehyde as the stabilized products, the ratio of [butene oxide + isobutyraldehyde]/methane has the maximum value of 0.1 at a pressure of about 3 cm, whereas in the reaction of oxygen atoms with butene, yields of products were independent of pressure above 10 cm. However, if as suggested earlier, an abstraction reaction, independent of pressure, occurs simultaneously with the insertion reaction, the ratio given above does not represent the true ratio of stabilization to dissociation of the excited molecules formed by insertion. In fact, for these energy differences it is reasonable to assume, as already suggested, that in the addition of methylene to aldehydes stabilization may be complete at rather low pressures.

Another difference in the two sets of reactions is in the relative yields of the isomers of the stabilized molecule. These differences are most pronounced when the comparison is made with the reaction of ground state ^3P oxygen atoms with olefins. For example, with propylene, propylene oxide and propionaldehyde were formed in equal quantities, along with very small amounts of acetone, while the reaction of methylene radicals with acetaldehyde gave only propylene oxide and no propionaldehyde. Similarly, the stabilized products of the reaction of ^3P oxygen atoms with butene-1 were nearly equal yields of α-butene oxide and n-butyraldehyde, with small amounts of ketone. In the methylene radical reaction, the α-butene oxide predominated, and the aldehyde formed was isobutyraldehyde. In these systems methylene radicals were formed in the singlet state, and although some degradation to the triplet may have occurred in the presence of carbon dioxide, most of the radicals probably reacted in the singlet state. The difference in electronic state probably implies a fundamental difference in the mode of attack of the radical on the reactant and in the structure of the complex formed. For example, the addition of a ^3P oxygen atom to the double bond in an olefin forms a diradical complex, which, to form a stable molecule, may undergo migration of groups or may close the ring to form an epoxide. Excess energy may be lost before the structural changes occur. Insertion of singlet methylene, on the other hand, forms a singlet complex, which must lose energy by collisions to form a stable molecule. It is not surprising that the distribution of stabilized products is different from the two reactions.

In the reaction of ^1D oxygen atoms with butene-1 (15) the relative yield of α-butene oxide was increased to about three times that of n-butyraldehyde. The main stabilization product was thus the same for the reaction of ^1D oxygen atoms with butene-1 and the reaction of singlet methylene with propionaldehyde. However, the aldehyde from the oxygen atom reaction was exclusively n-butyraldehyde while from the methylene reaction only isobutyraldehyde was formed. This indicates there is still a difference in the mode of attack of the radicals even when both are in the singlet state and both therefore form singlet addition complexes. The oxygen atom attacks the molecule at one point only—the double bond—and subsequent products are formed by rearrangement or decomposition of the one excited molecule. Thus the excited α-butene oxide molecule initially formed may rearrange to n-butyraldehyde or methyl ethyl ketone (which was observed in small quantities), but not to isobutyraldehyde. Addition of methylene radicals, on the other hand, may occur at any bond in the molecule, usually with little discrimination. However, attack on a secondary C—H bond is usually faster than on a primary C—H bond and therefore isobutyraldehyde would be expected to predominate over n-butyraldehyde. Thus the differences between the oxygen atom reactions and the methylene radical

Can. J. Chem. Downloaded from www.nrcresearchpress.com by 210.87.254.40 on 09/05/12
For personal use only.

reactions are for the most part the result of differences in the mode of attack of each on the reactant, rather than in the subsequent behavior of the isomeric complex.

Formaldehyde

At the beginning of this research a few experiments were done with formaldehyde as reactant. No conclusive evidence for stabilization products was observed and the main reaction of the methylene radicals appeared to be the initiation of the chain decomposition of formaldehyde. The main products were carbon monoxide, methane, and hydrogen in the approximate proportion, 70%, 20%, and 10%, respectively. Small amounts of acetaldehyde were observed but these may have been formed by radical combination. Ethylene oxide was not found.

TABLE II

Rate of product formation from the photolysis of ketene in the presence of carbon dioxide at 44 °C

	Pressure (cm)			Rate of product formation (μmole/s $\times 10^3$)							
Expt.	Ketene	CO_2	Time ($s \times 10^{-3}$)	CH_4	CO	C_2H_6	C_2H_4	CH_3COCH_3	CH_3CHO	Total product	CO/total product
1	1.1	39.2	68.7	.041	0.995	.040	.129	.0041	.008	0.659	1.51
2	1.0	50.0	72.1	.036	0.845	.0366	.111	.0029	.015	0.594	1.42
3	1.0	26.0	65.7	.0391	1.02	.0410	.155	.0033	.011	0.710	1.44
4	1.0	15.0	62.5	.034	1.18	.0474	.224	.0021	.005	0.841	1.40
5	1.0	5.7	58.5	.025	1.35	.0446	.276	.003	.007	0.904	1.49
6	1.0	6.0	26.0	.039	1.82	.084	.450	—	—	1.476	1.23

Carbon Dioxide

A few experiments were done with ketene and carbon dioxide, and these are summarized in Table II. Although the present conditions were somewhat different, the results are consistent with those found by Kistiakowsky and Sauer (9) and with their suggestion that the initial products are carbon monoxide and formaldehyde. The products formaldehyde and ethylene will be attacked more rapidly than carbon dioxide, and the minor products methane, ethane, acetaldehyde, and acetone probably arise by such secondary reactions. The number of moles of carbon monoxide which accompany each mole of minor product depends somewhat on an assumed mechanism. However, the simplest stoichiometry leads to the following. $CH_4 = 4CO$; $C_2H_6 = 5CO$; $CH_3CHO = 2CO$; $CH_3COCH_3 = 5CO$. The ratio of carbon monoxide to total products $[2C_2H_4 + 4CH_4 + 5C_2H_6 + 2CH_3CHO + 5CH_3COCH_3]$ is given in the table. The excess carbon monoxide indicates a loss of some product, which may be formaldehyde. However, the ratio increased with time of reaction (experiments 5 and 6) and extrapolated to one at zero time. This probably indicates the increasing formation of higher products which were not observed in the analysis. Loss of product as formaldehyde would be expected to be reduced at longer times of reaction, as formaldehyde is consumed by secondary reactions, so that this is not the main source of the discrepancy. Formaldehyde is probably converted to other products at very short times of reaction and has a low steady-state concentration in the reaction mixture.

ACKNOWLEDGMENTS

The author wishes to thank Professor K. J. Laidler for his advice and encouragement and Dr. R. A. Back for many helpful discussions. The work was supported by a grant from the National Research Council of Canada.

Can. J. Chem. Downloaded from www.nrcresearchpress.com by 210.87.254.40 on 09/05/12
For personal use only.

REFERENCES

1. H. M. FREY. Reactions of methylene and some simple carbenes. *In* Progress in reaction kinetics. Vol. 2. Pergamon Press. 1964.
2. T. INOUE and Y. TAKEZAKI. Bull. Inst. Chem. Res. Kyoto Univ. **41**, 190 (1963).
3. H. M. FREY. J. Am. Chem. Soc. **80**, 5005 (1958).
4. J. H. KNOX and A. F. TROTMAN-DICKENSON. Chem. Ind. London, 731 (1957).
5. VON FRANZEN and L. FIKENTSHER. Ann. **617**, 1 (1958).
6. W. VON E. DOERING, L. H. KNOX, and M. JONES. J. Org. Chem. **24**, 136 (1959).
7. H. OGOSHI and Y. TAKEZAKI. Bull. Inst. Chem. Res. Kyoto Univ. **38**, 299 (1960).
8. T. B. WILSON and G. B. KISTIAKOWSKY. J. Am. Chem. Soc. **80**, 2934 (1958).
9. G. B. KISTIAKOWSKY and K. SAUER. J. Am. Chem. Soc. **80**, 1066 (1958).
10. G. J. FISHER, A. F. MACLEAN, and A. W. SCHNIZER. J. Org. Chem. **18**, 1055 (1953).
11. H. M. FREY. Trans. Faraday Soc. **56**, 1201 (1960).
12. R. K. BRINTON and D. H. VOLMAN. J. Chem. Phys. **20**, 1053 (1952).
13. A. N. STRACHAN and W. A. NOYES. J. Am. Chem. Soc. **76**, 3261 (1954).
14. R. J. CVETANOVIC. Can. J. Chem. **36**, 623 (1958).
15. S. SATO and R. J. CVETANOVIC. Can. J. Chem. **36**, 1668 (1958).

Can. J. Chem. Downloaded from www.nrcresearchpress.com by 210.87.254.40 on 09/05/12
For personal use only.

Can. J. Chem. Downloaded from www.nrcresearchpress.com by 210.87.254.5 on 09/05/12
For personal use only.

THE CHEMISTRY OF THE AMINOCHROMES

PART VI. THE REACTION OF ADRENOCHROME WITH GLUTATHIONE[1,2,3]

G. L. MATTOK AND R. A. HEACOCK

Psychiatric Research Unit, University Hospital, Saskatoon, Saskatchewan

Received August 10, 1964

ABSTRACT

The reaction between adrenochrome and glutathione has been studied. The main products result from the 1,4-addition of glutathione to the C_5 unsaturated carbonyl systems in adrenochrome involving the C_6—C_7 and the C_4—C_9 double bonds, and are probably 7-*S*-glutathionyl-5,6-dihydroxy-*N*-methylindole and 9-*S*-glutathionyl-2,3,6,9-tetrahydro-3,5-dihydroxy-6-oxo-*N*-methylindole respectively. 5,6-Dihydroxy-*N*-methylindole is also formed during the interaction of glutathione and adrenochrome. The mechanisms by which these compounds are formed are discussed.

INTRODUCTION

Thiols, such as glutathione, generally react with quinones by 1,4-addition across one of the α,β-unsaturated carbonyl systems. Much of the early work, dating back to 1888 (1), was reviewed by Snell and Weissberger in 1939 (2). The reaction of thiols, including glutathione, with 2-methyl-1,4-naphthoquinone has been described by several workers as a 1,4-addition process (3, 4, 5), although it has recently been suggested that this reaction proceeds by a simple nucleophilic substitution of the quinone ring by the mercaptide anion (6). Most of the previously reported additions of this type involved *p*-quinones; however, there have been a number of examples of the reported addition of thiols, including glutathione, to oxidized catechol derivatives (cf. 7–11) and recently the 1,4-addition of a thiol (1-phenyl-5-mercaptotetrazole) to several quinones, including some *o*-quinones, has been described (12, 13).

Preliminary paper chromatographic studies on the interaction of adrenochrome (I) with glutathione (free acid) in aqueous solution indicated that 5,6-dihydroxy-*N*-methylindole (II) and two other products (non-ether extractable) were formed; the major product (III) had an R_f value* of ca. 0.60 and appeared to have retained the indole nucleus and to contain an α-amino acid grouping (14, 15). Bouchilloux and Kodja subsequently reported that dopachrome solutions were decolorized by glutathione (phosphate buffer, pH = 5.5) with the formation of 5,6-dihydroxyindole, 5,6-dihydroxyindole-2-carboxylic acid, and compounds described as 4-*S*-glutathionyl-5,6-dihydroxyindole and its 2-carboxy derivative (10, 11). These latter two compounds were also reported to be obtained by the enzymatic oxidation of 5,6-dihydroxyindole or 5,6-dihydroxyindole-2-carboxylic acid respectively in the presence of glutathione (10, 11). This paper reports the results of an extensive spectroscopic and paper chromatographic examination of the products obtained by the interaction of adrenochrome and glutathione.

EXPERIMENTAL

Materials

Adrenochrome (16), *N*-ethylnoradrenochrome (17), *N*-isopropylnoradrenochrome (17), adrenochrome methyl ether (17), adrenochrome ethyl ether (17), and 5,6-dihydroxy-*N*-methylindole (18) were prepared

[1]*This investigation was supported by grants from the Department of National Health and Welfare (Ottawa) and the Government of Saskatchewan (Department of Public Health).*

[2]*Part V. Can. J. Chem. 41, 139 (1963).*

[3]*A preliminary report of part of this investigation appeared in Arch. Biochem. Biophys. 107, 352 (1964).*

**All the R_f values referred to in this paper were obtained using 2% acetic acid in water as the running solvent (see Experimental section for details).*

by the methods described in the literature. Glutathione, its monosodium salt, and oxidized glutathione were obtained from the Nutritional Biochemicals Corporation.

Spectroscopy

The spectra were recorded on either a Beckman DK-2 or Unicam SP-800 recording spectrophotometer. The reaction mixtures studied were prepared from adrenochrome (5.0 mg) and glutathione (free acid or monosodium salt) (25.0 mg) dissolved in water (1.0 ml). Suitable dilutions were prepared for measurement of the spectra. When required, ether extractions were carried out with peroxide-free ether (4 × 1 ml). In experiments designed to study the effects of added reagents, the reaction mixture was prepared by the method described above; ether extracted (if necessary) and a slight excess of the solid reagent (i.e. silver oxide, sodium hydrosulfite, sodium bisulfite, or sodium acetate) were added directly to the solution. In the experiments designed to find the optimum pH for the formation of a given product the reaction mixture was prepared as described above, except that a suitable acetate or phosphate buffer was used as the reaction medium in place of water.

Paper Chromatography

The aminochrome (10 mg) was dissolved in water (1.0 ml) and the solution was treated with a slight excess of glutathione (free acid or monosodium salt).* When the red color of the aminochrome had been completely discharged the reaction mixture was filtered and a sample (ca. 25–50 μl) of the clear filtrate applied to the chromatographic paper (acid-washed Whatman No. 1 paper). The chromatography was carried out by the descending technique, using 2% acetic acid in water as the running solvent. In all cases the solvent was allowed to descend about 15 to 16 in. (this required approximately 2.5–3 h running time). After drying (in air, at room temperature), the developed chromatograms were examined for fluorescence in ultraviolet light and individual chromatograms were sprayed with one of the following chromogenic reagents:† (*a*) Ehrlich's reagent, (*b*) cinnamaldehyde, (*c*) *p*-dimethylaminocinnamaldehyde, (*d*) Gibb's reagent, (*e*) diazotized *p*-nitroaniline, (*f*) ninhydrin/pyridine, and (*g*) ferric chloride.

In some cases the aqueous solution of the aminochrome reduction products (prepared as described above, 1.0 ml) was extracted, after filtration, with peroxide-free ether (4 × 1.0 ml). Spots consisting of ca. 120–150 μl of the dried (Na_2SO_4) ethereal extract and ca. 40–60 μl of the aqueous mother liquors were applied to the paper separately and the chromatography carried out as described above.

In the experiments designed to obtain relatively pure solutions of the individual products, the reaction mixture was prepared in the manner described above and a sample (ca. 500 μl) was applied as a "streak" across the origin on acid-washed Whatman 3 MM paper (23 cm × 57 cm). After development with 2% acetic acid, the appropriate zones were located by spraying a narrow strip, cut from the edge of the chromatogram. The zones were cut out and eluted with water.

To ascertain if any reaction occurred between 5,6-dihydroxy-*N*-methylindole (II) and glutathione (or oxidized glutathione), an aqueous solution of (II) (10 mg in 1 ml) was treated with an excess of the amino-acid and the reaction mixture examined chromtographically in the manner described above, after it had been allowed to stand at room temperature for a period of time comparable to that required for the adrenochrome–glutathione reaction to go to completion.

RESULTS

Addition of glutathione (monosodium salt) to an aqueous solution of adrenochrome (I) resulted in the discharge of the red color of the solution; the resulting pale yellow solution showed well-defined absorption maxima of approximately equal intensity in the regions of 300 mμ and 350 mμ (see Fig. 1). When the reaction was carried out using glutathione, as the free acid rather than its monosodium salt, the absorbance at 300 mμ was ca. 70% greater than that at 350 mμ (see Fig. 1). In view of the higher absorbances in the 350 mμ region of reaction mixtures obtained using the sodium salt of glutathione. the effect of pH on the relative intensities of the main absorption peaks was investigated, Reaction mixtures containing adrenochrome (I) and glutathione were prepared in a series of acetate and phosphate buffers in the pH range 1–7, and it was observed that formation of the product (λ_{max} = ca. 350 mμ) (i.e. (IV)) occurred optimally at pH = 4.7 (see Fig. 2); the amount of (IV) formed fell off sharply at pH values above and below 4.7 and did not form at all at pH values > 6.

Paper chromatograms of these reaction mixtures on Whatman No. 1 paper with 2%

**An analogous experiment was carried out using oxidized glutathione in place of glutathione, but the red color of the adrenochrome solution was not discharged in a comparable period of time.*

†The chromogenic reagents were prepared by the methods commonly described in the literature (cf. (19)).

Can. J. Chem. Downloaded from www.nrcresearchpress.com by 210.87.254.5 on 09/05/12
For personal use only.

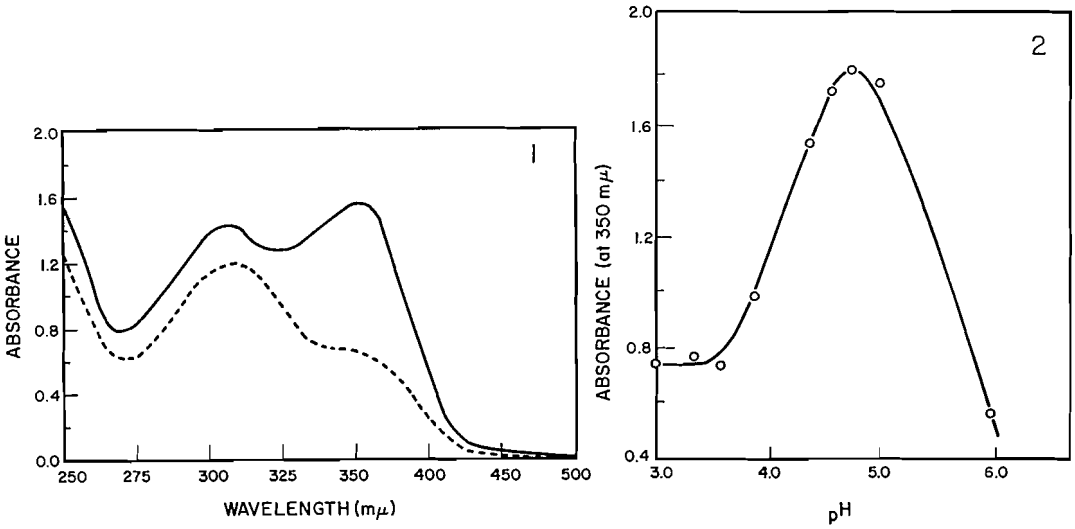

FIG. 1. Absorption spectra of (*a*) adrenochrome/glutathione reaction mixture (broken line) and (*b*) adrenochrome/glutathione (monosodium salt) reaction mixture (solid line).
FIG. 2. The effect of pH on the absorbance at 350 mμ of buffered glutathione/adrenochrome reaction mixtures.

acetic acid as the developing solvent (cf. 14, 15) showed three spots (which gave blue colors after spraying with Ehrlich's reagent) with R_f values of 0.43, 0.64, and 0.85 respectively (see Table I). A yellow spot (R_f = ca. 0.90), which appeared overnight on the sprayed chromatograms, was probably due to unchanged glutathione. The substance with an R_f of 0.85 showed a distinct yellow fluorescence in ultraviolet light; the substance with an R_f of 0.64 (i.e. (III)) did not fluoresce and the product with an R_f of 0.43 showed the weak "blue-mauve" fluorescence in "long wavelength" ultraviolet light characteristic of (II). The absorption maxima for the products were obtained by elution of the appropriate zones from a developed chromatogram of the adrenochrome–glutathione reaction mixture; these were as follows: R_f, 0.64 (i.e. (III)), 303 mμ and R_f, 0.85 (i.e. (IV)), 352 mμ. The unidentified product (III) exhibited color reactions expected for (i) an indole, (ii) a phenol, and (iii) an α-amino acid (see Table I). The color reactions of the product (IV) were a little less certain, due to the contamination of the zone (R_f, 0.80–0.90) on the chromatograms with unchanged glutathione; however, it did appear to react slowly with Ehrlich's reagent, cinnamaldehyde, diazotized *p*-nitroaniline, and ferric chloride (see Table I). The colors obtained from (IV) were similar to those given by the adrenochrome – sodium bisulfite addition product with these reagents (20).

N-Ethylnoradrenochrome and *N*-isopropylnoradrenochrome behaved similarly to adrenochrome on treatment with glutathione in aqueous solution. Paper chromatographic examination of the reaction mixtures showed that three products were formed in each case; the expected *N*-alkyl-5,6-dihydroxyindole and products probably analogous to (III) and (IV). Adrenochrome methyl ether and adrenochrome ethyl ether also behaved in a similar manner to adrenochrome on treatment with glutathione (see Table I). These results suggest that the 1- and 3-positions of the adrenochrome nucleus are not materially involved in any of the reaction sequences. There was no reaction between adrenochrome and oxidized glutathione; consequently, the thiol group of glutathione must have been involved in all these reactions. The possibility of secondary product formation by the

Can. J. Chem. Downloaded from www.nrcresearchpress.com by 210.87.254.5 on 09/05/12
For personal use only.

TABLE I

Paper chromatography of the products obtained from the reaction of some aminochromes with glutathione

Aminochrome reduced	Average R_f values (×100) of the major products				
Adrenochrome	43*		64†,‡	85§,‖	90¶
N-Ethylnoradrenochrome		51**	66	84	90¶
N-Isopropylnoradrenochrome		55††	69	85	90¶
Adrenochrome methyl ether	44*		65†	85	90¶
Adrenochrome ethyl ether	45*		66†	85	92¶

*5,6-Dihydroxy-*N*-methylindole (II).
†7-*S*-Glutathionyl-5,6-dihydroxy-*N*-methylindole (III).
‡Color reactions of (III). Ehrlich's reagent, blue–violet; cinnamaldehyde, red–pink → grey–violet; *p*-dimethylaminocinnamaldehyde, blue–green → grey–blue; diazotized *p*-nitroaniline, magenta → violet–brown; Gibb's reagent, brown; ninhydrin/pyridine, blue–grey (slow at room temperature).
§9-*S*-Glutathionyl-2,3,6,9-tetrahydro-3,5-dihydroxy-6-oxo-*N*-methylindole (IV).
‖Color reactions of (IV). Ehrlich's reagent, blue; cinnamaldehyde, violet–brown; *p*-dimethylaminocinnamaldehyde, grey–blue; diazotized *p*-nitroaniline, yellow → brown; Gibb's reagent, brown; ferric chloride, grey–brown; ninhydrin/pyridine, probably blue–grey, but this area is confused by the proximity of excess glutathione.
¶Excess glutathione (and possibly oxidized glutathione).
**N*-Ethyl-5,6-dihydroxyindole.
††5,6-Dihydroxy-*N*-isopropylindole.

interaction of 5,6-dihydroxy-*N*-methylindole (II) with glutathione (or oxidized glutathione) was also ruled out, since no reaction occurred between (II) and either glutathione or oxidized glutathione in aqueous solution, over periods of time comparable with those required for the adrenochrome/glutathione (or monosodium salt) reactions to go to completion.

It was shown by paper chromatography that ether extraction of the adrenochrome–glutathione reaction mixtures completely removed the substance with an R_f of 0.43 (i.e. (II)). The ultraviolet spectrum of the aqueous mother liquors, still showed peaks at ca. 300 mμ and 350 mμ, although the intensity of the 300 mμ peak was much reduced, because of the removal of (II) which also absorbs in this region. The reaction mixture, after removal of (II) by ether extraction, was initially yellow, but on the addition of solid sodium acetate or on the cautious addition of aqueous sodium hydroxide the solution became red. Dilution (ca. 100 times) of the ether-extracted reaction mixture with water, also led to the formation of an orange–red product, after 2 h at room temperature; the color intensified on standing overnight. These color changes did not appear to be affected by bubbling oxygen through the solution. The change in color of the solution was accompanied by a modification of the absorption spectrum; the intensity of the absorption at ca. 350 mμ was markedly reduced, and eventually disappeared; at the same time there was an increase in the absorbance at 300 mμ and a new peak at 485 mμ appeared. The red color of the modified reaction mixture was discharged on addition of excess sodium hydroxide, with the formation of a yellow product which exhibited an intense yellow–green fluorescence, usually associated with adrenolutin (5,6-dihydroxy-*N*-methylindoxyl), in ultraviolet light (cf. 21). The red product was also decolorized by the addition of sodium hydrosulfite or sodium bisulfite. In the former case an ether extractable product was obtained which was shown by paper chromatography and spectroscopy to be identical with 5,6-dihydroxy-*N*-methylindole (II), and in the latter case the red color could be restored by the cautious addition of alkali; addition of excess alklai resulted in the discharge of the red color and the formation of a fluorescent product similar to that described above. These reactions with sodium bisulfite and alkali suggests that the red product is derived from (IV) and that it is probably adrenochrome (I) (λ_{max} 300 mμ and 487 mμ (cf. 22)). The ether extracted adrenochrome–glutathione reaction mixture is capable of further modification by oxidizing and reducing agents. After treatment of the ether

Can. J. Chem. Downloaded from www.nrcresearchpress.com by 210.87.254.5 on 09/05/12
For personal use only.

extracted reaction mixture with silver oxide, the solution became deep yellow and the original peaks at ca. 300 mμ and ca. 350 mμ were replaced by peaks at 285 mμ* and 399 mμ; this suggests that both compounds can undergo oxidation. The peak at ca. 350 mμ (due to (IV)) disappeared and the 300 mμ peak increased in intensity on treatment of the original reaction mixture (ether extracted) with sodium hydrosulfite. Paper chromatography showed that reduction with this reagent resulted in the elimination of the faster running substance (i.e. (IV)) and the formation of (II) which could be extracted with ether and identified by chromatography and spectroscopy.

DISCUSSION

On the basis of the observed spectroscopic, paper chromatographic, and chemical data, it is possible to propose likely structures for the products obtained by the action of glutathione on adrenochrome; the formation of all the reaction products can also be explained by reasonable mechanisms.

It is well known that 5,6-dihydroxy-*N*-methylindole (i.e. (II)) is usually produced, to some extent, when adrenochrome reacts with a reducing agent (cf. 22), and it has previously been suggested that the product with an R_f value of 0.43 (i.e. (II)) was, in fact, 5,6-dihydroxy-*N*-methylindole; the results of the present investigation are in agreement with this suggestion. The paper chromatographic and spectroscopic properties of (II) were identical to those of pure 5,6-dihydroxy-*N*-methylindole. The formation of 5,6-dihydroxy-*N*-methylindole (II) could result from the direct reduction of adrenochrome (I) by glutathione. It could also result from the reduction of (I) by (III) (or possibly its immediate precursor (i.e. (VI)); the reduction of a quinone by the corresponding hydroquinone containing an electron-donating group is well known (cf. 23). To test the plausibility of the latter type of reaction occurring, a solution of *N*-isopropylnoradrenochrome was treated with (II); paper chromatography of this reaction mixture showed that interaction had, in fact, occurred, with the formation of 5,6-dihydroxy-*N*-isopropylindole (i.e. the dehydrated reduction product of *N*-isopropylnoradrenochrome). In view of the difficulty of detecting oxidized glutathione, in the presence of glutathione (with the chromatographic system used in this investigation), and the uncertainty that its presence, if found, was not merely due to autoxidation, it is not possible to be sure if the direct reduction mechanism is operating to any extent in the adrenochrome–glutathione system. However, since 5,6-dihydroxy-*N*-methylindole (II) is not the major product of the adrenochrome/glutathione reaction and the *N*-isopropylnoradrenochrome/5,6-dihydroxy-*N*-methylindole interaction resulted in appreciable formation of 5,6-dihydroxy-*N*-isopropylindole, in a time comparable to that required for the completion of the adrenochrome/glutathione reaction, it is most probable that the majority of the (II) present in the glutathione/adrenochrome system resulted from the reduction of adrenochrome by (III) or (VI) which gave "leuco-adrenochrome" (VII) which is known to dehydrate spontaneously and form 5,6-dihydroxy-*N*-methylindole (II) (cf. 24).

There are two possible ways by which glutathione could add, by a 1,4-addition mechanism, to adrenochrome. Addition could occur across the α,β-unsaturated C_5-carbonyl system, which includes the C_6—C_7 double bond, to form the adduct (V); subsequently this product could undergo an "enolization" of the polarized C_6-carbonyl

**The position of the 285 mμ peak could not be precisely determined since end absorption due to oxidized glutathione is significant below 290 mμ; this was partially compensated by the addition of oxidized glutathione to the solution in the reference beam of the spectrophotometer.*

Can. J. Chem. Downloaded from www.nrcresearchpress.com by 210.87.254.5 on 09/05/12
For personal use only.

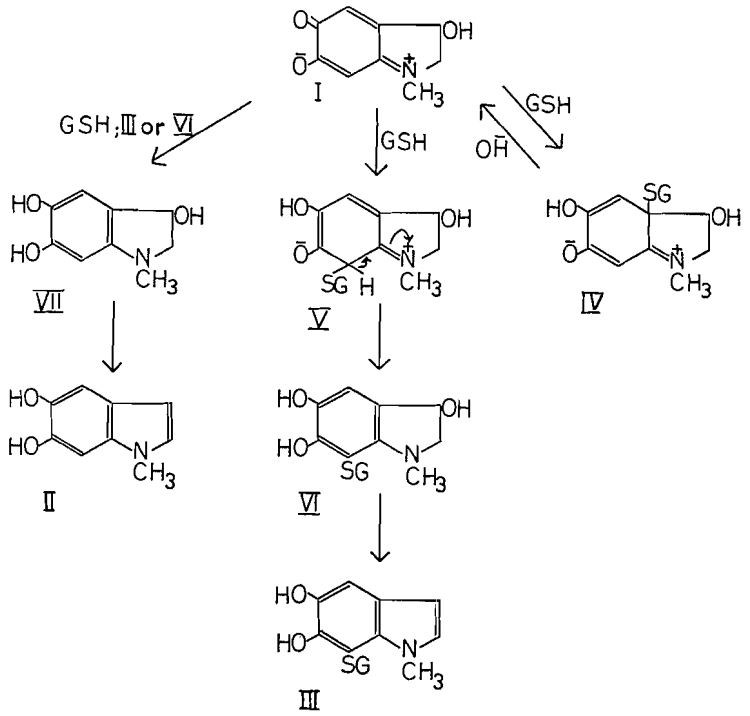

group to give 7-*S*-glutathionyl-3,5,6-trihydroxy-*N*-methylindoline (VI). The 3,5,6-trihydroxyindoline structure is known to rapidly undergo an intramolecular dehydration to give the 5,6-dihydroxyindole structure (cf. 24), consequently, (VI) would be expected to dehydrate to give 7-*S*-glutathionyl-5,6-dihydroxy-*N*-methylindole (III). This structure is quite compatible with the observed properties of (III), i.e. the typical indole absorption maximum at ca. 300 mμ and the color reactions expected for an indole, catechol, and an α-amino acid. It is also water soluble and was not extracted from its aqueous solutions by ether as would have been expected for a molecule containing a large amino acid residue. This structure is similar to that postulated by Bouchilloux and Kodja for one of the products obtained from dopachrome by the action of glutathione, except that the French authors suggested that the glutathione residue was attached to the 4-position of the indole nucleus (11). Alternatively, 1,4-addition of glutathione to the α,β-unsaturated C_5-carbonyl system, with the double bond between the C_9-bridge-head carbon atom and C_4 would result in structure (IV), i.e. 9-*S*-glutathionyl-2,3,6,9-tetrahydro-3,5-dihydroxy-6-oxo-*N*-methylindole. This structure is similar to that proposed by Tse and Oesterling for the adrenochrome – sodium bisulfite addition product (25) and is compatible with the properties of the glutathione/adrenochrome interaction product (IV) with $R_f = 0.85$ and $\lambda_{max} = 352$ mμ. There are a number of chemical similarities between (IV) and the bisulfite addition product (cf. 25, 26) although the glutathione adduct would appear to be less stable. In the first place, there is the apparent regeneration of adrenochrome (λ_{max}, ca. 300 and 487 mμ) on treatment with mild alkali (cf. 14, 26); both products exhibit an absorption maximum in the 350–360 mμ range; both compounds show a weak yellow fluorescence in ultraviolet light and (IV) and the adrenochrome – sodium bisulfite addition product show similar paper chromatographic behavior, e.g. they both have high

Can. J. Chem. Downloaded from www.nrcresearchpress.com by 210.87.254.5 on 09/05/12
For personal use only.

R_f's in 2% acetic acid and they both react relatively slowly with indole reagents, such as Ehrlich's reagent and cinnamaldehyde.

Reactions between thiols and aminochromes, such as those described above may be of considerable significance in several biological processes. A possible mode of attachment of melanins to proteins could be by a sulfide linkage formed by an interaction of one of the thiol groups in the latter with one of the indole-5,6-quinone units in the melanin structure (cf. 27, 28); such interactions could also occur with the distinct aminochrome units which are considered by some workers to be present in the melanin structure (cf. 29, 30). It has been suggested that the sulfide linkage occurs at the 4-position in the indole nucleus (11, 31), however, the present investigation would suggest that the possibility of such linkages occurring at the 7-position of the indole nucleus should not be overlooked.

The formation of aminochrome–thiol addition products such as the compound (IV) offers the intriguing possibility that some thiols could conceivably act as "aminochrome-carriers", which could readily regenerate the aminochrome under the appropriate conditions. Hadler *et al.* have recently described the somewhat analogous conjugation of cysteine during its oxidation by 2,6-dichlorophenolindophenol, and suggested that reactions of this type maybe of biological significance (32, 33).

ACKNOWLEDGMENTS

The assistance of Mrs. B. D. Scott and Mrs. D. L. Wilson with some of the paper chromatographic work is gratefully acknowledged.

REFERENCES

1. J. Bongartz. Ber. **21**, 483 (1888).
2. J. M. Snell and A. Weissberger. J. Am. Chem. Soc. **61**, 450 (1939).
3. L. F. Fieser and M. Fieser. Organic chemistry. D. C. Heath and Co., Boston, Mass. 1944. p. 738.
4. L. F. Fieser and R. B. Turner. J. Am. Chem. Soc. **69**, 2335 (1947).
5. E. Friedman, D. H. Marrian, and I. Simon-Reuss. Brit. J. Pharmacol. **3**, 335 (1948).
6. W. J. Nickerson, G. Falcone, and G. Strauss. Biochemistry, **2**, 537 (1963).
7. H. S. Mason. Nature, **175**, 771 (1955).
8. E. A. H. Roberts. Chem. Ind. London, 955 (1959).
9. A. Kodja and S. Bouchilloux. Compt. Rend. Soc. Biol. **154**, 737 (1960).
10. S. Bouchilloux and A. Kodja. Compt. Rend. **251**, 1920 (1960).
11. S. Bouchilloux and A. Kodja. Bull. Soc. Chim. Biol. **42**, 69 (1960).
12. R. F. Porter, W. W. Rees, E. Frauenglass, H. S. Wilgus, G. H. Nawn, P. P. Chiesa, and J. W. Gates. J. Org. Chem. **29**, 588 (1964).
13. H. S. Wilgus, E. Frauenglass, E. T. Jones, R. F. Porter, and J. W. Gates. J. Org. Chem. **29**, 594 (1964).
14. R. A. Heacock and B. D. Laidlaw. Chem. Ind. London, 1510 (1958).
15. R. A. Heacock and B. D. Scott. Can. J. Biochem. Physiol. **37**, 1087 (1959).
16. R. A. Heacock, C. Nerenberg, and A. N. Payza. Can. J. Chem. **36**, 853 (1958).
17. R. A. Heacock and B. D. Scott. Can. J. Chem. **38**, 516 (1960).
18. G. L. Mattok and R. A. Heacock. Can. J. Chem. **42**, 484 (1964).
19. R. A. Heacock, M. E. Mahon, and B. D. Scott. Can. J. Chem. **39**, 231 (1961).
20. R. A. Heacock and B. D. Scott. Unpublished results.
21. R. A. Heacock and G. L. Mattok. Can. J. Chem. **41**, 139 (1963).
22. R. A. Heacock. Chem. Rev. **59**, 181 (1959).
23. R. Cecil and J. R. McPhee. Advan. Protein Chem. **14**, 255 (1959).
24. J. Harley-Mason. J. Chem. Soc. 1276 (1950).
25. R. L. Tse and M. J. Oesterling. Clin. Chim. Acta, **8**, 393 (1963).
26. J. van Espen. Pharm. Acta Helv. **33**, 207 (1958).
27. H. S. Mason. Advan. Enzymol. **16**, 122 (1955).
28. H. S. Mason. *In* Pigment cell biology. *Edited by* Myron Gordon. Academic Press Inc., New York. 1959. p. 580.
29. R. A. Nicolaus. Rass. Med. Sper. **9**, Suppl. No. 1 (1962).
30. G. A. Swan. Ann. N.Y. Acad. Sci. **100**, 1005 (1963).
31. J. L. Stoves. Research London, **6**, 29S (1953).
32. H. I. Hadler, M. J. Erwin, and H. A. Lardy. J. Am. Chem. Soc. **85**, 458 (1963).
33. H. I. Hadler and M. J. Erwin. Biochemistry, **2**, 954 (1963).

Can. J. Chem. Downloaded from www.nrcresearchpress.com by 210.87.254.5 on 09/05/12
For personal use only.

Can. J. Chem. Downloaded from www.nrcresearchpress.com by 210.87.254.5 on 09/05/12
For personal use only.

ESTER HYDRAZONES AS POSSIBLE PRECURSORS TO ALKOXYDIAZOALKANES[1]

I. THE SYNTHESIS OF ESTER (*p*-TOLYLSULFONYL)HYDRAZONES AND THEIR DECOMPOSITION IN PROTIC SOLVENTS TO GIVE MIXED ACETALS

ROBERT J. CRAWFORD AND RINTJE RAAP[2]
Department of Chemistry, University of Alberta, Edmonton, Alberta
Received July 10, 1964

ABSTRACT

Methyl benzoate (*p*-tolylsulfonyl)hydrazone (I) was prepared from the reaction between (*p*-tolylsulfonyl)hydrazide and either methyl benzimidate hydrochloride or methyl orthobenzoate. When the potassium or sodium salt of this hydrazone was decomposed, thermally or photochemically, in the presence of alcohols, benzaldehyde mixed acetals could be isolated in good yields and of high purity. When the decomposition was carried out in the presence of piperidine, there was produced 1-(α-methoxybenzyl)piperidine (II) and α,α-dipiperidinotoluene (III). The reaction products can be explained by assuming the initial formation of phenylmethoxydiazomethane.

INTRODUCTION

Diazo compounds have proved extremely useful in synthetic organic chemistry (1). There are, however, limited types of diazo compounds available, and as an extension to this useful class of reactants, an investigation into the possible synthesis of alkoxydiazoalkanes has been undertaken. Examination of the stabilities of known diazoalkanes (2) would lead one to predict that the alkoxydiazoalkanes may be unstable, thus only *in situ* synthesis may be possible. Such *in situ* generation of alkoxydiazoalkanes would in itself be of synthetic value and thus our initial investigations have been directed at the use of the Bamford–Stevens reaction (3) on ester (*p*-tolylsulfonyl)hydrazones.

Synthesis of Ester (p-Tolylsulfonyl)hydrazones

Orthoesters have frequently been used to prepare imidate esters and Ainsworth (4) has produced ester semicarbazones from orthoesters and semicarbazide.

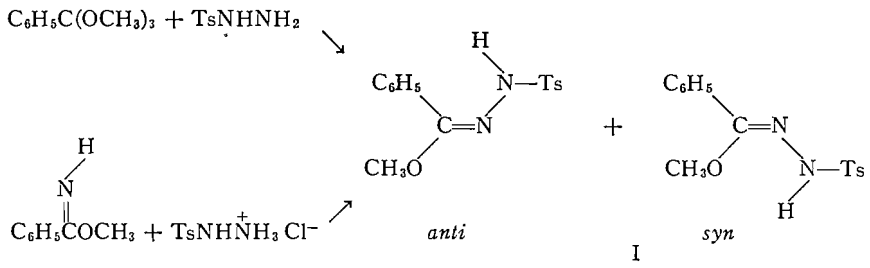

I

Upon refluxing an equimolar mixture of trimethyl orthobenzoate and (*p*-tolylsulfonyl)-hydrazide in methanol, methyl benzoate (*p*-tolylsulfonyl)hydrazone (I) was isolated in a 72% yield. The product consisted of a mixture of *syn* and *anti* isomers as was indicated by the presence of two signals for the methoxy protons at τ 6.22 and 6.33 in the nuclear

[1]*Presented at the 47th Canadian Chemical Conference, Kingston, Ontario, June 1–3, 1964.*
[2]*National Research Council of Canada Scholarship holder 1963–1964. Present address: R & L Molecular Research Ltd., Edmonton, Alberta.*

magnetic resonance (n.m.r.) spectrum. Upon further purification a pure isomer, m.p. 98–99°, with the signal for methoxy protons at τ 6.33, was produced.*

A second method of preparation was developed. Schmidt (6) has shown that imido esters react rapidly with hydrochloride salts of amines and hydrazines to give Schiff bases and hydrazones respectively. Methyl benzoate (*p*-tolylsulfonyl)hydrazone could be prepared in a 41% yield by adding a cold solution of methyl benzimidate in ethanol to a cold suspension of (*p*-tolylsulfonyl)hydrazide hydrochloride. The product was again a mixture of *syn* and *anti* isomers. Both methods are of general applicability, the former being preferred because of the superior yields.

Decompositions in Protic Solvents

The sodium or potassium salt of I was prepared in good yield from solutions of I (mixture of isomers) and sodium or potassium ethoxide in dimethoxyethane. These salts are stable and can be isolated in a high degree of purity as indicated by their n.m.r. spectra. Thus they were used for the majority of the reactions investigated. When the sodium salt of I was refluxed in ethanol, a reaction took place that required a 67 h reflux

$$\text{Na salt of I} + \text{ROH} \rightarrow \text{C}_6\text{H}_5\text{CH(OCH}_3\text{)OR} + \text{Na}^+ {}^-\text{O}_2\text{SC}_6\text{H}_4\text{—CH}_3(p) + \text{N}_2$$

period to complete. The only products found to be present were sodium *p*-toluenesulfinate and benzaldehyde methyl ethyl acetal. At higher temperatures the decomposition occurred much faster and in the presence of different alcohols fairly good yields of mixed acetals were obtained. A summary of these experiments is given in Table I.

The potassium salt of I decomposed photochemically in 2 h at room temperature to similarly produce benzaldehyde methyl ethyl acetal (70%).

TABLE I

Mixed acetals of benzaldehyde prepared by the thermal decomposition of salts of I

R	Boiling point (°C (mm))	C_6H_5 OCH_3* / C / H OR n_D^{25}	Yield (%)	Conditions
C_2H_5-†	58–59 (2.5)	1.4831	37	Na salt, ethanol, 67 h at 78°
C_2H_5-†	58–59 (2.5)	1.4831	70	Photochemical decomposition, ethanol, 25°
n-C_3H_7-	67–68 (2.0)	1.4809	65	Na salt, 1-propanol, 23 h at 95°
$(CH_3)_2CH—CH_2$-	66–67 (0.8)	1.4765	61	Na salt, 2-methyl-1-propanol, 7 h at 105°
$(C_2H_5)_2CH$-‡	87–88 (1.0)	1.4796	35	K salt, 3-pentanol, 6 h at 116°
$C_6H_5—CH_2$-‡	116–117 (0.3)	1.5460	63	K salt, benzyl alcohol, 3.5 h at 116°

*The acetals were characterized by elemental analysis, n.m.r. spectra, and by the formation of the 2,4-dinitrophenylhydrazone of benzaldehyde upon treatment with a methanolic solution of 2,4-dinitrophenylhydrazine sulfate.
†Reported (B. Wladislaw and A. M. J. Ayres. J. Org. Chem. 27, 281 (1962).) b.p. 205° (760), n_D^{19} 1.4878.
‡1,2-Diethoxyethane was used as a solvent.

It seemed of interest to see whether the decomposition of methyl benzoate (*p*-tolylsulfonyl)hydrazone in the presence of secondary amines might give rise to compounds of the type represented by II. When the potassium salt of I was refluxed for 11 h in piperidine, the decomposition was complete. The only product that was isolated, in a 82% yield, was α,α-dipiperidinotoluene (III). It was believed that this product resulted from a reaction

**Studies by Karabatsos and Taller (5) on the n.m.r. spectra of phenylhydrazones would suggest that the isomer melting at 98–99° and having a signal at τ 6.33 should be assigned the syn configuration, using the convention outlined in ref. 5.*

Can. J. Chem. Downloaded from www.nrcresearchpress.com by 210.87.254.5 on 09/05/12
For personal use only.

between initially formed 1-(α-methoxybenzyl)piperidine (II) and piperidine. In order to test this assumption the decomposition was carried out photochemically at room temperature. When the reaction mixture was worked up, special care was taken that the temperature was kept as low as possible and II was isolated, in a yield of 30%. However

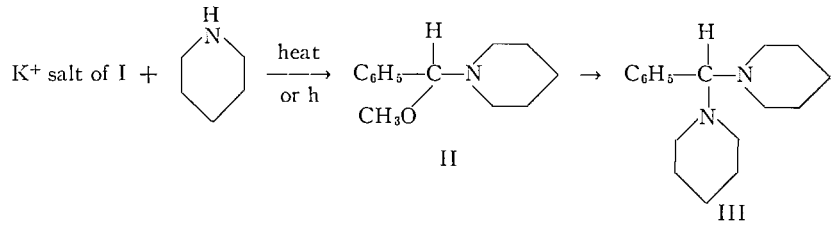

III was still the principal reaction product. The proof of structure of 1-(α-methoxybenzyl)piperidine (II) is based upon an elemental analysis, spectral data, and its conversion into α,α-dipiperidinotoluene upon heating with piperidine. Compound II is an unstable high-boiling liquid (b.p. 81–85° at 0.2 mm). Even at 0° it slowly decomposes and the smell of benzaldehyde becomes apparent. The infrared spectrum of a solution on standing also develops a carbonyl band at the same frequency as benzaldehyde (1 708 cm^{-1}). The n.m.r. spectrum shows singlets at τ 2.76, 5.33, and 6.66 ascribed to the aromatic protons, the methinyl hydrogen, and the methoxy hydrogens respectively, and broad bands at τ 7.3–7.8 and τ 8.3–8.8 ascribed respectively to the α- and β,γ-hydrogens of the piperidine ring. The ratio of integrated areas is the same as that predicted for II.

When the decomposition of the potassium salt of I was carried out in diglyme at 125–130° in the presence of a trace of water, a 15% yield of a crystalline compound, melting at 147–149°, was isolated. The infrared spectrum showed a strong absorption at 1 619 cm^{-1}, which was attributed to a carbon–nitrogen double bond, and further strong bands at 1 165 cm^{-1} and in the 1 300 – 1 350 cm^{-1} region. These latter absorptions suggested the presence of a sulfonylamido group (7). The n.m.r. spectrum showed a complicated signal pattern of aromatic protons at τ 2.0–3.3 and singlets at τ 4.14, 6.23, 7.05, and 7.59 with relative areas 14:1:3:3:3. The compound was found to have a molecular weight of 440 and to fit the empirical formula $C_{23}H_{24}N_2O_4S$ (molecular weight 424.5). The only structure that readily fits all the requirements is that of methyl benzoate (α-methoxybenzyl)-(*p*-tolylsulfonyl)hydrazone (IV).* When the experiment was repeated with a trace of

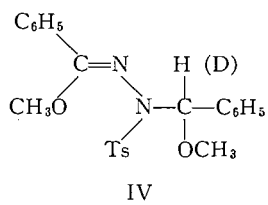

IV

D_2O instead of H_2O, the n.m.r. spectrum of IV showed that the singlet at τ 4.14 was present in only one-fifth of its original intensity, thus indicating that the proton responsible for this signal originates from the water. This type of product has recently been isolated by Nozaki *et al.* in an investigation of the reaction of phenylcarbene formed from benzaldehyde (*p*-tolylsulfonyl)hydrazone in various solvents (8).

**When an equimolar mixture of I and its potassium salt were heated in diglyme at 130° a 36% yield of IV was obtained.*

Can. J. Chem. Downloaded from www.nrcresearchpress.com by 210.87.254.5 on 09/05/12
For personal use only.

Can. J. Chem. Downloaded from www.nrcresearchpress.com by 210.87.254.5 on 09/05/12
For personal use only.

CONCLUSIONS

Salts of ester (*p*-tolylsulfonyl)hydrazones may be decomposed in protic solvents, both thermally and photochemically, to give rise to those products expected from alkoxydiazoalkanes. The results described herein are similar to those obtained by Bamford and Stevens (3) in the thermal decomposition (*p*-tolylsulfonyl)hydrazone salts of aromatic aldehydes and ketones. Therefore it seems reasonable to assume that the decomposition of an ester (*p*-tolylsulfonyl)hydrazone salt produces initially an alkoxydiazoalkane (V) which by virtue of its reactivity undergoes an immediate reaction with the solvent. However on basis of the present experiments alone the possibility of product formation via an intermediate such as VI can not be excluded.

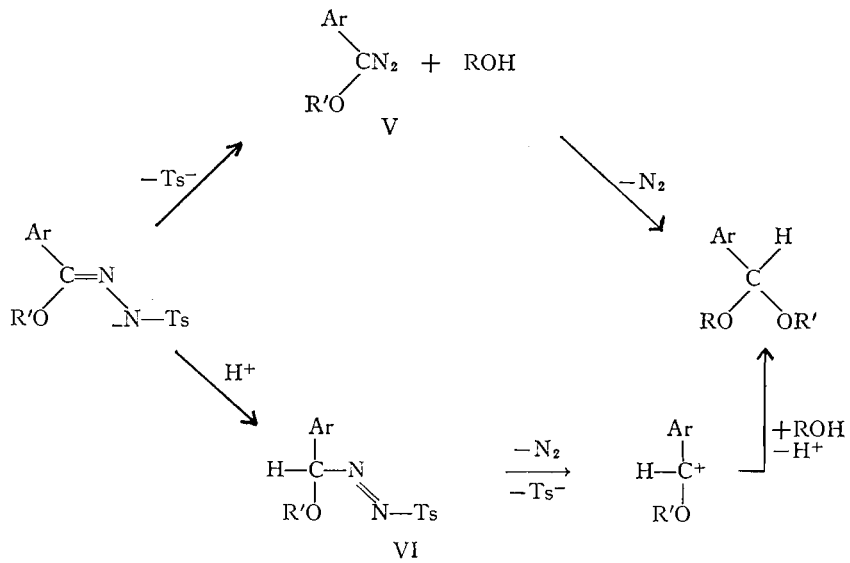

EXPERIMENTAL

All melting points and boiling points are uncorrected.

The infrared spectra were obtained on a Perkin–Elmer Model 421 spectrophotometer equipped with grating optics. Nuclear magnetic resonance spectra were measured using a Varian Associates Model A-60 spectrometer, with tetramethylsilane as a reference. Ultraviolet spectra were obtained using a Cary Model 14M recording spectrophotometer.

Vapor phase chromatography was carried out with a Perkin–Elmer Model 154 vapor fractometer or a F. & M. Model 500 temperature-programmed gas chromatograph.

The photochemical decompositions were all carried out in a quartz reaction vessel, cooled by running tap water, with an internally situated 250 W Hanovia ultraviolet source.

The microanalyses were performed by Pascher Mikroanalytisches Laboratorium (Bonn, West Germany), Daessle Organic Microanalyses (Montreal), and the Microanalytical Laboratory of the Department of Chemistry, University of Alberta (Edmonton).

Methyl Benzimidate was prepared as described by Wheeler (9); yield, 90%; b.p. 73–74° (2.4 mm); n_D^{25} 1.5420. Reported b.p. 95–97° (14 mm).

Methyl Benzoate (p-Tolylsulfonyl)hydrazone (I) from Methyl Benzimidate

A solution of methyl benzimidate (12.2 g, 90.4 mmole) in 20 ml of absolute ethanol was added to a cold suspension of (*p*-tolylsulfonyl)hydrazide hydrochloride (20.0 g, 89.9 mmole) in 60 ml of absolute ethanol. Ammonium chloride precipitated slowly from the obtained homogeneous reaction mixture. After 3 h at room temperature the ammonium chloride was filtered off and most of the ethanol removed under reduced pressure. Diethyl ether and water were added to the residue. The ether solution was again washed with water and dried and the ether evaporated. The residue was dissolved in a mixture of 60 ml of benzene and 25 ml of *n*-hexane and cooled in the refrigerator for 2 days. The solid amounted to 8.2–11.2 g (30–41%). The n.m.r. spectrum showed that it was a mixture of the *syn* and *anti* isomer (methoxy signals at 6.23 and

6.34 with an integration ratio of 1:4 respectively). Two additional recrystallizations from a benzene – *n*-hexane mixture gave a product, m.p. 93–97°, consisting of only one isomer. However the crystals contained some benzene, as indicated by the n.m.r. spectrum and an analysis, which could not be readily removed. A pure product, believed to be the *syn* isomer, was obtained by recrystallization from diethyl ether; m.p. 98–99°.

Anal. Calcd. for $C_{15}H_{16}N_2O_3S$: C, 59.19; H, 5.30; N, 9.21; S, 10.54. Found: C, 58.87; H, 5.06; N, 9.41; S, 10.71.

When the product was heated for 0.5 h at 100–102°, a mixture of the two isomers was obtained (the integration ratio of the methoxy signals at 6.23 and 6.33 in the n.m.r. spectrum was 1:2 respectively).

Potassium Salt of Methyl Benzoate (p-Tolylsulfonyl)hydrazone

Methyl benzoate (*p*-tolylsulfonyl)hydrazone (10.0 g, 32.9 mmole) was added to a solution of potassium (1.3 g, 33.3 mg-atom) in a mixture of 6 ml of anhydrous ethanol and 70 ml of 1,2-dimethoxyethane. The solution was heated to its boiling point, then cooled. The potassium salt was filtered off and washed with ether. Yield 7.3 g (65%) of slightly yellow-colored salt which decomposes above 170°. The n.m.r. spectrum (in D_2O) indicated a complex signal pattern from the aromatic protons at 2.2–3.3, and sharp singlets at 6.55 and 8.25.

Methyl Benzoate (p-Tolylsulfonyl)hydrazone from Methyl Orthobenzoate

A solution of methyl orthobenzoate (10.0 g, 55 mmole, prepared by the method of McElvain and Venerable (10)) and (*p*-tolylsulfonyl)hydrazide (10.0 g, 54 mmole) in 60 ml of methanol was refluxed for 4 h. The solvent was removed under reduced pressure, the residual oil dissolved in 50 ml of benzene, and 25 ml of *n*-hexane added. The solution thus obtained was cooled for 2 days in the refrigerator before the crystals were filtered off. Yield, 12.2 g (73%) of white crystals, m.p. 85–95°. By an examination of the n.m.r. spectrum (in $CDCl_3$) it was clear that the solid consisted only of a mixture of the *syn* and *anti* isomer (apart from a small amount of benzene that could not be removed), as indicated by methoxy singlets at 6.22 and 6.33 (integration ratio 2:3 respectively) and aromatic methyl singlets at 7.58 and 7.63.

The Preparation of Benzaldehyde Acetals from the Thermal or Photochemical Decomposition of Alkyl Benzoates (p-Tolylsulfonyl)hydrazones (Benzaldehyde Dimethyl Acetal)*

Methyl benzoate (*p*-tolylsulfonyl)hydrazone (5.0 g, 16.4 mmole) and sodium methoxide (0.90 g, 16.6 mmole) were refluxed for 47 h in 35 ml of 1,2-dimethoxyethane. The solid (3.3 g) was collected by filtration and found to be a mixture of sodium *p*-toluenesulfinate and sodium methyl benzoate (*p*-tolylsulfonyl)-hydrazone. The filtrate was concentrated and the residue was dissolved in ether, washed with water, and dried ($MgSO_4$). The liquid residue obtained after removal of the ether consisted of only benzaldehyde dimethyl acetal (as shown by n.m.r. spectroscopy); yield, 0.8 g (50%, based on 60% starting material that had reacted); b.p. 56–57° (3.5 mm). Reported (11) b.p. 207° at atmospheric pressure.

Benzaldehyde Methyl Ethyl Acetal

(a) Methyl benzoate (*p*-tolylsulfonyl)hydrazone (10.0 g, 32.9 mmole) was added to a solution of sodium (0.8 g, 34.8 mg-atom) in 50 ml of absolute ethanol and the mixture was refluxed for 67 h. Gas evolution took place very slowly. The ethanol was distilled off and the residue was taken up in ether, washed with water, and dried with anhydrous magnesium sulfate. A vacuum distillation of the residue, obtained after removal of the ether, gave 2.0 g (37%) of the acetal; b.p. 58–59° (2.5 mm); n_D^{25} 1.4831. Reported (12) b.p. 205° (atmospheric pressure); n_D^{19} 1.4878.

Anal. Calcd. for $C_{10}H_{14}O_2$: C, 72.26; H, 8.49. Found: C, 72.48; H, 8.40.

(b) Potassium methyl benzoate (*p*-tolylsulfonyl)hydrazone (9.0 g, 26.3 mmole) was suspended in 180 ml of absolute ethanol and irradiated at room temperature. Gas evolution took place rapidly and the potassium salt slowly dissolved. After 2 h the gas evolution ceased (calcd. amount of nitrogen at 25° and 700 mm: 693 ml; observed: 695 ml). The solution was treated as described above and yielded 3.1 g (70%) benzaldehyde methyl ethyl acetal; b.p. 60–61° (2.6 mm); n_D^{25} 1.4832.

Benzaldehyde Methyl n-Propyl Acetal

Methyl benzoate (*p*-tolylsulfonyl)hydrazone (10.0 g, 32.9 mmole) was added to a solution of sodium (0.8 g, 34.8 mg-atom) in 40 ml of 1-propanol, and the mixture was refluxed for 23 h, at which time the nitrogen evolution had ceased. Part of the sodium *p*-toluenesulfinate (4.5 g, 77%; its infrared and n.m.r. spectra were identical with those of an authentic sample) crystallized out upon cooling and was filtered off. The 1-propanol was distilled off and the residue was taken up in ether, washed with water, and dried. Removal of the ether and a vacuum distillation of the residue yielded 3.85 g (65%) of the acetal; b.p. 67–68° (2.0 mm); n_D^{25} 1.4809.

Anal. Calcd. for $C_{11}H_{16}O_2$: C, 73.29; H, 8.95. Found: C, 73.72; H, 8.57.

Benzaldehyde Methyl Isobutyl Acetal

The same procedure as described above was used except that 40 ml of isobutyl alcohol was used as

**All the acetals prepared reacted with a methanolic 2,4-dinitrophenylhydrazine sulfate solution to give benzaldehyde 2,4-dinitrophenylhydrazone, m.p. 241–242°.*

Can. J. Chem. Downloaded from www.nrcresearchpress.com by 210.87.254.5 on 09/05/12
For personal use only.

solvent and a reflux time of only 7 h was required to effect complete decomposition. Yield, 3.9 g (61%); b.p. 77–78° (2.4 mm); n_D^{25} 1.4769.

Anal. Calcd. for $C_{12}H_{18}O_2$: C, 74.20; H, 9.34. Found: C, 75.24; H, 9.45.

Benzaldehyde Methyl 3-Pentyl Acetal

Potassium (1.3 g, 33.3 mg-atom) was added to a mixture of 3-pentanol (10.0 g, 0.114 mole) and 50 ml of 1,2-diethoxyethane. Methyl benzoate (*p*-tolylsulfonyl)hydrazone (10.0 g, 32.9 mmole) was added and the mixture was refluxed for 6 h. The solvent was removed under reduced pressure and the residue was taken up in ether, washed with water, and dried. The residue, obtained after removal of the solvent, was distilled *in vacuo* to give 2.4 g (35%) of the acetal; b.p. 87–88° (1.0 mm); n_D^{25} 1.4796.

Anal. Calcd. for $C_{13}H_{20}O_2$: C, 74.96; H, 9.68. Found: C, 75.18; H, 9.77.

Benzaldehyde Methyl Benzyl Acetal

Methyl benzoate (*p*-tolylsulfonyl)hydrazone (10.0 g, 32.9 mmole) was added to a solution of potassium (1.3 g, 33.3 mg-atom) in benzyl alcohol (10.0 g, 92.6 mmole) and 1,2-diethoxyethane (50 ml). The mixture was refluxed for 3.5 h and cooled, potassium *p*-toluenesulfinate (6.15 g, 97%) was filtered off and the solvent removed under reduced pressure. The residue was fractionally distilled *in vacuo* to yield 4.7 g (63%) of the product; b.p. 116–117° (0.3 mm); n_D^{25} 1.5460.

Anal. Calcd. for $C_{15}H_{16}O_2$: C, 78.91; H, 7.06. Found: C, 78.67; H, 6.91.

The Thermal Decomposition of Potassium Methyl Benzoate (p-Tolylsulfonyl)hydrazone in Diglyme in the Presence of a Trace of Water to Produce IV

Potassium methyl benzoate (*p*-tolylsulfonyl)hydrazone (2.0 g, 5.8 mmole) was heated for 1 h at 125–130° in 20 ml of diglyme, to which a small amount of water (0.100 g, 5.5 mmole) had been added. The reaction mixture was cooled and filtered. Addition of 50 ml of water and 75 ml benzene followed. The benzene layer was separated, after vigorous shaking, washed twice with water, and dried with magnesium sulfate. The benzene was removed and pentane was added to the residue. Upon cooling, methyl benzoate (α-methoxybenzyl)(*p*-tolylsulfonyl)hydrazone (IV) (0.18 g, 15%) slowly crystallized. The product was recrystallized from a 5:1 *n*-hexane – benzene mixture, to give white prisms, m.p. 147–149°.

Anal. Calcd. for $C_{23}H_{24}N_2O_4S$ (molecular weight 424.5): C, 65.07; H, 5.70; N, 6.60; S, 7.55. Found: C, 65.35; H, 5.76; N, 6.72; S, 7.71. Molecular weight (osmometric), 440.

The experiment was repeated using D_2O (0.093 g, 4.6 mmole) instead of H_2O. Investigation of the n.m.r. spectrum of the methyl benzoate (α-methoxybenzyl)(*p*-tolylsulfonyl)hydrazone (0.12 g, 10%; m.p. 146–148°) thus obtained revealed that the singlet at 4.14 was present in only one-fifth of its original intensity, indicating that the proton responsible for this signal had originated from the water.

The Thermal Decomposition of Potassium Methyl Benzoate (p-Tolylsulfonyl)hydrazone in Piperidine

The potassium salt (10.0 g, 29.2 mmole) was refluxed for 11 h in 50 ml of predistilled piperidine (b.p. 103–105°), at which time the gas evolution had ceased. The reaction mixture was cooled, potassium *p*-toluenesulfinate (5.5 g, 97%) was filtered off, and the solvent removed under reduced pressure. The residue was dissolved in ether, washed with water, and dried with magnesium sulfate. Removal of the ether left 6.2 g (82%), α,α-dipiperidinotoluene (III) that slowly solidified, m.p. 76–79°. Recrystallization from acetone produced white needles, m.p. 81–83°. Reported (13) m.p. 80–81°; mixture m.p. 81–83°. The infrared spectrum was also identical with that of an authentic sample.

The Photochemical Decomposition of Potassium Methyl Benzoate(p-Tolylsulfonyl)hydrazone in the Presence of Piperidine

A suspension of the potassium salt of I (9.2 g, 26.9 mmole) in a mixture of 150 ml of 1,2-dimethoxyethane and 30 ml of piperidine was irradiated for 7.5 h. The solution was filtered, the solvent mixture removed under reduced pressure and the residue taken up in ether and dried. The liquid residue obtained after removal of the ether was distilled *in vacuo* to give 1.6 g distillate, b.p. 85–100° (0.25 mm). A high-boiling residue (3.0 g) solidified upon cooling and a n.m.r. spectrum showed that it consisted mainly of α,α-dipiperidinotoluene. The distillate was almost pure 1-(α-methoxybenzyl)piperidine (II), and only a small amount of benzaldehyde dimethyl acetal was present as impurity, as was shown by n.m.r. spectroscopy. Redistillation afforded pure α,α-dipiperidinotoluene; b.p. 81–85° (0.2 mm); n_D^{25} 1.5202.

Anal. Calcd. for $C_{13}H_{19}ON$: C, 76.05; H, 9.33; N, 6.82. Found: C, 76.02; H, 9.13; N, 7.01.

A small amount of 1-(α-methoxybenzyl)piperidine (0.19 g) was dissolved in 3 ml of piperidine, heated to the boiling point of the solution, and then immediately cooled. Removal of the solvent yielded 0.24 g of a solid, m.p. 75–78°, identical in all respects with α,α-dipiperidinotoluene.

ACKNOWLEDGMENTS

The research described here was supported by the National Research Council of Canada grant to R. J. Crawford. The n.m.r. and infrared spectra were measured by R. N. Swindlehurst and Mrs. Gail B. Conway of this Department.

Can. J. Chem. Downloaded from www.nrcresearchpress.com by 210.87.254.5 on 09/05/12
For personal use only.

REFERENCES

1. H. ZOLLINGER. Azo and diazo chemistry. Interscience publishers, Inc., New York. 1961.
2. H. ZOLLINGER. Azo and diazo chemistry. Interscience Publishers, Inc., New York. 1961. p. 43.
3. W. R. BAMFORD and T. S. STEVENS. J. Chem. Soc. 4735 (1952).
4. C. AINSWORTH. J. Am. Chem. Soc. **78**, 1973 (1956).
5. G. J. KARABATSOS and R. A. TALLER. J. Am. Chem. Soc. **85**, 3624 (1963).
6. E. SCHMIDT. Ber. **47**, 2545 (1914).
7. L. J. BELLAMY. The infrared spectra of complex molecules. John Wiley and Sons, Inc., New York. 1959. p. 363.
8. H. N. NOZAKI, R. NOYON, and K. SISIDO. Tetrahedron, **20**, 1125 (1964).
9. H. L. WHEELER. Am. Chem. Soc. J. **17**, 397 (1895).
10. S. M. MCELVAIN and J. T. VENERABLE. J. Am. Chem. Soc. **72**, 1661 (1950).
11. E. W. ADAMS and H. ADKINS. J. Am. Chem. Soc. **47**, 1358 (1925).
12. B. WLADISLAW and A. M. J. AYRES. J. Org. Chem. **27**, 281 (1962).
13. W. LAUN. Ber. **17**, 675 (1884).

Can. J. Chem. Downloaded from www.nrcresearchpress.com by 210.87.254.5 on 09/05/12
For personal use only.

BIOSYNTHETIC INCORPORATION OF ONE-CARBON UNITS INTO BERBERINE AND HYDRASTINE[1]

RAM NATH GUPTA AND IAN D. SPENSER
Department of Chemistry, McMaster University, Hamilton, Ontario
Received July 23, 1964

ABSTRACT

The utilization of one-carbon precursors in the biosynthesis of hydrastine and berberine was investigated by tracer experiments with plants of *Hydrastis canadensis* L. The lactone group of hydrastine and the bridge carbon of berberine are shown to be derived from the *S*-methyl group of methionine.

Recent tracer studies have established several intermediates of the pathway leading to the phthalideisoquinoline and the protoberberine alkaloids. By systematic carbon-by-carbon degradation of the labelled products which were isolated after administration of specifically tagged precursors to intact plants, it was shown that two tyrosine (I) units are incorporated into hydrastine (VIII) (2, 3), into narcotine (IX) (4), and into berberine (VII) (3, 5), that dopamine (III) is utilized in the biosynthesis of hydrastine (3, 6) and berberine (7), and that norlaudanosoline (V) serves as a precursor of narcotine (4). Incorporation of radioactivity from dopa (II) into berberine has also been reported (8). These findings, summarized in Fig. 1, are in remarkable agreement with the biogenetic speculations which were first put forward, mainly on the basis of structural considerations, almost half a century ago (9). They establish a source of all but one of the carbon atoms in the nucleus of the phthalideisoquinoline and protoberberine alkaloids. The remaining carbon atom in the skeletons of these alkaloids, the carbonyl carbon of hydrastine and narcotine (* in VIII and IX) and the so-called bridge carbon of berberine (* in VII), has long been postulated to arise from a one-carbon unit, which was presumed to enter at the oxidation level of formaldehyde (9). In agreement with this hypothesis, radioactivity from labelled formate has been found in the carbonyl group of narcotine (4).

We have tested the incorporation of ^{14}C-formate and of methyl-^{14}C-methionine into hydrastine and berberine in intact plants of *Hydrastis canadensis* L. (Golden Seal). The results indicate that the carbonyl group of hydrastine and the bridge carbon of berberine are indeed derived from one-carbon precursors. The methyl group of methionine is incorporated into these sites more efficiently than is formate. The findings lead to the inference that the one-carbon unit, from which the carbonyl carbon of hydrastine and the bridge carbon of berberine are ultimately derived, is introduced into a precursor molecule by a transmethylation step.

In a series of seven feeding experiments, sodium ^{14}C-formate (expts. 1–3) and L-methyl-^{14}C-methionine (expts. 4–7) were administered to plants of *Hydrastis canadensis* L., either via the roots or by infusion into the stem (3). In each experiment radioactive berberine and hydrastine was isolated from roots and rhizomes. Chemical and radiochemical yields are summarized in Table I. As observed previously with other precursors (3), berberine isolated from a particular experiment invariably had a higher specific activity than hydrastine (Table I). It is noteworthy that hydroponic administration of methionine led to more efficient incorporation of tracer than wick feeding, whereas wick

[1]*A preliminary account of parts of this work has been published (1).*

Can. J. Chem. Downloaded from www.nrcresearchpress.com by 210.87.254.5 on 09/05/12
For personal use only.

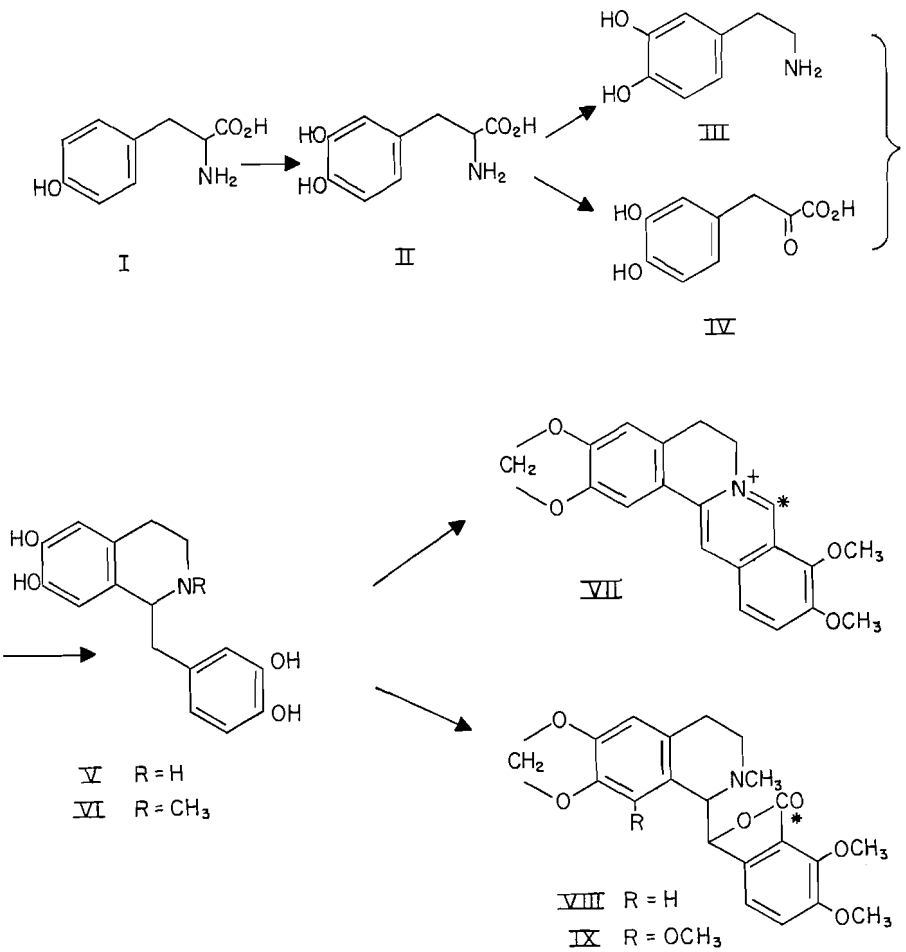

FIG. 1. Biosynthesis of berberine and hydrastine.

feeding was more efficient in the case of formate, in experiments conducted over the same time span. In terms of specific radiochemical yield, as well as in terms of recovery in the products of administered radioactivity (% incorporation), methionine was more efficiently incorporated than formate (Table II).

It was anticipated that incorporation of one-carbon precursors would yield hydrastine labelled at five centers (C=O, NCH_3, 2 × OCH_3, and CH_2O_2) and berberine labelled at four centers (bridge, 2 × OCH_3, and CH_2O_2). For an unequivocal interpretation of such multi-site incorporation of radioactivity, the labelled carbon atoms in each product had to be separated from one another, so that the extent of radioactivity at each labelled site could be determined. A method for degrading the alkaloids was worked out by pilot experiments with inactive material. The degradation sequences shown in Figs. 2 and 3 permitted determination of the radioactivity at the predicted one-carbon sites.

The labelled samples of hydrastine and berberine, obtained from six of the experiments, were degraded. The specific activities of the intermediates in the degradation sequences are shown in Tables III and IV. (Indicated limits are standard deviations of the mean.)

Can. J. Chem. Downloaded from www.nrcresearchpress.com by 210.87.254.5 on 09/05/12
For personal use only.

Can. J. Chem. Downloaded from www.nrcresearchpress.com by 210.87.254.5 on 09/05/12
For personal use only.

TABLE I

Chemical and radiochemical yields

Expt. No.	Precursor (total activity, counts $min^{-1} \times 10^{-7}$; specific activity, counts min^{-1} $mmole^{-1} \times 10^{-9}$)	Mode and duration of feeding (days)		Plants		Hydrastine			Berberine		
				No.	Dry weight (g)	Yield (mg)	Specific activity (counts min^{-1} $mmole^{-1} \times 10^{-4}$)	Total activity (counts min^{-1} $\times 10^{-4}$)	Yield (mg)	Specific activity (counts min^{-1} $mmole^{-1} \times 10^{-4}$)	Total activity (counts min^{-1} $\times 10^{-4}$)
1	$H^{14}COO^{-}Na^{+}$ (4.81; 2.55)	Root	3	8	10.0	184	0.36	0.17	220	0.71	0.38
2	"	Root	6	8	9.4	190	0.67	0.33	208	1.43	0.73
3	"	Wick	6	6	24.0	303	1.14	0.90	481	3.90	4.60
4	L-$^{14}CH_3$-methionine (2.51; 2.50)	Root	6	8	9.0	250	15.81	10.30	344	20.51	17.30
5		Wick	6	5	36.0	460	2.80	3.36	749	4.53	8.32
6	L-$^{14}CH_3$-methionine (1.92; 2.39)	Root	$1\frac{1}{4}$	9	16.0	244	4.47	2.84	268	16.0	10.91
7		Root	3	9	12.0	165	19.21	8.27	305	39.2	29.54

TABLE II

Efficiency of incorporation of radioactive precursors

Expt. No.	Precursor	Specific radiochemical yield* × 10^4		% incorporation of activity†		
		Hydrastine	Berberine	Hydrastine	Berberine	Total
1	^{14}C-Formate	1.4	2.8	0.003	0.008	0.011
2		2.6	5.6	0.007	0.015	0.022
3		4.5	15.3	0.019	0.096	0.12
4	L-Methyl-^{14}C-methionine	63.4	82.3	0.41	0.69	1.10
5		11.3	18.1	0.13	0.33	0.46
6		18.7	69.5	0.15	0.57	0.72
7		80.3	165.3	0.43	1.54	1.97

*Specific radiochemical yield $= \frac{\text{specific activity of product}}{\text{specific activity of precursor}} \times 100.$

†% incorporation $= \frac{\text{total activity of isolated product}}{\text{total activity of administered precursor}} \times 100.$

From these values the activity at the predicted one-carbon sites was deduced, in the manner indicated in the legend of Figs. 2 and 3. In each case these sites fully account for the activity of the original molecule. In Table V the contribution which each of these carbon atoms makes to the specific activity of the alkaloids obtained in individual experiments is expressed as a percentage of the specific activity of the intact alkaloids. The sum of the specific activities of the individual sites agrees, within experimental error, with the specific activity of the intact molecule, indicating the self-consistency of the results.

The results show that the lactone-carbonyl carbon of hydrastine and the bridge carbon of berberine, as well as the *O*- and *N*-attached one-carbon units of the two alkaloids, are specifically derived from one-carbon precursors. It is evident (Table V) that in every experiment the contribution which each of the one-carbon sites makes to the total specific activity of hydrastine and of berberine is of similar magnitude. This indicates that in each of the alkaloids all one-carbon sites are derived from the same immediate precursor. For if one of the one-carbon sites had been derived from some other immediate precursor than the other one-carbon sites in the same molecule, a different order of magnitude of the specific activity at that site, in either the formate or the methionine experiments, would have resulted. It follows that the lactone-carbonyl carbon of hydrastine and the bridge carbon of berberine are derived from the same immediate precursor which yields the extra-nuclear *O*- and *N*-attached one-carbon units.

There can be little doubt that transmethylation processes are responsible for the introduction of the one-carbon centers into the skeletons of hydrastine and berberine.

The evidence is strong that *O*- and *N*-methyl groups of alkaloids and other plant products originate in this manner (10). In a number of cases the transfer of methionine-methyl to such groups has been established by multiple labelling (11); and in others, transmethylase activity leading to the formation of *N*-methyl (12) and *O*-methyl groups (13, 14) by methyl transfer from *S*-adenosyl methionine has been demonstrated. In many further instances the methyl group of methionine proved to be more efficient than formate as a precursor of *O*-methyl (15) and *N*-methyl groups (15, 16) of plant alkaloids.

A transmethylation step is also required in the formation of the methylenedioxy group, (13, 17) which has been shown to arise from the methoxy group of an *o*-methoxyphenol (8, 18).

The origin of the bridge carbon of berberine and of the lactone group of hydrastine by a

Can. J. Chem. Downloaded from www.nrcresearchpress.com by 210.87.254.5 on 09/05/12
For personal use only.

Can. J. Chem. Downloaded from www.nrcresearchpress.com by 210.87.254.5 on 09/05/12
For personal use only.

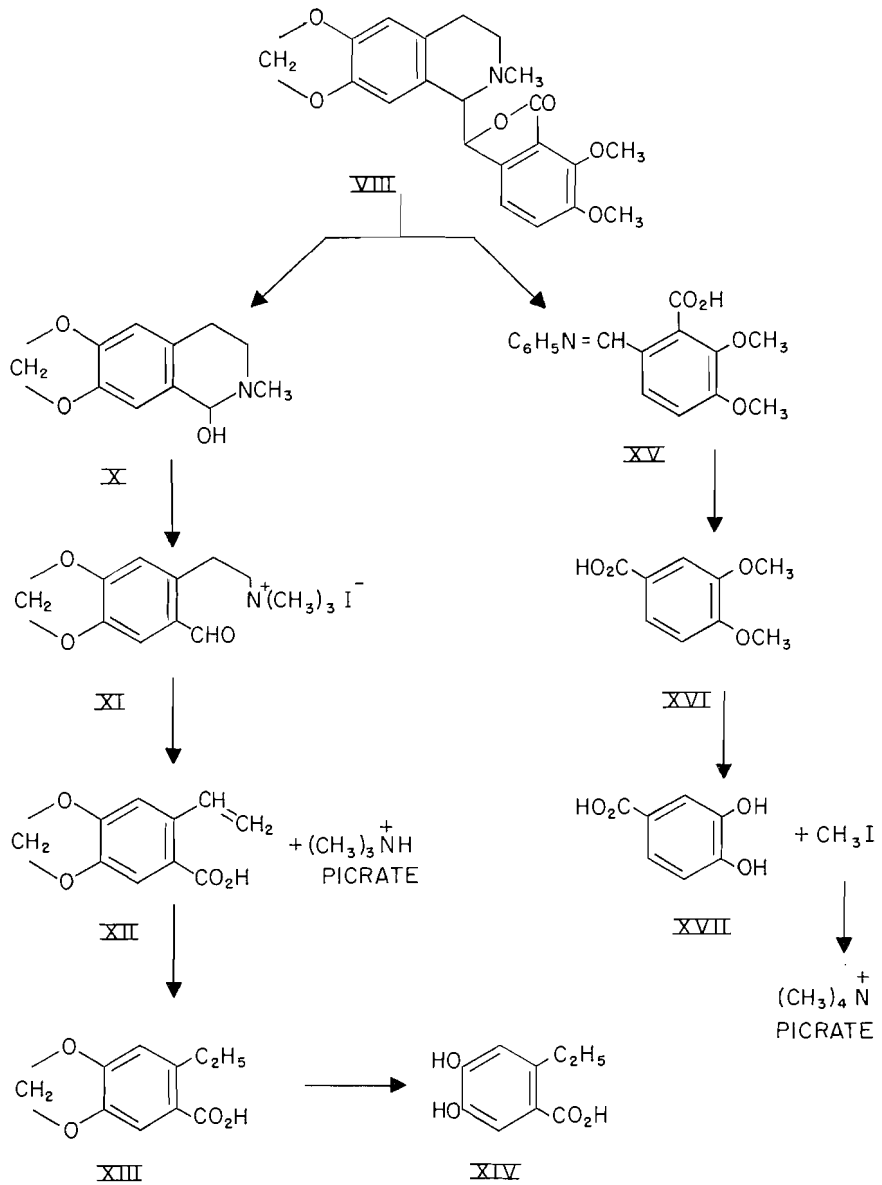

FIG. 2. Degradation of hydrastine, permitting isolation of one-carbon sites. NCH_3 = trimethylamine picrate; CH_2O_2 = 6-vinylpiperonylic acid (XII) minus 6-ethylprotocatechuic acid (XIV) (inactive) = 6-vinylpiperonylic acid (XII); $2 \times OCH_3$ = $2 \times$ tetramethylammonium picrate = veratric acid (XVI) minus protocatechuic acid (XVII) (inactive) = veratric acid (XVI); C=O = opianic acid anil (XV) minus veratric acid (XVI).

route involving transmethylation is less obvious. The early work of Sribney and Kirkwood (17) had indicated that radioactivity from methyl-labelled methionine entered the nucleus of protopine, an alkaloid structurally related to berberine. The site of activity was not determined but it was suggested that the label was located at a position corresponding to the berberine bridge. Recently it was shown that laudanosoline (VI) (19) and its di-*O*-methyl derivative, reticuline (8), are incorporated into berberine *in toto*, and that the

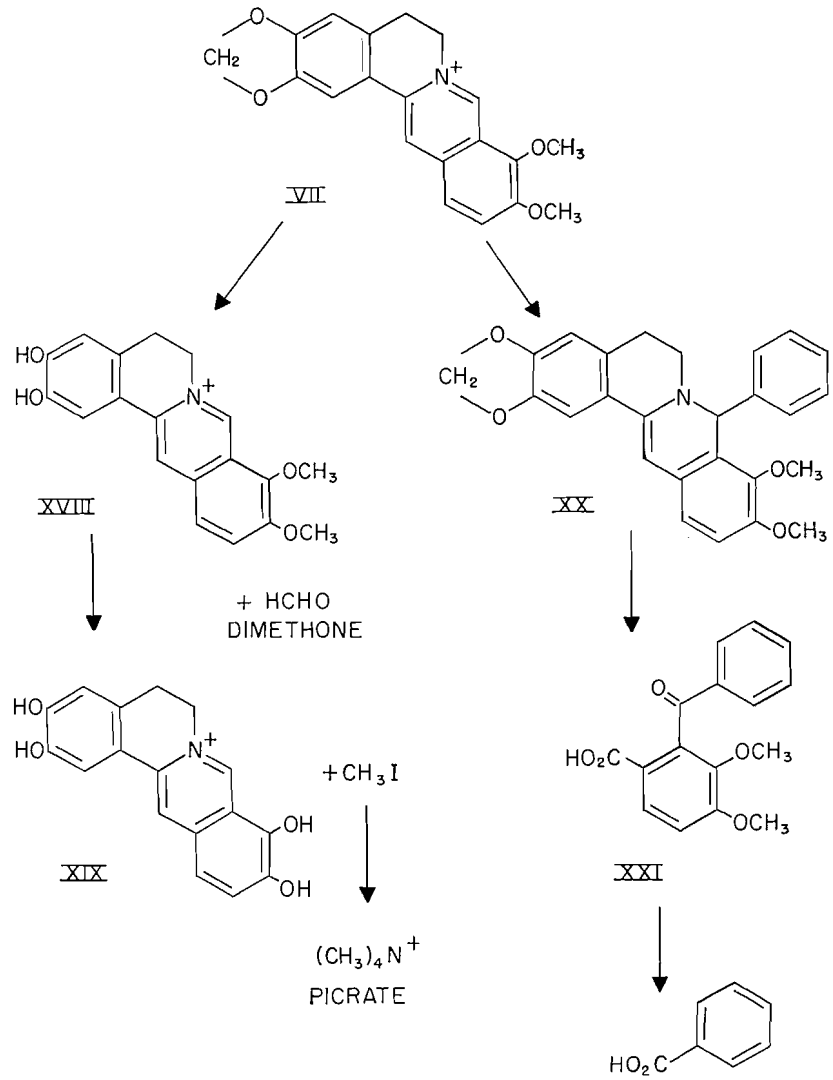

FIG. 3. Degradation of berberine, permitting isolation of one-carbon sites. CH_2O_2 = formaldehyde dimethone; 2 × OCH_3 = 2 × tetramethylammonium picrate; bridge = benzoic acid.

N-methyl group of these precursors is transformed into the bridge carbon of berberine. These results are consistent with the present findings, and with the view that the methyl group of methionine which gives rise to the bridge carbon of berberine enters the biosynthetic pathway by transmethylation onto the nitrogen atom of norlaudanosoline (V).

The present results indicate also that the lactone-carbonyl group of hydrastine, like the bridge carbon of berberine, is formed by modification of a methyl group, introduced into a precursor by transmethylation. Whether berberine and hydrastine arise from a common *N*-methylated precursor, laudanosoline (VI), by independent pathways, or whether hydrastine is formed by oxidative modification of berberine (20), or whether a *C*-methylated rather than an *N*-methylated derivative of norlaudanosoline is the intermediate of hydrastine biosynthesis, remains to be established.

Can. J. Chem. Downloaded from www.nrcresearchpress.com by 210.87.254.5 on 09/05/12
For personal use only.

Can. J. Chem. Downloaded from www.nrcresearchpress.com by 210.87.254.5 on 09/05/12
For personal use only.

TABLE III

Degradation of hydrastine

	Specific activity (counts min^{-1} $mmole^{-1}$ $\times 10^{-4}$)					
	Formate			Methionine		
	Expt. No. 1	Expt. No. 2	Expt. No. 3	Expt. No. 4	Expt. No. 5	Expt. No. 6
Hydrastine (VIII) (NCH_3, CH_2O_2, $2\times OCH_3$, C=O)	0.36±0.02	0.39±0.01*	0.66±0.02*	4.90±0.05*	2.80±0.04	1.56±0.01*
Hydrastinine (X)	0.11±0.01	0.13±0.01	0.25±0.01	2.14±0.02	1.28±0.04	0.74±0.01
Trimethylamine picrate (NCH_3)	0.064±0.007	0.081±0.007	0.10±0.01	1.21±0.02	0.86±0.02	0.33±0.01
6-Vinylpiperonylic acid (XII) (CH_2O_2)	0.070±0.004	0.084±0.008	0.16±0.01	0.98±0.01	0.48±0.01	0.32±0.01
6-Ethylprotocatechuic acid (XIV)	—	—	—	—	Inactive	—
Opianic acid anil (XV) ($2\times OCH_3$ + C=O)	0.21±0.01	0.24±0.01	0.40±0.04	2.88±0.06	1.52±0.02	0.98±0.02
Veratric acid (XVI) ($2\times OCH_3$)	0.14±0.01†	0.17±0.01	0.28±0.01	1.84±0.03	1.01±0.01	0.64±0.01
Tetramethylammonium picrate (OCH_3)	—	0.09±0.01	0.14±0.01	—	0.52±0.02	—
Protocatechuic acid (XVII)	Inactive	—	—	—	—	—

*Diluted with carrier.
†The sample of labelled opianic acid anil was diluted with carrier prior to decarboxylation. The value given for veratric acid so obtained takes into account the dilution factor.

Can. J. Chem. Downloaded from www.nrcresearchpress.com by 210.87.254.5 on 09/05/12
For personal use only.

TABLE IV

Degradation of berberine

	Specific activity (counts min^{-1} $mmole^{-1}$ $\times 10^{-4}$)					
	Formate			Methionine		
	Expt. No. 1	Expt. No. 2	Expt. No. 3	Expt. No. 4	Expt. No. 5	Expt. No. 6
Berberine picrate (CH_2O_2, 2×OCH_3, bridge)	0.71±0.03	1.43±0.02	1.90±0.02*	5.20±0.12*	4.53±0.11	8.20±0.19*
Formaldehyde dimethone (CH_2O_2)	0.15±0.01	0.33±0.01	0.43±0.02	1.27±0.04	1.13±0.03	2.07±0.10
Tetramethylammonium picrate (OCH_3)	0.17±0.01	0.35±0.01	0.43±0.02	1.36±0.04	1.17±0.04	1.95±0.09
Benzoic acid (bridge)	—	—	0.46±0.01	1.26±0.04	—	2.09±0.11

*Diluted with carrier.

TABLE V

Incorporation of one-carbon units into hydrastine and berberine

Expt. No.	Hydrastine					Berberine			
	Relative specific activity (%)*					Relative specific activity (%)			
	C=O	2 OCH_3	CH_2O_2	NCH_3	Total (%)†	Bridge	2 OCH_3	CH_2O_2	Total (%)‡
1	20±5	41±4	20±1	18±2	95±6		47±3‡	21±2‡	
2	18±4	41±3	21±2	20±2	103±5		49±2‡	23±1‡	
3	19±6	42±3	24±2	15±2	100±7	26±1*	49±1*	25±1*	92±2
4	21±1	36±1	19±1	24±1	103±3	24±1*	52±2*	24±1*	101±3
5	18±1	35±1	17±1	30±1	101±2		52±2‡	25±1‡	
6	21±1	39±1	20±1	20±1	104±3	26±1*	48±2*	26±1*	98±3

*Sum of specific activities of individual one-carbon sites = 100.
†Specific activity of intact hydrastine = 100.
‡Specific activity of intact berberine = 100.

Can. J. Chem. Downloaded from www.nrcresearchpress.com by 210.87.254.5 on 09/05/12
For personal use only.

EXPERIMENTAL

Degradation of Hydrastine

Conversion of Hydrastine (VIII) to Hydrastinine (X) and Opianic Acid Anil (XV) (3, 22)

Hydrastine (0.5 g) was suspended in 20% nitric acid (4 ml) and the mixture was kept at 40° for 16 h. The clear yellow solution was cooled, and cold 40% potassium hydroxide (3 ml) was added during stirring and cooling. The mixture was kept at 5° for 1 h, and the crystalline precipitate was filtered off and washed with a little cold water. Hydrastinine (227 mg, 84%), melting at 116–117° after recrystallization from ethyl acetate, was obtained; reported m.p. 116–117° (21).

Aniline (0.3 g) in ethanol (2 ml) was added to the filtrate and the solution was warmed for a few minutes at 60–70°. After the solution was cooled, cold 10% hydrochloric acid was added dropwise, with stirring, until the mixture was acidic to Congo red. The precipitate was filtered off, washed with water and with a little methanol, and crystallized from methanol. Opianic acid anil (170 mg, 45%), melting at 188–189°, was obtained; reported m.p. 191.5–192.5° (22).

Conversion of Hydrastinine to Hydrastinine Picrate (23)

Crude hydrastinine (10 mg) was dissolved in methanol (5 ml) and an excess of a hot saturated solution of picric acid in methanol was added. A red precipitate formed when the mixture was warmed and allowed to cool. This precipitate recrystallized from methanol as red crystals of hydrastinine picrate melting at 173° (reported m.p. 173° (23)).

Conversion of Hydrastinine (X) to β-[2-Formyl-4,5-methylenedioxyphenyl]-ethyltrimethylammonium Iodide (N-Methylhydrastinine Methiodide) (XI)

A one-step Hofmann degradation (3, 24) was not suitable for the present purpose, since, in the presence of excess methylating agent, methyl exchange on trimethylamine was likely to take place. Such an exchange would make the recovery of isotope in trimethylamine uncertain. *N*-Methylhydrastinine methiodide was therefore isolated.

Hydrastinine (105 mg) was suspended in water (2 ml), and potassium carbonate (100 mg) and methyl iodide (2 ml) were added. The mixture was shaken for 24 h and then kept at 40° for another 24 h. Methyl iodide was evaporated, the residue was cooled and filtered, and the product washed with a little cold water and recrystallized from aqueous methanol. *N*-Methylhydrastinine methiodide (135 mg, 75%), melting at 265–266°, was obtained; reported m.p. 267° (25) and 262–264° (26).

Hofmann Degradation of N-Methylhydrastinine Methiodide

A suspension of the above quaternary salt (180 mg) in 10% sodium hydroxide (5 ml) was kept on the steam bath for 1 h, during which time a current of nitrogen was passed through the suspension. The issuing gas was passed through an alcoholic solution of picric acid; from this solution, on concentration and recrystallization from methanol, trimethylamine picrate, melting at 216°, was isolated. Quantitative recovery of this picrate was not attempted.

The original reaction mixture was cooled, extracted with ether, and the ether extract was washed with water, dried, and evaporated. The residue was dissolved in a mixture of methanol (4 ml) and water (2 ml) and powdered silver nitrate (0.6 g) was added to the solution, followed by 20% sodium hydroxide (6 ml). The mixture was warmed on the steam bath, shaken for 2 h, filtered, and extracted with ether. The aqueous layer was warmed to remove ether and cooled and acidified with cold 50% (v/v) sulfuric acid. The precipitate, which was obtained on cooling, was washed with cold water and recrystallized from aqueous methanol. 6-Vinylpiperonylic acid (XII) (53 mg, 55%), melting at 167–168°, was obtained; reported m.p. 168° (3).

Reduction of 6-Vinylpiperonylic Acid (XII) to 6-Ethylpiperonylic Acid (XIII)

6-Vinylpiperonylic acid (100 mg) was dissolved in 10% sodium hydroxide (4 ml) and the solution maintained at 60–65°. Nickel–aluminium alloy (150 mg) was added in small portions with constant stirring. The addition of alloy was complete in 45 min. The temperature was raised to 75–80° and stirring was continued for 12 h. The catalyst was then filtered off and washed with water. The combined filtrate and washings were acidified with 50% hydrochloric acid and the product was filtered off, washed with a little cold water, and recrystallized from aqueous methanol. 6-Ethylpiperonylic acid (90 mg, 60%), melting at 125–126°, was obtained. (Found: C, 62.1; H, 5.2. $C_{10}H_{10}O_4$ requires C, 61.9; H, 5.2%.) Subsequent reductions were carried out at room temperature without affecting the yield or the nature of the reduction product. Cleavage of the methylenedioxy group, reported to take place in a number of other methylenedioxyphenyl derivatives (27), did not appear to occur with 6-vinylpiperonylic acid under these conditions.

Conversion of 6-Ethylpiperonylic Acid (XIII) to 6-Ethylprotocatechuic Acid (XIV)

6-Ethylpiperonylic acid (60 mg) and phosphorus pentachloride (180 mg) were sealed in a hard-glass test tube, which was then kept at 150–160° for 2 h. The tube was opened and the reaction mixture, after addition of water, was refluxed for 2 h in a current of nitrogen which had been purified by passing through potassium hydroxide solution. The exit gases were bubbled into *M* potassium hydroxide which was protected from atmospheric carbon dioxide by a trap of potassium hydroxide solution. The carbon dioxide

which had been swept out of the reaction mixture was converted to barium carbonate by addition of 17% barium chloride solution. The precipitate was washed with water and dried in air when barium carbonate (38 mg, 73%) was obtained.

The reaction mixture was cooled and extracted with ether. The ether extract was dried and evaporated and the residue sublimed at 130° and 1×10^{-3} mm. 6-Ethylprotocatechuic acid (24 mg, 40%), melting at 194–195°, was obtained; reported m.p. 164–165° (28). (Found: C, 59.2; H, 5.6. $C_9H_{10}O_4$ requires C, 59.3; H, 5.5%.)

Decarboxylation of Opianic Acid Anil (XV) (22)

A slow stream of nitrogen, which had been purified by passing through a saturated solution of potassium hydroxide and through sulfuric acid, was passed through the tube containing opianic acid anil (100 mg) and copper bronze (5 mg). The exit gases were bubbled through *M* potassium hydroxide, which was protected from the atmosphere by a trap of saturated potassium hydroxide solution. The reaction tube was placed in a bath of boiling ethyl benzoate (b.p. 212°) until the evolution of carbon dioxide ceased (10 min). Heating was discontinued, but passage of nitrogen was continued for another 0.5 h. Barium chloride (17%) was added to the potassium hydroxide trap which had absorbed the exit gases, to yield barium carbonate (60 mg, 90%).

The residue in the reaction tube, veratraldehyde anil, was hydrolyzed by refluxing with 5% acetic acid (1 ml) for 1 h (22). The mixture was cooled and extracted with ether. The ether extract was washed, in succession, with water, dilute potassium hydroxide solution, and water and was then dried and evaporated. The residue, veratraldehyde, was dissolved in a mixture of methanol (4 ml) and water (2 ml). Powdered silver nitrate (0.5 g) and 20% sodium hydroxide (5 ml) were added. The mixture was warmed on a steam bath for a few minutes, shaken for 2 h, and then filtered. Acidification of the filtrate with 50% (v/v) sulfuric acid yielded crude product, which was washed with water, dissolved in methanol, decolorized with charcoal, and recrystallized from aqueous methanol. Veratric acid (XVI) (34 mg, 50%), melting at 175–176°, was obtained; reported m.p. 179–181.5° (29).

Cleavage of the Methoxy Groups of Veratric Acid (cf. Ref. 30)

Veratric acid (200 mg) in freshly distilled hydriodic acid (density, 1.7, 10 ml) was gently refluxed in a current of dry nitrogen for 2 h. The exit gases were passed through a suspension of red phosphorus in 5% cadmium sulfate solution, passed over anhydrous potassium carbonate, and bubbled into a 5% methanolic solution of trimethylamine contained in a series of two tubes which were cooled in dry ice–acetone mixture. After 2 h passage of nitrogen was stopped, and the tubes containing trimethylamine solution were disconnected and allowed to stand at room temperature overnight. A crystalline precipitate of tetramethylammonium iodide was obtained. The solution was decanted and the precipitate repeatedly washed with dry methanol. The precipitate was dissolved in water, and a hot saturated aqueous solution of picric acid was added. The residue obtained on cooling was washed with ether and recrystallized twice from methanol, when pale red needles of tetramethylammonium picrate, melting at 312–313°, were obtained. No attempt was made to recover the picrate quantitatively.

The reaction mixture was diluted with water and extracted with ether. The extract was washed with cold dilute sodium thiosulfate solution to destroy iodine, and with water, dried, and evaporated. The residue sublimed at 125° and 3.5×10^{-3} mm when protocatechuic acid (XVII) (100 mg, 60%), melting at 200–202°, was obtained; reported m.p. 199°.

Degradation of Berberine

Conversion of Berberine Hydrochloride to Berberine Picrate

Berberine hydrochloride (10 mg) was dissolved in methanol and an excess of a hot saturated solution of picric acid in methanol was added. The mixture was heated and allowed to cool. An orange precipitate appeared which was filtered off, washed with methanol, and recrystallized from methanol–acetone, yielding orange needles of berberine picrate, melting at 238–239°; reported m.p. 239° (31).

Hydrolytic Cleavage of the Methylenedioxy Group of Berberine (cf. Ref. 17)

Berberine hydrochloride (100 mg) and dimedone (5,5-dimethyldihydroresorcinol) (300 mg) were suspended in dilute sulfuric acid (60 ml concentrated sulfuric acid in 100 ml water) (5ml) and the mixture was maintained at 98–100° for 18 h. The cooled reaction mixture was diluted with water (5 ml) and extracted with ether. The ether extract was washed with water, dried, and evaporated. The residue was crystallized from aqueous methanol when white silky needles of the dimedone derivative of formaldehyde (24 mg, 36%), melting at 190–191°, were obtained.

The aqueous layer, in which a precipitate had now appeared, was warmed to remove residual ether, and a saturated solution of potassium iodide (2 ml) was added. The mixture was cooled and filtered and the residue washed with a little sulfur dioxide water and dried. 2,3-Dihydroxy-9,10-dimethoxy-7,8,13,14-tetradehydroberbinium iodide (XVIII) (90 mg, 80%) was obtained (cf. ref. 32).

Cleavage of the Methoxy Groups

2,3-Dihydroxy-9,10-dimethoxy-7,8,13,14-tetradehydroberbinium iodide (XVIII) (90 mg) was refluxed with freshly distilled hydriodic acid (5 ml). Methyl iodide was isolated as tetramethylammonium picrate by the method described earlier for the cleavage of veratric acid.

Can. J. Chem. Downloaded from www.nrcresearchpress.com by 210.87.254.5 on 09/05/12
For personal use only.

The reaction mixture was diluted with water, decolorized with sulfur dioxide water, filtered, and dried. Berberoline iodide (XIX) (70 mg, 74%) was obtained. This compound could not be crystallized nor converted into a crystalline derivative (cf. ref. 33).

Isolation of the Bridge Carbon of Berberine as Benzoic Acid (cf. ref. 34)

Berberine hydrochloride (700 mg) was dried at 100° under vacuum for 2 h and then suspended in 10 ml ether. Excess of an ethereal solution of phenylmagnesium bromide, prepared from magnesium turnings (0.12 g) and bromobenzene (0.6 ml) in 5 ml anhydrous ether, was added. The mixture was stirred and refluxed for 2 h. Water (5 ml) and dilute hydrochloric acid (5 ml) was added and the resulting precipitate was washed with water and a little ether.

The crude phenyldihydroberberine hydrobromide (XX) was suspended in a solution of potassium carbonate (3 g) in water (150 ml). Potassium permanganate (3 g) was added in small portions over a period of 80 h with continuous stirring. Sulfur dioxide was passed through the solution until it was clear. The solution was then acidified and boiled to expel dissolved sulfur dioxide, cooled, and extracted with chloroform. The chloroform layer was washed with water and dilute acid and extracted with 10% sodium hydroxide. The basic extract was washed with ether, acidified with 50% hydrochloric acid, and extracted with ether. The ether extract was dried and evaporated. The residue was crystallized from 50% acetic acid. 2-Benzoyl-3,4-dimethoxybenzoic acid (XXI) (120 mg, 24%), melting at 193–194°, was obtained; reported m.p. 190–191° (34) and 192° (35).

2-Benzoyl-3,4-dimethoxybenzoic acid (XXI) (100 mg) was moistened with water (0.5 ml), potassium hydroxide (1 g) was added, and the mixture was fused for 2–3 min. The cooled melt was dissolved in water and the solution was acidified with 10% hydrochloric acid and extracted with chloroform. The chloroform layer was washed with water, dried, and evaporated. The residue was sublimed at 60–70° and 1×10^{-3} mm, yielding benzoic acid (35 mg, 83%) melting at 119–120°.

Administration of ^{14}C-labelled Compounds to Hydrastis canadensis L. and Extraction of Labelled Alkaloids

Methyl-^{14}C-methionine and sodium ^{14}C-formate were administered to 4-year-old plants of *Hydrastis canadensis* L., either hydroponically or by infusion into the stem, by reported methods (3). Hydrastine and berberine were extracted from roots and rhizomes by standard methods (3). Leaves and other aerial parts were rejected. Chemical and radioactive yields from all experiments are shown in Table I.

Degradation of Radioactive Alkaloids

The radioactive alkaloids were degraded by the reaction sequences described above. When the amount of material permitted, the alkaloid was degraded without dilution after crystallization to constant activity. In most cases, however, dilution with carrier was necessary to obtain sufficient material to carry out the complete degradation sequence. A minimum of 500 mg berberine and 350 mg hydrastine was desirable for this purpose.

The degradation products were solids, or were isolated as solid derivatives, and were crystallized to constant melting point. Their radioactivity was assayed on samples of finite thickness on aluminium planchettes, using a Model 1052 gas-flow counter with "micromil" window (Nuclear Chicago Corp.) in a low-background automatic sample changer (Nuclear Chicago Corp., Model C115). Counts were recorded on a printing timer (Nuclear Chicago Corp., C111B) in association with a scaler (Nuclear Chicago Corp., 181B).

The usual corrections for background and self-absorption were applied.

For plating, a 1% solution of collodion in dimethylformamide was used as the solvent. Only berberine hydrochloride and formaldehyde dimethone could not be plated in this way. Dissolution of these samples required prolonged contact with benzyl alcohol before application of the collodion dimethylformamide solution. In the case of benzoic acid, a drop of a 5% solution of sodium hydroxide in 50% aqueous methanol was required to avoid loss of benzoic acid by evaporation.

ACKNOWLEDGMENTS

We are greatly indebted to Mr. L. Laking, Director, and Mr. R. E. Halward, Propagator, of the Royal Botanical Gardens, Hamilton, for facilities and help in the cultivation of *Hydrastis canadensis* L.

This investigation was supported by Research Grant GM-10043 from the National Institute of General Medical Sciences, United States Public Health Service, and by a grant from the National Research Council of Canada.

REFERENCES

1. R. N. GUPTA and I. D. SPENSER. Biochem. Biophys. Res. Commun. **13**, 115 (1963).
2. J. R. GEAR and I. D. SPENSER. Nature, **191**, 1393 (1961).
3. J. R. GEAR and I. D. SPENSER. Can. J. Chem. **41**, 783 (1963).

Can. J. Chem. Downloaded from www.nrcresearchpress.com by 210.87.254.5 on 09/05/12
For personal use only.

4. A. R. BATTERSBY and D. J. MCCALDIN. Proc. Chem. Soc. 365 (1962).
5. I. D. SPENSER and J. R. GEAR. Proc. Chem. Soc. 228 (1962).
6. I. D. SPENSER and J. R. GEAR. J. Am. Chem. Soc. **84**, 1059 (1962).
7. I. MONKOVIĆ and I. D. SPENSER. Proc. Chem. Soc. 223 (1964).
8. D. H. R. BARTON, R. H. HESSE, and G. W. KIRBY. Proc. Chem. Soc. 267 (1963).
9. R. ROBINSON. J. Chem. Soc. **111**, 876 (1917). The structural relations of natural products. Clarendon Press, Oxford. 1955. p. 78.
10. K. MOTHES. Symp. Soc. Exptl. Biol. **13**, 258 (1959).
11. R. U. BYERRUM, J. H. FLOKSTRA, L. J. DEWEY, and C. D. BALL. J. Biol. Chem. **210**, 633 (1954). L. J. DEWEY, R. U. BYERRUM, and C. D. BALL. J. Am. Chem. Soc. **76**, 3997 (1954).
12. J. G. JOSHI and P. HANDLER. J. Biol. Chem. **235**, 2981 (1960). J. D. MANN and S. H. MUDD. J. Biol. Chem. **238**, 381 (1963). J. D. MANN, C. E. STEINHART, and S. H. MUDD. J. Biol. Chem. **238**, 676 (1963).
13. J. D. MANN, H. M. FALES, and H. S. MUDD. J. Biol. Chem. **238**, 3820 (1963).
14. B. J. FINKLE and R. F. NELSON. Biochim. Biophys. Acta, **78**, 747 (1963).
15. M. DUBECK and S. KIRKWOOD. J. Biol. Chem. **199**, 307 (1952). A. R. BATTERSBY and B. J. T. HARPER. Chem. Ind. London, 365 (1958).
16. S. A. BROWN and R. U. BYERRUM. J. Am. Chem. Soc. **74**, 1523 (1952). T. J. MATCHETT, L. MARION, and S. KIRKWOOD. Can. J. Chem. **31**, 488 (1953). E. LEETE and L. MARION. Can. J. Chem. **32**, 646 (1954). R. M. BAXTER, S. I. KANDEL, and A. OKANY. Chem. Ind. London, 1453 (1961).
17. M. SRIBNEY and S. KIRKWOOD. Nature, **171**, 931 (1953).
18. D. H. R. BARTON, G. W. KIRBY, and G. B. TAYLOR. Proc. Chem. Soc. 340 (1962).
19. A. R. BATTERSBY, R. J. FRANCIS, M. HIRST, and J. STAUNTON. Proc. Chem. Soc. 268 (1963).
20. E. LEETE. *In* Elucidation of structures by physical and chemical methods. *Edited by* K. W. Bentley. Interscience Publishers, New York. 1963. p. 440. *In* Biogenesis of natural compounds. *Edited by* P. Bernfeld. Pergamon Press, New York. 1963. p. 766.
21. M. FREUND and W. WILL. Ber. **20**, 88 (1887).
22. J. WEIJLARD, E. TASHJIAN, and M. TISHLER. J. Am. Chem. Soc. **69**, 2070 (1947).
23. H. DECKER. Ann. **395**, 321 (1913).
24. W. J. GENSLER, E. M. HEALY, I. ONSHUUS, and H. L. BLUHM. J. Am. Chem. Soc. **78**, 1713 (1956).
25. M. FREUND. Ber. **22**, 2329 (1889).
26. J. J. BROWN and G. T. NEWBOLD. J. Chem. Soc. 4397 (1952).
27. E. SCHWENK and D. PAPA. J. Org. Chem. **10**, 232 (1945).
28. T. KONDO and S. TANAKA. J. Pharm. Soc. Japan, **49**, 263 (1929).
29. J. HOUBEN and W. FISCHER. Ber. **60**, 1759 (1927).
30. A. ELEK. *In* Organic analysis. Vol. 1. *Edited by* J. Mitchell, Jr., I. M. Kolthoff, E. S. Proskauer, and A. Weissberger. Interscience Publishers, New York. 1953. p. 67.
31. A. PICTET and A. GAMS. Ber. **44**, 2480 (1911).
32. E. SPÄTH and H. QUIETENSKY. Ber. **58**, 2267 (1925).
33. M. OBERLIN. Arch. Pharm. **265**, 256 (1927).
34. F. FALTIS. Monatsh. **31**, 557 (1910).
35. CH. WEIZMANN and E. BERGMANN. J. Chem. Soc. 567 (1936).

Can. J. Chem. Downloaded from www.nrcresearchpress.com by 210.87.254.5 on 09/05/12
For personal use only.

OXYGEN-17 NUCLEAR MAGNETIC RESONANCE STUDY OF THE CHROMATE REACTION WITH DICHROMATE[1]

B. N. FIGGIS,[2] R. G. KIDD,[3] AND R. S. NYHOLM
William Ramsay and Ralph Forster Laboratories, University College, London, England

Received July 10, 1964

ABSTRACT

The ^{17}O n.m.r. spectra from aqueous solutions containing both chromate and dichromate ions have been obtained over a range of concentrations. Signals from both the bridging oxygen and the terminal oxygens in the dichromate ion have been observed. The line widths for the dissolved species were found to be concentration dependent. The variations in line width have been ascribed to a rapid reaction occurring at equilibrium between chromate and dichromate ions. The bimolecular rate constant for the reaction is $2.3 \pm 0.4 \times 10^3$ l mole^{-1} s^{-1} at 27 °C. The reaction mechanism is discussed in the general context of nucleophilic attack on dichromate ion. A comparison of this rate constant with those for the analogous reaction using different nucleophiles indicates that it is polarizability rather than basicity which determines nucleophilic reactivity towards $Cr_2O_7^=$.

INTRODUCTION

The direct reaction between $CrO_4^=$ and $Cr_2O_7^=$ ions at equilibrium in aqueous solution, without the involvement of solvent water molecules and leading to the rapid exchange of chromium atoms between one species and the other, has never been postulated. While carrying out a nuclear magnetic resonance (n.m.r.) study of chemical shifts of oxygen-17 atoms bonded to metal atoms, we have obtained experimental evidence for the reaction

$$Cr^*O_4^= + O_3Cr—O—CrO_3^= \rightarrow O_3Cr^*—O—CrO_3^= + CrO_4^=.$$

This evidence was obtained from the widths of ^{17}O resonance lines in the n.m.r. spectra of aqueous solutions of $Na_2Cr_2O_7$ containing varying concentrations of Na_2CrO_4. The kinetic rate constant for this reaction at 27 °C has been evaluated. The reaction is viewed in terms of a nucleophilic attack by $CrO_4^=$ on $Cr_2O_7^=$ leading to substitution at a chromium(VI) atom. Its mechanism is discussed in this context.

The nature of the kinetic processes occurring in both equilibrium and nonequilibrium solutions of $CrO_4^=$ and $Cr_2O_7^=$ ions has been the subject of considerable interest for the past 35 years. This interest has manifested itself in studies of the rate at which $CrO_4^=$ and $Cr_2O_7^=$ ions exchange oxygen atoms with solvent water molecules (1–5) and studies of the rate at which $CrO_4^=$ ions dimerize to give $Cr_2O_7^=$ ions (6–10). The exchange reaction newly reported in this paper proceeds independently of and at a rate considerably greater than either of these two reactions.

EXPERIMENTAL

The n.m.r. spectra were obtained using a Varian V-4300B fixed-frequency spectrometer adapted for the observation of quadrupolar-broadened ^{17}O signals by the addition of a lock-in amplifier and phase-sensitive detector. At a frequency of 6.000 Mc/s the signals were observed in the region of 10 400 gauss. Audiofrequency field modulation of 40 c.p.s. and peak-to-peak amplitude less than 45 mgauss was applied to the Helmholtz coils of the probe assembly. The output time constant of the phase-sensitive detector was variable between 2 and 140 s. A radiofrequency power level of about 50 mgauss was found to be below the saturation level and was used for all measurements. The spectra were calibrated by passing a measured

[1] *Presented at the 46th Annual Conference of the Chemical Institute of Canada, Toronto, June 6–8, 1963.*
[2] *Present address: Chemistry Department, University of Western Australia, Nedlands, Australia.*
[3] *Present address: Chemistry Department, University of Western Ontario, London, Ontario; to whom correspondence connected with this paper should be directed.*

Can. J. Chem. Downloaded from www.nrcresearchpress.com by 210.87.254.42 on 09/05/12
For personal use only.

d-c. biasing current through the Helmholtz coils of the probe, thereby shifting the position of one of the spectral signals by a known amount to provide a calibration point in each spectrum. The phase of the current leaked from the transmitter coil to the receiver coil within the probe was adjusted to give absorption mode presentation, and the signals obtained from the phase-sensitive detector were recorded in the absorption derivative form.

Water containing 2.1 atom per cent ^{17}O was obtained commercially from The Weizmann Institute, Israel. Hopkin & Williams $Na_2Cr_2O_7$ was twice recrystallized from water containing 0.1 *N* HCl. The product was dried for 6 h at 100 °C and 0.5 mm pressure. $Na_2Cr_2O_7$ (0.500 g) was placed in a 15 mm n.m.r cell and 0.870 g of the enriched water was distilled into the cell. The density of this solution was 1.42 g/cc, corresponding to a concentration of 1.98 *M* $Na_2Cr_2O_7$. Further solutions of increasing pH were prepared by the addition of weighed increments of solid NaOH to the initial solution.

In order to avoid loss of the enriched water, an identical series of solutions was prepared using natural water in place of the enriched water. The pH of each of these solutions was determined with a Cambridge potentiometer using glass and saturated calomel electrodes. The curve of *pH* vs. *weight of added NaOH* obtained from these measurements provided approximate pH values for the enriched solutions.

The sample temperature during measurement of the n.m.r. spectra was measured with a copper–constantan thermocouple and was found to be 27 ± 1 °C.

RESULTS

The ^{17}O linewidth data for the chromate and dichromate solutions are given in Table I.

TABLE I

^{17}O linewidths for $Cr_2O_7^=$ and $CrO_4^=$ solutions

Solution No.	Added NaOH, moles $\frac{NaOH}{Na_2Cr_2O_7}$	^{17}O linewidth, c.p.s.				Concentration, mole l^{-1}	
		Solvent H_2O	Terminal $Cr_2O_7^=$	Bridging $Cr_2O_7^=$	$CrO_4^=$	$[Cr_2O_7^=]$	$[CrO_4^=]$
1	0		115±15	198±9			
2	0.38		180±51	292±15			
3	0.67	199±41	321±54	872±57			0.49
4	0.84	209±17	452±12				0.86
5	1.02	227±12	534±82		554±1	1.38	1.25
6	1.11	230±10	826±61		603±56	1.27	1.45
7	1.32	230±24	923±199		570±50	1.05	1.89
8	1.40	249*			525±5	0.98	
9	1.60	245±16			380±15	0.76	
10	1.72	287±8			381±43	0.64	
11	1.95	302±14			276±67	0.39	
12	2.39	310±26			96±5		

Error limits are standard deviations.
*Single determination only.

Solution No. 1 is the initial solution containing 1.98 *M* $Na_2Cr_2O_7$ and the successive solutions were prepared from this one by addition of the amounts of NaOH indicated in the table. Each linewidth figure listed is an average value taken from at least three different spectra, except where otherwise noted.

The ionic concentration figures for the calculation of bimolecular rate constants are given in the last two columns of the table. They were obtained by a process of interpolation, making use of Fig. 1. The linewidth plots indicate that in the region between 50 and 180 mg added NaOH the concentrations of both $CrO_4^=$ and $Cr_2O_7^=$ are linear functions of the weight added. Since the initial $Cr_2O_7^=$ and the final $CrO_4^=$ concentrations are known, linear interpolation between them yields the values listed in the table. It is estimated that the inaccuracies in these figures are no greater than ±15%.

INTERPRETATION OF THE DICHROMATE ION ^{17}O SPECTRUM

The ^{17}O chemical shift for the terminal oxygen atoms in the dichromate ion has been shown (11) to be −1125 parts per million (p.p.m.) relative to water oxygens. A signal

Can. J. Chem. Downloaded from www.nrcresearchpress.com by 210.87.254.42 on 09/05/12
For personal use only.

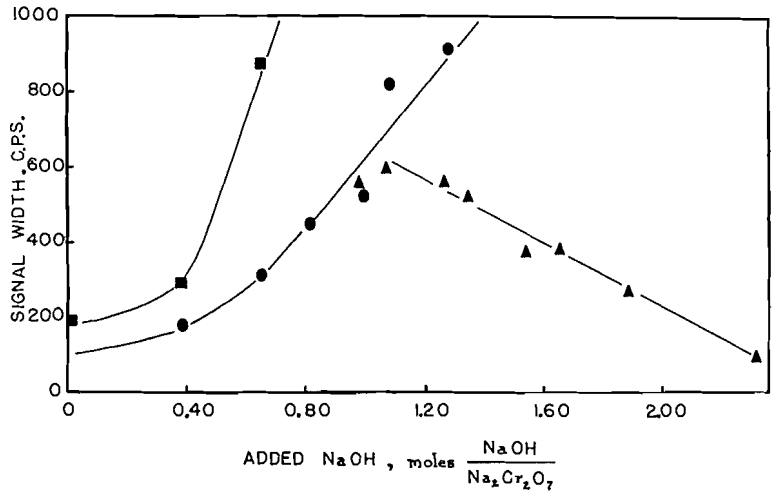

FIG. 1. ^{17}O signal widths for aqueous solutions of $Cr_2O_7^=$ and $CrO_4^=$; ■ bridging oxygen in $Cr_2O_7^=$; ● terminal oxygen in $Cr_2O_7^=$; ▼ oxygens in $CrO_4^=$.

from the bridging oxygen atom has not hitherto been reported. In order to detect the signal from the bridging oxygen it was necessary to enrich the $Cr_2O_7^=$ ion in ^{17}O. A 1.98 M aqueous solution of $Na_2Cr_2O_7$ enriched by a factor of 50 in ^{17}O yielded two ^{17}O signals apart from the solvent water line; a large signal at -1129 p.p.m. due to the terminal oxygens and a line of much lower intensity at -345 p.p.m. which was assigned to the bridging oxygens. The significant feature of this spectrum was the fact that the bridging-oxygen signal was approximately twice as wide as the terminal-oxygen signal.

The width of a nuclear resonance line having Lorentzian shape is determined by the effective transverse relaxation time T_2' of the nucleus, according to the equation (12)

$$[1] \qquad \Delta\nu = \frac{1}{\sqrt{3}\pi T_2'} \text{ s}^{-1}.$$

$\Delta\nu$ is the line width expressed in c.p.s. and defined as the horizontal separation between the points of maximum deflection of the absorption derivative curve. Where a chemical rate process causes a change in the magnetic environment of a nucleus due to exchange of the atom between two chemically different sites, then the lifetime of the spin state under investigation is limited by this process. If the lifetime of the spin state is long relative to the frequency separation of the two sites, then $\tau \cdot \Delta\omega > 1$, and the effective transverse relaxation time is given by (13)

$$[2] \qquad \frac{1}{T_2'} = \frac{1}{T_2} + \frac{1}{\tau}.$$

T_2 is the magnitude of the transverse relaxation time in the absence of any exchange process and τ is the mean lifetime for the stay of an atom at the site under investigation before it changes to another. $\Delta\omega$ is the frequency separation in radians per second between the two sites available to the nucleus. In the present study the lifetime value τ satisfies this slow exchange condition. The resonance linewidth for an ^{17}O nucleus which is not exchanged is obtained by substituting T_2 into eq. [1]. We will call this the static linewidth.

If one assumes that the static linewidths for oxygen atoms in both terminal and bridging positions of the dichromate ion are the same (and this assumption will be shown to

Can. J. Chem. Downloaded from www.nrcresearchpress.com by 210.87.254.42 on 09/05/12
For personal use only.

Can. J. Chem. Downloaded from www.nrcresearchpress.com by 210.87.254.42 on 09/05/12
For personal use only.

have a certain measure of validity), the fact that the bridging-oxygen signal is wider than the terminal-oxygen signal indicates that $\tau_B < \tau_T$. (In the following discussion, parameters with subscript T and B refer to oxygen atoms in dichromate ion terminal and bridging sites respectively.) The equilibrium constants for the existence of $Cr_3O_{10}^{=}$ (14) and $CrO_4^{=}$ (15) in equilibrium with $Cr_2O_7^{=}$ indicate that under the experimental conditions (pH $\approx$ 4), the concentrations of each of the former two ions will be less than 10^{-3} *M*. Accordingly, we consider the solution under study to consist primarily of $Cr_2O_7^{=}$ ions and H_2O molecules; concentrations of other oxygen-containing species in chemical equilibrium with these are relatively low, as is verified by the lack of further lines in the ^{17}O spectrum. A given oxygen atom spends only a very small fraction of its time in any one of these other environments, so the contribution of these environments to the shapes of the observed lines can be neglected. When an oxygen atom leaves a bridging position, it must transfer to either an H_2O site or to a terminal site. If it transfers to an H_2O site, then oxygen atoms must leave these sites at the same rate as bridging oxygens enter. This process would result in a correlated shortening of τ_{H_2O} leading to a broadening of the H_2O signal. With solution No. 7 as an example where the broadening of the dichromate terminal signal is most marked but still measureable, the linewidth which one calculates for the water signal, assuming that terminal oxygens are exchanging with H_2O oxygens, is 300 c.p.s. The observed linewidth for the solvent water line of solution No. 7 taken from Table I is, however, 230 c.p.s. Thus the broadening of the dichromate terminal oxygen signal cannot be ascribed to exchange of oxygen between terminal and solvent H_2O sites. Since ^{17}O linewidths are known to be dependent upon solution viscosity (16), we attribute the small monotonic increase in H_2O linewidth to increasing solution viscosity, which rises steadily from 1.9 cP for solution No. 1 to 5.6 cP for solution No. 12.

A more reasonable interpretation of the linewidth discrepancy can be made in terms of exchange of oxygen atoms between bridging and terminal positions. If this exchange occurs by some mechanism as yet unspecified, then the average lifetime of a terminal oxygen is longer than that of a bridging oxygen, and $\tau_T = 6\tau_B$ by considerations of detailed balancing. On this basis we set up a pair of simultaneous equations for the effective relaxation times of oxygen atoms at the two sites.

[3]
$$\frac{1}{T_{2T}'} = \frac{1}{T_{2T}} + \frac{1}{\tau_T}$$

$$\frac{1}{T_{2B}'} = \frac{1}{T_{2B}} + \frac{1}{\tau_B}.$$

T_{2T}' and T_{2B}' values can be obtained from the experimental linewidths using eq. [1] and $\tau_T = 6\tau_B$. Then, provided that static linewidths of terminal and bridging oxygens are the same, the equations can be solved for τ_B and T_2. Diehl and his co-workers (17) have examined the ^{17}O n.m.r. spectra of acetic and propionic anhydrides, both of which contain terminal and bridging oxygens. In these molecules, exchange between the two sites is not expected. In both cases, they found the linewidths for terminal and bridging sites in the same molecule to be identical, thereby supporting the contention that the oxygen linewidth is not particularly sensitive to differences in the nature of the bonding at the oxygen atom.

From the $Cr_2O_7^{=}$ ion spectrum we get $\Delta\nu_T = 115$ c.p.s. and $\Delta\nu_B = 198$ c.p.s. which gives $1/T_{2B}' = 1\,077\ s^{-1}$ and $1/T_{2T}' = 626\ s^{-1}$. Assuming that $T_{2T} = T_{2B} = T_2$ and eliminating τ_B and τ_T from eq. [3] we obtain $T_2 = 1.85 \times 10^{-3}$ s. This corresponds to a linewidth of 98 c.p.s. in the absence of exchange.

Can. J. Chem. Downloaded from www.nrcresearchpress.com by 210.87.254.42 on 09/05/12
For personal use only.

KINETIC PATHS LEADING TO OXYGEN EXCHANGE

Two different kinetic paths may lead to exchange of oxygen atoms between terminal and bridging positions in the dichromate ion. Both of them involve scission of one of the Cr—O—Cr bonds.

[4] 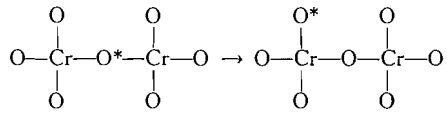

[5] 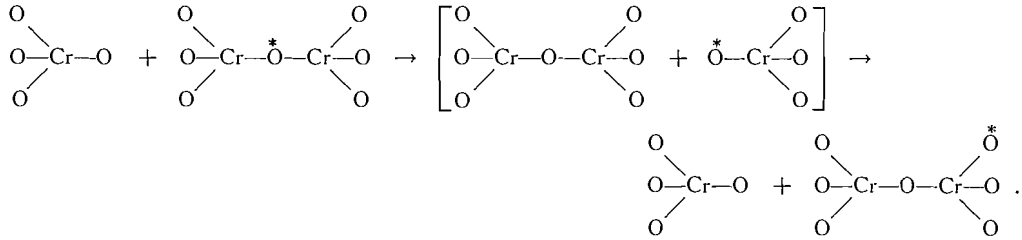

Path [4] is an intramolecular rearrangement and path [5] is a bimolecular process involving the low concentration of $CrO_4^=$ ions present in equilibrium with $Cr_2O_7^=$ ions. It should be stressed at this point that when detailed mechanisms are discussed in this paper, no distinction is drawn between the unprotonated chromium(VI) anions and their several protonated forms. Under the experimental conditions used in the study, it is not possible to distinguish between $CrO_4^=$, $HCrO_4^-$, and H_2CrO_4. Thus, the results of experimental observations made upon $CrO_4^=$ include the effects of any $HCrO_4^-$ and H_2CrO_4 present in the system.

In order to determine whether the second of these processes makes a significant contribution to the exchange process, the chromate–dichromate equilibrium in the ^{17}O-enriched solution

$$Cr_2O_7^= + 2OH^- \rightarrow 2CrO_4^= + HOH$$

was shifted to the right by adding increments of solid NaOH until the solution was alkaline, when all chromium(IV) was present in the form of $CrO_4^=$ ions. The ^{17}O spectrum was measured after the addition of each NaOH increment and the linewidth data for each solution are given in Table I.

As the $CrO_4^=$ ion concentration increases, both the terminal- and bridging-oxygen linewidths increase markedly indicating an increase in the exchange rate. In fact the bridging signal soon becomes so broad as to be undetectable. When the $CrO_4^=$ ion concentration reaches the level where a $CrO_4^=$ resonance line can be detected, the width of this line provides further evidence for the bimolecular process. Since the $CrO_4^=$ ion takes part in the exchange path [5], the width of this line also exhibits the effects of lifetime limiting. In the pH region where the dominant chromium(VI) species is $CrO_4^=$, the width of its ^{17}O signal decreases as the concentration of $Cr_2O_7^=$ drops, as is expected for a bimolecular process. The linewidth variations for the bridging signal, terminal signal, and chromate ion signal with change in solution pH can be seen in Fig. 1.

EVALUATION OF THE EXCHANGE RATE CONSTANT

The linewidth behavior illustrated in Fig. 1 indicates that the exchange rate is markedly dependent upon the relative concentrations of chromate and dichromate ions in solution

and that the exchange process is a bimolecular one governed by a rate law of the type

$$\pm\frac{d[Cr_2O_7^{=}]}{dt} = \pm\frac{d[CrO_4^{=}]}{dt} = k[Cr_2O_7^{=}][CrO_4^{=}].$$

If we direct our attention to the pH region where $CrO_4^{=}$ ions are the predominant chromium(VI) species, then the average lifetime of a chromate oxygen, τ_C, can be evaluated from the chromate linewidths. The rate at which chromate ions react is given by

$$\frac{[CrO_4^{=}]}{\tau_C} = \pm\frac{d[CrO_4^{=}]}{dt} = k[CrO_4^{=}][Cr_2O_7^{=}]$$

and

$$\frac{1}{\tau_C} = k[Cr_2O_7^{=}].$$

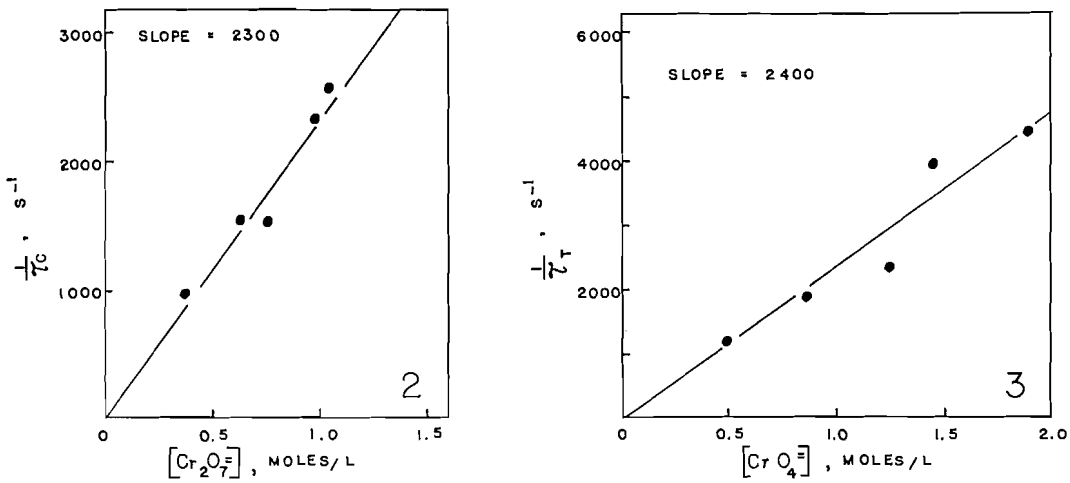

FIG. 2. Variation of $1/\tau_C$ with change in $[Cr_2O_7^{=}]$.
FIG. 3. Variation of $1/\tau_T$ with change in $[CrO_4^{=}]$.

When $1/\tau_C$ is plotted against $[Cr_2O_7^{=}]$ as in Fig. 2, a straight line with slope k and passing through the origin is obtained. The slope of Fig. 2 obtained by a least-squares treatment gives a rate constant value of $k = (2.3 \pm 0.4) \times 10^3$ l mole^{-1} s^{-1}, the error limits being the standard deviation.

The treatment of the dichromate ion linewidth data is not quite as straightforward. When a $CrO_4^{=}$ ion reacts with a $Cr_2O_7^{=}$ ion as in process [5], all four oxygens on $CrO_4^{=}$ assume new environments, but the same does not hold true for the $Cr_2O_7^{=}$ ion. Only four of these change environment to become $CrO_4^{=}$ oxygens, the other three remain as dichromate ion terminal oxygens. The average lifetime of a terminal-oxygen atom should then be twice that of a dichromate ion, since only half the terminal oxygens change their environment at each exchange event. This reasoning, however, is not confirmed by the experimental data. If one does assume that $\tau_T = \tau_{Cr_2O_7^{=}}$ then

$$\frac{[Cr_2O_7^{=}]}{\tau_T} = \pm\frac{d[Cr_2O_7^{=}]}{dt} = k[Cr_2O_7^{=}][CrO_4^{=}]$$

and

$$\frac{1}{\tau_T} = k[CrO_4^{=}].$$

Can. J. Chem. Downloaded from www.nrcresearchpress.com by 210.87.254.42 on 09/05/12
For personal use only.

The plot of $1/\tau_T$ vs. $[CrO_4^{=}]$ shown in Fig. 3 has the slope $k = (2.4 \pm 0.8) \times 10^3$ l mole^{-1} s^{-1}, thus lending substance to the assumption that $\tau_T = \tau_{Cr_2O_7^{=}}$. It must be concluded, therefore, that even though three of the terminal dichromate oxygens have the same environment before and after the reaction, the magnetic perturbation exerted upon them during the exchange event is sufficiently great to cause all of the terminal oxygens to lose their precessional phase correlation.

In connection with the rate constants given above, it should be mentioned that they were obtained under conditions of varying ionic strength. Since the measurements were made at electrolyte concentrations in excess of those where the ionic strength principle is applicable, it is impossible to estimate to what extent this variation affects the rate constants.

MECHANISM FOR THE EXCHANGE PROCESS

In the transfer of chromium atoms from $Cr_2O_7^{=}$ ions to $CrO_4^{=}$ ions, the ^{17}O linewidth data indicate that the largest, if not the only, contribution to the exchange process is through a mechanism the rate-determining step of which is the bimolecular reaction [5]. This being the case, the reaction can be considered as a specific example of the more general reaction

$$B + O_3Cr{-}O{-}CrO_3^{=} \xrightarrow{k_B^{II}} BCrO_3 + CrO_4^{=},$$

where B is a nucleophilic base. The case where $CrO_4^{=}$ acts as the nucleophile is unique, however, in that the products of the kinetic process are identical with the reactants. The reaction can therefore proceed with unvarying rate in a system at chemical equilibrium. Although no direct evidence concerning the detailed mechanism of this reaction has yet been obtained, the most likely reaction path involves an attack by B on the chromium atom at the center of the triangular face opposite the bridging oxygen. The transition state for this mechanism has three oxygens coplanar with the chromium atom being attacked.

The most familiar example of the general reaction is the hydrolysis of $Cr_2O_7^{=}$ with OH^- acting as the nucleophile. Saal (6) in 1928 pointed out on the basis of conductivity measurements made in a fast-flow system that the reaction

$$OH^- + Cr_2O_7^{=} \rightarrow CrO_4^{=} + HCrO_4^-$$

is a bimolecular one. However, LaMer and Read (7) two years later measured the enthalpy change accompanying the same reaction in a similar flow system and concluded that the reaction rate did not depend upon hydroxide ion concentration and obeyed a first-order rate law. This latter conclusion has been accepted until very recently when Lifshitz and Perlmutter-Hayman (9) established unambiguously, again by measurement of the enthalpy change, that the reaction is in fact bimolecular.

There is now available sufficient rate data for different donor groups reacting with $Cr_2O_7^{=}$ to attempt to assess which property of the donor determines its nucleophilic reactivity with this substrate. In Table II are listed, in order of decreasing reactivity towards $Cr_2O_7^{=}$, those nucleophiles whose rates have been determined, along with the bimolecular rate constants for these reactions. Although OH^- is the strongest base in the group listed, both NH_3 and $CrO_4^{=}$ are seen to be more reactive. Edwards and Pearson (18) have discussed recently the factors determining nucleophilic reactivity in its broadest context. They list those factors sufficient for a fundamental description of nucleophilic reactivity (defined in terms of the reaction rate with a given substrate) as being

(i) basicity, defined in terms of the equilibrium dissociation constant of the conjugate acid in water,

Can. J. Chem. Downloaded from www.nrcresearchpress.com by 210.87.254.42 on 09/05/12
For personal use only.

TABLE II

Rates for bimolecular nucleophilic attack on $Cr_2O_7^=$

Nucleophile, N	Rate constant		$\log\left(\frac{k_N}{k_{H_2O}}\right)$	Nucleophile parameters		
	k_N, l mole^{-1} s^{-1}	T, °C		H	R_N¶	P
$CrO_4^=$	2 300*	27	7.395	7.64††	6.70**	0.262
NH_3	740†	25	6.901	11.22‖	5.69	0.192
OH^-	460†	25	6.695	17.48‖	5.15	0.148
$CO_3^=$	~10†	25	5.073	12.1‖	4.05**	0.044
H_2O	9.3×10^{-5}‡	25	0.000	0.00	3.67	0.000

*This study.
†Reference 9.
‡R. H. Holyer and H. W. Baldwin, to be published.
‖J. O. Edwards. J. Am. Chem. Soc. 76, 1540 (1954).
¶Landolt-Bornstein, 6th edition, Springer-Verlag, Berlin. Band I, Teil 1, p. 402; Band I, Teil 3, p. 514.
**Values of R_N for the whole ion divided by the number of equivalent oxygens in the ion.
††Y. Sasaki. Acta Chem. Scand. 16, 719 (1962).

(ii) polarizability, defined in terms of the molar refractivity,

(iii) unshared electron pairs on the atom to which the donor atom is bonded.

It does not appear necessary to invoke the influence of unshared electron pairs in the present discussion of nucleophilic reactivity, so this factor will not be considered further.

If the relative rates for the different nucleophiles can be expressed as a linear combination of the polarizability and the basicity having the following form

$$\log \frac{k_N}{k_0} = \alpha P + \beta H, \qquad [6]$$

then it is possible to decide whether the polarizability or the basicity makes the dominant contribution to the nucleophilic reactivity towards $Cr_2O_7^=$. In this expression, (k_N/k_0) is the rate relative to water chosen as reference nucleophile, P is defined as $\log (R_N/R_{H_2O})$ with R representing molar refractivity, and H is a function of the basicity towards protons defined by the equation $H = pK_a + 1.74$. Values for all these parameters for the nucleophiles under discussion are listed in Table II. The coefficients α and β are variable parameters used to describe the substrate.

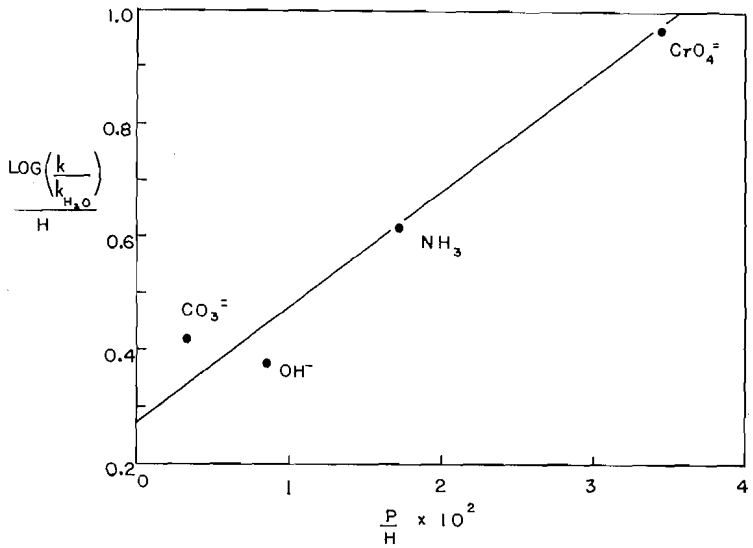

FIG. 4. Relative reactivity of nucleophiles with $Cr_2O_7^=$ as a function of basicity and polarizability.

Can. J. Chem. Downloaded from www.nrcresearchpress.com by 210.87.254.42 on 09/05/12
For personal use only.

By writing expression [6] in the form,

$$\frac{\log (k_N/k_{H_2O})}{H} = \alpha\frac{P}{H} + \beta,$$

and plotting $\log (k_N/k_{H_2O})/H$ against P/H, we obtain the linear relation shown in Fig. 4. From this the values for the variable coefficients are obtained; these turn out to be $\alpha = 18.3$ and $\beta = 0.3$. Since the polarizability coefficient is much larger than the basicity coefficient, it is suggested that polarizability of the nucleophile is of prime importance in determining nucleophilic reactivity toward $Cr_2O_7^=$.

ACKNOWLEDGMENTS

The authors are grateful to the Ministry of Aviation for financial support including a maintenance award to one of them (R. G. K.). They also wish to thank Dr. H. W. Baldwin for making available to them some rate data prior to publication.

REFERENCES

1. E. R. S. WINTER, M. CARLTON, and H. V. A. BRISCOE. J. Chem. Soc. 131 (1940).
2. G. A. MILLS. J. Am. Chem. Soc. **62**, 2833 (1940).
3. N. F. HALL and O. R. ALEXANDER. J. Am. Chem. Soc. **62**, 3455 (1940).
4. A. I. BRODSKII and E. I. DONTSOVA. Dopovidi Akad. Nauk Ukr. RSR No. 3, 6 (1940); Chem. Abstr. **37**, 4957 (1943).
5. M. R. BALOGA and J. E. EARLEY. J. Phys. Chem. **67**, 964 (1963).
6. R. N. J. SAAL. Rec. Trav. Chim. **47**, 264 (1928).
7. V. K. LAMER and C. L. READ. J. Am. Chem. Soc. **52**, 3098 (1930).
8. G. SCHWARZENBACK and J. MEIER. J. Inorg. Nucl. Chem. **8**, 302 (1958).
9. A. LIFSHITZ and B. PERLMUTTER-HAYMAN. J. Phys. Chem. **65**, 2098 (1961).
10. J. H. SWINEHART and G. W. CASTELLAN. Inorg. Chem. **3**, 279 (1964).
11. B. N. FIGGIS, R. G. KIDD, and R. S. NYHOLM. Proc. Roy. Soc. London, Ser. A, **269**, 469 (1962).
12. E. R. ANDREW. Nuclear magnetic resonance. Cambridge University Press, London. 1955. p. 105.
13. H. M. MCCONNELL. J. Chem. Phys. **28**, 430 (1958).
14. A. MARTENS and G. CARPENI. J. Chim. Phys. **60**, 534 (1963).
15. J. D. NEUSS and W. RIEMANN. J. Am. Chem. Soc. **56**, 2238 (1934).
16. H. A. CHRIST and P. DIEHL. Magnetic and electric resonance and relaxation. North-Holland Publishing Co., Amsterdam. 1963. p. 224.
17. H. A. CHRIST, P. DIEHL, H. SCHNEIDER, and H. DAHN. Helv. Chim. Acta, **44**, 865 (1961).
18. J. O. EDWARDS and R. G. PEARSON. J. Am. Chem. Soc. **84**, 16 (1962).

Can. J. Chem. Downloaded from www.nrcresearchpress.com by 210.87.254.42 on 09/05/12
For personal use only.

Can. J. Chem. Downloaded from www.nrcresearchpress.com by 210.87.254.40 on 09/05/12
For personal use only.

SOLVOLYSIS IN LIGHT AND HEAVY WATER

VI. THE ROLE OF INITIAL STATE STRUCTURE[1]

P. M. LAUGHTON[2]
Department of Chemistry, Carleton University, Ottawa, Canada
AND
R. E. ROBERTSON
Division of Pure Chemistry, National Research Council, Ottawa, Canada

Received August 14, 1964

ABSTRACT

The solubility data in light and heavy water of Swain and Thornton and of Taft and co-workers are reinterpreted to show that they support primarily the initial state origin for the kinetic solvent isotope effect. Other recent data, including the effect for *t*-butyl and α-phenethyl fluorides, are also shown to be compatible with the same hypothesis.

Papers from several different laboratories (1–4) have recently criticized our ideas ((5) and earlier papers quoted therein) attributing the major contributor to the origin of the kinetic solvent isotope effect k_{D_2O}/k_{H_2O} (KSIE) in solvolysis to differences between the initial states. The purpose of this paper is to dispose of those criticisms which have been based on solubility parameters of substrates in light and heavy water; in particular the analysis of the situation by Swain and Thornton (3), which recent reviewers (6) have accepted as negating our views.

As further evidence supporting our hypotheses, we also present solvent isotope effect data for two alkyl fluorides. These data differ little from those for other alkyl halides, while explanations based on solvation differences in the transition state would predict sharp differences between substrates generating fluoride ion and those producing other halide ions.

The main source of our disagreement with Swain and Thornton is that they have chosen as a standard state for their thermodynamic calculations one which by definition conceals any differences originally present in the solvents themselves before they undergo the change from initial state to transition state. Therefore, while relevant to the characterization of the reaction in general, their data are actually incapable of deciding the matter under contention, and in fact support our views. The same observation applies to the data of Taft and co-workers (4).

DISCUSSION

The usual practice of looking for reactivity differences only in the structures of substrates and in solvent interactions with transition states implies that differences between the various initial states may be considered negligible. Since relatively few data are available concerning the thermodynamic properties of initial states, it is hard to say how generally valid this implied approximation may be. There is, however, ample evidence that it is *not* true in water solutions ((7) and references quoted therein).

In fact, in the papers mentioned above (5), we have developed the theme that the solvent shell provides a source of structural free energy, relative changes in which during

[1]*Issued as N.R.C. No. 8202.*
[2]*Supported by a grant-in-aid of research from the National Research Council.*

the activation process account for the greater part of the KSIE. This explanation of the KSIE also implies that the structural free energy changes in the solvent during activation are themselves important parts of the free energy of activation. This view is further required by the small entropies yet large negative heat capacities of activation, which can only be generated with the involvement of many solvent molecules in processes resembling melting (8).

Arguments Based on Solubility Data

In rebuttal to our views, Swain and Thornton (3) and Taft (4) have recently offered the solubilities of several alkyl halides in light and heavy water. They confirm that the solubility ratios are near unity, representing values of $\Delta\Delta F$(gas → solution) smaller than the corresponding $\Delta\Delta F^{\ddagger}$ values for solvolysis. Their data are summarized in Table I.

TABLE I

Solubility and solvolysis parameters of alkyl halides in H_2O and D_2O

Alkyl halide	Solubility ratio D_2O/H_2O	$\Delta\Delta F^*$ (kcal/mole)	$\Delta\Delta H^*$ (kcal/mole)	$\Delta\Delta F^{\ddagger *}$,§ (kcal/mole)
MeF	1.02†	−0.01	−0.49	—
MeCl	0.96†	0.02	−0.04	−0.179
MeBr	0.93†	0.04	−0.08	−0.142
MeI	0.91†	0.06	−0.37	−0.152
t-BuCl	1.02‡	—	—	−0.172

*ΔΔ for Δ(H_2O) − Δ(D_2O).
†Reference 3; 29.4 °C.
‡Reference 4; 14.85 °C.
§Reference 14; at temperatures quoted.

Swain and Thornton evaluated their data as follows.

(1) $$\text{R—X}_{gas} + D_2O \rightleftharpoons \text{R—X in } D_2O,$$
$$\text{R—X}_{gas} + H_2O \rightleftharpoons \text{R—X in } H_2O.$$

The solubility ratio then corresponds to the equilibrium:

$$\text{R—X in } H_2O \rightleftharpoons \text{R—X in } D_2O,$$

with equilibrium constant K_{sol}.

(2) $$\text{R—X in } D_2O \rightleftharpoons \begin{matrix} D \\ D \end{matrix}\!\!>\!O\cdots R\cdots X \text{ in } D_2O;\ \text{rate constant } k_{D_2O},$$
$$\text{R—X in } H_2O \rightleftharpoons \begin{matrix} H \\ H \end{matrix}\!\!>\!O\cdots R\cdots X \text{ in } H_2O;\ \text{rate constant } k_{H_2O}.$$

(3) The kinetic solvent isotope effect is then K_{kin} for the equilibrium:

$$\begin{matrix} H \\ H \end{matrix}\!\!>\!O\cdots R\cdots X \text{ in } H_2O + \text{R—X in } D_2O + D_2O \text{ in } D_2O \rightleftharpoons$$
$$\begin{matrix} D \\ D \end{matrix}\!\!>\!O\cdots R\cdots X \text{ in } D_2O + \text{R—X in } H_2O + H_2O \text{ in } H_2O.$$

(4) They then identify as "transition state isotope effect" the equilibrium constant for the reaction:

$$\begin{matrix} H \\ H \end{matrix}\!\!>\!O\cdots R\cdots X \text{ in } H_2O + D_2O \text{ in } D_2O \rightleftharpoons \begin{matrix} D \\ D \end{matrix}\!\!>\!O\cdots R\cdots X \text{ in } D_2O + H_2O \text{ in } H_2O,$$

which is the product of K_{sol} and K_{kin}.

Can. J. Chem. Downloaded from www.nrcresearchpress.com by 210.87.254.40 on 09/05/12
For personal use only.

Since K_{kln} is farther from unity than is K_{sol}, these authors then attribute the solvent isotope effect to differences in the respective transition states.

It is true that the transition states have different solubilities in the two waters. This fact does not, however, demonstrate that the transition states themselves are different. The flaw in this argument is that it ignores the differences in free energies of the two solvents, which, because K_{sol} is near unity, still exist in the two initial states. That is, the substrates have nearly the same free energies in each case, but the other reactants, the solvents, have quite different free energies. Swain and Bader (1) have estimated that nearly 1 kcal/mole of the 4.3 kcal/mole excess in free energy of H_2O over D_2O can be attributed to structural factors, i.e. libration and translation energies.

Translating equilibrium constants into free energies:

$$\delta_I\Delta F \equiv \Delta\Delta F(\text{solubility}) = -RT \ln K_{sol} = -10 \text{ to } +60 \text{ cal/mole},$$

where $\Delta\Delta F$ is the relative free energy change for the equations:

$$\Delta F_{D_2O} = F(\text{solution of RX in } D_2O) - F(\text{RX gas}) - F(D_2O),$$

$$\Delta F_{H_2O} = F(\text{solution of RX in } H_2O) - F(\text{RX gas}) - F(H_2O).$$

Since $\Delta\Delta F$ is small, F(RX gas) is common to both, and $(F_{D_2O} - F_{H_2O})$ is large and negative, then F(solution in D_2O) $-$ F(solution in H_2O) must also be large, and in the direction which is more than enough to account for K_{kln}. The solvation differences between the two transition states are therefore smaller than those between the initial states, as we have postulated.

The question of the interpretation of the solubility data is another and interesting problem. Swain and Thornton find it difficult to believe that so-called iceberg formation about a nonpolar solute can occur without a significant isotope effect on solubility. They suggest instead that these solutes utilize pre-existing holes in the water structure, especially since they are more concentrated in the aqueous than in the gas phase. Utilization of pre-existing holes would, however, imply partial molal volumes near zero for the solutes, whereas they are not, where they are known, very different from the molar volumes of the pure solutes (7). In any case, the situation is too complex to be treated on the basis of assumed H-bonding effects. The situation has been discussed by several authors, particularly Eley (9). For example, the cavitation energies $(\delta E/\delta V)_T$ of H_2O and D_2O are, of course, zero at their corresponding maximum densities, 4° and 11.2°, and appear to cross over near 100°. That is, over the whole temperature range of kinetic interest the energies required to generate holes for solutes in the two solvents lie close together. In any detailed explanation of solubilities in water, dispersion energies must be taken into account, in addition to H-bond energies and energies and entropies arising from any restricted translations and librations.

H-Bonding Models

We find it difficult to comment on the model proposed by Bunton and Shiner (2). They include in their calculations assumed frequencies for H bonds from water to neutral solutes such as alkyl halides and sulfides. More evidence will be needed to establish that such H bonds in fact exist.

Arguments from Data in Aqueous Mixtures

Recent data by Arnett and co-workers (10) highlight the role of initial state solvation in an aqueous system other than the isotopic systems considered above. They have

Can. J. Chem. Downloaded from www.nrcresearchpress.com by 210.87.254.40 on 09/05/12
For personal use only.

measured the heat of solution of *t*-butyl chloride in aqueous alcohol mixtures and shown that the changes in enthalpy of solution, $\Delta\Delta H_{sol}$, with increasing alcohol concentration over a considerable range parallel the corresponding values of $\Delta\Delta H^{\ddagger}$ for solvolysis, i.e. $\Delta\Delta H_{sol}/\Delta\Delta H^{\ddagger} \sim -1$. Hyne has recently shown (11) that this relation does not hold so exactly for all substrates, but its existence in any instance shows the danger of attributing all kinetic differences to transition states.

Our own data for the KSIE for *t*-butyl chloride in aqueous dioxane (12) also support an initial state interpretation. The effect changes from 0.70 to 0.74 in the pure waters to 0.95 in aqueous dioxane. This is just what one would expect if the KSIE arises from a loss of initial state water structure during activation, since several lines of evidence indicate that the structure of water is broken down by diluents such as dioxane in the concentration range studied.

Alkyl Fluorides, a Possible Test Case

In Swain and Thornton's paper, the so-called transition state isotope effect is discussed in terms of the solution isotope effect on the halide ions and relative bond breaking of RX at the transition state. They do not predict the effect with fluorides, but if solvation differences in the two transition states are responsible for the KSIE, then one might expect fluorides to be unusual. Fluoride ion is the only simple ion which has a *lower* free energy in D_2O than in H_2O (1), and since the KSIE is sensitive to the anionoid portion of these substrates rather than to the alkyl group (13), one might then expect a KSIE for fluorides nearer unity or perhaps even inverted. (Uncertainty in this prediction is introduced by the compensating inversion noted in the solubility of methyl fluoride.)

We have measured the KSIE for two fluorides with the requisite precision by using 2,6-lutidine in slight excess (0.005–0.01 *M*) to delay attack on the borosilicate conductance cells. The values of k_{D_2O} and k_{H_2O} redetermined (14) for *t*-butyl fluoride at 90.00° and newly determined for α-phenethyl fluoride at 55.01° are, respectively, $4.25_1 \pm 0.004$ and $5.17_7 \pm 0.016 \times 10^{-4}$ s^{-1}, and $2.46_3 \pm 0.014$ and $2.95_4 \pm 0.004 \times 10^{-4}$ s^{-1}, leading to KSIE values of 0.82_1 and 0.83_4, respectively. These differ negligibly from those for other alkyl halides in the same temperature ranges (14).

CONCLUSIONS

We therefore believe that all the relevant data so far support our hypothesis that differences in initial state solvation energies are often significant, and should particularly not be considered negligible where the solvent is structurally ordered.

However, our hypothesis is essentially qualitative. The lack of sensitivity of the KSIE to nucleophilic involvement remains unexplained. The effect of substituents which interact with the solvent is only imperfectly understood (15). This parameter has helped to define our picture of solvent involvement near the seat of reaction, but more sensitive parameters are needed to sharpen the focus.

EXPERIMENTAL

Materials

t-Butyl fluoride was prepared in the usual way (16).

α-Phenethyl fluoride was prepared by the method of Henne and Midgely (17), using 10 g α-phenethyl bromide and mercuric oxide in 50 ml carbon tetrachloride in a Polythene bottle, and passing in HF. After careful removal of the solvent, the product was purified by Späth bulb distillation. Absence of kinetically significant impurities was evidenced by the excellent linearity of all rate plots used.

2,6-Lutidine was distilled from commercial material. Heavy water (99.7–9.8 atom % deuterium) was obtained from Merck, Sharp and Dohme of Canada Ltd.

Can. J. Chem. Downloaded from www.nrcresearchpress.com by 210.87.254.40 on 09/05/12
For personal use only.

Method

The conductance method of obtaining the solvolytic rates was that used previously.

Although the presence of 0.005 (α-phenethyl fluoride) or 0.01 (t-butyl fluoride) M 2,6-lutidine delayed attack on the cell walls such that the effect on conductance during a run was negligible, we were unable to carry on our usual practice of conditioning cells for long periods with the electrolyte to be studied without ultimate damage to the cells.

α-Phenethyl fluoride has been studied in water over the range 45–70°, but the data are not yet of the quality required for evaluation of the heat capacity of activation.

ACKNOWLEDGMENTS

We are indebted to Mr. S. Sugamori for expert technical assistance. Drs. D. N. Glew and H. S. Frank have been most generous in advising us on the properties of aqueous solutions.

REFERENCES

1. C. G. Swain and R. F. W. Bader. Tetrahedron, **10**, 182 (1960).
2. C. A. Bunton and V. J. Shiner, Jr. J. Am. Chem. Soc. **83**, 3207 (1961).
3. C. G. Swain and E. R. Thornton. J. Am. Chem. Soc. **84**, 822 (1962).
4. G. A. Clarke, T. R. Williams, and R. W. Taft. J. Am. Chem. Soc. **84**, 2292 (1962).
5. R. E. Robertson. Can. J. Chem. **42**, 1707 (1964).
6. B. Capon and C. W. Rees. Reaction mechanisms. *In* Annual reports on the progress of chemistry. The Chemical Society, London. 1962. p. 218.
7. D. N. Glew. J. Phys. Chem. **66**, 605 (1962).
8. E. A. Moelwyn-Hughes, R. E. Robertson, and S. Sugamori. J. Chem. Soc. In press.
9. D. D. Eley. Trans. Faraday Soc. **40**, 184 (1944).
10. E. M. Arnett, P. M. Duggleby, and J. J. Burke. J. Am. Chem. Soc. **85**, 1350 (1963).
11. J. B. Hyne. Chemical Institute of Canada Annual Meeting, Kingston, Ont. May, 1964.
12. W. G. Craig, L. Hakka, P. M. Laughton, and R. E. Robertson. Can. J. Chem. **41**, 2118 (1963).
13. R. E. Robertson and P. M. Laughton. Can. J. Chem. **35**, 1319 (1957).
14. P. M. Laughton and R. E. Robertson. Can. J. Chem. **37**, 1491 (1959).
15. P. M. Laughton and R. E. Robertson. Can. J. Chem. **39**, 2155 (1961).
16. K. A. Cooper and E. D. Hughes. J. Chem. Soc. 1183 (1937).
17. A. L. Henne and T. Midgely, Jr. J. Am. Chem. Soc. **58**, 884 (1936).

Can. J. Chem. Downloaded from www.nrcresearchpress.com by 210.87.254.40 on 09/05/12
For personal use only.

Can. J. Chem. Downloaded from www.nrcresearchpress.com by 210.87.254.6 on 09/05/12
For personal use only.

A PULSED ION SOURCE FOR THE STUDY OF UNIMOLECULAR AND BIMOLECULAR REACTIONS OF GAS-PHASE IONS[1]

T. W. SHANNON, F. MEYER, AND A. G. HARRISON[2]
Department of Chemistry, University of Toronto, Toronto, Ontario

Received August 21, 1964

ABSTRACT

A pulsed ion source has been constructed for use with a magnetic-deflection mass spectrometer. With this source the time between ion formation and withdrawal for analysis can be controlled and varied in a known manner. The design and operating characteristics of the source are discussed and a technique is described for the measurement of ion withdrawal times using the pulsing technique.

The rate constant for the ion molecule reaction

$$CH_4^+ + CH_4 \rightarrow CH_5^+ + CH_3$$

has been determined for the reaction of thermal energy ions using reaction time as the experimental variable. The equivalent reactions in the deuteriomethanes have also been studied. Preliminary results obtained in the study of the unimolecular fragmentation of the cyclohexadiene, toluene, and spiroheptadiene parent ions are presented.

INTRODUCTION

The quasi-equilibrium theory of mass spectra (1) considers that the fragment ions observed in the mass spectra of polyatomic molecules are formed by a series of competing and consecutive unimolecular reactions similar to the rate processes of ordinary chemical kinetics. The evidence that these fragmentation reactions can be considered as rate processes has depended almost entirely on indirect evidence and it is desirable to attempt direct measurements of the reaction rates to provide experimental tests of the theory. Such measurements require that the time between ion formation and mass analysis be varied. Some success has been achieved in varying this time by varying the repeller field which pushes the ions out of the ionization chamber and information has been obtained (2–5) on the rates of fragmentation reactions leading to metastable ion formation. However, the results obtained are not in complete agreement (5). A more difficult approach, which is not necessarily limited to the observation of fragmentation reactions leading to metastable ion formation, consists of pulsing the ionizing electron beam and varying the time between ion formation and application of the fields which abstract the ions for mass analysis. Using this technique with a time-of-flight mass spectrometer, Wahrhaftig (6), in a preliminary study, has observed directly the fragmentation reaction [1] in propane.

[1] $$C_2H_5^+ \rightarrow C_2H_3^+ + H_2.$$

In addition to unimolecular fragmentation reactions, the ions formed in the mass spectrometer ion source may undergo bimolecular reactions with neutral molecules, particularly at higher ion source concentrations. Such reactions have been extensively studied in the past 10 years (7, 8, 9). The usual technique has been to operate the ion source at a relatively high pressure with the consequence that the ions formed by the primary processes undergo reactive collisions with neutral molecules as they move out of the ionization chamber under the influence of electric fields. By varying these electric fields (particularly the repeller field) the ion-residence time can be varied and kinetic data obtained. In addition, for the bimolecular reactions kinetic data can be obtained from

[1]*Presented in part at the ASTM Committee E-14 Conference on Mass Spectrometry, Montreal, June 1964.*
[2]*Alfred P. Sloan Fellow, 1962–1964.*

pressure variation. The results obtained refer to the reactions of ions accelerated by electric fields and it is known that the cross sections for such reactions are velocity dependent. It is obviously desirable to have kinetic data for the reactions of thermal energy ions, particularly for application in radiation chemistry (8) and in combustion and discharge phenomena (10).

In 1960 Tal'roze and Frankevich (11) reported the development of a pulsed source magnetic-deflection mass spectrometer with which the time between ion formation and ion withdrawal could be varied. Using this source they studied the reactions of thermal energy ions in methane and in water vapor. While the present work was in progress Hand and von Weyssenhoff (12) briefly reported on similar experiments in methane using a time-of-flight mass spectrometer.

The present communication reports the adaptation of a commercial magnetic-deflection mass spectrometer to permit operation in the pulsed manner. The design of the pulsed source and its operating characteristics will be discussed and preliminary results obtained in the study of both unimolecular and bimolecular reactions of gas-phase ions will be presented.

DESIGN AND OPERATION OF PULSED SOURCE

The modifications necessary for operation with a pulsed ion source were made to an A.E.I. MS-2 Mass Spectrometer. The basic mass spectrometer is a 6 in. radius of curvature 90° sector-field instrument. The major changes were made to the ion source and the potentials supplied to the source. The modified source, similar in many respects to that used by Tal'roze and Frankevich (11), is shown schematically in Fig. 1. The voltages

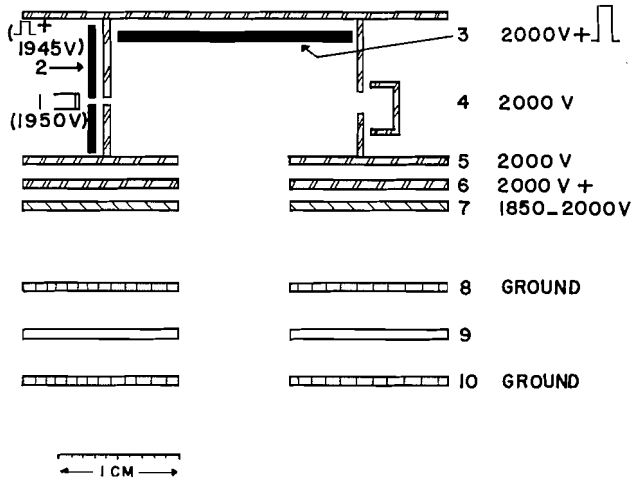

FIG. 1. Schematic diagram of ion source: 1, filament; 2, electron beam control plate; 3, repeller; 4, trap; 5, cage; 6, withdrawal plate; 7, focus; 8, 10, beam-defining plates; 9, beam centering.

given in Fig. 1 represent typical operating conditions. Essentially the modifications consisted of the installation of an electron beam control plate (plate 2) in the electron gun and the enlargement of the ionization chamber. The electrons, emitted from a directly heated tungsten or rhenium cathode, enter the ionization chamber through slits 3.0 × 0.5 mm in the two electron gun plates and are focussed by an auxiliary permanent magnet. The distances from the center of the electron beam to the exit slit and to the repeller are each

Can. J. Chem. Downloaded from www.nrcresearchpress.com by 210.87.254.6 on 09/05/12
For personal use only.

4.8 mm, while the distance to the side walls of the ionization chamber is 6.9 mm. The ionizing region is approximately 18 mm long with the ion exit slit having the dimensions 10×0.76 mm.

In operation, the spectrometer first was focussed on an ion beam of interest during continuous operation. The electron beam was then arrested (as indicated by the disappearance of the ion current) by applying a bias, negative with respect to the filament, to the electron beam control plate (plate 2). A positive pulse, supplied by a Datapulse Model 102 Pulse Generator, was then applied to plate 2 to provide the pulsed electron beam. With the electron beam pulsing, a small positive potential was applied to the ion withdrawal plate (plate 6) to prevent withdrawal of the ions by the main accelerating field. This potential was approximately 6 V, the magnitude being determined by the disappearance of the recorded ion current. With the present source design the main acceleration occurs between plates 7 and 8, while in the original MS-2 design the main acceleration occurred between plates 6 and 7 (plate 7 at +150 V). Under these latter conditions a positive bias of approximately 90 V on plate 6 was necessary to prevent ion withdrawal by the accelerating field and with this potential the ions were lost rapidly from the sampling region during the delay period presumably due to penetration of the field from plate 6.

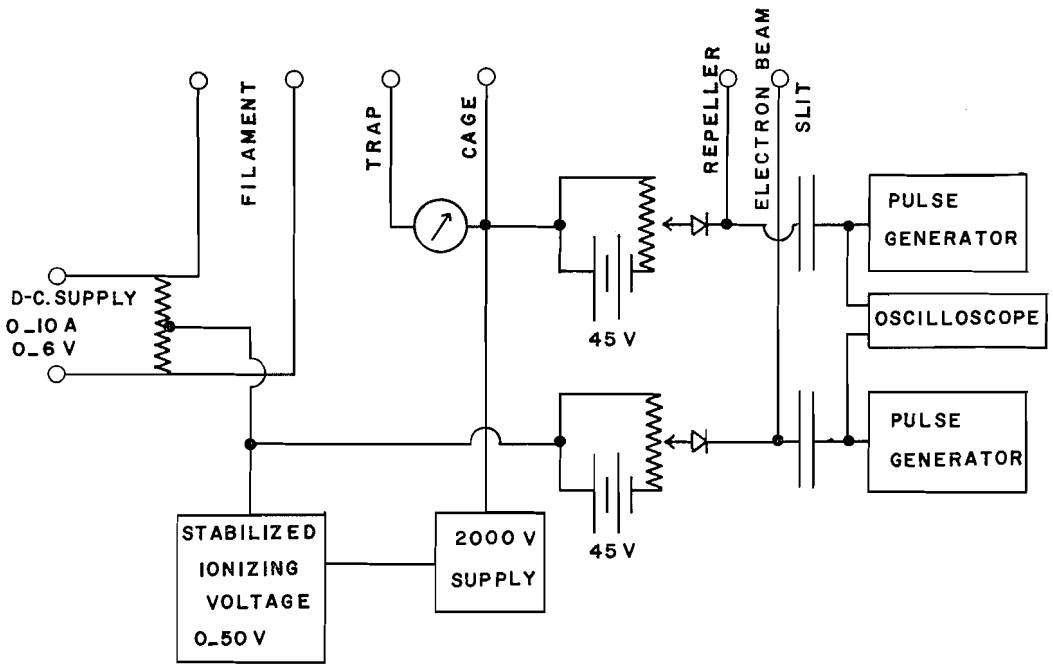

FIG. 2. Potential supplies to ion source.

The ions were pushed out of the ionization chamber by a positive pulse applied to the repeller plate (plate 3). This pulse was supplied by a Datapulse Model 100 Pulse Generator triggered by the first pulse generator with a variable time delay. The time between the ionizing and repelling pulses was determined by displaying the pulses on a two-channel oscilloscope (Tektronix Model 516). A schematic diagram of the potential supplies for the ion source is shown in Fig. 2. The filament current was initially supplied by a 6 V storage battery or, more recently, by a stabilized d-c. power supply. The ion current reaching the collector was amplified by a Cary Model 31 Vibrating Reed Electrometer.

Can. J. Chem. Downloaded from www.nrcresearchpress.com by 210.87.254.6 on 09/05/12
For personal use only.

The operating characteristics were found to be primarily dependent on the potentials and pulses applied to the electron beam control plate and to the repeller plate and these points deserve more detailed comment.

Electron Beam Control Plate

A bias of 3–5 V, negative with respect to the filament, was sufficient to arrest the electron beam completely. The positive pulse applied to admit the electrons usually had an amplitude of 5–10 V and a duration of 0.1 to 1.0 μs with a rise and decay time of approximately 40 ns each. The recorded ion current was a linear function of the pulse width. However, the dependence of ion current on the pulse amplitude was somewhat variable. Usually the ion current was found to increase with the difference between the pulse amplitude and the bias voltage up to approximately 3–4 V difference and then to decrease slowly with greater differences. When operating near this maximum the major part of the electron acceleration occurs between the two plates of the electron gun and under these conditions satisfactory ionization efficiency curves, yielding appearance potentials in agreement with the literature, were obtained. Application of higher pulse amplitudes (20–30 V) frequently resulted in long tails on the ionization efficiency curves possibly because of space charge effects in the electron gun. The maximum repetition rate was limited by the duty cycle of the pulse generator to approximately 2×10^5 pulses s^{-1}.

Repeller Plate

The recorded ion current was found to depend on both the duration and amplitude of the repeller pulse. For a constant pulse amplitude the ion current increased with pulse duration up to 1.2–1.4 μs and then began to drop off slowly with longer durations, although the maximum ion current could be regained at these longer times by decreasing the pulse amplitude. Consequently the duration and amplitude of the pulse were adjusted for maximum ion current; normal operating conditions were a pulse duration of 1.4–2.0 μs and a pulse amplitude of 5–10 V.

The settings of the repeller pulse and the focus half-plate for maximum ion current were mass dependent. This fact coupled with the possibility of preferential loss of low-mass ions from the sampling region makes scanning of complete mass spectra both inconvenient and inaccurate when using the pulsed mode of operation. Consequently complete mass spectra were recorded using continuous ionization and ion withdrawal yielding mass spectra in agreement with those previously obtained.

Some experiments were carried out using a U-shaped repeller in place of the flat repeller shown in Fig. 1. The operating characteristics remained unaltered with the exception that some improvement in ion decay curves was noted presumably due to an increase in the volume sampled by the analyzing system when the repeller pulse was applied.

ION DECAY CURVES AND DISCRIMINATION EFFECTS

The usefulness of the present ion source in the study of the reactions of ions with time as the experimental variable depends on the rate at which ions are lost from the volume sampled by the analyzing system when the repeller pulse is applied. The ions will be lost from this volume due to thermal kinetic energy and under the influence of fields arising from surface potentials, space charge, and field penetration. All of these effects will lead to a more rapid loss of lighter-mass ions with increasing delay times and hence to discrimination effects which may obscure the changes anticipated from the chemical reaction under study.

Typical decay curves are shown for m/e = 16 (CH_4^+), 40 (A^+), 92 ($C_7H_8^+$), and 132

Can. J. Chem. Downloaded from www.nrcresearchpress.com by 210.87.254.6 on 09/05/12
For personal use only.

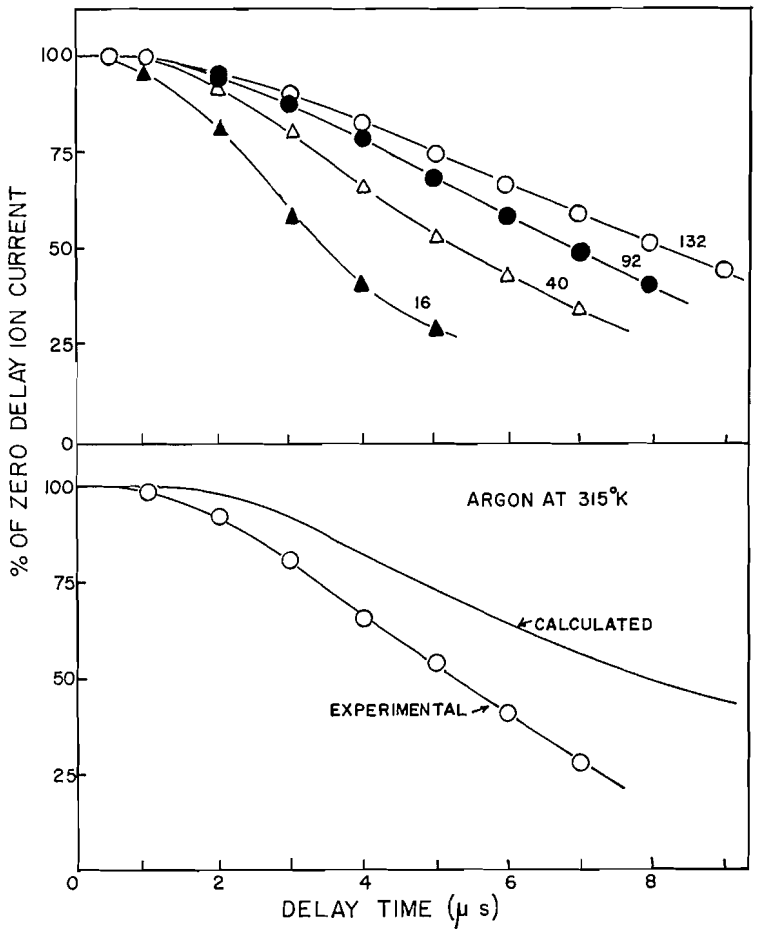

FIG. 3. (*a*) Experimental ion decay curves; (*b*) comparison of experimental and theoretical decay curves $m/e = 40$.

(Xe^+) in Fig. 3*a* where the results are plotted as percent of the zero delay ion current versus the delay time between the ionizing and repelling pulses. The mass effect is clearly demonstrated in the rather rapid loss of CH_4^+ (50% value, 3.5 μs) compared to Xe^+ (50% value, 8.3 μs).

Figure 3*b* compares the experimental decay curve for A^+ with that calculated assuming the loss of ions from the sampling region to be due to thermal kinetic energy only and assuming a Maxwell–Boltzmann distribution of energies with a temperature of 315 °K, the temperature of the ionization chamber as measured directly by a thermocouple. In view of the increased interest in the use of a pulsed source we present the details of the calculation in an appendix. It is clear from comparison of the experimental and theoretical curves that the ions are lost from the sampling volume more rapidly than would be expected from thermal effects alone indicating that small stray fields are present. To reproduce the experimental curve would require an average ion velocity about 1.8 times the thermal velocity at the temperature of the ion source. This velocity, however, would still be less than 10% of the velocity imparted to an argon ion from acceleration by a potential of 10 V (a situation common in the study of ion–molecule reactions by conventional techniques).

Can. J. Chem. Downloaded from www.nrcresearchpress.com by 210.87.254.6 on 09/05/12
For personal use only.

Can. J. Chem. Downloaded from www.nrcresearchpress.com by 210.87.254.6 on 09/05/12
For personal use only.

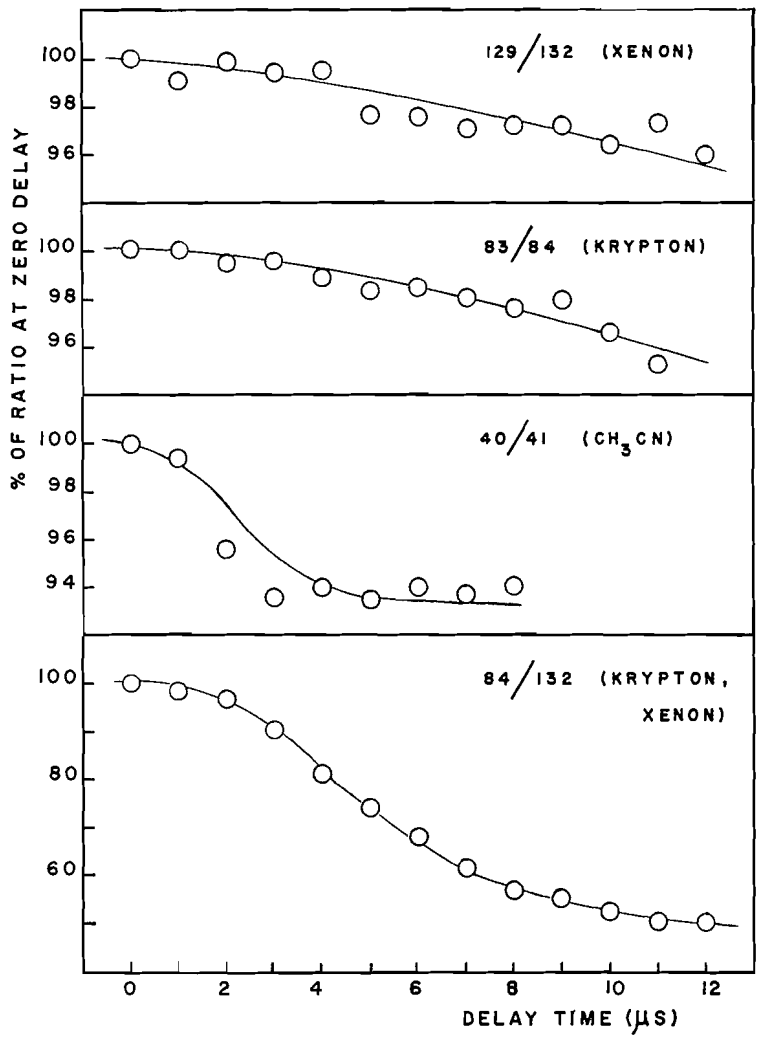

FIG. 4. Mass discrimination as a function of mass difference and delay time.

The decay curves of Fig. 3 show a much more rapid loss of the lighter-mass ions, an effect which will lead to increasing discrimination against such ions with increasing delay times. The magnitude of this discrimination effect is indicated for a number of mass regions and mass differences in Fig. 4 and also for a lower mass region in the ratio plots of Fig. 7 discussed in more detail in the section on ion–molecule reactions. For the highest masses studied the 129/132 ratio in xenon changes by less than 4% in a total of 12 μs. However, for krypton and CH_3CN the ratio of adjacent masses changes by this amount in about the same time. For a large ΔM, the 84/132 ratio in xenon–krypton mixtures, a change of 40% in the ratio is observed in 12 μs. However, in all cases the change during the first microsecond is quite small and we have found it possible to study ion–molecule reactions where the product and reactant ions differ considerably in mass by restricting the total delay time to less than 1 μs.

During operation for a period of months, the decay curves gradually deteriorated in that

the drop-off in intensity was considerably more rapid. This deterioration was presumably due to a buildup of nonconducting deposits on the electrodes. It was found that coating the surface of the ion source with colloidal graphite considerably improved the decay curves although gradual deterioration after this treatment has been observed.

MEASUREMENT OF ION RESIDENCE TIMES AND WITHDRAWAL TIMES

For the study of unimolecular fragmentation reactions the effective reaction time is the total elapsed time from initial formation of the reactant ion until it enters the main accelerating field. Any product ions formed after the reactant ion enters the accelerating field will not appear at the m/e of the product ion. Similarily a reactant ion which decomposes during acceleration, in the first drift region, or in the magnetic field will not be detected as a reactant ion nor as a product ion and, ideally, a correction should be applied to the reactant ion intensity to allow for this effect. However, calculations show that such a correction is small and lies within experimental error. To a good approximation with the present source we can take the average reaction time as the average time from formation of the ions until they reach the focus plate.

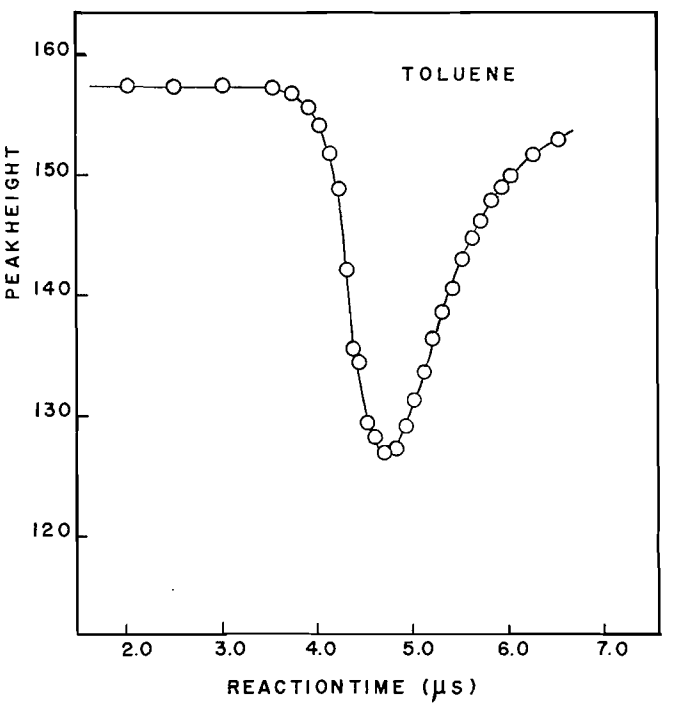

FIG. 5. Peak height vs. focus pulse delay, m/e = 92 toluene (1 μs ionizing pulse, 2 μs repeller pulse, 1 μs delay between pulses).

It was found that this time could be measured in the following manner. With the ion source operating in the pulsed mode a third pulse of short duration was applied to one-half of the focus plate. Ions passing the focus plate at the time the pulse is applied suffer a deflection and do not reach the collector causing a decrease in the recorded peak intensity. By varying the time between the ionizing and deflecting pulses a time profile of the ions passing the focus plate can be obtained. A typical deflection curve for m/e = 92 of toluene

Can. J. Chem. Downloaded from www.nrcresearchpress.com by 210.87.254.6 on 09/05/12
For personal use only.

is shown in Fig. 5. This curve was obtained with a 1 μs ionizing pulse and a delay of 1 μs between the ionizing and repelling pulses. The time scale represents the time between the center of the ionizing pulse and the deflecting pulse and we have taken the minimum in the curve as the average reaction time. The width of the curve is determined by the kinetic energy of the ions, the amplitude of the repeller pulse and the spatial distribution of the ions when the repeller pulse is applied. It was found that the time from application of the repeller pulse to the minimum in the deflection curve increased slightly with increasing delay time suggesting that the ion cloud was slowly drifting away from the exit slit during the field-free time. For accurate estimation of reaction time this necessitates experimental determination of the time for each repeller pulse delay setting.

The deflection brought about by the focus plate pulse, contrary to our original expectations, does not depend primarily on the pulse amplitude but rather on the rate of voltage change during the leading and trailing edge of the pulse. With the pulses used the rate of change is approximately 10^8 V s^{-1} and it appears probable that the deflection is caused by the magnetic field associated with this potential change.

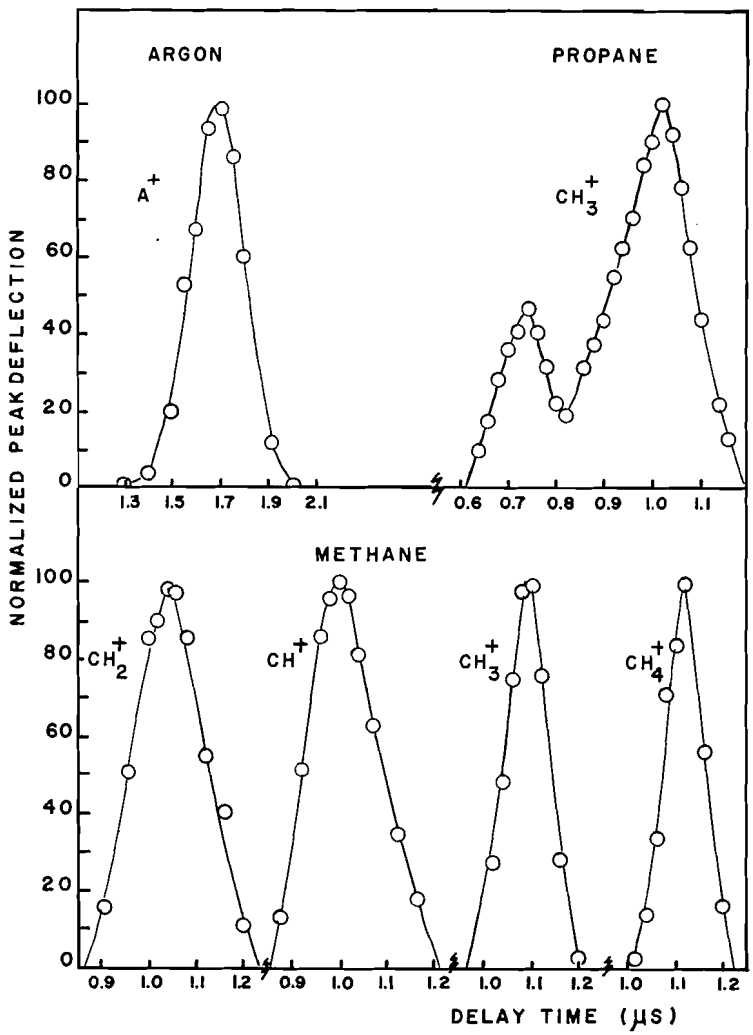

FIG. 6. Ion withdrawal curves.

Can. J. Chem. Downloaded from www.nrcresearchpress.com by 210.87.254.6 on 09/05/12
For personal use only.

The width of the curve in Fig. 5 is determined in part by the initial velocity distribution of the ions along the axis of ion withdrawal. This suggested that the technique might have application in the determination of initial ion kinetic energy and led us to make further studies of ion withdrawal times. Results obtained for the ions from methane, A^+, and CH_3^+ from propane are shown in Fig. 6 where the normalized peak deflection is plotted against the time between the ionizing and deflecting pulses. These results were obtained with an electron pulse of approximately 0.1 μs, a constant repeller voltage of 20 V and a deflecting pulse on the focus plate which was sufficiently broad that only the voltage change at the leading edge interacted with the ions. The CH_4^+ and CH_3^+ ions from CH_4 and the A^+ ions are thermal energy ions and the half-widths observed are therefore typical of such ions and indicates that the half-width increases with increasing mass. On the other hand, the CH_2^+ and CH^+ ions show a considerably larger half-width (0.17 μs compared to 0.10 μs for CH_4^+) which must be indicative of the higher initial kinetic energy of these ions. Using a rather similar technique, Taubert (13) has demonstrated that the CH_2^+ and CH^+ ions from methane do have an initial kinetic energy greater than thermal energy. The CH_3^+ ion from propane is of particular interest since it is well known (13, 14) that this ion consists of a thermal energy component in addition to a component of high initial kinetic energy. The withdrawal curve for CH_3^+ from propane shows two maxima, one at 1.02 μs which, by comparison with CH_3^+ from CH_4, corresponds to the thermal energy ion and a smaller maximum at shorter withdrawal times which must correspond to the high kinetic energy ions. This second maximum disappeared at 25–30 V electron energy consistent with a mechanism of formation from a doubly charged parent (14).

It is obvious from the foregoing that the width of the ion withdrawal curves can lead to at least qualitative information on initial ion kinetic energies. Further studies are in progress to determine whether quantitative estimates can be obtained by this method and to determine the sensitivity of the method.

ION–MOLECULE REACTIONS

The decay curves of Fig. 3 indicate that with the present ion source it is feasible to vary the ion residence time by varying the time delay between the ionizing and repelling pulses and that during this delay time the ions are in a relatively field-free region. Thus it should be possible to obtain the rates of bimolecular reactions of thermal energy ions using reaction time as the experimental variable. The total reaction time which can be used will depend on the magnitude of the discrimination between the product and reactant ion which will be determined by the decay curves for the two species.

For the general ion–molecule reaction

[2] $$P^+ + M \rightarrow S^+ + N$$

where P^+ and S^+ are the reactant and product ions respectively the integrated rate expression with time as the experimental variable becomes

[3] $$\log (1 + I_S/I_P) = k[M]t/2.303,$$

assuming the concentration of M to remain constant and assuming equal collection efficiencies for the product and reactant ion.

As a first study of ion–molecule reactions by the pulsing technique we have redetermined the rate constant for the hydrogen transfer reaction [4] in methane and have extended this work to the equivalent hydrogen and deuterium transfer reactions in the deuteriomethanes

[4] $$CH_4^+ + CH_4 \rightarrow CH_5^+ + CH_3.$$

Can. J. Chem. Downloaded from www.nrcresearchpress.com by 210.87.254.6 on 09/05/12
For personal use only.

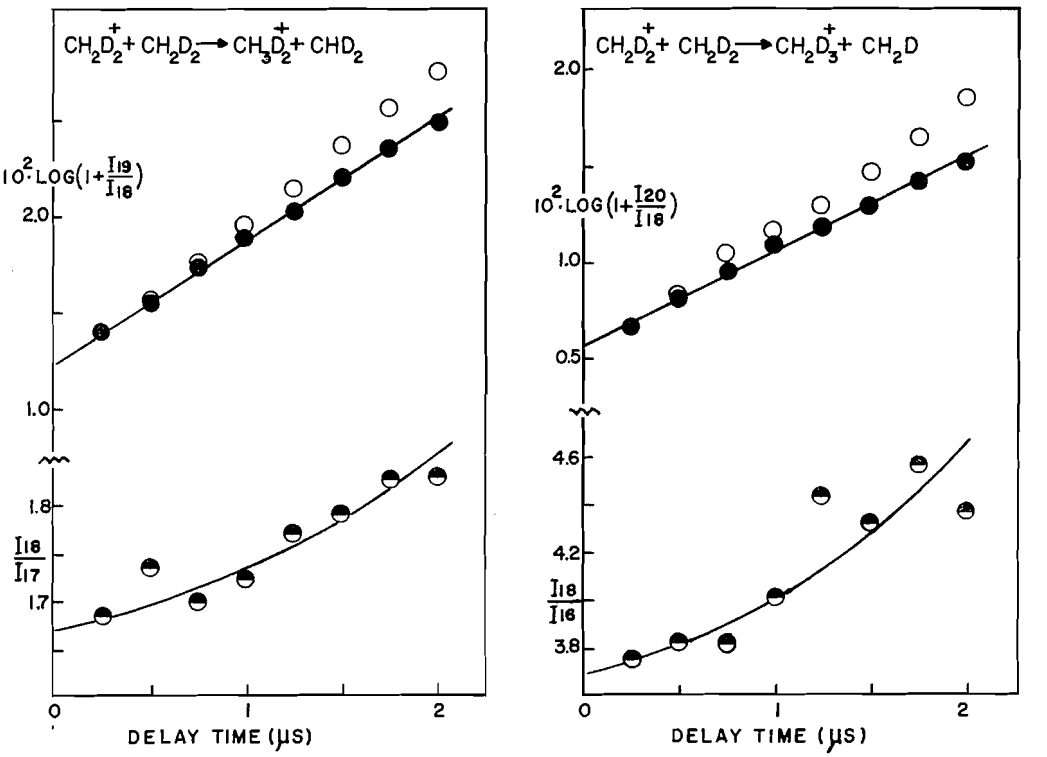

FIG. 7. Ion-molecule reactions in CH_2D_2; [M] = 5.70×10^{13} molecules cc^{-1}.

Typical plots of log $(1 + (I_S/I_P))$ versus delay time between the ionizing and repelling pulses are shown in Fig. 7 for the transfer of H and of D in CH_2D_2. The length of the ionizing pulse in this work was 0.2 μs and the electron energy was 50 V. The open circles are the log plot of the experimental I_S/I_P ratio as a function of the delay time. In general these plots showed an upward curvature which undoubtedly can be attributed to discrimination effects. The magnitude of these discrimination effects are indicated by the I_{18}/I_{17} and I_{18}/I_{16} ratios also plotted in Fig. 7. Since at the pressures used only a small fraction of the ions are reacting, we can use the change in these ratios to correct the observed I_S/I_P ratios. The log plot of the corrected data are shown by the solid points. The maximum correction amounted to about 8% for the H transfer and 17% for the D transfer. Although the corrected data in Fig. 7 possibly show a slight downward curvature which might be taken to indicate overcorrection, the points still define a reasonable straight line within experimental error and, further, such downward curvature was not observed in other cases indicating that the method of correction does not lead to serious error.

From the slopes of the corrected plots, which give k[M]/2.303, we have determined the rate constants summarized in Table I. The concentration of neutral molecules in the ion source was related to the pressure in the sample inlet system in the usual manner by total ionization measurement at 75 eV using continuous ionization. The sample inlet pressure was read by an Atlas Type MCT capacitance micromanometer, calibrated against a dibutylphthalate manometer, while the total ion current collected on the repeller was measured with a General Radio Type 1230-A d-c. Amplifier. Ionization cross sections for the methane and argon used were taken from Lampe *et al.* (15).

Can. J. Chem. Downloaded from www.nrcresearchpress.com by 210.87.254.6 on 09/05/12
For personal use only.

TABLE I
Hydrogen transfer reaction in methanes

Molecule	Rate constant $\times 10^{10}$ (cc molecule^{-1} s^{-1}) k (per H)	k (per D)	k (total)	$k_{CH_4} \times (\mu_H/\mu_D)^{1/2}$
CH_4	1.53		6.12	6.12
CH_3D	1.49	1.30	5.77	5.94
CH_2D_2	1.35	1.08	4.84	5.77
CHD_3	1.64	1.12	5.01	5.61
CD_4		1.18	4.71	5.46

Each rate constant reported is the average of at least three determinations. The overall rate constant for the reaction in methane is almost a factor of two lower than previous values of 11.6×10^{-10} and 11.0×10^{-10} cc molecule^{-1} s^{-1} obtained by Tal'roze and Frankevich (11) and Hand and von Weyssenhoff (12) respectively using similar techniques. The accuracy of the rate constant is dependent on the accuracy of the measurement of the source concentration and the delay times. A reasonable estimate of this error in both the present and previous work is 25%. Even allowing for this error the agreement is not good. It might be noted, however, that the previous workers have not made allowance for discrimination effects nor is it possible to estimate the magnitude of the discrimination from their published data. Further the results of Tal'roze and Frankevich were obtained at 370 °K compared to 315 °K in the present work and the discrepancy may indicate a small temperature coefficient. No temperature measurement was reported in the work of Hand and von Weyssenhoff. With the present instrument it is not possible to vary the temperature over a significant range. It might be noted that although absolute values of rate constants may have considerable error, relative values obtained on one instrument can be compared with greater confidence.

From columns 2 and 3 of Table I it is seen that the rate constant per H (k_H) and the rate constant per D (k_D) remain essentially constant through the series of methanes and lead to $k_H/k_D = 1.28$. Thus the total rate constant for H plus D transfer decreases with increasing deuterium substitution as shown in column 4. This decrease is considerably greater than that predicted by the effect of reduced mass on the number of collisions. This is shown by comparison of the observed total rate constants with the values calculated in column 5 by multiplying $k(CH_4)$ by the appropriate ratio of the reduced masses. We would suggest that this large effect of deuterium substitution may indicate that an appreciable fraction of the initial collision complex reverts to the reactant species (eq. [5]).

$$[5] \qquad CH_xD_y^+ + CH_xD_y \rightleftharpoons CH_xD_y \overset{+}{\ldots} CH_xD_y \begin{cases} \nearrow CH_{x+1}D_y^+ + CH_{x-1}D_y \\ \searrow CH_xD_{y+1}^+ + CH_xD_{y-1} \end{cases}.$$

With increasing deuterium substitution the transfer step in the collision complex is slowed down with the consequence that a larger fraction of the complex reverts to reactants. This implies an activation barrier in the transfer step and thus a possible temperature coefficient for the thermal rate constant. Further speculation does not appear to be justified from the limited data presently available.

While the results obtained for the methanes show that the pulsing technique can provide kinetic data for the bimolecular reactions of ions, they also serve to point out the problems encountered. As the results in Fig. 4 show, discrimination effects cause a significant

Can. J. Chem. Downloaded from www.nrcresearchpress.com by 210.87.254.6 on 09/05/12
For personal use only.

increase in the I_S/I_P ratio with increasing delay time. For greater percentage mass differences this discrimination effect will increase and, in the extreme cases, may completely mask the changes attributed to the occurrence of ion–molecule reactions.

The pulsing technique would appear to be ideally suited for the study of charge transfer reactions of the general type

[6] $$A^+ + B \rightarrow A + B^+.$$

In principle one should be able to observe increases in the ratio B^+/A^+ with increasing reaction time which can be attributed to the charge transfer reaction. However, B^+ will also be formed by the primary electron impact process and changes in the B^+/A^+ ratio may be anticipated due to discrimination effects. Thus to obtain quantitative data one must know accurately the decay curves for A^+ and B^+. In our experience these curves cannot be obtained in separate experiments since they are quite sensitive to minor changes in operating conditions. For those cases where a third ion, C^+, with a m/e near that of B^+, is formed by the primary impact process only, simultaneous observation of the C^+/A^+ ratio should permit correction of the B^+/A^+ ratio for discrimination effects.

UNIMOLECULAR ION FRAGMENTATIONS

As mentioned previously Wahrhaftig (6), using a time-of-flight mass spectrometer in which the time between ion formation and ion analysis could be varied, observed increases in the I_{27}/I_{29} ratio in propane with increasing reaction time which he attributed to the unimolecular fragmentation of the $C_2H_5^+$ ion (reaction [1]). In a brief study we did not observe increases in this ratio probably because of excessive discrimination. To minimize such effects we have chosen to study only those reactions which involve loss of H and, in addition, we have confined our attention to reactant ions of relatively high mass.

Increases in the $(\text{parent—H})^+/\text{parent}^+(R^+/RH^+)$ ratio with increasing delay time were observed for 1,4-cyclohexadiene, spiro[2.4]hepta-1,3-diene, and toluene. Typical results for these compounds at low electron energy are shown in Fig. 8 where the ratio $R^+/(R^+ + RH^+)$ is plotted versus the delay time between the ionizing and repelling pulses. At the electron energies used, only the R^+ and RH^+ ions are present in the spectrum and the ratio plotted therefore represents the fraction of the parent ion which has undergone fragmentation in the total time available. Reproducible increases of 5–10% in the ratio were observed over the range of reaction time studied. These increases cannot be due to discrimination since the lighter $(R)^+$ ion should be lost more rapidly nor can they be caused by bimolecular reactions since the extent of the change was independent of source pressure. Therefore we conclude that we are observing directly the unimolecular fragmentation of the parent molecule–ion.

[7] $$RH^+ \rightarrow (R)^+ + H.$$

As discussed previously the total time available for fragmentation, with the event still observable experimentally, corresponds to the time taken for the ion to reach the main accelerating field in the vicinity of plate 7. Therefore zero delay time between the ionizing and repelling pulses corresponds to a finite minimum reaction time. With a repeller pulse which optimized the observed ion current, this minimum reaction time was approximately 4 μs for $m/e = 92$ (toluene or spiroheptadiene). By an increase in the amplitude of the repeller pulse and a shortening of the ionizing pulse, this minimum reaction time could be reduced to approximately 2 μs. With a minimum reaction time of 2 μs any reaction with a half-life of 0.2 μs or less will be completed before the first observations can be made. It is apparent from the curves shown that the major fraction of the ions having sufficient energy to dissociate have done so before we are able to make observations and that the

Can. J. Chem. Downloaded from www.nrcresearchpress.com by 210.87.254.6 on 09/05/12
For personal use only.

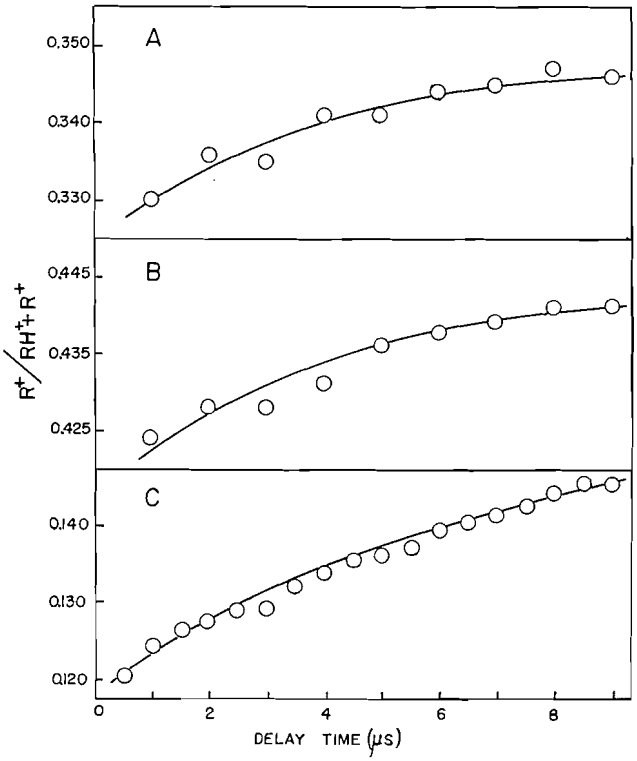

FIG. 8. Unimolecular fragmentation: (A) 1,4-cyclohexadiene 16.0 eV; (B) spiro[2.4]hepta-1,3-diene 14.0 eV; (C) toluene 13.0 eV. (All electron energies uncorrected.)

increases we are observing correspond to fragmentation of ions with a half-life of a few microseconds. Quantitative interpretation of the results is made difficult by the fact that a large and unknown fraction of the parent ions have not received sufficient energy to fragment. A more detailed study of the reaction in toluene and deuteriated toluenes will be presented elsewhere.

A considerable improvement in the minimum reaction time could be achieved by decreasing the distance from the electron beam to the exit slit. However, such a change is incompatible with the study of ion–molecule reactions where longer reaction times are required. In the time scale of unimolecular ion fragmentations, the present technique appears suitable only for those reactions which are slow. For the faster reactions the approach suggested recently by Tal'roze (16) appears more promising.

ACKNOWLEDGMENTS

The authors are indebted to the National Research Council of Canada and to the Alfred P. Sloan Foundation for financial support. Part of this work was carried out while one of the authors (T. W. S.) was the recipient of a C.I.L. Graduate Fellowship.

APPENDIX

Calculation of Decay Curves[3]

Essentially, the problem is to calculate the number of ions remaining in the volume sampled by the analyzing system at time τ, having initially produced ions in a volume

[3]*We are indebted to Professor J. P. Valleau for his assistance in formulating this problem.*

Can. J. Chem. Downloaded from www.nrcresearchpress.com by 210.87.254.6 on 09/05/12
For personal use only.

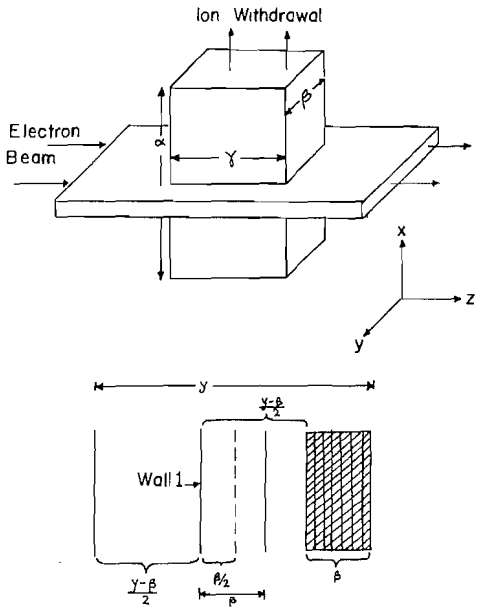

FIG. 9. (*a*) Ion formation and sampling zones. (*b*) Cross section of zones along *y*-axis.

defined by the electron beam where this initial volume intersects the sampling volume symmetrically (Fig. 9*a*). We assume free molecular flow with a temperature T.

The dimensions of the box representing the volume of initial ion formation we can take to be the dimensions of the electron beam entrance slit plus the length of the ionizing region, i.e. $x = 0.05$ cm, $y = 0.30$ cm, $z = 1.80$ cm. For the box representing the volume sampled by the analyzing system we have taken the dimension along the axis of ion withdrawal, α, to be 0.954 cm, the distance from repeller to exit slit, the dimension, γ, along the long axis of the exit slit to be 1.0 cm, the length of the exit slit, and the dimension, β, along the short axis of the exit slit to be twice the slit width or 0.152 cm. This dimension is rather arbitrary since the ions follow a curved trajectory out of the source. However, the resulting decay curves were not strongly dependent on the value chosen for β.

With the dimensions chosen $x < \alpha$, $y > \beta$, and $z > \gamma$, we have the result that ions will be lost from the sampling region by three processes:

(*a*) Loss across the plane at $-\alpha/2$. All ions travelling in $+\alpha$ direction will be collectable.

(*b*) Deficit in flow across plane at $\pm\beta/2$.

(*c*) Deficit in flow across plane at $\pm\gamma/2$.

The number of ions which survive will be given by $N_t = N_o F_a F_b F_c$ where F_i represents the fraction of ions surviving process i.

F_a

We need consider only the velocity component, u, in the $-x$ direction. All ions with $|u| > (x + \alpha)/2\tau = u_n$ will be lost while all ions with $|u| < (\alpha - x)/2\tau = u_m$ will survive. For ions where $u_m < |u| < u_n$, ions initially in a slab of thickness $((\alpha + x)/2) - u\tau$ will survive or a fraction $((\alpha + x)/2x) - (u\tau/x)$ will survive.

F_a is thus given by the equation:

$$F_a = \frac{1}{2} + \int_0^{u_m} f(u)\,du + \int_{u_m}^{u_n} \left(\frac{(\alpha + x)}{2x} - \frac{u\tau}{x}\right) f(u)\,du,$$

Can. J. Chem. Downloaded from www.nrcresearchpress.com by 210.87.254.6 on 09/05/12
For personal use only.

where $f(u)$ is the one-dimensional Maxwell distribution, $f(u)\,du = \pi^{-1/2}\exp(-y^2)\,dy$, $y = (M/2RT)^{1/2}u$.

Integration leads to the final expression:

$$F_a = 1/2 + 1/2[\operatorname{erf}(\sqrt{2}u_m') + \operatorname{erf}(\sqrt{2}u_n') + (\alpha/x)[\operatorname{erf}(\sqrt{2}u_n') - \operatorname{erf}(\sqrt{2}u_n')] - (2RT/\pi M)^{1/2}\tau/x[\exp(-u_m'^2) - \exp(-u_n'^2)]],$$

where $u_m' = (M/2RT)^{1/2}(\alpha - x)/2\tau$, $u_n' = (M/2RT)^{1/2}(\alpha + x)/2\tau$,

and $\operatorname{erf}(t) = \dfrac{1}{\sqrt{2}\pi^{1/2}}\displaystyle\int_0^t e^{-x^2/2}\,dx.$

F_b

The problem in this case is to calculate the net flow out of the region of length β (Fig. 9*b*), having initially produced ions in the total length y. The flow inwards across wall 1 (Fig. 9*b*) will be exactly balanced, by symmetry, by the outward flow of ions from a region of thickness $(y - \beta)/2$ to the right of the wall. The *net* flow across the wall will therefore be that arising from the region of length β, shaded in the diagram. The problem therefore is to calculate the fraction of ions in the length β which do not cross the wall in the time τ.

All ions with velocities $v_n > (y + \beta)/2\tau$ will cross wall 1 while all ions with velocities $v_m < (y - \beta)2\tau$ will be retained. For ions with velocities intermediate between v_n and v_m those in the segment of length $((y + \beta)/2) - v\tau$ will survive or a fraction $((y + \beta)/2\beta) - (v\tau/\beta)$ will survive. The formulation is thus similar to the calculation of F_a and the solution in terms of the reduced velocities

$$v_m' = (M/2RT)^{1/2}(y - \beta)/2\tau \text{ and } v_n' = (M/2RT)^{1/2}(y + \beta)/2\tau$$

becomes

$$F_b = \operatorname{erf}(\sqrt{2}v_m') + \operatorname{erf}(\sqrt{2}v_n') + (y/\beta)[\operatorname{erf}(\sqrt{2}v_n') - \operatorname{erf}(\sqrt{2}v_m')] - (2RT/\pi M)^{1/2}(\tau/\beta)[\exp(-v_m'^2) - \exp(-v_n'^2)].$$

F_c

The calculation for F_c is identical to that for F_b and leads in terms of the reduced velocities

$$w_m' = (M/2RT)^{1/2}(z - \gamma)/2\tau \quad \text{and} \quad w_n' = (M/2RT)^{1/2}(y + \gamma)/2\tau$$

to

$$F_c = \operatorname{erf}(\sqrt{2}w_n') + \operatorname{erf}(\sqrt{2}w_m') + (z/\gamma)[\operatorname{erf}(\sqrt{2}w_n') - \operatorname{erf}(\sqrt{2}w_m')] - (2RT/\pi M)^{1/2}(\tau/\gamma)[\exp(-w_m'^2) - \exp(-w_n'^2)].$$

REFERENCES

1. H. M. Rosenstock, M. B. Wallenstein, A. L. Wahrhaftig, and H. Eyring. Proc. Natl. Acad. Sci. U.S. **38**, 667 (1952). H. M. Rosenstock and M. Krauss. Mass spectrometry of organic ions. Academic Press, New York. 1963. Chap. 1.
2. J. Momigny. Bull. Soc. Chim. Belges, **70**, 291 (1961).
3. N. D. Coggeshall. J. Chem. Phys. **37**, 2167 (1962).
4. G. A. Muccini, W. H. Hamill, and R. Barker. J. Phys. Chem. **68**, 261 (1964).
5. J. C. Schug. J. Chem. Phys. **40**, 1283 (1964).
6. A. L. Wahrhaftig. *In* Advances in mass spectrometry. Pergamon Press, London. 1959. p. 274.
7. C. E. Melton. Mass spectrometry of organic ions. Academic Press, New York. 1963. Chap. 2.
8. D. P. Stevenson. Mass spectrometry. McGraw-Hill, New York. 1963. Chap. 13.
9. F. W. Lampe, J. L. Franklin, and F. H. Field. Progress in reaction kinetics. Vol. 1. Pergamon Press, London. 1961. Chap. 3.
10. P. F. Knewstubb. Mass spectrometry of organic ions. Academic Press, New York. 1963. Chap. 6.
11. V. L. Tal'roze and E. L. Frankevich. Russ. J. Phys. Chem. English Transl. **34**, 1275 (1960).
12. C. W. Hand and H. von Weyssenhoff. Can. J. Chem. **42**, 195 (1964).

Can. J. Chem. Downloaded from www.nrcresearchpress.com by 210.87.254.6 on 09/05/12
For personal use only.

13. R. TAUBERT. *In* Advances in mass spectrometry. Pergamon Press, London. 1959. p. 489. R. FUCHS and R. TAUBERT. Z. Naturforsch. **19a**, 494 (1964).
14. F. L. MOHLER, V. H. DIBELER, and R. M. REESE. J. Chem. Phys. **22**, 394 (1954). H. E. STANTON. J. Chem. Phys. **30**, 1116 (1959). T. TSUCHIYA. J. Chem. Phys. **36**, 568 (1962). J. OLMSTEAD, K. STREET, and A. S. NEWTON. J. Chem. Phys. **40**, 2114 (1964).
15. F. W. LAMPE, J. L. FRANKLIN, and F. H. FIELD. J. Am. Chem. Soc. **79**, 6129 (1957).
16. C. V. KARACHEVTEV and V. L. TAL'ROZE. Kinetika i Kataliz, **4**, 923 (1963).

Can. J. Chem. Downloaded from www.nrcresearchpress.com by 210.87.254.6 on 09/05/12
For personal use only.

Can. J. Chem. Downloaded from www.nrcresearchpress.com by 210.87.254.105 on 09/05/12
For personal use only.

EVIDENCE FOR $ZnF_2.2H_2O$

DEHYDRATION AND X-RAY DIFFRACTION STUDIES

E. A. Secco and Ronald R. Martin

Chemistry Department, Saint Francis Xavier University, Antigonish, Nova Scotia

Received July 22, 1964

ABSTRACT

Evidence for a dihydrate of zinc fluoride $ZnF_2.2H_2O$ from dehydration studies is reported. The structural changes accompanying the decomposition of the hydrate were followed by X-ray diffraction. The heating of the dihydrate in air was found to yield as residues (*a*) mixture of ZnF_2 and its hemihydrate, (*b*) mixture of ZnF_2 and ZnO, (*c*) the hemihydrate, and (*d*) ZnO.

INTRODUCTION

Our interest in the dehydration of zinc fluoride hydrate has been aroused by the acquisition of zinc fluoride, C.P. grade, from two independent suppliers.* These fluorides gave diffraction patterns distinct from those patterns for ZnF_2 and $ZnF_2.4H_2O$ as recorded in the ASTM file index. Our observed diffractions did show many peaks common to the reported tetrahydrate pattern and infrared spectra confirmed the presence of water. Furthermore, repeated efforts to obtain the pure anhydrous fluoride by heating in air at 100 °C as reported (1, 2, 3) and accepted as routine procedure have failed. In a literature survey on the dehydration of the tetrahydrate we were able to uncover only the early work reported in the Mellor treatise. It was desirable therefore to follow up the dehydration reactions of this unidentified zinc fluoride hydrate and to reconcile the obvious disparity between our observations and the reported data in the literature.

EXPERIMENTAL

Each fluoride sample† used for dehydration studies was placed in an aluminium weighing dish or pyrex weighing bottle, weighed, heated at the appropriate temperature for a given time interval, cooled in a dessicator containing P_2O_5, reweighed, and its resulting weight loss determined. In the reverse reaction, i.e., hydration, the product from dehydration was placed in a dessicator, without dessicant, containing distilled water at room temperature and the weight increase was measured as a function of time.

The method of preparation of the hydrate powder for the X-ray diffractometer and the procedure for recording its diffractogram after annealing have already been described (4).

The infrared spectra of the powder were obtained by using the standard KCl disc technique in a Beckman IR.8 spectrophotometer.

RESULTS

For comparison purposes the *d*-spacings corresponding to the observed peaks on the diffractograms and their relative intensities obtained with the untreated fluoride hydrate as received from the suppliers are given in Table I with those of $ZnF_2.4H_2O$.

The infrared absorption spectrum of the untreated fluoride hydrate, Fig. 1 shows the presence of the characteristic water bands in addition to bands observed with the monohydrate of HF (5) and aqueous solutions of HF (6) at −195 °C. These bands are also present in the spectrum of the residue from 20% weight loss but with their intensities reduced.

**A. D. MacKay, Inc., 198 Broadway, New York 38, N.Y. This hydrate is made by slurring zinc oxide and treating with aqueous hydrofluoride acid. City Chemical Corporation, New York, Lot G-212.*

†MacKay hydrate was used as the main source of our studies; City Chemical was used only to check what may have been judged as an anomalous result.

Can. J. Chem. Downloaded from www.nrcresearchpress.com by 210.87.254.105 on 09/05/12
For personal use only.

TABLE I

A. D. MacKay			City Chemical			ASTM index	
2θ	d	I/I_0	2θ	d	I/I_0	d	I/I_0
18.2	4.89	95	18.3	4.88	100	4.91	100
—	—	—	19.0	4.67	65	—	—
20.9	4.24	100	20.8	4.26	90	4.30	4
—	—	—	21.5	4.12	25	4.13	50
21.8	4.07	40	21.8	4.07	30	—	—
—	—	—	22.5	3.93	7	—	—
23.6	3.76	15	23.7	3.75	3	3.79	3
25.0	3.55	12	25.3	3.51	22	3.61	1
25.9	3.43	12	25.8	3.44	10	—	—
27.0	3.30	12	27.1	3.29	15	—	—
—	—	—	27.8	3.21	15	—	—
28.4	3.13	50	28.4	3.13	20	3.16	25
—	—	—	29.6	3.02	25	3.05	3
30.0	2.97	35	20.0	2.97	50	2.99	37
32.6	2.75	50	32.6	2.75	45	2.77	13
33.8	2.65	35	33.8	2.65	35	—	—
34.6	2.59	12	34.7	2.59	20	—	—
35.4	2.54	40	—	—	—	2.55	4
35.7	2.51	95	35.7	2.51	80	—	—
36.7	2.45	15	36.7	2.45	15	2.43	1
—	—	—	38.3	2.35	5	—	—
39.0	2.31	25	39.0	2.31	20	2.32	4
40.4	2.23	25	40.4	2.23	25	2.23	8
41.3	2.18	15	41.3	2.18	15	2.17	13
41.9	2.15	20	42.0	2.15	25	—	—
42.5	2.13	10	42.5	2.13	15	—	—
44.0	2.06	15	44.0	2.06	5	—	—
44.8	2.02	18	44.8	2.02	25	2.03	10
46.6	1.95	18	46.6	1.95	15	1.95	8
49.3	1.85	15	49.0	1.86	10	1.89	4
—	—	—	49.5	1.84	10	—	—
50.8	1.80	15	50.7	1.80	12	1.79	8
51.3	1.78	20	—	—	—	—	—
51.9	1.76	50	51.9	1.76	45	1.76	15
53.0	1.73	20	53.0	1.73	20	—	—
—	—	—	—	—	—	1.70	1
55.0	1.67	10	—	—	—	1.66	3
55.5	1.65	10	55.0	1.65	18	—	—
56.0	1.64	15	56.0	1.64	12	—	—
57.3	1.61	30	57.5	1.60	25	1.62	4
59.4	1.55	18	59.5	1.55	20	1.56	1
—	—	—	60.2	1.53	10	—	—
—	—	—	61.8	1.50	10	1.50	3
62.3	1.48	20	62.5	1.48	18	1.47	4
63.7	1.46	18	63.5	1.46	10	—	—
65.4	1.42	10	—	—	—	—	—
67.5	1.39	10	67.5	1.39	8	1.38	3
—	—	—	68.3	1.37	20	—	—
69.3	1.35	15	69.5	1.35	10	—	—

Table II gives the weight loss data expressed in percentage of the original sample weight at different temperatures for uncrushed and crushed samples. Fig. 2 gives the average weight loss as a function of time for three crushed samples.

Heating the crushed powder on the specimen stage of the high-temperature gonimeter for 10 min at 120 °C or in an oven at 150 °C i.e., corresponding to weight loss of 20.0 ± 0.6%, produced a diffractogram given in Fig. 3. This diffractogram remained unchanged when heated in air in the gonimeter up to 250 °C, but above 250 °C the characteristic pattern of zinc oxide was obtained. The product corresponding to Fig. 3 when left in an ambient of water vapor overnight regained the peaks observed in the original diffractograms, but with slightly lower intensities.

Can. J. Chem. Downloaded from www.nrcresearchpress.com by 210.87.254.105 on 09/05/12
For personal use only.

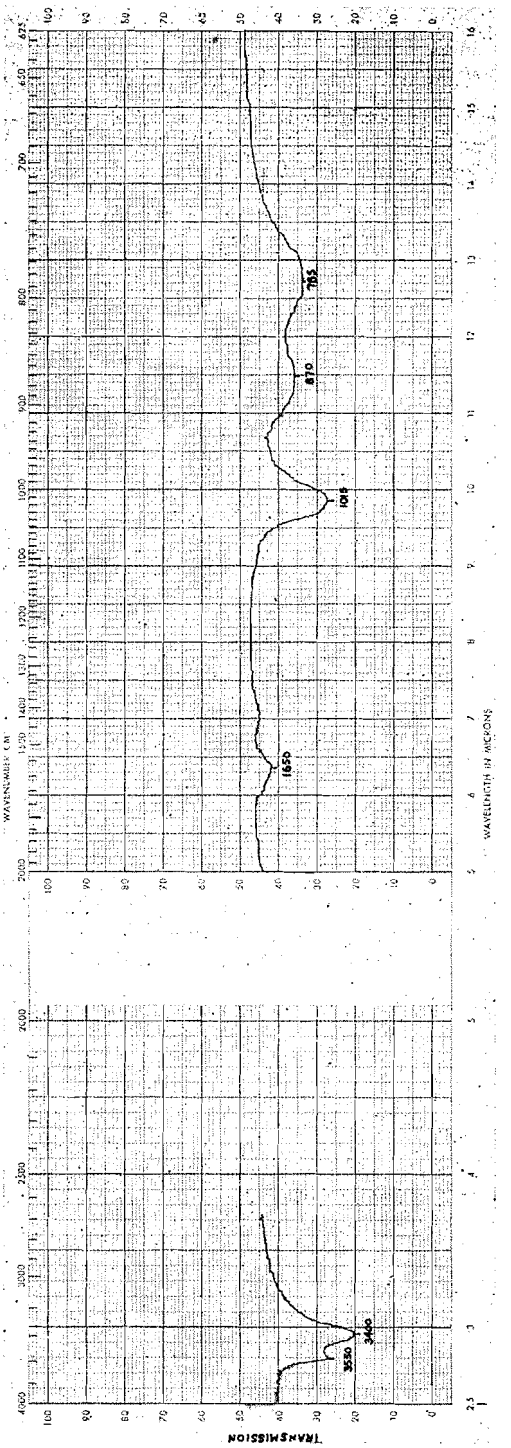

FIG. 1. Infrared spectrum of the untreated fluoride hydrate.

TABLE II

Uncrushed				Crushed			
Run	T (°C)	Time (h)	% wt. loss	Run	T (°C)	Time (h)	% wt. loss
1–6	150	3	20.4±0.6	19	250	1	26.0
7–10	150	ca. 15	20.8±0.5	20–22	250	3	29.9±0.3
11–13	250	3	20.2±0.5	23–25	250	3	25.9±0.4
14	230	1	21.4	26–27	100	40 min	21.0±0.2
15	350	1	25.5				
	500	1	29.3				
16–18	250	3	29.8±0.8				

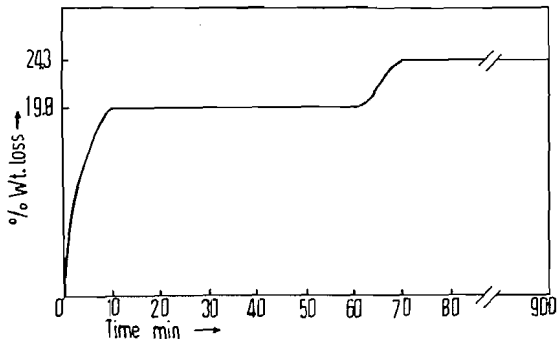

FIG. 2. Average weight loss as a function of time for three crushed samples.

The product of dehydration corresponding to ca. 26% weight loss gave a diffractogram consisting of a mixture predominant in anhydrous zinc fluoride along with evidence of zinc oxide. The product from ca. 30% weight loss gave a similar diffractogram but with stronger oxide peak intensities. On the other hand, the product from less than 26% weight loss showed a diffractogram consisting of a mixture of Fig. 3 and anhydrous zinc fluoride.

TABLE III

Run	T (°C)	Time (h)	% wt. loss	Time (h)	% wt. loss	Time (h)	% wt. gain	Time (h)	% wt. gain
28	150	2	19.4	24	93.0	72	100.2	120	102.0
29	150	2	19.8	24	91.8	72	100.1	120	101.8
30	150	2	19.7	24	92.6	72	100.1	120	101.7

Table III shows the weight losses of three samples in percentage of total water of a dihydrate along with the weight increases for those residues in an ambient of saturated water vapor. The extra weight increase, i.e., above the original, was believed due to condensation on the powder or weighing dish. These samples lost weight on exposure to the atmosphere.

Untreated fluoride was allowed to stand in distilled water at room temperature overnight with the object of preparing the reported tetrahydrate. The insoluble fluoride was filtered on No. 1 filter paper (Whatman) and allowed to dry in air for 24 h. The product gave the diffractogram in Fig. 4 and a weight loss of 20.7% was observed on heating. Another sample left in distilled water overnight, filtered, and allowed to dry in air for 1 week produced the diffractogram of Fig. 5.

Can. J. Chem. Downloaded from www.nrcresearchpress.com by 210.87.254.105 on 09/05/12
For personal use only.

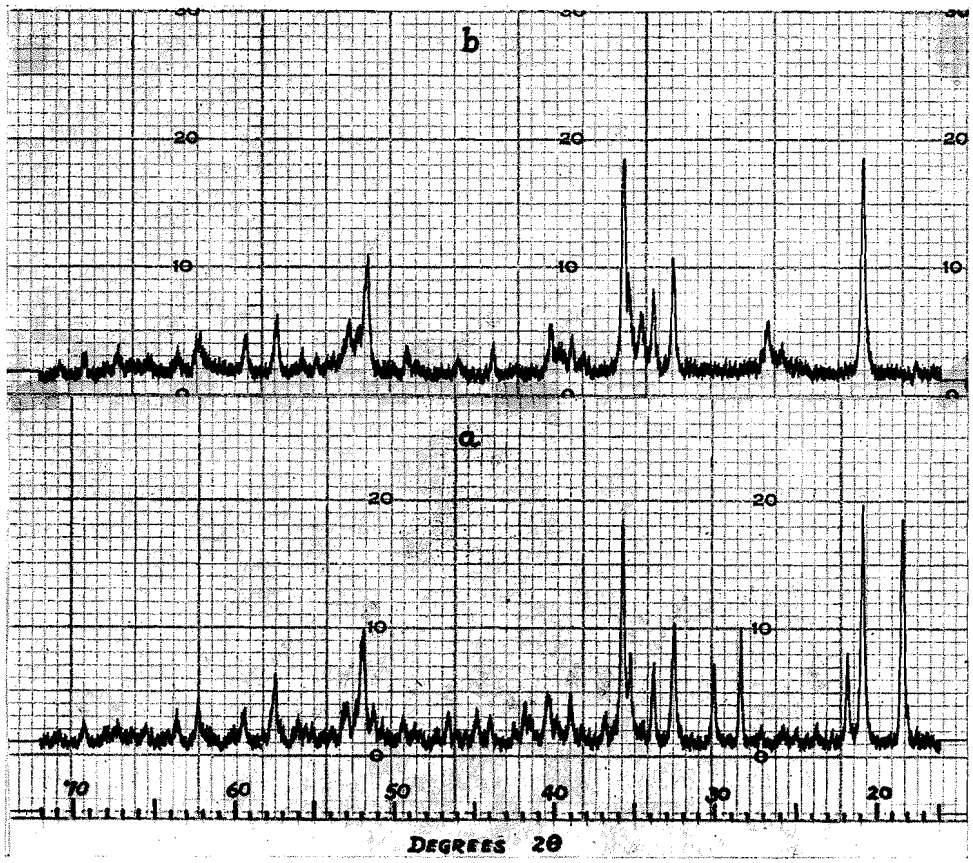

FIG. 3. Diffractograms (*a*) of untreated fluoride hydrate, for comparison purposes, and (*b*) of product after heating for 10 min at 150 °C with 20% weight loss.

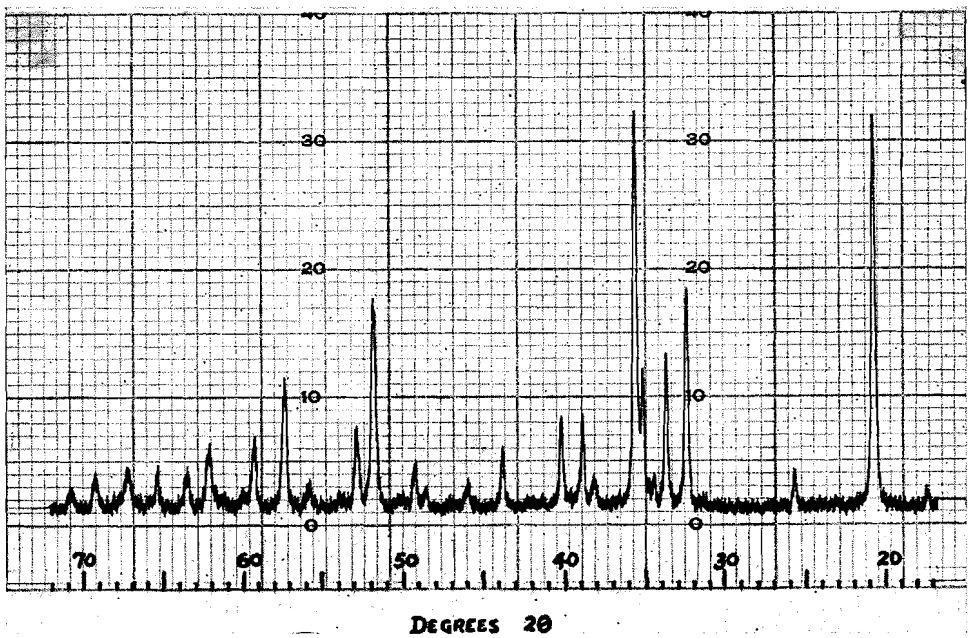

FIG. 4. Diffractogram of the untreated fluoride hydrate allowed to stand in distilled water for 18 h at room temperature, filtered, and dried in air for 24 h.

Can. J. Chem. Downloaded from www.nrcresearchpress.com by 210.87.254.105 on 09/05/12
For personal use only.

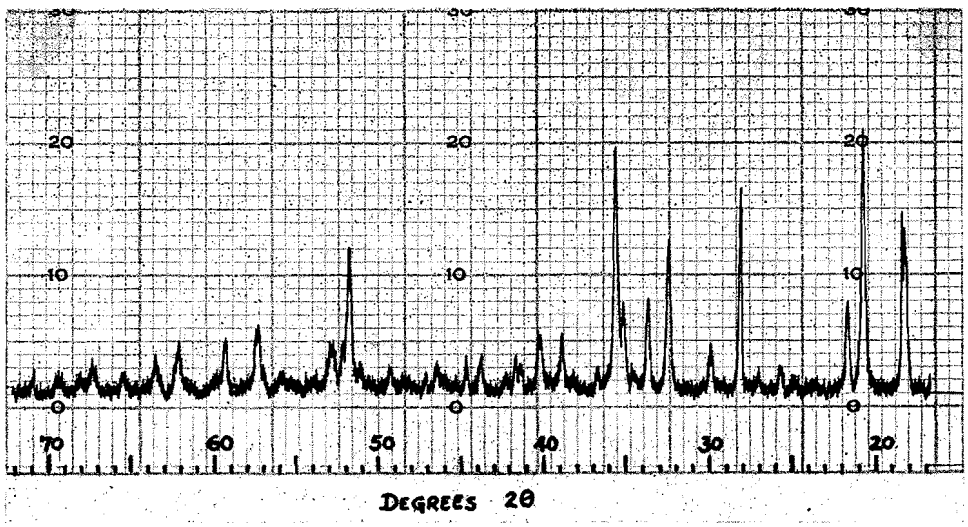

FIG. 5. Diffractogram of the untreated fluoride hydrate allowed to stand in distilled water at room temperature overnight and dried in air for 1 week.

DISCUSSION

It is not possible on the evidence available to elucidate completely the process of dehydration of the zinc fluoride hydrate. The dehydration of the hydrate will be discussed, however, in the light of the major points of our results.

The first important point is the variation in weight loss percentages from 100 °C to 500 °C. Since the residue from ca. 26% dehydration consists mainly of anhydrous zinc fluoride, this suggests the original compound to be a dihydrate, $ZnF_2.2H_2O$, i.e.,

$$ZnF_2.2H_2O \rightarrow ZnF_2 + 2H_2O.$$

For weight losses greater than 26%, the residue contained some zinc oxide which resulted from the reaction between the fluoride and water (1, 7). The extent of oxidation was not constant and presumably is a function of particle size, rate of heating, and humidity of the air. The oxidation reaction can conceivably go to completion under proper conditions (7). In the event of complete oxidation of the dihydrate, i.e.,

$$ZnF_2.2H_2O \rightarrow ZnO + 2HF + H_2O,$$

the stoichiometric weight loss is 41.6%, which is fortuitously identical to the value expected for the dehydration of zinc fluoride tetrahydrate.

The dehydration of 20% suggests an intermediate or lower hydrate of zinc fluoride, most probably a hemihydrate, i.e.,

$$ZnF_2.2H_2O \rightarrow ZnF_2.\tfrac{1}{2}H_2O + \tfrac{3}{2}H_2O.$$

The postulated hemihydrate is stable to 250 °C up to 3 h and its diffraction pattern is that given in Figs. 3 and 4. Mikhailov (7) has postulated an intermediate Zn(OH)F from oxidation studies. Our intermediate cannot be Zn(OH)F from two arguments. Firstly, the return of the intermediate to the original hydrate in an ambient of water vapor is not expected to be possible with Zn(OH)F. Secondly, our value of 20% weight loss is too low compared to 27.2% demanded for Zn(OH)F.

The 20.7% weight loss determined for the product after ageing in distilled water and

Can. J. Chem. Downloaded from www.nrcresearchpress.com by 210.87.254.105 on 09/05/12
For personal use only.

the diffractogram of Figs. 4 and 5 indicate that ageing promoted growth of preferred crystallographic faces of the dihydrate.

The X-ray diffractograms and thermogravimetric data were reproduced by treating anhydrous ZnF_2 in water. However, the infrared spectrum did not show the additional bands of the HF hydrate indicating that a trace of excess HF must have been present in the supplier's hydrate.

The heating of zinc fluoride dihydrate in air has yielded as residues (*a*) mixture of zinc fluoride and its hemihydrate, (*b*) mixture of zinc fluoride and zinc oxide, (*c*) the hemihydrate, and (*d*) zinc oxide. It was practically impossible to obtain pure anhydrous zinc fluoride by heating zinc fluoride hydrate in air up to 500 °C. The kinetics of the dehydration reaction in N_2 or vacuum and of hydration in controlled ambients of water vapor is planned as the subject of a future study.

REFERENCES

1. J. W. MELLOR. A comprehensive treatise on inorganic and theoretical chemistry. Vol. IV. Longmans Green and Co. 1923. p. 533.
2. N. SIDGWICK. Chemical elements and their compounds. Vol. I. Oxford. 1950. p. 271.
3. HANDBOOK OF CHEMISTRY AND PHYSICS. 44th ed. Chemical Rubber Publishing Company.
4. E. A. SECCO. Can. J. Chem. **42**, 2143 (1964).
5. C. C. FERRISO and D. F. HORNIG. J. Chem. Phys. **23**, 1464 (1955).
6. P. A. GIGUÈRE. Private communication.
7. M. A. MIKHAILOV. Chem. Abstr. **56**, 5615*g* (1962); Trudy Tomsk. Gosudarst. Univ. im. V. V. Kuibysheva, Ser. Khim., 5-ya Nauch. Konf. No. 145, 11–24 (1954).

Can. J. Chem. Downloaded from www.nrcresearchpress.com by 210.87.254.105 on 09/05/12
For personal use only.

Can. J. Chem. Downloaded from www.nrcresearchpress.com by 210.87.254.6 on 09/05/12
For personal use only.

SOME ANOMALOUS CARBONYL STRETCHING FREQUENCIES IN STEROID INFRARED SPECTRA[1]

R. NORMAN JONES AND J. B. DIGIORGIO[2]
Division of Pure Chemistry, National Research Council, Ottawa, Canada
Received June 22, 1964

ABSTRACT

Abnormal C=O and C=C stretching frequencies in the infrared spectra of Δ^4-3-ketosteroids containing a 19,8-lactone bridge are discussed in relation to possible conformational structures. The C=O stretching frequencies of 1,11,17-triketo-5β-steroids and Δ^2-1,11,17-triketo-5β-steroids are reported. It is noted that the anomalous C=O stretching band position previously recorded for the 11-ketone in 11,17-diketosteroids is also observed in these triketones, but no additional perturbation results from the introduction of the 1-ketone group, in spite of its proximity to the carbonyl at C_{11}.

The C=O stretching frequencies in the infrared spectra of ketosteroids and steroid esters in carbon disulfide, carbon tetrachloride, and chloroform solutions have been used extensively to characterize the type of carbonyl function. The spectra–structure correlations were summarized in 1954 (1) and again in 1958 (2). Subsequent investigations have confirmed the general applicability of these correlations to a wide range of steroids and derivatives.

This paper deals with a few recently examined cases in which the infrared carbonyl frequencies exhibit unusual features. These involve the 19:8-bridged lactone structure I and the triketones II and III. The spectra of Δ^4-3-ketosteroids containing the 8:19-epoxide bridge (IV), the 19:8-hemiacetal group (V), and the 19-methoxy-8:19-epoxide bridge (VI) will also be discussed.

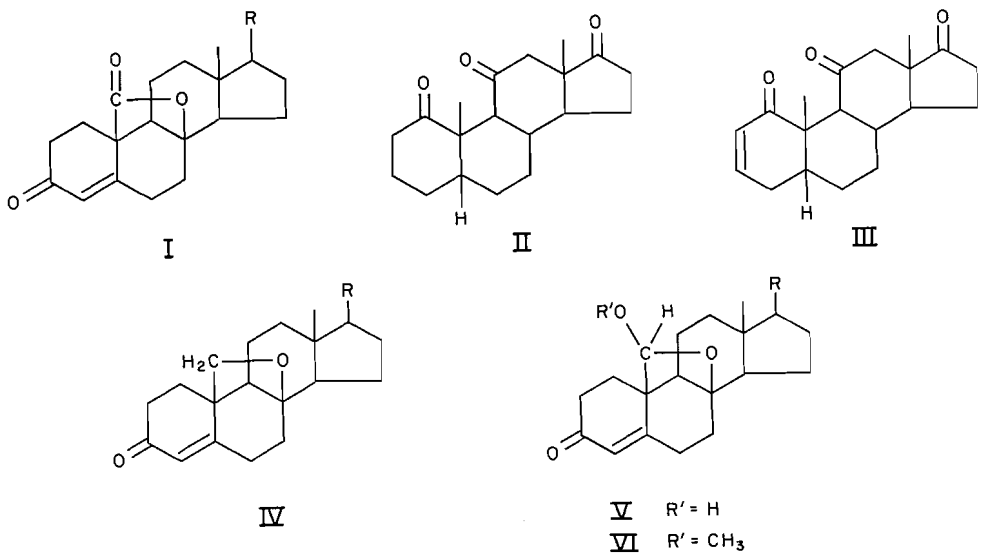

[1]*Issued as N.R.C. No. 8142.*
[2]*National Institutes of Health Research Fellow (1961–1962). National Research Council of Canada Postdoctoral Fellow (1962–1963).*

Δ^4-3-Ketosteroids Containing 8:19-Bridges

Several Δ^4-3-ketosteroids containing the 8:19-bridges I, IV–VI have been synthesized by Ehrenstein *et al.* (3–7). The positions of $\nu_{C=O}$ and $\nu_{C=C}$ for the Δ^4-3-ketone system in the infrared spectra are summarized in Table I. The values for the individual compounds

TABLE I

Summary of infrared spectral data and optical rotatory dispersion data for 8:19-bridged Δ^4-3-ketosteroids

Structure	$\nu_{C=O}$(cm^{-1})	$\nu_{C=C}$(cm^{-1})	Solvent	O.r.d.
Unbridged (2)	1 681 – 1 677	—	CS_2	(+)
	1 668 – 1 660	1 619 – 1 613	$CHCl_3$	
I (3)	1 686	—	CCl_4	(+)*
	1 680 – 1 675	1 635	$CHCl_3$	
IV (4)	1 675	—	CS_2	(−)*
	1 664	1 620	Nujol mull	
V (5, 7)	1 665 – 1 659	1 623 – 1 622	$CHCl_3$	
VI (5, 7)	1 665	1 623 – 1 621	$CHCl_3$	(−)†

*Solvent: dioxane.
†Solvent: methanol.

have already been published (3–6). The spectra were measured on Perkin–Elmer Model 21 and Model 421 spectrophotometers with wavenumber scales calibrated with indene (8, 9) and are accurate to ± 1 cm^{-1}. The significant feature of Table I is the displacement of the C=O and C=C stretching bands by +14 and +19 cm^{-1} in chloroform solution on introduction of the lactone bridge. The spectra of I (R(β) = CO—CH_2OH) and V (R(β) = CO—CH_2OH) are compared in Fig. 1. The displacement on introduction of the epoxide or hemiacetal bridges, in contrast to that of the lactone bridge, is barely significant. These

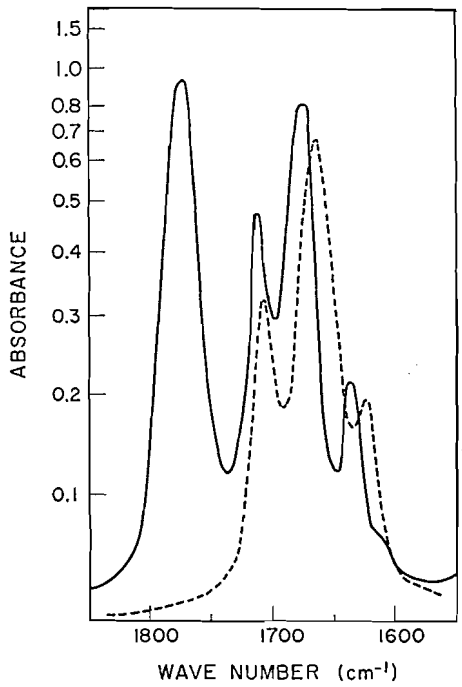

FIG. 1. Infrared spectra in chloroform solution. Concentration ~ 0.12 *M*; path length 0.1 mm; solid line, spectra of I (R(β) = CO—CH_2OH); dashed line, spectra of V (R(β) = CO—CH_2OH).

Can. J. Chem. Downloaded from www.nrcresearchpress.com by 210.87.254.6 on 09/05/12
For personal use only.

results acquire additional interest when compared with the optical rotatory dispersion (o.r.d.) curves. Djerassi has shown that the K-band Cotton effect curve for the lactone I ($R(\alpha) = COOCH_3$, and $R(\beta) = COOH$) resembles that of the unbridged Δ^4-3-ketone (3), whereas the 8:19-bridges of IV ($R(\beta) = COOH$) (4) and VI ($R(\beta) = COOCH_3$) (7) induce an inversion in the sign of the K-band Cotton effect curves. We therefore have the curious result that the type of bridge closure that induces an anomalous infrared spectrum does not perturb the o.r.d. and vice versa.

The C=C—C=O system in ring A in Δ^4-3-ketosteroids is not coplanar, and the sign of the K-band Cotton effect curve has been shown by Djerassi *et al.* (10) and by Whalley (11) to depend on the chirality of the conjugated system. The chirality is determined by the angle θ between the C_2—C_3 bond and the C=C bond. We have measured θ in Dreiding models for a variety of limiting conformations (Table II). In these measurements, the conjugated system is viewed along the axis of the C_3—C_4 bond with the C=O bond forward, horizontal, and to the left.* The o.r.d. data require that θ be positive in the lactone I and in the unbridged ketone, but negative in the other bridged compounds (IV–VI).† One cannot be so specific as to the cause of the anomalous infrared band positions of I, but the fact that both the C=O and the C=C stretching frequencies are displaced upwards could most simply be explained by a decrease in the planarity of the conjugated system: viz. an increase in the absolute value of θ without respect to sign. This would diminish the resonance coupling and increase the force constants of both the C=O and C=C bonds. It is therefore of interest to examine the effect of the bridge closure on the sign and magnitude of θ for different conformations of the A/B ring system.

The cyclohexanoid ring B can have a chair or boat form, and with each is associated two limiting conformations of ring A which we designated "C_2-up" and "C_2-down", having regard to the relation between C_2 and C_3 when the model is viewed in the conventional orientation with the angular methyl groups up and ring A to the left. The closure of the 8:19-bridge causes the C/D rings to tilt upwards and the C_{10}—C_{19} bond to deflect to the right. The flexibility of ring A is also affected in the Dreiding model, and the inter-hydrogen distances associated with C_1, C_2, C_{11}, and C_{19} are altered. In Table II the non-bonded hydrogen–hydrogen and hydrogen–oxygen distances that may influence the relative stability of the conformers are listed. These are averaged values from measurements on four sets of Dreiding models.

The following conclusions can be drawn concerning the relative stability of the four conformers of the various bridged structures.

The unbridged Δ^4-3-ketone.—The nuclear magnetic resonance (n.m.r.) coupling constants (12) and the o.r.d. data (13) indicate that ring B is in the chair form except possibly in some derivatives containing bulky substituents at the $C_6(\beta)$ position (12, 14). The ring A conformation with C_2-up is favored since the alternative C_2-down structure brings the $C_1(\alpha)$ and $C_{11}(\alpha)$ hydrogen atoms within 1.7 Å. The conformation with ring B chair and C_2-up satisfies the chirality requirements for the o.r.d. curve, and the small angle ($\theta \approx +8°$) indicates strong conjugation consistent with the observed spectrum.

The 19:8-lactone (I).—Closure of the lactone bridge in the B ring chair / C_2-up form brings the hydrogen atoms on C_1 and C_{11} into partial eclipse and 2.1–2.2 Å apart. These interactions are reduced in the C_2-down form where the hydrogens are staggered, but the $C_1(\beta)$ hydrogen and the C_{19} oxygen are then eclipsed at 2.5 Å and a choice is problematic.

*To observe this angle the model must be inverted from its conventional orientation so that the angular methyl groups point downwards.

†The o.r.d. measurements were obtained only for IV and VI, but it is tacitly assumed that V will behave similarly.

Can. J. Chem. Downloaded from www.nrcresearchpress.com by 210.87.254.6 on 09/05/12
For personal use only.

TABLE II

Characteristics of conformations of Δ^4-3-ketosteroids as evaluated from Dreiding models

Conformation	Chirality angle*	Significant interatomic distances (Å)	
Unbridged			
Ring B chair / C_2-up	+8°	1β H/11α H	2.2
		2β H/19Me	2.7†
		6β H/19Me	3.2†
		8β H/19Me	2.7†
		11β H/19Me	2.3†
Ring B chair / C_2-down	−35°	1α H/11α H	1.7
		1β H/19Me	2.5†
		11β H/19Me	2.5†
		6β H/19Me	2.7†
		8β H/19Me	2.5†
19:8-Lactone bridge			
Ring B chair / C_2-up	+27°	1α H/11α H	2.1
		1β H/11β H	2.2
		1β H/19O	2.5
Ring B chair / C_2-down	−24°	1α H/11β H	2.2
		1β H/19O	2.5
Ring B boat / C_2-up	+6°	1β H/11β H	2.2
		2β H/19O	2.2
		6α H/9α H	2.3
Ring B boat / C_2-down	−43°	1α H/11α H	2.0
		1β H/19O	2.4
		6α H/9α H	2.1
8:19-Epoxide bridge			
Ring B chair / C_2-up	+23°	1α H/11α H	2.1
		1β H/11β H	2.3
		1β H/19H	2.2
		6β H/19H	2.4
Ring B chair / C_2-down	−22°	1α H/11β H	2.2
		6β H/19β H	2.3
Ring B boat / C_2-up	+3°	1β H/11β H	2.2
		2β H/19H	2.6
		6α H/9α H	2.2
Ring B boat / C_2-down‡	−36°	1α H/2α H	2.3
		1β H/2β H	2.3
		1α H/11α H	2.1
		1β H/11β H	2.5
		1β H/19H	2.1
		6α H/9α H	2.2

*The chirality angle was measured on the model with a protractor and the estimated precision is ±3°.

†These distances are measured to the C_{19} carbon atom and the van der Waals radius of the methyl group (2.0 Å) is subtracted.

‡This conformation is not very stable and in some of the Dreiding models it inverts spontaneously to the C_2-up form.

If ring B is in the boat form, the model indicates much greater flexibility for the A ring. With C_2-up, the $C_2(\beta)$ hydrogen and the C_{19} oxygen are eclipsed with a 2.2 Å separation, and the C_2-down conformation would probably be favored.

The o.r.d. curve requires the same chirality as for the unbridged ketone, while the infrared frequency shift, if due to diminished resonance, necessitates an increase in $|\theta|$. Both requirements are compatible with the form having ring B chair and C_2-up, since the distortion of ring A consequent to the closure of the lactone bridge changes θ from +8° to +27° in the Dreiding model. None of the other conformations is compatible with both the spectrum and the o.r.d. curve.

The 8:19-epoxide IV.—With ring B in a chair form, the hydrogen interactions on C_1 and C_{11} are similar to those in the lactone (I) and are more favorable with C_2-down than

Can. J. Chem. Downloaded from www.nrcresearchpress.com by 210.87.254.6 on 09/05/12
For personal use only.

C_2-up. Interaction between C_1 and C_{19} is different from the lactone case and the $C_1(\beta)$ hydrogen and the C_{19} hydrogen atoms are staggered. The Dreiding model therefore suggests that of the two ring B chair forms, the C_2-down is favored. If ring B is a boat, ring A is very flexible. Of the limiting forms the C_2-up is preferred since it avoids the partial eclipsing of the hydrogens on C_2, C_1, and C_{11} which occurs with C_2-down. However the flexibility of the A ring makes intermediate structures plausible.

The o.r.d. curve requires a minus sign for θ, and the infrared spectrum, on the basis of the resonance hypothesis, requires that $|\theta|$ be approximately the same as in the unbridged ketone ($\approx 8°$). These requirements cannot be met by any of the limiting conformers. The o.r.d. measurements would fit the form with ring B chair and C_2-down ($\theta \approx -22°$), or ring B boat and C_2-down ($\theta \approx -36°$), but the large values of $|\theta|$ would be unacceptable spectroscopically. The form with ring B boat and C_2-up ($\theta \approx +3°$) would fit the spectrum best. In view of the flexibility of ring A in this conformation small repulsive forces would suffice to invert the chirality of ring A and such a distorted conformation with ring B boat and ring A "nearly up" would reconcile both the spectroscopic and o.r.d. requirements. More detailed quantitative studies of the o.r.d. spectrum and the proton magnetic resonance coupling constants should settle this question.*

Structures V and VI.—The conformations of ring A and ring B of the other 8:19-bridged structures V and VI probably resemble that of the epoxide, with the R′ substituent oriented vertically. It is not known whether the forward- or rearward-directed hydrogen atom of the C_{19} methylene group of IV is substituted in V and VI. In none of the conformations can the C_{19} hydroxyl group of V approach within hydrogen-bonding distance of the C_3 carbonyl oxygen atom, though, in the forward position, it could bond with the π-electrons of the Δ^4-double bond.

Although the arguments presented above are only rationalizations of the observed optical phenomena, they suggest that with closure of the 8:19-bridge there can be little difference between the energies of the A/B ring systems with ring B in chair or boat form and that secondary repulsive forces between C_1 and C_{11} and between C_2 and C_{19} may tip the scales in favor of one or other of the ring B conformations.

Interactions Between Carbonyl Groups

It is alternatively possible that the infrared frequency shifts for the lactone (I) result from a transannular interaction between the 3-ketone and lactone carbonyl groups, but there are reasons for thinking this effect less important than the planarity factor considered above. There are few, if any, well-established instances of carbonyl shifts in steroid infrared spectra that can be attributed to non-bonded carbonyl–carbonyl interactions. Ketone and acetate carbonyl groups in a 1:3 relation give rise to upward frequency displacements of both C=O frequencies, as has been observed in 21-acetoxy-20-ketones, 17-acetoxy-16-ketones, 16-acetoxy-17-ketones, 11-acetoxy-12-ketones, and 12-acetoxy-11-ketones and in 17*a*-acetoxy-17-ketones of D-homo steroids (2). These shifts appear to be independent of steric factors and probably result from inductive effects acting through the bond system. A mutual interaction between remote carbonyl groups in the 1:4 relation is seen in 11,17-diketosteroids, where both the C=O stretching bands are displaced to higher frequency (15); this will be discussed further below. If the 19:8-lactone

**In a personal communication, Professor Djerassi has pointed out that the inherently asymmetric nature of the α,β-unsaturated ketone is probably a function of the angle of skew and the larger the angle, the larger the intrinsic optical asymmetry; conversely, if the angle is very small, then other factors, such as vicinal effects from other substituents, may play an important part or even governing role in controlling the sign of the Cotton effect. This being the case, it is conceivable that a small amount of one conformer may control the sign of the Cotton effect by having a much more powerful rotational strength in one direction than the dominant conformer may have in the opposite one.*

Can. J. Chem. Downloaded from www.nrcresearchpress.com by 210.87.254.6 on 09/05/12
For personal use only.

carbonyl group of I were interacting transannularly with the Δ^4-3-ketone system, either by mutual dipole repulsion or π-orbital overlap, the ultraviolet spectrum would also be expected to show abnormality. The positions of the K bands in the ultraviolet spectra of similarly substituted steroids containing 19:8-lactone and 8:19-epoxide bridges are compared in Table III from which it is evident that any such effect must be quite small

TABLE III

Position of the K-band maximum in the ultraviolet spectra of 8:19-bridged Δ^4-3-ketosteroids*

Side chain	8:19-Epoxide		19:8-Lactone	
	max.(Å)	max.(Å)	max.(Å)	max.(Å)
R(β) = —CO—CH_3	2 430	16 130	2 440	14 900
R(β) = —CO—CHN_2	2 465	23 660	2 470	23 400
R(β) = —COOH	2 435	16 100	2 440	13 800
R(β) = —CO—CH_2OH	2 430	15 970	2 440	14 000
R(β) = —CO.CH_2.O.CO.CH_3	2 430	16 480	2 440	12 900

*These data are taken from refs. 3 and 4. The spectra were measured on a Beckman Model DU spectrophotometer in 95% ethanol solution.

since the untraviolet shift does not exceed 10 Å. Braude has noted (16) that *small* changes in the planarity of conjugated systems have a negligible effect on the position of the K band, but do produce a diminution of the band intensity and there is some evidence for that in the data in Table III. A transannular interaction would also be expected to perturb the C=O stretching frequency of the lactone carbonyl, but this band is observed at 1 774 ± 3 cm^{-1} in chloroform solution and is within the normal range of 1 777 ± 5 cm^{-1} established for various types of γ-lactones (17).

For the 19:11-lactone bridged Δ^4-3-ketosteroid VII, Barton and Beaton (18) report infrared bands at 1 765, 1 675, and 1 620 cm^{-1} in chloroform solution. Here $\nu_{C=O}$ for the Δ^4-3-ketone group is displaced upwards but $\nu_{C=C}$ is not. The band at 1 765 cm^{-1} must be an unresolved doublet with contributions from the lactone carbonyl and the C_{21} acetate group. A γ-lactone at the normal position of 1 777 ± 5 cm^{-1} should be separated from the ester carbonyl band, and there is a suggestion here that the lactone maximum is displaced downwards. For VII the Dreiding model allows only one stable conformation, which

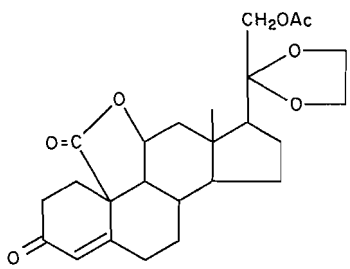

VII

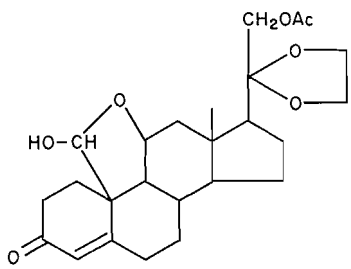

VIII

is rigid, with ring B in the chair form and has the two carbonyl groups approximately parallel and 3.2 Å apart.* The chirality is negative with $\theta \approx -15°$. The ultraviolet K-band maximum of VII is at 2 410 Å in methanol and is shifted some 50 Å from the 2 460 Å

**For I the closest approach of the C_3 and lactone carbonyl groups is 4.2 Å in the ring B boat / C_2-down conformation. In the other conformations the separation is 4.8–5.6 Å.*

Can. J. Chem. Downloaded from www.nrcresearchpress.com by 210.87.254.6 on 09/05/12
For personal use only.

position observed for the hemiacetal VIII in the same solvent. There is therefore stronger support for a transannular effect for the carbonyl shift in VII than in I.

TABLE IV

Infrared group frequencies for 1,11,17-triketosteroids and related compounds (cm^{-1})*

	Δ^2 C=C	1 C=O	11 C=O	17 C=O	Solvent
1-Keto-5α-steroid	—	1 709 – 1 704	—	—	CCl_4
Δ^2-1-Ketosteroid	1 630(vw)	1 682	—	—	CCl_4
11-Ketosteroid	—	—	1 710 – 1 704	—	CS_2, CCl_4
11-Ketosteroid	—	—	1 705 – 1 698	—	$CHCl_3$
17-Ketosteroid	—	—	—	1 745 – 1 741	CS_2, CCl_4
17-Ketosteroid	—	—	—	1 737 – 1 733	$CHCl_3$
11,17-Diketosteroid	—	—	1 719 – 1 713	1 752 – 1 748	CS_2, CCl_4
11,17-Diketosteroid	—	—	1 711 – 1 707	1 742 – 1 738	$CHCl_3$
1,11,17-Triketo-5β-steroid	—	1 715†		1 745	CS_2
1,11,17-Triketo-5β-steroid	—	1 714†		1 738	$CHCl_3$
Δ^2-1,11,17-Triketo-5β-steroid	—	1 682	1 718	1 745	CS_2
Δ^2-1,11,17-Triketo-5β-steroid	1 635(vw)	1 675	1 714	1 738	$CHCl_3$

*The data for the mono- and di-ketones are taken from the sources cited in ref. 2.
†Unresolved doublet.
Abbreviation: vw, very weak band.

Ketosteroids with Carbonyl Groups at 1, 11, and 17

The triketones II and III have recently been synthesized by Schneider (19) and the positions of the C=O and C=C stretching bands, as measured on a Perkin–Elmer 421 spectrophotometer are reported in Table IV together with relevant data for the 1-, 11-, and 17-monoketones and the 11,17-diketone in the same solvents. It is notable that the triketones exhibit the same displacements of the 11-carbonyl band as do the 11,17-diketones, but the introduction of the 1-carbonyl or the Δ^2-1-carbonyl group has little additional displacement effect. This is in spite of the fact that the oxygen atoms on C_1 and C_{11} are separated by only 2.8 Å and 3.7 Å in II and III respectively, as evaluated from Dreiding models. These figures are based on the conformations that maximize the oxygen–oxygen distance. For II this is a ring B chair conformation, but for III a ring B boat conformation must be postulated, otherwise the oxygen–oxygen distance is reduced to 2.4 Å. Both II and III are 5β-steroids. In the 5α-series the maximum C_1,C_{11} oxygen–oxygen separations are 2.4 Å for the analogue of II and 2.2 Å for the analogue of III, and the interaction effects should therefore be more severe. It would be interesting to examine these compounds.

The perturbations of the group frequencies of the 11- and 17-carbonyls in the 11,17-diketones probably depend mainly on the change in the geometry of the C and D rings. The normal coordinate analyses of Overend and Scherer (20) indicate that, for simple ketones, the C=O frequency is very sensitive to changes in the angle opposite the O=C bond, independently of any change in the C=O force constant. A small enlargement of these angles in the 11,17-diketone could bring about the observed effect.

CONCLUSION

The above results illustrate that, in dealing with small perturbations of "group" frequencies in complex molecules, the infrared spectroscopist cannot at present distinguish unequivocally among the various electronic and steric influences that can modify the band position. It must be emphasized however that the anomalies of the type discussed here are exceptional. It is important that they be noted, both to avoid errors of

Can. J. Chem. Downloaded from www.nrcresearchpress.com by 210.87.254.6 on 09/05/12
For personal use only.

interpretation when applying infrared spectroscopy to the determination of molecular structure, and to alert those investigating other physical properties of the molecules concerned.

ACKNOWLEDGMENTS

We wish to thank Dr. M. Ehrenstein and Dr. J. J. Schneider for providing the compounds discussed in this paper, and Mr. R. Lauzon for technical assistance in measuring the infrared spectra. We also wish to acknowledge the opportunity of discussing the rotatory dispersion aspects of the problem with Professor C. Djerassi.

REFERENCES

1. R. N. JONES and F. HERLING. J. Org. Chem. **19**, 1252 (1954).
2. G. ROBERTS, B. S. GALLAGHER, and R. N. JONES. Infrared absorption spectra of steroids—an atlas. Vol. II. Interscience Publishers, Inc., New York and London. 1958. pp. 22–28.
3. G. W. BARBER and M. EHRENSTEIN. J. Org. Chem. **26**, 1230 (1961).
4. K. OTTO and M. EHRENSTEIN. J. Org. Chem. **26**, 2871 (1961).
5. T. KUBOTA and M. EHRENSTEIN. J. Org. Chem. **29**, 345 (1964).
6. T. KUBOTA and M. EHRENSTEIN. J. Org. Chem. **29**, 342, 351 (1964).
7. T. KUBOTA and M. EHRENSTEIN. J. Org. Chem. **29**, 357 (1964).
8. R. N. JONES, N. B. W. JONATHAN, M. A. MACKENZIE, and A. NADEAU. Spectrochim. Acta, **17**, 77 (1961).
9. R. N. JONES and A. NADEAU. Spectrochim. Acta, **20**, 1175 (1964).
10. C. DJERASSI, R. RECORDS, E. BUNNENBERG, K. MISLOW, and A. MOSCOWITZ. J. Am. Chem. Soc. **84**, 870 (1962).
11. W. B. WHALLEY. Chem. Ind. 1024 (1962).
12. K. TORI and K. KURIYAMA. Chem. Ind. 1525 (1963).
13. C. DJERASSI, R. RINIKER, and B. RINIKER. J. Am. Chem. Soc. **78**, 6377 (1956).
14. C. DJERASSI, O. HALPERN, V. HALPERN, and B. RINIKER. J. Am. Chem. Soc. **80**, 4001 (1958).
15. R. N. JONES, P. HUMPHRIES, and K. DOBRINER. J. Am. Chem. Soc. **71**, 241 (1949).
16. E. A. BRAUDE, E. R. H. JONES, H. P. KOCH, R. W. RICHARDSON, F. SONDHEIMER, and J. B. TOOGOOD. J. Chem. Soc. 1890 (1949).
17. R. N. JONES and B. S. GALLAGHER. J. Am. Chem. Soc. **81**, 5242 (1959).
18. D. H. R. BARTON and J. M. BEATON. J. Am. Chem. Soc. **84**, 199 (1962).
19. J. J. SCHNEIDER. Federation Proc. **23**, 276 (1964).
20. J. OVEREND and J. R. SCHERER. Spectrochim. Acta, **16**, 773 (1960).

Can. J. Chem. Downloaded from www.nrcresearchpress.com by 210.87.254.6 on 09/05/12
For personal use only.

Can. J. Chem. Downloaded from www.nrcresearchpress.com by 210.87.254.6 on 09/05/12
For personal use only.

CONCERNING THE EXISTENCE OF 2-(2-NITROVINYL)BENZOIC ACID

A CONTRIBUTION TO THE ALKALINE ELIMINATION IN β-SUBSTITUTED NITRO COMPOUNDS

HANS HELMUT BAER AND FRANK KIENZLE
Department of Chemistry, University of Ottawa, Ottawa, Canada

Received August 21, 1964

ABSTRACT

Action of aqueous alkali upon 3-phthalidylnitromethane (I) is shown to produce unstable 2-(2-nitrovinyl)benzoate ion (II*a*) which rapidly adds hydroxyl ion to form the dianion IV*a* of 2-(1-hydroxy-2-nitroethyl)benzoic acid. Both II*a* and IV*a* revert to I upon acidification. Substitution of methoxide for aqueous alkali converts I via II*a* into 2-(1-methoxy-2-nitroethyl)benzoate (V*a*), which is isolated as crystalline, free acid (V).

Condensations with nitromethane of isophthalaldehydic acid and terephthalaldehydic acid lead, respectively, to 3- and 4-(2-nitrovinyl)benzoic acids (1). On the other hand, *o*-phthalaldehydic acid under similar conditions has been known for many years to give a colorless compound (m.p. 130–131°) recognized to be 3-phthalidylnitromethane (I) rather than 2-(2-nitrovinyl)benzoic acid (II) (2, 3, 4). Recent work in this laboratory (5) demonstrated that the condensation of *o*-phthalaldehyde with nitromethane afforded, among other products, 2-(1-hydroxy-2-nitroethyl)benzaldehyde lactol (III). Dichromate oxidation of III gave I. The structure of I was also supported by a detailed discussion (6) of its infrared spectrum and by further chemical evidence (5).

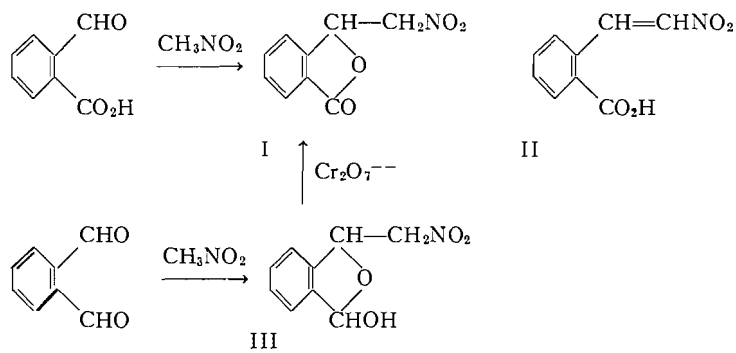

Apparently unaware of the previous work, Hashimoto and Nagase (7) also studied the nitromethane condensation of *o*-phthalaldehydic acid and obviously obtained the same colorless product (m.p. 129–130°). They assumed, however, that it was 2-(2-nitrovinyl)-benzoic acid (II). Their assignment of this structure was based on reduction of the nitro group followed by conversion of the product into isocarbostyril. In our opinion, the experiments as described would not corroborate formula II but would in fact favor formula I. In view of this discrepancy it seemed that additional work was needed to establish the possible existence of II.

The ultraviolet spectrum of I closely resembles that of phthalide, but is completely different from the spectra reported (1) for the isomeric 3- and 4-(2-nitrovinyl)benzoic acids in that it does not exhibit the characteristic β-nitrostyrene peak in the 315 mμ

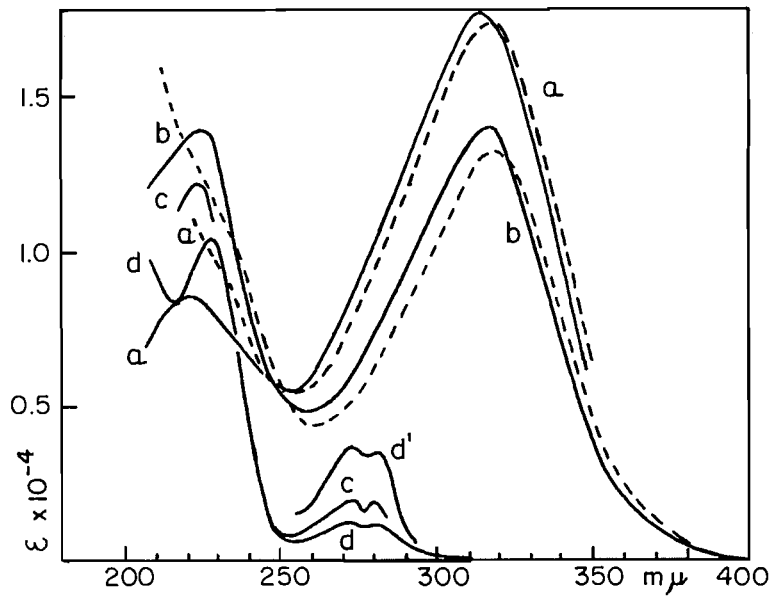

FIG. 1. Curves *a*: 4-(2-nitrovinyl)benzoic acid (solid line) and its anion (broken line) in water. Curves *b*: 3-(2-nitrovinyl)benzoic acid (solid line) and its anion (broken line) in water. Curve *c*: phthalide in methanol. Curve *d*: 3-phthalidylnitromethane, 10^{-4} *M* in methanol; in water the maxima are at about 2 mμ longer wavelengths. Curve *d'*: same as *d* but without reference to the ordinate; measured at somewhat higher concentration.—Curves *a* and *b* are redrawn from ref. 1, curve *c* from Stadtler Standard Spectrum No. 13929U.

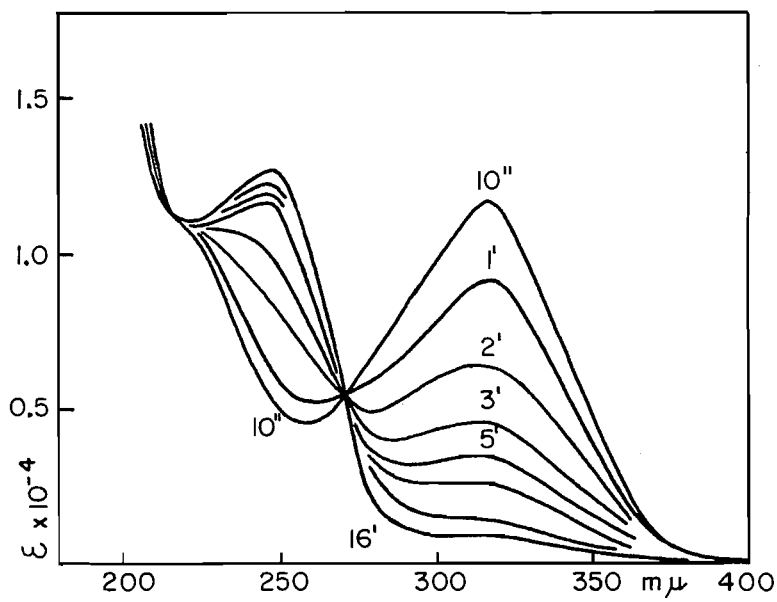

FIG. 2. Spectral changes observed in an alkalized solution of 3-phthalidylnitromethane (*c*, 10^{-4} *M*). Solvent, 1 part of methanol and 9 parts of *N*/100 aqueous sodium hydroxide.

region (Fig. 1). A β-nitrostyrene chromophore is, however, instantaneously generated when aqueous alkali is added to a solution of I. The spectrum (Fig. 2) then becomes very similar to the spectra of the anions of 3- and 4-(2-nitrovinyl)benzoic acids, suggesting

Can. J. Chem. Downloaded from www.nrcresearchpress.com by 210.87.254.6 on 09/05/12
For personal use only.

that a β-nitrostyrene carboxylate is present at this point. In $N/100$ sodium hydroxide solution the new peak at 319 mμ disappears rapidly, its half-life at 28° being about 2 min. The peak decreases more slowly in M sodium hydrogen carbonate solution at pH 8.5 (half-life, about 2 h). In phosphate buffers of pH 7.8 and 7.1 the decrease in intensity in 2 h was 9 and 6%, respectively. The spectral change occurring in alkaline solution is characterized by an isosbestic point at 271 mμ (Fig. 2). Acidification following the completion of the spectral change restores the original spectrum of I without observable recurrence of nitrostyrene absorption, and in a preparative experiment resulted in recovery of unchanged, crystalline I in 77% yield. The process may be represented by the following cyclic sequence.

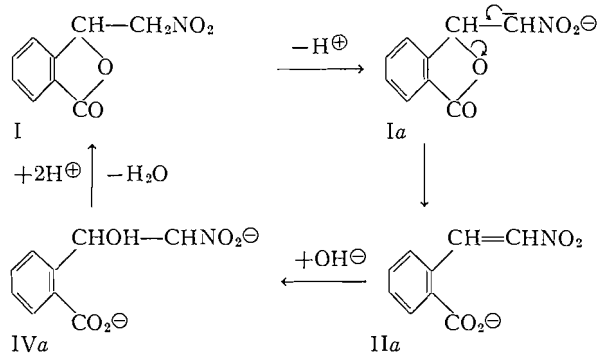

This sequence involves an eliminative opening of the lactone ring in I*a*, the nitronate ion of I, which as a β-acyloxynitro compound should be unstable toward alkali.[1] The resulting product, the 2-(2-nitrovinyl)benzoate II*a*, is evidently also rather unstable in an alkaline reaction medium. Depending on the alkalinity of the solution, nucleophilic attack by hydroxyl ion takes place more or less rapidly, leading to disappearance of the nitrostyrene chromophore and the formation of the dianion IV*a* of 2-(1-hydroxy-2-nitroethyl)benzoic acid. This dianion is characterized by nitronate absorption at 248 mμ (ε, 12 500 in $N/100$ NaOH). The dianion appears to be reasonably stable in dilute alkali, but on acidification reverts to the starting compound, lactone I. There are precedents in the literature for this type of hydroxylation of β-nitrostyrene derivatives.[2]

Numerous attempts were made to liberate and, if possible, isolate 2-(2-nitrovinyl)-benzoic acid (II) by acidifying freshly alkalized solutions of I while the absorption peak at 319 mμ indicated that II*a* was still present. Acidification with hydrochloric acid or acetic acid, deionization with cation exchange resin, or indeed even addition of potassium dihydrogen phosphate to pH 4.5 resulted in instant restoration of the spectrum of I with concomitant, complete disappearance of the nitrostyrene peak. Crystalline I was the only isolable product. In phosphate buffer of pH 5 it was possible to observe spectrophotometrically that the 319 mμ peak almost disappeared within 2 min (Fig. 3). At pH 6 the peak decreased, also within a few minutes, and then remained fairly constant at a low optical density approximately equalling that of I concurrently generated. It appears, therefore, that in a narrow range around pH 6 an equilibrium I ⇌ II ⇌ II*a* is established in which an appreciable amount of II*a* is present. The molar extinction coefficient of I

[1]*The elimination of acetic acid from β-acetoxynitroalkanes leading to nitroolefins is referred to as the Schmidt–Rutz reaction (8) and is usually effected by bicarbonate in an inert solvent.*

[2]*Examples reported include β-nitrostyrene itself (9), 4-hydroxy-3-methoxy-β-nitrostyrene (10), and 2-hydroxy-1-nitroindene (5).*

Can. J. Chem. Downloaded from www.nrcresearchpress.com by 210.87.254.6 on 09/05/12
For personal use only.

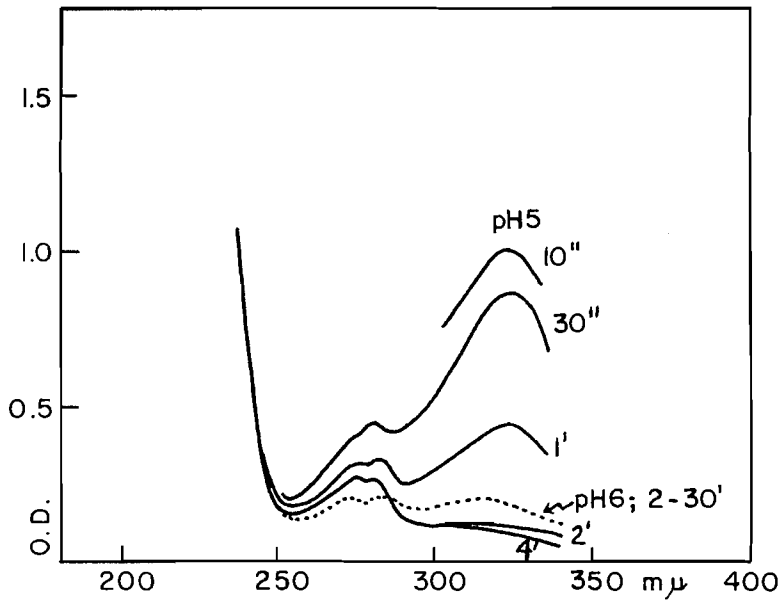

FIG. 3. Solid lines: spectral changes in a solution of 3-phthalidylnitromethane (c, approx. 2×10^{-4} M) that had been alkalized and immediately thereafter brought to pH 5 (phosphate buffer, cf. Experimental). Dotted line: final curve (after 2 and 30 min) of a similar experiment at pH 6.

(1 500) being roughly one-tenth of the values estimated[3] for II and IIa, it is evident that in this equilibrium the lactone I predominates about tenfold over the nitrostyrene system II $\rightleftharpoons$ IIa. Since any significant departure from pH 6 results in a complete shift to I (on the acid side) or to IVa (on the alkaline side), it becomes understandable that none of our attempts at isolating II was successful.

That the action of alkali upon I consists of an eliminative lactone ring opening with subsequent addition of base (I $\rightarrow$ Ia $\rightarrow$ IIa $\rightarrow$ IVa) was proved, further to the spectral evidence, by performing the same reaction with sodium methoxide in absolute methanol. Under these conditions, i.e., in the absence of aqueous hydroxide, no starting material (I) was isolated upon subsequent acidification. Instead, a colorless product melting at 140–141° was obtained in high yield. On the basis of its infrared and ultraviolet spectra, elemental analyses, and its acidic reaction toward litmus, the substance was assigned structure V, 2-(1-methoxy-2-nitroethyl)benzoic acid. This methoxy compound is stable as the free acid since, in contrast to the hydroxy analogue IV, it cannot lactonize.

If the action of methoxide upon I had consisted of lactone opening by transesterification, the methyl ester of IV would have been formed. The reaction mixture displayed transient, strong absorption at 310 mμ ascribable to IIa.[4] This intermediate, having a half-life of about 1.5 h in N/10 $NaOCH_3$, then adds methanol to give the methoxy acid V (Fig. 4). Interestingly, the final product, V, does not show nitronate absorption in the 245 mμ region in the presence of *methanolic methoxide*; it has short wavelength end absorption only. One has to conclude, therefore, that under the reaction conditions the product

[3]*By extrapolation to zero time of the IIa peak (Fig. 2) and by comparison with the ε-values given (1) for the m- and p-acids (13 900 and 18 000) and their anions (13 400 and 17 200).*

[4]*The hypsochromic shift of 9 mμ noted in methanol is explained as a solvent effect. It is in line with the fact that 4-(2-nitrovinyl)benzoic acid has* λ_{max} *307 mμ in methanol (11) and* λ_{max} *313 mμ in water (1); 2-hydroxy-1-nitroindene shows* λ_{max} *340 mμ in ethanol and* λ_{max} *355 mμ in water (5).*

Can. J. Chem. Downloaded from www.nrcresearchpress.com by 210.87.254.6 on 09/05/12
For personal use only.

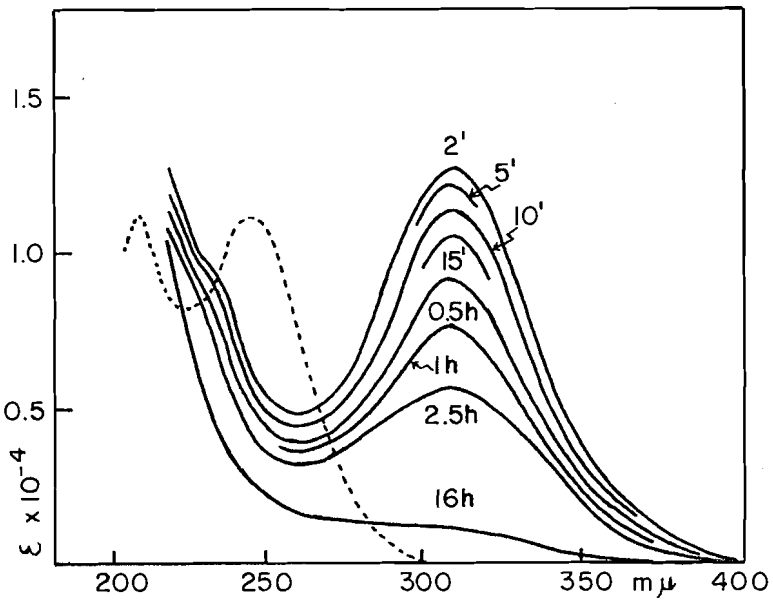

FIG. 4. Solid lines: spectral changes in a 10^{-4} *M* solution of 3-phthalidylnitromethane in *N*/10 methanolic sodium methoxide. Dotted line: a 10^{-4} *M* solution of 2-(1-methoxy-2-nitroethyl)benzoic acid in *N*/100 aqueous sodium hydroxide.

exists as carboxylate V*a* but not as a carboxylate-nitronate like IV*a*. For this reason there is no isosbestic point associated with the transformation depicted in Fig. 4, although the isolated acid (V) does produce nitronate absorption (λ_{max} 246 mμ; ε, 11 000) in the presence of *aqueous hydroxide*.

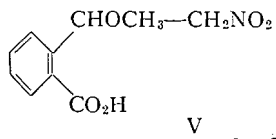

V

V*a*, $CO_2\ominus$ instead of CO_2H

Similar facile eliminations, combined with replacement by methoxyl, of substituents adjacent to a nitro group have been observed in carbohydrate chemistry (12) and have more recently been utilized for the synthesis of aliphatic nitroalkyl ethers (13). In these cases, too, there was evidence for nitroolefins playing a role as intermediates. On the other hand the lactol III when treated with aqueous or ethanolic alkali is converted instantly into a 1,3-dihydroxy-2-*aci*-nitroindane salt, with no nitroolefin intermediate observed (5). Apparently, shift in III of the mobile equilibrium toward the hydroxy aldehyde and internal Henry condensation of the latter giving the indane derivative take preference over an alternative elimination process.

EXPERIMENTAL

Spectral Determinations

The ultraviolet spectra were obtained with a Beckman DK-2 recording spectrophotometer and rechecked with a Perkin–Elmer 202 apparatus. For the runs involving action upon I of aqueous base (*N*/100 NaOH, *M* $NaHCO_3$) and (or) phosphate buffer (0.15 *M*), one part of a standard 0.001 *M* solution of I in methanol (A) was diluted with nine parts of the aqueous reagent; thus, the concentration of I was 10^{-4} *M*. The small

Can. J. Chem. Downloaded from www.nrcresearchpress.com by 210.87.254.6 on 09/05/12
For personal use only.

changes in reagent pH that were due to the introduction of 1/9 volume of solvent methanol were neglected. The spectral curves at pH 7.8, 7.1, 6.0, 5.0, and 4.5 were taken after 0.3 ml of A had been alkalized with Na_2HPO_4 buffer component and, after a few seconds, had been made up to a volume of 3 ml with KH_2PO_4 buffer component in such proportions as to provide the desired final pH value.

3-Phthalidylnitromethane (I)

Samples of I prepared (3, 4, 7) from *o*-phthalaldehydic acid and from *o*-phthalaldehyde via III (5) were found to be identical. The identity was established by mixed melting point (130.5–132°, undepressed) and infrared (6) and ultraviolet spectra; λ_{max} in methanol, 273 mμ (ϵ, 1 550), 281 mμ (ϵ, 1 500); λ_{max} in water containing 10% of methanol, 275 and 282 mμ.

Action of Aqueous Base on I

A solution of I (96.5 mg, 0.5 mmole) in 3 ml of warm methanol was allowed to cool to about 25°, with care being taken to avoid crystallization. Then 50 ml of *N*/100 sodium hydroxide and 1 ml of *N*/1 sodium hydroxide were added quickly. After half an hour the solution was checked spectroscopically for absence of high-intensity absorption in the near ultraviolet region,[5] then acidified with 2 ml of *N*/1 acetic acid and concentrated *in vacuo* at 35° to a small volume. Excess methanol was added and sodium ions were removed by stirring with 3 ml of Rexyn RG-50(H^+). Evaporation of the filtrate gave a residue that crystallized from a small amount of aqueous methanol and was collected after standing overnight at 0°. The washed and dried, colorless crystals were identified as starting material; m.p. 131–132°. The recovery was 74 mg (77%). The mother liquor was inspected in the ultraviolet and found to exhibit absorption due to I only.

An identical experiment in which the acidification was done after 10 s furnished 78 mg (81%) of starting material. No significantly different results were obtained when ice-cold solutions were used nor when sodium bicarbonate was substituted for sodium hydroxide.

2-(1-Methoxy-2-nitroethyl)benzoic Acid (V)

3-Phthalidylnitromethane (I) (300 mg, 1.55 mmole) was dissolved in 30 ml of methanol, and 200 mg of sodium methoxide (3.12 mmole) in 10 ml of methanol was added. The slightly yellowish mixture was allowed to stand at room temperature for 24 h and then was deionized at 0° with 10 ml of methanol-washed Rexyn RG-50(H^+). The filtrate gave upon evaporation a crystalline residue which was recrystallized from 5 ml of water with the addition of a few drops of ethanol. The solution showed a pH of about 2 (indicator paper) and deposited compound V as fine needles (202 mg, m.p. 135–137°); a second crop (25 mg, m.p. 128–130°) was obtained on concentration of the mother liquor. The total yield was 64%. A recrystallization from ethanol-containing water, with activated carbon treatment, raised the m.p. to 138–139° and a further recrystallization to 140–141°. There was left 145 mg of pure V the melting point of which did not change upon further recrystallization.

Anal. Calcd. for $C_{10}H_{11}NO_5$ (225.2): C, 53.33; H, 4.92; N, 6.22; OCH_3, 13.80. Found: C, 53.29; H, 4.83; N, 6.31; OCH_3, 14.25.

The pK_a value was 3.68 (method of half titration at 25°).

Ultraviolet spectrum.—In methanol, λ_{max} 277.5 mμ (ϵ, 1 000); in *N*/10 methanolic sodium methoxide, end absorption only; in *N*/100 aqueous sodium hydroxide, λ_{max} 245 mμ (ϵ, 11 000).

Characteristic infrared bands (in cm^{-1}).—Aromatic carboxyl, 2 700 to 2 500 (group of small bands), 1 680 (strong), 920 (broad, medium). Primary nitro, 1 555 (asym., strong), 1 370 (sym., medium, superimposed on Nujol band). Methoxyl, 1 120 (strong). *o*-Substituted phenyl, 1 620, 1 600, and 1 480 (weak), 1 300, 1 285, 1 270, and 1 065 (strong), 1 030 (medium), 765 (strong).

In comparison, 3-phthalidylnitromethane (I) shows the phthalide carbonyl band at 1 760 cm^{-1} and the strained-ring =C—O—C stretching modes at 1 215 cm^{-1} (asym.) and 1 090 cm^{-1} (sym.).

ACKNOWLEDGMENT

This work was supported by the Ontario Research Foundation.

REFERENCES

1. R. STEWART and L. G. WALKER. Can. J. Chem. **35**, 1561 (1957).
2. T. SZÉKI. Ber. ungar. pharm. Ges. **13**, 680 (1937); Chem. Abstr. **31**, 6644 (1937).
3. B. B. DEY and T. K. SRINIVASAN. Arch. Pharm. **275**, 397 (1937).
4. G. E. ULLYOT, J. J. STEHLE, C. L. ZIRKLE, R. L. SHRINER, and F. J. WOLF. J. Org. Chem. **10**, 429 (1945).
5. H. H. BAER and B. ACHMATOWICZ. J. Org. Chem. In press; Angew. Chem. **76**, 50 (1964) (Intern. Ed. **3**, 224 (1964)).
6. K. NAKANISHI. Infrared absorption spectroscopy. Holden-Day, Inc., San Francisco. 1962. p. 183.
7. T. HASHIMOTO and S. NAGASE. Yakugaku Zasshi, **80**, 1637 (1960); Chem. Abstr. **55**, 7415*d* (1961).

[5] *For this check an aliquot was diluted with N/100* NaOH *to approximately 10^{-4} M concentration; low-intensity absorption causing a slight yellow color in the undiluted solution is of no significance.*

Can. J. Chem. Downloaded from www.nrcresearchpress.com by 210.87.254.6 on 09/05/12
For personal use only.

8. E. SCHMIDT and G. RUTZ. Ber. **61**, 2142 (1928). W. E. Noland. Chem. Rev. **55**, 137 (1955).
9. G. KORTÜM. Z. physik. Chem. B, **43**, 279 (1939).
10. R. STEWART. J. Am. Chem. Soc. **74**, 4531 (1952).
11. Spectrum No. 3326 U. *In* The Stadtler standard spectra. Philadelphia, Pa.
12. H. O. L. FISCHER and H. H. BAER. Ann. **619**, 53 (1958).
13. H. FEUER and S. MARKOFSKY. J. Org. Chem. **29**, 929 (1964).

Can. J. Chem. Downloaded from www.nrcresearchpress.com by 210.87.254.6 on 09/05/12
For personal use only.

Can. J. Chem. Downloaded from www.nrcresearchpress.com by 210.87.254.42 on 09/05/12
For personal use only.

ELECTROCHEMICAL STUDIES ON TITANIUM IN MOLTEN LiCl–KCl EUTECTIC

R. Baboian,[1] D. L. Hill,[2] and R. A. Bailey
Department of Chemistry, Rensselaer Polytechnic Institute, Troy, New York

Received August 7, 1964

ABSTRACT

The methods of potentiometry and polarography have been used to study the Ti(II) and Ti(III) ions in solution in the LiCl–KCl eutectic at 450 °C and 550 °C. Solutions of Ti(II) were prepared by anodic dissolution of Ti metal, and Ti(III) solutions by coulometric titration of Ti(II) by Pt(II). Apparent standard electrode potentials were measured for the Ti(II)/Ti and Ti(III)/Ti(II) couples against the Pt(II)/Pt and Ag(I)/Ag reference electrodes. Values obtained on the mole fraction scale with a Pt(II)/Pt reference electrode were

Ti(II)/Ti, −1.74 V at 450 °C; −1.73 V at 550 °C;

Ti(III)/Ti(II), −1.43 V at 450 °C; −1.43 V at 550 °C.

Polarographic waves for oxidation and reduction of Ti(II), and for reduction of Ti(III), were observed.

INTRODUCTION

The technological importance of titanium metal has led to its study at elevated temperatures and in molten salt systems. Disproportionation equilibria in alkali halide melts were studied by Mellgren and Opie (1) and Kreye and Kellogg (2) by direct analysis, and by Flengas (3) and Smirnov (4) using potential measurements in molten KCl–NaCl mixtures. These studies showed the importance of the lower states Ti(II) and Ti(III) in these systems.

Redox potential measurements of the Ti(III)/Ti(II) couple in the LiCl–KCl eutectic melt were carried out by Menzies *et al.* (5) and by Smirnov (6). Although both groups used essentially the same technique, their values differ by 0.6 V at 500 °C. Bockris *et al.* (7) studied solutions of titanium chlorides in the same melt polarographically. At 400 °C they obtained the polarographic wave for the reduction of Ti(III) to Ti(II), but no wave for the Ti(II)–Ti(0) reduction was seen at potentials less negative than that for decomposition of the melt. However, under the same conditions Okada (8) has obtained polarograms for both of these reduction processes.

The object of this work was to make a further investigation of the redox potentials of the titanium system in the LiCl–KCl eutectic melt in which the lower oxidation states of titanium were prepared *in situ*. Our approach was by way of anodic dissolution of the metal, rather than by direct addition of titanium chloride as had been done previously. In addition to the metal, three oxidation states are of importance: Ti(II), Ti(III), and Ti(IV). The last of these is volatile as the chloride and was not investigated.

Electrode potentials in this work are referred to the cells

[A]

Ti	Ti(II),C_1	glass frit	Pt(II),C_2	Pt
	LiCl–KCl eutectic		LiCl–KCl eutectic	

or

Ti	Ti(II),C_1	glass frit	Ag(I),C_2	Ag
	LiCl–KCl eutectic		LiCl–KCl eutectic	

[1]*Present address: Department of Metallurgical and Material Science, University of Toronto, Toronto, Ontario.*
[2]*Present address: Department of Chemistry, University of Hong Kong, Hong Kong.*

for the metal ion – metal system, and

[B]	Pt	Ti(II),C_1 Ti(III),C_1' LiCl–KCl eutectic	glass frit	Pt(II),C_2 LiCl–KCl eutectic		Pt

or

	Pt	Ti(II),C_1 Ti(III),C_1' LiCl–KCl eutectic	glass frit	Ag(I),C_2 LiCl–KCl eutectic		Ag

when two oxidation states of titanium are present. The concentration on the mole fraction or molality scale is represented by C.

In the first case where the cell reaction is Ti + Pt(II) = Ti(II) + Pt, the cell potential is given by

$$[1] \qquad E_{\text{cell}} = E^0_{\text{Pt(II)/Pt}} - E^0_{\text{Tl(II)/Tl}} - \frac{2.303RT}{nF} \log \frac{\gamma_1 C_1}{(\gamma_2 C_2)^{n/2}},$$

where E^0 refers to the standard potential. The activity coefficient is represented by γ. Signs follow the Stockholm convention. If the Pt(II)/Pt electrode is taken as the reference, its standard potential is set at zero at all temperatures. Then, referring the cell potential to unit concentration of the reference electrode, and assuming the activity coefficients to be constant over the concentration range considered, one can rewrite for eq. [1],

$$[2] \qquad -E'_{\text{cell}} = E^{0'}_{\text{Tl(II)/Tl}} + \frac{2.303RT}{nF} \log C_1.$$

$E'_{\text{Tl(II)/Tl}}$ is the apparent standard electrode potential, referred to unit concentration but containing a term involving the activity coefficients.

When two oxidation states are present (cell B), the equation for the cell potential would reduce to

$$[3] \qquad -E'_{\text{cell}} = E^{0'}_{\text{Tl}(n')/\text{Tl}(n)} + \frac{2.303RT}{(n'-n)F} \log \frac{C_1'}{C_1}.$$

The cell reaction concerned here is Ti(II) + $\frac{1}{2}$Pt(II) = Ti(III) + $\frac{1}{2}$Pt. When $C_1' = C_1$, $-E'_{\text{cell}}$ equals the apparent standard potential of the couple.

A similar treatment would apply to the Ag(I)/Ag reference electrode.

From a theoretical point of view, the best reference electrode for chloride melts would be the chlorine electrode. Measurements referred to the platinum or silver electrodes can easily be converted to the chlorine electrode scale, since their potentials are known on this scale. For the cell

$$\text{M}\,|\,\text{MCl}_n\,|\,\text{Cl}_2,$$

the cell potential can be calculated from the free energy of formation of the pure metal chloride. Thus, one can calculate $E^0_{\text{Tl(II)/Tl}}$ on a mole fraction scale. If the activity coefficient of the reference electrode ion is known (that for Ag(I) is known to be unity

Can. J. Chem. Downloaded from www.nrcresearchpress.com by 210.87.254.42 on 09/05/12
For personal use only.

in this melt (9, 10)), the activity coefficient γ_1 of the Ti(II) ion can be calculated; using this, γ_1', for Ti(III), can be found also. Potentiometric data will lead to further thermodynamic quantities through standard relations.

EXPERIMENTAL

The LiCl–KCl eutectic mixture was prepared from Baker Analyzed chemicals, purified by the method of Hill *et al.* (11). The most serious impurity was water. The oven-dried eutectic mixture was placed in a tube with a fritted glass bottom beneath which was a collecting tube. The whole was encased in an outer glass jacket and surrounded by a furnace. Dry HCl gas was passed through the mixture as the temperature was raised until the salt melted. Pure argon was then passed into the melt to remove excess HCl; magnesium turnings were added to reduce heavy metal impurities, and the salt was filtered into the collecting tube. Transfer of the purified eutectic was carried out in a dry-box.

Electrochemical measurements were carried out in a cylindrical furnace made of a steel-lined copper cylinder 20 in. long, with a $2\frac{1}{2}$ in. bore and a 1 in. wall thickness. This was electrically heated by five balanced resistance windings and enclosed in several inches of asbestos felt for insulation. Two slots for observation were cut in the furnace walls and closed with evacuated pyrex tubes imbedded in the insulation to reduce heat loss. Temperature was controlled to ± 0.5 °C by an iron–constantan thermocouple, which was enclosed in a glass sheath in the melt, and controlled a Barber-Coleman Wheelco furnace regulator.

The electrochemical cell and reference electrodes were as described by Hill *et al.* (11). The electrodes were inserted into the cell through O-ring glands which permitted them to be raised or lowered during a run. The reference electrodes consisted of a Pt or Ag foil in a pyrex compartment separated from the bulk of the melt by a glass frit. The Pt(II) or Ag(I) was prepared coulometrically using a second Pt foil in a similar compartment as cathode. The exact concentration was determined from the number of coulombs passed and the chloride content of the electrode compartment as determined at the end of the experiment. The junction potential across the frit should not be significant since the LiCl–KCl eutectic melt was present in all compartments in great excess. A check of thermal potentials arising in the electrode connections and leads showed that these were negligible in our arrangement.

Solutions of Ti(II) were prepared by anodic dissolution of a titanium rod (purity > 99.9%). Successive periods of anodization, accompanied by argon stirring, were used to give a series of Ti(II) concentrations. Concentrations were known from the number of coulombs passed and the weight of the eutectic. Equilibrium potentials were measured on unstirred solutions.

Titanium(II) was oxidized to Ti(III) by coulometric titration, using Pt(II) generated from an immersed platinum foil. Potentials were measured at intervals against a reference electrode. The Ti(III)/Ti(II) apparent standard potential could be taken from the titration curves.

Polarographic behavior was studied using platinum microelectrodes made from 15 mil Pt wire sealed into pyrex tubing. About 0.8 to 1.0 mm^2 of wire projected from the seal; the actual exposure of each one was determined with a microscope. Polarography was also used to monitor the purity of the melt.

In all experiments, a weighed amount of eutectic (about 160 g) was placed in the cell in the dry-box, and fused under *vacuo*. The electrodes were kept above the level of the salt but in the hot zone of the furnace for outgassing. The cell was then flushed with purified argon, which was also used for stirring, and the electrodes lowered to the desired depth.

The measuring equipment included a Sargent Model IV coulometric current source, a Sargent XXI recording polarograph, and a Leads and Northrup Type K-3 Universal potentiometer with electronic d-c. null detector.

Solubility of TiO_2, TiO, or Ti metal in the melt could alter the true concentrations of Ti species present. Consequently, solubilities of these substances were studied by stirring the substance in the melt for several hours, sucking a portion into a fritted glass tube, and cooling. Titanium could then be tested for by chemical analysis.

The LiCl–KCl eutectic is well known to be hygroscopic and to be appreciably hydrolyzed if melted in the presence of moisture. The presence of impurities from this source can be indicated grossly by etching of pyrex containers, and more precisely by a polarographic wave at -1.6 to -1.7 V using a platinum microelectrode and Pt(II)/Pt reference electrode. A small polarographic current (<1.5 $\mu A/cm^2$ at -2.0 V) was observed even with the most carefully purified melts; but this very small current indicates a negligible amount of impurity and compares favorably with the results of other workers (10).

When present in significant amounts, these impurities can have an important effect on the behavior of titanium metal. With inadequately purified melts, corrosion of the rod yielded a dark insoluble product immediately upon its insertion into the melt. This reaction ceased after a period of time which depended on the purity of the melt. It was more rapid at higher temperatures. In adequately purified melts, the effect was slight but still noticeable.

Henrie (12) has suggested that reaction of Ti ions with SiO_2 could take place in these systems. This did not seem to be significant in our case, since the corrosion of the rod ceased after a short time, the Ti(II) solutions prepared seemed quite stable for some time (according to their potentiometric and polarographic

Can. J. Chem. Downloaded from www.nrcresearchpress.com by 210.87.254.42 on 09/05/12
For personal use only.

behavior), there was no trace of attack of the glass when properly purified melts were used, and there was no trace of any silicon-containing residue in the melt (by emission spectrography).

The blackish corrosion product was recovered by leaching the solidified melt with water. X-ray diffraction of the final product showed it to be a mixture of titanium dioxide and titanium monoxide. This precipitate should have no bearing on the electrochemical measurement, since independent studies showed both TiO_2 and TiO to be insoluble in the melt. Solubility studies of powdered Ti metal similarly gave no trace of a soluble corrosion product.

RESULTS AND DISCUSSION

At 450 °C, a plot of cell potential vs. log (mole fraction Ti(II)) (calculated from the number of coulombs passed on anodic dissolution of the Ti rod) was a straight line in the low-concentration region, and had a slope here of 0.06 V, close to that calculated for a two-electron transfer (0.07 V). The plot leveled out at a concentration corresponding to about 5×10^{-5} mole fraction of Ti(II). Further anodization produced a black cloudiness in the melt. Presumably this marks the limit of solubility of $TiCl_2$ in the LiCl–KCl eutectic at this temperature. These results are shown in Fig. 1.

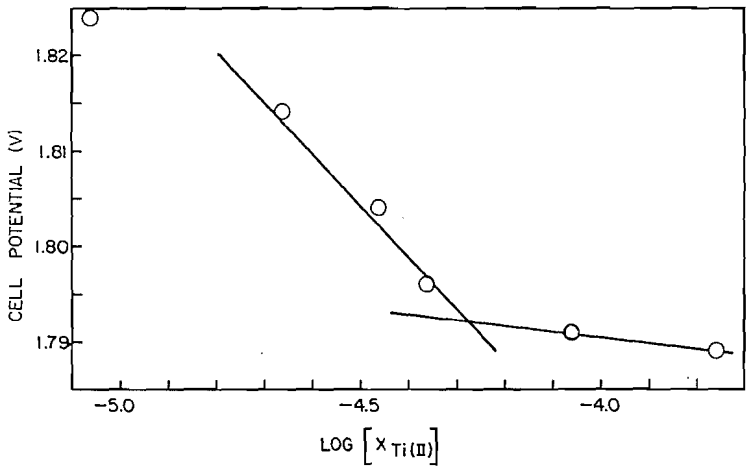

FIG. 1. Ti(II)/Ti potential in LiCl–KCl eutectic at 450 °C. Pt(II)/Pt reference electrode, 2.42×10^{-3} mole fraction of Pt(II).

Polarograms for the oxidation of Ti(II) at this temperature are shown in Fig. 2. At a fixed potential, the polarographic current increases until a Ti(II) concentration of about 5×10^{-5} mole fraction is reached, and then levels off as did the cell potential.

Similar plots of cell potential at 550 °C are shown in Figs. 3 and 4. Again, the plots are linear with a slope of 0.080V, close to the calculated value of 0.082 V for a two-electron transfer. The $TiCl_2$ was more soluble at this temperature. The calculated apparent standard potential averaged over several runs is given in Table I. Solutions of Ti(II) at this temperature were light green in color. Admission of oxygen immediately resulted in the formation of a grey precipitate.

Table I lists the apparent standard potentials determined in this work. The Ti(II)/Ti and Ti(III)/Ti(II) systems were measured directly. The uncertainties indicated here represent the observed variation from the mean of the different experiments. The Ti(III)/Ti potential is calculated from the other values. Also included are results of the Ag(I)/Ag potential against the Pt(II)/Pt electrode to aid in comparison; our value agrees very well with that of Laitinen and Liu (13), −0.637V at 450 °C on the mole fraction scale.

Can. J. Chem. Downloaded from www.nrcresearchpress.com by 210.87.254.42 on 09/05/12
For personal use only.

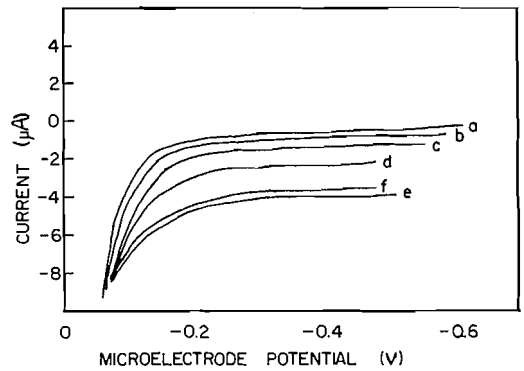

FIG. 2. Polarograms for the oxidation of Ti(II) in LiCl–KCl eutectic at 450 °C. Pt(II)/Pt reference electrode, 1.65×10^{-3} mole fraction of Pt(II). Ti(II) generated in equivalents per 100 g of melt; (*a*) 0, (*b*) 0.31×10^{-4}, (*c*) 1.6×10^{-4}, (*d*) 2.4×10^{-4}, (*e*) 3.1×10^{-4}, (*f*) 6.3×10^{-4}.

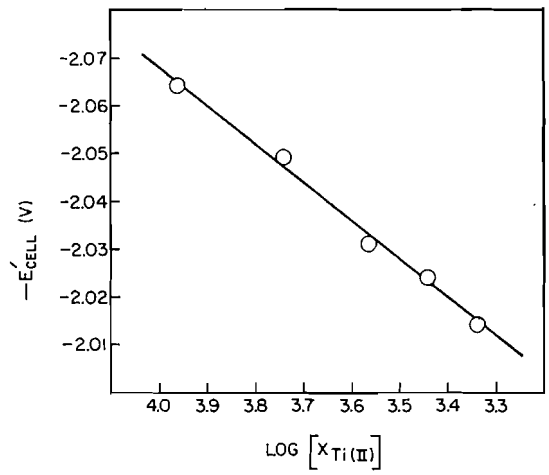

FIG. 3. Ti(II)/Ti potential in LiCl–KCl eutectic at 550 °C. Pt(II)/Pt reference electrode, 2.03×10^{-3} mole fraction of Pt(II).

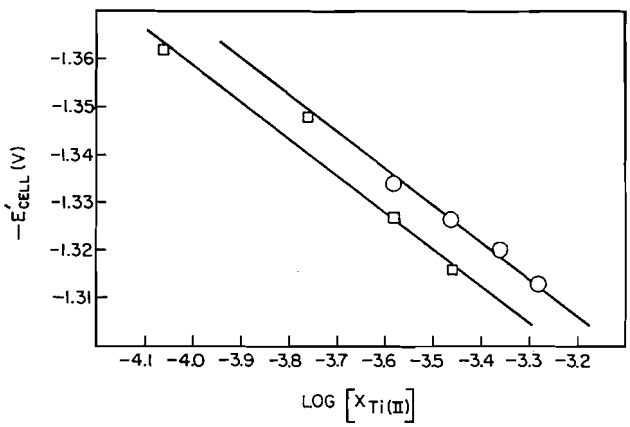

FIG. 4. Ti(II)/Ti potential in LiCl–KCl eutectic at 550 °C. Ag(I)/Ag reference electrode; (○) 1.35×10^{-3} mole fraction of Ag(I), (□) 2.13×10^{-3} mole fraction of Ag(I).

Can. J. Chem. Downloaded from www.nrcresearchpress.com by 210.87.254.42 on 09/05/12
For personal use only.

TABLE I

Apparent standard electrode potentials

Cell	T (°C)	Apparent standard potential (V)	
		Mole fraction scale	Molality scale
Ti|Ti(II)||Pt(II)|Pt	450	−1.74†	−1.74†
	550	−1.73 ±0.01	−1.73
Ti|Ti(II)||Ag(I)|Ag	550	−1.04 ±0.01	−0.94
Pt|Ti(II), Ti(III)||Pt(II)|Pt	450	−1.43†	−1.34†
	550	−1.43 ±0.02	−1.33
Pt|Ti(II), Ti(III)||Ag(I)|Ag	550	−0.75 ±0.01	−0.55
Ti|Ti(III)||Pt(II)|Pt	450	−1.64*	−1.61*
	550	−1.63*	−1.60*
Ag|Ag(I)||Pt(II)|Pt	450	−0.635±0.005	−0.725
	550	−0.667±0.005	−0.770

*Calculated values.
†Extrapolated from higher temperatures.

The temperature dependence of the apparent standard potential of the Ti(II)/Ti system against the Ag(I)/Ag electrode was strictly linear over the range 500–600 °C. (Table II).

TABLE II

Temperature dependence of apparent standard potentials

Cell	T range (°C)	$\Delta E^{0\prime}/\Delta T$ (Volts per degree)
Ag|Ag(I)||Pt(II)|Pt	450–550	3.20×10^{-4}
Ti|Ti(II)||Ag(I)|Ag	500–600	4.0×10^{-4}
Pt|Ti(II), Ti(III)||Pt(II)|Pt	500–600	0

With a given concentration of Ti(II) in the melt, Ti(III) was generated in the system by the reaction

$$2\text{Ti(II)} + \text{Pt(II)} \rightarrow 2\text{Ti(III)} + \text{Pt(0)},$$

using Pt(II) generated coulometrically. A plot of the potential of the immersed platinum foil vs. a reference electrode gave a typical potentiometric titration curve. The greenish color of the Ti(II) changed to a lemon yellow, while finely divided platinum metal was formed. The Ti(III)/Ti(II) apparent standard potential could be taken from the mid-portion of the upper branch of the titration curve, which was comparatively flat. An example of such a titration is shown in Fig. 5. The results of these titrations are listed in Table III; the uncertainty represents that involved in reading the potential from the titration curve. Similar titrations could be carried out using coulometrically generated Cu(I). Each value in Table III represents the mean of several experiments.

The observed end-points of these titration curves usually occurred before the theoretical end-points which could be calculated by the number of coulombs used to generate each reactant. This effect was most significant when small concentrations of Ti(II) were used and probably was caused by reaction of the Ti(II) with traces of impurities. The initial Ti(II) content of the experiment shown in Fig. 5 was only 5×10^{-4} equivalents. Use of larger amounts of Ti(II) reduced this effect, but introduced other problems from the larger amount of platinum metal formed, and from anodic current limitations. This discrepency did not affect the reading of the Ti(III)/Ti(II) potential from the curve, nor would it have influenced the Ti(II)/Ti potential measurements since the concentrations were higher.

Can. J. Chem. Downloaded from www.nrcresearchpress.com by 210.87.254.42 on 09/05/12
For personal use only.

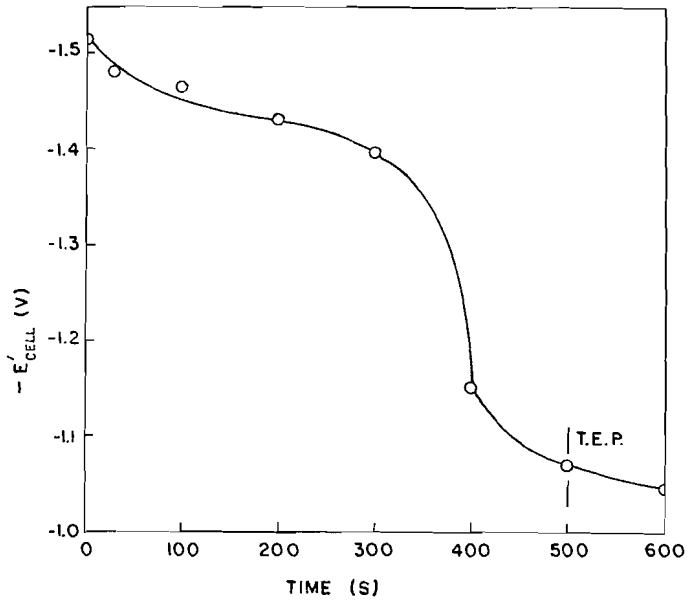

FIG. 5. Coulometric titration of Ti(II) with Pt(II) in LiCl–KCl eutectic at 550 °C. T.E.P. = theoretical end-point.

TABLE III

Standard potentials for the Ti(III)–Ti(II) couple

Cell	T (°C)	Initial concentration Ti(II) (mole fraction)	$E^{0}_{Ti(III)/Ti(II)}$ (V)	Method
(−)Pt | Ti(III), Ti(II) || Pt(II) | Pt(+)	500	9.13×10^{-5}	-1.43 ± 0.02	Back titration
(−)Pt | Ti(III), Ti(II) || Pt(II) | Pt(+)	550	8.59×10^{-5}	-1.43 ± 0.01	Coulometric titration
(−)Pt | Ti(III), Ti(II) || Pt(II) | Pt(+)	550	1.60×10^{-4}	-1.42 ± 0.02	Coulometric titration
(−)Pt | Ti(III), Ti(II) || Pt(II) | Pt(+)	600	8.26×10^{-5}	-1.43 ± 0.02	Coulometric titration
(−)Pt | Ti(III), Ti(II) || Pt(II) | Pt(+)	600	8.26×10^{-5}	-1.43 ± 0.02	Back titration
(−)Pt | Ti(III), Ti(II) || Ag(I) | Ag(+)	550	9.11×10^{-6}	-0.75 ± 0.01	Coulometric titration
(−)Cu | Ti(III), Ti(II) || Ag(I) | Ag(+)	550	3.49×10^{-4}	-0.75 ± 0.02	Coulometric titration

At the end of the titration, it was observed that immersion of the titanium rod back into the melt caused the color to revert back to green, presumably from the reaction

$$Ti + 2Ti(III) \rightarrow 3Ti(II).$$

Consequently, the potential of the platinum foil was measured against the reference electrode at successive times while the titanium rod was immersed in the argon-stirred melt, and a plot of cell potential vs. time again yielded a characteristic titration curve. The Ti(III)/Ti(II) potentials from this "back titration" procedure are also listed in Table III.

Menzies (5) has observed that the equilibrium for the above reaction lies to the right. The free energy change and equilibrium constant calculated for this reaction from the potential data, at 550 °C, are

$$\Delta G \text{ (kcal/mole)} \quad -13.4,$$
$$K_{eq} \quad 3.61 \times 10^{3}.$$

Can. J. Chem. Downloaded from www.nrcresearchpress.com by 210.87.254.42 on 09/05/12
For personal use only.

Thus, the equilibrium does lie far to the right. The reaction Ti(III) + $e^- \rightarrow$ Ti(II) is electrochemically reversible.

Activity coefficients and partial molar free energies of solution for $TiCl_2$ and $TiCl_3$ were calculated from the potential data and are given in Table IV. Activity coefficients increase with temperature, but remain significantly less than unity. They are essentially constant over the concentration range studied. That for Ti(III) is considerably lower than the value for Ti(II); this is at variance with the conclusions of Menzies *et al.* (5) who found $(\gamma_{TiCl_2}/\gamma_{TiCl_3})_{500\,°C} = 2.7$.

TABLE IV

Activity coefficients and partial molal free energies of solution of titanium chlorides in the molten LiCl–KCl eutectic

Salt	Range of mole fraction ($\times 10^5$)	Activity coefficient (γ)		$\Delta\bar{G}_s$ (kcal/mole)	
		450 °C	550 °C	450 °C	550 °C
$TiCl_2$	5–50	0.5	0.8	−9.2	−0.46
$TiCl_3$	3–20	0.1	0.2	−2.8	−2.8

One explanation for low activity coefficients is found in the existence of complex species. Indeed, Gruen and McBeth (14) have spectroscopic evidence for Ti(III) chloride complexes in this melt at these temperatures. The more highly charged Ti(III) would be expected to be more extensively complexed than Ti(II).

The polarographic behavior of Ti(II) and Ti(III) in this melt at 550 °C is shown in Fig. 6. Polarograms (*b*) and (*c*) show waves for the oxidation of Ti(II) to Ti(III) for two concentrations of Ti(II). At a fixed potential, the polarographic currents for successive

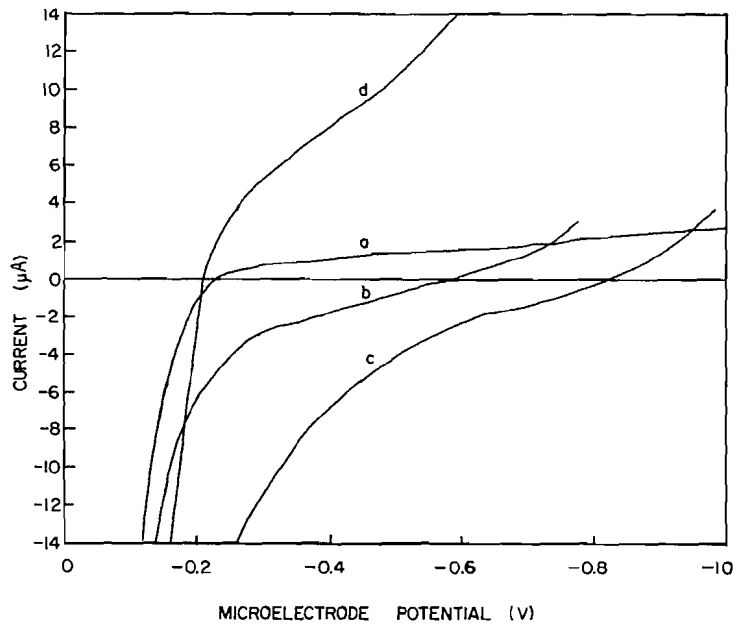

FIG. 6. Polarograms of Ti(II) and Ti(III) in LiCl–KCl eutectic at 550 °C. Pt(II)/Pt reference electrode; 2.10×10^{-3} mole fraction of Pt(II). (*a*) Residual current; (*b*) Ti(II) oxidation (4.3×10^{-5} mole fraction); (*c*) Ti(II) oxidation (8.6×10^{-5} mole fraction); (*d*) Pt(II) reduction, Ti(III) reduction.

Can. J. Chem. Downloaded from www.nrcresearchpress.com by 210.87.254.42 on 09/05/12
For personal use only.

additions of Ti(II) increased in magnitude, but no quantitative relation was observed because of the absence of well-defined plateaus. The potential at which the polarographic current attained the residual value became more negative as the Ti(II) concentration was increased.

Polarogram (*d*) in Fig. 6 shows the combined Pt(II) and Ti(III) reduction waves in solutions, prepared by coulometric titration of Ti(II) with Pt(II) beyond the end-point.

Polarographic waves for the reduction of Ti(II) to Ti(0) were not well defined or reproducible; the waves appeared at about -1.7 to -1.8 V. An approximate fit of the Ti(II) reduction waves to a linear plot of log $(i/(i_d - i))$ vs. E_{me} (where i is the current at any point on the wave, i_d is the limiting diffusion current, and E_{me} is the potential of the platinum microelectrode) was found. This is the sort of behavior expected if the reduced Ti(0) atoms diffuse into the platinum electrode. The oxidation waves fit neither this nor a log $(i_d - i)$ plot.

ACKNOWLEDGMENT

Technical assistance was provided by Mr. Eugene A. Grossi. This work was supported by the United States Atomic Energy Commission under Contract No. At(30-1)-2787.

REFERENCES

1. S. MELLGREN and W. OPIE. J. Metals, **9**, 266 (1957).
2. W. C. KREYE and H. H. KELLOGG. J. Electrochem. Soc. **104**, 504 (1957).
3. S. N. FLENGAS. Ann. N.Y. Acad. Sci. **79**, 853 (1960).
4. M. V. SMIRNOV, L. A. TSIOVKINA, and N. A. LOGENOV. Dokl. Akad. Nauk SSSR, **136**, 1388 (1961).
5. I. A. MENZIES, G. J. HILLS, L. YOUNG, and J. O'M. BOCKRIS. Trans. Faraday Soc. **55**, 1580 (1954).
6. M. V. SMIRNOV, L. IVANOVSKII, and N. A. LOGENOV. Dokl. Akad. Nauk SSSR, **121**, 685 (1958).
7. J. O'M. BOCKRIS, G. J. HILLS, I. A. MENZIES, and L. YOUNG. Nature, **178**, 654 (1956).
8. S. OKADA, M. KAWANE, and T. HASHINO. Z. Elektrochem. **62**, 437 (1958).
9. S. N. FLENGAS and T. R. INGRAHAM. Can. J. Chem. **35**, 1139 (1957).
10. J. B. RAYNOR. Z. Elektrochem. **67**, 360 (1963).
11. D. L. HILL, J. PERANO, and R. A. OSTERYOUNG. J. Electrochem. Soc. **107**, 698 (1960).
12. T. A. HENRIE. The physical chemistry of process metallurgy. Vol. 2. Interscience Publishers, New York. 1961. p. 942.
13. H. A. LAITINEN and C. H. LIU. J. Am. Chem. Soc. **80**, 1015 (1958).
14. D. M. GRUEN and R. L. MCBETH. Pure Appl. Chem. **6**, 23 (1963).

Can. J. Chem. Downloaded from www.nrcresearchpress.com by 210.87.254.42 on 09/05/12
For personal use only.

Can. J. Chem. Downloaded from www.nrcresearchpress.com by 210.87.254.42 on 09/05/12
For personal use only.

SYNTHESIS OF SOME ALPHA-SUBSTITUTED CYSTINES

R. J. THIBERT, J. F. G. DIEDERICH,* AND K. G. RUTHERFORD
Department of Chemistry, University of Windsor, Windsor, Ontario
Received July 14, 1964

ABSTRACT

The synthesis of α-ethyl-, α-*n*-propyl-, α-*n*-butyl-, and α-phenyl-DL-cystine via hydantoin intermediates is reported.

INTRODUCTION

Results in this laboratory on the reduction of α-methyl-DL-cystine at the dropping mercury electrode (1) have prompted further investigation into this area with other alpha-substituted cystines. It became of interest to study the steric effects of various groups in the alpha position of the cystine molecule on the half-wave potential, the diffusion current, the diffusion coefficient, and on the general shapes of the polarograms. Again, the metabolic behavior of alpha-substituted cystines and cysteines (which can be readily obtained from the corresponding cystines by reduction) should be of interest. Umbreit (2), for example, found that α-methyl-DL-glutamic acid is inert to dehydrogenation and transamination and inhibits glutamine breakdown. It has long been known, of course, that alpha-substituted amino acids such as alanine and valine are inert to metabolic reactions (2).

DISCUSSION OF EXPERIMENTAL RESULTS

Several attempts to prepare other alpha-substituted cystines in our laboratory by the Strecker route failed. However, the sequence shown here has proved quite successful for the synthesis of α-ethyl-, α-*n*-propyl-, α-*n*-butyl-, and α-phenyl-DL-cystine.

The only alpha-substituted cystine known to have been synthesized prior to this report is α-methyl-DL-cystine which was prepared by Arnstein (3) and simultaneously in this laboratory by Ottenbrite (4). The Strecker synthesis was employed in both cases. Stapleton and Swan (5) later synthesized this compound via the Bucherer-Bergs route, which involves the isolation of an intermediate hydantoin. α-Methyl-DL-cysteine hydrochloride was first reported by Connors and Ross (6). These authors reduced S-benzyl-α-methyl-DL-cysteine with sodium in liquid ammonia and isolated the final product under nitrogen. Potts (7) synthesized S-benzyl-α-methyl-DL-cysteine by the Bucherer-Bergs route but did not prepare the free mercapto-amino acid.

EXPERIMENTAL

The alpha-haloketones used as starting materials were prepared by methods previously described in the literature. 1-Bromo-2-butanone was obtained via the bromination of 2-butanone according to the procedure of Catch *et al.* (8). Both 1-chloro-2-pentanone and 1-chloro-2-hexanone were prepared by the method of Haworth (9), which involves the reaction of the appropriate acid chlorides with diazomethane followed by decomposition of the diazoketones with hydrochloric acid. Phenacyl chloride was obtained commercially.

The alpha-haloketones were condensed with the sodium salt of α-toluenethiol to yield the corresponding benzylmercaptomethyl ketones. Treatment of these ketones with potassium cyanide and ammonium carbonate in aqueous ethanol (50%) at 60–70° for several hours afforded good yields of the respective

**Taken in part from the thesis submitted by J. F. G. Diederich to the Faculty of Graduate Studies, University of Windsor, Windsor, in partial fulfillment of the requirements for the degree of Master of Science, October, 1963.*

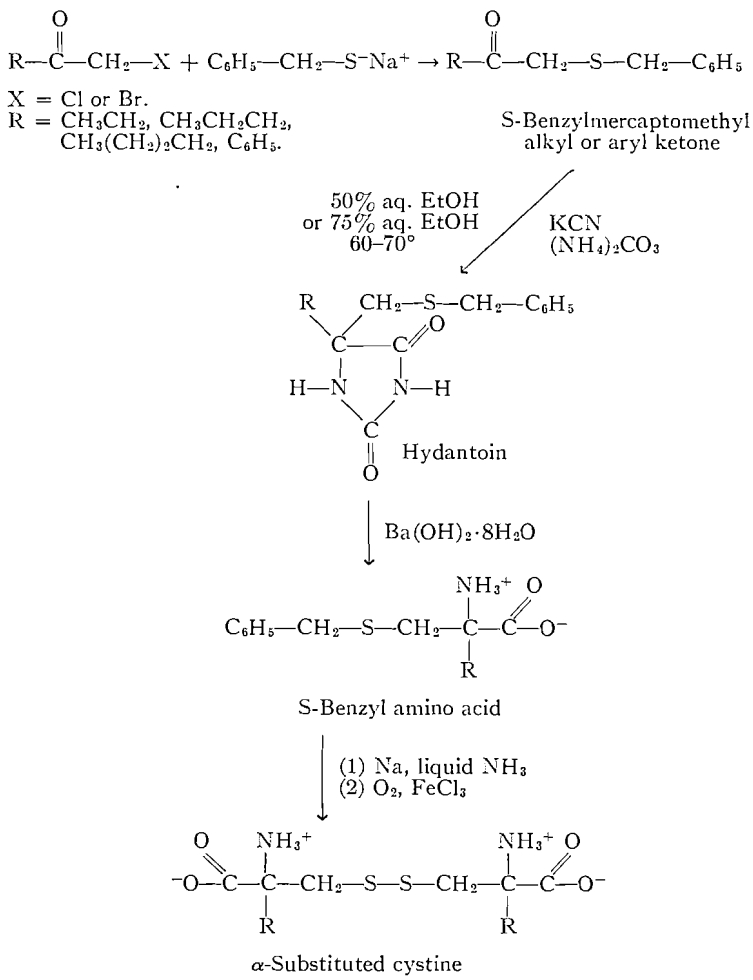

hydantoins when R consisted of ethyl, *n*-propyl, and *n*-butyl groups. A much longer heating period (several days) and 75% alcohol were required for the preparation of the phenyl-substituted hydantoin.

Hydrolysis of the hydantoins with barium hydroxide afforded the S-benzyl amino acids. These compounds were then reduced with sodium in liquid ammonia to the corresponding sulfhydryl amino acids. Subsequent air oxidation of these latter compounds yielded the disulfides (cystines). This route then afforded α-ethyl-, α-*n*-propyl-, α-*n*-butyl-, and α-phenyl-DL-cystine in overall yields of 47%, 45%, 35%, and 31%, respectively, from the starting alpha-haloketones. It is interesting to note that Arnstein (3) obtained a 20% overall yield of α-methyl-DL-cystine via the Strecker route.

Analyses were performed by the Schwarzkopf Microanalytical Laboratory, 56–19 37th Avenue, Woodside 77, New York. Melting points are uncorrected. Some properties of all compounds prepared are presented in Table I.

Benzylmercaptomethyl Ketones

These compounds were prepared according to the procedure of Wahl (10). The preparation of benzylmercaptomethyl-*n*-propyl ketone is typical of the method used in the synthesis of ketones with R = ethyl, *n*-propyl, *n*-butyl, and phenyl. The sodium salt of α-toluenethiol was prepared by extracting α-toluenethiol (130 g, 1.05 mole) in ether (500 ml) with 10% sodium hydroxide solution (400 g). The mixture was shaken intermittently at room temperature for 2 h. The aqueous phase was then separated and heated at reflux temperature with 1-chloro-2-pentanone (60 g, 0.50 mole) overnight. The light-yellow top phase was washed with several 25 ml portions of water until it was free of chloride ions as tested by 10% silver nitrate solution. The heavy oil thus obtained (101 g) was dried over anhydrous sodium sulfate. Fractional distillation yielded benzylmercaptomethyl-*n*-propyl ketone as a colorless oil (93.5 g, 90%), b.p. 163–166° (9.5 mm).

Anal. Calcd. for $C_{12}H_{16}OS$: C, 69.19; H, 7.74; S, 15.39. Found: C, 69.17; H, 7.90; S, 15.53.

Can. J. Chem. Downloaded from www.nrcresearchpress.com by 210.87.254.42 on 09/05/12
For personal use only.

Can. J. Chem. Downloaded from www.nrcresearchpress.com by 210.87.254.42 on 09/05/12
For personal use only.

TABLE I

Properties of compounds prepared*

Type of compound	R	% yield (crude)	Melting point or [boiling point] (°C)	Analysis							
				Found				Calculated			
				%C	%H	%N	%S	%C	%H	%N	%S
Benzylmercapto-methyl ketone	Ethyl	98	[126–128 at 3.5 mm]	68.13	7.19	—	16.28	68.02	7.23	—	16.51
	n-Propyl	90	[163–166 at 9.5 mm]	69.17	7.90	—	15.53	69.19	7.74	—	15.39
	n-Butyl	97	[166–167 at 6 mm]	70.25	8.30	—	14.50	70.21	8.15	—	14.42
	Phenyl†	97	85	—	—	—	—	—	—	—	—
Hydantoin	Ethyl	90	130–131	59.09	6.05	10.40	11.85	59.03	6.10	10.65	12.12
	n-Propyl	97	154	60.50	6.74	10.17	11.70	60.37	6.51	10.11	11.51
	n-Butyl	71	169	61.56	6.64	9.29	—	61.61	6.89	9.58	—
	Phenyl‡	71	175–176	65.61	5.26	8.63	10.50	65.34	5.17	8.97	10.27
S-Benzyl-DL-cysteine	Ethyl	74	224–226 (decomp.)	60.50	7.00	5.93	13.64	60.20	7.15	5.88	13.31
	n-Propyl	72	229 (decomp.)	61.47	7.62	5.56	12.87	61.61	7.56	5.56	12.65
	n-Butyl	73	229–230 (decomp.)	62.73	7.96	5.05	12.22	62.99	7.89	5.22	11.97
	Phenyl	79	236–240 (decomp.)	67.12	5.67	5.09	11.13	66.80	5.96	4.88	11.16
DL-Cystine	Ethyl§	72	254–258 (decomp.)	34.64	6.15	8.13	18.64	35.06	5.87	8.18	18.73
	n-Propyl	72	260 (decomp.)	44.11	7.54	8.50	—	44.42	7.46	8.63	—
	n-Butyl	70	245–249 (decomp.)	47.52	7.86	7.84	17.89	47.70	8.01	7.95	18.16
	Phenyl‖	57	243–245 (decomp.)	54.84	4.94	7.33	16.92	55.08	5.14	7.10	16.34

*All compounds in the table, except for the two indicated, have not been reported in the literature.
†Prepared previously by Wahl (10).
‡Prepared previously by Long (12).
§Obtained as the disodium salt by a final precipitation at a pH of 7.5.
‖Purified by dissolution in hot 2 *N* hydrochloric acid, followed by filtration and precipitation at a pH of about 5 by concentrated ammonium hydroxide.

Benzylmercaptomethyl Alkyl Hydantoins

These compounds were prepared according to the method of Bucherer (11). The preparation of 5-benzylmercaptomethyl-5-*n*-propyl hydantoin is an example of the method used in the synthesis of the alkylated hydantoins. A mixture of benzylmercaptomethyl-*n*-propyl ketone (90 g, 0.43 mole), potassium cyanide (40 g, 0.61 mole), and ammonium carbonate (135 g, 1.40 mole) dissolved in 400 ml of 50% ethanol was heated in a 1 l, three-necked, round-bottomed flask (equipped with a condenser and mechanical stirrer) on a water bath at 60–70° for 7 h. The dark-yellow solution was allowed to partially evaporate overnight. The residue was then poured on crushed ice. The white precipitate was separated by filtration, washed with water and small quantities of ether, and dried in a vacuum dessicator. This procedure gave 52 g (97%) of hydantoin, m.p. 148–151°. After one crystallization from hot ethanol, white plates, m.p. 154°, were obtained.

Anal. Calcd. for $C_{14}H_{18}N_2O_2S$: C, 60.37; H, 6.51; N, 10.11; S, 11.51. Found: C, 60.50; H, 6.74; N, 10.17; S, 11.70.

5-Benzylmercaptomethyl-5-phenyl Hydantoin

The Bucherer-Bergs method described above was modified slightly, the reaction time was increased, and a higher percentage of ethanol was used.

A mixture of benzylmercaptomethyl phenyl ketone (125 g, 0.52 mole) and 1 500 ml of absolute ethanol was stirred at 60° until all the solid had dissolved. A solution of potassium cyanide (50 g, 0.77 mole) dissolved in 500 ml of water was added with stirring. Ammonium carbonate (300 g, 3.13 mole) was then added. A clear, light-yellow solution was obtained after this mixture had been stirred at 60–70° for about 20 h. This was allowed to react for another 28 h, decanted into a beaker, and allowed to stand at room temperature for several hours whereupon a white solid precipitated. This was recovered by filtration, m.p. 164–168°. The filtrate was poured on a mixture of ice and hydrochloric acid. The solid which separated was recovered by filtration.

All of the solid material obtained was crystallized from hot ethanol to yield 110 g of pure 5-benzylmercaptomethyl hydantoin, m.p. 175–176°. More hydantoin, 5 g, m.p. 175–176°, was recovered by partial evaporation of the combined filtrates. A total yield of 115 g (71%) of hydantoin, m.p. 175–176°, was thus obtained. Long (12) reported a melting point of 174° and a 90% yield.

Anal. Calcd. for $C_{17}H_{16}N_2O_2S$: C, 65.34; H, 5.17; N, 8.97; S, 10.27. Found: C, 65.61; H, 5.26; N, 8.63; S, 10.50.

*S-Benzyl-α-alkyl-*DL*-cysteines*

The preparation of S-benzyl-α-*n*-propyl-DL-cysteine is typical of the procedure used, where R = ethyl, *n*-propyl, or *n*-butyl.

A mixture of 5-benzylmercaptomethyl-5-*n*-propyl hydantoin (60 g, 0.27 mole), barium hydroxide (315 g, 1.0 mole) and 1 500 ml of water was heated at reflux temperature for 40 h in a 2 l round-bottomed flask. Barium was precipitated as barium carbonate at 100° using carbon dioxide generated from the reaction of marble chips with hydrochloric acid. The barium carbonate was separated by filtration and washed with boiling water and then acetone. When the filtrate was allowed to cool, unreacted hydantoin (13 g) precipitated and was removed by filtration. The filtrate was then allowed to evaporate at room temperature whereupon S-benzyl-α-*n*-propyl-DL-cysteine precipitated after several hours. It was separated by filtration and washed with small amounts of acetone. A crude yield of 72% (39 g), m.p. 218–220° (decomp.) was obtained. After the product was recrystallized from hot water, washed with acetone, and dried over phosphorous pentoxide in a vacuum dessicator, the melting point of the white powder was 229° (decomp.). The ninhydrin test gave a reddish-purple color.

Anal. Calcd. for $C_{13}H_{19}NO_2S$: C, 61.61; H, 7.56; N, 5.56; S, 12.65. Found: C, 61.47; H, 7.62; N, 5.56; S, 12.87.

*S-Benzyl-α-phenyl-*DL*-cysteine*

A mixture of 5-benzylmercaptomethyl-5-phenyl hydantoin (42 g, 0.13 mole), and 860 ml of water was heated at reflux temperature with stirring. Only part of the hydantoin dissolved. After a reaction time of 7 days a large quantity of a white solid appeared in the reaction flask. This was recovered by filtration. The barium in the filtrate was precipitated as barium carbonate and was separated by filtration. The filtrate was partially evaporated on a hot plate whereupon some S-benzyl-α-phenyl-DL-cysteine precipitated. This was separated by filtration and washed with acetone, m.p. 236–240° (decomp.). However, only a few grams of material were obtained in this manner. The solid removed previously from the reaction flask was added with stirring into 3 l of boiling water. Carbon dioxide was then passed into the mixture to precipitate barium as barium carbonate. The latter was then removed by filtration. Evaporation of the filtrate yielded a few grams of desired product, m.p. 235–239° (decomp.). Most of the amino acid was apparently adsorbed to the barium carbonate. This could be recovered by stirring the mixture of inorganic and organic materials with several 3 l quantities of boiling water, followed by filtration and evaporation of the filtrate. This process yielded a total of 30.5 g (79%) of the cysteine, m.p. 236–240° (decomp.).

The cysteine is very insoluble in hot water. In order to purify it, it was dissolved in 3 *N* sulfuric acid. Insoluble impurities were removed by filtration. Dropwise addition of concentrated ammonium hydroxide caused the amino acid to precipitate. Precipitation began at about pH 2. The final pH was 5. The material melted at 242–243° (decomp.).

Can. J. Chem. Downloaded from www.nrcresearchpress.com by 210.87.254.42 on 09/05/12
For personal use only.

Anal. Calcd. for $C_{16}H_{17}NO_2S$: C, 66.80; H, 5.96; N, 4.88; S, 11.16. Found: C, 67.12; H, 5.67; H, 5.09; S, 11.13.

α-Alkyl Cystines

A method used by Arnstein (3) and Wood and du Vigneaud (13) was followed with slight modifications. The preparation of α-*n*-propyl-DL-cystine is typical of the procedure used. Sodium metal (7.5 g, 0.33 mole), cut into small pieces and freshly dried S-benzyl-α-*n*-propyl-DL-cysteine (25 g, 0.077 mole) were added alternatively in small amounts with stirring to about 500 ml of liquid ammonia over a period of 30 min. After 1 h the blue color of the mixture was discharged with 3 g of ammonium chloride. The reaction mixture was left at room temperature overnight to allow the ammonia to evaporate. The white paste which remained was dissolved in 350 ml of cold water. The insoluble material was removed by filtration. The filtrate was then extracted with 35 ml of ether. The pH of the filtrate was adjusted to 7.5 with concentrated hydrochloric acid and a trace (about 5 mg) of ferric chloride was added. The dark-violet solution was aerated for 30 h. After this period no sulfhydryl groups were present as tested by sodium nitroprusside. The pH was then adjusted to 6. When this solution was evaporated on a steam bath to a volume of about 200 ml the α-*n*-propyl-DL-cystine precipitated as a yellow, amorphous powder. After recrystallization from boiling water which contained a small amount of decolorizing charcoal, a white solid was obtained, m.p. 260° (decomp.). The melting point was found to vary with variation in rate of heating. A yield of 11.6 g (72%) was obtained.

Anal. Calcd. for $C_{12}H_{24}N_2O_4S_2$: C, 44.42; H, 7.46; N, 8.63. Found: C, 44.11; H, 7.54; N, 8.50.

ACKNOWLEDGMENT

The authors gratefully acknowledge the continued financial support from the National Research Council of Canada.

REFERENCES

1. R. J. THIBERT and R. M. OTTENBRITE. Anal. Chem. **32**, 106 (1960).
2. W. W. UMBREIT. Symposium on Amino Acid Metabolism, Merck Inst., Rahway, N.J. 1955. pp. 48–62.
3. H. R. V. ARNSTEIN. Biochem. J. **68**, 333 (1958).
4. G. W. KOSICKI, R. M. OTTENBRITE, and R. J. THIBERT. Chemistry Dept., University of Windsor, Windsor, Ont. Unpublished studies.
5. I. W. STAPLETON and J. M. SWAN. Australian J. Chem. **13**, 416 (1960).
6. T. A. CONNORS and W. C. J. ROSS. Chem. Ind. London, 366 (1958).
7. K. P. POTTS. J. Chem. Soc. 1632 (1955).
8. J. R. CATCH, D. F. ELLIOT, D. H. HEY, and E. R. H. JONES. J. Chem. Soc. 272 (1948).
9. R. D. HAWORTH. J. Chem. Soc. 3617 (1954).
10. R. WAHL. Ber. **55**, 1449 (1922).
11. H. T. BUCHERER. J. Prakt. Chem. **141**, 28 (1934).
12. L. M. LONG. J. Am. Chem. Soc. **68**, 2159 (1946).
13. J. L. WOOD and V. DU VIGNEAUD. J. Biol. Chem. **131**, 267 (1939).

Can. J. Chem. Downloaded from www.nrcresearchpress.com by 210.87.254.42 on 09/05/12
For personal use only.

Can. J. Chem. Downloaded from www.nrcresearchpress.com by 210.87.254.42 on 09/05/12
For personal use only.

AN ELECTRON IMPACT STUDY OF SOME C_8H_{10} ISOMERS

F. MEYER, P. HAYNES,[1] STEWART MCLEAN, AND A. G. HARRISON[2]
Department of Chemistry, University of Toronto, Toronto, Ontario

Received August 4, 1964

ABSTRACT

The mass spectra of 1-, 2-, and 6-methylspiro[2.4]hepta-1,3-diene have been measured and found to be very similar to the spectra of 7-methylcycloheptatriene and the isomeric alkyl benzenes. It is concluded that in all cases the major part of the fragmentation occurs by identical paths involving identical intermediates. This conclusion is supported by deuterium labelling and appearance potential data. On the other hand the mass spectrum of 2,5-dimethyl-1,5-hexadien-3-yne, an acyclic C_8H_{10} isomer, shows a number of significant differences in its fragmentation pattern. These differences are reflected in the energetics of ion formation and it is concluded that in this case the fragmentation proceeds through different intermediates.

INTRODUCTION

It was pointed out recently (1, 2) that the mass spectra of a number of C_7H_8 isomers are very similar and this was explained by the assumption that all compounds decompose largely via a common intermediate, probably a seven-membered ring. The C_7H_8 isomers included toluene and cycloheptatriene (1), bicyclo[2.2.1]hepta-2,5-diene, spiro[2.4]hepta-1,3-diene, 1- and 3-ethinylcyclopentene, and quadricyclene (3). More recently the mass spectrum of bicycylo[3.2.0]hepta-2,6-diene has been recorded (4) and is again very similar. Extensive deuterium labelling has supported the assumption of a symmetrical seven-membered ring intermediate, presumably the tropylium ion (5).

We report now the mass spectra of a number of methyl-substituted analogues of these compounds, the C_8H_{10} isomers. The mass spectra of 1-, 2-, and 6-methylspiro[2.4]hepta-1,3-diene (I, II, III) have been compared with three other C_8H_{10} compounds: 7-methylcycloheptatriene, *m*-xylene, and an acyclic compound 2,5-dimethylhexa-1,5-dien-3-yne (IV). The spectra of the 1- and 2-methyl spiro compounds are identical while the 6-methyl compound shows only minor differences. The spectra of the methyl-substituted spiroheptadienes are very similar to the spectra of the xylenes and methylcycloheptatriene. Furthermore the spectra of the deuterium-labelled methylspiroheptadienes show extensive hydrogen-deuterium scrambling in the formation of $C_8H_9^+$ and $C_7H_7^+$, similar to the results reported previously for *p*-xylene (6). On the other hand the spectrum of the acyclic isomer, 2,5-dimethyl-1,5-hexadien-3-yne, differs significantly from the spectra of the other C_8H_{10} isomers and these differences are reflected in the energetics of formation of the $C_8H_9^+$ and $C_7H_7^+$ fragments.

The further decomposition of the $C_8H_9^+$ ion is shown from deuterium labelling in the methylspiroheptadienes and methylethylbenzene to involve complete scrambling of all hydrogens.

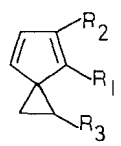

I. R_1 = Me; R_2 = R_3 = H.
II. R_2 = Me; R_1 = R_3 = H.
III. R_3 = Me; R_1 = R_2 = H.

IV. $H_2C{=}C(CH_3){-}C{\equiv}C{-}C(CH_3){=}CH_2$.

[1]*Holder of an N.R.C. Studentship 1963–1964.*
[2]*Alfred P. Sloan Research Fellow 1962–1964.*

Can. J. Chem. Downloaded from www.nrcresearchpress.com by 210.87.254.42 on 09/05/12
For personal use only.

EXPERIMENTAL

All mass spectra were obtained with an A.E.I. MS-2 mass spectrometer which has been described previously (7). Mass spectra were recorded at 50 V electron energy, 20 μA ionizing current, and a repeller voltage of 3 V (7 V/cm). Appearance potentials were measured as described previously (8) using xenon to calibrate the voltage scale.

1-(I) and 2-(II)Methylspiro[2.4]hepta-1,3-diene

The synthesis of these compounds by the reaction of 1,2-dibromoethane with sodium methylcyclopentadienide in the presence of sodium amide in liquid ammonia is described elsewhere (9).

1- and 2-Methylspiro[2.4]hepta-1,3-diene-6,6,7,7-d_4

These were synthesized in the same way using 1,2-dibromoethane-d_4.

1- and 2-Methyl-d_3-spiro[2.4]hepta-1,3-diene

These were prepared by the reaction in liquid ammonia of 1,2-dibromoethane with sodium methyl-d_3-cyclopentadienide which had been prepared *in situ* by treatment of sodium cyclopentadienide with bromomethane-d_3 and then sodium amide.

6-Methylspiro[2.4]hepta-1,3-diene (III)

6-Methylspiro[2.4]hepta-1,3-diene (III) was synthesized from sodium cyclopentadienide and 1,2-dibromopropane by the procedure described for I and II (9). The product, retention time 1.65 (relative to spiroheptadiene = 1.00 (9)), $\lambda\lambda_{max}^{MeOH}$ 257, 227 mμ, formed an N-phenylmaleimide adduct, m.p. 170–171 (sealed tube). (Found: C, 77.31; H, 6.03; N, 5.13. $C_{18}H_{17}O_2N$ requires C, 77.39; H, 6.13; N, 5.01.)

2,5-Dimethyl-1,5-hexadien-3-yne(IV)

2,5-Dimethyl-1,5-hexadien-3-yne(IV) was prepared from 2,5-dihydroxy-2,5-dimethyl-3-hexyne by Nazarov's method (10). Purification of the yellow product by gas–liquid chromatography led to the isolation of its principal component as a *colorless* liquid, $\lambda\lambda_{max}^{heptane}$ 250 mμ (ϵ 14 250), 233 mμ (shoulder, ϵ 11 800), 262 mμ (shoulder, ϵ 12 100), which showed absorption at 1 613 and 895 cm^{-1} in the infrared and a complex multiplet (at least 10 narrowly spaced lines) centered at 4.78 τ (area 2) and a narrowly spaced multiplet (at least 3 lines) at 8.12 τ (area 3) in the nuclear magnetic resonance (n.m.r.) spectrum. The material rapidly became an intensely yellow oil on standing in air.

7-Methylcyclohepta-1,3,5-triene

7-Methylcyclohepta-1,3,5-triene was very kindly supplied by Mr. R. B. Medz and Professor H. J. Dauben, Jr. of the University of Washington.

Compounds used in the present study were purified by gas–liquid chromatography using a 9 ft. $\times$ $\frac{1}{4}$ in. column of 20% MEEE($(MeOCH_2CH_2OCH_2CH_2)_2O$) on Chromosorb P (60–80 mesh), typically at 75 °C with 80 ml/min helium as carrier gas.

RESULTS AND DISCUSSION

Table I shows the major peaks in the spectra of six C_8H_{10} isomers expressed as percentage of total ionization. The peaks shown account for approximately 85% of the total ionization.

TABLE I

Partial mass spectra of C_8H_{10} compounds

m/e	1- and 2-Methyl-spiroheptadiene	6-Methyl-spiroheptadiene	7-Methyl-cycloheptatriene	*m*-Xylene	2,5-Dimethyl-1,5-hexadien-3-yne
106	11.66	10.09	10.88	18.30	19.71
105	6.57	5.05	4.48	7.96	4.40
103	2.24	1.51	1.66	1.89	1.42
91	31.10	31.20	37.84	31.40	17.01
79	4.11	3.84	3.04	2.39	4.22
78	2.67	6.34	3.58	2.16	6.43
77	4.85	4.22	4.39	4.18	3.73
65	4.10	4.28	4.64	2.49	8.99
63	1.86	2.42	1.91	1.98	3.67
52	1.92	2.41	1.66	1.83	2.07
51	4.42	4.26	3.86	3.57	3.59
50	1.93	1.86	1.48	1.21	1.83
41	0.88	1.35	0.67	0.63	1.46
39	5.06	6.41	4.56	4.24	6.43

Can. J. Chem. Downloaded from www.nrcresearchpress.com by 210.87.254.42 on 09/05/12
For personal use only.

The mass spectrum of 1-methylspiro[2.4]hepta-1,3-diene was found to be identical with the spectrum of the 2-methyl isomer, while the only significant difference in the spectrum of the 6-methyl isomer is the higher intensity for $m/e = 78$ (parent-28). This higher intensity may correspond to the simple loss of $CH_3CH\langle$ from the 6-methyl isomer, a fragmentation which is not possible for the other isomers without rearrangement. The spectra of the spiro compounds bear a very close resemblance to the spectra of 7-methylcycloheptatriene and the C_8H_{10} alkylbenzene isomers, of which *m*-xylene has been chosen as representative. On the other hand the spectrum of the acyclic isomer shows a greatly reduced parent-CH_3 ($m/e = 91$) intensity and an increased $C_5H_5^+$ ($m/e = 65$) intensity. The close similarity of the spectra of the monocyclic and spiro isomers suggests that for these isomers fragmentation occurs by common paths involving common intermediates. The same fragmentation paths undoubtedly apply for the acyclic isomer as well; however, the intermediates formed in this case have different structures.

For all compounds the same metastable transitions were observed (Table II), indicating the same fragmentation paths. The major decomposition path is the sequence [1]:

[1] $$C_8H_{10}^+ \rightarrow CH_3 + C_7H_7^+ \rightarrow C_2H_2 + C_5H_5^+ \rightarrow C_2H_2 + C_3H_3^+$$

TABLE II

Metastables in C_8H_{10} compounds

Reaction	Metastable
$105^+ \rightarrow 103^+ + 2$	101.0
$106^+ \rightarrow 91^+ + 15$	78.1
$105^+ \rightarrow 79^+ + 26$	59.4
$105^+ \rightarrow 78^+ + 27$	57.9*
$106^+ \rightarrow 78^+ + 28$	57.4
$91^+ \rightarrow 65^+ + 26$	46.4
$65^+ \rightarrow 39^+ + 26$	23.5

*Only one metastable observed.

A second minor path proceeds through the $C_8H_9^+$ ion to form ions in the C_6 and C_4 region. In addition several other minor paths are possible, such as that suggested above for formation of $m/e = 78$ in 6-methylspiroheptadiene.

Table III records the appearance potentials of the $C_8H_{10}^+$, $C_8H_9^+$, and $C_7H_7^+$ ions from seven C_8H_{10} isomers in addition to the appearance potential of $C_8H_9^+$ from *p*-ethyl

TABLE III

Appearance potentials and heats of formation of $C_8H_{10}^+$, $C_8H_9^+$, and $C_7H_7^+$

Compound	Appearance potential (±0.1 eV)			ΔH_f (kcal/mole)		
	$C_8H_{10}^+$	$C_8H_9^+$	$C_7H_7^+$	$C_8H_{10}^+$	$C_8H_9^+$	$C_7H_7^+$
1-Methylspiroheptadiene	8.02	9.9	9.8	229	220	237
2-Methylspiroheptadiene	8.07	9.9		230	220	
6-Methylspiroheptadiene	8.40	10.65	9.7	240	239	238
7-Methylcycloheptatriene	8.39	11.0	10.0	231	240	235
m-Xylene	8.85	11.85*	11.6	208	225	240
2,5-Dimethyl-1,5-hexadien-3-yne	8.95	10.4	10.5	275	252	278
Spiroheptadiene			10.45			241
Ethylbenzene	9.17†	11.4	11.2	218	223	234
p-Methylethylbenzene		11.2			225	

*Reference 7.
†Tables of ionization potentials by R. W. Kiser, U.S. Atomic Energy Commission TID-6142.

toluene. The last three columns show the ionic heats of formation calculated from these data. The heats of formation for several of the isomers are not known and were estimated as outlined in a later section. For the cyclic isomers the appearance potential data are consistent with the spectral intensities given in Table I. Thus *m*-xylene has the highest parent ion intensity, as would be predicted since the activation energy (A(fragment) − A(molecule ion)) for further fragmentation is highest in this case. The high parent ion intensity for 2,5-dimethyl-1,5-hexadien-3-yne cannot be explained in this fashion since the activation energy for further fragmentation is lower than for any other compound studied. If fragmentation occurred through the same intermediates, one might well expect the lowest parent ion intensity for the acyclic isomer.

The $\Delta H_f(C_7H_7^+)$ from the spiroheptadienes, methylcycloheptatriene, xylene, and ethylbenzene all lead to a value of 237 ± 3 kcal/mole, suggesting that in all cases the same ion is formed through the same intermediate. For ethylbenzene, deuterium labelling (11) strongly suggests a tropylium ion structure for the $C_7H_7^+$ ion. The identity of the heat of formation suggests a tropylium structure for the $C_7H_7^+$ ion from the other isomers as well. However, in all cases the ion must be formed with excess energy, since the true heat of formation for a tropylium ion is probably considerably lower (12). The excess energy may be viewed as the energy required to raise the molecule to an excited ionized state capable of dissociating to give the cyclic $C_7H_7^+$. For 2,5-dimethyl-1,5-hexadien-3-yne a much higher value for $\Delta H_f(C_7H_7^+)$ = 278 kcal/mole is obtained. This suggests either a different (acyclic) structure or a more complicated rearrangement to form the cyclic $C_7H_7^+$ ion which requires a greater excess energy. In the absence of labelling evidence a definite conclusion cannot be reached although the former appears more likely. In any event it is evident that the fragmentation does not proceed through the same intermediate ionic state in this case.

Although the appearance potential data for the $C_7H_7^+$ ion serve to point out the similar behavior of the cyclic compounds and the rather striking difference for the acyclic isomer, the data for the $C_8H_9^+$ ion are much less clear-cut. As shown by the data in Table III the appearance potential of $C_8H_9^+$ from 1- and 2-methylspiroheptadiene, ethylbenzene, and *m*-xylene lead to $\Delta H_f(C_8H_9^+)$ = 220–225 kcal/mole, in agreement with values in this same range obtained from appearance potential measurements in the xylenes (7), the diethylbenzenes (13), the methyl-*n*-propylbenzenes (13), and *p*-ethyltoluene. On the other hand $A(C_8H_9^+)$ from 6-methylspiroheptadiene and 7-methylcycloheptatriene give a $\Delta H_f(C_8H_9^+)$ = 239–240 kcal/mole, in agreement with a value of 236 kcal/mole reported for $C_8H_9^+$ from mesitylene (13). Both these sets are much higher than the value of 202 ± 3 kcal/mole derived from the directly measured ionization potentials of the xylyl radicals (14) and from the appearance potential of $C_8H_9^+$ from the xylylbromides (7). In the latter case it was suggested, from the absence of observable substituent orientation effects, that the $C_8H_9^+$ ion had the methyltropylium structure. If such is the case the $C_8H_9^+$ formed by dissociation of the alkylbenzenes and spiroheptadienes must be formed with excess energy which, in contrast with the results for $C_7H_7^+$ formation, varies with the compound studied.

The appearance potential of $C_8H_9^+$ from 2,5-dimethyl-1,5-hexadien-3-yne leads to $\Delta H_f(C_8H_9^+)$ = 252 kcal/mole. One would expect this to correspond to an acyclic ion and the heat of formation is indeed considerably higher than that obtained from any of the cyclic isomers. However, since the total spread in values for $\Delta H_f(C_8H_9^+)$ is rather large it is probably premature to reach any definite conclusions in the absence of more conclusive evidence.

The similarity in behavior of the spiro compounds and the alkylbenzenes upon electron

Can. J. Chem. Downloaded from www.nrcresearchpress.com by 210.87.254.42 on 09/05/12
For personal use only.

impact is shown further by comparison of the spectra of deuterium labelled methylspiroheptadienes and labelled alkylbenzenes (particularly *p*-xylene (6)). Two deuterium-labelled spiro compounds methyl-d_3-spiroheptadiene and methylspiroheptadiene-6,6,7,7-d_4 were studied. In both cases spectra were obtained for mixtures of the 1- and 2-methyl-substituted isomers. Partial mass spectra in the C_8 and C_7 region are given in Table IV. The spectra are corrected for naturally occurring ^{13}C.

TABLE IV

Partial mass sepctra of 1- and 2-methylspiroheptadienes

	Methylspiroheptadiene				Methylspiroheptadiene		
m/e	d_0	Methyl-d_3	6,6,7,7-d_4	*m/e*	d_0	Methyl-d_3	6,6,7,7-d_4
110			36.26	102	1.06		
109		36.10	13.93	95			43.88
108		15.82	7.06	94		30.57	12.50
107		6.16	2.97	93		10.52	22.58
106	35.64	2.96	3.00	92		11.30	12.56
105	21.02	3.96	1.80	91	100.0	51.12	2.39
104	1.34	1.28		90	0.57	0.69	0.46
103	7.10			89	2.00	0.99	

The C_8 region is formed from the parent ion with essentially complete scrambling of the deuterium and hydrogen just as in *p*-xylene (6). There is a preference for loss of H over loss of D, probably due to an isotope effect. The loss of D compared with the total loss of hydrogen and deuterium from the parent is 26% and 32% in the d_3- and the d_4-compound respectively compared with calculated percentages of 30% and 40% assuming complete scrambling and no isotope effect. The ratios are corrected for a small contribution for loss of H_2 which gives a peak at the same mass as loss of deuterium.

As is the case for *p*-xylene (6), the loss of methyl from the methylspiroheptadienes is a very complicated process as shown by the large intensities at *m/e* 91 to 94 in the d_3-compound and 92 to 95 in the d_4-compound. The labelling results clearly are not in accord with a simple loss of the CH_3 group and indeed they cannot be explained by any simple fragmentation scheme. Low energy scans in the C_7 region for the methylspiroheptadiene-d_4 suggested that there is more than one process for the loss of methyl from the parent ion. With lower energy the intensity at *m/e* = 95 ($C_7H_3D_4^+$) decreases with respect to 92, 93, and 94. It is interesting to note that although the 95 peak corresponds to straight loss of the original methyl group and is the biggest peak in the spectrum; it is energetically the least favored process for loss of methyl. Combining the data at 50 V for the two deuterated spectra the percentages given in Table V can be assigned to the loss of CH_3 containing hydrogen from different parts of the molecule. H_m stands for hydrogen from the original methyl group, H_r for hydrogen from the five-membered ring, and H_s for hydrogen from the three-membered ring. The solution is given between two limiting values because it was not possible to solve the equations completely. $CH_mH_rH_s + CH_rH_rH_s = 2.56\%$ and this gives the limits $CH_mH_rH_s = 2.56\%$ and $CH_rH_rH_s = 2.56\%$. Because there are probably different processes with slightly different energy requirements it is not possible to propose any general reaction mechanism but it might be noted that the results indicate a high degree of mixing of the methyl hydrogens and three-membered ring hydrogens ($CH_mH_sH_s$ and $CH_mH_mH_s$).

As mentioned previously the structure of the $C_8H_9^+$ ion is not certain. A methyl-substituted tropylium structure has been proposed for the $C_8H_9^+$ ion formed by dissociative

Can. J. Chem. Downloaded from www.nrcresearchpress.com by 210.87.254.42 on 09/05/12
For personal use only.

TABLE V

Loss of methyl from 1- and 2-methylspiroheptadiene between two limiting values

Methyl group	% loss	Methyl group	% loss
$CH_mH_mH_m$	49.40–49.40	$CH_mH_rH_s$	0–2.56
$CH_mH_sH_s$	10.15–7.60	$CH_rH_rH_s$	2.56–0
$CH_rH_sH_s$	13.45–16.00	$CH_mH_rH_r$	0–0
$CH_mH_mH_s$	10.91–10.91	$CH_mH_mH_r$	0–0
$CH_sH_sH_s$	13.53–13.53	$CH_rH_rH_r$	0–0

ionization of the xylylbromides (7), based on the lack of effects due to substituent orientation. Labelling studies (15) on the loss of methyl from *p*-methylethylbenzene are also best explained on the assumption of a methyltropylium structure for the $C_8H_9^+$ ion. However, the results obtained for the further decomposition of the $C_8H_9^+$ ion, both in this work and in previous studies (5), cannot be reconciled with a simple methyltropylium structure for those $C_8H_9^+$ ions which undergo further frgamentation.

The $C_8H_9^+$ ion loses C_2H_2 to form the $C_6H_7^+$ ion which further loses H_2 to form $C_6H_5^+$ as shown from the metastable peaks at 59.4 and 75.1 corresponding to reactions [2] and [3] respectively.

[2] $$C_8H_9^+ \rightarrow C_6H_7^+ + C_2H_2$$

[3] $$C_6H_7^+ \rightarrow C_6H_5^+ + H_2.$$

These decomposition paths have been observed previously for *p*-xylene (6) and ethylbenzene (16) and it was observed that essentially complete scrambling of the hydrogens in $C_8H_9^+$ occurred in the formation of the C_6 ions. Similar results have been obtained for the labelled methylspiroheptadienes in the present work. Table VI compares the measured intensities in the C_6 region of the labelled methylspiroheptadienes with the intensities calculated assuming complete loss of identity in the precursor $C_8H_9^+$ ion (or deuterated equivalent). The reasonable agreement between measured and calculated intensities indicates that the assumption of complete scrambling is valid and further indicates the similarity of behavior upon electron impact of the spiro compounds and the isomeric alkyl benzenes.

TABLE VI

Mass spectra in the C_6 region for methylspiroheptadienes

		Methyl-d_3		6,6,7,7-d_4				Methyl-d_3		6,6,7,7-d_4	
m/e	d_0	Meas.	Calcd.	Meas.	Calcd.	*m/e*	d_0	Meas.	Calcd.	Meas.	Calcd.
83		0.18	—	1.93	2.40	79	12.72	8.13	8.95	9.31	8.10
82		4.21	3.93	5.24	7.10	78	7.58	6.35	6.89	4.43	3.56
81		8.29	7.99	4.95	6.93	77	15.52	2.00	1.64	1.50	0.58
80	0.14	6.79	7.30	6.04	7.42	76	1.06	1.05	—	0.65	—

In the spectrum of *p*-methylethylbenzene, $C_8H_9^+$ forms the base peak. In the fragmentation forming this ion, loss of both the α-methyl and the β-methyl occurs in the ratio 1:5 as was shown from the spectra of methylethylbenzene-α-methyl-d_3 and -β-methyl-d_3 (15). Both reactions have the same energy requirements and it was concluded that the $C_8H_9^+$ has the same structure in both cases. The mechanism for this reaction is discussed elsewhere (15).

In the spectra of the two deuterated methylethylbenzenes, $C_8H_9^+$ and $C_8H_6D_3^+$ ions

Can. J. Chem. Downloaded from www.nrcresearchpress.com by 210.87.254.42 on 09/05/12
For personal use only.

are formed which further fragment to form the C_6 ions. In *p*-methyl-d_3-ethylbenzene, metastable peaks for reactions [4], [5], and [6] are observed.

[4] $C_8H_6D_3^+ \rightarrow C_6H_4D_3^+ + C_2H_2$, metastable 62.3

[5] $C_8H_6D_3^+ \rightarrow C_6H_5D_2^+ + C_2HD$, metastable 60.8

[6] $C_8H_6D_3^+ \rightarrow C_6H_6D^+ + C_2D_2$, metastable 59.4.

The metastable peak at mass 59.4 also corresponds to reaction [2]. In *p*-methylethyl-β,β,β-d_3-benzene only the metastable peak at 59.4 was observed because of the much lower intensity of the $C_8H_6D_3^+$ ion. Calculations based on complete scrambling of the hydrogen and deuterium atoms in $C_8H_6D_3^+$ in forming the C_6 region are in reasonable agreement with the measured intensities as shown in Table VII. In Table VII are given also the major peaks in the spectra of the two deuterated methylethylbenzenes and the corresponding intensities in methylethylbenzene-d_0.

TABLE VII

Partial mass spectra of *p*-methylethylbenzenes

		Methylethylbenzene						Methylethylbenzene			
		Methyl-d_3		Ethyl-β,β,β-d_3				Methyl-d_3		Ethyl-β,β,β-d_3	
Mass	d_0	Meas.	Calcd.	Meas.	Calcd.	Mass	d_0	Meas.	Calcd.	Meas.	Calcd.
123		38.8		35.5		80		3.25	3.52	1.35	0.68
120	36.9					79	10.50	7.86	7.12	8.47	8.45
108		100.0		20.0		78	4.23	4.66	4.58	4.51	3.70
105	120.0	18.9		100.0		77	14.49	3.74	2.78	9.04	10.27
82		2.90	3.16	0.70	0.61	76	0.83	0.48	0.18	0.68	0.58
81		4.13	4.53	1.20	0.87						

The above evidence indicates that, for those $C_8H_9^+$ ions which have sufficient internal energy to undergo further decomposition, a simple methyltropylium structure is not adequate since all hydrogens and also all carbons (6) become equivalent. It is possible to accommodate the results by postulating a number of isomerizations from a tropylium to a benzyl structure accompanied by hydrogen shifts or alternatively by expansion to an eight-membered ring with a number of intramolecular hydrogen shifts before decomposition.

Estimation of Heats of Formation

ΔH_f(7-mecylcoheptatriene) has been previously estimated (12) to be 37.2 kcal/mole using Franklin's group equivalent method (17). By the same method ΔH_f(spiro[2.4]-hepta1,3-diene) can be calculated as follows using ΔH_f(cyclo-C_5H_6) = 31.9 kcal/mole (18). ΔH_f(spiroheptadiene) = ΔH_f(cyclo-C_5H_6) − ΔH_f(—CH_2—) + ΔH_f(—$\overset{|}{\underset{|}{C}}$—) + $2\Delta H_f$(—CH_2—) + (correction for cyclopropane ring) = 52.0 kcal/mole. In a similar manner values of 44.1 kcal/mole and 45.4 kcal/mole for the 1- and 2-methyl- and the 6-methylspiroheptadienes were obtained. By Franklin's method ΔH_f(2,5-dimethyl-1,5-hexadien-3-yne) = 68.2 kcal/mole. The heats of formation of *m*-xylene, ethylbenzene, and *p*-methylethylbenzene necessary for the calculations of Table III were taken from the literature (18).

ACKNOWLEDGMENTS

The authors are indebted to the National Research Council and to the Alfred P. Sloan Foundation for financial support.

Can. J. Chem. Downloaded from www.nrcresearchpress.com by 210.87.254.42 on 09/05/12
For personal use only.

REFERENCES

1. S. MEYERSON and P. N. RYLANDER. J. Chem. Phys. **27**, 901 (1957).
2. V. HANUS and Z. DOLEJSEK. Collection Czech. Chem. Commun. **28**, 652 (1963).
3. Z. DOLEJSEK, V. Hanus, and H. PRINZBACH. Angew. Chem. **74**, 902 (1962).
4. C. H. LIFSHITZ and S. H. BAUER. J. Phys. Chem. **67**, 1629 (1963).
5. H. M. GRUBB and S. MEYERSON. Mass spectra of alkyl benzenes. *In* Mass spectrometry of organic ions. Academic Press, New York. 1963.
6. S. MEYERSON and P. N. RYLANDER. J. Phys. Chem. **62**, 2 (1958).
7. J. M. S. TAIT, T. W. SHANNON, and A. G. HARRISON. J. Am. Chem. Soc. **84**, 4 (1962).
8. A. G. HARRISON and T. W. SHANNON. Can. J. Chem. **40**, 1730 (1962).
9. S. MCLEAN and P. HAYNES. To be published.
10. I. N. NAZAROV and S. S. BAKHMUTSKAYA. Zh. Obshch. Khim. **18**, 1077 (1948).
11. P. N. RYLANDER, S. MEYERSON, and H. M. GRUBB. J. Am Chem. Soc. **79**, 842 (1957).
12. A. G. HARRISON, L. R. HONNEN, H. J. DAUBEN, and F. P. LOSSING. J. Am. Chem. Soc. **82**, 5593 (1960).
13. F. H. FIELD and J. L. FRANKLIN. J. Chem. Phys. **22**, 1895 (1954).
14. J. B. FARMER, F. P. LOSSING, D. G. H. MARSDEN, and C. A. MCDOWELL. J. Chem. Phys. **24**, 52 (1956).
15. F. MEYER and A. G. HARRISON. To be published.
16. S. MEYERSON and P. N. RYLANDER. J. Am. Chem. Soc. **79**, 1058 (1957).
17. J. L. FRANKLIN. Ind. Eng. Chem. **41**, 1070 (1949).
18. F. D. ROSSINI *et al.* Selected values of physical and thermodynamic properties of hydrocarbons and related compounds. Carnegie Press, Pittsburg, Pennsylvania. 1953.

Can. J. Chem. Downloaded from www.nrcresearchpress.com by 210.87.254.42 on 09/05/12
For personal use only.

Can. J. Chem. Downloaded from www.nrcresearchpress.com by 210.87.254.5 on 09/05/12
For personal use only.

FORMATION DES DÉRIVÉS PENTAFLUOROSULFURES ÉTHYLÈNIQUES, DIÈNIQUES ET ACÉTYLÈNIQUES

MÉÜDE TREMBLAY
Centre Canadien de Recherches et Perfectionnement des Armes (CARDE) Québec, Québec

Reçu le 12 août 1964

ABSTRACT

The reaction of disulfur decafluoride with olefins, dienes, and acetylenes has been studied under pressure at 125–140 °C. The gases formed have been separated and identified with a gas chromatograph coupled to a time-of-flight mass spectrometer. Liquid pentafluorosulphur derivatives, studied by mass spectrometry, were attributed the following structures: $CH_2FCHClSF_5$, $CH_2FCHBrSF_5$, $CH_2FCHBrCH_2CHBrSF_5$, $CH_2FCHFCH_2CHFSF_5$, and $CH_2{=}CHCHFCH_2SF_5$. Addition compounds of dienes or acetylenes have structures assumed to be $FCH_2CF_2CH_2SF_5$ from propadiene and $C_2H_5CF_2CHFSF_5$ from ethyl acetylene.

RÉSUMÉ

Nous avons étudié la réaction du décafluorobisulfure (S_2F_{10}) avec les oléfines, les dièns et les acétylènes sous pression à 125–140 °C. Nous avons séparé les gaz formés par chromatographie gazeuse et les avons identifiés à l'aide d'un spectrographe de masse à temps de vol. Nous avons aussi isolé les liquides formés, qui étaient des dérivés pentafluorosulfures monosubstitués. L'étude de leur structure au moyen de la spectrographie de masse suggère que nous avons obtenu les composés suivants: $CH_2FCHClSF_5$, $CH_2FCHBrSF_5$, $CH_2FCHBrCH_2$-$CHBrSF_5$, $CH_2FCHFCH_2CHFSF_5$ et $CH_2{=}CHCHFCH_2SF_5$. A partir des dièns et des acétylènes, nous croyons avoir isolé les composés de structures suivantes: $FCH_2CF_2CH_2SF_5$ du propadiène et $C_2H_5CF_2CHFSF_5$ de l'éthylacétylène.

INTRODUCTION

Récemment, Roberts (1) a signalé l'addition du S_2F_{10} sur les oléfines. Les rendements obtenus étaient faibles. Nous nous sommes proposés d'étudier les conditions expérimentales, l'influence du substituant sur le carbone non saturé et la structure du composé d'addition. La formation de radicaux $\cdot SF_5$ à partir de S_2F_{10} a lieu sous l'action des rayons ultraviolets ou par décomposition catalytique à 150 °C. Nous avons choisi la méthode catalytique où S_2F_{10} est chauffé sous pression en présence des éthylènes, dièns ou acétylènes. Dans ces conditions, S_2F_{10} forme en premier lieu des radicaux $\cdot SF_5$ qui se décomposent rapidement en SF_4 et SF_6 (2). Ces mêmes radicaux SF_5 peuvent réagir avec les composés non saturés pour donner des produits fluorés gazeux, tel CH_2FCHF_2 isolé dans les gaz ou des produits d'oxydation comme SO_2F_2. Et, enfin, nous obtenons des dérivés pentafluorosulfures liquides qui sont partiellement ou totalement fluorés:

$$\rangle C{=}C\langle + S_2F_{10} \rightarrow \rangle \underset{\displaystyle SF_5}{\overset{\displaystyle |}{C}}{-}CF\langle$$

DISCUSSION

1. Réaction de S_2F_{10} avec les éthylènes

La réaction de S_2F_{10} avec les éthylènes substitués démontre que la liaison S—S est très faible (3), et qu'il y a rupture facile pour former des radicaux libres $\cdot SF_5$. La masse obtenue à 175 ($CHClSF_5$) dans le cas du dérivé SF_5 du chlorure de vinyle nous porte à croire que le radical $\cdot SF_5$ attaque plus aisément le centre électropositif du chlorure de vinyle,

$$\cdot SF_5 + CH_2{=}CHCl \rightarrow \cdot CH_2CHClSF_5,$$

ou que le groupe pentafluorosulfure est plus stable lorsque substitué sur un carbone déjà porteur d'halogène. Le produit isolé se formerait par décomposition du produit bisubstitué.

$$SF_5CH_2CHClSF_5 \rightarrow CH_2FCHClSF_5 + SF_4.$$

En plus d'isoler des produits partiellement fluorés, le radical $\cdot CH_2CHClSF_5$ peut ajouter une deuxième molécule d'halogénure de vinyle.

$$\cdot CH_2CHClSF_5 + CH_2{=}CHCl \rightarrow \cdot CH_2CHClCH_2CHClSF_5$$

$$\cdot CH_2CHClCH_2CHClSF_5 + \cdot SF_5 \rightarrow FCH_2CHClCH_2CHClSF_5 + SF_4.$$

En présence du radical $\cdot SF_5$, les halogénures de vinyle ont tendance à se polymériser. D'où la possibilité d'isoler un grand nombre de produits lorsque l'halogénure de vinyle est en excès. Il peut même y avoir substitution du brome ou du chlore par le fluor, pour former des vinyles fluorés, tel CH_2FCHF_2 isolé dans les gaz. Nous avons même retrouvé $ClSF_5$ à partir du chlorure de vinyle et de S_2F_{10}.

$$CH_2{=}CHCl + 4\cdot SF_5 \rightarrow CH_2FCHF_2 + ClSF_5 + 3SF_4.$$

La réaction du bromure de vinyle et de S_2F_{10} donne le 1,1,2-trifluoroéthane de la même façon. Cependant, le bromure de pentafluorosulfure qui est connu (4) n'a pas été isolé. Le fluorure de vinyle réagit avec S_2F_{10} pour donner aussi CH_2FCHF_2, ce qui indiquerait la décomposition rapide des dérivés pentafluorosulfures des halogénures de vinyle à la température de la réaction:

$$SF_5CH_2CHFSF_5 \rightarrow CH_2FCHF_2 + 2SF_4.$$

Les produits liquides obtenus sont donnés dans le Tableau I. A partir de S_2F_{10} et du chlorure de vinyle, un seul produit liquide partiellement fluoré a été isolé, i.e., $CH_2FCHClSF_5$. L'ion moléculaire dans le spectre de masse de ce produit n'est pas visible à la masse 208, mais les fragments suivants sont visibles: FCH_2CHCl, CH_2F, SF_5ClCH, Cl et SF_5. Le dérivé bisubstitué est possible et a été préparé par H. L. Roberts (1) qui lui a attribué la structure suivante: $F_5SCHClCH_2SF_5$. Il ne se forme pas dans les conditions expérimentales employées ici ou encore se décompose à la température de la réaction.

TABLEAU I

Dérivés pentafluorosulfurés (S_2F_{10}, 0.1 mole)

Réactifs				Temps de rétention sur le Prep-Partitioner à 80 °C (min)
Formule	Mole	Temp. (°C)	Structure proposée	
$CH_2{=}CHCl$	0.2	125–140	$CH_2FCHClSF_5$	67
$CH_2{=}CHBr$	0.3	125–140	$CH_2FCHBrSF_5$	38
			$CHF_2CHBrCH_2CHBrSF_5$	146
$CH_2{=}CHF$	0.3	140–150	$CH_2FCHFCH_2CHFSF_5$	27
			$CH_2{=}CHCH_2CHFSF_5$	43
$CH_2{=}C{=}CH_2$	0.3	125	$FCH_2CF_2CH_2SF_5$	8
$C_2H_5C{\equiv}CH$	0.3	125	$C_2H_5CF_2CHFSF_5$	28

Du bromure de vinyle et S_2F_{10}, nous avons isolé deux produits liquides: $CH_2FCHBrSF_5$ et $CH_2FCHBrCH_2CHBrSF_5$. L'ion moléculaire du premier n'est pas visible dans le spectre de masse, mais plusieurs fragments ont été identifiés, CH_2FCHBr, $CH_2CHBrSF_5$, CH_2CHBr, SF_5, etc. La masse 360 du deuxième composé qui est l'ion moléculaire a été identifiée ainsi que nombre de fragments: CH_2F, CH_2FCHBr, $CH_2CHBrSF_5$, $CH_2FCHCH_2CHBrSF_5$, SF_5, etc.

Can. J. Chem. Downloaded from www.nrcresearchpress.com by 210.87.254.5 on 09/05/12
For personal use only.

Le fluorure de vinyle et le S_2F_{10} donnent les produits liquides suivants: $CH_2FCHFCH_2$-$CHFSF_5$ et $CH_2{=}CHCH_2CHFSF_5$. Le premier est le dimère du fluorure de vinyle sur lequel s'est ajouté un groupe pentafluorosulfure et un fluor. Le second produit serait peut-être formé du précédent par défluoruration dans la colonne chromatographique du Prep-Partitioner. Une troisième fraction a été isolée mais n'a pas pu être identifiée d'après son spectre de masse.

La réaction de l'éthylène avec S_2F_{10} donne de grandes quantités de carbone et d'acide fluorhydrique et aucun produit d'addition.

2. Réaction avec les dienes

L'action du pentafluorobisulfure sur le propadiène, l'isoprène et le chloroprène sous pression à 125–150 °C a été étudiée. Nous avons trouvé que la température de réaction est très critique, alors qu'entre 125 et 140 °C, il se produit une polymérisation rapide en présence des radicaux libres $\cdot SF_5$ et formation d'huiles ou gommes contenant des groupes SF_5. Il se produit même dans certains cas formation de carbone et d'acide fluorhydrique. Les systèmes conjugués, tels que le chloroprène et l'isoprène, ont montré plus de tendance à se polymériser qu'à ajouter des groupes pentafluorosulfures sur les carbones 1 et 4. Le propadiène, qui possède deux doubles liaisons accumulées, a moins de tendance à se polymériser et nous avons pu isoler en trace un dérivé pentafluorosulfure. Selon toute apparence, ce dérivé se formerait de la façon suivante par l'attaque du carbone 1 et 2

$$CH_2{=}C{=}CH_2 + 2\cdot SF_5 \rightarrow CH_2{=}CFCH_2SF_5 + SF_4$$
$$CH_2{=}CFCH_2SF_5 + 2\cdot SF_5 \rightarrow CH_2FCF_2CH_2SF_5 + 2SF_4.$$

La structure ci-dessus la plus probable est en accord avec le spectre de masse qui montre une masse de 205 très intense et attribuable à l'ion $CH_2CF_2CH_2SF_5$.

3. Dérivés acétylèniques

La réaction de S_2F_{10} avec les acétylènes donne plus facilement des produits d'addition. De plus, la réactivité des acétylènes substitués croît dans l'ordre suivant:

$$H < CH_3 < C_2H_5 < C_3H_7.$$

L'acétylène non substitué donnerait le dérivé le plus intéressant ($SF_5CH{=}CHSF_5$), mais l'acétylène est décomposé en carbone. C'est pourquoi notre attention s'est portée surtout sur les dérivés méthylés et éthylés.

L'étude du spectre de masse du produit obtenu à partir de l'éthylacétylène et S_2F_{10} montre que le dérivé fluoré, $C_2H_5CF_2CHFSF_5$ de poids moléculaire 236 a été isolé selon tout probabilité. La méthode de formation serait la suivante:

$$C_2H_5{\equiv}CH + S_2F_{10} \rightarrow C_2H_5CF{=}CHSF_5 + SF_4$$
$$C_2H_5CF{=}CHSF_5 + S_2F_{10} \rightarrow C_2H_5CF_2CHFSF_5 + 2SF_4,$$

où S_2F_{10} sert d'agent fluorant.

Le radical libre $\cdot SF_5$ peut abstraire un proton pour former l'unité HSF_5 instable qui donne SF_4 et HF. Ceci explique la formation de carbone et d'acide fluorhydrique sous certaines conditions:

$$\cdot SF_5 + CH{\equiv}CH \rightarrow \cdot CH{=}CHSF_5$$
$$S_2F_{10} + \cdot CH{=}CHSF_5 \rightarrow SF_5CH{=}CHSF_5 + \cdot SF_5$$
$$SF_5CH{=}CHSF_5 \rightarrow 2C + 2SF_4 + 2HF.$$

La réaction de S_2F_{10} est beaucoup plus rapide avec les acétylènes et éthylènes ne contenant pas d'halogènes. La réaction, par exemple, de S_2F_{10} avec l'éthylacétylène est

Can. J. Chem. Downloaded from www.nrcresearchpress.com by 210.87.254.5 on 09/05/12
For personal use only.

complète à 125 °C, alors qu'avec le fluorure de vinyle, la réaction a lieu à 140–160 °C.

Cependant, la présence d'halogène dans la molécule, après addition de SF_5, stabilise le produit formé et empêche la formation de SF_4 à partir de $\cdot SF_5$ et de l'hydrogène. Ceci explique l'isolation plus facile des dérivés des halogénures de vinyle.

PARTIE EXPÉRIMENTALE

La réaction de S_2F_{10} avec les oléfines, les diènes et les acétylènes se fait dans une bombe d'acier au chrome–vanadium de 300 ml de capacité. Après l'addition du S_2F_{10} (25.4 g, 0.1 mole) sous forme liquide, la bombe est fermée, refroidie dans l'azote liquide et évacuée à la pompe à vide. Les oléfines, diènes et acétylènes (0.2 à 0.3 mole) sont condensés dans la bombe à −196 °C. Après chauffage à la température désirée, un échantillon des produits gazeux est séparé par chromatographie et les gaz individuels identifiés par leur spectre de masse.

Le temps de rétention d'un gaz donné dépend de plusieurs facteurs dont la température, la longueur de la colonne, le débit du gaz vecteur, etc. Mais cette valeur du temps de rétention peut être donnée comme valeur relative à un gaz de référence, soit SOF_2 dans le cas présent, et en calculant le temps à partir du pic de l'air. Si tous les facteurs variables, tels que température, vitesse du gaz vecteur, etc., sont gardés constants pendant la durée de l'expérience, le temps de rétention relatif à SOF_2 est alors donné par la formule,

$$T_r = \frac{(t_x - t_{air})100}{(t_{SOF_2} - t_{air})},$$

où T_r = temps de rétention relatif à SOF_2 du gaz en question, t_x = temps de rétention du gaz en question en min, t_{air} = temps de rétention de l'air en min, t_{SOF_2} = temps de rétention de SOF_2 ou SF_4 en min.

Nous avons utilisé un chromatographe Perkin–Elmer, modèle 154 pour la séparation du mélange gazeux. Ce chromatographe possède deux colonnes consécutives. La première colonne, qui est en cuivre, mesure 9 pieds de long par 1/4 pouce de diamètre. Elle est remplie de chromosorb A (Perkin–Elmer) qui contient du diisodécyl phtalate comme phase stationnaire liquide. La deuxième colonne est aussi en cuivre, mesure 20 pieds de long par 1/4 pouce de diamètre et est remplie de brique refractaire C-22 de granulosité 35 à 80 (Johns-Manville Co.) contenant de l'huile Kel-F (Grade No. 10, Minnesota Mining and Manufacturing Co.).

Les gaz, à leur sortie du chromatographe, sont introduits avec le gaz vecteur, l'hélium, dans un spectromètre de masse à temps de vol, Bendix, Modèle 12-101, où ils sont identifiés individuellement sur l'écran d'un oscilloscope.

Les spectres de masse des liquides sont obtenus par introduction dans le spectromètre de masse à l'aide d'un appareil à introduction d'échantillon moléculaire (No. 919, Bendix Corporation) et leur spectre enregistré avec une caméra Polaroid placée devant l'écran d'un oscilloscope ou à l'aide d'un Visicorder qui enregistre le spectre sur papier photographique.

Les liquides obtenus ont été rectifiés à l'aide d'un chromatographe (Fisher Scientific Co., Prep-Partitioner, modèle 24) dont la colonne est maintenue à 80 °C, remplie de chromosorb A contenant du diisodécyl phtalate, et balayée avec de l'azote. Les liquides purifiés à l'aide de cet appareil sont donnés dans le tableau I avec les temps de rétention observés.

1. Réaction de S_2F_{10} avec le chlorure de vinyle

La réaction du décafluorobisulfure avec le chlorure de vinyle à 125–140 °C sous pression donne les gaz suivants: SF_6, SO_2F_2, SF_4, CH_2FCHF_2 et $ClSF_5$, à des temps de rétention relatifs à SOF_2 de 32, 63, 100, 141 et 209 et en pourcentage de 20.6, 5.6, 36.7, 17.8 et 2.0 respectivement. Le liquide obtenu contient le produit monosubstitué, $CH_2FCHClSF_5$, qui fut purifié à l'aide du Prep-Partitioner; temps de rétention, 67 min. Environ 2 ml (3 g) de ce liquide furent obtenus à partir de 25 g de S_2F_{10} et d'un excès de chlorure de vinyle; rendement $\simeq 7.5\%$. Son spectre de masse est donné ci-dessous, par ordre d'intensité décroissante des pics en opérant l'appareil à 50 eV. Les ions positifs identifiés sont entre parenthèses, près de leur masse respective: 81 (FCH_2CHCl), 89 (SF_3), 46 ($CH_2{=}CHF$), 27 ($CH_2{=}CH$), 127 (SF_5), 62 (CH_2CH_2Cl), 175 ($CHClSF_5$), 70 (SF_2), 51 (SF), 35 (Cl), 189 ($CH_2CHClSF_5$), 33 (CH_2F).

Anal. Calc. pour $CH_2FCH_2ClSF_5$: S, 15.4; F, 54.9. Trouvé: S, 15.4; F, 54.6.

2. Réaction de S_2F_{10} avec le bromure de vinyle

La réaction du bromure de vinyle avec S_2F_{10} dans les mêmes conditions a donné les gaz suivants, SF_6, SO_2F_2, SF_4, CH_2FCHF_2, à des temps de rétention relatifs et pourcentages respectivement de 32 et 12.8%, 63 et 5.9%, 100 et 38.3%. 141 et 8.4%. Le produit liquide séparé avec le Prep-Partitioner a donné à 38 et 146 min respectivement $CH_2FCHBrSF_5$ et $CH_2FCHBrCH_2CHBrSF_5$. Rendement: 2 ml (3 g) par 25 g de S_2F_{10}, soit environ 6%. L'analyse spectrale de masse donna les pics suivants par ordre d'intensité décroissante pour le dérivé monosubstitué: 126 (CH_2FCHBr), 127 (SF_5), 46 ($CH_2{=}CHF$), 27 ($CH_2{=}CH$), 107 (CH_2-$CHBr$), 80 (Br), 89 (SF_3), 70 (SF_2), 51 (SF), 33 (CH_2F).

Can. J. Chem. Downloaded from www.nrcresearchpress.com by 210.87.254.5 on 09/05/12
For personal use only.

Anal. Calc. pour $CH_2FCHBrSF_5$: S, 12.6; F, 45.1. Trouvé: S, 12.0; F, 44.8.

Le dérivé isolé à 146 min donna le spectre de masse suivant: 27 (CH_2=CH), 127 (SF_5), 126 (CHFCHBr), 107 (CH_2FHBr), 89 (SF_3), 360 ($CH_2FCHBrCH_2CHBrSF_5$), 70 (SF_2), 234 ($CH_2CHBrSF_5$), 80 (Br), 154 (CH_2CHSF_5), 51 (SF), 280 ($CHF{=}CHCH_2CHBrSF_5$).

Anal. Calc. pour $CH_2FCHBrCH_2CHBrSF_5$: S, 8.89; F, 31.7. Trouvé: S, 8.74; F, 29.6.

3. Réaction de S_2F_{10} avec le fluorure de vinyle

Du fluorure de vinyle et S_2F_{10}, nous avons obtenu à 140–150 °C sous pression les gaz aux temps de rétention relatifs et pourcentages respectifs suivants: SF_6, 32, 23%; SO_2F_2, 65, 0.9%; SF_4, 100, 42.1%; CH_2FCHF_2, 140, 29%. Le liquide obtenu, 5 ml (7.5 g) par 25 g de S_2F_{10} (rendement $\simeq$ 19%), se sépare en deux constituants à l'aide du chromatographe Prep-Partitioner passant respectivement à 27 et 43 min. Le spectre de masse du composé isolé à 27 min est donné par ordre d'intensité décroissante des pics: 65 ($CHFCH_2F$), 89 (SF_3), 45 (CHCHF), 127 (SF_5), 173 ($CHFCH_2SF_5$), 46 (CH_2CHF), 70 (SF_2), 51 (SF), 33 (CH_2F), 27 (CH_2=CH), 154 (CH_2CHSF_5). Ce produit donne l'analyse élémentaire calculée pour $CH_2FCHCFH_2CHFSF_5$: C, 21.9; H, 2.74; S, 14.6; F, 60.7. Trouvée: C, 22.9, H, 2.08; S, 14.2; F, 60.9. Le liquide obtenu à 43 min sur le Prep-Partitioner donne le spectre de masse suivant: 47 (CH_2CH_2F), 65 (CH_2FCHF), 51 (SF), 27 (CH_2=CH), 89 (SF_3), 33 (CH_2F), 127 (SF_5), 70 (SF_2), 154 (CH_2CHSF_5), 173 (F_5SCH_2CHF). L'analyse élémentaire calculée pour $CH_2{=}CHCHFCH_2SF_5$: C, 24.0; H, 3.00; S, 16.0; F, 56.0. Trouvée: C, 24.9; H, 2.14; S, 17.4; F, 56.1.

La réaction de S_2F_{10} avec d'autres dérivés vinylés, tel le méthyl vinyl éther donne des produits difficilement isolables et contenant de grandes quantités d'acide fluorhydrique.

4. Réaction de S_2F_{10} avec le propadiène

Lorsqu'un excès de S_2F_{10} réagit sur le propadiène à 125° sous pression, nous obtenons les gaz suivants aux temps de rétention relatifs à SOF_2 et pourcentages respectifs: SF_6, 32, 26.5%; SO_2F_2, 63, 1.0%; SF_4, 100, 10.8%. De faibles quantités de liquides, qui seraient les produits substitués, sont été isolés à l'état brut, mais un seul produit siolé en trace du Prep-Partitioner donne le spectre du produit monosubstitué: 59 ($CH_2{=}CFCH_2$ ou $CH_2{=}CCH_2F$), 40 ($CH_2{=}C{=}CH_2$), 39 ($CH_2{=}C{=}CH$), 89 (SF_3), 51 (SF), 27 (CH_2=CH), 33 (CH_2F), 70 (SF_2), 205 ($CH_2CF_2SF_5$), 127 (SF_5).

5. Réaction de S_2F_{10} avec le méthylacétylène et l'éthylacétylène

Un excès de méthylacétylène sur S_2F_{10} donne SF_6, 32, 28.5%; SO_2F_2, 63, 1.1%; SF_4, 100, 31.6% et $CH_3C{\equiv}CH$, 210, 31.1%, aux temps de rétention et pourcentage respectifs ci-dessus. Le produit d'addition liquide du méthylacétylène se décompose dans la colonne du Prep-Partitioner à 80 °C.

L'éthylacétylène en excès sur S_2F_{10} donne le gaz suivants aux temps de rétention relatifs et ppurcentages dans l'ordre suivant: SF_6, 32, 43.4%; SO_2F_2, 63, 1.3%; SF_4, 100, 30.9% et éthylacétylène, 550, 23.9%. La réaction laisse un produit qui donne le spectre de masse suivant: 28 (C_2H_4), 27 (C_2H_3). 55 ($C_2H_5CH{=}CH$), 29 (C_2H_5), 127 (SF_5), 54 ($C_2H_5C{=}CH$), 236 ($C_2H_5CF_2CHFSF_5$), 89 (SF_3), 70 (SF_2), 111 ($C_2H_5CF_2CHF$), 182 ($SF_5CH{=}CHC_2H_5$).

BIBLIOGRAPHIE

1. H. L. ROBERTS. J. Chem. Soc. 3183 (1962).
2. W. R. TROST et R. L. MCINTOSH. Can. J. Chem. **29**, 508 (1951).
3. R. B. HARVEY et S. H. BAUER. J. Am. Chem. Soc. **75**, 2840 (1953).
4. B. COHEN et A. G. MACDIARMID. Chem. Ind. London, 1866 (1962).

Can. J. Chem. Downloaded from www.nrcresearchpress.com by 210.87.254.5 on 09/05/12
For personal use only.

Can. J. Chem. Downloaded from www.nrcresearchpress.com by 210.87.254.5 on 09/05/12
For personal use only.

ELECTRON SPIN RESONANCE STUDIES OF RADICAL ANIONS AND ION PAIRS IN THE PYRAZINE SERIES

C. A. McDowell and K. F. G. Paulus
Department of Chemistry, University of British Columbia, Vancouver, British Columbia
Received August 4, 1964

ABSTRACT

The alkali metal hyperfine interaction in ion pairs of sodium and potassium cations with the radical anions of some methyl-substituted pyrazines and pyridines has been investigated. The electrostatic, electronic, and steric interactions which influence the metal hyperfine splitting are discussed in detail. It is proposed that the variation of the observed hyperfine splitting is due, in some cases, to steric effects, but in the series of *m*-xylene, 3,5-dimethylpyridine, and 2,6-dimethylpyrazine, the variation is caused by a change in the energy of electronic excitations from the anion to the cation.

The results of molecular orbital calculations of the spin densities in tetramethylpyrazine and 3,5-dimethylpyridine are compared with experiment and found to give reasonable agreement.

1. INTRODUCTION

In electron spin resonance (e.s.r.) investigations of radical anions prepared by chemical reduction with alkali metals in polyethers, it is often assumed that the anions can be considered essentially as free, being surrounded individually by solvent shells. Recently improved methods of detecting free radicals have made it necessary to revise this picture. It has been found in many cases that aromatic anions prepared in the above way are associated as ion pairs with the cations of the alkali metals used in the reduction reaction. The electronic spectra of the anions exhibit this association by observed shifts of the absorption maxima, the shifts being different for different metals (1, 2). The formation of ion pairs is detectable also by e.s.r. techniques because the unpaired electron on the anion can, by various mechanisms, create unpaired electron spin density at the cation nucleus, and the resulting hyperfine interaction with the nuclear spin angular momentum appears as an additional splitting in the e.s.r. spectrum of the anion (3–8, 11).

In certain cases the e.s.r. spectra of the ion pairs can give information about their structure. Thus in the ion pairs formed by alkali metals with pyracene the cation was found to be situated near the methylene bridges of the anion (4, 5). When *m*-dinitrobenzene is reduced with alkali metals in polyethers the cation is associated with only one of the nitro groups, making the two nitro groups non-equivalent (6).

For the ion pair of 2,2′-dipyridyl with sodium, Zahlan and co-workers (7) have proposed that the cation is in proximity to the nitrogen non-bonding electron pairs. On the other hand, McDowell *et al.* (8) have suggested that in the pyrazine–sodium ion pair the sodium ion is located above the center of the ring, as in the case of the corresponding pairs with hydrocarbon anions (3). In what follows this particular viewpoint will be discussed more fully.

2. EXPERIMENTAL AND RESULTS

The preparation of the radical anions with sodium or potassium was accomplished as previously described (8, 9). The solvents were purified by distillation from anthracene and sodium–potassium alloy. The e.s.r. spectra were recorded on a Varian spectrometer with a 12 in. magnet and with 100 kc field modulation. Field measurements were made with a proton resonance magnetometer in conjunction with a frequency counter.

Can. J. Chem. Downloaded from www.nrcresearchpress.com by 210.87.254.5 on 09/05/12
For personal use only.

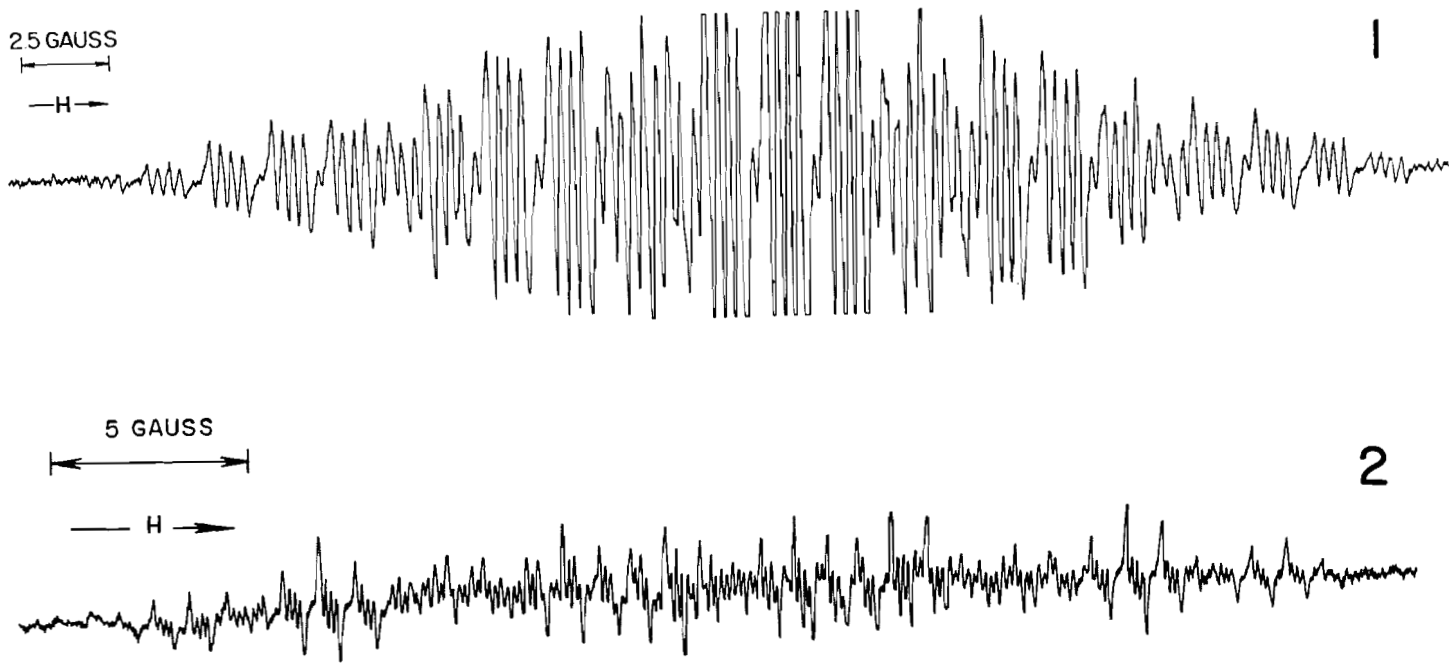

FIG. 1. Electron spin resonance (e.s.r.) spectrum of the potassium–tetramethylpyrazine ion pair in DME.
FIG. 2. Electron spin resonance (e.s.r.) spectrum of the potassium-3,5-dimethylpyridine ion pair in DME.

Figure 1 shows the spectrum obtained from the radical anion of tetramethylpyrazine when prepared with potassium in dimethoxyethane (DME). The e.s.r. spectra of the ion pairs with potassium in tetrahydrofuran (THF) and 2-methyltetrahydrofuran (MeTHF), and with sodium in DME and THF were also recorded. All the alkali metal hyperfine splittings are listed in Table I. The complexes with potassium in 1,4-dioxane and with

TABLE I

Alkali metal hyperfine coupling constants (G) at 20°

Compound	Potassium		Sodium	
	DME	THF	DME	THF
2,5-Dimethylpyrazine	<0.025	<0.035	0.15	0.200
2,6-Dimethylpyrazine	~0.07	~0.09	0.36	0.45
Pyrazine	0.09	0.11	0.54	0.580
3,5-Dimethylpyridine	0.14	0.15	0.39	0.47
m-Xylene	~0.23*	—	—	—
Tetramethylpyrazine	0.31	0.25 0.21 (MeTHF)	0.72	0.72

*From ref. 11. Values quoted are probably correct to ±0.01 G.

sodium in MeTHF were not sufficiently soluble to give a detectable e.s.r. spectrum. In all cases, the nitrogen and methyl proton coupling constants are as follows

$$a_N = 6.18 \text{ G}, a_{CH_3} = 1.73 \text{ G}.$$

The e.s.r. spectrum of the 3,5-dimethylpyridine negative ion has been investigated previously (10). We have reexamined this compound and resolved the alkali metal hyperfine structure for both the sodium and potassium complexes. Atherton *et al.* (10) have given the sodium hyperfine splitting as 0.35 G in this case. Figure 2 shows the e.s.r. spectrum of the ion pair with potassium in DME. The alkali metal hyperfine coupling constants are listed in Table I. From the above spectrum the coupling constants of the anion itself are found to be

$$a_N = 6.12 \text{ G}, a_{H_2} = 3.27 \text{ G}, a_{H_4} = 8.70 \text{ G}, a_{CH_3} = 0.92 \text{ G}.$$

These are slightly different from the previous values (10).

Table I gives a list of the alkali metal hyperfine splitting constants found in the ion pairs with the two compounds above, and also the ion pairs of pyrazine, 2,6-dimethylpyrazine, and 2,5-dimethylpyrazine with sodium or potassium in DME and THF, and of *m*-xylene with potassium only in DME (11). The e.s.r. spectra of the radical anions of pyrazine and the dimethylpyrazines have already been discussed elsewhere (8, 9).

With 2,6-dimethylpyrazine the potassium hyperfine splitting is derived from measurements of the linewidth at the onset of further resolution of the individual components of the anion spectrum. With 2,5-dimethylpyrazine the potassium hyperfine splitting is likely to be smaller than indicated. This splitting was derived from measurements of the lowest linewidth achieved in the spectrum, which was 0.075 G. Since this is near the limiting linewidth of the 100 kc instrument the splitting could possibly be less than one-third of this value. Because the potassium hyperfine splitting is detectable in all other cases and because sodium hyperfine splitting is present with 2,5-dimethylpyrazine we are confident that an ion pair is formed with potassium also, though in this case the hyperfine interaction may be too small to be resolved by our experimental apparatus at the present time.

Can. J. Chem. Downloaded from www.nrcresearchpress.com by 210.87.254.5 on 09/05/12
For personal use only.

Can. J. Chem. Downloaded from www.nrcresearchpress.com by 210.87.254.5 on 09/05/12
For personal use only.

3. DISCUSSION

(a) Anion Radicals

The e.s.r. spectra of the pyrazine and dimethylpyrazine radical anions have been discussed in earlier communications (8, 9). 3,5-Dimethylpyridine has been investigated previously by Atherton and co-workers (10) who used the e.s.r. data for the anion to derive empirically the hyperfine coupling parameters of the ring nitrogen. The tetramethylpyrazine radical anion has not been studied previously.

TABLE II

Calculated and experimental hyperfine coupling constants (G)

Compound	Substitution position	Hückel	McLachlan	Experiment
Tetramethylpyrazine	1 (N)	6.55	7.18	6.18
	2 (CH_3)	2.99	2.05	1.73
3,5-Dimethylpyridine	1 (N)	7.16	7.95	6.12
	2 (H)	3.74	4.13	3.27
	3 (CH_3)	(+)0.86	(−)0.66	(±)0.92
	4 (H)	6.62	8.73	8.70

In Table II we compare the experimental hyperfine coupling constants with those calculated using both the Hückel l.c.a.o. method, and the McLachlan method for calculating spin densities (12). In both approaches the simple inductive model was used for the methyl groups, with the Hückel parameters employed earlier (9). To reproduce the ring proton, methyl proton, and ring nitrogen coupling constants we employ here only the single constants $Q_H = -22.5$ G, $Q_{CH_3} = +19.0$ G, $Q_N = +25.3$ G.

Although the agreement between calculated and experimental hyperfine coupling constants leaves something to be desired, the calculations do at least give a fairly good approximation for the spin density distribution in the two ring systems. It is to be noted, of course, that both the Q's, and the empirical parameters of the Hückel calculations are not necessarily the best ones for the particular cases at hand. The calculations give less good results for 3,5-dimethylpyridine radical anion than for tetramethylpyrazine radical anion, and it appears likely that the parameters used previously for substituted pyrazines (9) may not be quite appropriate for the substituted pyridine radical anions.

It is noteworthy that the calculations using McLachlan's method for the pyridine radical anion indicate a negative spin density at one of the ring positions. This is in contrast to the assumption of Atherton *et al.* (10) that the spin density is everywhere positive in this radical anion.

(b) Electrostatic Interaction within the Ion Pairs

Several considerations lead us to believe that the configuration of the ion pairs formed in the present series must be such that the cation moves in a plane parallel to the plane of the anion. In the first place, the steric effect of the methyl groups would be expected to tend to keep the cation out of the plane of the ring atoms. This viewpoint is supported by the fact that the alkali metal hyperfine splitting is largest for the tetramethylpyrazine radical anion case, where the separation of cation and anion will be greatest, so that the interaction observed experimentally is unlikely to be an in-plane one.

A second point supporting our contention is that the electronic charge in the anion is distributed in orbitals of π-symmetry, so that the electrostatic interaction should be largest out-of-plane. Furthermore, the observation of a large potassium-39 interaction in

the case of the *m*-xylene ion pair by Bolton and Carrington (11) indicates that an out-of-plane interaction is taking place, assuming that the *m*-xylene radical anion can be placed in the present series by reason of the symmetry of its electron distribution.

The effect of the electrostatic interaction between cations and anions on the energy levels of the anion has been considered in detail by McClelland (1) and Hush and Rowlands (2). The energy E_j^0 of orbital j is changed by the electrostatic interaction to

$$[1] \qquad E_j = E_j^0 - e^2 \sum_s \frac{q_s^j}{r_s} + \frac{e^4}{2} \sum_{s,t} \frac{\pi_{ss,tt}^j}{r_s r_t} + 0(e^4),$$

where $\pi_{ss,tt}^j$ are the bond polarizabilities. For an approximate treatment of the electrostatic interaction between cation and anion we assume that the total electrostatic energy of interaction ϵ, can be written simply as

$$[2] \qquad \epsilon = -e^2 \sum_s \frac{q_s}{r_s},$$

where q_s is the excess π-electron charge density on atom s in the anion, and r_s is the distance between nucleus s and the center of the cation.

Making use of charge densities calculated with the inductive Hückel model we have calculated ϵ for the ion pairs of potassium with all the compounds listed in Table I. In doing so we have assumed that the cation moves at a distance of $(2.5 + r_K)$ Å above the plane of the anion (2), where r_K is the crystal radius of potassium, 1.33 Å. For simplicity, we have further assumed that in all cases the dimensions of the radical anion were the same as those of the pyrazine molecule, with the bond lengths and angles as given by Wheatley (13). We have found that the comparatively large changes in bond lengths taking place from pyrazine to tetramethylpyrazine (14) do not in any case change ϵ appreciably.

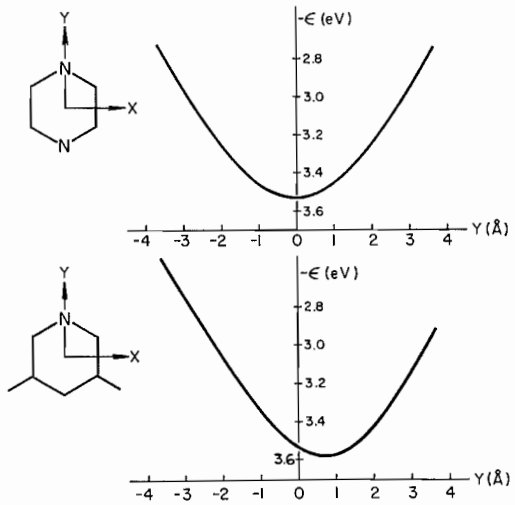

FIG. 3. Electrostatic interaction within the potassium–pyrazine (top) and the potassium–3,5-dimethylpyridine (bottom) ion pairs.

In the top portion of Fig. 3 we give the electrostatic interaction as a function of distance the cation moves along the *y*-axis. Almost identical curves are obtained for the cases of the 2,5-dimethylpyrazine and tetramethylpyrazine radical anions. The interaction as a

Can. J. Chem. Downloaded from www.nrcresearchpress.com by 210.87.254.5 on 09/05/12
For personal use only.

function of x is similar and also has a minimum at the center of the ring. The lower half of Fig. 3 shows ϵ as a function of y, with the axes indicated on the figure, for the 3,5-dimethylpyridine radical anion. The greatest attraction between cation and anion still takes place along the y-axis but the minimum is now shifted toward the nitrogen atom. ϵ as a function of y is almost identical for both the 2,6-dimethylpyrazine and the *m*-xylene radical anions, but the shift of the cation from the center of the ring along the y-axis is not as large as in the case of the 3,5-dimethylpyridine radical anion.

If the electrostatic interaction between the cation and the anion is out-of-plane it is thus clear that the most likely position for the cation will be above the center of the ring, or only slightly displaced from it along the twofold axis of symmetry of the anion. It should be noted that this follows from a consideration of the electrostatic interaction alone. In the 2,5-dimethylpyrazine and tetramethylpyrazine radical anions the effect of the methyl groups will be to increase the vertical separation of the cations and the anions compared to the pyrazine radical anion itself, while in the remaining three cases this steric effect will increase the vertical separation as well as shifting the cation horizontally in the same direction as does the electrostatic effect.

(c) Alkali Metal Hyperfine Interaction

If Ψ_0 represents the electronic ground state of the ion pair where the 4s electron is completely transferred from the potassium atom to the aromatic π-electron system, and Ψ_t represents the excited states formed when an electron is "back-donated" to the 4s level of the metal, then the potassium hyperfine splitting constant, a_K, can be written as

$$[3]\quad a_K = \frac{16\pi}{3} g_K \beta_K \left\{ \langle \Psi_0 | \sum{}' | \Psi_0 \rangle + 2 \sum_i \frac{\langle \Psi_0 | \mathscr{H} | \Psi_i \rangle}{E_0 - E_i + \epsilon} \langle \Psi_i | \sum{}' | \Psi_0 \rangle + \sum_i \left(\frac{\langle \Psi_0 | \mathscr{H} | \Psi_i \rangle}{E_0 - E_i + \epsilon} \right)^2 \langle \Psi_i | \sum{}' | \Psi_i \rangle \right\},$$

where $\sum'$ is the spin operator defined by McConnell (15), and the remaining symbols follow the usual conventions.

Excited states which could be taken into consideration are those found when an electron is promoted from any of the π-orbitals to the 4s level. Other possibilities are excitations from the nitrogen non-bonding orbital to this level or from lower levels on the metal ion itself. A similar situation exists for the other alkali metal ions.

It is expected that the zero-order term in eq. [3] will give little contribution to a_K because it depends on the probability density of the π-orbital containing the unpaired electron at the potassium nucleus, which will generally be small. It is not so straightforward to estimate the relative importance of the higher-order terms. For the naphthalene–sodium ion pair, Aono and Oohashi (16) have indeed estimated the magnitude of the second term to be only about one-tenth that of the third term and they have retained the third term only in their calculation of the sodium hyperfine splitting. It is apparent that the third term in eq. [3] will be the largest one for the integral $\langle \Psi_i | \sum' | \Psi_i \rangle$ is proportional to $|ns(r_k)|^2$, the density of the ns orbital at the alkali-metal nucleus, whereas the integrals $\langle \Psi_0 | \sum' | \Psi_0 \rangle$ and $\langle \Psi_i | \sum' | \Psi_0 \rangle$ in the other terms depend on the π-electron density at the metal nucleus. These latter are, of course, quite small.

Intuitively we may expect the exchange integrals $\langle \Psi_0 | \mathscr{H} | \Psi_i \rangle$ to decrease as the number of methyl groups increases, because the bulkiness of the methyl substituents will tend to keep anion and cation separated. The same may be said for the integrals $\langle \Psi_t | \sum' | \Psi_0 \rangle$ while

Can. J. Chem. Downloaded from www.nrcresearchpress.com by 210.87.254.5 on 09/05/12
For personal use only.

integrals of the type $\langle\Psi_i|\sum'|\Psi_i\rangle$ should be independent of the degree of methyl substitution. It therefore appears likely that the variation of the alkali metal hyperfine splitting in the series is not solely due to variations in these integrals, but that considerable importance must be attached to the excitation energies which occur in the denominator of both the second and third terms of eq. [3].

With respect to the excitation energies several comments may be made. If only those excitations from the π-orbitals of the anions are considered, and in particular from the π-orbital containing the unpaired electron, then it would seem reasonable that the excitation energy will decrease with increasing methyl group substitution. This should be a consequence of the decreasing electron affinity of the neutral molecules on increasing methyl substitution.

This argument, however, gives only a partial answer to the question. It is indeed seen that, as one might expect, the alkali metal hyperfine splitting increases considerably from the pyrazine radical anion to the tetramethylpyrazine radical anion. The metal hyperfine splitting constant for the dimethylpyrazines is smaller, however, than for the pyrazine radical anion itself, and the intermediate position of the pyrazine radical anion in the series remains a puzzle. A consideration of the Hückel energy levels in the series of the pyrazine radical anions is not helpful since the inductive effect of the methyl groups on the Hückel eigenvalues is very small. Steric interactions may here play some part in the variation of the hyperfine splitting constants.

If one considers the series of *m*-xylene, 3,5-dimethylpyridine, and 2,6-dimethylpyrazine radical anions, it is tempting to suggest that the increasing number of nitrogen atoms in the ring will lower the energy of the π-orbitals, and hence increase the energy of excitation from these orbitals. It is indeed found that the Hückel eigenvalues decrease considerably from *m*-xylene to 2,6-dimethylpyrazine. The change in these energies is such that the highest filled level in the neutral molecule has practically the same eigenvalue for all three molecules, while the lower filled levels and the lowest unfilled one decrease in energy with respect to this level. These considerations would then lead to the prediction that the alkali metal hyperfine splitting constant should decrease in this series, as is found experimentally.

(d) Solvent Effects

Hoijtink and co-workers (17) have made a study of ion association in solution and have found that the degree of association increases with increasing radius of the metal cation and with decreasing dielectric constant of the solvent. The dielectric constant of the solvents used in the present study decreases in the order dimethyoxyethane, tetrahydrofuran, and 2-methyltetrahydrofuran (18).

It is found in most cases (3, 5, 17) that little or no alkali metal hyperfine splitting is observable in DME, the solvent of highest dielectric constant, while larger splitting constants appears in THF and MeTHF. This observation is made also in the present investigations where the larger alkali metal splitting in the pyrazines and 3,5-dimethylpyridine is found in THF. The only exceptions to this observation are the ion pairs formed with the tetramethylpyrazine radical anion and various alkali metal cations. Here the potassium hyperfine splitting decreases in going from DME to MeTHF, in contrast to the other results. The hyperfine splitting could not be measured in 1,4-dioxane as a solvent, which has an even lower dielectric constant than MeTHF, presumably because the ion pair did not have sufficient solubility in this solvent. The sodium hyperfine splitting could be measured in DME and THF only, and the same value was obtained for the hyperfine splitting, within the limits of experimental error, in both solvents.

Can. J. Chem. Downloaded from www.nrcresearchpress.com by 210.87.254.5 on 09/05/12
For personal use only.

If the alkali metal hyperfine splitting is divided by the atomic hyperfine coupling constant to obtain the spin density at the metal nucleus it is found that in the case of the pyrazine radical anion and the dimethylpyrazine radical anions, the spin denisty is higher for sodium than for potassium, while for the tetramethylpyrazine and 3,5-dimethylpyridine radical anions the opposite takes place. The degree of ion association is not immediately derivable from the alkali metal hyperfine splittings, however, since the unpaired electron in sodium and potassium will be preferentially in the 3s and 4s levels, respectively, which have different densities at the nucleus.

4. CONCLUSIONS

The variation of the alkali metal hyperfine splitting constants in the series of compounds investigated is rather unusual and contrary to expectations. It appears that steric effects are not the main determining factors throughout the series, nor are electrostatic effects very important as far as the magnitude of the interaction between the cation and the anion is concerned.

The hyperfine splitting in the pyrazine radical anion and the two dimethylpyrazine radical anions appears to be normal in that the effect of the methyl groups on the separation of the anion and the cation will be to lower the alkali metal hyperfine splitting in the substituted pyrazines compared to the pyrazine radical anion itself.

A different situation is found in the series *m*-xylene, 3,5-dimethylpyridine, and 2,6-dimethylpyrazine. Here the decrease of the metal hyperfine splitting is probably caused by an increase in the energies of excitation from the anion to the cation with increasing substitution by nitrogen in the ring of the radical anion.

The special position of the tetramethylpyrazine radical anion in the series is not understood at the present time. Both the magnitude of the metal hyperfine splitting, and its variation with solvent are contrary to expectation, except for a small increase in splitting above that of the pyrazine radical anion which would be expected on the basis of a decrease in the excitation energies.

5. ACKNOWLEDGMENTS

We should like to thank the National Research Council for generous financial aid in support of this research work. C. A. McD. is much indebted to the same body for the award of a Senior Research Fellowship during the 1963–1964 academic year. One of us (K. F. G. P.) wishes to acknowledge the award of a predoctoral fellowship by the Imperial Oil Company. We also thank Mr. J. A. Hebden for performing some of the experiments reported.

REFERENCES

1. B. J. McLELLAND. Trans. Faraday Soc. **57**, 1458 (1961).
2. N. S. HUSH and J. R. ROWLANDS. Mol. Phys. **6**, 201 (1963).
3. N. M. ATHERTON and S. I. WEISSMAN. J. Am. Chem. Soc. **83**, 1330 (1961).
4. E. DE BOER and E. L. MACKOR. Proc. Chem. Soc. 23 (1963).
5. E. DE BOER and E. L. MACKOR. J. Am. Chem. Soc. **86**, 1513 (1964).
6. R. L. WARD. J. Am. Chem. Soc. **83**, 1297 (1961).
7. A. ZAHLAN, F. W. HEINEKEN, M. BRUIN, and F. BRUIN. J. Chem. Phys. **37**, 683 (1962).
8. C. A. McDOWELL, K. F. PAULUS, and J. R. ROWLANDS. Proc. Chem. Soc. 60 (1962).
9. C. A. McDOWELL and K. F. G. PAULUS. Mol. Phys. **7**, 541 (1964).
10. N. M. ATHERTON, F. GERSON, and J. N. MURRELL. Mol. Phys. **5**, 509 (1962).
11. J. R. BOLTON and A. CARRINGTON. Mol. Phys. **4**, 497 (1961).
12. A. D. McLACHLAN. Mol. Phys. **3**, 233 (1960).
13. P. J. WHEATLEY. Acta Cryst. **10**, 182 (1957).
14. D. T. CROMER, A. J. IHDE, and H. L. RITTER. J. Am. Chem. Soc. **73**, 5587 (1951).
15. H. M. McCONNELL. J. Chem. Phys. **28**, 1188 (1958).
16. S. AONO and K. OOHASI. Progr. Theoret. Phys. Kyoto, **30**, 162 (1963).
17. A. C. ATEN, J. DIELEMEN, and G. J. HOITJTINK. Discussions Faraday Soc. **29**, 182 (1960).
18. J. L. DOWN, J. LEWIS, B. MOORE, and G. WILKINSON. J. Chem. Soc. 3767 (1957).

Can. J. Chem. Downloaded from www.nrcresearchpress.com by 210.87.254.5 on 09/05/12
For personal use only.

Can. J. Chem. Downloaded from www.nrcresearchpress.com by 210.87.254.105 on 09/05/12
For personal use only.

STUDIES ON THE RANGE OF ^{140}Ba IN PROTON-INDUCED FISSION OF ^{238}U AND A SEMI-EMPIRICAL DERIVATION OF A GENERAL RANGE–ENERGY RELATION[1]

S. MUKHERJI[2] AND L. YAFFE
Department of Chemistry, McGill University, Montreal, Quebec
Received February 14, 1964

ABSTRACT

Ranges of ^{140}Ba have been measured in the forward and backward directions with respect to the proton beam by bombarding uranium foils of normal isotopic composition with protons of 15, 30, and 60 MeV energies. Successive thin layers of aluminium were removed from the front and back catchers by an electrochemical technique, and the ranges were calculated from the relative distribution of ^{140}Ba activity in the different layers. The calculations indicate that full momentum transfer of the incident protons has taken place, suggesting that the compound nucleus mechanism is predominant at these energies.

An analysis of the existing range and energy data for fission fragments has shown that the 'effective charge' of a fission fragment, first postulated by Bohr, can be expressed as a function of the charge and the mass of the medium being penetrated. The original range–velocity relation of Bohr has been modified to include the above fact and has led to a general range–velocity relation for ranges in different metallic catchers. Similar equations seem to be applicable to the range data in gaseous media.

INTRODUCTION

Much experimental work has been done on the ranges of fragments from the thermal neutron fission of ^{235}U and ^{239}Pu and from the high-energy proton-induced fission of Bi and Ta. The thin-target thin-catcher differential technique was used by Katcoff, Miskel, and Stanley (1) for the ranges of ^{239}Pu fragments in air and by Brown and Oliver (2) for some ^{235}U fission fragments in aluminium. Finkle *et al.* (3) used a thin-target thin-catcher integral method and determined the range of ^{140}Ba in aluminium from the equation of Segrè and Wiegand (4). Thin-target methods are suitable for fragments produced from the fission of ^{235}U and ^{239}Pu by thermal neutrons because of the high fission cross sections and the fact that the targets can be conveniently irradiated inside the reactors for a long period of time.

Where the ranges of fragments from materials like ^{238}U with smaller fission cross sections are to be measured, especially if fission is induced by charged particles, thin-target thin-catcher methods become unsuitable because of the low yields of the recoils. Hence thick targets with thick or thin catchers have been used for studying the ranges of fragments from comparatively high-energy fission. Porile and Sugarman (5) used thick targets sandwiched between thick aluminium catchers for the study of fragment ranges from the fission of bismuth and tantalum. Niday (6) used the same technique for the ranges of fragments from thermal neutron fission of ^{235}U. From the ratios of the activities in the catcher foils to those in the total assembly, the ranges were calculated in terms of the target material. Sugarman, Campos, and Wielgoz (7) used thick targets and comparatively thin catchers for differential experiments to calculate the ranges in aluminium. Alexander and Gazdik (8) used a moderately thick target with comparatively thin catchers and by differential experiments calculated ranges in aluminium and in gold.

The recently developed electrochemical techniques of Davies *et al.* (9) for the removal of very thin layers of aluminium of accurately known thicknesses opened up the possibility

[1]*This work received financial assistance from the National Research Council of Canada.*
[2]*Present address: Enrico Fermi Institute for Nuclear Studies, University of Chicago, Chicago, Illinois.*

of performing differential experiments with an unprecedented degree of differentiation. The present work is essentially a thick-target thin-catcher differential experiment in which the uncertainties in the thicknesses of the commercially available foils of aluminium have been avoided.

Very few experimental data are available on the variation of the range of ^{140}Ba with energy in the low-energy proton-induced fission of ^{238}U. Douthett and Templeton (10) determined the ranges of ^{140}Ba in ^{238}U fission induced by 18 MeV deuterons and 335 MeV protons. The energies used differed widely and the fission mechanism would be presumably different so that the ranges cannot be compared on a common basis. Bombarding energies of 15, 30, and 60 MeV were chosen in the present work to see whether any change, due to reactions proceeding via mechanisms other than compound nucleus formation, could be found.

EXPERIMENTAL

(a) Target Preparation and Irradiation

A uranium foil (thickness 0.0006 in.) of normal isotopic composition was gently warmed with 6 *N* nitric acid to remove the oxide layer. A piece (1 in. × 1½ in.) was sandwiched between two 'super-pure' electropolished aluminium foils from each of which a 100 V 'thick' oxide layer had previously been removed by the technique to be described later. The aluminium foils were of slightly larger dimensions than the uranium foil. One edge of the sandwich assembly was fixed to the target holder. The other edge was vertically sheared so as to align the edges of the three foils exactly in the same vertical plane. The assembly was then attached to the water-cooled probe of the McGill Synchrocyclotron, and the foil assembly was placed perpendicular to the internally circulating proton beam. The radial distance was so chosen as to intercept the proton beam of the desired energy.

(b) Electropolishing, Anodizing, and Stripping

'Super-pure' aluminium foils of thickness 0.02 in. were first electropolished by the perchloric acid – acetic anhydride prescription of Tegart (11). The foil was anodized by dipping it for 10 min in a citrate buffer solution (3% ammonium citrate) contained in an aluminium beaker. A d-c. voltage was applied, the aluminium beaker serving as the cathode and the foil itself as the anode. The potential was always maintained at 100 V from an assemblage of 7.5 V dry batteries connected in series. The stripping of the oxide layer was carried out according to the method of Davies *et al.* (9) by a 2-min treatment with a chromium trioxide – phosphoric acid mixture maintained at 90 °C. From each catcher foil at each bombarding energy 92 layers were removed at a 100 V potential. Because of the low activity of ^{140}Ba in a single layer, two such layers were taken together and these are designated as double layers. The activity in a double layer has been assumed to be concentrated in the second of the two layers.

(c) Chemical Separation

Ba^{++} carrier, 20 mg, was added to the solution containing each alternate double layer, and the solution was then evaporated to about 4 ml. Barium was separated from the solution by the ether – hydrochloric acid method of Glendenin (12). The barium was then purified by alternate scavenging with ferric hydroxide and precipitating as barium chloride. Barium was finally precipitated as barium chromate, filtered onto glass fiber discs, dried at 110 °C, and weighed. No absolute chemical yields were determined, since only relative activities were essential for the range determination. Likewise, no activity measurement was made on the target foil itself.

(d) Measurement of Radioactivity

All the activities were determined by gross beta ray measurement, and the purity of the samples was checked by following the decay of the 12.8-d half-life activity of ^{140}Ba. Because of the low activities involved (maximum number of counts of ^{140}Ba in the 15 MeV experiment was only 40 c.p.m.) a Sharp Low Beta counter with a background of 0.5 c.p.m. was used. The counter was operated as an end-window flow type proportional counter with P-10 as the circulating gas. No self-absorption corrections were made as the weights of barium chromate did not differ appreciably in the various samples. The activities were normalized to the same sample weights, and decay corrections were made where applicable.

RESULTS

The plots of the activity of double layer against the number of the double layers removed are shown in Figs. 1 to 6 inclusive. Each double layer represents 54.3 $\mu g/cm^2$ aluminium removed from the exposed surface. The activity increases initially with increasing depth

Can. J. Chem. Downloaded from www.nrcresearchpress.com by 210.87.254.105 on 09/05/12
For personal use only.

from the surface and then decreases linearly with perfect regularity. The two plots at 15 MeV show considerable scatter because of the low activities involved. Extrapolation of the linear portion of the curve to zero activity gives the value of the range in any particular catcher. These are shown in Table I along with the ratios of the actual total activities in the forward and the back catchers.

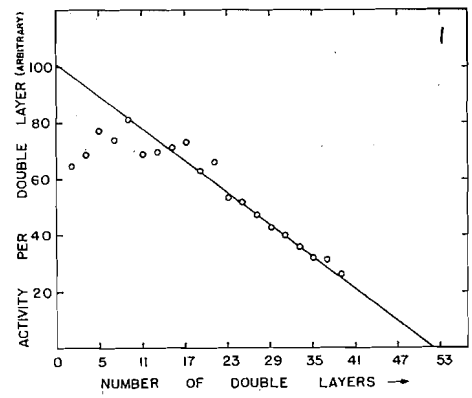

FIG. 1. Plot of activity of each double layer against the double layer number in front catcher (15 MeV protons).

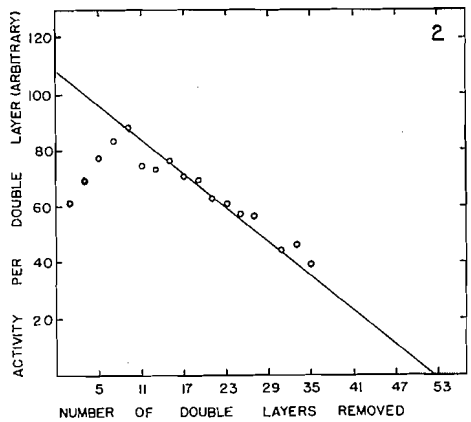

FIG. 2. Plot of activity of each double layer against the double layer number in back catcher (15 MeV protons).

The statistical errors in activity measurements and in the weight of aluminium removed by stripping are $\pm 3\%$ and $\pm 4\%$ respectively, while the error in chemical yield is $\pm 1\%$. The error in the range values is estimated to be only $\pm 3\%$, since these values are obtained by extrapolation of straight lines passing through a large number of points representing the mean values of the activities per double layer.

If one assumes that the activities should ideally have decreased linearly starting with the first double layer, then the total activity in any catcher foil can be calculated by extrapolating the linear portion backward to the original surface of the foil. The values of the ideal activities of the first few double layers were calculated by interpolation from the extrapolated initial part of the straight lines. The total ideal activities and their ratios are shown in Table I.

Can. J. Chem. Downloaded from www.nrcresearchpress.com by 210.87.254.105 on 09/05/12
For personal use only.

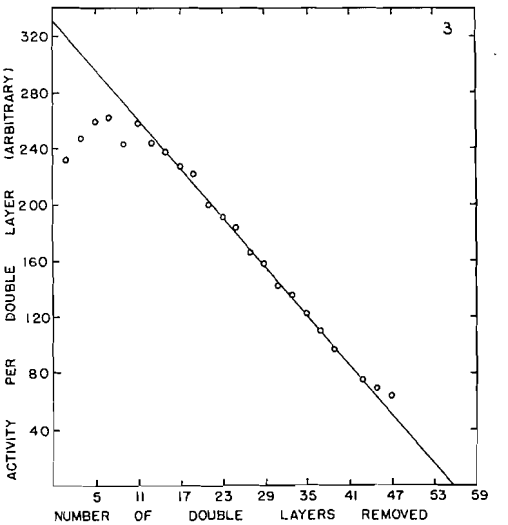

FIG. 3. Plot of activity of each double layer against the double layer number in front catcher (30 MeV protons).

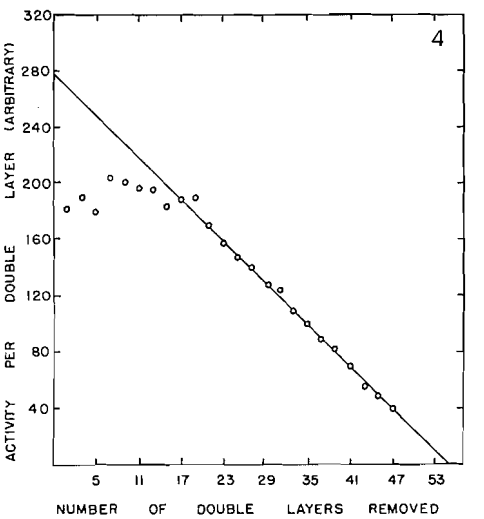

FIG. 4. Plot of activity of each double layer against the double layer number in back catcher (30 MeV protons).

DISCUSSION

(a) Evidence for Compound Nucleus Formation

As can be seen from Table I, the difference between the ranges in the front and the back catcher increases with increasing bombarding energy. If these ranges reflected fully the transfer of momentum to the struck nucleus then one could calculate quantitatively the transferred momentum. However, for reasons mentioned later, an alternative method of calculating the transferred momentum from the ratio of the activities in the front and back catchers has been used. From a modified form (Appendix B) of the equation of Sugarman *et al.* (7) we have the absorption equation

Can. J. Chem. Downloaded from www.nrcresearchpress.com by 210.87.254.105 on 09/05/12
For personal use only.

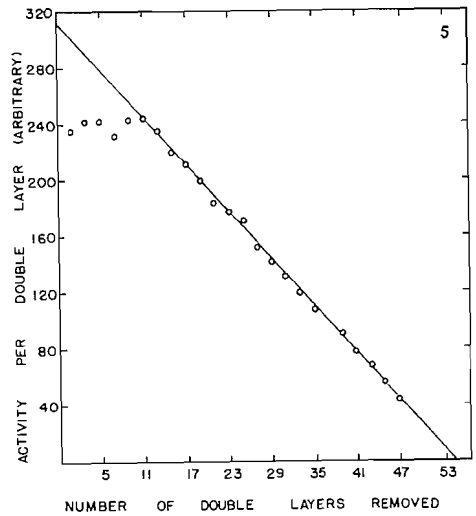

FIG. 5. Plot of activity of each double layer against the double layer number in front catcher (60 MeV protons).

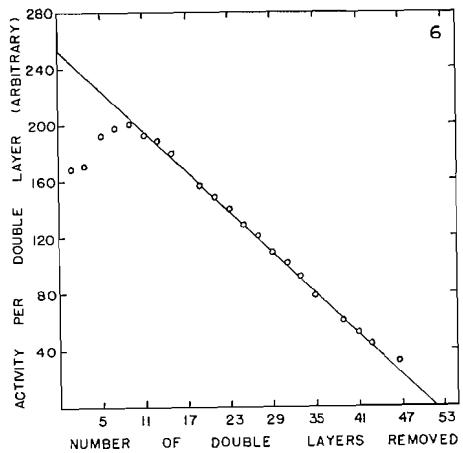

FIG. 6. Plot of activity of each double layer against the double layer number in back catcher (60 MeV protons).

$$[1] \qquad N(t) = K'(1 \pm \eta - \eta')^2 \left[1 - \frac{t}{R\left(1 \pm \frac{\eta}{1-\eta'}\right)}\right]^2,$$

where

$N(t)$ = number of recoils penetrating beyond a thickness t of the catcher material,
$\eta = v/V$,
$\eta' = v_0/V$,
v = velocity imparted to the struck nucleus by the projectile,
v_0 = velocity of the electron in the hydrogen orbit and represents the velocity at which the fission fragment essentially comes to a stop,

Can. J. Chem. Downloaded from www.nrcresearchpress.com by 210.87.254.105 on 09/05/12
For personal use only.

Can. J. Chem. Downloaded from www.nrcresearchpress.com by 210.87.254.105 on 09/05/12
For personal use only.

TABLE I

Range and activity data

E = Bombarding energy (MeV)	R_f = Range in front catcher (mg/cm² Al)	R_b = Range in back catcher (mg/cm² Al)	$A_f = (I_f \times R_f)/2$ = Total activity in front catcher (arb. units)	$A_b = (I_b \times R_b)/2$ = Total activity in back catcher (arb. units)	A_f' = Actual total A front catcher (arb. units)	A_b' = Actual total A back catcher (arb. units)	$R_M = (R_f + R_b)/2$ (mg/cm² Al)
15	2.813	2.813					
30	3.062	2.986	9 136	7 535	8 433	6 659	3.024
60	2.953	2.834	8 268	6 498	7 688	5 920	2.893

TABLE II

Velocity data

E = Bombarding energy (MeV)	A_f/A_b	A_f'/A_b'	V^*	η'	η	$v_{calc}^* = \eta V$	$v_{th}^* = \sqrt{(2E)/239}$	v_{th}/v_{calc}
30	1.212±0.05	1.267±0.05	0.9604	0.234	0.0362±0.008	0.034±0.0076	0.032	0.94±0.20
60	1.272±0.05	1.298±0.05	0.9285	0.242	0.0456±0.008	0.042±0.0074	0.045	1.07±0.20

*In units of (Mev/nucleon mass)$^{1/2}$.

V = velocity of the escaping fragment,
R = range of the fragment in the catcher material from a stationary target, and
K' = constant.

The plus and minus signs refer to the front and the back catcher respectively. If R_f and R_b are the ranges in the forward and backward directions with respect to the proton beam, then

$$R_f = \frac{R(1 + \eta - \eta')}{1 - \eta'}, \qquad R_b = \frac{R(1 - \eta - \eta')}{1 - \eta'}.$$

Hence

$$\frac{R_f}{R_b} = \frac{1 + \eta - \eta'}{1 - \eta - \eta'}. \tag{2}$$

The absorption equation in the front catcher becomes

$$N_f(t) = K'(1 + \eta - \eta')^2\left[1 - \frac{t}{R_f}\right]^2. \tag{3}$$

The activity ΔN_f retained by a layer of the catcher material of thickness Δt is given by

$$\frac{\Delta N_f(t)}{\Delta t} \approx \frac{dN_f(t)}{dt} = -\frac{2K'}{R_f}(1 + \eta - \eta')^2\left[1 - \frac{t}{R_f}\right]$$

and similarly for the back catcher

$$\frac{\Delta N_b(t)}{\Delta t} \approx \frac{dN_b(t)}{dt} = -\frac{2K'}{R_b}(1 - \eta - \eta')^2\left[1 - \frac{t}{R_b}\right].$$

These relations show that the plot of the activity per double layer of aluminium against the depth of the layer should give a straight line as has been experimentally found. The total activities in the front and back catchers are obtained from the areas under the straight lines (Figs. 3–6). Hence

$$\frac{A_f}{A_b} = \frac{I_f \times R_f}{I_b \times R_b}, \tag{4}$$

where A_f and A_b are the total activities in the front and back catchers respectively, and I_f and I_b represent corresponding activities at $t = 0$ (intercepts on the activity axis). It follows (Appendix A) that

$$\frac{A_f}{A_b} = \frac{(1 + \eta - \eta')^2}{(1 - \eta - \eta')^2}. \tag{5}$$

Calculation of η from eq. [5] requires a knowledge of η'. Assuming that the mean range R_M ($= (R_f + R_b)/2$) represents the range of ^{140}Ba from a stationary target, the value of V can be calculated from eq. [19] and hence η' is known (Appendix C). The calculation of V from R_M is justified by the fact that the latter is in good agreement with the values of Douthett and Templeton (10) and of Alexander and Gazdik (8).

The value of v is then calculated from the relation $v = \eta V$. These values of v have an associated error of $\pm 20\%$ arising out of the error of $\pm 3\%$ in the values of A_f and A_b. The theoretically expected values of v, assuming full momentum transfer, have also been calculated and the relevant data are shown in Table II. The ratios of v (theoretical) to v (calculated), apart from the experimental error, are very close to unity. The calculated

Can. J. Chem. Downloaded from www.nrcresearchpress.com by 210.87.254.105 on 09/05/12
For personal use only.

value of v obviously cannot be expected to exceed the theoretical value, and thus the calculated values of v will essentially have an error limit of -20%. Thus, at bombarding energies of 30 and 60 MeV, at least as much as 80% of the momentum of the impinging proton is transferred to the fissioning nucleus, and fission at these energies seems to proceed predominantly through the compound nucleus mechanism (13).

The calculation of η from eq. [2] has not been made for the following reasons. (*a*) The absolute values of the extrapolated ranges obtained graphically are very sensitive to the slopes of the lines (Figs. 3–6). Experimental errors of the order of $\pm 3\%$ would cause considerable error in the value of η. The total areas under the straight lines, however, are much less sensitive to these errors. (*b*) Equation [5] is independent of the straggling and scattering phenomena inside the catcher, which might add to the experimental errors in altering the slopes of the lines.

As a check on the validity of eq. [5] we have used the range values of Douthett and Templeton (10) to calculate the velocity v imparted by 18 MeV deuterons to the (^{238}U + d) nucleus. These range values have been corrected for straggling and source thickness, have a precision of 1%, and represent averaged values of R_f and R_b. The value of η' has been calculated as previously (Appendix C). The values of v obtained from $v = \eta V$ and from theoretical calculations, assuming full momentum transfer, are 0.033 and 0.0353 respectively in appropriate units. Assuming $R_f/R_b = (1 + \eta)/(1 - \eta)$, the value of v comes out to be 0.0579.

(b) Scattering and Thermal Diffusion

If one assumes isotropic distribution of the fragments, the activity per double layer should decrease linearly with increasing depth of the layer. The activity in the first few double layers is found to be consistently low in all the catcher foils, rising to a maximum in the ninth double layer and then decreasing linearly. The effect might be due to a combination of scattering and thermal diffusion. Although scattering plays a large role near the interface between the catcher and the target, because of the increasing number of nuclear collisions (14), one would expect anomalously high activities in the first few double layers rather than the opposite. In the case of ^{140}Ba produced in the range of 30–60 MeV bombarding energies, thermal diffusion of the ^{140}Xe precursor is quite likely. Significant errors may arise when ranges are calculated from the ratio of the total activities in the front and back catchers in a thick-target thick-catcher type of experiment. The corrected total activities A_f and A_b obtained by extrapolating the straight lines to zero layer and their ratios are shown in Table II. The summed total activities A_f' and A_b' and their ratios are also shown in Table II.

(c) Range–Energy Relation for Fission Fragments

Bohr (14) dealt comprehensively with the problem of the energy loss of charged particles passing through matter and derived the following equation:

$$[6] \qquad \frac{dV}{dR} = \frac{4\pi N \epsilon^4 (Z_1^{eff})^2}{m_0 M V^3} \sum_s \ln \frac{m_0 V^3}{2\pi \nu_s \epsilon^2 Z_1^{eff}} + \frac{4\pi \epsilon^4 Z_1^2 Z_2^2}{mMV^3} \ln \left[\left(\frac{mM}{m+M} \right) \frac{V^2 a_{sc}}{Z_1 Z_2 \epsilon^2} \right],$$

where

dV/dR = rate of velocity loss per unit path length,
N = number of atoms of the absorber per unit volume,
m_0 = electronic mass,
ϵ = electronic charge,
M = mass of the penetrating particle,

Can. J. Chem. Downloaded from www.nrcresearchpress.com by 210.87.254.105 on 09/05/12
For personal use only.

m = mass number of the absorber,
Z_1 = nuclear charge of the penetrating particle,
Z_2 = nuclear charge of the absorber,
V = velocity of the penetrating particle,
ν_s = frequency of the sth electron,
Z_1^{eff} = effective charge of the penetrating particle (which is related to the rate of capture and loss of electrons by the penetrating particle), and
a_{sc} = screening constant.

The first term on the right-hand side of the equation represents the energy loss due to electronic collision while the second is that due to nuclear collisions. For fission fragment ranges in solid absorbers, as a first approximation, we may neglect the second term in comparison to the first and write

$$[7] \qquad \frac{dV}{dR} = \frac{4\pi\epsilon^4 N(Z_1^{eff})^2}{m_0 M V^3} \sum_s \ln \frac{m_0 V^3}{2\pi\nu_s \epsilon^2 Z_1^{eff}}.$$

It was further argued by Bohr (14) that the effective charge of the fission fragments is given by

$$[8] \qquad Z_1^{eff} = K\frac{V}{V_0},$$

where

V = velocity of the fragment,
V_0 = velocity of the electron in the hydrogen orbit, and
$K = kZ_1^{1/3} = kZ_p^{1/3}$, where
k = a constant and was taken by Bohr (14) as unity for gaseous absorbers, and
Z_1 = probable nuclear charge of the fragment and equals the most probable charge Z_p.

Since the logarithmic term within the summation bracket would be proportional to V, by substituting the value of Z_1^{eff} from eq. [8], we have

$$\frac{dV}{dR} = C' \times \frac{Z_p^{2/3}}{M}$$

where C' is a constant and, since $V = \sqrt{(2E/M)}$, we can write

$$[9] \qquad R = C \times \frac{E^{1/2}M^{1/2}}{Z_1^{2/3}},$$

where C is a constant and E is the kinetic energy of the fission fragment. Brown and Oliver (2) utilized this form of Bohr's equation to calculate the kinetic energies of some ^{235}U fission fragments. The constant C was first evaluated. The kinetic energy values for some nuclides were taken from the velocity data of Milton and Fraser (15) and the range data were taken from the work of Niday (6) for ranges in uranium and those in air from the data of Katcoff, Miskel, and Stanley (1). The 'constancy' of the constant C was then checked by plotting the value of C for the different nuclides obtained from eq. [9] against the mass number of the nuclides. The constant was found to show a definite drift, the values for mass numbers 92 and 134 being approximately 0.295 and 0.275 respectively. However, the plot gives a straight line up to mass number 133 for the range data in air, and the value of C for a particular nuclide could be obtained by suitable interpolation from the straight

Can. J. Chem. Downloaded from www.nrcresearchpress.com by 210.87.254.105 on 09/05/12
For personal use only.

line. This form of the range–energy equation cannot be regarded as a general one, as the value of the constant must be determined for each absorber material, and there is no way of theoretically comparing the range values of the same nuclide in different absorbers.

Alexander and Gazdik (8), by a different procedure, showed that the range could be related to the energy by the expression:

$$R = KE^{2/3}, \tag{10}$$

where K is not a true constant in the sense that it depends both on the absorber and on the fission product being considered. To determine the value of the constant, K, known values of the kinetic energies of some nuclides were taken from the data of Stein (16). The known ranges were taken from their own data in aluminium and the range data in air from Katcoff, Miskel, and Stanley (1). The values of K, obtained from these and from eq. [10], were plotted against the mass number of the nuclides. The plot shows that, like the constant C of the previous equation, K also does not have a unique value for all the nuclides penetrating a particular medium, although it seems to be a smooth function of the mass number of the nuclides. Consequently, to determine the kinetic energy of a nuclide from its experimentally determined range, the value of K has to be determined first by proper interpolation from the plot of the known values of K against the mass number and substituted in eq. [10].

Niday (6) determined the ranges of a large number of nuclides from the slow neutron fission of ^{235}U. From a simplification of another form of Bohr's (14) energy-loss equation, he obtained a relation between the range in uranium and the initial fragment velocity:

$$R_U = \frac{A(v_i - v_0)}{2.411(K + 4.7622K^{5/3})} \tag{11}$$

where

R_U = the range in uranium in mg/cm^2,
v_i = velocity of the nuclide in units of 10^8 cm/s,
A = mass number of the nuclide, and
v_0 = electron velocity in the hydrogen orbit in units of 10^8 cm/s.

The constant K for a particular nuclide is the same as that described previously (i.e. $K = kZ_p^{1/3}$). By an empirical choice of $k = 1$, Niday found that all his range data could be accurately reproduced when Stein's (16) kinetic energy values were substituted in this equation. This disagrees with the suggestion of Bohr and Lindhard (17) that a value of $K = 1.5 \times Z_p^{1/3}$ should be chosen for fragments passing through solids, which is close to the value of $1.4 \times Z_p^{1/3}$ found by Lassen (18) and Cohen *et al.* (19). This fact pointed towards the possibility that the value of k may not be a constant for all the absorbers but may be a function of the catcher material itself.

To investigate the applicability of eq. [11] in the case of absorbers other than U, it may be rearranged to bring out the dependence on the nuclear charge and mass number of the absorber:

$$R = \frac{A(v_i - v_0)}{126\left(\frac{Z^{1/3}}{A}\right)[K + 4.7622K^{5/3}]}. \tag{12}$$

For ease of manipulation, K was neglected in comparison to $4.7622K^{5/3}$ in the denominator of the right-hand side of eq. [12].

Can. J. Chem. Downloaded from www.nrcresearchpress.com by 210.87.254.105 on 09/05/12
For personal use only.

[13] $$R = \frac{A(v_i - v_0)}{126\left(\frac{Z^{1/3}}{A}\right)_{abs}(4.7622K^{5/3})}.$$

To find out if there is a unique value of k for aluminium as in the case of uranium, a set of nuclides was chosen with known range values in aluminium (8). Their energies were taken from ref. 14, after correction for neutron emission, with the exception of that for ^{111}Ag which is taken from ref. 8. These values were substituted in eq. [13] and values of K were calculated for each nuclide. The ratio of $K/Z_p^{1/3}$ is tabulated in Table III. The

TABLE III

Values of k calculated from the equations

$$k = \frac{K}{Z_p^{1/3}} \text{ and } K^{5/3} = \frac{A(v_i - v_0)}{126 \times 4.7622\left(\frac{Z^{1/3}}{A}\right)_{cat} \times R_{cat}}$$

	U catcher		Al catcher		Au catcher	
Nucl.	K	k	K	k	K	k
^{89}Sr	3.55	1.082	2.655	0.809	3.420	1.042
^{97}Zr	3.64	1.073				
^{99}Mo	3.75	1.096				
^{111}Ag			2.837	0.808	3.703	1.054
^{131}I			2.970	0.803	3.892	1.051
^{140}Ba	4.02	1.060	3.074	0.813	3.902	1.032
^{143}Ce	4.06	1.060				
	Mean = 1.077		Mean = 0.808		Mean = 1.044	

value of Z_p for ^{111}Ag was obtained from Milton (20). All other values are those of Wahl (21). It seems that for aluminium there is a constant k value for all the nuclides. With range data in gold (8) a similar calculation gave constant k values, as shown in Table III. Range data in some gases were then chosen from the work of Petrzhak *et al.* (22). In spite of the fact that Bohr's equation was derived for particles penetrating into heavy media and consequently no unique value ought to have been expected, Table IV shows that k, for

TABLE IV

Values of k calculated from the equations

$$k = \frac{K}{Z_p^{1/3}}, \qquad K^{5/3} = \frac{A(v_i - v_0)}{126 \times 4.7622\left(\frac{Z^{1/3}}{A}\right)_{abs} \times R_{abs}}$$

	A as absorber		Ne as absorber		He as absorber		N_2 as absorber		H_2 as absorber	
Nucl.	K	k	K	k	K	k	K	k	K	k
^{91}Sr			2.297	0.694	1.586	0.479	3.656	1.104	1.580	0.477
^{92}Y	2.977	0.896	2.295	0.691	1.597	0.481	3.724	1.120	1.583	0.476
^{97}Zr	3.070	0.905	2.383	0.703	1.617	0.476	3.78	1.110	1.607	0.474
^{140}Ba	3.430	0.907			1.773	0.469			1.730	0.457
^{143}Ce	3.422	0.895			1.740	0.455	4.15	1.086	1.692	0.443
	Mean = 0.901		Mean = 0.696		Mean = 0.472		Mean = 1.105		Mean = 0.465	

each of the gases H_2, N_2, He, Ne, and Ar, has a constant value for all the nuclides considered. In the light of the preceding facts, we can express the range of a nuclide in any absorber by

Can. J. Chem. Downloaded from www.nrcresearchpress.com by 210.87.254.105 on 09/05/12
For personal use only.

[14] $$R = \frac{A(v_i - v_0)}{126\left(\frac{Z^{1/3}}{A}\right)_{abs} 4.7622(k \times Z_p{}^{1/3})^{5/3}},$$

provided the value of k, which is a constant for a particular absorber, is empirically determined. The next step was to find out if k could be related to some fundamental constants of the absorbers. Such a relation would eliminate the arbitrariness involved in the choice of k by empirical means. An intuitive guess was that k might be a function of $(Z^{1/3}/A)$ of the catcher material, and the values of log k for uranium, gold, and aluminium were plotted against the log $(Z^{1/3}/A)$ value of the corresponding catcher. All the three points were found to fall on a straight line. Values of log k plotted against log $(Z^{1/3}/A)$ for the other absorbers are also shown in Fig. 7. The points for the rare gases fall on a straight line

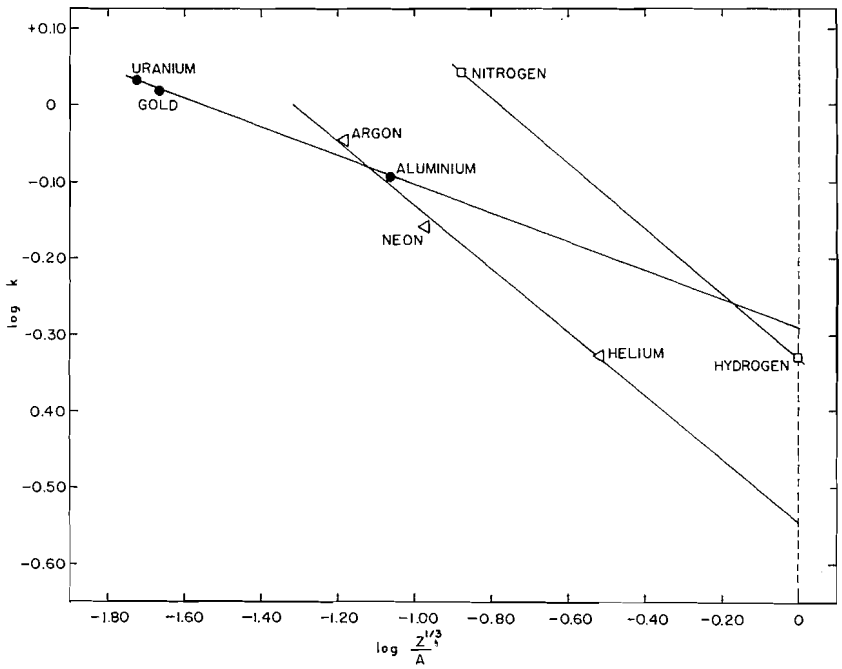

FIG. 7. Plot of log k vs. log $(Z^{1/3}/A)$ of the catcher.

whose slope is almost the same as that of the line joining the points for nitrogen and hydrogen. Thus the difference in the nature of the absorbers appears to be visibly reflected in their alignment along three different straight lines. The relation between k and $Z^{1/3}/A$ can now be expressed as:

[15] $$k_{met} = c\left(\frac{Z^{1/3}}{A}\right)^{\alpha}_{cat}$$

$$k_{mon} = c'\left(\frac{Z^{1/3}}{A}\right)^{\beta}_{cat}$$

$$k_{dl} = c''\left(\frac{Z^{1/3}}{A}\right)^{\gamma}_{cat}$$

where met = metal, cat = catcher, mon = monatomic gas, and di = diatomic gas. If

Can. J. Chem. Downloaded from www.nrcresearchpress.com by 210.87.254.105 on 09/05/12
For personal use only.

these are substituted in eq. [14], we have the generalized form of range–velocity relation for the three different types of catcher materials:

$$[16] \qquad R_{\text{met}} = \frac{A(v_i - v_0)}{(c^{5/3} \times 126) \times \left(\frac{Z^{1/3}}{A}\right)_{\text{cat}}^{(5\alpha/3)+1} \times 4.7622 Z_p^{5/9}}$$

$$[17] \qquad R_{\text{mon}} = \frac{A(v_i - v_0)}{126(c')^{5/3} \times \left(\frac{Z^{1/3}}{A}\right)_{\text{cat}}^{(5\beta/3)+1} \times 4.7622 Z_p^{5/9}}$$

$$[18] \qquad R_{\text{dl}} = \frac{A(v_i - v_0)}{126(c'')^{5/3} \times \left(\frac{Z^{1/3}}{A}\right)_{\text{cat}}^{(5\gamma/3)+1} \times 4.7622 Z_p^{5/9}}.$$

Evaluations of c, c', and c'' were made by taking the intercepts of the three lines in Fig. 7, on the log k axis. The values of α, β, and γ are the slopes of the straight lines. These values were substituted into eqs. [16], [17], and [18] to obtain the final forms of the general range–velocity relations, from which the kinetic energies may be conveniently calculated.

$$[19] \qquad R_{\text{met}} = \frac{A(v_i - v_0)}{195\left(\frac{Z^{1/3}}{A}\right)_{\text{cat}}^{0.6870} Z_p^{5/9}}$$

$$[20] \qquad R_{\text{mon}} = \frac{A(v_i - v_0)}{74\left(\frac{Z^{1/3}}{A}\right)_{\text{cat}}^{0.3097} Z_p^{5/9}}$$

$$[21] \qquad R_{\text{dl}} = \frac{A(v_i - v_0)}{168\left(\frac{Z^{1/3}}{A}\right)_{\text{cat}}^{0.2880} Z_p^{5/9}}.$$

From these equations, and the known energy values used previously, the ranges have been recalculated and are shown in Table V. A good correlation is evident.

(d) Interconversion of Range Values

From eq. [19] for ranges in metallic catchers, we have

$$[22] \qquad \frac{R_2}{R_1} = \left(\frac{Z_1^{1/3}}{Z_2^{1/3}} \cdot \frac{A_2}{A_1}\right)^{0.6870},$$

where R_1 and R_2 represent the ranges of the same nuclide in catchers of nuclear charges Z_1 and Z_2 and mass numbers A_1 and A_2 respectively. It was interesting to see if this formula holds for range ratios in fission at higher energies. Panontin and Sugarman (23) have determined the range values in aluminium and in the target materials of some fission fragments in the fission of ^{238}U, ^{209}Bi, and ^{181}Ta induced by 450 MeV protons. The ratios of the ranges in the target materials to those in aluminium are shown in Table VI. The same ratios calculated from eq. [22] are also shown. The agreement is fairly good.

ACKNOWLEDGMENTS

The authors are deeply indebted to Dr. J. A. Davies for his advice on electropolishing and to Mr. D. Marsden for a great deal of assistance in various ways. One of us (S. M.)

Can. J. Chem. Downloaded from www.nrcresearchpress.com by 210.87.254.105 on 09/05/12
For personal use only.

TABLE V

Experimental ranges and those calculated from eqs. [19]–[21]

Nucl.	Uranium R_{exp}, mg/cm²	Uranium R_{calc}, mg/cm²	Uranium % deviation	Gold R_{exp}, mg/cm²	Gold R_{calc}, mg/cm²	Gold % deviation	Aluminium R_{exp}, mg/cm²	Aluminium R_{calc}, mg/cm²	Aluminium % deviation
^{89}Sr	11.55	11.88	+3	10.80	10.88	+0.8	4.12	4.17	+1
^{92}Y	11.40	11.84	+3						
^{97}Zr	11.36	11.63	+2						
^{99}Mo	11.17	11.65	+4						
^{111}Ag	9.74	10.09	+4	9.00	9.18	+2	3.51	3.54	+1
^{131}I				8.60	8.74	+2	3.37	3.37	0
^{140}Ba	8.74	8.64	−1	8.00	7.85	−2	2.98	3.03	+1.5
^{143}Ce	8.42	8.30	−1						

Nucl.	Argon R_{exp}, mg/cm²	Argon R_{calc}, mg/cm²	Argon % deviation	Neon R_{exp}, mg/cm²	Neon R_{calc}, mg/cm²	Neon % deviation	Helium R_{exp}, mg/cm²	Helium R_{calc}, mg/cm²	Helium % deviation
^{91}Sr	4.64	4.74	+2.5	4.32	4.08	−6	2.81	2.95	+5
^{92}Y	4.60	4.76	+4	4.35	4.09	−7	2.80	2.96	+5
^{97}Zr	4.44	4.68	+5	4.19	4.02	−4	2.79	2.91	+5
^{140}Ba	3.29	3.47	+5				2.13	2.16	+1.5
^{142}Ce	3.23	3.34	+4				2.14	2.08	−3

Nucl.	Nitrogen R_{exp}, mg/cm²	Nitrogen R_{calc}, mg/cm²	Nitrogen % deviation	Hydrogen R_{exp}, mg/cm²	Hydrogen R_{calc}, mg/cm²	Hydrogen % deviation
^{91}Sr	1.61	1.61	0	0.898	0.899	+1
^{92}Y	1.58	1.62	+2.5	0.898	0.903	+1
^{97}Zr	1.56	1.59	+2	0.858	0.887	+3
^{140}Ba				0.677	0.658	−3
^{143}Ce	1.16	1.13	−3	0.686	0.633	−8

TABLE VI

Ranges and range ratios in 450 MeV proton fission of ^{238}U, ^{209}Bi, and ^{181}Ta

Nucl.	$\left(\frac{R_{^{238}U}}{R_{Al}}\right)_{exp}$	$\left(\frac{R_{^{238}U}}{R_{Al}}\right)_{calc}$	$\left(\frac{R_{^{209}Bi}}{R_{Al}}\right)_{exp}$	$\left(\frac{R_{^{209}Bi}}{R_{Al}}\right)_{calc}$	$\left(\frac{R_{^{181}Ta}}{R_{Al}}\right)_{exp}$	$\left(\frac{R_{^{181}Ta}}{R_{Al}}\right)_{calc}$
^{67}Cu	2.65±0.01	2.850	2.62±0.01	2.673	2.57±0.01	2.490
^{89}Sr	2.72±0.01					
^{91}Sr					2.63±0.01	
^{99}Mo	2.73±0.01		2.71±0.01		2.67±0.01	
^{115}Cd	2.76±0.01		2.73±0.01			
^{115m}Cd	2.75±0.01		2.73±0.01			

wishes to express his gratitude to the National Research Council of Canada for the award of a Studentship (1962–63).

REFERENCES

1. S. KATCOFF, J. A. MISKEL, and C. W. STANLEY. Phys. Rev. **74**, 631 (1948).
2. F. BROWN and B. H. OLIVER. Can. J. Chem. **39**, 616 (1961).
3. B. FINKLE, E. J. HOAGLAND, S. KATCOFF, and N. SUGARMAN. National nuclear energy series. Div. IV, Book 1. McGraw-Hill Publishing Co., New York. 1951. pp. 463, 471.
4. E. SEGRÈ and C. WIEGAND. Phys. Rev. **70**, 808 (1946).
5. N. T. PORILE and N. SUGARMAN. Phys. Rev. **107**, 1410 (1957).
6. J. B. NIDAY. Phys. Rev. **121**, 1471 (1961).
7. N. SUGARMAN, M. CAMPOS, and K. WIELGOZ. Phys. Rev. **101**, 388 (1956).

Can. J. Chem. Downloaded from www.nrcresearchpress.com by 210.87.254.105 on 09/05/12
For personal use only.

8. J. M. ALEXANDER and M. GAZDIK. Phys. Rev. **120**, 874 (1960).
9. J. A. DAVIES, J. FRIESEN, and J. D. MCINTYRE. Can. J. Chem. **38**, 1526 (1960).
10. E. M. DOUTHETT and D. H. TEMPLETON. Phys. Rev. **94**, 128 (1954).
11. W. J. MCG. TEGART. Electrolytic and chemical polishing of metals. The Pergamon Press Limited, London. 1956.
12. L. E. GLENDENIN. National nuclear series. Vol. 9. McGraw-Hill Publishing Co., New York. 1951. Paper 288.
13. N. BOHR. Nature, **137**, 344 (1936).
14. N. BOHR. Kgl. Danske Videnskab. Selskab Math.-fys. Medd. **18**, No. 8 (1948).
15. J. C. D. MILTON and J. S. FRASER. *Quoted in* Can. J. Chem. **39**, 616 (1961).
16. W. E. STEIN. Phys. Rev. **108**, 94 (1957).
17. N. BOHR and J. LINDHARD. Kgl. Danske Videnskab. Selskab Math.-Fys. Medd. **28**, No. 7 (1954).
18. N. O. LASSEN. Proceedings of the International Conference on the Peaceful Uses of Atomic Energy, Geneva. 1955. Vol. 2. United Nations, New York. 1956. p. 215.
19. B. L. COHEN, A. F. COHEN, and C. D. COLEY. Phys. Rev. **104**, 1046 (1956).
20. J. C. D. MILTON. University of California Report, U.C.R.L. 9883. 1962.
21. A. C. WAHL. J. Inorg. Nucl. Chem. **6**, 263 (1958).
22. K. A. PETRZHAK, G. PETROV, and J. SHLYAMIN. Exptl. Theor. Phys. U.S.S.R. **38**, 1723 (1960).
23. J. PANONTIN and N. SUGARMAN. J. Inorg. Nucl. Chem. **25**, 1321 (1963).

APPENDIX A

Niday (6) has given a generalized expression for calculating the number of fission fragments escaping from a thick target:

$$[1] \qquad N_c = \frac{1}{4\pi}\int_{x=0}^{R}\int_{\theta=0}^{\cos^{-1}(x/R)}\int_{\phi=0}^{2\pi} I(x)J(\theta,\phi)\sin\theta\,\mathrm{d}\phi\,\mathrm{d}x,$$

where

$I(x) \propto$ beam intensity,
$J(\theta,\phi)$ = factor to take into account any anisotropy in the emission of the fragments,
R = range of the fragments in target matter,
x = perpendicular distance between the point of origin of the fragment and the catcher surface,
$\mathrm{d}\theta$ = angle increment with respect to the normal to the foil surface, and
$\mathrm{d}\phi$ = angle increment with respect to the plane of the foil surface.

Assuming uniform beam intensity over the target area undergoing fission and isotropic emission of fragments:

$$[2] \qquad N_c = \frac{1}{2}\int_{x=0}^{R}\int_{\theta=0}^{\cos^{-1}(x/R)} I\,\mathrm{d}x\,\mathrm{d}\theta\sin\theta$$

$$= \frac{I}{2}\int_{x=0}^{R}\int_{\theta=0}^{\cos^{-1}(x/R)} \sin\theta\,\mathrm{d}\theta.$$

In the case of a moving target there would be no unique range since the forward momentum would be shared to varying extents by the fragments depending on the angle θ at which they are emitted. Hence the new range $R'(\theta')$ would have an angular dependence. Further, the modified equation has to take into account the range–velocity relationship of the type $R = k(V - v_0)$ which has been found to hold for a wide number of fission fragments (eq. [19]). The modification is simple as seen from the diagram below.

From a stationary target, fragments from a thin layer $\mathrm{d}x$ situated at distance x from the catcher surface would have escaped if $R\cos\theta = 0\mathrm{A}\cos\theta \geq x$, or $k(V - v_0)\cos\theta \geq x$. Because of the forward momentum, in the case of a moving target, fragments situated at a depth x' and making an angle θ' would be just able to escape. If v is the velocity imparted to the struck nucleus in the beam direction, then

$$R'(\theta')\cos\theta' = k[(V - v_0)\cos\theta + v].$$

Can. J. Chem. Downloaded from www.nrcresearchpress.com by 210.87.254.105 on 09/05/12
For personal use only.

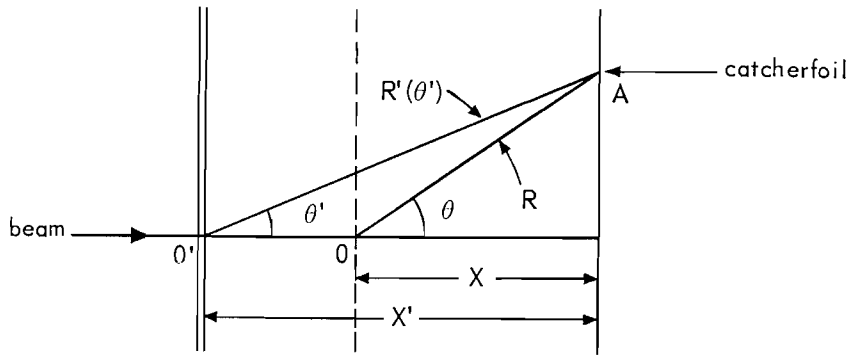

Hence

$$\cos\theta = \frac{\frac{R'}{k}\cos\theta' \pm v}{(V - v_0)},$$

$$\sin\theta\,\mathrm{d}\theta = -\mathrm{d}(\cos\theta) = -\frac{1}{k(V - v_0)}\,\mathrm{d}[R'(\theta')\cos\theta'].$$

Using this in eq. [2] and shifting to appropriate limits of integration, we have

$$N_c = -\frac{I}{2k(V - v_0)}\int_{x'=0}^{R'(0)}\int_{\theta'=0}^{\cos^{-1}(x'/R'(\theta'))}\mathrm{d}[R'(\theta')\cos\theta']\mathrm{d}x'$$

$$= \frac{I}{4k(V - v_0)}[x'^2]_{x'=0}^{R'(0)},$$

where $R'(0)$ indicates range at zero angle to the beam direction. If A_f and A_b are the total activities in the front and the back catcher respectively, then

$$A_f = \frac{I}{4k(V - v_0)}[x'^2]_{x'=0}^{R'(0)=k(V+v-v_0)}$$

$$A_b = \frac{I}{4k(V - v_0)}[x'^2]_{x'=0}^{R'(0)=k(V-v-v_0)}.$$

Hence

$$\frac{A_f}{A_b} = \frac{(V + v - v_0)^2}{(V - v - v_0)^2} = \frac{(1 + \eta - \eta')^2}{(1 - \eta - \eta')^2},$$

where $\eta = v/V$ and $\eta' = v_0/V$.

APPENDIX B

Assuming $R = kV$, the absorption equation of Sugarman *et al.* (7) is given by

$$N(t) = K[1 \pm \eta - (t/R_0')],$$

where

$N(t)$ = number of fragments penetrating beyond a thickness t of the catcher material,
R_0' = range of the fragment in the catcher material if the target were stationary,
K = constant,
$\eta = v/V$,

Can. J. Chem. Downloaded from www.nrcresearchpress.com by 210.87.254.105 on 09/05/12
For personal use only.

V = velocity of the fragment from a stationary target, and
v = velocity imparted to the struck nucleus by the projectile.

Assuming $R = k(V - v_0)$, the above equation takes the form

$$N(t) = K'\left[1 \pm \eta - \eta' - \frac{t}{\left(\frac{R}{1-\eta'}\right)}\right]^2$$

$$= K'(1 \pm \eta - \eta')^2\left[1 - \frac{t}{R\left(1 \pm \frac{\eta}{1-\eta'}\right)}\right]^2,$$

where R = range in the catcher material from a stationary target and K' = a constant.

APPENDIX C

(i) From eq. [19] we have $R = k(V - v_0)$. From known values of R and V, the value of k in aluminium for ^{140}Ba is found to be 0.42. Putting

$$R = R_M \qquad \left(R_M = \frac{R_t + R_b}{2}\right),$$

$$V = \frac{R_M}{0.42} + v_0 = 2.381\,R_M + v_0$$

$$\eta' = \frac{v_0}{2.381\,R_M + v_0} = \frac{2.2}{2.381\,R_M + 2.2}.$$

The velocities are all in units of cm/s $\times 10^8$.

(ii) Calculation of v from conservation of momentum is straightforward. If E is the energy of the proton in MeV, m_p is its mass, and M is the mass of the struck nucleus, then from conservation of momentum,

$$\frac{1}{2}(m + M)v^2 = \frac{E}{m_p + M}$$

$$v = \frac{\sqrt{2E}}{m_p + M},$$

where v is in units of (MeV/nucleon mass)$^{1/2}$.

Can. J. Chem. Downloaded from www.nrcresearchpress.com by 210.87.254.105 on 09/05/12
For personal use only.

Can. J. Chem. Downloaded from www.nrcresearchpress.com by 210.87.254.6 on 09/05/12
For personal use only.

MASS DISTRIBUTION IN THERMAL NEUTRON FISSION OF ^{239}Pu[1]

D. A. MARSDEN AND L. YAFFE
Department of Chemistry, McGill University, Montreal, Quebec
Received July 6, 1964

ABSTRACT

Improved radiochemical techniques have been used to study the distribution in mass of the fission fragments resulting from thermal neutron fission in ^{239}Pu.

Disintegration rates and half-lives were determined by measurement with a $4\pi\beta$ gas flow proportional counter. Further identification of the nuclides was obtained by gamma scintillation spectrometry. The flux intensity during irradiation was monitored by the $^{59}Co(n,\gamma)^{60}Co$ reaction.

The absolute fission yields of ^{89}Sr, ^{90}Sr, ^{91}Y, ^{95}Zr, ^{99}Mo, ^{103}Ru, ^{106}Ru, ^{105}Rh, ^{109}Pd, ^{112}Pd, ^{111}Ag, and ^{115}Cd in the light mass peak and ^{127}Sb, ^{131}I, ^{133}I, ^{132}Te, ^{137}Cs, ^{140}Ba, ^{141}Ce, ^{143}Ce, ^{144}Ce, ^{147}Nd, and ^{156}Eu in the heavy mass peak have been measured. In addition, the independent yields of ^{82}Br, ^{124}Sb, ^{126}Sb, and ^{136}Cs were obtained.

INTRODUCTION

The results of the only comprehensive radiochemical study of the fission product yields of ^{239}Pu were summarized by Steinberg and Freedman (1) in 1951. In this study Geiger-Müller counters had been used for activity measurements; the number of fission events were not determined directly in each experiment and the yields were often expressed relative to an internal standard—usually ^{140}Ba. The estimated accuracy was of the order of 10–20%. Since that time Bunney *et al.* (2) have determined relative yields radiochemically for the heavy rare earths with an accuracy of better than $\pm 10\%$ and Bartholomew *et al.* (3) have radiochemically determined relative yields for ^{89}Sr, ^{91}Sr, ^{139}Ba, and ^{141}La with an accuracy comparable to that obtained by using mass spectrometric techniques. Absolute cumulative yields obtained by the latter technique have been published by Fickel and Tomlinson (4, 5), Fritze *et al.* (6) and Anikina *et al.* (7).

Evaluations of all published yield data have been made by Steinberg and Glendenin in 1955 (8) and by Katcoff in 1958 (9) and 1960 (10).

The purpose of the present work was to reexamine carefully the cumulative chain yields from the thermal neutron fission of ^{239}Pu by using improved measurement techniques and by determining absolute yields.

EXPERIMENTAL

(a) Irradiation

The ^{239}Pu was in the form of a plutonium–aluminium alloy containing 3.81% ^{239}Pu by weight. Amounts of this alloy equivalent to ~1 mg ^{239}Pu were accurately weighed and then sealed in quartz vials. Weighed amounts (0.5 to 1.00 mg) of "spec. pure" (0.005 in. diameter) cobalt wire were sealed into similar vials to serve as flux monitors. The capsules containing the Pu–Al alloy and the cobalt wire were then irradiated together for a period of 48 h in a position in the NRX reactor at Chalk River where the neutron flux was predominantly thermal.

(b) Treatment of Pu–Al Alloy

On account of the low concentration of ^{239}Pu in the alloy, ~0.5 atom %, recoil losses of fission products into the quartz tube were expected to be small. Nevertheless, during the dissolution of the alloy, the quartz vial was leached as described below. The quartz tube was covered with conc. hydrochloric acid to which was added 1 ml of a solution containing 1 μg each of Cs^+, Ba^{++}, La^{+3}, and I^- ions. The quartz capsule was crushed and the alloy allowed to dissolve. When bromine or iodine were to be separated, dissolution was carried out in the cold by immersing the solution in ice water; otherwise dissolution was allowed to proceed

[1]*This work received financial assistance from the National Research Council of Canada.*

at room temperature. After the sample had dissolved, the solution was transferred to a volumetric flask. The crushed pieces of the quartz tube were washed several times with small portions of conc. hydrochloric acid, the washings being transferred each time to the volumetric flask. Several washings with distilled water were done in a similar manner. Aliquots were removed from the fission product stock solution and the fission products of interest were separated by standard radiochemical procedures (Appendix I) and their activities measured. Chemical yield recoveries in general were determined spectrophotometrically by standard methods (Appendix I).

(c) Treatment of Flux Monitor

The irradiated cobalt wire was removed from the quartz capsule and dissolved in nitric acid. The crushed vial was repeatedly leached with small volumes of dilute nitric acid until the remaining activity was negligible. The combined solutions were made up to volume and known aliquots were removed for disintegration rate determinations.

(d) Disintegration Rate Determinations and Identification of Nuclides

All disintegration rates were determined using the $4\pi\beta$-counting techniques described by Pate and Yaffe (11–15). Aliquots of the samples were deposited on calibrated gold-coated VYNS films (15–20 $\mu g/cm^2$) and dried under infrared radiation. The films were pretreated with a 5% insulin solution to ensure even deposition of the source on a known area. Corrections for absorption of radiation in the source mount and self-absorption losses were determined from absorption curves of Pate and Yaffe (13, 15) and Yaffe and Fishman (16). The half-lives of the nuclides were determined by $4\pi\beta$-counting and the nuclides were further identified by γ scintillation spectrometry both with respect to γ-ray energies and the half-lives of γ-ray decay.

RESULTS

(a) Neutron Flux Determinations

The neutron flux was calculated by means of the equation

$$(N\lambda)_{^{60}Co} = N_{^{59}Co} I\sigma_c(1 - e^{-\lambda T})e^{-\lambda t},$$

where $(N\lambda)_{^{60}Co}$ = ^{60}Co disintegration rate at a time t after an irradiation, $N_{^{59}Co}$ = no. of ^{59}Co atoms, I = thermal neutron flux, σ_c = thermal neutron capture cross section for ^{59}Co, and T = time of irradiation. The half-life of ^{60}Co was taken as 5.26 yr (17). The neutron flux is attenuated to 0.97 of its initial value by the 0.005 in. diameter cobalt wire (18) and corrections were made for this. The thermal neutron capture cross section used for ^{59}Co was 37.5 barns (19, 20).

(b) Fission Rate Determinations

On account of the low atom concentration, ~0.5% of ^{239}Pu in the alloy, the attenuation of the neutron flux in the fissile material was small enough to be neglected. The fission rates were calculated from the equation

$$R = N_{^{239}Pu} I\sigma_f,$$

where N = no. of ^{239}Pu atoms, I = thermal neutron flux, and σ_f = thermal neutron fission cross section for ^{239}Pu. The value of σ_f used was 742 barns (21).

(c) Activities Isolated

1. Bromine

The decay data for the bromine sample could be resolved into a 34-h activity with longer-lived components having half-lives of 4.2 d and 37 d and of roughly equal activities at time of separation. It was not possible to identify the longer-lived activities by γ-ray spectrometry.

^{82}Br, a shielded nuclide, occurs in very low yield and this undoubtedly accounts for the divergence from the 36-h literature value.

2. Strontium

The elapsed time from the end of bombardment to the time of separation was such

Can. J. Chem. Downloaded from www.nrcresearchpress.com by 210.87.254.6 on 09/05/12
For personal use only.

Can. J. Chem. Downloaded from www.nrcresearchpress.com by 210.87.254.6 on 09/05/12
For personal use only.

that only ^{89}Sr and ^{90}Sr were expected to be present. The decay data were resolved into 50-d ^{89}Sr and a long-lived component, which was taken to be ^{90}Sr (27.7 yr) and ^{90}Y (64 h) in equilibrium.

3. Yttrium

Yttrium samples were measured several days after the radiochemical separation so that all the 64-h ^{90}Y had decayed. The remaining yttrium activity decayed with a half-life of 59 d over a period of 5 half-lives and corresponded to ^{91}Y.

4. Zirconium

The zirconium activity decay curve was observed to increase to a maximum at about 30 d then to die away into a long-lived tail. The amount of this long-lived activity was estimated and subtracted from the gross counting rates to give a decay curve which grew to a maximum and then decayed with a 65-d half-life. A gamma ray spectrum of the zirconium fraction showed a prominent photopeak at 728 keV which shifted to 767 keV as the decay was followed. The decay of this gamma peak also increased to a maximum and then died away with a 65-d half-life. This was consistent with the growth of ^{95}Nb from a freshly separated ^{95}Zr parent. The long-lived activity was not identified. Disintegration rates to determine fission yields were obtained by extrapolating the $4\pi\beta$-counting data back to the time of separation, where the ^{95}Nb daughter was absent.

5. Niobium

The niobium fraction decayed with a half-life of 36.5 d measured over a period of 6 half-lives. The gamma spectrum contained a very prominent 758 keV photopeak which decayed with a 34.2-d half-life. This is consistent with the decay of ^{95}Nb. The 90-h ^{95m}Nb was not detected. In the β^--disintegration measurements, very large absorption corrections had to be applied because of the large amount of oxalic acid necessary to keep the niobium oxide in solution. Since ^{95}Nb is only one charge unit away from stability, its independent yield will be extremely small and all the niobium activity results from the decay of ^{95}Zr during and after the irradiation up to the time of separation. The ^{95}Nb disintegration rates were therefore used in growth and decay equations to calculate the ^{95}Zr fission yields.

6. Molybdenum

Freshly separated molybdenum activities showed an initial growth followed by decay with a half-life of 68.2 h lasting for about 6 half-lives. Thereafter the decay curves began tailing off, indicating the presence of a long-lived activity. These data together with gamma spectra and the decay of the gamma peaks were consistent with the growth of ^{99m}Tc and ^{99}Tc from a freshly separated ^{99}Mo parent. Since the complexity of the decay schemes involved did not allow direct calculation of ^{99}Mo disintegration rates, counting data were obtained as soon after separation as possible, and the ^{99}Mo disintegration rates were then obtained by extrapolating back to the time of separation.

7. Ruthenium

The gross decay curve obtained from $4\pi\beta$-measurements was resolved graphically into two components, one with a 1.01-yr half-life and the other with a 38-d half-life. The gamma spectrum of the ruthenium fraction showed a very prominent 508-keV gamma peak. The decay curve of this peak could be resolved into a 1.0-yr half-life and a 37-d half-life. These two activities were assigned to ^{103}Ru and ^{106}Ru respectively.

To determine the disintegration rate of ^{103}Ru, corrections have to be made for the contribution of the conversion electrons from 57-min ^{103m}Rh to the counting rate. Similarly the $4\pi\beta$-counter will measure the contributions from both ^{106}Ru (1 yr) and ^{106}Rh (30 s)

and corrections have to be made. Details for obtaining these corrections are given in Appendix II.

8. Rhodium

The β^--decay curve of the rhodium activity, measured on the $4\pi\beta$-counter, showed a single component with a half-life of 36 h measured over 7 half-lives. The gamma spectrum contained one photopeak at 315 keV which decayed with a half-life of 36 h, confirming the fact that the rhodium activity was ^{105}Rh.

9. Silver

The decay curve of the silver activity fraction was resolved into a 7.5-d component (over 7 half-lives) and a 3.2-h component (over 4 half-lives). The energy and decay of gamma peaks observed in the gamma spectra were consistent with the assignment to ^{111}Ag and ^{112}Ag respectively. Since the separation of the silver activity had taken place when all the independently formed ^{112}Ag had already decayed, this activity results from the decay of ^{112}Pd.

10. Palladium

The gross β^--decay curve was resolved into a 21-h component and a 12-h component. The early portion of the decay due to the 21-h component was calculated assuming that the later section of the decay represented an equilibrium mixture of ^{112}Pd (21 h) and ^{112}Ag (3.2 h). The resolved decay curve and the original data are shown in Fig. 1. A gamma ray spectrum of the palladium activities showed gamma peaks at 20, 90, and 626 keV. The decay of the 626-keV peak showed an initial growth and subsequent decay with a 21-h half-life. The decay of the 20-keV peak was resolved into a 12.5-h component and a 21-h component, while the 90-keV peak decayed with a half-life of 12.8 h. These data confirmed the presence of ^{109}Pd and ^{112}Pd.

In determining the disintegration rate of ^{109}Pd, it was necessary to take into account the conversion electrons emitted by ^{109m}Ag; the calculations for this are shown in Appendix II*c*.

For ^{112}Pd it was necessary to consider the growth of ^{112}Ag which contributes to the equilibrium counting rate. The data and calculations are given in Appendix II*d*.

11. Cadmium

The gross β^--decay curve was resolved graphically into a 43-d component and a 53.4-h component (over 9 half-lives). This corresponded to ^{115m}Cd and ^{115g}Cd. A gamma ray spectrum taken several hours after the separation showed an X-ray to be present, together with gamma rays of energies 255, 333, and 526 keV. This was almost identical with the gamma spectrum for 54-h ^{115}Cd in equilibrium with 4.5-h ^{115}In given by Heath (22) and compared well with gamma rays for ^{115}Cd listed in the Nuclear Data Sheets (23). The 333-keV gamma ray was observed to grow and then to decay with a half-life of 54 h, while the 527-keV gamma ray decayed with a similar half-life. The absence of gamma rays characteristic of ^{115m}Cd resulted from the very small amount of this activity present in the sample and from the fact that about 97% of the beta disintegrations (23) lead directly to the ground state of ^{115}In.

Since ^{115g}Cd decays to metastable ^{115m}In (4.5 h), the measured disintegration rate had to be corrected for the additional counts registered as a result of conversion electron emission. The details of this calculation are shown in Appendix II*e*.

12. Antimony

The gross β^--decay curve was resolved into 3.73-d ^{127}Sb, 12.8-d ^{126}Sb, 61-d ^{124}Sb, and a long-lived activity considerably above the background rate, probably due to ^{125}Sb.

Can. J. Chem. Downloaded from www.nrcresearchpress.com by 210.87.254.6 on 09/05/12
For personal use only.

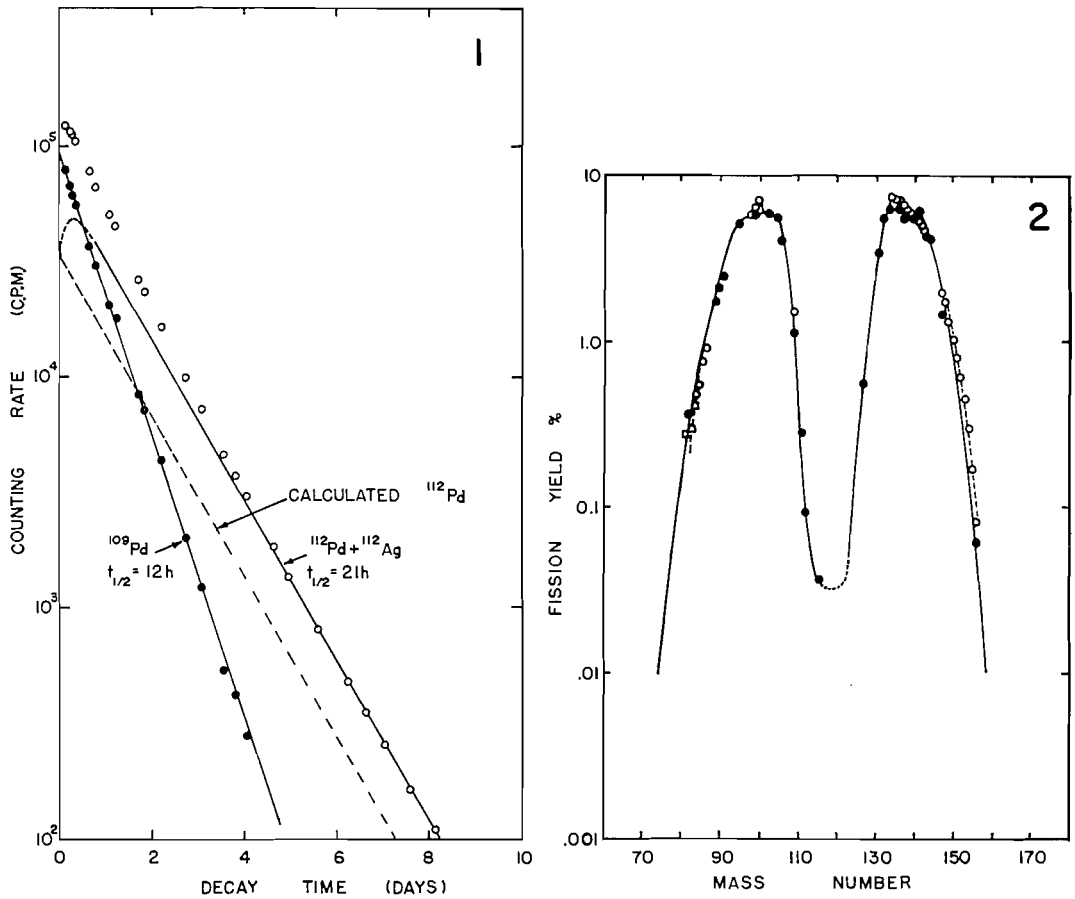

FIG. 1. Palladium activity decay curve.
FIG. 2. Mass distribution curve for thermal neutron fission of ^{239}Pu. ●This work, ○Fickel and Tomlinson (4, 5), □Croall and Willis (29).

Identification by means of gamma ray spectra was not attempted because of the complexities of the decay schemes involved.

Disintegration rate determinations for ^{124}Sb and ^{126}Sb are straightforward. These are shielded nuclides and thus are primary fission products. For ^{127}Sb it was necessary to take into account the amount of the ^{127}Te activity which would be in equilibrium with its parent. The calculations and data used in the correction factors are shown in Appendix II*f*.

13. Tellurium

The decay curve for the tellurium fraction was resolved into 105-d, 33-d, and 3.27-d components corresponding to ^{127m}Te, ^{129m}Te, and ^{132}Te in equilibrium with ^{132}I respectively. The ^{132}Te was identified by the decay of the ^{132}Te 230-keV gamma peak and the growth and decay of the 675-keV gamma peak of ^{132}I. The disintegration rate of ^{132}Te was calculated using standard growth and decay equations. No yield data were calculated for ^{127m}Te and ^{129m}Te since not sufficient information about conversion coefficients was available.

Can. J. Chem. Downloaded from www.nrcresearchpress.com by 210.87.254.6 on 09/05/12
For personal use only.

14. Iodine

Sources for beta disintegration determinations were prepared by pipetting aliquots of the final lithium iodide solution on to gold-coated VYNS films and drying them under an infrared lamp. Kjelberg *et al.* (24) have used this technique in preparing iodide sources for $4\pi\beta$-measurements. The lithium iodide continuously released the xenon formed by the decay of iodine activity, and no measurable evaporation losses of iodine activity were found.

The decay curve was resolved graphically into 8.05-d ^{131}I, 21-h ^{133}I, and 2.4-h ^{132}I, and the assignments were confirmed by following the decay of the 360-keV γ-ray of ^{131}I, the 530-keV γ-ray of ^{133}I, and the 675-keV γ-ray of ^{132}I.

The ^{132}I disintegration rates were used to calculate ^{132}Te fission yield data since all independently formed ^{132}I had decayed at the time of the iodine separation.

15. Cesium

The gross β^--decay curve of the cesium activity was resolved graphically into a 12.9-d component and a long-lived component which had a counting rate considerably above background. A gamma ray spectrum taken a few hours after separation showed gamma peaks consistent with the presence of 12.9-d ^{136}Cs. A subsequent spectrum taken about 100 d after the first showed only a 662-keV gamma peak indicating the presence of ^{137}Cs. In determining the disintegration rate of ^{137}Cs it is necessary to take into account the internal conversion of the 662-keV gamma ray. The data and calculations are shown in Appendix II*g*.

16. Barium

The barium activity was measured immediately after separation, at half-hour intervals during the first 5 h after separation, and then less frequently. Since the growth of ^{140}La is linear during the first few hours, accurate back-extrapolation to the separation time to determine the ^{140}Ba disintegration rates could be made.

The decay curve was seen to rise to a maximum and then die away with a half-life of 12.8 d. Gamma ray energies and the decay of the gamma peaks were consistent with the decay of ^{140}Ba and the growth of ^{140}La from this parent.

17. Cerium

The gross β^--decay curve was resolved by subtracting a long-lived background activity from the experimental counting rates. A 33-d component and a 35.4-h component were then observed. The background activity, as drawn, had a half-life of about 2 yr and by trial and error was resolved into a long-lived activity considerably above background and a 285-d component. The 35.4-h activity was taken to be ^{143}Ce, the 33-d to be ^{141}Ce, and the 285-d to be ^{144}Ce. The γ-ray spectra of the cerium fraction were quite complex, and therefore γ-ray decays were not followed. For ^{144}Ce it was necessary to correct for the contribution of ^{144}Nd (17 min) daughter activity. Because of the short half-life of the latter, at equilibrium the disintegration rates of parent and daughter are equal. Furthermore, since absorption in the source mount and source material of both activities was negligible, the observed counting rates are equal.

18. Rare Earths

(i) Neodymium.—The β^--decay curve of the neodymium fraction was seen to die away with an 11-d half-life and then to tail off into a long-lived activity. The neodymium activity expected to be present at the time of separation occurs in the chain

$$\text{short-lived } ^{147}\text{Nd}(11.1\text{ d}) \rightarrow ^{147}\text{Pm}(2.6\text{ yr}) \rightarrow ^{147}\text{Sm}(1.3 \times 10^{11}\text{ yr}).$$

Can. J. Chem. Downloaded from www.nrcresearchpress.com by 210.87.254.6 on 09/05/12
For personal use only.

The time required for the ^{147}Pm daughter to reach maximum activity is 72 d. From the decay curve this time was about 44 d. Thus some other long-lived activity was present, in an amount estimated to be 4% of the counting rate of ^{147}Nd at separation time. This was subtracted from the ^{147}Nd counting rate for the disintegration rate determination. A gamma ray spectrum of the neodymium fraction showed photopeaks with 33, 93, 308, 416, 530, and 685-keV energies. This compared well with the gamma ray spectrum given by Heath (22) for ^{147}Nd. The 530-keV peak was seen to decay with a half-life of 11.5 d.

(ii) Europium.—The β^--decay of the europium activity was resolved into a 71.5-d component and a 15.3-d component. The activities expected to be present were 1.7-yr ^{155}Eu and 15.4-d ^{156}Eu. Since, at the end of the counting period, 120 d, the ^{156}Eu activity would have decayed through about 8 half-lives, its contribution to the counting rate would be negligible at that time. It would seem then that an activity with a half-life between 15 d and 1.7 yr, in addition to the 1.7-yr ^{155}Eu, remained in the europium sample. A gamma ray spectrum of the europium activities showed photopeaks with energies of 45, 93, 624, 806, 1160, and 1940 keV respectively, consistent with gamma ray spectra of ^{155}Eu and ^{156}Eu shown by Heath (22).

ERRORS

(a) Systematic Errors

These errors arise in weighing, diluting, and pipetting and in chemical yield analyses. A sensitive microbalance was used for all weighings, while calibrated volumetric glassware and micropipettes were used for dilutions and pipetting. Chemical yield determinations were done either by spectrophotometry, by titration, or by weighing. A Beckman DU spectrophotometer was used in making the absorbance measurements, while in the titrations calibrated pipettes and microburettes were used. The estimated errors from the above causes were less than ±3%. By the use of very thin films the source mount absorption errors were kept to ±0.2%. In order to make self-absorption losses as small as possible, only 5 to 10 mg of carrier was added before the chemical separations, the amount used depending upon the reported efficiency of the separation scheme employed. Errors associated with self-absorption losses were assessed at 0.1 to 2%, depending upon the energy of the β^--radiations. The loss of activity due to fission recoil was assumed to be negligible because of the low concentration of plutonium in the alloy used and the chemical treatment of the quartz vial.

(b) Statistical Errors

For all measurements on the 4π proportional counter, more than 10 000 counts were recorded per counting period, so that these errors were less than ±1%. Sources were prepared at least in duplicate, and only those whose counting rates agreed within 1% were used for disintegration rate determinations.

(c) External Errors

These arise in the decay schemes and decay constants of the nuclides of interest and influence the fission yields when used. Each fission yield was determined using the observed half-life and the decay scheme, as discussed.

In connection with saturation activity calculation, the pile power was constant during all the irradiations.

The calculated fission yields depend upon the ratio of the capture cross section for cobalt and the thermal neutron fission cross section for ^{239}Pu. The values used for these were obtained from the literature. Where several values were obtained for a fission yield,

Can. J. Chem. Downloaded from www.nrcresearchpress.com by 210.87.254.6 on 09/05/12
For personal use only.

an average value was calculated assuming equal statistical 'weights' for the individual values. The error quoted for the average fission yield is the standard deviation.

Where a single determination of a fission yield was made an error of ±5% is quoted, while for two yield values the calculated average is given with the limits of the two values as the quoted error.

DISCUSSION

The fission yields are given in Table I along with previous literature values for the yields of masses measured in this work. Isobaric yields were determined for the non-shielded nuclides by calculating Z_p, the most probable nuclear charge, according to the equal charge displacement hypothesis (25) for the mass numbers concerned and then interpolating on the charge distribution curve of Wahl *et al.* (26) to obtain the fractional cumulative yield. The isobaric yields calculated in this way were identical with the experimental values except in the case of ^{133}I where the isobaric value is 6.14%.

TABLE I

Absolute thermal neutron fission yields for ^{239}Pu

Nuclide	Absolute yield, %			
	This work	Refs. 4,* 5*	Ref. 8†	Refs. 2,† 3,† 7*
^{82}Br	0.0036±0.0002‡			
^{89}Sr	1.74±0.05	1.71	1.8	1.71 (3)
^{90}Sr	2.05±0.04	2.16		2.31 (7)
^{91}Y	2.41±0.11	2.59 (^{91}Zr)	2.8	2.45 (^{91}Sr)(3)
^{95}Zr (^{95}Nb)	5.06±0.33	4.99 (^{95}Mo)	5.6	
^{99}Mo	5.61±0.33	6.44§	6.1	
^{103}Ru	5.79±0.37	5.63	5.5	
^{105}Rh	5.47±0.06	5.50	3.7	
^{106}Ru	4.04±0.22	4.53	4.7	
^{109}Pd	1.13±0.06		1.0	
^{111}Ag	0.28±0.04		0.27	
^{112}Pd (^{112}Ag)	0.093±0.003		0.10	
^{115m}Cd	0.003±0.0006		0.003	
^{115}Cd	0.033±0.002		0.045	
Total ^{115}Cd	0.036	0.041§	0.048	
^{124}Sb	0.088±0.004‡			
^{126}Sb	0.069±0.003‡			
^{127}Sb	0.55±0.03			
^{131}I	3.80±0.14	3.77	3.6	
^{132}Te (^{132}I)	5.51±0.27	5.26	4.9	
^{133}I	5.53±0.06	6.90	5.0	
^{136}Cs	0.083±0.007	6.62		
^{137}Cs	5.40±0.39	6.48	5.8	6.50 (7)
^{140}Ba	5.47±0.32	5.58	5.36	
^{141}Ce	6.11±0.31	5.23	4.9	
^{143}Ce	4.28±0.21	4.56	5.1	
^{144}Ce	4.09±0.20	3.84	3.7	3.6 (2)
^{147}Nd	1.46±0.08	1.99		2.8 (^{147}Pm)(7) 2.2 (2)
^{156}Eu	0.062±0.004	0.08	0.12	0.10 (2)

*Mass spectrometrically determined yields.
†Radiochemically determined yields.
‡Independent yields.
§Interpolated yields.

Independent yields for four shielded nuclides, ^{82}Br, ^{124}Sb, ^{126}Sb, and ^{136}Cs, have been measured. Of these only the ^{136}Cs yield has been measured previously. The value obtained, 0.083%, is in excellent agreement with that of Glendenin (0.089%) reported by Steinberg and Glendenin (8) and that of Grummitt and Milton (27) (0.0835%). The independent

Can. J. Chem. Downloaded from www.nrcresearchpress.com by 210.87.254.6 on 09/05/12
For personal use only.

yields were converted to isobaric yields by obtaining the fractional yields from the charge distribution curve (26). The isobaric yields for ^{82}Br and ^{136}Cs were found to be 0.35% and 6.30% respectively. However, the values obtained for ^{124}Sb and ^{126}Sb are too high by several orders of magnitude when plotted on the mass distribution curve. This seems to be in accord with the observation of Kennett and Thode (28) that, for masses A = 128–132, Z_p remains near 50. The influence of the 50-proton shell seems to maintain itself in the case of antimony (Z = 51).

In general, the agreement with other radiochemically determined yields is good. The yield values in column 4 have an associated error of ±10–20% (8). The agreement with mass spectrometric data is good on the rising and falling wings of each peak but poor at the maxima of the peaks. The ^{99}Mo yield of 5.61% is some 1% lower than the yield obtained by interpolation from the mass spectrometric data. This interpolated value is, however, a reflection of the very high yield, 7.05%, obtained mass spectrometrically for ^{100}Mo. It was not possible in this work to determine radiochemically the yield at mass 100 since the radioactive members of the chain are short-lived.

Discrepancies in the yields of ^{133}I, ^{136}Cs, ^{137}Cs, and ^{141}Ce occur in the heavy peak. The chain yield for masses 133 and 136 depend upon the fractional yields interpolated from the charge distribution hypothesis and would reflect the uncertainties involved in determining Z_p. The ^{137}Cs yield of Fickel and Tomlinson (5) was obtained using 26.6 yr for the half-life of this nuclide. A recently reported value for this half-life is 29.68 yr (17), but this should only affect their result very slightly. The ^{141}Ce yield reported in the present work is only the result of a single determination and cannot be regarded as confirmed.

The isobaric yields obtained in the present work are plotted as a function of the mass number to give the mass distribution curve shown in Fig. 2. Also included are the results of the mass spectrometric determinations (4, 5) at masses where the yields differ. Recent data for masses 81, 83, and 84 by Croall and Willis (29) are also included in order to delineate better the wing of the curve. The mass distribution is seen to be symmetrical about mass 118 with the two maxima representative of asymmetric fission. The width at half height is approximately 16 mass units for both peaks, and the peak-to-valley ratio is about 160. The sum of the yields in the light peak is 97%, while that of the heavy peak is 93%. The yields in each peak should sum up to 100%. The difference is seen to be mainly in the yields at the top of the peaks.

APPENDIX I
CHEMICAL TREATMENT OF SAMPLES

(a) Bromine

Bromine was separated by the method of Glendenin *et al.* (30). Bromate and iodate carriers were added to an aliquot of the fission product solution, which was then treated with hydrogen sulfide to ensure exchange between active bromine and the carrier. The bromine was oxidized with potassium permanganate and extracted with carbon tetrachloride; several oxidation–reduction cycles were performed together with extractions into and out of carbon tetrachloride to purify the bromine. Finally, the bromine was reduced to bromide by sulfurous acid, warmed to remove excess sulfur dioxide, and then neutralized with dilute lithium hydroxide solution. The active solution was made up to a known volume. Chemical yields were determined according to Volhard's method.

(b) Strontium

The method of Glendenin (31) was used to separate strontium. Barium and strontium carriers were added to an aliquot of the fission product solution and their mixed nitrates

Can. J. Chem. Downloaded from www.nrcresearchpress.com by 210.87.254.6 on 09/05/12
For personal use only.

were precipitated with fuming nitric acid. Barium was removed as the chromate after the nitrates had been dissolved in water, leaving the strontium behind in solution. The strontium was purified by precipitating the oxalate from ammoniacal solution, dissolving the oxalate precipitate in dilute nitric acid, and again precipitating the nitrate. The nitrate was washed with ethyl alcohol, dissolved in water, and made up to volume. The chemical yield was determined by titration with EDTA (ethylenediaminetetraacetic acid) in a 50% alcoholic solution, using phthalein complexone as indicator (32).

(c) Yttrium

Yttrium was separated from an aliquot of the fission product solution by the method of Ballou (32). Carriers for cerium, yttrium, lanthanum, and zirconium were added to the solution from which yttrium and the rare earths were precipitated as fluorides. After the fluorides were dissolved in a boric acid – nitric acid mixture, cerium was removed, as recommended by Boldridge and Hume (33), by oxidation with sodium bromate and precipitation of the iodate. The rare earths were removed from the supernate by precipitating the potassium – rare earth carbonates. The yttrium, left in solution, was precipitated as the hydroxide, dissolved in dilute hydrochloric acid, and made up to volume. Chemical yields were determined spectrophotometrically using the sodium alizarin sulfonate method (34).

(d) Zirconium

With slight modifications, Moore's solvent extraction method (35), which makes use of the solubility of zirconium–TTA (2-thenoyltrifluoroacetone) complexes in xylene was used. A preliminary separation of barium fluozirconate (36) was necessary since plutonium is extracted along with zirconium in this method. Zirconium was recovered from the $BaZrF_6$ precipitate by dissolving it in dilute H_3BO_3–HNO_3 mixture, removing the barium as sulfate, and precipitating zirconium hydroxide. The hydroxide was dissolved in dilute nitric acid and extracted into a xylene solution of TTA. The organic phase was scrubbed with 1 *M* nitric acid and the zirconium removed with 0.25 *M* hydrofluoric acid. Barium fluozirconate was again precipitated and the zirconium was recovered as before. The precipitate was dissolved in dilute nitric acid and made up to a volume of 10 ml. Chemical yield was determined by developing the colored zirconium–'Thoron' [1-(*O*-arsonophenylazo)-2-naphthol-3,6-disulfonic acid] complex (37).

(e) Niobium

Niobium was separated by Glendenin's method (38) in which the oxide is precipitated from an oxalic acid solution with chloric acid. Purification from zirconium was achieved by adding zirconium hold-back carrier and repeatedly precipitating the oxide. The final precipitate was dissolved in saturated oxalic acid solution and made up to volume. Chemical yields were determined on the spectrophotometer by the thiocyanate method (34) in which the yellow niobium thiocyanate complexes are extracted into peroxide-free ethyl ether.

(f) Molybdenum

The method of Scadden (39) was used to separate molybdenum from the other fission products. Molybdenum carrier was added to an aliquot of the fission product mixture. The acidity was adjusted to about 1 *M* and molybdenum precipitated with α-benzoinoxime in ethanol. The precipitate was dissolved in fuming nitric acid and the molybdenum reprecipitated as before, after the acid solution was diluted and partially neutralized.

Can. J. Chem. Downloaded from www.nrcresearchpress.com by 210.87.254.6 on 09/05/12
For personal use only.

The α-benzoinoxime was destroyed by dissolving the precipitate in fuming nitric acid and fuming with perchloric acid. After a ferric hydroxide scavenge was made, the molybdenum was precipitated as lead molybdate from the buffered solution. The precipitate was dissolved in dilute nitric acid and made up to volume. Chemical yields were determined spectrophotometrically on the colored molybdenum thiocyanate complex extracted with a carbon tetrachloride – *n*-amyl alcohol mixture (34).

(g) Ruthenium

Ruthenium was separated from the other fission products by distilling the volatile ruthenium oxide, RuO_4 (40). Ruthenium(III) iodide and bromide carriers were added, and ruthenium was oxidized to volatile RuO_4 with sodium bismuthate and perchloric acid. The ruthenium oxide was then distilled into a sodium hydroxide solution from which it was precipitated by adding ethanol. Further purification was obtained by repeated precipitations of the RuO_4 from alkaline solution with ethanol. The final precipitate was dissolved in 6 *M* hydrochloric acid and made up to volume. Chemical yields were determined by developing the strongly colored ruthenium–thiourea complex (34).

(h) Rhodium

By a method of Ballou (41) the pyridine complex of rhodium was extracted into pyridine from a strongly alkaline solution to separate rhodium from a fission product aliquot. Decontamination from tellurium is achieved by adding Te^{+4} hold-back carrier along with Rh^{+3} carrier before the extraction. The rhodium was recovered from the pyridine layer by precipitating the sulfide. The precipitate was dissolved in aqua regia, ruthenium was removed by adding Ru^{+3} carrier and distilling the ruthenium by fuming with perchloric acid, and finally halogens were removed by adding iodide carrier and again fuming with perchloric acid. Rhodium sulfide was again precipitated, dissolved in a minimum of aqua regia, and made up to volume. Chemical yields were determined spectrophotometrically by the stannous chloride method (42).

(i) Silver

The method of Glendenin (43) was used to separate silver. Silver chloride was precipitated by adding silver carrier to an aliquot of the fission product solution which had been diluted so that the chloride concentration was about 0.3 *M*. Exchange between the carrier and any silver activity was ensured by gentle boiling and brisk stirring. After the silver chloride was dissolved in ammonium hydroxide, purification was achieved by performing two cycles of ferric hydroxide scavenging followed by precipitation of silver sulfide, the sulfide being dissolved in nitric acid between cycles. Silver was finally precipitated as silver chloride, dissolved in ammonium hydroxide, and made up to volume. Chemical yields were determined by titrating with EDTA the Ni^{+2} liberated on reacting Ag^+ with tetracyanonickelate ion, $[Ni(CN)_4]^{-2}$, in ammoniacal solution, muroxide being used as indicator (44).

(j) Palladium

A method of Seiler (45) was used to separate palladium from the other fission products. Palladium dimethylglyoxime was precipitated from acid solution. Repeated scavenging with lanthanum and zirconium hydroxides and silver chloride provided further purification. The final dimethylglyoxime precipitate was dissolved by boiling with a small amount of aqua regia and made up to volume. Chemical yields were determined in a procedure similar to that used for silver (44).

Can. J. Chem. Downloaded from www.nrcresearchpress.com by 210.87.254.6 on 09/05/12
For personal use only.

(k) Cadmium

Cadmium was separated from an aliquot of the fission product solution by the method of Glendenin (46). This consisted of repeated precipitations of cadmium sulfide interspersed with ferric hydroxide and palladium sulfide scavenging precipitations. The final cadmium sulfide precipitate was dissolved in a small amount of dilute hydrochloric acid. The solution was boiled to remove hydrogen sulfide and then made up to volume. Chemical yield determinations were made by titrating aliquots of the solution with EDTA using Eriochrome Black T (+ methyl red) as an indicator (44).

(l) Antimony

Exchange between carrier and the antimony activity was assured by adding Sb^{+3} carrier to an aliquot of the fission product solution and then oxidizing Sb^{+3} to Sb^{+5} with bromine water. Metallic antimony was precipitated with chromous chloride (47). The precipitate was dissolved in aqua regia and further purified by precipitating the sulfide. The final precipitate was dissolved in a minimum of hydrochloric acid, boiled to remove excess hydrogen sulfide, and made up to volume. Chemical yields were determined by precipitating metallic antimony with chromous chloride and weighing.

(m) Tellurium

Tellurium was recovered by precipitating the metal with sulfur dioxide in acid solution. The precipitate was dissolved in 6 *M* nitric acid and fumed with hydrobromic acid to volatilize selenium. Further decontamination was achieved by repeated ferric hydroxide scavenges. The tellurium was finally recovered as the metal, dissolved in nitric acid, and made up to volume. Chemical yields were determined by precipitation of the metal and weighing.

(n) Iodine

Iodine was separated from the fission products by the solvent extraction method of Glendenin and Metcalf (48). Iodine carrier was added and the iodide was oxidized to periodate by sodium hypochlorite in alkaline solution. Exchange between active iodine and the carrier was ensured by heating or by allowing oxidation to proceed at room temperature followed by reduction to I_2 with hydroxylamine hydrochloride in acid solution. The iodine was then extracted with carbon tetrachloride followed by extraction with sulfurous acid. Another oxidation–reduction cycle followed in which sodium nitrite was used to oxidize I^- to I_2 and sulfurous acid was used to reduce I_2 to I^-. The solution was then boiled to remove excess sulfur dioxide, after which the I^- was neutralized with a dilute lithium hydroxide solution and made up to volume. The chemical yield was determined by oxidizing the I^- to I_2 from an aliquot of the solution, extracting with a fixed volume of CCl_4, and measuring the absorbance at 517 mμ (49).

(o) Cesium

Cesium activity was separated from an aliquot of the fission product mixture by the method of Glendenin and Nelson (50). Cesium carrier was added and a silicotungstate precipitation was performed. The precipitate was dissolved in sodium hydroxide and the cesium converted to the perchlorate by boiling the solution with perchloric acid. Upon dilution, silica and tungstic acid were precipitated and removed by centrifugation. The supernate was again fumed with perchloric acid from which, after cooling, the cesium perchlorate was precipitated by the addition of absolute alcohol. The cesium perchlorate was dissolved in water, and the resulting solution was scavenged by precipitating ferric hydroxide with ammonia from the heated solution. After removing the ferric hydroxide,

Can. J. Chem. Downloaded from www.nrcresearchpress.com by 210.87.254.6 on 09/05/12
For personal use only.

the supernate was boiled with a small amount of sodium hydroxide to remove ammonia completely. From this solution the cesium was precipitated as perchlorate. The precipitate was washed several times with absolute alcohol, dissolved in water, and made up to volume. Chemical yields were obtained by precipitating the cesium as chloroplatinate and weighing.

(p) Barium

Barium was separated from the fission product mixture by the method of Glendenin (31). After the addition of carriers, barium and strontium were isolated by precipitation of the nitrates with fuming nitric acid. The barium was then separated from strontium by precipitating the chromate from a buffered solution of the mixed nitrates. Further purification was obtained by repeated precipitations of barium chloride with an HCl–ether mixture. The final chloride precipitate was dissolved in water and made up to volume. Chemical yields were determined by titration with EDTA in a 50% alcoholic solution using *o*-cresolphthalein complexone as indicator (44).

(q) Cerium

Cerium was isolated from the other fission products by oxidation with bromate in nitric acid and precipitation of the iodate with iodic acid (33). Repeated cycles of this operation were performed to separate cerium from the other rare earths. Further purification was obtained by reducing Ce^{+4} to Ce^{+3} and precipitating zirconium iodate. The cerium was finally precipitated as the hydroxide, dissolved in a minimum of hydrochloric acid, and made up to volume. Chemical yields were determined by the alizarin sulfonate method (34).

(r) Rare Earths

The rare earth activities, europium and neodymium, were separated by a combination of the methods of Nervik (51) and Smith and Hoffmann (52). Europium and neodymium carriers were added and the rare earth fluorides were precipitated. These were dissolved, scavenged by zirconyl phosphate and barium sulfate precipitations, and separated by elution from a Dowex-1 anion exchange column with conc. hydrochloric acid. After elution, the rare earth hydroxides were precipitated and dissolved in a small amount of conc. hydrochloric acid. Europium and neodymium were separated by elution at room temperature from a Dowex-50 cation exchange column with a 0.3 *M* α-hydroxyisobutyric acid solution adjusted to pH 4.1 with concentrated ammonia. The individual rare earths were then precipitated as the hydroxides, dissolved in a minimum of dilute hydrochloric acid, and made up to volume. Chemical yields were determined on the spectrophotometer by the sodium alizarin sulfonate method (34).

APPENDIX II

DETERMINATION OF DISINTEGRATION RATES

(a) Correction for Contribution of the Conversion Electrons from 57-min ^{103m}Rh to the Determination of the ^{103}Ru Disintegration Rate

The number of extra events counted per beta disintegration of ^{103}Ru is given by

$$N_{e^-} = \left(\frac{\alpha_T}{1+\alpha_T}\,\text{B.R.}\right) + \left(e\,\frac{1}{1+\alpha_T}\,\text{B.R.}\right),$$

where α_T = total internal conversion coefficient, e = efficiency for detecting the unconverted gamma rays, and B.R. = branching ratio. From the following data α_T is calculated to be 484. The value of α_K is 40 and $\alpha_K/\alpha_L = 0.09$ (53), where α_K and α_L are the

Can. J. Chem. Downloaded from www.nrcresearchpress.com by 210.87.254.6 on 09/05/12
For personal use only.

conversion coefficients for the K and L shells respectively. The efficiency for detecting the unconverted 40-keV gamma rays is less than 0.14% (54) so that the second term can be neglected. Therefore

$$N_{e^-} = \left(\frac{484}{485} \times 0.995\right) = 0.993.$$

The energies of these conversion electrons are given by

$$E_{e^-} = E_\gamma - \text{B.R.},$$

the difference between the gamma ray energy and the binding energy of the electron in the K or L shell. Strominger *et al.* (55) gives 23.2 and 3.4 keV for the K and L electron binding energies respectively. This results in 9% of the conversion electrons having energies of 17 keV and 91% having 37-keV energy. Since these conversion electrons are monoenergetic, they will be absorbed to a different extent in the source mount and in the source itself than β^--rays of the same maximum energies. It was assumed that the absorption of conversion electrons was equivalent to the absorption of β^--rays having maximum energies of twice the energy of the conversion electrons (56). If ^{103}Ru and ^{103m}Rh are represented by subscripts 1 and 2 respectively, then since $\lambda_1 < \lambda_2$, at equilibrium

$$N_1\lambda_2 + N_2\lambda_2 = N_1\lambda_1(1.993)$$

that is

$$N_2\lambda_2 = 0.993\ N_1\lambda_1.$$

Putting $A_1 = c_1N_1\lambda_1$ and $A_2 = c_2N_2\lambda_2$, where A_1 and A_2 are the observed counting rates of ^{103}Ru and ^{103m}Rh and c_1 and c_2 are detection efficiencies given by the product of the self-absorption factor and the source mount absorption factor, then

$$\frac{A_1 + A_2}{A_1} = \frac{c_1N_1\lambda_1 + c_2N_2\lambda_2}{c_1N_1\lambda_1}$$

$$= \frac{c_1N_1\lambda_1 + 0.993\ c_2N_1\lambda_1}{c_1N_1\lambda_1}$$

$$= 1 + 0.993\frac{c_2}{c_1},$$

and

$$A_1 = \frac{A_1 + A_2}{1 + 0.993\frac{c_2}{c_1}}.$$

That is, the counting rate of ^{103}Ru is given by dividing the observed counting rate of ^{103}Ru + ^{103m}Rh by the factor $1 + 0.993\ c_2/c_1$. From this, $N_1\lambda_1$, the disintegration rate, for ^{103}Ru is given by

$$N_1\lambda_1 = \frac{A_1}{c_1} = \frac{A_1 + A_2}{c_1 + 0.993\ c_2}.$$

(b) Determination of the Disintegration Rate of ^{106}Ru

A computation, similar to the above, where subscripts 1 and 2 refer to ^{106}Ru (1 yr) and ^{106}Rh (30 s), gives the following:

$$\frac{A_1 + A_2}{A_1} = \frac{c_1N_1\lambda_1 + c_2N_2\lambda_2}{c_1N_1\lambda_1}.$$

Can. J. Chem. Downloaded from www.nrcresearchpress.com by 210.87.254.6 on 09/05/12
For personal use only.

In this case, at equilibrium, since $\lambda_1 \ll \lambda_2$,

$$N_1\lambda_1 = N_2\lambda_2,$$

and therefore

$$\frac{A_1 + A_2}{A_1} = \frac{c_1N_1\lambda_1 + c_2N_1\lambda_1}{c_1N_1\lambda_1} = 1 + \frac{c_2}{c_1}.$$

The β^--rays of ^{106}Rh all have energies >2 meV and would therefore be absorbed to a negligible extent. Thus $c_2 = 1$ and

$$\frac{A_1 + A_2}{A_1} = 1 + \frac{1}{c_1}$$

$$N_1\lambda_1 = \frac{A_1}{c_1} = \frac{A_1 + A_2}{1 + c_1}.$$

The disintegration rate for ^{106}Ru is therefore given by dividing the observed counting rate of ^{106}Ru + ^{106}Rh by the factor $1 + c_1$.

(c) Correction for Contribution of Conversion Electrons from ^{109m}Ag to the Determination of the Disintegration Rate of ^{109}Pd

From the K shell conversion coefficient of 10.5 and the K/LM ratio of 0.84 for the 88-keV gamma ray (23), the total conversion coefficient, α_T, is calculated to be 22.6. This gives a value of 0.958 for the number of conversion electrons emitted per beta disintegration:

$$N_{e^-} = \frac{\alpha_T}{1 + \alpha_T} = 0.958.$$

The detection efficiency for the 88-keV unconverted gamma rays is less than 0.1% (54). The energy of these conversion electrons is the difference between the gamma ray energy and the electron binding energy. Strominger *et al.* (55) list the following for Ag: K electron binding energy 25.5 keV, L_1 and M_1 electron binding energy 5.8 and 0.7 keV respectively. Therefore 44% of the conversion electrons have energies of about 62 keV and 56% have energies of about 84 keV. The absorption determined as being equivalent to β^--rays with maximum energies of double the conversion electron energies gives a detection efficiency of 0.964 for the ^{109m}Ag disintegrations while the ^{109}Pd 1.025-keV β^--rays are negligibly absorbed, so that

$$\frac{\text{observed counting rate}}{^{109}\text{Pd counting rate}} = 1 + (0.958 \times 0.964) = 1.924.$$

(d) Correction for Growth of ^{112}Ag

For the determination of the disintegration rate of ^{112}Pd it was necessary to consider the growth of ^{112}Ag, which contributes to the equilibrium counting rate. At equilibrium the ratio of the disintegration rates is given by

$$\frac{N\lambda_{^{112}Ag}}{N\lambda_{^{112}Pd}} = \frac{\lambda_{^{112}Ag}}{\lambda_{^{112}Ag} - \lambda_{^{112}Pd}}.$$

If the half-life values are substituted, then

$$\frac{N\lambda_{^{112}Ag}}{N\lambda_{^{112}Pd}} = 1.180.$$

Can. J. Chem. Downloaded from www.nrcresearchpress.com by 210.87.254.6 on 09/05/12
For personal use only.

Now putting $A = cN$, where A is the observed activity and c is the detection efficiency,

$$\frac{A_{^{112}Ag} + A_{^{112}Pd}}{A_{^{112}Pd}} = \frac{c_{^{112}Ag}N\lambda_{^{112}Ag} + c_{^{112}Pd}N\lambda_{^{112}Pd}}{c_{^{112}Pd}N\lambda_{^{112}Pd}}$$

$$= 1 + \frac{c_{^{112}Ag}}{c_{^{112}Pd}}\frac{N\lambda_{^{112}Ag}}{N\lambda_{^{112}Pd}}$$

$$= 1 + 1.180\frac{c_{^{112}Ag}}{c_{^{112}Pd}}.$$

Since the efficiency for detecting ^{112}Ag is 1.00 and for ^{112}Pd is 0.991,

$$A_{^{112}Pd} = \frac{\text{observed counting rate}}{2.191}.$$

(e) Contribution of Conversion Electrons from ^{115m}In to the Determination of the Disintegration Rate of ^{115}Cd

From the data $\alpha_K = 0.83$ and $K/L_1M = 3.85$ (57), the total internal conversion coefficient, α_T, is calculated to be 1.05. From this the number of conversion electrons is given by

$$N_{e^-} = \frac{\alpha_T}{1 + \alpha_T} = 0.512,$$

and the number of unconverted gamma rays is therefore 0.488. Since ^{115m}In decays 94.5% by isomeric transition to ^{115}In and 5.5% by 840-keV β^--emission to ^{115}Sn, the observed β^--disintegration rate is related to the ^{115}Cd disintegration rate by

$$\text{observed D.R.} = {}^{115}\text{Cd D.R.}[1 + (0.512 \times 0.945) + 0.055].$$

Therefore

$$^{115}\text{Cd D.R.} + {}^{115m}\text{In D.R.} = {}^{115}\text{Cd D.R.}(1.539).$$

The efficiency of the 4π-counter for the 333-keV unconverted gamma rays is less than 0.14% (54), and the contribution due to these may therefore be neglected. At equilibrium, the disintegration rates of ^{115}Cd and ^{115m}In are related by

$$\frac{N_2\lambda_2}{N_1\lambda_1} = \frac{\lambda_2}{\lambda_2 - \lambda_1} = 1.093.$$

Here the subscripts 1 and 2 refer to ^{115}Cd and ^{115m}In respectively. Putting $A = cN\lambda$, where A is the observed counting rate and c is the detection efficiency,

$$\frac{A_1 + A_2}{A_1} = \frac{c_1N_1\lambda_1 + c_2N_2\lambda_2}{c_1N_1\lambda_1}$$

$$= 1 + \frac{c_2}{c_1} \times \frac{N_2\lambda_2}{N_1\lambda_1}$$

$$= 1 + \frac{c_2}{c_1} \times \frac{\lambda_2}{\lambda_2 - \lambda_1}.$$

The value of c_1 is 1.00 and c_2 is given by the product of the factor 0.539, calculated above, and the absorption factor of the conversion electrons which was estimated to be 0.996. Therefore

$$(A_1 + A_2)/A_1 = 1 + (0.539 \times 0.996 \times 1.093) = 1.587.$$

Can. J. Chem. Downloaded from www.nrcresearchpress.com by 210.87.254.6 on 09/05/12
For personal use only.

The observed counting rate for $^{115}Cd + {}^{115m}In$ was divided by this factor to give the ^{115}Cd counting rate.

(f) Correction for Contribution by ^{127}Te to the Determination of the Disintegration Rate of ^{127}Sb

From growth and decay considerations

$$\frac{N\lambda_{^{127}Te}}{N\lambda_{^{127}Sb}} = \frac{\lambda_{^{127}Te}}{\lambda_{^{127}Te} - \lambda_{^{127}Sb}} = 1.116.$$

From a consideration of actual activities measured on the 4π-counter,

$$\frac{A_1 + A_2}{A_1} = \frac{c_1N_1\lambda_1 + c_2N_2\lambda_2}{c_1N_1\lambda_1},$$

where subscripts 1 and 2 refer to ^{127}Sb and ^{127}Te respectively, A is the observed activity, and c is the detection efficiency, so that

$$\frac{A_1 + A_2}{A_1} = 1 + \left(\frac{c_2}{c_1} \times 1.116\right).$$

Since only 80% of the ^{127}Te activity assumes equilibrium with ^{127}Sb (the other 20% results from the isomeric transition from 105-d ^{127m}Te) and since both ^{127}Sb and ^{127}Te activities are negligibly absorbed in the source mount and the source material, then

$$(A_1 + A_2)/A_1 = 1 + (0.80 \times 1.116) = 1.895.$$

The observed counting rate of the combined activities was divided by this factor to give the counting rate of ^{127}Sb.

(g) Correction for Conversion Electrons from ^{137}Ba to Determination of Disintegration Rate of ^{137}Cs

The number of conversion electrons per disintegration of ^{137}Cs is given by $\alpha_T/(1 + \alpha_T)$, which is calculated to be 0.1066 from $\alpha_K = 0.0976$, $\alpha_K/\alpha_L = 5.66$, $\alpha_L/\alpha_{M,N} = 3.85$ (58). From this the number of unconverted gammas is 0.8934. The disintegration rate of ^{137}Cs is then given by

$$\text{observed D.R.} = {}^{137}\text{Cs D.R.}[1 + (0.1066 \times 0.95) + (0.8934 \times 0.95 \times 0.0018)],$$

where 0.95 is the branching ratio and 0.0018 is the estimated detection efficiency of the 4π-counter for the unconverted gamma rays. Thus

$$\text{observed D.R.} = 1.1028 \times {}^{137}\text{Cs D.R.}$$

Since the observed disintegration rate is the sum of the ^{137}Cs and the ^{137m}Ba disintegration rates, then

$$N\lambda_{^{137m}Ba} = 0.1028\, N\lambda_{^{137}Cs}.$$

But

$$\frac{A_1 + A_2}{A_1} = 1 + \frac{c_2N_2\lambda_2}{c_1N_1\lambda_1},$$

where the subscripts 1 and 2 refer to ^{137}Cs and ^{137m}Ba respectively, A is the observed counting rate, and c is the detection efficiency of the 4π-counter determined from the total absorption in the source mount and the source itself. Therefore

Can. J. Chem. Downloaded from www.nrcresearchpress.com by 210.87.254.6 on 09/05/12
For personal use only.

$$\frac{A_1 + A_2}{A_1} = 1 + \frac{0.1028\, c_2}{c_1}$$

and the ^{137}Cs counting rate is given by

$$A_1 = \frac{\text{observed counting rate}}{1 + (0.1028\, c_2/c_1)}.$$

Hence the ^{137}Cs disintegration rate is given by

$$N_1\lambda_1 = \frac{A_1}{c_1} = \frac{\text{observed counting rate}}{c_1 + 0.1028\, c_2}.$$

ACKNOWLEDGMENTS

1. We express our appreciation to Atomic Energy of Canada Ltd. for loan of the Pu–Al alloy used in this investigation.

2. One of us (D. A. M.) wishes to record his appreciation to Canadian Industries Ltd. for Fellowships given in 1959–1960 and 1961–1962 and to the Graduate Faculty of McGill University for award of the Alexander McFee Fellowship in 1960–1961.

REFERENCES

1. E. P. Steinberg and M. S. Freedman. *In* Radiochemical studies: the fission products. Nationa Nuclear Energy Series, Div. IV. McGraw-Hill Book Co., Inc., New York. 1951. Paper 219.
2. L. R. Bunney, E. M. Scadden, J. O. Abriam, and N. E. Ballou. Proceedings of the Second International Conference on the Peaceful Uses of Atomic Energy, Geneva. 1958. Paper 644.
3. R. M. Bartholomew, J. S. Martin, and A. P. Baerg. Can. J. Chem. **37**, 660 (1959).
4. H. R. Fickel and R. H. Tomlinson. Can. J. Phys. **37**, 916 (1959).
5. H. R. Fickel and R. H. Tomlinson. Can. J. Phys. **37**, 926 (1959).
6. K. Fritze, C. C. McMullen, and H. G. Thode. Proceedings of the Second International Conference on the Peaceful Uses of Atomic Energy, Geneva. 1958. Paper 187.
7. M. P. Anikina, P. M. Aron, V. N. Gorshov, R. N. Ivanov, L. M. Krizhansky, C. M. Kukavadze, A. N. Mourin, I. A. Reformatsky, and B. V. Ershler. Proceedings of the Second International Conference on the Peaceful Uses of Atomic Energy, Geneva. 1958. Paper 2040.
8. E. P. Steinberg and L. E. Glendenin. Proceedings of the International Conference on the Peaceful Uses of Atomic Energy, Geneva. 1955. Paper 614.
9. S. Katcoff. Nucleonics, **16**, 78 (1958).
10. S. Katcoff. Nucleonics, **18**, 201 (1960).
11. B. D. Pate and L. Yaffe. Can. J. Chem. **33**, 15 (1955).
12. B. D. Pate and L. Yaffe. Can. J. Chem. **33**, 610 (1955).
13. B. D. Pate and L. Yaffe. Can. J. Chem. **33**, 929 (1955).
14. B. D. Pate and L. Yaffe. Can. J. Chem. **33**, 1656 (1955).
15. B. D. Pate and L. Yaffe. Can. J. Chem. **34**, 265 (1956).
16. L. Yaffe and J. B. Fishman. Can. J. Chem. **38**, 1113 (1960).
17. S. C. Cobrics, W. E. Kunz, and A. E. Nash. Nucleonics, **21**, 63 (1963).
18. T. A. Eastwood and R. D. Werner. Nucl. Sci. Eng. **13**, 385 (1962).
19. C. H. Westcott. Atomic Energy of Canada Ltd., Chalk River, Ontario. A.E.C.L.-1101. 1960.
20. R. C. Hawkins. A.E.C.L., Chalk River. Private communication.
21. D. J. Hughes. Nucleonics, **17**, 132 (1959).
22. R. L. Heath. U.S. Atomic Energy Commission Report, Idaho Falls, Idaho. IDO-16408. 1957.
23. Nuclear Data Sheets. National Academy of Sciences, National Research Council, Washington, D.C.
24. A. Kjelberg, H. Taniguchi, and L. Yaffe. Can. J. Chem. **39**, 635 (1961).
25. L. E. Glendenin, C. D. Coryell, and R. R. Edwards. *In* Radiochemical studies: the fission products. National Nuclear Energy Series, **9**, Div. IV. McGraw-Hill Book Co., Inc., New York. 1951. Paper 52, p. 489.
26. A. C. Wahl. J. Inorg. Nucl. Chem. **6**, 263 (1958).
27. W. E. Grummitt and G. M. Milton. J. Inorg. Nucl. Chem. **20**, 6 (1961).
28. T. J. Kennett and H. G. Thode. Phys. Rev. **103**, 323 (1956).
29. I. F. Croall and H. H. Willis. J. Inorg. Nucl. Chem. **25**, 1213 (1963).
30. L. E. Glendenin, R. R. Edwards, and H. Gest. *In* Radiochemical studies: the fission products. National Nuclear Energy Series, **9**, Div. IV. McGraw-Hill Book Co., Inc., New York. 1951. Paper 232.
31. L. E. Glendenin. *In* Radiochemical studies: the fission products. National Nuclear Energy Series, **9**, Div. IV. McGraw-Hill Book Co., Inc., New York. 1951. Paper 236.
32. N. E. Ballou. *In* Radiochemical studies: the fission products. National Nuclear Energy Series, **9**, Div. IV. McGraw-Hill Book Co., Inc., New York. 1951. Paper 292.

Can. J. Chem. Downloaded from www.nrcresearchpress.com by 210.87.254.6 on 09/05/12
For personal use only.

33. W. F. BOLDRIDGE and D. N. HUME. *In* Radiochemical studies: the fission products. National Nuclear Energy Series, **9**, Div. IV. McGraw-Hill Book Co., Inc., New York. 1951. Paper 294.
34. E. B. SANDELL. Colorimetric determination of trace metals. 3rd ed. Interscience Publishers, Inc., New York. 1959.
35. H. L. MOORE. Anal. Chem. **28**, 997 (1956).
36. D. N. HUME. *In* Radiochemical studies: the fission products. National Nuclear Energy Series, **9**, Div. IV. McGraw-Hill Book Co., Inc., New York. 1951. Paper 245.
37. A. D. HORTON. Anal. Chem. **25**, 1331 (1953).
38. L. E. GLENDENIN. *In* Radiochemical studies: the fission products. National Nuclear Energy Series, **9**, Div. IV. McGraw-Hill Book Co., Inc., New York. 1951. Paper 253.
39. E. M. SCADDEN. Nucleonics, **15**, 102 (1957).
40. L. E. GLENDENIN. *In* Radiochemical studies: the fission products. National Nuclear Energy Series, **9**, Div. IV. McGraw-Hill Book Co., Inc., New York. 1951. Paper 260.
41. N. E. BALLOU. *In* Radiochemical studies: the fission products. National Nuclear Energy Series, **9**, Div. IV. McGraw-Hill Book Co., Inc., New York. 1951. Paper 263.
42. J. O. KARTUNEN and H. B. EVANS. Anal. Chem. **32**, 917 (1960).
43. L. E. GLENDENIN. *In* Radiochemical studies: the fission products. National Nuclear Energy Series, **9**, Div. IV. McGraw-Hill Book Co., Inc., New York. 1951. Paper 267.
44. H. J. WELCHER. The analytical uses of ethylenediaminetetraacetic acid. D. Van Nostrand Co., Inc., New York. 1957.
45. J. A. SEILER. *In* Radiochemical studies: the fission products. National Nuclear Energy Series, **9**, Div. IV. McGraw-Hill Book Co., Inc., New York. 1951. Paper 264.
46. L. E. GLENDENIN. *In* Radiochemical studies: the fission products. National Nuclear Energy Series, **9**, Div. IV. McGraw-Hill Book Co., Inc., New York. 1951. Paper 265.
47. W. F. BOLDRIDGE and D. N. HUME. *In* Radiochemical studies: the fission products. National Nuclear Energy Series, **9**, Div. IV. McGraw-Hill Book Co., Inc., New York. 1951. Paper 272.
48. L. E. GLENDENIN and R. P. METCALF. *In* Radiochemical studies: the fission products. National Nuclear Energy Series, **9**, Div. IV. McGraw-Hill Book Co., Inc., New York. 1951. Paper 278.
49. A. G. COLLINS and J. W. WATKINS. Anal. Chem. **31**, 1182 (1959).
50. L. E. GLENDENIN and C. M. NELSON. *In* Radiochemical studies: the fission products. National Nuclear Energy Series, **9**, Div. IV. McGraw-Hill Book Co., Inc., New York. 1951. Paper 283.
51. W. E. NERVIK. *In* The radiochemistry of the rare earths, scandium, yttrium and actinium. P. C. STEVENSON and W. E. NERVIK. Nuclear Science Series, National Research Council, U.S.A.E.C. 1961. p. 186.
52. H. L. SMITH and D. C. HOFFMANN. J. Inorg. Nucl. Chem. **3**, 243 (1956).
53. P. AVIGNON, A. MICHALOWICS, and R. BOUCHEZ. J. Phys. Radium, **16**, 404 (1955).
54. A.E.C.L. 1711 PROGRESS REPORT. Atomic Energy of Canada Ltd., Chalk River, Ontario. 1962.
55. D. STROMINGER, J. M. HOLLANDER, and G. T. SEABORG. Rev. Mod. Phys. **30**, 585 (1958).
56. J. H. DAVIES and L. YAFFE. Can. J. Phys. **41**, 762 (1963).
57. J. VARMA and C. R. MANDEVILLE. Phys. Rev. **99**, 977 (1955).
58. Y. YOSHIZAWA. Nucl. Phys. **5**, 122 (1958).

Can. J. Chem. Downloaded from www.nrcresearchpress.com by 210.87.254.6 on 09/05/12
For personal use only.

Can. J. Chem. Downloaded from www.nrcresearchpress.com by 210.87.254.105 on 09/05/12
For personal use only.

KINETICS AND MECHANISMS OF THE THERMAL DECOMPOSITION OF PROPIONALDEHYDE

PART I. THE UNINHIBITED REACTION

K. J. LAIDLER AND M. EUSUF
Department of Chemistry, University of Ottawa, Ottawa, Canada

Received May 4, 1964

ABSTRACT

The propionaldehyde pyrolysis was studied in the temperature range 520–560 °C and at pressures from 20 to 360 mm Hg. The reaction was followed by pressure change and by gas chromatography. The overall order was between 1.25 and 1.30 over the whole range of temperatures and pressures studied. Inert gases have no effect on the rates of formation of the products of reaction. The results are consistent with a mechanism consisting of first-order initiation, $C_2H_5CHO \rightarrow C_2H_5 + CHO$, and second-order termination, $C_2H_5 + C_2H_5 \rightarrow C_4H_{10}$ or $C_2H_6 + C_2H_4$. The overall rate can be expressed as $v = k[C_2H_5CHO]^{3/2} + k'[C_2H_5CHO]^{1/2}$. The molecular reaction, $C_2H_5CHO \rightarrow C_2H_6 + CO$, appears to be of minor importance. The reaction $C_2H_5 \rightarrow C_2H_4 + H$ was found to take place in its first-order high-pressure region under the conditions of the present investigations.

INTRODUCTION

Hinshelwood and Thompson (1) studied the thermal decomposition of propionaldehyde in the temperature range 450–600 °C; they reported that the reaction was completely homogeneous and approximately first-order with respect to propionaldehyde. Winkler, Fletcher, and Hinshelwood (2) also reported that the reaction was approximately first order. They analyzed the products of decomposition and found that the major products were CO and C_2H_6, and that considerable amounts of C_2H_4, H_2, and CH_4 were also produced. Sworski and Burton (3), studying this decomposition in the temperature range 850–950 °C, detected both CH_3 and C_2H_5 radicals and concluded that the C_2H_5 radicals are the principal chain carriers. Boyer and Niclause (4) investigated the thermal decomposition of propionaldehyde at somewhat lower temperatures (427–486 °C) and reported that the overall order of the decomposition was three-halves with respect to propionaldehyde. In a recent investigation Márta (5) observed that the overall order of decomposition was three-halves in the temperature range 515–565 °C and pressure range 100–250 mm Hg; he suggested a simple mechanism of the Rice–Herzfeld (6) type to explain his results. Recently Ho (7) compared the thermal decompositions of different aldehydes. His results show that the order of the propionaldehyde decomposition is significantly lower than that of acetaldehyde, which is known to be accurately three-halves (8). The presence of appreciable amounts of C_2H_4 and H_2 (2) shows that the C_2H_5 radical may not be as stable as suggested by Márta (5); in that case, since the chain carrier has some μ-character, the order of the propionaldehyde decomposition is expected to be lower than that of acetaldehyde, whereas in the latter case the stable CH_3 radical is the principal chain carrier.

In view of these uncertainties in the overall order of the decomposition and the stability of the C_2H_5 radical a reinvestigation of the thermal decomposition of propionaldehyde (both uninhibited and inhibited by NO) was felt to be desirable. The present experimental work was mainly concerned with establishing the order of reaction and the effect of inert gas. Other matters, such as mass balances, have been adequately dealt with by previous investigators.

EXPERIMENTAL

The apparatus used was essentially the same as described in a previous paper (8). The reaction was carried out in a quartz vessel 20 cm long and 4 cm wide having a dead space of about 1% of the total volume. The vessel was confined in a metal block, the temperature of which was controlled to within 0.2 °C. Analyses were made using a Perkin–Elmer Vapor Fractometer containing a thermal conductivity detector and a 4-metre silica gel column; dry helium was used as carrier gas.

The propionaldehyde was an Eastman Kodak product; it was purified by several distillations from 0 to −76 °C and stored in the dark. The inert gases used were Matheson research grade chemicals and were purified by several distillations.

RESULTS

Rates of Carbon Monoxide Formation

Several previous investigations (1, 2, 4, 7) have shown that the rate of pressure increase is a good measure of the rate of disappearance of propionaldehyde, and it was not considered necessary to confirm this. It was thought to be of interest, however, to relate the rate of pressure increase to the rate of carbon monoxide formation; since this substance is the only oxygen-containing product that has been detected, the rate of its formation should be equal to the rate of disappearance of the aldehyde. Figure 1 shows a plot of the

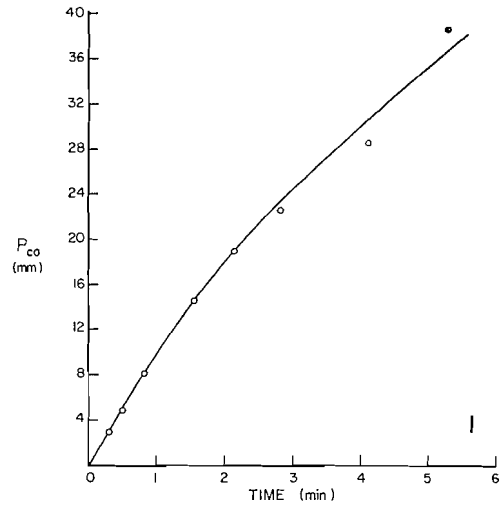

FIG. 1. Plot of the pressure of carbon monoxide formed against time with 100 mm of propionaldehyde at 540 °C.

pressure of the CO formed against time, at 540 °C and 100 mm pressure. The initial rate of appearance of CO is found from these results to be 0.154 mm per s, and this agrees satisfactorily (within 6%) with the value of 0.145 mm per s for the rate calculated from the pressure increase under the same conditions.

Ratios of Other Decomposition Products

Table I shows ratios of decomposition products corresponding to 6% decomposition at an initial pressure of 100 mm Hg. It is to be seen that there is a significant variation of the ratios with temperature and that ethane is a much more important product than ethylene and hydrogen over the entire temperature range. The fact that the ratios vary with temperature means that the correlations between pressure change and amount of aldehyde decomposed cannot be strictly valid over the entire range; however, since C_2H_4 and H_2 are minor products, the variation in their relative importance does not have a significant effect on the correlations.

Can. J. Chem. Downloaded from www.nrcresearchpress.com by 210.87.254.105 on 09/05/12
For personal use only.

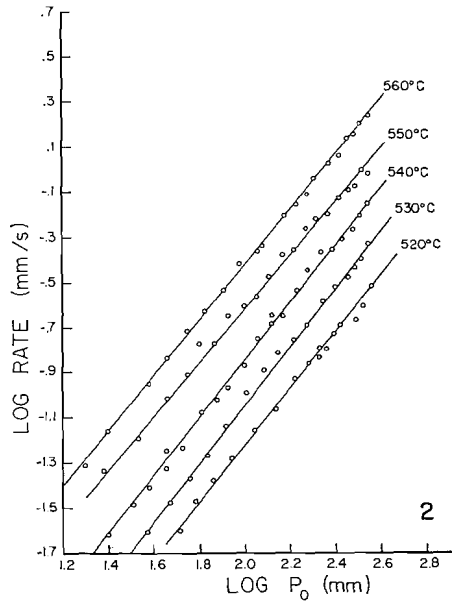

FIG. 2. Double logarithmic plots of initial rate against initial pressure of propionaldehyde at different temperatures.

TABLE I

Ratios of decomposition products
Initial pressure = 100 mm Hg; 6% decomposition

Temperature (°C)	C_2H_6/C_2H_4	H_2/C_2H_4
560	5.86	1.80
560	5.73	1.80
540	7.47	1.33
540	7.56	1.50
540	8.50	1.50
520	10.25	1.25
520	10.62	1.30

Some *n*-butane was detected in the products by the use of a 2,5-hexanedione column; the quantity formed is very small, being about 0.05% of the total products.

Order of Reaction

In view of the above results it is justifiable to determine the order of reaction and related parameters on the basis of pressure measurements. Figure 2 shows a double logarithmic plot of initial rates against initial pressures of propionaldehyde at different temperatures. The order is between 1.25 and 1.30. This result is in apparent disagreement with the work of Márta (5), but is consistent with the results of Ho (7). Our results are not directly comparable with those of Boyer and Niclause (4) because of the much lower temperature used by the latter. Figure 3 shows that added CO_2 and C_2H_6 has no effect on the rate at 520 °C. This is in agreement with the results of Márta (5) and of Hinshelwood and Thompson (1) at high pressure. Figure 4 shows the effect of 100 mm of CO_2 added to 100 mm C_2H_5CHO on the rate of formation of ethylene and ethane at 540 °C. It is clear that added inert gas has little effect on the rate of formation of ethylene and ethane. In this connection, it may be mentioned that in a study of the pyrolysis of *n*-butane by Purnell and

Can. J. Chem. Downloaded from www.nrcresearchpress.com by 210.87.254.105 on 09/05/12
For personal use only.

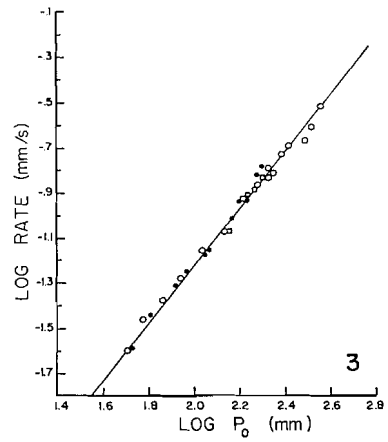

FIG. 3. Plot of log (rate) against log (pressure of propionaldehyde) showing the effects of adding CO_2 and C_2H_6. Rates with no inert gas are shown as ○, those with CO_2 added (CO_2/C_2H_5CHO = 0.5) as □, and those with C_2H_6 added (C_2H_6/C_2H_5CHO = 0.5–2.0) as ●. Temperature = 520 °C.

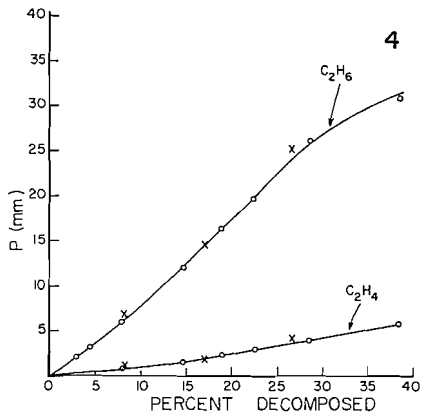

FIG. 4. Plots of the pressures of C_2H_6 and C_2H_4 formed against the percentage of propionaldehyde decomposed showing the effect of adding 100 mm of CO_2 to 100 mm of propionaldehyde. Without CO_2, ○; with CO_2, ×. Temperature = 540 °C.

Quinn (9) the ratio $v_{C_2H_4}/v_{C_2H_6}$, was found to increase with the addition of inert gas at *n*-butane pressures below 24 mm Hg.

Figure 5 shows a plot of $P_{C_2H_6}/P_{C_2H_4}$ against $P_{C_2H_5CHO}$ at 540 °C and 6% decomposition. The curve shows a slight negative curvature. In Fig. 6 is shown a plot of $v_{C_2H_6}/v_{C_2H_4}$ $[C_2H_5CHO]^{1/2}$ against $[C_2H_5CHO]^{1/2}$. At the initial stage of decomposition $P_{C_2H_6}/P_{C_2H_4}$ will be equal to $v_{C_2H_6}/v_{C_2H_4}$.

It will be shown later that the overall reaction can be divided into two parts, one in which the rate varies as $[C_2H_5CHO]^{1/2}$ and the other as $[C_2H_5CHO]^{3/2}$. Figure 7 shows a plot of $v_0/P^{1/2}_{C_2H_5CHO}$ against $P_{C_2H_5CHO}$ at different temperatures. The intercepts give the rate constants corresponding to one-half order and the slopes give those corresponding to three-halves order. In Fig. 8 is shown an Arrhenius plot, the rate constants being obtained from Fig. 7. The activation energy corresponding to the one-half-order reaction is 70.8 kcal per mole and that corresponding to the three-halves-order reaction is 57.1 kcal per mole.

Can. J. Chem. Downloaded from www.nrcresearchpress.com by 210.87.254.105 on 09/05/12
For personal use only.

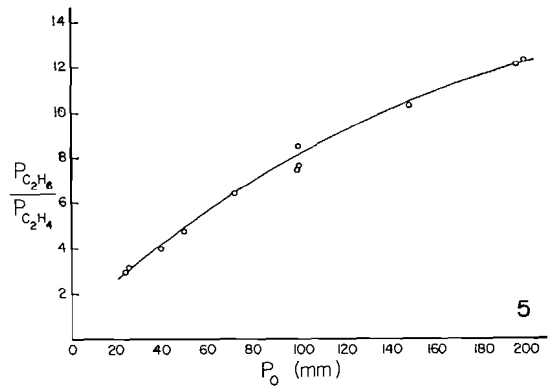

FIG. 5. Plot of the ratio $P_{C_2H_6}/P_{C_2H_4}$ against the initial pressure of propionaldehyde for 6% decomposition

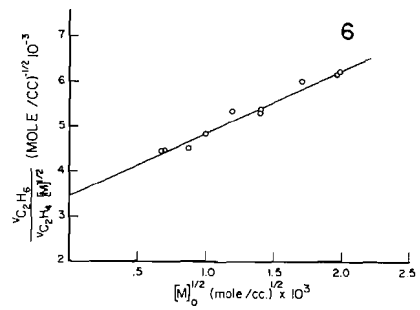

FIG. 6. Plot of $v_{C_2H_6}/v_{C_2H_4}[C_2H_5CHO]^{1/2}$ against $[C_2H_5CHO]^{1/2}$ at 540 °C.

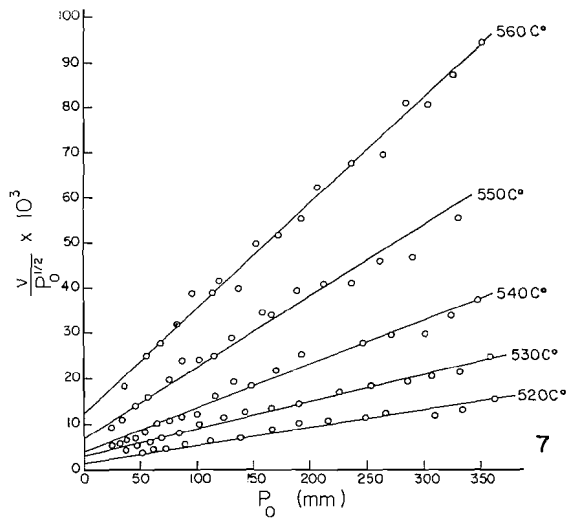

FIG. 7. Plots of $v/P^{1/2}_{C_2H_5CHO}$ against $P_{C_2H_5CHO}$ at different temperatures.

Can. J. Chem. Downloaded from www.nrcresearchpress.com by 210.87.254.105 on 09/05/12
For personal use only.

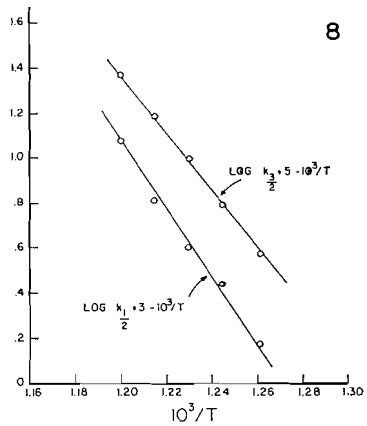

FIG. 8. Arrhenius plots. The lower curve shows the plot of $10^3 k_{1/2}$ $mm^{1/2}$ s^{-1} and the upper one that of $10^5 k_{3/2}$ $mm^{-1/2}$ s^{-1}, $k_{1/2}$ and $k_{3/2}$ being the one-half and the three-halves order rate constants respectively.

DISCUSSION

The Overall Mechanism

It is generally agreed (3–5, 7) that in the thermal decomposition of propionaldehyde C_2H_5 is the most abundant radical and that the combination of C_2H_5 radicals is the predominant chain-ending step. Since the combination of C_2H_5 radicals is a pressure-independent process (10, 11) and inert gas has no effect on the rate of decomposition (Figs. 3 and 4), chain initiation must be the first-order process

[1] $$C_2H_5CHO \rightarrow C_2H_5 + CHO.$$

Since the ratio $[C_2H_6]/[C_2H_4]$ decreases with a decrease in pressure (Fig. 5), but increases with a decrease in temperature (Table I), the two reactions producing ethane and ethylene must be in competition with each other. The same conclusion has been drawn by Purnell and Quinn (9) from their experimental results on the pyrolysis of *n*-butane.

The mechanism to which the above considerations lead is

[1] $$C_2H_5CHO \rightarrow C_2H_5 + CHO$$

[2] $$X + CHO \rightarrow CO + H + X$$

[3] $$C_2H_5 + C_2H_5CHO \rightarrow C_2H_6 + C_2H_5CO$$

[4] $$C_2H_5CO \rightarrow C_2H_5 + CO$$

[5] $$H + C_2H_5CHO \rightarrow H_2 + C_2H_5CO$$

[6] $$C_2H_5 \rightarrow C_2H_4 + H$$

[7] $$C_2H_5 + C_2H_5 \rightarrow C_4H_{10} \text{ or } C_2H_6 + C_2H_4.$$

This mechanism, without reaction [6], is very similar to that proposed by Boyer and Niclause (4) and Márta (5). Application of the steady-state treatment to this mechanism gives rise to the following expressions for the radical concentrations:

[i] $$[C_2H_5] = \left(\frac{k_1}{k_7}\right)^{1/2} [C_2H_5CHO]^{1/2}$$

[ii] $$[H] = \frac{k_1}{k_5} + \frac{k_6}{k_5}\left(\frac{k_1}{k_7}\right)^{1/2} [C_2H_5CHO]^{-1/2}.$$

Can. J. Chem. Downloaded from www.nrcresearchpress.com by 210.87.254.105 on 09/05/12
For personal use only.

With the assumption of large chain lengths (see below) the rate of disappearance of C_2H_5CHO is given by

[iii] $$v = k_3\left(\frac{k_1}{k_7}\right)^{1/2}[C_2H_5CHO]^{3/2} + k_6\left(\frac{k_1}{k_7}\right)^{1/2}[C_2H_5CHO]^{1/2}.$$

A similar rate equation has been suggested by Ho (7) to fit his experimental results for the pyrolysis of isobutyraldehyde.

The Chain Length

The fact that the amount of *n*-butane formed is 0.05% of the total products indicates, if reaction [7] is the main chain-ending step, a chain length of $\sim 1 \times 10^3$. Márta (5) has given a value for the rate constant of reaction [1], and, using his value, the chain length at 100 mm *P* and 540 °C is 8.5×10^3. There seems therefore to be no doubt that the chains are long.

Formation of Ethane and Ethylene

In equation [iii] the first term represents the rate of formation of ethane and the second that of ethylene. The ratio of the two terms at 540 °C and 100 mm pressure is

[iv] $$\frac{v_{C_2H_6}}{v_{C_2H_4}} = \frac{k_3}{k_6}[C_2H_5CHO] = 2.9,$$

the values for the rate constants k_3 and k_6 being taken from Volman and Brinton (12) and Bywater and Steacie (13), respectively. The agreement of this calculated result with the experimental value 8.1 (Fig. 5) within a factor of less than 3 must be considered satisfactory in view of the fact that a change of 1 kcal per mole in the value of *E* changes this ratio by a factor of about 2.

The predominance of the chain-termination reaction $X + H + C_2H_5 \rightarrow C_2H_6 + X$ over $2C_2H_5 \rightarrow C_4H_{10}$ at low pressures does not affect the order of ethane formation. The former process is regarded as being in its pressure-dependent region, because the excited species $C_2H_6^*$ has at least 12 kcal more than required to form two CH_3 radicals (14). If the decomposition of the C_2H_5 radical is a pressure-dependent process, the order of ethylene formation will tend towards 3/2 as the pressure is lowered, and a plot of $P_{C_2H_6}/P_{C_2H_4}$ against $P_{C_2H_5CHO}$ should show a positive curvature. The reverse character of such a plot (slight negative curvature, see Fig. 5) is attributed to the formation of some ethane by the molecular process

[1*m*] $$C_2H_5CHO \rightarrow C_2H_6 + CO.$$

The contribution of this reaction may be estimated in the following way:

[v] $$v_{C_2H_6} = k_{1m}[C_2H_5CHO] + k_3\left(\frac{k_1}{k_7}\right)^{1/2}[C_2H_5CHO]^{3/2}$$

[vi] $$v_{C_2H_4} = k_6\left(\frac{k_1}{k_7}\right)^{1/2}[C_2H_5CHO]^{1/2}$$

[vii] $$v_{C_2H_6}/v_{C_2H_4} = \frac{k_{1m}}{k_6}\left(\frac{k_7}{k_1}\right)^{1/2}[C_2H_5CHO]^{1/2} + \frac{k_3}{k_6}[C_2H_5CHO]$$

[viii] $$\frac{v_{C_2H_6}/v_{C_2H_4}}{[C_2H_5CHO]^{1/2}} = \frac{k_{1m}}{k_6}\left(\frac{k_7}{k_1}\right)^{1/2} + \frac{k_3}{k_6}[C_2H_5CHO]^{1/2}.$$

Can. J. Chem. Downloaded from www.nrcresearchpress.com by 210.87.254.105 on 09/05/12
For personal use only.

From Fig. 6, at 540 °C,

[ix] $$\frac{k_{1m}}{k_6}\left(\frac{k_7}{k_1}\right)^{1/2} = 3.4 \times 10^3.$$

If the values of k_1 (5), k_6 (13, 15), and k_7 (16, 17) are inserted into this equation, k_{1m} is calculated to be 11.7×10^{-5} s^{-1}. On the basis of this value the contribution of the molecular reaction to the rate is found to be less than 10% under the conditions of the present experiments. Because of uncertainties in the mechanism and in the rate constants, however, this conclusion could be in serious error.

Formation of Hydrogen

The fact that, as shown in Table I, the rate of production of hydrogen is significantly greater than that of ethylene requires some comment. Reaction [8*b*] gives rise to H_2, and the radical CH_3CHCHO can give rise to H_2 following a split into $CH_2CHCHO + H$. Also, radicals will add on to ethylene formed in the reaction,

$$C_2H_4 + R \rightarrow CH_2CH_2R,$$

and the resulting radical may abstract a hydrogen atom to form a hydrocarbon; alternatively it will split off a hydrogen atom or other radical which will subsequently abstract a H atom to form H_2 or a hydrocarbon. The net effect is to increase H_2 and diminish C_2H_4.

Activation Energies

The predicted activation energies for the one-half and three-halves-order reactions are given by the expressions

[x] $$E_{1/2} = E_6 + \tfrac{1}{2}(E_1 - E_7)$$

[xi] $$E_{3/2} = E_3 + \tfrac{1}{2}(E_1 - E_7).$$

Insertion of the values for E_1 (5), E_3 (12), E_6 (13), and E_7 (16, 17) leads to 80.9 kcal per mole for $E_{1/2}$ and 49.0 kcal per mole for $E_{3/2}$. The experimental values are 70.8 and 57.1, so that the agreement is not good. The mechanism proposed is necessarily oversimplified, and the inclusion of other possible chain-ending steps appears to explain the discrepancy. At lower pressures the reaction

[7*a*] $$X + H + C_2H_5 \rightarrow C_2H_6 + X$$

will become more and more important. If, hypothetically, this reaction were predominant, the rate expression would become

$$v = k_3\left(\frac{k_1k_5}{k_6k_{7a}}\right)^{1/2}[C_2H_5CHO]^{3/2} + \left(\frac{k_1k_5k_6}{k_{7a}}\right)^{1/2}[C_2H_5CHO]^{1/2}.$$

With E_5 taken as 8 kcal per mole, E_{7a} as zero and with the other values taken from Table I of Part II it is found that $E_{1/2} = 65.1$ kcal per mole and $E_{3/2} = 33.3$ kcal per mole. The experimental value of $E_{1/2}$ is between the two values given on the basis of the two chain-ending steps, and this suggests that [7*a*] does play some role. The $E_{3/2}$ values predicted by both of the mechanisms are lower than the experimental value. This suggests that ethane is formed by some other process which has a high activation energy and a low order in C_2H_5CHO. A possible process is the molecular process, which has been seen to contribute perhaps 10% of the rate; this contribution will increase with temperature.

Comparison with Acetaldehyde Pyrolysis

The overall rate of decomposition of propionaldehyde is significantly lower than that of

Can. J. Chem. Downloaded from www.nrcresearchpress.com by 210.87.254.105 on 09/05/12
For personal use only.

acetaldehyde (7, 8), and the activation energy for the overall propionaldehyde decomposition is about 7 kcal higher than that of the acetaldehyde decomposition. The following suggestions may be made to explain the above facts.

(1) The chain-termination reaction in the acetaldehyde pyrolysis is a third-order process, whereas that with propionaldehyde is a second-order process and therefore more rapid.

(2) C_2H_5 and H radicals may abstract hydrogen atoms other than those attached to the carbonyl groups, e.g.

$$C_2H_5 + CH_3CH_2CHO \xrightarrow{[8a]} C_2H_6 + CH_3CHCHO$$

$$H + CH_3CH_2CHO \xrightarrow{[8b]} H_2 + CH_3CHCHO.$$

The CH_3CHCHO radical will mainly be involved in a chain-ending step because of its higher stability. Higher temperature may, however, favor the following reactions

$$CH_3CHCHO \overset{[9]}{\rightleftarrows} CH_3CH_2CO \xrightarrow{[10]} CH_3CH_2 + CO$$

$$CH_3CHCHO \overset{[11]}{\rightleftarrows} CH_2CH_2CHO \xrightarrow{[12]} C_2H_4 + CHO$$

which will lead to a larger chain length and consequently a higher activation energy than predicted.

One important difference between the present reaction and the decomposition of acetaldehyde is that initiation is first-order rather than second-order. It has been suggested (8) that the abstraction reaction

$$CH_3CHO + CH_3CHO \rightarrow CH_3CHOH + CH_3CO$$

is an important initiation reaction in the acetaldehyde pyrolysis, and it might be asked why the corresponding reaction

[1a] $$C_2H_5CHO + C_2H_5CHO \rightarrow C_2H_5CHOH + C_2H_5CO$$

does not play a role in the propionaldehyde pyrolysis. Using thermal data quoted by Steacie (18), Szwarc (19), and Benson (14) and estimating entropies using Benson's procedure (14), we conclude that

$$\frac{v_1}{v_{1a}} = \frac{e^{29.6/R} e^{-27000/RT}}{[C_2H_5CHO]}.$$

This ratio is 8.6 at 800 °K and 1 atm, and 18.1 at 800 °K and 360 mm (the highest pressure of the present investigation); it is higher at highest temperatures. These estimates are undoubtedly crude, but may be significant in throwing light on the difference between the initiation processes in the two reactions.

General Conclusions

It is evident from the preceding discussion that the propionaldehyde pyrolysis is even more complex than decompositions of acetaldehyde and the lower paraffins. The mechanism arrived at as representing the main features of the reaction is undoubtedly an oversimplification, and other reactions should be included. In particular, the discussion of activation energies has suggested that an additional chain-ending step is needed. The steady-state equations become quite intractable, however, if more than one chain-ending step is included. The point of view of the present paper is that it is most useful to propose an oversimplified mechanism, as a basis for discussion, and later to amend it in various particulars.

Can. J. Chem. Downloaded from www.nrcresearchpress.com by 210.87.254.105 on 09/05/12
For personal use only.

ACKNOWLEDGMENTS

The authors are indebted to Drs. Margaret H. Back, T. M. Bell, and K. O. Kutchke for extremely valuable comments and discussions relating to this work. The work was supported by a grant from the American Petroleum Fund, and M. E. wishes to thank the Canadian Commonwealth Scholarships and Fellowships Committee for a scholarship under the tenure of which this work was carried out.

REFERENCES

1. C. N. HINSHELWOOD and H. W. THOMPSON. Proc. Roy. Soc. London, Ser. A, **113**, 221 (1926).
2. C. A. WINKLER, C. J. FLETCHER, and C. N. HINSHELWOOD. Proc. Roy. Soc. London, Ser. A, **146**, 345 (1934).
3. J. J. SWORSKI and M. J. BURTON. J. Am. Chem. Soc. **73**, 3194 (1951).
4. A. BOYER and M. NICLAUSE. J. Chim. Phys. **49**, 354 (1952).
5. F. MÁRTA. Acta Chim. Hung. **31**, 415 (1962).
6. F. O. RICE and K. F. HERZFELD. J. Am. Chem. Soc. **56**, 284 (1934).
7. S. K. HO. Proc. Roy. Soc. London, Ser. A, **276**, 278 (1963).
8. M. EUSUF and K. J. LAIDLER. Can. J. Chem. **42**, 1851 (1964).
9. J. H. PURNELL and C. P. QUINN. Proc. Roy. Soc. London, Ser. A, **270**, 267 (1962).
10. K. J. LAIDLER and B. W. WOJCIECHOWSKI. Proc. Roy. Soc. London, Ser. A, **260**, 91 (1961).
11. N. H. SAGERT and K. J. LAIDLER. Can. J. Chem. **41**, 838 (1963).
12. D. H. VOLMAN and R. K. BRINTON. J. Chem. Phys. **22**, 929 (1954).
13. S. BYWATER and E. W. R. STEACIE. J. Chem. Phys. **19**, 326 (1951).
14. S. W. BENSON. The foundations of chemical kinetics. McGraw-Hill Book Co., Inc. 1960. pp. 662–671.
15. H. W. MELVILLE and J. C. ROBB. Proc. Roy. Soc. London, Ser. A, **196**, 494 (1949).
16. K. J. IVIN and E. W. R. STEACIE. Proc. Roy. Soc. London, Ser. A, **208**, 25 (1951).
17. A. SHEPP and K. O. KUTSCHKE. J. Chem. Phys. **26**, 1020 (1957).
18. E. W. R. STEACIE. Atomic and free radical reactions. Reinhold Publ. Corp. New York. 1954.
19. M. SZWARC. Chem. Rev. **47**, 75 (1950).

Can. J. Chem. Downloaded from www.nrcresearchpress.com by 210.87.254.105 on 09/05/12
For personal use only.

Can. J. Chem. Downloaded from www.nrcresearchpress.com by 210.87.254.6 on 09/05/12
For personal use only.

KINETICS AND MECHANISMS OF THE THERMAL DECOMPOSITION OF PROPIONALDEHYDE

PART II. THE REACTION IN THE PRESENCE OF NITRIC OXIDE

K. J. LAIDLER AND M. EUSUF
Department of Chemistry, University of Ottawa, Ottawa, Canada

Received May 4, 1964

ABSTRACT

The decomposition of propionaldehyde in the presence of various amounts of nitric oxide has been studied in the temperature range 520–560 °C and at propionaldehyde pressures from 30 to 300 mm Hg. The reaction is inhibited by small amounts of nitric oxide, and larger amounts give rise to strong catalysis. The order of the maximally inhibited reaction is 1.5 and the degree of inhibition decreases with an increase of propionaldehyde pressure. In the catalytic region the order of the overall reaction is 1.25 with respect to propionaldehyde, and the relative rate (the ratio of rates in the presence and absence of nitric oxide) is independent of propionaldehyde pressure. The overall rate in the catalytic region can be expressed as

$$v = 8.38 \times 10^{12}\, e^{-36800/RT}[C_2H_5CHO][NO] + 2.35 \times 10^{14}\, e^{-42300/RT}[C_2H_5CHO]^{3/2}[NO]^{1/2}\ s^{-1},$$

the unit of concentration being mole per cc. A mechanism in which nitric oxide initiates chains by the reaction $C_2H_5CHO + NO \rightarrow C_2H_5CO + HNO$, propagates them by $C_2H_5NO + C_2H_5CHO \rightarrow C_2H_6 + C_2H_5CO + NO$, and terminates them by $C_2H_5 + C_2H_5NO \rightarrow C_4H_{10} + NO$ and $C_2H_5 + C_2H_4 + NO$ and $C_2H_5NO + C_2H_5NO \rightarrow C_4H_{10} + 2NO$ or $C_2H_6 + C_2H_4 + 2NO$ is proposed and is shown to be consistent with the results.

INTRODUCTION

Although a number of investigations have been carried out on the thermal decomposition of propionaldehyde in the presence of nitric oxide, the mechanism of the reaction has been a matter of controversy. Staveley and Hinshelwood (1) investigated the thermal decomposition of propionaldehyde; they found that the reaction was inhibited by small amounts of nitric oxide and that there was catalysis at high nitric oxide pressures. They suggested that the maximally inhibited reaction was a non-chain molecular process. Smith and Hinshelwood (2) found that both nitric oxide and propylene reduced the rate by the same amount, and also concluded that the maximally inhibited reaction was a molecular process. A recent investigation by Szabó and Márta (3, 4) showed that the overall order of the reaction in the presence of nitric oxide was three-halves with respect to propionaldehyde and approximately one-half with respect to nitric oxide at high nitric oxide pressures. These workers attempted to explain the above facts by adding the reactions

[8]	$C_2H_5 + NO \rightarrow C_2H_5NO$
[3*i*]	$C_2H_5NO + C_2H_5CHO \rightarrow C_2H_6 + C_2H_5CO + NO$
[7*i*]	$C_2H_5NO + C_2H_5 \rightarrow$ products
[7*i*′]	$C_2H_5NO + C_2H_5NO \rightarrow$ products

to the scheme of the uninhibited reaction originally suggested by Boyer and Niclause (5). Analysis of the results of Szabó and Márta (3, 4) on the basis of their mechanism reveals that $E_{7i} - E_{3i} = 2.4$ kcal per mole and $E_{7i} - 2E_{3i} = -2.9$ kcal per mole. These relationships indicate unreasonably high activation energies for the chain-ending steps, and suggest that the mechanism does not represent the complete picture. Recently Ho (6) studied the thermal decomposition of different aldehydes in the presence of nitric oxide, propylene,

and isobutene and found that in the thermal decomposition of propionaldehyde the limiting rate was lower with nitric oxide than with isobutene and propylene, in disagreement with the results of Smith and Hinshelwood (2).

Wojciechowski and Laidler (7, 8) have suggested that in the thermal decomposition of organic substances nitric oxide starts chains by abstracting a hydrogen atom and ruptures them by being involved in chain-ending reactions. The thermal decompositions of various compounds (9–14) have been explained satisfactorily on the basis of the above suggestion. Aldehydes present an additional interesting feature in that they contain a labile aldehyde hydrogen atom. It has been shown (14) on the basis of experimental results and of calculated activation energies that the following chain-propagating reaction involving a species containing nitric oxide,

$$RNO + M \rightarrow RH + R' + NO,$$

is significantly more important in the acetaldehyde pyrolysis than in that of the hydrocarbons. Szabó and Márta have suggested this reaction in the thermal decomposition of propionaldehyde, but their omission of the chain initiation by nitric oxide leads, as shown above, to unreasonably high activation energies for the chain-ending steps in order for their mechanism to be consistent with their experimental results.

The present paper describes an experimental reinvestigation of the pyrolysis of propionaldehyde in the presence of nitric oxide and interprets the results on the basis of the above ideas.

EXPERIMENTAL

The apparatus used was the same as that described in the preceding paper (15). The reaction was carried out in the same vessel as was used for the uninhibited reaction. The nitric oxide used was Matheson C.P. grade and was purified by the method of Hughes (16). The procedure followed to ensure complete mixing of propionaldehyde and nitric oxide was the same as described previously (14).

RESULTS

Rate of Carbon Monoxide Formation

It has been shown by Staveley and Hinshelwood (1) and Ho (6) that in the maximally inhibited region 1 mm pressure increase corresponds to the reaction of 1 mm of propionaldehyde. In Fig. 1 is shown a plot of the pressure of carbon monoxide formed against time, with 100 mm propionaldehyde and 14 mm nitric oxide at 540 °C. The rate of formation of carbon monoxide (0.149 mm per s) obtained from Fig. 1 agrees within 3% with the overall rate (0.145 mm per s) obtained from the pressure increase. All of the rate measurements were therefore made from the pressure increases, which were recorded automatically.

Methane Formation

A few measurements were made on the rate of methane production. Very little is formed in the uninhibited reaction, and the rate is increased by addition of nitric oxide. Table II shows the ratios of the amounts of CH_4 and CO produced, at different percentages of conversion at 540 °C; the ratio is seen to be independent of the extent of decomposition.

Orders With Respect to Propionaldehyde and Nitric Oxide

Figure 2 shows the effect of nitric oxide on the products of reaction in the catalytic region at 540 °C. The overall rate is equal to that in the absence of nitric oxide. Ethylene production shows a marked increase and hydrogen production appears to decrease slightly.

In Fig. 3 is shown a plot of relative rate, v_{NO}/v_{uninh}, against the pressure of nitric oxide

Can. J. Chem. Downloaded from www.nrcresearchpress.com by 210.87.254.6 on 09/05/12
For personal use only.

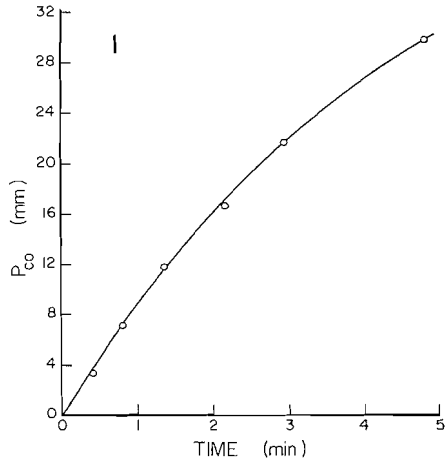

FIG. 1. Plot of the pressure of carbon monoxide formed against time with 14 mm nitric oxide added to 100 mm propionaldehyde. Temperature = 540 °C.

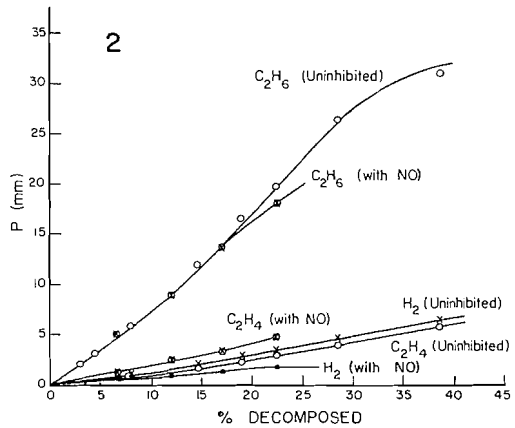

FIG. 2. Analytical results for the decomposition of propionaldehyde in the absence and presence of 14 mm of nitric oxide. Propionaldehyde pressure = 100 mm Hg, temperature = 540 °C.

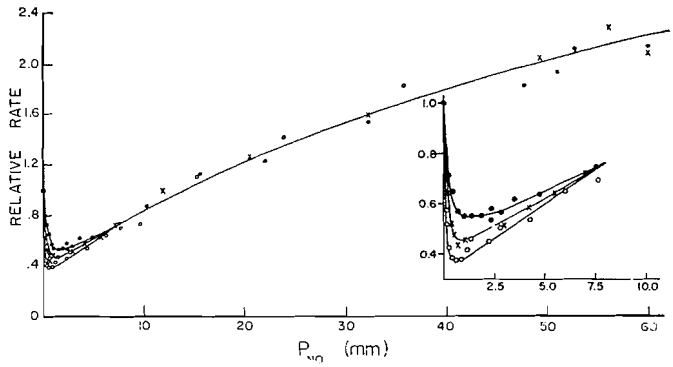

FIG. 3. Plots of relative rate against nitric oxide pressure. Relative rates with 50 mm propionaldehyde are shown as ○, those at 100 mm as ×, and those at 200 mm as ●. Temperature = 540 °C.

Can. J. Chem. Downloaded from www.nrcresearchpress.com by 210.87.254.6 on 09/05/12
For personal use only.

at different propionaldehyde pressures and at 540 °C. It is seen that small amounts of nitric oxide inhibit the reaction but that larger amounts produce strong catalysis. The ratio v_{min}/v_{uninh} increases with an increase of propionaldehyde pressure; this result does not agree with the results of Szabó and Márta (3, 4) but is in agreement with those of Ho (6). At higher nitric oxide pressures the relative rate is approximately independent of the propionaldehyde pressure. This result is in agreement with the results of Szabó and Márta (3, 4) but apparently in disagreement with those of Ho (6).

Figure 4 shows a double logarithmic plot of initial rates against initial pressures of

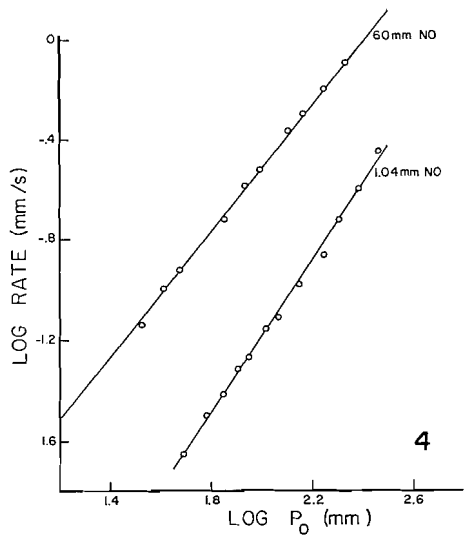

FIG. 4. Plots of log (rate) against log (pressure of propionaldehyde) showing the effect of nitric oxide pressure on the order with respect to propionaldehyde. Temperature = 540 °C.

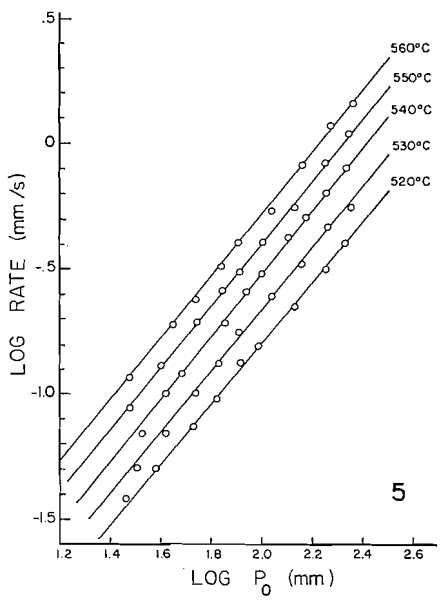

FIG. 5. Plots of log (rate) against log (pressure of propionaldehyde) with 60 mm of nitric oxide at different temperatures.

Can. J. Chem. Downloaded from www.nrcresearchpress.com by 210.87.254.6 on 09/05/12
For personal use only.

propionaldehyde at 1 mm and 60 mm of nitric oxide at 540 °C. The lower curve with 1 mm of nitric oxide represents approximately the maximally inhibited rate and gives an order of 1.5. From the upper curve, with 60 mm nitric oxide, an order of 1.25 is obtained. Figure 5 shows a double logarithmic plot of initial rates against initial pressures of propionaldehyde with 60 mm NO. The order of the reaction is seen to be 1.25 with respect to propionaldehyde. Since the orders of the reaction in the absence (Part I) and presence of large amounts of nitric oxide are the same, the relative rate must be independent of propionaldehyde pressure (Fig. 3) in contrast to the conclusion of Ho (6). In Fig. 6 is shown a plot of log (relative rate) against log (pressure of nitric oxide) at 50, 100, and 200 mm pressures of propionaldehyde. The order of the reaction is seen to be about 0.65 with respect to nitric oxide.

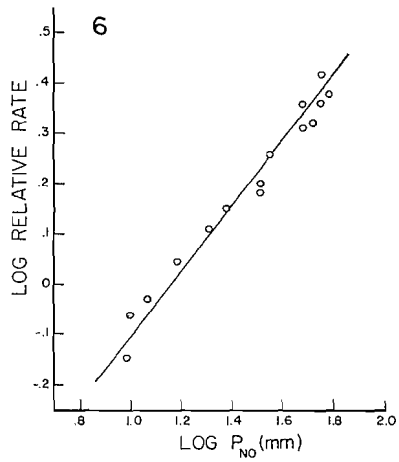

FIG. 6. Plot of log (relative rate) against log (pressure of nitric oxide) in the region where relative rates are independent of propionaldehyde pressures (Fig. 3). Temperature = 540 °C.

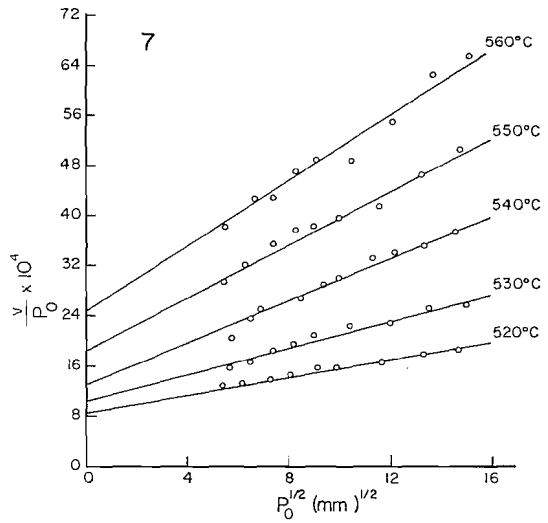

FIG. 7. Plot of $v/P_{C_2H_5HO}$ against $P^{1/2}_{C_2H_5CHO}$ with 60 mm of nitric oxide at different temperatures.

Can. J. Chem. Downloaded from www.nrcresearchpress.com by 210.87.254.6 on 09/05/12
For personal use only.

The overall rate at higher nitric oxide pressures can be represented as

[i] $$v = 2k_{1i}[C_2H_5CHO][NO] + k[C_2H_5CHO]^{3/2}[NO]^{1/2}.$$

The dependence on $[C_2H_5CHO]$ is demonstrated in Fig. 7, which is a plot of $v/P_{C_2H_5CHO}$ against $P^{1/2}_{C_2H_5CHO}$ with 60 mm of nitric oxide at different temperatures; $P_{C_2H_5CHO}$ is the initial pressure of propionaldehyde in mm. Plots of this kind were made at four nitric oxide concentrations, ranging from 0 to 100 mm; as shown in Fig. 8 the intercepts vary approximately with the first power of the nitric oxide concentration and the slopes with the one-half power. From these results values of k_{1i} and k were calculated, and Fig. 9 shows Arrhenius plots for the rate constants. The rate constants k_{1i} and k can be expressed as

$$k_{1i} = 4.19 \times 10^{12}\ e^{-36800/RT}\ \text{cc mole}^{-1}\ \text{s}^{-1}$$

$$k = 2.35 \times 10^{14}\ e^{-42300/RT}\ \text{cc mole}^{-1}\ \text{s}^{-1}.$$

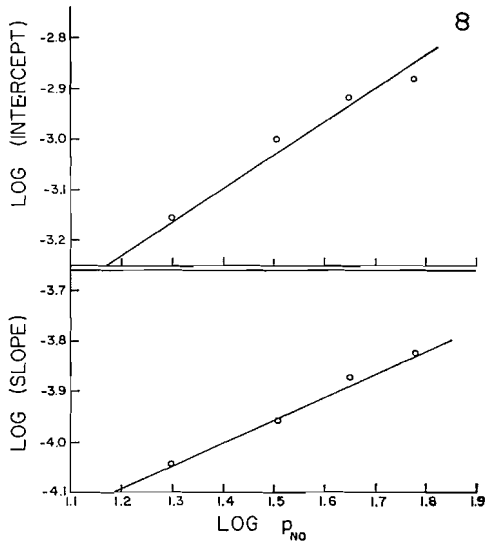

FIG. 8. Plots of log (intercept), upper curve, and log (slope), lower curve, against log (pressure of nitric oxide). Temperature = 540 °C.

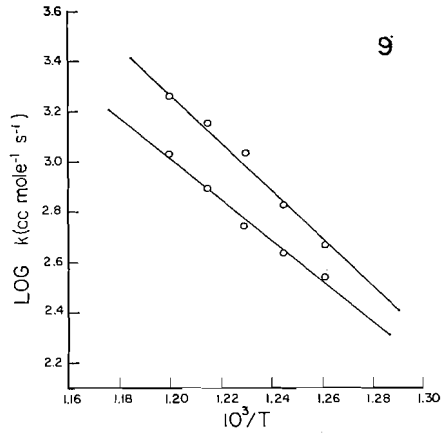

FIG. 9. Arrhenius plots. The upper curve shows a plot of $k_{3i}(k_{1i}/k_{7i}')^{1/2}$ and the lower one that of k_{1i} (cf. eq. [vii]), the rate constants being those obtained from Fig. 7.

Can. J. Chem. Downloaded from www.nrcresearchpress.com by 210.87.254.6 on 09/05/12
For personal use only.

Can. J. Chem. Downloaded from www.nrcresearchpress.com by 210.87.254.6 on 09/05/12
For personal use only.

DISCUSSION

Overall Reaction Mechanism

That the maximally inhibited reaction is not a simple non-chain unimolecular process is suggested by the following facts.

(1) The maximally inhibited reaction has a non-integral order (1.5).

(2) The degree of inhibition decreases with increase of propionaldehyde pressure.

(3) In the catalytic region, the order of the reaction is non-integral with respect to both propionaldehyde and nitric oxide, indicating that the latter must be involved in the chain reaction. The maximally inhibited reaction must, therefore, be the resultant of two opposing reactions—acceleration as well as inhibition by nitric oxide.

(4) The increase of the ratio C_2H_4/H_2 with increase in nitric oxide pressure is consistent with a chain mechanism.

(5) In the uninhibited reaction (cf. Part I), the contribution of a molecular process appears to be unimportant in comparison with that of a chain reaction.

In line with previous work in this laboratory (7–14) it is suggested that nitric oxide initiates chains by the reaction

[1*i*] $$C_2H_5CHO + NO \rightleftarrows C_2H_5CO + HNO.$$

and that the most abundant radical C_2H_5 is involved in the following equilibrium:

[8] $$C_2H_5 + NO \rightleftarrows C_2H_5NO.$$

In order for the overall order of the maximally inhibited reaction to be three-halves, an important chain-ending step must be

[7*i*] $$C_2H_5 + C_2H_5NO \rightarrow C_4H_{10} + NO \quad \text{or } C_2H_6 + C_2H_4 + NO.$$

In the catalytic region the order of the reaction with respect to propionaldehyde falls below three-halves and a plot of relative rate against nitric oxide concentration gives a negative curvature. In line with previous suggestions (14) and the work of Szabó and Márta (3, 4) it is proposed that the reactions

[3*i*] $$C_2H_5NO + C_2H_5CHO \rightarrow C_2H_6 + C_2H_5CO + NO$$

[7*i*] $$C_2H_5NO + C_2H_5NO \rightarrow \text{products}$$

become important at high nitric oxide pressures.

As in the case of acetaldehyde, in the present decomposition there is no flat region when rate is plotted against nitric oxide concentration. One must, therefore, take into consideration all the processes in the uninhibited reaction in addition to those involving nitric oxide.

The complete scheme may be written as

[1] $$C_2H_5CHO \rightarrow C_2H_5 + CHO$$

[1*i*] $$C_2H_5CHO + NO \rightarrow C_2H_5CO + HNO$$

[2] $$X + CHO \rightarrow CO + H + X$$

[2*i*] $$X + HNO \rightarrow NO + H + X$$

[3] $$C_2H_5 + C_2H_5CHO \rightarrow C_2H_6 + C_2H_5CO$$

[3*i*] $$C_2H_5NO + C_2H_5CHO \rightarrow C_2H_6 + C_2H_5CO + NO$$

[4] $$C_2H_5CO \rightarrow C_2H_5 + CO$$

[5] $$H + C_2H_5CHO \rightarrow H_2 + C_2H_5CO$$

[6] $$C_2H_5 \rightarrow C_2H_4 + H$$

$$C_2H_5 + NO \overset{[8]}{\rightleftarrows} C_2H_5NO \overset{[9]}{\rightleftarrows} C_2H_4{=}NOH \overset{[10]}{\rightarrow} \text{products}$$

[7] $C_2H_5 + C_2H_5 \rightarrow C_4H_{10}$ or $C_2H_6 + C_2H_4$

[7i] $C_2H_5 + C_2H_5NO \rightarrow C_4H_{10} + NO$ or $C_2H_6 + C_2H_4 + NO$

[7i'] $C_2H_5NO + C_2H_5NO \rightarrow C_4H_{10} + 2NO$ or $C_2H_6 + C_2H_4 + 2NO$

The numbering is consistent with the mechanism in Part I; X represents a third body, which may be propionaldehyde itself. The same type of mechanism has been used to explain the results of the acetaldehyde pyrolysis (14). Without reactions [1i], [2i], and [6] the above mechanism is very similar to that proposed by Szabó and Márta (3, 4) in the thermal decomposition of propionaldehyde.

Application of the steady-state treatment, with the usual approximations, leads to the following expressions for the radical concentrations and for the rate of decomposition:

$$[C_2H_5] = \left(\frac{k_1 + k_{1i}[NO]}{k_7 + k_{7i}k_8[NO] + k_{7i'}k_8^2[NO]^2}\right)^{1/2}[C_2H_5CHO]^{1/2}$$

$$[C_2H_5CO] = \frac{[C_2H_5CHO]k_1 + 2k_i[NO] + k_3[C_2H_5] + k_{3i}[C_2H_5NO] + k_6[C_2H_5]}{k_4}$$

$$[C_2H_5NO] = K_8[C_2H_5][NO] \qquad (K_8 = k_8/k_{-8})$$

[ii] $$v = 2k_1[C_2H_5CHO] + 2k_{1i}[C_2H_5CHO][NO] + k_3[C_2H_5][C_2H_5CHO] + k_{3i}[C_2H_5NO][C_2H_5CHO] + k_6[C_2H_5]$$

$$= 2k_{1i}[C_2H_5CHO][NO] + k_3\left(\frac{k_1}{k_7}\right)^{1/2}[C_2H_5CHO]^{3/2}\frac{\left(1 + \frac{k_{3i}}{k_3}K_8[NO]\right)\left(1 + \frac{k_{1i}}{k_1}[NO]\right)^{1/2}}{\left(1 + \frac{k_{7i}}{k_7}K_8[NO] + \frac{k_{7i'}}{k_7}K_8^2[NO]^2\right)^{1/2}}$$

$$+ k_6\left(\frac{k_1}{k_7}\right)^{1/2}[C_2H_5CHO]^{1/2}\frac{\left(1 + \frac{k_{1i}}{k_1}[NO]\right)^{1/2}}{\left(1 + \frac{k_{7i}}{k_7}K_8[NO] + \frac{k_{7i'}}{k_7}K_8^2[NO]^2\right)^{1/2}}$$

Important special cases follow.

(1) If [NO] is zero, eq. [ii] reduces to

[iii] $$v = k_3\left(\frac{k_1}{k_7}\right)^{1/2}[C_2H_5CHO]^{3/2} + k_6\left(\frac{k_1}{k_7}\right)^{1/2}[C_2H_5CHO]^{1/2},$$

which is the rate expression for the uninhibited reaction (cf. Part I).

(2) In the presence of nitric oxide, ethylene production increases but not at the expense of ethane production (Fig. 2); in the uninhibited reaction, on the other hand, the ethane and ethylene productions are in competition with each other. In the uninhibited reaction the rates of formation of ethylene and hydrogen are within a factor of two, but in the presence of nitric oxide the rate of formation of hydrogen is much less than that of ethylene (Fig. 2). These facts suggest that the reaction

[6] $$C_2H_5 \rightarrow C_2H_4 + H$$

is unimportant in the presence of nitric oxide. This is understandable in view of the fact that using the kinetic parameters of Table I the equilibrium constant K_8 is calculated to

Can. J. Chem. Downloaded from www.nrcresearchpress.com by 210.87.254.6 on 09/05/12
For personal use only.

be 1.7×10^{10} at 540 °C, and of the fact that the relative concentrations of C_2H_5NO and C_2H_5 increase with an increase in NO concentration. Thus, at 540 °C and with 1 mm NO, the ratio $[C_2H_5]/[C_2H_5NO] = 1/340$. It is suggested therefore that most of the ethylene formed in the presence of nitric oxide comes from the chain-ending steps [7*i*] and [7*i'*]. On the basis of the above considerations eq. [ii] reduces to

$$[iv] \qquad v = 2k_{1i}[C_2H_5CHO][NO] + k_3\left(\frac{k_1}{k_7}\right)^{1/2}[C_2H_5CHO]_{3/2}\frac{\left(1+\frac{k_{3i}}{k_3}K_8[NO]\right)\left(1+\frac{k_{1i}}{k_1}[NO]\right)^{1/2}}{\left(1+\frac{k_{3i}}{k_7}K_8[NO]+\frac{k_{7i'}}{k_7}K_8^2[NO]^2\right)^{1/2}}.$$

(3) At sufficiently low nitric oxide concentrations

$$1 \gg \frac{k_{3i}}{k_3}K_8[NO], \qquad \left(1+\frac{k_{7i}}{k_7}K_8[NO]\right) \gg \frac{k_{7i'}}{k_1}K_8^2[NO]^2.$$

Equation [iv] then reduces to

$$[v] \qquad v = 2k_{1i}[C_2H_5CHO][NO] + k_3\left(\frac{k_1}{k_7}\right)^{1/2}[C_2H_5CHO]^{3/2}\frac{\left(1+\frac{k_{1i}}{k_1}[NO]\right)^{1/2}}{\left(1+\frac{k_{7i}}{k_7}K_8[NO]\right)^{1/2}}.$$

Approximately 1 mm of nitric oxide gives maximum inhibition and the first term of the above equation can then be neglected. In the maximally inhibited region the rates of the chain-initiating steps [1] and [1*i*] and chain-terminating steps [7] and [7*i*] may be compared on the basis of the following ratios, which refer to 540 °C and 1 mm of NO and are based on the rate constants in Table I:

$$\frac{v_{1i}}{v_1} = \frac{k_{1i}}{k_1}[NO] \approx 130,$$

$$\frac{v_{7i}}{v_7} = \frac{k_{7i}k_8[NO]}{k_7} \approx 20,$$

$$\frac{v_{7i}}{v_{7i'}} = \frac{k_{7i}}{k_{7i'}k_8[NO]} \approx 5.$$

TABLE I

Kinetic parameters for elementary reactions

Reaction	Frequency factor (s^{-1} or cc $mole^{-1}$ s^{-1})	Activation energy (kcal $mole^{-1}$)	Reference
[1]	1.7×10^{15}	82.8	Marta (18)
[1*i*]	4.19×10^{12}	36.8	See text
[3]	2.36×10^{11}	7.6	Volman and Brinton (19)
[3*i*]	1×10^{13}	26.0	Estimated
[8]	3.0×10^{11}	0	Estimated
[−8]	5.0×10^{14}	50.0	Estimated
[7]	1.6×10^{13}	0	Ivin and Steacie (20) Shepp and Kutschke (21)
[7*i*]	1×10^{12}	0	Estimated
[7*i'*]	9.0×10^{9}	4.2	*A* estimated; for *E* see text

Can. J. Chem. Downloaded from www.nrcresearchpress.com by 210.87.254.6 on 09/05/12
For personal use only.

These ratios justify one in writing the expression for the maximally inhibited rate as

[vi] $$v \approx k_3 \left(\frac{k_{1i}}{k_{7i}k_8}\right)^{1/2} [C_2H_5CHO]^{3/2},$$

which is in complete agreement with experiment (Fig. 4.).

(4) At high nitric oxide pressures

$$\frac{k_{1i}}{k_1}[NO] \gg 1, \qquad \frac{k_{7i'}}{k_7}K_8{}^2[NO]^2 \gg \left(1 + \frac{k_{7i}K_8[NO]}{k_7}\right),$$

and

$$\frac{k_{3i}}{k_3}K_8[NO] \gg 1.$$

Equation [iv] reduces to

[vii] $$v = 2k_{1i}[C_2H_5CHO][NO] = k_{3i}\left(\frac{k_{1i}}{k_{7i'}}\right)^{1/2}[C_2H_5CHO]^{3/2}[NO]^{1/2}.$$

The inequalities imply that at high nitric oxide pressures reactions [3] and [7*i*] are unimportant in comparison with [3*i*] and [7*i*'] respectively, and the justification for this is as follows:

$$\frac{v_{3i}}{v_3} = \frac{k_{3i}}{k_3}\frac{[C_2H_5NO][C_2H_5CHO]}{[C_2H_5][C_2H_5CHO]} = \frac{k_{3i}K_8}{k_3}[NO],$$

$$\frac{v_{7i'}}{v_{7i}} = \frac{k_{7i'}[C_2H_5NO]^2}{k_{7i}[C_2H_5NO][C_2H_5]} = \frac{k_{7i'}K_8}{k_{7i}}[NO].$$

Insertion of the values of the rate constants from Table I gives, at 540 °C and 60 mm NO,

$$v_3/v_{3i} \approx 10 \text{ and } v_{7i'}/v_{7i} \approx 12.$$

The validity of eq. [vii] was demonstrated above (cf. Fig. 7).

Activation Energies

Further support for eq. [vii] can be obtained from a comparison of the observed and predicted activation energies. Activation energies corresponding to the first and the second terms of eq. [vii] are 36.8 and 42.3 kcal per mole respectively (Fig. 8). The observed activation energy of 36.8 kcal for reaction [1*i*] compares well with its endothermicity, which is 36.4 kcal per mole (calculated on the basis of D(H—NO) = 48.6 kcal and D(C_2H_5CO—H) = 85 kcal per mole; the latter value is assumed by comparison with D(CH_3CO—H) = 85 kcal per mole (17)). The activation energy expression for the second term is

$$E_{3i} + \tfrac{1}{2}(E_{1i} - E_{7i'}) = 42.3 \text{ kcal (experimental value)}.$$

Insertion of values of E_{3i} and E_{1i} from Table I leads to 4.2 kcal per mole for $E_{7i'}$. This value may be compared with 3.9 kcal per mole obtained for the similar reaction

$$CH_3NO + CH_3NO \rightarrow C_2H_6 + 2NO$$

in the pyrolysis of acetaldehyde (14).

The Production of Methane

In the uninhibited reaction only a trace of methane was detected, and it was observed that nitric oxide increases the rate of production of methane. This fact may be explained

Can. J. Chem. Downloaded from www.nrcresearchpress.com by 210.87.254.6 on 09/05/12
For personal use only.

through the occurrence of the following reactions:

$$NO + CH_3CH_2CHO \rightarrow CH_3NO + CH_2CHO$$
$$CH_2CHO \rightarrow CH_3 + CO.$$

Inclusion of these reactions in the scheme of reactions suggested above leads to the same overall kinetics.

According to Norrish and Pratt (22) methane may arise from the oxime decomposition in the following way:

$$C_2H_5NO \rightarrow CH_3CHNOH$$
$$CH_3CHNOH + NO \rightarrow CH_3CHN + HNO_2$$
$$CH_3CHN \rightarrow CH_3 + HCN$$
$$HNO_2 \rightarrow OH + NO.$$

The data in Table II, however, show that methane is produced mainly as a primary product, so that an explanation other than that of Norrish and Pratt is required to account for its formation.

TABLE II

Ratios of CH_4 produced to CO produced
Temperature = 540 °C, $P_{C_2H_5CHO}$ = 100 mm, P_{NO} = 14 mm

% decomposed	CH_4/CO
7.0	0.048
11.7	0.055
16.5	0.044
21.6	0.052
29.7	0.054

The Termination Steps

An important feature of the proposed mechanism is that chain termination in the presence of nitric oxide involves interaction between C_2H_5 and C_2H_5NO, reaction [7*i*], and between two C_2H_5NO molecules, reaction [7*i*']. It has been shown by Pratt and Purnell (23) that, in the decomposition of tetraethyl lead in the presence of nitric oxide at 252 °C, reaction [7*i*] is unimportant in comparison with reactions [9] and [10] and that reaction [10] is entirely heterogeneous. Szabó and Márta (3, 24) have found that nitric oxide is not consumed in the pyrolysis of propionaldehyde at 55 °C; they found that after a reaction was completed a new dose of aldehyde was inhibited to the same extent. This fact suggests that, under the conditions of the pyrolysis of propionaldehyde, reactions [9] and [10] are unimportant in contrast to the suggestion of Pratt and Purnell (23) and that nitric oxide is regenerated in some way. The occurrence of the surface reaction [10] to any significant extent in the pyrolysis of propionaldehyde is also excluded by the fact that the contribution of any heterogeneous reaction in this pyrolysis is negligible (6). Figure 2 shows that the ratio C_2H_4/C_2H_6 is increased by the addition of nitric oxide. Since reaction [6] is, as shown above, unimportant in the presence of nitric oxide, the increase of C_2H_4/C_2H_6 in the presence of nitric oxide and the regeneration of the latter are attributed to the occurrence of reactions [7*i*] and [7*i*']; in other words the removal of ethyl radicals in the presence of nitric oxide takes place by the radical–molecule complex mechanism which has recently been considered theoretically by Eusuf and Laidler (25).

General Conclusions

As in the case of the uninhibited reaction the propionaldehyde pyrolysis in the presence of nitric oxide is a very complex process, and the mechanism proposed is necessarily an

Can. J. Chem. Downloaded from www.nrcresearchpress.com by 210.87.254.6 on 09/05/12
For personal use only.

oversimplification. In our view the general behavior can be explained on the basis of the type of mechanism first proposed by Wojciechowski and Laidler (7), in which initiation involves H abstraction by NO and termination involves species like HNO, CH_3NO, and C_2H_5NO.

A completely different theory of the effect of NO has been proposed by Norrish and Pratt (22), emphasis being placed on the part played by the decomposition of oximes formed as intermediates. In our view this theory is inconsistent with the experimental results on the aldehyde decompositions and does not lead to any general interpretation of the many results that have been obtained on the effect of NO in pyrolysis. In particular it seems impossible to explain, on the basis of the Norrish and Pratt theory, the following important results:

(1) The activation energies for pyrolysis in the presence of excess NO, for a whole series of compounds, are consistent with the view that they relate to the H atom abstraction process, $NO + M \rightarrow HNO + R$.

(2) The fact that a number of clear-cut equations are obtained under various conditions and that these fall into a definite pattern.

(3) The fact that in the aldehyde pyrolyses there is no consumption of NO.

All of these facts have been explained in a self-consistent manner on the basis of the mechanisms put forward from this laboratory.

ACKNOWLEDGMENTS

The authors thank Drs. Margaret H. Back, T. M. Bell, and K. O. Kutschke for extremely valuable comments and discussions. The work was supported by a grant from the American Petroleum Fund, and M. E. wishes to thank the Canadian Commonwealth Scholarships and Fellowships Committee for a scholarship under the tenure of which this work was carried out.

REFERENCES

1. L. A. K. Staveley and C. N. Hinshelwood. J. Chem. Soc. 812 (1936).
2. J. R. E. Smith and C. N. Hinshelwood. Proc. Roy. Soc. London, Ser. A, **180**, 237 (1942).
3. Z. G. Szabó and F. Márta. J. Am. Chem. Soc. **83**, 768 (1961).
4. Z. G. Szabó and F. Márta. Acta Chim. Hung. **32**, 81 (1962).
5. A. Boyer and M. Niclause. J. Chim. Phys. **49**, 354 (1952).
6. S. K. Ho. Proc. Roy. Soc. London, Ser. A, **276**, 278 (1963).
7. B. W. Wojciechowski and K. J. Laidler. Can. J. Chem. **38**, 1027 (1960).
8. B. W. Wojciechowski and K. J. Laidler. Trans. Faraday Soc. **59**, 369 (1963).
9. K. J. Laidler and B. W. Wojciechowski. Proc. Roy. Soc. London, Ser. A, **260**, 103 (1963).
10. K. J. Laidler, N. H. Sagert, and B. W. Wojciechowski. Proc. Roy. Soc. London, Ser. A, **270**, 254 (1962).
11. N. H. Sagert and K. J. Laidler. Can. J. Chem. **41**, 848 (1963).
12. D. J. McKenney, B. W. Wojciechowski, and K. J. Laidler. Can. J. Chem. **41**, 1993 (1963).
13. K. J. Laidler and D. J. McKenney. Proc. Roy. Soc. London, Ser. A, **278**, 517 (1964).
14. M. Eusuf and K. J. Laidler. Can. J. Chem. **42**, 1851 (1964).
15. M. Eusuf and K. J. Laidler. Can. J. Chem. **42**, 1861 (1964).
16. E. E. Hughes. J. Chem. Phys. **35**, 1531 (1961).
17. E. W. R. Steacie. Atomic and free radical reactions. Reinhold Publ. Corp., New York. 1954.
18. F. Márta. Acta Chim. Hung. **31**, 415 (1962).
19. D. H. Volman and R. K. Brinton. J. Chem. Phys. **22**, 929 (1954).
20. K. J. Ivin and E. W. R. Steacie. Proc. Roy. Soc. London, Ser A. **208**, 25 (1951).
21. A. Shepp and K. O. Kutschke. J. Chem. Phys. **26**, 1020 (1957).
22. R. G. Norrish and G. L. Pratt. Nature, **197**, 143 (1963).
23. G. L. Pratt and J. H. Purnell. Trans. Faraday Soc. **60**, 371 (1964).
24. Z. G. Szabó and F. Márta. Acta Chim. Hung. **32**, 69 (1962).
25. M. Eusuf and K. J. Laidler. Trans. Faraday Soc. **59**, 2750 (1963).

Can. J. Chem. Downloaded from www.nrcresearchpress.com by 210.87.254.6 on 09/05/12
For personal use only.

Can. J. Chem. Downloaded from www.nrcresearchpress.com by 210.87.254.105 on 09/05/12
For personal use only.

HYDROLYSIS CONSTANTS OF SOME PLATINUM(II) CHLORO COMPLEXES CONTAINING UNSATURATED LIGANDS

A. D. Allen and T. Theophanides[1]
Lash Miller Laboratories, University of Toronto, Toronto, Ontario
Received August 13, 1964

ABSTRACT

Hydrolysis equilibrium constants have been determined for a series of compounds of the general form $K[LPtCl_3]$, where L is a substituted dialkyl acetylene. The hydrolysis equilibrium position is only slightly affected by the nature of L, indicating that the *trans* metal–chlorine and metal–water bonds are similar in character.

It is now well established that in complexes of bivalent platinum the presence of a strongly *trans*-directing group may or may not lead to weakening of the bond in the *trans* position to this group (1). For ions of the form $[LPtCl_3]^-$, where L is an unsaturated organic ligand, the chlorine *trans* to the ligand L is extremely readily displaced by nucleophilic reagents (2, 6), and infrared studies have shown (3, 4) that the platinum–chlorine bond is weaker than the bonds to the *cis* chlorines. However, it has been found (2, 5) that the hydrolysis equilibrium constant for the reaction

$$[LPtCl_3]^- + H_2O \rightleftharpoons \textit{trans}\text{-}[LPtCl_2H_2O] + Cl^-$$

is smaller for L = ethylene than it is for L = ammonia, a weakly *trans*-directing group, showing that the extent of the hydrolysis does not necessarily depend on the lability of the chlorine displaced.

We have investigated the behavior of a series of related complexes in which L is an acetylenic ligand (ac.). When Zeise salt is dissolved in water hydrolysis occurs and an initial equilibrium is established which involves only the chlorine *trans* to ethylene. On standing, hydrolysis of the *cis* chlorines also occurs, but at a rate which is much slower than that of the *trans* chlorine (2, 14). Preliminary experiments were designed to check whether acetylenic complexes react in a similar manner. Titration of the complexes with standard alkali gives a typical weak acid – strong base titration curve with an end point corresponding to the titration of the aquo complex, *trans*-$[ac.PtCl_2.OH_2]$. This cannot be taken as an indication that one chlorine is completely displaced by water at equilibrium, since the coordinated water is converted to the hydroxide ligand during the titration and further hydrolysis takes place to restore the equilibrium. Important conclusions from this are that the equilibrium position shifts much more rapidly than one can titrate, and that the end point corresponds to the hydrolysis of only one chlorine. From these titrations an estimated value for pK_a of 7.5 was found for the aquo complex *trans*-$(Me_2C(OH)C{\equiv}CC(OH)Me_2)PtCl_2H_2O$. Direct titration with silver nitrate also gives an end point corresponding to the displacement of one chlorine, again confirming the inertness of the *cis* chlorines and the lability of the equilibrium involving the *trans* chlorine.

Equilibrium data for the hydrolysis of the *trans* chlorine were obtained by measuring the concentration of chloride ions displaced from the complex, by a potentiometric method.

[1]*Present address: Department of Chemistry, Howard University, Washington, D.C.*

Can. J. Chem. Downloaded from www.nrcresearchpress.com by 210.87.254.105 on 09/05/12
For personal use only.

EXPERIMENTAL

Materials

The compounds potassium trichloro(2,5-dimethyl-3-hexyne-2,5-diol)platinum(II), potassium trichloro-(2,5-dimethyl-2,5-dimethoxy-3-hexyne)platinum(II), and Zeise salt were prepared as reported previously (4). The following compounds were prepared in a similar manner.

Potassium trichloro(3,6-dimethyl-4-octyne-3,6-diol)platinum(II), yellow crystals 128–130° (decomp.) (lit. (6) 122–124° (decomp.)

Anal. Calcd. for $C_{10}H_{18}O_2Cl_3KPt$: C, 23.5; H, 3.55. Found: C, 23.8; H, 3.56.

Potassium trichloro(3,6-diethyl-4-octyne-3,6-diol)platinum(II), orange–yellow crystals, 114–117° (decomp.)

Anal. Calcd. for $C_{12}H_{22}O_2Cl_3KPt$: C, 26.75; H, 4.1. Found: C, 26.1; H, 4.05.

Equilibrium Measurements

The following cell was used.

$$Ag/AgCl/[ac.PtCl_3]^-, KCl, HClO_4(0.2\ M)//HClO_4(0.2\ M)//KCl, HClO_4(0.2\ M)/AgCl/Ag.$$

Solutions of the complexes in 0.2 *M* perchloric acid do not decompose during the time necessary to perform the experiments and are stable for long periods in the presence of added chloride. In the above cell the added chloride ion concentration was always the same in both half cells, so that any difference in electromotive force was due to chloride ion liberated by hydrolysis of the complex. The cell compartments were separated by small ultrafine porosity sintered glass discs. The silver – silver chloride electrodes were prepared in the manner described by MacInnes and Parker (7), with the modifications, precautions, and improvements suggested by Carmody (8) and Brown (9). The electrodes so prepared were not affected by sunlight, and they gave very low differences in e.m.f. (0.01–0.05 mV) when placed in the same solution.

The cell voltage was measured by a Leeds and Northrup K-2 potentiometer. The cell was immersed in a constant temperature bath during the measurements. "Analar" perchloric acid (70%), (1.66 specific gravity) was diluted with doubly distilled water to give a 0.4 *N* solution. It was found that this solution contained about 3×10^{-5} *M* chloride ions, and this was allowed for in the calculations. Potassium chloride was "Analar" grade, dried for 3 h at 150 °C or 1 h at 300 °C. Stock chloride solutions of 10×10^{-3}, 6×10^{-3}, and 3×10^{-3} *M* were prepared with doubly distilled water.

Determination of the Hydrolysis Constants (K_{aq})

The solutions of the complexes were prepared in small vials by pipetting known volumes of solutions of potassium chloride in 0.2 *N* perchloric acid (10 ml) onto a weighed amount of the complex. The solution was well mixed and was then transferred to one of the cell compartments. To the second compartment was added the same solution of potassium chloride in 0.2 *N* perchloric acid (10 ml). All solutions had previously been kept in the thermostat to reach the appropriate temperature.

The total chloride concentration of the cell was calculated from the formula

$$E = \frac{RT}{F} \ln \frac{(a + x)}{a},$$

where a = concentration of added chloride, and x = chloride derived from the hydrolysis. It was assumed that the activity coefficients of the chloride ion in each half cell were equal since the ionic strengths were almost the same.

The e.m.f. of the cell was measured as soon as possible (about 1 min after mixing) and every minute thereafter for 10 min. In some cases the potential was not constant but drifted slowly downwards and an extrapolation to zero time was used to obtain the e.m.f. of the cell. In most cases, changes were small and the e.m.f. did not drift, so that an average of 8 or 9 readings could be taken.

The cell was checked every time an experiment was performed, using appropriate potassium chloride solutions in 0.2 *N* perchloric acid. The e.m.f. was compared with the theoretical e.m.f. calculated from the formula

$$E = \frac{RT}{F} \ln \frac{a_1}{a_2},$$

where a_1 and a_2 are the potassium chloride concentrations in the two compartments. A small correction for the bias of the electrodes used was applied to these results and the corrected values were used to determine the chloride concentrations. Measurements were made at three temperatures, 10° or 15°, 25°, and 40°.

Equilibrium constants for the hydrolysis were calculated from the equation

$$K_{aq} = \frac{[ac.PtCl_2H_2O]^0[Cl^-]}{[ac.PtCl_3^-]} = \frac{([Cl^-]_{total} - [Cl^-]_{KCl})[Cl^-]_{total}}{([Cpx] + [Cl^-]_{KCl} - [Cl^-]_{total})},$$

where [Cpx] = initial concentration of complex.

Can. J. Chem. Downloaded from www.nrcresearchpress.com by 210.87.254.105 on 09/05/12
For personal use only.

RESULTS AND DISCUSSION

Detailed results and calculated hydrolysis constants are given in Tables I–V. These results are summarized in Table VI, and are compared with data for other platinum(II) chloro complexes in Table VII. The most obvious conclusion to be drawn from Table VII is that all the hydrolysis constants are very similar, showing that the ligand L has little effect on the extent of hydrolysis of the *trans* chlorine. In their paper on the hydrolysis of Zeise's salt (2), Leden and Chatt predicted that this situation might occur. The labilizing effect of a *trans*-directing group is obviously a kinetic one and both the *trans* chloro group in the complex and the *trans*-aquo group in the product are highly susceptible to nucleophilic displacement. The equilibrium position would be changed drastically only if the chloro and aquo groups were very differently affected by the ligand L, which would be the case if, for example, there were substantial π-bonding with one group and not with the other. Absence of large effects shows that the bonding of the chloro and aquo groups to the platinum in these compounds is similar in character.

TABLE I

Equilibrium constants for the hydrolysis of the ion $[Me_2C(OH)C \equiv CC(OH)Me_2PtCl_3]^-$ in 0.2 M $HClO_4$

Temp. (°C)	[Complex] ($\times 10^{-3}$ M)	$[Cl^-]_{KCl}$ ($\times 10^{-3}$ M)	$[Cl^-]_{total}$ ($\times 10^{-3}$ M)	E.m.f. (mV)	10^3 K_{aq} (mole l^{-1})
10	10.26	3.35	5.51	12.16	1.48
	10.65	3.35	6.66	16.84	1.37
	25.40	3.35	7.53	19.80	1.49
25	2.0	3.00	3.70	5.50	1.99
	5.0	3.15	4.66	10.06	2.05
	5.0	3.00	4.60	10.96	2.16
	9.85	3.00	5.46	15.23	1.84
	10.0	3.00	5.74	16.70	2.15
	10.0	3.00	5.62	16.10	1.98
	10.0	3.00	5.60	16.02	1.96
	10.0	4.00	6.32	11.75	1.91
	15.0	5.00	8.08	12.31	2.08
	20.0	4.00	7.64	16.60	1.70
40	5.00	3.00	4.82	12.80	2.80
	8.20	3.35	5.84	15.00	2.55
	10.00	3.35	6.56	18.08	3.00
	21.35	3.35	8.84	25.00	2.65

TABLE II

Equilibrium constants for the hydrolysis of the ion $[EtMeC(OH)C \equiv CC(OH)MeEtPtCl_3]^-$ in 0.2 M $HClO_4$

Temp. (°C)	[Complex] ($\times 10^{-3}$ M)	$[Cl^-]_{KCl}$ ($\times 10^{-3}$ M)	$[Cl^-]_{total}$ ($\times 10^{-3}$ M)	E.m.f. (mV)	10^3 K_{aq} (mole l^{-1})
15	2.00	1.50	2.30	10.58	1.54
	2.00	1.50	2.37	11.41	1.82
	5.00	1.50	3.25	19.20	1.75
	5.00	3.00	4.20	8.33	1.34
25	2.58	3.00	3.97	7.16	2.39
	4.27	3.00	4.46	10.13	2.32
	5.05	3.00	4.64	11.15	2.32
	5.95	3.00	4.85	12.32	2.19
	10.10	3.00	5.73	16.58	2.13
40	5.00	1.50	3.52	23.00	2.40
	6.70	1.50	4.05	26.71	2.46
	10.00	1.50	4.82	31.41	2.40

Can. J. Chem. Downloaded from www.nrcresearchpress.com by 210.87.254.105 on 09/05/12
For personal use only.

TABLE III

Equilibrium constants for the hydrolysis of the ion $[Et_2CO(H)C \equiv CC(OH)Et_2PtCl_3]^-$ in 0.2 M $HClO_4$

Temp. (°C)	[Complex] ($\times 10^{-3}$ M)	$[Cl^-]_{KCl}$ ($\times 10^{-3}$ M)	$[Cl^-]_{total}$ ($\times 10^{-3}$ M)	E.m.f. (mV)	10^3 K_{aq} (mole l^{-1})
10	10.00	3.35	8.11	21.59	7.36
	10.00	3.00	7.71	23.08	6.90
	10.08	3.35	8.09	21.57	7.18
25	5.00	3.00	5.84	17.10	7.68
	10.00	3.00	7.96	25.12	7.85
	10.00	3.00	7.86	24.72	7.44
	10.00	5.00	7.80	24.50	7.21
40	5.00	3.00	5.86	18.06	7.84
	5.00	3.00	5.97	18.53	8.74
	5.64	3.00	6.23	19.69	8.35
	10.00	3.00	8.37	27.94	9.70

TABLE IV

Equilibrium constants for the hydrolysis of the ion $[Me_2C(OMe)C{\equiv}CC(OMe)Me_2PtCl_3]^-$ in 0.2 M $HClO_4$

Temp. (°C)	[Complex] ($\times 10^{-3}$ M)	$[Cl^-]_{KCl}$ ($\times 10^{-3}$ M)	$[Cl^-]_{total}$ ($\times 10^{-3}$ M)	E.m.f. (mV)	10^3 K_{aq} (mole l^{-1})
15	1.96	1.50	2.07	8.05	0.85
	2.37	3.00	3.48	3.66	0.88
	2.62	3.00	3.57	4.31	0.99
	4.25	3.00	3.86	6.26	0.98
25	2.00	1.50	2.25	10.46	1.35
	2.04	1.50	2.31	11.15	1.52
	3.41	3.00	4.01	7.51	1.68
	3.68	3.00	4.06	7.75	1.64
	5.00	3.00	4.25	8.95	1.42
40	1.50	1.50	2.16	9.80	1.70
	1.57	1.50	2.19	10.20	1.70
	2.54	1.50	2.55	14.26	1.80
	3.39	3.00	3.95	7.40	1.55
	6.32	3.00	4.74	12.40	1.80

TABLE V

Equilibrium constants for the hydrolysis of the ion $[C_2H_4PtCl_3]^-$ in 0.2 M $HClO_4$

Temp. (°C)	[Complex] ($\times 10^{-3}$ M)	$[Cl^-]_{KCl}$ ($\times 10^{-3}$ M)	$[Cl^-]_{total}$ ($\times 10^{-3}$ M)	E.m.f. (mV)	10^3 K_{aq} (mole l^{-1})
25	1.91	1.50	2.46	12.72	2.48
	1.91	1.50	2.49	12.95	2.70
	4.76	1.50	3.45	21.43	2.40
	5.00	1.50	3.27	20.00	2.50
	9.52	3.00	5.79	16.90	2.40

We have been interested in the role of the hydroxyl groups in the bonding of the ligand $Me_2C(OH)C{\equiv}CC(OH)Me_2$ to the metal atom. Chatt *et al.* (10) originally attributed the unexpectedly high stability of these complexes to an interaction between the metal and the hydroxyl groups, either via hydrogen bond or by coordination of oxygen to the metal. More recently Chatt *et al.* (6) have proposed a structure in which the hydroxyl groups are linked by hydrogen bonds to the *cis* chlorines. If the formation of hydrogen bonds is an important part of the link between the unsaturated ligand and the metal, we would

TABLE VI

Complex	Temp. (°C)	$10^3 K_{aq}$ (mole l^{-1})
$K[Pt(Me_2C(OH)C{\equiv}CC(OH)Me_2)Cl_3]$	10	1.5
	25	2.0
	40	2.8
$K[Pt(MeEtC(OH)C{\equiv}CC(OH)MeEt)Cl_3]$	15	1.6
	25	2.3
	40	2.4
$K[Pt(Et_2C(OH)C{\equiv}CC(OH)Et_2)Cl_3]$	10	7.1
	25	7.5
	40	8.6
$K[Pt(Me_2C(OMe)C{\equiv}CC(OMe)Me_2)Cl_3]$	15	0.9
	25	1.5
	40	1.7
$K[Pt(C_2H_4)Cl_3]$	25	2.5

TABLE VII

Equilibrium hydrolysis constants of some platinum(II) complexes in aqueous solution at 25 °C

Complex ion	$10^3 K_{aq}$ (mole l^{-1})	Ref.
$PtCl_4^=$	18.0	11
$Pt(H_2O)Cl_3^-$	1.0	12
$Pt(NH_3)Cl_3^-$	14.4	5
$Pt(C_2H_4)Cl_3^-$	2.5*	
$Pt(Me_2C(OH)C{\equiv}CC(OH)Me_2)Cl_3^-$	2.0	
$Pt(MeEtC(OH)C{\equiv}CC(OH)MeEt]Cl_3^-$	2.3	
$Pt(Me_2C(OMe)C{\equiv}CC(OMe)Me_2)Cl_3^-$	1.5	
$Pt(Et_2C(OH)C{\equiv}CC(OH)Et_2)Cl_3^-$	7.5	

*Leden and Chatt (2) report a value of $3.0 \pm 0.5 \times 10^{-3}$ for this compound.

expect the dimethyl ether of this glycol to form a less stable complex. It not surprising that our equilibrium results do not reveal any significant differences between the two complexes, but the complex containing the dimethyl ether of the glycol is actually the more stable in air, has a slightly higher decomposition temperature, and is just as stable in the solutions used in this work. While these observations provide only qualitative indications, it is clear that the absence of hydrogen bonding does not seriously effect the stability of the compounds.

From the variation of the equilibrium constants with temperature it is possible to obtain approximate values for the enthalpy, free energy, and entropy of these reactions. For the hydrolysis of the complex of the glycol $Me_2C(OH)C{\equiv}CC(OH)Me_2$ we find $\Delta H^0 = 3.4$ kcal, $\Delta F^0 = 3.7$ kcal, and $\Delta S^0 = -1$ entropy unit at 25°. These values are similar to those found for the hydrolysis of $[Pt(NH_3)Cl_3]^-$ (5). For the complex of the above glycol the effect of ionic strength was also determined, giving values of K_{aq} (25°) $= 2.0 \times 10^{-3}$ at 0.02 M $HClO_4$, 2.0×10^{-3} at 0.04 M $HClO_4$, and 1.0×10^{-3} at 2 M $HClO_4$. This slight decrease with increase of ionic strength is in accordance with the expected dependence of the activity coefficients on ionic strength (13).

REFERENCES

1. D. M. Adams, J. Chatt, J. Gerratt, and A. D. Westland. J. Chem. Soc. 734 (1964).
2. I. Leden and J. Chatt. J. Chem. Soc. 2936 (1955).
3. D. M. Adams and J. Chatt. J. Chem. Soc. 2821 (1961).
4. A. D. Allen and T. Theophanides. Can. J. Chem. **42**, 1551 (1964).
5. T. S. Elleman, J. W. Reishus, and D. S. Martin, Jr. J. Am. Chem. Soc. **80**, 536 (1958).
6. J. Chatt, R. G. Guy, L. A. Duncanson, and D. T. Thompson. J. Chem. Soc. 5170 (1963).
7. D. A. MacInnes and K. Parker. J. Am. Chem. Soc. **37**, 1445 (1915).

Can. J. Chem. Downloaded from www.nrcresearchpress.com by 210.87.254.105 on 09/05/12
For personal use only.

8. W. R. CARMODY. J. Am. Chem. Soc. **51**, 2901 (1929).
9. A. S. BROWN. J. Am. Chem. Soc. **56**, 646 (1934).
10. J. CHATT, L. A. DUNCANSON, and R. G. GUY. Nature, **184**, 526 (1959).
11. L. F. GRANTHAM, T. S. ELLEMAN, and D. S. MARTIN, JR. J. Am. Chem. Soc. **77**, 2965 (1955).
12. C. I. SANDERS and D. S. MARTIN, JR. J. Am. Chem. Soc. **83**, 807 (1961).
13. G. D. PINCHING and R. G. BATES. J. Research Natl. Bur. Standards, **40**, 405 (1948).
14. S. J. LOKKEN and D. S. MARTIN, JR. Inorg. Chem. **2**, 562 (1963).

Can. J. Chem. Downloaded from www.nrcresearchpress.com by 210.87.254.105 on 09/05/12
For personal use only.

Can. J. Chem. Downloaded from www.nrcresearchpress.com by 210.87.254.42 on 09/05/12
For personal use only.

THERMAL INDOLIZATION OF ARYLHYDRAZONES

A. H. KELLY, D. H. MCLEOD, AND J. PARRICK
Department of Chemistry, Rutherford College of Technology, Newcastle-upon-Tyne, England

Received June 22, 1964

ABSTRACT

Thermal cyclization of arylhydrazones in the absence of acid catalyst has been investigated. Indole was not obtained from acetaldehyde phenylhydrazone; aniline, N-ethylaniline, and an unidentified compound were isolated. Phenylhydrazones of cyclohexanone and cyclopentanone and their 2-substituted derivatives were cyclized, often in good yield, to the indole and indolenine; the nature of the substituent markedly influences the ratio of the two products. Gas–liquid chromatographic analysis of the reaction mixture from indolization of two arylhydrazones revealed no crossed products. Nitrophenylhydrazones do not cyclize in good yield, but thermal indolization of some pyridylhydrazones is a good method for the preparation of pyrrolopyridines.

One of the most useful methods available for the preparation of indoles is the acid-catalyzed cyclization of phenylhydrazones discovered by Fischer (1). Many Brønsted and Lewis acids have been used as catalysts. The mechanism of the reaction was investigated by Robinson and the proposed intramolecular cyclization process has been accepted by later workers, with some slight modification. A review of the mechanism and some aspects of the synthetic utility of the reaction has appeared recently (2).

Early work led to the idea that an acid catalyst and a high temperature were essential for a successful Fischer indole synthesis. However, later work (3) has shown that the acid may assist in the first stage of the reaction, i.e. the tautomerization of the hydrazone to the enehydrazine, but is not generally essential for this or later stages of the cyclization. The early ideas may explain why an observation (4) that distillation of acetophenone phenylhydrazone gave some 2-phenylindole was ignored, until Fitzpatrick and Hiser (5) reported several phenylhydrazones were converted into the corresponding indoles on boiling a solution of the phenylhydrazone in a suitable high-boiling solvent. The reaction occurred in the absence of any acid catalyst and, indeed, in one case, in the presence of sodium hydroxide. The examples quoted by Fitzpatrick and Hiser were somewhat limited in variety. Since the reaction has obvious interest and application due to the experimental simplicity, we have investigated this thermal indolization reaction.

Indole cannot be prepared by the acid-catalyzed cyclization of acetaldehyde phenylhydrazone, though propionaldehyde and higher aldehyde phenylhydrazones do give the 3-alkylindoles (2). Fitzpatrick and Hiser (5) report the thermal cyclization of propionaldehyde *p*-tolylhydrazone but make no mention of attempts to cyclize acetaldehyde phenylhydrazone. Our efforts to obtain indole in this way were unsuccessful, though ammonia was evolved from the reaction mixture. The product consisted of a steam-volatile fraction and a nonvolatile black residue. Fractional distillation of the volatile material yielded N-ethylaniline, aniline, and an unidentified component. Since our experiments were completed, Robinson (2) has recorded that he was unable to obtain indole by this technique, though the formation of ammonia was again noted. The evolution of ammonia (possibly accompanied by other basic gas) is not a reliable indication of the formation of an indole, nor is the rate of evolution of the basic gas always a trustworthy criterion on which to judge the optimum reaction time. It seems likely that, in certain cases, two competing reactions may occur; one leading to the indole and the other giving polymeric products. Both reactions involve the evolution of basic gas.

TABLE I

Phenylhydrazone of:	Thermal cyclization		Acetic acid (7)	Sulfuric acid (7)
	Indolenine (II) (%)	Indole (III) (%)	Indole (%)	Indole (%)
Cyclohexanone	0	100	100	100
2-Methylcyclohexanone	51	49	9	68
2-*n*-Propylcyclohexanone	28	72	—	—
2-Phenylcyclohexanone	13	87	28	73
2-Cyclohexylcyclohexanone	4	96	10	63

Acid-catalyzed cyclization of phenylhydrazones from aldehydes or ketones having only one hydrogen on the α-carbon atoms give indolenines (I). Robinson (6) has used the thermal cyclization technique to prepare such compounds. Pausacker (7) has shown that the ratio of 1,2,3,4-tetrahydrocarbazolenine (II, $n = 4$, R = alkyl or aryl) to 1,2,3,4-tetrahydrocarbazole (III, $n = 3$, R = H, R′ = alkyl or aryl), formed by acid-catalyzed cyclization of 2-substituted cyclohexanone phenylhydrazones, depends on the nature of the acid catalyst: glacial acetic acid favored the formation of the tetrahydrocarbazolenine, while dilute sulfuric acid gave the tetrahydrocarbazole preferentially. We find that 1,2,3,4-tetrahydrocarbazole (III, $n = 3$, R = R′ = H) (83% yield) is obtained by boiling a solution of cyclohexanone phenylhydrazone in diethylene glycol. Thermal cyclization of 2-methyl-, 2-*n*-propyl-, 2-phenyl-, and 2-cyclohexyl-cyclohexanone phenylhydrazones gave mixtures of the corresponding 1,2,3,4-tetrahydrocarbazolenine (II, $n = 4$, R = CH_3, C_3H_7, C_6H_5, and C_6H_{11}) and 1,2,3,4-tetrahydrocarbazole (III, $n = 3$, R = H, R′ = CH_3, C_3H_7, C_6H_5, and C_6H_{11}) in the proportions shown in Table I. The high proportion of tetrahydrocarbazole resembles the results for the dilute sulfuric acid catalyzed cyclizations (7), but the steric size of the substituent has a more marked effect on the ratio of products from the thermal cyclizations than in the acid-catalyzed indolization.

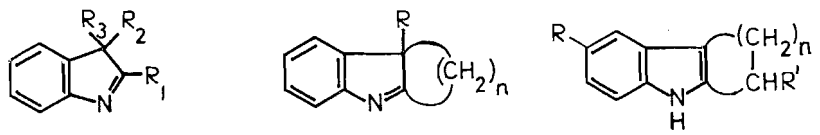

I II III

When an indole shows exceptional acid sensitivity, the thermal cyclization technique appeared to offer advantages over the acid-catalyzed procedure. For example, 1,2,3,4-tetrahydrocyclopent[*b*]indole (III, $n = 2$, R = R′ = H) rapidly forms a red gum in the presence of an acid, and previous preparations (8) have used dilute sulfuric acid catalyzed indolization of cyclopentanone phenylhydrazone and extraction of the indole from the gum. 8*b*-Alkyl-1,2,3,8*b*-tetrahydrocyclopent[*b*]indoles (II, $n = 3$, R = alkyl) were not known; a reported attempt to cause indolization of 2-ethylcyclopentanone phenylhydrazone by acid-catalyzed procedure failed (9). 1,2,3,8*b*-Tetrahydrocyclopent[*b*]indole (III, $n = 2$, R = R′ = H) was now obtained in high yield by the thermal cyclization technique and was more stable than that obtained by the acid-catalyzed process. Further, 1,2,3,8*b*-tetrahydro-8*b*-methylcyclopent[*b*]indole (II, $n = 3$, R = CH_3) and the indole (III, $n = 2$, R = H, R′ = CH_3) were obtained, though in poor yield, by thermal cyclization of 2-methylcyclopentanone phenylhydrazone, while attempts to cause indolization

Can. J. Chem. Downloaded from www.nrcresearchpress.com by 210.87.254.42 on 09/05/12
For personal use only.

in the presence of glacial acetic acid, dilute sulfuric acid or zinc chloride gave only intractable material. However, attempts to obtain 1,4-dihydro-4-methyl-1-phenylcyclopent[*b*] indole (V) by thermal cyclization of 3-phenylcyclopent-2-en-1-one α-methylphenylhydrazone failed.

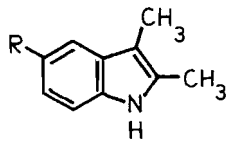

IV

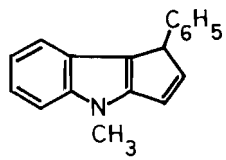

V

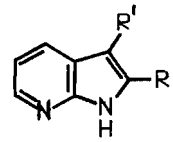

VI

It has been suggested (10), on the basis of the isolation of crossed products, that the acid-catalyzed formation of indoles may occur by a free radical mechanism. This idea was later shown to be erroneous (11): crossed products having been formed by hydrolysis of the arylhydrazones and formation of crossed arylhydrazones, or direct transhydrazonation (12), and subsequent cyclization. Any tendency towards a free radical type of mechanism would be expected to be favored by the purely thermal cyclization technique. Consequently we have analyzed the products of the thermal cyclization of two separate pairs of arylhydrazones.

1,2,3,4-Tetrahydrocarbazole (III, $n = 3$, R = R′ = H), 1,2,3,4-tetrahydro-6-methylcarbazole (III, $n = 3$, R = CH_3, R′ = H), 1,2,3,8*b*-tetrahydrocyclopent[*b*]indole (III, $n = 2$, R = R′ = H) were prepared in high yield by thermal cyclization of the corresponding arylhydrazones. An analytical separation of these three was achieved by gas–liquid chromatography, but (III, $n = 2$, R = CH_3, R′ = H) was not separated from (III, $n = 3$, R = R′ = H). Gas–liquid chromatographic analysis of the reaction product from the thermal indolization of a mixture of cyclopentanone phenylhydrazone and cyclohexanone *p*-tolylhydrazone in diethylene glycol showed the presence of neither (III, $n = 2$, R = CH_3, R′ = H) nor (III, $n = 3$, R = R′ = H), only the expected (III, $n = 2$, R = R′ = H) and (III, $n = 3$, R = CH_3, R′ = H) were found. A similar experiment involving the indolization of cyclohexanone phenylhydrazone and ethyl methyl ketone *p*-tolylhydrazone in the same reaction mixture gave only 2,3,5-trimethylindole (IV, R = CH_3) and 1,2,3,4-tetrahydrocarbazole, no 2,3-dimethylindole (IV, R = H) or 1,2,3,4-tetrahydro-6-methylcarbazole (III, $n = 3$, R = CH_3, R′ = H) were present: in this experiment all four possible products were resolved by gas–liquid chromatography. These results, together with the high yields frequently obtained, indicate that thermal indolization of arylhydrazones does not proceed by free radical mechanism.

Arylhydrazones containing an electron-deficient aromatic nucleus undergo acid-catalyzed indolization much less rapidly than the corresponding phenylhydrazones (2). Thus, nitrophenylhydrazones cyclize with some difficulty and the choice of catalyst is critical (13). We find that thermal cyclization of cyclohexanone *p*-nitrophenylhydrazone to the nitrotetrahydrocarbazole (III, $n = 3$, R = NO_2, R′ = H) occurs in only poor yield. Addition of cuprous chloride to the reaction mixture caused a more rapid evolution of ammonia, but no increase in the yield of (III, $n = 3$, R = NO_2, R′ = H).

Pyridylhydrazones also contain an electron-deficient nucleus, but have the additional feature that in acid solution further deactivation occurs due to protonation of the pyridyl nucleus. Attempts to use acid catalysts in the cyclization of these compounds have had little success, and Robison (14) concluded that only those 2-pyridylhydrazones cyclize

Can. J. Chem. Downloaded from www.nrcresearchpress.com by 210.87.254.42 on 09/05/12
For personal use only.

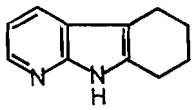

VII

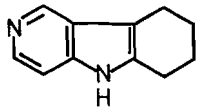

VIII

to the pyrrolo[2,3-*b*]pyridine (VI, R = R′ = H), where the corresponding phenylhydrazones cyclize with extreme ease. Cyclohexanone and benzyl phenyl ketone 2-pyridylhydrazones have been cyclized, using polyphosphoric acid as catalyst, to 6,7,8,9-tetrahydro-α-carboline (VII) and 2,3-diphenylpyrrolo[2,3-*b*]pyridine (VI, R = R′ = C_6H_5); the yields were 53% and 12%. Thermal cyclization in diethylene glycol gave yields of 70% and 56% respectively.

Indolization of pyridylhydrazones by fusion with zinc chloride has been reported in some cases, the product being first obtained as the chlorozincate. Mann *et al.* (15) obtained a chlorozincate (2.8 g) on fusion of cyclohexanone 4-pyridylhydrazone (2 g) with an excess of zinc chloride, and then obtained 6,7,8,9-tetrahydro-γ-carboline (VIII) in unspecified yield. Thermal cyclization afforded the tetrahydro-γ-carboline (VIII) directly in 95% yield. The high yields obtained in these thermal cyclizations of pyridylhydrazones are surprising, and in marked contrast to the results with nitrophenylhydrazones. Details of further applications of thermal indolization to the preparation of pyrrolopyridines will be reported elsewhere.

EXPERIMENTAL

Infrared spectra were recorded on a Grubb Parsons GS3 spectrophotometer. Gas–liquid chromatography apparatus was a Pye Argon Chromatograph.

Attempted Indolization of Acetaldehyde Phenylhydrazone

Acetaldehyde phenylhydrazone (65 g) in diethylene glycol (300 ml) was boiled under reflux for 5 days. Ammonia was evolved during this time and the mixture darkened. The mixture was steam distilled to give a volatile fraction and much residual black tar, which was not investigated further. The distillate was extracted with ether and dried (Na_2SO_4), the ether removed, and the pale yellow oil (11.4 g) fractionally distilled to give fraction (i), b.p. 44–50° at 2.5 mm (3.7 g), redistilled and collected over the range 64–66° at 8 mm, n_D^{21} 1.5840, and identified as aniline by conversion to acetanilide; fraction (ii), b.p. 62–68° at 2.5 mm (5.5 g), was found to contain basic and neutral components. The basic compound was separated by extraction with acid in the usual way and distilled, b.p. 86–90° at 10 mm (0.6 g), n_D^{23} 1.5536, and identified as mainly N-ethylaniline by formation of a picrate and melting point mixed melting point with an authentic sample, 130–132°. The non-basic component was distilled, b.p. 84–88° at 10 mm (1.7 g) n_D^{21} 1.5998.

Anal. Calcd. for C_6H_6N: C, 78.3; H, 6.5; N, 15.2. Found: C, 78.2; H, 6.3; N, 15.2.

The infrared spectrum showed absorption at 3 413 cm^{-1}. The Ehrlich test was positive, but the compound was not investigated further.

Thermal Indolization of Phenyl- and p-Tolylhydrazones

The general method adopted was to prepare the arylhydrazone from the corresponding arylhydrazine and ketone by standard procedure, and to purify the product by distillation under reduced pressure or crystallization. A 10–20% solution of the arylhydrazone, in ethylene glycol or diethylene glycol, was boiled under reflux for a few hours and then poured into ice water. The solid was filtered off and recrystallized. Reaction conditions and yields are recorded in Table II. The indoles, with one exception (III, *n* = 2, R = CH_3, R′ = H), were known compounds and had melting points in accordance with the literature values.

1,2,3,4-Tetrahydro-7-methylcyclopent[b]indole (III, n = 2, R = CH_3, R′ = H) crystallized from petroleum ether (b.p. 60–80°) as colorless prisms, m.p. 116–118°.

Anal. Calcd. for $C_{12}H_{13}N$: C, 84.3; H, 7.6. Found: C, 84.6; H, 7.8.

It gave a *picrate* as brown needles from aqueous ethanol, m.p. 145–147° (decomp.).

Anal. Calcd. for $C_{18}H_{16}N_4O_7$: C, 54.0; H, 4.0. Found: C, 53.6; H, 4.2.

Indolization of 2-Substituted Cyclohexanone Phenylhydrazones

Phenylhydrazones of 2-methyl-, 2-*n*-propyl-, 2-phenyl-, and 2-cyclohexyl-cyclohexanone were prepared from the corresponding 2-substituted cyclohexanones and phenylhydrazine. The indolization procedure

Can. J. Chem. Downloaded from www.nrcresearchpress.com by 210.87.254.42 on 09/05/12
For personal use only.

TABLE II

R.C_6H_4.-NH.NH_2	Ketone	Solvent*	Time (h)	Product	Yield (%)
R = H	Cyclohexanone	DEG	1	III, n = 3, R = R′ = H	83†
R = H	Cyclopentanone	DEG	1	III, n = 2, R = R′ = H	78‡
R = H	Ethyl methyl ketone	EG	3	IV, R = H	65‡
R = *p*-CH_3	Cyclohexanone	DEG	12	III, n = 3, R = CH_3, R′ = H	73‡
R = *p*-CH_3	Cyclopentanone	DEG	1	III, n = 2, R = CH_3, R′ = H	56‡
R = *p*-CH_3	Ethyl methyl ketone	EG	3	IV, R = CH_3	68‡

*Abbreviations: EG = ethylene glycol; DEG = diethylene glycol.
†Crystallization from ethanol.
‡Crystallization from light petroleum.

adopted was that a phenylhydrazone (10 g), in diethylene glycol (30 ml), was gently boiled under reflux for 2 h. After pouring into water, the mixture was extracted with ether, and the ethereal solution washed with dilute hydrochloric acid (3 × 25 ml). The acid washings were added to an excess of ice-cold, dilute sodium hydroxide solution. Any solid product was filtered off and recrystallized. When an oil was formed, it was extracted with ether and the indolenine distilled under reduced pressure. The above acid-washed, ethereal solution was washed with water, dried (Na_2SO_4), and filtered, the ether distilled off, and the indole crystallized.

2-Methylcyclohexanone phenylhydrazone gave 1,2,3,4-tetrahydro-11-methylcarbazolenine (II, $n = 4$, $R = CH_3$) (3.5 g), b.p. 120–126° at 1 mm, crystallized from alcohol, m.p. 68–69° (lit. m.p. 69° (9)) and 1,2,3,4-tetrahydro-1-methylcarbazole (III, $n = 3$, R = H, R′ = CH_3) (3.4 g), recrystallized from aqueous ethanol, m.p. 66–68° (lit. m.p. 69° (7)).

2-*n*-Propylcyclohexanone phenylhydrazone yielded 1,2,3,4-tetrahydro-11-*n*-propylcarbazolenine (II, $n = 4$, R = *n*-C_3H_7) (1.2 g), b.p. 120–144° at 0.5–1 mm, crystallized from petroleum ether (b.p. 60–80°), m.p. 137–139° (lit. m.p. 139° (10)) and *1,2,3,4-tetrahydro-1-n-propylcarbazole (III, n = 3, R = H, R′ =* *n*-C_3H_7) (3.1 g), recrystallized as colorless needles from benzene, m.p. 151–152°.

Anal. calcd. for $C_{15}H_{19}N$: C, 84.6; H, 8.9. Found: C, 84.5; H, 8.9.

Picrate crystallized as brown plates from ethanol, m.p. 116–118°.

Anal. Calcd. for $C_{21}H_{22}N_4O_7$: C, 57.1; H, 5.0. Found: C, 56.8; H, 4.8.

2-Phenylcyclohexanone phenylhydrazone afforded 1,2,3,4-tetrahydro-11-phenylcarbazolenine (II, $n = 4$, R = C_6H_5), b.p. 175–186° at 1.5 mm (0.6 g), crystallized from petroleum ether (b.p. 60–80°), m.p. 122–124° (lit. m.p. 125° (7)) and 1,2,3,4-tetrahydro-1-phenylcarbazole (III, $n = 3$, R = H, R′ = C_6H_5) (3.9 g), recrystallized from petroleum ether (b.p. 40–60°), m.p. 97–99° (lit. m.p. 99° (7)).

2-Cyclohexylcyclohexanone phenylhydrazone gave 11-cyclohexyl-1,2,3,4-tetrahydrocarbazolenine (II, $n = 4$, R = C_6H_{11}) (0.2 g), recrystallized from petroleum ether (b.p. 60–80°), m.p. 76–78° (lit. m.p. 79° (7)) and 1-cyclohexyl-1,2,3,4-tetrahydrocarbazole (III, $n = 3$, R = H, R′ = C_6H_{11}) (4.9 g), b.p. 201–206° at 1 mm, crystallized from petroleum ether (b.p. 60°–80°) m.p. 137–139° (lit. m.p. 140° (7)).

1,2,3,8b-Tetrahydro-8b-methylcyclopent[b]indole (II, n = 3, R = CH_3) and 1,2,3,4-tetrahydro-3-methylcyclopent[b]indole (III, n = 2, R = H, R′ = CH_3)

2-Methylcyclopentanone (2.64 g) and phenylhydrazine (2.9 g) were mixed, and, after the initial exothermic reaction had slackened, the mixture was warmed on a water bath for 30 min. The water produced was removed by azeotropic distillation with benzene. The hydrazone, in diethylene glycol (20 ml), was boiled under reflux for 2 h and then poured into ice water. The oil was extracted with ether and quickly separated into basic and neutral fractions by extraction with dilute hydrochloric acid in the usual way. The basic fraction was distilled, b.p. 94–96° at 0.5 mm, as a colorless oil (0.57 g). Treatment with ethanolic picrolonic acid afforded *1,2,3,8b-tetrahydro-8b-methyl-cyclopent[b]indole picrolonate* as yellow prisms, m.p. 219–221° (decomp.).

Anal. Calcd. for $C_{22}H_{21}N_5O_5$: C, 60.1; H, 4.8; N, 16.1. Found: C, 59.7; H, 5.0; N, 15.6. The neutral fraction was distilled, b.p. 116–124° at 0.8 mm, as a colorless oil (0.12 g). Addition of ethanolic picric acid gave *1,2,3,4-tetrahydro-3-methylcyclopent[b]indole picrate*, recrystallized as dark-red needles from aqueous ethanol, m.p. 132–134°.

Anal. Calcd. for $C_{18}H_{16}N_4O_7$: C, 54.0; H, 4.0. Found: C, 54.2; H, 4.1.

Attempted Preparation of 1,4-Dihydro-4-methyl-1-phenylcyclopent[b]indole (V)

3-Phenylcyclopent-2-en-1-one (3.2 g) and α-methylphenylhydrazine (2.4 g) were mixed and, after the addition of glacial acetic acid (2 drops), warmed on a water bath for 30 min. Benzene was added and the water removed by azeotropic distillation. The *phenylhydrazone* was crystallized from ethanol as yellow prisms (4.4 g), m.p. 113–114°.

Anal. Calcd. for $C_{18}H_{18}N_2$: C, 82.5; H, 6.8. Found: C, 82.2; H, 7.0.

When a solution of this phenylhydrazone in ethylene glycol (or diethylene glycol) was boiled under reflux in a nitrogen atmosphere a basic gas was evolved, but, after pouring the reaction mixture into water, the only product isolated was a black, friable amorphous solid.

Can. J. Chem. Downloaded from www.nrcresearchpress.com by 210.87.254.42 on 09/05/12
For personal use only.

Indolization of Mixtures of Arylhydrazones

(i) A mixture of freshly prepared cyclopentanone phenylhydrazone (1 g) and cyclohexanone *p*-tolylhydrazone (1 g), in diethylene glycol (10 ml), was boiled under reflux for 1 h and then poured into water. The oil was extracted with benzene, washed with water, and dried (Na_2SO_4). The benzene solution was submitted to gas–liquid chromatography in a column of 4% silicone oil on celite 545 (80–100 mesh) at 150°, packed in 4 ft of 5 mm (outside diameter) glass tubing, and using argon as the carrier gas at a flow rate of 20 ml/min. Retention times were measured relative to that for 1,2,3,4-tetrahydrocarbazole (III, $n = 3$, R = R′ = H) (15 min). The two peaks obtained had relative retention time (r.r.t.) of 0.68 and 1.54 and were shown to be due to 1,2,3,4-tetrahydrocyclopent[b]indole (III, $n = 2$, R = R′ = H) and 1,2,3,4-tetrahydro-6-methylcarbazole (III, $n = 3$, R = CH_3, R′ = H). 1,2,3,4-Tetrahydro-7-methylcyclopent[b]indole (III, $n = 2$, R = CH_3, R′ = H) had r.r.t. 1.02.

(ii) A similar reaction was performed with a mixture of cyclohexanone *p*-tolylhydrazone and ethyl methyl ketone phenylhydrazone. Gas–liquid chromatography in a column of 4% Apiezon L on celite 545 at 200°, in a tube of the dimensions mentioned above and at the same gas flow rate, gave two peaks, r.r.t. 0.23 and 1.27, identified as due to 1,2,3,4-tetrahydro-6-methylcarbazole (III, $n = 3$, R = CH_3, R′ = H) and 2,3-dimethylindole (IV, R = H). 1,2,3,4-Tetrahydrocarbazole had a retention time of 22.5 min and 2,3,5-trimethylindole (IV, R = CH_3) had r.r.t. 0.59.

1,2,3,4-Tetrahydro-6-nitrocarbazole (III, $n = 3$, R = NO_2, R′ = H)

Cyclohexanone *p*-nitrophenylhydrazone (3 g), in diethylene glycol (20 ml), was boiled under reflux until evolution of ammonia ceased (10 h) and then poured into water. The solid (2.1 g) was extracted with boiling benzene (2 × 50 ml). The benzene solution was passed down an alumina column and afforded an upper brown band and a lower yellow band. The latter was eluted with more benzene, and the benzene solution concentrated to give yellow prisms (0.1 g), m.p. 176–178° (lit. m.p. 177° (13)).

6,7,8,9-Tetrahydro-α-carboline (VII)

Cyclohexanone 2-pyridylhydrazone (14) (4.25 g) in diethylene glycol (20 ml) was boiled under reflux for 7 h. Ammonia was evolved and the solution became red-brown. After cooling, the mixture was poured into ice water and the solid (2.7 g) filtered off. Recrystallization from petroleum ether (b.p. 60–80°) gave pale cream needles, m.p. 153.5–154.5° (lit. m.p. 156° (14)).

2,3-Diphenylpyrrolo[2,3-b]pyridine (VI, R = R′ = C_6H_5)

Benzyl phenyl ketone 2-pyridylhydrazone (14) (6.5 g) in diethylene glycol (20 ml) was boiled under reflux for 7 h. After cooling, the solid was filtered off and washed with water. The dry solid (3.4 g, 56%) was sublimed, 230° at 1.5 mm, to give a pale cream solid m.p. 293–295° (lit. m.p. 293.5° (14)).

6,7,8,9-Tetrahydro-γ-carboline (VIII)

Cyclohexanone 4-pyridylhydrazone (15) (3 g), in diethylene glycol (20 ml), was boiled under reflux for 11 h. After cooling, the mixture was poured into water and the solid filtered off. The light brown solid (2.6 g, 95%) was recrystallized from aqueous ethanol (charcoal) to give colorless prisms, m.p. 268.5–270° (lit. m.p. 272° (15)).

ACKNOWLEDGMENTS

Part of this work was done as a project for the diploma in Technology while employed (D. H. McL.) by Winthrop Laboratories Ltd. We gratefully acknowledge the award (A. H. K.) of a research studentship by Newcastle-upon-Tyne Education Committee and our indebtedness to Mr. R. Hindson for technical assistance.

REFERENCES

1. E. Fischer and F. Jourdan. Ber. **16**, 2241 (1883). E. Fischer and O. Hess. Ber. **17**, 559 (1884).
2. B. Robinson. Chem. Rev. **63**, 373 (1963).
3. N. N. Suvorov and N. P. Sorokina. Doklady Akad. Nauk S.S.S.R. **136**, 840 (1961).
4. L. Wolff. Ann. **394**, 86 (1912).
5. J. T. Fitzpatrick and R. D. Hiser. J. Org. Chem. **22**, 1703 (1957).
6. B. Robinson. Tetrahedron Letters, 139 (1962).
7. K. H. Pausacker. J. Chem. Soc. 621 (1950).
8. W. H. Perkin and S. G. P. Plant. J. Chem. Soc. 3242 (1923).
9. N. P. Buu-Hoï, P. Jacquignon, and T. B. Loc. J. Chem. Soc. 738 (1958).
10. K. H. Pausacker and C. I. Schubert. J. Chem. Soc. 1384 (1949).
11. P. H. Gore, G. K. Hughes, and E. Ritchie. Nature, **164**, 835 (1949).
12. A. E. Arbuzov and Y. P. Kitaev. Tr. Kazansk. Khim. Tekhnol. Inst. **23**, 60 (1957).
13. D. S. Deohra and S. S. Joshi. J. Org. Chem. **26**, 3527 (1961).
14. S. Okuda and M. M. Robison. J. Am. Chem. Soc. **81**, 740 (1959).
15. F. G. Mann, A. F. Prior, and T. J. Wilcox. J. Chem. Soc. 3830 (1959).

Can. J. Chem. Downloaded from www.nrcresearchpress.com by 210.87.254.42 on 09/05/12
For personal use only.

Can. J. Chem. Downloaded from www.nrcresearchpress.com by 210.87.254.5 on 09/05/12
For personal use only.

NOTES

THE OPTICAL ACTIVITY OF FUCOXANTHIN

N. J. Antia

Fucoxanthin has been shown to be the predominant plastid carotenoid pigment of brown algae (Phaeophyceae), diatoms, and Chrysophyceae, with evidence for direct participation in photosynthesis by light activation (1). Although extensively studied by several investigators (see Jensen (2) for the most recent work and citation of the earlier literature), its chemical structure has remained undetermined and the question of its optical activity unresolved. Karrer *et al.* (3) reported the compound to be optically active ($[\alpha]_C$ +72.5°) but subsequent investigators (4) have claimed it to be inactive. The discrepancy appears to be due to the problem of making measurements in the spectral region dictated by standard polarimetric equipment but where fucoxanthin shows strong light absorption thereby necessitating the use of concentrations too low to register reliable activity readings. The recent development of spectropolarimeters has now offered an excellent opportunity to reexamine the problem by measuring the optical activity of fucoxanthin over the widest possible spectral range especially in regions where light absorption of the compound is low enough not to interfere.

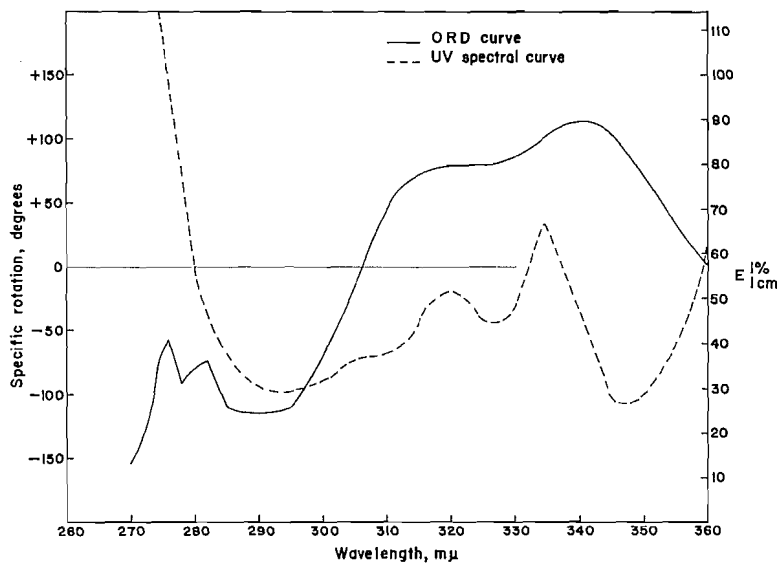

FIG. 1. The rotatory dispersion and ultraviolet absorption of fucoxanthin.

Crystalline fucoxanthin isolated from *Sargassum muticum* by Parsons and Strickland (5) was used in the present study. A sample was scanned in *p*-dioxane solution (*c*, 0.0175)

from 600 to 240 mμ and the only region showing measurable rotation was that between 360 and 270 mμ. The optical rotatory dispersion (o.r.d.) curve for this region, depicted in Fig. 1, shows a multiple Cotton effect with close correspondence between its *extrema* and the ultraviolet absorption maxima. The nature of the rotatory dispersion observed suggests the proximity of elements of asymmetry in the molecule of fucoxanthin to chromophores with λ_{max} at 334, 320, 307, and 264 mμ. The molecular asymmetry may stem from one or more carbon atoms carrying a secondary or tertiary hydroxyl or acetoxy group or from the location of the allene group in the carotenoid chain. The ultraviolet-absorbing chromophores may be carbonyl functions of the ester group and keto group conjugated with the polyene chain (or with the allene group). Evidence for the occurrence of these groups in the fucoxanthin molecule has been recently presented (2, 6). In the absence of o.r.d. studies on other carotenoids or allenes, it is not possible to make comparative inferences on the structure of fucoxanthin from the present study, which does show, however, that any structure proposed for this carotenoid will henceforth require to take cognizance of molecular asymmetry. Similar o.r.d. studies on other carotenoids are desirable to resolve controversies on their optical activity (e.g. zeaxanthin (7)).

EXPERIMENTAL

The fucoxanthin sample of Parsons and Strickland (5) was recrystallized twice from ether – light petroleum (30–60°); m.p. 151–153° (uncorrected, Kofler block).

Anal. Calcd. for $C_{42}H_{62}O_6$: C, 76.13; H, 9.36; mol. wt., 662. Found: C, 75.69; H, 9.07; mol. wt. (Rast), 649.

Solutions of the compound scanned for light absorption in the region 350–700 mμ showed maxima at the following wavelengths: ethanol, 450 mμ ($E_{1\ cm}^{1\%}$ = 1 140); chloroform, 458 mμ; light petroleum (60–80°), (426), 448, 476 mμ. The infrared spectrum (KBr disc) was identical with that of a specimen of fucoxanthin from *Fucus vesiculosus* (6) kindly supplied by Dr. B. C. L. Weedon; no band was observed in the acetylenic grouping absorption region 2 100 to 2 200 cm^{-1}, indicating the absence of any allene → acetylene rearrangement during the isolation of the pigment. Paper chromatography by the method and solvent systems of Jeffrey (8) showed the pigment to be homogeneous with the following R_F values: 4% propan-1-ol in light petroleum, 0.78; 30% chloroform in light petroleum, 0.54.

The o.r.d. was measured on a Cary Model 60 recording spectropolarimeter, with a path length of 1 cm, temperature of 25°, slit width of 25 Å (spectral band pass), and scan speed of 1 Å per second. The specific rotation at 589 mμ was too low for measurement with the high light absorption obtained at this wavelength and appears to be less than +25°. The ultraviolet absorption was measured with a Cary Model 14 recording spectrophotometer on the same solution used for o.r.d. measurement.

ACKNOWLEDGMENTS

Grateful acknowledgment is hereby made to Dr. T. R. Parsons for supplying the fucoxanthin from *S. muticum* used in this investigation as well as to Mr. N. Mitchell of Applied Physics Corporation, Monrovia, California, for making the o.r.d. measurement.

1. T. W. Goodwin. Advances in enzymology. Vol. 21. *Edited by* F. F. Nord. Interscience Publishers. 1959. p. 295.
2. A. Jensen. Acta Chem. Scand. **15**, 1604, 1605 (1961); **18**, 840 (1964).
3. P. Karrer, A. Helfenstein, H. Wehrli, B. Pieper, and R. Morf. Helv. Chim. Acta, **14**, 614 (1931).
4. I. M. Heilbron and R. F. Phipers. Biochem. J. **29**, 1369 (1935).
5. T. R. Parsons and J. D. H. Strickland. J. Marine Res. Sears Found. Marine Res. **21**, 155 (1963).
6. F. G. Torto and B. C. L. Weedon. Chem. Ind. London, 1219 (1955).
7. P. Karrer and E. Jucker. Carotenoids. Elsevier Publishing Co., Inc., New York. 1950. p. 185.
8. S. W. Jeffrey. Biochem. J. **80**, 336 (1961).

Received August 24, 1964.
Fisheries Research Board of Canada,
Technological Research Laboratory,
Vancouver, British Columbia.

Can. J. Chem. Downloaded from www.nrcresearchpress.com by 210.87.254.5 on 09/05/12
For personal use only.

UREA INCLUSION COMPOUNDS OF ALKENOIC ACIDS AND ALKYL ALKENOATES

JACK RADELL AND B. W. BRODMAN

Can. J. Chem. Downloaded from www.nrcresearchpress.com by 210.87.254.6 on 09/05/12
For personal use only.

Commercially obtained samples of alkenoic acids and alkyl alkenoates were examined in the infrared region to determine the geometric isomerism around the double bond. This information was required because in an earlier study (1) it was found that the effect of *cis* and *trans* isomerism on the ability of a molecule to form a urea inclusion compound was very significant. The geometric isomerism of all endocytes selected were the same, so that their behavior under complexing conditions could be compared. The *trans* rather than the *cis* isomers were chosen because it made it possible to deal with the more readily available shorter molecules which are capable of forming complexes. This would not be true of the corresponding *cis* molecules.

Some of the pertinent peaks obtained from the infrared analysis are listed in Table I.

TABLE I

Summary of infrared data

n-Compounds	Wave numbers (cm^{-1}) and intensity*			
$H(CH_2)_3CH{=}CHCOOH$	685m	985s	1 310s	1 650s
$H(CH_2)_4CH{=}CHCOOH$	688m	982s	1 305s†	1 648s
$C(CH_2)_5CH{=}CHCOOH$	680m	980s	1 300s	1 640s
$H(CH_2)_6CH{=}CHCOOH$	685w	970m	1 300m	1 642m
$H(CH_2)_2CH{=}CHCH_2COOH$	—	965m	—	1 650m†
$H(CH_2)_3CH{=}CHCOOMe$	—	975m	1 318m	1 655m
$H(CH_2)_4CH{=}CHCOOMe$	—	978s	1 308s	1 650s
$H(CH_2)_5CH{=}CHCOOMe$	—	973s	1 310s	1 650s
$H(CH_2)_6CH{=}CHCOOMe$	—	970s	1 308s	1 650s
$H(CH_2)_3CH{=}CHCOOEt$	—	975s	1 310s	1 650s
$H(CH_2)_2CH{=}CHCH_2COOMe$	—	964m	1 315m 1 308m	1 660w
$H(CH_2)_2CH{=}CHCH_2COOEt$	—	963m	1 300m	1 655w

*Intensity of peaks are described as s (strong), m (medium), and w (weak).
†Shoulder.

Most significant is the *trans* out-of-plane =CH deformation reported (2) as a strong band at 965–980 cm^{-1} for unconjugated acids with some shifts to higher frequencies observed for the α,β-unsaturated acids. This band was observed in this range for all the acids and esters, although the frequency of the absorption was consistently higher for the conjugated acids and esters than for the unconjugated acids and esters, respectively. This band alone is not conclusive evidence for the presence of the *trans* structure. The *trans* in-plane deformation which reportedly (2) appears at 1 295 to 1 310 cm^{-1} appears in all the acids and esters in Table I except for 3-*n*-hexenoic acid which has the hint of a shoulder around 1 308 cm^{-1}. The remaining absorption bands present are consistent with the structure of the molecules and have been omitted.

In Table II are listed the compounds treated by an urea–methanol solution as described in the experimental section. All compounds treated formed urea-inclusion compounds except 3-*n*-hexenoic and 3-*n*-octenic acids. All other alkenoic acids differed from these two by the presence of a double bond in the 2-position. This trend is similar to one observed in earlier studies of alkynes (3). The triple bond did not prevent complex formation in 1-, 2-, or 3-nonyne and 2- and 3-decyne but did prevent complex formation in 4-nonyne and 5-decyne. The fact that all the 3-*n*-alkenoic acid esters formed urea complexes is

TABLE II

X-ray powder patterns of alkenoic acids and alkenoates* and weight data

n-Compounds	3.24–3.30†	3.35–3.41	3.53–3.57	3.84–3.87	4.00–4.02	4.09–4.15	4.34–4.38	7.04–7.19	Weight‡ (g)
$H(CH_2)_3CH{=}CHCOOH$	0.06§	0.11	0.54	0.07	—	1.00	0.07	0.15	0.10
$H(CH_2)_4CH{=}CHCOOH$	—	0.08	0.06	—	—	1.00	—	—	0.10
$H(CH_2)_5CH{=}CHCOOH$	0.09	0.32	0.50	0.08	—	1.00	0.10	0.10	0.32
$H(CH_2)_6CH{=}CHCOOH$	—	0.07	1.00	—	—	0.22	—	0.25	0.25
$H(CH_2)_3CH{=}CHCOOMe$	0.07	0.26	1.00	0.09	0.17	0.76	0.05	0.53	0.28
$H(CH_2)_4CH{=}CHCOOMe$	0.05	1.00	0.56	—	—	0.50	—	0.41	0.35
$H(CH_2)_5CH{=}CHCOOMe$	—	0.13	0.72	0.06	—	1.00	—	0.24	0.30
$H(CH_2)_6CH{=}CHCOOMe$	0.07	0.24	1.00	0.09	—	—	—	0.48	0.42
$H(CH_2)_3CH{=}CHCOOEt$	—	0.07	1.00	—	0.05	0.20	—	0.37	0.34
$H(CH_2)_2CH{=}CHCH_2COOMe$	—	0.07	1.00	—	0.17	0.15	—	0.37	0.26
$H(CH_2)_2CH{=}CHCH_2COOEt$	0.07	0.07	1.00	0.06	—	0.51	—	0.54	0.17
Urea‖	—	—	—	—	1.00	—	—	—	—

*3-*n*-Hexenoic acid and 3-*n*-octenoic acid formed no crystalline material.
†Interplanar spacings in Å using Cu K_α radiation.
‡Weight of urea-inclusion compound isolated by procedure in the experimental.
§Relative intensities; 1.00 being the strongest. A dash has been used for spacing of intensity less than 0.05.
‖Other interplanar spacings for urea occurred at 2.00, 2.53, and 2.83 Å.

attributable to the added van der Waals stabilization resulting from the alkyl groups of the ester. In general for two identical compounds differing in the location and not in the geometric isomerism of the double bond, the isomer with the more centrally located double bond is less stable and forms less or no complex under the same conditions.

The interplanar spacings listed in Table II indicate that all compounds which formed crystals when treated with an urea–methanol solution formed urea-inclusion compounds. This is demonstrated by the following three most generally intense interplanar spacings 3.53–3.57 Å, 4.09–4.15 Å, and 7.04–7.19 Å. The urea–methanol-treated samples are all generally free from dissociated tetragonal urea except the 2-*n*-hexenoic acid methyl ester and 3-*n*-hexenoic acid methyl ester, both of which have a low-intensity interplanar spacing characteristic of free tetragonal urea. The 3-*n*-hexenoic and 3-*n*-octenoic acids formed no crystalline product and are therefore not listed in Table II.

EXPERIMENTAL

Urea-Inclusion Compounds

Urea-inclusion compounds of the alkenoic acids and alkyl alkenoates were prepared by a previously described procedure (4). The only exception was that 1 g of the guest compound was used in place of 30 drops.

X-Ray Powder Diffraction Measurements

The X-ray diffraction patterns were obtained by a previously described method (4).

Alkenoic Acids and Alkyl Alkenoates

The acids and esters were all obtained from the Gallard-Schlesinger Mfg. Corp., Long Island, N.Y., and their purity was established by elemental analysis and infrared data.

1. J. RADELL, J. W. CONNOLLY, and W. R. COSGROVE, JR. J. Org. Chem. **26**, 2960 (1961). E. MULLER. Methoden der organischen Chemie (Houben-Weyl), I/1. George Thieme Verlag, Stuttgart. 1958. pp. 408–409.
2. L. J. BELLAMY. The infra-red spectra of complex molecules. 2nd ed. John Wiley and Sons, Inc., New York. 1958.
3. J. RADELL, J. W. CONNOLLY, and L. D. YUHAS. J. Org. Chem. **26**, 2022 (1961).
4. J. RADELL, B. W. BRODMAN, and E. D. BERGMANN. Can. J. Chem. **42**, 1069 (1964).

RECEIVED SEPTEMBER 11, 1964.
PITMAN-DUNN INSTITUTE FOR RESEARCH,
FRANKFORD ARSENAL,
PHILADELPHIA, PENNSYLVANIA.

Can. J. Chem. Downloaded from www.nrcresearchpress.com by 210.87.254.6 on 09/05/12
For personal use only.

3,5,8,4′-TETRAMETHOXYFLAVONE AND THE CONSTITUTION OF PRATOLETIN

JASWINDER SINGH CHADHA[1]

Pratoletin, a flavone, was isolated from the flowers of *Trifolium pratense* by Hattori, Hasegawa, and Simokoriyama (1). It was considered to be either (i) 3,5,6,4′-tetrahydroxy flavone or (ii) 3,5,8,4′-tetrahydroxyflavone. This was based on the following considerations: pratoletin gave an orange red color with magnesium and hydrochloric acid and produced a greenish-brown color with ferric chloride. The analysis of pratoletin and its derivatives corresponded to a tetrahydroxy flavone. It was considered to have an ortho- or a para-dihydroxylic system because an alcoholic solution of pratoletin gave a black precipitate with an aqueous solution of chloropentaaminocobaltic chloride. From a comparison of the ultraviolet spectra of pratoletin and its tetramethyl ether, it was considered to be a flavonol (1).

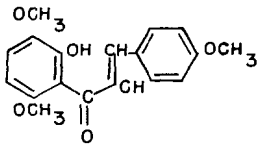

I

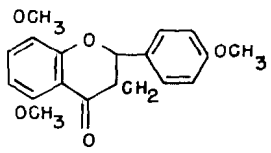

II

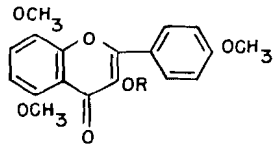

III, R = H

IV, R = CH_3

Because of war time difficulties, the above publication (1) was for a long time not fully known; it was abstracted in the Chemical Abstracts only in 1951 (2). Meanwhile, during studies relating to nuclear oxidation in the flavone series, Rajagopalan, Row, and Seshadri (3) prepared 3,5,6,4′-tetrahydroxyflavone and its derivatives. These do not agree with those of pratoletin and its derivatives. Consequently pratoletin has been considered to be 3,5,8,4′-tetrahydroxyflavone (4).

During work carried out relating to leucoanthocyanidins, 3-hydroxy-5,8,4′-trimethoxyflavone was prepared and methylated to yield 3,5,8,4′-tetramethoxyflavone. The synthesis was carried out following the procedure of Ahluwalia and Seshadri (5), who prepared the closely related 3,5,8,3′,4′-pentahydroxyflavone and derivatives. 2-Hydroxy-3,6,4′-trimethoxychalcone I (6) was cyclized to the corresponding flavanone II and the flavanone was converted into the flavonol III by the amylnitrite method (7). Final methylation yielded the tetramethoxyflavone IV.

3,5,8,4′-Tetramethoxyflavone IV has a m.p. 158° (anhydrous sample) and λ_{max}: 272 mμ(log ε 4.11), 299 mμ(log ε 4.13), and 321 mμ(log ε 4.16). Pratoletin tetramethyl ether is recorded to have m.p. 109° (hydrate) and 138° (anhydrous) and λ_{max}: 266 mμ and 329 mμ (1). It seems, therefore, necessary to reinvestigate the constitution of pratoletin.

EXPERIMENTAL

5,8,4′-Trimethoxyflavanone (II)

2-Hydroxy-3,6,4′-trimethoxychalcone (1 g) was dissolved in ethanol (60 ml) and aqueous hydrochloric acid (3%) was added till there was a permanent turbidity and the solution refluxed for 24 h. On cooling, part of the chalcone separated. This was filtered and the filtrate heated to expel most of the alcohol. On

[1]*Present address: Unilever Research Laboratory, The Frythe, Welwyn, Herts, England.*

Can. J. Chem. Downloaded from www.nrcresearchpress.com by 210.87.254.5 on 09/05/12
For personal use only.

cooling, a mixture of the chalcone and the flavanone separated. It was filtered (600 mg) and treated with cold aqueous sodium hydroxide (1%) to dissolve the unchanged chalcone. On filtration, crude flavanone (500 mg) was obtained. It was crystallized from methanol yielding light yellow rods, m.p. 178°.

Anal. Calcd. for $C_{18}H_{18}O_5$: C, 68.8; H, 5.8. Found: C, 68.6; H, 5.8.

The mixture of the chalcone and the flavanone could also be separated by fractional crystallization from carbondisulfide.

3-Hydroxy-5,8,4'-trimethoxyflavone (III)

The trimethoxyflavanone (120 mg) was dissolved in ethanol (20 ml) and to the boiling solution concentrated hydrochloric acid (10 ml) was added. To this isoamyl nitrite (1 ml) in ethanol (10 ml) was added in small portions and with constant shaking during 3 min. The color of the reaction mixture changed to orange. It was allowed to stand for 2 h with occasional shaking. Part of the alcohol was distilled and water added. On cooling, the flavonol separated as needles (50 mg) and on crystallization from methanol, it came out as light yellow needles, m.p. 188°.

Anal. Calcd. for $C_{18}H_{16}O_6$: C, 65.8; H, 4.9. Found: C, 65.3; H, 5.3.

3,5,8,4'-Tetramethoxyflavone (IV)

A mixture of 3-hydroxy-5,8,4'-trimethoxyflavone (70 mg), dimethyl sulfate (0.1 ml), and potassium carbonate (500 mg) in dry acetone was refluxed for 6 h. The mixture was filtered and the acetone solution concentrated to small bulk and water added. On cooling, the product was obtained as a crystalline compound. It was filtered (50 mg) and crystallized from benzene – petroleum ether. It came out as light yellow needles, m.p. 158°.

Anal. Calcd. for $C_{19}H_{18}O_6$: C, 66.7; H, 5.3. Found: C, 66.3; H, 5.4.

ACKNOWLEDGMENTS

The author wishes to thank Professor T. R. Seshadri, for his helpful suggestions and interest. A Research Fellowship from the Council of Scientific and Industrial Research is gratefully acknowledged.

1. S. Hattori, M. Hasegawa, and M. Simokoriyama. Acta Phytochim. Japan, **13**, 99 (1943).
2. S. Hattori, M. Hasegawa, and M. Simokoriyama. Chem. Abstr. **45**, 5157a (1951).
3. S. Rajagopalan, L. R. Row, and T. R. Seshadri. Proc. Indian Acad. Sci. A, **23**, 97 (1946).
4. J. Gripenberg. Chemistry of flavonoid compounds. *Edited by* T. A. Geissman. Pergamon Press. 1962. p. 420.
5. V. K. Ahluwalia and T. R. Seshadri. Proc. Indian Acad. Sci. A, **39**, 296 (1954).
6. A. Ballio and F. Pocchiari. Ricerca Sci. **20**, 1301 (1950); Brit. Abstr. A, **II**, 763 (1951).
7. L. R. Row and T. R. Seshadri. Proc. Indian Acad. Sci. A, **21**, 130 (1945).

Received July 20, 1964.
Department of Chemistry,
University of Delhi,
Delhi, India.

THE PREPARATION OF THIOACETALS FROM ORTHOTHIOBORIC ESTERS

F. Bessette, J. Brault, and J. M. Lalancette

We have indicated that orthothioboric esters $(RS)_3B$ can be obtained by the action of mercaptans on boron sulfide (1). These esters were found to react with aldehydic or ketonic carbonyls to give the corresponding thioacetals and boric anhydride according to the following equation:

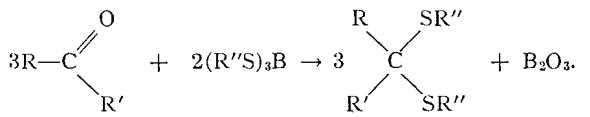

Can. J. Chem. Downloaded from www.nrcresearchpress.com by 210.87.254.5 on 09/05/12
For personal use only.

cooling, a mixture of the chalcone and the flavanone separated. It was filtered (600 mg) and treated with cold aqueous sodium hydroxide (1%) to dissolve the unchanged chalcone. On filtration, crude flavanone (500 mg) was obtained. It was crystallized from methanol yielding light yellow rods, m.p. 178°.

Anal. Calcd. for $C_{18}H_{18}O_5$: C, 68.8; H, 5.8. Found: C, 68.6; H, 5.8.

The mixture of the chalcone and the flavanone could also be separated by fractional crystallization from carbondisulfide.

3-Hydroxy-5,8,4'-trimethoxyflavone (III)

The trimethoxyflavanone (120 mg) was dissolved in ethanol (20 ml) and to the boiling solution concentrated hydrochloric acid (10 ml) was added. To this isoamyl nitrite (1 ml) in ethanol (10 ml) was added in small portions and with constant shaking during 3 min. The color of the reaction mixture changed to orange. It was allowed to stand for 2 h with occasional shaking. Part of the alcohol was distilled and water added. On cooling, the flavonol separated as needles (50 mg) and on crystallization from methanol, it came out as light yellow needles, m.p. 188°.

Anal. Calcd. for $C_{18}H_{16}O_6$: C, 65.8; H, 4.9. Found: C, 65.3; H, 5.3.

3,5,8,4'-Tetramethoxyflavone (IV)

A mixture of 3-hydroxy-5,8,4'-trimethoxyflavone (70 mg), dimethyl sulfate (0.1 ml), and potassium carbonate (500 mg) in dry acetone was refluxed for 6 h. The mixture was filtered and the acetone solution concentrated to small bulk and water added. On cooling, the product was obtained as a crystalline compound. It was filtered (50 mg) and crystallized from benzene – petroleum ether. It came out as light yellow needles, m.p. 158°.

Anal. Calcd. for $C_{19}H_{18}O_6$: C, 66.7; H, 5.3. Found: C, 66.3; H, 5.4.

ACKNOWLEDGMENTS

The author wishes to thank Professor T. R. Seshadri, for his helpful suggestions and interest. A Research Fellowship from the Council of Scientific and Industrial Research is gratefully acknowledged.

1. S. Hattori, M. Hasegawa, and M. Simokoriyama. Acta Phytochim. Japan, **13**, 99 (1943).
2. S. Hattori, M. Hasegawa, and M. Simokoriyama. Chem. Abstr. **45**, 5157a (1951).
3. S. Rajagopalan, L. R. Row, and T. R. Seshadri. Proc. Indian Acad. Sci. A, **23**, 97 (1946).
4. J. Gripenberg. Chemistry of flavonoid compounds. *Edited by* T. A. Geissman. Pergamon Press. 1962. p. 420.
5. V. K. Ahluwalia and T. R. Seshadri. Proc. Indian Acad. Sci. A, **39**, 296 (1954).
6. A. Ballio and F. Pocchiari. Ricerca Sci. **20**, 1301 (1950); Brit. Abstr. A, **II**, 763 (1951).
7. L. R. Row and T. R. Seshadri. Proc. Indian Acad. Sci. A, **21**, 130 (1945).

Received July 20, 1964.
Department of Chemistry,
University of Delhi,
Delhi, India.

THE PREPARATION OF THIOACETALS FROM ORTHOTHIOBORIC ESTERS

F. Bessette, J. Brault, and J. M. Lalancette

We have indicated that orthothioboric esters $(RS)_3B$ can be obtained by the action of mercaptans on boron sulfide (1). These esters were found to react with aldehydic or ketonic carbonyls to give the corresponding thioacetals and boric anhydride according to the following equation:

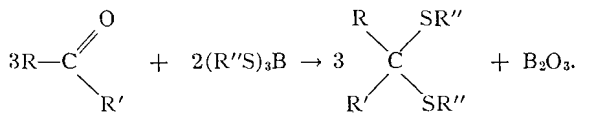

Can. J. Chem. Downloaded from www.nrcresearchpress.com by 210.87.254.105 on 09/05/12
For personal use only.

This reaction seems general for aliphatic and aromatic molecules. It has given good yields of the thioacetals without undesirable side reactions with the molecules studied (Table I). Contrary to the usual procedure leading to the formation of thioacetals (2), this reaction proceeds smoothly in neutral medium at room temperature.

TABLE I

Preparation of thioacetals

RCOR′	R″	Boiling point, °C (mm Hg)	n_D^{25}	Analysis (%) for C Calcd.	C Found	H Calcd.	H Found	S Calcd.	S Found
Benzaldehyde	Ethyl	118–120 (3.0–3.4)	1.5723	62.18	61.97	7.56	7.56	30.22	30.11
p-Tolualdehyde	Ethyl	125–130 (0.35)	1.5730	63.64	63.29	8.02	7.75	28.34	28.61
p-Chloro-benzaldehyde	Ethyl	140–144 (0.3–0.5)	1.5819	53.60	53.83	6.13	6.24	25.10	24.97
p-Nitro-benzaldehyde	Ethyl	173–176 (1.0)	1.5980	51.33	51.22	5.87	5.63	24.91	24.86
n-Butanal	Ethyl	219–220 (750)	1.4967	53.90	53.61	10.18	9.90	35.92	35.69
i-Butanal	Ethyl	216 (750)	1.4968	53.90	54.13	10.18	10.29	35.92	35.57
Propanal	Ethyl	196–198 (750)	1.5002	51.20	51.21	9.81	9.75	39.03	38.71
Benzophenone	Ethyl	165–171 (0.7–0.9)	1.6165	70.78	70.75	6.99	6.90	22.23	22.07
Butanone	Ethyl	205–208 (750)	1.4955	53.87	54.47	10.17	10.00	35.95	35.24
m-Nitro-benzaldehyde	*n*-Pentyl	213 (0.85)	1.5496	59.78	59.65	7.97	7.97	18.78	19.07
Benzaldehyde	*n*-Butyl	133–135 (0.3)	1.5453	67.10	67.43	9.01	8.89	23.88	23.94

With some reactive aldehydes like benzaldehyde, the speed of the reaction has to be controlled by working with a diluent, such as petroleum ether or benzene. In several cases, however, the thioacetal can be obtained merely by mixing the reactants and filtering off the boric anhydride, after a contact of a few hours at room temperature.

This reaction shows some analogy with the interchange of oxygen for sulfur on the boron atoms of B_2S_3, when this sulfide is allowed to react with aldehydic or ketonic carbonyls (3). The exchange is much favored, thermodynamically, by the difference in the heats of formation of B—S and B—O bonds. This should be, in fact, the driving factor of the reaction. The reaction proceeds in neutral medium and shows an induction period, the initiation of the process being indicated by the precipitation of boron oxide, highly insoluble in the petroleum ether or benzene used as solvents. These results can be interpreted as indications of a free radical mechanism for the reaction.

EXPERIMENTAL

Benzaldehyde Thioacetal

To an ice-cold solution of 16 g (0.083 mole) of ethyl orthothioborate in 150 ml of dry petroleum ether, b.p. 40–50°, a solution of 13.8 g (0.13 mole) of freshly distilled benzaldehyde in the same amount of petroleum ether is added slowly, under stirring and nitrogen atmosphere. As the addition proceeds, a white precipitate of boric anhydride slowly appears. The reaction is completed by heating under reflux for 2 h. By filtration, 2.82 g (0.041 mole) of B_2O_3 is obtained. This solid does not melt below 300° and yields boric acid, m.p. 175–177°, on treatment with boiling water.

The organic fraction, after evaporation of the petroleum ether, leaves a pink residue which is fractionated *in vacuo*. The main fraction, b.p. 125–127° at 0.22 mm, n_D^{25} 1.5731, 19.85 g (0.093 mole), is the benzaldehyde thioacetal.

Anal. Calcd. for $C_{11}H_{16}S_2$: C, 62.18; H, 7.56; S, 30.22. Found: C, 61.97; H, 7.56; S, 30.11.

By this technique, several aldehydes and ketones have been transformed into their thioacetal (Table I). Ethyl, butyl, and pentyl orthothioborates have been shown to give the expected reaction which should be general for all orthothioboric esters.

With carbonyls of moderate reactivity, the diluent—petroleum ether or benzene—can be omitted. In such an experiment, 5.7 g (0.079 mole) of butanone was mixed with 10.0 g (0.052 mole) of ethyl orthothioborate. After 5 to 10 min, the reaction mixture starts to exhibit a gel-like appearance. After a contact

Can. J. Chem. Downloaded from www.nrcresearchpress.com by 210.87.254.105 on 09/05/12
For personal use only.

time of 18 h, at room temperature, in a dessicator containing potassium hydroxide pellets, the mass is taken up by petroleum ether, b.p. 40–50°. The boric anhydride is filtered off and the usual techniques give the butanone thioacetal, b.p. 205–208° at 750 mm, n_D^{25} 1.4955, in 76% yield.

Anal. Calcd. for $C_8H_{18}S_2$: C, 53.87; H, 10.17; S, 35.95. Found: C, 54.47; H, 10.00; S, 35.24.

ACKNOWLEDGMENT

One of the authors (J. M. L.) thanks the Defence Research Board of Canada for its financial assistance. (Grant No. 9530-30.)

1. J. Brault and J. M. Lalancette. Can. J. Chem. To be published.
2. H. Hauptmann. J. Am. Chem. Soc. **69**, 562 (1947).
3. S. Jerumanis and J. M. Lalancette. Can. J. Chem. **42**, 1928 (1964).

Received September 10, 1964.
Department of Chemistry,
University of Sherbrooke,
Sherbrooke, Quebec.

Can. J. Chem. Downloaded from www.nrcresearchpress.com by 210.87.254.105 on 09/05/12
For personal use only.

THE ADSORPTION OF KRYPTON AND ETHYLENE ON EVAPORATED FILMS OF MAGNESIUM[1]

D. M. Young and C. D. Anderson

A study of the adsorptive behavior of boron halides on evaporated films of magnesium was initiated in the hope of throwing some light on the mechanism of formation of protective films on magnesium surfaces. The project was later abandoned, however, on finding that evaporated magnesium films sinter to a marked degree even at temperatures as low as −78 °C. The sintering behavior is reported here because no such information is available in the literature. Some unusual physical adsorption isotherms, obtained during surface area measurements, also merit publication.

EXPERIMENTAL

Magnesium wire of 0.025 in. diameter, extruded from sublimed magnesium of 99.96% purity, was obtained from the Metallurgical Laboratory, The Dow Chemical Co. Ethylene supplied by Imperial Oil, Ltd., was 99.99 mole % pure, the major impurity being 0.0047% ethane. Reagent grade helium and krypton supplied in glass flasks by Air Reduction Sales Co. were used as received. The only detectable impurity, according to the supplier, was 0.03 mole % nitrogen in the krypton.

The apparatus was of the constant volume type conventionally used for studies on evaporated metal films. Wide bore mercury cut-offs were used in place of stopcocks and a U trap, always kept at liquid air temperature, served to protect the metal film from mercury vapor. Measured amounts of adsorbate were admitted by means of a greaseless doser previously described (1). Equilibrium pressures were measured with a McLeod gauge for krypton or with a Pirani gauge calibrated against a McLeod gauge for helium (used for determining the dead space) and ethylene.

The temperatures of the liquid oxygen or nitrogen baths surrounding the adsorbent were measured with an oxygen vapor pressure thermometer. The correction for gas adsorbed on the walls was estimated by carrying out a blank run prior to evaporating a film, making allowance for the area later to be covered with magnesium. This correction, negligible for krypton at −195°, never exceeded 3% of the ethylene adsorbed on the film at −183°. It has been applied to the ethylene results given here. The effects of thermal transpiration, calculated by the methods of Bennett and Tompkins (2), were found negligible for all gases.

[1]*Contribution No. 89.*

time of 18 h, at room temperature, in a dessicator containing potassium hydroxide pellets, the mass is taken up by petroleum ether, b.p. 40–50°. The boric anhydride is filtered off and the usual techniques give the butanone thioacetal, b.p. 205–208° at 750 mm, n_D^{25} 1.4955, in 76% yield.

Anal. Calcd. for $C_8H_{18}S_2$: C, 53.87; H, 10.17; S, 35.95. Found: C, 54.47; H, 10.00; S, 35.24.

ACKNOWLEDGMENT

One of the authors (J. M. L.) thanks the Defence Research Board of Canada for its financial assistance. (Grant No. 9530-30.)

1. J. Brault and J. M. Lalancette. Can. J. Chem. To be published.
2. H. Hauptmann. J. Am. Chem. Soc. **69**, 562 (1947).
3. S. Jerumanis and J. M. Lalancette. Can. J. Chem. **42**, 1928 (1964).

Received September 10, 1964.
Department of Chemistry,
University of Sherbrooke,
Sherbrooke, Quebec.

Can. J. Chem. Downloaded from www.nrcresearchpress.com by 210.87.254.40 on 09/05/12
For personal use only.

THE ADSORPTION OF KRYPTON AND ETHYLENE ON EVAPORATED FILMS OF MAGNESIUM[1]

D. M. Young and C. D. Anderson

A study of the adsorptive behavior of boron halides on evaporated films of magnesium was initiated in the hope of throwing some light on the mechanism of formation of protective films on magnesium surfaces. The project was later abandoned, however, on finding that evaporated magnesium films sinter to a marked degree even at temperatures as low as −78 °C. The sintering behavior is reported here because no such information is available in the literature. Some unusual physical adsorption isotherms, obtained during surface area measurements, also merit publication.

EXPERIMENTAL

Magnesium wire of 0.025 in. diameter, extruded from sublimed magnesium of 99.96% purity, was obtained from the Metallurgical Laboratory, The Dow Chemical Co. Ethylene supplied by Imperial Oil, Ltd., was 99.99 mole % pure, the major impurity being 0.0047% ethane. Reagent grade helium and krypton supplied in glass flasks by Air Reduction Sales Co. were used as received. The only detectable impurity, according to the supplier, was 0.03 mole % nitrogen in the krypton.

The apparatus was of the constant volume type conventionally used for studies on evaporated metal films. Wide bore mercury cut-offs were used in place of stopcocks and a U trap, always kept at liquid air temperature, served to protect the metal film from mercury vapor. Measured amounts of adsorbate were admitted by means of a greaseless doser previously described (1). Equilibrium pressures were measured with a McLeod gauge for krypton or with a Pirani gauge calibrated against a McLeod gauge for helium (used for determining the dead space) and ethylene.

The temperatures of the liquid oxygen or nitrogen baths surrounding the adsorbent were measured with an oxygen vapor pressure thermometer. The correction for gas adsorbed on the walls was estimated by carrying out a blank run prior to evaporating a film, making allowance for the area later to be covered with magnesium. This correction, negligible for krypton at −195°, never exceeded 3% of the ethylene adsorbed on the film at −183°. It has been applied to the ethylene results given here. The effects of thermal transpiration, calculated by the methods of Bennett and Tompkins (2), were found negligible for all gases.

[1]*Contribution No. 89.*

RESULTS AND DISCUSSION

A reliable method of determining surface areas was required in order to study the effect of heat treatment on sintering and to measure the porosity of the films, i.e. to establish whether the surface area increased with increasing film thickness. A number of variants on the Brunauer, Emmett, Teller (B.E.T.) method are useful for small surface areas (3), notably the use of krypton at −195° and ethylene at −183°.

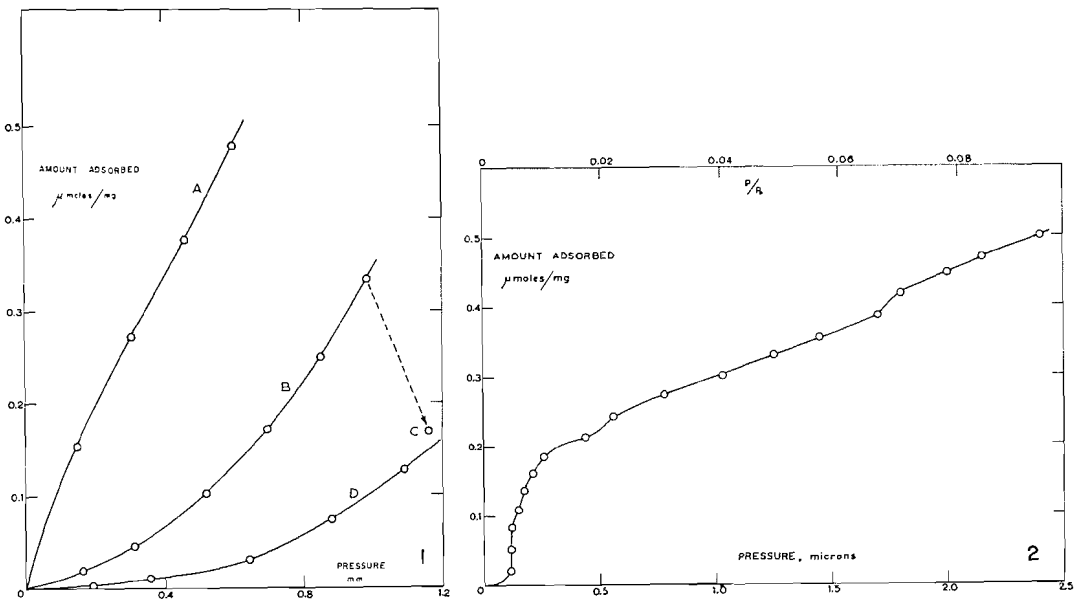

FIG. 1. Adsorption isotherms of krypton on film I at −195°, showing effects of sintering at −78°. Curve A, freshly formed film; curve B, after pumping at −78° for 2.5 h; curve C, after standing at −78° for 63.5 h; curve D, after pumping at −78° for 1 h.
FIG. 2. Adsorption isotherm for ethylene on film II at −183°.

The krypton method, due to Beebe, Beckwith, and Honig (4), was tried with film I (78.6 mg) and the results are shown in Fig. 1. Isotherm A was measured on the freshly formed film. It is characteristic of a B.E.T. type II isotherm with a very low value of the B.E.T. *c*-constant and is virtually useless for surface area determinations (3). Experiments with krypton were continued on film I, however, to determine its temperature stability. The film was warmed to −78° and pumped for 2.5 h to remove the krypton. A second krypton isotherm at −195° was measured (curve B). The diffuse knee-bend in the original isotherm has now disappeared and curve B is a typical B.E.T. type III isotherm. This, together with the lowered adsorptive capacity, shows that rapid sintering has occurred even at −78°. With the krypton left in the adsorption system, the temperature of the film was again raised to −78° and so maintained for 63.5 h. The film was then cooled to −195° and the equilibrium pressure of krypton again measured. The amount adsorbed had dropped from the final point of isotherm B to point C in Fig. 1. The adsorption vessel was warmed to −78° and evacuated for 1 h, then cooled to −195° and a third krypton isotherm measured (curve D).

Can. J. Chem. Downloaded from www.nrcresearchpress.com by 210.87.254.40 on 09/05/12
For personal use only.

The adsorption isotherms of ethylene at −183° were found suitable for B.E.T. surface area determination; this method was first suggested by Wooten and Brown (5). Equilibrium was established within a few minutes after each admission of gas and almost complete desorption occurred on pumping at −183°. A number of points were obtained at low relative pressures, revealing several "steps" in the isotherm (Fig. 2, film II). Some possible explanations for isotherms of this type are discussed elsewhere (3). In the pressure range used for the B.E.T. calculation ($p/p_0 = 0.05 - 0.3$) however, the isotherms have normal type II curvature and the B.E.T. equation fits quite accurately. The natural isotherm for film III, again showing an inflection, is plotted in Fig. 3 (upper curve) with the corresponding B.E.T. plot (lower curve).

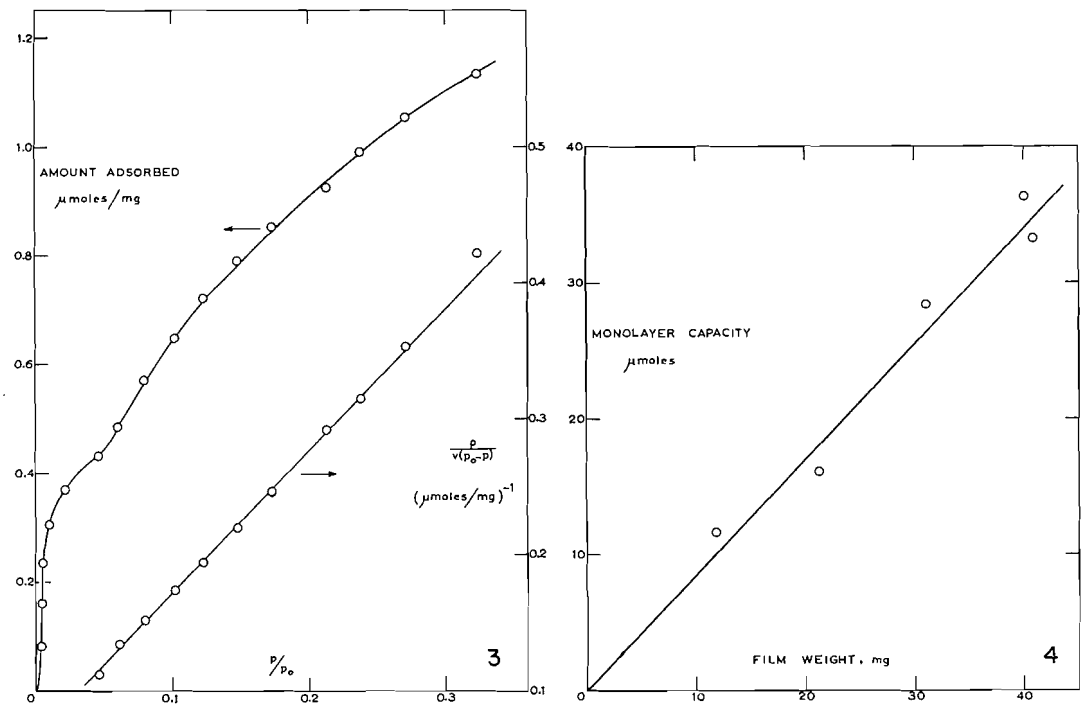

FIG. 3. The adsorption of ethylene on film III at −183°. Upper curve, natural isotherm; lower curve, plotted according to the B.E.T. equation.
FIG. 4. Monolayer capacity of films II–VI as a function of film weight.

Ethylene adsorption isotherms were measured on a series of magnesium films of different weights, and monolayer capacities calculated from the B.E.T. equation. The results are given in Fig. 4 in which the monolayer capacity is plotted against the film weight, for films II to VI inclusive. The linearity of this plot shows that the surface areas of the films are proportional to their weight and hence that the films are porous. Taking 17.55 Å² as the cross-sectional area of an ethylene molecule in the completed monolayer, following Wooten and Brown (5), the slope of the line in Fig. 4 corresponds to an average specific surface area of 89.8 m²/g for the five films studied.

Can. J. Chem. Downloaded from www.nrcresearchpress.com by 210.87.254.40 on 09/05/12
For personal use only.

1. D. M. YOUNG. Rev. Sci. Instr. **24**, 77 (1953).
2. M. J. BENNETT and F. C. TOMPKINS. Trans. Faraday Soc. **53**, 185 (1957).
3. D. M. YOUNG and A. D. CROWELL. Physical adsorption of gases. Butterworths. 1962.
4. R. A. BEEBE, J. B. BECKWITH, and J. M. HONIG. J. Am. Chem. Soc. **67**, 1554 (1945).
5. L. A. WOOTEN and C. BROWN. J. Am. Chem. Soc. **65**, 113 (1943).

RECEIVED DECEMBER 7, 1962.
EXPLORATORY RESEARCH LABORATORY,
DOW CHEMICAL OF CANADA, LIMITED,
SARNIA, ONTARIO.

Can. J. Chem. Downloaded from www.nrcresearchpress.com by 210.87.254.40 on 09/05/12
For personal use only.

THE AMMONOMERCURATION OF CYCLOHEXENE

D. CHOW, J. H. ROBSON, AND GEORGE F WRIGHT

This is a preliminary report of a reaction in which the acetamino group and the anionomercuri group are added to the double bond. It is not the first time that a double bond has been saturated by an anionomercuri group and a nitrogen function. Previously N-β-chloromercuriethylpiperidine has been prepared from ethylene, mercuric salt and piperidine (1), diethylamine (2), and mesidine (3). However the reagents in our transformation are unique, the yields are high, and the reaction ought to be useful in syntheses.

A solution of mercuric nitrate and absolute nitric acid in acetonitrile reacts with cyclohexene within 1 min to give a nearly quantitative yield, after conversion with mercuric chloride, of 2-acetaminocyclohexylmercuric chloride, I. No configuration has been assigned because we have as yet been unable to convert I to a mixture (4) from which the other diastereomer might be isolated, nor have we been able to find the other isomer in the nearly pure product of the reaction.

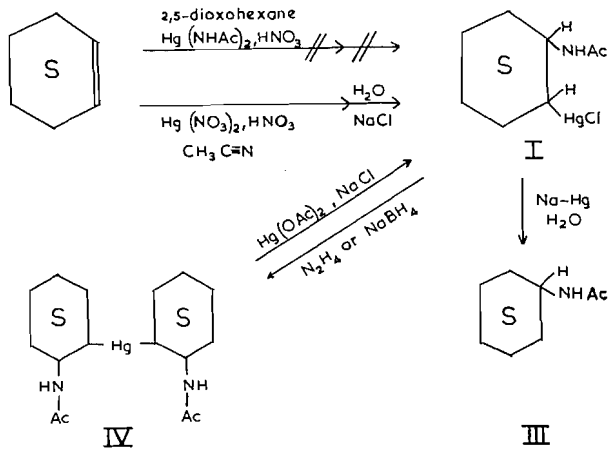

We are not prepared to suggest a mechanism for this reaction but we do not believe that it involves mercuric acetamide, II, or a mixed salt of it because I is not obtained when II and nitric acid are treated with cyclohexene in 2,5-dioxahexane, diethyl ether, methanol, or acetonitrile. In each case cyclohexene and acetamide have been recovered from the hydrolysate.

1. D. M. YOUNG. Rev. Sci. Instr. **24**, 77 (1953).
2. M. J. BENNETT and F. C. TOMPKINS. Trans. Faraday Soc. **53**, 185 (1957).
3. D. M. YOUNG and A. D. CROWELL. Physical adsorption of gases. Butterworths. 1962.
4. R. A. BEEBE, J. B. BECKWITH, and J. M. HONIG. J. Am. Chem. Soc. **67**, 1554 (1945).
5. L. A. WOOTEN and C. BROWN. J. Am. Chem. Soc. **65**, 113 (1943).

RECEIVED DECEMBER 7, 1962.
EXPLORATORY RESEARCH LABORATORY,
DOW CHEMICAL OF CANADA, LIMITED,
SARNIA, ONTARIO.

Can. J. Chem. Downloaded from www.nrcresearchpress.com by 210.87.254.5 on 09/05/12
For personal use only.

THE AMMONOMERCURATION OF CYCLOHEXENE

D. CHOW, J. H. ROBSON, AND GEORGE F WRIGHT

This is a preliminary report of a reaction in which the acetamino group and the anionomercuri group are added to the double bond. It is not the first time that a double bond has been saturated by an anionomercuri group and a nitrogen function. Previously N-β-chloromercuriethylpiperidine has been prepared from ethylene, mercuric salt and piperidine (1), diethylamine (2), and mesidine (3). However the reagents in our transformation are unique, the yields are high, and the reaction ought to be useful in syntheses.

A solution of mercuric nitrate and absolute nitric acid in acetonitrile reacts with cyclohexene within 1 min to give a nearly quantitative yield, after conversion with mercuric chloride, of 2-acetaminocyclohexylmercuric chloride, I. No configuration has been assigned because we have as yet been unable to convert I to a mixture (4) from which the other diastereomer might be isolated, nor have we been able to find the other isomer in the nearly pure product of the reaction.

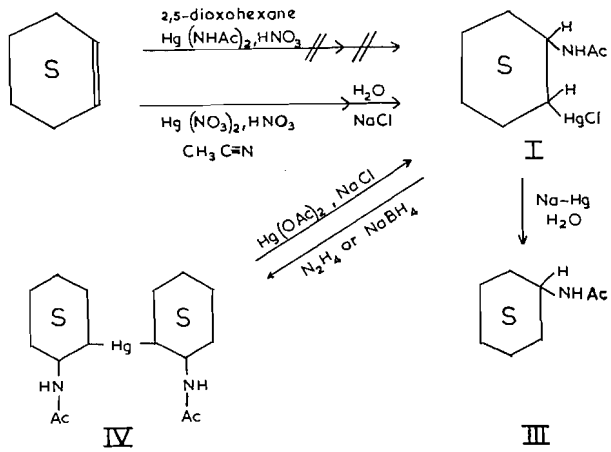

We are not prepared to suggest a mechanism for this reaction but we do not believe that it involves mercuric acetamide, II, or a mixed salt of it because I is not obtained when II and nitric acid are treated with cyclohexene in 2,5-dioxahexane, diethyl ether, methanol, or acetonitrile. In each case cyclohexene and acetamide have been recovered from the hydrolysate.

The ammonomercurial, I, is more stable than the analogous oxymercurials. It may be recovered unchanged after long treatment with 5% aqueous sodium hydroxide in which it dissolves. Also it dissolves initially in concentrated hydrochloric acid but a hydrochloride is precipitated shortly. When this hydrochloride after many hours is washed with water it reverts to I. Only in boiling concentrated hydrochloric acid is I decomposed to cyclohexene, acetamide, and mercuric chloride.

Reduction with sodium amalgam in alkaline solution leads cleanly to N-cyclohexylacetamide, III, and some of this is found upon treatment of an alkaline solution with sodium borohydride or hydrazine hydrate. However, the principal product with these reagents is the bis-mercurial, IV, even though conditions of reaction with the hydrazine hydrate have been arranged to cause diastereomeric equilibration via the mercuri linkage. The bis-mercurial has been reconverted quantitatively to I by treatment with mercuric salts. The bis-mercurial, IV, is only slightly soluble in 40% aqueous sodium hydroxide and is unchanged by it after a half-hour at 110°.

EXPERIMENTAL

Physical Constants

Melting points have been corrected against reliable standards. X-ray diffraction patterns have been obtained using Cu (Ni-filtered) radiation and are recorded as *d*-spacings in Å at intensities I/I_1.

Reagents

Cyclohexene was washed peroxide free with aqueous ferrous sulfate and after drying with magnesium sulfate was distilled under nitrogen. Acetonitrile was distilled under vacuum from phosphorus pentoxide and then at 82° and 755 mm. It was subsequently dried by means of drierite. Mercuric nitrate (Merck) was used as received. Absolute nitric acid (water white) was prepared by vacuum distillation of a nitric acid – sulphuric acid mixture.

2-Acetaminocyclohexylmercuric Chloride, I

From Cyclohexene

To a stirred suspension of 1.62 g (5 mmole) of freshly ground mercuric nitrate in 5 ml of acetonitrile was added 0.021 ml (0.5 mmole) of absolute nitric acid and then with cooling 0.5 ml (5 mmole) of cyclohexene. The suspension disappeared and after 2 min a test with alkali for inorganic mercuric salt was negative; a slight amount of mercurous salt was present. After 20 min the system was poured slowly into 10 ml of water at 4° and then 1.5 ml of 5 *M* aqueous sodium chloride was added. Filtration removed 1.75 g (94%), m.p. 199°. Crystallization from methanol (11 ml per g) and finally from dimethylformamide raised the m.p. to 201.5–202°.

Anal. Calcd. for $C_8H_{14}ClHgNO$: C, 25.5; H, 3.75. Found: C, 25.5; H, 3.72.

The reaction was completed within 1 min when the amount of nitric acid was doubled, and the yellow color characteristic of the reaction system appeared correspondingly earlier. When the reaction system was diluted with 2,5-dioxahexane the yield was decreased to 30% and much mercurous salt was formed.

From Bis-2-acetaminocyclohexylmercury

A 50 mg quantity (0.104 mmole) either of one pure diastereomer (m.p. 253°) or else of the diastereomeric mixture of bis-mercurials IV and 33 mg (0.104 mmole) of mercuric acetate was dissolved in 2 ml of methanol, warmed 5 min at 50°, then cooled, diluted with 4 ml of water and 0.1 ml of 5 *M* aqueous sodium chloride solution, and finally centrifuged to remove 0.76 g, m.p. 188–191°. Crystallization of this 86% yield raised its m.p. to 200–201°. A mixture melting point with I was not depressed.

N-Cyclohexylacetamide, III

A mixture of 15 ml of water, 3.75 g (10 mmole) of I, 2 ml of 6 *M* aqueous sodium hydroxide solution, and 20 mmole of 2% sodium amalgam was shaken for 3 h. Filtration of the aqueous suspension after decanting from mercury gave a grey solid which was extracted with 10 ml of hot ethyl acetate. Concentration of this extract yielded 0.75 g (66%) of III, m.p. 102–106°. Crystallization raised this m.p. to 105–106° and a mixture melting point with an authentic sample (5) was not depressed.

Bis-2-acetaminocyclohexylmercury, IV

A solution of 2.00 g (5.3 mmole) of I, 18.3 ml (0.26 mole) 100% hydrazine hydrate, and 5 ml of 5% aqueous sodium hydroxide quickly formed a white precipitate which became orange in color within a few minutes and then successively darker, because of the deposition of metallic mercury. The temperature was raised and maintained at 70–80° for 3 h. The system was cooled; the solid was filtered off and extracted

Can. J. Chem. Downloaded from www.nrcresearchpress.com by 210.87.254.5 on 09/05/12
For personal use only.

with 30 ml of hot methanol. Concentration of this extract yielded 12.7 g (99%) m.p. 213–215°. From this mixture of diastereomers was obtained 0.27 g (22%) m.p. 256–257° of one isomer by repeated crystallization from hot methanol (16 ml per g).

Anal. Calcd. for $C_{16}H_{28}HgN_2O_2$: C, 39.9; H, 5.87. Found: C, 40.0; H, 5.50.

The X-ray diffraction pattern was (10) 5.129; (6) 2.203; (5) 2.038; (4) 2.508; 1.925; (3) 2.640, 1.795, 1.591; (2) 2.508, 2.424.

Reduction with 2 equivalents of sodium borohydride in an otherwise identical system was much less satisfactory. The yield of the diastereomic mixture of IV was only 22% but the isomer, m.p. 253–254° was identified after isolation from methanol solution by its X-ray diffraction pattern.

Cyclohexene with Mercuric Acetamide, II

Systems comprised of cyclohexene and mercuric acetamide (m.p. 197–198°) (6) in equivalent amounts dispersed in 2,5-dioxahexane, diethyl ether, and acetonitrile gave none of I whether or not nitric acid was present. The odor of cyclohexene was strong when these systems were diluted with water. Extraction of the diluate with diethyl ether yielded unchanged acetamide. Similar results were obtained, when mercuric nitrate and acetamide were treated with cyclohexene (all equimolar) in dioxahexane.

The authors are grateful to the National Research Council for grants-in-aid which made this work possible.

1. R. K. Freidlina and N. S. Kochetkova. Bull. Acad. Sci. U.R.S.S. Classe Sci. Chim. 128 (1945).
2. N. S. Kochetkova, R. Kh. Freidlina, and A. N. Nesmayanov. Bull. Acad. Sci. U.R.S.S. Classe Sci. Chim. 347 (1947).
3. G. Sachs. J. Chem. Soc. 733 (1949).
4. G. F Wright. Can. J. Chem. **30**, 268 (1952).
5. A. Baeyer. Ann. **88**, 278 (1893).
6. W. Schoeller and W. Schrauth. Ber. **42**, 777 (1909).

Received September 1, 1964.
Department of Chemistry,
University of Toronto,
Toronto, Ontario.

HYDRATION OF PURINES, PYRIMIDINES, NUCLEOSIDES, AND NUCLEOTIDES[1]

Michael Falk

Hydration is a major factor determining the structure of deoxyribonucleic acid (DNA) (1–3). It was therefore of interest to examine the hydration of the molecular constituents of DNA (purines, pyrimidines, nucleosides, nucleotides, and related compounds) and to compare it with the hydration of DNA at comparable values of relative humidity.

The 37 compounds used in the present study were the best commercial grades available. Their melting points and their infrared and ultraviolet spectra were determined and compared whenever possible with the data reported in the literature. The weight of water taken up by each compound was determned as a function of relative humidity by the procedure reported in a recent study of DNA (4). Duplicate specimens of 50 to 100 mg, in pyrex weighing bottles, were exposed to atmospheres of constant relative humidity at 21.0 ± 0.5° in glass hygrostats and were weighed daily to 0.1 mg until the weight remained constant *for at least a week*. The dry weight of each sample was obtained by drying it to constant weight in a vacuum of 10^{-3} Torr at room temperature, followed by prolonged drying in vacuum at temperatures up to 100° for those compounds that were stable under such a treatment.

[1]*Issued as N.R.C. No. 8211.*

Can. J. Chem. Downloaded from www.nrcresearchpress.com by 210.87.254.5 on 09/05/12
For personal use only.

with 30 ml of hot methanol. Concentration of this extract yielded 12.7 g (99%) m.p. 213–215°. From this mixture of diastereomers was obtained 0.27 g (22%) m.p. 256–257° of one isomer by repeated crystallization from hot methanol (16 ml per g).

Anal. Calcd. for $C_{16}H_{28}HgN_2O_2$: C, 39.9; H, 5.87. Found: C, 40.0; H, 5.50.

The X-ray diffraction pattern was (10) 5.129; (6) 2.203; (5) 2.038; (4) 2.508; 1.925; (3) 2.640, 1.795, 1.591; (2) 2.508, 2.424.

Reduction with 2 equivalents of sodium borohydride in an otherwise identical system was much less satisfactory. The yield of the diastereomic mixture of IV was only 22% but the isomer, m.p. 253–254° was identified after isolation from methanol solution by its X-ray diffraction pattern.

Cyclohexene with Mercuric Acetamide, II

Systems comprised of cyclohexene and mercuric acetamide (m.p. 197–198°) (6) in equivalent amounts dispersed in 2,5-dioxahexane, diethyl ether, and acetonitrile gave none of I whether or not nitric acid was present. The odor of cyclohexene was strong when these systems were diluted with water. Extraction of the diluate with diethyl ether yielded unchanged acetamide. Similar results were obtained, when mercuric nitrate and acetamide were treated with cyclohexene (all equimolar) in dioxahexane.

The authors are grateful to the National Research Council for grants-in-aid which made this work possible.

1. R. K. Freidlina and N. S. Kochetkova. Bull. Acad. Sci. U.R.S.S. Classe Sci. Chim. 128 (1945).
2. N. S. Kochetkova, R. Kh. Freidlina, and A. N. Nesmayanov. Bull. Acad. Sci. U.R.S.S. Classe Sci. Chim. 347 (1947).
3. G. Sachs. J. Chem. Soc. 733 (1949).
4. G. F Wright. Can. J. Chem. **30**, 268 (1952).
5. A. Baeyer. Ann. **88**, 278 (1893).
6. W. Schoeller and W. Schrauth. Ber. **42**, 777 (1909).

Received September 1, 1964.
Department of Chemistry,
University of Toronto,
Toronto, Ontario.

HYDRATION OF PURINES, PYRIMIDINES, NUCLEOSIDES, AND NUCLEOTIDES[1]

Michael Falk

Hydration is a major factor determining the structure of deoxyribonucleic acid (DNA) (1–3). It was therefore of interest to examine the hydration of the molecular constituents of DNA (purines, pyrimidines, nucleosides, nucleotides, and related compounds) and to compare it with the hydration of DNA at comparable values of relative humidity.

The 37 compounds used in the present study were the best commercial grades available. Their melting points and their infrared and ultraviolet spectra were determined and compared whenever possible with the data reported in the literature. The weight of water taken up by each compound was determned as a function of relative humidity by the procedure reported in a recent study of DNA (4). Duplicate specimens of 50 to 100 mg, in pyrex weighing bottles, were exposed to atmospheres of constant relative humidity at 21.0 ± 0.5° in glass hygrostats and were weighed daily to 0.1 mg until the weight remained constant *for at least a week*. The dry weight of each sample was obtained by drying it to constant weight in a vacuum of 10^{-3} Torr at room temperature, followed by prolonged drying in vacuum at temperatures up to 100° for those compounds that were stable under such a treatment.

[1]*Issued as N.R.C. No. 8211.*

Can. J. Chem. Downloaded from www.nrcresearchpress.com by 210.87.254.5 on 09/05/12
For personal use only.

For the purpose of the experiment the compounds were divided into "hygroscopic", characterized by forming at least a tetrahydrate at high relative humidity, and "non-hygroscopic", forming no higher hydrate than a dihydrate. The non-hygroscopic compounds were only subjected to one series of measurements at gradually increasing values of relative humidity. The hygroscopic compounds were subjected to several cycles of increasing and decreasing relative humidity. "Adsorption" and "desorption" values obtained in this manner often did not coincide.

TABLE I

Hydration of purines, pyrimidines, nucleosides, and nucleotides
(moles H_2O per mole of compound)

		% relative humidity				
		5	49	75	87	93
Adenine*,†		0	0	0		0
Caffeine*		0	0	0		0
Guanine*,†		0	0	0		0
Hypoxanthine*,†		0	0	0		0.1
Theophylline*,†		0	0	0		1.0
Xanthine*,†		0	0	0		0
Cytosine*,†		0	0	0		0.9
Thymine*,†		0	0	0		0
Uracil*,†		0	0	0		0
Adenosine*,†		0	0	0		0
Cytidine†		0	0	0		0
Guanosine*,†		0.4	1.8	1.9		2.0
Inosine†		0				0
Thymidine†		0	0	0		0
Uridine†		0				0
Xanthosine†		0	0.2	0.4		1.0
Deoxyadenosine*		0.3	0.3	0.3	0.3	
Deoxyguanosine*			0			0
Deoxyuridine*						0
2′- and 3′-Adenylic acid*,‡			0.2		0.4	1.2
5′-Adenylic acid*	Ads.§	0.1	0.8	1.7	1.8	1.8
	Des.§	0.9	0.9		1.7	
2′- and 3′-Cytidylic acid*		0		0		0
2′- and 3′-Uridylic acid*			0.2		0.4	1.0

*California Corporation for Biochemical Research, Los Angeles.
†Nutritional Biochemicals Corporation, Cleveland.
‡Pabst Laboratories, Milwaukee.
§Abbreviations: ads. = adsorption; des. = desorption.

The degree of hydration of the compounds investigated at various relative humidities is shown in Tables I and II. Most of the values reported are averages from several determinations. The separate determinations agreed within 0.1 moles of water per mole of compound. The results may be summarized as follows. Purines, pyrimidines, their nucleosides and nucleotides (Table I) do not as a rule become hydrated even at 93% relative humidity, which was the highest relative humidity used in this study. Those few that do, form at the most a dihydrate. On the other hand, the salts of the nucleotides and other compounds containing the *ionic* phosphate group (Table II) begin to take up water at low relative humidity and usually become highly hydrated as relative humidity increases. At 93% relative humidity all but one of the compounds in this class form hydrates higher than a dihydrate, and more than half take up 20 or more molecules of water.

Of all the compounds in Table II the most appropriate for a rough comparison with DNA are the monosodium salts of the nucleotides. Figure 1 compares the hydration

Can. J. Chem. Downloaded from www.nrcresearchpress.com by 210.87.254.5 on 09/05/12
For personal use only.

Can. J. Chem. Downloaded from www.nrcresearchpress.com by 210.87.254.5 on 09/05/12
For personal use only.

TABLE II

Hydration of compounds containing an ionic phosphate group (moles H_2O per mole of compound)

		% relative humidity													
		5	11	23	33	39	44	49	54	59	65	75	80	87	93
Monosodium adenosine-5′-phosphate*	Ads.	0.7	0.9	1.3	2.7	4.1	5.3	6.1	5.6		5.8	9.4	12.2	17.4	29.9
	Des.		1.9	4.1	4.5	5.6	5.7	6.2		7.8		8.9	13.8		
Disodium guanosine-(2′ and 3′)-phosphate†	Ads.	0.7	1.9	3.0	4.1	4.3	4.6	4.9	5.3	5.7	6.3	9.6	10.9		28.0
	Des.	1.1	2.6		4.5		4.8			5.7		9.9		15.3	
Monoammonium deoxy-guanosine-5′-phosphate*	Ads.	0.5	0.6	0.8		1.0		1.7	2.1	2.3	2.6	3.4	4.1	5.7	8.9
	Des.		0.7					1.7				3.5			
Monosodium cytidine-5′-phosphate*	Ads.	1.7	1.9	4.0	4.7	4.9		5.0	5.1	5.2	5.7	7.0	7.1	7.5	29.0
	Des.		2.3				6.5			6.8		7.4			
Trisodium adenosine-5′-diphosphate‡	Ads.	1.7	2.0	3.5	4.8	5.6		7.6			11.2	14.7		20.8	34.5
	Des.	2.8	5.5			7.1				9.7			16.7		
Disodium adenosine-5′-triphosphate‡	Ads.	1.4	1.5	1.8	2.2	2.5		2.7			2.8	3.2		3.8	6.2
	Des.	2.0	2.1			2.9				3.6			4.1		
Barium ribose-5′-phosphate‡	Ads.	0.6	0.7	1.1	1.2	1.2		1.5	1.9	1.8	2.6	4.8	6.0	8.7	17.7
	Des.	0.8	0.9			1.6		1.9		2.1			6.1		
Disodium glucose-6-phosphate‡	Ads.	0.9	1.0	1.7	3.0	3.5	4.0	4.6	5.1	5.7	6.8	9.5	11.0	14.5	27.1
	Des.	3.0		3.5			4.1		5.2					14.5	
Barium glucose-6-phosphate‡	Ads.	0.1	0.2	0.5	0.6	0.7		0.7			1.0	1.6		2.8	3.9
	Des.	3.3	3.4			3.5				3.5			3.5		
Dipotassium glucose-6-phosphate‡	Ads.	2.0	2.0	2.0	2.0	2.0		2.0			2.0	2.0			2.0
Sodium dihydrogen hypophosphite§	Ads.		0	0.4	0.5	0.5		0.6		3.6		6.4		10.6	20.7
	Des.		0.3			0.9				3.6			7.9		
Sodium dihydrogen orthophosphate§	Ads.	0		0	0					1.0	1.0	4.4	6.6	9.6	20.7
	Des.	0.7	1.1	1.4			1.5	2.1			4.0			9.9	
Sodium monohydrogen orthophosphate§	Ads.	0		0			0.3		1.0	1.7	4.0	6.2	6.0	6.0	9.6
	Des.	1.9		1.8			1.8	1.9	6.0		5.9		9.7	11.6	
Sodium orthophosphate§	Ads.	0	0		0.4	0.8		3.9	4.0	3.9	6.8	7.0	7.1	14.5	26.7
	Des.	0			3.3		3.8	4.1	6.7		8.1			14.4	

*Nutritional Biochemicals Corporation, Cleveland.
†California Corporation for Biochemical Research, Los Angeles.
‡C. F. Boehringer & Soehne, Mannheim.
§Fisher Scientific Co., Fair Lawn, N.J.

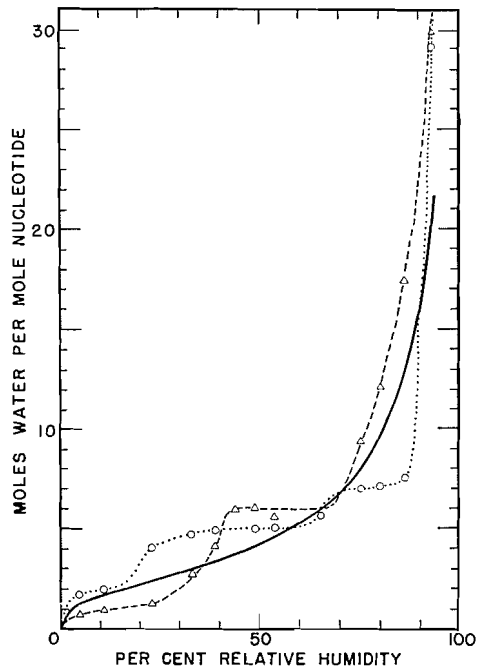

FIG. 1. Hydration curves of the sodium salt of deoxyribonucleic acid (full line), monosodium cytidine-5′-phosphate (circles, dotted line), and monosodium adenosine-5′-phosphate (triangles, broken line).

curves of the two compounds in this class with the hydration curve of the sodium salt of DNA from ref. 4, expressed in moles of water sorbed per mole of 'average nucleotide'. Figure 1 shows that the hydration of DNA is of the same order of magnitude at various relative humidities as that of the salts of single nucleotides. The hydration curves for various types of ribonucleic acid (RNA) and for several synthetic polynucleotides are similar to that for DNA (5). One difference between the hydration curves of polynucleotides and those of nucleotides may be noted; the latter often show plateaux indicating the existence of distinct hydrates, stable or metastable over certain ranges of relative humidity (cf. Fig. 1). Small environmental differences between the successive ionic phosphate groups of the polynucleotide chain can be expected to cause the merging of such plateaux. The complex sequence of four different nucleotides along the DNA or RNA chain may further smooth out the hydration curve.

The present results show that the hydration of nucleotides and of related compounds is very slight, while the hydration of their phosphate salts is high and is of the same order of magnitude as that of polynucleotides. These results suggest that the ionic phosphate groups are the primary sites for the hydration of nucleotides *and* polynucleotides and that these groups are easily accessible to water in the polynucleotides so far examined.

ACKNOWLEDGMENT

A part of this work was carried out at the Spectroscopy Laboratory, Massachusetts Institute of Technology, and was supported by Grant No. A-2262 (C3) from the U. S. National Institutes of Health.

Can. J. Chem. Downloaded from www.nrcresearchpress.com by 210.87.254.5 on 09/05/12
For personal use only.

1. R. E. FRANKLIN and R. G. GOSLING. Acta Cryst. **6**, 673 (1953).
2. M. H. F. WILKINS. J. Chim. Phys. **58**, 891 (1961).
3. M. FALK, K. A. HARTMAN, JR., and R. C. LORD. J. Am. Chem. Soc. **85**, 387, 391 (1963).
4. M. FALK, K. A. HARTMAN, JR., and R. C. LORD. J. Am. Chem. Soc. **84**, 3843 (1962).
5. M. FALK. Unpublished results.

RECEIVED SEPTEMBER 2, 1964.
ATLANTIC REGIONAL LABORATORY,
NATIONAL RESEARCH COUNCIL,
HALIFAX, NOVA SCOTIA.

ERRATUM: PRIMARY PROCESS STUDIES BY MONOISOTOPIC PHOTOSENSITIZATION ON THE REACTIONS OF Hg $6(^3P_1)$ ATOMS WITH ALKYL CHLORIDES

J. K. S. WAN,[1] O. P. STRAUSZ, W. F. ALLEN, AND H. E. GUNNING

(Ref. Can. J. Chem. **42**, 2056 (1964))

On page 2063, line 1, reference (12) should read (12*a*). In paragraph 2, line 2, Masson should read Raal; reference (12) should read (12*b*).

On page 2064, the following should replace references 1, 12, and 13.

1. G. L. LEE and D. J. LE ROY. Can. J. Res. B, **28**, 500 (1950).
12. (*a*) P. GOLDFINGER. Pure Appl. Chem. **5**, 423 (1962).
(*b*) F. A. RAAL and E. W. R. STEACIE. J. Chem. Phys. **20**, 578 (1952).
13. E. CREMER, J. CURRY, and M. POLANYI. Z. Physik. Chem. B, **23**, 445 (1933). See also ref. 1.

DEPARTMENT OF CHEMISTRY,
UNIVERSITY OF ALBERTA,
EDMONTON, ALBERTA.

Can. J. Chem. Downloaded from www.nrcresearchpress.com by 210.87.254.5 on 09/05/12
For personal use only.

Can. J. Chem. Downloaded from www.nrcresearchpress.com by 210.87.254.5 on 09/05/12
For personal use only.

Canadian Journal of Chemistry

Issued by THE NATIONAL RESEARCH COUNCIL OF CANADA

VOLUME 43 FEBRUARY 1965 NUMBER 2

REACTIONS OF OZONIDES

III. OZONOLYSIS OF ETHYL 10-UNDECENOATE IN ETHANOL[1,2]

D. G. M. DIAPER

Department of Chemistry, Royal Military College of Canada, Kingston, Ontario

AND

D. L. MITCHELL

Department of Chemistry, The University College of East Africa, Kampala, Uganda

Received August 12, 1964

ABSTRACT

Diethyl sebacate was the major product obtained by ethanolysis of the ozonization products of ethyl 10-undecenoate in the temperature range 28 to 170 °C. Mixed esters of sebacic acid were similarly obtained, in poor to moderate yields, by alcoholysis of the ozonization product from an alkyl ester of 10-undecenoic acid in the appropriate alcohol. Sebacic acid half esters are prepared by a similar treatment of the ozonization products from 10-undecenoic acid itself. Ester formation has been shown to proceed mainly by rearrangement of an alkoxyhydroperoxide, with oxidative esterification of an aldehyde intermediate contributing to a minor degree.

INTRODUCTION

Ozonolytic cleavage reactions have long been used to determine the positions of the double bonds in unsaturated natural products, but relatively little was known about the mechanism of product breakdown. Knowledge concerning this mechanism has greatly increased during the last decade, largely as a result of the discovery of the reacting solvent systems, particularly aliphatic alcohols. Their use has provided considerable stimulus for current study of the alkoxyhydroperoxides and related peroxidic compounds.

It has been established, largely by the work of Criegee, that ozonization of an olefin in a reacting solvent produces an aldehyde or a ketone, an alkoxyhydroperoxide, and other peroxidic compounds (1, 2, 3). Bailey has studied the formation and decomposition of the ozonization products of phenanthrene in methanol and has reported the formation of an aldehydo–ester in good yield under the appropriate conditions (4, 5). A methyl ester was also detected among the ozonization products of camphene (6), and acenaphthylene in methanol has been found to produce a 50% yield of methyl 8-formyl-1-naphthoate (7).

Isolation of esters from ozonolytic decomposition products has principally been used to gain insight into the possible mechanisms of intermediate product breakdown. For example, ozonization of 1,2-dibenzoylethene in methanol formed the intermediate, α-hydroperoxy-α-methoxyacetophenone, which was purified and subsequently decomposed

[1]*Part II. Can. J. Chem. 40, 1189 (1962).*

[2]*Presented in part at the Edmonton Conference of the Chemical Institute of Canada, June, 1962.*

in refluxing ethanol. Isolation of acids (formic and benzoic), esters (methyl and ethyl formate and ethyl benzoate), and methanol demonstrated the complexity of the decomposition but the quantitative estimation of the constituents suggested that one major and three minor decomposition mechanisms were simultaneously operating (8, 9).

Other instances of ester by-products from ozonization reactions have been reported (10, 11, 12) but the reaction has neither been specifically investigated as a preparative method for obtaining esters from olefinic compounds, particularly the naturally occurring unsaturated fatty acids, nor have optimum reaction conditions been described. The possibility of ester formation through an aldehyde intermediate has been suggested but not explored.

In the present work, we have studied the ozonization of ethyl 10-undecenoate in ethanol and find that moderate yields of diethyl sebacate (50%) can be obtained by the thermal decomposition of the ozonization product in the same alcohol that was used for the ozonization stage. We have attempted to assess the preparative utility of such procedures for preparation of half esters and mixed esters of sebacic acid.

EXPERIMENTAL

Ozonized oxygen was obtained from a Towers apparatus at a concentration of approximately 6%. Heptanal[3] was better than 98% pure; heptanoic acid, detected as the methyl ester, was the only impurity found. The methyl and ethyl esters of heptanoic acid[4] and the ethyl ester of hexanoic acid[4] were prepared by standard procedures and fractionally distilled through a short column (Raschig rings) to give products with a purity better than 98% (g.l.c.).[5] 10-Undecenoic acid[6] had m.p. 21.6–23.2 °C (thermometer immersed) and was esterified with the appropriate alcohols without further purification. The 10-undecenoic esters were distilled through a short column and were better than 99% pure (g.l.c.).

Gas–Liquid Chromatography

Gas–liquid chromatographic analyses were carried out using the Aerograph Hy-FI model with flame ionization detection. Separations were performed on columns (copper tubing, 10 ft. × $\frac{1}{8}$ in. outside diameter) filled with Celite (60–80 mesh) coated with Apiezon L grease (10% w:w) at an oven temperature of 128 °C and a carrier gas (N_2) flow rate of 20 ml/min. Samples were injected directly as neat liquids (0.1–0.3 μl) using a Hamilton syringe. Undecenoic ester solutions were analyzed in the Burrell K3 chromatograph using a hot-wire detector. Separations were performed on columns (copper, 9 ft. × $\frac{1}{4}$ in.) filled with Embacel coated with Apiezon T (10% w:w) at an oven temperature of 215–220 °C and using helium for the carrier gas. (Fig. 1, A and C; Fig. 2, A.) Percentage yields were calculated on the amounts of emerging components and were determined by weighing the respective excised peak traces. Calibration was achieved by comparing peak areas with syringe volume readings (pure liquids and solutions). The average value from 10 runs was quoted.

Under the above conditions, an equimolar synthetic mixture of heptanal, methyl heptanoate, and ethyl heptanoate gave three well-resolved peaks of equal area, showing that the response of the instrument was linear with respect to molar concentration. Mixtures of these three substances in different relative concentrations also gave well-resolved peaks of the expected areas.

Preliminary Experiments

An ethanolic solution of heptanal was diluted with ethereal diazomethane to give a solution with a yellow color persisting for 10 min. Evaporation of the solvents left an oil that gave only two peaks (g.l.c.) that were identified as heptanal (93%) and methyl heptanoate (7%). Repeated addition of ethereal diazomethane and storage up to 12 h increased the formation of the acid derivative to 50%.

Ethyl Ester Formation from Heptanoic Acid

(*a*) Heptanoic acid (5 g) in Analar grade ethanol (50 ml) was heated in a stainless steel pressure vessel at 150–155 °C for 4 h. The ethanol was removed under reduced pressure (75 °C bath temperature and 50 mm) and the residual acid was neutralized with a slight excess of ethereal diazomethane. After removal of the solvents, the mixture was analyzed (g.l.c.). Methyl heptanoate and ethyl heptanoate were the only two constituents detected (excluding the solvent peak) and their identities were confirmed by admixture experiments with authentic specimens. Yield of ethyl heptanoate 23.5%.

[3]*Fluka, A. G., Buchs, Switzerland. Purissima grade.*
[4]*The British Drug Houses Ltd., Poole, Dorset, England. Reagent Grade.*
[5]*Gas–liquid chromatography.*
[6]*Matheson, Coleman, and Bell.*

Can. J. Chem. Downloaded from www.nrcresearchpress.com by 210.87.254.5 on 09/05/12
For personal use only.

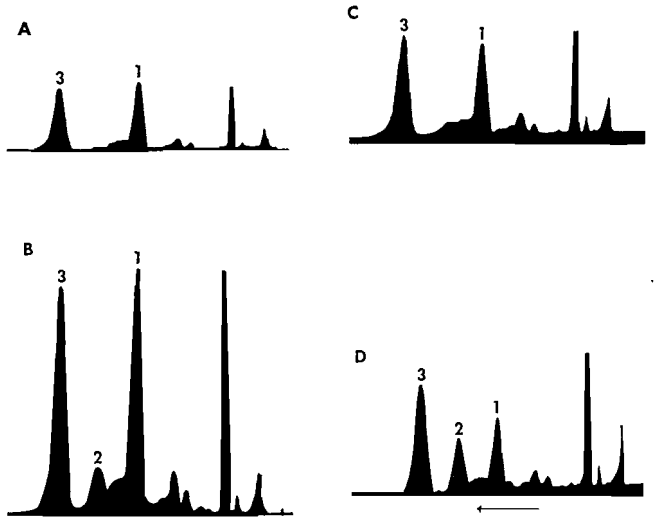

FIG. 1. A. Palladium-catalyzed hydrogenolysis of the ozonolysis products of ethyl 10-undecenoate in ethanol at room temperature (28 °C). B. Products of reaction A after esterification with ethereal diazomethane. C. Heating ozonolysis products of ethyl 10-undecenoate with Raney nickel in ethanol to 100–110 °C. D. Products of reaction C after esterification with ethereal diazomethane. Peak 1, 9-carbethoxynonanal; peak 2, methyl ethyl sebacate; peak 3, diethyl sebacate.

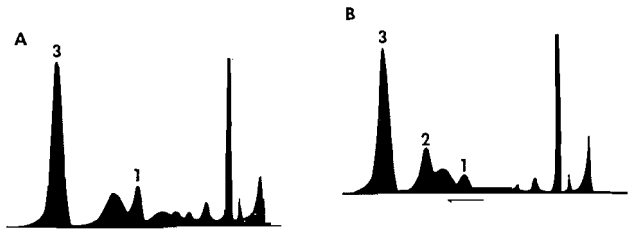

FIG. 2. A. Heating ozonolysis products of ethyl 10-undecenoate in ethanol to 150–155 °C. B. Products of reaction A after esterification with ethereal diazomethane. Peak 1, 9-carbethoxynonanal; peak 2, methyl ethyl sebacate; peak 3, diethyl sebacate.

(*b*) In a duplicate experiment, a stream of ozonized oxygen was passed through a chilled (ice bath) solution of ethanolic heptanoic acid (10% w:v) for 4 h then charged to the pressure vessel and heated as above. After an identical work-up, and analysis (g.l.c.), only the same two constituents were detected and identified. Yield of ethyl heptanoate 23.0%.

(*c*) A repeat experiment of (*b*) was carried out differing only by the heating conditions (200–220 °C, 3 h). No additional peaks were detected but the yield of ethyl heptanoate had increased to 33.9%.

Simulated Ozonolysis Products Decomposition Using a Model Aldehyde–Heptanal in Ethanol (Table I)

An ice-cold solution of heptanal (8 g, 10% w:v) in ethanol was subjected to a stream of ozonized oxygen for 2.5 h. The solution was transferred to the pressure vessel and heated at the above standardized conditions (150–155 °C, 3 h). After solvent removal, the residual oil was taken up in ether (100 ml, peroxide free). Sample 2 of Table I was a 1% aliquot of this solution treated with diazomethane and was found to contain the six components tabulated. Sample 3 was obtained from the main ether solution by sodium bicarbonate extraction followed by acid and diazomethane treatment. Sample 1 was the non-acidic fraction of the main ether solution (6.81 g after solvent removal).

Ozonization Products Decomposition Using a Model Aldehyde – Olefin Mixture – Heptanal and Ethyl 10-Undecenoate in Ethanol

Sample 4, Table I, was an ice-cold solution of ethyl 10-undecenoate (2 g) in ethanol (25 ml). It was subjected to a stream of ozonized oxygen until a test aliquot indicated the absence of unsaturation. The solution was then heated under the standardized conditions described above. Product analysis gave only a baseline trace in the region where products 1–6 (Table I) would have been expected.

Can. J. Chem. Downloaded from www.nrcresearchpress.com by 210.87.254.5 on 09/05/12
For personal use only.

TABLE I

Heptanal–ethanol–ozone reactions

Sample	Starting materials	Products* 1 (heptanal)	2	3	4 (methyl heptanoate)	5 (ethyl heptanoate)	6 (heptanal diethyl acetal)
1	Heptanal in ethanol	40	+†	31	–	14	15
2	Product from 1 treated with diazomethane	+	+	+	+	+	+
3	Methyl ester of acidic products from 1	–	–	–	+	–	–
4	Ethyl undecenoate in ethanol	–	–	–	–	–	–
5	Ethyl undecenoate and heptanal in ethanol	11.3	+	+	18.1‡	12.6	58.6

*Products 1, 4, 5, and 6 were identified as indicated by co-chromatography with authentic specimens. Product 2 was unidentified and appeared as a small shoulder on the heptanal peak. Product 3 had a retention time intermediate between that of methyl heptanoate (b.p. 172°) and ethyl hexanoate (167°) and was not identical with either; it was obtained only in small yield. The – sign means that the product was absent (below 1%); the + sign that it was present. The figures are percentage yields based on heptanal.

†Included in product 1.

‡This figure includes products 2 and 3 which were present only in small quantity.

TABLE II

Reaction conditions for ester formation

Run No.	Decomp. method	Major products*	Gas chromatogram
1	Hydrogenolysis at room temperature†	9-Carbethoxynonanal, diethyl sebacate, ethyl hydrogen sebacate (minor)	Fig. 1, traces A and B
2	Heating ethanolic solution to 100–110 °C (3 h)‡	9-Carbethoxynonanal, diethyl sebacate, ethyl hydrogen sebacate (minor)	Pattern of products similar to Fig. 1, traces C and D
3	Heating ethanolic solution to 150–155 °C (3 h)‡§	Maximum yield of diethyl sebacate, 9-carbethoxynonanal, and ethyl hydrogen sebacate (minor)	Fig. 2, traces A and B
4	Heating ethanolic solution to 170 °C (3 h)‡	Lower yield of diethyl sebacate with increased amounts of polymeric products	Pattern of volatile products similar to Fig. 2, traces A and B

*Products were detected by gas chromatography. Acids were detected as the derived methyl esters.

†Hydrogen at 60–70 p.s.i. over 5% palladium catalyst on calcium carbonate.

‡A duplicate experiment containing a stirred suspension of freshly prepared Raney nickel catalyst gave essentially an identica pattern of products (Fig. 1, A and B).

§A duplicate experiment containing a stirred suspension of powdered sodium sulfite gave an identical pattern of products and a comparable yield of diethyl sebacate.

Sample 5 was obtained from an experiment using heptanal (3 g) and ethyl 10-undecenoate (3 g) in ethanol (50 ml) ozonized and heated in the usual matter. Analysis of the syrupy product (g.l.c.) is shown in Table I.

Diethyl Sebacate

Reaction conditions and products formed in exploratory experiments on ethanolysis of ozonized ethyl 10-undecenoate are presented in Table II. In each case, 10 g samples of ethyl undecenoate in ethanol (50 ml) were ozonized to completion, purged with nitrogen, and hydrogenated as indicated. In this manner, the effect of presence and absence of catalyst and of hydrogen were explored, including trial runs employing Raney nickel W-2 catalyst (30 ml settled volume) or sodium sulfite as mild reducing agents.

A solution of ethyl 10-undecenoate (20 g, n_D^{20} 1.4390) in ethanol (200 ml) was ozonized at ice-bath temperatures. The end point of the reaction was detected by failure of a test sample to decolorize a dilute solution of bromine in glacial acetic acid. The solution was transferred to a top-stirred autoclave pressure

Can. J. Chem. Downloaded from www.nrcresearchpress.com by 210.87.254.5 on 09/05/12
For personal use only.

vessel[7] and heated to 125–150 °C for 4 h. When the vessel was opened, a strong odor of formaldehyde was detected. The solution gave a negative peroxide test with aqueous potassium iodide solution but gave a positive Schiff test, even after prolonged boiling to expel formaldehyde. Examination by g.l.c. gave a pattern of peaks very similar to the trace obtained in the above preliminary experiments (Fig. 2). The constituent corresponding to peak 1 was identified as 9-carbethoxynonanal by co-chromatography with an authentic specimen prepared from ethyl 10-undecenoate by ozonolysis and reduction (13). The constituent corresponding to peak 3 (Fig. 2) was present in greatest yield and was identified as diethyl sebacate, by co-chromatography and by further tests described below. From four experiments, differing only in the rate of heating the autoclave to the maximum temperature (150 °C), the following yields were obtained (excluding peaks assigned to low boiling solvents) 56%, 63%, 61%, and 68%. At this column temperature (220 °C), sebacic acid half ethyl ester did not emerge. Esterification of an aliquot sample with ethereal diazomethane formed the volatile methyl ethyl sebacate and the yield of the acidic constituent could be evaluated (Fig. 2B). The last three runs were combined and fractionally distilled to give diethyl sebacate (36.4 g, 50%) with a b.p. 180–183 °C (14 mm) and n_D^{23} 1.4355 (lit. n_D^{20} 1.4366) (14). The ester gave an infrared spectrum identical to that of an authentic specimen.

Anal. Calcd. for $C_{14}H_{26}O_4$: saponification equivalent, 129. Found: saponification equivalent, 130, 131.

Alkaline hydrolysis afforded sebacic acid which was identified by its melting point, mixed melting point, and infrared spectrum.

From the forerun of the distillation, a crude semicarbazone was obtained by reaction with semicarbazide acetate. Hydrolysis with ethanolic alkali liberated the semicarbazone of 9-carboxynonanal (sebacic semialdehyde) which was recrystallized from ethanol, m.p. 169–170 °C and mixed melting point 169–170 °C. The authentic specimen was prepared from the ozonolysis and reduction of 10-undecenoic acid (13).

Mixed Esters of Sebacic Acid

Mixed esters were prepared by essentially the same procedure as was described in the preceding experiment, by carrying out the ozonization of a 10-undecenoate ester in a series of aliphatic alcohols. The products were purified by fractional distillation and their physical constants have been summarized in Table III.

TABLE III

Mixed sebacic esters

Ester	Method*	Boiling point (°C)	n_D (T °C)	Saponification equivalent	Yield‖ (%)
Ethyl *n*-butyl sebacate	Ethyl 10-undecenoate in *n*-butyl alcohol,†	125 at 0.1 mm	1.4402 (22)	143.0, 145.0,‡ 143.0§	32
	n-Butyl undecenoate in ethanol	125 at 0.1 mm	1.4405 (21)		45
Ethyl *n*-amyl sebacate	Ethyl 10-undecenoate in *n*-amyl alcohol	108 at 0.02 mm	1.4416 (21)	146.0, 150.0, 150.0, 142.7	34
n-Butyl *n*-amyl sebacate	*n*-Amyl 10-undecenoate in *n*-butyl alcohol	105 at 0.03 mm	1.4447 (22)	164.0, 164.7, 164.0	30
Isopropyl isobutyl sebacate	Isopropyl 10-undecenoate in isobutyl alcohol	110 at 0.05 mm	1.4406 (22)	150.7, 155.0, 150.0	23

*Solutions were heated in a pressure vessel at 150 °C for 3 h.
†Crude reaction product contained ca. 5% di-*n*-butyl sebacate (g.l.c.).
‡Saponification equivalent, found.
§Saponification equivalent, calculated.
‖After fractional distillation *in vacuo*.

9-Carbethoxynonanoic Acid (Sebacic Acid Half Ethyl Ester)

An ethanolic solution of 10-undecenoic acid (20 g, 10% w:v) was ozonized to completion at −10 to −20 °C, and then heated to 150 °C in the usual manner. An aliquot portion was removed and analyzed as the derived methyl ester by g.l.c. (10% w:w Apiezon M on silver-coated firebrick at 225–230 °C). Three peaks were detected, excluding low boiling solvent peaks, and were identified by co-chromatography experiments with authentic specimens, as dimethyl sebacate (minor), methyl ethyl sebacate (major), and diethyl sebacate (minor) respectively. Area measurements indicated that these products were present in the ratio of 1.5:7.0:1.5 respectively. An authentic specimen of methyl ethyl sebacate was prepared from monoethyl sebacic acid, m.p. 34–35 °C, and ethereal diazomethane.

The alcoholic reaction solution was concentrated to a thin syrup under reduced pressure and diluted with ether. The ethereal solution was extracted with cold sodium bicarbonate solution. The bicarbonate extracts

[7] *Autoclave Hydrogenator, Superpressure Division of the American Instrument Company, Inc., Silver Springs, Maryland, U.S.A.*

Can. J. Chem. Downloaded from www.nrcresearchpress.com by 210.87.254.5 on 09/05/12
For personal use only.

were acidified and the liberated carboxylic acids were collected with ether. Concentration of the dried ether extract afforded crude 9-carbethoxynonanoic acid (12 g) as a hygroscopic semisolid. The syrupy impurity was partially separated on unglazed porcelain tile and a product of m.p. 36–40 °C was obtained. Analysis of the derived methyl ester by g.l.c. indicated a purity of 83 ± 5% with dimethyl sebacate being the major impurity.

Anal. Calcd. for $C_{12}H_{22}O_4$: acid equivalent, 230; calcd. for a 4:1 mixture of sebacic acid ethyl ester – sebacic acid: acid equivalent, 204. Found: acid equivalent, 202.

Hydrogenolysis of the Ethanolic Ozonization Product from Ethyl 10-Undecenoate

By the previously described method, a solution of ethyl 10-undecenoate (20 g) in ethanol (200 ml) was ozonized and hydrogenated using an aged sample of Raney nickel catalyst (19). Hydrogenation was initially carried out at 2 000 p.s.i. and at room temperature (4 h). The temperature was then raised to 140 °C and held there for a further 4 h. Relative yields of diethyl sebacate and ethyl 10-hydroxydecanoate were determined using gas chromatography (oven temperature, 170 °C). In synthetic admixture and in the hydrogenolysis sample, the peaks were imperfectly resolved, but their areas were estimated by triangular approximation to be in the ratio of 2 moles of diester to 1 mole of hydroxyester. In a second run, using freshly prepared Raney W-2 catalyst and a slow rate of heating the autoclave, the yield of hydroxyester predominated and the relative peak areas were almost exactly reversed.

DISCUSSION

Decomposition of ozonolysis products under the appropriate conditions has resulted in the preparation of satisfactory yields of carboxylic acids (90–100%) (15, 16), aldehydes (80–90%) (17), and alcohols (75–90%) by organohydride reductions (18, 19) while moderate yields of amines (40–60%) (11, 12), esters (ca. 50%) (4–7), and alcohols (ca. 50%, by pressure hydrogenolysis) (19) have been reported. In some cases improved yields have been attributed to the use of alcohols for the ozonization solvent (17). Decomposition at low temperature has been found necessary for reactions involving a hydrogenation stage if a pure product was to be obtained. In two previous investigations, the implication has been that elevated temperatures increased side reactions (11, 17) and direct evidence that the side reactions were significant was obtained from reductive amination experiments where by-products such as aldehydes (12), acids (12), and esters (11) were identified. Since high temperatures were also employed in the ozonolysis–pressure reduction of ethyl 10-undecenoate (19), reinvestigation of this reaction, using product analysis by g.l.c., demonstrated that the product was a mixture of ethyl 10-hydroxydecanoate and diethyl sebacate. The ratio of the products was dependent upon the activity of the Raney nickel catalyst and also upon the rate of heating of the pressure autoclave. Clearly, this experiment demonstrated that a competition between hydrogenation and ester formation takes place. Palladium-catalyzed hydrogenolysis of an ethanolic solution of ozonization products from ethyl 10-undecenoate gives predominantly 9-carbethoxynonanal at 0°. By the use of similar pressure, solvent, and catalyst conditions and a temperature (28°) only slightly elevated, significant amounts of diethyl sebacate and sebacic acid half ethyl ester were concurrently formed (Fig. 1, A and B). Although esters were initially observed in all of these reduction-type reactions, a systematic elimination of reaction variables indicated that heating the alcoholic ozonolysis solution at an elevated temperature was the major factor involved in ester formation. Optimum heating conditions were obtained where the ester (diethyl sebacate) was now predominantly formed (ca. 60%) and the respective aldehyde and half acid ethyl ester were present as comparatively minor constituents (Fig. 2, A and B).

The ozonolytic fission of ethyl 10-undecenoate (I), an unsymmetrically alkylated olefin, in ethanol can be expected to take place as a competition between two reactions I → II and III and I → IV and V. Other dimeric and polymeric peroxidic products may possibly be formed.

It can be reasonably assumed that the direction of ring opening in the postulated primary ozonization product VIII, should be controlled by the inductive effect of a

Can. J. Chem. Downloaded from www.nrcresearchpress.com by 210.87.254.5 on 09/05/12
For personal use only.

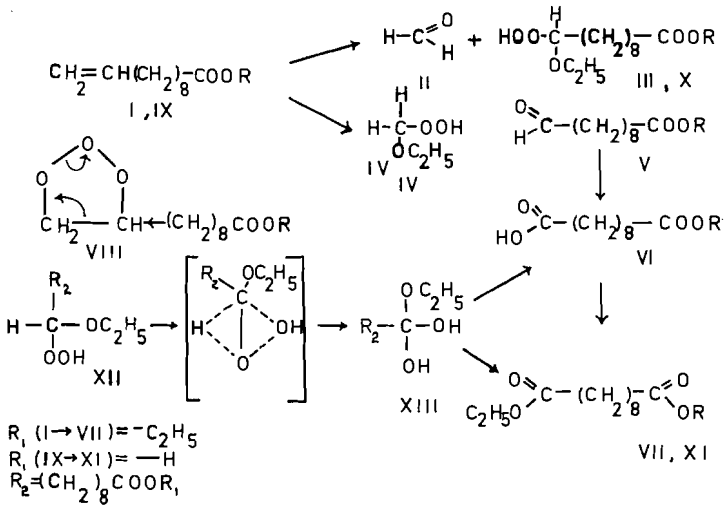

chain of eight methylene groups with negligible influence expected from the terminal carbethoxyl group. Nucleophilic attack at the 10-position yielding III or X rather than at the 11-position giving V are the two possible routes of attack. We favor the former route because it best explains the observations discussed below (see also ref. 3). Scission of the ring in the direction indicated by the arrows should favor the formation of II and III in preference to IV and V (20, 21).

Ester formation could theoretically also occur via 9-carbethoxynonanal (V) by oxygen/-ozone oxidation to 9-carbethoxynonanoic acid (VI) followed by esterification to diethyl sebacate (VII), during autoclaving of the ethanolic solution.

We have checked both steps of this route using heptanal and heptanoic acid as model compounds. Autoclaving an ethanolic solution of heptanoic acid under standardized conditions formed ethyl heptanoate in 23% yield with the remainder being unchanged heptanoic acid. This figure was probably not the equilibrium concentration of ester but rather the final yield to be expected under the alcoholysis experimental conditions. The ester yield was unaffected by pretreatment with ozone, but increased by temperature increase. Similarly, heptanal in ethanol solution was partially oxidized by the oxygen/-ozone mixture to heptanoic acid, even in admixture with a competitive olefin. Autoclaving this solution afforded a complex mixture of at least six constituents with ethyl heptanoate being formed in about 12.5% yield.

Assuming that the model aldehyde will exhibit a reactivity in the preceding reactions not significantly different from that of 9-carbethoxynonanal (V), it would appear that the yield of diethyl sebacate expected from this route (V → VI → VII) would be ca. 10–20%. Since ester yields of ca. 60% were obtained (Fig. 2), the major reaction route most likely proceeded via the preferred intermediate, the alkoxyhydroperoxide (III).

Support for decomposition of the intermediate alkoxyhyroperoxide was also obtained from the thermal decomposition of ozonolyzed ethanolic 10-undecenoic acid (IX). Product analysis after treatment with diazomethane indicated that dimethyl sebacate, 9-carbethoxynonanoic acid (sebacic acid half ethyl ester), and diethyl sebacate were formed in the ratio of 1.5:7.0:1.5 respectively. These results indicated that both aldehyde oxidation to carboxyl and ethyl ester formation were occurring as comparatively minor reactions, but the major product, the half ethyl ester, could have been obtained only by

Can. J. Chem. Downloaded from www.nrcresearchpress.com by 210.87.254.5 on 09/05/12
For personal use only.

selective ester formation at one end of the chain. Rearrangement and decomposition of (X) could provide a tentative explanation.

The preparation by classical means of half esters of such acids as sebacic offers some practical difficulty. Equilibrium partial esterification of the acid gives a low yield of half ester and it is difficult to purify because of further equilibration during isolation. The Grün and Wirth procedure of rapid partial saponification of the diester attempts to achieve kinetic control of the half-ester proportion but is only partially successful. Saponification of the diester by methanolic baryta gives good yields of insoluble barium salt of the half ester and is judged to be of comparable convenience with the method here described. The ozonide alcoholysis route is virtually independent of the vagaries of esterification equilibria, and, in the case of easily alcoholyzed ozonization products, may offer a preferred route for half-ester preparation. A suggested alternative half-ester preparation having similar advantages is oxidative work-up of ozonolysis products from esters of undecenoic acid.

Rearrangement of the alkoxyhydroperoxide (XII), according to Bailey's suggested mechanism (8), could take place through a concerted 1,2-hydrogen shift to form intermediate (XIII). Intermediate (XIII) could be decomposed by two possible routes to form the ester (VII), with loss of a molecule of water, or the carboxylic acid (VI), with loss of a molecule of ethanol. Decomposition entirely by route (XII) → (XIII) → (VI) would form the carboxylic acid (sebacic acid half ethyl ester) which has been demonstrated, by model experiments, to yield about 23% ethyl ester under standardized autoclaving conditions. Decomposition predominantly by route (XII) → (XIII) → (VII) would directly form the ethyl ester. This route of decomposition provides the only alternative, of the routes outlined, that avoids esterification of the carboxylic acid group and could possibly account most reasonably for the yields of diethyl sebacate obtained. An alternative route from the *gem*-diol (XIII) to the ester (VII) without passing through the acid (VI) is the replacement by —OEt of one of the —OH groups of (XIII). A large excess of ethanol would facilitate this process, which would if completed, give the ortho ester, $R_2C(OEt)_3$. Elimination of ethanol would then produce the ester (VII).

On the basis of this alternate route of ester formation, higher mixed esters from an unsaturated fatty acid could be prepared by esterification with the first alcohol, then the second ester group could be introduced at the double bond by ozonolysis and thermal decomposition in the second alcohol. We have selected the terminal unsaturated fatty acid, 10-undecenoic acid (IX), and have prepared a representative number of mixed esters in poor to moderate yield, by the suggested two-step synthesis.[8] Further examples of mixed and half esters will be the subject of another publication.

Our previous work on preparative ozonization has assumed that ozonization products may be regarded as aldehyde or ketone precursors. In reacting solvents this view must be somewhat modified, yet we have successfully employed the concept in synthesis of amino acids which will be the subject of a further communication.

ACKNOWLEDGMENTS

The authors wish to thank the Central Research Grants Committee, Makerere University College, for a maintenance grant. For valuable assistance in the laboratory, they wish to thank Mr. M. S. Schwemin and Mr. E. S. P. Wasula-Kyaze.

[8]*We have considered and rejected for this reaction the term "alcozonolysis" in conformity with the reactions named by Fields "cyanozonolysis" and "amozonolysis" (22, 23).*

Can. J. Chem. Downloaded from www.nrcresearchpress.com by 210.87.254.5 on 09/05/12
For personal use only.

REFERENCES

1. R. CRIEGEE. Record Chem. Progr. Kresge-Hooker Sci. Lib. **18**, 111 (1957).
2. R. CREIGEE. Ann. **560**, 127 (1948).
3. P. S. BAILEY. Chem. Rev. **58**, 925 (1958).
4. P. S. BAILEY. J. Am. Chem. Soc. **78**, 3811 (1956).
5. P. S. BAILEY and S. B. MAINTHIA. J. Org. Chem. **23**, 1089 (1958).
6. P. S. BAILEY. Ber. **88**, 795 (1954).
7. R. H. CALLIGHAN, M. F. TARKER, JR., and M. H. WILT. J. Org. Chem. **26**, 1379 (1961).
8. P. S. BAILEY and Y. G. CHANG. J. Org. Chem. **27**, 1192 (1962).
9. P. S. BAILEY, Y. G. CHANG, and W. W. L. KWIE. J. Org. Chem. **27**, 1198 (1962).
10. J. PASERO, J. CHOUTEAU, and M. NAUDET. Bull. Soc. Chim. France, 1717 (1960).
11. D. G. M. DIAPER and D. L. MITCHELL. Can. J. Chem. **40**, 1189 (1962).
12. K. A. POLLART and R. E. MILLER. J. Org. Chem. **27**, 2392 (1962).
13. C. R. NOLLER and R. ADAMS. J. Am. Chem. Soc. **48**, 1074 (1926).
14. A. I. VOGEL. J. Chem. Soc. 642 (1948).
15. P. S. BAILEY, R. H. PERRY, JR., C. A. COHEN, and L. K. BEACH. British Patent No. 844,825 (1960); Chem. Abstr. **55**, 5379 (1961).
16. R. G. ACKMAN, M. E. RETSON, L. R. GALLEY, and F. A. VANDENHEUVEL. Can. J. Chem. **39**, 1956 (1961).
17. E. H. PRYDE, D.E. ANDERS, H. M. TEETER, and J. C. COWAN. J. Org. Chem. **25**, 618 (1960).
18. J. A. SOUSA and A. L. BLUHM. J. Org. Chem. **25**, 108 (1960).
19. D. G. M. DIAPER and D. L. MITCHELL. Can. J. Chem. **38**, 1976 (1960).
20. P. S. BAILEY and S. S. BATH. J. Am. Chem. Soc. **79**, 3120 (1957).
21. P. S. BAILEY, S. B. MAINTHIA, and C. J. ABSHIRE. J. Am. Chem. Soc. **82**, 6136 (1960).
22. E. K. FIELDS. Talk presented at the 148th American Chemical Society national meeting.
23. M. I. FREMERY and E. K. FIELDS. J. Org. Chem. **29**, 2240 (1964).

Can. J. Chem. Downloaded from www.nrcresearchpress.com by 210.87.254.5 on 09/05/12
For personal use only.

Can. J. Chem. Downloaded from www.nrcresearchpress.com by 210.87.254.42 on 09/05/12
For personal use only.

STRUCTURAL STUDIES BY MASS SPECTROMETRY

DETERMINATION OF THE STRUCTURE OF LYCOFAWCINE (BASE L)

W. A. AYER, W. R. BOWMAN, AND P. KEBARLE
Department of Chemistry, University of Alberta, Edmonton, Alberta

AND

R. H. BURNELL
Department of Chemistry, Laval University, Quebec, Quebec

Received September 16, 1964

ABSTRACT

The mass spectra of lycofawcine (base L from *L. fawcettii*) and some of its derivatives are recorded and discussed. On the basis of the interpretation of the mass spectra a structure (IV) is proposed for lycofawcine. Experiments which confirm structure IV are described, and the stereochemistry of lycofawcine is discussed.

The isolation and characterization of an alkaloid designated base L from *Lycopodium fawcettii* was reported recently (1). At that time it was suggested that base L is a tricyclic tertiary base possessing a tertiary hydroxyl, a secondary equatorial hydroxyl, and a secondary axial O-acetyl grouping. An examination of the mass spectra of base L and some of the transformation products described previously (1) has now been carried out. The results, which are discussed below, permit the deduction of a structure for base L and this structure has been confirmed by means of chemical transformations. Since the relation between base O, another alkaloid of *L. fawcettii* (2), and base L has already been determined (1), this also establishes the structure of base O. For ease of reference we suggest the trivial name lycofawcine for base L, and acetyllycofawcine for base O.

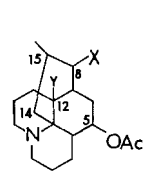

I X=Y=H
II X=OAc, Y=H

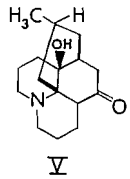

V

IV X=Y=OH

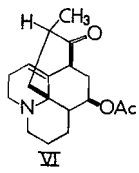

VI

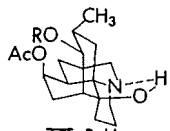

VII R=H
VIII R=Ac

The mass spectra of lycofawcine, desacetyllycofawcine, dehydrolycofawcine, and desacetyldehydrolycofawcine are shown in Figs. 1, 2, 3, and 4, respectively. The most obvious deduction to be made from the mass spectra is that the molecular formula $C_{18}H_{31}NO_4$ (molecular weight 325) originally suggested (1) for lycofawcine is incorrect and should be changed to $C_{18}H_{29}NO_4$ (molecular weight 323). This requires that the

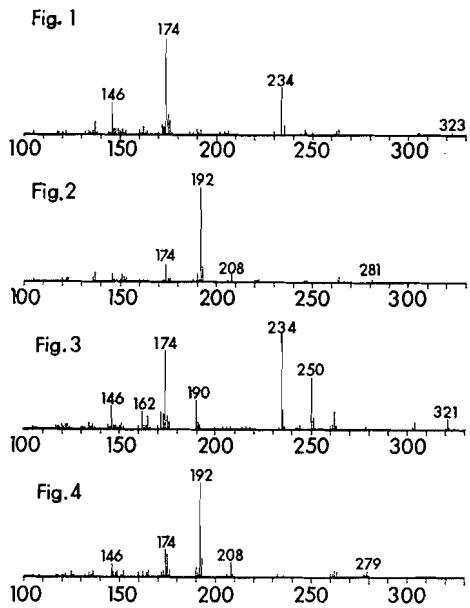

FIGS. 1–4. Mass spectra of lycofawcine and derivatives: 1, lycofawcine; 2, desacetyllycofawcine; 3, dehydrolycofawcine; 4, desacetyldehydrolycofawcine. Peaks with an intensity greater than 2% of the most intense peak are shown.

base be tetracyclic, nor tricyclic as originally suggested. Besides the weak molecular ion at *m/e* 323, the mass spectrum of lycofawcine (Fig. 1) shows strong peaks at *m/e* 234, 174 (base peak), and 146. This fragmentation pattern is reminiscent of that of O-acetyldihydrolycopodine (I) (3) and O-acetyllofoline (II) (4) and is consistent with structure A for lycofawcine, where two of the X's are hydroxyl and the other hydrogen, as shown in Scheme I. The appearance of a C-methyl doublet in the nuclear magnetic resonance (n.m.r.) spectra of derivatives of lycofawcine eliminates C-15 as a possible position for a hydroxyl group. Since elimination of water does not occur as readily as elimination of acetic acid (compare the mass spectra of dihydrolycopodine and O-acetyldihydrolycopodine (3)), the mass spectrum of desacetyllycofawcine (Fig. 2) has its base peak at *m/e* 192 (ion B, OH instead of OAc) rather than at 174.

Dehydrolycofawcine, in which one of the hydroxyl groups of lycofawcine is oxidized

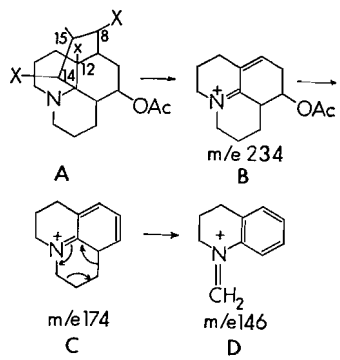

SCHEME 1

Can. J. Chem. Downloaded from www.nrcresearchpress.com by 210.87.254.42 on 09/05/12
For personal use only.

to a ketone (1), again displays strong peaks in its mass spectrum (Fig. 3) at *m/e* 234, 174, and 146 corresponding to ions B, C, and D in Scheme 1, suggesting that the keto group is located on the bridge at either C-8 or C-14. Provided the absolute configuration is as illustrated in A, a decision between the two positions can be made by application of the Octant rule (5). As predicted if the ketone is located at C-8, the optical rotatory dispersion curve for dehydrolycofawcine shows a negative Cotton effect curve. If the ketone were at C-14 a positive Cotton effect would be expected. In the mass spectrum of dehydrolycofawcine, besides the peaks at 234, 174, and 146, prominent peaks are also observed at *m/e* 250, 190, and 162. These peaks are easily accounted for if the remaining hydroxyl group is located at C-12 instead of C-14, fragmentation of dehydrolycofawcine (III) occurring as shown in Scheme 2 to give ions E, F, and G. On this basis we arrive at structure IV for lycofawcine.

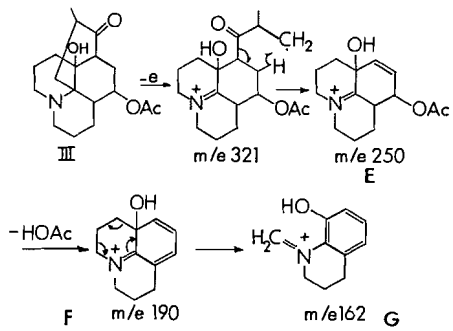

SCHEME 2

The mass spectrum of desacetyldehydrolycofawcine (III, OH in place of OAc) shows (Fig. 4) prominent peaks corresponding to ions of type B (*m/e* 192, OH in place of OAc), C, D, E (*m/e* 208, OH in place of OAc), and F.

In order to confirm the deductions made above dehydrolycofawcine (III) was dehydrated, using conditions similar to those used (6) in dehydrating lycodoline (V). The product was identical with O-acetylacrifoline (VI) (7), corroborating structure III for dehydrolycofawcine and hence IV for lycofawcine. Since the stereochemistry of acrifoline is known this result also establishes the stereochemistry of lycofawcine at all points except C-8, C-12, and C-15. Dehydrolycofawcine (III), like lycodoline (V), (6), has an intramolecularly hydrogen-bonded hydroxyl group (concentration independent band at 3 565 cm^{-1} in the infrared (CCl_4 solution)), and since none of the lycofawcine derivatives show "Bohlmann bands", characteristic of *trans*-quinolizidines (8), the stereochemistry at C-12 must be the same as in lycodoline (V) and as shown in the conformational drawing VII. The configuration at C-15 is not rigorously defined, but is assigned on the basis of analogy with other Lycopodium alkaloids which have, except in cases where there is a carbonyl group at C-8, the configuration shown. The assignment of configuration at C-8 is based on the earlier suggestion (1) that the secondary hydroxyl is equatorial. Base O, which is acetyllycofawcine (1), must have structure VIII.

EXPERIMENTAL

The mass spectra were determined on a AEI MS2-H mass spectrometer at an ionizing potential of 70 eV. Samples were introduced through a heated inlet system maintained at 200°. Infrared spectra were determined by Mr. R. N. Swindlehurst and his associates using a Perkin–Elmer Model 421 spectrophotometer.

Can. J. Chem. Downloaded from www.nrcresearchpress.com by 210.87.254.42 on 09/05/12
For personal use only.

Dehydrolycofawcine

Dehydrolycofawcine was prepared as previously described (1). Infrared spectrum (CCl_4): ν_{max} 3 565 (concentration independent, intramolecularly H-bonded hydroxyl), 1 736 (OAc), 1 703 cm^{-1} (ketone). Nuclear magnetic resonance spectrum ($CDCl_3$): τ 4.97 (1H, quartet, C*H*OAc), 8.02 (3H, singlet, $OCOCH_3$), 8.74 (3H, doublet, splitting 6 c.p.s.). Rotatory dispersion in methanol (*c* 0.10): $[\phi]_{589}$ −190°, $[\phi]_{400}$ −475°, $[\phi]_{305}$ −2025°, $[\phi]_{260}$ +825°.

Dehydration of Dehydrolycofawcine

Dehydrolycofawcine (55 mg) was dissolved in a 1:1 solution of phenylphosphoric dichloride : pyridine (6 ml) and maintained at 65° for 20 h. The excess phenylphosphoric dichloride was then decomposed by the slow addition of ice and water. Sodium hydroxide pellets were added until the solution was alkaline and the resulting solution was extracted with chloroform. Evaporation of the chloroform left a viscous oil (40 mg). Thin layer chromatography (t.l.c.) indicated the presence of O-acetylacrifoline as well as some starting material. The crude product was subjected to chromatography over basic alumina (4 g). Elution with ether–chloroform (7:3) yielded O-acetylacrifoline (25 mg) identical (infrared spectrum, t.l.c. behavior, mixed melting point undepressed), with an authentic sample.

The methiodide, prepared in methanol, and recrystallized from acetone–ether, melted at 278–279°. When admixed with an authentic sample of O-acetylacrifoline methiodide, m.p. 281–282°, it melted at 280–281°.

ACKNOWLEDGMENTS

We wish to thank Messrs. R. Taylor and W. Duholke for their assistance in determining the mass spectra, and the National Research Council for financial support.

REFERENCES

1. R. H. Burnell, C. G. Chin, B. S. Mootoo, and D. R. Taylor. Can. J. Chem. **41**, 3091 (1963).
2. R. H. Burnell, B. S. Mootoo, and D. R. Taylor. Can. J. Chem. **38**, 1927 (1960).
3. D. B. MacLean. Can. J. Chem. **41**, 2654 (1963).
4. W. A. Ayer, A. N. Hogg, and A. C. Soper. Can. J. Chem. **42**, 949 (1964).
5. W. Moffit, R. B. Woodward, A. Moscowitz, W. Klyne, and C. Djerassi. J. Am. Chem. Soc. **83**, 4013 (1961).
6. W. A. Ayer and G. G. Iverach. Can. J. Chem. **42**, 2514 (1964).
7. W. N. French and D. B. MacLean. Can. J. Chem. **39**, 2100 (1961).
8. F. Bohlmann. Chem. Ber. **91**, 2157 (1958).

Can. J. Chem. Downloaded from www.nrcresearchpress.com by 210.87.254.42 on 09/05/12
For personal use only.

Can. J. Chem. Downloaded from www.nrcresearchpress.com by 210.87.254.42 on 09/05/12
For personal use only.

β-AMINOCROTONONITRILE

I. GEOMETRICAL ISOMERISM AND SOME REACTIONS

E. BULLOCK AND B. GREGORY

Department of Chemistry, Memorial University, St. John's, Newfoundland

Received August 26, 1964

ABSTRACT

The low-melting form of β-aminocrotononitrile is a mixture of two components, one of which is the high-melting isomer. Isomerization reactions between the high- and low-melting forms occur very easily, reactions in solution being subject to acid–base catalysis. Self-condensation of β-aminocrotononitrile gives 4-amino-1,3-dicyano-2-methylpenta-1,3-diene which readily cyclizes to 2-amino-5-cyano-4,6-lutidine.

Condensation of β-aminocrotononitrile with 1,2-dichloroethyl ethyl ether gives the chloromethyldihydropyridine (I) and other products (1, 2). During attempts to increase the yield of (I) at the expense of by-products we examined the isomeric composition of the nitrile.

In connection with the nomenclature of the geometrical isomers of the title compound, double bonds carrying four different substituents cannot be described unambiguously by the terms *cis-* and *trans-*, without a definition. Conn and Taurins (3) define (II) as *cis-* and (III) as *trans-β*-aminocrotononitrile, presumably on the reasonable basis that CH_3— and H— are the 'most alike' of the substituents (4).

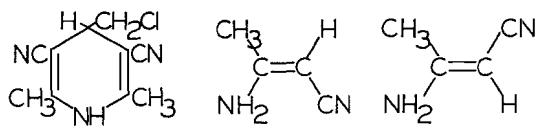

I II III

We wished to compare proton nuclear magnetic resonance (n.m.r.) spectra of the nitrile with those of crotonic acid derivatives, and it is possible to make a definition in terms of the parent nitriles. This leads to the description of (II) as *trans* and (III) as *cis* but is more convenient for the present purpose than the older nomenclature. Thus, in this paper the terms *cis-* and *trans-β*-aminocrotononitrile refer to formulas (III) and (II) respectively and are the reverse of those in ref. 3.

Two forms of β-aminocrotononitrile have been described (5, 6, 7), and recently it was suggested that the high-melting form (m.p. ca. 80°) was the *cis*-compound (III) and the low-melting material (m.p. ca. 50°) has the *trans*-configuration (II) (3).

The n.m.r. spectra of the two forms show that the low-melting material is a mixture of two components, one of which is the high-melting form. (The spectra are consistent with the assignment of structure (III) to the high-melting form; see detailed discussion of n.m.r. results.) The composition of the low-melting material is variable and depends on the method of preparation, the solvents used, and even the storage conditions. It has been noted that the melting point of the low-melting material rises on keeping in the solid phase (8) and this change corresponds to an increase in the proportion of the *cis*-isomer.

The high-melting form is isomerized on heating under reflux in benzene (6) or on attempted recrystallization from ethanol (3). The conversion is subject to acid–base

Can. J. Chem. Downloaded from www.nrcresearchpress.com by 210.87.254.42 on 09/05/12
For personal use only.

catalysis. Thus, acetic acid (0.1 *M* solution) in benzene accomplishes the change in less than 5 min at room temperature. A similar concentration of piperidine in benzene completes the same reaction in about 6 h. The final composition of the product of the reaction depends on the solvent used, but is insensitive to low concentrations of acid or base. If any β-aminocrotononitrile is allowed to stand in commercial chloroform for 2 days, it achieves a composition (which is somewhat concentration dependent) of about 65% of (II) and closely resembles material isolated by the literature preparation of the low-melting form (3). Melting point is a poor criterion of composition of β-aminocrotononitrile except for the very pure *cis*-form (m.p. 78–80°). In general, a material which melts below about 55° will have a preponderance of the *trans*-compound. Repeated fractional sublimation (40°, 0.1 mm) of the chloroform equilibration mixture gives material, m.p. 41–53°, which is about 90% *trans*-isomer. We have been unable to improve the purity of this isomer any further. This material rapidly equilibrates to the starting mixture when dissolved in chloroform.

The recorded solubility data for the nitrile (3) suggest that the *cis*-compound (III) is about 2.5 times more soluble in benzene in the presence of the *trans*-isomer than when it is pure. This fact, plus the marked sensitivity of the n.m.r. peak positions to concentration and the reasonably well-defined melting point of the equilibrated material, suggests that strong intermolecular complexing occurs when the two isomers are present in the same solution. Cryoscopic molecular weight determinations in benzene were limited by solubility, but even in 0.15 *M* solution, the molecular weight of the low-melting form is about 30% high. Infrared comparisons were limited (by solubility difficulties) to chloroform solutions and mulls. The only differences between the solution spectra of the high- and low-melting forms were in intensities of certain bands. The relative absorbances of these particular absorptions are noted in the Experimental section.

Clarification of the mechanism of the isomerization reactions in the solution and solid phases is being sought through rate studies.

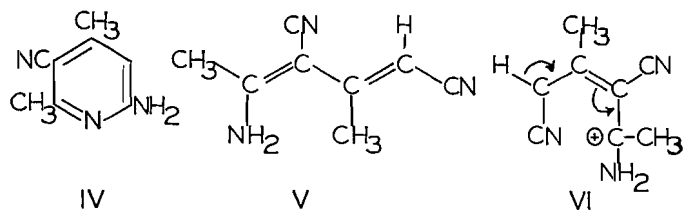

IV V VI

The main by-product from the preparation of (I) is a white, crystalline solid, $C_8H_9N_3$, which shows two intense nitrile absorptions in the infrared spectrum. The n.m.r. spectrum (partially shown in Fig. 1) indicates the presence of two methyl groups, one of which is coupled ($J \sim 0.9$ c.p.s.) to an olefinic proton. The compound yields 2-amino-5-cyano-4,6-lutidine (IV) (6) under a variety of conditions and is thus formulated as the pentadiene derivative (V). (This formula is not intended to imply a proved stereochemistry.) In pyridine solution (9) the n.m.r. absorptions are more complex (Fig. 1) and strongly suggest that the compound is a mixture of conformational (or, less likely, geometric or tautomeric) isomers. The NH region of the infrared spectrum (in chloroform) also supports this idea, though the melting point is very sharp. Recovery of the compound from pyridine solution gives a substance which is identical in all respects with starting material. Compounds with similar melting characteristics to those of (V) have been reported previously (10, 11) from reactions involving β-aminocrotononitrile and may be identical with our material. A

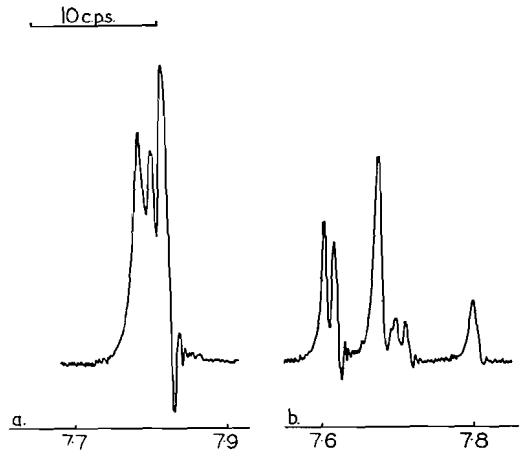

FIG. 1. Partial nuclear magnetic resonance spectra of (V): (*a*) in d_6-dimethylsulfoxide, (*b*) in pyridine.

mechanism for the self-condensation of β-aminocrotononitrile (to pyridine derivatives) has been proposed (12), and involves the formation of a carbonium ion intermediate (VI). Loss of a proton from this intermediate would give (V). This product contrasts with that from the acid-catalyzed dimerization of diphenylacetaldimine, $(C_6H_5)_2$—CH—CH=NH (or tautomer), in which attack of the enamine on the imine form gives a divinylamine $[(C_6H_5)_2C{=}CH]_2NH$ (13).

The use of pure *cis*-β-aminocrotononitrile in the preparation of (I) causes a marked decrease in the reaction rate (cf. ref. 8), but does not materially affect the composition of the product. Since formation of both (I) and (V) occurs with elimination (of the elements of ammonia) there may be a steric factor in the reaction which requires the presence of both isomers. Thus the rate of formation of products from pure *cis*-isomer would be slow and dependent largely on the rate of isomerization. A modified technique for the preparation of (I) using water as a moderator (14) gives a good yield of the desired product.

EXPERIMENTAL

Melting points (uncorrected) were determined in capillaries (for β-aminocrotononitrile samples) or on a Kofler block. Nuclear magnetic reso nance spectra were recorded on a Varian A-60 analytical spectrometer and peak positions are given on the τ-scale. Infrared spectra were recorded on a Perkin–Elmer Model 237B spectrometer.

Nuclear Magnetic Resonance Results

Nuclear magnetic resonance studies of *cis-/trans*-isomers of β-substituted crotonic acid derivatives (bibliography in ref. 15) have led to the generalization that the methyl signal of a *trans*-compound will occur to high field of the methyl signal of the corresponding *cis*-isomer. The position of the signal is relatively unaffected by the substituent on C-3. Further, olefinic protons of $CH_3.CX{=}CH.COOR$ (R = H, Me, etc.) isomers show the reverse order, i.e. the *trans*-olefinic proton occurs to low field of the corresponding *cis*-proton. This holds for a number of derivatives (15) but the position of the olefinic proton signal is very sensitive to the nature of X. In particular, the *trans*-proton appears to be more affected by electron-donating substituents on C-3 than does the *cis*-proton, through in no case is the difference large enough to reverse the generalization. The n.m.r. spectra of crotononitrile isomers have been analzyed (16) and the above generalizations still hold. In this example, however, the *cis*-2-proton is only 0.05 p.p.m. to high field of the corresponding *trans*-proton. (The corresponding difference in the methyl crotonates is 0.63 p.p.m. (17).) Table I shows that the resonance signals for the two forms of β-aminocrotononitrile do not follow the generalization for the esters since the isomer with the high field methyl signal also has the high field olefinic proton. Since chemical evidence favors (III) for the high-melting isomer (3), the n.m.r. results will be consistent with known effects if it is postulated that the primary amino-group reverses the expected order for the olefinic protons.

Can. J. Chem. Downloaded from www.nrcresearchpress.com by 210.87.254.42 on 09/05/12
For personal use only.

TABLE I

Compound	Solvent	Olefinic H	Methyl H	NH	J (c.p.s.)
cis-β-Aminocrotononitrile (III) (saturated solution)	Benzene	6.36	8.50	Not observed	$H/CH_3 = 0$
Equilibrium mixture (dilute solution)	Benzene				
(*a*) *cis* (III)		6.37	8.50	Not observed	$H/CH_3 = 0.8$
(*b*) *trans* (II)		6.64	8.97		
Equilibrium mixture (saturated solution)	Benzene				
(*a*) *cis* (III)		6.02	8.22	Broad, 5.35	$H/CH_3 = 0.8$
(*b*) *trans* (II)		6.51	8.68		
Compound (V) (see Fig. 1)	d_6-Dimethyl sulfoxide	4.70	(*a*) 7.80 (*b*) 7.82	Broad, 2.45	$H/CH_3(a) = 0.9$
Compound (V)	Pyridine				
(*a*) major component		4.30	(*a*) 7.60 (*b*) 7.65	Not observed	$H/CH_3(a) = 0.9$
(*b*) minor component		4.71	(*a*) 7.70 (*b*) 7.76		$H/CH_3(a) = 0.9$

The olefinic proton absorptions are about 1.5 p.p.m. to high field of the corresponding unsubstituted crotononitrile (16) and similar effects have been noted in vinyl ethers (18) and other enamines (19).

Molecular Weight of β-Aminocrotononitrile

The molecular weight of the low-melting form was determined cryoscopically in benzene. The variation of molecular weight with concentration is shown below.

Concentration (g/l)	Molecular weight
3.393	87.1
6.619	94.7
10.293	109.0
Theory	82.108

cis-β-Aminocrotononitrile (III)

The sodium salt was prepared by the method of Adkins and Whitman (20). The salt was decomposed with water at 0° and the product taken into ether which was washed twice with a small volume of water and dried (magnesium sulfate). The solvent was removed *in vacuo* at room temperature. It is important that all stages after decomposition of the salt are performed rapidly. The aminonitrile should not be left in solution over extended periods. The residue after removal of the majority of the ether (it is difficult to remove the ether completely) was cooled and the residual liquid decanted from the crystalline product. The solid was allowed to stand overnight at room temperature in a stoppered vessel and then recrystallized five times from benzene to give a white, crystalline solid, m.p. 78–80° (with preliminary softening above about 72°), which was homogenous (by n.m.r. spectrum in benzene).

Low-Melting β-Aminocrotononitrile

Decomposition of the above sodium salt at 30° yields material of m.p. 38–44° before crystallization and m.p. 44–46° after crystallization from a small volume of benzene (3). Alternatively, the pure *cis*-compound (above) may be kept in chloroform (10 mg/ml) for 64 h, after which removal of the solvent gives a clean, low-melting product which contains 65.4% *trans*-isomer (mean of nine integrations of n.m.r. spectrum; spread of values ±0.4%). Infrared spectrum of pure *cis*-compound (freshly prepared solution 8.1 mg per ml of chloroform) showed peaks at 3 516 (0.35), 3 417 (0.71), 3 357, 3 250, 3 219, 3 199, 2 918, 2 201, 1 637, 1 605, 1 434, 1 409, 1 365, (0.23) 1 298 (0.38) 1 123, and 1 020 cm^{-1}. After 3.5 days at room temperature, intensity changes occurred for the following bands 3 516 (0.44), 3 417 (0.54), 1 365 (0.30), 1 305 (0.16) cm^{-1}. Pure *cis*-compound (Nujol mull) showed peaks at 3 433, 3 339, 3 247, 3 219, 3 054, 2 180, 1 646, 1 594, 1 523, 1 311, 1 122, 1 023, 841, 760, and 719 cm^{-1}. The low-melting form (Nujol mull) showed peaks at 3 427, 3 332, 3 233, 3 207, 3 047, 2 172, 1 648, 1 591, 1 523, 1 309, 1 122, 1 026, 844, 764, and 722 cm^{-1}.

4-Amino-1,3-dicyano-2-methylpenta-1,3-diene (V)

(i) β-Aminocrotononitrile (29 g, 0.28 moles mixed isomers) was dissolved in benzene (30 ml) and cooled in ice, while 1,2-dichloroethyl ethyl ether (25 ml, 0.2 moles) was added. A vigorous exothermic reaction occurred. The mixture was kept for 2 h when the precipitated yellow solid (19.5 g) was separated, washed with ether and then water, and fractionally crystallized from aqueous ethanol. The more soluble product, m.p. 178–180°,

Can. J. Chem. Downloaded from www.nrcresearchpress.com by 210.87.254.42 on 09/05/12
For personal use only.

was 4-chloromethyl-3,5-dicyano-1,4-dihydro-2,6-lutidine (I:2). The less soluble compound (which was the major product) had m.p. 166–166.5° and resolidified at 167°, remelting with sublimation at 220–225°.

Anal. Calcd. for $C_8H_9N_3$: C, 65.28; H, 6.16; N, 28.55; molecular weight, 147. Found: C, 65.10; H, 6.01; N, 28.60; molecular weight (Rast), 178.

Light absorption (ethanol); λ_{max} at 219, 254, and 328 mμ; ϵ_{max} 11 300, 7 080, and 17 500 respectively. The infrared spectrum showed main maxima at 3 540, 3 511, 3 440, 3 405, 3 344, 3 244, 2 210, 2 196, 1 630, 1 598, 1 557, and 1 040 cm^{-1}.

(ii) The above reaction was repeated using pure *cis*-β-aminocrotononitrile. There was no exothermic reaction on removal of the mixture from the ice bath and development of a yellow precipitate required approximately 12 h. The same products were isolated.

4-Chloromethyl-3,5-dicyano-2,6-dimethyl-1,4-dihydropyridine (I)

β-Aminocrotononitrile (5 g, mixed isomers) was melted and then cooled almost to crystallization. 1,2-Dichloroethyl ethyl ether (5.04 g) was added and followed immediately by water (30 ml). After the reaction had subsided, the mixture was warmed on the steam bath for 5 min, cooled, and filtered. The solid was crystallized twice from aqueous ethanol to give the dihydropyridine, 3.0 g (47%), identical with that from (i) above.

2-Amino-5-cyano-4,6-lutidine (IV)

(i) The foregoing dinitrile (V) was heated to 170° and the product crystallized from ethanol to yield colorless needles, m.p. 227–228° (with sublimation).

(ii) A mixture of the dinitrile (100 mg) and potassium hydroxide (40 mg) in ethanol (5 ml) was heated under reflux for 20 min when the ethanol was removed and the residue treated with water. The crystalline solid thus obtained was crystallized from aqueous ethanol giving the product in almost quantitative yield as colorless needles, m.p. 227–228°.

(iii) The dinitrile (2.6 mg) was dissolved in ethanol (25 ml) and the solution was divided into two parts. The first was kept in the dark and the ultraviolet absorption spectrum was shown to be unchanged after 17 h. The second fraction was irradiated under an ultraviolet lamp and after 17 h, the light absorption showed maxima at 210, 271, and 295 mμ; ϵ_{max} 11 250, 17 300, and 7 470 respectively. Evaporation of the solvent gave colorless needles, m.p. 227–228°.

The same product (melting point and spectra) was obtained from all three reactions. (Calcd. for $C_8H_9N_3$: C, 65.28; H, 6.16; N, 28.55. Found: C, 65.00; H, 5.97; N, 28.40.) The infrared spectrum showed main maxima at 3 519, 3 415, 2 212, 1 615, 1 555, 1 472, 1 448, 1 378, 1 357, 1 173, and 846 cm^{-1}. Reaction of this product with sodium nitrite in dilute sulfuric acid gave 5-cyano-4,6-lutid-2-one (6, 7), m.p. 305–307° (sealed tube) with darkening ca. 280°. This was identical (melting point and spectra) with the product obtained from β-aminocrotononitrile with boiling water.

ACKNOWLEDGMENTS

This investigation was supported by an operating grant from the National Research Council. We are grateful to Memorial University for a Postdoctoral Fellowship (awarded to Brian Gregory).

REFERENCES

1. E. Benary and G. Lowenthal. Ber. **55**, 3429 (1922).
2. P. J. Brignell, E. Bullock, U. Eisner, B. Gregory, A. W. Johnson, and H. Williams. J. Chem. Soc. 4819 (1963).
3. J. J. Conn and A. Taurins. Can. J. Chem. **31**, 1211 (1953).
4. E. L. Eliel. Stereochemistry of carbon compounds. McGraw-Hill. 1962. p. 318.
5. R. Holtzwart. J. Prakt. Chem. Ser. 2, **39**, 230 (1889).
6. E. von Meyer. J. Prakt. Chem. Ser. 2, **52**, 83 (1895)
7. J. Moir. J. Chem. Soc. 101 (1902).
8. D. Hofmann, E. M. Kosower, and K. Wallenfels. J. Am. Chem. Soc. **83**, 3314 (1961).
9. G. Slomp and F. MacKellar. J. Am. Chem. Soc. **82**, 999 (1960).
10. P. Bruylants. Bull. Classe Sci. Acad. Roy. Belg. 5, **8**, 7 (1922); Chem. Zentr. I, 86 (1923).
11. L. Bary. Bull. Soc. Chim. Belges, **31**, 397 (1922); Chem. Zentr. III, 123 (1923).
12. F. Brody and P. R. Ruby. *In* Pyridine and derivatives. Part I. E. Klingsberg (*Editor*). Interscience Publishers, Inc., New York. 1960. p. 392.
13. B. Witkop. J. Am. Chem. Soc. **78**, 2873 (1956).
14. T. H. Curry. Dissertation Abstr. 18, 1615 (1958).
15. J. S. Pizey and W. E. Truce. J. Chem. Soc. 865 (1964).
16. G. S. Reddy, J. H. Goldstein, and L. Mandell. J. Am. Chem. Soc. **83**, 1300 (1961).
17. L. M. Jackman. Applications of n.m.r. spectroscopy in organic chemistry. Pergamon. 1959. p. 122.
18. L. M. Jackman. Applications of n.m.r. spectroscopy in organic chemistry. Pergamon. 1959. p. 62.
19. N. J. Leonard, C. K. Steinhart, and C. Lee. J. Org. Chem. **27**, 4027 (1962). H. Booth, A. W. Johnson, F. Johnston, and R. A. Langdale-Smith. J. Chem. Soc. 650 (1963).
20. H. Adkins and G. M. Whitmann. J. Am. Chem. Soc. **64**, 150 (1942).

Can. J. Chem. Downloaded from www.nrcresearchpress.com by 210.87.254.42 on 09/05/12
For personal use only.

Can. J. Chem. Downloaded from www.nrcresearchpress.com by 210.87.254.105 on 09/05/12
For personal use only.

A SERIES OF MODEL COMPOUNDS FOR THE STUDY OF AROMATIC REACTIONS[1]

S. Safe and R. Y. Moir
Department of Chemistry, Queen's University, Kingston, Ontario
Received September 22, 1964

ABSTRACT

A series of halogenated phthalides was prepared in which there was a systematic variation in the identity, position, and degree of activation of the halogen, and in the activation of the methylene group. A study was made of the selective reductive removal of halogen in the presence of another halogen, or of a nitro group.

Metameconine (I*a*) is admirably adapted to the study of competitive reactions. A rapid survey of its possibilities has shown that in several well-known aromatic reactions it could be used to drive currently favored theories into difficulties that were not easily resolved (1). The new compounds described in this paper formed a weapon that has since been used in a much more intensive attack upon two of these reactions.

One of these was the copper-catalyzed removal of halogen by aqueous hydroxide ion. Our previous work (1–6) had provided a set of compounds superbly suited to the study, as shown by the large number of new observations recorded in the next paper. More compounds needed in the investigation were provided in the present work. In particular, the synthesis of II*b*, II*c*, and II*d* was saved from triviality by two difficulties that had to be overcome. It was pointed out previously (1) that the nitro group in 4-amino-7-nitrometameconine (II*e*) was very easily extruded on diazotization. For example, when II*e* was diazotized in dilute aqueous hydrochloric acid, reduction of the diazonium solution gave 7-chlorometameconine (III*a*), and treatment of the diazonium solution with potassium iodide gave 4-iodo-7-chlorometameconine (III*d*) (1). The same diazonium solution has now been shown to give 4,7-dichlorometameconine (III*b*) with cuprous chloride. However, cuprous bromide gave a mixture of compounds instead of pure III*c*. Thus the diazonium cation III*e* was conventional in its relative reactivities towards chloride, bromide, and iodide under the conditions used.

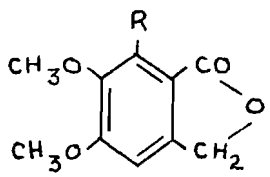

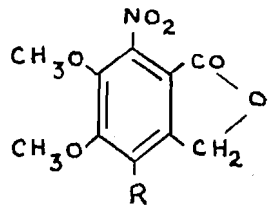

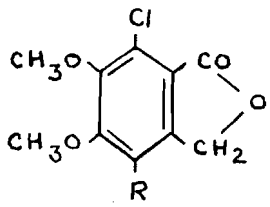

I*a*. R = H
I*b*. R = $NHCOCH_3$
I*c*. R = $N(COCH_3)_2$
I*d*. R = NHCHO

II*a*. R = H
II*b*. R = Cl
II*c*. R = Br
II*d*. R = I
II*e*. R = NH_2
II*f*. R = OH
II*g*. R = OCH_3
II*h*. R = NHCHO
II*i*. R = NO_2
II*j*. R = $NHCOCH_3$

III*a*. R = H
III*b*. R = Cl
III*c*. R = Br
III*d*. R = I
III*e*. R = N_2^+
III*f*. R = OH
III*g*. R = OCH_3

[1]*Most of the work was presented at the Annual Meeting of the Chemical Institute of Canada, in Toronto, June 7, 1963.*

Can. J. Chem. Downloaded from www.nrcresearchpress.com by 210.87.254.105 on 09/05/12
For personal use only.

When sulfuric acid was used in the diazotization of II*e* (in an attempt to avoid nucleophilic displacement of the nitro group) a diazonium salt was obtained whose resistance to thermal decomposition and to reduction has been recorded (1). The idea of using the poorly nucleophilic monovalent anions, nitrate and perchlorate, in place of sulfate, seemed most unattractive.[2] Fortunately, the diazonium sulfate prepared by the method of Hodgson and Walker (7, 8) was found to react under suitable conditions (8) with cuprous chloride, cuprous bromide, or potassium iodide to give good yields of the activated aromatic halides 4-chloro-7-nitrometameconine (II*b*), 4-bromo-7-nitrometameconine (II*c*), and 4-iodo-7-nitrometameconine (II*d*), respectively.

The study also required a knowledge of the products of hydroxydehalogenation, and these were characterized in the present work. The uncatalyzed reaction of 7-chloro-4-iodometameconine (III*d*) with aqueous potassium hydroxide gave 7-chloro-4-hydroxymetameconine (III*f*), with selective replacement of iodine. One might have expected II*b*, II*c*, and II*d* all to give 4-hydroxy-7-nitrometameconine (II*f*) in the same reaction, but in fact with one exception the reactions took a more complex course. However, the copper-catalyzed reaction of the iodo compound (II*d*) gave the expected hydroxy compound (II*f*), accompanied by some 7-nitrometameconine (II*a*); this competition between substitution and reduction is the main theme of the next paper. Phenols II*f* and III*f* and their methyl ethers II*g* and III*g* were synthesized for further comparative studies of anisoles and diphenyl ethers (9, 10).

It is odd that metameconine gives no 4-nitrometameconine on nitration (since 7-nitrometameconine readily gives 4,7-dinitrometameconine) (1), and we have now accumulated a considerable list of failures to nitrate at the 4-position. Over the course of 26 years, previous workers in this laboratory have repeatedly failed to nitrate 7-acetaminometameconine (I*b*) (3)[3] and 7-diacetylaminometameconine (I*c*) (3).[3] To this list of failures we have now added the known compound 7-chlorometameconine (III*a*) (5) and the new compound 7-formaminometameconine (I*d*). As a check, 4-formamino-7-nitrometameconine (II*h*) and 4-acetamino-7-nitrometameconine (II*j*) were made and found to be fairly stable. The difference between the 4- and 7-positions was also illustrated in another interesting way. The previous observations that 4- and 7-bromophthalides were subject to reductive dehalogenation (6) but that some related chloro compounds were not (5) led to the successful selective reduction of 7-chloro-4-iodometameconine (III*d*) to 7-chlorometameconine (III*a*) (1). We now find that 4,7-dichlorometameconine can also be selectively reduced in excellent yield, to the same 7-chlorometameconine (III*a*). Thus a difference in the identity of the two halogens is not required for selective removal of one of them.

The reductive removal of halogen in the presence of the easily reducible nitro group is of considerable interest, especially since the established method of Leslie and Turner (12) failed completely in the present series. Removal of the halogen of 4-iodo-7-nitrometameconine (II*d*) with copper and aqueous potassium hydroxide has already been mentioned; it was (in this case) overshadowed by the substitution reaction. Better, but still moderate, yields of the reduced product (II*a*) were obtained when 4-bromo-7-nitrometameconine (II*c*) was heated with copper and molten benzoic acid at about 160°, according to the

[2]*Diazotization of II*e *in hydrobromic acid gave a crystalline diazonium salt showing diazonium and nitro bands at 2 180 and 1 547 cm*$^{-1}$ *in the infrared spectrum. It failed to give the Sandmeyer reaction, and it survived attempted reduction with hypophosphorous acid. While one sample remained unmelted at 250°, another exploded with quite a lot of noise, smoke, and flame, when touched by a spatula on the Buchner funnel. An analogous salt was obtained by diazotization of II*e *in concentrated hydrochloric acid. Attempts to obtain fluoborates failed.*

[3]*Our early papers used the numbering scheme of Rây and Robinson (11), the later ones the scheme of Chemical Abstracts.*

method of Smith and Campanaro (13). In their examples bromine para to nitro was *not* removed. With the more delicate 4-iodo-7-nitrometameconine (II*d*), acetic acid was found to be preferable to benzoic acid as the source of hydrogen. Curiously, the addition of the very nucleophilic acetate ion did not appreciably lower the yield of the reduced product (II*a*); apparently the substitution reaction was much depressed in the acetic acid solvent.

Anbar, Guttman, and Friedman (14) recently found that cupric ion and ascorbic acid in neutral aqueous solutions were together very effective in the de-iodination of ortho-iodobenzoic acid. As is shown in the next paper, our experience differed sharply in nearly every respect from theirs. Nevertheless, 4-iodo-7-nitrometameconine (II*d*) was reduced smoothly and in good yield to 7-nitrometameconine (II*a*) by copper *metal* and ascorbic acid in alkaline solution. It is likely that this reduction system will prove very useful in preparative aromatic chemistry.

EXPERIMENTAL

Melting points marked (p) were determined on the precision capillary apparatus, the rest on the Kofler Micro Hot Stage; the values from the latter have been lowered 3–5° to bring them into agreement with the former (5), except for cases of polymorphism or decomposition at the melting point in which there is a real theoretical difference between the two methods. Infrared spectra for all of the new compounds and nuclear magnetic resonance (n.m.r.) spectra for some of them have been determined and are in agreement with the structures suggested.

*4,7-Dinitrometameconine (II*i*)*

The yield (70.5%) and quality (151.3–152.0°) of the crude material were considerably better than reported before (1), due to the use of relatively larger amounts of nitrating acid and of purer metameconine. Fuming nitric acid (80 ml, 90%) and concentrated sulfuric acid (20 ml) were mixed and chilled to 0°. Metameconine (16.5 g, m.p. 157.5–158.5°) was added with stirring over 45 min. More fuming nitric acid (75 ml) was added, and the stirring continued 5 h longer, the mixture then being poured onto ice and water (300 ml). Crude product was recovered, washed, and dried; yield 17.0 g.

*4-Iodo-7-nitrometameconine (II*d*)*

The method resembled that used by Chalmers, Dickson, Elks, and Hems in the synthesis of a precursor of thyroxine (8). Sodium nitrite (0.42 g) was warmed with concentrated sulfuric acid (8 ml). The solution was chilled, diluted with glacial acetic acid (8 ml), and then stirred and cooled in an ice bath while a second cold solution, made from 4-amino-7-nitrometameconine (II*e*) (1) (0.95 g, m.p. 230–231°), concentrated sulfuric acid (10 ml), and glacial acetic acid (10 ml), was added over a period of 1 h; stirring and cooling were continued for an additional 3 h. The cold *solution of diazotized 4-amino-7-nitrometameconine* was then added with stirring to a solution of potassium iodide (4 g), urea (2 g), and water (150 ml). The temperature rose to 58°. After being stirred for 0.5 h, the solution was treated with sodium bisulfite and chilled overnight; the light-yellow, crude product was recovered in a yield of 1.21 g (84%), m.p. 159.5–161.5°. When the cold solution of diazotized 4-amino-7-nitrometameconine from 3 g of the amine was poured into a mixture of water, chloroform, urea, potassium iodide, and iodine in the more elaborate procedure used in previous examples (8, 15), the total yield of once-crystallized product was only 76%. Three more recrystallizations of the first fraction of this material from ethanol gave the analytical sample, m.p. 161.3–161.9° (p).

Found: C, 32.96; 33.13; H, 2.27, 2.48; N, 3.66, 3.51; I, 35.00, 35.06. Calcd. for $C_{10}H_8O_6NI$: C, 32.88; H, 2.23; N, 3.83; I, 34.79.

4-Chloro-7-nitrometameconine (IIb)

A cold solution of diazotized 4-amino-7-nitrometameconine (made approximately as above from 2.5 g of the amine) was added with swirling to a fresh solution of cuprous chloride (made from 5 g of copper sulfate pentahydrate) in concentrated hydrochloric acid (10 ml). Urea and water were added to the dark-purple mixture which was then warmed to 60–70°. Crude product was recovered from the cooled solution in a yield of 2.41 g (94%), m.p. 130–131°. Four recrystallizations from butanol gave the pale-yellow needles of the analytical sample, m.p. 132.8–133.3° (p).

Found: C, 44.12, 44.11; H, 2.74, 2.91; N, 5.24, 5.15; Cl, 12.81, 12.71. Calcd. for $C_{10}H_8O_6ClN$: C, 43.88; H, 2.93; N, 5.12; Cl, 12.98.

4-Bromo-7-nitrometameconine (IIc)

A cold solution of diazotized 4-amino-7-nitrometameconine (made approximately as above from 1.0 g of the amine) was added with swirling to a solution of cuprous bromide (made from 2.5 g of copper sulfate pentahydrate) in hydrobromic acid (60%, 5 ml); urea was added and the mixture was warmed slightly,

Can. J. Chem. Downloaded from www.nrcresearchpress.com by 210.87.254.105 on 09/05/12
For personal use only.

diluted with water, and cooled. The recovered product after one recrystallization from butanol had a m.p. of 141.5–142.2°, yield 1.08 g (91%). Two more recrystallizations gave white plates, m.p. 140.5–141.5° (p).

Found: C, 38.12, 38.23; H, 2.50, 2.70; N, 4.44, 4.42; Br, 25.38, 25.09. Calcd. for $C_{10}H_8O_6NBr$: C, 37.74; H, 2.52; N, 4.40; Br, 25.16.

7-Chloro-4-iodometameconine (IIId) (1)

Pure 4-amino-7-nitrometameconine (3.0 g, m.p. 230–231°) was diazotized with sodium nitrite in aqueous hydrochloric acid (cf. ref. 1); the solution was poured into a rapidly stirred mixture of potassium iodide (10 g), urea (5 g), iodine (5 g), water (110 ml), and chloroform (140 ml). Crude product was recovered (in much the same way as in the second method used for 4-iodo-7-nitrometameconine above) in a yield of 3.08 g (74%), reduced after one recrystallization from methanol to 2.61 g (m.p. 140.5–145.5°). One more recrystallization raised the melting point to that of the pure material previously obtained (1), 148.5–153.5°, the range being due to the dimorphism observed on the Kofler hot stage (1), though usually not in the capillary method (1).

4,7-Dichlorometameconine (IIIb)

Pure 4-amino-7-nitrometameconine (2.0 g) was diazotized in aqueous hydrochloric acid approximately as above. The solution was treated with urea and then added to a fresh solution of cuprous chloride (made from 5 g of copper sulfate pentahydrate) in concentrated hydrochloric acid (10 ml). After effervescence had ceased, the mixture was warmed to 60–70° and then chilled. The pale-yellow product was recovered and recrystallized from aqueous ethanol with charcoal. Colorless flat plates were obtained in a yield of 1.38 g (90%), m.p. 141.3–141.8° (with a trace at 138.8°). Four recrystallizations from butanol gave the analytical sample, m.p. 141.6–142.2° (p).

Found: C, 45.54; 45.39; H, 3.23, 3.07; (on another sample) Cl, 27.32, 27.19. Calcd. for $C_{10}H_8O_4Cl_2$: C, 45.65; H, 3.04; Cl, 27.00.

An attempt to convert the amine to the corresponding bromo compound (IIIc), using cuprous bromide in hydrobromic acid in place of cuprous chloride in hydrochloric acid, but retaining the diazotization in hydrochloric acid, gave a product which after two recrystallizations from acetic acid and two from butanol had m.p. 154.6–157.2°.

Found: C, 40.21, 40.21; H, 2.82, 2.99; Cl, 15.20, 15.39; Br, 19.25, 19.28. Calcd. for $C_{10}H_8O_4ClBr$: C, 39.09; H, 2.61; Cl, 11.40; Br, 26.06.

Reduction of this mixture yielded 7-chlorometameconine (IIIa).

Selective Dehalogenation of 4,7-Dichlorometameconine (IIIb)

4,7-Dichlorometameconine (0.10 g, m.p. 141–142°) was heated under reflux with water (15 ml), potassium hydroxide (1.5 g), and zinc dust (0.50 g) for 10 h. The mixture was filtered, the filtrate acidified with hydrochloric acid, and the long, white needles isolated in a yield of 0.075 g (79%), m.p. 193–194°. A mixture melting point with an authentic sample of 7-chlorometameconine (IIIa) (m.p. 194–195°) (5) showed no depression (194–195°). The reaction was not complete in a reaction time of 4 h.

4-Hydroxy-7-nitrometameconine (IIf)

4-Iodo-7-nitrometameconine (0.70 g, m.p. 160–161°) was dissolved in boiling 3% aqueous potassium hydroxide (35 ml, made in the proportion of 30 g potassium hydroxide (85% minimum) in 100 ml of water). Copper bronze (Kahlbaum's No. 02219, 0.34 g) was added and the mixture heated under reflux for 3 h with periodic stirring. The catalyst was removed by filtration. Then the filtrate was acidified with concentrated hydrochloric acid and cooled. Fluffy, yellow crystals, m.p. 167–197°, were recovered in a yield of 0.41 g. These were extracted with aqueous sodium bicarbonate, the insoluble material removed, and the filtrate acidified to give a white precipitate in a yield of 0.30 g (56%), m.p. 217–218° (with decomp.). Three recrystallizations from water gave the analytical sample of 4-hydroxy-7-nitrometameconine, m.p. 218.2–219° (p) (decomp.).

Found: C, 47.06, 47.02; H, 3.49, 3.70; N, 5.36, 5.26. Calcd. for $C_{10}H_9O_7N$: C, 47.06; H, 3.53; N, 5.49.

The bicarbonate-insoluble material (0.07 g) had m.p. 172–179°, raised to 178–180° after one recrystallization from glacial acetic acid; mixture melting point with authentic 7-nitrometameconine (3, 11)[3] (m.p. 181–182°) (IIa), 178–181°. In several repetitions of the experiment, the crude 7-nitrometameconine showed the same low melting point, indicating a third reaction product (see next paper).

4-Methoxy-7-nitrometameconine (IIg)

Pure 4-hydroxy-7-nitrometameconine (m.p. 219–220°, 1.0 g) was treated in ethereal solution with an excess of diazomethane. Some solid (0.21 g, m.p. 115–116.3°) deposited; more (0.72 g) was recovered by evaporation of the solvent (total yield 89%). Four recrystallizations from aqueous methanol gave the *light-sensitive* analytical sample, m.p. 113.6–114.5° (p).

Found: C, 48.64, 48.38; H, 4.12, 4.22; N, 5.26, 5.37. Calcd. for $C_{11}H_{11}O_7N$: C, 49.07; H, 4.09; N, 5.26.

7-Chloro-4-hydroxymetameconine (IIIf)

Pure 7-chloro-4-iodometameconine (0.20 g, double m.p. 148.5–153.5°) was heated under reflux with potassium hydroxide (1.2 g) and water (15 ml) for 12 h. The cooled solution was acidified and the precipitate was recovered and treated with sodium bicarbonate solution. After filtration from a small amount

Can. J. Chem. Downloaded from www.nrcresearchpress.com by 210.87.254.105 on 09/05/12
For personal use only.

of insoluble material, the solution was acidified to give the product in a yield of 0.097 g (70%), m.p. 179.3–180.8°. Combined with a similar product from another reaction and thrice recrystallized from water, the sample gave short, white, stubby crystals, m.p. 179.3–180.0° (p).

Found: C, 48.91, 48.96; H, 3.84, 3.77; Cl, 13.93, 14.00. Calcd. for $C_{10}H_9O_5Cl$: C, 49.18; H, 3.64; Cl, 14.34.

7-Chloro-4-methoxymetameconine (IIIg)

Treatment of 7-chloro-4-hydroxymetameconine (1.0 g, m.p. 180–181°) with excess ethereal diazomethane gave glistening white plates, 0.55 g, m.p. 108–109.5° (p), and 0.44 g, m.p. 110.4–111.2° (p), a total yield of 93%. Two recrystallizations from absolute ether gave the analytical sample, m.p. 109.0–109.8° (p).

Found: C, 51.47, 51.53; H, 4.45, 4.62. Calcd. for $C_{11}H_{11}O_5Cl$: C, 51.16; H, 4.22.

4-Acetamino-7-nitrometameconine (IIj)

Pure 4-amino-7-nitrometameconine (II*e*) (1) (1.0 g, m.p. 233–234.5°) was dissolved in warm glacial acetic acid (20 ml). The solution was kept at 80–100° for 40 min with acetic anhydride (3 ml) and then diluted with water (7 ml). Long, fine, white needles were recovered in a yield of 0.94 g (85%), m.p. 187–189°. Three recrystallizations from water gave the analytical sample, m.p. 187.8–188.3° (p). The sample quickly turned purple on exposure to daylight, and poor analytical results were obtained on a sample sent away. Satisfactory results were found on a sample analyzed immediately after preparation.

Found: C, 48.71, 48.47; H, 4.36, 4.34. Calcd. for $C_{12}H_{12}O_7N_2$: C, 48.65; H, 4.18.

4-Formamino-7-nitrometameconine (IIh)

The pure amino compound (II*e*) (1.5 g, m.p. 230–231°) was heated under reflux with formic acid (90%, 25 ml) for 20 min, diluted with water (50 ml), and chilled. Fine, yellow needles were obtained in a yield of 1.42 g (86%), m.p. 188–188.5°. Three recrystallizations from water gave the analytical sample, m.p. 188.6–189.4° (p).

Found: C, 46.86, 47.01; H, 3.61, 3.67; N, 10.26, 10.03. Calcd. for $C_{11}H_{10}O_7N_2$: C, 46.83; H, 3.55; N, 9.93.

7-Formaminometameconine (Id)

7-Aminometameconine (3, 11)[3] (0.84 g, m.p. 160.5–161.5°) was heated under reflux with formic acid (90%, 15 ml) for 20 min. The solution was diluted with water (40 ml) and chilled. White crystals were recovered in a yield of 0.78 g (82%), m.p. 211.9–213.4°. Three recrystallizations from water gave the analytical sample as long, white needles, m.p. 213.2–214.0° (p).

Found: C, 55.97, 56.05; H, 4.50, 4.66; N, 6.16, 6.27. Calcd. for $C_{11}H_{11}O_5N$: C, 55.46; H, 4.20; N, 5.88.

Reductive Dehalogenations in the Presence of Nitro Groups

(a) With Copper and Benzoic Acid

The method is that of Smith and Companaro (13). Pure 4-bromo-7-nitrometameconine (0.20 g, m.p. 140–141°) (II*c*) and benzoic acid (0.61 g) were heated together on an oil bath at 150–175°. Kahlbaum's copper bronze (No. 02219, 1.0 g) was added over a period of 5–10 min. The melt soon solidified. Heating was continued for a short time. The greenish mixture was then cooled, extracted with aqueous sodium carbonate (1.0 g in 5 ml), and filtered. The insoluble material was extracted with several small portions of boiling acetone. The product was recovered by evaporation of the acetone and recrystallized from glacial acetic acid with charcoal. Light-yellow crystals, m.p. 178–180°, were recovered (some from mother liquors) in a total yield of 0.06 g (40%), mixture melting point with authentic 7-nitrometameconine (3, 11)[3] (m.p. 181–182°), 178–181°.

(b) With Copper and Acetic Acid

Pure 4-iodo-7-nitrometameconine (0.114 g, m.p. 160–161°) (II*d*) was heated under reflux for 12.5 h with glacial acetic acid (12 ml) and Kahlbaum's copper bronze (No. 02219, 0.15 g). The "catalyst" was then removed. The filtrate was concentrated to one-quarter of its original volume and diluted with water. The crude 7-nitrometameconine (II*a*) so obtained had m.p. 175–178°, undepressed by admixture with authentic material. The yield was 0.05 g (68%). No reaction occurred in the absence of the copper bronze.

(c) With Copper and Acetate

The same iodo compound (0.25 g, m.p. 160–161°) (II*d*) was heated under reflux for 6.5 h with glacial acetic acid (25 ml), potassium acetate (2.5 g), and Kahlbaum's copper bronze (0.25 g). The "catalyst" was removed. The markedly green filtrate was concentrated and then diluted with water to give a precipitate of crude 7-nitrometameconine in a yield of 0.086 g (53.5%). Its melting point of 177–179° was undepressed by admixture with authentic material.

(d) With Copper and Tetralin (12, 16)

The nitro-iodo compound (II*d*) (0.25 g) was heated about 40 min with tetralin (2.5 ml) and copper bronze (0.25 g); attempts to isolate the product gave only an intractible, green gum.

(e) With Copper and Ascorbic Acid

Pure 4-iodo-7-nitrometameconine (0.200 g) (II*d*), 4% aqueous potassium hydroxide (15 ml), ascorbic acid (0.100 g), and copper bronze (0.020 g) were heated together under reflux for 2 h. The reddish-orange solution was filtered from the catalyst (which was unchanged in appearance), and the product was isolated

Can. J. Chem. Downloaded from www.nrcresearchpress.com by 210.87.254.105 on 09/05/12
For personal use only.

in the usual way to give 7-nitrometameconine in a yield of 0.1025 g (78.6%), m.p. 179.5–182°, mixture melting point with authentic material (3, 11)[3] (m.p. 182–183°), 179–183.5°.

The method failed with the corresponding bromine compound (II*c*).

ACKNOWLEDGMENTS

The work was supported by the National Research Council of Canada with a Grant and with a Scholarship awarded to one of us. The vanillin which was the source of our compounds was donated by Dr. G. H. Tomlinson of the Howard Smith Paper Company division of Dominion Tar and Chemical Co., Ltd., Cornwall, Ontario.

REFERENCES

1. S. SAFE, M. ALLEN, and R. Y. MOIR. Can. J. Chem. **40**, 2402 (1962).
2. J. A. MCRAE, R. B. VANORDER, F. H. GRIFFITHS, and T. E. HABGOOD. Can. J. Chem. **29**, 482 (1951).
3. R. H. MANSKE, J. A. MCRAE, and R. Y. MOIR. Can. J. Chem. **29**, 526 (1951).
4. J. A. MCRAE, R. Y. MOIR, J. J. URSPRUNG, and H. H. GIBBS. J. Org. Chem. **19**, 1500 (1954).
5. J. A. MCRAE, M. ALLEN, and R. Y. MOIR. Can. J. Chem. **39**, 995 (1961).
6. M. ALLEN, A. L. PROMISLOW, and R. Y. MOIR. J. Org. Chem. **26**, 2906 (1961).
7. H. H. HODGSON and J. WALKER. J. Chem. Soc. 1620 (1933).
8. J. R. CHALMERS, G. T. DICKSON, J. ELKS, and B. A. HEMS. J. Chem. Soc. 3424 (1949).
9. W. D. CHANDLER, W. MACFARLANE SMITH, and R. Y. MOIR. Can. J. Chem. **42**, 2549 (1964).
10. S. SAFE and R. Y. MOIR. Can. J. Chem. **42**, 160 (1964).
11. J. N. RÂY and R. ROBINSON. J. Chem. Soc. **127**, 1618 (1925).
12. M. S. LESLIE and E. E. TURNER. J. Chem. Soc. 281 (1932).
13. W. T. SMITH and L. CAMPANARO. J. Am. Chem. Soc. **75**, 3602 (1953).
14. M. ANBAR, S. GUTTMAN, and C. FRIEDMAN. Proc. Chem. Soc. 10 (1963).
15. M. ALLEN and R. Y. MOIR. Can. J. Chem. **41**, 252 (1963).
16. H. KING. J. Chem. Soc. 1157, 1165 (1939).

Can. J. Chem. Downloaded from www.nrcresearchpress.com by 210.87.254.105 on 09/05/12
For personal use only.

Can. J. Chem. Downloaded from www.nrcresearchpress.com by 210.87.254.40 on 09/05/12
For personal use only.

RELATIVE REACTIVITY OF TOLUENE–BENZENE IN NITRONIUM TETRAFLUOROBORATE NITRATION

LIMITATION OF THE COMPETITIVE METHOD OF RATE DETERMINATION IN FAST REACTIONS*

W. S. TOLGYESI

Exploratory Research Laboratory, Dow Chemical of Canada, Limited, Sarnia, Ontario

Received August 14, 1964

ABSTRACT

A study was made to determine the relative reactivity of the toluene–benzene pair in a nitronium salt nitration, using the method of competitive rate determination. Despite difficulties encountered in ensuring homogeneous reaction conditions owing to the high speed of reaction the relative rates (toluene/benzene) obtained under certain conditions attained a range (25–30) which is considered to represent the range of relative reactivity and it corresponds to the known reactivity of toluene–benzene in nitric acid nitration. On the basis of these results there seems to be no reason to suppose that nitronium salt nitration involves a mechanism different from that of the nitric acid nitration.

INTRODUCTION

In recent years the method of competitive rate determination has been extensively used in connection with aromatic substitutions. Using nitronium salts as nitrating agents, Olah and co-workers (1–5) reported relative reactivity values much lower (e.g. toluene/benzene = 1.67 with NO_2BF_4 in tetramethylene sulfone) than those obtained with nitric acid (toluene/benzene = 21–27) (6, 7). At the same time the nitronium salt nitration retained the high positional selectivity of nitric acid nitrations, thereby invalidating the selectivity principle for these systems.

The possibility was suggested by Brown,[1] however, that non-kinetic factors had been responsible for the observed low substrate selectivity in the nitronium salt nitrations.

The competitive method, described by Francis (8) in 1926, consists of "adding to a mixture of two compounds an insufficient amount of a reagent which reacts with both; and by suitable analysis determining the extent of each reaction. From these the ratio of the two velocity constants can be calculated."

The method, though supplying less kinetic information than absolute rate measurement, has its advantages. Francis (8) applied it to determine relative reaction velocities when the rate constants were in the region of 10^6, making absolute rate determination impractical. According to Ingold and Shaw (9): "uncertainties arising from imperfect, and consequently unequal, temperature control are avoided." Another important advantage of the method was mentioned by Dewar (10) in connection with aromatic nitration: the concentration of the reagent added to the competing compounds does not need to be known. "It is of course necessary to ensure that appreciable amounts of each hydrocarbon remain unchanged." Furthermore, "the method does not require an accurate knowledge of the reaction kinetics, provided we assume that both hydrocarbons are nitrated by the same nitrating agent or agents, and that the rates of nitration are of the first order with respect to the hydrocarbon concentration" (10).

Competitive rate determination has limitations as well. The one with which the present work is concerned was first described by Francis (8), who tried to carry out competitive

*Contribution No. 123.

[1]*Reference 15 in the paper of Olah and co-workers. J. Am. Chem. Soc. 83, 4571 (1961).*

bromination using aqueous solutions of free bromine: "The difficulty arises of obtaining a homogeneous mixture of the reactants, since the reactions are so rapid that they take place at the point of entrance of the bromine water, the bromine perhaps not being properly divided between the competitors. Thus, if competitor A reacts much more rapidly than B, it would become impoverished in the layer of solution adjacent to the bromine water and allow competitor B to obtain more than its just share of the bromine. The error thus introduced would usually be on the side of making the competitors seem too nearly equal in speed and probably would be slight for well-matched competitors."

The explanation of Francis implies that in the limiting case when the rate of reaction of both competitors with reactant X is very much higher than the rate with which they are supplied in the layer adjacent to the reactant, the product ratio is equal to the concentration ratio of the competitors. Therefore the calculated relative rate is 1. One can use the two limiting values of a competitive reaction (relative reactivity under kinetic control on one end and unity under statistical control on the other) to calculate intermediate points when only portions of reactant X react according to statistical control. In Fig. 1 calculated reaction rates[2] of three hypothetical competitive reactions are plotted against percentage kinetic control of the reaction.

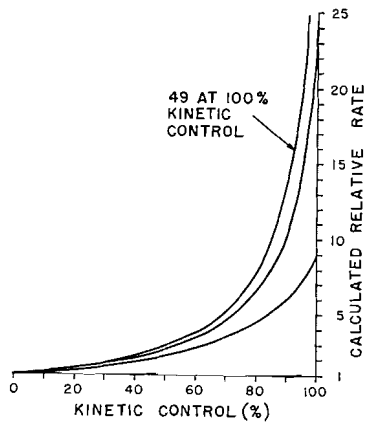

FIG. 1. Calculated relative rate: influence of statistical factors.

It is not intended to correlate the curves quantitatively with subsequent results, mainly because the assumption that the two limiting mechanisms operate simultaneously is certainly an oversimplification. However, some qualitative conclusions, drawn from these approximate calculations, seem plausible; of prime significance is the fact that even small deviations from kinetic control decrease the relative rate markedly. The higher the relative reactivity, the more marked is the decrease. On the other end, in the region nearer to statistical control, the value of the relative reactivity or the extent of influence of the statistical factor is less important in determining the relative rate.

It is known that the rate of nitration of reactive aromatics is very high in solutions

[2]*The following equation was used for the calculation of reaction rates shown in Fig. 1.*

$$\text{Reaction rate} = [y(R + 1) + 2Rx]/[y(R + 1) + 2x],$$

where R is the relative reactivity of the two competitors towards the reactant, while x and y (y = 100 − x) are % portions of the reactant consumed in kinetically and statistically controlled steps, respectively. One must, of course, assume that the concentrations of the competitors are equal and constant both in time and distribution in the reaction medium and the reactant can only be consumed according to either of the two extreme steps.

Can. J. Chem. Downloaded from www.nrcresearchpress.com by 210.87.254.40 on 09/05/12
For personal use only.

where nitronium ion, the active nitrating species, is readily available, as in nitric acid. According to Hughes and Ingold (11): "A direct kinetic observation of the mononitration of benzene in nitric acid is scarcely possible, because of the very high speed of nitration of benzene in this medium. In order to obtain a measurable reaction rate one has to introduce some strongly deactivating group such as a nitro group." Ciaccio and Marcus (12) measured the rate of nitration of nitrobenzene in nitric acid and found even this to be a fast reaction (k_2 = 1.0–10.0 l mole^{-1}min^{-1}). Using nitronium tetrafluoroborate the rate constants were 0.11 in acetonitrile, 0.5 in sulfuric acid, and 1.1 in methanesulfonic acid. Benzene is estimated to be 10^5–10^7 (11, 13) times as active as nitrobenzene in nitration. After the present work had been finished, it was learned that Ritchie and Win (14) carried out nitronium fluoroborate nitration of aromatics and found that: "these reactions may not be well-behaved kinetically."

According to these references, the rate coefficient of the nitration of aromatics like benzene and toluene is large, though unknown, and competitive experiments of high velocity reactions can yield relative rates not corresponding to relative reactivities.

EXPERIMENTAL

Materials

Benzene, toluene, and chlorobenzene. Reagent grade materials, dried over calcium chloride. Fluorobenzene. Technical grade material, fractionated on an Aldershaw column and dried with calcium chloride. Nitric acid. Reagent grade, red fuming nitric acid. Specific gravity, 1.59–1.60. Sulfuric acid. Reagent grade 96% sulfuric acid. Specific gravity: 1.84.

Tetramethylene sulfone. Development product of the Shell Chemical Company. The dark-brown material, solid at room temperature, was purified by fractional distillation from solid sodium hydroxide (15) at 106–115° and 1–2 mm. After discarding the first 10–15% of the distillate, the following 50–55% was collected. The distilled material was colorless, solid at room temperature. Its water content, analyzed according to the Karl-Fischer method, was always less than 7 p.p.m., the limit of detection being 5 p.p.m. A blank reaction with the solvent did not cause a measurable increase of its water content. The material was free of butadiene sulfone—an intermediate in the production of tetramethylene sulfone—according to nuclear magnetic resonance (n.m.r.) (sensitivity 1 000 p.p.m.) and gas chromatography (g.c.) (sensitivity 100 p.p.m.) analyses. Tetramethylene sulfone was further purified for reactions in which the concentration of the nitronium tetrafluoroborate was less than 2%. The once distilled material was fractionated on a Todd column at 98–103° and 0.8–1.2 mm with 5:1 reflux ratio and 0.3–0.4 ml/min takeoff. Analytical results are shown below.[3]

FREEZING POINT	26.7 °C
REFRACTIVE INDEX AT 30 °C	1.4816
SPECIFIC CONDUCTIVITY	6.45×10^{-6} cm/ohm

Nitronium tetrafluoroborate was prepared according to the method of Kuhn (16) from fuming nitric acid, hydrogen fluoride, and boron trifluoride in nitromethane solution. The white, powdery nitronium tetrafluoroborate was filtered on a sintered glass crucible, washed four times with nitromethane, then three times with Freon 113. The material was dried at room temperature at pressures below 0.1 mm until constant weight (10–12 h) and stored in a dessicator. Filtration and all subsequent handling was carried out in dry nitrogen atmosphere.

Preparation of Solutions

Tetramethylene sulfone was used as solvent in all the experiments. The solutions were prepared by weight for each set of experiments. Sulfuric and nitric acid solutions were prepared by slowly adding the measured amount of acid into tetramethylene sulfone with cooling because of the high heat of dissolution.

Nitronium tetrafluoroborate solutions were prepared by transferring a measured amount of nitronium tetrafluoroborate into a known amount of tetramethylene sulfone at 30–35°, in dry nitrogen atmosphere. The mixture was stirred for about 3 h with a magnetic stirrer because the rate of dissolution of the salt was rather low. For saturated solutions excess amount of nitronium salt was stirred in tetramethylene sulfone for 6–7 h then it was allowed to settle overnight. The concentration of the saturated solution was determined by the following methods:[3] (1) boron determination, 6.8% (w/w); (2) specific gravity, 7.8% (w/w); (3) refractive index, 7.8%(w/w); (4) hydrolysis, 7.55% (w/w).

The solutions had a pale-yellow color probably originating from some impurity of the solvent. In one case a colorless solution was obtained using freshly distilled tetramethylene sulfone.

[3]*The analyses were carried out by Mr. D. Choksi, Dow Chemical of Canada, Limited.*

Can. J. Chem. Downloaded from www.nrcresearchpress.com by 210.87.254.40 on 09/05/12
For personal use only.

Reactions

Employing Magnetic Stirring and Dropwise Addition of the Nitrating Solution (Tables I and IV)

The reactions were carried out in a 250 ml flat bottom flask equipped with thermometer, dropping funnel, and $CaCl_2$ tube in a 25 ± 1 °C water bath. Fifty milliliters of the toluene–benzene solution was measured in the flask and 25 ml of nitronium tetrafluoroborate solution in the dropping funnel. The aromatic solution was agitated with a Teflon-coated magnetic bar (9 × 38 mm) rotated by a magnetic stirrer. Electric input of the motor was regulated by a Powerstat Voltage Regulator. The rotating speed of the magnetic bar in the aromatic solution was calibrated with a stroboscope, and the results are shown below.

Setting of Powerstat, V	42.5	45	50	55	60	65	70	75
Revolutions of magnetic bar, rev/min	79	137	198	300	410	612	778	966

The nitronium tetrafluoroborate solution was added to the aromatic solution at a rate of 30–40 drops/min, the total time of addition being between 16 and 19 min. The tip of the dropping funnel was positioned slightly off the center of the revolving magnet. After the addition of all the nitronium salt, the dark-red reaction mixture was poured into water (150 ml) which turned its color to yellow. The organic layer of the mixture was diluted with 50 ml ether.

Magnetic Stirring and Syringe Addition of the Nitronium Salt Solution (Part of Table III)

The reactions were carried out in a 50 ml Erlenmeyer flask, having a short side arm closed with a serum cap, a baffle in the form of a flattened glass rod reaching vertically to about 3 mm above the tip of the rotating magnet, and a long wide neck closed with a $CaCl_2$ tube. Forty milliliters of the toluene–benzene solution was measured in the flask filling it to the bottom of the neck. High liquid level was necessary to prevent air reaching to the the magnetic bar at the high rate of stirring and making the solution "boil". Nitronium tetrafluoroborate solution (6 ml) was measured in the barrel of a 10 ml syringe connected to a nitrogen cylinder through a pressure regulator. The nitronium salt solution was injected into the aromatic solution in the form of a fine jet, at pressures 5–15 p.s.i., through a thin hypodermic needle (20G–24G). The tip of the hypodermic needle, entering through the serum cap on the side arm of the flask, was positioned between the rotating magnetic bar and the baffle. Addition time ranged from 0.5 to 2 min depending on the size of the needle, pressure, and concentration of the nitronium salt solution. These variants were constant in comparative experiments. The temperature was not controlled, but was measured to be between 23 and 26 °C.

Vibrator Disc Agitation and Syringe Addition of the Nitronium Tetrafluoroborate Solution (Tables II, Part of III and V)

The reactions were carried out under a blanket of dry nitrogen in a jacketed test tube (28 × 200 mm) having a short side arm, closed with a serum cap, near to the bottom of the vessel. Sixty milliliters of the aromatic solution was measured in the reaction vessel and it was agitated with a laboratory type, Model E-1 Vibro-Mixer.[4] The vibrating stainless steel disc (23 mm diameter) had five Venturi-type orifices (3 mm diameter) and it was positioned about 15 mm from the bottom of the reaction tube, the orifices pointing downwards. Electric input was controlled with a Powerstat Voltage Regulator. The frequency of vibration of the disc was 7 200 cycles/min and it was independent of the power input. Voltage regulation influenced only the amplitude of vibration. The amplitudes, measured with the aid of a stroboscope and cathetometer, are given below.

Setting of Powerstat, V	40	50	60	70	80	90	100	110	120
Amplitude of vibration, mm	0.35	0.45	0.70	1.15	1.55	2.00	2.40	2.85	3.40

The vibrator disc with Venturi tube type orifices ensured a very turbulent agitation. The turbulence originates in three separate characteristics of the agitator (*a*) Non-aerodynamic shape of the disc in the direction of movement, with small localized passages for the liquid; (*b*) continuously changing speed; (*c*) reciprocal movement of the disc (7 200 cycles/min). Nitronium tetrafluoroborate solution (20 ml) was added to the aromatic solution from a 25 ml syringe at 15–20 p.s.i. nitrogen pressure through a fine hypodermic needle (1 in. long, 24G except when stated otherwise) as described above. The tip of the needle, inserted through the serum cap was positioned 1–2 mm beneath the center of an orifice. Time of addition varied between 3.5 and 4.5 min depending on the concentration of the solution and the pressure applied. The temperature was regulated by circulating water (25 ± 1 °C) in the jacket of the reaction tube. After the addition of the nitrating solution the mixture was poured into 150 ml water and diluted with 50 ml ether. "Mixed acid" nitrations were all carried out according to the above method using the Vibro-Mixer and syringe addition of the acid solution.

In the first set of five parallel experiments 20 ml of a tetramethylene sulfone solution of nitric acid (1.3 *M* for HNO_3) was injected in 10–11 min at 25 °C. into 60 ml of a tetramethylene sulfone solution which was 2.1 *M* for both benzene and toluene and 1.7 *M* for sulfuric acid.

In the second set of five parallel experiments 20 ml of a tetramethylene sulfone solution of sulfuric acid

[4] *A. G. Fur Chemie-Apparatebau, Mannedorf-Zurich.*

Can. J. Chem. Downloaded from www.nrcresearchpress.com by 210.87.254.40 on 09/05/12
For personal use only.

(4.2 *M* for H_2SO_4) was injected in 10–11 min at 25 °C into 60 ml of a tetramethylene sulfone solution which was 2.3 *M* for both benzene and toluene and 0.5 *M* for nitric acid.

Nitric Acid Nitration

(a) With Dissolved Nitric Acid

A solution of 0.08 mole of nitric acid in 60 g of tetramethylene sulfone was added dropwise in the course of 20 min to a mixture of 0.25 mole of benzene and 0.25 mole of toluene dissolved in 70 g of tetramethylene sulfone, while it was agitated with a magnetic stirrer (60 V). The solution was agitated for 11 h or 6 h at 24–26°. The mixtures were poured into 250 ml water and were diluted with 50 ml ether.

(b) With Neat Nitric Acid

Nitric acid (0.07 mole) was added dropwise in 10 min to a solution of 0.25 mole of benzene and 0.25 mole of toluene in 120 g of tetramethylene sulfone while it was agitated as above. After 6 h of further agitation at 24–26° the solution was poured into 250 ml of water and was diluted with 50 ml of ether.

Washing and Concentrating of the Reaction Mixtures

The quenched reaction mixtures were filled up to about 450 ml with water in a 500 ml separatory funnel. The aqueous layer containing most of the tetramethylene sulfone was extracted three times with 35–40 ml portions of ether after separation. The combined organic solution was washed twice more with 250–300 ml water. Each portion of the washing water was extracted twice with 30–35 ml ether, which was added back to the organic solution. In the case of "mixed acid" and nitric acid nitration the solution had to be washed with water once more to ensure neutral pH. The solutions were dried with $CaCl_2$ and the ether and part of the excess benzene was distilled off on a 30 cm packed column. The head temperature of the distillation never exceeded 95 °C (for mixtures of very low conversion) and in most cases the distillation was carried only to 50 °C. The method of washing and concentrating—checked on synthetic mixtures—did not change the composition of the reaction products.

Analyses[5]

All analyses of the nitrated samples were carried out on an F and M Model 720 Dual Column Gas Chromatograph equipped with a thermal conductivity detector. The operating conditions were cell current: 100 mA (W-2 filaments); carrier gas: helium at 10 ml per 10 s; injection port temperature: 300 °C; detector block temperature: 340 °C; injection size: 15 μl, injected with 50 μl Hamilton syringe equipped with Chaney Adaptor.

Peak areas were determined either by triangulation or with a Disc Chart Integrator. Peak heights were measured when peaks were smaller than about 10 mm in height or were incompletely resolved from other large peaks (*m*-nitrotoluene).

Calibrating standards were prepared in volumetric flasks on an analytical balance. New standards were prepared and analyzed whenever a new set of samples contained nitrated compounds at concentrations not previously encountered. Sample concentrations were based on direct comparisons of samples and standards and expressed as moles of compound per 15 μl of sample solution.

Nitrobenzene and Nitrotoluene

These compounds were determined on a 4.5 ft column of 1/4 in. outside diameter copper tubing packed with 15 w/w % 6 ring poly-*m*-phenyl ether on Chromosorb W at 180 °C.

Dinitrotoluene

Dinitro compounds were analyzed either on a 9 ft column packed with 15 w/w % silicone gum rubber SE-30 on Chromosorb W at 230 °C or on the 4.5 ft poly-*m*-phenyl ether column at 225 °C. The resolving power of the columns changed rapidly and unknown impurities started to interfere after about 20 samples.

Other columns using polar-partitioning liquids (such as Carbowax 20M, Carbowax 4000 terephthalic acid, Carbowax 4000 monostearate) were tried but all were found to be unsuitable because of inadequate resolution of the dinitro compounds, interference from unknowns, or an insufficiently high maximum column temperature.

Nitrofluoro and Nitrochlorobenzenes

Analysis was carried out on the 4.5 ft poly-*m*-phenyl ether column at 175 °C. The nitrofluorobenzene isomers were separated from one another, eluting in 4–6 min in the sequence *m*-, *p*-, *o*-. The *o*-nitrofluorobenzene isomer, however, had the same retention time as nitrobenzene. For samples containing both of these compounds their combined concentration was found using the area response of nitrobenzene as calibration. Nitrochlorobenzenes eluted in about 12 min. The isomers were not adequately separated to permit their separate determination. The area response of the *p*-isomer was used to convert the combined nitrochlorobenzene peak area to concentration.

RESULTS

Toluene–Benzene

The purpose of the following set of experiments was to investigate the possible existence

[5]*The analyses were carried out by Mr. P. Kann, Dow Chemical of Canada, Limited.*

Can. J. Chem. Downloaded from www.nrcresearchpress.com by 210.87.254.40 on 09/05/12
For personal use only.

of non-kinetic conditions in competitive nitration of benzene and toluene with nitronium tetrafluoroborate. This point was approached by determining whether non-kinetic factors, like rate of stirring, and concentration of the solutions, influenced the product ratios of the reaction.

TABLE I

Nitration with the use of magnetic stirrer and dropwise addition of the nitrating agent* (Aromatic solution: 50 ml; 2.3 *M* for benzene and toluene each. NO_2BF_4 solution: 25 ml)

$[NO_2BF_4]$ (mole/l)	Voltage (V)	Product ratio†	Nitrotoluene†			
			ortho- (%)	meta- (%)	para- (%)	*o-/p-*
0.74	45	1.32±0.05	62.8±0.3	3.11±0.1	34.1±0.2	1.84±0.02
	50	1.46±0.03	63.0±0.2	2.98±0.03	33.9±0.2	1.86±0.01
	60	1.84±0.06	63.3±0.1	2.92±0.03	33.8±0.1	1.87±0.01
	75	2.2 ±0.1	63.0±0.1	2.98±0.04	34.0±0.1	1.85±0.01
0.41	45	1.72±0.03	63.6±0.2	3.03±0.04	33.4±0.2	1.91±0.02
	50	2.1 ±0.1	63.5±0.2	3.01±0.05	33.5±0.3	1.89±0.02
	60	2.5 ±0.0	63.6±0.1	2.97±0.06	33.4±0.1	1.90±0.01
	75	2.9 ±0.1	64.1±0.5	2.98±0.05	33.0±0.4	1.94±0.04
0.15	45	2.6 ±0.2	64.0±0.2	2.96±0.06	33.0±0.1	1.94±0.01
	50	3.2 ±0.1	64.0±0.3	2.97±0.10	33.0±0.2	1.94±0.02
	60	3.9 ±0.3	64.2±0.1	2.97±0.11	32.8±0.1	1.96±0.01
	75	5.1 ±0.3	63.8±0.5	3.16±0.14	33.1±0.4	1.93±0.04

*Data represent the average and maximum scatter of three parallel experiments.
†Estimated accuracy of analysis (determination of peak area on the chromatogram): ±5% for meta-nitrotoluene and ±3% for all other components using 0.74 and 0.41 *M* NO_2BF_4 solutions. ±10% for meta-nitrotoluene, ±5% for nitrobenzene, and ±3% for ortho- and para-nitrotoluene using 0.15 *M* NO_2BF_4 solution.

Results are given in Table I showing concentration of the nitronium salt solution, rate of stirring characterized by the voltage setting on the regulator, product ratio (NO_2-toluene/NO_2-benzene), and the isomer distribution of nitrotoluene. The definite and continuous dependence of product ratio on both the speed of agitation and the concentration of the nitrating solution was further investigated with a method ensuring a faster dispersion of the nitrating agent in the aromatic solution. Results of this series of experiments are given in Table II.

TABLE II

Nitration with the use of vibrator stirrer and syringe addition of the nitrating agent (Aromatic solution: 60 ml; 2.3 *M* for benzene and toluene each. NO_2BF_4 solution: 20 ml)

Number of parallel experiments	$[NO_2BF_4]$ (mole/l)	Voltage (V)	Product ratio*	Nitrotoluene*			
				ortho- (%)	meta- (%)	para- (%)	*o-/p-*
2	0.74	60	2.9±0.2	62.3±0.2	3.03±0.04	34.7±0.1	1.80±0.01
2		90	5.2±0.2	63.6±0.0	3.06±0.20	33.3±0.2	1.91±0.01
5		120	7.6±0.6	63.2±0.9	3.10±0.10	33.7±0.8	1.87±0.08
2	0.41	60	4.9±0.2	63.2±0.1	3.20±0.17	33.6±0.3	1.88±0.02
2		90	9.3±1.0	63.5±0.3	3.23±0.01	33.3±0.3	1.91±0.02
5		120	13.2±0.6	63.4±1.4	3.12±0.20	33.5±1.2	1.89±0.11
2	0.18	40	3.1±0.5	64.1±0.1	3.09±0.06	32.9±0.1	1.95±0.01
2		80	11.7±0.3	64.5±0.4	3.03±0.08	32.5±0.4	1.98±0.04
6		120	19.4±2.0	63.8±0.8	3.06±0.13	33.1±0.6	1.94±0.06
2	0.07	40	11.7±1.0	63.2±1.5	3.45±0.40	33.3±1.1	1.90±0.11
2		80	21.4±1.2	64.2±1.1	2.88±0.22	32.8±1.1	1.95±0.07
6		120	26.5±2.2	63.9±1.5	2.91±0.65	33.1±0.9	1.93±0.11
2	0.04	60	21.7±1.0	64.3±0.7	2.86±0.12	32.9±0.6	1.95±0.05
2		80	26.2±0.1	63.9±0.3	2.95±0.01	33.2±0.3	1.93±0.03
2		100	26.2±1.1	64.4±0.5	3.00±0.01	32.6±0.5	1.97±0.05
2		110	26.8±3.2	63.6±0.1	3.36±0.05	33.0±0.1	1.93±0.01
2		120	27.1±0.9	64.6±0.1	3.15±0.05	32.2±0.2	2.00±0.01

*Estimated accuracy of analysis: for the results obtained with 0.07 *M* NO_2BF_4 solution; meta-nitrotoluene ±25%, nitrobenzene and para-nitrotoluene ±10%, and ortho-nitrotoluene ±5%. For all others, nitrobenzene and meta-nitrotoluene ±10%, ortho- and para-nitrotoluene ±5%.

Can. J. Chem. Downloaded from www.nrcresearchpress.com by 210.87.254.40 on 09/05/12
For personal use only.

The results show the same general trend. Increased speed of agitation or decreased concentration of the nitrating agent results in an increase of the product ratio. At the same time, however, the data of Table II show some new characteristics which can be best represented graphically. Figures 2 and 3 show the product ratios, given in Tables I and II respectively, plotted against the voltage of agitation.

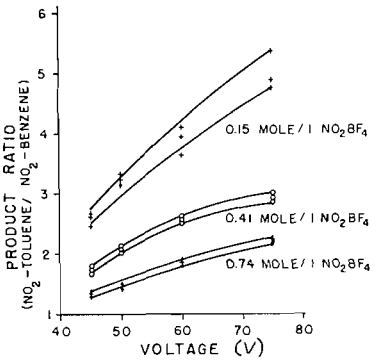

FIG. 2. Product ratio vs. voltage of magnetic stirrer using NO_2BF_4 solutions of different concentrations.

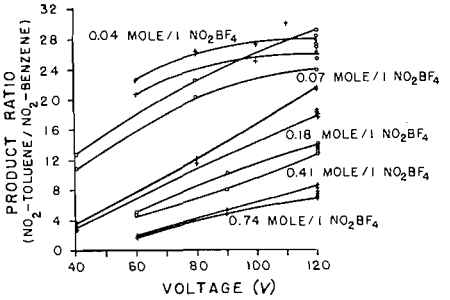

FIG. 3. Product ratio vs. voltage of vibrator motor using NO_2BF_4 solutions of different concentrations.

Two of the curves of Fig. 3 representing product ratios obtained with the two most dilute NO_2BF_4 solutions approach a constant and common value at high rate of agitation. Therefore it can be suggested that the product ratio approached independence from both stirring rate and concentration under the specific conditions. With the following set of experiments the effect of dilution of the aromatic solution was investigated. Pairs of reactions were carried out under different conditions. Within each pair, however, only the concentration of the aromatic solutions was changed. It is seen from the data of Table III that the more concentrated aromatic solution yields a higher product ratio than the less concentrated one under the investigated conditions. The change is opposite in direction to that observed when the concentration of the nitronium salt was varied.

As has already been indicated, a nitro group on the aromatic ring decreases its activity for further nitration by a factor of 10^5–10^7 (11, 13). Therefore, dinitration should not be observable in the present investigation as the conversion of the aromatics was always less than 10%. Reaction mixtures of low product ratio, however, contained measurable amounts of dinitrotoluene as identified by g.c. analysis. Amounts of dinitrotoluene found

Can. J. Chem. Downloaded from www.nrcresearchpress.com by 210.87.254.40 on 09/05/12
For personal use only.

TABLE III

Effect of concentration of the aromatic solution on the product ratio (Aromatic solution: 60 ml; 0.3*M* 3 or 2.3 for benzene and toluene each. NO_2BF_4 solution: 10 ml; syringe injection)

$[NO_2BF_4]$ (mole/l)	Type of stirrer	Voltage (V)	Size of hypodermic needle	Product ratio* in aromatic solutions† of: 0.33 *M*	2.3 *M*
0.35	Magnetic	120	24	3.3	6.2
			23	3.6	5.9
			22	3.7	6.5
	Vibrator	120	24	5.3	14.1
			23	6.7	13.5
			22	8.0	12.5
			20	5.9	9.7
0.15	Magnetic	115	24	5.5	8.1
	Vibrator	120	24	11.8	16.3
			20	8.0	15.9

*Estimated accuracy of analysis ±5%.
†No differences could be observed in the rate of agitation between the more or less concentrated solutions.

in reaction mixtures are shown in Table IV expressed as percentage of the mononitrotoluene. Dinitrotoluene was found in similar quantity in 37 additional reaction mixtures[6] with product ratios of the mononitro compounds ranging from 1.3 to 6.5.

TABLE IV

Extent of dinitration of toluene

Product ratio	Calculated conversion of toluene* (%)	Dinitrotoluene as % of mononitrotoluene: 2,4-Dinitro	2,6-Dinitro	Estimated accuracy of analysis (±%)
1.33	9	1.0	0.5	10
5.6	6	0.4	Less than limit of	25
7.4	6	0.3	quantitative	25
10.3	6	0.4	determination	25

*Calculated from the amount of NO_2BF_4 and product ratio.

Dinitrobenzene was not found in the reaction mixtures or at least it was present in quantities smaller than the limit of detection of the analytical method, about 0.1% of the mononitrobenzene under optimum conditions. Its absence can be explained by the facts that mononitrobenzene nitrates about 330 times slower than *p*-nitrotoluene (17), and its concentration was always lower than that of nitrotoluene.

The problem of fast distribution of the nitrating agent in the reaction mixture prior to considerable degree of conversion was investigated from a different angle in the following set of experiments. The rate of consumption of the nitronium salt was decreased by using aromatics (fluorobenzene and chlorobenzene) less reactive than benzene and toluene. Reactions were carried out with vibrator disc agitation and syringe addition of 20 ml of the nitronium salt solution to 60 ml of the aromatic solution which was 2.3 *M* for each competitor. Results are shown in Table V. Data represent the average and maximum scatter of three parallel experiments.

[6]*Dinitrotoluene and mononitrotoluene were determined from separate injections; therefore, they cannot be directly compared.*

Can. J. Chem. Downloaded from www.nrcresearchpress.com by 210.87.254.40 on 09/05/12
For personal use only.

TABLE V

Competitive nitration of different pairs of aromatics

Aromatic compounds	$[NO_2BF_4]$ (mole/l)	Product ratio	Isomer distribution		
			ortho- (%)	meta- (%)	para- (%)
			of fluoronitrobenzene		
Fluorobenzene–chlorobenzene	0.17	4.3±0.1	9.9±0.3	0.31±0.05	89.8±0.3
	0.74	4.2±0.1	9.5±0.3	0.30±0.01	90.2±0.3
Benzene–fluorobenzene	0.17	6.0±0.2			
	0.74	5.0±0.5			
Benzene–chlorobenzene	0.17	22.2±3.5			
	0.74	19.7±3.3			
			of nitrotoluene		
Toluene–fluorobenzene	0.17	101 ±1	63.5±0.2	3.06±0.08	33.5±0.1
	0.74	27.8±5	62.5±0.2	3.16±0.05	34.3±0.2

It is seen from Table V that the product ratio of the fluorobenzene–chlorobenzene pair is independent of the concentration of the nitronium salt. Furthermore it corresponds closely to the relative reactivity value (4.5) obtained by Bird and Ingold (18) using acetyl nitrate in acetic anhydride solution. In the case of the more reactive benzene–fluorobenzene pair the product ratios depend on the concentration of the nitronium fluoroborate solution only slightly and are still similar to the relative reactivity value of 6.7 (18) and 7.1 (19) obtained under different conditions. The product ratio for the still more active toluene–benzene pair (Table II), however, depends markedly on the nitronium salt concentration and is increasingly lower than the relative reactivity.

The results obtained for aromatic pairs of increasingly different reactivity show the same characteristics. The product ratio of the benzene–chlorobenzene pair depends on the nitronium salt concentration only slightly and is only moderately different from the reported (18) relative reactivity of 30. In the case of the faster toluene–fluorobenzene pair, the same conclusion cannot be drawn.

Isomer Distribution of Nitrotoluene

The isomer distribution data obtained from 151 nitration experiments with NO_2BF_4 are shown in Figs. 4 and 5. The bar graph (Fig. 4) shows the reproducibility of data. The amount of ortho- and para-isomers, seems to exhibit a slight dependence on the concentration of NO_2BF_4 as shown in Fig. 5. The small but perceptible decrease in the amount of ortho-isomer might be attributed to changes in steric hindrance with increasing concentration of the nitronium fluoroborate solution.

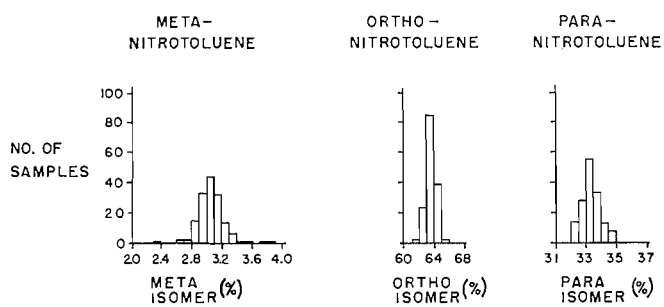

FIG. 4. Distribution diagram of the isomers of nitrotoluene in NO_2BF_4 nitration.

Can. J. Chem. Downloaded from www.nrcresearchpress.com by 210.87.254.40 on 09/05/12
For personal use only.

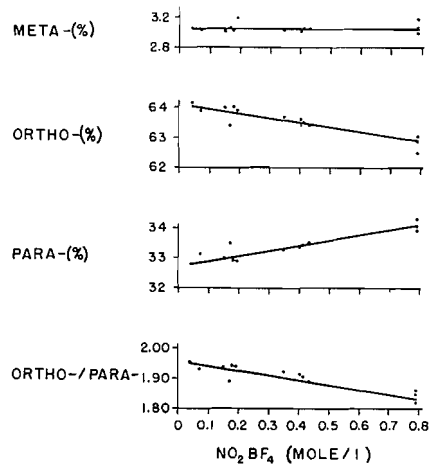

FIG. 5. Isomer distribution of nitrotoluene vs. concentration of NO_2BF_4 solution. (Each point represents the average of one set of experiments.)

As nitric acid or mixed acid nitration is reported (8, 9) to yield lower ortho-/para-values than the present ones a few further experiments were carried out with nitric acid as the nitrating agent in tetramethylene sulfone solution. In the first set of experiments a tetramethylene sulfone solution of nitric acid was added to the aromatic solution containing sulfuric acid. The product ratio was found to be 36.9 ± 2.2 while the isomer distribution of nitrotoluene (61.6 ± 0.8% *o*-, 2.91 ± 0.21% *m*-, and 35.5 ± 0.6% *p*-) gave an ortho-/para-value of 1.74 ± 0.06.

In the second set of experiments the nitric acid was dissolved in the aromatic solution and nitration was effected by the addition of a sulfuric acid solution. The product ratio was found to be 34.8 ± 4.3 in this case while the composition of nitrotoluene (61.6 ± 0.6% *o*-, 3.36 ± 0.47% *m*-, and 35.0 ± 0.5 *p*-) gave an ortho-/para-value of 1.76 ± 0.04.

Both types of nitration may be described as "mixed acid" nitration, because nitric acid alone did not yield measurable amounts of nitro aromatics under similar conditions.

The product ratio is surprisingly high in both cases even if we take into account that because of the low conversion the estimated accuracy of analysis of nitrobenzene is 10% and 20% in the first and second set of experiments, respectively.

The ortho-/para-value of nitrotoluene was checked further, using a tetramethylene sulfone solution of nitric acid in two parallel experiments omitting the sulfuric acid. The product ratio was found to be 24.7 ± 1.6 while the isomer distribution of nitrotoluene (60.2 ± 0.9% *o*-, 5.1 ± 0.9% *m*-, and 34.7 ± 0.1% *p*-) gave an ortho-/para-value of 1.73 ± 0.03. In spite of the prolonged reaction time, the conversion of the aromatics was very low and therefore the product ratio and the *m*-nitrotoluene value are indicative rather than quantitative data. Both *o*- and *p*-nitrotoluene were present, however, in easily measurable quantities (±5% estimated analytical accuracy) and show, similarly to the "mixed acid" nitration, a lower ortho-/para-value than NO_2BF_4.

The possibility of obtaining low product ratio even in nitric acid nitration was demonstrated with the following experiment. The above described experiment was repeated with the exception that neat nitric acid was added to the tetramethylene sulfone solution of benzene and toluene. After 6 h of reaction time the product ratio was found to be 3.4. The isomer distribution of nitrotoluene (59.6% *o*-, 4.7% *m*-, and 35.7% *p*-) gave an ortho-/para-value of 1.67.

Can. J. Chem. Downloaded from www.nrcresearchpress.com by 210.87.254.40 on 09/05/12
For personal use only.

Can. J. Chem. Downloaded from www.nrcresearchpress.com by 210.87.254.40 on 09/05/12
For personal use only.

DISCUSSION

On the basis of the results it is proposed that the competitive nitration of reactive aromatics with nitronium tetrafluoroborate does not proceed with kinetic control under the conditions described in the literature—magnetic stirring, dropwise addition of the reactant (1–5). Therefore, reported relative rates do not represent the relative reactivity of the competitors. The absence of kinetic control originates probably from the fact that the rate of nitration of benzene and aromatics of similar reactivity is very high with nitronium ion. Seemingly it is high enough to ensure a considerable consumption of the nitrating agent before it is homogenized in the aromatic solution. The reaction occurring prior to homogenization might be influenced by the non-kinetic factors described by Francis (8).

The absence of kinetic control and the correspondence to Francis' conclusions in the presently described nitration is shown by the following observations.

(1) Product ratios increased with increasing intensity of stirring.

(2) Product ratios increased with decreasing concentration of the nitrating solution. The two phenomena may be explained by a related effect. Both increased speed of distribution and lower concentration of the reactant decrease the extent of reaction occurring prior to homogenization in the layer adjacent to the entering nitronium salt solution.

(3) Product ratios decreased with decreasing concentration of the aromatic solution. The extent of the primary, selective depletion of the more reactive competitor in the reaction zone is higher when the concentration of the aromatic compound is low. Therefore the less reactive competitor obtains increasingly larger portions of the reactant, and the product ratio moves toward unity.

(4) Reaction mixtures of low product ratio contained measurable amounts of dinitrotoluene (Table IV). Though the extent of dinitration was small, one could calculate from the data a relative rate of nitration of toluene/nitrotoluene as being < 10 considering the low conversion. This low figure can hardly be considered as a kinetic value. The result can be explained by imperfect homogenization of the reaction mixture. If the aromatic solution were not exchanged fast enough in the layer surrounding the nitrating agent subsequent portions of the nitronium salt would be confronted with a layer rich in nitroaromatics. It seems plausible to suggest that the same factors might limit the applicability of the competitive method of rate determination for other fast reactions as well.

To diminish the influence of non-kinetic factors in the investigated system the effectiveness of agitation was increased by using a disc vibrator instead of a magnetic stirrer. By use of the vibrator stirrer in connection with nitronium salt solutions of low concentrations (0.07 and 0.04 M), the product ratios approached a range (between 25 and 30) where they became independent of both concentration and stirring rate. Because this range corresponds to that of the relative reactivity of toluene/benzene in nitric acid nitrations there seems to be no reason to suppose that nitronium salt nitration involves a mechanism different from that of nitric acid nitration, investigated in great detail by Ingold and co-workers (11). This proposal is supported further by the fact that when the absolute rate of the reaction was reduced by using aromatic pairs of lower reactivity (fluorobenzene/chlorobenzene and with certain limitations benzene/fluorobenzene) the product ratios remained independent of the concentration of the nitronium salt solution, in spite of the higher values, and corresponded to the known relative reactivities (18, 19) in nitric acid nitration as well. An alternative explanation of the results would imply the existence of separate nitrating species in the nitronium salt solutions; a highly reactive one, present when the concentration of the salt is high, and another, present in dilute solutions, with

decreased reactivity because of solvation. The former would show much lower substrate selectivity than the latter.

The validity of this type of explanation is, however, extremely doubtful considering the following.

(1) The concentration of tetramethylene sulfone is so high (93.2 mole %) even in a saturated nitronium fluoroborate solution, that further increase to 99.6 mole % seems to be insufficient to effect drastic changes in the environment of the nitronium salt.

(2) According to indicator and cryoscopic studies of Arnett and Douty (20), tetramethylene sulfone is a very weakly basic solvent, in which ions are poorly solvated. The electrical conductivity of nitronium tetrafluoroborate in tetramethylene sulfone (21), attributed to conducting ion triplets (4), varied linearly with the concentration in the range used in the present investigation.

(3) According to spectroscopic evidence the nitronium ion is insensitive to environmental changes (4, 22).

(4) Rate constants for the nitration of nitrobenzene (12) with nitronium tetrafluoroborate were independent of the concentration of the nitronium salt both in organic solution (acetonitrile) and in inorganic solution (sulfuric acid).

(5) Concentration changes of the nitronium salt affect the product ratios, in the present investigations, only in the case of highly reactive aromatics. Chlorobenzene–fluorobenzene was insensitive, benzene–fluorobenzene slightly sensitive, and toluene–benzene highly sensitive to the concentration.

(6) Dilute aromatic solution always yielded a lower product ratio than a more concentrated one.

(7) If dilution effected any change in the isomer distribution of nitrotoluene through solvation the ortho-/para-value would be expected to decrease. The results, however, point to the other direction. Toluene showed a somewhat greater ortho-steric hindrance against concentrated solutions of nitronium tetrafluoroborate than against dilute ones.

Apart from these facts solvation or some other kind of complex formation can not explain the dependence of product ratios on the rate of agitation.

Based on the foregoing arguments it seems highly improbable that separate nitronium ion species of highly different reactivities operate simultaneously in the reaction and that their relative concentration determined by dilution regulates the product ratios.

ACKNOWLEDGMENTS

It is a pleasure to thank Dr. J. W. Crump of Albion College, Michigan, and many of my colleagues for helpful discussions. I also wish to thank Mr. P. Kann for the gas chromatographic analysis.

REFERENCES

1. G. A. Olah, S. J. Kuhn, and S. H. Flood. J. Am. Chem. Soc. **83**, 4571 (1961).
2. G. A. Olah, S. J. Kuhn, and S. H. Flood. J. Am. Chem. Soc. **83**, 4581 (1961).
3. G. A. Olah and S. J. Kuhn. J. Am. Chem. Soc. **84**, 3684 (1962).
4. G. A. Olah, S. J. Kuhn, S. H. Flood, and J. C. Evans. J. Am. Chem. Soc. **84**, 3687 (1962).
5. G. A. Olah and S. J. Kuhn. J. Am. Chem. Soc. **86**, 1067 (1964).
6. H. Cohn, E. D. Hughes, M. H. Jones, and M. G. Peeling. Nature, **169**, 291 (1952).
7. C. K. Ingold, A. Lapworth, E. Rothstein, and D. Ward. J. Chem. Soc. 1959 (1931).
8. A. W. Francis. J. Am. Chem. Soc. **48**, 655 (1926).
9. C. K. Ingold and F. R. Shaw. J. Chem. Soc. 2918 (1927).
10. M. J. S. Dewar, T. Mole, and E. W. T. Warford. J. Chem. Soc. 3576 (1956).
11. E. D. Hughes, C. K. Ingold, and R. I. Reed. J. Chem. Soc. 2400 (1950).
12. L. L. Ciaccio and R. A. Marcus. J. Am. Chem. Soc. **84**, 1838 (1962).
13. F. H. Westheimer and M. S. Karasch. J. Am. Chem. Soc. **68**, 1871 (1946).

Can. J. Chem. Downloaded from www.nrcresearchpress.com by 210.87.254.40 on 09/05/12
For personal use only.

14. C. D. RITCHIE and H. WIN. J. Org. Chem. In press (private communication).
15. R. L. BURWELL and C. H. LANGFORD. J. Am. Chem. Soc. **81**, 3799 (1959).
16. S. J. KUHN. Can. J. Chem. **40**, 1660 (1962).
17. C. D. BRAND and R. P. PATON. J. Chem. Soc. 281 (1952).
18. M. L. BIRD and C. K. INGOLD. J. Chem. Soc. 918 (1938).
19. J. R. KNOWLES, R. O. C. NORMAN, and G. K. RADDA. J. Chem. Soc. 4885 (1960).
20. E. M. ARNETT and C. F. DOUTY. J. Am. Chem. Soc. **86**, 409 (1964).
21. S. J. KUHN and G. A. OLAH. J. Am. Chem. Soc. **83**, 4564 (1961).
22. R. A. MARCUS and J. M. FRESCO. J. Chem. Phys. **27**, 564 (1957).

Can. J. Chem. Downloaded from www.nrcresearchpress.com by 210.87.254.40 on 09/05/12
For personal use only.

Can. J. Chem. Downloaded from www.nrcresearchpress.com by 210.87.254.40 on 09/05/12
For personal use only.

ESTER HYDRAZONES AS POSSIBLE PRECURSORS TO ALKOXYDIAZOALKANES[1]

II. THE DECOMPOSITION OF ESTER (*p*-TOLYLSULFONYL)HYDRAZONE SALTS IN APROTIC SOLVENTS

ROBERT J. CRAWFORD AND RINTJE RAAP[2]
Department of Chemistry, University of Alberta, Edmonton, Alberta
Received July 10, 1964

ABSTRACT

The thermal and photochemical decomposition of methyl benzoate (*p*-tolylsulfonyl)hydrazone salts in 1,2-dimethoxyethane, 1,2-diethoxyethane, or diglyme gives rise to benzaldehyde dimethyl acetal, methyl benzoate azine (II), *meso*-1,2-diphenyl-1,2-dimethoxyethane, and methyl α-(*p*-tolylsulfonyl)benzyl ether. The thermal decomposition in the presence of diethyl fumarate produced diethyl 3-methoxy-3-phenyl-*trans*-1,2-cyclopropanedicarboxylate (XIV) in 62% yield; a low yield (4%) of the two isomeric forms of 1-methoxy-2-*n*-octyl-1-phenylcyclopropane (V) was formed in 1-decene. The thermal and photochemical decomposition of potassium 4-pentenyl benzoate (*p*-tolylsulfonyl)hydrazone (XVIII) produced 1-phenyl-2-oxabicyclo[4.1.0]heptane (XXI) in 14 and 21% yield respectively. These products provide additional evidence for the occurrence of alkoxydiazoalkanes and suggest alkoxycarbenes as possible intermediates in the decomposition of ester (*p*-tolylsulfonyl)hydrazone salts.

INTRODUCTION

Diazoalkanes undergo thermal and photochemical decomposition in aprotic solvents to give rise to a number of unique products (1). The reactions of the sodium salts of I in protic solvents was shown, in the preceding paper (2), to decompose in a manner reconcilable with an alkoxydiazoalkane intermediate. We have herein undertaken a study of the decomposition of the sodium salts of I in aprotic solvents in an attempt to gain information of a synthetic and mechanistic value.

I

DISCUSSION*

The sodium salt of I was prepared by dissolving the hydrazone I in DME with an equimolar amount of sodium methoxide. The methanol was distilled off and the resulting solution refluxed for 65 h, as judged sufficient by the decreased rate of nitrogen evolution. The products were benzaldehyde dimethyl acetal (34%) and a solid, m.p. 72–73°, that was isolated by chromatography, on alumina, of the nonvolatile fraction. The infrared spectrum of the solid showed an intense absorption at 1 615 cm^{-1}, indicative of C=N. The nuclear magnetic resonance (n.m.r.) spectrum indicated aromatic protons at τ 2.0 to 2.8 and a sharp —OCH_3 singlet at τ 6.18, with relative areas of 10:6 respectively. The compound has a molecular weight of 269 and its elemental composition fits the empirical formula

[1]*Presented at the 47th Canadian Chemical Conference, Kingston, Ontario, June 1–3, 1964.*
[2]*Holder of a National Research Council of Canada Scholarship, 1963–1964. Present address: R & L Molecular Research Ltd., Edmonton, Alberta.*
**Solvents such as 1,2-dimethoxyethane(DME), 1,2-diethoxyethane (DEE), and diglyme were freed, prior to use, from hydroxylic materials by distillation from potassium metal.*

$C_{16}H_{16}N_2O_2$ (molecular weight 268.3). There is little doubt that the product is methyl benzoate azine (II), as the same product was prepared from methyl benzoate (α-methoxybenzyl)(p-tolylsulfony)hydrazone (III) (2) by refluxing with sodium methoxide in DME.

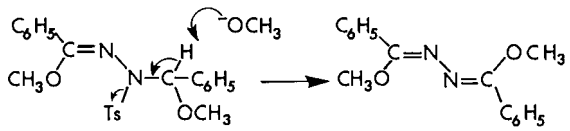

III II

An n.m.r. spectrum of the product mixture resulting from the decomposition of the potassium salt of I indicated that, apart from benzaldehyde dimethyl acetal and methyl benzoate azine (II), other products were present containing only aromatic hydrogens. Possible products such as benzonitrile, diphenylacetylene, and biphenyl could not be detected by infrared spectroscopy and (or) gas-liquid partition chromatography (g.l.p.c.), neither could any other product be isolated by elution chromatography on alumina.

When the decomposition was repeated in the presence of cyclohexene the product mixture was the same as that obtained in the absence of cyclohexene and there was no indication of the formation of 7-methoxy-7-phenylnorcarane (IV), which would have resulted from a reaction between phenylmethoxycarbene, a possible decomposition intermediate, and cyclohexene.

IV

The potassium salt, when heated alone in diglyme, dissolved at the boiling point, and was completely decomposed within 5 min. Benzaldehyde dimethyl acetal, although not isolated, was shown to be present by g.l.p.c. A very complicated product mixture had resulted from this decomposition as was indicated by n.m.r. spectroscopy, and only two products were isolated in small amounts, methyl benzoate azine (II) (2.5%) and *meso*-1,2-diphenyl-1,2-dimethyoxyethane (3%). That the solvent was not involved in the formation of the benzaldehyde dimethyl acetal was shown by the isolation of this product, in 30% yield, from the thermal decomposition of the potassium salt in DEE.

A further attempt to isolate a cyclopropane derivative was made by carrying out the decomposition in 1-decene. The boiling point of this olefin (168°) is such that it may be used as a 1:1 mixture with diglyme. The reaction product obtained when the potassium salt was decomposed at 158° had a n.m.r. spectrum very similar to that of the product that was obtained when the decomposition was carried out in diglyme alone. However, when the product mixture was repeatedly chromatographed on alumina, a 2.2% yield of a pure liquid was obtained. The molecular weight of the compound was found to be 260; this, together with an elemental analysis, established the empirical formula as $C_{18}H_{28}O$ (molecular weight 260.4). The infrared spectrum showed a weak band at 1 020 cm^{-1}, a position corresponding to a cyclopropane ring deformation frequency (3) and strong absorption in the region 1 050 to 1 080 cm^{-1}, indicative of an ether linkage. The n.m.r. spectrum contains singlets at τ 2.81 and 6.84 and a broad band at τ 8.3–9.4 (with a strong maximum at 8.72 and a weak maximum at 9.11) with relative areas 1.8:1.0:10.4. These findings led to the conclusion that the compound was indeed one of the isomers of the

Can. J. Chem. Downloaded from www.nrcresearchpress.com by 210.87.254.40 on 09/05/12
For personal use only.

desired cyclopropyl derivatives V. The mass spectrum provides further evidence as the major fragment, accounting for 13.8% of the fragmentation products, has a $m/e = 147$, which corresponds with the carbonium ion VI whose presence may arise by the following sequence:

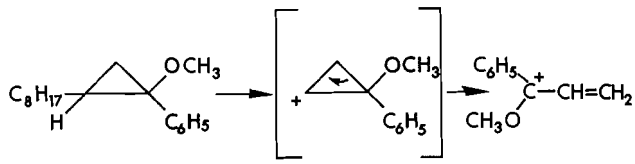

V VI

The fragment with $m/e = 259$ can similarly be explained by the initial loss of hydrogen, instead of the octyl group, to give the carbonium ion VII. The second largest fragment (6.8%), $m/e = 121$, is believed to be α-methoxybenzyl carbonium ion (VIII).

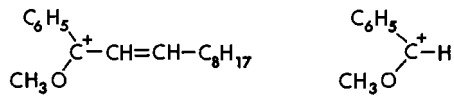

VII VIII

The configuration assignment of the isolated isomer, and the detection of the other isomer, required the synthesis of the isomers V*a* and V*b*. The mode by which this synthesis was accomplished is outlined in reaction Scheme 1, in which the yields of the individual steps are also indicated.

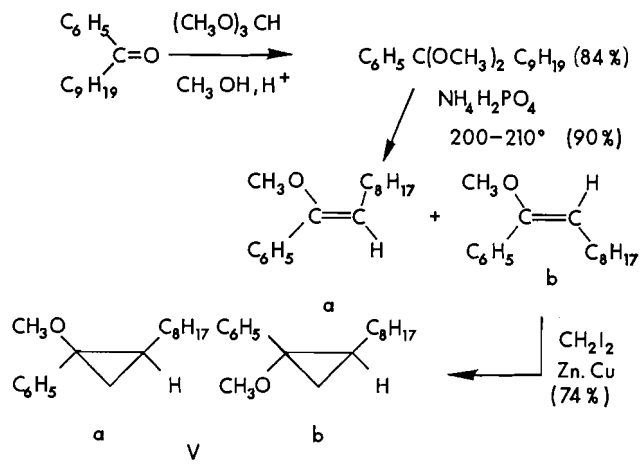

SCHEME 1

When the Simmons–Smith reaction (4) was carried out with the mixture of isomers of IX, a 5:3 mixture of the cyclopropyl isomers of V was obtained. The n.m.r. spectrum showed that the principal product has the same signal pattern as that isolated from the thermal decomposition of the potassium salt of I in the presence of 1-decene. The aromatic protons and the methoxy group appear in V*b* as singlets at τ 2.73 and 6.98 respectively, whereas the octyl group appears as a broad band at τ 8.6–9.2, with a strong maximum at

Can. J. Chem. Downloaded from www.nrcresearchpress.com by 210.87.254.40 on 09/05/12
For personal use only.

8.83 and a smaller maximum at τ 9.04. The position of the octyl group in the n.m.r. spectrum may serve as a means for the configuration assignment. The n.m.r. spectra displayed a distinct difference in the position of the two maxima of the octyl group in the two isomers. It was felt that, due to steric and electronic interactions, the proximity of a phenyl group to the octyl group, as in V*b* and IX*b*, would alter the position of the latter more than the *cis*-methoxy group would in structures V*a* and IX*a*. Thus the octyl maxima in V*a* and IX*a* were expected to be very much the same as in the unsubstituted *n*-octylcyclopropane (X).

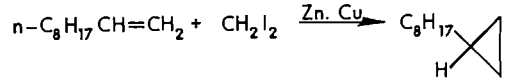

X

The n.m.r. spectrum of X shows the two octyl maxima at τ 8.78 and 9.11. As these maxima appear at the same positions in the principal product from either the dealcoholation or the methylene-transfer reaction, there is little doubt that they can also be attributed to the favored reaction products IX*a* and V*a*.

With the configurations established, it was thus possible to determine the isomeric ratio of the cyclopropanes that resulted from the thermal decomposition in 1-decene at 155–165°. The yield of 1-methoxy-2-*n*-octyl-1-phenylcyclopropane (V), determined by g.l.p.c.,* amounted to 4%; the relative ratio of V*a* and V*b* was 1.8:1 respectively.

It was thought that a more electron-rich olefin would give a better yield of cyclopropane derivative. Ketene diethylacetal has been shown to act as a very efficient carbene trap (5) and thus ketene dipropyl acetal, with a boiling point of 153°, was most suitable for the present purpose. No 1-methoxy-2,2-di-*n*-propyloxy-1-phenylcyclopropane (XI) could be isolated from the complex product mixture that was obtained when the potassium salt of I was decomposed at 150–155° in a 1:1 mixture of diglyme and ketene dipropyl acetal. Although the n.m.r. spectrum of a distillation fraction boiling at 90–125° (0.2 mm) showed a complicated signal pattern at τ 8.3–9.5, which could only be due to propyl groups, no separation could be effected by elution chromatography on alumina. However it could be concluded from the n.m.r. spectrum that compound XI is certainly not formed

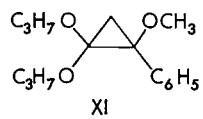

XI

in a yield exceeding 4%, and therefore the use of a ketene acetal does not seem to have much effect on the yield of the carbene adduct.

Diazo compounds and olefins, e.g. α,β-unsaturated carbonyl compounds, react to produce 1-pyrazolines (XII) which generally rapidly isomerize to 2-pyrazolines (XIII) and in certain instances decompose to cyclopropane derivatives (6).

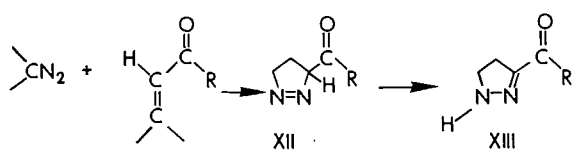

XII XIII

*A 4 ft Apiezon M column at 220° was used. It was shown that the product did not isomerize on the column, as an analysis of an authentic mixture of Va and Vb by g.l.p.c. and by n.m.r. spectroscopy gave the same result.

Can. J. Chem. Downloaded from www.nrcresearchpress.com by 210.87.254.40 on 09/05/12
For personal use only.

The formation of a pyrazoline from the decomposition of the potassium salt of I in the presence of an α,β-unsaturated carbonyl compound would provide additional evidence for the existence of the intermediate phenylmethoxydiazomethane. The potassium salt of I was decomposed at 130–135° in diethyl fumarate. A solid was isolated in 62% yield, by elution chromatography on alumina, m.p 40–41°. The infrared spectrum of the product showed an intense absorption in the carbonyl region at 1 720 cm^{-1}. The n.m.r. spectrum contained singlets at τ 2.77, 6.98, and 7.14, two methylene quartets (J = 7 c.p.s.) of the same intensity at 5.82 and 6.17, and two methyl triplets (J = 7 c.p.s.) of the same intensity at τ 8.69 and 9.02, the approximate relative areas were respectively 5:3:2:4:6. As the product did not contain any nitrogen and the infrared and n.m.r. spectra did not indicate the presence of an olefinic double bond or olefinic hydrogens, its structure was believed to be that of diethyl 3-methoxy-3-phenyl-*trans*-1,2-cyclopropanedicarboxylate (XIV), a conclusion in agreement with the elemental analysis. However a less ambiguous proof of structure appeared necessary, and therefore the cyclopropane derivative XIV was synthesized as shown in Scheme 2. Ethyl *trans*-β-methoxy cinnamate (XV), prepared by the procedure of Arndt and Loewe (7) for the methyl ester, was allowed to react with carbethoxycarbene, generated from ethyl diazoacetate under the catalytic influence of cuprous chloride. Diethyl 3-methoxy-3-phenyl-*trans*-1,2-cyclopropanedicarboxylate (XIV) and diethyl 3-methoxy-*trans*-3-phenyl-*cis*-1,2-cyclopropanedicarboxylate (XVI) were obtained in yields of 10% and 3% respectively. Compound XIV was identical in all respects with the solid obtained from the thermal decomposition of the potassium salt of I in diethyl fumarate.

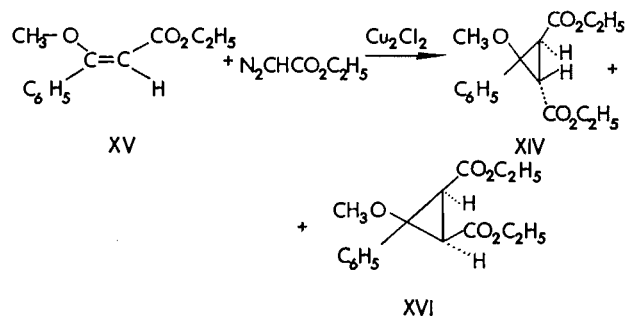

SCHEME 2

The photochemical decomposition of the potassium salt of I at room temperature in a 1:1 mixture of DME and cyclohexene was also investigated. Prior to the work-up the presence of a trace of methanol was demonstrated by g.l.p.c. Benzaldehyde dimethyl acetal was again isolated (36%), and treatment of the product mixture with *n*-hexane caused a solid to precipitate that was obtained as white needles, m.p. 101–103° (decomp.). The infrared spectrum showed strong absorption at 1 128 cm^{-1} and in the region 1 290 to 1 320 cm^{-1}, suggesting the presence of a sulfone group (7). The n.m.r. spectrum showed aromatic proton signals in the region τ 2.4–2.9, with a sharp singlet at 2.73, and further singlets at 4.82, 6.35, and 7.62, with integrated areas 9:1:3:3. The compound was found to have a molecular weight of 272 and to fit the emperical formula $C_{15}H_{16}O_3S$ (molecular weight 276.3). From this it is clear that the product is methyl α-(*p*-tolylsulfonyl)benzyl ether (XVII). This product was isolated in 3.2% yield; however, it could be isolated in as high as a 17% yield when the photochemical decomposition was carried out in DME

Can. J. Chem. Downloaded from www.nrcresearchpress.com by 210.87.254.40 on 09/05/12
For personal use only.

alone. Although a large number of other products were produced, as demonstrated both by n.m.r. spectroscopy and g.l.p.c., they could not be isolated in pure form by distillation and (or) elution chromatography.

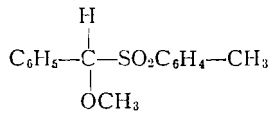

XVII

Since the phenylmethoxydiazomethane gave such such poor yields of cyclopropane products with 1-decene, it was decided to investigate the efficiency of an internally situated olefinic double bond to cyclopropane formation. Because of the availability of 4-pentenol the corresponding potassium 4-pentenol benzoate (*p*-tolylsulfonyl)hydrazone (XVIII) was prepared and reactions of it studied. Thus if cyclopropane ring formation occurred through the diazoalkane (XIX) or the carbene (XX), the olefinic double bond would be suitably disposed to trap the intermediate and lead to the formation of 1-phenyl-2-oxabicyclo[4.1.0.]heptane (XXI).

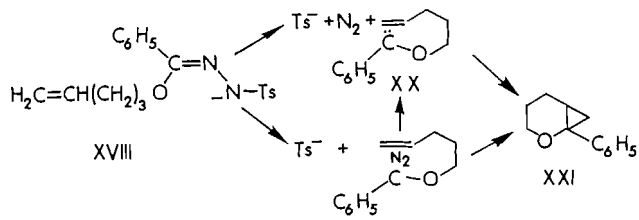

XVIII XX XXI XIX

In order to facilitate the isolation and quantitative determination of XXI it was first synthesized by a Simmons–Smith reaction on 2-phenyl-2-dihydropyran (XXII) in 72% yield. The infrared spectrum of the product shows an absorption of medium intensity at 1 024 cm^{-1}, characteristic of a cyclopropyl group (3). The n.m.r. spectrum contains a singlet at τ 2.09 and complex absorption at τ 6.1–7.0 and 7.8–9.2, with relative areas 5:2:7 respectively.

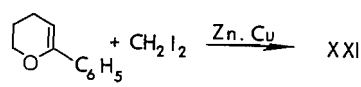

XXII XXI

The thermal decomposition of XVIII was carried out in diglyme at 140–150°, at which temperature the salt readily decomposed. The amount of XXI in the product mixture was quantitatively determined by g.l.p.c. To establish its identity it was also isolated by elution chromatography. The pyran (XXI) was the major product in the thermal decomposition, its yield amounting to 11–14%. Although several modifications in the decomposition procedure were investigated in order to improve this yield, they were without success. When a dilute solution of XVIII in anhydrous diethyl ether was photolyzed at room temperature, the product XXI was formed in 20–21% yield. The photochemical decomposition also produced an appreciable amount (15%) of 4-pentenyl α-(*p*-tolylsulfonyl)benzyl ether (XXIII), as a white crystalline solid, m.p. 90–91°.

Can. J. Chem. Downloaded from www.nrcresearchpress.com by 210.87.254.40 on 09/05/12
For personal use only.

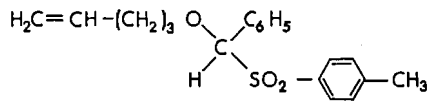

XXIII

The presence of another expected product, benzaldehyde 4-pentenyl acetal (XXIV), was shown by g.l.p.c. and its yield was estimated at 3–6% from the thermal decomposition and 1–4% in the photochemical decomposition. As this low yield did not permit an effective isolation it was only characterized by its retention time on an Apiezon M column. Authentic benzaldehyde 4-pentenyl acetal was prepared in 80% yield by the thermal decomposition of XVIII in DEE in the presence of 4-pentenol.

$$C_6H_5CH(O(CH_2)_3CH{=}CH_2)_2$$

XXIV

The possibility of carbene insertion into the allylic 3-position of the alkyl group in XVIII to form the vinyl furan (XXV) was seriously considered since the vapor phase chromatogram, of the product mixture from the decomposition of XVIII, displayed a relatively large amount (estimated at 3 to 4% in the thermal and at 5 to 7% in the photochemical decomposition) of a product with a similar retention time to that of XXI. However it was later found that this product resulted from the thermal decomposition of the sulfone XXIII, and the idea was abandoned as the chromatogram indicated that the insertion product XXV had not been formed, if at all, in a yield greater than 1%.

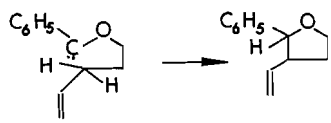

XXV

CONCLUSIONS

The production of benzaldehyde dimethylacetal in aprotic solution along with the formation of methanol suggests that the salts are decomposing by routes as yet not elucidated. The methanol formed in this process would appear to occur via alkoxy radicals abstracting from the solvent, since the methanol can be detected by g.l.p.c. on the anhydrous solutions before work-up.

Three possible reaction paths which may explain the cyclopropane formation with 1-decene and diethyl fumarate, are shown in Scheme 3.

Mechanism A involves a nucleophilic attack on the olefin which although reasonable for diethyl fumarate, seems less likely for 1-decene. Mechanism B involves a 1,3-dipolar addition of the diazocompound to the olefin, but requires that the loss of nitrogen be more rapid than the rate of tautomerization of 1-pyrazoline (6). Mechanism C involves the thermal decomposition of the alkoxydiazoalkane to an alkoxy carbene which may have nucleophilic properties similar to the carbene species investigated by Wanzlick (9) and Kirmse (10). Thus diethyl fumarate is a superior trap to any of the other olefins. It is not possible on the basis of existing data to discriminate among these three mechanisms, and minor variations thereof, but since phenyldiazomethane can be prepared, and isolated, by

Can. J. Chem. Downloaded from www.nrcresearchpress.com by 210.87.254.40 on 09/05/12
For personal use only.

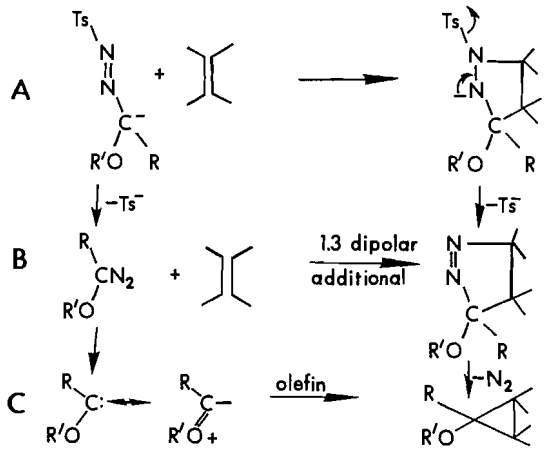

SCHEME 3

this method and since nucleophilic addition to 1-decene does not seem likely,* mechanisms B and C are favored.

EXPERIMENTAL

All melting points and boiling points are uncorrected.

The infrared spectra were obtained on a Perkin–Elmer Model 421 spectrophotometer equipped with grating optics. Nuclear magnetic resonance spectra were measured using a Varian Associates Model A-60 spectrometer, with tetramethylsilane as a reference. Ultraviolet spectra were obtained using a Cary Model 14M recording spectrophotometer. Mass spectra were obtained on a A.E.I. MS2-H mass spectrometer.

Vapor phase chromatography was carried out with a Perkin–Elmer Model 154 vapor fractometer or a F. & M. Model 500 temperature-programmed gas chromatograph.

The photochemical decompositions were all carried out in a quartz reaction vessel, cooled by running tap water, with an internally situated 250 W Hanovia ultraviolet source.

The microanalyses were performed by Pascher Mikroanalytisches Laboratorium (Bonn, West Germany), Daessle Organic Microanalyses (Montreal), and the Microanalytical Laboratory of the Department of Chemistry, University of Alberta (Edmonton).

The Decompositon of α-Alkoxy(p-tolylsulfonyl)hydrazone Salts

Solvents

1,2-Dimethoxyethane was distilled from potassium metal, b.p. 82°. A technical grade of *1,2-diethoxyethane* was distilled. The fraction boiling at 116–120° was left with potassium overnight and fractionally distilled. The fraction with b.p. 116–117° consisted of pure 1,2-diethoxyethane as was shown by g.l.p.c. *Diglyme* (diethylene glycol dimethyl ether) was left over potassium metal overnight and distilled, b.p. 157–159°.

The Thermal Decomposition of Sodium Methyl Benzoate (p-Tolylsulfonyl)hydrazone in 1,2-Dimethoxyethane

Methyl benzoate (*p*-tolylsulfonyl)hydrazone (10.0 g, 32.9 mmole) (1) was dissolved in 60 ml of 1,2-dimethoxyethane, and sodium methoxide (1.8 g, 33.3 mmole) was added. Solvent was distilled (approximately 20 ml) until the boiling point reached that of pure 1,2-dimethoxyethane. The mixture was stirred and refluxed for 65 h. After cooling, the sodium *p*-toluenesulfinate (5.3 g, 90%) was filtered off and the solvent of the orange-colored solution was removed. The residue was dissolved in ether, washed with water, and dried. Removal of the ether gave 3.1 g liquid residue. A vacuum distillation produced 0.9 g (34%) benzaldehyde dimethyl acetal, b.p. 56–57° (3.5 mm); n_D^{25} 1.4960. The high-boiling point liquid residue was chromatographed on Harshaw alumina. The product obtained by elution with a 5% ether in pentane solution was recrystallized from a small amount of *n*-hexane to give 0.5 g (12%) of methyl benzoate azine (II) as white needles, m.p. 72–73°. The ultraviolet spectrum shows a broad band with a maximum at 2 700 Å (log = 4.09).

Anal. Calcd. for $C_{16}H_{16}N_2O_2$ (molecular weight, 268.3); C, 71.62; H, 6.01; N, 10.44. Found: C, 71.87; H, 5.99; N, 10.49; molecular weight (osmometric), 269.

Although other products were formed that contained only aromatic protons, as was shown by n.m.r. spectroscopy, no other compounds could be isolated and characterized. When the experiment was repeated

**The rate of nitrogen evolution appears to be independent of the presence of the olefin substrate which would not seem reasonable for mechanism A.*

Can. J. Chem. Downloaded from www.nrcresearchpress.com by 210.87.254.40 on 09/05/12
For personal use only.

in the presence of 15 ml cyclohexene, the same product mixture was obtained and there was no indication for the formation of 7-methoxy-7-phenylnorcarane as the n.m.r. spectrum of the reaction products showed no absorption above 7.0.

The Reaction of Methyl Benzoate (α-Methoxybenzyl)(p-tolylsulfonyl)hydrazone with Sodium Methoxide

Methyl benzoate (α-methoxybenzyl)(*p*-tolylsulfonyl)hydrazone (0.500 g, 1.18 mmole) (2) and sodium methoxide (0.072 g, 1.33 mmole) were refluxed in 20 ml of 1,2-dimethoxyethane. A precipitate formed slowly and after 5.5 h the mixture was cooled and sodium *p*-toluenesulfinate (0.16 g, 76%) was filtered off. The solvent was removed and the residue was dissolved in ether, washed with water, and dried. Removal of the ether produced 0.33 g of residue that slowly solidified. An infrared spectrum was identical with that of a mixture of starting material and methyl benzoate azine. Addition of *n*-hexane caused the starting material (0.08 g, 16%) to precipitate. The remaining product was chromatographed on alumina. The pure azine was obtained by elution with a 5% ether in pentane solution and amounted to 0.14 g (46%), m.p. 72–73°; mixture m.p. 72–73°.

The Thermal Decomposition of Potassium Methyl Benzoate (p-Tolylsulfonyl)hydrazone in 1-Decene

A suspension of the potassium salt (1.50 g, 4.4 mmole) in 15 ml of 1-decene was heated, while being stirred, at 155–165° until the gas evolution had ceased, which required approximately 40 min. The reaction mixture was cooled and water and diethyl ether were added. The organic layer was dried, and the ether and 1-decene distilled off, the latter under reduced pressure. It was shown by g.l.p.c. that the residue contained at least 13 different products, all present in relatively low concentrations. In order to be able to analyze for the two isomeric 1-methoxy-2-*n*-octyl-1-phenylcyclopropanes (V), the mixture was added to an alumina column and eluted with *n*-pentane until all of the desired product was removed from the column. This operation required approximately 700 ml of *n*-pentane. The pentane was removed and an accurately known amount of 2-ethoxynaphthalene was added as an internal standard. The total amount of 1-methoxy-*trans*-2-*n*-octyl-1-phenylcyclopropane and 1-methoxy-*cis*-2-*n*-octyl-1-phenylcyclopropane was determined by g.l.p.c. using a 4 ft Apiezon M column. In two separate experiments the total amount of these two isomers was 47 mg (4.1%) and 42 mg (3.8%). the isomer ratio *trans/cis* being 1.9 and 1.7 respectively. It was shown that the product did not isomerize at the column temperature (220°) as the analysis of an authentic mixture of the two isomers by n.m.r. spectroscopy and by g.l.p.c. gave the same result.

The decomposition was repeated on a larger scale in a 1:1 mixture of diglyme and 1-decene: The potassium salt (10.0 g, 29.2 mmole) was decomposed by refluxing for 10 min in a mixture of 30 ml diglyme and 30 ml 1-decene. Prior to the work-up an appreciable amount of benzaldehyde dimethyl acetal was shown to be present in the reaction mixture by g.l.p.c. on an Apiezon L column. A quantitative amount of potassium *p*-toluenesulfinate was filtered off and the solvent mixture was distilled off under reduced pressure. The highly colored residue was passed through a short alumina column with 300 ml of *n*-pentane. The pentane was removed and the residue distilled *in vacuo*. After a small amount of a low-boiling fraction, which was not further investigated, 1.35 g of a fraction with a boiling range of 110–140° (0.3 mm) distilled over. Upon addition of a small amount of *n*-hexane and cooling overnight at −15°, 0.1 g (3%) of crystals with m.p. 138–140° were obtained, identical in all respects (mixture melting point, infrared and n.m.r. spectra) with *meso*-1,2-diphenyl-1,2-dimethoxyethane. The hexane solution was chromatographed on alumina. The product that was eluted with a 5% ether in pentane solution was recrystallized from a small amount of *n*-hexane to give 0.1 g (2.6%) of methyl benzoate azine. The *n*-pentane fraction contained 1-methoxy-2-*n*-octyl-1-phenylcyclopropane. The product mixture from this fraction was again chromatographed on alumina and eluted with *n*-pentane. The first fraction contained 0.17 g (2.2%) of pure 1-methoxy-*trans*-2-*n*-octyl-1-phenylcyclopropane.

Anal. Calcd. for $C_{18}H_{28}O$ (molecular weight, 260.4): C, 83.02; H, 10.84. Found: C, 83.21; H, 11.11; molecular weight 260 (mass spectrometrically).

The following chromatographic fractions contained smaller amounts of a mixture of the two isomers and also other products.

The Photochemical Decomposition of Potassium Methyl Benzoate (p-Tolylsulfonyl)hydrazone in 1,2-Dimethoxyethane and Cyclohexene

A stirred suspension of the potassium salt (10.0 g, 29.2 mmole) in a mixture of 90 ml 1,2-dimethoxyethane and 100 ml cyclohexene was irradiated for 9 h, at which time the gas evolution had become almost negligible. A total of 570 ml of gas had evolved (theoretically 770 ml of nitrogen). The solution was filtered, the solvent removed under reduced pressure, and the residue taken up in ether. The ether solution was washed with water and dried and the ether removed. A n.m.r spectrum showed the residue was a mixture of many products. Addition of a small amount of *n*-hexane caused 0.26 g of a white solid to precipitate, that could be recrystallized from a 5:1 mixture of *n*-hexane and benzene to give white needles, m.p. 101–103°. Because of decomposition no sharp melting point could be obtained.

Anal. Calcd. for methyl α-(*p*-tolylsulfonyl)benzyl ether (XVII), $C_{15}H_{16}O_3S$ (molecular weight 276): C, 65.19; H, 6.83; S, 11.61. Found: C, 65.34; H, 6.29; S, 11.45; molecular weight (osmometric) 272, 274.

The *n*-hexane was removed and the residue distilled *in vacuo* to give 0.8 g (36%) benzaldehyde dimethyl

Can. J. Chem. Downloaded from www.nrcresearchpress.com by 210.87.254.40 on 09/05/12
For personal use only.

acetal (b.p. 58–59° at 3.6 mm), 0.9 g of a fraction with b.p. 102–109° (1.0 mm), and 0.55 g of a fraction boiling at 110–116° (0.15 mm). Both these last fractions showed a very complicated n.m.r. signal pattern. An attempt was made to separate the fraction with b.p. 102–109° (1.0 mm) into its components by elution chromatography on alumina, however no separation could be effected and each fraction that was eluted from the column contained several components as was shown by n.m.r. spectroscopy and g.l.p.c.

When the photochemical decomposition was carried out in 1,2-dimethoxyethane alone, methyl α-(*p*-tolylsulfonyl)benzyl ether was isolated in 17% yield. Prior to the work-up benzaldehyde dimethyl acetal was shown to be present by g.l.p.c., using a 2 m Apiezon L column. A trace of methanol could also be detected. It was characterized by its retention time on two columns, packed with Apiezon L, and Ucon LB-550-X respectively.

The Decomposition of Potassium Methyl Benzoate (p-Tolylsulfonyl)hydrazone in Diethyl Fumarate

The potassium salt (4.0 g, 11.7 mmole) was suspended in 40 ml of diethyl fumarate (a center distillation cut, b.p. 66–67° at 1.8 mm, of Eastman white label material) and heated, while stirred, at 130–135° for 1.5 h. The mixture was cooled, 100 ml ether added, and the ether solution washed four times with water. The pale yellow-colored ether solution was dried, the ether evaporated, and the diethyl fumarate distilled off *in vacuo*. Upon addition of a small amount of *n*-pentane to the residue, methyl benzoate (α-methoxybenzyl)(*p*-tolylsulfonyl)hydrazone (III) (0.43 g, 18%; m.p. 147–149°) precipitated. The pentane was removed and the residue purified by elution chromatography on alumina. Elution with benzene produced 2.15 g of an oil that slowly solidified to a white solid, m.p. 37–39°. The product was twice recrystallized from a small amount of *n*-hexane to give fine white needles, m.p. 40–41°, of analytical purity. The melting point was not depressed by diethyl 3-methoxy-3-phenyl-*trans*-1,2-cyclopropanedicarboxylate. The infrared and n.m.r. spectra were identical with those of an authentic sample of diethyl 3-methoxy-3-phenyl-*trans*-1,2-cyclopropane dicarboxylate. No other reaction products were detected either by n.m.r. spectroscopy or elution chromatography.

4-Pentenyl Benzimidate

Dry hydrogen chloride (25.5 g, 0.70 mole) was added to a mixture of 4-pentenol (60.0 g, 0.70 mole) and benzonitrile (68.0 g, 0.66 mole) and cooled in an ice–salt mixture. The reaction mixture was left in the refrigerator for 24 h, at which time it had almost solidified, and 200 ml of ether was added. The hydrochloride salt was collected and mounted to 77.7 g (0.36 mole, 52%), m.p. 122–123° (decomp.). Under vigorous stirring this salt was added to a solution of potassium carbonate (120 g 0.87 mole) in 300 ml of water covered with 150 ml of ether, followed by the further extraction of the aqueous layer with 60 ml of ether. The combined ether solutions were dried and the residue was distilled *in vacuo* to give 59.8 g (92%) of colorless product, b.p. 86–87° (0.3 mm); n_D^{25} 1.5252. The infrared spectrum (in CCl_4) shows an N—H band at 3 340 cm^{-1} and a strong band at 1 630 cm^{-1} due to the C=N.

Anal. Calcd. for $C_{12}H_{15}NO$: C, 76.15; H, 7.99; N, 7.40. Found: C, 76.41; H, 8.12; N, 7.38.

4-Pentenyl Benzoate (p-Tolylsulfonyl)hydrazone

A solution of 4-pentenyl benzimidate (15.9 g, 84.1 mmole) in 35 ml of absolute ethanol was added to a cold suspension of (*p*-tolylsulfonyl)hydrazide hydrochloride (18.7 g, 84.0 mmole) in 75 ml of absolute ethanol and the mixture was left at room temperature for 3 h. The ammonium chloride was filtered off, the ethanol removed under reduced pressure, and the residue dissolved in 120 ml of methylene chloride. The methylene chloride solution was washed twice with water, dried ($MgSO_4$), and filtered, and the solvent removed. The residue was immediately dissolved in 100 ml of anhydrous diethyl ether and cooled at −15° overnight to yield 14.4 g (48%) of crystals, m.p. 87–89°. One additional recrystallization produced an analytical sample, m.p. 89–90°. The infrared spectrum (in $CHCl_3$) shows N—H stretching at 3 300 cm^{-1} and a C=N— stretching band of medium intensity at 1 620 cm^{-1} with a shoulder at 1 635 cm^{-1}.

Anal. Calcd. for $C_{19}H_{22}N_2O_3S$: C, 63.66; H, 6.19; N, 7.82; S, 8.95. Found: C, 63.75; H, 6.38; N, 7.68; S, 8.81.

Potassium 4-Pentenyl Benzoate (p-Tolylsulfonyl)hydrazone (XVIII)

A solution of 4-pentenyl benzoate (*p*-tolylsulfonyl)hydrazone (10.0 g, 27.9 mmole) in 40 ml of 1,2-dimethoxyethane was added to a solution of potassium (1.1 g, 28.2 mgram-atom) in a mixture of 6 ml absolute ethanol and 40 ml of 1,2-dimethoxyethane. Cooling and the addition of *n*-pentane did not cause any salt to precipitate. Thus the solvent was removed and the residue kept *in vacuo* for 30 min, at which time the syrup had crystallized completely. The slightly yellow-colored salt, soluble in water and in most organic solvents, amounted to 11.0 g.

Benzaldehyde Di-(4-pentenyl) Acetal XXIV

Potassium 4-pentenyl benzoate (*p*-tolylsulfonyl)hydrazone (11.0 g, 27.7 mmole) was refluxed in a mixture of 10 ml 4-pentenol and 40 ml of 1,2-diethoxyethane for 3 h. Potassium *p*-toluenesulfinate (5.5 g, 100%) was filtered off, the solvent removed under reduced pressure, and the residue taken up in ether, washed with water, and dried ($MgSO_4$). Removal of the solvent, followed by a vacuum distillation, yielded 5.8 g (80%) of the product, b.p. 102–103° (0.2 mm); n_D^{25} 1.4905. The infrared spectrum shows the olefinic double bond stretching as a band of medium intensity at 1 637 cm^{-1}.

Anal. Calcd. for $C_{17}H_{24}O_2$: C, 78.42; H, 9.29. Found: C, 78.47; H, 9.19.

Can. J. Chem. Downloaded from www.nrcresearchpress.com by 210.87.254.40 on 09/05/12
For personal use only.

The Thermal Decomposition of Potassium 4-Pentenyl Benzoate (p-Tolylsulfonyl)hydrazone in Diglyme to Produce XXI

The potassium salt (1.31 g, 3.3 mmole) was dissolved in 20 ml diglyme and heated for 10 min at 145–150°. After cooling there was added 50 ml water and 75 ml *n*-pentane and the mixture was vigorously shaken. The pentane layer was again washed with water and then dried. The pentane was removed, 0.091 g of 2-ethoxynaphthalene was added as an internal standard, and the absolute amount of 1-phenyl-2-oxabicyclo[4.1.0]heptane (XXI) was determined by g.l.p.c. using a 4 ft Apiezon M column, yield 0.071 g (12.3%). The experiment was repeated, with the potassium salt slowly added, either as the solid or as a diglyme solution, to diglyme at 140–150°. The yield of XXI was 13.7% and 10.8% in two separate experiments. By carrying out the experiment on a somewhat larger scale and by eluting the product mixture with *n*-pentane from an alumina column, a pure sample of XXI could be isolated (even though the overall separation was poor) and characterized by its retention time and by comparing its infrared and n.m.r. spectra with those of an authentic sample.

The Photochemical Decomposition of Potassium 4-Pentenyl Benzoate (p-Tolylsulfonyl)hydrazone in Diethyl Ether

The potassium salt (1.571 g, 4.0 mmole) was dissolved in 190 ml of diethyl ether and irradiated for 45 min, at which time the gas evolution had ceased. The ether solution was washed with water and dried. The residue (1.0 g) obtained after removal of the ether, solidified slowly. Upon the addition of a small amount of *n*-pentane, 0.220 g of a white solid, m.p. 81–85°, was obtained. Two recrystallizations from *n*-hexane produced an analytical sample, m.p. 90–91°. The infrared spectrum (in CCl_4) showed a band of medium intensity at 1 640 cm^{-1} and strong bands at 1 320 and 1 139 cm^{-1}.

Anal. Calcd. for 4-pentenyl α-(*p*-tolylsulfonyl)benzyl ether (XXIII), $C_{19}H_{22}O_3S$: C, 69.06; H, 6.71; S, 9.70. Found: C, 68.86; H, 6.70; S, 10.01.

The pentane was removed, 2-ethoxynapthalene (0.100 g) was added as an internal standard, and the amount of XXI was determined by g.l.p.c.; yield 0.137 g (19.9%). When the experiment was repeated, the product was formed in a 20.6% yield.

The Preparation of Some Authentic Samples

Decanophenone

This compound was prepared in 77% yield by a Friedel–Crafts reaction between decanoyl chloride and benzene, according to the procedure of Breusch and Oguzer (11); m.p. 35–36°. Reported (11) m.p. 34.4–35.4°.

Decanophenone Dimethyl Ketal

Decanophenone (70.0 g, 0.30 mole), methyl orthoformate (32.0 g, 0.30 mole), and a small amount of anhydrous *p*-toluenesulfonic acid (0.40 g) were dissolved in a mixture of 200 ml of methanol and 25 ml of diethyl ether. This mixture was left at room temperature for 3 days, after which the acid was neutralized by adding sodium methoxide. The solvent was distilled off, the residue dissolved in ether, washed with water, and dried with magnesium sulfate. The ether was removed and the residue distilled *in vacuo* to give 71.4 g (84%) of the colorless liquid; b.p. 115–118° (0.3 mm); n_D^{25} 1.4804.

Anal. Calcd. for $C_{18}H_{30}O_2$: C, 77.65; H, 10.86. Found: C, 77.85; H, 10.95.

β-n-Octyl-α-methoxystyrene

Decanophenone dimethyl ketal (27.0 g, 0.097 mole) was stirred and heated with ammonium dihydrogen phosphate (2.0 g) at 200–210° for 45 min, under slightly reduced pressure. Initially, the pressure could be reduced only slightly because of foaming. After approximately 0.5 g the foaming ceased, probably indicating the complete removal of methanol. The liquid was distilled *in vacuo* to give 21.4 g (90%) of a 2:3 mixture of the isomeric products, b.p. 107–110° (0.2 mm); n_D^{25} 1.5035. The infrared spectrum of the neat liquid shows the olefinic double bond as a band of medium intensity at 1 641 cm^{-1}. The compound was found to have a molecular weight of 241 (osmometric); calcd. for $C_{17}H_{26}O$: molecular weight 246.4.

1-Methoxy-2-n-octyl-1-phenylcyclopropane

A crystal of iodine was added to a stirred suspension of a Zn–Cu couple (3) (7.2 g, 0.11 gram-atom) in 60 ml of anhydrous ether. As soon as the brown color had disappeared, methylene iodide (29.5 g, 0.110 mole) and an isomeric mixture of β-*n*-octyl-α-methoxystyrene (18.0 g, 0.073 mole) was added. The reaction mixture was refluxed for 13 h, after which the solid was filtered off. The ether solution was washed twice with a saturated aqueous ammonium chloride solution, twice with a saturated aqueous sodium bicarbonate solution, and finally twice with water. The residue obtained after drying and removal of the ether was distilled *in vacuo* to give 14.0 g (74%) of colorless product, b.p. 114–118° (0.3 mm); n_D^{25} 1.4926. The infrared spectrum shows a cyclopropyl ring deformation band at 1 020 cm^{-1}. The n.m.r. spectrum indicated that a small amount of β-*n*-octyl-α-methoxystyrene was still present which could not be removed by either distillation or elution chromatography on alumina. The n.m.r. spectrum showed that 1-methoxy-*cis*-2-*n*-octyl-1-phenylcyclopropane and 1-methoxy-*trans*-2-*n*-octyl-1-phenylcyclopropane were present in a ratio of 3:5.

Can. J. Chem. Downloaded from www.nrcresearchpress.com by 210.87.254.40 on 09/05/12
For personal use only.

n-Octylcyclopropane

To a suspension of a Zn–Cu couple (3) (10.6 g, 0.163 gram-atom) in 75 ml of anhydrous ether was added methylene iodide (43.7 g, 0.163 mole) and 1-decene (15.0 g, 0.107 mole), and the mixture was refluxed for 20 h. After filtration and washing with a saturated ammonium chloride solution, a saturated sodium bicarbonate solution, and water, the ether solution was dried over magnesium sulfate. Removal of the ether gave a residue that still contained a large amount of 1-decene. Enough bromine was added to convert all the 1-decene into the dibromo compound. The mixture was again dissolved in ether, washed twice with an aqueous sodium thiosulfate solution, and dried. The ether was removed and the residue distilled *in vacuo* to give 4.1 g (25%) of the product, b.p. 65–66° (5.0 mm); n_D^{25} 1.4280. A large amount of a higher boiling product, that partially decomposed, was left behind in the flask. The infrared spectrum of a neat sample of *n*-octylcyclopropane shows sharp absorption bands at 3 070 and 1 009 cm^{-1} respectively due to cyclopropyl hydrogen stretching and cyclopropyl ring deformation. The n.m.r. spectrum is described in the text.

Anal. Calcd. for $C_{11}H_{22}$: C, 85.63; H, 14.37. Found: C, 85.68; H, 14.33.

1-Phenyl-2-oxabicyclo[4.1.0]heptane (XXI)

A crystal of iodine was added to a suspension of a Zn–Cu couple (13.0 g, 0.20 mole) in 80 ml anhydrous diethyl ether. As soon as the brown color had disappeared, methylene iodide (53.6 g, 0.20 mole) and 2-phenyl-Δ^2-dihydropyran (12) (25.0 g, 0.156 mole) were added and the mixture was stirred and refluxed for 20 h. A finely divided black suspension was filtered off and the ether solution successively washed with saturated aqueous ammonium chloride, saturated aqueous sodium bicarbonate, and water. After drying and removal of the ether, a yellow-colored liquid residue was obtained, that was distilled *in vacuo* to give 19.5 g (72%) of the colorless product, b.p. 75–76° (0.25 mm); n_D^{25} 1.5487. No starting material was recovered from the reaction. The infrared and n.m.r. spectra are compatible with that required by the structure XXI.

Anal. Calcd. for $C_{12}H_{14}O$: C, 82.72; H, 8.10. Found: C, 82.44; H, 8.04.

Diethyl 3-Methoxy-3-phenyl-1,2-cyclopropanedicarboxylate

A solution of ethyl diazoacetate (5.5 g, 0.048 mole; prepared in 63% yield by the method of Searle (13); n_D^{25} 1.4616; reported (12) n_D^{25} 1.4616) in 10 ml of *n*-hexane was added dropwise, in approximately 30 min, to a refluxing solution of ethyl-*trans*-β-methoxycinnamate (6) (8.0 g, 0.039 mole) in 10 ml of *n*-hexane to which a small amount of cuprous chloride (0.25 g) had been added. A vigorous nitrogen evolution took place during the addition. Some ether was added and the solution was filtered. Upon removal of the ether a darkly colored liquid residue was obtained. A n.m.r. spectrum suggested that it contained mainly diethyl fumarate and ethyl *trans*-β-methoxycinnamate. Most of these products were removed by a vacuum distillation which yielded 1.3 g of a fraction boiling at 65–80° (1.7 mm) and 4.2 g of a fraction with b.p. 95–103° (0.3 mm). The residue (4.6 g) was chromatographed on alumina. A mixture of ethyl *trans*-β-methoxycinnamate and diethyl 3-methoxy-3-phenyl-*trans*-1,2-cyclopropanedicarboxylate was eluted with a *n*-hexane–benzene (1:1) mixture. Relatively pure diethyl 3-methoxy-3-phenyl-*trans*-1,2-cyclopropanedicarboxylate was eluted with benzene. The oil was dissolved in a small amount of *n*-hexane and cooled in a dry ice–acetone mixture. The solid thus obtained was twice recrystallized from a small amount of *n*-hexane to give an analytical sample of fine white needles, m.p. 40–41°. The total amount produced in the reaction was estimated at 1.1 g (10%).

Anal. Calcd. for $C_{16}H_{20}O_5$: C, 65.74; H, 6.90. Found: C, 65.49; H, 6.73.

Diethyl 3-methoxy-*trans*-3-phenyl-*cis*-1,2-cyclopropanedicarboxylate (0.33 g, 3%) was eluted with a *n*-hexane – diethyl ether (1:1) mixture. A relatively pure sample was obtained when this chromatography fraction was again chromatographed on alumina. The oily material, n_D^{25} 1.505, did not solidify at room temperature. Its infrared and n.m.r. spectra indicated that it was structurally similar to the isomeric material, and that it contained no olefinic hydrogens.

Anal. Calcd. for $C_{16}H_{20}O_5$: C, 65.74; H, 6.90. Found: C, 65.56; H, 6.89.

ACKNOWLEDGMENTS

The research described herein was supported by a National Research Council of Canada grant to R. J. Crawford. The n.m.r. and infrared spectra were measured by R. N. Swindlehurst and Mrs. Gail B. Conway of this Department.

REFERENCES

1. H. ZOLLINGER. Azo and diazo chemistry. Interscience Publishers, Inc., New York, N.Y. 1961. Chap. 6. P. YATES. Abstracts of the 18th National Organic Symposium of the American Chemical Society, Columbus, Ohio. 1963. p. 93.
2. R. J. CRAWFORD and R. RAAP. Can. J. Chem. **43**, 126 (1965).

Can. J. Chem. Downloaded from www.nrcresearchpress.com by 210.87.254.40 on 09/05/12
For personal use only.

3. L. J. BELLAMY. The infrared spectra of complex molecules. John Wiley and Sons, Inc., New York. 1959. p. 29. M. HANACK, H. EGGENSPERGER, and S. KANG. Chem. Ber. **96**, 2532 (1963).
4. R. D. SMITH and H. E. SIMMONS. Org. Syn. **41**, 72 (1961).
5. U. SCHOLLKOPF and E. WISKOTT. Angew. Chem. Intern. Ed. **2**, 485 (1963). U. SCHOLLKOPF and G. J. LEHMANN. Tetrahedron Letters, No. 4, 165 (1962). S. M. MCELVAIN and P. L. WEYNA. J. Am. Chem. Soc. **81**, 2579 (1959).
6. R. HUISGEN. Angew. Chem. Intern. Ed. **2**, 575, 633 (1963). W. M. JONES, T. H. GLENN, and D. G. BAARDA. J. Org. Chem. **28**, 2887 (1963).
7. F. ARNDT and L. LOEWE. Ber. **71**, 1631 (1938).
8. P. YATES. Abstracts of the 18th National Organic Symposium of the American Chemical Society, Columbus, Ohio. 1963. p. 360.
9. W. H. WANZLICK. Angew. Chem. Intern. Ed. **1**, 75 (1962). H. W. WANZLICK and H. J. KLEINER. Angew. Chem. Intern. Ed. **3**, 65 (1964).
10. W. KIRMSE. Ann. **666**, 9 (1963).
11. F. L. BREUSCH and M. OGUZER. Chem. Ber. **87**, 1225 (1954).
12. H. NORMANT. Compt. Rend. **231**, 909 (1950); Chem. Abstr. **46**, 3492 (1952).
13. N. E. SEARLE. Org. Syn. **36**, 25 (1956).

Can. J. Chem. Downloaded from www.nrcresearchpress.com by 210.87.254.40 on 09/05/12
For personal use only.

Can. J. Chem. Downloaded from www.nrcresearchpress.com by 210.87.254.6 on 09/05/12
For personal use only.

THE LIFETIME OF THE A.$^3\Sigma_u^+$ STATE OF N_2

L. F. PHILLIPS
Chemistry Department, University of Canterbury, Christchurch, New Zealand

Received September 14, 1964

ABSTRACT

The decay of the blue emission from the active nitrogen – iodine flame has been measured at iodine pressures down to 1.4×10^{-4} torr. Extrapolation of the decay rate to zero iodine pressure yields a value of 0.89 ± 0.41 s^{-1} for the first-order rate constant in absence of iodine, corresponding to a mean lifetime of 1.1 s for the A.$^3\Sigma_u^+$ state of N_2. The rate constants for the reactions

[1] $$N + I_2 \rightarrow NI + I$$

and

[6] $$N_2(^3\Sigma_u^+) + I_2 \rightarrow N_2(^1\Sigma_g^+) + I_2^*$$

are $(2.6 \pm 0.3) \times 10^{-11} \exp(-68 \pm 34/RT)$ and $(8.3 \pm 1.2) \times 10^{-11}$ cm^3 molecule^{-1} s^{-1} respectively.

INTRODUCTION

In a recent photometric study of the reaction of iodine with active nitrogen (1) it was found that the characteristic blue reaction flame is largely the result of energy transfer to molecular iodine during collisions with a metastable species that is produced by the reaction. It was suggested that the metastable species involved is a nitrogen molecule in the A.$^3\Sigma_u^+$ state, and the present results provide further support for this identification. An alternative possibility (2), that the metastable species is a nitrogen molecule in the $^3\Delta_u$ state, appears to be ruled out by the agreement between the present results and other recent estimates of the lifetime of the A state (3, 4, 5).

It has now been shown that the decay of the iodine emission in the flame does not depend markedly on the surface area of the reaction vessel, has a negligible temperature coefficient between 15 and 50 °C, and is the same whether the intensity is measured at 2 600 Å or 4 600 Å. An error due to the use of a faulty iodine saturator in the previous work has been corrected, and the lifetime of the metastable species which is responsible for most of the iodine emission has been determined by means of a short extrapolation of the decay rate to zero iodine pressure. From the variation of the decay rate with iodine pressure an improved rate constant for deactivation of the metastable species by molecular iodine has been obtained, while from the decay of the nitrogen afterglow the rate constant for reaction [1] has been redetermined in the interval 10–50 °C.

[1] $$N + I_2 \rightarrow NI + I.$$

EXPERIMENTAL

The apparatus was essentially the same as that described previously (1), except that the length of the reaction tube was 1.5 m instead of 30 cm. Active nitrogen from a microwave discharge passed a light trap and entered one end of the 18.4 mm i.d. reaction tube. Iodine vapor, carried by a stream of argon, entered through a spherical inlet jet nearby. Photometric observations were made on the last 100 cm of the reaction tube, this part being enclosed in a black box. For observations of the ultraviolet emission a plain thin-walled pyrex tube was used; otherwise the reaction tube was water-jacketed for temperature control, although most measurements were in fact carried out at room temperature (18 °C). For several sets of measurements the surface-to-volume ratio of the tube was increased by inserting a central pyrex rod of diameter 7.9 mm. From the reaction tube the gases passed to a small rotary vacuum pump protected by a cold trap.

Flow velocities in the reaction tube were between 1 and 3 m/s at pressures between 1 and 12 torr. The velocity was usually calculated from the total gas flow and the pressure in the tube, but could also be

measured directly by determining the time required for a light front to travel the length of the reaction tube when the discharge was turned on or off. For this purpose two photomultipliers were mounted 100 cm apart with their outputs connected via a capacitance to the input of a Tektronix type 564 storage oscilloscope. The oscilloscope was triggered by the signal from a photocell placed near the discharge. The flow time was obtained from the distance on the oscilloscope screen between the differentiated signals from the photomultipliers. Velocities obtained by the two methods agreed to within 3%.

Light intensities were measured with a 1P28 photomultiplier enclosed in a box which could be slid along rails parallel to the reaction tube. The photomultiplier box was fitted with collimating windows and a holder for filters. For the iodine emission a Wratten number 50 filter (λ_{max} = 4 600 Å), or a Baird-Atomic type A11 interference filter, of 100 Å half-width at 2 600 Å, was used. For the nitrogen afterglow a Spectrolab type P interference filter of 15 Å half-width at 6 250 Å was used. At the highest iodine flows the emission could only be measured in the first 20 cm or less of the reaction tube inside the black box, while at the lowest iodine flows the decay of the blue emission was affected by the presence of unreacted nitrogen atoms except in the last 15 or 20 cm.

Analytical reagent grade iodine, welding grade dry argon ($O_2 < 5$ p.p.m.) and Matheson prepurified nitrogen ($O_2 < 8$ p.p.m.) were used. The nitrogen was dried further at −196 °C and the argon at −80 °C, although the results did not seem to be affected by failure to do this. All-glass connections were used to convey nitrogen and argon to their flowmeters. With ordinary commercial nitrogen a film of I_2O_5 formed on the walls of the reaction tube near the iodine inlet and decay rates at low iodine pressures were markedly less than usual, showing that some iodine had been removed. Since oxygen is likely to be the most serious impurity, as far as the lifetime of the A state is concerned, the ability of iodine to remove it in this way is an advantage. With prepurified nitrogen the 'pink afterglow' (6) was always present but did not extend as far as the iodine inlet.

Two different iodine saturators were used. In the first the argon stream passed down a tube containing iodine crystals at ca. 50°, through a sintered glass disc and then through a glass spiral immersed in a water bath at between 0 and 20 °C, before going to the inlet jet. The walls of the spiral were coated with iodine and the emerging argon stream was assumed to be saturated at the temperature of the water bath. The second saturator consisted simply of a vertical tube of 12 mm i.d. which contained a 15 cm depth of powdered iodine packed around the stem of a thermometer, the whole being immersed in the water bath at between 0 and 20 °C. The vapor pressure data of Gillespie and Fraser (7) were used. The two saturators gave the same results within experimental error. When the iodine from the second saturator was collected in a cold trap for a known time, extracted with KI solution, and titrated with thiosulfate, the result agreed to within 2% with that predicted from the argon flow, the saturator temperature, and the pressure in the reaction tube. (The argon flow was always so small that the pressure drop across the iodine inlet to the reaction tube could be neglected.) In the present work much lower values than those obtained previously were found for the rate constant of reaction [1] and for the decay rate of the blue emission at any given iodine pressure. In the previous work saturation of the argon stream was assumed to take place above a sintered glass disc and the partial pressure of iodine in the gas which had passed through the disc was calculated by multiplying the vapor pressure by a factor for the pressure drop across the disc. It now appears that this was wrong, and that with this type of saturator the pressure at which saturation with iodine vapor actually takes place is not well defined, but may even be closest to the pressure on the exit side of the disc. Fortunately a different type of saturator was used for the recent work with chlorine and bromine (2).

Typical partial pressures in the reaction tube were: N_2 5.0 torr, Ar 0.1 torr, and I_2 0.005 torr. Nitrogen atom concentrations were not usually determined, but would have been about 0.1 torr at the iodine inlet. As in the previous work, iodine was assumed to be present almost entirely in the form of I_2 because of the speed with which iodine atoms are able to recombine on a glass surface (8).

RESULTS

1. *Iodine Emission*

Some typical graphs of log intensity vs. time for the iodine emission are shown in Figs. 1 and 2. These particular graphs show that the decay rate is the same for the blue and ultraviolet emissions and is independent of temperature.

In Fig. 3 the apparent first-order rate constant for the decay of the iodine emission is plotted against the iodine pressure in the reaction tube. Three kinds of experimental points are distinguished: those obtained with the blue filter, those obtained with the ultraviolet filter, and those obtained with the blue filter with the surface-to-volume ratio increased by the insertion of the central glass rod. There appear to be no systematic differences between the three sets of results. Nor was there any apparent effect due to variation of the nitrogen pressure in the range 1 to 12 torr.

Can. J. Chem. Downloaded from www.nrcresearchpress.com by 210.87.254.6 on 09/05/12
For personal use only.

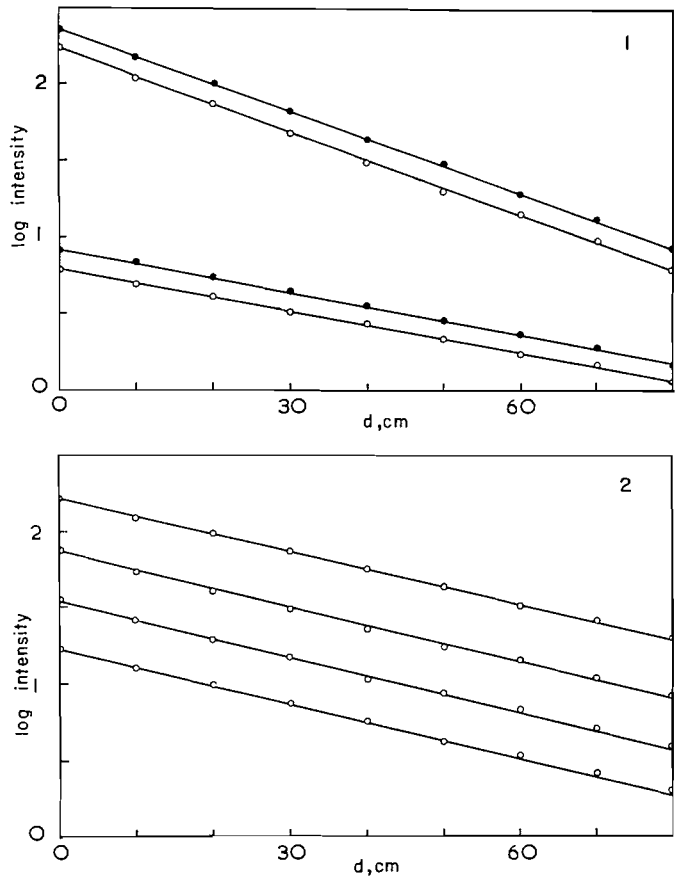

FIG. 1. Graphs of log intensity vs. time (in terms of distance along the reaction tube) for the iodine emission. ○, blue emission; ●, ultraviolet emission. Upper pair of lines 7.5 torr N_2, lower pair of lines 1.5 torr N_2.

FIG. 2. Graphs of log intensity vs. time for the iodine emission at different temperatures, at constant iodine pressure and flow velocity. Jacket temperatures, from top to bottom: 52, 38, 29, and 15 °C.

The least-squares line for the points of Fig. 3 (the regression line for $[I_2]$ in terms of k) has the equation

$$k = 0.89 + (2.72 \times 10^{-3})P_{I_2} \qquad [2]$$

so that the mean lifetime of the metastable species at zero iodine pressure is 1.1 s. The standard error of k is 0.41 s^{-1}, corresponding to an upper limit of 2.1 s and a lower limit of 0.77 s for the lifetime. The lowest observed value of k was 1.1 s^{-1}, in an experiment with impure nitrogen. The iodine pressure in this case was unknown because of formation of I_2O_5. With pure nitrogen the lowest observed value of k was 1.3 s^{-1} at an iodine pressure of 1.4×10^{-4} torr.

From eq. [2] the rate constant for deactivation of the metastable species by I_2 is $(8.3 \pm 1.2) \times 10^{-14}$ cm^3 $molecule^{-1}$ s^{-1}, where the limits of error are estimated from the possible variation of the slope of the line in Fig. 3.

2. Nitrogen Afterglow

Graphs of log intensity vs. time for the nitrogen afterglow are linear in the presence

Can. J. Chem. Downloaded from www.nrcresearchpress.com by 210.87.254.6 on 09/05/12
For personal use only.

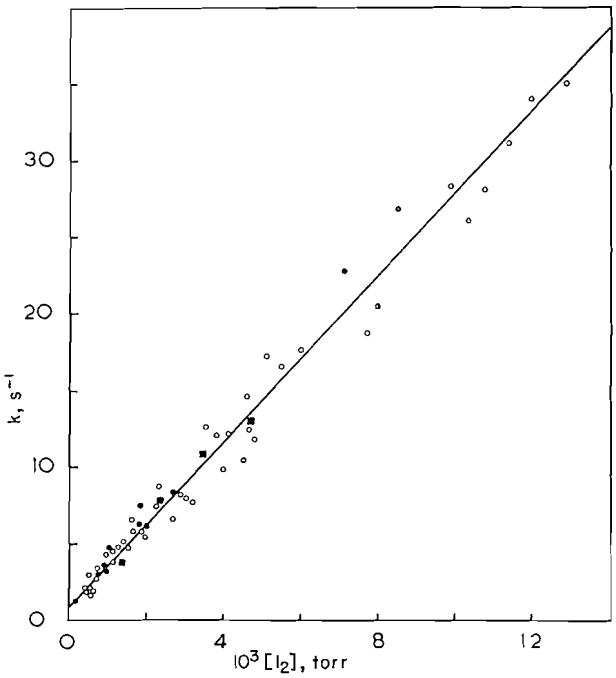

FIG. 3. Variation of the rate of decay of the iodine emission with iodine pressure. ○, blue filter; ●, ultraviolet filter; ■, blue filter with increased surface to volume ratio.

of iodine. Nitrogen atoms are believed to be removed by reaction [1], followed mainly by [3] at high atom concentrations and by [4] at low atom concentrations (1).

[3] $$N + NI \rightarrow N_2^* + I,$$

[4] $$NI + \text{wall} \rightarrow \tfrac{1}{2}N_2 + \tfrac{1}{2}I_2 + \text{wall}.$$

By the time the part of the reaction tube inside the black box is reached, the nitrogen atom concentration is expected to be so low that reaction [3] can be neglected in comparison with [4]. In all cases ordinary termolecular recombination is negligible in comparison with [1]. Results for the decay of the afterglow at low nitrogen atom concentrations are given in Table I, together with corresponding values of the rate constant for reaction [1].

The temperature coefficient of this reaction is remarkably small. In a typical experiment

TABLE I

Results for the decay of the nitrogen afterglow

$[N_2]$, torr	$10^3[I_2]$, torr	$d(\log_{10} I)/dt$, s^{-1}	k_1, cm^3 molecule^{-1} s^{-1}
3.7	1.01	3.88	2.55×10^{-14}
4.5	2.50	8.03	2.12×10^{-14}
5.3	1.92	7.04	2.42×10^{-14}
6.15	1.71	6.32	2.46×10^{-14}
3.45	0.62	2.17	2.33×10^{-14}
2.9	0.80	2.58	2.15×10^{-14}
4.1	0.80	2.78	2.29×10^{-14}

Mean $k_1 = 2.33\times10^{-14}$ cm^3 molecule^{-1} s^{-1} at 15 °C

Can. J. Chem. Downloaded from www.nrcresearchpress.com by 210.87.254.6 on 09/05/12
For personal use only.

the slope of the log intensity vs. time graph increased by (6 ± 3)% when the temperature of the water jacket was changed from 12 to 38 °C. Incorporation of the temperature coefficient into the results of Table I gives finally

[5] $$k_1 = 2.6 \times 10^{-14} \exp(-68/RT) \text{ cm}^3 \text{ molecule}^{-1} \text{ s}^{-1}$$

with an estimated error of ±15% in the range 10–50 °C.

DISCUSSION

The value of 1.1 s which has been obtained for the mean lifetime of the metastable species is identical, within the experimental error, with the values of 2.0 ± 0.9 s and ca. 0.9 s found by Carleton and Oldenberg (3) and Zipf (4) respectively for the lifetime of the $A.^3\Sigma_u^+$ state of N_2. The lower values found by several previous workers (9, 10, 11) probably result either from the presence of deactivating species or from the A state molecules being in other than the ground vibrational level. (It might be expected that the nitrogen molecules produced by reaction [3] would possess vibrational as well as electronic excitation, but this does not have to be the case, as shown for example by the work of Del Greco and Kaufman (12) on the reaction of H with NO_2.)

The agreement between these lifetime values suggests very strongly that it is the A state that is produced by reaction [3], as was previously supposed. It seems unlikely that the other metastable species that might be produced by reaction [3], namely the $^3\Delta_u$ state of N_2, should have the same lifetime as the A state. If the $^3\Delta_u$ state lies above $B.^3\Pi_g$, then it should readily undergo collision-induced transitions to the B state, even if the rate of the allowed radiative transitions is low because of the ν^3 factor in the transition probability, and its lifetime should be pressure dependent and probably quite short. If, on the other hand, the $^3\Delta_u$ state lies below the B state, then the failure of spectroscopists to discover a band system analogous to the Vegard–Kaplan bands of the A state (13) would indicate that its lifetime is considerably longer than that of the A state. (It is notable that both of the possible transitions, to $A.^3\Sigma_u^+$ and $X.^1\Sigma_g^+$, are forbidden by two selection rules, and not just by one as is the case with the Vegard–Kaplan system.) The results of Kenty (14), if they do refer to the $^3\Delta_u$ state, suggest that its lifetime is several seconds even in the presence of deactivating species. Our attempts to obtain a conclusive identification of the metastable species, by observing its absorption spectrum in that of the reaction flame, have so far been unsuccessful.

We have found that reactions [1] and [6] both have very small temperature coefficients. This is not unexpected for

[6] $$N_2(^3\Sigma_u^+) + I_2 \rightarrow N_2(^1\Sigma_g^+) + I_2^*,$$

which is an energy transfer process, but reaction [1] is a simple bimolecular reaction with a rate constant 10^3 times smaller than the collision frequency, and the lack of a corresponding energy of activation indicates that the entropy of activation ($\Delta S^* = -13$ cal/mole deg) is unusually large. A factor of 50 in the rate constant can be accounted for by the loss of translational freedom on forming the activated complex; the remaining factor of 20 could be a steric factor.

ACKNOWLEDGMENTS

This work was supported by grants from the New Zealand Universities Research Committee and the United States Air Force Office of Scientific Research.

Can. J. Chem. Downloaded from www.nrcresearchpress.com by 210.87.254.6 on 09/05/12
For personal use only.

REFERENCES

1. C. G. FREEMAN and L. F. PHILLIPS. J. Phys. Chem. **68**, 362 (1964).
2. K. S. RAXWORTHY and L. F. PHILLIPS. Can. J. Chem. **42**, 2928 (1964).
3. N. P. CARLETON and O. OLDENBERG. J. Chem. Phys. **36**, 3460 (1962).
4. E. C. ZIPF. J. Chem. Phys. **38**, 2034 (1963).
5. J. F. NOXON. J. Chem. Phys. **36**, 926 (1962).
6. G. E. BEALE and H. P. BROIDA J. Chem. Phys. **31**, 1030 (1959).
7. L. J. GILLESPIE and L. H. D. FRASER. J. Am. Chem. Soc. **58**, 2260 (1936).
8. E. A. OGRYZLO. Can. J. Chem. **39**, 2556 (1961).
9. P. G. WILKINSON and R. A. MULLIKEN. J. Chem. Phys. **31**, 674 (1959).
10. A. N. WRIGHT, R. L. NELSON, and C. A. WINKLER. Can. J. Chem. **40**, 1082 (1962).
11. H. B. DUNFORD. J. Phys. Chem. **67**, 258 (1963).
12. F. P. DEL GRECO and F. KAUFMAN. Discussions Faraday Soc. **33**, 128 (1962).
13. Y. TANAKA, M. OGAWA, and A. S. JURSA. J. Chem. Phys. **40**, 3690 (1964).
14. C. KENTY. J. Chem. Phys. **35**, 2267 (1961); **37**, 1567 (1962).

Can. J. Chem. Downloaded from www.nrcresearchpress.com by 210.87.254.6 on 09/05/12
For personal use only.

REACTIONS OF AMIDES AND RELATED COMPOUNDS

I. N.M.R. (PROTON) INVESTIGATION OF *N,N*-DIMETHYLFORMAMIDE – LEWIS ACID ADDUCTS AND REMARKS ON THE RELATIVE STRENGTH OF LEWIS ACIDS[1]

STEPHEN J. KUHN AND JOHN S. MCINTYRE
Exploratory Research Laboratory, Dow Chemical of Canada, Limited, Sarnia, Ontario
Received March 16, 1964

ABSTRACT

The proton resonance spectra of a number of Lewis acid – *N,N*-dimethylformamide adducts in 2-nitropropane and methylene chloride solutions have been investigated and an attempt has been made to correlate the relative strength of Lewis acids with the chemical shift of the methyl protons. The order obtained for the relative strength of Lewis acids shows good agreement with the results obtained by other methods. The complex formation has taken place on the carbonyl oxygen of the *N,N*-dimethylformamide in all cases. The DMF – Lewis acid mole ratios were 1:1 in $ZnCl_2$, $AlCl_3$, PF_5, $BiCl_3$, $InCl_3$, AsF_5, $SbCl_5$, SbF_5, BF_3, BCl_3, BBr_3. The 2:1 DMF – Lewis acid complexes of $ZnCl_2$, $SnCl_4$, $SnBr_4$, SnI_4, $TiCl_4$, $ZrBr_4$ have also been investigated.

INTRODUCTION

During recent years a considerable effort has been made by a number of investigators to obtain additional information about the chemical reactions and structure of carboxylic amides (1). The structure of DMF (*N,N*-dimethylformamide) has been well established by infrared and proton magnetic resonance spectroscopy (1, 2, 3). The n.m.r. spectrum shows two different kinds of methyl protons (*cis* and *trans* to carbonyl oxygen). These arise from the restricted rotation about the carbon–nitrogen bond due to its partial double bond character.

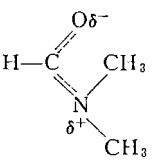

At higher temperatures the rate of rotation becomes sufficiently fast that only one type of methyl proton can be observed. The methyl peak located towards higher field has been assigned as *cis* to the aldehyde proton. Although both methyl peaks are split by the aldehyde proton (4), no definite split has been observed in the aldehyde proton but broadening indicates complex structure.

The retention of the two separate signals for the methyl protons in the n.m.r. spectra of strong acid solutions of DMF (5, 6) shows the preservation of the partial double bond character of the C—N bond and indicates oxygen coordination. The proton resonance spectrum of the $DMF \cdot BCl_3$ adduct has also shown the presence of the two chemically different methyl proton peaks (7).

The infrared spectra of *N,N*-dialkylamide complexes strongly support coordination (1, 7) at the oxygen atom. Such coordination would tend to increase the single bond character of the carbonyl group and thus shift the carbonyl stretching vibration to lower frequencies. Also, the double bond character of the C—N group would be increased, with consequent shifting of its stretching vibration to higher frequencies. If N coordination took place, the frequency shifts would be in the opposite direction to those cited

[1]*Contribution No. 108.*

above. Quite recently Cook (8) has convincingly demonstrated that protonation occurs on the carbonyl oxygen by preparing compounds from aliphatic acylhalides and tertiary amines, as shown in [1], and comparing their infrared spectra with alpihatic amide salts.

[1] 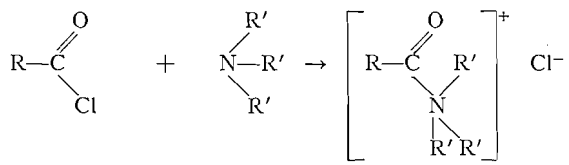

The compounds prepared in this manner are the same as would be expected if the coordination were to take place on the N atom of the amides. Their infrared spectra show that the carbonyl stretching vibrations occur at a much higher frequency (near 1 800 cm^{-1}) than in the protonated amides.

Crystallographic studies have also shown that in complexes with metal salts the amides are bonded to the metal atom through the carbonyl oxygen (9).

In the present work a number of DMF – Lewis acid complexes have been prepared in solution and the proton resonance spectra of these compounds have been investigated.

EXPERIMENTAL

Solutions of DMF – Lewis acid adducts

(*a*) *N,N*-Dimethylformamide (0.1 mole), dissolved in 40 g of 2-nitropropane, was added in small portions to a solution of 0.1 mole of Lewis acid in 40 g of 2-nitropropane. The temperature was kept around 0 °C during the addition.

(*b*) If the Lewis acids were gases, 0.1 mole of Lewis acid gas was introduced into a solution of 0.1 mole of the amide in 80 g of 2-nitropropane.

(*c*) The $ZnCl_2$ complex was prepared by shaking a solution of 0.1 mole of dimethylformamide in 80 g of 2-nitropropane with 0.1 mole of $ZnCl_2$ until all the $ZnCl_2$ was dissolved.

(*d*) The SbF_5 salt, prepared in Freon 113, and the AsF_5 and PF_5 salt, prepared in ether, were isolated and then dissolved in 2-nitropropane.

The CH_2Cl_2 solutions were prepared in a similar manner: 0.1 mole of complex was dissolved in 80 g of CH_2Cl_2.

From $ZnCl_2$, $SnCl_4$, $SnBr_4$, $TiCl_4$, SnI_4, $ZrBr_4$, the $2DMF \cdot MX_n$ complexes have also been prepared as described above.

Nuclear Magnetic Resonance

The nuclear magnetic resonance spectra were recorded on a Varian A-60 spectrometer operating at room temperature. In the series using 2-nitropropane as solvent, the chemical shifts of the methyl protons were measured relative to the second band of the nitropropane septuplet (Fig. 1), and in the series using methylene chloride, the shifts were relative to an external reference of acetonitrile (Fig. 2). These shifts were determined on the 100 cycle sweep width except in the few cases where the shift was greater than 100 c.p.s., when measurement was on the 250 cycle sweep width. The aldehyde shifts were measured relative to tetramethylsilane in both solvents.

RESULTS AND DISCUSSION

The n.m.r. results obtained in 2-nitropropane and methylene chloride solvents are summarized in Tables I and II.

The data show that the methyl protons are separated in all of the DMF – Lewis acid complexes investigated. The arguments used to substantiate O protonation in acid solutions of dimethylformamide can be used to deduce the site of coordination in DMF – Lewis acid adducts. If the coordination were to take place on the N atom of the molecule, the partial double bond character of DMF would be destroyed and the difference between the methyl protons would disappear. In coordination on the oxygen atom of the molecule, the carbon–nitrogen bond would retain its double bond character and the methyl protons

TABLE I

Proton shifts of DMF – Lewis acid complexes in 2-nitropropane

Complex	*cis* Methyl*	*trans* Methyl*	Aldehyde†
DMF	102	94	474
$ZnCl_2 \cdot 2DMF$	91	82	487
$SnI_4 \cdot 2DMF$	89	79	483
$InCl_3 \cdot 1DMF$	87	77	493
$ZnCl_2 \cdot 1DMF$	85	75	489
$ZrBr_4 \cdot 2DMF$	84	75	503
$BiCl_3 \cdot 1DMF$	82	69	507
$TiCl_4 \cdot 2DMF$	78	69	518
$SnCl_4 \cdot 2DMF$	80	69	500
$SnBr_4 \cdot 2DMF$	80	68	502
$BF_3 \cdot 1DMF$	78	68	487
$TiCl_4 \cdot 1DMF$	75	65	512
$PF_5 \cdot 1DMF$	75	64	502
$AlCl_3 \cdot 1DMF$	74	64	493
$AsF_5 \cdot 1DMF$	72	60	507
$SbF_5 \cdot 1DMF$	70	60	505
$BCl_3 \cdot 1DMF$	68	57	506
$SbCl_5 \cdot 1DMF$	68	56	519

*The shifts are in c.p.s. upfield from second peak in nitropropane septuplet. The *cis* or *trans* is with respect to aldehyde proton.
†The shifts are in c.p.s. downfield from internal tetramethylsilane.

TABLE II

Proton shifts of DMF – Lewis acid complexes in methylene chloride

Complex	*cis* Methyl*	*trans* Methyl*	Aldehyde†
DMF	75	80	475
$ZnCl_2 \cdot 2DMF$	89	97	488
$ZnCl_2 \cdot 1DMF$	92	100	488
$BiCl_3 \cdot 1DMF$	88	98	501
$TiCl_4 \cdot 2DMF$	92	98	
$SnCl_4 \cdot 2DMF$	93	100	505
$BF_3 \cdot 1DMF$	96	103	484
$SnCl_4 \cdot 1DMF$	96	104	498
$TiCl_4 \cdot 1DMF$	99	107	507
$PF_5 \cdot 1DMF$	96	105	490
$AlCl_3 \cdot 1DMF$	100	107	489
$BCl_3 \cdot 1DMF$	104	112	502
$BBr_3 \cdot 1DMF$	106	113	510
$SbCl_5 \cdot 1DMF$	105	114	512

*The shifts are in c.p.s. downfield from external acetonitrile reference. The *cis* or *trans* is with respect to aldehyde proton.
†The shifts are in c.p.s. downfield from internal tetramethylsilane.

would remain separated. One can conclude from the data obtained that in DMF – Lewis acid adducts the interaction takes place on the carbonyl oxygen of the molecule.

It was anticipated that some data on the strength of Lewis acids could also be obtained by comparing the n.m.r. spectra of DMF – Lewis acid complexes. This was based on the assumption that with the individual Lewis acids the strength of the interaction with the carbonyl oxygen should be different. This interaction would affect the magnetic shielding of the methyl protons through the participation of the unshared electron pair of the nitrogen in the formation of the C=N double bond.

For the stoichiometric adducts studied no peaks were observed for the uncomplexed DMF. In the case of the $DMF \cdot BF_3$ adduct in methylene chloride solution, an excess of DMF gave two pairs of methyl signals: one pair corresponds to the methyls of the

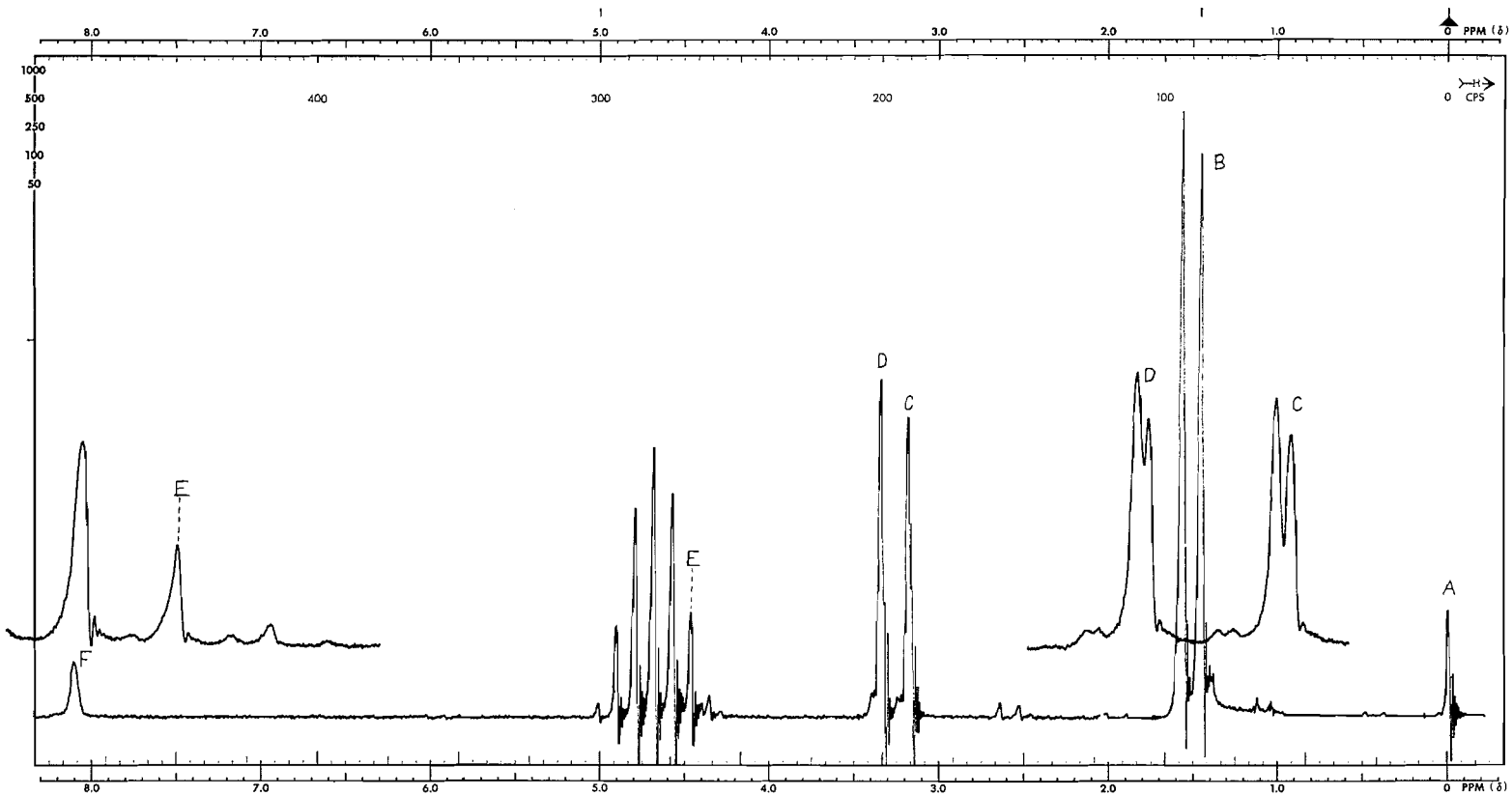

FIG. 1. The $BF_3 \cdot DMF$ complex in 2-nitropropane. The 100 and 500 c.p.s. sweep width are shown on the upper and lower spectra respectively. A, tetramethyl silane; B, 2-nitropropane doublet; C, *cis* methyl; D, *trans* methyl; E, second peak in nitropropane septuplet; F, aldehyde proton.

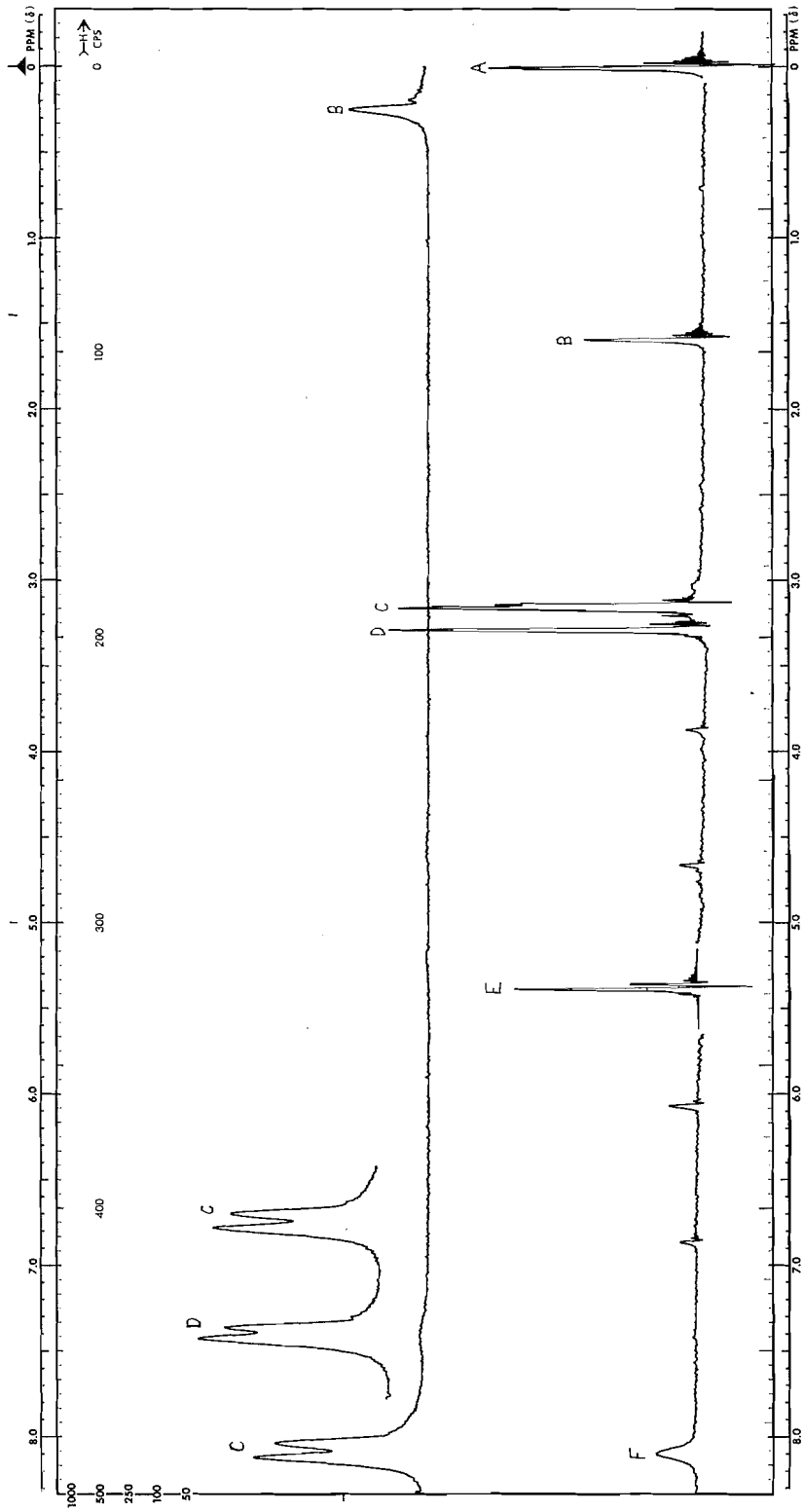

FIG. 2. The $BF_3 \cdot DMF$ complex in methylene chloride. The 100 and 500 c.p.s. sweep width are shown on the upper and lower spectra respectively. A, tetramethylsilane; B, external acetonitrile; C, *cis* methyl; D, *trans* methyl; E, methylene chloride; F, aldehyde proton.

complex and the other to the uncomplexed methyls of DMF. This shows that the equilibrium strongly favors the complex structure and allows a comparison of the Lewis acid strengths with methyl proton shifts. The relative perturbation of the stretching frequency of a carbonyl group by different Lewis acids has been used to measure Lewis acid strength: Susz and Chalandon (10) used acetophenone as a donor, Lappert (11) used ethyl acetate, and Cook (12) used xanthone. The relative order obtained for the strength of Lewis acids in this investigation shows close agreement to the order obtained by the infrared technique (Table III).

TABLE III

Comparison of Lewis acid strength* obtained by infrared and n.m.r. methods

DMF – Lewis acid† (n.m.r.)	Xanthone – Lewis acid (12) (infrared)	Acetophenone – Lewis acid (10) (infrared)	Ethylacetate – Lewis acid(11) (infrared)
$ZnCl_2$(2DMF)	$HgCl_2$	$HgCl_2$	$ZrCl_4$
SnI_4(2DMF)	$ZnCl_2$	$ZnCl_2$	$InCl_3$
$InCl_3$	$BiCl_3$	BF_3	$AlCl_3$
$ZnCl_2$	$InCl_3$	$TiCl_4$	BF_3
$ZrBr_4$(2DMF)	$SnCl_4$	$SnCl_4$	$SnBr_4$
$BiCl_3$	$SnBr_4$	$AlCl_3$	$TiCl_4$
$TiCl_4$(2DMF)	BF_3	$FeCl_3$	$TiBr_4$
$SnCl_4$(2DMF)	$FeCl_3$	$AlBr_3$	$AlBr_3$
$SnBr_4$(2DMF)	$AlBr_3$		BCl_3
BF_3	PF_5		BBr_3
$SnCl_4$	$ZrCl_4$		
$TiCl_4$	$TiCl_4$		
PF_5	BCl_3		
$AlCl_3$	SbF_5		
SbF_5	$SbCl_5$		
BCl_3	BBr_3		
$SbCl_5$			
BBr_3			

*Acid strength increases downward.
†Mole ratios in the complexes are 1:1 unless otherwise indicated.

Tables I and II also show that there is a definite difference in the methyl proton shift of complexes of $TiCl_4$, $SnCl_4$, etc. depending upon the mole ratio of $DMF \cdot MX_n$. According to these results $TiCl_4$, for example, seems to be a stronger Lewis acid in $TiCl_4 \cdot 1DMF$ complex than in $TiCl_4 \cdot 2DMF$ adducts. A number of possible structures can be written to explain this fact, but only through an X-ray investigation can the correct structure be determined.

REFERENCES

1. R. A. Y. Jones and A. R. Katrizky. Chem. Ind. London, 722 (1961).
2. H. S. Gutowsky and C. H. Holm. J. Chem. Phys. **32**, 1272 (1960).
3. W. D. Phillips. J. Chem. Phys. **23**, 1363 (1955).
4. V. J. Kowalewski and D. G. Kowalewski. J. Chem. Phys. **32**, 1272 (1960).
5. G. Fraenkel and C. Niemann. Proc. Natl. Acad. Sci. U.S. 44, 688 (1958).
6. R. J. Gillespie and T. Birchall. Can. J. Chem. **41**, 148 (1963).
7. W. Gerrard, M. F. Lappert, H. Pyszora, and J. W. Wallis. J. Chem. Soc. 2144 (1960).
8. D. Cook. Can. J. Chem. **40**, 2362 (1962).
9. M. Nardelli. Gazz. Chim. Ital. **89**, 1616 (1959).
10. B. P. Susz and P. Chalandon. Helv. Chim. Acta, **41**, 1322 (1958).
11. M. F. Lappert. J. Chem. Soc. 542 (1962).
12. D. Cook. Can. J. Chem. **40**, 522 (1962).

Can. J. Chem. Downloaded from www.nrcresearchpress.com by 210.87.254.6 on 09/05/12
For personal use only.

THE RADIOLYSIS OF ETHANOL

III. LIQUID PHASE

J. J. J. Myron and G. R. Freeman
Chemistry Department, University of Alberta, Edmonton, Alberta

Received September 11, 1964

ABSTRACT

The G values of the major products of the γ-radiolysis of liquid ethanol at a dose of 2×10^{20} eV/g are: hydrogen, 4.2; acetaldehyde, 1.9; 2,3-butanediol, 2.2; $G(-C_2H_5OH) = 7.5$. At progressively lower doses $G(H_2)$ increases to a maximum of 5.0. The yield of water, $G(H_2O) = 0.5$, is equal to the sum of the yields of the C_2 fragments found in the other products.

The approximate yields of three kinetically distinguishable sources of hydrogen were found to be $G(e^-_{solv}$, free ion$) = 0.9$, $G(H) = 2.7$ and G(unscavengeable $H_2) = 1.5$. The half-life of solvated electrons with respect to reactions such as

$$e^-_{solv} \rightarrow C_2H_5O^- + H$$

is 3 μs.

Both 1,3-pentadiene and benzene inhibit hydrogen and glycol formation but neither affect the high dose yield of acetaldehyde. Pentadiene reacts with H atoms and other radicals and possibly also with e^-_{solv}. Benzene appears to inhibit hydrogen and glycol formation mainly by an unidentified activation transfer process.

INTRODUCTION

The yields of products of the γ-radiolysis of liquid ethanol that are reported in the literature show poor agreement (1–5). Values of $G(H_2)$ range from 3.7 to 5.5 and the yields of acetaldehyde and 2,3-butanediol show a similarly wide variation. The ratios of the reported yields of the products also vary greatly; for example, the value of the ratio G(acetaldehyde)/G(2,3-butanediol) has been reported to be 1.8 (3) and 0.7 (5). The discrepancies between the several sets of results are probably due partly to different experimental conditions (dose, dose rate, etc.) and partly to the presence of small amounts of impurities that act as inhibitors.

Three products, hydrogen, acetaldehyde, and 2,3-butanediol, account for 85% of the observed decomposition. Proposed mechanisms have included free radical, molecular, and ionic reactions (1–8).

The present work was done to obtain further information about the yields of the products, including water, and about the reaction mechanism.

EXPERIMENTAL

Materials

Benzene-free absolute ethanol from Reliance Chemical Company was used. The only impurity detectable by gas chromatography (g.c.) was water (0.1%). The water content was reduced to $\leqslant 0.005\%$ by treatment with sodium and diethylphthalate followed by distillation (9). The purification system was protected from atmospheric moisture. For low-dose samples ($< 1 \times 10^{20}$ eV/g), the drying was preceded by a modification of the procedure outlined by Wild (10) for the preparation of 2,4-dinitrophenylhydrazones, to remove any aldehyde present. The purified ethanol was thoroughly degassed and distilled under vacuum into a Pyrex reservoir.

Phillips Research Grade benzene was distilled, the middle third being retained and stored in the vacuum system; g.c. analysis showed no detectable hydrocarbon impurities and $<0.001\%$ water.

The 1,3-pentadiene (Columbia Organic Chemicals Company) was purified by vacuum distillation, and g.c. analysis showed it to be 95% pure.

Sample Preparation

The sample cells were cleaned with hot sulfonitric acid, rinsed several times with dilute sodium carbonate solution, then rinsed many times with doubly distilled water.

Most of the samples were 1.0–2.2 ml of liquid contained in 15 mm O.D. tubes of about 4 ml capacity.

However, for water analysis, very thin-walled spherical bulbs (capacity $\approx$ 0.5 ml) were used to contain 0.1 ml samples.

Irradiation

Co^{60} γ-irradiations were done with three different sources; the approximate dose rates were 0.9, 5, and 60×10^{18} eV/g h. The dosimetry was done with the Fricke dosimeter. Dose rates for ethanol and ethanol–inhibitor solutions were calculated using the assumption that the dose rate was proportional to the electron density of the solution. To obtain the dose rates for the 0.1 ml samples, a plot of sample volume vs. dose rate was extrapolated from 0.5 ml to 0.1 ml.

The temperature during irradiation was 25 $\pm$ 4 °C.

The ethanol–benzene solutions were given a dose of 1.5×10^{20} eV/g and the ethanol–1,3-pentadiene solutions were given 3.5×10^{20} eV/g.

Product Analysis

Gaseous products were separated into two fractions by successive distillations of the samples through traps at different temperatures (−196° and −112°). The total amount of each fraction was measured in a gas burette and each fraction was analyzed by g.c. with either a charcoal or a silica gel column.

The glycols, *sec*-butyl alcohol, and acetal were measured by g.c. using a di-*n*-decyl phthalate on Fluoropak 80 column. The glycols used were separated from each other in the following order; ethylene glycol, 1,2-propanediol, 2,3-butanediol, 1,3-propanediol, 1,3-butanediol, and 1,4-butanediol.

Acetaldehyde was determined polarographically using a 0.1 *M* aqueous lithium hydroxide supporting electrolyte solution at 0 °C. The total acetaldehyde yield was determined by adding the yields of acetaldehyde and acetal. In some samples part of the acetaldehyde reacted with ethanol to produce acetal and water. Although the amounts of acid present in the samples were less than that required to affect the radiolysis mechanism (11), only a small trace of acid is required (12) to catalyze the reaction

$$CH_3CHO + 2C_2H_5OH \rightarrow CH_3CH(OC_2H_5)_2 + H_2O.$$

Formaldehyde was analyzed by the chromotropic acid method (13).

Water analysis was effected by crushing the thin-walled bulbs directly in the carrier gas stream above the chromatographic column. After water analysis on a Carbowax 1500 on Fluoropak 80 column, the sample was led from the first detector cell *via* a heated stainless steel capillary tube to a second column (di-*n*-decyl phthalate on Fluoropak) and detector, by which the acetal yield was determined. The value of $G(H_2O)$ was obtained by subtracting the amount of acetal from the total amount of water.

RESULTS

Pure Ethanol

Gaseous Products

The yield of hydrogen decreased rapidly with increasing dose at low doses, then decreased more slowly as the dose increased above about 3×10^{19} eV/g (Fig. 1). The value of $G(H_2)$ extrapolated to zero dose was $G_i(H_2) = 5.0$. The hydrogen yield was independent of dose rate and was the same for samples that contained 0.005% or 0.2% water.

The yields of methane, carbon monoxide, ethane, ethylene, and propane are shown as a function of dose in Fig. 2. Only G(ethylene) shows an appreciable dependence on dose and dose rate (Fig. 2D). Variations in the yields of the other products with dose rate were random and were within experimental error of each other.

The initial G values of these products are given in Table I.

Liquid Products

The yields of acetaldehyde ($G = 1.9$), formaldehyde ($G = 0.13$), 2,3-butanediol ($G = 2.2$), and 1,2-propanediol ($G = 0.13$) were independent of dose over the ranges studied (Fig. 3). However, analytical difficulties prevented the measurement of liquid product yields in the dose region where the hydrogen yield increased rapidly with decreasing dose (i.e., $<10^{19}$ eV/g).

At high doses ($>5 \times 10^{20}$ eV/g) the 2,3-butanediol g.c. peak was resolved into a doublet. With the aid of authentic samples of meso- and *d,l*-2,3-butanediol[1] it was established that the doublet peak was due to approximately equal amounts of the two diasterioisomers.

[1]*We are grateful to Dr. F. A. L. Anet of the University of Ottawa for a sample of d,l-2,3-butanediol.*

Can. J. Chem. Downloaded from www.nrcresearchpress.com by 210.87.254.6 on 09/05/12
For personal use only.

Can. J. Chem. Downloaded from www.nrcresearchpress.com by 210.87.254.6 on 09/05/12
For personal use only.

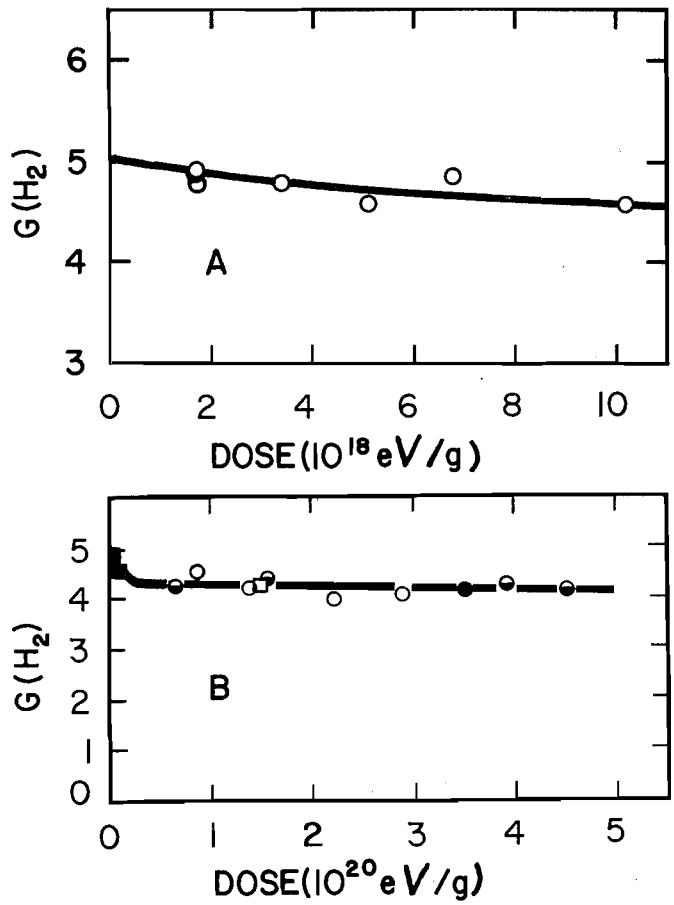

FIG. 1. Hydrogen yield as a function of dose. A: Dose rate = 5×10^{18} eV/g h and H_2O content of ethanol = 0.005%; the curve represents equation [iii]. B: ■ Taken from plot A (above), ◒ dose rate = 0.9×10^{18} eV/g h and H_2O content = 0.2%; ○ dose rate = 0.9×10^{18} eV/g h and H_2O content = 0.005%, □ dose rate = 5×10^{18} eV/g h and H_2O content = 0.005%, ● average of four values at three different dose rates, 0.9, 5, and 60×10^{18} eV/g h, the four values being too close to each other to plot separately.

TABLE I

Product yields

Product	G	Lowest dose used (10^{19} eV/g)	Dose rate (10^{18} eV/g h)
Hydrogen	5.0	0.2	0.9–60
Acetaldehyde	1.9	1.1	5–60
2,3-Butanediol	2.2	9.0	5–60
Water	0.5	58	5
Methane	0.6	0.2	0.9–60
Carbon monoxide	0.06	1.0	0.9–60
Ethane	0.24	4.0	0.9–60
Ethylene	0.14	4.0	0.9
Acetylene	$\leqslant$0.02	35	60
Propane	0.009	6.5	0.9–60
Butane	0.0004	25	5
sec-Butanol	0.08	92	5
Formaldehyde	0.13	2.2	5
Ethylene glycol	0.01	300	5
1,2-Propanediol	0.13	22	0.9–60
1,3-Propanediol	0.002	300	5
1,3-Butanediol	0.05	300	5
1,4-Butanediol	0.01	300	5

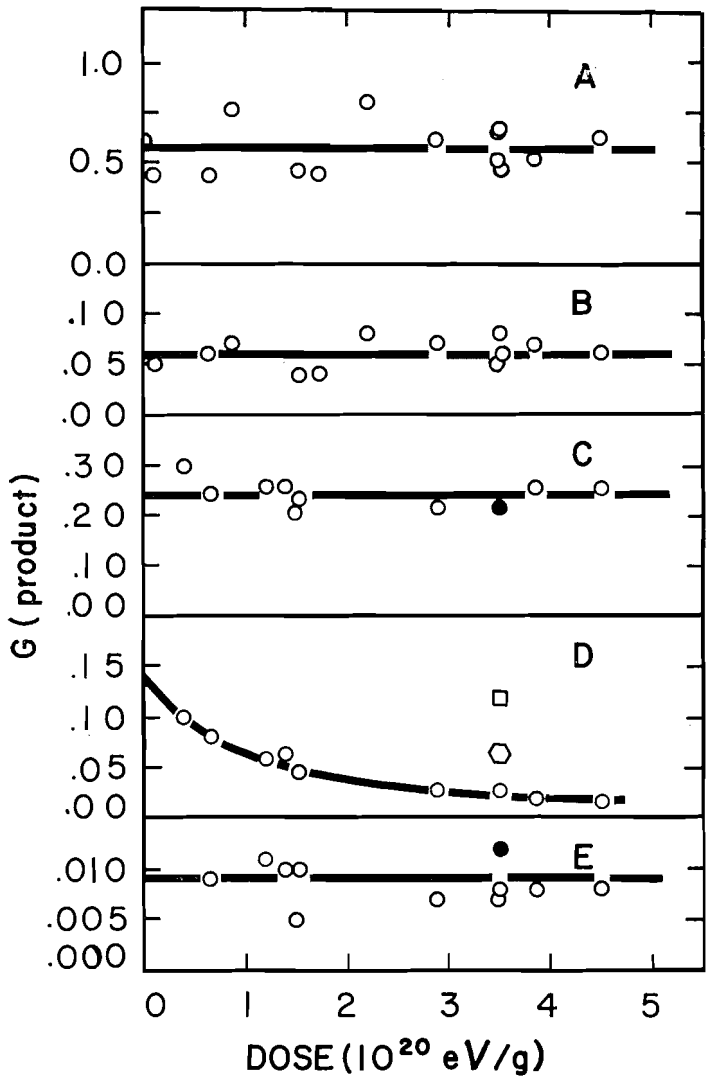

FIG. 2. Various gaseous product yields as a function of dose. A: Methane. B: Carbon monoxide. C: Ethane, ● average of four values at three different dose rates (0.9, 5, and 60 × 10^{18} eV/g h). D: Ethylene, ○ dose rate = 0.9 × 10^{18} eV/g h, ⬭ dose rate = 5 × 10^{18} eV/g h, □ dose rate = 60 × 10^{18} eV/g h (average of two values). E: Propane, ● average of two values at a dose rate of 60 × 10^{18} eV/g h.

Small yields of 1,3-butanediol, 1,4-butanediol, 1,3-propanediol, ethylene glycol, and *sec*-butanol were measured at doses greater than 10^{21} eV/g (see Table I).

The determination of the value of $G(H_2O)$ was difficult because of the hygroscopic nature of pure ethanol and because of the conversion of varying amounts of the acetaldehyde into acetal and water. For these reasons, previous values of $G(H_2O)$ from liquid phase (8) and vapor phase (13) radiolyses of ethanol were probably too high. Under the present conditions, the water yield could not be measured accurately at doses below 6×10^{20} eV/g; $G(H_2O) = 0.5$ (see Fig. 4 and Table I).

Ethanol–Inhibitor Solutions

The yields of the three major products, hydrogen, acetaldehyde, and 2,3-butanediol, are plotted as functions of the electron fraction of inhibitor, ϵ, in Figs. 5 and 6. The

Can. J. Chem. Downloaded from www.nrcresearchpress.com by 210.87.254.6 on 09/05/12
For personal use only.

Can. J. Chem. Downloaded from www.nrcresearchpress.com by 210.87.254.6 on 09/05/12
For personal use only.

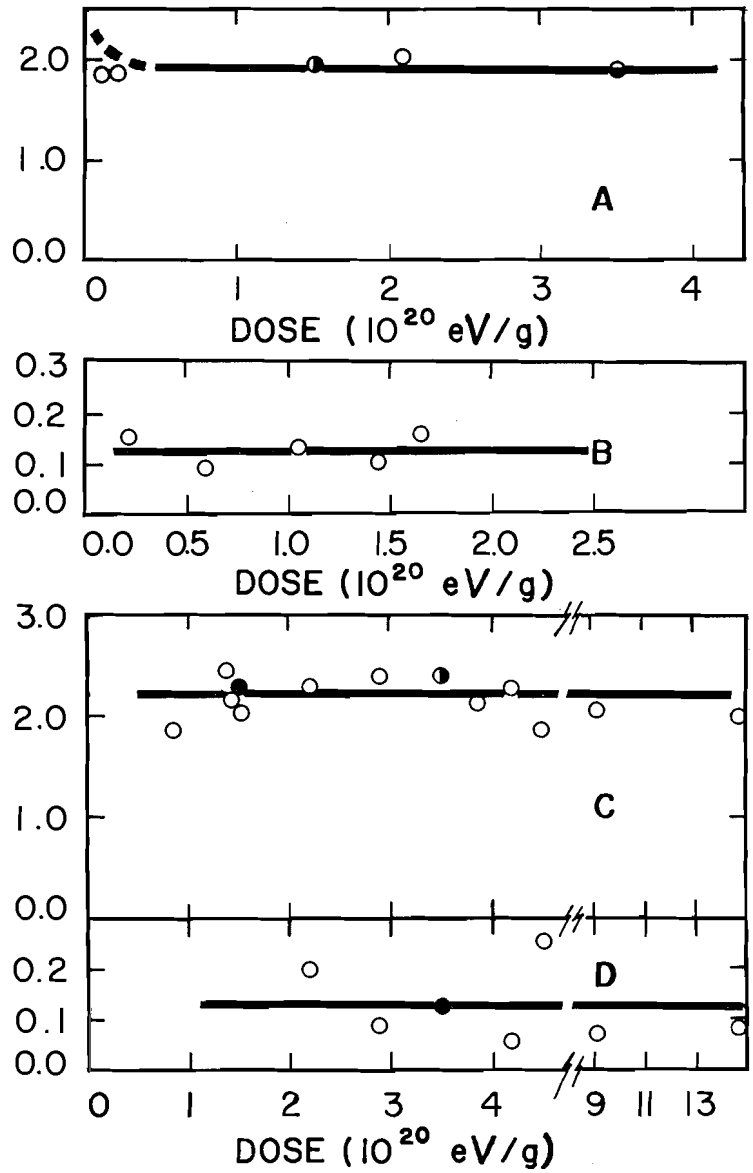

FIG. 3. Liquid product yields as a function of dose. A: Acetaldehyde, ◑ average of two values, ◒ average of three values, - - - theoretical yield. B: Formaldehyde. C: 2,3-Butanediol, ● average of two values, ◑ average of four values. D: 1,2-Propanediol, ● average of four values.

broken lines in the figures represent values of G(product) that would be expected if the radiolysis of the inhibitor and of ethanol were unaffected by the presence of each other. The most remarkable result is that both benzene and 1,3-pentadiene inhibit the formation of hydrogen and of 2,3-butanediol (Figs. 5, 6B, 6C) but neither additive appreciably inhibits the formation of acetaldehyde (Fig. 6A). Methane formation is also inhibitable by both additives (Fig. 7). Where inhibition effects occur, 1,3-pentadiene is a more efficient inhibitor than is benzene.

Three new products were measured in the pentadiene–ethanol solutions. The g.c. peaks of these products appeared in the region where C_{10} hydrocarbon peaks appeared from

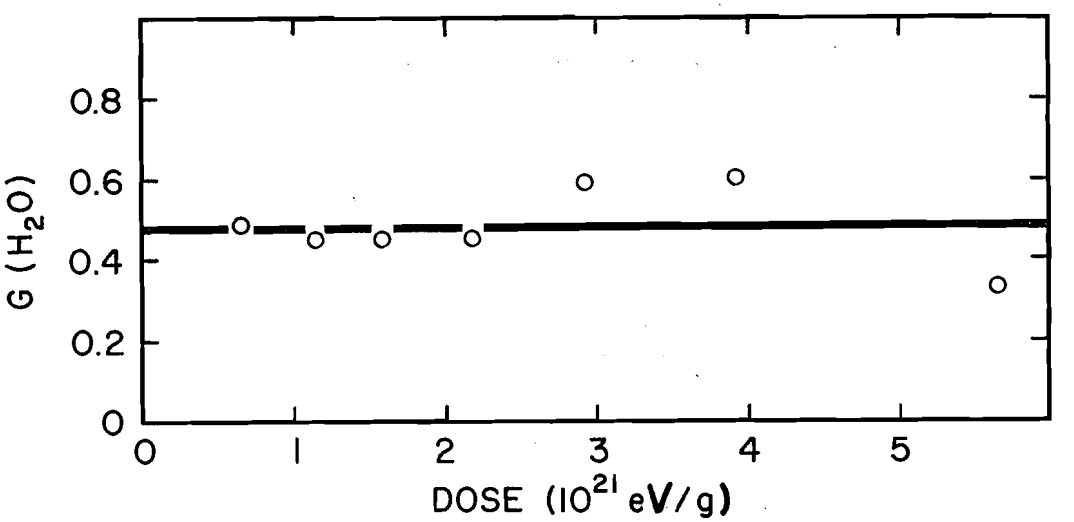

FIG. 4. Water yield as a function of dose.

the same column. The areas of the peaks are plotted against the electron fraction of 1,3-pentadiene, ϵ_p, in Fig. 8. Using a calibration factor estimated from those of other compounds that appeared in the same region, 1 area unit corresponds to a G value of 0.12 ± 0.02. Thus the maximum G value of product A (Fig. 8) was 1.8 ± 0.3, of product B was 0.5 ± 0.1, and of C was 0.7 ± 0.1. The yield of product A increased approximately linearly with increasing ϵ_p, whereas B and C passed through maxima at $\epsilon_p = 0.04$ and then decreased linearly with increasing ϵ_p.

DISCUSSION

Mass Balance

A mass balance for carbon, hydrogen, and oxygen, using product yields obtained from the graphs at a dose of 2×10^{20} eV/g, gave an empirical formula of $C_{2.00}H_{6.11}O_{1.01}$ and $G(-C_2H_6O) = 7.5$. There was a slight stoichiometric excess of hydrogen over the carbon and oxygen in the products. The excess corresponds to $G(H_2) = 0.4$.

Reaction Mechanism

The present results are consistent with many of the features of the mechanism proposed for the radiolysis of liquid ethanol by Adams and Sedgwick (4). A similar mechanism had been proposed earlier by Baxendale and Mellows for the radiolysis of methanol (14).

The main features of the overall radiolysis are: (*a*) there are three precursors of hydrogen that are distinguishable by their ease of reaction with inhibitors; (*b*) most of the butanediol is scavengeable; (*c*) the acetaldehyde produced at high doses is not scavengeable, although part of the larger yield of acetaldehyde produced at low doses is probably scavengeable.

Hydrogen

Adams and Sedgwick (4) suggested that solvated electrons and hydrogen atoms were kinetically distinguishable precursors of hydrogen and that there was also a "molecular yield" of hydrogen. The following is a refinement of their mechanism that is suggested by the present results and consideration of the yields of free ions in various kinds of liquids (15). The square brackets indicate that the entities are within a spur.

Can. J. Chem. Downloaded from www.nrcresearchpress.com by 210.87.254.6 on 09/05/12
For personal use only.

Can. J. Chem. Downloaded from www.nrcresearchpress.com by 210.87.254.6 on 09/05/12
For personal use only.

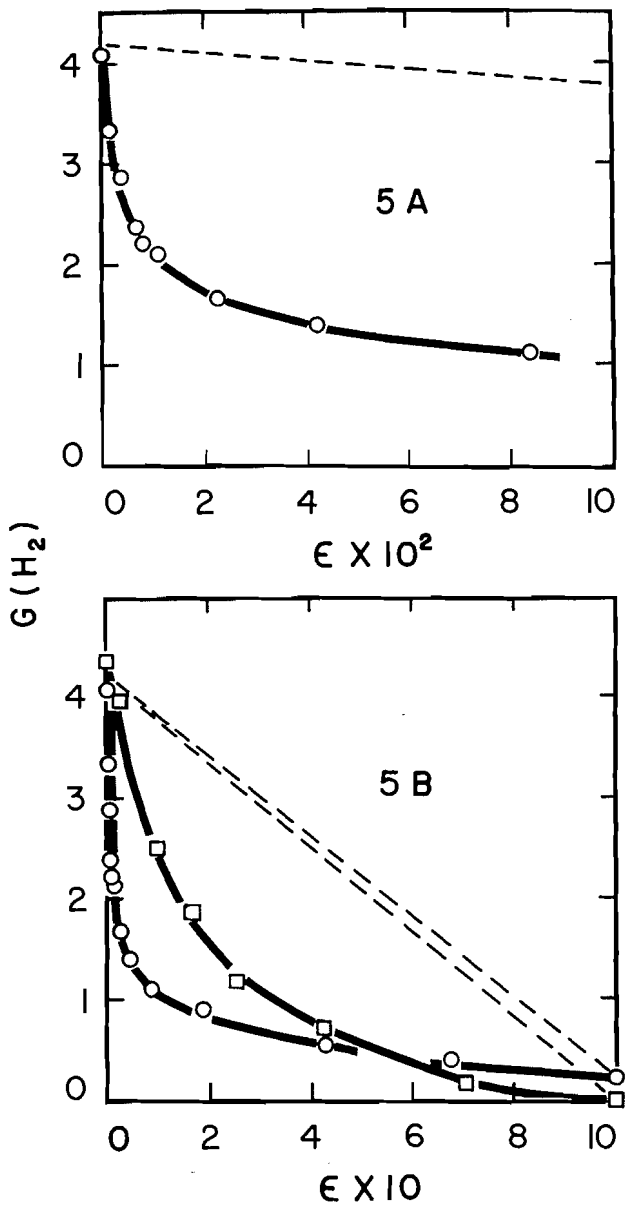

FIG. 5. Hydrogen yield as a function of additive concentration, where ϵ = electron fraction of additive; ○ 1,3-pentadiene, □ benzene.

[1] $C_2H_5OH \longrightarrow [C_2H_5OH^+ + e^-]$

[2] $\longrightarrow [CH_3CHOH^+ + H + e^-]$

[3] $[C_2H_5OH^+ + C_2H_5OH] \rightarrow [C_2H_5OH_2^+ + CH_3CH_2O]$

[4] $[CH_3CHOH^+ + C_2H_5OH] \rightarrow [CH_3CHO + C_2H_5OH_2^+]$

[5] $[e^- + mC_2H_5OH] \rightarrow [e^-_{solv}]$

[6] $[e^-_{solv} + C_2H_5OH_2^+] \rightarrow [nC_2H_5OH + H]$

[7] $\rightarrow e^-_{solv} + C_2H_5OH_2^+$ (free ions)

Can. J. Chem. Downloaded from www.nrcresearchpress.com by 210.87.254.6 on 09/05/12
For personal use only.

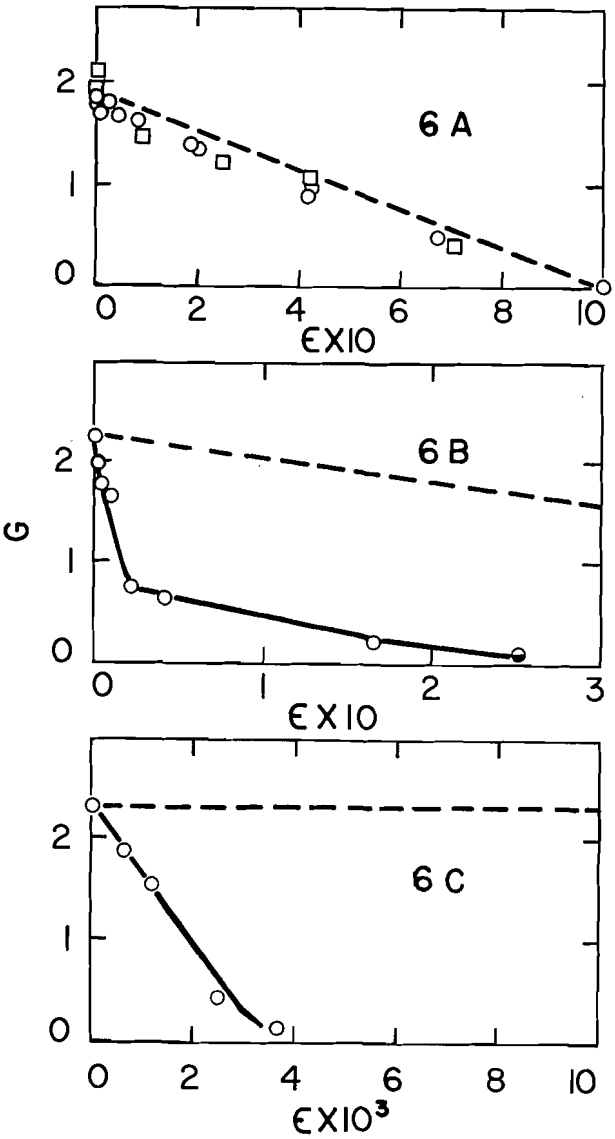

FIG. 6. Acetaldehyde and 2,3-butanediol yields as functions of additive concentration, where ϵ = electron fraction of additive. A: Acetaldehyde yield, O 1,3-pentadiene solutions, □ benzene solutions. B: Butanediol from benzene solutions. C: Butanediol from pentadiene solutions.

[8] $$e^-_{solv} \rightarrow CH_3CH_2O^- + H$$

[9] $$H + C_2H_5OH \rightarrow H_2 + CH_3CHOH.$$

At doses $>10^{18}$ eV/g, reactions [10] and [11] become important.

[10] $$e^-_{solv} + CH_3CHO \rightarrow CH_3CHO^-$$

[11] $$CH_3CHO^- + C_2H_5OH_2^+ \rightarrow CH_3CHOH + C_2H_5OH.$$

The mechanism does not involve excited molecules as such; however, reaction [2] is simply reaction [1] involving a more energetic precursor. Excited neutral molecule reactions cannot be excluded, but they appear to contribute less than do the ionic reactions

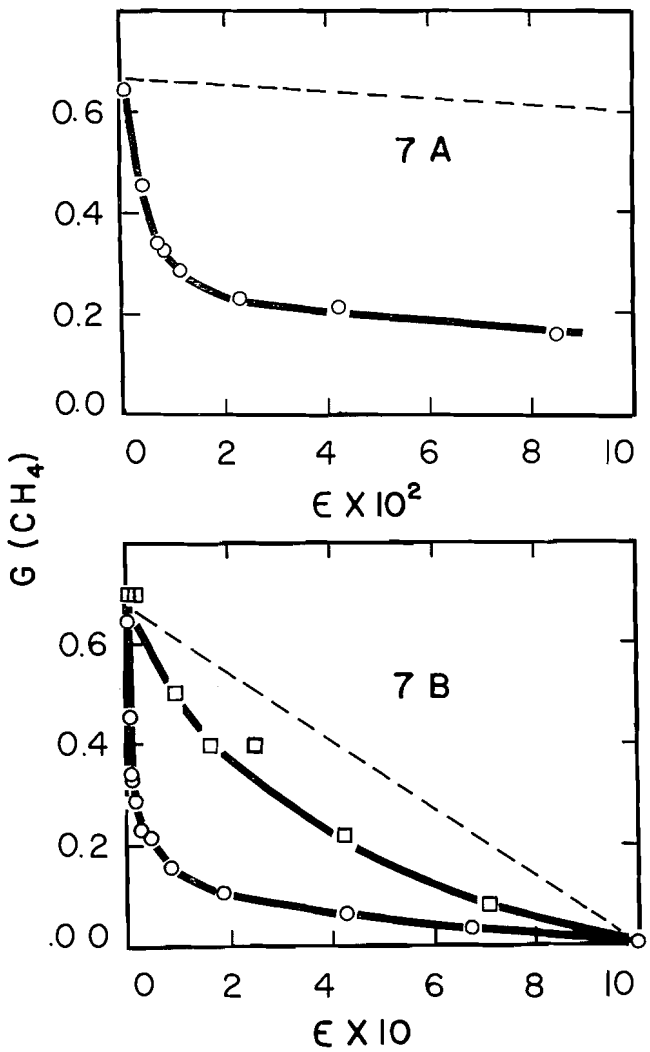

FIG. 7. Methane yield as a function of additive concentration, where ϵ = electron fraction of additive; ○ 1,3-pentadiene, □ benzene.

to the present system. The results indicate that reactions [1] and [2] occur to similar extents if G(total ionization) = 3–4.

In a mass spectrometric study of ion–molecule reactions, Ryan *et al.* (16) found that CH_3CHOH^+ was the important precursor for the formation of $CH_3CH_2OH_2^+$. Reaction [3] probably involves the shift of a hydrogen atom along a hydrogen bond in the liquid phase.

Reactions similar to [5], [6], and [7] will be discussed elsewhere (15).

An alternative to reaction [8] as a fate for the solvated electrons, e^-_{solv}, that exist as free ions in the bulk solution might be

$$[6'] \qquad e^-_{solv} + C_2H_5OH_2^+ \rightarrow nC_2H_5OH + H.$$

However, Adams and Sedgwick (4) found that reaction [6'] was not important in neutral ethanol. This conclusion is confirmed by kinetic calculations (17) involving the dose rate,

Can. J. Chem. Downloaded from www.nrcresearchpress.com by 210.87.254.6 on 09/05/12
For personal use only.

Can. J. Chem. Downloaded from www.nrcresearchpress.com by 210.87.254.6 on 09/05/12
For personal use only.

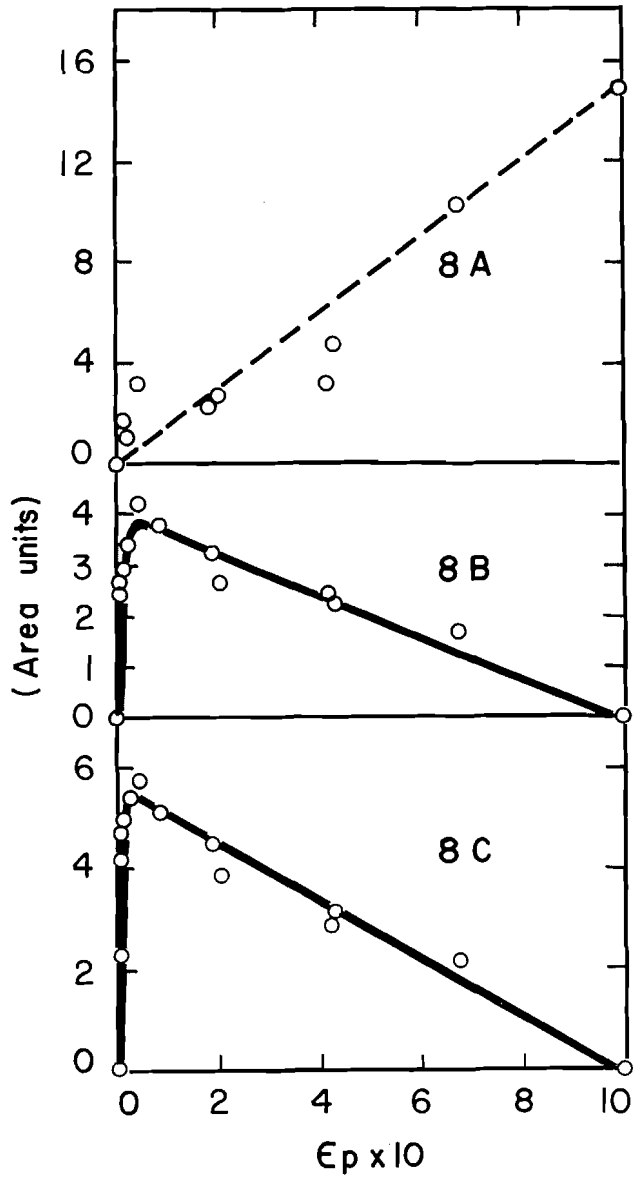

FIG. 8. C_{10} hydrocarbon products as functions of pentadiene concentration, ϵ_p. The ordinate, area units, refers to the g.c. peak area of the product. Using an estimated calibration factor, 1.0 area unit corresponds to a G value of 0.12 ± 0.02.

$G(\text{free } e^-_{solv}) = 1$, the value of the autodissociation constant of ethanol ($pK = 19.1$, ref. 18), $k_{6'} = 2.0 \times 10^{10}$ l/mole s (19*a*), $k_{10}/k_{6'} = 0.080$ (4), and the curves in Fig. 1. Briefly, the concentration of $C_2H_5OH_2^+$ from the autodissociation of ethanol (3×10^{-10} M) is more than an order of magnitude greater than that from the "free ions" generated by radiolysis. The total $[C_2H_5OH_2^+]$ is four or five orders of magnitude too small to explain the curve in Fig. 1A by a competition between reactions [10] and [6′].

The decrease in $G(H_2)$ from 5.0 to 4.2 with increasing dose can be explained by competition between reactions [8] and [10]. Thus, $G(H_2)$ is given by

[i] $$G(H_2) = 5.0 - \frac{0.8\, k_{10}\,[CH_3CHO]}{k_8 + k_{10}\,[CH_3CHO]}$$

at a particular value of $[CH_3CHO]$. Since the acetaldehyde concentration increases with increasing dose, the observed hydrogen yield at dose D is an average value:[2]

[ii] $$G(H_2)_D = \frac{1}{D}\int_0^D \left(5.0 - \frac{0.8\, k_{10}\,[CH_3CHO]}{k_8 + k_{10}\,[CH_3CHO}\right) dD$$

[iii] $$= 4.2 + \frac{0.8\ln(1+r)}{r},$$

where

[iv] $$r = k_{10}[CH_3CHO]_D/k_8,$$

and

[v] $$[CH_3CHO]_D = \int_0^D \frac{d[CH_3CHO]}{dD}\, dD.$$

The halfway point between $G(H_2) = 5.0$ and 4.2 occurs at $r = 2.6$ and $D = 1.1 \times 10^{19}$ eV/g. Equation [v] was solved graphically by assuming that $G(CH_3CHO)$ varied[3] from 2.8 to 1.9 as $G(H_2)$ varied from 5.0 to 4.2 (see later discussion). At 1.1×10^{19} eV/g, $[CH_3CHO] = 3.4 \times 10^{-4}\ M$ and

[vi] $$k_8 = k_{10} \times 3.4 \times 10^{-4}/2.6 = 2.1 \times 10^5\ s^{-1}.$$

Thus the half-life of the solvated electron in ethanol is 3.3 μs. Taub *et al.* (19*a*) measured the half-life of the solvated electron in neutral ethanol and found it to be 3 μs. They suggested that this half-life was partly due to reaction [6′]. An estimate of 4.0 μs for the half-life of the solvated electron can be obtained by combining data of Adams (4) with Taub's value of $k_{6'}$ (19*a*). It therefore appears likely that the contribution of reaction [6′] to the decay of the solvated electrons was small, even at the high dose rate in the pulse used by Taub (2×10^{23} eV/g s (19*a*)).

The value $G(e^-_{solv}) = 0.8$ is obtained from the data in Fig. 1. Adams and Sedgwick (4) reported a value of 1.02 which included a contribution of $G = 0.07$ for the reaction (transcribed into the present symbolism)

[12] $$e^-_{solv} \rightarrow C_2H_5 + OH^-.$$

Addition of this contribution to the present yield gives $G(e^-_{solv}) = 0.9$. Taub *et al.* (19*b*) reported $G(e^-_{solv}) = 1.0 \pm 0.3$. The three values are in reasonably good agreement.

The inhibition studies were done at high doses (to give measureable concentrations of liquid products) where reaction [10] was proceeding to the exclusion of reaction [8].

Pentadiene was a more effective inhibitor of hydrogen formation than was benzene in the low concentration region (Fig. 5). The shapes of the pentadiene curves in Figs. 5A and 5B indicate that there are scavengeable ($G \approx 2.7$) and unscavengeable ($G \approx 1.5$) precursors of hydrogen in addition to the solvated electrons discussed above. The results are consistent with the suggestion of Adams and Sedgwick (4) that the scavengeable precursor is atomic hydrogen (they reported $G(H) = 2.25$ and $G_m(H_2) = 1.65$). The

[2]*The following is a refinement of the treatment originally presented and was suggested by one of the referees.*

[3]*The variation in the acetaldehyde yield is expected to occur at such low doses (see Fig. 3) that the present method of analysis could not measure it. The good agreement between the two yields measured at 0.1 and 0.2 $\times$ 10^{20} eV/g is fortuitous because they were measured near the detection limit of the method.*

Can. J. Chem. Downloaded from www.nrcresearchpress.com by 210.87.254.6 on 09/05/12
For personal use only.

source of the unscavengeable hydrogen is possibly a combination of direct decomposition of ethanol to form molecular products,

[13a] $$CH_3CH_2OH^* \rightarrow CH_3CHO + H_2$$

[13b] $$\rightarrow CH_2{=}CHOH + H_2,$$

and reaction of hot hydrogen atoms generated by reactions [2] and [6].

Low concentrations of 1,3-pentadiene are roughly 20 times as efficient as benzene in inhibiting hydrogen formation and about 30 times as efficient as benzene in inhibiting methane formation. The value of the ratio of the methyl affinity of 1,3-pentadiene to that of benzene in alkane solutions is about 3 000 (20, 21) and it seems unlikely that this value would be reduced 100-fold by changing the solvent from alkane to ethanol. It therefore appears that benzene affects the product yields mainly by an activation transfer process. The activated species with which benzene interacts has several possible identities ($C_2H_5OH^+$, e^-, $[e^-_{solv}]$) among which it is not yet possible to choose. The gas phase proton affinity of benzene (6.26 eV) is much smaller than that of ethanol (8.4 eV) (22) so the species is probably not $C_2H_5OH_2^+$.

Kinetic analysis of the data according to the general mechanism[4]

[14] $$h \rightarrow \text{hydrogen}$$

[15] $$h + C_6H_6 \rightarrow \text{no hydrogen}$$

gave $k_{15}/k_{14} = 0.54$ l/mole. Other values obtained for this rate constant ratio are 0.58 for methylcyclohexane–benzene solutions (23), 0.78 for cyclohexane–benzene (24), 0.54 for cyclohexane–cyclohexene (25), 0.2 for cyclohexanone–benzene (26), and 0.2 for cyclohexene–benzene (27).

Acetaldehyde and 2,3-Butanediol

Acetaldehyde is formed by reactions [4] and [13], and both acetaldehyde and butanediol are products of reactions such as [16]–[18].

[16] $$2CH_3CHOH \rightarrow (CH_3CHOH)_2$$

[17a] $$CH_3CHOH + CH_3CH_2O \rightarrow CH_3CHO + CH_3CH_2OH$$

[17b] $$\rightarrow CH_3CH(OH)OCH_2CH_3 \text{ (hemiacetal)}$$

[18] $$2CH_3CH_2O \rightarrow CH_3CHO + CH_3CH_2OH$$

The hemiacetal from reaction [17*b*] is equivalent to acetaldehyde in the present analytical system.

Pentadiene inhibited the formation of butanediol but not the net rate of formation of acetaldehyde at the high dose used. Hayon and Weiss (3) found G(acetaldehyde) = 3.1 at a low dose (1×10^{17} eV/g), which is higher than the value found at doses in the vicinity of 10^{20} eV/g. Although reported product yields vary too much to confidently draw conclusions from differences between them, the present work indicates that a high acetaldehyde yield ($G \approx 2.8$) would be found in neutral ethanol at low doses. At high doses, solvated electrons destroy 0.9 units of the aldehyde. Since the high dose yield of aldehyde is not inhibited by pentadiene, either (i) the diene reacts both with free radicals that generate aldehyde in the bulk solution and with the solvated electrons that exist as free ions, or (ii) if the diene does not react with solvated electrons, reactions [17] and [18] occur mainly in the spurs. It appears that (i) is more likely because reaction [16] occurs mainly in the bulk medium and is readily inhibitable by the diene. It is improbable that reaction [16] would occur mainly in the bulk solution if reactions [17] and [18] occurred mainly in the spurs.

[4]*Unknown hydrogen precursors are symbolized by h.*

Can. J. Chem. Downloaded from www.nrcresearchpress.com by 210.87.254.6 on 09/05/12
For personal use only.

Methane

The results from the pentadiene solutions (Fig. 7) show that about 70% of the methane is scavengeable. Methyl radicals are probably the precursors of the scavengeable methane.

Ethane, Ethylene, and Water

Ethane is probably formed by the reaction

[19] $$C_2H_5 + C_2H_5OH \rightarrow C_2H_6 + CH_3CHOH.$$

Ethyl radicals have been detected in photolyzed solid ethanol by electron spin resonance spectroscopy (28). Possible sources of ethyl radicals in the radiolysis are reactions [12] and

[20] $$C_2H_5OH^* \rightarrow C_2H_5 + OH$$

[21] $$e^-_{solv} + C_2H_5OH_2^+ \rightarrow C_2H_5 + H_2O.$$

Ethylene may be formed by

[22] $$CH_3CH_2OH^* \rightarrow C_2H_4 + H_2O.$$

Some ethane and ethylene might also be formed by the disproportionation of ethyl radicals with other radicals.

The decrease in G(ethylene) with increasing dose can be ascribed to the reaction

[23] $$R + C_2H_4 \rightarrow RC_2H_4\cdot.$$

The average lifetime of the radicals with respect to radical–radical reactions decreases with increasing dose rate, so the dose dependence of the ethylene yield decreases with increasing dose rate.

Water can be formed by reactions [21] and [22] and by

[24] $$OH + C_2H_5OH \rightarrow H_2O + CH_3CHOH$$

[25] $$OH^- + C_2H_5OH_2^+ \rightarrow H_2O + C_2H_5OH.$$

The water yield ($G = 0.5$) equals the sum of the C_2 hydrocarbon fragments found in the other products:

$$G(C_2H_6 + C_2H_4 + C_2H_2 + C_3H_8 + C_4H_9OH + 2C_4H_{10}) = 0.48.$$

C_{10} Hydrocarbons from the Pentadiene Solutions

The maximum yield of two of the C_{10} products occurs at $\epsilon_p = 0.04$ (Figs. 8B and 8C). The hydrogen atoms are essentially completely scavenged at the same diene concentration (Fig. 5A). It appears that these C_{10} compounds are formed by the reactions

[26] $$H + CH_2{=}CH{-}CH{=}CH{-}CH_3 \rightarrow CH_3{-}\overset{\displaystyle I}{CH\cdots CH\cdots CH}{-}CH_3$$

[27] $$2I \rightarrow C_{10} \text{ isomers}$$

There is evidence that allylic radicals do not disproportionate to an appreciable extent (26). Thus,

$$G(H) \approx 2G(C_{10}) \approx 2.4 \pm 0.4,$$

where $G(C_{10})$ refers to the maximum yield of the compounds represented in Figs. 8B and 8C. This value is in good agreement with the estimates of G(H) mentioned earlier.

The C_{10} hydrocarbon represented in Fig. 8A is apparently a product of the direct radiolysis of pentadiene.

The products of reactions such as

[28] $$CH_3CHOH + C_5H_8 \rightarrow \cdot C_7H_{12}OH$$

[29] $$2 \cdot C_7H_{12}OH \rightarrow (C_7H_{12}OH)_2$$

would not have been observed with the present analytical system.

Can. J. Chem. Downloaded from www.nrcresearchpress.com by 210.87.254.6 on 09/05/12
For personal use only.

Free Radicals and Glycol Formation

The ratio of $CH_3CHOH:CH_2CH_2OH$ radicals contained in the glycols is 69:1. These figures roughly reflect the relative ease of abstraction of hydrogen from the α- and β-carbons in ethanol. If this difference is attributed to the difference in the activation energies of the two abstraction reactions, then $\Delta E = 2.7$ kcal/mole. This is similar to the value $(E_{31} - E_{30}) = 2.0$ kcal/mole (29) found for the reactions

[30] $$CH_3 + C_3H_8 \rightarrow CH_4 + CH_3CHCH_3$$

[31] $$\rightarrow CH_4 + CH_2CH_2CH_3.$$

ACKNOWLEDGMENTS

This work received financial assistance from the National Research Council.

NOTE ADDED IN PROOF:

G. Dobson and L. I. Grossweiner (Radiation Res. **23**, 290 (1964)) have recently photolyzed potassium iodide in ethanol solution, and their results indicate that the solvated electrons so produced have a half-life of 21 μs. The difference between this half-life and those reported in the present paper might be due to the difference in reaction conditions, although the size of the difference is surprising.

F. S. Dainton, J. P. Keene, T. J. Kemp, G. A. Salmon and J. Teply (Proc. Chem. Soc. 265 (1964) found a half-life of 1.9 μs for solvated electrons in methanol at 20°. This is in general agreement with the present results.

REFERENCES

1. J. G. BURR. J. Phys. Chem. **61**, 1477 (1957).
2. G. E. ADAMS, J. H. BAXENDALE, and R. D. SEDGWICK. J. Phys. Chem. **63**, 854 (1959).
3. E. M. HAYON and J. WEISS. J. Chem. Soc. 3962 (1961).
4. G. E. ADAMS and R. D. SEDGWICK. Trans. Faraday Soc. **60**, 865 (1964).
5. R. H. JOHNSEN. J. Phys. Chem. **65**, 2144 (1961).
6. T. F. WILLIAMS. Nature **194**, 348 (1962).
7. J. H. BAXENDALE and R. D. SEDGWICK. Trans. Faraday Soc. **57**, 2157 (1961).
8. A. S. NEWTON and W. R. MCDONELL. J. Am. Chem. Soc. **78**, 4554 (1956).
9. L. F. FIESER. Experiments in organic chemistry. 3rd ed. D. C. Heath and Co., Boston. 1955.
10. F. WILD. Characterization of organic compounds. 2nd ed. Cambridge University Press. 1960.
11. J. W. FLETCHER. Unpublished results.
12. E. R. ROYALS. Advanced organic chemistry. Prentice-Hall Inc., New York. 1958.
13. J. M. RAMARADHYA and G. R. FREEMAN. Can. J. Chem. **39**, 1836 (1961).
14. J. H. BAXENDALE and F. W. MELLOWS. J. Am. Chem. Soc. **83**, 4720 (1961).
15. G. R. FREEMAN. To be published.
16. K. R. RYAN, L. W. SIECK, and J. H. FUTRELL. J. Chem. Phys. **41**, 111 (1964).
17. J. J. J. MYRON. Ph.D. Thesis, University of Alberta. 1964.
18. L. P. HAMMETT. Physical organic chemistry. McGraw-Hill, New York. 1940.
19*a*. I. A. TAUB, M. C. SAUER, JR., and L. M. DORFMAN. Discussions Faraday Soc. **36**, 206 (1963).
19*b*. I. A. TAUB, D. A. HARTREE, M. C. SAUER, JR., and L. M. DORFMAN. J. Chem. Phys. **41**, 979 (1964).
20. A. RAZBENBACH and M. SZWARC. Proc. Roy. Soc. London, Ser. A, **251**, 394 (1959).
21. M. LEVY and M. SZWARC. J. Chem. Phys. **22**, 1621 (1954).
22. F. W. LAMPE, J. L. FRANKLIN, and F. H. FIELD. *In* Progress in reaction kinetics. Vol. 1. *Edited by* G. Porter. Pergamon Press, London. 1961.
23. G. R. FREEMAN. J. Chem. Phys. **36**, 1542 (1962).
24. G. R. FREEMAN. J. Chem. Phys. **33**, 71 (1960).
25. G. R. FREEMAN. Can. J. Chem. **38**, 1043 (1960).
26. A. SINGH and G. R. FREEMAN. Can. J. Chem. **42**, 1877 (1964).
27. B. R. WAKEFORD. Unpublished results.
28. P. J. SULLIVAN and W. S. KOSKI. J. Am. Chem. Soc. **86**, 159 (1964).
29. E. W. R. STEACIE. Atomic and free radical reactions. 2nd ed. Reinhold Publishing Corp., New York. 1954.

Can. J. Chem. Downloaded from www.nrcresearchpress.com by 210.87.254.6 on 09/05/12
For personal use only.

Can. J. Chem. Downloaded from www.nrcresearchpress.com by 210.87.254.40 on 09/05/12
For personal use only.

PAPER CHROMATOGRAPHY OF SOME AMINE HYDROCHLORIDES AND ACETATES IN ACIDIC SOLVENT SYSTEMS[1]

R. A. B. BANNARD AND A. A. CASSELMAN
Defence Chemical Biological and Radiation Laboratories, Ottawa, Canada

Received September 4, 1964

ABSTRACT

The chromatography of piperidine, cyclohexylamine, benzylamine, and morpholine hydrochlorides on unwashed Whatman No. 1 and No. 17 papers in *t*-butanol : acetic acid : water (2:1:1) leads in each case to partial conversion to the acetate salt, the mobility of which differs from that of the hydrochloride. The interconversion is reduced but is not prevented by the use of acid-washed papers and is increased again when the acid-washed papers are treated with sodium, potassium, calcium, or magnesium acetate prior to chromatography. The salt interconversion is continuous during development of the chromatograms, extended development leading to complete disappearance of the hydrochloride. Quantitative chromatography of piperidine and morpholine hydrochlorides revealed that the extent of salt interconversion is ca. 12% on unwashed and calcium ion washed Whatman No. 17 papers, ca. 6% on sodium ion washed papers, and ca. 1% on acid-washed papers. Piperidinium ions become bound to unwashed, acid-washed, and salt-washed Whatman No. 17 papers during chromatography in aqueous solution just as they do to the hydrogen, sodium, and calcium forms of the carboxylate ion exchanger Amberlite IRC-50 under similar conditions, indicating that a cation exchange mechanism involving carboxyl groups in the paper is responsible for the observed salt interconversion.

The chromatography of ethylenediamine dihydrochloride on unwashed Whatman No. 17 paper in *t*-butanol : acetic acid : water (2:1:1) gave two ninhydrin-positive bands, R_F 0.28 and 0.51, which were identified as ethylenediamine dihydrochloride (98%) and diacetate (1%) respectively (1). The multiple zoning was not observed on papers which had been deashed by acid washing but reappeared if acid-washed papers were treated with a solution of an alkaline earth metal prior to chromatography. The chromatography of ethylenediamine diacetate on unwashed or acid-washed Whatman No. 17 paper in *t*-butanol : 0.5% hydrochloric acid (3:1), on the other hand, led to quantitative conversion to the dihydrochloride due to displacement of the weak acid in the substrate by the strong acid in the solvent system.

There are numerous examples in the literature in which ion exchange properties have been attributed to paper by virtue of the carboxyl groups contained in the cellulose (e.g. refs. 2–7) and in fact ion exchange processes generally form the basis for estimation of the carboxylic content of paper (e.g. refs. 8–10). Two possible ion exchange mechanisms involving carboxylic acid groups and alkaline earth metal ash constituents (11) in the papers were therefore proposed (1) to account for the observed dihydrochloride to diacetate conversion on the unwashed paper. Both mechanisms were consistent with the experimental facts but it was not possible to distinguish between them from the data at hand. In the first mechanism (which is subsequently referred to as the acetolysis – anion exchange mechanism) it was suggested that the carboxylate salt I could be converted to the mixed salt II by partial acetolysis under the influence of the solvent system. Sites of the latter type could then readily effect the observed interconversion by anion exchange. Alternatively, the dicarboxylate salt I could undergo direct cation exchange with the ethylenediammonium ion, with formation of III and liberation of the alkaline earth metal cation (M^{++}). A second cation exchange with the protons of the acidic solvent would

[1]*Issued as DCBRL Report No. 449.*

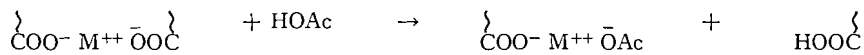

I II

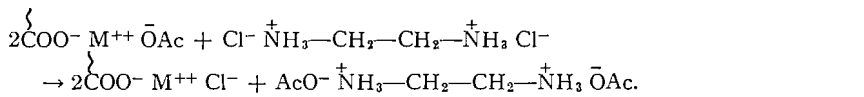

free the ethylenediammonium cation again for combination with the acetate ion in the solvent. This reaction sequence is subsequently referred to as the cation exchange mechanism.

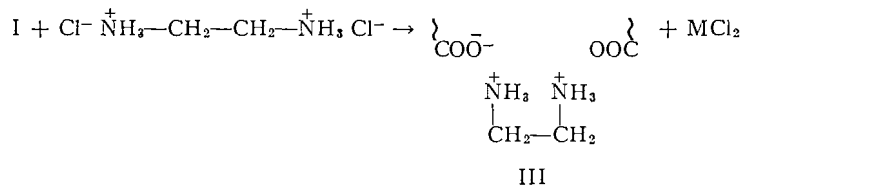

III

If ion exchange is responsible for the salt interconversion there appeared to be no reason why monoacid base hydrochlorides should not exhibit analogous behavior. Furthermore, if the acetolysis – anion exchange mechanism is operating, it should be possible to prevent the exchange reaction by replacing the divalent cationic impurity in the paper with a monovalent alkali metal. On the other hand, the cation exchange mechanism should be capable of functioning in the presence of either an alkali metal or an alkaline earth metal, although there could be a considerable difference in the extent of conversion because of the difference in ion exchange potential between these cations (12). If the cation exchange mechanism is valid, the aminium ions undergoing exchange should become temporarily bound to the carboxyl groups of the paper, accompanied by a release of cations from the binding groups; two conditions which do not obtain for the alternative mechanism. It seemed of interest, therefore, to examine the validity of these mechanisms by determining the qualitative and quantitative paper chromatographic behavior of some monofunctional amine hydrochlorides and acetates in both of the solvent systems mentioned earlier, using unwashed, acid-washed, and salt-washed papers.

Chromatography of each amine hydrochloride shown in Table I on unwashed Whatman No. 1 and No. 17 paper in *t*-butanol : acetic acid : water (2:1:1) gave two ninhydrin-positive spots, the faster moving of which is identical in R_F with the single spot resulting from similar chromatography of the corresponding acetate (Table II). Thus, the double-spotting phenomenon observed with ethylenediamine dihydrochloride in this solvent system (1) is quite general for monoacid bases and in each case examined the acetate salt has the higher R_F. Similar experiments conducted in *t*-butanol : 0.5% hydrochloric acid (3:1) demonstrated that only one ninhydrin-positive spot is obtained regardless of whether the amine hydrochloride or acetate is used. It is therefore concluded that, as in the case of ethylenediamine (1), acetate salts of monoacid bases are converted to hydrochlorides by simple acid displacement in this strongly acidic solvent system. This conclusion was readily confirmed since the quantitative chromatography of piperidine and morpholine acetates on Whatman No. 17 paper under these conditions led to recovery of the respective hydrochlorides in 97.5% and 97.0% yields.

Can. J. Chem. Downloaded from www.nrcresearchpress.com by 210.87.254.40 on 09/05/12
For personal use only.

Can. J. Chem. Downloaded from www.nrcresearchpress.com by 210.87.254.40 on 09/05/12
For personal use only.

TABLE I

Preparation of amine hydrochlorides and acetates

Compound	Reaction solvent	Solvent for recrystallization	% yield	Melting point (°C) Observed	Melting point (°C) Reported		Analysis (%)	C	H	N	Cl
Piperidine hydrochloride	Ether	Acetone–ethanol	83.0	244–245	244–245	(19)	Calcd. 49.38	9.95	11.52	29.16
							Found 49.58	9.85	11.70	29.11
Piperidine acetate	Ether	Acetone	75.6	104–106	106	(20)	Calcd. 57.90	10.41	9.65	—
							Found 57.99	10.50	9.78	—
Cyclohexylamine hydrochloride	Ether	Acetone–ethanol	86.5	205.5–207.5	206–207	(21)	Calcd. 53.14	10.40	10.33	26.14
							Found 53.24	10.36	10.31	26.08
Cyclohexylamine acetate	Ether	Acetone–ethanol	95.4	144–146	143.5–145	(22)	Calcd. 60.34	10.76	8.80	—
							Found 60.41	10.51	8.62	—
Benzylamine hydrochloride	Acetone	Ethanol–ether	77.6	260–261	258	(23)	Calcd. 58.53	7.02	9.76	24.69
							Found 58.78	7.00	9.74	24.52
Benzylamine acetate	Ether	Acetone–ether	75.0	98–100	97.5–98.5	(24)	Calcd. 64.65	7.84	8.38	—
							Found 64.40	7.70	8.44	—
Morpholine hydrochloride	Ether	Ethanol–ether	74.0	174.5–175.5	175–176	(25)	Calcd. 38.87	8.16	11.33	28.69
							Found 39.03	8.31	11.33	28.54
Morpholine acetate	Acetone	Acetone	75.0	112–114	112	(26)	Calcd. 48.96	8.90	9.52	—
							Found 49.03	8.83	9.46	—

TABLE II

Qualitative paper chromatography of amine salts

Compound	Whatman No. 1 R_F in solvent systems of: t-BuOH : HOAc : H_2O (2:1:1)	Whatman No. 1 R_F in solvent systems of: t-BuOH : 0.5% HCl (3:1)	Whatman No. 17 R_F in solvent systems of: t-BuOH : HOAc : H_2O (2:1:1)	Whatman No. 17 R_F in solvent systems of: t-BuOH : 0.5% HCl (3:1)
Piperidine acetate	0.76	0.51	0.77	0.48
hydrochloride	0.60 0.75	0.51	0.63 0.74	0.48
Cyclohexylamine acetate	0.80	0.69	0.81	0.64
hydrochloride	0.68 0.78	0.69	0.70 0.81	0.64
Benzylamine acetate	0.78	0.62	0.80	0.55
hydrochloride	0.67 0.77	0.62	0.66 0.79	0.55
Morpholine acetate	0.72	0.38	0.72	0.33
hydrochloride	0.57 0.68	0.38	0.56 0.70	0.33

Can. J. Chem. Downloaded from www.nrcresearchpress.com by 210.87.254.40 on 09/05/12
For personal use only.

The R_F values shown in Table II were not changed significantly when acid-washed or salt-washed papers were used. However, in contrast to the results reported for ethylenediamine dihydrochloride (1) and clam poison dihydrochloride (13) the use of acid-washed papers did not eliminate the double spotting from chromatograms of these base hydrochlorides in the acetic acid solvent system, although the extent of acetate formation was greatly reduced by the use of acid-washed papers and restored by the use of salt-washed papers, judging from the areas of the ninhydrin-positive spots. These observations confirmed that the presence of metallic ions in the paper does have an important influence on the degree of interconversion. During the chromatography of the amine hydrochlorides on unwashed paper (both No. 1 and No. 17) in the acetic acid system, silver nitrate reagent revealed the majority of the chloride ion to be coincident with the slower-moving, ninhydrin-positive spot, but there was also a diffuse chloride ion tail. It was concluded that the aminium ion and chloride ion migrate as an ion pair (cf. ref. 1) and that the diffuse tail represents chloride ion which has been released during the salt interconversion. It was found by the use of the lanthanum nitrate reagent that the acetate ion is coincident with the faster-moving, ninhydrin-positive spot. Furthermore, a diffuse ninhydrin- and acetate-positive tail extended from the faster- to the slower-moving ninhydrin-positive spot. These results were considered indicative that the aminium ion and acetate ion also migrate as an ion pair and that the interconversion is continuous during chromatographic development. That the interconversion is indeed continuous was demonstrated by prolonged chromatography of the piperidine and morpholine salts on unwashed Whatman No. 17 paper in the acetic acid solvent system, under which conditions the area of the acetate spot gradually increased with increasing time of development at the expense of the hydrochloride spot, until the latter disappeared entirely.

Piperidine and morpholine hydrochlorides were also chromatographed quantitatively on unwashed, acid-washed (0.01 *N* HCl), and salt-washed (0.01 *N* HCl, Na^+ and Ca^{++}) papers in *t*-butanol : acetic acid : water (2:1:1). Since the qualitative experiments had indicated the slower-moving hydrochloride spot to contain acetate as well, the entire ninhydrin-positive area was recovered by aqueous elution and the respective hydrochlorides and acetates were isolated by fractional sublimation *in vacuo*. From the results given in Table III it is clear that on unwashed paper 11–12% of the hydrochlorides are converted to the acetates and that the conversion is decreased by an order of magnitude when acid-washed paper is used. Thus, the extent of conversion is independent of the strength of the base, within the range of basicities examined (14). It is also evident that the conversion on calcium ion washed paper is identical with that on unwashed paper and that sodium ion washed paper is only about half as effective as calcium ion washed paper in promoting the conversion. It thus appears that alkaline earth metal impurities are more important in the conversions on unwashed papers than are alkali metal impurities. The fact that sodium ion washed papers are capable of effecting significant conversions of monoacid base hydrochlorides to acetates suggests that the cation exchange mechanism is more probable than the acetolysis – anion exchange mechanism. The much greater conversion observed on the calcium ion washed papers was unexpected, since although the ability of one cation to displace another from a carboxylic exchanger (the exchange potential) normally increases with increasing atomic number and with increasing valence (12, 15), when the ease of displacement of divalent and monovalent cations from the carboxylate group by another monovalent ion (e.g. an aminium ion) is considered, the latter are generally much more readily displaced than the former (cf. refs. 12 and 16 and the experiments with Amberlite IRC-50 resin mentioned below). That this reversal of the normal exchange potential seems general for cellulosic carboxyl groups

is shown in experiments described later on the aqueous chromatography of piperidine hydrochloride on the variously treated papers.

The occurrence of a small amount of hydrochloride to acetate conversion on the acid-washed paper was unexpected because this phenomenon had not been observed with the diacid base hydrochlorides and because of the exceedingly high affinity of the carboxylate group in resinous carboxylic exchangers (12) for protons in the presence of neutral salts such as alkali and alkaline earth metal chlorides. However, the study of methods for the estimation of carboxyl groups in paper (4–10) has revealed that protons bound to such groups will exchange to a small extent due to the equilibrium reaction

$$\text{[1]} \qquad \text{COOH} + \text{M}^+ \rightarrow \text{COO}^- \text{M}^+ + \text{H}^+$$

which is kept well shifted in favor of the undissociated acid unless the protons freed in the exchange are continuously removed (17). Thus, the fact that a small but measurable conversion is observed with monoacid base hydrochlorides during chromatography is consistent with an ion exchange mechanism. The apparent failure of ethylenediamine dihydrochloride to yield the diacetate under similar conditions is readily explicable when differences in the extent of conversion of the mono- and di-acid bases on unwashed paper are considered. Calculation of the probable concentration (10 γ/in.^{2}) of ethylenediamine diacetate produced by exchange from the dihydrochloride revealed that it would have been insufficient for detection by the ninhydrin reagent. This interpretation does not explain why the extent of exchange with ethylenediamine dihydrochloride is so much lower than that observed with the monoacid base hydrochlorides and no firm explanation can be offered at this time. However, the presence of a third ninhydrin positive spot corresponding to a mixed salt (e.g. ethylenediamine monohydrochloride monoacetate) or a mixture of ethylenediamine dihydrochloride and diacetate has never been observed on chromatograms on unwashed paper. Moreover, the recovery in these experiments of 98% dihydrochloride and 1% diacetate virtually excludes the possibility of the presence of mixed salt or salt mixtures. The suggestion is offered, therefore, that conversion of the diacid base dihydrochloride to diacetate may require simultaneous exchange at the two aminium ions. Such a requirement would clearly reduce markedly the extent of the phenomenon because the chances of obtaining simultaneous collisions between the reactive centers would depend on the distribution of carboxylic sites in the paper relative to the geometry of the aminium ions, a condition which would not need to be satisfied for the monoacid bases.

Evidence in support of the cation exchange mechanism was sought by experiments designed to show that a portion of the piperidinium ion remains bound to the variously treated Whatman No. 17 papers during chromatography. Since the much greater affinity of carboxyl groups for protons than for aminium ions would render the retention of the latter by carboxylate groups in the paper very small in the acidic solvent normally employed, water was used as the developing solvent. Piperidine hydrochloride was applied to strips of the variously pretreated papers as for normal descending chromatography and was eluted with freshly boiled, distilled water until no further salt could be extracted. The strips were then eluted with carbon dioxide – saturated water to displace any piperidinium ion which had remained bound to the papers and the latter was converted to piperidine hydrochloride for recovery by sublimation *in vacuo*.[2] It is quite

[2]*In experiments in which unwashed or calcium ion washed papers were used, it was necessary to basify the eluate and extract with ether prior to regeneration of the hydrochloride to effect quantitative recovery, due presumably to complex formation between the amine and calcium chloride (18).*

Can. J. Chem. Downloaded from www.nrcresearchpress.com by 210.87.254.40 on 09/05/12
For personal use only.

Can. J. Chem. Downloaded from www.nrcresearchpress.com by 210.87.254.40 on 09/05/12
For personal use only.

TABLE III

Hydrochloride to acetate conversion in *t*-butanol : acetic acid : water (2:1:1) on Whatman No. 17 paper

Hydrochloride applied	Weight applied (mg)	Type of paper	Acetate recovered (mg)	Hydrochloride recovered (mg)	% recovered	% conversion to acetate
Piperidine	1 000	Unwashed	133	798	96.4	12.1
	500	Acid washed (0.01 *N* HCl)	6.0	451	96.6	1.1
	500	Salt washed (0.01 *N* HCl, Na^+)	36.8	434	98.5	6.7
	400	Salt washed (0.01 *N* HCl, Ca^{++})	51.0	323	96.8	11.7
Morpholine	500	Unwashed	60.5	411	97.8	11.1
	500	Acid washed (0.01 *N* HCl)	5.4	462	98.8	1.0
	500	Salt washed (0.01 *N* HCl, Na^+)	32.0	438	98.7	5.8
	500	Salt washed (0.01 *N* HCl, Ca^{++})	61.6	406	97.2	11.4

clear from the results shown in Table IV that a significant quantity of the aminium ion remains bound to each of the papers. Furthermore, the quantity of aminium ion bound parallels the extent of hydrochloride to acetate conversion observed during chromatography on the same papers in the acetic acid solvent system (Table III) when the results from the binding experiments are calculated on the basis of an 18 × 22 in. sheet of paper (Table IV, column 5). Thus, the greater ease of displacement of calcium than of sodium ion from the cellulosic carboxylates noted in the acidic solvent system is also observed during aqueous chromatography. The amount of piperidinium ion bound during aqueous chromatography of piperidine hydrochloride on a column prepared from mechanically dispersed acid-washed Whatman No. 17 paper was an order of magnitude greater than that bound by the same weight of this paper in strip chromatograms. This result strongly suggests that many of the exchange sites in the paper are made less accessible during the sheeting process.

TABLE IV

Aqueous chromatography of piperidine hydrochloride on Whatman No. 17 paper

Paper pretreatment	Salt bound (meq)	Ion liberated (meq)	% salt bound	% salt bound (18 × 22 in. sheet basis)
Unwashed	0.070	0.140 Ca^{++} 0.112 Na^{+}	2.8	11.2
Acid washed	0.021	0.031 H^{+}	0.8	3.2
Sodium ion washed	0.041	0.102 Na^{+}	1.7	6.8
Calcium ion washed	0.076	0.170 Ca^{++}	3.1	12.4

For comparison with the results mentioned above, the behavior of piperidine hydrochloride during aqueous chromatography on the hydrogen, sodium, and calcium forms of the carboxylic cation exchanger Amberlite IRC-50 was also examined, and the unbound and bound salt was recovered as mentioned earlier. It is evident from Table V that a significant amount of piperidinium ion exchanges with the protons of the carboxyl groups and that, as anticipated, much more exchange occurs with the calcium and sodium forms of the resin. As predicted from the cation exchange potential series (12, 15), sodium ion is much more readily displaced from the resin than is calcium ion. These results contrast sharply with those given in Tables III and IV for chromatography of amine hydrochlorides on the variously pretreated papers.

That ion exchange involving carboxyl groups is indeed involved in the binding of piperidinium ions to acid-washed papers as well as to the hydrogen form of Amberlite IRC-50 appears certain since during both processes the pH of the effluent at first fell abruptly, indicating the liberation of protons in agreement with eq. [1], then slowly increased to a pH more alkaline than that of the water used for elution, signifying the anticipated slow hydrolysis of the salt of a weak acid and a weak base formed during the cation exchange. Only the cation exchange mechanism could lead to the observed binding of piperidinium ions to acid-washed paper since this paper would be virtually free of the divalent metallic impurity required for intervention of the acetolysis – anion exchange mechanism. That cation exchange is also involved on unwashed, sodium ion washed, and calcium ion washed papers is supported by the concomitant liberation of metal ions and the binding of piperidinium ions during the experiments on the chromatography of piperidine hydrochloride in aqueous solution which are summarized in Table IV. It is, therefore, concluded that the cation exchange mechanism is the only one which receives

Can. J. Chem. Downloaded from www.nrcresearchpress.com by 210.87.254.40 on 09/05/12
For personal use only.

support from the quantitative data available. The reversal of exchange potential observed for sodium and calcium ions on cellulosic carboxyl groups does not invalidate the conclusion reached regarding the mechanism of the salt interconversion since numerous examples of such behavior are known (ref. 16, p. 57).

TABLE V

Aqueous chromatography of piperidine hydrochloride on Amberlite IRC-50 resin

Form of resin	Recovery from aqueous elution (mg)	Recovery from acid elution (mg)	Total recovery (%)	% bound to resin
H^+	228	12.0	98.4	4.9
Na^+	42.0	196	97.6	80.4
Ca^{++}	192	45.6	97.6	18.7

As a result of these studies the following practical considerations should be borne in mind during the paper chromatography of amine salts. It is essential not to use a solvent which contains an acid weaker than that in the salt if double zoning is to be prevented. A solvent system which contains an acid much stronger than that present in the salt will cause complete conversion to the salt of the stronger acid, but the minimal difference in acid strength necessary to produce this effect has not been delineated. It is, therefore, highly desirable to use a solvent system which contains the same acid as is present in the salt if complications are to be avoided.

EXPERIMENTAL[3,4]

Preparation of Amine Salts

The amine hydrochlorides and acetates were prepared by dropwise addition of a solution of the appropriate acid (0.12 mole) in ether or acetone to a stirred cold (0°) solution of the amine (0.10 mole) in the same solvent. The reaction mixture was allowed to come to room temperature and was evaporated to dryness *in vacuo* and the resultant solid was purified by recrystallization from a suitable solvent. Analytical and pertinent experimental data for these compounds are given in Table I.

Pretreatment of Papers for Chromatography

The Whatman No. 1 and No. 17 papers used in these studies were either unwashed, acid washed, or salt washed. Acid-washed papers ($18\frac{1}{4} \times 22\frac{1}{2}$ in.) were prepared from unwashed papers by chromatographic elution with (*a*) 0.01 *N* hydrochloric acid (3 days) and water (3 days) or (*b*) 0.6 *N* acetic acid (3 days) and water (3 days). Salt-washed papers were prepared by similarly washing *each* type of acid-washed paper with a 0.1% solution of sodium, potassium, calcium, or magnesium acetate (2 days) and water (2 days).

Qualitative Paper Chromatography

(1) Normal Development

Whatman No. 17 papers were supported by means of a Whatman 3MM stirrup (27) and a single wick of the latter paper was used as solvent feed. The amine salts were spotted from 4% aqueous solutions, 200 γ and 1 mg being applied per spot on the No. 1 and No. 17 papers respectively. After chromatographic development with either *t*-butanol : acetic acid : water (2:1:1) or *t*-butanol : 0.5% hydrochloric acid (3:1) by descending flow, the No. 1 papers were dried in a forced air oven at 55° for 30 min (No. 17 papers, 1.5 h), sprayed with ninhydrin reagent (1), and heated for 5 min (No. 17 papers, 10 min) for detection of the amines. For detection of chloride ion, the chromatograms, dried as mentioned above, were sprayed with 5% aqueous silver nitrate and exposed to ultraviolet light to develop the color. Acetate ion was detected by the lanthanum nitrate reagent (1) after chromatograms on No. 1 paper (acetic acid solvent system only) had been air dried for 96 h at room temperature to remove excess acetic acid. Acetate ion was not detectable in this manner when the hydrochloric acid solvent system was used due to interference by chloride ion with the lanthanum nitrate test. The results of these experiments are given in Table II.

(2) Extended Development

On two separate sheets ($18\frac{1}{4} \times 22\frac{1}{2}$ in.) of unwashed No. 17 paper, 1 mg spots of piperidine and morpholine were each applied as pairs of their hydrochloride and acetate salts and developed for 7 h in a

[3] *Melting points are uncorrected.*

[4] *Microanalyses by J. Helie of these laboratories.*

Can. J. Chem. Downloaded from www.nrcresearchpress.com by 210.87.254.40 on 09/05/12
For personal use only.

Chromatocab using *t*-butanol : acetic acid : water (2:1:1). A strip containing one pair of salt spots was then removed, dried, and sprayed with ninhydrin. The remaining portion of the chromatogram was developed for a further 20 h, following which a second strip was removed and sprayed with ninhydrin. The remaining spots on the unsprayed portion of the chromatogram were removed in a horizontal strip, to which was sewn a new 3MM stirrup and a new long strip of unwashed No. 17 paper. This paper was developed for two additional periods of 20 h following each of which a strip was removed and sprayed with ninhydrin. Upon completion of the final development, each chromatogram contained only acetate spots, i.e. the hydrochlorides had been completely converted to the acetates.

Quantitative Paper Chromatography

(a) Amine Acetate to Amine Hydrochloride Conversion, Chromatography in t-Butanol : 0.5% Hydrochloric Acid (3:1)

Piperidine or morpholine acetate was applied as a 100 mg streak from 20% aqueous solution to the start line of each of two or three sheets ($18\frac{1}{4} \times 22\frac{1}{2}$ in.) of unwashed Whatman No. 17 paper. The papers were developed simultaneously in a Model A 300 Chromatocab by the descending method in *t*-butanol : 0.5% hydrochloric acid (3:1) for 60 h, using a single wick of Whatman 3MM paper as solvent feed. The papers were air dried for removal of the solvent and 1 in. reference strips were cut and sprayed with ninhydrin (0.4% in water-saturated *n*-butanol). The band bearing the salt was removed and eluted chromatographically with water (200 ml). The eluate was taken to dryness *in vacuo* and the residue was sublimed at 1×10^{-3} mm pressure at 110–120° for piperidine hydrochloride and at 80–90° for morpholine hydrochloride. The sublimates were identified by their melting points alone and in admixture with authentic specimens (see Table I) and also by their infrared spectra (KBr pellet). Piperidine and morpholine hydrochlorides were obtained in 97.5% and 97.0% yield respectively.

(b) Amine Hydrochloride to Amine Acetate Conversion, Chromatography in t-Butanol : Acetic Acid : Water (2:1:1)

Experiments were conducted in the same manner as described in (*a*) above except that unwashed, acid-washed (0.01 *N* HCl), and salt-washed (0.01 *N* HCl, Na^+ and Ca^{++}) papers were used; 400–500 mg of piperidine or morpholine hydrochloride was applied per paper, and development was for 40 h in *t*-butanol : acetic acid : water (2:1:1). Since qualitative chromatograms had indicated that the slower-moving hydrochloride band contains some of the acetate, the entire ninhydrin-positive area was eluted with water (400 ml). The eluates were taken to dryness *in vacuo* and the residues were fractionally sublimed at 1×10^{-3} mm pressure. Under these conditions piperidine acetate and hydrochloride sublimed at 40–50° and 110–120° respectively and morpholine acetate and hydrochloride at 35–45° and 80–90° respectively. The sublimates were identified by their melting points, alone and in admixture with authentic specimens, and by their infrared spectra (KBr pellet). Results are given in Table III.

(c) Evidence for the Binding of Piperidinium Ions to the Paper During Chromatography of Piperidine Hydrochloride in Water

Piperidine hydrochloride (300 mg) was applied as a single streak from 10% aqueous solution to a strip of unwashed Whatman No. 17 paper (6.0 × 16.7 in., 100 sq. in.) to one 6 in. edge of which a Whatman 3 MM stirrup and single wick had been affixed. The paper was eluted with freshly boiled distilled water (pH 6.4, 4 × 100 ml) in a nitrogen atmosphere. The unbound salt (290 mg) was all contained in the first 100 ml of eluate and was recovered by sublimation at 1×10^{-3} mm pressure at 100–120°. However, when the residue from the sublimation was taken up in water (10 ml), basified to pH 11–12 with sodium hydroxide, and extracted with ether and the dried ether solution treated with dry hydrogen chloride, a small amount of precipitate resulted. Removal of the ether *in vacuo* followed by sublimation as before gave a further 5.6 mg of piperidine hydrochloride. Further elution of the paper with carbon dioxide saturated water (pH 3.95, 100 ml) followed by evaporation to dryness *in vacuo* furnished an additional 5 mg of piperidine hydrochloride. Identifications were made by comparison of melting points and infrared spectra.

The experiment was repeated using acid-washed, sodium ion washed, and calcium ion washed papers. It was not necessary to resort to basification and ether extraction to recover all of the amine when sodium ion washed or acid-washed papers were used, but was quite essential to effect quantitative recovery in the presence of calcium ions. An aliquot of the eluate containing the unbound salt was removed and (*a*) titrated to pH 6.3 with 0.02 *N* sodium hydroxide in a carbon dioxide free atmosphere to determine the acid liberated during binding of the salt, or (*b*) analyzed for sodium ion content by the micro magnesium uranyl acetate method (28), or (*c*) analyzed for calcium ion content by the complexon method (ref. 28, p. 117). Results are given in Table IV.

Acid-washed Whatman No. 17 paper (100 sq. in.) was dispersed in 0.001 *N* hydrochloric acid by mechanical stirring and transferred to a chromatographic column 3.1 cm in diameter. After elution with freshly boiled distilled water until the pH of influent and effluent were identical (6.4), piperidine hydrochloride (300 mg) was added and the column was washed with freshly boiled distilled water (300 ml) to remove the unbound salt. During this process the pH of the effluent first decreased rapidly to 4.10, then rose again slowly to 6.86. Elution was resumed with carbon dioxide saturated distilled water (500 ml) to remove the bound salt and the latter was recovered in the usual manner, yielding 14.1 mg of piperidine hydrochloride.

Can. J. Chem. Downloaded from www.nrcresearchpress.com by 210.87.254.40 on 09/05/12
For personal use only.

Column Chromatography on Amberlite IRC-50 Resin with Piperidine Hydrochloride

(a) With Amberlite IRC-50 (H^+)

An Amberlite IRC-50 (H^+) column (7.5 × 0.75 cm) containing 3 ml (9 meq) of the resin was prepared and washed with distilled water at the rate of 10 drops per min until the pH of influent and effluent were identical (5.8). Piperidine hydrochloride (244 mg, 2 mmoles in 10 ml of distilled water) was started through the column, followed by distilled water. The pH of the effluent dropped rapidly to 2.0, then rose gradually to 6.4, at which point the fraction was cut (20 ml) and collection was resumed in a second receiver. As elution was continued, the pH rose gradually to 6.7, then fell again and leveled off at 6.0. This eluate was designated as fraction 2 (70 ml). The column was then eluted with 0.01 *N* hydrochloric acid until the effluent pH decreased to 2.0 (20 ml, fraction 3). The fractions were taken to dryness *in vacuo* after acidification to pH 1 with hydrochloric acid and the residues were sublimed *in vacuo* yielding 244, 4.1, and 12 mg of piperidine hydrochloride respectively. Identifications were made by comparison of melting points and infrared spectra.

(b) With Amberlite IRC-50 (Na^+)

An Amberlite IRC-50 (Na^+) column containing 3 ml (9 meq) of the resin was prepared and washed with distilled water. Piperidine hydrochloride (244 mg, 2 meq) was added in 10 ml of distilled water and the column was washed with distilled water (50 ml). The eluate was taken to dryness *in vacuo* yielding 42 mg of piperidine hydrochloride. The column was washed with 0.1 *N* hydrochloric acid until the pH of the effluent decreased to 1. The solution thereby collected (150 ml) was evaporated to dryness *in vacuo*, yielding 196 mg of piperidine hydrochloride.

(c) With Amberlite IRC-50 (Ca^{++})

The above-described experiment was repeated using 3 ml (9 meq) of Amberlite IRC-50 (Ca^{++}) resin. The aqueous eluate furnished piperidine hydrochloride (161 mg) by sublimation as in the experiment described above but the acidic eluate failed to give any sublimate under the normal conditions used. However, when the dry residue was dissolved in water (10 ml), basified, and extracted with ether, and the extract dried and treated with dry hydrogen chloride, a colorless precipitate was obtained. Removal of the ether *in vacuo*, followed by sublimation *in vacuo* yielded 45.6 mg of piperidine hydrochloride. Similar treatment of the residue from vacuum sublimation of the aqueous eluate furnished a further 30.7 mg of piperidine hydrochloride. Results of all the experiments with Amberlite IRC-50 resin are given in Table V.

ACKNOWLEDGMENTS

The authors are indebted to Professors C. B. Purves and J. K. N. Jones for helpful discussions.

REFERENCES

1. R. A. B. Bannard and A. A. Casselman. Can. J. Chem. **41**, 92 (1963).
2. G. F. Davidson and T. P. Nevell. J. Textile Inst. **39**, T59 (1948).
3. J. B. Schute. Nature, **171**, 839 (1953).
4. K. H. Schroder. Chemiker Ztg. **81**, 558 (1957).
5. G. Ackermann and G. Kruger. Z. Anal. Chem. **191**, 17 (1962).
6. W. F. Pickering. J. Chromatog. **4**, 477 (1960).
7. J. Yamamoto and T. Miyata. Seni-i Gakkaishi, **15**, 805 (1959); Chem. Abstr. **54**, 1843*h* (1960).
8. G. F. Davidson. J. Textile Inst. **39**, T65 (1948).
9. M. A. Millett, J. S. Schultz, and J. F. Saeman. Tappi, **41**, 560 (1958).
10. W. K. Wilson and J. Mandel. Tappi, **44**, 131 (1961).
11. C. B. Purves. Cellulose and cellulose derivatives. *In* High polymers. Vol. V. *Edited by* E. Ott. Interscience Publishers, Inc., New York. 1946. p. 123.
12. R. Kunin and R. E. Barry. Ind. Eng. Chem. **41**, 1269 (1949).
13. A. A. Casselman, R. Greenhalgh, H. H. Brownell, and R. A. B. Bannard. Can. J. Chem. **38**, 1277 (1960).
14. H. K. Hall. J. Am. Chem. Soc. **79**, 5441 (1957).
15. R. Kunin. Ion exchange resins. 2nd ed. John Wiley and Sons, Inc., New York, N.Y. 1958. Chap. 3.
16. C. Calmon and T. R. E. Kressman. Ion exchangers in organic and biochemistry. Interscience Publishers, Inc., New York, N.Y. 1957. p. 507.
17. J. C. Winters and R. Kunin. Ind. Eng. Chem. **41**, 460 (1949).
18. A. A. Morton. Laboratory technique in organic chemistry. McGraw-Hill Book Co., Inc., New York, N.Y. 1938. p. 4.
19. A. Skita and W. Brunner. Ber. **49**, 1597 (1916).
20. E. B. R. Prideaux and R. N. Coleman. J. Chem. Soc. 1346 (1936).
21. P. Sabatier and J. B. Senderens. Compt. Rend. **138**, 457 (1904).
22. J. F. Carson. J. Am. Chem. Soc. **75**, 4337 (1953).
23. B. Reichert and W. Dornis. Arch. Pharm. **282**, 100 (1944).
24. R. Boudet. Bull Soc. Chim. France, 390 (1948).
25. L. Knorr. Ber. **22**, 2081 (1889).
26. J. Cymerman-Craig, W. P. Rogers, and M. E. Tate. Australian J. Chem. **9**, 397 (1956).
27. H. H. Brownell, J. G. Hamilton, and A. A. Casselman. Anal. Chem. **29**, 550 (1957).
28. C. J. Van Nieuwenburg and J. W. L. Van Ligten. Quantitative chemical micro-analysis. Elsevier Publishing Co., New York. 1963. p. 68.

Can. J. Chem. Downloaded from www.nrcresearchpress.com by 210.87.254.40 on 09/05/12
For personal use only.

SIMULTANEOUS POLAROGRAPHIC DETERMINATION OF SMALL AMOUNTS OF BISMUTH AND LEAD IN COPPER-BASE ALLOYS

C. H. McMaster

Mineral Sciences Division, Department of Mines and Technical Surveys, Ottawa, Canada

Received September 22, 1964

ABSTRACT

The extraction of metal diethyldithiocarbamate complexes into chloroform from an alkaline solution containing cyanide and citrate ions is a convenient means of separating small amounts of bismuth and lead from copper and uranium, and from the elements normally found in copper-base alloys. After the separation, bismuth and lead are determined polarographically using an acidic tartrate solution as the supporting electrolyte.

The method is applicable to the determination of bismuth and lead, in the concentration range from 0.0005–0.05%, in copper-base alloys of widely different composition.

INTRODUCTION

Small amounts of bismuth and lead seriously affect the hot workability of copper and brass by producing a characteristic known as "hot shortness". Generally, this condition exists when the impurity has a low melting point and is insoluble in the base material; during cooling the impurity segregates at the grain boundaries and causes cracking. As little as 0.005% bismuth and 0.02% lead can cause hot shortness in brass (1). During an investigation into the uses of depleted uranium, carried out by the Physical Metallurgy Division of the Mines Branch and the Canadian Uranium Research Foundation, it was found that uranium metal added to molten brass baths acts as a scavenger for bismuth and lead and results in the restoration of normal hot working conditions (2). In the course of this project, samples of brass containing up to 0.5% uranium were submitted for bismuth and lead analyses.

Polarography is a particularly attractive technique for the analysis of small amounts of bismuth and lead as the two metals can be determined simultaneously by using a slightly acidic tartrate solution as the supporting electrolyte (3). In this medium copper and uranium interfere and must be removed by chemical separation. The separation technique must result in complete elimination of uranium since the reduction of uranyl ion occurs at the same potential as lead. Copper is reduced at a more positive potential and interferes by limiting the amounts of bismuth and lead that can be determined with a conventional direct current polarograph. It is necessary, therefore, to decrease the amount of copper to about the same order as the bismuth and lead.

The usual methods of separation, involving precipitation of the hydroxides from ammoniacal solution (4) or coprecipitation with manganese dioxide (5), are not applicable in the present case as part or all of the uranium remains with the bismuth and lead. Uranium also interferes in the methods proposed by Eve and Verdier (6) in which bismuth is precipitated with ammonium carbonate and lead is separated from copper by controlled potential electrolysis.

A colorimetric procedure for the determination of bismuth is based on the extractability of the yellow-colored complex of bismuth diethyldithiocarbamate with chloroform or carbon tetrachloride (7, 8). Many interfering elements are rendered innocuous by carrying out the extraction from an alkaline solution containing cyanide ions and citrate or tartrate ions. Under these conditions lead diethyldithiocarbamate is also extracted. The utilization

Can. J. Chem. Downloaded from www.nrcresearchpress.com by 210.87.254.6 on 09/05/12
For personal use only.

of this extraction procedure as a means of isolating small amounts of bismuth and lead from cast iron, prior to the polarographic determination of the two elements, is described by Rooney (9). After extraction of the bulk of the iron with ethyl acetate, bismuth and lead are separated from the remaining iron, and other impurities by extraction of the diethyldithiocarbamates.

In the work described herein, the diethyldithiocarbamate separation technique is applied to the polarographic determination of small amounts of bismuth and lead in samples of brass containing uranium. Investigations also show that the method is applicable to copper-base alloys of widely different composition.

EXPERIMENTAL

Apparatus

Polarograph: Leeds and Northrup Electrochemograph, Type E.

Polarographic cell: An H-type cell was used with a saturated calomel electrode (s.c.e.) serving as the reference electrode, and a dropping mercury electrode as the indicating electrode (10). All polarographic measurements were made at 25 ± 0.1 °C. pH meter: Leeds and Northrup.

Reagents

Ammonium citrate: 40% (w/v) aqueous solution.

Potassium cyanide: 20% (w/v) aqueous solution. The salt used to prepare this solution should contain little or no sulfide. Analar potassium cyanide (British Drug Houses) was found to be suitable.

Sodium diethyldithiocarbamate: 0.1% (w/v) aqueous solution (freshly prepared).

Wash solution: Mix 50 ml of 40% ammonium citrate solution with 50 ml of 20% potassium cyanide solution and dilute with water to about 425 ml. Adjust the pH to 10.1 with ammonium hydroxide and make up to 500 ml with water.

Chloroform: c.p. grade.

Supporting electrolyte: Dissolve 23 g sodium tartrate in about 150 ml of water, adjust the pH to 4.5 with hydrochloric acid, add 2 ml of 0.1% Triton X-100, and dilute to 200 ml with water.

Procedure

Weigh out 1 g of the sample and dissolve in 5 ml of hydrochloric acid and about 10 ml of 30% hydrogen peroxide added in small portions. Heat the solution in a covered beaker to drive off the excess peroxide, and evaporate to a small volume. Cool and add 25 ml of ammonium citrate solution. Adjust the pH to 10.1 with ammonium hydroxide. Add 25 ml of potassium cyanide solution and transfer quantitatively to a 250 ml separatory funnel. Add 20 ml of sodium diethyldithiocarbamate solution and mix. Add 10 ml of chloroform, shake for 1 min, allow the layers to separate, and transfer the chloroform layer to a 125 ml separatory funnel containing 50 ml of wash solution. Shake for about 15 s, allow the layers to separate, and transfer the chloroform layer to a 50 ml beaker. Carry out a total of three extractions in identical fashion, and evaporate the combined fractions to dryness. Add 3 ml of nitric acid and 3 ml of perchloric acid, cover the beaker, and heat until fumes of perchloric acid are evolved. Remove the cover and evaporate to dryness. Cool and dissolve the residue in exactly 5 ml of supporting electrolyte solution, added from a pipette, and transfer to a polarographic cell. Deaerate with nitrogen gas and electrolyze at the dropping mercury electrode from 0.1 to 0.7 V.

In 0.5 M tartrate solution of pH 4.5 bismuth is reduced at −0.29 V and lead at −0.48 V vs. s.c.e.

RESULTS AND DISCUSSION

Dissolution of Sample

The mixture of hydrochloric acid and hydrogen peroxide, used to dissolve the samples, was selected in order to prevent the precipitation of metastannic acid when dealing with copper-base alloys containing tin.

Samples containing appreciable amounts of silicon, such as silicon bronzes, should be treated with a few drops of hydrofluoric acid to achieve complete dissolution.

Extraction

The extraction of bismuth and lead diethyldithiocarbamates with chloroform is quantitative at any pH between 9 and 10.5. The extraction at pH values outside of this range was not investigated.

The extraction of bismuth and lead is complete up to at least 0.05% of each, using the

Can. J. Chem. Downloaded from www.nrcresearchpress.com by 210.87.254.6 on 09/05/12
For personal use only.

quantities of sodium diethyldithiocarbamate and chloroform specified in the procedure. Above this value it is preferable to decrease the size of the sample. An excess of sodium diethyldithiocarbamate does not present any problems as the reagent is not extracted above a pH of 8 (11).

Washing of the chloroform layer was implemented as a means of obtaining more complete isolation of bismuth and lead from copper. The chloroform extract, before washing, was found to contain as much as 0.05% copper; after washing, the amount of copper was decreased to less than 0.0005%.

Inteferences

The extraction procedure provides a satisfactory separation of bismuth and lead from copper and uranium. Typical recoveries, obtained with synthetic samples, are shown in Table I.

TABLE I

Recovery of bismuth and lead

Composition of synthetic sample	Bismuth (%)		Lead (%)	
	Added	Found	Added	Found
Cu, 70%, Zn, 29.5%, U, 0.5%	0.0020	0.0021	0.020	0.020
	0.0050	0.0051	0.010	0.011
	0.010	0.010	0.0050	0.0052
	0.020	0.020	0.0020	0.0021

The combination of cyanide and citrate ions prevents the precipitation or extraction of a large number of elements including the major alloying constituents, viz. silver, zinc, aluminium, tin, manganese, iron, and nickel. Iron appears to be partially extracted as evidenced by the dark-amber color of the initial chloroform extract. This coloration, however, disappears on washing the organic layer.

Of the many elements associated with copper, only antimony(III) and tellurium(IV) are extracted from an alkaline cyanide solution (11).

Trivalent antimony forms a white precipitate with diethyldithiocarbamate that is extracted by chloroform at pH 9–9.5. In the present procedure antimony is oxidized to the pentavalent state during dissolution of the sample and does not interfere.

Tellurium(IV) is extracted completely from an alkaline cyanide solution at pH 8.5. Tests carried out in this laboratory showed that tellurium is partially extracted up to pH 9.6, but is without effect at pH 10–10.5. Since tellurium interferes with the polarographic determination of bismuth and lead, it is essential that the extraction be performed at a pH of 10 or above.

Application to Copper-Base Alloys

There appears to be a lack of standard copper-base alloys containing certificate values for both bismuth and lead. Three bronze samples and a copper–nickel–zinc alloy from the National Bureau of Standards contained lead in the desired range, but none of the samples contained bismuth. Instead of preparing completely synthetic samples, the above-mentioned N.B.S. alloys were used and known amounts of bismuth were added to each. The bismuth was added during dissolution of the sample and was carried through the entire procedure. Table II shows the results obtained with the N.B.S. alloys and with a sample of cupro-nickel (British Chemical Standards) in which the bismuth was reported as $< 0.0005\%$ and the lead as $< 0.01\%$.

Can. J. Chem. Downloaded from www.nrcresearchpress.com by 210.87.254.6 on 09/05/12
For personal use only.

TABLE II

Analysis of standard copper-base alloys

Description of sample	Lead (%)	Bismuth (%)	
	Found	Added	Found
N.B.S. Aluminum bronze, 164*a*, Pb = 0.04% (Provisional Certificate)	0.036	Nil	Nil
	0.036	0.0020	0.0021
	0.038	0.010	0.010
	0.036	0.020	0.021
N.B.S. Cast bronze, 52*c*, Pb = 0.011% (range: 0.009–0.015%)	0.011	Nil	Nil
	0.011	0.0020	0.0021
	0.012	0.010	0.011
	0.012	0.020	0.021
N.B.S. Silicon bronze, 158, Pb = 0.004% (range: 0.002–0.005%)	0.005	Nil	Nil
	0.005	0.0020	0.0021
	0.006	0.010	0.010
	0.007	0.020	0.020
N.B.S. Cu–Ni–Zn, 157*a*, Pb = 0.03% (range: 0.029–0.043%)	0.033	Nil	Nil
	0.036	0.0020	0.0020
	0.036	0.010	0.011
	0.039	0.020	0.020
B.C.S. Cupro-nickel, 180–1, Pb < 0.01% (0.003–0.010%) Bi < 0.0005% (0.0002–0.0005%)	0.008	Nil	0.0005

TABLE III

Composition of standard copper-base alloys (%)

Sample	Cu	Zn	Ni	Al	Sn	Fe	Si	Mn
N.B.S. 164*a*	82.25	—	3.72	9.59	—	4.05	—	0.22
N.B.S. 52*c*	89.25	2.12	0.76	—	7.85	—	—	—
N.B.S. 158	90.86	2.07	—	0.54	0.97	1.48	2.72	1.31
N.B.S. 157*a*	58.60	29.06	11.82	—	—	0.17	—	0.18
B.C.S. 180–1	67.36	—	30.85	—	—	0.82	—	0.81

The copper-base alloys listed in Table II contain wide ranges of alloying elements and, thus, are ideally suited to illustrate the application of the proposed method. Table III shows the percentages of the constituents that are present in these alloys in amounts greater than 0.1%.

The procedure, as described in this report, can be used for the determination of bismuth and lead in the concentration range from 0.0005–0.05%. Reagent blanks are negligible at 0.002% and above, but should be taken into consideration at lower concentrations. The elements normally found in copper-base alloys do not interfere in the proposed method.

REFERENCES

1. W. W. Kee. J. Inst. Metals, **82**, 307 (1954).
2. R. Thomson and J. O. Edwards. Metal Ind. London, **102**, 82 (1963).
3. J. J. Lingane. Ind. Eng. Chem. Anal. Ed. **16**, 147 (1944).
4. D. T. Englis and B. B. Burnett. Anal. Chim. Acta, **13**, 574 (1955).
5. Y. L. Yao. Ind. Eng. Chem. Anal. Ed. **17**, 114 (1945).
6. A. J. Eve and E. T. Verdier. Anal. Chem. **28**, 537 (1956).
7. J. Kinnunen and B. Wennerstrand. Chemist-Analyst, **43**, 88 (1954).
8. K. L. Cheng, R. H. Bray, and S. W. Melsted. Anal. Chem. **27**, 24 (1955).
9. R. C. Rooney. Analyst, **83**, 83 (1958).
10. J. J. Lingane and H. A. Laitinen. Ind. Eng. Chem. Anal. Ed. **11**, 504 (1939).
11. E. B. Sandell. Colorimetric determination of traces of metals. 3rd ed. Interscience Publishers, Inc., New York. 1959. p. 192.

Can. J. Chem. Downloaded from www.nrcresearchpress.com by 210.87.254.6 on 09/05/12
For personal use only.

Can. J. Chem. Downloaded from www.nrcresearchpress.com by 210.87.254.5 on 09/05/12
For personal use only.

PYRROLE CHEMISTRY

IV. THE PREPARATION AND SOME REACTIONS OF BROMINATED PYRROLE DERIVATIVES

HUGH J. ANDERSON AND SHU-FAN LEE
Department of Chemistry, Memorial University of Newfoundland, St. John's, Newfoundland

Received September 21, 1964

ABSTRACT

Methyl 2-pyrrolecarboxylate and 2-pyrrolecarboxaldehyde have been brominated under a variety of conditions and the isomer ratios determined. The products have been identified as the 4-bromo, 5-bromo, and 4,5-dibromo derivatives and their structures proved. It has been shown that the bromine group in these products is not easily displaced by nucleophiles although this has been accomplished with the cyanide ion. The bromine has been removed easily by catalytic hydrogenation.

In our survey of the reactions of relatively simple pyrrole derivatives (1) it appeared likely that bromination might prove both useful and interesting. A selection of types of brominating agents including molecular bromine, the bromonium ion, and the bromine atom is available (2). In turn it might prove possible to replace the bromine group by others such as cyanide or methoxyl as has been done in the thiophene and furan series (3, 4, 5). The most satisfactory starting materials appeared to be methyl 2-pyrrolecarboxylate and 2-pyrrolecarboxaldehyde. The electron-withdrawing groups would provide a 4-directing effect. Thus a mixture of 4- and 5-isomers would be formed (1, 6) which might be made to favor one or the other position by a choice of the type of brominating agent. In addition, both ester and aldehyde can be converted to the acid group which then might be removed by decarboxylation. Finally, the deactivation of an electron-withdrawing group would be necessary to allow the isolation of monobrominated products in reasonable yields (7). From the reaction products we isolated 4-bromo, 5-bromo, and 4,5-dibromo derivatives for both the 2-ester and the 2-aldehyde. A small amount of the 3,4,5-tribromo-2-ester (8) was also found in one reaction. Methyl 4,5-dibromo-2-pyrrolecarboxylate (9) has been reported previously.[1]

Identification of the monobrominated-2-esters (I) was accomplished by a series of reactions. First, nucleophilic displacement of the bromine group was carried out using cuprous cyanide in hot dimethyl sulfoxide. The yields of methyl 4- and 5-cyano-2-pyrrolecarboxylate (II) were not good but in each case a single product was obtained and characterized. Then methyl 2-pyrrolecarboxylate was formylated by the Vilsmeier-Haack technique (3) producing a mixture (III), containing mostly the 4-formyl-2-ester along with some of the 5-formyl-2-ester. Pinder (10) has formylated the corresponding ethyl ester but obtained a considerably greater proportion of 5-formylation. Each formyl-2-ester was then subjected to two operations. First, it was oxidized (IV) and esterified (V) to the known methyl 2,5- or 2,4-pyrroledicarboxylate (11), thus proving the orientation of substituents. A second portion of each formyl-2-ester was converted to the oxime (VI), dehydrated to the corresponding 4- or 5-cyano-2-ester and used for mixed melting point and comparison of infrared spectrum with the products (II) obtained above. Further

[1]*Dr. R. W. Rickards of the University of Manchester has kindly informed us that he and P. Hodge have brominated the 2-ester with bromine in acetic acid and obtained and identified the same products. The physical properties of the products are in agreement with ours.*

bromination of either monobrominated ester led to the same dibrominated product. The same was true for the monobrominated aldehydes. The monobromo-2-aldehydes were oxidized and esterified to the corresponding monobromo-2-esters (I) for identification. The dibromo-2-aldehyde was treated similarly.

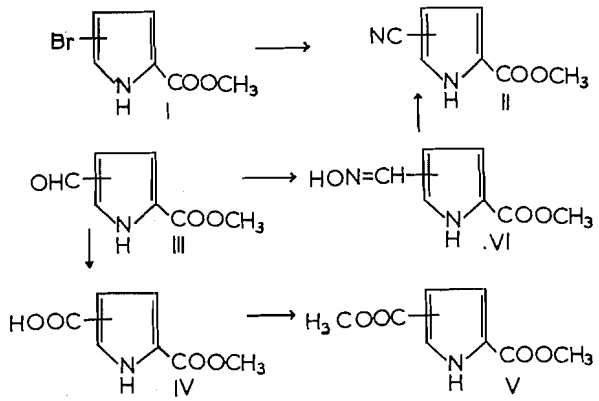

In addition, the nuclear magnetic resonance (n.m.r.) spectra of the brominated esters and aldehydes had already provided quite adequate identification. As has been observed for the benzene series (12), bromination does not greatly alter the positions of the signals of the remaining aromatic protons from those of the parent compounds. These results will be discussed in a forthcoming paper.

After isolation of all the pure substances from the bromination reactions using column chromatography on alumina and fractional crystallization, further trials were analyzed by gas–liquid partition chromatography. A series of trials with known mixtures showed that the triangulation method of analysis could be applied to the gas chromatograms with an accuracy of about 2%. The results were converted to mole % and are recorded in the tables. It was soon found that from a preparative point of view bromination in carbon tetrachloride, with a trace of iodine, was by far the best reaction. No other method approached the greater than 90% conversions possible for the ester. Although the acetic acid reaction was satisfactory the work-up was more laborious.

Several conclusions may be drawn from Table I, which lists a representative selection from a large number of trials on ester and aldehyde. Bromination at the 4-position predominates at room temperature and below, where the 4- : 5- substitution ratio is usually from 6:1 to 10:1. At the boiling point of carbon tetrachloride the attack is much less selective and the amount of 5-bromo product present approaches that of the 4-bromo. The former may then be isolated easily by column chromatography. Increasing the relative amount of bromine raises the percentage of dibrominated product and may produce almost a quantitative yield of it if desired. Conversions are generally lower for the aldehyde brominations than for those of the ester. There is little destruction of the pyrrole nucleus under these conditions.

Of the variety of other reagents listed in Table II none proved to be a selective reagent for attack at the 5-position. The only satisfactory procedures found by us for obtaining 5-bromo derivatives involve the most vigorous reagents and conditions. Under these circumstances the amounts of 4- and 5-bromination are about equal. The free radical reagent N-bromosuccinimide in carbon tetrachloride, with some benzoyl peroxide, was equally random. No 3-bromination was detected in any of our experiments.

Can. J. Chem. Downloaded from www.nrcresearchpress.com by 210.87.254.5 on 09/05/12
For personal use only.

TABLE I

Brominations in carbon tetrachloride

t (min)	Temp.	Conversion*	4-Bromo*	5-Bromo*	4,5-Dibromo*
		(*a*) Methyl 2-pyrrolecarboxylate			
90	0°	74.9	68.4	6.5	—
10	28°	69.6	58.4	9.5	1.7
30	28°	84.9	74.1	7.6	3.2
60	28°	96.9	83.1	11.9	1.9
90	28°	97.6	82.8	12.5	2.3
90	70°	84.3	46.5	31.4	6.4
120	28°	100.0†	15.6	2.3	82.1
20	70°	100.0†	49.0	38.1	12.9
90	70°	100.0†	46.3	35.0	18.7
120	28°	100.0‡	2.0	—	98.0
		(*b*) 2-Pyrrolecarboxaldehyde			
90	0°	62.8	60.7	2.1	—
90	28°	74.7	62.3	11.0	1.4
90	70°	66.0	26.0	24.0	16.0
120	28°	100.0§	5.2	0.4	94.4

*Values in mole %, mole ratio 1:1 (except †, ‡, and §).
†Mole ratio ester : bromine = 1:1.25.
‡Mole ratio ester : bromine = 1:2.
§Mole ratio aldehyde : bromine = 1:2.

TABLE II

Bromination of methyl 2-pyrrolecarboxylate*

Reagent†	Conversion	4-Bromo	5-Bromo	4,5-Dibromo
(*a*) Br_2/Fe	69.6	47.5	16.7	5.4
(*b*) $Br_2/AlCl_3$	64.5	29.1	29.7	5.7
(*c*) Br_2/dioxane	68.0	38.0	16.4	13.6
(*d*) Br_2/HOAc	36.3	12.3	3.3	20.7
(*e*) NBS/peroxide	40.7	15.3	14.2	11.2
(*f*) $Br_2/AgClO_4/HClO_4$	35.3	14.9	5.2	15.2
(*g*) $HOBr/H_3O^+$	6.2	4.7	0.4	1.1
(*h*) Pyridinium bromide perbromide	55.7	49.1	1.8	4.8
(*i*) NaOBr/NaOH	22.2	20.5	1.7	—
(*j*) CuBr/DMF	6.3	3.3	3.0	—

*Values in mole %, mole ratio ester : reagent = 1:1 throughout.
†See Experimental for description of reagent, time, and temperature.

The bromonium ion from acidified hypobromous acid (13) or from bromine and silver perchlorate in perchloric acid (prepared analogously to the chloronium ion of ref. 14), was neither very selective nor very successful. Basic reagents such as bromine in dilute aqueous sodium hydroxide and pyridinium bromide perbromide in pyridine (15) favored 4-substitution fairly strongly. The latter reagent was quite successful for the preparation of the 4-bromo-2-ester, although less so for the corresponding aldehyde. The only similar monobrominated pyrrole has been prepared by Ciamician (16) through the action of bromine in acetic acid on 2-acetylpyrrole, and later identified as the 4-bromo derivative by n.m.r. (17). The same compound has also been obtained by the action of the dioxane–bromine complex (18). It seems surprising that although some dibrominated product was isolated none of the 5-isomer was found. The contrast with the thiophene series, where bromination of the 2-aldehyde (19) and the 2-acid (20) using bromine produced the 5- but not the 4-bromo derivative, points up the selectivity of the bromination reaction.

It was found in general that nucleophilic substitution of the bromine in these compounds

Can. J. Chem. Downloaded from www.nrcresearchpress.com by 210.87.254.5 on 09/05/12
For personal use only.

Can. J. Chem. Downloaded from www.nrcresearchpress.com by 210.87.254.5 on 09/05/12
For personal use only.

was difficult. The displacement of bromine by cyanide in the ester series was not a satisfactory conversion. This is in agreement with results reported for thiophene derivatives (3). Attempts to replace the bromine with methoxyl by refluxing the monobromo-2-ester with sodium methoxide in methanol for 30 h were unsuccessful. It appears that much more drastic conditions would be necessary to make this conversion successful. The reaction takes place moderately well in the thiophene and furan series (4, 5).

It was found that the bromines could be removed from the ring by reduction. Catalytic hydrogenation was much more successful than zinc and acetic acid or other chemical means. The 5-bromine was removed more rapidly than the 4-bromine. It was thus possible to reduce the 4,5-dibromo compounds to a mixture in which the 4-bromo compound predominated. However, this seemed to have little preparative value since some complete reduction also took place. Bromine was less readily removed from the aldehydes than from the corresponding esters. Although the corresponding bromo-2-acids were obtained, from the ester and from the aldehyde, it was found that their purification was very difficult and they rapidly blackened. Various attempts to isolate the products of decarboxylation using a variety of conditions were all unsuccessful. These included dry distillation from a mixture with copper–bronze and from a mixture with soda–lime, as well as distillation from quinoline and copper powder.

EXPERIMENTAL

General

Melting points were determined on a Fisher–Johns apparatus and are uncorrected. Infrared spectra were recorded by a Perkin–Elmer 237-B grating spectrophotometer using the potassium chloride disc technique (2 mg of sample in 200 mg KCl). Ultraviolet spectra were determined with a Beckman DK-2A recording spectrophotometer at a concentration of 10 mg per liter in ethanol (95%). Elemental analyses were determined by Alfred Bernhardt, Mülheim (Ruhr), Germany.

Analyses of reaction mixtures were carried out by means of gas–liquid partition chromatography using a Beckman GC-2A gas chromatograph, equipped with an 18 in. column (No. 70008) packed with Apiezon L on fire brick. For the pyrrole esters operation was at 220° using helium as carrier gas at 20 p.s.i.g. inlet pressure. Retention times established for pure compounds were: methyl 2-pyrrolecarboxylate, 0.9 min; 5-bromo derivative, 2.1 min; 4-bromo derivative, 3.5 min; 4,5-dibromo derivative, 6.5 min. For the pyrrole aldehydes operation was at 190° using helium as carrier gas at 20 p.s.i.g. inlet pressure. Retention times established for pure compounds were: 2-pyrrolecarboxaldehyde, 1.3 min; 5-bromo derivative, 3.3 min; 4-bromo derivative, 4.7 min; 4,5-dibromo derivative, 12.5 min.

Starting Materials

Methyl 2-pyrrolecarboxylate was prepared and purified as described in ref. 1. 2-Pyrrolecarboxaldehyde was prepared by the method of Silverstein, Ryskiewicz, and Willard (21).

General Procedure for Bromination with Bromine

In a 100 ml three-necked round bottom flask equipped with a sealed stirrer, a condenser, and a dropping funnel, was placed 0.004 mole of starting material along with 2–3 mg of iodine dissolved in 30 ml of carbon tetrachloride. A solution of bromine (0.004 mole) in 10 ml of carbon tetrachloride was added dropwise, with stirring. The mixture was neutralized with 20% sodium carbonate solution, the layers separated, and the aqueous layer extracted with ether. The combined organic layers were dried over sodium sulfate and the solvents were removed by flash evaporation. The residue was injected into the gas chromatograph in ether solution. The results of the analyses, together with conditions of time, temperature, and concentration are listed in Table I.

Isolation of Bromination Products

The solid material, after flash evaporation of solvents, was chromatographed on neutral alumina (Woelm, No. 1), following the progress of elution by means of gas chromatography. Homogeneous fractions were isolated, and the solids sublimed and recrystallized from petroleum pentanes to obtain purified products.

Methyl 4-bromo-2-pyrrolecarboxylate, m.p. 98–99°. Calcd. for $C_6H_6NO_2Br$: C, 35.32; H,2.96; N, 6.87; Br, 39.16. Found: C, 35.52; H, 2.93; N, 7.01; Br, 39.21. Methyl 5-bromo-2-pyrrolecarboxylate, m.p. 102–103°. Calcd. for $C_6H_6NO_2Br$: C, 35.32; H, 2.96; N, 6.87; Br, 39.16. Found: C, 35.15; H, 3.07; N, 6.55; Br 39.31. Methyl 4,5-dibromo-2-pyrrolecarboxylate, m.p. 158–159°. Calcd. for $C_6H_5NO_2Br_2$: C, 25.47; H, 1.78; N. 4.95; Br, 56.49. Found: C, 25.30; H, 1.65; N, 4.86; Br, 56.71. 4-Bromo-2-pyrrolecarboxaldehyde, m.p. 123–124°. Calcd. for C_5H_4NOBr: C, 34.51; H, 2.32; N, 8.05; Br, 45.93. Found: C, 34.68; H, 2.39; N, 7.87;

Can. J. Chem. Downloaded from www.nrcresearchpress.com by 210.87.254.5 on 09/05/12
For personal use only.

Br, 46.04. 5-Bromo-2-pyrrolecarboxaldehyde, m.p. 93–94°. Calcd. for C_5H_4NOBr: C, 34.51; H, 2.32; N, 8.05. Found: C, 34.67; H, 2.51; N, 7.80. 4,5-Dibromo-2-pyrrolecarboxaldehyde, m.p. 155–156°. Calcd. for $C_5H_3NOBr_2$: C, 23.75; H, 1.11; N, 5.54. Found: C, 23.66; H, 1.43; N, 5.71.

Bromination with Other Reagents

In each trial 0.004 mole of starting material was treated with 0.004 mole of the brominating reagent. The reaction time was usually judged on the basis of a color change. Working-up involved standard procedures for the removal of by-products, depending on the reagent. This was followed by flash evaporation of the solvent, and gas chromatographic analysis. The results are listed in Table II. (*a*) The bromination in carbon tetrachloride was carried out at 70° for 60 min using a small amount of iron powder as catalyst. (*b*) The bromination was carried out in carbon tetrachloride at room temperature for 120 min in the presence of an excess (0.008 mole) of anhydrous aluminium chloride. (*c*) The bromine–dioxane complex (22) was used in dioxane solution at 60° for 30 min. (*d*) Bromination was carried out at 60° in a solution of 30 ml glacial acetic acid containing 0.75 g sodium acetate. (*e*) N-Bromosuccinimide was used at the boiling point of the carbon tetrachloride solution and in the presence of about 0.1 g benzoyl peroxide. Reaction time was 90 min. (*f*) The bromonium ion was prepared by the action of bromine on silver perchlorate (0.012 mole) in aqueous perchloric acid solution (3 ml, 72%). The reaction proceeded at room temperature over 30 min. (*g*) Hypobromous acid solution (0.079 *N*) was prepared by the action of freshly prepared mercuric oxide on bromine in an excess of water (23). The reaction was carried out at room temperature in the presence of 72% perchloric acid (0.10 mole) over 30 min (13). (*h*) Pyridinium bromide perbromide was used in pyridine solution at room temperature over 1 h (15). (*i*) The sodium hypobromite solution was prepared by dissolving bromine in 40 ml 6 *N* aqueous sodium hydroxide. (*j*) The mixture of cupric bromide and starting material together with 0.0005 mole of lithium bromide was heated at 150° for 2 h in 25 ml of dimethylformamide (24).

Preparation of Brominated Acids and Their Esterification

(*a*) The brominated ester (0.008 mole) was refluxed with a mixture of 25 ml of 20% aqueous potassium hydroxide and 20 ml of methanol for 2 h. The methanol was removed under vacuum and unreacted ester extracted with ether. The aqueous layer was acidified with dilute hydrochloric acid and extracted with ether. After drying, the ether solution was evaporated and the crude solid was sublimed and recrystallized.

(*b*) The brominated aldehyde (0.0002 mole) in 2 ml of ethanol was added to a suspension of silver oxide (from 50 mg of silver nitrate, 5 ml of water, and 10 ml of 1 *N* sodium hydroxide solution). The mixture was shaken mechanically for 1 h at room temperature and filtered (25). The filtrate was acidified and extracted with ether. The extract was dried and the product was isolated by evaporation.

Products obtained by methods (*a*) and (*b*) were: 4-bromo-2-pyrrolecarboxylic acid, m.p. 155–165°; 5-bromo-2-pyrrolecarboxylic acid, which decomposed in air after a short time; 4,5-dibromo-2-pyrrolecarboxylic acid, m.p. 165–175°. All attempts to purify these compounds caused extensive decomposition.

The addition of an ethereal solution of diazomethane (26) to the ethereal solution obtained by method (*b*), followed by keeping overnight at room temperature converted the crude acids directly to the corresponding esters. The products were proved identical to those from direct bromination of the 2-ester by mixed melting points and comparison of infrared spectra.

Reductive Removal of Bromine

(*a*) A solution of methyl 4,5-dibromo-2-pyrrolecarboxylate (0.004 mole) in 30 ml of glacial acetic acid was refluxed gently while zinc dust (0.001 mole) was added slowly. After a further 3 h heating the solution was cooled, neutralized with base, and extracted with ether. Gas-chromatographic analysis of the dried extract indicated: methyl 2-pyrrolecarboxylate, trace; methyl 4-bromo-2-pyrrolecarboxylate, 5.9%; methyl 5-bromo-2-pyrrolecarboxylate, 2.1%; starting material, 92%.

(*b*) A solution of brominated ester or aldehyde (50 mg) was dissolved in 25 ml of glacial acetic acid containing 10 mg sodium acetate. After adding 20 mg of 5% palladium-on-charcoal catalyst the reaction mixture was shaken in a heavy-wall glass bottle under 3 atm of hydrogen at 60° for from 10 min to 2 h depending on the compound. After removal of the catalyst, neutralization, extraction, and drying, gas-chromatographic analysis showed quantitative removal of bromine.

(*c*) With the same starting materials the reductions were carried out at room temperature and pressure while agitating the reaction mixture with a magnetic stirrer. Again quantitative reduction was observed over times ranging from 15 min to 3 h.

Products were isolated from all these reductions and identified.

Replacement of Bromine with Cyanide

A mixture of the bromopyrrole ester (0.01 mole) and freshly prepared cuprous cyanide (0.015 mole) (27) in 50 ml of dimethyl sulfoxide was refluxed for 5 h. Most of the solvent was removed by vacuum distillation and the dark residue was washed with 30 ml of 20% aqueous ammonium chloride and extracted with ether. The ether extract was washed with water and dried over anhydrous sodium sulfate. After evaporation of the ether the nitrile was obtained by crystallization from petroleum pentanes and sublimation. Yields averaged about 20%. The products were: methyl 5-cyano-2-pyrrolecarboxylate, m.p. 165–166°. Calcd. for $C_7H_6O_2N_2$: C, 56.00; H, 4.03; N, 18.66. Found: C, 55.82; H, 4.11; N, 18.57. Methyl 4-cyano-2-pyrrolecarboxylate, m.p. 169–170°. Calcd. for $C_7H_6N_2O_2$: C, 56.00; H, 4.03; N, 18.66. Found: C, 55.96; H, 4.19; N, 18.71.

Formylation of Methyl 2-Pyrrolecarboxylate

Following the procedure of Silverstein *et al.* (21) methyl 2-pyrrolecarboxylate (0.04 mole) was formylated with 3.5 g of dimethylformamide and 7.0 g of phosphorus oxychloride in 25 ml of ethylene chloride. After working-up, the product was distilled at 120° and 5 mm giving a product which, after sublimation, melted at 92–93°. The undistilled residue was purified by recrystallization from pentane, and sublimation, to m.p. 121–122°. Over 90% of the ester was converted to products.

Identification of Formylated Pyrrole Esters

Each of the formyl-2-esters was oxidized with alkaline silver oxide following the procedure outlined above for the brominated aldehydes. Each crude acid in ether was then esterified by the addition of an ethereal solution of diazomethane. Yields were very good. From the formyl-2-ester, m.p. 92–93°, was obtained: methyl 2,4-pyrroledicarboxylate, m.p. 126–127°; λ_{max} 264 mμ (ϵ 13 700). (Reference 11 gives m.p. 126–127°; λ_{max} 267 mμ in aqueous solution.) Calcd. for $C_7H_7NO_3$: C, 54.90; H, 4.61; N, 9.15. Found: C, 54.97; H, 4.71; N, 9.21; From the formyl-2-ester, m.p. 121–122°, was obtained methyl 2,5-pyrroledicarboxylate, m.p. 128.5–129.5°; λ_{max} 274 mμ (ϵ 24 400). (Reference 11 gives m.p. 129–130°; λ_{max} 277 mμ in aqueous solution.) Calcd. for $C_7H_7NO_3$: C, 54.90; H, 4.61; N, 9.15. Found: C, 54.97; H, 4.72; N, 9.32.

Conversion of Formyl Derivatives to Cyano Derivatives

The now proven methyl 4-formyl-2-pyrrolecarboxylate (m.p. 92–93°) was converted to its oxime, m.p. 204–205°, and dehydrated with hot acetic anhydride (28) to the corresponding methyl 4-cyano-2-pyrrolecarboxylate. Similarly the 5-formyl-2-ester was converted by way of its oxime, m.p. 123–124°, to methyl 5-cyano-2-pyrrolecarboxylate. These compounds were then used to prove the structures of the same compounds obtained above by displacement of bromine by cyanide. Mixed melting points were undepressed and infrared spectra corresponded.

ACKNOWLEDGMENT

The authors acknowledge with thanks the continued financial support of the National Research Council.

REFERENCES

1. H. J. Anderson and L. C. Hopkins. Can. J. Chem. **42**, 1279 (1964).
2. P. B. D. de la Mare and J. H. Ridd. Aromatic substitution. Butterworths, London. 1959. Chap. 8.
3. S. Nishimura, R. Motoyama, and E. Imoto. Chem. Abstr. **53**, 4248 (1959). S. Nishimura and E. Imoto. Chem. Abstr. **59**, 3860 (1963).
4. J. Sicé. J. Am. Chem. Soc. **75**, 3697 (1953).
5. N. K. Kochetkov and E. E. Nifant'ev. Chem. Abstr. **53**, 12267 (1959). D. G. Manly and E. D. Amstutz. J. Org. Chem. **21**, 516 (1956).
6. J. Tirouflet and P. Fournari. Bull. Soc. Chim. France, 1651 (1963).
7. F. Richter (*Editor*). Beilstein's Handbuch der organischen Chemie. Vol. XX. Springer-Verlag, Berlin. 1935. p. 160.
8. G. L. Ciamician and P. Silber. Ber. **17**, 1152 (1884).
9. I. J. Rinkes. Rec. Trav. Chim. **60**, 303 (1941).
10. W. A. M. Davies, A. R. Pinder, and I. G. Morris. Tetrahedron, **18**, 405 (1962).
11. M. Scrocco and R. A. Nicolaus. Atti Accad. Nazl. Lincei, Rend. Classe Sci. Fis. Mat. Nat. **22**, 500 (1957). R. A. Nicolaus and L. Mangoni. Chem. Abstr. **52**, 2833 (1958).
12. J. A. Pople, W. G. Schneider, and H. J. Bernstein. High-resolution nuclear magnetic resonance. McGraw-Hill, New York, 1959. p. 259.
13. P. B. D. de la Mare and J. T. Harvey. J. Chem. Soc. 36 (1956).
14. D. R. Harvey and R. O. C. Norman. J. Chem. Soc. 3604 (1961).
15. K. Piers, C. Meimaroglou, R. V. Jardine, and R. K. Brown. Can. J. Chem. **41**, 2399 (1963).
16. G. L. Ciamician and M. Dennstedt. Ber. **16**, 2348 (1883).
17. A. D. Josey, R. J. Tuite, and H. R. Snyder. J. Am. Chem. Soc. **82**, 1597 (1960).
18. A. P. Terent'ev, L. I. Belen'kiĭ, and L. A. Yanovskaya. Chem. Abstr. **49**, 12327 (1955).
19. S. Gronowitz. Chem. Abstr. **50**, 11312 (1956).
20. W. Steinkopf, H. Jacob, and H. Penz. Ann. **512**, 136 (1934).
21. R. M. Silverstein, E. E. Ryskiewicz, and C. Willard. Organic syntheses. Vol. 36. *Edited by* N. J. Leonard. John Wiley and Son, New York. 1956. p. 74.
22. L. F. Fieser. Experiments in organic chemistry. D. C. Heath and Co., Boston. 1955. p. 306.
23. J. R. Partington. A textbook of inorganic chemistry. Macmillan and Co., London. 1943. p. 359. (Modified by Prof. J. M. W. Scott. Personal communication.)
24. E. M. Kosower, W. J. Cole, G.-S. Wu, D. E. Cardy, and G. Meisters. J. Org. Chem. **28**, 630 (1963).
25. E. Compaigne and W. M. LeSeur. Organic syntheses. Vol. 33. *Edited by* C. C. Price. John Wiley and Son, New York. 1953. p. 94.
26. A. I. Vogel. Textbook of practical organic chemistry. Longmans, Green and Company, London. 1957. p. 971.
27. A. I. Vogel. Textbook of practical organic chemistry. Longmans, Green and Company, London. 1957. p. 191.
28. H. J. Anderson. Can. J. Chem. **37**, 2053 (1959).

Can. J. Chem. Downloaded from www.nrcresearchpress.com by 210.87.254.5 on 09/05/12
For personal use only.

Can. J. Chem. Downloaded from www.nrcresearchpress.com by 210.87.254.105 on 09/05/12
For personal use only.

THE OXYGENATED FATTY ACIDS FROM THE OIL OF THE SPORES OF LYCOPODIUM SPECIES[1,2]

A. P. TULLOCH
National Research Council of Canada, Prairie Regional Laboratory, Saskatoon, Saskatchewan
Received October 1, 1964

ABSTRACT

The oil from the spores of commercial *Lycopodium*, mainly *L. complanatum*, contains *cis*-9,10-epoxyoctadecanoic acid (2%), (+)-8-hydroxyhexadecanoic acid (7%), and (±)-*threo*-9,10-dihydroxyoctadecanoic acid (4%). Smaller amounts of 8-oxohexadecanoic acid and an epoxyhexadecanoic acid also seem to be present.

The oil from the spores of species of the clubmoss *Lycopodium* has been examined by a number of workers, most of whom (1–5) agreed that it contained a small amount of a 9,10-dihydroxyoctadecanoic acid. The present investigation of the spore oil was undertaken because it was thought that the dihydroxy acid might have been produced in the spore by enzymatic hydrolysis of a hitherto unobserved epoxyoctadecanoic acid. The enzymatic conversion of *cis*-9,10-epoxyoctadecanoic acid to (+)-*threo*-9,10-dihydroxyoctadecanoic acid had earlier been found to occur in the uredospores of the wheat stem rust fungus (6). It was hoped that *Lycopodium* spores might prove to be a more convenient source of epoxide-hydrolyzing enzyme than wheat stem rust spores.

A further reason for reinvestigating *Lycopodium* spore oil was that the early workers disagreed about the melting point of the dihydroxy acid. Thus Bukowsky (1) gave 92 °C, Rathje (2) 140 °C, Bauer and Piners (3) 98 °C, Riebsomer and Johnson (4) 93 °C, and Hirai and Toyama (5) 130 °C. These melting points indicate that different stereoisomers had been isolated; the higher melting acids probably were *erythro* forms (racemic form has melting point 130 °C and the (+) or (−) form 140 °C) and the lower melting probably *threo* forms (racemic form has melting point 95 °C and the (+) or (−) form 99 °C). One possible explanation for these results is that the spores had been obtained from different species of *Lycopodium*. The above workers seem to have used commercial "lycopodium powder", and though it has been assumed that this consists of the spores of *L. clavatum*, it is most probable that other species are also present in considerable proportions. The spores of the "lycopodium powder" used in the present work belonged to the species *L. complanatum*.

Methyl esters of the oil were prepared, and analyzed by gas–liquid chromatography (g.l.c.) using a silicone SE-30 column. The g.l.c. separation of the esters is shown in Fig. 1A and the separation, after the esters had been treated with acetic acid to open epoxide rings and acetylated to convert hydroxy esters to acetates (6, 7), is shown in Fig. 1B. The small peak in the C_{20} region in A is still smaller in B, indicating the presence of C_{18} epoxy ester (7). A diacetate peak has appeared in B, part of which should be derived from epoxy ester and the rest from dihydroxy ester in the original oil. Also in B an acetoxy palmitate peak has appeared just beyond the C_{18} peak. In A the original hydroxy palmitate would be obscured by the larger C_{18} peak, since previous work has shown that the

[1]*Presented at the 47th Canadian Chemical Conference of the Chemical Institute of Canada, Kingston, June 1964.*
[2]*Issued as N.R.C. No. 8236.*

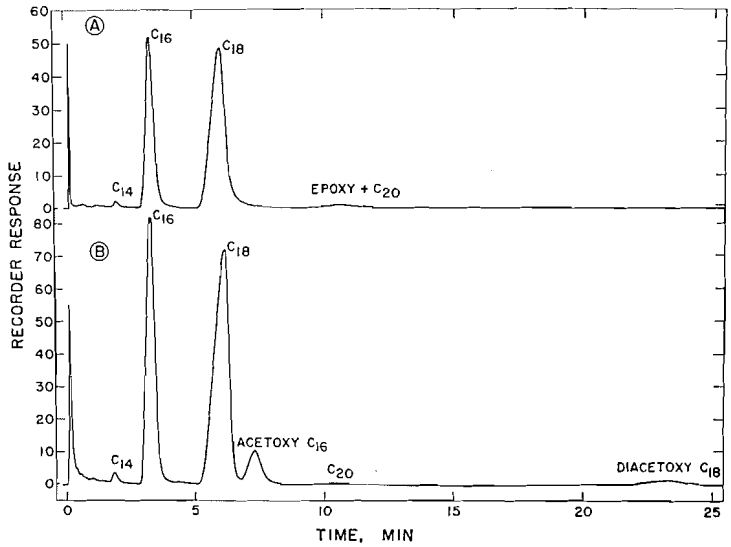

FIG. 1. (A) Gas–liquid chromatographic separation of the methyl esters of *Lycopodium* spore oil; (B) g.l.c. separation of esters after treatment with acetic acid and acetylation.

carbon number (8) of a hydroxy ester changes by 0.5 to 1.0 units on acetylation, the size of the change depending on the location of the hydroxyl group on the fatty acid chain (9).

Using a silicic acid column the esters were separated into non-oxygenated, epoxy, hydroxy, and dihydroxy ester fractions (10). The non-oxygenated esters were examined by g.l.c. and separated into saturated monoene and diene fractions by chromatography on a silver nitrate – silicic acid column (11, 12) and the fractions oxidized to determine the positions of the double bonds. 9-Hexadecenoic acid was present in the unusually large amount of 29%, as found by Riebsomer and Johnson (4), the other acids were oleic (21%) and linoleic (19%). The less common 11-octadecenoic acid, the presence of which was suggested by Riebsomer and Johnson, was also found (8%). The infrared spectra indicated that these unsaturated acids had the *cis* configuration.

Saponification of the epoxy ester fraction yielded an epoxy acid identical with the optically active *cis*-9,10-epoxyoctadecanoic acid previously isolated from the oil of wheat stem rust uredospores (13). Since the specific rotation of the epoxy ester was lower than that of epoxy ester derived from rust spores some racemic ester may also have been present in *Lycopodium* spore oil. The epoxy ester fraction also contained a lesser amount of a slightly more polar second component which was isolated after conversion of the accompanying epoxy ester to dihydroxy acid. The infrared spectrum indicated that it was an oxo ester (14); the carbon number, using a silicone QF-1 column, was 21.03 which suggested an 8- or 9-oxohexadecanoate (9). The acid could not be isolated in a sufficiently pure form for comparison with synthetic 8-oxohexadecanoic acid, but chromic acid oxidation yielded suberic and pimelic acids, confirming that it was 8-oxohexadecanoic acid. The fraction also contained a very small amount of a methyl epoxyhexadecanoate which had about the same carbon number, using the SE-30 column, as the above oxo ester but, using the QF-1 column, the carbon number was 20.2 (methyl *cis*-9,10-epoxyoctadecanoate had a carbon number of 22.2 using this column). This component could not be detected after acetic acid treatment (7).

Gas–liquid chromatography showed that the hydroxypalmitate fraction contained only

Can. J. Chem. Downloaded from www.nrcresearchpress.com by 210.87.254.105 on 09/05/12
For personal use only.

a single component. The ester was optically active and chromic acid oxidation at 100 °C yielded suberic and pimelic acids, indicating that the hydroxyl group was at carbon 8. Chromic acid oxidation at 25 °C gave an oxo ester which was shown to be methyl 8-oxopalmitate by comparison with the synthetic ester prepared by chain elongation of 6-oxotetradecanoic acid (9). The hydroxy ester is thus (+)-methyl 8-hydroxyhexadecanoate; (±)-methyl 8-hydroxyhexadecanoate was synthesized for comparison by reduction of the oxo ester. This hydroxy acid does not seem to have been isolated previously. The (±) ester has been synthesized before (15), but the route used and the physical properties of the ester and acid have apparently not been disclosed. The other hydroxyhexadecanoic acids which have been found in nature are 3-D-hydroxyhexadecanoic in the extracellular glycolipids produced by species of *Rhodotorula* (16), (+)-11-hydroxyhexadecanoic in the seeds and roots of convolvulaceous plants (17), 14- and (or) 15-hydroxyhexadecanoic in beeswax (18, 19), and 15- and 16-hydroxyhexadecanoic acids in the glycolipid produced by *Torulopsis magnoliae* (20).

The dihydroxy ester fraction was shown by comparison with synthetic material to be racemic methyl *threo*-9,10-dihydroxyoctadecanoate. Since the residue obtained after crystallization of the racemic *threo* ester had a low rotation ($[\alpha]_D$ +4°), the amount of (+)-*threo*-dihydroxy acid isomer ($[\alpha]_D$ +24° (13)) present in the oil, if any, must have been very small. The finding of a *threo* dihydroxy acid is in agreement with the results of Riebsomer and Johnson (4), who carried out the most thorough of the previous investigations.

The overall percentage fatty acid composition of the oil was calculated to be: myristic, 1; palmitic, 6; 9-hexadecenoic, 29; stearic, 1; 9-octadecenoic, 21; 11-octadecenoic, 8; linoleic, 19; *cis*-9,10-epoxyoctadecanoic, 2; 8-oxohexadecanoic, 0.4; (+)-8-hydroxyhexadecanoic, 7; *threo*-9,10-dihydroxyoctadecanoic, 4; and unidentified, 1.6.

The presence of racemic dihydroxy acid is surprising, particularly since the other two oxygenated acids are optically active. This acid could not have been produced by enzymatic hydrolysis of the epoxy acid as occurs in wheat stem rust spores unless it is assumed that some type of racemizing enzyme is also present in *Lycopodium* spores. The dihydroxy acid could not have arisen by hydrolysis of epoxy acid during preparation of methyl esters from the oil since it was previously shown that methanolysis with a weak solution of sodium methoxide in methanol did not affect the epoxide group (7, 26). It is unlikely that the oxygenated acids are produced by autoxidation since some are optically active and since only a few specific acids are produced. If random autoxidation occurred epoxy- and dihydroxy-hexadecanoic acids derived from 9-hexadecenoic acid would be expected.

It is interesting that about 2% of racemic *threo*-9,10-dihydroxyoctadecanoic acid was recently found in the oil of *Onguekoa gore* (isano oil) (21). This oil was also reported to contain 1.4% of *cis*-9,10-epoxyoctadecanoic acid, apparently mainly as the racemic form (22). The epoxy acid also occurs in small quantity in the seed oil of *Tragopogon porrifolius* (23). However, no explanation of the presence of these small amounts of oxygenated acid has been put forward. Epoxy and hydroxy acids have also been found in sulfur olive oil and it has been suggested that they are produced by the action of microorganisms (24, 25). At least some of the oxygenated acids in *Lycopodium* spore oil and the other oils may have been produced in the same way.

EXPERIMENTAL

Optical rotations were measured at 25 °C in a 1 dm tube. Light petroleum refers to a fraction of boiling range 60–80 °C.

Can. J. Chem. Downloaded from www.nrcresearchpress.com by 210.87.254.105 on 09/05/12
For personal use only.

Can. J. Chem. Downloaded from www.nrcresearchpress.com by 210.87.254.105 on 09/05/12
For personal use only.

Isolation of the Oil

The *Lycopodium* spores were purchased from Canadian Laboratory Supplies, Ltd., Winnipeg, and were found to consist mainly of spores of *Lycopodium complanatum* by Dr. M. Steeves of the Department of Geology, University of Saskatchewan. The spores were extracted by grinding in a ball mill with light petroleum for 48 h, the yield of oil was about 50%. The oil was treated with diazomethane to esterify free fatty acids, and, using methyl eicosanoate as a marker, the free fatty acids were estimated by g.l.c. to be less than 0.5%. Methyl esters were prepared by methanolysis with 0.02 *N* sodium methoxide in methanol (26)

Gas–liquid Chromatographic Analysis

Silicone SE-30 and QF-1 columns were prepared and operated as described earlier (9), and the ethylene glycol phthalate column used to analyze the esters and their oxidation products was employed as described by Tulloch and Craig (27).

Column Fractionation of the Methyl Esters of the Oil

Methyl esters (24.8 g) were dissolved in light petroleum and applied to a column (5 × 40 cm) of silica gel (Davison, 60–200 mesh). Non-oxygenated esters (20.5 g) were eluted with light petroleum containing 3% ether, and an epoxy ester fraction (1.1 g) with light petroleum containing 4% acetone; increasing the acetone content to 8% eluted a hydroxy ester fraction (1.5 g), and to 15% gave a dihydroxy ester fraction (1.1 g).

The Non-Oxygenated Ester Fraction

The following composition (in weight %) was obtained by g.l.c.: 14:0, 0.8; 14:1, 0.2; 16:0, 7.5; 16:1, 31.0; 16:2, 0.4; 18:0, 0.6; 18:1, 34.4; 18:2, 23.4; 20:0, 0.4; 20:1, 0.3; 22:0, 0.4; 22:1, 0.3. Chromatography on a silver nitrate – silicic acid column (11, 12) gave saturated esters (9.0), monoenes (65.9), and dienes (25.1%). Gas–liquid chromatography showed that the diene fraction contained some 16 carbon monoene but rechromatography on a shorter column yielded an almost pure diene fraction. The monoene fraction was separated, in batches, into C_{16} and C_{18} monoenes by g.l.c., using the SE-30 column. A portion of the C_{16} monoene was converted to *threo*-9,10-dihydroxyhexadecanoic acid by performic acid oxidation (26); the acid had melting point and mixed melting point 88–89 °C. The two monoene fractions and the diene fraction were oxidized with the permanganate periodate reagent (28) and the oxidation fragments analyzed by g.l.c. (27). The results are summarized below, only the major products are shown.

	C_{16} monoene (mole %)	C_{18} monoene (mole %)	Diene (mole %)
Dibasic acids			
C_9	94.2	69.4	93.6
C_{11}	1.2	26.9	1.3
Monobasic acids			
C_6	1.6	—	89.5
C_7	95.9	27.7	6.2
C_9	1.2	72.3	—

Epoxy Ester Fraction

Ester (0.90 g) was rechromatographed on a short silicic acid column and elution with light petroleum containing 6% ether gave almost pure epoxy ester (0.54 g). After crystallization from light petroleum the ester had melting point 22.5–24.5 °C and $[\alpha]_D$ +0.4° (*c*, 12.5, MeOH). A freshly prepared sample of methyl *cis*-9,10-epoxyoctadecanoate from the oil of wheat stem rust uredospores had melting point 23–25 °C and $[\alpha]_D$ +0.7° (*c*, 17.5, MeOH). The *Lycopodium* epoxy ester was saponified and the acid obtained after acidification was crystallized from acetone. The melting point and mixed melting point with *cis*-9,10-epoxyoctadecanoic acid from wheat stem rust was 57.5–58.5 °C and the mixed melting point with synthetic racemic *cis*-9,10-epoxyoctadecanoic acid was 53–57 °C. The infrared spectra of the acid from *Lycopodium* spores and the acid from wheat stem rust spores were indistinguishable.

A later fraction (0.21 g), obtained during the rechromatography of the epoxy ester, which seemed from g.l.c. analysis to be a mixture of an oxo C_{16} ester (40%) and the epoxy ester, was refluxed with acetic acid, the product hydrolyzed, and the acids isolated. The oxo acid was extracted with light petroleum and had melting point 72–77 °C, oxidation with chromic acid at 100° gave pimelic and suberic acids. The dihydroxy acid produced from the epoxy acid was crystallized from ethyl acetate and the melting point and mixed melting point with synthetic racemic *threo*-9,10-dihydroxyoctadecanoic acid was 93–94.5 °C.

Hydroxy Ester Fraction

Saponification of the ester yielded (+)-8-hydroxyhexadecanoic acid which, after crystallization from acetone, had melting point 78.5–79.5 °C and $[\alpha]_D$ +0.3° (*c*, 19.5, $CHCl_3$).

Anal. Calcd. for $C_{16}H_{32}O_3$: C, 70.5; H, 11.8. Found: C, 70.5; H, 11.9.

Methyl (+)-8-hydroxyhexadecanoate was prepared by treating the acid with diazomethane. Crystallization from light petroleum gave the pure ester with melting point 44–45.5 °C and $[\alpha]_D$ +0.8° (*c*, 14, MeOH).

Anal. Calcd. for $C_{17}H_{34}O_3$: C, 71.3; H, 12.0. Found: C, 71.4; H, 12.1.

The mixed melting point with the racemic ester was 42.5–45 °C.

Methyl ester (0.01 g) was oxidized with a solution of chromic acid in glacial acetic acid (2%, 1 ml) for 30 min at 100°. Sodium metabisulfite and dilute sulfuric acid were added and the products extracted with ether and converted to methyl esters with diazomethane. Gas–liquid chromatographic analysis on the polyester column showed that the major dibasic products were pimelic and suberic acids.

Methyl 8-oxohexadecanoate was prepared by oxidation of the hydroxy ester with chromic acid in acetic acid at 25 °C. The melting point of the oxo ester and the mixed melting point with synthetic methyl 8-oxohexadecanoate was 36–36.5 °C. 8-Oxohexadecanoic acid was obtained on hydrolysis and had melting point and mixed melting point 75.5–77 °C.

Synthesis of 8-Oxo- and 8-Hydroxyhexadecanoic Acids

6-Oxotetradecanoic acid (6 g) (9) and methyl hydrogen succinate (6.6 g) were electrolyzed in 0.022 *N* sodium methoxide solution (30 ml). After 1.5 h a further 3 g of half ester was added in sodium methoxide solution (10 ml) and the electrolysis continued for another 1.5 h when the solution was alkaline. Methanol was added to give a volume of 75 ml and insoluble dioxohexacosane was filtered off. The residue was acidified with acetic acid, the methanol removed, and the product taken up in ether and washed with sodium bicarbonate. After removal of the ether the esters were distilled and crude oxo ester collected at 130–150 °C and 0.1 mm. The distillate was saponified and crystallization of the acid from acetone yielded 8-oxohexadecanoic acid (1.35 g) with melting point 76–77 °C (lit. (29) gives 77.4–78.9 °C). The methyl ester had melting point 36–36.5 °C (lit. (29) gives 36.5–37.1 °C).

Hydrogenation of the oxo acid (30) yielded 8-hydroxyhexadecanoic acid with melting point 73.5–74.5 °C.

Anal. Calcd. for $C_{16}H_{32}O_3$: C, 70.5; H, 11.8. Found: C, 70.5; H, 12.0.

The methyl ester had melting point 45–46 °C.

Anal. Calcd. for $C_{17}H_{34}O_3$: C, 71.3; H, 12.0. Found: C, 71.5; H, 12.0.

Dihydroxy Ester Fraction

Crystallization from light petroleum gave methyl *threo*-9,10-dihydroxyoctadecanoate with melting point 67.5–68.5 °C, undepressed by admixture with the synthetic ester of melting point 68–69 °C. After removal of several optically inactive crops of crystals from the mother liquors the residue (0.17 g from 1.16 g) had $[\alpha]_D$ +4° (*c*, 3.4, MeOH). *threo*-9,10-Dihydroxyoctadecanoic acid was obtained by saponification of the ester and had melting point and mixed melting point of 93–94.5 °C.

ACKNOWLEDGMENTS

The author is grateful to Dr. M. Steeves for the identification of the *Lycopodium* spores. The author also thanks Mr. L. L. Hoffman for able technical assistance, Mr. M. Mazurek for the microanalyses, and Mr. W. C. Haid for the infrared spectra.

REFERENCES

1. A. Bukowsky. Chemiker Ztg. **21**, 174 (1889).
2. A. Rathje. Arch. Pharm. **246**, 692 (1908).
3. K. H. Bauer and W. Piners. Pharm. Zentralhalle, **71**, 33 (1930).
4. J. L. Riebsomer and J. R. Johnson. J. Am. Chem. Soc. **55**, 3352 (1933).
5. H. Hirai and Y. Toyama. J. Chem. Soc. Japan, Ind. Chem. Sect. **52**, 212 (1949) (National Research Council Tech. Transl. 1126).
6. A. P. Tulloch. Can. J. Biochem. Physiol. **41**, 1115 (1963).
7. A. P. Tulloch, B. M. Craig, and G. A. Ledingham. Can. J. Microbiol. **5**, 485 (1959).
8. F. P. Woodford and C. M. van Gent. J. Lipid Res. **1**, 188 (1960).
9. A. P. Tulloch. J. Am. Oil Chemists' Soc. In press.
10. L. J. Morris, H. Hayes, and R. T. Holman. J. Am. Oil Chemists' Soc. **38**, 316 (1961).
11. B. De Vries. J. Am. Oil Chemists' Soc. **40**, 184 (1963).
12. M. K. Bhatty and B. M. Craig. J. Am. Oil Chemists' Soc. **41**, 508 (1964).
13. A. P. Tulloch. Can. J. Chem. **38**, 204 (1960).
14. I. Fischmeister. Arkiv Kemi, **18**, 101 (1961).
15. J. S. O'Brien and G. Rouser. Anal. Biochem. **7**, 288 (1964).
16. A. P. Tulloch and J. F. T. Spencer. Can. J. Chem. **42**, 830 (1964).
17. C. R. Smith, L. H. Niece, H. F. Zobel, and I. A. Wolff. Phytochemistry, **3**, 289 (1964).
18. Y. Toyama and H. Hirai. Fette, Seifen, Anstrichmittel, **53**, 556 (1951).
19. D. H. S. Horn, Z. H. Kranz, and J. A. Lamberton. Australian J. Chem. **17**, 464 (1964).
20. A. P. Tulloch, J. F. T. Spencer, and P. A. J. Gorin. Can. J. Chem. **40**, 1326 (1962).
21. F. D. Gunstone and A. J. Sealy. J. Chem. Soc. 5772 (1963).

Can. J. Chem. Downloaded from www.nrcresearchpress.com by 210.87.254.105 on 09/05/12
For personal use only.

22. L. J. MORRIS. J. Chem. Soc. 5779 (1963).
23. M. CHISHOLM and C. Y. HOPKINS. Chem. Ind. London, 1154 (1959).
24. E. VIOQUE, L. J. MORRIS, and R. T. HOLMAN. J. Am. Oil Chemists' Soc. **38**, 489 (1961).
25. E. VIOQUE and M. P. MAZA. Grasas Aceites Seville, Spain, **15**, 66 (1964).
26. A. P. TULLOCH and G. A. LEDINGHAM. Can. J. Microbiol. **6**, 425 (1960).
27. A. P. TULLOCH and B. M. CRAIG. J. Am. Oil Chemists' Soc. **41**, 322 (1964).
28. E. VON RUDLOFF. Can. J. Chem. **34**, 1413 (1956).
29. F. L. BREUSCH and A. KIRKALI. Fette, Seifen, Anstrichmittel, **65**, 995 (1963).
30. M. SKOGH. Acta Chem. Scand. **6**, 809 (1952).

Can. J. Chem. Downloaded from www.nrcresearchpress.com by 210.87.254.105 on 09/05/12
For personal use only.

Can. J. Chem. Downloaded from www.nrcresearchpress.com by 210.87.254.40 on 09/05/12
For personal use only.

CONSTITUTION OF AN ARABINOGALACTOMANNAN FROM HONEY[1]

I. R. SIDDIQUI
Food Research Institute, Canada Department of Agriculture, Ottawa, Canada
Received August 14, 1964

ABSTRACT

An arabinogalactomannan isolated from honey consisted of D-mannose, L-arabinose, and D-galactose in molar proportions of 1.0:2.04:4.04 respectively. Electrophoretic and sedimentation results indicated that the arabinogalactomannan was homogeneous. Methylation studies showed a highly branched structure. Hydrolysis of the methylated polysaccharide gave 2,3,4,6-tetra-*O*-methyl-D-mannose (3 molecular proportions); 2,3,4,6–tetra-*O*-methyl-D-galactose (2 molecular proportions); 2,3,5-tri-*O*-methyl-L-arabinose (1 molecular proportion); 2,3,4-tri-*O*-methyl-D-galactose (6 molecular proportions); 2,3-di-*O*-methyl-L-arabinose (4 molecular proportions); 2,5-di-*O*-methyl-L-arabinose (1 molecular proportion); 2,4-di-*O*-methyl-D-galactose (5 molecular proportions). The general structural features of the arabinogalactomannan are discussed.

Although many extensive investigations have been made on the composition of honey, practically nothing is known about its polymeric constituents. The presence of polysaccharide in honey has been recognized for many years and it has been pointed out that the removal of these colloidal components results in the elimination of turbidity and production of brilliant clarity; caramelization and tendency to crystallization are also greatly lessened (1, 2, 3). The only report on the nature of these colloidal constituents appeared in 1953. On the basis of electrophoretic and sedimentation analyses of buckwheat honey the presence of three polymeric constituents has been claimed (4); the major components were proteins and the minor component appeared to be a polysaccharide.

In the present investigation, a number of honey samples were examined for their polysaccharide content. The polymeric material, in every instance, on hydrolysis produced small amounts of sugars and large amounts of amino acids. Among the sugars, glucose, galactose, mannose, arabinose, and xylose were invariably present; in some cases rhamnose and traces of uronic acids were also detected. Following this preliminary investigation, a detailed study was made of the polysaccharide isolated from honey collected at the Central Experimental Farm, Ottawa.

The crude polymer was precipitated from a 50% aqueous solution of honey by ethanol in a yield of about 0.2% of honey. Attempts to fractionate the crude material by the conventional methods such as precipitation with Fehling solution (5), precipitation with Cetavlon and borate (6), and phenol–water partition (7), were largely unsuccessful. The procedure which proved successful consisted of acetylation (8) of the crude material, extraction with acetone, and deacetylation to yield two fractions (I and II yield; ca. 1% based on the crude polymer and 0.002% of honey respectively).

There was undoubtedly more polysaccharide present in the acetylated acetone-insoluble residue as was evident by the paper chromatographic analysis of the deacetylated hydrolyzed product. However, the present technique did not permit its isolation. Fraction I on acid hydrolysis yielded galactose, glucose, mannose, arabinose, xylose, and rhamnose. Fraction II produced galactose, mannose, and arabinose, and showed a single symmetrical mobile peak on boundary electrophoresis (9) and sedimentation analysis (10) (Figs. 1 and

[1]*Issued as Contribution No. 18 of the Food Research Institute.*

2). On the basis of these observations, this material appeared to be a chemically homogeneous polysaccharide and was the subject of further investigations as reported in this paper.

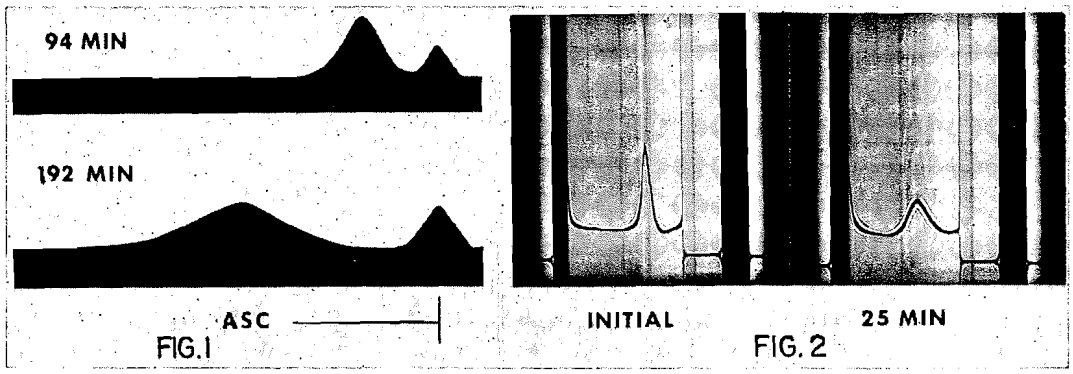

FIG. 1. Electrophoretic pattern of polysaccharide in borate buffer pH 9.2.
FIG. 2. Sedimentation pattern of polysaccharide in borate buffer pH 9.2.

After acid hydrolysis of the polysaccharide, mannose, arabinose, and galactose were found (11) in a ratio of 1.0:2.04:4.04. From the hydrolysis products, D-galactose and L-arabinose were obtained in the crystalline form and D-mannose was identified as *N*-*p*-nitrophenyl-β-D-mannosylamine, dihydrate (12).

The polysaccharide was methylated and the fully methylated product was subjected to methanolysis and hydrolysis. The *O*-methyl sugars were quantitatively determined, in a portion of the hydrolysate, by gas–liquid partition chromatography (13) of their methyl glycosides. The overall quantitative ratio of (di-*O*-methyl-hexosides) to (di-*O*-methyl-pentosides and tri-*O*-methyl-hexosides) to (tri-*O*-methyl-pentosides and tetra-*O*-methyl-hexosides) was 1:2:1. Analytical data are summarized in the following table.

Hydrolysis products from methylated arabinogalactomannan

Component No.	Component	Molar ratio	Structural feature indicated
1	2,3,4,6-Tetra-*O*-methyl-D-mannose	3	D-Man*p* 1 →
2	2,3,4,6-Tetra-*O*-methyl-D-galactose	2	D-Gal*p* 1 →
3	2,3,5-Tri-*O*-methyl-L-arabinose	1	L-Ara*f* 1 →
4	2,3,4-Tri-*O*-methyl-D-galactose	6	→ 6-D-Gal*p* 1 →
5	2,3-Di-*O*-methyl-L-arabinose	4	→ 5-L-Ara*f* 1 → and (or) → 4-L-Ara*p* 1 →
6	2,5-Di-*O*-methyl-L-arabinose	1	→ 3-L-Ara*f* 1 →
7	2,4-Di-*O*-methyl-D-galactose	5	→ 3 → 6 -D-Gal*p* 1 →

All of these sugars, with the exception of 2,3,5-tri-*O*-methyl-L-arabinose and 2,5-di-*O*-methyl-L-arabinose, were characterized by the isolation of crystalline aniline derivatives. The ratio of mannose : arabinose : galactose calculated from the proportion of methylated sugars was 1.0:2.0:4.3 in good agreement with that found for the original polysaccharide. All of the mannose was accounted for as nonreducing terminal units and, therefore, could not have arisen from an admixed mannan.

The methylation analysis showed that the molecule had a highly branched structure. Thus, of the 22–23 sugar residues which make up an average unit of the polysaccharide

Can. J. Chem. Downloaded from www.nrcresearchpress.com by 210.87.254.40 on 09/05/12
For personal use only.

there are 6 terminal nonreducing end groups consisting of 3 units of mannose, 2 of galactose, and 1 of arabinose. There are also 5–6 residues of galactose at which branching occurs, in the polysaccharide, through the 3 and 6 positions. The remaining 11 nonterminal residues consist of 6, 1 → 6 linked galactose units; 4, 1 → 5 and (or) 1 → 4 linked and 1, 1 → 3 linked arabinose units.

Although no attempt was made to determine the molecular weight of the polysaccharide, the rapid rate of diffusion (Fig. 2) indicated a low molecular weight. The use of a synthetic boundary cell for sedimentation analysis suggested this to be less than 10 000. The value quoted (4) for the molecular weight of buckwheat honey polysaccharide is 9 000.

The present data do not permit formulation of a unique structure, as the sugar residues can be arranged in several different ways. At present only the linkages between the various sugars are known with certainty. Fragmentation studies are necessary to reveal the detailed structure of the polysaccharide. Such a study might also be useful in providing additional evidence for the triheteropolymer nature of this polysaccharide.

EXPERIMENTAL

Paper chromatography was performed by the descending method on Whatman No. 1 paper using the organic phases of the following solvent systems: (A) 1-butanol : acetic acid : water (4:1:5); (B) ethyl acetate : pyridine : water (8:2:1); (C) 1-butanol : ethanol : water (40:11:19); (D) 2-butanone saturated with water containing 2% ammonia. Chromatograms were sprayed with (A) aniline hydrogen phthalate for reducing sugars (14) and (B) ninhydrin (15) for amino acids. Evaporations were carried out at 35 °C using a rotary film evaporator. Melting points are corrected and rotations are equilibrium values.

Isolation of the Polymer

Honey (100 lb) diluted with an equal volume of water was added to 95% ethanol (50 gal) agitated mechanically. The precipitate was removed using a Sharples centrifuge, suspended in water, and dialyzed for 3 days against running tap water. The soluble and insoluble material (80 g) was recovered by ethanol precipitation. The polymer (80 g) was extracted successively with benzene, ether, and chloroform. The resulting material (73 g) showed N, 11.02% and ash, 2.4%. Chromatography of a hydrolysate (solvents A and B) (sprays A and B) showed galactose, mannose, arabinose, xylose, small amounts of rhamnose, and large amounts of amino acids.

Acetylation of the Polymer

Honey polymer (53 g) in formamide (500 ml) was shaken for 3 days. The gel-like product was warmed to 68 °C and pyridine (700 ml) was added with vigorous shaking followed by acetic anhydride (600 ml) in ten 60 ml portions. After shaking for 3 days the reaction mixture was poured into a mixture of water and ice (20 l). The insoluble material was removed by decantation and centrifugation and was extracted with acetone in a Soxhlet for 24 h. Evaporation of the acetone-soluble material gave the acetylated product. The residue was treated in this manner altogether four times, giving a total of acetylated product (6.3 g).

Deacetylation and Fractionation of the Polysaccharide

The acetylated product (6.3 g) was dissolved in acetone (1 500 ml), *N* sodium hydroxide (150 ml) was added, and the mixture was stirred magnetically for 20 h. The mixture was neutralized with glacial acetic acid, with cooling, and an oily precipitate was separated from the solution. This oily precipitate which was still alkaline was dissolved in water (200 ml) and the solution was mixed with methanol (4 volumes). The solution on neutralization with glacial acetic acid gave a precipitate and a supernatant solution A. The precipitate was dissolved in *N* sodium hydroxide and the solution was mixed with methanol (1 volume). The precipitate which formed was removed from the supernatant solution B, was suspended in water, dialyzed, and freeze dried to yield fraction I, 560 mg.

The acetone extract left after removal of the oily precipitate as described above was freed from the solvent by distillation and the residual solution (150 ml) was made *N* with respect to sodium hydroxide and mixed with methanol (4 volumes). A small amount of precipitate was discarded and the supernatant liquid was combined with supernatants A and B. The combined supernatant was adjusted to pH 7, concentrated to 200 ml, and dialyzed. The dialyzed solution was centrifuged to remove small amounts of insoluble material and the dark turbid solution was mixed with methanol (1 volume). The precipitate (145 mg) was centrifuged off and the clear solution was decolorized with charcoal, filtered, concentrated, and freeze dried to yield fraction II, 520 mg.

Paper chromatography of the hydrolysates prepared from the two fractions showed the presence of galactose, mannose, glucose, arabinose, xylose, and rhamnose in fraction I and galactose, arabinose, and mannose in fraction II.

Can. J. Chem. Downloaded from www.nrcresearchpress.com by 210.87.254.40 on 09/05/12
For personal use only.

Analysis of Arabinogalactomannan (Fraction II)

The arabinogalactomannan $[\alpha]_D^{22}$ −21.4° (*c*, 0.84 water) on analysis gave the following: N, 1%; ash, nil. Electrophoretic examination of a 1% solution in a Spinco apparatus model H in 0.5 *M* borate buffer pH 9.2 showed a single symmetrical peak (Fig. 1). The sedimentation pattern, using a synthetic boundary cell, of a 1% solution in borate buffer pH 9.2; ionic strength, 0.2; rotational speed 59 780 rev/min is shown in Fig. 2. The polysaccharide (2.5 mg) was hydrolyzed with 2 *N* sulfuric acid for 3 h at 100 °C. The sugars were recovered and determined quantitatively according to Nelson (11), giving a ratio of mannose : arabinose : galactose of 1.0:2.04:4.04.

Acid Hydrolysis of Arabinogalactomannan

Polysaccharide (250 mg) was hydrolyzed with 2 *N* sulfuric acid (5 ml) for 3 h at 100 °C. After neutralization with barium carbonate, filtration, and evaporation, the sugars were recovered and separated on paper chromatograms in solvent B. Location and elution of appropriate strips gave galactose, mannose, and arabinose as syrups.

(i) D-*Galactose.*—The syrup crystallized from ethanol to give D-galactose, m.p. 164–165 °C and $[\alpha]_D^{22}$ +81.05 ± 1° (*c*, 0.95 water).

(ii) L-*Arabinose.*—The syrup crystallized from ethanol to give L-arabinose, m.p. 150–152 °C and $[\alpha]_D^{22}$ +105.8 ± 2° (*c*, 0.51 water).

(iii) D-*Mannose.*—The syrup was refluxed for a total of 12 h with an aliquot (1 ml) of a solution containing *p*-nitroaniline (9 g), methanol (200 ml), and concentrated hydrochloric acid (0.14 ml). The *N*-*p*-nitrophenyl-β-D-mannosylamine dihydrate, which settled out from the solution, was washed with methanol and had m.p. 219 °C and $[\alpha]_D^{22}$ −335° (*c*, 0.1 dry pyridine). Reported values (12): m.p. 219 °C, $[\alpha]_D^{22}$ −333°.

Methylation of Arabinogalactomannan

An ice-cooled solution of arabinogalactomannan (250 mg) in water (5 ml) was methylated by adding 30% sodium hydroxide (14 ml) and dimethyl sulfate (5 ml). The reagents were added at such a rate that the reaction mixture remained alkaline but as close to neutral as possible for the first few hours. The additions took place over 2 h after which the solution was stirred for 24 h. After four such methylations the reaction mixture was cooled and neutralized with glacial acetic acid to pH 7.0 and the solution extracted with chloroform (7 × 100 ml portions). The chloroform extract was dried (sodium sulfate), filtered, and evaporated to a syrup. The chloroform-soluble fraction gave some methanol-insoluble material (100 mg) which was combined with the residue recovered by freeze drying from the dialyzed aqueous solution. The combined material after nine further additions of 30% sodium hydroxide (7 ml) and dimethyl sulfate (3 ml) was recovered in the usual way. The partially methylated product (175 mg) was methylated 10 times by Purdie's method, using methyl iodide (30 ml) and silver oxide (3 g) per methylation, to yield a product (150 mg), $[\alpha]_D^{22}$ −42.0° (*c*, 1.0 chloroform), which showed no hydroxyl absorption in its infrared spectrum.

Hydrolysis Products from Methylated Arabinogalactomannan

The methylated polysaccharide (150 mg) was refluxed with 3% methanolic hydrogen chloride (25 ml) for 24 h. The solution was neutralized with silver carbonate, filtered, and evaporated to a syrup, which was hydrolyzed with *N* sulfuric acid (10 ml) at 100 °C for 24 h. The hydrolysate was neutralized with barium carbonate, filtered, and evaporated to a syrup (90 mg). A portion of this syrup was refluxed with 2% methanolic hydrogen chloride for 6 h, neutralized with silver carbonate, and the resulting methyl glycosides in the solution were examined by gas–liquid partition chromatography (13) using a 4 ft column of 10% neopentylglycol sebacate on Chromosorb W at 180 °C and an argon flow rate of 100 ml/min. The areas under the peaks, measured by triangulation, gave the overall quantitative ratios of di-*O*-methyl-hexosides to (di-*O*-methyl-pentosides and tri-*O*-methyl-hexosides) to (tri-*O*-methyl-pentosides and tetra-*O*-methyl-hexosides) to be 1:2:1. Molar ratios of individual components were determined by gas–liquid partition chromatography of *O*-methyl-glycosides with the exception of 2,3,4-tri-*O*-methyl-galactose and 2,3-di-*O*-methyl-arabinose. The ratio for the latter components was evaluated from the combination of gas–liquid partition chromatography data and the actual weights of the fractions isolated. These ratios converted to the nearest whole number were 2,3,4,6-tetra-*O*-methyl-D-mannose, [3]; 2,3,4,6-tetra-*O*-methyl-D-galactose, [2]; 2,3,5-tri-*O*-methyl-L-arabinose, [1]; 2,3,4-tri-*O*-methyl-D-galactose, [6]; 2,3-di-*O*-methyl-L-arabinose, [4]; 2,5-di-*O*-methyl-L-arabinose, [1]; 2,4-di-*O*-methyl-D-galactose, [5].

The remaining mixture of sugars was separated on eight chromatograms (7 × 22 in.) using solvent C. Location and elution of appropriate strips gave the following fractions:

Fraction 1

The syrup showed two components having R_f values (solvent D) and color reactions identical with authentic specimens of 2,3,4,6-tetra-*O*-methyl mannose and 2,3,5-tri-*O*-methyl arabinose. It was separated on three chromatograms (6 × 22 in.) giving

*(a) 2,3,4,6-Tetra-O-methyl-*D-*mannose.*—The syrup (4 mg) in ethanol (0.25 ml) containing aniline (2 mg) was refluxed for 5 h. On evaporation of ethanol at room temperature crystals appeared which after recrystallization from ether in the cold gave 2,3,4,6-tetra-*O*-methyl-*N*-phenyl-D-mannosylamine m.p. 153–155 °C. Reported value: 142–143 °C (19). An authentic sample of 2,3,4,6-tetra-*O*-methyl-D-mannose was treated

Can. J. Chem. Downloaded from www.nrcresearchpress.com by 210.87.254.40 on 09/05/12
For personal use only.

with aniline in exactly the same manner. The resulting crystals showed the same melting point undepressed on admixture with the former sample.

*(b) 2,3,5-Tri-O-methyl-*L*-arabinose.*—The syrup (ca. 3 mg) was oxidized with bromine. The resulting lactone was recovered in amounts too small to permit identification.

Fraction 2

The syrup on paper chromatography in solvent D showed a mixture of 2,3,4,6-tetra-*O*-methyl galactose and 2,5-di-*O*-methyl arabinose (one spot) and faint traces of an unidentified component. It was purified on two chromatograms (6 × 22 in.) using solvent D. The mixture of sugars (6 mg) was refluxed with aniline (3 mg) in ethanol (0.5 ml) for 5 h. Evaporation of ethanol gave crystals which were recrystallized from ethanol giving 2,3,4,6-tetra-*O*-methyl-*N*-phenyl-D-galactosylamine, melting point and mixed melting point 195–197 °C. Reported value: 196 °C (16).

Fraction 3

The syrup showed two components, R_f values (solvent D) and color reactions identical to those given by authentic samples of 2,3,4-tri-*O*-methyl galactose and 2,3-di-*O*-methyl arabinose. The mixture was separated on four chromatograms (6 × 22 in.) using solvent D. Location and elution of appropriate strips gave

*(a) 2,3,4-Tri-O-methyl-*D*-galactose.*—The syrup (10 mg) was refluxed with aniline (5 mg) in ethanol (1 ml) for 5 h. On cooling, crystals separated which after recrystallization from ethanol gave 2,3,4-tri-*O*-methyl-*N*-phenyl-D-galactosylamine melting point and mixed melting point 167–168 °C. Reported value: 167 °C (17).

*(b) 2,3-Di-O-methyl-*L*-arabinose.*—The syrup (6 mg) in ethanol (0.5 ml) was refluxed with aniline (3 mg) for 5 h. Crystallization of the ether-soluble portion in the cold gave 2,3-di-*O*-methyl-*N*-phenyl-L-arabinosylamine having m.p. 135–138 °C. Reported value: 138 °C (18).

Fraction 4

Fraction 4 (15 mg) showed R_f value (solvent D) and color reactions identical with an authentic sample of 2,4-di-*O*-methyl galactose. The syrup was mixed with aniline (8 mg) in ethanol (1 ml) and the solution was refluxed for 4 h. Slow evaporation gave crystals which were washed and recrystallized from ethanol giving 2,4-di-*O*-methyl-*N*-phenyl-D-galactosylamine melting point and mixed melting point 216–217 °C. Reported value: 214-217 °C (16).

ACKNOWLEDGMENT

The author is grateful to Mr. F. P. Cooper for the gas–liquid chromatographic analysis.

REFERENCES

1. H. S. Paine and R. E. Lothrop. Am. Bee J. **71**, 28 (1931).
2. H. S. Paine and R. E. Lothrop. Am. Bee J. **72**, 444 (1932).
3. H. S. Paine and R. E. Lothrop. Am. Bee J. **73**, 53, 57 (1933).
4. T. C. Helvey. Food Res. **18**, 197 (1953).
5. W. N. Haworth, E. L. Hirst, and F. A. Isherwood. J. Chem. Soc. 784 (1937).
6. S. A. Barker, M. Stacey, and G. Zweifel. Chem. Ind. London, 330 (1957).
7. O. Westphal, O. Luderitz, and F. Bister. Z. Naturforsch. **7b**, 320 (1952).
8. J. F. Carson and W. D. Maclay. J. Am. Chem. Soc. **70**, 293 (1948).
9. D. H. Northcote. Biochem. J. **58**, 353 (1954).
10. T. Svedberg and K. O. Pederson. The ultracentrifuge. Oxford. 1940.
11. N. Nelson. J. Biol. Chem. **153**, 375 (1944).
12. F. Weygand, W. Perkow, and P. Kuhner. Chem. Ber. **84**, 594 (1951).
13. A. G. McInnes, D. H. Ball, F. P. Cooper, and C. T. Bishop. J. Chromatog. **1**, 556 (1958).
14. S. M. Partridge. Nature, **164**, 443 (1949).
15. R. J. Bayly and E. J. Bourne. Nature, **171**, 385 (1953).
16. E. Baldwin and D. J. Bell. J. Chem. Soc. 1461 (1938).
17. F. Smith. J. Chem. Soc. 1724 (1939).
18. F. Smith. J. Chem. Soc. 753 (1939).
19. J. C. Irvine and D. McNicoll. J. Chem. Soc. **97**, 1449 (1910).

Can. J. Chem. Downloaded from www.nrcresearchpress.com by 210.87.254.40 on 09/05/12
For personal use only.

Can. J. Chem. Downloaded from www.nrcresearchpress.com by 210.87.254.105 on 09/05/12
For personal use only.

ADDITION COMPOUNDS OF TITANIUM(IV) CHLORIDE CONTAINING ELEMENTS OF GROUPS V AND VI AS DONOR ATOMS

ALAN D. WESTLAND AND LIESELOTTE WESTLAND
Department of Chemistry, University of Ottawa, Ottawa, Canada
Received August 20, 1964

ABSTRACT

Complexes $TiCl_4.L$ where L is a mono- or bi-dendate ligand having P, As, S, or Se as donor atom were prepared. Triphenylphosphine and dialkyl sulfide also form complexes $TiCl_4.2L$. Far infrared data are presented for certain of the complexes.

Organo derivatives of the heavier elements of groups V and VI, that is, phosphorus, arsenic, antimony, sulfur, selenium, and tellurium serve frequently as ligands in addition complexes with transition elements in low valence states. Few complexes of these elements have been reported in which the central atom is a transition element from one of the earlier groups in its highest valence state. However, H. Rose (1) reported over a century ago that phosphine forms an adduct with titanium(IV) chloride and hydrogen sulfide is known to form an adduct at low temperatures (2). Challenger and Pritchard (3) reported in 1924 that triphenylarsine forms an addition compound with $TiCl_4$ but they did not identify the resulting substance. In recent years, Clarke and co-workers (4) have shown that *o*-phenylenebisdimethylarsine forms the complexes MCl_4.dias and MCl_4.2dias where M = Ti, Zr, Hf. Fairbrother and Nixon (5) have shown that alkyl sulfides, R_2S, where R = CH_3, C_2H_5, will form complexes with pentahalides of niobium and tantalum. Chatt and Hayter (6) have prepared a few complexes of titanium(IV) chloride and mono- and di-tertiary phosphines. We have extended the list of known adducts formed by tertiary phosphines and arsines with tetrahalides of group IV elements and have shown that even the very weak Lewis bases, dialkyl sulfide and dialkyl selenide, form stable complexes with these elements. The present paper deals with complexes of titanium(IV) chloride.*

RESULTS AND DISCUSSION

All of the alkyl and aryl compounds of the elements N, P, As, Sb, O, S, Se, and Te which were tested were found to react with $TiCl_4$. Fowles has reported an investigation of the reaction of tertiary amines with $TiCl_4$ (7). We shall restrict ourselves here to the behavior of tertiary phosphine, arsine, and stibine and organo-sulfide, -selenide, and -telluride.

When pure components were allowed to react, fairly exothermic reactions occurred. The reaction of $TiCl_4$ with pure triethylphosphine is violent. For preparative purposes, the components were dissolved in dry benzene and allowed to react. In all cases, a yellow or deep-red coloration appeared. In one case studied more closely, that of triphenylarsine, the red color did not obey Beer's law indicating that the equilibrium,

$$TiCl_4 + AsPh_3 \rightleftharpoons TiCl_4.AsPh_3,$$

does not lie strongly to the right at low concentrations. It follows that the complex formed is not particularly stable with respect to the solvating effect of benzene upon the

**Note added in proof: Professor G. W. A. Fowles described the dialkyl sulfide complexes at the 8th International Conference on Coordination Chemistry, Vienna, September 1964.*

component substances. This solvation energy is presumably not large in the case of each component as there is no sensible heat effect when they are dissolved alone. However, Elliot, Evans, and Owen (8) report that $TiCl_4$ forms a 1:1 complex with benzene but it is a very weak one.

The compounds which were prepared are listed with colors, melting points, and analyses in Table I. It may be seen that 1:1 complexes only are found with monodentate arsine and selenide while triphenylphosphine and alkylsulfide formed 2:1 addition compounds. We have found a 1:1 complex as well with triphenylphosphine. This gave a Debye–Scherrer X-ray pattern which was almost identical with that of the corresponding arsine but which differed from that of the 2:1 complex. The 2:1 phosphine complex has been reported by Chatt and Hayter (6).

TABLE I

Properties and analyses of complexes of $TiCl_4$

Compound	Color	Melting point (°C)	Percentage composition			
			Found		Calcd.	
			Ti	Cl	Ti	Cl
$(Ph_3P)TiCl_4$	Red–violet	147.5–149	11.2	31.1	10.6	31.4
$(Ph_3P)_2TiCl_4$	Red–black	149–151	6.77	19.4	6.75	19.8
$(Ph_4P_2C_2H_4)_2Ti_3Cl_{12}$	Dark red	139–143	9.84	29.2	10.5	31.1
$(Ph_4P_2C_2H_4)TiCl_4$	Red	178 (decomp.)	7.97	25.2	8.14	24.1
$(Ph_4P_2C_2H_4)_3Ti_2Cl_8$	Red	138–140	6.38	19.0	6.08	18.0
$(Ph_3As)TiCl_4$	Red–black	126–128	9.67	28.4	9.66	28.6
$(Ph_4As_2C_2H_4)_3Ti_2Cl_8$	Red–orange	145–149	5.60	15.4	5.21	15.4
$(Me_2S)_2TiCl_4$	Orange	95–99	15.4	44.1	15.3	45.2
$(Et_2S)_2TiCl_4$	Bright red	55–57	13.2	37.9	12.9	38.3
$(Ph_2S_2C_2H_4)TiCl_4$	Bright red	69.5–70	11.3	32.0	11.0	32.5
	Dark	122–132	11.1	32.1	11.0	32.5
$(Et_2Se)TiCl_4$	Red–black	55 (decomp.)	14.7	42.6	14.7	43.4
$(Ph_2Se_2C_3H_6)TiCl_4$	Red–black	83 (decomp.)	8.20	25.3	8.81	26.1

Triphenylstibine and diethyltelluride reacted with $TiCl_4$ in two stages. A deep-violet color was observed in each case, upon mixing benzene solutions of the components. After some seconds or minutes a black, somewhat gummy solid appeared. Evaporation of the mother liquor yielded a gum which crystallized poorly upon standing for a few days. Benzene solutions of these gums were brown rather than violet. Although the chlorine to titanium ratio in these residues was 4:1, the products were thought to consist of a complex or mixture of $TiCl_2$ and dichlorinated diethyltelluride. That it was not a simple mechanical mixture was indicated by the failure to remove tellurium, e.g. as dichlorodiethyltellurium, by extraction with carbon tetrachloride.

The possibility that all of the compounds contained titanium in a reduced valence state was considered, for all of the ligand substances are reducing agents to some degree. The molar magnetic susceptibility of one of the compounds, $TiCl_4.AsPh_3$, was found to be $\chi_M = -0.26 \times 10^{-3}$ c.g.s. units. The estimated value for the compound assuming an oxidation state of +4 for the titanium is -0.27×10^{-3}. The similar color and behavior of the remaining compounds allows us to extend analogous formulations to them.

Attempts were made to discover compounds with apparently different coordination numbers. The use of a ditertiary arsine and a selenodiether allowed us to produce complexes with two donor atoms in the coordination shell. Variation of the proportions of the components in the reaction mixture led to the formation of more than one product in

Can. J. Chem. Downloaded from www.nrcresearchpress.com by 210.87.254.105 on 09/05/12
For personal use only.

the cases of triphenylphosphine and the ditertiary phosphine. As Clarke and co-workers (4) were successful in preparing an eight-coordinate complex of $TiCl_4$ with o-$C_6H_4(AsMe_2)_2$, similar complexes with $C_2H_4(PPh_2)_2$ and $C_2H_4(AsPh_2)_2$ were sought. However, addition occurred in each case only to the extent of 3 moles of ligand to 2 moles of $TiCl_4$ which, if the compounds are not molecular mixtures, indicates a coordination greater than six. The 3:2 phosphine compound was formed when a benzene solution containing n moles of $TiCl_4$ was mixed with a solution containing $5n$ moles of the base. The 3:2 and the 2:3 adducts appear from the analyses to be somewhat contaminated with the 1:1 compound. The ditertiary arsine formed only the 3:2 complex.

It remains undecided whether the 1:1 complexes are five-coordinate monomers or more highly coordinated polymers. Many of the complexes are not sufficiently stable to yield definitive results from molecular weight determinations. It is likely that both 1:1 and 2:1 complexes occur in varying proportions in solution. Attempts to detect spectrophotometrically the existence of a 2:1 complex in the system Ph_3As–$TiCl_4$ were limited, because of the intense color, to work on systems containing very low concentrations of the components and perhaps for this reason were unsuccessful.

The dialkyl sulfide complexes were sufficiently soluble in benzene to measure depression of the freezing point. Good agreement with the molecular weights indicated that these complexes are stable monomers in benzene solution. The chelated compounds were all too sparingly soluble to afford sufficient accuracy in freezing point determinations.

An examination of far infrared spectra provided values of various metal–ligand stretching frequencies and thereby some comparison of the bonding was possible. Sulfide and selenide complexes gave broad absorptions of little interpretive value. About all that could be seen with certainty was the fact that this absorption reached a maximum at ca. 410 cm^{-1} for sulfur compounds and continued to lower frequencies while the maximum was reached at 395 cm^{-1} for the ethyl selenide complex. The upper limit is certainly associated with sulfur and selenium stretching rather than chlorine stretching.

TABLE II

Infrared absorption frequencies for complexes of $TiCl_4$ in the region 525–260 cm^{-1}

Compound										
$(Ph_3P)TiCl_4$	514w	499.5s	*463*s	426w		393sh	380sh	357vs		
$(PhP_3)_2TiCl_4$	516s	496s	489sh	*445*s		*434*s	431s	418w	381s, b	365–302s, b
$(Ph_4P_2C_2H_4)TiCl_4$	506sh	499s	479s	*453*w	*414*w		343vs	325vs	313vs	
$(Ph_4P_2C_2H_4)_3Ti_2Cl_8$	447w	*436.5*w	*416*s	393vs	389vs		374vs	363vs	359sh	312sh
$(Ph_4P_2C_2H_4)_2Ti_3Cl_{12}$	514s	499.5s	493.5s	465s						
$(Ph_3As)TiCl_4$	470s	452sh	396sh	383s, b		322vs				
$(Ph_4As_2C_2H_4)_3Ti_2Cl_8$	477s	457w	400sh	391s		381.5s	375s	350s	345s	316.5w

Titanium–phosphorus stretches, where identifiable, are shown in italics.
Abbreviations: s, strong; vs, very strong; w, weak; sh, shoulder; b, broad.

It was possible to identify stretching bands with reasonable certainty in the case of the simpler phosphine complexes. A summary of frequencies in the region 260–520 cm^{-1} is given in Table II and where possible titanium–phosphorus stretching frequencies are shown in italics. These were assigned easily because of their relative isolation in compounds of various transition metals.* A sample spectrum is shown in Fig. 1. A single phosphorus stretch appears in the spectrum of $(Ph_3P)TiCl_4$ as expected but two bands are found for $(Ph_3P)_2TiCl_4$. The conclusion drawn is that these are symmetric and antisymmetric

**Unpublished work.*

Can. J. Chem. Downloaded from www.nrcresearchpress.com by 210.87.254.105 on 09/05/12
For personal use only.

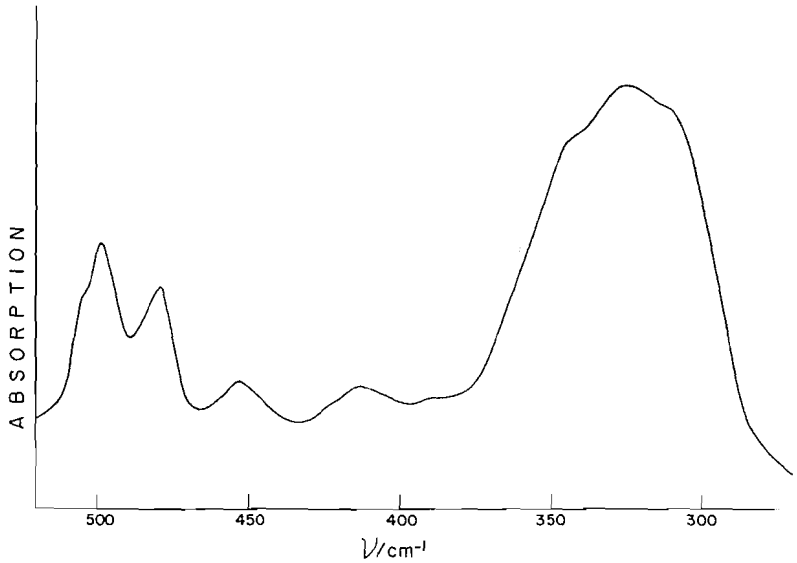

FIG. 1. Infrared spectrum of the compound $(Ph_4P_2C_2H_4)TiCl_4$.

modes which arise in the case of complexes having the *cis* configuration. The frequency values reported by Coates and Parkin (9) for the bonds formed between phosphorus and palladium, platinum, and gold are comparable with those found here. A force constant calculation which takes account only of the two atoms forming the bond shows that the values for the Ti—P bond in $(Ph_3P)_2TiCl_4$ are just about the same as for the Pt—P bond in *cis*-$(Me_3P)_2PtCl_2$, a typical phosphine complex of high stability. Table III presents the force constants so estimated for the symmetric and antisymmetric modes of these compounds. The force constants are designated k_1 and k_2 because it is not certain which belongs to the symmetric and which to the antisymmetric mode. The comparison

TABLE III

Comparison of force constants

	Force constants (dyne $cm^{-1} \times 10^{-5}$)	
Compound	k_1	k_2
$(Ph_3P)_2TiCl_4$	2.18	2.07
$(Ph_4P_2C_2H_4)TiCl_4$	2.27	1.90
cis-$(Me_3P)_2PtCl_2$	2.22	2.05
$(Ph_4P_2C_2H_4)PtCl_4$	2.96	2.87

shows that $TiCl_4$ is just as effective as an acceptor toward a phosphine as $PtCl_2$. It will be remembered that platinum is regarded as one of the most strongly bonding elements towards phosphines. However, it is seen that when the valence state of the platinum is made to equal that of the titanium, platinum is then the better acceptor.

It is interesting to observe that the Ti—P stretching frequency is greater for $(Ph_3P)TiCl_4$ than for either mode of the 2:1 adduct. A similar but rough comparison can be made for the 2:3 and the 3:2 complexes. Although it is not certain how many bands in each case should be attributed to metal–phosphorus and metal–chlorine stretching, it is at

Can. J. Chem. Downloaded from www.nrcresearchpress.com by 210.87.254.105 on 09/05/12
For personal use only.

least likely that the band at 465 cm^{-1} for $L_2Ti_3Cl_{12}$ is due to Ti—P stretching and this is higher than the highest corresponding frequency, 436 cm^{-1}, for $L_3Ti_2Cl_8$. In the latter compound, additional bands, e.g. at 416 and 393 cm^{-1} are evidently due to Ti—P stretching, which indicates the complexity of the compound structure. A similar complexity is observed for the arsine $(Ph_4As_2C_2H_4)_3Ti_2Cl_8$.

EXPERIMENTAL

Infrared spectra of Nujol mulls between caesium iodide plates were obtained with a Perkin–Elmer Model 13G spectrometer set for double beam operation and fitted with a 30 micron grating. The fore-prism index was adjusted continuously throughout the spectral range. Analyses of complexes were carried out gravimetrically following preparation of the sample by Parr bomb combustion.

Titanium(IV) chloride was purified by the method of Clabaugh and co-workers (10). Triphenylphosphine, triphenylarsine, and triphenylstibine, obtained from M and T Chemicals, Inc., were recrystallized from ethanol until the melting points were constant. Dimethylsulfide and diethylsulfide, supplied by Distillation Products Industries, were distilled prior to use. The compounds 1,2-bis(diphenylphosphino)ethane and 1,2-bis(diphenylarsino)ethane were prepared by the method of Chatt and Hart (11).

1,3-Bis(phenylseleno)propane.—Phenylselenol (55.4 g) was added to a solution prepared by adding sodium (8.18 g, 1 mole) to ethanol (50 cc). To this, 1,3-dibromopropane (71.6 g, 0.5 mole) dissolved in ethanol (50 cc) was added dropwise with stirring. The solution was heated under reflux in a nitrogen atmosphere for 2 h. The solution was separated from sodium bromide by filtration and the alcohol removed by distillation. The resulting brown oil was distilled at 0.1 mm Hg pressure to yield an amber oil (37.2 g, 59%) with b.p. 185–188 °C.

Anal. Found: C, 50.7; H, 4.32. Calcd. for $C_{15}H_{16}Se_2$: C, 50.9; H, 4.55.

Preparation of complexes.—The addition complexes were all prepared by essentially the same procedure of which the following is representative.

Tetrachlorotriphenylphosphinetitanium.—The content of an ampoule of titanium(IV) chloride (3.84 g) was introduced to a nitrogen-filled Schlenk tube containing carefully dried, sulfur-free benzene (8 cc). To this solution was added triphenylphosphine (2.7 g, 0.5 mole) dissolved in benzene (10 cc). There was immediate appearance of a dark-red coloration with the formation of dark crystals. These were removed by filtration in an apparatus similar to that described by Fritz and co-workers (12). The product (2.3 g) was washed on the filter with a small quantity of benzene and dried at room temperature under vacuum. As the compound was attacked by moist air, it was stored in ampoules. This was true of all other complexes as well.

The other complexes were best prepared from stoichiometric quantities of the components except in the cases of the 3:2 and 2:3 compounds of the diphosphine. For the former, a fivefold excess of diphosphine was used and for the latter, a fivefold excess of $TiCl_4$.

It was possible to recrystallize the compounds prepared from monodentate ligands by dissolving in benzene and removing the solvent by distillation under reduced pressure. The bidentate ligands formed compounds which were only sparingly soluble. However, the analyses reported in Table I refer to preparations which had not been recrystallized.

One compound, $(Ph_2S_2C_2H_4)TiCl_4$, appeared as a mixture of bright-red needles and darker-red granules. As shown in Table I these forms when separated melt at different temperatures, the darker one under non-equilibrium conditions, of course.

ACKNOWLEDGMENTS

The authors wish to express their gratitude to Mrs. Astrid Benn for assistance in obtaining the infrared spectra and to the National Research Council for financial aid.

REFERENCES

1. H. Rose. Poggendorff's Ann. Phys. **24**, 141, 159, 259 (1832).
2. W. Biltz and E. Keunecke. Z. Anorg. Chem. **147**, 171 (1925).
3. F. Challenger and F. Pritchard. J. Chem. Soc. 864 (1924).
4. R. J. H. Clarke, J. Lewis, R. S. Nyholm, P. J. Pauling, and G. B. Robinson. Nature, **192**, 222 (1961).
5. F. Fairbrother and J. F. Nixon. J. Chem. Soc. 150 (1962).
6. J. Chatt and R. Hayter. J. Chem. Soc. 1343. (1963).
7. G. W. A. Fowles and R. A. Hoodless. J. Chem. Soc. 33 (1963).
8. B. Elliot, A. G. Evans, and E. D. Owen. J. Chem. Soc. 689 (1962).
9. G. E. Coates and C. Parkin. J. Chem. Soc. 421 (1963).
10. N. S. Clabaugh, R. T. Leslie, and R. Gilchrist. J. Res. Natl. Bur. Std. **55**, 261 (1955).
11. J. Chatt and F. A. Hart. J. Chem. Soc. 1378 (1960).
12. G. Fritz, D. Habel, D. Kummer, and G. Teichmann. Z. Anorg. Allgem. Chem. **302**, 60 (1959).

Can. J. Chem. Downloaded from www.nrcresearchpress.com by 210.87.254.105 on 09/05/12
For personal use only.

Can. J. Chem. Downloaded from www.nrcresearchpress.com by 210.87.254.40 on 09/05/12
For personal use only.

DIFFUSION IN MULTICOMPONENT GASEOUS MIXTURES

PART 2. DIFFUSION OF XENON-133 IN BINARY MIXTURES OF XENON WITH HELIUM, NEON, ARGON, AND KRYPTON

HARRY WATTS[1]

South Australian Institute of Technology, Adelaide, South Australia

Received September 21, 1964

ABSTRACT

The diffusion coefficient of trace amounts of xenon-133 has been measured in binary mixtures of xenon with helium, neon, argon, and krypton. Measurements were made over the complete composition range in the pressure range 10–300 Torr at 302.6 °K. These systems are the first studied in which the results do not agree with the equation:

$$\frac{1}{D_{iM}} = \sum_{j \neq i} \frac{x_j}{\mathscr{D}_{ij}},$$

which relates the effective diffusion coefficient of a trace in an ideal gas mixture to binary diffusion coefficients and the composition of the mixture. Deviation from this equation can not be accounted for in terms of the known deviation of xenon from ideal gas behavior.

The self-diffusion coefficient of xenon was 0.060 and the binary diffusion coefficients Xe–He 0.535, Xe–Ne 0.230, Xe–Ar 0.127, Xe–Kr 0.0823, in $cm^2\ s^{-1}$ corrected to 1 atm pressure.

INTRODUCTION

Kinetic theory predicts, and several recent experimental investigations confirm (1–4), that the effective diffusion coefficient D_{iM} of a trace component i in a dilute gas mixture is given by the equation:

[1] $$\frac{1}{D_{iM}} = \sum_{j \neq i} \frac{x_j}{\mathscr{D}_{ij}}.$$

In eq. [1] the x_j are mole fractions and the $\mathscr{D}_{ij}$ are binary diffusion coefficients. This paper presents results of a further experimental investigation in which xenon-133 is the diffusing trace component in binary mixtures of xenon with the other group 0 gases. These systems are a special case of diffusion in a three-component mixture. Equation [1] then takes the form:

[2] $$\frac{1}{D_{A^*M}} = \frac{x_A}{\mathscr{D}_{A^*A}} + \frac{x_B}{\mathscr{D}_{A^*B}},$$

where x_A, x_B are the mole fractions of xenon and the second major component, $\mathscr{D}_{A^*A}$ is the self-diffusion coefficient of xenon and $\mathscr{D}_{A^*B}$ is the binary diffusion coefficient of xenon-133 with the other major component. This last quantity is approximated by the binary diffusion coefficient of normal xenon with the other major component.

RESULTS

All measurements were made in the same apparatus and by the same technique as previously described (4). Xenon-133 was obtained from the Radiochemical Centre, Amersham, England through the Australian Atomic Energy Commission.

The effective diffusion coefficient of xenon-133 in mixtures of xenon with each of the other group 0 gases was measured at several mole fractions. The self-diffusion coefficient of xenon and the binary diffusion coefficient of xenon with each of the other gases were also measured. All measurements were made at pressures in the range 10–300 Torr and

[1]*Present address: Exploratory Research Laboratory, Dow Chemical of Canada, Limited, Sarnia, Ontario.*

at 302.6 °K. The diffusion coefficients listed in Table I have been converted to 1 atm pressure assuming that the diffusion coefficient is inversely proportional to pressure; the actual experimental pressures are recorded in the table. It was previously shown that there is a significant difference of 2.5% between the results of duplicate experiments performed in the two diffusion cells (4). (This was shown by the application of "Student's *t* test", see, for example, Youden (5).)

Further, over the pressure range used, results obtained in the same cell may differ by 1.5%. The standard deviations given in Table I are those calculated for a single experiment; they vary from under 5% to over 10%. When allowance is made for the difference between cells and pressures, the standard deviations vary from about 1 to 6%. The standard deviation on the means should thus be better than 6%.

DISCUSSION

The predictions of eq. [2] are: (i) $1/D_{A^*M}$ varies linearly with x_A; (ii) at $x_{Xe} = 0$, $1/D_{A^*M} = 1/\mathscr{D}_{AB}$; (iii) at $x_{Xe} = 1$, $1/D_{A^*M} = 1/\mathscr{D}_{A^*A}$. Figure 1 shows that the reciprocal of the effective diffusion coefficient is a linear function of mole fraction over the greater part of the composition range for each system. The intercepts at $x_{Xe} = 0$ are given by the experimental binary diffusion coefficients. Straight lines through the points for each system extrapolate to the same intercept at $x_{Xe} = 1$. This intercept, however, does not agree with the experimental value of the self-diffusion coefficient of xenon from which it differs by 10%; this difference is significantly greater than the measuring error.

Before concluding that eq. [2] is invalid for these systems it is well to be certain that systematic experimental errors are not present. Errors in making up gas mixtures or contamination of the gases with impurities could lead to the observed results. It is unlikely that the same errors could have been made consistently with each mixture to give a common intercept at $x_{Xe} = 1$. Further, the technique for making mixtures was as used in the previous measurements (4) of the effective diffusion coefficient of krypton-85 in mixtures. Three different samples of xenon-133 and several different samples of normal xenon and the other gases were used in preparing mixtures, so errors due to impurities are unlikely.

The observed self-diffusion coefficient of xenon may be in error. The six measurements tabulated, however, were not all performed with the same sample of normal xenon or of xenon-133. The results in Table I*e* have a standard deviation of about 5%, less than 2% when allowance is made for the difference between cells and pressures. Thus these measurements are self-consistent. In Table II a comparison is made between the self and binary diffusion coefficients of xenon found in this work and values recorded in the literature.

The self-diffusion coefficient of xenon is consistent with those of Visner (6) and Amdur and Schatzki (7), but not with that of Groth and Harteck (8). The value of Groth and Harteck, however, is even less in agreement with that calculated from the intercept of Fig. 1. The binary diffusion coefficients agree with those in the literature. Thus it must be concluded that eq. [2] is not valid for the present systems. A detailed investigation in the composition range 0.8–1.0 mole fraction of xenon would be necessary to discover the relation between diffusion coefficient and composition.

The observed self-diffusion coefficient is significantly smaller than the value given by extrapolation of the concentration dependence; 0.06 $cm^2\ s^{-1}$ compared with 0.07 $cm^2\ s^{-1}$. A possible cause of this lower value is association of the diffusing species. Bernardes and Primakoff (10) investigated the possibility of stable diatomic molecule formation in the group 0 gases and derived an equation from which the degree of association might be calculated. Their equation predicts about 0.4% association in xenon under the conditions of these experiments. This is insufficient to affect the diffusion results significantly.

Can. J. Chem. Downloaded from www.nrcresearchpress.com by 210.87.254.40 on 09/05/12
For personal use only.

TABLE I

Diffusion coefficient of xenon-133 in mixtures, corrected to 1 atm, in units $cm^2 s^{-1}$ (where only one pressure is mentioned one experiment was performed in each cell at that pressure. The standard deviations are those for a single experiment)

Composition	Pressure (Torr)	Diffusion coefficient Cell 1	Diffusion coefficient Cell 2	Pressure (Torr)
(*a*) Xenon–helium				
$x_{Xe} = 0.80$	27.83	0.1059	0.1100	50.99
	109.20	0.1226	0.1078	173.02
	135.65	0.0898	0.0946	239.30
			Mean 0.1051±0.0116	
$x_{Xe} = 0.50$	70.70	0.1184	0.1045	38.45
	117.07	0.1136	0.1291	172.95
	193.60	0.1415	0.1299	271.95
			Mean 0.1228±0.0140	
$x_{Xe} = 0.25$	25.62	0.1696	0.1739	50.51
	107.50	0.1795	0.1976	190.74
			Mean 0.1801±0.0123	
$x_{Xe} = 0.125$	37.52	0.2643	0.2621	184.46
	87.09	0.2538	0.2609	366.76
			Mean 0.2603±0.0045	
Binary	18.99	0.5335	0.4653	34.54
	79.53	0.5993	0.5417	143.12
			Mean 0.5350±0.055	
(*b*) Xenon–neon				
$x_{Xe} = 0.50$	35.28	0.08721	0.0987	39.93
	68.43	0.1095	0.1181	110.82
	133.68	0.1176	0.1140	209.83
			Mean 0.1075±0.0122	
$x_{Xe} = 0.25$	31.19	0.1335	0.1351	
	65.34	0.1388	0.1278	
	127.43	0.1523	0.1526	
			Mean 0.1400±0.0103	
Binary	38.35	0.2382	0.1900	54.07
	87.43	0.2409	0.2120	155.75
	262.11	0.2649	0.2320	184.60
			Mean 0.2297±0.0268	
(*c*) Xenon–argon				
$x_{Xe} = 0.75$	35.84	0.09148	0.08612	
	83.82	0.09569	0.07881	
	102.33	0.08629	0.07847	
			Mean 0.08614±0.00682	
$x_{Xe} = 0.50$	19.88	0.07838	0.08266	35.80
	80.56	0.1261	0.09239	129.14
	116.00	0.1005	0.08935	181.04
			Mean 0.09490±0.0173	
$x_{Xe} = 0.25$	27.80	0.09956	0.08749	
	62.90	0.09800	0.09912	
	102.40	0.1124	0.1288	
			Mean 0.1042±0.0144	
Binary	32.12	0.1173	0.1140	
	111.39	0.1440	0.1254	
	117.86	0.1113	0.1486	
			Mean 0.1268±0.0158	
(*d*) Xenon–krypton				
$x_{Xe} = 0.75$	42.40	0.06947	0.07160	63.35
	112.43	0.06961	0.08171	199.79
			Mean 0.07311±0.0058	
$x_{Xe} = 0.25$	45.65	0.07221	0.08887	82.01
	106.96	0.07577	0.07864	152.77
			Mean 0.07887±0.00716	
$x_{Xe} = 0.10$	27.57	0.07301	0.08652	50.32
	80.86	0.07315	0.09069	137.23
	129.35	0.08947	0.09749	201.27
			Mean 0.08506±0.0313	
Binary	From ref. 4.		Mean 0.0823±0.0014	
(*e*) Xenon self-diffusion				
	13.97	0.06387	0.05792	32.81
	115.33	0.06172	0.05680	63.79
	117.86	0.06121	0.05840	117.86
			Mean 0.05999±0.00270	

Can. J. Chem. Downloaded from www.nrcresearchpress.com by 210.87.254.40 on 09/05/12
For personal use only.

TABLE II
Diffusion coefficients

System	This work, 302.6 °K ($cm^2\ s^{-1}$)	Other workers ($cm^2\ s^{-1}$)
Xe (self-diffusion)	0.0600	0.0576±0.0009* 0.0443±0.0022† 0.0480 (273.2°)‡ 0.0684 (329.9°)‡
Xe–He	0.535	0.604§
Xe–Ne	0.230	
Xe–Ar	0.127	0.114§ 0.0962 (273.2 °K)‡
Xe–Kr	0.0823	0.1366 (329.9 °K)‡

*Visner (6), 300.5 °K.
†Groth and Harteck (8), 293 °K.
‡Amdur and Schatzki (7).
§Srivastava (9), 303 °K.

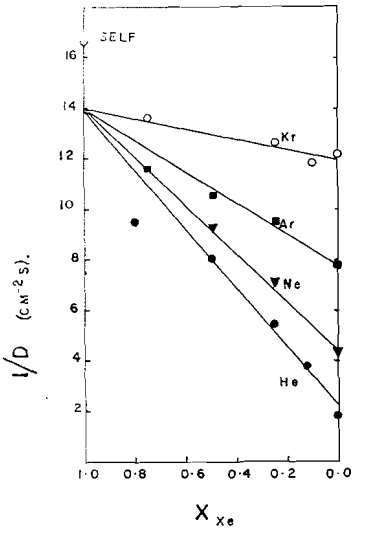

FIG. 1. Reciprocal of the effective diffusion coefficient of xenon-133 in the various mixtures plotted against mole fraction.

The formation of diatomic molecule ions, such as Xe_2^+, caused by ionizing radiation from the decay of xenon-133, was calculated to occur to less than 1 part in 10^{14}. This would not influence the diffusion results. The calculation was made on the basis of data in the literature (11–13) and the known amount of xenon-133 used in an experiment.

The effect of nonideal gas behavior was calculated to be insufficient to cause deviations from eq. [2]. The calculation was performed on the basis of the association model for the second virial coefficient given by Fowler and Guggenheim (14) and the second virial coefficients tabulated by Beattie (15).

The systems reported here are the first for which eq. [2] is not valid. No simple explanation for the failure of this equation can be offered. The need for further investigation of these systems in the xenon-rich region is obvious. The author is no longer in a position to carry out such an investigation and suggests that others may care to do so.

Can. J. Chem. Downloaded from www.nrcresearchpress.com by 210.87.254.40 on 09/05/12
For personal use only.

REFERENCES

1. L. MILLER and P. C. CARMAN. Trans. Faraday Soc. **57**, 2143 (1961); **60**, 33 (1964).
2. B. N. SRIVASTAVA and R. PAUL. Physica, **28**, 646 (1962).
3. R. PAUL. Indian J. Phys. **36**, 464 (1962).
4. H. WATTS. Trans. Faraday Soc. **60**, 1745 (1964).
5. W. J. YOUDEN. Statistical methods for chemists. John Wiley and Sons, New York. 1957.
6. S. VISNER. Phys. Rev. **82**, 297 (1951).
7. I. AMDUR and T. F. SCHATZKI. J. Chem. Phys. **27**, 1049 (1957).
8. W. GROTH and P. HARTECK. Z. Elektrochem. **47**, 167 (1941).
9. K. P. SRIVASTAVA. Physica, **25**, 571 (1959).
10. N. BERNARDES and H. PRIMAKOFF. J. Chem. Phys. **30**, 691 (1959).
11. J. A. HORNBECK and J. P. MOLNAR. Phys. Rev. **84**, 621 (1951).
12. W. F. EDGELL. *In* Argon, helium and the rare gases, Vol. I. *Edited by* G. A. Cook. Interscience Publishers, New York. 1961. p. 99.
13. E. F. WESTRUM and J. M. PLANEIX. *In* Argon, helium and the rare gases. Vol. I. *Edited by* G. A. Cook. Interscience Publishers, New York. 1961. p. 87.
14. SIR R. FOWLER and E. A. GUGGENHEIM. Statistical thermodynamics. Cambridge University Press. 1949. p. 269.
15. J. A. BEATTIE. *In* Argon, helium and the rare gases. Vol. I. *Edited by* G. A. Cook. Interscience Publishers, New York. 1961. p. 273.

Can. J. Chem. Downloaded from www.nrcresearchpress.com by 210.87.254.40 on 09/05/12
For personal use only.

Can. J. Chem. Downloaded from www.nrcresearchpress.com by 210.87.254.40 on 09/05/12
For personal use only.

THE CRYSTAL STRUCTURE OF α-$Zn_3(PO_4)_2$

CRISPIN CALVO
Department of Chemistry, McMaster University, Hamilton, Ontario
Received July 28, 1964

ABSTRACT

α-$Zn_3(PO_4)_2$ crystallized in the monoclinic space group $C2/c$ with lattice parameters $a = 8.14 \pm 0.02$ Å, $b = 5.63 \pm 0.01$ Å, $c = 15.04 \pm 0.04$ Å, $\beta = 105°08' \pm 05'$, and $Z = 4$. The cations are found in two types of tetrahedrally coordinated sites. One-third of the cations lie on twofold axes within an oxygen tetrahedron. The remaining cations are found in a pair of edge-sharing oxygen atom tetrahedra. The green emission of Mn^{++} in α-$Zn_3(PO_4)_2$ is consistent with Mn^{++} substituting for Zn^{++} in either tetrahedral site.

INTRODUCTION

The probable phase diagram of anhydrous zinc orthophosphate has been determined by Hummel and co-worker (1). The α-phase was shown to be stable below 942 °C and to transform above this temperature to a new phase, labelled β. No further transitions occur between 942 °C and the melting temperature (1 060 °C). Upon the addition of Mn^{++} (2), Mg^{++} (3, 5), Cd^{++} (4) as orthophosphates a third phase was found. This phase, generally called γ, has been shown to be in fact a solid solution (2). The composition range over which the γ-phase is stable varies with the nature of the added cation. The crystal structure of γ-$Zn_3(PO_4)_2$ has been resolved (6) and, in addition, it appears to be isostructural with the end member $Mg_3(PO_4)_2$. Some crystallographic data are available on other phases that may be important in understanding the phase behavior of $Zn_3(PO_4)_2$. Mackay has discussed the crystallography of $Ca_3(PO_4)_2$ (7) and unpublished data have been obtained for $Mn_3(PO_4)_2$, $Cd_3(PO_4)_2$, and β-$Zn_3(PO_4)_2$ (8).

Studies related to the luminescence of suitably activated $M_3(PO_4)_2$ has led to the discovery of a large number of polymorphs. Here temperature and composition are to be regarded as the variables. Two stable phases are reported to occur in each of $Zn_3(PO_4)_2$ (1), $Sr_3(PO_4)_2$ (9), $Ca_3(PO_4)_2$ (7), and $Pb_3(PO_4)_2$ (10). Recently two phases of $Mn_3(PO_4)_2$ have been identified and a third is suspected on crystallographic grounds. Similarly a second phase is suspected to occur in $Cd_3(PO_4)_2$ at high temperatures. $Ba_3(PO_4)_2$ on the other hand shows only one phase up to its melting temperature. Additional new compounds of the type $Ba_2Y(PO_4)_2$, $BaY_2(PO_4)_2$, and $SrY_2(PO_4)_2$ for Y = Zn or Mg (9, 11) have been reported. Differential thermal analysis studies of these phases indicate new polymorphic forms in the zinc-containing members at high temperature. In addition three distinct solid solutions are found in the $(Cd,Zn)_3(PO_4)_2$ system. One of these phases appears to be an isostructure of γ-$Zn_3(PO_4)_2$ (4). In contrast only a limited number of anhydrous orthophosphates are found as minerals in nature. These minerals are whitlockite, graftonite (12), scarscopside, and hurlbutite. Crystal structures of the last two have been published (13, 14). Finally the crystal structures of the room-temperature forms $Ba_3(PO_4)_2$ and $Sr_3(PO_4)_2$ have been determined and are identical (15). It is clear that a great deal of crystallographic information remains unresolved and that without such a resolution the crystal chemistry of the orthophosphates will remain a bibliographic indexing.

It has been widely suggested that the emission energy of Mn^{++} is related to its coordination number. The luminescence of α-$Zn_3(PO_4)_2$:Mn is green whereas both

β-$Zn_3(PO_4)_2$:Mn and γ-$Zn_3(PO_4)_2$:Mn emit red when suitably excited. In detail a green emission is said to arise from tetrahedrally coordinated Mn^{++} while the red emission arises from an octahedrally coordinated environment. The theoretical basis for this proposed correlation lies in the Sugano–Tanabe (16) diagram of the energy level splittings versus the ratio of the octahedral component of the crystal field energy to the electron correlation as measured by the parameter DQ/B. Assuming that the crystal field term DQ increases with the number of ligands and further that a similar diagram is also valid for the emission states, one can understand the proposed correlation. In γ-$Zn_3(PO_4)_2$ one finds both tetrahedral and octahedral cation sites and some evidence exists for the preferential solubility of Mn^{++} into the octahedral site. Thus a consistent model can be obtained in this system.

The present crystal structure study has been undertaken, in part, to determine whether the tetrahedrally coordinated cation sites, as suggested by the emission, actually exist. The consequences of direct Mn^{++} substitution for Zn^{++} are considered and this manner of substitution is the basis for a discussion of the relative free energies of the α- and γ-phases.

EXPERIMENTAL

Single crystals of α-$Zn_3(PO_4)_2$ suitable for X-ray crystallographic studies were grown from $ZnCl_2$ melt (17). A mix containing about tenfold molar excess of the solvent was placed in an open vycor tube plugged at the open end with quartz wool. At 650 °C all the zinc orthophosphate had dissolved. Crystals were then grown by slow cooling of this mix from 650 °C to room temperature. The α-$Zn_3(PO_4)_2$ crystals were easily recovered from the slurry formed upon the addition of water. The crystals were needle-shaped with the needle axis coinciding with the crystallographic b-axis. Since X-ray reflections indexed as $h0l$ with l = odd and hkl with $h + k$ = odd were not observed, the space group choice then lay between $C2/c$ and Cc. The centered space group was chosen as the trial space group.

Lattice parameters were obtained from rotation photographs calibrated for the effective camera radius by superimposing NaCl powder lines. The parameters so obtained were $a = 8.14 \pm 0.02$ Å, $b = 5.63 \pm 0,01$ Å, $c = 15.04 \pm 0.04$ Å, $\beta = 105°08' \pm 05'$. These values are in good agreement with those obtained by Amick from powder data (18). The measured density of 3.88 g/cm³ compares well with the calculated density of 3.85 g/cm³ for a unit cell containing four molecules. Since the $C2/c$ space group requires that atoms in the general position occur in the unit cell as multiples of 8, at least 4 of the 12 Zn^{++} must occur in special positions. The available sites of fourfold multiplicity are on the twofold axis and at the center of symmetry.

Intensity data visually estimated from Weissenberg photographs were obtained for the 0th and 1st layer lines about the b-axis. These data were taken with Cu K_α radiation using a crystal of breath 0.1 mm × 0.1 mm perpendicular to the needle axis and 0.3 mm along this axis. Patterson function projections were prepared from these intensity data after suitable corrections for Lorentz and polarization effects. These functions were readily interpreted for the x- and z-parameters of Zn and P atoms. The ambiguity with regards to the special site occupied by one-third of the cations was resolved in favor of a twofold axis site by the interpretation of the generalized Patterson function, prepared with the data from the 1st layer line, together with the trial x- and z-parameters; x- and z-parameters from the oxygen atoms were determined from Fourier and difference Fourier projections. Trial y-parameters for the oxygen atoms were found by distributing these atoms tetrahedrally about the P atom on a spherical shell of radius equal to 1.5 Å. Subsequent refinement of these parameters yielded a value for the reliability index of 0.18 for the $h0l$ and 0.27 for the $h1l$ data. At this stage the dispersions in the value of the P—O and O—O bond distances about the PO_4 group suggested the need for additional data. Therefore $hk0$ and $0kl$ data were taken with Mo K_α radiation on the precession camera and in addition the first three layer lines about the b-axis were also recorded with this radiation using the Weissenberg camera. No absorption corrections were necessary for the data taken with Mo K_α radiation. Additional refinements using difference Fourier series and least-squares procedures with this new data included has led to the atomic parameters tabulated in Table I. A modified Busing, Martin, and Levy program (19) for the IBM 7040 (20K) was used in this least-squares refinement. The overall reliability index for the 750 independent observations including unobserved reflections is 0.12. The reliability index for the individual zones is shown in Table II and the observed and calculated structure factors are compared in Table III.

THE CRYSTAL STRUCTURE

The crystal structure is seen in projection onto the $x - z$-plane in Fig. 1. The Zn^{++} in the special site and the one in the general position show tetrahedral coordination to surrounding oxygen atoms. However, only in the former case is the symmetry of a

Can. J. Chem. Downloaded from www.nrcresearchpress.com by 210.87.254.40 on 09/05/12
For personal use only.

TABLE I

Atomic parameters

	A. Positional		
	x/a	y/b	z/c
Zn_I	0	0.7448±0.0009	1/4
Zn_{II}	0.2678±0.0002	0.5548±0.0007	0.0675±0.0001
P	0.1592±0.0004	0.0634±0.0014	0.1286±0.0002
O_I	0.2929±0.0014	0.0607±0.0039	0.2211±0.0008
O_{II}	0.1197±0.0016	0.3092±0.0043	0.0770±0.0008
O_{III}	0.2129±0.0014	0.9021±0.0041	0.0625±0.0007
O_{IV}	0.9935±0.0013	0.9676±0.0033	0.1429±0.0006

	B. Thermal (mean square atomic displacement, Å²)					
	U_{11}	U_{22}	U_{33}	U_{12}	U_{13}	U_{23}
Zn_I	0.004	0.009	0.005	—	0.000	—
Zn_{II}	0.007	0.009	0.010	0.000	0.002	0.003
P	0.004	0.007	0.004	−0.005	0.001	−0.001
O_I	0.009	0.008	0.014	0.001	−0.005	−0.025
O_{II}	0.017	0.011	0.013	−0.027	0.004	0.000
O_{III}	0.017	0.010	−0.031	−0.007	0.000	−0.007
O_{IV}	0.011	0.013	0.006	0.011	−0.001	0.010

TABLE II

Residual value per each zone

Zone	Total number of $\|F_{obs}\|$	(Unobserved reflections not included) $R = \frac{\sum\|F_{obs}\| - \|F_{calcd}\|}{\sum\|F_{obs}\|}$
*h*0*l*	215	0.098
*h*1*l*	220	0.098
*h*2*l*	232	0.105
*hk*0	34	0.082
0*kl*	52	0.072

regular tetrahedron actually approached. These zinc ions (Zn_I^{++}) lie on twofold axes and share one oxygen atom with each of four neighboring phosphorus atoms. The average Zn_I—O bond distance is found to be 1.98 ± 0.05 Å and the O—O near neighbor distance around this cation is 3.27 ± 0.13 Å. The near neighbor oxygen atom distribution about Zn_{II}^{++} is quite irregular but still roughly tetrahedral. The Zn_{II}—O bond distances range from 1.86 to 2.03 Å with an average of 1.96 ± 0.05 Å. Again each oxygen atom is shared with an unique phosphorus atom. The Zn_{II}^{++} occur as a centered pair of edge-sharing tetrahedra with O_{III} as the common oxygen atom. Only one oxygen atom (O_{IV}) is shared between the cations in the general position and the special site.

The phosphate groups are slightly irregular independent tetrahedron with each of its oxygen atoms coordinated with at least one Zn^{++}. The average P—O bond distance is 1.53 Å with an estimated standard deviation (e.s.d.) of 0.03 Å in agreement with the accepted value of 1.54 Å for a P—O bond with a double bond order of 0.5 (20). However, the values obtained range from 1.50 to 1.58 Å. There is no doubt that the lack of high resolution along the *y*-direction will limit the accuracy with which these oxygen atoms can be located. The relatively large e.s.d. on all the *y*-parameters illustrates this point. The O—O bond distances around the tetrahedron average 2.52 Å and the bond angles

Can. J. Chem. Downloaded from www.nrcresearchpress.com by 210.87.254.40 on 09/05/12
For personal use only.

Can. J. Chem. Downloaded from www.nrcresearchpress.com by 210.87.254.40 on 09/05/12
For personal use only.

TABLE III

Observed and calculated structure factors

H	K	L	|F(O)|	F(C)	H	K	L	|F(O)|	F(C)	H	K	L	|F(O)|	F(C)	H	K	L	|F(O)|	F(C)
0	0	4	26.9	-23.6	14	0	-8	24.0	20.8	3	1	1	14.9	12.7	2	2	21	<19.0	-9.0
0	0	6	160.7	-151.4	14	0	-6	37.9	-36.3	3	1	2	93.9	-81.5	2	2	22	38.2	32.8
0	0	8	20.3	-19.0	14	0	-4	<10.4	-13.7	3	1	3	31.7	-27.8	4	2	-24	42.1	-40.2
0	0	10	96.3	-92.3	14	0	-2	27.0	-21.3	3	1	4	40.7	-38.9	4	2	-23	<16.3	4.6
0	0	12	25.8	27.2	14	0	0	23.6	21.5	3	1	5	61.3	63.0	4	2	-22	<16.1	2.6
0	0	14	54.1	55.4	14	0	2	<10.6	-8.7	3	1	6	<5.6	3.8	4	2	-21	<15.4	17.4
0	0	16	78.8	81.0	14	0	4	32.0	33.7	3	1	7	20.0	-16.1	4	2	-20	<15.1	-9.6
0	0	18	15.9	-21.3	14	0	6	<10.8	4.9	3	1	8	6.5	10.3	4	2	-19	<14.6	3.2
0	0	20	16.0	-19.9	14	0	8	<7.2	9.1	3	1	9	54.7	58.9	4	2	-18	19.7	24.7
0	0	22	30.4	-30.3	14	0	10	36.9	-39.1	3	1	10	51.6	51.7	4	2	-17	<13.5	4.2
0	0	24	<10.1	2.1	14	0	12	<10.6	-4.5	3	1	11	30.9	-33.3	4	2	-16	13.0	-8.0
0	0	26	17.3	-18.2	14	0	14	<10.3	-2.5	3	1	12	40.7	41.2	4	2	-15	<10.2	7.2
0	0	28	18.4	19.4	14	0	16	9.8	14.8	3	1	13	<7.8	1.2	4	2	-14	77.2	76.4
0	0	30	<10.8	7.6	14	0	18	<9.1	-2.3	3	1	14	<8.1	7.5	4	2	-13	17.6	-21.0
0	0	32	15.4	18.0	14	0	20	<8.3	15.3	3	1	15	41.7	-40.1	4	2	-12	12.8	-15.5
2	0	-30	28.8	-31.0	16	0	-20	35.1	29.3	3	1	16	57.2	-49.2	4	2	-11	29.4	-42.3
2	0	-28	<10.8	2.2	16	0	-18	<10.8	1.8	3	1	17	32.1	24.7	4	2	-10	15.5	-20.8
2	0	-26	<10.4	5.2	16	0	-16	<10.8	2.0	3	1	18	29.7	-24.1	4	2	-9	17.0	-20.3
2	0	-24	29.3	29.2	16	0	-14	20.9	-19.0	3	1	19	<11.9	-7.7	4	2	-8	103.6	-110.2
2	0	-22	<9.3	-4.1	16	0	-12	<15.4	6.5	3	1	21	17.7	15.3	4	2	-7	49.8	51.7
2	0	-20	40.9	36.3	16	0	-10	25.1	-26.3	-5	1	21	22.7	25.5	4	2	-6	17.6	24.2
2	0	-18	25.6	-23.3	16	0	-8	<10.8	3.4	-5	1	20	17.2	-18.3	4	2	-5	40.7	52.4
2	0	-16	14.0	-15.9	16	0	-6	<10.8	4.1	-5	1	19	<11.0	-8.9	4	2	-4	21.0	-23.7
2	0	-14	100.6	-99.6	16	0	-4	32.8	37.2	-5	1	18	45.8	-45.3	4	2	-3	<6.6	8.5
2	0	-12	25.0	25.5	16	0	-2	10.8	-5.2	-5	1	17	<10.2	8.0	4	2	-2	62.6	76.8
2	0	-10	10.9	9.7	16	0	0	14.0	-1.5	-5	1	16	<13.2	7.1	4	2	-1	8.7	-6.2
2	0	-8	155.1	135.0	16	0	2	17.1	-19.3	-5	1	15	42.5	-41.2	4	2	1	27.9	-27.9
2	0	-6	16.5	15.3	16	0	-18	22.3	-23.8	-5	1	14	67.7	65.9	4	2	2	95.6	72.6
2	0	-4	58.0	60.6	18	0	-12	20.3	19.2	-5	1	13	14.1	16.0	4	2	3	37.4	-37.1
2	0	-2	55.4	-66.3	18	0	0	18.3	21.3	-5	1	12	50.8	49.1	4	2	4	59.2	-54.6
2	0	0	89.1	-89.2	3	1	0	39.9	-39.1	-5	1	11	18.4	-23.5	4	2	5	61.7	-53.8
2	0	2	159.8	-161.8	5	1	0	58.2	59.8	-5	1	10	14.1	-13.1	4	2	6	38.2	-40.0
2	0	4	30.7	27.2	7	1	0	10.5	-11.5	-5	1	9	33.4	32.4	4	2	7	35.7	29.7
2	0	6	101.6	89.9	9	1	0	17.8	17.4	-5	1	8	27.8	-27.8	4	2	8	68.9	-63.2
2	0	8	110.3	106.3	11	1	0	22.7	-25.2	-5	1	7	16.0	-16.8	4	2	9	46.2	52.6
2	0	10	28.6	-27.3	13	1	0	30.8	37.9	-5	1	6	24.9	-23.2	4	2	10	22.5	26.0
2	0	12	16.9	21.3	15	1	0	25.9	-24.0	-5	1	5	62.9	68.0	4	2	11	25.8	27.3
2	0	14	63.1	-51.7	0	2	0	86.0	88.0	-5	1	4	93.8	-86.7	4	2	12	<12.1	8.8
2	0	16	25.6	-28.8	2	2	0	122.8	-125.7	-5	1	3	38.5	-40.7	4	2	13	21.1	-16.1
2	0	18	46.6	-49.4	4	2	0	34.3	31.7	-5	1	2	26.2	-26.4	4	2	14	42.4	40.9
2	0	20	57.2	54.2	6	2	0	42.3	-40.2	-5	1	1	7.9	7.9	4	2	15	<14.0	-13.9
2	0	22	16.8	20.8	8	2	0	12.5	-9.0	5	1	1	77.2	79.0	4	2	16	<15.0	-7.1
2	0	24	19.0	16.5	10	2	0	39.9	-31.8	5	1	2	109.3	108.5	6	2	-24	<17.3	3.0
2	0	26	15.8	-20.2	12	2	0	<16.5	-0.	5	1	3	46.4	-37.7	6	2	-23	<16.9	-7.8
2	0	28	16.0	10.1	1	3	0	45.5	38.9	5	1	4	14.0	13.5	6	2	-22	24.1	33.9
2	0	30	16.8	-17.9	3	3	0	9.3	-9.2	5	1	5	11.4	13.1	6	2	-21	23.4	-26.2
4	0	-28	32.9	33.8	5	3	0	11.7	18.4	5	1	6	21.1	-23.2	6	2	-20	22.7	-22.1
4	0	-26	31.7	-26.5	7	3	0	<9.5	3.6	5	1	7	52.5	-44.3	6	2	-19	<15.0	-8.6
4	0	-24	25.5	-27.8	9	3	0	18.5	16.8	5	1	8	21.3	-26.2	6	2	-18	<14.6	-19.8
4	0	-22	36.6	-33.0	0	4	0	49.2	48.8	5	1	9	12.8	13.6	6	2	-17	16.6	13.5
4	0	-20	35.2	32.8	2	4	0	53.4	54.8	5	1	10	37.1	-33.5	6	2	-16	31.5	-32.5
4	0	-18	14.5	-7.1	4	4	0	44.9	42.3	5	1	11	31.2	-27.1	6	2	-15	13.7	11.2
4	0	-16	38.5	43.3	6	4	0	23.2	28.9	5	1	12	24.7	-28.0	6	2	-14	18.1	17.6
4	0	-14	31.4	37.0	8	4	0	21.3	28.0	5	1	13	28.0	27.7	6	2	-13	13.7	13.6
4	0	-12	38.0	39.6	1	5	0	12.3	-12.9	5	1	14	<10.9	-0.9	6	2	-12	25.1	-28.3
4	0	-10	111.6	-107.1	3	5	0	18.8	22.4	5	1	15	<11.3	3.0	6	2	-11	12.6	16.3
4	0	-8	49.7	-62.7	5	5	0	<11.6	-1.9	5	1	16	43.8	40.9	6	2	-10	30.3	35.8
4	0	-6	30.8	-39.1	5	5	0	<11.1	-4.0	5	1	17	26.9	21.0	6	2	-9	14.6	15.2
4	0	-4	56.6	72.5	0	6	0	62.8	-62.9	5	1	18	30.4	24.2	6	2	-8	20.3	22.5
4	0	-2	11.6	-10.9	2	6	0	16.4	16.6	5	1	19	32.8	-24.1	6	2	-7	39.9	-43.8
4	0	0	120.5	118.1	4	6	0	39.7	-31.2	-7	1	16	<10.5	-1.2	6	2	-6	44.8	56.7
4	0	2	3.7	-0.6	6	6	0	16.5	-16.1	-7	1	15	<8.3	-7.4	6	2	-5	39.3	-41.2
4	0	4	30.3	31.5	1	7	0	<10.8	-4.7	-7	1	14	29.3	-34.6	6	2	-4	62.5	-68.1
4	0	6	121.4	-123.2	3	7	0	20.2	24.8	-7	1	13	24.9	27.3	6	2	-3	10.2	-13.9
4	0	8	9.4	-8.9	0	2	1	43.9	-43.6	-7	1	12	68.7	-64.3	6	2	-2	17.8	-19.0
4	0	10	24.3	-26.7	0	2	2	69.8	70.5	-7	1	11	51.6	-44.1	6	2	-1	27.2	32.8
4	0	12	58.3	57.0	0	2	3	24.0	-22.2	-7	1	10	<7.3	-5.5	6	2	1	23.0	26.1
4	0	14	<8.0	-3.1	0	2	4	76.0	-80.0	-7	1	9	13.1	17.0	6	2	2	21.7	25.4
4	0	16	27.6	31.5	0	2	5	18.5	-17.9	-7	1	8	44.5	51.9	6	2	3	15.7	15.9
4	0	18	<9.3	-2.8	0	2	6	9.5	4.8	-7	1	7	17.3	-25.0	6	2	4	31.6	-36.7
4	0	20	<9.9	3.7	0	2	7	14.0	12.5	-7	1	6	46.8	51.0	6	2	5	19.0	18.8
4	0	22	33.0	-34.5	0	2	8	60.9	-57.0	-7	1	5	24.8	31.4	6	2	6	75.9	67.3
4	0	24	10.7	-5.9	0	2	9	<7.5	3.4	-7	1	4	18.5	23.7	6	2	7	10.2	-8.9
4	0	26	10.9	1.4	0	2	10	8.0	-9.0	-7	1	3	30.2	-31.7	6	2	8	17.2	15.2
4	0	28	16.8	20.8	0	2	11	9.1	10.0	-7	1	2	<6.8	7.5	6	2	9	29.0	-30.9
6	0	-30	19.8	-16.9	0	2	12	39.3	-42.5	-7	1	1	34.7	36.0	6	2	10	22.8	21.4
6	0	-28	<10.8	-2.3	0	2	13	33.4	29.6	7	1	1	9.7	11.1	6	2	11	32.3	-31.8
6	0	-26	<8.0	-10.4	0	2	14	71.8	71.7	7	1	3	20.2	-23.0	6	2	12	60.3	-58.1
6	0	-24	34.2	39.2	0	2	15	<12.7	2.8	7	1	2	75.9	-81.2	6	2	13	<14.9	6.3
6	0	-22	18.6	24.5	0	2	16	25.5	15.0	7	1	4	46.9	-48.3	6	2	14	<15.4	6.0
6	0	-20	<9.0	10.8	0	2	17	19.4	-21.7	7	1	5	39.1	38.1	6	2	15	24.2	23.6
6	0	-18	63.9	-55.5	0	2	18	22.0	22.7	7	1	6	30.3	25.5	6	2	16	17.0	-17.9
6	0	-16	12.5	-8.0	0	2	19	20.8	-21.2	7	1	7	16.9	-16.9	8	2	-24	21.2	-25.2
6	0	-14	35.9	-39.7	0	2	20	37.3	-34.6	7	1	8	69.2	58.7	8	2	-23	<17.4	-1.9
6	0	-12	<13.7	19.3	0	2	21	<10.1	5.2	7	1	9	10.6	18.4	8	2	-22	<17.0	-4.8
6	0	-10	<5.3	-4.2	0	2	22	<23.3	7.5	7	1	10	17.0	17.8	8	2	-21	22.8	25.4
6	0	-8	114.5	135.8	0	2	23	<17.1	10.4	7	1	11	20.2	-20.7	8	2	-20	<16.2	-4.6
6	0	-6	8.9	5.1	0	2	24	19.9	-25.3	-9	1	13	<10.7	11.8	8	2	-19	<16.1	23.1
6	0	-4	22.3	-27.1	0	4	1	55.3	-52.8	-9	1	12	51.5	46.1	8	2	-18	43.2	44.0
6	0	-2	101.4	-125.4	0	4	2	32.4	-34.3	-9	1	11	10.3	-6.7	8	2	-17	14.6	-6.4
6	0	0	14.4	16.2	0	4	3	73.1	-76.6	-9	1	10	10.2	5.2	8	2	-16	14.7	3.3
6	0	2	23.9	-27.9	0	4	4	30.8	27.6	-9	1	9	45.8	42.9	8	2	-15	39.0	-38.1
6	0	4	27.8	29.7	0	4	5	39.6	-41.7	-9	1	8	42.4	-41.8	8	2	-14	17.8	15.8
6	0	6	27.1	29.8	0	4	6	28.6	-30.5	-9	1	7	15.1	-17.9	8	2	-13	17.4	-17.9
6	0	8	87.3	74.2	0	4	7	13.4	9.5	-9	1	6	50.7	-49.6	8	2	-12	39.3	-40.8
6	0	10	29.6	-28.5	0	4	8	20.8	30.3	-9	1	5	9.8	4.1	8	2	-10	<12.9	5.1
6	0	12	33.0	-35.6	0	4	9	26.9	29.0	-9	1	4	16.0	-14.4	8	2	-9	<10.3	0.7
6	0	14	36.1	-34.0	0	4	10	40.1	-38.9	-9	1	3	36.9	-36.7	8	2	-8	42.5	-48.5
6	0	16	19.9	23.3	0	4	11	36.0	27.0	-9	1	2	14.5	14.9	8	2	-7	18.2	23.5
6	0	18	14.7	-12.7	0	4	12	29.5	26.4	-9	1	1	22.2	24.9	8	2	-6	16.3	19.9
6	0	20	21.8	19.6	0	4	13	48.5	44.0	9	1	1	21.9	24.8	8	2	-5	34.7	43.2
6	0	22	<10.7	2.9	0	4	14	15.3	-14.3	9	1	2	40.4	38.8	8	2	-4	9.9	-7.1
6	0	24	18.5	20.4	0	4	15	<13.4	-7.0	9	1	3	22.6	-25.4	8	2	-3	27.7	21.4
6	0	26	16.9	-22.6	0	4	16	15.9	17.8	9	1	4	19.4	23.7	8	2	-2	77.3	73.4
8	0	-32	19.3	18.0	0	4	17	35.0	-31.5	9	1	5	<10.8	9.5	8	2	-1	40.9	-39.6
8	0	-30	<10.8	-8.4	0	6	1	29.0	-29.5	9	1	6	<11.1	0.4	8	2	1	45.6	-43.8
8	0	-28	<10.8	11.2	0	6	2	<11.9	10.1	9	1	7	25.3	-30.5	8	2	2	<12.8	2.6
8	0	-26	<10.6	-9.1	0	6	3	37.9	-31.4	9	1	8	42.2	-46.2	8	2	3	<13.0	-5.8
8	0	-24	<10.3	-1.2	0	6	4	<11.4	-8.6	9	1	9	23.4	27.0	8	2	4	35.3	-46.7
8	0	-22	46.3	-41.2	0	6	5	36.5	-36.5	9	1	10	23.3	-28.4	8	2	5	<13.9	3.2
8	0	-20	16.0	15.4	0	6	6	33.5	39.1	-11	1	13	26.6	18.6	8	2	6	<13.9	13.0
8	0	-18	12.4	13.9	0	6	7	<13.4	5.8	-11	1	12	24.5	-18.5	8	2	7	<14.2	11.8

TABLE III (*Concluded*)

8	0 -16	50.2	49.5	0	6	8	<13.4	-11.5	-11	1	11	24.2	-19.5	8	2	8	28.4	-25.0
8	0 -14	14.7	-17.3	0	6	9	<12.1	7.2	-11	1	10	17.0	-11.0	8	2	9	15.0	13.8
8	0 -12	10.8	9.0	0	6	10	23.5	21.6	-11	1	9	<11.4	6.4	8	2	10	15.3	7.9
8	0 -10	41.8	-39.5	0	6	11	20.8	24.7	-11	1	8	29.3	22.3	8	2	11	33.1	28.0
8	0 -8	16.1	-17.1	-1	1	24	19.0	19.9	-11	1	7	35.8	-29.4	8	2	12	<16.1	6.8
8	0 -6	57.6	-53.1	-1	1	23	<12.5	6.1	-11	1	6	58.3	56.6	8	2	13	<16.6	-7.0
8	0 -4	37.8	41.1	-1	1	22	<12.1	-7.8	-11	1	5	31.2	27.4	8	2	14	40.2	36.2
8	0 -2	51.4	46.8	-1	1	21	26.1	25.0	-11	1	4	<19.2	11.0	8	2	15	21.2	-20.4
8	0 0	71.7	60.6	-1	1	20	23.7	-27.1	-11	1	3	<11.3	-2.7	10	2	-18	<16.6	-8.4
8	0 2	53.9	-46.7	-1	1	19	25.2	-27.2	-11	1	2	35.2	-29.6	10	2	-17	<16.8	-7.1
8	0 4	9.2	-7.6	-1	1	18	22.0	-23.1	-11	1	1	31.7	23.2	10	2	-16	48.6	-46.6
8	0 6	45.1	-40.3	-1	1	17	<10.0	4.2	11	1	1	19.1	22.2	10	2	-15	32.7	26.2
8	0 8	12.4	6.9	-1	1	16	< 9.6	-1.6	11	1	2	<11.8	-12.1	10	2	-14	20.3	21.0
8	0 10	35.8	-34.8	-1	1	15	39.7	-35.6	11	1	3	<12.0	-10.7	10	2	-13	35.0	31.2
8	0 12	56.5	51.4	-1	1	14	10.9	12.2	11	1	4	<12.1	-9.9	10	2	-12	<15.0	13.0
8	0 14	18.5	17.8	-1	1	13	20.1	18.3	11	1	5	20.1	19.4	10	2	-11	<14.8	3.2
8	0 16	14.7	15.1	-1	1	12	21.3	16.5	11	1	6	<12.5	-2.3	10	2	-10	40.8	35.1
8	0 18	33.7	-40.3	-1	1	11	30.0	-34.9	11	1	7	<12.7	-6.4	10	2	-9	15.0	-14.6
8	0 20	<10.8	3.8	-1	1	10	57.9	67.7	11	1	8	27.8	33.1	10	2	-8	<14.3	-9.6
8	0 22	<10.8	-7.5	-1	1	9	82.0	79.8	11	1	9	<13.1	12.7	10	2	-7	21.4	-18.8
8	0 24	<10.6	2.6	-1	1	8	27.5	29.0	11	1	10	20.3	22.0	10	2	-6	24.8	21.2
8	0 26	<10.1	-5.2	-1	1	7	6.6	-6.5	11	1	11	24.5	-23.5	10	2	-5	15.6	-15.9
10	0 -28	17.7	23.1	-1	1	6	33.6	-36.4	-13	1	6	32.8	-27.7	10	2	-4	38.6	-33.8
10	0 -26	<10.8	3.0	-1	1	5	62.6	51.5	-13	1	5	<12.7	11.5	10	2	-3	25.5	-24.9
10	0 -24	<10.6	8.3	-1	1	4	152.9	-145.6	-13	1	4	25.0	-20.5	10	2	-2	22.3	-22.0
10	0 -22	<10.3	-4.0	-1	1	3	98.6	-108.1	-13	1	3	26.6	-23.5	10	2	-1	19.0	15.7
10	0 -20	16.9	18.0	-1	1	2	11.2	-8.4	-13	1	2	<12.8	12.9	10	2	1	43.4	37.7
10	0 -18	39.2	-36.4	-1	1	1	33.2	26.2	-13	1	1	<12.9	9.4	10	2	2	39.3	37.7
10	0 -16	20.7	-21.2	1	1	1	58.6	59.6	13	1	1	18.5	7.2	10	2	3	29.2	27.6
10	0 -14	< 8.9	-7.5	1	1	2	29.3	26.4	13	1	2	<13.2	14.1	10	2	4	15.7	13.2
10	0 -12	61.1	54.4	1	1	3	47.2	-44.1	13	1	3	19.7	-20.5	10	2	5	17.8	-15.2
10	0 -10	< 8.4	-4.9	1	1	4	48.3	44.8	2	2	-26	21.1	23.2	10	2	6	36.6	27.6
10	0 -8	18.5	21.9	1	1	5	38.4	30.4	2	2	-25	<14.6	3.2	10	2	7	17.4	-21.5
10	0 -6	15.0	-17.3	1	1	6	55.2	62.0	2	2	-24	14.4	1.9	10	2	8	16.5	-18.7
10	0 -4	15.8	16.2	1	1	7	60.5	-64.4	2	2	-23	14.6	-6.7	10	2	9	<16.8	-7.7
10	0 -2	71.9	-66.6	1	1	8	6.1	4.9	2	2	-22	24.5	25.8	10	2	10	<13.0	7.3
10	0 0	<10.8	2.3	1	1	9	9.5	10.6	2	2	-21	15.2	0.4	10	2	11	<16.6	-10.6
10	0 2	< 8.6	-0.6	1	1	10	96.4	-101.7	2	2	-20	15.9	-1.5	10	2	12	25.8	-29.7
10	0 4	51.8	54.2	1	1	11	23.0	-23.0	2	2	-19	14.5	-8.8	12	2	-18	22.5	14.8
10	0 6	< 9.2	-8.1	1	1	12	37.2	-44.8	2	2	-18	13.9	8.3	12	2	-17	<17.7	7.3
10	0 8	14.0	11.1	1	1	13	34.8	43.0	2	2	-17	20.1	-23.1	12	2	-16	<17.3	3.4
10	0 10	9.9	-16.8	1	1	14	17.3	19.5	2	2	-16	61.0	-58.3	12	2	-15	16.7	-14.5
10	0 12	< 10.2	-1.2	1	1	15	17.5	-15.1	2	2	-15	13.2	-13.4	12	2	-14	18.8	20.6
10	0 14	20.4	-25.7	1	1	16	29.2	28.7	2	2	-14	19.2	-23.6	12	2	-13	19.8	-21.4
10	0 16	<10.8	4.1	1	1	17	21.3	22.1	2	2	-13	48.2	52.4	12	2	-12	33.2	-33.4
10	0 18	<10.9	7.0	1	1	18	10.0	6.3	2	2	-12	20.0	-25.5	12	2	-11	<16.6	-8.5
10	0 20	20.1	24.9	1	1	19	17.2	-16.1	2	2	-11	32.2	36.9	12	2	-10	<16.4	-13.6
12	0 -26	19.5	-28.8	1	1	20	17.8	16.8	2	2	-10	83.2	81.7	12	2	-9	16.9	19.3
12	0 -20	23.5	21.9	1	1	21	17.2	15.4	2	2	-9	7.6	-5.0	12	2	-8	13.5	-16.5
12	0 -18	<10.3	-5.6	1	1	22	16.1	15.2	2	2	-8	33.1	34.0	12	2	-7	16.7	15.4
12	0 -16	38.9	34.5	1	1	23	21.0	-23.6	2	2	-7	42.5	-46.5	12	2	-6	31.2	31.9
12	0 -14	13.5	-8.1	1	1	24	20.8	-22.1	2	2	-6	64.6	74.5	12	2	-5	<16.6	5.1
12	0 -12	13.8	-15.9	-3	1	24	18.0	-22.0	2	2	-5	16.3	-17.8	12	2	-4	<16.2	-10.1
12	0 -10	59.9	-55.8	-3	1	23	25.7	-26.3	2	2	-4	53.9	-74.0	12	2	-3	<16.1	5.7
12	0 -8	24.2	20.2	-3	1	22	<12.0	7.9	2	2	-3	16.0	-20.4	12	2	-2	27.5	29.8
12	0 -6	17.1	13.8	-3	1	21	<11.6	-2.6	2	2	-2	4.6	3.0	12	2	-1	< 15.3	-3.1
12	0 -4	32.0	26.4	-3	1	20	38.1	37.6	2	2	-1	29.7	-26.4	12	2	1	19.7	-17.0
12	0 -2	< 9.5	-3.4	-3	1	19	20.1	-23.3	2	2	2	7.5	4.9	12	2	2	17.9	11.9
12	0 0	27.3	28.3	-3	1	18	34.0	30.2	2	2	3	84.7	65.8	12	2	3	23.1	-22.0
12	0 2	22.0	-22.1	-3	1	17	49.7	46.3	2	2	4	23.7	-27.6	12	2	4	46.8	-48.5
12	0 4	26.5	-28.1	-3	1	16	21.3	-23.1	2	2	5	25.2	22.0	12	2	5	<17.5	2.9
12	0 6	25.4	-28.9	-3	1	15	< 9.1	-2.8	2	2	6	129.4	131.1	12	2	6	<17.6	-0.1
12	0 8	31.2	32.9	-3	1	14	31.0	-29.3	2	2	7	64.0	-47.4	12	2	7	18.2	18.8
12	0 10	<10.7	5.0	-3	1	13	41.9	38.6	2	2	8	9.0	-2.3	14	2	-10	25.3	30.3
12	0 12	<10.8	17.4	-3	1	12	20.0	-23.0	2	2	9	35.5	-34.6	14	2	-9	<18.3	-14.0
12	0 14	<10.8	-9.2	-3	1	11	30.1	-35.5	2	2	10	16.2	19.2	14	2	-8	<17.8	-9.6
12	0 16	<10.7	16.5	-3	1	10	32.9	-36.2	2	2	11	10.9	-3.6	14	2	-7	<18.0	-22.3
12	0 18	18.1	-26.8	-3	1	9	9.2	12.2	2	2	12	38.2	-39.2	14	2	-6	<17.8	-3.1
12	0 20	10.4	-3.2	-3	1	8	< 2.4	2.8	2	2	13	<14.2	-8.7	14	2	-5	<18.0	-2.4
14	0 -22	19.8	-17.0	-3	1	7	95.3	-89.6	2	2	14	<14.9	11.3	14	2	-4	26.2	-29.1
14	0 -20	10.8	-5.9	-3	1	6	45.3	48.6	2	2	15	<15.4	9.7	14	2	-3	<18.0	9.5
14	0 -18	20.8	-17.2	-3	1	5	< 7.1	2.3	2	2	16	50.5	-48.3	14	2	-2	<18.0	8.0
14	0 -16	10.7	4.7	-3	1	4	88.5	98.6	2	2	17	17.8	15.9	14	2	-1	<18.0	7.6
14	0 -14	10.7	-11.7	-3	1	3	6.5	-0.5	2	2	18	<17.4	0.5	16	2	-6	25.3	25.0
14	0 -12	24.2	25.5	-3	1	2	< 5.1	4.7	2	2	19	23.7	24.3					
14	0 -10	16.3	17.4	-3	1	1	114.8	114.5	2	2	20	<18.7	11.7					

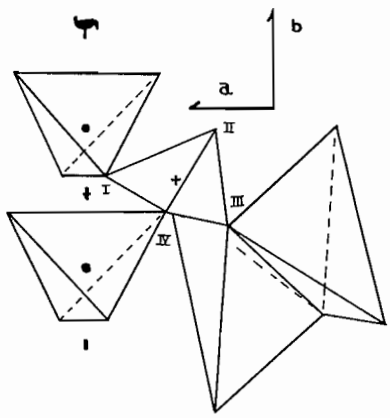

FIG. 1. α-$Zn_3(PO_4)_2$ crystal. Structure projected onto the $x = 0$ plane. The PO_4 group and Zn_IO_4 are represented by tetrahedra and the $Zn_{II_2}O_6$ group is depicted as an edge-shared pair of tetrahedra. The oxygen positions are at the corners of these polyhedra. The positions of the phosphorus atoms are shown by the crosses, and the full circles are the positions of Zn_I^{++}.

Can. J. Chem. Downloaded from www.nrcresearchpress.com by 210.87.254.40 on 09/05/12
For personal use only.

range from 105 to 118°. These distances and angles together with other pertinent values are found in Table IV.

TABLE IV

Bond distances and angles

Bond distances, Å				Bond angles, °	
A. PO_4 group					
P—O_I	1.53	O_I—O_{II}	2.66	O_I—P—O_{III}	117.5
P—O_{II}	1.58	O_I—O_{III}	2.47	O_I—P—O_{III}	109.7
P—O_{III}	1.50	O_I—O_{IV}	2.47	O_I—P—O_{IV}	108.4
P—O_{IV}	1.52	O_{II}—O_{III}	2.44	O_{II}—P—O_{III}	105.3
		O_{II}—O_{IV}	2.50	O_{II}—P—O_{IV}	107.9
		O_{III}—O_{IV}	2.43	O_{III}—P—O_{IV}	107.6
B. Zn_I—O_4 group					
		Zn_I—O_I	1.93	O_I—Zn—O_I	115.0
		Zn_I—O_{IV}	2.03	O_I—Zn—O_{IV}	108.2
		O_{IV}—O_{IV}	3.19	O_I—Zn—$O_{IV'}$	113.6
		O_I—O_I	3.26	O_{IV}—Zn—O_{IV}	103.0
		O_I—O_{IV}	3.21		
		O_I—$O_{IV'}$	3.26		
C. Zn_{II}—O_4 group					
		Zn_{II}—O_{II}	1.86	O_{II}—O_{III}	3.19
		Zn_{II}—O_{III}	2.00	O_{II}—$O_{III'}$	3.23
		Zn_{II}—O_{IV}	1.95	O_{II}—O_{IV}	3.08
		Zn_{II}—$O_{III'}$	2.03	O_{III}—$O_{III'}$	3.06
				O_{III}—O_{IV}	3.19

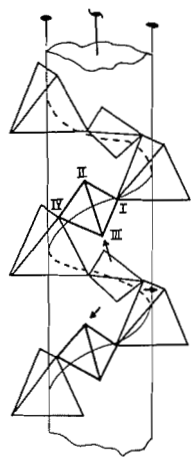

FIG. 2. The coordination among the PO_4 and Zn_IO_4 groups. The axis of the cylinder corresponds to the 2_1 axes of the structure whereas the twofold axes lie in the surface. The smaller tetrahedron represents the PO_4 group. The oxygen atoms are labelled for one of these tetrahedra. The three oxygen atoms which are bonded to a given Zn_{II}^{++} are indicated by arrows.

The phosphate ion and the $Zn_{II}O_4$ group alternate in generating the spiral unit shown in Fig. 2. This spiral has a pitch equal to the length of the *b*-axis and its axis coincides with the twofold screw axis. The structure near the $c/4$-planes parallel to the *a*-axis and containing the twofold axes consists of spirals of this sort. The spirals in this plane are related by the twofold axes lying in the conceived surface that encloses the spiral. Adjacent sheets of these spirals are generated by the centers of symmetry lying in the $z = 0$ plane. These near neighbor sheets are joined by the coordination of the Zn_{II}^{++}. Of the

Can. J. Chem. Downloaded from www.nrcresearchpress.com by 210.87.254.40 on 09/05/12
For personal use only.

four oxygen atoms bonded to a given Zn_{II}^{++} three are shared with phosphorus atoms in one set of spirals. The arrows in Fig. 2 indicate these oxygen atoms. Zn_{II}^{++} can be considered to control the pitch of the spiral. The fourth oxygen atom (O_{III}') is used to join adjacent spirals. An alternate description of the structure is presented below where the α- and γ-phase structures are compared.

α- TO γ-PHASE BOUNDARY

For temperatures near but below 900 °C and upon the addition of 5 or more mole % of the orthophosphates of Mn, Mg, or Cd to $Zn_3(PO_4)_2$, the γ-phase is found to be stable. In the case of added Mn^{++} this phase boundary has a negative temperature versus composition slope. The α-phase on the other hand is stable to the addition of only a very small percentage of Mn^{++}. Any composition between these limits of solubility of Mn^{++} in the two phases results in fact in a mixture of α-$(Zn,Mn)_3(PO_4)_2$ and γ-$(Zn,Mn)_3(PO_4)_2$. The low solubility of Mn^{++} must mean that the free energy of the α-phase must increase rapidly upon adding Mn^{++}, for finite concentration of the added impurity. This in turn indicates a relatively unfavorable site for the added Mn^{++}. The phase diagram of $Cd_3(PO_4)_2$ or $Mg_3(PO_4)_2$ with $Zn_3(PO_4)_2$ leads one to a similar conclusion in these cases. We will examine the differences in the two structures in some detail in the hope of gaining some understanding of the large dependence of the chemical potential of Mn^{++} on its concentration in the α-phase.

These structures have the following points of similarity. The phosphate groups occur as independent tetrahedra with each oxygen atom shared with at least one Zn^{++}. The cations are found in two different types of sites with the less symmetrically coordinated cation (Zn_{II}^{++}) occurring at twice the frequency of the more symmetrically bonded cation (Zn_I^{++}). The cations in the low symmetry site are found as a discrete centered pair of edge-sharing ZnO_4 groups. In each phase a pair of symmetry-related oxygen atoms (O_I) are shared only between phosphorus atoms and the higher symmetry cations site.

The near neighbor bonding in the two structures differ on the following points. Zn_I^{++} in the α-phase lies on a twofold axis and is tetrahedrally coordinated with each of the four oxygen atoms shared with a different phosphorus atom. In contrast the more symmetrical cation site in the γ-phase lies on a center of symmetry and is octahedrally coordinated with each of the six oxygen atoms contributed by a different PO_4 group. In the α-phase only one oxygen atom is shared between the type I and type II cations while in the γ-phase two oxygen atoms are so shared.

We would expect that if the transition between α and γ were to be direct, the structural features that these phases have in common would be preserved. Thus the tetrahedrally coordinated Zn_I^{++} in the α-phase would transform into the octahedrally coordinated Zn_I^{++} in the γ-$Zn_3(PO_4)_2$. The two new oxygen atoms coordinated with Zn_I^{++} must have been contributed by two PO_4 groups not previously sharing oxygen atoms with the particular cation site under consideration. Unfortunately when we consider further neighbors we find that a more drastic rearrangement is necessary than that required to transform the tetrahedrally to the octahedrally coordinated site. In each structure the Zn_2O_6 groups about the type II cation site share oxygen atoms with two pair of PO_4 to form a linear hexagonal chain (Fig. 3*a*). In the α-phase these ribbons are joined through O_{III} to form the set of steps shown in Fig. 3*b*. Adjacent sheets are generated by the twofold axes passing through the cations. Thus in one sheet the steps run along the

Can. J. Chem. Downloaded from www.nrcresearchpress.com by 210.87.254.40 on 09/05/12
For personal use only.

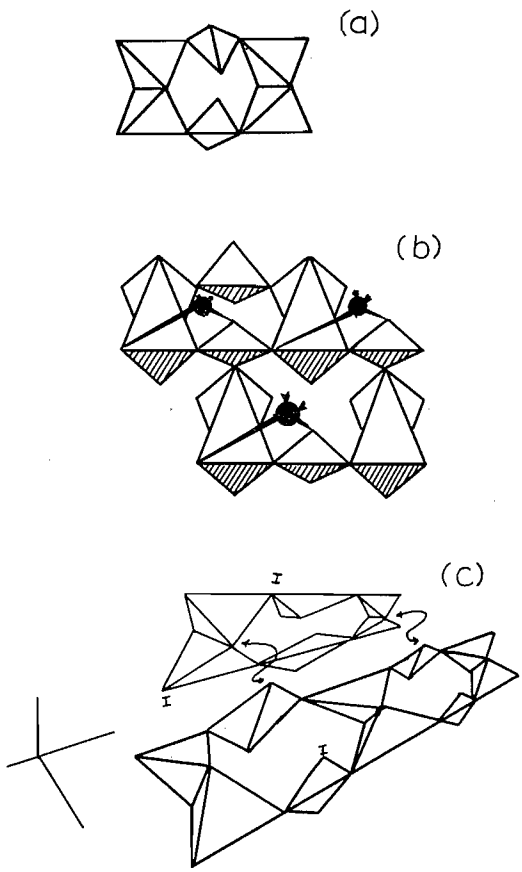

FIG. 3. A comparison of the structures of γ- and α-$Zn_3(PO_4)_1$. (*a*) Coordination of PO_4 and $Zn_{II_2}O_6$ groups. The edge-shared tetrahedra represented by the $Zn_{II_2}O_6$ groups and the tetrahedra represented by the PO_4 groups form a one dimensional ribbon. (*b*) The arrangement of adjacent ribbons in the α-$Zn_3(PO_4)_2$ structure. The special site cation is represented by the open circle. (*c*) The arrangement of adjacent ribbons in the γ-$Zn_3(PO_4)_2$ structure. Two ribbons are shown and these are bond through sharing the common O_{III} indicated by the arrows. The cations at the special site is coordinated to the oxygen atoms at the positions indicated by I and those related to it by the center of symmetry at the cation.

$\vec{a} + \vec{b}$ direction while in the next neighboring sheet they run in the $\vec{a} - \vec{b}$ direction. The bonding across adjacent sheets is solely through these special site ions.

Similar ribbons occur in the γ-phase but here they all run parallel. The bonding of adjacent ribbons in the γ-phase is depicted in Fig. 3*c*. The cations at the center of symmetry lie within tubes of diamond cross section formed from four of these $(Zn_2O_6PO_2)_n$ chains. Here adjacent sheets are bonded both by the special site cations and by O_{III}. The conceived phase transformation therefore must involve a change from the crossed ribbons of the α-form to the parallel ones of the γ-form. This requires that alternate cations break Zn_{II}^{++}—O_{IV} bonds in alternate sheets of the α-phase and that these bonds reform with O_{IV} in adjacent cells translated one unit along the *b*-axis. Such a transformation would require such large cooperative motions that a solid state transformation is to be judged as unlikely although the structural similarity suggests a small free energy difference between the phases.

Can. J. Chem. Downloaded from www.nrcresearchpress.com by 210.87.254.40 on 09/05/12
For personal use only.

Can. J. Chem. Downloaded from www.nrcresearchpress.com by 210.87.254.40 on 09/05/12
For personal use only.

DISCUSSION

Divalent manganese substituted in either cation site would be consistent with the Linwood–Weyl–Schulman (21, 22) proposal that the green emission of Mn^{++} indicates that it is tetrahedrally coordinated. Unfortunately at present we do not know which site, if either, is occupied by the Mn^{++}. Although the crystallographic studies of the γ-phases did indicate a large relative nonpreference on the part of Mn^{++} for the edge-shared tetrahedral site, we can not deduce from this any reason for a preferred site in the α-phase. Fortunately this question can be answered by the examination of the electron paramagnetic resonance (e.p.r.) spectra of α-$Zn_3(PO_4)_2$:Mn. If Mn^{++} dissolves into the site on the twofold axis one should see one e.p.r. active site and further, one of the magnetic axes of the spin Hamiltonian tensor should lie along the twofold axis in this space group as in β-$Zn_2P_2O_7$ (23) and β-$Mg_2P_2O_7$ (24). Note that a positive result would confirm the space group chosen here. This study is presently in progress.

The role of divalent metal ions (Ca^{++}, Cd^{++}, Mn^{++}, or Mg^{++}) in causing the instability of the α-phase must involve a chemical specificity of either the Zn^{++} or the impurity ion, since a scalar variable like temperature as a perturbing influence results in yet another phase (β-$Zn_3(PO_4)_2$). This role, because of the diverse nature of the impurities, cannot be simply attributed to a "single" cause such as the difference in ionic radii or electronegativity between the added divalent metal ion and the Zn^{++}. Unfortunately the crystal structure of α-$Zn_3(PO_4)_2$ offers no clear-cut clue to indicate why this structure is so critically sensitive to the characteristics of the Zn^{++}. The fact that the spiral consisting of the Zn_IO_4 and PO_4 tetrahedra is locked laterally and vertically by the Zn_{II}^{++} may preclude the substitution of divalent cations into the general cation site. On the other hand the strain introduced by the cations substituting into the special site seems readily relaxable. The structure regarded as steps of ribbons joined by these special site cations seems easily adaptable to distortions. Unfortunately the crystallographic method emphasizes just geometric considerations and one must speculate about other factors, such as electron effects, which probably are very important in this question.

In contrast γ-$Zn_3(PO_4)_2$ appears to be a "compromise" structure since it appears so often as a solid solution. Thus ions such as Mg^{++} and Mn^{++} that have a high site preference for the octahedral site, can gain enough stabilization to compensate for the relatively unfavorable tetrahedra site. This suggests that entropy of mixing in the γ-$(Zn,Mn)_3(PO_4)_2$ will be near ideal and this further suggests, because of the nature of the phase diagram, that the α- and γ-$Zn_3(PO_4)_2$ have free energies of formation nearly the same. In particular assuming $Mn_3(PO_4)_2$ to dissolve ideally into the γ-phase, one would expect the α-phase to be stable by about 0.2 kcal/mole at the temperature of interest in the limit that the Mn concentration goes to zero. Inexact phase boundary curves, however, prevent one from directly determining the composition or temperature dependence of the chemical potential of $Mn_3(PO_4)_2$ in this phase. It is hoped that the study of the crystal structures of β-$Zn_3(PO_4)_2$, $Mn_3(PO_4)_2$, and $Cd_3(PO_4)_2$ will shed light upon site sensitivity of the ions.

ACKNOWLEDGMENTS

The early portions of this work were performed while the author was associated with the Radio-Corporation of America at Princeton, N.J. Special thanks are extended to Dr. W. H. McCarrol of that corporation who helped with the growing of the crystals and to the National Research Council of Canada which supported this work.

REFERENCES

1. F. L. KATNACK and F. A. HUMMEL. J. Electrochem. Soc. **105**, 125 (1958).
2. F. A. HUMMEL and F. L. KATNACK. J. Electrochem. Soc. **105**, 528 (1958).
3. J. F. SARVER, F. L. KATNACK, and F. A. HUMMEL. J. Electrochem. Soc. **106**, 960 (1959).
4. J. J. BROWN and F. A. HUMMEL. J. Electrochem. Soc. **110**, 1218 (1963).
5. A. L. SMITH. J. Electrochem. Soc. **98**, 363 (1951).
6. C. CALVO. J. Phys. Chem. Solids, **24**, 141 (1963).
7. A. D. MACKAY. Acta Cryst. **6**, 743 (1953).
8. J. S. STEPHENS and C. CALVO. To be published.
9. J. F. SARVER, F. A. HUMMEL, and M. V. HOFFMAN. J. Electrochem. Soc. **108**, 1103 (1961).
10. J. R. ARGLE and F. A. HUMMEL. J. Am. Ceram. Soc. **43**, 453 (1960).
11. M. V. HOFFMAN. J. Electrochem. Soc. **110**, 1223 (1963).
12. E. S. DANA and W. E. FORD. Text-book of mineralogy. John Wiley and Sons. 1932. p. 703.
13. M. E. MROSE and D. E. APPLEMAN. Am. Cryst. Assoc. Program and Abstracts, Boulder, Colorado, July, 1961.
14. V. V. BAKKIN and N. V. BELOV. Soviet Phys. "Doklady" English transl. **5**, 1141 (1961).
15. W. H. ZACHARIASEN. Acta Cryst. **1**, 263 (1948).
16. Y. TANABE and S. SUGANO. J. Phys. Soc. Japan, **9**, 753 (1954).
17. J. W. MELLOR. A comprehensive treatise on inorganic and theoretical chemistry. Longmans, Green and Co., London. 1923.
18. J. A. AMICK. Private communication.
19. W. R. BUSING, K. O. MARTIN, and H. A. LEVY. ORNL-TM-305 (1962).
20. D. W. J. CRUICKSHANK. J. Chem. Soc. 5486 (1961).
21. S. H. LINWOOD and W. A. WEYL. J. Opt. Soc. Am. **32**, 443 (1942).
22. J. H. SCHULMAN. J. Appl. Phys. **17**, 902 (1947).
23. J. G. CHAMBERS, W. R. DATARS, and C. CALVO. J. Chem. Phys. **41**, 806 (1964).
24. LEUNG JURG SUN. Private communication.

Can. J. Chem. Downloaded from www.nrcresearchpress.com by 210.87.254.40 on 09/05/12
For personal use only.

Can. J. Chem. Downloaded from www.nrcresearchpress.com by 210.87.254.5 on 09/05/12
For personal use only.

CONSIDERATIONS OF ADSORBED IONIC INTERMEDIATES ON THE AgO/Ag_2O ELECTRODE IN AQUEOUS ALKALINE SOLUTION

R. G. BARRADAS AND G. H. FRASER[1]
Department of Chemistry, University of Toronto, Toronto, Ontario
Received July 21, 1964

ABSTRACT

An experimental study of the kinetics for the electrochemical formation of AgO from Ag_2O in aqueous alkaline solutions was reported in an earlier paper (1). The proposed mechanism for the rate-determining step was suggested to be the transfer of oxide ions across the mixed oxide interface. Further theoretical possibilities under Langmuir and Temkin conditions of surface coverages are considered here in the light of the previously obtained experimental data. In particular we examine the possibilities of the rate-determining step involving adsorbed ionic intermediates on the AgO/Ag_2O electrode at the oxide/electrolyte interface. For the Temkin conditions, the intrinsic and induced heterogeneity models of Conway and his co-workers have been applied to our calculation of Tafel slopes. None of the mechanisms at the oxide/electrolyte interface were found to be rate-controlling.

INTRODUCTION

In a previous paper (1) the relations between current and potentials were obtained by galvanostatic and potentiostatic experiments for the anodic oxidation of Ag_2O to AgO in normal and $N/40$ aqueous potassium hydroxide solutions. The stoichiometric reaction is

[1] $$2OH^- + Ag_2O = 2AgO + H_2O + 2e.$$

At high overpotentials a Tafel relation was obtained:

[2] $$\eta = a + 2.303(RT/F) \log i.$$

The results were fitted over the entire range of overpotentials studied (1 to 170 mV) to a hyperbolic sine relationship

[3] $$i = 2i_0 \sinh (\eta F/RT).$$

No dependence of rate on the extent of conversion of Ag_2O to AgO was noted, indicating that the rate-determining step occurs at an interface and is not a migration process within one of the oxides.

From these results it was concluded that the rate-determining step occurred at the AgO/Ag_2O interface, and was either

[4] $$Ag^+ = Ag^{+3} + 2e$$

or, more probably, the transfer of O^{-2} ions across the mixed oxide interface.

It was proposed that oxide ions were formed from adsorbed hydroxyl ions according to

[5] $$(OH^-)_{aq} = (OH^-)_s$$

followed by either proton abstraction

[6] $$(OH^-)_{aq} + (OH^-)_s = H_2O + (O^{-2})_s$$

or surface recombination

[7] $$2(OH^-)_s = H_2O + (O^{-2})_s$$

[1]*Holder of a Province of Ontario Government Fellowship for 1963–1964.*

or surface dissociation

[8] $$(OH^-)_s = (H^+)_{aq} + (O^{-2})_s, \qquad (H^+)_{aq} + (OH^-)_{aq} = H_2O.$$

The subscripts "aq" and "s" refer to an ion dissolved in solution and adsorbed on the electrode surface. It must be emphasized that our mechanisms involve adsorbed *ionic* intermediates. We do not consider intermediates covalently adsorbed on the electrode surface, e.g. OH and O species formed by the discharge of hydroxyl ions. It is improbable that O atoms would migrate through a semiconductor film independently of the electrons removed from the ion.

REACTION MECHANISMS AT THE OXIDE/ELECTROLYTE INTERFACE

We now examine the possibility that either reactions [5], [6], [7], or [8] occurring at the AgO/electrolyte interface is the correct rate-determining step of reaction [1]. For Langmuir conditions, i.e. limitingly low or limitingly high surface coverage by the intermediates, the Tafel slopes to be expected if any of the steps [5] to [8] were rate-controlling can be easily calculated. Reactions [5], [6], and [7] can be treated analogously to

[9] $$M + OH^- = MOH + e,$$

[10] $$OH^- + MOH = MO + H_2O + e,$$

and

[11] $$2MOH = MO + M + H_2O$$

respectively. Reactions [9] to [11] concern formation and reaction of covalently adsorbed surface species by neutralization of the adsorbing ions. In reactions [5] to [8], however, the surface species contain ionic and not covalent bonds, i.e. the adsorbing ions are not neutralized. Similar rate equations can be applied to both cases (2). Hence, we can calculate the Tafel slopes reported in Table I. The calculations show that under Langmuir conditions none of the reactions listed except [8] could be the rate-controlling step. However, in alkaline solutions it is rather unlikely that reaction [8] should occur. For this reason we rule out [8] as a possible rate-determining step.

TABLE I

Langmuir conditions of surface coverage

Rate-determining step	Slope	Analytical condition
[5]	$2RT/F$	$[OH^-]_s \rightarrow 0$
[6]	$2RT/3F$	$[OH^-]_s \rightarrow 0$
	$2RT/F$	$[OH^-]_s \rightarrow 1$
[7]	$RT/2F$	$[OH^-]_s \rightarrow 0$
	∞	$[OH^-]_s \rightarrow 1$
[8]	RT/F	$[OH^-]_s \rightarrow 0$
	∞	$[OH^-]_s \rightarrow 1$

TEMKIN CONDITIONS OF SURFACE COVERAGE

When the surface coverage (θ) is neither limitingly high nor limitingly low, the Tafel slopes can be calculated using two models proposed by Conway and Gileadi (3). For an induced surface heterogeneity model, the variation of the heat of adsorption is given by

[12] $$\Delta H_A = \Delta H^0{}_A - r_A\theta_A - r_B\theta_B, \qquad \Delta H_B = \Delta H^0{}_B - r_A\theta_A - r_B\theta_B,$$

Can. J. Chem. Downloaded from www.nrcresearchpress.com by 210.87.254.5 on 09/05/12
For personal use only.

whereas for the intrinsic heterogeneity model,

[13] $$\Delta H_A = \Delta H^0{}_A - r_A(\theta_A + \theta_B), \qquad \Delta H_B = \Delta H^0{}_B - r_B(\theta_A + \theta_B),$$

where $\Delta H^0{}_A$ and $\Delta H^0{}_B$ refer to the heat of adsorption of species A and B respectively at zero coverage. In our mechanisms r_A and r_B refer to O^{-2} and OH^- species. In the intrinsic heterogeneity model r is directly associated with the variation of the forces of interaction between adsorbent and adsorbate with coverage as preferred sites for adsorption are occupied. In the induction model it is associated with the variation with coverage of the effect of the adsorbed dipole double-layer on the surface potential of the electrode. Hence the r terms are not the same in the two models.

Equations [12] and [13] assume a linear variation of the heat of adsorption with surface coverage (Temkin isotherm). However, the actual form of the variation does not affect the kinetic parameters for the induced model nor, if the form of the variation is the same for all intermediates, for the intrinsic model (3, 4). Equations [12] and [13] were originally proposed by Conway and Gileadi (*loc. cit.*) for reactions involving the chemisorption of neutral species at a metal electrode. The interactions between the adsorbent and adsorbate will be quite different in the case of ions adsorbed on the surface layers of an oxide such as AgO. Nevertheless, the nature of the interaction can reasonably be expected to fall into one or other of the categories described by [12] and [13].

Using the two models mentioned above we can calculate the slopes which are listed in Table II. Except for steps [5] and [7] in Table II it will be noted that the other slopes do not correspond to the observed experimental slope of RT/F (1), and hence cannot be rate-controlling. It may be further noted that eq. [2] would be obeyed if

$$r_{[OH^-]_s} > 5r_{[O^{-2}]}$$

and that eq. [3] would be valid if the surface coverage of $(O^{-2})_s$ as well as that of $(OH^-)_s$ is appreciable. The parameter r may differ for two intermediates for steric reasons alone (5). In the case of O^{-2} and OH^-, however, these will have a negligible effect, since the *radii* of the two ionic species are nearly the same (6).

TABLE II

Temkin conditions of surface coverage

Rate-determining step	Slope	
	Induced heterogeneity model	Intrinsic heterogeneity model
[5]	$2RT/F$	$2RT/F$
[6]	$2RT/F$	$(RT/F)\ 2r_{[OH^-]_s}/(2r_{[OH^-]_s} - r_{[O^{-2}]_s})$
[7]	$2RT/F$	$(RT/F)\ 2r_{[OH^-]_s}/(2r_{[OH^-]_s} - r_{[O^{-2}]_s})$
[8]	∞	$(RT/F)\ 2r_{[OH^-]_s}/(r_{[OH^-]_s} - r_{[O^{-2}]_s})$

The following arguments can be applied (7, 8) to resolve the probable contributions to the r parameters from the adsorption of O^{-2} and OH^-. When ions adsorb on a uniform ionic dielectric, the most important contribution to the energy of interaction is due to the electrostatic induction of the dielectric (7, 8)

[14] $$E = -(n_1{}^2e^2/4R_0)(K - 1)/(K + 2),$$

where K is the static polarizability of the dielectric, e is the charge on the electron, n_1 is the valency of the adsorbing ion and R_0 is the equilibrium distance from the ion to the

Can. J. Chem. Downloaded from www.nrcresearchpress.com by 210.87.254.5 on 09/05/12
For personal use only.

surface. Assuming that R_0 is reasonably constant, the variation of heat of adsorption with coverage will be in the term $(K - 1)/(K + 2)$. This type of interaction will obviously make

$$r_{[O^{-2}]_s} > r_{[OH^-]_s}$$

since n_1 is twice as great for O^{-2} as for OH^-. It follows therefore that steps [6] and [7] cannot be rate-determining ones.

The properties of the oxide are not uniform as implied in the intrinsic heterogeneity model which we are using here. In this case the value of K varies from site to site on the surface. The energy of interaction (E) is greater at large values of K since E represents the energy of the bond between the adsorbed ion and the surface. Preferential adsorption will occur at those sites for which E is higher (i.e. K large). The value of K which appears in eq. [14] is not the average value for the oxide but is that for the site at which adsorption is taking place. When the most favorable sites are covered, adsorption then takes place at sites with lower K values. Therefore, as coverage increases, the value of K to be used in eq. [14] decreases. This means that E (and also the heat of adsorption) decreases as surface coverage increases. The properties of the surface, i.e. the K values of individual adsorption sites, do not change with coverage; only the value of K to be used in eq. [14] changes with coverage.

In summary, it appears that none of the reactions involving adsorbed ionic intermediates taking place at the oxide/electrolyte interface are rate-controlling steps for the electrolytic formation of AgO from Ag$_2$O. This supports our original conclusion (1) that the rate-determining step occurs at the mixed oxide interface.

ACKNOWLEDGMENTS

We wish to thank the National Research Council of Canada and the University of Toronto for generous financial support.

REFERENCES

1. R. G. Barradas and G. H. Fraser. Can. J. Chem. **42**, 2488 (1964).
2. T. P. Hoar. Modern aspects of electrochemistry. No. 2. *Edited by* J. O'M. Bockris. Butterworths, London. 1959. p. 279.
3. B. E. Conway and E. Gileadi. Trans. Faraday Soc. **58**, 2493 (1962).
4. B. E. Conway, E. Gileadi, and M. Dzieciuch. Electrochim. Acta, **8**, 143 (1963).
5. B. E. Conway and M. Dzieciuch. Can. J. Chem. **41**, 21 (1963).
6. J. D. Bernal and R. H. Fowler. J. Chem. Phys. **1**, 515 (1933). Landolt-Börnstein. Phys. chem. tabellen. Vol. 1, Part 4. 6th ed. Springer-Verlag, Berlin. 1955. p. 524. A. F. Kapustinskii. Compt. Rend. Acad. Sci. U.R.S.S. **32**, 59 (1941). H. Trichés. Compt. Rend. **217**, 687 (1943).
7. J. H. de Boer. Advan. Catalysis, **VIII**, 17 (1956).
8. A. C. Zettlemoyer. Chem. Rev. **59**, 937 (1959).

Can. J. Chem. Downloaded from www.nrcresearchpress.com by 210.87.254.5 on 09/05/12
For personal use only.

Can. J. Chem. Downloaded from www.nrcresearchpress.com by 210.87.254.40 on 09/05/12
For personal use only.

THE *C*- AND *O*-BENZYLATION OF L-ASCORBIC ACID

K. G. A. JACKSON AND J. K. N. JONES
Chemistry Department, Queen's University, Kingston, Ontario
Received May 11, 1964

ABSTRACT

Alkylation of sodium L-ascorbate with benzyl chloride yielded a 2-*C*-benzyl-3-keto-hexulosonic acid lactone and 3-*O*-benzyl-L-ascorbic acid, the yield of each being dependent on reaction conditions. Other products obtained from the alkylations were 2,3-di-*O*-benzyl-L-ascorbic acid and a 1-deoxy-1-*C*-phenyl-2-hexulose. Treatment of 3-*O*-methyl-5,6-*O*-isopropylidene-L-ascorbic acid with benzyl chloride and sodium methoxide yielded the 2-*O*-benzyl derivative.

INTRODUCTION

A 2-*O*-methyl-3-hexulose has been prepared from L-ascorbic acid (1). It was argued that preparation of the corresponding *O*-benzyl derivative and subsequent hydrogenolysis of the resultant 2-*O*-benzyl-3-hexulose should yield the parent 3-hexulose.

The reaction of sodium-L-ascorbate with benzyl chloride in aqueous acetone resulted in a mixture of products; the two major components of which were identified as syrupy 3-*O*-benzyl-L-ascorbic acid (I, R = Ph—CH_2, R′ = H) and a crystalline 2-*C*-benzyl-3-keto-hexulosonic acid lactone (III). Derivatives of I, II, and III were prepared.

The lactone (III) did not affect ferric chloride solution and therefore did not contain enolic hydroxyl groups. Aqueous solutions of III were acidic to litmus and gave an instantaneous positive test with Wallenfels reagent (2). The infrared spectrum of III indicated the presence of a lactone and a benzene ring; the absorption of the ascorbate structure was absent. Periodate oxidation revealed the uptake of 5 moles of periodate and the release of 3 moles of titratable acid per mole of lactone. The detection and characterization of phenylacetic acid in the reaction mixture indicated the presence of a *C*-benzyl residue which was attached as a tertiary carbinol. Reduction of III with sodium borohydride provided a neutral product which gave a negative test with Wallenfels reagent. This new crystalline compound showed an absorption corresponding to lactone carbonyl in the infrared and was formulated as a 2-*C*-benzyl-hexonic acid lactone (IV). The amide (VI) of IV was prepared, as well as the amide (V) of III. The optical rotation of each was positive, lending weight to the assignment of the L-*lyxo* configuration to III by Hudson's rules (3). Furthermore the optical rotation of sodium L-ascorbate in acetone–water did not change appreciably over a period of 2 days, indicating that change of configuration at C_4, as experienced by Brenner *et al.*, did not occur (4).

The methyl glycoside (VII) of III was formed in methanolic hydrogen chloride. It did not react with sodium metaperiodate. Molecular models show that only one strain-free glycoside (alpha-L) can be produced. Reaction of the glycoside (VII) in ether with lithium aluminium hydride produced two crystalline compounds, one of which analyzed correctly for the expected alcohol (VIII). Periodate oxidation of VIII caused the formation of 0.6 mole of formaldehyde per mole of VIII; a small amount of acid was also produced. These results indicated that III was 2-*C*-benzyl-3-keto-L-*lyxo*-hexulosonic acid lactone and ruled out the isomeric structure, a 3-*C*-benzyl-2-keto-hexulosonic acid lactone. On treatment with acetic anhydride in pyridine, VIII readily gave a crystalline triacetate in which all of the secondary groups were acetylated.

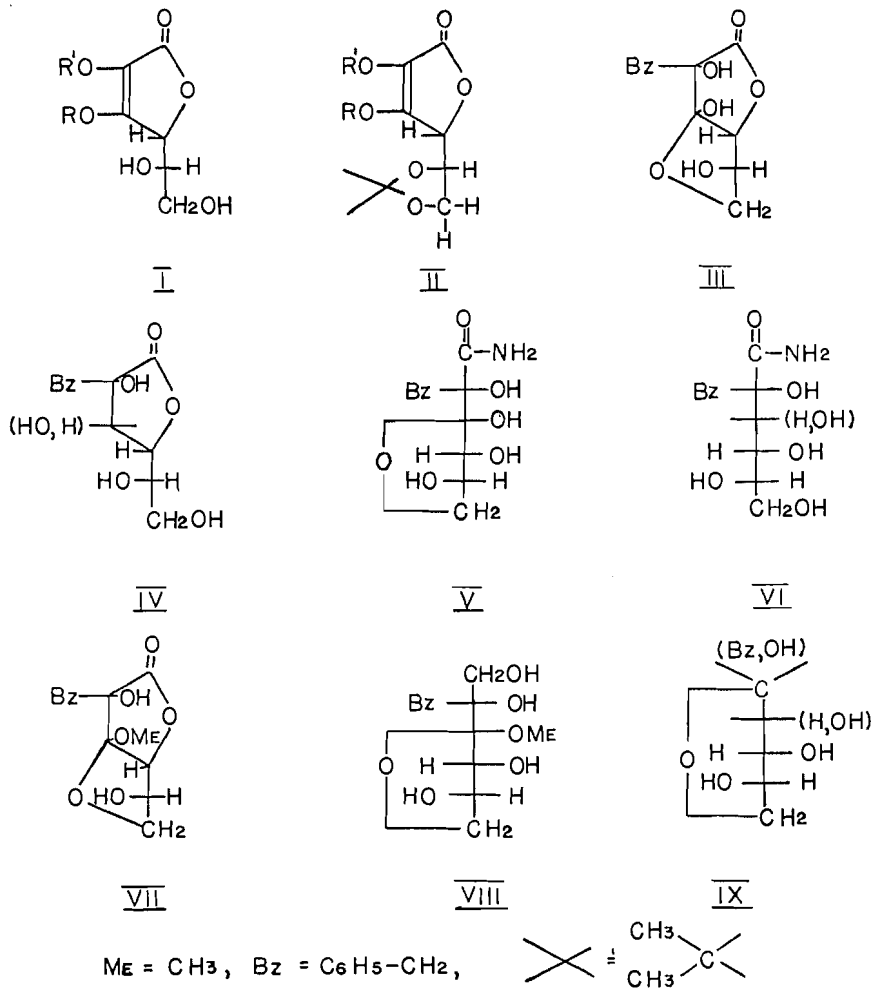

The sodium salt of III spontaneously decomposed in water giving a crystalline 1-deoxy-1-*C*-phenyl-2-hexulose (IX). This was more easily prepared on a larger scale when L-ascorbic acid and 2 moles of sodium hydroxide per mole were stirred with benzyl chloride. The product was neutral to litmus paper, reduced Fehling's solution, and showed no absorption in the infrared in the interval 1 605 to 2 000 cm^{-1}. Quantitative periodate oxidation of IX resulted in the uptake of 3 moles of periodate per mole and the release of 2 moles of acid per mole. Analysis of the product revealed the presence of glycolaldehyde phenylacetate, both alcohol and acid portions of which were characterized. This substance originates presumably from a 3-hexulose derivative which isomerizes to the 2-hexulose under the influence of base. This wandering of the keto group has been observed to occur in other furano-ketoses and in acyclic ketoses (unpublished results) when a stable ring derivative can be produced.

3-*O*-Benzyl-L-ascorbic acid (I, R = Ph—CH_2, R′ = H) was isolated from the reaction mixture containing 2-*C*-benzyl-3-keto-L-*lyxo*-hexulosonic acid lactone. The separation of I (R = Ph—CH_2, R′ = H) from the amide of III was effected by cellulose column chromatography. On weighing the concentrated fractions of 3-*O*-benzyl-L-ascorbic acid

Can. J. Chem. Downloaded from www.nrcresearchpress.com by 210.87.254.40 on 09/05/12
For personal use only.

and V, the amide of III, we found the relative amounts of *C*-benzylation and *O*-benzylation to be in the approximate ratio of 1:1.

A solution of III in chloroform–acetone, after an interval of 3 weeks, crystallized to yield a new lactone which was considered to be an isomorph of III. The isomorph had a lower melting point and a lactone absorption in the infrared (KBr disc) 15 cm^{-1} higher than that of III. Both compounds had similar optical rotations in water, as well as in methanol, and had similar rates of movement on thin layer chromatograms. It was found that the isomorph could be recovered from deuterium oxide by evaporation of the solvent at room temperature. Furthermore, recrystallization of the isomorph from chloroform–acetone solution at 60° gave III only, whereas recrystallization from chloroform–acetone solution at room temperature yielded starting material. The nuclear magnetic resonance (n.m.r.) spectra of each were indistinguishable from one another.

Alkylation reactions in which there is a choice between two reactive sites have been investigated (5–8). It has, in general, been found that *C*-alkylation is favored in media of high hydrogen-bonding power and that *O*-alkylation is favored in media of low hydrogen-bonding power and high dielectric constant such as dimethylsulfoxide and dimethylformamide (9). When dimethylsulfoxide was used as a reaction solvent, a high yield of 3-*O*-benzyl-L-ascorbic acid was obtained.

The crude product so obtained partially crystallized but the crystals proved to be the isomorph of III. Higher substituted derivatives of L-ascorbic acid were removed from the residue by chloroform extraction and 3-*O*-benzyl-L-ascorbic acid (I, R = Ph—Ch_2, R′ = H) was separated from the remaining material by formation of the amide (V) from any III present, followed by chromatography of the mixture on a cellulose column. The weights of *C*-benzylated amide (V) and 3-*O*-benzyl-L-ascorbic acid were in the ratio of 1:3. Syrupy 3-*O*-benzyl-L-ascorbic acid gave a light green color with ferric chloride reagent and showed absorptions at 1 675 and 1 750 cm^{-1} in the infrared. These absorptions were present in all the ascorbic acid derivatives examined. The crystalline isopropylidene derivative (II, R = Ph—CH_2, R′ = H) was readily formed in anhydrous acetone – zinc chloride. 3-*O*-Benzyl-L-ascorbic acid, in excess ethereal diazomethane, gave a syrupy product that did not affect ferric chloride reagent. This was assumed to be 2-*O*-methyl-3-*O*-benzyl-L-ascorbic acid (I, R = Ph—CH_2, R′ = CH_3) and was proved to be such by conversion to crystalline II (R = Ph—CH_2, R′ = CH_3) with anhydrous acetone-zinc chloride reagent.

2-*O*-Benzyl-3-*O*-methyl-5,6-*O*-isopropylidene-L-ascorbic acid (II, R = CH_3, R′ = Ph—CH_2) was prepared from syrupy 3-*O*-methyl-5,6-*O*-isopropylidene-L-ascorbic acid (II, R = CH_3, R′ = H) by treatment of the latter with sodium methoxide followed by benzyl chloride. The melting point and optical rotation of the product obtained (II, R = CH_3, R′ = Ph—CH_2) were found to be significantly different from those of the compound assumed to be 3-*O*-benzyl-2-*O*-methyl-5,6-*O*-isopropylidene-L-ascorbic acid. The infrared spectra were indistinguishable from each other.

EXPERIMENTAL

Paper chromatography was carried out on Whatman No. 1 filter paper by the descending method using the following solvent systems (v/v): (A) butan-1-ol – ethanol – water (3:1:1); (B) butan-1-ol – pyridine – water (10:3:3); (C) ethyl acetate – acetic acid – formic acid – water (18:3:1:4). The sugars were located on paper chromatograms using the following spray reagents: (O) a spray solution of 1% silver nitrate in acetone followed by 2% sodium hydroxide in ethanol (10); (P) a spray solution of 3% *p*-anisidine hydrochloride in butan-1-ol (11) followed by heating the chromatogram in an oven at 115° for 2 min; (Q) a spray solution of 0.01 *M* sodium metaperiodate in water. After 5 min the sugars were located with spray reagent (P). Also used was (R), a spray solution of 2% ninhydrin in butan-1-ol (12). The final detection system, (S) consisted of a glass tank filled with iodine vapor. The chromatograms were suspended in the vapor.

Can. J. Chem. Downloaded from www.nrcresearchpress.com by 210.87.254.40 on 09/05/12
For personal use only.

Can. J. Chem. Downloaded from www.nrcresearchpress.com by 210.87.254.40 on 09/05/12
For personal use only.

Thin layer chromatography was carried out on glass plates coated with Silica Gel G (Research Specialties Co.). The plate was developed in benzene–isopropanol (2:1, v/v) solvent and then dried in air. Compounds were located as black spots by spraying the plate with concentrated sulfuric acid, followed by heating it at 140–170° in an oven.

Infrared spectra were determined on a Perkin–Elmer Model 21 infrared spectrophotometer. Formaldehyde formation in periodate oxidations was measured by the chromotropic acid method (13). All periodate oxidations were carried out using sodium metaperiodate solutions. Melting points were taken on a Fisher block and are uncorrected. All evaporations were carried out under reduced pressure at 40–60° on a water bath.

C-Benzylation of L-*Ascorbic Acid*

*2-C-Benzyl-3-keto-*L-*lyxo-hexulosonic Acid Lactone (III)*

L-Ascorbic acid (20 g, 0.113 mole) dissolved in water (200 ml) and partially neutralized by potassium hydroxide (5.8 g, 0.105 mole) in water (50 ml) was treated with benzyl chloride (14.4 g, 0.114 mole) in acetone (200 ml). The mixture was shaken mechanically for 60 h at room temperature and concentrated to remove acetone and the residue was washed with petrol (b.p. 60–80°). The residue was then exhaustively extracted with hot ethyl acetate. The extracts were dried (magnesium sulfate), filtered, and the filtrate was concentrated to yield a light-yellow oil. Yields varied from 8.1 g (27% theoretical) to 21.85 g (69% theoretical). The syrup crystallized in one preparation and on recrystallization from chloroform–acetone (8:1) the product had m.p. 156–156.5° with solvent of crystallization eliminated between 70 and 80° and $[\alpha]_D^{23} = +7 \pm 1°$ (*c*, 1.0 in methanol). The crystalline material had R_f 0.76, R_{Rh} 2.50 (spray reagent (O), (P), (Q)) in solvent (A) and R_f 0.82, R_{Rh} 2.04 (spray reagent (O)) in solvent (B). A strong absorption at 1 775 cm^{-1} (lactone carbonyl) was present in the infrared. The material was acidic to litmus; it gave an instantaneous Wallenfels test (2) but did not affect ferric chloride.

Anal. Calcd. for $C_{13}H_{14}O_6$: C, 58.6; H, 5.3. Found: C, 58.5; H, 5.4.

The analysis was performed on solvent-free material, obtained by heating the lactone at 80° for 10 min.

*The Periodate Oxidation of 2-C-Benzyl-3-keto-*L-*lyxo-hexulosonic Acid Lactone (III)*

Oxidations were carried out quantitatively and qualitatively on solvent-free material. In the qualitative oxidation 2-*C*-benzyl-3-keto-L-*lyxo*-hexulosonic acid lactone (200 mg) was dissolved in 0.10 *M* sodium metaperiodate solution (25 ml) in the absence of light. After 4 h the solution was extracted with chloroform (50 ml) and the extracts were evaporated to a gum that crystallized immediately. After recrystallization from petrol (b.p. 60–80°) thin plates of m.p. 74–76° were obtained. The mixed melting point with authentic phenylacetic acid was 75–77°. The infrared spectrum was indistinguishable from that of phenylacetic acid (KBr disc).

In the quantitative oxidation, periodate uptake and acid release were determined from an unbuffered aqueous solution shielded from light. The results are tabulated below.

TABLE I

The periodate oxidation of 2-*C*-benzyl-3-keto-L-*lyxo*-hexulosonic acid lactone

Time (h)	Periodate uptake (moles/mole)	Acid release (moles/mole)
0.25	2.80	1.65
0.75	3.30	2.09
2.33	4.15	2.62
5.25	4.73	2.83
8.25	5.00	3.03
11.00	5.00	3.03

*2-C-Benzyl-3-keto-*L-*lyxo-hexulonamide (V)*

2-*C*-Benzyl-3-keto-L-*lyxo*-hexulosonic acid lactone (1.87 g) in anhydrous methanolic ammonia was kept at −20° for 7 h. Paper chromatography of the solution at the end of this time revealed only one component, moving at R_f 0.62, R_{Rh} 2.00 (solvent (A), spray reagents (Q), (R)) and at R_f 0.74, R_{Rh} 1.50 (solvent (C)). Crystallization occurred when the solution was concentrated to 20 ml and the amide was recrystallized from methanol to give needle-shaped crystals (1.91 g) of m.p. 137–138.5° and $[\alpha]_D^{23} = +7 \pm 1°$ (*c*, 1.0 in methanol).

Anal. Calcd. for $C_{13}H_{17}O_6N \cdot MeOH$: C, 53.3; H, 6.7; N, 4.4. Found: C, 53.3; H, 6.7; N, 4.5.

*2-C-Benzyl-(*L-*idono or* L-*talono)-lactone (IV)*

2-*C*-Benzyl-3-keto-L-*lyxo*-hexulosonic acid lactone (2.69 g, 1.01×10^{-2} mole) in water (100 ml) was added dropwise over a period of 4 h to sodium borohydride (0.404 g, 1.3×10^{-2} mole) in water (100 ml). After it had been stirred for 14 h the solution was still reducing to Benedict's reagent although paper chromatography (solvent (A)) revealed mainly one component of R_f 0.70, R_{Rh} 2.06 with spray reagent

(O). The reaction mixture was treated with acetone (10 ml) and passed through a column of IR-120 (acidic) resin. The effluent was evaporated to a syrup and treated with successive portions of hot methanol (3 × 50 ml) followed by evaporation of the methanol in order to remove boric acid. The syrup so obtained crystallized and recrystallization from chloroform afforded needle-shaped crystals, neutral to litmus and of m.p. 174–175° and $[\alpha]_D^{23} = +39 \pm 2°$ (*c*, 1.0 in methanol).

Anal. Calcd. for a 2-*C*-benzyl-hexonolactone, $C_{13}H_{16}O_6$: C, 58.2; H, 6.0. Found: C, 58.5; H, 6.1. The infrared spectrum was almost identical with the spectrum of the starting material, except for a new absorption at 3 200 cm^{-1} (hydroxyl).

2-C-Benzyl-(L-idonamide or L-talonamide) (VI)

2-*C*-Benzyl-(L-idono or L-talono)-lactone (100 mg) in methanolic ammonia (25 ml) was kept at 0° for 48 h. Paper chromatography (solvent A) revealed the gradual disappearance of starting material and the appearance of a new slower moving component R_f 0.62 and R_{Rh} 1.70 (spray (O), (Q), (R)). The solution was filtered and concentrated to give a light-yellow syrup of $[\alpha]_D^{23} = +24 \pm 2°$ (*c*, 1.0 in methanol).

The Optical Rotation of Sodium L-Ascorbate in Aqueous Acetone (4)

L-Ascorbic acid (1.0 g) was titrated to equivalence (phenolphthalein) with aqueous sodium hydroxide (2.0 *N*) and the solution was diluted with water to a volume of 30 ml. Acetone (30 ml) was then added to bring the total volume to 60 ml. The optical rotation of this solution was measured at various times over a period of 2 days at room temperature.

TABLE II

Optical rotation of sodium L-ascorbate in aqueous acetone

Time (h)	$[\alpha]_D^{23}$
0.16	+132
1.5	+129
24	+127
48	+129

Thin layer chromatography (4) of the product showed the presence only of L-ascorbic acid.

Methyl Glycoside of 2-C-Benzyl-3-keto-L-lyxo-hexulosonic Acid Lactone

A solution of 2-*C*-benzyl-3-keto-L-*lyxo*-hexulosonic acid lactone (1.87 g) in methanolic hydrogen chloride (2% w/v, 100 ml) was heated for 11 h at 55–60°. The solution was neutralized with silver carbonate, filtered, and the filtrate was evaporated to yield a light-yellow syrup that crystallized. The product was recrystallized from hot water to give 0.96 g of needle-shaped crystals of $[\alpha]_D^{23} = +12 \pm 1°$ (*c*, 1.0 in methanol) and m.p. 139–140°.

Anal. Calcd. for $C_{14}H_{16}O_6$: C, 60.0; H, 5.8; OMe, 11.1. Found: C, 59.8; H, 5.6; OMe, 9.0.

The glycoside was not detectable on paper chromatograms (sprays (O), (P), (Q), or in iodine vapor (S)).

Methyl 2-C-Benzyl-L-lyxo-3-hexuloside (VIII)

A solution of the methyl glycoside of 2-*C*-benzyl-3-keto-L-*lyxo*-hexulosonic acid lactone (0.90 g) in anhydrous ether was added slowly to lithium aluminium hydride (1.0 g) in ether (50 ml). Reaction took place immediately with the formation of a precipitate. After 5 min ethyl acetate (5 ml) was added followed by distilled water (50 ml) and the mixture was filtered through Celite. The filtrate was extracted exhaustively with ethyl acetate, to yield, on evaporation of the extracts, a light-yellow oil (0.73 g). This crystallized and recrystallization was effected with ether–petrol b.p. 60–80° (85:15). Two different crops were collected, the first crop (150 mg) having m.p. 144–148° and the second crop (110 mg) having m.p. 115–117°. The product having m.p. 115–117° was recrystallized from ether–petrol b.p. 60–80° (85:15) to give long needles of m.p. 116–118° and $[\alpha]_D^{23°} = -23 \pm 1°$ (*c*, 1.0 in methanol).

Anal. Calcd. for $C_{14}H_{20}O_6$: C, 59.1; H, 7.1. Found: C, 59.4; H, 6.9.

The infrared spectrum showed absorptions at 3 420 and 3 550 cm^{-1} (hydroxyl) and no absorption in the region 1 605 to 1 800 cm^{-1}.

The initial crop of crystals having the melting point 144–148° were recrystallized from water, to give plates of m.p. 149–150° and $[\alpha]_D^{23} = -5 \pm 2°$ (*c*, 1.0 in methanol).

Anal. Calcd. for $C_{14}H_{20}O_6$: C, 59.1; H, 7.1. Found: C, 60.3; H, 6.8.

The infrared spectrum was practically identical with that of the alcohol m.p. 116–118° except for the absence of the absorption at 3 550 cm^{-1} (hydroxyl). The structure of this compound remained unknown.

Periodate Oxidation of Methyl 2-C-Benzyl-L-lyxo-3-hexuloside (VIII)

After 18 h the periodate uptake was determined as 2 moles/mole and formaldehyde release as 0.7 mole/mole. Slow overoxidation resulted in a total periodate consumption of 2.56 moles/mole and an acid realse of 0.63 mole/mole after 60 h.

Can. J. Chem. Downloaded from www.nrcresearchpress.com by 210.87.254.40 on 09/05/12
For personal use only.

Methyl 1,4,5-Tri-O-acetyl-2-C-benzyl-L-lyxo-3-hexuloside

The triacetate was prepared by dissolving VIII (100 mg) in pyridine (50 ml) and acetic anhydride (1 ml) and storing the solution at 0° for 10 h. Water (300 ml) was then added and the solution was extracted with chloroform (100 ml). The extract was washed successively with sulfuric acid solution (2 *N*, 2 × 50 ml), saturated sodium bicarbonate solution (50 ml), and water (100 ml) and then dried over calcium sulfate. Concentration of the dried solution afforded a syrup that crystallized immediately. After two recrystallizations from methanol–water the crystals had m.p. 152–154° and $[\alpha]_D^{23} = +14 \pm 1°$ (*c*, 0.62 in chloroform).

Anal. Calcd. for $C_{20}H_{26}O_9$: C, 58.5; H, 6.4. Found: C, 58.3; H, 6.2.

The infrared spectrum (KBr disc) revealed a single hydroxyl absorption at 3 600 cm^{-1}.

Decarboxylation of 2-C-Benzyl-3-keto-L-lyxo-hexulosonic Acid Lactone (III)

The lactone (III) (3.0 g, 1.1 × 10^{-2} mole) in water, was titrated to 77% equivalence (phenolphthalein) with aqueous sodium hydroxide (15 ml, 1.02 *N*). Paper chromatography in solvent (A) revealed mainly one component; R_f 0.19, R_{Rh} 0.60 (spray reagents (O), (P)). The component of R_f 0.19 gradually disappeared over a period of 2 days and was replaced by a substance with R_f 0.62, R_{Rh} 2.15 (solvent (A), spray (O)). After 3 days the solution was evaporated to dryness, extracted with butan-1-ol, and the butan-1-ol solution was filtered, and the solvent evaporated. The heavy oil so obtained was passed through a cellulose column (eluent; butan-1-ol – water, 10:1) and fractions of ca. 6 ml were collected automatically every 15 min. The fractions on which paper chromatographic examination (solvent (A), spray (O)) were shown to contain only the component of R_f 0.62, R_{Rh} 2.15, were combined and evaporated to a light-yellow syrup (1.28 g). The syrup crystallized after 3 weeks and on recrystallization from chloroform–acetone, crystals of m.p. 126–128° were obtained. This was subsequently shown to be a 1-deoxy-1-*C*-phenyl-2-hexulose.

1-Deoxy-1-C-phenyl-L-(lyxo or xylo)-2-hexulose (IX)

L-Ascorbic acid (20 g, 0.113 mole) in water (150 ml) was treated with aqueous potassium hydroxide, (12.8 g, 0.228 mole, 50 ml) benzyl chloride (28 g), and acetone (250 ml) and the system was shaken for 8 h at room temperature. After this interval paper chromatography (solvent A) and spray (O) revealed the presence of only one main component, with R_f 0.62, R_{Rh} 2.15. The solution was evaporated to remove the acetone and washed with petrol (b.p. 60–80°). Exhaustive extraction with hot ethyl acetate and evaporation of the combined extracts provided a syrup, yields of which varied from 11 to 14 g. The syrup crystallized spontaneously only once and further crystallizations were effected by dissolving the syrup in hot acetone (7.1 ml per gram of syrup) and chloroform (1.2 ml per gram of syrup) and seeding the solution. After recrystallization the melting point increased from 115–117° to 127–128° with $[\alpha]_D^{23} = -31 \pm 1°$ (*c*, 1.0 in methanol). The infrared spectrum showed no absorption in the region 1 605 to 1 800 cm^{-1} and was indistinguishable from that of the crystalline product isolated from the decarboxylation of 2-*C*-benzyl-3-keto-L-*lyxo*-hexulosonic acid lactone with alkali.

Anal. Calcd. for $C_{12}H_{16}O_5$: C, 60.0; H, 6.7. Found: C, 59.9; H, 6.8.

Periodate Oxidation of 1-Deoxy-1-C-phenyl-L-(lyxo or xylo)-2-hexulose (IX) and Isolation of Products

The quantitative oxidation on 100 mg of the hexulose (IX) resulted in 3 moles/mole of periodate uptake and 2 moles/mole of acid release after 0.25 h. Little further oxidation occurred after 36 h and no formaldehyde was detected.

In order to isolate the oxidation products the hexulose (0.63 g) was oxidized with sodium metaperiodate solution (0.2 *M*, 7.0 ml) in the absence of light. Chloroform extraction of the reaction mixture after 12 h afforded, after concentration of the extracts, a light-yellow fragrant oil (440 mg) that did not crystallize. The infrared spectrum showed absorptions at 1 740 and 1 720 cm^{-1} (ester, carbonyl). A portion of the syrup (58 mg) was saponified with sodium hydroxide (0.01 *N*, 2.92 ml), acidified with hydrochloric acid, and then extracted with chloroform. The extracts on concentration crystallized immediately and recrystallization from petrol (b.p. 60–80°) afforded plates of m.p. 74–76°. The infrared spectrum was indistinguishable from that of phenylacetic acid (0.8% KBr). A second portion of the syrup (200 mg) was hydrolyzed in aqueous sulfuric acid (0.5 *N*, 10 ml) for 2.5 h, neutralized with sodium hydroxide (phenolphthalein), and evaporated to dryness. Extraction of the salts and organic material with hot acetone yielded, on concentration, a brown gum. A portion of the gum so obtained was dissolved in hot ethanol (60°) containing 2,4-dinitrophenylhydrazine reagent, to give a red-orange product of m.p. 310–320°. The melting point of glycolaldehyde-bis-2,4-dinitrophenylhydrazone prepared from authentic glycolaldehyde was 320–325°. The infrared spectra of the product and of the authentic specimen were indistinguishable from each other.

Isolation of an Isomorph of 2-C-Benzyl-3-keto-L-lyxo-hexulosonic Acid Lactone (III)

The syrupy product from the reaction of L-ascorbic acid with sodium hydroxide and benzyl chloride was dispersed in chloroform–acetone and allowed to stand. After 3 weeks large needle-shaped crystals had formed, with m.p. 142–143° and $[\alpha]_D^{23} = +6 \pm 1°$ (*c*, 0.6 in methanol), $[\alpha]_D^{23} = 13.5 \pm 1°$ (*c*, 2.0 in water) in the unrecrystallized state. The isomorph gave an instantaneous Wallenfels test (2), was acidic to litmus, and revealed an absorption at 1 788 cm^{-1} (lactone) in the infrared and had the same rate of movement as III on thin layer chromatograms. The n.m.r. spectrum, taken with a Varian A-60 spectrometer, D_2O solvent, was found to be identical to that of 2-*C*-benzyl-3-keto-L-*lyxo*-hexulosonic acid lactone. Evaporation of D_2O at room temperature afforded crystals that had m.p. 142–145° with instantaneous

Can. J. Chem. Downloaded from www.nrcresearchpress.com by 210.87.254.40 on 09/05/12
For personal use only.

solidification at 145° to a glass that melted at 154–156°. When the isomorph was recrystallized by cooling a solution in hot chloroform–acetone the melting point rose to 154–155° with solvent of crystallization being given off at 70–80°. *Analysis* of the isomorph. Found: C, 58.9; H, 5.5. 2-*C*-Benzyl-3-keto-L-*lyxo*-hexulosonic acid lactone has the following constants. *Analysis*: C, 58.6; H, 5.3; m.p. 156–156.5°, $[\alpha]_D^{23} = +7 \pm 1°$ (*c*, 1.0 in methanol), $[\alpha]_D^{23} = +15.5 \pm 1°$ (*c*, 2.0 in water).

*Isolation of 3-O-Benzyl-*L*-ascorbic Acid (I, R = Ph—CH₂, R′ = H)*

The filtrate after isolation of 2-*C*-benzyl-3-keto-L-*lyxo*-hexulosonic acid lactone gave a light-green color with ferric chloride solution. In a typical separation 5.8 g of crude reaction product gave 0.83 g of crystalline lactone. The filtrate was concentrated, dissolved in methanolic ammonia (100 ml) and left at 0° for 4 days. On concentration of the solution a dark-brown syrup (4.55 g) was recovered. A portion of the syrup (1.77 g) was fractionated on a cellulose column (usual eluent) to yield two main fractions considered to be 3-*O*-benzyl-L-ascorbic acid (800 mg) and 2-*C*-benzyl-3-keto-L-*lyxo*-hexulonamide (580 mg). The infrared spectrum of the former fraction was indistinguishable from that of 3-*O*-benzyl-L-ascorbic acid. The percentage of 3-*O*-benzyl-L-ascorbic acid calculated from the above data was 50%.

O-Benzylation of L-*Ascorbic Acid*

*3-O-Benzyl-*L*-ascorbic Acid (I, R = Ph—CH₂, R′ = H)*

The sodium salt of L-ascorbic acid (17.84 g, 0.09 mole) was dissolved in dimethylsulfoxide (350 ml) containing benzyl chloride (11.43 g, 0.09 mole) and shaken for 1 week at room temperature. Dimethylsulfoxide was removed at 70° *in vacuo* to yield a dark gum. This was dissolved in water (300 ml), washed with petrol (b.p. 60–80°, 100 ml), and exhaustively extracted with hot ethyl acetate. The extracts on evaporation gave a light-brown syrup (19.45 g). Absorptions at 1 690, 1 730, 1 760, and 1 790 cm^{-1} were present in the infrared and indicated the presence of two or more components.

Chloroform extraction of a solution of crude 3-*O*-benzyl-L-ascorbic acid (7.44 g) in water (200 ml) and evaporation of the extracts yielded 1.13 g of dark gum assumed to contain higher substituted derivatives of L-ascorbic acid. The aqueous layer on evaporation gave a syrup of $[\alpha]_D^{23} = +8 \pm 1°$ (*c*, 1.0 in methanol). A portion of the syrup (1.34 g) was dissolved in anhydrous methanolic ammonia and kept at 0° for 48 h. The solution was then concentrated and passed through a cellulose column (usual eluent) to yield two syrupy fractions of total weight 800 mg. The first fraction; R_f 0.77, R_{Rh} 2.63 in solvent (A) (spray (O)) was assumed to be 3-*O*-benzyl-L-ascorbic acid and the second fraction to be 2-*C*-benzyl-3-keto-L-*lyxo*-hexulonamide. 3-*O*-Benzyl-L-ascorbic acid had $[\alpha]_D^{23} = +15 \pm 2°$ (*c*, 1.0 in methanol) and showed absorptions at 1 760 and 1 685 cm^{-1} in the infrared (typical pattern for ascorbate derivatives). There was no shoulder at 1 790 cm^{-1}. The syrup gave a light-green to light-blue color with ferric chloride in methanol and was acidic to litmus. In the above fractions the ratio of 3-*O*-benzyl-L-ascorbic acid to amide was 3:1.

*2,3-Di-O-benzyl-5,6-O-isopropylidene-*L*-ascorbic Acid (II, R = R′ = Ph—CH₂)*

The chloroform extract (1.13 g) (see above) was dispersed in anhydrous acetone (30 ml) containing crushed zinc chloride sticks (2.0 g) and the solution was shaken for 24 h at room temperature. After neutralization with 10% aqueous potassium carbonate (75 ml), extraction of the aqueous solution with diethyl ether, and evaporation of the ether, a light-yellow oil that crystallized immediately was obtained. Recrystallization from ether afforded needle-shaped crystals (0.052 g) of m.p. 125–126° and $[\alpha]_D^{23} = +23 \pm 1°$ (*c*, 1.15 in chloroform). The infrared spectrum showed strong absorptions at 1 755 and 1 675 cm^{-1}. No absorption was present in the region 3 100 to 3 600 cm^{-1}.

Anal. Calcd. for $C_{23}H_{24}O_6$: C, 69.7; H, 6.1. Found: C, 69.4; H, 6.3.

*3-O-Benzyl-5,6-O-isopropylidene-*L*-ascorbic Acid (II, R = Ph—CH₂, R′ = H)*

The isopropylidene derivative was prepared in the usual way (see above) from 3-*O*-benzyl-L-ascorbic acid (1.0 g, $[\alpha]_D^{23} = +8 \pm 1°$). The product crystallized and after recrystallization from diethyl ether – petrol (b.p. 60–80°) afforded needle-shaped crystals (374 mg) of m.p. 109–111° and $[\alpha]_D^{23} = +36 \pm 1°$ (*c*, 1.0 in methanol). The infrared spectrum (KBr disc) showed strong absorptions at 1 750 and 1 690 cm^{-1} with a medium absorption at 3 310 cm^{-1} (enolic hydroxyl).

Anal. Calcd. for $C_{16}H_{18}O_6$: C, 62.7; H, 5.9. Found: C, 62.6; H, 6.0.

*Isolation of the Isomorphous Form of 2-C-Benzyl-3-keto-*L*-lyxo-hexulosonic Acid Lactone (III) from the Experiment with Dimethylsulfoxide*

On standing 4 weeks, the crude reaction product ($[\alpha]_D^{23} = +8 \pm 1°$, (*c*, 1.0 in methanol)) had partially crystallized. The syrupy crystalline mass was dispersed in chloroform – ethyl acetate (4:1) and allowed to crystallize further to yield needles of m.p. 142–144° showing an absorption at 1 790 cm^{-1} (lactone) in the infrared. Except for the lactone peak the infrared spectrum was indistinguishable from that of 2-*C*-benzyl-3-keto-L-*lyxo*-hexulosonic acid lactone.

*3-O-Benzyl-2-O-methyl-*L*-ascorbic Acid (I, R = Ph—CH₂, R′ = CH₃)*

Crude 3-*O*-benzyl-L-ascorbic acid (3.42 g) was dissolved in absolute methanol (25 ml) containing excess ethereal diazomethane and kept at 0° for 2 days. The solution on evaporation yielded a syrup. The syrup was dispersed in chloroform and washed with water. The chloroform layer was dried and evaporated to yield a neutral gum (1.73 g) of $[\alpha]_D^{23} = +21 \pm 2°$ (*c*, 1.0 in methanol). The infrared spectrum of the gum showed strong peaks at 1 758 and 1 672 cm^{-1}.

Can. J. Chem. Downloaded from www.nrcresearchpress.com by 210.87.254.40 on 09/05/12
For personal use only.

3-O-Benzyl-2-O-methyl-5,6-O-isopropylidene-L-ascorbic Acid (II, R = Ph—CH_2, R' = CH_3)

The isopropylidene derivative was prepared from 3-*O*-benzyl-2-*O*-methyl-L-ascorbic acid in the usual way. The product was recrystallized from diethyl ether to give needles of m.p. 99.5–100.5° and $[\alpha]_D^{23}$ = +36 ± 1° (*c*, 1.0 in methanol).

Anal. Calcd. for $C_{17}H_{20}O_6$: C, 63.7; H, 6.3. Found: C, 63.9; H, 6.3.

Two strong absorptions at 1 675 and 1 750 cm^{-1} and no hydroxyl absorption were present in the infrared spectrum.

3-O-Methyl-5,6-O-isopropylidene-L-ascorbic Acid (II, R = CH_3, R' = H)

The isopropylidene derivative was prepared from 2.0 g of 3-*O*-methyl-L-ascorbic acid (14) in the usual way except that the product was extracted with ethyl acetate. The yield was 1.32 g of a colorless syrup of $[\alpha]_D^{23}$ = +18 ± 1° (*c*, 1.0 in methanol). Paper chromatography (solvent (A)) revealed one component moving at R_f 0.84, R_{Rh} 2.81 (spray (O), iodine vapor).

2-O-Benzyl-3-O-methyl-5,6-O-isopropylidene-L-ascorbic Acid (II, R = CH_3, R' = Ph—CH_2)

3-*O*-Methyl-5,6-*O*-isopropylidene-L-ascorbic acid (1.32 g) in anhydrous methanol (50 ml) was treated with sodium methoxide (0.7 ml, 4.0 *N*) and the solution was concentrated to a syrup. Benzyl chloride (30 ml) was added and the mixture heated for 1 h to give a dark-brown solution. The reaction system was removed from the bath, treated with water (200 ml), and steam distilled to remove the benzyl chloride. Crystallization commenced after the removal of the benzyl chloride and after recrystallization from ether the product had m.p. 86–87° and $[\alpha]_D^{23}$ = +41 ± 1° (*c*, 1.0 in methanol).

Anal. Calcd. for $C_{17}H_{20}O_6$: C, 63.7; H, 6.3. Found: C, 63.45; H, 6.3.

The infrared spectrum was indistinguishable from that of 3-*O*-benzyl-2-*O*-methyl-5,6-*O*-isopropylidene-L-ascorbic acid.

ACKNOWLEDGMENTS

The authors thank the National Research Council for a Scholarship (to K. G. A. J.) and for a Grant (N.R.C. T-19) and Queen's University for financial assistance. They also thank Dr. E. Buncel for his interest and advice.

REFERENCES

1. J. K. N. Jones. J. Am. Chem. Soc. **78**, 2855 (1956).
2. K. Wallenfels, E. Bernt, and G. Limburg. Angew. Chem. **65**, 581 (1953).
3. C. S. Hudson. J. Am. Chem. Soc. **40**, 813 (1918).
4. G. S. Brenner, D. F. Hinkley, L. M. Perkins, and S. Weber. J. Org. Chem. **29**, 2389 (1964).
5. N. Kornblum and A. Lurie. J. Am. Chem. Soc. **81**, 2705 (1959).
6. D. Y. Curtin, R. J. Crawford, and M. Wilhelm. J. Am. Chem. Soc. **80**, 1391 (1958).
7. D. Y. Curtin and D. H. Dybvig. J. Am. Chem. Soc. **84**, 225 (1962).
8. D. Y. Curtin and R. R. Fraser. J. Am. Chem. Soc. **80**, 6016 (1958).
9. N. Kornblum, R. Seltzer, and P. Haberfield. Report on 142nd Am. Chem. Soc. Meeting, Chem. Eng. News, **40**, Sept. 24 (1962).
10. W. E. Trevelyan, D. P. Proctor, and J. S. Harrison. Nature, **166**, 444 (1950).
11. L. Hough, J. K. N. Jones, and W. H. Wadman. J. Chem. Soc. 1702 (1950).
12. H. K. Berry and L. Cain. Arch. Biochem. **24**, 179 (1949).
13. J. F. O'Dea and R. A. M. Gibbons. Biochem. J. **55**, 580 (1953).
14. W. N. Haworth, E. L. Hirst, and F. Smith. J. Chem. Soc. 1558 (1934).

Can. J. Chem. Downloaded from www.nrcresearchpress.com by 210.87.254.40 on 09/05/12
For personal use only.

Can. J. Chem. Downloaded from www.nrcresearchpress.com by 210.87.254.5 on 09/05/12
For personal use only.

ION–SOLVENT INTERACTION IN MIXED SOLVENTS

PART III. THE MOLAR REFRACTION OF ELECTROLYTES

J. PADOVA[1]

The Northern Polytechnic, London, England, and
Soreq Research Establishment, Israel Atomic Energy Commission, Yavne, Israel

Received July 13, 1964

ABSTRACT

The apparent Lorenz–Lorentz molar refractions of Na_2SO_4, $MgSO_4$, $MnCl_2$, $NaOCOCH_3$, $Ba(OCOCH_3)_2$, $Mg(OCOCH_3)_2$, and $KOCOCH_3$ have been determined at 25 °C in mixtures of ethanol and acetone with water. The molar refraction of the solvated ions has been defined, and the values were calculated and found to be a linear function of the reciprocal of the dielectric constant of the bulk solvent.

INTRODUCTION

The refractive indices of sodium sulfate, magnesium sulfate, manganese chloride, sodium acetate, barium acetate, magnesium acetate, and potassium acetate have been determined at 25 °C with a view to investigating the variation of the molar refraction of the salts with the composition of the mixed solvents. These determinations may be expected to give some indication of the ion–solvent interaction in the immediate vicinity of the ions, since the refractivity of the salt is determined by the polarizability of the ions themselves and the change in the polarizability of the solvent produced by their presence. Although a large amount of data is available in aqueous solutions, only little is known on mixed solvents. Butler and Lees (1) have previously investigated the behavior of lithium chloride in ethanol–water mixtures using the Lorenz–Lorentz expression, whereas Bottcher (2) used glycerol–water mixtures as solvents to confirm his modified Lorenz–Lorentz equation. A number of references (unavailable to the writer) to work on molar refractions of salts may be found in the article on "Refractometry" (3).

EXPERIMENTAL

The solutions examined were the same as before (4), and were placed in a thermostat at 25° for half an hour before measurements were commenced. The refractive indices were then determined using a thermostated Abbé refractometer at 25 °C. The refractometer was checked using water and standard test specimens.

RESULTS AND DISCUSSION

For all the salts examined the refractive index increases with the concentration of the salts and of the organic components of the mixed solvents. On the assumption that the apparent molar refraction of electrolytes is given by the Lorenz–Lorentz expression for mixtures, Geffcken (5) derived relation [1] for the apparent molar refraction R

$$[1] \qquad R = \frac{n_0^2 - 1}{n_0^2 + 2} \cdot \left[\frac{1\,000}{c} \left(\frac{n^2 - 1}{n^2 + 2} \cdot \frac{n_0^2 + 2}{n_0^2 - 1} - 1 \right) + \phi_v \right],$$

where n_0 is the refractive index of the solvent, n is the refractive index of the solution, c is the molar concentration of solute, and ϕ_v is the apparent molar volume of solute. The molar refraction R is called the apparent molar refraction as it is calculated on the assumption that solution of the electrolyte causes no change in the solvent. Equation [1]

[1]*Present address: Radiochemistry Department, Soreq Research Establishment, Israel Atomic Energy Commission, Yavne, Israel.*

may be reduced to the form

$$[2] \qquad R = \frac{3\,000(n^2 - n_0^2)}{c(n^2 + 2)(n_0^2 + 2)} + \frac{n_0^2 - 1}{n_0^2 + 2}\,\phi_v.$$

Merland (6) has shown that in electrolyte solutions the relation

$$[3] \qquad n - n_0 = a(1 - e^{-bc})$$

is sometimes valid up to saturation. Here a and b are constants for the salt considered, where a is specific to the wavelength used and b is suggested to be the volume of the dissolved ions (6). Using [3] in eq. [2] when $c \rightarrow 0$,

$$[4] \qquad R^0 = \frac{6\,000abn_0}{(n_0^2 + 2)^2} + \frac{n_0^2 - 1}{n_0^2 + 2}\,\phi_v^0.$$

Table I compares the values of R^0 at 18 °C calculated using eq. [4] with those from the literature. The agreement is especially good for potassium salts and justifies the use of eq. [4] in the calculation of R^0 from Merland's expression.

TABLE I

Apparent molar refraction at infinite dilution

Salt	R^{0a}	R^{0b}
KNO_3	13.30	13.28
KCl	11.03	11.31
$BaCl_2$	21.37	22.00
$MgCl_2$	16.00	16.52
K_2SO_4	19.00	19.03
KBr	14.87	14.73
KI	21.28	21.55
$KOCOCH_3$	16.41 (25 °C)	16.53

[a]From eq. [4].
[b]See refs. 11 and 7.

For all electrolytes used in the experiments it has been found possible to extend the application of eq. [3] to mixed solvents. For a given salt, the constant a is the same irrespective of the nature of the solvent but the constant b varies with the solvent, usually decreasing with increasing concentration of non-aqueous solvent in the mixture (see Table II). The agreement between the calculated and experimental values of $(n - n_0)$ was well within the accuracy obtainable with the refractometer (± 0.0001).

It is proposed to use the solvated molar volume ϕ_s to arrive at a better representation of the molar refraction of the solvated complex R_s.

Assuming no further interaction between the solvation shell and the rest of the solvent, the Lorenz–Lorentz equation may be used and one obtains an equation similar to eq. [2],

$$[5] \qquad R_s = \frac{3\,000(n^2 - n_0^2)}{c(n_0^2 + 2)(n^2 + 2)} + \frac{n_0^2 - 1}{n_0^2 + 2}\,\phi_s.$$

Comparing [5] and [2], the relation between R_s and R at any concentration is

$$[6] \qquad R_s = R + h\,\frac{M_0}{d_0}\,\frac{n_0^2 - 1}{n_0^2 + 2},$$

where M_0 is the molar weight of solvent, d_0 is the density of pure solvent, and h is the

Can. J. Chem. Downloaded from www.nrcresearchpress.com by 210.87.254.5 on 09/05/12
For personal use only.

TABLE II

Constants a and b of the Merland equation $n = n_0 + a(1 - e^{-bc})$

	b (liter/mole)						
Solvent	Na_2SO_4 $a=0.1064$	$MgSO_4$ $a=0.1650$	$MnCl_2$ $a=0.4889$	NaAc $a=0.1520$	$Ba(Ac)_2$ $a=0.2020$	$Mg(Ac)_2$ $a=0.2300$	KAc $a=0.1810$
Ethanol–water							
Wt. % ethanol							
0	0.1860	0.1380	0.0525	0.0664	0.1600	0.1080	0.0616
8.5	0.1860	0.1380	0.0532	0.0685	0.1600	0.1080	0.0760
18.5	0.1436	0.1290	0.0513	0.0648	0.1460	0.1040	0.0520
29.5		0.1150	0.0499	0.0567	0.1360	0.1040	0.0460
40.4				0.0500	0.1180	0.0924	0.0440
52.0				0.0500		0.0880	0.0392
60.2				0.0457		0.0846	0.0384
70.3						0.0788	0.0384
79.8						0.0768	0.0348
89.9							0.0372
99.6							0.0464
Acetone–water							
Wt. % acetone							
8.5	0.1640	0.1524	0.0523	0.0673	0.1540	0.1120	0.0580
21.2	0.1580	0.1270	0.0507	0.0634	0.1430	0.1070	0.0540
30.8			0.0495	0.0609	0.1338	0.1000	0.0500
40.9			0.0495	0.0500	0.1256	0.0908	0.0448
52.0				0.0553		0.0744	0.0328

solvation number corresponding to the relation between ϕ_s and ϕ_v:

[7] $$\phi_s = \phi_v + h\frac{M_0^2}{d_0}.$$

Let

$$\frac{M_0}{d_0}\frac{n_0^2 - 1}{n_0^2 + 2} = R_0'.$$

Then at infinite dilution

[8] $$R_s^0 = R^0 + h^0 R_0'.$$

The molar refractions were calculated for sodium sulfate, magnesium sulfate, manganese chloride, potassium acetate, sodium acetate, barium acetate, and magnesium acetate in ethanol–water and acetone–water mixtures. In Figs. 1 and 2 the results are plotted against the reciprocal of the dielectric constant of the solvent. It is seen that the molar refraction of solvated ions varies linearly, in a similar manner to the solvated molar volume (3).

According to Merland (6) the constant b should be regarded as the volume of the ions. However, since

$$R_s^0 = \phi_s^0 \frac{n_s^2 - 1}{n_s^2 + 2},$$

where n_s is the refractive index of the solvated complex,

[9] $$\phi_s^0 \frac{n_s^2 - 1}{n_s^2 + 2} = \frac{6\,000abn_0}{(n_0^2 + 2)^2} + \phi_s^0 \frac{n_0^2 - 1}{n_0^2 + 2}$$

or

[10] $$b = \phi_s^0 \frac{(n_s^2 - n_0^2)(n_0^2 + 2)}{2\,000an_0(n_s^2 + 2)}$$

and is only proportional to ϕ_s^0.

Can. J. Chem. Downloaded from www.nrcresearchpress.com by 210.87.254.5 on 09/05/12
For personal use only.

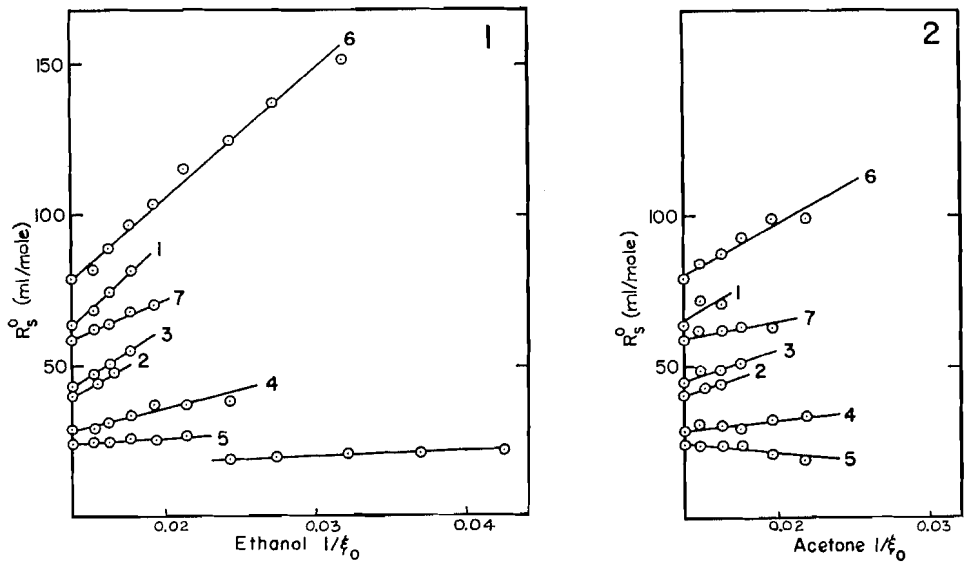

FIG. 1. Molar refraction in ethanol–water mixtures. (1) $MgSO_4$, (2) Na_2SO_4, (3) $MnCl_2$, (4) $NaOCOH_3$, (5) $KOCOCH_3$, (6) $Mg(OCOCH_3)_2$, (7) $Ba(OCOCH_3)_2$.

FIG. 2. Molar refraction in acetone–water mixtures. (1) $MgSO_4$, (2) Na_2SO_4, (3) $MnCl_2$, (4) $NaOCOCH_3$, (5) $KOCOCH_3$, (6) $Mg(OCOCH_3)_2$, (7) $Ba(OCOCH_3)_2$.

The polarizability data compiled from the published values of the apparent molar refraction data for electrolytes are not accurate (2), and only from eq. [9] is it possible to obtain the correct polarizability of the solvated ion complex. Bottcher (2) proposed a corrected Lorenz–Lorentz expression to account for the deviation in the apparent molar electrolyte refraction, and its application entails the assumption that the polarizability of Li^+ is zero. Fajans and his coworkers (7) tried to explain the deviations by assuming that the polarizability of a particle would depend to a large extent upon the properties of the surrounding media. The polarizability of water molecules which are subjected to polarization from surrounding ions has been calculated (8), but a later analysis did not indicate whether the Bottcher or Lorenz–Lorentz method is more appropriate (9), although theoretical considerations (10) seem to favor the former method. The above relation shows that the polarizability of solvated complex changes with the mixed solvent used. From the various values of ϕ_s and R it has been found that in a given solvent, the refractive index of the solvated complex is constant, in like manner to the constancy found for the dielectric constant (11) of the solvated complex determined assuming the additivity of the molar polarization at infinite dilution.

These data tend to show that with respect to certain properties, a solvated complex seems to behave as if it were a true particle and not merely an effective entity.

ACKNOWLEDGMENT

The experimental work was carried out in the laboratories of the Chemistry Department, The Northern Polytechnic, London. The author wishes to express his sincere appreciation for the help and encouragement he received from Dr. C. G. Smith during the course of this work.

Can. J. Chem. Downloaded from www.nrcresearchpress.com by 210.87.254.5 on 09/05/12
For personal use only.

REFERENCES

1. J. A. V. BUTLER and A. D. LEES. Proc. Roy Soc. London, Ser. A, **131**, 382 (1931).
2. C. J. BOTTCHER. Theory of electric polarisation. Elsevier Publishing Co. 1952. C. J. F. BOTTCHER and TH. G. SCHOLTE. Rec. Trav. Chim. **70**, 209 (1961).
3. N. BAUER and K. FAJANS. *In* Physical methods of organic chemistry. Vol. I, Part 2. 3rd ed. *Edited by* Weisberger. Interscience Publ. 1960.
4. J. PADOVA. J. Chem. Phys. **38**, 2635 (1963); **39**, 2599 (1963).
5. W. GEFFCKEN. Z. Physik. Chem. B, **5**, 81 (1929).
6. A. MERLAND. Compt. Rend. **227**, 189 (1948).
7. K. FAJANS. Z. Elektrochem. **34**, 502 (1928).
8. T. SATOB and K. HAYASHI. J. Phys. Soc. Japan, **15**, 1658 (1960).
9. W. H. ORTTUNG. J. Phys. Chem. **67**, 503 (1963).
10. W. F. BROWN, JR. Handbuch der physik. Vol. XVII. Springer Verlag, Berlin. 1956. pp. 1–153.
11. J. PADOVA. J. Chem. Phys. **40**, 691 (1964).
12. A. HEYDWEILLER. Z. Physik, **26**, 526 (1925).

Can. J. Chem. Downloaded from www.nrcresearchpress.com by 210.87.254.5 on 09/05/12
For personal use only.

Can. J. Chem. Downloaded from www.nrcresearchpress.com by 210.87.254.40 on 09/05/12
For personal use only.

MOLECULAR FORCE FIELD FOR SULFUR TETRAFLUORIDE

M. G. KRISHNA PILLAI, K. RAMASWAMY,[1] AND R. PICHAI
Department of Physics, Annamalai University, Annamalainagar, South India

Received September 1, 1964

ABSTRACT

An attempt has been made to modify the UBFF for SF_4 by taking into account the presence of the lone pair of electrons. It has been found that the bond pair – lone pair interactions become of importance only when the angle between the bond pair and the lone pair approaches 90°. The equatorial S—F stretching force constant (4.0146 mdyn/Å) is greater than the axial stretching force constant (3.6237 mdyn/Å), which is consistent with the form of the relationship between the force constant and bond length.

INTRODUCTION

Gillespie (1) has shown that the shapes of molecules of the non-transition elements can be readily understood in terms of the repulsive interactions between the electron pairs in the valency shell of the central atom. On this basis all molecules of the type AX_4E, where X is a ligand and E is a lone pair, will have a general shape based on a trigonal bipyramidal arrangement. SF_4, which has one lone pair of electrons, belongs to this category. The microwave spectral data for SF_4 determined by Tolles and Gwinn (2)—namely, that the equatorial bonds (1.545 Å) are shorter than the axial bonds (1.646 Å) and the angle between the equatorial bonds is 101° 33′ while the angle between the axial bonds is 186° 56′—was satisfactorily, at least qualitatively, explained on the basis of the valency shell electron pair repulsion theory (3).

It is of interest to see whether the presence of the lone pair has any influence on the bond force constants and also to determine the lone pair interactions. This can be effected by suitably modifying the molecular force field for SF_4 by taking into account the presence of lone pair of electrons. Such an attempt was made by Pariseau *et al.* for NH_3 (4) and for ClF_3 by the authors (5).

The Raman and infrared spectra of SF_4 was reported by Dodd *et al.* (6) and a tentative assignment was given on the basis of a C_{2v} model. The vibrational wave numbers are

$$a_1 = 889, 715, 557, 235 \text{ cm}^{-1}$$

$$a_2 = 401 \text{ cm}^{-1}$$

$$b_1 = 867, 532 \text{ cm}^{-1}$$

$$b_2 = 728, 463 \text{ cm}^{-1}.$$

Using this assignment a force field calculation was made by Chantry and Ewing (7). They concluded that the relation between the bond force constant and the internuclear distance was not affected by the introduction of d-electrons as in SF_4. They also indicated the possibility of inversion in sulfur tetrafluoride.

In the present study an attempt was made to calculate the molecular force constants for SF_4, taking into account the presence of the lone pair of electrons, in the usual Urey–Bradley force field (UBFF).

[1]*Scientist Pool Officer.*

Can. J. Chem. Downloaded from www.nrcresearchpress.com by 210.87.254.40 on 09/05/12
For personal use only.

MODIFIED UBFF FOR SF_4

As pointed out earlier (1) SF_4 will have a trigonal bipyramidal arrangement with the lone pair occupying one of the equatorial positions as shown in Fig. 1. The internuclear distances (a, d, and R) and the interbond angles (α, β, η, and γ) used for the construction of F and G matrices are as defined in Fig. 1. The numerical values were taken from ref. 2.

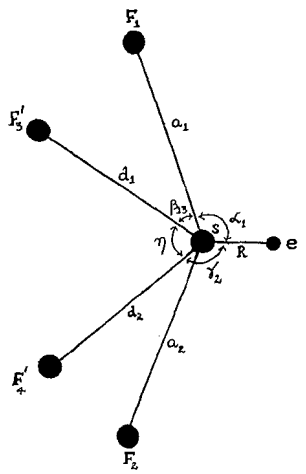

FIG. 1. Internal coordinates for SF_4.

In the usual UBFF for SF_4, there are six force constants (K_a, K_d, H_β, H_η, $F_{F'F'}$, and $F_{FF'}$ (see Fig. 1) and nine vibrational frequencies. Hence they can be determined uniquely. Therefore, it is not difficult to extend the UBFF to take into account the non-bonded interactions between the lone pair of electrons and the fluorine atoms. The coordinates R and α for the lone pair may be noted.

Using the internal coordinates defined in Fig. 1, the complete expression for the potential energy was written in the usual way (4, 5) and the expressions for the valence force constants were obtained. They are:

$$f_a = K_a + 2(S_{FF'}^2 F_{FF'} + t_{FF'}^2 F_{FF'}') + (S_{Fe}^2 F_{eF} + t_{Fe}^2 F_{eF}')$$

$$f_d = K_d + 2(S_{F'F}^2 F_{F'F} + t_{F'F}^2 F_{F'F}') + (S_{F'F'}^2 F_{F'F'} + t_{F'F'}^2 F_{F'F'}') + (S_{F'e}^2 F_{eF'} + t_{F'e}^2 F_{eF'}')$$

$$f_R = K_R + 2(S_{eF}^2 F_{eF} + t_{eF}^2 F_{eF}') + 2(S_{eF'}^2 F_{eF'} + t_{eF'}^2 F_{eF'}')$$

$$f_\alpha = H_\alpha - S_{eF} S_{Fe} F_{eF}' + t_{eF} t_{Fe} F_{eF}$$

$$f_\beta = H_\beta - S_{FF'} S_{F'F} F_{FF'}' + t_{FF'} t_{F'F} F_{FF'}$$

$$f_\gamma = H_\gamma - S_{eF'} S_{F'e} F_{eF'}' + t_{eF'} t_{F'e} F_{eF'}$$

$$f_\eta = H_\eta - S_{F'F'}^2 F_{F'F'}' + t_{F'F'}^2 F_{F'F'}$$

$$f_{aR} = S_{Fe} S_{eF} F_{eF} - t_{Fe} t_{eF} F_{eF}'$$

$$f_{dR} = S_{F'e} S_{eF'} F_{eF'} - t_{F'e} t_{eF'} F_{eF'}'$$

$$f_{ad} = S_{FF'} S_{F'F} F_{F'F} - t_{FF'} t_{F'F} F_{F'F}'$$

$$f_{dd} = S_{F'F'}{}^2 F_{F'F'} - t_{F'F'}{}^2 F_{F'F'}'$$
$$f_{R\alpha} = t_{eF} S_{Fe} F_{eF} + t_{Fe} S_{eF} F_{eF}'$$
$$f_{R\gamma} = t_{eF'} S_{F'e} F_{eF'} + t_{F'e} S_{eF'} F_{eF'}'$$
$$f_{a\beta} = t_{FF'} S_{F'F} F_{F'F} + t_{F'F} S_{FF'} F_{F'F}'$$
$$f_{a\alpha} = t_{Fe} S_{eF} F_{eF} + t_{eF} S_{Fe} F_{eF}'$$
$$f_{d\gamma} = t_{F'e} S_{eF'} F_{eF'} + t_{eF'} S_{F'e} F_{eF'}'$$
$$f_{d\beta} = t_{F'F} S_{FF'} F_{FF'} + t_{FF'} S_{F'F} F_{FF'}'$$
$$f_{d\eta} = t_{F'F'} S_{F'F'} F_{F'F'} + t_{F'F'} S_{F'F'} F_{F'F'}'$$

$$S_{ij} = \frac{r_i - r_j \cos \alpha_{ij}}{q_{ij}}$$

and

[1] $$t_{ij} = \frac{r_j \sin \alpha_{ij}}{q_{ij}}.$$

Here the subscripts refer to pairs of atoms; the qs represent the non-bonded distances; the symbols K, H, and F represent, respectively, the stretching, bending, and repulsive force constants. The Ks represent the linear terms which vanish in the equilibrium configurations. The constants F' were set equal to -0.1 times the corresponding F values, assuming that the energies associated with the qs are proportional to q^{-9}.

The following set of symmetry coordinates was formed from the internal coordinates.

For a_1 species.—$S_1 = (\Delta a_1 + \Delta a_2)/\sqrt{2}$
$S_2 = (\Delta d_1 + \Delta d_2)/\sqrt{2}$
$S_3 = \Delta\eta$
$S_4 = (\Delta\beta_{13} + \Delta\beta_{23} + \Delta\beta_{14} + \Delta\beta_{24})/2$
$S_5 = \Delta R$
$S_6 = (\Delta\gamma_1 + \Delta\gamma_2)/\sqrt{2}$
$S_7 = (\Delta\beta_{13} + \Delta\beta_{23} + \Delta\beta_{14} + \Delta\beta_{24} + \Delta\alpha_1 + \Delta\alpha_2)/\sqrt{6}$

For b_1 species.—$S_8 = (\Delta d_1 - \Delta d_2)/\sqrt{2}$
$S_9 = (\Delta\beta_{13} + \Delta\beta_{23} - \Delta\beta_{14} - \Delta\beta_{24})/2$
$S_{10} = (\Delta\gamma_1 - \Delta\gamma_2)/\sqrt{2}$

For a_2 species.—$S_{11} = (\Delta\beta_{13} - \Delta\beta_{23} - \Delta\beta_{14} + \Delta\beta_{24})/2$

For b_2 species.—$S_{12} = (\Delta a_1 - \Delta a_2)/\sqrt{2}$
$S_{13} = (\Delta\beta_{13} - \Delta\beta_{23} + \Delta\beta_{14} - \Delta\beta_{24})/2$

[2] $S_{14} = (\Delta\alpha_1 - \Delta\alpha_2)/\sqrt{2}.$

The coordinate S_7 is redundant and S_4 and S_7 are not orthogonal.

Can. J. Chem. Downloaded from www.nrcresearchpress.com by 210.87.254.40 on 09/05/12
For personal use only.

This set of symmetry coordinates gives a non-orthogonal U matrix and the unsymmetrized G matrix is constructed by the standard methods. The matrices are then symmetrized by the following transformations.

[3] $$\boldsymbol{F} = (U^{-1})' f U^{-1}$$

[4] $$\boldsymbol{G} = U G U'.$$

Owing to the presence of the atom of zero mass (electron) certain elements of G are infinite. The rows and columns containing these elements are now dropped from G and the residue G^0 is taken with modified F^0 matrix to give for each symmetry block a reduced secular equation by the method outlined earlier (4, 5, 8). The modified F^0 matrix elements thus obtained are as follows.

For a_1 species.—$$F_{11}^{\,0} = f_a - \frac{2f_{aR}^{\,2}}{f_R}$$

$$F_{12}^{\,0} = 2f_{ad} - \frac{2f_{aR}f_{dR}}{f_R} - \frac{f_{aR}f_{d\gamma}}{f_{R\gamma}}$$

$$F_{13}^{\,0} = 0$$

$$F_{14}^{\,0} = \sqrt{2}(f_{a\beta} - f_{a\alpha}) + \frac{2\sqrt{2}f_{aR}f_{R\alpha}}{f_R}$$

$$F_{22}^{\,0} = f_a + f_{dd} - \frac{2f_{dR}^{\,2}}{f_R} - \frac{f_{d\gamma}^{\,2}}{f_\gamma} - \frac{2f_{dR}f_{d\gamma}}{f_{R\gamma}}$$

$$F_{23}^{\,0} = \sqrt{2}f_{d\eta}$$

$$F_{24}^{\,0} = \sqrt{2}f_{d\beta} + \frac{2\sqrt{2}f_{dR}f_{R\alpha}}{f_R} \frac{\sqrt{2}f_{d\gamma}f_{R\alpha}}{f_{R\gamma}}$$

$$F_{33}^{\,0} = f_\eta$$

$$F_{34}^{\,0} = 0$$

$$F_{44}^{\,0} = f_\beta + 2f_\alpha - \frac{4f_{R\alpha}^{\,2}}{f_R}$$

For b_1 species.—$$F_{55}^{\,0} = f_d - f_{dd} - \frac{f_{d\gamma}^{\,2}}{f_\gamma}$$

$$F_{56}^{\,0} = \sqrt{2}f_{d\beta}$$

$$F_{66}^{\,0} = f_\beta$$

For a_2 species.—$$F_{77}^{\,0} = f_\beta$$

For b_2 species.—$$F_{88}^{\,0} = f_a - \frac{f_{a\alpha}^{\,2}}{f_\alpha}$$

$$F_{89}^{\,0} = \sqrt{2}f_{a\beta}$$

[5] $$F_{99}^{\,0} = f_\beta.$$

After removing the coordinates which have infinite values for the G matrix, we are left with the usual G^0 matrix and an F^0 matrix which contains extra terms involving the lone pair.

Can. J. Chem. Downloaded from www.nrcresearchpress.com by 210.87.254.40 on 09/05/12
For personal use only.

To facilitate computations the F^0 matrix given above was modified to a new $\mathfrak{F}$ matrix through the transformation

[6] $$\mathfrak{F} = U' F^0 U,$$

where U is the matrix of transformation from the real internal coordinates (without considering the lone pair) to the symmetry coordinates. The $\mathfrak{F}$ elements are given by

$$\bar{f}_a = f_a - \frac{f_{aR}^2}{f_R} - \frac{f_{a\alpha}^2}{2f_\alpha}$$

$$\bar{f}_d = f_d - \frac{f_{dR}^2}{f_R} - \frac{f_{d\gamma}^2}{f_\gamma} - \frac{f_{dR}f_{d\gamma}}{f_{R\gamma}}$$

$$\bar{f}_{dd} = f_{dd} - \frac{f_{dR}^2}{f_R} - \frac{f_{dR}f_{d\gamma}}{f_{R\gamma}}$$

$$\bar{f}_{ad} = f_{ad} - \frac{f_{aR}f_{dR}}{f_R} - \frac{f_{aR}f_{d\gamma}}{2f_{R\gamma}}$$

$$\bar{f}_\eta = f_\eta$$

$$\bar{f}_{d\eta} = f_{d\eta}$$

$$\bar{f}_\beta = f_\beta + \frac{f_\alpha}{2} - \frac{f_{R\alpha}^2}{f_R}$$

$$\bar{f}_{d\beta} = f_{d\beta} + \frac{f_{dR}f_{R\alpha}}{f_R} + \frac{f_{d\gamma}f_{R\alpha}}{2f_{R\gamma}}$$

[7] $$\bar{f}_{a\beta} = f_{a\beta} - \frac{f_{a\alpha}}{2} + \frac{f_{aR}f_{R\alpha}}{f_R}.$$

With these expressions for the force constants, the problem was treated as a simple UBFF calculation, but with the following modified Urey–Bradley force constant (UBFC),

[8] $$\bar{K}_a = K_a + (S_{Fe}^2 F_{eF} + t_{Fe}^2 F_{eF}') - \frac{f_{aR}^2}{f_R} - \frac{f_{a\alpha}^2}{2f_\alpha}$$

[9] $$\bar{K}_d = K_d + (S_{F'e}^2 F_{eF'} + t_{F'e}^2 F_{eF'}') - \frac{f_{dR}^2}{f_R} - \frac{f_{d\gamma}^2}{f_\gamma} - \frac{f_{dR}f_{d\gamma}}{f_{R\gamma}}$$

[10] $$\bar{H}_\beta = H_\beta + \frac{f_\alpha}{2} - \frac{f_{R\alpha}^2}{f_R}$$

[11] $$\bar{H}_\eta = H_\eta$$

[12] $$\bar{F}_{FF'} = F_{FF'}$$

[13] $$\bar{F}_{F'F'} = F_{F'F'},$$

and with additional non-Urey–Bradley cross terms,

[14] $$\bar{F}_{dd} = -\frac{f_{dR}^2}{f_R} - \frac{f_{dR}f_{d\gamma}}{f_{R\gamma}}$$

[15] $$\bar{F}_{ad} = -\frac{f_{aR}f_{dR}}{f_R} - \frac{f_{aR}f_{d\gamma}}{2f_{R\gamma}}$$

Can. J. Chem. Downloaded from www.nrcresearchpress.com by 210.87.254.40 on 09/05/12
For personal use only.

[16] $$\bar{F}_{d\beta} = \frac{f_{dR}f_{R\alpha}}{f_R} + \frac{f_{d\gamma}f_{R\alpha}}{2f_{R\gamma}}$$

[17] $$\bar{F}_{a\beta} = -\frac{f_{a\alpha}}{2} + \frac{f_{aR}f_{R\alpha}}{f_R}.$$

The force constants in eqs. [8]–[17] were adjusted by Danielewsky's method of successive approximation (9). The set which gives the best reproduction of frequencies was obtained. The agreement between the observed and calculated frequencies may be seen from Table I. The vibrational assignments and the microwave data given earlier were used in the present calculations. The distance between the nucleus and the lone-pair electrons (R) was assumed to be 0.54 Å.

The modified Urey–Bradley force constants obtained using the transformation equations are presented in Table II along with F^0 matrix elements.

TABLE I

Observed and calculated wave numbers for SF_4

Species	Observed frequencies, cm^{-1}	Calculated frequencies, cm^{-1}
a_1	889, 715, 557, 235	902, 717, 546, 241
a_2	401	401
b_1	867, 532	867, 532
b_2	728, 463	728, 463

TABLE II

Potential energy constants for SF_4

F^0 matrix elements[a] in symmetry coordinates		Modified UBFF constants in internal coordinates		Modified UBFF constants	
F_{11}^0	6.4072[b]	$\bar{f}_a$	4.7237	$\bar{K}_a$	3.6237
F_{22}^0	5.3768	$\bar{f}_d$	5.1347	$\bar{K}_d$	4.0146
F_{33}^0	0.7364	$\bar{f}_\eta$	0.7364	$\bar{H}_\eta$	0.5731
F_{44}^0	6.2097	$\bar{f}_\beta$	3.4467	$\bar{H}_\beta$	2.7845
F_{55}^0	4.8926	$\bar{f}_{dd}$	0.2421	$\bar{F}_{dd}$	0.0150
$\bar{F}_{66}^0$	4.6097	$\bar{f}_{a\alpha}$	0.6324	$\bar{F}_{ad}$	0
F_{77}^0	1.4037	$\bar{f}_{d\eta}$	0.1565	$\bar{F}_{d\beta}$	0
F_{88}^0	3.0401	$\bar{f}_{d\beta}$	0.5893	$\bar{F}_{a\beta}$	0.0791
F_{99}^0	1.5635	$\bar{f}_{a\beta}$	0.5789		
F_{12}^0	1.2645				
F_{13}^0	0				
F_{14}^0	0.9306				
F_{23}^0	0.2213				
F_{24}^0	0.8334				
F_{34}^0	0				
F_{56}^0	0.8334				
F_{89}^0	0.7068				

[a]The F^0 matrix elements containing only stretching constants are in mdyn/Å, those containing only angle–angle constants are in mdyn Å/rad^2 and those containing bond angle interaction constants are in mdyn/rad.

[b]This number of significant figures is retained to secure internal consistency in the calculations and to obtain the best agreement with the observed wave numbers.

DISCUSSION

It is seen from Table II that the S—F axial stretching force constant is less than that for the equatorial bond. The magnitude is consistent with the variation in the bond

Can. J. Chem. Downloaded from www.nrcresearchpress.com by 210.87.254.40 on 09/05/12
For personal use only.

length. The S—F stretching force constants ($\bar{K}_a$ and $\bar{K}_d$) for axial and equatorial bonds (1.646 Å and 1.545 Å) are 3.6237 mdyn/Å and 4.0146 mdyn/Å respectively. Hiraishi *et al.* (10) reported the UBFC for S—F stretch in SF_6 to be 3.75 mdyn/Å. The S—F bond length in SF_6 is 1.58 Å (11). This value is intermediate between the values obtained in the present study for the axial and equatorial S—F bonds. This is to be expected on the basis of the empirical relations suggested for the variation of bond force constant with internuclear distance (12, 13).

It is possible to calculate the value of the lone pair – bond pair interaction constants ($F_{eF'}$ equatorial and F_{eF} axial) and stretching force constant (K_R) of the lone pair. The values obtained for the lone pair – bond pair interactions ($F_{eF'} = -0.2056$ mdyn/Å and $F_{eF} = -0.6167$ mdyn/Å) indicate that the lone pair – bond pair interactions become of importance only when the angle between them approaches 90°. This result is consistent with earlier statements (11). The value for K_R (2.0179 md/Å) seems to be in agreement with the value reported by Pariseau *et al.* (4) for ammonia (3.62 mdyn/Å).

The value of the equatorial $\overset{\frown}{F\ S\ F}$ bending constant ($\bar{f}_\eta$) as well as $F_{F'F'}$ equatorial non-bonded interaction constant are considerably lower than those for the axial $\overset{\frown}{F\ S\ F}$ bending constant ($\bar{f}_\beta$) and $F_{FF'}$ axial–equatorial non-bonded interaction constant. This shows that there is lack of strain in the trigonal plane due to fluorine–fluorine repulsion as pointed out by Ewing and Chantry.

ACKNOWLEDGMENT

Two of the authors (K. R.) and (R. P.) are grateful to the C.S.I.R. and Ministry of Education and Cultural Affairs, Govt. of India, for financial assistance through the Scientist Pool and Senior Research Scholarship.

REFERENCES

1. R. J. Gillespie. Can. J. Chem. **39**, 318 (1961).
2. W. M. Tolles and W. D. Gwinn. J. Chem. Phys. **36**, 1119 (1962).
3. R. J. Gillespie. J. Chem. Phys. **37**, 2498 (1962).
4. M. Pariseau, E. Wu, and J. Overend. J. Chem. Phys. **39**, 217 (1963).
5. M. G. Krishna Pillai, K. Ramaswamy, and R. Pichai. Australian J. Chem. In press.
6. R. E. Dodd, L. A. Woodward, and H. L. Roberts. Trans. Faraday Soc. **52**, 1052 (1956).
7. G. W. Chantry and V. C. Ewing. Mol. Phys. **5**, 209 (1962).
8. E. B. Wilson, J. C. Decius, and P. C. Cross. Molecular vibrations. McGraw-Hill, New York. 1955. p. 75.
9. H. Wayland. Quart. Appl. Math. **2**, 282 (1945).
10. J. Hiraishi, I. Nakagawa, and T. Shimanouchi. Spectrochim. Acta, **20**, 819 (1964).
11. H. J. M. Bowen *et al.* Tables of interatomic distances and configuration in molecules and ions. Chem. Soc. London, Spec. Publ. 11. 1958. p. 72.
12. R. M. Badger. J. Chem. Phys. **2**, 128 (1934).
13. W. Gordy. J. Chem. Phys. **14**, 305 (1946).

Can. J. Chem. Downloaded from www.nrcresearchpress.com by 210.87.254.40 on 09/05/12
For personal use only.

Can. J. Chem. Downloaded from www.nrcresearchpress.com by 210.87.254.6 on 09/05/12
For personal use only.

REACTIONS OF PALLADIUM COMPOUNDS WITH ACETYLENES

II. TETRAKIS(*p*-CHLOROPHENYL)CYCLOBUTADIENE PALLADIUM COMPLEXES

P. M. MAITLIS, D. POLLOCK, M. L. GAMES, AND W. J. PRYDE
Department of Chemistry, McMaster University, Hamilton, Ontario

Received September 30, 1964

ABSTRACT

It is found that both diphenylacetylene and bis(*p*-chlorophenyl)acetylene on reaction with bis(benzonitrile)palladium chloride in benzene give the benzenoid trimer (R_6C_6) as well as a new type of cyclobutadiene complex $[(R_4C_4)(PdCl_2)_x]_2$ (R = Ph and *p*-ClC_6H_4) for which structure IV is proposed. *p,p'*-Dichlorotolan reacts with bis(benzonitrile)palladium chloride in ethanol – methylene chloride to give a complex $[(R_4C_4OC_2H_5)PdCl]_2$ (II) which is converted into the normal cyclobutadiene complex $[(R_4C_4)PdBr_2]_2$ (V) on treatment with hydrogen bromide. This can also be obtained from IV. The tetrakis(*p*-chlorophenyl)cyclobutadiene palladium halides on treatment with tri-*n*-butylphosphine give a dimer of tetrakis(*p*-chlorophenyl)cyclobutadiene which is probably octakis(*p*-chlorophenyl)cyclooctatetraene. Tetrakis-(*p*-chlorophenyl)cyclobutadiene iron tricarbonyl has also been prepared from IV and V by a ligand-transfer reaction.

INTRODUCTION

We recently communicated (1) the results of a reinvestigation of the reaction between diphenylacetylene (tolan) and palladium(II) compounds originally discovered by Malatesta *et al.* (2). This reaction we found to give products, the nature of which depended largely on the conditions and solvent used for the reaction. For example, tolan and bis(benzonitrile)palladium chloride in benzene gave mainly hexaphenylbenzene, while the same reaction carried out in ethanol–chloroform or with sodium chloropalladite and tolan in aqueous ethanol gave mainly a complex $[C_{30}H_{25}OPdCl]_2$. This was originally assigned structure I, but an X-ray structure determination by Dahl and Oberhansli (3) has now shown it to be the *endo*-4-ethoxy-π-1,2,3,4-tetraphenylcyclobutenyl palladium chloride dimer (II, R = Ph).

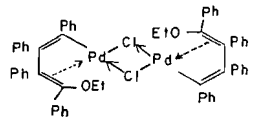

I

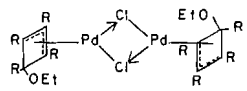

II

Reaction of II, R = Ph with hydrogen halides gave the π-tetraphenylcyclobutadiene palladium halides, $[\pi\text{-}Ph_4C_4]PdX_2$ (III). It was originally hoped that this reaction would lead to a simple general synthesis of cyclobutadiene palladium complexes from the appropriate acetylenes. However, it is now well established that acetylenes react with palladium(II) compounds to give a wide variety of oligomers and complexes, the nature of which depends largely on the acetylene used (4). We are currently, therefore, engaged on a detailed investigation of these reactions with the aim of correlating the structure of the acetylene with the nature of the products obtained and hope, on completion of this project, to be able to present a comprehensive theory of the reaction of acetylenes with palladium(II) and other transition metal compounds. Since there is such a wide variation in the nature of the reaction of palladium compounds with acetylenes we decided to start by examining the effect of a very simple change in the structure of the acetylene used, i.e., by using *p,p'*-dichlorotolan in place of tolan. The effect of this will be almost entirely

electronic since the para-chlorines will not be expected to exert any appreciable steric influence on the course of the reaction. We find that *p,p'*-dichlorotolan reacts qualitatively in a very similar fashion to tolan, but a sufficient number of points of interest have arisen during the course of this work to prompt us to publish our results now.

RESULTS

The reaction of tolan with bis(benzonitrile)palladium chloride in non-hydroxylic solvents gave, as mentioned, mainly hexaphenylbenzene. A careful reexamination of this reaction has now, however, shown that some tetraphenylcyclobutadiene palladium chloride is also formed in addition. The amount of this and the exact structure of the complex, however, vary with the ratio of tolan:bis(benzonitrile)palladium chloride used and with the method of addition. Thus, using a 2:1 ratio, 18% of a cyclobutadiene complex was obtained, whereas with a 1:1 ratio and slow addition of the tolan to the bis(benzonitrile) palladium chloride in high dilution a 34% yield of a related complex was obtained. The former complex analyzed for $[(Ph_4C_4)(PdCl_2)_{2.5}]_2$, the latter for $[(Ph_4C_4)(PdCl_2)_3]_2$.[1] As these were both definitely complexes of tetraphenylcyclobutadiene palladium chloride from their infrared spectra and their reactions, we conclude that their structure must involve the existence of two $(Ph_4C_4)PdCl_2$ units bridged by a series of $PdCl_2$ units as in IV, R = Ph, the former complex having $n = 3$ and the latter $n = 4$. This structure is

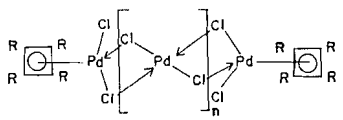

IV

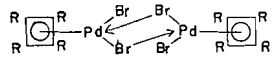

V, R = *p*-ClC_6H_4

similar to that for solid palladium chloride itself and can be thought of as a short segment of the palladium chloride polymer terminated by a $(Ph_4C_4)PdCl_2$ group at each end. The formation and also the stability of such structures is quite surprising.

This type of complex is also formed by reaction of *p,p'*-dichlorotolan and bis(benzonitrile)palladium chloride in benzene, but the yields of the cyclobutadiene complexes under comparable conditions are rather better for the *p,p'*-dichlorotolan (43%) than for tolan (34%). In this case complexes of type IV, R = *p*-ClC_6H_4 with analyses corresponding to $n = 2$ and $n = 4$ have been obtained, depending on the conditions, together with hexakis-(*p*-chlorophenyl)benzene. Attempts to remove the excess palladium chloride from these complexes (e.g., by treatment with Cl^-, benzonitrile, or other solvents) were not successful, and the complex was either recovered unchanged or else had been completely destroyed. However, IV, R = *p*-ClC_6H_4 could be converted into tetrakis(*p*-chlorophenyl)cyclobutadiene palladium bromide (V) by treatment with hydrogen bromide in methylene chloride.

The presence of a π-bonded cyclobutadiene ring in these complexes was also indicated by their conversion to the known tetrakis(*p*-chlorophenyl)cyclobutadiene iron tricarbonyl (VI) by the ligand-transfer reaction recently described by Maitlis and Games for the tetraphenylcyclobutadiene complexes (5). The complex VI had originally been prepared by Braye and Hübel (6) and the infrared spectrum has been studied by Fritz (7).

Tetrakis(*p*-chlorophenyl)cyclobutadiene palladium bromide (V) was found to be a

[1]*Since these complexes are too insoluble for molecular weight determinations, the dimeric structures which we are assigning to them are by analogy with other structures described below.*

Can. J. Chem. Downloaded from www.nrcresearchpress.com by 210.87.254.6 on 09/05/12
For personal use only.

stable red crystalline solid, decomposing only above 300°. The solubility of this complex was sufficient for an osmometric molecular weight determination to be possible in chloroform; this showed that V was dimeric even in a 0.0053 *M* solution and hence must have the bromine-bridged structure (V). This is similar to that of Criegee's tetramethylcyclobutadiene nickel chloride (8), an X-ray structure determination of which showed it to be dimeric with bridging halogens and formally five-coordinate Ni(II) (9).

Reaction of *p*,*p*′-dichlorotolan with bis(benzonitrile)palladium chloride in ethanol – methylene chloride yielded the ethoxy-π-cyclobutenyl complex (II, R = *p*-ClC_6H_4) by analogy to the tolan reaction already described above. The ethoxy complex (II, R = *p*-ClC_6H_4) on treatment with hydrogen bromide in methylene chloride also gave the tetrakis(*p*-chlorophenyl)cyclobutadiene palladium bromide (V) and, as in the tetraphenylcyclobutadiene series, this represents the best route to V. Attempts to prepare II, R = *p*-ClC_6H_4 by using aqueous ethanolic sodium chloropalladite and acetylene were not successful, and other variations in the method invariably gave low yields of II, R = *p*-ClC_6H_4 together with hexakis(*p*-chlorophenyl)benzene from which it was difficult to separate.

As reported previously (1), tetraphenylcyclobutadiene palladium chloride can be converted by treatment with ethanol into a geometric isomer of II which has now been shown (3) to have the structure VII, R = Ph, the isomers only differing in the orientation of the ethoxy and phenyl groups on the saturated carbon of the four-membered ring with respect to the metal.

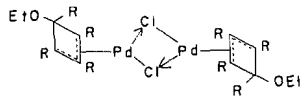

VII

In a similar manner the *p*-chlorophenyl complex (VII, R = *p*-ClC_6H_4) was formed by treatment of IV, R = *p*-ClC_6H_4 with ethanol. As in the tetraphenylcyclobutadiene series, VII, R = *p*-ClC_6H_4 could be reconverted into the tetrakis(*p*-chlorophenyl)cyclobutadiene palladium bromide by treatment with hydrogen bromide in methylene chloride. However, neither II nor VII, R = *p*-ClC_6H_4 formed the simple tetrakis(*p*-chlorophenyl)cyclobutadiene palladium chloride (IV, R = *p*-ClC_6H_4, $n = 0$) by reaction with hydrogen chloride or hydrochloric acid under a variety of conditions. The reactions and interconversions are summarized in the chart.

Maitlis and Stone (10) showed that reaction of tetraphenylcyclobutadiene palladium halides with *t*-phosphines gave high yields of the tetraphenylcyclobutadiene dimer, previously described by Freedman and Petersen (11). The latter authors suggested that this dimer was octaphenylcubane (VIII*a*, R = Ph) on the evidence of the absence of a C=C stretching mode in the Raman spectrum at ca. 1 650 cm^{-1} and on the preliminary results of an X-ray structure determination (but see below). Tetrakis(*p*-chlorophenyl) cyclobutadiene palladium halides (IV, R = *p*-ClC_6H_4) on treatment with *t*-phosphines, especially tri-*n*-butylphosphine, gave bis(tributylphosphine)palladium chloride and 54–73% yields of the tetrakis(*p*-chlorophenyl)cyclobutadiene dimer (VIII, R = *p*ClC_6H_4). This was at first also assumed to have the cubane skeleton. However, although this compound had no double-bond peak in the infrared, a very strong band was found in the solid state Raman spectrum at 1 642 cm^{-1}, in the region expected for a C=C stretching mode in these compounds (11) as well as a phenyl band at 1 597 cm^{-1} (corresponding to the one

Can. J. Chem. Downloaded from www.nrcresearchpress.com by 210.87.254.6 on 09/05/12
For personal use only.

CHART I

Reactions of *p,p'*-dichlorotolan and the complexes derived from it (R = *p*-ClC_6H_4)

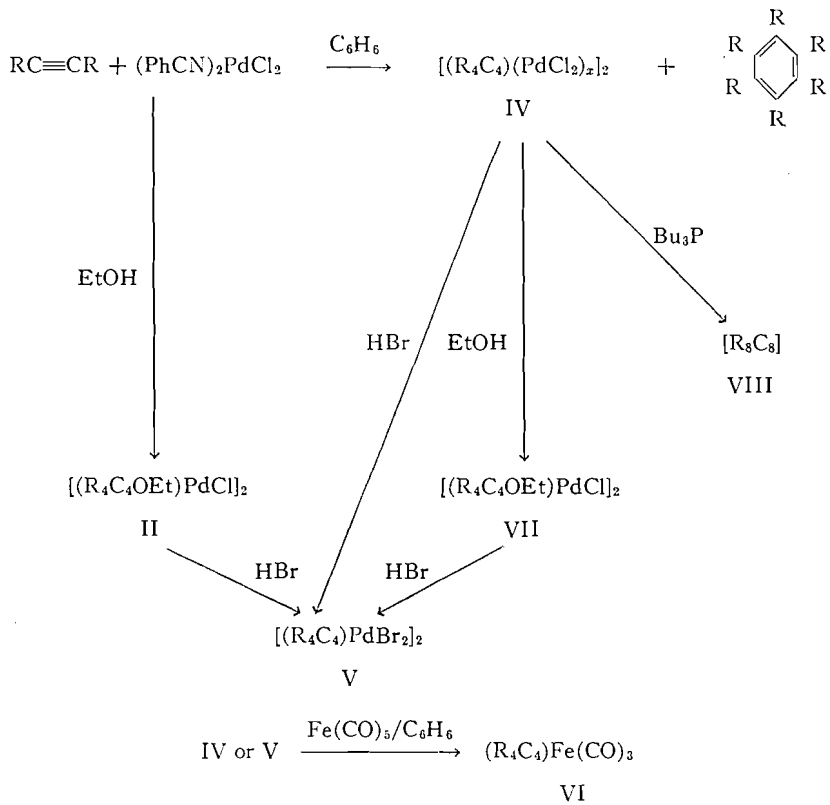

observed in "octaphenylcubane" at 1 605 cm^{-1}). The ultraviolet spectrum of our dimer showed a single band centered around 2 730 Å (ϵ = 34 000) and a plateau at about 2 375 Å (ϵ = 42 100), and is reminiscent of that of the *cis*-stilbene chromophore (bands at ~2 800 Å, ϵ = 10 500 and 2 240 Å, ϵ = 24 400 (12)). These results suggest strongly that our dimer has not the cubane skeleton.

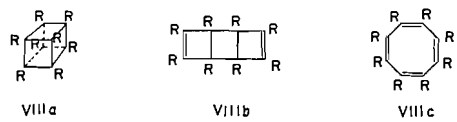

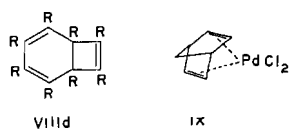

DISCUSSION

Because we have as yet no quantitative data on other substituted tolans with which to compare these results, this discussion is confined to some of the novel structural features encountered in this work.

Can. J. Chem. Downloaded from www.nrcresearchpress.com by 210.87.254.6 on 09/05/12
For personal use only.

Due to their insolubility in solvents with which they do not react, molecular weight determinations for the tetraphenylcyclobutadiene palladium halides have not been possible. However, this insolubility and the fact that tetraphenylcyclobutadiene palladium chloride readily dissolves in chloroform saturated with hydrogen chloride, an obvious halogen-bridge-splitting reaction (1), together with the known dimeric structure for V and tetramethylcyclobutadiene nickel chloride, suggests that they are all halogen-bridged dimers with 5-coordinate Pd(II). This tendency for cyclobutadiene palladium and nickel complexes to achieve 5-coordination and, incidentally, the electronic configuration of xenon and krypton respectively, deserves some comment since it is at first sight surprising in view of the known 4-coordinate monomeric structures for diene palladium dihalides. The crystal structure of one of these, norbornadiene palladium chloride (IX), has been determined and shown unambiguously to have a square planar arrangement of the four ligands about the palladium (13). However, in this complex the diene system subtends an angle of 72° at the metal, whereas it can easily be shown that in tetramethylcyclobutadiene nickel chloride (9) the angle subtended by the four-membered ring is only about 45°. This angle will, of course, be even somewhat less for the tetraphenylcyclobutadiene palladium complexes. As a result there will be less crowding around the metal in a cyclobutadiene complex than in a "normal" diene complex (since the phenyl rings are bent back (14), they will not interfere greatly) and thus to achieve the desired highest coordination number, halogen bridges with another molecule will be formed. This argument may also partly explain the high stability of the similarly 5-coordinated π-tetraphenylcyclobutadiene iron tricarbonyl and (π-cyclopentadienyl)(π-tetraphenylcyclobutadiene)cobalt complexes by comparison with the very reactive diene iron tricarbonyl and diene (π-cyclopentadienyl)cobalt analogues.

Since this paper was originally prepared we have been informed by Lipscomb (15) that a complete X-ray structure determination of Freedman and Petersen's "octaphenylcubane" (VIII*a*, R = Ph) now shows it to be octaphenylcyclooctatetraene (VIII*c*, R = Ph). This suggests that our tetrakis(*p*-chlorophenyl)cyclobutadiene dimer will also have this structure, in agreement with the observed presence of a C=C stretching mode in the Raman spectrum. More conclusive evidence is necessary, however, since structures VIII*b*, VIII*c*, and VIII*d* would all be expected to show this band. Since chemical evidence is difficult to obtain because of the steric hindrance of the phenyl groups, the best evidence would be from the intensities of the main peaks in the ultraviolet spectrum. Braye, Hübel, and Caplier (16) already observed some years ago that the ratio of the extinction coefficient for the tetraphenylcyclobutadiene dimer to that of *cis*-stilbene is nearly 4, and on this basis suggested the octaphenylcyclooctatetraene structure for it. Unfortunately such a direct comparison is not possible for our dimer (VIII, R = *p*-ClC_6H_4) since *cis*-*p*,*p*′-dichlorostilbene is unknown. Even using a "reasonable" value for the expected extinction coefficient (extrapolated from the difference between *trans*-stilbene and *trans*-*p*,*p*′dichlorostilbene) a result suggesting the presence of three double bonds is obtained for our molecule. While such a structure is quite possible (VIII*d*, R = *p*-ClC_6H_4, for example) we still prefer the cyclooctatetraene (VIII*c*, R = *p*-ClC_6H_4). Freedman and Petersen (11) also obtained an isomer of octaphenylcyclooctatetraene, which showed a strong Raman-active C=C stretching mode at 1 650 cm^{-1}, from the reaction of 3,4-dibromo-1,2,3,4-tetraphenylcyclobutene with butyl-lithium. This was an unstable material which on standing at room temperature isomerized to the octaphenylcyclooctatetraene. This compound is probably now best regarded as the *syn*- or anti-isomer of octaphenyltricyclooctadiene (VIII*b*, R = Ph), and the reaction

VIII*b*, R = Ph → VIII*c*, R = Ph

Can. J. Chem. Downloaded from www.nrcresearchpress.com by 210.87.254.6 on 09/05/12
For personal use only.

exactly parallels the reactions recently described by White and Dunathan (17). These authors found that in reactions in which diphenylcyclobutadienes were plausible products, tetraphenyltricyclooctadienes were isolated when the reactions were run at low temperatures, while at higher temperatures the products were tetraphenylcyclooctatetraenes. The latter were also formed by thermal isomerization of the tetraphenyltricyclooctadienes. That our dimer (VIII, R = p-ClC_6H_4) is not the one corresponding to Freedman and Petersen's unstable isomer is shown by it being unchanged even after melting at 375° or vacuum sublimation over a free flame. This again suggests that our dimer is the "stable" isomer and hence octakis(p-chlorophenyl)cyclooctatetraene. We are, however, unable to account for the fact that VIII*c*, R = Ph shows no Raman active C=C stretching mode whereas VIII*c*, R = p-ClC_6H_4 does.

NOTE ADDED IN PROOF:

Hüttel and Neugebauer (20) have also recently reported a tetraphenylcyclobutadiene palladium chloride complex with high Pd and Cl analyses. They propose a structure for it with one bridging $PdCl_2$ group, identical with that proposed here, IV, R = Ph, n = 1.

EXPERIMENTAL

Preparation of p,p'-Dichlorotolan

This was conveniently prepared in a 2 g scale by a modification of the method of Jonas (18) from the readily available insecticide 1,1-bis(p-chlorophenyl)-2,2-dichloroethane (DDD).

An amount of 10 g of DDD (0.312 moles) was mixed with 10 g potassium hydroxide in a 2 l flask. This was arranged horizontally, so that the product could be recovered more easily, and carried a glass tube which came nearly to the base of the flask and through which a slow stream of nitrogen was passed. The contents of the flask were heated with a flame until an oil distilled out; this oil was washed out, the flask was dried, and the contents were reheated vigorously. A white solid now sublimed out into the neck and was collected. This was the fairly pure p,p'-dichlorotolan. Additional quantities were obtained by reheating twice more. After crystallization from methanol, a total of 1.8 g (23%) was usually obtained. This had m.p. 174.5–176° (lit. 175–176° (18)) and analyzed correctly.

Anal. Calcd. for $C_{14}H_8Cl_2$: C, 68.07; H, 3.26; Cl 28.79%. Found: C, 68.19; H, 3.39; Cl, 28.65%.

Attempts to improve the yield by changing conditions or by the use of other bases were not successful. For example refluxing DDD with a large excess of potassium t-butoxide in t-butanol for 14 h only gave 2,2-bis(p-cholorophenyl)-1-chloroethylene in 47% yield.

Tetrakis(p-chlorophenyl)cyclobutadiene Palladium Chloride Complexes (IV, R = p-ClC_6H_4)

(1) A solution of 6 g (24.2 mmoles) of p,p'-dichlorotolan in 550 ml benzene was added slowly with stirring over 10–15 h to a solution of 3.88 g (10.1 mmoles) bis(benzonitrile)palladium chloride in 275 ml benzene. After about 50 ml of the solution had been added, a red-brown precipitate began to form. On completion of the reaction this precipitate was filtered off and digested thoroughly with two portions of 150 ml of boiling benzene to remove any trimer present. A crystalline residue of 1.91 g of the cyclobutadiene complex (IV, R = p-ClC_6H_4, n = 2) remained, m.p. 244–248° decomp.[2]

Anal. Calcd. for $[(C_{28}H_{16}Cl_4)(PdCl_2)_2]_2$: C, 39.58; H, 1.90; Cl, 33.38; Pd, 25.12%. Found: C, 39.65; H, 1.86; Cl, 33.30; Pd, 25.20%.

A molecular weight determination was not possible due to the insolubility of the compound. The yield of complex, based on the amount of acetylene used, was 18%. Evaporation of the benzene solution gave the crude trimer which was chromatographed on silica in benzene – light petroleum to remove other impurities and then crystallized from benzene as colorless prisms. Yield of analytically pure hexakis(p-chlorophenyl)-benzene 2.95 g (45%), m.p.[2] 433° (lit. 404–405° (19)).

Anal. Calcd. for $C_{42}H_{24}Cl_6$: C, 68.03; H, 3.26; Cl, 28.68%; mol. wt. 741. Found: C, 68.16; H, 3.36; Cl, 28.91%; mol. wt. (mass-spectroscopically) 740.

(2) A solution of 3.21 g (13 mmoles) of p,p'-dichlorotolan in 800 ml benzene was added to 5 g (13 mmoles) bis(benzonitrile)palladium chloride dissolved in 800 ml benzene, with stirring over 15 h. After the crystalline precipitate had been washed with benzene as above, it weighed 2.80 g and had m.p.[2,3] 232–234° (decomp). The compound analyzed correctly for the complex IV, R = p-ClC_6H_4, n = 4 and had identical infrared spectrum in the 2–16 μ range.

Anal. Calcd. for $[(C_{28}H_{16}Cl_4)(PdCl_2)_3]_2$: Pd, 31.1%. Found: Pd, 30.4; 31.0%. Yield, based on the amount of acetylene used: 43%.

From the benzene mother liquors 1.02 g (32%) of hexakis(p-chlorophenyl)benzene was obtained.

[2]*Melting point taken in an evacuated capillary.*

[3]*The melting point obtained depends on rate of heating and values as high as 256–258° have been obtained.*

Can. J. Chem. Downloaded from www.nrcresearchpress.com by 210.87.254.6 on 09/05/12
For personal use only.

Reaction of Tolan with Bis(benzonitrile)palladium Chloride

A solution of 0.5 g (2.81 mmoles) diphenylacetylene in 50 ml of benzene was added to a solution of 0.54 g (1.40 mmoles) bis(benzonitrile)palladium chloride in 50 ml benzene, and the solution was stirred for 16 h at 25°. A pinkish solid was slowly formed which consisted of a mixture of mainly hexaphenylbenzene and a little tetraphenylcyclobutadiene palladium chloride complex. The former was removed by repeatedly boiling the mixture with benzene until the residue was homogeneous. This left 0.20 g of the tetraphenylcyclobutadiene palladium chloride complex (IV, R = Ph, $n = 3$).

Anal. Calcd. for $[(C_{28}H_{20})(PdCl_2)_{2.6}]_2$: Pd, 33.2%. Found: Pd, 33.2%.

The infrared spectra (KBr disc, 2–16 μ) was identical to that of an authentic sample of tetraphenylcyclobutadiene palladium chloride. The yield of IV based on the amount of tolan used was 18%.

A solution of 1.0 g (5.56 mmoles) of diphenylacetylene in 345 ml benzene was added to a solution of 2.16 g (5.56 mmoles) bis(benzonitrile)palladium chloride in 345 ml benzene over 4 h at 25°. The solid product was filtered off and was boiled repeatedly with benzene until all the hexaphenylbenzene had been removed. This left 0.84 g of a red solid, (IV, R = Ph, $n = 4$).

Anal. Calcd. for $[(C_{28}H_{20})(PdCl_2)_3]_2$: Pd, 33.9%. Found: Pd, 33.6%. Yield, based on the amount of acetylene used: 34%.

Di-μ-chloro-di[π-(endo-4-ethoxy-1,2,3,4-tetrakis(p-chlorophenyl)cyclobutenyl)palladium] (II, R = p-ClC$_6$H$_4$)

A solution of 0.78 g (2.03 mmoles) of bis(benzonitrile)palladium chloride in 50 ml methylene chloride was added with stirring to a suspension of 1.00 g (4.05 mmoles) of *p,p'*-dichlorotolan in 100 ml of ethanol. After stirring for 30 min a clear solution resulted which slowly began to deposit a copious yellow precipitate. This was filtered off after a further hour at room temperature and was recrystallized from methylene chloride – ethanol. Yield: 0.90 g (66%). Thin-layer chromatography showed the material to be homogeneous and different to the exo-isomer (VII). The pure material gradually decomposed above 280° and finally melted[2] about 310°. The n.m.r. spectrum showed the presence of phenyl (2.58 τ), CH_2 (5.72 τ), and CH_3 (8.50 τ) protons in the expected ratio.

Anal. Calcd. for $[C_{30}H_{21}Cl_5OPd]_2$: C, 52.82; H, 3.11; Cl, 25.99; Pd, 15.7%; mol. wt. 1 362. Found: C, 52.99; H, 3.38; Cl, 26.06; Pd, 15.5%; mol. wt. 1 380.

Tetrakis(p-chlorophenyl)cyclobutadiene Palladium Bromide (V)

(1) Dry hydrogen bromide gas was bubbled through a solution of 0.50 g of di-μ-chloro-di[π-endo-4-ethoxy-1,2,3,4-tetrakis(p-chlorophenyl)cyclobutenyl]palladium (II, R = p-ClC$_6$H$_4$) in 100 ml of methylene chloride for 10 min. There was an immediate darkening of the color. On completion of the reaction the solution was evaporated to dryness, and the resultant solid was redissolved in methylene chloride, filtered, and crystallized by the addition of ligroin (b.p. 80–100°). Yield of tetrakis(*p*-chlorophenyl)cyclobutadiene palladium bromide: 0.46 g (82%). The red, crystalline complex was stable in air and had no sharp melting point[2] but slowly decomposed on heating to above 300°.

Anal. Calcd. for $[(C_{28}H_{16}Cl_4)PdBr_2]_2$: C, 44.22; H, 2.12; Br, 20.95; Cl, 18.65; Pd, 14.0%; mol. wt. 1 521. Found: C, 43.89; H, 2.05; Br, 21.37; Cl, 18.30; Pd, 14.0%; mol. wt. 1 517 (0.0053 *M* in chloroform).

(2) Dry hydrogen bromide gas was passed into a suspension of 0.84 g of the tetrakis(*p*-chlorophenyl)-cyclobutadiene palladium chloride complex (IV, R = p-ClC$_6$H$_4$, $n = 4$) in methylene chloride for 10 min. The suspended solid mostly dissolved after a few minutes and was replaced by a precipitate of $PdBr_4^{2-}$ which was then filtered off. The solvent and excess hydrogen bromide were removed on a rotary evaporator, and the residue was crystallized from methylene chloride – ligroin. Yield of pure tetrakis(*p*-chlorophenyl)-cyclobutadiene palladium bromide (V) was 0.17 g (23%), and was shown to be identical to the above prepared sample by thin-layer chromatography and infrared spectra.

Tetrakis(p-chlorophenyl)cyclobutadiene Dimer (VIII, R = p-ClC$_6$H$_4$)

A solution of 0.63 g (3.2 mmoles) of tri-*n*-butylphosphine in 10 ml benzene was added to a well-stirred refluxing suspension of 0.60 g (0.71 mmoles) of the tetrakis(*p*-chlorophenyl)cyclobutadiene palladium chloride complex (IV, R = p-ClC$_6$H$_4$, $n = 2$) in 90 ml of benzene under nitrogen. The red suspension rapidly dissolved to give a green solution which then turned yellow and finally pale yellow on refluxing. It was refluxed for a total of 30 min and then filtered and the solvent was taken off. Addition of ethanol to the oily residue gave 0.26 g (73%) colorless crystals of the dimer, whicle concentration of the ethanol solution yielded 0.443 g of yellow crystals of bis(tributylphosphine)palladium chloride identified by comparison with an authentic sample. The dimer was purified by crystallization from benzene–ligroin, and had m.p.[2] 371°. A slightly higher m.p. (373–375°) was obtained after vacuum sublimation of the sample over a free flame; the compound analyzed correctly for the dimer (VIII, R = p-ClC$_6$H$_4$).

Anal. Calcd. for $C_{56}H_{32}Cl_8$: C, 68.03; H, 3.26; Cl, 28.68%; mol. wt. 988.5. Found: C, 68.07; H, 3.29; Cl, 28.59%; mol. wt. 1 038 (osmometric in benzene) 982 (mass spectroscopic). The compound underwent no significant change on vacuum sublimation. The same compound, VII, was also obtained in 54% yield by an identical reaction from the tetrakis(*p*-chlorophenyl)cyclobutadiene palladium chloride complex (IV, R = p-ClC$_6$H$_4$, $n = 4$). The tetrakis(*p*-chlorophenyl)cyclobutadiene dimer (VIII) shows the following spectral bands.

Can. J. Chem. Downloaded from www.nrcresearchpress.com by 210.87.254.6 on 09/05/12
For personal use only.

(i) Ultraviolet: peak at 2 730 Å (ϵ = 34 000); plateau at 2 375 Å (ϵ = 42 100) in hydrocarbon solvent.
(ii) Infrared (KBr disc): 491(s), 769(s), 787(s), 829(s), 1 013(s), 1 092(s), 1 398(m), 1 487(vs), and 1 588(m) cm^{-1}.
(iii) Raman (solid state): 621, 641, 854, 869, 1 000, 1 036, 1 161, 1 196, 1 292, 1 341, 1 447, 1 498, 1 542, 1 597, and 1 642 cm^{-1}.

Tetrakis(p-chlorophenyl)cyclobutadiene Iron Tricarbonyl (VI, R = p-ClC_6H_4)

A solution of 1.0 g (0.975 mmoles) of the tetrakis(*p*-chlorophenyl)cyclobutadiene palladium chloride complex (IV, R = *p*-ClC_6H_4, n = 4) was refluxed in 100 ml benzene under nitrogen for 10 min. An amount of 6 ml (44.5 mmoles) iron pentacarbonyl was added and refluxing was continued for a further 10 min.[4] The solution was then filtered, all the solvent was removed, and the residue was taken up in 5 ml benzene and chromatographed in alumina in 15% benzene – 85% light petroleum (b.p. 30–60°). The first, yellow, fraction to be eluted contained the desired compound which after crystallization from methylene chloride – ethanol gave 0.27 g of yellow crystals of tetrakis(*p*-chlorophenyl)cyclobutadiene iron tricarbonyl (VI) (44%). This had m.p.[2] 242°, showed terminal carbonyl bands in the infrared at 1 978 and 2 025 cm^{-1} (CCl_4 solution) and 2 040, 1 986, and 1 965 cm^{-1} (KBr disc); the whole spectrum was identical with that of a sample prepared by Braye (6).

Anal. Calcd. for $C_{31}H_{16}Cl_4O_3Fe$: C, 58.71; H, 2.54; Fe, 8.81; Cl, 22.36%; mol. wt. 634. Found: C, 58.72; H, 2.88; Fe, 8.79; Cl, 22.26%; mol. wt. 647 (osmometric). The same compound was also obtained in an identical ligand-transfer reaction from tetrakis(*p*-chlorophenyl)cyclobutadiene palladium bromide (V) in 46% yield, identified by m.p. and mixed m.p. as well as infrared spectra.

Di-μ-chloro-di-[π-exo-(4-ethoxy-1,2,3,4-tetrakis(p-chlorophenyl)cyclobutenyl)palladium] (VII, R = p-ClC_6H_4)

A suspension of 1 g (0.975 mmoles) of the tetrakis(p-chlorophenyl)cyclobutadiene palladium chloride complex (IV, R = *p*-ClC_6H_4, n = 4) in 150 ml absolute ethanol was stirred for 48 h at 25°. This gave 0.61 g of the crude complex (VII) contaminated with some palladium metal. The complex was dissolved in methylene chloride, filtered, and crystallized by the addition of ligroin to give 0.35 g (53%) of the yellow π-cyclobutenyl complex (VII, R = *p*-ClC_6H_4), m.p. 201–202° decomp.[2]

Anal. Calcd. for $[C_{30}H_{21}Cl_5OPd]_2$: C, 52.82; H, 3.11; Cl, 25.99; Pd, 15.65%; mol. wt. 1 362. Found: C, 53.16; H, 3.25; Cl, 26.21; Pd, 15.44%; mol. wt. 1 347 (osmometric). The n.m.r. spectrum agreed with this formulation and showed the presence of C_6H_5 (2.70 τ), CH_2 (6.51 τ), and CH_3 (9.02 τ) protons. Treatment of this complex with hydrogen bromide in methylene chloride solution in a similar manner tp that used above converted it into tetrakis(*p*-chlorophenyl)cyclobutadiene palladium bromide (V) in 62% yield, identified by infrared spectrum and thin-layer chromatography with an authentic sample. Attempts to convert the complex into tetrakis(*p*-chlorophenyl)cyclobutadiene palladium chloride were unsuccessful. Even under very drastic conditions products were obtained for which the n.m.r. spectra still showed the presence of ethoxy groups, showing that neither hydrogen chloride nor hydrochloric acid is a powerful enough reagent to cleave the ether link here.

ACKNOWLEDGMENT

We wish to thank the National Research Council of Canada and the Research Corporation of New York for supporting this research, and Mr. D. Clugston for determining some of the n.m.r. spectra and mass-spectroscopic molecular weights.

REFERENCES

1. A. T. Blomquist and P. M. Maitlis. J. Am. Chem. Soc. **84**, 2329 (1962). P. M. Maitlis and M. L. Games. Can. J. Chem. **42**, 183 (1964).
2. L. Malatesta, L. Vallarino, G. Santerella, and F. Zingales. Atti Accad. Naz. Lincei, Rend. Classe Sci. Fis. Mat. Nat. **27**, 230 (1959); Angew. Chem. **72**, 34 (1960).
3. L. F. Dahl and W. E. Oberhansli. Proceedings of the VIII International Conference on Coordination Chemistry, Vienna. 1964. p. 242. L. F. Dahl. Private communication.
4. F. Zingales. Ann. Chim. Rome, **52**, 114 (1962). O. N. Temkin, S. M. Brailousky, R. M. Flyd, M. P. Strukova, B. V. Belyunin, and M. G. Zaitseva. Kinetika i Kataliz, **5**, 192 (1964). P. M. Maitlis. Unpublished observations.
5. P. M. Maitlis and M. L. Games. J. Am. Chem. Soc. **85**, 1887 (1963).
6. E. H. Braye. Private communication.
7. H. P. Fritz. Z. Naturforsch. **16b**, 415 (1961).
8. R. Criegee. Angew. Chem. Intern. Ed. Engl. **1**, 519 (1962).
9. J. D. Dunitz, H. C. Mez, O. S. Mills, and H. M. M. Shearer. Helv. Chim. Acta, **45**, 647 (1962).
10. P. M. Maitlis and F. G. A. Stone. Proc. Chem. Soc. 330 (1962).
11. H. H. Freedman and D. R. Petersen. J. Am. Chem. Soc. **84**, 2837 (1962).

[4]*Heating for a longer period of time severely reduced the amount of desired product. The main product then was the cyclobutadiene dimer (VIII, R = p-ClC_6H_4).*

Can. J. Chem. Downloaded from www.nrcresearchpress.com by 210.87.254.6 on 09/05/12
For personal use only.

12. R. N. BEALE and E. M. F. ROWE. J. Chem. Soc. 2757 (1953). M. CALVIN and H. W. ALTER. J. Chem. Phys. **19**, 766 (1951).
13. N. C. BAENZIGER, J. R. DOYLE, and C. CARPENTER. Acta Cryst. **14**, 303 (1961).
14. R. P. DODGE and V. SCHOMAKER. Nature, **186**, 798 (1960).
15. G. S. PAWLEY, W. N. LIPSCOMB, and H. H. FREEDMAN. J. Am. Chem. Soc. **86**, 4725 (1964).
16. E. H. BRAYE, W. HÜBEL, and I. CAPLIER. J. Am. Chem. Soc. **83**, 4406 (1961).
17. E. H. WHITE and H. C. DUNATHAN. J. Am. Chem. Soc. **86**, 453 (1964).
18. H. JONAS. Z. Naturforsch. **7b**, 132 (1952).
19. W. HÜBEL and C. HOOGZAND. Chem. Ber. **93**, 111 (1960).
20. R. HÜTTEL and H. J. NEUGEBAUER. Tetrahedron Letters, 3541 (1964).

Can. J. Chem. Downloaded from www.nrcresearchpress.com by 210.87.254.6 on 09/05/12
For personal use only.

Can. J. Chem. Downloaded from www.nrcresearchpress.com by 210.87.254.6 on 09/05/12
For personal use only.

^{13}C N.M.R. STUDIES

PART III.[1] CARBON-13 N.M.R. SPECTRA OF SUBSTITUTED ACETOPHENONES[2]

K. S. DHAMI[3] AND J. B. STOTHERS

Department of Chemistry, University of Western Ontario, London, Ontario

Received September 24, 1964

ABSTRACT

The 15.1 Mc/s ^{13}C n.m.r. spectra of 55 substituted acetophenones have been examined and the chemical shifts of the various carbon nuclei determined. This series included a variety of monosubstituted cases (ortho, meta, and para) as well as several polysubstituted examples. The factors contributing to the observed shieldings of all carbon nuclei are considered. The aromatic shieldings are compared with previous results for other aromatic derivatives. The application of the carbonyl shifts to the study of steric inhibition of resonance in these derivatives is examined critically. The shieldings of the acetyl methyl and para-carbon nuclei are found to offer confirmatory evidence for the existence of steric hindrance to coplanarity of the acetyl group in several ortho-substituted cases.

INTRODUCTION

Earlier papers in this series have presented the data and our interpretations of the carbon-13 nuclear magnetic resonance (n.m.r.) signals of carbonyl groups in a wide variety of organic carbonyl compounds (1) and some ortho-substituted acetophenones (2). To investigate some of the features noted in these studies in more detail, a series of 55 substituted acetophenones has been examined by ^{13}C n.m.r. spectroscopy at 15.1 Mc/s. Examples of a number of monosubstituted derivatives (ortho, meta, and para) as well as several polysubstituted compounds having at least one ortho-substituent have been included. Chemical shift values for all carbon nuclei in these compounds have been obtained except for a few cases in which the upper solubility limit was insufficient to obtain a satisfactory signal:noise ratio to allow measurements in the aromatic region. Analyses of the aromatic portions of the spectra were accomplished by intercomparisons of the variously substituted derivatives and by assuming an additive relation for the substituent effects on the aromatic nuclei on the basis of the careful studies by Lauterbur (3*a*–*e*). The resonances of the alkyl carbons were readily identified by comparisons of the observed positions with those observed for the simpler benzenoid hydrocarbons or monosubstituted benzene derivatives. The assignment of the carbonyl peaks, of course, is the easiest of all and presents no difficulty (1).

The results of this study afford a further test of the additivity of substituent effects on aromatic shieldings, first noted by Lauterbur (3*b*). Since the series includes 36 compounds with at least one ortho-grouping, the variations in the spectral parameters with increasing steric hindrance are easily followed and potential application of ^{13}C n.m.r. techniques to the study of hindered systems is clearly indicated. In particular, an extensive test is possible for our proposed method (2) of estimating angles of twist between the planes of the aromatic ring and the carbonyl group based on the variation of the carbonyl carbon resonance position with ortho-substitution. Variations of the acetyl methyl and para-carbon shieldings also follow the trends expected for sterically hindered systems on the basis of the most probable changes in the π-electron distributions with increasing steric

[1]*Part I, ref. 1. Part II, ref. 2.*

[2]*These results were reported in part at the 46th Annual Conference of the Chemical Institute of Canada, Toronto, June, 1963.*

[3]*Petroleum Research Fund Predoctoral Fellow, 1962–1964.*

interference of the acetyl grouping. Further evidence for the effects of hydrogen bonding by both intra- and inter-molecular mechanisms are presented and, since the latter may involve the solvent, some results of more detailed studies of solvent effects are given to support our arguments, although a fuller discussion of these is deferred for a later publication. The spectral data for a few alkylbenzenes were required to provide estimates of the shielding properties of the ethyl, isopropyl, and *t*-butyl groups and are reported in full for the first time, although their spectra have been published (4).

EXPERIMENTAL

Nuclear Magnetic Resonance Spectra

All spectra were obtained at 15.085 Mc/s using compounds containing carbon-13 in natural abundance. In most cases, the reference was either external CH_3I (enriched to 58% ^{13}C) or CS_2 contained in a 5 mm outside diameter tube inserted in the larger 15 mm sample tube, although in a few instances CS_2 was used as both solvent and internal reference. The spectra were calibrated by the generation of audio side bands of the reference signal on the spectrum so that peak positions could be measure by interpolation (5). The output of the audio oscillator was continuously monitored with a Hewlett Packard 522B counter. A minimum of eight separate spectra were measured in each case. The position of the CS_2 resonance signal was assigned as the origin of the chemical shift scale and no corrections for bulk susceptibility differences were included. The data are judged to be accurate to within ±0.5 p.p.m. Other details of the experimental procedure have been reported (3*a*). Where possible the spectra were obtained on the neat liquids, otherwise solutions in appropriate solvents were used as noted in the text and tables. These conditions were employed to produce a maximum signal:noise ratio and sufficient model studies have been carried out to show that solvent effects, although not always negligible, are of secondary importance for any of the comparisons discussed herein.

In a few cases, double irradiation experiments were performed to assist in the spectral analysis. In these experiments, the protons coupled to the carbon nuclei under examination were irradiated at their resonance frequency near 60 Mc/s to reduce the carbon signals to singlets by heteronuclear spin-decoupling. The technique has been reviewed (6) and a detailed description of the procedure has been given (7). In the present case, a NMR Specialties, Inc. Model SD-60 decoupler was employed.

Typical traces are illustrated in Fig. 1 to show the general features of the 15.085 Mc/s carbon-13 spectra obtained.

Materials

Acetophenone was a B.D.H. Ltd. product and the following substituted acetophenones were obtained from the Aldrich Chemical Company, Inc.: 2-hydroxy, 4-hydroxy, 2,4-dihydroxy, 2,6-dihydroxy, 2,4,6-trihydroxy, 4-methoxy, 2,4-dimethoxy, 2,4,5-trimethyl, 2,6-dimethyl-4-*t*-butyl, 4-bromo, 2,4-dichloro, 2-nitro, and 2-amino. The 3-nitro- and 4-nitro-acetophenones were Eastman-Kodak products. A sample of 2,5-di-*t*-butylacetophenone was kindly supplied by Professor L. R. C. Barclay. The rest of the materials examined in this investigation are known compounds, with one exception, and all were prepared by established procedures. In each case, infrared and proton spectra were obtained to check their purity. Their physical properties and the syntheses employed are outlined in Table I together with the previously reported physical constants. All melting points were determined on a Kofler hot stage and are uncorrected. For the most part, the liquids were purified by distillation through an 18 in. Nester-Faust platinum-plated spinning band column and the refractive indices were determined on a Bausch and Lomb refractometer. The microanalysis of 2,6-diisopropylacetophenone was performed by Alfred Bernhardt and Associates, Mulheim, Germany.

DISCUSSION

To facilitate the discussion and to emphasize their similarities the results for the meta- and para-substituted acetophenones are discussed together, while the ortho-substituted compounds are considered in a separate section. To permit an easier intercomparison of the figures for the various compounds, each type of carbon nucleus is discussed under a separate subheading. Finally, considerations of the application of the ^{13}C n.m.r. technique to the study of sterically hindered ketones are described in the last section.

meta- and para-Substituted Acetophenones

(a) Aromatic Carbons

The shieldings observed for the aromatic carbons in acetophenone itself may be compared with those reported previously by Spiesecke and Schneider (35) and which are

Can. J. Chem. Downloaded from www.nrcresearchpress.com by 210.87.254.6 on 09/05/12
For personal use only.

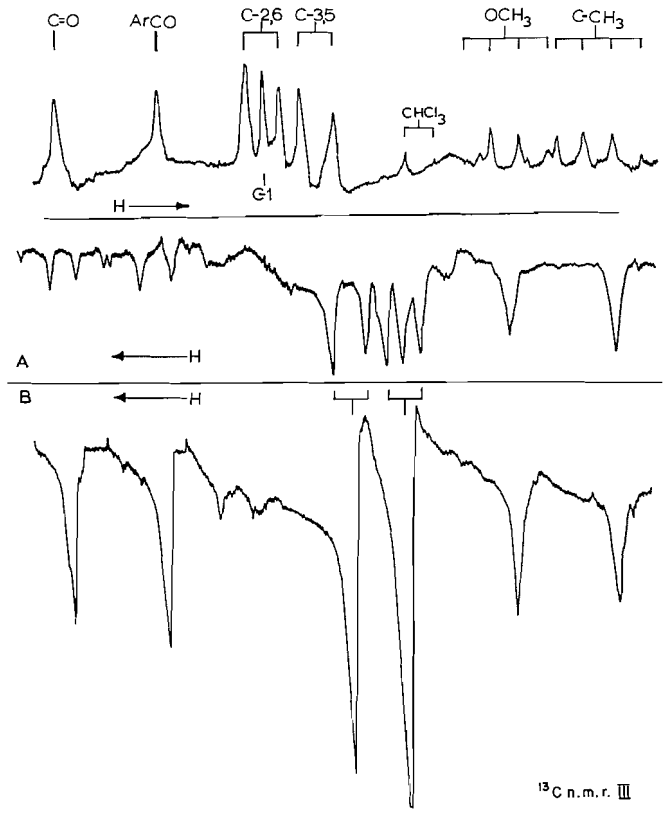

FIG. 1. Spectra at 15.085 Mc/s for *p*-methoxyacetophenone (field direction as shown) direction of sweep is from left to right for these examples. (*a*) Normal spectrum with the assignments indicated; (*b*) ^{13}C spectrum with simultaneous irradiation of ^{1}H nuclei at their respective resonance frequencies.

included in Table II in parentheses. The agreement is within experimental error and it may be noted that the earlier data were measured using a concentric spherical cell arrangement which eliminates bulk susceptibility differences. Part of the difference between the two sets of data may be due to this factor. While these authors have unequivocally established the assignments for acetophenone by deuterium labelling, the method used for assigning specific bands in the spectra of the substituted compounds requires some explanation. The problem is twofold, (i) the bands which form portions of multiplets must be distinguished from the singlet peaks and all chemical shifts measured and (ii) the observed shifts must be assigned to specific carbon nuclei. For the first distinction, the problem is simplified by virtue of the fact that, in general, only direct ^{13}C—^{1}H spin couplings are resolved in the spectra obtained under these experimental conditions. Thus, bands due to the aromatic nuclei bearing substituents appear as singlets, while the unsubstituted carbons give rise to doublets having coupling constants in the range, 161 ± 3 c/s.[3] A further aid for selecting the components of a multiplet within a spectrum is given by the relative intensities of the bands, since the multiplets are generally skewed owing to magnetization transfer (36) so that the first peak of a doublet, for example, is more intense than the second. A scan in the opposite direction gives the reverse behavior, while

[3]*No specific coupling constants have been included in the tables, since all were within the expected range and the present experimental method does not allow their measurement to better than ±8 c/s.*

Can. J. Chem. Downloaded from www.nrcresearchpress.com by 210.87.254.6 on 09/05/12
For personal use only.

TABLE I

Physical data for the substituted acetophenones prepared for this study

Substituent	Method of preparation	Physical constants: Observed b.p./mm (m.p.)	Observed n_D (t^0)	Reported b.p./mm (m.p.)	Reported n_D (t^0)	Ref.
4-CH_3	A	94/7	1.5343 (20)	60/3	1.5328 (22)	8
4-C_2H_5	A	82–84/0.5	1.5280 (22)	125/20	1.5298 (20)	9
4-$(CH_3)_2CH$	A	89–91/0.6	1.5222 (23)	68–72/0.8	1.5211 (25)	10
4-$(CH_3)_3C$	A	98–99/1.4	1.5195 (25)	97–98/0.9	—	11
4-CH_3O	A	(38–39)	—	(38–39)	—	12
4-Cl	A	103–104/10	1.5551 (20)	138–139/15	1.5558 (20)	8
4-$(CH_3)_2N$	B1	(104–105)	—	83/4 (105.5) 108–110/12	—	13
3-CH_3	C	73–74/2.9	1.5296 (25)	116–117/26	1.5300 (23.5)	14
3-CH_3O	B2	99/4	1.5415 (20)	141/23	1.5371 (23)	14
3-Cl	D	88–89/4	1.5478 (26)	88/4	1.5494 (23)	8
3-Br	D	90/11	1.5740 (26.5)	135–136/26	1.5755 (21)	14
3-OH	D	(94–95)	—	(95)	—	15
2-CH_3	C	51–53/1	1.5305 (25)	70/4	1.5310 (20)	8
2-C_2H_5	E1	117–120/30	1.5215 (26)	99–103/13	1.5222 (25)	16
2-$(CH_3)_2CH$	E1	77–78/3.3	1.5150 (25.5)	72–73/2	1.5225 (20)	17
2-C_6H_5	F	103–104/0.9	1.6110 (20)	104–105/1	—	18
2-CH_3O	B2	131–132/18	1.5380 (23.5)	131–132/18	1.5383 (23.5)	19
2-C_2H_5O	B2	77–78/0.5 (40–41)	—	(43)	—	20
2-Cl	G	107/14		75/4	1.5147 (23)	8
2-Br	C	71–72/0.8	1.5669 (25)	80–84/2	1.5683 (19.5)	8
2-I	G	135–139/5–6	1.6145 (24)	144/15 112/4	1.6180 (20)	21*a* 21*b*
2,3-$(CH_3)_2$	E1	70–71/1.1	1.5310 (25)	108/13	1.5334	9
2,4-$(CH_3)_2$	A	117–118/24	1.5325 (25)	122–123/27	1.5319 (24)	22
2,5-$(CH_3)_2$	A	113/17	1.5137 (25)	52/0.1	1.5290 (22)	22
2,4-$(CH_3O)_2$	A	120–121/0.5 (40)	—	156–161/9	—	23
2,5-$(CH_3O)_2$	A	122–124/1	1.5405 (26)	155–159/15	—	23
2,6-$(CH_3)_2$	E1	110–112/23	1.5160 (22)	111–112/23	1.5162 (20)	24
2,4,6-$(CH_3)_3$	A	100–102/7	1.5137 (25)	100–102/7	1.5155 (20)	25
2,3,4,6-$(CH_3)_4$	A	91–93/1	1.5245 (22)	74/0.3	1.5248 (21)	26
2,3,5,6-$(CH_3)_4$	A	(74–75)	—	(75)	—	27
2,3,4,5,6-$(CH_3)_5$	A	(85–86)	—	(87)	—	27
2,6-$(C_2H_5)_2$	E1	85–86/4	1.5105 (26)	86/4	1.5110 (21)	28
2,6-$(i\text{-}C_3H_7)_2$*	E1	81–82/0.8 (49–50)	—	—	—	
2,4,6-$(i\text{-}C_3H_7)_3$	A	(86–87)	—	(87.5–88)	—	29
2,6-$(CH_3O)_2$	E2	(70–71) 110–111/1.1	—	118–120/11.5	—	30
2,6-Cl_2	H	73/1 (41–42)	—	(44)	—	31
2,4,6-Br_3	E2	(90–91)	—	(92)	—	32
2-OH-6-CH_3O	B3	(57–58)	—	(60)	—	33

*Found for the ketone: C, 82.17; H, 9.90. Calcd. for $C_{14}H_{20}O$: C, 82.35; H, 9.80.

Methods employed: (A) acetylation via Friedel–Crafts reaction with CH_3COCl, RH → $RCOCH_3$ (28);
(B1) methylation using CH_3I/Na_2CO_3, Ar-NH_2 → Ar-$N(CH_3)_2$ (13);
(B2) methylation using $(CH_3)_2SO_4/NaOH$, ArOH → $ArOCH_3$ (19);
(B3) methylation using $(CH_3)_2SO_4/K_2CO_3$, $Ar(OH)_2$ → $Ar(OH)OCH_3$ (34);
(C) Grignard reaction of CH_3MgI on the nitrile, ArCN → $ArCOCH_3$ (9);
(D) reaction of HX with a diazonium salt, ArN_2^+ → ArX (8);
(E1) reaction from the aniline, $ArNH_2 \rightarrow ArBr \xrightarrow[2.CO_2]{1.Mg} ArCOOH \xrightarrow{SOCl_2} ArCOCl \xrightarrow{(CH_3)_2Cd} ArCOCH_3$ (35);
(E2) reaction from the acid, $ArCOOH \xrightarrow{SOCl_2} ArCOCl \xrightarrow{(CH_3)_2Cd} ArCOCH_3$ (35);
(F) from *o*-aminobiphenyl (18);
(G) via reaction of the ortho-substituted benzoyl chloride with diethyl malonate (21*b*);
(H) from the aldehyde, ArCHO → $ArCH(OH)CH_3$ → $ArCOCH_3$ (32).

Can. J. Chem. Downloaded from www.nrcresearchpress.com by 210.87.254.6 on 09/05/12
For personal use only.

the singlet peaks are unaffected. Since the intensity of a band is directly proportional to the number of contributing nuclei, measurements of relative intensities offer an additional aid. In each case, the carbonyl peak serves as a reference, representing one carbon nucleus. Many of the general features of a typical 15.085 Mc/s ^{13}C spectrum are illustrated in Fig. 1*a* for *p*-methoxyacetophenone. Finally, confirmation of which particular bands constitute multiplets may be gained by heteronuclear spin-decoupling experiments to eliminate the effects of spin coupling with protons in the observed carbon spectrum. A typical result is shown in Fig. 1*b*. Thus, the observed chemical shifts for the various nuclei may be determined.

TABLE II

^{13}C n.m.r. data for some para-substituted acetophenones (p.p.m.from CS_2)

Substituent	Acetyl group		Aromatic nuclei				Others
	C=O	CH_3	C-1	C-2,6	C-3,5	C-4	
H	−3.2	167.9	56.2 (55.7)*	64.4 (64.8)*	64.4 (64.8)*	61.2 (60.8)*	—
Me	−3.2	166.9	59.1	64.3	64.3	49.8†	171.6
Et	−3.2	167.3	59.6	64.9	64.9	43.9	164.6 177.9
i-Pr	−3.4	167.4	57.4	64.7	66.4	38.8†	159.0 169.9
t-Bu	−2.4	167.1	59.5	65.2	68.3†	37.8	158.3 162.4
OMe‡	−2.9	167.3	63.0	62.7	79.5	29.7	137.9
Cl	−3.0	168.0	58.2	63.7	63.7	54.6	—
Br†	−3.8	166.3	58.1	62.0	62.0	66.2	—
NO_2†	−3.3	165.9	51.7†	63.5	68.7	42.4	—
$N(Me)_2$†	−2.6	167.5	67.7	62.6	82.7†	39.8	153.5
OH§	−4.6	167.7	62.9	61.6	77.3	30.7†	—

*Values given by Spiesecke and Schneider (35).
†(Calcd. − obsd.) more than 1.3 p.p.m. (see text).
‡Saturated solution in $CHCl_3$.
§Saturated solution in 1,4-dioxane.

The assignment of particular shieldings to specific nuclei within the molecule is based primarily on the previous results of extensive investigations of several aromatic series. Lauterbur (3*a*–*e*) has been the principal contributor to this field and was the first to point out the apparent additivity of substituent effects on aromatic carbon shieldings (3*b*). His studies of several polysubstituted benzenes show that the combined effects of a methyl group with other methyls (3*a*), methoxyl (3*b*), iodo (3*c*), amino and dimethylamino (3*d*), and nitro groups (3*e*) are additive to a high degree of precision (ca. ±1 p.p.m.) provided the substituents are not ortho with respect to each other. (It may be noted that the aromatic carbons for these various series absorb over a total range of almost 70 p.p.m.) More recently, Savitsky (37) has shown that comparable results are obtained for some para-disubstituted benzenes, *p*-X-C_6H_4-X, where X = F, Cl, Br, and Ac, and with somewhat less precision (ca. 2 p.p.m. maximum deviation) for some para-substituted anisoles, *p*-Y-C_6H_4OMe, where Y = Br, Cl, CHO. Comparable results were obtained from an extensive survey of the spectra of 40 substituted anisoles (38), the full details of which will be published in due course.

Assuming that an additive relation holds for the meta- and para-substituted acetophenones, we have assigned the observed shifts as shown in Tables II and III utilizing the substituent effects which are available for the appropriate monosubstituted benzenes

Can. J. Chem. Downloaded from www.nrcresearchpress.com by 210.87.254.6 on 09/05/12
For personal use only.

TABLE III

^{13}C chemical shifts for some meta-substituted acetophenones (in p.p.m.from CS_2)

Substituent	Acetyl group		Aromatic nuclei						Others
	C=O	CH_3	C-1	C-2	C-3	C-4	C-5	C-6	
H	−3.2	167.9	56.2	64.4	64.4	61.2	64.4	64.4	—
Me	−2.7	167.7	55.9	65.5	55.9	60.3	65.5	68.3	172.3
OMe	−3.3	167.3	55.1	81.1*	34.0	74.0*	64.1	74.0	138.5
Cl	−2.6	167.0	54.8	63.7	58.7	60.3	63.7	66.0	—
Br	−2.6	166.7	55.0	62.9*	71.2	57.3	62.9	66.0	—
NO_2†	−2.8	—	—	—	—	—	—	—	—
OH‡	−4.9	—§	(53.9)	(78.6)	(35.1)	—	(62.6)	(72.9)	—

*(Calcd. − obsd.) more than 1.3 p.p.m. (see text).
†Saturated solution in $CHCl_3$, but too dilute to obtain aromatic chemical shifts.
‡Saturated solution in 1,4-dioxane, but too dilute to measure aromatic shifts precisely.
§Absorption lost in solvent signals.

(3*b*, 35). For the effects of the acetyl group, we have employed values obtained by averaging the present results and those reported by Spiesecke and Schneider (35). Since the necessary shielding data for the alkylbenzenes, R—C_6H_5 where R = Et, *i*-Pr and *t*-Bu, were not available, although their spectra have been published (4), these spectra were determined and the figures appear in Table IV. For the most part, the deviations between the calculated and observed shifts are less than ±1.3 p.p.m. and those cases for which the differences are larger are indicated in the tables. It may be that a part of these discrepancies arises from the fact that our observed shieldings are not corrected for bulk susceptibility differences. In general, however, it appears that the combined substituent effects on the aromatic carbon nuclei for the meta- and para-substituted acetophenones are additive to a reasonable approximation. Some typical results for this comparison are shown in Fig. 2 in which the difference between the calculated and observed shifts is given beside the various aromatic nuclei.

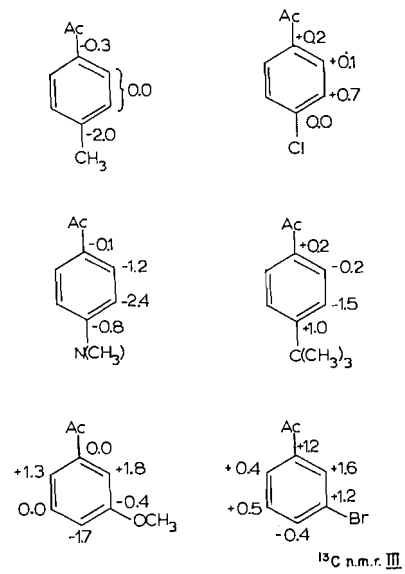

FIG. 2. Deviations between observed and calculated shielding data for aromatic carbon nuclei in some meta- and para-substituted acetophenones.

Can. J. Chem. Downloaded from www.nrcresearchpress.com by 210.87.254.6 on 09/05/12
For personal use only.

TABLE IV

^{13}C chemical shifts of monosubstituted benzenes (in p.p.m. from CS_2)

Substituent	Aromatic nuclei				Others
	C—X	ortho	meta	para	
H	65.0	65.0	65.0	65.0	—
Et*	48.9	(67.7	63.4)	67.3	164.8 177.7
i-Pr*	45.2	67.6	65.7	67.6	159.8 169.5
t-Bu*	42.8	68.3	65.3	68.3	158.1 162.1

*The reader is referred to ref. 4 for typical spectra of these compounds.

(b) Carbonyl Carbons

The assignment of the carbonyl peak in these spectra is straightforward in all cases since it appears as a clear single band at the lowest field position. The most striking feature of the carbonyl carbon resonance positions for the meta- and para-substituted acetophenones is the apparent lack of sensitivity toward the variety of polar substituent groups examined. All carbonyl peaks fall in the range, -3.2 ± 0.6 p.p.m., with the exception of the two hydroxy derivatives at -4.6 and -4.9 p.p.m. which constitute separate cases and are discussed in conjunction with their corresponding ortho-derivatives in a later section. While the present series is more extensive, our earlier reports (1, 2) have noted the absence of substituent effects on the carbonyl resonance position and this feature has been discussed in detail (2). Although it is conceivable that solvent effects may mask a weak substituent effect, the influence of the substituent on the carbonyl shielding must be very small since the observed difference between the *p*-NO_2 and *p*-NMe_2 derivatives is only 0.7 p.p.m. (both in $CHCl_3$). An indication that chloroform tends to lower the carbonyl shielding relative to that in a less polar medium has been given for acetophenone (1) and, as a further example, we find the carbonyl peak for the *p*-NMe_2 derivative at 0.8 p.p.m. higher field in benzene solution relative to chloroform solution. Thus, it is clear that our original observation of no pronounced substituent effect holds.

(c) Acetyl Methyl Carbons

In all of these spectra a quartet appears centered at 167 ± 1.0 p.p.m. with a coupling constant of 127 ± 2 c/s (the highest field multiplet in Fig. 1*a*, for example) and for most cases an unambiguous assignment of this multiplet to the acetyl methyl carbon nucleus can be made directly. Since the compounds bearing polar groups exhibit no large changes in the resonance position for the acetyl methyl quartet, it follows that its shielding is also unaffected by alkyl groups in the meta- and para-positions. In the case of alkylated derivatives with other bands in this region, the acetyl methyl resonance was assigned to correspond with the other cases. The increased shielding of the acetyl methyl carbon in conjugated ketones by ca. 4 p.p.m. relative to saturated analogues has been noted and discussed (1). It is possible that the total range of these shifts listed in Tables II and III is increased somewhat by a small effect of the chloroform solvent relative to the pure liquids but this effect would not appear to exceed ca. 1 p.p.m. (see Table VII, ref. 1).

(d) Other Carbons

The observed shieldings and coupling constants for the various nuclei in the substituent groupings are found to be in close agreement with the data obtained for the corresponding

Can. J. Chem. Downloaded from www.nrcresearchpress.com by 210.87.254.6 on 09/05/12
For personal use only.

monosubstituted benzenes. The figures in Table II for the ethyl, isopropyl, and *t*-butyl groups may be compared with those in Table IV while the results for the different types of methyl carbons agree closely with those given by Lauterbur for toluene, 171.8 (3*a*), anisole, 138.4 (3*b*), and N,N-dimethylaniline, 152.6 p.p.m. (3*d*). The observed coupling constants for these various carbons were OCH_3, 147 ± 2; $N—CH_3$, 134 ± 2; $C—CH_3$, $C—CH_2—C$, and C—CH—, 127 ± 2 c/s, in close agreement with other results (3*a*–*e*).

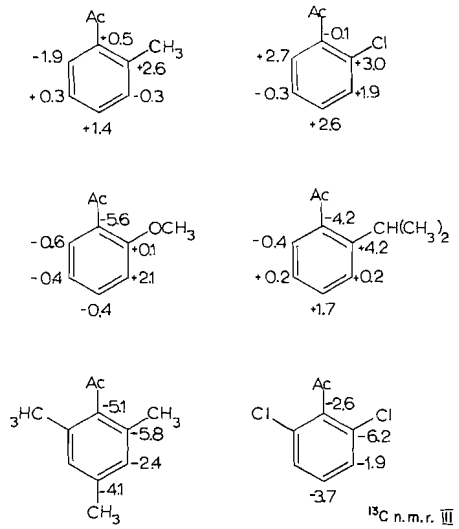

FIG. 3. Deviations between observed and calculated shielding data for aromatic carbon nuclei in some ortho-substituted acetophenones.

ortho-Substituted Acetophenones

(a) Aromatic Carbons

Following the procedure outlined above for the meta- and para-substituted cases, the assignments of the observed spectral bands to the various aromatic carbons in the ortho derivatives have been made as listed in Tables V and VI. As Lauterbur has established for several other examples, the additivity of the indirect effects of substituents on the ring carbons appears to break down with ortho substitution. In the present series of monosubstituted acetophenones the differences between the observed and calculated shifts are appreciably larger, on the average, than those discussed for the meta- and para-derivatives. In addition these differences appear to increase with increasing size of the group ortho to acetyl, clearly suggesting the existence of steric interference between substituent groups. To indicate the magnitude of these differences, some examples are shown in Fig. 3 together with a few more highly substituted compounds. While the larger deviations from the calculated values tend to introduce a greater uncertainty in the specific assignments, intercomparison of the data for the monosubstituted derivatives with those for the more highly substituted cases provide some support for our assignments. Examination of ortho-derivatives labelled with deuterium would, of course, allow unequivocal assignments but this has not been done. The assignments for the symmetrically substituted cases (i.e., 2,6-disubstituted) are unambiguous.

Four of the examples, having similarly positioned substituents, display particularly striking deviations of the observed chemical shifts from those calculated by the additivity relation. These are 2,3-dimethyl-, 2,3,4,6-tetramethyl-, 2,3,5,6-tetramethyl-, and 2,3,4,5,6-pentamethylacetophenone, each of which has three or more contiguous, substituted

Can. J. Chem. Downloaded from www.nrcresearchpress.com by 210.87.254.6 on 09/05/12
For personal use only.

aromatic carbons. It can be seen that for each of these compounds, at least one of the aromatic nuclei bearing a methyl group absorbs at considerably higher field than the less highly methylated compounds. For the four examples, these signals appear at 58.5, 59.9, 64.8, and 65.1 p.p.m., respectively. The last two figures are virtually the same as that of benzene itself although the effect of a methyl group is usually ca. −9 p.p.m. Lauterbur has noted this remarkable change in durene and hexamethylbenzene (*3a*). While this particular case is perhaps an extreme example, it serves to illustrate the complexity of the problem which must be solved before a rational explanation of the origins of these substituent effects can be offered.

Apart from the changes in chemical shift for the para-carbon (C-4), the observed trends are difficult to interpret on the basis of present knowledge and further discussion does not seem warranted. A detailed discussion of the para-carbon shieldings is included in the section on steric inhibition of conjugation below.

TABLE V

^{13}C chemical shifts for substituted acetophenones bearing one ortho-substituent (in p.p.m. from CS_2)

	Acetyl group		Aromatic nuclei						
Substituent(s)	C=O	CH_3	C-1	C-2	C-3	C-4	C-5	C-6	Others
2-CH_3	−6.5	164.2	56.1	56.1	64.0	62.4	67.7	62.4	172.5
2-C_2H_5	−6.9	164.3	57.0	49.8		62.5	68.7	62.5	166.5 177.6
2-*i*-C_3H_7	−8.0	164.3	55.1	46.6	68.1	63.0	68.1	66.3	164.4 170.0
2-C_6H_5	−9.6	163.0							
2-CH_3O	−5.0	161.8	65.1	34.3	81.4	59.7	73.1	63.2	138.2
2-C_2H_5O*	−5.9	160.9	64.5	34.3	80.2	59.2	72.7	62.2	
2-Cl	−5.9	163.3	55.7	61.2	66.3	62.6	66.3	66.3	—
2-Br	−6.5	163.1	52.6	70.5	61.0	61.0	65.1	65.1	—
2-I*	−8.0	163.8	47.4	102.2	54.4	61.1	64.5	64.5	—
2-NO_2	−5.5	164.4	57.1	47.8	70.0	62.7	59.5	66.2	—
2-OH	−11.6	167.1	73.6	31.0	74.2	57.0	74.2	62.8	—
2-NH_2	−7.5	165.7	75.3	42.7	77.8	59.2	75.7	61.1	—
2,3-$(CH_3)_2$	−7.8	163.7	53.4	58.5	55.8	61.2	68.6	68.6	173.0 177.2
2,4-$(CH_3)_2$	−5.8	164.9	52.0	58.7	63.1	55.2	67.6	63.1	173.0 173.0
2,5-$(CH_3)_2$	−5.7	164.4	57.1	59.2	64.2	64.2	59.2	64.2	172.8 172.8
2,4,5-$(CH_3)_3$	−5.5	164.7	59.6	57.9	61.8	53.9	57.9	60.2	174.5
2,5-(*t*-$C_4H_9)_2$†	−15.3	161.6							157.5 161.6
2,4-$(CH_3O)_2$*	−2.8	161.8	72.7	32.3	95.7	29.2	88.0	61.3	137.9 137.9
2,5-$(CH_3O)_2$*	−4.5	162.2	65.3	40.1	79.9	74.1	40.1	79.9	138.3 138.3
2,4-Cl_2	−3.9	162.9	60.8	56.8	63.1	56.8	66.1	63.1	—
2,4-$(OH)_2$‡	−10.1	168.9	78.6	27.4	89.0	27.4	83.9	58.6	—

*Saturated solution in $CHCl_3$.
†In $CHCl_3$ solution.
‡Saturated solution in 1,4-dioxane.

(b) Carbonyl Carbons

The striking feature of the carbonyl shieldings for the ortho-substituted acetophenones is the wide range over which these peaks absorb, −2.8 to −15.3 p.p.m., in direct contrast to the results for the meta- and para-derivatives. The values listed in Tables V and VI serve to extend the number of examples included in our previous report (2) in which a detailed discussion of the earlier observations was presented. The application of these

Can. J. Chem. Downloaded from www.nrcresearchpress.com by 210.87.254.6 on 09/05/12
For personal use only.

TABLE VI

^{13}C chemical shifts for substituted acetophenones bearing two ortho-substituents (in p.p.m. from CS_2)

	Acetyl groups		Aromatic nuclei						
Substituents	C=O	CH_3	C-1	C-2	C-3	C-4	C-5	C-6	Others
2,6-$(CH_3)_2$	−12.9	162.0	50.8	61.0	65.6	65.6	65.6	61.0	174.8
2,4,6-$(CH_3)_3$	−13.4	161.7	53.1	60.8	64.4	55.4	64.4	60.8	174.0
2,3,4,6-$(CH_3)_4$	−13.5	161.0	57.9	59.9	52.3	52.3		59.9	173.6(2) 169.3
2,3,5,6-$(CH_3)_4$*	−14.2	159.4	48.3	64.8	58.6	60.8	58.6	64.8	176.0(2) 172.1(2)
2,3,4,5,6-$(CH_3)_5$*	−14.1	158.1	50.4	65.1	59.2	59.2	59.2	65.1	174.4
2,6-$(CH_3)_2$-4-(t-C_4H_9)*	−13.3	160.0	52.1	60.5	67.0	41.6	67.0	60.5	158.2 174.7
2,6-$(C_2H_5)_2$	−13.0	161.5	51.1	54.8	67.2	64.4	67.2	54.8	167.1 177.4
2,6-(i-$C_3H_7)_2$*	−13.5	160.8	51.3	49.5	69.3	63.3	69.3	49.5	158.5 166.8
2,4,6-(i-$C_3H_7)_3$†	−13.8	160.8	53.7	49.8	72.4	43.9	72.4	49.8	159.6 168.9
2,6-$(CH_3O)_2$*	−6.8	161.2	51.3	36.2	88.4	61.4	88.4	36.2	137.3
2,6-Cl_2†	−5.2	162.6	53.1	63.4	64.5	62.7	64.5	63.4	—
2,4,6-Br_3‡	−7.2	162.4	50.5	74.0	58.5	69.2	58.5	74.0	—
2,6-$(OH)_2$†	−12.0	160.6	84.5	31.1	86.0	58.0	86.0	31.1	—
2-OH-6-CH_3O‡	−11.9	159.3	81.8	28.5	82.6	56.7	91.6	31.7	137.3
2,4,6-$(OH)_3$†	−10.4	160.4	88.5	27.4	98.0	27.4	98.0	27.4	—

*Saturated solution in CS_2.
†Saturated solution in 1,4-dioxane.
‡Saturated solution in $CHCl_3$.

carbonyl results to the estimation of the extent of steric inhibition of conjugation in these hindered systems is illustrated in the final section of this paper.

Further comments, however, regarding the different media employed are in order. Since it was impossible to obtain all of the spectra using the neat liquid, solutions in various solvents were required for examination. Since preliminary solvent studies had indicated that data obtained in either dioxane or carbon disulfide solution are in close agreement with the neat liquid values (1), these were the solvents employed, if possible. In the case of the former, recent work has confirmed our conclusion (39). To examine the effect of chloroform, which was employed in a few cases to obtain concentrations sufficient for detection of the spectra, on the carbonyl carbon resonance position, some compounds were measured in different solvents. These figures in Table VII indicate clearly that, although there is a small but definite deshielding of the carbonyl carbon, the effect of chloroform as a solvent is much smaller than the changes caused by ortho-substitution. It seems likely that the effect of chloroform is due to hydrogen bonding of the carbonyl oxygen and the proton of the solvent.

(c) Acetyl Methyl Carbons

The shieldings of the acetyl methyl carbons in the ortho-substituted acetophenones follow trends similar to those exhibited by the carbonyl carbon nuclei as the results in Tables V and VI show. The resonance position of these nuclei moves to lower field, relative to that of acetophenone, as the bulk and (or) number of the ortho-substituents increases such that this carbon absorbs over the range, 159.3–168.9 p.p.m. The variation of these shifts roughly follows that of the carbonyl carbon for this series of ortho-substituted compounds. The trend is illustrated in Fig. 4, for a number of the alkyl-substituted

Can. J. Chem. Downloaded from www.nrcresearchpress.com by 210.87.254.6 on 09/05/12
For personal use only.

TABLE VII

^{13}C carbonyl shieldings of various acetophenones in different solvents (p.p.m. from CS_2)

Substitution	Solvents			Other
	$CHCl_3$	$C_4H_8O_2$*	CS_2	
Nil	−4.5	−3.1		−2.9(C_6H_6) −3.2(neat)
4-N(CH_3)$_2$	−2.6			−1.8(C_6H_6)
2,6-Cl_2	−6.0	−5.2		
2,6-(CH_3O)$_2$	−7.8		−6.8	
2,6-(C_2H_5)$_2$	−14.0	−13.2	−13.1	−12.2(C_6H_6)
2,4,6-(*i*-C_3H_7)$_3$	−15.1	−13.8		
2,6-(CH_3)$_2$-4-(*t*-C_4H_9)	−13.3		−12.3	
2,3,5,6-(CH_3)$_4$	−15.3		−14.2	
2,3,4,5,6-(CH_3)$_5$	−15.7		−14.1	

*1,4-Dioxane.

acetophenones examined. The apparent slope of this plot indicates that the shielding of the acetyl methyl carbon is somewhat less sensitive to the influence of the ortho-grouping than the carbonyl carbon shielding. The possible significance of the variation of the acetyl methyl chemical shift with the nature of the ortho-group is discussed in a later section.

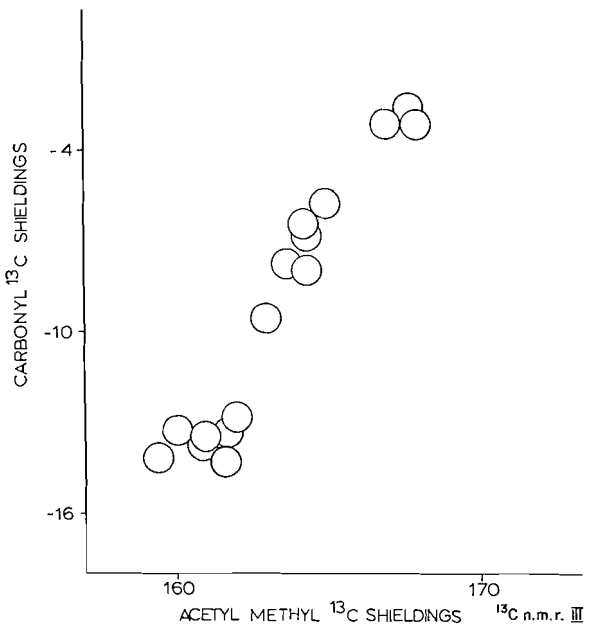

FIG. 4. Plot of observed resonance positions of carbonyl carbon nuclei vs. those of the acetyl methyl carbon nuclei for a number of ortho-alkylated acetophenones.

(d) Other Carbons

The observed chemical shifts for the methoxyl carbon nuclei are in the range, 137.8 ± 0.5 p.p.m. in agreement with the data for the meta- and para-derivatives above and with the results reported by Lauterbur previously (3*b*). Apparently there is no effect of

Can. J. Chem. Downloaded from www.nrcresearchpress.com by 210.87.254.6 on 09/05/12
For personal use only.

ortho-substitution on these shieldings. A more extensive study of the spectra of substituted anisoles has shown that substitution at both positions ortho to the methoxyl group is required to change its shielding from the typical value near 138 p.p.m. (38).

In the case of the alkyl substituent groups, however, the chemical shifts of the carbons bonded directly to the aromatic ring and flanked by one or more ortho-groups show small but significant differences from those in the corresponding meta- and para-substituted compounds. In general, the effect of ortho-substitution is one of shielding at these α-carbons. Intercomparisons of the figures in Tables V and VI with those in Tables II, III, and IV show that this effect on primary carbon is ca. 1 p.p.m., on secondary carbon, ca. 2 p.p.m., and on tertiary carbon ca. 4 p.p.m. for methyl, ethyl, and isopropyl groups, respectively. In the last two cases, the β-carbons do not appear to be affected. For the more highly substituted compounds, the data indicate that this trend is accentuated in compounds bearing three substituents on contiguous aromatic carbons (i.e., 1,2,3-trisubstitution). For example, for 2,3-dimethylacetophenone, the two aromatic methyl carbons appear at 177.2 and 173.0 p.p.m., the first of which may be assigned to the 2-methyl carbon flanked by two substituents. Similar shifts were found for acetyldurene (2,3,5,6-tetramethylacetophenone).

Hydroxy-Substituted Acetophenones

A number of derivatives bearing hydroxyl groups have been included in this series and the results obtained differ somewhat from those found for the other examples. One would expect that hydrogen bonding involving the hydroxyl proton and the carbonyl oxygen is probably responsible for these differences. In the monosubstituted cases, the ortho-hydroxyl group is seen to lower the carbonyl shift substantially (by ca. 7 p.p.m.) relative to the meta- and para-derivatives, while the acetyl methyl shielding is unaffected. Presumably the slightly lower carbonyl peak position in the meta- and para-derivatives relative to acetophenone is due to electron-withdrawing intermolecular hydrogen bonding while much more effective intramolecular interaction occurs in the ortho-case. The carbonyl carbon absorbs at significantly lower field for the ortho-amino derivative relative to acetophenone. Although the appropriate model compounds (3-NH_2— and 4-NH_2—) were not examined, it is reasonable that the intramolecular hydrogen bonding of the type, N—H---O=C, is responsible, at least in part, for the observed shift. In those compounds bearing two ortho-hydroxyl groups, the acetyl methyl shielding is reduced indicating steric interference between the acetyl methyl and the second substituent. The carbonyl resonance position is little affected by the second ortho-hydroxyl grouping. It does seem reasonable that hydrogen bonding between a carbonyl group and an ortho-hydroxyl would not be seriously affected if the carbonyl group was hindered from attaining coplanarity with the ring provided it was not twisted too far from this plane. For reasons that are presented in detail below, we would suggest that the second hydroxyl group does not cause a severe twist of the carbonyl group away from the aromatic ring plane although there is little doubt that these two groups are not coplanar. While both inter- and intramolecular H bonding will contribute to the shift of the carbonyl carbon nucleus in these cases, it is not possible to show with the present evidence the extent of the contribution of the former factor for the ortho-substituted cases. Studies of the dilution effect on these shifts are required but these present a practical difficulty due to the low sensitivity of the present technique.

Steric Inhibition of Conjugation

In the preceding section, some spectral features pointing to the existence of steric interference between substituent groupings in the compounds having ortho-substitution

Can. J. Chem. Downloaded from www.nrcresearchpress.com by 210.87.254.6 on 09/05/12
For personal use only.

Can. J. Chem. Downloaded from www.nrcresearchpress.com by 210.87.254.6 on 09/05/12
For personal use only.

have been mentioned. A number of these observations suggested the possibility of a semiquantitative approach to the estimation of the extent of steric inhibition of conjugation in these derivatives. In the preceding part of this series (2), a method has been proposed which is alternative to, and possesses certain advantages over, the more usual means of predicting angles of twist between the carbonyl group and the aromatic ring. With the results for a larger number of derivatives now in hand, a critical assessment of this proposed method may be undertaken.

We have already demonstrated the variation of the carbonyl carbon shielding with the size of the ortho-grouping, as estimated by van der Waal's radii or covalent radii (see Fig. 2, ref. 2) and the additional data in Tables V and VI offer further support for this relation. The rationale of the arguments leading to the conclusion that the carbonyl resonance position reflects the degree of steric interference in these ketones has been given and need not be reiterated. Secondary and confirmatory evidence for these ideas derived from other observed trends in these spectra was not presented in detail previously, however, and requires further amplification.

The deviations from additivity of substituent effects on the aromatic carbon shieldings in the ortho-substituted acetophenones were noted above and the difficulty of presenting a clear evaluation of all of these differences was mentioned. One possible exception, however, is the variation of the para-carbon (i.e. C-4) chemical shifts with changes in the substituent group. There are two reasons which suggest that a rational interpretation of these shieldings is possible. First, Spiesecke and Schneider (35) have demonstrated that there is a good correlation of the para-carbon shifts with the Hammett σ_P parameter for a number of monosubstituted benzenes. This result indicates that these ^{13}C shifts reflect the π-electron density distribution at this position and Lauterbur has confirmed this conclusion by comparing the calculated π-electron densities with the para-carbon shifts for several examples (3*a*–*e*, 40). Secondly, the effect of various substituents at the meta-carbon in monosubstituted benzenes is small, less than 1 p.p.m. for the substituents included in our series with the exception of the halogens and hydroxyl. These two facts suggest that the shielding of the para-carbon in the acetophenones will reflect variations in the extent of electron withdrawal at this position by the acetyl group, which would be caused by steric hindrance to co-planarity of the carbonyl group and the aromatic ring. In acetophenone, the para-carbon absorbs ca. 4 p.p.m. toward lower field from the resonance position of pure benzene and it is reasonable that this low field shift is primarily due to conjugative electron withdrawal by acetyl from the para-position. Thus, any factor hindering this conjugation would be expected to reduce the effect of the acetyl group at the para-carbon which would mean an increased shielding and, therefore, a shift to a value closer to that of pure benzene.

An examination of the data for the para-carbon nuclei, however, does not necessarily support this proposal unless the effects of the other substituents are taken into account. To allow an easier comparison, the pertinent shielding data are collected in Tables VIII and IX and the "corrected" figures, allowing for the effects of the other substituents, are included. In general, the para-carbon shifts move to higher field with increasing size and (or) number of ortho-groups, in agreement with expectations. Probably the most reliable data are those for the mono- and 2,6-di-substituted compounds, since the "corrections" for the substituents in these positions are relatively small. Because of the breakdown of the additivity relation for ortho-substituted derivatives, the significance of the "corrections" used for the examples having groups at the 3-, 4-, and 5-positions is questionable. As an example, the corrected figures for tetramethyl- and pentamethyl-acetophenone do not agree well with those for less highly substituted examples. It is interesting that this

TABLE VIII

^{13}C chemical shifts of certain nuclei in some ortho-alkyl acetophenones (p.p.m. from CS_2)

	C-4		$CH_3C{=}O$	C=O	
Substituent(s)	Obsd.	Corr.	Obsd.	Obsd.	Corr.
H	61.2	61.2	167.9	−3.2	−3.2
2-CH_3	62.4	62.7	164.2	−6.5	−7.5
2,3-$(CH_3)_2$	61.2	61.8	163.7	−7.8	−8.8
2,4-$(CH_3)_2$	55.2	64.6	164.9	−5.8	−6.8
2,5-$(CH_3)_2$	64.2	64.8	164.4	−5.7	−6.7
2,4,5-$(CH_3)_3$	53.9	63.6	164.7	−5.5	−6.5
2,6-$(CH_3)_2$	65.6	66.2	162.0	−12.9	−14.9
2,4,6-$(CH_3)_3$	55.4	65.0	161.7	−13.4	−15.4
2,6-$(CH_3)_2$-4-(t-C_4H_9)*	41.6	64.4	160.0	−13.3	−15.3
2,3,4,6-$(CH_3)_4$	52.3	62.3	161.0	−13.5	−15.5
2,3,5,6-$(CH_3)_4$*	60.8	62.0	159.4	−14.2	−16.2
2,3,4,5,6-$(CH_3)_5$*	50.4	60.7	158.1	−14.1	−16.1
2-C_2H_5	62.5	62.6	164.3	−6.9	−7.9
2,6-$(C_2H_5)_2$	64.4	64.6	161.5	−13.0	−15.0
2-i-C_3H_7	63.0	62.7	164.3	−8.0	−9.0
2,6-(i-$C_3H_7)_2$*	63.3	62.7	160.8	−13.5	−15.5
2,4,6-(i-$C_3H_7)_3$†	43.9	63.2	160.8	−13.8	−15.8
2,5-(t-$C_4H_9)_2$‡	—		161.6	−15.3	
2-C_6H_5	—		163.0	−9.6	

*Saturated solution in CS_2.
†Saturated solution in 1,4-dioxane.
‡In $CHCl_3$.

TABLE IX

^{13}C chemical shifts of specific nuclei in some ortho-substituted acetophenones (in p.p.m. from CS_2)

	C-4		$CH_3C{=}O$	C=O	
Substituent(s)	Obsd.	Corr.	Obsd.	Obsd.	Corr.
H	61.2	61.2	167.9	−3.2	−3.2
2-CH_3O	59.7	60.0	161.8	−5.0	−9.8
2-C_2H_5O*	59.2		160.9	−5.9	−10.7
2,4-$(CH_3O)_2$*	29.2	60.3	161.8	−2.8	−7.6
2,5-$(CH_3O)_2$*	74.1	60.3	162.2	−4.5	−9.3
2,6-$(CH_3O)_2$†	61.4	63.2	161.2	−6.8	−11.6
2-Cl	62.6	63.6	163.3	−5.9	−7.1
2,4-Cl_2	56.8	64.2	162.9	−3.9	−5.1
2,6-Cl_2‡	62.7	64.7	162.6	−5.2	−7.6
2-Br	61.0	63.2	163.1	−6.5	−5.8
2,4,6-Br_3*	69.2	67.2	162.4	−7.2	−5.8
2-I*	61.1	63.7	163.8	−8.0	
2-NO_2	62.7	63.5	164.4	−5.5	−6.4

*Saturated solution in $CHCl_3$.
†Saturated solution in CS_2.
‡Saturated solution in 1,4-dioxane.

analysis of the data for the 2-methoxyl derivatives indicates no steric interference between the acetyl and methoxyl groups, but there is an indication of crowding for the 2,6-dimethoxyl case. Another feature is that the "corrected" para-carbon shielding is similar for each of the three mono-halo derivatives (Cl, Br, I), but the "corrections" for two of these cases are relatively large (i.e., 2.2 p.p.m. for Br, 2.6 p.p.m. for I) and these could be in error, although there is no obvious way to check this point. A further disadvantage to the use of the para-carbon shifts for estimating the extent of steric hindrance in these systems is the relatively small range of 4 p.p.m. over which one can expect to observe

Can. J. Chem. Downloaded from www.nrcresearchpress.com by 210.87.254.6 on 09/05/12
For personal use only.

changes. This consideration of para-carbon shieldings, however, does show that the general trends are consistent with those expected for steric inhibition of conjugation and that the observed shifts might be used to support evidence from other spectral features.

The observed shifts for the acetyl methyl carbons have been included in Tables VIII and IX to show more clearly the regular reduction in shielding with increasing bulk and number of ortho-groups mentioned above (see Fig. 4). While this trend to lower field is qualitatively reasonable, the maximum change observed is larger than expected, if the extent of conjugation of the carbonyl group with the aromatic ring were the dominant factor, indicating that longer range substituent effects contribute to these shieldings as well. Approximate estimates of the ring anisotropic effects indicate a maximum difference of 0.2 p.p.m. between the planar and perpendicular orientation of an acetyl methyl carbon with the ring, following the method of Johnson and Bovey (41) and, of course, this change is in the opposite direction to that observed.

Qualitatively, however, the observed variation of the acetyl methyl shieldings appears to indicate the extent of steric interference of the ortho-substituents with the acetyl group. In contrast to the para-carbon shieldings, these data indicate appreciable steric hindrance by *one* ortho-methoxyl group which is only slightly increased by the introduction of a second ortho-methoxyl.

While a full discussion of the probable significance of the carbonyl shieldings has been presented (2), further evidence in support of these ideas is given by the data in Tables VIII and IX for 30 examples and which are completely consistent with our original interpretation. The empirical expression, $\cos^2\theta = (\delta_C{}^X + 23.2)/20$ (where θ is the angle of twist for the acetophenone bearing the X substituent and $\delta_C{}^X$ is its ^{13}C carbonyl chemical shift), which was developed previously, permits one to estimate the dihedral angle between the planes of the carbonyl group and the aromatic ring and the calculated angles for the examples included in this study are given in Table X.

TABLE X

Estimated angles of twist, θ, for some ortho-substituted acetophenones (in degrees)

Substituent(s)	θ	Corr.	Substituent(s)	θ	Corr.
2-CH_3	24	28	2-C_6H_5	34	—
2,3-$(CH_3)_2$	29	32			
2,4-$(CH_3)_2$	21	25	2-CH_3O	17	35
2,5-$(CH_3)_2$	21	25	2-C_2H_5O	22	38
2,4,5-$(CH_3)_3$	20	24	2,4-$(CH_3O)_2$	0	28
			2,5-$(CH_3O)_2$	15	34
2,6-$(CH_3)_2$	44	50			
2,4,6-$(CH_3)_3$	46	51	2,6-$(CH_3O)_2$	25	40
2,6-$(CH_3)_2$-4-(t-C_4H_9)	45	51			
2,3,4,6-$(CH_3)_4$	46	52	2-Cl	22	26
2,3,5,6-$(CH_3)_4$	48	54	2,4-Cl_2	11	18
2,3,4,5,6-$(CH_3)_5$	48	53			
			2,6-Cl_2	18	28
2-C_2H_5	25	29			
			2-Br	24	21
2,6-$(C_2H_5)_2$	44	50			
			2,4,6-Br_3	27	21
2-i-C_3H_7	29	33			
			2-I	29	—
2,6-(i-C_3H_7)$_2$	46	52			
2,4,6-(i-C_3H_7)$_3$	47	53	2-NO_2	20	24
2,5-(t-C_4H_9)	51				

Can. J. Chem. Downloaded from www.nrcresearchpress.com by 210.87.254.6 on 09/05/12
For personal use only.

Can. J. Chem. Downloaded from www.nrcresearchpress.com by 210.87.254.6 on 09/05/12
For personal use only.

On the basis of Lauterbur's results for several aromatic series, there seems little doubt that closely neighboring groups can exert certain "ortho" effects on the shielding of the carbonyl nuclei which are independent of, and simultaneously operative with, any effects whose origins are steric in nature. The cause or causes of this mysterious effect are obscure. Although the most popular interpretation attributes these "ortho" effects to neighbor–anisotropy phenomena, it appears unlikely that this is the sole, or even the most important, factor for all cases. The problem has been discussed for particular cases, e.g. I (3*c*). The estimation of the magnitude of the non-steric "ortho" effect presents a difficult problem but, as a first approximation, we have examined the possibility of using estimates based on the data for various substituted toluenes (42, 43). At first, this approach seemed a reasonable one since the variation of the ^{13}C methyl shift with polar substitution is very small for meta- and para-substituted toluenes but there are significant changes from these in the ortho-derivatives. We assumed that this change is primarily due to a non-steric "ortho" effect of uncertain origin. By taking the difference between the observed methyl carbon shift for an ortho-substituted toluene and the averaged methyl shift for the corresponding meta- and para-substituted toluenes, we calculated "correction" factors for the various substituents. Applying these factors to the observed carbonyl carbon shielding data, we obtained "corrected" shielding values which are listed in the last column of Tables VIII and IX. Because of the unavailability of the required ethyl-, isopropyl-, and *t*-butyltoluenes, the "correction" factor for methyl carbons, found from the xylene data, were used for the first two cases since both can adopt conformations which would tend to minimize steric interactions and which would be approximately similar to those for methyl substitution. A factor for the *t*-butyl group, however, is more difficult to estimate and we hesitate to hazard a guess as to its magnitude. For the same reasons, "correction" factors for the ortho-phenyl and iodine nuclei have been omitted. For the tables, the following "correction" factors were employed: CH_3, -1 p.p.m., Cl, -1.2 p.p.m., Br, $+0.7$ p.p.m., NO_2, -0.9 p.p.m., and CH_3O, -4.8 p.p.m. Two immediate surprises in these figures appear to be the value for the methoxyl group and the opposite signs of the factors for chlorine and bromine. Substitution of the "corrected" carbonyl shieldings in the expression given above yielded the angles of twist, θ, listed in Table X and termed "corr." For most cases, the "corrected" angles are only slightly different from the original values. These estimates seem to be satisfactory for the alkyl groups, but some of the results for the polar groups are dubious.

Support for the inclusion of the "correction" factor for methyl groups in the ortho-position(s) was noted in our earlier report, based on the results for substituted benzaldehydes. In the present series, the results give no reason to change this conclusion for the alkyl groups. No supporting evidence, however, can be put forward for the other substituents. In fact, in view of the apparent discrepancies in the results obtained using the "corrected" carbonyl data, it would seem more desirable to accept the uncorrected figures as a better indication of the geometry of the molecules. Clearly more information on the nature of the indirect effects of these polar groups on the shielding of carbon nuclei is required to allow a full understanding of the present results. The main difficulty which must be overcome is by no means trivial and clear approaches to its resolution are difficult to suggest. This problem is the estimation of the contribution to the observed effect of that portion which is operative through space, the so-called field effect. The usual approach employed is an application of the point dipole model (44) to evaluate the so-called neighbor–anisotropy contribution (44, 45) due to the field induced circulation of electrons on the X atom. Several examples, however, are known for which inclusion of the neighbor–anisotropy effect is insufficient to rationalize the observed data, the case of iodine, for

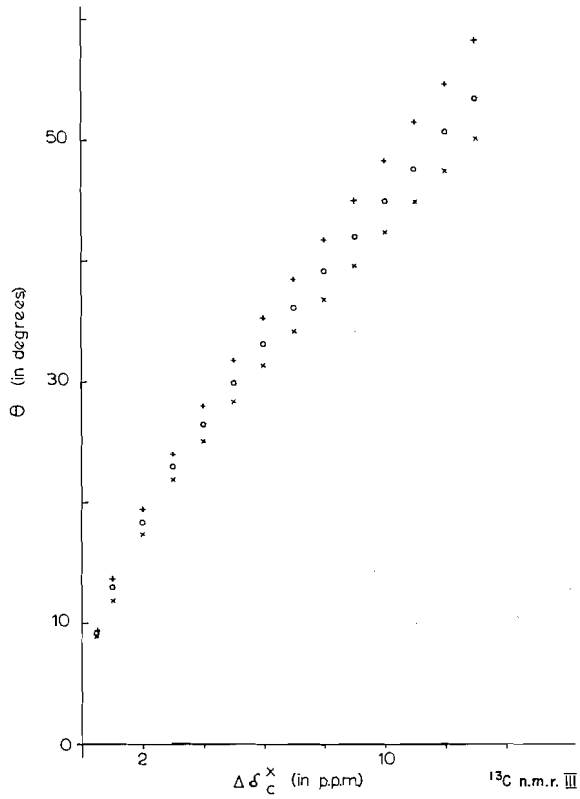

FIG. 5. Variation of the calculated angle of twist, θ, with $\delta_C{}^X$ values for various ortho-substituted acetophenones, assuming different values for the contribution by the phenyl group on the carbonyl chemical shifts (+, 15 p.p.m.; ○, 17 p.p.m.; ×, 19 p.p.m.).

example (3*c*). With the present state of knowledge, we would favor neglecting these "correction" factors until a more rational method for their estimation is suggested.

A weakness of this overall approach to θ values may appear to be the estimation of the shielding of the carbonyl carbon nucleus for the 90° case. To show that an estimated value of 17 p.p.m. for the conjugative shielding effect of the phenyl group is not extremely critical, we have plotted the variation of θ with $\delta_C{}^X$, the difference between the carbonyl shielding in acetophenone and that for an X-substituted compound, for other values of the phenyl conjugative effect, viz. 15 and 19 p.p.m. (see Fig. 5). Only for the highly hindered cases is there an appreciable change in θ, although $< 8°$ at 50°. Hence, we feel that this weakness is not a strong objection to the proposed approach to estimates of angles of twist.

An examination of the data in Table X indicates that the estimates of θ based on the observed shieldings are in substantial agreement with simple stereochemical considerations. In general, these estimates tend to be somewhat smaller than those obtained from analyses of ultraviolet spectral data or dipole moments (22, 46), comparisons with which were given previously (2). Estimates of θ for the 2,4,6-trimethyl- and 2,3,5,6-tetramethylacetophenones have recently appeared derived from determinations of the Kerr constants (47) and are found to be 90° for each of these cases. Clearly, these values are greatly different from any of the previous estimates and seem to be much too large.

An additional example of the buttressing effect of a second methyl group has been found

Can. J. Chem. Downloaded from www.nrcresearchpress.com by 210.87.254.6 on 09/05/12
For personal use only.

(2,3-dimethylacetophenone) and the observed change in θ by ca. 4° is comparable to that found for acetyldurene. No additional hindrance appears to be associated with the introduction of a fifth methyl group in the latter case.

The order observed for the three ortho-haloacetophenones using the uncorrected data also is in agreement with that expected on steric grounds but, since the observed carbonyl ^{13}C shielding may be strongly affected by an "ortho" effect of iodine (3*c*), the internal agreement of these estimates may be fortuitous. The results for the group of compounds bearing the methoxyl group in the ortho-position(s) may also be suspect. It was pointed out above that the other trends indicating steric interference in most of the cases (the acetyl methyl and para-carbon shieldings) are in direct contradiction and, in addition, the non-steric "ortho" effect of oxygen nuclei (from the toluene data) is appreciably larger than that for the other groupings examined. The estimates using the observed carbonyl data (i.e. uncorrected) appear reasonable with the exception of the 2,4-dimethoxy-derivative, but the "corrected" values seem unduly large (note especially the 2,6-$(CH_3O)_2$ case). At the present time, no clear explanation of these discrepancies can be offered apart from the suggestion that a smaller angle of twist might be expected for a compound bearing a para-methoxyl group due to conjugative electron release by oxygen. The slightly reduced θ in the alkylated examples having para-methyl groups may be ascribed to a similar electron release by the methyl group.

In general, the proposed method for the estimation of angles of twist in these carbonyl-containing systems yields reasonable and, most importantly, consistent results for the alkylated examples and for a number of other polar substituents. The approach possesses distinct advantages over the method based on the intensities of electronic transitions since the observed spectral band is characteristic of the ground state of the molecule. Furthermore, this transition can be assigned unambiguously and measured accurately. In addition, confirmatory evidence is provided by measurements of two other transitions in the spectrum. The results of an extension of our study of carbonyl compounds and a consideration of this approach for the estimation of steric hindrance in a series of alkyl phenyl ketones and the results of a detailed examination of several aliphatic conjugated carbonyl compounds will be reported shortly.

ACKNOWLEDGMENTS

We gratefully acknowledge the support of the Petroleum Research Fund, administered by the American Chemical Society, in the form of operating funds and the Ontario Research Foundation for a grant to purchase the 15.1 Mc/s rf unit. We also thank Professor L. R. C. Barclay for a sample of 2,5-di-*t*-butylacetophenone.

REFERENCES

1. J. B. Stothers and P. C. Lauterbur. Can. J. Chem. **42**, 1563 (1964).
2. K. S. Dhami and J. B. Stothers. Tetrahedron Letters, No. 12, 631 (1964).
3. (*a*) P. C. Lauterbur. J. Am. Chem. Soc. **83**, 1838 (1961); (*b*) J. Am. Chem. Soc. **83**, 1846 (1961); (*c*) J. Chem. Phys. **38**, 1406 (1963); (*d*) J. Chem. Phys. **38**, 1415 (1963); (*e*) J. Chem. Phys. **38**, 1432 (1963).
4. R. A. Friedel and H. L. Retcofsky. J. Am. Chem. Soc. **85**, 1300 (1963).
5. J. T. Arnold and M. E. Packard. J. Chem. Phys. **19**, 1608 (1951).
6. J. D. Baldeschwieler and E. W. Randall. Chem. Rev. **63**, 81 (1963).
7. J. B. Stothers and J. R. Robinson. Can. J. Chem. **42**, 967 (1964).
8. W. F. Forbes and W. A. Mueller. Can. J. Chem. **35**, 488 (1957).
9. S. F. Birch, R. A. Dean, F. A. Fidler, and R. A. Lowry. J. Am. Chem. Soc. **71**, 1362 (1949).
10. J. D. Matlock, S. N. Chinai, R. A. Guzzi, and D. W. Levi. J. Polymer Sci. **49**, 533 (1961).
11. J. W. Baker. J. Chem. Soc. 445 (1938).
12. E. H. Man and C. R. Hauser. J. Org. Chem. **17**, 397 (1952).
13. L. Weil. Monatsh. **29**, 905 (1908).

Can. J. Chem. Downloaded from www.nrcresearchpress.com by 210.87.254.6 on 09/05/12
For personal use only.

14. R. STEWART and K. YATES. J. Am. Chem. Soc. **80**, 6355 (1958).
15. H. RUPE and K. VON MAJEWSKI. Chem. Ber. **33**, 3401 (1900).
16. B. VAN ZANTEN and W. TH. NAUTA. Rec. Trav. Chim. **79**, 1211 (1960).
17. B. N. CAMPBELL and E. C. SPAETH. J. Am. Chem. Soc. **81**, 5933 (1959).
18. E. CAMPAIGNE and WM. B. REID. J. Am. Chem. Soc. **68**, 1663 (1946).
19. K. V. AUWERS, A. BOENNECKE, F. KROLLPFEIFFER, and G. PETERS. Ann. **408**, 212 (1915).
20. E. BESTHORN, E. BANZHAF, and G. JAEGLE. Chem. Ber. **27**, 3035 (1894).
21. (*a*) W. S. RAPSON and R. G. SHUTTLEWORTH. J. Chem. Soc. 487 (1941). (*b*) R. G. R. BACON and W. S. LINDSAY. J. Chem. Soc. 1382 (1958).
22. E. A. BRAUDE and F. SONDHEIMER. J. Chem. Soc. 3754 (1955).
23. E. R. SHEPARD, H. D. PORTER, J. F. NOTH, and C. K. SIMMANS. J. Org. Chem. **17**, 568 (1952).
24. L. H. SCHWARTZMAN and B. B. CORSON. J. Am. Chem. Soc. **76**, 781 (1954).
25. W. M. SCHUBERT and H. K. LATOURETTE. J. Am. Chem. Soc. **74**, 1829 (1952).
26. E. A. BRAUDE, B. F. GOFTON, G. LOWE, and E. S. WAIGHT. J. Chem. Soc. 4054 (1956).
27. W. F. FORBES and W. A. MUELLER. Can. J. Chem. **33**, 1145 (1955).
28. V. R. REMISCHNEIDER and B. DIEDRICH. Ann. **646**, 18 (1961).
29. R. C. FUSON, E. M. BOTTORFF, and S. B. SPECK. J. Am. Chem. Soc. **64**, 1450 (1942).
30. S. SUGASAWA. J. Chem. Soc. 1483 (1934).
31. G. LOCK and E. BÖCK. Chem. Ber. **70**, 916 (1937).
32. R. C. FUSON, J. H. VAN CAMPEN, and D. E. WOLF. J. Am. Chem. Soc. **60**, 2269 (1938).
33. W. BAKER. J. Chem. Soc. 956 (1939).
34. I. M. HUNSBERGER, D. LEDNICER, H. S. GUTOWSKY, D. L. BUNKER, and P. TAUSSIG. J. Am. Chem. Soc. **77**, 2466 (1955).
35. H. SPIESECKE and W. G. SCHNEIDER. J. Chem. Phys. **35**, 731 (1961).
36. P. C. LAUTERBUR. Nuclear magnetic resonance spectra of elements other than hydrogen and fluorine. *In* Determination of organic structures by physical methods. *Edited by* F. C. Nachod and W. D. Phillips. Academic Press. 1962. Chap. 7.
37. G. B. SAVITSKY. J. Phys. Chem. **67**, 2723 (1963).
38. K. S. DHAMI and J. B. STOTHERS. Abstr. 47th Conference Chem. Inst. of Canada, Kingston. 1964. p. 60.
39. G. E. MACIEL and G. C. RUBEN. J. Am. Chem. Soc. **85**, 3903 (1963).
40. P. C. LAUTERBUR. Tetrahedron Letters, No. 8, 274 (1961).
41. C. E. JOHNSON and F. A. BOVEY. J. Chem. Phys. **29**, 1012 (1958).
42. P. C. LAUTERBUR. Ann. N.Y. Acad. Sci. **70**, 841 (1958).
43. K. S. DHAMI and J. B. STOTHERS. Unpublished observations.
44. H. M. MCCONNELL. J. Chem. Phys. **27**, 226 (1957).
45. J. A. POPLE. Proc. Roy. Soc. London, Ser. A, **239**, 550 (1957).
46. W. F. FORBES. Can. J. Chem. **38**, 1104 (1960).
47. M. J. ARONEY, M. G. CORFIELD, and R. J. W. LEFEVRE. J. Chem. Soc. 648 (1964).

Can. J. Chem. Downloaded from www.nrcresearchpress.com by 210.87.254.6 on 09/05/12
For personal use only.

Can. J. Chem. Downloaded from www.nrcresearchpress.com by 210.87.254.5 on 09/05/12
For personal use only.

^{13}C N.M.R. STUDIES

PART IV.[1] CARBON-13 N.M.R. SPECTRA OF SOME ALKYL PHENYL KETONES[2]

K. S. DHAMI[3] AND J. B. STOTHERS
Department of Chemistry, University of Western Ontario, London, Ontario

Received September 24, 1964

ABSTRACT

The 15.1 Mc/s ^{13}C n.m.r. spectra of 21 substituted alkyl phenyl ketones, ArCOR, have been determined and the ^{13}C chemical shifts measured. This group of compounds included examples of each of the ethyl, isopropyl, and *t*-butyl phenyl ketone series. Variations of the chemical shifts with structure are analyzed and compared with the results for substituted acetophenones. The study of steric inhibition of conjugation in these compounds by means of their ^{13}C data is discussed in detail. The parameters for the acetyl carbons for a few methyl aryl ketones have been determined as well to examine the effect of orientation of this group on a polycyclic aromatic skeleton.

INTRODUCTION

As an extension of our investigations of the carbon-13 nuclear magnetic resonance spectra of organic carbonyl groups (1, 2, 3), we have prepared a number of alkyl phenyl ketones and determined their ^{13}C spectra at 15.085 Mc/s. Seven examples in each of the propiophenone, isobutyrophenone, and pivalophenone series have been included and, since our interest has centered primarily on the ^{13}C shieldings in hindered systems, most of these compounds bear at least one ortho-substituent. As models for comparison with the results for these hindered systems, the parent ketone of each series and its para-methoxyl derivative were examined. Analyses of the spectra were carried out by the methods which have been described in detail in Part III of this series (3). The aromatic shieldings for the methoxyl derivatives permit an additional test of the additive relation of combined substituent effects on the chemical shifts of these nuclei (4).

The results for the hindered ketones show that variations of the ^{13}C chemical shift parameters for the carbonyl carbon, the para-carbons, and the α-carbon of the acyl group provide indications of the existence of steric interference to coplanarity of the acyl grouping. Application of the carbonyl shieldings to semiquantitative estimates of the angles of twist in these systems has been attempted, using an approach similar to that described for the analysis of the carbonyl data for the acetophenones. The limitations of the approach for these compounds place greater uncertainties on the calculated values, but the results are reasonable and appear to yield satisfactory estimates as a first approximation.

EXPERIMENTAL

Nuclear Magnetic Resonance Spectra

All spectra were determined at 15.085 Mc/s using the compounds described below containing ^{13}C in natural abundance. Details of the experimental procedure have been presented (3).

Materials

All of the compounds were prepared from readily available commercial products. Most of the ketones are well known and all were obtained by established procedures. In each case, infrared and proton spectra were determined to check their purity. The observed physical constants and the syntheses employed are collected

[1]*Part III, ref. 3.*
[2]*These results were reported in part at the 46th Annual Conference of the Chemical Institute of Canada, Toronto, June 1963.*
[3]*Petroleum Research Fund Predoctoral Fellow, 1962–1964.*

in Table I together with the reported constants. The analytical data are included for the new compounds: 2,3,4,5,6-pentamethylpropiophenone, 2,3,5,6-tetramethyl-, 2,3,4,5,6-pentamethyl-, and 2,4,6-triisopropylisobutyrophenone. The microanalyses were performed by Alfred Bernhardt and Associates, Mulheim, Germany. All melting points, determined on a Kofler hot stage, are uncorrected. The liquids were purified by distillation through a platinum-plated, spinning band column. The solvents used for spectral studies were Fisher "Spectro-Grade" reagents.

TABLE I

Physical data for the substituted alkyl phenyl ketones, ϕCOR, prepared for this study

Parent compound (R)	Substituent(s)	Method of preparation	Physical constants: Observed b.p./mm (m.p.)	Observed n_D (t°)	Reported b.p./mm (m.p.)	Reported n_D (t°)	Ref.
C_2H_5	Nil	A1	61/0.4	1.5260 (23)	85/7.5	1.5274 (20)	5
	4-CH_3O	A1	108–110/2	1.5450 (25)	143–144/12	1.5484 (20)	6
	2-CH_3	B	102/18	1.5250 (20)	127/38	1.5250 (20)	7
	2,4,6-$(CH_3)_3$	A1	120/6	1.5112 (21)	125/13	—	8
	2,3,5,6-$(CH_3)_4$	A1	(78–79)	—	(79)	—	
	2,3,4,5,6-$(CH_3)_5$*	A1	(84–85)	—			9
	2,4,6-(i-$C_3H_7)_3$	A1	145–146/11 (80–81)	—	123–126/3 (81–83)	—	10
i-C_3H_7	Nil	A2	73–75/1.2	1.5170 (25)	115/29	1.5180 (20)	5
	4-CH_3O	A2	112–114/2.1	1.5355 (25)	149–150/14	1.5390 (16.6)	6
	2-CH_3	B	103–104/15	1.5135 (19.5)	230/758	—	11
	2,4,6-$(CH_3)_3$	A2	117/8	1.5085 (25)	142–143/19	—	12
	2,3,5,6-$(CH_3)_4$†	A2	(40–41)	—			
	2,3,4,5,6-$(CH_3)_5$‡	A2	(42–43)	—			
	2,4,6-(i-$C_3H_7)_3$§	A2	106–107/0.9 (47–49)	—			
t-C_4H_9	Nil	C	97–98/16	1.5080 (20)	98/11.5	1.5102 (20)	5
	4-CH_3O	A3	116–118/2	1.5260 (26)	138–140/8	—	13
	2-CH_3	C	75/1.4	1.5057 (25)	110/110	—	14
	2,4,6-$(CH_3)_3$	A3	129–130/11	1.5092 (20)	120–122/8	1.5150 (25)	15
	2,3,4,6-$(CH_3)_4$	A3	92–93/0.4	1.5192 (24)	117–119/2	1.5170 (25)	15
	2-CH_3-4-CH_3O	A3	100/0.8		126–128/4	—	15
	2-CH_3-5-CH_3O	A3	(51–52)		(50–51)	—	15

*Found: C, 81.94; H, 9.88. Calcd. for $C_{14}H_{20}O$: C, 82.30; H, 9.87.
†Found: C, 82.04; H, 9.87. Calcd. for $C_{14}H_{20}O$: C, 82.30; H, 9.87.
‡Found: C, 82.38; H, 10.00. Calcd. for $C_{15}H_{22}O$: C, 82.38; H, 10.09.
§Found: C, 83.10; H, 10.99. Calcd. for $C_{19}H_{30}O$: C, 83.15; H, 11.02.
Methods used: (A1) acetylation via Friedel–Crafts reaction with CH_3COCl, ArH → $ArCOCH_3$ (10);
(A2) Friedel–Crafts acylation with $(CH_3)_2CHCOCl$, ArH → $ArCOCH(CH_3)_2$ (12);
(A3) Friedel–Crafts acylation with $(CH_3)_3CCOCl$, ArH → $ArCOC(CH_3)_3$ (15);
(B) Grignard reaction of RMgI (R = Me or Et) on the appropriate nitrile, ArCN → $ArCOCH_3$ (7);
(C) Grignard reaction of $(CH_3)_3CMgBr$ with the aldehyde, followed by CrO_3/HOAc oxidation, ArCHO → $ArCH(OH)CH_3$ → $ArCOCH_3$ (16).

DISCUSSION

The results for the three closely related series of alkyl phenyl ketones are considered together to facilitate discussion and to emphasize the common features. The observed chemical shifts for each type of carbon nucleus are discussed under separate subheadings to allow ready intercomparison of the data from each series. The shieldings of the carbons of the acetyl group in a few polycyclic aryl methyl ketones are presented in a separate section. In the final section, the application of these ^{13}C spectral results to the estimation of the extent of steric inhibition of conjugation of the acyl grouping is considered in detail.

The majority of the data have been obtained using the neat liquids or solutions of the ketones in carbon disulfide. In the latter cases, however, the maximum concentrations attainable were not sufficient to permit satisfactory measurements for all band positions and consequently certain data do not appear in the tables. Measurements for some of

Can. J. Chem. Downloaded from www.nrcresearchpress.com by 210.87.254.5 on 09/05/12
For personal use only.

these bands were possible in chloroform solution and these figures are indicated in the tables. On the basis of our previous results (1, 3), it seemed unlikely that chloroform causes appreciable changes in the shielding of any but the carbonyl carbons, but, to confirm this point, a few examples were studied in both carbon disulfide and chloroform solutions.

TABLE II

^{13}C chemical shifts for some substituted propiophenones (in p.p.m. from CS_2)

	R—C=O			Aromatic nuclei*				
Substituent(s)	C=O	—CH_2—	—CH_3	C-1	C-2,6	C-3,5	C-4	Others
Nil	−5.6	162.2	185.8	56.5	65.6	65.6	61.7	—
4-CH_3O	−4.7	162.3	185.4	63.3 (64.6)	63.4 (64.7)	79.9 (80.3)	30.2 (31.5)	138.1
2-CH_3	−9.7	159.3	185.1	56.0	56.0 (C-2) 61.9 (C-6)	61.9(C-3) 67.5(C-5)	64.5	172.1
2,4,6-$(CH_3)_3$	−15.0	156.2	185.3	53.7	61.5	65.3	56.2	173.6 175.4
2,3,5,6-$(CH_3)_4$†	−16.7	(154.4)‡		49.2	64.9	58.7	61.9	173.4 (176.7)‡
2,3,4,5,6-$(CH_3)_5$†	−16.9	(154.7)‡		51.1	65.3	59.2	59.2	175.1
2,4,6-$(i\text{-}C_3H_7)_3$†	−16.3	(153.1)‡		53.8	49.0	71.3	43.6	160.0 168.4 176.8

*Data in parentheses are the calculated values assuming additivity of substituent effects.
†Saturated solution in CS_2, but owing to low concentration some data obtained in $CHCl_3$.‡
‡Data for saturated $CHCl_3$ solutions.

TABLE III

^{13}C chemical shifts for some substituted isobutyrophenones (in p.p.m. from CS_2)

	R—C=O			Aromatic nuclei*				
Substituent(s)	C=O	—CH—	—CH_3	C-1	C-2,6	C-3,5	C-4	Others
Nil	−10.3	157.9	174.4	56.7	64.6	64.6	60.1	—
4-CH_3O	−8.5	158.2	173.7	64.3 (64.8)	62.9 (63.7)	79.6 (79.3)	30.1 (29.9)	138.1
2-CH_3	−13.9	155.2	174.6	56.1	56.1(C-2) 61.8(C-6)	61.8(C-3) 67.0(C-5)	65.1	172.6
2,4,6-$(CH_3)_3$	−18.2	151.4	174.9	53.4	60.2	64.7	55.7	173.2
2,3,5,6-$(CH_3)_4$†	−19.8	148.0	(175.0)‡	49.4	63.1	57.6	60.1	172.4
2,3,4,5,6-$(CH_3)_5$†	−20.1	149.0	(174.5)‡	52.3	64.4	59.8	59.8	174.5
2,4,6-$(i\text{-}C_3H_7)_3$†	−19.5	149.9	(175.7)‡	54.7	48.2	71.4	43.5	175.7

*Data in parentheses are the calculated values assuming additivity of substituent effects.
†Saturated solution in CS_2 but owing to low concentration methyl shifts obtained in $CHCl_3$.‡
‡Data for saturated $CHCl_3$ solutions.

Alkyl Phenyl Ketones

(a) Aromatic Carbons

The chemical shifts of the aromatic carbon nuclei in the propiophenone, isobutyrophenone, and pivalophenone series are given in Tables II, III, and IV, respectively. The analyses and assignments in the aromatic regions of these spectra were accomplished by the methods which were described in detail in the preceding part of this series (3). The data for the parent ketone for each of these series show that the substituent effects of the three acyl groups are similar and not greatly different from those caused by an acetyl group. To compare the effects of various carbonyl-containing groups on the aromatic shieldings, the relevant data are listed in Table V in which the substituent

Can. J. Chem. Downloaded from www.nrcresearchpress.com by 210.87.254.5 on 09/05/12
For personal use only.

TABLE IV

^{13}C chemical shifts for some substituted pivalophenones (in p.p.m. from CS_2)

	R—C=O			Aromatic nuclei*				
Substituent(s)	C=O	—C—	CH_3	C-1	C-2,6	C-3,5	C-4	Others
Nil	−14.4	149.0	164.6	54.7	65.2	65.2	62.4	—
4-OCH_3	−11.0	149.7	164.8	63.6 (62.8)	62.5 (64.3)	80.1 (79.9)	31.5 (32.2)	138.2
2-CH_3	−19.2	148.6	166.0	52.3	59.1(C-2) 65.3(C-6)	65.3(C-3) 68.2(C-5)	62.8	174.3
2-CH_3-5-CH_3O†	−19.2	148.2	164.6	62.6	60.4(C-2) 81.3(C-6)	65.1(C-3) 39.3(C-5)	81.3	136.7
2-CH_3-4-CH_3O†	−18.8	148.4	165.1	52.7	60.7(C-2) 66.0(C-6)	76.4(C-3) 80.6(C-5)	37.3	137.8
2,4,6-$(CH_3)_3$	−23.0	149.2	165.0	53.9	61.8	64.9	56.7	173.2
2,3,4,6-$(CH_3)_4$	−22.9	149.2	165.7	35.0	64.3(C-3) 59.2(C-6)	62.2 64.7(C-5)	62.2	178.6

*Data in parentheses are the calculated values assuming additivity of substituent effects.
†Saturated solution in CS_2.

effects are given relative to benzene. The figures for the formyl group are from Spiesecke and Schneider (17). The effects of the acyl groups at the ortho- and meta-positions are slightly less than those of the formyl and the differences between the effects for the various R—C(=O)— groups are within experimental error. For these acyl groups, appreciable differences are found, however, at the C-1 and C-4 nuclei, but there is no apparent trend for these changes at either position. No explanation can be offered to account for the small, but distinct, variations.

TABLE V

^{13}C chemical shifts of the aromatic nuclei in some monosubstituted benzenes (in p.p.m. relative to C_6H_6)

	Chemical shifts			
Substituent	C-1	C-2,6 (ortho)	C-3,5 (meta)	C-4 (para)
—CHO*	−9.0	−1.2	−1.2	−6.0
—$COCH_3$†	−9.0	−0.4	−0.4	−4.0
—$COCH_2CH_3$	−8.5	+0.6	+0.6	−3.3
—$COCH(CH_3)_2$	−8.3	−0.4	−0.4	−4.9
—$COC(CH_3)_3$	−10.3	+0.2	+0.2	−2.6

*Reference 17.
†Averaged values of data reported in refs. 1 and 17.

The para-methoxyl derivative of each parent ketone was examined to test for additivity of substituent effects, since an additive relation has been found to hold to a good approximation for several meta- and para-substituted aromatic compounds (3, 4, 18, 19). The methoxyl group was chosen since the effect of this grouping differs considerably at the various aromatic nuclei and thus provides a more definitive test. The agreement between the observed and calculated chemical shifts for the ring carbons was found to be within 1.3 p.p.m. with one exception, the 2- and 6-positions (which are equivalent) in 4-methoxypivalophenone. These differences are comparable to those found for acetophenones (3). We have assumed that these results confirm our peak assignments.

Can. J. Chem. Downloaded from www.nrcresearchpress.com by 210.87.254.5 on 09/05/12
For personal use only.

Can. J. Chem. Downloaded from www.nrcresearchpress.com by 210.87.254.5 on 09/05/12
For personal use only.

The remaining compounds were examined primarily to study the variations of the chemical shifts of nuclei in the substituent groups of other hindered systems to compare with our previous results and to test conclusions drawn therefrom. The shieldings of the aromatic carbon nuclei of these compounds are listed in the tables (II, III, and IV) but little comment can be offered at this time. As before, ortho-positioning of substituent groupings on the ring produces marked deviations of the observed shifts from the values calculated by assuming an additive relation. Remarkable differences are also observed for those cases in which an aromatic methyl group is flanked on both sides by substituents. The acyl derivatives of durene and pentamethylbenzene exhibit this behavior as does 2,3,4,6-tetramethylpivalophenone. For each of these examples, one of the methyl-substituted aromatic nuclei absorbs in the range, 63.1–65.3 p.p.m., indicating that the usual deshielding effect of ca. 9 p.p.m. due to methyl substitution is largely overcome by some other factor. As before (3), we have assigned this signal to the aromatic carbon(s) bearing the most crowded methyl group(s) which for the durene derivatives are the C-2 and C-6 nuclei. The other methyl-substituted aromatic nuclei in these derivatives are also abnormally shielded but to a lesser degree. Evidence suggesting that this shielding effect is due, at least in part, to the acyl group comes from the observation that only *two* aromatic carbons absorb near 65 p.p.m. in the pentamethyl derivatives. Thus, this effect would not appear to arise merely from a simple crowding of the methyl substituents and consequently the highest field signal in the aromatic region has been assigned to the C-2 and C-6 nuclei in these compounds. By the same reasoning, the signal at 64.3 p.p.m. in the spectrum of 2,3,4,6-tetramethylpivalophenone has been assigned to carbon-2. Similar effects have been noted for the polymethylated acetophenones (3). Further indication that the acyl group is largely responsible for this up-field shift is given by the shieldings for the aromatic nuclei of hexamethylbenzene at 60.4 p.p.m. (20) and pentamethylbenzene in which the substituted ring carbons appear at 60.8 p.p.m. (21). Clearly both show a shift to higher field relative to less highly substituted compounds, but the relative change is considerably less than that observed for the ketones.

The chemical shifts for the C-4 aromatic nuclei in the ortho-substituted derivatives exhibit variations similar to those found for the acetophenone series (3) in that substitution at the ortho-position(s) tends to reduce the deshielding effect of the acyl group at the para-position. A comparison of the observed C-4 shifts for propiophenone or isobutyrophenone and the corresponding 2-methyl derivative illustrates the trend without allowing for the small effect of the methyl group at C-4. The observed changes are consistent with previous observations in the acetophenone series, even the exceptions are similar (i.e. the 2,3,4,5,6-pentamethylated derivatives) and these have been discussed (3). We attribute the increased shielding at the para-carbon to steric inhibition of conjugation in the ortho-substituted compounds relative to compounds lacking ortho-substituents.

Apart from the observations and interpretations noted above, present knowledge of aromatic shieldings in general does not permit a fuller evaluation of our results.

(b) Acyl Groups

(i) Carbonyl carbons.—The easily recognized singlet peaks due to the carbonyl carbon nuclei are the lowest field bands in all of these spectra and the observed resonance positions (Tables II, III, and IV) clearly show that methyl substitution on the α-carbon of the acyl group tends to deshield the carbonyl carbon. These bands appear at -3.2, -5.6, -10.3, and -14.4 p.p.m. for the acetyl, propionyl, isobutyryl, and pivaloyl groups, respectively. These changes are in *qualitative* agreement with those found for

the comparable series of alkyl methyl ketones (1) as well as the differences in chemical shift of the unsaturated carbon in the system =C—R, where R = ethyl, isopropyl, *t*-butyl for both aromatic (3) and aliphatic (22) hydrocarbons. In the latter case, the assignments for the appropriate olefinic carbon nuclei have not been made by the original authors, but, by analogy with their other results the most probable assignment supports the above claim. There are significant *quantitative* differences, however, between these effects and those found for methyl substitution in the aliphatic and aromatic ketones. In the present series, successive substitution on the α-carbon tends to deshield the carbonyl nucleus by ca. 4 p.p.m. per methyl group whereas, in the aliphatic ketones the carbonyl carbon shift difference between the isopropyl methyl and *t*-butyl methyl ketones is only 0.8 p.p.m. Further discussion of this point is presented in the final section.

In each series, there are distinct variations in the carbonyl shieldings with substitution on the aromatic ring. In contrast to the results for the acetophenone series, the para-methoxyl group shifts the carbonyl resonance to higher field relative to its position for the parent ketone. These differences of 0.9, 1.8, and 3.4 p.p.m. for the propiophenone, isobutyrophenone, and pivalophenone derivatives, respectively, appear to increase with increasing size of the acyl group suggesting that the origin of the effect is probably steric. The results of the study of the acetophenone series established that the polar nature of substituent groups was of minor effect on the carbonyl shieldings in planar systems while some evidence for a shielding effect operative in hindered systems was obtained for certain electron-releasing groups in the para-position. The present results, therefore, seem consistent with the latter condition.

The remaining examples in each of the three series bear one or two ortho-substituents and a comparison of the changes in carbonyl chemical shift with substitution shows that similar variations are found for each series. For example, introduction of an ortho-methyl group produces an average change of -4.2 ± 0.6 p.p.m. for each carbonyl carbon shift relative to that observed for the parent ketone, while a second ortho-methyl substituent gives an additional average change of -4.5 ± 0.7 p.p.m. The observed changes for these and other substitutions are collected in Table VI. The average effects are given in the last column of Table VI, and, although the deviations are slightly larger than experimental error, the effects are closely similar. A more important observation is probably the fact that the order throughout each series is the same. This order follows that expected on the grounds of increasing steric interference of the substituents with the acyl groups thus hindering the carbonyl group from attaining coplanarity with the aromatic ring.

(ii) Alkyl carbons.—The observed chemical shifts of the alkyl carbon nuclei of the three acyl groups of the parent ketones (Tables II, III, and IV) may be compared to the shifts observed for ethyl, isopropyl, and *t*-butyl groups directly bonded to aromatic

TABLE VI

Substituent effects on the carbonyl shieldings of some alkyl phenyl ketones, $RCOC_6H_{(5-n)}R_n'$ (in p.p.m. relative to shift of parent compound)

	R group			
Substituent(s) (R′)	Et	*i*-Pr	*t*-Bu	Average effects
2-CH_3	−4.1	−3.6	−4.8	−4.2±0.6
2,4,6-$(CH_3)_3$	−9.4	−7.9	−8.6	−8.6±0.7
2,3,5,6-$(CH_3)_4$	−11.1	−9.5	—	−10.3±0.8
2,3,4,5,6-$(CH_3)_5$	−11.3	−9.8	—	−10.5±0.7
2,4,6-(*i*-$C_3H_7)_3$	−10.7	−9.2	—	−9.9±0.7

Can. J. Chem. Downloaded from www.nrcresearchpress.com by 210.87.254.5 on 09/05/12
For personal use only.

TABLE VII

^{13}C chemical shifts of alkyl carbons in some substituted benzenes (p.p.m. from CS_2)

	Chemical shifts					
	α-Carbon			β-Carbon		
Alkyl group	C_6H_5-	C_6H_5CO-	Δδ*	C_6H_5-	C_6H_5CO-	Δδ*
CH_3-	171.8	167.9	−3.9	—	—	
CH_3CH_2-	164.8	162.2	−2.6	177.7	185.5	+7.8
$(CH_3)_2CH$-	159.8	157.9	−1.9	169.5	174.4	+4.9
$(CH_3)_3C$-	158.1	149.0	−9.1	162.1	164.6	+2.5

*Difference between shifts for ketone and hydrocarbon.

rings (3). In each case, the α-carbon is deshielded and the β-carbons (methyl) are shielded for the ketone relative to the values for the corresponding alkylbenzene. These figures are collected in Table VII for comparison. The largest difference for the α-carbon shielding is found for the *t*-butyl group and is much greater than any of the others. Indeed, this difference appears to break the trend (compare the figures in Table VII). The shielding effect at the β-methyl carbons decreases with increasing size of the alkyl group. Apart from this variation for the β-methyl carbon shifts, however, the shielding of these nuclei is relatively insensitive to the introduction of substituents in the aromatic ring. It appears that the methyl carbon shieldings are not sensitive to changes in the polarization of the carbonyl bond, at least in the first approximation. With the exception of the pivalophenone series, a similar behavior is not observed for the α-carbon shieldings. One would expect the α-carbon shift to reflect changes in the carbonyl polarization since this nucleus is directly bonded thereto. The fact that the α-carbon shieldings are decreased with increasing ortho-substitution is completely consistent with the existence of steric interference to coplanarity of the carbonyl group and the observed changes are strikingly similar to those observed for the acetyl methyl carbon in similarly substituted acetophenones (3). For example, the average change caused by the introduction of a 2-methyl group is -3.2 ± 0.5 p.p.m. for the acetophenone, propiophenone, and isobutyrophenone systems, while substitution of a second ortho-methyl group (from the results for the 2,4,6-trimethyl derivatives) produces an average shift of -6.25 ± 0.25 p.p.m. relative to the parent ketone in each of these three systems. It is reasonable to suggest that these changes arise from a common origin which is steric inhibition of conjugation of the carbonyl grouping.

Other Carbons

The observed chemical shifts for the various types of carbon nuclei in the substituent alkyl groups are similar to those reported earlier in the acetophenone series. As before, an increased crowding of the methyl groups on an aromatic ring tends to shift the methyl carbon resonance toward higher field. It is important to note that in view of considerable overlapping of the bands for the various alkyl carbons in these spectra, their data are the least precise. The methoxyl carbons, however, absorb in a region of the spectrum which is uncluttered and their signals are easily measured. The shieldings of 138.1 ± 0.1 p.p.m. are unexceptional (3, 4).

Methyl Polycyclic Aryl Ketones

The shieldings of the carbonyl carbon nuclei for a few methyl aryl ketones having polycyclic aryl groupings have been reported (3) and these data together with those for the methyl carbon nuclei are collected in Table VIII. The figures for acetophenone are

Can. J. Chem. Downloaded from www.nrcresearchpress.com by 210.87.254.5 on 09/05/12
For personal use only.

TABLE VIII

^{13}C shieldings of the acetyl group of some methyl aryl ketones (in p.p.m. from CS_2)

Aryl group	Chemical shifts	
	C=O	CH_3
Phenyl	−3.2	167.9
2-Naphthyl	−3.0	167.0
1-Naphthyl	−6.7	164.0
3-Phenanthranyl*	−2.9	167.0
9-Phenanthranyl*	−7.5	163.0
9-Anthranyl*	−14.5	159.0

*Saturated solution in $CHCl_3$.

included for comparison. The variations in these results clearly indicate that there are steric interactions between the acetyl group and the aromatic ring system for those cases in which *peri*-hydrogens could interfere with the rotation of the acetyl group, namely, 1-naphthyl, 9-phenanthranyl, and 9-anthranyl. The latter case exhibits the most pronounced deshielding effect at both the carbonyl and methyl carbons presumably owing to the fact that two *peri*-hydrogen interactions may be involved. Although three of these examples were studied in chloroform solution only, the observed chemical shifts would not be expected to differ greatly from values for comparable concentrations in less polar media. An upper limit for the solvent effect on the resonance positions of these carbons would, in all probability, not exceed 2 p.p.m. on the basis of previous results (1, 3). The chemical shifts of certain nuclei in chloroform solution relative to those in carbon disulfide are listed in Table IX, and it is evident that the solvent effects are relatively small. Thus, there is clear evidence for steric inhibition of conjugation for these three cases. Owing to the complexity of the aromatic regions in these spectra, and, for the solids, the relatively low concentrations of the solutions obtainable, satisfactory analyses of the aromatic patterns were not possible and the chemical shift measurements are limited to the carbons of the acetyl grouping. In the case of 9-acetylanthracene, spin-decoupling experiments were carried out to locate and measure the position of the acetyl methyl signal.

Steric Inhibition of Conjugation

A number of the variations in the chemical shift results for alkyl aryl ketones which provide evidence for the existence of steric inhibition of conjugation in several cases

TABLE IX

Solvent effects on certain ^{13}C shieldings in alkyl phenyl ketones ($\delta_C^{CS_2} - \delta_C^{CHCl_3}$, in p.p.m.*)

Parent compound	Substituents	Acyl group		Aromatic carbons			
		C=O	α-C	C-1	C-2,6	C-3,5	C-4
$\phi COCH_2CH_3$	2,3,5,6-$(CH_3)_4$	−1.7	†	−0.4	−0.5	−0.1	−0.8
	2,3,4,5,6-$(CH_3)_5$	−1.3	†	−1.4	−0.3	−1.1	−1.0
	2,4,6-(*i*-$C_3H_2)_3$	−1.5	†	−0.8	−0.3	−0.5	−0.5
$\phi COCH(CH_3)_2$	2,3,5,6-$(CH_3)_4$	−0.8	−2.0	−1.3	−1.4	−1.4	−2.2
	2,3,4,5,6-$(CH_3)_5$	0.0	−1.4	−1.1	−0.9	−0.7	−1.6
	2,4,6-(*i*-$C_3H_7)_3$	−1.7	†	−0.5	−0.6	−0.2	−0.1
$\phi COC(CH_3)_3$	2-CH_3-4-CH_3O	0.9	+0.1	−0.2	−0.3	−0.7(C-3) −1.2(C-5)	−0.2

*Chemical shift difference for saturated $CHCl_3$ solutions relative to saturated CS_2 solution.
†Concentration in CS_2 solution was too low to permit measurements.

Can. J. Chem. Downloaded from www.nrcresearchpress.com by 210.87.254.5 on 09/05/12
For personal use only.

have been noted in the preceding sections. Our previous studies of the ^{13}C spectra of substituted acetophenones permitted the development of a semiquantitative approach to an estimation of the magnitude of the steric interference in terms of the angles of twist, θ, between the planes of the carbonyl group and the aromatic ring. The present series affords an opportunity to investigate the use of this method for similar estimates in some closely related systems.

Of the four series of compounds included in this study, the polycyclic aryl methyl ketones are perhaps the least different from the acetophenones, if one is to judge on the basis of the observed chemical shifts of the acetyl carbon nuclei. These shieldings for the 2-naphthyl and 3-phenanthranyl systems are the same, within experimental error, as those found for acetophenone (Table VIII). The other examples exhibit deshielding effects which we attribute to steric interference with the *peri*-hydrogens. Assuming that the empirical expression (2, 3) relating θ with the carbonyl carbon shift is applicable, substitution of the observed values yields the following angles of twist for these hindered cases: 1-naphthyl, 25°; 9-phenanthranyl, 28°; 9-anthranyl, 49°. All of these values seem to be reasonable estimates although figures with which comparisons might be made are lacking. The effect of varying contributions due to ring currents in these aromatic skeletons have been neglected in these calculations but any differences arising from this effect are small relative to the overall changes observed for the hindered and planar cases. An estimate, using the calculated values for ring current contributions from Johnson and Bovey (23) and assuming independent contributions by each ring in the polycyclic system (24), of the additional ring current effect for the most extreme case, 9-acetylanthracene, relative to acetophenone is calculated to be -1.02 p.p.m. for the carbonyl carbon shielding. Clearly, the ring current contributions, as estimated by the generally accepted models, are of secondary importance, although the calculated angles of twist may be somewhat larger than the actual angles. Differences due to varying ring current contributions at the various acetyl methyl carbons will be even smaller than those at the carbonyl nuclei owing to their greater distance from the aromatic ring systems and the fact that these methyl groups are not in the plane of the aromatic skeleton.

A direct comparison of the carbonyl carbon shifts for acetophenone, propiophenone, isobutyrophenone, and pivalophenone clearly shows that the effect of methyl substitution on the α-carbon is substantial, as pointed out above. Since the ethyl and isopropyl groups in propiophenone and isobutyrophenone, respectively, can adopt conformations which have the same non-bonded interactions as the methyl group in acetophenone, it is generally assumed that the carbonyl group is coplanar with the aromatic ring in each of these compounds (25, 26). The observed differences in the shieldings, therefore, must be primarily due to polar effects of methyl substitution. Attention has been drawn to the similarities of these changes with those observed for the corresponding methyl alkyl ketones and olefins, although no clear explanation for these changes can be offered. Assuming that these effects are entirely due to the alkyl substituents bonded to the carbonyl groups, the variations in carbonyl carbon shielding caused by alkyl substitution on the ring may be employed to calculate the angles of twist, θ, for the hindered systems. For this purpose, the original expression must be modified to, $\cos^2\theta = (\delta_C{}^X + 20)/20$ where $\delta_C{}^X$ represents the difference in carbonyl shielding for the X-substituted compound relative to the corresponding parent ketone. The necessary data are given in the first two columns of Table VI. Using these figures, angles of twist have been calculated for the propiophenone and isobutyrophenone series and these are listed in Table X. As

Can. J. Chem. Downloaded from www.nrcresearchpress.com by 210.87.254.5 on 09/05/12
For personal use only.

described in previous papers (2, 3), there is evidence that an ortho-methyl substituent tends to shield the carbonyl carbon nucleus by ca. 1 p.p.m. and, taking this effect into account, "corrected" estimates of θ have been calculated and included in Table X. A detailed discussion of the significance of these "corrections" has been presented (3) and need not be repeated. The estimates in this table seem reasonable although, again, other estimates for these systems are not available for comparison. Two interesting features are apparent from these results: (*a*) the hindrance of two ortho-isopropyl groups is apparently slightly greater than that caused by two ortho-methyls, and (*b*) there are indications of a buttressing effect by the additional methyl groups in durene and pentamethylbenzene derivatives relative to the acylmesitylenes. Both of these observations are in agreement with the results from the acetophenone study.

TABLE X

Estimated angles of twist, θ, for some hindered alkyl phenyl ketones (given in degrees)

	Alkyl group			
	C_2H_5		i-C_3H_7	
Substituents		Corrected		Corrected
Nil	0	0	0	0
2-CH_3	27	30	25	28
2,4,6-$(CH_3)_3$	43	49	39	45
2,3,5,6-$(CH_3)_4$	48	55	44	49
2,3,4,5,6-$(CH_3)_5$	49	55	44	50
2,4,6-(i-C_3H_7)$_3$	47	53	43	48

As noted in a previous section, the carbonyl shielding of pivalophenone is towards lower field by −4.1 p.p.m. relative to isobutyrophenone, while the difference in carbonyl carbon shifts for methyl isopropyl and methyl *t*-butyl ketones is only 0.8 p.p.m. and this difference is even less (0.2 p.p.m.) for diisopropyl and di-*t*-butyl ketones. This distinct difference for pivalophenone indicates that its carbonyl carbon is deshielded by an effect in addition to that of the *t*-butyl group. The most probable interpretation of this observation appears to be the presence of steric inhibition of conjugation due to interference between the aromatic protons and the β-methyls of the *t*-butyl grouping since it cannot assume a conformation having non-bonded interactions similar to those of methyl, ethyl, or isopropyl. If this is a valid explanation, the magnitude of the angle of twist for this system may be estimated using the empirical expression given above and the figure −3.6, for δ_C^X, since this is the difference between the observed change in pivalophenone and the average of the two *t*-butyl aliphatic examples, all relative to the corresponding isopropyl derivatives. In this way, the angle of twist is found to be 25° which may be compared to the value of 34°, estimated from ultraviolet spectral data (25). Both of these estimates agree well with those found for ortho-methylacetophenone by the corresponding methods (3, 25). Although this analysis of the ^{13}C chemical shift data is crude, it is interesting that the estimated angle is not unreasonable for this system. For the substituted pivalophenones, the observed variations of the carbonyl shieldings are comparable to those for the related series and estimates of the extent of steric inhibition can be made in a similar fashion. In view of the uncertainties of the approach to the estimated value for the parent compound, however, the significance of such estimates is questionable. For the 2-methyl and 2,4,6-trimethyl derivatives, the

Can. J. Chem. Downloaded from www.nrcresearchpress.com by 210.87.254.5 on 09/05/12
For personal use only.

calculated angles are found to be 40° and 51°, respectively, and the figures for the other derivatives correspond closely with these values, for the mono- and di-ortho-substituted examples, respectively. In any event, the differences in the carbonyl shieldings for the pivalophenone series are qualitatively consistent with the other findings.

Another feature of these spectra of the alkyl phenyl ketones, which was mentioned earlier but deserves further comment, is the effect of the para-methoxyl group on the carbonyl carbon shieldings. For each of the three series, a shift of the resonance position of the carbonyl carbon toward higher field is observed upon the introduction of this substituent and is most pronounced for pivalophenone (3.4 p.p.m.). This change provides supporting evidence of steric interference in pivalophenone itself since it may reasonably be attributed to an increased conjugation of the carbonyl group with the ring due to the strong electron-releasing tendency of the methoxyl group. In other words, it is suggested that the conjugative interaction of the methoxyl oxygen with the carbonyl group, acting through the aromatic ring, reduces the angle of twist in the substituted case relative to the parent ketone. Support for this conclusion is provided by the very much reduced effect of the methoxyl group on the carbonyl shielding in 2-methyl-4-methoxypivalophenone (relative to that for the 2-methyl derivative) for which it would appear that any conjugative interaction is not sufficient to overcome the more pronounced nonbonded interactions. The effect of the para-methoxyl substituent on the isobutyrophenone carbonyl shielding (1.8 p.p.m.) is appreciable and it follows, therefore, that there is some hindrance to coplanarity of the carbonyl group in the unsubstituted ketone. Some evidence for minor steric interference in secondary alkyl phenyl ketones has been noted from ultraviolet studies (25), but no appreciable hindrance to coplanarity would be expected since conformations similar to those for acetophenone may be adopted. In the event there is some interference, the estimated angles of twist collected in Table X for the isobutyrophenone series will be low by a few degrees. There is no compelling evidence to suggest that steric inhibition of conjugation occurs in propiophenone, since the observed effect of the para-methoxyl group, while directionally similar to the other series, is much smaller, 0.9 p.p.m., and is not outside the limits of experimental uncertainty. No evidence from other sources which would indicate deviations from coplanarity has been found.

In summary, the ^{13}C spectral results for the present examples of alkyl phenyl ketones and methyl aryl ketones support the conclusions drawn from the previous results for the acetophenones and are in good agreement with expectations based on simple steric considerations. Although the proposed semiquantitative approach to estimates of the angles of twist in these systems may be subject to some error due to presently unrecognized effects, there is no question that the variations of the chemical shifts are qualitatively reasonable and provide a potentially useful method for investigating related systems.

ACKNOWLEDGMENTS

We are grateful to the donors of the Petroleum Research Fund, administered by the American Chemical Society, for providing operating funds and to the Ontario Research Foundation for a major equipment grant.

REFERENCES

1. J. B. Stothers and P. C. Lauterbur. Can. J. Chem. **42**, 1563 (1964).
2. K. S. Dhami and J. B. Stothers. Tetrahedron Letters, No. 12, 631 (1964).
3. K. S. Dhami and J. B. Stothers. Can. J. Chem. This issue.
4. P. C. Lauterbur. J. Am. Chem. Soc. **83**, 1846 (1961).

Can. J. Chem. Downloaded from www.nrcresearchpress.com by 210.87.254.5 on 09/05/12
For personal use only.

5. G. D. HEDDON and W. G. BROWN. J. Am. Chem. Soc. **75**, 3733 (1953).
6. K. v. AUWERS, A. BOENNECKE, F. KROLLPFEIFFER, and G. PETERS. Ann. **408**, 212 (1915).
7. S. F. BIRCH, R. A. DEAN, F. A. FIDLER, and R. A. LOWRY. J. Am. Chem. Soc. **71**, 1362 (1949).
8. A. KLAGES. Ber. **35**, 2262 (1902).
9. F. BAUM and V. MEYER. Ber. **28**, 3212 (1895).
10. R. C. FUSON, E. M. BOTTORFF, and S. B. SPECK. J. Am. Chem. Soc. **64**, 1450 (1942).
11. J. B. SENDERENS. Compt. Rend. **152**, 90 (1911).
12. P. L. BAYLESS and C. R. HAUSER. J. Am. Chem. Soc. **76**, 2306 (1954).
13. E. ROTHSTEIN and R. W. SAVILLE. J. Chem. Soc. 1950 (1949).
14. M. RAMART-LUCAS and M. J. HOCH. Bull. Soc. Chim. France, 220 (1952).
15. D. V. NIGHTINGALE, R. L. SUBLETT, R. A. CARPENTER, and H. D. RADFORD. J. Org. Chem. **16**, 655 (1951).
16. H. A. NEIDIG, D. L. FUNCK, R. UHRICH, R. BAKER, and W. KREISER. J. Am. Chem. Soc. **72**, 4617 (1950).
17. H. SPIESECKE and W. G. SCHNEIDER. J. Chem. Phys. **35**, 731 (1961).
18. P. C. LAUTERBUR. J. Chem. Phys. **38**, 1406, 1415, 1432 (1963).
19. G. B. SAVITSKY. J. Phys. Chem. **67**, 2723 (1963).
20. P. C. LAUTERBUR. J. Chem. Soc. **83**, 1838 (1961).
21. K. S. DHAMI and J. B. STOTHERS. Unpublished observations.
22. R. A. FRIEDEL and H. L. RETCOFSKY. J. Am. Chem. Soc. **85**, 1300 (1963).
23. C. E. JOHNSON and F. A. BOVEY. J. Chem. Phys. **29**, 1012 (1958).
24. H. J. BERNSTEIN, W. G. SCHNEIDER, and J. A. POPLE. Proc. Roy. Soc. London, Ser. A, **236**, 515 (1956).
25. E. A. BRAUDE and F. SONDHEIMER. J. Chem. Soc. 3754 (1955).
26. B. M. WEPSTER. Steric effects on mesomerism. *In* Progress in stereochemistry. Vol. 2. W. Klyne and P. B. D. de la Mare (*Editors*). Butterworth and Co., London. 1958. Chap. 4.

Can. J. Chem. Downloaded from www.nrcresearchpress.com by 210.87.254.5 on 09/05/12
For personal use only.

Can. J. Chem. Downloaded from www.nrcresearchpress.com by 210.87.254.6 on 09/05/12
For personal use only.

^{13}C N.M.R. STUDIES

PART V.[1] CARBON-13 SPECTRA OF SOME SUBSTITUTED STYRENES[2]

K. S. DHAMI[3] AND J. B. STOTHERS
Department of Chemistry, University of Western Ontario, London, Ontario

Received September 30, 1964

ABSTRACT

The 15.1 Mc/s ^{13}C n.m.r. spectra of 23 substituted styrenes have been examined and the shieldings of the various carbon nuclei determined. Several meta- and para-substituted derivatives were included to study the effects of polar substituents on the vinyl carbon chemical shifts. In agreement with previous proposals, a linear correlation with the Hammett σ parameter is found for the β-carbon shieldings, but not for those of the α-carbons. Nine ortho-substituted examples and two α-substituted compounds were investigated to compare their chemical shifts with results for related carbonyl compounds. While the ^{13}C data exhibit marked differences in the hindered compounds, the variations differ from those observed in the more polar carbonyl systems.

INTRODUCTION

In previous papers of this series we have presented the results of an extensive survey of organic carbonyl compounds by carbon-13 nuclear magnetic resonance (n.m.r.) spectroscopy (1, 2, 3). These investigations have revealed a number of factors which contributed to the shieldings of carbon nuclei in groups bonded to aromatic rings. To gain a fuller understanding, and to test previous interpretations (1), of the effects of polar substituents on these chemical shifts, we have chosen to study a series of substituted styrenes which will allow an examination of two unsaturated centers in a group capable of conjugative interaction with the ring. Ten monosubstituted meta- and para-derivatives were included to compare variations of the vinyl carbon shieldings with the polar character of substituents covering the range p-NMe_2 to p-NO_2. Another facet of this investigation was the examination of the chemical shift parameters for nine compounds, bearing one or two ortho-groups, and two examples with α-substituents. The analyses of these spectra were performed by methods which have been described (2). More extensive use of spin-decoupling experiments, however, was required than in the previous work, particularly to establish the location of the vinyl carbon signals with certainty for several cases.

The results for the meta- and para-substituted styrenes show that the β-carbon shieldings are sensitive to the effects of polar substituents and a linear correlation of these values is obtained with the Hammett σ parameters. These shifts also correlate with the ^{19}F shieldings for similarly substituted fluorobenzenes (4), although different slopes are found for the meta- and para-cases. While the variation in the shieldings for the α-carbon nuclei are slightly larger than the experimental uncertainty, no similar correlations were found. The ortho-substituted examples extend our studies of hindered systems and the results are qualitatively comparable to those found for the carbonyl compounds. There are significant quantitative differences, however, and estimates of the extent of steric inhibition of conjugation for these styrenes are not possible by the methods previously proposed (2, 3, 5). An approximate correlation has been found for the chemical shifts of the β-carbon nucleus in the hindered compounds with the molar extinction coefficient of

[1]*Part IV. Reference 3.*
[2]*These results were reported in part at the 47th Annual Conference of the Chemical Institute of Canada, Kingston, June 1964.*
[3]*Petroleum Research Fund Predoctoral Fellow, 1962–1964.*

the electronic transition involving the conjugated chromophore (6, 7). In addition, these examples provide further tests of the applicability of the additive relation of substituent effects on aromatic carbon shieldings, originally noted by Lauterbur (8). Since the only previously reported study of unsaturated hydrocarbons did not include styrene (9), this paper represents the first investigation of aromatic olefins.

EXPERIMENTAL

Nuclear Magnetic Resonance Spectra

The ^{13}C spectra were obtained at 15.085 Mc/s using samples which contained carbon-13 in natural abundance. The detailed procedure employed in this study has been described (2).

Materials

Most of the substituted styrenes were obtained from commercial sources as listed in the following: Matheson, Coleman and Bell, styrene and α-methylstyrene; Aldrich Chemical Co. Inc., the 4-methyl-, 3-nitro-, 2,4-dimethyl-, 2,5-dimethyl-, 2,6-dimethyl-, 2,4,6-trimethyl-, and 2,3,5,6-tetramethyl-derivatives; Columbia Organic Chemicals, 2-bromo-, 3-bromo-, 4-bromo-, 2-chloro-, 3-chloro-, 4-chloro-, 2-methyl-, and 3-methyl-derivatives. A sample of 3,4-dichlorostyrene was kindly provided by Prof. K. Yates. The remaining examples included in this investigation, one of which is a new compound, were prepared by well-known methods. The physical constants (uncorrected) and the syntheses employed for these materials are outlined in Table I together with their reported physical data and the analytical results for 2,4,6-triisopropylstyrene. The microanalysis was performed by Alfred Bernhardt and Associates, Mulheim, Germany. Infrared and proton spectra were determined for each sample before its ^{13}C spectrum was obtained as a check of the purity. The ultraviolet spectra for a few examples were determined to measure their molar extinction coefficients. These were obtained with a Bausch and Lomb 505 spectrophotometer.

TABLE I

Physical properties of some substituted styrenes prepared for this study

		Physical constants				
		Observed		Reported		
Substituent	Method of preparation†	b.p./mm (m.p.)	n_D (t^0)	b.p./mm (m.p.)	n_D (t^0)	Ref.
4-$N(CH_3)_2$	A-1	45–50/0.05	1.6112 (20)	—	1.6110 (20)	10
4-CH_3O	B	57–58/0.9	1.5885 (24)	76–80/8	1.5586 (20)	11
4-NO_2	C	(~20)	—	(21.5)	—	10
2,4,6-(i-C_3H_7)$_3$*	A-2	85–86/0.4	1.5045 (25)			
α-C_2H_5	D	177–180/atm	1.5262 (22)	177–180/742	1.5262 (22)	12, 13

*Found: C, 88.35; H, 11.45. Calcd. for $C_{17}H_{26}$: C, 88.62; H, 11.30.

†Methods used: A-1, Grignard reaction of MeMgI + ArCHO, spontaneous dehydration of carbinol (10). A-2, Grignard reaction of MeMgI + ArCHO, followed by dehydration on $KHSO_4$ (14). B, dehydration of carbinol on $KHSO_4$ (14). C, from ϕCH_2CH_2Br, following the method of Strassbourg, Gregg, and Walling (10). D, from $CH_3CH_2CH(\phi)COOH$ by reduction followed by dehydration over KOH (12, 13).

RESULTS AND DISCUSSION

The observed chemical shifts for the carbon nuclei in the meta- and para-substituted styrenes are listed in Table II, while the data for the ortho-derivatives appear in Table III. For purposes of the discussion, these will be considered separately. For clarity, the various types of nuclei will be discussed under individual subheadings in the following. Finally, the evidences provided by the spectra of the ortho- and α-substituted cases for the existence of steric inhibition of conjugation of the vinyl group in the hindered systems are considered.

Meta- and Para-Substituted Styrenes

Aromatic Carbons

The assignments of chemical shifts for the aromatic nuclei in styrene shown in Table II have been made by analogy with the results for other aromatic hydrocarbons (2, 15, 16).

Can. J. Chem. Downloaded from www.nrcresearchpress.com by 210.87.254.6 on 09/05/12
For personal use only.

TABLE II

^{13}C chemical shifts of some meta- and para-substituted styrenes (in p.p.m. from CS_2)

	Vinyl carbons		Aromatic carbons				
Substituent	α-C	β-C	C-1	C-2,6	C-3,5	C-4	Others
H	57.0	80.5	56.4	56.4	65.8	67.5	—
4-CH_3	56.2	79.7	56.0	64.8	64.8	56.0	172.4
4-CH_3O	57.2	82.3	62.4	66.0	79.2	33.8	138.7
4-$N(CH_3)_2$	56.4	85.0	68.2	66.8	81.0	43.4	153.4
4-Cl	57.0	78.9	56.2	64.7	64.7	59.3	—
4-Br	57.5	78.6	56.3	65.4	61.7	70.6	—
3,4-Cl_2*	61.1	78.0	55.9	—‡	—‡	—‡	
4-NO_2†	57.8	74.7	48.9	66.5	69.4	46.0	—
3-CH_3	56.4	81.1	56.3	65.3 (C-2)	56.3 (C-3)	65.3	172.5
				70.0 (C-6)	65.3 (C-5)		
3-Cl	59.1	78.7	55.0	66.9 (C-2)	59.1 (C-3)	66.9	—
				69.1 (C-6)	64.5 (C-5)		
3-Br	60.6	78.3	54.5	63.6 (C-2)	69.1 (C-3)		
				68.4 (C-6)	63.6 (C-5)	63.6	—
3-NO_2	58.8	77.1	56.1	71.9 (C-2)	45.3 (C-3)		
				58.8 (C-6)	64.1 (C-5)	71.9	—

*In CS_2 solution (saturated).
†In 1,4-dioxane solution.
‡Reliable data could not be obtained due to the low concentration attainable.

TABLE III

^{13}C chemical shifts of some ortho-substituted styrenes (in p.p.m. from CS_2)

	Vinyl group		Aromatic nuclei						Other
Substituent(s)	α-C	β-C	C-1	C-2	C-3	C-4	C-5	C-6	nuclei
H	57.0	80.5	56.4	65.8	65.8	67.5	65.8	65.8	—
2-Cl	58.2	77.7	58.6	61.2	64.2	66.0	66.0	64.2	—
2-Br	56.2	76.5	56.2	70.1	60.8	65.0	65.0	65.0	—
2-CH_3	57.3	79.1	59.1	58.2	65.1	67.5	67.5	65.1	174.0
2,4-$(CH_3)_2$	58.1	80.4	58.7	58.7	62.7	58.7	67.5	62.7	172.9
2,5-$(CH_3)_2$	58.8	80.0	58.7	58.7	64.2	66.4	58.7	64.2	173.5
2,6-$(CH_3)_2$	58.3	74.3	56.8	58.5	65.4	65.4	65.4	58.5	172.4
2,4,6-$(CH_3)_3$	58.0	74.7	58.5	58.5	64.0	58.5	64.0	58.5	172.5
2,3,5,6-$(CH_3)_4$	58.6	74.2	55.6	61.0	61.0	62.8	61.0	61.0	173.1
									177.3
2,4,6-$(i\text{-}C_3H_7)_3$	58.0	74.6	59.6	47.6	73.3	47.6	73.3	47.6	163.3
									169.5
									167.4
α-CH_3	50.6	81.3	52.1	65.8	65.8	67.8	65.8	65.8	
α-C_2H_5	43.7	82.8	52.0	66.1	66.0	67.1	66.0	66.0	

While the assignment for C-1 is unambiguous, the others are not unequivocal although support for the present assignment is provided by the results for the meta-substituted cases. The values for styrene indicate that the substituent effect of the vinyl group on the aromatic shieldings is very similar to that of the methyl group. At the para-position, an up-field shift of 2.5 p.p.m. relative to benzene is observed, whereas the C-1 nucleus is deshielded by 8.6 p.p.m. The comparable figures for the methyl group are +2.8 and −9.1 p.p.m., respectively, (16). Directionally the effects at the ortho- and meta-positions are opposite for these two groups but the changes are less than 1 p.p.m. and, therefore, within experimental uncertainty. According to previous results (16, 17), the observed shielding for the para-carbon indicates an increased π-electron density at this position which is due, presumably, to electron release by the vinyl group to the ring.

An examination of the aromatic shieldings for the meta-derivatives given in Table II

Can. J. Chem. Downloaded from www.nrcresearchpress.com by 210.87.254.6 on 09/05/12
For personal use only.

shows that bands are observed whose positions are in good agreement with calculated values assuming additivity of substituent effects at these nuclei. The latter values may be calculated from the substituent effects found for monosubstituted cases (16) and the present styrene data. In general, the differences are less than 1.5 p.p.m. with two exceptions, the C-4 and C-3 nuclei in the 3-methyl and 3-bromo derivatives, respectively. The present assignments are based on the assumption that additivity of substituent effects holds. For the para-derivatives, the situation is significantly different. In general, the observed transitions appear at positions which are up to 3.5 p.p.m. from those calculated. To compare the results for the meta- and para-substituted systems, the deviations between the observed and calculated chemical shifts are shown in Fig. 1 for the methyl, bromo, and nitro groups. The assignments indicated in Table II for the aromatic nuclei have been made by assuming a minimum difference between the calculated and observed values, since no other approach is available without resorting to the use of labelled compounds. It is possible, of course, that the deviations are even larger than these but evidence is lacking.

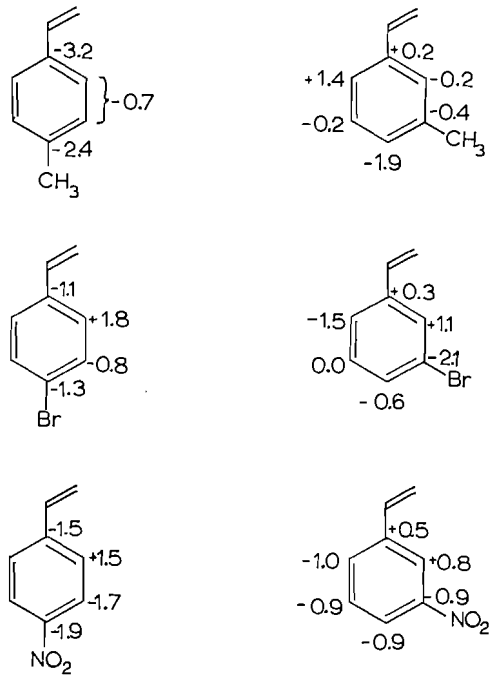

FIG. 1. Differences between the observed and calculated chemical shifts for the aromatic carbon nuclei of some meta- and para-substituted styrenes.

The fact that much better agreement is found for the meta-substituted compounds seems entirely reasonable, since conjugative interactions between the vinyl group and a meta-substituent will be minimal. In cases with significant resonance interaction between two groups on an aromatic ring, it would not be surprising to find greater deviations for the aromatic shieldings, since one or both of the substituent effects could be altered by conjugation. This situation has been discussed in general (18). In the present system, the vinyl group is capable of either electron release to, or withdrawal from, the ring depending on the influence of other polar substituents in conjugation with it. Consequently, the

Can. J. Chem. Downloaded from www.nrcresearchpress.com by 210.87.254.6 on 09/05/12
For personal use only.

substituent effects of the vinyl group at the aromatic carbon nuclei would be expected to depend strongly on the demands of para-substituents. In styrene itself, it appears that the vinyl group releases electrons to the ring, but this tendency may be reversed if an electron-releasing group is at the para-position such that the vinyl group tends to gain electrons from the ring. Support for this argument is provided by the chemical shift results for the β-carbon of the vinyl group discussed below. Since the electronic characteristics of the vinyl substituent are subject to these two extremes, it is hardly surprising that the observed values for the aromatic carbons in the para-substituted examples differ from those calculated by substantially greater amounts than the corresponding figures for the meta-systems. For each example having a para-substituent capable of electron release by resonance, the deviations at the C-4 nucleus are large, ranging up to 3.5 p.p.m. for the para-methoxyl case, and all are negative (i.e. the observed shift is at *lower* field than that calculated). This observation is consistent with the reversal of the polar tendencies of the vinyl group in these compounds relative to styrene and reflects a reduced π-electron density at this position.

Vinyl Carbons

The first investigation of ^{13}C spectra of olefins, reported by Holm (19), established that olefinic carbons absorb in the same general region as aromatic carbon nuclei. A recent detailed study of ^{13}C olefinic n.m.r. absorption (9) in aliphatic compounds has clearly defined the effects of alkyl substitution on these shieldings. Since the conjugated systems examined in the aliphatic series showed no marked differences from the corresponding non-conjugated cases, these results suggest the most probable regions of absorption for the vinyl carbons in styrene. Without exception, the bands overlap with the aromatic signals but the patterns due to spin coupling provide an essential clue for the detection of the β-carbon absorption since it is a triplet with a coupling constant in the range 161 ± 4 c/s. The α-carbon band is a doublet with a similar spacing. In most instances, the triplet is readily distinguished since it appears in the higher field portion of this spectral region and overlap with other bands was found to be less serious. The α-carbon resonances, however, present a problem in several instances, due to their appearance in a more congested region of the spectrum and the presence of other doublets with comparable coupling constants. Spin-decoupling experiments proved to be extremely valuable in aiding identifications and allowing more precise measurements of these bands. Owing to the above complications, it is necessary to note that the assignments given in Table II appear to be the most reasonable and internally consistent, but they are not unequivocal for all cases, and, lacking measurements of labelled materials, it is conceivable that a few of these figures may be interchanged with certain of the aromatic shifts, the rationale for which was discussed in the previous section. To illustrate the type of spectrum which is obtained for these compounds, that of 4-methoxystyrene is illustrated in Fig. 2 and the assignments are indicated. This case was chosen to show an example in which the β-carbon signals are not well separated and to illustrate the effect of double irradiation at the proton resonance frequency for the aromatic region (Fig. 3). The origins of the singlets in the decoupled spectrum are indicated since the two traces were obtained at slightly different sweep rates. The effect of sweep direction on the shapes of multiplets is apparent in Fig. 2 and the signal enhancement due to a nuclear Overhauser effect (20) may be seen in Fig. 3 by comparison of the intensities of the absorption due to the C-4 and α-C nuclei, for example. Both of these effects prove to be useful as aids for the analyses of these spectra.

The chemical shift values for the vinyl carbons in styrene have been found to be 57.0

Can. J. Chem. Downloaded from www.nrcresearchpress.com by 210.87.254.6 on 09/05/12
For personal use only.

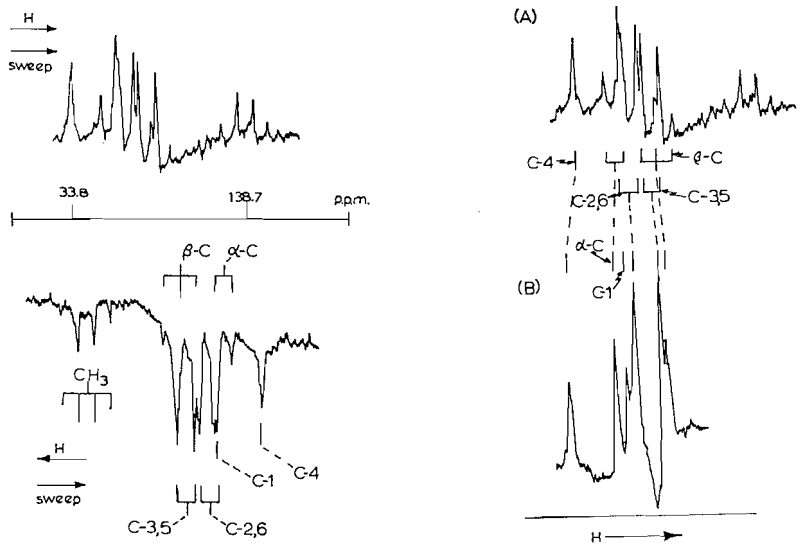

FIG. 2. 15.085 Mc/s ^{13}C spectra of para-methoxystyrene.
FIG. 3. (A) Normal 15.085 Mc/s ^{13}C spectrum of para-methoxystyrene; (B) decoupled ^{13}C spectrum of aromatic region obtained by simultaneous irradiation at the resonance frequencies of the various protons (near 60 Mc/s).

(α-C) and 80.5 (β-C) p.p.m., which may be compared to shifts of 55.2 and 79.3 p.p.m. for the C-2 and C-1 nuclei, respectively, of 1-pentene and 55.6 and 76.2 p.p.m. for C-2 and C-1 in 1,3-butadiene (9). Clearly, the aliphatic shifts are comparable with those for the aromatic system although the latter appear at slightly higher field. Any contribution from a ring-current effect in styrene, an effect which is absent in the other systems, would tend to decrease the vinyl shieldings; thus these data provide another piece of evidence indicating that ring-current effects in carbon spectra are of secondary importance.

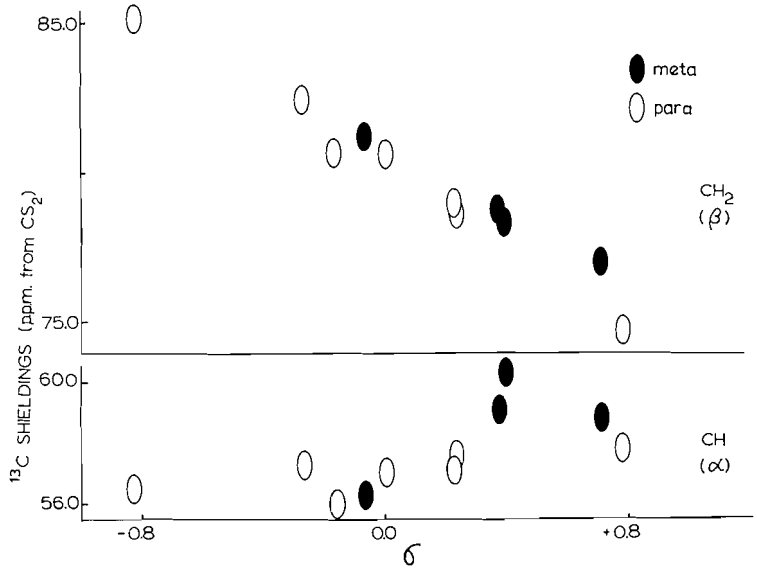

FIG. 4. Plot of vinyl ^{13}C shieldings of meta- and para-substituted styrenes vs. Hammett σ parameters.

Can. J. Chem. Downloaded from www.nrcresearchpress.com by 210.87.254.6 on 09/05/12
For personal use only.

Can. J. Chem. Downloaded from www.nrcresearchpress.com by 210.87.254.6 on 09/05/12
For personal use only.

An inspection of the β-carbon shieldings for the meta- and para-substituted compounds reveals that these nuclei absorb over a total range of 10.3 p.p.m. and that the shifts appear to be dependent on the polar characteristics of the substituent groups. A reasonably linear correlation of the β-carbon chemical shifts with the Hammett σ parameters is obtained as illustrated in Fig. 4. The variation of the α-carbon shifts with the same parameters is included to show the marked difference for this nucleus. The scatter of the α-carbon shielding values is significantly larger than the experimental error of the measurements but there is no apparent trend with polarity of substituent. In fact, the total variation for the para-derivatives is just greater than the experimental uncertainty while the meta-substituted examples exhibit somewhat larger differences. Perhaps this indicates the presence of a field effect operative at the α-carbon due to groupings at the meta-position. The uniform change in the β-carbon shifts, however, fits well with our previous interpretation of the observed absence of substituent effects on carbonyl carbon shifts in acetophenones (1, 2). The explanation of the latter result was based on a consideration of the contributions to the ground state of conjugated molecules by various resonance forms. As an example, consider a conjugated molecule (I) bearing an electron-releasing group in the para-position. Resonance form II (as well as others) will contribute to the

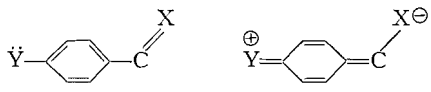

I II

electronic distribution in the ground state. Analogous structures with reversed charges may be written for examples bearing electron-withdrawing substituents. The polarized form (II) illustrates an important difference between the α- and β-nuclei of the sidechain (i.e. C and X, respectively) in that the latter nucleus is at a terminus of the resonance system while the α-carbon is not. It appears reasonable to suggest, therefore, that the electron density changes will be most pronounced at the β-position and minimal at the α-nucleus. Our present investigation was prompted by this proposal which was used to explain the carbonyl shieldings of acetophenones, since the styrene series provides a close analogy to the carbonyl systems and permits ^{13}C studies of the β-nucleus. ^{19}F spectral studies (4, 21) on an extensive series of substituted fluorobenzenes has established the marked dependence of ^{19}F shieldings on substituent polarities. It is interesting to compare the β-carbon chemical shift values with the ^{19}F results for the corresponding fluorobenzene derivatives as illustrated in Fig. 5. The meta and para cases appear to follow different correlations. Taft (4) has shown that ^{19}F data for the two types of substituted systems require different correlation equations using the separated parameters σ_I and σ_R, and therefore, the present result is not unexpected, although difficult to explain. One surprising feature is the excellent plot obtained for the para-substituted derivatives except for the result for styrene itself. The range of values which the meta-series includes is small. The available evidence, however, indicates that the β-carbon shieldings are approximately one-third as sensitive to substituent polarity as the ^{19}F nuclei in the para-derivatives, but in the meta-compounds the β-carbon and ^{19}F nuclei respond similarly.

Other Carbons

The observed chemical shifts for the methyl carbon nuclei in the various substituents agree well with those reported previously by Lauterbur for the corresponding mono-substituted benzenes: toluene, 171.8 (15), anisole, 138.4 (4), and N,N-dimethylaniline, 152.6 p.p.m. (22). It is evident that the vinyl group exerts no significant effect on these

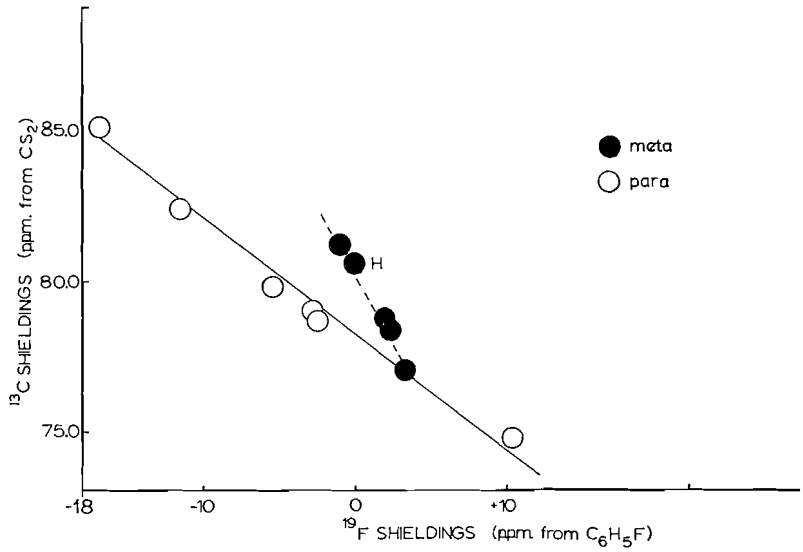

FIG. 5. Plot of β-carbon shieldings for meta- and para-substituted styrenes vs. ^{19}F shieldings of similarly substituted fluorobenzenes.

nuclei for the meta- and para-derivatives. The observed coupling constants are also similar to the earlier results (4, 15, 22).

Ortho-Substituted Styrenes

Aromatic Carbons

We have assigned the chemical shifts for the aromatic carbons as listed in Table III by again assuming an additive relation for substituent effects. Since the deviations are greater for ortho-substituted compounds in general (2, 3, 8, 15, 22, 23), there is more uncertainty in all of these cases. Qualitatively, two features are consistent with previous results for the carbonyl systems. Ortho-substitution tends to reduce the deshielding effect of the vinyl group at C-1. To show this for each example it is necessary to allow for the effects of the other substituents but, having done this, it can be seen that for most cases the observed shift is at higher field than that calculated. While the opposite effect is not found consistently for the C-4 nucleus, its absence is not particularly surprising in view of the relatively small change at this position in styrene itself relative to benzene. The second point concerns the aromatic shieldings in vinyldurene for which the "normal" deshielding effect of methyl at the substituted aromatic nuclei is absent. It is curious that the shielding at the C-1 nucleus, however, is very close to that expected if the substituent effects were additive. As in our other recent investigations, present knowledge does not permit an adequate explanation of these aromatic shieldings to be offered.

Vinyl Carbons

From the data for the first four entries in Table III, it can be seen that the α-carbon chemical shifts for the ortho-substituted styrenes show small variations with the nature of the ortho-group relative to the value for styrene itself, but no pronounced changes are found. These results are similar to those for the meta- and para-derivatives. The α-carbon shieldings for the compounds bearing two or more alkyl substituents are the same within experimental error and indicate that these nuclei are slightly shielded by the ortho-alkyl

Can. J. Chem. Downloaded from www.nrcresearchpress.com by 210.87.254.6 on 09/05/12
For personal use only.

carbons, although to a lesser extent than carbonyl or methyl carbons in corresponding environments (2, 15). The situation at the β-carbon in these compounds is distinctly different, since the signals due to these nuclei appear at lower fields than those for the β-carbon in styrene. For the 2-chloro-, 2-bromo-, and 2-methyl-derivatives the observed shieldings are reduced by 0.5–2 p.p.m. relative to the corresponding 3- and 4-substituted examples. In the diortho-substituted systems, a further reduction of ca. 5 p.p.m. is apparent. This trend is consistent with the presence of steric interference to coplanarity of the vinyl group in this series. In the alkylated cases, for example, the aromatic ring is electron-rich relative to styrene due to electron release by the alkyl substituents and, in the absence of steric inhibition of conjugation, the vinyl group would be expected to act as an electron-withdrawing substituent from the results discussed above for the meta- and para-derivatives. In this event, the β-carbon nucleus should exhibit an increased shielding with the signal shifted to higher field. In fact, the observed effect is the reverse and, therefore, would appear to indicate that there is steric inhibition of resonance in these systems. It is unfortunate that ^{13}C data are not available for lower molecular weight olefins with which the values for the hindered styrenes might be compared.

A closer examination of the trends exhibited by the β-carbon shifts of the methylated derivatives shows the following pattern. The β-carbon nucleus in 2-methylstyrene appears at 79.1 p.p.m., which is 1.4 p.p.m. to lower field from its position in styrene. The introduction of the 4-methyl group tends to increase its shielding by 1.3 p.p.m. suggesting that this substituent increases the conjugative interaction of the ring with the vinyl group, an effect that was found for the carbonyl carbon resonances in similarly substituted aromatic ketones. A second ortho-methyl group (e.g. 2,6-dimethylstyrene) shifts the β-carbon signal to 74.3 p.p.m. Further methyl substitution on the ring does not affect the observed shift, nor does this shielding differ for the 2,4,6-triisopropyl derivative. These variations of the β-carbon shieldings are similar to those observed for the carbonyl carbon in the corresponding acetophenones with two important differences. These two nuclei are in different positions relative to the aromatic ring and the carbonyl carbon in the poly-substituted cases is affected by increased substitution. The α-carbon shielding which might be expected to undergo changes similar to those exhibited by the carbonyl carbon nucleus remains essentially constant for this series. In the case of the ketones, however, the α-nucleus (carbonyl carbon) is doubly bonded to an electronegative element, oxygen, whose polarizing effect on the C=O bond will be more pronounced at the α-position for the hindered ketones since the electron supply from the ring is reduced by steric inhibition of conjugation. In the styrene system, both nuclei of the vinyl carbon have comparable electronegativities and no strong polarization of the C=C bond would result from a reduced conjugative interaction with the ring, instead, the shielding at the β-carbon would be decreased relative to the unhindered systems since the conjugative electron release by the ring to the vinyl group is less efficient. We suggest, therefore, that the nature of the double bond in conjugation with the aromatic system is the major controlling factor for determining the shieldings at these side-chain nuclei in the hindered systems and is responsible for the observed differences between the carbonyl and olefinic systems.

Correlations of the shieldings of the β-carbon vinylic grouping with other physical properties would be expected if the above interpretations are valid. In particular, the intensities of the electronic transitions for the fully conjugated chromophores are believed to reflect the extent of steric inhibition of resonance in hindered systems such as these (6, 7, 24). While only limited data are available, an approximate correlation between these two parameters is found as illustrated in Table IV. There is a marked decrease in the

Can. J. Chem. Downloaded from www.nrcresearchpress.com by 210.87.254.6 on 09/05/12
For personal use only.

TABLE IV

Comparison of β-^{13}C shielding and ultraviolet data for some substituted styrenes

Substitution	$\delta_c^{\beta-C}$ (p.p.m.)	ϵ_{max}	Estimated angle of twist* (°)	
Nil	80.6	15 600	0	0
2-CH_3	79.1	12 000	28	31
2,6-$(CH_3)_2$	74.3	5 400	—	54
2,4,6-$(CH_3)_3$	74.7	7 000	54	49
2,3,5,6-$(CH_3)_4$	74.2	4 000	—	—
2,4,6-(*i*-Pr)$_3$	74.6	5 800	—	—

*First column from ref. 6, second column, ref. 24.

extinction coefficients with increased ortho-substitution which roughly parallels the change in β-carbon chemical shifts, although the ϵ_{max} values vary somewhat for the various diortho-substituted derivatives. All of the latter variation may not be real due to the difficulty in locating and measuring the appropriate ultraviolet band precisely. A few of the intensity figures were not available in the literature and were determined for this comparison. The ultraviolet spectral data have been utilized by others to calculate the angles of twist for sterically hindered systems (6, 24) and these estimates are included in Table IV. Lacking the figures for suitable model compounds, we hesitate to perform a similar analysis of the ^{13}C data. Qualitatively, however, the observed ^{13}C shifts provide strong evidence of steric inhibition of conjugation of the vinyl group.

Other Carbons

The chemical shifts for the carbon nuclei of the substituent groups are found to correspond well with those observed for the corresponding substituted acetophenones (2). The carbons bonded directly to the ring and ortho to the vinyl group tend to absorb at slightly higher field than those in less hindered positions. The most striking example of this feature is provided by vinyldurene for which two methyl groups appear at 177.3 p.p.m. and these signals have been assigned to the 2- and 6-groups, for reasons discussed previously (2).

α-Substituted Styrenes

Aromatic Carbons

The effects of the isopropenyl and 2-butenyl groups on the aromatic shieldings are found to be closely similar to those exhibited by the vinyl group (last two entries in Table III). The major difference is a greater decrease in shielding at the substituted carbon (C-1) which is found to be 13 p.p.m. for these two groups compared to the −8.6 p.p.m. decrease caused by the vinyl substituent. Apart from this change, the effects at the other aromatic nuclei are the same within experimental error.

Vinyl Carbons

The shielding effects at the olefinic carbon nuclei by methyl substitution on double bonds have been established by Friedel and Retcofsky (9) for aliphatic systems. In general, the changes are opposite at the two centers with the signal for the substituted nucleus moving to lower field and the β-carbon absorption to higher. Qualitatively, the vinyl carbon shifts for 2-methylstyrene undergo similar changes. The closest model system included in the aliphatic series, is that of 1,3-butadiene and 2,3-dimethyl-1,3-butadiene for which the shift of the internal olefinic carbon (C-2 and C-3) change by −5.2 p.p.m. and the terminal nuclei (C-1 and C-4) are shielded by +5.0 p.p.m. by methyl substitution

Can. J. Chem. Downloaded from www.nrcresearchpress.com by 210.87.254.6 on 09/05/12
For personal use only.

(9). For α-methylstyrene relative to styrene, the corresponding changes are −6.4 and +0.8 p.p.m. Introduction of the ethyl group instead of methyl was found to cause changes of -6.5 ± 1.3 and $+1.1 \pm 1.1$ p.p.m. for the substituted and β-carbon nuclei, respectively, relative to the shifts in the methyl derivative, in some aliphatic olefinic systems (9). Although none of these are closely related to the present cases, the observed changes for α-ethylstyrene are remarkably close to these values, −6.9 and +1.5 p.p.m., respectively. The two α-substituted styrenes, therefore, are additional examples showing the same general variations as aliphatic olefins.

The most interesting feature of these observations is the very much reduced shielding at the β-carbon caused by α-methyl substitution. A possible explanation of this could invoke steric inhibition of conjugation such that there is a reduced effect of the aromatic ring at this center. Suzuki has concluded this to be the case from the ultraviolet spectra and has estimated the angle of twist to be 33°(24). Our study of the ^{13}C results for this system, however, is not nearly extensive enough to corroborate or refute his conclusion.

ACKNOWLEDGMENTS

We thank the donors of the Petroleum Research Fund, administered by the American Chemical Society, for generous support of this investigation through the provision of operating funds and the Ontario Research Foundation for a grant to purchase the 15.1 Mc/s oscillator unit.

REFERENCES

1. J. B. Stothers and P. C. Lauterbur. Can. J. Chem. **42**, 1563 (1964).
2. K. S. Dhami and J. B. Stothers. Can. J. Chem. This issue.
3. K. S. Dhami and J. B. Stothers. Can. J. Chem. This issue.
4. R. W. Taft, S. Ehrenson, I. C. Lewis, and R. E. Glick. J. Am. Chem. Soc. **81**, 5353 (1959).
5. K. S. Dhami and J. B. Stothers. Tetrahedron Letters, No. 12, 631 (1964).
6. E. A. Braude and F. Sondheimer. J. Chem. Soc. 3773 (1955).
7. J. C. D. Brand and A. I. Scott. Applications of ultraviolet spectroscopy. *In* Elucidation of structures by physical and chemical methods. Pt. 1, Vol. XI, Technique of organic chemistry. *Edited by* A. Weissberger. Interscience, New York. 1963. pp. 61–131.
8. P. C. Lauterbur. J. Am. Chem. Soc. **83**, 1846 (1961).
9. R. A. Friedel and H. L. Retcofsky. J. Am. Chem. Soc. **85**, 1300 (1963).
10. R. W. Strassbourg, R. A. Gregg, and C. Walling. J. Am. Chem. Soc. **69**, 2141 (1947).
11. W. J. Dale and H. E. Hennis. J. Am. Chem. Soc. **81**, 2143 (1959).
12. C. G. Overberger and D. Tanner. J. Am. Chem. Soc. **77**, 369 (1955).
13. S. Sabety. Bull. Soc. Chim. France, [4] **47**, 614 (1930).
14. L. A. Brooks. J. Am. Chem. Soc. **66**, 1295 (1944).
15. P. C. Lauterbur. J. Am. Chem. Soc. **83**, 1838 (1961).
16. H. Spiesecke and W. G. Schneider. J. Chem. Phys. **35**, 731 (1961).
17. P. C. Lauterbur. Tetrahedron Letters, No. 8, 274 (1961).
18. G. B. Savitsky. J. Phys. Chem. **67**, 2723 (1963).
19. C. H. Holm. J. Chem. Phys. **26**, 707 (1957).
20. J. D. Baldeschwieler and E. W. Randall. Chem. Rev. **63**, 81 (1963).
21. H. S. Gutowsky, D. A. McCall, B. R. McGarvey, and L. H. Meyer. J. Am. Chem. Soc. **74**, 4805 (1952).
22. P. C. Lauterbur. J. Chem. Phys. **38**, 1415 (1963).
23. P. C. Lauterbur. J. Chem. Phys. **38**, 1406 1432 (1963).
24. H. Suzuki. Bull. Chem. Soc. Japan, **33**, 619 (1960).

Can. J. Chem. Downloaded from www.nrcresearchpress.com by 210.87.254.6 on 09/05/12
For personal use only.

Can. J. Chem. Downloaded from www.nrcresearchpress.com by 210.87.254.5 on 09/05/12
For personal use only.

ESSENTIAL OILS AND THEIR CONSTITUENTS

XXVII.[1] COMPOSITION OF OIL OF GINGERGRASS

M. C. NIGAM,[2] ISHWAR C. NIGAM, AND LEO LEVI
Pharmaceutical Chemistry Division, Food and Drug Directorate, Ottawa, Canada

Received September 2, 1964

ABSTRACT

Oil of gingergrass was found to contain the following as yet unreported constituents: *trans-p*-menthene-8-diol-1,2; *cis*- and *trans*-carveol; *cis*- and *trans*-dihydrocarvone; piperitenone and limonene oxide. The presence of an aromatic compound for which gas chromatographic and infrared criteria of identity were determined was also demonstrated. Limonene oxide is probably the most important precursor of these and related monoterpenoids of the essential oil.

INTRODUCTION

Oil of gingergrass (*Cymbopogon martini* Stapf var. *sofia*) has been the subject of a number of chemical investigations (1, 2, 3). These established the presence of the following constituents: limonene, dipentene, α-phellandrene, perillyl alcohol, carvone, and geraniol. Recently Naves and Grampoloff, studying a genuine sample of Indian origin, established the occurrence of four alcohols: *cis*- and *trans-p*-menthadiene-2,8-ol-1, *cis-p*-menthadiene-1(7),8-ol-2, and isopiperitenol. They did not detect the presence of geraniol (4, 5). Swaleh, Bhushan, and Sidhu confirmed subsequently the occurrence of several compounds already reported (6). The present investigation was undertaken to identify hitherto unknown constituents, establish the presence or absence of geraniol and reflect on the biogenesis of some of the components of the essential oil.

EXPERIMENTAL

Column Chromatography of the Essential Oil

An authentic sample (2 g) was chromatographed over alumina (Woelm Grade I; 40 g) using as eluants petroleum ether (b.p. 40–60 °C), benzene, ether, and methanol. Effluents (50 ml) were collected and elutions continued until evaporation of fractions left no residue. Following removal of solvent each fraction was examined by gas chromatography. Recoveries are shown in Table I.

TABLE I

Column chromatography of oil of gingergrass

Fraction No.	Eluant	Volume of eluant (ml)	Weight of fraction (%)
A	Hexane	200	13.5
B	Benzene	200	3.0
C	Ether	50	37.5
D	Ether	150	42.0
	Methanol	100	
		(Recovery	96.0%)

Rechromatography of Fraction D

Fraction D (0.84 g) was chromatographed over neutral grade II alumina (40 g). Ether was used as eluant and subfractions were recovered by evaporating 10 ml portions of effluents collected. Product yields are shown in Table II.

[1]*Paper XXVI: J. Org. Chem. (In press.)*
[2]*National Research Council of Canada Postdoctorate Fellow, 1964.*

TABLE II

Rechromatography of fraction D

Fraction No.	Weight of fraction (g)	Essential oil (%)
D-1	0.19	9.5
D-2	0.22	11.0
D-3	0.18	9.0
D-4	0.13	6.5
D-5	0.08	4.0
D-6	0.02	2.0

Gas Chromatography of Essential Oil and Isolated Fractions

Apparatus and general procedures have been described (7). Reoplex 400 (20%) deposited on Chromosorb W (acid washed; 60–80 mesh size) was used as column packing. Analyses were carried out at the following column temperatures: fraction A: 110 °C; fractions B, C, and D-1 to D-4: 170 °C; fractions D-5, D-6, and the essential oil: 200 °C.

Identification and Determination of Constituents

Constituents were identified by the serial dilution technique and comparison of infrared spectra of effluents (deposited directly on a salt plate (8) or collected in carbon tetrachloride and purified by rechromatography) with those of pure reference standards or published data. Quantitative estimations were carried out by the sigma method (9, 10).

Isomerization of Limonene Oxide to Terpenoids Present in Oil of Gingergrass

Limonene oxide (180 mg) and pyridinium bromide were refluxed for 1 h with 3 ml of pyridine. The reaction mixture was cooled, diluted with excess of ether, and filtered. Following evaporation of the filtrate 125 mg of material was recovered and analyzed by gas chromatography. Effluents corresponding to main peaks and shoulders were collected in carbon tetrachloride following repeated sample injections, the fractions repurified by chromatography, and constituents identified on the basis of gas chromatographic and infrared spectral data.

RESULTS AND DISCUSSION

The gas chromatogram of the essential oil is reproduced in Fig. 1A. It is more complex than one would expect on the basis of existing compositional data. The presence of compounds already reported was confirmed and some constituents giving rise to distinct peaks and shoulders were identified for the first time.

Constituents

Limonene.—This terpene was identified as the only constituent of fraction A.

cis- and trans-Dihydrocarvone, carvone, and piperitenone.—These ketones were found to be present in fraction B.

Isopiperitenol and cis-p-Menthadiene-1(7),8-ol-2.—These two alcohols made up fraction C. They were also present in sub-fractions D-1 to D-4. Small quantities of isopiperitenol were also found to occur in fraction B.

trans-p-Menthadiene-2,8-ol-1, cis- and trans-carveol, and perillyl alcohol.—These compounds were present in varying proportions in sub-fractions D-1 to D-4.

trans-p-Menthene-8-diol-1,2.—This glycol formed the chief constituent of sub-fraction D-5 and was also present in sub-fraction D-6.

Aromatic compound.—Sub-fraction D-6 contained, in addition to the glycol, an aromatic compound, displaying characteristic infrared absorptions at 3 420, 1 680, 1 615, 1 508, 1 095, 968, 930, 910, and 895 cm^{-1}.

Limonene oxide.—A small peak (relative retention time 0.72; reference, isopiperitenol) (see Fig. 1A) was identified as limonene oxide by the serial dilution technique. The terpenoid (2.1% of the oil) could, however, not be recovered in any chromatographic fraction which observation suggested its decomposition during column chromatography on active alumina.

Can. J. Chem. Downloaded from www.nrcresearchpress.com by 210.87.254.5 on 09/05/12
For personal use only.

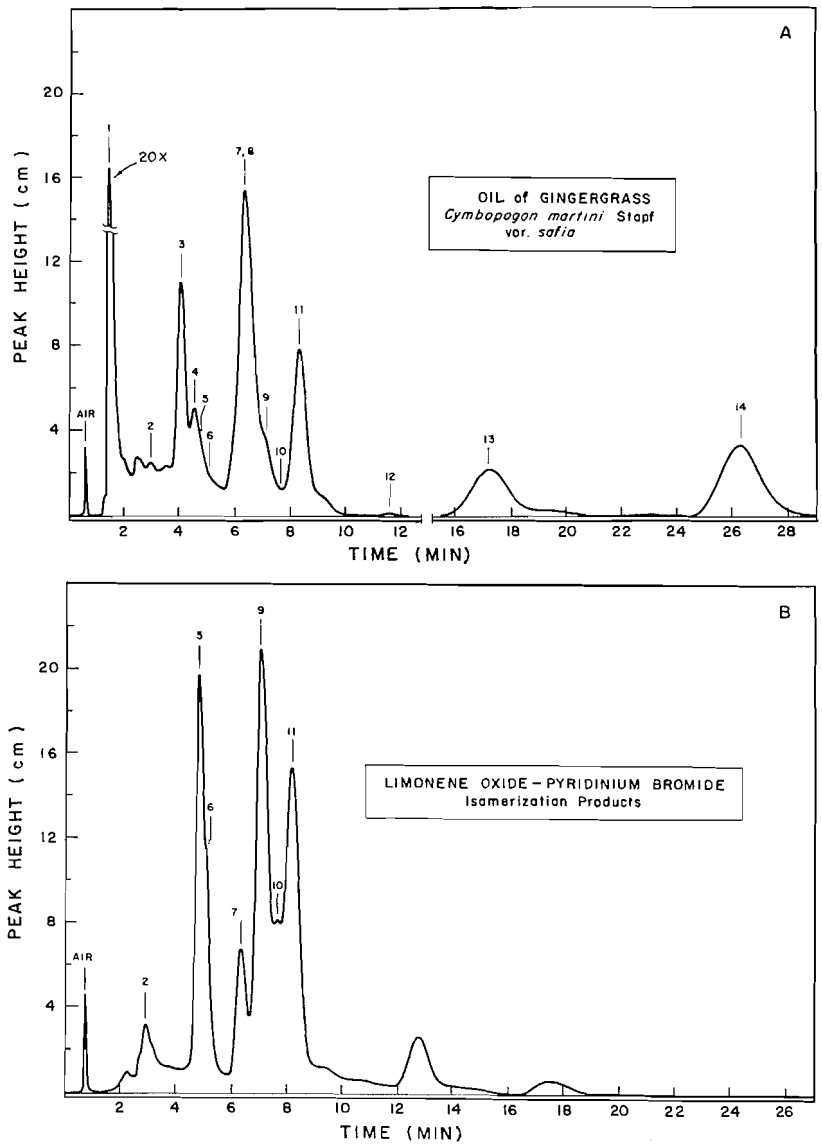

FIG. 1. Gas chromatograms: A, oil of gingergrass; B, limonene oxide–pyridinium bromide isomerization products. Column temperature, 200 °C; helium, 75 ml/min.

Geraniol.—The presence of geraniol in oil of gingergrass reported by earlier workers was questioned by Naves and Grampoloff (4, 5), who showed that the alcohol does not occur in the essential oil at concentration greater than 0.25%. Using preparative gas and thin layer chromatography, the present authors failed to detect even minute traces ($< 0.001\%$) of the alcohol in the essential oil. Evidently, genuine gingergrass oil does not contain geraniol. Quite likely the occurrence of small amounts of the alcohol in the essential oil is due to contamination with trace amounts of palmarosa oil which admixture may occur if plants are not raised or harvested under expert supervision (11).

Can. J. Chem. Downloaded from www.nrcresearchpress.com by 210.87.254.5 on 09/05/12
For personal use only.

Composition of Essential Oil

Quantitative results were obtained by correlation of gas chromatographic data assembled for the various fractions isolated. They are shown in Table III.

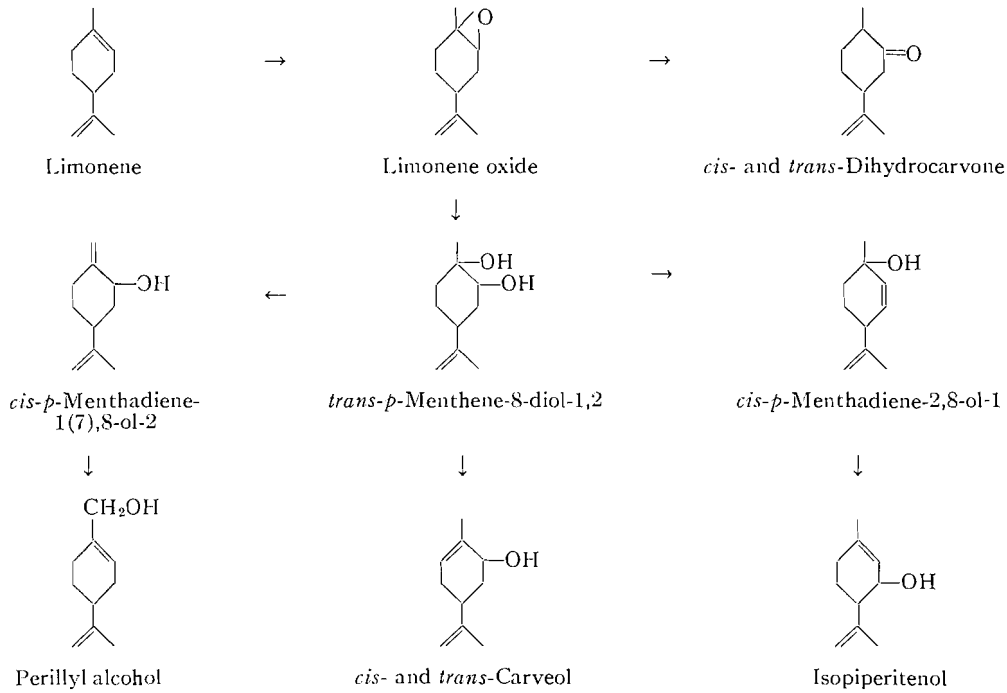

FIG. 2. Biogenetic relationships of monoterpenoids derived from limonene oxide.

TABLE III

Composition of gingergrass oil

Peak No.	Constituent	Relative retention time	% (w/w)
1	Limonene	0.36	13.5
2	Limonene oxide	0.72	2.1
3	Isopiperitenol	1.00	13.4
4	*trans*-*p*-Menthadiene-2,8-ol-1	1.12	8.6
5	*trans*-Dihydrocarvone	1.18	0.3*
6	*cis*-Dihydrocarvone	1.28	
7	*cis*-*p*-Menthadiene-1(7),8-ol-2	1.53	31.1
8	Carvone	1.65	1.1
9	*trans*-Carveol	1.71	2.7*
10	*cis*-Carveol	1.90	
11	Perillyl alcohol	2.05	15.0
12	Piperitenone	2.81	0.1
13	Aromatic compound	4.23	0.6
14	*trans*-*p*-Menthene-8-diol-1,2	6.46	2.4
	Unidentified		9.1

*These pairs of isomers were not sufficiently resolved by column and gas chromatography to permit quantitative measurements of either component.

Biogenetic Significance of Analytical Data

Epoxy compounds of mono- and sesqui-terpenes occur in many essential oils (12) and they have been considered as precursors of related constituents. Oil of gingergrass is of

Can. J. Chem. Downloaded from www.nrcresearchpress.com by 210.87.254.5 on 09/05/12
For personal use only.

particular interest in this regard since it was shown to contain limonene oxide as well as a number of structurally closely related monoterpenes. Biogenetic transformations of the epoxide to other constituents may take place in accordance with the scheme of rearrangements outlined in Fig. 2. The ease with which such transformations can be brought about was demonstrated by the authors who succeeded in synthesizing a mixture containing most of these compounds by merely refluxing the epoxide with pyridinium bromide. The resulting product was found to be composed of *cis*- and *trans*-dihydrocarvone, *cis*-*p*-menthadiene-1(7),8-ol-2, *cis*- and *trans*-carveol as well as perillyl alcohol, as shown in Fig. 1B.

ACKNOWLEDGMENTS

The authors are indebted to Excel Traders, Bombay, Sri. G. N. Gupta, H. B. Technological Institute, Kanpur, Manaunlal Ram Narain, Kannauj, and Dr. M. Swaleh, Regional Research Laboratory, Hyderabad, India, for courteously supplying authentic samples of oil of gingergrass for this study.

REFERENCES

1. BER. SCHIMMEL & Co. 52 (April 1904); 41 (October 1904); 34 (April 1905); 33 (October 1906). GILDEMEISTER and HOFFMAN. Die Ätherishcen Öle, 3rd. ed. Vol. I. Verlag der Schimmel & Co., A. G., Miltitz b. Leipzig, 1928. p. 544.
2. H. WALBAUM and O. HÜTHIG. J. Prakt. Chem. Ser. 2, **71**, 459 (1905).
3. E. GILDEMEISTER and K. STEPHAN. Arch. Pharm. **234**, 326 (1896).
4. Y. R. NAVES and A. V. GRAMPOLOFF. Compt. Rend. **249**, 306 (1959).
5. Y. R. NAVES and A. V. GRAMPOLOFF. Bull. Soc. Chim. France, 37 (1960).
6. M. SWALEH, B. BHUSHAN, and G. S. SIDHU. Perfumery Essent. Oil Record, **54**, 295 (1963).
7. I. C. NIGAM and L. LEVI. Can. J. Chem. **40**, 2083 (1962).
8. I. C. NIGAM *et al.* Perfumery Essent. Oil Record, **53**, 614 (1962).
9. J. C. BARTLET and D. M. SMITH. Can. J. Chem. **38**, 2057 (1960).
10. D. M. SMITH and L. LEVI. J. Agr. Food Chem. **9**, 230 (1961).
11. E. GUENTHER. The essential oils. Vol. IV. D. Van Nostrand Company Inc., New York. 1950. p. 5.
12. A. D. CROSS. Quart. Rev. London, **14**, 317 (1960).

Can. J. Chem. Downloaded from www.nrcresearchpress.com by 210.87.254.5 on 09/05/12
For personal use only.

Can. J. Chem. Downloaded from www.nrcresearchpress.com by 210.87.254.5 on 09/05/12
For personal use only.

NOTES

REARRANGEMENT STUDIES WITH ^{14}C. XXII. SOLVOLYSES OF 1-^{14}C-ETHYL *p*-TOLUENESULFONATE

C. C. Lee and Moira K. Frost

Roberts and Yancey (1) have reported that the nitrous acid deamination of 1-^{14}C-ethylamine gave rise to 1.5% 2-^{14}C-ethanol resulting from 1,2-hydride shift. This finding has been confirmed by Sixma and Hendriks (2). It is of interest to ascertain whether any analogous 1,2-shift would take place in solvolytic reactions with 1-^{14}C-ethyl *p*-toluenesulfonate (I). Solvolysis of I was carried out in 75% dioxane – 25% water (by volume), glacial acetic acid, or anhydrous formic acid. The ethanol produced from the reaction in aqueous dioxane, or obtained after hydrolysis of the ethyl acetate or formate from acetolysis or formolysis, was degraded to iodoform. The activity in the iodoform would be a measure of the extent of rearrangement of the ^{14}C-label from the C-1 to the C-2 positions of the ethyl group. The results, summarized in Table I, show that there were no significant amounts of ^{14}C-rearrangement, indicating the absence of 1,2-hydride shift, in any of the solvolyses studied. These results are consistent with the expectation that such solvolyses with the primary ethyl system likely proceed by a direct displacement or an S_N2 mechanism. The present findings are also in agreement with the conclusion of Winstein and Marshall (3), arrived at from kinetic studies, that solvolysis of ethyl *p*-toluenesulfonate is not close to "limiting" in type.

TABLE I

Data from solvolyses of 1-^{14}C-ethyl *p*-toluenesulfonate

	Specific activity (c.p.m./mmole) × 10^{-3}					
	C_2H_5OTs		CHI_3		% rearrangement	
Solvent	Run 1	Run 2	Run 1	Run 2	Run 1	Run 2
None (blank degradation)	300	830	0.2	0.2	0.07	0.02
Dioxane–water	300	830	0.3	0.3	0.1	0.04
Acetic acid	300	830	0.3	0.4	0.1	0.05
Formic acid	300	830	0.4	0.6	0.1	0.07

EXPERIMENTAL

1-^{14}C-Ethyl *p*-toluenesulfonate (I), m.p. 32 °C (lit. (4) m.p. 32 °C), was prepared from 1-^{14}C-ethanol* by treatment with *p*-toluenesulfonyl chloride in pyridine (4).

A solution of 10 g (0.05 mole) of I in 20 ml of 75% dioxane – 25% water, glacial acetic acid, or anhydrous formic acid was heated under reflux for 24 h. For the reaction in aqueous dioxane, an ethanol–water solution was distilled directly from the reaction mixture, 6–7 ml of distillate being collected. For acetolysis and formolysis, the reaction mixture was cooled in an ice bath, 50 ml of water added, and the solution neutralized with solid sodium carbonate. The product was recovered by continuous extraction with alcohol-free ether for 48 h. After the extract was dried over magnesium sulfate and the ether removed, the residual ester was hydrolyzed directly by heating over a steam bath for 2 h with 10 ml of 20% sodium hydroxide solution. The ethanol produced, together with water, was distilled from the hydrolysate, 6–7 ml of distillate being collected. In preliminary trials, the yields of ethyl acetate or formate were found to be in the order of 50%.

**Purchased from New England Nuclear Corp.*

The aqueous ethanol obtained from each solvolysis run was degraded to give iodoform according to a procedure previously described (5).

The activities of I and of iodoform were measured using a liquid scintillation counter. Samples weighing about 10 mg dissolved in 20 ml of toluene were counted. The iodoform solutions caused considerable quenching and correction factors were determined with ^{14}C-toluene as internal standard. The actual observed activities, together with background, of all the iodoform samples recorded in Table I were less than twice background.

ACKNOWLEDGMENT

The financial support given by the National Research Council of Canada is gratefully acknowledged.

1. J. D. ROBERTS and J. A. YANCEY. J. Am. Chem. Soc. **74**, 5943 (1952).
2. F. L. J. SIXMA and H. HENDRIKS. Koninkl. Ned. Akad. Wetenschap. Proc. Ser. B, **59**, 61 (1956).
3. S. WINSTEIN and H. MARSHALL. J. Am. Chem. Soc. **74**, 1120 (1952).
4. R. S. TIPSON. J. Org. Chem. **9**, 235 (1944).
5. I. S. BHARDWAJ and C. C. LEE. Can. J. Chem. **41**, 2368 (1963).

RECEIVED SEPTEMBER 21, 1964.
DEPARTMENT OF CHEMISTRY,
UNIVERSITY OF SASKATCHEWAN,
SASKATOON, SASKATCHEWAN.

Can. J. Chem. Downloaded from www.nrcresearchpress.com by 210.87.254.5 on 09/05/12
For personal use only.

Can. J. Chem. Downloaded from www.nrcresearchpress.com by 210.87.254.105 on 09/05/12
For personal use only.

Canadian Journal of Chemistry

Issued by THE NATIONAL RESEARCH COUNCIL OF CANADA

VOLUME 43 MARCH 1965 NUMBER 3

THE IONIZATION BEHAVIOR OF AMIDES IN CONCENTRATED SULFURIC ACIDS

II. APPLICATIONS OF THE H_A FUNCTION TO RATES AND EQUILIBRIA

KEITH YATES AND JOAN B. STEVENS

Department of Chemistry, University of Toronto, Toronto, Ontario

Received October 16, 1964

ABSTRACT

The newly determined H_A scale of acidity has been tested against ionization ratio data for 33 amides. Twenty-nine of these compounds give log I vs. H_A slopes of 0.9–1.1 and most are within 0.95–1.05. The average slope for these is 1.001 ± 0.051. The H_A function is thus considered to be generally applicable to the ionization of this type of base, and the significance of previously reported amide pK values is discussed in the light of these results. Previously reported basicity – substituent constant relations have been reexamined using thermodynamically significant pK data and earlier conclusions confirmed. Appropriate equations are derived in an attempt to explain the rate–acidity dependence of amide hydrolysis directly in terms of the water activity of the reaction medium. The picture of the hydrolysis transition state which results is in accord with that obtained using methods described by other workers.

INTRODUCTION

In Part I of this series (1) values of a new acidity function H_A were reported. This scale was based on a set of structurally related amide indicators. The usefulness of such a scale depends on the extent to which it can be applied to the ionization of other bases, therefore any tests of ionization behavior with respect to the H_A scale are important. Although it is not expected that the applicability of the H_A function will be any wider than is that of the H_0 function (2) for example, it is important for any such function that it be obeyed at least by bases of similar structural type to those used to establish the scale. Only in this way can the function be expected to yield quantitative information about base strengths. In the present paper we wish to report the results of such tests of the H_A scale using all presently available data on the ionization of amides in sulfuric acid.

Two of the principal uses of the acidity function approach have been in the study of structure–reactivity relations and rate–acidity correlations. We have therefore reexamined such relations involving amide protonation and hydrolysis in the light of information provided by the new amide acidity scale.

EXPERIMENTAL

Measurement of Ionization Ratios

Ionization ratios ($I = [BH^+]/[B]$) for the following amides were obtained spectrophotometrically as described previously (1): *p*-bromobenzamide, *p*-toluamide, 4-bromo-3-nitrobenzamide, 3,5-dinitrobenzamide, and 3-hydroxyphenylurea. These were all commercially available compounds which were recrystallized to constant melting point before use.

Calculation of pK Values and Indicator Slopes

All pK values and slopes of log I versus H_A plots were obtained by the standard least mean squares treatment. Only values of log I in the range ± 1.0 were selected since the experimental uncertainty in this quantity increases very rapidly outside this range (3). At least 6 and up to 20 experimental points were used to calculate each pK value and indicator slope. Values of log I were measured in the present work or taken directly from the literature, or, where the log I values were not actually reported, they were supplied by the authors. We are very grateful to Professors R. Stewart and J. T. Edward and Dr. R. B. Moodie for access to unpublished material. The log I versus H_A plots showed good linearity in most cases, correlation coefficients in the range 0.980–0.999 being obtained. In one case only, that of N,N-dimethyl-*p*-phenylbenzamide, were the points too widely scattered ($r = 0.925$) to allow estimates of pK and the slope to be made. In cases where the necessary log I data was not available, estimates of pK were made by converting the reported pK values (based on the H_0 scale) to values based on the new H_A scale by simple interpolation.

RESULTS AND DISCUSSION

The Generality of the H_A Scale and Significance of Derived pK Values

The basicities of a large number of amides have been measured previously. These were based on spectrophotometric determination of ionization ratios ($I = [BH^+]/[B]$) and plots of log I against the Hammett acidity function H_0. However, as Arnett (4) has pointed out, unless the base in question can be demonstrated to adhere to the H_0 function in its ionization behavior, any pK value so derived has no thermodynamic significance. Such pK values are simply equal numerically to the H_0 value of the acid in which they are half protonated and are not true equilibrium constants. That amides as a class do not follow H_0 even approximately has been shown previously (5) by the fact that slopes of log I vs. H_0 plots for amides are far from unity, as required by the defining equation for H_0.

$$H_0 = pK_{BH^+} - \log I = -\log a_{H^+} f_B / f_{BH^+}.$$

The H_0 slopes for a large number of amides for which data is available are in the range 0.4–0.8 (5, 6). Thus all previously reported pK values for amides cannot be considered as valid thermodynamic equilibrium constants.

In order to investigate the possibility of obtaining amide pK values of thermodynamic significance and at the same time to test the validity of the recently determined H_A scale of acidity, we have plotted log I versus H_A using all the data presently available on the ionization of this type of base. The H_A function is defined in an analogous way to H_0, except that A and AH^+ refer to an amide and its conjugate acid,

$$\begin{aligned} H_A &= pK_{AH^+} - \log [AH^+]/[A] \\ &= pK_{AH^+} - \log I = -\log a_{H^+} f_A / f_{AH^+}, \end{aligned}$$

where $K_{AH^+} = a_{H^+} a_A / a_{AH^+}$ is the thermodynamic dissociation constant of the conjugate acid. Values of this function were based on a set of eight primary amide indicators, using the standard stepwise technique (2). It is therefore of importance to investigate the adherence of other amides to this function to determine how adequately it represents the ionization behavior of amides in general. We have obtained slopes of log I versus H_A for 25 amides which were not used as indicators in establishing the scale. These slopes are listed in Table I. It can be seen that they are generally close to unity, as required by the defining equation for H_A. Excluding for now four widely deviating cases, the slope values are all in the range 0.9–1.1. If one includes the 8 amides used as H_A indicators, which naturally have slopes close to unity, 29 out of 33 amides listed have slopes within this range and most are in the range 0.95–1.05. The average value for these 29 bases is 1.001 with a standard deviation of ± 0.051. Thus the H_A function appears to be quite generally

Can. J. Chem. Downloaded from www.nrcresearchpress.com by 210.87.254.105 on 09/05/12
For personal use only.

applicable to the ionization of amide type bases. A similar test of the behavior of aniline type bases with respect to H_0 has not been carried out. However, if the 10 new aniline indicators used in the recent re-investigation of the H_0 scale (7) are subjected to the same treatment, it is found that their log I vs. H_0 slopes are in the range 0.94–1.06, with a mean value and standard deviation of 0.995 $\pm$ 0.040. Since these anilines were actually used as indicators in determining H_0, the comparable degree of agreement of the large majority of the amides with respect to H_A is very satisfactory evidence that this function represents the ionization behavior of aromatic amides as well as H_0 represents that of anilines.

Taking a log I – acidity function slope of 0.95–1.05 as a reasonable criterion of whether a particular base is following that particular function, we can assess the quantitative significance of the pK values listed in Table I. These fall into several groups. Those listed for compounds having log I vs. H_A slopes within the above range can be considered to be valid thermodynamic pK values based on dilute aqueous solution as standard state, within the usual limits of experimental uncertainty. In a few cases where the slopes are outside this range, but still fairly close to unity (0.9–1.1), the pK values have less significance but can be taken as approximate pK values. Those for which no slope is given may be valid pK's, but this remains to be demonstrated. In the cases where the slope deviates widely from unity, the pK value has no thermodynamic significance and only corresponds numerically to the H_A value of the acid in which the base is half protonated.

Although the criterion of unit slope is a necessary condition for a derived pK value to be taken as a valid equilibrium constant, Arnett (4) has pointed out that this is not always in itself a sufficient condition. The possibility cannot be ruled out that a given base may exhibit anomalous activity coefficient behavior in an acid region where ionization ratios are too small to be experimentally accessible. This has been observed for at least two supposedly Hammett type bases, with the result that although their indicator curves have unit slope, the pK values are not referred to the same standard state as the H_0 scale, and hence are not true pK values. We are at present investigating the activity coefficient behavior of typical amides and have not yet observed any similar cases of anomalous solubility increase. Thus in the absence of evidence to the contrary, we are assuming that the criterion of unit slope is a satisfactory one.

The only amides so far investigated which do not follow H_A very closely are propionamide (0.70), *p*-nitrobenzamide (0.75), *o*-toluamide (0.81), and N,N-dimethyl-2-naphthamide (0.77). The deviation of propionamide is perhaps not surprising since this is an aliphatic compound and it is now evident that Hammett-type acidity functions can be quite sensitive to large changes in base structure. The anomalous behavior of *p*-nitrobenzamide is probably attributable to uncertainty in the spectrophotometric determination of ionization ratios. The ultraviolet absorption characteristics of this compound are not very suitable for obtaining precise log I data, since both forms of the amide absorb at almost the same wavelength and the increase in absorption on protonation is not very large. The reason for the deviation of *o*-toluamide is less easy to account for. It is difficult to see how the steric effect of an *o*-methyl group on solvation of the amide group could produce this effect, since both 2,6-dimethylbenzamide (0.95) and 2,4,6-trimethylbenzamide (0.92) do not show similar large deviations. We are unable to explain this at present. In view of a recent study of the non-Hammett-type behavior of N,N-disubstituted anilines (8), it might be expected that alkyl substitution on the amide nitrogen would produce similar large deviations from an acidity function based on primary amides. However, of the seven secondary and tertiary amides in Table I for which indicator ratio

Can. J. Chem. Downloaded from www.nrcresearchpress.com by 210.87.254.105 on 09/05/12
For personal use only.

TABLE I

Collected data on the ionization of amides in sulfuric acid*

Amide	$-pK_{AH^+}$†	Slope of log I vs. H_A	% H_2SO_4‡ to half-ionize	Ref.
Substituted benzamides				
Benzamide	1.74	0.99	35.2	10
	1.68§	0.98§		14
m-Bromo-	2.13	1.00	42.6	10
p-Bromo-	2.02	1.03	40.8	
m-Chloro-	2.09		42.4	10
p-Chloro-	1.97	1.00	39.5	10
p-Fluoro-	1.80		36.1	10
m-Methoxy-	1.90	1.03	38.7	10
p-Methoxy-‖	1.44	1.00	28.8	1
	1.48	1.01§		14
o-Methyl-	1.8	0.81	37.5	17
m-Methyl-	1.76	0.95	35.7	10
p-Methyl-	1.67	1.04	33.6	
m-Nitro-‖	2.42	1.01	48.6	1
p-Nitro-	2.7	0.75	53.8	5
p-Phenyl-	1.84	1.01	36.8	6
4-Bromo-3-nitro-	2.63	0.95	52.6	
2,6-Dimethyl-	1.96	0.95	39.6	17
3,5-Dinitro-	3.26	1.05	61.3	
2,3,6-Trichloro-‖	3.30	1.05	63.6	1
3,4,5-Trimethoxy-‖	1.82	1.00	36.7	1
2,4,6-Trimethyl-	1.70	0.92	34.4	17
2,4,6-Trinitro-‖	4.08	1.05	74.3	1
3,5-Dinitro-4-methyl-‖	2.69	1.01	53.8	1
2,4-Dichloro-3,5-dinitro-‖	3.73	0.95¶	69.8	1
Other primary amides				
Acetamide	0.6		13.0	18
2-Furamide	2.10		42.5	10
Glycinamide	3.3**		63.4	18
3-Hydroxyphenylurea	1.31	0.99	26.4	
1-Naphthamide	2.04	0.98	41.2	6
2-Naphthamide	2.04	0.97¶	41.2	6
Propionamide	0.8	0.70	16.6	18
2-Pyrrolecarboxamide‖	1.23	1.00	24.8	1
N-Substituted amides				
Aceturic acid	2.3		46.9	18
N-*n*-Butylacetamide	0.4		11.4	18
N-*i*-Butylacetamide	0.6		14.2	18
N-Methylacetamide	1.2		23.3	18
N-Methylbenzamide	1.7	1.02	34.2	10
N-Methyl-1-naphthamide	1.75	1.11	35.2	6
N-Methyl-2-naphthamide	1.74	1.11	35.0	6
N-Methyl-*p*-phenylbenzamide	1.76	1.07	35.3	6
N,N-Dimethylbenzamide	1.4	0.90	28.6	10
N,N-Dimethyl-1-naphthamide	1.57	0.90	31.7	6
N,N-Dimethyl-2-naphthamide	1.5	0.77	29.6	6
N,N-Dimethyl-*p*-phenylbenzamide	1.3††		24††	6

*Data obtained at 25 °C unless noted.
†Dissociation constant of amide conjugate acid.
‡Acid whose H_A value is numerically equal to pK_{AH^+}.
§Data obtained at 18 ± 3 °C.
‖Used as indicator to establish H_A scale.
¶Omitting one widely deviating experimental point.
**For first dissociation of $[NH_3CH_2COHNH_2]^{++}$.
††Estimated by method described in ref. 6.

slopes are available, only one deviates widely from unity. This provides a further indication (1) that hydration of the protonated carbonyl oxygen of the amide group is much more important that hydration of the $—NH_2$ group. It is interesting that the four secondary amides in Table I have indicator slopes somewhat greater than unity (1.02–1.11), whereas the three tertiary amides show less than unit slope (0.77–0.90). Considering

Can. J. Chem. Downloaded from www.nrcresearchpress.com by 210.87.254.105 on 09/05/12
For personal use only.

the number of acidic protons available for hydrogen bonding to solvent molecules, and making the usual assumption that hydration of the conjugate acid forms is more important than that of the neutral bases, it would be predicted that f_{AH^+}/f_A would rise most rapidly with acid strength (i.e. diminishing water activity) for primary, less rapidly for secondary, and least rapidly for tertiary amides. Thus the rate of change of log $[AH^+]/[A]$ with acidity would be in the order tertiary > secondary > primary. Plots of log I against H_A should therefore give greater than unit slopes for both secondary and tertiary amides with the latter having the highest slopes. It can be seen from Table I that the secondary amides behave as predicted but the tertiary amides do not. Although the data on N-substituted amides is somewhat limited, it is again evident that differences in activity coefficient behavior cannot be explained solely in terms of the *number* of acidic protons available for hydration, even in a qualitative way. A similar conclusion has been reached by Moodie (9) on the basis of the water activity dependence of ionization ratios.

In conclusion, the results of the above tests show that aromatic amides follow the H_A function remarkably well in view of the large differences in structure of some of the bases investigated. This agreement is probably due in part to the fact that the H_A function is not based too heavily on polynitro-substituted indicators. This is a consequence of the inherently weaker basicity of amides when compared with anilines. However, there are indications that aliphatic amides do not follow H_A with anything like the same precision, but further work is needed to test this.

Linear Free Energy Relations

A good linear correlation between Hammett σ-values and pK values of *m*- and *p*-substituted benzamides was reported previously (10). Since this was better than the correlation between σ^+ and pK, it was taken as evidence of a lack of conjugation between the protonated carboxamide group and phenyl ring. However, as pointed out in the previous section, the pK values used were not true equilibrium constants, and this conclusion might not be valid. We have therefore re-investigated these relations using the pK values in Table I. Using only the pK data for which the log I vs. H_A slope is 1.00 ± 0.05, a fairly good linear relation ($r = 0.978$) between pK and σ still holds. The corresponding plot of pK versus σ^+ shows poor linearity ($r = 0.896$) and further, all seven points for *p*-substituted benzamides deviate in the same direction from a line drawn through the points for non-conjugating substituents. This confirms the earlier conclusion. Several suggestions have been advanced (6, 10) to explain this lack of conjugation in amides but as yet there is no evidence to indicate which, if any, is correct. From the above pK–σ relation, the correct Hammett ρ-value for the equilibrium is -0.92, which is appreciably lower than previously reported. This is a more reasonable value for an

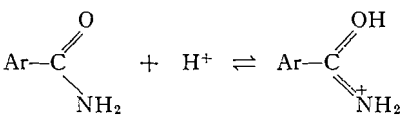

ionization in which unit positive charge is developed and essentially localized at a distance of two atoms from the phenyl ring (11).

It was suggested in Part I of this series that the last indicator of the H_A set might not be too reliable due to the small spectral changes produced by protonation. The pK of this base, 2,4,6-trinitrobenzamide, was found experimentally to be -4.08. Using the above linear free energy relation, one can estimate roughly the effect of three nitro groups on the basicity of benzamide. Assuming additivity of substituent effects and that

Can. J. Chem. Downloaded from www.nrcresearchpress.com by 210.87.254.105 on 09/05/12
For personal use only.

Can. J. Chem. Downloaded from www.nrcresearchpress.com by 210.87.254.105 on 09/05/12
For personal use only.

o-nitro has a similar electronic effect to *p*-nitro, the equation $\log K/K_0 = \rho\sum\sigma$ yields a rough pK value of -3.9 for 2,4,6-trinitrobenzamide, which is in good agreement with the experimental value.

Rate–Acidity Correlations

Bunnett (12) has shown for a large number of reactions in moderately concentrated acids that the following relation between the rate constant, acidity, and water activity is generally obeyed,

$$\log k + H_0 = w \log a_{H_2O} + \text{constant}.$$

The values of w obtained can be used to classify reactions according to mechanism. Although this relation is empirical, Bunnett (13) has also shown that by considering hydration of all species involved, these w-parameters can be related to the change in hydration in going from reactants to transition state. However, this hydration treatment involves the extreme assumption that activity coefficient ratios* for species of like charge are medium independent. This assumption results in cancellation of a term $f_{S(H_2O)_s} f_{BH(H_2O)_c^+}/f_{B(H_2O)_b} f_{\ddagger(H_2O)_t^+}$ (Bunnett's notation (13)) which appears in the rate expression derived on the basis of transition state theory. In this activity coefficient ratio S and ‡ refer to a wide variety of substrates and their transition states and B and BH^+ refer to the Hammett indicators used to measure the acidity of the reaction medium. For substrates such as amides, whose ionization behavior does not follow H_0, the similar ratio $f_{S(H_2O)_s} f_{BH(H_2O)_c^+}/f_{B(H_2O)_b} f_{SH(H_2O)_p^+}$ is clearly strongly medium dependent and it is therefore extremely unlikely that the Bunnett assumption is valid for acid-catalyzed reactions of this type of substrate. Hence the w-parameters for reactions of substrates which have not been demonstrated to follow H_0 as bases cannot be simply related to the hydration changes involved in the rate-determining step. It is possible, however, to obtain direct information about the nature of the transition state in the following way. The generalized mechanism for acid-catalyzed reactions, in terms of fully hydrated species, can be written

$$S(H_2O)_s + H(H_2O)_n^+ \rightleftharpoons SH(H_2O)_p^+ + (s + n - p)H_2O$$
$$SH(H_2O)_p^+ + rH_2O \rightleftharpoons S^{\ddagger}(H_2O)_t \rightarrow \text{products}.$$

For reactions in which the protonation step is rapidly reversible, this scheme leads to the rate equation

$$[1] \qquad v = k/K_{SH^+} \cdot [S(H_2O)_s] f_{S(H_2O)_s}/f_{S^{\ddagger}(H_2O)_t} \cdot a_{H(H_2O)_n^+} \cdot a_{H_2O}^{r-(s+n-p)} = k_{obs}[S]_{st},$$

where K_{SH^+} is the dissociation constant of the substrate conjugate acid, k_{obs} is the observed pseudo-first-order rate constant (the acidity remaining effectively constant in any given kinetic experiment) and $[S]_{st}$ is the stoichiometric substrate concentration. Consider now the generalized indicator equilibrium, also in terms of fully hydrated species

$$In(H_2O)_b + H(H_2O)_n^+ \rightleftharpoons InH(H_2O)_c^+ + (b + n - c)H_2O.$$

This can be used to define the acidity of the medium in terms of a general acidity function:

$$[2] \qquad h_x = a_{H(H_2O)_n^+}/a_{H_2O}^{b+n-c} \cdot (f_{In(H_2O)_b}/f_{InH(H_2O)_c^+}).$$

If we now substitute for the hydronium ion activity in eq. [1] in terms of the relation given in eq. [2] and indicate by a subscript h that each species referred to is fully hydrated, we obtain the rate expression

$$[3] \qquad v = k/K_{SH^+} \cdot [S_h](f_{S_h} f_{InHh^+}/f_{S^{\ddagger}h} f_{In_h}) \cdot h_x \cdot a_{H_2O}^{r+(b-c)-(s-p)}.$$

**All activity coefficients in this section refer to fully hydrated and not formal species.*

This gives a general relation between the rate, acidity, and water activity similar to that derived by Bunnett (13). Now if the substrates and indicators are of the same structural type, i.e. if both are amides, this expression can be simplified by a much less extreme assumption. The terms f_{S_h} and f_{In_h} refer to the same type of species and will approximately cancel in all solutions. For the same reason $(b - c) - (s - p)$ will be effectively zero. Since the amide conjugate acid and the transition state have the same charge and are very similar structurally, it is reasonable to assume that the ratio of their activity coefficients will be nearly medium independent. Thus the rate equation for amide hydrolysis becomes

$$v \approx (k/K_{SH^+}) \cdot [S_h] h_A a_{H_2O}{}^r.$$

For weakly basic amides which are protonated to a very small extent in the reaction medium, $[S_h] = [S]_{st}$ and the rate constant is given by

$$k_{obs} = k/K_{SH^+} h_A a_{H_2O}{}^r.$$

Taking logarithms and rearranging, this gives

$$\log k_{obs} + H_A = r \log a_{H_2O} + \text{constant}. \quad [4]$$

For more basic substrates which are protonated to an appreciable extent, $[S_h] = [S]_{st} \times (h_A/K_{SH^+} + h_A)$, and the rate constant is given by $k_{obs} = k(h_A/K_{SH^+} + h_A)a_{H_2O}{}^r$. The corresponding logarithmic relation between rate, acidity, and water activity is thus

$$\log k_{obs} - \log (h_A/K_{SH^+} + h_A) = r \log a_{H_2O} + \text{constant}. \quad [5]$$

Equations [4] and [5] are formally very similar to the empirical relations discovered by Bunnett (12), except that an acidity function strictly appropriate to the substrate is involved and r can now be more directly related to the number of water molecules needed to convert protonated substrate to its transition state.

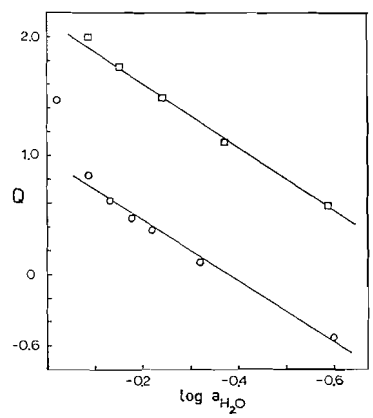

FIG. 1. Plot of $Q(= [\log k_{obs} - \log(h_A/h_A + K_{SH^+})] + 3)$ against $\log a_{H_2O}$ for the hydrolysis of benzamide (circles) and *p*-nitrobenzamide (squares) in sulfuric acid at 25 °C. Data taken from refs. 1, 12, and 14.

In Fig. 1 the quantity $\log k_{obs} - \log (h_A/K_{SH^+} + h_A)$ is plotted against $\log a_{H_2O}$ for the hydrolysis of benzamide (15) in sulfuric acid. The plot is reasonably linear over a wide range of acid giving a slope $r = 2.6$ (correlation coefficient = 0.994) if the point in dilute acid is omitted. This deviation may be due to the fact that in the dilute region

Can. J. Chem. Downloaded from www.nrcresearchpress.com by 210.87.254.105 on 09/05/12
For personal use only.

there is plenty of "free" water available for solvation. Average hydration numbers in this region may be significantly different from those in more concentrated acids where competition for available water is more serious. The only other amide for which appropriate data (14) is available is *p*-nitrobenzamide, and although this base does not follow H_A as well as benzamide, a similar plot is also linear with slope $r = 2.7$ (correlation coefficient = 0.998). These results suggest that over a wide range of acidity an amide conjugate acid is converted to its transition state by the attack of three additional water molecules on the average. This transition state can be reasonably represented by the following structure.

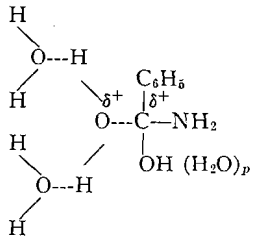

Moodie (15) has already reached a similar conclusion concerning the nature of this transition state using a different treatment which involves the water activity but does not involve either the pK of the base or any acidity function values. An alternative approach is the recent ϕ-parameter treatment of Bunnett (16), which does not involve any water activity data. In this method quantities such as the left hand sides of eqs. [4] or [5] are plotted against (log $[H^+] + H_0$) as a reference standard for all reactions and equilibria. By this approach excellent linear plots are also obtained in the present case, yielding ϕ-values of 0.71 (correlation coefficient 0.993) and 0.69 (correlation coefficient 1.000) for the hydrolysis of benzamide and *p*-nitrobenzamide respectively. On the basis of acidity – water activity variation over a wide range of hydrochloric, sulfuric, and perchloric acids, Bunnett (16) assigns a value of 4.5 ϕ to the average hydration change accompanying any reaction. This again indicates that three additional water molecules are involved in the rate-determining step of amide hydrolysis. Thus all three approaches described above yield essentially the same picture of the transition state.

At present the scarcity of appropriate acidity function and kinetic data does not allow the present approach to be tested further to see if similar results are obtained for other amides. We are at present evaluating the H_A function in other acids in an attempt to test the general usefulness of this method of obtaining detailed information about transition states.

ACKNOWLEDGMENTS

The financial assistance of the National Research Council of Canada is gratefully acknowledged. We are also grateful for the award of a Province of Ontario Graduate Fellowship to one of us (J. B. S.) and to the President's Advisory Committee on Scientific Research for continued financial support.

REFERENCES

1. K. YATES, J. B. STEVENS, and A. R. KATRITZKY. Can. J. Chem. **42**, 1957 (1964).
2. L. P. HAMMETT and A. J. DEYRUP. J. Am. Chem. Soc. **54**, 2721 (1932). M. A. PAUL and F. A. LONG. Chem. Rev. **57**, 1 (1957).
3. W. M. SCHUBERT and R. H. QUACCHIA. J. Am. Chem. Soc. **84**, 3778 (1962).
4. E. M. ARNETT. *In* Progress in physical organic chemistry. Vol. 1. *Edited by* S. G. Cohen, A. Streitwieser, Jr., and R. W. Taft. Interscience, New York. 1963. p. 233 ff.

Can. J. Chem. Downloaded from www.nrcresearchpress.com by 210.87.254.105 on 09/05/12
For personal use only.

5. A. R. KATRITZKY, A. J. WARING, and K. YATES. Tetrahedron, **19**, 465 (1963). J. T. EDWARD and I. C. WANG. Can. J. Chem. **40**, 966 (1962).
6. R. B. HOMER and R. B. MOODIE. J. Chem. Soc. 4377 (1963).
7. M. J. JORGENSON and D. R. HARTTER. J. Am. Chem. Soc. **85**, 878 (1963).
8. E. M. ARNETT and G. MACH. J. Am. Chem. Soc. **86**, 2671 (1964).
9. R. B. MOODIE. Unpublished results.
10. J. T. EDWARD, H. S. CHANG, K. YATES, and R. STEWART. Can. J. Chem. **38**, 1518 (1960).
11. R. W. TAFT and I. C. LEWIS. J. Am. Chem. Soc. **80**, 2436 (1958).
12. J. F. BUNNETT. J. Am. Chem. Soc. **83**, 4956, 4968, 4978 (1963).
13. J. F. BUNNETT. J. Am. Chem. Soc. **83**, 4973 (1963).
14. J. T. EDWARD and S. C. R. MEACOCK. J. Chem. Soc. 2000 (1957).
15. R. B. MOODIE, P. D. WALE, and T. J. WAITE. J. Chem. Soc. 4273 (1963).
16. J. F. BUNNETT. J. Am. Chem. Soc. To be published.
17. K. YATES and B. F. SCOTT. Can. J. Chem. **41**, 2320 (1963).
18. J. T. EDWARD and I. C. WANG. Can. J. Chem. **40**, 966 (1962). A. R. GOLDFARB, A. MELE, and N. GUTSTEIN. J. Am. Chem. Soc. **77**, 6194 (1955).

Can. J. Chem. Downloaded from www.nrcresearchpress.com by 210.87.254.105 on 09/05/12
For personal use only.

CONTRIBUTION A L'ÉTUDE DU MÉCANISME D'OXYDATION CHROMIQUE DES ALCOOLS SECONDAIRES[1]

JEAN-CLAUDE RICHER ET CLAUDE GILARDEAU[2]
Département de Chimie, Université de Montréal, Montréal, Québec

Reçu le 28 septembre 1964

RÉSUMÉ

Cette étude montre que lorsqu'il n'y a que des effets stériques qui influencent les vitesses de réaction d'oxydation chromique d'alcools secondaires, toutes les réactions passent par un état de transition semblable et que l'enthalpie et l'entropie d'activation se compensent; d'autre part le rapport des vitesses d'oxydation d'alcools épimères est égal au rapport de la concentration de ces derniers à l'équilibre.

INTRODUCTION

Le mécanisme d'oxydation chromique des alcools secondaires a fait l'objet de nombreux travaux (1–10). Au cours des années récentes, deux relations linéaires ont été proposées (6, 9) pour relier les vitesses d'oxydation chromique d'alcools secondaires épimères et la stabilité relative des alcools oxydés. Les résultats rapportés dans le présent travail indiquent que la différence d'énergie libre entre deux alcools épimères (ΔF_{ox}) est reliée aux vitesses d'oxydation des alcools d'après l'équation [1] proposée par Sicher et ses collaborateurs (6).

$$[1] \qquad \Delta F_{ox} = RT \ln k_a/k_e.$$

RÉSULTATS ET DISCUSSION

Les vitesses d'oxydation par l'acide chromique, de plusieurs monoalcools alicycliques secondaires ont été mesurées et les résultats obtenus sont résumés au Tableau I.

TABLEAU I

Vitesses d'oxydation par l'acide chromique*

Alcool	17 °C	25 °C	33 °C
tert-Butyl-4 cyclohexanol *trans* (I)	1.266	2.50	4.95
Triméthyl-3,3,5 cyclohexanol *cis* (II)	1.864	4.25	7.42
Cyclohexanol (III)	2.02	3.72	6.58
Diméthyl-4,4 cyclohexanol (IV)	2.24	4.22	7.23
tert-Butyl-4 cyclohexanol *cis* (V)	5.46	9.70	16.15
Cyclopentanol (VI)	3.86	6.96	11.79
Triméthyl-3,3,5 cyclohexanol *trans* (VII)	100.8	143.2	198.4
tert-Butyl-4 diméthyl-2,2 cyclohexanol *trans* (VIII)		11.73	
tert-Butyl-4 diméthyl-2,2 cyclohexanol *cis* (IX)		19.5	
Diméthyl-3,5 cyclohexanol *cis,cis* (X)		3.30	
Diméthyl-3,5 cyclohexanol *trans,trans* (XI)		18.4	
Diméthyl-3,3 cyclohexanol (XII)		6.82	

*10^3 k_2 (l mole^{-1} s^{-1}). Les vitesses d'oxydation rapportées sont la moyenne de 3–4 mesures; l'erreur moyenne sur ces mesures est de ±0.6%.

A l'aide des vitesses d'oxydation à plusieurs températures, les paramètres thermodynamiques d'activation, $\Delta H^{\ddagger}$, $\Delta S^{\ddagger}$ et $\Delta F^{\ddagger}$, ont été calculés. Ces valeurs sont rapportées au Tableau II.

[1]*Communication présentée en partie lors du XIXeme Congrès de l'Union Internationale de Chimie Pure et Appliquée, Londres, juillet 1963.*
[2]*Détenteur de la Bourse C.I.L. pour les années 1963–1965.*

TABLEAU II

Facteurs thermodynamiques d'activation

Alcool*	$\Delta H^{\ddagger}$†	$\Delta S^{\ddagger}$‡	$\Delta F^{\ddagger}$†
I	13.80	24.20	21.02
II	13.23	25.17	20.74
III	12.14	28.95	20.78
IV	12.06	29.01	20.71
V	10.91	31.20	20.22
VI	10.35	33.73	20.41
VII	5.79	42.49	18.46

*Les alcools auxquels on se réfère ici sont nommés dans le Tableau I.
†En kcal/mole, l'erreur moyenne sur ces valeurs est de 0.05 kcal/mole.
‡En unités entropiques, erreur moyenne de 0.03 u.e.

Dans le présent travail, tous les facteurs thermodynamiques ne dépendent que de la structure des alcools employés, c'est-à-dire que les effets polaires des substituants alkyles sont nuls ou négligeables (11). De plus l'enthalpie et l'entropie d'activation sont reliés d'une façon linéaire. Cette relation qui peut être décrite par une équation (éq. [2]) du type proposé par Leffler (12) indiquerait que, dans tous les cas étudiés ici, les états de transition sont semblables.

[2] $$\Delta H = \Delta H_0 + B\Delta S.$$

Dans une étude rapportée récemment, Wilcox (9) a proposé une corrélation linéaire entre les $\Delta(\Delta F^{\ddagger})$ d'oxydation des alcools et la stabilité relative calculée de ces alcools. Grâce aux vitesses d'oxydation de ces alcools et utilisant l'éq. [1] proposée par Sicher (6), il est possible d'évaluer la différence d'énergie libre entre deux alcools épimères. Les valeurs (ΔF_{ox}) calculées de cette manière à l'aide des résultats rapportés ici ainsi que dans le travail de Richer, Pilato et Eliel (3) sont rapportées dans le Tableau III en regard des différences d'énergie libre (ΔF) mesurées par équilibration des alcools par l'isopropylate d'aluminium. Ces données présentées sous forme de graphique montrent une relation linéaire avec pente de 0.97 et passant par l'origine. Ce résultat indique que les états de transition des oxydations des alcools épimères examinés ont atteint une équivalence énergétique dépassant même la valeur de 90% proposée par Wilcox (9) et confirme la validité de l'éq. [1] pour déterminer la différence d'énergie libre entre deux alcools épimères.

TABLEAU III

Équilibre *cis–trans*

Cyclohexanols	ΔF_{ox}	ΔF
Méthyl-2*	0.83	1.03
Méthyl-3*	0.81	0.84
Méthyl-4*	0.62	0.62
tert-Butyl-3*	1.07	1.24
tert-Butyl-4†	0.80	0.92
Triméthyl-3,3,5†	2.08	1.94
tert-Butyl-4 diméthyl-2,2†	0.30	0.29
cis-Diméthyl-3,5†	1.03	1.22

*Richer, Pilato, Eliel.
†Ce travail.

PARTIE EXPÉRIMENTALE

Préparation des alcools

Les diméthyl-3,5 cyclohexanols nous ont été gracieusement fournis par le Dr. E. L. Eliel, Département de Chimie, Notre Dame University, alors que les *tert*-butyl-4 diméthyl-2,2 cyclohexanols ont été synthétisés

par M. Guy Perrault de ce département (13). Les autres alcools utilisés dans cette étude ont été préparés et purifiés par des méthodes connues. Leur pureté a été vérifiée par c.p.g. (Colonne de 2.5 m de Carbowax 20 M sur Chromat FB à 20% et à une température variant entre 160 et 170°) et par spectrophotométrie infrarouge.

Cinétique

La méthode employée ici est semblable à celle d'Eschenmoser (4). Une solution d'acide acétique 75% v/v et environ 10^{-3} M en $HCrO_4^-$ est gardée dans un bain à température constante. L'alcool est pesé de façon à obtenir une solution environ 10^{-2} M en alcool. Les mesures cinétiques sont effectuées spectrophotométriquement à 348 mμ. L'enregistrement automatique de la disparition de l'acide chromique en fonction du temps est fait sur un appareil Perkin-Elmer, modèle 4000A. La constante de vitesse est trouvée en faisant le graphique du log $(a - x)$ en fonction du temps. Une relation linéaire est obtenue au delà de 60% de la réaction.

REMERCIEMENTS

Les auteurs remercient sincèrement la compagnie C.I.L. (1954) et le Conseil National de Recherches pour l'aide financière apportée sous forme de bourse prédoctorale (C. G.) et d'octrois de recherches (J. C. R.)

BIBLIOGRAPHIE

1. H. KWART. Suomen Kemistilehti, A, **34**, 173 (1961).
2. H. KWART. Chem. Ind. London, 610 (1962).
3. J. C. RICHER, L. A. PILATO et E. L. ELIEL. Chem. Ind. London, 2007 (1961).
4. J. ROCEK, F. H. WESTHEIMER, A. ESCHENMOSER, L. MOLDOVANYI et J. SCHREIBER. Helv. Chim. Acta, **45**, 2554 (1962).
5. J. SCHREIBER et A. ESCHENMOSER. Helv. Chim. Acta, **38**, 1529 (1955).
6. F. SIPOS, J. KRUPICHA, M. TICHY et J. SICHER. Collection Czech. Chem. Commun. **27**, 2079 (1962).
7. R. STEWARD et D. G. LEE. Can. J. Chem. **42**, 439 (1964).
8. N. VENKATASUBRAMANIAN. Proc. Indian Acad. Sci. Sect. A, **53**, 80 (1961).
9. C. F. WILCOX, M. SEXTON et M. F. WILCOX. J. Org. Chem. **28**, 1079 (1963).
10. S. WINSTEIN et N. J. HOLNESS. J. Am. Chem. Soc. **77**, 5562 (1955).
11. H. KWART et T. TAKESHITA. J. Am. Chem. Soc. **86**, 1161 (1964).
12. J. E. LEFFLER. J. Org. Chem. **20**, 1202 (1955).
13. J. C. RICHER et G. PERRAULT. Can. J. Chem. À paraître.

Can. J. Chem. Downloaded from www.nrcresearchpress.com by 210.87.254.105 on 09/05/12
For personal use only.

THE REACTION OF SOME AROMATIC ACIDS WITH SODIUM AZIDE IN A TRIFLUOROACETIC ACID - TRIFLUOROACETIC ANHYDRIDE MEDIUM

K. G. RUTHERFORD, SANDRA YUEN-SHUN ING (YU), AND R. J. THIBERT
Department of Chemistry, University of Windsor, Windsor, Ontario

Received October 26, 1964

ABSTRACT

Some commercially available aromatic acids have been treated with sodium azide using a mixture of trifluoroacetic acid and trifluoroacetic anhydride as the reaction medium. Benzoic, ortho-, meta-, and para-toluic, ortho-bromo-, and ortho-nitro-benzoic acids were converted to corresponding N-substituted trifluoroacetamides in good yields. 1-Naphthoic acid was converted to N-(1-naphthyl)-trifluoroacetamide in near quantitative yield. Meta- and para-bromobenzoic and meta- and para-nitrobenzoic acids did not undergo this modified Schmidt reaction under these conditions. The conversion of aromatic acids to N-substituted trifluoroacetamides is discussed and evidence is presented for the mechanism.

INTRODUCTION

The normal Schmidt reaction involves the conversion of an organic acid to an amine with the use of sodium azide in a sulfuric acid medium. The mechanism of the reaction has been well established and is known to involve the following sequence of steps (1):

$$\mathrm{RCOOH} \xrightarrow{HN_3} \mathrm{RCON_3} \xrightarrow{H^{\oplus}} \mathrm{R{-}N{=}C{=}O} \xrightarrow[H_2O]{H^{\oplus}} \mathrm{R{-}\overset{H}{\overset{|}{N}}{-}COOH} \longrightarrow \mathrm{RNH_2} + \mathrm{CO_2}$$

Rutherford and Newman (2) reported that 4-phenanthroic acid underwent sulfonation under the normal conditions of the Schmidt reaction but was converted in almost quantitative yield to 4-phenanthryl isocyanate when a mixture of trifluoroacetic acid (TFA) and trifluoroacetic anhydride (TFAn) was used as the reaction medium. It was decided then to investigate the scope and limitations of these modified Schmidt conditions with some commercially available aromatic acids.

RESULTS AND DISCUSSION

Table I indicates the organic acids which were subjected to the modified Schmidt reaction. Wherever possible a comparison with the normal Schmidt reaction is shown. As can be seen from the table, trifluoroacetyl derivatives of the corresponding amines were obtained in all cases of those acids which proved amenable to the TFA–TFAn system with the exception of 2-naphthoic acid which afforded the azide in quantitative yield. The N-substituted trifluoroacetamides could be readily hydrolyzed in excellent yields to afford the amines. It is important to note, however, that these modified conditions of the Schmidt reaction are not to be considered general, since attempted conversion of meta- and para-bromobenzoic and the analagous nitrobenzoic acids failed. The normal Schmidt reaction proves ideal for the conversion of the nitrobenzoic acids to amines.

The presence of trifluoroacetic anhydride in the reaction medium is as previously reported (2) imperative. In no case did the reaction proceed in 100% trifluoroacetic acid. Table II indicates the effect on the yield of N-(1-naphthyl)-trifluoroacetamide with varying amounts of TFA and TFAn. Even the presence of 10% (by volume) of TFAn has a pronounced effect on the success of the reaction. The yields, however, are reduced quite drastically when the amount of TFAn exceeds 60%.

Can. J. Chem. Downloaded from www.nrcresearchpress.com by 210.87.254.105 on 09/05/12
For personal use only.

TABLE I

Comparison of products and yields in the normal and modified Schmidt reaction with some aromatic acids

Parent acid	Reaction temp. (°C)	Product of modified reaction	Melting point (°C)	Yield % Modified reaction	Yield % Normal reaction (amine)
Benzoic	R.T.	N-Phenyl-trifluoroacetamide	87–89	72	69
1-Naphthoic	R.T.	N-(1-naphthyl)-trifluoroacetamide	96–97	97	
2-Naphthoic	40–45	2-Naphthoic acid azide	80–82	Quant.	
o-Toluic	R.T.	N-(*o*-Tolyl)-trifluoroacetamide	81–82	87	46
m-Toluic	R.T.	N-(*m*-Tolyl)-trifluoroacetamide	67–68	79	42
p-Toluic	R.T.	N-(*p*-Tolyl)-trifluoroacetamide	112–113	71	70
o-Bromobenzoic	R.T.	N-(*o*-Bromophenyl)-trifluoroacetamide	70–71	85–95	
m-Bromobenzoic	35–40	Starting material	—	—	Not reported
p-Bromobenzoic	35–40	Starting material	—	—	Not reported
o-Nitrobenzoic	35–40	N-(*o*-Nitrophenyl)-trifluoroacetamide	89–90	62	83
m-Nitrobenzoic	35–40	Starting material	—	—	83
p-Nitrobenzoic	35–40	Starting material	—	—	83

TABLE II

The influence on the yields of the Schmidt reaction with 1-naphthoic acid with a varying ratio of trifluoroacetic acid and its anhydride

Volume % CF_3COOH	% yield of trifluoroacetyl 1-naphthylamine	% acid recovered
100	—	100
90	75.8	—
80	84.7	—
70	97.8	—
60	97.0	—
50	97.6	—
40	92.3	—
30	57.0	30
20	27.6	59.3
10	19.1	78.4
0	—	100

Of special interest to us was the formation of the trifluoroacetamide derivatives in all cases in which the reaction was successful, especially in view of the fact that 4-phenanthroic acid yielded an isocyanate which was stable in the reaction medium. Evidently, the isocyanate intermediates arising from the acids studied in this investigation underwent rapid reaction with trifluoroacetic acid according to the well-known sequence:

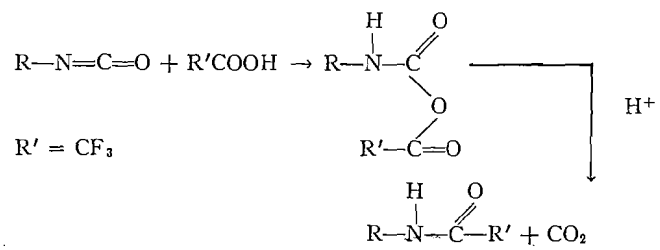

Fry (3) had previously shown that the CO_2 which is liberated in such a reaction contains the carbon atom which is adjacent to the R—NH group of the mixed anhydride. The acid-catalyzed breakdown of the mixed anhydride can be rationalized in the following two ways:

[1]

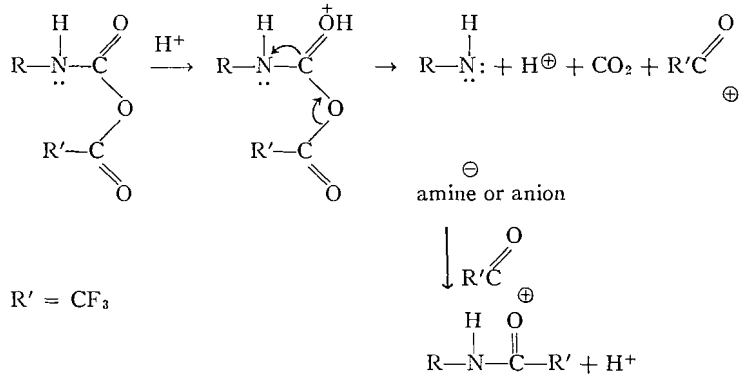

[2]

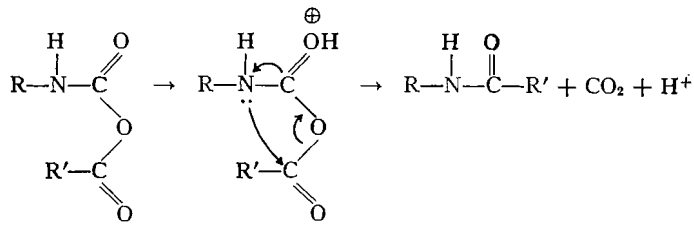

Although it is obvious that either the free amine or its anion (path [1]) could result from a slightly different route from the one depicted above, there is a distinct difference between paths [1] and [2]. The latter route involves a concerted path which would be independent of the presence of extraneous anhydride. Although intuitively one might expect path [1] to be operative, it was found that when phenyl isocyanate was treated with trifluoroacetic acid in the presence of an equimolar amount of acetic anhydride, N-phenyl-trifluoroacetamide was obtained in 84% yield. None of the expected acetanilide was obtained. Under the same conditions, 1-naphthyl isocyanate afforded the trifluoroacetyl derivative of 1-naphthylamine in 91% yield. The expected N-(1-naphthyl)-acetamide was not detected.

The reaction of these isocyanates with trifluoroacetic acid to yield N-substituted trifluoroacetamides via the concerted process (path [2]) is probably unique, since, when phenyl isocyanate was treated with an equimolar mixture of trichloroacetic acid and acetic anhydride, only acetanilide was isolated (92%). Again, when phenyl isocyanate was treated with an equimolar mixture of acetic acid and trifluoroacetic anhydride only trifluoroacetanilide was obtained (87%). Clearly, in these latter cases then, the formation of the intermediate amine or its anion (path [1]) is evident.

The uniqueness of the concerted path in the case of the reaction of phenyl and naphthyl isocyanates with trifluoroacetic acid is undoubtedly a manifestation of the exceptional carbonyl character of the trifluoroacetyl group of the mixed anhydride. Other analogous mixed anhydride intermediates may be expected to undergo decomposition under the reaction conditions to yield the transient amine or its anion prior to amide formation. A study of the reaction of substituted aryl and alkyl isocyanates with strong organic acids

Can. J. Chem. Downloaded from www.nrcresearchpress.com by 210.87.254.105 on 09/05/12
For personal use only.

in order to determine electrical and steric effects on the course of the reaction is in progress.

It is of interest to note that acetophenone was converted to acetanilide in 80% yield using sodium azide in the TFA–TFAn medium. This compares quite favorably with that reported by Briggs and De Ath (4) who obtained a yield of 70% using the sulfuric acid medium.

EXPERIMENTAL

Melting points were taken on the Fisher-Johns melting point apparatus and are uncorrected. Analyses were performed by the Schwarzkopf Microanalytical Laboratory, 56–19 37th Avenue, Woodside 77, New York.

The Schmidt Reaction in the Trifluoroacetic Acid – Anhydride Medium

The reaction apparatus used throughout consisted of a 100 ml, three-necked, round-bottomed flask which was equipped with a mercury-sealed stirrer, a small oblong flask which allowed the portionwise addition of sodium azide simply by rotation of the flask at the appropriate angle, and a reflux condenser. The outlet of the condenser was connected via a rubber tube to an inverted graduated cylinder which was used to collect gas by the downward displacement of water. When required, the reaction flask was immersed in an oil bath which was heated to facilitate reaction. The conversion of benzoic acid to N-phenyl-trifluoroacetamide exemplifies the reaction.

Benzoic acid (3.0 g, 0.0246 mole) was dissolved in a solution of trifluoroacetic acid (25 ml) and trifluoroacetic anhydride (10 ml). Sodium azide (1.6 g, 0.0492 mole) was added portionwise with stirring over a period of 48 h whereupon 700 ml of gas was collected. The volatile materials were removed *in vacuo* and the remaining portion of the reaction mixture was poured on crushed ice. The crude N-phenyl-trifluoroacetamide was collected by filtration, washed with cold water, and air dried. Recrystallization from a chloroform – petroleum ether (b.p. 60–110°) solvent pair gave colorless crystals (3.3 g, 72%), m.p. 87–89°, recorded 87–89° (5).

Anal. Calcd. for $C_8H_6F_3NO$: C, 50.81; H, 3.19; F, 30.11; N, 7.40. Found: C, 50.92; H, 3.19; F, 30.39; N, 7.42.

An authentic sample of N-phenyl-trifluoroacetamide was prepared by the addition of trifluoroacetic anhydride to freshly distilled aniline at ice-bath temperature. The mixture was allowed to stand for 20 min and was poured on crushed ice. Recrystallization from chloroform – petroleum ether (b.p. 60–110°) yielded colorless crystals, m.p. 87–89°. There was no depression in melting point on admixture with the N-phenyl-trifluoroacetamide isolated from the Schmidt reaction with benzoic acid.

The following analytical data is recorded for the N-substituted trifluoroacetamides listed in Table I.

N-(ortho-Tolyl)-trifluoroacetamide

Anal. Calcd. for $C_9H_8F_3NO$: C, 53.20; H, 3.96; N, 6.89; F, 28.05. Found: C, 53.17; H, 4.21; N, 6.59; F, 27.77.

N-(para-Tolyl)-trifluoroacetamide

Anal. Calcd. for $C_9H_8F_3NO$: C, 53.20; H, 3.96; N, 6.89; F, 28.05. Found: C, 53.34; H, 4.17; N, 7.05; F, 28.02.

N-(meta-Tolyl)-trifluoroacetamide

Anal. Calcd. for $C_9H_8F_3NO$: C, 53.20; H, 3.96; N, 6.89; F, 28.05. Found: C, 53.46; H, 3.98; N, 6.73; F, 28.11.

N-(ortho-Bromophenyl)-trifluoroacetamide

Anal. Calcd. for $C_8H_5F_3NOBr$: C, 35.43; H, 1.88; Br, 29.82; N, 5.22; F, 21.22. Found: C, 35.57; H, 2.02; Br, 30.06; N, 5.19; F, 21.13.

N-(ortho-Nitrophenyl)-trifluoroacetamide

Anal. Calcd. for $C_8H_5F_3N_2O_3$: C, 41.03; H, 2.15; N, 11.96; F, 24.34. Found: C, 41.33; H, 2.33; N, 11.82; F, 24.18.

N-(1-Naphthyl)-trifluoroacetamide

Anal. Calcd. for $C_{12}H_8F_3NO$: C, 60.21; H, 3.42; N, 5.81; F, 23.92. Found: C, 60.28; H, 3.52; N, 5.74; F, 23.80.

The above N-substituted trifluoroacetamides were prepared independently from the reaction of the corresponding amine with trifluoroacetic anhydride. The corresponding infrared spectrograms were identical as were melting points of appropriate admixtures with the corresponding derivatives obtained from the Schmidt reaction.

Can. J. Chem. Downloaded from www.nrcresearchpress.com by 210.87.254.105 on 09/05/12
For personal use only.

The Reaction of Phenyl Isocyanate with Trifluoroacetic Acid

Phenyl isocyanate (2.97 g, 0.025 mole) was dissolved in 10 ml of anhydrous chloroform. The solution was placed in a filter flask (100 ml) which was fitted with a dropping funnel. The side outlet was connected to a rubber tube which was led into an inverted graduated cylinder (1 000 ml) such that gas could be collected by the downward displacement of water. A solution of trifluoroacetic acid (2.7 g, slightly less than 0.025 mole) and chloroform (10 ml) was added dropwise over a period of 20 min through the funnel with occasional shaking while the reaction flask was maintained at a temperature of −20° by means of dry-ice – acetone bath. The resultant yellow solution was allowed to warm to room temperature whereupon gas evolved quite rapidly. The volatile material was removed *in vacuo* and the residue was poured on crushed ice whereupon N-phenyl-trifluoroacetamide solidified. The compound was recovered by filtration and air dried (3.13 g, 67.3%), m.p. 85–87°. A mixture melting point determination with an authentic sample was not depressed.

Reaction of Phenyl Isocyanate with a Mixture of Trifluoroacetic Acid and Acetic Anhydride

A solution of phenyl isocyanate (5.0 g, 0.042 mole), freshly distilled acetic anhydride (4.28 g, 0.042 mole), and 10 ml of anhydrous chloroform was cooled externally by means of an ice-water bath. Trifluoroacetic acid (4.8 g, 0.042 mole) was added dropwise with stirring over a period of 30 min. The reaction mixture was allowed to stir for an additional 30 min whereupon the chloroform was removed *in vacuo* and the remaining portion was poured on crushed ice. The N-phenyl-trifluoroacetamide was collected by filtration, air dried, and recrystallized from chloroform – petroleum ether (b.p. 60–110°). A yield of 6.67 g (84.1%), m.p. 89–90°, was obtained. The melting point was not depressed on admixture with an authentic sample of N-phenyl-trifluoroacetamide. The infrared spectrograms were identical.

Reaction of 1-Naphthyl Isocyanate with a Mixture of Trifluoroacetic Acid and Acetic Anhydride

A solution of 1-napthyl isocyanate (5.0 g, 0.0296 mole), freshly distilled acetic anhydride (3.38 g, 0.0296 mole), and 10 ml of anhydrous chloroform was mechanically stirred while trifluoroacetic acid (3.38 g, 0.0296 mole) was added dropwise rapidly at room temperature. The reaction mixture was allowed to stand overnight whereupon the volatile components were removed *in vacuo*. The residue was poured on crushed ice and N-(1-naphthyl)-trifluoroacetamide was collected by filtration. Recrystallization from a chloroform – petroleum ether (b.p. 60–110°) solvent pair afforded 6.4 g (90.6%) of pure material, m.p. 96–97°. The melting point was not depressed on admixture with an authentic sample.

Reaction of Phenyl Isocyanate with a Mixture of Trichloroacetic Acid and Acetic Anhydride

A three-necked, round-bottomed flask (250 ml) was equipped with a stirrer, a dropping funnel, and a reflux condenser outfitted with a rubber tube which led to a gas-measuring cylinder. Phenyl isocyanate (5.0 g, 0.042 mole) was added to the flask. Stirring was commenced and a solution of trichloroacetic acid (6.84 g, 0.042 mole) and 10 ml of anhydrous chloroform was added. The reaction mixture was heated to 40° by means of a water bath and was allowed to stir at this temperature for 24 h. The chloroform was removed *in vacuo* and the remaining contents of the flask were poured on crushed ice. The product which precipitated was collected by filtration, washed twice with cold water, and air dried. Recrystallization from a chloroform – petroleum ether (b.p. 60–110°) solvent pair afforded 5.2 g (92%) of pure acetanilide, m.p. 114–115°. The melting point was not depressed on admixture with an authentic sample. The infrared spectrograms were identical.

Reaction of Phenyl Isocyanate with a Mixture of Acetic Acid and Trifluoroacetic Anhydride

A solution of trifluoroacetic anhydride (8.8 g, 0.042 mole) acetic acid (2.35 g, 0.042 mole), and phenyl isocyanate (5.0 g, 0.042 mole) was stirred at 45–50° for 24 h. The volatile components were removed *in vacuo* and the remaining contents were poured on crushed ice. The resultant precipitate was collected by filtration, washed with cold water, and air dried. Recrystallization from a chloroform – petroleum ether (60–110°) solvent pair gave pure N-phenyl-trifluoroacetamide (6.9 g, 87.2%), m.p. 89–90°. The melting point was not depressed on admixture with an authentic sample. The infrared spectrograms were identical.

Reaction of Acetophenone with Sodium Azide in a Mixture of Trifluoroacetic Acid and Trifluoroacetic Anhydride

A solution of acetophenone (3.0 g, 0.024 mole), trifluoroacetic acid (25 ml), and trifluoroacetic anhydride (10 ml) was placed in a reaction flask. Sodium azide (3.16 g, 0.048 mole) was added portionwise with stirring over a period of 15 min. The reaction mixture was allowed to stir for an additional 4 h whereupon the volatile components were removed *in vacuo* and the remaining portion was poured on crushed ice. The acetanilide was recovered by filtration and recrystallized from chloroform – petroleum ether (b.p. 60–110°). A yield of 2.72 g (80.4%), m.p. 114–115° was obtained. The melting point was not depressed on admixture with an authentic sample.

ACKNOWLEDGMENTS

The authors express deep appreciation for a Province of Ontario Fellowship received by Mrs. Ing. They also wish to express gratitude to the National Research Council for support of this work.

Can. J. Chem. Downloaded from www.nrcresearchpress.com by 210.87.254.105 on 09/05/12
For personal use only.

REFERENCES

1. H. WOLFF. The Schmidt reaction. *In* Organic reactions. Vol. III. John Wiley and Sons, Inc., New York. 1946. pp. 307–336.
2. K. G. RUTHERFORD and M. S. NEWMAN. J. Am. Chem. Soc. **79**, 213 (1957).
3. A. FRY. J. Am. Chem. Soc. **75**, 2686 (1953).
4. L. H. BRIGGS and G. C. DE ATH. J. Chem. Soc. 456 (1937).
5. R. REED. J. Am. Chem. Soc. **78**, 801 (1956).

Can. J. Chem. Downloaded from www.nrcresearchpress.com by 210.87.254.105 on 09/05/12
For personal use only.

Can. J. Chem. Downloaded from www.nrcresearchpress.com by 210.87.254.42 on 09/05/12
For personal use only.

SOLVOLYSIS OF ALKYL CHLOROSULFATES

PART I. REACTION OF *n*-PROPYL CHLOROSULFATE WITH NUCLEOPHILES[1]

E. BUNCEL AND J. P. MILLINGTON
Department of Chemistry, Queen's University, Kingston, Ontario

Received July 31, 1964

ABSTRACT

The effect of various reagents on the rate of hydrolysis of *n*-propyl chlorosulfate in 10 *M* aqueous dioxane is reported. Halide ions increase the rate of reaction ($I^- > Br^- > Cl^-$) but perchlorate is without effect. Hydroxide and pyrrolidine have a strong accelerating effect, but only at higher concentrations. These observations support a bimolecular mechanism: rate-determining displacement by nucleophile on carbon, with OSO_2Cl^- as the leaving group. The present results are not in accord with a previous proposal that alkyl chlorosulfates react by rate-determining sulfur–chlorine bond fission followed by fast displacement by nucleophile on carbon.

INTRODUCTION

Alkyl chlorosulfates,[2] $ROSO_2Cl$, comprise a class of acyl halide which has been only slightly studied in the past, in comparison with, for example, the structurally related chlorosulfites, ROSOCl, or the sulfonyl chlorides, RSO_2Cl. It is only recently that the diverse reactions of chlorosulfates have been utilized in organic synthesis, by Jones and co-workers (1) of this laboratory in the field of carbohydrate chemistry. The complexity of these reactions have pointed to the necessity of detailed studies of relatively simple compounds and it is with this purpose that this series of studies was initiated. The present paper reports the results of perhaps the simplest and most basic study, that of aqueous hydrolysis of a typical primary alkyl chlorosulfate.

Early studies (2) of the hydrolysis of methyl chlorosulfate in water ascribed three concurrent modes of reaction to the ester, to give the hydrogen sulfate, chloride, and methanol (eqs. [1]–[3]); in addition some dimethyl ether was often observed. These reactions were heterogeneous, due to insolubility of the chlorosulfates in water.

$$[1] \qquad CH_3OSO_2Cl + H_2O \rightarrow CH_3OSO_3H + HCl,$$

$$[2] \qquad CH_3OSO_2Cl + H_2O \rightarrow CH_3Cl + H_2SO_4,$$

$$[3] \qquad CH_3OSO_2Cl + 2H_2O \rightarrow CH_3OH + H_2SO_4 + HCl.$$

More recently Hall (3) found that under homogenous conditions, in a medium of aqueous dioxane, reaction occurred only according to eq. [3]. Hall also carried out the first kinetic study on this class of acyl halide and compared their reactivity with the related sulfonyl chlorides and sulfamyl chlorides. He studied methyl and ethyl chlorosulfates and came to certain conclusions concerning their mechanism of reaction. However, these conclusions needed a reevaluation in view of the recent work by Jones *et al.* (1). In the present work, carried out in 10 *M* aqueous dioxane, the effect of a variety of reagents has been investigated to ascertain the intimate nature of the hydrolysis.

RESULTS

Rate of Neutral Hydrolysis

The products of reaction of a 0.01 *M* solution of *n*-propyl chlorosulfate in 10 *M* aqueous dioxane were first examined. The ionic products are H_2SO_4 and HCl, formed in

[1]*Presented in part at the 47th Annual Conference of the Chemical Institute of Canada, Kingston, Ontario, June 1964.*

[2]*Also known as alkyl chlorosulfonates or alkoxysulfonyl chlorides.*

quantitative yield. The only organic product detected by vapor-phase chromotography was *n*-propyl alcohol. The stoichiometry of reaction is hence that of a simple hydrolysis, as in eq. [3].

The rate of neutral hydrolysis in 10 *M* aqueous dioxane at 25° was measured conductimetrically; the pseudo-first-order rate constant calculated from the usual plot, linear over 90% reaction,[3] is $(38.6 \pm 0.3) \times 10^{-4}$ s^{-1}. As a check, the rate was also determined by electrochemical measurement of chloride ion; this gave the rate constant value $(37.4 \pm 2.8) \times 10^{-4}$ s^{-1}.

Effect of Added Nucleophiles

In Table I are presented the effects of added perchloric acid, sodium perchlorate, some halide ions, sodium hydroxide, and pyrrolidine on the rate of hydrolysis of *n*-propyl chlorosulfate in 10 *M* aqueous dioxane at 25 °C. These data were obtained by the conductivity method. In the presence of halide, hydroxide, and pyrrolidine the first-order plot was linear over 1–2 half-lives but showed a moderate deviation from linearity thereafter. The variation in the individual rate constants during a given run was also markedly greater than in the absence of added reagents (±1%), particularly at the higher ionic strengths. Thus with added halide the highest error was ±5%, with added hydroxide, pyrrolidine, and perchloric acid, ±10%; with added perchlorate, a smaller error was observed.

TABLE I

Hydrolysis of *n*-propyl chlorosulfate in 10 *M* aqueous dioxane at 25 °C in presence of added reagents

$[ROSO_2Cl] \times 10^2$ (*M*)	Added reagent	Conc. $\times 10^2$ (*M*)	$k \times 10^4$ (s^{-1})
1.00	—	—	38.6
1.00	$HClO_4$	0.453	40.7
		1.00	40.1
		5.12	40.3
1.00	$NaClO_4$	0.538	38.8
		0.959	39.5
		5.29	40.1
1.00	NaCl	0.685	46.0
		0.824	49.3
		5.09	74.7
1.00	NaBr	0.551	52.6
		1.02	68.5
		4.98	222
1.00	NaI	0.423	44.6
		1.33	145
		5.22	541
0.50	NaOH	—	37.7
1.02		0.54	40.7
0.94		1.08	35.7
1.04		4.5	42.0
0.537		4.0	61.5
0.510		4.5	105
0.604		9.0	145
1.28	C_4H_8NH	1.55	44.0
1.78		2.55	47.0
1.62		2.60	46.2
1.73		3.27	75.3
1.35		3.40	198

[3]*At higher concentration of chlorosulfate (0.05–0.10 M) deviation from linearity is observed much sooner, due to reaction of the liberated chloride ion with substrate (vide infra).*

Can. J. Chem. Downloaded from www.nrcresearchpress.com by 210.87.254.42 on 09/05/12
For personal use only.

Can. J. Chem. Downloaded from www.nrcresearchpress.com by 210.87.254.42 on 09/05/12
For personal use only.

DISCUSSION

Mechanism of Hydrolysis

In early work with methyl and ethyl chlorosulfate a variety of products was observed, which would suggest rather complex reactions with water. The more recent work of Hall (3) showed that in dilute solution in aqueous dioxane the only products are the alcohol, H_2SO_4, and HCl. Hall's results are confirmed in the present study. The principal reaction is therefore that of a simple hydrolysis (eq. [3]). The other products in the early work were due in part to heterogeneous reaction conditions. At the same time the early studies used very vigorous conditions, e.g. heating to 100° for several hours when the present work shows that hydrolysis at 25° would be complete in several minutes. In the acidic reaction mixture the alcohol formed in the primary reaction would give rise to alkyl hydrogen sulfate, alkyl chloride, and dialkyl ether by straightforward reaction paths.

Discussion of the mechanism of hydrolysis must consider whether the sulfur or the carbon of the alkyl chlorosulfate suffers attack by a water molecule, and also the nature of the leaving group. In the case of displacement on sulfur, there are two possible leaving groups, chloride and alkoxide. Since it is known that chloride ion is a much better leaving group than alkoxide (4), the latter possibility is extremely unlikely. Attack on sulfur with chloride as the leaving group would yield the intermediate alkyl hydrogen sulfate, which may subsequently hydrolyze to ROH and H_2SO_4. However, it is known (5) that alkyl hydrogen sulfates are hydrolyzed with difficulty and would certainly be stable under the reaction conditions. Hence this reaction path can be eliminated.

A variation of the above pathway is possible, if it is postulated that the rate-determining step is ionization at the sulfur–chlorine bond to give an intermediate alkoxysulfonylium ion, $ROSO_2^+$, followed by a fast step involving reaction of the nucleophile at carbon (eq. [4]). The displaced SO_3 would react instantaneously with the water of the medium.

[4*a*] $$ROSO_2Cl \xrightarrow{\text{slow}} Cl^- + R{-}O{-}\overset{\overset{O}{\|}}{\underset{\underset{O}{\|}}{S^+}} \xrightarrow{\text{fast}} \begin{cases} \xrightarrow{H_2O} HOR + H^+ + SO_3 \\ \xrightarrow{Y^-} Y{-}R + SO_3 \end{cases}$$

[4*b*]

An alternative to the reaction paths considered above is a rate-determining displacement on carbon by a water molecule or a nucleophile (eq. [5]). The leaving group in this displacement would be OSO_2Cl^- which is expected to react with a water molecule in a fast step with formation of $SO_4^=$, Cl^-, and $2H^+$.

[5] $$Y^- + ROSO_2Cl \rightarrow Y{-}R + {}^-OSO_2Cl.$$

Hall concluded (3) that although methyl and ethyl chlorosulfates may undergo some reactions which are S_N2 displacements on carbon, the usual reaction mode is the ionization mechanism at sulfur (eq. [4]). The main evidence on which Hall based this conclusion was that hydrolysis of ethyl chlorosulfate in presence of pyrrolidine in concentrations "too low to affect the rate significantly" yielded 20% of 1-ethylpyrrolidine as reaction product. Reaction sequence [4], with Y^- = pyrrolidine, was proposed to account for this result.

Our data on the effect of added reagents (Table I) are consistent with bimolecular displacement on carbon (eq. [5]). Perchloric acid and sodium perchlorate have no effect on the rate of hydrolysis of *n*-propyl chlorosulfate. A lack of acid catalysis or salt effect

has been noted in other bimolecular solvolytic reactions (6), even though theory (7) would predict a small accelerating affect. On the other hand, chloride, bromide, and iodide ions have a substantial accelerating effect on the rate (Fig. 1). The relative rate sequence $I^- > Br^- > Cl^-$ has been observed in many past studies of displacement reactions at carbon in aqueous media (4). Clearly in presence of these nucleophiles there are two competing reactions at hand: solvolysis and bimolecular displacement at carbon by the added nucleophile.

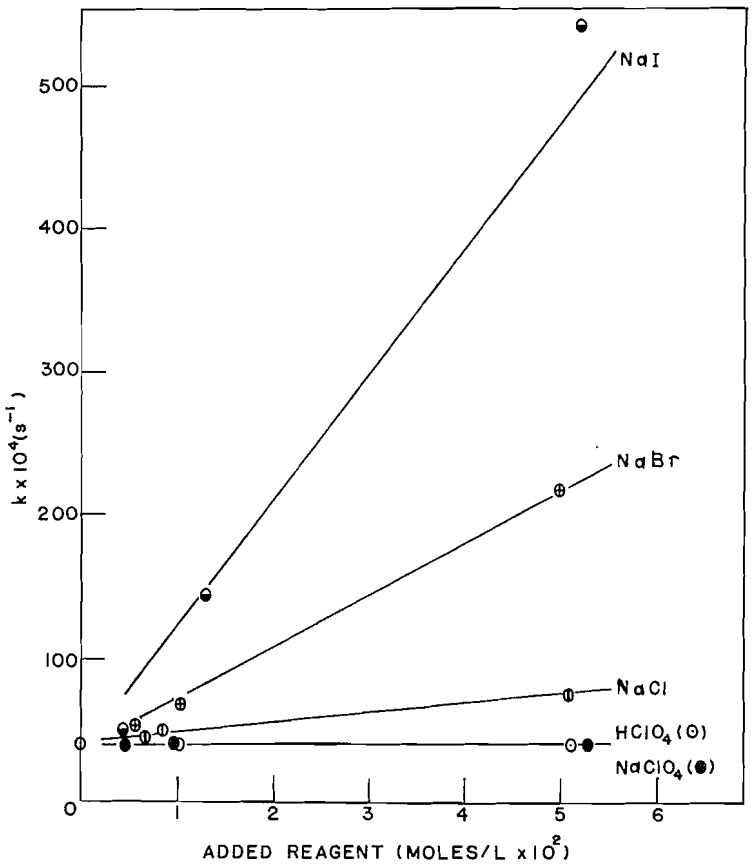

FIG. 1. Effect of added reagents on rate of hydrolysis of *n*-propyl chlorosulfate.

The effect of hydroxide ion and of pyrrolidine on the rate of hydrolysis of *n*-propyl chlorosulfate (Fig. 2) follow a different pattern from the effect of halide ions. No effect on the rate is observed at low concentrations, but a very large accelerating effect is observed at higher concentrations of these reagents. Figure 2 shows the results with hydroxide ion and pyrrolidine, expressed as rate constants as a function of the concentration ratios $[OH^-]/[ROSO_2Cl]$ and $[C_4H_8NH]/[ROSO_2Cl]$. Pyrrolidine is seen to have a much greater effect on the rate than does hydroxide. An explanation of these results must first consider the derivation of the rate constants. As stated previously, the rate data are obtained by the conductivity method, which clearly is based on the number and type of ions formed in the reaction. When neutral solvolysis is studied, these ions are H_3O^+, Cl^-, and $SO_4^=$ (or HSO_4^-). When the reaction is conducted in presence of added

Can. J. Chem. Downloaded from www.nrcresearchpress.com by 210.87.254.42 on 09/05/12
For personal use only.

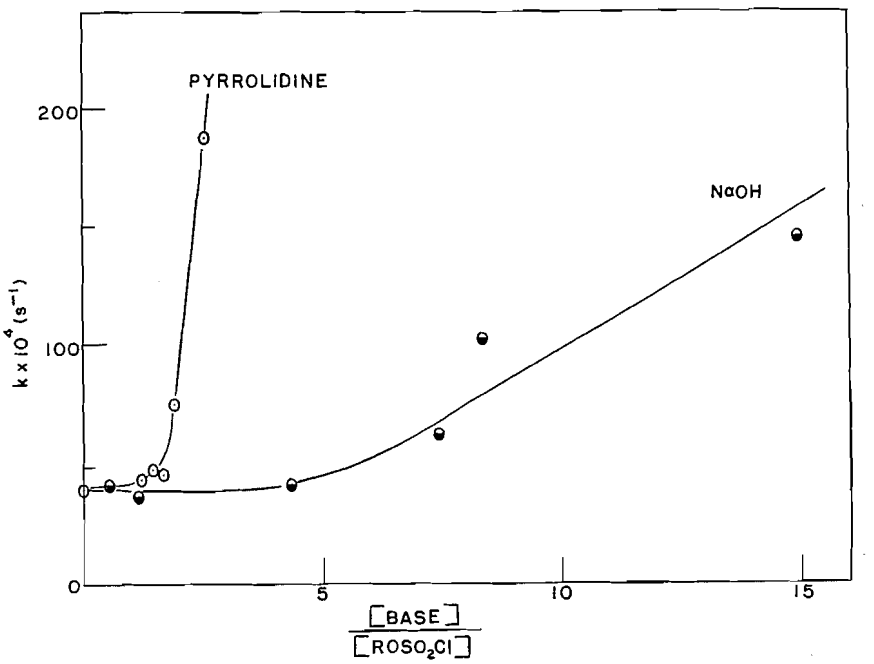

FIG. 2. Effect of added sodium hydroxide and pyrrolidine on rate of hydrolysis of *n*-propyl chlorosulfate.

hydroxide ions these make themselves felt in several ways. Firstly, they will have an effect on the neutral solvolysis, by neutralizing the hydrogen ions thus liberated. In this process three hydroxyl ions are consumed and a chloride and a sulfate ion are formed; this has no effect on the conductimetrically measured neutral solvolytic rate constant. Secondly, hydroxyl ions themselves undergo nucleophilic displacement on the substrate, the stoichiometry of this reaction being given by eq. [6].[4]

$$[6] \qquad 3HO^- + ROSO_2Cl \rightarrow ROH + SO_4^{=} + Cl^- + H_2O.$$

Since hydroxide ion is a more effective nucleophile than water, this reaction will manifest itself in an increased rate constant. At sufficiently low concentrations hydroxide ion cannot effectively compete with neutral solvolysis, but as the hydroxide ion concentration is increased it is increasingly able to compete with the neutral solvolytic reaction, until eventually this reaction (eq. [6]) becomes dominant. This accounts for the greatly increasing rate at higher concentrations of hydroxide. Since three hydroxyl ions are consumed according to each act of the hydroxide displacement (eq. [6]) and three more in neutral solvolysis (eq. [3]), the reaction is strongly dependent on the hydroxide ion concentration and the ratio $[OH^-]/[ROSO_2Cl]$ must be considered when the chlorosulfate concentration is varied, as in this series of runs.

The lyate ion effect, k_{OH^-}/k_{H_2O}, calculated by means of eq. [7] from the last three points of Fig. 2, is 380 ± 30.

$$[7] \qquad \text{Rate} = k_{H_2O}[ROSO_2Cl] + k_{OH^-}[ROSO_2Cl][OH^-].$$

A lyate ion effect of this magnitude is added evidence for the normal solvolytic nature of this reaction. Typical values for other solvolytic reactions range between about 10 and several thousand, depending on the nature of substrate and solvent (e.g. ethyl bromide

Can. J. Chem. Downloaded from www.nrcresearchpress.com by 210.87.254.42 on 09/05/12
For personal use only.

in 80% aqueous ethanol, 1 230 (9); 1-bromohexane in 50% aqueous dioxane, 124 (10); ethyl *p*-toluenesulfonate in 60.7% aqueous dioxane, 45 (11)).

In the presence of added pyrrolidine a parallel situation arises. In neutral solvolysis the liberated hydrogen ions are again neutralized in formation of pyrrolidinium ions, and the conductimetric rate constant remains unaltered since it now reflects the formation of sulfate, chloride, and pyrrolidinium ions. Competing with neutral solvolysis is the displacement of pyrrolidine on carbon of $ROSO_2Cl$ with formation of N-propylpyrrolidine and HSO_3Cl. Since the latter will be hydrolyzed by water to H_2SO_4 and HCl, three more moles of pyrrolidine will be consumed in neutralization of the acids. The stoichiometry of the process is given in eq. [8].

$$[8] \qquad 4C_4H_8NH + ROSO_2Cl + H_2O \rightarrow R{-}NC_4H_8 + 3C_4H_8NH_2^+ + SO_4^{=} + Cl^-.$$

The pyrrolidine displacement is able to compete with neutral solvolysis more effectively than in the case of hydroxide displacement, since pyrrolidine is expected to be the better nucleophile (4); this in turn is reflected in a greater accelerating effect by pyrrolidine than by hydroxide, for a given [base]/[$ROSO_2Cl$] concentration ratio, as shown in Fig. 2.

According to Hall's observations added hydroxide significantly affected the rate of hydrolysis of ethyl chlorosulfate and pyrrolidine was without detectable effect, yet the product contained 20% of 1-ethylpyrrolidine. Our data, however, would indicate that with the concentrations used (3), $[C_4H_8NH]/[C_2H_5OSO_2Cl] = 2.3$, one would have expected a significant increase in rate. Although the effect of the amine : chlorosulfate concentration ratio on the rate may vary with the alkyl group and with the medium, methyl chlorosulfate in 86.1% water – 13.9% dioxane was found (3) to exhibit a significant increase in rate constant at $[C_4H_8NH]/[CH_3OSO_2Cl] = 1.5$. According to our work (12) ethyl chlorosulfate fits well into the reaction series of primary chlorosulfates, and a change in mechanism between methyl and propyl is extremely unlikely.[5]

The evidence presented in this paper supports a solvolytic mechanism analogous to that of other alkyl derivatives, except that in chlorosulfate solvolysis the leaving group, OSO_2Cl, is composite. That this leaving group, although unfamiliar, should be a chemically feasible one is shown by the stability of salts having OSO_2Cl as the anionic portion, e.g., $NaSO_3Cl$, Me_4NSO_3Cl, PCl_4SO_3Cl; the infrared assignments are fully in accord with the $^-O{-}SO_2{-}Cl$ structure (13). The ionization of these salts into M^+ and OSO_2Cl^- is also shown by conductivity data in liquid hydrogen chloride (13). Chlorosulfonic acid in sulfuric acid also ionizes in this manner (14). In aqueous medium the anion OSO_2Cl^- is unstable and becomes rapidly hydrolyzed to $SO_4^{=}$, Cl^-, and $2H_3O^+$.

Further discussion of the mechanism of solvolysis of alkyl chlorosulfates is presented in Part II of this series (12).

EXPERIMENTAL

Materials

n-Propyl chlorosulfate was prepared after the method of Binkley (15). Dioxane, analytical reagent grade, was purified by refluxing over sodium for 24 h, followed by fractional distillation. The fraction having a boiling point of 101.5° was collected. The dioxane was stored in the absence of light and was used within 2 weeks of distillation. The pyrrolidine was a commercial sample and was fractionally distilled twice, b.p. 88.5°. Water was distilled and deionized using a commercial mixed bed ion-exchange resin. All inorganic

[4]*Although one would expect the conductivity to decrease during this process, it actually increases, due to the very low conductance of hydroxide ion in the medium 85.3% dioxane – 14.7% water (8).*

[5]*Experimental difficulties in measuring rate constants for ethyl chlorosulfate were reported by Hall (3), apparently due to incomplete solubility of the compound in the more aqueous medium. It is possible that this accounted for the insensitivity of rate to pyrrolidine concentration with ethyl chlorosulfate. Methyl chlorosulfate was completely soluble in that medium and gave good rate constants (3).*

Can. J. Chem. Downloaded from www.nrcresearchpress.com by 210.87.254.42 on 09/05/12
For personal use only.

salts used were of analytical reagent quality. The 10 *M* aqueous dioxane was made up by weight (85.3 wt. % dioxane – 14.7 wt. % water).

Product Analysis

The ionic products were analyzed by standard methods. The concentrations used for the product analysis were the same as those in the kinetic experiments, 0.01 *M* in the chlorosulfate. The reaction mixtures were allowed to stand in the thermostat bath for at least six half-lives.

The total acid was determined by titrating aliquots (5 ml) with standard sodium hydroxide (0.01 *N*). The chloride was determined by adding an aliquot (5 ml) to distilled water containing finely powdered barium carbonate, which neutralized the acid, bringing the solution to the correct pH for titration, and removed sulfate ions as barium sulfate. The solution was then titrated with standard silver nitrate (0.01 *N*) using Mohr's method. Sulfate was obtained as the difference between the total acid and the chloride concentrations.

The determination of the alcoholic product of reaction was done by vapor-phase chromatography (v.p.c.). The reaction product was saturated with sodium chloride and extracted exhaustively with ether. Evaporation of the ether yielded a solution of the alcohol in dioxane, carried from the original reaction mixture. This solution was diluted to the original volume with dioxane and was analyzed by v.p.c. using calibration curves prepared from the authentic alcohol. The recovery of product ranged between 75 and 90%. No olefinic product could be detected by the method of Davis *et al.* (16).

Measurement of Rates

The reaction vessel was placed in a thermostat which gave temperature control to ±0.01°. Temperature was measured using an N.B.S. calibrated thermometer. In all the determinations, unless stated otherwise, the reaction solution was initially in the range of 0.01 *M* chlorosulfate in 10 *M* aqueous dioxane. All volumes and concentrations were measured at the temperature of the reaction.

Conductivity Method

A commercial direct-reading conductivity bridge, accurate to 1%, and a dip-type conductivity cell (cell constant approximately 0.6) were used.

A calibration curve (Fig. 3) of conductivity as function of concentration was determined as follows. As the chlorosulfate under the conditions of the hydrolysis yields 1 mole of sulfuric acid and 1 mole of hydrochloric acid, a standard solution of 0.01 *M* hydrochloric acid and 0.01 *M* sulfuric acid in 10 *M* aqueous dioxane was successively diluted. The measurement of the conductivity of these diluted solutions gave a plot of concentration of total ionic product (derived from the chlorosulfate) as a function of conductivity. From this curve values of concentration at various time intervals of any run could be interpolated.

It was found that, over the conductivity range measured during the runs, concentration was a linear function of conductivity. Hence rates calculated from conductivity were within the limits of experimental error, the same as those calculated from the interpolated values of concentration. A typical result is shown in Table II. Thereafter rates were normally determined graphically. The error in determining rates in the presence of added ions is rather large due to the small relative increase in conductivity during a run at the higher ionic strengths.

The experimental values of the specific conductivity obtained from rate measurements in the presence of hydroxide and pyrrolidine were related to concentration in a similar manner as described above for

TABLE II

Rates of hydrolysis of *n*-propyl chlorosulfate in 10 *M* aqueous dioxane, calculated from specific conductivity and from concentration (temperature = 24.97°; initial concentration of *n*-propyl chlorosulfate 0.00935 mole/l)

Time (s)	$\kappa^* \times 10^5$ ($ohm^{-1}\,cm^{-1}$)	$k \times 10^4$ (s^{-1}) from κ	$c^\dagger \times 10^2$ (mole/l)	$k \times 10^4$ (s^{-1}) from c
120	7.13	38.2	0.178	40.1
180	9.17	38.8	0.317	38.4
240	10.6	38.5	0.450	39.2
300	11.9	39.0	0.545	39.1
360	12.8	38.8	0.615	38.2
420	13.6	39.3	0.682	38.8
480	14.2	38.8	0.730	39.0
540	14.7	38.7	0.770	39.0
600	15.0	38.6	0.800	39.0
	16.4		0.913	
	Mean value	38.57±0.35		38.72±0.63
	Graphical value	38.5		38.6

*κ is the specific conductivity.
†c is expressed in mole/l of $ROSO_2Cl$ which is equivalent to 1 mole of H_2SO_4 plus 1 mole of HCl.

Can. J. Chem. Downloaded from www.nrcresearchpress.com by 210.87.254.42 on 09/05/12
For personal use only.

neutral solvolysis (Fig. 3). Again it was found that concentration was approximately proportional to conductivity. With added hydroxide, as with other reagents, the conductivity of the reaction solution during a run increased continuously with time. This rather surprising result is due to the very small conductance of hydroxide ion in 10 *M* aqueous dioxane (8).

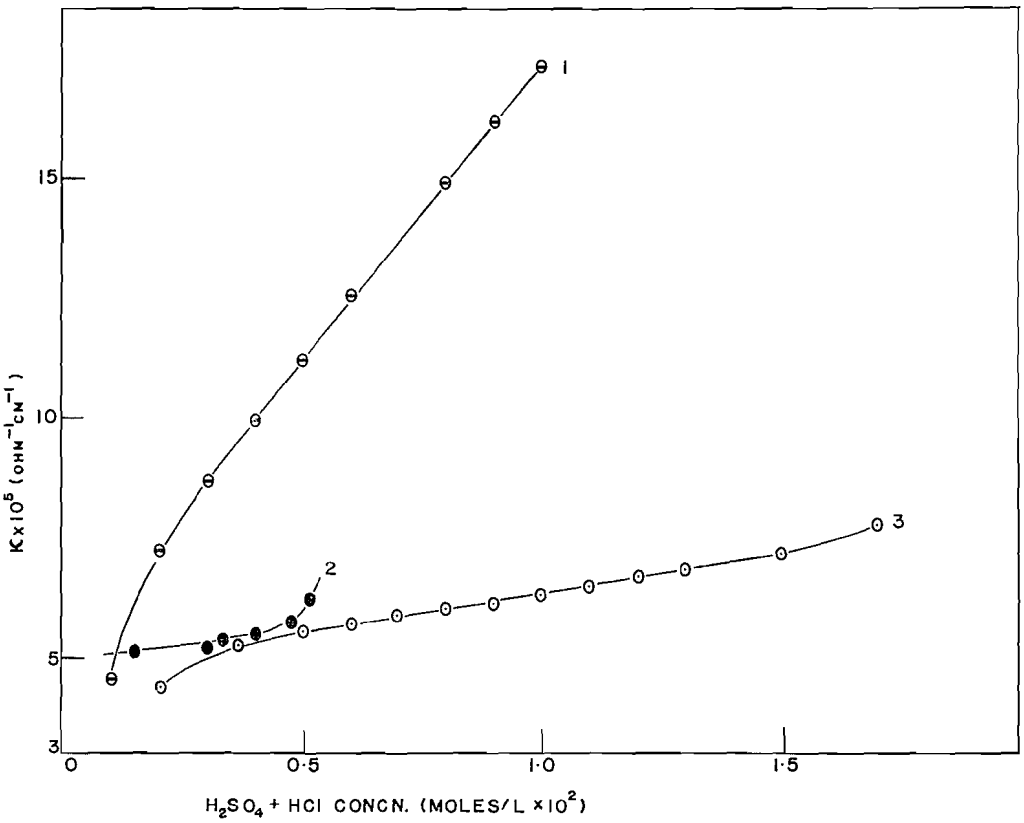

FIG. 3. Typical calibration curves of conductivity as function of added reagent for solvolysis of *n*-propyl chlorosulfate in 10 *M* aqueous dioxane: 1, H_2SO_4 + HCl only, with no added reagent; 2, with added NaOH (0.045 *M*); 3, with added pyrrolidine (0.0327 *M*).

Electrochemical Method for Chloride

A modification of the end-point cell described by Swain and Scott (17) was used. The cell was an H-type electrochemical cell with two compartments separated by an agar – potassium perchlorate salt bridge. Each compartment contained a silver / silver chloride electrode and a small air-driven stirrer. Several electrodes were prepared initially and before each run the two electrodes which had the least potential difference were chosen. The run was initiated by the addition of the chlorosulfate by means of a weight pipette to one compartment of the cell. A solution of hydrochloric acid in the same solvent equivalent to one-quarter half-life was then added to the other compartment. The potential difference (p.d.) between the two electrodes was then measured and when this approached zero the electrodes were shorted across the galvanometer; the time at which the p.d. was zero was noted. A further volume of the acid was then added and the time at which the p.d. was zero was again noted. Hence at these times the concentrations of chloride ion present in the reaction mixture was known, and the rate constant could be calculated.

ACKNOWLEDGMENTS

The authors are indebted to Professor J. K. N. Jones for his interest and encouragement. The National Research Council is thanked for financial support and a Studentship to J. P. M. The award by Queen's University of a R. Samuel McLaughlin Resident Fellowship to J. P. M. (1962–1963) is gratefully acknowledged.

Can. J. Chem. Downloaded from www.nrcresearchpress.com by 210.87.254.42 on 09/05/12
For personal use only.

REFERENCES

1. H. J. JENNINGS and J. K. N. JONES. Can. J. Chem. **41**, 1151 (1963); Can. J. Chem. **40**, 1408 (1962). J. K. N. JONES, M. B. PERRY, and J. C. TURNER. Can. J. Chem. **38**, 1122 (1960). P. D. BRAGG, J. K. N. JONES, and J. C. TURNER. Can. J. Chem. **37**, 1412 (1959).
2. C. M. SUTER. The organic chemistry of sulfur. J. Wiley and Sons, N.Y. 1944. Chap. 1.
3. H. K. HALL, JR. J. Am. Chem. Soc. **78**, 1450 (1956).
4. E. S. GOULD. Mechanism and structure in organic chemistry. Holt, Rinehart and Winston. N.Y. 1959. Chap. 8.
5. R. L. BURWELL. J. Am. Chem. Soc. **74**, 1462 (1952). J. ZAWIDSKI and J. SAYKOWSKI. Anzeiger Akad. Wiss. Krakau. 75 (1916); Chem. Abstr. **11**, 2294 (1917).
6. R. FOON and A. N. HAMBLY. Australian J. Chem. **15**, 668 (1962).
7. C. K. INGOLD. Structure and mechanism in organic chemistry. Bell and Sons, London. 1953. Chap. 7.
8. E. BUNCEL and J. P. MILLINGTON. Unpublished work.
9. L. C. BATEMAN, K. A. COOPER, E. D. HUGHES, and C. K. INGOLD. J. Chem. Soc. 925 (1940).
10. S. C. J. OLIVIER. Rec. Trav. Chim. **56**, 247 (1937).
11. H. R. MCLEARY and L. P. HAMMETT. J. Am. Chem. Soc. **63**, 2254 (1951).
12. E. BUNCEL and J. P. MILLINGTON. Can. J. Chem. This issue.
13. T. C. WADDINGTON and F. KLANBERG. J. Chem. Soc. 2332, 2339 (1960).
14. J. BARR, R. J. GILLESPIE, and E. A. ROBINSON. Can. J. Chem. **39**, 1266 (1961).
15. W. W. BINKLEY. J. Am. Chem. Soc. **60**, 2810 (1938).
16. H. S. DAVIS, G. S. CRANDALL, and W. E. HIGBEE. Ind. Eng. Chem. Anal. Ed. **3**, 108 (1931).
17. C. G. SWAIN and C. B. SCOTT. J. Am. Chem. Soc. **75**, 141 (1953).

Can. J. Chem. Downloaded from www.nrcresearchpress.com by 210.87.254.42 on 09/05/12
For personal use only.

Can. J. Chem. Downloaded from www.nrcresearchpress.com by 210.87.254.105 on 09/05/12
For personal use only.

HYDROLYSIS OF A SERIES OF PRIMARY ALKYL CHLOROSULFATES

ENTROPY OF ACTIVATION AS A CRITERION OF FRAGMENTATION IN SOLVOLYTIC REACTIONS[1,2]

E. BUNCEL AND J. P. MILLINGTON
Department of Chemistry, Queen's University, Kingston, Ontario

Received October 13, 1964

ABSTRACT

The solvolysis of the series of alkyl chlorosulfates, $ROSO_2Cl$, where R = methyl, ethyl, *n*-propyl, isobutyl, and neopentyl, has been studied in 10 *M* aqueous dioxane. The relative reactivities fit well a solvolytic mechanism involving displacement by water on carbon, with OSO_2Cl as the leaving group. The change in mechanism of solvolysis from bimolecular with the straight-chain chlorosulfates to unimolecular with neopentyl chlorosulfate is shown by the absence of the lyate ion effect and the observation of rearrangement in the latter case.

The entropies of activation in chlorosulfate solvolysis appear to be abnormally large. It is proposed that the abnormal $\Delta S^{\ddagger}$ indicates a transition state in which both carbon–oxygen and sulfur–chlorine bond weakening occurs. It is shown that some other solvolytic reactions that are characterized by abnormally high entropies of activation may be interpreted on the basis of multiple bond fission (fragmentation). The mechanism of S_Ni reactions is considered in this context.

The preceding paper (1) considered in detail the reaction of a typical primary alkyl chlorosulfate with nucleophiles. Here we report the results of a solvolytic study on the series of primary alkyl chlorosulfates $ROSO_2Cl$, where R is methyl, ethyl, *n*-propyl, isobutyl, and neopentyl.

The products of reaction of dilute solutions (0.01 *M*) of the alkyl chlorosulfates in 10 *M* aqueous dioxane were determined (Table V, Experimental section). The ionic products are H_2SO_4 and HCl, formed in quantitative yield. The major organic product in each case was the alcohol, with a trace of olefin as side product. The major reaction is therefore that represented by eq. [1], i.e. a simple hydrolysis, the olefin being formed most probably by a minor competing elimination reaction. In the case of neopentyl chlorosulfate, the alcohol formed is that from rearrangement, viz. *t*-pentyl alcohol.

$$ROSO_2Cl + 2H_2O \rightarrow ROH + H_2SO_4 + HCl. \quad [1]$$

The kinetic data were measured in 10 *M* aqueous dioxane, 85.3% dioxane – 14.7% water, by weight. The concentration of chlorosulfate employed was 0.01 *M*. Rates were measured conductimetrically. The half-lives of the hydrolyses were found to vary from the order of a minute in the case of the methyl compound to several hours for the neopentyl. The pseudo-first-order rate constants were calculated from usual plots which were linear over at least 75% of reaction and usually over 90% of reaction. Results for hydrolysis at several temperatures are given in Table I. Rate constants when calculated for each point individually within a run agreed to ±1% (standard deviation). The reproducibility between runs was generally also ±1%. The rate constants given in Table I are the values from two separate runs. E_a and log *A* were obtained from a least-square plot. The error in E_a is estimated as ±0.35 kcal/mole, and in $\Delta S^{\ddagger}$, ±1.0 entropy units (e.u.).

The Bimolecular and the Unimolecular Mechanism

One of the criteria used in evaluating the mechanism of solvolysis is the lyate ion

[1]*Part II in series of solvolysis of alkyl chlorosulfates. Part I, preceding paper.*
[2]*Presented in part at the 47th Annual Conference of the Chemical Institute of Canada, Kingston, Ontario, June 1964.*

TABLE I

Hydrolysis of chlorosulfates (0.01 *M*) in 10 *M* aqueous dioxane

	$k \times 10^4$ (s^{-1})						E_a	Log *A*
$ROSO_2Cl$	9.94 °C	14.95 °C	19.95 °C	24.97 °C	34.99 °C	45.01 °C	(kcal)	(s^{-1})
Methyl	57.0 56.7	82.3 83.2	143 143	210 210			14.4	8.85
Ethyl	21.7 22.5	33.5 33.1	48.9 48.5	72.2 71.2			13.2	7.54
n-Propyl	10.5 10.6	17.5 17.5	27.6 27.6	39.5 40.1			14.2	7.97
Isobutyl				3.10 3.08	8.90 9.05	21.8 22.1	18.2	9.83
Neopentyl				0.167 0.169	0.640 0.650	2.22 2.21	24.6	13.24

effect (2). The large lyate ion effect with *n*-propyl chlorosulfate ($k_{OH^-}/k_{H_2O} = 380 \pm 30$) was strongly indicative of a bimolecular mechanism of solvolysis. Since a change in mechanism along the series might be anticipated, it was of interest to determine how the lyate ion effect might vary. The rate of hydrolysis of neopentyl chlorosulfate was totally unaffected by base. The absence of a lyate ion effect in this case is indicative of a unimolecular carbonium ion mechanism (2). This is confirmed by the observation of rearrangement; *t*-pentyl alcohol was the only product formed, apart from a trace of olefin, in solvolysis of neopentyl chlorosulfate.

The relative reactivities of the series of alkyl chlorosulfates studied is informative. The results, relative to ethyl chlorosulfate as standard, are shown in Table II which also gives the results of some other nucleophilic substitutions of primary compounds containing displaceable groups. The reactions are arranged in a decreasing order of magnitude of the rate ratio of methyl (or ethyl) to neopentyl.

Reactions 1 and 6 represent two extremes in the effect of environment on reactivity. In reaction 1, which is a bimolecular displacement reaction, steric hindrance plays a dominant role and is responsible for the extremely low relative reactivity of the neopentyl compound. In reaction 6, solvolysis of the neopentyl compound actually proceeds at a faster rate than that of the methyl, so that clearly steric hindrance has now no importance; a limiting mechanism is indicated, that is a unimolecular carbonium ion mechanism with no participation by nucleophile in the transition state. However, even in formolysis some nucleophilic participation in the transition state must occur, since optically active 1-deutero primary systems react with inversion (3). In solvolysis of neopentyl derivatives there is no evidence for nucleophilic participation, but whether or not a migrating methyl group participates in the rate-determining transition state has not been settled (4, 5). An excellent discussion of this topic has been given (6).

The hydrolysis of alkyl chlorosulfates appears between the solvolysis of alkyl *p*-toluenesulfonates in pure ethanol and the solvolysis of alkyl bromides in 50% aqueous ethanol, in the reactivity order of Table II. Now solvolysis in ethanol (reaction 2) is considered (6) to be closely similar to the bimolecular displacement with ethoxide ion (reaction 1), so that in ethanolysis participation by the solvent molecule in the transition state must be very extensive (with the exception of the neopentyl case). By analogy, in the hydrolysis of alkyl chlorosulfates in 85.3% aqueous dioxane, solvent must likewise play an important role in the rate-determining transition state. Thus the above constitutes strong evidence in support of our view that alkyl chlorosulfates react with water in aqueous dioxane by

Can. J. Chem. Downloaded from www.nrcresearchpress.com by 210.87.254.105 on 09/05/12
For personal use only.

TABLE II

Relative rate of substitution of some primary compounds

Reaction	Relative rate					Ref.
	CH_3	CH_3CH_2	$CH_3CH_2CH_2$	$(CH_3)_2CHCH_2$	$(CH_3)_3CCH_2$	
1. RBr + EtO^- in EtOH, 55°	17.6	1.0	0.281	0.0297	0.00000423	7
2. ROTs, EtOH, 75°	2.3	1.0	—	0.046	0.00057	4
3. $ROSO_2Cl$, 85.3% aq. dioxane,* 25°	2.93	1.0	0.555	0.0431	0.00235	This work
4. RBr, 50% aq. EtOH,† 95°	1.94	1.0	—	0.075	0.00625	5
5. RBr, 70% aq. EtOH,† Ag^+, 64°	0.81	1.0	—	0.085	0.013	5
6. ROTs, HCOOH, 75°	0.56	1.0	—	1.22	1.0	4

*Expressed as weight %. On a volume % basis this would be 82%.
†Expressed as volume %.

bimolecular displacement on carbon, with the exception of neopentyl chlorosulfate which reacts by a unimolecular carbonium ion mechanism.

It is also noteworthy that the sequence of reactions 2–6, obtained by arranging these in the order of decreasing magnitude of the rate ratio methyl:neopentyl, also represents the order of increasing ionizing power of the medium, and the chlorosulfate hydrolysis fits exactly into this sequence on both accounts. This gives added weight to the above argument.

Activation Parameters

In the series ethyl, *n*-propyl, isobutyl, neopentyl, there is a steady change in both $\Delta H^{\ddagger}$ and $\Delta S^{\ddagger}$, the former increasing in magnitude and the latter becoming more positive (Table III). A plot of $\Delta H^{\ddagger}$ against $\Delta S^{\ddagger}$ is shown in Fig. 1. The slope of the straight line drawn through the points representing the above compounds, but excluding methyl, is 443.4 °K, which is the isokinetic temperature. Since the isokinetic temperature has a value far above the temperature of the experimental, interpretation of the data is free from the uncertainties arising when the isokinetic temperature is close to the experimental range (8). The enthalpy–entropy compensation effect observed in this reaction series is paralleled by the behavior of many other solvolytic reactions, for instance the solvolysis in water of alkyl methanesulfonates and bromides (9*a*). For one member of the series to deviate from this relationship is also not uncommon and in the present could be caused by the greatly reduced steric requirements of the transition state of the methyl case. It is also noteworthy that the neopentyl case falls on the isokinetic line with the alkyl chlorosulfates, methanesulfonates, and bromides (9*a*), even though neopentyl derivatives hydrolyze with rearrangement. Thus neopentyl derivatives seem to provide an exception to the general rule that a change in mechanism along a reaction series should be reflected by a deviation from the isokinetic relationship.

Entropy of Activation as a Criterion of Fragmentation

Further insight into the mechanism of chlorosulfate solvolysis is gained by consideration of the actual magnitudes of the activation parameters. A discussion of activation parameters must consider their dependence on the medium and on the mechanism of reaction. Thus the entropy of activation of solvolytic reactions conducted in aqueous organic solvents becomes rapidly more negative as the water content of the medium decreases (10) and a unimolecular mechanism is in general associated with a more positive entropy of activation, by 20 or more e.u., than a bimolecular reaction (11). The last point is well illustrated in the present series; $\Delta S^{\ddagger}$ for neopentyl chlorosulfate is 20–26 e.u. more positive than for the straight-chain chlorosulfates.

Can. J. Chem. Downloaded from www.nrcresearchpress.com by 210.87.254.105 on 09/05/12
For personal use only.

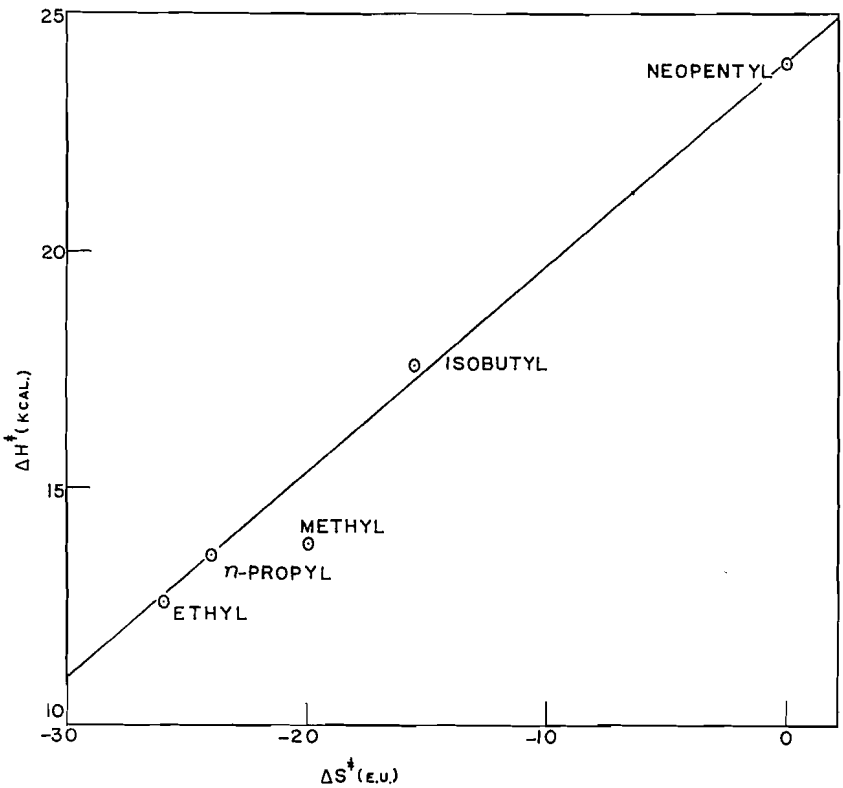

FIG. 1. Plot of $\Delta H^{\ddagger}$ vs. $\Delta S^{\ddagger}$ for solvolysis of chlorosulfates.

Comparison of the rates and activation parameters in chlorosulfate solvolysis with other solvolytic reactions, in the same reaction medium (Table III), shows at first glance that chlorosulfates react considerably faster and that in general lower enthalpies and greater entropies of activation are responsible for this enhanced reactivity. For a more searching comparison heed must be taken that two compared substrates should solvolyze by the same mechanism. It then becomes apparent that chlorosulfate solvolysis is associated with a more positive $\Delta S^{\ddagger}$, by 10–15 e.u. Considering first unimolecular solvolysis, *t*-butyl chloride, *t*-butyl bromide, α-phenylethyl chloride, α-phenylethyl bromide, and benzhydryl chloride all solvolyze with $\Delta S^{\ddagger}$ varying between −11 and −15 e.u., while $\Delta H^{\ddagger}$ varies between 20 and 22 kcal (12). Similarly, isopropyl benzenesulfonate, with $\Delta S^{\ddagger} = -13.3$ e.u. and $\Delta H^{\ddagger} = 22.0$ kcal, reacts by the unimolecular mechanism (13). No data have been found for neopentyl derivatives in this medium. For a comparison with activation parameters in bimolecular solvolysis, fewer data are available in the literature covering the present reaction medium. The solvolysis of a number of sulfonyl chlorides (14) provides comparable data: a typical example is ethane sulfonyl chloride, with $\Delta S^{\ddagger} = -37.4$ e.u. and $\Delta H^{\ddagger} = 12.8$ kcal. It appears then that in unimolecular as well as in bimolecular solvolysis, when $\Delta H^{\ddagger}$ is comparable ($EtOSO_2Cl$ vs. $EtSO_2Cl$) or when the reverse order obtains (neoPeOSO_2Cl vs. *t*-BuCl), chlorosulfates react with a more positive $\Delta S^{\ddagger}$. While this relationship has not been rigorously established, particularly in view of the many factors which can influence entropies of activation (9, 11, 12), yet it seems to be sufficiently well documented to warrant consideration of its possible mechanistic significance.

Can. J. Chem. Downloaded from www.nrcresearchpress.com by 210.87.254.105 on 09/05/12
For personal use only.

TABLE III

Rates and activation parameters for solvolysis in 10 *M* aqueous dioxane

	$k \times 10^4$ (25°) (s^{-1})	$\Delta H^{\ddagger}$ (kcal)	$\Delta S^{\ddagger}$ (25°) (e.u.)	$\Delta F^{\ddagger}$ (25°) (kcal)	Ref.
CH_3OSO_2Cl	211	13.8	−20.0	19.7	This work
$C_2H_5OSO_2Cl$	71.6	12.6	−26.0	20.4	
n-$C_3H_7OSO_2Cl$	39.8	13.6	−24.0	20.7	
i-$C_4H_9OSO_2Cl$	3.09	17.6	−15.5	22.2	
neo-$C_5H_{11}OSO_2Cl$	0.168	24.0	0.1	24.0	
CH_3SO_2Cl	0.13	15.3	−29.8	24.0	14
$C_2H_5SO_2Cl$	0.11	12.8	−37.4	24.2	14
i-$C_3H_7OSO_2C_6H_5$	0.0025	22.4	−14.6	26.7	13
$(CH_3)_3CCl$	0.010	21.9	−12.7	25.7	12*a*
$C_6H_5CH(CH_3)Cl$	0.0030	22.0	−14.7	26.3	12*b*

The relative reactivities, the lyate ion effect and the effect of added nucleophiles (1) in chlorosulfate solvolysis are entirely consistent with a normal solvolytic mechanism, which can be unimolecular or bimolecular, with the leaving group being —OSO_2Cl. On this basis, the transition state, for the unimolecular mechanism, would be as shown in eq. [2]. For comparison, the transition state of solvolysis of alkyl benzene sulfonates is shown in eq. [3], which is chosen due to the similarity of the two structures.

[2] $$R{-}O{-}\overset{\overset{O}{\|}}{\underset{\underset{O}{\|}}{S}}{-}Cl \rightarrow R{\cdots}O{-}\overset{\overset{O}{\|}}{\underset{\underset{O}{\|}}{S}}{-}Cl \rightarrow R^+ + {}^-O{-}\overset{\overset{O}{\|}}{\underset{\underset{O}{\|}}{S}}{-}Cl$$

[3] $$R{-}O{-}\overset{\overset{O}{\|}}{\underset{\underset{O}{\|}}{S}}{-}Ar \rightarrow R{\cdots}O{-}\overset{\overset{O}{\|}}{\underset{\underset{O}{\|}}{S}}{-}Ar \rightarrow R^+ + {}^-O{-}\overset{\overset{O}{\|}}{\underset{\underset{O}{\|}}{S}}{-}Ar$$

One would predict a slightly greater charge separation in the chlorosulfate than in the arenesulfonate on account of the electronegative chlorine, though this could be to some extent counteracted by the conjugating ability of the aryl group in the sulfonate. On the whole then, the polarities of the two ground states are rather similar and the same would be expected for the two transition states. Since the differential solvation of initial and transition states is generally accepted (10) as the major factor governing entropies of activation, one would expect both reactions to have similar $\Delta S^{\ddagger}$ values, which is not the case.

Another transition state may be considered for chlorosulfate solvolysis, one in which carbon–oxygen as well as sulfur–chlorine bond weakening occurs (eq. [4]):

[4] $$R{-}O{-}\overset{\overset{O}{\|}}{\underset{\underset{O}{\|}}{S}}{-}Cl \rightarrow R{\cdots}O{-}\overset{\overset{O}{\|}}{\underset{\underset{O}{\|}}{S}}{\cdots}Cl \rightarrow R^+ + SO_3 + Cl^-.$$

In this transition state there is a greater charge separation and also an incipient sulfur trioxide molecule is forming, to a degree which depends on progress along the reaction coordinate. Both these factors should give rise to an increased solvation of the transition state, and consequently a more negative $\Delta S^{\ddagger}$ compared with the situation in eq. [2]. However, the simultaneous fission of two bonds with formation of three fragments would

Can. J. Chem. Downloaded from www.nrcresearchpress.com by 210.87.254.105 on 09/05/12
For personal use only.

result in an increased $\Delta S^{\ddagger}$ due to the gain of translational, rotational, and vibrational degrees of freedom. The balance of the two effects, a smaller $\Delta S^{\ddagger}$ due to solvation and a larger $\Delta S^{\ddagger}$ due to dissociation, is difficult to estimate a priori. Gas-phase reactions provide a parallel: abnormally high entropies of activation, by 10–20 e.u., are believed to be due to simultaneous rupture of two bonds (15). The fragmentation process in chlorosulfate solvolysis may, therefore, well result in an abnormally large entropy of activation. On this basis the transition state in chlorosulfate solvolysis may be represented by the following resonance structures:

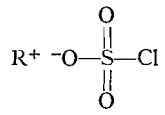

I

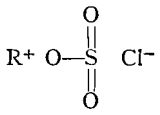

II

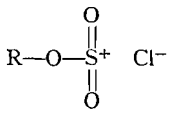

III

Analogous structures may be written for the bimolecular mechanism. The importance of structures II and III is indicated by the reported (16) relative inertness of alkyl fluorosulfates.[3] That I and II are contributing structures is further suggested by the fact that there are only very few examples of simple secondary chlorosulfate in the literature and that a tertiary chlorosulfate has never been reported.

Application to Other Systems

The hypothesis of the fragmentation process in chlorosulfate solvolysis is germane to the problem of the possible generality of multiple bond fission. The classical S_Ni reaction provides an example of this possibility. For instance, the decomposition of alkyl chlorosulfites and chloroformates to alkyl halides may in theory proceed by alkyl–oxygen fission, by acyl–chlorine fission, or by both modes simultaneously. There is considerable evidence that in inert solvents these processes have a predominantly carbonium ion character (alkyl–oxygen fission) (17), and that in the gas phase a cyclic four-centered, possibly polar, transition state obtains (18). The entropies of activation of these processes appear to be normal, generally ranging between -10 and -20 e.u. A recent study (19) of another S_Ni reaction, the decomposition of aralkyl thiocarbonates ROCOSR′ to RSR′ and CO_2, has provided evidence for simultaneous fission of the alkyl–oxygen and acyl–sulfur bonds, through the observation of specific electronic effects of R and R′ on the rate of reaction. No entropies of activation were reported for the reaction.

The solvolysis of alkyl chloroformates in formic acid appears to be associated with an unusually high $\Delta S^{\ddagger}$: ethyl and isopropyl chloroformates have $\Delta S^{\ddagger}$ values of -1.8 and -0.4 e.u. respectively (20). In contrast formolysis of the corresponding arenesulfonates proceeds with more negative $\Delta S^{\ddagger}$, by 5–15 e.u. (4). It is therefore noteworthy that in the solvolysis of alkyl chloroformates there is evidence of both alkyl–oxygen and acyl–chlorine bond fission (20, 21).

The solvolysis of γ-aminoalkyl halides (IV) yields products of substitution, elimination, cyclization, and fragmentation at the C_β—C_γ bond (22). The proposed mechanism (22) is rate-determining ionization of the C—X bond to give V, followed by fast product-forming steps.

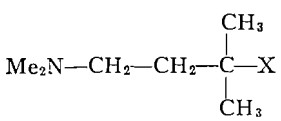

IV

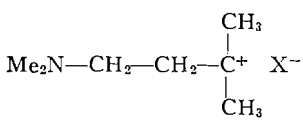

V

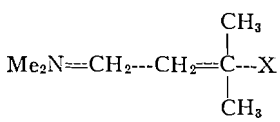

VI

[3]*Work is in progress to establish this point on a quantitative basis.*

Can. J. Chem. Downloaded from www.nrcresearchpress.com by 210.87.254.105 on 09/05/12
For personal use only.

The entropies of activation in 80% ethanol – 20% water, −1.2 e.u. for X = Cl, and 1.6 e.u. for X = Br are 4 e.u. greater than for the corresponding *t*-butyl halides (12*a*, 12*c*). Further, on substitution of the Me_2N group of IV (X = Cl) by Me_2CH, $\Delta S^{\ddagger}$ becomes again 5 e.u. smaller and only products from substitution and elimination are obtained. Now the Me_2N group does not play a role in the transition state by anchimerically assisting ionization of C—X, since there is no rate acceleration compared with the isopropyl analogue. If significance can be attached to a difference in $\Delta S^{\ddagger}$ of only 4–5 e.u., an explanation for the greater $\Delta S^{\ddagger}$ with IV is that in the transition state for solvolysis there is partial C_β—C_γ bond weakening (VI).

The hypothesis that entropies of activation may provide an indication of multiple bond fission in solution processes must be advanced with considerable caution, in view of the intricate nature of the activation process (23) and the many factors which can influence activation parameters. Further entropy data, for S_Ni and other solvolytic processes, are needed and corroboration by other criteria which afford a direct measure of the extent of bond weakening (e.g. isotope effects) is desirable before the validity of this hypothesis can be fully evaluated.

EXPERIMENTAL

Preparation of Chlorosulfates

The chlorosulfates were prepared by a modification of the method described by Binkley (24). Sulfuryl chloride (1 mole) was placed in a three-necked flask equipped with a gas inlet tube, a dropping funnel, and a drying tube. The flask was cooled in a bath of solid carbon dioxide and acetone and the solution agitated by means of a stream of dry nitrogen, which also removed most of the hydrogen chloride produced in the subsequent reaction. The anhydrous alcohol (1 mole) was then added by means of the dropping funnel, over a period of 1 h; in the neopentyl case the alcohol was dissolved in anhydrous ether before addition. At the end of this time the mixture was allowed to warm up to approximately 0 °C. The crude product was then washed three times with ice water, and dried over magnesium sulfate. The products were all purified by repeated fractional distillation under reduced pressure. The chlorosulfates were stable for prolonged periods at 0 °C but at room temperature they gradually decomposed.

The physical properties are shown in Table IV. The infrared spectrum of each compound showed the characteristic absorption bands in the region of 1 190 and 1 410 cm^{-1} due to the —OSO_2Cl group (25); there was no hydroxyl absorption. The nuclear magnetic resonance spectrum of neopentyl chlorosulfate showed only two peaks, one at τ = 8.97, of area 9 units corresponding to the methyl group and one at τ = 5.80, of area 2 units corresponding to the methylene group. This proved that no rearrangement had occurred during the synthesis.

TABLE IV

Physical properties of the alkyl chlorosulfates

	$ROSO_2Cl$	Methyl	Ethyl	*n*-Propyl	Isobutyl	Neopentyl
Boiling point (°C/mm)	Found	40/14	42/10	52/10	30/1	33/1
	Lit. (24)	48/29	43/10	53/10		
Density (25°)	Found	1.483	1.348	1.281	1.218	1.173
	Lit. (24)	1.48	1.35	1.28		
Refractive index	Found	1.412/22°	1.413/25°	1.420/20°	1.420/25°	1.422/25°
	Lit. (24)	1.414/20°	1.416/20°	1.422/20°		
Anal. S %	Found				18.29, 18.56	16.78, 17.15
	Calcd.				18.55	17.15
Cl %	Found				20.0, 20.3	18.7, 18.7
	Calcd.				20.57	19.04

Product Analysis

This was carried out as previously (1), Table V. It was found (vapor-phase chromatography (v.p.c.)) that methyl, *n*-propyl, isobutyl, and neopentyl chlorosulfates yielded methyl, *n*-propyl, isobutyl, and *t*-pentyl alcohol, respectively. No *t*-butyl alcohol was detected in the hydrolysis of isobutyl chlorosulfate. Whether reaction of neopentyl chlorosulfate also yielded some unrearranged neopentyl alcohol could not be determined by v.p.c., since neopentyl alcohol had the same retention time as dioxane under the conditions

Can. J. Chem. Downloaded from www.nrcresearchpress.com by 210.87.254.105 on 09/05/12
For personal use only.

TABLE V

Products of the hydrolysis of chlorosulfates (0.01 *M*) in 10 *M* aqueous dioxane

Chlorosulfate	H_2SO_4 produced (Mole %)	HCl produced (Mole %)	Olefin produced (Mole %)
Methyl	96.8	99.5	—
Ethyl	101.4	97.7	—
n-Propyl	99.4	99.6	—
Isobutyl	99.4	98.3	—
Neopentyl	98.8	98.3	4.5

used. To obtain information on this point a method of estimating a mixture of neopentyl and *t*-pentyl alcohol from their infrared spectra was developed.

The infrared spectrum of *t*-pentyl alcohol in dioxane showed a strong band at 940 cm^{-1} while neopentyl alcohol under the same conditions showed strong absorption at 1 017 cm^{-1}. Infrared spectra of mixtures of these alcohols in varying ratios but with the same total concentration (0.02 *M*) gave a calibration curve of concentration against % absorbance for each alcohol. Three reaction mixtures were then analyzed in this way and showed a total recovery of 88%, 87%, and 90% respectively of *t*-pentyl alcohol and 0% neopentyl alcohol, with an error in estimation of ±5%.

Measurement of Rates

The kinetic data were obtained by the conductivity method already described (1). The data for the lyate ion effect with neopentyl chlorosulfate are as follows:

$[ROSO_2Cl] \times 10^2$ (*M*)	$[NaOH] \times 10^2$ (*M*)	$k \times 10^4$ (25 °C) (s^{-1})
1.00	0.54	0.174
1.00	0.90	0.171
1.00	5.4	0.172
1.02	9.0	0.170
0.50	4.5	0.171
0.52	9.0	0.172

ACKNOWLEDGMENTS

The authors wish to thank Dr. R. E. Robertson for a stimulating discussion and the National Research Council for a Studentship (to J. P. M.) and a grant.

REFERENCES

1. E. BUNCEL and J. P. MILLINGTON. Can. J. Chem. This issue.
2. C. K. INGOLD. Structure and mechanism in organic chemistry. Bell and Sons, London. 1953. Chap. 7.
3. A. STREITWIESER, JR. J. Am. Chem. Soc. **77**, 1117 (1955).
4. S. WINSTEIN and H. MARSHALL. J. Am. Chem. Soc. **74**, 1120 (1952).
5. I. DOSTROVSKY, E. D. HUGHES, and C. K. INGOLD. J. Chem. Soc. 173 (1946).
6. A. STREITWIESER, JR. Solvolytic displacement reactions. McGraw-Hill, N.Y. 1962. pp. 73, 135.
7. I. DOSTROVSKY and E. D. HUGHES. J. Chem. Soc. 157 (1946).
8. J. F. BUNNETT. *In* Rates and mechanisms of reactions, part I. *Edited by* S. L. Friess, E. S. Lewis, and A. Weissberger. Interscience Publishers, N.Y. 1961. p. 177. O. EXNER. Nature, **201**, 488 (1964).
9. (*a*) R. E. ROBERTSON, R. L. HEPPOLETTE, and J. M. W. SCOTT. Can. J. Chem. **37**, 803 (1959).
   (*b*) G. KHONSTAM. The transition state. Special Publication No. 16. The Chemical Society, Lo ndon. 1962. p. 179.
10. A. A. FROST and R. G. PEARSON. Kinetics and mechanism. John Wiley, N.Y. 1961. Chap. 7.
11. L. L. SCHALAGER and F. A. LONG. Advan. Phys. Org. Chem. **1**, 1 (1963).
12. (*a*) S. WINSTEIN and A. H. FAINBERG. J. Am. Chem. Soc. **79**, 5937 (1957).
   (*b*) A. H. FAINBERG and S. WINSTEIN. J. Am. Chem. Soc., **79**, 1597 (1957).
   (*c*) A. H. FAINBERG and S. WINSTEIN. J. Am. Chem. Soc. **79**, 1602 (1957).
   (*d*) S. WINSTEIN, A. H. FAINBERG, and E. GRUNWALD. J. Am. Chem. Soc. **79**, 4146 (1957).
13. E. TOMMILA and E. MERIKALLIO. Suomen Kemistilehti B, **26**, 79 (1953). E. TOMMILA. Acta Chem. Scand. **9**, 975 (1955).
14. R. FOON and A. N. HAMBLY. Australian J. Chem. **15**, 668 (1962).
15. B. G. GOWENLOCK. Quart. Rev. London, **14**, 133 (1960). C. STEEL and K. J. LAIDLER. J. Chem. Phys. **34**, 1827 (1961).
16. J. MEYER and G. SCHRAMM. Z. Anorg. Allgem. Chem. **206**, 24 (1932).

Can. J. Chem. Downloaded from www.nrcresearchpress.com by 210.87.254.105 on 09/05/12
For personal use only.

17. C. E. BOOZER and E. S. LEWIS. J. Am. Chem. Soc. **76**, 794 (1954). D. J. CRAM. J. Am. Chem. Soc. **75**, 332 (1953). K. B. WIBERG and T. M. SHRYNE. J. Am. Chem. Soc. **77**, 2774 (1955). A. STREITWIESER, JR. and W. D. SCHAEFFER. J. Am. Chem. Soc. **79**, 379 (1957). K. L. OLIVIER and W. G. YOUNG. J. Am. Chem. Soc. **81**, 5813 (1959).
18. E. S. LEWIS and W. C. HERNDON. J. Am. Chem. Soc. **83**, 1961 (1961).
19. J. L. KICE and R. A. BARTSCH. Tetrahedron Letters, No. 25, 1693 (1963).
20. E. W. CRUNDEN and R. F. HUDSON. J. Chem. Soc. 3748 (1961).
21. M. GREEN and R. F. HUDSON. J. Chem. Soc. 1076 (1962).
22. C. A. GROB and F. A. JENNY. Tetrahedron Letters, No. 23, 25 (1960). C. A. GROB, F. OSTERMAYER, and W. RAUDENBUSCH. Helv. Chim. Acta, **45**, 1672 (1962).
23. R. E. ROBERTSON. Can. J. Chem. **42**, 1707 (1964).
24. W. W. BINKLEY. J. Am. Chem. Soc. **60**, 2810 (1938).
25. E. A. ROBINSON. Can. J. Chem. **39**, 247 (1961).

Can. J. Chem. Downloaded from www.nrcresearchpress.com by 210.87.254.105 on 09/05/12
For personal use only.

Can. J. Chem. Downloaded from www.nrcresearchpress.com by 210.87.254.42 on 09/05/12
For personal use only.

FREE RADICALS BY MASS SPECTROMETRY

XXXII. THERMAL DECOMPOSITION OF CYCLOPENTYL RADICALS[1]

T. F. PALMER[2] AND F. P. LOSSING
Division of Pure Chemistry, National Research Council, Ottawa, Canada

Received July 15, 1964

ABSTRACT

At low pressures and elevated temperatures cyclopentyl radicals are found to dissociate mainly by two modes of reaction: about 34% by loss of H atom to form cyclopentene, and about 66% by a C—C bond rupture to form ethylene and allyl radicals. Under the conditions employed no evidence for a third possible mode, the loss of H_2 to form cyclopentenyl radical, could be found. It is estimated that an incidence of 2% of the latter could have been detected.

INTRODUCTION

Three modes have been postulated for the thermal decomposition of cyclopentyl radicals:

[1]

[2] 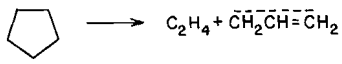

[3]

The occurrence of reaction [2] for cyclopentyl radicals produced by abstraction of H from cyclopentane has been observed (1). In later work (2) reaction [3] was proposed, on the basis of the CD_3H/CD_4 ratios found when CD_3 radicals were used as the abstracting species. The occurrence of reaction [2] above 250° has recently been confirmed (3) and a value of 36.9 ± 1 kcal/mole for its activation energy has been obtained. In the same work the occurrence of reaction [1] at about 300° has been proposed.

In the present work the modes of thermal decomposition of cyclopentyl radicals have been investigated, using a low-pressure thermal reactor coupled to a mass spectrometer (4). Although this apparatus is not suitable for accurate measurements of rate parameters, it enables a direct observation to be made on unstable intermediates and their decomposition products. It was thought therefore that a search for allyl and cyclopentenyl radicals, and measurements on the non-radical products of the decomposition of cyclopentyl radicals would provide information on the relative rates of reactions [1]–[3].

EXPERIMENTAL

The cyclopentyl radicals were generated by the thermal decomposition of cyclopentyl methyl nitrite in a fused-silica furnace leading directly to the ionization chamber of a mass spectrometer (4). The purified nitrite was held in a trap immersed in a freezing bath of suitable temperature, and admitted to the reactor through an adjustable stainless-steel valve. Also connected to the reactor was a conventional "leak" backed by a sample-handling system and micromanometer, by which calibration of the sensitivity coefficients for the nitrite and the stable reaction products could be made.

[1]*National Research Council Contribution No. 8143.*
[2]*National Research Council Postdoctorate Fellow, 1960–1962.*

The reactions leading to the formation of cyclopentyl radicals were:

[4] 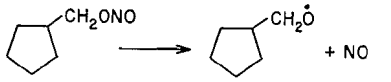

[5] 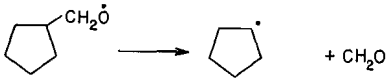

The partial pressure in the reactor was kept as low as practicable ($\sim 10^{-3}$ mm) to minimize the occurrence of bimolecular radical reactions in the contact time (~ 1 ms) available. No evidence for a significant lifetime for the cyclopentylmethoxy radical could be found even at the lowest temperature (300°) at which the nitrite began to decompose. Evidently reaction [5] occurs very rapidly at this temperature.

A special problem was posed in measuring the ethylene and cyclopentene yields in the presence of the cyclopentyl radical, whose mass spectral contributions at mass 68 and 28 could not be determined. To avoid this difficulty, all analyses were made using an ionizing electron beam of sufficiently low energy that the peaks at *m/e* 68 and 28 contained no contributions from the ionized cyclopentyl radicals. Since under these conditions the sensitivity coefficients are extremely dependent on small changes in ion-source contact potential, it was necessary to perform a calibration *in situ* for each measurement. Each measurement of the peak height of the product at mass 68 and 28 was accompanied by a calibration made by means of additions to the reaction stream of known partial pressures of cyclopentene and ethylene from the sample-handling system. The increase in peak height caused by the known increase in partial pressure of the component could then be used to calculate the equivalent partial pressure of product. This method of calibration was found to be rapid and accurate. A correction of $M^{1/2}$ for molecular flow in the reactor was required in order to express equivalent partial pressures in the reactor in terms of the known partial pressures in the sample-handling system. The reason for this is clear if one considers a component AB entering the reactor at a diffusion rate corresponding to a molecular weight M_{AB}, and dissociating there to A and B, which are then pumped out of the reactor independently at rates corresponding to M_A and M_B. The observed amounts of A and B in the reactor must therefore be multiplied by the ratios $(M_{AB}/M_A)^{1/2}$ and $(M_{AB}/M_B)^{1/2}$ to place them on the same basis as standard gases A and B admitted through the leak from the sample-handling system. The standard gases A and B flow through the leak into the reactor at rates corresponding to M_A and M_B and are pumped away unchanged.

TABLE I

Confirmation of calibration procedure: acetone yield from the thermal decomposition of di-*t*-butyl peroxide (DTBP)

Electron accel. potential (V)	DTBP decomposed (equiv. microns)	Acetone formed (equiv. microns)	Acetone yield % Ac/2DTBP × 100
50.0	24.6	50.0	101.6
12.0	24.6	49.7	101.0
50.0	62.9	127	101.0
11.5	62.9	124	98.6
50.0	107	224	104.7
11.2	107	213	99.5

This assumption of molecular flow, and the method of calibration, were checked by measuring the yield of acetone formed by the thermal decomposition of di-*t*-butyl peroxide. As shown in Table I, the yield of acetone measured, using the low electron energy method, agreed closely with the yield measured using 50 V electrons, and is within ±2% of the theoretical yield. The yield is independent of pressure, showing that no flow interaction occurred between the peroxide and the added acetone standard over the pressure interval employed. The observed amounts of acetone have been corrected by $(146/58)^{1/2}$ to give the values in Table I.

Materials

Cyclopentylmethyl nitrite was prepared from a commercial sample of cyclopentylmethanol by the action of sodium nitrite and dilute sulfuric acid. The nitrite was washed with water, dried over anhydrous sodium sulfite, and purified by repeated distillation at reduced pressure.

Can. J. Chem. Downloaded from www.nrcresearchpress.com by 210.87.254.42 on 09/05/12
For personal use only.

RESULTS AND DISCUSSION

Preliminary investigation showed that the major products of the decomposition of cyclopentylmethyl nitrite at 300–800° were NO, formaldehyde, and cyclopentyl radicals, and that the latter decomposed to form ethylene, allyl radicals, cyclopentene, and hydrogen. Small amounts of propylene, bi-allyl, cyclopentane, and bi-cyclopentyl were also detected using higher concentrations of the nitrite. With low energy ionizing electrons used for detection, the parent peak for the cyclopentyl radical (mass 69) rose from zero at 250° to a maximum at about 450°, and then fell with increasing temperature to nearly zero at 708°. No evidence for the formation of cyclopentenyl radical (mass 67) could be found over this temperature range, although it might be expected to be quite stable at these temperatures and contact times.

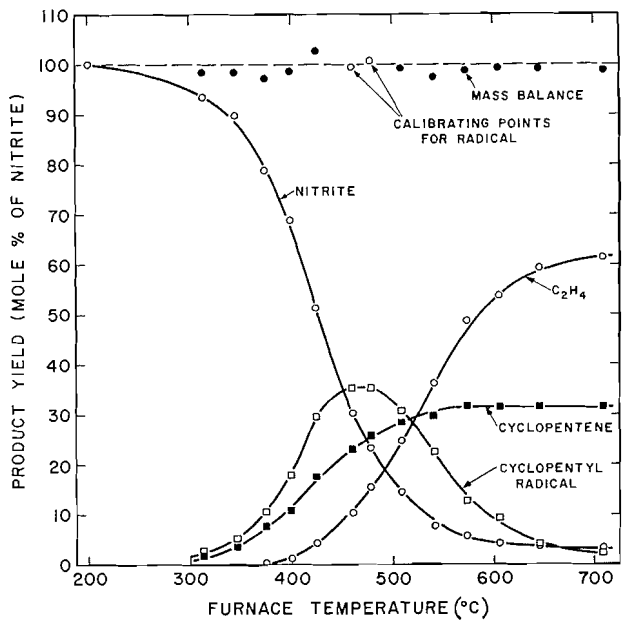

FIG. 1. Product yields in the thermal decomposition of cyclopentylmethyl nitrite.

The extent of decomposition of the nitrite as a function of furnace temperature, and the yields of ethylene, cyclopentene, and cyclopentyl radicals are shown in Fig. 1. It is evident that the nitrite decomposes to give cyclopentyl radicals (reactions [4] and [5]) and that the cyclopentyl radicals decompose subsequently by reaction [1] to give cyclopentene (and a hydrogen atom) and by reaction [2] to give ethylene and an allyl radical. Although allyl radicals were easily detected, the yield was not measured since it would be very nearly equal to that of ethylene. At the partial pressure of nitrite used in this experiment the amounts of cyclopentane and bi-cyclopentyl were too small to be shown in Fig. 1, although they are included in the calculation of mass balance. The cyclopentylmethyl nitrite, ethylene, and cyclopentene were measured by the calibration procedure described above. The sensitivity coefficient for cyclopentyl radicals was derived as follows. At 708°, at which temperature nearly all cyclopentyl radicals were decomposed,

Can. J. Chem. Downloaded from www.nrcresearchpress.com by 210.87.254.42 on 09/05/12
For personal use only.

the amounts of ethylene and cyclopentene (and including about 1% made up of cyclopentane and bi-cyclopentyl) amounted to 98% of the nitrite decomposed. It could be assumed consequently that at any temperature:

[original nitrite] − [nitrite decomposed] = [cyclopentyl] + [cyclopentene] + [ethylene] + 2[bi-cyclopentyl] + [cyclopentane].*

Since all these quantities except [cyclopentyl] could be determined by calibrations with standard gases, a solution for the sensitivity coefficient for cyclopentyl could be made at any temperature. For greatest accuracy this was done for the two temperatures (463° and 479°) at which the cyclopentyl concentration was greatest. At these temperatures the cyclopentyl yields were 34.8% and 34.5% respectively of the original nitrite. From the sensitivity coefficient (peak height / partial pressure) derived from the average yield at these two temperatures the observed peak heights for cyclopentyl radical were converted to the radical yield curve shown. The mass balance was found to be 100 ± 2% over the whole temperature range as shown at the top of Fig. 1. Since the radical yield varies from 0% to 35%, the constancy of the mass balance shows that a correct value for the sensitivity coefficient for the radical has been chosen.

These results indicate that at the lower temperatures cyclopentyl radicals dissociate faster by reaction [1] than by reaction [2], but with increasing temperature reaction [2] predominates.† The implication that the activation energy E_1 is less than E_2 is not in accord with estimates from thermochemistry. From ΔH_f(cyclopentane) = −18.46 kcal/mole and ΔH_f(cyclopentene) = 7.87 kcal/mole (5) and ΔH_f(H) = 52.1 kcal/mole, the sum of the two bonds $D(c\text{-}C_5H_9\text{—H}) + D(c\text{-}C_5H_8\text{—H}) = 130.5$ kcal/mole. There seems no reason why $D(c\text{-}C_5H_9\text{—H})$ should be much different from other secondary C—H bonds in alkanes, i.e. 93 kcal/mole at 25 °C (6). $D(c\text{-}C_5H_8\text{—H})$ in cyclopentyl radical is therefore close to 37.5 kcal/mole. The activation energy E_1 will be 37.5 kcal/mole plus the activation energy for the reverse reaction. A lower value for E_1 can be assigned only at the expense of increasing D(C—H) in cyclopentane by a corresponding amount. For example, $E_1 = 28$ kcal/mole (7) would require $D(c\text{-}C_5H_9\text{—H}) = 102.5 + E_{-1}$. Values of 4–5 kcal/mole for E_{-1} in gas phase reactions have been generally found (8), although the reaction of H atoms with olefins in the solid state suggest a lower value of 1.5 kcal/mole (9). Even with this lower value, D(C—H) in cyclopentane would have to be 104 kcal/mole. This seems unreasonably high.

The overall heat of reaction [2] to give C_2H_4 + allyl is about 22 kcal/mole, assuming ΔH_f(allyl) ~ 32 kcal/mole. E_2, presumably corresponding to the initial ring rupture, has, however, been found experimentally to be 37–38 kcal/mole by Gunning and Stock (3) and by Gordon (7). From these considerations it would appear that E_1 should be somewhat larger than E_2. Two possible reasons for the apparent reversal of this order in the present work may be considered. The first is that reaction [1] is accompanied at low temperatures by an abstraction of H by NO formed by the nitrite decomposition:

[6] $$c\text{-}C_5H_9 + NO \rightarrow HNO + c\text{-}C_5H_8.$$

A significant contribution by this reaction seems improbable, however, since [NO] ≈ [cyclopentyl] and even the presumably faster combination and disproportionation reactions of two cyclopentyl radicals are negligibly slow at the low pressures employed in the

*Assuming the cyclopentane to be formed from disproportionation of two cyclopentyl radicals.

†The flattening of the cyclopentene yield curve above 575° suggests that some cyclopentene may be disappearing by a secondary reaction. However, no evidence for products such as cyclopentadiene could be found.

Can. J. Chem. Downloaded from www.nrcresearchpress.com by 210.87.254.42 on 09/05/12
For personal use only.

present experiment. A second possibility is that reaction [1] is considerably accelerated by reaction at the wall. The pressure in the reactor is so low ($\sim 10^{-3}$ mm) that most radicals have several collisions with the wall. Any catalytic activity favoring a C—H split over a C—C split would cause a large increase in k_1/k_2 at the lower furnace temperatures. It is possible therefore that the ratio of k_1/k_2 observed at the highest temperature is also larger than would be observed at higher reaction pressures. With this reservation, the present findings show that at 700°, in a reaction time of around 1 ms some 66% of cyclopentyl radicals decomposing do so by reaction [2], about 34% by reaction [1], and less than 2% by reaction [3].* The uncertainties in contact time and temperature in the present apparatus preclude calculation of the rates on any but a relative basis.

REFERENCES

1. J. R. McNesby and A. S. Gordon. J. Am. Chem. Soc. **79**, 825 (1957).
2. J. R. McNesby and A. S. Gordon. J. Am. Chem. Soc. **79**, 4593 (1957).
3. H. E. Gunning and L. R. Stock. Can. J. Chem. **42**, 357 (1964).
4. J. B. Farmer and F. P. Lossing. Can. J. Chem. **33**, 861 (1955).
5. F. D. Rossini *et al.* Selected values of physical and thermodynamic properties of hydrocarbons and related compounds. Carnegie Press, Pittsburgh. 1953.
6. G. C. Fettis and A. F. Trotman-Dickenson. J. Am. Chem. Soc. **81**, 5260 (1959).
7. A. S. Gordon. Cited in ref. 3 as private communication.
8. A. F. Trotman-Dickenson. Gas kinetics. Butterworths Scientific Publications, London. 1955.
9. R. Klein and M. D. Scheer. J. Phys. Chem. **62**, 1011 (1958).

**Elsewhere in this issue, A. S. Gordon has concluded from experiments at higher pressures and lower temperatures that a much larger proportion of cyclopentyl radicals decompose by reaction [3].*

Can. J. Chem. Downloaded from www.nrcresearchpress.com by 210.87.254.42 on 09/05/12
For personal use only.

Can. J. Chem. Downloaded from www.nrcresearchpress.com by 210.87.254.105 on 09/05/12
For personal use only.

A STUDY OF SOME REACTIONS OF THE CYCLOPENTYL RADICAL

ALVIN S. GORDON
Chemistry Division, Research Department, USNOTS, China Lake, California
Received October 26, 1964

ABSTRACT

The specific rate constant for opening the cyclopentyl radical has been determined to be $10^{14.5}$ exp $-37\,700/RT$ s^{-1}. The energy of activation indicates that any eclipsed pairs of H atoms in the cyclic radical are not de-eclipsed in the activated complex. No evidence for the resulting five-membered linear radical can be found, only evidence for its breakdown products, allyl radical and ethylene.

The disproportionation/combination ratio for methyl and cyclopentyl radicals is about 0.3. The energy of activation for methyl abstracting a hydrogen atom from cyclopentane has been confirmed as about 9.5 kcal/mole.

Cyclopentyl radical also loses a hydrogen atom to form cyclopentene. The kinetic parameters are difficult to obtain because of radical–radical reactions which form cyclopentene. An analysis of the results indicates an energy of activation at least equal to that for opening the cyclopentyl ring.

Evidence is presented to support the view that the cyclopentyl radical loses a molecule of hydrogen to form the resonance-stablized cyclopentenyl radical with an energy of activation close to that for opening the ring, and a pre-exponential factor about 1/10 of that for the opening of the ring.

INTRODUCTION

In a study of cyclopentyl radicals from the Hg-sensitized photolysis of cyclopentane, Gunning and Stock (1) have recently published a value of 36.9 ± 1.4 kcal/mole for the E_{act} for opening the cyclopentyl radical. By use of a different experimental approach, the value found in this work is in excellent agreement. Also, the experiment makes it possible to monitor other reactions of the cyclopentyl radical.

In this study the cyclopentyl radicals are generated via abstraction of H from cyclopentane by methyl radicals.

MATERIALS AND PROCEDURE

Cyclopentane purchased from Phillips Company was at least 99.9% pure. There is a cyclopentene impurity which barely shows above the baseline of our gas chromatography unit at concentrations of cyclopentane used in this work. The acetone is Eastman Spectroscopic Grade with no detectible impurity. Merck acetone-d_6 has a D/D + H = 0.995.

Experiments were made in a 45 cc cylindrical quartz reaction cell set into a furnace with a quartz window. Full intensity medium pressure mercury arc, Hanovia SC-100, was the photolysis source, although the effect of intensity and wavelength were checked by using a filter which filtered linearly starting at 2 900 Å, cutting out about 65% of the 3 130 Å radiation.

Portions of a master mix of acetone and cyclopentane were metered into the reaction vessel to a desired pressure. The mix was photolyzed for a time such that less than 10% reacted. The reacted mixture was transferred to a gas chromatographic unit. Two 5% anthracene on silane columns in tandem were used to separate the constituents. The first column was held at 100 °C which retains the ketones in the products but had no effect on the remaining constituents. These constituents were then separated on the second column which was temperature programmed from −195 to 100 °C. Provision was made so that any fraction could be trapped for identification by a mass spectrometric analysis.

The mass spectrometer was also employed to analyze for hydrogens (H_2, HD, and D_2), and methanes by introducing the sample via a trap of copper wool at 77 °K.

RESULTS AND DISCUSSION

Disproportionation/Combination of Methyl and Cyclopentyl Radicals

The following reaction scheme accounts for the major products at temperatures up to 325 °C.

[1] $$CD_3COCD_3 \xrightarrow{h\nu} 2\dot{C}D_3 + CO$$

[2] $$\dot{C}D_3 + \bigcirc \rightarrow CD_3H + \bigcirc\cdot$$

[3] $$\dot{C}D_3 + CD_3COCD_3 \rightarrow CD_4 + \dot{C}D_2COCD_3$$

[4] $$\bigcirc\cdot + \dot{C}D_3 \rightarrow \bigcirc\!\!\!\!\begin{matrix}CD_3\end{matrix}$$

[5] $$\bigcirc\cdot + \dot{C}D_3 \rightarrow CD_3H + \bigcirc\!\!=$$

As seen in Table I, at temperatures up to about 300° cyclopentyl radical mostly reacts with other radicals since neither C_2H_4 nor H_2 (products of the cyclopentyl radical pyrolysis) appear in the products.

The ratio k_5/k_4 = cyclopentene / methyl cyclopentane is shown in Table II. Up to 220 °C the ratio is a constant ($\simeq 0.3$). At higher temperatures other radicals build up relative to methyl radical and give cyclopentene by disproportionation with cyclopentyl radical. At still higher temperatures, as will be discussed in a later section, cyclopentene is produced by loss of an H atom from a cyclopentyl radical, which rapidly becomes an important source for cyclopentene with increasing temperature.

Abstraction of an H Atom from Cyclopentane by Methyl Radical

The energy of activation for abstraction of H from cyclopentane by methyl radical has previously been published (2) using the method of competitive methyl radical abstraction from cyclopentane and acetone-d_6. In this work the experimental results contain the methane data necessary to determine the E_{act} reported above, as well as the ratio of pre-exponential factors for the methyl abstracting from cyclopentane and from acetone. The Arrhenius plot for the methane data is shown in Fig. 1. From the data, $E_D - E_H = 2.1$ kcal/mole where E_D is the abstraction of D from acetone-d_6 and E_H is the abstraction of H from cyclopentane. Since E_D has been established (3) as 11.6 kcal/mole, $E_H = 9.5$ kcal/mole, in excellent agreement with the previously published value. The ratio of pre-exponential factors $A_H/A_D = 1.2$; the value based on the number of H atoms and D atoms in the two compounds would give $A_H/A_D = 1.7$. The results indicate that the pre-exponential factor for a methyl radical to abstract an H atom is 50% of that for the abstraction of a D atom. Since the volume of a D atom is somewhat smaller than that of an H atom, the results cannot be explained by the cross-sectional area of the attacked atom. The eclipsing of the hydrogen atoms in the cyclic compound and the position of D atoms α to the carbonyl group are probably unimportant, since McNesby and Gordon (4) studied the abstraction of H and D from 2,2,3,3-butane-d_4 by methyl radicals and reported that the pre-exponential factor for abstraction is also about 50% higher for D than H. The writer is not able to offer any explanation for the pre-exponential ratio.

Can. J. Chem. Downloaded from www.nrcresearchpress.com by 210.87.254.105 on 09/05/12
For personal use only.

Can. J. Chem. Downloaded from www.nrcresearchpress.com by 210.87.254.105 on 09/05/12
For personal use only.

TABLE I

Products (μmoles) from photolysis of 1:1 mix of cyclopentane and acetone-d_6

T (°C)	P of mix (cm)		Time (s)	Total methanes	C_2H_4			H_2	*	1–5-Hexadiene	Allyl	†/C_2H_4
162	6.7	52	480	1.0	0.0	0.6	0.2	0.01	0.02			—
207	7.0	49	480	2.3	0.0	1 0	0.3	0.02	0.01			—
268	7.8	52	480	4.8	0.0	1.0	0.6	0.02	0.3			—
290.5	8.2	52	480	5.4	0.0	0.9	0.8	—	0.5			—
313	9.2	56	480	7.0	0.3	0.8	1.0	0.2	0.7	—	—	2.8
333.5	8.8	52	480	6.5	0.8	0.5	1.0	0.4	0.8	—	—	1.0
352	12.1	70	480	7.9	1.8	0.4	1.4	—	1.2	—	—	0.7
353	9.3	54	480	5.7	1.7	0.3	1.1	0.6	1.0	0.17	0.08	0.6
353†	9.3	54	3 600	0.9	0.6	0.0	0.3	0.2	0.3	0.13	—	0.5
355	4.8	27	600	2.1	0.8	0.07	0.5	—	0.5	0.11	0.18	0.6
370	9.7	50	480	7.0	2.7	0.2	1.3	0.8	1.2	0.24	0.58	0.5
384.5	6.5	37	480	2.1	1.5	0.04	0.6	—	0.6	—	—	0.4
385	9.6	52	480	6.9	3.4	0.13	1.3	0.9	1.3	0.48	0.48	0.4
394.5	9.1	48	600	3.6	2.5	0.04	1.0	—	1.0	—	—	0.4
396	9.6	52	600	3.7	2.6	0.03	1.0	—	1.0	—	—	0.4
403	9.7	52	480	7.2	4.4	0.07	1.4	1.1	1.4	0.75	0.41	0.3
407	9.0	48	480	3.6	2.7	0.03	0.8	—	0.8	—	—	0.3
420	8.9	47	480	3.6	2.8	0.02	0.9	—	0.9	—	—	0.3
440	9.2	47	480	4.0	3.1	0.02	0.9	—	0.9	—	—	0.3
445	8.0	40	360	2.95	2.3	0.02	0.8	0.6	0.8	—	—	0.3

*Corrected for methyl radical disproportionation with cyclopentyl to form cyclopentene.
† > 3 000 Å and relatively low flux compared to full intensity of lamp.

TABLE II

Ratios of cyclopentene and methyl cyclopentane over a temperature range

T (°C)	$\frac{\text{Cyclopentene}}{\text{Methyl cyclopentane}} = \frac{k_5}{k_4}$
132	0.30
160	0.32
180	0.30
190	0.34
198.5	0.28
207	0.31
217.5	0.32
268	0.62
290.5	0.86
313	1.27

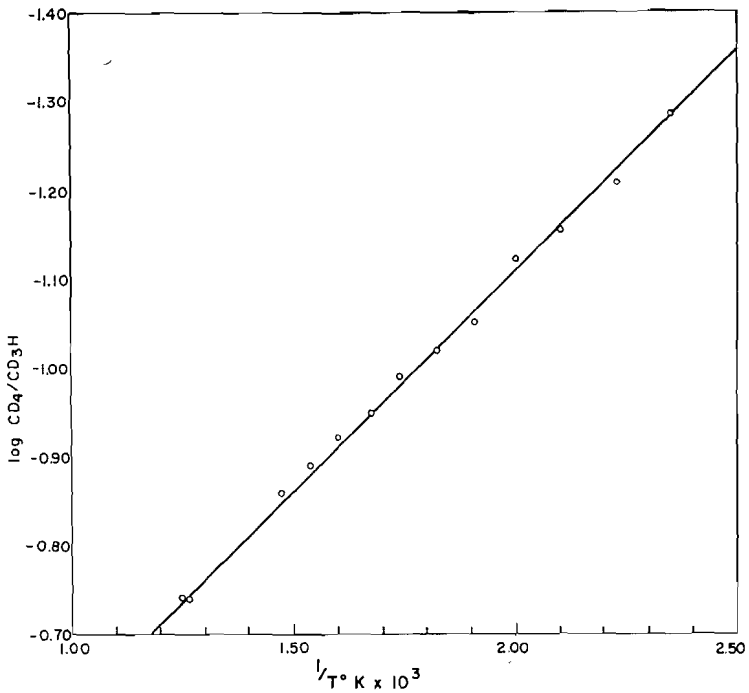

FIG. 1. Arrhenius plot for competitive abstraction of D from acetone-d_6 and H from cyclopentane.

Opening of the Cyclopentyl Radical

Starting at about 300° the cyclopentyl radical decomposes to an allyl radical and ethylene.

[6] 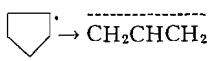 $\rightarrow \overline{\text{CH}_2\text{CHCH}_2} + \text{C}_2\text{H}_4.$

The products of the reaction never contain evidence that a linear C_5 pentenyl radical existed long enough to be stabilized to form hexene-1 by addition of a methyl radical, or to form pentene-1 by abstraction of H. Thus we may conclude that at temperatures where the cyclopentyl radical opens, the resultant pentenyl radical decomposes very

Can. J. Chem. Downloaded from www.nrcresearchpress.com by 210.87.254.105 on 09/05/12
For personal use only.

rapidly compared to the cyclopentyl radical breaking a C—C bond. The most likely reason for the above behavior is that the activated complex for decomposing the linear pentenyl radical has a portion of the resonance energy of the allyl radical; the energy of activation for decomposition is lowered by the amount of resonance energy in the complex.

The kinetic parameters for the opening of the cyclopentyl radical may be monitored by reactions [2], [4], and [6]. Using acetone-d_6 as the source for methyl radicals:

[I] $$r_6 = \frac{d[C_2H_4]}{dt} = k_6\left[\bigcirc\cdot\right]$$

[II] $$r_4 = \frac{d\left[\bigcirc CD_3\right]}{dt} = k_4 \left[\bigcirc\right][\dot{C}D_3]$$

[III] $$r_2 = \frac{d[CD_3H]}{dt} = k_2[\dot{C}D_3]\left[\bigcirc\right].$$

The photolyses are carried to small percentage decomposition and r_2, r_4, and r_6 do not vary with time. Under this condition:

[IV] $$\frac{r_2 r_6}{r_4\left[\bigcirc\right]} = \frac{k_2 k_6}{k_4}.$$

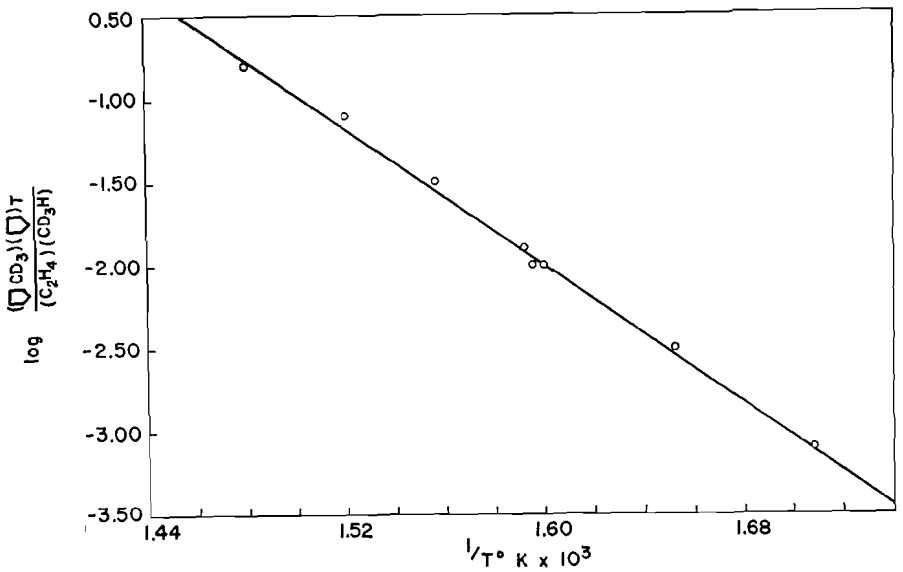

FIG. 2. Arrhenius plot for monitoring the opening of the cyclopentyl radical. T is the reaction time in seconds.

All the rates which determine the right-hand side of eq. [IV] were obtained from the results reported in Table I. The resulting ratio has been plotted in an Arrhenius plot (Fig. 2). From the slope the overall energy of activation for $E_6 + E_2 - E_4$ is determined to be 45.3 kcal/mole with a standard deviation of 1.4 kcal/mole. Since $E_4 = 0$ and $E_2 =$ 9.5 kcal/mole, $E_6 = 37.7$ kcal/mole in excellent agreement with Gunning and Stock (1).

Can. J. Chem. Downloaded from www.nrcresearchpress.com by 210.87.254.105 on 09/05/12
For personal use only.

The overall pre-exponential factor is

$$A_0 = \frac{A_2 A_6}{A_4} = 10^{13.5}.$$

Trotman-Dickenson and Steacie (6) report that the pre-exponential factor for the methyl radical abstraction of cyclopentane is about 10^{-2} of that for methyl radical combination. The combination of a methyl radical and a cyclopentyl radical is probably less favorable than the combination of two methyls, a relative factor of about 10^{-1} is considered to be reasonable and leads to a value for A_6 of $10^{14.5}$, consistent with the pre-exponential factors of many first order processes.

Loss of H Atom from Cyclopentyl Radical

It is possible, in principle, to monitor the loss of an H atom from cyclopentyl radical,

[7] 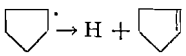

[6] 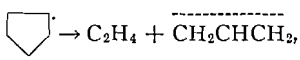

by measuring the products from competitive reactions [6] and [7]. Both cyclopentene and ethylene may be measured with good precision from our gas chromatogram records. The amount of cyclopentene may be corrected for the cyclopentene formed in the disproportionation reaction of methyl and cyclopentyl radicals by the methyl cyclopentane formed in the addition reaction of the same radicals. These corrected cyclopentene/ethylene ratios, when plotted in an Arrhenius graph (Fig. 3), are seen to increase with temperature from 300° to 400° and then remain constant to 445°.

The author has indicated in private communication (1, 7) that the low temperature slope indicated the E_{act} for reaction [7] to be as low as 28 kcal/mole. Based on thermodynamic values for the heat of formation for cyclopentane and for cyclopentene, with any realistic value for the C—H bond strength in cyclopentane, Palmer and Lossing (7) have shown clearly that this value is much too low. The products in Table I show an interesting trend for the hydrogen and cyclopentane. At temperatures up to 268° only small amounts of hydrogen appear in the products, probably associated with excited molecule reactions. Although there is essentially no hydrogen at 268°, substantial amounts of cyclopentene (which have been corrected for disproportionation of methyl and cyclopentyl radicals) appear in the product. The cyclopentene cannot be formed from loss of H from cyclopentyl radicals, since no hydrogen is present. The only reasonable source for the cyclopentene is via disproportionation of cyclopentyl with cyclopentyl. Above 300° H atoms, shown by the products H_2 and HD, and allyl radicals, shown by the production of ethylene from reaction [6], also participate in disproportionation reactions leading to formation of cyclopentene. Examination of the CD_3H/CD_4 ratios indicates that even at the highest temperatures, CD_3H is 85% of the total methane. Thus the rate of formation of the methanes is a good indicator of the rate of formation of cyclopentyl radicals. Against the above background the results in Table I show that methyl and cyclopentyl radicals decrease in steady-state concentration with increasing temperature since the rate of methyl cyclopentane is quite insignificant by 400 °C. Similarly the steady state concentration of H atoms probably follows the same trend. However, the steady state concentration of allyl radical, which is resonance stabilized, increases with temperature, as can

Can. J. Chem. Downloaded from www.nrcresearchpress.com by 210.87.254.105 on 09/05/12
For personal use only.

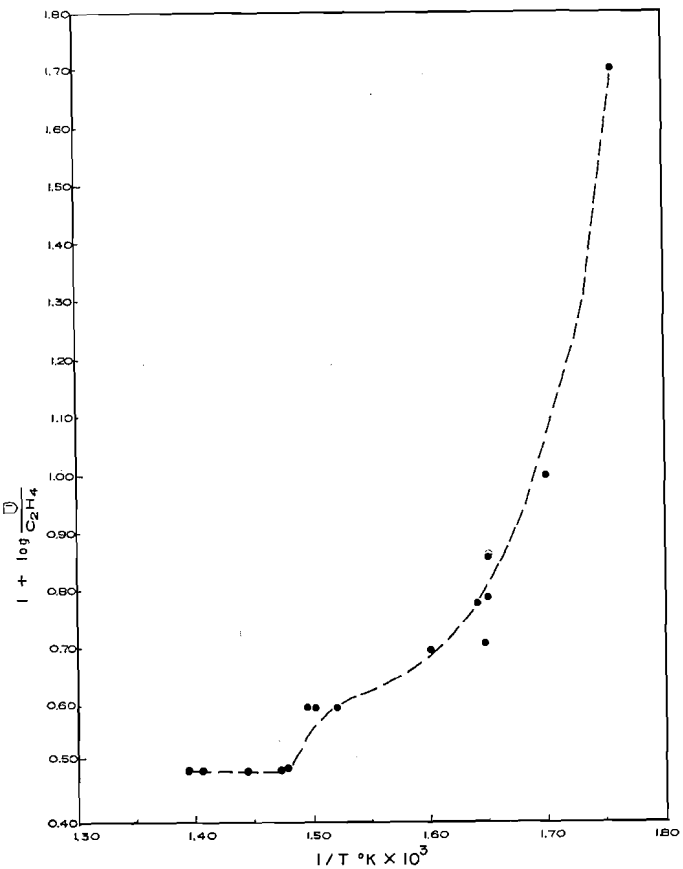

FIG. 3. Arrhenius plot for loss of H atom from the cyclopentyl radical.

be seen by the increasing rate of formation of 1.5 hexadiene, which results from the combination of two allyl radicals. Allyl cyclopentane, from the combination of allyl and cyclopentyl radicals, also increases with temperature until between 370 and 385°, and then decreases. Since the allyl radical is probably the radical of highest steady state concentration in this higher temperature range, the disproportionation formation of cyclopentene from allyl and cyclopentyl radicals also increases to 370–385° and then decreases. The rate of hydrogen (H_2 + HD) relative to the rate of formation of cyclopentene, agrees with the above analysis. The formation of hydrogen will be discussed in the next section. If we assume that the H atoms from reaction [7] will abstract H and D, then the rate of hydrogens should equal the rate of cyclopentene. The results in Table I show that the cyclopentene is always greater than the hydrogen, and that the discrepancy decreases with temperature. The results above 400 °C are probably more correct than the results at lower temperatures, and the energy of activation for reaction [7] is at least equal to 38 kcal/mole.

Loss of Molecular Hydrogen from the Cyclopentyl Radical

Gordon and Smith (8) have reported that molecular hydrogen could be eliminated from a hydrocarbon radical if an allylic radical results. According to the postulated reaction,

Can. J. Chem. Downloaded from www.nrcresearchpress.com by 210.87.254.105 on 09/05/12
For personal use only.

cyclopentyl radical could lose molecular hydrogen to form cyclopentenyl radical. The possibility for this reaction has been surveyed over a temperature range, and evidence will be presented below which provides support for the reaction.

In a mix of acetone-d_6 and cyclopentane, the hydrogens and methanes were analyzed for various deuterium marking and rate of formation as a function of temperature. The results in Table I show that starting at 300 °C the rate of total hydrogens (HD and H_2) formation progressively increases as a function of temperature, and at 350° is 10% of the methanes.

TABLE III

Ratios of H_2/HD and CD_3H/CD_4 as a function of temperature

P of mix (cm)	*T* (°C)	Time (min)	Micron H_2	Micron HD	H_2/HD	CD_3H/CD_4
6.6	161	8	0.14	0.07	2.0	18.8
6.7	182	8	0.26	0.06	4.3	16.9
7.0	204	8	0.26	0.05	5.2	15.3
6.4	227	8	0.33	0.06	5.5	13.8
7.4	249.5	8	0.37	0.03	12.3	12.6
7.8	269	8	0.48	0.04	12.0	11.7
9.2	314	8	2.94	0.11	26.7	9.9
5.0	325	8	5.3	0.28	18.9	9.0
8.8	333.5	8	6.13	0.27	22.7	9.4
6.5	350	6	10.5	0.55	19.2	8.2
9.1*	353	120	4.93	0.19	26.0	8.7
9.4	355	8	10.07	0.41	24.6	8.8
9.5	370	8	13.28	0.54	24.6	8.4
6.9	375	5	14.98	0.62	24.2	7.6
9.6	385	8	14.06	0.53	26.5	8.2
9.7	396	8	17.10	0.74	23.1	7.9
7.1	399.5	4	16.08	0.76	21.2	7.2
7.52	424	4	19.6	0.95	20.6	6.8
12.03	439.5	4	25.68	1.40	18.3	6.6
11.98	440	¼	7.68	0.45	17.1	6.5
7.8	450	2	13.49	0.74	18.2	6.3
8.11	475	2	16.0	0.97	16.5	6.0
12.00	475	¾	8.92	0.58	15.4	6.1

*$\lambda > 3\,000$ Å; low flux relative to full intensity of mercury arc.

The H_2/HD ratios are considerably larger than the CD_3H/CD_4 ratios generated in the same media, as may be seen in Table III. In unreported work on H atoms and methyl-d_3 radicals in the same media (9) it has been noted that the two species show the same difference in energies of activation for abstracting H and D; however, the H_2/HD ratios from the abstraction reactions may be as much as 1.5 times the corresponding CD_3H/CD_4 ratios. The H_2/HD ratios in Table III are 2.5 to 3.0 times the corresponding CD_3H/CD_4 ratios, suggesting that molecular hydrogen may be formed without intermediate formation of H atoms.

Time of reaction does not have a large effect on the ratios of H_2/HD or CD_3H/CD_4 reported in Table III. The ratios of hydrogens are not as precise as the methane ratios since comparatively small quantities of HD appear in the products. Errors from small quantities of HD from excited molecule processes cause significant errors in the amount of HD. These errors are reflected in the calculated molecular hydrogen / ethylene ratios in Table IV.

Figure 4 shows the Arrhenius plot of the H_2/HD ratios and the CD_3H/CD_4 ratios. If only H atoms were involved, as previously noted, two parallel lines would result. The CD_3H/CD_4 ratios are well behaved, but the H_2/HD ratios may be interpreted as due to

Can. J. Chem. Downloaded from www.nrcresearchpress.com by 210.87.254.105 on 09/05/12
For personal use only.

Can. J. Chem. Downloaded from www.nrcresearchpress.com by 210.87.254.105 on 09/05/12
For personal use only.

TABLE IV

Molecular hydrogen / ethylene ratios corrected for H atom abstraction. Corrections were made for H_2/HD ratios either 1.5 or 1.0 times the corresponding CD_3H/CD_4 ratios

T (°C)	H_2/C_2H_4 (1.5)	H_2/C_2H_4 (1.0)
300	0	5.2
325	7.2	16.7
350	12.4	18.7
375	13.1	18.3
400	11.1	15.4
425	11.1	15.7
450	10.8	15.7
450	9.3	14.7
475	12.1	18.6
475	9.9	15.5

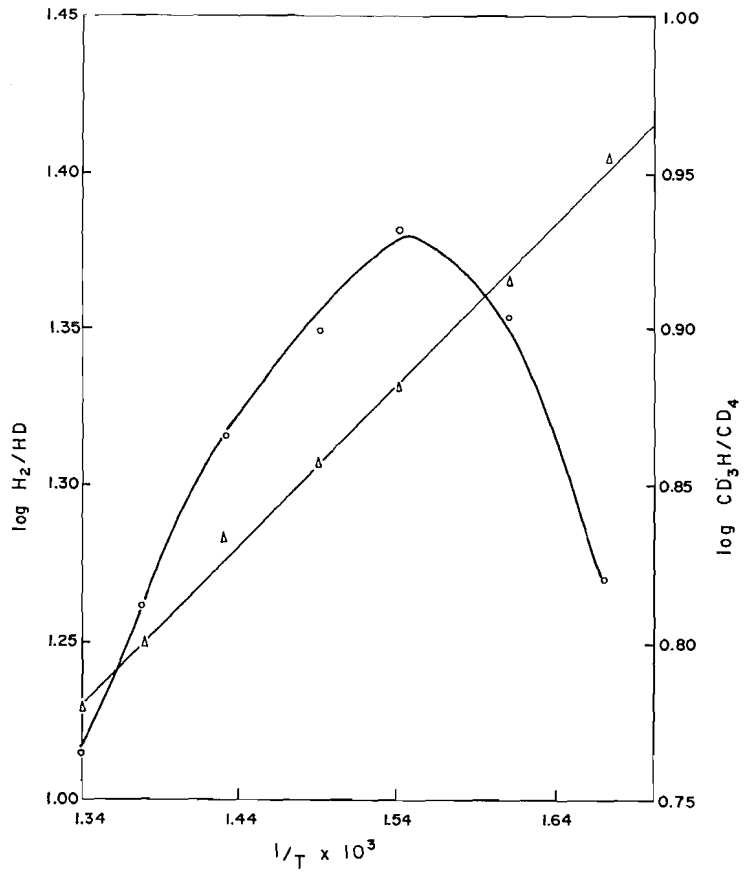

FIG. 4. Arrhenius plot of the methane ratios (△) and the corresponding hydrogen ratios (○).

H atoms as well as H_2 being introduced into the medium. The maximum in the H_2/HD ratio may be interpreted as resulting from a new source of H atoms at higher temperatures and increasingly important with increasing temperature. The new sources could be due to the radical reactions:

[8] $$\overline{CH_2CHCH_2} \rightarrow CH_2{=}C{=}CH_2 + H$$

[9] 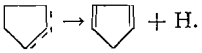 + H.

If molecular hydrogen is eliminated from the cyclopentyl radical, then evidence for the cyclopentenyl radical should be seen in the products. Methyl cyclopentene is identified as such a product. However, it could be argued that the product arose from methyl radical addition to cyclopentene with subsequent elimination of an H atom from the radical. The appearance of methyl cyclopentene when only relatively small amounts of cyclopentene appear argues against the latter interpretation. Cyclopentene-d_1 is also identified in the product, and this is a strong argument that cyclopentenyl radical is present because there are no free D atoms in the reaction media; the only D in the product is that abstracted from acetone-d_6. The cyclopentenyl radical can be formed by abstraction of one of the allylic hydrogens in the cyclopentene as well as by the elimination of molecular hydrogen from the cyclopentyl radical.

An experiment to choose between the two possibilities was performed at 475 °C by generating the smallest quantity of cyclopentene that could be reliably measured. A mix of 1 cyclopentane to 3 acetone-d_6 was employed in the reaction so that the chance to form cyclopentene-d_1 by abstraction was enhanced. The gas chromatographic cut of the cyclopentene product has a small amount of cyclopentane impurity, arising from the large cyclopentane peak preceding the cyclopentene peak. To maximize the accuracy of the analysis for cyclopentene-d_1, the mass spectrometer was calibrated with pure samples of cyclopentene and cyclopentane just prior to the analysis of the gas chromatographic cut. The reaction mix consisted of 28.9 μmoles of cyclopentane. CD_3H (0.2 μmole) was formed and thus the same number of μmoles of cyclopentane are attacked. It is realistic to assume that the energy of activation of H abstracted from cyclopentene is not more than 4 kcal/mole more favorable than the abstraction of H from cyclopentane. Bearing in mind that there are 4 allylic H atoms in cyclopentene which can be abstracted to form the cyclopentenyl radical as against 10 H atoms in cyclopentane which can be abstracted to form cyclopentyl radical, then the Arrhenius calculation indicates that the H atom in cyclopentene should be abstracted five times as rapidly as the H atom in cyclopentane. Since cyclopentene is formed during the reaction, its average concentration is only one-half of the final concentration and, thus, the ratio of the rates of attack on cyclopentene and cyclopentane during the time interval is 2.5. Since 0.7% of the cyclopentane is attacked, 1.8% of the cyclopentene product should be attacked, to form cyclopentenyl radical. Experimentally 1.4% of cyclopentene-d_1 is found in the cyclopentene product.

The energy of activation for methyl radical attack on an H atom bound to carbon increases with increasing C—H bond strength even though the reactions are all exothermic. For a resonance stabilized radical the reactions are endothermic for attack on saturated compounds and the energy of activation for abstraction should be ordered the same way with bond strengths as for the methyl radical; the difference in the energies of activation for abstraction should be at least as large as that for methyl radical. The ratio of pre-exponential factors for abstractions should be quite independent of the radical, and the relative rates of abstraction have been taken to be independent of the radical. Based on

Can. J. Chem. Downloaded from www.nrcresearchpress.com by 210.87.254.105 on 09/05/12
For personal use only.

the CD_3 radical attack, the abstraction of H atom is about twice the rate for D atom abstraction. Thus, about 4.2% of the cyclopentene has been formed by abstraction, which is more than twice the calculated cyclopentenyl radical that could be formed from the cyclopentene. Also the rate of abstraction of the resonance stabilized cyclopentenyl radical is less than that for methyl radical and radical–radical processes are important in removing the cyclopentenyl radical, e.g. allyl radical steady state concentration has been noted to increase with temperature, while methyl and cyclopentyl decrease. Thus only a fraction of the calculated 1.8% cyclopentenyl radical formed from cyclopentene would abstract H or D to re-form cyclopentene.

The normal experimental errors, including the analytical error and the lack of temperature equilibration in the reaction vessel because of the small reaction time, cannot provide an escape from the conclusion that very little of the cyclopentene-d_1 results from cyclopentenyl radical generated from cyclopentene.

The molecular hydrogen is monitored from the HD concentration, since it must form from a free H atom abstracting a D atom from acetone-d_6; the H_2 which is formed by the concurrent abstraction of H atom abstracting an H atom from cyclopentane is calculated from the CD_3H/CD_4 ratio at the same temperature multiplied by a factor. As previously mentioned, the H_2/HD ratio could be as much as 1.5 times the corresponding CD_3H/CD_4 ratio. The difference between the H_2 calculated above and the total H_2 found is taken to be molecularly eliminated.

Two reactions may be used to monitor the molecular elimination process:

[10] 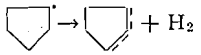

[6] 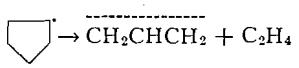

and $k_{10}/k_6 = H_2/C_2H_4$.

The resulting ratios are shown in Table IV over a temperature range. In one column the corrected H_2/C_2H_4 ratios are calculated assuming the H_2/HD ratios are 1.5 times the CD_3H/CD_4 ratios, and in the other column that the ratio of the ratios is unity. It may be seen that for both columns there is no trend in the ratio with temperature, suggesting that the E_{act} for molecular H_2 elimination is 35–40 kcal/mole, and the pre-exponential factor about 10% that for the opening of the cyclopentyl radical, or about $10^{13.5}$.

The large amounts of molecular hydrogen formed relative to the formation of ethylene may result from the eclipsing of the hydrogen on the carbon atoms α and β to the carbon atom with the odd electron. The hydrogen atoms are held in excellent position to form a molecule of H_2.*

PYROLYSIS OF CYCLOPENTANE

Gunning and Stock (1) report that cyclopentane pyrolyzes appreciably in 240 min at temperatures starting at 350 °C, and a concentration of 5.6×10^{-3} moles/l. Our reactions were done in 8 min or less and at a pressure of about 1×10^{-3} moles/l, except for one run of 1 h at 350° with filtered light. The product distribution for the long-time runs were

**Note added in proof: Palmer and Lossing (7) do not see any evidence of cyclopentenyl radical from the pyrolysis of cyclopentyl methyl nitrite at low pressures.*

The arguments for cyclopentenyl radical in this work are based on indirect evidence. The evidence against its appearance is direct but may be due to the special conditions of the work. For example, if cyclopentyl radical is the homogeneous source for ethylene and cyclopentene, the amounts of these products should increase with temperature, possibly at different rates. Since the experimental distribution of products does not conform to the prediction, it may be determined by the hot wall of the reactor.

Can. J. Chem. Downloaded from www.nrcresearchpress.com by 210.87.254.105 on 09/05/12
For personal use only.

quite in line with the short-time runs, although it is possible that some of the products were formed in pyrolysis.

Cyclopentane was pyrolyzed for 10 min over a temperature range at the pressure employed in this work. Up to 475 °C, no hydrogen was noted above the very small background hydrogen seen at low temperatures. Above this temperature hydrogen shows in the products in increasing amounts. At 520 °C the rate of production of ethylene from cyclopentane pyrolysis is about 5% of the rate of ethylene formed in the photolysis of the 1:1 acetone–cyclopentane mix at the same partial pressure of cyclopentane. In this work experiments involving hydrocarbon products were performed below 450°, and experiments with the marked hydrogens and marked methanes, at or below 475°, so that pyrolysis of the cyclopentane does not cloud the interpretation of the results.

ACKNOWLEDGMENTS

The author wishes to express his gratitude to Joseph H. Johnson for performing the experiments, and to Mrs. Helen R. Young for reducing the data.

REFERENCES

1. H. E. Gunning and R. L. Stock. Can. J. Chem. **42**, 357 (1964).
2. J. R. McNesby and A. S. Gordon. J. Am. Chem. Soc. **79**, 4593 (1957).
3. E. Whittle and E. W. R. Steacie. J. Chem. Phys. **21**, 993 (1953).
4. J. R. McNesby and A. S. Gordon. J. Am. Chem. Soc. **78**, 3570 (1956).
5. J. R. McNesby and A. S. Gordon. J. Am. Chem. Soc. **79**, 824 (1957).
6. A. F. Trotman-Dickenson and E. W. R. Steacie. J. Chem. Phys. **19**, 329 (1951).
7. T. Palmer and F. Lossing. This issue.
8. A. S. Gordon and S. R. Smith. J. Chem. Phys. **34**, 331 (1961).
9. A. S. Gordon and S. R. Smith. Unpublished data.

Can. J. Chem. Downloaded from www.nrcresearchpress.com by 210.87.254.105 on 09/05/12
For personal use only.

Can. J. Chem. Downloaded from www.nrcresearchpress.com by 210.87.254.105 on 09/05/12
For personal use only.

CARBON-13 ISOTOPE EFFECTS IN SYSTEMS CONTAINING CARBON DIOXIDE, BICARBONATE, CARBONATE, AND METAL IONS

H. G. THODE, M. SHIMA, C. E. REES, AND K. V. KRISHNAMURTY
McMaster University, Hamilton, Ontario

Received October 19, 1964

ABSTRACT

The fractionation of ^{13}C between $CO_2(g)$ and $CO_3^{=}$--$HCO_3^{-}(aq)$ in solution has been studied in single stage experiments using carbonic anhydrase to catalyze the hydration of CO_2. Added metal ions, pH of the equilibrium mixture, and temperature are found to play important roles in the overall fractionation process. Theoretical evaluation of the $^{13}CO_2(g)$--$^{12}CO_3^{=}(aq)$ equilibrium constant (K_2) has been made using the most recent spectroscopic data on the exchanging species. The variation of the equilibrium constant K_2 with temperature has been calculated for each 25 deg interval from 0 to 975 °C with the help of the McMaster University IBM 7040 computer. It is shown that the overall ^{13}C fractionation in the system may be treated as contributions due mainly to three exchange equilibria whereby $^{13}CO_2(g)$ independently exchanges with $^{12}CO_2(aq)$, $H^{12}CO_3^{-}(aq)$, and $^{12}CO_3^{=}(aq)$, the corresponding equilibrium constants being K_0, K_1, and K_2 respectively. The best fit values for the equilibrium constants are $K_0 = 1.0009$, $K_1 = 1.0077$, and $K_2 \geqslant 1.013$, indicating the order $K_0 < K_1 < K_2$.

INTRODUCTION

The fractionation of carbon-13 between gaseous carbon dioxide and solution carbon species such as $CO_2(aq)$, HCO_3^{-} $CO_3^{=}$, has been of considerable interest since the early thirties when Urey and his co-workers (1–4) showed that carbon-13 enrichment can be achieved via the following exchange reactions:

[1] $$^{13}CO_2(g) + {}^{12}CO_2(aq) \rightleftharpoons {}^{12}CO_2(g) + {}^{13}CO_2(aq),\ K_0;$$

[2] $$^{13}CO_2(g) + H^{12}CO_3^{-}(aq) \rightleftharpoons {}^{12}CO_2(g) + H^{13}CO_3^{-}(aq),\ K_1;$$

[3] $$^{13}CO_2(g) + {}^{12}CO_3^{=}(aq) \rightleftharpoons {}^{12}CO_2(g) + {}^{13}CO_3^{=}(aq),\ K_2.$$

The exchange studies reported until now make use of two phase gas–liquid column experiments and the single stage separation factor α is obtained from the familiar expression:

[4] $$\alpha^k = \frac{n/(1-n)_{\text{bottom}}}{N/(1-N)_{\text{top}}},$$

where k is the number of theoretical plates and n and N are the mole fractions of carbon-13 in solution and gas phase respectively. Apparently no attempt is made to obtain α independently from single stage equilibrium experiments. It is, however, shown in this study that α can be related to the individual equilibrium constants K_0, K_1, and K_2.

Among the numerous experimental problems the most formidable one perhaps is the slowness of the hydration reaction:

[5] $$CO_2 + H_2O \rightleftharpoons [H_2CO_3] \rightleftharpoons CO_2 + H_2O.$$

Urey, Aten, and Keston (2), in their pioneer column experiments, demonstrated that the hydration reaction [5], in fact, can be catalyzed enzymatically using carbonic anhydrase which was just then discovered by Meldrum and Roughton (5). The enzyme used was a crude solution of bovine carbonic anhydrase and the results were not encouraging. Interest in the use of enzyme-catalyzed CO_2 hydration as a means of isotope enrichment was revived when Scott and Mendive (6) succeeded in preparing carbonic anhydrase in

a pure crystalline form. Hawkings, Graham, Harkness, and Thode (7) used this preparation of the enzyme in their study of oxygen-18 enrichment in the hydration reaction:

[6] $$\tfrac{1}{2}C^{16}O_2 + H_2{}^{18}O \rightleftharpoons \tfrac{1}{2}C^{18}O_2 + H_2{}^{16}O.$$

The problem was reopened with a view to studying it from two directions: (i) a theoretical evaluation of the equilibrium constants K_0, K_1, and K_2 using more recent spectroscopic data on the exchanging species and (ii) experimental determination of the equilibrium constants from single stage fractionation experiments using carbonic anhydrase to speed up isotopic exchange

THEORY AND CALCULATIONS

For the isotope exchange reaction:

$$aA_1 + bB_2 = aA_2 + bB_1,$$

it may be shown (4, 8) that the equilibrium constant may be expressed in terms of ratios of partition functions,

$$K_{eq} = \left(\frac{Q_{A_2}}{Q_{A_1}}\right)^a \Big/ \left(\frac{Q_{B_2}}{Q_{B_1}}\right)^b$$

and that

[7] $$\frac{Q_2}{Q_1} = \prod_i^{3n-6} \left(\frac{u_{2i}}{u_{1i}}\right)\left(\frac{e^{-u_{2i}/2}}{e^{-u_{1i}/2}}\right)\left(\frac{1 - e^{-u_{1i}}}{1 - e^{-u_{2i}}}\right),$$

where $u_i = h\nu_i/kT$ and ν_i is the i-th fundamental vibrational frequency of the molecule. The use of eq. [7] implies a number of assumptions, but since calculations are usually made by employing approximate versions of this equation, when it is used in the form quoted above it will be referred to as the "exact" expression for the ratio of partition functions.

One of the main assumptions in the derivation of [7] is that the vibrations of molecules are harmonic. The approximation is not greatly in error when considering the ratios of partition functions for isotopic molecules, provided the observed fundamental frequencies are used rather than the zero order frequencies, and that the temperature is low enough so that only low lying vibrational levels have appreciable populations. Hulston (9) has shown how anharmonicity corrections can be of significance at high temperatures.

For the majority of the molecules, only the observed fundamentals are available. In the case of CO_2(g) the anharmonicity constants have been determined, but since the corresponding information has not been reported for the $CO_3^=$ ion or CO_2(aq), calculations have been performed using only the observed frequencies rather than applying corrections to only one member of a pair involved in exchange. It has been suggested (10) that the procedure will minimize the errors involved.

Several approximations (4, 7, 25, 26) exist for expression [7], the most widely used being those of Urey (4) and Bigeleisen (8) which may be written:

[8] $$\ln (Q_2/Q_1) = \sum_i^{3n-6} \ln \frac{u_{2i}}{u_{1i}} + \sum_i^{3n-6} \delta_i \coth x_i,$$

where $$x_i = \frac{u_{1i} + u_{2i}}{4} \quad \text{and} \quad \delta_i = \frac{u_{1i} - u_{2i}}{2}$$

Can. J. Chem. Downloaded from www.nrcresearchpress.com by 210.87.254.105 on 09/05/12
For personal use only.

and

$$[9] \qquad Q_2/Q_1 = 1 + \sum_i^{3n-6} G(u_i)\,\Delta u_i,$$

where

$$G(u_i) = \frac{1}{2} - \frac{1}{u_{2i}} + \frac{1}{e^{u_{1i}} - 1}$$

$$\Delta u_i = u_{1i} - u_{2i}.$$

While Bigeleisen's expression [9] is somewhat more convenient for purposes of computation, especially in view of the fact that values of the function $G(u)$ are tabulated (8), Urey's expression is, in fact, a more accurate approximation. Both expressions involve power series expansions in terms of a Δ_i, a number proportional to $(\nu_{1i} - \nu_{2i})$ the frequency shift, in the i-th fundamental frequency of the molecule, caused by isotopic substitution, and normally these expressions are terminated at the first-order term in Δ_i. However, in the logarithmic expansion developed by Urey, the term in Δ^2 has a zero coefficient so that the errors involved are due to terms in Δ^3 and higher, while the expansion developed by Bigeleisen has a non-zero term in Δ^2.

To demonstrate the improved accuracy of the Urey expression over the more generally used one due to Bigeleisen a sample set of calculations has been performed for the exchange reaction [3] and K_2 has been evaluated in three different ways, using expressions [7], [8], and [9]. The results of the calculations are shown in Table I.

TABLE I

Calculation of partition function ratios by the three main methods

25 °C	Exact	Urey	Bigeleisen
$Q(^{13}CO_3^=)/Q(^{12}CO_3^=)$	1.1926	1.1926	1.1750
$Q(^{13}CO_2)/Q(^{12}CO_2)$	1.1837	1.1837	1.1678
K_2	1.0075	1.0075	1.0062

In all further calculations reported below, the exact method of evaluation has been employed, using the computer program developed by Hulston (9).

Frequency Assignments for Gaseous Carbon Dioxide, $CO_2(g)$

The fundamental frequencies used in the calculations are shown in Table II and are those collected by Wentink (11). Estimates of anharmonicity constants have been made for both $^{12}CO_2$ and $^{13}CO_2$ but were not used, for the reasons discussed above.

Frequency Assignments for Dissolved Carbon Dioxide, $CO_2(aq)$

Jones and McLaren (12) measured the value of ν_3 for $^{12}CO_2$ dissolved in water. There are no experimental values available for ν_1 and ν_2 under the same conditions since ν_1 is not active in the infrared and presumably ν_2 was too low to measure on the instrument used by Jones and McLaren. ν_1 and ν_2 were estimated by assuming them to be displaced from the gaseous $^{12}CO_2$ values by the same fractional amount as in ν_3. The values for ν_1, ν_2, ν_3, for dissolved $^{13}CO_2$ were estimated by assuming the same fractional isotope shifts as for gaseous $^{13}CO_2$. These frequencies are listed in Table II.

Frequency Assignments for the Carbonate Ion, $CO_3^=$

For $^{12}CO_3^=$ the frequencies quoted by Kujumzelis (13) were used, and the $^{13}CO_3^=$ frequencies were calculated using the orbital valence force field (o.v.f.f.) treatment of Heath and Linnett (14). Both sets of frequencies are listed in Table II.

Can. J. Chem. Downloaded from www.nrcresearchpress.com by 210.87.254.105 on 09/05/12
For personal use only.

TABLE II

Vibrational frequency assignments for CO_2 and $CO_3^=$

Molecule	Frequency* (cm^{-1})			
	ν_1	ν_2	ν_3	ν_4
$^{12}CO_2$(g)	1 342.86	667.30 (2)	2 349.30	
$^{13}CO_2$(g)	1 344.66	648.65 (2)	2 283.46	
$^{12}CO_2$(aq)	1 338.70	665.20 (2)	2 342.00	
$^{13}CO_2$(aq)	1 340.49	646.61 (2)	2 276.37	
$^{12}CO_3^=$	1 063.00	1 415.00	680.00 (2)	879.00 (2)
$^{13}CO_3^=$	1 063.00	1 375.75	677.49 (2)	851.38 (2)

Degeneracy indicated in parentheses.
*Although the quoted frequencies are not by any means accurate to the degree implied by the quoted values, the computer program was designed to accommodate two places of decimals in the frequencies, and the numbers quoted above were placed straight into the expression.

Frequency Assignments for the Bicarbonate Ion, HCO_3^-

The only frequency assignments available for the bicarbonate are due to Duval, Duval, and Le Comte (15) who studied the infrared absorption spectra by the pellet method for the bicarbonates of ammonium, sodium, potassium, rubidium, and cesium. It is not possible to determine the fundamental frequencies of the ionic species from this work and since further, a force constant analysis on a XYZ_2 type molecule is difficult, no attempt was made to estimate partition function ratios in this case.

Results of Calculations

The partition function ratios for the carbonate ion and gaseous and dissolved carbon dioxide are presented in Table III together with the equilibrium constants for the exchange between $CO_3^=$ and CO_2(g) and for that between CO_2(g) and CO_2(aq).

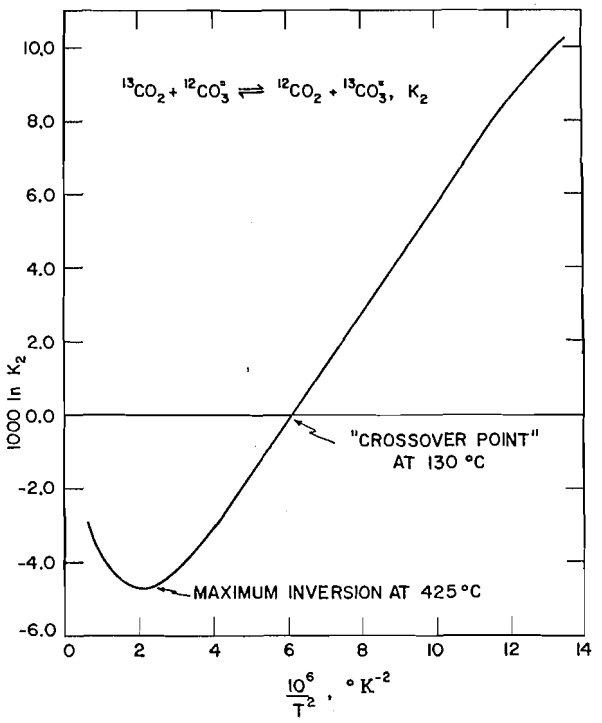

FIG. 1. Calculated temperature dependence of equilibrium isotope effect (K_2). Calculations made on McMaster University IBM 7040 Computer.

Can. J. Chem. Downloaded from www.nrcresearchpress.com by 210.87.254.105 on 09/05/12
For personal use only.

TABLE III

Calculated isotopic partition function ratios and ^{13}C exchange equilibrium constants for $CO_2(g)$–$CO_3^=$ (K_2), and $CO_2(g)$–$CO_2(aq)$ (K_0)

Temp. (°C)	$\frac{Q(^{13}CO_3^=)}{Q(^{12}CO_3^=)}$	$\frac{Q(^{13}CO_2(g))}{Q(^{12}CO_2(g))}$	K_2	$\frac{Q(^{13}CO_2(aq))}{Q(^{12}CO_2(aq))}$	K_0
0	1.2086	1.2211	1.0103	1.2077	1.0008
5	1.2032	1.2149	1.0098	1.2023	1.0008
10	1.1980	1.2090	1.0092	1.1971	1.0008
15	1.1930	1.2033	1.0086	1.1922	1.0008
20	1.1883	1.1978	1.0081	1.1874	1.0008
21	1.1873	1.1967	1.0080	1.1865	1.0008
22	1.1864	1.1957	1.0079	1.1856	1.0008
23	1.1855	1.1946	1.0078	1.1846	1.0008
24	1.1846	1.1936	1.0077	1.1837	1.0008
25	1.1837	1.1926	1.0076	1.1828	1.0008
26	1.1828	1.1915	1.0075	1.1819	1.0008
27	1.1819	1.1905	1.0074	1.1811	1.0008
28	1.1810	1.1895	1.0073	1.1802	1.0008
29	1.1801	1.1885	1.0072	1.1793	1.0008
30	1.1793	1.1875	1.0071	1.1785	1.0007
35	1.1750	1.1827	1.0066	1.1742	1.0007
40	1.1710	1.1781	1.0061	1.1702	1.0007
45	1.1670	1.1736	1.0057	1.1663	1.0007
50	1.1633	1.1693	1.0052	1.1625	1.0007
55	1.1596	1.1651	1.0048	1.1589	1.0007
60	1.1561	1.1612	1.0044	1.1554	1.0007
65	1.1527	1.1573	1.0040	1.1520	1.0007
70	1.1495	1.1536	1.0036	1.1488	1.0007
75	1.1463	1.1500	1.0033	1.1456	1.0006
80	1.1433	1.1465	1.0029	1.1426	1.0006
85	1.1403	1.1432	1.0026	1.1396	1.0006
90	1.1374	1.1400	1.0023	1.1368	1.0006
95	1.1347	1.1368	1.0019	1.1341	1.0006
100	1.1320	1.1338	1.0016	1.1314	1.0006

Figure 1 shows the wide temperature range behavior of K_2. In accordance with theory there is an extensive linear region in the curve and the high temperature limit for K_2 unity. Of particular interest is the fact that the equilibrium constant for this exchange undergoes inversion, is greater than unity at low temperatures and approaches unity from below at high temperatures. The "cross-over point" is 130 °C and the maximum inversion corresponding to the minimum on the curve occurs at 425 °C.

EXPERIMENTAL

A. Materials

The water used in this study was from Lake Ontario and distilled twice over $KMnO_4$. Both Na_2CO_3 (anhydrous) and $NaHCO_3$, as well as other chemicals, are of reagent grade purity. Pure crystalline bovine carbonic anhydrase was supplied to this laboratory by Professor D. A. Scott nearly 22 years ago and found to be still active as an enzyme. Stock solutions of carbonic anhydrase were prepared as and when needed by dissolving 2.16 mg of the crystalline enzyme in 1.00 ml of distilled water and 1.00 ml of 0.08% peptone solution. A working solution of the enzyme was made by diluting 0.50 ml of the stock solution with 12.25 ml of 0.08% peptone solution and 12.25 ml of water to give a concentration of 21.6 μg/ml carbonic anhydrase in 0.04% peptone solution. The 0.08% peptone nutrient solutions were prepared by dissolving 0.2 g each of the proteose–peptones in 250 ml of water. The proteose–peptones, Nos. 1, 2, 3, 4, and bactopeptone were supplied by Difco Laboratories, Inc., Detroit, Michigan.

B. Apparatus

Two different experimental procedures (I and II) were employed in the determination of the equilibrium constants.

I. Normal carbon dioxide of known isotopic composition was allowed to equilibrate with solutions of known carbonate concentration in a 60 ml round-bottom flask with a ground glass attached rotatable mixing sidearm for transfer of carbonic anhydrase solutions. The flask was thermostated while the admitted CO_2

Can. J. Chem. Downloaded from www.nrcresearchpress.com by 210.87.254.105 on 09/05/12
For personal use only.

attained isotopic equilibrium with solution species. The gas phase was removed from the flask in the usual way as described under Procedure.

II. The apparatus used in the second procedure is shown in Figs. 2*a* and 2*b*. No carbon dioxide was let into the system. Rapid sampling of small amounts of gaseous carbon dioxide without too much perturbation of equilibrium was accomplished by increasing both the size of the reaction vessel and concentrations of carbonate solutions. The reaction vessel and the vacuum line were considerably different from those used by Cragg and Thode (16) in their preliminary studies.

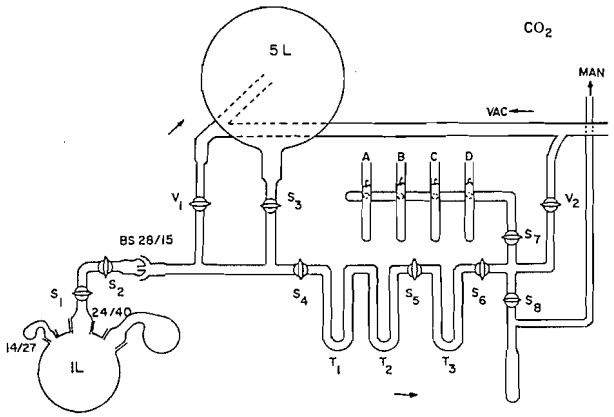

FIG. 2*a*. Gas phase sampling system.

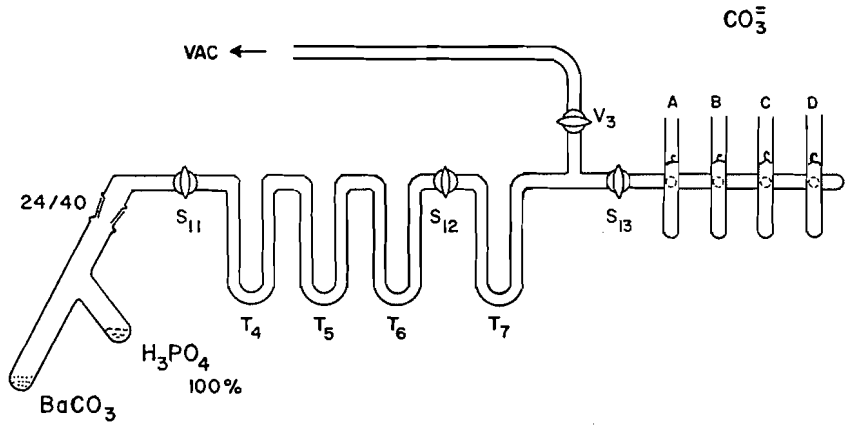

FIG. 2*b*. Solution phase sampling system.

The high precision isotope ratio mass spectrometer used in this investigation was built by Wanless and Thode (17) in 1953 and over the years it underwent several modifications to permit a good deal of flexibility in the collector system for measuring carbon, nitrogen, oxygen, and sulfur isotope ratios. Isotope ratio to an accuracy of $\pm 0.02\%$ was measured routinely on this machine using carbon dioxide samples. The 45/44 and 46/(45 + 44) peak ratios were measured in all samples against tank CO_2 as standard. Necessary corrections for differences in the O-17 content in all carbon analyses were applied using Craig's correction formulas (18).

C. Procedure

Enzymatic Activity and Choice of Stabilizer

The rates of evolution of carbon dioxide from carbonic acid – bicarbonate solutions were determined in the presence and absence of carbonic anhydrase with and without the peptone stabilizer.

In a 60 ml round-bottom reaction flask were placed 5 ml 0.4 *M* $NaHCO_3$ and 10 ml water, in the mixing sidearm 5 ml of phosphate buffer prepared by mixing equal volumes of 0.4 *M* Na_2HPO_4 and 0.4 *M* NaH_2PO_4, and the flask connected to a manometer through a stopcock. The contents of the flask were magnetically stirred at 25.0° and the phosphate buffer from the sidearm allowed to mix and react gently. The rates of CO_2

Can. J. Chem. Downloaded from www.nrcresearchpress.com by 210.87.254.105 on 09/05/12
For personal use only.

evolution were determined manometrically. In the catalyzed reaction 1.00 ml of carbonic anhydrase (10 μg/ml) was added to the buffer solution before mixing. Similar experiments were performed using the peptone stabilizers since dilute aqueous solutions of carbonic anhydrase were found to be unstable. The effect of five different peptones on carbonic anhydrase activity was studied repeating the experiments with 5.00 ml 0.4 *M* $NaHCO_3$ and 10.00 ml of 0.08% aqueous peptone solutions and following the CO_2 evolution rates as before.

Procedure I

All experiments on the effect of metal ions, particularly Mg^{2+} ion, were carried out using this procedure as also some preliminary experiments on the effect of pH of the equilibrium mixtures. The reaction vessel as described earlier was a 60 ml round-bottom flask with sidearm for transfer of enzyme solution, and a side finger attached through a stopcock for freeze-collection of CO_2.

Varying volumes of standard Na_2CO_3, HCl, and $MgCl_2$ (or other metal chlorides) were mixed to give stock solutions that are essentially HCO_3^-–$CO_3^=$ mixtures with or without added metal ions—Mg^{2+}, Mn^{2+}, Fe^{2+}, Co^{2+}, Ni^{2+}, Al^{3+}, Cr^{3+}. Twenty milliliters each of the mixtures were placed in the reaction vessel with the sidearm containing 1.00 ml carbonic anhydrase (21.6 μg/ml) and the solution was degassed by a repeated freezing, pumping, and thawing process. About 4.8×10^{-5} moles of previously equilibrated (with saturated Na_2CO_3 solution) CO_2 was admitted into the flask and the flask thermostated with shaking at 25.0° for ~5 h. The gaseous CO_2 after equilibration was collected in the side finger kept at liquid air temperature by opening and closing the attached stopcock. It was further purified by passing it through a trap at −80° and metered into a sample tube.

The solution in the reaction vessel was frozen to liquid air temperature and 1.00 ml 4 *N* HCl added and evacuated again. The frozen mass was allowed to melt and mix when CO_2 evolved. This was sampled as before for analysis to give the isotopic composition of solution carbon species.

Procedure II

The reaction vessel was a 1 l round-bottom flask with or without mixing sidearms connected to the vacuum line as shown in Fig. 2*a* through a detachable ball and socket joint (BS 28/15). About 500 ml of standard solutions ranging from 1 *M* to lower concentrations of $NaHCO_3$ and(or) Na_2CO_3 were taken in the flask to which 1.00 ml carbonic anhydrase stock solution was added with magnetic stirring. A small quantity of the solution was removed quickly to measure the initial pH and quench-precipitate the carbonate in solution for isotopic analysis. The reaction vessel was slowly chilled at dry ice – acetone temperature and air removed from the contents by alternately opening S_1, S_2, S_3 to the 5 l flask and evacuating the large flask with S_1, S_2 closed but V_1 open. This step was repeated several times. The reaction vessel was isolated and allowed to warm slowly, after pumping on the frozen mass for a few minutes. Thawing was accomplished by jacketing the flask with warm water. To ensure minimal mechanical and thermal strains on the reaction vessel it was replaced every two or three experiments.

The thawed contents were magnetically stirred at (27 ± 1°) room temperature and the gas phase containing the equilibrium CO_2 was sampled as follows: with S_2, S_3 open, S_1 was rapidly opened (< 6 s) to allow the gas to diffuse into the evacuated 5 l flask instantaneously. (Gas samples were thus collected in some experiments at intervals ranging from 2 to 40 h.) The collected CO_2 was transferred to the traps T_1, T_2 and kept at liquid air temperature by opening S_3, S_4 gradually until condensation in T_1 showed that the gas was slowly escaping from the large flask. With S_3, S_4, S_5, S_6, and V_2 open, the large flask and the traps were opened to the pumps for a few minutes and S_4, S_6 closed, confining the frozen CO_2 to T_1. It was purified from water by three successive distillations from T_1 to T_3 via T_2 kept at dry ice – acetone temperature. The first distillation was carried out rather slowly (1½ to 2 h) as this was found necessary to prevent interference of water contamination in the mass spectrometric analysis. After the final distillation, a suitably sized portion of CO_2 was metered into one of the break-seal sample tubes A, B, C, D.

Samples of the solution were obtained before and after the experiment to measure pH and for conversion of the carbonate to CO_2 for mass spectrometric analysis. A 2 ml aliquot of the solution was quenched in a saturated $BaCl_2$ solution and the precipitated $BaCO_3$ was centrifuged, washed successively with CO_2-free water and absolute alcohol, dried in filter paper folds, and transferred rapidly into the Y tube, shown in Fig. 2*b*, for vacuum drying. The dried $BaCO_3$ was then cautiously allowed to react with 2.5 ml 100% H_3PO_4 (prepared by dissolving P_2O_5 in 85% H_3PO_4), already taken in the sidearm, by gentle rotation-mixing. With S_{11} closed, the contents of the Y tube were left for an hour for equilibration of the evolved CO_2. The CO_2 was then condensed in T_4, T_5 at liquid air temperature by repeatedly opening and closing S_{11}. T_4 was allowed to warm to room temperature and T_5 to dry ice – acetone temperature while T_6 was kept at liquid air temperature. S_{12} was opened, T_7 kept at liquid air temperature, and T_6 allowed to warm. When the transfer was complete S_{12} was closed and a suitably sized sample was sealed in the sample tube for mass spectrometric analysis. Several Y tubes were used to facilitate rapid batch sampling of carbonate precipitates.

RESULTS AND DISCUSSION

Enzymic Activity and Choice of Stabilizer

The results calculated according to Meldrum and Roughton's method (5) from our rate data are presented in Table IV and the CO_2 evolution rates in Fig. 3. From these

Can. J. Chem. Downloaded from www.nrcresearchpress.com by 210.87.254.105 on 09/05/12
For personal use only.

experiments it is concluded that the carbonic anhydrase preparation, although 22 years old, is still active and is effectively stabilized in aqueous solution in presence of proteose–peptone No. 4 ("Difco").

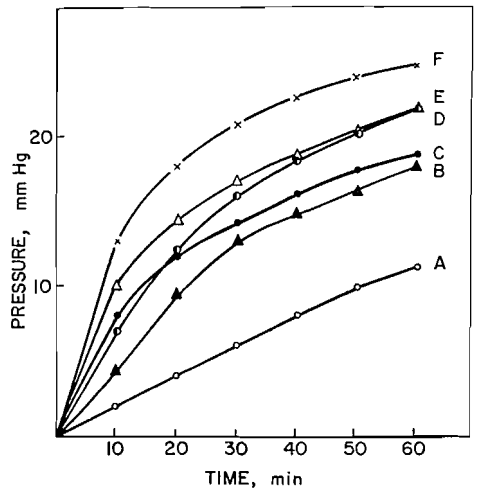

FIG. 3. Carbon dioxide evolution rates in carbonic anhydrase reactions. (A) Without enzyme; (B) enzyme + proteose–peptone No. 2; (C) with enzyme alone, and enzyme + proteose–peptone No. 1; (D) enzyme + bactopeptone; (E) enzyme + proteose–peptone No. 3; (F) enzyme + proteose–peptone No. 4.

TABLE IV

Carbonic anhydrase enzymic activity

No.	Experiment	Activity in arbitrary units per milligram	
		Initial	Final (20 h)
1	No enzyme added	1	1
2	Enzyme added	3 250	0
3	Enzyme + proteose peptone No. 1	3 450	2 950
4	Enzyme + proteose peptone No. 2	3 000	2 550
5	Enzyme + proteose peptone No. 3	—	4 700
6	Enzyme + proteose peptone No. 4	5 650	6 150
7	Enzyme + bactopeptone	2 850	3 600

Effect of Cations

Table V shows the effect of cations on the overall C-13 enrichment and the apparent equilibrium constant, K, is listed under varying experimental conditions.

Except in the case of Mg^{2+} ion, the other cations do not seem to suggest any specific effect although the K values are lower than the one with just Na^{+} ion present. The experimental difficulties are numerous when working with the transitional metal ions; one such difficulty is the extra element of heterogenity introduced into the equilibrium system as a result of precipitating hydroxides, basic carbonates, and carbonates. The same is true at higher concentrations of Mg^{2+} ion and at elevated pH's. However, with the available experimental data it can be shown that Mg^{2+} ion does participate in some way in the overall fractionation of ^{13}C, as illustrated in Fig. 4.

Furthermore, interest in the study of Mg^{2+} ion effect on ^{13}C fractionation derives mainly from its occurrence as the third major constituent in sea water. Any chemical model for sea water (19) must therefore take into consideration the various chemical species in

Can. J. Chem. Downloaded from www.nrcresearchpress.com by 210.87.254.105 on 09/05/12
For personal use only.

TABLE V

Effect of cations on equilibrium isotope effect at 25 °C

Added metal ion	Initial concentration (M)	K	pH
Mg^{2+}	0.0	1.0071	7.9
	4.9×10^{-3}	1.0075	7.9
	4.9×10^{-2}	1.0090	7.9
	5.0×10^{-1}	1.012	7.9
Mn^{2+}	2.5×10^{-2}	1.0010	8.1
Fe^{2+}	2.5×10^{-2}	0.9970	7.4
Co^{2+}	2.5×10^{-2}	0.9988	7.6
Ni^{2+}	2.5×10^{-2}	0.9999	7.6
Al^{3+}	2.0×10^{-2}	1.000	8.6
Cr^{3+}	2.5×10^{-2}	0.9976	7.7

Na^+ ion present in all cases.

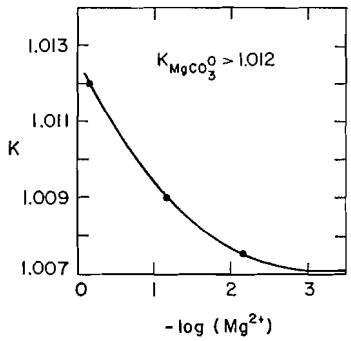

FIG. 4. Magnesium ion dependence of equilibrium isotope effect: temperature 25°; pH 7.9; Na^+, 2.48×10^{-2} M.

which magnesium is present. Recently Thode (20) summarized the carbonate ion anomaly in sea water and Garrels, Thompson, and Siever (21) calculated that of the total $CO_3^=$ in sea water nearly 75% is present as a neutral complex, $MgCO_3^0$. Magnesium is known to exhibit hexa-coordination, for example, in $Mg(H_2O)_6^{2+}$ (22) and $Mg(C_2O_4)_2(H_2O)_2^{2-}$ (23). A reasonable structure for the neutral complex of magnesium and carbonate in solution is

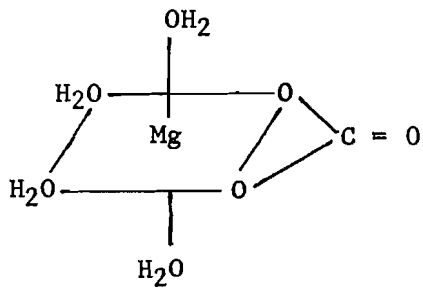

although some type of protonated carbonato complex might alter the bidentate character of the carbonate ligand. However, if we assume the neutral complex is so stable as to discriminate between free carbonate and bound carbonate then the symmetrical XY_3 form of free carbonate changes to what is in effect an XYZ_2 type of structure, resulting

Can. J. Chem. Downloaded from www.nrcresearchpress.com by 210.87.254.105 on 09/05/12
For personal use only.

in altered symmetry and perhaps changes in the characteristic vibrational frequencies. This therefore leads to isotopic discrimination and ^{13}C may be favored in the complex. Experimentally it is found to be so, as shown by the increased value of K in the presence of Mg^{2+} ions. It would be interesting, however, to make computer calculations of the normal coordinate treatment for this model and obtain band assignments and force constants which might permit evaluation of the partition function ratio, $Q_{Mg^{13}CO_3^0}/Q_{Mg^{12}CO_3^0}$, and calculation of the equilibrium constant for

[10] $$^{13}CO_2(g) + Mg^{12}CO_3^0(aq) = {}^{12}CO_2(g) + Mg^{13}CO_3^0(aq)$$

and also comparison with the experimental value ($K_{MgCO_3^0} > 1.012$). Mention may be made of an unsuccessful attempt to treat the complexed carbonate as an XYZ_2-type molecule using the vibrational frequencies of carbonyl fluoride, $^{12}COF_2$ (expt.) and $^{13}COF_2$ (calcd.) to represent $Mg^{12}CO_3^0$ and $Mg^{13}CO_3^0$ respectively for calculating $K_{MgCO_3^0}$. The calculated value gave an inverse isotope effect (0.935) indicating enrichment of carbon-13 in $CO_2(g)$. The COF_2 model may not be adequate to represent fully the bound carbonate.

Effect of pH

Preliminary experiments on the effect of pH on the carbon-13 fractionation carried out by procedure I consistently indicated a gradual, followed by steep and again gradual depletion of carbon-13 in the gas phase with increasing pH of the solution in the range 7–11. Figure 5 illustrates the trend when one plots ($^{12}C/^{13}C$) ratio in the $CO_2(g)$ vs. pH of the solution. The pH's were measured in these experiments from the change in color of the indicator present in the 60 ml reactor flask in two different sets of experiments and are less accurate than those measured by a pH meter in procedure II. Nevertheless, the S-shaped depletion curve was the case in all the experiments. A more detailed investigation was undertaken to study the effect of pH on the equilibrium isotope effect in general.

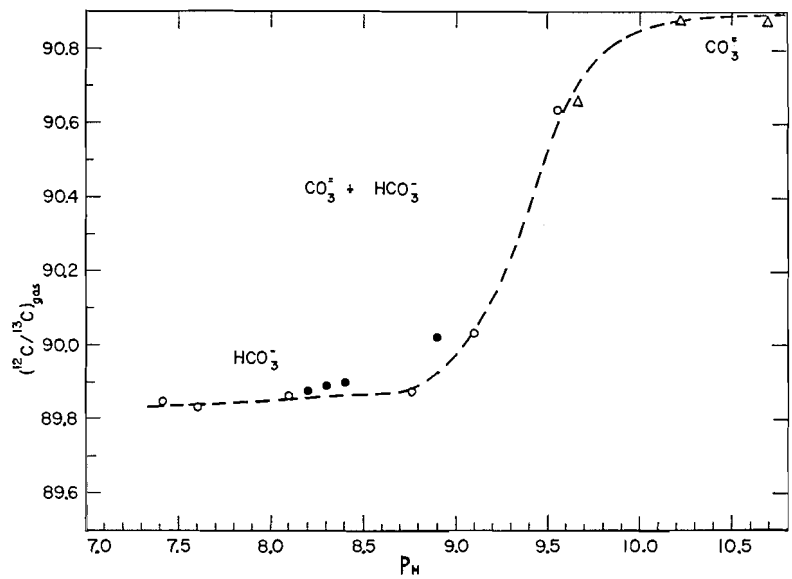

FIG. 5. Carbon-13 depletion curve: open circles and triangles indicate experimental data obtained using procedure I; solid circles are (normalized) points obtained using procedure II.

Can. J. Chem. Downloaded from www.nrcresearchpress.com by 210.87.254.105 on 09/05/12
For personal use only.

The wide fluctuations in the reported values for the single stage enrichment factor, α, obtained from column experiments are shown in Table VI. Earlier investigators have not taken into account the effect of pH nor has any further analysis been made in terms of three separate equilibria, [1], [2], and [3]. Since the magnitudes of K_0, K_1, and K_2 play an important role in the observed overall enrichment of ^{13}C in solution in a given experiment, a systematic study of the effect of pH seemed desirable and was undertaken.

TABLE VI

Summary of single stage ^{13}C-enrichment factors reported for $CO_2(g)$--$HCO_3^-(aq)$--$CO_3^=(aq)$ system

α	Temp. (°K)	Cation present	Method	pH	Authors
1.013 1.014	298 (?)	K^+	*, ‖	Unknown	Urey, Aten, and Keston (1936)
1.013 1.014	298 (?)	K^+	†	Unknown	Reid and Urey (1943)
1.0070 1.0120 1.0159 1.0132	298 (?)	NH_4^+	‡	Unknown	Reid and Urey (1943)
1.046	(?)	K^+	*	Unknown	Semiokhin, Panchenkov, and Zhurov (1963)
1.0083	298	Na^+	§	—	Abelson and Hoering (1960)
1.0071	298	Na^+	‖, ¶	$\leqslant 8.7$	This work
1.0083	300	Na^+	‖, **	8.4	This work
1.0096	300	Na^+	‖, **	8.9	This work
1.0125	300	Na^+	‖, **	9.3	This work
1.0131	300	Na^+	‖, **	9.3	This work
1.0166	300	Na^+	‖, **	9.9	This work

*Column experiments.
†Static bomb experiments.
‡Carbon dioxide bubbling experiments.
§Ion-exchange experiments.
‖Carbonic anhydrase enzyme-catalyzed experiments.
¶This study using procedure I.
**This study using procedure II.

Figure 6 shows the relation between K and pH; the calculated curves are based on the following considerations. The $^{13}CO_2(g)$ can exchange with the solution carbon species as follows:

$$^{13}CO_2(g) + \begin{Bmatrix} l\,^{12}CO_2(aq) \\ m\,H^{12}CO_3^-(aq) \\ n\,^{12}CO_3^=(aq) \end{Bmatrix} = {}^{12}CO_2(g) + \begin{Bmatrix} l\,^{13}CO_2(aq) \\ m\,H^{13}CO_3^-(aq) \\ n\,^{13}CO_3^=(aq) \end{Bmatrix}$$

and the apparent equilibrium constant K is given by

$$K = \frac{lK_0 + mK_1 + nK_2}{l + m + n}, \qquad [11]$$

where l, m, and n represent each fraction of the total carbon present as $CO_2(aq)$, $HCO_3^-(aq)$, and $CO_3^=(aq)$ respectively and are determined by the pH of the solution. Using the ionization constants of carbonic acid it is possible to calculate $CO_2(aq)/HCO_3^-/CO_3^=$ ratios at a given pH. Also by using the best available experimental values for K_0, K_1, and K_2, the apparent equilibrium constant, K, can be calculated at different pH's with the help of eq. [11]. The values used in calculating the curves in Fig. 6 are: $K_0 = 1.0009$, obtained experimentally by Abelson and Hoering (24); $K_1 = 1.0083$ (curve I), obtained by Abelson and Hoering (24); and $K_1 = 1.0071$ (curve II) obtained by us, using

Can. J. Chem. Downloaded from www.nrcresearchpress.com by 210.87.254.105 on 09/05/12
For personal use only.

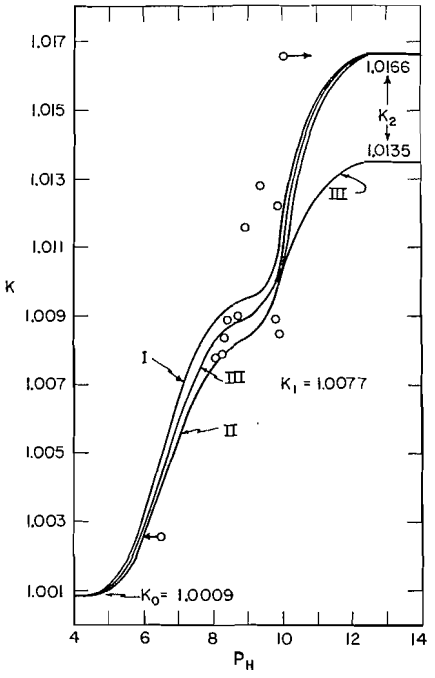

FIG. 6. pH dependence of equilibrium isotope effect. Curves are calculated using eq. [11] and for values, $K_0 = 1.0009$, $K_1 = 1.0083$ (curve I), $K_1 = 1.0071$ (curve II), $K_1 = 1.0077$ (curve III); $K_2 = 1.0166$ and 1.0135. Points shown in circles are those obtained experimentally using procedure II in all cases except the one at pH 6.5. Temperature 27 ± 1 °C.

procedure I in preliminary studies, as also a mean value 1.0077 (curve III); also two values of K_2 were used, 1.0166 the highest value obtained in our experiments and $K_2 = 1.0135$, the average value obtained (see curves in Fig. 6). The numerical values for these constants are further discussed.

At pH's greater than 7 the species in solution are predominantly HCO_3^- and $CO_3^=$ and eq. [11] becomes

$$K' = \frac{mK_1 + nK_2}{m + n}, \qquad [12]$$

where K' is the new overall equilibrium constant. If we define $c = m/n$, eq. [12] is further reduced to

$$K' = \frac{cK_1 + K_2}{c + 1}. \qquad [13]$$

The wide divergence in the apparent equilibrium constant reported from column experiments shown in Table VI is thus explained in part as due to different values of c (different pH's), in other words, mixtures of HCO_3^- and $CO_3^=$ present in the scrubbing solution. Knowing K', K_1, and K_2 it should be possible to fix the composition of the scrubbing solution used by various investigators in their column experiments.

$CO_2(g)$---$CO_2(aq)$ Equilibrium Constant, K_0

The value reported by Abelson and Hoering (24), 1.0009 at 25° and used by us in Fig. 6, agrees well with our calculated value, 1.0008 at 25° shown in Table III. It may

Can. J. Chem. Downloaded from www.nrcresearchpress.com by 210.87.254.105 on 09/05/12
For personal use only.

be pointed out that dissolved carbon dioxide in water is essentially present as $CO_2(aq)$ and no attention is paid to the questionable species $H_2CO_3(?)$. If the latter is at all present the ratio $(H_2CO_3)/(CO_2)$ at equilibrium is indeed small and hence its contribution to K_0 is negligible.

$CO_2(g)$---$HCO_3^-(aq)$ Equilibrium Constant, K_1

A direct measurement of K_1 is more difficult to make in view of the fact that bicarbonate solutions are never purely bicarbonate in their composition. Abelson and Hoering (24) report a value for $K_1 = 1.0083$ at 25° from their ion-exchange experiments assuming no isotope fractionation on the Dowex-1 resin used. Starting with purely bicarbonate solutions we obtained $K_1 = 1.0071$ by procedure I and somewhat higher values by procedure II (see Table VI). However, from an analysis of pH dependence data we recommend a value for $K_1 = 1.0077$. No theoretical calculation of K_1 was attempted for reasons discussed earlier.

$CO_2(g)$---$CO_3^=(aq)$ Equilibrium Constant, K_2

Although theoretical calculations have been made with a fair degree of success for this equilibrium constant over a wide range of temperature, 0 to 975 °C, there is considerable lack of reproducibility in experimental determinations and equal lack of agreement with the theoretical value. The calculated value for $K_2 = 1.0074$ at 27° seems to agree with only the lower limit set in this study. By using procedure II the observed equilibrium constant ranges from 1.0066 to 1.0166 in all the experiments at room temperature (27 ± 1 °C). The reason is not apparent. Although the experiments were intended to obtain K_2 directly, in reality, however, under the experimental conditions reported here we are not dealing with purely carbonate solutions but solutions containing significant concentrations of bicarbonate ion. In the presence of carbonic anhydrase and its nutrient solution the pH of a 1 *M* Na_2CO_3 solution was always found to be lower than the expected value of ~ 12. The problem is further complicated by the possibility of CO_2 absorption, in the course of pH measurements, which would yield spuriously low pH's. Equally important are (i) poor accuracy in analyzing small size $CO_2(g)$ samples from the gas phase, (ii) the possibility of rapid deterioration of carbonic anhydrase at pH's where $CO_3^=$ is the predominant species, and (iii) perhaps certain unknown kinetic problems associated with the hydration–dehydration reactions of carbon dioxide which are so vital in assuming isotopic equilibrium of elementic carbon between $CO_2(g)$ and $CO_3^=(aq)$. At best, therefore, one can give only an approximate value for $K_2 \geqslant 1.013$ indicating the order $K_0 < K_1 < K_2$. This is also supported by our preliminary experiments on carbon-13 depletion observed in the gas phase.

REFERENCES

1. H. C. Urey and L. Greiff. J. Am. Chem. Soc. **57**, 321 (1935).
2. H. C. Urey, A. H. W. Aten, Jr., and A. S. Keston. J. Chem. Phys. **4**, 622 (1936).
3. A. F. Reid and H. C. Urey. J. Chem. Phys. **11**, 403 (1943).
4. H. C. Urey. J. Chem. Soc. 562 (1947).
5. N. V. Meldrum and F. W. J. Roughton. J. Physiol. London, **80**, 113 (1933).
6. D. A. Scott and J. R. Mendive. J. Biol. Chem. **139**, 663 (1941).
7. R. C. Hawkings, R. L. Graham, A. L. Harkness, and H. G. Thode. National Research Council, Montreal Laboratory Report, MC 31. 1943.
8. J. Bigeleisen and M. G. Mayer. J. Chem. Phys. **15**, 261 (1947).
9. J. R. Hulston. Ph.D. Thesis, McMaster University. 1964.
10. M. Wolfsberg. Private communication.
11. T. Wentink, Jr. J. Chem. Phys. **30**, 105 (1959).
12. L. H. Jones and E. McLaren. J. Chem. Phys. **28**, 995 (1958).
13. T. G. Kujumzelis. Physik. Z. **39**, 665 (1938).
14. D. F. Heath and J. W. Linnett. Trans. Faraday Soc. **44**, 873 (1948).

Can. J. Chem. Downloaded from www.nrcresearchpress.com by 210.87.254.105 on 09/05/12
For personal use only.

15. R. DUVAL, C. DUVAL, and J. LE COMTE. Soc. Chim. France, Bull. V, **10**, 517 (1943).
16. B. CRAGG and H. G. THODE. Unpublished results. 1963.
17. R. K. WANLESS and H. G. THODE. J. Sci. Instr. **30**, 395 (1953).
18. H. CRAIG. Geochim. et Cosmochim. Acta, **12**, 133 (1957).
19. R. M. GARRELS and M. E. THOMPSON. Am. J. Sci. **260**, 57 (1962).
20. H. G. THODE. Henry Ford Hosp. Med. Bull. **10**, 501 (1962).
21. R. M. GARRELS, M. E. THOMPSON, and R. SIEVER. Am. J. Sci. **259**, 24 (1961).
22. J. P. MATHIEU. Compt. Rend. **231**, 896 (1950). R. L. FONT. Compt. Rend. **244**, 1481 (1957). R. E. HESTER and R. A. PLANE. Inorg. Chem. **3**, 768 (1964).
23. D. P. GRADDON. J. Inorg. Nucl. Chem. **3**, 308 (1956).
24. P. H. ABELSON and T. C. HOERING. Ann. Rep. Director Geophys. Lab. **59**, 158 (1960).
25. V. M. TATEVSKY and A. V. FROST. Bull. Moscow State Univ. **12**, 113 (1947). S. Z. ROGINSKY. Theoretical principles of isotopic methods for investigating chemical reactions. Academy of Sciences USSR Press, Moscow. 1956. United States AEC-tr-2873. Technical Information Service, Oak Ridge, Tenn., U.S.A.
26. E. M. KUZNETSOVA, Z. V. GRYAZNOVA, and G. M. PANCHENKOV. Doklady Phys. Chem. **148**, 18 (1963).
27. I. A. SEMIOKHIN, G. M. PANCHENKOV, and YU. A. ZHUROV. Vestn. Mosk. Univ. Ser. II Khim. **15** (5), 6 (1960); Chem. Abstr. **56**, 3083*h* (1962).

Can. J. Chem. Downloaded from www.nrcresearchpress.com by 210.87.254.105 on 09/05/12
For personal use only.

Can. J. Chem. Downloaded from www.nrcresearchpress.com by 210.87.254.105 on 09/05/12
For personal use only.

^{13}C N.M.R. STUDIES

PART VI.[1] CARBON-13 SPECTRA OF α,β-UNSATURATED CARBONYL COMPOUNDS[2]

D. H. MARR AND J. B. STOTHERS
Department of Chemistry, University of Western Ontario, London, Ontario

Received October 19, 1964

ABSTRACT

The 15.1 Mc/s ^{13}C n.m.r. spectra of 34 α,β-unsaturated carbonyl compounds have been obtained and the chemical shifts of the olefinic and carbonyl carbon nuclei are reported. Examples were drawn from the acyclic and five- and six-membered ring alicyclic series. A few aldehydes are included although most of the compounds are ketones. In the case of compounds assumed to be planar, variations of the olefinic shieldings with alkyl substitution parallel those observed previously for olefinic hydrocarbons. The key factor governing the chemical shifts of the carbonyl-carbon nuclei appears to be the extent of conjugation in a given system. Consequently, the ^{13}C results provide evidence for steric interference to coplanarity in the hindered systems. This approach is compared with other methods of estimating the extent of steric inhibition of conjugation and its merits are assessed.

INTRODUCTION

The investigation of the carbon-13 nuclear magnetic resonance (n.m.r.) spectra of a wide variety of organic carbonyl compounds was presented as the first part of this series (1) and included some results from a few aliphatic conjugated systems. To study in more depth the general features revealed by the earlier work, we have assembled a series of 15 acyclic and 19 alicyclic α,β-unsaturated aldehydes and ketones and measured the chemical shifts of their olefinic and carbonyl carbon nuclei. The alicyclic series included examples of the five- and six-membered cycloalkenones and a few acetylated cyclohexenes. The prime objective of the study of the effects of methyl substitution on these shieldings has been to allow a detailed comparison of chemical shift variations with those reported previously for acyclic olefins (2). No polar substituents were included. The analyses of the spectral data were, for the most part, straightforward. Intercomparisons of the chemical shift variations within a particular group generally provided a clear indication of the more reasonable assignment for the olefinic nuclei in those cases in which an unambiguous choice could not be made directly. The signals from the carbonyl carbon nuclei are at lowest field in all cases and present no difficulty (1).

The results of this study bear out the marked similarities for the olefinic shieldings in both the aliphatic (2) and aromatic olefins (3). Additivity of the effects of methyl substitution on or close to the double bond is noted for the olefinic shieldings and is compared with the earlier observations for the acyclic olefins (2). The carbonyl carbon shieldings are compared with our previous results for the acetophenones (4) and alkyl phenyl ketones (5) and similar trends found. Coplanarity of the components of the conjugated system appears to be the most important single factor governing the position of absorption of the carbonyl carbon in these systems, and, consequently, evidence for steric inhibition of conjugation in the hindered systems is given by the observed carbonyl shifts. The shieldings of the olefinic nuclei in these cases offer supporting evidence for this feature. Although no semiquantitative estimation of the extent of steric interference is attempted, the qualitative approach to the problem is compared with previous results for these

[1]*Part V, ref. 3.*
[2]*These results were reported in part at the 14th Conference on Analytical Chemistry and Applied Spectroscopy, Pittsburgh, March 1963.*

compounds obtained by the more usual techniques based on ultraviolet, infrared, and Raman spectroscopic data (6–13). The advantages and limitations of the ^{13}C method are discussed.

EXPERIMENTAL

N.M.R. Spectra

All spectra were obtained at a spectrometer frequency of 15.085 Mc/s using the pure compounds containing ^{13}C in natural abundance. The details of the experimental procedure have been given (4). The chemical shift data are judged to have a precision of ± 0.5 p.p.m. and are given on a scale relative to CS_2 (0 p.p.m.).

Materials

Some of the compounds employed are commercially available and were obtained from the following sources: Aldrich Chemical Co., Inc., isophorone, 2-cyclopentenone, 1-indanone, 9-fluorenone, 1-acetylcyclohexene; Eastman-Kodak, acrolein, crotonaldehyde, tiglaldehyde, pulegone; Louis Light and Co., piperitone. Samples of a number of the materials included in this survey were kindly supplied by Dr. Klaus Noack, who had prepared them for investigations of their infrared and ultraviolet spectra (9). The physical data for the following have been reported (9): methyl vinyl ketone; methyl isopropenyl ketone; 3-methyl-, 4-methyl-, and 3-ethyl-3-pentene-2-one; 3,4-dimethyl-3-hexen-2-one; 2-ethylidenecyclohexanone; 3-methyl-, 2,3-dimethyl-, 3,5-dimethyl-, and 3,5,5-trimethyl-2-cyclohexenone. A sample of piperitenone was donated by Mr. J. Cooper. The remaining compounds were prepared by well-known methods. The observed physical constants and the syntheses employed are outlined in Table I. In these cases the boiling points and melting points are uncorrected. One of the compounds, 3-pentenone, was isolated and purified by preparative scale vapor-phase chromatography (v.p.c.) and its boiling point was not determined. For all compounds, a small sample was examined by analytical v.p.c. before its ^{13}C spectrum was determined. These analyses were performed on a F-M model 700 instrument using a 10 ft column (outside diameter 0.25 in.) of 10% Apiezon on firebrick. The purity of most of the samples exceeded 98%, but a minimum of 96% was deemed acceptable for a few cases. Proton spectra were also obtained for most samples to check for the absence of gross amounts of impurities.

TABLE I

Physical data for α,β-unsaturated ketones prepared for this study

Compound	Method of preparation	Physical constants				
		Observed		Reported		
		b.p./mm	n_D^{25}	b.p./mm	n_D (t°)	Ref.
3-Methyl-3-butenone	A1	93–94/atm	1.4182	96–97/atm	1.4190 (25)	14
3-Pentenone	A2	*	1.4370	124/atm	1.4390 (20)	15
3-Hexen-2-one	A2	40/16	1.4446	198/atm	1.4400 (16)	15
3-Methyl-3-hexen-2-one	A2	52/15	1.4510	55–60/14	—	16
3-Hepten-2-one	A2	65/10	1.4420	62/15	1.4430 (20)	17
2-Cyclohexenone	B	47–48/9	1.4850	67/25	1.4879 (20)	18
2-Methyl-2-cyclohexenone	C	62–63/14	1.4900	66–66.5/14	1.4836 (25)	19
1-Acetyl-2-methylcyclohexene	D	Purified and characterized as the semicarbazone†				
1-Acetyl-6,6-dimethylcyclohexene	E	86–88/14	1.4786	116/47	1.4815 (25)	20
1-Acetyl-2,6,6-trimethylcyclohexene	E	98–100/17	1.4742	88–90/20	1.4775 (20)	21
2-Methyl-2-cyclopentenone	F	71/10	—	157/atm	1.4762 (25)	22
3-Methyl-2-cyclopentenone	G	64/9.5	1.4854	63/10	1.4868 (25)	8
2,3-Dimethyl-2-cyclopentenone	H	82/20	1.4844	90–92/25	1.4830 (20)	23
2-Isopropylidenecyclopentanone	A3	74/12	1.4891	88–88.5/21	1.4961 (22)	8

*Purified by preparative scale v.p.c.
†Semicarbazone, m.p. 225.5–226; reported (6), 227–227.5 °C.
Methods employed:
A1, aldol reaction of butanone + $(CH_2O)_3$ (14);
A2, aldol reaction of acetone + appropriate aldehyde (15);
A3, aldol reaction of acetone + cyclopentanone (24);
B, CrO_3 oxidation of cyclohexene (18);
C, chlorination of 2-methylcyclohexanone, followed by HCl removal (19);
D, Friedel–Crafts acetylation of 1-methylcyclohexene (6);
E, reaction of alkyl ketones with LiC≡CH, followed by elimination and hydration (25);
F, Grignard reaction, MeMgI + 1,2-cyclopentanedione (26);
G, base-catalyzed ring closure of 2,5-hexanedione (27);
H, rearrangement of 4-methyl-4-ethyl-4-butyrolactone with P_2O_5 (23).

DISCUSSION

The chemical shift results for the acyclic α,β-unsaturated ketones are collected in Table II, while the data for the cycloalkenones and acetylcyclohexenes are presented in Tables

Can. J. Chem. Downloaded from www.nrcresearchpress.com by 210.87.254.105 on 09/05/12
For personal use only.

III and IV, respectively. The results for the few aldehydes and cross-conjugated ketones examined appear in Table V. The tabulated data are restricted to the observed shieldings of the olefinic and carbonyl carbon nuclei. Since the complexity of the spectra in the saturated carbon region does not permit a precise analysis and any assignments would be uncertain, except for the simplest derivatives, we have not attempted a detailed analysis of these absorption bands. For purposes of discussion, the carbonyl and olefinic carbon shieldings are considered separately. In the last section, the application of these results to the investigation of steric inhibition of conjugation is discussed and compared with the more usual approaches to this problem. All of the data in Tables II–V were obtained using the neat liquids, but to examine the effect of hydrogen bonding at the carbonyl oxygen on the shieldings of these nuclei some compounds were examined in methanol solution as well (Table VII).

TABLE II

^{13}C chemical shifts of the carbonyl and olefinic carbons of some acyclic α,β-unsaturated ketones (in p.p.m. from CS_2)

Compound	Chemical shifts		
	C=O	C-3 (α-C)	C-4 (β-C)
Butenone	−4.4	56.2	65.1
3-Methyl-3-butenone	−4.8	49.2	68.5
3-Penten-2-one	−3.7	60.3	50.0
4-Methyl-3-penten-2-one (mesityloxide)	−3.4	69.8	40.0
3-Methyl-3-penten-2-one	−5.2	54.3	54.8
3-Ethyl-3-penten-2-one	−3.6	49.3	56.3
3,4-Dimethyl-3-penten-2-one	−8.9	62.0	56.3
3-Hexen-2-one	−2.8	63.3	45.0
3-Methyl-3-hexen-2-one	−4.4	56.6	50.5
3,4-Dimethyl-3-hexen-2-one	−8.8	62.5	51.6
3-Hepten-2-one	−2.8	61.9	46.3

TABLE III

^{13}C chemical shifts of the carbonyl and olefinic carbons of some alicyclic α,β-unsaturated ketones (in p.p.m. from CS_2)

Compound	Chemical shifts		
	C=O	C-2 (α-C)	C-3 (β-C)
2-Cyclohexenone	−4.3	64.4	43.0
2-Methyl-2-cyclohexenone	−4.7	57.9	48.2
3-Methyl-2-cyclohexenone	−3.7	67.2	31.5
2,3-Dimethyl-2-cyclohexenone	−3.6	62.8	39.1
3,5-Dimethyl-2-cyclohexenone	−3.2	67.8	32.8
3,5,5-Trimethyl-2-cyclohexenone (isophorone)	−3.8	68.2	34.3
3-Methyl-6-isopropyl-2-cyclohexenone (piperitone)	−5.1	66.6	33.4
2-Ethylidenecyclohexanone	−4.9	55.6	60.4
2-Isopropylidene-5-methylcyclohexanone (pulegone)	−7.8	61.5	52.4
2-Cyclopentenone	−15.3	59.9	28.6
2-Methyl-2-cyclopentenone	−14.9	51.9	35.4
3-Methyl-2-cyclopentenone	−15.1	63.6	14.3
2,3-Dimethyl-2-cyclopentenone	−13.5	58.1	24.8
2-Isopropylidene-2-cyclopentanone	−11.8	62.6	48.3

Carbonyl Carbon Chemical Shifts

For purposes of discussion it is convenient to consider the acyclic aldehydes and ketones and the cyclohexenone derivatives as a group, before examining the data for the cyclopentenones, acetylated cyclohexenes, and cross-conjugated examples. For this first group

Can. J. Chem. Downloaded from www.nrcresearchpress.com by 210.87.254.105 on 09/05/12
For personal use only.

of compounds, the ketonic carbonyl carbon signal appears over the range, −2.8 to −12.7 p.p.m., while the aldehydes exhibit this peak at 0.0–1.4 p.p.m. A comparison of the values for the simplest examples in each of these series shows that methyl substitution on the carbonyl group, i.e. RCHO → $RCOCH_3$, tends to deshield the carbonyl nucleus by ca. 5 p.p.m. as was noted previously (1). Certain consistent trends can be seen for the effects of further alkyl substitution on the α,β-unsaturated carbonyl system by comparing the rest of the data.

Methyl substitution on the β-olefinic carbon seems to increase the shielding at the carbonyl carbon nucleus by ca. 1 p.p.m. for both the aldehydes and ketones (cf. butenone with 3-pentenone; acrolein with crotonaldehyde). The effect of ethyl substitution at the β-position appears to be somewhat larger (ca. 2 p.p.m., butenone and 3-hexenone), although further extension of the chain causes no additional change. Similarly, methyl substitution at C-5 in the 2-cyclohexenone derivatives is without effect at the carbonyl carbon. Since it is well established that conjugation tends to shield carbonyl carbons (1) and that the carbonyl shieldings reflect the extent of conjugation (4, 5, 28), it is not surprising that β-methyl substitution tends to shift the carbonyl absorption toward higher field. The introduction of a second β-methyl group produces an additional shielding effect as illustrated by the values for mesityl oxide and 3-methyl-2-cyclohexenone relative to 3-pentenone and 2-cyclohexenone, respectively. For all of these comparisons, the observed effect is of the order of the experimental error but the consistency of the changes lends support to the idea that the trend may be real. The shielding at the carbonyl carbon nucleus of 2-cyclohexenone will be the resultant of the two opposing factors noted in the acyclic examples, namely, the deshielding effect of alkyl substitution on the carbonyl carbon and the shielding effect of β-alkyl substitution, and its carbonyl absorption position is virtually the same as that of butenone.

The replacement of α-hydrogens by alkyl groups tends to produce an effect opposite to that discussed above at the carbonyl carbon. For each of the five possible comparisons within this group of compounds, the α-methyl substituent reduces the carbonyl shielding by 0.4–1.6 p.p.m. Again, these changes are not large but the trend is observed for all examples without exception. The lone example bearing an α-ethyl group, 3-ethyl-3-pentenone, exhibits carbonyl absorption at −3.6 p.p.m. or 1.6 p.p.m. up-field from the 3-methyl derivative. An explanation of this observation is not evident. For the various α-methyl derivatives, however, it would appear that this grouping decreases the conjugative interaction between the olefinic and carbonyl bonds.

Marked low-field shifts of the carbonyl carbon absorption are found for the cases in which the double bond is fully substituted. Clearly the effects of the α- and β-methyl substituents at the carbonyl carbon are not additive, but rather produce an overall deshielding effect of 5.2–6.0 p.p.m. The most reasonable interpretation of this observation appears to be a pronounced interference to coplanarity for the conjugated system. We shall return to this point in the final section of the paper.

In the cyclopentenone series, the carbonyl absorption appears at much lower field than that for the six-membered cases, and the effects of monomethyl substitution on the double bond are very small, if indeed real. In addition, the carbonyl carbon for the 2,3-dimethyl derivative is 2.2 p.p.m. *more shielded* than that in 2-cyclopentenone itself. These variations would appear to reflect the geometrical differences between the five- and six-membered rings and will be considered in more detail below. We are still without explanation for the low-field position of the carbonyl absorption for five-membered ring compounds, although the problem was considered earlier (1) and further work is in progress.

Can. J. Chem. Downloaded from www.nrcresearchpress.com by 210.87.254.105 on 09/05/12
For personal use only.

TABLE IV

^{13}C chemical shifts of the carbonyl and olefinic carbons of some substituted 1-acetyl-1-cyclohexenes (in p.p.m. from CS_2)

Compound	Chemical shifts		
	C=O	C-1 (α-C)	C-2 (β-C)
1-Acetylcyclohexene	−4.6	54.1	52.4
1-Acetyl-6,6-dimethylcyclohexene	−4.7	46.7	54.4
1-Acetyl-2-methylcyclohexene	−7.6	60.6	52.5
1-Acetyl-2,6,6-trimethylcyclohexene	−12.7	65.2	49.9

The carbonyl shieldings for the four acetylated cyclohexenes (Table IV) depend strongly on the number of methyl substituents. Apparently substitution at C-6 does not alter the electronic environment about the carbonyl carbon nucleus unless the double bond is fully substituted, in which case the carbonyl shielding is decreased by 5.0 p.p.m. The effect of β-methyl substitution in this series is similar to that observed for the acyclic compounds, since this example possesses a fully substituted double bond and exhibits its carbonyl peak at 3.0 p.p.m. lower field than 1-acetyl-1-cyclohexene. Steric inhibition of conjugation would appear to be responsible for these variations in the observed carbonyl shieldings (see below).

Two ketones, phorone and piperitenone, having cross-conjugated systems were examined and both exhibit carbonyl carbon signals at considerably higher field than the simpler α,β-unsaturated derivatives. Clearly, any contribution to the carbonyl shielding arising from the magnetic anisotropy of the olefinic groups must be small, since this effect would tend to deshield in the olefinic plane (29, 30). Presumably, additional electron supply to the carbonyl group by the second double bond is responsible for the observed shift. Since few other types of carbonyl carbon nuclei absorb in this particular region, it appears that the ^{13}C spectrum may provide diagnostic evidence for the identification of cross-conjugated carbonyl systems, although several more examples are required to confirm this point. At the present time, it is known that α-halo ketones give rise to carbonyl peaks in this region (1) as do a number of substituted benzaldehydes (31). The latter would present no problem since the carbonyl band is a doublet, and there is little difficulty in distinguishing between haloketones and conjugated ketones by other means.

TABLE V

^{13}C chemical shifts of carbonyl and olefinic carbons of some α,β-unsaturated aldehydes and two cross-conjugated ketones (in p.p.m. from CS_2)

Compound	Chemical shifts		
	C=O	C-2 (α-C)	C-3 (β-C)
Propenal (acrolein)	0.4	56.4	56.8
2-Butenal (crotonaldehyde)	1.4	60.0	40.7
2-Methyl-2-butenal (tiglaldehyde)	0.0	53.5	45.2
3-Methyl-6-isopropylidene-2-cyclohexenone (piperitenone)	3.5	63.8	34.0
2,6-Dimethyl-3,6-heptadien-4-one (phorone)	4.9	68.1	41.3

Olefinic Carbons

As in the preceding section, it is convenient to discuss the acyclic carbonyl compounds and the cyclohexenones as a group. The data in Tables II, III, and V show that the

Can. J. Chem. Downloaded from www.nrcresearchpress.com by 210.87.254.105 on 09/05/12
For personal use only.

olefinic carbon nuclei absorb over a total range of 38.3 p.p.m. (31.5 → 69.8 p.p.m.) which is comparable to the 42.9 p.p.m. range (44.4 → 87.3 p.p.m.) reported for the acyclic olefins (2). Presumably the presence of the carbonyl group in conjugation with the double bond is responsible for the overall shift towards lower field for these chemical shifts. Except for the simplest cases, butenone and propenal, the first problem in the analysis of these results is the differentiation between the signals for the α- and β-olefinic carbons in the unsubstituted cases (cyclohexenone, pentenone, etc.). Due to the electron-withdrawing effect of the carbonyl grouping, however, it is reasonable to suggest that the lower field signals arise from the β-nucleus, since resonance forms of the type, II, contribute to the electronic distribution in the ground state. A shift toward lower field has

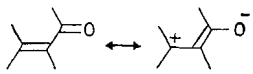

I II

been consistently observed for carbon nuclei in comparable environments [e.g. C-4 aromatic nuclei in monosubstituted benzenes (32, 33, 34), β-vinyl carbons in substituted styrenes (3)]. Closer inspection of the olefinic shieldings reveals variations caused by methyl substitution which are very similar to those observed for the olefinic hydrocarbons (2). These findings lend support to the above suggestion and provide reasonable evidence for the present assignments.

A comparison of the results for 3-methylbutenone and butenone itself shows that introduction of the methyl group tends to deshield C-3 (the α-C) by 7.0 p.p.m. and to shield C-4 (the β-C) by 3.4 p.p.m. There is no doubt about the assignments for these particular nuclei since the observed multiplicities provide a definite distinction. Similarly, the effect of the methyl group on the β-C can be found by comparing the results for acrolein and crotonaldehyde, which shows that the α- and β-carbons are shifted by +3.6 and −16.1 p.p.m., respectively. The observation that the olefinic carbon being substituted is deshielded by the introduction of a methyl group while the adjacent olefinic nucleus is shielded was found to be quite general in the hydrocarbon series (2). Further comparisons of this sort for the other monomethylated derivatives of the present series indicate that there are no exceptions to this behavior, although the magnitude of the effects differs for terminal and internal olefinic bonds. Again, this difference was found for the hydrocarbons. A summary of the changes arising from monomethyl substitution is presented in Table VI. The observed ranges are indicated and are found to be close to the experimental uncertainty except for one notable exception. The effect of methyl substitution on the β-position appears to be quite different in acyclic and alicyclic systems, but only one comparison was possible in the former case and perhaps it is anomalous. In any event, it is important to note that the consistency of these results appears to be limited to the monomethylated compounds. These trends break down for the examples having fully substituted double bonds. The possible significance of this observation is considered in more detail in the final section.

For the cyclopentenones, it is found that the effects of methyl substitution on the olefinic shieldings are qualitatively similar to those discussed above, but differ in magnitude. At both the α- and β-positions, the deshielding effect of a methyl substituent is greater (almost 50% greater for the β-methyl) than that found in the six-membered rings or the acyclic cases. Perhaps this enhancement is due to greater conjugative interactions in the more planar system, but the origin of these differences may be some unrecognized factor, since it is known that the five-membered ring affects carbonyl shieldings in a

Can. J. Chem. Downloaded from www.nrcresearchpress.com by 210.87.254.105 on 09/05/12
For personal use only.

TABLE VI

Effects of monomethyl substitution on olefinic shieldings in conjugated systems

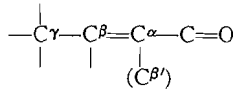

Position of substitution	$\Delta\delta_c$* (C—H → C—CH_3)		No. of examples
	α-C=	β-C=	
α	−6.5±0.5	+4.3±0.9	5
β'	−5.0	+1.5	1
β Terminal C=C	+3.8±0.2	−15.6±0.5	2
Internal C=C	+6.2±2.8	−10.1±1.4	4
γ	+3.0	−5.0	1

*In p.p.m.

unique manner (1). Little can be said about the olefinic shifts for 2-ethylidenecyclohexanone since no comparisons similar to the previous ones can be drawn. The methyl groups in 6,6-dimethyl-1-acetyl-1-cyclohexene appear to exert an effect at the olefinic nuclei which is appreciable for the α-C (−7.4 p.p.m.) but weak at the β-C (+2.0 p.p.m.). The remaining examples possess fully substituted olefinic bonds and a discussion of these is included in the final section.

While the overall consistency of the effects of methyl substitution tends to support the present assignments, a potential method of confirming our conclusions seemed worth investigating. It has been established that hydrogen-bonding solvents tend to reduce the shielding of carbonyl carbon nuclei relative to that measured for the pure liquid or in nonpolar solvents (1, 4, 5, 35). This reduction, although not particularly large unless protonation occurs (35), is significant and, furthermore, in aromatic systems the effect appears to be reflected at the terminal carbon nucleus as well [i.e., C-4 in acetophenone (1)]. The latter change is not unexpected since hydrogen bonding will enhance the contribution of polarized forms analogous to II. If a similar situation obtains for the aliphatic conjugated systems, one could distinguish the β-olefinic carbon from the α-nucleus by comparison of the olefinic shieldings measured for the neat liquid (or a solution in a nonpolar solvent) with those in a hydrogen-bonding solvent such as methanol. To test this idea, several samples were examined in the latter solvent and the difference in shielding for the olefinic and carbonyl carbons are listed in Table VII relative to the values for the pure liquids. Without exception, the carbonyl carbon absorption appears at lower field in methanol and the β-carbons are affected similarly, although to a lesser extent. These changes are consistent with the foregoing but the principal difficulty is that the shieldings of the α-nuclei are affected in a random fashion. With only one exception, however, the down-field shift is greater for the nucleus in the β-position and thus, further support for the present assignments is gained for the compounds having symmetrically substituted double bonds. The assignments for the lone exception, propenal, are unambiguous since the multiplicity of the absorption band differs for each olefinic carbon. While the solvent effects in several of these examples are small, within experimental error for some, it is interesting that the observed changes are qualitatively consistent with expectations based on the simple hydrogen-bonding explanation.

Steric Inhibition of Conjugation

The question of steric effects in conjugated carbonyl compounds has been the object of several investigations employing spectroscopic techniques and, although much of the

Can. J. Chem. Downloaded from www.nrcresearchpress.com by 210.87.254.105 on 09/05/12
For personal use only.

TABLE VII

Relative ^{13}C chemical shifts of olefinic and carbonyl carbons of some α,β-unsaturated compounds in methanol solutions (in p.p.m. relative to shifts of pure liquids)

Compound	Relative chemical shifts		
	C=O*	C-3† (α-C)	C-4† (β-C)
Butenone	−2.1	0.0	0.0
3-Pentenone	−1.3	+1.0	−0.2
3,4-Dimethyl-3-pentenone	−1.9	+0.8	−0.4
3-Hexen-2-one	−4.1	−0.7	−1.0
2-Cyclohexenone	−2.5	−0.6	−2.0
3,5-Dimethyl-2-cyclohexenone	−3.8	+0.1	−2.8
Propenal	−1.4	−0.9	−0.7
2-Butenal	−2.3	+0.1	−1.5

*For 25% (w/v) solutions in MeOH.
†For 50% (w/v) solutions in MeOH.

attention has been focussed on aromatic systems, a considerable effort has been expended on the study of aliphatic systems, a brief review of which has appeared (11). While the principal steric effect concerns the interference to coplanarity of the components of the conjugated systems, a secondary consideration is the orientation of these components about the single bond which joins them. This is perhaps a more important feature in the aliphatic systems since two, quite different, planar conformations are possible while differences between the planar conformations in aromatic compounds are less marked. For example, III and IV represent the planar conformations for a 2-substituted acetophenone while V and VI are the corresponding conformations for *trans*-3-penten-2-one. The latter are designated s-*trans* and s-*cis*, respectively. Since the absorption spectra of

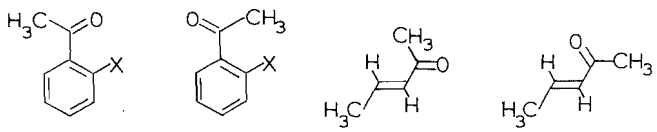

III IV V VI

these two aromatic conformations (III and IV) would be expected to be very similar, provided each was planar or had the same degree of nonplanarity, any conclusions regarding the preferred conformation must be based on some other consideration(s) such as the space-filling characteristics of the interfering groups (a subject that is not without controversy) or measurements of another physical property. At the present time, a clear choice between these two conformations is often difficult. In the aliphatic systems, however, the optical absorption spectra for the two planar forms (V and VI) were expected to be quite distinct on the basis of studies of model compounds in which the s-*trans* and s-*cis* configurations are fixed. Recently, Noack and Jones (10*b*) have described the infrared and Raman spectra of *trans*-3-penten-2-one obtained over a temperature range and their results show that this ketone exists as an equilibrium mixture of these two conformers with the s-*trans* form predominant at room temperature. It has been well established that the ultraviolet spectra of *cis* and *trans* forms of conjugated systems exhibit different characteristics, the most striking difference being the reduced intensity of the absorption band for the *cis* isomer with or without a shift in the position of the band. These differences have been discussed in detail and a classification system for the observed effects has been proposed (13), although its acceptance has not been universal.

Can. J. Chem. Downloaded from www.nrcresearchpress.com by 210.87.254.105 on 09/05/12
For personal use only.

Similar effects in the ultraviolet spectra of conjugated carbonyl compounds and certain differences in the infrared and Raman spectra of compounds of known geometry (7–12) have been suggested to distinguish between the two planar comformations. The general characteristics of the two forms are summarized in Table VIII. The principal difficulty of these approaches is a clear distinction between the planar s-*cis* conformation and possible nonplanar conformers, since the optical absorption characteristics of these forms are very similar. The present data indicate that a determination of the ^{13}C chemical shifts in these systems provides an alternative approach which yields more striking differences between the planar and nonplanar forms.

TABLE VIII

General characteristics of α,β-unsaturated carbonyl systems

	s-*trans*	s-*cis*
Ultraviolet		
$10^{-3}\epsilon_{max}^{(\pi\rightarrow\pi^*)}$	12–20	6–9
Infrared		
$\nu^{C=O} - \nu^{C=C}$	<70 cm^{-1}	>70 cm^{-1}
$\epsilon_a{}^{C=O}/\epsilon_a{}^{C=C}$	>6	0.5–3.5
Raman		
$\epsilon_a{}^{C=O}$	135–263*	17–46*

*Units given in Can. J. Chem. 39, 2201 (1961).

On the basis of the results from extensive series of acetophenones and related compounds (4, 5, 28), it was concluded that the degree of planarity of a conjugated carbonyl system is a most important factor affecting the shielding of the carbonyl carbon nuclei. Steric interference to coplanarity of the carbonyl group is clearly shown by a down-field shift of the carbonyl absorption band, while polar factors appear to be of minor importance, as are neighbor-anisotropy effects. Thus, one would expect little or no difference in the resonance position of carbonyl carbons in s-*cis* and s-*trans* conformations of α,β-unsaturated systems. The observed carbonyl shifts for mesityl oxide and 2-ethylidenecyclohexanone, which are closely similar to the values for 3-penten-2-one and 2-cyclohexenone, support this expectation. There is no question regarding the configurations for these alicyclic compounds, while mesityl oxide is generally believed to exist largely in the s-*cis* conformation and trans-3-penten-2-one mainly as the s-*trans* form. Thus, at least as a first approximation, it would appear that the shielding of the carbonyl carbon in the *planar* form is independent of the configuration about the connecting single bond. Several of the compounds having fully substituted double bonds, however, exhibit carbonyl bands at appreciably lower fields than the less highly alkylated examples. The most reasonable explanation for these trends seems to be a departure from coplanarity of the unsaturated groups due to steric interference of the substituents. The 3,4-dimethyl derivatives of 3-penten-2-one and 3-hexen-2-one are examples showing this behavior. It is unlikely that a fully substituted double bond in the five- or six-membered rings could cause a marked departure from coplanarity for the fixed s-*trans* cases and the observed carbonyl shieldings are not greatly different from those for the unsubstituted compounds. In the fixed s-*cis* configurations for the alicyclic cases, however, there will be an effect of ring size since one of the β-methyl substituents can more closely approach the carbonyl oxygen in the six-membered ring than in the five-membered system. The carbonyl chemical shift for pulegone indicates that this conjugated system is subject to interference since the peak

Can. J. Chem. Downloaded from www.nrcresearchpress.com by 210.87.254.105 on 09/05/12
For personal use only.

Can. J. Chem. Downloaded from www.nrcresearchpress.com by 210.87.254.105 on 09/05/12
For personal use only.

appears at −7.8 p.p.m. relative to the carbonyl absorption at −4.9 p.p.m. in 2-ethylidenecyclohexanone and at −4.3 p.p.m. in 2-cyclohexenone. On the other hand, the carbonyl peak at −11.8 p.p.m. for 2-isopropylidenecyclopentanone is at *higher* field than that of 2-cyclopentenone (−15.3 p.p.m.) indicating that there is substantial polarization of the system by the two β-methyl substituents. The observed carbonyl shielding for piperitone could, perhaps, be interpreted to mean that the 6-isopropyl grouping disturbs the planarity of the conjugated system but such a conclusion would be rash since we know little of the effects of alkyl substitution at this position on carbonyl carbon chemical shifts.

Further support for our present proposal was obtained from an examination of the ^{13}C spectra of the series of substituted 1-acetyl-1-cyclohexenes listed in Table IV. Members of this series have been employed previously as models to illustrate the spectral characteristics of hindered conjugated aliphatic systems (7, 11, 36). From the carbonyl results for the examples studied in this work, it follows that both the parent compound and its 6,6-dimethyl derivative are essentially planar (although probably in different conformations), while the 2-methyl compound is nonplanar as illustrated by the change of −3 p.p.m. for the carbonyl shielding. Apparently the interference in the 2,6,6-trimethyl derivative is more severe since the carbonyl signal is ca. 8 p.p.m. to low field relative to the planar compounds. These conclusions based on the observed carbonyl chemical shifts are completely consistent with those drawn from the optical spectral data or an examination of molecular models for the various members of the series.

A consideration of the carbonyl carbon shieldings for the entire series, therefore, points to a valuable application of the ^{13}C technique to the study of these systems. The basic assumption that the carbonyl carbon chemical shifts for both planar conformations are the same may be an oversimplification since only a few examples of the fixed s-*cis* configuration have been examined. Recent studies have been reported to show that unsaturated carbon nuclei exhibit chemical shifts which are somewhat dependent on the configuration of substituents about the double bond (37). These effects were observed, however, for compounds of the type XCH=CHX (where X = Cl, Br, I or COOEt) and the influence of the polar substituents may well be larger than that of alkyl groups. The two available comparisons for olefinic hydrocarbons (2) show that the differences between the *cis* and *trans* isomers are indeed small. Until more results for the fixed *cisoid* configuration become available, the present assumption seems reasonable since the effects of steric interference to coplanarity appear to be larger than the differences one would expect to arise for the *cis* and *trans* configurations.

An examination of the results for the olefinic carbons in the examples exhibiting lower field carbonyl peaks indicates that these olefinic shieldings offer supporting evidence for a departure from coplanarity in these compounds. In the earlier discussion of the observed olefinic shieldings it was noted that the introduction of a methyl group on the β-carbon of the double bond produced a marked deshielding effect at that nucleus and the effect was more pronounced than the methyl effect at the α-position (Table VI). The β-carbon shieldings for 3,4-dimethyl-3-penten-2-one, 3,4-dimethyl-3-hexen-2-one, 2-methyl-1-acetyl-1-cyclohexene, and its 2,6,6-trimethyl derivative are not shifted by the amounts indicated in Table VI. In fact, with one exception, the trend is toward slightly *higher* field if these shifts are compared with the values for the compounds bearing one less methyl group (i.e., 3-methyl-3-penten-2-one, 3-methyl-3-hexen-2-one, and 1-acetyl-1-cyclohexene, respectively). 2,6,6-Trimethyl-1-acetyl-1-cyclohexene is the exception for which the β-olefinic carbon is found at −2.5 p.p.m. lower field than the parent compound, a shift which is markedly reduced from that observed for less hindered systems (−10

p.p.m.). While the assignments for the olefinic carbons in the fully methylated compounds are not obtained directly, the reverse assignment seems very unlikely and the trends just described would be even more pronounced by 6–15 p.p.m. The absence of the strong deshielding effect of the β-methyl groups for these substituted cases, is fully consistent with the existence of steric inhibition of conjugation. It was noted above that the carbonyl group tends to produce an overall deshielding effect on the olefinic chemical shifts relative to the olefinic hydrocarbons and it follows that any factor which reduces the effect of the carbonyl group will tend to produce an up-field shift of the signals for these nuclei. Since the effect of the carbonyl group at the β-position must be largely due to conjugative interactions, any factor which influences the extent of conjugation should be reflected by the β-carbon shieldings.

TABLE IX

Ranges of ^{13}C chemical shifts in α,β-unsaturated ketones (p.p.m. from CS_2)

	Conformation of molecules*	
Carbon nucleus	Planar	Nonplanar
C=O†	−5.0 to −2.5	−12.7 to −5.5
α-C	50 to 70	56 to 72
β-C	14 to 65	50 to 56

*Relative orientation of olefinic and carbonyl bonds.
†Excluding cyclopentenones.

In summary, the present results indicate that ^{13}C n.m.r. spectroscopy provides a method for distinguishing hindered α,β-unsaturated carbonyl compounds from those capable of attaining planar conformations. The distinction is based on the carbonyl carbon chemical shift and the shieldings of the olefinic carbon nuclei provide confirmatory evidence. The principal differences are listed in Table IX in a brief form. An extension of the previously proposed approach (4, 28) to the estimation of angles of twist in these systems has not been attempted owing to the scarcity of data for suitable systems, but remains as a potential refinement when the necessary data become available.

ACKNOWLEDGMENTS

The authors wish to thank the donors of the Petroleum Research Fund, administered by the American Chemical Society, and the Ontario Research Foundation for operating funds and a major equipment grant, respectively. We also thank Dr. Klaus Noack for his generous donation of a number of samples which provided sufficient results to show that a more complete study of the system would be worthwhile.

REFERENCES

1. J. B. Stothers and P. C. Lauterbur. Can. J. Chem. **42**, 1563 (1964).
2. R. A. Friedel and H. L. Retcofsky. J. Am. Chem. Soc. **85**, 1300 (1963).
3. K. S. Dhami and J. B. Stothers. Can. J. Chem. **43**, 510 (1965).
4. K. S. Dhami and J. B. Stothers. Can. J. Chem. **43**, 479 (1965).
5. K. S. Dhami and J. B. Stothers. Can. J. Chem. **43**, 498 (1965).
6. R. B. Turner and D. M. Voitle. J. Am. Chem. Soc. **73**, 1403 (1951).
7. E. A. Braude and C. J. Timmons. J. Chem. Soc. 3766 (1955).
8. R. L. Erskine and E. S. Waight. J. Chem. Soc. 3425 (1960).
9. R. Mecke and K. Noack. Ber. **93**, 210 (1960).
10. (*a*) K. Noack and R. N. Jones. Can. J. Chem. **39**, 2201 (1961). (*b*) K. Noack and R. N. Jones. Can. J. Chem. **39**, 2225 (1961).
11. E. S. Waight and R. L. Erskine. Absorption spectra of conjugated carbonyl compounds. Chap. **7** *in* Steric effects in conjugated systems. *Edited by* G. W. Gray. Butterworth. London. 1958.

Can. J. Chem. Downloaded from www.nrcresearchpress.com by 210.87.254.105 on 09/05/12
For personal use only.

12. C. J. TIMMONS, B. P. STRAUGHAN, W. F. FORBES, and R. SHILTON. Advances in molecular spectroscopy. Vol. 2. Pergamon Press. 1962. p. 934.
13. W. F. FORBES. Classification of steric effects in ultraviolet absorption spectra. Chap. 6 *in* Steric effects in conjugated systems. *Edited by* G. W. Gray. Butterworth. London. 1958.
14. E. F. LANDAU and E. P. IRANY. J. Org. Chem. **12**, 422 (1947).
15. A. L. WILDS and C. DJERASSI. J. Am. Chem. Soc. **68**, 1718 (1946).
16. E. BENARY. Ber. **64**, 2544 (1931).
17. E. N. ECOTT and R. P. LINSTEAD. J. Chem. Soc. 914 (1930).
18. F. C. WHITMORE and G. W. PEDLOW. J. Am. Chem. Soc. **63**, 758 (1941).
19. E. W. WARNHOFF and W. S. JOHNSON. J. Am. Chem. Soc. **75**, 494 (1953).
20. J. D. CHANCEY. J. Am. Chem. Soc. **70**, 244 (1948).
21. H. B. HENBEST and G. WOODS. J. Chem. Soc. 1150 (1952).
22. M. GODCHOT. Compt. Rend. **158**, 506 (1914).
23. R. L. FRANK, R. ARMSTRONG, J. KWIATEK, and H. A. PRICE. J. Am. Chem. Soc. **70**, 1379 (1948).
24. G. VAVON and A. APCHIE. Bull. Soc. Chim. France, **43**, 667 (1928).
25. A. HALLER and R. CORNUBERT. Bull. Soc. Chim. France, **41** [4], 367 (1927).
26. H. H. INHOFFEN and H. KRAMER. Ber. **87**, 498 (1954).
27. R. M. ACHESON and R. ROBINSON. J. Chem. Soc. 1127 (1952).
28. K. S. DHAMI and J. B. STOTHERS. Tetrahedron Letters, No. 12, 631 (1964).
29. R. R. FRASER. Can. J. Chem. **40**, 78 (1962).
30. W. A. AYER, C. E. MCDONALD, and J. B. STOTHERS. Can. J. Chem. **41**, 1113 (1963).
31. K. S. DHAMI and J. B. STOTHERS. Unpublished observations.
32. P. C. LAUTERBUR. J. Am. Chem. Soc. **83**, 1838, 1846 (1961).
33. P. C. LAUTERBUR. J. Chem. Phys. **38**, 1406, 1415, 1432 (1963).
34. H. SPIESECKE and W. G. SCHNEIDER. J. Chem. Phys. **35**, 731 (1961).
35. G. E. MACIEL and G. C. RUBIN. J. Am. Chem. Soc. **85**, 3903 (1963).
36. H. P. KOCH. Chem. Ind. London, 273 (1942).
37. G. B. SAVITSKY and K. NAMIKAWA. J. Phys. Chem. **67**, 2754 (1963).

Can. J. Chem. Downloaded from www.nrcresearchpress.com by 210.87.254.105 on 09/05/12
For personal use only.

Can. J. Chem. Downloaded from www.nrcresearchpress.com by 210.87.254.40 on 09/05/12
For personal use only.

SPECTROSCOPIC STUDIES OF ORGANOPHOSPHORUS COMPOUNDS

PART I. THE CONSTITUTION OF ALKYLPHOSPHINE – CARBON DISULFIDE ADDUCTS

M. ARSHAD A. BEG AND M. S. SIDDIQUI
Central Laboratories, P.C.S.I.R., Karachi, Pakistan

Received May 19, 1964

ABSTRACT

The constitution of the alkylphosphine – carbon disulfide adducts has been investigated by the study of their infrared spectra. Certain definite features of the spectra of the adducts are the shift of the P—C asymmetric vibrations to higher frequencies and the large shifts in the fundamentals of the acceptor molecule. These features are attributed to the formation of a quadruply connected phosphorus compound. From a comparison of the spectra of the carbon disulfide adducts with those of the corresponding phosphonium compounds, phosphine oxides and phosphines, evidence is provided for the structure of these compounds which has been suggested to be of the phosphonium type.

INTRODUCTION

During an investigation on the chemistry of the trifluoromethylphosphines it was noted that the spectra of the boron trifluoride adducts of the phosphines had all the absorptions corresponding to the phosphines but those of boron trifluoride were shifted to lower frequencies on complex formation (1, 2). Similar shifts have also been observed for other BF_3 adducts (3). The other notable feature is the shift of the P—C stretching vibration to higher frequencies, and from a study of the spectra of the other organophosphorus compounds this may be associated with the formation of a quadruply connected structure. In order to further establish these features the study of the spectra of the addition compounds of carbon disulfide and alkylphosphines has been taken up. Carbon disulfide, which is also a Lewis acid, is expected to behave similarly to BF_3 and hence it was of interest to see if the change in frequency followed a similar trend.

Alkylphosphines react with carbon disulfide to form deep-red solids which can be hydrolyzed with alcoholic potassium hydroxide to give pure phosphines (4). Considerable controversy has existed regarding the nature of the bonding in these adducts (4, 5, 6). Recently the crystal structure of the triethylphosphine – carbon disulfide addition compound has been obtained from X-ray data (5) and it has been shown to be a phosphonium compound $R_3P^+CSS^-$ having the CS_2 moiety in the form of dithioformate anion. Jensen (6) has recently given a short account of the spectra of these compounds but no detailed discussion. We have furnished additional evidence in support of the idea of phosphonium compound formation and have also made tentative assignments of the absorption spectra.

EXPERIMENTAL

The phosphines, trimethylphosphine, triethylphosphine, and tripropylphosphine, were prepared by the Grignard method, using an inert atmosphere throughout the reaction. The reaction vessel was kept in a dry ice – acetone bath during the addition of phosphorus trichloride or phenyldichlorophosphine for the preparation of phenyldimethylphosphine. The yields of the phosphines were thus quite improved and ranged from 60–75% compared with 40–50% without the use of refrigerants. The CS_2 adducts were prepared by adding stoichiometric amounts of the reactants. The deep-red crystals so obtained were further purified by washing with ether, maintaining an inert atmosphere. The purity was checked from the melting point reported in the literature (6). The infrared spectra were recorded on a PE234 spectrophotometer, using both Nujol mulls and KBr pellets. For comparison purposes we have also prepared tetramethylphosphonium iodide, trimethylphosphine oxide, and phenyltrimethylphosphonium iodide.

TABLE I

Vibrational frequencies of triply and quadruply connected phosphorus compounds

	$(CH_3)_3P$	$(CH_3)_3PO$	$(CH_3)_4PI$	$(CH_3)_3P.CS_2$
C—H antisymmetric	2 970 m	2 995 m	2 970 m	2 970 m
C—H symmetric	2 920 m	2 935 m	2 920 m	2 920 m
C—H symmetric	2 850 m			
C—H antisymmetric bending	1 430 m	1 486 vw		
	1 417 m	1 443 w		
		1 435 m	1 427 m	
		1 418 m		1 415 m
		1 411 m		1 405 m
C—H symmetric bending	1 310 m	1 336 m		
	1 298 w	1 299 m	1 305 m	
		1 282 m	1 290 w	1 290 m
		1 259 m		
P—O		1 180 w		
		1 160 vs		
		1 102 w		
CH_3 rock	1 067 m			
C=S stretch				1 045 vs
CH_3 rock	960 m	960 m	990 m	980 sh
	947 w	944 m	975 wsh	978 vs
				958 vs
CH_3 rock		870 msh		877 s
		863 s		870 s
		805 s		862 s
				805 vw
P—C antisymmetric	717 s	777 m	785 m	772 m
	707 s	741 s	776 m	
P—C symmetric	652 m	664	571	678 m

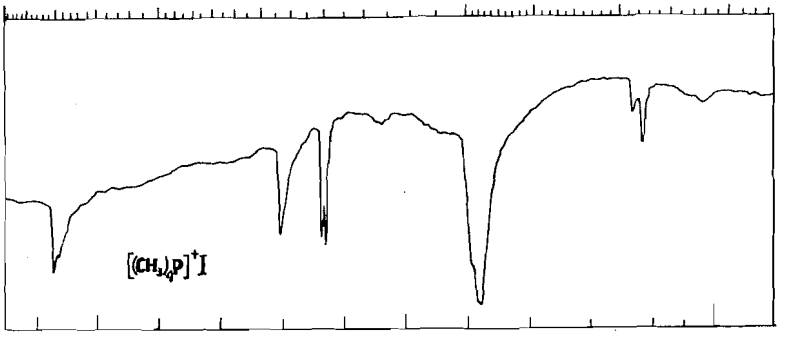

FIG. 1.

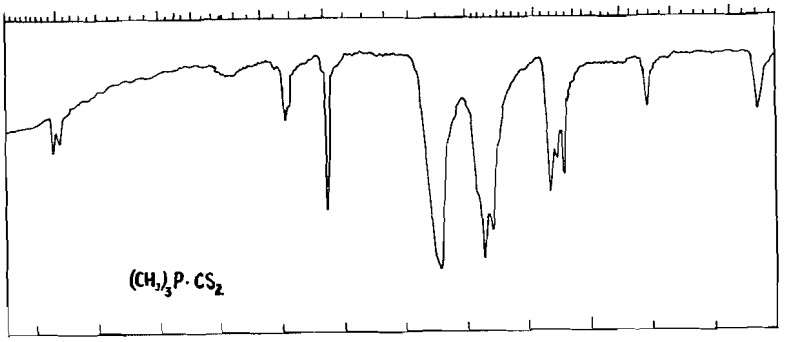

FIG. 2.

Can. J. Chem. Downloaded from www.nrcresearchpress.com by 210.87.254.40 on 09/05/12
For personal use only.

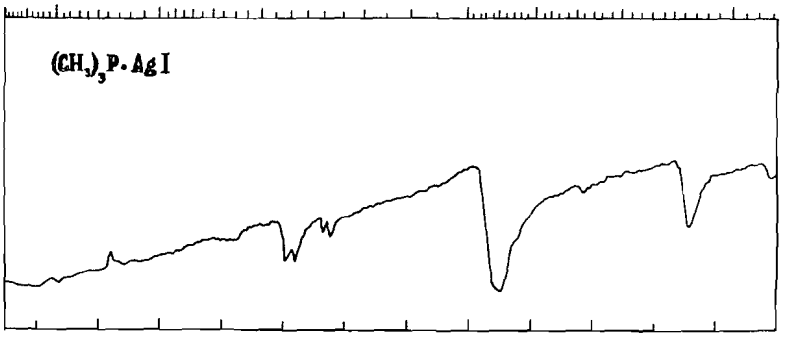

FIG. 3.

The spectra of tetramethylphosphonium iodide and the trimethylphosphine complex of carbon disulfide and silver iodide are shown in Figs. 1–3 and their infrared bands are listed in Table I. The infrared absorptions of phenyldimethylphosphine and phenyltrimethylphosphonium iodide and the CS_2 addition compounds of phenyldimethylphosphine are depicted in Figs. 4–6 and their bands are listed in Table IV.

DISCUSSION

The C—H stretching and bending vibrations in the quadruply connected compounds show small shifts in their positions compared with the corresponding triply connected structures. Shifts observed in the skeletal modes, however, are more marked than the others. The CH_3 rocking and the P—C asymmetric vibrations are seen to be quite sensitive to structural changes as would be evidenced by Table II.

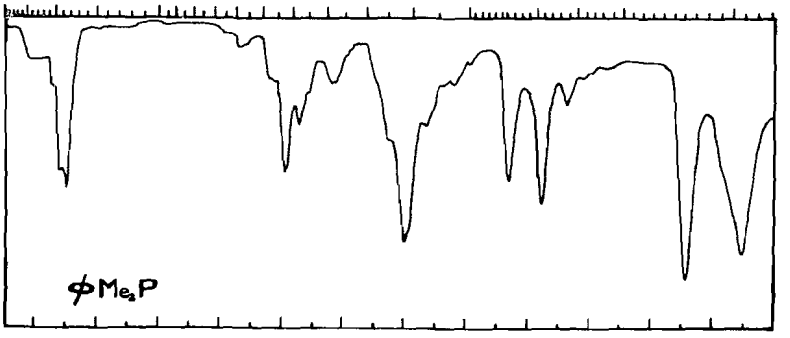

FIG. 4.

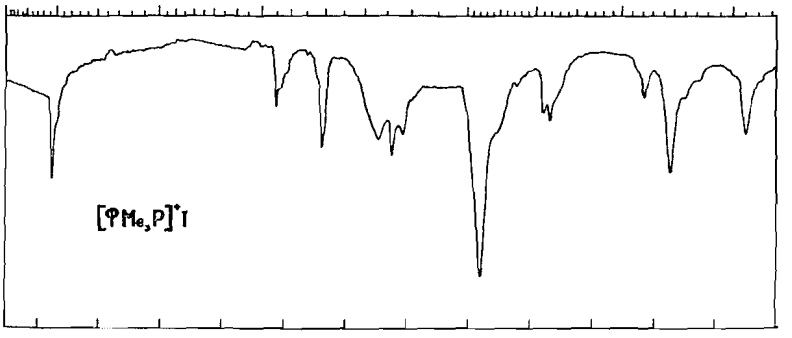

FIG. 5.

Can. J. Chem. Downloaded from www.nrcresearchpress.com by 210.87.254.40 on 09/05/12
For personal use only.

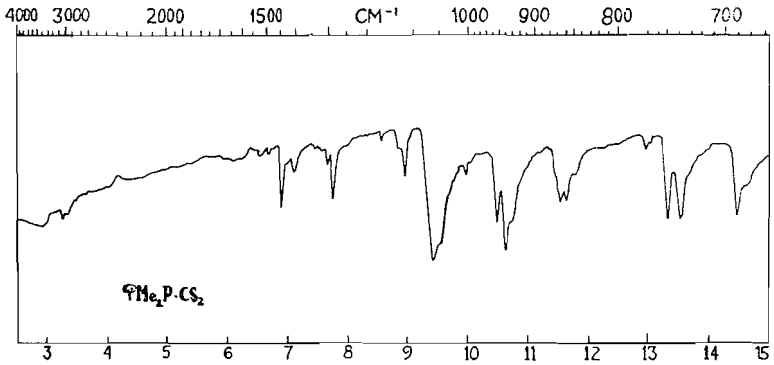

FIG. 6.

TABLE II

Comparison of the sensitive frequencies in trimethylphosphine and its compounds

	Me_3P	$Me_3P.AgI$	$Me_4P^+I^-$	$Me_3P.CS_2$	Me_3PO	$Me_3PhP^+I^-$	$Me_2PhP.CS_2$
	1 067						
	960	955	990	980		982	982
CH_3 rock	947	Broad, unresolved	975	978		955	955
				958	960	930	940
					944		930
				877		890	
				870		885	867
				862		875	855
							850
P—C antisymmetric	717	735	785	772	777	780	773
	707		776		741		
P—C symmetric	653			678	664		

In the spectra of phenyltrimethylphosphonium iodide, trimethylphosphine – carbon disulfide adduct, and the phosphine oxide (7) there are two bands corresponding to the CH_3 rocking vibration, one at 860 and the other at 950 cm^{-1}. The spectrum of trimethylphosphine also records splitting but at higher frequencies. Tetramethylphosphonium iodide on the other hand does not have such split bands. It is possible that the splitting is due to the lowering of symmetry from a completely symmetrical molecule Me_4P^+ (which by analogy with molecules and cation of this type may have T_d symmetry) to a less symmetrical molecule Me_3PO or Me_3P, having an axial symmetry. In $Me_3P.CS_2$ the splitting may also be due to a lowering of symmetry. Splittings are usually the result of interaction of another species, which in the present case is the CS_2 moiety, and which in the case of $PhMe_3P^+$ is the phenyl group and in the case of Me_3P, the lone-pair electrons.

For the P—C antisymmetric vibration characteristic shifts have been found in all quadruply connected structures as compared with the corresponding phosphine. The absorption in $Me_3P.CS_2$ occurs at 772 cm^{-1} and in the Me_4P^+ the absorption occurs as a doublet at 785 and 776 cm^{-1}. It may, however, be noted here that the P—C antisymmetric stretching vibrations for the quadruply connected compounds have shifted to higher frequencies, compared with Me_3P. Such shifts are usually associated with changes in symmetry and have been reported (9) for the amine complexes containing sulfates, carbonates, etc. as ligands. The P—C symmetric vibration occurs at 678 cm^{-1} for $Me_3P.CS_2$ and at 664 cm^{-1} for Me_3PO. The P—C symmetric vibration for Me_4P^+ is reported at 571 cm^{-1} (8). It is quite likely that the intense absorption at 678 cm^{-1} in $Me_3P.CS_2$ is a

Can. J. Chem. Downloaded from www.nrcresearchpress.com by 210.87.254.40 on 09/05/12
For personal use only.

result of the C—S single bond stretching or a possible coupling of this vibration with the P—C symmetric mode.

The most conspicuous difference between the spectrum of $Me_3P.CS_2$ and Me_4P^+ or Me_3PO is the occurrence of an intense absorption at 1 045 cm^{-1}, which is due to the C=S stretching mode and has been confirmed by a study of the spectra of the zanthates (10) and of the thiocyanates (11). The readily observable antisymmetric stretching frequency for the CS_2 molecule is totally absent in the addition compounds. If the CS_2 moiety were to preserve its identity an intense absorption would have been expected at 1 523 cm^{-1} in the infrared spectrum. However, it is noted from the X-ray data that the CS_2 group is no longer linear but has a triangular structure. Thus there is a change from $D_{\infty h}$ to C_{2v}. Such a change is also noted for the carbonyl group, e.g. from the CO_2 to the formate ion when the C=O frequency is seen to move to higher wavelengths (12). Also, in the case of the BF_3 addition compounds a similar change is noted (2). The large shifts in the characteristic frequencies of the acceptor molecule may thus be used as one of the evidences for the formation of a quadruply connected structure. The spectra of the adducts of the other trialkylphosphines also have the same features and are listed with tentative assignments in Table III.

TABLE III

Vibrational frequencies of $Et_3P.CS_2$ and n-$Pr_3P.CS_2$

	$Et_3P.CS_2$	n-$Pr_3P.CS_2$
C—H antisymmetric	2 975 m	2 965 m
C—H symmetric	2 945 m	2 930 m
	2 905 m	2 875 m
C—H antisymmetric bending	1 458 m	1 457 m
	1 447 m	
C—H symmetric bending	1 417 w	
	1 405 m	1 390 w
	1 393 w	1 370 w
	1 380 w	1 340 wv
CH_2 wag	1 259 w	
	1 240 w	1 225 w
CH_3 rock	1 065 s	1 075 ssh
C=S stretch	1 044 vs	1 050 vs
C—C antisymmetric stretch	1 015 s	1 025 ssh
CH_3 rock	983 m	900 vw
	886 w	835 w
P—C antisymmetric stretch	772 vs	770 w
	745 vs	
C—C symmetric stretch	723 m	720 m

The spectrum of the addition compound $PhMe_2P.CS_2$ is also quite interesting and one of the important features deserves to be mentioned. The single band at 739 cm^{-1} observed for phenyldimethylphosphine is split into two sharp and strong bands at 750 and 737 cm^{-1} in the case of $PhMe_2P.CS_2$ and into a sharp band at 754 and a weak one at 740 in the case of phenyltrimethylphosphonium iodide. This type of splitting seems to be characteristic of a quadruply connected aromatic phosphorus compound. Thus triply connected compounds like phenylphosphine, phenyldichlorophosphine, diphenylphosphine, diphenylchlorophosphine, and triphenylphosphine do not show any splitting in the 750 cm^{-1} region. It is only in the case of quadruply connected structures that this band is split, as is shown by a comparison with the reported spectra (13) of such compounds.

The similarity of the spectra of the phosphonium compounds and those of the carbon disulfide adducts of the alkylphosphines leads to the conclusion that the latter are phosphonium compounds with a tetrahedral structure having the constitution $R_3P^+CSS^-$.

Can. J. Chem. Downloaded from www.nrcresearchpress.com by 210.87.254.40 on 09/05/12
For personal use only.

TABLE IV

Vibrational frequencies of $PhMe_2P.CS_2$ and $PhMe_3P^+I^-$

	$PhMe_2P.CS_2$	$PhMe_3P^+I^-$
C—H aromatic stretch antisymmetric	3 030 m	3 030 m
C—H aliphatic stretch antisymmetric	2 960 m	3 000 m
C—H stretch symmetric	2 860 w	2 860 w
C—C skeletal	1 585 w	1 570 w
	1 490 w	1 482 w
	1 450 m	1 452 m
CH_3 asymmetric bending	1 410 w	1 410 w
CH_3 symmetric bending	1 340 w	1 312 m
	1 310 m	1 300 w
	1 228 w	
C—H in-plane vibrations	1 170 w	1 170 m
	1 135 w	1 147 s
X-sensitive	1 118 m	1 118 m
C═S stretch	1 060 svs	—
Ring breathing	1 005 m	1 005 sh
CH_3 rock	982 w	982 svs
	955 s	
	940 vs	955 sh
	930 ssh	930 w
CH_3 rock	867 s	890 m
	855 s	885 m
	850 m	875 sh
P—C antisymmetric stretch	773 m	780 m
C—H out-of-plane deformation	750 vs	754 s
	737 vs	740 w
Out-of-plane ring deformation	692 vs	690 s

ACKNOWLEDGMENTS

The assistance of Mr. A. R. Qureshi and Rahmat Khan in recording the infrared spectra is acknowledged with thanks.

REFERENCES

1. M. A. A. Beg and H. C. Clark. Can. J. Chem. **40**, 393 (1962).
2. M. A. A. Beg. Ph.D. Thesis, University of British Columbia. 1961.
3. P. Chalandon and B. P. Susz. Helv. Chim. Acta, **41**, 697 (1958).
4. K. Issleib and A. Brack. Z. Anorg. Allgem. Chem. **277**, 271 (1954).
5. T. N. Margolis and D. H. Templeton. J. Chem. Phys. **36**, 2311 (1962).
6. K. A. Jensen and P. M. Neilsen. Acta Chem. Scand. **17**, 547 (1963).
7. J. Goubeau and W. Berger. Z. Anorg. Allgem. Chem. **304**, 147 (1960).
8. G. B. Deacon, R. A. Jones, and P. E. Rogasch. Australian J. Chem. **16**, 360 (1963).
9. K. Nakamoto, J. Fujita, S. Tanaka, and M. Koboyashi. J. Am. Chem. Soc. **79**, 4904 (1957).
10. L. H. Little, G. W. Poling, and J. Leja. Can. J. Chem. **39**, 745 (1961).
11. C. N. R. Rao and R. Venkataraghavan. Spectrochim. Acta, **18**, 541 (1962).
12. G. Herzberg. Molecular spectra and molecular structure. Vol. II. Infrared and raman spectra of polyatomic molecules. D. Van Nostrand Co., Inc., Princeton, N.J. 1945. p. 302.
13. L. W. Daasch and D. C. Smith. Anal. Chem. **23**, 853 (1951).

Can. J. Chem. Downloaded from www.nrcresearchpress.com by 210.87.254.40 on 09/05/12
For personal use only.

Can. J. Chem. Downloaded from www.nrcresearchpress.com by 210.87.254.6 on 09/05/12
For personal use only.

RADIATION CHEMISTRY OF ALKALI THIOSULFATES

R. L. EAGER AND D. S. MAHADEVAPPA[1]

Department of Chemistry and Chemical Engineering, University of Saskatchewan, Saskatoon, Saskatchewan

Received June 29, 1964

ABSTRACT

The salts $Na_2S_2O_3$, $Na_2S_2O_3 \cdot 5H_2O$, $K_2S_2O_3$, and $K_2S_2O_3 \cdot \frac{5}{3}H_2O$ were irradiated at room temperature with ^{60}Co gamma rays. When the irradiated salts were dissolved in water, sulfite and sulfate ions, H_2S gas, colloidal sulfur, and a relatively small quantity of acid were found among the irradiation products. The dependence of yields on the absorbed dose was studied. *G*-values of approximately unity were found. Using ^{35}S as a label, it was found that the inner sulfur (the central, oxygen-bonded sulfur atom of the complex) appears in the sulfite and sulfate whereas the outer sulfur (the sulfur linked only to the central sulfur and not to oxygen) appears in the H_2S and colloidal sulfur. Annealing experiments using irradiated $Na_2S_2O_3$ and $K_2S_2O_3$ showed that the yields of sulfite, sulfate, and H_2S were decreased by heating. The sodium salts were also irradiated at 77 °K. The yields of sulfate and H_2S were higher for the low temperature irradiations as compared to room temperature irradiations, whereas the yields of sulfite were lower. A tentative mechanism which partially explains the results is proposed.

INTRODUCTION

A review of the literature shows that only limited information is available about the radiation chemistry of the inorganic compounds of sulfur. The radiation chemistry of aqueous solutions of ferrous ammonium sulfate has been extensively investigated (1–8), mainly because of the use of these solutions for dosimetry. Johnson (9) irradiated ferrous ammonium sulfate crystals with ^{60}Co gamma rays after which they were dissolved in water. Ferric and sulfite ions and hydrogen gas were found to be irradiation products. Mahlman (10) studied the yield of hydrogen from degassed concentrated solutions of sodium sulfate irradiated with ^{60}Co gamma rays. He concluded that all of the energy absorbed by the solution was effective in decomposing the water and that bisulfate and sulfate ions are not effective H-atom scavengers. Hochanadel *et al.* (11) have investigated the production of sulfur dioxide by the irradiation of sulfuric acid solutions with ^{60}Co gamma rays. Abellan (12) investigated the effect of ^{60}Co gamma rays on alkaline solutions of sodium thiosulfate. He suggested the following overall radiolytic reaction to explain the effects he observed.

$$2S_2O_3^{=} + 4OH + 2H \rightarrow HS^- + 3SO_3^{=} + 3H^+ + H_2O.$$

The present studies were undertaken to investigate the effect of ^{60}Co gamma rays on the crystalline sodium and potassium thiosulfates.

EXPERIMENTAL

Reagents

The sodium thiosulfate pentahydrate used was of reagent grade. The composition of the salt was checked by iodometric titration and by the weight loss upon dehydration. The results indicated that the sample used was quite pure. Reagent grade potassium thiosulfate was further purified by recrystallization from a hot aqueous solution. The tritapentahydrate, $K_2S_2O_3 \cdot \frac{5}{3}H_2O$, was obtained, as indicated by the weight loss upon dehydration. Crystalline anhydrous sodium thiosulfate and potassium thiosulfate were obtained by evaporating to dryness at 80 °C saturated solutions of the corresponding hydrates (13). That the salts were anhydrous was shown by the absence of a loss of weight when they were heated to 100 °C. The crystalline nature of the anhydrous sodium thiosulfate was shown by its X-ray diffraction pattern which was in good agreement with that reported elsewhere (14). Inner labelled and outer labelled sodium thiosulfates were obtained from Atomic Energy of Canada Limited. They were diluted with inactive sodium thiosulfate so as to give approximately 10^6 counts per min per g, assuming a 20% counting efficiency. Distilled water, again

[1]*Present address: Department of Chemistry, Manasagangothri, University of Mysore, Mysore, India.*

distilled from alkaline permanganate and then from an acid dichromate solution, was used for dissolving the irradiated samples. All other solutions used were prepared with deaerated double-distilled water.

Irradiations and Dosimetry

The irradiation source was a Gamma Cell 220 ^{60}Co Irradiation Unit manufactured by Atomic Energy of Canada Limited. The dose rates were of the order of 1 200 rad per min. The absorbed dose was measured using ferrous sulfate dosimetry, a *G*-value of 15.5 was used for the production of ferric ion. Allowance was made for the difference in the electron densities of the sample and the dosimeter. The samples were irradiated in the presence of air. The temperature of the samples was 25 ± 5 °C.

Counting of Radioactivity

A liquid scintillation counter was used. The scintillator used was a toluene solution of 2,5-diphenyloxazole (PPO) and 1,4-bis-2-[(5-phenyloxazolyl)]benzene (POPOP). As aqueous solutions were to be counted, a constant amount of water was always used in the counting solution. Similarly, as the H_2S was dissolved in "hyamine hydroxide" (*p*-(diisobutyl-cresoxyethoxyethyl)dimethylbenzylammonium hydroxide) prior to counting it, a constant amount of hyamine hydroxide was always used.

Analytical Procedures

The irradiated salt was dissolved in water and analyzed for acid, sulfite, sulfate, hydrogen sulfide, and colloidal sulfur. Prior to the determination of acid, sulfite, sulfate, and colloidal sulfur the hydrogen sulfide present was removed by bubbling nitrogen through the solution.

Acid was determined by a micro-titration with a standard sodium hydroxide solution using phenolphthalein as an indicator. A blank was done on a solution of the unirradiated thiosulfate.

Sulfite was determined by the decolorization of fuchsin (15). To the solution of the irradiated thiosulfate was added 0.2 to 0.3 g of sodium bicarbonate after which nitrogen was bubbled through the solution for a further 5–10 min (16). Fuchsin solution was added and the optical density of the solution was read at 542 mμ. A calibration curve was prepared by analyzing mixtures containing known amounts of sulfite and thiosulfate.

Sulfate was determined by difference using a nephelometric method (17) in which a barium sulfate precipitate is formed. Thiosulfate interferes when it is present in relatively large quantities due to the precipitation of barium thiosulfate. This interference was eliminated by oxidizing the thiosulfate to tetrathionate with iodine. The iodine also oxidized the sulfite present to sulfate. Hence the nephelometric determination gave sulfate plus sulfite and the amount of sulfate was calculated by difference. A calibration curve was prepared by analyzing solutions containing known amounts of sulfate, sulfite, and thiosulfate.

Hydrogen sulfide was estimated by the methylene blue method of Sands *et al.* (18). When hydrogen sulfide is passed into a solution containing the sulfate or hydrochloride of *p*-amino-*N*,*N*-dimethylaniline and ferric chloride, methylene blue is formed. The optical density of the solution is taken at 670 mμ. The apparatus used was similar to that described by Budd and Bewick (19). In experiments with labelled thiosulfates the hydrogen sulfide was absorbed from the nitrogen stream by bubbling it through 2 ml of hyamine hydroxide. The resulting solution was used in making up the counting solution for the scintillation counter.

The amount of colloidal sulfur present in the solutions of the irradiated salts was estimated as follows. As shown later it seems fairly definite that the colloidal sulfur is derived from the "outer" sulfur of the thiosulfates. Irradiated outer labelled $Na_2S_2O_3$ and $Na_2S_2O_3 \cdot 5H_2O$ was dissolved in water. After the removal of hydrogen sulfide the solution was filtered through a 0.22 μ pore size Millipore filter. The filter was washed free of labelled undecomposed thiosulfate by passing 500 ml of a 0.8 *M* inactive $Na_2S_2O_3$ solution through it. The dried paper was added to the scintillation counting solution and the resulting mixture counted. The paper disintegrated in the counting solution yielding a transparent gelatinous mass. A filter paper was similarly added when standard active thiosulfate solutions and when background solutions were counted.

The presence of oxygen in the irradiation products was checked using gas chromatography methods. A Linde 5A molecular sieve was used as a column packing. No oxygen was detected; the method was sensitive enough so that the presence of one μmole would have been detected.

RESULTS

The salts upon irradiation underwent the following color changes. At room temperature $Na_2S_2O_3 \cdot 5H_2O$ first turned yellow which then deepened to a dark-brown color at high doses. At 77 °K the pentahydrate turned a greenish-brown color which rapidly turned to a brown color when the solid was warmed to room temperature. The anhydrous salt, $Na_2S_2O_3$, showed little color effect at room temperature, a yellow tinge only being observed at high doses. At 77 °K the anhydrous salt assumed a violet color which was bleached upon the salt being warmed to room temperature. The potassium salts showed a yellow coloration upon irradiation. In annealing experiments with $K_2S_2O_3$ the yellow color persisted at 50 °C but it was completely bleached at 100 °C.

Can. J. Chem. Downloaded from www.nrcresearchpress.com by 210.87.254.6 on 09/05/12
For personal use only.

Comparison of the infrared spectra of irradiated samples with those of unirradiated samples showed that the irradiation had produced no detectable changes in the spectra. The lack of any change may be due to the small amount of decomposition undergone by the compounds, which was less than 1%. Cunningham and Heal detected new infrared bands in KNO_3 when the salt was irradiated with a sufficient dose of gamma rays to bring about 4 to 24% decomposition (20).

When the irradiated samples were powdered the odor of H_2S could be detected. Upon solution in water an effervescence was observed, and the odor of H_2S was given off. At the same time a white turbidity developed in the solution. Attempts to identify the material causing the turbidity were not successful, presumably due to the very small amounts present. It was assumed that the turbidity was due to sulfur as had been observed by Abellan (12) when solutions of thiosulfates were irradiated.

Yields of Products Formed Upon Solution of Irradiated Thiosulfates in Water

The yields of sulfite, sulfate, and H_2S, in μmoles, and of acid, in μequivalents, produced per mole of salt are shown plotted against absorbed dose in eV per mole in Figs. 1, 2, 3, and 4 for $Na_2S_2O_3 \cdot 5H_2O$, $Na_2S_2O_3$, $K_2S_2O_3 \cdot \frac{5}{3}H_2O$, and $K_2S_2O_3$, respectively. In Table I are given some *G*-values for the products. These were calculated from the curves given in Figs. 1, 2, 3, and 4.

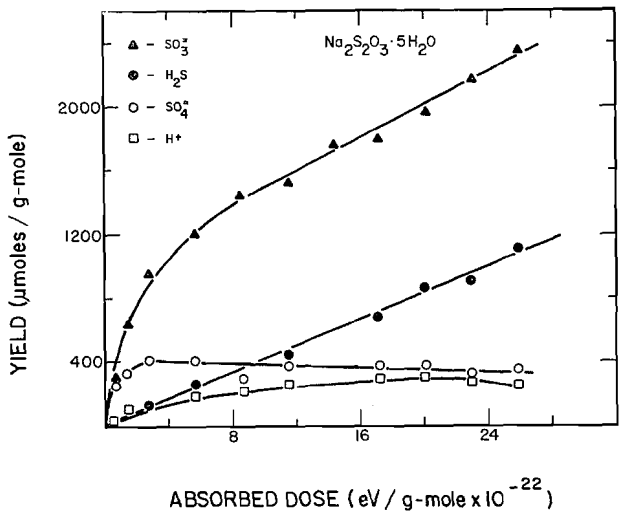

FIG. 1. Yields of $SO_3^=$, $SO_4^=$, H_2S, and acid as a function of dose for $Na_2S_2O_3 \cdot 5H_2O$.

Low Temperature Irradiations

Samples of $Na_2S_2O_3 \cdot 5H_2O$ and $Na_2S_2O_3$ were irradiated at liquid nitrogen temperatures. The salts received doses of 5.1×10^{22} and 3.1×10^{22} eV per g-mole, respectively. The results of the analyses of their aqueous solutions are given in Table II. Also given in Table II are the corresponding yields for room temperature irradiations. These yields were taken from Figs. 1 and 2.

Irradiations of ^{35}S-labelled $Na_2S_2O_3 \cdot 5H_2O$ and $Na_2S_2O_3$

The hydrogen sulfide liberated upon solution of irradiated $Na_2S_2O_3 \cdot 5H_2O$ and $Na_2S_2O_3$ labelled in the "outer" sulfur position was found to be radioactive. For both compounds

Can. J. Chem. Downloaded from www.nrcresearchpress.com by 210.87.254.6 on 09/05/12
For personal use only.

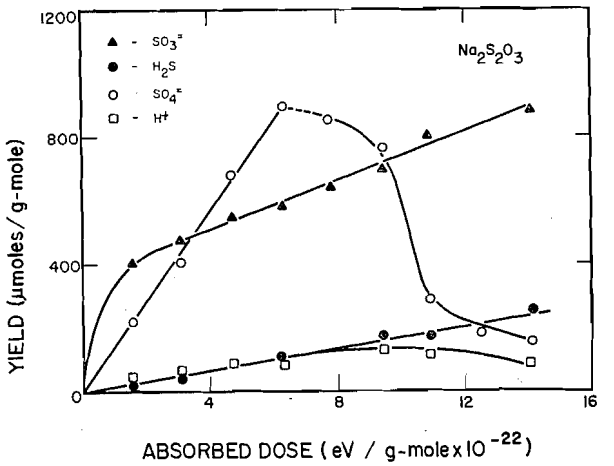

FIG. 2. Yields of $SO_3^=$, $SO_4^=$, H_2S, and acid as a function of dose for $Na_2S_2O_3$.

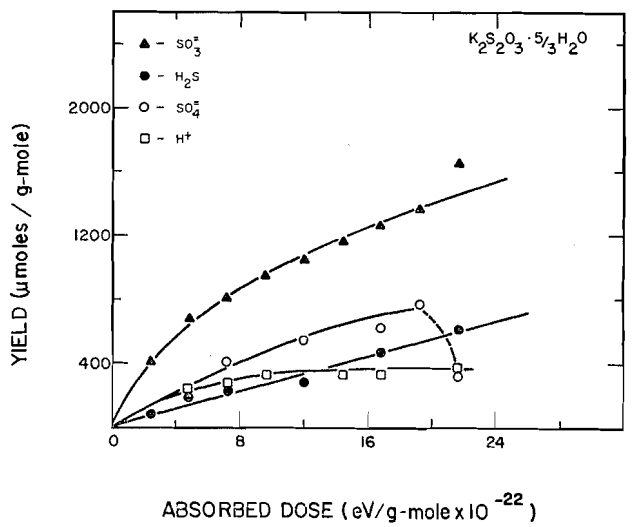

FIG. 3. Yields of $SO_3^=$, $SO_4^=$, H_2S, and acid as a function of dose for $K_2S_2O_3 \cdot \frac{5}{3}H_2O$.

it was calculated from the measured radioactivity of the H_2S and the specific activity of the outer labelled thiosulfates that the amount of H_2S possessing the label was approximately 90% of the amount of H_2S found by chemical analyses. The H_2S from inner labelled thiosulfates was found to be inactive, the observed "counts" being identical with the background. Hence, it is concluded that the only source of H_2S sulfur is from the outer sulfur atoms of the thiosulfates. The discrepancy of about 10% observed in the experiments with the outer labelled compounds must be due to errors either in the radioactivity measurements or in the chemical analyses, or in both.

Sulfite and Sulfate from outer labelled $Na_2S_2O_3 \cdot 5H_2O$ and $Na_2S_2O_3$ yielded $BaSO_4$ which was found to be nonradioactive. When inner labelled compounds were used the $BaSO_4$ was radioactive.

Can. J. Chem. Downloaded from www.nrcresearchpress.com by 210.87.254.6 on 09/05/12
For personal use only.

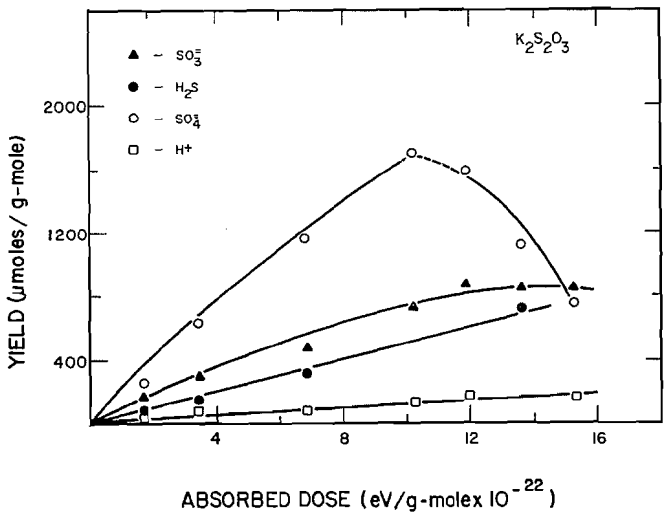

FIG. 4. Yields of $SO_3^=$, $SO_4^=$, H_2S, and acid as a function of dose for $K_2S_2O_3$.

TABLE I

G-values of products

Product	Dose, eV per mole × 10^{-22}	$Na_2S_2O_3 \cdot 5H_2O$	$Na_2S_2O_3$	$K_2S_2O_3 \cdot \frac{5}{3}H_2O$	$K_2S_2O_3$
$SO_3^=$	6.0	1.3	0.58	0.75	0.50
	12.0	0.80	0.42	0.55	0.41
$SO_4^=$	6.0	0.41	0.85	0.33	1.1
	12.0	0.20	0.11	0.29	0.77
H_2S	6.0	0.28	0.10	0.20	0.30
	12.0	0.25	0.11	0.18	0.30
Acid	6.0	0.20	0.10	0.28	0.08
	12.0	0.13	0.06	0.18	0.07

TABLE II

Dependence of yields of products upon irradiation temperature

Compound	Dose, eV per mole × 10^{-22}	Temp., °K	$SO_3^=$, μmoles per mole	$SO_4^=$, μmoles per mole	H_2S, μmoles per mole	Acid, μequiv. per mole
$Na_2S_2O_3 \cdot 5H_2O$	5.1	298	1 150	400	210	180
		77	186	670	360	102
$Na_2S_2O_3$	3.1	298	475	440	50	50
		77	67	600	51	31

TABLE III

Sulfur analyses

Compound	Dose, eV per mole × 10^{-22}	S, μatoms per mole	H_2S, μmoles per mole	$SO_3^=$, μmoles per mole	$SO_4^=$, μmoles per mole	$\frac{S + H_2S}{SO_3^= + SO_4^=} \times 100$
$Na_2S_2O_3 \cdot 5H_2O$	11.2	870	490	1 580	390	69
	22.4	1 100	940	2 150	360	81
$Na_2S_2O_3$	6.4	720	110	600	900	55

Can. J. Chem. Downloaded from www.nrcresearchpress.com by 210.87.254.6 on 09/05/12
For personal use only.

Can. J. Chem. Downloaded from www.nrcresearchpress.com by 210.87.254.6 on 09/05/12
For personal use only.

The colloidal sulfur retained by the 0.22 μ pore size millipore filter was found to be radioactive when outer labelled $Na_2S_2O_3 \cdot 5H_2O$ and $Na_2S_2O_3$ were used but to be non-radioactive when the inner labelled compounds were used. It was thought that this could be used as a method of determining the amount of colloidal sulfur produced. In Table III are given some of the results obtained when outer labelled compounds were used. Also given in Table III are the corresponding yields of H_2S, sulfite, and sulfate taken from Figs. 1 and 2. The last column of Table III gives the sum of the sulfur found as colloidal sulfur and H_2S as a percentage of that found as sulfite and sulfate. Since it appears that the outer sulfur of the thiosulfates forms colloidal sulfur or H_2S whereas the inner sulfur forms sulfite or sulfate, the low values in the last column suggest that some of the outer sulfur was not being found. It is possible that not all of the colloidal sulfur was retained by the 0.22 μ filter paper. When 0.45 μ filter papers were used, only about one-quarter as much colloidal sulfur was retained. An attempt was made to use 100 mμ filter papers, but with the slow filtration rates the paper could not be washed free of the radioactive thiosulfate. An attempt was made to carry down the colloidal sulfur with $Al(OH)_3$ precipitate but this did not prove to be very successful. The use of some solvent, immiscible with water, was considered for extracting the sulfur. However the method was not tried since considerable difficulty was anticipated in preventing a carry over of even a very small fraction of the relatively large amount of radioactivity present in the solution. The tendency for emulsion formation in such systems would also have caused difficulties. It should be noted that, for sample weights of 1 g, the weights usually used, the amount of sulfur unaccounted for is less than 0.0001 g.

Annealing Experiments

Irradiated samples of the anhydrous salts were annealed for varying lengths of time at 50 °C and at 100 °C. At the end of the annealing period, the salts were dissolved in water and the resulting solutions analyzed. Sodium thiosulfate samples were irradiated to a

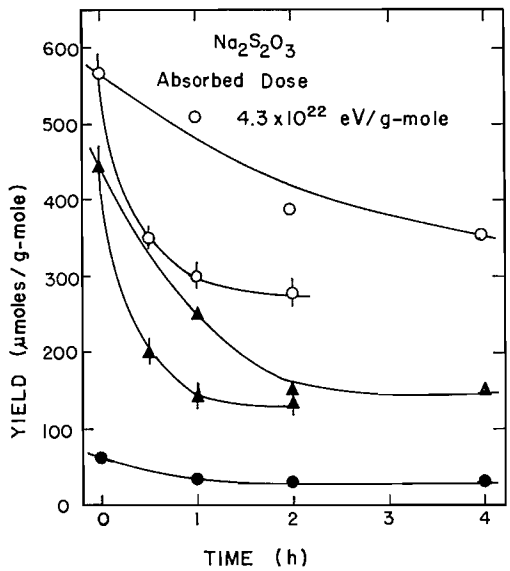

FIG. 5. Yields of $SO_3^=$, $SO_4^=$, H_2S, and acid as a function of time of annealing at 50 °C and 100 °C for $Na_2S_2O_3$ irradiated to a total dose of 4.3×10^{22} eV per g-mole: ▲, $SO_3^=$ for 50 °C; ○, $SO_4^=$ for 50 °C; ●, H_2S for 50 °C; a vertical line through symbol is for 100 °C.

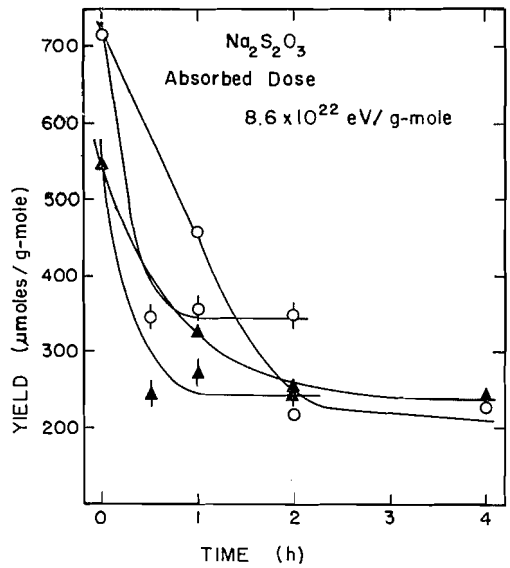

FIG. 6. Yields of $SO_3^=$ and $SO_4^=$ as a function of time of annealing at 50 °C and 100 °C for $Na_2S_2O_3$ irradiated to a total dose of 8.6×10^{22} eV per g-mole: ▲, $SO_3^=$ for 50 °C; ○, $SO_4^=$ for 50 °C; a vertical line through symbol is for 100 °C.

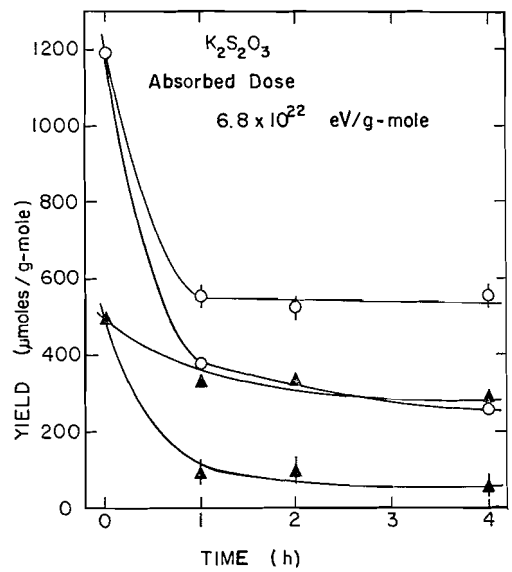

FIG. 7. Yields of $SO_3^=$ and $SO_4^=$ as a function of time of annealing at 50 °C and 100 °C for $K_2S_2O_3$ irradiated to a total dose of 6.8×10^{22} eV per g-mole: ▲, $SO_3^=$ for 50 °C; ○, $SO_4^=$ for 50 °C; a vertical line through symbol is for 100 °C.

dose of 4.3×10^{22} and 8.6×10^{22} eV per g-mole, the results being shown in Figs. 5 and 6, respectively. Potassium thiosulfate samples were irradiated to a dose of 6.8×10^{22} eV per g-mole; the results are shown in Fig. 7.

Can. J. Chem. Downloaded from www.nrcresearchpress.com by 210.87.254.6 on 09/05/12
For personal use only.

DISCUSSION

The experiments with labelled compounds indicate that the colloidal sulfur and the H_2S originate from the outer sulfur of the thiosulfate group whereas the sulfite and sulfate originate from the inner sulfur. An implication of the above is that the sum of the yields of colloidal sulfur and H_2S should be equal to the sum of the yields of sulfite and sulfate. The fact that a sulfur balance was not obtained may be due to not all of the collidal sulfur being retained by the filter paper.

The annealing experiments show that the yields of all of the products determined decrease when the samples are heated to 50 °C or to 100 °C. After approximately 2 h at either temperature the yields of all of the products are reduced to values which remain constant at a level about one-half of those found prior to annealing. An explanation of this behavior may be that at least some of the species produced in the crystals upon irradiation remain in close proximity of one another and so may recombine to form thiosulfate ions, or perhaps some other product which was not determined. Alternately, or in addition, excited thiosulfate ions may be formed by the radiation and these may be deactivated during the annealing process.

From the information presently available it does not appear to be possible to offer a detailed mechanism for the reactions which occur when the alkali thiosulfates are irradiated with gamma rays. The following tentative scheme is proposed to account for some of the observed behavior.

Ionization and Excitation

[1] $S_2O_3^{=} \sim\sim\sim\sim\rightarrow S_2O_3^{=*}$

[2] $S_2O_3^{=} \sim\sim\sim\sim\rightarrow S_2O_3^{-}$, S_2O_3, and electrons

[3] $H_2O \sim\sim\sim\sim\rightarrow H + OH.$

Primary Dissociation

[4] $S_2O_3^{=*} \longrightarrow S + SO_3^{=}$

[5] $S_2O_3^{=*} \longrightarrow S + SO_3 + 2e$

[6] $S_2O_3^{=*} \longrightarrow S^{=} + SO_3.$

Electron Capture

[7] Na^+ or $K^+ + e \longrightarrow$ Na or K

[8] S + electrons $\longrightarrow S^-$ and $S^{=}$

[9] SO_3 + electrons $\longrightarrow SO_3^-$ and $SO_3^{=}$.

The sulfur sesquioxide, whose formation is indicated in eq. [2], would upon solution of the sample react with water to form the observed products; sulfur, sulfite, and sulfate (21).

With the hydrates the yields of sulfate are considerably lower than for the anhydrous salts whereas the sulfite yields are increased. When the salts are irradiated at liquid nitrogen temperature the yield of sulfate is markedly increased over that at room temperature. It would seem reasonable to postulate that the primary interaction of gamma rays and of at least the high energy electrons with the thiosulfate group would be the same regardless of the presence of water or of a difference in temperature. It would thus appear that the precursor for at least some of the sulfate may either survive in the solid, and eventually produce sulfate, or it may undergo reactions in the solid, or upon solution, which leads to sulfite. As an example, such a sulfate precursor may be the SO_3 molecule

Can. J. Chem. Downloaded from www.nrcresearchpress.com by 210.87.254.6 on 09/05/12
For personal use only.

(either in the ground state or in some excited state). The SO_3 molecule may undergo an electron capture reaction [9] leading to the appearance of sulfite ions. If a large fraction of the SO_3 molecules did not undergo reaction [9] then a relatively low yield of sulfite would result, as is the case for the anhydrous salts. If, on the other hand, a further reducing agent is present when the hydrates are irradiated the rather large decrease in sulfate ions yields would be explained. Such a reducing agent may be H atoms, formed according to reaction [3]; these could react as follows,

$$SO_3 + H \longrightarrow SO_2 + OH. \quad [10]$$

Another source of hydrogen atoms in the hydrates would result from the reaction of electrons with the water of hydration. The increased yield of sulfate in the low temperature irradiations would follow from the decreased rate of diffusion of electrons and of hydrogen atoms and also from the reduced rates of reactions [9] and [10].

None of the reactions proposed so far would result in the formation of any acid in excess of that required for the formation of H_2S. A yield of acid would result if some of the sulfide ions, or their precursors, were converted into some substance which was not a volatile acid. Since this substance could not be sulfite or sulfate, as shown by the experiments with the outer labelled compounds, the sulfide would have to be changed into some product not determined in the scheme of analysis used.

Electron spin resonance spectra indicate the presence of the free radical ion SO_2^- in the irradiated salts (22). This radical could arise as the result of some dissociation reaction such as

$$S_2O_3^{-*} \longrightarrow SO_2^- + \text{other products}. \quad [11]$$

At high doses the fall-off of yield of sulfate, especially for the andhyrous salts, is very pronounced and occurs quite suddenly. Since there is no corresponding increase in the yield of sulfite the sulfate precursor, SO_3 perhaps, must disappear without being reduced to the sulfite precursor. A similar decrease was found by Johnson (9) for the yields of products from the irradiation of ferrous ammonium sulfate with ^{60}Co gamma rays. No explanation was offered as to the cause for the fall-off in yields. In the present work a simple recombination of ions or radicals to remove the sulfate precursor would only result in a leveling off of the yield of sulfate. If, however, after a certain amount of radiation had been absorbed by the crystal the recombination suddenly became more rapid, without a corresponding increase in the rate of formation of the precursor, then such a fall-off in the yield of sulfate would result. This increase in the rate of the reverse reaction might occur as a result of an increase in the rate of diffusion of electrons in the crystal after a certain threshold of "damage" has been produced in the crystal. For example, if reaction [5] were reversible then a sudden increase in the number of electrons reaching the sulfur atom – SO_3 molecule pair would result in a decrease in the amount of SO_3 present in the crystal. The sulfur atom and the SO_3 molecule could very likely be held in a cage and they may even be bonded together in an excited molecule. An alternative mechanism for the marked decrease in the yield of sulfate is that the following overall reaction becomes important in a crystal of a thiosulfate which has been subjected to high doses:

$$2SO_3 + 2e \longrightarrow S_2O_6^=.$$

Due to the lack of suitable analytical techniques no attempt was made to detect dithionate among the products.

Can. J. Chem. Downloaded from www.nrcresearchpress.com by 210.87.254.6 on 09/05/12
For personal use only.

ACKNOWLEDGMENT

Grateful acknowledgment is made to the National Research Council for financial support.

REFERENCES

1. H. FRICKE and S. MORSE. Am. J. Roentgenol and Radium Therapy, **18**, 430 (1927).
2. H. FRICKE and E. J. HART. J. Chem. Phys. **3**, 60 (1935).
3. N. MILLER. Nature, **162**, 448 (1948).
4. H. A. DEWHURST. Trans. Faraday Soc. **48**, 905 (1952).
5. F. S. DAINTON and H. C. SUTTON. Trans. Faraday Soc. **49**, 1011 (1953).
6. M. LEFORT. Compt. Rend. **237**, 159 (1953).
7. D. V. CORMACK, R. W. HUMMEL, H. E. JONES, and J. W. T. SPINKS. J. Chem. Phys. **22**, 6 (1954).
8. J. WEISS, A. O. ALLEN, and H. A. SCHWARZ. Proc. Intern. Conf. Peaceful Uses At. Energy, United Nations, New York. **14**, 179 (1956).
9. E. R. JOHNSON. J. Am. Chem. Soc. **78**, 5196 (1956).
10. H. A. MAHLMAN. J. Chem. Phys. **28**, 1256 (1958).
11. C. J. HOCHANADEL, J. A. GHORMLEY, and T. J. SWORSKI. J. Am. Chem. Soc. **77**, 3215 (1955).
12. J. ORTEGA ABELLAN. Anales Real Soc. Espan. Fis. Quim. Madrid, Ser. B, **57**, 773 (1961).
13. J. W. MELLOR. A comprehensive treatise on inorganic and theoretical chemistry. Vol. 10. Longmans, Green and Co., London. 1930. p. 520.
14. Index to X-ray powder data file. The American Society for Testing Materials, Philadelphia. 1962.
15. F. FEIGL. Qualitative analysis by spot tests. Elsevier Publishing Co., New York. 1946. p. 235.
16. A. DESGREZ, L. LESCOEUR, and S. MANJEAN. Comp. Rend. **183**, 1244 (1926).
17. B. J. HEINRICH, M. D. GRIMES, and J. E. PUCKETT. *In* Treatise on analytical chemistry. Part II, Vol. 7. *Edited by* I. M. Kolthoff and P. J. Elving. Interscience Publishers, New York, N.Y. 1961. p. 104.
18. G. D. PATTERSON, JR. *In* Colorimetric determination of non-metals. *Edited by* D. F. Boltz. Interscience Publishers, New York, N.Y. 1958. p. 285.
19. M. S. BUDD and A. H. BEWICK. Anal. Chem. **24**, 1536 (1952).
20. J. CUNNINGHAM and H. G. HEAL. Trans. Faraday Soc. **54**, 1355 (1958).
21. I. VOGEL and J. R. PARTINGTON. J. Chem. Soc. **127**, 1514 (1925).
22. R. L. EAGER and D. S. MAHADEVAPPA. Can. J. Chem. **41**, 2106 (1963).

Can. J. Chem. Downloaded from www.nrcresearchpress.com by 210.87.254.6 on 09/05/12
For personal use only.

Can. J. Chem. Downloaded from www.nrcresearchpress.com by 210.87.254.105 on 09/05/12
For personal use only.

A QUANTUM-THEORETICAL STUDY OF SOME AROMATIC NITRILES BY THE SEMIEMPIRICAL LCAO-SCF-MO METHOD

H. E. POPKIE AND J. B. MOFFAT
Department of Chemistry, University of Waterloo, Waterloo, Ontario
Received September 9, 1964

ABSTRACT

Semiempirical LCAO–SCF–MO calculations have been carried out on some aromatic nitriles in an attempt to predict spectral transitions. Mataga's approximation has been applied to the Coulomb repulsion integrals and a set of parameter values which gives a reasonable prediction of the observed singlet–singlet transition energies of pyridine and benzonitrile was used. The calculations were applied to pyridine, benzonitrile, 2-, 3-, and 4-cyanopyridine, 1,2-, 1,3-, and 1,4-dicyanobenzene, 2,6-dicyanopyridine, and 1,2,4,5-tetra cyanobenzene. Computed singlet–singlet transition energies are in fair agreement with experiment. However, calculated singlet–triplet transition energies are, in general, lower than the experimental values by about 1 eV. The SCF ground state MO's and orbital energies are reported together with the wave functions for the four lowest-energy excited singlet states for each molecule.

INTRODUCTION

The most successful application of the semiempirical LCAO–MO method as applied to π-electronic systems has been the quantitative prediction of the positions and intensities of the low-lying electronic spectral bands (1). Most of the work has been done on hydrocarbon molecules, especially alternant ones, but numerous computations on molecules containing heteroatoms are being reported. However, predicted transition energies for hetero molecules do not in general agree with experimental values as well as in the case of hydrocarbons, and Parr (1) notes that discrepancies of 0.5 eV are not uncommon. The main problem has been a judicious choice of parameter and integral values.

Several semiempirical SCF calculations have been done on aromatic nitrogen-containing molecules. The azabenzene series has been studied by Pariser and Parr (2), McWeeny and Peacock (3), and Mataga and Nishimoto (4); the azanaphthalenes by Peacock (5), Mataga (6), and Favini *et al.* (7). In addition, individual members such as pyridine and *s*-triazine have been subjected to treatments by many workers such as Anno (8), Kon (9), and Brown and Heffernan (10). Recently aniline and polysubstituted aminobenzenes have received attention from Fischer-Hjalmers (11), Bloor *et al.* (12), and Mataga (13).

A small amount of work seems to have been reported for aromatic nitriles. Peacock and Wilkinson (14) have done a semiempirical SCF study of benzonitrile and have calculated spectral transitions. Polansky and Grassberger (15) have attempted to predict the spectra of the cyanobenzenes using a Hückel-type procedure. It seemed worth while to attempt to apply a semiempirical SCF calculation to several cyanobenzenes and cyanopyridines to determine the extent to which transition energies could be predicted using the Mataga approximation (4) for Coulomb repulsion integrals and a set of parameter values which gave a reasonable prediction of the observed singlet–singlet transition energies of pyridine and benzonitrile. The molecules studied were pyridine, benzonitrile, 2-, 3-, and 4-cyanopyridine, 1,2-, 1,3-, and 1,4-dicyanobenzene, 2,6-dicyanopyridine, and 1,2,4,5-tetracyanobenzene.

METHOD OF CALCULATION

The LCAO–SCF–MO method with the simplifications introduced by Pariser, Parr (2), and Pople (16) was used. A brief outline of the principles and assumptions involved is given below.

The method begins with the assumption that the π-electrons of an unsaturated molecule can be treated apart from the σ-electrons. They are allowed to move in an effective field due to the core region composed of the σ-electrons and nuclei. Parr (1) has given a set of sigma–pi separability conditions which the wave functions of a set of molecular states must satisfy in order that the π-electrons can be treated separately. In this π-electron approximation, correlation energies between σ- and π-electrons are necessarily neglected and the σ-parts of the wave functions are assumed not to change from state to state.

The Hamiltonian for a system containing $2n$ π-electrons is written:

$$[1] \qquad H_\pi = \sum_{i=1}^{2n} H_{\text{core}}(i) + \sum_{i<j=1}^{2n} \frac{e^2}{r_{ij}},$$

where $H_{\text{core}}(i) = T(i) + U_{\text{core}}(i)$ is the kinetic energy operator for electron i plus its potential energy in the field of the core.

The ground state wave function for a molecule with a closed shell structure is represented by a single normalized Slater determinant:

$$[2] \qquad \Psi_0 = \det |\Phi_1\bar{\Phi}_1\Phi_2\bar{\Phi}_2 \ldots \Phi_n\bar{\Phi}_n|,$$

where $\Phi_i = \psi_i\alpha$ and $\bar{\Phi}_i = \psi_i\beta$ are molecular spin orbitals.

In the LCAO approximation, the molecular orbitals (MO's) ψ_i are assumed to be linear combinations of a basis set of m atomic orbitals (AO's) ϕ_μ:

$$[3] \qquad \psi_i = \sum_{\mu=1}^{m} c_{i\mu}\phi_\mu.$$

The AO's ϕ_μ are centered, one to an atom, on the various atoms contributing π-electrons to the system under consideration. They are mutually orthogonal orbitals of such a nature that differential overlap is negligible. Although their exact analytical form is unknown, they may be expected to resemble (somewhat) deformed 2p π-orbitals.

A procedure for the determination of the coefficients $c_{i\mu}$ which minimize the total π-electronic energy $E_0 = \int \Psi_0^* H_\pi \Psi_0 \, d\tau$ has been given by Roothaan (17).

However, the calculations are quite tedious. The equations can be simplified considerably by the introduction of the zero differential overlap (ZDO) approximation as suggested by Pariser, Parr (2), and Pople (16). The ZDO approximation can be expressed as:

$$[4] \qquad \phi_\mu^*(i)\phi_\nu(i) \, dv(i) = 0; \; (\mu \neq \nu).$$

It is rather difficult to determine theoretically whether or not the ZDO assumption is a justifiable approximation. For conjugated hydrocarbons it appears to be a good first approximation, but for heteroatomic molecules where the distribution of electrons is not so uniform one would expect overlap effects to play a greater role (1). Nevertheless, as Dewar (18) points out, calculations using the ZDO assumption have proved useful for extracting experimental data, as has been shown by actual quantitative applications.

With the ZDO approximation, the coefficients $c_{i\mu}$ and the MO energies ϵ_i are the eigenvectors and eigenvalues of the Hartree–Fock matrix h^F whose elements are given by:

Can. J. Chem. Downloaded from www.nrcresearchpress.com by 210.87.254.105 on 09/05/12
For personal use only.

$$h_{\mu\mu}^{\mathrm{F}} = \alpha_\mu + \tfrac{1}{2}P_{\mu\mu}\gamma_{\mu\mu} + \sum_{\nu\neq\mu} P_{\nu\nu}\gamma_{\mu\nu}; \quad [5]$$

$$h_{\mu\nu}^{\mathrm{F}} = \beta_{\mu\nu} - \tfrac{1}{2}P_{\mu\nu}\gamma_{\mu\nu}; \ (\mu \neq \nu). \quad [6]$$

In these equations α_μ is the Coulomb integral

$$\alpha_\mu = \int \phi_\mu^*(1) H_{\mathrm{core}}(1) \phi_\mu(1)\, dv(1), \quad [7]$$

the quantity $\beta_{\mu\nu}$ is the resonance integral

$$\beta_{\mu\nu} = \int \phi_\mu^*(1) H_{\mathrm{core}}(1) \phi_\nu(1)\, dv(1), \quad [8]$$

the quantity $\gamma_{\mu\nu}$ is the Coulomb repulsion integral

$$\gamma_{\mu\nu} = \iint \phi_\mu^*(1)\phi_\nu^*(2)\frac{e^2}{r_{12}}\phi_\mu(1)\phi_\nu(2)\, dv(1)\, dv(2), \quad [9]$$

and $P_{\mu\nu}$ is an element of the charge and bond order matrix P defined by

$$P_{\mu\nu} = 2\sum_i C_{i\mu}^* C_{i\nu}, \quad [10]$$

where the sum is over all occupied MO's.

The integral α_μ [7] can be expanded according to Goeppert-Mayer and Sklar (19) as:

$$\alpha_\mu = W_\mu - \sum_{\nu\neq\mu} [(\mu\mu:\nu) + Z_\nu\gamma_{\mu\nu}], \quad [11]$$

where Z_ν is the number of π-electrons contributed by atom ν. In this paper, the penetration integrals $(\mu\mu:\nu)$ are neglected.

Furthermore, the energy zero for the MO energies ϵ_i is chosen as $W_{\mathrm{C}} + \frac{1}{2}\gamma_{\mathrm{CC}}^{(0)}$ as suggested by McWeeny and Peacock (3).

The form finally adopted for the H–F Hamiltonian h^{F} can be written:

$$h_{\mu\mu}^{F} = \delta w_\mu + \tfrac{1}{2}P_{\mu\mu}\gamma_{\mu\mu} - \tfrac{1}{2}\gamma_{\mathrm{CC}}^{(0)} + \sum_{\nu\neq\mu} (P_{\nu\nu} - Z_\nu)\gamma_{\mu\nu}, \quad [12]$$

$$h_{\mu\nu}^{\mathrm{F}} = \beta_{\mu\nu} - \tfrac{1}{2}P_{\mu\nu}\gamma_{\mu\nu}; \ (\mu \neq \nu), \quad [13]$$

where

$$\delta w_\mu = W_\mu - W_{\mathrm{C}}. \quad [14]$$

Because h^{F} depends on P, an iterative calculation must be used to determine the $c_{i\mu}$'s and ϵ_i's. A procedure for the direct iteration of the matrix R $(= \frac{1}{2}P)$ utilizing the method of steepest descent has been proposed by McWeeny (20). As it only involves the manipulation of matrices, it is particularly adaptable for electronic computation. The entire procedure was programmed in SPS and run on an IBM 1620 computer. The input data required consisted of numerical values for Z_μ, δw_μ, $\beta_{\mu\nu}$, and $\gamma_{\mu\nu}$ defined in equations [11], [14], [8], and [9] and an initial estimate of R. At the end of each descent the idempotency of R was restored according to McWeeny's procedure (20). The procedure was regarded as self-consistent when successive iterations did not change any of the elements of R by more than 10^{-4}. If Huckel MO's were used as starting orbitals, 6 to 8 iterations on the average were required in order to reach self-consistency. The program running time was approximately proportional to n^3, where n is the number of atoms donating π-electrons in the system under consideration. A typical run for a 10-atom molecule took approximately 4 min per descent. The eigenvectors and eigenvalues of

Can. J. Chem. Downloaded from www.nrcresearchpress.com by 210.87.254.105 on 09/05/12
For personal use only.

the self-consistent Hamiltonian h^F were determined using an SPS subroutine which diagonalized the matrix utilizing the Jacobi method of rotations.

When an electron is excited from an occupied MO ψ_i to an unoccupied MO $\psi_{k'}$, the resulting singly excited configuration, which may be a singlet or triplet, can be represented by the determinantal wave function.

$$[15] \qquad {}^{1,3}X_{i\to k'} = \frac{1}{\sqrt{2}}\left(|\Phi_1\bar{\Phi}_1 \ldots \Phi_i\bar{\Phi}_{k'} \ldots \Phi_n\bar{\Phi}_n| \mp |\Phi_1\bar{\Phi}_1 \ldots \bar{\Phi}_i\Phi_{k'} \ldots \Phi_n\bar{\Phi}_n|\right).$$

The excited states of the molecule are expressed as a linear combination of singly excited configurations:

$$[16] \qquad S_I = \sum_{i,k'} c_{S_I,ik'}\,{}^1X_{i\to k'},$$

$$[17] \qquad T_I = \sum_{i,k'} c_{T_I,ik'}\,{}^3X_{i\to k'},$$

where i is summed over all occupied MO's, and k' is summed over all unoccupied MO's.

The coefficients $c_{S_I,ik'}$, $c_{T_I,ik'}$ and the electronic excitation energies are obtained by diagonalizing a configuration interaction (CI) matrix with elements given by (21):

$$[18] \qquad ({}^1X_{i\to k'}|H_\pi|{}^1X_{j\to l'}) = \delta_{ij}\delta_{kl}(\epsilon_{k'} - \epsilon_i) + 2\langle ik|jl\rangle - \langle ij|kl\rangle,$$

$$[19] \qquad ({}^3X_{i\to k'}|H_\pi|{}^3X_{j\to l'}) = \delta_{ij}\delta_{kl}(\epsilon_{k'} - \epsilon_i) - \langle ij|kl\rangle,$$

where ϵ_i is the orbital energy of MO ψ_i and $\langle ij|kl\rangle$ is a molecular repulsion integral which can be computed from:

$$[20] \qquad \langle ij|kl\rangle = \sum_{\mu,\nu} c_{i\mu}c_{k\mu}c_{j\nu}c_{l\nu}\gamma_{\mu\nu}.$$

An SPS program was set up to calculate all the elements of the singlet and triplet CI matrices. The required input data consisted of the MO coefficients $c_{i\mu}$, the MO energies ϵ_i, and the Coulomb repulsion integrals $\gamma_{\mu\nu}$.

All configurations which did not interact to an appreciable extent with any of the four lowest-energy configurations were not included in the final diagonalization of the CI matrix. "Important" configurations $X_{j\to l'}$ were arbitrarily selected as those which satisfied:

$$[21] \qquad |(X'_{i\to k'}|H_\pi|X_{j\to l'})|/[|(X_{j\to l'}|H_\pi|X_{j\to l'}) - (X'_{i\to k'}|H_\pi|X'_{i\to k'})|] \geqslant 0.1,$$

where $X'_{i\to k'}$ is one of the four lowest-energy configurations.

CALCULATION OF INTEGRAL AND PARAMETER VALUES

The one-center core parameters δw_μ were estimated using the relationship

$$[22] \qquad \delta w_\mu = I_C - I_\mu.$$

The necessary valence-state ionization potentials I_μ were taken from the recently compiled tables of Hinze and Jaffé (22):

$$I_C(trtrtr\pi) = 11.16 \text{ eV},$$

$$I_N(di^2di\pi\pi) = 14.18 \text{ eV},$$

$$I_N(tr^2trtr\pi) = 14.12 \text{ eV}.$$

Can. J. Chem. Downloaded from www.nrcresearchpress.com by 210.87.254.105 on 09/05/12
For personal use only.

Carbon–carbon resonance integrals were evaluated with an exponential fit

[23] $$\beta_{CC}(r) = -2\,500\exp(-5r)\text{ eV} \qquad (r \text{ in Å}).$$

The two carbon–nitrogen resonance integrals were chosen so as to best reproduce the observed singlet–singlet transition energies of pyridine and benzonitrile. The values adopted were:

$$\beta_{CN}\,(\text{aza}) = -2.6\text{ eV},$$

$$\beta_{CN}\,(\text{nitrile}) = -3.5\text{ eV}.$$

One-center Coulomb integrals were evaluated according to the method suggested by Pariser (23):

[24] $$\gamma_{\mu\mu}^{(0)} = I_\mu - A_\mu.$$

The required valence-state ionization potentials I_μ and electron affinities A_μ were taken from Hinze and Jaffé (22). These gave:

$$\gamma_{CC}^{(0)} = 11.13\text{ eV},$$

$$\gamma_{NN}^{(0)}\,(\text{aza}) = 12.34\text{ eV},$$

$$\gamma_{NN}^{(0)}\,(\text{nitrile}) = 12.52\text{ eV}.$$

Two-center Coulomb integrals were computed according to the scheme proposed by Mataga and Nishimoto (4):

[25] $$\gamma_{\mu\nu}(r) = e^2/(a_{\mu\nu} + r).$$

Of course, application of Mataga's approximation to atoms that are not uniformly charged +1 in the core is not readily justifiable.

The constants $a_{\mu\nu}$ were determined from the values of $\gamma_{\mu\mu}^{(0)}$ and $\gamma_{\nu\nu}^{(0)}$ according to:

[26] $$a_{\mu\nu} = \tfrac{1}{2}e^2\left(\frac{1}{\gamma_{\mu\mu}^{(0)}} + \frac{1}{\gamma_{\nu\nu}^{(0)}}\right).$$

The interatomic distances for the various molecules studied were estimated from the molecular geometrics of pyridine (24) and benzonitrile (25).

RESULTS AND DISCUSSION

The SCF ground state MO's and orbital energies of all the molecules studied are given in Appendix I. Charge densities and bond orders computed from these orbitals are shown in Fig. 1. The wave functions for the four lowest-energy excited singlet states for each molecule are listed in Appendix II. In addition, the four lowest-energy excited triplet states of pyridine and benzonitrile are given. Table I presents a summary of the computed transition energies and compares them with experimental values. Observed transition energies were taken to correspond to the position of the band maxima and were determined from the data given in the references listed below Table I. The nature of the solvent is indicated. Appendices I and II have been placed in the depository of unpublished data.

It can be seen from Table I that computed singlet–singlet transition energies are in fair agreement with experiment. In general, singlet levels are predicted to be somewhat higher (0.1 to 0.4 eV) than is observed. However, the spacing amongst the various levels is in good accord with observed spacings. As might be expected, the largest differences

Can. J. Chem. Downloaded from www.nrcresearchpress.com by 210.87.254.105 on 09/05/12
For personal use only.

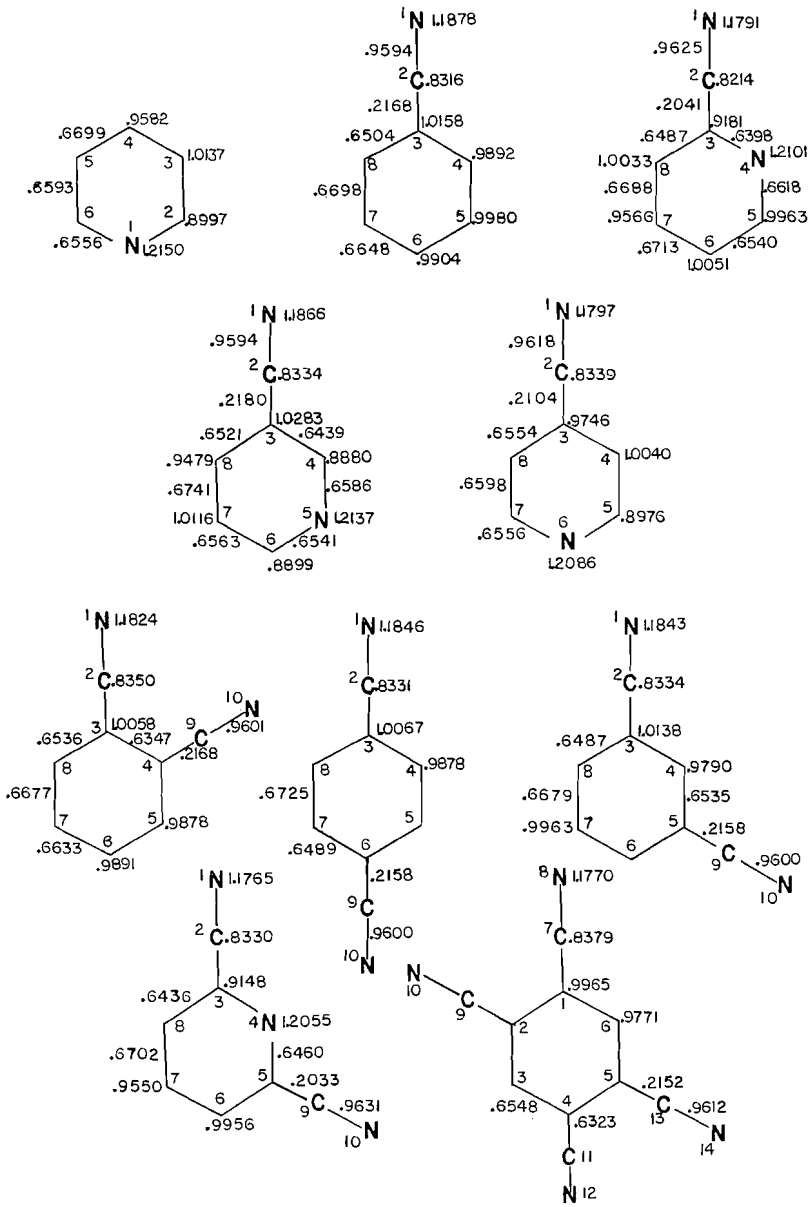

FIG. 1. SCF charge densities and bond orders.

between theory and experiment occur for the most highly substituted molecule studied, namely 1,2,4,5-tetracyanobenzene. It should be noted that the observed transition energies were not corrected for solvent effects. Such corrections would raise the observed singlet levels and bring them in closer agreement with theory. The calculated energy sequences for the first two singlet levels in the isomeric cyanopyridines and isomeric dicyanobenzenes agree with experiment with one notable exception. The second singlet level in 4-cyanopyridine is calculated to lie 0.2 eV above the second levels in 2- and 3-cyanopyridine, whereas experimentally it is observed to lie 0.05 eV below.

Can. J. Chem. Downloaded from www.nrcresearchpress.com by 210.87.254.105 on 09/05/12
For personal use only.

TABLE I

Calculated and observed transition energies

Molecule		Transition energies (eV) Calcd.	Obsd.
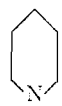	S_4	7.13	7.22[a]
	S_3	7.10	—
	S_2	6.15	6.17[a]
	S_1	4.90	4.94[b]
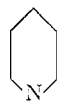	T_4	4.87	—
	T_3	4.02	—
	T_2	3.73	—
	T_1	2.51	3.68[c]
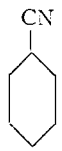	S_4	6.56	6.52[d]
	S_3	6.47	—
	S_2	5.68	5.59[e]
	S_1	4.63	4.48[e]
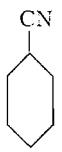	T_4	4.61	—
	T_3	3.72	3.96[f]
	T_2	3.70	3.84[f]
	T_1	2.26	3.33[c]
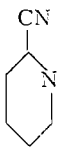	S_4	6.84	—
	S_3	6.81	—
	S_2	5.80	5.69[e]
	S_1	4.80	4.68[e]
	S_4	6.86	—
	S_3	6.71	—
	S_2	5.75	5.69[e]
	S_1	4.80	4.68[e]

Molecule		Transition energies (eV) Calcd.	Obsd.
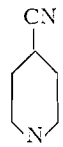	S_4	6.85	—
	S_3	6.55	—
	S_2	5.95	5.64[e]
	S_1	4.72	4.58[e]
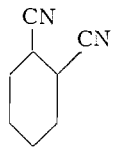	S_4	6.40	—
	S_3	6.14	—
	S_2	5.44	5.34[g]
	S_1	4.55	4.38[g]
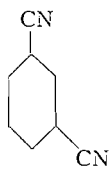	S_4	6.40	—
	S_3	6.04	—
	S_2	5.55	5.42[g]
	S_1	4.55	4.41[g]
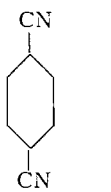	S_4	6.45	—
	S_3	6.44	—
	S_2	5.36	5.27[g]
	S_1	4.52	4.37[g]
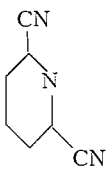	S_4	6.68	—
	S_3	6.40	—
	S_2	5.64	—
	S_1	4.69	4.51[b]
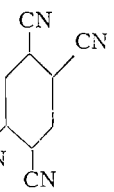	S_4	6.20	—
	S_3	5.80	5.56[h]
	S_2	5.12	4.84[h]
	S_1	4.45	4.02[h]

[a]Vapor, ref. 26.
[b]Cyclohexane, ref. 27.
[c]Chloroform, ref. 28.
[d]Vapor, ref. 29.
[e]Cyclohexane, ref. 30.
[f]Cyclohexane, ref. 31.
[g]Methanol, ref. 15.
[h]Ethanol, ref. 32.

The greatest conflict between theory and experiment occurs for the lowest singlet–triplet transition energy. In pyridine, the computed energy is 1.2 eV too low, while in benzonitrile it is 1.1 eV too low. This seems to be characteristic of the use of the Mataga

Can. J. Chem. Downloaded from www.nrcresearchpress.com by 210.87.254.105 on 09/05/12
For personal use only.

approximation for the two-center repulsion integrals. In benzene (4) it is possible to get an excellent fit with experiment for the three singlet levels by varying the carbon–carbon resonance integral β_{CC}. However, use of the "optimum" value of β_{CC} causes the calculated lowest triplet level to lie approximately 1 eV below the observed level. It is not surprising that this discrepancy lingers in calculations on substituted benzenes.

In CI calculations, the question arises as to whether or not it is sufficient to take into consideration only the singly excited configurations involving the two highest occupied and two lowest unoccupied ground state MO's. For the molecules studied, there is little change ($\approx$0.1 eV) in the singlet levels by considering all singly excited configurations. However, singly excited configuration involving the third and fourth highest occupied and lowest unoccupied orbitals were found to be important in the calculation of triplet levels, especially the lowest level as the following data illustrates:

Pyridine:—1st approximation,

$$^3E_1 = 3.11 \text{ eV},$$
$$T_1 = 0.857\ ^3X_{1\to 2'} - 0.516\ ^3X_{2\to 1'};$$

2nd approximation,

$$^3E_1 = 2.51 \text{ eV},$$
$$T_1 = 0.766\ ^3X_{1\to 2'} - 0.579\ ^3X_{2\to 1'} + 0.129\ ^3X_{2\to 3'} + 0.248\ ^3X_{3\to 3'}.$$

Benzonitrile:—1st approximation,

$$^3E_1 = 3.06 \text{ eV},$$
$$T_1 = 0.785\ ^3X_{1\to 1'} + 0.620\ ^3X_{2\to 2'};$$

2nd approximation,

$$^3E_1 = 2.26 \text{ eV},$$
$$T_1 = 0.668\ ^3X_{1\to 1'} + 0.620\ ^3X_{2\to 2'} + 0.158\ ^3X_{3\to 3'} - 0.174\ ^3X_{4\to 4'} + 0.200\ ^3X_{1\to 3'} - 0.174\ ^3X_{3\to 4'}.$$

In summary, it appears as though use of the Mataga approximation for two-center Coulomb repulsion integrals together with a judicious choice of core parameters will give a fairly reasonable prediction of singlet–singlet transition energies in aromatic nitriles. Treatment of δw_N as an empirical parameter and a careful selection of resonance integrals could undoubtedly improve the agreement between theory and experiment over that which is reported here. However, the lowest singlet–triplet transition energies are not predicted very well and lie around 1 eV below the observed energies.

ACKNOWLEDGMENTS

The authors are indebted to the National Research Council of Canada for financial support. The generous provision of computer time by the Computation Center of the University of Waterloo is gratefully acknowledged.

REFERENCES

1. R. G. Parr. Quantum theory of molecular electronic structure. W. A. Benjamin, Inc., N.Y. 1963. Chap. III. Note especially Sections 13, 14, and 16 and the references contained therein.
2. R. Pariser and R. G. Parr. J. Chem. Phys. **21**, 466, 767 (1953).
3. R. McWeeny and T. E. Peacock. Proc. Phys. Soc. London, A, **70**, 41 (1957).
4. N. Mataga and K. Nishimoto. Z. Physik. Chem. Frankfurt, **12**, 335 (1957); **13**, 140 (1957).
5. T. E. Peacock. J. Chem. Soc. 2308, (1959); Proc. Phys. Soc. London, A, **70**, 654 (1957).
6. N. Mataga. Z. Physik. Chem. Frankfurt, **18**, 285 (1958); Bull. Chem. Soc. Japan, **31**, 459 (1958).
7. G. Favini, S. Carrà, V. Pierpaoli, S. Polezzo, and M. Simonnetta. Nuovo Cimento, **8**, 60 (1958).
8. T. Anno. J. Chem. Phys. **32**, 867 (1960).
9. H. Kon. Bull. Chem. Soc. Japan, **28**, 275 (1955).

Can. J. Chem. Downloaded from www.nrcresearchpress.com by 210.87.254.105 on 09/05/12
For personal use only.

10. R. D. BROWN and M. L. HEFFERNAN. Australian J. Chem. **10**, 211 (1957).
11. I. FISCHER-HJALMERS. Arkiv Fysik, **21**, 123 (1962).
12. J. E. BLOOR, P. N. DAYKIN, and P. BOLTWOOD. Can. J. Chem. **42**, 121 (1964).
13. N. MATAGA. Bull. Chem. Soc. Japan, **36**, 1607 (1963).
14. T. E. PEACOCK and P. T. WILKINSON. Proc. Phys. Soc. London, **79**, 105 (1962).
15. O. E. POLANSKY and M. A. GRASSBERGER. Monatsh. Chem. **94**, 647 (1963).
16. J. A. POPLE. Trans. Faraday Soc. **49**, 1375 (1953).
17. C. C. J. ROOTHAAN. Rev. Mod. Phys. **23**, 69 (1951).
18. M. J. S. DEWAR. Rev. Mod. Phys. **35**, 586 (1963).
19. M. GOEPPERT-MAYER and A. K. SKLAR. J. Chem. Phys. **6**, 645 (1938).
20. R. MCWEENY. Proc. Roy. Soc. London, Ser. A, **235**, 496 (1956).
21. J. A. POPLE. Proc. Phys. Soc. London, A, **68**, 81 (1955).
22. J. HINZE and H. H. JAFFÉ. J. Am. Chem. Soc. **84**, 540 (1962).
23. R. PARISER. J. Chem. Phys. **21**, 568 (1953).
24. B. BAK, L. HANSEN-NYGAARD, and J. RASTRUP-ANDERSEN. J. Mol. Spectry. **2**, 361 (1958).
25. B. BAK, D. CHRISTENSEN, W. B. DIXON, L. HANSEN-NYGAARD, and J. RASTRUP-ANDERSEN. J. Chem. Phys. **37**, 2027 (1962).
26. M. F. A. EL-SAYED. J. Chem. Phys. **36**, 552 (1962).
27. S. F. MASON. J. Chem. Soc. 1247 (1959).
28. D. F. EVANS. J. Chem. Soc. 2753 (1959).
29. W. C. PRICE and A. D. WALSH. Proc. Roy. Soc. London, Ser. A, **191**, 32 (1947).
30. C. LEANDRI and D. SPINELLI. Boll. Sci. Fac. Chim. Ind. Bologna, **15**, 90 (1957).
31. R. C. HIRT and F. T. KING. J. Chem. Phys. **20**, 1821 (1952).
32. A. ZWEIG, J. E. LEHNSEN, W. G. HODGSON, and W. H. JURA. J. Am. Chem. Soc. **85**, 3937 (1963).

Can. J. Chem. Downloaded from www.nrcresearchpress.com by 210.87.254.105 on 09/05/12
For personal use only.

Can. J. Chem. Downloaded from www.nrcresearchpress.com by 210.87.254.6 on 09/05/12
For personal use only.

REACTIONS OF THE ETHYL RADICAL

IV. ADDITION TO VINYL MONOMERS

D. G. L. JAMES

Department of Chemistry, The University of British Columbia, Vancouver, British Columbia

AND

DUNCAN MACCALLUM[1]

Department of Chemistry, Queen's College of the University of St. Andrews, Dundee, Scotland

Received October 19, 1964

ABSTRACT

The Arrhenius parameters have been measured for the addition of the ethyl radical to a representative selection of vinyl monomers in the gas phase. The wide range of reactivity observed was almost entirely due to the variation of the energy of activation, from 3.4 ± 0.4 kcal/mole for acrylonitrile to 6.9 ± 0.5 kcal/mole for vinyl acetate. No significant variation was found among the values of the pre-exponential factors, indicating uniformity of steric conditions at the site of radical attack. The rate constant for the addition of the ethyl radical is considered as an alternative to the copolymerization parameter Q_0 as an index of the intrinsic reactivity of a monomer at a given temperature.

INTRODUCTION

The effect of structure upon the reactivity of monoolefins towards the addition of the ethyl radical was discussed in Part II of this series (1). This study has now been extended to vinyl monomers of the type CH_2=CHX, chosen so that diverse combinations of Q and e values should be included. The values of e for the olefins of Part II all lie within a narrow range, but in this study e varies from +1.11 for acrylonitrile to −1.64 for vinyl *n*-butyl ether (2, 3). Such a wide variation in e introduces a particular difficulty into any attempt to relate the intrinsic reactivity of the monomer to the rate constant for the addition of a chosen reference species. This is particularly clear if we consider the diverse patterns of response shown by the monomers of this study towards homogeneous polymerization under cationic, radical, and anionic conditions. Although none of these monomers is entirely unreactive towards attack by the polystyrene radical, kinetic measurements (4) reveal that vinyl *n*-butyl ether (Q = 0.014, e = −1.64) reacts far more rapidly with the polystyrene cation whereas acrylonitrile (Q = 0.58, e = 1.11) is more reactive towards the polystyrene anion. Selectivity varies from styrene (Q = 1.00, e = −0.80) which reacts freely with the polystyrene cation, radical, or anion, to vinyl acetate (Q = 0.026, e = −0.22) which reacts appreciably with the radical only. Parallel results are obtained in attempts to initiate homogeneous homopolymerization of these monomers with cationic, radical, and anionic catalysts. Selectivity is lowest with styrene, intermediate with acrylonitrile, which responds to anionic and radical catalysts but is inert to the strong cationic catalyst boron trifluoride etherate in a pure form (5), and highest with vinyl *n*-butyl ether and vinyl acetate, which yield appreciable amounts of high polymer only with cationic (6, 7) and radical (8, 9) catalysts respectively.

The examples given above show that the monomers chosen for this study encompass a wide diversity of behavior. Polar effects dominate the response of these monomers to the reaction conditions. A reliable index of the intrinsic reactivity of the monomer, independent of polar effects, is required before the reactivity of a given monomer can be

[1]*Present address: Plastics Division, Central Research Department, The Distillers Co. Ltd., Epsom, Surrey, England.*

related to its molecular structure. The rate constant for the addition of a common reference species to the monomer at a standard temperature provides a valid index of intrinsic reactivity only if this reference species is well chosen. The polyethylene radical has the virtue of possessing both a high ionization potential and a low electron affinity, so that polar effects in the addition of this radical should be particularly low. Indeed Burkhart and Zutty have recently proposed that the Q_0 value of the monomer should be used as an index of intrinsic reactivity (10). Q_0 values are based upon the choice of ethylene as the reference monomer, and the assignment to ethylene of the values: $Q_0 = 1.00$ and $e_0 = 0.00$. The Q_0 value of a monomer is then directly proportional to the rate constant for the addition of the polyethylene radical to the monomer molecule and thus provides a direct measure of monomer reactivity. The Q_0 value of a monomer (B) should be directly determined from the relationship $Q_{0B} = 1/r_A$, where r_A is the reactivity ratio of the copolymerization of monomer (B) with ethylene (A), but this has been measured accurately for only a few monomers (10, 11). Significantly these values of Q_0 are calculated on the assumption that the reactivity of the polyethylene radical is entirely determined by the terminal ethylene unit. In fact the model polyethylene radical is no more than the substituted ethyl radical, $YCH_2CH_2\cdot$, in which the nature of Y has no effect upon the reactivity. It is therefore reasonable to propose that at common temperature the rate constant for the addition of the ethyl radical itself to the monomer B should be proportional to Q_{0B}, and should therefore provide an alternative measure of the intrinsic reactivity of the monomer B. The ethyl radical also possesses a high ionization potential and a low electron affinity, so that polar effects in the addition reactions of the ethyl radical should be particularly small.

Ethyl radicals were generated in the presence of monomer molecules by the illumination of a gaseous mixture of diethyl ketone and the monomer with 3 130 Å radiation. To obtain more comprehensive information we have measured the rate constant for the addition of the ethyl radical to the various monomer molecules over a range of about 100 deg; values of the energy of activation and the pre-exponential factor can then be compared for the different monomers and the reactivity considered upon a more detailed basis.

EXPERIMENTAL PROCEDURE

The apparatus and method have been described in two earlier papers (1, 12). The kinetic analysis requires that the ethyl radical shall always be present in great excess over all other radicals. Acrylonitrile and styrene are far more reactive than the olefins towards the ethyl radical, and it was therefore necessary to use much lower initial concentrations than previously for these monomers, and to correct for consumption during the experiment. With these precautions the calculated rate constants were insensitive to variation of composition or intensity, and polymer was not formed in the reacting system.

The analysis followed the initial pattern of separation into CO, ($C_2H_6 + C_2H_4$), and C_4H_{10} fractions, each of which was estimated by the gas burette. The kinetic analysis requires a knowledge of the composition of the C_2 fraction, and this was obtained using the value of the ratio $\Delta = R(C_2H_4)/R(C_4H_{10})$ appropriate to the system, where $R(Z)$ denotes the rate of formation of the product Z. Many values of Δ have been measured for the photolysis of diethyl ketone in the presence of a wide variety of substrates; for all such systems under our prescribed conditions Δ is independent of temperature and has a mean value lying within the range 0.13 ± 0.01. The application of the appropriate value of Δ to the calculation of the rate constants is discussed in the next section.

THE KINETIC ANALYSIS

The mechanism proposed for the photolysis of a gaseous mixture of diethyl ketone and the vinyl monomers $CH_2{=}CHX$ by 3 130 Å radiation and under the conditions given above is analogous to that adopted for the olefinic systems (1, 12).

[1] $$CH_3CH_2COCH_2CH_3 + h\nu \rightarrow 2CH_3CH_2\cdot + CO$$

Can. J. Chem. Downloaded from www.nrcresearchpress.com by 210.87.254.6 on 09/05/12
For personal use only.

[2] $$2CH_3CH_2^{\cdot} \rightarrow C_4H_{10}$$

[3] $$2CH_3CH_2^{\cdot} \rightarrow C_2H_6 + C_2H_4$$

[4] $$CH_3CH_2^{\cdot} + CH_3CH_2COCH_2CH_3 \rightarrow CH_3CH_3 + CH_3\dot{C}HCOCH_2CH_3$$

[5] $$CH_3CH_2^{\cdot} + CH_3\dot{C}HCOCH_2CH_3 \rightarrow CH_3CH(CH_2CH_3)COCH_2CH_3$$

[6] $$CH_3CH_2^{\cdot} + CH_2{=}CHX \rightarrow CH_3CH_3 + V^{\cdot}$$

[6a] $$CH_3CH_2^{\cdot} + V^{\cdot} \rightarrow CH_3CH_2V$$

[7] $$CH_3CH_2^{\cdot} + CH_2{=}CHX \rightarrow CH_3CH_2CH_2\dot{C}HX$$

[7a] $$CH_3CH_2^{\cdot} + CH_3CH_2CH_2\dot{C}HX \rightarrow CH_3CH_2CH_2CH(CH_2CH_3)X$$

The symbol V$^{\cdot}$ indicates a radical formed by the abstraction of one hydrogen atom from the molecule of the vinyl monomer. The rate constants for metathesis (k_6) and addition (k_7) between the ethyl radical and the monomer molecule may be calculated from the equations:

$$\frac{k_6}{k_2^{1/2}} = \left(\frac{R(C_2H_6) - R(C_2H_4)}{R(C_4H_{10})^{1/2}}\right)\frac{1}{[B]} - \frac{[D]}{[B]}\frac{k_4}{k_2^{1/2}} = \left(\frac{R(C_2)}{R(C_4)} - 2\Delta\right)\frac{R(C_4)^{1/2}}{[B]} - \frac{[D]}{[B]}\frac{k_4}{k_2^{1/2}},$$

$$\frac{k_7}{k_2^{1/2}} = \frac{R(CO) - R(C_2H_6) - R(C_4H_{10})}{[B]R(C_4H_{10})^{1/2}} = \frac{R(CO) - R(C_2) - (1 - \Delta)R(C_4)}{[B]R(C_4)^{1/2}},$$

where [D] and [B] represent the concentration of diethyl ketone and the vinyl monomer respectively in molecules/cm^3; $R(Z)$ is the rate of formation of product Z in molecules/cm^3 s; C_2 and C_4 denote the product fractions with the specified carbon number; $\Delta = R(C_2H_4)/R(C_4H_{10})$; and $k_4/k_2^{1/2}$ has been previously determined (12).

The C_2 fractions were not normally analyzed for C_2H_4 and C_2H_6 content in this investigation, and so the right-hand form of each equation was used. A value of Δ is therefore required for each monomer system investigated. For the octene-1 system the value of 0.136 was used previously (12); this system has recently been reinvestigated using analytical gas chromatography and yielded the result: $\Delta = 0.137 \pm 0.010$, independent of temperature (13). The value of 0.136 was retained for heptene-1 and also used for the closely related monomer vinyl *n*-butyl ether. The acrylonitrile system has also been independently investigated using gas chromatography (14) yielding the value $\Delta = 0.127 \pm 0.014$, independent of temperature, and so the value of 0.127 was uniformly applied to the results of this study. No independent values of Δ exist for either the styrene or the vinyl acetate systems. The value of 0.136 was employed in the preliminary communication (15) and the results have since been recalculated using $\Delta = 0.127$. For neither monomer was the change in the value of $E_7 - \frac{1}{2}E_2$ or of $\log A_7/A_2^{1/2}$ greater than 0.1 unit, which is much less than the uncertainty in each case. The negligible effect of a 7% change in the value of Δ is not accidental, as all the experiments were planned to make the results insensitive to the value of Δ.

The results given for acrylonitrile in Fig. 1 belong to two distinct sets. The filled circles represent results of this investigation, and were calculated using a uniform value of 0.127 for Δ. The open circles are results of James and Ogawa (14); in each of these experiments the C_2 fraction was analyzed by gas chromatography for C_2H_4 and C_2H_6 and the result calculated directly from the analysis. The two sets form a single statistical population, and the Arrhenius parameters were calculated on this basis.

The molecules of acrylonitrile and styrene contain the formally unsaturated nitrile and phenyl groups respectively. The analytical method does not distinguish addition to the vinyl group from addition to an unsaturated group in the same molecule, but

Can. J. Chem. Downloaded from www.nrcresearchpress.com by 210.87.254.6 on 09/05/12
For personal use only.

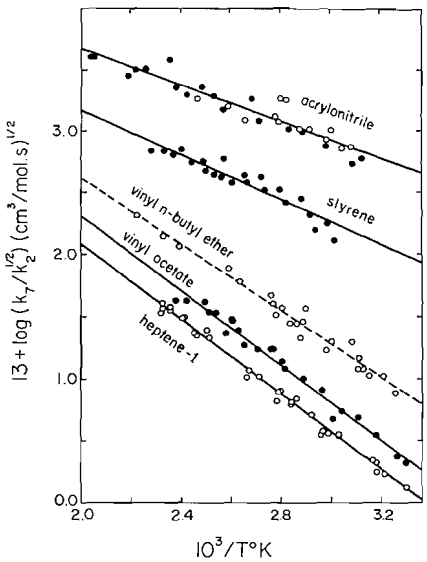

FIG. 1. Addition of the ethyl radical to vinyl monomers. The points and the line for vinyl *n*-butyl ether have been moved uniformly upwards by 0.5 units to avoid confusion.

independent attempts have been made to detect addition to the nitrile group of acetonitrile (14) and to the phenyl group of benzene (13). No addition could be detected to either substance, and it was estimated that $k_7(CH_3CN)/k_7(CH_2{=}CHCN) < 0.001$ and $k_7(C_6H_6)/k_7(C_6H_5CH{=}CH_2) < 0.001$ over the whole temperature range of this study. Appreciable addition of the ethyl radical to the substituent groups of acrylonitrile or styrene therefore appears to be unlikely.

The metathetical reaction [6] does not occur rapidly enough to be measured for any of the vinyl monomers by the method of this investigation.

RESULTS AND DISCUSSION

The Arrhenius plots for the addition of the ethyl radical to the four vinyl monomers $CH_2{=}CHX$ and the reference olefin heptene-1 are given in Fig. 1, and the Arrhenius parameters are listed in Table I.

TABLE I

Addition of the ethyl radical to vinyl monomers

Monomer	Number of expts.	Δ	C	B	$13 + \log A_7/A_2^{1/2}$	$E_7 - \frac{1}{2}E_2$ (kcal/mole)	$10^{13}k_7/k_2^{1/2}$ (at 100 °C)
Acrylonitrile	31	0.127	5.162	0.743	5.2±0.3	3.4±0.4	1 480
Styrene	22	0.127	4.980	0.905	5.0±0.3	4.1±0.6	360
Vinyl *n*-butyl ether	23	0.136	4.787	1.336	4.8±0.3	6.1±0.5	16
Vinyl acetate	23	0.127	5.341	1.512	5.3±0.3	6.9±0.5	19
Heptene-1 (ref. 1)	34	0.136	5.156	1.530	5.2±0.1	7.0±0.2	11

The constants B and C are the coefficients of the straight lines $13 + \log (k_7/k_2^{1/2}) = C - 10^3B/T$ fitted to the experimental results. The rate constants are expressed in units of cm³/molecule s; the limits of error are calculated at the 5% probability level.

None of the values of $13 + \log A_7/A_2^{1/2}$ deviates significantly from 5.1; this value is apparently insensitive to the substituent group X, and is probably characteristic of the

Can. J. Chem. Downloaded from www.nrcresearchpress.com by 210.87.254.6 on 09/05/12
For personal use only.

structural unit $CH_2{=}CH{-}$ which is common to all the molecules. In contrast, the energy of activation $E_7 - \frac{1}{2}E_2$ varies widely with the nature of the substituent group, and therefore the wide range of values of k_7 at a given temperature is almost entirely due to the variation in E_7. Reactivity is conferred upon the vinyl group by the substituent in the order $CN > C_6H_5 > OR > OCOR > R$, where R denotes an alkyl group.

The rate constants for the addition of the ethyl radical to a series of monomers in the gas phase may be compared with the corresponding rate constants for the addition of other free radicals. The wide range of values makes a log–log plot necessary, but the degree of linear correlation between the sets of rate constants may be judged by the closeness of the points to a reference line of unit gradient. Figure 2 shows such an attempt with the polyethylene radical, and is discussed in detail below. It is not truly representative of this kind of test because most of the values of Q_0 had to be calculated from the results of other copolymerizing systems and are therefore subject to more than the usual degree of error. Similar diagrams have been drawn for both the polystyrene radical (14) and the methyl radical (13) using directly determined results only. These show a reasonable degree of linear correlation in each case and indicate that radicals of widely differing intrinsic reactivity are capable of revealing a consistent pattern of reactivity among monomers if the polar effects are similar.

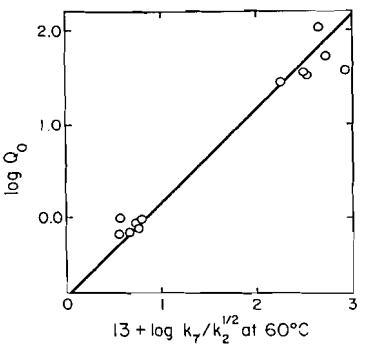

FIG. 2. Correlation of the rate constant k_7 with the parameter Q_0; the reference line has unit gradient.

Vinyl *n*-butyl ether seems to be more selective than the other monomers in its reactivity towards free radicals. The degree of reactivity shown by acrylonitrile, styrene, and vinyl acetate is consistent with the response of these monomers towards free radical polymerization (4). Vinyl *n*-butyl ether fails to yield high polymer under free radical conditions although the ether is nearly as reactive as vinyl acetate towards the ethyl radical, and this failure cannot be explained by an easy chain transfer process of the type that prevents the polymerization of heptene-1. On the other hand, the ready addition of the ethyl radical to vinyl *n*-butyl ether is paralleled by numerous examples of the addition of the rather electrophilic perhaloalkyl radicals to vinyl alkyl ethers (16). These observations indicate a higher electron density at the β-carbon atom of the vinyl group in vinyl *n*-butyl ether than in vinyl acetate, a conclusion which is supported by recent spectroscopic studies.

The nuclear magnetic resonance spectra of certain vinyl alkyl ethers have recently been discussed (17), and the most striking feature of the results is the extreme high-field position of the β-protons of the ethers, at about 80 c.p.s. above ethylene. This indicates conjugation between the lone pair of the oxygen atom and the π-electrons of the vinyl group, resulting in an increased charge density at the β-position. Certain doublets in the

Can. J. Chem. Downloaded from www.nrcresearchpress.com by 210.87.254.6 on 09/05/12
For personal use only.

vibrational spectra of the vinyl alkyl ethers reveal the presence of two rotational isomers, and a recent detailed study of vinyl methyl ether shows that the *cis* form lies 1.15 ± 0.25 kcal/mole below the *trans* form (18). Non-bonded interaction between the oxygen lone pair and the vinyl group is again indicated in the unsubstituted vinyl alkyl ethers. However this characteristic doublet is replaced by a singlet in the spectra of vinyl α,α-difluoroalkyl ethers (19); the fluorine atoms appear to inhibit the flow of charge from the oxygen atom to the vinyl group by virtue of their electronegativity. By the same reasoning we should expect the interaction between the non-carbonyl oxygen atom and the vinyl group to be much less in vinyl acetate than in vinyl *n*-butyl ether, giving to the latter the greater electron density at the β-carbon atom of the vinyl group. This would be consistent with the observations that vinyl *n*-butyl ether responds more readily to cationic polymerization and has the lower energy of activation for the addition of the ethyl radical.

In the introduction we have suggested that the addition rate constant k_7 may be an acceptable alternative to the copolymerization parameter Q_0 as an index of the intrinsic reactivity of a monomer at a given temperature. To find whether Q_0 and k_7 are linearly related, we have calculated values of Q_{0B} for each substrate from the Q_B and e_B values based upon styrene, using the equation:

$$\log Q_{0B} = -\log r_A = \log (Q_B/Q_A) + e_A(e_A - e_B)/2.303,$$

and the values $Q_A = 0.03$ and $e_A = -0.43$ for ethylene (10). The results are listed in Table II. For two of the substrates the Q and e values were not available, so those for a closely related monomer were used instead. Values of Q_0 have been directly determined for vinyl acetate at 90 °C and for *n*-butyl acrylate at 70 °C (10) and are included in Table II for comparison. Values of Q_0 may also be estimated for methyl acrylate and methyl methacrylate from the corresponding reactivity ratios for the copolymerization of these monomers with ethylene at 150 °C (11); they have not been included in this correlation as the reaction temperature was 90 deg higher than our standard of 60 °C, and the kinetic behavior of these systems was rather unusual.

TABLE II

Correlation of the rate constants for the addition of the ethyl radical to certain substrates in the gas phase with Q_0 values based upon ethylene as the reference monomer; each at 60 °C

Monomer (B)	Q_B	e_B	$\log Q_{0B}$	$13 + \log k_7/k_2^{1/2}$	Substrate
Ethylene (A) (10)	0.03	−0.43	0.00	0.57*	Ethylene (21)
Hexene-1 (3)	0.019	−0.28	−0.17	0.56	Heptene-1 (1)
Allyl acetate (3)	0.028	−1.13	−0.16	0.68	Allyl acetate (22)
Vinyl ethyl ether (3)	0.032	−1.17	−0.11	0.77	Vinyl *n*-butyl ether
Vinyl acetate (10)			−0.03†	0.80	Vinyl acetate
Vinyl acetate (3)	0.026	−0.22	−0.02	0.80	Vinyl acetate
Isobutene (3)	0.033	−0.96	−0.06	0.73	2-Methyl pentene-1 (23)
Styrene (3)	1.00	−0.80	+1.45	2.26	Styrene
Methyl methacrylate (20)	0.75	0.37	+1.55	2.51	Methyl methacrylate (23)
Butyl acrylate (10)			+1.52†	2.54	Methyl acrylate (23)
Methyl acrylate (3)	0.43	0.61	+1.35	2.54	Methyl acrylate (23)
2,3-Dimethyl butadiene-1,3 (3)	5.86	−1.81	+2.03	2.66	2,3-Dimethyl butadiene-1,3 (13)
Methacrylonitrile (3)	0.81	+1.12	+1.72	2.73	Methacrylonitrile (14)
Acrylonitrile (2)	0.58	+1.11	+1.57	2.93	Acrylonitrile

*Measured by a different method (21) than that used for the other substrates (1).
†Directly measured by copolymerization with ethylene (10).

Figure 2 is a plot of $\log Q_0$ against $13 + \log k_7/k_2^{1/2}$ at 60 °C, with a straight line of unit gradient added for reference. The points cluster fairly closely about this line, with

Can. J. Chem. Downloaded from www.nrcresearchpress.com by 210.87.254.6 on 09/05/12
For personal use only.

vinyl *n*-butyl ether and acrylonitrile showing the greatest deviation; otherwise the correlation is reasonably satisfactory for a range of values of k_7 of over 100-fold. In particular there is no systematic connection between the deviation and the value of e. Some of the values of Q and e may be subject to appreciable error, and indeed those for ethylene are average values obtained from three somewhat divergent sets; it is therefore difficult to judge the reliability of the derived Q_0 values of Table II. It seems reasonable to conclude that the directly determined values of k_7 offer an alternative index of intrinsic reactivity which is no less reliable than the set of derived values of Q_0.

ACKNOWLEDGMENT

We wish to thank the University of St. Andrews for a scholarship to D. M.

REFERENCES

1. D. G. L. James and E. W. R. Steacie. Proc. Roy. Soc. London Ser. A, **244**, 297 (1958).
2. B. R. Thompson and R. H. Raines. J. Polymer Sci. **41**, 265 (1959).
3. L. J. Young. J. Polymer Sci. **54**, 411 (1961).
4. F. R. Mayo. J. Chem. Educ. **36**, 157 (1959).
5. T. W. Campbell. J. Polymer Sci. **28**, 87 (1958).
6. C. E. Schildknecht, A. O. Zoss, and C. McKinley. Ind. Eng. Chem. **39**, 180 (1947).
7. J. M. Bruce and D. W. Farren. Polymer, 4, 407 (1963).
8. C. E. Schildknecht, A. O. Zoss, and F. Grosser. Ind. Eng. Chem. **41**, 2891 (1949).
9. M. Frankel, A. Ottolenghi, M. Albeck, and A. Zilkha. J. Chem. Soc. 3858 (1959).
10. R. D. Burkhart and N. L. Zutty. J. Polymer Sci. A, **1**, 1137 (1963).
11. F. E. Brown and G. E. Ham. J. Polymer Sci. A, **2**, 3623 (1964).
12. D. G. L. James and E. W. R. Steacie. Proc. Roy. Soc. London Ser. A, **244**, 289 (1958).
13. A. C. R. Brown and D. G. L. James. Unpublished results.
14. D. G. L. James and T. Ogawa. Can. J. Chem. This issue.
15. D. G. L. James and D. MacCallum. Proc. Chem. Soc. 259 (1961).
16. P. Tarrant and E. C. Stump, Jr. J. Org. Chem. **29**, 1198 (1964).
17. R. T. Hobgood, Jr., G. S. Reddy, and J. H. Goldstein. J. Phys. Chem. **67**, 110 (1963).
18. N. L. Owen and N. Sheppard. Proc. Chem. Soc. 264 (1963); Trans. Faraday Soc. **60**, 634 (1964).
19. M. L. Brey and P. Tarrant. J. Am. Chem. Soc. **79**, 6533 (1957).
20. R. H. Wiley and B. Davis. J. Polymer Sci. **62**, S132 (1962).
21. J. A. Kerr and A. F. Trotman-Dickenson. J. Chem. Soc. 1161 (1960).
22. D. G. L. James and G. E. Troughton. J. Polymer Sci. In press.
23. D. G. L. James and S. M. Kambanis. Unpublished data.

Can. J. Chem. Downloaded from www.nrcresearchpress.com by 210.87.254.6 on 09/05/12
For personal use only.

Can. J. Chem. Downloaded from www.nrcresearchpress.com by 210.87.254.5 on 09/05/12
For personal use only.

REACTIONS OF THE ETHYL RADICAL

V. ADDITION TO THE MONOMETHYL ACRYLONITRILES

D. G. L. James and Takeshi Ogawa[1]

Department of Chemistry, University of British Columbia, Vancouver, British Columbia

Received October 19, 1964

ABSTRACT

The Arrhenius parameters have been measured for the addition of the ethyl radical to methacrylonitrile and to the *cis* and *trans* isomers of crotononitrile. The energy of activation for each of these derivatives is significantly greater than for acrylonitrile. There is no significant variation among the values of the energy of activation for the monomethyl acrylonitriles, so that the introduction of a methyl group into the acrylonitrile molecule appears to raise the energy of activation by an amount which is insensitive to the position of the group. The pre-exponential factor is significantly smaller for each of the crotononitrile isomers than for methacrylonitrile; the partial shielding of the β-carbon atom of crotononitrile is thus expressed by a steric factor rather than by an energy term. The *cis–trans* isomerization of crotononitrile is photosensitized by diethyl ketone illuminated by 3 130 Å radiation in both the liquid and gaseous phases; a mechanism of triplet state energy transfer is proposed for the process.

INTRODUCTION

In Part IV of this series we have considered the effect of the substituent group upon the reactivity of a vinyl monomer CH_2=CHX towards the addition of the ethyl radical (1). A wide range of reactivity was discovered; thus acrylonitrile proved to be 80 times as reactive as vinyl acetate at 100 °C. The energy of activation varied greatly among the monomers, and this variation determined the differences in reactivity almost exclusively. No significant variation was found among the values of the pre-exponential factors, suggesting uniformity of steric conditions at the site of radical attack.

In this paper we consider the effect upon the reactivity of the molecule CH_2=CHX of the introduction of a second substituent group. We have chosen to examine this phenomenon with the three monomethyl derivatives of acrylonitrile. Acrylonitrile owes its low energy of activation to the influence of the electrophilic nitrile group upon the reactivity of the vinyl group. In the monomethyl acrylonitriles the electrostatic influence of the nitrile group is partially offset by the electron-donating capacity of the methyl group, and the corresponding change in the reactivity of the vinyl group towards addition should be observable as an increase in the energy of activation. Moreover, the steric factor for the addition reaction should be different for the geminal and vicinal patterns of substitution of methacrylonitrile and the crotononitriles respectively, and the effect should be observable as a difference in the pre-exponential factors. Finally, the easy separation of crotononitrile into *cis* and *trans* forms offers the possibility of finding a difference of reactivity between the isomers and of detecting the photosensitization of isomerization by diethyl ketone.

EXPERIMENTAL PROCEDURE

Ethyl radicals were formed in the presence of monomer molecules by the illumination of a gaseous mixture of diethyl ketone and the monomer with 3 130 Å radiation. The apparatus and general method have been described previously (2). The diethyl ketone and the monomers were purified by passage through the 2 m "Ucon polar" column of the Beckman Megachrom preparative gas chromatograph at 110 °C. Crotononitrile

[1]*Present address: Department of Chemistry, Birkbeck College (University of London), Malet Street, London W.C.1. England.*

Can. J. Chem. Downloaded from www.nrcresearchpress.com by 210.87.254.5 on 09/05/12
For personal use only.

was separated quantitatively into *cis* and *trans* isomers in this way. The isomers were identified by their nuclear magnetic resonance spectra (3).

Acrylonitrile and methacrylonitrile are very reactive towards the ethyl radical, and it was therefore necessary to use a low initial concentration for these reactants, and to correct for consumption during each experiment. With these precautions the calculated rate constants were insensitive to variation of composition or intensity, and no polymer was formed. The analysis followed the initial pattern of separation into CO, ($C_2H_4 + C_2H_6$), and C_4H_{10} fractions, each of which was estimated by the gas burette. The fractions were examined on a Perkin–Elmer Model 154 C gas chromatograph using helium as a carrier gas and a 2 m column J at 80 °C. No impurities were found in the fractions and the composition of each C_2 fraction was determined from the peak areas, using an appropriate sensitivity factor (2).

The products of the gas-phase reaction were also analyzed to determine whether the geometrical isomerization of the crotononitriles was photosensitized by diethyl ketone under the action of 3 130 Å radiation. After photolysis and removal of the CO, C_2, and C_4 fractions, the residue was condensed and analyzed on the Perkin–Elmer Model 154 C gas chromatograph, using the 2 m column R.

The photosensitized isomerization of the crotononitriles in the liquid phase was examined by illuminating a deaerated liquid mixture of diethyl ketone and the *cis* or the *trans* isomer with 3 130 Å radiation at constant intensity for different periods at 85 °C. A small sample of the product was analyzed using the 4 m column R. Control experiments were performed on the thermal isomerization of deaerated samples of the pure isomers at 85, 190, and 260 °C; these indicated that no correction for a thermal reaction was necessary in the evaluation of the photosensitized isomerization at 85 °C.

THE KINETIC ANALYSIS

The mechanism proposed for the photolysis of a gaseous mixture of diethyl ketone and a monomethyl acrylonitrile by 3 130 Å radiation under the specified conditions is given below for the case of methacrylonitrile; the crotononitriles will show analogous reactions.

[1] $$CH_3CH_2COCH_2CH_3 + h\nu \rightarrow 2CH_3CH_2\cdot + CO$$

[2] $$2CH_3CH_2\cdot \rightarrow C_4H_{10}$$

[3] $$2CH_3CH_2\cdot \rightarrow C_2H_6 + C_2H_4$$

[4] $$CH_3CH_2\cdot + CH_3CH_2COCH_2CH_3 \rightarrow CH_3CH_3 + CH_3\dot{C}HCOCH_2CH_3$$

[5] $$CH_3CH_2\cdot + CH_3\dot{C}HCOCH_2CH_3 \rightarrow CH_3CH(CH_2CH_3)COCH_2CH_3$$

[6] $$CH_3CH_2\cdot + CH_2{=}C(CN)CH_3 \rightarrow CH_3CH_3 + CH_2{=}C(CN)CH_2\cdot$$

[6a] $$CH_3CH_2\cdot + CH_2{=}C(CN)CH_2\cdot \rightarrow CH_2{=}C(CN)CH_2CH_2CH_3$$

[7] $$CH_3CH_2\cdot + CH_2{=}C(CN)CH_3 \rightarrow CH_3CH_2CH_2\dot{C}(CN)CH_3$$

[7a] $$CH_3CH_2\cdot + CH_3CH_2CH_2\dot{C}(CN)CH_3 \rightarrow CH_3CH_2CH_2C(CH_2CH_3)(CN)CH_3$$

The rate constants for metathesis (k_6) and addition (k_7) between the ethyl radical and the monomer molecule may be calculated from the equations:

[I] $$\frac{k_6}{k_2^{1/2}} = \left(\frac{R(C_2H_6) - R(C_2H_4)}{R(C_4H_{10})^{1/2}}\right)\frac{1}{[B]} - \frac{[D]}{[B]}\frac{k_4}{k_2^{1/2}}$$

[II] $$\frac{k_7}{k_2^{1/2}} = \frac{R(CO) - R(C_2H_6) - R(C_4H_{10})}{[B]R(C_4H_{10})^{1/2}} = \frac{(1 - M)R(CO)}{[B]R(C_4H_{10})^{1/2}},$$

where [D] and [B] represent respectively the concentration of diethyl ketone and the monomer in molecules/cm^3; R(Z) is the rate of formation of the product Z in molecules/cm^3 s; $k_4/k_2^{1/2}$ has been previously determined (4); and $M = [R(C_2H_6) + R(C_4H_{10})]/R(CO)$.

The addition of the ethyl radical to the carbon–carbon triple bond of heptyne-1 proceeds at an easily measurable rate (5). To complete this study we have attempted to detect the addition of the ethyl radical to the carbon–nitrogen triple bond of acetonitrile. Experiments were performed between 90 and 203 °C at relatively low ethyl radical

concentrations, but yielded no evidence for the addition reaction. The values of M fluctuated unsystematically about unity between limits of 0.95 and 1.03, which are unusually widely spaced for this type of study. Accordingly the lower limit of 0.95 was adopted as the critical value of M at which addition would become perceptible. For each experiment $M = 0.95$ corresponds to a certain value of $10^{13}k_7/k_2^{1/2}$; this is taken as the maximum value that $10^{13}k_7/k_2^{1/2}$ may attain under the conditions of that experiment without addition becoming perceptible. In this way we can show that

$$k_7(\text{acetonitrile})/k_7(\text{heptyne-1}) < 0.05 \text{ at } 108°, \text{ and } < 0.04 \text{ at } 142°; \text{ also that}$$

$$k_7(\text{acetonitrile})/k_7(\text{acrylonitrile}) < 0.0003 \text{ at } 108° \text{ and } < 0.0004 \text{ at } 142°.$$

Clearly the nitrile group has a low reactivity towards the addition of the ethyl radical, and is unlikely to contribute appreciably to the reactivity of acrylonitrile or its methyl derivatives in this respect.

The low reactivity of the hydrogen atoms of acetonitrile towards metathesis may be inferred from the same series of experiments. Values of $10^{13}k_6/k_2^{1/2}$ calculated from these results were small in magnitude even in comparison with those for *n*-heptane (5), and variable in sign, indicating a very small rate constant for abstraction. An upper limit for $k_6/k_2^{1/2}$ was obtained from the results of each experiment by assuming that metathesis would be just perceptible if

$$\frac{k_6}{k_2^{1/2}} = \frac{1}{10}\frac{[\text{D}]}{[\text{B}]}\frac{k_4}{k_2^{1/2}}.$$

This assumption was tested by comparing the calculated and limiting values for $k_6/k_2^{1/2}$ for each experiment; with one exception the calculated value was considerably smaller. By this method we can show that

$$k_6(\text{acetonitrile})/k_6(\text{heptyne-1}) < 0.03 \text{ at } 108° \text{ and } < 0.02 \text{ at } 142°; \text{ whereas}$$

$$k_6(\text{acetonitrile})/k_6(n\text{-heptane}) < 0.23 \text{ at } 108° \text{ and } < 0.15 \text{ at } 142°.$$

Clearly the nitrile group does not share with the ethynyl group the property of activating the hydrogen atoms of an adjacent methylene group. Wijnen found that metathesis between the $CD_3\cdot$ radical and acetonitrile was also slow, but still measurable (6), probably by virtue of the greater reactivity of the $CD_3\cdot$ radical. The metathetical reaction [6] does not occur rapidly enough to be measured for any of the unsaturated nitriles by the method of this investigation.

RESULTS AND DISCUSSION

The Arrhenius plots for the addition of the ethyl radical to the unsaturated nitriles are given in Figs. 1 and 2. The two vinyl compounds are compared in Fig. 1; as the reactivities of acrylonitrile and methacrylonitrile are similar one set of results has been uniformly displaced 0.2 units with respect to the other, as shown by the vertical scales. The results for acrylonitrile were obtained in two independent investigations; the open circles represent the results of this study, whereas black circles denote those of James and MacCallum (1). All the results for acrylonitrile were treated as a single set for the statistical analysis. Figure 2 shows the results for the *cis* and *trans* isomers of crotononitrile; the points for the reactive monomer vinyl acetate were added for comparison (7).

Statistical analysis of these data yields the values listed in Table I. Similar data for octene-1 (8) and 2-methyl pentene-1 (9) have been included to assist the interpretation.

Can. J. Chem. Downloaded from www.nrcresearchpress.com by 210.87.254.5 on 09/05/12
For personal use only.

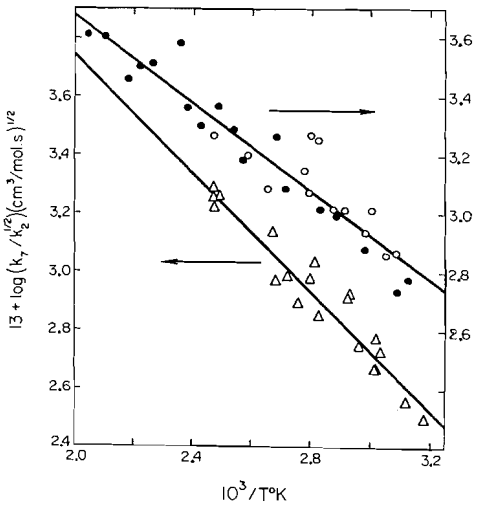

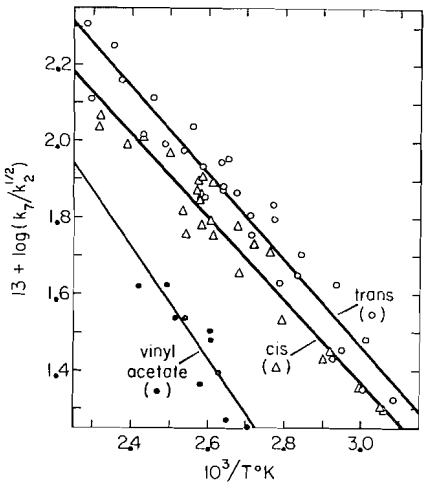

FIG. 1. Addition of the ethyl radical to vinyl compounds. Circles, acrylonitrile; $E_7 - \frac{1}{2}E_2 = 3.4 \pm 0.4$ kcal/mole; triangles, methacrylonitrile; $E_7 - \frac{1}{2}E_2 = 4.6 \pm 0.7$ kcal/mole.

FIG. 2. Addition of the ethyl radical to the crotononitrile isomers; the values of $E_7 - \frac{1}{2}E_2$ are *cis*, 5.0 ± 0.5; *trans*, 5.2 ± 0.6 kcal/mole.

All the values of Table I are based consistently upon the direct analysis of the C_2 fraction of each experiment, rather than upon an indirect estimate as used previously (5). The Arrhenius parameters for octene-1 are therefore revised values, and differ from the original parameters; this deviation will be discussed in Part VI of this series (8).

Acrylonitrile is reduced at the dropping mercury electrode, whereas the 1-alkenes are not reduced. The nitrile group activates the double bond towards reduction by its capacity to withdraw electron density, but in the crotonitrile isomers this tendency is partially offset by the capacity of the substituent methyl groups to increase the electron density at the double bond. These ideas are confirmed by the polarographic half-wave potentials measured for 1.0 mM solutions of these nitriles in acetonitrile containing 0.1 M tetrabutyl ammonium iodide (8). The half-wave potentials were -1.67, -1.94, and -1.95 V for acrylonitrile, *cis*-crotononitrile, and *trans*-crotononitrile, respectively, relative to the mercury pool at 25 °C. The influence of the methyl group as an electron density donor is clearly significant, and we shall suggest below that it has a significant influence upon the comparative reactivity of the nitriles towards the addition of the ethyl radical.

THE ARRHENIUS PARAMETERS AND REACTIVITY

The monomethyl acrylonitriles are distinguished as a class from acrylonitrile by the values of the energy of activation, $E_7 - \frac{1}{2}E_2$. The substitution of a methyl group for one of the hydrogen atoms of acrylonitrile increases the energy of activation for the addition reaction by an amount which is significant for each of the monomethyl acrylonitriles. There is no significant variation among the values of $E_7 - \frac{1}{2}E_2$ for the three monomethyl acrylonitriles, so that the introduction of the methyl group appears to raise the energy of activation by an amount which is independent of its position. The values of $E_7 - \frac{1}{2}E_2$ for the monomethyl acrylonitriles are still low in comparison with the value for octene-1; it is clear that the activation of the double bond by the nitrile group remains the dominant factor, whereas the deactivating effect of the methyl group is significant, uniform but

Can. J. Chem. Downloaded from www.nrcresearchpress.com by 210.87.254.5 on 09/05/12
For personal use only.

Can. J. Chem. Downloaded from www.nrcresearchpress.com by 210.87.254.5 on 09/05/12
For personal use only.

TABLE I

Addition of the ethyl radical to the monomethyl acrylonitriles and related species

Monomer	Number of expts.		C	B	$13 + \log A_7/A_2^{1/2}$	$E_7 - \frac{1}{2}E_2$ (kcal/mole)	$13 + \log k_7/k_2^{1/2}$ (at 100 °C)	$10^{13}k_7/k_2^{1/2}$ (at 100 °C)
Acrylonitrile	31	0.127±0.014	5.162	0.743	5.2±0.3	3.4±0.4	3.17±0.17	1 480
Methacrylonitrile	20	0.138±0.016	5.756	1.008	5.8±0.4	4.6±0.7	3.05±0.14	1 130
cis-Crotononitrile	26	0.126±0.012	4.623	1.084	4.6±0.3	5.0±0.5	1.72±0.12	52
trans-Crotononitrile	29	0.128±0.021	4.867	1.135	4.9±0.3	5.2±0.6	1.83±0.15	67
Octene-1	11	0.137±0.010	5.485	1.664	5.5±0.1	7.6±0.2	1.02±0.03	11
2-Methyl pentene-1	13	0.133±0.008	5.541	1.605	5.5±0.2	7.3±0.3	1.24±0.03	17

The constants B and C are the coefficients of the straight lines $13 + \log (k_7/k_2^{1/2}) = C - 10^3B/T$ fitted to the experimental results. The rate constants are expressed in units of cm^3/molecule s; the limits of error are calculated at the 5% probability level.

Can. J. Chem. Downloaded from www.nrcresearchpress.com by 210.87.254.5 on 09/05/12
For personal use only.

minor. The degree of activation conferred upon the double bond by the substituent alkyl and nitrile groups when present singly may be inferred from the values of $E_7 - \frac{1}{2}E_2$: ethylene, 8.6 kcal/mole (10); octene-1, 7.6 kcal/mole; and acrylonitrile, 3.4 kcal/mole. A single alkyl group activates the double bond by increasing the stability of the adduct radical by hyperconjugation, and two geminal alkyl groups cooperate to give a still greater reactivity, as in 2-methyl pentene-1. A single nitrile group activates the double bond by increasing the stability of the adduct radical by conjugation, and two geminal nitrile groups cooperate so effectively that methylene malononitrile polymerizes spontaneously. However, a comparison of the values of $E_7 - \frac{1}{2}E_2$ for styrene (4.1 kcal/mole (1)), methacrylonitrile (4.6 kcal/mole), and acrylonitrile (3.4 kcal/mole) indicates that the reactivity conferred upon the double bond of acrylonitrile by the highly electrophilic nitrile group may be due in part to a favorable polar effect. Polar effects are normally negligible in the addition reactions of the ethyl radical (1), but its ionization potential of 8.78 V is probably not high enough to prevent an appreciable contribution from ionic forms to the stability of the transition state in such a favorable case as acrylonitrile (7). The adverse polar effect introduced by the methyl group of methacrylonitrile appears from the value of the energy of activation to be much greater than the favorable effect of hyperconjugation. The β-carbon atom of the double bond is the preferred site for addition for each of the monomethyl acrylonitriles. Hyperconjugation should favor this addition for methacrylonitrile, but have no effect in the case of the crotononitrile isomers. The lack of any significant variation among the values of the energy of activation for these three nitriles indicates that hyperconjugation does not make a significant contribution to their reactivity.

The monomethyl acrylonitriles may form a single set in respect to the energy of activation, but they are split into two distinct sets when the pre-exponential factor is considered: the crotononitriles and methacrylonitrile, with vicinal and geminal patterns of substitution respectively. Table I shows that the values of $13 + \log A_7/A_2^{1/2}$ for methacrylonitrile are significantly higher than those for each of the crotononitriles, whereas the values for the *cis* and *trans* isomers are indistinguishable from each other. Such results may be interpreted in terms of steric effects at the carbon atom in the β-position with respect to the nitrile group, which is the most probable site for addition. This carbon atom is relatively unobstructed in methacrylonitrile, but it is partially shielded by the methyl group in crotononitrile, and to a similar degree in each of its isomers. A parallel difference in steric factors appears to govern the reactivity of 2-methyl pentene-1 and *trans*-octene-4 towards the ethyl radical; addition to the geminal compound 2-methyl pentene-1 is easily measured (9), but addition to the vicinal compound *trans*-octene-4 proceeds too slowly to be detected (5). The whole pattern of reactivity shown by acrylonitrile and its monomethyl derivatives is paralleled by the methyl esters of acrylic acid and its monomethyl derivatives (9).

COPOLYMERIZATION PARAMETERS AND REACTIVITY

One purpose of this investigation was to detect any difference between the reactivities of the *cis* and *trans* isomers of crotononitrile towards the addition of free radicals. It would appear from Fig. 2 that the *trans* isomer is the more reactive towards the addition of the ethyl radical. However statistical analysis reveals no significant differences for the two isomers between the respective values for the energy of activation, pre-exponential factor, or rate constant at 100 °C, as is clear from Table I. On the other hand, Fig. 2 reveals that the crotononitriles are much more reactive towards the addition of the ethyl

radical than the well-known monomer vinyl acetate (5). This suggested that the crotononitrile isomers (B) might copolymerize with styrene (A) under free radical conditions, offering an opportunity to detect a difference in reactivity from the values of the reactivity ratio r_A. Preliminary results show that the copolymerization is governed by the penultimate unit effect, and that the reactivity ratios to be compared are: $r_{AA}(trans) = 20$ and $r_{AA}(cis) = 18$; these values suggest that the *cis* isomer is the more reactive in homogeneous radical copolymerization (11).

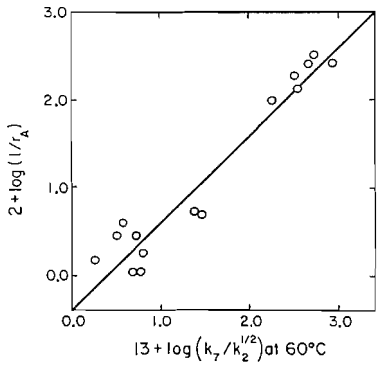

FIG. 3. Correlation of the rate constants for the addition of the polystyrene radical and the ethyl radical to various monomers at 60 °C. A line of unit gradient has been drawn for reference.

The rate constants for the addition of the ethyl radical to a series of monomers in the gas phase at 60 °C have been compared with the corresponding rate constants for the addition of the polystyrene radical in solution in Fig. 3; a line of unit slope has been drawn for reference. The wide range of values makes a plot of log $(1/r_A)$ against log $(k_7/k_2^{1/2})$ necessary; r_A is the reactivity ratio for the copolymerization of styrene (A) with a monomer (B) either identical with, or closely allied to, the substrate of the ethyl radical addition. The values used in the correlation are listed in Table II. The scatter of the points from the reference line is small, and not systematically related to the *e* value of the monomer. We conclude that there is reasonably good linear correlation between the rate constants for the addition of the ethyl radical in the gas phase and of the polystyrene radical in solution. A similar degree of correlation has been found between the rate constants for the addition of the ethyl radical in the gas phase and of the methyl radical in solution (8).

THE PHOTOSENSITIZED *cis–trans* ISOMERIZATION OF CROTONONITRILE

Photosensitization of the *cis–trans* isomerization of crotononitrile is observed when diethyl ketone is added to one of the isomers and the mixture is illuminated with 3 130 Å radiation. The isomerization occurs in both liquid and gaseous systems. No isomerization occurs in the absence of either diethyl ketone or the sensitizing radiation at the temperatures of this study, although thermal isomerization occurs at much higher temperatures (17).

The liquid phase experiments were conducted at 85 °C and constant intensity upon a deaerated binary mixture of diethyl ketone and one of the pure isomers of crotononitrile at an initial molar ratio of 1:1.3. The results are shown in Fig. 4, and indicate that the concentration c of the chosen isomer at time t is related to its initial value c_0 by the equation:

$$\ln ((2c/c_0) - 1) = -k^*t, \qquad [III]$$

where the constant k^* has the same value for both the *cis* and the *trans* isomer.

Can. J. Chem. Downloaded from www.nrcresearchpress.com by 210.87.254.5 on 09/05/12
For personal use only.

TABLE II

Correlation of the rate constants for the addition of the polystyrene radical and the ethyl radical to various monomers at 60 °C; A = styrene

Monomer (B)	$2 + \log (1/r_A)$	$13 + \log (k_7/k_2^{1/2})$	Substrate
Hexyne-1 (12)	0.18	0.25	Heptyne-1 (5)
Hexene-1 (12)	0.46	0.49	Octene-1 (8)
Ethylene (13)	0.60	0.57	Ethylene (10)
Allyl acetate (12)	0.05	0.68	Allyl acetate (16)
Isobutene (12)	0.46	0.72	2-Methyl pentene-1 (9)
Vinyl ethyl ether (12)	0.05	0.77	Vinyl *n*-butyl ether (1)
Vinyl acetate (12)	0.26	0.80	Vinyl acetate (7)
cis-Crotononitrile (11)	0.74	1.37	*cis*-Crotononitrile
trans-Crotononitrile (11)	0.70	1.46	*trans*-Crotononitrile
Styrene (12)	2.00	2.26	Styrene (7)
Methyl methacrylate (14)	2.28	2.51	Methyl methacrylate (9)
Methyl acrylate (12)	2.13	2.54	Methyl acrylate (9)
2,3-Dimethyl Butadiene-1,3 (12)	2.42	2.66	2,3-Dimethyl Butadiene-1,3 (8)
Methacrylonitrile (12)	2.52	2.73	Methacrylonitrile
Acrylonitrile (15)	2.43	2.97	Acrylonitrile (1)

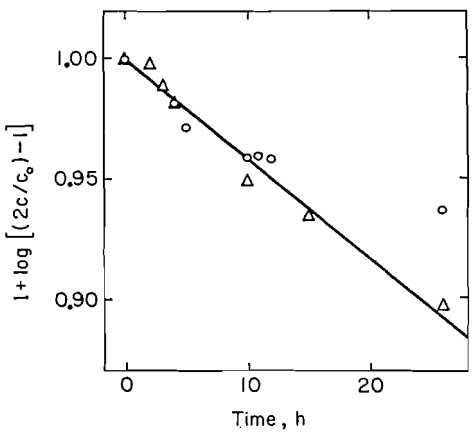

FIG. 4. Photosensitized isomerization of crotononitrile by diethyl ketone in the liquid phase with 3 130 Å radiation: triangles, the *cis* isomer; circles, the *trans* isomer.

Illumination of a gaseous mixture of diethyl ketone and one of the isomers of crotononitrile by 3 130 Å radiation also causes a slow isomerization to occur in addition to the normal range of reactions [1] to [7*a*]. The rate of isomerization is approximately equal to the rate of the addition reaction [7].

We propose that the photosensitized isomerization of crotononitrile proceeds by the transfer of triplet state energy from an excited molecule of diethyl ketone to a molecule of either isomer of crotononitrile. Molecules of crotononitrile in the triplet state will undergo rapid geometrical isomerization before deactivation stabilizes them in the *cis* or *trans* form. The literature of photosensitization provides comparable examples of systems where *cis–trans* isomerization proceeds through promotion to the triplet state, and where the triplet state of diethyl ketone is the effective donor in a photosensitization process.

The *cis–trans* isomerization of butene-2 in the gas phase can be effected with a variety of photosensitizers, including mercury atoms (18, 19) and benzene and pyridine molecules (18, 20, 21, 22). The essential step in the mechanism of photosensitization is the transfer

Can. J. Chem. Downloaded from www.nrcresearchpress.com by 210.87.254.5 on 09/05/12
For personal use only.

of triplet state energy from the excited sensitizer to the olefin molecule. This transfer of energy occurs at almost every collision between the donor and acceptor species. The molecules of the olefin in the triplet state may undergo repeated geometrical isomerization by internal rotation before their configuration is stabilized by deactivation to the ground state (22).

Diethyl ketone has been shown to photosensitize the conversion of *cis*-piperylene to the *trans* form in solution (23). The capacity of excited molecules of diethyl ketone to act as donors in a triplet–triplet energy interchange in the gas phase has been established in a study of the fluorescence of biacetyl photosensitized by diethyl ketone illuminated by 3 130 Å radiation (24).

The mechanism proposed for the *cis–trans* isomerization of crotononitrile (B) photosensitized by diethyl ketone (D) is given in outline below; a molecule in the triplet state is distinguished by an asterisk.

$$D^* + B(cis) \rightarrow D + B^* \qquad (k_c)$$
$$D^* + B(trans) \rightarrow D + B^* \qquad (k_t).$$

Configurations of the triplet state are not distinguished as many cycles of internal rotation are expected during the lifetime of B*. Deactivation of the triplet state regenerates the isomers:

$$B^* \rightarrow B(cis) \qquad (k_c')$$
$$B^* \rightarrow B(trans) \qquad (k_t').$$

At constant intensity of illumination [D*] may be taken as constant. The kinetics are particularly simple if $k_c = k_t = k$ and $k_c' = k_t'$; these assumptions are paralleled in the kinetic analysis of the *cis–trans* isomerization of butene-2 photosensitized by benzene and pyridine (22). The rate equation then becomes

$$\ln ((2c/c_0) - 1) = -k[D^*]t, \qquad [IV]$$

which is identical with eq. [III] if $k^* = k[D^*]$. The experimental results of Fig. 4 are therefore consistent with the simple form of the mechanism given above.

An alternative mechanism for the photosensitized isomerization of crotononitrile would exist if the addition of the ethyl radical to the crotononitrile molecule were reversible. Certainly the *cis–trans* isomerization of butene-2 can be sensitized by the reversible addition of iodine atoms (25, 26) or of thiyl radicals (27) and the *cis-trans* isomerization of crotononitrile can be sensitized by the reversible addition of bromine atoms (28). The kinetic study of the *cis–trans* isomerization of methyl crotonate photosensitized by diethyl ketone under 3 130 Å illumination yields evidence that the reversible addition mechanism becomes predominant above 200 °C (9). However, over the temperature range of the present study (51 to 165 °C) the methyl crotonate system appears to isomerize by the triplet state energy transfer mechanism. The kinetic behavior of both the methyl crotonate and the crotononitrile systems is very similar in this temperature range; indeed for none of the four substrates does the value of $E_7 - \frac{1}{2}E_2$ deviate significantly from 4.7 kcal/mole, or the value of $13 + \log A_7/A_2^{1/2}$ from 4.6. We should therefore expect the crotononitrile system to resemble the methyl crotonate system in isomerizing by the triplet energy transfer mechanism in the temperature range of this study, but possibly by the reversible addition mechanism at much higher temperatures.

ACKNOWLEDGMENTS

We wish to thank the National Research Council of Canada for the financial support of this work.

Can. J. Chem. Downloaded from www.nrcresearchpress.com by 210.87.254.5 on 09/05/12
For personal use only.

Can. J. Chem. Downloaded from www.nrcresearchpress.com by 210.87.254.5 on 09/05/12
For personal use only.

REFERENCES

1. D. G. L. James and D. MacCallum. Can. J. Chem. This issue.
2. A. C. R. Brown and D. G. L. James. Can. J. Chem. **40**, 796 (1962).
3. G. S. Reddy, J. H. Goldstein, and L. Mandell. J. Am. Chem. Soc. **83**, 1300 (1961).
4. D. G. L. James and E. W. R. Steacie. Proc. Roy. Soc. London Ser. A, **244**, 289 (1958).
5. D. G. L. James and E. W. R. Steacie. Proc. Roy. Soc. London Ser. A, **244**, 297 (1958).
6. M. H. J. Wijnen. J. Chem. Phys. **22**, 1074 (1954).
7. D. G. L. James and D. MacCallum. Proc. Chem. Soc. 259 (1961).
8. A. C. R. Brown and D. G. L. James. Unpublished results.
9. D. G. L. James and S. M. Kambanis. Unpublished results.
10. J. A. Kerr and A. F. Trotman-Dickenson. J. Chem. Soc. 1161 (1960).
11. D. G. L. James and T. Ogawa. J. Polymer Sci. B, **2**, 991 (1964).
12. L. J. Young. J. Polymer Sci. **54**, 411 (1961).
13. R. D. Burkhart and N. L. Zutty. J. Polymer Sci. A, **1**, 1137 (1963).
14. R. H. Wiley and B. Davis. J. Polymer Sci. **62**, S132 (1962).
15. B. R. Thompson and R. H. Raines. J. Polymer Sci. **41**, 265 (1959).
16. D. G. L. James and G. E. Troughton. J. Polymer Sci. In press.
17. J. N. Butler and R. D. McAlpine. Can. J. Chem. **41**, 2487 (1963).
18. R. B. Cundall and T. F. Palmer. Trans. Faraday Soc. **56**, 1211 (1960).
19. R. J. Cvetanovic, H. E. Gunning, and E. W. R. Steacie. J. Chem. Phys. **31**, 573 (1959).
20. S. Sato, K. Kikuchi, and M. Tanaka. J. Chem. Phys. **39**, 239 (1963).
21. R. B. Cundall, F. J. Fletcher, and D. G. Milne. J. Chem. Phys. **39**, 3536 (1963).
22. R. B. Cundall, F. J. Fletcher, and D. G. Milne. Trans. Faraday Soc. **60**, 1146 (1964).
23. G. S. Hammond, N. J. Turro, and P. A. Leermakers. J. Phys. Chem. **66**, 1144 (1962).
24. D. S. Weir. J. Am. Chem. Soc. **83**, 2629 (1961).
25. M. H. Back and R. J. Cvetanovic. Can. J. Chem. **41**, 1396 (1963).
26. S. W. Benson and A. N. Bose. J. Am. Chem. Soc. **85**, 1385 (1963).
27. C. Walling and W. Helmreich. **81**, 1144 (1959).
28. J. W. Crump. J. Org. Chem. **28**, 953 (1963).

Can. J. Chem. Downloaded from www.nrcresearchpress.com by 210.87.254.105 on 09/05/12
For personal use only.

ENTHALPIES OF INTRAMOLECULAR HALOGEN–HYDROXYL INTERACTIONS

A. W. BAKER AND A. T. SHULGIN
Dow Chemical Company, Walnut Creek, California
Received August 28, 1964

ABSTRACT

Enthalpies of halogen–hydroxyl interactions have been evaluated for the 2-halophenols in carbon tetrachloride. These values, in −kcal/mole, corrected for the temperature dependence of absorptivity coefficients, are Cl = 1.44, Br = 1.21, and I = 1.08. From enthalpy differences measured in unsymmetrical 2,6-dihalophenols, it is shown that the interaction in 2-fluorophenol lies between those in 2-bromophenol and 2-iodophenol, thus reaffirming the order Cl > Br > F > I.

The nature of halogen–hydroxy interactions is still open to conjecture despite intensive investigations (1–21) during the past several years. The investigations have been pursued by the use of several different techniques and have encompassed both intra- and intermolecular interactions of various phenols and alcohols. However, despite this attention, many aspects of the interactions are inadequately understood. For example, there has been no general agreement as to accepted values of these energies of interaction, nor has the relative order of energies within the halogen series been unambiguously determined.

For both 2-haloethanols and 2-halophenols, it is generally agreed that in "inert" solvents, 1, the difference ($\Delta\nu_{OH}$) between the frequencies of the free and bonded O—H configurations increases in the order F < Cl < Br < I, and 2, the proportion of the compound existing in the free (or *trans*) form increases in the same order. In addition, for the 2-halophenols, it is accepted that the O—H group is constrained to two coplanar positions by resonance interaction with the aromatic π-system and that it spends negligible time in residence between them. On the other hand, there is disagreement over the following points concerning these interactions. 1. Can these interactions be considered to be hydrogen bonds in the usual sense? 2. If we consider that these interactions embrace all contributions, such as from orbital basicity, atomic diameter, polarizability, and dipole moment, which halogen admits of the largest energy of interaction? 3. What is the relative order within the halogen series of the energies of interaction? 4. Does the Badger–Bauer rule (3), which states that the enthalpy of interaction (ΔH) is proportional to $\Delta\nu_{OH}$, apply to this interaction in which the O—H $\cdots$ X is highly bent away from the preferred rectilinear orientation?

Disagreement on question 1 stems from the fact that half-band widths and absorptivities of the O—H bands of 2-halophenols are only slightly larger than those of phenol- and alkyl-substituted phenols. In analogy with intermolecular hydrogen bonding, it would have been expected that both should show marked increases (9, 22). Explanations for this unexpected behavior have been offered previously (13, 15) and shall be the subject of subsequent discussions. However, this paper will deal only with the remaining three questions by the critical evaluation of enthalpies of these interactions, specifically, in the 2-halophenols in the single solvent, carbon tetrachloride.

Since 2-fluorophenol and 2-fluoroethanol each exhibit but a single O—H band, the enthalpy of interaction cannot be evaluated directly by these spectroscopic techniques. These bands are grossly unsymmetric, indicating that the two components occur so close

Can. J. Chem. Downloaded from www.nrcresearchpress.com by 210.87.254.105 on 09/05/12
For personal use only.

together that they contribute to a single band envelope. It has been observed previously (13), however, that unsymmetrical 2,4,6-trihalophenols exhibit two bands, each displaying a frequency characteristically assignable to the appropriate ortho-halide, regardless of the combination specifically represented. In the three possible unsymmetric 2-fluoro-6-halophenols (with or without a 4-halogen substituent), the O—H · · · · F band has the higher frequency in each case and is much broader than any of those involving the other halogens. Enthalpy differences can be measured accurately, thus allowing the relative strengths of the interactions to be determined. These data, combined with the measured enthalpies for 2-chloro-, 2-bromo-, and 2-iodo-phenol, determine the enthalpy of the fluorine–hydroxyl interaction to within perhaps a tenth of a kcal per mole. Obviously, the solvent is participating in these interactions and the *cis* and *trans* forms might be solvated or stabilized by different amounts. Therefore, enthalpies determined for one solvent system need not necessarily apply to a second, nor need the relative order established in one solvent system be the same as in a second. This is a moot question and will be investigated later in detail.

EXPERIMENTAL

The enthalpy calculations in this study required that the experimental data be obtained from compounds of high purity. If an ortho-halophenol displaying a *cis* to *trans* absorbance ratio[1] of 40 were contaminated by as little as 2½% of non-ortho-halogenated phenol (which would absorb at approximately the same frequency as the *trans*-isomer) the apparent ratio would be halved. Consequently, an undetermined but relatively large error would be embodied in any calculation involving that ratio. The same problem exists in the corresponding unsymmetrical dihalophenols but to a smaller degree since the absorbance ratios are more nearly unity. To meet the demands of purity, frequent use was made of gas–liquid chromatography (g.l.c.) in the course of synthesis, isolation, and purification of all compounds.

The separations were performed on a Wilkins Aerograph A-700 Autoprep, using helium as a carrier gas. Three 5 ft, 3/8 in. diameter columns were necessary: Apiezon L (7% on 50–60 mesh Anakrom), ethylene glycol succinate (5% on 60–80 mesh acid-washed Chromosorb W), and 20 *M* Carbowax (10% on the Chromosorb support). These columns are abbreviated in the following discussion as A-L, EGS, and 20 *M*, respectively.

The four monohalophenols were obtained from commercial sources. 2-Fluoro-(Aldrich Chemical Company), 2-chloro-, and 2-iodo-phenols (Eastman Kodak) were purified by preparative separation on the 20 *M* column. Analyses by reinjection verified the absence of both free phenol and the para-isomer. 2-Bromophenol (Dow Chemical Company) required the Apiezon L column. A small phenolic contaminant, although well separated at 112 °C and 300 ml/min gas flow (phenol at 2.3 min, 2-bromophenol at 5.0 min, and air at 0.5 min) was still present in the purified sample. The residual impurity (0.05%) was undoubtedly due to unsuspected tailing either from the column or from the collection technique. A second pass reduced this to an acceptable level. For the other monohalophenols, a single separation achieved adequate purity.

None of the unsymmetrical 2,6-dihalophenols have heretofore been described in the literature. They were synthesized by the halogenation of an appropriate, purified monohalo compound, and separated from the congeneric para- and di-substitution products as described in Table I. The corresponding trihalophenols also investigated have been described earlier (13). (See below.)

The solvent employed in these studies, carbon tetrachloride, was dried by suspended P_2O_5, and filtered directly into the sample cell in which the desired phenol had previously been captured from the Autoprep. This technique was employed when weighed samples were not required, as it effectively precluded the absorption of water. It has been observed here, as previously (23), that when small amounts of liquid phenols are weighed for dissolution, water pickup appears severe despite the employment of an acceptably dry solvent and an inert atmosphere. It must be concluded that the initial absorption of water by certain phenols, when dry, is extremely rapid.

The spectra were recorded directly in absorbance on a Beckman IR-7 prism-grating spectrophotometer at an effective resolution of 1.8 cm^{-1}. The absorbance potentiometer was calibrated by a set of linearity discs over the optical density (o.d.) range of 0.05 to 0.91, and found, after a zero adjustment, to be linear to within ±0.005 o.d. units. The temperature runs were obtained in 1 cm cells at phenol concentrations of approximately 5×10^{-3} *M*. The temperature of both sample and reference cells was controlled and measured by thermistors. The read-out thermistor was in contact with the solution inside the cell; we believe the temperature to be accurate to within 0.1 °C, described previously (23).

[1]*The cis and trans names apply to the two coplanar conformers in which the hydroxyl group is directed toward, and away from, respectively, the halide.*

TABLE I

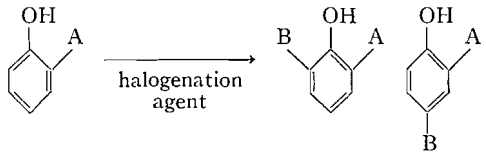

I II III

A, B	Agent	Ratio III/II	Column†	Time of emergence, min I	II	III	Melting point of II
F, Cl	$Cl_2(CCl_4)$	1.4	20 *M* (180°)	2.2	4.4	6.4	63–64°
F, Br	$Br_2(CCl_4)$	26	EGS (110°)	2.3	9.0	12.8	47–48°
F, I	ICl(HOAc)	11	20 *M* (180°)	2.2	12.9	18.6	Oil
Cl, Br	$Br_2(CCl_4)$	14	20 *M* (175°)	3.0	10.2	13.4	55–56°
I, Cl	$Cl_2(CCl_4)$‡	3.3	EGS (140°)	2.6	5.2	6.9	38–39°
I, Br	$Br_2(CCl_4)$	4.9	EGS (155°)	2.3	7.2	10.8	60–61°

*Determined by planimetry of the appropriate chromatographic scan.
†All were adjusted to a carrier gas flow of about 300 ml/min at the oven temperatures indicated.
‡In the chlorination of *o*-iodophenol, there was generation of free iodine. The 5.2 min peak proved, however, to be the desired chloroiodo isomer and its homogeneity was established by rechromatography on the 20 *M* column (emergence at 17.2 min, 180° 300 cc He/min of the injected sample; it was observed as a single peak of unchanged infrared spectrum).

TABLE II

ν_{OH} frequencies and half-band widths, cm^{-1}

	ν_{OH} 1	ν_{OH} 2	$\frac{1}{2}\Delta\nu_{OH}$ 1	$\frac{1}{2}\Delta\nu_{OH}$ 2
2-Fluorophenol		3 591.0	—	22.0
2-Chlorophenol	3 603.2	3 547.1	~23	18.4
2-Bromophenol	3 602.7	3 527.8	~23	18.5
2-Iodophenol	3 600.0	3 505.1	19.0	20.0
2-Fluoro-6-chlorophenol	3 580.5	3 543.8	28.4	20.5
2-Fluoro-6-bromophenol	3 578.6	3 524.9	28.5	20.0
2-Fluoro-6-iodophenol	3 578.7	3 501.9	32.0	25.1
2-Chloro-6-bromophenol	3 535.1	3 521.6	—	—
2-Chloro-6-iodophenol	3 532.9	3 494.8	19.1	—
2-Bromo-6-iodophenol	3 513.4	~3 490	—	—

The ν_{OH} band referred to as 1 is the band due to the O—H group oriented *trans* or, for the dihalophenols, toward the 2-position substituent. The half-band widths lined out could not be determined accurately because of inadequate band separation.

The spectra were obtained at temperatures ranging from 25 to 75 °C; in order to assure the necessary accuracy, a minimum of three repeat runs at the temperature extremes and two at intermediate points were taken. Band areas were measured repeatedly with a rolling disc planimeter until it was felt that the areas of these somewhat arbitrarily divided bands had been established to within 0.3%. The spectral data are given in Table II.

DISCUSSION

The energy of intramolecular halogen–hydroxyl interactions has always been considered to be less than that of intermolecular hydrogen bonds. Early attempts to evaluate this energy employed qualitative arguments (24), based either on measured free energies (2) and estimated entropies (25) or on relative peak heights of competitive halogens (13). The former arguments indicated that the bond strengths increased parallel to the increase in frequency shift in going from fluorine to iodine. This established the order I > Br > Cl > F. In contrast, the latter arguments (13), employing peak heights, indicated

Can. J. Chem. Downloaded from www.nrcresearchpress.com by 210.87.254.105 on 09/05/12
For personal use only.

that the order was Cl > Br > F > I. The early direct measurements of enthalpies of halophenols in the vapor state (6, 26) tended to support the latter order although the quantitative results were questioned (26) because of impure samples. More recent quantitative work is in general agreement that iodine forms the weakest bond of any halogen, but there is yet uncertainty concerning the strengths of interactions to the remaining halogens. Regarding intermolecular effects, there is now apparent agreement that the order of decreasing strength is F > Cl > Br > I. All of these data are summarized in Table III.

TABLE III

Literature enthalpies of halogen–hydroxyl interaction

Molecular environment	Compound	Technique	Halide F	Cl	Br	I	Ref.
Vapor state	2-Chlorophenol	Infrared		3.9			6
	2-Iodophenol	Infrared				3.2	26
Intramolecular, liquid	2-Halophenols	Infrared		1.27	1.86	1.00	27
	2-Halophenols	Nuclear magnetic resonance		2.3	2.0	1.5	28
	2-Haloethanols	Infrared	2.1	1.2	1.2	0.8	17
Intermolecular, liquid	Phenol vs. aliphatic halides	Infrared	3.1	2.2	2.0	1.7	20
	Phenol vs. cyclohexyl halides	Infrared	2.6	2.4	1.8	2.0	19

Other techniques have also been used but, unfortunately, have added further disagreement over the relative order of the halogens. The nuclear magnetic resonance (n.m.r.) values quoted in Table III are larger than those obtained from infrared, but nonetheless, maintain the order most generally accepted for the three heavier halogens, namely, Cl > Br > I. However, no interaction at all involving fluorine could be detected and it was assumed to be zero. This assumption was modified in a subsequent paper wherein the authors inferred that there was indeed interaction, but weaker than that involving iodine. Qualitative arguments employing dipole moment measurements of these phenols have led to conflicting assignments for fluorine. One report (29) attributes to fluorine the strongest interaction of any halogen; another (14) places it between bromine and iodine as suggested in the work below. Finally a qualitative infrared investigation of competitive hydrogen bonding (16) concluded that fluorine does indeed enter into an interaction in 2-fluorophenol but that its energy of interaction is the smallest of any halogen.

Enthalpies of 2-Halophenols

The enthalpies reported in this study have been obtained from area measurements of the two competitive hydroxyl bands displayed by each halophenol. These bands are shown in Fig. 1 for the 2-halophenols and in Fig. 2 for the unsymmetrical 2,6-dihalophenols. Enthalpy values derived in this way are based upon the assumption that the ratio of the band absorptivity coefficients is temperature independent. This assumption is inherent in all of the infrared data quoted above. We have examined this premise in a previous publication (30) and have found that corrections amounting to several percent of the measured enthalpies must be applied to obtain more accurate values.

Can. J. Chem. Downloaded from www.nrcresearchpress.com by 210.87.254.105 on 09/05/12
For personal use only.

Can. J. Chem. Downloaded from www.nrcresearchpress.com by 210.87.254.105 on 09/05/12
For personal use only.

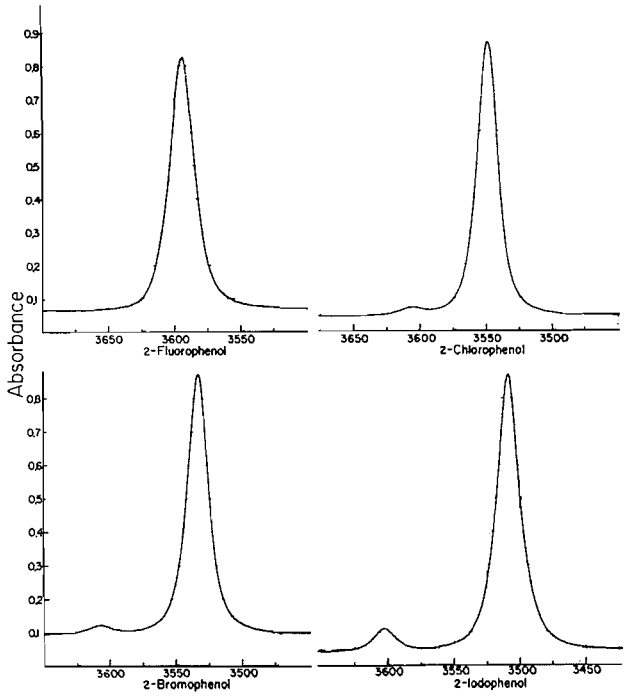

FIG. 1. ν_{OH} bands of the 2-halophenols. Solvent CCl_4.

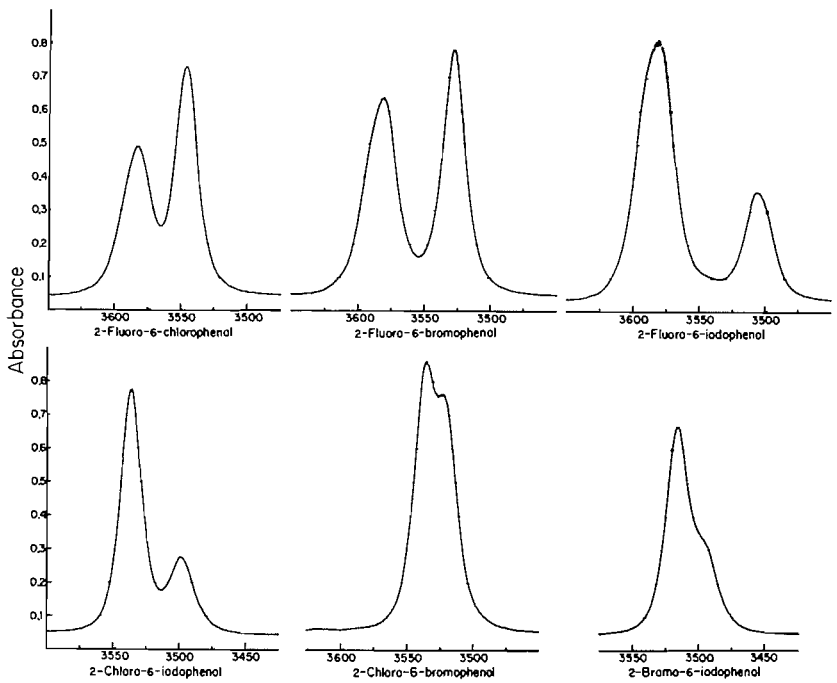

FIG. 2. ν_{OH} bands of the unsymmetrical 2,6-dihalophenols. Solvent CCl_4.

These corrections are obtained from the absorptivities of phenol and of symmetrical 2,6-dihalophenols measured at 25 and 75 °C. For these compounds, only a single O—H band exists; the temperature dependency of phenol should parallel that of the *trans*-component of the 2-halophenols and the temperature dependency of the dihalophenols that of the *cis*-component. This assumption appears to be reasonable and it is consistent with the behavior of the other band parameters such as the temperature shifts of frequencies and of half-band widths. The temperature corrections were calculated by the relationship

$$\Delta H_c = -4.571 \frac{\partial \log \frac{\alpha_1}{\alpha_2}}{\partial 1/T},$$

where α_1 and α_2 are the absorptivity coefficients of the two bands in each compound. As shown previously (30), this can be put into the form

$$\Delta H_c = -4.571 \left[\frac{\log \frac{\alpha_1^{25}}{\alpha_1^{75}} - \log \frac{\alpha_2^{25}}{\alpha_2^{75}}}{0.483 \times 10^{-3}} \right] \text{cal/mole}$$

for temperature limits of 25 and 75 °C. The ratios, α^{25}/α^{75} for phenol, dichloro-, dibromo-, and diiodo-phenols were found (30) to be 1.075, 1.056, 1.055, and 1.053, respectively. The value of this ratio for the fluoro group, measured here from 2,6-difluorophenol, is 1.066. Since the enthalpy for *o*-fluorophenol must be derived indirectly, this ratio can be utilized only in obtaining corrections for the enthalpy differences in the mixed fluoro–halophenols. The corrections for the other 2-halophenols are, in kcal/mole, −0.07, Cl; −0.08, Br; and −0.09, I. The addition of these corrections to the measured enthalpies of the 2-halophenols results in an increase of absolute magnitude in each case.

TABLE IV

Enthalpy values of halophenols, kcal/mole (solutions in carbon tetrachloride)

			Area			Peak height		
			Correction	$-\Delta H$ measured	$-\Delta H$ corrected	Correction	$-\Delta H$ measured	$-\Delta H$ corrected
2-Halophenols								
F					1.19*			
Cl			0.07	1.37	1.44	0.39	1.24	1.63
Br			0.08	1.13	1.21	0.52	1.10	1.62
I			0.09	0.99	1.08	0.50	0.94	1.44
Polyhalophenols†								
(2)	(4)	(6)						
F	H	Cl	0.04(+)	0.14	0.18	0.24	0.03	0.27
F	H	Br‡	0.04(+)	0.06	0.10	0.36	−0.03	0.33
F	H	I	0.05(−)	0.41	0.36	0.35	0.58	0.93
Cl	H	Br		§		0.12	0.06	0.18
Cl	H	I	0.01(−)	0.56	0.55	0.11	0.66	0.77
Br	H	I		§		0.00	0.33	0.33
F	Br	Br‡	0.04(+)	0.04	0.08	0.36	0.14	0.50
F	I	I	0.05(−)	0.38	0.33	0.35	0.70	1.05
Cl	Cl	I	0.01(−)	0.57	0.56	0.11	0.61	0.72

*Derived value, not directly measurable.
†Favored halide is underlined.
‡Bromo group favored by area, fluoro by peak height.
§Not measurable with accuracy.

Can. J. Chem. Downloaded from www.nrcresearchpress.com by 210.87.254.105 on 09/05/12
For personal use only.

Can. J. Chem. Downloaded from www.nrcresearchpress.com by 210.87.254.105 on 09/05/12
For personal use only.

A summary of these corrections, together with the measured and corrected enthalpies, is given in Table IV. Also listed are the corresponding values for the unsymmetrical di- and tri-halophenols. Results obtained by the use of optical densities are included for comparison. It can be seen that these values are much less consistent than those from band areas and that the corrections are so large as to have little meaning. This behavior indicates that temperature dependencies of optical densities cannot be transferred from one molecular system to another and that enthalpies based upon peak heights are not as reliable as those from band areas. Therefore, only the latter values will be considered in the following discussion. The enthalpies and ranking of the 2-halophenols that admit of direct measurement are, from Table IV, Cl (1.44) > Br (1.21) > I (1.08). A value can now be obtained for 2-fluorophenol by considering the following data from the mixed dihalophenols.

Unsymmetrical Di- and Tri-halophenols

All of the 2-halophenols except 2-fluorophenol have two well-resolved bands, thereby permitting enthalpies to be determined directly. However, due to the occurrence of only a single band in 2-fluorophenol, the enthalpy of interaction must be evaluated indirectly, i.e., by use of the unsymmetrical 2-fluoro-6-halophenols. The two bands in each of these three compounds are resolved adequately to permit the determination of relative band areas.

The bands were separated into the respective areas by arbitrary graphical techniques. Fortunately, as shown previously (31), the calculated enthalpy is virtually insensitive to the way the bands are separated (within reasonable limits) as long as any assumptions are applied consistently throughout a temperature run. Results corresponding to those discussed above for 2-halophenols are also listed in Table IV. Since the absorptivity temperature ratios are in the order F > Cl > Br > I, the pairing of the halogens acts to increase the enthalpy correction of the heavier with respect to the lighter. In the case of F ↔ Cl and F ↔ Br, the numerical value of the observed enthalpy difference is increased in each case because the interaction energy is larger for the heavier two halogens. However, in the remaining four comparisons (F ↔ I, Cl ↔ Br, Cl ↔ I, and Br ↔ I), the reverse occurs because the lighter atom dominates the interaction.

These relationships are diagrammed for clarity in Fig. 3 and are shown for both area and optical density measurements. The arrows point to the halogen forming the stronger

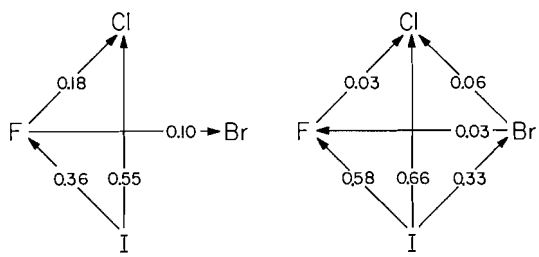

FIG. 3. Enthalpy differences, in kcal/mole, of the halogen–hydroxyl interaction as determined (A) from corrected area measurements, and (B) from uncorrected optical density values. Arrow points in direction of stronger association. Compounds examined

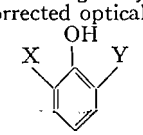

X, Y = F, Cl, B, I; X ≠ Y.

interaction (with the O—H group), and the enthalpy differences in kcal/mole are recorded on each arrow. The values missing from the diagram, for 2-bromo-6-iodophenol and for 2-bromo-6-chlorophenol, were not obtained due to inadequate band separation. This prevented accurate assignment of areas to the appropriate bands.

For the area diagram (Fig. 3) there is remarkable good internal agreement in the ΔH difference between chlorine and iodine by the two different routes. The direct value is 0.55 kcal/mole, and the value obtained by adding I → F and F → Cl is 0.54 kcal/mole. For the trihalophenols, the corresponding direct value is 0.56 kcal/mole. The two-step value is not available since the F → Cl compound was not run; however, the I → F value is 0.33 kcal/mole compared to 0.36 kcal/mole found for the dihalophenol. Due to the internal consistency of these results and to the reproducibility of the values obtained in duplicate runs, we believe the accuracy of these data to be better than ±0.05 kcal/mole.

Direct comparisons of energies obtained from the mixed dihalophenols give the following order for the decreasing enthalpy of the halogen–hydroxyl interaction: Cl > Br > F > I. Fluorine is definitely placed to the right of bromine by area measurements, although by only a small amount. It is placed to the left of bromine by use of peak height calculations, but not when the corrections are added. Such values that are obtained through the employment of peak heights become yet less reliable as the band separations become very small. Under these conditions, the temperature dependence of each band is diluted by the temperature dependence of the other, and as $\Delta\nu$ approaches zero, the enthalpy measured by peak heights will also approach zero. This effect is observed in the optical density diagram for the compounds 2-bromo-6-iodophenol and 2-bromo-6-chlorophenol, the two specific compounds not amenable to area measurement. The band separations are approximately 17 cm^{-1} and 14 cm^{-1}, respectively; in the former case, the band shows only an inflection point but no double maximum. The sum I → Br and Br → Cl is 0.39 kcal/mole, only two-thirds of the well-resolved I → Cl value of 0.66 kcal/mole.

From the excellent agreement in the enthalpy differences between the di- and trihalphenols, one must conclude that the presence of the additional halogen in the 4-position has no effect on these values. However, as correctly pointed out by the referee, there could conceivably be an appreciable difference in solvent effects for the 2-halo- and 2,6-dihalo-phenols. In the former compounds, the *trans*-conformer affords greater opportunity for solvent interaction, whereas in the latter compounds, the hydroxyl group in either conformer should be shielded from the solvent by approximately equal amounts. This could result in an internal inconsistency in transferring data between the mono- and di-substituted phenols. For this reason, the direct comparison of the interaction to fluorine and to bromine in 2-bromo-6-fluorophenol is given first preference. Thus, since this comparison shows that the ΔH to bromine is unequivocally larger than to fluorine, the enthalpy value for the fluorine–hydroxyl interaction is taken as 1.19 kcal/mole, slightly lower than that of O—H · · · Br.

Analogous Interactions in the 2-Haloethanols

Some intersting comparisons can be made between the data given here for the 2-halophenols and those recently published for the 2-haloethanols (17). Although these families are chemically dissimilar, the many spectral features they display in common strongly suggest that the actual physical interactions between the —OH and halo groups are qualitatively similar in both. Since band separations are small in these latter compounds, the use of peak heights for enthalpy evaluations was mandatory; therefore, it was necessary for the previous authors to accept the concomitant inaccuracies discussed above.

Can. J. Chem. Downloaded from www.nrcresearchpress.com by 210.87.254.105 on 09/05/12
For personal use only.

The enthalpies found (Table III) for the O—H · · · I and O—H · · · Br interactions were −0.8 and −1.2 kcal/mole, values surprisingly close to those given here for the 2-halophenols. The value for the O—H · · · Cl interaction was considered to be equal to, or slightly less than, that of the O—H · · · Br interaction. This is at variance with the increase found in the 2-halophenols and can readily be explained by the inherent decrease in measured ΔH as $\Delta\nu$ approaches zero. More disturbing is the placement of the O—H · · · F interaction as the largest of the four. This is based on the premise that the very unsymmetrical band shown by 2-fluoroethanol can be graphically resolved into two separate components and that the individual temperature dependency of each band can be determined. The procedure is, at best, questionable since many infrared bands are unsymmetric in compounds where only a single conformer can exist.

Compounds demonstrating this type of band dissymmetry are the unsymmetrical 2,6-dihalophenols. As discussed above, two ν_{OH} bands occur due to interactions with the two proximal halogens. Each band can be produced by only a single conformer; rotation around the C—O bond is restricted by at least 4 kcal/mole so that the O—H group is constrained to an in-plane residence. In the two compounds 2-fluoro-6-iodophenol and 2-fluoro-4,6-diiodophenol, the band due to the O—H · · · F interaction is grossly unsymmetric, as is readily observed for the former compound in Fig. 2. In order to assess the extent of this dissymmetry, two parameters are evaluated. These are defined as follows: the band is divided left and right by a vertical line drawn through the band maximum. The high-frequency part of the half-band width lying to the left of this line is divided by that to the right. This ratio is a measure of band dissymmetry and is unity for a symmetric band.

Values of this ratio found at 25 and 75° for the above two compounds are

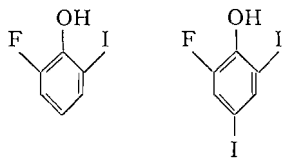

25° 1.42	1.32
75° 1.12	1.37.

In the first compound, the symmetry of the band increases with temperature. In the second, however, the dissymmetry increases in a manner similar to that observed in the single band in 2-fluoroethanol, and from which an apparent ΔH had been calculated (17). Despite this difference in temperature behavior of band shape, the ΔH's (F ↔ I) measured in the two phenols are identical. This supports the obvious conclusions that the O—H · · · F bands in these phenols consist of only one conformer and that the dissymmetry is due to other factors. Calculated ΔH values predicated upon assumed symmetry must therefore be discounted.

ACKNOWLEDGMENT

We thank Dr. Finger of Illinois State Geological Survey for a generous sample of the 2,6-difluorophenol employed in this study.

REFERENCES

1. O. R. Wulf and U. Liddel. J. Am. Chem. Soc. **57**, 1464 (1935).
2. L. Pauling. J. Am. Chem. Soc. **58**, 94 (1936).
3. R. M. Badger and S. H. Bauer. J. Chem. Phys. **5**, 839 (1937).
4. M. M. Davies. Trans. Faraday Soc. **34**, 1427 (1938).

Can. J. Chem. Downloaded from www.nrcresearchpress.com by 210.87.254.105 on 09/05/12
For personal use only.

5. M. M. DAVIES. Trans. Faraday Soc. **36**, 333 (1940).
6. L. R. ZUMWALT and R. M. BADGER. J. Am. Chem. Soc. **62**, 305 (1940).
7. R. MECKE. Z. Elektrochem. **52**, 107 (1948).
8. A. W. BAKER and A. T. SHULGIN. J. Am. Chem. Soc. **80**, 5358 (1958).
9. M. KUHN, W. LÜTTKE, and R. MECKE. Z. Anal. Chem. **170**, 106 (1959).
10. M. OKI and H. IWAMURA. Bull. Chem. Soc. Japan, **33**, 717 (1960).
11. L. W. REEVES, E. A. ALLEN, and K. O. STRØMME. Can. J. Chem. **38**, 1249 (1960).
12. A. W. PROSS and F. VAN ZEGGEREN. Spectrochim. Acta, **16**, 563 (1960).
13. A. W. BAKER and W. W. KAEDING. J. Am. Chem. Soc. **81**, 5904 (1959).
14. J. H. RICHARDS and S. WALKER. Trans. Faraday Soc. **57**, 412 (1961).
15. E. A. CUTMORE and H. E. HALLAM. Trans. Faraday Soc. **58**, 40 (1962).
16. H. BOURASSA-BATAILLE, P. SAVAGEAU, and C. SANDORFY. Can. J. Chem. **41**, 2240 (1963).
17. P. J. KRUEGER and H. D. METTEE. Can. J. Chem. **42**, 326 (1964).
18. L. J. BELLAMY and H. E. HALLAM. Trans. Faraday Soc. **55**, 220 (1959).
19. MARIE-LOUISE JOSIEN. Pure Appl. Chem. **4**, 33 (1962).
20. R. WEST, D. L. POWELL, L. S. WHATLEY, M. K. T. LEE, and P. VON SCHLEYER. J. Am. Chem. Soc. **84**, 3221 (1962).
21. C. G. CANNON. Mikrochim. Acta, 555 (1955).
22. M. ST. C. FLETT. Spectrochim. Acta, **10**, 21 (1957).
23. A. W. BAKER, H. O. KERLINGER, and A. T. SHULGIN. Spectrochim. Acta, **20**, 1477 (1964).
24. L. PAULING. The nature of the chemical bond. 2nd ed. Cornell University Press, Ithaca, N.Y. 1948. Chap. 9.
25. H. H. JAFFE. J. Am. Chem. Soc. **79**, 2373 (1957).
26. G. ROSSMY, W. LÜTTKE, and R. MECKE. J. Chem. Phys. **21**, 1606 (1953).
27. D. A. K. JONES and J. G. WATKINSON. Chem. Ind. London, 661 (1960).
28. E. A. ALLAN and L. W. REEVES. J. Phys. Chem. **66**, 613 (1962); **67**, 591 (1963).
29. W. F. ANZILLOTI and B. C. CURRAN. J. Am. Chem. Soc. **65**, 607 (1943).
30. A. W. BAKER, H. O. KERLINGER, and A. T. SHULGIN. Spectrochim. Acta, **20**, 1467 (1964).
31. A. W. BAKER and A. T. SHULGIN. Spectrochim. Acta, **19**, 1611 (1963).

Can. J. Chem. Downloaded from www.nrcresearchpress.com by 210.87.254.105 on 09/05/12
For personal use only.

Can. J. Chem. Downloaded from www.nrcresearchpress.com by 210.87.254.42 on 09/05/12
For personal use only.

THE REACTIVITY OF THE CYCLIC POLYENES TOWARDS FREE RADICALS

II. METATHESIS WITH THE ETHYL RADICAL

A. C. R. BROWN[1] AND D. G. L. JAMES

Department of Chemistry, University of British Columbia, Vancouver, British Columbia

Received August 27, 1964

ABSTRACT

Arrhenius parameters have been measured for metathesis between the ethyl radical and certain cyclic polyenes, chosen to reveal the extent to which particular structural features in a cyclic molecule may influence its reactivity towards metathesis. The highest reactivity was observed in cyclohexadiene-1,4 and is associated with the greatest increase in the delocalization of the π-electron system, which is only slightly offset by a minor change in the conformation of the carbon ring. Intermediate reactivity was displayed by the conjugated molecules cyclohexadiene-1,3 and cycloheptatriene, whereas cyclooctatetraene, which possesses no methylenic hydrogen atoms, was much less reactive. Very low reactivity was found in bicyclo[2.2.1]heptadiene-2,5; this molecule possesses the carbon ring structure of cyclohexadiene-1,4 symmetrically bridged by a methylene group, and the constraint imposed by this bridge upon the geometry of the ring appears to limit the reactivity of the molecule decisively.

The ratio of the rate constants for disproportionation and combination between the cyclohexadienyl radical and the ethyl radical is $k_d/k_c = 0.38 \pm 0.03$. The nature of the interaction between these two radicals is discussed, and the significance of this ratio is considered.

INTRODUCTION

The kinetic study of metathesis between the ethyl radical and certain hydrocarbons of simple structure was discussed in an earlier paper (1). Arrhenius parameters were measured with sufficient precision to reveal significant differences in reactivity due to bond order (*n*-heptane, heptene-1, and heptyne-1). A comparison of corresponding rate constants for cyclohexene and for *trans*-octene-4 indicated that a cyclic structure may significantly increase the reactivity per active hydrogen atom.

This study has now been extended to include cyclic polyenes of various classes chosen to investigate effects peculiar to cyclic systems. Firstly the class: cyclohexadiene-1,3, cyclohexadiene-1,4, and cyclooctadiene-1,5, chosen to reveal any cumulative enhancement of reactivity due to two double bonds present in $\Delta^{1,3}$, $\Delta^{1,4}$, or $\Delta^{1,5}$ relationship in a cyclic molecule. Secondly the class: bicyclo[2.2.1]heptadiene-2,5 and cyclohexadiene-1,4, which should show the effect of geometrical constraint imposed by a methylene bridge upon the reactivity of a cyclic $\Delta^{1,4}$ system. Finally the diverse class: cycloheptatriene, cyclooctatetraene, and benzene, which were included to study reactivity in systems characterized by multiple conjugation, an absence of methylene groups, or aromaticity.

The rates of metathesis between the polyacrylonitrile radical and certain cyclic polyenes appear to be very sensitive to the detailed structure of the latter. Metathesis with cycloheptatriene is so rapid that this substance completely inhibits the free radical polymerization of acrylonitrile, whereas under equivalent conditions cyclohexadiene-1,3 forms high copolymer with acrylonitrile (2). The factors which determine the reactivity of a molecule towards metathesis with a radical have been discussed in recent review articles (3–8). Polar effects are potentially important in metathesis between the electrophilic polyacrylonitrile radical and the cyclic polyenes, but the wide variation in electrical nature of these polyenes (2) renders the corresponding rate constants an uncertain measure of their

[1]*Present address: Petrochemical and Polymer Laboratory, Imperial Chemical Industries Ltd., Runcorn, Cheshire, England.*

intrinsic reactivity. Polar effects are seldom large in the reactions of the ethyl radical, and so the results of this study should give a better measure of the intrinsic reactivity of the cyclic polyenes. The cyclohexadienyl radical is generated by metathesis between the ethyl radical and either of the cyclohexadienes, and so the interaction of the cyclohexadienyl and ethyl radicals can be conveniently studied. The particular interest of this system arises from the formation of benzene as a product of one of the disproportionation reactions, and therefore allows us to see to what extent the peculiar stability of this product may influence the ratio of disproportionation to combination.

EXPERIMENTAL PROCEDURE

The apparatus and general method were described in two earlier papers (1, 9). The techniques of purification of reactants and analysis of products were later improved by the use of the Beckman Megachrom preparative gas chromatograph and the Perkin–Elmer Vapour Fractometer model 154C respectively (10), and the application of gas chromatography has been extended in this study. The reagents were of the purest grade commonly obtainable commercially. Each was further purified by the preparative chromatograph and the purity of the selected fraction was then examined by the analytical chromatograph. The only evidence of residual impurities was found for cyclooctatetraene (0.2% styrene) and for the cyclohexadienes (0.1% benzene). Such a concentration of styrene in cyclooctatetraene would have a negligible effect upon the observed rates of addition or metathesis with the ethyl radical (11), but benzene is an important product of the interaction of the ethyl radical with the cyclohexadienes, and a small correction of the apparent rate of formation of benzene was necessary.

The analysis followed the pattern of separation and measurement of CO, C_2, and C_4 fractions, supplemented by analysis by gas chromatography (10). The CO fraction was pure and free from traces of hydrogen and methane. The C_2 fraction consisted entirely of C_2H_4 and C_2H_6, except for systems containing cyclooctatetraene, when C_2H_2 was also present. Each component of the C_2 fraction of every run was estimated, following the calibration of the instrument by standard mixtures. The C_4 fraction was pure butane.

Special Procedure for Cyclohexadiene-1,4

The photolysis of diethyl ketone in the presence of cyclohexadiene-1,4 gave benzene and a less volatile hydrocarbon, both in significant quantity. No cyclohexadiene-1,3 was found among the products of this system. After the removal of the CO, C_2, and C_4 fractions the residue was normally analyzed for benzene on the Perkin–Elmer 6-ft column R at 50 °C in a stream of helium. If a column temperature of 100° was used, and the benzene, cyclohexadiene-1,4, and diethyl ketone were allowed to pass through, then two further peaks were observed. One of these peaks was also found when the products of the photolysis of pure diethyl ketone were examined, but the other was observed only when cyclohexadiene-1,4 was also present in the reacting system. The substance of the latter peak was accumulated in a series of experiments, separated by the chromatograph, and trapped by passing the effluent gas at the appropriate time through a hypodermic needle into 5 ml of 100% ethanol. The ultraviolet absorption spectrum of the resulting solution was obtained with the Cary model 11 spectrophotometer. The spectrum was very closely similar to that of cyclohexadiene-1,3 but of course could not be this substance. We shall suggest in the discussion that the cyclohexadienyl radical is generated in this system, and that the absorption band is due to 1-ethylcyclohexadiene-2,4 from the combination of cyclohexadienyl and ethyl radicals. This combination should also form 1-ethylcyclohexadiene-2,5, but the column failed to separate the isomers. Benzene is also formed during the photolysis of diethyl ketone in the presence of cyclohexadiene-1,3, but cyclohexadiene-1,4 was not found among the products. The failure of each cyclohexadiene to isomerize to the other under the reaction conditions indicates that mutual interaction of cyclohexadienyl radicals is negligible in these systems.

THE KINETICS OF METATHESIS WITH THE ETHYL RADICAL

Under the experimental conditions of this investigation, the photolysis of diethyl ketone conforms to the simple mechanism (12–15):

[1] $$CH_3CH_2COCH_2CH_3 + h\nu \rightarrow 2CH_3CH_2\cdot + CO,$$

[2] $$2CH_3CH_2\cdot \rightarrow C_4H_{10},$$

[3] $$2CH_3CH_2\cdot \rightarrow C_2H_6 + C_2H_4,$$

[4] $$CH_3CH_2\cdot + CH_3CH_2COCH_2CH_3 \rightarrow CH_3CH_3 + CH_3\dot{C}HCOCH_2CH_3,$$

[5] $$CH_3CH_2\cdot + CH_3\dot{C}HCOCH_2CH_3 \rightarrow CH_3CH(CH_2CH_3)COCH_2CH_3.$$

Can. J. Chem. Downloaded from www.nrcresearchpress.com by 210.87.254.42 on 09/05/12
For personal use only.

One molecule of carbon monoxide is equivalent to two ethyl radicals and hence to one molecule of either ethane or butane. If reactions [1–5] account for all the products, then

$$[I] \qquad M = [R(C_2H_6) + R(C_4H_{10})]/R(CO) = 1,$$

where $R(X)$ is the rate of formation of the product X in units molecules/cm^3 s. A new series of photolyses of pure gaseous diethyl ketone gave the result:

$$M = 1.005 \pm 0.005;$$

the values of $k_4/k_2^{1/2}$ calculated from the equation:

$$[II] \qquad k_4/k_2^{1/2} = [R(C_2H_6) - R(C_2H_4)]/[D]R(C_4H_{10})^{1/2},$$

where [D] is the concentration of diethyl ketone in molecules/cm^3, support the previous result (1):

$$k_4/k_2^{1/2} = 10^{(-7.5\pm0.1)} \exp(-7\,800 \pm 200)/RT \text{ (cm}^3\text{/molecule s)}^{1/2}.$$

These experiments also gave the result:

$$k_3/k_2 = R(C_2H_4)/R(C_4H_{10}) = 0.123 \pm 0.008$$

which, although somewhat lower than the previous value of 0.136 (1), is supported by the values obtained from the photolyses of diethyl ketone in the presence of cyclic polyenes (Table I).

The ethyl radicals formed by the photolysis of diethyl ketone may be expected to abstract hydrogen atoms from any hydrocarbon species present in the reacting system. Representing the cyclic polyene by RH_2, the initial metathetical reaction forms ethane:

$$[6] \qquad CH_3CH_2\cdot + RH_2 \rightarrow CH_3CH_3 + RH\cdot.$$

Mutual interaction of RH· radicals can be neglected in this study, as the light intensity was always high enough to ensure that the ethyl radical was present at a much higher concentration than the RH· radical. The RH· radical is therefore removed by interaction with the ethyl radical, and both combination and disproportionation must be considered:

$$[c] \qquad RH\cdot + \cdot CH_2CH_3 \rightarrow RHCH_2CH_3,$$

$$[d] \qquad \rightarrow R + CH_3CH_3,$$

$$[e] \qquad \rightarrow RH_2 + CH_2{:}CH_2.$$

The kinetics are particularly simple if we can neglect the disproportionation reactions [*d*] and [*e*], and if addition of the ethyl radical to the double bond of the polyene RH_2 is also negligible. Then the quantities k_3/k_2 and M should have the same values in the presence of the polyene as they have for the photolysis of pure diethyl ketone. This agreement is observed when RH_2 is cyclooctadiene-1,5. In this study the photolysis of pure diethyl ketone vapor was characterized by the values: $k_3/k_2 = 0.123 \pm 0.008$ and $M = 1.005 \pm 0.005$; when cyclooctadiene-1,5 vapor was also present the values were: $k_3/k_2 = 0.122 \pm 0.007$ and $M = 0.997 \pm 0.012$. Significant participation of reaction [*d*] would yield an excess of ethane and raise the value of M above unity; whereas reaction [*e*] would yield an excess of ethylene and raise the value of $R(C_2H_4)/R(C_4H_{10})$, which is assumed to measure k_3/k_2. Clearly both reaction [*d*] and reaction [*e*] can be neglected in the case of cyclooctadiene-1,5. Reaction [*d*] would yield the conjugated product cyclooctatriene-1,3,5, and therefore the suppression of this reaction in favor of the combination process [*c*] is perhaps rather surprising. It will be apparent later that the product R must

Can. J. Chem. Downloaded from www.nrcresearchpress.com by 210.87.254.42 on 09/05/12
For personal use only.

possess a very high delocalization energy in order that reaction [*d*] may compete significantly with reaction [*c*]; indeed in this investigation the only examples of such competition occurred with the cyclohexadienes, which yielded benzene by the sequence of reactions [6] and [*d*]. We can dismiss the possibility that the value of M for the cyclooctadiene-1,5 system is due to a fortuitous cancelling of opposed effects due to simultaneous participation of reaction [*d*] and addition of the ethyl radical to the double bond; this would cause M to vary with the temperature and the relative concentration of the reactants, and such variation is not observed. Moreover the reactivity of an isolated double bond in a cyclic hydrocarbon towards addition of the ethyl radical has been shown to be very low in the case of cyclohexene (9). We have assumed that reaction [*d*] may also be neglected both for cycloheptatriene and for cyclooctatetraene. In each case the nature of the product R renders the significant participation of reaction [*d*] far less probable than in the case of cyclooctadiene-1,5. The diagnostic use of the value of M is invalidated by the addition of the ethyl radical to both cycloheptatriene and cyclooctatetraene (9).

The ethylene-forming reaction [*e*] normally regenerates the original substrate RH_2 and can be detected only by observation of the ratio $R(C_2H_4)/R(C_4H_{10})$. The value of this ratio for pure diethyl ketone is 0.123 ± 0.008, and is not significantly altered in the presence of cyclic polyenes, as is apparent from Table I. Clearly reaction [*e*] is negligible for each of these cyclic polyenes, all the ethylene being formed by the disproportionation of ethyl radicals. We conclude that both reactions [*d*] and [*e*] can be neglected for each of the substrates, cyclooctadiene-1,5, cycloheptatriene, and cyclooctatetraene. The rate constant for reaction [6] is then given by the simple relationship (1):

$$\text{[III]} \qquad \frac{k_6}{k_2^{1/2}} = \frac{R(C_2H_6) - R(C_2H_4)}{[B]R(C_4H_{10})^{1/2}} - \frac{[D]}{[B]}\frac{k_4}{k_2^{1/2}},$$

where [D] and [B] represent the concentrations of diethyl ketone and the hydrocarbon respectively.

Benzene is formed during the illumination of a gaseous mixture of diethyl ketone with either of the cyclohexadienes, indicating the reaction sequence:

$$\text{[6]} \qquad CH_3CH_2\cdot + C_6H_8 \rightarrow CH_3CH_3 + C_6H_7\cdot,$$

$$\text{[}d\text{]} \qquad CH_3CH_2\cdot + C_6H_7\cdot \rightarrow CH_3CH_3 + C_6H_6.$$

Kinetic analysis shows that less than 30% of the cyclohexadienyl radicals react as [*d*], the remainder combining with ethyl radicals:

$$\text{[}c\text{]} \qquad CH_3CH_2\cdot + C_6H_7\cdot \rightarrow C_6H_7CH_2CH_3.$$

The adduct was detected by gas chromatography, but the column used failed to separate the adduct into the two isomers expected: 1-ethylcyclohexadiene-2,4 and 1-ethylcyclohexadiene-2,5. It was shown above that the values of $R(C_2H_4)/R(C_4H_{10})$ eliminate the significant participation of the ethylene-forming reaction:

$$\text{[}e\text{]} \qquad CH_3CH_2\cdot + C_6H_7\cdot \rightarrow CH_2{=}CH_2 + C_6H_8.$$

This was confirmed by a more sensitive test. Any cyclohexadiene formed by the disproportionation reaction [*e*] is almost certain to be a mixture of the two isomers. The same cyclohexadienyl radical is formed by abstraction of hydrogen from either cyclohexadiene-1,3 or cyclohexadiene-1,4, and it has been established (16) that the mutual disproportionation of cyclohexadienyl radicals gives cyclohexadiene-1,3 and cyclohexadiene-1,4 in the ratio of 1:2.7. Thus a reacting system that initially contained only one of the cyclohexadiene isomers would continuously form the other isomer if reaction [*e*] were appreciable,

Can. J. Chem. Downloaded from www.nrcresearchpress.com by 210.87.254.42 on 09/05/12
For personal use only.

and the detection of a trace of the second isomer in the presence of major amounts of the first is readily accomplished by gas chromatography. No such trace was found in either system, and we conclude that reaction [*e*] is negligible.

Each molecule of benzene formed in reaction [*d*] is accompanied by a molecule of ethane. Addition of the ethyl radical to either of the isolated double bonds of cyclohexadiene-1,4 is inappreciable, and so we expect, and find, that

$$M = [R(C_2H_6) + R(C_4H_{10})]/R(CO) > 1.$$

However, if ethane is formed solely by reactions [3], [4], [6], and [*d*], it follows that

$$M^* = [R(C_2H_6) + R(C_4H_{10}) - R(C_6H_6)]/R(CO) = 1, \qquad [IV]$$

and the observed value of M^* is 1.015 ± 0.021, independent of temperature, confirming the mechanism. The rate constant of reaction [6] for cyclohexadiene-1,4 is given by the appropriate modification of eq. [III]:

$$\frac{k_6}{k_2^{1/2}} = \frac{R(C_2H_6) - R(C_2H_4) - R(C_6H_6)}{[B]R(C_4H_{10})^{1/2}} - \frac{[D]}{[B]}\frac{k_4}{k_2^{1/2}}. \qquad [V]$$

The same equation may be used for cyclohexadiene-1,3, as the generation and consumption of the cyclohexadienyl radical is common to the two cyclohexadienes.

TABLE I

Abstraction of the hydrogen atom by the ethyl radical*

	No. of runs	$13 + \log A_6/A_2^{1/2}$	$E_6 - \frac{1}{2}E_2$	$R(C_2H_4)/R(C_4H_{10})$
Cyclohexadiene-1,3	17	5.0±0.3	5.4±0.5	0.120±0.010
Cycloheptatriene	8	5.3±0.3	6.5±0.5	0.119±0.005
Cyclooctatetraene	13	6.0±0.7	8.6±1.2	0.123±0.006
Cyclohexadiene-1,4	7	5.7±0.1	5.8±0.1	0.118±0.003
Cyclooctadiene-1,5	7	5.3±0.4	6.8±0.7	0.122±0.007
Cyclohexene	12	5.6±0.2	7.5±0.4	(0.122)
Octene-1	12	5.0±0.3	7.5±0.5	0.137±0.010
trans-Octene-4	9	5.9±0.6	8.7±1.0	(0.136)

*The units of A are cm^3/molecule s; the units of E are kcal/mole. The limits of error are calculated at the 5% probability level.

DISCUSSION

The results of this investigation are relevant to two aspects of chemical kinetics: the general problem of the relationship between reactivity and molecular structure, and the particular topic of the relative importance of combination and disproportionation in the reactions of the cyclohexadienyl radical. Each of these subjects will be discussed separately under an appropriate heading.

I. Structure and Reactivity

The principal aim of this section is to enquire whether the kinetic results reveal any general pattern of reactivity. The cyclic olefins fall naturally into three classes.

(1) The first class contains cyclic olefins which possess one or more reactive methylene groups. Reactivity in this class follows the order: cyclohexadiene-1,4 > cyclohexadiene-1,3 > cycloheptatriene > cyclooctadiene-1,5 > cyclohexene.

(2) The second class consists of cyclooctatetraene, which has no methylene groups, but shows moderate reactivity.

(3) In the third class are the unreactive polyenes: bicycloheptadiene and benzene.

Can. J. Chem. Downloaded from www.nrcresearchpress.com by 210.87.254.42 on 09/05/12
For personal use only.

The reactivity of a particular cyclic olefin may be strongly influenced by one or more of several factors.

(*a*) The extent of delocalization of the π-electron systems may differ in the molecule and in its derived radical, as in the sequence: cyclohexadiene-1,4 > cyclohexene > benzene.

(*b*) There may be a difference in strain energy in the molecule and its derived radical. Such strain may originate in the limitations imposed by the cyclic structure upon the conformation of the ring, and appears to govern the difference in reactivity: cyclohexadiene-1,4 $\gg$ bicyclo[2.2.1]heptadiene-2,5.

(*c*) Another factor may be the number and relative position of equivalent reactive hydrogen atoms.

Delocalization and Reactivity

The order of reactivity towards metathesis: cyclohexene < cycloheptatriene < cyclohexadiene-1,3 < cyclohexadiene-1,4, is shown by the Arrhenius plots of Figs. 1 and 2. We propose that the principal cause of this order of reactivity is that the gain in the delocalization energy attending metathesis increases in the same order. Certainly the most reactive olefin, cyclohexadiene-1,4, shows the greatest formal increase in delocalization in the change from the two isolated double bonds of the molecule to the π-electron system delocalized over five carbon atoms in the cyclohexadienyl radical. A much smaller change in delocalization attends the formation of the cyclohexenyl radical from cyclohexene, and the reactivity of cyclohexene is correspondingly low.

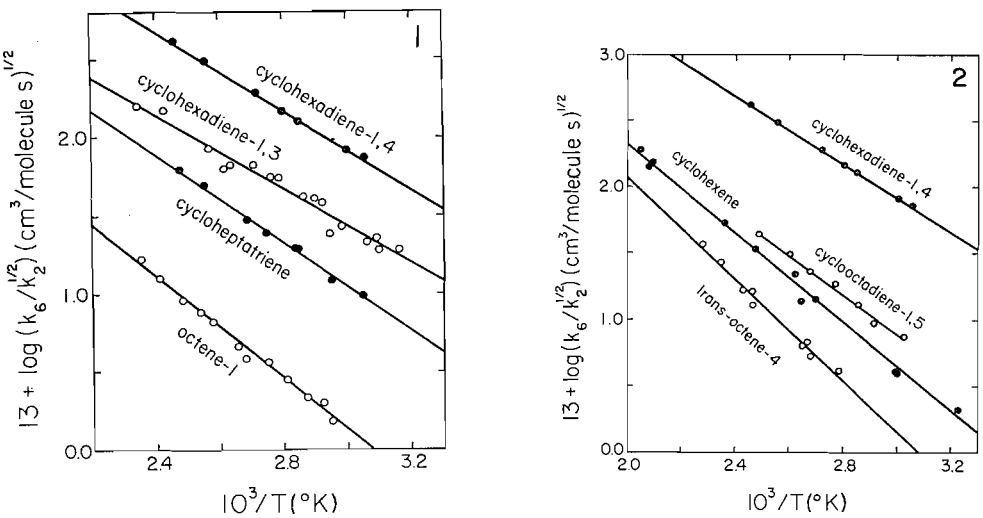

FIG. 1. Metathesis between the ethyl radical and cyclic polyenes, showing how the reactivity of the polyene may be influenced by the increase in the delocalization of the π-electron system attending metathesis. Octene-1 is included for reference.

FIG. 2. Metathesis between the ethyl radical and unconjugated cyclic olefins; *trans*-octene-4 is included for reference.

Cyclohexadiene-1,4 and cyclohexadiene-1,3 each yield the cyclohexadienyl radical as a product of metathesis, and thereby offer a special opportunity to test the proposition that the reactivity of such compounds is dominated by the increase in delocalization attending metathesis. Formally, the proposition is valid for this pair; the less reactive

Can. J. Chem. Downloaded from www.nrcresearchpress.com by 210.87.254.42 on 09/05/12
For personal use only.

Can. J. Chem. Downloaded from www.nrcresearchpress.com by 210.87.254.42 on 09/05/12
For personal use only.

polyene cyclohexadiene-1,3 suffers the smaller increase in delocalization from a four-carbon to a five-carbon system. However, this argument is inconclusive unless the change in the geometry of the carbon ring accompanying the formation of the cyclohexadienyl radical from the parent molecule is minimal, or at least equivalent, for each of the cyclohexadienes. Recent structural studies indicate that the change in geometry is indeed minimal, and are discussed below.

The electron spin resonance spectrum of the cyclohexadienyl radical shows that the six carbon atoms are coplanar and that the unpaired electron is delocalized over five carbon atoms (17). The pure rotational Raman spectrum of cyclohexadiene-1,4 vapor reveals that the molecule behaves as a very nearly symmetric top rotor; the small deviation of the carbon atoms from coplanarity is towards C_{2v} symmetry (18). The four carbon atoms of the conjugated system of cyclohexadiene-1,3 are probably coplanar; the other two carbon atoms may be expected to oscillate symmetrically through this plane in opposite phase.

We conclude that the geometry of the carbon ring of each of the cyclohexadienes departs only slightly from the planar form of the cyclohexadienyl ring, and therefore that the greater reactivity of cyclohexadiene-1,4 may properly be linked with the greater increase in the delocalization of the π-electron system attending metathesis.

Cycloheptatriene lies between cyclohexene and cyclohexadiene-1,3 in its reactivity towards metathesis. The reactivity of the hydrogen atoms of the methylene group of cycloheptatriene is associated with a change in delocalization from a slightly non-planar six-carbon system to a planar seven-carbon system. The pure rotational Raman spectrum of cycloheptatriene vapor shows that the molecule behaves as a nearly symmetric top rotor (18). The low-temperature proton magnetic resonance spectrum of cycloheptatriene in trifluorobromomethane reveals that the deviation of the ring from coplanarity is towards the boat form, and that cycloheptatriene is a mixture of two such rapidly equilibrating non-planar conformers (19). The geometry of the carbon ring of the cycloheptatriene molecule therefore departs only slightly from the planar, regular heptagonal structure of the tropyl radical. The structure of the tropyl radical has been deduced from the electron resonance spectrum of solid cycloheptatriene bombarded by electrons at -196 °C (20) and of a dilute solid solution of cycloheptatriene in a single crystal of naphthalene irradiated by X-rays at room temperature (21), and also from the ultraviolet absorption spectrum of the radical formed by the flash photolysis of ditropyl vapor at low pressure (22). The results indicate that the unpaired electron of the tropyl radical occupies a largely antibonding degenerate orbital and confers a uniform time-average spin distribution upon the radical (21). The tropyl radical therefore possesses an unusually high degree of symmetry, which may explain why cycloheptatriene is so much more reactive than cyclohexene, although metathesis extends delocalization over only one additional carbon atom in each case.

The molecule of benzene possesses a high delocalization energy associated with the six π-electron system delocalized over a planar, symmetrical six-carbon ring. A much smaller degree of delocalization is associated with the π-electron systems of either the phenyl radical (23) or the cyclohexadienyl radical (17); so that a considerable loss in delocalization energy will attend both the metathetical and the addition reactions of the ethyl radical with benzene. Benzene should therefore be much less reactive than cyclohexene towards the ethyl radical, and indeed neither metathesis nor addition could be detected for benzene in this study. The rate constant for metathesis was estimated as no more than 2% of the value for octene-1 between 100 and 120 °C, and ethyl benzene could not be

found among the products. A recent study of the interaction of toluene with the methyl radical at 60 °C is largely concerned with the reactivity of the aromatic ring (24). The products of addition of the methyl radical to the ring are easily found after reaction in the liquid phase, but cannot be detected after reaction in the gas phase. Metathesis with toluene is observed in the gas phase, and 15% of the hydrogen is abstracted from the aromatic ring. It was suggested that the transition state for interaction between the methyl group and the aromatic ring is a loose addition complex which may yield the products either of addition or of metathesis according to its environment. The reactivity of the aromatic ring towards the alkyl radicals seems to be marginal, and the reactivity of the methyl radical may well be only just sufficient to form the loose addition complex at a kinetically appreciable concentration in the gas phase; it is perhaps not surprising that the rather less reactive ethyl radical fails to perturb the stable aromatic system appreciably in the gas phase.

Ring Conformation and Reactivity

The high reactivity of cyclohexadiene-1,4 towards metathesis is associated with the $\Delta^{1,4}$ double bond distribution of its six-membered carbon ring. Bicyclo[2.2.1]heptadiene-2,5 possesses a similar structural unit in its molecule, but it is so unreactive towards metathesis that no reaction could be detected in our systems. The reactivities of cyclohexadiene-1,4 and bicycloheptadiene may be compared as follows. An estimate can be made, for each experiment performed, of the maximum value (U) that the abstraction rate constant could have while remaining undetectable. It was assumed that the rate of abstraction should be detectable if:

$$[VI] \qquad \frac{k_6}{k_2^{1/2}} > \frac{1}{10}\frac{[D]}{[B]}\frac{k_4}{k_2^{1/2}} = U.$$

Each value of U was compared with the value (A) of $k_6/k_2^{1/2}$ for cyclohexadiene-1,4 at the same temperature, obtained from the observed results by interpolation. Table II shows that the ratio U/A may be as low as 0.003.

TABLE II

Comparison of the reactivity of bicycloheptadiene (C_7H_8) and cyclohexadiene-1,4 (C_6H_8) towards metathesis with the ethyl radical*

Temp. (°K)	U (C_7H_8)	A (C_6H_8)	U/A
323	0.20	63	0.0031
336	0.35	90	0.0039
341	0.61	102	0.0060
360	1.10	160	0.0069
366	1.39	183	0.0076
382	4.53	255	0.018
398	5.72	347	0.016
404	8.02	388	0.021

*The variables U and A represent respectively an estimated upper limit and an actual value of $k_6/k_2^{1/2}$ for the species named, in units $(cm^3/molecule\ s)^{1/2}$.

The low reactivity of bicycloheptadiene may be ascribed to restrictions imposed by the methylene bridge upon the geometry of the $C_7H_7^{\cdot}$ radical formed by the removal of a hydrogen atom from one of the bridgehead carbon atoms. Firstly, the six-carbon ring cannot become planar as in the cyclohexadienyl radical, and so the associated gain in delocalization is no longer available to facilitate metathesis. Secondly, the carbon atom

Can. J. Chem. Downloaded from www.nrcresearchpress.com by 210.87.254.42 on 09/05/12
For personal use only.

with the free valence cannot easily even approach coplanarity with the three other carbon atoms to which it is bonded, and therefore the bridgehead carbon–hydrogen bond should be much stronger than the normal tertiary carbon–hydrogen bond. Nuclear magnetic resonance studies have shown that this bridgehead bond has a much higher degree of s-character than is found in a normal sp^3 bond (25). All other hydrogen atoms of the bicycloheptadiene molecule are likely to show low reactivity towards metathesis, but the double bonds are reactive towards the addition of free radicals in general, and the ethyl radical in particular. The same series of experiments yielded both a satisfactory Arrhenius plot for the addition of the ethyl radical (26), and the evidence that bicycloheptadiene is unreactive towards metathesis, thereby affirming the validity of this evidence.

Cyclooctadiene-1,5 was chosen as a cyclic polyene likely to conform closely to the ideal of a strainless system of non-interacting double bonds which are unreactive towards the addition of the ethyl radical. The last assumption is confirmed by the value $M = 0.997 \pm 0.012$, and the values of M and $R(C_2H_4)/R(C_4H_{10})$ indicate that reactions [6] and [*c*] are the only significant reactions of the cyclooctadiene-1,5 system. Figure 2 shows the Arrhenius plots for abstraction of a hydrogen atom from cyclooctadiene-1,5 and certain structurally related molecules. These were chosen as likely to reveal, by comparison with cyclooctadiene-1,5, any effects upon the reactivity of the molecule which might be endued by:

(*a*) an unstrained ring structure (*trans*-octene-4),
(*b*) a strained ring structure (cyclohexene),
(*c*) cumulative interaction of double bonds in a $\Delta^{1,4}$ system (cyclohexadiene-1,4).

Results for abstraction of a hydrogen atom from *trans*-octene-4 and from cyclohexene have been published previously (1), and were calculated from the equation:

$$[\text{VII}] \qquad \frac{k_6}{k_2^{1/2}} = \left(\frac{R(C_2H_6) + R(C_2H_4)}{R(C_4H_{10})} - \frac{2k_3}{k_2}\right)\frac{R(C_4H_{10})^{1/2}}{[B]} - \frac{[D]}{[B]}\frac{k_4}{k_2^{1/2}},$$

using $k_3/k_2 = 0.136$ throughout. In the present study we have reinvestigated the reactions of the ethyl radical with octene-1, and have obtained a value of k_3/k_2 for each run from the ratio $R(C_2H_4)/R(C_4H_{10})$, measured by gas chromatographic analysis. The original results have been confirmed in general, and in particular the new value of k_3/k_2 is 0.137 ± 0.010; but a slight systematic change in the values of $k_6/k_2^{1/2}$ leads to small changes in A_6 and E_6 giving the values listed in Table I. Accordingly we have retained 0.136 for the calculation of $k_6/k_2^{1/2}$ for the closely related olefin *trans*-octene-4. However, inspection of Table I reveals that the value $k_3/k_2 = 0.12$ is appropriate to systems containing cyclic olefins, and of these cyclooctadiene-1,5 seems to be most closely related to cyclohexene. Accordingly we have used the value of 0.122 uniformly for k_3/k_2 in eq. [VII] for the recalculation of the results obtained earlier with cyclohexene; this change has little effect upon the individual values of the rate constants, but reduces the energy of activation slightly to $E_6 - \frac{1}{2}E_2 = 7.5 \pm 0.4$ kcal/mole.

Inspection of Table I shows that the precision of the values of the Arrhenius parameters is insufficient to reveal systematically the separate effects of ring structure and ring strain upon the reactivity of cyclooctadiene-1,5, cyclohexene, and *trans*-octene-4, although Fig. 2 reveals an enhanced reactivity for the cyclic olefins. On the other hand, the very high reactivity of cyclohexadiene-1,4 is apparent both from Table I and from Fig. 2; this is associated with the large increase in delocalization that attends the formation of the

Can. J. Chem. Downloaded from www.nrcresearchpress.com by 210.87.254.42 on 09/05/12
For personal use only.

cyclohexadienyl radical from the molecule of cyclohexadiene-1,4, and is discussed elsewhere in this paper.

The Equivalence of Hydrogen Atoms in Metathesis

If n denotes the number of equivalent reactive α-methylenic hydrogen atoms present in each molecule, then the values of $13 + \log (A_7/A_2^{1/2}n)$ are: cycloheptatriene, 5.0 ± 0.3; cyclohexene, 5.0 ± 0.2; cyclohexadiene-1,4, 5.1 ± 0.1; cyclohexadiene-1,3, 4.4 ± 0.2; and cyclooctadiene-1,5, 4.4 ± 0.4. There is no characteristic value for this quantity if the cyclic olefins are regarded as members of a single set. However, the set seems to divide naturally into two subsets: those with isolated activated methylene groups (cycloheptatriene, cyclohexene, and cyclohexadiene-1,4) having a characteristic value of 5.0, and those with two adjacent activated methylene groups (cyclohexadiene-1,3 and cyclooctadiene-1,5) having a characteristic value of 4.4. The higher value is associated with the subset of molecules which offer the more favorable steric conditions for metathesis. In the other subset we might expect mutual crowding of the four hydrogen atoms in the two adjacent activated methylene groups to create less favorable steric conditions and thereby to depress the value of $13 + \log (A_7/A_2^{1/2}n)$. However, the average values of the pre-exponential factor per reactive hydrogen atom for the two subsets stand in the ratio 4:1, which is far too great to be explained by mutual crowding. Delocalization and ring strain are more likely sources of reactivity differences of this order, and indeed delocalization appears to govern the difference in reactivity of the cyclohexadienes. Further experiments are being carried out to determine whether the harmony observed within the subsets is fortuitous or part of a general pattern of reactivity.

Cyclooctatetraene

Cyclooctatetraene is the only hydrocarbon of this study to be decomposed directly by the 3 130 Å light used to generate the ethyl radicals from diethyl ketone. The direct photolysis of cyclooctatetraene vapor by 2 537 Å light has been reported to yield equimolar amounts of acetylene and benzene with a quantum yield of 0.10 for a pressure of 6 mm cyclooctatetraene (27). These products were also obtained in equimolar ratio in this study with 3 130 Å light. As cyclooctatetraene absorbs fairly strongly at 3 130 Å, with $\log \epsilon = 2.4$ (27), it was not practicable to reduce its concentration to a level at which direct photolysis would be negligible, and indeed the ratio $R(C_2H_2)/R(CO)$ varied between the limits 0.025 and 0.095. The kinetic analysis of this system is based upon the assumption that the direct photolysis proceeds independently of the other reactions of cyclooctatetraene.

The kinetic evidence indicates that the ethyl radical undergoes both metathetical and addition reactions with cyclooctatetraene. In our kinetic analysis we have assumed that the only significant reactions involving cyclooctatetraene are:

[6] $$CH_3CH_2^{\cdot} + C_8H_8 \rightarrow CH_3CH_3 + C_8H_7^{\cdot},$$

[c] $$CH_3CH_2^{\cdot} + C_8H_7^{\cdot} \rightarrow C_{10}H_{12},$$

[7] $$CH_3CH_2^{\cdot} + C_8H_8 \rightarrow C_{10}H_{13}^{\cdot},$$

[7c] $$CH_3CH_2^{\cdot} + C_{10}H_{13}^{\cdot} \rightarrow C_{12}H_{18},$$

[8] $$C_8H_8 + h\nu \rightarrow C_6H_6 + C_2H_2.$$

Partial support for this simple scheme is provided by the ratio $R(C_2H_4)/R(C_4H_{10}) = 0.123 \pm 0.006$ which is typical for the photolysis of diethyl ketone in the presence of a cyclic polyene (Table I). Further support was provided by the self-consistency of the results obtained. Thirteen experiments were performed, and each experiment yielded a

Can. J. Chem. Downloaded from www.nrcresearchpress.com by 210.87.254.42 on 09/05/12
For personal use only.

result for both the rate of metathesis and the rate of addition. Rate constants for metathesis were calculated from eq. [III] and those for addition (9) from the equation:

$$[\text{VIII}] \qquad \frac{k_7}{k_2^{1/2}} = \frac{R(\text{CO}) - [R(\text{C}_2\text{H}_6) + R(\text{C}_4\text{H}_{10})]}{[\text{B}]R(\text{C}_4\text{H}_{10})^{1/2}}.$$

The Arrhenius plots for addition and metathesis are given in Fig. 3. Addition occurs

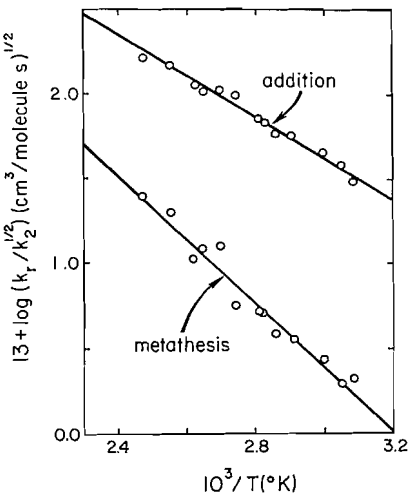

FIG. 3. Reactions of the ethyl radical with cyclooctatetraene; metathesis, $k_r = k_6$, $E_6 - \frac{1}{2}E_2 = 8.6 \pm 1.2$ kcal/mole; addition, $k_r = k_7$, $E_7 - \frac{1}{2}E_2 = 5.6 \pm 0.6$ kcal/mole.

much more rapidly by virtue of a much lower energy of activation; thus $E_7 - \frac{1}{2}E_2 = 5.6 \pm 0.6$ kcal/mole, which is significantly lower than $E_6 - \frac{1}{2}E_2 = 8.6 \pm 1.2$ kcal/mole. The latter value is the highest found for a metathetical reaction in this study, but cyclooctatetraene is the only molecule to give evidence of metathesis and yet to possess no methylene group. We should consider whether the independent sequences of reactions: [6], [*c*] and [7], [7*c*] ought to be replaced by the competitive scheme:

$$[7] \qquad \text{CH}_3\text{CH}_2\cdot + \text{C}_8\text{H}_8 \rightarrow \text{C}_{10}\text{H}_{13}\cdot,$$

$$[7c] \qquad \text{CH}_3\text{CH}_2\cdot + \text{C}_{10}\text{H}_{13}\cdot \rightarrow \text{C}_{12}\text{H}_{18},$$

$$[7d] \qquad \text{CH}_3\text{CH}_2\cdot + \text{C}_{10}\text{H}_{13}\cdot \rightarrow \text{CH}_3\text{CH}_3 + \text{C}_{10}\text{H}_{12},$$

where reaction [7*d*] gives the additional ethane originally attributed to reaction [6] and also forms the partially conjugated 1-ethylcyclooctatetraene-1,3,5,7. This alternative scheme is paralleled by a mechanism which has been proposed to explain the formation of CF_3H by the interaction of trifluoromethyl radicals with benzene (28, 29, 30):

$$[7'] \qquad \text{CF}_3\cdot + \text{C}_6\text{H}_6 \rightarrow \text{CF}_3\text{C}_6\text{H}_6\cdot,$$

$$[7d'] \qquad \text{CF}_3\cdot + \text{CF}_3\text{C}_6\text{H}_6\cdot \rightarrow \text{CF}_3\text{H} + \text{CF}_3\text{C}_6\text{H}_5.$$

However, reaction [7*d*'] is much more strongly favored energetically than reaction [7*d*], since the resonance energy of a benzene system is about five times as great as for a cyclooctatetraene system (31).

The strongest evidence against the alternative scheme rests upon the reasonable assumption that the energy of activation for the disproportionation reaction [7*d*] is unlikely to be appreciably larger than for the combination reaction [7*c*], and therefore the apparent

Can. J. Chem. Downloaded from www.nrcresearchpress.com by 210.87.254.42 on 09/05/12
For personal use only.

Can. J. Chem. Downloaded from www.nrcresearchpress.com by 210.87.254.42 on 09/05/12
For personal use only.

difference $E_6 - E_7$ should lie near zero. The observed value $E_6 - E_7 = 3.0 \pm 1.8$ kcal/mole indicates clearly that most of the additional ethane must be formed by a route other than the sequence of [7] and [7*d*].

We conclude that reactions [6] and [7] are independent. The value of $13 + \log (A_6/A_2^{1/2}) = 6.0 \pm 0.7$ is the highest observed in this study, but no other molecule possesses the steric advantages of having eight equivalent reactive hydrogen atoms singly bonded to the carbon atoms of the ring.

Finally, the internal self-consistency of the results indicates that they do reflect the reactivity of the ground electronic state of cyclooctatetraene rather than that of the metastable triplet state, which has been suggested as the precursor of the decomposition products (32). The observed rate constants for addition and metathesis are not abnormal for the ground state configuration, so that the contribution of the ground state to the observed reactivity can scarcely be negligible. The energies of activation appropriate to the triplet and ground states would be quite different, so that the Arrhenius plots for an effectively composite reaction would show curvature. The observed linearity indicates that the corresponding parameters represent the reactivity of the ground state of cyclooctatetraene.

II. The Cyclohexadienyl Radical

The generation and consumption of the cyclohexadienyl radical in the cyclohexadiene-1,4 system is adequately described by the mechanism:

[6] $$CH_3CH_2^{\cdot} + C_6H_8 \rightarrow CH_3CH_3 + C_6H_7,$$

[*c*] $$CH_3CH_2^{\cdot} + C_6H_7^{\cdot} \rightarrow C_8H_{12},$$

[*d*] $$CH_3CH_2^{\cdot} + C_6H_7^{\cdot} \rightarrow CH_3CH_3 + C_6H_6.$$

In this system ethane is formed only in reactions [3], [4], [6], and [*d*], and so the rate of reaction [6] is given by:

[IX] $$R_6 = R(C_2H_6) - R(C_2H_4) - R(C_6H_6) - k_4[D]R(C_4H_{10})^{1/2}/k_2^{1/2}.$$

Measurement of the ratio k_d/k_c is therefore possible, and yielded the result:

[X] $$k_d/k_c = R(C_6H_6)/[R_6 - R(C_6H_6)] = 0.38 \pm 0.03,$$

independent of temperature in the range 50 to 120 °C. Adopting the symbol Δ for the ratio of the rate constant for disproportionation to that for combination, we can express the results of this study in the form:

[XI] $$\Delta(C_6H_7^{\cdot} + {}^{\cdot}CH_2CH_3) = 0.38 \pm 0.03$$

[XII] $$\Delta(CH_3CH_2^{\cdot} + {}^{\cdot}CH_2CH_3) = 0.123 \pm 0.008.$$

A meaningful comparison of these values is possible only if the mechanism of the disproportionation and combination reactions is understood. Bradley (33) and Kerr and Trotman-Dickenson (7) have suggested that the paths of these two reactions pass through a common transition state. Thus two ethyl radicals will interact to form a highly activated molecule of butane, and this molecule is the common activated complex for both combination and disproportionation. Considerable bending of the carbon–carbon bond will occur and will lead to the type of interaction suggested in Fig. 4*a*, which represents the activated complex in terms of a four center model. Disproportionation can arise from the transfer of the newly-bonded hydrogen atom and the simultaneous cleavage of the central carbon–carbon bond, whereas combination results from the deactivation of the entire

Can. J. Chem. Downloaded from www.nrcresearchpress.com by 210.87.254.42 on 09/05/12
For personal use only.

complex. As each hydrogen atom in the two methyl groups is equivalent, it follows that the number of hydrogen atoms available for disproportionation is given by $n_d = 6$, whereas the number of modes of association leading to combination is $n_c = 1$. The significant quotient for the interaction of two ethyl radicals is $(n_c\Delta/n_d) = 0.020 \pm 0.001$. The validity of the theory of a common activated complex has been discussed recently by Dixon, Stefani, and Szwarc in the light of new experimental evidence (34). We shall discuss how this treatment may be applied to the interaction of the cyclohexadienyl radical with the ethyl radical.

The structure of the cyclohexadienyl radical has been inferred from the electron spin resonance spectrum of liquid (17) and solid (35) cyclohexadiene-1,4 during irradiation with 2.8 MeV electrons. The six carbon atoms are coplanar; the electron spin density at the methylene group is close to zero, and at the other positions is given by: ortho, 0.35; meta, −0.10; para, 0.50. Clearly, the ortho and para positions are the only sites in the cyclohexadienyl radical at which the initial interaction with the ethyl radical is probable, and the configuration of the corresponding activated complexes are represented in Figs. 4*b* and 4*c*. As the reaction

[*e*] $$C_6H_7\cdot + \cdot CH_2CH_3 \rightarrow C_6H_8 + CH_2{=}CH_2$$

has been shown to be negligible, only the two methylene hydrogen atoms of the cyclohexadienyl radical may be transferred during disproportionation. From Fig. 4*b* we assign $n_d^o = 4$ and $n_c^o = 2$ since the two ortho positions are equivalent; but from Fig. 4*c* it appears that the appropriate carbon–hydrogen distance is so great that $n_d^p = 0$, and clearly $n_c^p = 1$. The actual mechanism of interaction is probably related to the separate configurations of Figs. 4*b* and 4*c*, but the problem of superposition remains. The two extreme models for the overall interaction would represent the three configurations as either independent or indistinguishable. In the former case the ethyl radical would become specifically associated with one of the three sites in the cyclohexadienyl radical at an early stage; the activated complex would be quite strongly bonded and resemble the resultants rather than the reactants. If each configuration were to contribute independently and with equal weight, summation would give the effective values: $n_d = 4$, $n_c = 3$, and $(n_c\Delta/n_d) = 0.29 \pm 0.02$.

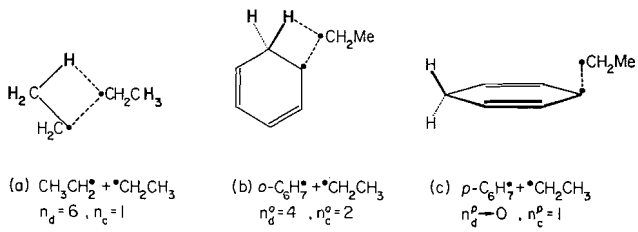

FIG. 4. Models for the transition state for disproportionation and combination of the cyclohexadienyl and ethyl radicals.

On the other hand, the three separate configurations of the activated complex may be kinetically indistinguishable, possibly by the operation of the uncertainty principle (36). The ethyl radical may become associated with the cyclohexadienyl radical as a whole, without causing much perturbation of its electronic structure; such an activated complex would be rather loosely bonded and resemble the reactants fairly closely. The assignment of an effective value to n_c is more difficult in this case; it may well be 3, but clearly cannot

be less than 1. Accordingly the minimum possible value of $(n_c\Delta/n_d)$ is 0.19 ± 0.02, with $n_c = 1$ and $n_d = 2$.

The behavior of the system may lie between these extreme models; however, this minimum value is substantially greater than the corresponding value of 0.020 ± 0.001 for the interaction of two ethyl radicals. The marked tendency of the cyclohexadienyl radical towards disproportionation presumably arises from the large delocalization energy of the product, benzene.

ACKNOWLEDGMENT

We wish to thank the National Research Council of Canada for financial support of this work and for a studentship to A. C. R. B.

REFERENCES

1. D. G. L. James and E. W. R. Steacie. Proc. Roy. Soc. London, Ser. A, **244**, 289 (1958).
2. E. S. Ferdinandi, W. P. Garby, and D. G. L. James. Part I of this series. Can. J. Chem. **42**, 2568 (1964).
3. M. Szwarc and J. H. Binks. Theoretical organic chemistry. Butterworths Scientific Publications, London. 1959. p. 262.
4. A. F. Trotman-Dickenson. Free radicals. Methuen, London. 1959. p. 61.
5. C. H. Bamford, A. D. Jenkins, and R. Johnston. Trans. Faraday Soc. **55**, 418 (1959).
6. J. M. Tedder. Quart. Rev. London, **14**, 336 (1960).
7. J. A. Kerr and A. F. Trotman-Dickenson. Progr. Reaction Kinetics, **1**, 105 (1961).
8. G. C. Fettis and J. H. Knox. Progr. Reaction Kinetics, **2**, 1 (1964).
9. D. G. L. James and E. W. R. Steacie. Proc. Roy. Soc. London, Ser. A, **244**, 297 (1958).
10. A. C. R. Brown and D. G. L. James. Can. J. Chem. **40**, 796 (1962).
11. D. G. L. James and D. MacCallum. Proc. Chem. Soc. 259 (1961).
12. L. M. Dorfmann and Z. D. Sheldon. J. Chem. Phys. **17**, 511 (1949).
13. K. O. Kutschke, M. H. J. Wijnen, and E. W. R. Steacie. J. Am. Chem. Soc. **74**, 714 (1952).
14. R. K. Brinton and E. W. R. Steacie. Can. J. Chem. **33**, 1840 (1955).
15. D. S. Weir. J. Am. Chem. Soc. **83**, 2629 (1961).
16. M. K. Eberhardt. J. Phys. Chem. **67**, 2856 (1963).
17. R. W. Fessenden and R. H. Schuler. J. Chem. Phys. **38**, 773 (1963).
18. B. J. Monostori and A. Weber. J. Mol. Spectry. **12**, 129 (1964).
19. F. R. Jensen and L. A. Smith. J. Am. Chem. Soc. **86**, 956 (1964).
20. S. Arai, S. Shida, K. Yamaguchi, and Z. Kuri. J. Chem. Phys. **37**, 1885 (1962).
21. D. E. Wood and H. M. McConnell. J. Chem. Phys. **37**, 1150 (1962).
22. B. A. Thrush and J. J. Zwolenik. Discussions Faraday Soc. **35**, 196 (1963).
23. K. Morokuma, S. Ohnishi, T. Masuda, and K. Fukui. Bull. Chem. Soc. Japan, **36**, 1228 (1963).
24. M. Cher. J. Phys. Chem. **68**, 1316 (1964).
25. K. Tori, R. Muneyuki, and H. Tanida. Can. J. Chem. **41**, 3142 (1963).
26. A. C. R. Brown and D. G. L. James. Part III of this series. To be published.
27. H. Yamazaki. Bull. Chem. Soc. Japan, **31**, 677 (1958).
28. S. W. Charles and E. Whittle. Trans. Faraday Soc. **56**, 794 (1960).
29. J. L. Holmes and K. O. Kutschke. Trans. Faraday Soc. **58**, 333 (1962).
30. S. W. Charles, J. T. Pearson, and E. Whittle. Trans. Faraday Soc. **59**, 1156 (1963).
31. G. W. Wheland. Resonance in organic chemistry. John Wiley and Sons, New York. 1955. pp. 8 and 98.
32. H. Yamazaki and S. Shida. J. Chem. Soc. Japan, Pure Chem. Sect. **77**, 500 (1956); J. Chem. Phys. **24**, 1278 (1956).
33. J. N. Bradley. J. Chem. Phys. **35**, 748 (1961).
34. P. S. Dixon, A. P. Stefani, and M. Szwarc. J. Am. Chem. Soc. **85**, 2551 (1963).
35. R. W. Fessenden and R. H. Schuler. J. Chem. Phys. **39**, 2147 (1963).
36. O. K. Rice. J. Phys. Chem. **65**, 1588 (1961).

Can. J. Chem. Downloaded from www.nrcresearchpress.com by 210.87.254.42 on 09/05/12
For personal use only.

Can. J. Chem. Downloaded from www.nrcresearchpress.com by 210.87.254.6 on 09/05/12
For personal use only.

FAST REARRANGEMENT OF *exo*-NORBORNANOL IN STRONG ACID SOLUTIONS

GIDEON FRAENKEL, PHILLIP D. RALPH,[1] AND JOHN P. KIM
Evans Chemical Laboratory, The Ohio State University, Columbus, Ohio
Received September 23, 1964

ABSTRACT

Nuclear magnetic resonance spectra have been obtained at several temperatures for solutions of 2-*exo*-norbornanol in strong acids. The spectra change with temperature reversibly. It is concluded that the 2-*exo*-norbornanol undergoes very rapid rearrangement, the fast steps being 2,6 and 3,2 hydride shifts, respectively.

INTRODUCTION

There is a vast literature which concerns carbonium ion rearrangements of bicyclic compounds (1–3). Of the many systems studied none has been the subject of such intensive investigation as the reactions of 2-substituted norbornanes. These detailed kinetic (4) and isotopic (5) studies of solvolysis and deamination reactions reveal the operation of 3,2 and 6,2 hydride shifts, respectively, and Wagner–Meerwein rearrangements and imply the intermediacy of several different carbonium ions. Hitherto these rearrangements have been observed in irreversible systems. In this work it will be shown by the methods of nuclear magnetic resonance (n.m.r.) spectroscopy that 2-*exo*-norbornanol is stable in strong acid solutions and at the same time undergoes fast skeletal rearrangements.

RESULTS AND DISCUSSION

The n.m.r. spectrum of 2-*exo*-norbornanol in methylene chloride is shown in Fig. 1. The absorptions at 6.19 tau and 7.87 tau arise from C*H*OH and the bridgehead hydrogens respectively. The remaining hydrogens on C_3, C_5, C_6, and C_7 give the multiplets in the region of 8.8 tau; the line for OH appears at 8.21 tau. The same spectrum is obtained using dimethyl sulfate and methanol as solvents with the exception that the chemical shift of the OH proton changes with solvents due to differences in hydrogen bonding. The chemical shifts of the solvent protons are as listed in the literature (6). In all these solutions the n.m.r. absorption for the OH hydrogen consisted of a single line. Thus O—H exchange was too fast to permit observation of C_2H, OH coupling. However, using trifluoroacetic acid as solvent, the line for C_2H appears at 5.40 tau and the rest of the spectrum (Fig. 2A) has a slightly different appearance from those obtained with the other solvents. Furthermore, due to fast proton exchange, the OH resonances in the acid and alcohol are merged. Since 2-*exo*-norbornanol was quantitatively recovered from trifluoroacetic solution, these changes must be due to a specific solvent effect.

When 2-*exo*-norbornanol is dissolved in 97% sulfuric acid or mixtures of trifluoroacetic acid and sulfuric acid the peak due to C*H*OH disappears and the remaining spectrum consists of two broad lines at 7.8 tau and 8.8 tau (Fig. 2E). The starting material was quantitatively recovered from these solutions also. Hence the effects found here do not arise from unusual chemical reactions. On heating the solutions of 2-*exo*-norbornanol in H_2SO_4–CF_3CO_2H between 0 and 60° the resonance due to C*H*OH broadens and disappears

[1]*Present address: Chemistry Department, Imperial College of Science and Technology, London, S.W.1, England.*

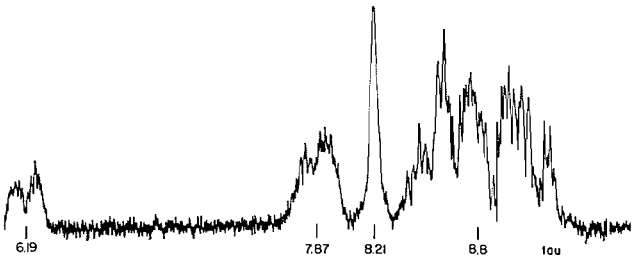

FIG. 1. Nuclear magnetic resonance spectrum, 60 Mc, 35°, of 2-*exo*-norbornanol 5% in CH_2Cl_2.

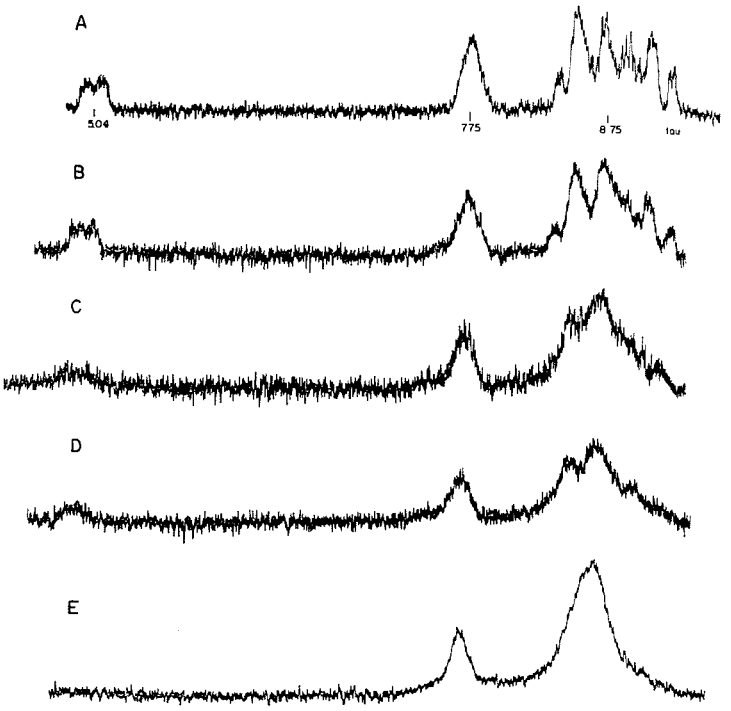

FIG. 2. Nuclear magnetic resonance spectra of 2-*exo*-norbornanol 5% in mixtures of H_2SO_4–CF_3CO_2H, 35°: (A) pure CF_3CO_2H; (B) 15% H_2SO_4; (C) 20% H_2SO_4; (D) 30% H_2SO_4; (E) 60% H_2SO_4. Acid concentrations are in volume %.

whilst the multiplets at 7.8 tau and 8.8 tau coalesce to single lines (Fig. 3), the effect being reversible with temperature. The same results were obtained at 40° with increasing sulfuric acid concentration (Fig. 2). The similarity of the low temperature spectra of the acid solutions to the spectrum of 2-*exo*-norbornanol in trifluoroacetic acid together with the quantitative recovery of the norbornanol from all these solutions strongly implies that the alcohol was the predominant species in solution. Furthermore, it is unlikely that norbornene was involved in these systems since similar experiments with norbornene yielded only tars.

These results do not originate from solvent effects or unusual chemical transformations. However, the disappearance of the peak at 5.04 tau together with the coalescence of the two multiplets at 7.8 tau and 8.8 tau to broad lines observed in these n.m.r. spectra of

Can. J. Chem. Downloaded from www.nrcresearchpress.com by 210.87.254.6 on 09/05/12
For personal use only.

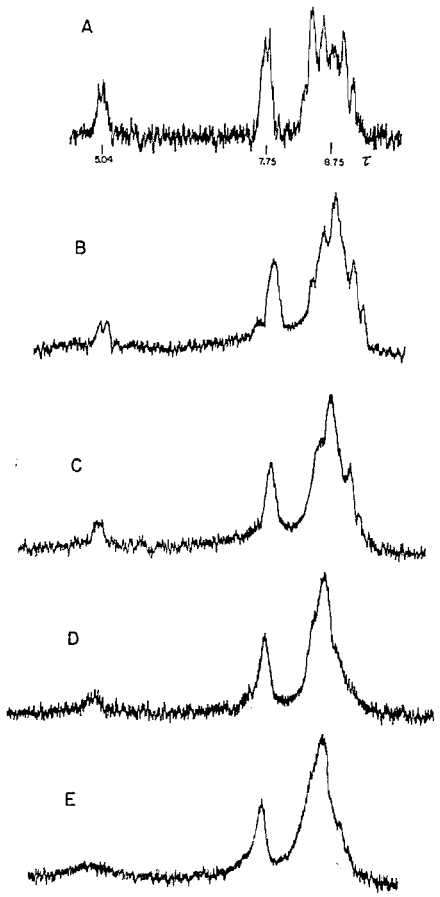

FIG. 3. Nuclear magnetic resonance spectra of 2-*exo*-norbornanol 5% in H_2SO_4–CF_3CO_2H at different temperatures: (A) 100% CF_3CO_2H, 35°; (B) 40% H_2SO_4, 0°; (C) 40% H_2SO_4, 10°; (D) 40% H_2SO_4, 30°; (E) 40% H_2SO_4, 40°.

acidified 2-*exo*-norbornanol solutions is most satisfactorily accounted for by fast hydrogen exchanges between magnetically non-equivalent sites (7).* Such processes occur in the well-known carbonium ion rearrangements which 2-*exo* derivatives of norbornane undergo, see steps [1], [2], and [3] below.

Fast skeletal rearrangement would have the effect of averaging several chemical shifts and coupling constants, the details depending on the nature of the fast steps in the reaction. At the higher acidities and temperatures employed in this work, the ratio of the integrals of the two peaks at 7.8 tau and 8.8 tau was 2/9. From the positions of these peaks and the way the line shapes changed with acidity at different temperatures, it is evident that the peak at 7.8 tau corresponds to both bridgehead hydrogens whilst that at 8.8 represents all the remaining *hydrogens* including C_2H.

It is now worthwhile to attempt to identify the fast rearrangement steps responsible for changing the n.m.r. spectrum of norbornanol in strong acid solution. If only one step were responsible for fast rearrangement, [1], [2], or [3], the final chemical shift of C_2H

**Solutions of 2-exo-norbornanol in 100% H_2SO_4 allowed to stand several hours yield derivatives of cyclohexene (8).*

Can. J. Chem. Downloaded from www.nrcresearchpress.com by 210.87.254.6 on 09/05/12
For personal use only.

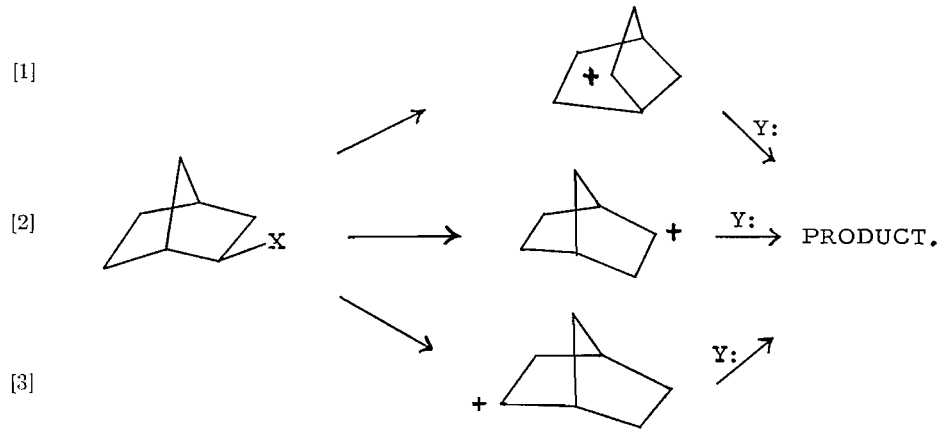

should lie in the region 4.5 to 7.0 tau and thus be resolvable from the other structure. Average shifts, δH_2 at the limit of fast rearrangement for different steps are:

step [1] $$\delta_{H_2} = \frac{\delta_{H_1}^{0} + \delta_{H_2}^{0}}{2}$$

step [2] $$\delta_{H_2} = \frac{\delta_{H_2}^{0} + \delta_{H_3 exo}^{0} + \delta_{H_3 endo}^{0}}{3}$$

step [3] $$\delta_{H_2} = \frac{\delta_{H_2}^{0} + \delta_{H_6 exo}^{0} + \delta_{H_6 endo}^{0}}{3}.$$

Zero superscripts indicate chemical shifts of hydrogens at slow exchange. However, the final shift of H_2 lies in the region 8.8 tau. Thus the shift of H_2 must be averaged with those of more than 3 other hydrogens, and more than one fast step is involved in the rearrangement. The fact that the n.m.r. absorption due to the bridgehead hydrogens in 2-*exo*-norbornanol changes relatively little as the rate of rearrangement increases strongly suggests that the bridgehead hydrogens are not *rapidly* undergoing exchange with other positions and implies that the Wagner–Meerwein shift is not one of the fast steps.

The operation of steps [2] and [3], a Namenkin rearrangement and a 6,2 hydride shift respectively would cause averaging of the chemical shifts of the hydrogens on C_2, C_3, C_5, and C_6. The resultant averaged shift would not be expected to differ greatly from that for the hydrogens on C_7, the peak at 8.8 tau would correspond to 9 hydrogens, that at 7.8 tau to 2. Such a mechanism qualitatively accounts for the results reported here.* It is not possible to describe the order in which these rearrangements occur or to determine the rates themselves. To do so would require a complete analysis of the n.m.r. spectrum of 2-*exo*-norbornanol.

In view of the results from previous work (2) it is surprising that the Wagner–Meerwein rearrangement in the present system is so much slower than the 3,2 and 6,2 hydride shifts. However, among all the rearrangements reported for derivatives of 2-*exo*-norbornanol only the present example represents a system in equilibrium. Schleyer and Olah (9) have found that the norbornyl cation in SbF_5 gives rise to resolvable absorption which integrates 1:4:6 at low temperatures and a single broad line at higher temperatures. Under

The absence of net chemical change in the system precludes the detection of intermolecular hydride exchange steps.

Can. J. Chem. Downloaded from www.nrcresearchpress.com by 210.87.254.6 on 09/05/12
For personal use only.

these conditions the Wagner–Meerwein and 6,2 hydride shift are fast throughout whilst changes in the n.m.r. spectra with temperature must be ascribed to different rates of the 3,2 hydride shift. That the relative rates of these rearrangement steps in the present work and other researches cited above should be so different can only be ascribed to the effects of solvents.

EXPERIMENTAL

Nuclear Magnetic Resonance Spectra

All spectra were determined with the Varian A60 NMR spectrometer equipped with a variable temperature probe. The resolution of the instrument always exceeded 0.15 c.p.s.

Chemicals

The 2-*exo*-norbornanol was kindly supplied by Professor Paul G. Gassman of this department. The material was sublimed immediately before use. The trifluoroacetic acid came from Eastman Kodak and sulfuric acid 100% was prepared by mixing the appropriate amounts of Dupont 97% sulfuric acid with stabilized sulfur trioxide from Baker and Adams.

Isolation of Norbornanol from Acid Solutions

The acid solution of norbornanol was slowly added by means of a Teflon syringe to aqueous sodium bicarbonate at 0°. The mixture was extracted with ether, the ether layer dried with magnesium sulfate, and the solvent removed. Norbornanol was identified by its n.m.r. spectrum.

ACKNOWLEDGMENTS

This work was supported by the National Institutes of Health and the Petroleum Research Fund of the American Chemical Society.

REFERENCES

1. J. SIMONSEN and L. N. OWEN. The terpenes. Vol. II. Cambridge University Press. 1949.
2. J. BERSON. *In* Molecular rearrangements. Vol. I. *Edited by* P. de Mayo. Interscience, New York. 1963. Chap. 3.
3. H. MEERWEIN and K. VAN EMSTER. Ber. **53**, 1815 (1920); **55**, 2500 (1922).
4. S. WINSTEIN and D. TRIFAN. J. Am. Chem. Soc. **71**, 2953 (1949); **74**, 1147, 1154 (1952). S. WINSTEIN and G. C. ROBINSON. J. Am. Chem. Soc. **80**, 169 (1958).
5. J. D. ROBERTS, C. C. LEE, and W. H. SAUNDERS. J. Am. Chem. Soc. **76**, 4501 (1954); **77**, 3034 (1955). J. D. ROBERTS and C. C. LEE. J. Am. Chem. Soc. **73**, 5009 (1951).
6. G. V. D. TIERS. Nuclear resonance shielding values. Minnesota Mining and Manufacturing Co. 1958.
7. J. A. POPLE, W. G. SCHNEIDER, and H. J. BERNSTEIN. High resolution nuclear magnetic resonance. McGraw-Hill. New York, 1959. Chap. 10.
8. NORMAN DENO. Pennsylvania State University. Private communication.
9. GEORGE OLAH. Research Laboratory, Dow Chemical Company, Farmingham, Mass. Private communication.

Can. J. Chem. Downloaded from www.nrcresearchpress.com by 210.87.254.6 on 09/05/12
For personal use only.

Can. J. Chem. Downloaded from www.nrcresearchpress.com by 210.87.254.40 on 09/05/12
For personal use only.

A CHEMICAL STUDY OF BOCCONIA LATISEPALA WATS.

XORGE ALEJANDRO DOMINGUEZ, JESÚS GARCIA DELGADO, ALBERTO MONROY C., LUIS G. ARMENDARIZ, ABRAHAM ALCALA, JOSEFINA QUEVEDO, AND PAULINO ROJAS

Departamento de Quimica, Escuela de Ciencias, Instituto Tecnológico de Monterrey, Monterrey, N.L. Mexico

Received October 26, 1964

ABSTRACT

The *Bocconia latisepala* Wats., has been chemically studied. Each part was extracted separately with petroleum ether and with ethanol. The extracts were crystallized and purified by chromatographic methods. Cerylic alcohol was isolated from petroleum ether extracts of the bark, stems, and leaves. The bark and stems, leaves, roots, and seeds afforded the alkaloids chelerythrine, sanguinarine, protopine, α-allocryptopine, and oxysanguinarine, identified by their physical and chemical properties.

The *Bocconia* genera of the alkaloid-rich Papaveraceae family contains nine species most of which are native to Mexico. They were used by the Indians as dyes and, of more interest, in a variety of medicinal preparations (1, 2).[1]

Armendariz (3) and later Manske (4, 5) in chemical studies on *B. arborea* reported the presence of chelerythrine (3–6), sanguinarine (3, 6), protopine (3, 4, 6), and allocryptopine (4) as well as other unidentified substances. Studies of *B. cordata* Wild (formerly *Macleya cordata*) (7, 8, 9), *B. frutescens* L. (10), and *B. parcei* Hecht (11) have also been reported. No chemical studies of *B. latisepala* Wats., a common medicinal plant of northeastern Mexico, have been made so it was selected for study. Pulverized samples of the roots, bark and stems, leaves, and seeds were each extracted with petroleum ether and then ethanol. The course of the extraction and later fractionations were followed by thin-layer chromatography (t.l.c.) (12).

The petroleum ether extracts of the bark and stems and the leaves afforded a precipitate shown to be cerylic alcohol. The filtrate from the extract of the bark and stems on alumina chromatography afforded more cerylic alcohol, chelerythrine (yellow, m.p. 205° decomp.), and sanguinarine (orange, m.p. 255–258° decomp.) identified by their infrared spectra, pseudocyanides, and t.l.c. R_f values. A white compound, m.p. 360–363°, was not further investigated since it gave negative results in the usual alkaloid tests. In addition to these two alkaloids, the alcoholic extract of the leaves and the roots afforded oxysanguinarine, protopine, and α-allocryptopine.

The petroleum ether extract of the seeds afforded a reddish, fluorescent oil (33.5%) shown upon saponification to contain principally stearic and palmitic acids and smaller amounts of oleic and lauric acids. From the non-saponifiable fraction was isolated a small amount of chelerythrine and sanguinarine. Thin-layer chromatography indicated that α-allocryptopine and oxysanguinarine were also present.

EXPERIMENTAL

Melting points (uncorr.) were determined on a Kofler hot stage. Ultraviolet spectra were determined on a Beckman DU spectrophotometer and infrared spectra on a Beckman IR-5 spectrophotometer or a Perkin–Elmer Infracord. Micronalyses were by Dr. A. Bernhardt, Mülheim/Ruhr, Germany. Identification methods and reactions were those of Cheronis (13), Feigl (14), and Cromwell (15).

[1]*These plants known locally as "llora sangre" (weeping blood), "tlacoxihuitl" "palo del diablo" (devil's stick), and "cocoxihuitl" were used by early Indians as healing agents (1). Hernández (2) mentioned that the stems were used to dissipate films and ulcers of the eyes. The "juices", fruits, and crushed leaves were applied as cataplasms to heal old wounds and dissolve warts.*

Plant Materials

Samples of *Bocconia latisepala* Wats. (16) were collected in Chipinque, Nuevo León, México at an altitude of 1 500 meters in July 1960, November 1961, and August 1963.

Thin-Layer Chromatography

Glass plates (20 × 20 × 0.3 cm) were used to support films of silica gel G (Merck) or aluminium oxide G coated with a DESAGA applicator. Plates were developed with *n*-butanol – acetic acid – water (75:15:10 v/v).

Extraction of Bark and Stems

General Procedure

The powdered, dry bark and stems of *B. latisepala* (800 g) were extracted first with petroleum ether (b.p. 30–60°) and then with ethanol. The marc was discarded. After t.l.c. examination, each extract was concentrated at 40–50° under reduced pressure to 250 ml, a quarter of its original volume. After cooling, any precipitate present was collected and the filtrate evaporated to dryness and worked up separately.

Petroleum Ether Extract

On concentration of the petroleum ether extract 2.5 g (0.31%) of a greenish precipitate *ITP* (m.p. 72–76°) was obtained. Crystallization from petroleum ether raised the m.p. to 79–80°. Evaporation of the filtrate (five fluorescent spots on t.l.c.) afforded 0.99 g (0.12%) of a greenish, resinous material. This was dissolved in 20 ml of petroleum ether, placed on chromatographic column of 80 g of neutral alumina (Merck), and eluted with solvents of increasing polarity. Fractions with similar t.l.c. characteristics were combined for attempts to separate their components. From fractions 1–12 an orange precipitate, principally of chelerythrine and sanguinarine (t.l.c.), was obtained. From fractions 13–20, there was obtained 140 mg of a white precipitate (*ITC*), m.p. 79–80°, later identified as cerylic alcohol. The second crop, a brown precipitate (32 mg) on fractional crystallization from cyclohexane gave 8 mg of yellowish needles (*2TC*, m.p. 205–207°, decomp.) and a second crop of 20 mg of orange crystals (*3TC*, m.p. 255–258°, decomp.). On treatment with acids *2TC* acquired a golden-yellow color and *3TC* an orange–red color. They were subsequently identified as chelerythrine and sanguinarine. From fractions 21–25, the same yellow and orange precipitates (58 mg) were obtained. A white precipitate (10 mg, *4TC* m.p. 330–333°) was isolated from fractions 26–31. It was subsequently identified as oxysanguinarine by its color reactions and R_f value on t.l.c.

ITP, on crystallization from chloroform or methanol (Norite), afforded white crystals, m.p. 79–80°. The infrared spectrum exhibited bands at 2.83 μ (OH), 3.45 μ (C—H), and 6.85 μ (CH_2). *ITP* was optical inactive (chloroform or methanol), contained one C-methyl group (Kuhn-Roth), no double bands (tetranitromethane), and one active hydrogen (Zerewitinoff). The reduction test with chromic acid was positive and the molecular weight (Rast, in camphor) was 346 (calcd. 382). *ITP* was identified as cerylic alcohol.

Anal. Calcd. for $C_{26}H_{54}O$: C, 81.60; H, 14.2; O, 4.18. Found: C, 81.49; H, 13.91; O, 4.01.

ITP, when treated with acetyl chloride in pyridine and worked up in the usual way, afforded an acetyl derivative, m.p. 64–65° (lit. (17) 65°), infrared 5.77 and 8.05 μ.

Anal. Calcd. for $C_{28}H_{56}O_2$: C, 79.18; H, 13.29; O, 7.53. Found: C, 79.12; H, 13.36; O, 7.65.

Similarly *ITP* afforded a benzoate when treated with benzoyl chloride in the presence of petroleum ether and sodium hydroxide. Crystallization from petroleum ether afforded white crystals, m.p. 47–49°. The infrared spectrum indicated absence of hydroxyl groups and the presence of an ester function (5.80 μ and 7.92 μ).

Anal. Calcd. for $C_{33}H_{58}O_2$: C, 71.42; H, 12.01. Found: C, 81.36; H, 11.95.

Compound *2TC*, m.p. 205–207°, gave a yellow color with acids or with potassium persulfate. The ultraviolet spectrum of *2TC* in ethanol (violet solution) shows absorption with λ_{max} (log ϵ) = 255 mμ (4.6), 298 (4.68). Its infrared spectrum (KBr) shows λ_{max} = 3.30, 3.35, 6.25, 6.40, 6.60, 6.90, 7.10, 7.50, 7.90, 8.30, 9.40, 9.65, and 10.60 μ.

Anal. Calcd. for $C_{21}H_{19}NO_5$: C, 69.03; H, 5.24; N, 3.83. Found: C, 69.12; H, 5.28; N, 3.71.

A mixed melting point with an authentic sample of chelerythrine was undepressed. The R_f of *2TC* and chelerythrine on t.l.c. were similar as were their fluorescence under ultraviolet light and their behavior with modified Dragendorff's reagent.

Compound *3TC*, m.p. 255–258°, exhibits ultraviolet absorption in ethanol at λ_{max} (log ϵ) = 259 (4.34), 312 (4.61), and 338 (4.18). Its infrared spectrum (KBr) shows bands at λ_{max} = 3.32, 6.15, 6.20, 6.44, 6.75, 8.45, 9.30, and 9.42 μ.

Anal. Calcd. for $C_{20}H_{15}NO_5$: C, 68.76; H, 4.33; N, 4.01. Found: C, 68.75; H, 4.25; N, 4.15.

A mixed melting point with sanguinarine was undepressed. The R_f of *3TC* and sanguinarine were identical as was their behavior under ultraviolet light and with modified Dragendorff's reagent.

Compound *4TC*, was identified by a mixed melting point with oxysanguinarine and by comparison of their R_f's on t.l.c.

The concentrated petroleum ether extract of 759 g of dried leaves afforded 5 g (0.66%) of impure cerylic alcohol. The greenish filtrate (negative tests for alkaloids) was discarded. The marc from the leaves yielded an ethanol extract which gave a positive alkaloid test. On concentration to a quarter of its volume, a precipitate (*11-HP-1*, 10.0 g, 1.33%) was obtained which gave a strong positive test for alkaloids. The filtrate

Can. J. Chem. Downloaded from www.nrcresearchpress.com by 210.87.254.40 on 09/05/12
For personal use only.

(positive test for alkaloids) was evaporated to dryness and the residue (*11-HR*, 8.32 g, 1.1%) was dissolved in chloroform and chromatographed on 400 g of alumina. The fractions containing the two components with the lowest R_f values on t.l.c. (*2HC* and *3HC*), were combined for separation by the pseudocyanide procedure (4, 18, 19, 20). Fractional crystallization from acetone gave 40 mg of white crystals (*A*), m.p. 256–257° (reported (4, 20) for the pseudocyanide of chelerythrine, m.p. 258°), which was not changed after three recrystallizations from acetone. Concentration of the filtrate gave 70 mg of white crystals (*B*) m.p. 234–236° (reported (4, 18) for the pseudocyanide of sanguinarine, m.p. 237–238°). On hydrolysis of *A* with diluted hydrochloric acid, the hydrochloride of chelerythrine, m.p. 256–258° (reported (6) 254–256°, yellow needles), was obtained. Thin-layer chromatography showed only one component which had the same R_f value as a simultaneously run sample of the authentic alkaloid. (*B*) was recrystallized twice from acetone, to give a product, m.p. 225–226°, identical with that reported (20) for sanguinarine pseudocyanide. On hydrolysis with dilute hydrochloric acid, sanguinarine hydrochloride was obtained as dark-red crystals, m.p. 204–206° (reported (17) 203–205°). Thin-layer chromatography showed only one orange spot having the same R_f value as an authentic specimen of sanguinarine. A methanol solution of 100 mg of a mixture of *2HC* and *3HC* was chromatographed on 60 g of silica gel. On development with chloroform there was observed an upper red band and a lower yellow band which after elution with chloroform was shown to be chelerythrine. Ethyl acetate eluted the red band (sanguinarine). Thin-layer chromatography of each fraction showed a single spot and comparison with authentic samples of the alkaloids established their identity.

The precipitate (*11-HP-1*) showed four fluorescent spots on t.l.c. It was dissolved in chloroform and chromatographed on 300 g of alumina. Fractions 6–12 afforded two different alkaloids, 65 mg of white crystals (*11-HP-2*), m.p. 160°, subsequently identified as α-allocryptopine and 459 mg of a tan precipitate (*11-HP-3*), m.p. 330°, later identified as oxysanguinarine. From fractions 13–34, after fractional crystallization, compounds *11-P-4*, m.p. 75–78° (identified as impure cerylic alcohol), *11-HP-5*, m.p. 155–159°, and *11-HP-6*, m.p. 171–174°, weighing 184 mg, compound *11-HP-7*, m.p. 206–207°, were obtained. Compound *11-HP-7* was identified as protopine, on the basis of t.l.c. and mixed melting point determination. Compounds *11-HP-5* and *11-HP-6* did not give positive alkaloid tests and so it was not further examined.

Compound *11-HP-2* (α-allocryptopine), m.p. 160°, showed a single violet spot on t.l.c. when observed under ultraviolet light. The color of the spot slowly changed to yellow on standing. *11-HP-2* in ethanol exhibit λ_{max} mμ (log ε) 236 (4.2) and 288 (3.6). The infrared spectrum (KBr) showed bands max. = 3.0, 3.5, 5.83, 6.25, 6.8, 7.9, and 9.7 μ.

Anal. Calcd. for $C_{21}H_{23}O_5N$: C, 68.24; H, 6.28; O, 21.66; N, 3.79. Found: C, 68.48; H, 5.95; O, 21.90; N, 3.77.

Compound *11-HP-3* (oxysanguinarine), m.p. 330°, gave a salmon or brownish spot on t.l.c. when observed under ultraviolet light. Its ultraviolet spectrum in ethanol exhibited λ_{max} mμ (log ε) = 256 (4.33) 286 (3.82), 310 (4.0), and 330 (3.8). Its infrared spectrum exhibited bands λ_{max}^{KBr} at 2.96, 3.45, 6.05, 6.75, 7.6, and 7.9 μ.

Anal. Calcd. for $C_{20}H_{13}O_5N$: C, 69.16; H, 3.77; O, 23.03; N, 4.03. Found: C, 70.57; H, 3.54; O, 23.23; N, 3.66.

The dried, powdered roots (500 g) were extracted and worked up by the general isolation procedure. The reddish petroleum ether solution left, on evaporation, 5.5 g (1.1%) of a reddish residue (*IRP*). A 5 g sample of *IRB* was chromatographed on alumina; from the eluates 150 mg of chelerythrine was obtained, besides two other non-alkaloidal fractions, *IRB* (brownish-red precipitate), m.p. 140–145°, and *IRC* (light-brown precipitate) m.p. 165–175°. They were not further investigated.

From the ethanolic extracts of the roots 40 g (8%) of a dark resin (*11-RR*) was obtained. This residue gave positive alkaloid tests. A chloroform solution of the residue was chromatographed on alumina and from the eluate; α-allocryptopine, chelerythrine, sanguinarine, protopine, and oxysanguinarine were isolated and identified.

Petroleum Ether Extract of the Seeds

From 906 g of ground, dried seeds a reddish ethereal extract was obtained. It gave weakly positive alkaloid tests. Evaporation to a quarter of its volume gave 0.85 g of a reddish, greasy precipitate (0.94%). On evaporation of the filtrate there remained 305 g (33.5%) of a reddish fluorescent oil, specific gravity, 0.935 at 31°; $n_D^{37°}$ 1.4326; iodine index 69.02; saponification index 176. A t.l.c. of a sample of the oil showed the presence of chelerythrine and sanguinarine. The oil was saponified and by chromatography of the liberated fatty acids, principally stearic and palmitic acids were isolated with smaller amounts of oleic and lauric acids.

The marc was extracted, first with acetone and then with ethanol. Both extracts were chromatographed on alumina yielding sanguinarine, chelerythrine, and oxysanguinarine.

ACKNOWLEDGMENTS

This research was made possible by a grant (GM 11332-01) from the U.S. Public Health Service, National Institutes of Health. We thank Dr. R. H. Manske, Dominion Rubber Company Ltd. (Canada) and Dr. J. Slavick, Prague, Czechoslovakia, who furnished several reference alkaloids.

Can. J. Chem. Downloaded from www.nrcresearchpress.com by 210.87.254.40 on 09/05/12
For personal use only.

REFERENCES

1. M. MARTÍNEZ. Las plantas medicinales de México. 4a ed. Ediciones Botas México. 1959. p. 197.
2. F. HERNÁNDEZ. Historia de las plantas de Nueva España. Imprenta Universitaria México 2. 1946. p. 610.
3. E. ARMENDARIZ. Datos para la materia medica Mexicana. Vol. 1. Sría. de Fomento, México. 1895. p. 15.
4. R. H. F. MANSKE. Can. J. Research B, **21**, 140 (1943).
5. R. H. F. MANSKE. Alkaloids, **4**, 147, 255 (1954).
6. T. A. HENRY. The plant alkaloids. 4th ed. Churchill, London. 1949.
7. J. F. EIJKMANN. Rec. Trav. Chim. **3**, 12 (1884).
8. P. MURRILL and J. O. SCHLOTTERBECK. Ber. **33**, 2802 (1900).
9. K. HOFFGARTHER. Monatsh. **19**, 179 (1898).
10. E. R. EMERSON and R. MILLER. J. Am. Pharm. Assoc. Sci. Ed. **18**, 12 (1929).
11. I. MACCIO. Arch. Farm. y Bioquím. Tucumán, **3**, 27 (1946); Chem. Abstr. **41**, 3507 (1947).
12. X. A. DOMÍNGUEZ. Rev. Soc. Quím. Méx. **7**, 151 (1963).
13. N. CHERONIS and J. B. ENTRIKEN. Semimicro qualitative organic analysis. 2nd ed. Interscience, N.Y. 1957.
14. F. FEIGL. Spot tests in organic chemistry. 6th ed. Elsevier, N.Y. 1960.
15. R. T. CROMWELL. *In* Moderne Methoden der Pflanzenanalyse. Vol. 4. *Edited by* K. Pech and M. V. Tracey. Springer-Verlag, Berlin. 1955. p. 967.
16. P. STANLEY. Trees and shrubs of Mexico. Vol. 1. Smithsonian Institute, Washington. 1923. p. 299.
17. J. HEILBRON and H. M. BUNBURY. Dictionary of organic compounds. Oxford Press, N.Y. 1953.
18. J. SLAVIK and L. SLAVIKOVA. Collection Czech. Chem. Commun. **20**, 17 (1955).
19. P. KARRER. Ber. **50**, 212 (1917).
20. E. SPATH and F. KUFFNER. Ber. **64**, 1123 (1931).

Can. J. Chem. Downloaded from www.nrcresearchpress.com by 210.87.254.40 on 09/05/12
For personal use only.

Can. J. Chem. Downloaded from www.nrcresearchpress.com by 210.87.254.42 on 09/05/12
For personal use only.

A SIMPLIFIED PROCEDURE FOR THE ANALYSIS OF COMPLEX NUCLEAR MAGNETIC RESONANCE SPECTRA

II. THE ANALYSIS OF SYMMETRICAL TRIFLUOROBENZENE, THE AA'A''XX'X'' SYSTEM[1]

R. G. JONES,[2] R. C. HIRST,[3] AND H. J. BERNSTEIN
Division of Pure Chemistry, National Research Council, Ottawa, Canada

Received October 8, 1964

ABSTRACT

The analysis of the six spin AA'A''XX'X'' system consisting of two sets of three chemically equivalent nuclei with spin $\frac{1}{2}$ and four coupling constants J_{AA}, J_{XX}, J_{AX}, and J_{AX}' has been developed with the use of group theory and the appropriate Hamiltonian. It is found that there will be differences in the A and X spectra if $J_{AX} \neq J_{AX}'$ and simultaneously $J_{AA} \neq J_{XX}$. If $J_{AA} = J_{HH}$ the A and X spectra become identical. If $J_{AX} = J_{AX}'$ each spectrum of course becomes trivial.

The complex n.m.r. spectrum of the AA'A''XX'X'' can be decomposed into subspectra, and the analysis of the nuclear magnetic resonance spectra of symmetrical trifluorobenzene has been carried out in this manner. The experimental proton and fluorine spectra of this molecule exhibit marked differences. Calculated spectra have been fitted to the experimental spectra and the following values of the coupling constants have been found:

$|J_{HH}| = 2.30 \pm 0.03$ c.p.s., $\quad |J_{FF}| = 5.83 \pm 0.03$ c.p.s.,
$|J_{HF}| = 8.96 \pm 0.03$ c.p.s., $\quad |J_{HF'}| = 1.68 \pm 0.03$ c.p.s.

The sign of J_{HH} is the same as the sign of J_{FF}. J_{HF} and J_{HF}' have opposite signs. It is not possible to relate the signs of J_{HH} and J_{FF} to the signs of J_{HF} and J_{HF}' in this type of spectrum. However, comparison of the signs of couplings in related molecules suggest that J_{HF}, J_{HH}, and J_{FF} have the same sign.

INTRODUCTION

The high-resolution n.m.r. spectrum of the A_2X_2 system with four distinct coupling constants, i.e., AA'XX', has been studied and a number of experimental spectra of this type have been analyzed (1–4). This problem presents no difficulties in the construction of the basic symmetry wave functions and the matrix elements of the Hamiltonian can be derived without much labor.

The next higher homologue in the A_nX_n series is the AA'A''XX'X'' system, symmetrical trifluorobenzene for example, consisting of two sets of three chemically equivalent nuclei with spin $\frac{1}{2}$ and having four distinct coupling constants J_{AA}, J_{XX}, J_{AX}, and J_{AX}' as in the AA'XX' system. By analogy with the AA'XX' system we might expect the AA'A'' and XX'X'' parts of the spectrum to be identical, but it will be shown that this is not so in general.

Wilson (5) illustrated the group theoretical procedures for utilizing molecular symmetry in setting up the equations for calculating the n.m.r. spectra resulting from spin–spin coupling in such molecules. The basic symmetry wave functions and the corresponding matrix elements of the Hamiltonian, essential to the analysis of the spectrum of symmetrical trifluorobenzene, were derived (5). The emphasis was, however, placed on the formulation of the problem rather than the detailed analysis.

It is intended in this paper that the emphasis shall be on the analysis of spectra of AA'A''XX'X'' systems in general and the symmetrical trifluorobenzene problem in

[1]*Issued as N.R.C. No. 8242.*
[2]*National Research Council Postdoctorate Fellow 1962–1964.*
[3]*National Research Council Postdoctorate Fellow 1963–1964.*

particular. The systematic simplifications that arise from direct application of the procedures outlined by Diehl, Jones, and Bernstein (6) (hereafter referred to as Part I) or from inspection of the tables of matrix elements, will be used as an aid in the interpretation of the spectra.

The AA′A″XX′X″ system with a fixed configuration can belong to one of the two symmetry classifications denoted by D_{3h} and C_{3v}. The geometry of the C_{3v} point group is either two staggered or two eclipsed equilateral triangles of different size and out of plane. The point group D_{3h} corresponds to two staggered equilateral triangles in a plane (e.g. symmetrical trifluorobenzene). All configurations with either D_{3h} or C_{3v} symmetry can be treated, however, under the C_{3v} classification. For symmetrical trifluorobenzene one may also use D_3 symmetry. The four coupling constants which arise in symmetrical trifluorobenzene are indicated below where A = ^{1}H and X = ^{19}F.

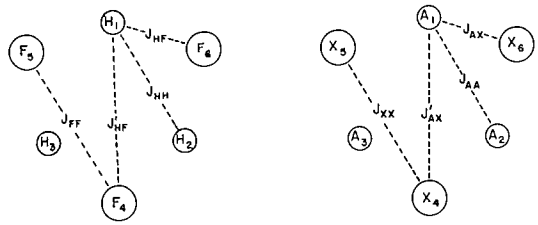

All of the 64 basic symmetry wave functions are presented here, together with the corresponding diagonal elements of the Hamiltonian and the off-diagonal elements between functions which mix.

THE METHOD OF ANALYSIS OF THE AA′A″XX′X″ SYSTEM

The procedures outlined in Part I will be used to sort out, where possible, the transition patterns of the A and X nuclear species of the AA′A″XX′X″ system. Information concerning coupling between the groups AA′A″ and XX′X″ will first be derived from examination of the subspectra corresponding to the maximum values of $|F_z(\mathrm{AA'A''})|$ and $|F_z(\mathrm{XX'X''})|$. Then any other simple patterns which can be recognized will be investigated in detail.

THE BASIC SYMMETRY WAVE FUNCTION DIAGRAM AND THE ENERGY LEVEL DIAGRAM FOR THE AA′A″XX′X″ SYSTEM

The eight basic symmetry wave functions of three equivalent nuclei are well known (2). The 64 molecular basic symmetry functions of the AA′A″XX′X″ system can be constructed from the 64 product wave functions obtained by taking the product of each of the AA′A″ functions with the eight XX′X″ functions, in turn, as indicated by Wilson (5).

However, following the procedure of Part I, it is not necessary at this stage to write out the 64 molecular symmetry wave functions in their entirety. It is of more importance to know at this stage the relevant quantum numbers characterizing the wave functions, i.e., $F_z(\mathrm{AA'A''})$ and $F_z(\mathrm{XX'X''})$, and the molecular symmetry species to which they belong. It has been shown (5) that there are 20 molecular wave functions belonging to the A_1 symmetry species. Sixteen are formed from ($A_1 \times A_1$) type products and four from ($E \times E$) products. There are four ($E \times E$) type wave functions belonging to the A_2 symmetry species. The 20 degenerate pairs of wave functions belonging to the E symmetry species are made up from eight ($A_1 \times E$) type, eight ($E \times A_1$) type and four ($E \times E$) type

Can. J. Chem. Downloaded from www.nrcresearchpress.com by 210.87.254.42 on 09/05/12
For personal use only.

product functions. The basic group symmetry wave functions and the molecular product functions are given in Table I. In this table $\underline{F_z(\mathrm{AA'A''})}$ is used to represent the eight basic symmetry wave functions of the three A nuclei, for example, $\underline{F_z(\tfrac{1}{2})}$ in the A_1 symmetry species represents $(\alpha\alpha\beta + \alpha\beta\alpha + \beta\alpha\alpha)/3^{-1/2}$ (and similarly for the X nuclei). The molecular product functions formed from products, $\underline{F_z(\mathrm{AA'A''})} \times \underline{F_z(\mathrm{XX'X''})}$, are represented by $\underline{F_z(\mathrm{AA'A''}),F_z(\mathrm{XX'X''})}$.

It should be noted here that, since for the purpose of deriving an energy level diagram we require only the overall symmetry of the wave functions and not intimate details of their construction, we need consider only one wave function of each of the degenerate pairs of (AA'A'') and (XX'X'') wave functions.

The procedure as set out in Part I then allows us to write down an energy level diagram picking out the A nuclear species and X nuclear species transitions from Table I. The energy level diagram is schematically represented in Fig. 1.

It is apparent from Fig. 1 that the energy levels for $F_z(\mathrm{XX'X''}) = \frac{3}{2}$ in the A_1 symmetry species together with the levels for $F_z(\mathrm{XX'X''}) = \frac{3}{4}$ in the E symmetry species constitute an energy level diagram similar to that for three, isolated, equivalent nuclei (2). The same can be said for the energy levels corresponding to $F_z(\mathrm{XX'X''}) = -\frac{3}{2}$. These diagrams give rise to subspectra which we denote a_3. In the AA'A'' part of the spectrum these a_3 subspectra appear as two intense lines, symmetrically spaced about ν_H and separated by the sum of coupling constants $2J_{AX} + J_{AX}'$ (see Part I). Each line has one eighth of the total AA'A'' intensity. The XX'X'' spectrum has equivalent features arising from two x_3 subspectra.

In Fig. 1 the $F_z(\mathrm{XX'X''}) = +\frac{1}{2}$ pattern in the A_1 and A_2 symmetry species is identical with that for an AB_2 system. This is true also for the corresponding $F_z(\mathrm{XX'X''}) = -\frac{1}{2}$ pattern. The corresponding subspectra will each have one eighth of the intensity of the relevant part of the spectrum (AA'A'' or XX'X''). They are designated as ab_2 in the AA'A'' part and xy_2 in the XX'X'' part.

Each of the $F_z(\mathrm{XX'X''}) = \pm\frac{1}{2}$ patterns (one for $+\frac{1}{2}$ and one for $-\frac{1}{2}$) of the E symmetry species (Fig. 1) is identical with the energy level diagram characteristic of an ABC system. and its spectrum is denoted by *abc*. The energy levels within the E symmetry species are doubly degenerate and hence the intensity of each transition between E symmetry species energy levels must be counted twice. As a result each of the *abc* subspectra will acount for a quarter of the intensity of either the AA'A'' or XX'X'' spectrum.

We expect therefore to be able to identify in the AA'A'' part of the spectrum of AA'A''XX'X'', subspectra of the types a_3, ab_2, and *abc*, and in the XX'X'' part, subspectra of the types x_3, xy_2, and *xyz*. Therefore, the solution to the six spin AA'A''XX'X'' system has been reduced in complexity to a problem involving the solution of three spin systems with spectra of the types a_3, ab_2, and *abc*.

The remarks made so far apply equally well to both the AA'A'' and XX'X'' parts of the AA'A''XX'X'' system and therefore as yet there is no indication that the spectra of the two parts will be different.

BASIC SYMMETRY WAVE FUNCTIONS, ENERGY LEVELS, TRANSITION ENERGIES, AND INTENSITIES FOR THE AA'A''XX'X'' SYSTEM

The AA'A''XX'X'' problem is, in general, characterized by four spin coupling constants J_{AA}, J_{XX}, J_{AX}, and J_{AX}' and two parameters H_A and H_X which represent the magetic fields at the two types of nuclei. It will be convenient to define new quantities,

Can. J. Chem. Downloaded from www.nrcresearchpress.com by 210.87.254.42 on 09/05/12
For personal use only.

Can. J. Chem. Downloaded from www.nrcresearchpress.com by 210.87.254.42 on 09/05/12
For personal use only.

TABLE I

Basic product symmetry wave function diagram for the AA′A″XX′X″ system[a]

	F_z(AA′A″)		F_z(X′XX″)		F_z(AA′A″),F_z(XX′X″)					
F_z(AA′A″XX′X″)	A_1 species	E species	A_1 species	E species	$A_1\times A_1 = A_1$	$E\times E = A_1$	$E\times E = A_2$	$A_1\times E = E$	$E\times A_1 = E$	$E\times E = E$
3					$\frac{3}{2},\frac{3}{2}$					
$\frac{5}{2}$										
2					$\frac{3}{2},\frac{1}{2}$ $\frac{1}{2},\frac{3}{2}$			$\frac{3}{2},\frac{1}{2}$	$\frac{1}{2},\frac{3}{2}$	
$\frac{3}{2}$	$\frac{3}{2}$		$\frac{3}{2}$							
1					$\frac{3}{2},-\frac{1}{2}$ $\frac{1}{2},\frac{1}{2}$ $-\frac{1}{2},\frac{3}{2}$	$\frac{1}{2},\frac{1}{2}$	$\frac{1}{2},\frac{1}{2}$	$\frac{3}{2},-\frac{1}{2}$ $\frac{1}{2},\frac{1}{2}$	$\frac{1}{2},\frac{1}{2}$ $-\frac{1}{2},\frac{3}{2}$	$\frac{1}{2},\frac{1}{2}$
$\frac{1}{2}$	$\frac{1}{2}$ $\frac{1}{2}$ $\frac{1}{2}$		$\frac{1}{2}$	$\frac{1}{2}$ $\frac{1}{2}$						
0					$\frac{3}{2},-\frac{3}{2}$ $\frac{1}{2},-\frac{1}{2}$ $-\frac{1}{2},\frac{1}{2}$ $-\frac{3}{2},\frac{3}{2}$	$\frac{1}{2},-\frac{1}{2}$ $-\frac{1}{2},\frac{1}{2}$	$\frac{1}{2},-\frac{1}{2}$ $-\frac{1}{2},\frac{1}{2}$	$\frac{1}{2},-\frac{1}{2}$ $-\frac{1}{2},\frac{1}{2}$	$\frac{1}{2},-\frac{1}{2}$ $-\frac{1}{2},\frac{1}{2}$	$\frac{1}{2},-\frac{1}{2}$ $-\frac{1}{2},\frac{1}{2}$
$-\frac{1}{2}$	$-\frac{1}{2}$ $-\frac{1}{2}$ $-\frac{1}{2}$		$-\frac{1}{2}$	$-\frac{1}{2}$ $-\frac{1}{2}$						
-1					$\frac{1}{2},-\frac{3}{2}$ $-\frac{1}{2},-\frac{1}{2}$ $-\frac{3}{2},\frac{1}{2}$	$-\frac{1}{2},-\frac{1}{2}$	$-\frac{1}{2},-\frac{1}{2}$	$-\frac{1}{2},-\frac{3}{2}$ $-\frac{3}{2},\frac{1}{2}$	$\frac{1}{2},-\frac{3}{2}$ $-\frac{1}{2},-\frac{1}{2}$	$-\frac{1}{2},-\frac{1}{2}$
$-\frac{3}{2}$	$-\frac{3}{2}$		$-\frac{3}{2}$							
-2					$-\frac{1}{2},-\frac{3}{2}$ $-\frac{3}{2},-\frac{1}{2}$			$-\frac{3}{2},-\frac{1}{2}$	$-\frac{1}{2},-\frac{3}{2}$	
$-\frac{5}{2}$										
-3					$-\frac{3}{2},-\frac{3}{2}$					

[a]The degeneracy of the molecular wave functions in the E species is not shown.

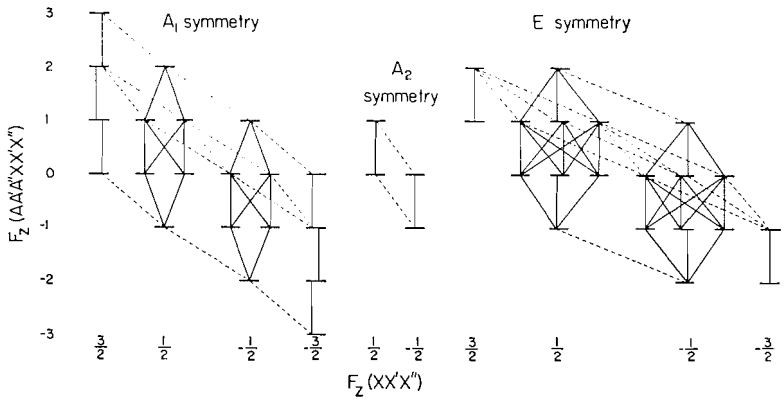

FIG. 1. Energy level diagram for the AA'A''XX'X'' system. The solid tie lines indicate AA'A'' transitions i.e., transitions permitted by the selection rule $\Delta F_z(\mathrm{AA'A''}) = \pm 1$, $\Delta F_z(\mathrm{XX'X''}) = 0$. The broken tie lines indicate XX'X'' transitions, i.e., transitions permitted by the selection rule $\Delta F_z(\mathrm{AA'A''}) = 0$, $\Delta F_z(\mathrm{XX'X''}) = \pm 1$. For clarity, only some of the X transitions have been sketched in. If $F_z(\mathrm{AA'A''})$ were plotted as abscissa instead of $F_z(\mathrm{XX'X''})$, the solid tie lines would represent X transitions and the dotted tie lines A transitions.

$$K = J_{\mathrm{AA}} + J_{\mathrm{XX}}, \qquad L = 2J_{\mathrm{AX}} - J_{\mathrm{AX}}',$$
$$M = J_{\mathrm{AA}} - J_{\mathrm{XX}}, \qquad N = 2J_{\mathrm{AX}} + J_{\mathrm{AX}}',$$

and

$$\nu_{\mathrm{A}} = \frac{\gamma_{\mathrm{A}} H_{\mathrm{A}}}{2\pi}, \qquad \nu_{\mathrm{X}} = \frac{\gamma_{\mathrm{X}} H_{\mathrm{X}}}{2\pi},$$

where γ_{A} and γ_{X} are the magnetogryric ratios of the two types of nuclei.

The basic symmetry wave functions for the AA'A''XX'X'' system have been discussed qualitatively above. The product functions of the type $(\mathrm{A_1} \times \mathrm{A_1}) = \mathrm{A_1}$, $(\mathrm{A_1} \times \mathrm{E}) = \mathrm{E}$, and $(\mathrm{E} \times \mathrm{A_1}) = \mathrm{E}$ give rise directly to basic symmetry wave functions, but the $\mathrm{E} \times \mathrm{E}$ products have to be combined to give linear combinations of species $\mathrm{A_1}$, $\mathrm{A_2}$, and E. There are four $\mathrm{E} \times \mathrm{E}$ products characterized by $F_z(\mathrm{AA'A''}) = F_z(\mathrm{XX'X''}) = \frac{1}{2}$ which can be combined to give linear combinations, using a group theoretical formula (5) of the type

$$\psi(\mathrm{A_1}) = (\mathrm{E}_{1/2}(\mathrm{A})\mathrm{E}_{1/2}(\mathrm{X}) + \mathrm{E}_{1/2}'(\mathrm{A})\mathrm{E}_{1/2}'(\mathrm{X}))2^{-1/2}$$
$$\psi(\mathrm{A_2}) = (\mathrm{E}_{1/2}(\mathrm{A})\mathrm{E}_{1/2}'(\mathrm{X}) - \mathrm{E}_{1/2}'(\mathrm{A})\mathrm{E}_{1/2}(\mathrm{X}))2^{-1/2}$$
$$\psi(\mathrm{E}) = (\mathrm{E}_{1/2}(\mathrm{A})\mathrm{E}_{1/2}(\mathrm{X}) - \mathrm{E}_{1/2}'(\mathrm{A})\mathrm{E}_{1/2}'(\mathrm{X}))2^{-1/2}$$
$$\psi(\mathrm{E}') = (\mathrm{E}_{1/2}(\mathrm{A})\mathrm{E}_{1/2}'(\mathrm{X}) + \mathrm{E}_{1/2}'(\mathrm{A})\mathrm{E}_{1/2}(\mathrm{X}))2^{-1/2},$$

where E and E' are a degenerate pair in the E symmetry species.

The matrix elements of the Hamiltonian,

$$= \frac{\gamma_{\mathrm{A}} H_{\mathrm{A}}}{2\pi} F_z(\mathrm{A}) + \frac{\gamma_{\mathrm{X}} H_{\mathrm{X}}}{2\pi} F_z(X) + \sum_{i<j}^{\mathrm{A}} J_{ij} I_i \cdot I_j$$
$$+ \sum_{i<j}^{\mathrm{X}} J_{ij} I_i \cdot I_j + \sum_{i}^{\mathrm{A}} \sum_{j}^{\mathrm{X}} J_{ij} I_i \cdot I_j,$$

have been derived and are presented in Table II together with the molecular basic symmetry wave functions.

Can. J. Chem. Downloaded from www.nrcresearchpress.com by 210.87.254.42 on 09/05/12
For personal use only.

Can. J. Chem. Downloaded from www.nrcresearchpress.com by 210.87.254.42 on 09/05/12
For personal use only.

TABLE II

Basic symmetry functions and matrix elements for AA′A″XX′X″

State, S_{Fz}	Basic function, A×X	Diagonal matrix elements	Off-diagonal matrix elements
A_1 species			
$A_{1,3}$	$A_{3/2}$ $A_{3/2}$	$\frac{3}{2}\nu_A+\frac{3}{2}\nu_X+\frac{3}{4}K+\frac{3}{4}N$	
$1A_{1,2}$	$A_{3/2}$ $A_{1/2}$	$\frac{3}{2}\nu_A+\frac{1}{2}\nu_X+\frac{3}{4}K+\frac{1}{4}N$	
$2A_{1,2}$	$A_{1/2}$ $A_{3/2}$	$\frac{1}{2}\nu_A+\frac{3}{2}\nu_X+\frac{3}{4}K+\frac{1}{4}N$	
$1A_{1,1}$	$A_{3/2}$ $A_{-1/2}$	$\frac{3}{2}\nu_A-\frac{1}{2}\nu_X+\frac{3}{4}K-\frac{1}{4}N$	
$2A_{1,1}$	$A_{-1/2}$ $A_{3/2}$	$-\frac{1}{2}\nu_A+\frac{3}{2}\nu_X+\frac{3}{4}K-\frac{1}{4}N$	
$3A_{1,1}$	$A_{1/2}$ $A_{1/2}$	$\frac{1}{2}\nu_A+\frac{1}{2}\nu_X+\frac{3}{4}K+\frac{1}{12}N$	$3A_{11}H'4A_{11} = -\frac{\sqrt{2}}{12}[3L-N]$
$4A_{1,1}$	$(2)^{-1/2}(E_{1/2}E_{1/2}+E_{1/2}'E_{1/2}')$	$\frac{1}{2}\nu_A+\frac{1}{2}\nu_X-\frac{3}{4}K+\frac{1}{12}[2N-3L]$	
$1A_{1,0}$	$A_{3/2}$ $A_{-3/2}$	$\frac{3}{2}\nu_A-\frac{3}{2}\nu_X+\frac{3}{4}K-\frac{3}{4}N$	
$2A_{1,0}$	$A_{-3/2}$ $A_{3/2}$	$-\frac{3}{2}\nu_A+\frac{3}{2}\nu_X+\frac{3}{4}K-\frac{3}{4}N$	
$3A_{1,0}$	$A_{1/2}$ $A_{-1/2}$	$\frac{1}{2}\nu_A-\frac{1}{2}\nu_X+\frac{3}{4}K-\frac{1}{12}N$	$3A_{10}H'4A_{10} = \frac{\sqrt{2}}{12}[3L-N]$
$4A_{1,0}$	$(2)^{-1/2}(E_{1/2}E_{-1/2}+E_{1/2}'E_{-1/2}')$	$\frac{1}{2}\nu_A-\frac{1}{2}\nu_X-\frac{3}{4}K-\frac{1}{12}[2N-3L]$	
$5A_{1,0}$	$A_{-1/2}$ $A_{1/2}$	$-\frac{1}{2}\nu_A+\frac{1}{2}\nu_X+\frac{3}{4}K-\frac{1}{12}N$	$5A_{10}H'6A_{10} = \frac{\sqrt{2}}{12}[3L-N]$
$6A_{1,0}$	$(2)^{-1/2}(E_{-1/2}E_{1/2}+E_{-1/2}'E_{1/2}')$	$-\frac{1}{2}\nu_A+\frac{1}{2}\nu_X-\frac{3}{4}K-\frac{1}{12}[2N-3L]$	
$1A_{1,-1}$	$A_{-3/2}$ $A_{1/2}$	$-\frac{3}{2}\nu_A+\frac{1}{2}\nu_X+\frac{3}{4}K-\frac{1}{4}N$	
$2A_{1,-1}$	$A_{1/2}$ $A_{-3/2}$	$\frac{1}{2}\nu_A-\frac{3}{2}\nu_X+\frac{3}{4}K-\frac{1}{4}N$	
$3A_{1,-1}$	$A_{-1/2}$ $A_{-1/2}$	$-\frac{1}{2}\nu_A-\frac{1}{2}\nu_X+\frac{3}{4}K+\frac{1}{12}N$	$3A_{1-1}H'4A_{1-1} = -\frac{\sqrt{2}}{12}[3L-N]$
$4A_{1,-1}$	$(2)^{-1/2}(E_{-1/2}E_{-1/2}+E_{-1/2}'E_{-1/2}')$	$-\frac{1}{2}\nu_A-\frac{1}{2}\nu_X-\frac{3}{4}K+\frac{1}{12}[2N-3L]$	
$1A_{1,-2}$	$A_{-3/2}$ $A_{-1/2}$	$-\frac{3}{2}\nu_A-\frac{1}{2}\nu_X+\frac{3}{4}K+\frac{1}{4}N$	
$2A_{1,-2}$	$A_{-1/2}$ $A_{-3/2}$	$-\frac{1}{2}\nu_A-\frac{3}{2}\nu_X+\frac{3}{4}K+\frac{1}{4}N$	
$A_{1,-3}$	$A_{-3/2}$ $A_{-3/2}$	$-\frac{3}{2}\nu_A-\frac{3}{2}\nu_X+\frac{3}{4}K+\frac{3}{4}N$	

TABLE II *(Concluded)*

Basic symmetry functions and matrix elements for AA′A″XX′X″ *(Concluded)*

State, S_{Fz}	Basic function, A×X	Diagonal matrix elements	Off-diagonal matrix elements
A_2 species			
$A_{2,1}$	$(2)^{-1/2}(E_{1/2}E_{1/2}'-E_{1/2}'E_{1/2})$	$\frac{1}{2}\nu_A+\frac{1}{2}\nu_X-\frac{3}{4}K+\frac{1}{4}L$	
$1A_{2,0}$	$(2)^{-1/2}(E_{1/2}E_{-1/2}'-E_{1/2}'E_{-1/2})$	$\frac{1}{2}\nu_A-\frac{1}{2}\nu_X-\frac{3}{4}K-\frac{1}{4}L$	
$2A_{2,0}$	$(2)^{-1/2}(E_{-1/2}E_{1/2}'-E_{1/2}'E_{-1/2})$	$-\frac{1}{2}\nu_A+\frac{1}{2}\nu_X-\frac{3}{4}K-\frac{1}{4}L$	
$A_{2,-1}$	$(2)^{-1/2}(E_{-1/2}E_{-1/2}'-E_{-1/2}'E_{-1/2})$	$-\frac{1}{2}\nu_A-\frac{1}{2}\nu_X-\frac{3}{4}K+\frac{1}{4}L$	
E species			
$1E_2$	$A_{3/2}\quad E_{1/2}$	$\frac{3}{2}\nu_A+\frac{1}{2}\nu_X+\frac{3}{4}M+\frac{1}{4}N$	
$2E_2$	$E_{1/2}\quad A_{3/2}$	$\frac{1}{2}\nu_A+\frac{3}{2}\nu_X-\frac{3}{4}M+\frac{1}{4}N$	
$1E_1$	$A_{3/2}\quad E_{-1/2}$	$\frac{3}{2}\nu_A-\frac{1}{2}\nu_X+\frac{3}{4}M-\frac{1}{4}N$	
$2E_1$	$E_{-1/2}\quad A_{3/2}$	$-\frac{1}{2}\nu_A+\frac{3}{2}\nu_X-\frac{3}{4}M-\frac{1}{4}N$	
$3E_1$	$A_{1/2}\quad E_{1/2}$	$\frac{1}{2}\nu_A+\frac{1}{2}\nu_X+\frac{3}{4}M+\frac{1}{12}N$	$3E_1H'4E_1=-\frac{1}{12}[3L-N]$
$4E_1$	$E_{1/2}\quad A_{1/2}$	$\frac{1}{2}\nu_A+\frac{1}{2}\nu_X-\frac{3}{4}M+\frac{1}{12}N$	$3E_1H'5E_1=\frac{1}{12}[3L-N]$
$5E_1$	$(2)^{-1/2}(E_{1/2}E_{1/2}-E_{1/2}'E_{1/2}')$	$\frac{1}{2}\nu_A+\frac{1}{2}\nu_X-\frac{3}{4}K+\frac{1}{12}N$	$4E_1H'5E_1=\frac{1}{12}[3L-N]$
$1E_0$	$A_{1/2}\quad E_{-1/2}$	$\frac{1}{2}\nu_A-\frac{1}{2}\nu_X+\frac{3}{4}M-\frac{1}{12}N$	$1E_0H'2E_0=\frac{1}{12}[3L-N]$
$2E_0$	$E_{1/2}\quad A_{-1/2}$	$\frac{1}{2}\nu_A-\frac{1}{2}\nu_X-\frac{3}{4}M-\frac{1}{12}N$	$1E_0H'3E_0=-\frac{1}{12}[3L-N]$
$3E_0$	$(2)^{-1/2}(E_{1/2}E_{-1/2}-E_{1/2}'E_{-1/2}')$	$\frac{1}{2}\nu_A-\frac{1}{2}\nu_X-\frac{3}{4}K-\frac{1}{12}N$	$2E_0H'3E_0=-\frac{1}{12}[3L-N]$
$4E_0$	$A_{-1/2}\quad E_{1/2}$	$-\frac{1}{2}\nu_A+\frac{1}{2}\nu_X+\frac{3}{4}M-\frac{1}{12}N$	$4E_0H'5E_0=\frac{1}{12}[3L-N]$
$5E_0$	$E_{-1/2}\quad A_{1/2}$	$-\frac{1}{2}\nu_A+\frac{1}{2}\nu_X-\frac{3}{4}M-\frac{1}{12}N$	$4E_0H'6E_0=-\frac{1}{12}[3L-N]$
$6E_0$	$(2)^{-1/2}(E_{-1/2}E_{1/2}-E_{-1/2}'E_{1/2}')$	$-\frac{1}{2}\nu_A+\frac{1}{2}\nu_X-\frac{3}{4}K-\frac{1}{12}N$	$5E_0H'6E_0=-\frac{1}{12}[3L-N]$
$1E_{-1}$	$A_{-3/2}\quad E_{1/2}$	$-\frac{3}{2}\nu_A+\frac{1}{2}\nu_X+\frac{3}{4}M-\frac{1}{4}N$	
$2E_{-1}$	$E_{1/2}\quad A_{-3/2}$	$\frac{1}{2}\nu_A-\frac{3}{2}\nu_X-\frac{3}{4}M-\frac{1}{4}N$	
$3E_{-1}$	$A_{-1/2}\quad E_{-1/2}$	$-\frac{1}{2}\nu_A-\frac{1}{2}\nu_X+\frac{3}{4}M+\frac{1}{12}N$	$3E_{-1}H'4E_{-1}=-\frac{1}{12}[3L-N]$
$4E_{-1}$	$E_{-1/2}\quad A_{-1/2}$	$-\frac{1}{2}\nu_A-\frac{1}{2}\nu_X-\frac{3}{4}M+\frac{1}{12}N$	$3E_{-1}H'5E_{-1}=\frac{1}{12}[3L-N]$
$5E_{-1}$	$(2)^{-1/2}(E_{-1/2}E_{-1/2}-E_{-1/2}'E_{-1/2}')$	$-\frac{1}{2}\nu_A-\frac{1}{2}\nu_X-\frac{3}{4}K+\frac{1}{12}N$	$4E_{-1}H'5E_{-1}=\frac{1}{12}[3L-N]$
$1E_{-2}$	$A_{-3/2}\quad E_{-1/2}$	$-\frac{3}{2}\nu_A-\frac{1}{2}\nu_X+\frac{3}{4}M+\frac{1}{4}N$	
$2E_{-2}$	$E_{-1/2}\quad A_{-3/2}$	$-\frac{1}{2}\nu_A-\frac{3}{2}\nu_X-\frac{3}{4}M+\frac{1}{4}N$	

Can. J. Chem. Downloaded from www.nrcresearchpress.com by 210.87.254.42 on 09/05/12
For personal use only.

Can. J. Chem. Downloaded from www.nrcresearchpress.com by 210.87.254.42 on 09/05/12
For personal use only.

There are no off-diagonal matrix elements between functions of different symmetry or between functions of different total spin. This divides the total matrix into submatrices as indicated by the solid horizontal lines. Further simplification follows if we neglect off-diagonal matrix elements between functions whose diagonal elements differ by an amount involving the large chemical shift between the A and X nuclei. This is the simplification which follows when we proceed from AA'A''BB'B'' to AA'A''XX'X''. Further subdivision of the matrix is indicated by broken lines, the largest order of the secular equation to be solved now being two in the A_1 symmetry species and three in the E symmetry species. Explicit energies for the interacting A_1 states can be derived by defining two positive quantities C, D and angles θ, ϕ $[0 < \theta, \phi < \pi]$ by,

$$C \cos 2\theta = \tfrac{3}{4}K + \tfrac{1}{24}(3L - N)$$

$$C \sin 2\theta = -\frac{\sqrt{2}}{12}(3L - N)$$

$$D \cos 2\phi = \tfrac{3}{4}K - \tfrac{1}{24}(3L - N)$$

$$D \sin 2\phi = \frac{\sqrt{2}}{12}(3L - N)$$

The corresponding wave functions and energies are given in Table III.

The stationary state wave functions for the E states that interact are given in Table IV. The elements of the $[a]$, $[b]$ eigenvector matrices are evaluated from the corresponding energy matrix and the matrix of the elements of the Hamiltonian.

TABLE III

Stationary state wave functions and energy levels for the A_1 species of AA'AA''XX'X''

State	Wave function	Energy
$3A_{1,1}^*$	$\cos\theta\,[A_{1/2}A_{1/2}] + \sin\theta\,(2)^{-1/2}[E_{1/2}E_{1/2} + E_{1/2}'E_{1/2}']$	$\frac{1}{2}\nu_A + \frac{1}{2}\nu_X + \frac{1}{8}[N-L] + C$
$4A_{1,1}^*$	$-\sin\theta\,[A_{1/2}A_{1/2}] + \cos\theta\,(2)^{-1/2}[E_{1/2}E_{1/2} + E_{1/2}'E_{1/2}']$	$\frac{1}{2}\nu_A + \frac{1}{2}\nu_X + \frac{1}{8}[N-L] - C$
$3A_{1,0}^*$	$\cos\phi\,[A_{1/2}A_{-1/2}] + \sin\phi\,(2)^{-1/2}[E_{1/2}E_{-1/2} + E_{1/2}'E_{-1/2}']$	$\frac{1}{2}\nu_A - \frac{1}{2}\nu_X - \frac{1}{8}[N-L] + D$
$4A_{1,0}^*$	$-\sin\phi\,[A_{1/2}A_{-1/2}] + \cos\phi\,(2)^{-1/2}[E_{1/2}E_{-1/2} + E_{1/2}'E_{-1/2}']$	$\frac{1}{2}\nu_A - \frac{1}{2}\nu_X - \frac{1}{8}[N-L] - D$
$5A_{1,0}^*$	$\cos\phi\,[A_{-1/2}A_{1/2}] + \sin\phi\,(2)^{-1/2}[E_{-1/2}E_{1/2} + E_{-1/2}'E_{1/2}']$	$-\frac{1}{2}\nu_A + \frac{1}{2}\nu_X - \frac{1}{8}[N-L] + D$
$6A_{1,0}^*$	$-\sin\phi\,[A_{-1/2}A_{1/2}] + \cos\phi\,(2)^{-1/2}[E_{-1/2}E_{1/2} + E_{1-/2}'E_{1/2}']$	$-\frac{1}{2}\nu_A + \frac{1}{2}\nu_X - \frac{1}{8}[N-L] - D$
$3A_{1,-1}^*$	$\cos\theta\,[A_{-1/2}A_{-1/2}] + \sin\theta\,(2)^{-1/2}[E_{-1/2}E_{-1/2} + E_{-1/2}'E_{-1/2}']$	$-\frac{1}{2}\nu_A - \frac{1}{2}\nu_X + \frac{1}{8}[N-L] + C$
$4A_{1,-1}^*$	$-\sin\theta\,[A_{-1/2}A_{-1/2}] + \cos\theta\,(2)^{-1/2}[E_{-1/2}E_{-1/2} + E_{-1/2}'E_{-1/2}']$	$-\frac{1}{2}\nu_A - \frac{1}{2}\nu_X + \frac{1}{8}[N-L] - C$

TABLE IV

Stationary state wave functions for the E species, $\pm\frac{1}{2},\pm\frac{1}{2}$ blocks

State	Wave function
$3E_1^*$	$a_{11}(3E_1) + a_{12}(4E_1) + a_{13}(5E_1)$
$4E_1^*$	$a_{21}(3E_1) + a_{22}(4E_1) + a_{23}(5E_1)$
$5E_1^*$	$a_{31}(3E_1) + a_{32}(4E_1) + a_{33}(5E_1)$
$1E_0^*$	$b_{11}(1E_0) + b_{12}(2E_0) + b_{13}(3E_0)$
$2E_0^*$	$b_{21}(1E_0) + b_{22}(2E_0) + b_{23}(3E_0)$
$3E_0^*$	$b_{31}(1E_0) + b_{32}(2E_0) + b_{33}(3E_0)$
$4E_0^*$	$b_{11}(4E_0) + b_{12}(5E_0) + b_{13}(6E_2)$
$5E_0^*$	$b_{21}(4E_0) + b_{22}(5E_0) + b_{23}(6E_0)$
$6E_0^*$	$b_{31}(4E_0) + b_{32}(5E_0) + b_{33}(6E_0)$
$3E_{-1}^*$	$a_{11}(3E_{-1}) + a_{12}(4E_{-1}) + a_{13}(5E_{-1})$
$4E_{-1}^*$	$a_{21}(3E_{-1}) + a_{22}(4E_{-1}) + a_{23}(5E_{-1})$
$5E_{-1}^*$	$a_{31}(3E_{-1}) + a_{32}(4E_{-1}) + a_{33}(5E_{-1})$

The transition patterns derived from Table I and shown in Fig. 1 can now be picked out from Table II using the symmetry selection rule and,

$$\Delta F_z(\mathrm{AA'A''}) = \pm 1, \quad \Delta F_z(\mathrm{XX'X''}) = 0 \qquad \text{for A transitions,}$$

$$\Delta F_z(\mathrm{XX'X''}) = \pm 1, \quad \Delta F_z(\mathrm{AA'A''}) = 0 \qquad \text{for X transitions.}$$

The results are shown in Fig. 2. For the AA'A'' portion of the spectrum there are 22 transitions between A_1 symmetry species energy levels, 2 transitions between A_2 symmetry species energy levels and 32 doubly degenerate transitions between E symmetry species energy levels. This gives a total of 56 transitions. The breakdown is the same for the 56 XX'X'' transitions.

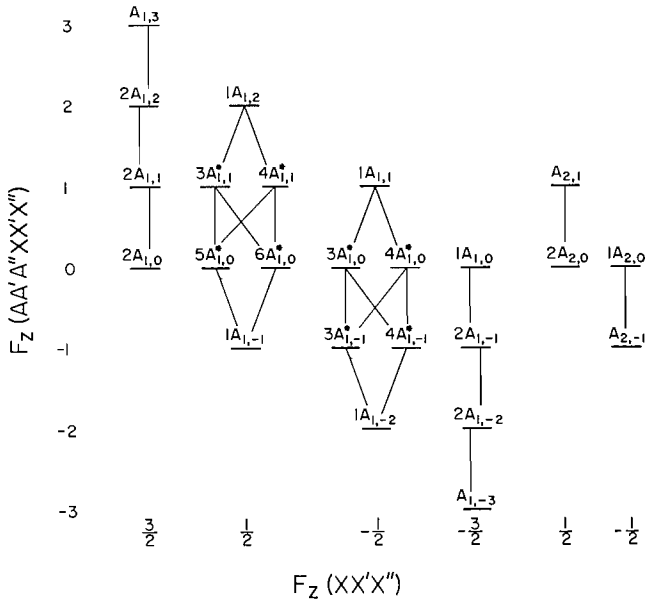

FIG. 2*a*. A schematic representation of the AA'A'' transitions within the A_1 and A_2 symmetry species. A similar schematic diagram can be constructed for XX'X'' transitions.

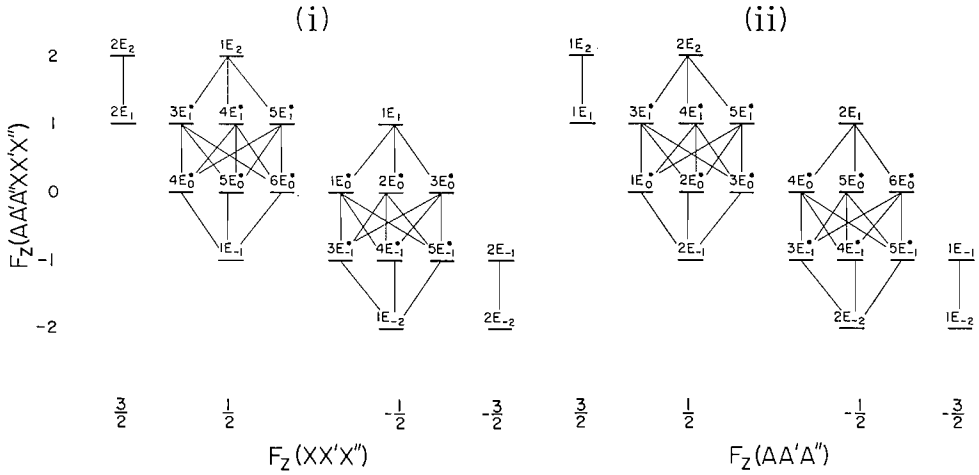

FIG. 2*b*. A schematic representation of (i) the AA'A'' transitions and (ii) the XX'X'' transitions within the E symmetry species. In order to simplify the appearance, not all of the transitions between the energy levels of the 3 × 3 determinants have been shown.

Can. J. Chem. Downloaded from www.nrcresearchpress.com by 210.87.254.42 on 09/05/12
For personal use only.

The energies and relative intensities of one half of the AA'A'' transitions belonging to the A_1 and A_2 symmetry species are given in Table V. For each of the 1 to 12 transitions given in Table V there is an exactly similar line reflected across ν_A (transitions 13–24). An exactly similar set of transitions (centered about ν_X) is obtained for the 22 A_1 and 2 A_2 transitions of the XX'X'' group.

Explicit expressions for the transition energies can be written for only two AA'A'' and two XX'X'' transitions occurring in the E symmetry species (49 to 52). These are given in Table VI.

TABLE V

Transition energies and relative intensities of the A_1 and A_2 symmetry species A transitions[a]

No.	Transition	Energy relative to ν_A	Relative intensity
1	$4A_{1,1}-1A_{1,2}$	$\frac{3}{4}K+\frac{1}{6}[N+L]+C$	$3\sin^2\theta$
2	$6A_{1,0}-3A_{1,1}$	$\frac{1}{4}[N-L]+C+D$	$[2\cos\theta\sin\phi+\sin\theta\cos\phi]^2$
3	$2A_{2,0}-A_{2,1}$	$\frac{1}{2}L$	1
4	$1A_{1,-1}-6A_{1,0}$	$-\frac{3}{4}K+\frac{1}{6}[N+L]+D$	$3\cos^2\phi$
5	$5A_{1,0}-3A_{1,1}$	$\frac{1}{4}[N-L]+C-D$	$[2\cos\theta\cos\phi-\sin\theta\sin\phi]^2$
6	$3A_{1,1}-1A_{1,2}$	$+\frac{3}{4}K+\frac{1}{6}[N+L]-C$	$3\cos^2\theta$
7	$6A_{1,0}-4A_{1,1}$	$\frac{1}{4}[N-L]-C+D$	$[2\sin\theta\sin\phi-\cos\theta\cos\phi]^2$
8	$1A_{1,-1}-5A_{1,0}$	$-\frac{3}{4}K+\frac{1}{6}[N+L]-D$	$3\sin^2\phi$
9	$5A_{1,0}-4A_{1,1}$	$\frac{1}{4}[N-L]-C-D$	$[2\sin\theta\cos\phi+\cos\theta\sin\phi]^2$
10	$2A_{1,2}-A_{1,3}$	$\frac{1}{2}N$	3
11	$2A_{1,1}-2A_{1,2}$	$\frac{1}{2}N$	4
12	$2A_{1,0}-2A_{1,1}$	$\frac{1}{2}N$	3

[a]Transitions 13 to 24 are mirror reflections of 1 to 12 respectively, about ν_A, the center of the spectrum. The 24 XX'X''transitions, 25–48, have similar energies relative to ν_X (see text).

TABLE VI

Explicit E symmetry species transition energies and relative intensities

No.	Transition	Energy	Rel. intensity
49	$2E_1-2E_2$	$\nu_A+\frac{1}{2}N$	2
50	$2E_{-2}-2E_{-1}$	$\nu_A-\frac{1}{2}N$	2
51	$1E_1-1E_2$	$\nu_X+\frac{1}{2}N$	2
52	$1E_{-2}-1E_{-1}$	$\nu_X-\frac{1}{2}N$	2

For the AA'A'' spectrum inspection of Fig. 2 and Tables V and VI indicates that the transitions numbered 10, 11, 12, 49 (one a_3 subspectrum) and 22, 23, 24, 50 (the other a_3 subspectrum) give rise to two strong lines with 12 units of relative intensity each and separated by $|2J_{AX}+J_{AX}'|=|N|$ as was predicted using the principles of Part I. An identical set of lines is found in the XX'X'' spectrum.

In the AA'A'' spectrum transitions numbered 1 to 9 give rise to one ab_2 subspectrum and transitions 13 to 21 give rise to the second ab_2 subspectrum. Comparison of the transition energies and intensities of either ab_2 subspectrum, as given in Table V, with those of the well known AB_2 system (2) gives the following relations between the parameters of either ab_2 subspectrum and the parameters of the AA'A''XX'X'' problem:

$$|J_{ab}|=|J_{AA}+J_{XX}|=|K| \quad \text{and} \quad |\nu_0\delta_{ab}|=|J_{AX}-J_{AX}'|.$$

The separation of lines 3 and 15 (i.e., the separation of the a chemical shifts in the ab_2 subspectra) is $|L|=2J_{AX}-J_{AX}'$. Also the separation of the mean of lines 5 and 7 and the

Can. J. Chem. Downloaded from www.nrcresearchpress.com by 210.87.254.42 on 09/05/12
For personal use only.

mean of lines 17 and 19 (i.e., the separation of the b chemical shifts in the two ab_2 subspectra) is $|N - L|/2 = |J_{AX}'|$.*

The remaining parameter to be determined, $|M| = |J_{AA} - J_{XX}|$, appears only in the E symmetry species matrices, and only the transitions within the *abc* energy level diagrams are affected by M. The parameter M cannot be obtained explicitly from the *abc* subspectra because of the third-order determinants that appear. However, a closer examination of these E symmetry transitions is worthwhile since it is here that any differences between the AA'A'' and XX'X'' spectra must arise.

It is possible to detect the differences between AA'A'' and XX'X'' by using Fig. 2*b*, (i) and (ii), as a guide and the corresponding diagonal matrix elements (see Table II). We are concerned with the $F_z(XX'X'') = \pm\frac{1}{2}$ and $F_z(AA'A'') = \pm\frac{1}{2}$ patterns respectively. We may write the energies, E_i, of a given third-order determinant as $E_i = H_i + P_i$, where H_i is the diagonal element and P_i is a diagonalization constant. The property of trace invariance requires that $\sum_i P_i = 0$. When these energies are defined for each third-order determinant in Fig. 2*b*, (i) and (ii), and the transition energies are written down for both the AA'A'' and XX'X'' parts, it is found that J_{AA} appears independently of J_{XX} in some transition energies of the AA'A'' part. Correspondingly J_{XX} appears independently of J_{AA} in some of the XX'X'' transition energies. From inspection of the transition energies, the differences in positions of the lines arise in transitions between the solutions of the third-order determinants and the stationary state energy levels ($1E_2$, $1E_1$, $1E_{-1}$, $1E_{-2}$ in (i) and $2E_2$, $2E_1$, $2E_{-1}$, $2E_{-2}$ in (ii)). Even so, these differences cannot arise unless $J_{AA} \neq J_{XX}$ and $J_{AX} \neq J_{AX}'$. The nine lines arising from transitions between the third-order determinants in the *abc* subspectra will have the same positions relative to ν_A and ν_X in the AA'A'' and XX'X'' spectra, respectively.

The intensities must next be considered in order to account for all the differences between the A and X spectra. It is possible to express the intensities of the transitions within the E symmetry species in terms of the first-order breakdown ($J_{AX} = J_{AX}'$) relative intensity distribution and the eigenvector matrix elements which determine mixing within the 3×3 determinants (see Table IV). The results are given in Table VII for the AA'A'' transitions of E symmetry species and in Table VIII for the XX'X'' transitions of E symmetry species. The six lines which have different positions in corresponding *abc* subspectra also have different intensities. The nine lines which have the same positions in corresponding subspectra can also have different intensities. Therefore the AA'A'' and XX'X'' spectra appear quite different.

In the special case that $J_{AA} = J_{XX}$, i.e., $M = 0$, the *abc* transitions in the AA'A'' group are identical to the *abc* transitions in the XX'X'' group.

THE ANALYSIS OF THE N.M.R. SPECTRUM OF SYMMETRICAL TRIFLUOROBENZENE

Symmetrical trifluorobenzene is a good example of the AA'A''XX'X'' system in which the differences between the two parts of the spectrum A (^{1}H) and X (^{19}F) are quite clear.

EXPERIMENTAL

The sample of symmetrical trifluorobenzene [n_D^{25}, 1.4110; b.p. 76 °C at 744 mm] was kindly supplied by Dr. G. C. Finger. It was used without further purification and the n.m.r. spectra showed no unexplained

**Inspection of Figs. 1 or 2 shows that the energy level diagrams of the two ab_2 subspectra taken together are identical in form to the energy level diagram of an AB_2X system (7, 8). Thus these two ab_2 subspectra could be designated as an ab_2x subspectrum, and relationships between the two ab_2 subspectra could be defined in terms of the coupling constants J_{ax} and J_{bx} ($\nu_0\delta_{AB} = 0$ here). When this is done the formulae for the transitions and intensities for AB_2X give all the ab_2 transition frequencies and intensities and the x transition frequencies. However, some of the x transition intensities are not given correctly, and for this reason the ab_2x analogy has not been used here.*

The two abc energy level diagrams may be considered together to form an abcx subspectrum, but because of the non-analytical character of abc systems, the abcx analogy was not helpful in this work.

Can. J. Chem. Downloaded from www.nrcresearchpress.com by 210.87.254.42 on 09/05/12
For personal use only.

TABLE VII

Relative intensities of E symmetry species, A transitions[a] for one *abc* subspectrum

No.	Transition origin	Relative intensities[b]
53	$3E_1^*-1E_2$	$3a_{11}^2$
54	$4E_1^*-1E_2$	$3a_{21}^2$
55	$5E_1^*-1E_2$	$3a_{31}^2$
56	$4E_0^*-3E_1^*$	$[2a_{11}b_{11}-a_{12}b_{12}-a_{13}b_{13}]^2$
57	$5E_0^*-3E_1^*$	$[2a_{11}b_{21}-a_{12}b_{22}-a_{13}b_{23}]^2$
58	$6E_0^*-3E_1^*$	$[2a_{11}b_{31}-a_{12}b_{32}-a_{13}b_{33}]^2$
59	$4E_0^*-4E_1^*$	$[2a_{21}b_{11}-a_{22}b_{12}-a_{23}b_{13}]^2$
60	$5E_0^*-4E_1^*$	$[2a_{21}b_{21}-a_{22}b_{22}-a_{23}b_{23}]^2$
61	$6E_0^*-4E_1^*$	$[2a_{21}b_{31}-a_{22}b_{32}-a_{23}b_{33}]^2$
62	$4E_0^*-5E_1^*$	$[2a_{31}b_{11}-a_{32}b_{12}-a_{33}b_{13}]^2$
63	$5E_0^*-5E_1^*$	$[2a_{31}b_{21}-a_{32}b_{22}-a_{33}b_{23}]^2$
64	$6E_0^*-5E_1^*$	$[2a_{31}b_{31}-a_{32}b_{23}-a_{33}b_{33}]^2$
65	$1E_{-1}-4E_0^*$	$3b_{11}^2$
66	$1E_{-1}-5E_0^*$	$3b_{21}^2$
67	$1E_{-1}-6E_0^*$	$3b_{31}^2$

[a]One half of the transitions are presented in this table. For each transition given there is a corresponding transition (transitions 68 to 82) with identical intensity reflected about ν_A.
[b]These intensities are to be multiplied by 2 to account for the degeneracy.

TABLE VIII

Relative intensities of E symmetry species, X transitions[a] for one *abc* subspectrum

No.	Transition origin	Relative intensities[b]
83	$3E_1^*-2E_2$	$3a_{12}^2$
84	$4E_1^*-2E_2$	$3a_{22}^2$
85	$5E_1^*-2E_2$	$3a_{32}^2$
86	$1E_0^*-3E_1^*$	$[-a_{11}b_{11}+2a_{12}b_{12}-a_{13}b_{13}]^2$
87	$2E_0^*-3E_1^*$	$[-a_{11}b_{21}+2a_{12}b_{22}-a_{13}b_{23}]^2$
88	$3E_0^*-3E_1^*$	$[-a_{11}b_{31}+2a_{12}b_{32}-a_{13}b_{33}]^2$
89	$1E_0^*-4E_1^*$	$[-a_{21}b_{11}+2a_{22}b_{12}-a_{23}b_{13}]^2$
90	$2E_0^*-4E_1^*$	$[-a_{21}b_{21}+2a_{22}b_{22}-a_{23}b_{23}]^2$
91	$3E_0^*-4E_1^*$	$[-a_{21}b_{31}+2a_{22}b_{32}-a_{23}b_{33}]^2$
92	$1E_0^*-5E_1^*$	$[-a_{31}b_{11}+2a_{32}b_{12}-a_{33}b_{13}]^2$
93	$2E_0^*-5E_1^*$	$[-a_{31}b_{21}+2a_{32}b_{22}-a_{33}b_{23}]^2$
94	$3E_0^*-5E_1^*$	$[-a_{31}b_{31}+2a_{32}b_{32}-a_{33}b_{33}]^2$
95	$2E_{-1}-1E_0^*$	$3b_{12}^2$
96	$2E_{-1}-2E_0^*$	$3b_{22}^2$
97	$2E_{-1}-3E_0^*$	$3b_{32}^2$

[a]One half of the transitions are presented in this table. For each transition given there is a corresponding transition (transitions 98 to 112) with identical intensity reflected about ν_X.
[b]These intensities are to be multiplied by 2 to account for the degeneracy.

lines. A 30% by volume solution in carbon disulfide, with tetramethylsilane (TMS) internal standard, was degassed and sealed under vacuum into a 5 mm O.D. sample tube.

Preliminary ^1H and ^{19}F spectra were run on a standard Varian 60 Mc/s high resolution n.m.r. spectrometer. Final spectra were obtained using the Varian unit and an RSI "spin decoupler". The field was locked to the TMS internal standard using the method of Freeman and Whiffen (9). The positions of each of the reported peaks in the ^1H spectrum were measured with a reproducibility of ± 0.02 c.p.s., or better, by manually sweeping the scanning audio oscillator across each peak and noting the frequency for maximum recorder deflection. This frequency as well as the frequency of the 1 000 c.p.s. tuning fork oscillator locking frequency was accurately monitored with a Hewlett-Packard 522B electronic counter using a 526C multiperiod average plug-in unit.

In the ^{19}F spectrum the field was locked to one of the two "tall" peaks in the spectrum. The positions of about two thirds of the lines were measured directly as above, and the positions of the remaining lines were obtained by interpolation on recorded spectra. The lower field half of the ^{19}F spectrum was obtained by

Can. J. Chem. Downloaded from www.nrcresearchpress.com by 210.87.254.42 on 09/05/12
For personal use only.

locking onto the upfield "tall" peak, and the upfield half of the spectrum was obtained by locking onto the low field peak. These two halves were joined to give the complete experimental ^{19}F spectrum.

The experimental ^{1}H and ^{19}F spectra are given in Figs. 3 (*a*) and 4 (*a*), respectively, and the corresponding experimental line positions are in Tables IX, X, and XI. The similarities and differences between the two spectra can be seen quite clearly from these experimental results. Observed intensities are not given because of the difficulty of accurately measuring intensities when so many lines overlap. However, Figs. 3 and 4 show good agreement of calculated intensities and experimental peak heights.

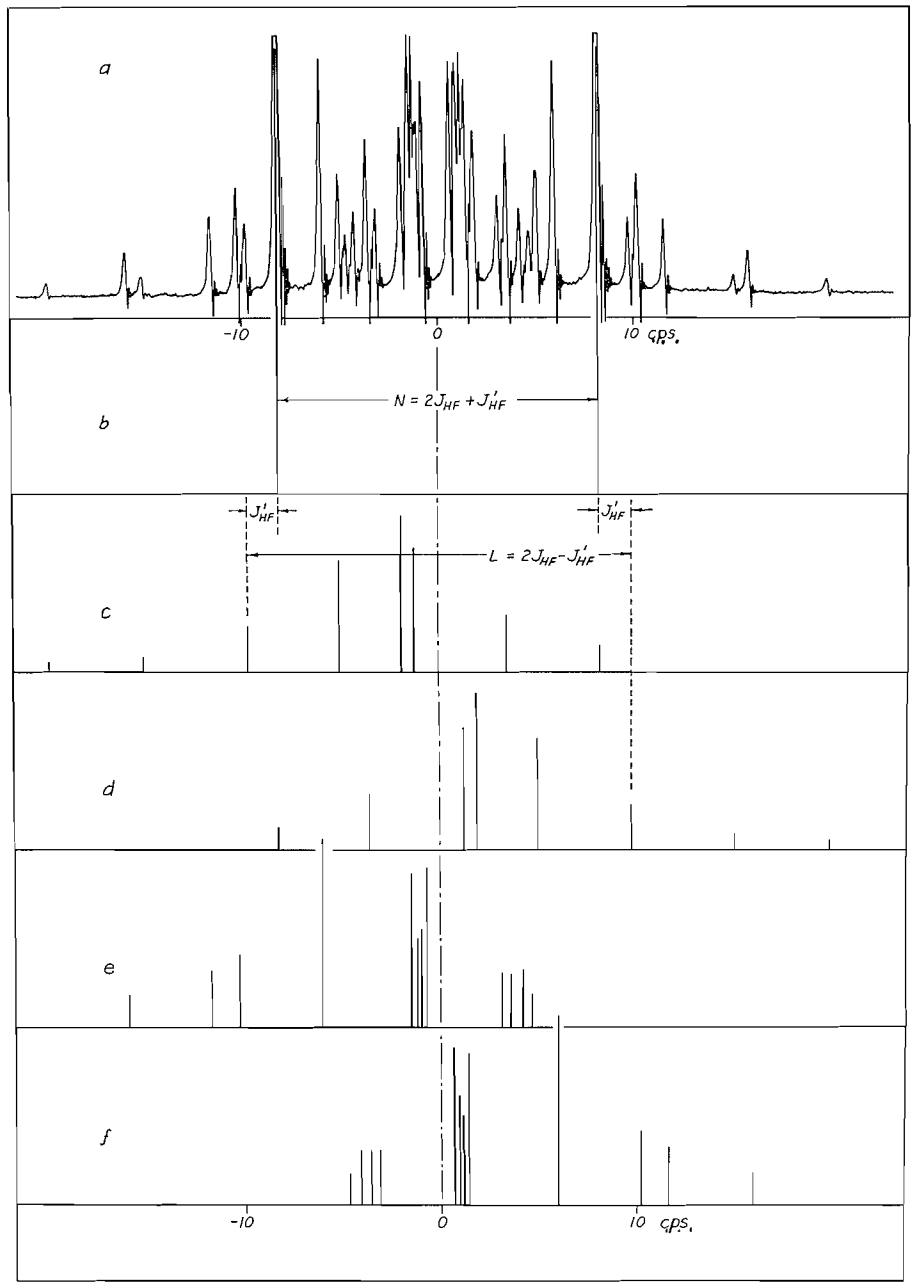

FIG. 3. Experimental and calculated 60 Mc/s ^{1}H n.m.r. spectra of *sym*-trifluorobenzene, 30% by volume in carbon disulfide: (*a*) experimental, (*b*) two calculated a_3 subspectra, (*c*) and (*d*) calculated ab_2 subspectra, (*e*) and (*f*) calculated *abc* subspectra.

Can. J. Chem. Downloaded from www.nrcresearchpress.com by 210.87.254.42 on 09/05/12
For personal use only.

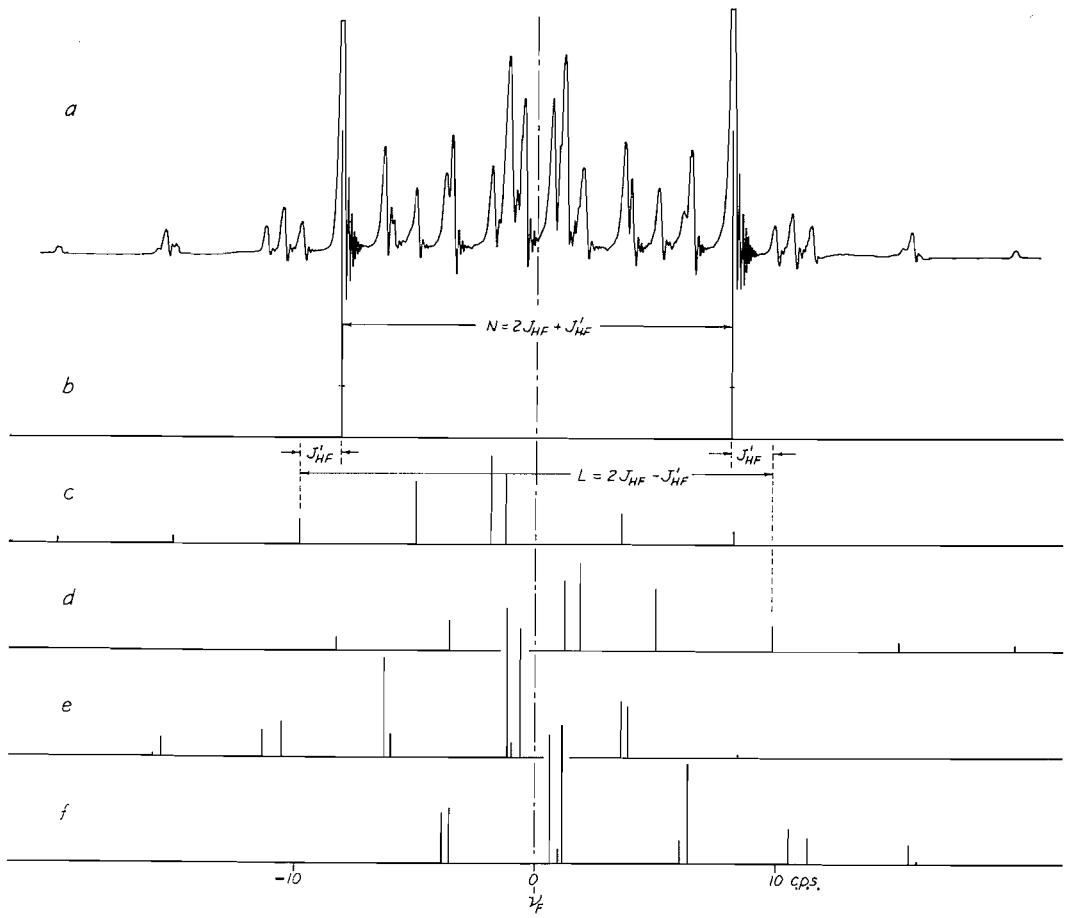

FIG. 4. Experimental and calculated 56.4 Mc/s ^{19}F n.m.r. spectra of *sym*-trifluorobenzene, 30% by volume in carbon disulfide: (*a*) experimental, (*b*) two calculated a_3 spectra, (*c*) and (*d*) calculated ab_2 subspectra, (*e*) and (*f*) calculated *abc* subspectra. Fig. 4 (*b*), (*c*), (*d*) is identical with Fig. 3 (*b*), (*c*), (*d*). The differences between the ^1H and ^{19}F spectra result from differences between Fig. 3 (*e*) and (*f*) and Fig. 4 (*e*) and (*f*).

METHOD OF ANALYSIS

The method of analysis follows from the arguments and results set out above. Therefore we have looked for the a_3 (and x_3) and ab_2 (and xy_2) subspectra in both parts of the spectrum and verified that for this case they are identical. The a_3 lines, with 12 units of intensity each, are the most distinctive features of both spectra. They appear as very intense lines 16.24 c.p.s. apart and symmetrical about the center of each spectrum. They are given in Figs. 3 (*b*) and 4 (*b*) where the A lines are numbered 10, 11, 12, 49 and 22, 23, 24, 50 and the X lines are numbered 34, 35, 36, 51 and 46, 47, 48, 52 in accordance with Tables V, VI, VII, and VIII. Hence we know that $N = 2J_{HF} + J_{HF}' = 16.24$ c.p.s.

The ab_2 subspectra were not picked out quite as easily. However, inspection of the observed line positions given in Tables IX–XI, together with the consideration of the relative intensity distribution and the knowledge that the two ab_2 subspectra in each part, taken together, must form a pattern of lines symmetrical about the center, led us to the assignment of the transitions 1 to 7 and 13 to 19 in the proton spectrum as indicated in Fig. 3 (*c* and *d*). Transitions 8 and 20 were hidden by the a_3 lines, and transitions 9 and 21

Can. J. Chem. Downloaded from www.nrcresearchpress.com by 210.87.254.42 on 09/05/12
For personal use only.

TABLE IX

Calculated and observed line positions and relative intensities of transitions within the A_1 and A_2 symmetry species (i.e., the a_3 and ab_2 lines) for both ^1H and ^{19}F

Transition No.		Calcd. line position[a]	Calcd. rel. intensity	Obsd. line position[a]
^1H	^{19}F			
1	25	19.90	0.235	19.90
2	26	15.10	0.306	15.10
3	27	9.80	1.000	9.80
4	28	5.00	2.470	5.01
5	29	1.87	3.459	1.87
6	30	1.25	2.765	1.24
7	31	−3.55	1.224	−3.56
8	32	−8.23	0.530	—
9	33	−16.78	0.011	—
10	34	8.12	3.000	
11	35	8.12	4.000	8.12
12	36	8.12	3.000	

[a]Line positions are in c.p.s. from center of either the ^1H or ^{19}F spectra. A negative sign indicates line is downfield from center of spectrum. The ^1H transitions 13 to 25 and the ^{19}F transitions 37 to 48 are reflections about the center of the spectra of lines 1 to 12 and 25 to 36, respectively.

TABLE X

Calculated and observed line positions and relative intensities of proton transitions within the E symmetry species

Transition No.	Calcd. line position[a]	Calcd. rel. intensity	Obsd. line position
49	8.12	2	8.12
50	−8.12	2	−8.12
61	15.90	0.740	15.90
66	11.64	1.300	11.64
59	11.34	0.004	—
58	10.55	0.036	—
55	10.25	1.680	10.25
56	6.00	4.252	6.00
65	1.44	3.468	1.43
60	1.14	2.004	1.15
64	0.98	2.454	0.98
53	0.69	3.572	0.69
67	−3.12	1.230	−3.12
62	−3.57	1.216	−3.55
57	−4.21	1.284	−4.20
54	−4.66	0.748	−4.66
63	−13.78	0.012	—

[a]Line positions are in c.p.s. from center of spectrum, ν_H. A negative sign indicates downfield displacement from ν_H. The line positions 53 to 67 are the 15 lines of one of the *abc* subspectra. The line positions of the second proton *abc* subspectrum, 68 to 82, are mirror reflections about ν_H.

were too small to be observed. An identical assignment was made for transitions 25 to 33 and 37 to 45, respectively, in the fluorine spectrum (Fig. 4 (*c* and *d*)). The positions of lines which were either not observed or were hidden by coincidence were calculated. The line positions and intensities of one complete ab_2 subspectrum and the position and intensity of one a_3 subspectrum are given in Table IX along with the measured line positions. Line positions are relative to the center of the spectrum. The data in Table IX apply to both the ^1H and ^{19}F spectra.

The parameters which can be calculated from these a_3 and ab_2 subspectra have been

Can. J. Chem. Downloaded from www.nrcresearchpress.com by 210.87.254.42 on 09/05/12
For personal use only.

TABLE XI

Calculated and observed line positions and relative intensities of fluorine transitions within the E symmetry species

Transition No.	Calcd. line position[a]	Calcd. rel. intensity	Obsd. line position
51	8.12	2	8.12
52	−8.12	2	−8.12
91	15.90	0.124	—
85	15.53	0.774	15.53
89	11.34	1.066	11.36
88	10.55	1.416	10.54
96	6.36	3.902	6.37
86	6.00	0.724	6.02
83	5.95	0.180	—
90	1.14	5.854	1.15
94	0.98	0.574	—
84	0.62	5.048	0.62
92	−3.57	2.194	−3.57
95	−3.87	1.984	−3.83
87	−4.21	0.042	—
97	−8.39	0.112	—
93	−13.78	0.006	

[a]Line positions are in c.p.s. from center of spectrum, ν_F. Negative sign indicates downfield displacement from ν_F. The line positions 83–97 are the 15 lines of one of the *abc* subspectra. The line positions of the second fluorine *abc* subspectrum, 98 to 112, are mirror reflections about ν_F.

described above. The values are as follows: $|N| = 2J_{HF} + J_{HF}' = 16.24$ c.p.s., $|L| = 2J_{HF} - J_{HF}' = 19.60$ c.p.s., and $|K| = J_{HH} + J_{FF} = 8.13$ c.p.s. The ortho H–F coupling constant, J_{HF}(ortho), is identified as J_{HF}, and J_{HF}' is identified as the para H–F coupling constant by observing the statistical weights with which these two couplings appear. Hence $J_{HF} = J_{HF}$(ortho) $= 8.96 \pm 0.02$ c.p.s. and $J_{HF}' = J_{HF}$(para) $= -1.68 \pm 0.02$ c.p.s. It is assumed that J_{HF}(ortho) is positive on the basis of the absolute sign determination of Buckingham and McLaughlan (10) that J_{HH}(ortho) is positive in aromatic compounds and the fact that J_{HH}(ortho) is the same sign as J_{HF}(ortho) in fluorobenzene (11). Actually the magnitudes and relative signs of J_{HF} and J_{HF}' can be obtained directly from the spectrum, once the ab_2 spectra are assigned, as shown in Fig. 3 (*c*, *d*) and Fig. 4 (*c*, *d*) (see Table V also).

The only transitions that are affected by the remaining parameter, $M = |J_{AA} - J_{XX}|$, are those involving the E symmetry 3 × 3 determinants. The value of M is obtained by guessing various values of M, solving the 3 × 3 determinants numerically, and calculating the transition frequencies and intensities. Since in the case of symmetrical trifluorobenzene, variation of the single parameter M must give a satisfactory fit in position and intensity of 12 *abc* type ^{1}H transitions and 8 resolvable *abc* type ^{19}F transitions, a unique fit seems assured. The calculated proton transition frequencies and intensities of E symmetry are given in Table X along with the experimental line positions. The corresponding fluorine data are in Table XI. Figure 3 (*e* and *f*) shows a plot of the ^{1}H lines, and Fig. 4 (*e* and *f*) shows the ^{19}F lines. The best value of $|M|$ is 3.53 ± 0.02 c.p.s. Since $|K| > |M|$, J_{HH} and J_{FF} have the same sign and their magnitudes are 2.30 ± 0.02 c.p.s. and 5.83 ± 0.02 c.p.s., but no information is obtained from the spectrum as to which value corresponds to which coupling. Also the spectra are independent of the signs of J_{HF}(ortho) and J_{HF}'(para) relative to J_{HH} and J_{FF}. However, in the present case, these last two couplings can be assigned and the signs related to J_{HF}(ortho) and J_{HF}'(para) by comparison with the coupling constants in similar molecules.

Can. J. Chem. Downloaded from www.nrcresearchpress.com by 210.87.254.42 on 09/05/12
For personal use only.

In a large number of aromatic compounds the proton–proton couplings lie in the ranges 7–9 c.p.s. and 1–3 c.p.s. for ortho and meta protons (2), respectively. Other workers (4, 12) have shown ortho and meta aromatic couplings to be of the same sign. Meta fluorine–fluorine couplings have been found in the few cases studied to have values in the range 2–4 c.p.s. (2) with no signs known. These data, combined with that in Table XII of the couplings in some 1,3,5-trisubstituted benzenes, strongly suggest that J_{HH} and J_{FF} are positive and should be assigned the values 2.30 c.p.s. and 5.83 c.p.s., respectively.

TABLE XII

Coupling constants for some 1,3,5-trisubstituted benzenes[a]

Molecule	Ref.	J_{HH}(meta), c.p.s.	J_{HF}(ortho), c.p.s.	J_{HF}(para), c.p.s.
1,3,5-$(CH_3)_3C_6H_3$	(13)	$\|2.2\pm0.5\|$		
1,3,5-$(CF_3)_3C_6H_3$	(13)	$\|1.9\pm0.5\|$		
1,3,5-$FCl_2C_6H_3$	(14)	$+1.8\pm0.1$	$+8.8\pm0.1$	-1.2 ± 0.1
1,3,5-$F(CH_3)_2C_6H_3$	(14)	$+1.5\pm0.1$	$+9.1\pm0.3$	-0.9 ± 0.3
1,3,5-$F_3C_6H_3$	This work	$\|2.30\pm0.02\|$	$+8.96\pm0.03$	-1.68 ± 0.03

[a]Signs, where given, are relative to J_{HF}(ortho) taken as positive in the same molecule.

ACKNOWLEDGMENT

The authors with to thank S. Bauer for originally suggesting this problem and C. J. Finger for furnishing a highly purified sample of symmetrical trifluorobenzene. We wish to thank also P. Diehl for several helpful discussions, and S. S. Danyluk for carrying out for us two general six spin calculations on *sym*-trifluorobenzene on an IBM 7090 computer.

REFERENCES

1. H. M. McConnell, A. D. McLean, and C. A. Reilly. J. Chem. Phys. **23**, 1152 (1955).
2. J. A. Pople, W. G. Schneider, and H. J. Bernstein. High-resolution nuclear magnetic resonance. McGraw-Hill Book Company, Inc. New York. 1959.
3. G. W. Flynn and J. D. Baldeschweiler. J. Chem. Phys. **38**, 226 (1963); **38**, 2295 (1963).
4. D. M. Grant, R. C. Hirst, and H. S. Gutowsky. J. Chem. Phys. **38**, 470 (1963).
5. E. B. Wilson. J. Chem. Phys. **27**, 60 (1957).
6. P. Diehl, R. G. Jones, and H. J. Bernstein. Can. J. Chem. **43**, 81 (1964).
7. P. Diehl and J. A. Pople. Mol. Phys. **3**, 547 (1960).
8. R. C. Hirst. Ph.D. Thesis, Univ. of Utah. 1963.
9. R. Freeman and D. H. Whiffen. Proc. Phys. Soc. London, **79**, 794 (1962).
10. A. D. Buckingham and K. A. McLaughlan. Proc. Chem. Soc. 144 (1963).
11. B. Bak, J. N. Shoolery, and G. A. Williams. J. Mol. Spectry. **2**, 525 (1958).
12. R. Freeman, N. S. Bhacca, and C. A. Reilly. J. Chem. Phys. **38**, 293 (1963).
13. J. V. Acrivos. Mol. Phys. **5**, 1 (1962).
14. R. G. Jones. Unpublished results.

Can. J. Chem. Downloaded from www.nrcresearchpress.com by 210.87.254.42 on 09/05/12
For personal use only.

Can. J. Chem. Downloaded from www.nrcresearchpress.com by 210.87.254.5 on 09/05/12
For personal use only.

NOTES

NUCLEOPHILIC ADDITION OF TRIETHYLAMINE TO DIMETHYL ACETYLENEDICARBOXYLATE

ROBERT J. ALAIMO[1] AND DONALD G. FARNUM[2]

During our studies concerning 1,3-dipolar additions involving dimethyl acetylenedicarboxylate as the dipolarophile and triethylamine as the base used to generate the 1,3-dipole, an interesting side reaction was observed.

In all cases, a dark-red polymeric material and a viscous, pale-yellow oil were obtained in addition to the product of 1,3-dipolar cycloaddition. The pale-yellow oil analyzed for a composition $C_{10}H_{17}NO_4$, and its infrared, ultraviolet, and nuclear magnetic resonance (n.m.r.) spectra were consistent with structure I, dimethyl α-diethylaminomaleate (or fumarate).

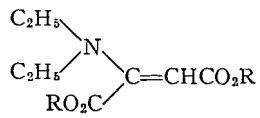

I, R = CH_3.
II, R = CH_3CH_2.

The infrared spectrum showed two non-equivalent carbonyl functions at 1 750 and 1 700 cm^{-1} and a very intense double bond peak at 1 575 cm^{-1}. The ultraviolet spectrum had a maximum at 287 mμ (extinction coefficient 35 400) which compares favorably with the model compound ethyl β-dimethylaminocrotonate with an ultraviolet maximum at 275 mμ (extinction coefficient 22 400) (1).

The n.m.r. spectrum showed two sharp singlets at τ 6.2 and 6.5 p.p.m. which were assigned to the protons of the non-equivalent methyl ester groups; a triplet centered at τ 8.9 assigned to the methyl protons of the ethyl group; a quartet centered at τ 6.8 assigned to the methylene protons of the ethyl group; and a sharp singlet at τ 5.5 assigned to the vinyl proton, the relative areas being consistent with these assignments.

This amino ester was prepared in quantitative yield when equimolar quantities of dimethyl acetylenedicarboxylate, triethylamine, and triethylamine hydrobromide were heated together for 4 h in refluxing methylene chloride, the same conditions as those used in the 1,3-dipolar additions. Triethylamine hydrobromide alone also reacts with dimethyl acetylenedicarboxylate to give an 80% yield of the same product, but triethylamine alone with dimethyl acetylenedicarboxylate gave none of the desired amino ester I. Thus a proton source seems to be necessary. The structure of the product was also confirmed by reaction of diethylamine with dimethyl acetylenedicarboxylate to give the same amino ester in 85% yield.

Reppe (2) reported that tertiary amines or their salts reacted with acetylene or its monosubstituted derivatives in the presence of water to yield quaternary vinyl-ammonium

[1]*Dow Chemical Company Summer Research Fellow, 1962–1963.*
[2]*Fellow of the Alfred P. Sloan Foundation.*

bases. Ruhemann and Cunnington (3) studied the reaction of diethyl acetylenedicarboxylate with diethylamine in ethereal solution at room temperature. They identified the amino ester formed as "Ethylic diethylamidomaleate" II. Vassiliades and Capatos (4), on the other hand, reported that diethylamine and dimethyl acetylenedicarboxylate reacted in alcohol solution at −10° to yield a mixture of the ester amide III and the diamide IV. In our work, no indication of ester-amide or diamide was found in any of the reactions.

$C_2H_5O_2C—C\equiv C—CON(C_2H_5)_2$ III

$(C_2H_5)_2NOC—C\equiv C—CON(C_2H_5)_2$ IV

EXPERIMENTAL

Dimethyl α-Diethylaminomaleate (I)

(a) With Triethylamine Hydrobromide

To a solution of 2.0 g (0.014 mole) of dimethyl acetylenedicarboxylate (Eastman 7235) in 15 ml of methylene chloride heated to reflux was added dropwise a suspension of 2.7 g (0.014 mole) of triethylamine hydrobromide* in 45 ml of methylene chloride. The addition took about 30 min, but the rate of addition did not appear to be critical. The mixture was refluxed for 4 h after addition and the clear solution changed to pale yellow. The solution was then cooled, washed once with 50 ml of water, and dried over anhydrous sodium sulfate.

The reaction mixture was then filtered and the solvent removed *in vacuo*, yielding 2.95 g of yellow–red oil (98%). The amino-ester was purified by molecular distillation at 70° and 5 mm to give a pale-yellow viscous oil (80% recovery). λ_{max} 287 mμ (ϵ = 35 400) (ethanol). ν_{max} 1 750, 1 700, 1 575 cm^{-1} (neat). τ 5.5 (relative area 1.1) singlet; 6.2 (3.2) singlet; 6.5 (2.9) singlet; 6.8 (3.9) quartet; 8.9 (6.0) triplet (carbon tetrachloride).

Anal. Calcd. for $C_{10}H_{17}NO_4$: C, 55.80; H, 7.96; N, 6.51. Found: C, 55.63; H, 7.93; N, 6.41.

Gas chromatographic analysis showed two peaks of areas 987 to 13. The retention time of the smaller peak corresponded to that of dimethyl acetylenedicarboxylate.

(b) With Diethylamine

To a stirred solution of 3.0 g (0.021 mole) of dimethyl acetylenedicarboxylate in 50 ml of methylene chloride chilled in an ice bath was added dropwise a solution of 1.6 g (0.021 mole) of diethylamine in 20 ml of CH_2Cl_2. The stirring in the ice bath was continued for 3 h after addition. The solvent was removed *in vacuo*, yielding 4.5 g (100%) of a pale-yellow oil whose infrared spectrum was identical with that of I. Gas chromatography of this sample under the same conditions as in (*a*) again gave two peaks with the same retention times as those in (*a*). The peak corresponding to the amino-ester accounted for 85% of the total area.

(c) With Triethylamine

With the procedure used in (*a*) but using 3.0 g (0.021 mole) of dimethyl acetylenedicarboxylate in 35 ml of methylene chloride and 2.1 g (0.021 mole) of triethylamine in place of triethylamine hydrobromide in 15 ml of methylene chloride, only starting materials and non-volatile red polymeric material were obtained.

(d) With Triethylamine and Triethylamine Hydrobromide

With the procedure used in (*a*) but using 3.0 g (0.021 mole) of dimethyl acetylenedicarboxylate in 30 ml of methylene chloride and a suspension of 2.1 g (0.021 mole) triethylamine and 3.7 g (0.021 mole) triethylamine hydrobromide in 75 ml of methylene chloride a quantitative yield (4.5 g) of the amino-ester I was obtained.

1. R. L. Shriner, R. C. Fuson, and D. Y. Curtin. The systematic identification of organic compounds. John Wiley & Sons, Inc., New York, N.Y. 1960. p. 183.
2. J. W. Reppe. Acetylene chemistry. Charles Meyer and Co., Inc., New York, N.Y. 1949.
3. S. Ruhemann and A. V. Cunnington. J. Chem. Soc. **75**, 954 (1899).
4. C. Vassiliades and L. Capatos. Compt. Rend. **194**, 1830 (1932).
5. I. F. Halverstadt, W. R. Hardie, and A. R. Williams. J. Am. Chem. Soc. **81**, 3618 (1959).
6. Sadtler Standard Spectra. Sadtler Research Laboratories, Philadelphia, Pa. 1959. No. 9771.
7. C. S. Rondestvedt and P. K. Chang. J. Am. Chem. Soc. **77**, 6532 (1955).

Received October 5, 1964.
Baker Laboratory of Chemistry,
Cornell University
Ithaca, New York.

**Prepared by treating an ethereal solution of triethylamine (Eastman 616) with excess 48% hydrobromic acid. The white, crystalline precipitate, after filtration and drying at 110°, had m.p. 247–251° (corrected) (lit. m.p. 250°, 253° (5, 6); diethylamine hydrobromide lit. m.p. 213–214° (7)).*

Can. J. Chem. Downloaded from www.nrcresearchpress.com by 210.87.254.5 on 09/05/12
For personal use only.

PYROLYSIS STUDIES. XIV.[1] THE PYROLYSIS OF *t*-BUTYL BENZOATES

GRANT GILL SMITH AND BRIAN L. YATES

In an attempt to determine accurate σ^0 values we have studied the intramolecular gas-phase elimination of benzoic acids from ethyl (1) and isopropyl (2) benzoates. Meta- and para-substituent effects in these reactions follow a Hammett σ^0 relationship and it is believed that proximity effects are a minimum for this intramolecular vapor-phase reaction. The values of ρ obtained for the ethyl and *i*-propyl benzoate (0.20 and 0.33 respectively) were rather small and it was thought that a study of the thermal elimination of the acid from *t*-butyl benzoate esters would prove to follow the upward trend and be larger than 0.33 and therefore more suitable for a determination of σ^0 values. Because of the larger *t*-butyl group there was also the possibility that interesting steric effects may alter the rates for certain ortho-substituents.

From the results reported in this paper, it is clear that the thermal decomposition of *t*-butyl benzoates is not a simple intramolecular homogeneous reaction but rather the reaction is subject to occurring also on the walls which activate the reactor and cause an increasing amount of heterogeneous reaction. Since all efforts failed to avoid the heterogeneous reaction, it is apparent that pyrolyzing of *t*-butyl benzoate is not suitable for studying linear free energy relationships.

EXPERIMENTAL

Preparation of the t-Butyl Benzoates

The esters were prepared by refluxing the benzoyl chloride with *t*-butyl alcohol in the presence of pyridine. The benzoyl chlorides were either purchased or prepared by refluxing the benzoic acid with thionyl chloride. The physical constants of the esters are given in Table I.

TABLE I

The physical constants of substituted *t*-butyl benzoates

Substituent	Boiling point °C(mm))	n_D^{20}	Formula	Analyses: Calcd. (%) C	Calcd. (%) H	Found (%) C	Found (%) H
H	116(18)	1.4910*	—	—	—	—	—
m-F	62–63(0.6)	1.4748	$C_{11}H_{13}O_2F$	67.5	6.90	67.3	6.68
p-Cl	94(0.33)	1.5070†	—	—	—	—	—
p-MeO	93–94(0.5)	1.5080	$C_{12}H_{16}O_3$	69.2	7.75	69.0	7.65

*Lit. n_D^{25} 1.4896 (S. G. Cohen and A. Schneider. J. Am. Chem. Soc. 63, 3382 (1941)).
†Lit. b.p. 158.5 at 3 mm, n_D^{25} 1.5041 (R. Altschul. J. Am. Chem. Soc. 70, 2569 (1948)).

Method of Pyrolysis

All of the esters were pyrolyzed at 271.7° in a stainless steel reactor of constant volume (200 ml), whose design and operation have been described (2*b*). The reaction was followed automatically by measuring the increase in pressure inside the reactor by using a stainless steel diaphragm closing one end of the reactor as a null gauge, and a pressure transducer connected to a strip chart recorder. The temperature was maintained to within 0.02° with a large glass wool lagged aluminium block which was electrically heated. Before each ester was introduced care was taken that the surface of the reactor was completely deactivated (3); this was done by leaving the products of pyrolysis of 3-butenoic acid inside the reactor at 400° for at least 1 day, and verifying that the rate constant obtained for the pyrolysis of 1-phenylethyl methyl carbonate in the reactor was 1.85×10^{-3} at 307.2 °C, the value obtained in a reactor with a completely deactivated surface (see Part XIII of this series). Since all esters could be injected into the evacuated reactor as liquids it was

[1]*Part XIII. J. Org. Chem. To be published.*

Can. J. Chem. Downloaded from www.nrcresearchpress.com by 210.87.254.42 on 09/05/12
For personal use only.

not necessary to dissolve them in an inert solvent, although the effects of such radical-inhibiting solvents as cyclohexene and toluene were also determined.

Product Analyses

The pyrolysis products from the pyrolysis of the *p*-methoxy and unsubstituted *t*-butyl benzoates were collected in a liquid nitrogen trap. Vapor-phase chromatographic analysis of the products on a silica gel column at 150 °C revealed only the presence of nitrogen and *i*-butylene, while the acids were reclaimed from the trap as solids.

RESULTS AND DISCUSSION

It would be expected on the basis of the results for the *i*-propyl benzoates that good first-order kinetics would be obtained in the pyrolysis of the *t*-butyl benzoates, and that substituent effects would follow a σ^0 relationship. The results actually obtained for the pyrolysis of the *t*-butyl benzoates are given in Table II; the four rate constants given for each ester was the result of four consecutive runs on that ester, the reactor having a completely deactivated surface before the start of the measurements on that ester. The results given are those for just one set of runs; on *three* completely separate occasions the same four esters were pyrolyzed with the same care to make sure that the surface of the reactor was completely deactivated before the start of the pyrolyses and the same results were obtained as those given in Table II.

TABLE II

Rates of pyrolysis of *t*-butyl benzoates at 271.7 °C

Substituent	$k \times 10^{-3}$, s^{-1}
p-MeO	3.0, 4.0, 6.9
H	3.08, 3.15, 3.25, 3.37
m-F	4.85, 4.89, 4.80, 4.86
p-Cl	5.40, 5.48, 5.52, 5.65

The degree of adherence to the expected first-order kinetics and the reproducibility of the results were found to depend on the ester being studied. Thus, for the *m*-fluoro ester, good first-order plots of $(P_\infty - P_t)$ against time were obtained, and the results were reproducible to the extent of $\pm 2\%$. This is the usual reproducibility obtained for pyrolyses in this apparatus. However, this reproducibility was not shown in the rates of pyrolysis of the other *t*-butyl esters, for each succeeding run of the ester the first-order plots became increasingly curved, and as can be seen from Table II, the rate constants obtained from the plots became greater in magnitude.This behavior was shown to the greatest extent by the *p*-methoxy ester, and only to a small extent by the *p*-chloro ester.

A comparison of the rates of pyrolysis of the *t*-butyl esters also reveals an anomaly, namely that the rate of pyrolysis of the *m*-fluoro ester is slower than that of the *p*-chloro, whereas if substituent effects in the pyrolysis of the *t*-butyl benzoates followed a σ^0 relationship, as was found for the ethyl and *i*-propyl benzoates, the rates should be in the opposite order. On this account and because of the unreproducibility of the data for the pyrolysis of some of the *t*-butyl benzoates it is obvious that this reaction is not very suitable for a determination of substituent constants, but it is of interest as to why this behavior is shown in the pyrolysis of the *t*-butyl benzoates.

It is well recognized (4) that in studying homogeneous gas-phase reactions it is necessary to deactivate the surface of the reactor before reproducible results can be obtained. This may be done either by pyrolyzing the compound to be studied many times or by leaving the products of pyrolysis of allyl bromide (4) or 3-butenoic acid for some time in the

Can. J. Chem. Downloaded from www.nrcresearchpress.com by 210.87.254.42 on 09/05/12
For personal use only.

reactor. This deactivation process seems to involve covering the surface of the reactor with an inert carbon layer which prevents surface catalysis. Under these conditions the gas-phase intramolecular decomposition of carboxylic esters and other types of compounds have been studied and reproducible data obtained. The presence of oxygen or free radicals, however, leads to reactivation of the surface of the reactor, giving fast rates and, generally, curved first-order plots.

The behavior shown by some of the *t*-butyl benzoates, namely that with each succeeding run the first-order plots became more curved and the magnitude of the rate constants became greater, is characteristic of that which would be shown if the previously deactivated surface of the reactor was becoming increasingly activated with each succeeding run. The most likely way in which this could occur would be if the ester was decomposing partially by a surface-catalyzed reaction leaving the surface more and more active. It would appear then, on the basis of this evidence, that some *t*-butyl benzoates under the present conditions can pyrolyze in two ways, one by the normal cyclic elimination reaction that is well known in ester pyrolysis (5), and the other by a surface-catalyzed reaction. It is doubtful that the wall reaction goes by way of a chain mechanism because the products of pyrolysis of *t*-butyl *p*-methoxy benzoate were shown to be exclusively *i*-butylene and *p*-methoxybenzoic acid, and also no effect on the rate of pyrolysis of any of the *t*-butyl benzoates was noted when the pyrolyses were carried out in a threefold excess of such radical inhibitors as toluene and cyclohexene. Because reproducible data were obtained for the pyrolysis of the *m*-fluoro ester it must be concluded that there is very little wall reaction in the pyrolysis of this ester. It would appear then that the relative importance of the normal *cis*-elimination reaction and the wall reaction depends on the substituent, i.e. the wall reaction becomes more important the more electron releasing the substituent in the benzene ring, hence it is greatest for the *p*-methoxy ester and least or non-existent for the *m*-fluoro ester. The *t*-butyl group is also more electron releasing than the *i*-propyl group. Further, if the *t*-butyl *p*-chlorobenzoate partially decomposes by a wall reaction while the *m*-fluoro ester does not, this is probably the reason why the *m*-fluoro ester decomposes more slowly than the *p*-chloro ester, when as stated earlier it would be expected that the reverse would be true. On the basis of this work it would seem then that in the pyrolysis of the carboxylic ester RCO_2R' if the groups R and R′ are too electron releasing, the ester will decompose by a wall reaction as well as the normal *cis*-elimination reaction.

ACKNOWLEDGMENTS

This work was supported in part by the United States Air Force through the Air Force Office of Scientific Research of the Air Research and Development Command under Grant No. AF-AFOSR 62-268. Grateful acknowledgment is given for this support, and for the postdoctoral research fellowship for Brian L. Yates. David Brown assisted in the syntheses of these esters.

1.(*a*) G. G. Smith and D. F. Brown. Can. J. Chem. **42**, 294 (1964). (*b*) G. G. Smith, D. A. K. Jones, and D. F. Brown. J. Org. Chem. **28**, 403 (1963).
2.(*a*) D. A. K. Jones and G. G. Smith. J. Org. Chem. **29**, 3531 (1964). (*b*) G. G. Smith and D. A. K. Jones. J. Org. Chem. **28**, 3496 (1963).
3. R. Taylor, G. G. Smith, and W. H. Wetzel. J. Am. Chem. Soc. **84**, 4817 (1962).
4. A. Maccoll. Technique of organic chemistry. Vol. VIII, Pt. 1. *Edited by* A. Weissberger. Interscience Publishers, Inc. 1961. p. 431
5. C. H. DePuy and R. W. King. Chem. Rev. **60**, 431 (1960).

Received October 1, 1964.
Department of Chemistry,
Utah State University,
Logan, Utah.

Can. J. Chem. Downloaded from www.nrcresearchpress.com by 210.87.254.42 on 09/05/12
For personal use only.

Can. J. Chem. Downloaded from www.nrcresearchpress.com by 210.87.254.105 on 09/05/12
For personal use only.

ISOMERIC 1,3-CYCLOPENTANEDICARBOXYLIC ACIDS FROM THE OXIDATIVE OZONIZATION OF NORBORNENE[1]

SAMUEL C. TEMIN AND MELVIN E. BAUM

We wish to report an unexpected *cis–trans* isomerization which occurs when the ozonization product of bicyclo[2.2.1]heptene-2(norbornene), (I), is oxidized to 1,3-cyclopentanedicarboxylic acid, (II).

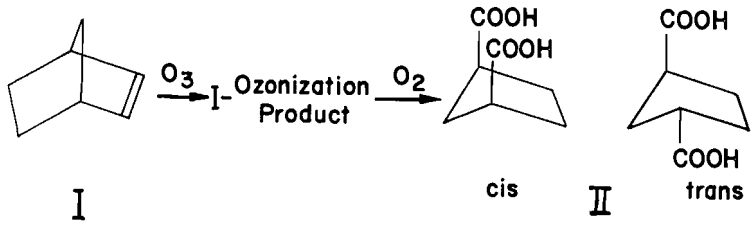

Several oxidative procedures have been reported to convert norbornene to pure *cis*-1,3-cyclopentanedicarboxylic acid (norcamphoric acid). These include oxidation of norbornene with permanganate (1) as well as the action of chlorine (2) and hydrogen peroxide (3) on I-ozonization products prepared in methanol. By use of a newly developed chromatographic technique (4) for the quantitative estimation of *cis* II and *trans* II in mixtures of the isomers, it was discovered (Table I) that the procedures involving oxidation of I-ozonization product yielded small amounts of *trans* II, previously undetected. Isomer distribution was not influenced by ageing the ozonization product (Table I, expt. 3) or preparing it at either −70 or 25 °C (Table I, expts. 2 and 4).

TABLE I
cis/trans Acid ratios

Expt. No.	Ozonization		Oxidation		Yield (%)		*cis/trans* Ratio*
	Solvent	Temp.(°C)	Solvent	Oxidant	*cis*	*trans*	
1†	MeOH	−70	MeOH–H_2O	Cl_2	85.5	Trace	>29
2‡	MeOH	−70	85% HCOOH	H_2O_2	63.3	0.9	67
3‡,§	MeOH	−70	85% HCOOH	H_2O_2	66.4	0.9	72
4	MeOH	25	85% HCOOH	H_2O_2	62.6	0.9	72
5	MeOH	−70	85% HCOOH	Air‖	56.0	5.8	10
6	MeOH	−70	85% HCOOH	Air‖	55.2	6.2	9
7	*t*-BuOH	25	85% HCOOH	Air	56.4	6.6	9
8	*t*-BuOH–H_2O	25	85% HCOOH	Air	49.5	5.4	9
9	H_2O	25	H_2O	Air	45.2	4.7	10
10	Permanganate oxidation¶						97

*Determined by chromatography (4).
†Duplication of ref. 2.
‡Duplication of ref. 3.
§Ozonate solution allowed to stand at room temperature 2 weeks before oxidation.
‖Small amount of potassium persulfate added to oxidation mixture.
¶Duplication of ref. 1.

As much as 10% of *trans* II was obtained, however, when norbornene ozonization product prepared in water or an alcohol as solvent was oxidized with air (5) (Table I, expts. 5 and 6). The ratio of *cis* to *trans* obtained by this procedure was essentially the

[1]*Contribution No. RD-63-13.*

same over a temperature range of −70 to 25 °C during ozonization. Norcamphoric acid (*cis* II) is known to isomerize to the *trans* isomer under acidic conditions (6, 7, 8). However, extended treatment of pure norcamphoric acid under the conditions used for oxidation of the ozonization product—bubbling air through a hot formic acid solution— caused no isomerization. This experiment serves to substantiate that the *trans* acid observed in these experiments did not result from isomerization of already formed norcamphoric acid.

The isomeric ratios were determined by a liquid–liquid chromatographic technique (4) utilizing a silicic acid column. It was demonstrated that interconversion of the isomers does not occur on the column, and that elution of both acids is essentially quantitative. The chromatographic technique permitted high purity *trans* II to be obtained free from *cis* isomer. The chromatographically purified *trans* acid had a melting point of 98–99 °C, several degrees higher than previous reported values. Pospischill (6) reported m.p. 87–88.5° for *trans* II, Ingold and Mohrhenn (9) reported m.p. 89°, and Birch and Dean (8) reported m.p. 95.5–96.5°. Chromatographically pure *cis* II melted at 121.5–122.5 °C.

The equilibrium isomer composition of II under acidic conditions was also determined. In previous HCl-catalyzed isomerizations (6, 8) the crude product obtained was estimated to consist of about equal parts of the two isomers. In all cases, however, the separation of isomers was incomplete and only impure *trans* II was isolated. In this work quantitative analysis of the isomers in the product mixtures permitted determination of a definite value, for the equilibrium isomer composition of II, of 1.0:1.0 at 110 °C. The equilibrium was approached from both sides, i.e., both mixtures rich in *cis* and *trans* II were isomerized by refluxing in concentrated HCl. The rate of isomerization was slow since equilibrium was not reached in 48 h.

EXPERIMENTAL

Norbornene Ozonization

The low temperature ozonization products were prepared as described by Perry (3). During ozonization at room temperature, if conducted by passing the ozone–oxygen stream through a solution of norbornene (I) in a solvent, there were rapid losses of the highly volatile olefin by entrainment in the gas stream. To minimize the loss of I during ozonization at 25°, norbornene dissolved in the appropriate solvent (15% solution) and ozone (2.3% in oxygen) were simultaneously added, at equimolar rates, to the reactor containing the same amount of solvent as used for the norbornene solution. The norbornene solution was metered to the reactor by means of a small pump. When water was employed as the reaction medium, an emulsion of norbornene in water was used. A solution of 66 g of norbornene in 14 ml of *n*-heptane was added slowly to 630 ml of water, containing 3.5 ml of Tergitol NP-14 and 1.5 ml of Triton X-405, with rapid stirring in a home blender. Stirring was continued for several minutes. The emulsion, which was stable for about 24 h, was added simultaneously with ozone to water in the reactor. The ozonization product formed was soluble in water.

Oxidations

The hydrogen peroxide oxidations of norbornene ozonization products were carried out as described by Perry (3). The air oxidations were performed by adding 85% formic acid (100 ml per 0.1 mole norbornene) to the ozonization solution, and then bubbling air (0.5 l/min) through the well-stirred, heated mixture (70–80° water bath) for 10 to 14 h. During this time the alcohol, if used as ozonization medium, was allowed to slowly evaporate. To maintain constant volume, the solvent loss was replenished by adding additional 85% formic acid. Finally, the solvents were removed *in vacuo* at 70 to 80° to give a residue suitable for chromatographic analysis.

Infrared Spectra of Acids

Characteristic absorption bands for *cis*-1,3-cyclopentanedicarboxylic acid (Nujol mull) were found at 7.76 (s), 8.01 (m), 8.25 (m), 9.78 (w), and 10.32 (w) microns. The *trans* acid has characteristic absorption bands at 8.17 (s) and 8.79 (w) microns. The absorption spectra of the *trans* acid in a Nujol mull containing water changed, particularly in the 10.3 to 11.3 micron region associated with the acid OH groups. Under these conditions, the *cis*-acid spectrum was unchanged. Apparently hydrogen bonding occurred with the *trans* acid but not with the *cis* acid which is internally bonded (4).

Can. J. Chem. Downloaded from www.nrcresearchpress.com by 210.87.254.105 on 09/05/12
For personal use only.

Equilibration of Acids

A solution of 3.0 g of *cis*-1,3-cyclopentanedicarboxylic acid in 60 ml of 20.2% hydrochloric acid was refluxed for 112 h at 110°. The solvent was removed *in vacuo* at room temperature, and the residue was analyzed by chromatography. The *cis/trans* ratio was 1.00:1.00. Similarly, a mixture of 2.7 g of the *trans* acid and 0.5 g of the *cis* acid was refluxed with 60 ml of 20.2% hydrochloric acid for 112 h. The *cis/trans* ratio in the product was 1.04:1.00 according to chromatographic analysis. A solution of 10 g of the *cis* acid in 85% formic acid was heated at 85° for 28 h while air was bubbled through at about 0.5 l/min. Solvent was removed *in vacuo* at 80°. The residue, analyzed chromatographically, showed the presence of less than 1% *trans* isomer.

Chromatographic Analysis

A detailed description of the chromatographic procedure has been published (4).

ACKNOWLEDGMENT

The authors wish to thank Dr. R. D. Hinkel and his associates of the Chemical and Instrumental Analysis Group of this laboratory for the chromatographic analyses. The infrared spectral data were furnished by Mr. R. Mainier.

1. S. F. Birch, W. J. Oldham, and E. A. Johnson. J. Chem. Soc. 818 (1947).
2. L. C. King and H. Farber. Abstracts, 136th National Meeting of American Chemical Society, Atlantic City. September 1959. p. 89P.
3. R. H. Perry, Jr. J. Org. Chem. **24**, 829 (1959).
4. E. C. Bossert, A. Donmoyer, R. D. Hinkel, and R. Mainier. Anal. Chem. **36**, 1213 (1964).
5. S. C. Temin and M. E. Baum. U.S. Patent No. 3,126,410. Mar. 24, 1964.
6. K. T. Pospischill. Ber. **31**, 1950 (1898).
7. W. L. Truett, D. R. Johnson, I. M. Robinson, and B. A. Montague. J. Am. Chem. Soc. **82**, 2337 (1960).
8. S. F. Birch and R. A. Dean. J. Chem. Soc. 2477 (1953).
9. C. K. Ingold and H. G. G. Mohrhenn. J. Chem. Soc. 949 (1935).

Received October 6, 1964.
Research Department,
Koppers Company, Inc.,
Pittsburgh, Pennsylvania.

THE CHEMICAL SHIFT OF THE HYDROXYL PROTON OF PHENOLS IN DIMETHYL SULFOXIDE

Robert J. Ouellette

The effect of ring substituents on the spectral properties of phenols has been examined by several groups of workers (1). The infrared stretching frequency of the phenolic hydroxyl group has been shown to vary linearly with σ^- values for 4-substituents in both the simple series and the 2,6-di-*t*-butyl series (2). The identical ρ has been found for both series. The effect of substituents on the nuclear magnetic resonance (n.m.r.) signal of the phenolic proton might also be expected to correlate with σ^- if the chemical shift is dependent on both inductive and resonance factors. However, the observed resonance signal represents a time average of all possible phenolic aggregates at the concentration under consideration. Therefore, it is necessary to extrapolate to infinite dilution in order to obtain the chemical shift of a definable species: that of the monomeric phenol. Dilution studies on phenols have led to inconclusive results as the extrapolated values of the chemical shifts are closely similar and only a trend with σ is noted (3). The reason for this lack of a correlation is unknown at present. The introduction of bulky substituents

Can. J. Chem. Downloaded from www.nrcresearchpress.com by 210.87.254.105 on 09/05/12
For personal use only.

Equilibration of Acids

A solution of 3.0 g of *cis*-1,3-cyclopentanedicarboxylic acid in 60 ml of 20.2% hydrochloric acid was refluxed for 112 h at 110°. The solvent was removed *in vacuo* at room temperature, and the residue was analyzed by chromatography. The *cis/trans* ratio was 1.00:1.00. Similarly, a mixture of 2.7 g of the *trans* acid and 0.5 g of the *cis* acid was refluxed with 60 ml of 20.2% hydrochloric acid for 112 h. The *cis/trans* ratio in the product was 1.04:1.00 according to chromatographic analysis. A solution of 10 g of the *cis* acid in 85% formic acid was heated at 85° for 28 h while air was bubbled through at about 0.5 l/min. Solvent was removed *in vacuo* at 80°. The residue, analyzed chromatographically, showed the presence of less than 1% *trans* isomer.

Chromatographic Analysis

A detailed description of the chromatographic procedure has been published (4).

ACKNOWLEDGMENT

The authors wish to thank Dr. R. D. Hinkel and his associates of the Chemical and Instrumental Analysis Group of this laboratory for the chromatographic analyses. The infrared spectral data were furnished by Mr. R. Mainier.

1. S. F. Birch, W. J. Oldham, and E. A. Johnson. J. Chem. Soc. 818 (1947).
2. L. C. King and H. Farber. Abstracts, 136th National Meeting of American Chemical Society, Atlantic City. September 1959. p. 89P.
3. R. H. Perry, Jr. J. Org. Chem. **24**, 829 (1959).
4. E. C. Bossert, A. Donmoyer, R. D. Hinkel, and R. Mainier. Anal. Chem. **36**, 1213 (1964).
5. S. C. Temin and M. E. Baum. U.S. Patent No. 3,126,410. Mar. 24, 1964.
6. K. T. Pospischill. Ber. **31**, 1950 (1898).
7. W. L. Truett, D. R. Johnson, I. M. Robinson, and B. A. Montague. J. Am. Chem. Soc. **82**, 2337 (1960).
8. S. F. Birch and R. A. Dean. J. Chem. Soc. 2477 (1953).
9. C. K. Ingold and H. G. G. Mohrhenn. J. Chem. Soc. 949 (1935).

Received October 6, 1964.
Research Department,
Koppers Company, Inc.,
Pittsburgh, Pennsylvania.

THE CHEMICAL SHIFT OF THE HYDROXYL PROTON OF PHENOLS IN DIMETHYL SULFOXIDE

Robert J. Ouellette

The effect of ring substituents on the spectral properties of phenols has been examined by several groups of workers (1). The infrared stretching frequency of the phenolic hydroxyl group has been shown to vary linearly with σ^- values for 4-substituents in both the simple series and the 2,6-di-*t*-butyl series (2). The identical ρ has been found for both series. The effect of substituents on the nuclear magnetic resonance (n.m.r.) signal of the phenolic proton might also be expected to correlate with σ^- if the chemical shift is dependent on both inductive and resonance factors. However, the observed resonance signal represents a time average of all possible phenolic aggregates at the concentration under consideration. Therefore, it is necessary to extrapolate to infinite dilution in order to obtain the chemical shift of a definable species: that of the monomeric phenol. Dilution studies on phenols have led to inconclusive results as the extrapolated values of the chemical shifts are closely similar and only a trend with σ is noted (3). The reason for this lack of a correlation is unknown at present. The introduction of bulky substituents

Can. J. Chem. Downloaded from www.nrcresearchpress.com by 210.87.254.5 on 09/05/12
For personal use only.

in the ortho positions, such as exists in 2,6-di-*t*-butyl-*p*-cresol, leads to a stabilized resonance signal which is independent of concentration (4). It has been shown that the effect of substituents in the 4-position on the hydroxyl resonance signal of 4-substituted 2,6-di-*t*-butyl phenols is proportional to σ^{-1}. The necessity of utilizing bulky groups to stabilize the hydroxyl resonance signal can be avoided by employing a solvent which serves as a good hydrogen acceptor. Phenolic aggregates can be eliminated with a hydrogen acceptor, and the resultant resonance signal will reflect the effect of substituents on the phenol ring. Dimethyl sulfoxide is utilized in this study to stabilize the hydroxyl resonance (5).

EXPERIMENTAL

Dimethyl sulfoxide (Crown Zellerbach) was distilled from calcium hydride under reduced pressure and stored over Linde molecular sieves. Uptake of atmospheric moisture was reduced by working under a nitrogen atmosphere in the preparation of samples. All phenols utilized in this study were available in this laboratory.

The solutions were approximately 1 mole % in phenol. The hydroxyl resonance signal was independent of concentration in the 0.005 to 0.02 mole fraction range. All spectra were obtained on a Varian A-60 spectrometer. The probe temperature was maintained at 40°. All resonances appeared at lower field than the 221 c.p.s. low field C_{13}—H satellite of dimethyl sulfoxide. The satellite was utilized as the internal standard and the τ values for the hydroxyl resonances were calculated in the standard manner.

TABLE I

Number	Compound	Chemical shift (τ)*
1	*p*-Aminophenol	1.72
2	3,4,5-Trimethylphenol	1.22
3	*p*-Methoxyphenol	1.17
4	3,4-Dimethylphenol	1.10
5	*p*-*t*-Butylphenol	1.04
6	*p*-Cresol	1.01
7	*p*-Isopropylphenol	0.99
8	3,5-Dimethylphenol	0.97
9	*m*-Cresol	0.88
10	Phenol	0.78
11	*p*-Fluorophenol	0.72
12	*m*-Methoxyphenol	0.59
13	3-Methyl-4-chlorophenol	0.55
14	*p*-Chlorophenol	0.44
15	*p*-Bromophenol	0.40
16	*m*-Fluorophenol	0.30
17	*m*-Acetylphenol	0.26
18	*m*-Chlorophenol	0.22
19	*m*-Bromophenol	0.21
20	*p*-Trifluoromethylphenol	−0.02
21	*p*-Acetylphenol	−0.41
22	*p*-Nitrophenol	−0.97

*The τ values were calculated utilizing the 221 c.p.s. low field C_{13}—H satellite of dimethyl sulfoxide as the internal standard.

RESULTS AND DISCUSSION

The positions of the hydroxyl resonance signals of 22 phenols, expressed in τ values, are given in Table I. The correlation between the observed resonance signals and σ^- values (6) is represented in Graph 1. The range of hydroxyl resonances is much larger than that observed from dilution work (3). The calculated ρ is 1.29. This value is higher than that of 0.73 which was obtained for the 4-substituted 2,6-di-*t*-butylphenols.* The sensitivity of the infrared stretching frequencies (2) of both the simple and the hindered series of 4-substituted phenols indicates that the hydroxyl group is coplanar with the aromatic nucleus. Furthermore, the use of σ^- in the correlation of the hydroxyl resonance signals of the hindered phenols also suggests that the hydroxyl group is coplanar with the

**The ρ was calculated from the data in ref. 1.*

Can. J. Chem. Downloaded from www.nrcresearchpress.com by 210.87.254.5 on 09/05/12
For personal use only.

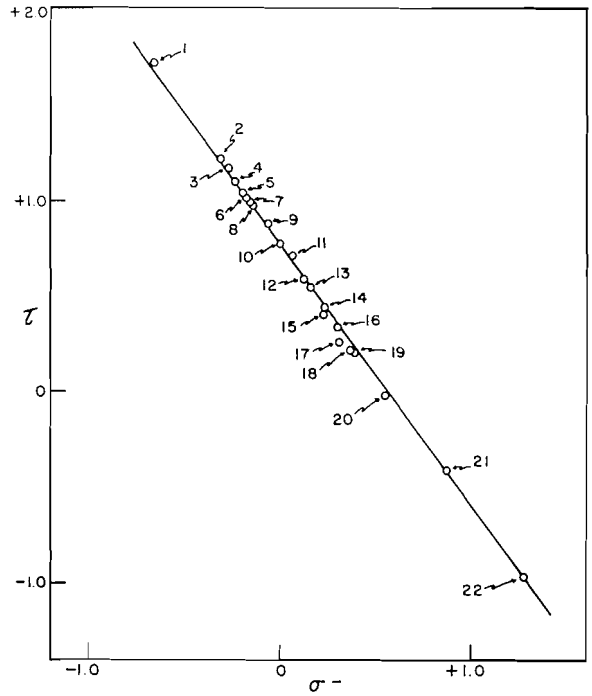

GRAPH 1. Correlation of n.m.r. chemical shift of phenolic hydroxyl with σ^-.

aromatic nucleus. The enhanced sensitivity of substituents on the hydroxyl resonance signals in this study, therefore, must be a reflection of the effect of solvent. The phenolic hydrogen must be effectively bonded to dimethyl sulfoxide. That a specific hydrogen bonded species is present in solution is supported by the absence of a concentration dependence of the resonance signal. Therefore, phenols in dimethyl sulfoxide more closely resemble an ionizing process in which the effect of substituents on the developing charge is reflected.

1. L. A. COHEN and W. M. JONES. J. Am. Chem. Soc. **85**, 3402 (1963).
2. K. U. INGOLD. Can. J. Chem. **38**, 1092 (1960).
3. W. G. PATERSON and N. R. TIPMAN. Can. J. Chem. **40**, 2122 (1962).
4. I. YAMAGUCHI. Bull. Chem. Soc. Japan, **34**, 451 (1961).
5. O. L. CHAPMAN and R. W. KING. J. Am. Chem. Soc. **86**, 1256 (1964).
6. H. H. JAFFE. Chem. Rev. **53**, 191 (1953).

RECEIVED OCTOBER 14, 1964.
CHEMISTRY DEPARTMENT,
OHIO STATE UNIVERSITY,
COLUMBUS, OHIO.

BIOSYNTHESIS OF COLCHICINE. TRACER STUDIES WITH CINNAMATE-3-^{14}C, METHANOL-^{14}C, AND ORNITHINE-2-^{14}C

R. D. HILL AND A. M. UNRAU

The biogenesis of the plant alkaloid colchicine (I) has been the subject of a number of investigations due to its unique chemical structure. Feeding experiments with acetate-1-^{14}C

Can. J. Chem. Downloaded from www.nrcresearchpress.com by 210.87.254.5 on 09/05/12
For personal use only.

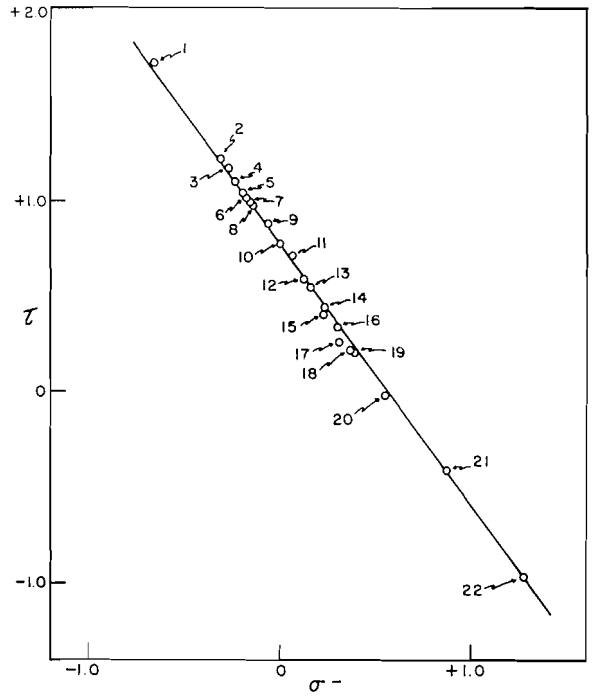

GRAPH 1. Correlation of n.m.r. chemical shift of phenolic hydroxyl with σ^-.

aromatic nucleus. The enhanced sensitivity of substituents on the hydroxyl resonance signals in this study, therefore, must be a reflection of the effect of solvent. The phenolic hydrogen must be effectively bonded to dimethyl sulfoxide. That a specific hydrogen bonded species is present in solution is supported by the absence of a concentration dependence of the resonance signal. Therefore, phenols in dimethyl sulfoxide more closely resemble an ionizing process in which the effect of substituents on the developing charge is reflected.

1. L. A. COHEN and W. M. JONES. J. Am. Chem. Soc. **85**, 3402 (1963).
2. K. U. INGOLD. Can. J. Chem. **38**, 1092 (1960).
3. W. G. PATERSON and N. R. TIPMAN. Can. J. Chem. **40**, 2122 (1962).
4. I. YAMAGUCHI. Bull. Chem. Soc. Japan, **34**, 451 (1961).
5. O. L. CHAPMAN and R. W. KING. J. Am. Chem. Soc. **86**, 1256 (1964).
6. H. H. JAFFE. Chem. Rev. **53**, 191 (1953).

RECEIVED OCTOBER 14, 1964.
CHEMISTRY DEPARTMENT,
OHIO STATE UNIVERSITY,
COLUMBUS, OHIO.

BIOSYNTHESIS OF COLCHICINE. TRACER STUDIES WITH CINNAMATE-3-^{14}C, METHANOL-^{14}C, AND ORNITHINE-2-^{14}C

R. D. HILL AND A. M. UNRAU

The biogenesis of the plant alkaloid colchicine (I) has been the subject of a number of investigations due to its unique chemical structure. Feeding experiments with acetate-1-^{14}C

Can. J. Chem. Downloaded from www.nrcresearchpress.com by 210.87.254.105 on 09/05/12
For personal use only.

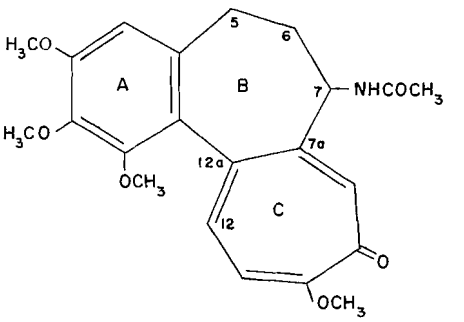

I

and methionine-methyl-^{14}C (1, 2) have shown that the ring structure is not derived from acetate and, in particular, that the tropolone ring is not synthesized in a similar manner to stipitatic acid (3). Acetate-1-^{14}C was incorporated into the N-acetyl group while methionine-methyl-^{14}C was incorporated into the O-methyl positions only. Further experiments have ascertained that the A ring and carbon atoms 5 and 6 of the B ring are derived from phenylalanine (4, 5) but not tyrosine (2). The non-equivalence of phenylalanine and tyrosine suggested that ring A and carbons 5, 6, and 7 were derived from a C_6—C_3 fragment via the cinnamic acid pathway. The results of Battersby and co-workers (6) with phenylalanine-1-^{14}C and cinnamate-3-^{14}C have shown this hypothesis to be correct. In the same paper, the incorporation of tyrosine-3-^{14}C into the tropolone ring of colchicine is reported. Additional experiments with tyrosine-3-^{14}C (7) indicated that colchicine elaborated under these conditions was specifically labelled at position 12.

The present investigations using ornithine-2-^{14}C and methanol-^{14}C were an attempt to ascertain whether the tropolone ring of colchicine might possibly be derived from ornithine, as in the tropane alkaloids (8, 9), and a three-carbon fragment not derived directly from acetate. Ornithine was considered as a remote possibility in the ring-C synthesis since at the time these experiments were conducted no positive results had been reported regarding the biosynthetic pathway for the elaboration of the tropolone ring in colchicine. The feeding experiments with cinnamate-3-^{14}C were performed prior to the publication of Battersby and co-workers (6) and substantiate their results. Table I is a summary of the incorporation data for the administered tracers. The low incorporation of label from ornithine-2-^{14}C conclusively indicates that this amino acid is not a precursor of colchicine. Table II presents the specific activities of the degradation products of colchicine derived from the cinnamate-3-^{14}C and methanol-^{14}C feeding experiments. Colchicine was labelled only in the O-methyl groups by methanol-^{14}C and in the case of cinnamate-3-^{14}C, the label appeared at C_5 as was found by Battersby and co-workers (6). The specific incorporation of methanol-^{14}C was high and is presumed to be mediated by the established one-carbon metabolic pathway involving L-methionine and S-adenosylmethionine (10).

EXPERIMENTAL

Aqueous solutions of the tracers were administered via wicks to *Colchicum autumnale* corms during the vegetative stage of the plants. Ten plants each were used for the cinnamate and ornithine feedings while two plants were used for the methanol experiment. The plants were fed over a 10 day period and stored at −20 °C after 14 days. Colchicine was isolated from the plant tissue using a method described by Leete (5). Radioactive samples were counted in duplicate using either a Nuclear Chicago Model 725 liquid scintillation spectrometer or a Tracerlab Mylar window continuous gas flow counter. Allowance was made for a counting error of 5% or less in each determination.

The radioactive colchicine was diluted with cold material to the specific activities indicated in Table II before degradation. Degradation of the colchicine was performed using previously described methods (1, 4).

Can. J. Chem. Downloaded from www.nrcresearchpress.com by 210.87.254.105 on 09/05/12
For personal use only.

TABLE I

Results of tracer experiments with *Colchicum autumnale*

	Compound fed to plants		Colchicine recovered		
	Weight (mg)	Activity (d.p.m.)	Percentage incorporation	Weight (mg)	Activity (d.p.m./mmole)
Cinnamate-3-^{14}C	9.86	2.1×10^8	0.1	114	2.2×10^5
Ornithine-2-^{14}C	14.9	2.0×10^8	0.003	327	6.9×10^3
Methanol-^{14}C	0.4	2.0×10^8	1.0	25	2.0×10^6*

*Counted as barium carbonate with a Tracerlab Mylar window continuous gas flow counter and converted to d.p.m./mmole of compound.

TABLE II

Degradation of colchicine from feeding experiments

Compound	Specific activity (d.p.m./mmole)
(*a*) Cinnamate-3-^{14}C experiment	
Colchicine	1.1×10^5
Trimethoxyphthalic anhydride	0.92×10^5
3,4,5-Trimethoxybenzoic acid	0.81×10^5
Barium carbonate	0.88×10^5
(*b*) Methanol-^{14}C experiment	
Colchicine	5.0×10^5*
Colchiceine	2.9×10^5*
Trimethoxyphthalic anhydride	2.7×10^5
Gallic acid	0

*Counted as barium carbonate with a Tracerlab Mylar window continuous gas flow counter and converted to d.p.m./mmole of compound.

1. E. Leete and P. E. Németh. J. Am. Chem. Soc. **83**, 219 (1961).
2. A. R. Battersby and J. J. Reynolds. Proc. Chem. Soc. 346 (1960).
3. R. Bentley. Biochim. Biophys. Acta, **29**, 666 (1958).
4. E. Leete and P. E. Németh. J. Am. Chem. Soc. **82**, 6055 (1960).
5. E. Leete. J. Am. Chem. Soc. **85**, 3666 (1963).
6. A. R. Battersby, R. Binks, and D. A. Yeowell. Proc. Chem. Soc. 86 (1964).
7. A. R. Battersby and R. B. Herbert. Proc. Chem. Soc. 260 (1964).
8. E. Leete. J. Am. Chem. Soc. **84**, 55 (1962).
9. E. Leete, L. Marion, and I. D. Spenser. Nature, **174**, 650 (1954); Can. J. Chem. **32**, 1116 (1954).
10. S. H. Mudd. Biochim. Biophys. Acta, **38**, 354 (1960).

Received October 15, 1964.
Department of Plant Science,
University of Manitoba,
Winnipeg, Manitoba.

REACTION OF ARALKYL KETONE OXIMES WITH CARBON MONOXIDE AND HYDROGEN TO YIELD FORMAMIDES AND SECONDARY AMINES

Alex Rosenthal and M. Yalpani

This note summarizes the principal results (shown in Table I) obtained when aromatic and aralkyl ketone oximes were reacted with carbon monoxide and hydrogen using dicobalt octacarbonyl as a catalyst. Prior work (1) showed that aromatic ketone oximes containing a C=N group conjugated to an aromatic ring cyclized with carbon monoxide to yield substituted phthalimidines. Under similar conditions, aralkyl ketone oximes

Can. J. Chem. Downloaded from www.nrcresearchpress.com by 210.87.254.105 on 09/05/12
For personal use only.

TABLE I

Results of tracer experiments with *Colchicum autumnale*

	Compound fed to plants		Colchicine recovered		
	Weight (mg)	Activity (d.p.m.)	Percentage incorporation	Weight (mg)	Activity (d.p.m./mmole)
Cinnamate-3-^{14}C	9.86	2.1×10^8	0.1	114	2.2×10^5
Ornithine-2-^{14}C	14.9	2.0×10^8	0.003	327	6.9×10^3
Methanol-^{14}C	0.4	2.0×10^8	1.0	25	2.0×10^6*

*Counted as barium carbonate with a Tracerlab Mylar window continuous gas flow counter and converted to d.p.m./mmole of compound.

TABLE II

Degradation of colchicine from feeding experiments

Compound	Specific activity (d.p.m./mmole)
(*a*) Cinnamate-3-^{14}C experiment	
Colchicine	1.1×10^5
Trimethoxyphthalic anhydride	0.92×10^5
3,4,5-Trimethoxybenzoic acid	0.81×10^5
Barium carbonate	0.88×10^5
(*b*) Methanol-^{14}C experiment	
Colchicine	5.0×10^5*
Colchiceine	2.9×10^5*
Trimethoxyphthalic anhydride	2.7×10^5
Gallic acid	0

*Counted as barium carbonate with a Tracerlab Mylar window continuous gas flow counter and converted to d.p.m./mmole of compound.

1. E. Leete and P. E. Németh. J. Am. Chem. Soc. **83**, 219 (1961).
2. A. R. Battersby and J. J. Reynolds. Proc. Chem. Soc. 346 (1960).
3. R. Bentley. Biochim. Biophys. Acta, **29**, 666 (1958).
4. E. Leete and P. E. Németh. J. Am. Chem. Soc. **82**, 6055 (1960).
5. E. Leete. J. Am. Chem. Soc. **85**, 3666 (1963).
6. A. R. Battersby, R. Binks, and D. A. Yeowell. Proc. Chem. Soc. 86 (1964).
7. A. R. Battersby and R. B. Herbert. Proc. Chem. Soc. 260 (1964).
8. E. Leete. J. Am. Chem. Soc. **84**, 55 (1962).
9. E. Leete, L. Marion, and I. D. Spenser. Nature, **174**, 650 (1954); Can. J. Chem. **32**, 1116 (1954).
10. S. H. Mudd. Biochim. Biophys. Acta, **38**, 354 (1960).

Received October 15, 1964.
Department of Plant Science,
University of Manitoba,
Winnipeg, Manitoba.

REACTION OF ARALKYL KETONE OXIMES WITH CARBON MONOXIDE AND HYDROGEN TO YIELD FORMAMIDES AND SECONDARY AMINES

Alex Rosenthal and M. Yalpani

This note summarizes the principal results (shown in Table I) obtained when aromatic and aralkyl ketone oximes were reacted with carbon monoxide and hydrogen using dicobalt octacarbonyl as a catalyst. Prior work (1) showed that aromatic ketone oximes containing a C=N group conjugated to an aromatic ring cyclized with carbon monoxide to yield substituted phthalimidines. Under similar conditions, aralkyl ketone oximes

Can. J. Chem. Downloaded from www.nrcresearchpress.com by 210.87.254.42 on 09/05/12
For personal use only.

Can. J. Chem. Downloaded from www.nrcresearchpress.com by 210.87.254.42 on 09/05/12
For personal use only.

TABLE I

Reactions of aromatic ketoximes with carbon monoxide and hydrogen

Expt. No.	Substrate	Substrate (mole)	Catalyst (mole)	Solvent (ml)	CO (p.s.i.)	H_2 (mole)	Reaction temp. (°C)	Reaction time (h)	Products	Yield (%)
1	$(PhCH_2)_2C{=}NOH$	0.04	0.005	45	2 020*	1%*	235	3	$(PhCH_2)_2CO$	20
									$(PhCH_2)_2CHNHCHO$	15
									$[(PhCH_2)_2CHNH]_2CO$†	20
2	$(PhCH_2)_2C{=}NOH$	0.02	0.003	30	2 000	0.055	235	3	$(PhCH_2)_2CHNHCHO$	35
									$[(PhCH_2)_2CH]_2NH$	39
3	$PhCH_2CH_2C(=NOH)CH_3$	0.02	0.003	25	1 900	0.055	235	3	$PhCH_2CH_2CH(CH_3)NHCHO$	30
									$(PhCH_2CH_2CH(CH_3))_2NH$	40
4	$Ph_2C{=}NOH$	0.07	0.02	25	2 070*	1%*	235	3	3-Phenylphthalimidine‡	75
5	$Ph_2C{=}NOH$	0.05	0.005	50	1 900	0.07	230	3	3-Phenylphthalimidine	5
									Diphenylmethane	50
									Benzophenone	12
6	$Ph_2C{=}NOH$	0.025	0.005	30	2 000	0.07	230	3	Diphenylmethane	55
									Diphenylcarbinol	About 5
									No carbonyl compounds	

*Commercial carbon monoxide contained about 1% hydrogen.
†Melting point 158–159°; mixed melting point with authentic sample (3) was 157–159°.
‡Melting point 218–220°; mixed melting point with authentic sample (9) was 218–220°.

might be expected to undergo ring closure to afford six- and seven-membered heterocyclic substances.

Reaction of 1,3-diphenyl-2-propanone oxime with commercial carbon monoxide (containing about 1% hydrogen) under conditions similar to those used in the synthesis of 3-phenylphthalimidine from benzophenone oxime (1) gave 2-formamido-1,3-diphenylpropane (15% yield) and N,N^1-di(1,3-diphenylisopropyl) urea (20%), identified by direct comparison with authentic samples. These products were accompanied by traces of three different crystalline substances exhibiting carbonyl stretching frequencies in their infrared spectra, possibly indicating that some cyclization had occurred. When the mole ratio of hydrogen to substrate was increased to 3:1, as shown in experiment 2, then the yield of the formamide was doubled and in addition, di(1,3-diphenylisopropyl) amine was produced in 39% yield (no primary amine (2) was produced). Application of the same reaction to 4-phenyl-2-butanone oxime (experiment 3) gave 2-formamido-4-phenylbutane (identified by direct comparison with an unambiguously synthesized authentic sample (4)) and di(4-phenyl-2-butyl) amine.

It is probable, as shown in reaction sequences [1] and [2], that the primary amine (II) was the precursor of the formamide (III), and the former compound also condensed with the imine intermediate (I) to yield the intermediate imine (IV) which subsequently was reduced to yield the secondary amine (V). Evidence for these reactions exists in the recent literature (5, 6).

[1] $$(PhCH_2)_2C{=}N{-}OH \xrightarrow[-H_2O]{H_2} \underset{I}{\left[(PhCH_2)_2C{=}NH\right]} \xrightarrow{H_2} \underset{II}{(PhCH_2)_2CHNH_2}$$

$$\downarrow CO$$

$$\underset{III}{(PhCH_2)_2CHNHCHO}$$

[2] $$I + II \xrightarrow[-NH_3]{} \underset{IV}{\left[(PhCH_2)_2C{=}NCH(CH_2Ph)_2\right]} \xrightarrow{H_2} \left[\underset{V}{(PhCH_2)_2CH}\right]_2NH$$

Since the products from the aralkyl ketone oximes were markedly dependent on the mole ratio of hydrogen to substrate, we re-investigated the direct cyclization of benzophenone oxime with carbon monoxide containing various quantities of hydrogen. Treatment of 1 mole of benzophenone oxime with 1.5 moles of hydrogen and 30 moles of carbon monoxide yielded mainly diphenylmethane and about 5% of 3-phenylphthalimidine. Further increase in the mole ratio of hydrogen caused complete elimination of 3-phenylphthalimidine.

In the reaction of 2-ethoxy-1-naphthaldehyde oxime with commercial carbon monoxide, ring closure to the 8-position was expected since the 2-position was blocked. However, no cyclization occurred. From these results, as well as those of other workers (7), evidently only five-membered heterocycles can be formed in significant yields from aromatic compounds containing the C=N group.

EXPERIMENTAL

General Considerations

These have been described previously (1, 8).

Reaction of 1,3-Diphenyl-2-propanone Oxime with Commercial Carbon Monoxide

Chromatographic separation of the product on alumina afforded the compounds shown in experiment 1, Table I, and compounds A, B, and C.

Compound A (1% yield) was recrystallized from ethanol, m.p. 197–198°.

Anal. Calcd. for $C_{16}H_{13}NO$: C, 81.62; H, 5.57; N, 5.95. Found: C, 81.63; H, 5.84; N, 6.01.

Can. J. Chem. Downloaded from www.nrcresearchpress.com by 210.87.254.42 on 09/05/12
For personal use only.

Infrared spectrum of compound A (KBr): 1 665(S), 1 640(S). Nuclear magnetic resonance (given in δ units; spectrum obtained in deuterated chloroform): 3.09 (singlet, area = 2H), 6.25 (singlet, area = 1H), 7.4 (multiplet, area = 8H), and 8.4 (doublet, area = 1H). A possible structure for compound (A) is 3-benzyl-1-isoquinolone.*

Compound B (about 2% yield) was recrystallized from ethanol, m.p. 275–276°. Anal. Found: C, 81.28; H, 5.73; N, 8.58; O, 4.90. The infrared spectrum of compound B showed a strong carbonyl peak at 1 675 cm^{-1}; its ultraviolet spectrum exhibited a peak at 270 mμ. A possible molecular formula for compound (B) is $C_{22}H_{18}N_2O$.

Compound C (2% yield) was recrystallized from chloroform, m.p. 233–234°. Anal. Found: C, 71.12, H, 5.17; N, 8.94. The infrared spectrum showed a strong peak at 1 720 cm^{-1}. A possible molecular formula for compound (C) is $C_{19}H_{16}N_2O_3$.

Reaction of 1,3-Diphenyl-2-propanone Oxime with Carbon Monoxide and Hydrogen to Yield Di(1,3-diphenyl-isopropyl) amine and 2-Formamido-1,3-diphenylpropane

The following compounds were obtained:

(1) Di(1,3-diphenylisopropyl) amine (isolated as the hydrochloride and recrystallized from ethanol), m.p. 245–246°.

Anal. Calcd. for $C_{30}H_{32}NCl$; C, 81.60; H, 7.25; N, 3.17. Found: C, 81.58; H, 7.48; N, 3.01.

(2) 2-Formamido-1,3-diphenylpropane, m.p. 88–89°; mixed melting point with authentic sample (2) m.p. 88–89°, 88–89°; n.m.r. (in $CDCl_3$): 7.8 (CHO, area = 1H), 7.28 (aromatic H, area = 10H), 6.28 (NH, area = 1H), 4.38 (N—CH, area = 1H), 2.88 (CH_2, area = 4H).

Reaction of 4-phenyl-2-butanone Oxime with Carbon Monoxide and Hydrogen to Yield 2-Formamido-4-phenyl-butane and Di(4-phenyl-2-butyl) amine

Work-up of the product by alumina chromatography afforded compounds (A) and (B). Treatment of compound (A) with anhydrous hydrogen chloride in ether yielded 1.7 g of di(4-phenyl-2-butyl) amine hydrochloride which was recrystallized from ethanol, m.p. 198–199°.

Anal. Calcd. for $C_{20}H_{28}NCl$: C, 75.53; H, 8.88; N, 4.42. Found: C, 75.13; H, 8.68; N, 4.37.

Compound (B) was directly compared with an unambiguously synthesized authentic sample of 2-formamido-4-phenylbutane (4) and shown to be the same. Infrared spectrum of compound (B): 3 250(S), 3 020(m), 2 900(S), 2 840 (m), 1 655(s), 1 600(W). Nuclear magnetic resonance (in $CDCl_3$): 8.8 (CHO, area = 1H), 7.5 (NH, area = 1H), 7.1 (aromatic H, area = 5H), 4.8 (C—C—H, area = 1H), 2.68 (CH_2, area = 2H), 1.88 (CH_2, area = 2H), 1.18 (CH_3, area = 3H).

Reaction of 2-Ethoxy-1-naphthaldehyde Oxime with Carbon Monoxide and Hydrogen

2-Ethoxy-1-naphthaldehyde oxime (5 g) was allowed to react with 2 000 p.s.i. of commercial carbon monoxide in the presence of dicobalt octacarbonyl (1.2 g) at a temperature of 235° for 2.5 h. The product (freed of catalyst) contained no cyclic carbonyl group.

ACKNOWLEDGMENTS

Grateful acknowledgment is made to the National Research Council of Canada and to the Petroleum Research Fund administered by the American Chemical Society for the support of this work.

1. A. Rosenthal, R. F. Astbury, and A. Hubscher. J. Org. Chem. **23**, 1037 (1958).
2. S. Rajagopalan. Proc. Indian Acad. Sci. Sect. A, **14**, 126 (1941); Chem. Abstr. **36**, 1604 (1942).
3. L. W. Jones and A. W. Scott. J. Am. Chem. Soc. **44**, 407 (1922).
4. M. L. Moore. *In* Organic reactions. Vol. V. *Edited by* R. Adams. John Wiley and Sons. 1949. p. 30.
5. H. W. Sternberg, I. Wender, R. A. Friedel, and M. Orchin. J. Am. Chem. Soc. **75**, 3148 (1953).
6. H. Shechter, S. S. Rawalay, and M. Tubis. J. Am. Chem. Soc. **86**, 1701 (1964).
7. S. Murahashi, S. Horiie, and T. Jo. Bull. Chem. Soc. Japan, **33**, 81 (1960).
8. A. Rosenthal and S. Millward. Can. J. Chem. **41**, 2504 (1963).
9. R. E. Rose. J. Am. Chem. Soc. **33**, 388 (1911).

Received September 4, 1964.
Department of Chemistry,
University of British Columbia,
Vancouver, British Columbia.

*Suggested by the referee.

Can. J. Chem. Downloaded from www.nrcresearchpress.com by 210.87.254.42 on 09/05/12
For personal use only.

SUR LES PRODUITS DE SUBSTITUTION DU DIMÉTHOXY-1,7 NAPHTALÈNE

JEAN-CLAUDE RICHER ET CLAUDE LAMARRE

Au cours d'une étude récente, Bell et Buck (1) ont rapporté que la nitration du diméthoxy-1,7 naphtalène (I) conduit au diméthoxy-1,7 dinitro-4,8 naphtalène (III*a*) alors que la bromuration de I conduit à un mélange de dibromo-2(?),4(?) et de dibromo-4,8 diméthoxy-1,7 naphtalènes (IV et III*b*). Ces travaux ont été repris; des produits de disubstitution dont les propriétés physiques correspondent à celles rapportées ont été obtenus. De plus les produits de monosubstitution II*a* et II*b* ont pu être isolés en utilisant des conditions expérimentales ménagées.

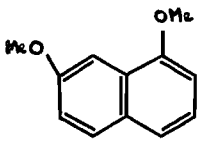

I

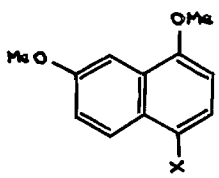

II a) X = NO_2

b) X = Br

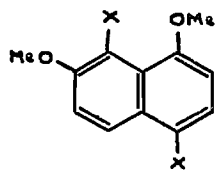

III a) X = NO_2

b) X = Br

Les spectres de résonance magnétique nucléaire (r.m.n.) de ces divers dérivés ont été examinés et les caractéristiques spectrales résumées au Tableau I ont permis d'en établir la structure.

TABLEAU I

Déplacements chimiques des protons aromatiques*

Diméthoxy-1,7 naphtalènes	H_2	H_3	H_5	H_6	H_8
Nitro-4[b] (II*a*)	7.11 (8.7)	8.26 (8.7)	8.57 (9.3)	7.63	7.44 (1.7)
Dinitro-4,8[b] (III*a*)	7.37 (8.5)	8.38 (8.5)	8.82 (9.5)	8.08 (9.5)	—
Bromo-4[a] (II*b*)	6.62 (8.3)	7.53 (8.3)	8.06 (9.3)	7.26	7.56 (2.8)
Dibromo-2,4[a] (IV)	—	7.72 (singulet)	8.04 (9.2)	7.16	7.34 (2.6)
Dibromo-3,4[a] (V)	6.95 (singulet)	—	8.10 (9.4)	7.17	7.47 (2.7)

*Les spectres r.m.n. ont été déterminés à l'aide d'un appareil Varian A-60 pour des solutions dans le chloroforme deutéré (produits marqués *a*) ou la diméthylacétamide (produits marqués *b*) suivant la technique décrite par Wells (4). Les déplacements chimiques ont été mesurés par rapport au benzène utilisé comme standard interne et sont rapportés en p.p.m. (échelle δ et tétraméthylsilane utilisé comme zéro). Les valeurs entre parenthèses indiquent les constantes de couplage entre protons ortho (H_2 vs. H_3, H_5 vs. H_6) ou les protons méta (H_6 vs. H_8). Ces constantes sont exprimées en c.p.s.

1. Les spectres r.m.n. des produits de monosubstitution correspondent à la superposition des éléments d'un système AB sur un système ABX et sont cohérents avec les structures II*a* et II*b* attendues.
2. Le spectre r.m.n. du dérivé dinitré comporte deux paires de doublets (J = 8.5 et J = 9.5 c.p.s.) et confirme la structure III*a* proposée (1) pour ce dérivé.
3. La structure IV proposée mais non prouvée (1) pour le dérivé dibromé de point de fusion 67.5° est confirmée par r.m.n. Le spectre comporte en effet un singulet (H_3) superposé aux éléments d'un système ABX (H_5, H_6 et H_8).

Can. J. Chem. Downloaded from www.nrcresearchpress.com by 210.87.254.5 on 09/05/12
For personal use only.

4. Pour le dérivé dibromé p.f. 124–126°, la r.m.n. suggère la structure V au lieu de la structure III*b* proposée (1). Le spectre de ce dérivé montre en effet *un* et *un seul* singulet (H_2) superposé aux éléments d'un système ABX. A cause de la proximité du groupe méthoxy, la position du singulet correspondant à l'hydrogène (H_2) est déplacée vers les champs magnétiques plus élevés par rapport au singulet (H_3) du dérivé IV.

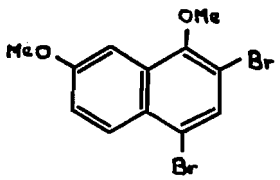

IV

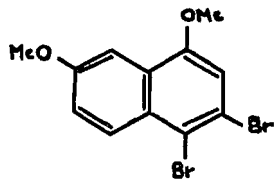

V

La formation des dérivés dibromés IV et V n'était pas prévue considérant que l'introduction d'un atome de brome sur un cycle devrait avoir tendance à désactiver ce cycle et prévenir l'introduction d'un substituant sur le même cycle. La formation prépondérante de IV indique que la désactivation du cycle A par l'introduction d'un atome de brome en position 4 n'est pas grande; la formation de V en quantités mineures n'est plus alors aussi surprenante si l'on considère les effets combinés du méthoxy en position 7 qui active légèrement les réactions en position *amphi* (position 3) et du brome en position 4 qui "oriente" les substitutions vers la position 3.

PARTIE EXPÉRIMENTALE

Les points de fusion ont été déterminés en tubes capillaires ouverts au moyen d'un thermomètre étalonné avec des substances pures de points fusion connus. Les chromatographies ont été réalisées selon la méthode de Stahl (2) à l'aide de couches de 250 microns de Silcia gel G. Les chromatogrammes ont été développés à l'aide de benzène ou d'éther de pétrole 60–110. La présence des taches est révélée à l'aide d'une lampe ultraviolette. Les analyses sont de C. Daesslé, Organic Microanalysis, Montréal.

Diméthoxy-1,7 nitro-4 naphtalène (IIa)

L'action de l'acide nitrique sur I selon le processus expérimental de Thomson *et al.* (3) conduit avec un rendement de 69% au dérivé II*a*, p.f. 127–128°; R_f 0.75 (benzène).

Anal. Calc. pour $C_{12}H_{11}NO_4$: C, 61.80; H, 4.75; N, 6.01. Trouvé: C, 61.84; H, 4.96; N, 6.02.

Diméthoxy-1,7 dinitro-4,8 naphtalène (IIIa)

La dinitration de I selon les indications de Bell et Buck (1) ou de Thomson *et al.* (3) conduit toujours au même dérivé III*a*, p.f. 213° (litt. (1) 209°); R_f 0.49 (benzène).

Bromo-4 diméthoxy-1,7 naphtalène (IIb)

L'action de 1 mole de brome en solution dans le chloroforme sur 1 mole de I fournit avec un rendement de 71% le dérivé monobromé II*b*, p.f. 71°; R_f 0.44 (éther de pétrole).

Anal. Calc. pour $C_{12}H_{11}O_2Br$: C, 53.93; H, 4.15; Br, 29.93. Trouvé: C, 53.84; H, 4.15; Br, 29.57.

Dibromo-2,4 et dibromo-3,4 diméthoxy-1,7 naphtalènes IV et V

La méthode de Bell et Buck (1) est fidèlement suivie et les deux dérivés attendus (IV et V) sont obtenus. Le dibromo-2,4 diméthoxy-1,7 naphtalène (IV) fond à 67.5° (litt. (1) 65–67°); R_f 0.45 (éther de pétrole). Le dibromo-3,4 diméthoxy-1,7 naphtalène (V) fond à 127° (litt. (1) 124–126°); R_f 0.48 (éther de pétrole).

REMERCIEMENTS

Les auteurs remercient le Conseil National de Recherches pour l'aide financière apportée sous forme d'octroi de recherches.

Can. J. Chem. Downloaded from www.nrcresearchpress.com by 210.87.254.5 on 09/05/12
For personal use only.

1. F. Bell et K. R. Buck. J. Chem. Soc. 4626 (1963).
2. E. Stahl. Angew. Chem. **73**, 646 (1961).
3. R. H. Thomson, E. Race et F. A. Rowe. J. Chem. Soc. 350 (1947).
4. P. R. Wells et P. G. E. Alcorn. Australian J. Chem. **16**, 1108 (1963).

Reçu le 6 octobre 1964.
Département de Chimie,
Université de Montréal,
Montréal, Québec.

PHOTOCHEMICAL SYNTHESIS OF VINYLTHIOLS

O. P. Strausz, T. Hikida, and H. E. Gunning

Vinyl mercaptan and its simple derivatives, like the vinyl alcohols, were assumed to be unstable until quite recently, although occasional references in the patent literature (1) can be found to their alleged preparation. It was only last year that Stacey and Harris (2) reported the first successful synthesis through the X-ray-induced chain addition of H_2S to various substituted acetylenes. These authors described the preparation of five compounds: 1-propene-1-thiol, 2-butene-2-thiol, 3,3,3-trifluoropropene-1-thiol, hexafluoro-2-butene-2-thiol, and 2-phenylethene-1-thiol. Vinyl mercaptan itself, however, was not mentioned.

Our interest in vinylic mercaptans arose from the fact that we have found them to be a major product of the reaction of singlet D sulfur atoms with olefins (3). Thus with ethylene, vinyl fluoride, 1,1-difluoro ethylene, propylene, and isobutylene as substrates the corresponding vinylic mercaptan comprises ca. 10–45% of the condensable fraction of the reaction products.

In the present communication, however, we would like to report the synthesis of vinyl mercaptan and 1-propene-1-thiol by another photochemical route, namely the ultraviolet light induced chain addition of H_2S to the corresponding acetylene. Thus when H_2S admixed with acetylene or methyl acetylene, in the liquid phase at −78 °C, in a quartz or Vycor 7910 reaction cell, was exposed to the unfiltered radiation of a medium pressure mercury arc, CH_2:CHSH and CH_3CH:CHSH were respectively formed in good yields. Minor products were H_2, polymer, CS_2, the saturated mercaptan, and possibly some olefins and dithiols. The reaction proceeds in the gas phase as well at room temperature, but with a much smaller yield. In addition secondary processes set in at an earlier stage in the gas-phase reactions.

The reaction mechanism is represented by the familiar scheme:

$$[1] \quad H_2S + h\nu \rightarrow H + SH,$$

$$[2] \quad RC{\equiv}CH + SH \rightarrow R\dot{C}{=}CHSH,$$

$$[3] \quad R\dot{C}{=}CHSH + H_2S \rightarrow RHC{=}CHSH + SH,$$

$$[4] \quad R\dot{C}{=}CHSH + SH \rightarrow RCSH{=}CHSH,$$

$$[5] \quad 2SH \rightarrow H_2S_2,$$

$$[6] \quad 2R\dot{C}{=}CHSH \rightarrow (RC{=}CHSH)_2,$$

$$[7] \quad H + H_2S \rightarrow H_2 + SH,$$

$$[8] \quad H + RC{\equiv}CH \rightarrow RH_2\dot{C}_2,$$

$$[9] \quad RH_2\dot{C}_2 + H_2S \rightarrow RH_3C_2 + SH.$$

Can. J. Chem. Downloaded from www.nrcresearchpress.com by 210.87.254.5 on 09/05/12
For personal use only.

1. F. Bell et K. R. Buck. J. Chem. Soc. 4626 (1963).
2. E. Stahl. Angew. Chem. **73**, 646 (1961).
3. R. H. Thomson, E. Race et F. A. Rowe. J. Chem. Soc. 350 (1947).
4. P. R. Wells et P. G. E. Alcorn. Australian J. Chem. **16**, 1108 (1963).

Reçu le 6 octobre 1964.
Département de Chimie,
Université de Montréal,
Montréal, Québec.

PHOTOCHEMICAL SYNTHESIS OF VINYLTHIOLS

O. P. Strausz, T. Hikida, and H. E. Gunning

Vinyl mercaptan and its simple derivatives, like the vinyl alcohols, were assumed to be unstable until quite recently, although occasional references in the patent literature (1) can be found to their alleged preparation. It was only last year that Stacey and Harris (2) reported the first successful synthesis through the X-ray-induced chain addition of H_2S to various substituted acetylenes. These authors described the preparation of five compounds: 1-propene-1-thiol, 2-butene-2-thiol, 3,3,3-trifluoropropene-1-thiol, hexafluoro-2-butene-2-thiol, and 2-phenylethene-1-thiol. Vinyl mercaptan itself, however, was not mentioned.

Our interest in vinylic mercaptans arose from the fact that we have found them to be a major product of the reaction of singlet D sulfur atoms with olefins (3). Thus with ethylene, vinyl fluoride, 1,1-difluoro ethylene, propylene, and isobutylene as substrates the corresponding vinylic mercaptan comprises ca. 10–45% of the condensable fraction of the reaction products.

In the present communication, however, we would like to report the synthesis of vinyl mercaptan and 1-propene-1-thiol by another photochemical route, namely the ultraviolet light induced chain addition of H_2S to the corresponding acetylene. Thus when H_2S admixed with acetylene or methyl acetylene, in the liquid phase at −78 °C, in a quartz or Vycor 7910 reaction cell, was exposed to the unfiltered radiation of a medium pressure mercury arc, CH_2:CHSH and CH_3CH:CHSH were respectively formed in good yields. Minor products were H_2, polymer, CS_2, the saturated mercaptan, and possibly some olefins and dithiols. The reaction proceeds in the gas phase as well at room temperature, but with a much smaller yield. In addition secondary processes set in at an earlier stage in the gas-phase reactions.

The reaction mechanism is represented by the familiar scheme:

$$[1] \quad H_2S + h\nu \rightarrow H + SH,$$

$$[2] \quad RC{\equiv}CH + SH \rightarrow R\dot{C}{=}CHSH,$$

$$[3] \quad R\dot{C}{=}CHSH + H_2S \rightarrow RHC{=}CHSH + SH,$$

$$[4] \quad R\dot{C}{=}CHSH + SH \rightarrow RCSH{=}CHSH,$$

$$[5] \quad 2SH \rightarrow H_2S_2,$$

$$[6] \quad 2R\dot{C}{=}CHSH \rightarrow (RC{=}CHSH)_2,$$

$$[7] \quad H + H_2S \rightarrow H_2 + SH,$$

$$[8] \quad H + RC{\equiv}CH \rightarrow RH_2\dot{C}_2,$$

$$[9] \quad RH_2\dot{C}_2 + H_2S \rightarrow RH_3C_2 + SH.$$

Can. J. Chem. Downloaded from www.nrcresearchpress.com by 210.87.254.5 on 09/05/12
For personal use only.

The competition between steps [2] and [3] on one hand and [4], [5], and [6] on the other is largely responsible for the observed difference in yield in the gas and liquid phase reactions.

Product identifications were performed by infrared, nuclear magnetic resonance (n.m.r.), and mass spectrometric analyses on the gas chromatographically refined products.

TABLE I

The mass spectra of 1-propen-1-thiol and vinyl mercaptan compared to those for the isomeric episulfides*

	Relative intensity			Relative intensity	
m/e	Propenethiol	Propylene sulfide	*m/e*	Vinyl mercaptan	Ethylene sulfide
76	9.9	5.6	62	8.8	4.6
75	4.0	3.9	61	9.9	6.4
74	81.1	100.0	60	100.0	100.0
73	15.7	11.1	59	95.5	79.5
72	1.9	—	58	47.0	25.3
71	9.0	3.9	57	32.7	11.5
70	1.4	—	56	9.3	2.5
69	8.4	3.3	47	7.7	4.3
68	2.6	—	46	3.4	5.4
61	1.8	—	45	76.4	89.1
59	12.7	32.4	44	7.2	3.8
58	8.0	11.0	34	26.4	9.9
57	4.8	4.2	33	12.2	3.2
48	2.4	3.6	32	14.1	5.1
47	22.2	16.1	30	1.1	—
46	18.3	49.2	29	6.2	2.9
45	70.5	55.5	28	4.1	4.5
44	4.0	2.6	27	50.8	22.1
43	5.3	1.3	26	19.8	8.9
42	7.8	5.8	25	7.3	2.0
41	100.0	97.0	24	2.0	—
40	6.4	5.8	15	2.1	1.2
39	55.5	42.4	14	2.2	2.8
38	8.5	6.4	13	1.6	1.5
37	7.0	3.9	12	1.6	—
36	1.9	1.9			
35	4.2	1.5			
34	2.5	1.4			
33	3.4	1.1			
32	3.4	3.4			
29	2.7	2.7			
28	2.9	3.0			
27	11.8	12.6			
26	4.9	5.7			
15	3.0	3.8			

*The spectra were obtained on a Metropolitan-Vickers Model MS-2 spectrometer at 70 eV.

The mass spectra of the two mercaptans in comparison with the isomeric episulfides are given in Table I. It can be seen from the data that while the cracking patterns for the two types of compounds are quite similar, the mercaptans show a greater tendency for the vinylic split, $(RHC{=}CH)^+ + SH$, as evidenced by their higher mass ratios 27/60 and 41/74 for the C_2 and C_3 compounds respectively.

The infrared spectrum (in CCl_4) of the vinyl mercaptan showed strong absorption at 1 580 cm^{-1} (—C=C—) and the characteristic SH absorption at 2 580 cm^{-1}. The corresponding absorption bands for the propene-1-thiol appeared at 1 620 and 2 590 cm^{-1} respectively.

Can. J. Chem. Downloaded from www.nrcresearchpress.com by 210.87.254.5 on 09/05/12
For personal use only.

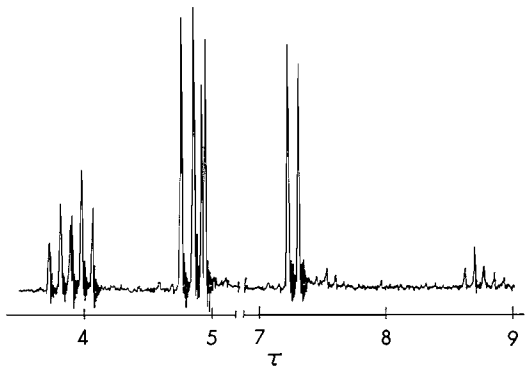

FIG. 1. The n.m.r. spectrum of vinylmercaptan in a CCl_4 solution. The weak resonances at τ = 8.6–9 are probably due to the trimer of the tautomeric thio-acetaldehyde.

The n.m.r. spectrum of vinyl mercaptan, shown in Fig. 1, as obtained in a CCl_4 solution using TMS as a standard gave a doublet in the SH resonance region at τ-values of 7.2 and 7.3, a quartet in the terminal $=CH_2$ region at τ-values of 4.72, 4.82, 4.90, and 4.84. A multiple $=CH_2$ resonance centered on a τ-value of 3.90 also appeared.

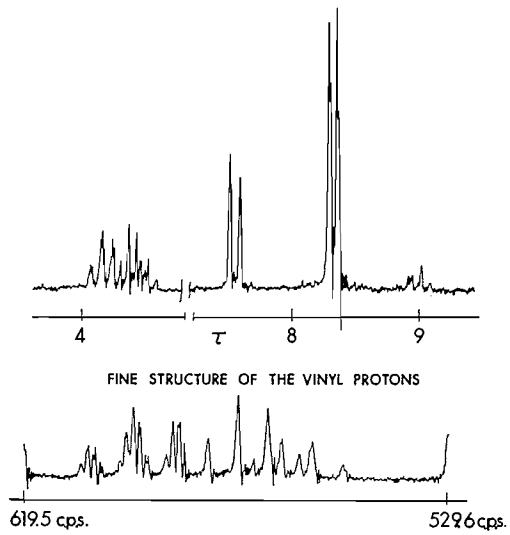

FIG. 2. The n.m.r. spectrum of 1-propene-1-thiol in CCl_4 solution. The weak signals centered at τ-value of 9 are probably due to the trimer of the tautomeric thio-propionaldehyde.

Similarly the n.m.r. spectrum of the propene-1-thiol, given in Fig. 2, showed a poorly resolved double doublet in the CH_3 resonance region at τ-values of 8.34 and 8.28, while the SH resonances appeared at τ-values of 7.59 and 7.51. The multiplet for vinyl protons was found centered at a τ-value of 4.3. The spin–spin coupling between the two vinylic protons is 9.1 c.p.s., an order of magnitude larger than would be expected for terminal vinyl protons. Consequently the structure must be 1-propene-1-thiol. Furthermore, the fine structure of the vinylic proton multiplet at τ = 4.3 indicates that of the two possible geometrical isomers only one is present; that is, one of the two vinyl doublets is split to

Can. J. Chem. Downloaded from www.nrcresearchpress.com by 210.87.254.5 on 09/05/12
For personal use only.

a quadruplet–quintuplet–quadruplet configuration through coupling to the SH and CH_3 protons, while the other gives two overlapping quadruplets through coupling to the methyl protons. The integrated peak areas were in the right proportion in each spectrum.

Both the infrared and n.m.r. spectra of the propene-1-thiol agree in the main with those reported by Stacey and Harris. One significant difference, however, is that according to the n.m.r. data the 1-propene-1-thiol obtained here consists of only one geometrical isomer, while Stacey and Harris (2) obtained a mixture of the *cis* and *trans* isomers. Now, Skell and Allen (4) have shown that the radical-chain addition of HBr to methyl acetylene is a stereospecific process. At higher conversions, however, the Br atom catalyzed *cis* → *trans* isomerization of the 1-bromo-1-propene product occurs readily, leading to equilibrium mixtures. In our experiment the conversion of methyl acetylene was 11%, while in Stacey and Harris' experiment it was 22% or greater and therefore it would appear that similar considerations apply to the H_2S—C_2H_2 system as was found for the HBr addition reaction (4).*

Both thiols synthesized here are colorless liquids with the characteristic mercaptan odor. They readily undergo polymerization on standing at room temperature to colorless oils and (or) white solids. There is no evidence for isomerization to the episulfide structure but a slow tautomeric conversion to the corresponding thio-aldehydes is probable (5).

EXPERIMENTAL

A cylindrical quartz reaction vessel, 5 cm in diameter and 2 cm in length was used for the liquid phase reactions. It was immersed in a dry ice–acetone bath with the liquid level in the cell below that of the coolant. Irradiation was effected through the flat window of the cell above the bath by a Hanovia, model 30620, medium-pressure mercury arc, positioned ca. 10 in. above the cell. To prevent warming of the cell by infrared emission from the lamp, a quartz plate was interposed between the cell and lamp.

Several runs were done on both systems under slightly different conditions, a representative example of which will be given below.

$CH_3C{\equiv}CH + H_2S$

Liquid methyl acetylene (5 ml) and 15 ml of liquid H_2S was introduced to the above cell and irradiated for 20 min. The noncondensable product, hydrogen, which amounted to 0.065 mmoles was removed at −196 °C. After distilling off the excess reactants at −98 °C, 0.6 ml of liquid remained. This could be distilled at −64 °C, with only a small amount of oily residue remaining. The volatile fraction was then transferred to the sample tube of a gas chromatographic unit by *in vacuo* distillation and analyzed on an 8 ft tricresylphosphate-on-firebrick column at 35 °C. The separated components were trapped from the gas chromatographic effluents and collected for identification. In addition to traces of substrates dissolved in the product three components appeared on the chromatogram. The first peak, a C_4H_6 hydrocarbon, which was an impurity in the methylacetylene, eluted in 5.2 min from the column, the second, CS_2, in 8.0 min, and the third peak, the propene-1-thiol, in 12.3 min. The composition for the whole sample in peak area percentage was: C_4H_6 (12%), CS_2 (1%), and $CH_3CH{=}CHSH$ (87%).

Thus, the total yield of the propenethiol, assuming a density of 0.8 g ml^{-1}, is about 0.4 g or 5×10^{-3} mole. From the lamp characteristics (140 W input, max 2 W output in the H_2S-absorbing region, i.e. $\lambda < 3\,000$ Å) and the geometrical arrangement of the cell-lamp assembly, the quantum yield may be estimated to be in the order of 100.

$C_2H_2 + H_2S$

The experiments with acetylene were carried out as with methyl acetylene, but here the whole cell was immersed in the cooling bath to minimize the danger of explosion. Since acetone absorbs strongly below $\lambda = 3\,000$ Å the yields were generally lower than with methyl acetylene. Also the acetylene to hydrogen sulfide ratio had to be kept low, $\leqslant$ 1:10 by liquid volume, although no explosion occurred in one run with a volume ratio of 1:5. On the other hand with 1:1 mixtures, explosion resulted on irradiation.

In a 1.5 h irradiation of a 1:5 $C_2H_2H_2S$ mixture with a total volume of 18 ml, 1.0 ml of liquid remained after the excess reactants were distilled off at −130 °C. This was distilled at −64 °C and analyzed by gas

**Note added in proof: Drs. F. W. Steacey and J. F. Harris of DuPont (ref. 2) have kindly informed us that further n.m.r. studies of their propene-1-thiol have shown the compound to be a single isomer, probably the trans, rather than a mixture of cis and trans as originally reported (2). Thus the apparent discrepancy between the two studies has been resolved.*

Can. J. Chem. Downloaded from www.nrcresearchpress.com by 210.87.254.5 on 09/05/12
For personal use only.

chromatography on the above column. Three peaks appeared on the chromatogram which were identified as C_2H_5SH (retention time 7.5 min), C_2H_3SH (9.2 min), and acetone (14.2 min). The acetone was an impurity in the acetylene. The vinyl mercaptan fraction was rerun on a 16 ft silicone-550 with 2% stearic acid on Kromat CE column which allowed the separation of the small amount of CS_2 present from the vinyl mercaptan. The percentage peak area composition of the 1 ml of liquid was: 62% acetone, 33% vinyl mercaptan, 4.5% C_2H_5SH, and 0.5% CS_2. A very small amount of nonvolatile oil was also formed.

The n.m.r. spectra were obtained on a Varian 100 Mc instrument.

ACKNOWLEDGMENT

We thank Mr. G. Bigam for the n.m.r. spectra. This work was supported by a grant from Imperial Oil Limited and the National Research Council of Canada.

1. E. E. Reid. Organic chemistry of bivalent sulfur. Vol. 1. Chemical Publishing, New York. 1958. p. 21.
2. F. W. Stacey and J. F. Harris. J. Am. Chem. Soc. **85**, 963 (1963).
3. H. A. Wiebe, A. R. Knight, O. P. Strausz, and H. E. Gunning. To be published.
4. P. S. Skell and R. G. Allen. J. Am. Chem. Soc. **86**, 1559 (1964).
5. E. Campaigne. Addition of thiols or hydrogen sulfide to carbonyl compounds. *In* Organic sulfur compounds. *Edited by* N. Kharasch. Pergamon. 1961. p. 143.

Received September 3, 1964.
Department of Chemistry,
University of Alberta,
Edmonton, Alberta.

DECOMPOSITION OF THE ETHYL RADICAL AND THE MECHANISM OF THE PYROLYSIS OF *n*-BUTANE

J. H. Purnell and C. P. Quinn

As a result of a detailed analytical study of the kinetics of formation of the products in the initial stages of the pyrolysis of *n*-butane we have offered support (1) for the homogeneous mechanism:

[1] $$\left.\begin{array}{l} C_4H_{10} \rightarrow C_2H_5\cdot + C_2H_5\cdot \\ C_4H_{10} \rightarrow CH_3\cdot + C_3H_7\cdot \end{array}\right\},$$

[2] $$C_4H_9\cdot \rightarrow C_2H_4 + C_2H_5\cdot,$$

[3] $$C_4H_9\cdot \rightarrow C_3H_6 + CH_3\cdot,$$

[4] $$C_2H_5\cdot + C_4H_{10} \rightarrow C_2H_6 + C_4H_9\cdot,$$

[5] $$CH_3\cdot + C_4H_{10} \rightarrow CH_4 + C_4H_9\cdot,$$

[6] $$H\cdot + C_4H_{10} \rightarrow H_2 + C_4H_9\cdot,$$

[7] $$C_2H_5\cdot \rightarrow C_2H_4 + H\cdot,$$

[8] $$\left.\begin{array}{l} C_2H_5\cdot + C_2H_5\cdot \rightarrow C_4H_{10} \\ C_2H_5\cdot + C_2H_5\cdot \rightarrow C_2H_4 + C_2H_6 \end{array}\right\}.$$

In order to explain several unusual features of the results, we proposed that the unimolecular decomposition of the ethyl radical [7] was in its pressure-dependent region under the conditions of our experiments. It has now been suggested (2) that an alternative interpretation of our results is possible. This alternative involves the assumption that the decomposition of the ethyl radical, [7], is strictly first order for the conditions of our study, and that a molecular process,

[M] $$C_4H_{10} \rightarrow C_2H_4 + C_2H_6,$$

Can. J. Chem. Downloaded from www.nrcresearchpress.com by 210.87.254.5 on 09/05/12
For personal use only.

chromatography on the above column. Three peaks appeared on the chromatogram which were identified as C_2H_5SH (retention time 7.5 min), C_2H_3SH (9.2 min), and acetone (14.2 min). The acetone was an impurity in the acetylene. The vinyl mercaptan fraction was rerun on a 16 ft silicone-550 with 2% stearic acid on Kromat CE column which allowed the separation of the small amount of CS_2 present from the vinyl mercaptan. The percentage peak area composition of the 1 ml of liquid was: 62% acetone, 33% vinyl mercaptan, 4.5% C_2H_5SH, and 0.5% CS_2. A very small amount of nonvolatile oil was also formed.

The n.m.r. spectra were obtained on a Varian 100 Mc instrument.

ACKNOWLEDGMENT

We thank Mr. G. Bigam for the n.m.r. spectra. This work was supported by a grant from Imperial Oil Limited and the National Research Council of Canada.

1. E. E. Reid. Organic chemistry of bivalent sulfur. Vol. 1. Chemical Publishing, New York. 1958. p. 21.
2. F. W. Stacey and J. F. Harris. J. Am. Chem. Soc. **85**, 963 (1963).
3. H. A. Wiebe, A. R. Knight, O. P. Strausz, and H. E. Gunning. To be published.
4. P. S. Skell and R. G. Allen. J. Am. Chem. Soc. **86**, 1559 (1964).
5. E. Campaigne. Addition of thiols or hydrogen sulfide to carbonyl compounds. *In* Organic sulfur compounds. *Edited by* N. Kharasch. Pergamon. 1961. p. 143.

Received September 3, 1964.
Department of Chemistry,
University of Alberta,
Edmonton, Alberta.

DECOMPOSITION OF THE ETHYL RADICAL AND THE MECHANISM OF THE PYROLYSIS OF *n*-BUTANE

J. H. Purnell and C. P. Quinn

As a result of a detailed analytical study of the kinetics of formation of the products in the initial stages of the pyrolysis of *n*-butane we have offered support (1) for the homogeneous mechanism:

[1] $$\left.\begin{array}{l} C_4H_{10} \rightarrow C_2H_5\cdot + C_2H_5\cdot \\ C_4H_{10} \rightarrow CH_3\cdot + C_3H_7\cdot \end{array}\right\},$$

[2] $$C_4H_9\cdot \rightarrow C_2H_4 + C_2H_5\cdot,$$

[3] $$C_4H_9\cdot \rightarrow C_3H_6 + CH_3\cdot,$$

[4] $$C_2H_5\cdot + C_4H_{10} \rightarrow C_2H_6 + C_4H_9\cdot,$$

[5] $$CH_3\cdot + C_4H_{10} \rightarrow CH_4 + C_4H_9\cdot,$$

[6] $$H\cdot + C_4H_{10} \rightarrow H_2 + C_4H_9\cdot,$$

[7] $$C_2H_5\cdot \rightarrow C_2H_4 + H\cdot,$$

[8] $$\left.\begin{array}{l} C_2H_5\cdot + C_2H_5\cdot \rightarrow C_4H_{10} \\ C_2H_5\cdot + C_2H_5\cdot \rightarrow C_2H_4 + C_2H_6 \end{array}\right\}.$$

In order to explain several unusual features of the results, we proposed that the unimolecular decomposition of the ethyl radical [7] was in its pressure-dependent region under the conditions of our experiments. It has now been suggested (2) that an alternative interpretation of our results is possible. This alternative involves the assumption that the decomposition of the ethyl radical, [7], is strictly first order for the conditions of our study, and that a molecular process,

[M] $$C_4H_{10} \rightarrow C_2H_4 + C_2H_6,$$

Can. J. Chem. Downloaded from www.nrcresearchpress.com by 210.87.254.6 on 09/05/12
For personal use only.

Can. J. Chem. Downloaded from www.nrcresearchpress.com by 210.87.254.6 on 09/05/12
For personal use only.

plays a significant role in *n*-butane pyrolysis. Because reaction [7] seems likely to be involved in many organic pyrolyses, it is clearly essential to establish whether or not this recently proposed alternative mechanism is compatible with the experimental results we have already published. Three tests may be applied.

First, it may be observed that, unlike our original mechanism, the alternative does *not* predict that an inert gas would increase the production of ethylene at the expense of ethane. In our earlier paper, we included a diagram clearly demonstrating the occurrence of this effect.

A second test of the alternative mechanism lies in a study of the product ratio,

$$\beta = \frac{[C_2H_4] + [C_2H_6]}{[CH_4]}.$$

From the results already presented (1) it can be deduced that, at constant temperature, over the pressure range 12.5 to 151 mm Hg of *n*-butane, β is constant to $\pm 6\%$ at the 96% confidence limit. This result is entirely compatible with our original explanation but only compatible with the alternative mechanism if the molecular process [M] contributes less than 19% of the total C_2 products under these conditions. This maximum value is almost half the 33% contribution envisaged by Laidler *et al.* (2) in proposing the alternative mechanism.

Finally, a steady state treatment of the alternative mechanism composed of reactions [1]–[8] and [M], yields

$$\frac{1}{(\alpha - 1)[C_4H_{10}]} = \frac{k_4}{2k_7} + \frac{k_M}{2k_7}\sqrt{\frac{k_8}{k_1[C_4H_{10}]}}$$

where

$$\alpha = \frac{[C_2H_4]}{[C_2H_6]}.$$

If k_7 were independent of pressure, this result would demand linearity of a plot of $\{(\alpha - 1)[C_4H_{10}]\}^{-1}$ against $[C_4H_{10}]^{-1/2}$, with a finite and positive *y*-intercept and positive slope. Figure 1 illustrates such a plot formed from the experimental results presented in our earlier paper. It is clear that the data may be taken either to fall on a line of positive curvature passing through the origin or on a straight line of *negative* *y*-intercept. The first possibility is incompatible with the alternative mechanism while the latter, absurdly, implies a negative rate constant. In contrast, our original interpretation (1) gives an excellent quantitative description of these same results.

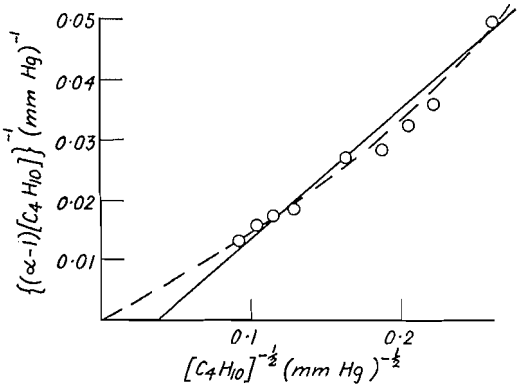

FIG. 1. Experimental values of $\{(\alpha - 1)[C_4H_{10}]\}^{-1}$ as a function of $[C_4H_{10}]^{-1/2}$ for *n*-butane pyrolysis at 518 °C.

These considerations confirm us in the view, which we have already expressed (3), that no molecular processes are important in *n*-butane pyrolysis. The suggested alternative mechanism does *not*, therefore, describe our experimental results, and we are forced, again, to the conclusion that the unimolecular decomposition of the ethyl radical is pressure dependent in the conditions of many organic pyrolyses. Confirmation of this view comes from recent work on ethane pyrolysis (4, 5), and from preliminary studies of hydrogen atom addition to ethylene in titration flow experiments (6).

1. J. H. PURNELL and C. P. QUINN. Proc. Roy. Soc. London Ser. A, **270**, 267 (1962).
2. M. H. BACK, K. EUSUF, and K. J. LAIDLER. Symposium on the Kinetics of Pyrolytic Reactions, Chemical Institute of Canada, Ottawa. 1964.
3. J. H. PURNELL and C. P. QUINN. Nature, **189**, 656 (1961).
4. C. P. QUINN. Proc. Roy. Soc. London Ser. A, **275**, 190 (1963).
5. (*a*) A. S. GORDON. (*b*) M. H. BACK and M. C. LIN. Symposium on the Kinetics of Pyrolytic Reactions, Chemical Institute of Canada, Ottawa. 1964.
6. F. S. LARKIN and B. A. THRUSH. Private communication.

RECEIVED OCTOBER 9, 1964.
DEPARTMENT OF PHYSICAL CHEMISTRY,
UNIVERSITY CHEMICAL LABORATORY,
LENSFIELD ROAD, CAMBRIDGE,

Can. J. Chem. Downloaded from www.nrcresearchpress.com by 210.87.254.6 on 09/05/12
For personal use only.

Can. J. Chem. Downloaded from www.nrcresearchpress.com by 210.87.254.6 on 09/05/12
For personal use only.

Canadian Journal of Chemistry

Issued by THE NATIONAL RESEARCH COUNCIL OF CANADA

VOLUME 43 APRIL 1965 NUMBER 4

AROMATIC SUBSTITUTION

PART VIII.[1] SOME ASPECTS OF THE MECHANISM OF THE TSCHITSCHIBABIN REACTION[2]

R. A. ABRAMOVITCH, F. HELMER, AND J. G. SAHA

Department of Chemistry, University of Saskatchewan, Saskatoon, Saskatchewan

Received October 16, 1964

ABSTRACT

The mechanism of the direct amination of pyridines is discussed in terms of both addition–elimination and elimination–addition pathways. The absence of deuterium kinetic isotope effects as well as the orientations observed in such reactions rule out the intervention of 2,3- or 2,6-dehydropyridines. The effect of a 3-methyl group upon the reactivities towards the amide ion of the various nuclear positions in pyridine has been determined. Predictions based on molecular orbital (m.o.) calculations are discussed in terms of the detailed mechanism of this reaction and of the orientations observed.

The direct amination of pyridine and its derivatives by means of alkali metal amides—the Tschitschibabin reaction—was, until recently, thought to involve a two-step addition–elimination process with the formation of a σ-complex (1–3). The mechanism proposed which accounts for the evolution of hydrogen (path *a*) is illustrated in Scheme 1 (4). An alternative, and probably competing, pathway is the thermal decomposition mode *b*, which would be rendered more facile [as is observed (2)] by the presence of

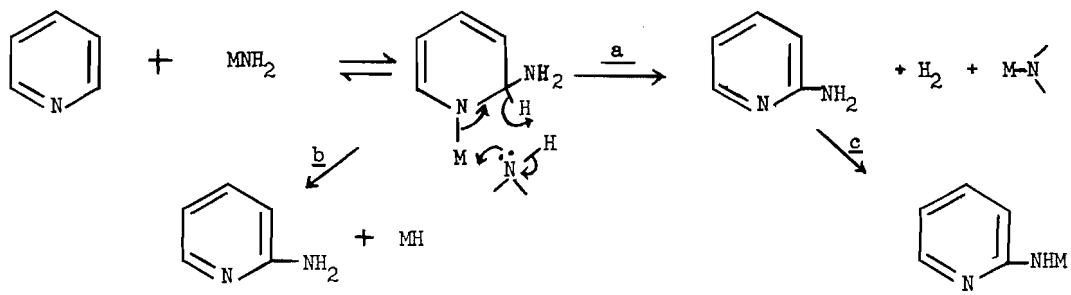

SCHEME 1.

oxidizing agents such as potassium nitrate (elimination of MOH instead of MH). Ammonia could be formed in step *c* which would also lead to the pyridyl-substituted alkali metal amide which, in turn, could attack pyridine to give the 2,2′-dipyridylamines sometimes observed in such reactions (2).

[1]*Part VII. R. A. Abramovitch and Choo-Seng Giam. Can. J. Chem. 42, 1627 (1964).*

[2]*Part of this work has been published in preliminary form (R. A. Abramovitch, F. Helmer, and J. G. Saha, Chem. Ind. London, 659 (1964)).*

In general, attack at C_2 of the pyridine nucleus is usually observed if this position is vacant. If substituents are present at both C_2 and C_6 then the amide ion enters at the 4-position. Some attack at C_4 leading to 4-aminopyridine was also observed with pyridine itself under forcing conditions (1, 2). When pyridine is heated at 80–130° with sodium in toluene in the presence of ammonia, a mixture of 2-amino- and 4-amino-pyridine is said to be formed together with some 4,4′-dipyridyl (5). Formation of the latter from pyridine and sodium metal is unexceptional (4).

On the other hand, Levitt and Levitt (6) suggested that the observations could be better accommodated by an elimination–addition mechanism which would involve the

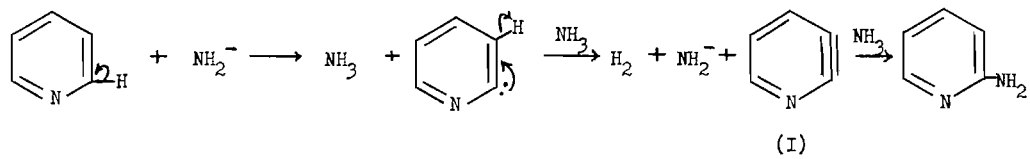

SCHEME 2.

formation of a 2,3-pyridyne (I) (or, in some cases, of a 3,4-pyridyne) (Scheme 2). In support of this, it was stated that amination of 5-ethyl-2-methylpyridine gave the 4-amino derivative instead of the expected 2-amino-3-ethyl-6-methylpyridine. Also, the formation of 2,6-diaminopyridine from the reaction of 3-hydroxypyridine with an excess of sodamide at 210° (7), and attributed (7) to the reduction of the phenolic function by nascent hydrogen, was said (6) to provide instead evidence for the intermediacy of (I) in this reaction:

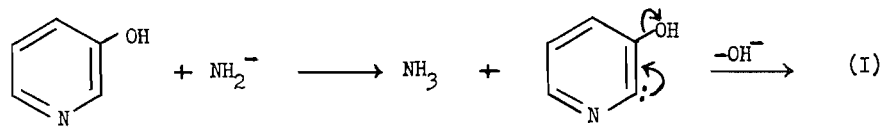

This proposed general mechanism has been attacked strongly (8, 9). In the first place, a number of reports in the literature indicate that many 3-substituted pyridines undergo direct amination predominantly, if not exclusively, at C_2. Examples include 3-picoline (10), 3-*n*-butylpyridine (11), nicotine (12), 3-ethylpyridine (13), 3-aminopyridine (14), nicotinamide (15), nicotyrine (16), anabasine and *N*-methylanabasine (17), and 5,6,7,8-tetrahydroisoquinoline (18). Secondly, the amination of 5-ethyl-2-methylpyridine does, in fact, give the expected 2- and not the 4-amino derivative (19) as claimed (6), and this has been confirmed recently both for 5-ethyl-2-methyl- as well as for 2-methyl-5-*n*-propyl-pyridine (20). The intervention of (I) in the reaction with 3-hydroxypyridine is rendered less probable by the report that 3,4-dihydroxypyridine gave 2-amino-3,4-dihydroxypyridine in the Tschitschibabin reaction (21). Again, if a 2,3-dehydropyridine intermediate were really involved one would have expected addition of a nucleophile to give a 3-substituted pyridine mainly, due to the electron-attracting character of the ring-nitrogen atom (22). Hence, some 3-aminopyridine would be expected in the amination of 3-hydroxypyridine, but was not obtained.

Confirmation of previous data as well as the obtention of new evidence concerning the mechanism of this reaction made the object of the work described here. No *quantitative* data on the effect of substituents upon the orientation of the entering amide ion and the reactivity of the pyridine nucleus have been published. The reaction of 3-picoline with

Can. J. Chem. Downloaded from www.nrcresearchpress.com by 210.87.254.6 on 09/05/12
For personal use only.

Can. J. Chem. Downloaded from www.nrcresearchpress.com by 210.87.254.6 on 09/05/12
For personal use only.

sodamide in boiling toluene has now been studied quantitatively. It was first established once again that 2-amino-3-picoline is the main product formed, the 2,3-/2,5-isomer ratio being 91:9. It was also shown that under the reaction conditions used no 4-amino-3-picoline was detectable by gas chromatography in the product. In fact, in none of the experiments carried out in our laboratory was this compound found to be present. Clearly, these results cannot be interpreted in terms of a 2,3-pyridyne intermediate mechanism, at least not as a major pathway for the reaction.

In the reaction of phenyllithium with 3-picoline, in which once again the 2-phenyl isomer is formed predominantly, it has been shown that the 3-methyl group activates the 2-position towards nucleophilic attack compared with the same position in pyridine itself (23). It was of interest to find out whether a similar situation prevailed in the sodamide reaction and competitive runs were carried out in which an excess of a mixture of 3-picoline and pyridine in boiling toluene was allowed to react with sodamide. Gas-chromatographic analysis of the reaction products gave a value of ${}^{CH_3}{}_HK = 0.22$ for the total rate ratio and values of ${}^{CH_3}{}_HF_2 = 0.40$ and ${}^{CH_3}{}_HF_6 = 0.039$ for the partial rate factors for attack at C_2 and C_6, respectively, compared with attack at C_2 in pyridine itself. Thus, in this case, the 3-alkyl substituent deactivates the nucleus quite unexceptionally towards nucleophilic attack, though the reasons for the predominant attack at C_2 are not clear yet (for a discussion of the similar orientation observed in the reaction of 3-alkylpyridines with phenyllithium see ref. 23).

The intervention of a pyridyne intermediate mechanism was tested for by a study of the reaction of sodamide with an excess of a mixture of pyridine and pyridine-3*d*. Unreacted pyridine was recovered and analyzed for its deuterium content by mass spectroscopy. If, as it would appear likely to be, the hydride-ion elimination step in Scheme 2 were the rate-determining one then, assuming a minimum deuterium isotope effect of 1.5 (24), one would have expected an increase in the pyridine-3*d* content of the recovered starting material of at least 1%, an increase which would be quite easily measured by the analytical method used. In actual practice the isotopic content of the recovered pyridine – pyridine-3*d* from the reaction mixture was identical within experimental error with that recovered from the blank. This eliminates a mechanism in which elimination of the hydrogen atom at C_3 is rate determining.

A way which might possibly circumvent the above experimental objections to a pyridyne intermediate mechanism was proposed in the form of the very interesting concept of lone-pair interaction in a dehydropyridine intermediate, a concept which was bolstered by molecular orbital calculations (25). According to this theory a 2,3-dehydropyridine may be stabilized by interaction of the vacant sp^2 carbon orbitals with the sp^2 hybrid orbital containing the nitrogen lone pair of electrons (II). This, it is calculated, would explain the lack of formation of any 3-aminopyridine derivatives (expected from the reaction of amide ion with a 2,3-pyridyne not stabilized by lone-pair interaction) and the absence of 4-aminopyridine (the latter is obtained, however, under more vigorous conditions as has been pointed out above). To account for substitutions at C_2 in 3-substituted pyridines it was postulated that a 2,6-dehydropyridine intermediate (III) could be formed readily. (It was pointed out, however, that in the amination of pyridine a 2,3-pyridyne was more likely to form than a 2,6-dehydropyridine since the 3-position is more favorable for the hydride-ion elimination (26)—a possibility negated by our results unless one assumes that it is the proton-elimination step in Scheme 2 that is rate determining.)

Unfortunately, this interesting proposal also goes contrary to a number of already published observations and to the present results. Thus, the well-established amination

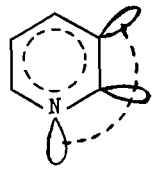
(II)

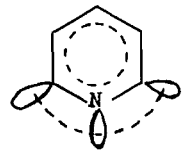
(III)

of 5-ethyl-2-methyl- and 2-methyl-5-*n*-propyl-pyridine at C_6 (20) cannot be accounted for by either a 2,3- or by a 2,6-dehydropyridine intermediate. The possibility that it was the proton-elimination stage in an elimination–addition mechanism which was the rate-determing step was tested very readily by repeating the experiment using 3-picoline and sodamide but with 3-picoline-2*d* and determining the 2,3-/2,5-isomer ratio quantitatively. This ratio was unchanged within experimental error, namely 92:8, and hence a 2,6-dehydropyridine intermediate was again discounted. It was ruled out completely by carrying out the amination on a mixture of pyridine – pyridine-2*d* and analyzing for the isotopic composition of the recovered starting material. If a 2,6-dehydropyridine were formed by a mechanism in which either the proton or the hydride-ion elimination step is rate determining a deuterium kinetic isotope effect would have been expected. With the concentrations used here and assuming a minimum isotope effect of 1.5 the pyridine-2*d* percentage in the recovered starting material should have increased from 26.6% to about 30.5% of the total. In actual practice, the *maximum* value of k_H/k_D observed was 1.05, ruling out the formation of dehydropyridine intermediates as a general mechanism for the Tschitschibabin reaction. It is also of interest to note that when a 3-halopyridine unsubstituted at C_4 is treated with potassium amide in liquid ammonia only the 3,4-pyridyne appears to be generated (26), whereas the m.o. calculations including lone-pair interaction predict that the 2,3-pyridyne would be the more stable intermediate (25). A reaction described in the literature which undoubtedly needs confirmation but which may actually involve a 3,4-pyridyne intermediate is that of 2-picoline with sodamide at a relatively high temperature. Under these conditions it was reported (27) that 3,6-diamino-2-picoline was one of the products isolated, together with 4,6-diamino-2-picoline. These could arise by the addition of ammonia to a 6-amino-2-methyl-3,4-pyridyne intermediate formed from 6-amino-2-picoline, the normal product of reaction under milder conditions. Alternatively, this may be another example of the type of orientation recently observed in the phenylation of pyridine with phenylcalcium iodide, which gave rise to some 2,5-diphenylpyridine (28).

The reactions with 3-picoline-2*d* and with pyridine-2*d* also throw some light upon another aspect of the mechanism of this reaction as well as upon a fundamental concept in the theory of nucleophilic substitution in the pyridine series in general. The absence of a primary deuterium isotope effect in the reactions illustrated in a simplified manner in Scheme 3 can be explained in one of two ways: (i) the addition steps leading to (V) and (VI) are the rate-determining ones, while the second, hydride-ion elimination step is relatively fast. This would seem to be rather unlikely since the amide ion should be more stable than a hydride ion; (ii) the hydride-ion elimination steps (V → VII and VI → VIII) are rate determining and *the addition stages are virtually irreversible*[3] *or the equilibria lie far on the product side and are not rapidly reversible.* Such a situation was found to obtain in the related reaction of phenyllithium with pyridine derivatives (29). Further work

[3]*This might be due to the formation of an N-sodio-derivative.*

Can. J. Chem. Downloaded from www.nrcresearchpress.com by 210.87.254.6 on 09/05/12
For personal use only.

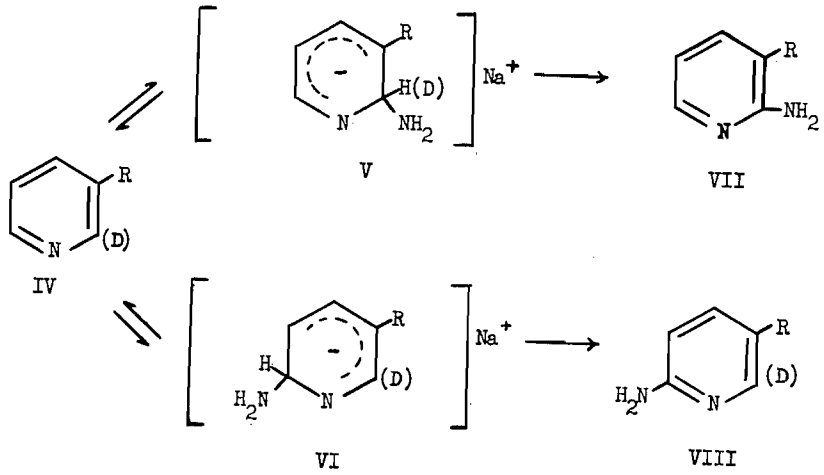

SCHEME 3.

is in progress to determine which of these two alternatives is, indeed, the correct one in the present case. In either case, the first i.e., *the addition step would be product determining* and the orientation would be governed by the effect of the substituent upon the ease of attack by the amide ion, and *not* by its effect upon the relative ease of elimination of a hydride ion from C_2, C_4, or C_6. On the basis of certain molecular orbital calculations of nucleophilic localization energies (30) and ground state π-electron densities (31, 32) it has been suggested (32) that the addition of the amide ion to pyridine should give predominantly the 4-amino σ-complex rather than the 2-amino derivative. The fact that 2-aminopyridine is formed mainly (if not exclusively) was attributed to a rate-determining elimination of hydride ion (presumably following a rapidly reversible addition step); the orientation would then depend on the relative ease of elimination of H^- from C_2 and C_4, respectively, and not upon the relative ease of attack at the two positions (32). The present results rule out this suggestion. Alternative possibilities are that the ground state π-electron densities for the various nuclear positions are actually in the order $2 < 4 < 3$ (4, 33) and that the non-crossing rule does not hold (33), or that the pyridine molecule that undergoes attack is actually complexed at nitrogen so that the values of the localization energies for the pyridinium ion (4, 33) should be employed for predictive purposes. One weak aspect of predictions based on calculations for the isolated molecule is that they do not take into account the fact that the reactions are actually being carried out in solution, where solvation effects may be very marked. There is, indeed, some evidence that solvation of the lone pair of electrons on nitrogen plays a fundamental, if not dominant, role in the determination of the relative reactivities of various nuclear positions in pyridine (34) as well as in the preferential orientation imposed by a 3-substituent upon an attacking nucleophile (35). This aspect is being explored further.

EXPERIMENTAL

Commercial 2° pyridine (Reilly Tar and Chemical Co.) was dried (KOH) and fractionally distilled; the fraction b.p. 110–112° at 720 mm was used. Commercial synthetic 3-picoline was similarly treated; the fraction b.p. 138–140° at 720 mm was used.

The preparation of pyridine-2*d* and 3-picoline-2*d* has already been described (36). Pyridine-3*d* was prepared similarly from 3-bromopyridine and *n*-butyllithium (15% solution in *n*-hexane). Commercial

Can. J. Chem. Downloaded from www.nrcresearchpress.com by 210.87.254.6 on 09/05/12
For personal use only.

2-amino-3-picoline and 2-amino-5-methylpyridine (Reilly Tar and Chemical Co.) were purified, the first to constant boiling point (100–103° at 11 mm), the second to constant melting point (77–78°). 2-Aminopyridine, purified by repeated recrystallization from light petroleum (b.p. 40–60°), had m.p. 55–56°.

Amination of 3-Picoline

3-Picoline (0.968 g, 0.01 mole) and sodamide (0.44 g, 0.011 mole) in toluene (0.4 ml) were boiled gently under reflux for 20 h, the reaction mixture was cooled in ice, and 5% aqueous sodium hydroxide (25 ml) followed by water (10 ml) carefully added. Sodium hydroxide pellets were now added so as to saturate the aqueous solution which was then extracted with benzene. The combined organic layers were dried ($MgSO_4$), the solvent removed under vacuum, and the oily residue analyzed quantitatively by gas chromatography using the following conditions: a column of 10 ft × ¼ in. silicone nitrile on Gas-Chrom P (1:6 w/w), column temperature 132°, injector temperature 190°, and helium inlet pressure 40 p.s.i., resulting in a flow-rate of 60 ml/min. Under these conditions 2-amino-3-picoline had a retention time of 36 min 30 s, and the 2-amino-5-methylpyridine 43 min 45 s. Duplicate runs were carried out in all cases. Identical conditions were used in the experiments with 3-picoline-2*d*. The average value of the 2,3-/2,5-isomer ratio was 91:11 in the case of 3-picoline and 92:8 with 3-picoline-2*d*.

Reaction of Pyridine and 3-Picoline with Sodamide under Competitive Conditions

Pyridine (1.439 g, 0.018 mole), 3-picoline (1.534 g, 0.016 mole), and sodamide (0.144 g, 0.0037 mole) in toluene (3 ml) were placed in a three-necked flask in a thermostat at 103° and the suspension stirred under reflux for 24 h. The reaction mixture was cooled in ice, treated with 5% sodium hydroxide solution and worked up as above. After drying over magnesium sulfate, the solvent and excess pyridines were distilled up to 130° at atmospheric pressure and the residue was transferred quantitatively to a volumetric flask which was filled up to the mark with toluene. Aliquots of this solution were then analyzed quantitatively by gas chromatography on a 9 ft × ¼ in. silicone nitrile on Gas-Chrom P (1:6 w/w) column operated at 163° and a helium inlet pressure of 20 p.s.i. Under these conditions 2-aminopyridine had a retention time of 24 min 15 s, 2-amino-3-picoline a retention time of 29 min 10 s, and 2-amino-5-methylpyridine a retention time of 35 min 45 s. Calibration curves (concentration vs. area of peak) were prepared for all three compounds. Runs were carried out using different relative amounts of pyridine and 3-picoline and the total rate ratios calculated by making the necessary corrections.

Reaction of Sodamide with Pyridine – Pyridine-3d Mixture

A mixture of pyridine and pyridine-3*d* (10.0 g, 0.127 mole) was dissolved in purified *N,N*-dimethylaniline (10.0 g), sodamide (0.247 g, 0.0063 mole; sodamide : pyridine ratio = 1:20) was added and the suspension was heated at 105–110° for 24 h. Some ammonia was evolved during the early part of the reaction. The yellow reaction mixture was treated with 10% aqueous sodium hydroxide with cooling, and then with concentrated sodium hydroxide solution. It was then extracted with ether and the ether layer dried (KOH) and distilled. The fraction b.p. 90–120° was collected and redistilled through a Vigreux column, the pure pyridine fraction, b.p. 114–115° (7.85 g), being collected. This was now treated again as above with a fresh batch of sodamide (0.195 g) and the reaction mixture heated and worked up. The recovered purified pyridine – pyridine-3*d* mixture (6.13 g) was reacted once again with fresh sodamide (0.148 g) as above and the unreacted pyridine recovered (3.85 g). A sample of this material was used for the mass spectroscopic analysis.

A blank run was carried out with a portion of the same pyridine – pyridine-3*d* mixture as was originally used above. This mixture (3.0 g) in *N,N*-dimethylaniline (3 g) was heated at 105–110° for 72 h and the pyridine recovered. A sample of this was used to obtain a value for the isotopic composition of the starting material and analyzed mass spectroscopically. A sample of ordinary purified pyridine, as was used in making up the original mixture with pyridine-3*d*, was analyzed as well to determine the contribution due to ^{13}C and ^{15}N in this material. The percentage of C_5H_4DN in the recovered pyridine used as the blank was 37.05%. The percentage of C_5H_4DN in the recovered pyridine from the reaction mixture was 37.15%. A duplicate run gave % C_5H_4DN = 37.12%.

Reaction of Sodamide with Pyridine – Pyridine-2d Mixture

A mixture of pyridine – pyridine-2*d* (2.513 g) and sodamide (0.413 g) in dimethylaniline (5 ml) was reacted and worked up as described in the pyridine-3*d* experiment. The recovered pyridine – pyridine-2*d* mixture was purified by preparative gas chromatography on a 5 ft × ¼ in. column packed with GE-SF-96 silicone on Gas-Chrom P (60-80 mesh) (20% by weight) operated at 100° with a helium inlet pressure of 40 p.s.i. The collected material (retention time 7 min 50 s) was distilled and analyzed by mass spectroscopy. Duplicate runs were carried out. A blank run using the same mixture as above but omitting the sodamide gave a value for the isotopic composition of the starting pyridine (26.6% C_5H_4DN). The pyridine recovered from reaction mixture No. 1 had a C_5H_4DN content of 26.4%, that from reaction mixture No. 2 a C_5H_4DN content of 27.0%. On the basis of this second figure k_H/k_D could be calculated to be 1.05. Assuming a kinetic deuterium isotope effect of 1.5 one would have expected the recovered pyridine from the two reaction mixtures to contain 30.80 and 30.19% of C_5H_4DN, respectively.

Can. J. Chem. Downloaded from www.nrcresearchpress.com by 210.87.254.6 on 09/05/12
For personal use only.

ACKNOWLEDGMENTS

The authors are grateful to the University of Saskatchewan for the award of a Demonstratorship (F. H.), to the National Research Council for financial support of this work, to Reilly Tar and Chemical for the gift of chemicals, and to Dr. E. L. Eliel for the mass-spectroscopic determinations.

REFERENCES

1. A. E. TSCHITSCHIBABIN and O. A. SEIDE. J. Russ. Phys.-Chem. Soc. **46**, 1216 (1914); Chem. Abstr. **9**, 1901 (1915).
2. M. LEFFLER. *In* Organic reactions. Vol. I. *Edited by* R. Adams. John Wiley & Sons, New York. 1942. p. 91.
3. J. EISCH and H. GILMAN. Chem. Rev. **57**, 525 (1957).
4. R. A. BARNES. *In* Pyridine and its derivatives. Pt. 1. *Edited by* E. Klingsberg. Interscience Publishers, New York. 1960. Chap. 1.
5. E. SCHERING. Ger. Patent No. 358,397; Chem. Abstr. **17**, 2118 (1923).
6. L. S. LEVITT and B. W. LEVITT. Chem. Ind. London, 1621 (1963).
7. E. PLAZEK. Roczniki Chem. **16**, 403 (1936).
8. G. C. BARRETT and K. SCHOFIELD. Chem. Ind. London, 1980 (1963).
9. R. A. ABRAMOVITCH, F. HELMER, and J. G. SAHA. Chem. Ind. London, 659 (1964).
10. E. PLAZEK, A. MARCINIKOW, and CH. STAMMER. Roczniki Chem. **15**, 505 (1935); Chem. Abstr. **30**, 1377 (1936). O. SEIDE. Ber. **57**, 1802 (1924).
11. E. HARDEGGER and E. NIKLES. Helv. Chim. Acta, **39**, 505 (1956).
12. A. E. TSCHITSCHIBABIN and A. W. KIRSSANOW. Ber. **57**, 1163 (1924).
13. Y. BAN and T. WAKAMATSU. Chem. Ind. London, 710 (1964). M. M. ROBISON and B. L. ROBISON. J. Am. Chem. Soc. **77**, 457 (1955).
14. A. KONOPNICKI and E. PLAZEK. Ber. **60**, 2045 (1927).
15. W. T. CALDWELL, F. T. TYSON, and L. LAUER. J. Am. Chem. Soc. **66**, 1479 (1944).
16. G. R. CLEMO and G. A. SWAN. J. Chem. Soc. 603 (1945). A. W. JOHNSON, T. J. KING, and J. R. TURNER. J. Chem. Soc. 1509 (1960).
17. M. I. KABATCHNIK and M. M. KATZNELSON. Bull. Soc. Chim. France, **2**, 576 (1935). G. MENSHIKOV, A. GRIGOROVICH, and A. ORECHOV. Ber. **67**, 289 (1934).
18. R. GREWE, A. MONDON, and E. NOLTE. Ann. **564**, 161 (1949).
19. A. E. TSCHITSCHIBABIN and M. S. VIDONOVA. Ger. Patent No. 398,204; Chem. Abstr. **18**, 2342 (1924).
20. R. F. CHILDS and A. W. JOHNSON. Chem. Ind. London, 542 (1964).
21. I. S. BELONOSOV. Zh. Prikl. Khim. **22**, 1103 (1949); Chem. Abstr. **45**, 5650 (1951).
22. J. D. ROBERTS, D. A. SEMENOW, H. E. SIMMONS, JR., and L. A. CARLSMITH. J. Am. Chem. Soc. **78**, 601 (1956). J. D. ROBERTS, C. W. VAUGHAN, L. A. CARLSMITH, and D. A. SEMENOW. J. Am. Chem. Soc. **78**, 611 (1956).
23. R. A. ABRAMOVITCH and C. S. GIAM. Can. J. Chem. **42**, 1627 (1964).
24. C. G. SWAIN, R. A. WILES, and R. F. W. BADER. J. Am. Chem. Soc. **83**, 1945 (1961).
25. H. L. JONES and D. L. BEVERIDGE. Tetrahedron Letters, 1577 (1964).
26. M. J. PIETERSE and H. J. DEN HERTOG. Rec. Trav. Chim. **80**, 1376 (1961). M. J. PIETERSE. Ph.D. Thesis, Amsterdam University. 1962. W. CZUBA. Rec. Trav. Chim. **82**, 997 (1963).
27. H. J. SCHNEIDERWIRTH. U.S. Patent No. 2,068,353; Chem. Abstr. **31**, 1959 (1937).
28. D. BRYDE-SMITH and A. C. SKINNER. J. Chem. Soc. 577 (1963).
29. R. A. ABRAMOVITCH and C. S. GIAM. Can. J. Chem. **41**, 3127 (1963).
30. R. A. BARNES. J. Am. Chem. Soc. **81**, 1935 (1959).
31. H. C. LONGUET-HIGGINS and C. A. COULSON. J. Chem. Soc. 971 (1949).
32. G. COPPENS and J. NASIELSKI. Tetrahedron, **18**, 507 (1962).
33. R. D. BROWN and M. L. HEFFERNAN. Australian J. Chem. **10**, 211 (1957); **9**, 83 (1956).
34. M. LIVERIS and J. MILLER. J. Chem. Soc. 3486 (1963).
35. R. A. ABRAMOVITCH, F. HELMER, and L. KLASSEN. Unpublished results.
36. R. A. ABRAMOVITCH, D. G. KROEGER, and B. STASKUN. Can. J. Chem. **40**, 2030 (1962).

Can. J. Chem. Downloaded from www.nrcresearchpress.com by 210.87.254.6 on 09/05/12
For personal use only.

Can. J. Chem. Downloaded from www.nrcresearchpress.com by 210.87.254.105 on 09/05/12
For personal use only.

THE ORTON REARRANGEMENT IN APROTIC SOLVENTS

PART II.[1] THE ACID-CATALYZED BROMINATION OF ANISOLE BY A SERIES OF 4-SUBSTITUTED N-BROMOACYLANILIDES

JOHN M. W. SCOTT AND JUNE G. MARTIN
Department of Chemistry, Memorial University of Newfoundland, St. John's, Newfoundland

Received October 28, 1964

ABSTRACT

Anisole has been brominated using a sequence of brominating reagents generated by the reaction of a series of 4-substituted N-bromoacylanilides 4-RC_6H_4NBrAc (R = Ph, H, Cl, and NO_2) with a series of carboxylic acids R'COOH (R' = CF_3, CCl_3, CH_2Cl, and CH_3). The isomer distributions of the bromoanisoles produced have been measured for each N-bromoacylanilide–carboxylic acid pair and their variation with both the structure of the N-bromoacylanilide and the carboxylic acid provides a useful basis for a discussion of the mechanism of the bromine migration.

Israel, Tuck, and Soper (2) have demonstrated the acid-catalyzed intermolecular transfer of bromine from N-bromoacetanilide to anisole (R = Me) and phenetole (R = Et):

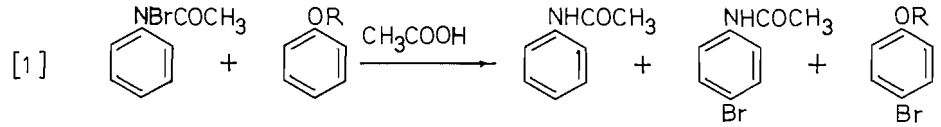

From the observation that the above reaction was zero order with respect to the aromatic ether they concluded that both the bromine transfer reaction and the concurrent rearrangement proceeded via the intermediate production of acetyl hypobromite according to the following scheme:

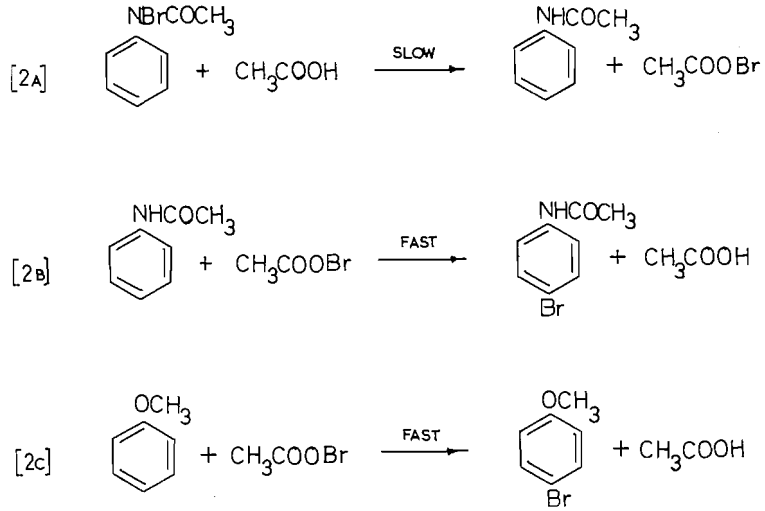

Dewar and Scott (3) and Scott (1) have observed similar transfers of bromine to chlorobenzene when N-bromo-2-nitroacetanilide or N-bromo-4-nitroacetanilide are treated with

[1]*The communication ref. 1 is to be considered as Part I of the present series.*

Can. J. Chem. Downloaded from www.nrcresearchpress.com by 210.87.254.105 on 09/05/12
For personal use only.

trichloroacetic acid in chlorobenzene. These particular experiments indicate that the bromine transfer reaction is not confined to situations in which the solvent is activated towards electrophilic attack.

In a more detailed investigation of the bromine transfer reaction Dewar and Couzens (4, 5) were able to demonstrate that such processes are not always zero order with respect to the aromatic ether. This important observation led Dewar and Couzens to reject the Soper mechanism (eqs. 2*a*, 2*b*, and 2*c*) but, in an alternative scheme which was offered, the acid hypobromites were retained as "complexed" rather than kinetically free intermediates. Dewar (4) has described intermolecular bromine transfer as an 'intra-complex reaction' but the nature of the complexes involved was not definitely established. The present communication is primarily concerned with the nature of these complexes as revealed by a detailed examination of the products obtained in a series of bromine transfer reactions. Soper and his co-workers (2) were only able to detect 4-bromoanisole when they treated N-bromoacetanilide with acetic acid and anisole dissolved in chloroform. By treating N-bromoacetanilide with a series of carboxylic acids in anisole and analyzing the products of these reactions by vapor-phase chromatography we have been able to detect both 2- and 4-bromoanisole in the reaction products. Isomer distributions in aromatic substitutions are well known to be sensitive to the structure of the attacking electrophile (6); consequently an examination of the variation of the isomer distribution in the bromine transfer reaction with the structure of both the N-bromoacylanilide (NBAA) and acid catalyst might be expected to provide some insight into the mechanism of this reaction. The results of such an investigation in which 16 unique NBAA – carboxylic acid pairs were used to brominate anisole are described below.

EXPERIMENTAL

Melting points were determined on a Fisher-Johns apparatus and are uncorrected. The thermostat used was of conventional design and experiments were carried out at 25 ± 0.02 °C.

The product analyses were determined by vapor-phase chromatography using an Aerograph AP-90 instrument equipped with a 10 ft × ¼ in. stainless steel column packed with 5% fluorinated silicone (QF 1) on Chromosorb W/HMDS 60–80. For the isomer distribution analyses the operating conditions were: injection oven 193 °C, detector oven 163 °C, and column oven 100 °C. The inlet pressure was 20 p.s.i. and the flow rate 25 ml He min^{-1}. Under these conditions the following retention times were observed: 2-bromoanisole 14.9 min, 3-bromoanisole 11.86 min, 4-bromoanisole 13.14 min, and 2,4-dibromoanisole 68.2 min. For the analysis of the yield of bromoanisoles biphenyl was used as an internal standard and the column oven was raised to 133 °C, whilst the other instrument parameters were identical to those given above. Under these conditions 4-bromoanisole had a retention time of 4.01 min and biphenyl a retention time of 8.73 min. Both yield and isomer distribution estimations were carried out using calibration curves constructed by correlating chromatograph peak areas determined by triangulation with the composition of synthetic mixtures.

The concentrations of the acid solutions were determined by titration with standard sodium hydroxide solution and the purity of the NBAA's determined by active bromine analysis in the usual way.

Materials

Acetanilides

Acetanilide and 4-nitroacetanilide were commercial samples and were used without further purification. 4-Aminobiphenyl and 4-chloroaniline were acylated with acetic anhydride. The melting points of all the anilides were in satisfactory agreement with those previously reported.

N-Bromoacylanilides

N-Bromo-4-nitroacetanilide, N-bromo-4-phenylacetanilide, and N-bromoacetanilide were all prepared by the route previously described for N-bromo-4-phenylacetanilide (1). Provided that the sodium hypobromite – bicarbonate solution used to effect the N-bromination was maintained in the vicinity of 0 °C during the addition of anilide, we were able to isolate relatively pure samples of each of the above substances. The routine preparation of N-bromoacetanilide by an alternative procedure (7) proved very erratic (see also ref. 5). N-Bromo-4-chloroacetanilide was prepared as before (1).

Can. J. Chem. Downloaded from www.nrcresearchpress.com by 210.87.254.105 on 09/05/12
For personal use only.

Acid Solutions

A purified sample of anisole was distilled with liberal rejection of initial and tail fractions, b.p. 152°. Trifluoroacetic acid was distilled, b.p. 73°, and A. R. grade acetic acid was fractionally frozen twice. A. R. grade trichloroacetic acid and monochloroacetic acids were used without further purification. The acid solutions were prepared from pure anisole and the appropriate acid as rapidly as possible to avoid contamination with atmospheric moisture and were stored in ruby-red glass flasks placed in a desiccator containing calcium chloride.

Miscellaneous Compounds

The 2- and 4-isomeric bromoanisoles were commercial samples which were distilled prior to their use; 2-bromoanisole had b.p. 217° and 4-bromoanisole had b.p. 215°. The 3-isomer was prepared from 3-anisidine in the usual way and distilled, b.p. 110° at 25 mm. 2,4-Dibromoanisole was prepared by brominating 2-bromoanisole in acetic acid. Recrystallization of the product from ethanol and then light petroleum gave prisms, m.p. 59–59.5° (lit. 61°). Biphenyl was recrystallized from light petroleum (b.p. 30–60°); m.p. 66° (lit. 69°).

Method

In a typical run the N-bromoacylanilide (ca. 0.01 mole) was dissolved in a 10 ml aliquot of the acid solution in a conical flask (50 ml) equipped with a ground-glass stopper. The flask was then wrapped in foil to exclude light and placed in the thermostat until the reaction was complete, as indicated by either the reaction of a portion of the reaction mixture with acid potassium iodide solution or the appearance of crystals of the parent anilide. Reaction times varied from a few hours to a maximum of 2 days. If the parent anilide separated during the course of reaction it was collected by filtration, the filtrate removed to avoid dilution prior to washing the solid with light petroleum (b.p. 40–60). The crystals were then dried and weighed and their melting point determined. The ratio of 2-bromoanisole to 4-bromoanisole (R) was determined as described above, the results recorded in Tables I–IV being the mean from at least three injections. It was observed that the brominations became more selective with decrease in acid strength as well as with decrease in the basic strength of the amine related to the NBAA. As the selectivity of the brominations increased there was a paralleled decrease in the accuracy with which the isomer distributions could be measured. The results for N-bromo-4-nitroacetanilide represent the limit of usefulness of the present method of analysis and this is reflected in the relatively large standard deviations in the measured isomer distributions for this compound. The results are, however, sufficiently accurate to establish definite trends in the isomer distribution with the structure of the acid and the NBAA in all cases. Three acid concentrations were used in the experiments employing trifluoroacetic acid as a catalyst to ascertain if the R parameter was dependent on the catalyst concentration. With N-bromo-4-chloroacetanilide and N-bromo-4-phenylacetanilide the R values showed a small increase with decrease in the acid concentration, but with the other two NBAA's of interest the results were random. It was concluded that until a more sensitive method of analysis could be developed for measuring small R values the small variation of this parameter with acid concentration was of little importance and would not alter any conclusions which we wish to draw at the present time. For the analysis of the total bromoanisoles present in the reaction mixture two 4 ml aliquots of the filtrate were added to two separate conical flasks (5 ml) containing known weights of biphenyl. At least three injections of the resulting solutions were made and the percentage yield of bromoanisoles was based on the active bromine analysis of the N-bromoacylanilide and is expressed with a standard deviation. The recovery of nitrogen bound bromine as 2- and 4-bromoanisoles averaged in the region of 80–90% (see Tables I–IV). The fate of the remaining bromine was not established, but the possibility of some rearrangement accompanying the bromine transfer reaction cannot be ruled out (cf. ref. 2).

Free Radical Reactions

The possibility that the observed isomer distributions might be derived from simultaneous acid-catalyzed and free radical reactions was considered and investigated. N-Bromoacetanilide, N-bromo-4-phenylacetanilide, and N-bromo-4-nitroacetanilide (ca. 0.01 mole) were allowed to react with anisole (10 ml) in daylight and the products examined as previously. The R values were found to be very small (ca. 0.01) being very close to the acid-catalyzed R values for N-bromo-2-nitroacetanilide; consequently this compound was selected for some further experiments. Suitable weights of this substance were added to three flasks A, B, and C, two of which contained anisole (50 ml) whilst the third (C) contained anisole and acetic acid (50 ml, 0.377 N). Flasks B and C were protected from the light with metal foil and the three flasks were then placed in the thermostat and active bromine analyses carried out on the contents of each flask at suitable time intervals. Within 4 h the flask exposed to the light contained no active bromine but flask B displayed only a 2.5% loss of active bromine over a period of ca. 100 h. On the other hand, the active bromine content of flask C demonstrated a steady reduction with time and a first-order plot gave an excellent straight line up to 70% of the reaction; ($k = 6.2 \times 10^{-5}$ s^{-1}) which corresponds to a half-life of 3.1 h and a complete reaction time (10 half-lives) of 31 h. These experiments, combined with the fact that any reasonable free radical mechanism would predict the isomer distributions to be independent of both the nature of the acid catalyst and NBAA, strongly suggest that results in Tables I–IV correspond to acid-catalyzed reactions with no important free radical component.

Can. J. Chem. Downloaded from www.nrcresearchpress.com by 210.87.254.105 on 09/05/12
For personal use only.

TABLE I

Isomer distributions and product analyses for the acid-catalyzed brominations of anisole with N-bromo-4-phenylacetanilide (purity of N-bromo-4-phenylacetanilide 100%)

Acid	C_a (M)	Wt. of NBAA (g)	Recovery of anilide			Analysis of 2- and 4-bromoanisoles†		R
			Wt. of anilide (g)	% yield	Melting point* (°C)	Wt. (g)	% yield	
	0.443	1.204	0.281	32.1	168–172	0.65±0.03	83±5	‡0.107±.002
CF_3COOH (*a*)	0.363	1.203	0.500	57.1	169	0.66±.01	85±2	‡0.116±.002
	0.207	1.202	0.850	97.1	169–170	0.67±.01	86±2	‡0.121±.002
CCl_3COOH (*b*)	0.535	1.205	Trace		164–165	0.62±.02	80±3	0.142±.002
$CH_2ClCOOH$ (*c*)	0.509	1.205	0.796	90.7	169–170	0.69±.03	89±5	0.036±.003
CH_3COOH (*d*)	0.377	1.213	0.751	85.1	169–169.5	0.70±.03	90±4	0.015±.002

pK_a (*a*) 0.23, pK_a (*b*) 0.65, pK_a (*c*) 2.86, and pK_a (*d*) 4.76 (taken from ref. 8).
*Lit. 171 °C.
†No 3-bromoanisole or 2,4-dibromoanisole was detected in any of these experiments.
‡Mean value of these quantities used in the correlation displayed in Fig. 1.

TABLE II

Isomer distributions and product analyses for the acid-catalyzed brominations of anisole with N-bromoacetanilide (purity of N-bromoacetanilide 97.8%)

Acid	C_a (M)	Wt. of NBAA (g)	Analysis of 2- and 4-bromoanisoles*		R
			Wt. (g)	% yield	
	0.443	1.032	0.76±.03	86±4	†0.092±.004
CF_3COOH	0.363	1.019	0.74±.03	85±4	†0.099±.002
	0.207	1.032	0.73±.03	83±4	†0.089±.003
CCl_3COOH	0.535	1.011	0.71±.02	82±3	0.120±.003
$CH_2ClCOOH$	0.509	1.049	0.71±.01	79±1	0.022±.004
CH_3COOH	0.377	1.026	0.73±.01	83±2	0.018±.003

*No 3-bromoanisole or 2,4-dibromoanisole was detected in any of these experiments.
†Mean value of these quantities used in the correlation displayed in Fig. 2.

DISCUSSION

The present series of experiments show that the isomer distributions obtained in the acid-catalyzed bromination of anisole by a series of NBAA's depend on the structure of both the catalyst and the brominating reagent. The Soper mechanism requires that these isomer distributions should be independent of the NBAA and consequently our results are not compatible with this mechanism. They are, however, consistent with the idea that transition states leading to the formation of 2- and 4-bromoanisole contain an anisole molecule together with an acid and NBAA molecule, i.e. the bromine transfer reaction has at least a termolecular transition state at the product-determining stage. The manner in which these species are linked or reorganized in the transition state is uncertain but structures I and II represent useful working hypotheses.

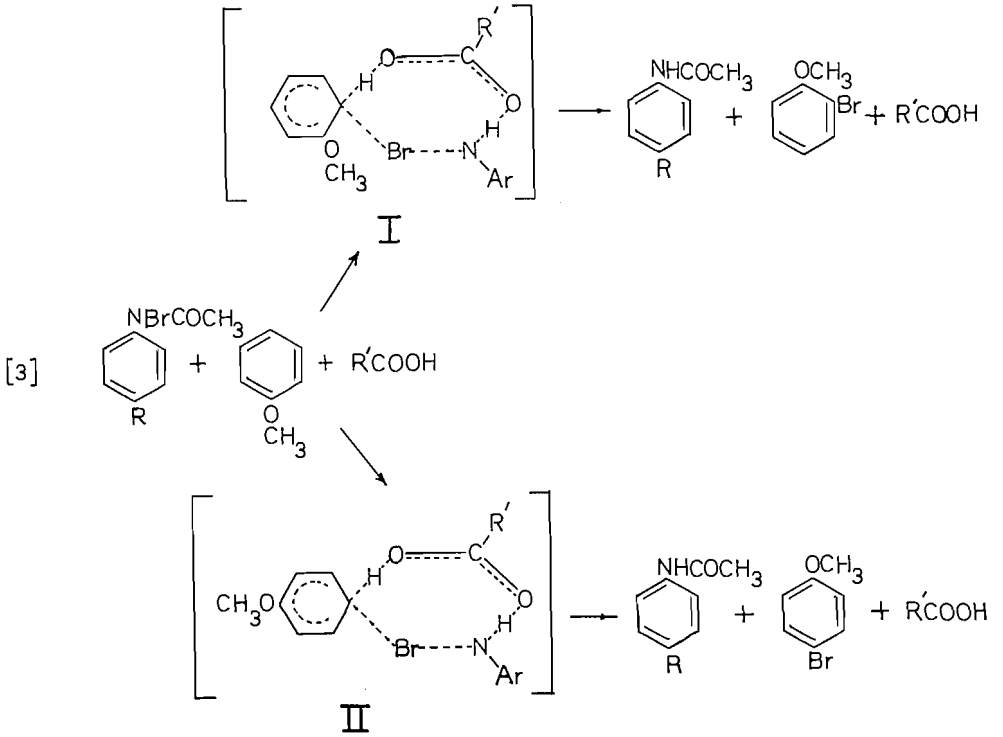

Can. J. Chem. Downloaded from www.nrcresearchpress.com by 210.87.254.105 on 09/05/12
For personal use only.

Can. J. Chem. Downloaded from www.nrcresearchpress.com by 210.87.254.105 on 09/05/12
For personal use only.

TABLE III

Isomer distributions and product analyses for the acid-catalyzed brominations of anisole with N-bromo-4-chloroacetanilide (purity of N-bromo-4-chloroacetanilide 99.3%)

Acid	C_a (M)	Wt. of NBAA (g)	Recovery of anilide: Wt. of anilide (g)	Recovery of anilide: % yield	Recovery of anilide: Melting point* (°C)	Analysis of 2- and 4-bromoanisoles†: Wt. (g)	Analysis of 2- and 4-bromoanisoles†: % yield	R
	0.443	1.160	0.455	57.0	177–177.5	0.75±.03	86±4	‡0.048±.008
CF_3COOH	0.363	1.173	0.448	55.4	177–178	0.71±.02	80±3	‡0.057±.002
	0.207	1.173	0.612	76.2	178–178.5	0.75±.02	85±2	‡0.061±.002
CCl_3COOH	0.535	1.170	0.419	51.9	177–178	0.77±.02	87±3	0.056±.001
$CH_2ClCOOH$	0.509	1.170	0.702	87.7	177.5–178	0.77±.02	87±2	0.018±.002
CH_3COOH	0.377	1.161	0.735	92.5	179	0.79±.01	90±1	0.010±.001

*Lit. 179 °C.
†No 3-bromoanisole or 2,4-dibromoanisole was detected in any of these experiments.
‡Mean value of these quantities used in the correlation displayed in Fig. 1.

TABLE IV

Isomer distributions and product ratios for the acid-catalyzed brominations of anisole with N-bromo-4-nitroacetanilide (purity of N-bromo-4-nitroacetanilide 94.9%)

Acid	C_a (M)	Wt. of NBAA (g)	Recovery of anilide: Wt. of anilide (g)	Recovery of anilide: % yield	Recovery of anilide: Melting point* (°C)	Analysis of 2- and 4-bromoanisoles†: Wt. (g)	Analysis of 2- and 4-bromoanisoles†: % yield	R
	0.443	1.201	0.756	83.7	211–212	0.71±.01	87±2	‡0.028±.002
CF_3COOH	0.363	1.201	0.794	87.2	211–214	0.75±.02	91±3	‡0.036±.009
	0.207	1.204	0.779	86.3	211–212	0.72±.02	87±3	‡0.022±.003
CCl_3COOH	0.535	1.203	0.733	80.7	211–212.5	0.74±.01	90±2	0.028±.003
$CH_2ClCOOH$	0.509	1.200	0.726	80.2	212–213	0.77±.01	93±1	0.020±.004
CH_3COOH	0.377	1.201	0.792	88.0	211	0.75±.03	91±4	0.017±.002

*Lit. 216 °C.
†No 3-bromoanisole or 2,4-dibromoansiole was detected in any of these experiments.
‡Mean value of these quantities used in the correlation displayed in Fig. 2.

The relative stabilities of structures I and II will reasonably depend on the nature of the alkyl and aryl groups (R′ and Ar) leading to different isomer distributions as the nature of these groups is varied. Structures I and II also represent favorable reaction paths in a medium of poor ionizing power such as anisole in that they involve no extensive charge separation. The results reported here are also consistent with the composition of complex given by Dewar and Couzens (ref. 4, p. 190).

The rate constants for the electrophilic attack of anisole at the 2- and 4-positions, (respectively k_o and k_p) are related to the R parameter by the equation:

$$R = 2k_o/k_p \qquad [4]$$

The logarithm of the R parameter demonstrates rough correlations with the pK_a's* of the catalyzing acids, separate curves being obtained for each NBAA as shown in Figs. 1 and 2. The scatter of the individual points in the case of N-bromoacetanilide is con-

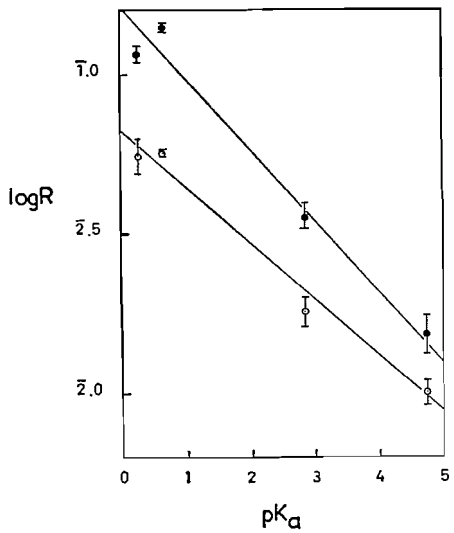

FIG. 1. Correlation between the isomer distribution parameter (R) and the pK_a of the catalyzing acid. ○, N-Bromo-4-phenylacetanilide; ●, N-bromo-4-chloroacetanilide.

siderable and the standard deviations of the individual points are large in the case of N-bromo-4-nitroacetanilide, reflecting the difficulty of measuring small R values accurately. The least-squares slopes of these lines, which are a kind of Brönsted exponent, vary with the nature of the substituent attached to the 4-position of the NBAA and they correlate with the Brown and Okamoto σ^+ parameter (Fig. 3 and Table V). In view of the large probable error (10) in the slopes (see Table V) the choice of the σ^+ parameter, rather than the Hammett σ or the pK_b's of the amines related to the NBAA's is rather arbitrary and will not be considered further.

To a first approximation the relationships between R and pK_a can be expressed in the form:

$$\log R = \alpha_s \mathrm{p}K_a + C, \qquad [5]$$

The use of pK_a values appropriate to water for linear free energy correlations in aprotic solvents such as anisole has ample precedent (see ref. 11, Chap. VI and also refs. 12, 13, and 14).

Can. J. Chem. Downloaded from www.nrcresearchpress.com by 210.87.254.105 on 09/05/12
For personal use only.

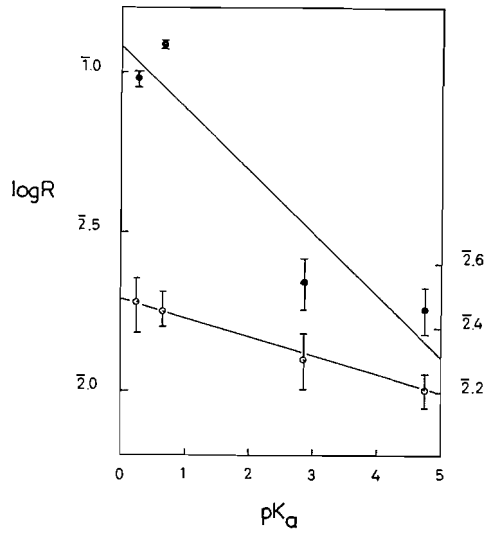

FIG. 2. Correlation between the isomer distribution parameter (R) and the pK_a of the catalyzing acid. ○, N-Bromoacetanilide; ●, N-bromo-4-nitroacetanilide. The scale on the right-hand y-axis refers to the latter substance.

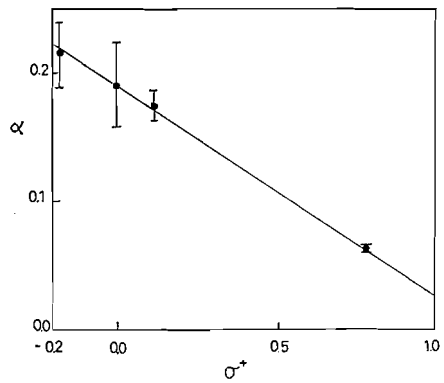

FIG. 3. Correlation between the σ^+ parameter and the Brönsted exponents (α) obtained from acid-catalyzed brominations.

TABLE V

Brown and Okamoto σ^+ substituent constants and related Brönsted exponents from acid-catalyzed brominations

Substituent	σ^+ (*a*)	α (*b*)*
Ph-	−0.179	0.216±0.025
H-	0	0.191±0.033
Cl-	0.114	0.174±0.011
NO_2-	0.77	0.060±0.003

(*a*) Taken from ref. 9.
(*b*) Expressed with a probable error; see ref. 10.
*In the plot Fig. 3 the negative slopes from the log R vs. pK_a correlations have been plotted against σ^+. The negative slopes are equivalent to the Brönsted exponents, since log k = α log K_a + const. = $-\alpha_s pK_a$ + const., i.e. $\alpha = -\alpha_s$.

Can. J. Chem. Downloaded from www.nrcresearchpress.com by 210.87.254.105 on 09/05/12
For personal use only.

where α_s and C are constants. Using eq. [4] it is possible to resolve eq. [5] into two separate Brönsted equations of the form:

[6] $$k_o = G_o K_a^{\alpha o}$$

and

[7] $$k_p = G_p K_a^{\alpha p}.$$

The meaning of the symbols in eqs. [6] and [7] follows the usual convention (11) and the subscripts o and p refer respectively to ortho and para attack. Combining eqs. [4], [6], and [7] gives

[8] $$\log 2k_o/k_p = \log R = (\alpha_p - \alpha_o)\mathrm{p}K_a + \log 2G_o/G_p,$$

which on comparison with eq. [5] gives

[9] $$\alpha_s = \alpha_p - \alpha_o$$

and

[10] $$C = \log 2G_o/G_p.$$

The experimental slopes are all negative which means that $\alpha_o > \alpha_p$. The enhanced value of α_o as compared to α_p implies a steeper intersection of the substrate–electrophile potential energy curves for attack at the 2-position of anisole. This might result from either a higher localization energy at the 2-position or steric repulsion between the attacking electrophile and the methoxy group. Both of these factors acting together probably contribute to the higher value of α_o.

ACKNOWLEDGMENTS

One of us (J. G. M.) wishes to thank the University for the award of a Summer Studentship (1963) and thanks are also extended to the National Research Council for financial support.

REFERENCES

1. J. M. W. Scott. Can. J. Chem. **38**, 2441 (1960).
2. G. C. Israel, A. W. N. Tuck, and F. G. Soper. J. Chem. Soc. 547 (1945).
3. M. J. S. Dewar and J. M. W. Scott. J. Chem. Soc. 1445 (1957).
4. M. J. S. Dewar. Kekule Symposium. International Union of Pure and Applied Chemistry. Butterworths Scientific Publications, London. 1959. p. 179.
5. P. J. Couzens. Ph.D. Thesis, University of London. 1959.
6. H. C. Brown and L. M. Stock. Advances in physical organic chemistry. *Edited by* V. Gold. Academic Press, London and New York. 1963. p. 35.
7. A. Slosson. Ber. **28**, 3266 (1894).
8. H. C. Brown, D. H. MacDaniel, and O. Hafliger. Determination of organic structures by physical methods. *Edited by* E. A. Braude and F. C. Nachod. Academic Press, Inc., New York. 1955. Chap. 14. p. 579.
9. H. C. Brown and Y. Okamoto. J. Am. Chem. Soc. **79**, 1045 (1957). H. C. Brown and L. M. Stock. Advances in physical organic chemistry. *Edited by* V. Gold. Academic Press, Inc., New York. 1963. p. 35.
10. H. Margenau and G. M. Murphy. Mathematics of physics and chemistry. D. Van Nostrand Co., Inc., 1956. Chap. 13. p. 519.
11. R. P. Bell. Acid–base catalysis. Oxford University Press. 1949. Chap. 7.
12. R. P. Bell and P. V. Dankwerts. J. Chem. Soc. 1774 (1939).
13. R. P. Bell and J. F. Brown. J. Chem. Soc. 1520 (1936).
14. R. P. Bell and O. M. Lidwell. J. Chem. Soc. 1096 (1936).

Can. J. Chem. Downloaded from www.nrcresearchpress.com by 210.87.254.105 on 09/05/12
For personal use only.

Can. J. Chem. Downloaded from www.nrcresearchpress.com by 210.87.254.40 on 09/05/12
For personal use only.

α-PYRIDONE COMPLEXES AND THEIR INFRARED SPECTRA[1]

DENYS COOK[2]
Exploratory Research Laboratory, Dow Chemical of Canada, Limited, Sarnia, Ontario
Received October 28, 1964

ABSTRACT

The infrared spectra of complexes of 1-methyl-2-pyridone and 1-methyl-2-quinolone with Lewis acids are consistent with interaction at the carbonyl group. The stretching frequency of this group, ν_{CO}, is lowered on complex formation, the change being proportional to the Lewis acidity. Two other bands, at 1 670 and 1 380 cm^{-1} move to lower frequency in much smaller steps and are associated with ring modes.

INTRODUCTION

The spectroscopic consequences of forming complexes between electron-deficient species and molecules containing carbonyl groups are well known (1–5). The size of the downward displacement of ν_{CO} is governed by many factors and can vary from 21 cm^{-1} in *m*-nitrobenzaldehyde:$HgCl_2$ (1) to 263 cm^{-1} in xanthone:BI_3 (6). The properties of the organic molecule which determine the size of $\Delta\nu_{CO}$ have to do with the polarity (and polarizability) of the C═O group but these have not, as yet, been put on a quantitative basis. With an understanding of these facts it is possible to make certain deductions about assignments of bands to carbonyl-stretching vibrations. This has been done in the case of γ-pyrones (4) and γ-pyridones (7) and resulted in a reversal of previous assignments for ν_{CO} and ν_{CC}, confirming suggestions to this effect by Bellamy and Rogasch (8), after measuring solvent shifts in absorption bands in γ-pyridones.

A study of complex formation in α-pyridones was undertaken to see if the above behavior was consistent; to find out whether the method might be applicable to tautomeric dihydroxypyridines; and to help in the understanding of some of the features in the spectra of α-pyridone salts (9).

RESULTS

The bands in the spectra of 1-methyl-2-pyridone complexes are shown in Table I and those of 1-methyl-2-quinolone complexes in Table II. Table III lists some bands due to the coordinate bond stretching vibration.

DISCUSSION

Vibration ν_{8a} and the Carbonyl-Stretching Vibration

Assignments in 1-methyl-2-pyridone have been considered by Katritzky and Jones (10), who along with Bellamy and Rogasch (8) attribute the 1 670 cm^{-1} band to the carbonyl-stretching frequency. Neither comment on the fact that there is a shoulder to this band at slightly lower frequency (in $CHCl_3$ solution) but its absence may be due to instrumental limitations. In the solvent shift studies (8) no separation took place even in the most perturbing solvent which suggests that both bands move together. The two bands are distinguished much more clearly of course when complex formation occurs. The carbonyl

[1]*Contribution No. 128.*
[2]*Present address: Department of National Health and Welfare, Food and Drug Directorate, Tunney's Pasture, Ottawa.*

Can. J. Chem. Downloaded from www.nrcresearchpress.com by 210.87.254.40 on 09/05/12
For personal use only.

TABLE I

Absorption bands in spectra of 1-methyl-2-pyridone complexes

	Base	$HgCl_2$	$CdCl_2$	$ZnCl_2$	BF_3	$SnBr_4$	BCl_3	BBr_3	$SbCl_5$
	3130m				3132m, sh				
	3085m			3080w	3122m	3084m	3092w		3088w
	3030m			3035w					
	2982m								
	2952m								
	2920m								
		1650s	1651s	1642s, sh	1643m, sh	1632s, sh		1632s, sh	1630m, sh
ν_{CC}	1664vs, sh	1645s	1646s	1635s	1638s	1628s	1630s	1625s	1622s
ν_{CO}	1660vs	1558s	1558vs	1520vs	1524s	1505vs	1502vs	1494vs	1492vs
	1618m, sh	1632m, sh				1615m, sh	1612m, sh	1612m, sh	1612m, sh
	1600vs			1563s, sh					
ν_{CC}	1585vs	1568s, sh	1567s, sh	1555s	1578s	1558s	1570s	1568s	1562m
	1538s, sh		1539m, sh		1568m, sh		1553m, sh	1552m, sh	1553m, sh
ν_{CC}	1529s	1540s	1535s, sh	1538m, sh	1532m, sh	1530m	1528m, sh	1519m, sh	1535w, sh
		1515m	1527m, sh			1520m, sh	1520m, sh		
	1502m, sh		1503m, sh	1501m, sh			1512s, sh		1502s, sh
	1482m					1495s, sh		1504m, sh	
ν_{CC}	1459m	1452m	1455m	1452m, sh	1462m	1455m	1454m	1456m	1453m
δ_{CH_3}	1450m, sh	1435w, sh		1425m	1448m	1443m	1435m	1430m	1435m, sh
	1436m								
δ_{CH_3}	1416m	1418m	1420m	1418w	1422m	1425m	1420m, sh		1420m
					1382w, sh	1362m, sh			1387w, sh
ν_{CC}	1389m	1382m	1382m	1379m	1370m	1355s	1347vs	1342s	1328m
				1368m, sh					
								1324m, sh	
δ_{CH}	1318s	1321m	1324m	1318m	1332m	1312m	1312s	1318m	1302s
								1310m, sh	
					1305w, sh	1302w, sh		1304m, sh	
δ_{CH}	1240m	1260w	1272w	1271w	1290m	1272m	1280m	1288w	1273m
ρ_{CH_3}	1180m	1178m	1181m	1180m	1188m	1182m	1179m	1180m	1180m
δ_{CH}	1151s	1165m	1169m	1164m, sh		1168m	1164m	1162m	1162m
		1152m		1159m					
ρ_{CH_3}	1134m	1140m	1142w	1140w		1148m, sh	1147m	1150m	1145m
δ_{CH}	1050m	1059m	1060m	1060m		1069m	1068m	1045m	1069w
							1032m		1025w
ν_{CC}	1000w	1018vw	1022w	1020w		1030w			
ν_{CC}	978w	990w		998w		1000w			
	921w	940w	944w	943w		950w			952w
γ_{CH}	873s	879m	885s	883m	880vs	885s		865m	882s
	837s	845m	849m	857w		866w		840m	
		775m, sh	778m		790s, sh	778s, sh	774s, sh	785s, sh	798m, sh
γ_{CH}	755vs	769s	769s	780s	784s	772vs	766s	768s	775vs
	745m, sh	763m, sh		773s					
				768m, sh					
				760w	750w				750m
	720s	731m	732m	735w	740m	739w		730w	736w

Lewis acid bands. BF_3: 1 095vs, 1 118vs, 1 150s, sh. BCl_3: 888s, 730s, 668s. BBr_3: 632m?

Can. J. Chem. Downloaded from www.nrcresearchpress.com by 210.87.254.40 on 09/05/12
For personal use only.

frequency in the $HgCl_2$ complex of 1-methyl-2-pyridone is displaced to 1 558 cm^{-1} and a slightly less intense doublet at 1 645 cm^{-1} and 1 650 cm^{-1} remains. One or both of the latter must clearly be the highest frequency ring mode (ν_{8a}) and not the 1 590 cm^{-1} band so designated by Katritzky and Jones (10).* The situation is entirely analogous in 1-methyl-2-quinolone and its $HgCl_2$ complex. Here the 1 650 and 1 640 cm^{-1} bands are assigned to the ring mode and carbonyl frequency in the free base, which move to 1 622 and 1 543 cm^{-1} in the $HgCl_2$ complex. The changes in ν_{CO} on complex formation with $HgCl_2$, both about 100 cm^{-1}, are somewhat larger than previously recorded for heterocyclic carbonyl compounds (4, 6, 7), but of the right order.

The doublet at 1 645 and 1 650 cm^{-1} in the $HgCl_2$ complex of 1-methyl-2-pyridone is also present in the $CdCl_2$ complex, but in the other complexes the higher frequency component slowly becomes less intense and subsides to a weaker shoulder. The assignment of this band to an overtone or combination tone in Fermi resonance with the ring-stretching mode (ν_{8a}) seems quite reasonable therefore. Since ν_{8a} belongs to the a' species, Fermi resonance is permitted between this mode and the combination tone of the two out-of-plane hydrogen-deformation modes ν_{11} and ν_{10b}. Equally probable would be a combination tone of an in-plane hydrogen-deformation mode in the 1 150 cm^{-1} region and a planar skeletal deformation mode, ν_{6a} or ν_{6b}. Inaccessibility of the region below 650 cm^{-1} prevents speculation about the skeletal modes.

Consideration of alternative assignments does not yield any improvement but the reverse. For example, assignment of the 1 585 cm^{-1} band to ν_{CO} is not only inconsistent with our experience of carbonyl-stretching frequencies but would mean a drop of only 23 cm^{-1} between free base and $SbCl_5$ complex, which is far too small. Reversal of the 1 664 and 1 660 cm^{-1} bands in the free base is trivial since they are so close.

Vibration ν_{8b}

The doublet near 1 606 and 1 590 cm^{-1} in CCl_4 solution referred to by Bellamy and Rogasch (8) as of variable intensity seems to be chiefly at 1 580 cm^{-1} in $CHCl_3$ solution with indeterminate high and low frequency shoulders and is assigned to ν_{8b}. Katritzky and Jones (10) with prism resolution find only one band at 1 590 cm^{-1}. The solid state spectrum is similar to the $CHCl_3$ solution spectrum in this region. Again it seems plausible to invoke Fermi resonance to explain the two bands of variable intensity. The fact that

**The nomenclature for ring vibrations is derived from that used originally for benzene (11) and by subsequent authors for other six-membered rings, e.g. pyridine (12), diazines (13). Very approximate normal coordinate displacements are shown in the accompanying figures. (The drawings become similar to those published by Katritzky and Jones if the (10) z-axis is changed from 1,4 to 3,6.)*

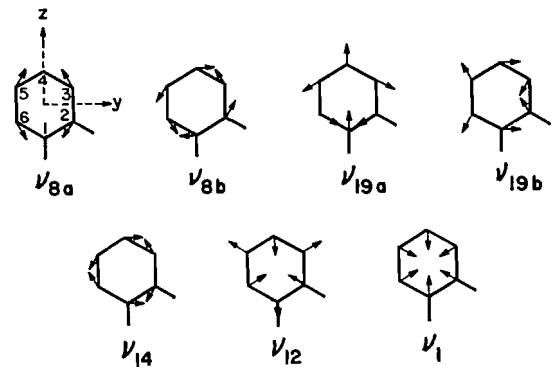

TABLE II

Absorption bands in spectra of 1-methyl-2-quinolone complexes

	Base	$HgCl_2$	$ZnCl_2$	BF_3	$SnCl_4$	BCl_3	BBr_3	$SbCl_5$
		1635m, sh						
		1627s, sh			1622s, sh	1616s, sh	1615s	1615s
ν_{CC}	1650s	1622s	1620s	1620s	1618s	1607s	1601s	1602s
		1610m, sh			1610m, sh			
				1530s, sh	1530s, sh	1540w, sh		1519s, sh
ν_{CO}	1640s	1543vs	1535s	1525s	1522s	1520s	1513s	1514s
	1612m, sh							
	1590m	1590w	1590w, sh					
			1570m, sh					
ν_{CC}	1580s	1568s	1567s	1582s	1570m	1580m	1578m	1572m
	1560m		1552m, sh			1540w, sh		
	1492w	1493m	1494m	1495m	1487m	1480s	1478s	1473s
	1450m, sh			1454m, sh	1454m			
ν_{CC}	1442m	1441m	1440m	1440s	1438s	1438m	1435m	1435s
	1422m	1425m	1422m	1428w, sh	1432m, sh			
ν_{CC}	1402m	1400m	1408m	1402s	1400s	1389s	1381s	1380s
			1400m			1370s	1366s	1375s, sh
	1335m	1343m	1348m	1376m	1360m	1358m	1355s	1355s
	1316m			1321m	1322m	1310s	1309s	1306m
	1270m	1281m	1280w	1284m	1286m	1282m	1280s	1279m
					1262vw	1265w	1270m, sh	1267m, sh
	1229m	1230m	1229m	1235m	1236m	1238m	1235m	1231m
	1176m	1165m	1170m	1170s, sh	1168m	1170s	1164s	1164s
	1162w, sh	1159w, sh	1159m	1160s	1163m, sh	1166m, sh	1155m, sh	1153m
ρ_{CH_3}	1140m	1146m	1144m	1140vs, sh	1130w	1130m	1128m	1123m
	1124m	1123m	1122m					
	1060w	1065m	1060w	1069s	1068w	1064m	1063m	1061w
	1039m	1041m	1040w	1040m			1040w, sh	
	1008w			1022m				
	970w	981w	978w		988w			988w
	942m	950w	948w		952w		938vw	944m
	924m							
	868m	866w, sh	863m	865vs	869m		866s	868m
	854w	860w	857w		860w		850s	855m
	844m	832s	830s	835m	834m	831s	822s	835s
			823m	828m				822m
				784m		787m	786s	788m
				773m				
	768w		768m, sh	768m		768s, sh		
γ_{CH}	750vs	761vs	759s	764m	761s	762vs	766s	768s
	740m, sh	754m	748m	748s	752m, sh			752m
				714m, sh				
	688w	700vw	700w	710m	703m		715s	700m
				682w			668s	

Lewis acids bands. BF_3: 1 130, 1 116, 904, 880 cm^{-1}. BCl_3: 720, 702, 695, 675 cm^{-1}.

in the complexes there is only one strong band (ν_{8b}) which appears between 1 555 and 1 570 cm^{-1} depending on the Lewis acid supports this assumption. ν_{11}, at about 766 cm^{-1} to 784 cm^{-1} in the complexes, is most probably the band whose first overtone interacts with ν_{8b}. The species of $2\nu_{11}$ is a', the same as the planar vibration ν_{8b}, and therefore the resonance condition is satisfied. In the free base though 755 (ν_{11}) + 837 (?) = 1592 would give a value more in keeping with the 1 606 / 1 590 cm^{-1} doublet. The assignment and species of the 837 cm^{-1} band are not known.

Vibration ν_{19a}

The third skeletal mode is found at 1 529 cm^{-1} in the free base with little shift on complex formation, and with quite a constant frequency in the different complexes. It is not a strong band except when in proximity to other strong bands.

Can. J. Chem. Downloaded from www.nrcresearchpress.com by 210.87.254.40 on 09/05/12
For personal use only.

Vibration ν_{19b}

In the 1 460 cm^{-1} region two medium intensity bands can be found in the free base and in the complexes. A ring-stretching mode (ν_{19b}) and an asymmetric CH_3 deformation mode would be expected in this region, and the higher frequency band at $\sim$ 1 455 cm^{-1} is assigned to the ring mode and the $\sim$ 1 435 cm^{-1} band to the CH_3 asymmetric deformation. A band at 1 416 cm^{-1} is assigned to the symmetric CH_3 deformation. The interpretation given here differs from that of Katritzky and Jones (10). One of the ring modes was overlooked by not observing ν_{8a} in coincidence with ν_{CO} (10); and the weak shoulder at 1 500 cm^{-1} was attributed to a ring mode. A more probable explanation for the 1 500 cm^{-1} band in the free base is as the first overtone of the CH out-of-plane deformation (ν_{11}) at 758 cm^{-1} (CS_2).

Vibration ν_{14}

The absorption at 1 389 cm^{-1} in the free base moving to progressively lower frequency as the Lewis acid gets stronger presents an aspect of complex formation not seen before. Previous observations of progressive shifts with increasing Lewis acidity have been either a gentle rise ($\sim$ 20 cm^{-1}) in some bands (ν_1) in complexes formed by coordination at a heterocyclic nitrogen atom (14, 15) or a large decrease in ν_{CO} ($\sim$ 100–250 cm^{-1}) on complex formation at a C=O group in a heterocyclic molecule (4, 6, 7) (plus a small relaxation ($\sim$ 35 cm^{-1}) in an interacting ring vibration of similar frequency, generally ν_{8a}) (4). Since the lowering in frequency in the 1 389 cm^{-1} band parallels that in the 1 664 and 1 660 cm^{-1} band thus following the order of relative Lewis acidity, and since there is no trend in the mass of the Lewis acid, it follows that the change in frequency must reflect a change in force constant in the bonds whose motion results in this vibration. This change in force constant must be induced by the alteration in the C=O bond structure on complex formation. The absorption at 1 389 cm^{-1} must therefore belong to a ring mode of some description, and the only one in this region is the vibration ν_{14}. For many years there was much confusion over the assignment of ν_{14} in benzene, but a recent decision in favor of the 1 309 cm^{-1} band seems to be acceptable (16). In pyridine the 1 375 cm^{-1} band assignment to ν_{14} is supported by normal coordinate calculation (17), and so is the 1 346 cm^{-1} band in pyrazine (18). The vibration is inactive in the infrared spectrum of benzene but is permitted in pyridine and the diazines; it also increases in intensity as more polar atoms are introduced into the ring. It should produce a bond with more intense absorption in 1-methyl-2-pyridone as the vibration involves stretching the polar CH_3N—CO bond. The problem of its bathochromic shift cannot be solved by an appeal to various valence bond structures, but is probably connected with electron depletion from the ring as a whole.

Vibrations ν_{12} *and* ν_1

The ring-breathing modes, ν_{12} and ν_1, are rarely of appreciable intensity in infrared spectra, though usually intense in Raman spectra. Two weak bands occur in the proper region of the spectra. These are at 1 000 cm^{-1} and 978 cm^{-1} in the free base, and about 1 020 and 1 000 cm^{-1} in the complexes.

Vibrations ν_3, ν_{9a}, ν_{15}, *and* ν_{18a}

There should be four in-plane hydrogen-bending vibrations associated with the ring hydrogens. Katritzky and Jones (10) have these at 1 318, 1 154, 1 138, and unassigned, respectively. The 1 154 cm^{-1} band has a more plausible assignment (*vide infra*) so the preferred assignments are 1 318, 1 240, 1 151, and 1 050 cm^{-1} respectively.

Can. J. Chem. Downloaded from www.nrcresearchpress.com by 210.87.254.40 on 09/05/12
For personal use only.

Vibrations ν_5, ν_{10b}, ν_{11}, *and* ν_{17b}

The in-phase out-of-plane hydrogen-bending mode gives rise to a strong infrared-active band and the 755 cm^{-1} band is thus assigned to ν_{11}. Three other bands occur in this region which could be assigned to these vibrations, and are at 873, 837, and 720 cm^{-1}. It is unlikely that the carbon out-of-plane modes could give rise to bands of such high frequency. The precise assignment of the 873, 837, and 720 cm^{-1} bands cannot at the moment be attempted.

Methyl Group Vibrations

The deformation vibrations have already been discussed. Authority for higher than usual methyl group symmetric deformation frequencies in NCH_3 groups comes from normal coordinate analyses of N-methyl amides (19, 20). The rocking modes are also at higher frequencies in NCH_3 groups (19, 20) compared with CCH_3 groups (21). Accordingly the bands at 1 180 and 1 134 cm^{-1} are assigned to the a' and a'' rocking modes.

Miscellaneous Vibrations

A weak band is observed in 1-methyl-2-quinolone at 1 492 cm^{-1}. This band also appears at 1 493 cm^{-1} in the $HgCl_2$ complex but is still of only moderate intensity. As the Lewis acidity increases, and the absorption of the carbonyl-stretching vibration moves to lower frequency this band becomes steadily more intense and also retreats to lower frequency. This could be explained as a case of Fermi resonance between the 1 492 cm^{-1} band, assigned to 2×750 cm^{-1} or the first overtone of an in-phase out-of-plane hydrogen deformation and the perturbed carbonyl group.

Ligand Group Vibrations

Most of the MX stretching bands due to the Lewis acid are below the rock salt region. Exceptions are the BF_3 and BCl_3 complexes. In the BF_3 complex of 1-methyl-2-pyridone bands at 1 118 and 1 095 are identified with a' and a'' asymmetric stretching modes of the $^{11}BF_3$ group, respectively. The shoulder at 1 150 cm^{-1} has been assigned to the a'' $^{10}BF_3$ asymmetric stretching vibration. The symmetric $^{11}BF_3$ stretching vibration probably gives rise to the strong absorption at 932 cm^{-1}. These frequencies are consistent with other values in BF_3 complexes, and are a measure of the very good donor characteristics of the α-pyridone molecule (22). Vibrations involving B—Cl bond stretching are observed in the 650–840 cm^{-1} region (23–25) and several appropriate frequencies are listed in the table.

TABLE III

B—O stretching vibrations

	1-Methyl-2-pyridone		1-Methyl-2-quinolone	
	^{11}B	^{10}B	^{11}B	^{10}B
BF_3	955	970	973	990
BCl_3	967	980	988	1 002
BBr_3	982	995	999	1 025

A strong band occurring only in the boron halide complexes near 980 cm^{-1} should be appropriate for the BO stretching vibration (see Table III). Although higher frequencies have been assigned to such bands (23, 24) for nitrogen–boron bonds these have not been without criticism (26), and values near 785 cm^{-1} (in $H_3N{:}BH_3$) suggested. One anomaly with the higher frequency assignments (24) was the absence of a component due to the ^{10}B isotope which should give a band of one fourth the intensity of the ^{11}B component

Can. J. Chem. Downloaded from www.nrcresearchpress.com by 210.87.254.40 on 09/05/12
For personal use only.

displaced some 20–40 cm^{-1} to higher frequency. The assignments in the α-pyridone:BX_3 series are all made more plausible by the presence of a shoulder some 13–26 cm^{-1} higher than the main component. Overlapping prevents an estimate of the relative intensities. The shift to higher frequency in the series $BF_3 \rightarrow BCl_3 \rightarrow BBr_3$ parallels the increasing order of Lewis acidity. The α-pyridone:BF_3 assignments are not perhaps quite as clear as the other complexes in this area because of overlapping bands.

EXPERIMENTAL

1-Methyl-2-pyridone and 1-methyl-2-quinolone were obtained as crystalline solids from The Aldrich Chemical Company.

1-Methyl-2-pyridone Complexes

$HgCl_2$ complex.—1-Methyl-2-pyridone (1.09 g, 0.01 mole) in 5 ml acetone was mixed with 2.72 g (0.01 mole) $HgCl_2$ in 5 ml acetone giving an immediate white solid, m.p. 130–133 °C.

Anal. Calcd. for $C_6H_7NO.HgCl_2$: C, 18.93; H, 1.85; N, 3.68. Found: C, 19.04; H, 2.24; N, 3.38.

$CdCl_2$ complex.—1-Methyl-2-pyridone (1.09 g, 0.01 mole) in 5 ml absolute ethanol on mixing with 1.83 g (0.01 mole) $CdCl_2$ in 150 ml absolute ethanol gave a white precipitate, m.p. > 290°.

Anal. Calcd. for $C_6H_7NO.CdCl_2$: Cl, 24.3. Found: Cl, 24.5.

$ZnCl_2$ complex.—$ZnCl_2$ (1.36 g, 0.01 mole) in 60 ml acetone and 1.09 g (0.01 mole) 1-methyl-2-pyridone in 5 ml acetone gave, on mixing and evaporation of the solvent, a white solid, m.p. 124–127°.

Anal. Calcd. for $(C_6H_7NO)_2.ZnCl_2$: Cl, 20.0. Found: Cl, 20.4.

$SnBr_4$ complex.—1-Methyl-2-pyridone (1.143 g, 0.011 mole) in 150 ml CCl_4 was treated with 0.69 ml $SnBr_4$ (0.005 mole). The resulting white solid was not hygroscopic; m.p. 225–227°.

Anal. Calcd. for $(C_6H_7NO)_2.SnBr_4$: Br, 48.7. Found: Br, 46.2.

BF_3 complex.—This has been previously described (27); m.p. 124–126°.

Anal. Calcd. for $C_6H_7NO.BF_3$: C, 40.72; H, 3.99; N, 7.92. Found: C, 40.46; H, 4.11; N, 7.67.

BCl_3 complex.—Gaseous BCl_3 passed into a CCl_4 solution of 1-methyl-2-pyridone resulted in a white hygroscopic solid, m.p. 115–123°. Due to their hygroscopic nature there are no analytical data for this and subsequent complexes. They are assumed to have 1:1 stoichiometry. They were also handled in a dry box.

BBr_3 complex.—Liquid BBr_3 was dropped into a CCl_4 solution of 1-methyl-2-pyridone giving a slightly viscous solid which soon hardened; m.p. 106–109°.

$SbCl_5$ complex.—Same procedure gave a white hygroscopic solid, m.p. 85–87°.

1-Methyl-2-quinolone Complexes

$HgCl_2$ complex.—1-Methyl-2-quinolone (1.59 g, 0.01 mole) in 30 ml acetone and 2.72 g (0.01 mole) $HgCl_2$ in 5 ml acetone were mixed, and after 30 s white platelets separated; m.p. 197–198°.

Anal. Calcd. for $C_{10}H_9NO.HgCl_2$: C, 27.88; H, 2.11; N, 3.25. Found: C, 27.80; H, 2.19; N, 2.95.

$ZnCl_2$ complex.—$ZnCl_2$ (0.68 g, 0.005 mole) in 50 ml acetone (filtered) added to 1.59 g (0.01 mole) 1-methyl-2-quinolone in 30 ml acetone. A solid slowly formed after standing a short while; m.p. 228–229°.

Anal. Calcd. for $(C_{10}H_9NO)_2.ZnCl_2$: C, 52.83; H, 3.99; N, 6.16. Found: C, 52.70; H, 4.10; N, 5.86.

$SnCl_4$ complex.—A stable non-hygroscopic solid was formed when $SnCl_4$ was dropped onto a solution of the base in CCl_4; m.p. > 290°.

Anal. Calcd. for $(C_{10}H_9NO)_2.SnCl_4$: Cl, 24.5. Found: Cl, 24.5.

BF_3 complex.— BF_3 gas when passed into a CCl_4 solution of 1-methyl-2-quinolone gave a white solid; m.p. 197–200°. This and subsequent BX_3 complexes were too hygroscopic to permit analytical determination. They are assumed to have 1:1 stoichiometry.

BCl_3 complex.—A white solid formed on passing BCl_3 gas into the base in CCl_4; m.p. 254–256°.

BBr_3 complex.—BBr_3 (0.78 ml, 0.08 mole) dropped onto CCl_4 solution of the base (1.298 g, 0.08 mole) gave a pale-yellow solid; m.p. 254–257°.

$SbCl_5$ complex.—1-Methyl-2-quinolone (0.786 g, 0.005 mole) in CCl_4 treated with 0.63 ml (0.005 mole) $SbCl_5$ gave a white solid; m.p. 220–222°.

Anal. Calcd. for $C_{10}H_9NO.SbCl_5$: Cl, 38.7. Found: Cl, 39.9.

Microanalyses were by Mr. L. E. Swim (Dow Chemical Company, Midland, Michigan, U.S.A.). Zn, Cd, and Hg halide complexes were estimated by argentimetric titration; Sn and Sb halides by acid–base titration. Melting points (in sealed tubes) are uncorrected. Spectra were obtained as described previously (7).

ACKNOWLEDGMENTS

The assistance of Mrs. R. H. Veach in preparing many of the complexes and recording their spectra is gratefully acknowledged. Mr. L. E. Swim and his associates (Dow Chemical Company, Midland, Michigan, U.S.A.) are thanked for the microanalyses.

Can. J. Chem. Downloaded from www.nrcresearchpress.com by 210.87.254.40 on 09/05/12
For personal use only.

REFERENCES

1. L. PAOLONI. Gazz. Chim. Ital. **87**, 408 (1957).
2. B.-P. SUSZ and I. COOKE. Helv. Chim. Acta, **37**, 1273 (1954).
3. A. TERENIN, W. FILIMONOW, and D. BYSTROW. Z. Elektrochem. **62**, 180 (1958).
4. D. COOK. Can. J. Chem. **39**, 1184 (1961).
5. M. F. LAPPERT. J. Chem. Soc. 542 (1962).
6. D. COOK. Can. J. Chem. **41**, 522 (1963).
7. D. COOK. Can. J. Chem. **41**, 515 (1963).
8. L. J. BELLAMY and P. E. ROGASCH. Spectrochim. Acta, **16**, 30 (1960).
9. D. COOK. Can. J. Chem. This issue.
10. A. R. KATRITZKY and R. A. JONES. J. Chem. Soc. 2947 (1960).
11. E. B. WILSON. Phys. Rev. **45**, 706 (1934).
12. C. H. KLINE and J. TURKEVITCH. J. Chem. Phys. **12**, 300 (1944).
13. R. C. LORD, A. L. MARSTON, and F. A. MILLER. Spectrochim. Acta, **9**, 113 (1957).
14. V. N. FILIMONOV and D. S. BYSTROV. Opt. Spectry. USSR English Transl. **12**, 31 (1962).
15. D. COOK. Can. J. Chem. **42**, 2523 (1964).
16. J. R. SCHERER and J. OVEREND. Spectrochim. Acta, **17**, 719 (1961).
17. D. A. LONG, F. S. MURFIN, and E. L. THOMAS. Trans. Faraday Soc. **59**, 12 (1963).
18. D. B. SCULLY. Spectrochim. Acta, **17**, 233 (1961).
19. T. MIYAZAWA, T. SHIMANOUCHI, and S. MIZUSHIMA. J. Chem. Phys. **29**, 611 (1958).
20. I. SUZUKI. Bull. Chem. Soc. Japan, **35**, 540 (1962).
21. I. SUZUKI. Bull. Chem. Soc. Japan, **35**, 1279 (1962).
22. D. COOK. *In* Proceedings of the Xth Colloquium Spectroscopicum Internationale. *Edited by* E. R. Lippincott and M. Margoshes. Spartan Books, Washington, D.C. 1963, p. 539.
23. A. R. KATRITZKY. J. Chem. Soc. 2049 (1959).
24. N. N. GREENWOOD and K. WADE. J. Chem. Soc. 1130 (1960).
25. T. C. WADDINGTON and F. KLANBERG. J. Chem. Soc. 2339 (1960).
26. R. C. TAYLOR and C. L. CLUFF. Nature, **182**, 390 (1958).
27. D. COOK. Chem. Ind. London, 1259 (1964).

Can. J. Chem. Downloaded from www.nrcresearchpress.com by 210.87.254.40 on 09/05/12
For personal use only.

Can. J. Chem. Downloaded from www.nrcresearchpress.com by 210.87.254.5 on 09/05/12
For personal use only.

PROTONATED CARBONYL GROUPS

V. α-PYRIDONE SALTS[1]

DENYS COOK[2]
Exploratory Research Laboratory, Dow Chemical of Canada, Limited, Sarnia, Ontario
Received October 28, 1964

ABSTRACT

Salts of 1-methyl-2-pyridone and 1-methyl-2-quinolone with strong acids have been prepared and their infrared spectra recorded between 4 000 and 650 cm^{-1}. Protonation of the carbonyl group occurs giving rise to OH stretching, in-plane and out-of-plane bending vibrations which absorb in characteristic regions of the spectrum, namely 1 900 – 3 300 cm^{-1} (depending on the anion), $\sim$ 1 250 cm^{-1}, and $\sim$ 800 cm^{-1} respectively, with appropriate shifts on deuteration. Other tentative assignments are made.

INTRODUCTION

The first article in this series gave an interpretation of the infrared spectra of protonated γ-pyrones (1). The simplicity of the spectra, in particular the absence of deuteration shifts in bands other than those due to the OH group, made the assignments relatively straightforward. Subsequent articles have dealt with increasingly complex systems (2, 3, 4) and the consistent behavior of the vibrational aspects of the protonated carbonyl group has justified attempts to deal with even more complicated systems.

1-Alkyl-2-pyridones fall into this category, and an initial survey of several salts of 1-methyl-2-pyridone seemed to show several inconsistencies, some of which, however, were removed when 1-methyl-2-quinolone salts were examined. It has been previously claimed, after an examination of the vibrational spectrum of the hydrochloride (5), that 2-pyridone protonates at the nitrogen atom but proton magnetic resonance spectra of 2-pyridone cations and deuterated analogues indicated O protonation (6). A more recent study of the infrared spectrum of the solid hexachloroantimonate was also put forward as supporting this concept (7).

RESULTS AND DISCUSSION

The bands in the spectra of salts of 1-methyl-2-pyridone and 1-methyl-2-quinolone are shown in Table I and II respectively. Those due to OH vibrations are summarized in Table III.

Vibrations of the OH Group

Strong absorptions at 2 272 and 1 902 cm^{-1} in the HCl salts of the pyridone (I) and quinolone (II) respectively, moving to progressively higher frequency with increasing anionic complexity, are associated with the OH-stretching vibration of the protonated carbonyl group. The band is very broad and strong and has not been found too useful in giving information on protonation sites. Deuteration shifts and half bandwidths are similar to previous observations (Table III). The very low value of ν_{OH} in 1-methyl-2-quinolone.HCl is noteworthy.

[1]*Contribution No. 129.*
[2]*Present address: Department of National Health and Welfare, Food and Drug Directorate, Tunney's Pasture, Ottawa.*

Can. J. Chem. Downloaded from www.nrcresearchpress.com by 210.87.254.5 on 09/05/12
For personal use only.

TABLE I

Absorption bands in infrared spectra of 1-methyl-2-pyridone salts

	HCl	DCl	HBr	DBr	HI	DI	$HSbCl_4$	$DSbCl_4$	H_2SnBr_6	D_2SnBr_6	H_2SnCl_6	D_2SnCl_6	$HSbCl_6$	$DSbCl_6$
ν_{CH}	3080m	3080w		3080w			3083m						3094w	3096w
ν_{CH}		3055m,sh	3065m	3060m	3062m			3072w		3067w		3068m	3078w,sh	3080w,sh
ν_{CH}		3035m		3048m		3050w,sh	3030m,sh	3050w		3040w		3042w		3050w,sh
ν_{CH}	3011m	3010m	3011m	3010m	3025w	3010w								
ν_{CH_3}	2956m	2950w	2950m	2950m										
			2235m	2070m										
			2160s,b	2024m		2245w								
ν_{OH}	2272vs,b	1795s,b	2565s,b	1914s	2790s,vb	2100s	2055s,b	2288m,b	3070m,b	2310m,b	3078s,vb	2305s,b	3320s,b	2490s,b
		1745m	2468s			1880w								
			2382m											
	1670m	1211m												
	1640s,sh		1640s,sh											
ν_{CC}	1632vs	1630s	1636s	1639s	1635vs	1634s	1640s	1638s	1632s	1630s	1633vs	1630vs	1638s	1635vs
	1622m,sh	1620s,sh	1630s,sh	1630s,sh	1630s,sh	1630s,sh	1638m,sh	1625m,sh	1620m,sh	1620m,sh	1630vs	1620s,sh	1630s,sh	1630m,sh
ν_{CC}	1588vs	1578vs	1596s	1586vs	1539vs	1539s	1596s	1588s	1590s	1580s	1591vs	1581vs	1592vs	1585s
	1580vs,sh	1565s,sh				1572m,sh	1575m,sh		1570m,sh	1570m,sh	1579w,sh	1570w,sh	1570m,sh	1570m,sh
	1570s,sh		1570w,sh	1572m,sh	1572m,sh				1562w,sh	1562m,sh		1562w,sh		1562w,sh
	1553w,sh	1553m,sh												
ν_{CC}	1535m	1534m	1530m	1530m,sh	1525w,sh	1530w,sh	1531m	1527m,sh	1550w,sh	1552m,sh	1539w,sh		1518m,sh	1515s,sh
	1515s,sh	1515m,sh	1515m,sh	1512s,sh										
ν_{CO}	1510vs,sh	1510m,sh	1510s,sh	1506vs	1505s	1508s	1512s	1510s	1505s	1500s	1507vs	1502s	1509s	1509vs
	1506vs	1495vs	1500s	1500vs,sh	1501s,sh	1500s,sh	1502m	1502s	1500s,sh		1500m,sh	1500s,sh	1502m,sh	1500s,sh
ν_{CC}	1468vs	1460s	1469s	1462m	1462s	1450m	1471s	1465m	1463s	1458m	1467s	1458m	1467s	1462m
	1450m,sh	1450s,sh	1450m,sh	1450m,sh	1450m,sh	1450m,sh	1448m		1458m,sh	1450m,sh	1448m	1450m,sh	1450m,sh	1450m,sh
	1440m,sh	1432s,sh	1432m,sh	1442m,sh	1435m	1430m	1425m	1431m	1450m,sh		1438m,sh	1440m,sh	1440m,sh	1438m,sh
	1402s	1396m	1396m	1400w	1410m,sh	1403m	1402w,sh		1425m	1438m,sh			1425w,sh	1416w,sh
ν_{CC}	1380m,sh	1321m	1385m	1312m	1380m	1295m?	1385m	1352m	1375m	1318w	1375m	1292m,sh	1365m	1322w
	1356vs	1355s	1351s	1352m	1338m	1342m	1345s	1342m	1339m	1342m	1340s	1346m	1339m	1341m
	1310s	1296s,sh	1307s	1302s	1300s	1295m	1305s	1302m	1295m	1296m	1300s	1299s	1298s	1295s
δ_{OH}	1260w	992m	1248m	978m	1240w	950m	1240m	980m	1220m	962m	1228m	951m	1193m	933m
	1183s	1184s	1180m	1185m	1176m	1176m	1183m	1183m	1173m	1178m	1180m	1179m	1180m	1178m
	1168s	1167s	1168m	1170m	1152m	1155m	1166m	1169m	1159m	1162m	1160m	1163m	1161m	1162m
			1160m,sh	1155w,sh				1162m,sh		1160m,sh				1150w,sh
	1149m	1146m	1145m	1100m	1141m	1148m,sh	1144m	1152m	1138m	1140m,sh	1140m	1160m,sh	1132m	1131w
	1112w		1110vw		1120w									
ν_{CC}	1065m	1065m	1065m	1069m	1068m	1069m	1075w	1075m	1067w	1068m	1070w	1070w	1070vw	1072w
ν_{CC}	1032w	1035m	1032w	1035w	1038m	1035m	1036w	1035m	1025w	1030w	1031w	1030w	1031w	1031w
	868s	878m	865m	863m	871m	863w	874m	860m	860m	858m	870m	863m	861m,sh	
	860m	860m	860m,sh	860m,sh	860m,sh	859m	865m	855w	852w,sh	852m,sh	860m	858m	856m	855m
γ_{OH}	842m	756m					692m				667m			
γ_{CH}	780vs	780vs	778vs	776vs	779s	778s	770vs	770vs	780m,sh	780s	786vs	780vs	779vs	769vs
						772m,sh	765w,sh		768s	770s	759m	772m,sh	760s	759s
						764m			756s,sh			761w		
	725m	725w	720m	724w	729w	725w	738w	730w			730w	716w		
													660m	660m

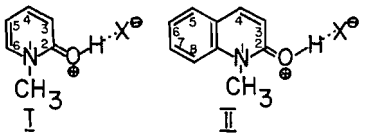

I II

In-plane deformation modes (δ_{OH}) of the OH group have previously been located near 1 260 cm^{-1} (1–4). Occasionally splitting into two components is observed (correlation field splitting) which can sometimes be ascribed to unit cell coupling (8, 9) when crystal data are available (1). In 1-methyl-2-pyridone salts there are four bands which seem to disappear, or decrease in intensity, on deuteration, and this effect is more marked in the HCl salt. These bands are at 1 468, 1 380, 1 260, and 1 112 cm^{-1}. Correlation field splitting into four components seems unlikely even though the average value, 1 305 cm^{-1}, is reasonably close to the average value of δ_{OH}, 1 260 cm^{-1} (4). On the other hand perturbation of ring vibrations on deuteration substitution is not observed in γ-pyrone or γ-pyridone salts, though it does occur quite markedly in pyridinium salts (10), and other protonated heterocyclic bases (11).

It was assumed, and the study of 1-methyl-2-quinolone salts later confirmed, that the 1 468, 1 380, and 1 112 cm^{-1} bands were not associated with the in-plane hydrogen-bending mode. This mode thus gives rise to one single absorption band at 1 260 cm^{-1} which is equivalent to a medium intensity band present in the deuterated salt at 992 cm^{-1}, the isotopic ratio being 1.27. Furthermore this is the only new band to occur in this region of the spectrum. Thus α-pyridone salts turn out to be consistent with other protonated carbonyl groups in having δ_{OH} near 1 260 cm^{-1}. In the 1-methyl-2-pyridone hydrohalides there is a trend towards higher values of δ_{OH} with decreasing anionic size. In the 1-methyl-2-quinolone salts this trend is not noticeable. The α-pyridone salts are not consistent though in having a single band for δ_{OH}, for most salts studied previously have two components (3).

The position of δ_{XH} has been used diagnostically to indicate protonation site, and tertiary amine groups have been found to have δ_{NH} near 1 402 cm^{-1} (12). The presence of the two bands near 1 468 and 1 380 cm^{-1} could have indicated a split band (average 1 424 cm^{-1}) due to correlation field effects, in quite a realistic position for a protonated N atom as in III.

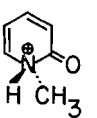

III

This possibility must be discounted since no split ND deformations are found in the appropriate region i.e. 1 468 / 1.35 = 1 087 and 1 380 / 1.35 = 1 022 cm^{-1}. In addition the effect of a positive charge on the N atom would have a large inductive effect on the carbonyl group significantly raising its stretching frequency to near 1 780 – 1 800 cm^{-1}, as has been described for N-aroyltrialkylammonium halides (13), 2,2-dimethyl-6-quinuclidone salts (14), and N-acyltrialkylammonium and N-acylpyridinium halides (15). Alternative explanations must be sought for the 1 468, 1 380, and 1 112 cm^{-1} bands as will be described below.

Vibrations of the Ring and Carbonyl Group

The six-membered conjugated ring in 1-methyl-2-pyridone should be capable of analysis in principle in terms of the vibrational characteristics of a perturbed benzene molecule,

Can. J. Chem. Downloaded from www.nrcresearchpress.com by 210.87.254.5 on 09/05/12
For personal use only.

Can. J. Chem. Downloaded from www.nrcresearchpress.com by 210.87.254.5 on 09/05/12
For personal use only.

TABLE II

Absorption bands in infrared spectra of 1-methyl-2-quinolone salts

	HCl	DCl	HBr	DBr	HI	$HSbCl_4$	$DSbCl_4$	H_2SnBr_6	D_2SnBr_6	H_2SnCl_6	D_2SnCl_6
ν_{CH}	3070w	3075w	3070w	3069w	3070w	3070m		3068s	3070w	3070s	3072m
ν_{CH}		3022w	3015w	3022w				3035s	3035w	3040s	
ν_{CH}	3002w	3000w			3006w						
	1970w		2560w	1968m,b							
ν_{OH}	1902m		2250vs,b	1795s,b	2608s,b	2965vs,b	2260s,b	3130s,b	2330m,b	3150s,b	2340m,b
			2200s,sh		2465m,b						
	1685m		2050m,sh		2360m,b						
			1650w,sh			1630m,sh					
ν_{CC}	1610s,sh	1618s,sh	1618s	1614s	1614vs	1620vs	1615vs	1625vs	1622vs	1621vs	1619vs
	1595s,sh	1610s	1602s	1604s	1604vs	1605vs	1605vs	1610vs	1610vs	1605vs	1605vs
	1584s	1588s	1598s	1596s	1596s,sh	1581m	1586m	1599m	1595m	1595m	1598m,sh
			1572m,sh		1588m,sh						
			1528s,sh	1519s,sh	1522s,sh	1528s,sh	1526s,sh	1530s,sh		1528s,sh	1528s,sh
											1521s,sh
ν_{CO}	1502s,sh	1510s	1517vs	1510s	1515s	1517vs	1519vs	1520vs	1520vs	1516vs	1517vs
	1490s	1493s	1491s	1490s	1500m,sh	1500m,sh	1488m	1501m	1494m	1500m,sh	1490m
					1485m,sh	1490w,sh		1490w,sh		1490w,sh	
						1458m	1450w			1460w,sh	1458w,sh
	1460s,sh	1460m,sh	1450m,sh		1454s			1462m	1450m,sh	1450m,sh	1450m,sh
	1425s	1432s	1437s	1433s	1435s	1434s	1434s	1440s	1439m	1438s	1435s
									1432m,sh		
			1406m	1398w,sh	1408m		1390w,sh	1410m,sh		1403m	1400w,sh
	1396m	1362s	1381vs	1362s	1379s	1380vs	1370s	1386m	1359vs	1383vs	1372s
										1365m,sh	
	1350s,b	1352s,sh	1351m	1350m,sh	1352m	1353m	1352m	1368vs		1352m	1353m
		1336m,sh	1338w, sh	1335w,sh	1335m,sh	1335w,sh		1339m	1340m	1335w	1333w,sh
	1310s,sh	1305m,sh	1314w	1305m	1310m	1312w	1304w	1322w,sh		1310w	1302m
	1302s,sh		1285m,sh		1298w			1298w	1293m		

Can. J. Chem. Downloaded from www.nrcresearchpress.com by 210.87.254.5 on 09/05/12
For personal use only.

TABLE II (*Concluded*)

	HCl	DCl	HBr	DBr	HI	$HSbCl_4$	$DSbCl_4$	H_2SnBr_6	D_2SnBr_6	H_2SnCl_6	D_2SnCl_6
	1271s	1277s	1280m	1274m	1278s	1280m	1278m	1269m	1270m	1280m	1278m
δ_{OH}	1265s,sh	989m	1262m,sh	970m	1258m	1252m	942m	1246m	956m	1259m	960m
	1250s,sh	1250m,sh									
	1220s	1226m	1230m	1229m	1223s	1223s	1230m	1218s	1220m	1229s	1228m
			1210w		1210m,sh	1212m,sh	1212m,sh	1210w,sh		1212w	1210m,sh
								1203w,sh	1203w	1202w,sh	
	1170m	1178m	1170w,sh	1175m,sh	1170m,sh	1170w,sh	1175w,sh			1170w,sh	1178w,sh
								1162w,sh			
	1156m	1162m	1162m	1160m	1158m	1158s	1159m	1153m	1153m	1160m	1162m
	1142s	1149s	1150m	1148m	1147s	1152m,sh	1151m	1149m,sh	1150m,sh	1155m,sh	1148m
									1145w,sh		
	1115s	1119m	1122w	1122m	1118s	1120m		1119w		1126w	1117w
					1062m						
	1052m	1057m	1060m	1056m	1055m	1060m	1059w	1053m	1056w	1059w	1058m
	1035m			1035w							
	992m		988w					998w	996w	1003vw	1003vw
										995vw	
	962m	965m	968w		973m	988w	985w	987w		982vw	988w
						963w	960w,sh	950vw		962w,sh	
γ_{OH}	936m	660m?	841vs			714m					
	926m	924m?	932w	928w			930w,sh	930vw	929w	932vw	932m,sh
				896w							
	860m	863m	858m,sh	856m	867m	870w		867w	866w	869w	869m
	854m,sh	857m,sh			855m	855m	852m	857w	855m	855m	854m
	828s	830s	841vs	825s	820vs	823vs	820s	830vs	830vs	833s	830s
								822w,sh	822m,sh	820m	
	763s	765s	780vs	768s	770s	766vs	766vs	768vs	769vs	775m	766s
					762m					768m	
	752s	755s	752w,sh	750m	752m			755vs	755vs	756s	759s
	730w	731w	733w	730w	730m	730m	730w	734w	732w	732m	731m
	698w	698vw	699w	692vw	697m					695w	
	675w		678w								
		660m			664m	668m	660m				

TABLE III

	ν_{OH}	ν_{OH}/ν_{OD}	$\Delta\nu_{1/2}$*	δ_{OH}	δ_{OH}/δ_{OD}	γ_{OH}	γ_{OH}/γ_{OD}
1-Methyl-2-pyridone salts							
HCl	2272	1.27	350	1260	1.27	842	
DCl	1795		200	992			
HBr	2565	1.27		1248	1.28	756	
DBr	2024			978			
HI	2790	1.33	300	1240	1.31		
DI	2100		150	950			
$HSbCl_4$	2955	1.29	400	1240	1.29	692	
$DSbCl_4$	2288		125	960			
H_2SnBr_6	3070	1.33	250	1220	1.27		
D_2SnBr_6	2310		180	962			
H_2SnCl_6	3078	1.34	250	1228	1.29	667	
D_2SnCl_6	2305		150	951			
$HSbCl_6$	3320	1.33	250	1205	1.28		
$DSbCl_6$	2490		140	939			
1-Methyl-2-quinolone salts							
HCl	1902			1265	1.28	936	1.42
DCl				989		660	
HBr	2250	1.26	360	1262	1.30	841	
DBr	1705		130	970			
HI	2608			1258			
DI							
$HSbCl_4$	2905	1.31		1252	1.33	714	
$DSbCl_4$	2260			942			
H_2SnBr_6	3130	1.34		1246	1.30		
D_2SnBr_6	2330			956			
H_2SnCl_6	3150	1.35		1259	1.31		
D_2SnCl_6	2340			960			

*Very approximate half bandwidth.

with the addition of carbonyl group and N-methyl group vibrations. 2-Pyridone itself is known to have alternate double (3,4 and 5,6) and single bonds (2,3 and 4,5) plus the lactam grouping mesomeric bonds (16). The changes these differences from hexagonal symmetry make in the vibrational characteristics, symmetry questions apart, are not known.

Seven planar vibrations of the ring are permitted, the approximate normal coordinate displacements being shown in the previous paper (17). The bands in the 1-methyl-2-pyridone salts at 1 632, 1 588, 1 535, 1 468, 1 380, 1 065, and 1 032 cm^{-1} are assigned to the vibrations ν_{8a}, ν_{8b}, ν_{19a}, ν_{19b}, ν_{14}, ν_{12}, and ν_1 respectively and a little arbitrarily. They are, however, in keeping with values in other six-membered heterocyclic rings.

The changes that take place on deuteration of the salts seem to be more pronounced than those in γ-pyrones (1) for example, where hardly any changes in ring vibrations were noticed, but less pronounced than in pyridine (10) or 1,4-diazines (11) where large changes in several bands take place. Part of the reason for the large change in the pyridine salts must be because protonation takes place directly on a ring atom and alters the ring bond force constants. In the γ-pyrone salts the ring is insulated from such effects by the carbonyl group. In α-pyridones too one would expect this insulating effect, but either for reasons of symmetry or π-electron interaction, it does not occur.

The assignments become a little clearer on consideration of the bands in 1-methyl-2-quinolone salts. In these salts the 1 460 cm^{-1} band moves only very slightly in position and changes little in intensity, and the 1 390 cm^{-1} band shifts only about 30 cm^{-1} to lower frequency instead of the 60–70 cm^{-1} in the 1-methyl-2-pyridone salts. It is thus possible to relate the bands in the two isotopic series in 1-methyl-2-quinolone salts with

Can. J. Chem. Downloaded from www.nrcresearchpress.com by 210.87.254.5 on 09/05/12
For personal use only.

Can. J. Chem. Downloaded from www.nrcresearchpress.com by 210.87.254.5 on 09/05/12
For personal use only.

greater assurance, and to extrapolate them to the 1-methyl-2-pyridone salts. The intensity changes on deuteration in the 1 460 cm^{-1} bands may also be due in part to their slight shift away from the strong 1 490 to 1 500 cm^{-1} band, from which they derive some of their intensity in the H salts.

No clear explanation for the larger than usual change in frequency on deuteration of the 1 390 cm^{-1} band seems possible. Because of the slow drift in this band as the Lewis acid in the complexes changes (17), a real alteration in the force constant of the bonds involved would be supposed, since mass or mechanical effects clearly could not be responsible with such a wide variety of Lewis acids. However a change in frequency associated with an isotopic change in the protonated base could only be due to a mass effect. Further work to clear up this anomaly is obviously desirable.

The assignment of the 1 112 cm^{-1} band which decreases in intensity on deuteration is also the subject of some uncertainty. No new band in the region near 1 112 / 1.37 = 812 cm^{-1} in the deuterated salts is apparent apart from the 980 cm^{-1} band due to δ_{OD}. It seems therefore likely that, as was assumed earlier, it is not connected with δ_{OH}. Whenever splitting of the OH in-plane deformation modes has been noted, both components have always been quite prominent in both isotopic species (1, 2, 3). The most probable assignment of the 1 112 cm^{-1} band, and one consistent with its intensity, would be to an overtone or combination tone. If it is due to a first overtone the fundamental would be near 556 cm^{-1}, beyond the range of the instrument used to record these spectra, but in the spectral region where the ring in-plane (ν_{6a} and ν_{6b}) and out-of-plane (ν_{16a} and ν_{16b}) bending modes would occur. If it is due to a combination tone then one probable participant would be the out-of-plane hydrogen-bending mode γ_{CH}, near 760 cm^{-1}. The other partner should then be near 352 cm^{-1}, which may be ascribed to a ring out-of-plane bending mode, or to $2\nu_L$ where ν_L is a lattice mode associated with the hydrogen bond.

Previous experience has indicated that the carbonyl-stretching frequency should be in the 1 500 cm^{-1} region (see Table III of ref. 3). Two exceptions are the salts of N,N-dimethylacetamide (4) and N,N-dicyclohexylacetamide (15) which have ν_{CO} at 1 386 and 1 400 cm^{-1} respectively, and it is believed that vibrational coupling, well known to occur in the free bases, is responsible for these low values. The situation in antipyrine, a cyclic amide, is not definite either, for though an assignment of a band at 1 496 cm^{-1} to the carbonyl-stretching vibration was made, it was noted that coupling very probably took place (3).

In the α-pyridones studied here the same conditions apply, for not only are the amide group vibrations coupled, but there may be interactions between these and the higher frequency ring modes. Identification of the carbonyl frequency is therefore not a simple matter. Some information may be obtained, however, from an examination of several complexes of α-pyridones with Lewis acids (17). In accordance with previous experience the carbonyl frequency would be expected to decrease on complex formation with a weak Lewis acid (18) and go to progressively lower values as the Lewis acidity increased (19, 20). The only band that fits this description in 1-alkyl-2-pyridone is at 1 662 cm^{-1} in the free base, at 1 561 cm^{-1} in the $HgCl_2$ complex, moving progressively to 1 492 cm^{-1} in the $SbCl_5$ complex. Two other bands which move gently to lower frequency as ν_{CO} decreases are at 1 670 cm^{-1} moving to 1 622 cm^{-1} in steps of $\sim$ 5–10 cm^{-1}, thus recalling the behavior of γ-pyrone complexes (20), and at 1 374 cm^{-1} moving to 1 328 cm^{-1}. In the α-pyridone salts therefore the 1 500 cm^{-1} band is most satisfactorily assigned to the

protonated carbonyl group stretching mode. It is not accidental either that this value is close to the carbonyl-stretching frequency in a complex of 1-methyl-2-pyridone with a strong Lewis acid, as both the proton and the strong Lewis acid seem to offer the same degree of perturbation to the carbonyl group (20, 21).

The symmetry of 1-methyl-2-pyridone is so low that all vibrational modes [$(3 \times 15) - 6 = 39$] are infrared active. This situation does not alter in the salts and the cation has 42 active modes. As only about 30 bands are listed in Table I it is obvious that many fundamentals are missing. Notwithstanding this it is suggested that part of the complexity of the 1 300 to 1 600 cm^{-1} region is due to the effect of mechanical interactions and Fermi resonances, and that many of the assignments must remain tentative till further data can substantiate them.

2 Base : 1 Acid Salts

The acids $HAsF_6$, HPF_6, and $HSbF_6$ gave only the 2:1 salts whose spectra show no absorption near 3 300 cm^{-1}, but broad strong absorption reaching a maximum in intensity near 900 cm^{-1}, with characteristic transmission windows (22). These salts are thought to contain short, possibly symmetrical hydrogen bonds (23, 24). Usually the anion is a large complex polyatomic molecule but sometimes the iodide ion seems to fit the required lattice conditions. The hemihydrochloride dihydrate of 1-methyl-2-quinolone, prepared by allowing the 1:1 salts to hydrate in air, seems to belong to this class. The water molecules probably form hydrogen-bonded bridges between successive Cl^- ions.

EXPERIMENTAL

1-Methyl-2-pyridone Salts

Hydrohalides were made by passing the appropriate gas through an ether solution of the base. Ethereal HI (from aqueous solution) gave the 2:1 salt, but the 1:1 salt was subsequently made from excess aqueous HI and the base giving the monohydrate, which was then dehydrated by gentle heating *in vacuo*. Salts of complex acids were made by dissolving the base in $CHCl_3$, saturating with the appropriate HX, then adding the Lewis acid SnX_4 or $SbCl_n$. Most of the salts were then handled in a dry box.

All salts were analyzed by titrimetric methods and gave satisfactory figures for 1:1 salts for monobasic acids, and 2:1 for dibasic acids. Melting points:* HCl, 170–172°; HBr, 175–176°; HI, monohydrate, 73–75°; anhydrous, 116–119°; $HSbCl_4$, 128–131°; H_2SnBr_6, 132–135°; H_2SnCl_6, 167–169°; $HSbCl_6$, 186–189°.

1-Methyl-2-quinolone Salts

The same procedures as for the 1-methyl-2-pyridone salts were used with the same results. Melting points: HCl, 151–153°; HBr, 198–200°; HI, 159–162°; $HSbCl_4$, 169–171°; H_2SnBr_6, 223–225°; H_2SnCl_6, > 290.

Replacement of the protonating hydrogen atom with deuterium was achieved with D_2O or DBr. Attempts to prepare the DI salts, however, yielded the 2:1 salt. All deuterated salts were prepared using vacuum line techniques and were subsequently handled in a dry box. Spectra were recorded as described previously (4).

ACKNOWLEDGMENT

The assistance of Mrs. R. H. Veach in preparing some of the compounds and recording their spectra is gratefully acknowledged.

REFERENCES

1. D. Cook. Can. J. Chem. **41**, 505 (1963).
2. D. Cook. Can. J. Chem. **41**, 2575 (1963).
3. D. Cook. Can. J. Chem. **41**, 2794 (1963).
4. D. Cook. Can. J. Chem. **42**, 2721 (1964).
5. E. Spinner. J. Chem. Soc. 1226 (1960).
6. A. R. Katritzky and R. E. Reavill. J. Chem. Soc. 753 (1963).
7. C. L. Bell, J. Shoffner, and L. Bauer. Chem. Ind. London, 1435 (1963).
8. R. S. Halford. J. Chem. Phys. **14**, 8 (1946).
9. D. F. Hornig. J. Chem. Phys. **16**, 1063 (1948).

**Sealed tube, uncorrected.*

Can. J. Chem. Downloaded from www.nrcresearchpress.com by 210.87.254.5 on 09/05/12
For personal use only.

10. D. Cook. Can. J. Chem. **39**, 2009 (1961).
11. D. Cook. Unpublished results.
12. D. Cook. Can. J. Chem. **42**, 2292 (1964).
13. R. Gompper and P. Altreuther. Z. Anal. Chem. **170**, 205 (1959).
14. H. Pracejus. Chem. Ber. **92**, 988 (1959).
15. D. Cook. Can. J. Chem. **40**, 2362 (1962).
16. B. R. Penfold. Acta Cryst. **6**, 591 (1953).
17. D. Cook. Can. J. Chem. This issue.
18. L. Paoloni. Gazz. Chim. Ital. **87**, 408 (1957).
19. B. P. Susz. Compt. Rend. **248**, 2569 (1961).
20. D. Cook. Can. J. Chem. **39**, 1184 (1961).
21. D. Cook. Can. J. Chem. **41**, 515 (1963).
22. J. C. Evans and N. Wright. Spectrochim. Acta, **16**, 352 (1960).
23. D. Cook. Chem. Ind. London, 607 (1963).
24. H. H. Mills and J. C. Speakman. Proc. Chem. Soc. 216 (1963).

Can. J. Chem. Downloaded from www.nrcresearchpress.com by 210.87.254.5 on 09/05/12
For personal use only.

A STUDY OF THE PECTIN PRESENT IN THE BARK OF AMABILIS FIR (ABIES AMABILIS)

S. S. BHATTACHARJEE[1] AND T. E. TIMELL[2]

Department of Chemistry, McGill University, and the Pulp and Paper Research Institute of Canada, Montreal, Quebec

Received November 9, 1964

ABSTRACT

A pectic material has been isolated from the bark of *Abies amabilis* (Dougl.) Forbes in a yield of 2%. On hydrolysis it yielded D-galacturonic acid, D-galactose, and L-arabinose in a ratio of 85:4:11, and also traces of rhamnose. The product, when submitted to several conventional fractionation methods, appeared homogeneous. Further resolution could be effected by acidification of an aqueous solution of the pectin, followed by ultracentrifugation. The insoluble portion (50%) was an electrophoretically homogeneous *galacturonan* with $[\alpha]_D$ +246°. The material remaining in solution (30%), here referred to as a *pectic acid*, had $[\alpha]_D$ +225° and on hydrolysis gave D-galacturonic acid, D-galactose, and L-arbabinose in a ratio of 74:7:19, as well as traces of rhamnose.

The structure of the galacturonan was established by partial hydrolysis and methylation. It consisted of α-D-galacturonic acid residues linked together by (1 → 4)-glycosidic bonds to a linear macromolecule. The same techniques were applied to the pectic acid. While a unique structural formula could not be assigned in this case, one probable alternative involved a framework of (1 → 4)-linked α-D-galacturonic acid residues together with a few residues of 1,2,4-linked L-rhamnose. Some of the galacturonic acid units carried at C-2 and C-3 side chains which were terminated by D-galactopyranose and L-arabinofuranose residues. A few of the latter also occurred as inner units, probably in the side chains. This appears to be the first time a pectic material has been resolved into a galacturonan and a pectic acid containing the four sugar residues usually found in pectins. It is probable that the pectin occurring to a limited extent in wood has a similar composition.

In previous investigations several polysaccharides were isolated from the bark of amabilis fir (*Abies amabilis*) (1), namely a cellulose (2), a galactoglucomannan (3), a glucomannan (4), and a xylan (5). The present study is concerned with the pectic substances also present in this bark. Pectin has previously been isolated from both wood and bark by Anderson and his co-workers (6–9). Painter and Purves (10) obtained pectin in a yield of 7% from white spruce inner bark. Similarly, inner bark of white birch has yielded a pectin in a yield of 3–4% (11). During the early stages of cell differentiation, the primary wall and the middle lamella consist largely of pectin. The pectic substances of cell walls in the phloem, cambial, sapwood, and heartwood regions have recently been studied by Thornber and Northcote (12).

The pectic group of polysaccharides is based on residues of D-galacturonic acid, D-galactose, L-arabinose, and L-rhamnose, with the galacturonic acid usually, albeit not always, predominating. A polymer containing only D-galacturonic acid residues (a galacturonan) seems to have been isolated only on one occasion, namely from sunflower heads (13). Lately, it has become evident that most of the so-called pectic acids probably also contain neutral sugar residues, such as D-galactose, L-arabinose, L-rhamnose, and L-fucose (14–18). The exact constitution of these heteropolymers is still unknown although the main features of one pectic acid have recently been established (17).

RESULTS AND DISCUSSION

When extractive-free fir bark was treated with chlorous acid for complete removal of polyphenolic material, a holocellulose was obtained in a yield of 50%. A mixture of

[1]*Present address*: *Department of Chemistry, Ohio State University, Columbus 10, Ohio.*
[2]*Present address*: *Department of Forest Chemistry, State University College of Forestry, Syracuse 10, N. Y.*

Can. J. Chem. Downloaded from www.nrcresearchpress.com by 210.87.254.5 on 09/05/12
For personal use only.

polysaccharides, including a galactoglucomannan (3) and pectic material, was removed by extraction with hot water, the amount corresponding to a yield of 1.8% of the bark. The extract on hydrolysis gave galacturonic acid, galactose, glucose, mannose, arabinose, and xylose in a ratio of 10:8:20:44:10:8. Free boundary electrophoresis indicated that it consisted of at least three components. The solid residue was treated with hot 0.5% ammonium oxalate in water to give a crude ammonium pectate with $[\alpha]_D$ +120° in water and in a yield of 6.0% of the bark. On hydrolysis the product gave the same sugars as above, the ratio being 38:8:10:22:12:10. Boundary electrophoresis showed that it consisted of one major, fast-moving and three or four slower components.

Anderson and co-workers (19) have recently claimed that decarboxylation can easily occur on isolation of pectin by techniques such as those used here. Using different times of treatment with both water and ammonium oxalate, 16 samples were isolated. Yields, specific rotations, and sugar compositions remained practically constant throughout, showing that in the present case the pectic material underwent no chemical change during its isolation. When the crude ammonium pectate was subjected to chromatography on diethylaminoethylcellulose (20), three fractions were obtained. Water eluted a galactoglucomannan (52%), phosphate buffer an acidic arabinoxylan (7%), and sodium hydroxide a pectic acid (28%), containing galacturonic acid, galactose, and arabinose residues. Obviously, the crude ammonium pectate was a mixture of at least three different components.

The pectic acid was separated from the other polysaccharides by forming the insoluble calcium pectate which was washed with alkali and water. The purified product, obtained in a yield of 30%, had $[\alpha]_D$ +230° in water and on hydrolysis gave galacturonic acid, galactose, and arabinose in a ratio of 85:4:11, and also traces of rhamnose. Boundary electrophoresis indicated that the product was not homogeneous. Several attempts were made to effect further resolution by renewed treatment with calcium chloride, precipitation with cetyltrimethylammonium hydroxide, fractional precipitation with ethanol from an aqueous solution, and ion exchange chromatography on diethylaminoethylcellulose. In each case, the fractions obtained were unchanged in composition and optical rotation.

Yean and Goring (21) have recently shown that sodium lignosulfonate can be conveniently separated from neutral polysaccharides by an electrophoresis–convection technique. When the crude ammonium pectate was subjected to this procedure, the upper layers in the electrolyte vessel contained the galactoglucomannan, while the pectic acid was located at the bottom. Very little resolution could be achieved, however, with the purified product.The repeated failure to resolve the purified ammonium pectate any further made it tempting to conclude that the product must be chemically homogeneous in spite of the electrophoretic evidence. At this stage, however, it was discovered that the product could actually be resolved into two fractions. While several procedures were found to be applicable, they were all based on the different solubility in water of the two components. When an aqueous solution of the purified ammonium pectate was passed through a column with a cation exchange resin in the acid form, a slightly cloudy, colloidal solution was obtained. Ultracentrifugation at 40 000 g gave in 50% yield a precipitate, the sodium salt of which had $[\alpha]_D$ +246° in water and which on hydrolysis gave only galacturonic acid. The portion remaining in solution amounted to 30%, had $[\alpha]_D$ +225°, and contained, in addition to traces of rhamnose, residues of galacturonic acid, galactose, and arabinose in a ratio of 74:7:19. The first polysaccharide was obviously a *galacturonan*. The second will, somewhat arbitrarily, be referred to here as a *pectic acid*.

Can. J. Chem. Downloaded from www.nrcresearchpress.com by 210.87.254.5 on 09/05/12
For personal use only.

The same fractionation was attained when a solution in water of the purified ammonium pectate was treated with dilute sulfuric acid or aqueous sodium chloride, respectively, followed by ultracentrifugation. On electrophoresis–convection of the ammonium pectate, a colloidal, viscous layer formed at the bottom of the vessel. When this layer was diluted with water and subjected to ultracentrifugation, the same two fractions were again obtained. Boundary electrophoresis showed that the galacturonan was homogeneous, while the pectic acid was probably still somewhat heterogeneous. Application of the four fractionation methods referred to above failed to effect any further resolution, showing that no separate galactan or araban was present. Gel filtration, using Sephadex G-200 was also of no avail, indicating the absence of low molecular weight material. The pectic acid was probably a mixture of closely related acidic polysaccharides, differing slightly in their content of galacturonic acid residues. Both polysaccharides were accordingly subjected to structural analysis.

When the galacturonan was hydrolyzed with a commercial pectinase enzyme, a series of four polymer-homologous oligomers of galacturonic acid were obtained, ranging from the di- to the penta-saccharide. The propylene glycol ester of the acidic polymer was reduced in water with sodium borohydride to the corresponding galactan (14). Reduction of the acetylated galacturonan with diborane in diglyme (22) proved less efficient. The reduced product, which still contained a few galacturonic acid residues, was methylated and hydrolyzed, giving, in a molar ratio of 1:350:1, 2,3-di-*O*-methyl-D-galacturonic acid, 2,3,6-tri-*O*-methyl-D-galactose, and 2,3,4,6-tetra-*O*-methyl-D-galactose, which were identified through crystalline derivatives. The number-average degree of polymerization of the *O*-methylgalactan was 450, as determined from osmotic pressure measurements. Only one nonreducing end group was thus present per average molecule.

These results show that the galacturonan was a linear polysaccharide containing at least 450 (1 → 4)-linked α-D-galacturonic acid residues. The unbranched nature of the galacturonan and its relatively high degree of polymerization are probably the reasons for its insolubility in water. When the pectic acid was subjected to a mild, partial acid hydrolysis, arabinose appeared immediately in the hydrolysate, soon followed by galactose. On prolonged hydrolysis, the four galacturonic acid oligomers, previously obtained from the galacturonan, were formed. In order to make available more of these compounds, the purified, but unfractionated, ammonium pectate was partially hydrolyzed. A combination of ion exchange and paper chromatography gave four pure oligomers. 4-*O*-(α-D-Galactopyranosyluronic acid)-D-galacturonic acid was tentatively identified by conversion to the known α-(1 → 4)-linked galactobiose (23). The corresponding galacturonotriose, on reduction, methylation, and hydrolysis, gave 1 mole of 2,3,4,6-tetra-*O*-methyl-D-galactose and 2 moles of 2,3,6-tri-*O*-methyl-D-galactose.

2-*O*-(α-D-Galactopyranosyluronic acid)-L-rhamnose was identified through its crystalline, fully methylated methyl glycoside dihydrate (17) and from the *O*-methyl sugars obtained on hydrolysis of the latter. The fourth oligosaccharide was a galacturonosyl rhamnosyl rhamnose. The nature of the linkage between the two rhamnose residues could not be determined with certainty. A similar trisaccharide has been isolated from alfalfa pectic acid (17). The nature of the first two oligosaccharides shows the presence of (1 → 4)-linked α-D-galacturonic acid residues. The isolation of the last two oligomers indicates that rhamnose was probably an integral part of the pectic acid.

A reduction of the pectic acid prior to its methylation would obviously make it impossible to distinguish between the galacturonic acid and the galactose residues. The polysaccharide was therefore methylated directly by the Haworth and the Purdie

Can. J. Chem. Downloaded from www.nrcresearchpress.com by 210.87.254.5 on 09/05/12
For personal use only.

methods, but under mild conditions in view of its lability towards alkali (24, 25). The mixture of *O*-methyl glycosides obtained on methanolysis was resolved into an acid and a neutral portion with the aid of exchange resin. The acid fraction was esterified, reduced with lithium aluminium hydride, and hydrolyzed. The neutral portion, finally, was also hydrolyzed. The neutral *O*-methyl sugars present in each fraction were separated by preparative paper chromatography. Seven of the compounds obtained were crystalline or were identified through crystalline derivatives. The remaining three were tentatively identified by other means. The methylation data are summarized in Table I.

TABLE I

Sugar constituents of the methylated pectic acid

Component	Mole %	Component	Mole %
Unknown sugars	1.8	D-Galacturonic acid	4.3
3-*O*-Methyl-L-rhamnose	2.6	2-*O*-Methyl-D-galacturonic acid	10.5
Di-*O*-methyl-L-arabinose	2.4	3-*O*-Methyl-D-galacturonic acid	9.7
2,3,5-Tri-*O*-methyl-L-arabinose	13.3	Di-*O*-methyl-D-galacturonic acid	0.3
2,3,4-Tri-*O*-methyl-D-galactose	1.2	2,3-Di-*O*-methyl-D-galacturonic acid	45.3
2,3,4,6-Tetra-*O*-methyl-D-galactose	7.2	2,3,4-Tri-*O*-methyl-D-galacturonic acid	1.4

The large amount of 2,3-di-*O*-methyl-D-galacturonic acid shows that the pectic acid contained a framework of (1 → 4)-linked D-galacturonic acid residues, probably, in view of the high specific rotation of the polysaccharide, in the α-D-modification. The presence of 2-*O*- and 3-*O*-methyl-D-galacturonic acid and of D-galacturonic acid indicates that the framework was partly branched through C-2 or C-3 or both, respectively. The 2,3,4-tri-*O*-methyl-D-galactose evidently originated from nonreducing end groups. The majority of the D-galactose and L-arabinose residues were present as nonreducing end groups, precluding the presence of a separate galactan or araban. Their number was only slightly less than that of galacturonic acid residues carrying branches. A small amount of inner arabinose and (1 → 6)-linked galactose residues were also present. The nature of the galacturonosyl rhamnose obtained on partial hydrolysis in conjunction with the presence of 3-*O*-methyl-L-rhamnose among the *O*-methyl sugars strongly indicate that a few rhamnose residues were an integral part of the galacturonan framework, with at least some of them serving as branching points through their 4-position. No evidence was obtained for the presence of (1 → 4)-linked galactose residues, such as those constituting the galactan occurring in seeds from *Lupinus albus* (26, 27).

It is not possible to assign a unique structural formula to the pectic acid on the basis of the present experimental evidence. One of several possibilities is a molecule consisting of a framework of (1 → 4)-linked α-D-galacturonic acid residues, carrying numerous branches containing D-galactopyranose and L-arabinofuranose residues, most of them present as end groups. Since partial acid hydrolysis produced no galacturonic acid oligomers containing (1 → 2)- or (1 → 3)-linkages, a direct attachment of side chain galacturonic acid residues to the backbone is not likely. The presence of (1 → 4)-linked galacturonic acid residues elsewhere in the side chains is, of course, not excluded.

The experimental evidence presented for the structure of the present pectic acid from fir bark is quite similar to that reported by Aspinall and Fanshawe (17) for their alfalfa pectic acid, and it is clear that these two polysaccharides are closely related. No other pectic acid has so far been studied in similar detail.

Can. J. Chem. Downloaded from www.nrcresearchpress.com by 210.87.254.5 on 09/05/12
For personal use only.

Can. J. Chem. Downloaded from www.nrcresearchpress.com by 210.87.254.5 on 09/05/12
For personal use only.

CONCLUSIONS

To the best of the authors' knowledge, the present investigation represents the first successful resolution of a pectic material into a galacturonan and a pectic acid. There is little reason to doubt that in the future pectins from other sources will also prove amenable to this treatment. The earlier conclusion of Aspinall and Cañas-Rodriguez (14) that pectin might consist of "a mixture of acidic polysaccharides, one composed solely of D-galacturonic acid residues and the other or others containing both neutral sugar and D-galacturonic acid residues" appears eminently justified in view of the present results.

Bark obviously contains much more pectin than wood. No wood pectin has so far been subjected to a structural analysis, mostly, no doubt, because of the small quantities present. It is known, however, that the primary wall and middle lamella in wood cells are rich in galacturonic acid, galactose, and arabinose residues (12, 28–30). An α-(1 $\rightarrow$ 2)-linked-D-galacturonosyl rhamnose has been isolated from pine (31, 32) and beech (33) woods. The presence in wood of pectic material similar to that found in the fir bark is therefore quite likely.

EXPERIMENTAL

General experimental conditions were the same as in a previous paper (34). The following solvent systems were used for paper chromatography: (A) ethyl acetate, acetic acid, water (9:2:2 v/v), (B) ethyl acetate, acetic acid, water (18:7:8), (C) ethyl acetate, acetic acid, formic acid, water (18:3:1:4), (D) ethyl acetate, pyridine, water (8:2:1), and (E) 2-butanone, water, ammonia (90:8:2). For preparative purposes, Whatman No. 3MM filter paper with a wick of No. 50 paper was used. R_{GalA} values refer to the rate of movement of the sugars relative to galacturonic acid. M_G values refer to the rate of movement of a sugar relative to glucose on paper electrophoresis in 0.05 M borate solution. Specific rotations were determined in water (c, 1.0), unless otherwise stated.

Isolation of Crude Pectin

For isolation of crude pectin, the bark was first treated with chlorous acid as described elsewhere (1). The average yield of holocelluloses in several experiments was 50 $\pm$ 2%.

Batches of holocellulose (50 g) were stirred at 75° with water (1 l) containing 6% of potassium acetate for 3, 6, 9, and 12 h, respectively. Each of the four residues was extracted at the same temperature with 0.5% aqueous ammonium oxalate, aliquots being withdrawn after 3, 6, 9, and 12 h. Each of the 16 fractions thus obtained was purified by washing the insoluble calcium pectate with water. The purified ammonium pectates were all essentially similar, with average yield from the holocellulose 3.5%, $[\alpha]_D$ +195°, and the ratio of galacturonic acid, galactose, and arabinose 77:6:17.

For large-scale recovery of pectin, holocellulose (1 200 g) was stirred in water (18 l) containing 6% potassium acetate at 75° for 12 h. The residue was recovered by filtration and washed with hot water (20 l). After concentration to 3 l, the extract was added to ethanol (15 l). The precipitate formed was recovered by filtration, washed successively with 70% aqueous ethanol, ethanol, and petroleum ether, and finally dried *in vacuo* to give a white powder (42 g, 3.5% of holocellulose). The solid residue was extracted with 0.5% aqueous ammonium oxalate at 75° for 12 h. The extract was recovered in the usual way to give a white product (145 g, 12% yield) with $[\alpha]_D$ +120°.

Purification of Crude Ammonium Pectate

Crude ammonium pectate (113 g) was dissolved in water (2 l) and a 10% aqueous solution of calcium chloride (1.5 l) was added. The precipitate formed was washed with water and then suspended in water (4 l) to which 8% aqueous sodium hydroxide (2 l) was added. The suspension was stirred, and the solids were recovered by filtration, and washed with dilute acetic acid and water. The calcium pectate was treated with ammonium oxalate, insoluble calcium oxalate was removed by centrifugation, and the supernatant solution was concentrated and added to ethanol. The precipitate was recovered as described above to give 37 g of material (33% of crude product); $[\alpha]_D$ +230°; OCH_3, 0.9%; ash, 2.3%.

Chromatography on Diethylaminoethylcellulose (16, 20)

Purified ammonium pectate (400 mg) in aqueous solution was added to the top of a column containing diethylaminoethylcellulose in the phosphate form. The column was eluted in succession with 500 ml each of water, 0.025 M, 0.05 M, 0.10 M, and 0.25 M sodium dihydrogen phosphate, and, finally, using gradient elution, with water – 0.3 M sodium hydroxide (2 l). The fractions (15 ml each) were analyzed polarimetrically and by the phenol – sulfuric acid method (35). After deionization with exchange resins, the pectic material was recovered in the usual way.

Electrophoresis–Convection

The apparatus used has been described elsewhere (21). Ammonium pectate (500 mg) was dissolved in water (400 ml) and subjected to electrophoresis. After 5 h, a turbid, viscous layer was observed at the bottom of the vessel used. The experiment was terminated after 8 h, and fractions were carefully removed with a syringe, starting with the top layer.

Resolution of Purified Ammonium Pectate

Acidification.—Purified ammonium pectate (500 mg) was dissolved in water, and the solution was passed through a column containing Amberlite IR-120 exchange resin (acid form). The turbid eluate was concentrated and subjected to ultracentrifugation at 40 000 g. The supernatant, clear solution was treated with more exchange resin until no more turbidity was observed. The final, clear solution was concentrated and added to ethanol. The precipitate formed was recovered in the usual way to give a water-soluble *pectic acid* (160 mg); $[\alpha]_D$ +225°; OCH_3, 2.7%; ash, 0.35%. The solid residue was washed with water and subjected to the same ultracentrifugation, a process which was repeated six times, after which the material was washed with acetone and petroleum ether and dried *in vacuo*, yielding 250 mg of the water-insoluble *galacturonan*; $[\alpha]_D$ +246°; OCH_3, 0.6%; ash, 0.16%.

Alternatively, *N* sulfuric acid was added slowly to an aqueous solution of the ammonium pectate until a pH of 4.0 had been reached. The precipitate and solution were recovered as described.

Addition of aqueous sodium chloride.—A saturated solution in water of sodium chloride (10 ml) was added slowly to an aqueous, 1% solution of ammonium pectate (100 ml). The precipitate formed and the solution were treated as above.

Electrophoresis–convection.—The turbid, viscous solution obtained at the bottom after electrophoresis was diluted with water and subjected to ultracentrifugation. The precipitate and solution gave the same products as the other two methods.

Partial Acid Hydrolysis of the Purified Ammonium Pectate

Purified ammonium pectate (40 g) was dissolved in water (972 ml) to which 28 ml of concentrated sulfuric acid was added. The solution was heated on a steam bath for 3.5 h. After cooling, an equal volume of acetone was added. The precipitate formed was recovered by filtration and washed with aqueous acetone. The degraded product (18 g) gave only galacturonic acid on complete hydrolysis.

The filtrate and washings were neutralized with barium carbonate, treated with a cation exchange resin, and added to the top of a column containing Amberlite CG-45 (formate form) anion exchange resin. After washing with water until a Molisch test was negative, elution was continued with increasing concentrations of formic acid (0.001 *N* to 2 *N*). Eight fractions were collected and examined by paper chromatography (solvents A to D). Further resolution was effected with solvent B, using preparative paper chromatography.

Identification of Oligosaccharides

Galacturonotriose.—This trisaccharide (60 mg) had $[\alpha]_D$ +187°, R_{GalA} 0.04, 0.39, and 0.05 in solvents A, B, and C, respectively, and melted with decomposition at 135–142°. Partial hydrolysis gave galacturonic acid, galacturonobiose, and some galacturonotriose. The methyl ester methyl glycoside was reduced with sodium borohydride, methylated, and hydrolyzed, giving two sugars which were separated by paper chromatography (solvent E). One of the components (35 mg) was identified as 2,3,6-tri-*O*-methyl-D-galactose by conversion to the corresponding galactonolactone, which had melting point and mixed melting point 97–98°. The second compound (20 mg) was shown to be 2,3,4,6-tetra-*O*-methyl-D-galactose through its aniline derivative which had melting point and mixed melting point 192–194°.

Galacturonosyl rhamnosyl rhamnose.—This trisaccharide (90 mg) had $[\alpha]_D$ +118°, had R_{GalA} 0.10 in solvent C, and gave 1 mole of galacturonic acid and 2 moles of rhamnose on prolonged hydrolysis. Partial hydrolysis yielded rhamnose, galacturonic acid, and galacturonosyl rhamnose. After prior reduction with borohydride, only galacturonosyl rhamnose and a trace of galacturonic acid were obtained on hydrolysis.

Galacturonobiose.—This disaccharide (700 mg) had $[\alpha]_D$ +154° and R_{GalA} 0.23, 0.60, and 0.20 in solvents A, B, and C, respectively. It melted with decomposition at 125–135°. After treatment with trimethylorthoformate, esterification with diazomethane, and reduction with lithium aluminium hydride (23), a neutral disaccharide was obtained which gave only galactose on hydrolysis and had $[\alpha]_D$ +175°. The compound could not be induced to crystallize but was chromatographically and ionophoretically identical with an authentic sample of 4-*O*-(α-D-galactopyranosyl)-D-galactose (36).

2-O-(α-D-Galactopyranosyluronic acid)-L-rhamnose.—This oligosaccharide (300 mg) had $[\alpha]_D$ +108° and gave equimolar amounts of galacturonic acid and rhamnose on prolonged hydrolysis. The methyl ester methyl glycoside, after reduction with sodium borohydride, on hydrolysis gave galactose and rhamnose. When the disaccharide was directly reduced, galacturonic acid was the only reducing sugar obtained on hydrolysis. The fully methylated aldobiouronic acid, after recrystallization from chloroform – ethyl ether, gave methyl 2-*O*-(2,3,4-tri-*O*-methyl-α-D-galactopyranosyluronic acid)-3,4-di-*O*-methyl-L-rhamnopyranoside dihydrate which had m.p. 66–68° and $[\alpha]_D$ +98° (*c*, 0.5 in chloroform) (17). The compound (50 mg) was reduced with diborane in diglyme and hydrolyzed, giving equimolar amounts of two compounds which on demethylation gave galactose and rhamnose, respectively. They were tentatively identified from their rates of movement in solvent E as 2,3,4-tri-*O*-methyl-D-galactose and 3,4-di-*O*-methyl-L-rhamnose.

Can. J. Chem. Downloaded from www.nrcresearchpress.com by 210.87.254.5 on 09/05/12
For personal use only.

Partial Enzymic Hydrolysis of the Galacturonan

An aqueous solution of the sodium salt of the galacturonan was treated with a commercial pectinase preparation (Nutritional Biochemical Corporation, Cleveland, Ohio) using the technique of Painter (37). The hydrolysate was resolved into five fractions using paper chromatography (solvent B). A plot of the degree of polymerization of each oligomer versus $R_{GalA}/(1 - R_{GalA})$ was linear.

Esterification and Reduction of the Galacturonan

The galacturonan (20 g) was esterified with propylene oxide and reduced with sodium borohydride as described earlier (11). After four such treatments, a product (13 g) was obtained which on hydrolysis gave galactose and galacturonic acid in a ratio of 94:6. When the fully acetylated galacturonan was reduced with diborane in diglyme (22) a product was obtained in 50% yield containing galacturonic acid and galactose residues in a ratio of 3:2. This method accordingly appeared to have no advantage in this case.

Methylation of the Galacturonan and Identification of Methylated Sugars

The reduced galacturonan (10 g) was methylated four times with dimethyl sulfate and alkali. The partly methylated product (8 g) was further methylated by the procedure of Kuhn and co-workers (38), yielding a product (3.5 g), which was further reduced with lithium aluminium hydride in tetrahydrofuran. After two further methylations with methyl iodide and silver oxide, the *O*-methylgalactan (2.0 g) had $[\alpha]_D$ +128° (*c*, 1.0 in chloroform) and OCH_3 42.7%. Methanolysis and hydrolysis gave a mixture containing one major and two minor constituents.

*2,3,6-Tri-O-methyl-*D*-galactose.*—The sirupy sugar (980 mg) had $[\alpha]_D$ +84°. The derived 2,3,6-tri-*O*-methyl-α-D-galactonolactone, on recrystallization from ethyl ether, had melting point and mixed melting point 97–98°.

*2,3,4,6-Tetra-O-methyl-*D*-galactose.*—This sirup (3 mg) had $[\alpha]_D$ +102°. It was converted to its aniline derivative which had melting point and mixed melting point 196–198°.

*2,3-Di-O-methyl-*D*-galacturonic acid.*—This compound (4 mg) was converted to its methyl ether methyl glycoside, reduced with lithium aluminium hydride, and hydrolyzed. The aniline derivative of the 2,3-di-*O*-methyl-D-galactose thus obtained had melting point and mixed melting point 130–132°.

Determination of the Molecular Weight of the Methylated Galactan

Osmotic pressure measurements were carried out with the *O*-methylgalactan dissolved in chloroform–ethanol (9:1 v/v) as described previously (39). Extrapolation to zero concentration gave a value of 0.28 for $(h/w)_{w\to 0}$, corresponding to a number-average molecular weight of 91 800 and a degree of polymerization of 450.

Methylation of the Pectic Acid

The pectic acid (8 g) was methylated for 20 h at 10° with dimethyl sulfate and alkali. Treatment with methyl iodide and silver oxide gave a product (1.5 g) which had $[\alpha]_D$ +118° (*c*, 1.0 in chloroform) and OCH_3 39.2%, not raised on further methylations. The methylated pectic acid (1.2 g) was directly hydrolyzed by refluxing with *N* sulfuric acid for 12 h. The neutralized (barium carbonate) and deionized solution was added to the top of a column containing Dowex 1-X4 (acetate form) anion exchange resin. Neutral sugars were removed with water. The eluate on concentration gave a sirup (270 mg) which was resolved by paper chromatography using solvent E. Acid sugars were eluted with 30% aqueous acetic acid, yielding a sirup (645 mg) which was treated with methanolic hydrogen chloride, reduced with lithium aluminuim hydride, and hydrolyzed. The mixture of neutral *O*-methyl sugars thus obtained was resolved as above.

Identification of Methylated Sugars

Neutral Series

*3-O-Methyl-*L*-rhamnose.*—This sugar (11 mg) had $[\alpha]_D$ +40° and gave rhamnose on demethylation. Crystals obtained from the sirup had m.p. 106–108°.

*Di-O-methyl-*L*-arabinose.*—This sugar (10 mg) had $[\alpha]_D$ +65° and gave arabinose on demethylation. The aniline derivative could not be induced to crystallize.

*2,3,5-Tri-O-methyl-*L*-arabinose.*—This sugar (60 mg) had $[\alpha]_D$ −36° and gave arabinose on demethylation. The 2,3,5-tri-*O*-methyl-L-arabonamide had melting point and mixed melting point 134–135°.

*2,3,4,6-Tetra-O-methyl-*D*-galactose.*—This sirupy compound (40 mg) had $[\alpha]_D$ +106°. The aniline derivative had melting point and mixed melting point 193–195°.

Acid Series

*2-O-Methyl-*D*-galactose.*—This compound (73 mg) gave no color reaction with triphenyltetrazolium hydroxide (40) and had $[\alpha]_D$ +80°. Crystals produced from the sirup had m.p. 145–146°. The aniline derivative had m.p. 159–161°.

Anal. Calcd. for $C_7H_{14}O_6$: OCH_3, 16.0. Found: OCH_3, 15.2.

*3-O-Methyl-*D*-galactose.*—This sugar (67 mg) had $[\alpha]_D$ +101° and gave a color reaction with triphenyltetrazolium hydroxide. Its M_G value was higher than that of 2-*O*-methylgalactose.

Anal. Calcd. for $C_7H_{14}O_6$: OCH_3, 16.0. Found: OCH_3, 15.2.

Can. J. Chem. Downloaded from www.nrcresearchpress.com by 210.87.254.5 on 09/05/12
For personal use only.

*2,3-Di-O-methyl-*D*-galactose.*—The sirupy sugar (336 mg) had $[\alpha]_D$ +78°. The aniline derivative had m.p. 130–131°.

Anal. Calcd. for $C_8H_{16}O_6$: OCH_3, 29.8. Found: OCH_3, 28.9.

*2,3,4-Tri-O-methyl-*D*-galactose.*—This compound (11 mg) had $[\alpha]_D$ +107° and gave a crystalline aniline derivative with melting point and mixed melting point 164–166°.

ACKNOWLEDGMENT

The authors wish to express their gratitude to Dr. C. T. Bishop and to Dr. R. L. Whistler for generous gifts of sugar samples. They are also thankful to Dr. H. I. Bolker and Dr. C. B. Purves for help and advice.

REFERENCES

1. T. E. Timell. Svensk Papperstid. **64**, 651 (1961).
2. T. E. Timell. Svensk Papperstid. **64**, 685 (1961).
3. T. E. Timell. Svensk Papperstid. **65**, 843 (1962).
4. T. E. Timell. Svensk Papperstid. **64**, 744 (1961).
5. T. E. Timell. Svensk Papperstid. **64**, 748 (1961).
6. E. Anderson. J. Biol. Chem. **112**, 531 (1935).
7. E. Anderson, L. W. Seigle, P. W. Krznarich, L. Richards, and W. W. Marteny. J. Biol. Chem. **121**, 165 (1937).
8. E. Anderson, R. B. Kaster, and M. G. Seeley. J. Biol. Chem. **144**, 767 (1942).
9. E. Anderson. J. Biol. Chem. **165**, 233 (1946).
10. T. J. Painter and C. B. Purves. Tappi, **43**, 729 (1960).
11. T. E. Timell and A. Jabbar Mian. Tappi, **44**, 788 (1961).
12. J. P. Thornber and D. H. Northcote. Biochem. J. **81**, 449, 455 (1961); **82**, 340 (1962).
13. C. T. Bishop. Can. J. Chem. **33**, 1521 (1955).
14. G. O. Aspinall and A. Cañas-Rodriguez. J. Chem. Soc. 4020 (1958).
15. U. K. Sen Gupta and C. V. N. Rao. Bull. Chem. Soc. Japan, **36**, 1683 (1963).
16. W. Heri, H. Neukom, and H. Deuel. Helv. Chim. Acta, **44**, 1939 (1961).
17. G. O. Aspinall and R. S. Fanshawe. J. Chem. Soc. 4215 (1961).
18. D. M. W. Anderson and N. J. King. J. Chem. Soc. 5333 (1961).
19. D. M. W. Anderson, A. M. Bews, S. Garbutt, and N. J. King. J. Chem. Soc. 5230 (1961).
20. H. Neukom, H. Deuel, W. J. Heri, and W. Kundig. Helv. Chim. Acta, **43**, 64 (1960).
21. W. Q. Yean and D. A. I. Goring. Tappi, **47**, 16 (1964).
22. F. Smith and A. M. Stephen. Tetrahedron Letters, **7**, 17 (1960).
23. J. K. N. Jones and W. W. Reid. J. Chem. Soc. 1361 (1954); 1890 (1955).
24. R. L. Whistler and J. N. BeMiller. Advan. Carbohydrate Chem. **13**, 289 (1958).
25. H. F. Launer and Y. Tomimatsu. J. Org. Chem. **26**, 541 (1961).
26. E. L. Hirst, J. K. N. Jones, and W. O. Walder. J. Chem. Soc. 1225 (1947).
27. P. Andrews, L. Hough, and J. K. N. Jones. J. Chem. Soc. 806 (1954).
28. R. F. Sultze, Jr. Tappi, **40**, 985 (1957).
29. H. Meier and K. C. B. Wilkie. Holzforschung, **13**, 177 (1959).
30. H. Meier. J. Polymer Sci. **51**, 11 (1961); Pure Appl. Chem. **5**, 37 (1962).
31. A. J. Roudier and L. Eberhard. Bull. Soc. Chim. France, 2074 (1960).
32. S. K. Banerjee and T. E. Timell. Tappi, **43**, 849 (1960).
33. H. Meier. Acta Chem. Scand. **16**, 2275 (1962).
34. E. C. A. Schwarz and T. E. Timell. Can. J. Chem. **41**, 1381 (1963).
35. M. Dubois, K. A. Gilles, J. K. Hamilton, P. A. Rebers, and F. Smith. Anal. Chem. **28**, 350 (1956).
36. R. L. Whistler and H. E. Conrad. J. Am. Chem. Soc. **76**, 1673 (1954).
37. T. J. Painter. Can. J. Chem. **37**, 497 (1959).
38. R. Kuhn, H. Trischmann, and I. Löw. Angew. Chem. **67**, 32 (1955).
39. C. P. J. Glaudemans and T. E. Timell. Svensk Papperstid. **61**, 1 (1958).
40. K. Wallenfels. Naturwissenschaften, **37**, 491 (1950).

Can. J. Chem. Downloaded from www.nrcresearchpress.com by 210.87.254.5 on 09/05/12
For personal use only.

Can. J. Chem. Downloaded from www.nrcresearchpress.com by 210.87.254.42 on 09/05/12
For personal use only.

ENTROPY DIFFERENCES FOR SOME RELATED PAIRS OF COMPLEX IONS[1]

J. LIN[2] AND W. G. BRECK
Department of Chemistry, Queen's University, Kingston, Ontario
Received November 3, 1964

ABSTRACT

The temperature coefficient of e.m.f. of a cell consisting of a saturated calomel electrode and a redox electrode of $K_4Fe(CN)_6$ and $K_3Fe(CN)_6$ has been determined by e.m.f. measurements at a series of equimolal concentrations of the above salts and at temperatures of 20, 25, 30, 35 °C. The results for this calomel–redox cell are expressed by the equation $E_{CR}^0 = 0.1200 - 0.00214(t - 25)$, or for the redox electrode against a hydrogen gas electrode, $E_{HR}^0 = 0.3644 - 0.00280(t - 25)$, with E in V and t in °C. Analogous results are available in the literature for other such pairs of complex ions; an examination of these data leads to the hypothesis that the following trichelated pairs: Fe $dip_3^{2+/3+}$, Fe $phen_3^{2+/3+}$, Ru $dip_3^{2+/3+}$, are respectively nearly isentropic.

To know the difference in entropy between a pair of complex ions such as $Fe(CN)_6^{4-}$ and $Fe(CN)_6^{3-}$, which have the same chemical composition but different charge, is equivalent to the evaluation of a single-ion entropy as can be seen by writing for the reaction,

$$[1] \qquad Fe(CN)_6^{3-} + \tfrac{1}{2}H_2 = Fe(CN)_6^{4-} + H^+;\ \Delta S^0 = S_1^0 - S_2^0 + S_{H^+}{}^0 - \tfrac{1}{2}S_{H_2}{}^0,$$

where the subscripts 1 and 2 on the S^0 terms refer respectively to the reduced and oxidized forms of the complex ion. The quantities ΔS^0, $\frac{1}{2}S_{H_2}{}^0$ and $S_1^0 - S_2^0 + S_{H^+}{}^0$ are in principle determinable by experiment. Thus the evaluation of $S_1^0 - S_2^0$ is equivalent to that of $S_{H^+}{}^0$; however, it is not at present clear how the absolute entropy of a single ion can be measured directly.

For the purpose of *assigning* entropies to single ions it is often assumed conventionally that $S_{H^+}{}^0 = 0$ at all temperatures. On the other hand the absolute evaluation of $S_{H^+}{}^0$ has been attempted according to various arguments (1); of these one of the most convincing, by Gurney (2), is based on effecting a coincidence for cations and anions of the correlation between entropies and viscosity B-coefficients, yielding the absolute result, $S_{H^+}{}^0 = -5.5$ e.u. Representation of ionic entropies by the use of equations both fundamental and empirical has had limited success. If the ion in solution is regarded in an approximate way as a charged sphere in a continuous dielectric medium, then the Born equation (3) may be applied to assess the free energy of solvation and differentiation with respect to temperature gives the electrostatic entropy of solvation, ΔS_S, which, for water at 25 °C as the medium, becomes (3)

$$[2] \qquad \Delta S_S = -9.4z^2/r,$$

where z is the valence of the particular ion and r the radius of the spherical boundary between ion and dielectric medium. Laidler (4) has shown that it is possible to fit the observed entropies of hydration of simple ions to the Born relation by adjustment of the coefficient of z^2/r to give the partially empirical relations:

$$[3] \qquad S_{abs}{}^0 = \tfrac{3}{2}R \ln M + 10.2 - 11.6z^2/r_u;$$

[1]*From part of the Ph.D. thesis of J. L.*
[2]*Holder of a Province of Ontario Fellowship. Present address: Institute for the Study of Metals, The University of Chicago, Chicago, Illinois.*

[4] $$S_{conv}^0 = 5.5z + \tfrac{3}{2}R \ln M + 10.2 - 11.6z^2/r_u.$$

In the above the term $\frac{3}{2}R \ln M$ is the usual contribution to the entropy by an uncharged atom of mass M/N_0; r_u is Pauling's univalent radius (5); the term z^2/r_u represents the electrostatic contribution according to the approximate Born model; and the term $5.5z$ adjusts the ion entropies from an absolute scale (based on $S_{H^+}^0 = -5.5$ e.u.) to the conventional scale (based on $S_{H^+}^0 = 0$).

Powell and Latimer (6) have obtained good agreement with experiment by use of the equation for simple ions,

[5] $$S_{conv}^0 = \tfrac{3}{2}R \ln M + 37 - 270z/r_e^2,$$

where r_e is an adjusted radius in a term which is notably not of the Born form. While this equation calculates values on the conventional scale it is absolute in the sense that in order to put values for cations and anions on the same line it is required to assume that $S_{H^+}^0$ is, in fact, close to zero. More recently Noyes (7) by a matching technique, and Glueckauf (8) by treating in more detail the nature of the dielectric, have refined the Born approach to the electrostatic entropy of hydration to obtain more complicated terms in z^2/r.

Equations have also been presented to represent entropies of complex ions, particularly oxy-anions. That of Couture and Laidler (9) contains the usual electrostatic term in z^2/r while others (10) do not. King (11) observes that for monatomic ions S^0 depends on z while for complex ions it depends on z^2. Of immediate interest is an empirical equation by George, Hanania, and Irvine (12),

[6] $$S^0 = A - B|z| + Cn,$$

where z is the numerical value of the valence, n the number of ligands; A is a function of the size of the ion and its effect on solvent structure; the coefficient B depends on the identity of the ligand and C is a contribution per ligand. For cyanide as the ligand, $A = 45$, $B = 43$, and $C = 18.5$ e.u. Accordingly, the entropy difference for the pair $Fe(CN)_6^{4-/3-}$ is given by B, viz. 43 e.u. (presumably on the conventional basis that $S_{H^+}^0 = 0$ although such is not stated). For dipyridyl (dip) as the ligand B is quite small at 3 ± 4 e.u., being the entropy difference for the pair $Fe\,dip_3^{2+/3+}$.

It is the intention here to compare values of the quantity $S_1^0 - S_2^0 + S_{H^+}^0$, which are experimentally determinable as, for example, in eq. [1], for related pairs of complex ions such as $Fe(CN)_6^{4-/3-}$, $Fe\,dip_3^{2+/3+}$, $Fe(CN)_4\,dip^{2-/1-}$, and others in the hope that some conclusions might be reached concerning the values of $S_1^0 - S_2^0$ (and of $S_{H^+}^0$) as well as their dependence on valence. Some such results have been obtained and are reported along with others by George, Hanania, and Irvine (12). However, since specific experimental data for the reaction in eq. [1] involving the pair $Fe(CN)_6^{4-/3-}$ were lacking, it was decided to determine these data by measurement of the temperature coefficient of e.m.f. of an appropriate cell.

EXPERIMENTAL

For the measurement of the temperature coefficient of e.m.f. of the cell,

Hg	Hg_2Cl_2, KCl sat'd.	KCl sat'd.	$K_4Fe(CN)_6$ m $K_3Fe(CN)_6$ m	Pt,

H cells were used with the saturated calomel electrode in one limb and the redox electrode in the other, separated by a 2% agar plug saturated with KCl. The calomel electrodes were prepared (13) 2 weeks before

Can. J. Chem. Downloaded from www.nrcresearchpress.com by 210.87.254.42 on 09/05/12
For personal use only.

use and allowed to stand in a thermostat regulated at the required temperature for at least 2 days before measurements were taken. The other half-cell containing the equimolal redox solutions at various concentrations (m) equillibrated much more rapidly in the bath. The bath temperatures of 20, 25, 30, 35 °C were controlled to within a few hundredths °C and for all except the two most dilute solutions the reproducibility was within 0.1 mV over a period of more than a day; for the most dilute, 0.2 mV over a period of 6 h.

RESULTS

The e.m.f. values, E, obtained at 20, 25, 30, 35 °C for the cell at various equimolal concentrations of $K_4Fe(CN)_6$ and $K_3Fe(CN)_6$ are shown in Fig. 1 plotted against the function $\mu^{1/2}/(1 + \mu^{1/2})$, where μ is the ionic strength. Extrapolating to zero ionic strength for each temperature and representing the results in an equation by least-squares yields for the calomel–redox cell (CR), with t in °C and E in V,

$$E_{CR}^0 = 0.1200 - 0.00214(t - 25), \quad [7]$$

and since in this temperature range the potential of the calomel electrode against the hydrogen gas electrode (HC) is given by (14)

$$E_{HC}^0 = 0.2444 - 0.00066(t - 25), \quad [8]$$

there is obtained for the cell reaction, $Fe(CN)_6^{3-} + \frac{1}{2}H_2 = Fe(CN)_6^{4-} + H^+$,

$$E_{HR}^0 = 0.3644 - 0.00280(t - 25); \ \Delta S^0 = -64.6 \text{ e.u.} \quad [9]$$

Taking $\frac{1}{2}S_{H_2}^0$ as 15.6 e.u. (15), $S_1^0 - S_2^0 + S_{H^+}^0 = -49.0$ e.u.

Data are available in the paper of George, Hanania, and Irvine (12) for calculation of the value of the same function for analogous reactions involving other related pairs

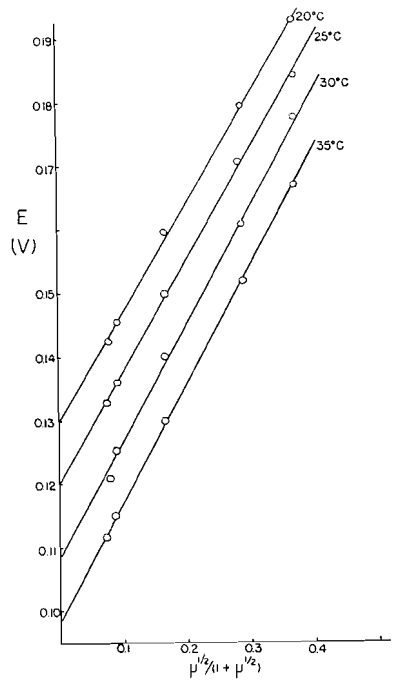

FIG. 1. Plot of e.m.f. (E) in V for calomel redox cell against the function $\mu^{1/2}/(1 + \mu^{1/2})$ at temperatures 20, 25, 30, 35 °C.

Can. J. Chem. Downloaded from www.nrcresearchpress.com by 210.87.254.42 on 09/05/12
For personal use only.

of complex ions. The results are in Table I where the subscripts 1 and 2 on the S^0 terms refer to the reduced and oxidized forms respectively; "dip" signifies a dipyridyl and "phen" an O-phenanthroline ligand.

TABLE I

Values of $S_1^0 - S_2^0 + S_{H^+}{}^0$ in e.u. for related pairs of complex ions

Pair 1/2	$S_1^0 - S_2^0 + S_{H^+}{}^0$	Reference
$Fe(CN)_6^{4-/3-}$	−49.0	This work
$Fe(CN)_4\,dip^{2-/1-}$	−34.6	12
$Fe\,dip_3^{2+/3+}$	−6.9*	12
$Fe\,phen_3^{2+/3+}$	−5.2	12
$Ru\,dip_3^{2+/3+}$	−5.1	12
$Os\,dip_3^{2+/3+}$	+0.8	12
$Fe(H_2O)_6^{2+/3+}$	+43.0	15

*This value recalculated. The value given (12) is 8.2 e.u.

DISCUSSION

In Table I the difference in values for $Fe(H_2O)^{2+/3+}$ and $Fe(CN)_6^{4-/3-}$ amounts to the enormous figure of 92 e.u. There is a good chance of accounting for much of this on the basis of valences and radii. But the difference in values for $Fe(H_2O)_6^{2+/3+}$ and, say, $Fe\,phen_3^{2+/3+}$ of 48.2 e.u. is also impressive and here the charges are the same. It appears that large, neutral ligands such as dipyridyl or O-phenanthroline are extremely effective in insulating the surrounding water structure from the effect of the charge on the central ions. On the assumption that $S_{H^+}{}^0$ is not very large, the difference in entropy, $S_1^0 - S_2^0$, for $Fe(H_2O)_6^{2+/3+}$ is notably large and positive. As large, neutral ligands such as O-phenanthroline are substituted the radii of the ions increase, becoming more nearly equal, and the surrounding water structure becomes shielded from the effect of charge on the central ions. If this shielding is completely effective, the entropy difference $S_1^0 - S_2^0$ should drop to zero; if the shielding is incomplete, $S_1^0 - S_2^0$ should become less positive, but not negative. This argument requires that $S_{H^+}{}^0$ must be somewhat negative. For example, in the case of $Fe\,phen_3^{2+/3+}$, if the shielding is complete, $S_1^0 - S_2^0 = 0$, and $S_{H^+}{}^0 = -5.2$ e.u. On the other hand, if the shielding is incomplete, $S_1^0 - S_2^0 > 0$, and $S_{H^+}{}^0$ is more negative than −5.2 e.u. If the argument is applied to the case of $Fe\,dip_3^{2+/3+}$, $S_{H^+}{}^0 \leqslant -6.9$ e.u.

When full coordination with negative ligands occurs, as for the pair $Fe(CN)_6^{4-/3-}$, the difference in entropy is considerably negative owing to the change in total charges on the complex ions. As dipyridyl ligands are substituted for cyanide the value of $S_1^0 - S_2^0 + S_{H^+}{}^0$ increases almost linearly to −6.9 e.u., or in the case of $Fe\,phen_3^{2+/3+}$, to −5.2 e.u. This substitution process differs from that in the previous paragraph in that changes in charge are involved. It is thus seen that the substitution of large, neutral ligands in the one case for water molecules reduces the large positive difference for $Fe(H_2O)_6^{2+/3+}$, in the other case for negative cyanide ligands reduces the large, negative entropy difference for $Fe(CN)_6^{4-/3-}$. At some point these different substitution processes must cause the entropy difference, $S_1^0 - S_2^0$, to pass through zero and the most likely point is where the shielding of central positive charge and replacement of negative ligands are at the same maximum, namely for the trichelated species.

It seems more than coincidental that the values −6.9, −5.2, −5.1 e.u. are so close

Can. J. Chem. Downloaded from www.nrcresearchpress.com by 210.87.254.42 on 09/05/12
For personal use only.

Can. J. Chem. Downloaded from www.nrcresearchpress.com by 210.87.254.42 on 09/05/12
For personal use only.

for the trichelated pairs. This should be the case, of course, if the shielding were completely effective so that in all three cases $S_1^0 - S_2^0 = 0$. As a matter of fact the above values of -6.9 for Fe $dip_3^{2+/3+}$ and -5.2 for Fe $phen_3^{2+/3+}$ have hardly been distinguished experimentally. George, Hanania, and Irvine (12) give $\Delta H^0 = -32.7$ kcal mole^{-1} for both cell reactions analogous to [1] and for the E_{cell}^0 values 1.141 and 1.120 V respectively; Dwyer and McKenzie (see ref. 12) obtained 1.120 and 1.096 V; Hume and Kolthoff (see ref. 12) measured the same e.m.f. for both cell reactions in 1 M sulfuric acid solution. The values of ΔS^0 are sensitive to such small differences in e.m.f., and George, Hanania, and Irvine estimate the error in ΔS^0 at ± 2 e.u., which covers the above deviations for the trichelated pairs.

TABLE II

Standard entropy differences, $S_1^0 - S_2^0$ in e.u.

Pair 1/2	$S_1^0 - S_2^0$	$-(z_1 - z_2)$	$-(z_1^2 - z_2^2)$
$Fe(CN)_6^{4-/3-}$	-43.3	1	-7
$Fe(CN)_4dip^{2-/1-}$	-28.9	1	-3
$Fe(CN)_2dip_2^{0/1+}$	-14.8*	1	$+1$
$Fe\,dip_3^{2+/3+}$	-1.0	1	$+5$
$Fe(H_2O)_6^{2+/3+}$	$+48.7$	1	$+5$

*By interpolation.

According to the arguments above, it is postulated that the related pairs, Fe $dip_3^{2+/3+}$, Fe $phen_3^{2+/3+}$, and Ru $dip_3^{2+/3+}$ are respectively isentropic, or very nearly so, and the values averaged to obtain the result, $S_{H^+}{}^0 = -5.7$ e.u. The value for Os $dip_3^{2+/3+}$ of 0.8 has been omitted as being too far off; if the data are accurate then the shielding is presumably incomplete for this largest element of the series. Taking $S_{H^+}{}^0 = -5.7$ e.u., values of $S_1^0 - S_2^0$ have been calculated and entered in Table II along with differences in z and z^2 for certain pairs.

It is difficult to see how the pattern of the various entropy differences can be explained in terms of differences in z whereas they are in good accord with differences in z^2 as shown in Table II or in Fig. 2 by the plot of values of $S_1^0 - S_2^0$ against $-(z_1^2 - z_2^2)$ for the complex ion species (for this purpose the aqueous ions are not considered as one of the series of complex ions). Little has been said in the foregoing about radii of ions,

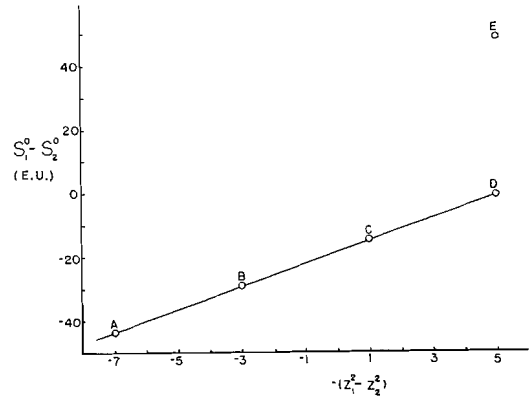

FIG. 2. Plot of $S_1^0 - S_2^0$ in e.u. against $-(z_1^2 - z_2^2)$ for complex ion pairs: (A) $Fe(CN)_6^{4-/3-}$; (B) $Fe(CN)_4\,dip^{2-/3-}$; (C) $Fe(CN)_2\,dip_2^{0/1+}$; (D) $Fe\,dip_3^{2+/3+}$; (E) $Fe(H_2O)_6^{2+/3+}$.

which also affect the electrostatic entropy term. However for the complex ion pairs considered this contribution cannot be important as the differences in radii involved must be relatively small.

If the present arguments are valid, they lend support to Gurney's result that $S_{H^+}{}^0 = -5.5$ e.u. On the other hand, if Gurney's result is accepted a priori, then it must be concluded that certain trichelated pairs are nearly isentropic. Apart from any theoretical importance attached to the evaluation of absolute ion entropies, it is of considerable experimental significance to have available well-behaved redox electrode systems with zero or very small temperature dependence of potential.

ACKNOWLEDGMENTS

We are indebted to the National Research Council of Canada for assistance in the form of grants and to the Provincial Government of Ontario for the provision of a Fellowship (held by J. Lin).

REFERENCES

1. J. O'M. Bockris and B. E. Conway. Modern aspects of electrochemistry. Butterworths, London. 1951.
2. R. W. Gurney. Ionic processes in solution. McGraw-Hill, New York. 1953.
3. K. S. Pitzer and L. Brewer. Thermodynamics. McGraw-Hill, New York. 1961.
4. K. J. Laidler. Can. J. Chem. **34**, 1107 (1956).
5. L. Pauling. The nature of the chemical bond. 3rd ed. Cornell University Press, N.Y. 1960.
6. R. E. Powell and W. M. Latimer. J. Chem. Phys. **19**, 1139 (1951).
7. R. M. Noyes. J. Am. Chem. Soc. **84**, 513 (1962).
8. E. Glueckauf. Trans. Faraday Soc. **60**, 572 (1964).
9. A. M. Couture and K. J. Laidler. Can. J. Chem. **35**, 202 (1957).
10. J. W. Cobble. J. Chem. Phys. **21**, 1446 (1953).
11. E. L. King. J. Phys. Chem. **63**, 1070 (1959).
12. P. George, G. I. H. Hanania, and D. H. Irvine. J. Chem. Soc. 2548 (1959); J. Chem. Phys. **22**, 1616 (1954).
13. F. Daniels, J. H. Mathews, and J. W. Williams. Experimental physical chemistry. Maple Press, York, Pa. 1956.
14. D. J. G. Ives and G. J. Janz. Reference electrodes. Academic Press, New York. 1961.
15. W. M. Latimer. Oxidation potentials. 2nd ed. Prentice-Hall, Englewood Cliffs, New Jersey. 1952.

Can. J. Chem. Downloaded from www.nrcresearchpress.com by 210.87.254.42 on 09/05/12
For personal use only.

Can. J. Chem. Downloaded from www.nrcresearchpress.com by 210.87.254.5 on 09/05/12
For personal use only.

SOME BASE-CATALYZED CONDENSATIONS OF SYSTEMS OF THE FORM $R_1R_2C{=}C(CN)_2$

MARY R. S. WEIR AND J. B. HYNE
Department of Chemistry, University of Alberta at Calgary, Calgary, Alberta
Received November 2, 1964

ABSTRACT

We have investigated the condensations of the systems $\phi CH_3C{=}C(CN)_2$, $\phi HC{=}C(CN)_2$, and $CH_3HC{=}C(CN)_2$ in the presence of organic bases. Proton nuclear magnetic resonance (n.m.r.) spectral evidence is presented in support of the suggested structures of the condensation products, and an attempt has been made to present diagrammatically the interrelation between these condensations and other known reaction pathways for condensations of this type.

INTRODUCTION

The reactive nature of methylenemalononitrile systems of the type $R_1R_2C{=}C(CN)_2$ in the presence of base has been known for some time (1, 2). In particular the tendency of such compounds to undergo condensations and dimerizations in the presence of base has been the subject of several recent investigations (3–7). The general mechanism of the base-catalyzed dimerizations of several alkylidenemalononitriles of the type $R_1R_2C{=}C(CN)_2$ has been described previously (6). We have now extended this study to some other methylenemalononitriles whose behavior under the basic reaction conditions appears to be somewhat more complex. Table I represents an attempt to show the interrelationships between the different reaction pathways, which we believe to be possible under various basic reaction conditions, leading to both carbocyclic and heterocyclic products.

Path A (Table I). Cyclodimerization of Alkylidenemalononitriles in the Presence of Organic Bases

When both R_1 and R_2 are alkyl groups, the critical first step is base abstraction of a proton from one of these groups. This is followed by attack of the anion so formed on a second monomer molecule, and then ring closure (4, 6). The same pathway is followed when $R_1 = \phi$ and $R_2 = CH_3$, the base abstracting a proton from the CH_3 group in the initial step.

Path B (Table I). Condensation of Benzalmalononitrile in Ethanolic Potassium Hydroxide Solution

The formation of substituted pyridines by the action of ethanolic potassium hydroxide solution on benzalmalononitrile has been reported previously (7). The reaction was shown to proceed via a reverse aldol cleavage of the diene to benzaldehyde and malononitrile anion, followed by attack on the β-carbon atom of a second diene molecule by the $^{(-)}CH(CN)_2$ anion, and subsequent ring closure.

Path C (Table I). Condensation of Benzalmalononitrile in the Presence of Organic Bases

In contrast to its behavior in ethanolic potassium hydroxide solution benzalmalononitrile appears to undergo more complex condensations in the presence of *n*-butyl amine in aqueous ethanol. The initial step here again seems to be cleavage to benzaldehyde, or the corresponding anil with the organic base, and malononitrile anion, followed by attack of the latter on a molecule of monomer. In this case, however, there is further

TABLE I

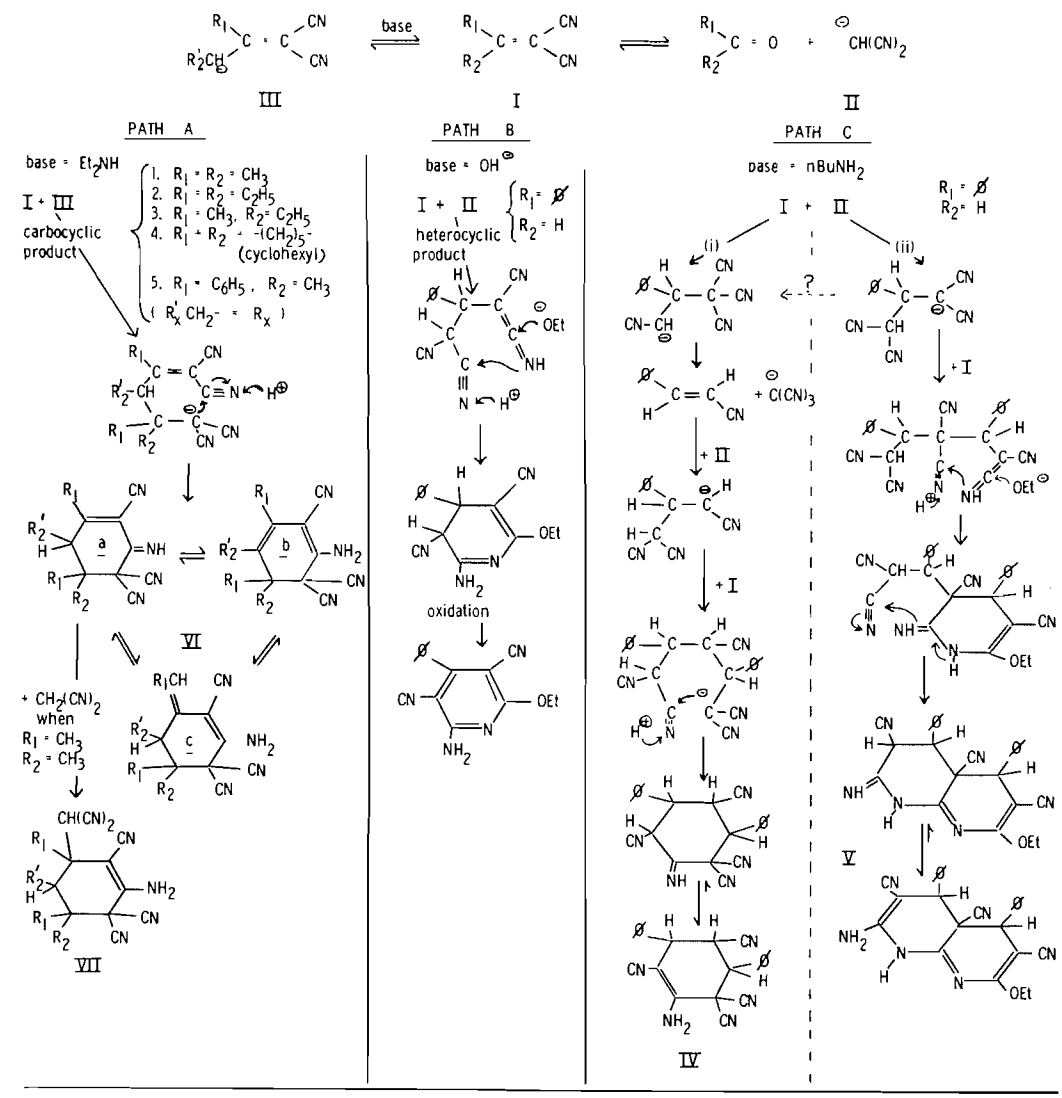

incorporation of a second monomer molecule into the products. Also, under conditions which are as nearly identical as possible, *two* products of m.p.'s 210–213 °C, IV, and 155–158 °C, V, are obtained, IV being produced in some cases and V in others. Suggested structures for these products and possible pathways leading to them are outlined in Table I.

It may be noted that pathways A and B represent mechanistically the two simplest modes of condensation available to the alkylidene- and arylidene-malononitrile systems respectively. Thus, if the β-carbon carries a group (e.g. $C_2H_5CH_3C{=}C(CN)_2$) from which a proton may be readily extracted by base, then this abstraction is in fact the first step: if the system (e.g. $\phi HC{=}C(CN)_2$) does not contain such a group, then the

Can. J. Chem. Downloaded from www.nrcresearchpress.com by 210.87.254.5 on 09/05/12
For personal use only.

condensation is forced to proceed via attack on the β-carbon by a $^{(-)}CH(CN)_2$ anion, i.e., via a Michael condensation.

Special Case (Table II). Condensation of Ethylidenemalononitrile in the Presence of Organic Bases

Although ethylidenemalononitrile might have been expected to follow path A and give the dimeric product VI on treatment with base, we found no evidence for this material being formed. The spectral data strongly suggested that the product isolated was in fact VIII (although in the absence of solvent a second condensation product was also formed —see structure proof section).

STRUCTURE PROOFS

1. β-Methylbenzalmalononitrile Dimer

Of the compounds listed as reacting according to path A, the condensation products of 1–4 have been discussed (4, 6). β-Methylbenzalmalononitrile, (III, 5), appears to undergo dimerization in the presence of base by a similar pathway (Table I, Path A) leading to compound IX (special case of VI*a*). This reaction has been studied previously by Anderson, Bell, and Duncan (3) who isolated the bright-yellow crystalline dimer from the condensation of acetophenone and malononitrile in the presence of base. They reported its infrared spectrum and noted that it "did not agree with the expected 4-amino-1,1,5-tricyano-2,6-diphenylhepta-1,3,5 triene" (3), but they did not suggest an alternative structure. The n.m.r. spectrum (Fig. 1.1) of the dimer is consistent with the cyclic imino structure shown, IX. The AB quartet at 6.8 τ rules out the possibility of the previously proposed (3) triene structure $\phi(CH_3)C{=}C(CN){-}C(NH_2){=}CH{-}C(\phi){=}C(CN)_2$, and its tautomer $\phi(CH_3)C{=}C(CN){-}C(=NH){-}CH_2{-}C(\phi){=}C(CN)_2$. The CH_2 group in the latter would be expected to give rise to a singlet signal rather than to an AB quartet. The large coupling constant (17 c.p.s.) of this quartet is similar to that noted by Calvin and co-workers (8) for the geminal coupling in the cyclic system XIII when the conformation of the molecule was fixed by cooling to −65 °C. The amino form of the cyclic dimer, X, is also inconsistent with the observed spectrum, since it again would not give rise to an AB quartet. The position of the CH_3 signal at 8.2 τ seemed somewhat low for a CH_3 on a saturated carbon. However, comparison of the two systems $CH_3CH{=}C(CN)_2$ and $\phi(CH_3)C{=}C(CN)_2$ indicated that the presence of a phenyl group on the carbon carrying the CH_3 significantly lowered the position of the CH_3 signal, the one in ethylidenemalononitrile appearing at 7.9 τ and that in β-methylbenzylmalononitrile at 7.5 τ.

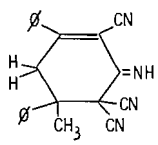

IX

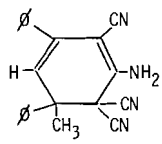

X

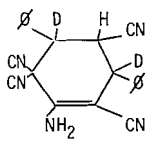

XI

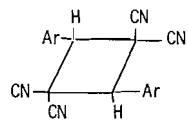

XII

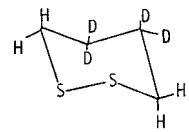

XIII

Apart from the apparently exclusive formation of the imino form here the dimerization of β-methylbenzalmalononitrile fits the pattern recently described (4, 6) for several alkylidenemalononitriles where both R_1 and R_2 are alkyl groups. In the present case the imino structure is presumably favored over the amino since straight conjugation from the phenyl group through to the imino group is possible only in the former, IX, the amino form, X, involving a cross-conjugated system. Also an examination of molecular models indicates that the ring strain in the cyclic amino form with two endocyclic

Can. J. Chem. Downloaded from www.nrcresearchpress.com by 210.87.254.5 on 09/05/12
For personal use only.

double bonds is greater than that in the imino form in which one double bond is outside of the ring.

2. Products from Benzalmalononitrile

Benzalmalononitrile, on treatment with *n*-butyl amine in ethanolic solution gave two crystalline products, of m.p.'s 210–213 °C and 155–158 °C respectively.

A. The structure which seems to best fit the n.m.r., infrared, and analytical data on the 210–213° compound is IV, Table I. The outstanding structural feature in the n.m.r. spectrum (Fig. 1.2) of this material is the partially split AB quartet with the superimposed split singlet centered around 5.8 τ. We have interpreted this as an ABC system (9), in which the A and B hydrogens are involved in mutual splitting while the C hydrogen is not split by A. Such a system is present in the structure proposed, hydrogens A and B being on adjacent carbons and the angle between the two C—H bonds being about 60°, while hydrogens B and C, also on adjacent carbons, are *trans* to each other, and the C—H bonds are at approximately 180°. (See diagram of model.) Consideration of the

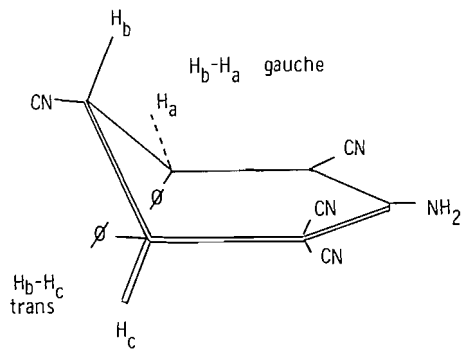

Projection drawing IV

Karplus curve (10, 11, 12) indicates that the expected coupling constants for such a system would be small in the case of the A and B hydrogens and large for the B and C hydrogens: the observed J values are in fact as follows: $J_{AB} = 2$ c.p.s.; $J_{BC} = 13$ c.p.s.; $J_{AC} = 0$ c.p.s.

The other compelling piece of evidence in favor of this structure was obtained from deuterium-labelling experiments. When benzalmalononitrile was replaced by $C_6H_5CD{=}C(CN)_2$ as starting material in the base-catalyzed condensation the 210–213° compound which was isolated had only 1 singlet at 5.1 τ (Fig. 1.2*b*) in the n.m.r., instead of the quartet with superimposed singlet. The rest of the spectrum was unchanged. This would fit the proposed structure if both carbons carrying phenyl groups were deuterated, the structure being XI: the 5.1 τ peak now lies *between* the two peaks in the quartet assigned to hydrogen B. On the other hand, if the reaction were run with unlabelled benzalmalononitrile but in C_2H_5OD as solvent we should expect to see two singlets (those due to hydrogens A and C) remaining in the quartet region of the spectrum. These in fact appear (Fig. 1.2*a*) at 5.5 τ (the position of the split singlet due to hydrogen A (Fig. 1.2)) and at 5.9 τ (between the two peaks in the AB quartet assigned to hydrogen C in Fig. 1.2). The nonexchangeability of the benzylic hydrogen of benzalmalononitrile under basic conditions was checked (see experimental section).

A possible mechanistic pathway leading to this product is outlined in Table I, Path C

Can. J. Chem. Downloaded from www.nrcresearchpress.com by 210.87.254.5 on 09/05/12
For personal use only.

(i). Here, instead of the "normal" Michael addition of malononitrile to benzalmalononitrile, we suggest that an "abnormal" Michael addition (13) takes place, involving the intramolecular shift of a CN group; the system then undergoes a reverse Michael reaction to give cinnamonitrile plus $^{(-)}C(CN)_3$. Such rearrangement retrogression products are not unknown in the literature (14, 15). The subsequent steps in the mechanism, addition of a malononitrile anion, and then of a second molecule of benzalmalononitrile and final ring closure, are indicated in Table I. The compound appears to contain one molecule of ethanol of crystallization, readily removed by heating under vacuum to 90°, or by heating at atmospheric pressure to 160°. Ethanol, or methanol, of crystallization could be reintroduced into the compound by crystallization of the de-ethanolated material from the appropriate solvent. The n.m.r. spectra of the ethanolate and of the de-ethanolated material were identical, except for the signals due to ethanol. Alkaline permanganate oxidation of IV gave benzoic acid in a yield which suggested the presence of two phenyl groups per molecule. Hydrolysis of IV in 30% sulfuric acid gave a ketone.

B. Consideration of the analytical and spectral data have lead us to suggest V as a likely structure for the 155–158° compound. The infrared spectrum of the material shows C=C, C=N, N—H and a strong conjugated CN band. The n.m.r. spectrum includes two single peaks at 5.2 τ and 5.4 τ, each of area 1 (the hydrogens on the carbons carrying phenyl groups), a signal at 3.6 τ of area 1.8 (the amino hydrogens), and a signal at 1.5 τ of area 0.8 (the hydrogen on the ring nitrogen), as well as the phenyl and the ethanolic CH_3CH_2 hydrogen signals (Fig. 1.3). The mechanism is outlined in Table I, Path C (ii). Hydrolysis of V in 30% aqueous sulfuric acid gave a ketone. Oxidation of the 155–158° compound with alkaline permanganate solution, or with dichromate, gave benzoic acid in a yield which suggested that each molecule of starting material contained two phenyl groups.

As isolated from the reaction medium this material contains one molecule of ethanol of crystallization, in addition to the bonded EtO, removable by heating under vacuum to 90° for several hours. This ethanol is reincorporated into the molecule by recrystallization of the de-ethanolated material from 95% ethanol (or it may be replaced by methanol by a similar procedure). The n.m.r. spectra of the ethanolate and the de-ethanolated material are identical, except for the signals due to ethanol. Both of these products from the condensation of benzalmalononitrile using *n*-butyl amine as catalyst, appear to be quite different from the cyclobutane dimers of the type XII, described recently by Patai and Rappoport (16), who stated that these can be produced by treatment of alkylidenemalononitriles with malononitrile under conditions similar to those used in some of the experiments here. The cyclobutane dimer of benzalmalononitrile was readily prepared by irradiation of the solid monomer for a few days with a sun lamp according to the method of Baker and Howes (17), but we were not able to produce this compound in solution media, either by using malononitrile, or malononitrile plus base, as catalyst. However, as Patai and Rappoport also state (16), these condensations are extremely sensitive to experimental conditions, so that even when the procedures given in the experimental part are followed closely the results are irreproducible. In many cases we isolated only tars or starting materials.

3. Products from Ethylidenemalononitrile

The extreme sensitivity of ethylidenemalononitrile to base is evident from the special precautions (20, 21) necessary in the preparation of the pure liquid. Contact with even the small amounts of alkali present in Pyrex glassware is sufficient to cause the liquid monomer to condense to a pale-yellow solid over a period of 1 or 2 days at room temperature. To determine whether this condensation of ethylidenemalononitrile followed

Can. J. Chem. Downloaded from www.nrcresearchpress.com by 210.87.254.5 on 09/05/12
For personal use only.

the general pattern recently described (4, 6) for the base-catalyzed condensation of alkylidenemalononitriles (Table I, Path A), we have now investigated the reaction under more controlled conditions in dilute solution, in the presence of added base. By analogy to the base-catalyzed dimerization of isopropylidenemalononitrile (4) ethylidenemalononitrile might have been expected to form the dimeric product VI. Also by analogy to the isopropylidene system (4) the other expected product here would have been of type VII, formed by 1,4 addition of malononitrile to the imino form of the dimer (VI) (see Table I).

However, all of the spectral and analytical evidence we have obtained strongly suggests that the product isolated from the treatment of ethylidenemalononitrile with base in solution, or from acetaldehyde plus malononitrile (the precursors of ethylidenemalononitrile) and base in solution, was in fact VIII. Furthermore, this material (15) was not the same as the yellow solid formed by the action of base on the pure liquid ethylidenemalononitrile.

The reaction mechanism leading to VIII is outlined in Table II, and the n.m.r. spectrum is given in Fig. 1.4.

TABLE II

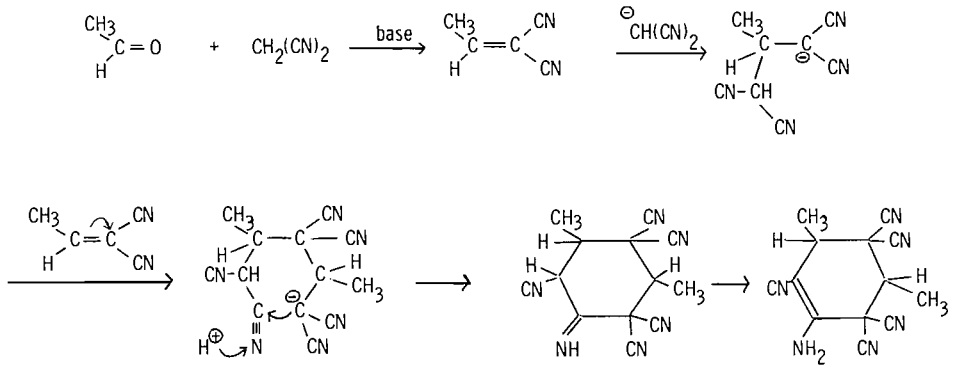

VIII

The area of the methyl doublets around 8.4 τ is in agreement with structure VIII and clearly indicates that the material is neither the simple dimer nor the dimer plus, malononitrile which might have been predicted by analogy to the isopropylidenemalononitrile system (4). Both the n.m.r. and the infrared spectra suggest that VIII is present almost exclusively in the amino form. Thus the infrared spectrum has a strong conjugated CN absorption which could not be accommodated in the imino structure; likewise the NH_2 signal of area 2 in the n.m.r. spectrum at 3.9 τ favors the amino form. The two sets of doublets centered around 8.4 τ and the overlapping quartets at 6.8 τ suggest that the compound exists as a mixture of two conformers.

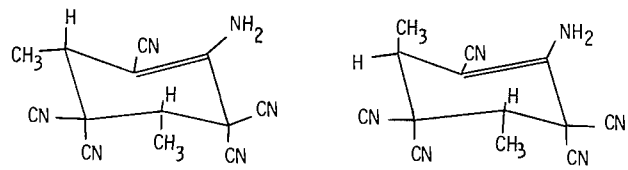

Can. J. Chem. Downloaded from www.nrcresearchpress.com by 210.87.254.5 on 09/05/12
For personal use only.

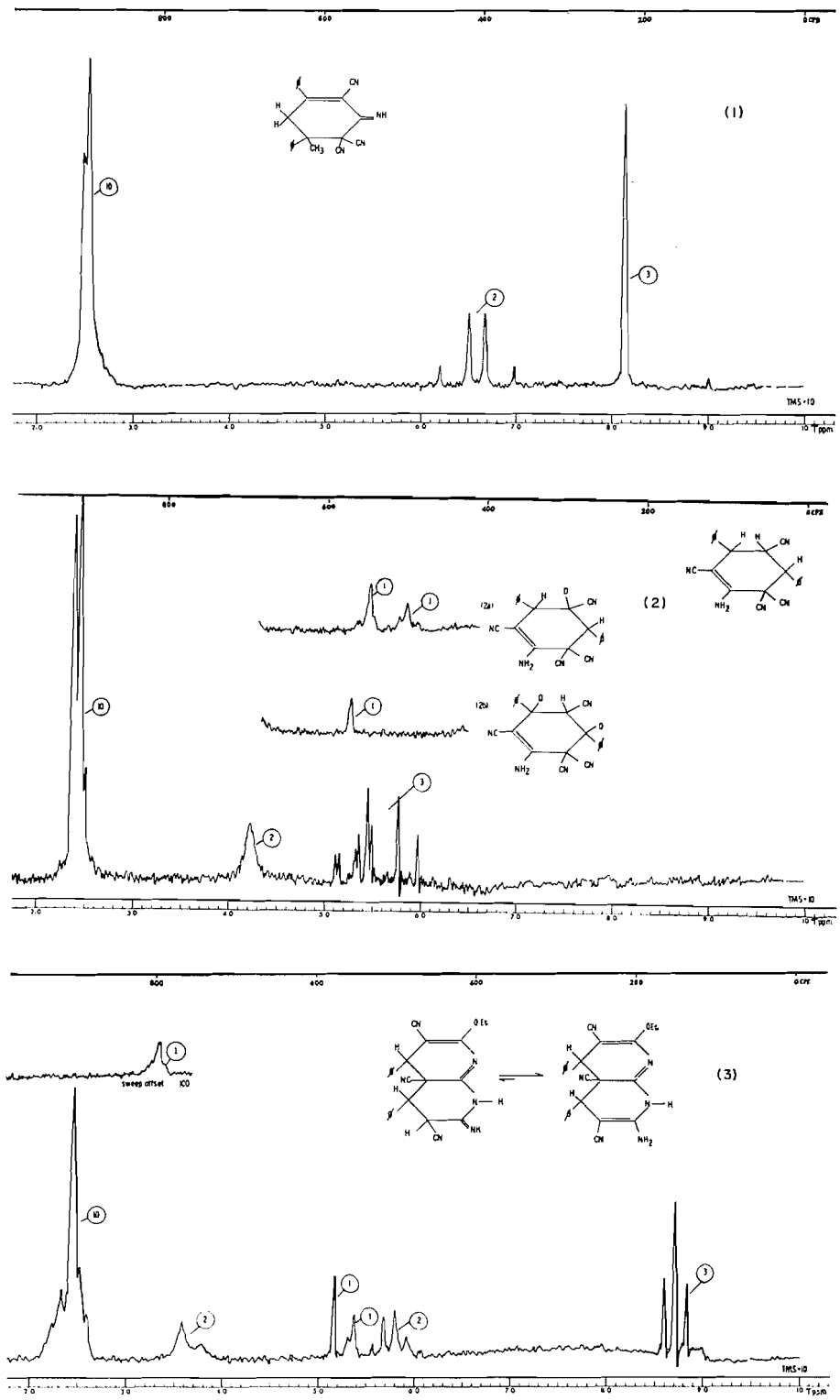

Can. J. Chem. Downloaded from www.nrcresearchpress.com by 210.87.254.5 on 09/05/12
For personal use only.

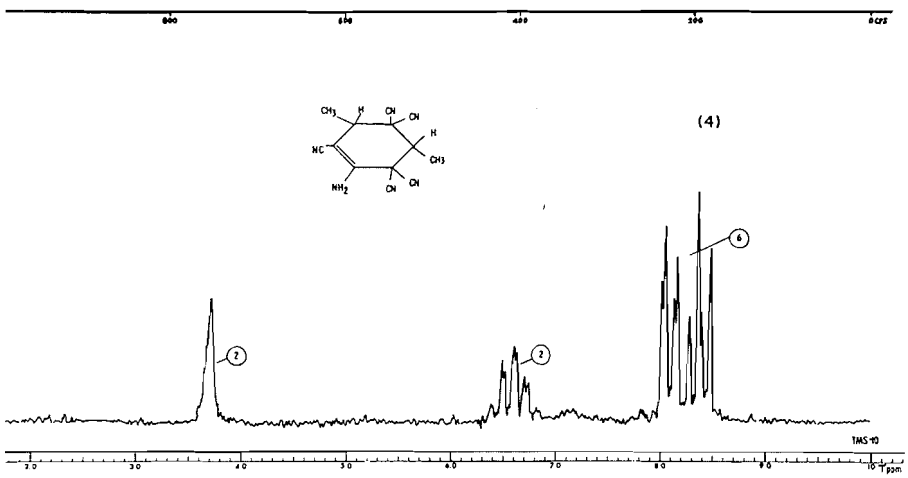

FIG. 1. (i) The spectra were run in the following solvents: (1) and (2) in acetonitrile and in benzonitrile; (3) in acetone and in benzonitrile; (4) in acetonitrile. All solutions approximately 10%. (ii) Relative peak areas are shown in the circled numbers. (iii) Tetramethylsilane internal standard.

The tendency of ethylidenemalononitrile to undergo condensation via attack on the β-carbon by a malononitrile anion in contrast to the pathway involving abstraction of a proton from a methyl in $(CH_3)_2C{=}C(CN)_2$ is possibly best explained on the basis of the inductive effects of the two methyl groups which reduce the effective polarization of the molecule and hence the net positive charge on the β-carbon, thereby making it less susceptible to attack by a malononitrile anion. Replacement of one of the CH_3 groups by a proton appears to diminish this effect sufficiently to favor condensation via initial attack on the β-carbon.

The other material isolated, the yellow solid formed by the action of base on liquid ethylidenemalononitrile, appears from the elemental analysis to be a simple polymer without any additional malononitrile incorporated into the structure. The infrared spectrum indicated that it did not contain any NH or conjugated CN. The n.m.r. spectrum showed two doublets around 8 τ and two shattered quartets between 6.5 and 7.5 τ. However, the low solubility of the material made good spectral determinations difficult. It seems possible that the yellow solid might be a mixture of cyclobutane dimers of the kind XII recently described by Patai and Rappoport (16) as being formed from systems of the type $ArCH{=}C(CN)_2$. However, molecular weight determinations were conflicting and failed to give clear evidence in favor of a dimeric structure.

General Remarks

Attempted base-catalyzed condensations of β-ethylbenzalmalononitrile, β-phenylbenzalmalononitrile, and β-naphthylmethylenemalononitrile, as well as of several ring-substituted benzalmalononitriles, have in our hands yielded only tarry products so far. It would appear that base-catalyzed condensations of arylmethylenemalononitriles are much more sensitive to reaction conditions than are those of the alkylidenemalononitriles studied here (with the exception of ethylidenemalononitrile). As we have already indicated, these condensations are not always reproducible even when the experimental procedures are followed closely. Also, when, as in the case of the arylmethylenemalononitriles, the first step in the reaction involves a Michael addition, in contrast to abstraction

Can. J. Chem. Downloaded from www.nrcresearchpress.com by 210.87.254.5 on 09/05/12
For personal use only.

of a proton from an alkyl group as in the alkylidenemalononitrile cases, the number of subsequent mechanistic pathways available to the system is greatly increased; hence the greater variety of products obtained from benzalmalononitrile under basic conditions.

EXPERIMENTAL

Preparation of β-Methylbenzalmalononitrile (18)

Acetophenone (60 g, 0.50 mole) and malononitrile (33 g, 0.50 mole) were added to 4 g (0.057 mole) of ammonium acetate plus 12 ml of glacial acetic acid in 200 ml of benzene. The mixture was heated to reflux with stirring and the water evolved was collected in a Dean-Stark trap. Refluxing overnight produced 14 ml of water. The benzene was then removed under vacuum leaving a yellow solid, which was crystallized from 50% ethanol. The product was obtained in the form of pale-yellow prisms of m.p. 93–94°. (Lit. (18) 94 °C.) Yield 75 g, 90%.

Preparation of Ethylidenemalononitrile

Two recent patent references (19, 20) are available for the preparation of this material. We found, however, that the following method worked for the preparation of the quantities we required.

Malononitrile (3.3 g, 0.05 mole) and acetaldehyde (3.0 g, 0.07 mole) were dissolved in 50 ml of benzene, and a few drops of diethylamine were added. The solution was left at room temperature for 2 h, and then washed with dilute hydrochloric acid and water, and dried over "Drierite". Removal of the solvent gave a clear liquid, which was vacuum distilled from glassware previously well washed with dilute hydrochloric acid. $n_D^{20} = 1.4571$; infrared (smear) 3.2, 3.3, 4.4, 6.2, 6.95, 7.25, 7.50, 8.35, 9.20, 9.50, 10.20, 11.50, in μ; n.m.r. in CCl_4, doublet, relative area 3, centered on 7.75 τ, quartet, relative area 1, centered on 2.25 τ.

Base-catalyzed Condensation of β-Methylbenzalmalononitrile

β-Methylbenzalmalononitrile (4 g) was dissolved in 95% ethanol with slight warming, and a few drops of diethylamine added. On standing overnight a solid was deposited from the mixture. On crystallization from ethanol this gave 2.9 g of bright-yellow needles of m.p. 206–207 °C. (Yield 72%.)

Anal. Calcd. for $C_{22}N_{10}N_4$: C, 78.57; H, 4.76; N, 16.65; molecular weight, 336. Found: C, 78.42; H, 5.02; N, 16.50; molecular weight, 330.

The main infrared peaks (in KBr) are 2.92, 4.43, 6.23, 6.32 (shoulder), 6.45, 6.70, 6.90, 7.00, 7.95, 13.10, 13.50, 14.40, in μ. λ_{max} values in the ultraviolet: 324 mμ and 250 mμ. This compound may also be prepared from acetophenone and malononitrile plus base by the method of Anderson, Bell, and Duncan (3).

Base-catalyzed Condensation of Benzalmalononitrile

Benzalmalononitrile (1 g, 0.0065 mole) was dissolved in 50 ml of 95% ethanol, and 0.2 g (0.0033 mole) of malononitrile added. The flask was then swept with nitrogen, and 0.4 g (0.0055 mole) of *n*-butylamine was added. After stirring in a stream of nitrogen gas for about 24 h the solid product was collected, washed with 95% ethanol, and recrystallized from ethanol. This reaction was not reproducible, an intractable tar being the only product on many occasions. Also the crystalline product formed was sometimes the material of m.p. 155–158 °C, and sometimes that of m.p. 210–213 °C. Average yields were 0.10 g for the 210–213° compound, and 0.1–0.2 g for the 155–158° material. The difficulty of drying the samples thoroughly without removal of some of the ethanol of crystallization complicated the analyses in both the 210–213° and the 155–158° compounds.

210–213° Melting Compound

Analyses: (a) ethanolate.—Calcd. for $C_{24}H_{19}N_5O$: C, 73.40; H, 4.84; N, 17.80; molecular weight, 393. Found: C, 73.25; H, 5.26; N, 17.52; molecular weight, 406.

(b) De-ethanolated sample.—Calcd. for $C_{22}H_{13}N_5$: C, 76.02; H, 3.75; N, 20.06. Found: C, 76.08; H, 3.69; N, 19.63.

Main bands in the infrared spectrum of the de-ethanolated compound (KBr): 2.80, 2.89, 3.00, 3.20, 3.24 (weak), 4.50, 6.08, 6.20 μ. There was also a broad absorption between 13.7 and 14.4 with peaks at 13.72, 13.99, and 14.32, in μ.

Permanganate Oxidation of Solid, M.P. 210–213°

The material (0.1 g) was refluxed overnight in a mixture of 0.3 g of potassium permanganate, 1 small pellet of sodium hydroxide, and 10 ml of water. After cooling, the mixture was acidified with dilute sulfuric acid and refluxed for a further 30 min. The manganese dioxide was then taken up with sodium bisulfite, and the aqueous solution cooled and extracted with ether; 0.05 g of benzoic acid was obtained from the ether extracts; m.p. 121–122 °C, mixed melting point with an authentic sample of benzoic acid, 122–124 °C.

Hydrolysis of Solid, M.P. 210–213°

The solid (0.1 g) was heated with 20 ml of 30% aqueous sulfuric acid overnight. The resulting white powder was washed with distilled water till free from acid and dried. Attempted recrystallization led to discoloration. A strong ketone absorption was now present in the infrared spectrum, whose main peaks (KBr) were at 3.35, 5.68, 6.69, 6.82, 13.73 (shoulder at 13.9), and 14.28 μ.

Can. J. Chem. Downloaded from www.nrcresearchpress.com by 210.87.254.5 on 09/05/12
For personal use only.

155–158° Melting Compound

Analyses: (a) ethanolate.—Calcd. for $C_{27}H_{26}N_6O_2$: C, 69.50; H, 5.58; N, 18.00; molecular weight, 466. Found: C, 69.81; H, 5.54; N, 18.54; molecular weight, 419.

(b) De-ethanolated sample.—Calcd. for $C_{25}H_{20}N_6O$: C, 71.50; H, 4.76; N, 20.00. Found: C, 71.18; H, 4.79; N, 20.13.

Main absorptions in the infrared spectrum of de-ethanolated compound (KBr): 2.90 (shoulder at 2.80 and 3.00), 3.30–3.40 (weak), 4.50, 6.10, 6.25 (shoulders at 6.00 and 6.32), 6.70, 6.90, 14.00, and 14.30 (shoulders at 3.76), in μ. The permanaganate oxidation and the sulfuric acid hydrolysis were carried out in the same manner as for the other compound described above. The main infrared peaks (KBr) in the hydrolysis product were at 2.90 (shoulder at 2.85), 3.20–3.40 (broad and weak), 4.50, 5.70, 6.15, 6.25, 7.73, 6.90, 13.80 (shoulder at 13.95), and 14.30 μ.

Base-catalyzed Condensation of Ethylidenemalononitrile in Solution

Ethylidenemalononitrile (1 g) was dissolved in 25 ml of benzene and a small amount of malononitrile and 3 drops of diethylamine were added. The mixture was left at room temperature for 2 h, washed with dilute hydrochloric acid and then with water, and dried over Drierite. Removal of the benzene left a glass which crystallized to a white solid overnight. On recrystallization from chloroform this yielded a finely crystalline white powder of m.p. 173–174 °C. The main absorptions in the infrared were at 2.79, 2.86, 2.98, 3.25, 4.47, 6.04, 6.16, and 6.83, in μ.

Anal. Calcd. for $C_{13}H_{10}N_6$: C, 62.40; H, 4.00; N, 33.60; molecular weight, 250. Found: C, 62.50; H, 4.33; N, 33.40; molecular weight, 229.

This compound could also be prepared by the following method: 2.4 g (0.055 mole) of acetaldehyde and 6.6 g (0.050 mole) of malononitrile were dissolved in 100 ml of benzene and 6 drops of diethylamine were added to the mixture. After standing at room temperature for 2 h the benzene solution was washed with dilute hydrochloric acid, and then with water. Removal of the solvent and crystallization from chloroform as above gave the white crystalline product.

Base-catalyzed Condensation of Ethylidenemalononitrile in Absence of Solvent

Ethylidenemalononitrile on standing in contact with glass for 1 or 2 days condensed to a yellow solid, which on crystallization from 95% ethanol gave a pale-yellow powder of m.p. 166–168°.

Anal. Calcd. for $C_{10}H_8N_4$: C, 65.30; H, 4.35; N, 30.41; molecular weight, 184. Found: C, 64.95; H, 4.53; N, 30.72; molecular weight, 180, 270 (on two separately prepared samples of material).

Preparation of Benzalmalononitrile-d_1

Ethyl benzoate was reduced with lithium aluminium deuteride to $C_6H_5CD_2OH$ (21) which was then oxidized with activated manganese dioxide to C_6H_5CDO (22). The benzaldehyde-d_1 was condensed with malononitrile following the method already described for the preparation of benzalmalononitrile.

1. To 1.7 g (0.041 mole) of lithium aluminium deuteride in 500 ml of dry ether was added, dropwise, 10 g (0.067 mole) of ethyl benzoate. After addition of the ester the mixture was refluxed for a further hour, the excess deuteride destroyed with wet ether, and the mixture poured into ice-cold 10% sulfuric acid. Extraction with ether and removal of the solvent gave 6.5 g (88%) yield of alcohol. The infrared spectrum of the product showed strong C—D absorptions at 4.5 and 4.7 μ. No ester absorption was apparent at this stage.

2. Activated manganese dioxide (22 g, 0.26 mole) was added to 250 ml of benzene and the mixture refluxed till no more water appeared to be coming off. The water evolved was collected in a Dean-Stark trap. $C_6H_5CD_2OH$ (6.5 g, 0.059 mole) was then added, and the refluxing continued till a further 1 ml (approximately) of water was collected. The mixture was then cooled and filtered and the solvent removed under vacuum. Benzaldehyde-d_1 (3.8 g, 67% yield) was isolated. This was distilled through a Nester/Faust micro spinning band column. The final product showed a strong carbonyl absorption in the infrared at 5.9 μ, and C—D absorptions at 4.5 and 4.7 μ. No alcohol or ester absorptions were apparent.

Control Experiment on Base-catalyzed Exchange of the Benzylic Hydrogen in Benzalmalononitrile

Benzalmalononitrile was dissolved in methanol-d_1 and the n.m.r. spectrum recorded. The benzylic hydrogen, appearing downfield from the aromatic hydrogens, is readily distinguishable from the latter. The addition of a drop of *n*-butyl amine or of ethanolic potassium hydroxide to the solution caused no appreciable change in the relative areas of the benzylic and aromatic hydrogens. Addition of several drops of base eventually caused the benzylic hydrogen peak to almost disappear, but not before the aromatic hydrogen absorptions had also decreased in intensity and sharpness, and the solution had turned brown, the latter presumably being due to condensation and tar formation.

Notes

Molecular weights were determined osmometrically. Melting points are uncorrected.

ACKNOWLEDGMENT

The research for this paper was supported in part by the Defence Research Board of Canada, Grant No. 2001-01.

Can. J. Chem. Downloaded from www.nrcresearchpress.com by 210.87.254.5 on 09/05/12
For personal use only.

REFERENCES

1. B. B. CORSON and R. W. STOUGHTON. J. Am. Chem. Soc. **50**, 2825 (1928).
2. A. C. COPE and K. E. HOYLE. J. Am. Chem. Soc. **63**, 733 (1941).
3. D. W. M. ANDERSON, F. BELL, and J. L. DUNCAN. J. Chem. Soc. 4705 (1961).
4. J. K. WILLIAMS. J. Org. Chem. **28**, 1054 (1963).
5. M. R. S. WEIR and J. B. HYNE. Can. J. Chem. **41**, 2905 (1963).
6. M. R. S. WEIR and J. B. HYNE. Can. J. Chem. **42**, 1440 (1964).
7. M. R. S. WEIR, K. E. HELMER, and J. B. HYNE. Can. J. Chem. **41**, 1042 (1963).
8. G. GLEASON, G. M. ANDROES, and M. CALVIN. J. Am. Chem. Soc. **82**, 4428 (1960).
9. J. A. POPLE, W. G. SCHNEIDER, and H. J. BERNSTEIN. High resolution nuclear magnetic resonance. McGraw-Hill Book Co. Inc., New York. 1959. p. 133.
10. K. B. WILBERG. Physical organic chemistry. John Wiley and Sons, Inc., New York. 1964. p. 207.
11. R. U. LEMIEUX, R. K. KULLNIG, and R. Y. MOIR. J. Am. Chem. Soc. **80**, 2237 (1958).
12. M. KARPLUS. J. Chem. Phys. **30**, 11 (1959).
13. E. D. BERGMAN, D. GINSBURG, and R. PAPPO. Organic reactions. Vol. 10. John Wiley and Sons, Inc., New York. 1959. p. 191.
14. A. MICHAEL and J. ROSS. J. Am. Chem. Soc. **55**, 1632 (1933).
15. R. CONNER and D. B. ANDREWS. J. Am. Chem. Soc. **56**, 2713 (1934).
16. S. PATAI and Z. RAPPOPORT. J. Chem. Soc. 377 (1962).
17. W. BAKER and C. S. HOWES. J. Chem. Soc. 119 (1953).
18. D. T. MOWRY. J. Am. Chem. Soc. **67**, 1050 (1945).
19. Brit. Patent No. 812,240 (April 1959).
20. U.S. Patent No. 2,971,977 (Feb. 14th, 1961).
21. R. F. NYSTROM and W. G. BROWN. J. Am. Chem. Soc. **69**, 1197 (1964).
22. E. F. PRATT and J. F. VAN DE CASTLE. J. Org. Chem. **26**, 2973 (1961).

Can. J. Chem. Downloaded from www.nrcresearchpress.com by 210.87.254.5 on 09/05/12
For personal use only.

Can. J. Chem. Downloaded from www.nrcresearchpress.com by 210.87.254.40 on 09/05/12
For personal use only.

COMPLEX FORMATION BETWEEN PROPARGYL CHLORIDE AND BENZENE

JAMES TYRRELL
Department of Chemistry, McMaster University, Hamilton, Ontario
Received November 5, 1964

ABSTRACT

The proton resonance signals of the methylene and ethynyl hydrogens in propargyl chloride shift upfield in going from cyclohexane to benzene as solvent. This is interpreted as being due to complex formation between propargyl chloride and benzene. Though the methylene proton resonance signal shifts farther upfield than does the ethynyl proton resonance signal, it is found that only a 1:1 complex exists between the two molecules. The complex is considered to be one in which the methylene protons "bond" to the π-electron system of the benzene ring. The ethynyl proton of the propargyl chloride is thought to lie close enough to the ring to interact with the "ring current", but not close enough to be a prime agent in complex formation.

INTRODUCTION

Nuclear magnetic resonance can be used to study the phenomenon of hydrogen bonding in solution and can allow very accurate determination of the extent of association between the complexing agents. Where the hydrogen involved is bonding to an oxygen or nitrogen the proton resonance signal moves downfield relative to that of the uncomplexed proton signal. Where the solvent is benzene or some other aromatic compound, the proton resonance signal is found to move upfield: this being explained by the large anisotropy in the magnetic susceptibility of aromatic molecules, commonly referred to as the "ring current" effect (1). In propargyl chloride, however, it was shown by Hatton and Richards (2) that both the methylene and the ethynyl proton resonance signals moved upfield in going from cyclohexane to benzene as solvent. In fact, the shift upfield of the proton resonance signal of the methylene group (27 c.p.s.) was greater than that of the ethynyl proton (18.6 c.p.s.). Though this difference was not commented on by the above authors, it was considered significant enough to be studied more closely.

EXPERIMENTAL

The propargyl chloride used was obtained commercially and fractionally distilled, the main fraction having a boiling point of 56 °C. The benzene and cyclohexane used were AnalaR reagents and were used without further purification. The investigation was carried out with a concentration of 0.2 mole/l of propargyl chloride, the solvent ranging from pure cyclohexane through various mole fractions of benzene in cyclohexane. As cyclohexane was used both as an inert solvent and as an internal reference from which to measure the chemical shift, it was impossible to obtain results in pure benzene.

The instrument used in these investigations was an Associated Electrical Industries R.S.2 nuclear magnetic resonator, the samples being studied at room temperature (25 °C) using a 60 Mc probe. To detect the proton resonance signal at the low concentrations used, it was necessary to operate at high power and at a fairly high filter setting. Calibration was obtained using an audio frequency unit in the spectrometer and side bands were taken from the internal reference to encompass the region being studied.

If the chemical shift in cycles per second from cyclohexane of the proton resonance signal in pure cyclohexane is denoted by δ_A, and the chemical shift in the mixed solvent by δ_1, then the chemical shift due to complex formation can be taken as $\delta = \delta_1 - \delta_A$. In addition, if x_B is taken as the mole fraction of the active solvent in cyclohexane, and δ_{AB} is taken to be the chemical shift if complex formation is complete, then it is possible to use the following equation to determine the association constant K_n:

$$[1] \qquad x_B/\delta = x_B/\delta_{AB} + 1/K_n\delta_{AB}.$$

The above formula assumes a 1:1 complex and was derived in the same manner as that given by Brand, Eglinton, and Morman (3). The position of the proton resonance signals were obtained with considerable accuracy by placing side bands of known frequency on either side of the proton signal. In the case of the methylene proton resonance signal where there are two peaks, the mid-point of these was taken.

To investigate the activating power of substituents on neighboring methylene groups, a number of compounds were studied in carbon tetrachloride and in benzene, with tetramethylsilane as the reference standard. The chemical shift of the methylene proton resonance signal on going from carbon tetrachloride to benzene as solvent was noted. Of the compounds studied propargyl chloride, methylene chloride, and chloroacetonitrile were commercial products which were dried and distilled before use. The 1,4-dichlorobut-2-yne was supplied by Dr. G. Eglinton. The concentration of solute in all cases was taken to be 0.2 mole/l of solvent.

RESULTS AND DISCUSSION

When x_B/δ was plotted against x_B for propargyl chloride in benzene–cyclohexane, a straight line graph was obtained from whose slope and intercept it was possible to obtain the values for K_n and δ_{AB}. The method of least squares was employed to obtain the limiting errors in the results. Tables I*a* and I*b* give the results obtained for the methylene

TABLE I*a*

Propargyl chloride in benzene–cyclohexane (CH_2 protons)
(shift measured relative to cyclohexane)

δ_1 (c.p.s.)	x_B (mole fraction)	δ (c.p.s.)	x_B/δ (mole fraction) $(c.p.s.)^{-1}$
150.3±0.2	0	0	0
144.4±0.2	0.1	5.9±0.3	0.0168±0.0008
135.4±0.2	0.3	15.0±0.3	0.0200±0.0004
128.6±0.2	0.5	21.7±0.3	0.0230±0.0003
123.6±0.2	0.7	26.8±0.3	0.0262±0.0003
120.0±0.2	0.9	30.4±0.3	0.0296±0.0003

TABLE I*b*

Propargyl chloride in benzene–cyclohexane (≡CH proton)
(shift measured relative to cyclohexane)

δ_1 (c.p.s.)	x_B (mole fraction)	δ (c.p.s.)	x_B/δ (mole fraction) $(c.p.s.)^{-1}$
48.8±0.2	0	0	0
45.5±0.1	0.1	3.3±0.2	0.0300±0.0017
40.4±0.2	0.3	8.5±0.3	0.0355±0.0011
36.2±0.3	0.5	12.6±0.4	0.0397±0.0011
33.3±0.3	0.7	15.5±0.4	0.0452±0.0011
32.1±0.2	0.9	16.7±0.2	0.0540±0.0008

protons and for the ethynyl proton respectively. These results led to the following constants.

(*a*) From the methylene protons: $K_n = 1.01 \pm 0.02$ (mole fraction)$^{-1}$; $\delta_{AB} = 63.8 \pm 1.3$ c.p.s.; degree of association ($x_B = 1$) $= 0.50 \pm 0.01$.

(*b*) From the ethynyl proton: $K_n = 0.96 \pm 0.06$ (mole fraction)$^{-1}$; $\delta_{AB} = 37.0 \pm 2.4$ c.p.s.; degree of association ($x_B = 1$) $= 0.49 \pm 0.04$.

The effect of different neighboring groups on the chemical shift of the methylene proton in going from carbon tetrachloride to benzene as solvent is shown in Table II. The results tended to suggest that the activating power of the neighboring groups followed the order: C≡C < Cl < C≡N.

The results obtained for propargyl chloride indicated that the δ_{AB} for the methylene protons was nearly twice that obtained for the ethynyl proton. This indicated that the

Can. J. Chem. Downloaded from www.nrcresearchpress.com by 210.87.254.40 on 09/05/12
For personal use only.

TABLE II

Methylene proton resonance signals—solvent effects (shift measured relative to tetramethylsilane)

Solute	Carbon tetrachloride (p.p.m.)	Benzene (p.p.m.)	Shift (p.p.m.)
Propargyl chloride	5.91	6.58	0.67
1,4-Dichloro-but-2-yne	5.83	6.57	0.74
Methylene chloride	4.65	5.55	0.90
Chloroacetonitrile	5.93	7.16	1.23

methylene protons were interacting to a greater extent with the ring current of the benzene than was the ethynyl proton. The results obtained from studying the chemical shift of the methylene protons gave a straight line graph indicating the presence of a 1:1 complex. However, the graph obtained from the ethynyl proton results was slightly curved at lower values of x_B. This curvature was not pronounced and was probably due to the increasing importance of experimental error when measuring small differences. However, within their stated errors all points lay on a straight line. The association constants obtained for both types of protons were identical within the limits of experimental error, indicating that the results obtained from the methylene and ethynyl protons referred to the same 1:1 complex. In this complex it would appear that the methylene protons were closer to the ring than the ethynyl proton, the axis of the molecule lying at an angle above the plane of the ring.

The work of Buckingham, Schaefer, and Schneider (4) provided the theoretical basis for interpreting the results obtained as being due to complex formation. The contributions to the chemical shift from the Van der Waals forces, the reaction field, and the bulk diamagnetic susceptibility were effectively eliminated by using cyclohexane both as an inert solvent and as the internal reference. This left only two contributions to the chemical shift arising from the presence of the solute in the solvent. These were the shift due to the solvent magnetic anisotropy and the shift arising from complex formation. Now Schneider (5) has shown that the latter contribution is usually negative while the former contribution, particularly in aromatic solvents, is large and positive. For propargyl chloride in benzene the ethynyl and methylene proton resonance signals were shifted upfield, which suggested that the small chemical shifts of the solute proton signal, arising from complex formation in aromatic solvents, were effectively amplified because of the large magnetic anisotropy of the active solvent. It was therefore assumed that the chemical shifts observed were the result of complex formation between propargyl chloride and benzene.

Though the foregoing allows one to assume complex formation between propargyl chloride and benzene it does not help to decide whether the association is due to a form of hydrogen bonding between the methylene protons and the π-electron system of benzene, or whether it is due to dipole-induced dipole effects produced by the solute dipole. Both forms of association would be strongly influenced by temperature. While it is now generally accepted that hydrogen bonding can occur between the C—H group of a molecule such as chloroform and the π-electrons of benzene (6), there is still considerable controversy as to whether hydrogen bonding can occur in a situation in which a CH_3 group or a CH_2 group is the hydrogen donor. Abrahams (7), for instance, has concluded that association between methyl halides and aromatic solvents is caused by

Can. J. Chem. Downloaded from www.nrcresearchpress.com by 210.87.254.40 on 09/05/12
For personal use only.

hydrogen bonding; whereas Schneider (5) attributes the complex formation to a dipole-induced dipole form of attraction. The present state of knowledge only allows one to conclude that propargyl chloride forms a 1:1 complex with benzene, in which the methyllene protons are closer to the plane of the ring than is the ethynyl proton.

ACKNOWLEDGMENTS

This work was carried out in the Department of Chemistry of the University of Glasgow. The author wishes to thank Dr. J. C. D. Brand for his encouragement and advice, and the Department of Scientific and Industrial Research for a Studentship.

REFERENCES

1. J. A. Pople. J. Chem. Phys. **24**, 1111 (1956).
2. J. V. Hatton and R. E. Richards. Trans. Faraday Soc. **57**, 28 (1961).
3. J. C. D. Brand, G. Eglinton, and J. F. Morman. J. Chem. Soc. 2526 (1960).
4. A. D. Buckingham, T. P. Schaefer, and W. G. Schneider. J. Chem. Phys. **32**, 1227 (1960).
5. W. G. Schneider. J. Phys. Chem. **66**, 2653 (1962).
6. C. J. Creswell and A. L. Allred. J. Phys. Chem. **66**, 1469 (1962).
7. R. J. Abrahams. Mol. Phys. **4**, 369 (1961).

Can. J. Chem. Downloaded from www.nrcresearchpress.com by 210.87.254.40 on 09/05/12
For personal use only.

Can. J. Chem. Downloaded from www.nrcresearchpress.com by 210.87.254.105 on 09/05/12
For personal use only.

COORDINATION COMPLEXES OF GROUP (IV) HALIDES

PREPARATION OF THE COMPLEXES OF TITANIUM TETRACHLORIDE, TITANIUM TETRABROMIDE, AND TIN TETRACHLORIDE WITH SOME THIO-, ISOTHIO-, AND ISO-CYANATE LIGANDS[1]

SUMER CHAND JAIN[2] AND ROLAND RIVEST
Department of Chemistry, University of Montreal, Montreal, Quebec

Received September 21, 1964

ABSTRACT

Coordination complexes between ethyl thiocyanate, ethyl isothiocyanate, ethylene dithiocyanate, ethyl isocyanate, and tetrachlorides of titanium and tin and titanium tetrabromide have been prepared. The analytical results indicate that under different experimental conditions one can obtain compounds of the following type:

$MX_4.L$	$2MX_4.L—L$	$MX_4.2L$	$MX_4.L—L$
a	*b*	*c*	*d*

where MX_4 is a Lewis acid and L, L—L are mono- and bi-dentate ligands respectively. The complexes obtained are compared with the dinitrile complexes prepared by us previously (1).

INTRODUCTION

After our study on the nitrile and dinitrile complexes of group (IV) halides (1) where coordination was reported to take place through the nitrogen atom of the CN group, it was considered interesting to study the thiocyanate, isothiocyanate, and isocyanate molecules as ligands having the sulfur and oxygen atoms respectively in addition to nitrogen atoms as donor atoms. Since these functional groups are linear, the two donor atoms present in the ligand molecule cannot coordinate to the same metal atom but can, without putting too great a strain on the ligand molecule, coordinate to two different metal atoms and form a bridge between them.

Some work has been reported on the inorganic thiocyanate complexes of Co, Ni, Cu, Cr, Pt, etc. (2), by Mitchell and Williams. In their article the authors had intended to use inorganic thiocyanates to diagnose the type of binding in terminal thiocyanate complexes. Taking into account all the factors influencing the vibration frequency of the CN group, they could not reach their original goal but could, however, make correlations between infrared band frequencies and structure. These correlations were: (*a*) the frequency was at higher wave numbers in the order M—NCS $\leqslant$ M—SCN $<$ B—SCN—M, where M was the central metal ion and B the cation used to neutralize the charge on anionic thiocyanate; (*b*) for a given arrangement of the thiocyanate ion, the more polarizing the cation the greater the frequency of the CN vibrations; (*c*) bridged thiocyanates could also be obtained.

Lewis and co-workers (3) using infrared together with X-ray and ultraviolet spectral studies have found that the bonding in the $[Mo(NCS)_6]^{3-}$ ion occurs through the nitrogen; inorganic thiocyanate and isothiocyanate have thus largely been studied as ligands, but very little is reported on the organic thiocyanates and isothiocyanates as ligands with group (IV) halides.

[1]*Paper presented at the 47th Chemical Institute of Canada Conference, Kingston, June 1, 1964.*
[2]*Present address: Postdoctorate Fellow, Chemistry Department, University of Western Ontario, London, Ontario, Canada.*

The purpose of this work was to investigate: (*a*) how the coordination of thiocyanates compares with nitriles in the complexes with group (IV) halides; (*b*) which of the two possible donor atoms, sulfur or nitrogen, are involved in coordination; and (*c*) how the coordination of thiocyanates compares with the coordination of isocyanates and isothiocyanates.

EXPERIMENTAL

The experimental setup and the method of preparation of the complexes were quite similar to the ones used previously (1, 4). The Lewis acids used were purified by appropriate methods as mentioned in a previous publication (1). The ligands were obtained from the Fisher Scientific Co. and were dried on molecular sieves before use. The reactions were performed in solutions in methylene chloride or hexane (Table I). The ethyl isothiocyanate complex with titanium tetrachloride was a liquid at room temperature and all the other complexes reported were solid, powdery products which were filtered, washed, and dried under vacuum at room temperature.

TABLE I

Analytical results

Complex	Solvent used	Color of the compound	Melting point (°C)	Metal (%)		Halogen (%)	
				Theor.	Found	Theor.	Found
$TiCl_4.2C_2H_5SCN$	C_6H_{12}	Yellow	88–89	13.16	13.18	38.95	38.80
$TiCl_4.C_2H_5SCN$	C_6H_{12}	Yellow	90–92	17.30	17.18	51.20	50.75
$TiCl_4.NCS(CH_2)_2SCN$	CH_2Cl_2	Yellow	158–160	14.35	14.20	42.46	43.70
$2TiCl_4.NCS(CH_2)_2SCN$	CH_2Cl_2	Yellow	178–180	18.29	18.10	54.15	55.29
$TiBr_4.2C_2H_5SCN$	C_6H_{12}	Red	85–87	8.84	9.20	58.99	59.10
$TiBr_4.NCS(CH_2)_2SCN$	CH_2Cl_2	Red	166–168	9.36	9.42	62.44	61.20
$SnCl_4.2C_2H_5SCN$	C_6H_{12}	White	49–51	27.30	26.63	32.61	32.90
$SnCl_4.NCS(CH_2)_2SCN$	CH_2Cl_2	White	115–117	29.33	28.30	35.03	35.70
$TiCl_4.C_2H_5NCS$*	C_6H_{12}	Dark orange	Liquid at room temp.	17.30	16.82	51.20	51.0
$TiCl_4.2C_2H_5NCO$	C_6H_{12}	Yellow	82–84	14.77	14.35	42.72	41.27

*This sample was sent for C, H, N analysis to the Microanalytical Laboratory, 164 Banbury Road, England. Theor.: C, 13.01; H, 1.81; N, 5.06. Found: C, 13.95; H, 2.44; N, 4.92.

The analysis of chlorine and of the metals have been described previously (5, 6). The results are included in Table I. The infrared spectral measurements were carried out on a Perkin–Elmer spectrophotometer Model 21, using a sodium chloride prism. The results obtained for the stretching frequency of the functional group are included in Table II.

TABLE II

Infrared spectra results (in Nujol mulls)

Complex	Stretching frequency of the functional group (cm^{-1})		Shift in stretching frequency (cm^{-1})
	Pure ligand	Compound	
$TiCl_4.2C_2H_5SCN$	2 160	2 190	30
$TiCl_4.C_2H_5SCN$	2 160	2 195	35
$TiCl_4.NCS(CH_2)_2SCN$	2 155	2 190	30
$2TiCl_4.NCS(CH_2)_2SCN$	2 155	2 195	40
$TiBr_4.2C_2H_5SCN$	2 160	2 180	20
$TiBr_4.NCS(CH_2)_2SCN$	2 155	2 180	25
$SnCl_4.2C_2H_5SCN$	2 160	2 190	30
$SnCl_4.NCS(CH_2)_2SCN$	2 155	2 190	35
$TiCl_4.C_2H_5NCS$	2 100	2 120	20
	2 180	2 220	40
			New peak at 1 605
$TiCl_4.2C_2H_5NCO$	2 272	Vanish	New peak at 1 845

Can. J. Chem. Downloaded from www.nrcresearchpress.com by 210.87.254.105 on 09/05/12
For personal use only.

INFRARED SPECTRA AND STRUCTURAL DISCUSSION

From the work of Lieber and Rao (7) organic thiocyanates exhibit a band at 2 140 cm^{-1} probably due to the C≡N frequency and another one in the 683–722 cm^{-1} region mostly due to C—S stretching. For our complexes of ethyl thiocyanate as monodentate

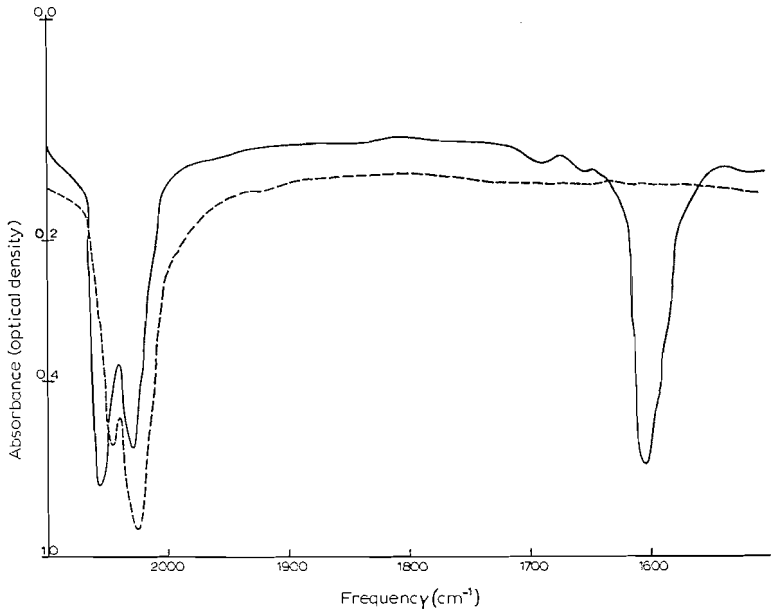

FIG. 1. Infrared spectra of pure C_2H_5NCS (- - -), complex $TiCl_4.C_2H_5NCS$ (—). (Both taken in Nujol mulls.)

and ethylene dithiocyanate as bidentate ligand, the infrared spectra indicate a positive shift of the CN-stretching frequency similar to the shift observed for dinitrile complexes. However, in the dinitrile series (1) the values of the frequency shifts in similar compounds were always lower for the $SnCl_4$ than for the $TiCl_4$ complexes. In our thiocyanate complexes they are about the same. Moreover, in the dinitrile series the frequency shifts were identical for the complexes of $TiCl_4$ and of $TiBr_4$ and in the thiocyanate series they are much smaller for the $TiBr_4$ complexes.

Since one would not expect any steric effect on the bonding to titanium when passing from R—SCN to R—CN if the bonding is done through nitrogen, one would then explain this effect by assuming that coordination is done through sulfur and thus explain the steric hindrance of the bromine compared to that of the chlorine in the titanium complexes. In the comparison between the complexes of dinitriles with the complexes of dithiocyanates, one point worth mentioning is that the thiocyanate complexes had relatively low true melting points and that they could be purified by sublimation. This was not the case for the dinitrile complexes which decomposed before melting.

The complex of $TiCl_4$ with ethyl isothiocyanate is quite different from the analogous complex with ethyl thiocyanate. 1. The color of the complex with ethyl isothiocyanate is dark orange whereas the color of the other one is yellow. 2. One is a liquid at room temperature, the other has a melting point of 90 °C. 3. The infrared spectrum of the thiocyanate complex is quite similar to the spectrum of the pure thiocyanate ligand except for the band assigned to the SCN group observed at 2 160 cm^{-1} in the pure

Can. J. Chem. Downloaded from www.nrcresearchpress.com by 210.87.254.105 on 09/05/12
For personal use only.

ligand and shifted to 2 195 cm^{-1} in the complex, whereas the infrared spectrum of the complex isothiocyanate is very different from the spectrum of the pure isothiocyanate ligand. According to Lieber (7) the infrared spectra of isothiocyanates exhibit a strong band in the region of 2 100 cm^{-1} due to the isothiocyanate group. This band shows its fine structure at smaller layer thickness and leads to two bands as we observed for the pure ligand. As one would expect on coordination these bands are increased by about 40 cm^{-1}. A new band at 1 605 cm^{-1} is particularly surprising. It indicates a great change of the electron distribution of the ligand in the complex and could be explained only by assuming that it is due to N=C bonding.

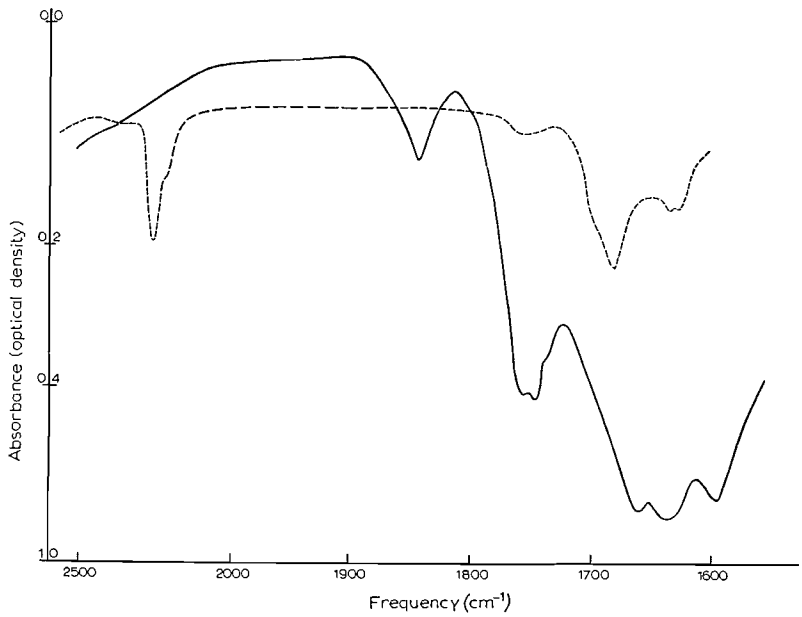

FIG. 2. Infrared spectra of pure C_2H_5NCO (- - -), complex $TiCl_4.2C_2H_5NCO$ (—). (Both taken in Nujol mulls.)

It is interesting to note that a similar effect has been observed in the case of isocyanate, Fig. 2. In the pure state isocyanate has a band at 2 272 cm^{-1}; this band vanishes in the $TiCl_4$ complex and a new band appears at 1 845 cm^{-1}, and a doublet at 1 700 cm^{-1} in the pure ligand is shifted to 1 750 cm^{-1} and intensified. The explanation of so many important changes in the spectrum of the ligand when coordinated can be qualitatively explained by assuming that coordination favors the following form C_2H_5—N=C=O over the other form C_2H_5—N—C≡O. Although this last form would contribute to a good description of the free ligand, it would not be favored in the adduct because it has a positive formal charge on oxygen.

The infrared spectrum of this compound in CH_2Cl_2 solutions shows both the original peaks and the new peaks indicating that the compound is considerably dissociated in solution. This is quite interesting since it indicates that through dissociation the original ligand is regenerated and may indicate that in the complex the molecular changes happening to the ligand are reversible if the ligand is liberated.

Can. J. Chem. Downloaded from www.nrcresearchpress.com by 210.87.254.105 on 09/05/12
For personal use only.

ACKNOWLEDGMENT

The authors are indebted to the National Research Council of Canada whose financial assistance made this work possible.

REFERENCES

1. S. C. JAIN and R. RIVEST. Can. J. Chem. **41**, 2130 (1963).
2. P. C. H. MITCHELL and R. J. P. WILLIAMS. J. Chem. Soc. 1912 (1960).
3. J. LEWIS, R. S. NYHOLM, and P. W. SMITH. J. Chem. Soc. 4590 (1961).
4. S. C. JAIN and R. RIVEST. Can. J. Chem. **40**, 2243 (1962).
5. J. ARCHAMBAULT and R. RIVEST. Can. J. Chem. **36**, 1461 (1958).
6. E. RIVET, R. AUBIN, and R. RIVEST. Can. J. Chem. **39**, 2343 (1961).
7. E. LIEBER, C. N. R. RAO, and J. R. CHANDRAN. Spectrochim. Acta, **13**, 296 (1959).

Can. J. Chem. Downloaded from www.nrcresearchpress.com by 210.87.254.105 on 09/05/12
For personal use only.

Can. J. Chem. Downloaded from www.nrcresearchpress.com by 210.87.254.6 on 09/05/12
For personal use only.

STEROIDS

IX.[1] THE SOLVOLYSIS OF 4,4-DIETHYLCHOLESTERYL METHANESULFONATE

D. N. GUPTA,[2] G. SCHILLING, AND G. JUST
Departments of Chemistry, McGill University and Ayerst, McKenna and Harrison

Received October 16, 1964

ABSTRACT

The acetolysis of 4,4-diethylcholesteryl mesylate gave 11% 3,4-dialkyl (A), 39% 3α,5-cyclo (C), and 50% A-norcholestene (B) derivatives. The corresponding yield for the 4-4,dimethyl series is 25, < 11.6, and > 61.4%.

Knowledge of the mechanism of solvolysis of cholesteryl derivatives does not permit one to predict with reasonable accuracy the solvolytic reactions of 4-monomethyl (2, 3) or 4,4-dimethyl (4, 5, 6) cholesteryl derivatives. Since small changes in structure seem to have a fairly large effect on the reactions, we undertook a study of the reactions of 4,4-diethylcholesteryl mesylate, expecting to obtain a product distribution similar to that observed in the solvolysis of 4,4-dimethylcholesteryl tosylate. In that reaction (6), one isolates products formally derived from carbonium ions A, B, and C in the yields indicated.

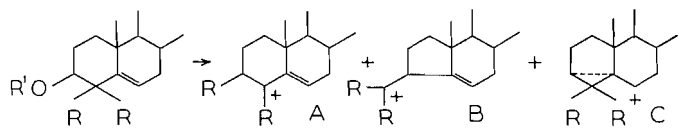

I, R=CH_3	25%	> 61.4%	< 11.6%
III, R=C_2H_5	11%	50%	39%

Since the results obtained are somewhat unexpected, we would like to report on them.

Cholest-4-en-3-one (7) was converted to 4,4-diethylcholest-5-en-3-one (II) by appropriately modifying the procedure described by Woodward, Barton, and co-workers (8). Lithium aluminium hydride reduction (8) of ketone II gave 4,4-diethylcholesterol (III) in quantitative yield. When ketone II was reduced with sodium borohydride in N,N-dimethylformamide (9) and the resulting mixture separated on alumina, there was obtained the starting material, 3α-alcohol IV, and 3β-alcohol III in 63.5, 1.2, and 15.1% yields respectively. The stereochemical assignment of the two epimeric alcohols was based on the relative yield of products obtained and the relative ease of elution on alumina (10).

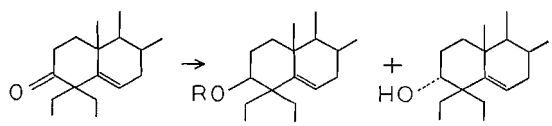

II III, R=H IV
III$_a$, R=Ms

[1]*For part VIII, see ref. 1.*
[2]*Abstracted from part of the Ph.D. thesis of D. N. G.*

Solvolysis of 4,4-Diethylcholesteryl Mesylate (IIIa)

Mesylate III*a* was prepared by treatment of 3β-alcohol III with methanesulfonyl chloride in pyridine for 2 h at 0°. Because of its instability, it could not be purified by crystallization. However, reasonably satisfactory analytical data could be obtained for it. Mesylate III*a* was solvolyzed in buffered aqueous acetone for 16 h at reflux temperature (4–6). Ether extraction and chromatography on silica gel gave a hydrocarbon fraction (56.2%) and an alcohol fraction (36.3%). The latter was roughly separated into three sub-fractions during elution with hexane–benzene mixtures.

Hydrocarbons

From the hydrocarbon fraction, the olefins IX, VIII, and XI were separated by preparative thin-layer chromatography (t.l.c.).

Hydrocarbon IX, $[M]_D$ −21.2°, did not absorb in the ultraviolet above 220 mμ. Its nuclear magnetic resonance (n.m.r.) spectrum showed a poorly resolved two-proton signal around 5 p.p.m. and a one-proton signal at 3 p.p.m. which could be assigned to the doubly allylic proton at C_3. A similar signal was observed in the n.m.r. spectrum of 3-isopropenyl-A-norcholest-5-ene (IX*a*), $[M]_D$ −31° (6). Gas–liquid chromatography (g.l.c.) (see Table I) showed one peak at 7.05 min and a 1.8% contamination of VIII at 8.6 min. When alcohol VI, the structure of which is proved below, was submitted to g.l.c., the major portion (65%) was pyrolyzed and gave a hydrocarbon having a retention time identical to that of IX. Hydrocarbon IX was also obtained from alcohol VI by treatment with phosphorus oxychloride – pyridine, thus confirming the structure assigned.

Diene VIII absorbed in the ultraviolet at 238, 245, and 253.5 mμ, a pattern characteristic for dienes of this type (6). Gas–liquid chromatography showed one single peak at 8.6 min. Its structure was established by comparison with an authentic sample prepared by reacting 4-ethylcholest-4-en-3-one with an ethyl Grignard reagent (11).

Hydrocarbon XI, $[M]_D$ −580°, did not absorb in the ultraviolet above 220 mμ, thus excluding the possibility of a conjugated diene structure. The purity of the compound was established by g.l.c., which showed one peak at 6.7 min and a 1% impurity at 5.9 min (probably dienes XII or XIII). The n.m.r. spectrum showed a poorly resolved quartet at 5.18 p.p.m. (2H, $HC_6{=}C_7H$) and signal at 2.5 p.p.m. (1H, $HC_8{-}C_7{=}$). A one-proton signal due to cyclopropyl methine proton in conjugation with $\Delta^{6,7}$ could not be detected. These protons were reported to absorb around 1.1 p.p.m. (12, 13). In the case of hydrocarbon XI, methylene and methyl absorption obscured this region and prevented identification of cyclopropyl proton resonance peaks. A band at 780 cm^{-1} in the infrared spectrum of XI confirmed the presence of a *cis*-disubstituted double bond. The shift to the higher region indicated some conjugation with the cyclopropane ring (14, 15). The molecular rotational change[3] of alcohol VII and hydrocarbon XI was compared with that of the analogous compounds in the cholesteryl series (16). The changes were in the same direction but quite different in magnitude, reflecting some unusual deformation which is probably steric in origin (17, 18). Hydrocarbon XI was also obtained by the acid-catalyzed demethoxylation (19) of 4,4-diethyl-6β-methoxy-3α,5-cyclocholestane (VII*a*). The only other hydrocarbon which could possibly fit some of the spectroscopic data is 3-(pent-2′-en-3′-yl)-A-norcholest-5-ene (IX). Its structure, however, has been proved conclusively and can therefore be excluded as an alternative.

No other hydrocarbons could be isolated by t.l.c., although g.l.c. of the crude solvolysis

[3] *3α,5-Cyclocholestane derivatives (16): alcohol, $[M]_D$ +98°; hydrocarbon, $[M]_D$ −173°; $\Delta[M]_D$, +271°. 4,4-Diethyl-3α,5-cyclocholestane derivatives: alcohol XI, $[M]_D$ +246°; hydrocarbon, $[M]_D$ −580°; $\Delta[M]_D$ +826°.*

Can. J. Chem. Downloaded from www.nrcresearchpress.com by 210.87.254.6 on 09/05/12
For personal use only.

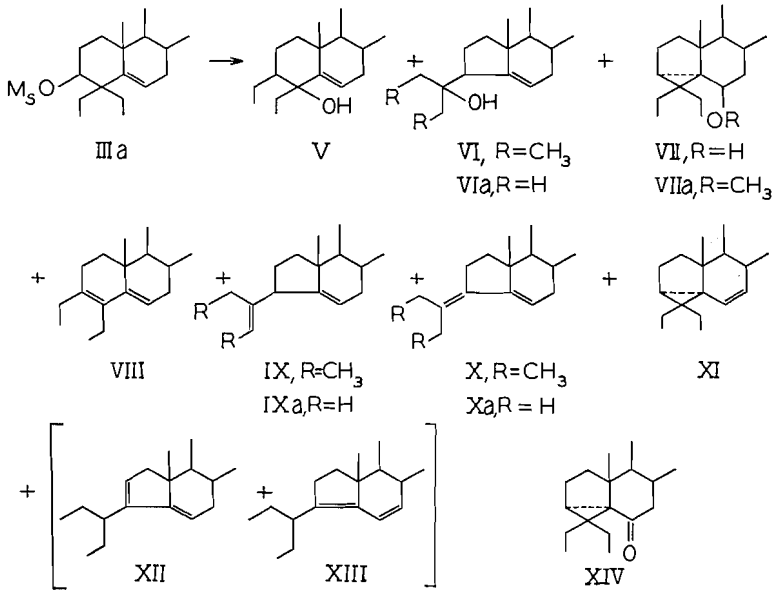

FLOWSHEET 1.

mixture indicated the presence of hydrocarbons having retention times of 7.5 (X) and 5.9 (XII, XIII) min. Hydrocarbons of identical retention time were also obtained when alcohol VI was submitted to g.l.c. It was noted that when the retention times of the structurally analogous hydrocarbons from the solvolyses of 4,4-dimethyl- (6) and 4,4-diethylcholesteryl sulfonates were plotted against each other, a straight line was obtained (except for hydrocarbons IX and IX*a*). This was taken as additional evidence for the presence of hydrocarbon X, and possibly XII and XIII.

Alcohols

Column chromatography and further purification by t.l.c. and crystallization gave alcohols V, VI, and VII.

The structure of alcohol VI was established as follows. The n.m.r. spectrum of the alcohol showed signals at 5.33 p.p.m. (1H, HC_6=) and 2.61 p.p.m. (1H, HC_3—C=C) (6). The alcohol was tertiary since it resisted acetylation at room or reflux temperature. Dehydration with phosphorus oxychloride – pyridine (6) gave a mixture of dienes. Separation on t.l.c. gave as major hydrocarbon olefin IX, and as minor product diene X, which absorbed in the ultrvaiolet at 251 mμ. Gas–liquid chromatography of X showed a major peak (70%) at 7.5 min in addition to minor peaks, which are either impurities or due to decomposition. A conjugated diene, 3-isopropylidene-A-norcholest-5-ene (X*a*), having identical ultraviolet spectrum and similar g.l.c. pattern, was also obtained in the 4,4-dimethyl series (6). It had been obtained directly from solvolysis of 4,4-dimethylcholesteryl tosylate or by treatment of 3-isopropanol-A-norcholest-5-ene (VI*a*) with phosphorous oxychloride in pyridine. There is therefore very little doubt about the structure of diene X.

Alcohol VII, $[M]_D$ +246°, was the major constituent of the alcohol fraction. Its infrared spectrum exhibited bands at 3 050 (inflection), 1 005 – 1 035, and 850 cm^{-1} and showed no absorption for C=C stretch around 1 600 – 1 650 cm^{-1}. Two vibrations at

Can. J. Chem. Downloaded from www.nrcresearchpress.com by 210.87.254.6 on 09/05/12
For personal use only.

1 000 – 1 020 and 860 cm^{-1} in the cyclopropane ring have been frequently used to indicate an *i*-steroidal structure (20–22). Slabey (23) found that the presence of two substituents on a cyclopropane ring raised the characteristic frequencies at 1 000 – 1 020 cm^{-1}. These findings and the observed frequencies in the infrared spectrum of alcohol VII indicated the *i*-steroidal structure for it. The n.m.r. spectrum showed no signal for olefinic protons and a one-proton signal at 4.76 p.p.m. was assigned to the proton α to the oxygen function.

Chemical evidence supporting the structural assignment of VII came from the oxidation of VII with chromium trioxide – pyridine (24) to ketone XIV, $[M]_D$ +472°, ν_{CCl_4} 1 690 cm^{-1} (cyclopropyl ketone). The ketone did not absorb in the ultraviolet above 220 mμ. Comparison of molecular rotational change[4] (XIV → VII) with that observed in the 3α,5-cyclocholestane series showed that the changes were in the same direction but quite different in magnitude.

The alcohol VII appeared quite stable to base but very labile to acid. It was transformed quantitatively to 6β-methyl ether VII*a* by simple crystallization from methanol (compare ref. 6).[5] Ether VII*a*, $[M]_D$ +433°, absorbed in the infrared at 3 040 (inflection) and 1 095 cm^{-1} and showed no absorption around 3 600 cm^{-1}. Josien and co-workers (25) had reported a band at 1 095 cm^{-1} for a number of *i*-steroid ethers which distinguished them from normal methyl ethers of steroids. The n.m.r. spectrum showed a sharp three-proton peak at 3.13 p.p.m. (OCH_3) and a one-proton signal at 4.18 p.p.m. characteristic of a proton α to an oxygen function. Treatment of VII*a* with 0.001 *M* *p*-toluenesulfonic acid in absolute ethanol (19) gave a mixture of dienes. Separation by t.l.c. gave 4,4-diethyl-3α,5-cyclocholest-6-ene (XI) and 3,4-diethylcholesta-3,5-diene (VIII) in 27% and 9% yields respectively.[6]

Alcohol V was isolated in lowest yield from the solvolysis of 4,4-diethylcholesteryl tosylate. Some doubts persisted about its purity. The structural assignment was based on the following observation. Alcohol V resisted acetylation with acetic anhydride – pyridine at room temperature. At reflux temperature, a small amount of 3,4-diethylcholesta-3,5-diene (VIII) was obtained. The n.m.r. spectrum of alcohol V showed a one-proton signal at 5.5 p.p.m. (=C_6H).

Quantitative Study of Hydrocarbon Mixtures by G.L.C.

Preparative t.l.c. was used to isolate the individual compounds from the solvolysis of 4,4-diethylcholest-5-en-3β-yl mesylate (III*a*) in a pure form. However, a quantitative product distribution could not be obtained since some of the compounds, in particular diene X, were not isolated. The losses of the products due to desorption difficulties and during crystallization also did not permit a quantitative estimation of various components of the mixture. The purity of some of the compounds was by no means certain since the compounds of this nature frequently co-crystallize.

In order to ascertain the purity of the isolated compounds and the percentage composition of the solvolysis products, the hydrocarbon fractions from acetolysis of 4,4-diethylcholesteryl mesylate (III*a*) were subjected to gas–liquid chromatography (5% DC 710 on silanized gaschrom P, 6 ft column at 265.3° ± 2). Wherever possible the retention times were correlated with the retention times of the authentic samples.

[4]*3α,5-Cyclocholestane derivatives (16): ketone, $[M]_D$ +157°; alcohol, $[M]_D$ +98°; $\Delta[M]_D$ +59°.*
4,4-Diethyl-3α,5-cyclocholestane derivatives: ketone XIV, $[M]_D$ +472°; alcohol VII, $[M]_D$ +246°; $\Delta[M]_D$ +226°.

[5]*When the reaction was repeated, it was found that more consistent results were obtained upon addition of traces of acids.*

[6]*The formation of VIII was completely unexpected and will be discussed in a forthcoming paper.*

Can. J. Chem. Downloaded from www.nrcresearchpress.com by 210.87.254.6 on 09/05/12
For personal use only.

Alcohols were excluded from the g.l.c. analyses when it was desired to determine the percentage composition of the solvolysis products, since they led to dehydration products.[7] All hydrocarbons were shown to be stable to the g.l.c. conditions used except for 3-(3′-isopentylidene)-A-norcholest-5-ene (X). The percentage yield for this diene hence represented a minimum value. No appropriate correction could be applied to compensate for its transformation during g.l.c. because the peaks due to the rearranged products were poorly resolved. The structural assignment of X was based completely on analogy with 3-isopropylidene-A-norcholest-5-ene (X*a*) (ultraviolet, g.l.c. retention times correlation and decomposition pattern, optical rotations). The g.l.c. results are summarized in Table I.

TABLE I

Hydrocarbon	Retention time* (min)	% yield acetolysis	Evidence
XII, XIII	5.9	4.7	Gas–liquid chromatography
XI	6.8	38.7	Isolated
IX	7.05	30.5	Isolated
X	7.50	14.6	Gas–liquid chromatography
VIII	8.70	11.3	Isolated

*5% DC 710 on silanized gaschrom P, 6 ft column at 265.3°.

DISCUSSION

The yields of the major types of products obtained are summarized on Flowsheet I and contrasted with the results from the 4,4-dimethyl series. It can be seen that substitution of ethyl for methyl groups resulted in the decrease of products of alkylshift (A) and an increase of cyclosteroids (C).

Since it has been demonstrated (6) that the products of alkylshift arise from a boat-like intermediate and that 4β-methylcholesteryl tosylate (2, 3) gave mainly products of type A due to hydride shift, it may be concluded that the conformation of the starting material or intermediate is not only governed by the 4β,10β-dialkyl interaction, but also by the presence of the 4α-alkyl groups, which tends to restore the boat into the chair form.

The difference in product distribution in the 4,4-dimethyl and 4,4-diethyl series is perhaps not significant, in particular since the solvolyses were performed on the tosylate in one case and on a noncrystalline mesylate in the other case. However, taken together with the results of the solvolysis of 4β-methylcholesteryl tosylate, the product yield reported might reflect the conformation of the intermediate(s).

Further work to determine the exact nature of the intermediate is in progress.

EXPERIMENTAL[8]

4,4-Diethylcholest-5-en-3-one (II)

A stirred solution of 25 g of cholest-4-en-3-one in 250 ml of dry *tert*-butanol was treated with a solution of 28 g of potassium metal in 750 ml of the same solvent at 40°. Ethyl iodide (10 ml) in 25 ml of *tert*-butanol was then added over a period of 5 min. The reaction mixture was refluxed for 2 h with constant stirring and was further stirred for 6 h at 60°. The bulk of the solvent was removed *in vacuo*. Ether extraction and washing with 2 *N* hydrochloric acid gave a yellow amorphous residue (27 g), which showed in the infrared bands at 1 710 cm^{-1} (saturated ketone), 1 675 (inflection), and 1 610 cm^{-1}. The ultraviolet, λ_{max}^{ETOH} 241 mμ (ε 1 000), showed the presence of nearly 10% of the starting material.

Chromatography on alumina (activity II–III) and elution with hexane gave 16 g (56%) of ketone II, m.p. 92–94°. Crystallization from chloroform–methanol raised the melting point to 95–96° (26).

[7]*The results for the acetolysis of IIIa were recorded since acetolysis gave mainly hydrocarbons and since the product composition of the acetolysis of 4,4-dimethylcholesteryl tosylate (6) had been recorded.*

[8]*For details in instrumentation and general procedures, see ref. 27.*

Can. J. Chem. Downloaded from www.nrcresearchpress.com by 210.87.254.6 on 09/05/12
For personal use only.

Reduction of Ketone II with Lithium Aluminium Hydride

A solution of 13.5 g of II in 1 l of anhydrous ether was reduced with lithium aluminium hydride (8). After extraction, the ethereal solution was concentrated to 100 ml, and diluted with methanol. A colorless crystalline product (13 g), m.p. 126–129°, was obtained. Crystallization from ether–methanol gave 10 g (73.7%) of 4,4-diethylcholest-5-en-3β-ol (III), m.p. 129–130°, $[\alpha]_D^{22}$ −55.9° (*c* 1.52). The alcohol gave a single spot on t.l.c., using benzene–ether (95:5) as the solvent system.

Anal. Calcd. for $C_{31}H_{54}O$: C, 84.09; H, 12.29. Found: C, 83.98; H, 12.09.

3,4-Diethylcholesta-3,5-diene (VIII)

A solution of 515 mg of 4-ethylcholest-4-en-3-one was added dropwise at 0° to a solution of ethyl magnesium iodide formed from 1.52 g of magnesium and 10 ml of ethyl iodide in 75 ml of anhydrous ether. The reaction mixture was refluxed for 24 h and cooled and the excess Grignard reagent destroyed by adding cold saturated solution of ammonium chloride. Ether extraction gave 635 mg of colorless residue. Two crystallizations from ether–acetone gave 250 mg (50%) of pure 3,4-diethylcholestadiene (VIII), m.p. 123–123.5°, $[\alpha]_D^{23}$ −63°, λ_{max}^{ETOH} 238 mμ (ϵ 13 800), 245 (14 900), 253.5 (9 600).

Anal. Calcd. for $C_{31}H_{52}$: C, 87.66; H, 12.34. Found: C, 87.74; H, 12.11.

4,4-Diethylcholesteryl Mesylate (IIIa)

A solution of 9.6 g of 4,4-diethylcholesterol (III) in 24 ml of freshly distilled pyridine was reacted with 12 ml of methanesulfonyl chloride for 2 h at 0° with continuous stirring. The reaction mixture was poured on crushed ice and extracted with cold ether. The ethereal solution was washed with cold dilute hydrochloric acid and with ice-cold water. It was dried over magnesium sulfate and the solvent removed *in vacuo* at room temperature. A colorless crystalline residue (14 g) was obtained. The crude mesylate III*a* absorbed in the infrared at 1 415, 1 380, 1 340, 1 175, 960, and 900 cm^{-1}. No absorption maxima were shown in the ultraviolet above 220 mμ. Further crystallization of mesylate III*a* could not be effected due to extreme instability.

Anal. Calcd. for $C_{32}H_{56}O_3S$: C, 71.15; H, 11.09; S, 6.29. Found: C, 71.14; H, 10.28; S, 6.49.

Solvolysis of Methanesulfonate IIIa

Methanesulfonate III*a* (14 g) was solvolyzed in 2.55 l of 90% acetone containing 14 g of anhydrous sodium acetate for 16 h at reflux temperature. Part of the solvent was distilled off and the remainder diluted with 2 l of water and extracted with ether. The ethereal solution was washed with 5% sodium bicarbonate and water and dried over magnesium sulfate and the solvent removed *in vacuo*. A colorless oily residue (8.9 g) was obtained. The product did not show absorption for the mesyl group in the infrared. Chromatography on silica gel and elution with hexane gave 5.01 g (56.2%) of hydrocarbon mixture. Further elution with hexane–benzene (1:1) gave 3 g (36.2%) of alcohol fraction which was roughly separated into three sub-fractions.

A. Purification of Hydrocarbon Fraction

Preparative t.l.c. was used to separate hydrocarbons VIII, IX, and XI from the mixture as described below.

The glass plates (8 in. × 8 in.) were covered with 3 mm thick silica gel G and air dried overnight. They were then sprayed with a 5% solution of silver nitrate and activated by heating at 120°; 200 mg of hydrocarbon mixture was applied on each plate and the chromatogram developed with hexane–ether (95:5). Two ultraviolet-active bands were detected with the ultraviolet lamp and gave, after desorption from silica gel by extraction with ether, hydrocarbons XI (R_f 1) and VIII (R_f 0.77) in 20 and 6.8% yields respectively. A third band (R_f 0.67) appeared when the plates were exposed to the atmosphere for 10–12 h and gave, after desorption with ether, hydrocarbon IX in 18% yield.

4,4-Diethyl-3α,5-cyclocholest-6-ene (XI)

Crystallization of 340 mg of hydrocarbon XI (R_f 1) from ether–acetone gave 128 mg of crystals, m.p. 90–90.5°, $[\alpha]_D^{23}$ −137° (*c*, 1.36), νKBr 1 020, 780 cm^{-1}.

Anal. Calcd. for $C_{31}H_{52}$: C, 87.64; H, 12.37. Found: C, 87.64; H, 12.70.

3,4-Diethylcholesta-3,5-diene (VIII)

The residue (110 mg) from the middle band, R_f 0.77, gave, after crystallization from ether–acetone, 60 mg of hydrocarbon VIII, m.p. 124°, $[\alpha]_D^{23}$ −63° (*c*, 2.16), $\lambda_{max}^{C_6H_{12}}$ 238 mμ (14 000), 245 (14 900), 253.5 (9 600). Gas liquid chromatography showed one peak at 8.6 min. The melting point was not depressed upon admixture of an authentic sample.

3-(Pent-2′-en-3′-yl)-A-norcholest-5-ene (IX)

The residue (300 mg), R_f 0.67, was crystallized from ether–acetone to give 170 mg of IX; m.p. 69–70°, $[\alpha]_D^{23}$ −5.03° (*c*, 1.53). Gas–liquid chromatography showed a peak at 7.0 min, and a 1.8% impurity at 8.7 min (VIII).

Anal. Calcd. for $C_{31}H_{52}$: C, 87.64; H, 12.37. Found: C, 87.64; H, 12.12.

B. Purification of Alcohols on T.L.C.

The plates (8 in. × 8 in.) coated with silica gel G (3 mm thick) were used for the separation of alcohols

Can. J. Chem. Downloaded from www.nrcresearchpress.com by 210.87.254.6 on 09/05/12
For personal use only.

V, VI, and VII. An ethereal solution containing 150–200 mg of the alcohol mixture was applied on each plate and the chromatogram developed with hexane–ether (85:15). The bands of identical R_f values were collected and desorbed from silica gel with ether. Filtration and removal of the solvent gave alcohols V, VI, and VII in 1.5, 7.5, and 13.7% yields respectively.

3-(3'-Hydroxypent-3-yl)-A-norcholest-5-ene (VI)

Crystallization of 600 mg of the residue from ether–acetone gave 170 mg of alcohol VI, m.p. 104–105°, $[\alpha]_D^{23}$ −8.1° (*c* 1.76).

Anal. Calcd. for $C_{31}H_{54}O$: C, 84.09; H, 12.39. Found: C, 84.17; H, 12.16.

Treatment of Alcohol VI with Phosphorus Oxychloride – Pyridine

A solution of 60 mg of alcohol VI in 0.6 ml of pyridine was heated under reflux with 0.6 ml of phosphorus oxychloride for 1 h. The excess reagent was destroyed by careful addition of iced water. The reaction mixture was extracted with ether and the ethereal solution washed neutral. It was dried over magnesium sulfate and the solvent removed *in vacuo* to give a brown oily residue. Thin-layer chromatographic separation, using hexane as solvent system, gave two hydrocarbons IX and X in 55 and 16% yields respectively. Crystallization of 32 mg of hydrocarbon IX from ether–acetone gave 9 mg of substance, m.p. 68–69.5°, $[\alpha]_D^{23}$ −5° (*c*, 0.7). The hydrocarbon did not absorb in the ultraviolet. Gas–liquid chromatography showed a single peak at 7.05 min. The n.m.r. spectrum showed signals at 5 p.p.m. (1H, HC_6) and 3 p.p.m. (1H, HC_3—C=). The identity of the compound was established by comparison of the physcial and spectral characteristics with a sample obtained in the solvolysis. The second, minor fraction (9 mg) from the fast-moving band gave, after crystallization from ether–acetone, 3 mg of X, m.p. 92–93°, $\lambda_{max}^{C_6H_{12}}$ 252 mμ (ε 10 400). Gas–liquid chromatography showed a complex pattern with peaks at 5 min (20%), 5.75 min (69.7%), and 7.05 min (10.4%).

Attempted Acetylation of Alcohol VI

Alcohol VI was recovered unchanged when treated with acetic anhydride and pyridine at room temperature. At reflux temperature, the product which was formed did not absorb in the infrared in the hydroxyl or carbonyl region. Too small a quantity of the product did not permit further purification and characterization.

4,4-Diethyl-3α,5-cyclocholestan-6β-ol (VII)

The alcohol residue (400 mg) from the silica gel gave, after crystallization from ether–acetone at 4–5°, 300 mg of VII, m.p. 89–90°, $[\alpha]_D^{22}$ +55.5° (*c*, 2.23).

Anal. Calcd. for $C_{31}H_{54}O$: C, 84.09; H, 12.29. Found: C, 84.33; H, 12.21.

Treatment of VII with Chromium Trioxide

To a solution of 92 mg of VII in 0.9 ml of pyridine was added 91 mg of chromium trioxide in 0.9 ml of pyridine (24). The reaction mixture was swirled and left overnight. The mixture was poured into water, extracted twice with ether–benzene (1:1) and filtered through supergel to break the emulsion. The combined organic solution was washed neutral and dried over magnesium sulfate and the solvent removed *in vacuo*. A brown oily residue (84 mg) was obtained. Thin-layer chromatographic separation and two crystallizations from ether–acetone gave ketone XIV, m.p. 99–100°, $[\alpha]_D$ +116.5° (*c*, 1.19).

Anal. Calcd. for $C_{31}H_{52}O$: C, 84.48; H, 11.87. Found: C, 84.20; H, 11.85.

4,4-Diethyl-6β-methoxy-3α,5-cyclocholestane (VIIa)

A part of the residue which gave alcohol VII was crystallized from ether–methanol to give crystalline ether VII*a*, m.p. 68°, $[\alpha]_D^{23}$ +94.85° (*c*, 1.77).

Anal. Calcd. for $C_{32}H_{56}O$: C, 84.14; H, 12.36; OCH_3, 6.80. Found: C, 84.33; H, 12.17; OCH_3, 5.82.

Treatment of Ether VIIa with Absolute Ethanol – p-Toluenesulfonic Acid

To a solution of 200 mg of ether VII*a* in 2 ml of absolute ethanol was added 1.8 ml of an ethanolic solution of *p*-toluenesulfonic acid (0.001 *M*) and the mixture refluxed for 30 min (19). It was neutralized with a few drops of 5% sodium bicarbonate and diluted with water and the organic material extracted with hexane. The crude product (190 mg) did not absorb around 1 100 cm^{-1}. Preparative t.l.c. (silica gel impregnated with 5% silver nitrate) using hexane as solvent system, gave hydrocarbons VIII and XI in 9 and 27% yields respectively.

3,4-Diethylcholest-5-en-4-ol (V)

Alcohol, m.p. 125–129°, $[\alpha]_D^{23}$ −36.3° (*c*, 1.256), was obtained in small quantity only. Repeated crystallizations from ether–acetone did not alter the melting point. The n.m.r. spectrum of the compound showed a one-proton signal at 5.5 p.p.m. (1H, C_6H).

Anal. Calcd. for $C_{31}H_{54}O$: C, 84.09; H, 12.29. Found: C, 84.38; H, 12.05.

Acetylation of V

Acetylation at room temperature gave starting material. When a mixture of 60 mg of alcohol V, 1 ml of acetic anhydride, and 1 ml of pyridine was refluxed, the product obtained showed no absorption for a

Can. J. Chem. Downloaded from www.nrcresearchpress.com by 210.87.254.6 on 09/05/12
For personal use only.

carbonyl group. Thin-layer chromatographic purification and crystallization from ether–methanol gave 10 mg of VIII, m.p. 121–122.5° $[\alpha]_D^{23}$ −62.5° (*c* 0.7), $\lambda_{max}^{C_6H_{12}}$ 238, 245, 253 mμ. The identity of the diene was established by melting point, mixed melting point, and by the comparison of ultraviolet absorption with a synthetic sample.

ACKNOWLEDGMENTS

We wish to thank Dr. Stammer for taking the n.m.r. spectra, and the National Research Council of Canada and Bristol Laboratories for financial support.

REFERENCES

1. G. Just and V. Di Tullio. Can. J. Chem. **42**, 2695 (1964).
2. R. M. Moriarty and R. M. de Sousa. J. Org. Chem. **28**, 3072 (1963).
3. S. Julia, J. P. Lavaux, S. R. Pathak, and G. H. Whitham. Compt. Rend. **256**, 1537 (1963).
4. Y. M. Y. Haddad and G. H. R. Summers. J. Chem. Soc. 769 (1959).
5. R. M. Moriarty and E. S. Wallis. J. Org. Chem. **24**, 1274, 1987 (1959).
6. G. Just, S. Winstein, R. Sneen, F. Shortland, and D. N. Gupta. Unpublished results.
7. J. F. Eastham and R. Teranishi. Organic syntheses. Vol. 35. John Wiley and Sons, Inc., N.Y. 1955. p. 39.
8. R. B. Woodward, A. A. Patchett, D. H. R. Barton, and D. A. J. Yves, and R. B. Kelly. J. Chem. Soc. 1131 (1957).
9. D. Taub, R. D. Hoffsommer, and N. L. Wendler. J. Am. Chem. Soc. **81**, 3291 (1959).
10. S. Winstein and E. M. Kosower. J. Am. Chem. Soc. **78**, 4347 (1956).
11. G. Just and K. St. C. Richardson. Can. J. Chem. **42**, 464 (1964).
12. G. Stork and J. Finici. J. Am. Chem. Soc. **83**, 4678 (1961).
13. V. Georgian, J. F. Kerwin, M. E. Wolff, and F. F. Owings. J. Am. Chem. Soc. **84**, 3594 (1962).
14. R. Kuhn, H. H. Inhoffen, H. A. Staab, and W. Otting. Chem. Ber. **86**, 965 (1953).
15. W. Oroshnik and A. D. Mebane. J. Am. Chem. Soc. **76**, 5719 (1954).
16. L. F. Fieser and M. Fieser. Steroids. Reinhold Publishing Corp. N.Y. 1959. pp. 315, 317.
17. D. T. Cropp, B. B. Dewhurst, and J. S. E. Holker. Chem. Ind. London, 209 (1961).
18. N. Allinger and M. A. DaRooge. Tetrahedron Letters, No. 19, 676 (1961); J. Am. Chem. Soc. **84**, 4561 (1962).
19. S. Winstein and A. H. Schlesinger. J. Am. Chem. Soc. **70**, 3328 (1948).
20. L. J. Bellamy. The infrared spectra of complex molecules. John Wiley and Sons, Inc., N.Y. 1960. p. 29.
21. C. W. Cannon, A. A. Santilli, and P. Shenian. J. Am. Chem. Soc. **81**, 1660 (1959).
22. C. F. H. Allen, T. J. Davis, W. J. Humphlett, and D. W. Stewart. J. Org. Chem. **22**, 1291 (1957).
23. V. A. Slabey. J. Am. Chem. Soc. **76**, 3604 (1954).
24. G. I. Poos, G. E. Arth, R. E. Beyler, and L. H. Sarett. J. Am. Chem. Soc. **75**, 422 (1953).
25. M. L. Josien, N. Fuson, and A. S. Cary. J. Am. Chem. Soc. **73**, 4445 (1951).
26. K. St. C. Richardson. Ph.D. Thesis, McGill University, Montreal. 1963.
27. G. Just and C. C. Leznoff. Can. J. Chem. **42**, 79 (1964).

Can. J. Chem. Downloaded from www.nrcresearchpress.com by 210.87.254.6 on 09/05/12
For personal use only.

DETERMINATION OF THE FIELD DEPENDENCE OF THE TAFEL SLOPE FOR THE STEADY-STATE ANODIC OXIDATION OF ALUMINIUM

M. J. DIGNAM, D. GOAD, AND M. SOLE
Department of Chemistry, University of Toronto, Toronto, Ontario
Received September 4, 1964

ABSTRACT

A novel and sensitive experimental technique has been developed and employed to measure the field variation of the Tafel slope at 25 °C for the steady-state anodic oxidation of aluminium. The data have been fitted to an equation of the form $I = \alpha \exp[\gamma E - \delta E^2]$ where I and E are the current density and field strength in the anodic film and α, γ, and δ are positive constants for isothermal conditions. Some information concerning the field variation of the interfacial potentials has also been obtained.

1. INTRODUCTION

In a recent publication (1) by one of us (M. J. D.) a theory was presented to explain the field and anomalous temperature dependence of Tafel slopes for processes occurring at high electrostatic fields. In this paper Tafel slope results for Ta, Nb, and Al were compared with the theory. The Al results were preliminary ones obtained during the investigation reported herein. The purpose of the present publication, in addition to presenting a novel experimental method, is to provide the experimental details, the data, and the calculations from which the Al results were obtained. In addition, some further information regarding interfacial potentials is presented.

The principle of the method is elementary; experimental complications arise, however, as a result of transient conduction phenomena (2), interfacial potentials, and space charge effects (3). If these phenomena did not exist, one can imagine carrying out an experiment in which the film was formed at a known field strength, E_1, to a potential V_1, following which the potential was suddenly changed to V_2 and held constant. The field strength immediately after switching, E_2, will then be $(V_2/V_1)E_1$. Since the cell currents can be measured, sufficient information is available to determine the Tafel slope ($\simeq \Delta E/\Delta \log I$, where I is the anodic current density). Because of the existence of transients, even pseudo steady-state conditions[1] would not be established for some time after changing the voltage, by which time the film would be thicker and hence E_2 would no longer be given by $(V_2/V_1)E_1$. To get around this difficulty, V_2 must be increased proportionally to the charge passed in order to compensate for film growth. This can be accomplished with the aid of electronic analogue computer equipment. This does not, however, overcome the difficulty introduced by the presence of unknown and most likely current-dependent interfacial potentials. One can overcome this problem, however, by in effect extrapolating the data to infinite film thickness for which the interfacial potentials become infinitesimal compared to the applied potential. The details of the equipment and procedure are given in the following sections. It is worth mentioning here, however, that the method is applicable only if film formation takes place with close to 100% current efficiency (strictly speaking, the current efficiency need only be independent of current density and film thickness). In addition, it is not absolute, in that it requires an independent determination of the field strength in the film for one set of conditions. Within

[1]*Under potentiostatic conditions, true steady-state conditions (i.e. $dE/dt = 0 = dI/dt$) can not be achieved since the field is changing as the film grows.*

these limitations, however, the method is very sensitive, allowing for example the Tafel slope to be determined with a precision of better than 2% for a change in field strength of only 3%. It is therefore ideally suited for obtaining the variation of Tafel slope with field strength. It is to this end that the method has been applied herein, the data being fitted to the following equation (cf. ref. 1, eq. [28])

$$I = i_0 \exp\{-[\phi - \mu^* E(1 - \mu^* E/C\phi)]/kT\}. \qquad [1.1]$$

For the purposes of the present paper, i_0, ϕ, μ^*, and C can simply be regarded as empirical constants to be determined from the data. A full discussion of the equation can be found in the original paper. A glossary of symbols used in Section 2 *et seq.* is given in the Appendix.

2. EXPERIMENTAL

Apparatus

The circuit, depicted in Fig. 1, was designed to satisfy the following equations:

$$\mathrm{d}V/\mathrm{d}t = Y, \qquad \text{for } t \leqslant t_0 \qquad [2.1]$$

$$(V + A) = y(V_0 + A) + y(Y/I_r)\int_{t_0}^{t} I \, \mathrm{d}t, \qquad \text{for } t > t_0. \qquad [2.2]$$

In these equations Y is a constant given by $e_1/100$ V/s, e_1 is a constant potential (cf. Fig. 1), V is the potential of the Al electrode with respect to the reference electrode, t is the time, t_0 is the specific time at which switches S_1 and S_2 are moved from positions 1 to positions 2, A is a constant voltage which may be altered from one experiment to the next, y is a constant factor, which may also be altered, and is equal to $1/(1 + R_y)$, where R_y is expressed in megohms, and I_r and V_0 are the values of I and V at time t_0, just before switching to circuit 2.

The triangular symbols represent high-gain, d-c., inverting, operational amplifiers, No. 3101 made by Donner Scientific Co.; the square symbol, a Keithley Instruments Inc. No. 610A electrometer-amplifier. The resistors are all 0.1% wire-wound; the capacitor, high quality polystyrene.

Referring all circuit potentials to ground and identifying the output of amplifier 2, say, as $V(2)$, etc., the circuit analysis proceeds as follows. With the switches in positions 1, the following equations can be written down immediately from a knowledge of conventional electronic analogue computer circuits:

$$-\mathrm{d}V(1)/\mathrm{d}t = e_1/100 = Y \qquad \text{for } t \leqslant t_0 \qquad [2.3]$$

$$-V(2) = V_{\mathrm{ref}} \qquad [2.4]$$

$$V(3) = -V(1) - V(2) - A \qquad \text{for } t \leqslant t_0 \qquad [2.5]$$

$$V = V(3) - V_{\mathrm{ref}} \qquad [2.6]$$

where V_{ref} is the potential of the reference electrode with respect to ground. From eqs. [2.3] to [2.6], eq. [2.1] is obtained.

At time t_0, just before the switches are connected to circuit 2, $V = V_0$, and hence, using eqs. [2.4] to [2.6] we obtain:

$$-V(1) = V_0 + A \qquad \text{at } t = t_0. \qquad [2.7]$$

Again, just before the switches are connected to circuit 2, the potentiometer, P, is adjusted so that:

$$V(\mathrm{P}) = e_1 \qquad \text{at } t = t_0, \qquad [2.8]$$

where $V(\mathrm{P})$ is the potential at the wiper arm of the potentiometer. Noting that $V(\mathrm{P})$ is proportional to the cell current, we may write:

$$V(\mathrm{P}) = \beta I_r \qquad \text{at } t = t_0 \qquad [2.9]$$

$$V(\mathrm{P}) = \beta I \qquad \text{at } t > t_0, \qquad [2.10]$$

where β is a constant for a given oxidation run. After the switches are connected to circuit 2 (i.e. for $t > t_0$) eqs. [2.4] and [2.6] are still valid. Equations [2.3] and [2.5], however, become

$$-\mathrm{d}V(1)/\mathrm{d}t = V(\mathrm{P})/100 \qquad \text{for } t > t_0 \qquad [2.11]$$

$$V(3) = -yV(1) - V(2) - A \qquad \text{for } t > t_0, \qquad [2.12]$$

where $y = [1 + R_y \text{ (in megohms)}]^{-1}$ as before. From eqs. [2.3] and [2.8]–[2.11], we obtain $-\mathrm{d}V(1)/\mathrm{d}t = RI/I_r$ which on integration using the boundary condition [2.7] gives:

$$-V(1) = V_0 + A + (Y/I_r)\int_{t_0}^{t} I\,\mathrm{d}t. \qquad [2.13]$$

From eqs. [2.4], [2.6], [2.12], and [2.13], eq. [2.2] is obtained.

The electrolysis cell, constructed of lucite, is shown diagramatically in Fig. 1. The electrolyte used was a 30% solution of ammonium pentaborate in ethylene glycol (4), as it has been shown by Bernard and Cook to lead to 100% current efficiencies for the formation of Al_2O_3. The reference electrode was a glass electrode, $E^0 = -0.657$ V (with respect to the reversible hydrogen electrode), which was positioned in a tube connected to the cell through a capillary-tipped sidearm adjacent to the anode.

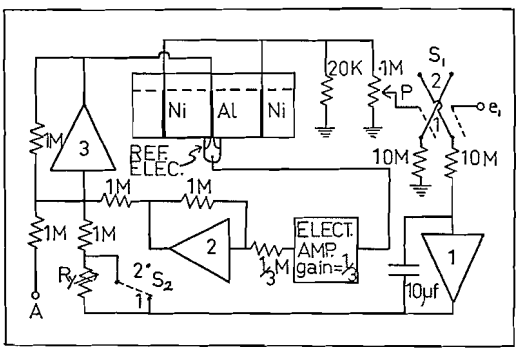

FIG. 1. Electronic circuit used to obtain steady-state conduction data.

Experimental Procedure

Aluminium sheet (99.996% Al, 0.04 in. thick) was formed into paddle-shaped electrodes of dimensions 1 in. × 0.25 in. for the paddle, 1 in. × 0.06 in. for the tab. Following routine cleaning procedures, the electrodes were electropolished at about 0.2 A/cm² and 25 °C in 5 parts ethyl alcohol to 1 part 70% perchloric acid by volume (5). The electrodes were rinsed briefly in ethyl alcohol, rinsed for 1 min in running distilled water, dried in a clean air jet, and stored in a desiccator over activated alumina.

A typical experimental run was carried out as follows. The cell was filled to just above the shoulders of the paddle-shaped aluminium electrode and was then connected into the circuit with S_1 and S_2 in positions 1, and e_1 set to zero. A value of e_1 of about 10 V was then applied to give a value of y of precisely 0.1 V/s. The cell current was then monitored (by measuring V(P) with a digital voltmeter) until no change in cell current with time could be detected. The cell current usually became constant by the time the cell potential reached about 20 V. No evidence of interference from electrolyte creeping up the electrode tab was found, in accord with a previous investigation (3). Following the attainment of a constant current, V(P) was adjusted to equal e_1, as mentioned previously, and then S_1 and S_2 (in that order) were switched to positions 2. The current, as measured by V(P), was then followed until it became constant. This current reading, the current reading before switching, and the potential $V(3)$ at the time of each of the current readings were then recorded.

In fact, the recording of $V(3)$ was an error in procedure, $V(1)$ being the required potential. Subsequent determinations of the potential V_{ref} at the current densities in question enabled the value of $V(1)$ to be deduced from the measured values of $V(3)$ with an uncertainty no greater than 2 V. This uncertainty is of no consequence, its effect on the intercepts in Fig. 2 and hence on μ^*, C, and ϕ being negligible. Its effect on the slopes of the lines in Fig. 1, and therefore on Z (see Section 3), is perhaps as great as 6%, which is likewise of little consequence.

After the second current reading, the switches were returned to positions 1 and the entire procedure was repeated from this point on. This procedure was continued until $V(3)$ exceeded 100 V, the limit of the capability of the amplifiers. In a typical run, 8 to 10 sets of readings would be obtained in this way, the value of A and y being held constant for any given run, but varied from run to run. From a single set of readings I_r/I and $V' = -V(1) - A$ were obtained, where $V(1)$ is determined at the time I is measured. Graphs of $\log I_r/I$ versus $1/V'$ were then constructed for each run. Figure 2 shows the data for one series of runs, each for the same value of y but different values of A, plotted in this way. The current ratios were measured with an accuracy of 1% or better, the value of $1 - y$ being known to 0.1%, and A to better than 1%. Similar sets of data to that presented in Fig. 2 were obtained for five different values of y. The pertinent results obtained from these sets are presented in Section 4 of this paper along with the discussion of the results. All of the data pertain to 25 °C.

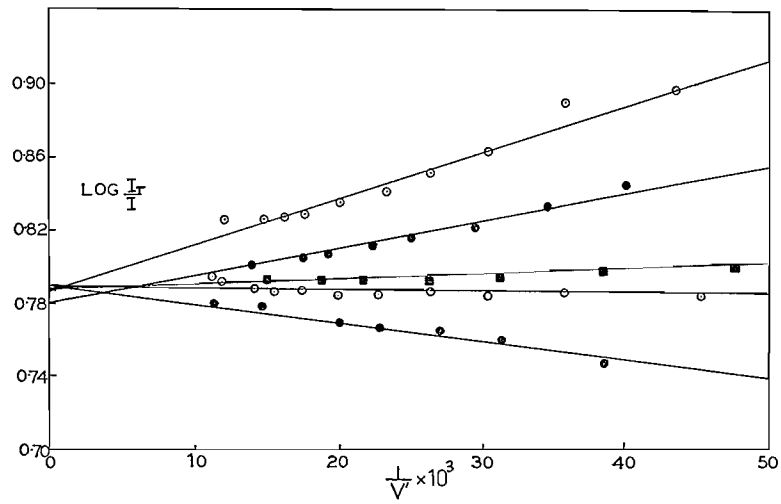

FIG. 2. Typical experimental data: dependence of log I_r/I on V' (in volts) for $y = 0.9524$ and various values of A.

3. THEORY OF METHOD

In analyzing the data obtained using the circuit illustrated in Fig. 1, we shall assume that all of the films on which measurements were performed were sufficiently thick so that there exists in the film a region which is essentially devoid of space charge. An essentially space charge free region will exist in a sufficiently thick film provided that both positively and negatively charged defects are present in the film, or alternatively for any thickness provided that the charged defect concentration is very low. Experimentally, the existence of a space charge free region is demonstrated by the lack of dependence of the differential field strength, dV/dX, on the film thickness, X, for films thicker than about 100 Å on Ta, Nb, and Al (2, 3). Since for Al the differential field strength does vary with film thickness below about 100 Å (3), the first alternative appears to be the correct one at least for this system, although such need not be assumed for the following argument.

We may now write

$$V = E_\infty X + \psi, \tag{3.1}$$

where V is the potential of the anode with respect to a reference electrode, X is the thickness of the oxide film, E_∞ is the field in the space charge free region of the film, and

$$\psi = \int_0^x (E_x - E_\infty)\, dx + \psi',$$

where ψ' is the sum of the electrostatic potential differences across the metal–oxide interface, the oxide–solution interface, and the solution – reference electrode interface. Since we are interested only in variations in ψ, the fact that it is indeterminate will not concern us. Accepting the condition that a space charge free region exists in the film, under steady-state oxide formation conditions ψ will be independent of X, the total film thickness. In general, however, it will be a function of electrolyte composition, temperature, and current density.

Assuming 100% current efficiency for film formation, the film thickness, X, is related

to the ion current density in the space charge free region of the film, I_∞, and the thickness at time t_1, X_1, by the equation:

$$X = X_1 + f\int_{t_1}^{t} I_\infty \, dt, \qquad [3.2]$$

where $f = W_e/\rho F$, W_e and ρ are the electrochemical equivalent weight and density of the oxide, and F is Faraday's constant. The external, observed current density, I, is made up of two terms, I_∞ and the current associated with the alteration of the space charge density in the oxide and of surface charge densities.

In rationalized units, the relevant Maxwell equation and the equation of continuity lead to the following equation for the one dimensional case:

$$(\partial^2 E_x/\partial t \partial x) = (-1/K\epsilon_0)\partial I_x/\partial x,$$

where K is the dielectric constant of the oxide and ϵ_0 is the permittivity of free space. Integration within the oxide from the metal–oxide interface to the space charge free region in the film, assuming K constant, gives:

$$\partial E_\infty/\partial t - \partial E_0/\partial t = (-1/K\epsilon_0)(I_\infty - I_0),$$

where E_0 and I_0 are the field strength and current density in the oxide at the metal–oxide interface. However, from Gauss's theorem, $E_0 = \sigma'/\epsilon_0 K$, and hence $\partial E_0/\partial t = (1/\epsilon_0 K)\partial\sigma'/\partial t$, where σ' is the surface charge density on the metal, so that we may write:

$$\partial E_\infty/\partial t = (1/K\epsilon_0)(I - I_\infty), \qquad [3.3]$$

where I, which equals $I_0 + \partial\sigma'/\partial t$, is the current in the metal per unit electrode area. From eqs. [3.1] to [3.3] we may now write:

$$V = E_\infty\left[X_1 + f\int_{t_1}^{t} I \, dt - fK\epsilon_0\Delta E_\infty\right] + \psi, \qquad [3.4]$$

where $\Delta E_\infty = E_\infty(t) - E_\infty(t_1)$, the change in E_∞ from time t_1 to time t. For Al_2O_3, $f \simeq 5 \times 10^{-5}$ cm^3/C, $K \simeq 10$, and $E_\infty \simeq 8 \times 10^6$ V/cm, so that for a change in field, ΔE_∞, as large as 20% of E_∞, $fK\epsilon_0\Delta E \simeq 0.0035$ Å, which may be neglected compared with X_1.

From eq. [3.4] we have that $dV/dt = fE_\infty I$ for I and hence E_∞ held constant. The circuit eqs. [2.1] and [2.2] can therefore be written:

$$dV/dt = Y = fE_r I_r \qquad \text{for } t \leqslant t_0 \qquad [3.5]$$

$$(V + A) = y(V_0 + A) + yfE_r\int_{t_0}^{t} I \, dt \text{ for } t > t_0. \qquad [3.6]$$

Applying eq. [3.4] to the conditions prevailing at time t_0 and $t > t_0$ respectively, we obtain (neglecting the charging term, $fK\epsilon_0\Delta E_\infty$)

$$V_0 = E_r X_0 + \psi_r \qquad [3.7]$$

$$V = E_\infty\left[X_0 + f\int_{t_0}^{t} I \, dt\right] + \psi, \qquad [3.8]$$

where ψ_r is the value of ψ for $E = E_r$, and X_0 is the value of X at $t = t_0$. Eliminating V_0 and X_0 from eqs. [3.6] to [3.8] we obtain:

$$(E_r - E_\infty)/E_r = (1 - y) + [(\psi_r + A)(1 - y) - (\psi_r - \psi)]/(V' - \psi_r), \qquad [3.9]$$

where $V' = (V + A)/y - A$. That this definition of V' is equivalent to that given in Section 2 (i.e. $V' = -V(1) - A$) follows from eqs. [2.4], [2.6], and [2.12]. Accepting the conduction equation, eq. [1.1], as applying to the space charge free region of the film, we may write:

$$[3.10] \qquad (E_r - E_\infty)/E_r = 2.303kT(\mu^* E_r)[1 - (\mu^*/C\phi)(E_r + E_\infty)]^{-1} \log (I_r/I).$$

Elimination of E_∞ from eqs. [3.9] and [3.10] leads to the desired equation:

$$[3.11] \qquad \log (I_r/I) = W[1 + Z/(V' - \psi_r)] + S/(V' - \psi_r)^2,$$

where

$$[3.12] \qquad W = (\mu^* E_r/2.303kT)[1 - (\mu^* E_r/C\phi)(1 + y)]\,(1 - y),$$

$$[3.13] \qquad Z = \left[\psi_r + A - \frac{\psi_r - \psi}{1 - y}\right]\left[\frac{1 - 2y\mu^* E_r/C\phi}{1 - (1 + y)\mu^* E_r/C\phi}\right],$$

and

$$S = \left(\frac{\mu^* E_r}{2.303kT}\right)\cdot\left(\frac{\mu^* E_r}{C\phi}\right)[(\psi_r + A)(1 - y) - (\psi_r - \psi)]^2.$$

For $V' \gg \psi, \psi_r$, and $A(1 - y)$, a condition readily satisfied, eq. [3.11] reduces to

$$[3.14] \qquad \log (I_r/I) \simeq W(1 + Z/V'),$$

where terms of the order of $(\psi/V')^2$ or smaller have been neglected compared with unity. A plot of $\log (I_r/I)$ versus $1/V'$ for fixed y and A should therefore be linear, yielding values of W and Z. Again, $W/(1 - y)$ should be linear in y, yielding values of $\mu^* E_r/2.303kT$ and $\mu^* E_r/C\phi$.

Finally, for fixed y, A should vary linearly with Z with a slope close to unity (since $2y \simeq 1 + y$) and have an intercept $A_0 = (\psi_r - \psi)/(1 - y) - \psi_r$, which will in turn be a function of y if ψ is a function of field strength.

4. DISCUSSION OF RESULTS

In Fig. 2, the data for a series of runs for fixed y and varying A have been plotted according to eq. [3.14]. As predicted, the data for a given run fall on a straight line with the intercepts, W, for the different runs the same within experimental error (since W is not a function of A). Two runs whose points gave poor linear plots were rejected. The cause of this anomalous behavior is not known, but is likely due to a faulty film, giving localized oxygen evolution. This effect was observed directly in a few runs.

From similar sets of runs, as shown in Fig. 2, mean values of W as a function of y were obtained and have been plotted in Fig. 3 according to eq. [3.12]. The lines through the points are equal in length to 4 times the standard deviation of the mean for each set of W values, representing therefore 95% confidence limits. The abscissa, $W/(1 - y)$, is proportional to the reciprocal Tafel slope, being in fact $E_r[\log (I_r/I)/(E_r - E_\infty)]$, with the ordinate, y, equal to E_∞/E_r. This follows from eq. [3.9] where it can be seen that as $V' \to \infty$, $E_\infty/E_r \to y$. Figure 3 represents, therefore, the variation of Tafel slope with field strength. It is worth noting that the direction of change of the Tafel slope is opposite to that which would occur if the effect arose from a decrease in current efficiency with decreasing current density. It is also a much larger variation than could be attributed to possible variation of current efficiency (4). The total range of field strength over which these measurements could be made was limited at the low end by the electronic equipment and at the high end by heating effects which occur at high current densities.

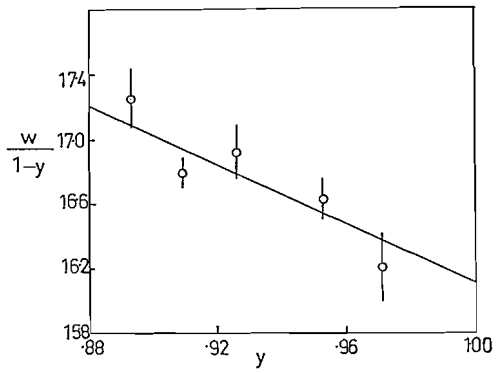

FIG. 3. Results plotted according to eq. [3.12], illustrating the variation of Tafel slope (related to $W/[1 - y]$) with field strength (related to y).

From the slope and intercept of Fig. 3, the following values were calculated:

$$E_r\mu^* = 2.04 \text{ eV}, \qquad \sigma = 14\%$$

$$C\phi = 7.65 \text{ eV}, \qquad \sigma = 3\%.$$

To obtain a value for μ^*, E_r must be known. By interpolation from the data of Bernard and Cook (4) the field in the oxide corresponding to a rate of voltage rise for formation of 0.1000 V/s (i.e. E_r) was calculated. Four values of E_r were obtained corresponding to the four different methods used by Bernard and Cook to determine the film thickness. These methods were measurements of total charge passed, weight of stripped oxide, anode weight gain, and optical interference. The values of E_r were, respectively, 0.086_6, 0.085_8, 0.085_4, and 0.083_7 V/Å. Weighting the final value 1/2, because of the lower precision of this measurement, we obtain $E_r = 0.085_6$ V/Å with a standard deviation of 1.3%. The corresponding current density was determined to be $I_r = 2.09_5 \times 10^{-4}$ A/cm² with a standard deviation of 0.7%. The actual uncertainty in E_r and I_r is probably around 5% because of interfacial potential effects and electrode surface roughness. Using these values in conjunction with the present values of $E_r\mu^*$ and $C\phi$ and eq. [1.1], we obtain:

$$\mu^* = 23.8\ e\text{Å}, \ C\phi = 7.65 \text{ eV}, \ i_0 \exp[-\phi/kT] = 10^{-29.0} \text{ A/cm}^2.$$

Numbers differing slightly from these have been reported earlier (1), as previously mentioned. The significance of these results is discussed in the earlier paper and will not be repeated here.

To test the validity of eq. [3.13], and also to obtain values of $A_0 = (\psi_r - \psi)/(1 - y) - \psi_r$, A has been plotted against Z for the various sets of runs (see Fig. 4), and the best straight line with unit slope has been drawn through each set. (The theoretical slope differs from unity by at most 4.5%.) Although there is considerable scatter, the results confirm eq. [3.13] well within experimental error.

The values of A_0 obtained from Fig. 4 have been plotted against $1/(1 - y)$ in Fig. 5, the lines through the points representing 95% confidence limits. Within experimental error, the points lie on a straight line with a non-zero slope. Actually the relation cannot be rigorously linear since it may be shown that the linearity condition, $dA_0/d(1 - y)^{-1} = \text{constant}$, can only be satisfied for A_0 independent of y. It might be hoped that considerable information concerning the variation of ψ with current density (or field strength) could be extracted from the results of Fig. 5. Unfortunately, this is not the case. One can

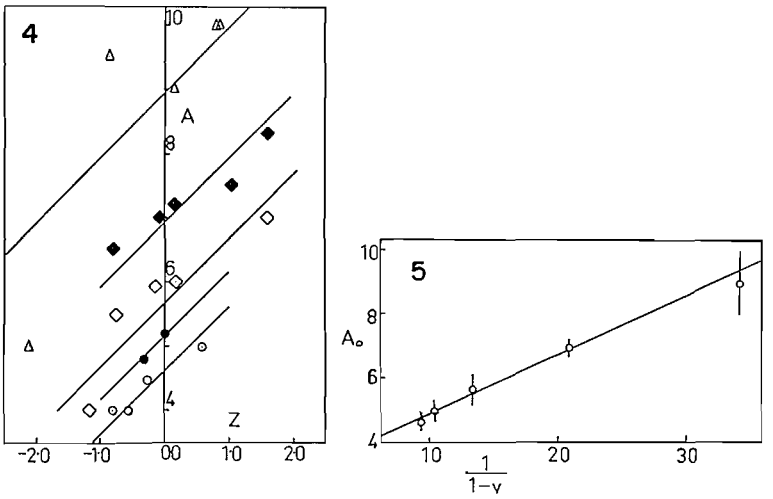

FIG. 4. Results plotted according to eq. [3.13] for various values of y (from top to bottom y = 0.9709, 0.9524, 0.9259, 0.9091, and 0.8929 respectively). The lines represent least square regression lines of unit slope (A and Z in volts).
FIG. 5. Variation of A_0 (volts) with y.

say, however, that ψ does not vary according to a Tafel equation, i.e. $\psi \neq a + b \log I$, since if this were so, A_0 would be independent of y to a very good approximation. This follows from the fact that $\psi_r - \psi$ would then be given by $b \log I_r/I$, which in turn is very nearly proportional to $1 - y$, the deviation from proportionality arising from the field dependence of the Tafel slope for ionic conduction. Provided that ψ contains a component which changes sufficiently rapidly with I (i.e. more rapidly than $\log I_r/I$) then an approximately linear relation between A_0 and $1/(1 - y)$ is predicted in accord with the results. For example, we might assume ψ to be made up of a constant term, Tafel terms, and resistive terms. Accordingly,

$$\psi = a + b \log I + dI, \qquad [3.15]$$

where a, b, and d are constants.

Substituting for ψ and ψ_r in the equation for A_0, we obtain:

$$A_0 = d(I_r - I)/(1 - y) + \text{constant} \qquad [3.16]$$

and since for all the experimental points, $I_r \gg I$, we predict a linear relation between A_0 and $1/(1 - y)$. Clearly, however, eq. [3.15] is not unique in giving rise to this prediction. More extensive data would be required in order to gain further information concerning the current dependence of the interfacial potentials.

ACKNOWLEDGMENTS

The authors are grateful to the National Research Council of Canada for supporting this research.

REFERENCES

1. M. J. DIGNAM. Can. J. Chem. **42**, 1155 (1964).
2. L. YOUNG. Anodic oxide films. Academic Press, London. 1961. pp. 26–31.
3. M. J. DIGNAM and P. J. RYAN. Can. J. Chem. **41**, 3108 (1963).
4. W. J. BERNARD and J. W. COOK. J. Electrochem. Soc. **106**, 643 (1959).
5. P. A. JACQUET. Met. Rev. **1**, 157 (1956).

APPENDIX

i_0, ϕ, μ^*, C = Constants in ionic conduction eq. [1.1], units: A/cm², eV, eÅ, and dimensionless, respectively.

I = Anodic current density (A/cm²).

E = Field strength (V/Å).

I_r, E_r = Current density (c.d.) and field strength (f.s.) respectively, in space charge free region of film corresponding to a rate of change of anodic overpotential of 0.1 V/s at 25 °C.

I_∞, E_∞ = c.d. and f.s. in space charge free regions of film.

I_x, E_x = c.d. and f.s. at distance x from metal–oxide interface.

I_0, E_0 = c.d. and f.s. in oxide at metal–oxide interface.

V = Anode potential with respect to reference electrode.

$V(\mathrm{i})$ = Potential at output of amplifier i with respect to ground.

V_{ref} = Potential of reference electrode with respect to ground.

$V(\mathrm{P})$ = Potential at wiper arm of potentiometer (point P in Fig. 1).

e_1, A = Potentials with respect to ground (see Fig. 1).

Y = Linear voltage rise of e_1 per 100 V/s.

$V' = -\mathrm{V}(1) - A$.

ψ' = Sum of electrostatic potential differences across metal–oxide, oxide–solution, and solution – reference electrode interfaces.

$$\psi = \int_0^X (\mathrm{E}_x - E_\infty)\, \mathrm{d}x + \psi'.$$

ψ_r = Value of ψ when $E_\infty = E_r$.

X = Thickness of oxide film.

t_0 = Time of switching from circuit 1 to circuit 2 (see Fig. 1).

R_y = Resistance (see Fig. 1).

$y = 1/(1 + R_y)$; R_y in megohms (see Fig. 1).

$f = W_e/\rho F$, where W_e = electrochemical equivalent weight of the oxide, ρ = density of the oxide, and F = Faraday's constant.

K = Dielectric constant of oxide.

ϵ_0 = Permittivity of free space.

σ' = Surface charge density on metal at metal–oxide interface.

Can. J. Chem. Downloaded from www.nrcresearchpress.com by 210.87.254.40 on 09/05/12
For personal use only.

CHARGE TRANSFER IN THE RADIOLYSIS OF DILUTE SOLUTIONS OF HYDROCARBONS IN KRYPTON MATRICES AT 77 °K[1]

J. A. STONE

Research Chemistry Branch, Chalk River Nuclear Laboratories, Atomic Energy of Canada Limited, Chalk River, Ontario

Received November 20, 1964

ABSTRACT

The radiolysis of dilute solutions (0.3 to 10 electron %) of saturated hydrocarbons in krypton matrices at 77 °K results in the production of much more hydrogen than that obtained in the absence of krypton. This enhanced hydrogen yield is independent of hydrocarbon concentration over the range studied. The cyclohexane–krypton system was studied in detail. The energy transferred from the krypton to the cyclohexane results in a large first-order yield of hydrogen with a corresponding large yield of cyclohexene. Cyclohexane-d_{12} irradiated at the same concentration in a krypton matrix has the same product yields. However, when mixtures of cyclohexane and cyclohexane-d_{12} are irradiated in a krypton matrix the hydrogen evolved has a high H_2 content which must be the result of an isotope effect in the energy transfer process. This isotope effect and the enhancement of product yields is consistent with a charge transfer mechanism.

INTRODUCTION

The chemical effects of energy transfer in the radiolysis of mixtures of hydrocarbons have been observed in both the liquid and solid phases (1, 2). In these experiments, the isotopic composition and deuterium atom content of the hydrogen evolved in the radiolysis of dilute solutions of a deuterated hydrocarbon (usually cyclohexane-d_{12}) in saturated hydrocarbons were measured. The method is limited to isotopically substituted molecules. When products other than hydrogen are examined complications arise due to secondary reactions, e.g. a change in identity of the initially formed radicals by hydrogen atom abstraction from the solvent (3). The use of a noble gas as the solvent was considered to be attractive since stable products can arise only from the solute. Energy transfer will therefore show up as a difference in the overall decomposition of the hydrocarbon solute from that which would be expected for the same amount of hydrocarbon in the absence of the noble gas.

Homogeneous mixtures of hydrocarbon and krypton were irradiated in the solid state since difficulties due to limited solubility could then be avoided. Krypton was chosen in the first series of experiments because of its ready availability and the fact that it is a solid at liquid nitrogen temperatures. The first ionization potential is 13.999 eV, well above that of any hydrocarbon molecule and the metastable level is 9.915 eV (4). By studying hydrocarbons with ionization potentials either above or below 9.9 eV a clear distinction can therefore be made between excitation transfer due to induced ionization by metastable atoms (Penning Effect) and other forms of transfer.

We have found that the amount of radiolytic decomposition observed when a saturated hydrocarbon is dispersed in a krypton matrix is far greater than that for the pure hydrocarbon alone.

EXPERIMENTAL PROCEDURE

Materials

The krypton (Matheson Research Grade) was distilled several times from trap to trap. Mass spectrometric analysis showed that some xenon ($\sim 0.02\%$) was present but oxygen was absent ($< 0.001\%$).

[1]*Issued as A.E.C.L. No. 2161.*

Cyclohexane-d_{12} and butane-d_{10} (Merck) were used as received. Cyclohexane was Fisher Spectro Grade and contained no cyclohexene. All other hydrocarbons were Philips' Research Grade and were used without further purification.

Sample Preparation and Irradiation

The krypton and appropriate hydrocarbon were degassed separately, mixed in the gas phase, and then condensed at 77 °K to give a homogeneous solid sample. Hoke valves with Teflon seats were used throughout the vacuum line to eliminate the use of greased stopcocks. Since the liquid hydrocarbon samples required were so small (0.005 to 0.100 ml in each experiment) a special degassing technique was used. A clean, dry micropipette containing the required volume of liquid hydrocarbon was placed in a narrow tube, closed at one end, which was attached to the vacuum line using a Teflon O-ring seal. The lower part of the tube was immersed in liquid nitrogen while the upper part was heated. After all the hydrocarbon was frozen in the bottom of the tube, degassing was by the usual freeze-pump-thaw technique. Gas–liquid chromatographic analysis after sample irradiation showed that this degassing technique led to no loss of sample. For isotopic experiments with mixtures of cyclohexane and cyclohexane-d_{12} the two liquids were degassed separately. Butane and butane-d_{10} were measured out separately in the gas phase before degassing.

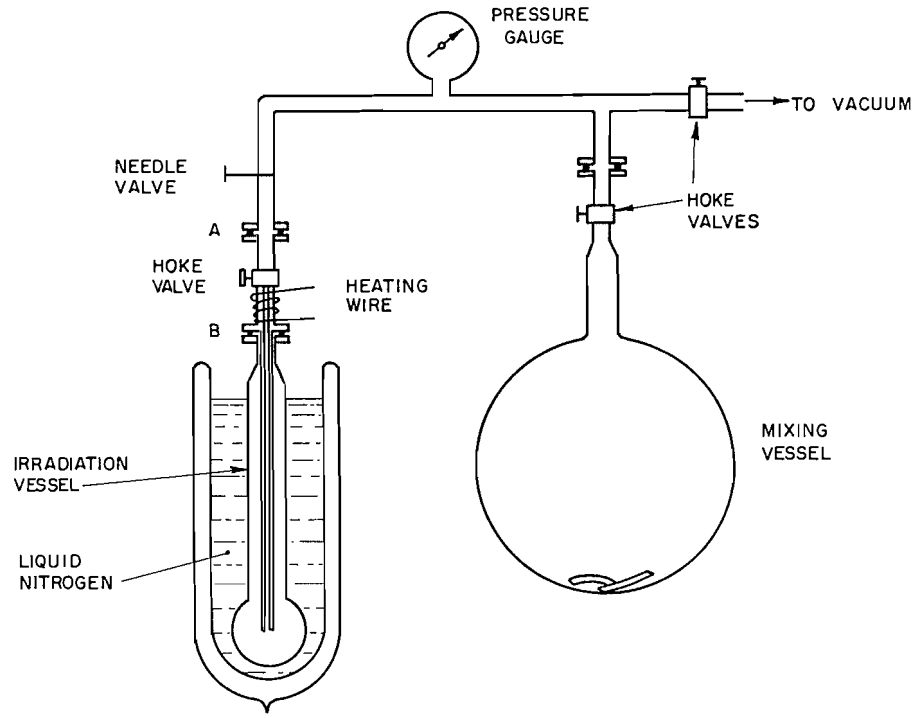

FIG. 1. Apparatus for preparing homogeneous mixtures of hydrocarbons and krypton in the solid phase at 77 °K.

A liter bulb containing a few, small Teflon chips was evacuated and flamed out. The degassed hydrocarbon was passed into the vessel and frozen in the bottom together with a measured volume of krypton (typically from 300 to 500 ml at N.T.P.). The flask was warmed to room temperature and shaken to ensure thorough mixing of hydrocarbon and noble gas. The gaseous mixture was then leaked slowly through a needle valve and condensed in the bottom of the irradiation vessel at 77 °K as shown in Fig. 1. The irradiation vessel was a tube with a bulb of $\sim$ 30 ml capacity blown at the lower end. To the upper end was attached, by means of an Edwards vacuum union, B, a Hoke valve with an extended brass tube. This tube was electrically heated during sample deposition to prevent hydrocarbon condensing in it. The pressure in the mixing flask was read with an all metal, aneroid pressure gauge and the needle valve was adjusted to ensure a constant sample flow of $\sim$ 6 ml/min. With this flow rate reasonably reproducible results could be obtained while the time for sample deposition was not excessively long. At higher flow rates lower product yields were obtained probably due to local melting and hence segregation of the sample during deposition. When all the sample had been condensed the valve was sealed and the vacuum was broken at A. The sample was irradiated at 77 °K

Can. J. Chem. Downloaded from www.nrcresearchpress.com by 210.87.254.40 on 09/05/12
For personal use only.

in a Co-60 γ source at a dose rate of 2.33×10^{22} eV/l h in cyclohexane as determined by Fricke dosimetry. All samples, unless otherwise stated, were irradiated to a total dose of 4.66×10^{22} eV/l. Energy absorption in the krypton was found by interpolation from the tables of Grodstein (5).

Analysis

After irradiation only $\sim 1\%$ of the hydrogen produced was in the gas phase, the remainder being trapped in the matrix. The sample was melted to release the hydrogen and was frozen again at 77 °K. An evacuated 250 ml bulb was attached to the sample tube at union A and the hydrogen, together with krypton at its vapor pressure at 77 °K, was equilibrated through the two vessels. The gas in the bulb was then analyzed mass spectrometrically for H_2 and ^{86}Kr, it being assumed that the amount of ^{86}Kr present in the gas phase did not vary from experiment to experiment. The method was calibrated by irradiating a known amount of cyclohexane (which yielded a known amount of hydrogen) then adding some krypton gas and repeating the above procedure. The reproducibility of this calibration procedure was better than 3%. The relative amounts of H_2, HD, and D_2 in experiments with deuterated hydrocarbons were also measured mass spectrometrically.

Samples for liquid product analysis were obtained by cooling the sample tube to 193 °K, releasing the krypton, and diluting the small amount of hydrocarbon left at the bottom of the sample vessel with 0.5 ml of a suitable solvent. The determination of cyclohexene and bicyclohexyl by gas–liquid chromatography has been described previously (3).

RESULTS

(1) Irradiation of Pure Cyclohexane in the Solid Phase at 77 °K

The yields of the major products in the radiolysis of solid cyclohexane were determined using large samples (5 ml) irradiated at the same dose rate as in all the other experiments. These yields, which were independent of dose over the range $1.1–2.8 \times 10^{22}$ eV/l, were $G(H_2) = 4.65$, G(cyclohexene) = 2.35, and G(bicyclohexyl) = 1.55.

The isotopic composition of the hydrogen evolved from two mixtures of cyclohexane and cyclohexane-d_{12} in the solid phase and one in the liquid phase was measured. These results are shown in Table I. Comparative figures for mixtures with 5.6 electron % total hydrocarbon concentration in krypton matrices are also included.

TABLE I

The isotopic composition of the hydrogen evolved from mixtures of cyclohexane and cyclohexane-d_{12} irradiated under various conditions

Phase	Mole % C_6D_{12}	% H_2	% HD	% D_2
Solid (77 °K)	50	54.5	32.3	13.2
Krypton matrix (77 °K)	50	66.0	17.0	17.0
Solid (77 °K)	75	28.7	38.2	33.1
Krypton matrix	75	42.0	24.0	34.0
Liquid (293 °K)	75	27.8	42.4	29.8

(2) Irradiation of Hydrocarbons in Krypton Matrices at 77 °K

All G values quoted in this paper have been calculated using the total energy absorbed in the samples.

(a) Hydrogen Yields

A blank run showed that no hydrogen was formed ($G < 0.02$) when pure krypton was irradiated in the absence of any hydrocarbon. If water was present as an impurity some hydrogen was produced. The mixing vessel and irradiation vessel were therefore always thoroughly flamed out between runs.

At 5.6 electron % cyclohexane in krypton $G(H_2)$ was, within experimental error, constant with dose up to at least 6×10^{22} eV/l. $G(H_2)$ had an almost constant value of ~ 2.4 for dilute solutions (0.3 to 12 electron %) of cyclohexane in krypton. Over a smaller hydrocarbon concentration range $G(H_2)$ for n-hexane was ~ 1.8 and for methylcyclohexane was ~ 1.3. These results are shown in Fig. 2. $G(D_2)$ values from cyclohexane-d_{12}

Can. J. Chem. Downloaded from www.nrcresearchpress.com by 210.87.254.40 on 09/05/12
For personal use only.

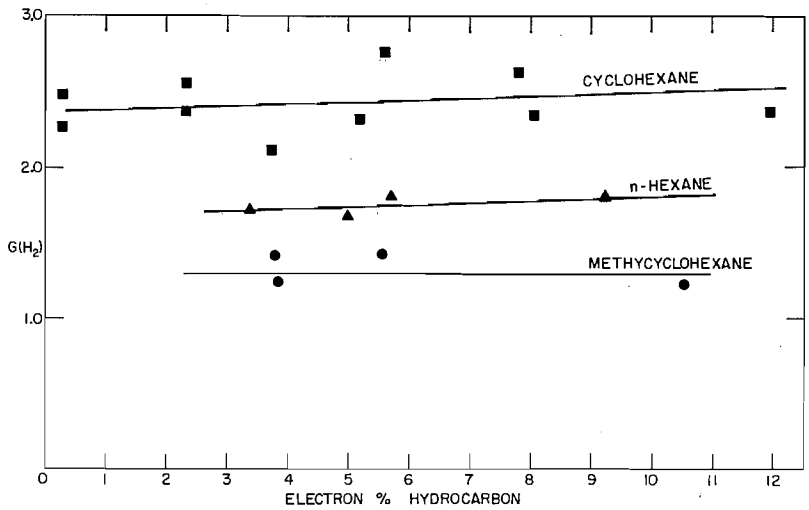

FIG. 2. Hydrogen production from cyclohexane, *n*-hexane, and methylcyclohexane irradiated in krypton matrices at 77 °K.

at concentrations from 3 to 8 electron % in krypton were as scattered as those for $G(H_2)$ from cyclohexane. $G(D_2)$ was independent of hydrocarbon concentration and had an average experimental value of 2.1. $G(H_2)$ from 4.8 electron % butane in krypton was determined in a single experiment to be 1.8.

(b) Isotopic Experiments

Mixtures of cyclohexane and cyclohexane-d_{12} at a constant hydrocarbon concentration of 5.6 electron % in krypton were irradiated. The isotopic composition of the hydrogen evolved is shown in Fig. 3 for the full range of hydrocarbon mixtures. Figure 2 shows that the reproducibility of $G(H_2)$ from cyclohexane–krypton mixtures is poor but since in Fig. 3 only % composition is given these variations in total yield have been ignored. It was found, however, that although the total hydrogen yield was not very reproducible the relative yields of H_2, HD, and D_2 in these mixed samples could be reproduced to better than 5%. It is to be noted that even from 99% isotopically pure cyclohexane-d_{12} irradiated in a krypton matrix 4.4% HD and 1.9% H_2 were produced.

Similar isotopic experiments were performed with mixtures of butane and butane-d_{10} in krypton at a constant hydrocarbon concentration of 4.8 electron %. These results are presented in Table II with results for cyclohexane taken from the smoothed curves of Fig. 3 for comparison.

TABLE II

The isotopic composition of hydrogen evolved from mixtures of butane and butane-d_{10} compared with that from mixtures of cyclohexane and cyclohexane-d_{12} all irradiated in krypton matrices

Mole % deuterated species	Butane			Cyclohexane		
	% H_2	% HD	% D_2	% H_2	% HD	% D_2
86.6	29.3	24.3	46.3	26.0	22.3	51.2
49.6	70.4	15.0	14.6	68.0	16.4	15.6
29.2	82.2	11.3	6.5	84.0	10.2	6.8

Can. J. Chem. Downloaded from www.nrcresearchpress.com by 210.87.254.40 on 09/05/12
For personal use only.

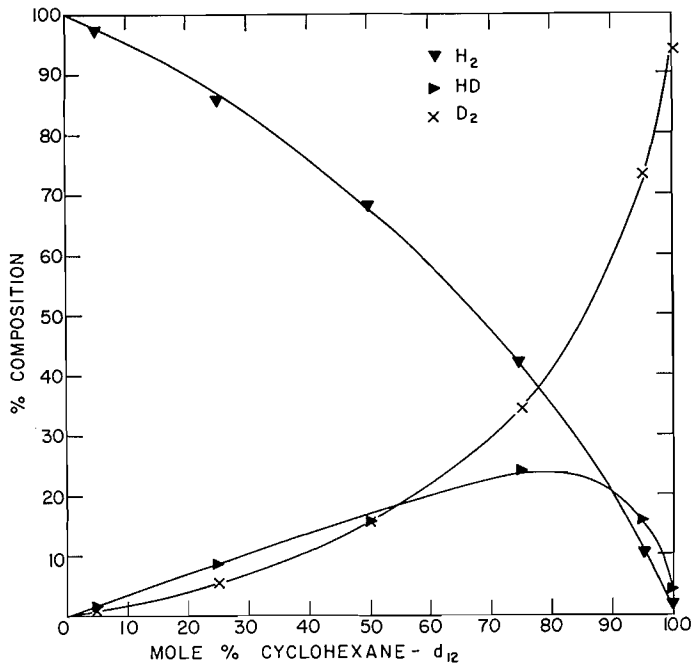

FIG. 3. The isotopic composition of the hydrogen evolved from mixtures of cyclohexane and cyclohexane-d_{12} irradiated in krypton matrices at 77 °K.

(c) Effect of Solutes

The effects of the solutes carbon tetrachloride and benzene on the yields of hydrogen, cyclohexene, and bicyclohexyl from 5.6 electron % cyclohexane in krypton were determined. The results are shown in Table III.

TABLE III

The effect of solutes on the yields of products from cyclohexane irradiated in a krypton matrix

Additive	$G(H_2)$	G(cyclohexene)	G(bicyclohexyl)
0	2.4	1.7	0.29
0.37 electron % CCl_4	0.9	0.6	0.055
0.30 electron % C_6H_6	1.6	1.10	0.070

G(cyclohexene-d_{10}) and G(bicyclohexyl-d_{22}) from 5.6 electron % cyclohexane-d_{12} in krypton mixtures were 1.56 and 0.36, respectively.

A mixture of 2.6 electron % cyclohexane, 2.6 electron % cyclohexane-d_{12}, and 0.37 electron % carbon tetrachloride irradiated in a krypton matrix yielded 68.6% H_2, 13.8% HD, and 17.5% D_2.

DISCUSSION

Energy transfer experiments of the chemical type described here can detect only that part of the energy absorbed from the incident radiation which is (*a*) transferable and (*b*) can then lead to chemical change. Since, presumably, energy can be transferred from the donor to the acceptor molecules only by certain specific paths not all the energy which

Can. J. Chem. Downloaded from www.nrcresearchpress.com by 210.87.254.40 on 09/05/12
For personal use only.

causes chemical decomposition in the donor (in the case of hydrocarbons) is available for transfer. Also, in the radiolysis of hydrocarbons, some of the energy is dissipated without leading to chemical decomposition. It will therefore be impossible to say absolutely how much of the energy, which is initially absorbed in the inert gas, causes decomposition in the hydrocarbon solute. The relative amounts of energy transferred in different systems may, however, be determined by comparing the observed product yields with those expected for the same amount of hydrocarbon in the absence of krypton.

The major portion of this work has been a study of the enhancement of product yields when dilute solutions of cyclohexane and cyclohexane-d_{12} are irradiated in krypton matrices at 77 °K. The main features of the energy transfer process will be established from four experimental observations: 1, the invariance of the chemical yields with hydrocarbon concentrations, 2, the nature of the hydrocarbon decomposition as shown by experiments with mixtures of light and deuterated hydrocarbons, 3, the effect of solutes on the product yields, and 4, the isotope effect in the energy transfer process. Finally, we will show that these experimental results are compatible with a charge transfer mechanism.

(1) Energy Transfer as a Function of Hydrocarbon Concentration

$G(H_2)$ from solid cyclohexane at 77 °K is 4.65. In a hydrocarbon–noble gas mixture if no energy transfer occurs $G(H_2)$ will be a linear function of the electron fraction of hydrocarbon, e.g. at 5 electron % the value will be 0.23 whereas the experimental value is 2.4. Figure 2 shows that energy transfer does occur in hydrocarbon–krypton matrices and is (*a*) considerable, (*b*) almost independent of hydrocarbon concentration over a 40-fold range, and (*c*) results in different hydrogen yields from different hydrocarbons.

As shown above $G(H_2)$ from 5 electron % cyclohexane in a krypton matrix is 10 times greater than expected in the absence of energy transfer. As the cyclohexane concentration decreases, the ratio of the actual hydrogen yield to the expected yield increases rapidly. The constancy of the hydrogen yield with hydrocarbon concentration leads us to conclude that over the range studied all available energy is transferred. At 12 electron % hydrocarbon there are 10 krypton atoms for each hydrocarbon molecule. Assuming a close-packed structure each krypton atom is adjacent to at least one hydrocarbon molecule. At the lowest concentration used (0.3 electron %) there are $\sim$ 400 krypton atoms for every cyclohexane molecule. Each krypton atom, although it may not be in contact with a hydrocarbon molecule will not be far removed (closer than 20 Å). Dyne and Denhartog (6) have shown that in hydrocarbons the range of energy transfer is $\sim$ 50 Å. In the present case complete transfer, independent of the hydrocarbon concentration over the limited range used, is not unreasonable since the range of transfer does not have to be large.

Figure 2 shows that different hydrocarbons produce different amounts of hydrogen as a result of energy transfer. This may seem surprising since in the liquid phase the $G(H_2)$ values for the pure hydrocarbons do not show such large differences (cyclohexane 5.55, *n*-hexane 5.0, and methylcyclohexane 4.4). However, hydrogen is formed in the radiolysis of hydrocarbons in more than one process (7). The relative efficiencies of energy utilization in these processes may be different for different molecules so that if energy transfer enhances only one mode of hydrogen formation large differences in $G(H_2)$ are possible.

(2) The Nature of the Hydrogen Yield

The isotopic composition of the hydrogen evolved from mixtures of cyclohexane and cyclohexane-d_{12} dispersed uniformly in a krypton matrix is markedly different from that observed in the radiolysis of mixtures of the two hydrocarbons in either the solid or liquid

Can. J. Chem. Downloaded from www.nrcresearchpress.com by 210.87.254.40 on 09/05/12
For personal use only.

phases (see Table I and Fig. 3). In particular the yield of HD is reduced by about a factor of two in the krypton matrix while the D_2 and in particular the H_2 yields are increased. This suggests that much of the hydrogen is formed in a reaction involving the elimination of two hydrogen atoms from the same molecule. This is supported by the fact that the yield of olefin is large, and the yield of bicyclohexyl is small (Table III). In a krypton matrix G(cyclohexene)/G(bicyclohexyl) $\simeq 6$ whereas in the radiolysis of solid or liquid cyclohexane the ratio is ~ 1.5. In summary, these isotopic results show that the transfer of energy from krypton to cyclohexane leads mainly to products (hydrogen and cyclohexene) characteristic of a first-order decomposition of cyclohexane. Energy transfer also leads to smaller concentrations of other products which must be formed in reactions involving the participation of more than one cyclohexane molecule. These products are bicyclohexyl and some of the hydrogen (demonstrated by a yield of HD from mixtures of cyclohexane and cyclohexane-d_{12} in krypton).

The transfer of energy from krypton to a hydrocarbon has also been reported by Bouldin and Gordy (8). Using electron spin resonance techniques they have observed the formation of both deuterium atoms and methyl-d_3 radicals in an irradiated krypton matrix containing methane-d_4. The experiments were performed at 4.2 °K. In agreement with the present work they found that above 0.3 electron % methane-d_4 the amount of energy transferred [in their case measured by G(D atoms)] did not show a great variation with hydrocarbon concentration. At 0.3 electron % CD_4 G(D) was 1 whereas in pure methane-d_4 G(D) was 1.9. In the present work at 0.3 electron % cyclohexane $G(H_2)$ is ~ 2.4 while for pure cyclohexane at 77 °K $G(H_2) = 4.65$. In both cases therefore the irradiated systems at 0.3 electron % hydrocarbon behave as if they were composed of $\sim 50\%$ hydrocarbon. Using electron spin resonance Bouldin and Gordy could only measure decomposition to atoms and radicals. By measuring $G(H_2)$ we believe that we have a more complete picture of the overall decomposition. $G(H_2)$ for the radiolysis of methane in the solid phase is not known and the value of 1.9 for G(D) given by Bouldin and Gordy would imply $G(D_2) < 1$ (since at these low temperatures D atoms can form D_2 only by combination which will be in competition with the recombination of D and CD_3 to yield CD_4 again). We think that this value is too low to represent the total hydrogen yield and that energy transfer must also lead to molecular hydrogen formed by the decomposition of single hydrocarbon molecules.

(3) The Effect of Solutes

$G(H_2)$ from cyclohexane krypton mixtures is decreased by the addition of small quantities of carbon tetrachloride and benzene, the former being the more effective (see Table III). These results have been compared in Table IV with the corresponding reductions in hydrogen yield obtained when the same concentrations of the two solutes are added to liquid cyclohexane (9, 10).

TABLE IV

The effect of solutes on hydrogen yields from cyclohexane in the presence and absence of a krypton matrix

	$\Delta G(H_2)$	
Solute	Liquid cyclohexane	5.6 electron % cyclohexane in krypton
0.37 electron % CCl_4	1.3	1.5
0.30 electron % C_6H_6	0.75	0.80

Can. J. Chem. Downloaded from www.nrcresearchpress.com by 210.87.254.40 on 09/05/12
For personal use only.

Can. J. Chem. Downloaded from www.nrcresearchpress.com by 210.87.254.40 on 09/05/12
For personal use only.

We have suggested earlier in this discussion that energy transfer from krypton to cyclohexane results in hydrogen formation by one method of decomposition which in the liquid phase accounts for only part of the hydrogen yield. From Table IV we see that values of $\Delta G(H_2)$ in the two systems are remarkably alike, i.e. the same small solute concentration depresses $G(H_2)$ by the same amount whether the environment is krypton or cyclohexane (it is to be noted however that the % decrease in $G(H_2)$ is very different in the two cases). This suggests that the same mechanism of inhibition of hydrogen formation occurs in both cases, i.e. that that part of the hydrogen yield which can be most easily inhibited in the liquid phase radiolysis of hydrocarbons is formed by the same mechanism as the whole yield produced by energy transfer in a krypton matrix. We have shown previously that energy transfer which occurs in mixtures of saturated hydrocarbons can be suppressed by the addition of small amounts of carbon tetrachloride (3). This energy transfer process has been interpreted in terms of charge transfer (11) while the action of carbon tetrachloride has been shown to be consistent with an electron capture mechanism (12). We will show later that a combination of charge transfer and electron capture is consistent with the results of radiolyses in krypton matrices.

Table III shows that G(cyclohexene) is reduced to the same extent as $G(H_2)$ by the addition of carbon tetrachloride or benzene but G(bicyclohexyl) is reduced to a much greater extent. Since the cyclohexane molecules are isolated in the matrix, bicyclohexyl must be formed on warming up the sample, i.e. by combination of two cyclohexyl radicals. Szwarc (13) has shown that cyclohexyl radicals are stable in solid cyclohexane at 77 °K and the same should hold for cyclohexyl radicals trapped in a krypton matrix at the same temperature. If solute is present on melting, radical scavenging will occur. In fact cyclohexyl chloride was detected among the products from the matrix containing carbon tetrachloride. Cyclohexene is not reduced in yield to the same extent as bicyclohexyl and therefore much of it must be produced in a reaction not involving the disproportionation of cyclohexyl radicals.*

(4) The Isotope Effect in the Energy Transfer Process

$G(H_2)$ from cyclohexane in krypton is ~ 2.4 while $G(D_2)$ from cyclohexane-d_{12} in krypton is ~ 2.1. The corresponding olefin yields are 1.70 and 1.56. With the assumption made earlier that all available energy is transferred this means that the efficiency of utilizing this energy to produce chemical decomposition is slightly greater for cyclohexane than for cyclohexane-d_{12}. The effect of isotopic substitution is not large. When, however, the two species are dispersed in the same krypton matrix a large isotope effect is observed, e.g. a 50/50 mixture of the two yields hydrogen containing 75 atom % H and 25 atom % D. The hydrogen present as H_2 accounts for 66% of the total. This means that the isotope effect occurs mainly in the energy transfer reaction since a kinetic isotope effect could not yield more than 50% H_2. This means that cyclohexane and cyclohexane-d_{12} are in competition for the available energy, the light hydrocarbon being favored. Exactly the same conclusion applies to the butane/butane-d_{10}/krypton system which yields hydrogen with almost the same isotopic composition as in the cyclohexane experiments (Table II).

(5) The Mechanism of Energy Transfer

The four main experimental conclusions that must be satisfied by any proposed mechanism are: 1, energy transfer over distances up to 20 Å is very efficient; 2, the

**Klots and Johnsen (14) have shown that k(disproportionation)/k(combination) for cyclohexyl radicals in the liquid phase is 1.3 so that for the radiolysis of pure cyclohexane in a krypton matrix only $\sim$ 22% of the cyclohexene yield could be accounted for by radical disproportionation.*

major products of the transfer of energy from krypton to cyclohexane are hydrogen and cyclohexene; 3, small concentrations of carbon tetrachloride or benzene reduce the yields of the products of energy transfer; 4, when mixtures of light and deuterated hydrocarbons are irradiated in a krypton matrix preferential energy transfer to the light hydrocarbon occurs.

Examples of the enhancement of the radiolytic decomposition of hydrocarbons in the gas phase upon addition of noble gases are well known (15, 16, 17). Explanations for this phenomenon in terms of charge transfer and ion molecule reactions have been advanced. It is of interest to see whether such mechanisms are consistent with the results obtained in the present study.

The action of γ-rays is to produce ions, electrons, and excited molecules. The ionization process is non-selective so that in the case of a krypton matrix containing a low concentration of hydrocarbon most of the energy will be deposited in the krypton and initially krypton ions will predominate. Magee (18) has discussed theoretically the mechanism of transfer of a positive charge from an ion to a neutral molecule or atom. He considers that the resonance charge transfer process, e.g.

[1] $$Kr^+ + Kr \rightarrow Kr + Kr^+,$$

involving the same atomic species may have a very large cross section "since the momenta of the heavy pair (ion and molecule) do not have to change as the electron jump occurs and a close collision is thus not necessary." In the case of a lattice where the krypton atoms are in close contact the movement of the electron hole should be facile and hence migration from the initial place of ionization is rapid. Transfer of charge by this mechanism to the proximity of a hydrocarbon molecule should proceed with high efficiency.

Mass spectrometric observation of charge transfer reactions from Kr^+ to methane has been reported by Melton (19) and Field, Head, and Franklin (20). The reactions involved both simple charge transfer and also dissociative charge transfer. The analogous, energetically allowed reactions for Kr^+ and C_6H_{12} are:

[2] $$Kr^+ + C_6H_{12} \rightarrow Kr + C_6H_{12}^+$$

[3] $$\rightarrow Kr + C_6H_{11}^+ + H$$

[4] $$\rightarrow Kr + C_6H_{10}^+ + H_2.$$

Hydrogen is produced directly in reactions [3] and [4] and could be produced from $C_6H_{12}^+$ upon charge neutralization.

[5] $$C_6H_{12}^+ + e \rightarrow C_6H_{12}^* \rightarrow \cdot C_6H_{11} + H$$

[6] $$\searrow C_6H_{10} + H_2.$$

The isotopic experiments showed that much of the energy transfer leads to hydrogen and olefin formed by the decomposition of a single molecule. This suggests that either reactions [4] or [2] and [6] predominate. However, reactions [3] and [5] need not necessarily be ruled out since Klein, Scheer, and Kelley (21) have shown that H atoms can take part in disproportionation reactions with radicals to yield H_2 and an olefin. In the present case for no isotopic mixing this would imply the reaction between an H atom and its geminate radical.

[7] $$H + \cdot C_6H_{11} \rightarrow H_2 + C_6H_{10}.$$

However, the same authors showed that diffusion of hydrogen atoms is very rapid at 77 °K so that in these cyclohexane–krypton experiments much more isotopic mixing of

Can. J. Chem. Downloaded from www.nrcresearchpress.com by 210.87.254.40 on 09/05/12
For personal use only.

the hydrogen isotopes should occur than that experimentally determined. Reactions [4] and [6] are therefore the most probable.

It has been shown that low concentrations of carbon tetrachloride in irradiated organic glasses can capture electrons with high efficiency (22).

$$[8] \qquad e + CCl_4 \rightarrow CCl_4^- \overset{?}{\rightarrow} CCl_3 + Cl^-.$$

The negative ion formed, CCl_4^- (or Cl^-), is very stable and is held rigidly until charge neutralization occurs upon melting. Since carbon tetrachloride reduces the hydrogen yield in the cyclohexane–krypton system much of the hydrogen cannot be formed before charge neutralization, i.e. major contributions from reactions [3] and [4] can be ruled out.

A charge transfer mechanism is therefore consistent with the experimental results that energy transfer is both rapid, practically independent of hydrocarbon concentration over the range studied, and that hydrogen is produced in a large part by a unimolecular decomposition of the hydrocarbon molecule. Assuming $G(Kr^+)$ is ~ 4.0 as in the gas phase (23) then for cyclohexane a $G(H_2)$ value of 2.4 corresponds to an efficiency of utilizing the transferred charge (assumed to be complete) of 60%. For other hydrocarbons, the calculated efficiencies are *n*-hexane 44%, methylcyclohexane 32.5%. These efficiencies are in the same order as the $G(H_2)$ yields in the liquid phase at ambient temperature. Since in the latter case hydrogen is formed by other processes as well, this could mean that the production of hydrogen upon charge neutralization is not 100% efficient and that the efficiency is different for different molecules. Since both cyclohexane and methylcyclohexane have ionization potentials equal to or lower than the metastable level of krypton (9.915 eV) a contribution to the hydrogen yield from the Penning effect might be possible:

$$[9] \qquad Kr^* + C_6H_{12} \rightarrow C_6H_{12}^+ + e + Kr.$$

However, both butane and hexane have ionization potentials above the krypton metastable level so that reactions analogous to [9] are not possible for these compounds. A major contribution of [9] to the observed phenomenon is most improbable.

The outstanding experimental result to be explained by this charge transfer hypothesis is the isotope effect, i.e. the fact that there is no isotope effect on total yields when deuterated and light hydrocarbons are irradiated separately in a krypton matrix but when mixtures of the two are used a large one does appear. Magee (18) has suggested that exothermic reactions of the type

$$[10] \qquad A^+ + B \rightarrow A + B^+$$

occur readily by passage through an excited electronic state $(A + B)^+$ to a lower state, the process being formally equivalent to a quenching process in photochemistry. The charge transfer complex may last for periods of many vibrations before either separating again or passing over to the form $B^+ + A$ with liberation of energy. It is during the lifetime of the collision complex that the possibility of an isotope effect exists. Bellas, Rousseau, Strausz, and Gunning (24) have shown that cyclohexane is much more effective than cyclohexane-d_{12} in competing with nitrous oxide to quench Hg $6(^3P_1)$ atoms. A similar observation was made for butane and butane-d_7. This was explained on the assumption that the transfer reaction proceeds through the formation of a well-defined transition complex involving both hydrocarbon molecule and excited mercury atom (25). For the radiolysis of the single hydrocarbons in a krypton matrix very little difference between $G(D_2)$ and $G(H_2)$ is to be expected since the frequency factor for the transition state will

Can. J. Chem. Downloaded from www.nrcresearchpress.com by 210.87.254.40 on 09/05/12
For personal use only.

not affect the final yield. However, when the light and deuterated hydrocarbons are in competition the higher frequency factor for the light hydrocarbon means that more of these molecules will produce H_2 at the expense of D_2 production from the deuterated hydrocarbon.

ACKNOWLEDGMENTS

The author wishes to thank Dr. P. J. Dyne for many helpful discussions during the preparation of this paper. Dr. R. H. Betts is thanked for his critical comments on the final draft of the paper.

REFERENCES

1. P. J. DYNE and J. DENHARTOG. Can. J. Chem. **40**, 1616 (1962).
2. P. J. DYNE and J. DENHARTOG. Nature, **202**, 1105 (1964).
3. J. A. STONE. Can. J. Chem. **42**, 2872 (1964).
4. A. C. JENKINS and G. A. COOK. *In* Argon, helium and the rare gases. Vol. I. Interscience, New York. 1961. p. 237.
5. G. W. GRODSTEIN. U.S. Natl. Bur. Std. Circular No. 583. 1957.
6. P. J. DYNE and J. DENHARTOG. Unpublished work.
7. L. J. FORRESTAL and W. H. HAMILL. J. Am. Chem. Soc. **83**, 1535 (1961).
8. W. V. BOULDIN and W. GORDY. Phys. Rev. **135**, A806 (1964).
9. J. A. STONE and P. J. DYNE. Can. J. Chem. **42**, 669 (1964).
10. J. A. STONE and P. J. DYNE. Radiation Res. **17**, 353 (1962).
11. T. J. HARDWICK. J. Phys. Chem. **66**, 2132 (1962).
12. J. ROBERTS and W. H. HAMILL. J. Phys. Chem. **67**, 2446 (1963).
13. H. SZWARC. J. Chim. Phys. 1067 (1962).
14. C. E. KLOTS and R. H. JOHNSEN. Can. J. Chem. **41**, 2702 (1963).
15. S. C. LIND. J. Phys. Chem. **56**, 920 (1952).
16. G. G. MEISELS, W. H. HAMILL, and R. R. WILLIAMS, JR. J. Phys. Chem. **61**, 1456 (1957).
17. C. F. SMITH, B. G. GAMAN, and F. W. LAMPE. J. Am. Chem. Soc. **83**, 3559 (1961).
18. J. L. MAGEE. J. Phys. Chem. **56**, 555 (1952).
19. C. E. MELTON. J. Chem. Phys. **33**, 647 (1960).
20. F. H. FIELD, H. N. HEAD, and J. L. FRANKLIN. J. Am. Chem. Soc. **84**, 1118 (1961).
21. R. KLEIN, M. D. SCHEER, and R. KELLEY. J. Phys. Chem. **68**, 598 (1964).
22. J. P. GUARINO, M. R. RONAYNE, and W. H. HAMILL. Radiation Res. **17**, 379 (1962).
23. W. P. JESSE and J. SADAUKIS. Phys. Rev. **107**, 766 (1957).
24. M. G. BELLAS, Y. ROUSSEAU, O. P. STRAUSZ, and H. E. GUNNING. J. Chem. Phys. **41**, 768 (1964).
25. Y. ROUSSEAU, O. P. STRAUSZ, and H. E. GUNNING. J. Chem. Phys. **39**, 962 (1963).

Can. J. Chem. Downloaded from www.nrcresearchpress.com by 210.87.254.40 on 09/05/12
For personal use only.

Can. J. Chem. Downloaded from www.nrcresearchpress.com by 210.87.254.5 on 09/05/12
For personal use only.

INTRAMOLECULAR HYDROGEN TRANSFER IN MERCURY PHOTOSENSITIZATION OF PENTENE-1[1]

D. W. PLACZEK[2] AND B. S. RABINOVITCH
Chemistry Department, University of Washington, Seattle, Washington

Received November 27, 1964

ABSTRACT

Upon photosensitization with Hg 6 ($^3P_1$), pentene-1 undergoes several reactions: the well-known C—C and C—H ruptures and the recently found isomerization consisting of an H-atom transfer and subsequent bond formation. We report two additional products formed by an H-transfer mechanism, 1,2-dimethylcyclopropane and cyclopentane, the former being a major product.

INTRODUCTION

Evidence for the existence of a hydrogen migration mechanism amongst the reactions of mercury photosensitized (Hg 6 ($^3P_1$)) olefin was first given by Callear and Cvetanović (1). They noted that photosensitization of *cis*-ethylene-d_2 yielded the *asymmetric* product as well as the expected *trans* species. A later study (2) of butene-1 again provided strong evidence that this mode of reaction is operative; methylcyclopropane was found to be a major product within an intermediate pressure range. The nature of the H-atom shift, whether 1,2 or 1,4, was, however, not established.[3] Further evidence for 1,2-migrations came from studies by Srinivasan of a trio of compounds: he reported that photosensitized 1,5-hexadiene yielded primarily allylcyclopropane (3), 1,4-pentadiene yielded vinylcyclopropane (4), and one of the products of photosensitized 1,5-cyclooctadiene was bicyclo-[5.1.0]octene-3 (4). A 1,2 migration process in ethylene-d_2 has also been verified in quantitative detail (5).

That possible products of 1,2 H-atom translocations occur to a negligible extent in the propylene (6), isobutene (2), and butene-2 (7) systems and that 1,3 shifts are minimal, if at all extant, in the butene-1 system (2, 8) evoked from Kebarle and Avrahami (7*b*) the suggestion that H-atom transfers are favored in the order 1,4 > 1,3 > 1,2.

To further clarify the situation, Majer, Pinkard, and Robb (9) have just published a restudy (10) of the reactions of photosensitized pentene-1. Possible migration processes and products of electronically excited triplet pentene-1 may be represented as follows:

$$H_3CCH_2CH_2\dot{C}H\dot{C}H_2\dagger \xrightarrow{1,3(1,3)} H_3CCH_2\dot{C}H\dot{C}HCH_3\dagger \rightarrow \textit{cis}\text{- and }\textit{trans}\text{-pentene-2}$$

$$\xrightarrow{1,4(1,4)} H_3C\dot{C}HCH_2\dot{C}HCH_3\dagger \rightarrow \textit{cis}\text{- and }\textit{trans}\text{-dimethylcyclopropane}$$

$$\xrightarrow{1,5(1,5)} H_2\dot{C}CH_2CH_2\dot{C}HCH_3\dagger \rightarrow \text{methylcyclobutane}$$

$$\xrightarrow{1,2(2,3)} H_3CCH_2\dot{C}HCH_2\dot{C}H_2\dagger \rightarrow \text{ethylcyclopropane}$$

$$\xrightarrow{1,3(2,4)} H_3C\dot{C}HCH_2CH_2\dot{C}H_2\dagger \rightarrow \text{methylcyclobutane}$$

$$\xrightarrow{1,4(2,5)} H_2\dot{C}CH_2CH_2CH_2\dot{C}H_2\dagger \rightarrow \text{cyclopentane}$$

[1]*Supported in part by the National Science Foundation.*
[2]*Abstracted from the Ph.D. thesis of D. W. Placzek, 1965.*
[3]*The 1,2 and 1,4 shift correspond, respectively, to the reverse processes for methylcyclopropane isomerization by H-atom migration within the ring or by H-atom migration from the methyl to the ring; see D. W. Setser and B. S. Rabinovitch. Can. J. Chem. 40, 1425 (1962).*

Here the first number pair refers to the nature of the shift and the second pair in parentheses refers to the particular carbon atoms involved. Majer *et al.* looked especially for ethyl cyclopropane and methyl cyclobutane, the products of 1,2(2,3) and 1,5(1,5) translocations; a 1,3(2,4) shift also gives rise to methylcyclobutane, but this mechanism was excluded by these authors. The 1,2(2,3) process is the analogue of the 1,2(2,3) shift in butene-1, but the mechanism most closely related to 1,4(1,4) migration in butene-1 is here the 1,4(1,4) process which would give rise to dimethylcyclopropane. Ethylcyclopropane was not found by Majer *et al.*, and dimethylcyclopropane was not reported; however, methylcyclobutane was a major product. The complete absence of ethylcyclopropane does indeed verify that, in this case, a 1,2 migration is not a preferred path. Some pentene-2 that was found was attributed by these workers to a radical mechanism, namely, the disproportionation of pentyl radicals formed by the addition of H atoms to the reactant pentene-1, rather than to a 1,3(1,3) H-atom migration.

At the time of publication of the work of Majer *et al.* (9) we had already in progress an investigation of the pentene-1 system. The products they looked for do not exhaust the list of possible products of migration mechanisms; cyclopentane and 1,2-dimethylcyclopropane are missing. The presence or absence of these products, some formed by singular reaction paths, can shed light on the validity of the empirical rule of Kebarle and Avrahami. This rule had a somewhat tenuous foundation at the time of its formulation in that several results forming its basis came from studies performed at a single, low pressure; this is an experimental condition not conducive to the formation of ring species. Indeed, a major contribution by Cvetanović and Doyle (2) was the re-emphasis of the important role of pressure effects in these systems and the concomitant correlation of possibly "conflicting" data so provided. Thus cyclopropane, which is an intermediate that must decline in amount at lower pressure, is actually formed (11) to the extent of 1.4% at the optimal pressure of 7 cm. This value is sevenfold larger than the 0.2% found by Avrahami and Kebarle (6) (although this does not substantially affect their conclusion that cyclopropane is a minor product).

EXPERIMENTAL

Pentene-1 was obtained from Phillips Petroleum Company. It was purified chromatographically until free of impurity peaks. Runs were carried out statically in a 5.3 cc Vycor tube, of diameter 0.9 cm, which was irradiated with a low pressure Hanovia quartz helical resonance lamp. Reactants were saturated with mercury, and reactions were run at the ambient temperature, 22 °C. Reaction times varied from 0.5 to 5.0 min.

Analyses were made with a 300 ft squalane-coated capillary column maintained at 0 °C, with an argon ionization detector. Peak height calibrations were known from various pure samples. Under these conditions, the *trans*-dimethylcyclopropane peak was submerged by the reactant pentene-1 peak. The amounts of *cis*- and *trans*-pentene-2 formed were the same within experiental error. The *trans*- and *cis*-cyclopropanes can undoubtedly be assumed to be produced in comparable, although not necessarily equal, amounts. Retention times and identities were calibrated by use of the pure compounds.

RESULTS AND DISCUSSION

The results (Table I) are in partial agreement with those of Majer *et al.*: methylcyclobutane is certainly a major product, and no ethylcyclopropane was found. But, by contrast, we find that both 1,2-dimethylcyclopropane and cyclopentane are formed, and the former in quantities comparable to the methylcyclobutane. The cyclopentane is produced in minor amounts; at 2 cm pressure, the lowest pressure used, the percentage of cyclopentane relative to methylcyclobutane is 2.6%; at higher pressures, the percentage seems reduced to ~1.0%. The corresponding relative values for *cis*-1,2-dimethylcyclopropane are identical, i.e. 40%, within experimental error at the two pressure extremes.

Can. J. Chem. Downloaded from www.nrcresearchpress.com by 210.87.254.5 on 09/05/12
For personal use only.

TABLE I

Products[a] of H-atom shifts in Hg ($^3P_1$) photosensitized pentene-1 (22 °C)

Pressure (cm)	*trans*-Pentene-2	*cis*-Pentene-2	*cis*-Dimethylcyclopropane[b]	Cyclopentane
2	[c]	4.9	41.2	2.7
2	4.8	4.7, 4.8 av.	37.8, 39.5 av.	2.4, 2.6 av.
5	1.2	1.2	22.7	1.4
10	1.4	1.4	33.3	0.8
15	2.2	2.0	46.5	1.0
15	1.4	1.6	33.3	0.8
15	1.4	1.5	31.3	1.1
15	4.6	6.0	43.7	1.4
15	2.7	3.4	41.4	[c]
15	[c]	[c]	42.2	[c]
15	[c]	[c]	42.6	[c]
15	[c], 2.5 av.	[c], 2.9 av.	41.9, 40.4 av.	[c], 1.1 av.
20	1.9	1.8	40.9	0.9

[a]Expressed in %, relative to methylcyclobutane product; the pentenes are not necessarily products of an H-migration process (10).
[b]The *trans* product was also formed, see text.
[c]Data retrieval precluded by small extent of reaction or loss of sample.

Majer *et al.* showed that methylcyclobutane product passed through a maximum at 3.5 cm total pressure, as does therefore dimethylcyclopropane; a cyclopentane maximum presumably occurs at a little lower pressure.

Noteworthy is the fact that both of these products are produced by single reaction paths and that both result from 1,4 shifts; but the cyclopentane is formed via a *primary* → *secondary* H transfer and the dimethylcyclopropane by a *secondary* → *primary* H migration. These data illustrate that any empirical rule used to predict the aptitude of a positional shift must be properly, and perhaps extensively, modified by the nature of the processes involved; and, in this, the diradical systems apparently behave much like monoradical systems as to relative ease of H-atom translocations (12). The modification is attributable to conventional interpretation in terms of relative stability of various types of radicals. Apart from these cautionary remarks, the data seem to substantiate the predictions of Kebarle and Avrahami.

In view of the above, it can be seen that methylcyclobutane is not produced in quantities which greatly exceed the amount of 1,2-dimethylcyclopropane for two reasons: on the one hand, one mode of production, 1,3(2,4) transfer, is not highly favored, and on the other, a *primary* → *primary* transfer is required for the preferred 1,5(1,5) mode, as opposed to the *secondary* → *primary* H shift which leads to the production of the dimethylcyclopropane. The total lack of ethylcyclopropane and the relatively minute yield of the pentene-2, some or all of which is undoubtedly due to disproportionation of pentyl radicals, demonstrates that 1,2 and 1,3 translocations are unlikely.

Srinivasan's findings (3, 4) remain a hindrance to the formulation of a complete mechanistic rationale for reactions of this genre. That some ordinarily favorable transfers are hindered in his system due to the presence of vinylic hydrogens fails to account for the fact that of the other possible, albeit less favorable, cases, the least preferred according to the prior considerations is the one that does indeed occur.

It appears desirable to reiterate (5) the relationship between reactions of mercury photosensitized electronically excited compounds† and the reactions of highly vibrationally excited ground singlet state cyclopropanes*:

[1*a*] $$\nabla\text{—C=C}^* \rightarrow \text{C=C—C—C=C} \qquad (13)$$

Can. J. Chem. Downloaded from www.nrcresearchpress.com by 210.87.254.5 on 09/05/12
For personal use only.

[1*b*]	$C{=}C{-}C{-}C{=}C\dagger \rightarrow \triangledown{-}C{=}C$	(4)
[2*a*]	$\triangledown{-}C^* \rightarrow C{-}C{-}C{=}C$	(15)
[2*b*]	$C{-}C{-}C{=}C\dagger \rightarrow \triangledown{-}C$	(2)
[3*a*]	$\triangledown^* \rightarrow C{-}C{=}C$	(16)
[3*b*]	$C{-}C{=}C\dagger \rightarrow \triangledown$	(6, 11)
[4*a*]	$CH_3CH^* \rightarrow C{=}C$	(17)
[4*b*]	$C{=}C\dagger \rightarrow CH_3CH.$	(5)

The last is the 2-carbon analogue of the preceding cyclopropane examples. The asterisk signifies the excited singlet state. In these examples, the rearrangements of vibrationally excited singlet cyclopropanes readily reverse (but not microscopically) the reactions of electronically excited triplet olefins. The reactions of triplet cyclopropanes differ from those of the singlet species. For example, triplet state cyclopropane undergoes polymerization (18, 19) and geometric isomerization (19) but not structural isomerization (in significant amount) to propylene. Similarly, Duncan and Cvetanović (20) have studied the reaction of presumably triplet state 1,2-dimethylcyclopropane and have obtained a product distribution which deviates considerably from that of vibrationally excited singlet dimethylcyclopropane (21).[4] The reactions of the two electronic states take place on distinctly different surfaces. The activated complex for reactions of the type (singlet cyclopropane) → (singlet propene) involves ring rupture and 1,2 H-atom transfer (22) in an α,γ-diradical. The triplet state cyclopropane, on the other hand, evidently leads to an α,β-diradical, which is presumably a relatively long-lived species; it can go through an activated complex characteristic of alkyl radicals, for which the non-adjacent H transfer, with a multi-membered ring intermediate, seems favored. The failure of triplet state cyclopropane to yield propylene readily is in this sense the microscopic concomitant of the low yield of cyclopropane which arises from triplet diradical propylene.

ACKNOWLEDGMENT

We wish to thank Dr. W. D. Walters for the gift of a sample of methylcyclobutane.

REFERENCES

1. A. B. Callear and R. J. Cvetanović. J. Chem. Phys. **24**, 873 (1956).
2. R. J. Cvetanović and L. C. Doyle. J. Chem. Phys. **37**, 543 (1962).
3. R. Srinivasan. J. Phys. Chem. **67**, 1367 (1963).
4. R. Srinivasan. J. Am. Chem. Soc. **86**, 3318 (1964).
5. D. W. Setser, B. S. Rabinovitch, and D. W. Placzek. J. Am. Chem. Soc. **85**, 862 (1963).
6. M. Avrahami and P. Kebarle. J. Phys. Chem. **67**, 354 (1963).
7. (*a*) R. J. Cvetanović, H. E. Gunning, and E. W. R. Steacie. J. Chem. Phys. **31**, 573 (1959).
   (*b*) P. Kebarle and M. Avrahami. J. Chem. Phys. **38**, 700 (1963).
8. R. B. Cundall and T. F. Palmer. Trans. Faraday Soc. **56**, 1211 (1960).
9. J. R. Majer, J. F. T. Pinkard, and J. C. Robb. Trans. Faraday Soc. **60**, 1247 (1964).
10. J. R. Majer, B. Mile, and J. C. Robb. Trans. Faraday Soc. **57**, 1336 (1961).
11. D. W. Placzek. Unpublished work.
12. A. Fish. Quart. Rev. London, **18**, 243 (1964).
13. M. C. Flowers and H. M. Frey. J. Chem. Soc. 3547 (1961). H. M. Frey. Trans. Faraday Soc. **58**, 516 (1962).

[4] *That the "pressure independent" production of certain olefins from triplet dimethylcyclopropane (ref. 20 and report by R. J. Cvetanović. Photochemistry Symposium, Rochester, 1963) takes place on a triplet surface, rather than via a very rapid internal conversion to a singlet cyclopropane surface, follows from the quasi-pressure independent character of this process and from the difference between these olefin products and those formed from hot singlet dimethylcyclopropane. It is further supported by the failure of analogous triplet cyclopropane to yield propylene at pressures at which vibrationally excited singlet cyclopropane, if formed by internal conversion, would do so readily (19).*

Can. J. Chem. Downloaded from www.nrcresearchpress.com by 210.87.254.5 on 09/05/12
For personal use only.

14. W. A. GIBBONS, W. F. ALLEN, adn H. E.GUNNING. Can. J. Chem. **40**, 568 (1962).
15. J. N. BUTLER and G. B. KISTIAKOWSKY. J. Am. Chem. Soc. **82**, 759 (1960).
16. T. S. CHAMBERS and G. B. KISTIAKOWSKY. J. Am. Chem. Soc. **56**, 399 (1934). G. B. KISTIAKOWSKY and K. SAUER. J. Am. Chem. Soc. **78**, 5699 (1956).
17. G. B. KISTIAKOWSKY and B. H. MAHAN. J. Am. Chem. Soc. **79**, 2414 (1957).
18. R. J. SCOTT and H. E. GUNNING. J. Phys. Chem. **56**, 156 (1952) *et seq.*
19. D. W. SETSER, B. S. RABINOVITCH, and E. G. SPITTLER. J. Chem. Phys. **35**, 1840 (1961).
20. F. J. DUNCAN and R. J. CVETANOVIĆ. J. Am. Chem. Soc. **84**, 3593 (1962). *See also, in this regard,* H. M. FREY. J. Am. Chem. Soc. **82**, 5947 (1960).
21. H. M. FREY. Proc. Roy. Soc. London, Ser. A, **251**, 575 (1959). M. C. FLOWERS and H. M. FREY. Proc. Roy. Soc. London, Ser. A, **257**, 122 (1960).
22. E. W. SCHLAG and B. S. RABINOVITCH. J. Am. Chem. Soc. **82**, 5996 (1960). D. W. SETSER and B. S. RABINOVITCH. J. Am. Chem. Soc. **86**, 564 (1964).

Can. J. Chem. Downloaded from www.nrcresearchpress.com by 210.87.254.5 on 09/05/12
For personal use only.

Can. J. Chem. Downloaded from www.nrcresearchpress.com by 210.87.254.40 on 09/05/12
For personal use only.

CHASMANINE AND ITS STRUCTURE[1]

O. ACHMATOWICZ, JR.,[2] Y. TSUDA,[2] AND LÉO MARION
Division of Pure Chemistry, National Research Council, Ottawa, Canada
AND
T. OKAMOTO, MITSUTAKA NATSUME, HONG-HSI CHANG, AND K. KAJIMA
Faculty of Pharmaceutical Sciences, University of Tokyo, Tokyo, Japan

Received December 3, 1964

ABSTRACT

The alkaloid chasmanine, $C_{25}H_{41}O_6N$, isolated from *A. chasmanthum* contains four methoxyl and two hydroxyl groups as well as an imino-ethyl. It undergoes the usual pyrolytic reaction and the unsaturated product, pyrochasmanine, $C_{25}H_{39}O_5N$, gives rise to an acid-catalyzed allylic rearrangement product, isopyrochasmanine. Pyrochasmanine, on treatment with lithium aluminium hydride, is demethoxylated. It can be concluded that the base, like bikhaconine, contains the sequence $\rangle C(OH)—CH_2—CH(OCH_3)—$. Chasmanine can be oxidized to a compound containing a cyclopentanone ring so that its second hydroxyl must be secondary and located on a five-membered ring. It is possible to benzoylate the secondary hydroxyl and acetylate the tertiary hydroxyl. The n.m.r. characteristics of the resulting double ester determine the location of these two groups and their stereochemistry. The relative position of two of the remaining methoxyl groups is established via a demethylation reaction resulting in the formation of a cyclic ether. All the chemical reactions studied are in agreement with structure IV (R = R′ = H) for chasmanine. There is, however, no positive proof for the location of the fourth methoxyl and it has been placed in ring A by analogy. An attempted correlation with bikhaconine is described.

Recently the isolation of five alkaloids from the roots of *Aconitum chasmanthum* Stapf has been reported (1). One of these, indaconitine I, the structure of which has already been established (2), had been isolated long ago from this source by Dunstan and Andrews (3). Two others, designated chasmaconitine and chasmanthinine, have been shown to have structures II and III respectively (1).

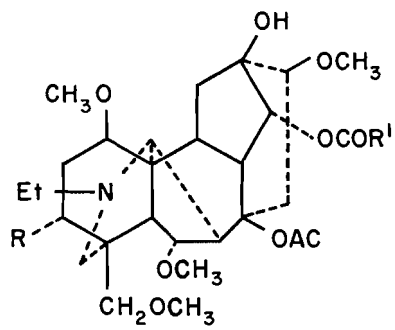

I, R = OH, R′ = C_6H_5

II, R = H, R′ = C_6H_5

III, R = H, R′ = -CH=CH-C_6H_5

We now wish to report on the fourth alkaloid, previously identified as base B (1), for which the name chasmanine is now suggested. Whereas chasmaconitine and chasmanthinine were isolated from the weak bases, chasmanine was obtained from the fraction containing the strong bases, of which it formed the main component.

Chasmanine (base B), $C_{25}H_{41}O_6N$, was earlier reported to melt at 84–88°. By further purification this has been raised to 90–91°. The base was optically active, $[\alpha]_D^{25}$ +23.6°.

[1]*Issued as N.R.C. No. 8313.*
[2]*National Research Council of Canada Postdoctorate Fellow.*

Can. J. Chem. Downloaded from www.nrcresearchpress.com by 210.87.254.40 on 09/05/12
For personal use only.

Although it crystallized readily, all attempts to prepare crystalline salts failed. Its infrared spectrum contained a broad absorption band with a small peak at 3 475 and two well-defined peaks at 3 365 and 3 263 cm^{-1} indicative of hydroxyl groups, but contained no carbonyl absorption, so that no ester group is present. The nuclear magnetic resonance (n.m.r.) spectrum revealed the presence of four methoxyl groups (δ 3.31, 3.21 corresponding to three protons each and δ 3.28 corresponding to six protons) and an N-ethyl group (triplet centered at δ 1.03). Acetylation of the base with acetic anhydride and *p*-toluenesulfonic acid produced a readily crystallized diacetate, the n.m.r. spectrum of which confirmed the introduction of two acetyl groups (δ 2.02, 1.97). Oxidation of chasmanine with chromium trioxide in acetone (3) gave rise to a gummy ketone characterized as its crystalline monoacetate. In the infrared the latter showed a band at 1 752 cm^{-1} attributable to a five-membered cyclic ketone, and one at 1 727 cm^{-1} indicative of an acetate carbonyl. In the n.m.r. spectrum only one acetyl group was indicated (δ 1.99). Both the ketone and its acetyl derivative were converted back to chasmanine by reduction with sodium borohydride and lithium aluminium hydride respectively.

Oxidation of chasmanine with chromium trioxide – pyridine complex (Sarett's reagent) went further than chromium trioxide in acetone and gave two products, one, m.p. 196°, $C_{23}H_{33}O_6N$, that contained a cyclopentanone ring, but had lost the imino-ethyl group and had the properties of an azomethine. It formed an ethiodide convertible into chasmanine by reduction with sodium borohydride. In the n.m.r. spectrum the azomethine showed a singlet at δ 3.72 attributable to the protons of a methylene adjacent to an oxygen (—CH_2—O—), and a singlet at δ 7.51 that can be ascribed to —CH=N—. The infrared spectrum contained bands at 1 655 cm^{-1} attributable to the latter function, and at 1 761 cm^{-1} indicative of a five-membered cyclic ketone. The second oxidation product is neutral, m.p. 206–207° ($C_{25}H_{37}O_7N$). It also contains a cyclopentanone ring, but its imino-ethyl group has been oxidized to an acetyl group. It is converted back into chasmanine by the action of lithium aluminium hydride.

Consequently, of the six oxygens in chasmanine, four are present in methoxyl groups, one is in a tertiary hydroxyl, and the sixth is in a secondary hydroxyl located on a five-membered ring.

Just as with lycoctonine ($C_{25}H_{41}O_7N$) and aconitine ($C_{34}H_{47}O_{11}N$), if all the oxygen-containing substituents in chasmanine are replaced by hydrogen, there is obtained the common empirical formula $C_{21}H_{33}N$. As a working hypothesis, therefore, we have assumed that chasmanine possessed the same carbon–nitrogen skeleton common to lycoctonine and aconitine, and that it could be represented by structure IV. Hence the diacetate would be V and the keto-monoacetate or 10-dehydrochasmanine VI. The oxidation products obtained by the action of Sarett's reagent would be N-deethyl-10-dehydrochasmanine-azomethine and N-acetyl-N-deethyl-10-dehydrochasmanine.

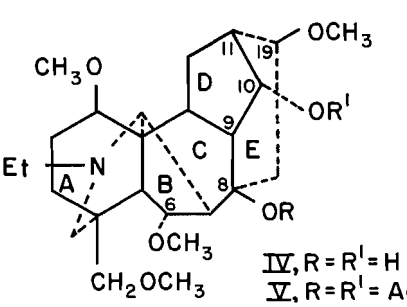

IV, R = R' = H
V, R = R' = Ac

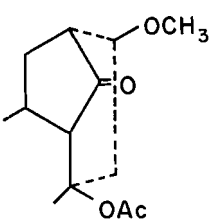

VI

The stereospecific course of the reduction of the ketone and the keto-monoacetate VI indicates the position of the secondary hydroxyl in the five-membered ring. There are two possible positions for a secondary hydroxyl in this ring. Whereas there is free access to the C-12 position, the C-10 position is hindered on one side and would thus account for a stereospecific reduction.

Diacetylchasmanine V when heated *in vacuo* gave rise to three products showing distinct spots in thin layer chromatography. The relative yield of each component varied with the condition of pyrolysis. The combined product was not crystalline and could not be separated by chromatography on alumina, although after saponification it separated readily into three crystalline components that proved to be pyrochasmanine VII, isopyrochasmanine VIII, and demethylisopyrochasmanine IX.

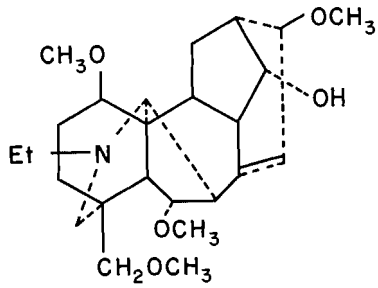

VII

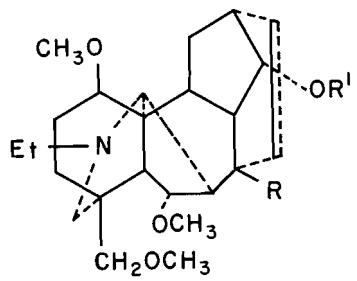

VIII, R = OCH_3, R' = H
IX, R = OH, R' = H
X, R = OAC, R' = AC
XIV, R = R' = H

Pyrochasmanine VII, the compound of intermediate mobility showed in the infrared an absorption band at 3 430 cm^{-1} attributable to a hydroxyl and one at 1 634 cm^{-1} characteristic of a double bond. Its n.m.r. spectrum contained signals for one olefinic proton (δ 5.43, J = 6 c.p.s.), for four methoxyl groups (δ 3.14, 3.28, 3.24, 3.21) and an imino-ethyl (triplet at δ 1.04). When pyrochasmanine was heated with methanolic perchloric acid, it was converted quantitatively to isopyrochasmanine VIII identical with the most mobile component of the hydrolyzed pyrolytic product. Isopyrochasmanine in its n.m.r. spectrum still showed the presence of four methoxyl groups and an imino-ethyl, but in the olefinic region the spectrum contained the signals of two protons (multiplet at δ 5.75–6.12). The acid-catalyzed allylic rearrangement involved in the conversion of pyrochasmanine to isopyrochasmanine has been observed in several highly oxygenated diterpenoid alkaloids (4–7).

The structure of the third compound, demethylisopyrochasmanine IX isolated from the hydrolyzed product of pyrolysis was verified as follows. The n.m.r. spectrum of the compound revealed the presence of three methoxyls only (δ 3.21, 3.30, 3.32), an imino-ethyl (triplet centered at δ 1.02), and two olefinic protons (multiplet at δ 5.67–5.91). The two olefinic protons indicate that the allylic shift has taken place and therefore that the new hydroxyl is at C-8. The presence of a double bond was confirmed by the formation of a dihydro derivative on catalytic hydrogenation. The low chromatographic mobility of IX suggested the presence of an additional hydroxyl, and this was confirmed by the preparation of a diacetyl derivative X (n.m.r. δ 1.93, 1.99) that could be hydrogenated

Can. J. Chem. Downloaded from www.nrcresearchpress.com by 210.87.254.40 on 09/05/12
For personal use only.

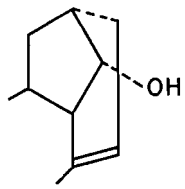

XII

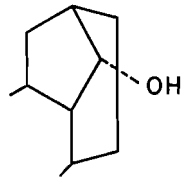

XIII

to a dihydrodiacetyl derivative XI also obtainable by acetylation of the dihydro derivative obtained from IX.

The dihydrodiacetyldemethylisopyrochasmanine XI was pyrolyzed *in vacuo* at 180–190° for 5 min. The crude pyrolytic product (single spot in thin layer chromatography) showed in the n.m.r. spectrum a single acetyl group (δ 2.02) and one olefinic proton (multiplet at δ 4.98–5.28). It could not be crystallized, but after hydrolysis was characterized as its crystalline perchlorate XII; catalytic hydrogenation of this salt produced a dihydro derivative XIII also characterized as its crystalline perchlorate. Since compound XI undergoes pyrolytic elimination of an *O*-acetyl group, it follows that the additional hydroxyl in IX must be located at C-8 as mentioned above.

Pyrochasmanine VII treated with lithium aluminium hydride in tetrahydrofurane at room temperature underwent the allylic shift and demethoxylation, giving rise to demethoxyisopyrochasmanine XIV ($C_{24}H_{37}O_4N$). The n.m.r. spectrum of XIV contained signals characteristic of an imino-ethyl (triplet centered at δ 1.02), of two olefinic protons (multiplet at δ 6.03–5.78), and of three methoxyl groups (δ 3.29, 3.28, 3.22), thus confirming the loss of one methoxyl as well as the shift in double bond in the course of the reaction. Catalytic hydrogenation of the perchlorate of XIV gave the corresponding dihydro derivative, isolated as the perchlorate. This salt was identical in every respect (melting point, that of the mixture, infrared spectra, X-ray powder patterns) with the perchlorate of the dihydro derivative XIII.

The above described formation of pyrochasmanine and its transformation products are characteristic of diterpenoid alkaloids containing the sequence $\rangle C(OH)—CH_2—CH(OCH_3)—$ in ring E as was well established in connection with delphinine (8), pseudaconitine (5), and bikhaconitine (7). What is unusual with these reactions in chasmanine is the formation of isopyrochasmanine and its demethyl derivative in the initial pyrolytic reaction. For instance, the pyrolysis of pseudaconitine produced pyropseudaconitine as the only identified base, while isopyropseudaconine was produced by an acid-catalyzed rearrangement of pyropseudaconine (5). As mentioned already, the relative proportions of the three compounds produced by the pyrolysis of chasmanine were dependent on the conditions of the experiment. Heating for less than 5 min at 170–180° favored the formation of pyrochasmanine VII while heating for a longer time (10 min) at higher temperatures (190–200°) produced mainly isopyrochasmanine VIII and demethylisopyrochasmanine IX. The production of a demethylisopyro compound as a direct product of pyrolysis had not been observed before in other diterpenoid alkaloids.

The product of the already described pyrolysis of diacetylchasmanine can also be worked up in a different way. When the crude pyrolyzed product was treated with lithium aluminium hydride in tetrahydrofurane, three compounds were obtained, i.e., isopyrochasmanine VIII, demethylisopyrochasmanine IX, and demethoxyisopyrochasmanine XIV. These compounds were separated readily by chromatography on alumina. In this

Can. J. Chem. Downloaded from www.nrcresearchpress.com by 210.87.254.40 on 09/05/12
For personal use only.

experiment, the yield of demethylisopyrochasmanine was higher than when the isolation was carried out after hydrolysis of the product. Surprisingly it was found that demethylisopyrochasmanine could be obtained in 30% yield by treatment of isopyrochasmanine with lithium aluminium hydride in tetrahydrofurane.

Treatment of chasmanine with benzoyl chloride in pyridine at room temperature gave a high yield of monobenzoylchasmanine XV; it was amorphous, but formed a crystalline hydrochloride. The benzoylated product in turn, when acetylated gave rise to crystalline acetylbenzoylchasmanine XVI. The n.m.r. spectrum of this diester showed, in addition

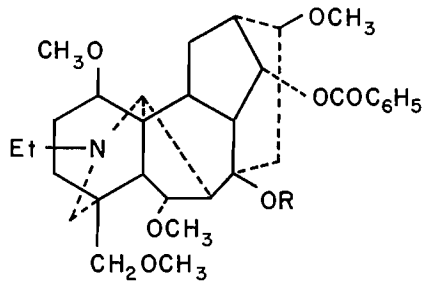

XV, R = H

XVI, R = Ac

to the main features already present in the spectrum of chasmanine, five aromatic protons (multiplet at δ 8.23–7.20) and a triplet centered at δ 5.07 that may be attributed to the C-10 hydrogen. That this signal is not a doublet as in the case of the other esterified aconite-type alkaloids examined (9) indicates that the C-10 proton must be flanked not by one but by two other protons. Consequently, the substituent at the bridgehead position C-11 must be a hydrogen and not a hydroxyl as in aconitine, pseudaconitine, etc. The signal for the acetyl group protons was at quite high field (δ 1.36). As pointed out previously (9) this shift to high field in esterified oxygenated diterpenoid alkaloids is due to the anisotropic effect of the benzene ring of the aromatic acid, and indicates the location and orientation of the benzoyl ester group. Hence the secondary hydroxyl present on a five-membered ring in chasmanine is the one that was esterified by the action of benzoyl chloride and must be located at C-10. Consequently, the substituents on rings D and E are located as required by structure IV and the stereochemistry of the hydroxyl at C-10 must be the same as that of the benzoyloxy group in aconitine.

Isopyrochasmanine VIII when heated for 40 min on the steam bath with 50% sulfuric acid gave a mixture of three products: a component that could not be purified completely (but appeared from its n.m.r. spectrum to contain two methoxyls only), some demethylisopyrochasmanine IX, and tridemethylanhydroisopyrochasmanine XVII, $C_{22}H_{31}O_4N$. If, however, the reaction was carried out for $2\frac{1}{4}$ h, two products only were obtained, i.e., IX and XVII. Jacobs and Sato (10) had found that isopyrooxodelphinine when heated at 40° with zinc chloride and 5% hydrochloric acid underwent a similar demethylation and gave rise to a didemethyl and a tridemethyl cyclic ether. Wiesner *et al.* (11) in a later interpretation of this result provided evidence that the two methyl groups that were removed with the resulting formation of a cyclic ether were located at C-6 and C-17. Consequently, the most probable structure of tridemethylanhydroisopyrochasmanine which contains only one methoxyl—n.m.r. δ 2.50 (3 H)—is XVII and affords strong evidence for the presence of a methoxyl at both C-6 and C-17 positions in the alkaloid (IV). The latter was already indicated by the n.m.r. spectrum of N-deethyl-10-dehydrochasmanine-azomethine (δ 3.72).

Can. J. Chem. Downloaded from www.nrcresearchpress.com by 210.87.254.40 on 09/05/12
For personal use only.

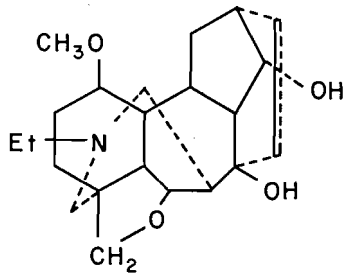

XVII

Neoline undergoes a similar demethylation (6). The structure suggested for neoline (6) differs from that suggested for chasmanine only in that it contains an α-hydroxyl at C-1 in ring A while chasmanine contains a C-1 β-methoxyl. In order to correlate the two through their cyclic ether derivatives, it is necessary to demethylate chasmanine at C-1. Jacobs and Sato (10) in their demethylation experiments had used neutral oxo-derivatives and had observed that by carrying out the reaction at 60° they could obtain a completely demethylated compound. Isopyrochasmanine was therefore oxidized with permanganate in aqueous acetone to remove the imino-ethyl group (12) and the resulting secondary base was acetylated to N-acetyl-N-deethylisopyrochasmanine. This N-acetyl derivative was heated with zinc chloride in 5% hydrochloric acid for 1 h at 70–75° and the crude product (single spot in thin layer chromatography) was reduced with lithium aluminium hydride in tetrahydrofurane. This series of reactions yielded exclusively the tridemethyl cyclic ether XVII already described. The failure of the reaction to remove the last remaining methoxyl, i.e., that in ring A, cannot be considered as militating against the presence of a C-1 methoxyl since an exactly parallel series of reactions carried out with isopyrobikhaconine XVIII gave rise to a product XIX still carrying a methoxyl.

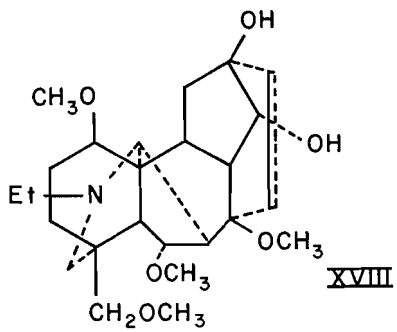

XVIII

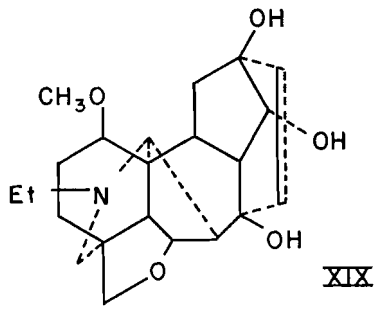

XIX

The location of the C-6 methoxyl has been derived from the formation of the cyclic ether. Not only is this position confirmed, but the orientation of the group is also determined by the course of the oxidation of chasmanine with potassium permanganate. It has been established that in the aconite type of diterpenoid alkaloids, in which the C-6 methoxyl is α, potassium permanganate oxidation under neutral (or basic) condition leads mainly to N-deethylation whereas in the lycoctonine type, in which the C-6 methoxyl is β, the same oxidizing agent leads to a lactam (12). The oxidation of chasmanine with permanganate, under these conditions, gives an excellent yield of N-deethylchasmanine, so that the alkaloid must contain a C-6 methoxyl in the α-configuration.

N-Deethylchasmanine when treated with ethyl iodide is converted back to chasmanine.

Can. J. Chem. Downloaded from www.nrcresearchpress.com by 210.87.254.40 on 09/05/12
For personal use only.

When treated with methyl iodide instead, it is converted to N-methyl-N-deethyl-chasmanine, $C_{24}H_{39}O_6N$, m.p. 90–92°. This new base, like the acetylated and benzoylated chasmanine described above, has not yet been reported to occur in nature.

Because of the ease with which the allylic rearrangement takes place in pyrochasmanine, it is highly probable that the configuration of the C-19 methoxyl is the same as in the other aconite alkaloids already investigated.

The location of all the substituents in the proposed chasmanine structure IV has been confirmed chemically except for the ring A methoxyl. Concerning the carbon skeleton, it is known that pyrodelphonine shows unexpected absorption in the ultraviolet (λ_{max} 245 mμ, log ϵ 3.8) and that this disappears on acidification. Wiesner *et al.* (6) noticed similar spectroscopic properties in pyroneoline and considered that this similarity indicated an analogy between the neoline and the delphonine structures. The ultraviolet spectra of pyrochasmanine and of pyrobikhaconine show absorption at λ_{max} 244 mμ, log ϵ 3.74 and λ_{max} 249 mμ, log ϵ 3.71 respectively. In both cases the peak disappeared on acidification. This parallel spectroscopic behavior of chasmanine and bikhaconine as well as delphonine and neoline supports the assumption of the same carbon skeleton in all four compounds.

There is a close relation between structure IV suggested for chasmanine and the structure of bikhaconine, the hydrolytic alkamine derived from bikhaconitine (7). The only difference is that bikhaconine contains a C-11 bridgehead hydroxyl that is absent in chasmanine. In an attempt to find a rigorous confirmation of the structure of chasmanine, we sought to correlate the base with bikhaconine. Such a correlation involved removing the C-11 hydroxyl from the latter, either by first opening ring E or by direct attack on the hydroxyl.

Although the initial opening of ring E prior to removal of the hydroxyl appeared to be the more promising, three different methods of achieving this proved unsuccessful and failed to yield the ultimate expected product.

After several fruitless attempts to remove the C-11 hydroxyl directly it was decided to try a recently described method. Okamoto *et al.* (13) have reported that a bridgehead *O*-mesylate group in a pseudokobusine derivative could be hydrogenolyzed by high pressure hydrogenation over Raney nickel. Although in pseudokobusine the hydroxyl thus removed is a carbinolamine the reaction might work with bikhaconine if it proceeded through radical formation.

Methanesulfonation of bikhaconitine gave the desired mesylate $C_{37}H_{53}O_{13}NS$ (XX) in a good yield. Deoxyindaconitine and deoxyaconitine were similarly smoothly mesylated to XXI and XXII respectively. The last compound was a monomesylate and it was the bridgehead hydroxyl that reacted; even forced conditions could not mesylate the second ring E hydroxyl. The hydrogenation of bikhaconitine mesylate at 41 atm and 120–130° for 15 h gave two products. The main product separated by chromatography represented a 60% yield; it still contained the mesylate and the veratroyl groups, but lacked the acetoxy group. Its structure has been confirmed by an alternative synthesis. Pyrobikhaconitine was hydrogenated over platinum to the dihydro derivative and this when mesylated gave the same mesylate XXIII previously obtained from XX.

The minor product of the hydrogenation over Raney nickel was obtained in 5% yield only. Although it could not be crystallized, its infrared and n.m.r. spectra revealed that it no longer contained the mesylate and acetoxy groups, but still contained an imino-ethyl, four methoxyl, and the veratroyl groups. It was assumed to possess structure XXIV, and was hydrolyzed into the corresponding hydroxy base XXV.

Pyrochasmanine VII prepared as described above was hydrogenated catalytically to

Can. J. Chem. Downloaded from www.nrcresearchpress.com by 210.87.254.40 on 09/05/12
For personal use only.

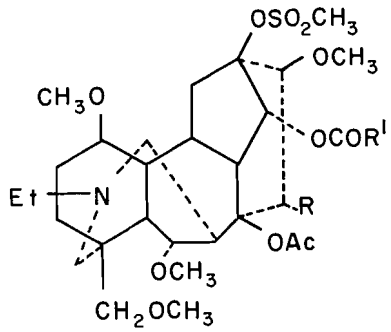

XX, R = H, R' = $C_6H_3(OCH_3)_2$
XXI, R = H, R' = C_6H_5
XXII, R = OH, R' = C_6H_5

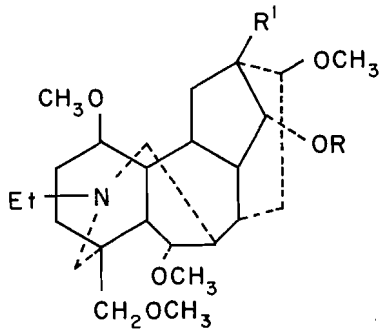

XXIII, R = $COC_6H_3(OCH_3)_2$, R' = OSO_2CH_3
XXIV, R = $COC_6H_3(OCH_3)_2$, R' = H
XXV, R = R' = H

its amorphous dihydro derivative. This derivative had exactly the same R_f value as the hydroxy base XXV in thin layer chromatography, thus suggesting their identity. All attempts to crystallize the two products or their salts failed, and the quantities available were too small for further comparison. The correlation work will be repeated but the present results are now reported as they do support the structure of chasmanine although they do not constitute a rigorous proof.

Ochiai, Okamoto, and Sakai (14) have reported the isolation from *Aconitum subcuneatum* Nakai and *Aconitum yesoensis* Nakai (both plants collected in the northern part of Japan) of an alkaloid designated Toroko-base II, m.p. 85–88°, $C_{24}H_{39}O_6N$, $[\alpha_D]$ +43°, containing an imino-methyl. Further purification and investigation by these authors has shown that the base had m.p. 90–91°, $[\alpha]_D$ +25.0° and contained an imino-ethyl instead of an imino-methyl, so that the empirical formula was corrected to $C_{25}H_{41}O_6N$. A direct comparison of chasmanine with Toroko-base II has shown the two to be identical in every respect (melting point, that of the mixture, infrared spectra, and X-ray powder patterns).

Undoubtedly the discovery of the occurrence of the base in *A. subcuneatum* antedates the report of its occurrence in *A. chasmanthum*. Since, however, the designation Toroko-base, meant to be tentative, refers to the place where the plant was collected, it is proposed to abandon it and retain the name chasmanine[3] derived from the specific name of one of the plants in which the base occurs.

EXPERIMENTAL

The infrared spectra were taken in Nujol mulls (unless otherwise mentioned) on a Perkin–Elmer double beam Model 21B spectrometer. The n.m.r. spectra were measured in chloroform solution containing

[3]*Professor E. Ochiai is in agreement with this proposal.*

Can. J. Chem. Downloaded from www.nrcresearchpress.com by 210.87.254.40 on 09/05/12
For personal use only.

tetramethylsilane as an internal reference, on a Varian A-60 instrument, and the chemical shifts are given in p.p.m. The ultraviolet spectra were measured on a Cary recording spectrometer Model 11.

The melting points were taken on a Kofler hot stage and were not corrected. For column chromatography Woelm grade IV neutral alumina was used, unless otherwise mentioned, and for thin layer chromatography the adsorbent was Merck silica gel G, and the developing solvent employed was cyclohexane – chloroform – diethyl amine. All extracts were dried and subsequently evaporated under reduced pressure.

Chasmanine

The alkaloid was isolated from the plant extract as previously described (1). After several recrystallizations from *n*-hexane it consisted of fine colorless needles, m.p. 90–91°, $[\alpha]_D^{25}$ +23.6° (*c*, 2.5 in EtOH), pK_a 6.3 (in 80% ethanol).

Anal. Calcd. for $C_{25}H_{41}O_6N$: C, 66.49; H, 9.15; N, 3.10. Found: C, 66.31; H, 9.09; N, 3.14.

ν_{max} 3 460, 3 365, 3 260 cm^{-1} (OH); 1 113, 1 095 cm^{-1} (OCH_3). In the n.m.r. spectrum: singlets at δ 3.31 (3H), 3.28 (6H), 3.21 (3H), triplet centered at δ 1.03 (3H). Chasmanine may be distilled at 150° and 5×10^{-5} mm without decomposition, but the pure crystalline base is somewhat unstable and after several months it contains a considerable amount of impurities (~10%).

Diacetyl Chasmanine

A mixture of chasmanine (109 mg) and *p*-toluenesulfonic acid (100 mg) in acetic anhydride (3 ml) was heated on a steam bath for 1 h. After cooling, the mixture was poured on ice and made basic with sodium carbonate, and the solution extracted with chloroform. Evaporation of the extract left a gum (128 mg) which was dissolved in *n*-hexane – benzene (1:1) and chromatographed on alumina. The column was eluted with the same solvent mixture and the eluate evaporated to dryness. There was left a residue (93 mg) which crystallized when triturated with *n*-hexane. After several recrystallizations from the same solvent, the diacetyl chasmanine produced consisted of colorless needles, m.p. 139–141°.

Anal. Calcd. for $C_{29}H_{45}O_8N \cdot \frac{1}{2}H_2O$: C, 63.96; H, 8.45; N, 2.57. Found: C, 63.76; H, 8.46; N, 2.79.

ν_{max} 1 725, 1 242 cm^{-1} (acetate). In the n.m.r. spectrum: singlets at δ 2.02 (3H), 1.97 (3H), 3.30 (3H), 3.28 (3H), 3.22 (6H), triplet centered at δ 1.05 (3H), poorly resolved triplet at δ 4.76 (1H).

Oxidation of Chasmanine with Chromic Oxide

(*a*) To a solution of chasmanine (640 mg) in acetone (15 ml) cooled in ice, a solution of chromic oxide (650 mg) in acetone (10 ml) also cooled in ice was added all at once. After having been left 48 h at room temperature, the acetone was evaporated, the residue was suspended in 2 *N* sulfuric acid (60 ml), and sodium sulfite was added until the green color persisted. The liquor was made basic with sodium carbonate and extracted with chloroform. Evaporation of the extract yielded the crude oxidation product (585 mg) which in thin layer chromatography was found to contain minor contaminating substances and some starting material as well. The crude product was therefore acetylated by the usual method. The resulting product was dissolved in benzene, chromatographed on alumina, and eluted with benzene. Fractions 2–7 of the eluate on evaporation left a crystalline acetyl ketone (480 mg), m.p. 151–159°. After several recrystallizations from acetone – *n*-hexane, it consisted of colorless needles, m.p. 158–160°.

Anal. Calcd. for $C_{27}H_{41}O_7N$: C, 65.96; H, 8.41. Found: C, 65.79; H, 8.83.

ν_{max} 1 751, 1 727, 1 242 cm^{-1}. In the n.m.r. spectrum: singlets at δ 1.99 (3H), 3.28 (9H), 3.19 (3H), triplet centered at δ 1.08 (3H).

Hydrolysis of the pure acetyl ketone (V) gave a colorless glass that failed to crystallize. ν_{max} 3 350 cm^{-1} (OH), 1 750 cm^{-1} (cyclic five-membered ketone). An attempt to prepare a crystalline salt also failed.

To a small quantity of the amorphous ketone in methanol, sodium borohydride was added. The reduction product, worked up as usual, was identical in every respect with chasmanine. Reduction of the crystalline monoacetyl ketone with lithium aluminium hydride also produced chasmanine shown by X-ray powder patterns to be identical with the original alkaloid.

(*b*) To a solution of chasmanine (243 mg) in pyridine (1 ml) was added chromium trioxide – pyridine complex, prepared from chromium trioxide (600 mg) and pyridine (9 ml), and the reaction mixture allowed to stand at room temperature for 90 h. The mixture was made basic with dilute ammonia and extracted thoroughly with chloroform. Evaporation of the extract left a brown syrup which was suspended in 5% hydrochloric acid and extracted with chloroform to remove the neutral product (extract A). The aqueous solution was rendered alkaline with sodium carbonate and extracted with chloroform. Evaporation of this previously dried extract left a syrup (112 mg); it was dissolved in chloroform, chromatographed over Florisil, and eluted with the same solvent, the eluate being collected in 10 ml fractions. Evaporation of the eluant left a number of crystalline fractions that were combined and recrystallized in ether from which N-deethyl-10-dehydrochasmanine-azomethine separated as colorless needles, m.p. 196°, wt. 20 mg. ν_{max}^{KBr} 1 761 cm^{-1} CO), 1 655 cm^{-1} (—CH=N—); $\nu_{max}^{CHCl_3}$ 1 756, 1 634 cm^{-1}. In the n.m.r. spectrum: singlet at δ 7.51 (1H, —CH=N—), δ 3.72 (2H, $\rangle$C—CH_2—OCH_3), δ 6.68, 6.74, 6.76 ($4OCH_3$).

Anal. Calcd. for $C_{23}H_{33}O_6N$: C, 65.85; H, 7.93; N, 3.34. Found: C, 65.86; H, 7.93; N, 3.37.

The extract A from the acid separation was washed with water, dried, and evaporated. The residual syrup (156 mg) was chromatographed over Florisil exactly as above. The crystalline fractions obtained

Can. J. Chem. Downloaded from www.nrcresearchpress.com by 210.87.254.40 on 09/05/12
For personal use only.

from the eluate were combined and recrystallized from *n*-hexane – acetone from which N-acetyl-N-deethyl-10-dehydrochasmanine separated as colorless scales, m.p. 206–207°, wt. 54 mg. ν_{max}^{KBr} 1 755 cm^{-1} (CO), 1 660 cm^{-1} (N—Ac). In the n.m.r. spectrum: signals at δ 6.68, 6.72, 6.75 ($4OCH_3$), singlet at δ 2.19 (N—Ac).

Anal. Calcd. for $C_{25}H_{37}O_7N \cdot H_2O$: C, 62.35; H, 8.16; N, 2.91. Found: C, 62.06; H, 7.89; N, 2.90.

Conversion of N-Deethyl-10-dehydrochasmanine-azomethine to Chasmanine

N-Deethyl-10-dehydrochasmanine-azomethine (23 mg) was dissolved in ethyl iodide (1 ml), the solution kept for 3 h at room temperature and evaporated to dryness under reduced pressure. The residue was crystallized twice from ethanol, m.p. 250–251° (decomp.), wt. 20 mg. ν_{max}^{KBr} 1 762, 1 672 cm^{-1}.

Anal. Calcd. for $C_{23}H_{33}O_6N—C_2H_5I$: C, 52.17; H, 6.66; N, 2.44. Found: C, 52.38; H, 6.71; N, 2.42.

To a solution of the ethiodide (18 mg) in methanol sodium borohydride (18 mg) was added and the solution was allowed to stand at room temperature for 16 h. The reduction product, worked up as usual, was a crystalline mass which after recrystallization from *n*-hexane consisted of colorless needles, m.p. 88–89°, wt. 4 mg. A further crop (8 mg) was obtained from the mother liquor. In admixture with chasmanine the melting point was unaltered, and the infrared spectra of both were superimposable.

Reduction of N-Acetyl-N-deethyl-10-dehydrochasmanine

This product (10 mg) was refluxed for 20 min with lithium aluminium hydride (40 mg) in tetrahydrofurane (5 ml). The reaction mixture, worked up as usual, yielded a crystalline substance (9 mg) which after recrystallization from *n*-hexane had m.p. 85°, wt. 5 mg. It was identical in every respect with chasmanine.

Benzoylchasmanine (XV)

A mixture of chasmanine (47 mg), freshly distilled benzoyl chloride (0.15 ml), and pyridine (1 ml) was kept at room temperature for 1 h. The reaction mixture was poured onto ice and made basic by the addition of potassium carbonate and the solution extracted with chloroform. Evaporation of the extract left the crude product (79 mg) which after chromatography in benzene on alumina afforded benzoylchasmanine (48 mg) which gave only one spot in thin layer chromatography. The product could not be induced to crystallize. It was distilled at 145° and 5×10^{-5} mm, but gave somewhat unsatisfactory analytical figures. ν_{max} 3 350 (OH), 1 710 cm^{-1} (CO). In the n.m.r. spectrum: multiplet at δ 8.10–7.30 (5H), triplets centered at δ 5.17 (1H) and 1.08 (3H), singlets at δ 3.30 (6H), 3.26 (3H), 3.17 (3H). It formed a hydrochloride that crystallized from acetone as colorless prisms, m.p. 248–249°, and gave good analytical results.

Anal. Calcd. for $C_{32}H_{45}O_7N \cdot HCl$: C, 64.86; H, 7.67. Found: C, 64.60; H, 7.76.

Acetylbenzoylchasmanine (XVI)

Benzoylchasmanine (264 mg) was heated on a steam bath for 1 h with *p*-toluenesulfonic acid (150 mg) and acetic anhydride (5 ml). The reaction mixture, worked up as usual, yielded acetylbenzoylchasmanine (260 mg) which solidified when triturated with *n*-hexane. After several crystallizations from the same solvent, it consisted of a microcrystalline solid, m.p. 148–156°.

Anal. Calcd. for $C_{34}H_{47}O_8N$: C, 68.32; H, 7.93. Found: C, 68.34; H, 7.84.

In the n.m.r. spectrum: singlets at δ 3.37 (3H), 3.27 (3H), 3.24 (3H), 3.16 (3H) (OCH_3 groups), 1.36 (OAc), triplets centered at δ 1.07 (3H), 5.07 (1H).

Acetylbenzoylchasmanine readily formed a perchlorate which after two crystallizations from ethanol consisted of colorless needles, m.p. 231–234°. ν_{max} 1 718, 1 600, 1 583 (weak), 719 cm^{-1} (strong).

Anal. Calcd. for $C_{34}H_{47}O_8N \cdot HClO_4$: C, 58.45; H, 6.88. Found: C, 58.24; H, 7.02.

Pyrolysis of Diacetylchasmanine

Diacetylchasmanine (264 mg) was heated under reduced pressure (10 mm) during 6 min at 185–190° (air bath). The product was dissolved in ether, chromatographed on a short column of alumina, and eluted with ether. Evaporation of the elutate left a gum (234 mg) which showed three spots in thin layer chromatography. The mixture could not be separated by column chromatography. It was dissolved in 2% methanolic potassium hydroxide (20 ml) and the solution refluxed for 1 h. The methanolic solution was evaporated to dryness, the residue dissolved in ice-cold water, and the aqueous solution extracted with chloroform. Evaporation of the extract left a gum (219 mg) which was dissolved in *n*-hexane and chromatographed on alumina. It was eluted with *n*-hexane, with benzene, with 50% chloroform–benzene and finally with chloroform, the eluate being collected in 10 ml fractions.

The *n*-hexane eluate (fractions 2–5) yielded isopyrochasmanine VIII (62 mg) which, after several crystallizations from *n*-hexane, was obtained as colorless elongated prisms, m.p. 177–179°. ν_{max} 3 450 (OH), 1 106, 1 087 cm^{-1} (OCH_3). In the n.m.r. spectrum: singlets at δ 3.31 (6H), 3.25 (3H), 3.21 (3H), triplet centered at δ 1.02, multiplet at δ 6.12–5.75.

Anal. Calcd. for $C_{25}H_{39}O_5N$: C, 69.25; H, 9.07. Found: C, 68.98; H, 9.28.

Fractions 6–10 made up the benzene eluate. Fractions 6 and 7 contained mainly pyrochasmanine VII but was contaminated with isopyrochasmanine. Fractions 8 and 9 yielded pure pyrochasmanine (74 mg) while fraction 10 contained mainly pyrochasmanine with an impurity of lower mobility in thin layer chromatography. Fractions 6, 7, and 10 were combined and rechromatographed thus affording a second crop of pure pyrochasmanine (35 mg). Pyrochasmanine, after crystallization from *n*-hexane, consisted of colorless prisms, m.p. 126–129°. ν_{max} 3 430 (OH), 1 634 cm^{-1} (double bond). In the n.m.r. spectrum: singlets at δ 3.14

Can. J. Chem. Downloaded from www.nrcresearchpress.com by 210.87.254.40 on 09/05/12
For personal use only.

(3H), 3.28 (3H), 3.24 (3H), 3.21 (3H), doublet at δ 5.43 (1H) (J = 6 c.p.s.), triplet centered at δ 1.04 (3H).

Anal. Calcd. for $C_{25}H_{39}O_5N$: C, 69.25; H, 9.07. Found: C, 69.16; H, 8.78.

The chloroform–benzene and chloroform eluates gave fractions 11–13. They contained demethylisopyrochasmanine IX (36 mg), homogeneous in thin layer chromatography. After several crystallizations from *n*-hexane – acetone, it consisted of colorless needles, m.p. 163–165°. ν_{max} 3 420, 3 418 cm^{-1} (OH), 743 cm^{-1} (double bond). In the n.m.r. spectrum: singlets at δ 3.32 (3H), 3.30 (3H), 3.21 (3H), triplet centered at 1.02 (3H), multiplet at δ 5.91–5.67 (2H). For analysis a sample was sublimed at 150° and 9×10^{-5} mm.

Anal. Calcd. for $C_{24}H_{37}O_5N$: C, 68.70; H, 8.89. Found: C, 68.56; H, 8.86.

Isopyrochasmanine VIII

Pyrochasmanine (20 mg) dissolved in methanol (5 ml) containing 1 drop of 70% perchloric acid was heated under reflux for 30 min. The reaction mixture was evaporated, the residue dissolved in water, and the solution made basic with sodium carbonate and extracted with chloroform. Evaporation of the extract left a residue of isopyrochasmanine that crystallized spontaneously. Recrystallized from *n*-hexane it separated as colorless elongated prisms, m.p. 177–179°, This product was identical with the sample obtained directly from the pyrolysis mixture (melting point, that of the mixture, infrared spectra, mobility in thin layer chromatography).

Demethoxyisopyrochasmanine XIV

A mixture of pyrochasmanine (32 mg) and lithium aluminium hydride (50 mg) in tetrahydrofurane (5 ml) was stirred for 15 h at room temperature. After decomposition of the excess hydride by the addition of wet ether, the mixture was diluted with methylene chloride and filtered. The inorganic material was washed with methylene chloride and the combined filtrate and washings were evaporated to dryness. The residue was dissolved in *n*-hexane and passed through a short column of alumina, and the solution evaporated to dryness. The residue was demethoxyisopyrochasmanine (29 mg) which crystallized when triturated with *n*-pentane. Recrystallized from *n*-hexane, it consisted of colorless fine needles, m.p. 84–88°. ν_{max} 3 410 (OH), 710, 690 cm^{-1} (double bond). In the n.m.r. spectrum: singlets at δ 3.29 (3H), 3.28 (3H), 3.22 (3H), a triplet at δ 1.02 (3H), a multiplet at δ 6.03–5.78.

Anal. Calcd. for $C_{24}H_{37}O_4N$: C, 71.43; H, 9.24. Found: C, 71.41; H, 9.37.

Demethoxyisopyrochasmanine formed a perchlorate which after several crystallizations from isopropanol gave colorless prisms, m.p. 207–210°.

Anal. Calcd. for $C_{24}H_{37}O_4N.HClO_4$: C, 57.14; H, 7.54. Found: C, 56.98; H, 7.66.

Dihydrodemethoxyisopyrochasmanine

The perchlorate of demethoxyisopyrochasmanine (55 mg) was dissolved in ethanol (10 ml) and hydrogenated in the presence of platinum oxide (22 mg). When the absorption of hydrogen had ceased, the catalyst was removed by filtration and the filtrate evaporated to dryness. The residue was dissolved in water and the solution was made basic with sodium carbonate and extracted with chloroform. Evaporation of the extract left a foam (54 mg) which was dissolved in benzene, chromatographed on alumina, and eluted with benzene. The eluate on evaporation yielded pure dihydrodemethoxyisopyrochasmanine (52 mg) which could not be induced to crystallize. Its n.m.r. spectrum contained no signal attributable to double bond protons. The base was converted to the perchlorate which crystallized from ethanol. After two recrystallizations from the same solvent, it consisted of colorless prisms, m.p. 173–174°.

Anal. Calcd. for $C_{24}H_{39}O_4N.HClO_4$: C, 56.92; H, 7.91. Found: C, 57.32; H, 7.68.

Demethylisopyrochasmanine IX

Isopyrochasmanine (48 mg) and lithium aluminium hydride (50 mg) were stirred overnight in tetrahydrofurane (5 ml) at room temperature. The reaction mixture was worked up as in the similar experiment with pyrochasmanine. Thin layer chromatography showed the presence in the product of starting material and several other substances of lower mobility. The product was dissolved in benzene, chromatographed on alumina, and eluted with benzene. Fractions 3–5 of the benzene eluate contained demethylisopyrochasmanine. The total yield obtained (20 mg) was crystallized twice from *n*-hexane – acetone from which the compound separated as colorless needles, m.p. 158–164°. After sublimation at 145° and 5×10^{-5} mm, it melted at 163–165°, and was identical in melting point, that of the mixture, infrared spectra, and behavior in thin layer chromatography with demethylisopyrochasmanine isolated in the pyrolysis reaction described above.

Reduction of Pyrolysis Product with Lithium Aluminium Hydride

Diacetylchasmanine (1.880 g) was pyrolyzed at 190° (air bath) for 8 min. The crude reaction mixture was dissolved in ether, chromatographed on alumina, and eluted with ether. Evaporation of the eluate left a foam (1.765 g) which was dissolved in tetrahydrofurane (25 ml) and stirred overnight at room temperature with lithium aluminium hydride ($\sim$ 0.5 g). The excess hydride was decomposed by the addition of wet ether and the product was worked up exactly as described above for the reduction of pyrochasmanine. The product (1.532 g) was found by thin layer chromatography to contain three compounds. It was dissolved in benzene and chromatographed on alumina. The column was eluted first with benzene, then with chloroform–benzene (1:4) and chloroform–benzene (1:1), and finally with chloroform and with chloroform containing 3% methanol, the eluate being collected in 50 ml fractions.

Can. J. Chem. Downloaded from www.nrcresearchpress.com by 210.87.254.40 on 09/05/12
For personal use only.

Fractions 2–6 (benzene eluate) contained isopyrochasmanine (658 mg) which after two crystallizations from *n*-hexane consisted of colorless needles, m.p. 177–179°.

Fractions 7–9 (chloroform–benzene (1:4)) and fractions 10–13 (chloroform–benzene (1:1)) both yielded demethoxyisopyrochasmanine (439 mg) which was slightly impure and was rechromatographed. The eluted material consisted of the homogeneous compound (407 mg) which crystallized from *n*-hexane as fine needles, m.p. 84–88°. It formed a perchlorate separating from isopropanol as colorless prisms, m.p. 207–210°.

The remaining fractions (14–17) eluted with chloroform and methanol–chloroform, yielded a residue (436 mg) which in thin layer chromatography showed one main spot and a few weaker, less mobile spots. Repeated chromatography in benzene on short alumina columns gave homogeneous demethylisopyrochasmanine (427 mg) which after crystallization from *n*-hexane – acetone melted at 163–165°.

All three products, isopyrochasmanine, demethoxyisopyrochasmanine, and demethylisopyrochasmanine, were identical in every respect with samples obtained in previous experiments described above.

Diacetyldemethylisopyrochasmanine X

Demethylisopyrochasmanine (60 mg) was heated on a steam bath with acetic anhydride (2 ml) and *p*-toluenesulfonic acid (50 mg). The reaction mixture, worked up as usual, yielded the product which was chromatographed on alumina in benzene solution and eluted with the same solvent. On evaporation, the eluate left the diacetyl compound (53 mg) which crystallized from *n*-hexane as colorless plates, m.p. 121–123°.

Anal. Calcd. for $C_{28}H_{41}O_7N$: C, 66.77; H, 8.21. Found: C, 66.57; H, 8.19.

ν_{max} 1728, 1716 (CO), 705 cm^{-1} (double bond). In the n.m.r. spectrum: triplet centered at δ 1.02 (3H), singlets at δ 1.93 (3H), 1.99 (3H), 3.29 (3H), 3.21 (6H), multiplet, at δ 6.60–5.83 (2H). Hydrogenation under the usual conditions gave the dihydrodiacetyl derivative (see below).

Dihydrodemethylisopyrochasmanine

Demethylisopyrochasmanine (213 mg) dissolved in ethanol (20 ml) containing a few drops of 70% perchloric acid was hydrogenated in contact with platinum oxide (57 mg). The reaction product, worked up as usual (see above hydrogenation of demethoxy compound), consisted of a gum (212 mg) which crystallized on contact with ether. After several recrystallizations from ether – *n*-hexane, dihydrodemethylisopyrochasmanine formed colorless prisms, m.p. 124–127°.

Anal. Calcd. for $C_{24}H_{39}O_5N.\frac{1}{2}H_2O$: C, 66.97; H, 9.37. Found: C, 67.34; H, 9.66.

Diacetyldihydrodemethylisopyrochasmanine XI

A mixture of dihydrodemethylisopyrochasmanine (200 mg) and *p*-toluenesulfonic acid (100 mg) was heated with acetic anhydride (5 ml) for 1 h on the steam bath. The diacetyl product (188 mg), isolated as usual from the reaction mixture, was crystallized from *n*-hexane from which it separated as colorless prisms, m.p. 123–125°.

Anal. Calcd. for $C_{28}H_{43}O_7N$: C, 66.51; H, 8.57. Found: C, 66.68, H, 8.73.

ν_{max} 1 730, 1 720 cm^{-1} (CO). The product was identical with that obtained by the catalytic hydrogenation of diacetyldemethylisopyrochasmanine.

Demethoxypyrochasmanine

Diacetyldihydrodemethylisopyrochasmanine (109 mg) was heated under reduced pressure (15 mm) for 5 min at 190° (air bath). The product was dissolved in benzene, chromatographed on alumina, and eluted with the same solvent. Evaporation of the eluate left a gum (80 mg) which gave a single spot in thin layer chromatography. ν_{max} 1 727 cm^{-1} (CO).

The gummy product (80 mg) thus obtained was refluxed with 3% methanolic potassium hydroxide (5 ml) for 30 min. The solvent was evaporated, water and ice were added, and the solution extracted with chloroform. Evaporation of the extract left a residue which was dissolved in *n*-hexane – benzene (1:1), chromatographed on alumina, and eluted with the same solvent. The eluate yielded homogeneous demethoxypyrochasmanine (61 mg) which failed to crystallize. It was converted to the perchlorate which crystallized from isopropanol as prisms with a slight yellowish cast, m.p. 198–202°. ν_{max} 3 475 cm^{-1} (OH).

Anal. Calcd. for $C_{24}H_{37}O_4N.HClO_4.\frac{1}{2}H_2O$: C, 56.21; H, 7.60. Found: C, 56.22; H, 7.60.

Dihydrodemethoxypyrochasmanine

Demethoxypyrochasmanine perchlorate (39 mg) was dissolved in ethanol (10 ml) and hydrogenated in contact with platinum oxide (25 mg). When hydrogen absorption had ceased, the catalyst was filtered off and the filtrate evaporated to dryness. The residue was dissolved in water, and the solution made basic with sodium carbonate and extracted with chloroform. Evaporation of the extract left a gum which was converted into the perchlorate. The salt crystallized from ethanol as colorless prisms, m.p. 173–174°. It was identical in melting point, that of the mixture, mobility in thin layer chromatography, infrared spectra, and X-ray powder patterns with the salt derived earlier from pyrochasmanine and designated dihydrodemethoxyisopyrochasmanine perchlorate (see above).

Demethylation of Isopyrochasmanine

Experiment 1

Isopyrochasmanine (141 mg) was dissolved in 50% sulfuric acid (5 ml) and heated on the steam bath for 40 min. The cooled solution was diluted by the addition of ice and alkalized with sodium carbonate. It

Can. J. Chem. Downloaded from www.nrcresearchpress.com by 210.87.254.40 on 09/05/12
For personal use only.

Can. J. Chem. Downloaded from www.nrcresearchpress.com by 210.87.254.40 on 09/05/12
For personal use only.

was extracted six times with chloroform and the combined extract evaporated to dryness. There was left a residue (121 mg) which gave three spots in thin layer chromatography. The residue was dissolved in benzene, chromatographed on alumina, and eluted first with benzene, then with benzene–chloroform (1:1), with chloroform, and finally with chloroform containing 2% methanol, the eluate being collected in fractions of 30 ml.

Fractions 1–3 (benzene eluate) afforded a compound (32 mg) which after crystallization from ether consisted of colorless needles, m.p. 164–167°. In the n.m.r. spectrum: singlet at δ 3.29 (6H), triplet centered at δ 1.02 (3H), multiplet at δ 5.90–5.62 (2H). For analysis a sample was sublimed at 145° and 10^{-4} mm.

Anal. Calcd. for $C_{23}H_{33}O_4N$: C, 71.29; H, 8.58. Found: C, 74.22; 9.18.

The analytical figures are unsatisfactory and indicate either the presence of an impurity or partial solvation with benzene even after sublimation (calcd. for $C_{23}H_{33}O_4N.C_6H_6$: C, 74.80; H, 8.44).

Fractions 4–6 eluted with benzene–chloroform (1:1) gave demethylisopyrochasmanine (35 mg) which, after crystallization from ether and sublimation, melted at 163–165°, undepressed by admixture with the product obtained in the pyrolysis. The infrared spectra of the two compounds were identical and so was their behavior in thin layer chromatography.

Fractions 7–10 eluted with chloroform and with chloroform containing 2% methanol yielded tridemethylanhydroisopyrochasmanine XVII (45 mg) which formed colorless prismatic crystals from methanol, m.p. 245–248° (decomp.). For analysis a sample was sublimed at 170° and 5×10^{-5} mm.

Anal. Calcd. for $C_{22}H_{31}O_4N$: C, 70.75; H, 8.27; N, 3.75. Found: C, 70.66; H, 8.27; N, 3.81.

Because of the low solubility of the product, its n.m.r. spectrum was obtained in pyridine solution, and for comparison the spectrum of isopyrochasmanine was taken in the same solvent. Compound XVII: singlet at δ 2.50 (3H), triplet centered at 0.25 (3H). Isopyrochasmanine: singlets at δ 2.63 (3H), 2.59 (3H), 2.49 (3H), 2.31 (3H), triplet centered at δ 0.30 (3H).

Experiment 2

Isopyrochasmanine (41 mg) dissolved in 50% sulfuric acid (2 ml) was heated on the steam bath for 2¼ h. The reaction mixture worked up as in Experiment 1 gave a product (27 mg) which crystallized spontaneously and in thin layer chromatography showed two spots: a more mobile one (weak) corresponding to demethylisopyrochasmanine, and a less mobile one (strong) corresponding to tridemethylanhydroisopyrochasmanine (XVII). The last compound was obtained in a pure condition by crystallization of the crude product from methanol, m.p. 245–248°.

Experiment 3

Tridemethylanhydroisopyrochasmanine was treated under the conditions described in Experiment 2. It was recovered unchanged in 70% yield.

Experiment 4

Isopyrochasmanine (210 mg) was dissolved in acetone (40 ml) and potassium permanganate (150 mg) in 50% acetone–water (40 ml) was added all at once. The mixture was stirred for 5 min at room temperature and the excess permanganate decomposed with sulfurous acid (sodium sulfite and dilute sulfuric acid). After evaporation of the acetone the remaining aqueous solution was made basic by the addition of aqueous sodium carbonate and extracted with chloroform. The extract was evaporated to dryness and the residue, which was homogeneous in thin layer chromatography, was heated on the steam bath for 90 min with acetic anhydride (2.5 ml) and pyridine (2.5 ml). The reaction mixture, worked up as usual, was dissolved in benzene, chromatographed on alumina, and eluted with benzene. Evaporation of the eluate left the residual gummy N,O-diacetyl-N-deethylisopyrochasmanine (250 mg) which gave a single spot in thin layer chromatography. Its infrared absorption spectrum indicated the presence of an N—Ac group (1 610 cm^{-1}) and an O—Ac group (1 715, 1 245 cm^{-1}). The compound was heated in a water bath (60–65°) for 1 h with zinc chloride (10 g) in 5% hydrochloric acid (3.5 ml). The solution, after cooling, was diluted with water (25 ml) and extracted continuously with chloroform for 50 h. The chloroform extract, on evaporation to dryness, left a gum (167 mg) which was dissolved in tetrahydrofurane (10 ml) and heated with lithium aluminium hydride under reflux for 2 h. The excess hydride was decomposed with wet ether and the solution diluted with chloroform and filtered. The inorganic filtered salt was washed with chloroform and the combined filtrate and washings were evaporated to dryness. There was left a residue (142 mg) which in thin layer chromatography produced only one spot identical in mobility with that produced by tridemethylanhydroisopyrochasmanine XVII. The product was dissolved in chloroform, chromatographed on alumina, and eluted with chloroform. The residue left after evaporation of the eluate was crystallized twice from methanol from which it separated as colorless prisms, m.p. 244–247° (decomp.). Its n.m.r. spectrum in pyridine solution showed a signal at δ 2.50 corresponding to three protons, identical with that of compound XVII.

Demethylanhydroisopyrobikhaconine

Isopyrobikhaconine (XVIII) (130 mg) after the same sequence of reactions as described in Experiment 4 above, yielded demethylanhydroisopyrobikhaconine (XIX) (112 mg) which after crystallization from ethanol was obtained as colorless prisms, m.p. 242–243°. For analysis it was sublimed at 190° and 6×10^{-5} mm. In the n.m.r. spectrum in pyridine solution it showed signals at δ 2.50 (3H) and a triplet centered at δ 0.25 (3H).

Anal. Calcd. for $C_{22}H_{31}O_5N$: C, 68.01; H, 7.96. Found: C, 68.24, H, 8.26.

N-Deethylchasmanine

To chasmanine (243 mg) in acetone (40 ml) potassium permanganate (152 mg) in 50% acetone–water (40 ml) was added all at once. After the mixture had been stored for 5 min at room temperature, the excess permanganate was reduced by the addition of sodium sulfite and dilute sulfuric acid. The liquor was concentrated until the acetone had evaporated, was made basic with sodium carbonate, and extracted with chloroform. The extract was evaporated to dryness, the residue dissolved in benzene, chromatographed on alumina, and eluted with the same solvent. Evaporation of the eluate left a residue which solidified when triturated with ether, and crystallized from benzene (152 mg). The mother liquor, when chromatographed on alumina, yielded a further crop of N-deethylchasmanine (60 mg). The product after two crystallizations from benzene, consisted of colorless needles, m.p. 232–234°. Its n.m.r. spectrum did not contain a triplet at $\delta \sim 1.0$.

Anal. Calcd. for $C_{23}H_{37}O_6N$: C, 65.22; H, 8.81. Found: C, 65.02; H, 8.82.

N-Methyl-N-deethylchasmanine

N-Deethylchasmanine (83 mg) in 50% ether–methanol (6 ml) was heated under reflux for 30 min with methyl iodide (1 ml) and powdered potassium carbonate (100 mg). The solvent was evaporated and the residue dissolved in water and extracted with methylene chloride. The extract was evaporated and the residue dissolved in *n*-hexane – benzene (1:1), chromatographed on alumina, and eluted with the same solvent. Evaporation of the eluate left a residue (78 mg) which crystallized spontaneously. After several crystallizations from *n*-hexane, N-methyl-N-deethylchasmanine formed fine colorless needles, m.p. 90–92°. In the n.m.r. spectrum: singlets at δ 3.31 (3H), 3.28 (6H), 3.23 (3H), and 2.29 (3H).

Anal. Calcd. for $C_{24}H_{39}O_6N$: C, 65.87; H, 8.98; N, 3.20. Found: C, 65.64; H, 9.10; N, 3.19.

When N-deethylchasmanine was treated similarly with ethyl iodide, it was converted back to chasmanine.

Bikhaconitine Methanesulfonate (XX)

Bikhaconitine perchlorate (1.2 g) with pyridine (10 ml) and methanesulfonyl chloride (2 ml) was kept at room temperature overnight. The resulting brown mixture was poured into ice water, made basic with potassium carbonate, and extracted with chloroform. The extract, after drying over magnesium sulfate, was evaporated to dryness. It left a brown gum that was dissolved in benzene, chromatographed on alumina, and eluted with benzene. Evaporation of the eluate left a residue that crystallized when triturated in the presence of ether. Recrystallized from methanol, it consisted of colorless prisms, m.p. 188–190°, yield, 0.9 g.

Anal. Calcd. for $C_{37}H_{53}O_{13}NS$: C, 59.10; H, 7.11. Found: C, 59.01; H, 7.16.

Deoxyaconitine methanesulfonate was also prepared exactly as above. It formed colorless prisms from methanol, m.p. 194–195°.

Anal. Calcd. for $C_{35}H_{49}O_{12}NS$: C, 59.39; H, 6.98. Found: C, 59.22; H, 7.00.

Further treatment with methanesulfonyl chloride failed to introduce a second group.

Hydrogenolysis of Bikhaconitine Mesylate

Bikhaconitine mesylate (900 mg) dissolved in dioxane (100 ml) was hydrogenated over Raney nickel at 120–130° and 41 atm for 15 h. The product, isolated as usual, was dissolved in benzene and extracted with 5% hydrochloric acid. The aqueous solution was alkalized with potassium carbonate and extracted with chloroform. The gummy residue (500 mg) left after evaporation of the extract showed two spots in thin layer chromatography; it was dissolved in benzene–hexane (1:1) and chromatographed on grade III alumina. Elution was done first with the same solvent mixture, then with benzene, with benzene–chloroform, and finally with chloroform. The first eluate yielded 290 mg of a mixture of components A and B while the benzene and benzene–chloroform eluates yielded pure B. Rechromatography of the first eluate gave pure A and pure B. Component B, recrystallized from ether, consisted of colorless prisms, m.p. 190–193°.

Anal. Calcd. for $C_{35}H_{51}O_{11}NS$: C, 60.60; 7.36. Found: C, 61.11; H, 7.45.

That this component is correctly designated by formula XXIII has been shown by its alternative preparation from pyrobikhaconitine (7). This compound was hydrogenated catalytically by the usual procedure over platinum oxide to dihydropyrobikhaconitine, colorless needles from ether, m.p. 181–183°.

Anal. Calcd. for $C_{34}H_{47}O_9N \cdot \frac{1}{2}H_2O$: C, 65.57; H, 7.47. Found: C, 65.71; H, 7.98.

Treatment with methanesulfonyl chloride as described above gave the *O*-mesylate, m.p. 191–194°, identical in every respect (mixture melting point, infrared, thin layer chromatography) with the hydrogenolysis component.

The minor component A separated by chromatography from the product of hydrogenolysis could not be obtained very pure because of paucity of material, and because it failed to crystallize. The infrared and n.m.r. spectra showed that it no longer contained the mesylate nor the acetoxy groups, but still contained an imino-ethyl, four methoxyls, and the two veratroyl methoxyls. It was assumed to have structure XXIV and it was hydrolyzed to the corresponding alkamine XXV.

Pyrochasmanine was hydrogenated catalytically to dihydrochasmanine. The product could not be induced to crystallize; it had the same behavior in thin layer chromatography as compound XXV. All attempts to prepare crystalline salts from the two products failed. It is probable that the two compounds were identical but there was insufficient material for further comparison.

Can. J. Chem. Downloaded from www.nrcresearchpress.com by 210.87.254.40 on 09/05/12
For personal use only.

ACKNOWLEDGMENTS

We express our thanks to Mr. M. Lesage who prepared the n.m.r. spectra, Mr. R. Lauzon for the infrared spectra, and Mr. H. Séguin for the microanalyses. We also thank Dr. M. Przybylska for preparing the X-ray powder patterns.

REFERENCES

1. O. ACHMATOWICZ, JR. and L. MARION. Can. J. Chem. **42**, 154 (1964).
2. R. E. GILMAN and L. MARION. Tetrahedron Letters, No. 20, 923 (1962).
3. W. R. DUNSTAN and A. E. ANDREWS. J. Chem. Soc. **87**, 1620 (1905).
4. W. A. JACOBS and C. F. HUEBNER. J. Biol. Chem. **170**, 209 (1947).
5. Y. TSUDA and L. MARION. Can. J. Chem. **41**, 1485 (1963).
6. K. WIESNER, H. W. BREWER, D. L. SIMMONS, D. R. BABIN, F. BICKELHAUPT, J. KALLOS, and T. BOGRI. Tetrahedron Letters, No. 3, 17 (1960).
7. Y. TSUDA and L. MARION. Can. J. Chem. **41**, 3055 (1963).
8. K. WIESNER, F. BICKELHAUPT, and Z. VALENTA. Tetrahedron, **4**, 418 (1958).
9. Y. TSUDA and L. MARION. Can. J. Chem. **41**, 1634 (1963).
10. W. A. JACOBS and Y. SATO. J. Biol. Chem. **180**, 133 (1949).
11. K. WIESNER, F. BICKELHAUPT, D. R. BABIN, and M. GÖTZ. Tetrahedron Letters, No. 3, 11 (1959).
12. O. ACHMATOWICZ, JR., Y. TSUDA, and L. MARION. In preparation.
13. T. OKAMOTO, M. NATSUME, H. ZENDA, and S. KAMOTO. Chem. Pharm. Bull. Tokyo, **10**, 883 (1962).
14. E. OCHIAI, T. OKAMOTO, and S. SAKAI. J. Pharm. Soc. Japan (Yakugaku Zasshi), **75**, 550 (1955).

Can. J. Chem. Downloaded from www.nrcresearchpress.com by 210.87.254.40 on 09/05/12
For personal use only.

Can. J. Chem. Downloaded from www.nrcresearchpress.com by 210.87.254.5 on 09/05/12
For personal use only.

A NOVEL SYNTHESIS FOR AMINODIDEOXY SUGARS

3-AMINO-2,3-DIDEOXY-D-ARABINO-HEXOSE

HANS HELMUT BAER AND THOMAS NEILSON
Department of Chemistry, University of Ottawa, Ottawa, Canada

Received August 20, 1964

ABSTRACT

The 4,6-*O*-benzylidene derivative II of methyl 3-nitro-3-deoxy-β-D-glucopyranoside (I) was prepared. Its 2-*O*-acetate (III) was converted by a Schmidt–Rutz reaction into methyl 4,6-*O*-benzylidene-2,3-dideoxy-3-nitro-β-D-*erythro*-hexos-2-enide (IV). Selective hydrogenation of the olefinic double bond in IV afforded methyl 4,6-*O*-benzylidene-2,3-dideoxy-3-nitro-β-D-*arabino*-hexopyranoside (V). The debenzylidenated derivative of V (VI) was reduced to methyl 3-amino-2,3-dideoxy-β-D-*arabino*-hexopyranoside hydrochloride (VII), from which the free reducing sugar (VIII), the *N*-acetyl glycoside (IX), the *N*-acetyl glycoside 4,6-di-*O*-acetate (X), and the *N*-acetyl glycoside 4,6-di-*O*-mesylate (XI) were obtained. The solvolysis of XI proceeded with neighboring group participation to give a product of either aziridine (XII) or pyrrolidine (XIII) structure.

More than a dozen amino sugars of unusual structures have been characterized as components of antibiotics (1). In the present paper is described the synthesis of a new amino dideoxy hexose, 3-amino-2,3-dideoxy-D-*arabino*-hexose (VIII). Although this particular sugar has not as yet been discovered in nature, it may well prove to become significant in further analytical and synthetic investigations in the field of carbohydrate antibiotics.

Methyl 3-nitro-3-deoxy-β-D-glucopyranoside (I), which is readily available (2, 3) by nitromethane cyclization from methyl β-D-glucopyranoside, was converted into its 4,6-*O*-benzylidene derivative II in 74% yield. Acetylation of II with acetic anhydride in pyridine gave methyl 2-*O*-acetyl-4,6-*O*-benzylidene-3-nitro-3-deoxy-β-D-glucopyranoside (III) in 90% yield. This is noteworthy because acetylations, in the presence of pyridine, of other cyclic nitro alcohols have been known (4) to lead to dehydration. Treatment of acetate III with solid sodium bicarbonate in refluxing benzene smoothly afforded nitroolefin IV, methyl 4,6-*O*-benzylidene-2,3-dideoxy-3-nitro-β-D-*erythro*-hexos-2-enide (Schmidt–Rutz reaction (5, 6)). This compound is the first sugar derivative possessing a nitroolefin grouping as part of a glycosidic ring; it is very reactive as far as addition reactions are concerned. Thus, it easily adds ammonia or ethanol. Catalytic hydrogenation of IV using 10% palladium on charcoal readily furnished methyl 4,6-*O*-benzylidene-2,3-dideoxy-3-nitro-β-D-*arabino*-hexopyranoside (V).[1] Proof of the configuration at C-3 is established below. Since V was obtained in 87% yield after recrystallization, this hydrogen addition appeared to be remarkably stereoselective. Gentle hydrolytic removal of the benzylidene blocking group in V produced methyl 2,3-dideoxy-3-nitro-β-D-*arabino*-hexopyranoside (VI). For preparative purposes, VI may be obtained from II in 50% overall yield without purification of the intermediates III, IV, and V. Catalytic reduction, with platinum in the presence of 1 molar equivalent of hydrochloric acid, converted VI into methyl 3-amino-2,3-dideoxy-β-D-*arabino*-hexopyranoside hydrochloride (VII) which, on acid hydrolysis, gave the corresponding free sugar, 3-amino-2,3-dideoxy-D-*arabino*-hexose hydrochloride (VIII).

[1]*The hydrogenation, which was carried out in ethyl acetate, showed a sharp decrease in rate after 1 mole of hydrogen had been consumed and therefore did not affect the nitro and benzylidene groups. Similar selective hydrogenations using palladium black in absolute ethanol have been reported, although with the latter catalyst in ethyl acetate the selectivity has been said to be less marked (cf. ref. 6, pp. 315–316).*

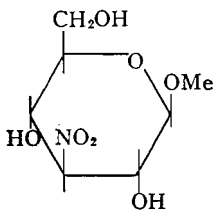

I

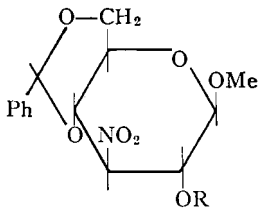

II, R = H.
III, R = Ac.

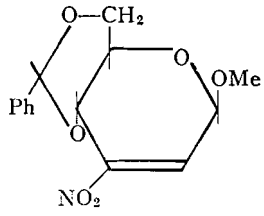

IV

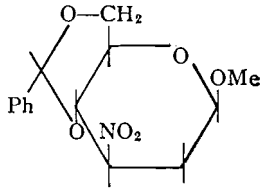

V

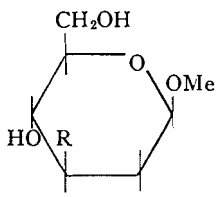

VI, R = NO_2.
VII, R = NH_3Cl.

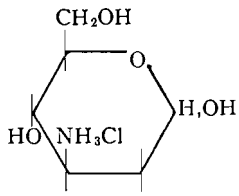

VIII

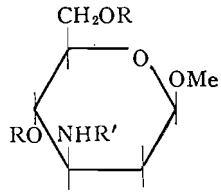

IX, R = H, R′ = Ac.
X, R = R′ = Ac.
XI, R = Ms, R′ = Ac.

The configuration at C-3, where the asymmetry had been relinquished and then regenerated in the course of the above synthetic pathway, was established by nuclear magnetic resonance (n.m.r.) spectroscopy and by experiments involving solvolysis with neighboring group participation. For these purposes the *N*-acetyl-4,6-di-*O*-acetyl derivative X, *N*-acetate IX, and *N*-acetyl-4,6-di-*O*-mesylate XI were prepared by standard procedures in crystalline condition and high yields from the amino glycoside hydrochloride VII.

The n.m.r. spectrum[2] of triacetate X showed methyl proton signals at 8.09, 7.95, and 6.50 τ in an intensity ratio 1:2:1. The signals were assigned to the *N*-acetyl, *O*-acetyl, and methoxy groups, respectively. In accord with the known stereochemistry at C-4 and C-5 the chemical shift of the *O*-acetyl signal indicated equatorial arrangement of the substituents at these carbons. (Cf. the ranges recorded (7, 8, 9) for equatorial (7.91–8.03 τ) and axial (7.78–7.88 τ) acetoxy groups in pyranose and inositol derivatives.) The τ-value of the signal attributed to the acetamido group agreed well with the values reported (7, 8, 9) for equatorial disposition (8.02–8.11 τ) but differed from those found (7) in cases of axial disposition (7.92, 7.94 τ). The spectrum, therefore, implied a configuration as shown in formulas X and X*a*.

An independent proof of configuration was provided by solvolysis of the dimesylate XI. When the dimesylate was solvolyzed in refluxing 95% ethanol in the presence of sodium acetate, a quantitative yield (2 moles) of sodium mesylate was produced. Since the solvolyzed glycoside could not be obtained in crystalline form, it was directly acetylated under two sets of conditions, viz., acetic anhydride – pyridine and acetic anhydride – sodium acetate. On both occasions a crystalline acetate (m.p. 110°, $[\alpha]_D$ −231° in ethanol) was isolated in 85–90% yield. Complete elemental analysis (C, H, N, O, and molecular weight) established the molecular formula $C_{11}H_{17}NO_5$ for this acetate. The infrared spectrum in carbon tetrachloride exhibited peaks at 1 740 cm^{-1} (ester carbonyl) and 1 660 cm^{-1}

[2]*Obtained with a Varian V-4302 High Resolution Spectrometer operating at 60 Mc/s. The solvent was deuterochloroform, and the spectra were calibrated by the side-band technique with tetramethylsilane as internal standard.*

Can. J. Chem. Downloaded from www.nrcresearchpress.com by 210.87.254.5 on 09/05/12
For personal use only.

(amide I[3]), but there were no amide II and N—H bands. The integrated n.m.r. spectrum[2] revealed the presence of *two* acetyl groups (8.02 and 7.95 τ) and one methoxy group (6.68 τ).

The analytical and spectral data of the acetylated solvolysis product are compatible only with structures XII and XIII. A decision between these two structures cannot be made as yet. However, the formation of either structure requires internal displacement of one mesyloxy group through attack by the acetamido nitrogen. An obvious steric condition that must be met in both cases is the orientation of the acetamido group as depicted in XI. The acetamido group in XI is *trans* to the C-4 mesyloxy group and thus suitably arranged for rearward attack leading to the aziridine XII; and it is *cis* to C-6 rendering possible a cyclization to the pyrrolidine XIII. The nitrogen ring that was engendered furnished proof, therefore, of the configuration at C-3, regardless of whether the acetylated solvolysis product was XII or XIII.[4]

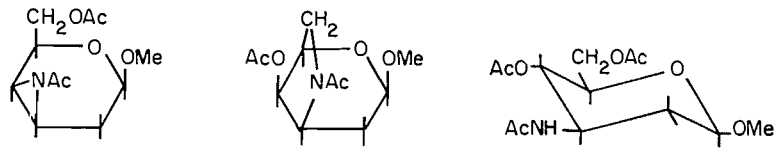

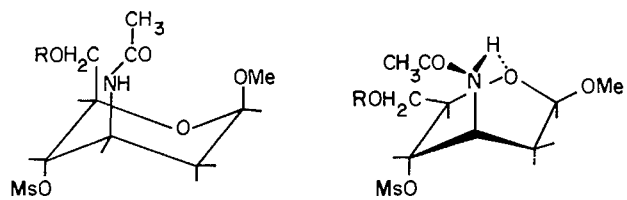

The formation in neighboring group reactions of sugar aziridines in competition with (thermodynamically favored) oxazolines or other five-membered heterocycles has been observed on several occasions (10–14); of particular relevance to the present work are instances involving benzamido (11, 12) and acetamido (13) sugar derivatives. There were no exceptions to the generally accepted mode of reaction which requires *trans* vicinal reactive groups. In the cases cited the three-membered rings arose under conditions of anionic displacement, however, and not by solvolysis with an acid acceptor. Aziridine formation under the latter conditions might nevertheless be possible if for any reason the formation of an oxazolidine intermediate[5] were impeded. Thus, in the case of XI, in conformations such as XI*a* or XI*b* which place the 3,4-substituents in the diaxial arrangement conducive to participation, the acetamido group might be prevented by steric hindrance or proton bonding from aligning suitably for *carbonyl* attack at C-4. Formation of the less strained structure XIII would perhaps seem more likely. However, one would then have to assume that the acetamido group would be able to assist anchimerically in the removal

[3]*In a solid state spectrum this peak occurred at a very similar frequency (1 643 cm^{-1}) suggesting absence of association.*

[4]*The substantially higher τ-value of the methoxyl signal given by the acetylated solvolysis product as compared to that of X may be interpreted (9a) in terms of an axial* OCH_3 *group in the former; conformational models taking this into account can be constructed for both XII and XIII.*

[5]*Solvolyses of trans vicinal acylamido–sulfonyloxy systems normally lead to cis acylamido alcohols via an oxazolidine which opens in the presence of water (cf. ref. 15).*

Can. J. Chem. Downloaded from www.nrcresearchpress.com by 210.87.254.5 on 09/05/12
For personal use only.

of the C-4 sulfonyloxy group; for in view of the general resistance to solvolysis, even under more drastic conditions, of isolated, secondary sulfonyloxy groups in sugars (16) the observed, facile displacement would be difficult to explain without invoking neighboring group participation.

It is anticipated that the new principle of synthesis involving nitroolefinic glycosides can be used to prepare further aminodideoxy sugars. Work along these lines is in progress.

EXPERIMENTAL

Methyl 4,6-O-Benzylidene-3-nitro-3-deoxy-β-D-glucopyranoside (II)

Methyl 3-nitro-3-deoxy-β-D-glucopyranoside (2) (7.8 g), zinc chloride (7.8 g), and benzaldehyde (50 ml) were stirred together at room temperature for 24 h. Water (400 ml) was added and the heterogeneous mixture was stirred for 15 min. Upon addition of petroleum ether (400 ml, b.p. 80–100°) a semi-crystalline mass separated, which was collected and washed twice with 100 ml of petroleum ether. Crystallization from aqueous ethanol gave the benzylidene derivative II (8.0 g, 74%) as needles of m.p. 181–182° and $[\alpha]_D^{23}$ −72.5° (*c*, 1 in ethanol).

Anal. Calcd. for $C_{14}H_{17}NO_7$ (311.3): C, 54.01; H, 5.51; N, 4.50. Found: C, 54.07; H, 5.57; N, 4.65.

Methyl 2-O-Acetyl-4,6-O-benzylidene-3-nitro-3-deoxy-β-D-glucopyranoside (III)

Benzylidene derivative II (7 g) was dissolved in pyridine (70 ml), and acetic anhydride (20 ml) was added with ice cooling. The reaction mixture was left overnight at room temperature and then poured into 500 ml of ice water. The crude acetate which separated was washed thoroughly with water to remove all traces of pyridine, and dried (yield 8 g). Crystallization from aqueous ethanol furnished the acetate III (7.2 g, 90%) as plates melting at 193–194° and showing $[\alpha]_D^{23}$ −77.7° (*c*, 0.99 in chloroform).

Anal. Calcd. for $C_{16}H_{19}NO_8$ (353.2): C, 54.40; H, 5.42; N, 3.97. Found: C, 54.41; H, 5.60; N, 4.15.

Methyl 4,6-O-Benzylidene-2,3-dideoxy-3-nitro-β-D-erythro-hexos-2-enide (IV)

The nitroolefin IV was obtained from the *O*-acetyl compound III by Schmidt–Rutz elimination of acetic acid, i.e., by refluxing in benzene in the presence of solid sodium hydrogen carbonate. In order to follow this heterogeneous phase reaction and to determine its point of completion, small test samples were withdrawn occasionally, cleared from suspended bicarbonate, allowed to evaporate, and inspected by infrared spectroscopy. A gradual decrease in the intensities of the acetyl and nitroalkane frequencies at 5.72 and 6.44 mμ, respectively, and a concomitant appearance of a nitroolefin peak at 6.55 mμ indicated proceeding of the reaction. Completion as shown by the absence of the former frequencies was usually attained within 2 days but sometimes required up to 4 days; difficultly controllable conditions such as stirring efficiency or traces of moisture may have been responsible for these variations which did not, however, seem to affect the yields.

For practical purposes acetate III (5 g) was refluxed, with magnetic stirring, with 25 g of dry sodium bicarbonate in 125 ml of reagent grade benzene. After completion of the reaction (see above) the mixture was allowed to cool, filtered, and the filtrate was evaporated leaving a near-colorless crystalline residue of IV (4.1 g). This material was suitable without further purification for the next synthetic step. An analytical sample of IV was obtained in a small-scale run (200 mg of III), the crude product of which was recrystallized from ethyl acetate – petroleum ether (30–60°) giving 110 mg (66%) of needles with m.p. 144–145° and $[\alpha]_D^{23}$ −192.5° (*c*, 1.2 in chloroform).

Anal. Calcd. for $C_{14}H_{15}NO_6$ (293.3): C, 57.33; H, 5.16; N, 4.78. Found: C, 57.19; H, 5.32; N, 4.91.

Attempted recrystallization of the compound from *ethanol* resulted in the formation of an ethoxy derivative (m.p. 122–123°), presumably arising from the addition of solvent across the double bond. Further work on this and similar addition reactions is currently being undertaken.

Methyl 4,6-Benzylidene-2,3-dideoxy-3-nitro-β-D-arabino-hexopyranoside (V)

Crude nitroolefin IV (4.1 g) from the previous experiment was dissolved in ethyl acetate (200 ml) and shaken under hydrogen (S.T.P.) with 500 mg of 10% palladium on charcoal (Matheson, Coleman & Bell) for 15 min. Gas uptake was rapid and showed a sharp decrease in rate after 300 ml had been consumed. The filtrate from the catalyst was evaporated to give a crystalline residue (4 g). Recrystallization from aqueous ethanol afforded compound V (3.6 g, 87%) as needles of m.p. 148–149° and $[\alpha]_D^{23}$ −95.5° (*c*, 1.1 in chloroform).

Anal. Calcd. for $C_{14}H_{17}NO_6$ (295.3): C, 56.94; H, 5.83; N, 4.74. Found: C, 57.19; H, 5.87; N, 4.80.

Methyl 2,3-Dideoxy-3-nitro-β-D-arabino-hexopyranoside (VI)

Benzylidene derivative V (1.5 g) in 200 ml of methanol–water (4:1, v/v) was refluxed and magnetically stirred with 6 g of Dowex 50 W – X8 (H^+) for 4 h. The resin was removed, and the filtrate on evaporation gave a crystalline residue which was freed from the last traces of water by two co-evaporations with 50 ml of ethanol. Recrystallization from ethyl acetate – petroleum ether (30–60°) afforded 610 mg (58%) of the debenzylidenated derivative VI; needles, m.p. 177–179°; $[\alpha]_D^{23}$ −33.3° (*c*, 0.96 in water).

Anal. Calcd. for $C_7H_{13}NO_6$ (207.2): C, 40.58; H, 6.33; N, 6.76. Found: C, 40.48; H, 6.39; N, 6.58.

Can. J. Chem. Downloaded from www.nrcresearchpress.com by 210.87.254.5 on 09/05/12
For personal use only.

Omitting the recrystallizations described above for compounds III, IV, and V it was possible to obtain 1.1 g of pure VI starting from 3.3 g of II (overall yield 50%).

In several later experiments debenzylidenation was effected by heating V in acetic acid – water (7:3, v/v) on a steam bath for precisely 30 min. This quicker procedure was at least as satisfactory, the yields in pure VI being 60–62%.

*Methyl 3-Amino-2,3-dideoxy-β-*D*-arabino-hexopyranoside Hydrochloride (VII)*

Nitroglycoside VI (1 g) was shaken under hydrogen (S.T.P.) with prereduced platinum oxide (200 mg) in water containing 1 molar equivalent of hydrogen chloride (48 ml of *N*/10 HCl added to excess water). Uptake of 3 moles of hydrogen (324 ml, corrected volume) was complete within approximately 2 h. Evaporation of the filtrate yielded a gum that could be crystallized from ethanol – ethyl acetate. The aminoglycoside hydrochloride VII thus obtained (640 mg, 62%) formed needles melting with decomposition at 145–150° and exhibiting $[\alpha]_D^{23}$ −41.0° (*c*, 0.83 in water).

Anal. Calcd. for $C_7H_{16}NO_4Cl$ (213.7): C, 39.35; H, 7.56; N, 6.56; Cl, 16.60. Found: C, 39.33; H, 7.46; N, 6.47; Cl, 16.5.

*3-Amino-2,3-dideoxy-*D*-arabino-hexose Hydrochloride (VIII)*

Aminoglycoside hydrochloride VII (500 mg) was refluxed overnight with 10 ml of *N* hydrochloric acid. The hydrolysate was decolorized with activated charcoal and evaporated with 10 consecutive additions of water (10 ml) to ensure removal of all excess hydrogen chloride. The amino sugar hydrochloride was finally obtained as a froth that was dried in a high vacuum; yield, 450 mg (96%). $[\alpha]_D^{23}$ +54° (*c*, 0.9 in water). A sample was found to reduce Fehling solution.

Anal. Calcd. for $C_6H_{14}NO_4Cl$ (199.6): C, 36.09, H, 7.06; Cl, 17.76. Found: C, 36.29; H, 7.31; Cl, 18.03.

Similar material was produced in good yield in the hydrolysis of compound IX, below.

*Methyl 3-Acetamido-2,3-dideoxy-β-*D*-arabino-hexopyranoside (IX)*

Nitroglycoside VI (1 g) was hydrogenated as described in a previous paragraph to give an aqueous solution of aminoglycoside hydrochloride VII. This was used for *N*-acetylation (17) without prior isolation of VII. After removal of the platinum catalyst, the filtrate (60 ml) was stirred with 25 ml of Dowex-1, carbonate form, and methanol (3 ml) and acetic anhydride (0.5 ml) were added. After 90 min the anion exchange resin was removed and the solution stirred briefly with 10 ml of Dowex-50W (H^+). The filtrate therefrom was evaporated giving a sirup which crystallized when treated with ethanol. The acetamide IX formed needles with m.p. 191–192° (from ethanol–ethyl acetate) and $[\alpha]_D^{23}$ −37.2° (*c*, 1.04 in ethanol). The yield was 950 mg (91%).

Anal. Calcd. for $C_9H_{17}NO_5$ (219.2): C, 49.30; H, 7.82; N, 6.39. Found: C, 49.27; H, 7.99; N, 6.49.

*Methyl 3-Acetamido-4,6-di-O-acetyl-2,3-dideoxy-β-*D*-arabino-hexopyranoside (X)*

Acetamide IX (150 mg) was dissolved in pyridine (5 ml) and acetic anhydride (0.5 ml) was added. The reaction mixture was left at room temperature for 24 h, then poured onto ice (25 g), and extracted three times with 20 ml of chloroform. The combined chloroform extracts were washed with water (2 × 20 ml), dried over anhydrous sodium sulfate, and evaporated, the last traces of pyridine being azeotropically removed with toluene (2 × 10 ml). Crystallization of the residue from ethyl acetate – petroleum ether (30–60°) gave the triacetate X (160 mg, 77%) as needles of m.p. 157.5–158° and $[\alpha]_D^{23}$ +9.9° (*c*, 0.61 in ethanol).

Anal. Calcd. for $C_{13}H_{21}NO_7$ (303.3): C, 51.47; H, 6.98; N, 4.62. Found: C, 51.56; H, 6.99; N, 4.80.

*Methyl 3-Acetamido-2,3-dideoxy-4,6-di-O-mesyl-β-*D*-arabino-hexopyranoside (XI)*

A solution of acetamide IX (500 mg) in pyridine (5 ml) was chilled to 0°, and methanesulfonyl chloride (0.70 ml, 4 molar equivalents) was added dropwise with stirring. The mixture was stirred a further 30 min and then left overnight at 0°. Upon addition of ice (25 g) dimesylate XI (350 mg) separated in the course of 2 h. Concentration and removal of pyridine from the filtrate by evaporation *in vacuo* produced a second crop (400 mg) of crude dimesylate. The combined crops were recrystallized from ethanol yielding 650 mg (75%) of XI as needles with m.p. 155–156° and $[\alpha]_D^{23}$ −5.5° (*c*, 0.9 in dimethylformamide).

Anal. Calcd. for $C_{11}H_{21}NO_9S_2$ (375.4): C, 35.19; H, 5.64; N, 3.73; S, 17.08. Found: C, 35.31; H, 5.60; N, 3.81; S, 17.05.

Solvolysis of the Dimesyl Derivative XI

Dimesyl derivative XI (275 mg) and anhydrous sodium acetate (300 mg) were refluxed in 95% ethanol (25 ml) for 48 h. The cooled solution was concentrated *in vacuo* and filtered from a crystalline solid which was identified by its infrared spectrum as sodium mesylate. The yield was 171.5 mg (calcd. for 2 molar equivalents, 173.5 mg). The filtrate was freed from ethanol *in vacuo*. As the nearly colorless residue could not be obtained in crystalline condition it was dissolved in pyridine (2 ml), and acetic anhydride (0.5 ml) was added. The reaction mixture was left overnight at room temperature. Ice (25 ml) was added and the mixture was extracted three times with 25 ml of chloroform. The combined extracts were washed twice with 10 ml of water, dried over magnesium sulfate, and evaporated to dryness to give gum, the last traces of pyridine being azeotropically removed by co-distillation with toluene (2 × 10 ml) *in vacuo*. Crystallization from ethyl acetate / petroleum ether (30–60°) gave prismatic needles (160 mg) melting at 102–104°. After recrystalliza-

Can. J. Chem. Downloaded from www.nrcresearchpress.com by 210.87.254.5 on 09/05/12
For personal use only.

tion from the same solvents the product melted at 105–107°, and after a further recrystallization from ethyl acetate – cyclohexane it showed m.p. 106–107°. (Slow crystallization by evaporation of solvent in the air afforded large prisms with m.p. 110°). $[\alpha]_D$ −231° (*c*, 0.7 in ethanol). The compound is to be assigned either structure XII or (isomeric) structure XIII; its yield based on XI was 90%. The analytical sample was dried at 56° and 0.1 mm.

Anal. Calcd. for $C_{11}H_{17}NO_5$ (243.3): C, 54.31; H, 7.04; N, 5.76; O, 32.89. Found: C, 54.27; H, 7.14; N, 5.70; O, 32.87; molecular weight, 236 (Rast method with camphor).

An analogous acetylation of the solvolyzed material using 2.5 ml of acetic anhydride in the absence of pyridine (the sodium acetate left over from the solvolysis being sufficient to serve as a catalyst) gave the same product in similar yield.

In some of the runs a few milligrams of a by-product was isolated which crystallized out as needles when the crude gum obtained in the acetylation was dissolved in ethanol (from which XII (or XIII) did not crystallize). The by-product (m.p. 171–172°) differed from the main product in that it exhibited infrared bands associated with a —NH—$COCH_3$ structure. The spectrum also differed from that of triacetate X. A mixture melting point with X was depressed (ca. 145°). No analytical or rotation data were obtained owing to lack of material.

Infrared Absorption Data

Unless otherwise stated the infrared spectra of the compounds listed were taken using the Nujol mull technique and a Perkin–Elmer Infracord instrument. Only the most characteristic absorption bands are given.

Compound	ν_{max} in cm^{-1} (group assignments in parentheses).
II	3 480 (OH); 1 560, 1 378 (NO_2); 1 075, 1 000 (C—O—C); 760, 697 (phenyl).
III	No OH; 1 748 (acetate CO); 1 553, 1 375 (NO_2); 1 223 (acetate C—O—C); 1 100, 1 040, 960 (ether C—O—C); 760, 695 (phenyl).
IV	No OH and acetate CO; 1 530, 1 370 (olefinic NO_2); 1 100, 995 (C—O—C); 752, 695 (phenyl).
V	1 553, 1 380 (NO_2); 1 090, 1 075, 985 (C—O—C); 760, 695 (phenyl).
VI	3 450 – 3 330 (OH); 1 550, 1 375 (NO_2); 1 090, 1 040, 1 000, 993 (C—O—C); no phenyl.
VII	3 430, 3 250 (OH, NH); 2 020, 1 590, 1 515 (—NH_3^+); 1 400 (CH_2 adjacent to N^+); 1 075 (C—O—C).
IX	3 400 (OH); 3 290 (NH); 1 635 (amide I); 1 545 (amide II); 1 065 (C—O—C).
X	3 330 (NH); 1 733 (acetate CO); 1 655 (amide I); 1 553 (amide II); 1 250, 1 227 (acetate C—O—C); 1 065 – 1 040 (ether C—O—C).
XI	3 330 (NH); 1 650 (amide I); 1 520 (amide II); 1 340, 1 320, 1 175, 1 155 (—SO_2—); 1 000 – 985, 965 (C—O—C).
XII or XIII	No OH or NH; 1 740 (acetate CO); 1 643 (amide I); no amide II; 1 230 (acetate C—O—C); 1 070, 1 060 (C—O—C). In carbon tetrachloride (Beckman IR8 instrument): no OH or NH; 1 745 (acetate CO); 1 660 (amide I); no amide II.
By-product m.p. 171–172°	3 380 (NH); 1 733 (acetate CO); 1 650 (amide I); 1 520 (amide II); 1 230 (acetate C—O—C); 1 065 (ether C—O—C).

ACKNOWLEDGMENT

This work was supported by research grant AI 4697 from the National Institute of Allergy and Infectious Diseases, United States Public Health Service.

REFERENCES

1. J. D. Dutcher. Advan. Carbohydrate Chem. **18**, 259 (1963).
2. H. H. Baer. Ber. **93**, 2865 (1960); J. Am. Chem. Soc. **83**, 1882 (1961).
3. H. H. Baer and F. Kienzle. Can. J. Chem. **41**, 1606 (1963).
4. J. M. Grosheintz and H. O. L. Fischer. J. Am. Chem. Soc. **70**, 1479 (1948). F. W. Lichtenthaler and H. O. L. Fischer. J. Am. Chem. Soc. **83**, 2005 (1961).
5. E. Schmidt and G. Rutz. Ber. **61**, 2142 (1928).
6. J. C. Sowden. Advan. Carbohydrate Chem. **6**, 291 (1951).
7. F. W. Lichtenthaler. Ber. **96**, 2047 (1963); earlier work by this and other authors cited there.
8. A. C. Richardson and K. A. McLauchlan. J. Chem. Soc. 2499 (1962).

Can. J. Chem. Downloaded from www.nrcresearchpress.com by 210.87.254.5 on 09/05/12
For personal use only.

9. H. H. BAER, L. D. HALL, and F. KIENZLE. J. Org. Chem. **29**, 2014 (1964).
9*a*. R. U. LEMIEUX and B. FRASER-REID. Can. J. Chem. **42**, 532 (1964).
10. L. GOODMAN and J. E. CHRISTENSEN. J. Am. Chem. Soc. **83**, 3823 (1961).
11. R. D. GUTHRIE and D. MURPHY. J. Chem. Soc. 5288 (1963).
12. D. H. BUSS, L. HOUGH, and A. C. RICHARDSON. J. Chem. Soc. 5295 (1963).
13. B. R. BAKER and T. NEILSON. J. Org. Chem. **29**, 1047 (1964).
14. B. R. BAKER and T. NEILSON. J. Org. Chem. **29**, 1051, 1057, 1063 (1964).
15. S. WINSTEIN and R. BOSCHAN. J. Am. Chem. Soc. **72**, 4669 (1950).
16. R. S. TIPSON. Advan. Carbohydrate Chem. **8**, 107 (1953).
17. S. ROSEMAN and J. LUDOWIEG. J. Am. Chem. Soc. **76**, 301 (1954).

Can. J. Chem. Downloaded from www.nrcresearchpress.com by 210.87.254.5 on 09/05/12
For personal use only.

Can. J. Chem. Downloaded from www.nrcresearchpress.com by 210.87.254.105 on 09/05/12
For personal use only.

REACTION MECHANISM STUDIES

3. SOLVENT EFFECTS AND THE NATURE OF THE TRANSITION STATE IN THE DIAXIAL → DIEQUATORIAL REARRANGEMENT

J. F. KING AND R. G. PEWS
Department of Chemistry, University of Western Ontario, London, Ontario

Received November 6, 1964

ABSTRACT

The rates of the diaxial → diequatorial rearrangement of 2β,3α-dibromocholestane (I*a*), and the analogous bromohydrin *p*-toluenesulfonates (I*d* and I*e*) and anisates (I*f* and I*g*) have been measured in various solvents. The change in rate with variation in solvent was found to correlate with the change in the ionizing power of the solvents. The sensitivity of the rate of rearrangement to changes in solvent ionizing power, as measured by the ratio of the rate of rearrangement in nitromethane to that in decalin, was found to be smaller for the dibromide (I*a*) than for the esters (I*d* to I*g*). A detailed discussion of the mechanism of the reaction is presented. It is proposed that the following factors (either singly or simultaneously) could lead to the smaller sensitivity to solvent change shown by the dibromide (I*a*) as compared with the esters (I*d* to I*g*): (*1*) a difference in a postulated change of the axial:equatorial opening ratio with change in solvent, and (*2*) the development of a smaller charge in the transition state for the rearrangement of the dibromide (I*a*) as compared with that in the rearrangement of the esters, when the reactions are carried out in the less polar solvents. It is argued that the operation of the latter factor would be most simply interpreted in terms of a merged ion-pair, cyclic-concerted mechanism, as initially suggested by Grob and Winstein.

A merged ion-pair, cyclic-concerted mechanism for the diaxial → diequatorial rearrangement of 5α,6β-dibromocholestane was suggested in 1952 by Grob and Winstein (1). Their proposal, which was a significant modification of an earlier mechanism put forward by Barton and Miller (2), stated, in effect, that the reaction takes place in solvents of high ionizing power via an ion pair, in solvents of lowest ionizing power through a cyclic nonpolar transition state, and in solvents of intermediate polarity through a transition state intermediate in character between these two extremes. The specific basis for

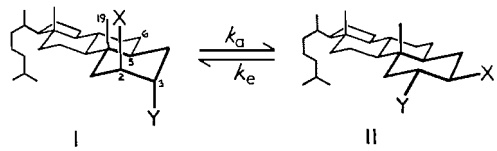

I II

a X, Y = Br

b X = Br, Y = OH

c X = OH, Y = Br

d X = Br, Y = CH_3–C$_6$H$_4$–SO_2O

e X = CH_3–C$_6$H$_4$–SO_2O, Y = Br

f X = Br, Y = CH_3O–C$_6$H$_4$–COO

g X = CH_3O–C$_6$H$_4$–COO, Y = Br

this suggestion was their observation that the change in the rate of rearrangement accompanying a change in the ionizing power of the solvent was larger than that expected of a cyclic, concerted process (typified by the Claisen or Cope rearrangements) and smaller than that expected of an ionic reaction, e.g. unimolecular solvolysis. Winstein has reiterated this proposal (3), and other discussions of the diaxial → diequatorial rearrangement have been in terms of this mechanism (4, 5, 6). Though the basic idea has gained credence through the presentation of evidence supporting a merged ion-pair, cyclic-concerted process in certain other reactions,* no additional data specifically concerned with the nature of the diaxial → diequatorial rearrangement have been reported. Some of our experiments connected with work reported in Part 1 of this series (6) suggested that further information on this reaction might be obtained by comparing the effect of solvents on the rate of rearrangement of a vicinal dibromide with the corresponding effect on the rate of rearrangement of the analogous bromohydrin sulfonate and carboxylate esters. It was hoped that by thereby comparing the solvent sensitivity of very closely related reactions that a more detailed analysis of the experimental results might be applied in order to assess the validity of the proposed merged ion-pair, cyclic-concerted mechanism.

RESULTS

2β,3α-Disubstituted 5α-cholestanes (I) were chosen for this investigation because these compounds had been subjected to considerable study already, and the amount of necessary preliminary work was correspondingly less than it would have been with another system. Whereas there is only one diaxial dibromide (I*a*) corresponding to structure I, there are two diaxial bromohydrins, I*b* and I*c*. For a meaningful comparison of the dibromide with the bromohydrin esters it was necessary to include the esters of both bromohydrins. The characterization and rearrangement of both of the tosylates (I*d* and I*e*) (6) and one of the anisates (I*f*) (5), as well as the dibromide (12), had been previously described. The other anisate (I*g*) was accordingly prepared and found to rearrange on heating in nitromethane at 99° to a mixture containing 95 ± 5% of the diequatorial isomer (II*g*), identified by comparison with an authentic specimen prepared from the bromohydrin (II*c*) (13, 14).

TABLE I

Rate constants ($\times 10^4$ s^{-1}) for the diaxial → diequatorial rearrangement under various conditions*

	CF_3COOH: $CHCl_3$ (1:1) at 25°	Triglyme at 135°	TMS–phenetole† at 135°	Decalin at 99°	Phenetole at 99°	Triglyme at 99°	Nitrobenzene at 99°	Nitromethane at 99°	$\frac{k_{CH_3NO_2}}{k_{decalin}}$
I*a* ⇌ II*a*	0.01 (0.01)	2.9 (2.8)	10 (9.5)	0.013 (0.012)	0.056 (0.053)	0.068 (0.065)	0.12 (0.11)	0.28 (0.27)	22
I*d* ⇌ II*d*	3.1 (2.9)	1.2 (1.1)	28 (26)	0.004 (0.004)	0.063 (0.049)	0.036 (0.033)	0.22 (0.20)	1.1 (1.0)	280
I*e* ⇌ II*e*	—	0.52 (0.45)	8.0 (7.0)	0.002 (0.002)	—	—	—	0.39 (0.34)	190
I*f* ⇌ II*f*	0.01 (?) (0.01)	—	—	0.011 (0.010)	0.12 (0.11)	—	—	1.3 (1.2)	110
I*g* ⇌ II*g*	—	—	—	0.0020 (0.0019)	—	—	—	0.22 (0.21)	110

*Values without parentheses give k_{equil}, the rate of formation of the equilibrium mixture. Values in parentheses give k_a the rate of the reaction I → II, obtained from the relation $k_a = k_{equil}K/(K+1)$ where K is the equilibrium constant of the reaction I ⇌ II. The following mean values of K (derived from data in Table II) were used: I*a* ⇌ II*a*, $K \sim 19$; I*d* ⇌ II*d*, $K \sim 12$; I*e* ⇌ II*e*, $K \sim 7$. I*f* ⇌ II*f*, $K \sim 19$; I*g* ⇌ II*g*, $K \sim 19$.
†Tetramethylene sulfone – phenetole 3:1.

**For example, the thermal decomposition of α-phenethyl chloroglyoxalate (7), diphenylmethanethiolsulfonates (8), and alkyl chloroformates (9), the rearrangement of allylic thionbenzoates (10), the neutral acetolysis of crotylmercuric acetate (11), and other examples referred to in the references cited.*

Can. J. Chem. Downloaded from www.nrcresearchpress.com by 210.87.254.105 on 09/05/12
For personal use only.

The rate constant for the formation of the equilibrium mixture, k_{equil}, was measured polarimetrically as previously described (5, 6). The variation of k_{equil} with change of solvent is summarized in Table I (the numbers without parentheses). The choice of solvent in these experiments was limited by (*a*) the solubility of the compounds, and (*b*) the tendency of some of the compounds (especially the tosylates) to undergo solvolysis; the greater ease of handling at elevated temperatures was also a factor leading to the use of comparatively high boiling solvents.

For the purposes of the discussion in the next section it is pertinent to consider the evaluation of k_a, the rate constant for the reaction I $\rightarrow$ II. If k_e is the rate constant for the reverse process II $\rightarrow$ I, and K the equilibrium constant for the reaction I $\rightleftharpoons$ II, then from simple kinetic theory $k_{equil} = k_a + k_e = k_a(K + 1)/K$; i.e. knowing K, one may obtain k_a from k_{equil} simply by multiplying by $K/(K + 1)$. The values of K listed in the footnote in Table I are only approximate, and since the variation in K with change in solvent for any single compound appears to be small in comparison with the uncertainty in the values (see Table II), a single approximate mean value of K for each compound was used to calculate the values of k_a listed in parentheses in Table I. Because of the uncertainty in the measurement of K, the values of k_a are less precise than those of k_{equil}; in fact it is by no means certain that this procedure is any more meaningful than merely assuming $k_a \sim k_{equil}$. In any event nothing in the Discussion of the Mechanism (in which the term "rate of rearrangement" will refer, in principle, to k_a) depends on any *experimental* distinction between k_a and k_{equil}.

To obtain the data in Table I it was necessary to know the specific rotations of the various equilibrium mixtures. The values used for these quantities are summarized in Table II. Some of these values are from previous work, the others were obtained by heating the diaxial isomer for five half-lives (or in most instances, longer) and determining the composition of the product polarimetrically. Though a reaction time of more than five half-lives would have been desirable in order to approximate the true equilibrium value more closely, the polarimetric analysis of products of longer heating was often rendered impracticable by slow side reactions and general decomposition. As a result some of the values in Table II for the percentage of the diequatorial isomer (II) in the equilibrium mixture may be low; it can be shown that the *maximum* error in the rate constants listed in Table I that is introduced by incomplete equilibration is less than 10% and in all probability is much less.

Notably absent from Table II are data for the rearrangements of the esters in decalin. These reactions are so slow that side reactions seriously hamper the analysis of mixtures from runs carried beyond 25% reaction; direct determination of the equilibrium mixture (which would have involved heating some of the specimens for many months) was deemed impracticable. In view of the negligible variation of the equilibrium composition with solvent (as manifest in Table II), it is believed that no important error is introduced by assuming that the equilibrium composition in decalin is much the same as in the other solvents. The use of decalin as solvent also presented some difficulties in preliminary experiments to obtain the data in Table I. Consistent results were obtained only after the solvent had been subjected to thorough treatment to remove aromatic impurities (presumably mostly tetralin). Addition of glass beads to the reaction vessel in the decalin experiments had no effect on the rate, indicating that surface reactions are not significant with this solvent, and hence presumably not with the more polar solvents either.

The ionizing powers of the solvents used in the experiments at 99° have been estimated according to various procedures; the values are summarized in Table III. The dielectric

Can. J. Chem. Downloaded from www.nrcresearchpress.com by 210.87.254.105 on 09/05/12
For personal use only.

TABLE II

Thermal equilibration experiments

Starting material	Solvent	Temp. (°C)	Time (h)	$[\alpha]_D$ of I	$[\alpha]_D$ of II*	$[\alpha]_D$ of pyrolysis product	Estimated % of II at equilibrium
Ia ⇌ IIa							
Ia	Decalin	150	10	+70	(−29)	−21	(90±5)
IIa	Decalin	150	10			−21	
Ia	Triglyme	135	4	+78	−30	−28, −26	95±5
IIa	Triglyme	135	4			−29	
Ia	Phenetole	150	4	+77	−33	−34, −30	95±5
IIa	Phenetole	150	4			−29	
Ia	Nitrobenzene	150	10	+78	(−29)	−23	(95±5)
IIa	Nitrobenzene	150	10			−24	
Ia	Nitromethane	99	30	+78	−29	−19, −20	95±5
IIa	Nitromethane	99	30			−23	
Ia	TMS–phenetole†	135	1.5	+84	−30	−28	95±5
IIa	TMS–phenetole†	135	1.5			−25	
Id ⇌ IId							
Id	Triglyme	—	—	+49	−26	—	95±5‡
Id	Phenetole	135	24	+54	−33	−30, −28	95±5
Id	Nitrobenzene	99	55, 75	52	(−28)	−22, −22	(90±5)
Id	Nitromethane	99	12		−28	−21, −21	90±5
Id	TMS–phenetole†	135	0.66	+62	−28	−16	90±5
IId	TMS–phenetole†	135	0.33			−15	
Ie ⇌ IIe							
—	Triglyme	—	—	+50	−26	—	85±8‡
Ie	Nitromethane	99	48	+48	−38.5	0	85±8
IIe	Nitromethane	98	48			−25	
Ie	TMS–phenetole†	135	1.5	+64	−24	−23	95±5
If ⇌ IIf							
If	Phenetole	99	100	+88	(−34)	−39, −37	(95±5)
If	Nitromethane	99	20	+83		−24, −25	
Ig ⇌ IIg							
IIg	Nitromethane	99	48	+36	(−44)	−40	(95±5)
IIg	Nitromethane	99	96			−40	

*Values in parentheses in the $[\alpha]_D$ column indicate an estimated value, the rotation of II not having been determined in the solvent used to measure the rotation of the equilibrium mixture. Parentheses around the estimated equilibrium % of II indicate that the $[\alpha]_D$ of II, on which this value depends, was estimated and not determined in that solvent.
†Tetramethylene sulfone – phenetole 3:1 (by volume).
‡Taken from ref. 6.

TABLE III

Measures of the ionizing power of some of the solvents used in this study

	$\epsilon_{25°}$*	$\frac{\epsilon - 1}{2\epsilon + 1}$	**Z** (kcal/mole)	$\Omega_{25°}$†	*G*	*S*
Decalin	2.20	0.222	60.1 (?)	0.537	63	−§
Phenetole	4.17	0.339	58.9‡	(0.513)‡	89	−§
Triglyme	7.6	0.41	61.3	(0.547)	90	—
Nitrobenzene	34.82	0.479	—	—	100	−0.218
Nitromethane	36.67	0.480	(71.2)†	0.685	98	−0.134

*The value for decalin is from ref. 15 and that for triglyme was determined by Dr. R. K. Chan in this department; the other values are taken from ref. 16.
†Values in parentheses are obtained from the equation $\mathbf{Z} = 71.7\ \Omega_{25°} + 22.1$ given in ref. 17.
‡0.075 *M* chloroform in phenetole.
§*S* values for decalin and phenetole have not been reported (18); values for the following structurally related compounds are: cyclohexane −0.324 and anisole −0.214.

constants in the first numerical column were used in the calculation of the values for the function $(\epsilon - 1)/(2\epsilon + 1)$. The **Z** values (19) for phenetole (containing a trace of chloroform to dissolve the 4-carbomethoxy-N-ethylpyridinium iodide) and triglyme were

Can. J. Chem. Downloaded from www.nrcresearchpress.com by 210.87.254.105 on 09/05/12
For personal use only.

Can. J. Chem. Downloaded from www.nrcresearchpress.com by 210.87.254.105 on 09/05/12
For personal use only.

determined directly; the value for nitromethane is that estimated by Berson *et al.* (17), the value agreeing well with an approximate value obtainable by direct measurement. Direct determination of **Z** values for decalin and nitrobenzene is not possible because of insolubility in the former case and solvent absorption in the latter; solvent absorption also interferes with an accurate determination of the **Z** value for nitromethane. Kosower indirectly estimated a **Z** value of 60.1 kcal/mole for isoöctane from a combination of the long wavelength absorption of pyridine N-oxide and a roughly linear plot of **Z** versus this band for other solvents (19). Our observation of a lower value for phenetole (58.9 kcal/mole) and also for tetrahydrofuran (58.8 kcal/mole), raises serious doubts about the accuracy of such a manoeuvre, since by any other mode of estimating solvent ionizing power saturated hydrocarbons are distinctly less polar than ethers. The values for $\Omega_{25°}$ are derived by interpolation from those given by Berson (17) for other temperatures; the *G* values (20) were obtained from the position of the carbonyl-stretching frequency of benzophenone (only). Included in Table III are values given by Brownstein (18) for his composite *S* values for nitrobenzene and nitromethane, together with those for compounds closely related to decalin and phenetole.

The agreement among the different ways of measuring solvent ionizing power is only approximate but does suffice to indicate the following order: decalin < phenetole $\leqslant$ triglyme < nitrobenzene $\leqslant$ nitromethane. For the rearrangement of I*a* and I*d* the rates (Table I) follow the same order with only the minor exception that the rearrangement of I*d* is slightly faster in phenetole than in triglyme (though the reverse order is found with I*a*). It would appear then that the rates of rearrangement qualitatively follow the ionizing power of the solvent, the agreement being about as good as that between the various methods of estimating ionizing power themselves. As it appeared extremely likely that the rates of rearrangement of the other esters (I*e*, I*f*, and I*g*) would show the same trend with change in solvent, the study of the rates of these reactions was limited to the solvents of highest and lowest ionizing power.

If we take the ratio of the rate constants (either k_{equil} or k_a) in nitromethane and decalin, i.e. $k_{CH_3NO_2}/k_{decalin}$, as an indicator of the sensitivity of the reaction to change in solvent ionizing power, it is apparent from Table I that the rearrangement of 2β,3α-dibromocholestane is distinctly less sensitive to such changes than the rearrangements of the esters. It should be noted that the rate constants for the rearrangements are sufficiently similar in magnitude that this difference in sensitivity to solvent results in the rearrangement of I*d*, I*e*, and I*f* being *slower* than that of I*a* in decalin, but *faster* in nitromethane.

Most of the solvents in this work have not been used extensively (if at all) in other studies of the effect of solvent on reactivity, but some sort of comparison between the present reactions and various others may be obtained by plotting log k_a vs. **Z** for the reactions in phenetole, triglyme, and nitromethane (the solvents for which the **Z** values in Table III are believed to be most meaningful). The slope of the best straight line for each of these plots may be converted by the equation $\mathbf{Z} = 104.2 + 8.11 \log k_1$ into Winstein's *a* parameter (21), which has been used to describe the solvent sensitivity of a number of reactions (10, 21). For the rearrangement of 2β,3α-dibromocholestane (I*a*) $a \sim 0.5$ and for that of 2β-bromocholestan-3α-yl tosylate (I*d*) $a \sim 1$. Approximate though the *a* values from this procedure are, they would indicate that the rearrangement of I*d* is about as sensitive to change in the ionizing power of the solvent as the solvolysis of *p*-methoxyneophyl tosylate itself (for which $a = 1$, by definition (21)).

The rearrangement of I*d*, and in smaller measure I*a*, when carried out in a 1:1 mixture of trifluoroacetic acid and chloroform is notably faster than in any of the other solvents.

Within 5 min of adding the solid tosylate I*d* to pure trifluoroacetic acid at room temperature, it is essentially completely converted to a mixture consisting of about 80% II*d* and less than 20% solvolysis products. Since I*d* does not dissolve instantaneously in trifluoroacetic acid, the actual time for complete reaction is even less. Just how much of this effect is due to enhanced solvent ionizing power and how much to the acidity of the medium is not clear. As indicated in Table I, the rearrangement of I*f*, in which protonation of either of the ester oxygen atoms would strongly retard the rearrangement by the usual mechanism (5), proceeds very slowly if at all in trifluoroacetic acid.

DISCUSSION OF THE MECHANISM

The mechanism of the diaxial → diequatorial rearrangement (at least in polar solvents) as proposed by Barton and Miller (2), and Grob and Winstein (1), may be generalized as in eq. [1], formula III representing the diaxial isomer and V the diequatorial isomer. From the known properties of the reactions of substituted cyclohexane derivatives, this description may be expanded further as in Scheme 1. If one takes each of the divisions of the ordinate in the energy diagram in Scheme 1 as equal to 10 kcal/mole then the diagram

[1]

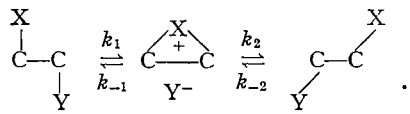

III IV V

may be taken as an approximate representation of the free energy changes in the rearrangement of the 2,3-dibromocholestanes (I*a* ⇌ II*a*) at 99°. There is no basis for assigning any quantity to ΔG_{VII} (except that it be less than ΔG_{TS1} or ΔG_{TS2}) and that portion of the diagram is indicated by a broken line. The diaxial opening rule (22, 23) requires that ΔG_{TS1} be less than ΔG_{TS2}, as drawn. This rule is commonly rationalized (see, for example, Valls and Toromanoff (24)) in terms of a reaction scheme in which attack at one carbon of the three-membered ring species gives a diaxial chair isomer, and attack at the other yields a diaxial twist-boat which in a subsequent rapid conformational inversion leads to the diequatorial chair isomer (cf. Scheme 1). With such a mechanism the difference between the free energies of activation for the formation of the diaxial (chair) and diequatorial (chair) isomers is governed by the free energy difference between a partly formed diaxial chair and a partly formed diaxial twist-boat. The free energy values for VIII and "TS3" indicated on the diagram for Scheme 1 are simply rough estimates based on the corresponding quantities measured in simpler systems (cf. Eliel (25) pp. 206 and 211); the value for $\Delta G_{\text{VI}} - \Delta G_{\text{IX}}$ is derived from the equilibrium constant, K (see footnote, Table I), and $\Delta G_{\text{TS2}} - \Delta G_{\text{VI}}$ from the rate constants in Table I.

The energy diagrams for the rearrangements of the bromohydrin tosylates (I*d* ⇌ II*d* and I*e* ⇌ II*e*) are in all likelihood qualitatively similar to that for the reaction I*a* ⇌ II*a*, but the rearrangement of the anisates may very well be distinctly different. It has been shown (5) that the transition state in the rearrangement of the carboxylic esters is polarized so that there is a negative charge on the halogen and a positive charge on the ester group, i.e. that if the reaction were to proceed through an ion pair it would be an acyloxonium bromide and not the alternative, a bromonium acylate. In this case the "onium" ion is part of a five-membered ring and the diaxial opening rule may no longer apply. Examination of molecular models indicates that there is considerable angle strain accompanying a *cis* fusion of an acyloxonium ion with a cyclohexane ring, and that attack on the carbon

Can. J. Chem. Downloaded from www.nrcresearchpress.com by 210.87.254.105 on 09/05/12
For personal use only.

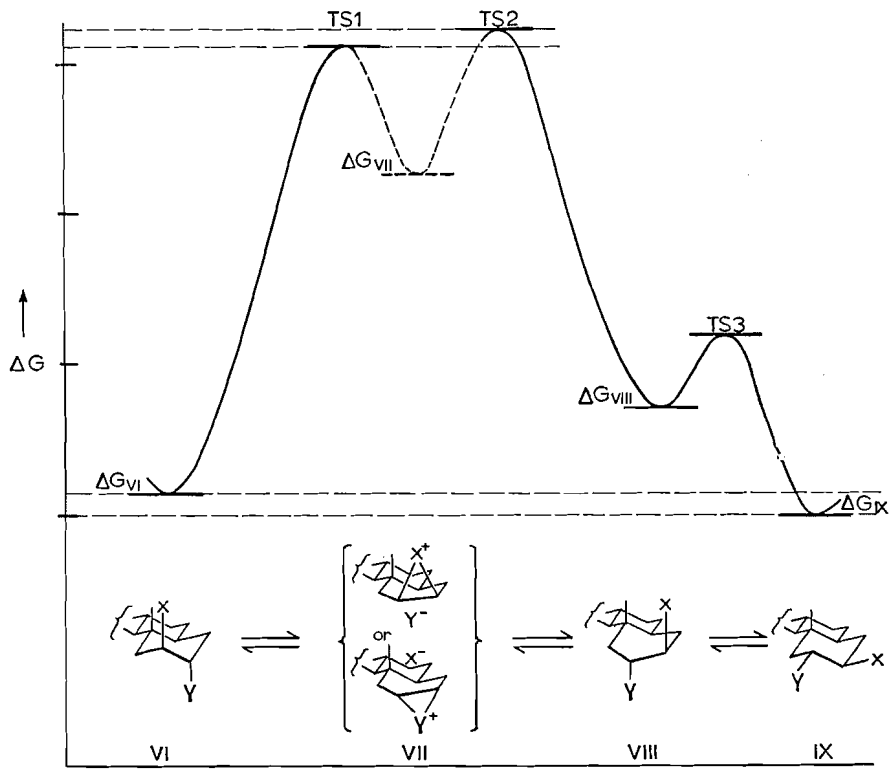

SCHEME 1.

bearing the equatorial oxygen (diaxial opening) would give a transition state in which this strain is somewhat relieved, while attack at the carbon bearing the axial oxygen (direct diequatorial opening) would lead to a transition state in which the angle strain is apparently increased. On the other hand substitution of an *axial* function in a simple cyclohexane system is normally faster* than that of the analogous equatorial function (cf. Eliel (25), pp. 223ff.). The two effects oppose each other and it is not evident which is stronger. But it would seem likely that the axial : equatorial opening ratio is much smaller with the acyloxonium ion than with a three-membered ring intermediate, and may well be < 1. Such is probably the case in the rearrangement I*f* $\rightleftharpoons$ II*f*, in which in addition to the above factors, any reagent attacking at C-2 (which would give diaxial opening) would be subjected to considerable steric compression with the hydrogens of the nearby axial methyl group (C-19).

In terms of the rate constants defined in eq. [1], we may (assuming steady-state conditions) express the measured rate for the reaction I $\rightarrow$ II (also III $\rightarrow$ V, and VI $\rightarrow$ IX) by $k_a = k_1/(1 + k_{-1}/k_2)$. From the discussion just given, for the reaction of I*a*, I*d*, or I*e*, $k_{-1} > k_2$ and hence $k_a < k_1$, and for the rearrangement of I*f* or I*g*, k_a is probably only slightly less than k_1. The question that now arises is how the observed solvent dependence of k_a may be rationalized in terms of k_1 and the ratio k_{-1}/k_2. Most of the remainder of this section will be devoted to this problem, beginning with the possible role of the axial : equatorial opening ratio, k_{-1}/k_2. To simplify matters the following treatment is

**Except for a bimolecular displacement in which the attacking group is significantly smaller than the leaving group, which would not appear to be the case here.*

Can. J. Chem. Downloaded from www.nrcresearchpress.com by 210.87.254.105 on 09/05/12
For personal use only.

based initially on an ionization mechanism; any conclusion derived in this way may be readily adapted to a "merged mechanism," which is examined later in the discussion.

Variation in the Axial: Equatorial Opening Ratio

Consider a hypothetical reaction $X \rightarrow Y \rightarrow Z$, in which the positions in the reaction coordinate of all three species and the free energies of X and Z are fixed (so that $\Delta G_Z > \Delta G_X$), and ΔG_Y (the free energy of Y) is variable (see Fig. 1). Let $\Delta\Delta G^{\ddagger}$ be defined as the difference between the free energies of the transition states, specifically, the free energy of the transition state in the reaction $Y \rightleftharpoons Z$ minus that for the transition state in the reaction $X \rightleftharpoons Y$. The question is what effect will variation of ΔG_Y have on $\Delta\Delta G^{\ddagger}$.

In the degenerate case in which Y is a transition state (curve *a* in Fig. 1), $\Delta\Delta G^{\ddagger}$ is obviously zero. As ΔG_Y is diminished, at some point Y will cease to be a transition state and will become a true intermediate so that there will be a transition state between X and Y and another between Y and Z. According to the Hammond postulate (26),* as

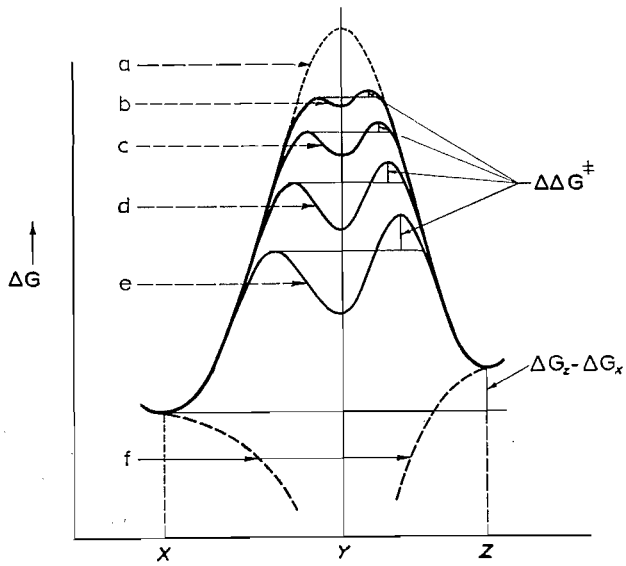

FIG. 1.

ΔG_Y is lowered still further an increasingly extensive atomic reorganization will be required on going from Y to either of the transition states. That is to say, as ΔG_Y decreases, the transition states move away from Y to resemble increasingly X and Z, respectively (cf. curves *b* to *e*, Fig. 1). If the lowering of the free energy of Y is continued to the extreme case (cf. curve *f*, Fig. 1), $\Delta\Delta G^{\ddagger}$ will become identical to the difference in free energy between X and Z, i.e. $\Delta G_Z - \Delta G_X$, this value presumably being approached asymptotically as ΔG_Y diminishes. Without attempting to describe the relation between $\Delta\Delta G^{\ddagger}$ and ΔG_Y exactly, we can see that $\Delta\Delta G^{\ddagger}$ is a non-linear function of ΔG_Y such that $\Delta\Delta G^{\ddagger}$ equals zero when ΔG_Y is large, and tends to increase to the value $\Delta G_Z - \Delta G_X$ as ΔG_Y becomes very small.

**Strictly speaking the Hammond postulate deals with potential energies rather than free energies. The discussion given here is essentially qualitative and is presented in terms of free energies in order to keep the argument and symbolism as simple as possible. For the species corresponding to potential energy maxima and minima, it is simply assumed that the potential energies and free energies will show sufficient correspondence for the conclusions drawn to be qualitatively valid.*

Can. J. Chem. Downloaded from www.nrcresearchpress.com by 210.87.254.105 on 09/05/12
For personal use only.

Can. J. Chem. Downloaded from www.nrcresearchpress.com by 210.87.254.105 on 09/05/12
For personal use only.

The conclusion of this general treatment may now be applied specifically to the diaxial → diequatorial rearrangement. If the discussion be restricted for the moment to an ion-pair mechanism, then since the ion pair has the greatest dipole moment of any species in the reaction, an increase in the ionizing power of the solvent would be expected to operate most significantly by lowering the free energy of the ion pair. To the extent that the effect of solvent on the completely covalent species of the reaction may be neglected, the diaxial → diequatorial rearrangement corresponds to the reaction X → Y → Z just discussed; thus VI corresponds to X, VII to Y, and VIII to Z, and the lowering of ΔG_Y is effected by solvation of the ion pair (VII) as the ionizing power of the solvent is increased. In terms of the rate constants defined in eq. [1], $\Delta\Delta G^{\ddagger} = RT \ln k_{-1}/k_2$. Therefore, increasing the ionizing power of the medium lowers the free energy of the ion pair (which corresponds to ΔG_Y), and this in turn is accompanied by a trend to an increase in $\Delta\Delta G^{\ddagger}$ and hence in k_{-1}/k_2, the axial : equatorial opening ratio. To summarize, on the assumption that the chief effect of a change in solvent polarity is on the free energy of the intermediate ion pair, *an increase in the solvent ionizing power would be expected to be accompanied by an increase in the axial : equatorial opening ratio* (k_{-1}/k_2).

As has been pointed out previously, k_a, the rate constant for the reaction I → II, is given by $k_a = k_1/(1 + k_{-1}/k_2)$. If the ionization is normal, k_1 will increase rapidly with an increase in solvent ionizing power. But from the above argument k_{-1}/k_2 is also expected to increase with solvent polarity and therefore any increase in rate constant accompanying an increase in the solvent ionizing power will be *smaller* for k_a than for k_1, i.e. the increase in k_{-1}/k_2 tends to damp the effect on k_a of the simultaneous increase in k_1. Such an effect may account for part—or, conceivably, even all—of the rather low sensitivity of k_a to a change in solvent in the rearrangement of 5α,6β-dibromocholestane (1). This rationalization, then, represents a possible supplementary, or even alternative, explanation for the data on which Grob and Winstein based their suggestion of a "merged mechanism" for the diaxial → diequatorial rearrangement of 5α,6β-dibromocholestane.

If the experimental observations reported in the *present* study are to be rationalized in terms of changes in the ratio k_{-1}/k_2, a further point must be considered. For a variation in the axial : equatorial opening ratio to account for the differences in solvent sensitivity of the rearrangement of the dibromide (I*a* ⇌ II*a*) as compared with that of the bromohydrin tosylate (I*d* ⇌ II*d*), it is necessary not only for k_{-1}/k_2 to vary with solvent but also for the variation in the case of the dibromide (I*a*) to be different from that with the tosylate (I*d*). It will be recalled that the greater the change in k_{-1}/k_2 with change in solvent polarity, the smaller the change in k_a (assuming the change in k_1 to be the same). Therefore it is necessary on this basis to devise a reason why the hypothetical variation in k_{-1}/k_2 might be greater for the dibromide than for the tosylate. The argument in the next paragraph indicates a way in which this might conceivably occur, though owing to current ignorance of the details of the energy diagrams in such complex reactions, this rationale can only be regarded as a plausible suggestion.

In the discussion of the generalized scheme X → Y → Z, it was concluded that as ΔG_Y becomes very small $\Delta\Delta G^{\ddagger}$ probably tends gradually to the value $\Delta G_Z - \Delta G_X$. Such an asymptotic approach to a limiting value bespeaks a non-linear relationship in which $\Delta\Delta G^{\ddagger}$ is more sensitive to a change in ΔG_Y at some region where ΔG_Y is comparatively large than at a region where it is comparatively small. This would suggest that in two *different* reactions a greater sensitivity to change in ΔG_Y would be more likely to be found when Y is in a comparatively shallow "energy well" (e.g. curve *b*, Fig. 1) rather than in a deep "energy well". Translating the symbolism of the general case to that of the diaxial

Can. J. Chem. Downloaded from www.nrcresearchpress.com by 210.87.254.105 on 09/05/12
For personal use only.

$\rightarrow$ diequatorial rearrangement, it would appear that the sensitivity of the ratio k_{-1}/k_2 to a change in solvent ionizing power might be expected to be greater in the case of an ion pair which is rapidly converted to the diaxial or the diequatorial isomer, than in that in which the formation of the nonionic compounds from the ion pair is slow. Since the bromide ion is found to exhibit greater nucleophilic activity than the tosylate anion (27), it is almost certain that the bromonium bromide ion pair would, in fact, more readily recombine to form the diaxial or the diequatorial compound, than would the bromonium tosylate. Hence, if the above argument holds, the ratio k_{-1}/k_2 in the case of the dibromide (I*a*) would be expected to increase more rapidly with an increase in solvent polarity than it would in the case of the bromohydrin tosylate (I*d*). This in turn would lead to what is observed experimentally, that is to say, to a greater sensitivity to a change in solvent ionizing power on the part of k_a for the rearrangement of the tosylate (I*d*), than that of k_a for the dibromide (I*a*). It is perhaps worth repeating at this point that it has been necessary to make some fairly extensive assumptions in order to derive an explanation for the variations in rate with change in solvent in terms of variations in the axial:equatorial opening ratio. The discussion is included, nonetheless, in order to show that *without invoking any differences in the behavior of* k_1 (the rate constant for the ionization step), it is possible to conceive of a set of circumstances which might possibly lead to a smaller sensitivity to solvent change in the rearrangement of the dibromide (I*a*) than in the case of the bromohydrin tosylate (I*d*).

Difference in the Sensitivity of the Rate of the First Step

As the possible sources and effects of a variation in the axial : equatorial opening ratio have been examined at some length, it is appropriate now to consider the significance of factors connected with k_1, the ionization rate constant. Again, making some drastic simplifications about the importance and nature of the solvation of the transition state, k_1 may be expressed by the following well-known equation (28) in terms of k_0, the rate of ionization of I in a vacuum, and a term dealing with the effect of solvent.

$$\ln k_1 = \ln k_0 + \frac{\mu_{\pm}^2}{kTr_{\pm}^3}\left(\frac{\epsilon - 1}{2\epsilon + 1}\right) = \ln k_0 + \frac{e_{\pm}^2 d_{\pm}^2}{kTr_{\pm}^3}\left(\frac{\epsilon - 1}{2\epsilon + 1}\right).$$

In the latter term $\mu_{\pm}$ is the dipole moment of the transition state and $r_{\pm}$ the radius of the solvent cavity (assumed to be spherical) occupied by the transition state; this term may be expanded by expressing the dipole moment in terms of the magnitude of the charge ($e_{\pm}$), and the distance ($d_{\pm}$) between the positive and negative centers of charge in the transition state. The factor $e_{\pm}^2 d_{\pm}^2/kTr_{\pm}^3$ defines the slope of the straight line obtained from a plot of ln k_1 vs. $(\epsilon - 1)/(2\epsilon + 1)$. For the rearrangements of I*a* and I*d* the ratio of the slopes is given by:

$$[2] \qquad \frac{\text{slope Ia}}{\text{slope Id}} = \frac{(e_{\pm})_{Ia}^2 (d_{\pm})_{Ia}^2 (r_{\pm})_{Id}^3}{(e_{\pm})_{Id}^2 (d_{\pm})_{Id}^2 (r_{\pm})_{Ia}^3}.$$

Since the tosylate (I*d*) is more bulky than the dibromide (I*a*), and the same relation presumably holds for analogous transition states, then $(r_{\pm})_{Id}^3/(r_{\pm})_{Ia}^3 > 1$. Temporarily assuming an ion-pair mechanism, we estimate the distance between the centers of the two bromine atoms in the ion pair from I*a* to be ~ 5.0 Å, and the distance from the positively charged bromine to the approximate center of charge for the tosylate anion in the ion pair from I*d* to be ~ 4.5 Å. From the Hammond postulate one would expect that the transition state would resemble the ion pair to the extent that the distances between the

charges in the transition state follow the same order, and therefore $(d_{\mp})_{Ia}^2/(d_{\mp})_{Id}^2 > 1$. But the rearrangement of I*a* has in fact been found to be *less* sensitive to solvent change than that of I*d*, viz., slope I*a* / slope I*d* $\sim$ 0.5 to 0.6. If any of this is due to differences in sensitivity of k_1, and if eq. [2] is even qualitatively valid, then *slope Ia / slope Id can be less than one only if there is a distinctly smaller value for the magnitude of the charge* ($e_{\mp}$) *in the transition state of the dibromide rearrangement* as compared with that of the bromohydrin tosylates. It remains now to see what the smaller value of $e_{\mp}$ means in terms of the mechanism of these reactions.

In contrast to the diaxial → diequatorial rearrangement, the solvolysis of primary and secondary bromides has been found by Winstein, Grunwald, and Jones (29) to be slightly more sensitive to solvent ionizing power than that of the corresponding tosylates or brosylates (*p*-bromobenzenesulfonates). These authors' investigations were carried out using a more polar range of solvents than that used in our study and it is conceivable that their results are not directly applicable to this discussion. They would suggest, however, that there is no reason to expect that the magnitude of the charge ($e_{\mp}$) in the transition state of a *true ionization* of an aliphatic bromide is less than that in the ionization of a corresponding sulfonate ester. But it was concluded in the above paragraph that $e_{\mp}$ for the *rearrangement* of the dibromide (I*a*) is less than that for the rearrangement of the tosylate (I*d*). It follows, therefore, that if the rearrangement of the tosylate (I*d*) is proceeding via an ion pair, the rearrangement of the dibromide (I*a*) cannot also be taking place through an ion pair but rather must be going through a species with a smaller development of charge. In other words if the observed differences in the effect of solvent stem to any degree from the behavior of k_1, the reaction of I*a* must proceed in some solvents at least, via a merged ion-pair, cyclic-concerted mechanism as suggested initially by Grob and Winstein (1) for the rearrangement of 5β,6α-dibromocholestane. There is nothing in this discussion which demands that the rearrangement of the tosylates (I*d* and I*e*) be taking place via fully formed ion pairs; it does require, however, that if the tosylates are also rearranging through a "merged mechanism" that the magnitude of the charge in the transition state be greater than that in the corresponding stage of the rearrangement of the dibromide, i.e. that the rearrangement of the tosylates be more like an ionic reaction than that of the dibromide.

It is perhaps of interest to take note of a curious feature of "merged-mechanism" reactions. With reference to Fig. 1 again, it would appear that as the energies of the transition states become higher accompanying a decrease in solvent ionizing power, the transition state comes to resemble the intermediate Y more closely. Hence $e_{\mp}$, the magnitude of the charge at either end of the dipole of the transition state, becomes *greater* as the solvent ionizing power is diminished. If the merged mechanism be defined as above, then this indicates the interesting possibility that a merged mechanism may show an increased, constant, or decreased value for $e_{\mp}$ with decrease in solvent ionizing power, though presumably the increase in $e_{\mp}$ must be less than that for the ion-pair extreme case.

Specific Solvation Effects

Much of the above discussion of mechanism has sought to find an explanation for our observations in terms of general phenomena. In any limited study the possibility exists that comparatively specific factors may actually be responsible. It might be suggested, for example, that in the rearrangement of the dibromide the two bromine atoms and the two attached carbon atoms (C-2 and C-3) form a four-membered ring in the transition state, whereas in the rearrangement of the esters the corresponding atoms may form a

Can. J. Chem. Downloaded from www.nrcresearchpress.com by 210.87.254.105 on 09/05/12
For personal use only.

six-membered ring; such a geometrical difference might conceivably (by an unspecified mechanism) be responsible for the lower solvent sensitivity of the rearrangement of the dibromide. Recent observations in this laboratory (30) indicate that a four-membered ring transition state does not have to be solvent insensitive. It has been found that the rearrangement of 2β-chloro-3α-thiophenoxycholestane, in which the chlorine, the two carbons, and the sulfur atom presumably form a four-membered ring in the transition state, is at least as sensitive to solvent change as the esters in the present investigation.

Though as mentioned already the effect of solvents in this study correlates acceptably with the ionizing power of the solvents, there might still remain the possibility that either the greater sensitivity to solvent change shown by the esters, or the smaller effect of the medium in the dibromide rearrangement, might be due to some sort of special interaction with some of the solvents. If there were a specific interaction with the incipient tosylate anion in I*d* and I*e*, there would also have to be an interaction of similar effect with the developing acyloxonium cation in I*f* and I*g* (and also with the sulfur or the chlorine of 2β-chloro-3α-thiophenoxycholestane), since these compounds show a sensitivity to the same solvents of the same order of magnitude. On the other hand any specific interaction of either the positively or the negatively charged bromine atoms in the rearrangement of I*a* would have to be manifest also in the rearrangement of either the tosylates or the anisates, since a positively charged bromine atom is formed in the former case and a negatively charged bromine in the latter. To devise a consistent system with the above data on such a basis would seem complicated; at this juncture we much prefer the alternative view that the observed phenomena reflect the operation of a few general effects rather than a number of specific interactions.

Concluding Summary

The aim of this study was to elucidate the detailed mechanism of the diaxial → diequatorial rearrangement, particularly with a view to establishing whether or not it belongs to the proposed class of merged ion-pair, cyclic-concerted reactions. It was found that the rates of the diaxial → diequatorial rearrangement of compounds I*a* and I*d* increase with increasing polarity of the solvent. The rate of rearrangement of the dibromide (I*a*) does not show as great an increase as that of the tosylate I*d* (or those of the other esters I*e* to I*g*). Because the dibromide (I*a*) and the esters (I*d* to I*g*) have similar structures, it is believed that the difference in solvent sensitivity shown by the rates is significant and warrants close analysis.

On the basis of a two-step mechanism, involving the formation of either an ion pair or of an intermediate with smaller charge separation than an ion pair, it is argued that the difference in behavior shown by the dibromide (I*a*) may be due either to a difference connected with the rate of the first step (k_1), or to a difference in the behavior of the intermediate, specifically in the variability of the ratio of axial to equatorial opening (k_{-1}/k_2). The assumptions required to make the latter factor workable are such as to suggest that it is probably the less important of the two, but it cannot be dismissed with the evidence at hand. If the different behavior of the dibromide should derive mainly from the first step, it is shown that this would most likely be due to a smaller magnitude of charge in the transition state ($e_{\pm}$) of the dibromide reaction, and that this in turn would indicate a "merged mechanism". The possibility that the observed differences reflect the operation of specific solvent effects is considered to be unlikely.

Though the avowed goal of clarifying the detailed mechanism of the diaxial → diequatorial rearrangement has not yet been reached, it is felt that the results and discussion

Can. J. Chem. Downloaded from www.nrcresearchpress.com by 210.87.254.105 on 09/05/12
For personal use only.

presented here give increased insight into the reaction and point the way to further experiments, which, it is hoped, will remove the remaining uncertainties. Such experiments are now being carried out.

EXPERIMENTAL

Melting points were determined using a Kofler block and are uncorrected. Optical rotations given in the characterization of compounds refer to solutions in chloroform ($c \sim 1.0$). Infrared spectra were obtained using Beckman IR-5 or IR-7 spectrophotometers equipped with sodium chloride optics. Thin-layer chromatography was carried out using Camag Kieselgel D5 or DF5. Petroleum ether refers to the fraction of boiling range 35–60°.

Phenetole and triglyme were purified as previously described (6). Commercial tetramethylene sulfone (supplied under the trade name "Sulfolane" by the Phillips Petroleum Company, Bartlesville, Oklahoma) was distilled under reduced pressure, first from potassium hydroxide and then from potassium permanganate; the distillate solidified on standing, m.p. 18–22°. Anhydrous chloroform free from alcohol was prepared by the method described by Vogel (31). Eastman Kodak white label trifluoroacetic acid was distilled before use. Fisher Certified Reagent grade nitrobenzene was twice partially frozen and separated from the unfrozen material; it was then fractionally distilled twice and the middle fraction from the second distillation redistilled under reduced pressure from calcium hydride. Commerical reagent grade nitromethane was washed three times each with (*a*) 20% of its volume of a solution containing sodium bicarbonate (25 g/l) and sodium bisulfite (25 g/l), (*b*) 5% sulfuric acid, and (*c*) water; the nitromethane was then dried over phosphorus pentoxide and distilled under reduced pressure from calcium hydride. BDH Laboratory Reagent grade decalin (mixed *cis* and *trans* isomers) was stirred vigorously with concentrated sulfuric acid at 90–100° for 24 h and then stirred with an alkaline 5% potassium permanganate solution at room temperature for 24 h; this was followed by drying with phosphorus pentoxide and distillation in an inert atmosphere under reduced pressure from lithium aluminium hydride. The preparation and properties of the dibromocholestanes (I*a* and II*a*) and the bromohydrin tosylates (I*d*, I*e*, II*d*, and II*e*) were as previously described (6, 32).

2β-Bromocholestan-3α-yl Anisate (If)

This compound was prepared as described by Barton and King (5); m.p. 136–138°, $[\alpha]_D$ +83°; reported m.p. 136–138°, $[\alpha]_D$ +83°.

3β-Bromocholestan-2α-yl Anisate (IIf)

This compound was isolated from the pyrolytic equilibrium experiments as previously described (5); m.p. 110–114°, $[\alpha]_D$ −34°; reported m.p. 114–115°, $[\alpha]_D$ −37°.

3α-Bromocholestan-2β-yl Anisate (Ig)

A slight excess of redistilled anisyl chloride was added to a solution of 3α-bromocholestan-2β-ol (12), and the mixture allowed to stand overnight at room temperature. After work-up the compound was recrystallized twice from 2-ethoxyethanol (ethyl cellosolve) and three times from a mixture of ether and methanol; m.p. 115–118°, $[\alpha]_D$ +36°.

Anal. Calcd. for $C_{35}H_{53}O_3Br$: C, 69.86; H, 8.88. Found: C, 70.29; H, 8.61.

2α-Bromocholestan-3β-yl Anisate (IIg)

2α-Bromocholestan-3β-ol (13, 14) was treated with anisyl chloride in pyridine as above. After four recrystallizations from ether–methanol the compound melted at 174–176°, $[\alpha]_D$ −44°.

Anal. Calcd. for $C_{35}H_{53}O_3Br$: C, 69.86; H, 8.88. Found: C, 69.98; H, 8.75.

Rate Measurements and Determination of the Composition of the Pyrolytic Equilibrium Mixtures

The rate measurements and the determination of the equilibrium composition of the reactions run above room temperature were carried out as before (6), except that the rate constants were calculated from the slope of the best straight line for the plot of $\log \alpha_o - \alpha/\alpha_o - \alpha_{eq}$ vs. time, as determined by the method of least squares. The following procedure was used for the experiments in trifluoroacetic acid – chloroform (1:1). The compound (20–30 mg) was weighed into a flask and dissolved in chloroform (0.5 ml); trifluoroacetic acid (0.5 ml) was added, the solution transferred to a polarimeter tube, and the rotation measured at intervals. Most of the data from these experiments are summarized in Tables I and II.

The rate of rearrangement of 2β-bromocholestan-3α-yl tosylate (I*d*) in decalin was obtained from the following data: initial $[\alpha]_D$ +52°; $[\alpha]_D$ after 137 h at 99°, +35°, +41°, +36°; $[\alpha]_D$ after 336 h at 99°, +24°, +22°, +21°; average $k_{equil} = 4 \times 10^{-7}$ s^{-1}.

On heating at 99° for 357 h in decalin the rotation of 3α-bromocholestan-2β-yl tosylate (I*e*) changed from +50° to +33° (average of three runs). Absorption at 995 cm^{-1} in the infrared spectrum and the presence of a spot corresponding to the diequatorial isomer (II*e*) in a thin-layer chromatogram established that rearrangement was occurring; the chromatogram, however, also indicated that some decomposition was taking place. Three further runs heated for 708 h showed much the same change in rotation as those run for 357 h; thin-layer chromatography of the mixtures from the longer reaction time indicated considerable decomposition.

Can. J. Chem. Downloaded from www.nrcresearchpress.com by 210.87.254.105 on 09/05/12
For personal use only.

Comparison of the relative intensities of the spots due to the diaxial and diequatorial isomers in the latter reaction mixture, with those obtained from mixtures of known composition indicated that the reaction mixture contained less than 30% but more than 20% rearranged product (II*e*). Based on the polarimetric reading at 357 h, $k_{equil} = 2 \times 10^{-7}$ s^{-1}. Taking the maximum value of 30%, as estimated by thin-layer chromatography of the mixture after heating for 708 h, $k_{equil} = 1.4 \times 10^{-7}$ s^{-1}.

Rearrangement of 2β-Bromocholestan-3α-yl Tosylate (Id) in Trifluoroacetic Acid

2β-Bromocholestan-3α-yl tosylate (I*d*) (22 mg) was added to trifluoroacetic acid (3 ml) at room temperature and the mixture shaken to dissolve the substrate. After 5 min the reaction mixture was poured into water and the aqueous mixture extracted with ether. The ether extract was washed with dilute sodium bicarbonate and water, dried over sodium sulfate, and the solvent evaporated. Examination of the infrared spectrum showed the product to be principally the diequatorial isomer (II*d*), with less than 20% solvolysis product (estimated from the intensity of the band at 1 786 cm^{-1}) and no starting material (I*d*). The above experiment was repeated with the addition of lithium trifluoroacetate (250 mg). (The salt was prepared from trifluoroacetic acid and lithium carbonate and was purified by recrystallization from anhydrous tetrahydrofuran.) The infrared spectrum of the crude product showed a large increase in the proportion of the solvolysis product, judged again by the band at 1 786 cm^{-1}.

Attempted Rearrangement of 2β-Bromocholestan-3α-yl Anisate (If) in Trifluoroacetic Acid

2β-Bromocholestan-3α-yl anisate (23 mg) was dissolved in trifluoroacetic acid (2 ml), the solution let stand at room temperature for 18 h, and then worked up in the same way as with the tosylate (I*d*), above. The infrared spectrum and specific rotation of the product were identical to those of the starting material. In another experiment, the anisate (I*f*) (31 mg) was heated in trifluoroacetic acid (1 ml) in a sealed ampoule at 99° for ½ h. The specific rotation of the product, isolated as described above, was found to be +33°, as compared with +85° for the pure starting material. Examination of the infrared spectrum indicated, in addition to starting material, some solvolysis product absorbing at 1 786 cm^{-1}. An attempt to detect the rearranged isomer (II*f*) by thin-layer chromatography was inconclusive because of the difficulty in finding a solvent system capable of resolving the diaxial and diequatorial isomers.

Solvent Polarity Measurements

At least three traces of the infrared spectrum in the carbonyl region of a solution of benzophenone (4–7 mg) in the solvent (0.2 ml) vs. the solvent, were run on a Beckman IR-7 spectrophotometer calibrated using the water vapor peak at 1 662.82 cm^{-1} (33). The following values for the carbonyl maxima (ν^s) were obtained: decalin 1 667.$_6$ cm^{-1}, phenetole 1 662.$_3$ cm^{-1}, triglyme 1 662.$_0$ cm^{-1}, nitromethane 1 660.$_5$ cm^{-1}, nitrobenzene 1 660.$_0$ cm^{-1}. The *G* values (20) were calculated from the relation $G = 7.90 \times 10^3 (1\,681 - \nu^s)/\nu^s$, and are listed in Table III.

The ultraviolet and visible spectra of solutions of 4-carbomethoxy-N-ethylpyridinium iodide (prepared by the method of Kosower (19)) in the solvents studied were determined on a Bausch and Lomb Spectronic 505 spectrophotometer calibrated with at least two Hg emission bands flanking the absorption maximum. The composition of the solutions, λ_{max} values, and the apparent extinction coefficients are as follows: 4-carbomethoxy-N-ethylpyridinium iodide (0.3 mg) in phenetole (5 ml) containing chloroform (41.3 mg), λ_{max} 486 mμ (ϵ_{app} 1 400); 4-carbomethoxy-N-ethylpyridinium iodide (0.3 mg) in phenetole (5 ml) containing chloroform (97.5 mg), λ_{max} 486 mμ (ϵ_{app} 1 100); 4-carbomethoxy-N-ethylpyridinium iodide (1.6 mg) in triglyme (10 ml) (*freshly* distilled from lithium aluminium hydride), λ_{max} 466 mμ (ϵ_{app} 1 030); 4-carbomethoxy-N-ethylpyridinium iodide (0.2 mg) in tetrahydrofuran (5 ml) containing chloroform (24.4 mg), λ_{max} 486.5 mμ (ϵ_{app} 2 200). The **Z** values (19) in Table III were obtained from the relation $\mathbf{Z} = 2.859 \times 10^4/\lambda_{max}$ (where λ_{max} is in mμ).

ACKNOWLEDGMENTS

This work was made possible by grants-in-aid and a scholarship from the National Research Council, by a Frederick Gardner Cottrell grant-in-aid from the Research Corporation, and a scholarship from Dow Chemical of Canada Limited. We thank Dr. R. K. Chan of this department for determining the dielectric constant of triglyme and Professor Jerome A. Berson (University of Wisconsin) for a stimulating discussion of the results described in this paper.

REFERENCES

1. C. A. GROB and S. WINSTEIN. Helv. Chim. Acta, **35**, 782 (1952).
2. D. H. R. BARTON and E. MILLER. J. Am. Chem. Soc. **72**, 1066 (1950).
3. S. WINSTEIN and G. C. ROBINSON. J. Am. Chem. Soc. **80**, 169 (1958).
4. D. H. R. BARTON. *In* Theoretical organic chemistry papers presented to the Kekulé Symposium. Butterworths, London. 1959. p. 127.
5. D. H. R. BARTON and J. F. KING. J. Chem. Soc. 4398 (1958).

Can. J. Chem. Downloaded from www.nrcresearchpress.com by 210.87.254.105 on 09/05/12
For personal use only.

6. J. F. KING, R. G. PEWS, and R. A. SIMMONS. Can. J. Chem. **41**, 2187 (1963).
7. S. J. RHOADS and R. E. MICHEL. J. Am. Chem. Soc. **85**, 585 (1963).
8. J. L. KICE and F. M. PARHAM. J. Am. Chem. Soc. **82**, 6168 (1960).
9. E. S. LEWIS and W. C. HERNDON. J. Am. Chem. Soc. **83**, 1955 (1961).
10. S. G. SMITH. J. Am. Chem. Soc. **83**, 4285 (1961).
11. P. D. SLEEZER, S. WINSTEIN, and W. G. YOUNG. J. Am. Chem. Soc. **85**, 1890 (1963).
12. G. H. ALT and D. H. R. BARTON. J. Chem. Soc. 4284 (1954).
13. E. J. COREY. J. Am. Chem. Soc. **75**, 4832 (1953).
14. L. F. FIESER and W.-Y. HUANG. J. Am. Chem. Soc. **75**, 4837 (1953).
15. W. F. SEYER and G. M. BARROW. J. Am. Chem. Soc. **70**, 802 (1948).
16. A. A. MARVOTT and E. R. SMITH. Table of dielectric constants of pure liquids. U.S. Department of Commerce, National Bureau of Standards Circular 514. 1951.
17. J. A. BERSON, Z. HAMLET, and W. A. MUELLER. J. Am. Chem. Soc. **84**, 297 (1962).
18. S. BROWNSTEIN. Can. J. Chem. **38**, 1590 (1960).
19. E. M. KOSOWER. J. Am. Chem. Soc. **80**, 3253 (1958).
20. A. ALLERHAND and P. v. R. SCHLEYER. J. Am. Chem. Soc. **85**, 371 (1963).
21. S. G. SMITH, A. H. FAINBERG, and S. WINSTEIN. J. Am. Chem. Soc. **83**, 618 (1961).
22. A. FÜRST and P. A. PLATTNER. Abstracts Papers 12th International Congress of Pure and Applied Chemistry, New York. 1951. p. 409.
23. D. H. R. BARTON and R. C. COOKSON. Quart. Rev. London, **10**, 44 (1956).
24. J. VALLS and E. TOROMANOFF. Bull. Soc. Chim. France, 758 (1961).
25. E. L. ELIEL. Stereochemistry of carbon compounds. McGraw-Hill, New York. 1962.
26. G. S. HAMMOND. J. Am. Chem. Soc. **77**, 334 (1955).
27. C. G. SWAIN and C. B. SCOTT. J. Am. Chem. Soc. **75**, 141 (1953).
28. S. GLASSTONE, K. J. LAIDLER, and H. EYRING. The theory of rate processes. McGraw-Hill, New York. 1941. p. 419.
29. S. WINSTEIN, E. GRUNWALD, and H. W. JONES. J. Am. Chem. Soc. **73**, 2700 (1951).
30. J. F. KING and K. ABIKAR. Unpublished observations.
31. A. I. VOGEL. A textbook of practical organic chemistry. 2nd ed. Longmans, Green and Co., London. 1951. p. 174.
32. J. F. KING and R. G. PEWS. Can. J. Chem. **42**, 1294 (1964).
33. E. K. PLYLER, A. DANTI, L. R. BLAINE, and E. D. TIDWELL. J. Res. Natl. Bur. Std. A, **64**, 29 (1960).

Can. J. Chem. Downloaded from www.nrcresearchpress.com by 210.87.254.105 on 09/05/12
For personal use only.

Can. J. Chem. Downloaded from www.nrcresearchpress.com by 210.87.254.6 on 09/05/12
For personal use only.

THE WALLACH REARRANGEMENT

PART II.[1] KINETICS AND MECHANISM OF THE ACID-CATALYZED REARRANGEMENT OF AZOXYBENZENE

E. BUNCEL AND B. T. LAWTON

Department of Chemistry, Queen's University, Kingston, Ontario

Received September 21, 1964

ABSTRACT

The rate of rearrangement of azoxybenzene to *p*-hydroxyazobenzene has been measured in 75.3–96.4% sulfuric acid at 25° and in 65.0–90.4% sulfuric acid at 75.5° by spectrophotometric methods. The pK_a of azoxybenzene in aqueous sulfuric acid has also been determined. It is found that although azoxybenzene is almost completely protonated over the entire range of acid concentration studied, the rate increases by more than 1 000-fold. A two-proton process is therefore indicated and mechanisms are proposed involving a dication (II) as the key intermediate. The rate data do not allow differentiation between two proposed mechanisms, one involving two equilibrium protonations, and the other a single equilibrium protonation followed by rate-determining proton transfer. Past mechanisms of the Wallach rearrangement are discussed.

INTRODUCTION

In 1880, Wallach and Belli (2) discovered that azoxybenzene on treatment with concentrated sulfuric acid isomerized to *p*-hydroxyazobenzene. This reaction is known as the Wallach rearrangement. Since then numerous studies have been made to elucidate the nature of this reaction but up to the present time (1) no kinetic study of the Wallach rearrangement has been reported. As an introduction to the present work the more recent studies on this topic will be reviewed.

Of particular interest to the early investigators was to determine whether the rearrangement is intramolecular or intermolecular, and the direction of migration of the oxygen function in the case of substituted azoxybenzenes. Angelli (3), who was the first to isolate two position isomers of a mono-substituted azoxybenzene, observed that both isomers of 4-nitroazoxybenzene gave the same rearranged product, 4-nitro-4′-hydroxyazobenzene (eq. 1). When both para positions are substituted, the oxygen enters one of the ortho positions (4*b*).

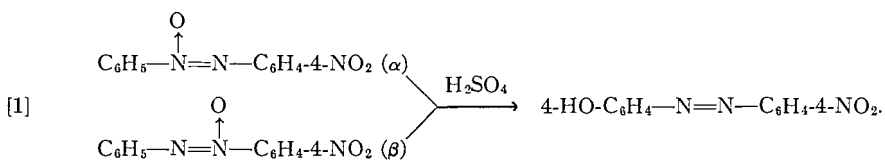

[1]

The most revealing studies on the mechanism of the acid-catalyzed para rearrangement have been the N-15 and O-18 tracer investigations of Shemyakin *et al.* (5, 6). Their main observations can be summarized by the following equations:

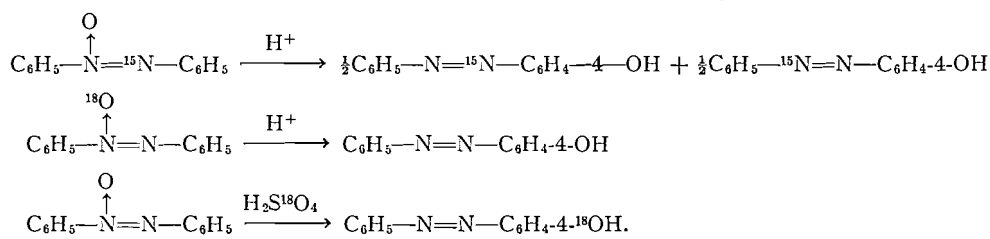

[1]*A preliminary communication on part of this work has appeared (ref. 1).*

In addition, azoxybenzene recovered from partial reaction in all three types of experiments contained the original label undisturbed. On the basis of the equalization of the nitrogen label during the rearrangement but not prior to it, Shemyakin *et al.* deduced that a symmetrical intermediate must be formed. They proposed that the symmetrical intermediate was the N,N-oxide (I) and suggested Scheme 1 for the mechanism of the Wallach rearrangement.

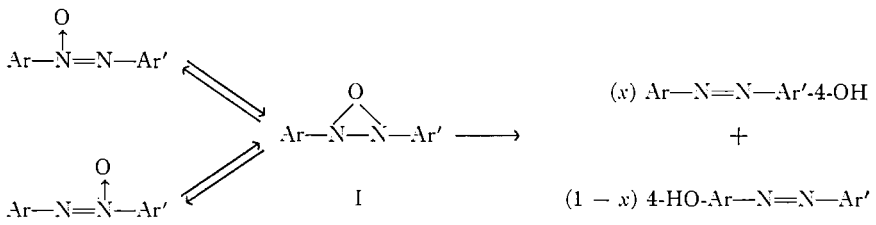

SCHEME 1.

The α and β isomerization was included in the scheme for the following reasons. Although azoxybenzene itself does not undergo this isomerization under the conditions of the rearrangement, as shown by the N-15 tracer experiments, Gore (7) found that β-4-nitroazoxybenzene underwent extensive conversion to the more stable α-isomer under rearrangement conditions.[2] Now the isomerization of β-4-nitroazoxybenzene in $H_2S^{18}O_4$ resulted in no O-18 enrichment in the recovered α-isomer (6). Shemyakin hence concluded that the N,N-oxide was a common intermediate in isomerization and rearrangement. Gore (7) suggested that the dicationic species (II) is also a possible intermediate in the Wallach rearrangement. He considered that II represents the major reaction route, with a minor route proceeding via the monocationic species (III).

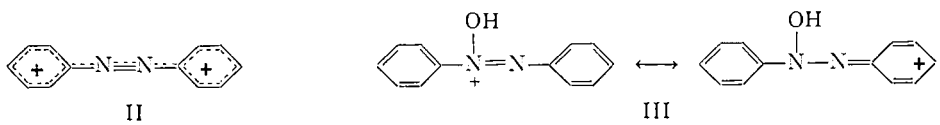

Oxygen-18 tracer studies on the azoxybenzene rearrangement have also been carried out, independently, by Oae *et al.* (9); the results are very similar to those of the Russian workers. The mechanism proposed by Oae *et al.* is shown in Scheme 2.

The value of kinetic data in the interpretation of the mechanism of acid-catalyzed reactions is well known (10). It was with the expectation that kinetic data would shed further light on the mechanism of the Wallach rearrangement that the present study was initiated.

RESULTS

Kinetic Data

Before a kinetic study of the acid-catalyzed rearrangement of azoxybenzene could be undertaken it was important to determine to what extent the reaction was quantitative and what was the nature of side products, if any, under the kinetic conditions. Previous work had shown that azobenzene, an azo-sulfonic acid, aniline, and polymer may all be formed as side products of reaction (4*a*). However, in the single reported study (11*a*) where the conditions were comparable to those planned for the kinetic work, i.e. low azoxybenzene concentrations (ca. 10^{-3} *M*), the yield of *p*-hydroxyazobenzene was found

[2]*The only other report of α–β isomerization under rearrangement conditions is due to Angelli (8) who found that a bisazoxybenzene isomerized as well as rearranged in cold sulfuric acid.*

Can. J. Chem. Downloaded from www.nrcresearchpress.com by 210.87.254.6 on 09/05/12
For personal use only.

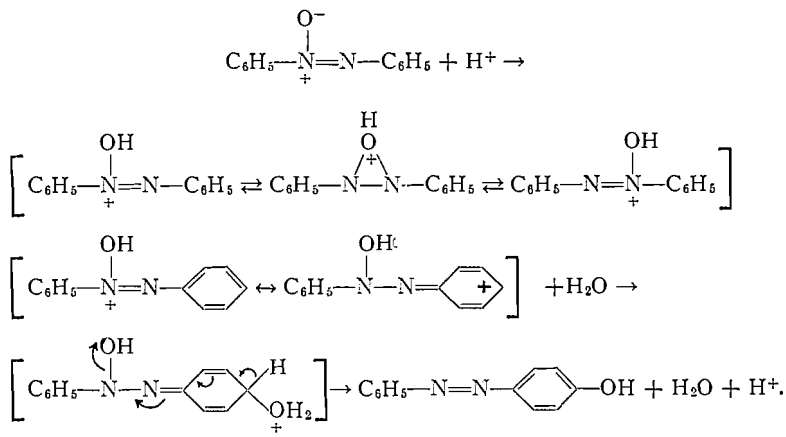

SCHEME 2.

to be quantitative by spectrophotometry and no side products were apparent. In contrast, the earlier work was carried out at much higher azoxybenzene concentrations, from 0.5 *M* to 3 *M*, and often at high temperatures and for long reaction times. Since it thus appeared that the formation of side products may be connected with the reactant concentration and the vigor of the reaction conditions, it was decided to carry out a trial run under favorable reaction conditions.

The data for the run ($1.87 \times 10^{-3}M$ azoxybenzene in 88.22% H_2SO_4 at 25° C) are shown in Table I. The rate of reaction was followed spectrophotometrically (12). Aliquots were removed periodically and quenched in ethanolic aqueous alkali, thus taking advantage of the long-wavelength absorption of the anion of *p*-hydroxyazobenzene (λ_{max} = 435 mμ) compared with azoxybenzene (λ_{max} = 323 mμ), as shown in Fig. 1 and Fig. 2. The spectra of the quenched solutions were both qualitatively and quantitatively identical with that of *p*-hydroxyazobenzene. After eight half-lives the spectra remained constant for several more half-lives. The pseudo-first-order rate constant, calculated from the linear plot of log (O.D.$_\infty$ − O.D.$_t$) at 435 mμ against time, is 5.20×10^{-5} s^{-1}. These results showed that under the kinetic conditions *p*-hydroxyazobenzene is produced quantitatively. However, as the acid concentration was increased it was observed that the absorbance of the "infinity solutions" was greater by a few percent than the calculated value and the absorption maximum was shifted slightly. This result was shown to be due to decomposition of *p*-hydroxyazobenzene. In 96.4% sulfuric acid this decomposition amounted to about 1.5% per half-life of the azoxybenzene reaction. Runs in over 92% sulfuric acid were corrected for this decomposition of *p*-hydroxyazobenzene.

In order to confirm the soundness of the rate data a check was made by another method. Instead of following the rate by a sampling procedure and spectrophotometric measurement of the quenched alkaline solutions, the rate was followed by direct spectrophotometric measurement of the acid solutions in a thermostatted cell of a spectrophotometer. Spectral sweeps were taken at various time intervals over the regions of protonated azoxybenzene (λ_{max} = 390 mμ) and protonated *p*-hydroxyazobenzene (λ_{max} = 463 mμ). The curves exhibited a regular decrease of the 390 mμ absorption and corresponding increase of the 463 mμ absorption, with a single well-defined isosbestic point. Rate constants were calculated both from the disappearance of the azoxybenzene absorption and the development of the *p*-hydroxyazobenzene absorption. The rate constants so obtained

Can. J. Chem. Downloaded from www.nrcresearchpress.com by 210.87.254.6 on 09/05/12
For personal use only.

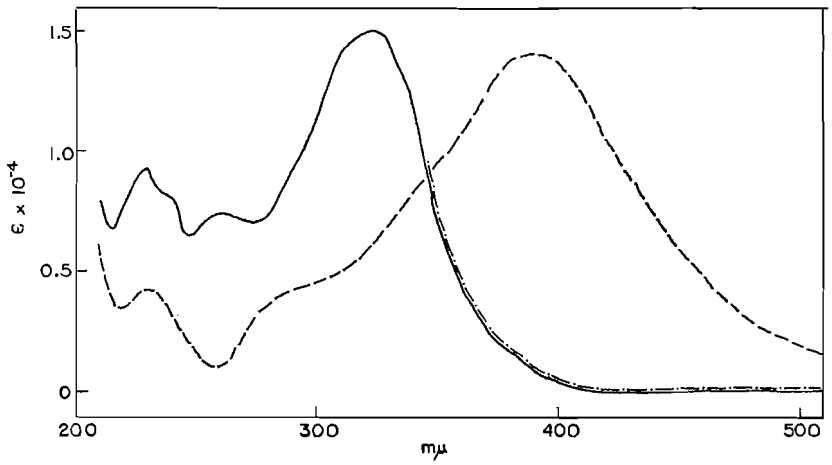

FIG. 1. Spectrum of azoxybenzene in 95% ethanol (—); 90% sulfuric acid (---); aqueous ethanolic alkali (1 *M*) (-·-·).

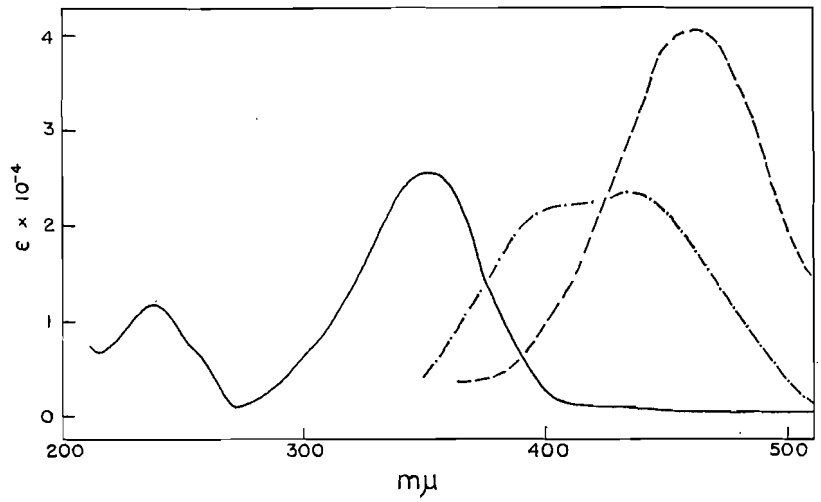

FIG. 2. Spectrum of *p*-hydroxyazobenzene in 95% ethanol (—); 90% sulfuric acid (---); aqueous ethanolic alkali (1 *M*) (-·-·).

were equal within experimental error and also agreed with the value obtained by the quenching method. These results are shown in Fig. 3.

The rate data at 25° and 75° and at various acid concentrations are recorded in Table II. The usual method of measurement was the dilution method. At 75°, some of the rates were determined by a sealed-tube method. The reproducibility of the rate data was about 2% when the same stock solution of sulfuric acid was used and about 10% between two different stock solutions of acid. The larger error in the latter case is evidently caused by the very steep rise in rate constant with acid concentration and the difficulty of reproducing exactly a given acid concentration by ordinary analytical techniques; thus at 95% H_2SO_4 the rate increases by 9% for an increment of 0.1% H_2SO_4 while at 80% H_2SO_4 the corresponding increase in rate constant is 30%.

Can. J. Chem. Downloaded from www.nrcresearchpress.com by 210.87.254.6 on 09/05/12
For personal use only.

TABLE I

Rearrangement of azoxybenzene in 88.22% H_2SO_4 at 25.0° by dilution method

Time (h)	O.D. at 435 mμ	$O.D._\infty - O.D._t$	$\log (O.D._\infty - O.D._t) + 2$
0	0.007	0.774	1.889
0.25	0.042	0.739	1.869
0.50	0.076	0.705	1.848
0.75	0.111	0.670	1.826
1.00	0.134	0.647	1.808
1.25	0.171	0.610	1.785
1.50	0.197	0.584	1.766
2.00	0.250	0.531	1.725
2.50	0.297	0.484	1.685
3.00	0.343	0.438	1.641
4.00	0.416	0.365	1.562
5.00	0.476	0.305	1.484
6.00	0.529	0.252	1.401
7.50	0.590	0.191	1.281
9.50	0.642	0.139	1.143
12.00	0.693	0.088	0.944
24.00	0.774	0.007	
48.00	0.781	0.000	

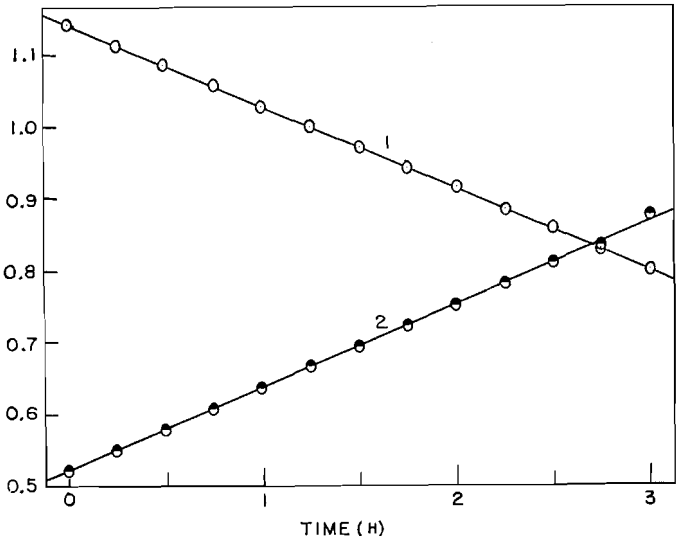

FIG. 3. First-order plots for rearrangement of $3.93 \times 10^{-5} M$ azoxybenzene in 90.37% H_2SO_4 by the "direct" method: (1) $1 + \log (O.D._\infty - O.D._t)$ vs. time, absorbances at 463mμ; (2) $-\log (O.D._t - O.D._\infty)$ vs. time, absorbances at 390 mμ. Rate constant from plot (1), 7.24×10^{-5} s^{-1}, from plot (2), 7.35×10^{-5} s^{-1}.

Product analysis was also carried out, at two acid concentrations, 90.4% H_2SO_4 and 77.5% H_2SO_4, in order to cover most of the range of the kinetic study. The azoxybenzene concentration was about $3 \times 10^{-2} M$. Unexpectedly it was found that the quantity of side products, mainly azobenzene, depended not only on the reaction time, as anticipated from the kinetic work, but also on the manner of isolation of products. The most satisfactory method was slow addition of the acidic reaction mixture to cooled aqueous sodium hydroxide, keeping the temperature below 0°. If during the neutralization the temperature was allowed to reach 50°, the side products increased by several percent. Also the exclusion of light was found to be necessary, both during reaction and work-up.

Can. J. Chem. Downloaded from www.nrcresearchpress.com by 210.87.254.6 on 09/05/12
For personal use only.

TABLE II

Kinetic data for azoxybenzene rearrangement*

$T = 25.0°$			$T = 75.5°$		
Stock solution	Wt. % H_2SO_4	10^5k, s^{-1}	Stock solution	Wt. % H_2SO_4	10^5k, s^{-1}
2	75.30	0.016	4	65.00	0.0854
2	77.45	0.048	4	65.00	0.0800‡
2	80.15	0.208	4	70.00	0.916
3	80.15	0.245	4	70.00	1.08
3	80.15	0.236	4	70.00	1.03‡
2	82.87	0.778	4	75.30	11.5
2	85.61	2.17	4	75.30	11.1
3	85.61	2.43	4	80.15	95.2
3	85.61	2.41	4	80.15	97.5
2	87.57	3.68	4	85.61	611
1	88.22	5.20	4	85.61	601
2	90.37	7.23	4	90.37	1 670
3	90.37	7.69	4	90.37	1 680
3	90.37	7.69			
3	90.37	7.35†			
3	90.37	7.24†			
2	92.81	11.6			
2	95.19	20.2			
3	95.19	21.2			
3	95.19	21.1			
2	96.40	26.1			

*Data were obtained by the dilution method unless otherwise stated.
†Direct method.
‡Sealed tube method.

When this precaution was not taken, small amounts of *o*-hydroxyazobenzene were obtained. The reaction at 90.4% H_2SO_4 after 5 half-lives yielded 3% of unchanged azoxybenzene, 1.5% of other neutral material, and 95% of *p*-hydroxyazobenzene. At 77.5% H_2SO_4 after 2.5 half-lives, the corresponding values were 17, 2, and 81% respectively. The product analyses were hence in full agreement with the kinetic data.

pK Determinations

Knowledge of the pK_a of azoxybenzene is essential for the interpretation of the kinetic data, since azoxybenzene is expected to be appreciably protonated in the acid concentrations employed. The pK_a of azoxybenzene in 20% ethanol and 80% sulfuric acid – water mixture was found to be −6.45 by Jaffé and Hahn (11*b*), based on the H_0 scale appropriate for this ethanolic aqueous acid medium (13*a*). Since the present study was carried out in aqueous medium, in which interpretation of rate data is less ambiguous than in mixed solvents (14*a*), determination of the pK_a of azoxybenzene in aqueous sulfuric acid was deemed necessary.

Spectra of azoxybenzene solutions of various sulfuric acid concentrations, covering the complete range of protonation, were recorded. The data, shown in Table III, were treated by the methods of Davis and Geissman (15) and Katritzky, Waring and Yates (16). The two methods gave pK_a values of −5.15 and -5.14 ± 0.05, respectively, rounded off to −5.15.

The Katritzky–Yates procedure also allows one to test whether or not a given substrate undergoes equilibrium protonation in the manner of a true Hammett base (understood to mean a primary aromatic amine (17)). Thus, since $H_0 = pK_a - \log [BH^+]/[B]$, a plot of log $[BH^+]/[B]$ against H_0 should be linear of unit slope, if in fact protonation of the base is governed by H_0. For azoxybenzene the value of this slope, calculated from the

Can. J. Chem. Downloaded from www.nrcresearchpress.com by 210.87.254.6 on 09/05/12
For personal use only.

ϵ_{383} and ϵ_{323} plots is 0.92 ± 0.10 and 1.01 ± 0.05 respectively. (The error depends directly on the gradient at the inflection point of the sigmoid curves.) It is therefore concluded that, within the error of the present measurements, the protonation of azoxybenzene is in fact governed by the Hammett acidity function H_0.

TABLE III

Data for determination of pK_a of azoxybenzene

% H_2SO_4	$-H_0$	O.D. at 383 mμ	O.D. at 323 mμ	(O.D.$_{383}$ − O.D.$_{323}$)
41.07	2.50	0.081	0.904	−0.823
50.77	3.48	0.100	0.905	−0.805
54.70	3.88	0.127	0.893	−0.766
60.31	4.50	0.264	0.847	−0.583
64.49	5.01	0.524	0.725	−0.201
67.24	5.38	0.760	0.619	+0.141
70.16	5.83	0.921	0.518	+0.403
71.07	5.97	0.953	0.490	+0.463
73.82	6.38	1.015	0.447	+0.568
76.18	6.75	1.040	0.434	+0.606
77.93	7.01	1.048	0.424	+0.624
85.17	8.16	1.060	0.385	+0.675
90.49	9.02	1.070	0.392	+0.678
96.54	10.12	0.956	0.353	+0.603

TABLE IV

Protonation and rate data for azoxybenzene rearrangement

% H_2SO_4	log C_{H^+}	$-H_0$	$\frac{C_{SH^+}}{C_S + C_{SH^+}}$	$\frac{C_S}{C_S + C_{SH^+}}$	$-\log a_{H_2O}$	$\log k + 7$
$T = 25.0°$						
75.30	1.108	6.61	0.967	0.0335	1.77	0.20
77.45	1.126	6.95	0.984	0.0156	1.97	0.68
80.15	1.149	7.37	0.994	0.00599	2.28	1.36
82.87	1.170	7.80	0.998	0.00223	2.69	1.89
85.61	1.191	8.22	0.999	0.000850	3.04	2.37
87.57	1.205	8.55	1.000	0.000399	3.28	2.57
88.22	1.210	8.64	1.000	0.000324	3.35	2.72
90.37	1.223	9.00	1.000	0.000141	3.66	2.87
92.81	1.237	9.45	1.000	0.000050	4.01	3.06
95.19	1.249	9.89	1.000	0.000018	4.44	3.32
96.40	1.256	10.10	1.000	0.000011	4.88	3.42
$T = 75.5°$						
65.00	0.999	5.07	0.454	0.546	1.05	0.82
70.00	1.060	5.80	0.817	0.183	1.35	2.00
75.30	1.096	6.61	0.966	0.0335	1.77	3.05
80.15	1.136	7.37	0.994	0.00599	2.28	3.98
85.61	1.178	8.22	1.000	0.000850	3.04	4.78
90.37	1.210	9.00	1.000	0.000141	3.66	5.22

DISCUSSION

Proposed Mechanism for Wallach Rearrangement

The kinetic data coupled with the pK measurement allow an interpretation of the mechanism of the rearrangement of azoxybenzene. The first deduction, that the reaction is acid catalyzed, is evident from the rapid increase in rate with acid concentration. Further insight on the manner of the acid catalysis is obtained by calculating the extent of monoprotonation of azoxybenzene ($C_{SH^+}/C_S + C_{SH^+}$) in the acid solutions used, from the relationship $\log C_{SH^+}/C_S = pK_a - H_0$. The unexpected result then becomes apparent that azoxybenzene is present almost entirely in the protonated form even in

Can. J. Chem. Downloaded from www.nrcresearchpress.com by 210.87.254.6 on 09/05/12
For personal use only.

the lowest acid concentrations used, and yet there is a great increase in the rate of reaction with increasing concentration. Thus the data of Table IV show that on increasing the sulfuric acid concentration from 75.3% to 85.6% the protonation changes only from 96.7% to 99.9%, yet the rate constant increases by 140-fold. From 85.6% to 96.4% sulfuric acid the extent of protonation remains virtually constant, but the rate constant increases by another 12-fold over this range.[3] This striking increase in rate constant with acidity while the amount of monoprotonated species remains virtually unchanged can only be explained on the basis that a second proton transfer is involved at some stage of the reaction.

With the knowledge that the transfer of two protons is a necessary feature in the reaction path of the conversion of azoxybenzene to *p*-hydroxyazobenzene (VIII), it is possible to formulate mechanisms which may then be tested by the experimental data. The proposed reaction paths are given in Schemes 3 and 4.

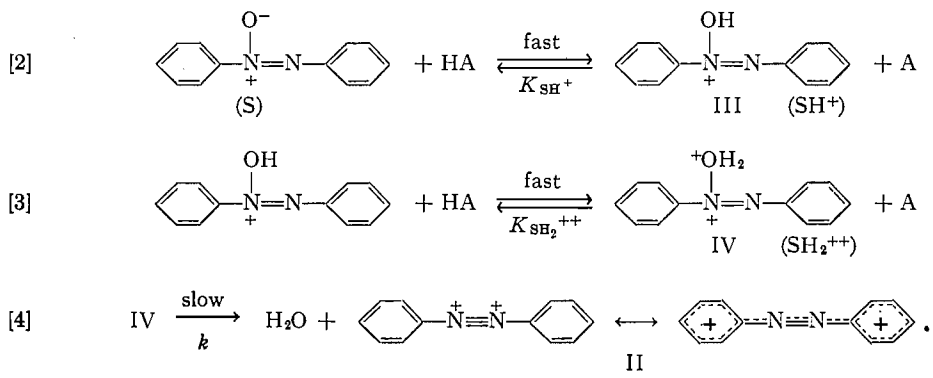

SCHEME 3.

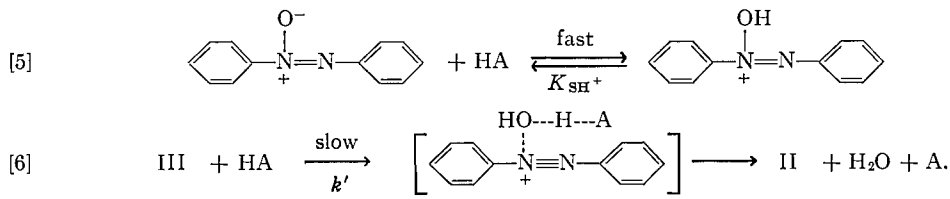

SCHEME 4.

Steps [4] and [6] are followed by [7], [8] or [8*a*], and [9] or [9*a*].

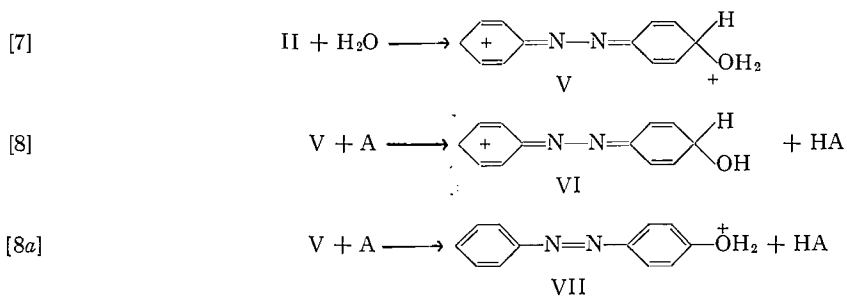

[3] *The degrees of protonation given in Table IV are slightly different from those reported in (1) due to the replacement of the H_0 values compiled by Paul and Long (14a) by the recently measured Jorgenson–Hartter H_0 scale (17). Use of the new H_0 scale has also changed the pK_a of azoxybenzene from −5.10 to −5.15.*

Can. J. Chem. Downloaded from www.nrcresearchpress.com by 210.87.254.6 on 09/05/12
For personal use only.

[9] $$VI + A \longrightarrow VIII + HA$$

[9a] $$VII + A \longrightarrow VIII + HA.$$

Scheme 3 begins with a rapid equilibrium protonation of azoxybenzene; the site for the proton has been shown to be the coordinated oxygen (11*b*). (The acid is depicted as HA in order to include all possible species present in the relatively concentrated acid, viz. H_3O^+, H_2SO_4; A is then the conjugate base of HA, which is also depicted without charge.) Next follows a second fast equilibrium protonation, again on the oxygen. The rate-determining step is the loss of a water molecule from the oxonium ion to give the dication (II). Steps [3] and [4] are analogous to the formation of a carbonium ion from an alcohol. Scheme 4 also begins with a rapid equilibrium protonation, but is followed directly by a rate-determining proton transfer to oxygen with simultaneous heterolysis of the nitrogen–oxygen bond. Thus step [6] of Scheme 4 combines step [3] and [4] of Scheme 3. The dication (II), formed by either of the two schemes, would then undergo further reactions as outlined in eq. [7]–[9], which for the present are assumed to be fast steps. According to the classical interpretation of acid-catalyzed reactions, Scheme 3 is the two-proton analogue of the A-1 case while Scheme 4 is similar to the A-S_E2 mechanistic case (14*b*). The following discussion on the correlation of the kinetic data with theoretical derivations will consider both these schemes.

Rate Expressions for Scheme 3

The rate of reaction is given by the Brönsted eq. [10], in which the symbols have their usual significance. Substitution for a_{H^+} is made in terms of h_+ since the second equilibrium protonation is governed by the h_+ acidity function ($h_+ = a_{H^+}f_{C^+}/f_{CH^{++}}$ where C^+ is the reference charged base and CH^{++} its conjugate acid), the resulting expression [11] can then be equated with $k_{obs}\cdot(C_S + C_{SH^+})$ where k_{obs} is the pseudo-first-order rate constant, assuming that there is negligible diprotonation ($C_{SH_2^{++}} \ll C_{SH^+}$) and yields the final rate expression [12].

[10] $$\text{Rate} = \frac{ka_{SH_2^{++}}}{f_{\neq}} = \frac{kC_{SH^+}f_{SH^+}a_{H^+}}{K_{SH_2^{++}}f_{\neq}}$$

[11] $$= \frac{kC_{SH^+}h_+f_{SH^+}f_{CH^{++}}}{K_{SH_2^{++}}f_{\neq}f_{C^+}}$$

[12] $$\log k_{obs} - \log \frac{C_{SH^+}}{C_S + C_{SH^+}} = -H_+ + \log \frac{k}{K_{SH_2^{++}}} + \log \frac{f_{SH^+}f_{CH^{++}}}{f_{\neq}f_{C^+}}.$$

An alternative rate expression can be derived by substitution for a_{H^+} in the expressions for K_{SH^+} and $K_{SH_2^{++}}$ in terms of h_0 and h_+, respectively, followed, as previously, by equating the Brönsted equation with $k_{obs}(C_S + C_{SH^+})$:

$$a_{SH^+} = \frac{a_S h_0 f_{BH^+}}{K_{SH^+}f_B}; \quad a_{SH_2^{++}} = \frac{a_{SH^+}h_+f_{CH^{++}}}{K_{SH_2^{++}}f_{C^+}}$$

$$\text{rate} = \frac{ka_{SH_2^{++}}}{f_{\neq}} = \frac{kC_S h_0 h_+ f_S f_{BH^+} f_{CH^{++}}}{K_{SH^+}K_{SH_2^{++}}f_{\neq}f_B f_{C^+}}$$

[13] $$\log k_{obs} - \log \frac{C_S}{C_S + C_{SH^+}} = -H_0 - H_+ + \log \frac{k}{K_{SH^+}K_{SH_2^{++}}} + \log \frac{f_S f_{BH^+} f_{CH^{++}}}{f_{\neq}f_B f_{C^+}}.$$

In order to test the experimental rate and equilibrium data according to eqs. [12] and [13], knowledge of the acidity function H_+ is required. The presently available measurements show that for the indicator 4-aminoacetophenone over the acid range 75–95%

Can. J. Chem. Downloaded from www.nrcresearchpress.com by 210.87.254.6 on 09/05/12
For personal use only.

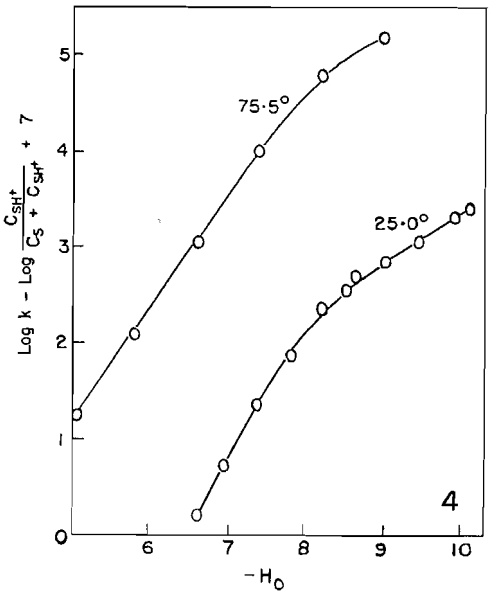

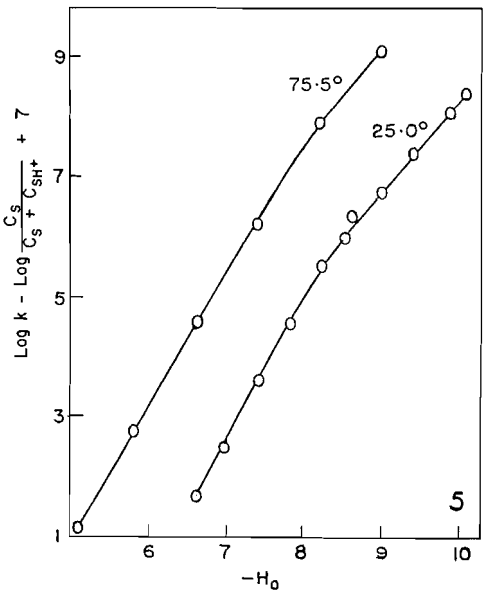

FIG. 4. Plot showing rate dependence based on rate expression [12].
FIG. 5. Plot showing rate dependence based on rate expression [13].

H_2SO_4 H_+ is a parallel function of H_0 (18). Although the generality of this relationship has not been proved, as has not the applicability to this particular system, it has, however, been found to hold in some other studies (19), and hence H_0 will be substituted for H_+ in these tests.[4] Hence the plots of the left sides of eqs. [12] and [13] against H_0 should be linear with slopes of 1 and 2 respectively if the activity coefficient terms are zero or constant. The plots are shown in Figs. 4 and 5 and the appropriate data are contained in Table IV. All the plots are curved downwards and the initial slopes are slightly in excess of the predicted values. Thus the 25° and 75° curves of Fig. 4 have initial slopes of 1.30 and 1.19, while the corresponding curves of Fig. 5 have slopes of 2.32 and 2.17.[5] The assumptions behind these plots must be critically examined. The pairs $C^+ - CH^{++}$ and $SH^+ - T.S.$ have the same charge characteristics and both differ by one proton. The ratios of the activity coefficients should then vary in a parallel manner with acid concentration, i.e. $f_{C^+}/f_{CH^{++}} = f_{SH^+}/f_{\pm}$. In the case of eq. [13], however, the argument concerning cancellation of activity coefficients cannot be made, so that this term would not be expected to cancel, unless fortuitously. Therefore the plot of Fig. 4 according to eq. [12] is considered to be the more sound one theoretically. A possible reason for the deviation from linearity at the higher acid concentrations will be considered later.

Rate Expressions for Scheme 4

Since all acid species present can fulfill the function of HA one should have general acid catalysis. In practice this is difficult to demonstrate in strongly acid solutions (14*b*)

[4]*The parallelism of H_+ and H_0 refers to H_0 values compiled by Long and Paul (14a) and will not be strictly correct when the recently measured Jorgenson–Hartter (17) values are used. However, in view of the scarcity of data on the H_+ function it seems to be desirable to continue assuming this parallelism with the new H_0 function (17) also, even though an error may be introduced. It is also noteworthy that for the medium 20% ethanol – 80% aqueous sulfuric acid H_0 and H_+ are equivalent functions (13b).*

[5]*If the H_0 values at 25° (17) are corrected to 75° using the data of Gelbstein et al. (20) then the 75° slopes become 1.25 and 2.44 respectively. Similarly, if the other plots involving H_0 are so corrected, the slopes of the 75° plots assume values closer to the 25° plots. This would indicate that there is no change in mechanism over this temperature range.*

Can. J. Chem. Downloaded from www.nrcresearchpress.com by 210.87.254.6 on 09/05/12
For personal use only.

and hence acidity function correlations are sought. The problem now arises whether to assign the H_2O of H_3O^+ a structural role in the transition state (14*b*). If a transition state free of H_2O is considered then the rate expressions [14] and [15] may be derived.

$$[14] \qquad \log k_{obs} - \log \frac{C_{SH^+}}{C_S + C_{SH^+}} = -H_0 + \log k' + \log \frac{f_{SH^+} f_{BH^+}}{f_{\neq}' f_B}$$

$$[15] \qquad \log k_{obs} - \log \frac{C_S}{C_S + C_{SH^+}} = -2H_0 + \log \frac{k'}{K_{SH^+}} + \log \frac{f_S f_{BH^+}^2}{f_{\neq}' f_B^2}.$$

Except for the activity coefficient terms, these equations are similar to [12] and [13], derived for Scheme 3, and in practice cannot be differentiated from them.

When water is considered to be present in the transition state one may derive eq. [16] and [17] for consideration.

$$[16] \qquad \log k_{obs} - \log \frac{C_{SH^+}}{C_S + C_{SH^+}} = \log C_{HA} + \log k' + \log \frac{f_{SH^+} f_{HA}}{f_{\neq}''}$$

$$[17] \qquad \log k_{obs} - \log \frac{C_S}{C_S + C_{SH^+}} = -H_0 + \log C_{HA} + \log \frac{k'}{K_{SH^+}} + \log \frac{f_S f_{HA} f_{BH^+}}{f_{\neq}'' f_B}.$$

The activity coefficient term in [16] is likely to change uniformly with acid concentration. In fact the $\log k_{obs} - \log (C_{SH^+}/C_S + C_{SH^+})$ vs. $\log C_{H^+}$ plots at 25° and 75° are curved with initial slopes of 27 and 25! No obvious assumption can be made concerning the activity coefficient term in [17]. A plot of $\log k_{obs} - \log (C_S/C_S + C_{SH^+})$ vs. $\log C_{H^+} - H_0$ is closely similar to that in Fig. 5, with initial slopes at 25° and 75° of 2.30 and 2.13 respectively.

In evaluation of the above tests of Schemes 3 and 4 it is apparent that the rate data do not fit exactly any of the derived rate expressions. Hence differentiation between the proposed schemes cannot be made. Also, yet other mechanisms cannot be excluded. In this regard the curvature of the plots provides a clue, since the break in most of the curves occurs very close to the monohydrate composition. A plausible explanation would appear to be that step [7] of the proposed scheme may become rate determining as the water activity decreases, which will become particularly crucial above the monohydrate composition. Alternatively, the curvature could be considered to lend support to Scheme 3. If, as is likely, catalysis by H_2SO_4 is less effective than by H_3O^+, then this decreasing dependence of rate on acidity would be expected, particularly above the monohydrate composition.

The Bunnett Criteria

According to the proposals of Bunnett (21, 22) $\log k_{obs} - \log (C_{SH^+}/C_S + C_{SH^+})$ was plotted (*i*) against $\log a_{H_2O}$ and (*ii*) against $\log C_{H^+} + H_0$. Plot (*i*) is curved; at 25° the initial slope is −2.1 decreasing to −0.5 while at 75° the slopes are −2.8 and −0.8. Plot (*ii*) is also curved; the corresponding slopes at 25° are −1.8 and −0.4 and at 75°, −1.5 and −0.5. Negative slopes in the Bunnett-type plots indicate that water is not involved in the rate-determining transition state, either as nucleophile or as proton-transfer agent. The Bunnett criteria are thus in accord with Scheme 3 but are subject to the qualification that they have not been extensively tested in the high acid regions used in this study and neither is it known whether they would apply to two proton processes. It has also been suggested (22) that curvature in these plots is indicative of more than one competing mechanism.

Can. J. Chem. Downloaded from www.nrcresearchpress.com by 210.87.254.6 on 09/05/12
For personal use only.

Activation Parameters

The activation parameters calculated from the rate data at 25° and 75° for the common acid concentrations from 75% to 90% H_2SO_4 are given in Table V. Long *et al.* (23) have proposed that entropies of activation may be used as criteria of mechanism in acid-catalyzed hydrolyses; thus reactions proceeding by the A-1 mechanism have in general $\Delta S^{\ddagger}$ values between 0 and +20, while A-2 reactions have $\Delta S^{\ddagger}$ values between −10 and −30. The $\Delta S^{\ddagger}$ values for azoxybenzene rearrangement fall somewhere in between the two ranges. However, most of the literature data refer to very dilute acid solutions, in contrast to the present work. The data (Table V) show a trend, that $\Delta S^{\ddagger}$ becomes more positive as the acid concentration decreases, so that a positive $\Delta S^{\ddagger}$ might well result in dilute acid solution. This would then be in accord with the A-1 mechanism of Scheme 3, though it is not known whether the entropy criterion would apply to two-proton processes.

TABLE V

Activation parameters for azoxybenzene rearrangement

% H_2SO_4	90.37	85.61	80.15	75.30
E_a(kcal)	22.1±0.2	22.7±0.2	24.7±0.3	26.8±0.5
Log A	12.08	12.03	12.47	12.86
$\Delta S^{\ddagger}$ (e.u.)	−5.3±0.5	−5.5±0.5	−3.5±0.9	−1.7±1.5

It was also hoped that the high temperature data might provide an indication of a competing mechanism proposed in the past (7, 9). The close similarity of the various curves at the two temperatures suggest that there is no change in reaction mechanism on increasing the temperature from 25° to 75°.[5]

Discussion of Previous Mechanisms of the Wallach Rearrangement

Shemyakin *et al.* (5) proposed that the Wallach rearrangement proceeds by way of the N,N-oxide intermediate as a means of explaining the equalization of the nitrogen label on rearrangement. As evidence of this intermediate, the Russian workers cited the formation of 50%–60% azobenzene when the rearrangement was carried out in chlorosulfonic acid in presence of potassium iodide (6). However, that chlorosulfonic acid may act in an anomalous manner is indicated by the finding that 4,4′-dichloro- and 4,4′-dibromoazoxybenzene in chlorosulfonic acid yielded only the corresponding azobenzenes (24), whereas in sulfuric acid the former yielded some 2-hydroxy-4,4′-dichloroazobenzene in addition to the azobenzene (4*b*). In view of the complex situation with respect to side products (4) under usual preparative conditions, a more extensive study of the effect of added iodide on the rearrangement of a number of azoxybenzenes, both in sulfuric acid and in chlorosulfonic acid, is required for such evidence to be decisive. It is doubtful that the role of the α-β isomerization in the scheme of the Wallach rearrangement can be considered as known in the absence of further tracer as well as kinetic studies.

The interpretation of Shemyakin *et al.* (5, 6) suffers from the disadvantage that it does not consider the participation of acid, even though the reaction is clearly acid catalyzed. The basic difficulty with the N,N-oxide intermediate is that it appears not to provide a path for further reaction on the basis of the theories of acid catalysis. Oae *et al.* (9) consider the protonated N,N-oxide to be intermediate in the interconversion of α- and β-isomers but not in the Wallach rearrangement. The difficulty now becomes that in order to explain the lack of equalization of label in the recovered azoxybenzene one has to postulate that protonation of azoxybenzene is not reversible, as shown in Scheme 2,

Can. J. Chem. Downloaded from www.nrcresearchpress.com by 210.87.254.6 on 09/05/12
For personal use only.

a situation which is not likely to obtain in view of the present equilibrium (pK) studies. Further, our data show that monoprotonated azoxybenzene is not the rate-limiting species, as is suggested by Scheme 2.

In conclusion it should be stated that the present work has not provided proof of the dication intermediate (II), although it is fully in accord with this intermediate. Definitive evidence may perhaps be found through kinetic and other physical studies, now in progress, in anhydrous acids where it is possible that (II) might become stabilized.

EXPERIMENTAL

Materials

Recrystallizations were carried out in the dark to exclude the possibility of *cis–trans* isomerization, and in the case of azoxybenzene the occurrence of the ortho-Wallach rearrangement. Ultraviolet and visible spectra were determined on a Beckmann DK1 recording spectrophotometer using 1 cm quartz cells. Commercial 95% ethanol was fractionally distilled using a Dufton column and the fraction boiling at 78.2 °C was collected. The following compounds were recrystallized at least twice from aqueous ethanol and their ultraviolet and visible spectra in 95% ethanol determined: *trans*-azoxybenzene, m.p. 35–36° (lit. (11*a*) m.p. 35°), log ϵ_{max} 4.17 (322 mμ), 3.87 (260 mμ), 3.95 (232 mμ) (lit. (25) log ϵ_{max} 4.16 (323 mμ), 3.85 (260 mμ), 3.92 (231 mμ)); *p*-hydroxyazobenzene; m p. 153–154° (lit. (26) m.p. 155–156°) log ϵ_{max} 4.40 (349 mμ) (lit. (27) log ϵ_{max} 4.39 (348 mμ)); *trans*-azobenzene; m.p. 67.5–68.5° (lit. (28) m.p. 68–69.5°); *o*-Hydroxyazobenzene was prepared by irradiating a 4% solution of azoxybenzene in 95% ethanol for 3 h using a Hanovia high pressure mercury lamp with a quartz insert. The product had m.p. 83–84° (lit. (29*a*) m.p. 82.5–83.5°), log ϵ_{max} 4.26 (323 mμ) (lit. (29*b*) log ϵ_{max} 4.26 (323 mμ).

Fisher C.P. Reagent grade sulfuric acid was used throughout this study. Concentrations were determined by titrating weighed samples with standard sodium hydroxide. The aqueous sulfuric acid solutions used for both the kinetic measurements and the pK studies were prepared by dilution by weight of a stock solution of known concentration. All concentrations of sulfuric acid are percent by weight.

Product Analysis

Azoxybenzene (1.2 g) was dissolved in 200 ml of 77.5% sulfuric acid contained in a stoppered, aluminium foil covered flask. The reaction was carried out for 1 000 h at room temperature, equivalent to 2.5–3.0 half-lives. The reaction mixture was then added slowly to a solution of 250 g of sodium hydroxide in 250 g of water cooled in ice–methanol. The temperature of the neutralization process was never allowed to rise above 0 °C. By a series of ether extractions from acidic and basic solutions, the products of the rearrangement and unreacted azoxybenzene were separated into neutral, basic, and acidic fractions which were then analyzed qualitatively by thin-layer chromatography, using 35–60° petroleum ether and benzene–methanol (10:1) as developers, and quantitatively by ultraviolet and visible spectroscopy.

A second rearrangement was similarly carried out by dissolving 1 g of azoxybenzene in 200 ml of 90.4% sulfuric acid. After 12.5 h at 25 °C, equivalent to 5 half-lives the reaction mixture was worked up as previously.

Kinetic Procedures

Dilution Method

The reaction solution was prepared by adding a 0.01 g accurately weighed sample of azoxybenzene to 25 ml of aqueous sulfuric acid of known concentration in a 50 ml round bottom glass stoppered flask wrapped in aluminium foil and immersed in the thermostatted bath. Samples were removed at regular intervals using a 1 ml fast delivery calibrated pipette and run into 40 ml of quenching solution, which had been precooled in ice–water, in a 50 ml graduated flask. The flasks were stored in the dark and after attaining room temperature were made up to mark with quenching solution and analyzed spectrophotometrically. Rate constants were calculated from absorbances at 435 mμ, the wavelength corresponding to maximum absorption of *p*-hydroxyazobenzene in the quenching solution, 1 M NaOH in 80% aqueous ethanol (ϵ = 22 830).

Sealed Tube Method at 75.5°

The reaction solution was prepared as for the dilution method except that 0.005 g of azoxybenzene was used. Two milliliter samples were pipetted into small tubes which were sealed, wrapped in foil, and placed in the thermostatted oil bath at 75.5 °C. The tubes were removed at intervals, cooled, and stored in a refrigerator. On completion of the run the contents were added to quenching solution, made up to 50 ml, and analyzed as previously. Studies on the decomposition of *p*-hydroxyazobenzene in aqueous sulfuric acid, where required, were carried out under the same conditions as the kinetic measurements.

Direct Method at 25 °C

The reaction solution was prepared by successive dilution: a 1 ml portion of a solution of 0.01 g azoxybenzene in 50 ml sulfuric acid was further diluted to 50 ml using sulfuric acid of the same concentration. This solution was placed in the thermostatted sample cell. Aqueous sulfuric acid of the same concentration

Can. J. Chem. Downloaded from www.nrcresearchpress.com by 210.87.254.6 on 09/05/12
For personal use only.

as the reaction solution was used in the reference cell. The spectrum of the reaction solution was recorded at regular time intervals from 500 mμ to 375 mμ.

pK Determination

A 1 ml sample of a 2×10^{-3} *M* solution of azoxybenzene in 95% ethanol was pipetted into a 50 ml flask and the solvent evaporated with a slow stream of dry nitrogen. Aqueous sulfuric acid (25 ml) of known concentration was added and the flask was agitated vigorously to ensure dissolution of the azoxybenzene. The spectrum of each solution was recorded over the range 300–500 mμ. For the 85, 90, and 95% sulfuric acid solutions, in which the rearrangement is relatively fast, the spectra were recorded at regular time intervals and extrapolated to zero time. In the case of the 85 and 90% sulfuric acid solutions, the extrapolated values did not differ by more than 5% from the first recorded values. In the case of the 95% sulfuric acid the difference was 12%. The results are shown in Table III.

ACKNOWLEDGMENTS

The authors wish to thank Drs. H. H. Jaffé and K. Yates for valuable comments and the National Research Council for financial support.

REFERENCES

1. E. Buncel and B. T. Lawton. Chem. Ind. London, 1835 (1963).
2. O. Wallach and L. Belli. Ber. **13**, 525 (1880).
3. A. Angelli and B. Valori. Atti. Accad. Lincei, **21**, 729 (1912); Chem. Abstr. **6**, 2747 (1912).
4. (*a*) P. H. Gore and G. K. Hughes. Australian J. Sci. Research Ser. A, **3**, 136 (1950); (*b*) **4**, 185 (1951).
5. M. M. Shemyakin, V. I. Maimind, and B. K. Vaichunaite. Chem. Ind. London, 755 (1958); J. Gen. Chem. USSR Engl. Transl. **28**, 1756 (1958); Izv. Akad. Nauk SSSR Otd. Khim. Nauk, 866 (1960).
6. M. M. Shemyakin, V. I. Maimind, and T. E. Agadzhanyan. Chem. Ind. London, 1223 (1961). M. M. Shemyakin and V. I. Maimind. *In* Chemistry of natural and synthetic colouring matters. *Edited by* T. S. Gore. Academic Press, N.Y. 1962. p. 441. M. M. Shemyakin, T. E. Agadzhanyan, V. I. Maimind, and R. V. Kudryavtsev. Izv. Akad. Nauk SSSR., Ser Khim., 1339 (1963).
7. P. H. Gore. Chem. Ind. London, 191 (1959).
8. A. Angelli. Atti. Accad. Lincei, **22**, 844 (1913).
9. S. Oae, T. Fukumoto, and M. Yamagami. Bull. Chem. Soc. Japan, **34**, 1873 (1961); **36**, 601 (1963).
10. R. P. Bell. The proton in chemistry. Cornell University Press, N.Y. 1959.
11. (*a*) C. S. Hahn and H. H. Jaffé. J. Am. Chem. Soc. **84**, 946 (1962); (*b*) **84**, 949 (1962).
12. J. F. Bunnett and E. Buncel. J. Am. Chem. Soc. **83**, 1117 (1961). J. F. Bunnett, E. Buncel, and K. V. Nahabedian. J. Am. Chem. Soc. **84**, 4136 (1962).
13. (*a*) H. H. Jaffé and R. W. Gardner. J. Am. Chem. Soc. **80**, 319 (1958). S. J. Yeh and H. H. Jaffé. J. Am. Chem. Soc. **81**, 3274 (1959). (*b*) M. Isaks and H. H. Jaffé. J. Am. Chem. Soc. **86**, 2209 (1964).
14. (*a*) M. A. Paul and F. A. Long. Chem. Rev. **57**, 1 (1957). (*b*) F. A. Long and M. A. Paul. Chem. Rev. **57**, 935 (1957).
15. C. T. Davis and T. A. Geissman. J. Am. Chem. Soc. **76**, 3507 (1954).
16. A. R. Katritzky, A. J. Waring, and K. Yates. Tetrahedron, **19**, 465 (1963).
17. M. J. Jorgenson and D. R. Hartter. J. Am. Chem. Soc. **85**, 878 (1963).
18. T. G. Bonner and J. C. Lockhart. J. Chem. Soc. 364 (1957).
19. M. W. Fuller and W. M. Schubert. J. Am. Chem. Soc. **85**, 108 (1963).
20. A. I. Gelbstein, G. G. Shcheglova, and M. I. Temkin. Zh. Neorgan. Khim. **1**, 506 (1956).
21. J. F. Bunnett. J. Am. Chem. Soc. **83**, 4956, 4968, 4973, 4978 (1961).
22. J. F. Bunnett. Abstracts, 145th American Chemical Society Meeting, New York. 1963. p. 41A; private communication.
23. F. A. Long, J. G. Pritchard and F. E. Stafford. J. Am. Chem. Soc. **79**, 2362 (1957). L. L. Schalager and F. A. Long. Advan. Phys. Org. Chem. **1**, 1 (1963).
24. V. O. Lukashevich and T. N. Khurdyumova. Zh. Obshch. Khim. **18**, 1963 (1948).
25. P. H. Gore and O. H. Wheeler. J. Am. Chem. Soc. **78**, 2160 (1956).
26. H. H. Jaffé and S. Y. Yeh. J. Am. Chem. Soc. **81**, 3274 (1959).
27. W. R. Brode, I. L. Seldin, P. E. Spoerri, and G. M. Wyman. J. Am. Chem. Soc. **77**, 2762 (1955).
28. H. H. Jaffé and R. W. Gardner. J. Am. Chem. Soc. **80**, 319 (1958).
29. (*a*) W. R. Brode, J. H. Gould, and G. M. Wyman. J. Am. Chem. Soc. **74**, 4642 (1952); (*b*) **75**, 1856 (1953).

Can. J. Chem. Downloaded from www.nrcresearchpress.com by 210.87.254.6 on 09/05/12
For personal use only.

AN ELECTRON SPIN RESONANCE STUDY OF TRAPPED ELECTRONS FORMED AT 77.5 °K BY GAMMA IRRADIATION OF AN ORGANIC GLASS[1]

D. R. SMITH AND J. J. PIERONI

Research Chemistry Branch, Chalk River Nuclear Laboratories, Atomic Energy of Canada Limited, Chalk River, Ontario

Received November 26, 1964

ABSTRACT

2-Methyltetrahydrofuran (MTHF) traps electrons and free radicals or radical-ions when irradiated with ^{60}Co gamma rays at 77.5 °K. The e.s.r. difference spectrum technique has been used to determine the microwave saturation properties and line shape parameters of the absorption due to "trapped" electrons. These measurements support the postulate that physically trapped electrons are present and indicate that trapped electrons and free radicals or radical-ions exist in local concentrations which are considerably greater than their average concentration in the sample. It is concluded that they are trapped in clusters. A study of the thermal decay of the trapped electrons supports the cluster model.

INTRODUCTION

Hamill and co-workers (1) have irradiated 2-methyltetrahydrofuran (MTHF) at 77 °K and observed a broad optical absorption band with a maximum at about 13 000 Å. This absorption band could be removed by photobleaching. Salmon (2) observed that both the near infrared optical absorption band and an electron spin resonance (e.s.r.) singlet could be photobleached with visible light and each disappeared fairly rapidly at 90 °K, suggesting that both are due to the same species.

When certain aromatic solutes are dissolved in MTHF, gamma radiolysis yields the optical absorption spectrum of the solute anion and the 13 000 Å band is diminished or eliminated depending on the solute concentration. If the solute concentration is such that both the solute anion spectrum and the 13 000 Å are observed, photochemical bleaching with light of wavelength greater than 6 000 Å removes the 13 000 Å band and enhances the intensity of the anion optical spectrum (1). These results suggest that solute anions are formed during bleaching by the capture of electrons and that the 13 000 Å band is due to solvated or trapped electrons. This identification is supported by the fact that in solutions of alkali metals in ammonia or amines, the "solvated electron" has a strong optical absorption band in the near infrared wavelength region (3).

The work of Hamill *et al.* provides strong evidence for the possibility that after ionization of a molecule, an electron and its parent ion can remain apart and can make significant contributions to the chemical reactions which occur as a result of subjecting solid organic material to ionizing radiation. In view of this, it was decided to attempt a closer examination of the nature of the solvated or trapped electron. With such a purpose in mind a study of microwave saturation properties and e.s.r. line shape parameters of paramagnetic species can be profitable. Such a study can yield information concerning magnetic interactions with other magnetic moments such as those due to hydrogen nuclei, or unpaired electrons, and can also lead to values for T_1 and T_2. A knowledge of T_1 enables one to ensure that a spectrum is being observed under slow passage conditions. This is a prerequisite for measurement of a true saturation curve. For convenience we shall henceforth refer to the solvated or trapped electron in MTHF as the trapped electron without implying anything regarding its nature.

[1]*A.E.C.L. No. 2165.*

Can. J. Chem. Downloaded from www.nrcresearchpress.com by 210.87.254.6 on 09/05/12
For personal use only.

A study of the kinetics of the thermal disappearance of trapped electrons in MTHF has also been carried out in an effort to gain more information concerning their spatial distribution.

THEORY

The reader is referred to Ingram's book (4) for a basic discussion of microwave saturation, T_1, T_2, etc.

Portis (5) and Castner (6) have provided a thorough description of line broadening associated with saturation phenomena. Saturation behavior depends on the mechanism of line broadening. Portis describes various phenomena which give rise to "homogeneous" and "inhomogeneous" line broadening. We shall only refer to those which concern this work. The homogeneous case can arise from dipolar interaction between unpaired electrons. The energy absorbed from the microwave field is distributed to all the electron spins and thermal equilibrium of the spin system is maintained. The inhomogeneous case occurs when the line width arises from variations (slow compared to the time for a spin transition) in the local magnetic field. Energy is transferred only to those spins whose local fields satisfy the conditions for resonance. Portis introduces the concept of "spin packets" which have very little interaction with each other and whose width is determined by the electron–electron spin–spin interaction. The observed response of the spin system will be a superposition of the spin packet absorptions. In other words a spin packet is a group of magnetically interacting unpaired electrons which see similar local fields due to nuclear magnetic moments. Each spin packet sees a slightly different local field and hence each absorbs at a slightly different value of H_z. The observed spectrum is the envelope of the spin packet absorptions and the shape of the envelope is the intensity distribution of the magnetic fields due to the magnetic moments of nearby nuclei (assuming no significant inhomogeneity in the external d-c. field H_z). To summarize, when pure homogeneous broadening occurs one observes the absorption due to a spin packet; when inhomogeneous broadening occurs one observes a line envelope due to superimposed spin packets. In the former case a plot of absorption intensity (V_R) vs. microwave field intensity (H_1) rises to a maximum and then decreases fairly rapidly. At the same time the absorption line appears to become wider (this is called "saturation broadening"). In the latter case, V_R increases to a maximum and then decreases so slowly that it often appears to have levelled off. The line width remains unchanged (i.e. no "saturation broadening" occurs). There are of course intermediate cases which reflect the ratio of the spin packet width to the envelope width.

The theory which Portis (5) has derived for saturation of an inhomogeneously broadened line assumes that the spin packet width is negligible compared to the line envelope width. Castner (6) has extended this theory to yield a general expression for the absorption component of the magnetic susceptibility χ'' without assuming that the spin packet width is small compared to the line envelope width. Two frequency distributions are used to describe a line; $g(\omega - \omega')$ is the assumed Lorentzian line shape function of the individual homogeneously broadened spin packet, $h(\omega - \omega_0)$ is the observed Gaussian distribution of static fields describing the envelope of the distribution of spin packets. Castner defines $A = \Delta\omega_L/\Delta\omega_G$ where $\Delta\omega_L$ is one half the frequency width for half maximum of $g(\omega - \omega')$ and $\Delta\omega_G$ is the width of the inhomogeneously broadened envelope $h(\omega - \omega_0)$. The line envelope width (ΔH_{pp}) between derivative maxima, in gauss (G), is given by $\sqrt{2}\Delta\omega_G/\gamma$. γ is the gyromagnetic ratio and has a value of 1.76×10^7 s^{-1} G^{-1}.

A saturation curve is a plot of V_R (height of absorption signal at ω_0) vs. microwave

Can. J. Chem. Downloaded from www.nrcresearchpress.com by 210.87.254.6 on 09/05/12
For personal use only.

field (H_1) or (microwave power)$^{1/2}$. Castner has plotted calculated saturation curves for various values of A. The value of A applicable to the experimental curve is determined by a curve-fitting procedure which Castner has outlined. $\Delta\omega_L$ is then calculated from $\Delta\omega_G$ and A. The equation $\Delta\omega_L T_2 = 1$ is used to obtained T_2.

$\Delta\omega_L$ is the spin packet half width at half maximum due to spin–spin dipolar interaction between unpaired electrons. In MTHF this would include both trapped electrons and unpaired electrons on free radicals. ΔH, the spin packet full width at half maximum in G, has been related to the molarity, M, of unpaired electrons by Smith and Wyard (7) who determined eq. [1] experimentally. After determining ΔH_{pp} and A, ΔH is obtained from eq. [2*a*] or [2*b*].

$$\Delta H = (60 \pm 30)M \qquad [1]$$

$$\Delta H = 2\Delta\omega_L/\gamma \qquad [2a]$$

$$\Delta H = \sqrt{2}A\Delta H_{pp}. \qquad [2b]$$

Again using curve-fitting techniques, Castner shows how to find the value of the microwave field H_1 at which eq. [3] applies.

$$H_1 = (1/\gamma)(T_1T_2)^{1/2}. \qquad [3]$$

Hence T_1 is calculated from H_1 and T_2.

EXPERIMENTAL

Samples were irradiated at liquid nitrogen temperature by gamma rays from ^{60}Co. The irradiation dose rate, obtained by ferrous sulfate dosimetry (11), was calculated to be 6.2×10^{18} eV l^{-1} s^{-1} in MTHF using a measured density of 1.06 g ml^{-1} for MTHF at 77.5 °K.

Spectra were obtained using the e.s.r. difference spectrum technique. This technique and the procedure for the preparation and handling of MTHF samples have been described previously (8). The scan rate was calibrated using the major hyperfine splitting of the tetracene positive ion (9). The total concentration of radicals and trapped electrons was determined by comparison of their doubly integrated e.s.r. spectrum with that of a free radical reference. Both samples were present in the dual cavity at the same time and both were at 77.5 °K. Their spectra were obtained consecutively without retuning the spectrometer. The reference was the stable free radical in nuclear reactor irradiated terphenyl coolant which had been stored at room temperature for 3 years. This was calibrated by the same procedure at room temperature by comparison with a solution of DPPH in CCl_4. The DPPH solution was calibrated by its optical absorption using an extinction coefficient $\epsilon = 1.31 \times 10^4$ l mole^{-1} cm^{-2} at 5 200 Å (10). The methods for cavity Q and cavity input power measurements were the same as those used by Castner (6).

It was found that 20 cycle modulation frequency and 2.0 G modulation amplitude ($\omega_m H_m = 250$) satisfied the slow passage requirement. To compensate for the lower spectrometer sensitivity at 20 cycle modulation frequency, the signal to noise ratio was increased by using the less "noisy" sample-cooling method of passing a flow of gaseous nitrogen through a coil at 77.5 °K and then over the sample tubes. The silica vacuum-jacketed cavity insert used for this purpose is shown in Fig. 1. The cooled nitrogen is passed through two vacuum-jacketed arms which are inserted into the two cavity sample positions. The unbleached sample is placed inside one arm and the bleached sample in the other. A copper–constantan thermocouple, calibrated against a N.B.S. Standard platinum resistance thermometer was placed in one arm at the top of the resonant cavity volume, i.e. about 0.25 in. above that part of the sample volume which generates most of the e.s.r. signal. If any error in determining the sample temperature occurs by this procedure, the temperature measured should be too high. Since our liquid nitrogen was at 77.5 °K (slightly contaminated by oxygen) and the temperature indicated by the thermocouple was 81 °K, the error must be less than 3.5 deg. The e.s.r. singlet, attributed to trapped electrons, was found to be stable for the duration of the experiment at this temperature. When results were obtained at 77.5 °K, the apparatus previously described (8) was used.

The spectroscopic g-values were measured by placing solid DPPH whose $g = 2.0036$ (4) in one cavity position and the unknown in the other cavity position. The magnetic field at which resonance for both DPPH and the unknown occurred was measured with a proton resonance gaussmeter.

RESULTS

(1) Difference Spectra

Figure 2*a* is the e.s.r. spectrum of unbleached MTHF which had been gamma irradiated for 90 min. Figure 2*b* is the spectrum of another sample of matched dimensions which

Can. J. Chem. Downloaded from www.nrcresearchpress.com by 210.87.254.6 on 09/05/12
For personal use only.

Can. J. Chem. Downloaded from www.nrcresearchpress.com by 210.87.254.6 on 09/05/12
For personal use only.

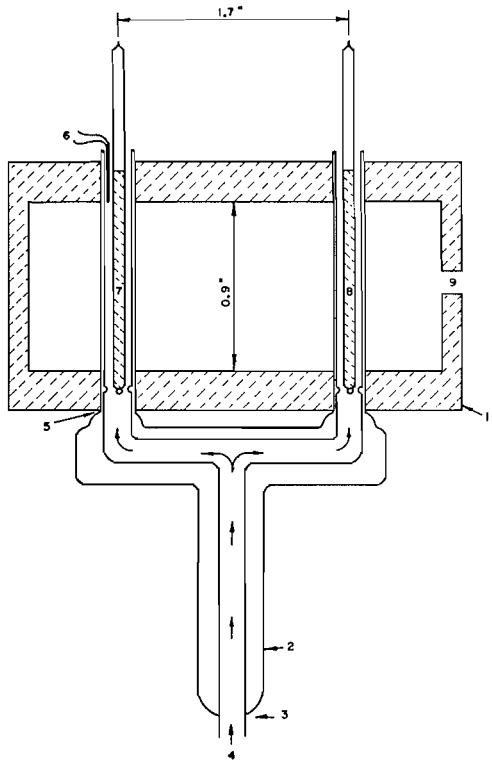

FIG. 1. Silica variable temperature dewar for TE104 cavity. (*1*) Varian dual cavity; (*2*) liquid N_2 level; (*3*) evacuated double-wall dewar above this point; (*4*) N_2 gas flow from a 40 ft copper coil submerged under liquid nitrogen; (*5*) the vacuum jacket silvered inside up to this point; (*6*) copper–constantan thermocouple; (*7*) unbleached, gamma-irradiated MTHF in a Spectrosil tube; (*8*) gamma-irradiated, bleached MTHF in a Spectrosil tube; (*9*) coupling to the waveguide.

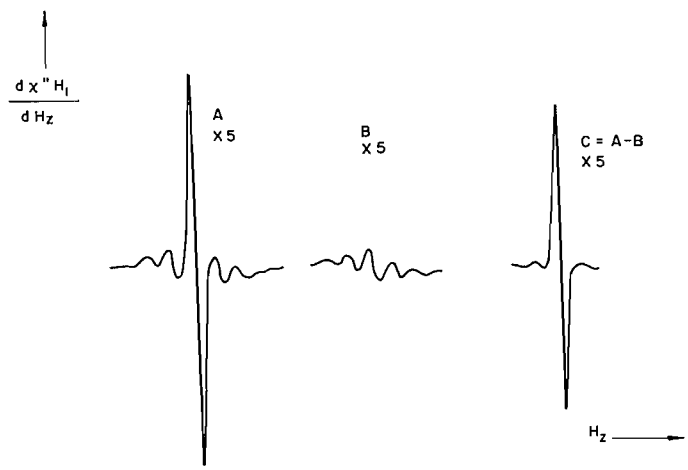

FIG. 2. First derivative e.s.r. spectra of gamma-irradiated MTHF. (A) unbleached, (B) photochemically bleached, (C) difference between A and B.

had also been gamma irradiated for 90 min, and bleached by visible light and was present in the dual cavity at the same time as the unbleached sample. Figure 2*c* is the difference between 2*a* and 2*b* obtained by the technique of measuring e.s.r. difference spectra described earlier (8). Figure 3 is the same as Fig. 2 but the spectra were measured at 10 times greater sensitivity. A, B, and C in Figs. 2 and 3 were obtained by consecutive scans, without retuning the spectrometer, at 77.5 °K. Figures 2*c* and 3*c* demonstrate that the singlet and about one-third of the intensity of the septet disappear during photobleaching. Consequently, to obtain the pure e.s.r. singlet due to trapped electrons, using the e.s.r. difference spectrum technique, the sample to be bleached was irradiated for 90 min and compared to a sample irradiated for 60 min, which remained unbleached (Results, section 2*a* and Fig. 4).

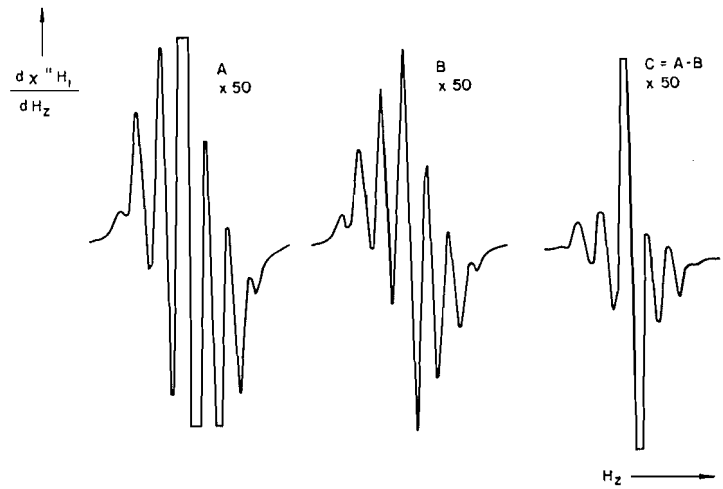

FIG. 3. Same as Fig. 2 but these spectra were obtained using a 10 times greater sensitivity.

The septet spectrum has a 20.5 G average hyperfine splitting and linewidths of about 10 G between derivative maxima. The integrated lines have relative intensities roughly equal to 1:3.9:6.7:8.2:6.7:3.9:1.

(2a) Line Shape and Width

The first derivative difference spectrum due to trapped electrons is shown in Fig. 4. The points represent calculated Gaussian and Lorentzian line shapes normalized to the maximum of the experimental line. The experimental line appears to be nearly Gaussian with a width between derivative maxima of 4.5 G. This spectrum was obtained at 77.5 °K using 100 kc/s modulation frequency and 1 G modulation amplitude. No fast passage distortion occurred because at the low value of H_1 (4.8×10^{-3} G) used no detectable saturation was occurring. Fast passage effects only occur when the signal is at least partly saturated.

(2b) g-Values

To obtain g for the trapped or solvated electron an unbleached sample was examined using $H_1 = 2.9 \times 10^{-3}$ G. At this low microwave intensity, the difference in saturation behavior between the radical or radical-ion and the electron (see Results, section 3) enabled observation of the electron singlet with little interference from the septet. Values

Can. J. Chem. Downloaded from www.nrcresearchpress.com by 210.87.254.6 on 09/05/12
For personal use only.

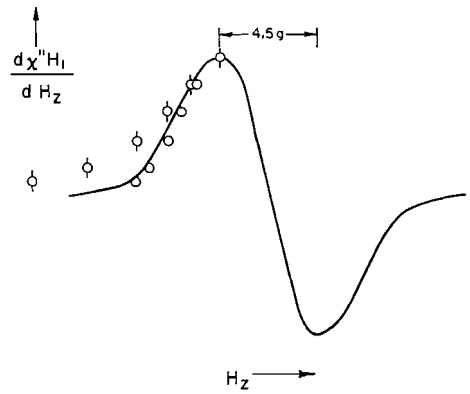

FIG. 4. The line is the first derivative e.s.r. spectrum of trapped electrons in MTHF. The points are calculated Gaussian (O) and Lorentzian (-O-) line shapes normalized to the observed derivative maximum.

of g for the radical or radical-ion were determined with a photochemically bleached sample. Both g-values were found to equal 2.003 ± 0.001 relative to $g = 2.0036$ for DPPH.

(3) Saturation Curve

Figure 5 is a plot of V_R vs. H_1 at 81 °K for trapped electrons and free radicals in MTHF. Both plots have been normalized to the maximum signal height. The line shape and width did not change in the range of H_1 used so V_R was taken to be proportional to the amplitude of the first derivative absorption signal. For the free radical, the central line intensity was measured.

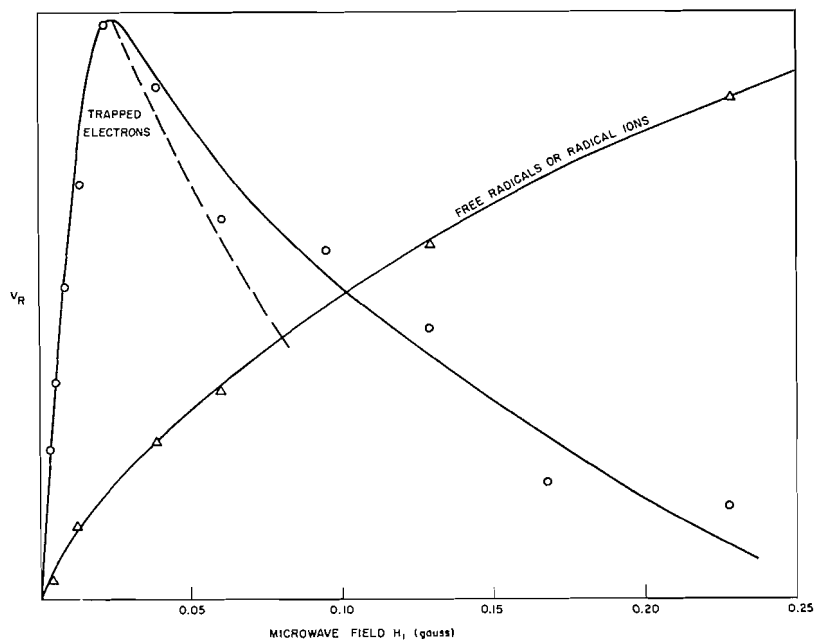

FIG. 5. Microwave saturation curves; O electrons and △ radicals or radical ions trapped in MTHF at 81 °K. ---- Theoretical for pure homogeneous broadening. Irradiation dose equals 2.25×10^{19} eV ml^{-1}.

Can. J. Chem. Downloaded from www.nrcresearchpress.com by 210.87.254.6 on 09/05/12
For personal use only.

(4) Thermal Decay Curves at 77.5 °K

At 77.5 °K using 100 kc modulation frequency and $H_1 = 4.8 \times 10^{-3}$ G, the signal intensity was followed as a function of time after irradiation. Since, at the low value of H_1 used, the septet intensity was negligible, accuracy was improved by observing an unbleached MTHF sample in one cavity position and a stable reference free radical sample in the other cavity position. The reference was used to monitor fluctuations in the spectrometer sensitivity. The septet intensity decreases somewhat during the thermal disppearance of trapped electrons, in fact, the observations seem analogous to those obtained by photobleaching. In this experiment, the small contribution by the septet to the intensity of the trapped electron singlet was graphically estimated and subtracted. Three radiation doses were used and the resulting decay curves are shown in Fig. 6. The normalized curves are fairly well superimposed as shown in Fig. 7. After an initially more rapid decay for about 50 h, the trapped electron concentration decayed more slowly and linearly. The data did not fit either first or second order kinetic plots.

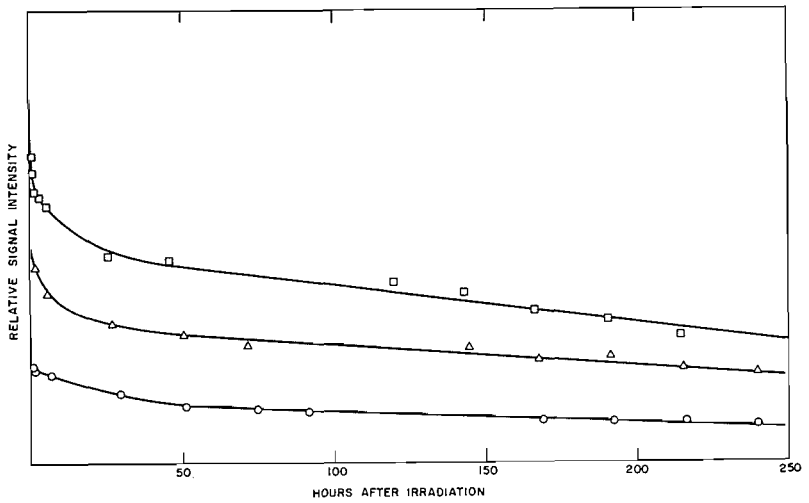

FIG. 6. Thermal decay of electrons trapped in MTHF at 77.5 °K. Irradiation dose equals ○ 9.8×10^{18} eV ml^{-1}, △ 1.74×10^{19} eV ml^{-1}, □ 3.43×10^{19} eV ml^{-1}.

(5) Thermal Decay at Temperatures Greater than 77.5 °K

These data suffice only to demonstrate the temperature at which trapped electrons or free radicals disappear rapidly, i.e. in 10–20 min. Small temperature increments were used but the sample was only kept for about 5 min at each temperature. The data were obtained as a graph of concentration vs. time. Figure 8 is a plot of the slope of this graph vs. the temperature at the point of measurement. It is seen that 92 to 95 °K is a very critical temperature range for the disappearance of trapped electrons. At the same time, the intensity of the septet decreased by roughly one-third. The remaining septet intensity remained stable up to 100 °K and disappeared in 5 min at 101 °K. In another sample, from which the trapped electrons had been bleached, the remaining free radicals or radical-ions did not disappear rapidly until 101 °K.

DISCUSSION AND CONCLUSIONS

(1) The Nature of the "Trapped Electron"

As discussed in the introduction, the e.s.r. singlet has been attributed to trapped

Can. J. Chem. Downloaded from www.nrcresearchpress.com by 210.87.254.6 on 09/05/12
For personal use only.

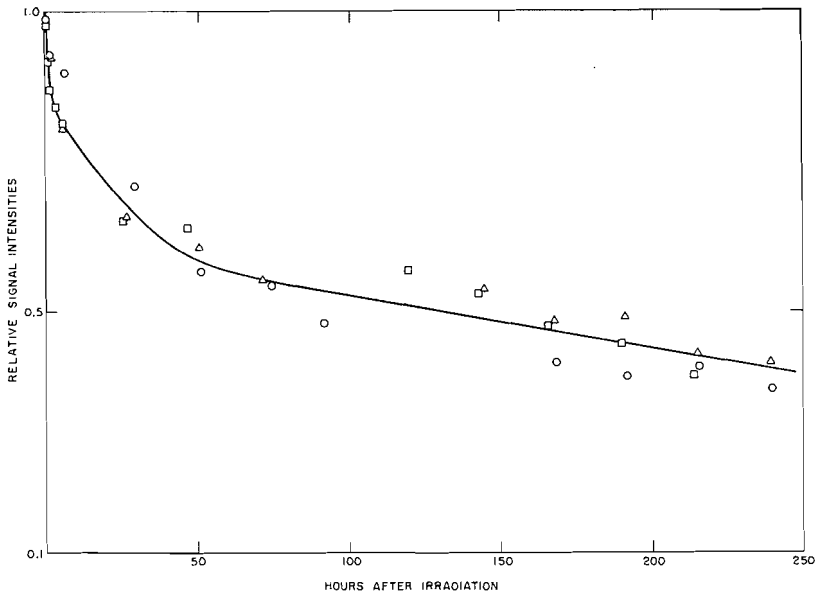

FIG. 7. The data of Fig. 6 normalized to unity. The symbols refer to the same irradiation doses as in Fig. 6.

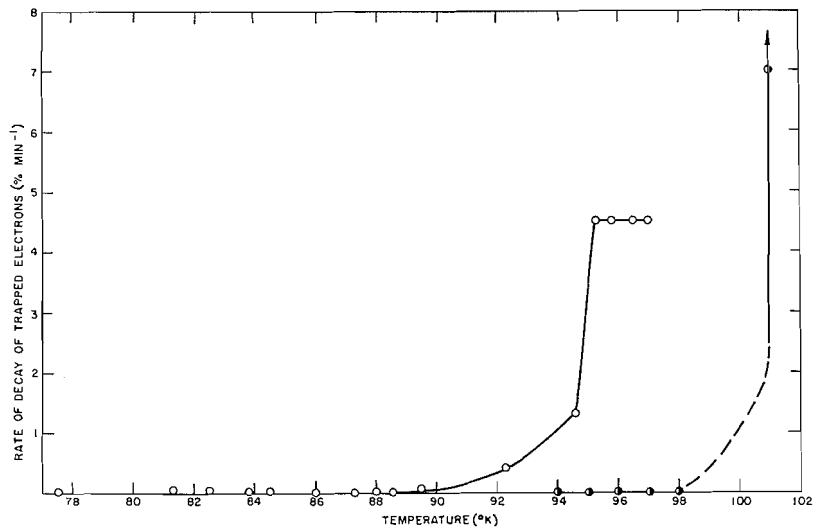

FIG. 8. MTHF irradiated to a dose of 4.5×10^{19} eV ml^{-1}. Approximate rate of thermal decay vs. temperature. ○ Trapped electrons, ◑ free radicals or radical-ions remaining after thermal or photochemical reaction of the trapped electrons.

electrons. This identification is supported by the e.s.r. line width and the microwave saturation measurements.

The e.s.r. singlet due to trapped electrons is essentially gaussian in shape and no saturation broadening occurs (the line width is independent of H_1) in the range of H_1 studied. This agrees with the theoretical picture of a line which is inhomogeneously broadened by either isotropic or anisotropic proton hyperfine interaction. The magnetic

Can. J. Chem. Downloaded from www.nrcresearchpress.com by 210.87.254.6 on 09/05/12
For personal use only.

interaction by protons has an intensity distribution which is approximately gaussian. The 4.5 G line width is unusually narrow compared to that observed in a hydrocarbon radical under the same conditions. In organic radicals trapped in a glassy or polycrystalline matrix at low temperature, an isotropic proton interaction of 20–40 G and a proton dipolar broadening interaction of 10 G are common. This shows that the trapped electron is experiencing weaker magnetic interactions due to protons than does an electron on a free radical.

The observed saturation curve for the septet absorption is a typical example (15) of a saturation curve for a hydrocarbon radical in a solid matrix whose e.s.r. lines exhibit considerable inhomogeneous broadening due to anisotropic proton hyperfine interaction, i.e. $\Delta\omega_L/\Delta\omega_G$ is fairly small. Comparison of the trapped electron saturation curve with that for the septet absorption confirms that the absorption due to trapped electrons is experiencing less inhomogeneous broadening than does the absorption due to an electron on a free radical. It is concluded that in MTHF the spin density of a trapped electron at any proton is less and its distance from any proton is greater than are the same parameters for an unpaired electron on a free radical. In other words the trapped electron orbital is relatively independent of molecular orbitals and it may be expected to behave as an independent chemical species. This is support, from physical measurements, of the conclusions reached by Hamill and co-workers (1) on the basis of chemical and optical absorption measurements.

(2) The Location of the Postitive Charge

The septet e.s.r. spectrum is interpreted as being due to one or both of the species I and II.

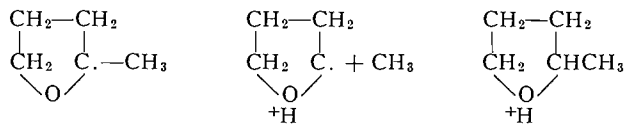

I II III

The three methyl protons and one of the beta CH_2 protons give a 20.5 G hyperfine splitting while the other beta CH_2 proton gives a 41 G hyperfine splitting. This would yield a septet with the observed splittings and with relative intensities of 1:4:7:8:7:4:1. Species I agrees with the interpretation of Dainton and co-workers (12).

The septet line splitting of 20.5 G is typical of the isotropic hyperfine splittings observed in saturated aliphatic radicals. The 10 G line width is typical of the e.s.r. spectra of saturated aliphatic radicals (at liquid nitrogen temperature) whose isotropic hyperfine structure is partly due to a rotating methyl group. This rotation somewhat reduces, by averaging, the anisotropic line broadening due to the methyl protons (14).

The ratio of the yield of trapped electrons to that of the species giving the septet absorption is 0.88 ± 0.04 (13). Therefore there is a positively charged species in the sample whose yield is nearly equivalent to that of the species represented by the septet. Dainton and co-workers suggest that the positive charge resides on a nearby solvent molecule (species III) but species II cannot be excluded because, by analogy with the $CH_3\dot{C}HOH$ radical, its e.s.r. spectrum should be the same as that of I. We found the spectra of $CH_3\dot{C}HOH$ and $CH_3\dot{C}HOD$ to be the same in C_2H_5OH and C_2H_5OD which had been gamma irradiated at liquid nitrogen temperature. Thus the hydroxyl hydrogen in the $CH_3\dot{C}HOH$ radical has little effect on its e.s.r. spectrum. Furthermore, formation of II compared to III involves less motion of a proton. There must be a limit to proton mobility, above which reaction with trapped electrons occurs. This should enhance the yield of I relative to

Can. J. Chem. Downloaded from www.nrcresearchpress.com by 210.87.254.6 on 09/05/12
For personal use only.

the yield of trapped electrons. Our yield ratio suggests that this occurs to a small extent.

The average energy absorbed per ion pair formed in organic gases is usually 25–30 eV and should be similar in solids. Consequently, assuming the absence of energy transfer effects the maximum possible yield of positive or negative species is about three per 100 eV compared to the observed yields, measured by e.s.r., $G(e) = 2.6$ and $G(I \text{ or } II) = 3.0$ (13).* Thus the magnitude and near equivalence of $G(e)$ and $G(I \text{ or } II)$ indicate nearly total efficiency of charge separation after the initial ionization of an MTHF molecule. This suggests little or no proton motion and favors species II as the site of the positive charge.

The yields and reactions of the species formed in irradiated MTHF will be discussed in a later paper.

(3) The Nature of the Electron Trap

The results indicate that the electrons are trapped as a separate chemical entity and should not be considered similar to an unpaired electron on a free radical. There are two clues regarding the nature of the trap. The first is that in the radiolysis of hydrocarbons, trapped electrons have only been observed in systems which form a glass at low temperatures. The second clue comes from some results in ethanol and methanol where broadening of the trapped electron e.s.r. line (identified by Chachaty and Hayon (16)) by electron–proton dipolar interaction is about three times as great as in MTHF. Zeldes and Livingston (17) have shown by deuterium substitution that the major interaction is with the hydroxyl hydrogen nucleus. In other words the trapped electrons are primarily surrounded by alcohol molecules which are oriented so that their hydroxyl group points at the electron. By analogy the electron in MTHF may be trapped in a field of oriented molecular electric dipoles. In a glass there may be some groups of molecules properly oriented to do this but it is far more likely that a thermalized electron's electric field induces its trap by causing a rotation of solvent molecules to a favorable orientation. Forces inhibiting molecular rotation must be weaker in a glassy hydrocarbon matrix than in a crystalline one, favoring this type of trapping.

Trapped electrons in MTHF disappear at 92–95 °K, apparently via reaction with free radicals or radical-ions, while the remaining free radicals or ions persist to 101 °K. If the sudden enhancement of reactivity were due to a phase change, both species should totally disappear at the same temperature. It is possible that 93–96 °K is the temperature above which the oriented solvent dipoles relax, releasing the electrons from their traps.

Since we cannot determine whether the inhomogeneous broadening of the trapped electron e.s.r. singlet arises from a weak isotropic interaction or from dipolar proton hyperfine interaction it is difficult to draw any conclusions regarding the delocalization of a trapped electron orbital. It is probably due to a mixture of the two types of interaction. In other words the trapped electron must be experiencing dipolar interaction with neighboring protons but its wave function probably has a low value on the nearest neighbor protons in the wall of the solvent "cage". Qualitatively, this is similar to the picture of an *F*-center in KCl interacting with nearest neighbor potassium nuclei (5, 18). Even though the magnetic moment of a proton is greater than that of a potassium nucleus, a trapped electron in MTHF experiences less inhomogeneous broadening than does an *F*-center in KCl as shown by the difference in their saturation curves and by the 10 times smaller width of the envelope of the e.s.r. line due to trapped electrons in MTHF compared to that due to *F*-centers in KCl (5). Presumably this means that the orbital motion of a trapped electron in MTHF is more localized than that of an *F*-center. In

G = number of species formed per 100 eV energy absorbed in the sample.

Can. J. Chem. Downloaded from www.nrcresearchpress.com by 210.87.254.6 on 09/05/12
For personal use only.

support of this proposal, the g-value for an electron in MTHF (2.003 ± 0.001) is close to the free spin value $g = 2.0023$. The g-value shift for an F-center in KCl compared to that of a free spin electron is -0.007 (19), suggesting a greater spin orbital coupling for the F-center.

T_1 (calculated in Discussion, section 4) seems to be rather short compared to what one might expect. T_1 is increased by decreasing temperature since this reduces the efficiency of spin lattice processes. However, $T_1 = 7.5 \times 10^{-5}$ s for trapped electrons in MTHF at 77.5 °K is similar to T_1 for amino acid radicals (15) and for KCl F-centers (5) at room temperature but is 75 times longer than T_1 for solvated electrons in liquid ammonia (20). Without a knowledge of the relaxation mechanism it is difficult to draw any conclusions from the value of T_1.

(4) Spatial Distribution of Trapped Electrons and Free Radicals or Radical Ions

The saturation curve for trapped electrons in MTHF reveals that this is a case where $\Delta\omega_L$ has a value of significant magnitude compared to $\Delta\omega_G$ in contrast to F-centers in which case $\Delta\omega_L$ is negligible compared to $\Delta\omega_G$. Using Castner's graphical techniques (6) it is found that the experimental saturation curve for trapped electrons corresponds to that obtained theoretically when $A = \Delta\omega_L/\Delta\omega_G = 0.2$. Since $\Delta\omega_G = 4.5\ \gamma/\sqrt{2}$ or $56. \times 10^7$, $\Delta\omega_L = 1.12 \times 10^7$ and $T_2 = 8.9 \times 10^{-8}$ s. The value of H_1 at which eq. [3] holds is 0.022 G so $T_1T_2 = 6.7 \times 10^{-12}$ and $T_1 = 7.5 \times 10^{-5}$ s. From eq. [2*a*] or [2*b*], $\Delta H = 1.27$ G and from eq. [1] the average local concentration of trapped electrons and free radicals surrounding a trapped electron is 0.02 ± 0.01 M. The overall total of the free radical and trapped electron concentrations in the sample has been measured and equals 0.0018 M. Thus the local concentrations of these species are 11 ± 5 times higher than the bulk concentration. It is concluded that electrons and free radicals are trapped in clusters. This agrees with the cluster model of the initial distribution of primary species along the track of a Compton electron. The electrons and free radicals are trapped before the volume which they occupy has expanded sufficiently to overlap with neighboring clusters. The 0.02 M cluster concentration indicates an average minimum separation of 44 ± 7 Å between a trapped electron and a neighboring trapped electron or free radical. If they were distributed homogeneously at 0.0018 M concentration the average minimum separation between neighboring unpaired spins would be 93 Å.

The fact that the normalized thermal decay curves of the trapped electrons are independent of total radiation dose (i.e. initial concentration) at 77.5 °K suggests that a trapped electron reacts with a primary species in the same cluster and this result therefore supports our postulate. At first one might predict first order decay kinetics based on this model but this would assume that the reaction rate within a cluster is the same for all clusters. If the "cluster reactivity" is assumed to vary then the results are as expected. Neither first nor second order kinetics are obeyed but the normalized decay curves (for different initial concentrations) are superimposed. In other words, varying the radiation dose varies the concentration of clusters and not the average concentration within a cluster.

Salmon (2) found second order decay kinetics at 90 °K. From this and other evidence, Dainton and co-workers (12) postulate that on warming or photochemical bleaching the trapped electron in MTHF reacts with a primary species from another track. This disagrees with our conclusions drawn from results obtained at 77.5 and 81 °K.

(5) Consequences of the Cluster Model

The average distance between neighboring unpaired electron spins suggests that an electron becomes trapped when separated by 40–50 Å from its parent ion. Hence when

Can. J. Chem. Downloaded from www.nrcresearchpress.com by 210.87.254.6 on 09/05/12
For personal use only.

trapped it may still experience a significant coulombic force of attraction from the parent ion. The dielectric constant of liquid MTHF is 4.6 (21) and it may be lower in the solid (22). If it equals 4.6, the parent ion's coulomb field at a point 50 Å distant would be 0.07 eV or 10 kT. It is possible that photochemical bleaching merely serves to free an electron from its trap and it is subsequently attracted back to the parent ion where charge neutralization must occur. We suggest the possibility that photochemical bleaching results in the electron reacting with a primary species in the same cluster rather than with one in another cluster as postulated by Dainton *et al.* (12).

We have concluded in section 4 (Discussion) that thermal disappearance of a trapped electron at 77.5 °K involves reaction within the same cluster. The mechanism of thermal escape from a trap is not known, but once this occurs, the coulombic field of the parent ion presumably draws the electron to it.

Our picture of clusters containing trapped electrons and free radicals or positive ion radicals with an average separation between neighboring species of about 50 Å merits examination in terms of solute competition for electrons before they become trapped. We have suggested that electrons induce their own trap via orientation of solvent molecule electric dipoles. The yield of trapped electrons in the absence of solute indicates that the probability of trapping is about unity. Addition of a solute which reacts at every encounter would require a concentration equal to or greater than the local (cluster) concentration of electrons to capture all the electrons before they become trapped. Since the ratio of the concentration of electrons and free radicals or radical ions is 0.88 ± 0.04 (12) this corresponds roughly to 0.009 M or 0.076 mole % of solute. Hamill *et al.* observe that at 0.08 mole % of biphenyl in MTHF, 60% of the limiting yield of anion is formed and that 0.15–0.2 mole % of solute is required to reach the limiting yield of anion (1). We regard this as good qualitative agreement with the proposed model.

ACKNOWLEDGMENTS

The authors wish to thank P. J. Dyne, R. H. Betts, and J. S. Geiger for their valuable criticism and advice. We are grateful to one of the referees for drawing refs. 21 and 22 to our attention.

REFERENCES

1. M. R. Ronayne, J. P. Guarino, and W. H. Hamill. J. Am. Chem. Soc. **84**, 4230 (1962).
2. G. A. Salmon. Discussions Faraday Soc. **36**, 284 (1963).
3. G. W. A. Fowles, W. R. McGregor, and M. C. R. Symons. J. Chem. Soc. London, 3329 (1957).
4. D. J. E. Ingram. Free radicals as studied by electron spin resonance. Butterworth Scientific Publications, London. 1958.
5. A. M. Portis. Phys. Rev. **91**, 1071 (1953).
6. T. G. Castner. Phys. Rev. **115**, 1506 (1959).
7. R. C. Smith and S. J. Wyard. Fifth International Symposium on Free Radicals. July 6–7, 1961. Paper 66.
8. D. R. Smith and J. J. Pieroni. Can. J. Chem. **42**, 2209 (1964).
9. J. S. Hyde and H. W. Brown. J. Chem. Phys. **37**, 368 (1962).
10. S. Ciborowski, N. Colebourne, E. Collinson, and F. S. Dainton. Trans. Faraday Soc. **57**, 1123 (1961).
11. J. Weiss, A. O. Allen, and H. A. Schwarz. Proc. Intern. Conf. Peaceful Uses At. Energy, United Nations, New York. **14**, 179 (1956).
12. F. S. Dainton, J. P. Keene, T. J. Kemp, G. A. Salmon, and J. Teply. Proc. Chem. Soc. London, 265 (August 1964).
13. D. R. Smith and J. J. Pieroni. To be published.
14. P. B. Ayscough and C. Thomson. Trans. Faraday Soc. **58**, 1477 (1962).
15. J. A. Simmons. J. Chem. Phys. **36**, 469 (1962).
16. C. Chachaty and E. Hayon. Nature, **200**, 59 (1963).
17. H. Zeldes and R. Livingston. J. Chem. Phys. **30**, 40 (1959).
18. G. Feher. Phys. Rev. **105**, 1122 (1957).
19. A. H. Kahn and C. Kittel. Phys. Rev. **89**, 315 (1953).
20. C. A. Hutchison, Jr. and R. C. Pastor. J. Chem. Phys. **21**, 1959 (1953).
21. J. L. Down, J. Lewis, B. Moore, and G. Wilkinson. J. Chem. Soc. London, 3767 (1959).
22. N. E. Hill. Proc. Roy. Soc. London, Ser. A, **240**, 101 (1957).

Can. J. Chem. Downloaded from www.nrcresearchpress.com by 210.87.254.6 on 09/05/12
For personal use only.

Can. J. Chem. Downloaded from www.nrcresearchpress.com by 210.87.254.42 on 09/05/12
For personal use only.

INFRARED SPECTRA OF TRIS-ETHYLENEDIAMINE COMPLEXES OF RUTHENIUM(II)

A. D. ALLEN AND C. V. SENOFF
Lash Miller Chemical Laboratories, University of Toronto, Toronto, Ontario

Received October 14, 1964

ABSTRACT

A number of complexes $[Ru(en)_3]X_2$, where X = I^-, Br^-, $PtCl_4^{2-}$, ClO_4^-, and PF_6^-, have been prepared and their infrared spectra measured in the solid state between 4 000–600 cm^{-1}. The effect of the various anions on the spectra and assignments for the observed fundamental vibrations are discussed.

The infrared spectra of ethylenediamine complexes have recently been reviewed (1). The available infrared data suggest that ethylenediamine coordinates to a metal with the *gauche* configuration (2). This has been substantiated by X-ray structural data for a number of ethylenediamine complexes (3, 4, 5). In this paper we report the preparation of a series of ruthenium(II) complexes, $[Ru(en)_3]X_2$, where en = ethylenediamine and X = I^-, Br^-, $PtCl_4^{2-}$, ClO_4^-, and PF_6^-. The infrared data for these complexes are given in Table I. Data for the N-deuterated complexes are found in Tables II and III.

TABLE I

Vibrational frequencies (cm^{-1}) and assignments for the absorption bands in the rock salt region of the complexes $[Ru(en)_3]X_2$[a]

Assignment	X = I^-	X = Br^-	X = $PtCl_4^{2-}$	X = ClO_4^-	X = PF_6^-
	3 294 s	3 332 s	3 323 s	3 354 vs	3 376 vs
$\nu(NH_2)$	3 246 s	3 286 s	3 307 s	3 302 vs	3 322 vs
	3 230 s	3 240 s	3 275 s,sh	3 179 w,br	(3 198) w
	3 142 s	3 156 s	3 269 s	—	(3 172) w
$\nu(CH_2)$	2 959 s,sh	2 953 s	2 948 s	2 947 m	2 951 m
	2 933 s	2 938 s	2 930 s	—	—
	2 884 s	2 885 s	2 880 s	2 893 m	2 899 m
$\delta(NH_2)$	1 578 s,sh	1 595 s,sh	1 594 m	(1 590) sh	—
	1 567 s	1 578 s	1 578 s	1 583 vs	1 578 vs
$\delta(CH_2)$	1 455 s	1 452 s	1 453 s	1 462 s	1 463 s
	—	—	—	—	—
$\omega(CH_2)$	1 392 w	1 389 w	1 385 w	1 394 w	1 396 w
	1 369 w	1 364 w	1 360 w	1 365 w	1 369 w
$\omega(NH_2)$	1 327 s	1 326 s	1 325 s	1 325 m	1 327 m
	1 128 s	1 143 s	1 121 w	b	1 141 m
$\gamma(CH_2)$	1 275 s	1 274 s	1 276 m	1 279 s	1 248 s
	—	—	—	—	1 258 m
$\gamma(NH_2)$	1 012 vs	1 021 s,sh	1 025 vs	1 025 vs	—
	964 s	975 s	961 s	964 s	967 s
ν(C—N)	1 106 m	1 102 m	1 107 m	b	1 102 m
	1 042 s	1 037 s,sh	1 038 vs	b	—
ν(C—C)	998 vs	1 008 vs	1 009 vs	1 001 vs	1 010 vs
$\rho(CH_2)$	873 vw	872 w	870 vw	871 w	b
	865 vw	860 w	859 vw	861 w	b
$\rho(NH_2)$	641 s	633 s	625 s	b	637 s
Combination?	—	1 166 m	1 156 w	—	—
	—	1 067 w	(1 070) vw		1 071 w
H_2O			3 551 s		
			1 630 m		

[a]s = strong; vs = very strong; w = weak; vw = very weak; b = anion absorbs in this region; m = medium; sh = shoulder; br = broad.

Can. J. Chem. Downloaded from www.nrcresearchpress.com by 210.87.254.42 on 09/05/12
For personal use only.

RESULTS AND DISCUSSION

Band Assignments for the Complexes $Ru(en)_3X_2$

(a) NH_2 Vibrations

There are six fundamental modes of vibration associated with the NH_2 group, viz., asymmetrical stretching, symmetrical stretching, bending, wagging, twisting, and rocking. Deuteration of the amino hydrogens confirmed the assignment of the absorption bands to NH_2 vibrations.

The NH_2 stretching vibrations were observed in the frequency range, 3 400–3 000 cm^{-1} shifted to 2 500–2 325 cm^{-1} in the spectra of the N-deuterated complexes (Tables II and III). The average value for the ratio, $\nu(NH)/\nu(ND)$ was 1.35, in reasonable agreement with the value of 1.37 calculated using the simple harmonic oscillator approximation. Most of the ruthenium(II) complexes exhibited four NH_2 stretching vibrations. In general, the absorption bands were broad for the simple halide salts (Figs. 1 and 2) but were much sharper in the salts of the complex anions (Figs. 3, 4, 5).

Two NH_2 bending motions were observed between 1 600–1 570 cm^{-1}. The corresponding bands in the N-deuterated complexes appeared at about 1 180–1 170 cm^{-1}, in agreement with published data for other ethylenediamine metal complexes (6, 7).

The strong band observed in all the spectra of the undeuterated complexes at about 1 330 cm^{-1} which disappeared in the spectra of the N-deuterated complexes has been assigned to the NH_2 wagging mode. Another NH_2 wagging vibration has been assigned to the weak to strong band occurring between 1 145–1 120 cm^{-1} depending upon the anion involved.

The NH_2 twisting modes have been shown to occur at lower frequency than the wagging modes when an NH_2 group is bound to two other atoms (8). Hence, the bands between 1 030–1 010 cm^{-1} and 980–960 cm^{-1} have been assigned to the twisting motions of the NH_2 groups.

The final NH_2 angle deformation mode to be observed is the NH_2 rocking mode which appears as a strong absorption band at about 630 cm^{-1}. The isotope ratio, $\nu(NH)/\nu(ND)$ has the smallest value for this vibration (about 1.20), indicating that there is probably a large amount of coupling with the metal–nitrogen motions occuring at lower frequencies.

(b) CH_2 Vibrations

The pattern of the CH_2 vibrations should closely parallel the NH_2 vibrations. The CH_2 stretching modes were observed between 3 000–2 750 cm^{-1} as medium to strong absorption bands and were not very much affected by N-deuteration (Table III). In general, three such absorption bands were observed in the spectra of most of the ruthenium(II) complexes.

The four types of CH_2 angle deformation modes should decrease in frequency in the order: bending > wagging > twisting > rocking (9). It was possible to observe only one CH_2 bending vibration, at about 1 465–1 450 cm^{-1}, but it is interesting to note that two such bands were detected in the spectra of the N-deuterated complexes at about 1 450–1 430 cm^{-1}. These vibrational modes were apparently not significantly shifted upon N-deuteration, indicating very little coupling with the corresponding NH_2 motions.

Two weak bands that appear in the spectra at about 1 390 and 1 370 cm^{-1} and which showed appreciable frequency shifts in the N-deuterated complexes have been assigned to the CH_2 wagging motions, which are apparently coupled with the corresponding NH_2 vibrations.

The CH_2 twisting vibration appears as a medium to strong band at about 1 275 cm^{-1}

Can. J. Chem. Downloaded from www.nrcresearchpress.com by 210.87.254.42 on 09/05/12
For personal use only.

TABLE II

Vibrational frequencies (cm^{-1}) and isotope ratios ($\nu(NH)/\nu(ND)$) of the NH_2 and ND_2 vibrations in undeuterated and N-deuterated $[Ru(en)_3]X_2$

X = $PtCl_4^{2-}$			X = Br^-			X = I^-		
$\nu(NH_2)$	$\nu(ND_2)$	$\nu(NH)/\nu(ND)$	$\nu(NH_2)$	$\nu(ND)_2$	$\nu(NH)/\nu(ND)$	$\nu(NH_2)$	$\nu(ND_2)$	$\nu(NH)/\nu(ND)$
3 323 s	2 483 s	1.34	3 332 s	2 450 s	1.36	3 294 s	2 463 s	1.34
3 307 s	2 456 s	1.35	3 286 s	2 425 s	1.36	3 246 s	2 434 s	1.33
3 275 s,sh	2 435 s	1.34	3 240 s	2 403 s	1.35	3 230 s	2 386 s	1.35
3 269 s	2 405 s	1.36	3 156 s	2 330 s	1.35	3 142 s	2 326 s	1.35
$\delta(NH_2)$	$\delta(ND_2)$		$\delta(NH_2)$	$\delta(ND_2)$		$\delta(NH_2)$	$\delta(ND_2)$	
1 594 m	1 182 s,sh	1.35	1 595 s,sh	1 180 s	1.35	1 578 s,sh	1 177 s	1.34
1 578 s	1 171 s	1.35	1 578 s	—	—	1 567 s	1 171 s	1.34
$\omega(NH_2)$	$\omega(ND_2)$		$\omega(NH_2)$	$\omega(ND_2)$		$\omega(NH_2)$	$\omega(ND_2)$	
1 325 s	1 053 s	1.26	1 326 s	1 056 s	1.26	1 327 s	1 058 s	1.25
1 121 w	885 s	1.27	1 143 s	897 s	1.27	1 128 s	886 s	1.27
$\gamma(NH_2)$	$\gamma(ND_2)$		$\gamma(NH_2)$	$\gamma(ND_2)$		$\gamma(NH_2)$	$\gamma(ND_2)$	
1 025 vs	791 m	1.30	1 021 s,sh	811 s	1.26	1 012 vs	770 s	1.31
961 s	765 s	1.26	975 s	770 s	1.27	964 s	752 s	1.28
$\rho(NH_2)$	$\rho(ND_2)$		$\rho(NH_2)$	$\rho(ND_2)$		$\rho(NH_2)$	$\rho(ND_2)$	
625 s	522 w	1.20	633 s	530 m	1.19	641 s	551 m	1.16

Can. J. Chem. Downloaded from www.nrcresearchpress.com by 210.87.254.42 on 09/05/12
For personal use only.

TABLE III

Vibrational frequencies (cm^{-1}) for the CH_2, C—N, and C—C absorption bands in the undeuterated and N-deuterated complexes $[Ru(en)_3]X_2$

Complex	Assignment	Undeut'd	N-Deut'd
$[Ru(en)_3]I_2$	$\nu(CH_2)$	2 959 s,sh	(2 952) sh
		2 933 s	2 932 s
		2 884 s	2 879 s
	$\delta(CH_2)$	1 455 s	1 454 s
		—	1 426 s
	$\omega(CH_2)$	1 392 w	1 376 m
		1 369 w	1 358 m
	$\gamma(CH_2)$	1 275 s	1 270 m
		—	—
	ν(C—N)	1 106 m	—
		1 042 s	—
	ν(C—C)	998 s	1 008 vs
	$\rho(CH_2)$	873 vw	—
		865 vw	—
$[Ru(en)_3]Br_2$	$\nu(CH_2)$	2 953 s	2 957 s
		2 938 s	2 937 s
		2 885 s	2 877 s
	$\delta(CH_2)$	1 452 s	1 454 s
		—	1 433 s
	$\omega(CH_2)$	1 389 w	1 369 m
		1 364 w	1 352 m
	$\gamma(CH_2)$	1 274 s	1 271 s
		—	—
	ν(C—N)	1 102 m	—
		1 037 s,sh	—
	ν(C—C)	1 008 vs	1 012 vs
	$\rho(CH_2)$	872 w	—
		860 w	—
$[Ru(en)_3]PtCl_4 \cdot H_2O$	$\nu(CH_2)$	2 948 s	2 947 s
		2 930 s	2 925 vs
		2 880 s	2 878 vs
	$\delta(CH_2)$	1 453 s	1 455 vs
		—	1 434 vs
	$\omega(CH_2)$	1 385 w	1 369 w
		1 360 w	1 354 m
	$\gamma(CH_2)$	1 276 m	1 269 m
		—	—
	ν(C—N)	1 107 m	—
		1 038 vs	—
	ν(C—C)	1 009 vs	1 008 vs
	$\rho(CH_2)$	970 vw	—
		859 vw	—

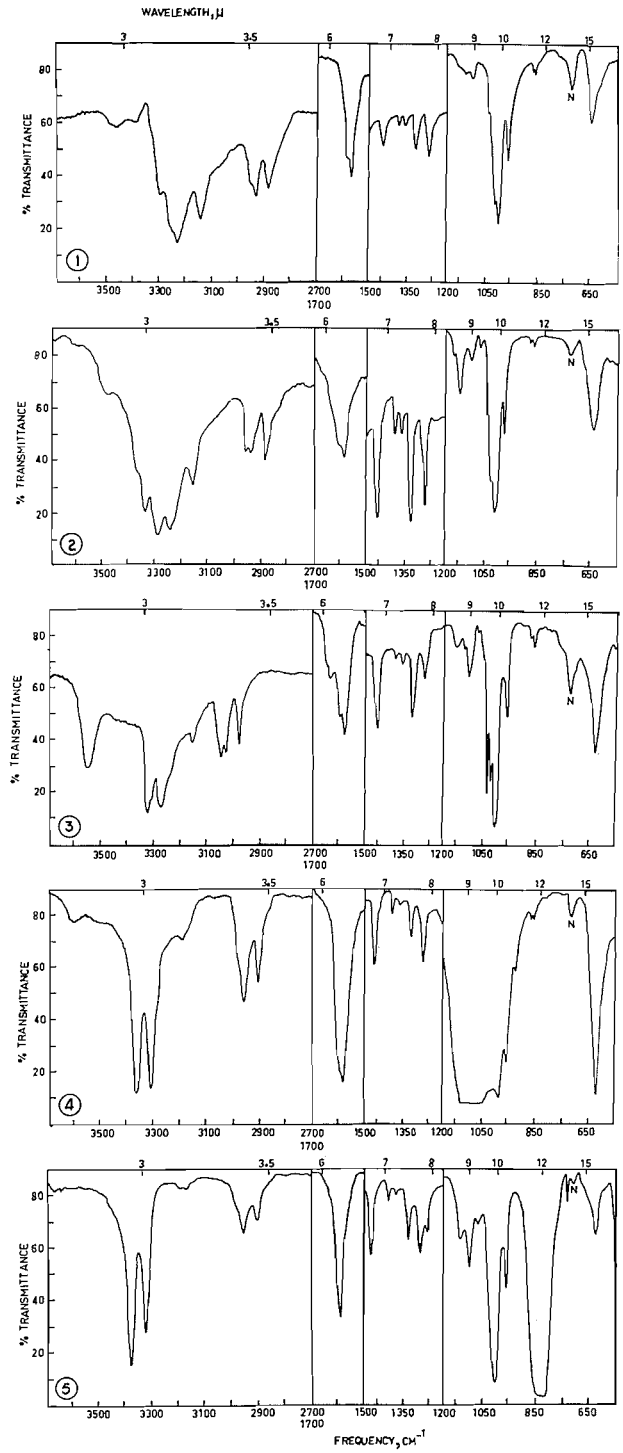

FIG. 1. Spectrum of $[Ru(en)_3]I_2$.
FIG. 2. Spectrum of $[Ru(en)_3]Br_2$.
FIG. 3. Spectrum of $[Ru(en)_3]PtCl_4 \cdot H_2O$.
FIG. 4. Spectrum of $[Ru(en)_3](ClO_4)_2$.
FIG. 5. Spectrum of $[Ru(en)_3](PF_6)_2$.

Can. J. Chem. Downloaded from www.nrcresearchpress.com by 210.87.254.42 on 09/05/12
For personal use only.

except for the hexafluorophosphate salt which has two bands at 1 284 and 1 258 cm^{-1} assigned to this deformation mode. The spectra of the N-deuterated salts indicate very little coupling with the NH_2 vibrations.

Finally, two weak bands at about 870–860 cm^{-1} have been assigned to the CH_2 rocking motions, but could not be detected in the spectra of the N-deuterated specimans since they were obscured by strong N—D absorptions that appeared in this region.

(c) C—C and C—N Vibrations

There are three possible types of motion associated mainly with the N—C—C—N chain of the ligand, viz., the C—C stretch, the C—N stretch, and the bending of the N—C—C—N chain (in plane bending and torsional motion). For the *cis* conformation, the C—N stretching vibrations for uncoordinated ethylenediamine have been observed at 1 104 and 1 065 cm^{-1} (10). It has been shown that the C—N frequency will probably be shifted in going from the *cis* to the *gauche* configuration, while the C—C stretching vibration should not be affected (11). It seems reasonable to assume that ethylenediamine coordinated to ruthenium(II) has the *gauche* configuration in view of the available X-ray structural data for other similar metal complexes (3, 4, 5). Hence, the medium to strong bands appearing at about 1 106 and 1 040 cm^{-1} have been assigned to the C—N stretching modes. The spectra of the N-deuterated complexes do not show these bands since they are apparently hidden under the N—D bands occurring in the same region. The C—C stretching mode has been assigned to the strong band at about 1 000 cm^{-1}, which is only slightly shifted upon N-deuteration. The C—C stretch for ethylenediamine occurs at 980 cm^{-1} (10). The bending vibrations of the N—C—C—N chain were not observed in the rock salt region of the spectra reported in this paper.

The Effect of Various Anions on the Spectra of the Complexes $[Ru(en)_3]X_2$

In the absence of X-ray structural data, it is difficult to arrive at any specific conclusions regarding the effect of a given anion on the infrared spectrum of the cation, $[Ru(en)_3]^{++}$. The data in Table I indicate that the NH_2 stretching region is quite sensitive to a change in the anion. Powell and Sheppard have stated that the observed spectral differences for the complexes $[M(en)_2]X_2$, where M = Pd or Pt and X = Cl^- or $PtCl_4^{2-}$, can be attributed to hydrogen bonding between the amino hydrogen atoms and a given anion (7). This explanation has recently been questioned by Klett, who has reinvestigated the infrared spectra of these salts (12). Klett has attributed the spectral differences to changes in crystal structure rather than hydrogen bonding. Examination of the data presented in Table I indicates that there is a gradual increase in frequency for the NH_2 stretching vibrations as the anion is varied in the order: I^-, Br^-, $PtCl_4^{2-}$, ClO_4^-, PF_6^-. If hydrogen bonding were the only factor causing the change in frequency of these vibrations, then the NH_2 stretching vibrations should occur at higher frequency for the iodide than the bromide salt. Clearly, this is not the case. There is also a change in the shapes of the NH_2 stretching bands (Figs. 1 to 5), which cannot be attributed solely to hydrogen bonding. The perchlorate and hexafluorophosphate salts each exhibit two very strong bands and one or two poorly resolved, weak, broad bands, while the other salts show four bands of comparable intensity. It seems quite probable that the bromide and iodide salts have similar crystal structures which are different from those salts with a relatively large anion. The similarity of the spectra for the perchlorate and hexafluorophosphate salts suggests that these two also have similar structures.

The assignments for the absorption bands in the infrared spectra of the complexes reported in this study agree very well with assignments made for a series of bis-ethylenediamine complexes of palladium(II) and platinum(II) by Klett (12). Analogous

Can. J. Chem. Downloaded from www.nrcresearchpress.com by 210.87.254.42 on 09/05/12
For personal use only.

osmium complexes are being prepared and their infrared spectra will be compared with those of the ruthenium complexes.

EXPERIMENTAL

(1) Infrared Spectra

All spectra were recorded on a Perkin-Elmer 521 grating spectrophotometer which was calibrated with polystyrene film in the NaCl region. The normal instrument settings were used: slit schedule 1 000, attenuator speed 11.00, amplifier gain 4.5, and scan suppression 5–6. The sharp bands were scanned at approximately 1 cm^{-1} per 5 s and at about 1 cm^{-1} per s for all other bands. Solid samples were prepared as Nujol and hexachlorobutadiene-1,3 mulls between NaCl or KBr plates. For comparison, the spectra of several complexes were determined with the KBr wafer technique and it was found that they did not substantially differ from those obtained with the mull technique. Reproducibility was ± 1 cm^{-1} and the precision of the band maxima is believed to be within ± 2 cm^{-1}.

*(2) The Complexes $[Ru(en)_3]X_2$**

The following general procedure was used to prepare these complexes. Commercial ruthenium trichloride (0.5 g) was dissolved in water (5 ml), and an excess of zinc powder and ethylenediamine (5 ml) were simultaneously added with mechanical stirring. The resulting mixture was warmed for 20 min and then filtered by gravity to remove the excess zinc and ruthenium metals. The appropriate anion (via the potassium, sodium, or ammonium salt) was then added to the filtrate at room temperature or at 0 °C to effect the precipitation of the desired complex. The yields were in the range 40–60%. The iodide, bromide, perchlorate, and hexafluorophosphate salts were recrystallized from hot water containing a small amount of their respective anions. All compounds were thoroughly dried *in vacuo* at 78 °C in the presence of P_2O_5. Analytical data are presented in Table IV.

TABLE IV

Analytical data for the complexes $[Ru(en)_3]X_2$[a]

	Calculated			Found		
X^-	% C	% H	% X	% C	% H	% X
I^-	13.46	4.49	47.47	14.02	4.88	47.4
Br^-	16.33	5.44	36.28	16.17	6.05	36.1
$PtCl_4^{2-}$ [b]	11.32	4.09	—	12.10	4.22	—
ClO_4	17.31	5.77	—	16.21	5.49	—
PF_6^-	12.61	4.20	—	12.70	4.27	—

[a]Microanalyses were carried out by Dr. A. Bernhardt, Mulheim, West Germany.
[b]Taken to be $[Ru(en)_3]PtCl_4 \cdot H_2O$.

(3) N-Deuterated Complexes

The N-deuterated iodide and bromide salts were prepared by dissolving the undeuterated samples in D_2O (99.78%) and allowing the exchange of the NH_2 hydrogen atoms to occur, followed by evaporation to dryness *in vacuo* in the presence of P_2O_5. The procedure was repeated until the infrared spectrum showed no NH_2 absorption bands. The chloroplatinate(II) salt was precipitated by the addition of a concentrated D_2O solution of K_2PtCl_4 to the N-deuterated iodide salt in D_2O. The N-deuterated salts were not further analyzed.

ACKNOWLEDGMENTS

Grateful acknowledgement is made to the National Research Council of Canada for financial support and to the Government of the Province of Ontario for a fellowship (to C. V. S.).

REFERENCES

1. K. NAKAMOTO. Infrared spectra of inorganic and coordination compounds. John Wiley, New York. 1963. p. 186.
2. D. M. SWEENY, S. MIZUSHIMA, and J. V. QUAGLIANO. J. Am. Chem. Soc. **77**, 6521 (1955).
3. A. NAKAHARA, Y. SAITO, and H. KWROYA. Bull. Chem. Soc. Japan, **25**, 331 (1952).
4. H. SCOULAND and C. H. CARLISLE. Acta Cryst. **6**, 651 (1953).

**Recently, Lever and Bradford have used a similar procedure to prepare* $[Ru(en)_3]ZnCl_4$ *(13).*

Can. J. Chem. Downloaded from www.nrcresearchpress.com by 210.87.254.42 on 09/05/12
For personal use only.

5. L. N. SWINK and M. ATOJI. Acta Cryst. **13**, 639 (1960).
6. M. E. BALDWIN. J. Chem. Soc. 4369 (1960).
7. D. B. POWELL and N. SHEPPARD. Spectrochim. Acta, **17**, 68 (1961).
8. S. MIZUSHIMA, I. NAKAGAWA, and D. M. SWEENY. J. Chem. Phys. **25**, 1006 (1956).
9. I. NAKAGAWA and S. MIZUSHIMA. Bull. Chem. Soc. Japan, **28**, 589 (1955).
10. A. SABATINI and S. CALIFANO. Spectrochim. Acta, **17**, 68 (1961).
11. S. MIZUSHIMA, I. ICHISHIMA, I. NAKAGAWA, and J. V. QUAGLIANO. J. Phys. Chem. **59**, 293 (1955).
12. D. S. KLETT. Ph.D. Thesis, University of Texas. 1963.
13. F. M. LEVER and C. W. BRADFORD. Platinum Metals Rev. **8**, 106 (1964).

Can. J. Chem. Downloaded from www.nrcresearchpress.com by 210.87.254.42 on 09/05/12
For personal use only.

Can. J. Chem. Downloaded from www.nrcresearchpress.com by 210.87.254.5 on 09/05/12
For personal use only.

SLIP FLOW IN LONG, SINGLE CAPILLARIES

PART II.[1] STEADY-STATE FLOW AND SPECULAR REFLECTION

R. M. BARRER AND D. NICHOLSON

Physical Chemistry Laboratories, Chemistry Department, Imperial College, London, England

Received October 16, 1964

ABSTRACT

The steady-state slip flow of the rare gases (He, Ne, Ar, Kr, and Xe) and of propane, CO_2, and SO_2 has been studied at different temperatures in long, single glass capillaries. The results give values of viscosity which are in agreement with literature values when Ar is used as a calibrating gas. The results can be expressed as a linear plot of the non-dimensional permeability ratio K/K_0 against reciprocal Knudsen number; the intercept on the K/K_0 axis is a. The value of this intercept depends on both gas and temperature being higher for light gases and high temperatures than for more condensable gases and low temperatures. The parameter a is therefore replaced by $((2 - \beta)/\beta)a_1$ where $(1 - \beta)$ is the so-called specular reflection coefficient and a_1 is a constant. The factors affecting $(1 - \beta)$ have been discussed. It is suggested that contributions to $(1 - \beta)$ will arise both from elastically and from inelastically scattered molecules, and the magnitude of these contributions is assessed in terms of the properties of the gas and the surface. The expression finally obtained is compared with experimental values of $(1 - \beta)$.

1. INTRODUCTION

The flow of gases in single capillaries has received considerable attention since the classical work of Knudsen (1), but the nature of the gas–wall interactions which influence the steady state, and of the transition from molecular to streamline flow, are not yet fully understood. It was therefore thought of interest to use long, glass capillaries of uniform bore to study steady and transient flow outside the molecular flow regime. In this paper we report the steady-state measurements and consider specular reflection. An early study of gas flow in metal capillaries by Adzumi (2) showed that the material of the capillary influenced the flow rate in the slip flow regime. He also found (3) that the differences between flow rates for hydrogen and ethylene could not be accounted for by kinetic theory considerations alone. Recently Huggill (4) and Berman and Lund (5) have shown that such differences between gases can also be observed in the transition and molecular flow regimes.

The equations governing gas flow are conveniently expressed in terms of the permeability K. For a single capillary this can be related to the flow rate, G, by

$$K = \frac{Gl}{\pi r^2 (p_1 - p_2)},$$

where $G = \partial(p_2 V)/\partial t$. p_1 is the pressure at the ingoing side, p_2 that at the outgoing side, r is the radius of the capillary of length l, and V is the volume of the outgoing side.

The permeability equation for slip flow is

$$K = \frac{r^2(p_1 + p_2)}{16\eta} + \delta D_K, \qquad [1]$$

where $D_K = \frac{4}{3}r(2RT/\pi M)^{\frac{1}{2}}$; T, M, and η are the gas temperature molecular weight and viscosity respectively, and δ is a coefficient. It is one of the purposes of this paper to investigate the nature of δ.

[1]*Part I is considered to be Z. Physik. Chem. Frankfurt, 37, 257 (1963).*

Can. J. Chem. Downloaded from www.nrcresearchpress.com by 210.87.254.5 on 09/05/12
For personal use only.

Equation [1] in dimensionless form (6) is

$$K/K_0 = (u + a), \qquad [2]$$

where $K_0 = 3\pi D_K/64$, and $u = r(p_1 + p_2)/\pi\eta\bar{v}$. u is equal to $r/\bar{\lambda}$ when $\eta = \frac{1}{2}\rho\lambda\bar{v}$, so that the value of u is an indication of the relative importance of different modes of transport (here $\bar{v}$ is $2(2RT/\pi M)^{\frac{1}{2}}$ and $\bar{\lambda}$ is a mean free path corresponding to the mean pressure). When $u \gg 1$, Poiseuille flow occurs and eq. [2] is valid; as u approaches unity, however, [2] no longer holds and for capillaries in which $l \gg r$ Knudsen was the first to show (1) that K passes through a minimum at $u \simeq 0.3$, and that $K = D_K$ for the limit when $u \to 0$.

An equation based on the work of Weber (7) should be applicable to the transition regime in long capillaries (6):

$$K = K_0\left\{u + a + \frac{a'}{u}\ln(1 + bu)\right\} \qquad [3]$$

Equation [3] differs appreciably from [2] only when u is less than 5; the difference is 2% when $u = 5$.

According to Weber the constants a, a', and b should have the values 5.33, 0.366, and 4.0, respectively; on the other hand Maxwell's slip theory for diffusely reflected molecules leads to a value of 4.0 for a in eq. [2]. The measurements discussed here mostly fall in the region $5 < u < 100$ which means that a contributes between 5 and 50% of the total permeability.

2. EXPERIMENTAL

(a) Apparatus and Flow Measurements

The capillaries were supplied by the British Petroleum Company as coils of helix radius about 5 cm, and in lengths of up to 50 m. They were mounted by sealing each end with 'Araldite' into a previously dried and etched tube which had been drawn out at its end. These seals were then surrounded by mercury cups, but even protected in this way they would not withstand cooling below about −80 °C, and had a limited lifetime when subjected to repeated cooling to this temperature. The capillaries used are listed in Table I. Series A refers to capillaries intended mainly to study transient flow, whilst series B were rather shorter and were used to augment the steady-state data. Mounted capillaries were protected from mercury vapor by traps cooled to 195 °K, and an appropriate correction was made to the outgoing volume for each gas used.

TABLE I

Ref. No.	Length (cm)	Radius from Ar flow (cm × 10^3)	Mean radius by microscope (cm × 10^3)	No. of readings	Maximum radius recorded (cm)	Minimum radius recorded (cm)
1A	1 587	5.25_3	5.56±0.3	44	6.35×10^{-3}	5.40×10^{-3}
2A	1 300	5.46_0	5.63±0.2	45	6.01×10^{-3}	5.39×10^{-3}
3A	1 486	11.04_5	10.92±0.2	53	11.70×10^{-3}	10.31×10^{-3}
4A	1 514	5.65_3	5.60±0.2	35	6.15×10^{-3}	5.15×10^{-3}
5A	2 549	4.97*				
1B	$407._0$	5.59_3†				
2B	$452._4$	5.59				

*Using CO_2 viscosity data of Johnston *et al.* (12).
†Using Ar at 25 °C.

Temperature control was achieved in a conventional thermostat near room temperatures, and with a stirred ice bath at 273 °K. For low temperature measurements an alcohol and 'Cardice' bath was used. It was found to be possible to maintain the temperature constant to within 0.3 °C with regular additions of crushed solid carbon dioxide although the mean temperature could be chosen between 195.5 and 196.5 °K. Temperatures were measured either by thermometer or with a thermocouple calibrated against a carbon dioxide vapor pressure thermometer at 195.5 °K (8).

When first mounted, a capillary was pumped out for several days at room temperature with a dynamic vacuum lower than 10^{-6} mm of mercury. Between each run the capillary system was outgassed for at least 4 h, and in most cases for a longer time, at room temperature. For series B measurements, in which transient state flow was not studied, degassing between runs required only a short time.

Flow rates were measured by noting the rate of change of p_2. p_2 was never allowed to rise to more than 0.1% of p_1 which was kept constant. Details of this type of measurement have been given elsewhere (9).

Gases used were either spectroscopically pure (He, Ne, Ar, Kr, Xe + 1% Kr, C_3H_8) or were prepared and purified in the laboratory (SO_2, CO_2). The length of the capillary was determined by making a large number of measurements of helix diameter on single turns. No regular deviation from circular could be detected in any of the capillaries and it is estimated that the absolute error in length was less than 0.2% for the long capillaries and less than 1% for the short capillaries.

(b) Internal Radius Measurement

Desty *et al.* (10) found that there was less than ±1% fluctuation from the mean radius for a capillary of 0.007 in. internal bore prepared by drawing from 'Veridia' tubing. Measurements on our capillaries indicated that the bore may be rather less consistent than this. The values obtained for 4 capillaries, cut into sections after use, are reported in Table I. Each reading had a reliability of ±2% and readings were made at regular intervals along the length of the capillary (capillary 1A had a slight taper). The third column of Table I gives values of the mean radius calculated from Poiseuille flow of argon (i.e. from the slope $\pi r^4/8\eta l$ of a plot of $G/(p_1 - p_2)$ against $\bar{p}$) and taking its viscosity (11) at 0 °C as $2.1001.10^{-4}$ P. The slight discrepancy between microscope and flow radii in capillaries 1A and 2A is probably due to geometrical factors discussed briefly below.

3. RESULTS

(a) Slopes of Slip Flow Lines

A value for the viscosity of any other flowing gas can be calculated from the slopes of K/K_0 plotted against p_1, using the radius obtained from the calibration with argon. For this purpose points with $u < 5$ were ignored and the best straight line, determined by a least mean square procedure, was used. Viscosity coefficients obtained in this way are compared with literature values in Table II. Typical data obtained at 0 °C for helium are illustrated in Fig. 1 as a plot of K/K_0 against u. At this temperature the viscosities agreed with Johnston's data (12) to within 2% or better. Low temperature results (Fig. 2) were rather more scattered, and viscosities may be reliable only to within 3%. Good independent viscosity data are not available in this region except for CO_2.

TABLE II

Viscosities

Gas	Temperature (°K)	Capillary No.	η (μP)	η from literature (μP)	Source
He	196.3	1B	147	147.8	*, †
	273.2	1A	189	185.9	*, †
		1B	185	185.9	
	313.2	1B	204	205.3	†
Ne	273.2	1A	230	232.7	*, †
Ar	196.3	1B	148	156.7	†
	328.2	2B	238	236	§
Kr	273.2	1A	297	296.8	*
Xe	195.7	2A	156	161	‡
	273.2	1A	205	210	*
	328.2	1B	244	251	§
SO_2	239.8	4A	116	102	§
CO_2	195.7	2A	98.8	99.6	§
C_3H_8	196.3	3A	53.0	56	‖
		4A	55.3		

*G. Cook *et al.*, "Helium, argon and the rare gases", ref. 11.
†Reference 12 (Johnston and Grilly).
‡Reference 13. Extrapolated from Sutherland's formula with C from International Critical Tables.
§Reference 14. Calculated using data and formulae from Hirschfelder *et al.*
‖Reference 13. Estimated from viscosities of methane, ethane, and propane in International Critical Tables.

Can. J. Chem. Downloaded from www.nrcresearchpress.com by 210.87.254.5 on 09/05/12
For personal use only.

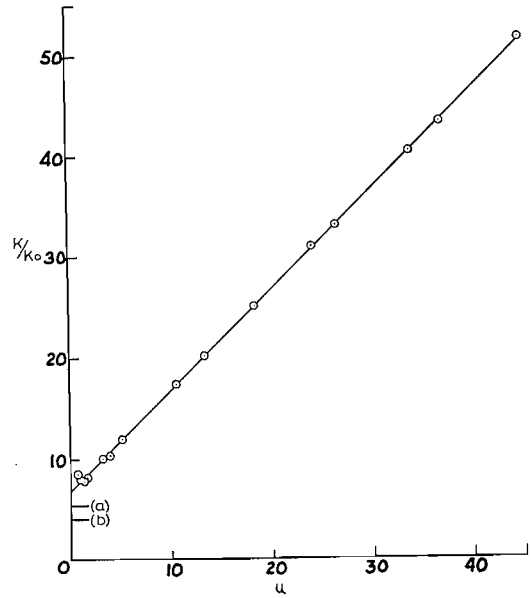

FIG. 1. Permeability ratio, K/K_0, for helium in capillary 1A as a function of $u = r/\bar{\lambda}$, and hence of mean pressure: (*a*) locates the theoretical intercept according to Weber; (*b*) locates this intercept according to Maxwell.

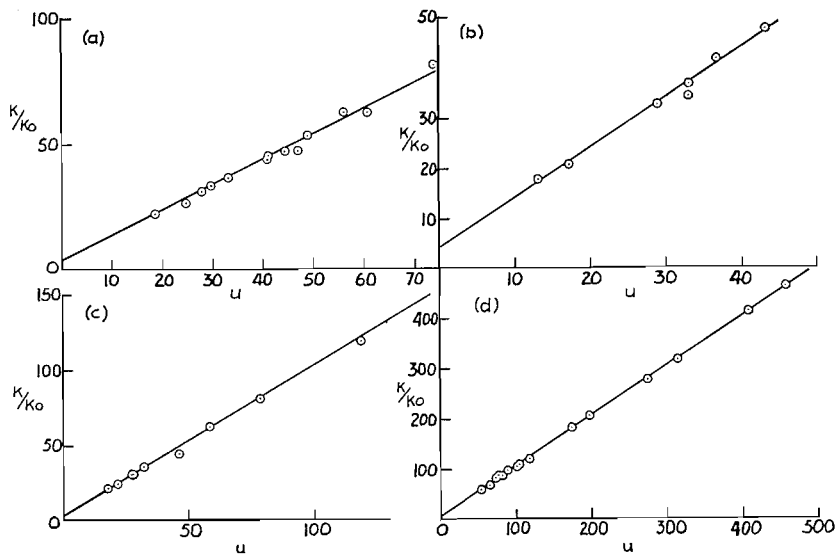

FIG. 2. Some permeability ratios, K/K_0, as functions of u at low temperatures: (*a*) CO_2 at 195.7 °K, in capillary 2A; (*b*) SO_2 at 239.8 °K, in capillary 4A; (*c*) C_3H_8 at 196.3 °K, in capillary 4A; (*d*) CO_2 at 196.3 °K, in capillary 5A.

The discrepancies between radii determined with the microscope and by flow, and between experimental viscosities and the literature values, led us to consider whether any correction of the Poiseuille term in eq. [1] was necessary.

Can. J. Chem. Downloaded from www.nrcresearchpress.com by 210.87.254.5 on 09/05/12
For personal use only.

Can. J. Chem. Downloaded from www.nrcresearchpress.com by 210.87.254.5 on 09/05/12
For personal use only.

(i) A reappraisal was made of the solution of the Navier Stokes equation (15) which gives the Poiseuille equation. The effect was considered of including first and second order derivatives of the mass velocity with respect to x (which may be important when $x \rightarrow l$). Secondly, the influence of helical curvature was examined by transforming the equation to suitable orthogonal coordinates (16) and solving it to obtain a corrected Poiseuille equation. In each instance the corrections were negligible.

(ii) Fluctuations in radius along the length of the capillary could also modify the flow. Thus if the mean fluctuation in radius found in capillary 1A (Table I) was repeated regularly along its length the measured flow rate would be $\sim 0.6\%$ less than that predicted from the 'flow' radius. In this estimate it was assumed that fluctuations in radius have no marked effect on the form of the pressure gradient. A consequence of this simplification is that the frequency of these fluctuations does not affect the final result. Under the microscope a slight departure from a circular cross section of the capillaries was also noted but it was estimated that this could change the flow rate by no more than 0.05%.

(b) Slip Flow Intercepts

Slip flow measurements allow the parameter a of eq. [2] to be calculated which, according to simple kinetic theory, should be a constant independent of gas and temperature. Results for capillaries of series A and B showed that this was not the case (Table III, column 4). The values of a were calculated for each point as $((K/K_0) - u)$, and their averages are quoted together with the mean standard deviations σ. In some cases, particularly for the series B capillaries, the deviation of a single point was more than 3σ and such data were discarded in order to calculate the final value. The values for helium are the most consistent and those for the heavy gases the least; in particular, the value of 0.8 for xenon at 0 °C in capillary 1A must be disregarded as in this case the results were widely scattered. From Table III it can be seen that values of a, among a similar series of molecules (He, Ne, Ar, Kr, Xe), tend to decrease with increasing molecular mass or boiling point. Values of a are also smaller for other molecules of higher boiling point

TABLE III

Values of a for $u > 5$

Gas	Temperature	Capillary	a	σ	β ($a_1 = 4.00$)	β ($a_1 = 4.50$)
He	196.$_3$	1B	6.1$_0$	0.3	0.75$_4$	0.84$_9$
	273.$_2$	1A	6.7$_2$	0.2	0.74$_7$	0.80$_3$
		1B	6.7	0.3	0.75	0.80
	313.$_2$	1B	6.8$_1$	0.3	0.74$_0$	0.79$_6$
Ne	273.$_2$	1A	5.7$_3$	0.1	0.82$_2$	0.87$_5$
Ar	196.$_3$	1B	4.1$_1$	0.6	0.99	1.05
	273.$_2$	1A	5.1	0.3	0.88	0.93$_7$
		3A	4.9	0.3	0.90$_0$	0.96$_8$
		4A	5.2	0.2	0.87$_0$	0.92$_8$
	298.$_2$	1B	5.6$_7$	0.2	0.83$_7$	0.88$_6$
	328.$_2$	2B	5.7	0.5	0.82	0.87
Kr	273.$_2$	1A	4.2	0.5	0.97	1.03
Xe	195.$_7$	2A	4.3	0.5	0.96$_5$	1.02
	273.$_2$	1A	0.8	>1.0		
	328.$_2$	1B	4.6	0.5	0.93	0.99$_0$
CO_2	195.$_7$	2A	3.5	0.5	1.1	1.12
	196.$_3$	5A	3.5	1.0	~1.1	1.12
SO_2	239.$_8$	4A	4.2	0.5	0.97	1.03
C_3H_8	196.$_3$	3A	4.5	1.0	~1.0	~1.0
		4A	3.4	0.5	1.1	1.13

(CO_2, SO_2, and C_3H_8) than for the gases He, Ne, and Ar. It is further seen that a decreases with falling temperature for the two gases for which the relevant data were obtained (He and Ar).

Such differences of intercept were anticipated by Maxwell in his theory of slip (17) and have been observed by Millikan (18). Maxwell equated the viscous drag across any plane in the flowing gas with momentum transferred to the walls. This results in the following expression for slip velocity, v_{os}:

$$[4] \qquad v_{os} = \frac{2 - \beta}{\beta} \frac{2\eta}{\rho\bar{v}} \frac{dv_{ox}}{dr},$$

where β is the fraction of diffusely reflected molecules, and therefore $(1 - \beta)$ is the fraction specularly reflected. If v_{os} is substituted as a boundary condition in the derivation of the Poiseuille equation, we obtain eqs. [1] and [2] with

$$[5] \qquad a = 4.00 \frac{2 - \beta}{\beta}.$$

β can be regarded as an indication of the extent to which momentum is exchanged with the surface. Complete exchange results in reflection according to the cosine law ($\beta = 1$) whereas no exchange results in a reversal of the perpendicular velocity component and a retention of the horizontal components ($\beta = 0$). In intermediate cases Nocilla (19) postulated two interaction parameters:

$$[6] \qquad \beta_T = \frac{\pi_i - \pi_r}{\pi_i}$$

$$[7] \qquad \beta_N = \frac{P_i - P_r}{P_i - P_w},$$

where the subscripts i, r, and w refer to 'incident', 'reflected', and 'wall' respectively, and π and P represent tangential and normal momenta. For gas flow in the x-direction along a tube only the first of these need be considered, so that $\beta = \beta_T$.

TABLE IV

a_1	Authors
4.80	Kramers (21) (1949)
4.0–5.1	Payne (22) (1953)
4.48	Mott-Smith (23) (1954)
4.54	Wang Chang and Uhlenbeck (24) (1956)
4.49	Willis (25) (1962)
4.68	Cercignani *et al.* (26) (1964)

It is clear from eqs. [4] and [5] that the values of β obtained from gas flow measurements depend on the value of the slip flow term. It has been pointed out by many authors that Maxwell's derivation cannot be considered rigorous because it assumes that the velocity distribution function at several mean free path lengths from the wall will be the same as that at the wall. Several attempts have been made to calculate a more realistic slip term than that of Maxwell by a solution of the Maxwell Boltzmann equation (20). Two unsatisfactory features of these treatments are, first, the division of molecules into two groups (those which undergo perfectly diffuse reflection and those which undergo perfectly specular reflection), and secondly, the use of unrealistic force laws between molecules (usually 'Maxwell molecules' are considered, which repel each other according to an

Can. J. Chem. Downloaded from www.nrcresearchpress.com by 210.87.254.5 on 09/05/12
For personal use only.

inverse fifth power law). The values of a_1 in the expression $a = a_1((2 - \beta)/\beta)$ which replaces Maxwell's value of $a_1 = 4.00$ are listed in Table IV for some recent treatments. However, no final verdict can yet be given concerning the best value of a_1.

4. SPECULAR REFLECTION

In the final columns of Table III values of β are given, calculated on the basis of $a_1 = 4.00$ and $a_1 = 4.50$. The so-called specular reflection coefficient, $1 - \beta$, has received some attention experimentally (2, 18), but little has been said regarding factors which may influence it. In the following section we have attempted to make an analysis of these factors. In doing so we have considered contributions from elastically and inelastically scattered molecules and the effect which surface forces and surface roughness will have on these: the final result is summarized in eq. [18]. The analysis has been set in quantitative terms as far as is possible in order that an assessment of the magnitudes of the factors involved can be made, but it must be emphasized at the outset that the complexities of gas–surface interactions do not allow a rigorous treatment of the problem.

The related problem of the accommodation coefficient, α, has received considerable attention (27, 28, 31). A classical treatment in which a single impinging atom exchanges energy with a three-dimensional lattice initially at 0 °K gave results for α quantitatively in agreement with experimental results (28). Two important assumptions are made in these theories of energy accommodation. The first is that atoms are incident normally on the surface; the second, that atoms are not trapped at the surface.* The first of these is clearly inadequate when dealing with the parameter β which, when it is less than unity, may indicate the persistence of a mass velocity component parallel to the surface.

De Boer (30) pointed out two factors which influence specular reflection. The first is the effect of surface roughness in scattering the molecules treated as de Broglie waves, and the second is adsorption. The following discussion is an expansion of these ideas.

(a) Elastic Scattering

An approximate treatment of scattering of de Broglie waves is given in Appendix 1. The result can be expressed in terms of the temperature, the molecular mass of the gas, and the height $\mu/2$ of an average surface serration, as

$$[8] \qquad 1 - \beta_1 = 1 - \exp\left[\frac{-h^2}{\mu^2 2mkT}\right],$$

where β_1 is the randomly scattered fraction of the molecules making elastic collisions with the surface. If one chooses μ in this expression to be about 10^{-5} cm, which is the order of magnitude of the irregularities on a polished surface, then eq. [8] becomes

$$\beta_1 = \exp\left[\frac{-9.58.10^{-4}}{MT}\right].$$

Thus $(1 - \beta_1)$ is approximately 1.10^{-6} for helium at 200 °K, which has the smallest value of MT encountered in these experiments.

It is probable, however, that elastic collisions with the surface will involve the impinging atom with a few surface atoms only, and from the viewpoint of collisions that the surface may be regarded as being composed of identical facets each having the area of a few atoms.

**Goodman (29) has developed a model which does not include this second restriction but he could find only qualitative agreement with experiment.*

Can. J. Chem. Downloaded from www.nrcresearchpress.com by 210.87.254.5 on 09/05/12
For personal use only.

In Appendix 2 we consider the effects of facets such as these on the net flow of molecules specularly reflected at the surface. An extra factor $(1 - \beta_2)$ multiplies the expression for the number of molecules which interact elastically with the surface and are specularly reflected:

$$[9] \qquad 1 - \beta_2 = \left\{1 - \frac{2\int_0^{\pi/2} \sin^2 \Psi\, h(\Psi)\, d\Psi}{\int_0^{\pi/2} h(\Psi)\, d\Psi}\right\},$$

where Ψ is the angle of inclination of a facet towards the direction of flow, and $h(\Psi)$ is a distribution function such that $h(\Psi)\, d\Psi$ gives the number of facets with Ψ between Ψ and $\Psi + d\Psi$.

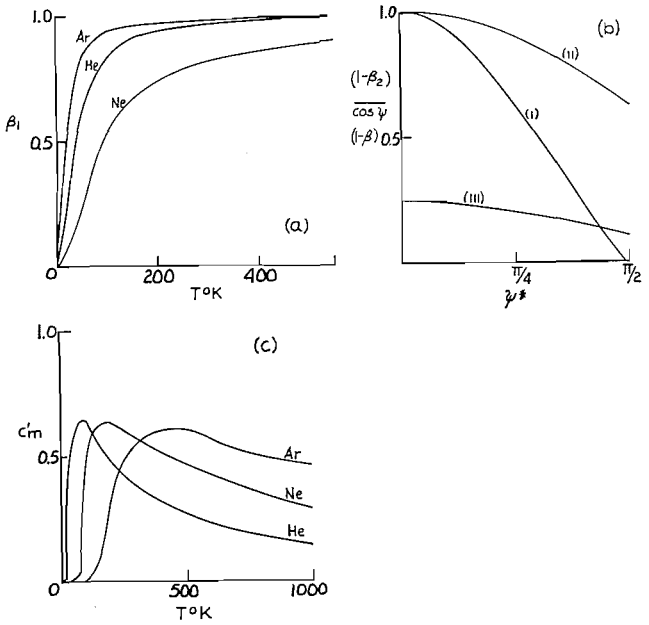

FIG. 3. (*a*) β_1 calculated from eq. [8] plotted against the absolute temperature for Ar, Ne, and He. (*b*) Curve *i*, $(1 - \beta_2)$ plotted against Ψ^* from eq. [19]; curve *ii*, $\overline{\cos \Psi}$ plotted against Ψ^* from eq. [19]; curve *iii*, $(1 - \beta)$ plotted against Ψ^* for He at 300 °K. (*c*) Values of c_m' calculated from eq. [14] plotted against the absolute temperature for Ar, Ne, and He.

On the basis of the foregoing argument we take μ in eq. [8] as being of the order of angstroms. The effect of T on β_1 calculated from this equation is illustrated in Fig. 3*a*, in which He, Ne, and Ar have been chosen as examples and μ taken as 2 Å.

It has been assumed that μ is not a function of temperature, but the increase in lattice vibration frequency with temperature could modify μ, particularly when the reflecting surface consists largely of adsorbed molecules with liquid-like properties, or is a liquid surface.

(b) Inelastic Gas–Surface Collisions

The division of molecules into those which, respectively, interact inelastically and

Can. J. Chem. Downloaded from www.nrcresearchpress.com by 210.87.254.5 on 09/05/12
For personal use only.

elastically with the surface necessitates choosing a rather arbitrary criterion for distinguishing these two groups. Such a criterion is a condensation coefficient

$$[10] \qquad c_\alpha = \left(1 - \exp -\frac{E}{RT}\right),$$

where E is the least energy required for an adsorbed atom to evaporate from the lowest adsorbed energy level and is equal to the exothermal adsorption energy but opposite in sign. This criterion is approximate because atoms with energies greater than E may well exchange energy quanta with the surface so that they are not undergoing elastic scattering. A quantitative study of condensation has been made by Lennard-Jones and Devonshire (32) but the perturbation method used makes values of c_α higher than 0.3 unreliable. In summary it may be said that $(1 - \exp -E/RT)$ is probably a rather low estimate for c_α.

If n molecules impinge on unit area in unit time and the mean time of adsorption is τ then the surface population for a very sparse coverage is $n\tau c_\alpha$. This population consists of $n\tau c_m$ molecules in energy levels where surface translation occurs and $n\tau c_1$ molecules in energy levels in which translational motion is not possible. When E_s is the height of the energy barrier to surface diffusion, we have

$$[11] \qquad \begin{aligned} n\tau c_\alpha &= n\tau c_m + n\tau c_1 \\ &= n\tau[\exp -E_s/RT - \exp -E/RT] + n\tau[1 - \exp -E_s/RT]. \end{aligned}$$

The population $n\tau c_1$ does not contain any molecules which retain a 'memory' of the mass flow velocity existing in the gas phase.

Of the molecules in the mobile level at any time, a fraction will have come from the immobile group; the remainder are molecules whose velocities still include the influence of the mass flow velocity existing in the gas phase.

In order to compute these fractions we consider the rate of entry, n_g, of molecules into the mobile population from the gas phase and their rate of entry, n_s, from the immobile level, and assume that there is detailed balancing for the reverse passage of molecules in the mobile levels into gas phase and immobile levels respectively. Then the fraction of molecules in the mobile population which may be considered as having a decaying drift velocity is $n_g/(n_g + n_s)$. If we designate k_a as the probability per second that a molecule in the immobile population will enter the mobile population then the number which undergo this transition is $n_s = n\tau c_1 \cdot k_a$ while from the gas phase $n_g = Nc_m$. The fraction of all molecules leaving the surface which retain a 'memory' of their original gas phase drift velocity is then

$$[12] \qquad c_m^{\,1} = \frac{c_m^{\,2}}{c_m + c_1\tau k_a}.$$

The quantities τ and k_a in this equation may be expressed in terms of E and E_s. The adsorption time is $\tau = \tau_0 e^{E/RT}$ where τ_0 is approximately the reciprocal of the vibration time of an adsorbed molecule and is $\sim 10^{-12}$ s. An expression for the transition probability k_a has been obtained by Lennard-Jones and Strachan (35) using a perturbation technique to solve the appropriate Schrödinger equation. The final expression was of the form

$$[13] \qquad k_a = A(\exp E_s/RT - 1)^{-1}.$$

A depends in a complex way on the parameters in the Morse equation used to express

Can. J. Chem. Downloaded from www.nrcresearchpress.com by 210.87.254.5 on 09/05/12
For personal use only.

the molecule–surface interaction, and on the number of energy levels below E_s. For Ar on KCl, A was found to be 10^{10}. Using this value, and the Morse parameters and combination rules given by Goodman (28), we find that A for He is about 2.5×10^{10}, and for Ne about 1.3×10^{10}. Inserting τ and k_a from [12] and [11], we obtain

$$[14] \qquad c_m^{\,1} = \frac{[e^{-E_s/RT} - e^{-E/RT}]^2[e^{E_s/RT} - 1]}{[e^{E_s/RT} - 1][e^{-E_s/RT} - e^{-E/RT}] + [1 - e^{-E_s/RT}]\, e^{E/RT}10^{-2}}$$

where it has been assumed that $A\tau_0 \sim 10^{-2}$ in all cases.

In Appendix 3 we derive an expression for the probability $(1 - \beta_3)\,\overline{\cos \Psi}$ that a molecule from the population $n\tau c_m^{\,1}$ will be specularly reflected. The mean time τ_s in eq. [3.6] is given by

$$[15] \qquad \tau_s = \tau_0 \exp \frac{E - E_s}{RT},$$

and k_b defined in Appendix 3 is given (35) by an expression similar to eq. [13] but with a different temperature dependence:

$$[16] \qquad k_b = B[1 - e^{-(E-E_s)/RT}]^{-1}$$

so that

$$[17] \qquad (1 - \beta_3) = \exp - \frac{B\tau_s}{1 - \exp -(E - E_s)/RT}$$

(c) Comparison of Theory with Experiment

We can now write the specular reflection coefficient as

$$[18] \qquad (1 - \beta) = (1 - \beta_1)(1 - \beta_2)(1 - c_a) + c_m^{\,1}(1 - \beta_3)\ \overline{\cos \Psi},$$

in which $c_m^{\,1}$, c_a, β_1, β_2, β_3, and $\overline{\cos \Psi}$, are given in eqs. [8], [9], [10], [14], [17], and [3.5]. Of these terms β_2 and $\overline{\cos \Psi}$ depend on the distribution and inclination of facets. Unfortunately it would be very difficult to obtain a reliable experimental measure of these quantities. However, their inclusion in eq. [18] indicates how surface roughening will affect $(1 - \beta)$. Thus $h(\Psi)$ would be expected to have a semi-Gaussian form exp $(-\text{const.}\ \Psi^2)$ in which the constant decreases as the surface becomes roughened. An approximation to this function is a step function with a sharp cut off at a value of $\Psi = \Psi^*$. This greatly simplifies the integrations in eqs. [2.8] and [3.6], and gives

$$[19] \qquad 1 - \beta_2 = \frac{\sin 2\Psi^*}{2\Psi^*} \quad \text{and} \quad \overline{\cos \Psi} = \frac{\sin \Psi^*}{\Psi^*}.$$

The variation of $(1 - \beta_2)$ and $\overline{\cos \Psi}$ with Ψ^* is illustrated in Fig. 3*b*, together with a graph of $(1 - \beta)$ against Ψ^* for He at 300 °K. The values used for the other quantities in this case are discussed below.

In the following calculations we have considered a surface rough on an atomic scale only, and have therefore taken both $(1 - \beta_2)$ and $\overline{\cos \Psi}$ as unity in all cases. The remaining parameters depend on the physical properties of the gas and surface. Possible values of E and E_s have been chosen (34) for Ar, Ne, and He in order to make the calculations (Table V). The values for Ar are those used by Lennard-Jones and Strachan (35) whilst E_s for He and Ne was chosen to be $E/10$, in keeping with these values, although this is probably a low estimate.

Can. J. Chem. Downloaded from www.nrcresearchpress.com by 210.87.254.5 on 09/05/12
For personal use only.

TABLE V

Gas	E (cal mole^{-1})	E_s (cal mole^{-1})	$a = 4.00$ ($B\tau_0$)	$a = 4.50$ ($B\tau_0$)
He	360	36	1.30	1.75
Ne	800	80	0.21	0.25
Ar	1 800	200	0.09	0.12

Calculations of the contribution of elastic scattering to $(1 - \beta)$ at 300 °K for Ar shows that even with $\mu = 1$ Å this is only 2×10^{-4} and therefore negligible. Hence the second term in [18], $c_m^1(1 - \beta_3)$, can be compared with the mean experimental value at 300 °K of $(1 - \beta)$ of 0.15 ($a_1 = 4.0$) or 0.09 ($a_1 = 4.5$), and $B\tau_0$ calculated. The values of $B\tau_0$ obtained suggest that B is about 10^{11} for Ar (if $\tau_0 \sim 10^{-12}$), which is the order of magnitude to be expected (35). In the case of He elastic scattering is quite important. For example, if $\beta_2 = 0.1$, and $\mu = 1$ Å, the contribution to $(1 - \beta)$ from the first term in [17] is larger than the experimental value of $(1 - \beta)$. A choice of $\mu = 2$ Å was therefore made and comparison of theory with experiment at 300 °K led to the values of $B\tau_0$ recorded in Table V. A increases with molecular weight so it might be expected that B will also: on the other hand τ_0 for He will be about the same or less than for Ar and the tenfold increase in B is unexpectedly large.†

$(1 - \beta)$ at other temperatures was calculated using these values of $B\tau_0$, and the theoretical and experimental points as well as the form of c_m^1 are shown in Figs. 3*c* and 4*a*, *b*, and *c*. For Kr and Xe only very slight variation of $(1 - \beta)$ with temperature is predicted.

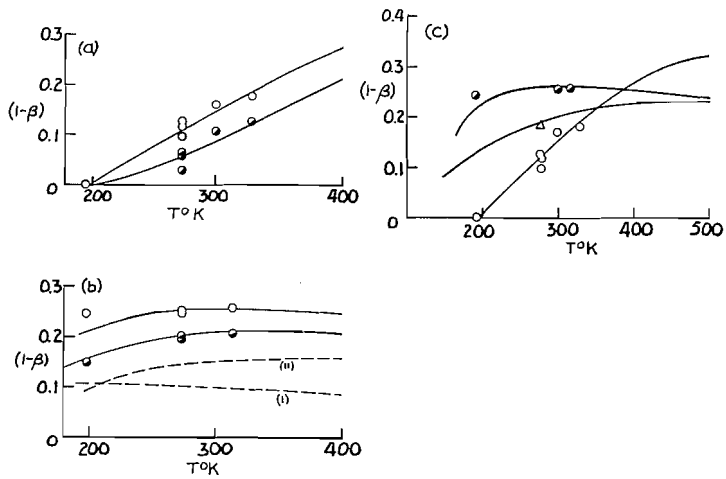

FIG. 4. In Figs. 4*a*, *b*, and *c*, the assumed values of E and E_s are those given in Table V. $\overline{\text{Cos}\,\Psi}$ and $(1 - \beta_2)$ are both taken to be unity. In Fig. 4*b* the roughness, μ, is taken as 2 Å. (*a*) Curves of $(1 - \beta)$ against T °K for Ar: ⊙ = experimental points for $a = 4.00$, ◑ = experimental points for $a = 4.50$. The full lines are theoretical curves taking $B\tau_0 = 0.09$ (upper line) and 0.12 (lower line). (*b*) Curves of $(1 - \beta)$ against T °K for He: ⊙ = experimental points for $a = 4.00$, ◑ = experimental points for $a = 4.50$. The full lines are theoretical curves taking $B\tau_0 = 1.30$ (upper line) and 1.75 (lower line). The curve (*i*) gives contributions from elastic and curve (*ii*) from inelastic scattering, both for $B\tau_0 = 1.30$. (*c*) $(1 - \beta)$ as a function of T °K for Ar (⊙), Ne (△), and He (◑). The full curves are theoretical and cover a wider temperature range, to show the crossing of the curves.

†*This suggests that A might also increase above the value of 10^{-2} adopted in [14]. However, an order of magnitude of 10 in this term has little effect on C_m^1 for He.*

Can. J. Chem. Downloaded from www.nrcresearchpress.com by 210.87.254.5 on 09/05/12
For personal use only.

Can. J. Chem. Downloaded from www.nrcresearchpress.com by 210.87.254.5 on 09/05/12
For personal use only.

5. DISCUSSION

Although the dependence of $(1 - \beta)$ on temperature is quite well reproduced, firm conclusions cannot be drawn at this stage. A more rigorous test of the views advanced here would require some means of assessing Ψ and $h(\Psi)$ and well-defined values of E, E_s, A, and B for the surface–gas pair.

In spite of these reservations the following points may be mentioned.

(i) Elastic scattering is apparently only important for light gases. Thus, even for Ne, $(1 - \beta_1)(1 - c_\alpha)$ is about 0.008 in the region 200–400 °K. This is because $(1 - c_\alpha)$ rapidly tends to zero for heavier gases and also because at constant temperature β_1 varies as $\exp(-\text{const.}/M^{1/2})$. On the other hand these terms do not depend on a mass flow velocity and so they are applicable to Knudsen flow as well as to slip flow.

(ii) Apparent specular reflection of heavier (easily condensed) gases indicates imperfect momentum exchange. A major factor is the time of stay on the surface although this is not related to $(1 - \beta)$ in any simple way. An interesting feature which appears from this analysis is that c_m^1 at high temperatures is bigger for heavy than for light gases because there is less interchange between mobile and immobile energy levels when E and E_s become large.

(iii) Surface roughness tends to increase the spread of $h(\Psi)$ towards higher values of Ψ but may also affect E by increasing the number of surface sites of high affinity.

It is notable that $(1 - \beta_2)$ (which depends on Ψ alone) can become negative and in principle it should be possible to reduce the flow rate of very light gases below the value for perfectly diffuse reflection by severe surface roughening.

ACKNOWLEDGMENTS

We would like to thank Mr. Ash of the Department for his interest in this work, and also Mr. L. E. Fraenkel of the Department of Mathematics for discussion of the Navier–Stokes equations. One of us (D. N.) is indebted to British Petroleum Limited for a postdoctoral fellowship.

REFERENCES

1. M. KNUDSEN. Ann. Phys. **28**, 75 (1909).
2. H. ADZUMI. J. Chem. Soc. Japan, **12**, 294 (1937).
3. H. ADZUMI. J. Chem. Soc. Japan, **14**, 346 (1939).
4. J. A. W. HUGGILL. Proc. Roy. Soc. London, Ser. A, **212**, 123 (1952).
5. A. S. BERMAN and L. M. LUND. 2nd Intern. Conf. on the Peaceful Uses of Atomic Energy. Vol. **4**. 1958. p. 359.
6. R. ASH, R. M. BARRER, and D. NICHOLSON. Z. Physik. Chem. Frankfurt, **37**, 257 (1963).
7. S. WEBER. Kgl. Danske Videnskab. Selskab, Mat.-Fys. Medd. **28**, No. 2 (1954).
8. R. B. SCOTT. Temperature, its measurement and control in science and industry. Rheinhold. 1941. p. 210.
9. R. M. BARRER and D. M. GROVE. Trans. Faraday Soc. **47**, 837 (1951).
10. D. H. DESTY, J. N. HARESNAPE, and B. H. F. WHYMAN. Anal. Chem. **32**, 304 (1960).
11. G. A. COOK. Helium, argon and the rare gases. Interscience. 1961.
12. H. L. JOHNSTON and E. R. GRILLY. J. Phys. Chem. **46**, 949 (1942). H. L. JOHNSTON and K. E. MCCLOSKEY. J. Phys. Chem. **44**, 1038 (1940).
13. INTERNATIONAL CRITICAL TABLES. McGraw-Hill. 1926.
14. J. O. HIRSCHFELDER, C. F. CURTISS, and R. B. BIRD. The molecular theory of gases and liquids. Wiley. 1954.
15. SHIH-I PAI. Viscous flow theory. Academic Press. 1956.
16. W. R. DEAN. Phil. Mag. 4, 208 (1927); **5**, 673 (1928).
17. J. C. MAXWELL. Scientific Papers. Vol. II. p. 705. C.U.P. (1290).
18. R. A. MILLIKAN. Phys. Rev. **21**, 218 (1923).
19. S. NOCILLA. Rarefied gas dynamics. Proc. 2nd Symp. Academic Press. 1961. p. 169.
20. S. CHAPMAN and T. G. COWLING. Mathematical theory of non-uniform gases. Cambridge. 1951.
21. H. A. KRAMERS. Nuovo Cimento, Suppl. **6**, 297 (1949).
22. H. PAYNE. J. Chem. Phys. **21**, 2127 (1953).

23. H. M. MOTT-SMITH. A new approach in the kinetic theory of gases. M.I.T. Lincoln Lab. Report, V-2. 1954.
24. C. S. WANG CHANG and G. E. UHLENBECK. Eng. Res. Inst., Univ. of Michigan Rept. 2457-I-T. 1956.
25. D. R. WILLIS. Phys. Fluids, **5**, 127 (1962).
26. S. ALBERTONI, C. CERCIGNANI, and L. GOTUSSO. Phys. Fluids, **6**, 993 (1963).
27. D. M. GILBEY. J. Phys. Chem. Solids, **23**, 1453 (1962).
28. F. O. GOODMAN. J. Phys. Chem. Solids, **24**, 1451 (1963).
29. F. O. GOODMAN. J. Phys. Chem. Solids, **23**, 1269 (1962).
30. J. H. DE BOER. Dynamical character of adsorption. Oxford. 1953.
31. A. F. DEVONSHIRE. Proc. Roy. Soc. London, Ser. A, **156**, 29 (1936).
32. J. E. LENNARD-JONES and A. F. DEVONSHIRE. Proc. Roy. Soc. London, Ser. A, **156**, 6 (1936).
33. P. L. BHATNAGER, E. P. GROSS, and M. KROOK. Phys. Rev. **94**, 511 (1954).
34. D. M. YOUNG and A. D. CROWELL. Physical adsorption of gases. Butterworths. 1962.
35. J. E. LENNARD-JONES and C. STRACHAN. Proc. Roy. Soc. London, Ser. A, **150**, 442 (1935).

APPENDIX 1

The number of molecules impinging on unit area in unit time from a Maxwellian population is, in terms of spherical polar coordinates, θ, ϕ, and v (Fig. 1.1),

$$[1.1] \qquad n = \int_0^{\pi/2} \int_0^{2\pi} \int_0^{\infty} C_g' \frac{v_r^3}{\pi^{3/2}} e^{-v_r^2} \cos\theta \sin\theta \, d\theta \, d\phi \, dv,$$

where C_g' is the number of molecules in unit volume, v the molecular speed, and $v_r = v(m/2kT)^{1/2}$.

For specular reflection the path difference between incident and reflected wave must

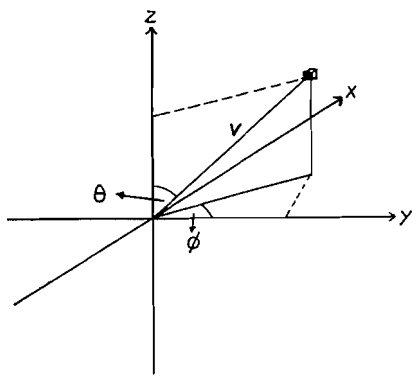

FIG. 1.1.

be such that $\Lambda \geqslant \mu \sin\theta$ where μ is twice the height of a surface discontinuity (30), and Λ is the de Broglie wavelength. For molecules we have $\Lambda = h/mv$. Hence for specular reflection

$$[1.2] \qquad v^* \leqslant \frac{h}{m\mu \cos\theta}.$$

Equation 1.2 defines a velocity v^* above which specular reflection of elastically scattered molecules will not occur. The number diffusely reflected is given by

$$[1.3] \qquad n_t = C_g' \frac{2}{\pi^{1/2}} \int_0^{\pi/2} \int_0^{v^*} v_r^3 e^{-v_r^2} \cos\theta \sin\theta \, d\theta \, dv,$$

where the integration over ϕ from 0 to 2π has been taken.

Can. J. Chem. Downloaded from www.nrcresearchpress.com by 210.87.254.5 on 09/05/12
For personal use only.

Because θ is the independent variable in [1.2] the integral over v can be taken and

$$[1.4] \qquad n_t = C_g' \left(\frac{2kT}{\pi m}\right)^{1/2} \int_0^{\pi/2} (1 + \delta^2 \sec^2\theta) \exp(-\delta^2 \sec^2\theta) \cos\theta \sin\theta \, d\theta$$

where $\delta = h/\mu\sqrt{2mkT}$.

The probability of specular reflection is thus

$$[1.5] \qquad (1 - \beta_1) = 1 - \frac{n_t}{\frac{1}{4}C_g'\bar{v}} = 1 - 2\delta^2 \int_\delta^\infty \frac{1 + x^2}{x^3} e^{-x^2} dx$$

$$= 1 - 2\delta^2 \int_\delta^\infty \frac{e^{-x^2}}{x^3} dx - 2\delta^2 \int_\delta^\infty \frac{e^{-x^2}}{x} dx$$

in which the substitution $x = \delta \sec\theta$ has been made. If we integrate the first integral by parts, eq. [1.5] leads to

$$[1.6] \qquad (1 - \beta_1) = 1 - e^{-\delta^2}.$$

APPENDIX 2

We consider the specular reflection of molecules from the elementary facets which are inclined at an angle Ψ to the direction of flow. WW' in Fig. 2.1*a* represents the cross section of a facet which is parallel to the direction of flow as indicated by the arrow. The net flow across plane A in the x-direction is

$$[2.1] \qquad n_0 = n_1 - n_r,$$

where n_1 is the number of molecules coming from the left and striking unit area in unit time, and n_r is the same number coming from the right.

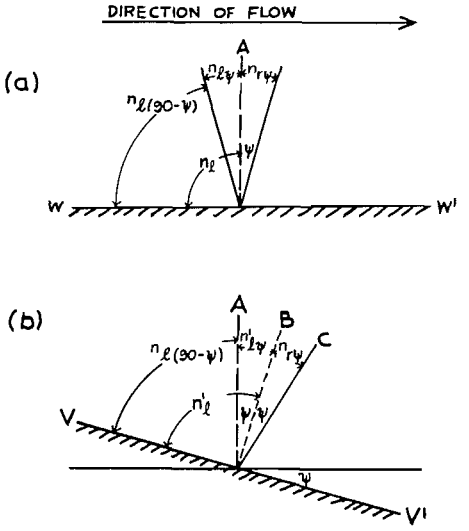

FIG. 2.1.

Figure 2.1*b* shows the cross section of a facet VV' inclined at angle Ψ towards the local direction of flow and B is a plane perpendicular to it. As in Fig. 2.1*a*, A is perpendicular to the flow direction. The molecules coming from the left of B are (*a*) $n_{1(90-\Psi)}$ in the

Can. J. Chem. Downloaded from www.nrcresearchpress.com by 210.87.254.5 on 09/05/12
For personal use only.

segment VA which is identical with the same number in Fig. 2.1*a*; (*b*) $n_{l\Psi}'$ in the segment AB which actually came from the right of A but are transferred in the direction of flow. As there are fewer molecules arriving from this side of A than from the left $n_{l\Psi}' < n_{l\Psi}$. The number of molecules transferred in the direction of flow is augmented by the number $n_{r\Psi}$ coming from the segment BC which will now be reflected to the right of plane A.

Hence the total number of molecules transferred to the left after reflection from VV' is

$$n_l' = n_{l(90-\Psi)} + n_{l\Psi}' + n_{r\Psi} = n_l - n_{l\Psi} + n_{l\Psi}' + n_{r\Psi}. \qquad [2.2]$$

By a similar argument we can also write

$$n_r' = n_r - n_{r\Psi} \qquad [2.3]$$

and the net flow across plane A is now

$$n_l' - n_r' = n_l - n_r - n_{l\Psi}' + 2n_{r\Psi}. \qquad [2.4]$$

The difference $n_{l\Psi} - n_{l\Psi}'$ is the number of molecules transferred across A which arrive from the segment of angle Ψ. We will denote this number by $n_{0\Psi}$ so that [2.4] is

$$n_l' - n_r' = n_0 - n_{0\Psi} + 2n_{r\Psi}. \qquad [2.4a]$$

We now postulate that for each facet of inclination Ψ to be found at a given cross section there is an identical facet of inclination $(180 - \Psi)$ at the same cross section. The flow across plane A through this facet is

$$n_l'' - n_r'' = n_0 - n_{0\Psi} - 2n_{l\Psi} \qquad [2.5]$$

and for the pair we have on summing [2.4*a*] and [2.5]

$$\begin{aligned} 2n_0{}^{\Psi} &= 2n_0 - 2n_{0\Psi} + 2n_{r\Psi} - 2n_{l\Psi} \qquad [2.6] \\ &= 2n_0 - 4n_{0\Psi}, \\ \text{i.e.} \quad n_0{}^{\Psi} &= n_0 - 2n_{0\Psi}, \end{aligned}$$

where $2n_0{}^{\Psi}$ is the total number of molecules transferred across the two planes which are inclined at angle Ψ.

From [1.1] the number of molecules striking unit area per second coming from segment 0 to Ψ in a Maxwellian gas at rest is

$$\begin{aligned} n_\Psi &= C_g' \int_0^\infty \frac{v_r^3}{\pi^{3/2}} e^{-v_r^2}\, dv \int_0^{2\pi} d\phi \int_0^\Psi \sin\theta \cos\theta\, d\theta \\ &= \frac{C_g'}{4} \bar{v} \cdot \sin^2 \Psi \\ &= n_0 \sin^2 \Psi, \end{aligned}$$

which is $\sin^2 \Psi$ times the number of molecules impinging on unit area in unit time. If we assume that this treatment will apply approximately to the flowing gas we can substitute in [2.6] to give

$$n_0{}^{\Psi} = n_0(1 - 2\sin^2 \Psi). \qquad [2.7]$$

Equation [2.7] predicts that $n_0{}^{\pi/2} = -n_0$ and that $n_0{}^{\pi/4} = 0$, as would be expected. When Ψ ranges from 0 to $\pi/2$, we must assume that the facets are distributed according to a function $h(\Psi)\, d\Psi$ and the modified flow is

Can. J. Chem. Downloaded from www.nrcresearchpress.com by 210.87.254.5 on 09/05/12
For personal use only.

$$[2.8] \qquad n_0^{\Psi} = n_0\left[1 - \frac{2\int_0^{\pi/2} \sin^2\Psi h(\Psi)\,d\Psi}{\int_0^{\pi/2} h(\Psi)\,d\Psi}\right] = n_0(1-\beta_2).$$

APPENDIX 3

We consider here those molecules which are adsorbed at a level in which they remain mobile, which exchange energy during their movements on the surface, and which finally evaporate again without becoming immobilized. On adsorption these molecules possess a component of mass velocity v_{0_x} in the direction of flow, the remaining components of $\mathbf{v}_0$ are zero (i.e. there is no net mass flow to the walls). We assume that collision between adsorbed molecules and substrate is the only mechanism which reduces mass velocity (i.e. that changes of direction in traversing facets do not affect this quantity).

On the surface molecules move across the facets with two-dimensional molecular velocities $\mathbf{v}_2$, which are distributed according to a (non-Maxwellian) distribution function $f_2(\mathbf{v}_2,t)$. It is assumed that f_2 does not change appreciably with position over the region of surface which a molecule can cover during its time of stay, and we designate the mean surface population (molecules cm^{-2}) over this region as C_s'.

If the probability per molecule that energy exchange, which is not large enough to bring about evaporation or condensation to the immobile level, occurs in unit time is k_b, and the surface population is so dilute that intermolecular collisions are not important, then we can apply a relaxation time approximation (33) to the Boltzmann equation (20) and write

$$[3.1] \qquad \frac{\partial f_2}{\partial t} = -k_b(f_2 - f_2^{0}),$$

where f_2^0 is the Maxwellian distribution which would be achieved at infinite time.

If k_b is independent of $\mathbf{v}_2$ and t then eq. [3.1] becomes

$$[3.2] \qquad \int \mathbf{v}_2 \frac{\partial f_2}{\partial t}\,d\mathbf{v}_2 = -k_b\int \mathbf{v}_2 f_2\,d\mathbf{v}_2 + k_b\int \mathbf{v}_2 f_2^{0}\,d\mathbf{v}_2.$$

Applying the customary transformation (20) to the left-hand side of [3.2] we have

$$[3.3] \qquad \int \mathbf{v}_2 \frac{\partial f_2}{\partial t}\,d\mathbf{v}_2 = \frac{\partial}{\partial t}\int \mathbf{v}_2 f_2\,d\mathbf{v}_2 - \int f_2 \frac{\partial \mathbf{v}_2}{\partial t}\,d\mathbf{v}_2$$

and as $\mathbf{v}_2$ is not a function of t the second integral on the right-hand side of [3.3] is zero.

Substituting [3.3] in [3.2] we have

$$\frac{\partial}{\partial t}\int \mathbf{v}_2 f_2\,d\mathbf{v}_2 = -k_b\int \mathbf{v}_2 f_2\,d\mathbf{v}_2 + k_b\int \mathbf{v}_2 f_2^{0}\,d\mathbf{v}_2.$$

Now $\int \mathbf{v}_2 f_2^0\,d\mathbf{v}_2 = 0$ and $\int \mathbf{v}_2 f_2\,d\mathbf{v}_2 = C_s'\mathbf{v}_{0_2}$ where $\mathbf{v}_{0_2}$ is the mass velocity of the molecules on the surface after a time t, hence

$$[3.4] \qquad \int \frac{d\mathbf{v}_{0_2}}{\mathbf{v}_{0_2}} = \int -k_b\,dt.$$

Can. J. Chem. Downloaded from www.nrcresearchpress.com by 210.87.254.5 on 09/05/12
For personal use only.

The boundary conditions in the integration of [3.4] are found as follows in order to obtain the mean drift momentum per molecule of the gas before (π_1) and after interaction (π_r). The ratio of these quantities is equated in [6] with the specular reflection coefficient.

Let τ_s be the mean lifetime of molecules adsorbed in the mobile levels. We consider a representative group of molecules which are desorbed in a short time interval about τ_s from the facets. The facets involved are also taken to be a representative group. We assume that all molecules leaving at $t = \tau_s$ arrived on the surface at $t = 0$ whence the value of π_1 is that appropriate to the flowing gas close to the surface which is mv_{0_x}. At τ_s, $\pi_r = mv_{0_x}(\tau_s)$ where $v_{0_x}(\tau_s)$ is the component of mass velocity in the plane of the facets, resolved in the x-direction, i.e. $v_{0_x}(\tau_s) = \mathbf{v}_{0_2}\,\overline{\cos\Psi}$. $\overline{\cos\Psi}$ is a mean value of the cosine of the angle of inclination of the facets, given by:

$$[3.5] \qquad \overline{\cos\Psi} = \frac{\int_0^{\pi/2} \cos\Psi\, h(\Psi)\, d\Psi}{\int_0^{\pi/2} h(\Psi)\, d\Psi}.$$

Using these boundary conditions in the integration of [3.4] we obtain

$$[3.6] \qquad (1 - \beta_3)\ \overline{\cos\Psi} = \frac{\mathbf{v}_{0_2}\,\overline{\cos\Psi}}{v_{0_x}} = \overline{\cos\Psi}\,.\,e^{-k_b\tau_s}.$$

Can. J. Chem. Downloaded from www.nrcresearchpress.com by 210.87.254.5 on 09/05/12
For personal use only.

Can. J. Chem. Downloaded from www.nrcresearchpress.com by 210.87.254.40 on 09/05/12
For personal use only.

SLIP FLOW IN LONG, SINGLE CAPILLARIES

PART III. THE TRANSIENT STATE OF FLOW

R. M. Barrer and D. Nicholson

Physical Chemistry Laboratories, Chemistry Department, Imperial College, London, England

Received October 16, 1964

ABSTRACT

The time lag in establishing steady-state slip flow in long, single capillaries has been measured for the rare gases at 0 °C, for CO_2, Xe, and propane at 196 °K, and for SO_2 at 240 °K. The results are presented as non-dimensional time-lag quotients and as the reciprocals of this quotient plotted against u the reciprocal Knudsen number. Attention is drawn to some properties of reciprocal time lags, in particular the fact that they often have the same form as the permeability function when plotted against concentration. When adsorption is not appreciable, agreement between experiment and theory is very good in the slip flow regime but becomes less so as the transition regime is approached. Experiments at the lower temperatures showed that the effect of adsorption could be detected for CO_2, Xe, and propane but not for SO_2. These results can be interpreted in terms of a Freundlich isotherm but it seems probable that the time lag is particularly sensitive to the presence of sites of high adsorption potential.

1. INTRODUCTION

In this paper measurements of time lag in single capillaries are reported and discussed. The measurements, made in the slip flow regime, were carried out in the series A capillaries described in Part II (1). The method of measuring time lags by extrapolating to zero pressure the linear part of the plot of outgoing pressure, P_2, against time, t, has been described elsewhere (2). In these experiments P_2 was always less than 0.05% P_1, and so $P_1 - P_2 \simeq P_1$.

The equation for non-steady-state slip flow can be formulated in a manner analogous to Fick's law as

$$\frac{\partial C_g'}{\partial t} = \frac{\partial}{\partial x}\left[D(C_g')\,\frac{\partial C_g'}{\partial x}\right],$$

where $D(C_g')$ is the concentration-dependent diffusion coefficient and C_g' is the gas phase concentration in molecules cm^{-3}. $D(C_g')$ is related to the integral diffusion coefficient or permeability K by

$$K = 1/C_0 \int_0^{C_0} D(C_g')\,dC_g',$$

where C_0 and O are the ingoing and outgoing concentrations.

When D depends on concentration a direct solution of the Fick's law equation can only be found in an approximate form (3). A general procedure due to Frisch is, however, available (4) for obtaining the time lag, and expressions have been developed for this parameter for cases when slip flow is occurring in single capillaries (Ash, Barrer, and Nicholson (5)). The physical conditions considered in this publication were slip flow and transition flow without adsorption, for which the permeability is given by eqs. [2] and [3] of Part I; and slip flow, with immobile adsorption, described by various isotherm equations, at the surface of the capillary. The results were expressed in dimensionless form, the quotient involving the time lag, which can be found from experimental data, being

$$\mathscr{L} = \frac{LK_0}{l^2},$$

where L is the measured time lag in seconds in a capillary of length l and radius r, and $K_0 = (\pi r/16)(2RT/\pi M)^{1/2}$, M and T being the molecular weight and absolute temperature of the gas. If the time-lag quotient with immobile adsorption is indicated by subscript 2 then it is found that $\mathscr{L}_2 = \mathscr{L} + (2u_m/r)\mathscr{L}_1$ where $\mathscr{L}$ here is the time-lag quotient without adsorption, and u_m is defined in terms of the monolayer capacity C_m as $u_m = (rC_m/2\eta)(2RTM/\pi)^{1/2}$. The form of $\mathscr{L}_1$ depends on the adsorption isotherm. The results of the earlier paper are summarized in Table I, in which non-dimensional time-lag quotients are expressed as functions of the dimensionless parameter u. As explained in Part II u can be identified approximately with $r/\bar{\lambda}$ where $\bar{\lambda}$ is the mean free path associated with $P_1/2$, and a is the slip flow intercept which is constant for a given gas and temperature.

One general feature of these equations is that $\mathscr{L}$ decreases as u increases, its value at the beginning of the slip flow regime being about 1/3 of that for Knudsen diffusion in the same capillary. This means that l must be large if suitable time lags are to be obtained. For example, in capillary 1A (l = 1 500 cm, $r = 5.10^{-3}$ cm) L was about 10 min for He with an ingoing pressure of 2 cm Hg at 273 °C and about 35 min for Kr under the same conditions; time lags below 5 min are difficult to measure accurately.

2. THEORY

Ash, Barrer, and Nicholson (5) have discussed ways in which the expressions of Table I might be compared with experimental results. An interesting property of these equations which was not discussed in that publication is the behavior of the reciprocal time lags. These have proved useful in assessing experimental data, and accordingly will be mentioned here.

The form of the curve of the time lag against u for slip flow with no adsorption is reminiscent of a rectangular hyperbola and suggests that reciprocal functions might be of interest. We can write for the slip flow regime

$$[1] \qquad \frac{1}{\mathscr{L}_2} = \frac{u^3(u+a)^3}{Q_0 + \nu Q_1},$$

where $\nu = 2u_m/r$. The denominator of [1] may be written in the form

$$[2] \qquad Q_0 + \nu Q_1 = \sum a_n u^n = a_5 u^5 + \text{----} + a_0 + \sum_1,$$

where a_n are coefficients and $\sum_1$ is the sum of terms with powers of u greater than 5, and will be negligible when $1/\mathscr{L}_2$ is a linear function of u.

(a) $Q_1 = 0$. No Adsorption

We find,

$$[3] \qquad 1/\mathscr{L} = 3.750u + 5.3906a\gamma = s_0 u + i_0,$$

where $\gamma = 1 + 0.0897(a/u) - 0.0696(a/u)^2 + \text{- - - - -}$ which converges when $u > a$; some values of γ are given in Table II which show that γ is not very variable over quite wide ranges of a/u. The function $u^3(u+a)^3/Q_0$ is plotted in Fig. 1 where it can be seen that there is no appreciable departure from linearity when $u > 10$.

Can. J. Chem. Downloaded from www.nrcresearchpress.com by 210.87.254.40 on 09/05/12
For personal use only.

TABLE I

Slip flow time lags

Conditions	$u^3(u+a)^3\mathscr{L}$	
No adsorption	$\frac{4}{15}u^5+\frac{5a}{12}u^4+\frac{a^2}{6}u^3=Q_0$	1*a*
Henry's law, $C_s'=k_sC_g'$	$\left(1+\frac{2k_s}{r}\right)Q_0$	
Conditions	$u^3(u+a)^3\mathscr{L}_1$	
Freundlich isotherm $\frac{C_s'}{C_m}=k_fC_g'^{1/n}$, $n>1$	$\frac{k_fn^2u^{2+(1/n)}}{(2n+1)}\left\{\frac{4u^2}{(4n+1)}+\frac{2(3n+2)au}{(3n+1)(n+1)}+\frac{a^2}{(n+1)}\right\}=Q_f$	1*b*
Langmuir isotherm	$\frac{1}{k_1^4}[\frac{1}{2}(uk_1)^4+\frac{1}{3}(3ak_1-4)(uk_1)^3+\frac{1}{2}(ak_1-2)(ak_1+1)(uk_1)^2$ $+(ak_1-2)(ak_1-1)uk_1+(ak_1-2)(1+uk_1)(1-ak_1-uk_1)\ln(1+uk_1)]$ $=Q_1$	1*c*
B.E.T. isotherm	$\left\{q(a+2q)(q-u)(a+q+u)\ln\left(1-\frac{u}{q}\right)\right\}$ $+\left\{\frac{q}{b^4}(ab-2q)(q+bu)(q-ab-bu)\ln\left(1+\frac{bu}{q}\right)\right\}-\frac{4}{3}\frac{k_bq}{b}u^3$ $+\frac{1}{2}\left[(a+2q)(q-a)+\frac{(ab-2q)(ab+q)}{b^2}\right]u^2$ $+q\left[(a+2q)(q+a)+\frac{(ab-2q)(ab-q)}{b^3}\right]u=Q_b$	1*d*
	$b=(k_b-1)$	
Hüttig isotherm	$Q_n=Q_1+\frac{Q_0}{q}-\frac{Q_1}{k_1q}$	1*e*
Transition to Knudsen flow	$\mathscr{L}_Tu^3\left[u+a+\frac{a'}{u}\ln(1+b'u)\right]^3$	
No adsorption, a, a', b' are constants (see Part II)	$=Q_0+\frac{a'}{b'}\left\{\frac{8b'}{9}u^3+\left(\frac{3ab'}{4}+\frac{1}{6}\right)u^2+b'\left(a'+\frac{a}{2b'}-\frac{1}{3b'^2}\right)u\right.$ $-\left[u^2+au+\left(a'+\frac{a}{2b'}-\frac{1}{3b'^2}\right)\right]\ln(1+b'u)$ $\left.-\frac{a'}{2}[\ln(1+b'u)]^2\right\}$	1*f*

TABLE II

a/u	1.0	0.70	0.50	0.30	0.05	0.03
γ	1.20	1.05	1.04	1.02	1.004	1.002

Can. J. Chem. Downloaded from www.nrcresearchpress.com by 210.87.254.40 on 09/05/12
For personal use only.

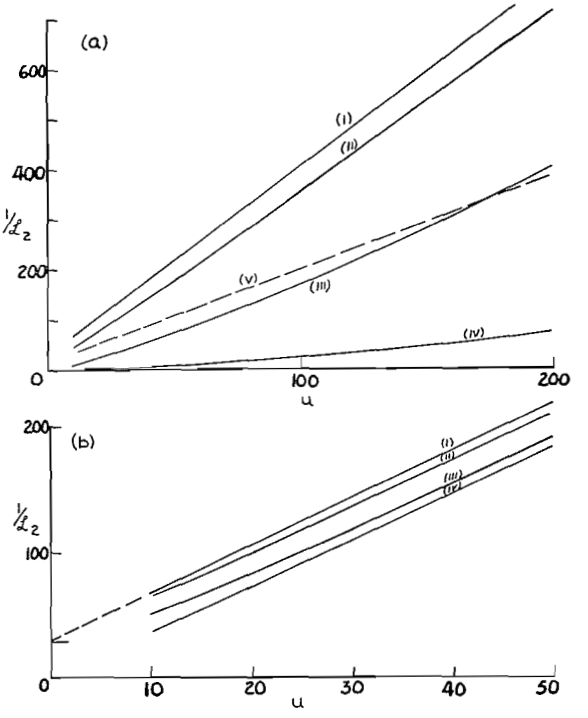

FIG. 1. Reciprocal time-lag quotients as functions of u. (*a*) Slip flow with Freundlich isotherm. (*i*) No adsorption ($a = 5.0$); (*ii*), (*iii*), (*iv*) Freundlich isotherm with $n = 2$ and $\nu k_f = 1.0$, 10.0, and 100 respectively; (*v*) Henry's law ($n = 1.0$) with $2k_s/r = 1.0$. (*b*) Slip flow with Langmuir isotherm. (*i*) No adsorption ($a = 5.3$); (*ii*), (*iii*), (*iv*) $k_1 = 0.01$, 0.10, and 1.00 respectively.

In the transition regime a much more complicated expression is obtained for the time lag (5) (see Table I). Its reciprocal and K/K_0 are both illustrated in Fig. 2 in which a value of $a = 6.0$ has been taken. It would be much more difficult to obtain an equation such as

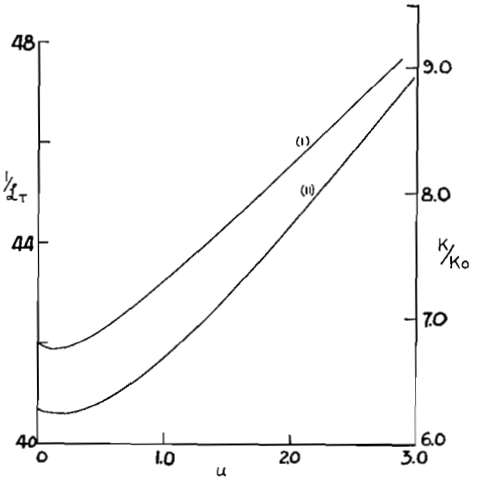

FIG. 2. Reciprocal time-lag quotients and relative permeabilities in the transition flow regime, as functions of u. (*i*) $1/\mathscr{L}_T$ vs. u; (*ii*) K/K_0 vs. u. $1/\mathscr{L}_T$ is calculated from eq. 1*f* from Table I; K/K_0 is obtained from the corresponding integrated form of Weber's equation (Part II); $a = 6.0$, $a' = 0.198$, $b' = 4.0$.

Can. J. Chem. Downloaded from www.nrcresearchpress.com by 210.87.254.40 on 09/05/12
For personal use only.

[3], in this case. Similarly no proof of this correspondence between reciprocal time lag and K/K_0, in the general case when K/K_0 is represented by a series, has yet been found.

(b) Q_1 Is Not Zero

b.1.—The simplest example is for Henry's law adsorption. Here,

$$[4] \qquad i_0/i_H = s_0/s_H = 1 + 2k_s/r,$$

where s_H and i_H are the slope and intercept of $1/\mathscr{L}_2$. The Freundlich isotherm (which reduces to Henry's law when $n = 1$) gives rise to curved plots of $1/\mathscr{L}_2$ against u (Fig. 1*a*).

b.2.—With Langmuir adsorption we can consider two extremes. (*i*) $uk_1 \gg 1.0$. The logarithmic term in Q_1 becomes negligibly small compared with the other terms and an equation similar to [3] is obtained in which γ is replaced by γ_1, a series which, like γ, does not depend markedly on u. Thus, as the monolayer is approached $1/\mathscr{L}_2$ against u tends to the same slope as $1/\mathscr{L}$ against u. It can also be shown that if this line is extrapolated back to $u = 0$ the intercept is

$$[5] \qquad i = i_0 - 7.031\nu.$$

(*ii*) $uk_1 < 1$. The logarithmic part of the expression for Q_1 can be expanded as a series of uk_1, and when uk_1 is sufficiently small the terms in $\sum_1$ (eq. [2]) become negligible. The ratio of the slopes is then

$$[6] \qquad \frac{s_0}{s_1} = \left[1 + \frac{\nu k_1}{16}(3ak_1 - 8)(ak_1 - 2)\right].$$

By definition $u_m k_1 = k_s$ so that [6] can also be written

$$[6a] \qquad \frac{s_0}{s_1} = \left[1 + \frac{2k_s}{r}\frac{(3ak_1 - 8)(ak_1 - 2)}{16}\right],$$

which reduces to [4] when k_1 is small. For intermediate values of uk_1 the terms in $\sum_1$ will no longer be negligible and no algebraic expression has been found for $1/\mathscr{L}_2$. The behavior of $1/\mathscr{L}_2$ with different values of k_1 is illustrated in Fig. 1*b*.

b.3.—When adsorption proceeds beyond the monolayer the expansion of the logarithmic term in u/q, where u is always less than q, must also be included in Q_1.

(i) $uk_1 < 1.0$. The expansion in terms of u/q for the B.E.T. and Huttig models are different only in powers of u/q greater than the fifth (5). Thus, if u/q is not very close to 1, eq. [6] can be replaced by the same expression in both cases, viz:

$$[7] \qquad \frac{s_0}{s_B} = \left[1 + \frac{\nu k_1}{16}(3ak_1 - 8)(ak_1 - 2) + \frac{\nu}{16q}((3a/q) - 8)((a/q) - 2)\right]$$

in which the term containing q tends to 0 when $a/q \to 0$.

(ii) $uk_1 > 1.0$. The ratio of slopes is

$$[8] \qquad \frac{s_0}{s_B} = \left[1 + \frac{\nu}{q} + \frac{1}{16q}\left(\frac{3a}{8q} + 3\left(\frac{a}{q}\right)^2\right)\right]$$

and the intercept can be written

$$i_B \simeq \frac{35a}{3(1 + \nu/q)} + \frac{\nu}{2}.$$

Calculations made previously (5) showed that ν would be about 5, and as q represents an upper limit to u this will usually be about 100 for the slip flow approximation to apply.

Can. J. Chem. Downloaded from www.nrcresearchpress.com by 210.87.254.40 on 09/05/12
For personal use only.

Thus the lines in Fig. 1*b* for Langmuir adsorption will have only slightly different slopes if the effect of multilayer adsorption is taken into account. Furthermore as $a \simeq \nu$ the terms in a/q in [8] are quite negligible compared with ν/q and so eq. [8] can be written

$$[8a] \qquad \frac{s_0}{s_B} = (1 + \nu/q).$$

3. RESULTS

(a) Adsorption Effects Negligible

The steady-state measurements discussed in Part I enable one to find a value of a, and also to calculate u for a particular value of the pressure. Hence a comparison of experimental values of $\mathscr{L}$ with those predicted from the steady state can be made. Such comparisons show good or very good agreement and provide a test of the Frisch method. Plots of $1/\mathscr{L}$ and of $\mathscr{L}$ against u for Ne at 0 °C in capillary 1A are shown in Fig. 3.

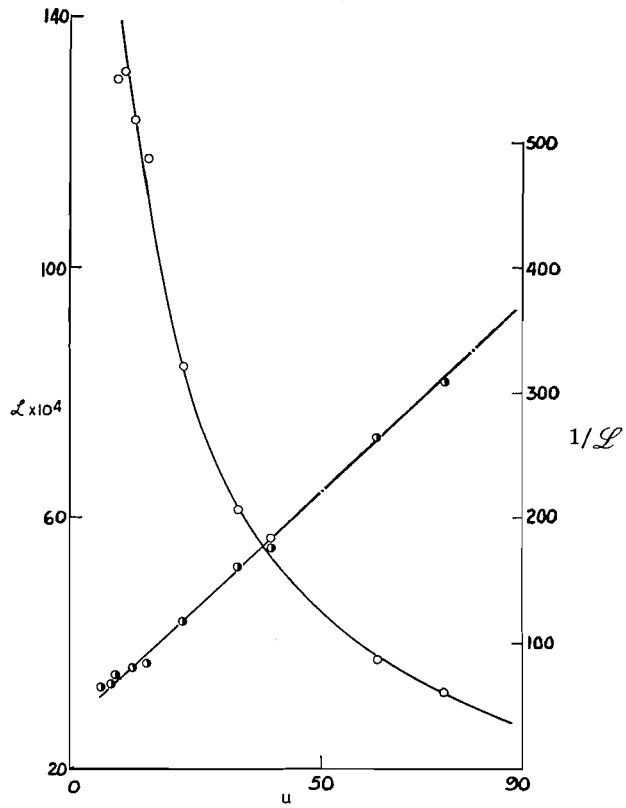

FIG. 3. Time-lag and reciprocal time-lag quotients in the slip flow regime for Ne at 0 °C, as functions of u. (*i*) Theoretical line and experimental points for $\mathscr{L}$ against u; (*ii*) theoretical line and experimental points for $1/\mathscr{L}$ against u; $a = 6.2$.

An alternative procedure is to assume that the expression for $\mathscr{L}$ is correct and to solve equation I*a* (Table I) for each experimental value of u and $\mathscr{L}$. This was done using an iterative method, on the London Mercury computer, and the results for steady state and transient state mean a values are given in Table III. The standard deviations quoted here

Can. J. Chem. Downloaded from www.nrcresearchpress.com by 210.87.254.40 on 09/05/12
For personal use only.

indicate that time-lag results are more scattered than steady state K values and reflect the fact that the time lag is more difficult to measure accurately.

TABLE III

Values of a in capillary 1A at 273 °K

Gas	Steady state	Transient state
He	$6.7_2 \pm 0.2$	$6.6_8 \pm 0.5$
Ne	$5.7_3 \pm 0.1$	6.2 ± 1.0
Ar	5.1 ± 0.3	5.8 ± 1.2
Kr	4.2 ± 0.5	4.1 ± 1.5

When u is < 5, $\mathscr{L}_T$ is lower than $\mathscr{L}$ by more than 5% of $\mathscr{L}$ (see ref. 5) and the equation for the transition regime should be more appropriate. This region is examined in detail in Fig. 4 where helium and neon results are compared with $\mathscr{L}_T$ which has been calculated using the a values already established for the slip flow regime. There is a considerable

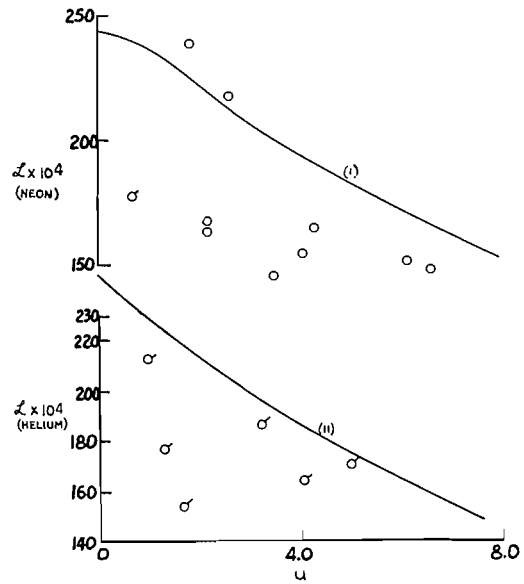

FIG. 4. Time-lag quotient in the transition regime as a function of u. ○ = Ne at 0 °C; ♂ = He at 0 °C. (*i*) Calculated with $a = 6.2$, from eq. 1*f* of Table I; (*ii*) calculated with $a = 6.7$, from eq. 1*f* of Table I.

scatter in time-lag points as this region is approached; in part this is because there is a lower limit to the pressure measurements which can be reliably made with the existing apparatus. Nevertheless it is clear that there is a definite tendency for experimental time lags to be low. One reason might be that a true steady state was not achieved when the time lag was large. However K/K_0 does not show the same marked deviation from Weber's equation (5) in the steady state. The absolute value of the time lag for He was quite low (about 10 min) and the runs were continued for more than 10 times L which should be ample time to establish the steady state.

(b) Systems with Adsorption

Because of experimental difficulties which arise at low temperature (1) most measure-

Can. J. Chem. Downloaded from www.nrcresearchpress.com by 210.87.254.40 on 09/05/12
For personal use only.

ments were made at 'cardice' temperature. This excludes measurements involving adsorption for a number of potentially interesting gases; e.g., Ar and Kr would not be expected to exhibit detectable differences in time lag in capillaries such as these, with radii of the order of 5×10^{-3} cm, until liquid oxygen or nitrogen temperature are reached. Four measurements on Kr at 'cardice' temperature confirmed that this was the case. A further restriction arises because otherwise suitable gases often condense at quite low u values.

In Fig. 5 the results obtained for adsorbable gases are illustrated as $\mathscr{L}_2$ and $1/\mathscr{L}_2$ plotted against u. For SO_2 at $\sim$ 240 °K adsorption is scarcely detectable but for all other cases time lags are definitely longer than would be expected if no adsorption occurred.

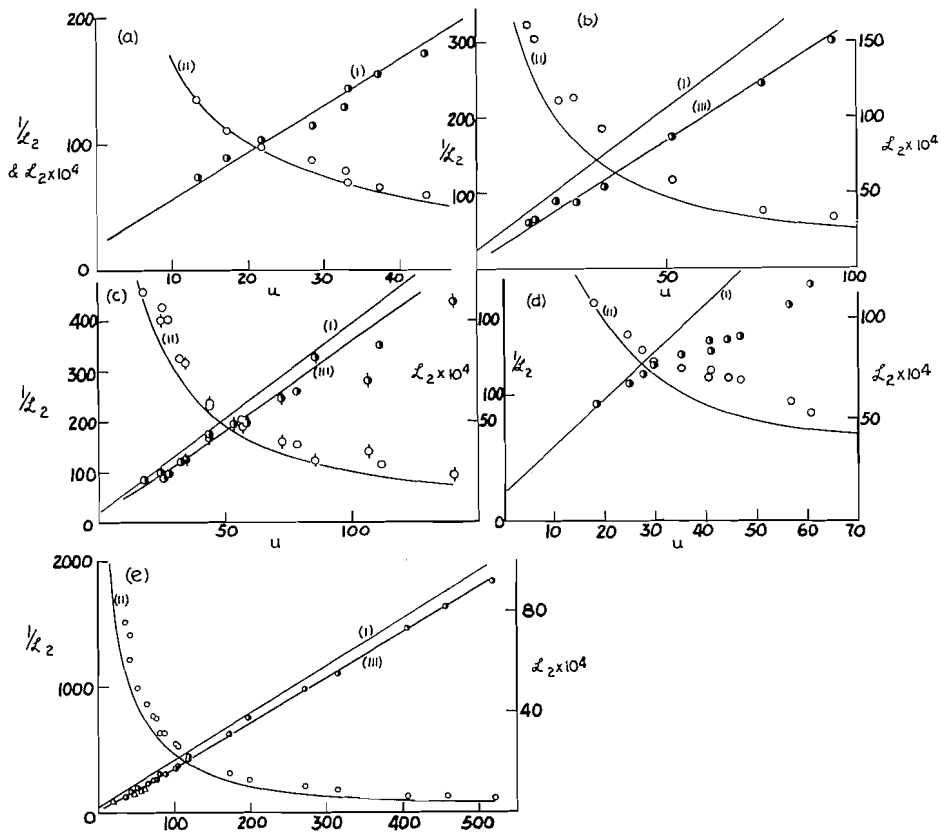

FIG. 5. Time-lag and reciprocal time-lag quotients for slip flow with adsorption, as functions of u. (*a*) SO_2 at 239.8 °K in capillary 4A; (*b*) Xe at 195.7 °K in capillary 2A; (*c*) Propane at 196.3 °K in capillaries 3A and 4A; (*d*) CO_2 at 195.7 °K in capillary 2A; (*e*) CO_2 at 196.3 °K in capillary 5A. Lines (*i*) and (*ii*) refer to $1/\mathscr{L}$ and $\mathscr{L}$ respectively, and line (*iii*) to $1/\mathscr{L}_2$ (calculated below). In Figs. 5 (*a*), (*b*), (*d*), and (*e*), ○ = $\mathscr{L}_2 \times 10^4$, ◑ = $1/\mathscr{L}_2$, while in Fig. 5 (*c*), ○ = $\mathscr{L}_2 \times 10^4$ and ◑ = $1/\mathscr{L}_2$, in capillary 4A; ⊖ = $\mathscr{L}_2 \times 10^4$ and ◐ = $1/\mathscr{L}_2$, in capillary 3A; △ = $1/\mathscr{L}_2$ for CO_2 in capillary 2A.

Although there was considerable experimental scatter, one feature emerged clearly from the results obtained in capillaries 1A, 2A, and 3A; this was that behavior characteristic of Langmuir adsorption (Fig. 1*b* and ref. 5) was not observed. To confirm this a series of experiments was performed with CO_2 in capillary 5A. This capillary was the longest one used (2 000 cm) and it was possible to obtain time lags of about 4 min at $u \simeq 500$. The value of u corresponding to saturation vapor pressure was $q = 1\ 260$ (Table IV) so that

Can. J. Chem. Downloaded from www.nrcresearchpress.com by 210.87.254.40 on 09/05/12
For personal use only.

adsorption beyond a completed monolayer would certainly be expected for points with u greater than about 150. Standard deviations for the three highest points calculated from the P_2 against t lines were about 1% of the time lag in each case.

TABLE IV

	q	$1 + \nu/q$	n	$k_t\nu$*	k_s (cm)
CO_2	1 260	1.004	1.1_1	0.13	
Propane	340	1.014	1.1_0	0.15	
Xe	5 600	1.0009	1.0	0.18	4.9×10^{-4}

*$k_t\nu = 2k_s/r$ when $n = 1.0$.

The theory discussed earlier (5) and the lines illustrated in Fig. 1*b* indicate that the behavior observed might be expected when uk_1 is less than 1.0. However, this criterion requires that the k_1 should be about 10^{-2} and it is unlikely that such low k_1 values would exist for the systems studied here, or that adsorption would be detectable in such instances (5). Again, it is possible that post-monolayer adsorption might be responsible for the divergence of $1/\mathscr{L}$ and $1/\mathscr{L}_2$. For CO_2, Xe, and propane values of q are given in Table IV; thus for propane $(1 + (\nu/q)) \simeq 1.014$, i.e. a 1% divergence in slope might be expected, but this is not sufficient to explain the results obtained. For propane $\mathscr{L}_2$ values were corrected by subtracting $\mathscr{L}/q$ (ref. 5) to account for post-monolayer adsorption.

It may be concluded that of the isotherms so far considered the Freundlich equation (Fig. 1*a*) would be expected to provide the best fit to the experimental results. To a good first approximation the time-lag quotient for this isotherm can be written

$$\mathscr{L}_2 = \mathscr{L}\left\{1 + \frac{15n^2\nu k_t u^{(1/n)-1}}{(4n+1)(2n+1)}\right\}$$

from which

$$[9] \qquad \log\left[\frac{\mathscr{L}_2}{\mathscr{L}} - 1\right] = \left(\frac{1}{n} - 1\right)\log u + \log\left[\frac{15n^2\nu k_t}{(4n+1)(2n+1)}\right].$$

From the plots of $\log(\mathscr{L}_2/\mathscr{L} - 1))$ against $\log u$ shown in Fig. 6, values of n and νk_t were calculated for Xe, propane, and CO_2. These results are summarized in Table IV and the reciprocal time-lag quotients calculated from them using eq. 1*b* of Table I are shown in Fig. 5 (curves *iii*).

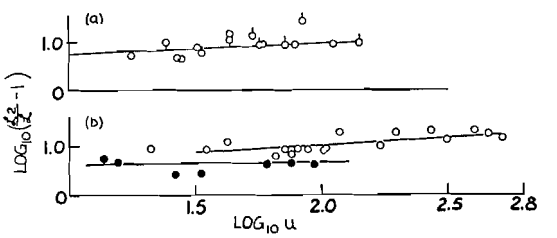

FIG. 6. Log $(\mathscr{L}_2/\mathscr{L} - 1)$ vs. log u. (*a*) ○ = propane in capillary 4A at 196.3 °K, ♂ = propane in capillary 3A at 196.3 °K; (*b*) ○ = CO_2 in 5A at 196.3 °K, ● = Xe in 2A at 195.7 °K.

In all these instances n does not differ significantly from the 'Henry's law' value of 1.0, and for Xe it would even appear that Henry's law is obeyed. On the other hand a calculation based on the value of k_s quoted in Table IV and taking the specific area of Xe at

Can. J. Chem. Downloaded from www.nrcresearchpress.com by 210.87.254.40 on 09/05/12
For personal use only.

196 °K to be 20 Å shows that monolayer coverage should have been achieved for the highest values of u. The reason for this behavior most probably originates in the nature of the time lag. Thus the theoretical consideration of the time lag (5) shows that processes involving large energies (adsorption of the first layer) are very much emphasized in comparison with those involving smaller energies (subsequent condensation of second, etc., layers). Similarly the part played by the most energetically sorbing sites in the adsorption process would be exaggerated in time-lag measurements.*

The Freundlich isotherm can be derived on the assumption that site energies are randomly distributed (7), and can therefore be taken as being associated with adsorption on an energetically heterogeneous surface. However, one of the weaknesses of this isotherm is that it does not reduce to Henry's law at low surface coverages. This suggests that n should actually be an increasing function of concentration, having a value of 1 at low concentrations (Henry's law), and therefore that the values of n we have obtained from the time-lag measurements are suitably weighted means for the surface concentration ranges studied. But, as explained above, the theory of the time lag shows that the mean value obtained for n will be weighted towards its value for lower concentrations and must thus give low values for n.

4. CONCLUSION

The experimental results for slip flow without adsorption are in excellent agreement with the theory based on Frisch's method and indicate that this procedure can be applied with confidence. The prediction that adsorption on the walls of single capillaries should be detectable from time-lag measurements in the slip flow regime has proved to be correct, although the interpretation of these results is less certain. One factor which cannot be fully accounted for at present is the possibility of surface flow. Although previous calculations have shown that this is unlikely to be important (5) there is some uncertainty in the estimation of surface diffusion coefficients. In most of the systems studied the surface flow is probably insignificant because time lags tend to be longer not shorter than would be expected; however, SO_2 is an exception and it may be that appreciable surface fluxes exist in this system.

One of the major difficulties of time-lag measurements is that they cannot yet be made with the degree of accuracy of permeability measurements. When more precise experimental results can be obtained time-lag measurements of the type discussed here and in ref. 5 may provide a means of investigating surface heterogeneity.

ACKNOWLEDGMENTS

We would like to thank Mr. R. Ash of this department for helpful discussions. One of us (D. N.) is indebted to the British Petroleum Company for a postdoctoral fellowship.

REFERENCES

1. R. M. Barrer and D. Nicholson. Can. J. Chem. This issue.
2. R. M. Barrer and D. M. Grove. Trans. Faraday Soc. **47**, 826 (1951).
3. A. Aitken and R. M. Barrer. Trans. Faraday Soc. **51**, 116 (1955).
4. H. L. Frisch. J. Phys. Chem. **61**, 93 (1957).
5. R. Ash, R. M. Barrer, and D. Nicholson. Z. Physik. Chem. Frankfurt, **37**, 257 (1963).
6. P. Clausing. Ann. Chim. Paris, **7**, 521 (1930).
7. G. D. Halsey and H. S. Taylor. J. Chem. Phys. **15**, 624 (1947).

**This conclusion is supported by the rather high value of heat of adsorption, 3 600 cal per mole, found by Clausing (6) in his measurements of adsorption times for* Ar *on glass.*

Can. J. Chem. Downloaded from www.nrcresearchpress.com by 210.87.254.40 on 09/05/12
For personal use only.

LIST OF IMPORTANT SYMBOLS

For a fuller discussion of the adsorption constants see ref. 5.

C_g' concentration in molecules cm^{-3} in the gas phase.

C_s' concentration in molecules cm^{-2} in the surface phase.

C_m concentration in molecules cm^{-2} in the surface phase at monolayer coverage.

K permeability in $cm^2\ s^{-1}$.

K_0 $\frac{\pi r}{16}\left(\frac{2RT}{\pi M}\right)^{1/2}$.

k_b B.E.T. isotherm constant, where $\frac{C_s'}{C_m} = \frac{k_b(w/q)}{(1-(w/q)(1+(1-k_b)(w/q))}$.

k_s Henry's law constant, where $C_s' = k_s C_g'$.

k_1 $\frac{2N_0}{r\eta RT}\left(\frac{2M}{\pi RT}\right)^{1/2} k_1'$, where k_1' is the constant in Langmuir isotherm $\frac{C_s'}{C_m} = \frac{k_1' C_g'}{1+C_g'}$.

$\mathscr{L}$ $Q_0/u^3(u+a)^3$, non-dimensional time-lag quotient for slip flow without adsorption.

$\mathscr{L}_2$ Non-dimensional time-lag quotient with adsorption $= \mathscr{L} + \nu\mathscr{L}_1$.

$\mathscr{L}_1$ Non-dimensional adsorption time lag $Q_1/u^3(u+a)^3$. Q_1 is given by the equations in Table I.

q Value of u corresponding to P_1 equal to P_0, the saturation pressure.

u $\frac{r}{\eta}\left(\frac{2M}{\pi RT}\right)^{1/2}\left(\frac{P_1+P_2}{2}\right)$.

w $\frac{r}{2\eta}\left(\frac{2M}{\pi RT}\right)^{1/2} P(x,t)$.

Can. J. Chem. Downloaded from www.nrcresearchpress.com by 210.87.254.40 on 09/05/12
For personal use only.

Can. J. Chem. Downloaded from www.nrcresearchpress.com by 210.87.254.40 on 09/05/12
For personal use only.

THE STRUCTURE OF A SYNTHETIC ARABINAN

G. G. S. DUTTON
Department of Chemistry, University of British Columbia, Vancouver, British Columbia
AND
A. M. UNRAU
Department of Plant Science, University of Manitoba, Winnipeg, Manitoba

Received April 27, 1964

ABSTRACT

Hydrolysis of the fully methylated synthetic arabinan showed it to have a highly branched structure in which about 16% of the terminal units were furanose and 2,3-di-*O*-methyl-L-arabinose was the principal di-*O*-methyl ether. A method has been developed whereby mixtures of isomeric di- or mono-*O*-methyl arabinoses may be qualitatively analyzed by successive borohydride reduction, periodate oxidation, and borohydride reduction. The resulting fragments may be separated directly by vapor phase chromatography or by paper chromatography after demethylation.

A variety of monosaccharides has been polymerized by Mora and his associates (1) and in previous papers we have reported on the structure of a synthetic glucan (2) and of a xylan (3). The present paper reports on the nature of an arabinan prepared by the polymerization of L-arabinose. The polysaccharide used in this study was prepared by Dr. Mora and was part of the same sample whose physical properties have already been reported (1). It has only been possible to carry out a methylation study owing to the small amount of polymer available. A novel method of qualitatively analyzing a mixture of isomeric methylated sugars has been developed and although the quantitative accuracy is not known some indication of the principal components, and hence linkages, may be obtained.

The arabinan was methylated three times by the method of Kuhn (4) and six times by Purdie's method (5) to give eventually a fully methylated product which was hydrolyzed with sulfuric acid (6). The methylated sugars were separated by paper chromatography into the fractions shown in Table I and indirect evidence for the presence of the majority of compounds was obtained by application of periodate degradation schemes similar to that shown in Table II.

Fraction 1, the fastest moving material, was characterized as 2,3,5-tri-*O*-methyl-L-arabinose by formation of the crystalline amide. The possible components of fraction 2

TABLE I

Hydrolysis products of methylated arabinan

Fraction	Components (L-arabinose ethers)	Wt. (mg)
1	2,3,5-Tri-*O*-methyl	65
2	2,3,4-Tri-*O*-methyl 2,5-Di-*O*-methyl 3,5-Di-*O*-methyl	410
3	2,3-Di-*O*-methyl 2,4-Di-*O*-methyl 3,4-Di-*O*-methyl	280
4	2-, 3-, 4-, and 5-mono-*O*-methyl	150
5	L-Arabinose	15
	Recovery	80%

Can. J. Chem. Downloaded from www.nrcresearchpress.com by 210.87.254.40 on 09/05/12
For personal use only.

were the 2,3,4-tri-*O*-methyl-, 2,5- and 3,5-di-*O*-methyl-L-arabinoses. Of these only the last would migrate on electrophoresis and examination in this way showed that 7–10% of fraction 2 was the 3,5-di-*O*-methyl ether. The overall composition of this fraction may be approximately determined by successive borohydride reduction, periodate oxidation, and borohydride reduction. The fragments produced may be demethylated with hydrobromic acid (7), the products separated by chromatography and estimated quantitatively. Under these conditions the 2,3,4-isomer will give arabinitol, the 3,5-isomer will give erythritol while the 2,5-ether will give an equimolecular mixture of ethylene glycol and glycerol as shown in Table II. Application of this method to fraction 2 gave arabinitol, erythritol, glycerol, and ethylene glycol in a molar ratio of 16:2:1:1. Although the quantitative nature of the demethylation step has not been examined in detail it should be noted that the sum of the weights of the demethylated glycitols recovered was almost quantitative for a mixture containing about 7% of 3,5-di-*O*-methyl-L-arabinose. Furthermore glycerol and ethylene glycol were obtained in equimolecular amounts which suggested that no selective decomposition had taken place. These results indicated that 2,3,4-tri-*O*-methyl-L-arabinose was the main component of fraction 2 and taken in conjunction with the weight of the 2,3,5-isomer isolated in fraction 1 showed that approximately 16% of the non-reducing end groups in the polysaccharide were furanose.

TABLE II

Periodate analysis of fraction 2

Components (L-arabinose ethers)	Reactions	Product	Demethylation product
2,3,4-Tri-*O*-methyl	(*i*) BH_4^-	2,3,4-Tri-*O*-methyl-L-arabinitol	L-Arabinitol
3,5-Di-*O*-methyl	(*ii*) IO_4^-	2,4-Di-*O*-methyl-L-erythritol	Erythritol
	(*iii*) BH_4^-	2-*O*-Methylglycerol	Glycerol
2,5-Di-*O*-methyl		+	+
		mono-*O*-methylethylene glycol	ethylene glycol

Fraction 3 was believed to consist of the 2,3-, 2,4-, and 3,4-di-*O*-methyl ethers. Electrophoretic examination showed one migrating component which amounted to about 15% of the fraction and corresponded to the 3,4-isomer. Periodate oxidation of fraction 3 gave a small amount of a sugar with a significantly higher R_f value than the bulk of the fraction which was unchanged. This fast moving material was isolated and was assumed to be 2,3-di-*O*-methylerythrose since reduction and demethylation gave erythritol according to the following scheme.

3,4-Di-*O*-methyl-L-arabinose $\xrightarrow{IO_4^-}$ 2,3-di-*O*-methyl-L-erythrose $\xrightarrow{BH_4^-}$ 2,3-di-*O*-methyl erythritol $\xrightarrow{HBr}$ erythritol.

Of the three possible isomers 2,4-di-*O*-methyl-L-arabinose cannot undergo cleavage with periodate, the 2,3-ether will undergo slow oxidation while the 3,4-isomer will be rapidly oxidized (8). Furthermore only the 3,4-isomer can give rise to erythritol and therefore the isolation of this glycitol confirms the electrophoretic assignment. The remaining material was reduced, oxidized, and reduced as shown,

2,3-di-*O*-methyl-L-arabinose, 2,4-di-*O*-methyl-L-arabinose $\xrightarrow[(ii)\ IO_4^-]{(i)\ BH_4^-}$ 2,3-di-*O*-methyl-L-threose, 2,4-di-*O*-methyl-L-arabinitol $\xrightarrow[(ii)\ HBr]{(i)\ BH_4^-}$ threitol, arabinitol,

and the glycitols obtained by demethylation were characterized thus proving the presence of the 2,3- and 2,4-di-*O*-methyl ethers in fraction 3. The ratio of threitol to arabinitol was 16:1 showing that 2,3-di-*O*-methyl-L-arabinose was the major constituent of fraction 3.

Fraction 4 contained the mono-*O*-methyl-L-arabinoses and reference to Table III shows that each monomethyl ether will form a characteristic glycitol when submitted to periodate degradation. Vapor phase chromatography showed the presence of each glycitol which, after demethylation, was characterized as its *p*-nitrobenzoate.

TABLE III

Periodate analysis of fraction 4

1 Mono-*O*-methyl ether of L-arabinose	2 Product formed by (*i*) IO_4^-, (*ii*) BH_4^-	3 Demethylation product	4 Melting point of *p*-nitrobenzoate of 3 (°C)
2-	2-*O*-Methylglycerol(II)*	Glycerol	190–192
	+	+	
	ethylene glycol (III)	ethylene glycol	143–144
3-	2-*O*-Methyl-L-erythritol(IV)	Erythritol	251–252
4-	2-*O*-Methylglycerol (II)	Glycerol	190–192
5-	1-*O*-Methyl-D-glycerol (I)	Glycerol	190–192

*The Roman numeral refers to the order of appearance on vapor phase chromatography.

The results presented here show that the arabinan was a highly branched polysaccharide in which there was a high proportion of furanosyl units. In these respects this polymer closely resembled the others examined.

Some of the analytical methods used to identify the components of a complex mixture of isomeric sugars represent a useful application of vapor phase chromatography where the original sugars, or their derivatives, themselves lack sufficient volatility. It is hoped that the application of the methods outlined here will be of general use in the study of other arabinose-containing polysaccharides especially those of natural origin.

EXPERIMENTAL

General methods have been described previously (2).

Methylation and Hydrolysis

The arabinan (1.60 g) was dissolved in dimethylformamide (25 ml) by warming to 55–60°. The solution was cooled and methyl iodide (5 ml) and silver oxide (5 g) were added. The mixture was shaken mechanically at room temperature for 3 days and the product recovered by extraction with chloroform. The Kuhn methylation was repeated twice more but a fully methylated arabinan (1.36 g, OMe, 39.8%, no hydroxyl band in the infrared) was only obtained after six treatments with Purdie's reagents. The final product was a yellow glass which could not be purified by fractional precipitation owing to its solubility in 95% petroleum ether (30–60°) and 5% chloroform. This probably explains the slightly high methoxyl value.

The fully methylated arabinan (1.25 g) was dissolved in 72% sulfuric acid (6) and after 1 h the thick solution was diluted with water to an acid concentration of 2 *N* and was boiled for 8 h. The solution was neutralized with barium carbonate and evaporated to give a mixture of methylated sugars (1.15 g). The mixture was resolved on Whatman 3MM paper using butanone–water azeotrope and gave the fractions shown in Table I.

Identification of Components

Fraction 1, 65 mg, $[\alpha]_D$ −38° (*c*, 1.5 in water) was oxidized with bromine and the acid lactonized. The lactone had $[\alpha]_D$ −24° (*c*, 1.5 in water) and vapor phase chromatography indicated only minor amounts of impurities. Reaction with methanolic ammonia gave the amide as a sirup $[\alpha]_D$ 20° (*c*, 1.5 in ethanol) from which a small quantity of 2,3,5-tri-*O*-methyl-L-arabonamide, melting point and mixed melting point 135–137°, was obtained.

Fraction 2 was subjected to the reactions shown in Table II. The sirup (410 mg) was dissolved in water (50 ml) and reduced for 24 h with sodium borohydride (1 g). Excess hydride was destroyed by the addition

Can. J. Chem. Downloaded from www.nrcresearchpress.com by 210.87.254.40 on 09/05/12
For personal use only.

of acetic acid and the solution made 0.1 *M* with respect to periodic acid. Periodate and iodate ions were removed 16 h later by the addition of barium carbonate and the filtrate again reduced overnight with borohydride (1 g). The solution was acidified with acetic acid and evaporated to dryness. The residue was dissolved in hydrobromic acid (45%, 10 ml) and refluxed for 35 min. The solution was deionized by passage through Amberlite IR-120 and Duolite A-4 resins and the components were resolved on Whatman 3MM paper in ethyl acetate – pyridine – water (9:2:2). Analysis showed arabinitol, erythritol, glycerol, and ethylene glycol in the molar ratio of 16:2:1:1. The individual compounds were characterized as follows: L-*arabinitol* (285 mg), pentaacetate melting point and mixed melting point 74–75°; *erythritol* (26 mg), tetra-*p*-nitrobenzoate melting point and mixed melting point 251–253°; *glycerol* (10 mg), tri-*p*-nitrobenzoate melting point and mixed melting point 190–192°; and *ethylene glycol* (7 mg), di-*p*-nitrobenzoate melting point and mixed melting point 143–145°. Paper electrophoresis of a sample of fraction 2 in borate buffer (0.07 *M*) showed non-migrating components and material with an M_G of 0.3. Using the phenol – sulfuric acid method the ratio of non-migrating to migrating material was 16:1.

Fraction 3, 280 mg, when subjected to electrophoresis indicated a component with M_G of 0.0 and a minor component with M_G of 0.40, the latter constituting 15% of the total. The mixture was subjected to the following series of reactions. The sirup was dissolved in cold periodic acid (0.1 *M*, 50 ml) and the solution stored at 5°. Excess periodate and iodate were precipitated (barium carbonate), the solution was evaporated, and the product was examined by paper chromatography using butanone–water azeotrope. A new component with R_f of about 0.7 was observed. The mixture was resolved, the new sugar (presumably 2,3-di-*O*-methyl-L-erythrose) was reduced, and the alcohol demethylated. The product (22 mg) was identified as erythritol by paper chromatography and by conversion to the tetra-*p*-nitrobenzoate, melting point and mixed melting point 251–253°. The non-degraded dimethyl sugar fraction was subjected to borohydride reduction, periodate oxidation, and a second borohydride reduction followed by demethylation with hydrobromic acid. The residue (165 mg), composed of threitol and arabinitol, molar ratio 16:1, was resolved by paper chromatography. Threitol (122 mg) was converted to the tetra-*p*-nitrobenzoate, melting point and mixed melting point 220–222°. Arabinitol (9.8 mg) was not further characterized.

Fraction 4, 150 mg, was subjected to periodate oxidation and borohydride reduction. The *O*-methyl glycitols and ethylene glycol were separated by vapor phase chromatography using an Aerograph instrument, model A90-P2, and a 3 ft column ($\frac{1}{4}$ in. I.D.) of 13% Versamid on Diatoport. The individual *O*-methyl glycitols were demethylated with hydrobromic acid and the products were characterized as their *p*-nitrobenzoates. These results are shown in Table III.

Fraction 5, 15 mg, $[\alpha]_D$ 102° (*c*, 0.5 in water) was identified as L-arabinose on conversion to the phenylosazone, melting point and mixed melting point 161–163°, by reaction with phenylhydrazine hydrochloride and sodium acetate in 80% ethanol.

ACKNOWLEDGMENTS

We gratefully acknowledge the financial support of the Public Health Service (GM 07652) and the skilful assistance of Miss J. Hunter. We are also indebted to Dr. M. C. Keith for some initial experiments on the arabinan and for the preparation of the fully methylated polysaccharide.

REFERENCES

1. P. T. MORA, J. W. WOOD, and V. W. MCFARLAND. J. Am. Chem. Soc. **82**, 3418 (1960).
2. G. G. S. DUTTON and A. M. UNRAU. Can. J. Chem. **41**, 2439 (1963).
3. G. G. S. DUTTON and A. M. UNRAU. Can. J. Chem. **40**, 2105 (1962).
4. R. KUHN, I. LOW, and N. TRISCHMAN. Ber. **90**, 203 (1957).
5. T. PURDIE and J. C. IRVINE. J. Chem. Soc. **83**, 1021 (1903).
6. I. CROON, G. HERRSTROM, G. KULL, and B. LINDBERG. Acta Chem. Scand. **14**, 1338 (1960).
7. L. HOUGH, J. K. N. JONES, and W. H. WADMAN. J. Chem. Soc. 1702 (1950).
8. G. W. HUFFMAN, B. A. LEWIS, F. SMITH, and D. R. SPRIESTERSBACH. J. Am. Chem. Soc. **77**, 4346 (1955).

Can. J. Chem. Downloaded from www.nrcresearchpress.com by 210.87.254.40 on 09/05/12
For personal use only.

Can. J. Chem. Downloaded from www.nrcresearchpress.com by 210.87.254.40 on 09/05/12
For personal use only.

STUDIES ON STOBBE CONDENSATION

REACTIONS OF ALDEHYDES AND KETONES WITH DIMETHYL METHYLSUCCINATE

A. M. EL-ABBADY AND H. H. MOUSA

Department of Chemistry, University College for Girls, Ain Shams University and National Research Centre, U.A.R.

Received August 7, 1964

ABSTRACT

Benzaldehyde, *o*-methoxybenzaldehyde, *p*-chlorobenzaldehyde, benzophenone, and acetophenone are condensed with dimethyl methylsuccinate in the presence of potassium *tert*-butoxide to give the corresponding β-half-esters. In the case of *o*-methoxybenzaldehyde the lactonic acid (IX) is also obtained. The β-half-esters are cyclized by sodium acetate and acetic anhydride to the corresponding acetoxynaphthoates which are converted into their methoxynaphthoates. Alkaline hydrolysis of the β-half-esters yields the corresponding itaconic acids, the anhydrides of which are converted to their α-half-esters.

In a preliminary communication (1, 2) the reaction of two representative ketones, benzophenone and fluorenone, with diethyl methylsuccinate in the presence of sodium ethoxide was shown to proceed by a Stobbe condensation giving the expected half-esters in good yields. In the present work we are reporting an extension of this study on both aldehydes and ketones. Benzaldehyde, *o*-methoxybenzaldehyde, *p*-chlorobenzaldehyde, benzophenone, and acetophenone were condensed with dimethyl methylsuccinate in the presence of potassium *tert*-butoxide (3); from the products were formed anhydrides, half-esters, indones, and naphthalene derivatives. In all these reactions, exact parallels were found with the corresponding products previously obtained from ethyl succinate itself (3).

Good yields (60–72%) of the β-half-esters (II) were obtained from the condensation of benzaldehyde, *o*-methoxybenzaldehyde, benzophenone, and acetophenone. However, the yield was only poor, as expected, with *p*-chlorobenzaldehyde, but a shorter period of reflux was found to increase this yield slightly and minimize resinification. In the case of acetophenone, the isomeric β-half-ester (VI; R = CH_3) was also obtained and separated.

The condensation of the aldehydes in general afforded, in addition to the expected half-esters, varying amounts of the corresponding itaconic acids.

o-Methoxybenzaldehyde gave also a small amount of an acidic non-ketonic substance, m.p. 217°, which was found to be the lactonic acid (IX). The constitution of (IX) as 2-*o*-anisyl-3-carboxy-4-*o*-methoxybenzylidene-3-methyl-5-oxotetrahydrofuran follows from the following observations: (*a*) the infrared spectrum (KBr) showed a strong band at 1 750 cm^{-1}, characteristic of the stretching frequencies of carbonyl groups of α,β-unsaturated-γ-lactones (4) and (*b*) alkaline hydrolysis of the substance gave the itaconic acid (II; $R_1 = R_3 = R_4 = H$, $R_2 = CH_3O$) and *o*-methoxybenzaldehyde which was characterized as the 2,4-dinitrophenylhydrazone. Analogs of (IX) have frequently been observed in the condensations of ethyl succinate with aromatic aldehydes. The formation of this lactonic acid at high temperature is evidence for (*a*) the relative stability of the intermediate paraconic ester (3) towards the *tert*-butoxide ions; and (*b*) the comparative reactivity of *o*-methoxybenzaldehyde. When *o*-methoxybenzaldehyde was condensed with dimethyl methylsuccinate in the presence of sodium ethoxide at −15°, the lactonic acid (IX) was obtained as the main product.

Benzaldehyde and *p*-chlorobenzaldehyde also gave different amounts of benzoic acid and *p*-chlorobenzoic acid arising from a Cannizzaro reaction, a common side reaction in Stobbe condensations (3). The difference in the yields of this side reaction, was confirmed by treating *p*-chlorobenzaldehyde, benzaldehyde, and *o*-methoxybenzaldehyde with potassium *tert*-butoxide under the same conditions of the Stobbe experiment but in the absence of the succinic ester, where the yields of the resulting benzoic acids, as expected, were found to be 45, 22, and 5% respectively. This is in agreement with the electronic structures of these aldehydes where the −I effect of the Cl atom in *p*-chlorobenzaldehyde favors the side reaction (by the transfer of a hydranion) while the +T effect of the methoxyl group in *o*-methoxybenzaldehyde opposes it.

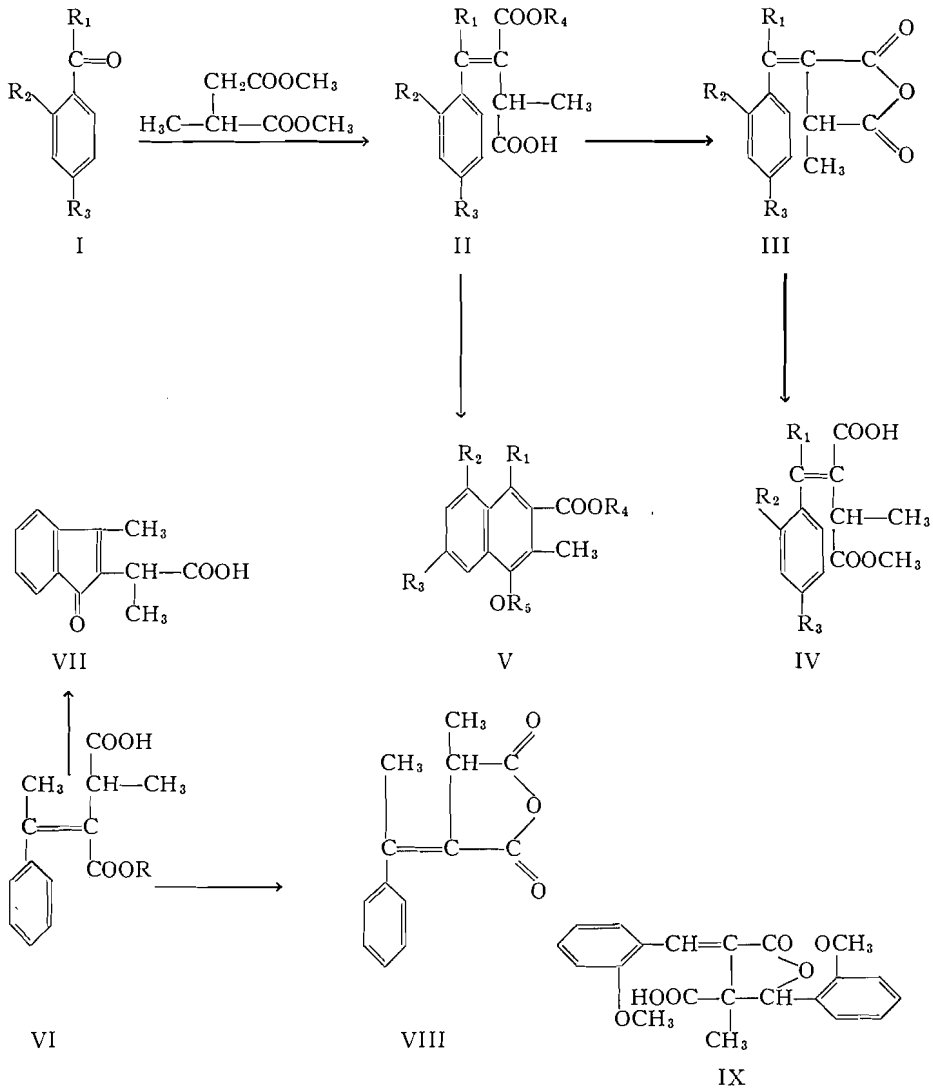

Hydrolysis of the half-esters using 10% sodium hydroxide solution gave very good yields of the corresponding itaconic acids except that from *p*-chlorobenzaldehyde which

Can. J. Chem. Downloaded from www.nrcresearchpress.com by 210.87.254.40 on 09/05/12
For personal use only.

Can. J. Chem. Downloaded from www.nrcresearchpress.com by 210.87.254.40 on 09/05/12
For personal use only.

gave a poor yield of the corresponding itaconic acid. This was improved by lowering the temperature of reflux (130°, oil bath) and by decreasing the concentration of the alkali (5%). The half-ester of benzaldehyde gave a purer product in higher yield when barium hydroxide was used. The two isomeric half-esters of acetophenone (II; $R_1 = R_4 = CH_3$, $R_2 = R_3 = H$ and VI; $R = CH_3$), separated by fractional crystallization after distillation, gave the corresponding itaconic acids which were found to be identical with those obtained from the hydrolysis of the crude undistilled mixture of the half-esters. This indicates that the two forms of the half-ester are stable to heat. The constitutions of the two isomeric itaconic acids of acetophenone as *cis*- and *trans*-α,γ-dimethyl-γ-phenylitaconic acid (II; $R_1 = CH_3$, $R_2 = R_3 = R_4 = H$ and VI; $R = H$ respectively) were demonstrated in the usual way (3); (*a*) the two acids gave acetophenone on oxidation with alkaline permanganate, showing the absence of double bond migration and (*b*) cyclization of both itaconic acids (m.p.'s 139° and 178–180°) with concentrated sulfuric acid (5) at room temperature was successful only in the case of the acid of m.p. 178–180°, yielding the indoneacetic acid (VII) as a yellow, crystalline solid, m.p. 127° (2,4-dinitrophenylhydrazone, m.p. 186–187°).

The structures and the *cis* configuration of the β-half-esters from the three aldehydes and benzophenone were confirmed in the usual way (3) by their cyclization with fused sodium acetate in acetic anhydride (6) to the corresponding methyl acetoxymethylnaphthoates (V) in good yields. Alkaline hydrolysis of the acetoxy esters gave the corresponding phenolic acids. Methyl 4-acetoxy-3-methyl-1-phenyl-2-naphthoate (V; $R_1 = C_6H_5$, $R_2 = R_3 = H$, $R_4 = CH_3$, $R_5 = CH_3CO$) afforded in addition to the expected phenolic acid (V; $R_1 = C_6H_5$, $R_2 = R_3 = R_4 = R_5 = H$) a phenolic solid which was found to be the phenolic ester (V; $R_1 = C_6H_5$, $R_2 = R_3 = R_5 = H$, $R_4 = CH_3$), as it showed bands in the infrared region (Nujol mull) at 3 500 (hydroxyl) and 1 715 cm^{-1} (aryl esters). The phenolic ester and acids when treated with dimethyl sulfate and anhydrous potassium carbonate in acetone afforded the corresponding methoxy esters. Methyl 4-methoxy-3-methyl-2-naphthoate (V; $R_1 = R_2 = R_3 = H$, $R_4 = R_5 = CH_3$) was obtained as a liquid and identified in the form of its solid methoxy acid (V; $R_1 = R_2 = R_3 = R_4 = H$, $R_5 = CH_3$). The itaconic acids were converted by acetyl chloride (7) into their anhydrides (III and VIII) in very good yields, except the itaconic acid from benzaldehyde (II; $R_1 = R_2 = R_3 = R_4 = H$) which failed completely to dehydrate and was recovered unchanged. The anhydrides on boiling with methanol (8) gave the corresponding α-half-esters (IV) in excellent yields. Thus in the formation of the α- and β-half-esters, and in the reactions of the latter, exact parallels are found with the analogous compounds from ethyl succinate in which the positions of the ester groups have been rigorously proved (3).

EXPERIMENTAL*

Condensation of Aldehydes or Ketones with Dimethyl Methylsuccinate (General Procedure)

A solution of the aldehyde or ketone (0.1 mole) and dimethyl methylsuccinate (0.1 mole) in dry *tert*-butanol (25 ml) was added under nitrogen atmosphere to a boiling solution of potassium *tert*-butoxide (from metallic potassium (0.12 mole) and *tert*-butanol (85 ml)). The addition took place in a period of 20 min, and the whole mixture was then refluxed under nitrogen for a further 45 min (the time of reflux was reduced to half an hour in case of *p*-chlorobenzaldehyde). The ice-cold mixture was acidified (litmus) with cold dilute hydrochloric acid. Distillation of alcohol under reduced pressure left a residue, which was diluted

**All melting points and boiling points are uncorrected, unless otherwise stated, the melting range of analytical samples was less than 1°. All yields refer to the yields of crude material. Infrared spectra were recorded on a Perkin–Elmer Infracord 137 spectrophotometer with a sodium chloride prism. Microanalyses are carried out by A. Bernhardt, Max-Plank-Institute, Mulheim (Ruhr).*

with water and extracted with ether. The ethereal solution was washed with water and repeatedly extracted with sodium bicarbonate solution which was then acidified with cold dilute hydrochloric acid to give the reaction product.

Benzaldehyde (10.6 g) gave a brown viscous oil (15.5 g), which failed to solidify. This when subjected to distillation under reduced pressure (140–150° at 0.3 mm, oil bath) gave a trace of benzoic acid (0.5 g) and most of the residue started to resinify. Saponification of the product (1 g) with a saturated solution of barium hydroxide (15 ml, 4 h heating at 100°) gave a barium salt which after filtration, washing with ethanol, and acidification with dilute hydrochloric acid yielded *cis*-α-methyl-γ-phenylitaconic acid (II; $R_1 = R_2 = R_3 = R_4 = H$) as colorless solid (0.8 g, 85% yield), m.p. 194° (from methanol).

Anal. Calcd. for $C_{12}H_{12}O_4$: C, 65.44; H, 5.49. Found: C, 65.44; H, 5.66.

When the above experiment was repeated but without the substituted succinic ester; benzoic acid, m.p. 122°, was obtained in about 22% yield.

o-Methoxybenzaldehyde (13.6 g) gave a viscous brown oil (25 g). Treatment of this oil with benzene in the cold, precipitated a solid (22 g) on standing. This solid after filtration was treated with boiling benzene in which it partly dissolved. The insoluble fraction (3.7 g) was found to be the itaconic acid (II; $R_1 = R_3 = R_4 = H$, $R_2 = CH_3O$), m.p. 198–199° (from water). This melting point was undepressed on admixture with a specimen of *cis*-γ-*o*-methoxyphenyl-α-methylitaconic acid obtained from the alkaline hydrolysis of the half-ester (II; $R_1 = R_3 = H$, $R_2 = CH_3O$, $R_4 = CH_3$) as shown later. Evaporation of the benzene solution gave the soluble fraction as a solid (17.6 g, 66% yield) which was crystallized from benzene, m.p. 168–170°. This was identified as β-methyl-α-hydrogen *cis*-γ-*o*-methoxyphenyl-α-methylitaconate (II; $R_1 = R_3 = H$; $R_2 = CH_3O$, $R_4 = CH_3$).

Anal. Calcd. for $C_{14}H_{16}O_5$: C, 63.62; H, 6.10. Found: C, 63.80; H, 6.28.

The original benzene mother liquor on long keeping gave a small amount of a solid acid (2.5 g), m.p. 217° (from methanol), which failed to give a 2,4-dinitrophenylhydrazone. This substance was found to be 2-*o*-anisyl-3-carboxy-4-*o*-methoxybenzylidene-3-methyl-5-oxo-tetrahydrofuran (IX). Infrared spectrum (KBr): 1 750 cm^{-1}.

Anal. Calcd. for $C_{21}H_{20}O_6$: C, 68.47; H, 5.4; CH_3O, 16.84; mol. wt. and equiv. wt., 368). Found: C, 68.59; H, 5.60; CH_3O, 17.08; mol. wt., 346; equiv. wt., 360.

Alkaline hydrolysis of this substance (0.4 g, 2 h refluxing with 10% sodium hydroxide solution) gave acid and neutral products. The acid (0.25 g), m.p. 196–198 (from water), on admixing with the previous specimen of *cis*-γ-*o*-methoxyphenyl-α-methylitaconic acid (II; $R_1 = R_3 = R_4 = H$, $R_2 = CH_3O$) gave no depression. The neutral semisolid (0.1 g) gave an orange 2,4-dinitrophenylhydrazone, m.p. 238° (from ethanol). This on admixing with an authentic specimen of *o*-methoxybenzaldehyde 2,4-dinitrophenylhydrazone (from B.D.H. *o*-methoxybenzaldehyde), m.p. 243–244° (from ethanol), gave no depression.

No *o*-methoxybenzoic acid was detected accompanying the Stobbe product. When the experiment was carried out under the same conditions, but in the absence of the methylsuccinic ester, *o*-methoxybenzoic acid (5% yield), m.p. 100°, was obtained and identified by its melting point and mixed melting point with a specimen of *o*-methoxybenzoic acid (B.D.H.).

Saponification of the half-ester (II; $R_1 = R_3 = H$, $R_2 = CH_3O$, $R = CH_3$) (1 g) with 10% sodium hydroxide solution (15 ml, 2 h refluxing), gave a colorless solid (0.8, 84.5% yield), m.p. 198–199° (from water). This was identified as *cis*-γ-*o*-methoxyphenyl-α-methylitaconic acid (II; $R_1 = R_3 = R_4 = H$, $R_2 = CH_3O$).

Anal. Calcd. for $C_{13}H_{14}O_6$: C, 62.39; H, 5.64. Found: C, 62.41; H, 5.66.

Alternative Preparation of 2-o-Anisyl-3-carboxy-4-o-methoxybenzylidene-3-methyl-5-oxotetrahydrofuran (IX)

A solution of *o*-methoxybenzaldehyde (12.1 g, 2 mole) and dimethyl methylsuccinate (4.4 g, 1 mole) in anhydrous ether (100 ml) was added dropwise with cooling (−15°) and shaking to a suspension of finally powdered alcohol-free sodium ethoxide (2 mole, from 1.12 g sodium in 50 ml dry ether). A precipitate rapidly separated. The mixture was kept for 2 days at −15° and then at 0 for another 2 days. The ice-cold mixture was acidified (litmus) with cold dilute hydrochloric acid. The ethereal layer was separated and the aqueous layer was extracted with ether. The ethereal layer and extracts were washed with water then repeatedly extracted with sodium carbonate solution. This was acidified to give an oil which was taken into ether and dried (Na_2SO_4). Evaporation of the solvent gave a semisolid (9.5 g) which solidified completely under benzene, m.p. 215–220°. This was crystallized from methanol as colorless crystals, m.p. 219–221°, and on admixing with a sample of the lactonic acid (IX, m.p. 217°) gave no depression.

p-Chlorobenzaldehyde (14 g) gave a deep-brown resinified oil (15 g). This was partly solidified after the addition of a little amount of benzene and standing. The solid fraction (about 2 g) melted over a wide range indicating that it was a mixture. Treatment of this mixture with boiling water gave two substances. The soluble one (1.4 g), m.p. 240° (from benzene), was found to be *p*-chlorobenzoic acid, and identified by its melting point and mixed melting point with an authentic specimen of *p*-chlorobenzoic acid (B.D.H.). The insoluble colorless substance (0.5 g), m.p. 206° (from methanol), was found to be *cis*-γ-*p*-chlorophenyl-α-methylitaconic acid (II; $R_1 = R_2 = R_4 = H$, $R_3 = Cl$)

Anal. Calcd. for $C_{12}H_{11}O_4Cl$: C, 56.27; H, 4.32; Cl, 13.95. Found: C, 56.22; H, 4.17; Cl, 14.56.

The benzene solution gave, after evaporation, an oily residue (about 13 g). A part of this oil (4 g) was

Can. J. Chem. Downloaded from www.nrcresearchpress.com by 210.87.254.40 on 09/05/12
For personal use only.

refluxed with 5% sodium hydroxide solution at 130° (oil bath) for 4 h. The solid product obtained after acidification, was treated repeatedly with boiling water. The insoluble part (1.1 g, m.p. 206° from methanol) was identified as *cis*-γ-*p*-chlorophenyl-α-methylitaconic acid (II; $R_1 = R_2 = R_4 = H$, $R_3 = Cl$) by its melting point and mixed melting point with the acid obtained directly from Stobbe reaction. The hot water washings gave after cooling a colorless solid (0.4 g, m p. 240°) which was found to be *p*-chlorobenzoic acid. When the Stobbe experiment was carried out normally but with no methylsuccinic ester; a solid acid, m.p. 240°, was obtained in about 45% yield and was identified as *p*-chlorobenzoic acid.

Benzophenone (18 g) gave a solid product (22 g, 72% yield). This was crystallized from benzene as colorless crystals, m.p. 152°, and identified as β-methyl-α-hydrogen-γ,γ-diphenyl-α-methylitaconate (II; $R_1 = C_6H_5$, $R_2 = R_3 = H$, $R_4 = CH_3$).

Anal. Calcd. for $C_{19}H_{18}O_4$: C, 73.53; H, 5.85. Found: C, 73.64; H, 5.73.

Saponification of this half-ester (1 g) resulted in the known γ,γ-diphenyl-α-methylitaconic acid (2) (II; $R_1 = C_6H_5$, $R_2 = R_3 = R_4 = H$) as colorless crystals, m.p. 178° (from water).

Anal. Calcd. for $C_{18}H_{16}O_4$: C, 72.96; H, 5.44. Found: C, 73.29, H, 5.41.

Acetophenone (12 g) gave a brown viscous oil (19 g, 76.6% yield). On distillation a heavy, pale-yellow oil, b.p. 158° at 0.7 mm, was obtained (12.2 g, 64.5% yield) which was partially solidified. The solid was separated by decantation, washed with little cold benzene, and crystallized from methanol as colorless needles (4.5 g), m.p. 106–108°. This was found to be β-methyl α-hydrogen *cis*-α,γ-dimethyl-γ-phenylitaconate (II; $R_1 = R_4 = CH_3$, $R_2 = R_3 = H$).

Anal. Calcd. for $C_{14}H_{16}O_4$: C, 67.73; H, 6.50. Found: C, 68.07; H, 6.11.

Saponification of this crystalline half-ester (1 g) gave a colorless solid (0.7 g) crystallizable from benzene, m.p. 139°, and was identified as *cis*-α,γ-dimethyl-γ-phenylitaconic acid (II; $R_1 = CH_3$, $R_2 = R_3 = R_4 = H$).

Anal. Calcd. for $C_{15}H_{14}O_4$: C, 66.65; H, 6.02. Found: C, 66.99; H, 6.42.

Alkaline hydrolysis of the oil fraction (1 g from about 7.5 g) gave a colorless solid (0.65 g), m.p. 178–180° (from water). This was identified later as *trans*-α,γ-dimethyl-γ-phenylitaconic acid (VI; R = H).

Anal. Calcd. for $C_{13}H_{14}O_4$: C, 66.65; H, 6.02. Found: C, 66.72; H, 6.16.

Saponification of the crude undistilled Stobbe product of acetophenone yielded a semisolid acid. This after treatment with charcoal gave colorless droplets of oil which solidified after cooling (42% yield), m.p. 124–157°, and was partly soluble in hot benzene. The insoluble fraction was found to be the acid (VI; R = H) of m.p. 178–180°, and the soluble fraction to be the acid (II; $R_1 = CH_3$, $R_2 = R_3 = R_4 = H$) of m.p. 139°.

Oxidation of α,γ-Dimethyl-γ-phenylitaconic Acids

α,γ-Dimethyl-γ-phenylitaconic acid (m.p. 139°, 0.5 g) was dissolved in 20% sodium carbonate solution (5 ml). Potassium permanganate solution (0.8 g in 45 ml water) was added dropwise with stirring until the color of permanganate persisted. The mixture was left for 2 h at room temperature, then extracted with ether. The ethereal layer after washing with water and drying (Na_2SO_4) was evaporated to give an oily residue (0.2 g). This oil gave a 2,4-dinitrophenylhydrazone, m.p. 229–230° (from ethanol), which on admixing with an authentic specimen of acetophenone 2,4-dinitrophenylhydrazone (from B.D.H. acetophenone) gave no depression. Repeating the above oxidation on the acid isomer (m.p. 178–180°) gave the same product.

Action of Concentrated Sulfuric Acid on the α,γ-Dimethylitaconic Acids

α,γ-Dimethyl-γ-phenylitaconic acid, m.p. 178–180°, (0.5 g) was treated with concentrated sulfuric acid (15 ml) at room temperature. The mixture was allowed to stand for 30 min, then poured on ice. 2-Methyl-2-(3-methyl-1-indone)-acetic acid (VII) was precipitated after cooling and crystallized from ether – petroleum ether (b.p. 40–60°) as long yellow needles (0.25 g), m.p. 127°. Infrared spectrum (Nujol mull): 1 790 and 1 740 cm^{-1}.

Anal. Calcd. for $C_{13}H_{12}O_3$: C, 72.21; H, 5.59. Found: C, 71.64; H, 5.52.

It gave a 2,4-dinitrophenylhydrazone as orange crystals, m.p. 186–187° (from ethanol).

Anal. Calcd. for $C_{19}H_{16}O_6N_4$: C, 57.57; H, 4.07; N, 14.14. Found: C, 57.73; H, 4.15; N, 13.89.

When the experiment was repeated on the acid isomer, m.p. 139°, a colorless solid was obtained which was found to be the starting material.

Cyclization of the β-Half-esters (General Procedure)

The β-half-ester (except that of *p*-chlorobenzaldehyde) (5 g) and anhydrous sodium acetate (2 g) in acetic anhydride (40 ml) were refluxed for 6 h, then worked up by removing the acetic anhydride under reduced pressure, adding water, then extracting the product with ether. The ethereal solution was washed with sodium bicarbonate solution and then water and dried (Na_2SO_4). Evaporation of the solvent left a neutral product.

The cis-β-half-ester from benzaldehyde (II; $R_1 = R_2 = R_3 = H$, $R_4 = CH_3$) gave a solid, crystallizable from benzene as colorless crystals, m.p. 120°, (69% yield) and was found to be methyl 4-acetoxy-3-methyl-2-naphthoate (V; $R_1 = R_2 = R_3 = H$, $R_4 = CH_3$, $R_5 = CH_3CO$).

Anal. Calcd. for $C_{15}H_{14}O_4$: C, 69.75; H, 5.46. Found: C, 70.33; H, 5.63.

Alkaline hydrolysis of this product (2 g, 2 h reflux in 10% sodium hydroxide solution, 50 ml) gave 4-hydroxy-3-methyl-2-naphthoic acid (V; $R_1 = R_2 = R_3 = R_4 = R_5 = H$; 90% yield) as dirty needles, m.p. 237–238° (from methanol).

Can. J. Chem. Downloaded from www.nrcresearchpress.com by 210.87.254.40 on 09/05/12
For personal use only.

Anal. Calcd. for $C_{12}H_{10}O_3$: C, 71.28; H, 4.99. Found: C, 71.27; H, 5.26.

The cis-β-half-ester from o-methoxybenzaldehyde (II; $R_1 = R_3 = H$, $R_2 = CH_3O$, $R_4 = CH_3$) afforded a neutral solid (61% yield), crystallizable from methanol as colorless needles, m.p. 123–125°, and was identified as methyl 4-acetoxy-8-methoxy-3-methyl-2-naphthoate (V; $R_1 = R_3 = H$, $R_2 = CH_3O$, $R_4 = CH_3$, $R_5 = CH_3CO$).

Anal. Calcd. for $C_{16}H_{16}O_5$: C, 66.66; H, 5.59; CH_3O, 21.52; CH_3CO, 14.93. Found; C, 67.03; H, 5.70; CH_3O, 20.98; CH_3CO, 15.52.

Saponification of this acetoxyester as usual gave a quantitative yield of 4-hydroxy-8-methoxy-3-methyl-2-naphthoic acid (V; $R_1 = R_3 = R_4 = R_5 = H$, $R_2 = CH_3O$) as dirty crystals, m.p. 243–245° (from methanol).

Anal. Calcd. for $C_{13}H_{12}O_4$: C, 67.23; H, 5.21. Found: C, 67.40; H, 5.27.

The cis-β-half-ester from p-chlorobenzaldehyde (II; $R_1 = R_2 = H$, $R_3 = Cl$, $R_4 = CH_3$) (4 g) and anhydrous sodium acetate (1.5 g) in a mixture of acetic anhydride (25 ml) and glacial acetic acid (25 ml) were heated at 130° (oil bath) for 3 h. The reaction mixture was then worked up as in the general procedure. The neutral product (3.8 g) as a brown viscous oil was saponified to give a semisolid product from which dirty crystals (20% yield) of 6-chloro-4-hydroxy-3-methyl-2-naphthoic acid (V; $R_1 = R_2 = R_4 = R_5 = H$, $R_3 = Cl$) were isolated, m.p. 275–276° (from aqueous methanol).

Anal. Calcd. for $C_{12}H_9O_3Cl$: C, 60.88; H, 3.80, Cl; 15.01. Found: C, 60.78; H, 3.88; Cl, 15.1.

The β-half-ester from benzophenone (II; $R = C_6H_5$, $R_2 = R_3 = H$, $R_4 = CH_3$) proceeded normally with a quantitative yield of methyl 4-acetoxy-3-methyl-1-phenyl-2-naphthoate (V; $R_1 = C_6H_5$, $R_2 = R_3 = H$, $R_4 = CH_3$, $R_5 = CH_3CO$) which was obtained as a colorless solid crystallizable from methanol, m.p. 137°.

Anal. Calcd. for $C_{21}H_{18}O_4$: C, 75.43; H, 5.43. Found: C, 75.28; H, 5.53.

This gave on alkaline hydrolysis a solid mixture which was dissolved in ether and the ethereal solution was extracted with sodium carbonate solution. The alkaline extract afforded a solid acid (40% yield) and the ethereal layer gave a phenolic solid (58% yield). The acid was crystallized from benzene as colorless light crystals, m.p. 232°, and identified as 4-hydroxy-3-methyl-1-phenyl-2-naphthoic acid (V; $R_1 = C_6H_5$, $R_2 = R_3 = R_4 = R_5 = H$).

Anal. Calcd. for $C_{18}H_{14}O_3$: C, 77.68; H, 5.07. Found: C, 77.94; H, 5.48.

The phenolic solid was crystallizable from benzene as colorless needles, m.p. 155°, and its infrared spectrum and analysis fitted for methyl 4-hydroxy-3-methyl-1-phenyl-2-naphthoate (V; $R_1 = C_6H_5$, $R_2 = R_3 = R_5 = H$, $R_4 = CH_3$). Infrared spectrum (Nujol mull): 3 500 and 1 710 cm^{-1}.

Anal. Calcd. for $C_{19}H_{16}O_3$: C, 78.06; H, 5.52. Found: C, 78.15; H, 5.43.

Methylation of Phenolic Acids (General Procedure)

The phenolic acid (1 g), dimethyl sulfate (3 g), and anhydrous potassium carbonate (4 g) in acetone (30 ml) were refluxed for 12 h on a water bath. Removal of acetone afforded a solid residue to which water was added to dissolve any inorganic material. The organic product was then filtered or extracted with ether.

4-Hydroxy-3-methyl-2-naphthoic acid (V; $R_1 = R_2 = R_3 = R_4 = R_5 = H$) gave a colorless oil (87.5% yield). This when refluxed with 10% sodium hydroxide solution (15 ml) for 2 h, afforded, after washing with ether and acidification with cold hydrochloric acid, 4-methoxy-3-methyl-2-naphthoic acid (V; $R_1 = R_2 = R_3 = R_4 = H$, $R_5 = CH_3$) (92% yield) as colorless crystals, m.p. 207° (from benzene).

Anal. Calcd. for $C_{13}H_{12}O_3$: C, 72.21; H, 5.59; CH_3O, 14.35. Found: C, 72.29; H, 6.20; CH_3O, 14.36.

4-Hydroxy-8-methoxy-3-methyl-2-naphthoic acid (V; $R_1 = R_3 = R_4 = R_5 = H$, $R_2 = CH_3O$) required a bigger amount of acetone (50 ml), and absolute methanol (20 ml) was added for its dissolution. The produced methyl 4,8-dimethoxy-3-methyl-2-naphthoate (V; $R_1 = R_3 = H$, $R_2 = CH_3O$, $R_4 = R_5 = CH_3$) was separated as colorless needles (95% yield), m.p. 108–110° (from methanol).

Anal. Calcd. for $C_{15}H_{16}O_4$: C, 69.21; H, 6.20. Found: C, 69.56; H, 6.25.

This after saponification as usual gave 4,8-dimethoxy-3-methyl-2-naphthoic acid (V; $R_1 = R_3 = R_4 = H$, $R_2 = CH_3O$, $R_5 = CH_3$) (87.7% yield) as a colorless solid, m.p. 209–211° (from acetic acid).

Anal. Calcd. for $C_{14}H_{14}O_4$: C, 68.28; H, 5.73; CH_3O, 25.16. Found: C, 67.73; H, 5.74; CH_3O, 24.22.

6-Chloro-4-hydroxy-3-methyl-2-naphthoic acid (V; $R_1 = R_2 = R_4 = R_5 = H$, $R_3 = Cl$) gave the corresponding methoxy ester (V; $R_1 = R_2 = H$, $R_3 = Cl$, $R_4 = R_5 = CH_3$) as colorless needles (99% yield), m.p. 100–102° (from methanol).

Anal. Calcd. for $C_{14}H_{13}O_3Cl$: C, 63.51; H, 4.9; Cl, 13.42. Found: C, 63.52; H, 4.89; Cl, 12.55.

4-Hydroxy-3-methyl-1-phenyl-2-naphthoic acid (V; $R_1 = C_6H_5$, $R_2 = R_3 = R_4 = R_5 = H$) gave methyl 4-methoxy-3-methyl-1-phenyl-2-naphthoate (V; $R_1 = C_6H_5$, $R_2 = R_3 = H$, $R_4 = R_5 = CH_3$) (88% yield) as colorless crystals, m.p. 113–115° (from methanol).

Anal. Calcd. for $C_{20}H_{18}O_3$: C, 78.41; H, 5.92. Found: C, 78.82; H, 5.99.

Methyl 4-hydroxy-3-methyl-1-phenyl-2-naphthoate (V; $R_1 = C_6H_5$, $R_2 = R_3 = R_5 = H$, $R_4 = CH_3$) gave a neutral solid, m.p. 113–115 (from methanol). This on admixing with a specimen of the above methoxy ester (V; $R_1 = C_6H_5$, $R_2 = R_3 = H$, $R_4 = R_5 = CH_3$) gave no depression.

Preparation of α-Half-esters (General Procedure)

The itaconic acid (1 g) was dissolved in the least amount of hot acetyl chloride (in case of the itaconic acid from *p*-chlorobenzaldehyde, a mixture of acetic anhydride and acetyl chloride was required). The mixture was refluxed for 2 h on a water bath and the excess acetyl chloride was then removed under reduced pressure

Can. J. Chem. Downloaded from www.nrcresearchpress.com by 210.87.254.40 on 09/05/12
For personal use only.

to give a solid itaconic anhydride. This anhydride (0.5 g) was then refluxed in dry methanol (10 ml) for 3 h. After the removal of excess methanol under reduced pressure, a solid residue was obtained.

The itaconic acid from o-methoxybenzaldehyde (II; $R_1 = R_3 = R_4 = H$, $R_2 = CH_3O$) proceeded normally to give the anhydride (III; $R_1 = R_3 = H$, $R_2 = CH_3O$) (0.8 g, 75% yield) as colorless needles, m.p. 149–150° (from benzene).

Anal. Calcd. for $C_{13}H_{12}O_4$: C, 67.23; H, 5.21. Found: C, 66.66; H, 5.29.

Treatment of this anhydride with methanol gave the α-half-ester (IV; $R_1 = R_3 = H$; $R_2 = CH_3O$) (70% yield) as colorless crystals, m.p. 162–163° (from methanol).

Anal. Calcd. for $C_{14}H_{16}O_5$: C, 63.62; H, 6.10. Found: C, 63.38; H, 6.22.

The itaconic acid from p-chlorobenzaldehyde (II; $R_1 = R_2 = R_4 = H$, $R_3 = Cl$) (1 g) was dissolved in acetic anhydride (10 ml). Acetyl chloride (15 ml) was then added to the solution, and the experiment was carried out as usual to give the anhydride (III; $R_1 = R_2 = H$, $R_3 = Cl$) (0.9 g, 89% yield). This was separated in yellow crystals from acetic anhydride, m.p. 175–177°.

Anal. Calcd. for $C_{12}H_9O_3Cl$: C, 60.88; H, 3.8; Cl, 15.01. Found: C, 60.34; H, 3.41; Cl, 16.15.

Treatment of this anhydride with methanol gave α-methyl β-hydrogen *cis*-γ-*p*-chlorophenyl-α-methyl-itaconate (IV; $R_1 = R_2 = H$, $R_3 = Cl$) (80% yield) as pale-yellow crystals, m.p. 143–144° (from benzene–benzine, b.p. 40–60°).

Anal. Calcd. for $C_{13}H_{13}O_4Cl$: C, 58.1; H, 4.42; Cl, 13.2. Found: C, 58.23; H, 4.75; Cl, 13.68.

The itaconic acid from benzophenone (III; $R_1 = C_6H_5$, $R_2 = R_3 = R_4 = H$), on dehydration, gave the known anhydride (1) (III; $R_1 = C_6H_5$, $R_2 = R_3 = H$) (0.7 g, 78% yield) as colorless crystals, m.p. 148° (from benzene).

Anal. Calcd. for $C_{18}H_{14}O_3$: C, 77.68; H, 5.07. Found: C, 78.17; H, 5.07.

This anhydride when treated with methanol yielded the α-half-ester (IV; $R_1 = C_6H_5$, $R_2 = R_3 = H$) (78% yield) as colorless solid crystallizable from ether – petroleum ether (b.p. 40–60°), m.p. 154–155°.

Anal. Calcd. for $C_{19}H_{18}O_4$: C, 73.53; H, 5.85. Found: C, 74.11; H, 5.81.

cis-α,γ-Dimethyl-γ-phenylitaconic acid (II; $R_1 = CH_3$, $R_2 = R_3 = R_4 = H$) gave on dehydration, *cis*-α,γ-dimethyl-γ-phenylitaconic anhydride (III; $R_1 = CH_3$, $R_2 = R_3 = H$) (0.8 g, 92% yield) as colorless needles, m.p. 94–95° (from benzene).

Anal. Calcd. for $C_{13}H_{12}O_3$: C, 72.21, H; 5.59. Found: C, 72.32; H, 5.68.

Treatment of this anhydride with methanol gave the α-half-ester (IV; $R_1 = CH_3$, $R_2 = R_3 = H$) as a colorless solid (85.5% yield) crystallizable from methanol, m.p. 121–123°.

Anal. Calcd. for $C_{14}H_{16}O_4$: C, 67.73; H, 6.50. Found: C, 67.79; H, 6.70.

trans-α,γ-Dimethyl-γ-phenylitaconic acid (VI; R = H) afforded, on dehydration, *trans*-α,γ-dimethyl-γ-phenylitaconic anhydride (VIII) (0.7 g, i.e. 84% yield) as colorless crystals, m.p. 89–90° (from benzene, petroleum ether, b.p. 40–60°).

Anal. Calcd. for $C_{13}H_{12}O_3$: C, 72.21; H, 5.59. Found: C, 72.60; H, 5.58.

ACKNOWLEDGMENT

The authors thank Dr. F. G. Baddar for the infrared spectral determinations.

REFERENCES

1. H. Stobbe and F. Gollücke. Ber. **39**, 1066 (1906).
2. H. Stobbe and M. Noetzel. Ber. **39**, 1070 (1906).
3. W. S. Johnson and G. H. Daub. Organic reactions. Vol. VI. J. Wiley and Sons, Inc. 1951. p. 1.
4. L. J. Bellamy. The infrared spectra of complex molecules. Methuen & Co. Ltd., London. 1956. p. 152.
5. H. Stobbe. Ber. **37**, 1619 (1904).
6. W. Borsche, S. Kettner, M. Gillies, H. Kuhn, and R. Manteuffel. Ann. **526**, 1 (1936).
7. W. S. Johnson *et al.* J. Am. Chem. Soc. **72**, 511 (1950).
8. A. M. El-Abbady and L. S. El-Assal. J. Chem. Soc. 1024 (1959).

Can. J. Chem. Downloaded from www.nrcresearchpress.com by 210.87.254.40 on 09/05/12
For personal use only.

Can. J. Chem. Downloaded from www.nrcresearchpress.com by 210.87.254.105 on 09/05/12
For personal use only.

THE REACTION OF ACTIVE NITROGEN WITH ETHANOL[1]

P. A. GARTAGANIS[2]

Physical Chemistry Department, Ontario Research Foundation, Toronto, Ontario

Received May 31, 1963

ABSTRACT

The reaction of active nitrogen with ethanol has been investigated in the range 300 to 593 °K using a modified condensed-discharge Wood–Bonhoeffer fast-flow system. The only condensable products found in appreciable amounts were hydrogen cyanide and water. Hydrogen was the main noncondensable product. A very small amount of acetaldehyde was also formed along with traces of ethane, ethylene, methane, acetonitrile, cyanogen, and probably carbon monoxide. The overall activation energy is 3.4 kcal/mole. It is postulated that the mechanism consists of the formation of two fragments NC_2H_5 and OH, from which the condensable products result as follows:

$$N + C_2H_5OH \rightarrow NC_2H_5 + OH,$$

$$NC_2H_5 \rightarrow CH_3 + HCN + H,$$

$$CH_3 + N \rightarrow HCN + 2H,$$

$$H + OH \rightarrow H_2O,$$

$$2H \rightarrow H_2.$$

A number of products found in trace quantities are produced by concomitant reactions of the hydrogen atoms with methyl radicals, and with ethanol as well as by disproportionation of ethyl radicals to produce ethane and ethylene. A preliminary study of the reaction of active nitrogen with isopropanol indicated that the energy of activation is in line with the energies of activation of methanol and ethanol.

INTRODUCTION

The reaction of active nitrogen with methanol has been discussed in a previous paper (*1*). The present investigation was initiated as a further step towards the study of the kinetics of the reactions between active nitrogen and various oxygen-containing organic compounds. The reaction with ethanol appeared to be of interest because of the opportunity for comparing the reactivity of the two lower members of the series. Some preliminary experiments were also performed with isopropanol to assess the trend of the reaction of active nitrogen with a higher alcohol.

EXPERIMENTAL

The apparatus and procedure used in carrying out the reactions were similar to those described by Gartaganis and Winkler (*2*), except that the spherical reaction vessel was replaced by a 100 cm reaction tube of 16 mm i.d. Thermocouple wells and observation windows were placed at regular intervals along the reaction tube. The products were identified by mass spectrometry and gas phase chromatography (Vapor Fractometer, Model 154, Perkin Elmer Corp. polyethylene glycol on Teflon powder; helium; 80 °C). Hydrogen cyanide was measured with silver nitrate and the water with Karl-Fischer reagent. The ratio of water to hydrogen cyanide was determined by the following method. The reaction products were trapped in methanol and titrated with Karl-Fischer reagent added to the trap through a septum from a microburette ending to a hypodermic needle. Ten milliliters 1 *N* potassium hydroxide were introduced with a syringe, the trap was then opened, 3 *N* ammonium hydroxide added, and the hydrogen cyanide determined with silver nitrate as usual.

RESULTS

The reaction was accompanied by a bright peach-colored flame, similar to those observed with hydrocarbons or methanol. As in the case of the latter compound the reaction of

[1]*Presented at the 46th Annual Conference of the Chemical Institute of Canada, Toronto, June 1963.*
[2]*Present address: Dominion Tar & Chemical Co. Ltd., Central Research Laboratories, Senneville, P.Q.*

active nitrogen with ethanol was found to be relatively simple inasmuch as very few products were produced and there seemed to be no extensive side reactions to complicate the kinetic considerations. Of course, intermediate steps of this type of reaction may be kinetically very complex. Hydrogen cyanide and water in approx. 2 to 1 ratio were the only condensable products found in appreciable amounts. Hydrogen was the main non-condensable product. A very small amount of acetaldehyde was formed along with small amounts (less than 2%) of ethane, ethylene, methane, acetonitrile, cyanogen, and probably carbon monoxide.

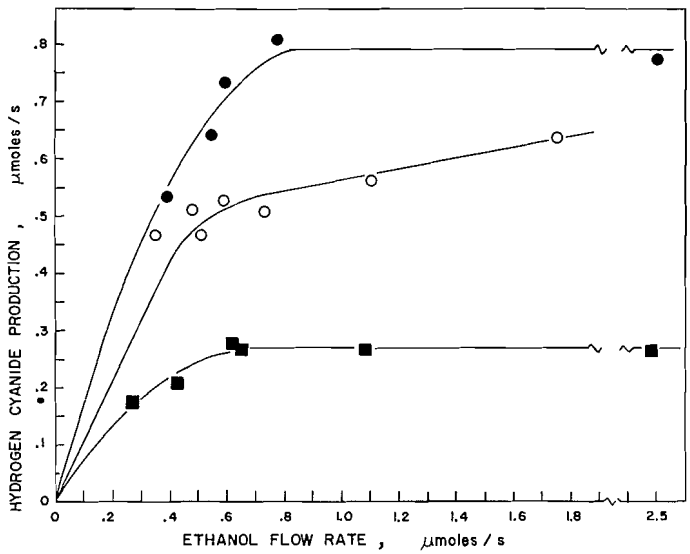

FIG. 1. Hydrogen cyanide production as a function of alcohol flowrate in the reaction of active nitrogen with ethanol. ●, 593 °K; ○, 428 °K; ■, 300 °K.

The yield of hydrogen cyanide, the only nitrogen-containing major product recovered at 300, 428, and 593 °K at various flow rates, is shown in Fig. 1. Since it is now recognized that the principal chemically reactive constituent present in active nitrogen is the nitrogen atom in the ^4S ground state (3), second-order rate constants for the nitrogen atom – ethanol reaction were calculated in a manner similar to that previously outlined for the methanol reaction (1).

A Reynolds-number calculation (4) showed that streamline flow prevailed in the reaction vessel and, therefore, the following integrated second-order expression was used for the calculation of the rate constants, assuming that one molecule of ethanol yields two molecules of hydrogen cyanide, i.e. assuming $n = 1/2$.

$$k_2 = \frac{(b + c)^2 R^2 T^2}{n(a - b/n) VP^2} \ln \frac{b(a - x)}{a(b - nx)}.$$

The pertinent kinetic data are shown in Table I. Another series of experiments with a different atomic nitrogen concentration was done earlier and the results agree with the information reported above.

A number of exploratory experiments were performed using the same apparatus and experimental conditions to study the general characteristics of the reaction of active nitrogen with isopropanol. The results are presented in Fig. 2 and Table I (in this case

Can. J. Chem. Downloaded from www.nrcresearchpress.com by 210.87.254.105 on 09/05/12
For personal use only.

n in the reaction rate formula is 1/3). The molecular nitrogen flow rate was 16.3 μmoles/s, and the atomic nitrogen flow rate, determined from the reaction with ethylene at 590 °K, was 1.06 μmoles/s.

TABLE I

Second-order rate constants at various temperatures and other kinetic data for the reactions of atomic nitrogen with ethanol and isopropanol (pressure, 0.5 mm Hg; atomic nitrogen flow, 1.06 μmoles/s; molecular nitrogen flow, 16.3 μmoles/s)

Alcohol flowrate (μmoles/s)	HCN production (μmoles/s)	k Streamline flow (l/mole s × 10^{-7})	Average log k	Temp. (°K)	E (kcal/mole)	P at 500 °K
Ethanol						
0.21	0.30	6.08				
0.28	0.40	6.65	7.822	593		
0.39	0.54	7.24				
0.27	0.30	2.04				
0.36	0.47	3.19				
0.48	0.52	2.53	7.379	428	3.4	3.6×10^{-3}
0.51	0.47	2.01				
0.27	0.18	0.46				
0.36	0.20	0.38	6.595	300		
0.43	0.21	0.35				
Isopropanol						
0.22	0.43	8.30				
0.28	0.48	7.29				
0.29	0.53	8.00	7.887	593		
0.31	0.52	7.31			3.5	3.8×10^{-3}
0.12	0.10	0.53				
0.17	0.12	0.46				
0.23	0.16	0.43	6.643	300		
0.28	0.17	0.36				

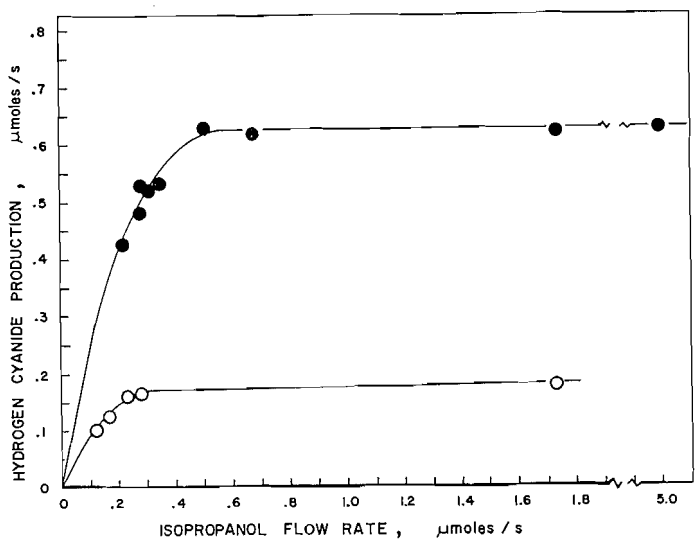

FIG. 2. Hydrogen cyanide production as a function of alcohol flowrate in the reaction of active nitrogen with isopropanol. ●, 593 °K; ○, 300 °K.

Can. J. Chem. Downloaded from www.nrcresearchpress.com by 210.87.254.105 on 09/05/12
For personal use only.

Can. J. Chem. Downloaded from www.nrcresearchpress.com by 210.87.254.105 on 09/05/12
For personal use only.

DISCUSSION

From the results of the present investigation, it is apparent that ethanol resembles methanol closely in its primary reaction with nitrogen atoms. The following steps account for the formation of hydrogen cyanide.

[1] $$N + C_2H_5OH \rightarrow NC_2H_5 + OH,$$

[2] $$NC_2H_5 \rightarrow HCN + CH_3 + H,$$

[3] $$CH_3 + N \rightarrow HCN + 2H.$$

It appears from spin considerations referred to earlier (1) that atomic rather than molecular hydrogen is produced by reactions [2] and [3]. Combination of the hydroxyl fragment of reaction [1] with this atomic hydrogen in the presence of a third body produces water:

[4] $$OH + H \rightarrow H_2O.$$

On the other hand the reaction $OH + N \rightarrow HNO$ does not seem to occur to any appreciable extent.

Recombination of hydrogen atoms by three-body collisions with ethanol molecules and with nitrogen (5) provide the only noncondensable product found in large amounts:

[5] $$H + H + N_2 \rightarrow H_2 + N_2.$$

It was again noticed that the limiting value of the rate of hydrogen cyanide formation does not correspond to the maximum nitrogen atom concentration indicated from the ethylene reaction and the same phenomenon was observed with isopropanol. It is probable that, in addition to the above reactions, homogeneous catalyzed recombination takes place with no product formation.

[6] $$N + N + C_2H_5OH \rightarrow N_2 + C_2H_5OH,$$

[7] $$N + NC_2H_5OH \rightarrow N_2 + C_2H_5OH.$$

It should be noted, however, that while reactions [6] and [7] are possible, catalytic recombination has fallen somewhat into disrepute in active nitrogen reactions. The earlier temperature dependence of hydrogen cyanide in the ethylene reaction, for example, now appears to have been an experimental artifact characteristic of the spherical reaction vessels used (7).

A reaction similar to eq. [7] has been postulated for ethylene by Kelly and Winkler (6). The formation of the small amounts of secondary hydrocarbon by-products probably resulted from reactions of various fragments with atomic hydrogen or with themselves, viz.

[8] $$CH_3 + H \rightarrow CH_4,$$

[9] $$C_2H_5 + H \rightarrow C_2H_6,$$

[10] $$2CH_3 \rightarrow C_2H_6,$$

[11] $$2C_2H_5 \rightarrow C_2H_4 + C_2H_6.$$

Conceivably ethyl radicals could be produced from the NC_2H_5 fragment directly or as a result of further attack by atomic nitrogen.

[12] $$NC_2H_5 \rightarrow N + C_2H_5,$$

[13] $$N + NC_2H_5 \rightarrow N_2 + C_2H_5.$$

Reaction [13] seems most unlikely, as there is no reason to expect the NC_2H_5 complex to have an appreciable existence before decomposing into hydrogen cyanide plus fragments.

Finally, hydrogen abstraction by hydrogen atoms or methyl radicals could account for the production of traces of acetaldehyde from ethanol.

CONCLUSION

As a result of the present investigation it can be concluded that ethanol molecules react with atomic nitrogen by C—O bond scission to form radicals that produce in a few simple steps hydrogen cyanide, water, and hydrogen, the principal products of this reaction. Some "wastage" of nitrogen atoms takes place and is probably due to homogeneous catalyzed recombinations, the alcohol and molecular nitrogen acting as the third body. The energy of activation for methanol, ethanol, and isopropanol reactions was calculated between 3.2 and 3.5 kcal/mole.

ACKNOWLEDGMENTS

The author is indebted to Dr. A. G. Harrison for mass spectrometric analyses, and to Messrs. M. J. Sole and S. M. Yee for assistance in the experimental work.

REFERENCES

1. M. J. Sole and P. A. Gartaganis. Can. J. Chem. **41**, 1097 (1963).
2. P. A. Gartaganis and C. A. Winkler. Can. J. Chem. **34**, 1457 (1956).
3. G. G. Mannella. Chem. Rev. **63**, 1 (1963).
4. J. R. Partington. An advanced treatise on physical chemistry. Vol. 1. Longmans, Green & Co. 1949.
5. H. Gesser, C. Luner, and C. A. Winkler. Can. J. Chem. **31**, 346 (1953).
6. R. Kelly and C. A. Winkler. Can. J. Chem. **37**, 62 (1959); **38**, 2514 (1960).
7. A. N. Wright, R. L. Nelson, and C. A. Winkler. Can. J. Chem. **40**, 1082 (1962).

Can. J. Chem. Downloaded from www.nrcresearchpress.com by 210.87.254.105 on 09/05/12
For personal use only.

Can. J. Chem. Downloaded from www.nrcresearchpress.com by 210.87.254.40 on 09/05/12
For personal use only.

AROMATIC SUBSTITUTION

PART IX.[1] ON THE MECHANISM OF THE PSCHORR CYCLIZATION

R. A. ABRAMOVITCH AND G. TERTZAKIAN
Department of Chemistry, University of Saskatchewan, Saskatoon, Saskatchewan

Received November 19, 1964

ABSTRACT

The decomposition of the diazonium salt from 3-(*o*-aminobenzoyl)pyridine has been studied under various conditions. A competitive-type cyclization of an equimolar mixture of the diazonium salts of 2-aminobenzophenone and 2-amino-3′-nitrobenzophenone has also been carried out. The results are interpreted in terms of a radical process in the copper-catalyzed reactions. It is suggested that the uncatalyzed thermal decompositions in aqueous acid solution give rise to a diradical cation intermediate in equilibrium with the aryl cation.

INTRODUCTION

The mechanism of the Pschorr and related cyclizations I → II has been the subject of much debate, without any definite conclusions being reached. Most of the arguments put forward have been based on analogies with the well-known intermolecular reactions

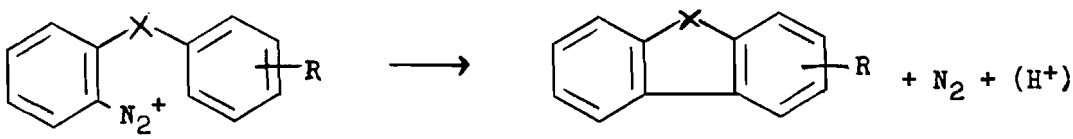

(I) (II)

of diazonium salts and on the effects (or lack of effects) of substituents present in the nucleus being attacked upon the yields of cyclized products. The reaction has been carried out under a variety of conditions ranging from the copper-catalyzed decomposition of the solid diazonium salts or of diazonium salt solutions in aqueous acid, through base-catalyzed decompositions and cyclizations to thermal decomposition in aqueous acid in the absence of a catalyst. Two recent reviews (1, 2) have summarized the conditions under which cyclization has been achieved and the various factors which affect the nature and yield of products obtained.

In general, two alternative mechanistic pathways have been proposed. The first of these is based essentially on the analogy between the Pschorr cyclization and the various intermolecular arylations which are known to involve the intermediacy of aryl radicals e.g. the Gomberg–Hey reaction, the decomposition of *N*-nitrosoacetanilides and of dimethyltriazens, and the Sandmeyer, Gattermann, and Waters (3) reactions, and on the fact that when conditions such as those used in the above reactions are employed to effect cyclization substituents seem to exert a minor influence upon the yield of cyclized products, unlike the situation which exists in the usual electrophilic substitution reactions. Such are the base-catalyzed reactions (see, however, (2)), the copper-catalyzed decompositions, and the thermal decomposition of *N*-nitrosoacetanilides. The second, involving mainly the uncatalyzed thermal decomposition in aqueous acid and analogous in many

[1]*Part VIII. R. A. Abramovitch, F. Helmer, and J. G. Saha. Can. J. Chem. This issue.*

Can. J. Chem. Downloaded from www.nrcresearchpress.com by 210.87.254.40 on 09/05/12
For personal use only.

ways to the decomposition of simple diazonium salts in aqueous acid (4), has been thought to involve a heterolytic process (1, 2).

A large number of observations are left unexplained, however. The copper-catalyzed reaction may involve the formation of radicals (probably not "free" but adsorbed at the surface of the catalyst) or a mechanism in which both aryl cations and radicals are participating may be operative (5). In the uncatalyzed decomposition, the absence of a marked substituent effect is perplexing if the reactions go through the formation of a phenyl cation intermediate. For example, the diazonium salt from *o*-aminobenzophenone gives a 65% yield of fluorenone, while cyclization of the corresponding 3′-nitro derivative gives a 33% yield of the mixed nitrofluorenones (6). This has been attributed (6) to the intermediacy of a highly reactive "hot" phenyl cation for, had an aryl radical been formed, the nitro group, it is argued, should have favored homolytic attack. On the other hand, one must assume that such a highly reactive cation is also selective to explain the ratio of angular to linear products formed in similar cyclizations onto a naphthalene ring (5). Unfortunately, no kinetic data are available to date on the effect of substituents upon the *rates of the cyclization step*, and most of the conclusions drawn have been based upon yields of products. DeTar and Relyea (6) have measured the effect of substituents upon the relative yields of cyclized products and phenols formed in the fluorenone synthesis. According to the heterolytic mechanism the aromatic nucleus and water would compete for the aryl cation, and the presence of a nitro substituent, which decreases considerably the nucleophilicity of the aromatic nucleus, should lead to a large increase in phenol formation relative to cyclization. Though such an effect was actually observed its magnitude was very small. Thus, with (I; X = CO, R = H) the ratio of fluorenone to phenol was 1.85, while with (I; X = CO, R = *m*-NO_2) this ratio was 0.5. This may be compared with the decrease by one nitro group of the reactivity of benzene towards nitration of the order of 10^6 (7), and with the fact that whereas the isopropyl cation is very reactive and non-discriminating in its attack upon toluene (8), nitrobenzene may be used as a solvent in Friedel–Crafts alkylations. The kinetics of the thermal decomposition of (I; X = CO) in aqueous acid solution have established that the rate-determining step is the S_N1 decomposition of the diazonium salt and that the substituent R has a small, predictable effect upon this step (6). But, contrary to what was implied (6), no information was available from these studies concerning the rates of cyclization of the intermediates once they are formed.

In the present study, two approaches were used to attempt to distinguish between a homolytic and a heterolytic mechanism for the cyclization. In the first approach, it was hoped to take advantage of the fact that the pyridine (and even more so the pyridinium) nucleus is highly resistant to electrophilic attack e.g. the Friedel–Crafts reaction does not take place with pyridine; the substitution of a $=N^+H-$ group for a ring $=CH-$ in benzene decreases the reactivity towards hydrogen exchange by a factor of ca. 10^{-18} (9). The copper-catalyzed decomposition of the diazonium salt of 2-amino-*N*-methyl-*N*-3′-pyridylaniline gave a mixture of carbolines (72%) while the thermal decomposition yielded 47% of cyclized products (10). The total yield of cyclized products in the copper-catalyzed reaction was comparable to that obtained (78%) (11) when *N*-(3-amino-2-pyridyl)-*N*-methylaniline was ring-closed to the α-carboline, i.e. a similar cyclization (with similar internuclear separation (12)) but onto a benzene ring. This showed that the pyridine ring in the above case was not deactivated towards nuclear attack and that the attacking species was probably a radical, bound in some way with the copper catalyst. The extent of attack upon the pyridine ring in the uncatalyzed thermal decomposition

was surprisingly high for a reaction involving a cationic intermediate. This *might* be accounted for by an activation of the pyridine nucleus by the 3-amino substituent. The argument is weakened by the fact that a positively charged aryl residue (produced in the S_N1 decomposition) attached to the 3-amino group would reduce considerably the latter's electron-donating capacity to the pyridine ring. In addition, in the acid medium used the pyridine ring would undoubtedly be protonated and be even less susceptible to electrophilic attack. To eliminate this possible source of ambiguity, however, the cyclization under a variety of conditions of the diazonium salt from 3-(*o*-aminobenzoyl)pyridine (III) was studied. Here an electron-attracting carbonyl group is present at C_3 rendering the pyridine ring even less susceptible than before to electrophilic attack.

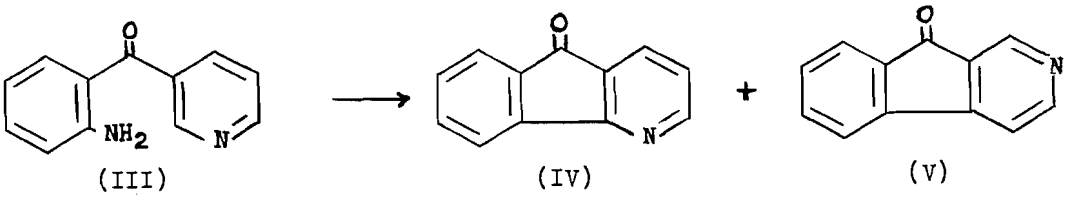

The reaction of 3-pyridyllithium with *o*-nitrobenzaldehyde at −70° gave the expected alcohol (VIII) in 45–55% yield, but since the latter exhibited a marked tendency to undergo aerial oxidation it was not purified but was oxidized directly to the ketone (IX). The results of the cyclization studies are summarized in Table I. The azafluorenones (IV)

and (V) were known compounds as was (VII). The structure of the phenol (VI) was confirmed by its physical and chemical properties and by its analysis and infrared spectrum.

The second approach attempted to gain a quantitative measure of the effects of substituents upon the actual *rate* of cyclization. Since the rate-determining step in these reactions is the S_N1 elimination of nitrogen, straightforward kinetic runs would not provide the information needed (13) and a "competitive-like" technique was used to

Can. J. Chem. Downloaded from www.nrcresearchpress.com by 210.87.254.40 on 09/05/12
For personal use only.

TABLE I

Decomposition of diazotized 3-(2′-aminobenzoyl)pyridine

Method of decomp.	Reaction temp. (°C)	Reaction time (h)	% yield of products: 4-Aza-fluorenone	2-Aza-fluorenone	3-Benzoyl-pyridine	Phenol*
Thermal (aq. acid)	80	2	3.5	2.9	0	67
Ultraviolet light	30	1	36.8	26.2	0	0
Gattermann copper	4	20 min	30.3	19.5	13.0	10
Silver powder	4, then r.t.†	48	2.2	1.6	11.1	—
Iron filings	4, then r.t.†	42	4.8	2.5	22	—
Zinc dust	4	6	16.3	9.3	15.4	—
Thermal (aq. NaOH)	40	4	9.4	4.0	3.2	0

*A dash indicates that the phenol was not estimated.
†r.t. = room temperature.

obtain semiquantitative estimates of relative rates of cyclization. For two consecutive first order reactions of the type

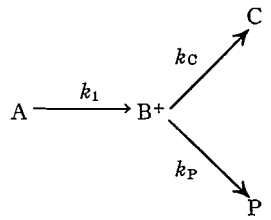

in which the formation of the carbonium ion B^+ is rate-determining it can be shown that

$$[1] \qquad \frac{k_{CS}}{k_{CH}} = \frac{C_S}{P_S} \cdot \frac{P_H}{C_H} \cdot \frac{k_{PS}}{k_{PH}},$$

where k_{CH} and k_{CS} are the rate constants for the cyclization of the intermediate carbonium ion onto unsubstituted and substituted aryl rings, respectively, k_{PH} and k_{PS} are the corresponding rate constants for the formation of the two phenols, C_H, C_S, P_H, and P_S are the concentrations of unsubstituted cyclized product, substituted cyclized product, unsubstituted phenol, and substituted phenol at any moment during the reaction (provided cyclized product and phenol are the only products formed and that the overall yields are almost quantitative). Whereas the concentrations of all the products can be determined at any time during the reaction the relative rates of cyclization k_{CS}/k_{CH} can only be obtained as a function of the relative rates of phenol formation k_{PS}/k_{PH}. While a substituent R in (I) has a small effect upon k_1 (6) its distance from the cationic site is relatively large and it should, therefore, not exert any appreciable inductive effect (and no direct mesomeric effect) upon it. Consequently, once the cation is formed in dilute aqueous acid solution, R should have a negligeable effect upon the hydroxylation reaction i.e. k_{PS}/k_{PH} may be assumed to be approximately one.

Preliminary attempts to effect the simultaneous decomposition of equimolar mixtures of the diazonium sulfates of 2-aminobenzophenone and 3-(*o*-aminobenzoyl)pyridine (III) followed by analysis of the reaction products failed. To isolate the azafluorenones from the acidic reaction medium it was necessary to basify it with ammonia (after chilling it); this led to the precipitation of undecomposed diazonium hydroxides which were extracted by chloroform or benzene together with the required products. When an excess

Can. J. Chem. Downloaded from www.nrcresearchpress.com by 210.87.254.40 on 09/05/12
For personal use only.

of cold alkaline β-naphthol solution was added to the cooled aliquot from the reaction mixture to destroy unreacted diazonium salts azo-dyes were formed immediately; but when the reaction mixture was extracted and the extract subjected to gas-chromatographic analysis none of the expected cyclized products could be detected. It would appear as though either the β-naphthol or the dyes are binding the products in such a way as to prevent their detection. These experiments were not pursued further. Instead, the "competitive" cyclization of mixtures of diazotized 2-aminobenzophenone and 2-amino-3′-nitrobenzophenone was studied since these compounds give almost quantitative yields of mixtures of cyclized products and phenols (6), and the gas-chromatographic analysis of the reaction products presented no difficulties.

EXPERIMENTAL

3-(2′-Nitrobenzoyl)pyridine

A solution of 3-bromopyridine (15 g) in dry ether (45 ml) was added under a nitrogen atmosphere over a period of 15 min to a stirred solution of *n*-butyllithium (7.6 g) in hexane (50 ml) and anhydrous ether (50 ml) at −70 to −80°. The mixture was stirred at that temperature for a further 15 min and then *o*-nitrobenzaldehyde (14.5 g) in dry ether (100 ml) was added dropwise during 25 min. Stirring was continued at −70° for 2 h and then at room temperature for a further 1¼ h. The light brown reaction mixture was poured into ice and water (2 l) saturated with salt, the ether layer was separated, and the aqueous phase was extracted with ether (6 × 200 ml). The combined extracts were evaporated and the residue steam distilled. The residue was salted out and extracted with ether (6 × 50 ml) and the combined extracts were dried (Na_2SO_4) and evaporated to yield crude 2′-nitrophenyl-3-pyridylmethanol (11 g, 48%) as a viscous brown oil. Infrared spectrum (liquid film): 3 180 (m)(br), 1 590(w), 1 535(s), 1 487(w), 1 435(m), 1 355(s), 1 030(m), 845(w), 785(m), and 705 cm^{-1}(s).

A solution of 2′-nitrophenyl-3-pyridylmethanol (11 g) in pyridine (80 ml) was added with shaking to a suspension of chromium trioxide (9 g) in pyridine (85 ml) and the mixture allowed to stand at room temperature overnight. It was then poured into water (1 l) saturated with salt. The black mixture was extracted with ether (6 × 100 ml), the ether evaporated, and the residue steam distilled until free of pyridine. The residue was salted out and extracted with ether (6 × 50 ml) and the extracts dried (Na_2SO_4) and evaporated to yield a viscous brown oil (7.8 g, 86%). A portion (1.2 g) of this product was chromatographed on alumina (50 g). A mixture of benzene – light petroleum (b.p. 36–48°) (2:1 v/v) eluted *3-(2′-nitrobenzoyl)pyridine* (0.612 g) as yellow crystals, m.p. 56–58°, which on recrystallization from aqueous ethanol had m.p. 60–60.5°. (Found: C, 63.52; H, 3.84. $C_{12}H_{18}N_2O_3$ requires C, 63.16; H, 3.53.) Infrared spectrum (Nujol mull): 1 670(s), 1 525(s), 1 420(m), 1 357(s), 1 290(s), 930 (m), 785(m), 722(m), and 693 cm^{-1}(w).

3-(2′-Aminobenzoyl)pyridine

3-(2′-Nitrobenzoyl)pyridine (7.8 g) was dissolved in ethanol (70 ml), 10% palladium–charcoal (1 g) was added, and the suspension boiled under reflux. Hydrazine hydrate (99%, 15 ml) was added and boiling continued for 1 h. The mixture was filtered and evaporated, eventually under reduced pressure. The residual viscous orange oil (7.2 g) was dissolved in benzene and chromatographed on a column of alumina (350 g). Benzene eluted *3-(2′-aminobenzoyl)pyridine* (2.5 g) as an orange oil which crystallized. This product proved difficult to purify but recrystallization from ethanol eventually gave analytically pure amine, m.p. 247–249°. (Found: C, 72.73; H, 5.06. $C_{12}H_{10}N_2O$ requires C, 72.71; H, 5.09.)

2- and 4-Azafluorenone

2-(3′-Aminobenzoyl)pyridine (1.3 g) in sulfuric acid (4 ml) and water (50 ml) was diazotized at 4° with sodium nitrite (0.52 g) in water (4 ml) with vigorous stirring. The solution was stirred for 15 min and the excess nitrous acid destroyed by the addition of solid urea. Gattermann copper (1 g) was added and stirring continued for 1 h. The mixture was filtered and the filtrate basified with concentrated ammonia solution and extracted with chloroform (6 × 40 ml). The organic layer was extracted with 5% aqueous sodium hydroxide (7 × 40 ml), dried (Na_2SO_4), and evaporated to yield a nearly black tar (0.96 g) which crystallized on cooling. This was dissolved in benzene and chromatographed on a column of alumina (100 g). Elution with a mixture of benzene and light petroleum (b.p. 36–48°) (2:1) yielded 4-azafluorenone (0.32 g, 27%) as a yellow solid, m.p. 140–141° from ethanol. The melting point was undepressed on admixture with an authentic sample (14). Kruber (15) reports m.p. 139–140° for this compound. Elution with benzene gave 3-benzoylpyridine (0.095 g, 8%) as an almost colorless oil, the retention time on gas chromatography and the infrared spectrum of which were identical with those of an authentic sample. Infrared spectrum (liquid film): 1 660(s), 1 585(s), 1 450(m), 1 418(m), 1 315(m), 1 280(s), 1 195(w), 1 055(w), 1 025(m), 935(m), 920(s), 780(m), 710(s), and 648 cm^{-1}(m). Further elution with benzene gave 2-azafluorenone (0.224

Can. J. Chem. Downloaded from www.nrcresearchpress.com by 210.87.254.40 on 09/05/12
For personal use only.

g, 20%) as a yellow solid, m.p. 155–158°. Sublimation at 110° and 0.3 mm and recrystallization from ethanol raised the melting point to 158.5°. Courts and Petrow give m.p. 156–158° for this compound (16). (Found: C, 79.49; H, 4.11. Calcd. for $C_{12}H_7NO_2$: C, 79.55, H, 3.89.)

Samples of the above three compounds were used to obtain calibration curves plotting weight of compound vs. area under peak to permit the quantitative analysis of mixtures using gas chromatography. A 2 ft × ¼ in. 15% Apiezon N on Fluoropak column operated at 200° and at a helium inlet pressure of 50 p.s.i. was used for the analysis.

Decomposition of Diazotized 3-(2′-Aminobenzoyl)pyridine

3-(2′-Aminobenzoyl)pyridine (0.100 g) in water (10 ml) containing sulfuric acid (0.4 ml) was cooled to 5° and diazotized with sodium nitrite (0.040 g) in water (2 ml). After 10 min the excess nitrous acid was decomposed with urea (starch–iodide paper) and the solution decomposed by one of the methods described below. Unless otherwise specified, the mixture was basified with concentrated ammonium hydroxide (2 ml) at the end of the reaction and extracted with chloroform (3 × 15 ml); the chloroform solution was extracted with 10% aqueous sodium hydroxide (3 × 15 ml), dried (Na_2SO_4), and evaporated down to a small volume. This was transferred to a 1 ml volumetric tube and made up to 1 ml with chloroform. Accurately measured aliquots were then analyzed by gas chromatography.

(i) Thermal Decomposition at 80°

The above diazotized solution was stirred at 80 ± 1° for 2 h. The average yields of cyclized products on two runs were: 4-azafluorenone, 3.5%; 2-azafluorenone, 2.85%. No 3-benzoylpyridine could be detected. The basic aqueous phase was brought to pH 7 with 50% aqueous acetic acid and the turbid solution extracted with chloroform; the extracts were dried (Na_2SO_4) and evaporated to give *3-(2′-hydroxybenzoyl) pyridine* as a pale-yellow oil which crystallized. On recrystallization from light petroleum it had m.p. 63–64°. (Found: C, 72.36; H, 4.63. $C_{10}H_9NO_2$ requires: C, 72.35; H, 4.55.) Infrared spectrum (CCl_4 solution): 3 100(w)(br), 3 050(w), 1 630(s), 1 487(m), 1 450(m), 1 416(m), 1 337(s), 1 310(s), 1 146(m), and 930 cm^{-1}(m). The average yield obtained in two runs was 67%.

(ii) With Ultraviolet Light at 30°

The solution of diazotized amine was placed in a Vitreosil beaker which was cooled by a current of air. The stirred solution was illuminated with a Hanovia type 30 600 ultraviolet lamp with a violet filter and the temperature maintained at 30°. Brisk effervescence set in after 10 min but began to subside after another 10 min. Stirring was continued for 1 h after which the solution was worked up and analyzed gas chromatographically as described above. Only two peaks, corresponding to 4- and 2-azafluorenone, were detected. The average yields obtained were: 4-azafluorenone, 36.8%; 2-azafluorenone, 26.2%. No phenol could be isolated from the aqueous phase.

(iii) With Gattermann Copper

The stirred diazonium salt solution (from 0.92 g of amine) was treated with Gattermann copper at 4°. Stirring was continued for 1 h and the suspension filtered and worked up. The average yields obtained were as follows: 4-azafluorenone, 30.3%; 2-azafluorenone, 19.5%; 3-benzoylpyridine, 13.0%; 2-(3′-hydroxybenzoyl)pyridine, 10%.

(iv) With Precipitated Silver

Freshly precipitated silver (0.10 g) was added to the stirred diazonium salt solution (from 0.092 g of amine) at 4° and stirring continued at this temperature for 6 h. As the decomposition was still incomplete the mixture was stirred at room temperature for 48 h, worked up, and analyzed. The average yields were: 4-azafluorenone, 2.2%; 2-azafluorenone, 1.6%; 3-benzoylpyridine, 1.1%. A large peak with a retention time of 21 min was also observed in the gas chromatogram and may be due to the dimer, but was not characterized further. Six minor peaks with retention times between 1 and 6 min were also detected.

(v) With Iron Filings

The diazonium salt solution was treated with iron filings (0.10 g, previously washed with glacial acetic acid, water, alcohol, and ether) at 4°, stirring continued at that temperature for 6 h and then at room temperature for 42 h. The solution obtained after filtration of the iron was deep red. The average yields were: 4-azafluorenone, 4.8%; 2-azafluorenone, 2.5%; 3-benzoylpyridine, 22%. Two other peaks with retention times of 1 and 19.5 min, respectively, were also observed in the chromatogram but were not identified.

(vi) With Zinc Dust

The use of reagent grade zinc dust (0.10 g) at 4° for 6 h gave 4-azafluorenone (16.3%), 2-azafluorenone (9.3%), and 3-benzoylpyridine (15.4%).

(vii) With Alkali at 40°

20% Aqueous sodium hydroxide (4 ml) was added to the diazotized amine solution, and the mixture stirred for 4 h with the temperature maintained at 40°. The mixture was extracted with chloroform and worked up to give 4-azafluorenone (9.4%), 2-azafluorenone (4.0%), and 3-benzoylpyridine (3.2%). Another peak with retention time 21 min (cf. decomposition with silver) was also observed but no phenol could be isolated from the basic solution.

Can. J. Chem. Downloaded from www.nrcresearchpress.com by 210.87.254.40 on 09/05/12
For personal use only.

Thermal Decomposition of Aqueous Acid Solutions of Equimolar Mixtures of the Diazonium Sulfates of 2-Aminobenzophenone and 2-Amino-3′-nitrobenzophenone

The preparations of 2- and 4-nitrofluorenones and of 2-hydroxy-3′-nitrobenzophenone have already been described (6). Standard solutions of these compounds as well as of fluorenone and 2-hydroxybenzophenone were prepared and calibration curves of weight of compound vs. area under chromatogram peak obtained independently for each one of them using a 2 ft × 1/4in. 15 % Apiezon N on Fluoropak column operated at 200° and a helium inlet pressure of 40 p.s.i. Under such conditions, 2- and 4-nitrofluorenone were not resolved from each other and the mixture of these two isomers, as obtained from a model Pschorr cyclization using 2-amino-3′-nitrobenzophenone, was used in preparing the calibration curve. The retention times were as follows: 2-hydroxybenzophenone, 7.5 min; fluorenone, 10 min; 2-hydroxy-3′-nitrobenzophenone, 33 min; 2- and 4-nitrofluorenone, 53 min.

A mixture of 2-aminobenzophenone (0.049 g) and 2-amino-3′-nitrobenzophenone (0.061 g) was placed in a 100 ml tall lipless beaker and dissolved in concentrated sulfuric acid (2 ml) and water (12 ml). The solution was cooled to 5° and solid sodium nitrite (0.040 g) slowly added with stirring while the temperature was maintained at 5°. As soon as the solution gave a positive starch–iodide test no more nitrite was added, the solution was stirred for a further 10 min and the excess nitrous acid decomposed by the addition of urea. The beaker was then transferred quickly to a thermostated water bath kept at 45° and vigorous stirring maintained for the required length of time (5, 10, or 18 min); the beaker and contents were then quickly chilled to 0° and the mixture transferred to a cold separatory funnel and quickly extracted with cold chloroform (2 × 15 ml). The extracts were dried (Na_2SO_4) and evaporated to a small volume (ca. 50 μl). The whole of the solution was then injected as quantitatively as possible into the gas chromatograph and the relative molar ratios of the products determined.

DISCUSSION

The relatively high proportion of cyclized product resulting from attack onto a pyridinium nucleus in the copper-catalyzed cyclization of the diazonium salt of (III), as well as the amount (13%) of deaminated product formed, suggests very strongly the intervention of a homolytic pathway under these conditions. It has been suggested (5) that the copper-catalyzed cyclization involves the formation of both aryl radicals and cations at the surface of the metal. This suggestion was based on a comparison of the ratios of angular to linear benzofluorenones formed on cyclization of the diazonium salt of 2-(*o*-aminobenzoyl)naphthalene under various reaction conditions. The thermal decomposition (presumed to proceed via a cationic intermediate) gave an angular:linear ratio of 2.2, the copper-catalyzed decomposition *and the thermal decomposition of the alkaline solution* gave a ratio of 4.4, while the alkaline decomposition in the presence of benzene and the decomposition of the *N*-nitrosoacylarylamine gave a ratio of 9.0–10. The high ratios in the last cases may well be due, however, to steric hindrance to the formation of the σ-complex with benzene on the α-side but not on the β-side: this could lead to one conformation cyclizing at the α-position of the naphthalene ring while the other could either cyclize at the β-position or react with benzene to give the phenylated product. This last alternative is not available when the alkaline decomposition is carried out in the absence of benzene. A similar argument may be used to explain the results obtained in the decomposition of benzophenone *o*-diazohydroxide in benzene (17). A good deal of evidence has accumulated in support of a radical mechanism for the alkaline decomposition of diazonium salts (1, 6). It must also be noted that the steric requirements of the copper-catalyzed reactions—where the reacting species is undoubtedly close to the surface of the metal—and those carried out in the absence of metal catalysts could well be different so that comparisons of examples of reactions in which one of the alternative modes of reaction involves steric crowding have to be viewed with caution. The formation of 10% of the phenol in our case may be a measure of the extent that the reaction goes via a cationic intermediate; however, a radical pathway for the formation of this product, though less likely, is not eliminated.

The photochemical decomposition of the acidic diazonium salt solution gave rise to

Can. J. Chem. Downloaded from www.nrcresearchpress.com by 210.87.254.40 on 09/05/12
For personal use only.

Can. J. Chem. Downloaded from www.nrcresearchpress.com by 210.87.254.40 on 09/05/12
For personal use only.

the highest yield of cyclized product, the 4- to 2-azafluorenone ratio being 1.4 as compared with 1.55 in the copper-catalyzed reaction. Neither 3-benzoylpyridine nor the phenol could be detected among the products under these conditions. The relatively high yield is consistent with a homolytic pathway in this case. The photo-catalyzed Pschorr-type reactions have also been investigated by Huisgen and Zahler (18). While these authors were able to obtain reasonably good yields of fluorenone and *N*-methylcarbazoles from the corresponding diazonium salts, the yields of dibenzofuran and of benzofluorenes starting with the appropriate amines were very poor. Decomposition of the aqueous acid solution of diazotized *o*-aminodiphenylether gave a 44% yield of the phenol and only a 1% yield of cyclized product. The conclusion reached by Boudreaux and Boulet (19), based on magnetic susceptibility measurements, that aryl radicals are formed by the photolysis of solutions of diazonium salts, has been questioned (20). It has been shown that when an aqueous solution of *p*-dimethylaminobenzenediazonium chloride at pH 5 is photolyzed in the presence of air or oxygen the *p*-dimethylaminophenoxy radical is formed and it has been suggested that the latter probably arises from a secondary reaction of the photolysis product, namely the phenol (20). The results do not necessarily extrapolate to pH values below 5 such as were used in the present work in which no phenol was apparently formed.

No phenol was obtained in the thermal decomposition of the diazonium salt of (III) under alkaline conditions and the overall yield of cyclized products was low (13.4%), probably due to the formation of "diazo-tars". The results are consistent with the intermediacy of radical but not of cationic intermediates. Silver, iron, and zinc metals were much less effective catalysts than was copper in the cyclization reaction and azo and dimeric products appeared to be formed though this was not confirmed. The formation of azo-compounds and of dimers has already been observed in Pschorr-type reactions (12). The main product obtained on thermal decomposition of the diazonium salt in aqueous acid solution was the phenol. In addition, however, a 6.4% yield of cyclized products was obtained. This result would be very surprising for a substitution involving an aryl cation, since the nucleophilicity of a pyridinium nucleus towards protons is about 10^{-18} smaller than that of a benzene ring and a 3-carbonyl group would be expected to decrease this nucleophilicity further still. Thus, in spite of the large increase in reactivity due to the intramolecular character of the reaction and, even assuming the formation of a "hot", unselective aryl cation, the pyridinium nucleus would hardly be expected to compete effectively with the surrounding water molecules for the positive center. In any event, the intermediate formed by the thermal decomposition of diazonium salts in organic solvents has been shown to be highly reactive *but selective* (21). It seems more probable, therefore, that most of the cyclized product results from the intervention of some type of homolytic mechanism. This is discussed further below.

The results of the "competitive" thermal decompositions of diazotized 2-aminobenzophenone and 2-amino-3′-nitrobenzophenone in aqueous acid solution are given in Table II. On the assumption that $k_{PS} = k_{PH}$, substitution of the experimentally found values for C_S/P_S and P_H/C_H into eq. [1] gives $k_{CS}/k_{CH} = 0.45$. Thus, if the rates of hydroxylation of the two reactive intermediates are presumed equal, cyclization onto the nitro-substituted benzene ring takes place only half as fast as that onto a ring not bearing the highly deactivating (towards electrophilic attack) nitro-group. If, on the other hand, the nitro-group has any effect upon the cationic center it should, if anything, slightly enhance the hydroxylation process by withdrawing electrons inductively. A twofold enhancement of the rate of hydroxylation in the nitro-compound would result in the

TABLE II

Relative yields of products from the simultaneous decomposition of diazotized 2-aminobenzophenone and 2-amino-3′-nitrobenzophenone

Reaction time (min)	Molar ratio of fluorenone to 2-hydroxybenzophenone	Molar ratio of nitrofluorenones to 2-hydroxy-3′-nitrobenzophenone
5	2.24	1.08
10	2.54	0.91
10	2.44	1.18
10	2.82	1.34
10	2.72	1.06
18	2.66	1.35
Average	2.58	1.15

relative rates of cyclization being about equal on the basis of our results. The above value for k_{CS}/k_{CH} is, therefore, a minimum one.

While there is no reason to doubt that the rate-determining step in the thermal decomposition is the S_N1 heterolysis with elimination of nitrogen, the above results are difficult to reconcile with the properties expected of a cationic intermediate, even of a "hot" one. A possible solution to this dilemma has been suggested on the basis of the results obtained in the thermal decomposition of dry benzenediazonium borofluoride in organic solvents (21). From both isomer ratio and total rate ratio as well as electron spin resonance (e.s.r.) studies it was proposed, following Taft (22), that the aryl cation initially formed isomerized to the diradical cation (X) and that it is this that attacks the

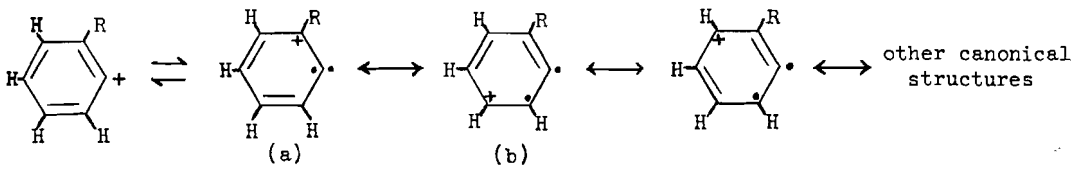

(X)

adjacent aromatic nucleus giving rise to cyclized product. The phenol could then arise from the aryl cation form. The diradical cation (X) (canonical structure (*a*) would give the species some of the properties of a triplet carbene) would be expected to behave as a strongly electrophilic free radical in substitution reactions, and this would account for both the low yield of azafluorenones in the cyclization of 3-(2′-aminobenzoyl)pyridine and for the slight deactivation observed in the cyclizations onto a nitro-substituted nucleus. While the pyridine ring is slightly more reactive than is benzene towards phenyl radicals, $^{C_5H_5N}_{C_6H_6}K$ is only 0.47 when the attacking reagent is the more electrophilic *o*-nitrophenyl radical (23) and this is even more marked when nitrobenzene is the substrate (24). Species (X) would be even more electrophilic than the nitrophenyl radical, but this should be compensated somewhat by the intramolecular character of the reactions. The participation of such an intermediate in the decomposition might rationalize many observations that have been made on the Pschorr reaction over the years. For example, the demethylation and deamination observed in suitable cases (25) may well be consistent with a hydrogen abstraction by the triplet carbene form (X*a*).

Can. J. Chem. Downloaded from www.nrcresearchpress.com by 210.87.254.40 on 09/05/12
For personal use only.

ACKNOWLEDGMENTS

This work was carried out during the tenure (1961–1962) of a C.I.L. Fellowship (by G. T.) and was supported generously by a grant from the National Research Council.

REFERENCES

1. G. H. WILLIAMS. Homolytic aromatic substitution. Pergamon Press, Oxford. 1960. p. 80.
2. D. F. DETAR. Org. Reactions, **9**, 409 (1957).
3. W. A. WATERS. J. Chem. Soc. 864 (1939). R. O. C. NORMAN and W. A. WATERS. J. Chem. Soc. 167 (1958). B. A. MARSHALL and W. A. WATERS. J. Chem. Soc. 381 (1959). P. S. JOHNSON and W. A. WATERS. J. Chem. Soc. 4652 (1962).
4. E. A. MOELWYN-HUGHES and P. JOHNSON. Trans. Faraday Soc. **36**, 948 (1940). D. F. DETAR and A. R. BALLENTINE. J. Am. Chem. Soc. **78**, 3916 (1956). D. F. DETAR and S. KWONG. J. Am. Chem. Soc. **78**, 3921 (1956).
5. R. HUISGEN and W. D. ZAHLER. Ber. **96**, 736 (1963).
6. D. F. DETAR and D. I. RELYEA. J. Am. Chem. Soc. **76**, 1680 (1954).
7. P. B. D. DE LA MARE and J. H. RIDD. Aromatic substitution. Nitration and halogenation. Butterworths Scientific Publications, London. 1959. p. 80.
8. H. C. BROWN and K. L. NELSON. J. Am. Chem. Soc. **75**, 6292 (1953).
9. A. R. KATRITZKY and B. J. RIDGEWELL. J. Chem. Soc. 3743 (1963).
10. R. A. ABRAMOVITCH. Can. J. Chem. **38**, 2273 (1960).
11. R. A. ABRAMOVITCH, D. H. HEY, and R. D. MULLEY. J. Chem. Soc. 4263 (1954).
12. D. H. HEY and R. D. MULLEY. J. Chem. Soc. 2276 (1952).
13. G. TERTZAKIAN. Ph.D. Thesis, University of Saskatchewan. 1962.
14. R. A. ABRAMOVITCH, C. S. GIAM, and A. D. NOTATION. Can. J. Chem. **38**, 761 (1960).
15. O. KRUBER. Ber. **82**, 199 (1949).
16. A. COURTS and V. PETROW. J. Chem. Soc. 1 (1952).
17. D. F. DETAR and S. V. SAGMANLI. J. Am. Chem. Soc. **72**, 965 (1950).
18. R. HUISGEN and W. D. ZAHLER. Chem. Ber. **96**, 747 (1963).
19. E. A. BOUDREAUX and E. BOULET. J. Am. Chem. Soc. **80**, 1588 (1958).
20. P. J. ZANDSTRA and E. M. EVLETH. J. Am. Chem. Soc. **86**, 2664 (1964).
21. R. A. ABRAMOVITCH, W. A. HYMERS, J. B. RAJAN, and R. WILSON. Tetrahedron Letters, 1507 (1963).
22. R. W. TAFT. J. Am. Chem. Soc. **83**, 3350 (1961).
23. R. A. ABRAMOVITCH and J. G. SAHA. J. Chem. Soc. 2175 (1964).
24. G. H. WILLIAMS. Chem. Ind. London, 1285 (1961).
25. T. COHEN, A. H. DINWOODIE, and L. D. MCKEEVER. J. Org. Chem. **27**, 3385 (1962).

Can. J. Chem. Downloaded from www.nrcresearchpress.com by 210.87.254.40 on 09/05/12
For personal use only.

Can. J. Chem. Downloaded from www.nrcresearchpress.com by 210.87.254.40 on 09/05/12
For personal use only.

AN EXOCELLULAR MANNAN, ALTERNATELY LINKED 1,3-β AND 1,4-β FROM RHODOTORULA GLUTINIS[1]

P. A. J. GORIN, K. HORITSU,[2] AND J. F. T. SPENCER
National Research Council of Canada, Prairie Regional Laboratory, Saskatoon, Saskatchewan
Received October 15, 1964

ABSTRACT

The yeast, *Rhodotorula glutinis*, gives an exocellular mannan containing 1,3-β- and 1,4-β-D-mannopyranose residues arranged in a straight chain of at least 90 units. Consecutive 1,3-β links are absent and although consecutive 1,4-β links may exist they are present at most in only a very small proportion. The 1,3-β- and 1,4-β-D-mannopyranose residues are therefore arranged alternately in the chain.

Mannans from *R. mucilaginosa*, *R. minuta*, and an unidentified *Rhodotorula* spp. 62-506 appear to have similar structures.

Rhodotorula glutinis, when grown on a 5% glucose – yeast nitrogen base medium, produced exocellular polysaccharides consisting mainly of mannan, in yields of up to 2.2 g per liter. Initially, the crude polysaccharide was oxidized with sodium periodate and the product then reduced with sodium borohydride. Hydrolysis gave mannose, erythritol, and glycerol, suggesting 1,3 and 1,4 links in the polysaccharide. It differed, therefore, from the mannans containing 1,2-α- and 1,6-α-pyranosyl links (with 1,3-α links in some cases) associated with certain yeasts (1, 2, 3), fungi (4), and bacteria (5, 6).

Hydrolysis of the crude polysaccharide gave another hexose and a methyl pentose in addition to mannose. Purification of the mannan was effected via its water-insoluble copper complex formed with Fehling's solution. The pure mannan had a specific rotation of −78° indicating β-linkages and on periodate oxidation it consumed oxidant rapidly, eventually after 2 days consuming 0.61 mole with the release of 0.07 mole of acid. These data suggest approximately equal amounts of 1,3-β and 1,4-β links in a straight chain structure, perhaps similar to the polysaccharide isolated by Smith and co-workers (7) from the uredospores of wheat stem rust. The latter polymer originally described as a glucomannan was fractionated later to yield a mannan (8).

Further structural data were obtained by methylation of the mannan. The *O*-methyl mannoses formed on acid hydrolysis of the methylated mannan were converted to their methyl glycosides which were separated by gas phase chromatography (g.l.c.). Methyl 2,3,6- and 2,4,6-tri-*O*-methyl mannosides were identified and occurred in almost equal amounts. These compounds had higher retention times than the 2,3,4- and 3,4,6-isomers. Some dimethyl methyl mannoside, probably formed because of undermethylation or demethylation (9), and methyl 2,3,4,6-tetra-*O*-methyl mannoside (1.1% of total signal) were also detected. The low proportion of nonreducing end groups should arise (barring cyclic polysaccharide structures) either from a slightly branched polymer or from the end unit of a straight chain polysaccharide containing approximately 90 mannose residues.

The sequence of 1,3 and 1,4 links in the mannan was elucidated by the Smith technique (10). The periodate-oxidized mannan was reduced with sodium borohydride and the modified polymer partially hydrolyzed with acid. Paper chromatography showed the presence

[1]*Issued as N.R.C. No. 8312.*
[2]*National Research Council of Canada Postdoctorate Fellow, 1963–1964.*

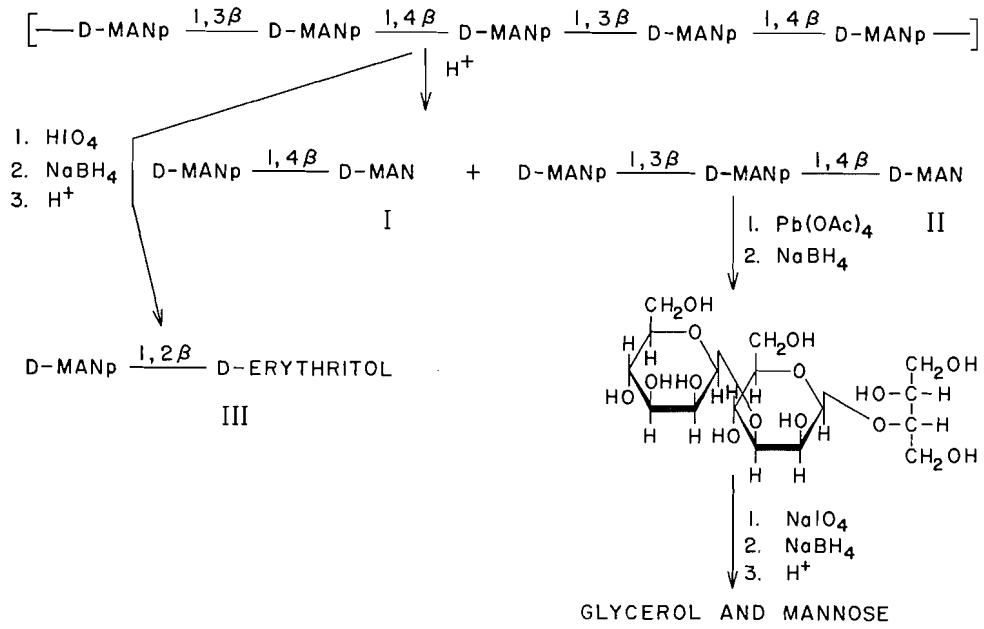

FIG. 1. Degradation products of *R. glutinis* mannan.

of 2-*O*-β-D-mannopyranosyl-D-erythritol (III), which should arise from D-mannopyranosyl residues alternately linked 1,3-β and 1,4-β. The absence of fragments of higher molecular weight negated the possibility of two or more consecutive 1,3 links. Periodate and methylation experiments pointed to approximately equal proportions of 1,3 and 1,4 linkages in the mannan. Exact determination of the amounts of 1,3 and 1,4 linkages was precluded by possible periodate overoxidation and lack of accurate conversion factors for the methylated methyl mannosides in the g.l.c. experiment. Evidence against the possibility of two or more consecutive 4-*O*-linked mannosyl units in the mannan was obtained by examination of the mannotriose fraction formed on partial hydrolysis.

A series of oligosaccharides from the mannan was isolated after treatment with *N* hydrochloric acid at 75 °C for 4 h. The disaccharide fraction, isolated chromatographically, consumed 1.76 moles of lead tetraacetate rapidly (11) and therefore contained at least 76% of 4-*O*-β-D-mannopyranosyl-D-mannose (I). This disaccharide was isolable as crystals in 67% yield. Since the mannosidic linkage attached to a 4-position is thus more stable than that attached to the 3-position, the presence of two or more consecutive 1,4 links should be reflected by occurrence of appreciable amounts of *O*-β-D-mannopyranosyl-(1 → 4)-*O*-β-D-mannopyranosyl-(1 → 4)-D-mannose in the trisaccharide fraction. Lead tetraacetate oxidation kinetics of this fraction showed a high proportion of 4-*O*-linked reducing end and reduction of the oxidation product gave an amorphous mannobiosyl erythritol fraction which consumed 2.8 moles of periodate with concomitant formation of 1.0 moles of acid in accord with a predominating O-β-D-mannopyranosyl-(1 → 3)-*O*-β-D-mannopyranosyl-(1 → 2)-D-erythritol structure (IV). This material arose from *O*-β-D-mannopyranosyl-(1 → 3)-*O*-β-D-mannopyranosyl-(1 → 4)-D-mannose (II). The oxidation product after reduction with sodium borohydride followed by hydrolysis gave mannose and glycerol. The presence also of a barely detectable amount of erythritol

Can. J. Chem. Downloaded from www.nrcresearchpress.com by 210.87.254.40 on 09/05/12
For personal use only.

showed that only a very small proportion of consecutive 1,4 links could be present. Alternately, the erythritol could have arisen from a trace amount of *O*-β-D-mannopyranosyl-(1 → 4)-*O*-β-D-mannopyranosyl-(1 → 2)-D-arabitol. The mannan can therefore be regarded as having alternate 1,3-β and 1,4-β pyranose links.

TABLE I

Specific rotations and periodate oxidation characteristics of mannans

Parent organism	$[\alpha]_D^{25}$ in water	Molar uptake of sodium periodate after 5 h	23 h	48 h
R. glutinis	−78° (*c*, 0.6)	0.52	0.55 (0.07)*	0.61 (0.07)
R. mucilaginosa	−79° (*c*, 0.1)	0.54	0.54 (0.07)	0.60 (0.07)
R. minuta	−88° (*c*, 0.1)	0.53	0.54 (0.04)	0.58 (0.06)
62-506	−80° (*c*, 0.1)	0.54	0.56 (0.07)	0.62 (0.07)

*Figures in parentheses refer to acid production in moles/mole.

Other *Rhodotorula* spp. gave rise to similar mannans, although in lesser yield than *Rhodotorula glutinis*. Mannans from *R. minuta*, *R. mucilaginosa*, and an unnamed species designated 62-506 were purified via their copper complexes. The products and specific rotations close to −80° and their periodate oxidation characteristics were similar to those obtained on purified *R. glutinis* polysaccharide (Table I). Reduction of the oxidized polysaccharides, followed by hydrolysis yielded mannose, erythritol, and a trace of glycerol. These polymers also appear to be 1,3-β;1,4-β-mannans and are quite different from the main exocellular polysaccharides of the related *Cryptococcus* genus. Those arising exocellularly from *C. laurentii* (12) and the capsule of *C. neoformans* (13) consist of glucuronic acid, mannose, and xylose.

EXPERIMENTAL

Culture Methods

Cultures of *Rhodotorula glutinis*, *R. mucilaginosa*, *R. minuta*, and an as yet unclassified species (62-506) isolated from fish gut contents obtained in Northern California, were grown in shaken flasks or in stirred fermentors. The medium contained Wickerham's chemically defined yeast nitrogen base (Difco) (14) and 5% glucose (this medium does not contain mannan). The shaken cultures were grown in 500 ml Erlenmeyer flasks containing 100 ml medium and incubated either on a New Brunswick rotary shaker, eccentricity 1/2 in., at a speed of about 250 r.p.m. at 20 °C or on a Gump shaker, eccentricity 1 in., a speed of 230 r.p.m. at 24 °C. When stirred fermentors were used, they were 5 l New Brunswick glass jar type fermentors, operated at 400 r.p.m. at a temperature of 24 °C, with an air flow rate of about 1 l/min/fermentor, or, for larger batches, they were 30 l stainless steel fermentors similar in design to the New Brunswick equipment. The progress of the fermentation was followed by determining the increase in drainage time of the culture from a 10 ml pipette. When the maximum drainage time was reached, the cells were removed by centrifugation and the polysaccharides were precipitated from the supernatant by the addition of 2 volumes of ethanol. The product from *R. glutinis* contained C, 39.7; H, 6.5; N, 1.2; ash, 3.7, and gave mannose and traces of another hexose and a methyl pentose on hydrolysis.

The yields, per liter of medium, of mannan were as follows: *R. glutinis*, 2.2 g; *R. mucilaginosa*, 0.8 g; *R. minuta*, 0.3 g; 62-506, 0.7 g.

Purification of Polysaccharides

The mannan could be precipitated from solution by Fehling's solution as its copper complex, either directly from the fermentation liquor or subsequent to ethanol precipitation. In a typical experiment mannan from *R. glutinis* (3.5 g) was dissolved in water (500 ml) and Fehling's solution added (200 ml). The precipitate was filtered off and washed with water and methanol. The product (2.6 g) was then decomposed by gradual addition of *N* hydrochloric acid to a stirred aqueous suspension (150 ml). When dissolution was complete and the light-blue color eliminated by a slight excess of acid 4 volumes of methanol were added to the slightly acidic solution. Yield, 2.1 g.

A sample (100 mg) of purified mannan was hydrolyzed in *N* sulfuric acid (10 ml) at 100 °C. The specific rotation of the solution after 18 h was +15° (based on hexose) and on further heating this value remained

Can. J. Chem. Downloaded from www.nrcresearchpress.com by 210.87.254.40 on 09/05/12
For personal use only.

unchanged. After 42 h the solution was neutralized ($BaCO_3$), filtered, and evaporated. Crystallization from ethanol provided α-D-mannose (52 mg) with m.p. 129–131 °C, undepressed on admixture with an authentic specimen, and $[\alpha]_D$ +26° → +14° (constant value; *c*, 1.05 H_2O).

The specific rotations and periodate oxidation characteristics of four purified mannans are listed in Table I.

Reduction of periodate oxidation products from the four polysaccharides with sodium borohydride followed by acid hydrolysis for 2 h with *N* HCl at 100 °C yielded mannose, erythritol, and a small amount of glycerol.

Methylation of R. glutinis Mannan

Purified mannan (1.00 g) was methylated at room temperature with dimethyl sulfate and sodium hydroxide by the Haworth procedure (15). Destruction of reagent followed by neutralization gave an insoluble partially methylated mannan (0.86 g) with —OCH_3, 42.4%. The mother liquor was continuously extracted with chloroform and a further 0.23 g of methylated mannan obtained. The two fractions were combined and methylated further using the Kuhn method (16) of silver oxide in dimethyl formamide – iodomethane.

The methylated mannan (1.08 g) was refluxed overnight in 5% methanolic hydrogen chloride (50 ml), neutralized (Ag_2CO_3), filtered, and evaporated. The product (1.13 g), now water soluble, was hydrolyzed with 2 *N* hydrochloric acid (10 ml) for 24 h at 100 °C. Removal of acid yielded the free methyl sugars. These were shown on paper chromatograms using the *p*-anisidine hydrochloride spray (17) to consist of tri-*O*-methyl mannoses and traces of di-*O*- and tetra-*O*-methyl mannoses. A portion (20 mg) was converted to a mixture of methyl mannosides by refluxing for 3 h in 5% methanolic hydrogen chloride (5 ml). The product was examined by g.l.c. using 2% neopentyl glycol succinate on HMDS Chromosorb W (80–100 mesh) in a 5 ft × 1/4 in. o.d. copper tube at 143 °C with helium (29 p.s.i.) as carrier gas (18). The g.l.c. unit was of conventional design using thermal conductivity detectors. The following glycosides were detected, their proportion being expressed as percentages of the total area under the peaks; the other figures in parentheses are the emergence times. Methyl 2,3,4,6-tetra-*O*-methyl mannoside (1.1%, 3.7 min); 2,4,6- (46.7%, 8.7 min); 2,3,6- (48.7%, 11.3 min);d i-*O*-methyl mannosides (2.4%, 16.7and 19.0 min; 0.5%, 22.7 and 26.3 min). 3,4,6-*O*- and 2,3,4-*O*-substituted mannosides had retention times of 6.9 and 7.0 min, respectively.

Partial Hydrolysis of R. glutinis Mannan

(i) Isolation of 2-O-β-D-Mannopyranosyl-D-erythritol Monohydrate

Purified mannan (4.0 g) was dissolved by stirring in water (500 ml) at 100 °C overnight. After cooling periodic acid (12.0 g) was added and oxidation allowed to proceed for 20 h. Excess oxidant was removed by addition of barium carbonate and after filtration the filtrate was treated with sodium borohydride (2.0 g). Two hours later acetic acid was added and the solution shaken with Amberlite IR120. The filtered solution was evaporated to dryness and residual boric acid removed by repeated evaporations of methanol. The modified polysaccharide was hydrolyzed with 0.01 *N* hydrochloric acid (100 ml) at 100 °C for 1 h. The methanol-soluble product, after removal of acid, gave spots on a paper chromatogram corresponding to mannosyl erythritol, smaller amounts of mannose and erythritol, and a trace of glycerol (solvents: acetone–water 4:1 (v/v) and butanol–ethanol–water, 40:11:19 (v/v); detector: silver nitrate – sodium hydroxide dip (19)). No oligosaccharides running more slowly than mannosyl erythritol were detected. Two faint spots were detectable in the butanol–ethanol–water solvent with rates compared with mannosyl erythritol (R_{ME}) of 1.7 and 2.1.

The 2-*O*-β-D-Mannopyranosyl-D-erythritol (0.83 g) was isolated by chromatography on cellulose using butanol saturated with water as eluant. The product after two crystallizations from ethanol had m.p. 87–90 °C and $[\alpha]_D$ −36° (*c*, 1.1 H_2O), and gave mannose and erythritol on hydrolysis. It consumed after 12 h 3.05 moles of sodium periodate with concomitant formation of 0.87 mole of acid.

Anal. Calcd. for $C_{10}H_{20}O_9 \cdot H_2O$: C, 39.7; H, 7.3. Found: C, 40.0; H, 7.3.

The specific rotation is close to −36° recorded for the syrupy 2-*O*-β-D-mannopyranosyl-D-erythritol in methanol (20).

The materials with R_{ME} 1.7 and 2.1 were obtained in yields of 0.80 g and 0.47 g and appeared to be side-products formed by molecular rearrangement of the modified polymer under the influence of acid. This conclusion was reached since treatment of each compound with 0.01 *N* hydrochloric acid at 100 °C for 3 h caused partial hydrolysis to mannosyl erythritol, as indicated on paper chromatograms.

Partial hydrolysis of the modified polymer with 0.1 *N* sulfuric acid at 100 °C for 1 h gave rise to mannosyl erythritol and trace spots with R_{ME} 1.7 and 2.1. Spots corresponding to mannobiosyl or mannotriosyl erythritol were not detected.

(ii) Isolation and Characterization of Mannobiose and Mannotriose Fractions

Preliminary experiments showed that the optimum yields of oligosaccharide from mannan were obtained using *N* hydrochloric acid at 75 °C for 4 h. Thus on partial hydrolysis of mannan (5.0 g) with acid (70 ml) the oligosaccharide products were fractionated on a cellulose column, after neutralization, using various solvents. Mannose (1.13 g) was obtained initially by use of *n*-butanol half saturated with water. Mannobiose (0.68 g) was eluted with acetone–water (6:1 (v/v)) and mannotriose (0.50 g) with acetone–water (3:1 (v/v)). Finally mannotetraose (0.44 g) and mannopentaose (53 mg) were eluted with acetone–water ((2:1 (v/v)).

Can. J. Chem. Downloaded from www.nrcresearchpress.com by 210.87.254.40 on 09/05/12
For personal use only.

The di-, tri- and tetra-saccharides moved on a paper chromatogram in ethyl acetate – acetic acid – water (9:2:2 (v/v)) at rates of 1.3, 0.5, and 0.3 respectively, compared with lactose.

The mannobiose fraction was oxidized with lead tetraacetate and consumed 1.42, 1.69, 1.71, and 1.76 moles of oxidant after 2, 5, 10, and 15 min respectively. Crystallization from methanol–ethanol yielded 4-*O*-β-D-mannopyranosyl-D-mannose (458 mg). The disaccharide had m.p. 195–199 °C, undepressed on admixture with an authentic specimen and $[\alpha]_D$ −11° (*c*, 1.8 H_2O). Its X-ray diffraction diagram was identical with that of an authentic specimen.

The mannotriose fraction had $[\alpha]_D$ −35° (*c*, 0.9 H_2O) and consisted mainly of material with a 4-*O*-linked reducing end. In this instance 1.47, 1.78, 1.74, and 1.98 moles of lead tetraacetate were consumed after 2, 5, 10, and 15 min respectively. Mannotriose (153 mg) was dissolved in water (0.5 ml) and acetic acid (25 ml) and treated with a 1% solution of 2 moles of lead tetraacetate in acetic acid. After 30 min oxalic acid (2 moles) in acetic acid was added, the precipitate of lead oxalate filtered off, and the solution evaporated. The residue was reduced with sodium borohydride (100 mg) in water (20 ml). After 2 h the solution was worked up as described previously in this section. Paper chromatographic examination showed mainly mannobiosyl erythritol and a smaller proportion of mannobiosyl arabitol. These were separated by cellulose column chromatography using acetone–water (6:1 (v/v)) as eluant. The mannobiosyl erythritol (49 mg) gave mannose and erythritol on hydrolysis and had $[\alpha]_D$ −50° (*c*, 1.1 H_2O). It consumed 2.6, 2.8, and 2.8 moles of sodium periodate after 4, 23, and 48 h respectively, and after 23 and 48 h, 1.0 mole of acid was formed. A portion was oxidized with excess sodium periodate for 24 h and the solution then deionized and reduced with sodium borohydride for 2 h. Hydrolysis of the product gave on a paper chromatogram mannose and glycerol with a barely detectable amount of erythritol.

ACKNOWLEDGMENTS

The authors thank Mr. N. Gardner for technical assistance, Mr. M. Mazurek for carrying out microanalyses, and Mr. W. C. Haid for preparation of X-ray diffraction patterns.

REFERENCES

1. W. N. Haworth, R. L. Heath, and S. Peat. J. Chem. Soc. 833 (1941).
2. P. A. J. Gorin and A. S. Perlin. Can. J. Chem. **34**, 1796 (1956).
3. C. T. Bishop, F. Blank, and P. E. Gardner. Can. J. Chem. **38**, 869 (1960).
4. L. Hough and M. B. Perry. J. Chem. Soc. 2807 (1962).
5. D. H. Ball and G. A. Adams. Can. J. Chem. **37**, 1012 (1959).
6. O. K. Orlova. Biokhimiya, **26**, 439 (1961).
7. N. Prentice, L. S. Cuendet, W. F. Geddes, and F. Smith. J. Am. Chem. Soc. **81**, 684 (1959).
8. W. Kloeker and A. S. Perlin. Unpublished results.
9. I. Croon, G. Herrstrom, G. Kull, and B. Lindberg. Acta Chem. Scand. **14**, 1338 (1960).
10. I. J. Goldstein, G. W. Hay, B. A. Lewis, and F. Smith. Abstracts of Papers, 135th Meeting of the American Chemical Society, Boston, Mass. April, 1959. p. 30.
11. A. J. Charlson and A. S. Perlin. Can. J. Chem. **34**, 1200 (1956).
12. M. J. Abercrombie, J. K. N. Jones, M. V. Lock, M. B. Perry, and R. J. Stoodley. Can. J. Chem. **38**, 1617 (1960).
13. T. Miyazaki. Chem. Pharm. Bull. Tokyo, **9**, 829 (1961).
14. L. J. Wickerham. U.S. Dept. Agr. Tech. Bull. No. 1029. 1951.
15. W. N. Haworth. J. Chem. Soc. 8 (1915).
16. R. Kuhn, H. Trischmann, and I. Low. Angew. Chem. **67**, 32 (1955).
17. L. Hough, J. K. N. Jones, and W. H. Wadman. J. Chem. Soc. 1702 (1950).
18. Y. C. Lee and C. E. Ballou. J. Biol. Chem. **239**, 1316 (1964).
19. W. E. Trevelyan, D. P. Procter, and J. S. Harrison. Nature, **166**, 444 (1950).
20. A. J. Charlson, P. A. J. Gorin, and A. S. Perlin. Can. J. Chem. **34**, 1811 (1956).

Can. J. Chem. Downloaded from www.nrcresearchpress.com by 210.87.254.40 on 09/05/12
For personal use only.

Can. J. Chem. Downloaded from www.nrcresearchpress.com by 210.87.254.40 on 09/05/12
For personal use only.

THE OXIDATION OF SUGAR ACETALS AND THIOACETALS BY ACETOBACTER SUBOXYDANS

D. T. Williams and J. K. N. Jones
Department of Chemistry, Queen's University, Kingston, Ontario

With an appendix by

N. J. Dennis, R. J. Ferrier, and W. G. Overend
Chemistry Department, Birkbeck College (University of London), London, England

Received November 18, 1964

ABSTRACT

The oxidation by *Acetobacter suboxydans* of several aldose dimethylacetals and diethyldithioacetals has been achieved. Isolation and characterization of the ketose products showed that the oxidations had followed the Bertrand–Hudson rules.

Previous workers (1, 2, 3) have reported unsuccessful attempts to adapt *A. suboxydans* to the oxidation of aldose dithioacetals and dimethylacetals. Bollenback and Underkofler (4) reported reducing values for aldose dithioacetals during an attempted oxidation, but Mitchell (3) has shown that these were most likely due to the oxidation of the sulfur atoms by the copper reagent used in the determination of the reducing values. We have now succeeded in oxidizing several aldose acetals and thioacetals (Table I) and have isolated the ketose products which were characterized as their 2,5-dichlorophenylhydrazones (except for compound C).

TABLE I

Substrate	Product	% yield	Time of oxidation (days)
D-Arabinose dimethylacetal	4-*keto*-D-Arabinose dimethylacetal	(A) 80	8
D-Arabinose diethyldithioacetal	4-*keto*-D-Arabinose diethyldithioacetal	(B) 70	19
D-Glucose dimethylacetal	5-*keto*-D-Glucose dimethylacetal	(C) 60	18
D-Glucose diethyldithioacetal	5-*keto*-D-Glucose diethyldithioacetal	(D) 60	15
D-Mannose diethyldithioacetal	5-*keto*-D-Mannose diethyldithioacetal	(E) 45	44
D-Galactose diethyldithioacetal	(3?)-*keto*-D-Galactose diethyldithioacetal	60	54

The usual technique used, when sugars are to be oxidized by *A. suboxydans*, is to inoculate the substrate broth with one drop of a culture of *A. suboxydans* grown on D-sorbitol. It was felt that this was insufficient inoculation, for the growth of the organism on unfavorable substrates, and in our work we have used 1–2 ml of the inoculation culture to promote the growth of the organism and thus to achieve oxidation. The oxidation of the sugar acetals and thioacetals followed the well-known Bertrand–Hudson rules (1, 5), although in the case of the *keto*-D-galactose diethyldithioacetal the position of the keto group has not yet been fully established and discussion of the structure of this compound will be left to a later publication.

Borohydride reduction of A followed by acid hydrolysis gave xylose and arabinose, indicating that the keto group was on C_4 of the parent compound. Periodate oxidation of the 2,5-dichlorophenylhydrazone (II*a*) of A showed a rapid uptake of 1 mole of periodate with neither liberation of formaldehyde or production of acid, and within a short

while a precipitate of hydroxypyruvaldehyde 2-(2,5-dichlorophenylhydrazone) (V) had formed. The 2,5-dichlorophenylhydrazone (II*b*, III, and IV) of B, D, and E, also gave V on treatment with periodate, thus confirming that the keto group in the parent compound had been formed adjacent to the primary hydroxyl group.

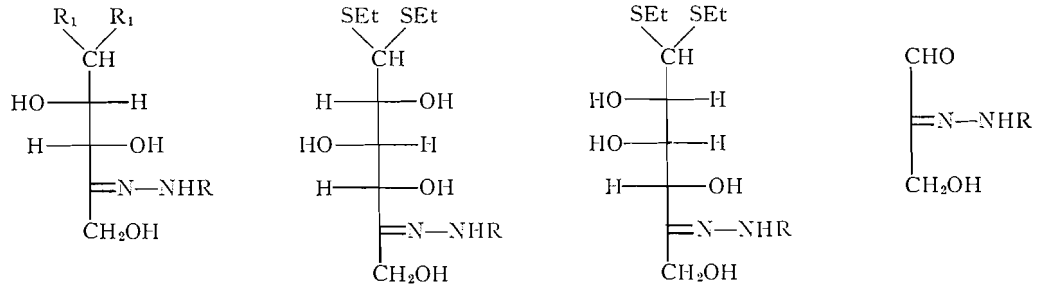

II III IV V

(*a*) $R_1 = OCH_3$
(*b*) $R_1 = SEt$

$R = C_6H_4Cl_2$

A crystalline hydrazone of C could not be obtained. However, borohydride reduction of C followed by acid hydrolysis gave idose and glucose, identified by gas chromatography, after reduction and acetylation, as iditol and sorbitol hexaacetates respectively. The extension of this work to the oxidation of other sugar acetals and the use of ketose products in the preparation of amino and branched chain sugars is being further nvestigated.

EXPERIMENTAL

All evaporations were carried out under reduced pressure and below 50°. Melting points were determined on a Fisher–Johns melting point apparatus and are uncorrected. Optical rotations were measured at 23 ± 3° with a Hilger Standard Polarimeter. Paper chromatography was carried out by the descending method at room temperature on Whatman No. 1 filter paper. The solvent system was butan-1-ol:ethanol:water, 3:1:1 (w/v). Sugars were detected on paper chromatograms by the following spray reagents: (i) alkaline silver nitrate (6), (ii) *p*-anisidine hydrochloride (7).

Preparation of Substrates

Diethyldithioacetals

The aldose (10 g) was dissolved in ice-cold concentrated hydrochloric acid (10 ml) and shaken with ethanethiol (10 ml). The temperature was maintained at 0° by immersion in ice water and by the addition of ice chips to the reaction mixture. Within 15 min the reaction mixture had usually solidified and the crystals were washed with ice-cold water until acid free and then recrystallized from ethanol or aqueous ethanol.

D-*Arabinose Dimethylacetal*

This was prepared by the general method of Wolfrom and Thompson (8).

D-*Glucose Dimethylacetal*

This was prepared by the method of Wolfrom and Thompson (8).

Acetobacter suboxydans (N.R.C. 471) was kindly supplied by the culture division of the National Research Council. The acetals to be oxidized were made up as a broth, containing the acetal (2.5%), yeast extract (0.5% w/v), potassium dihydrogen phosphate (0.05% w/v), and D-glucose (0.05% w/v) dissolved in tap water. After sterilization the solutions (25 ml), in 250 ml conical flasks, were inoculated with a vigorously growing culture of *A. suboxydans* (1–2 ml) grown on D-sorbitol. The flasks were stored in the dark, without agitation, at room temperature and the course of the oxidations was followed by paper chromatography. At a convenient time the oxidations were terminated by the addition of ethanol (2 vols.). After filtration and deionization the solutions were concentrated and the oxidation products separated by paper, column chromatography, or by continuous extraction from aqueous solutions by chloroform.

Can. J. Chem. Downloaded from www.nrcresearchpress.com by 210.87.254.40 on 09/05/12
For personal use only.

Preparation of 2,5-Dichlorophenylhydrazones

Molar ratios of the ketose and 2,5-dichlorophenylhydrazine were dissolved in a small volume of ethanol and left at room temperature overnight. Addition of water usually caused immediate crystallization and the product was recrystallized from ethanol by dropwise addition of water.

*4-keto-*D*-Arabinose Dimethylacetal*

D-Arabinose dimethylacetal was oxidized and gave a syrupy product with $[\alpha]_D = -41.3$ (*c*, 0.8, methanol). This ketose gave a crystalline 2,5 dichlorophenylhydrazone, m.p. 133° and $[\alpha]_D = -34.4$ (*c*, 0.44, methanol).

Anal. Calcd. for $C_{13}H_{18}O_5N_2Cl_2$: C, 44.19; H, 5.14; N, 7.93. Found: C, 43.93; H, 5.22; N, 8.20.

*4-keto-*D*-Arabinose Diethyldithioacetal*

D-Arabinose diethyldithioacetal gave on oxidation a crystalline ketose, m.p. 120–121° and $[\alpha]_D = -17.3°$ (*c*, 0.52, methanol).

Anal. Calcd. for $C_9H_{18}O_4S_2$: C, 42.54; H, 7.09; S, 25.19. Found: C, 42.35; H, 6.89; S, 25.36.

This ketose gave a crystalline 2,5-dichlorophenylhydrazone with m.p. 90–91° and $[\alpha]_D = -7°$ (*c*, 0.2, methanol).

Anal. Calcd. for $C_{15}H_{22}O_3S_2N_2Cl_2$: C, 43.60; H, 5.33; S, 15.49; N, 6.78. Found: C, 43.41; H, 5.33; S, 15.39; N, 6.86.

*5-keto-*D*-Glucose Dimethylacetal*

D-Glucose dimethylacetal gave on oxidation a syrupy ketose with $[\alpha]_D = +3.2°$ (*c*, 3.5, water), which did not give a crystalline hydrazone.

*5-keto-*D*-Glucose Diethyldithioacetal*

D-Glucose diethyldithioacetal gave on oxidation a syrupy ketose, $[\alpha]_D = -30°$ (*c*, 1.4, water), which yielded a crystalline 2,5-dichlorophenylhydrazone, m.p. 97° $[\alpha]_D = -24°$ (*c*, 0.5, methanol).

Anal. Calcd. for $C_{16}H_{24}O_4S_2N_2Cl_2$: C, 43.37; H, 5.42; N, 6.32; S, 14.44. Found: C, 43.53; H, 5.40; N, 6.48; S, 14.48.

*5-keto-*D*-Mannose Diethyldithioacetal*

D-Mannose diethyldithioacetal gave on oxidation a syrupy ketose, $[\alpha]_D = +28°$ (*c*, 1.67, water), which yielded a crystalline 2,5-dichlorophenylhydrazone, m.p. 129–130°, $[\alpha]_D = +40°$ (*c*, 0.25, methanol).

Anal. Calcd. for $C_{16}H_{24}O_4S_2N_2Cl_2$: C, 43.37; H, 5.42; N, 6.32; S, 14.44. Found: C, 43.24; H, 5.49; N, 6.50; S, 14.29.

Periodate Oxidations

Oxidations were carried out in the dark at room temperature in 50% aqueous ethanol containing excess sodium metaperiodate.

Hydroxy Pyruvaldehyde 2-(2,5-Dichlorophenylhydrazone)

The 2,5-dichlorophenylhydrazone of the ketose, when treated with periodate, gave an orange precipitate after a very short time. This precipitate was filtered off and after recrystallization from ethanol–water had m.p. 190–195° (decomp.).

Anal. Calcd. for $C_9H_8O_2N_2Cl_2$: C, 43.72; H, 3.24; N, 11.34. Found: C, 43.36; H, 2.95; N, 11.78.

*Sodium Borohydride Reduction of 4-keto-*D*-Arabinose Dimethylacetal*

4-*keto*-D-Arabinose dimethylacetal (100 mg) was reduced with sodium borohydride (100 mg) at 0° for 3 h. Excess sodium borohydride was converted to sodium borate which was removed as methyl borate after passage through Amberlite I.R. 120 (H^+) resin. The resultant syrup (90 mg) was hydrolyzed for 3 h at 80° with sulfuric acid (1 *N*, 1 ml). After neutralization of the acid, and concentration of the solution, paper chromatograms showed two components which co-chromatogrammed with xylose and arabinose and which were easily distinguished from lyxose and ribose.

*Sodium Borohydride Reduction of 5-keto-*D*-Glucose Dimethylacetal*

5-*keto*-D-Glucose dimethylacetal when subjected to the above procedure gave two components with $R_f = R_{glucose}$ and $R_f = 1.67\ R_{glucose}$. Borohydride reduction of this mixture followed by acetylation with acetic anhydride and pyridine gave a mixture of two hexaacetates identified by gas chromatography as sorbitol and iditol hexaacetates.

ACKNOWLEDGMENTS

The authors thank the National Research Council (N.R.C. T19) for a grant and Queen's University for financial assistance. They also thank Dr. H. G. Jones for the gas–liquid chromatographic analyses.

Can. J. Chem. Downloaded from www.nrcresearchpress.com by 210.87.254.40 on 09/05/12
For personal use only.

Can. J. Chem. Downloaded from www.nrcresearchpress.com by 210.87.254.40 on 09/05/12
For personal use only.

APPENDIX

In continuation of studies of methods for the synthesis of branched chain sugars (9) we are assessing a possible route in which one stage is the oxidation of aldose dithioacetals by the specific dehydrogenase system of *Acetobacter suboxydans*. To date our results are less complete than those of Williams and Jones (previous section) but some differences have been noted. Under the conditions of our experiments, a crystalline ketose derivative was obtained from the oxidation of D-glucose diethyldithioacetal, but the diethyldithioacetals of D-mannose, D-arabinose, and D-ribose were not oxidized by *A. suboxydans*. Very recent results indicate however that a bacterial suspension prepared under modified conditions will effect oxidation of these thioacetals.

The organism was grown on a medium containing D-glucose as the carbon source (10); the cells were washed from the agar surface and collected by centrifugation for 1 h at 2 000 *g*. D-Glucose diethyldithioacetal (5 g) was dissolved in a suspension of the bacterium (250 ml containing 15 ml wet-packed cells), the pH was adjusted to 6.8 by the addition of aqueous sodium hydrogen carbonate, and the suspension was shaken under an atmosphere of oxygen in a 1 l flask bearing a sidearm attached to a manometer. The oxygen was replenished at 24 h intervals and the uptake ceased after 4 days (total consumption 0.45 mole, 90%). After centrifugation, the solvent was removed at 40° and finally by azeotropic distillation with benzene, and the resultant syrup was extracted with warm methylene dichloride (100 ml). The extract was filtered and reduced in volume; addition of light petroleum (b.p. 40–60°) gave a crystalline product. Recrystallization from methylene dichloride / light petroleum (b.p. 40–60°) gave D-*xylo-hexos-5-ulose diethyldithioacetal* (3.1 g, 62%) m.p. 66–67°, $[\alpha]_D$ −30.5° (*c*, 2.1, in H_2O). (Found: C, 42.1; H, 7.2; S, 22.0. $C_{10}H_{20}O_5S_2$ requires C, 42.2; H, 7.1; S, 22.5.) The nuclear magnetic resonance (n.m.r.) spectrum was consistent with this structure. The derived 2,5-dichlorophenylhydrazone had m.p. 102–103°, $[\alpha]_D$ −15° → −58° (constant after 6 days) (*c*, 1.6, in MeOH). On periodate oxidation it yielded hydroxypyruvaldehyde 2-(2,5-dichlorophenylhydrazone), melting point and mixed melting point 190–191° (decomp.). The infrared spectrum of this derivative was identical with that of an authentic sample prepared from D-fructose 2,5-dichlorophenylhydrazone (11).

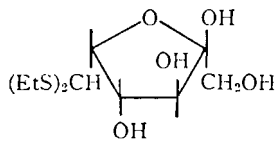

The ketose showed no carbonyl absorption in the infrared region, thereby suggesting that it exists in the crystalline form as a cyclic modification. Mutarotation was difficult to observe directly, but through the kindness of Dr. T. R. Emerson of Westfield College (University of London) and by the use of the Bellingham and Stanley / Bendix–Ericsson automatic recording spectropolarimeter, it was found that a rapid mutarotation did occur, $[\alpha]_{322}$ −57.5° (30 s) → −47° (2 min, const.) (*c*, 0.8, in H_2O). The compound therefore has structure I. On reduction with sodium borohydride D-glucose diethyldithioacetal was recovered together with a small amount of a second diethyldithioacetal which, on acidic hydrolysis, gave two products having the chromatographic mobilities of idose and its 1,6-anhydride.

REFERENCES

1. R. M. HANN, E. B. TILDEN, and C. S. HUDSON. J. Am. Chem. Soc. **60**, 1201 (1938).
2. B. ISELIN. J. Biol. Chem. **175**, 997 (1948).
3. L. HOUGH, J. K. N. JONES, and D. L. MITCHELL. Can. J. Chem. **37**, 725 (1959).
4. G. N. BOLLENBACK and L. A. UNDERKOFLER. J. Am. Chem. Soc. **72**, 741 (1950).
5. G. BERTRAND. Ann. Chim. Paris, **3**(8), 209, 287 (1904).
6. W. E. TREVELYAN, D. P. PROCTOR, and J. S. HARRISON. Nature, **166**, 444 (1950).
7. L. HOUGH, J. K. N. JONES, and W. H. WADMAN. J. Chem. Soc. 1702 (1950).
8. M. L. WOLFROM and A. THOMPSON. Methods in carbohydrate chemistry. Vol. II. Academic Press, Inc., New York. 1963. p. 427.
9. J. S. BURTON, W. G. OVEREND, and N. R. WILLIAMS. Chem. Ind. London, 175 (1961); Proc. Chem. Soc. 181 (1962); J. Chem. Soc. In press. S. W. GUNNER, W. G. OVEREND, and N. R. WILLIAMS. Chem. Ind. London, 1523 (1964). R. J. FERRIER. J. Chem. Soc. 3544 (1962).
10. V. MOSES and R. J. FERRIER. Biochem. J. **83**, 8 (1962).
11. I. MANDL and C. NEUBERG. Arch. Biochem. Biophys. **35**, 326 (1952).

Can. J. Chem. Downloaded from www.nrcresearchpress.com by 210.87.254.40 on 09/05/12
For personal use only.

Can. J. Chem. Downloaded from www.nrcresearchpress.com by 210.87.254.105 on 09/05/12
For personal use only.

REARRANGEMENT REACTIONS FOLLOWING ELECTRON IMPACT ON ETHYL AND ISOPROPYL ESTERS

A. G. HARRISON[1] AND E. G. JONES
Department of Chemistry, University of Toronto, Toronto, Ontario

Received November 5, 1964

ABSTRACT

The mass spectra of ethyl and isopropyl propionate and butyrate show rearrangement ions R_1COOH^+ and $R_1C(OH)_2^+$ formed by reactions [*a*] and [*b*]:

[*a*] $$R_1COOR_2^+ \rightarrow R_1COOH^+ + (R_2 - H),$$

[*b*] $$R_1COOR_2^+ \rightarrow R_1C(OH)_2^+ + (R_2 - 2H).$$

The mass spectra of ethyl-d_2 propionate and butyrate show that both [*a*] and [*b*] occur with essentially complete scrambling of the alkoxy hydrogens. For the isopropyl esters the mass spectra of the isopropyl-d_6 molecules show that reaction [*a*] occurs by transfer of one of the methyl hydrogens to the acid moiety while reaction [*b*] occurs predominately by transfer of two methyl hydrogens.

INTRODUCTION

The mass spectra of aliphatic esters of formula R_1COOR_2 show a number of characteristic rearrangement processes the general features of which have been elucidated (1, 2). When R_1 is three carbons or greater in length and contains hydrogen in the γ-position a rearrangement occurs to form the enol ion of the corresponding acetate (reaction [1]).

[1] $$RCH_2CH_2CH_2COOR_2^+ \rightarrow RCH{=}CH_2 + CH_2{=}C(OH)OR_2^+.$$

Deuterium labelling (3–6) has shown that reaction [1] involves a specific transfer of the γ-hydrogen to the oxygen, presumably through a cyclic intermediate (7).

When R_2 is ethyl or higher, further rearrangements may occur which lead not only to formation of the acid ion R_1COOH^+ (reaction [2]) but also to formation of the protonated acid ion $R_1C(OH)_2^+$ (reaction [3]). The formation of the latter ion has permitted estimation of the proton affinity of acids (8, 9). For the smaller R_1 groups reaction [2] occurs almost exclusively to give the charge on the $(R_2 - H)$ fragment.

[2] $$R_1COOR_2^+ \rightarrow R_1COOH^+ + (R_2 - H),$$

[3] $$R_1COOR_2^+ \rightarrow R_1C(OH)_2^+ + (R_2 - 2H).$$

The evidence concerning the hydrogens transferred in reactions [2] and [3] is neither as extensive nor as conclusive as the evidence for reaction [1]. From the mass spectra of *sec*-butyl acetates mono-deuterated in the C_2 and C_3 positions, McLafferty and Hamming (10) concluded that the hydrogens of C_1, C_3, and C_4 of the butyl group were involved in reaction [3]. While the present work was in progress two papers (11, 12) have appeared concerning rearrangement reaction [3] in butyl and pentyl acetates. From the mass spectra of selectively deuterated *n*-butyl acetates it was suggested (11) that the rearrangement occurred by a selective transfer of one hydrogen from the C_3 position of the alcohol followed by a random selection of the second hydrogen. On the other hand, the results for the *n*-pentyl acetates indicated (12) that the first hydrogen was selected practically equally from the C_3 and C_4 positions, followed by random selection of the second from the remaining hydrogens. Godbole and Kebarle (8) concluded from the

[1]*Alfred P. Sloan Fellow 1962–1964.*

mass spectra of labelled ethyl acetates and formates that the hydrogen transfer reactions to the acid portion of the molecule involved essentially complete scrambling of the ethyl hydrogens. On the other hand, their results for isopropyl acetate show a pronounced preference for transfer of the hydrogens from the 1 and 3 positions of the propyl group.

To obtain further information on the hydrogens transferred in reactions [2] and [3] and to obtain information on the relative importance of reactions [1] and [2] we have prepared ethyl-1,1-d_2 propionate and butyrate and 2-propyl-1,1,1,3,3,3-d_6 propionate and butyrate and compared the spectra of the labelled and unlabelled molecules. The results obtained not only provide information on the rearrangement reactions discussed above but also provide information on a number of other fragmentation processes in these esters.

EXPERIMENTAL

Mass spectra were obtained with an A.E.I. MS-2 mass spectrometer at 50 V electron energy and 10 V cm^{-1} repeller field strength. Appearance potentials were determined in the usual manner (13) using xenon or krypton to calibrate the voltage scale.

The ethyl esters, both labelled and unlabelled, were prepared by the acid-catalyzed esterification of the free acid by the appropriate alcohol following the procedure given by Vogel (14). For the isopropyl esters this procedure gave poor yields. Much better yields were obtained by reaction of the appropriate acid anhydride with the labelled or unlabelled alcohol using zinc chloride catalyst (15). Final purification in all cases was by gas–liquid chromatography (g.l.c.) using a diisodecylphthalate column.

The ethyl-d_2 alcohol and isopropyl-d_6 alcohol were obtained from Merck, Sharp and Dohme, Montreal and were of better than 98% isotopic purity (16).

RESULTS AND DISCUSSION

Partial mass spectra of ethyl-1,1-d_2 propionate and 2-propyl-1,1,1,3,3,3-d_6 propionate are compared with the spectra of the unlabelled esters in Table I, while the spectra of the

TABLE I

Partial mass spectra of propionate esters

Mass	Ethyl propionate	Ethyl-d_2 propionate	Isopropyl propionate	Isopropyl-d_6 propionate
122				0.59
116			0.30	
104		6.61		3.88
102	7.26			
101			4.04	
77		0.17		8.72
76		1.92		1.14
75	4.08	5.06	10.73	2.34
74	3.93	2.14	1.81	0.42
73	2.83	0.65	0.36	
65				4.48
59			3.54	
57	31.53	29.84	31.83	32.30
49				23.67
48				2.76
47		2.08		1.43
46		0.71		3.78
45	3.86	0.90	1.25	3.26
44	0.14	0.68	0.17	0.41
43	1.83	0.29	19.67	1.78
33		1.05		0.50
32		0.49		0.10
31	0.91	14.47	0.51	0.39
30	0.40	3.02	0.10	0.57
29	27.12	14.69	9.45	11.01
28	4.22	5.35	1.44	1.38

Can. J. Chem. Downloaded from www.nrcresearchpress.com by 210.87.254.105 on 09/05/12
For personal use only.

corresponding labelled and unlabelled butyrates are compared in Table II. In all cases the spectra have been corrected for naturally occurring ^{13}C and the intensities are expressed as a percentage of the total ionization.

TABLE II

Partial mass spectra of butyrate esters

Mass	Ethyl butyrate	Ethyl-d_2 butyrate	Isopropyl butyrate	Isopropyl-d_6 butyrate
136				1.19
130			1.10	
118		1.85		2.39
116	2.03			
115			2.60	
108				1.79
103		1.77		
102			1.06	
101	1.75			
91		0.16		6.57
90		12.29		0.82
89	2.54	1.84	9.65	4.67
88	11.82	0.92	4.09	0.23
87	0.45	0.16	0.15	
75		0.49		
74		0.72		2.13
73	3.72	2.70	2.11	0.15
72		1.07		
71	18.52	19.15	22.04	19.91
70	2.20	0.56		
65				4.56
63		0.17		
62		1.15		0.41
61	1.56	1.41		4.46
60	3.86	3.73	4.41	
59			4.04	
49				18.92
47		1.37		1.25
46		0.63		2.51
45	3.39	1.11	1.05	2.20
44	0.77	0.53	0.25	0.40
43	15.48	14.49	28.10	10.58
31	0.89	9.77	0.41	0.18
30	0.22	1.13	0.85	1.32
29	10.68	2.06	1.06	1.66

Of particular interest in the present context are the rearrangement ions formed by reactions [2] and [3] which occur at masses[3] 74 and 75 for the unlabelled propionates and masses 88 and 89 for the butyrates, although, as will be shown below, a large fraction of the mass 88 ion current in the ethyl butyrate spectrum corresponds to the $CH_2{=}C(OH)OC_2H_5^+$ ion formed by reaction [1]. The ion current at mass 102 in the spectrum of isopropyl butyrate moves to mass 108 in the d_6 compound and obviously corresponds to the $CH_2{=}C(OH)OC_3H_7^+$ ion formed by reaction [1].

The mass spectra of the labelled and unlabelled propionates in the mass 70–80 region are compared in Table III and the ionic contributions for the various masses presented in detail. For the isopropyl esters little confusion can arise. The mass 75 of the unlabelled ester moves to mass 76 and 77 in the labelled ester corresponding to transfer of HD and 2D to the acid moiety, while the mass 74 moves to mass 75 corresponding to transfer of D in reaction [2]. The small mass 73 moves to mass 74 and therefore cannot be the

[3]*Since only singly charged ions will be discussed the m/e ratio will be referred to as the mass throughout.*

Can. J. Chem. Downloaded from www.nrcresearchpress.com by 210.87.254.105 on 09/05/12
For personal use only.

$C_2H_5COO^+$ ion formed by loss of the isopropyl group but is probably the $C_2H_4COOH^+$ ion formed by loss of H from $C_2H_5COOH^+$. Such a decomposition is known (17) to proceed with retention of the acid hydrogen.

TABLE III

Contributions to mass spectra of propionates in mass 73–77 region

	Ethyl propionate		Ethyl-d_2 propionate	
Mass	Intensity	Contribution	Intensity	Contribution
77			0.19	$C_2H_5C(OD)_2^+$
76			2.10	$C_2H_5C(OH)(OD)^+$
75	4.08	$C_2H_5C(OH)_2^+$	5.52	2.12 = $COOC_2D_2H_3^+$ 1.59 = $C_2H_5COOD^+$ 1.81 = $C_2H_5C(OH)_2^+$
74	3.93	$C_2H_5COOH^+$	2.34	$C_2H_5COOH^+$
73	2.83	$C_2H_5COO^+$, $COOC_2H_5^+$	0.71	$C_2H_5COO^+$
	Isopropyl propionate		Isopropyl-d_6 propionate	
Mass	Intensity	Contribution	Intensity	Contribution
77			8.72	$C_2H_5C(OD)_2^+$
76			1.14	$C_2H_5C(OH)(OD)^+$
75	10.73	$C_2H_5C(OH)_2^+$	2.34	$C_2H_5COOD^+$
74	1.81	$C_2H_5COOH^+$	0.42	$C_2H_4COOD^+$
73	0.36	$C_2H_4COOH^+$		

The calculations for the ethyl esters are more complex since the total intensities for the labelled and unlabelled spectra differ slightly and, in addition, a number of the masses in the deuterated spectrum may have more than one contributor. To make the calculations possible we have multiplied all intensities in the labelled spectrum by 1.10 to make total intensities equal and we have further assumed that the ion at mass 73 in the unlabelled ester is formed by loss of C_2H_5 and is therefore either the $COOC_2H_5^+$ or the $C_2H_5COO^+$ ion. Undoubtedly a small amount may arise by loss of H from $C_2H_5COOH^+$, however, comparison with the spectrum of the isopropyl ester suggests that this contribution will be small. With these assumptions the ionic contributions detailed in the final column are calculated for the ethyl-d_2 propionate spectrum.

Similar calculations carried out for the mass 87–91 region of the labelled and unlabelled butyrates are presented in Table IV. Again the calculations for the isopropyl case are straightforward, however, the calculations for the ethyl esters are complex and it is not possible by equating intensities in the labelled and unlabelled spectra to solve directly for the ionic contributors at all masses. We have therefore made the logical assumption that the mass 88 intensity of the ethyl-d_2 spectrum corresponds entirely to $C_3H_7COOH^+$ formed by reaction [2] and that this reaction occurs by complete scrambling of the ethyl hydrogens as was found for the ethyl propionate. On this basis the contributions detailed in the last column of Table IV are obtained. The calculations show that approximately 92% of the mass 88 of the unlabelled ester has moved to mass 90 in the labelled spectrum and therefore must retain the two deuteriums. The major portion of the mass 88 therefore corresponds to the $CH_2{=}C(OH)OC_2H_5^+$ ion formed by reaction [1], while the remaining 8% corresponds to the $C_3H_7COOH^+$ ion formed by reaction [2]. This is in contrast to the results for isopropyl butyrate where reaction [1] produces an ion (mass 102) only 0.63 the intensity of the ion (mass 88) formed by reaction [2]. The presence of the isopropyl group appears to facilitate the rearrangement reaction [2].

Can. J. Chem. Downloaded from www.nrcresearchpress.com by 210.87.254.105 on 09/05/12
For personal use only.

TABLE IV

Contributions to mass spectra of butyrates in mass 87–91 region

	Ethyl butyrate		Ethyl-d_2 butyrate	
Mass	Intensity	Contribution	Intensity	Contribution
91			0.16	$C_3H_7C(OD)_2^+$
90			12.29	1.44 = $C_3H_7C(OD)(OH)^+$ 10.85 = $CH_2{=}C(OH)OCD_2CH_3^+$
89	2.54	$C_3H_7C(OH)_2^+$	1.84	0.29 = $CH_2COOCD_2CH_3^+$ 0.61 = $C_3H_7COOD^+$ 0.94 = $C_3H_7C(OH)_2^+$
88	11.82	$C_3H_7COOH^+$ $CH_2{=}C(OH)OC_2H_5^+$	0.92	$C_3H_7COOH^+$
87	0.45	$C_3H_7COO^+$ $CH_2COOC_2H_5^+$	0.16	$C_3H_7COO^+$

	Isopropyl butyrate		Isopropyl-d_6 butyrate	
Mass	Intensity	Contribution	Intensity	Contribution
91			6.57	$C_3H_7C(OH)_2^+$
90			0.82	$C_3H_7C(OH)(OD)^+$
89	9.65	$C_3H_7C(OH)_2^+$	4.67	$C_3H_7COOD^+$
88	4.09	$C_3H_7COOH^+$	0.23	$C_3H_6COOD^+$
87	0.15	$C_3H_6COOH^+$		

From the calculations of Tables III and IV for the deuterated esters one obtains the following results for the transfer of H and D to form the R_1COOH^+ and $R_1C(OH)_2^+$ ions by reactions [2] and [3].

Ethyl-d_2 propionate:

$$C_2H_5COOD^+ : C_2H_5COOH^+ = 1.59:2.59 = 0.41:0.59;$$
$$C_2H_5C(OD)_2^+ : C_2H_5C(OD)(OH)^+ : C_2H_5C(OH)_2^+ = 0.19:2.10:1.81 = 0.05:0.51:0.43.$$

Ethyl-d_2 butyrate:

$$C_3H_7COOD^+ : C_3H_7COOH^+ = 0.61:0.92 = 0.40:0.60 \text{ (assumed)};$$
$$C_3H_7C(OD)_2^+ : C_3H_7C(OD)(OH)^+ : C_3H_7C(OH)_2^+ = 0.16:1.44:0.94 = 0.06:0.57:0.37.$$

Isopropyl-d_6 propionate:

$$C_2H_5COOD^+ : C_2H_5COOH^+ = 2.34:0;$$
$$C_2H_5C(OD)_2^+ : C_2H_5C(OD)(OH)^+ = 8.72:1.14 = 0.88:0.12.$$

Isopropyl-d_6 butyrate:

$$C_3H_7COOD^+ : C_2H_5COOH^+ = 4.67:0;$$
$$C_3H_7C(OD)_2^+ : C_3H_7C(OD)(OH)^+ = 6.57:0.82 = 0.89:0.11.$$

These results clearly show that the transfer of one H in reaction [2] involves complete scrambling of the ethyl hydrogens, while transfer of two hydrogens in reaction [3] for the ethyl esters proceeds with extensive scrambling of the the ethyl hydrogens, the experimentally observed ratio for transfer of D_2:HD:H_2 being close to the ratio 0.10:0.60:0.30 calculated for complete equivalence of the two D and three H. The results for the ethyl esters are in agreement with the results obtained by Godbole and Kebarle (8) for the

Can. J. Chem. Downloaded from www.nrcresearchpress.com by 210.87.254.105 on 09/05/12
For personal use only.

similar rearrangements in ethyl acetate. The results for the isopropyl esters, on the other hand, show that transfer of one hydrogen in reaction [2] proceeds, within experimental error, exclusively by transfer of the methyl hydrogen. Reaction [3] for the isopropyl esters occurs predominately by transfer of two of the methyl hydrogens as shown by the ratios for transfer of D_2:DH = 0.88:0.12. Complete scrambling of the isopropyl hydrogens would lead to D_2:HD = 0.72:0.28 while transfer of one of the methyl hydrogens followed by random selection of the second hydrogen would lead to the ratio D_2:HD = 0.83:0.17. The present results are in agreement with the results obtained for reaction [3] in $CD_3COOCD(CH_3)_2$ which showed transfer of H_2 : transfer of HD = 0.88:0.12 (8). It has been noted (12, 18) that rearrangement reaction [2] in the acetates leads almost exclusively to formation of the $(R_2 - H)^+$ ion rather than the R_1COOH^+ ion since the ionization potential of the olefin fragment is lower. For the esters studied in the present work the ionization potentials of the R_1COOH fragments are comparable to the ionization potentials of the olefin fragments with the result that appreciable intensities are noted corresponding to the acid ion.

It has been suggested (7, 18) that reaction [2] may occur through formation of a cyclic intermediate (I) involving transfer of the β-hydrogen of the alcohol moiety.

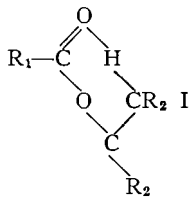

The results obtained in the present work for the isopropyl esters are clearly consistent with this interpretation since only the methyl (β) hydrogens are involved in reaction [2]. However, for the ethyl esters both the present results and previous work (8) show that the β-hydrogens are not transferred exclusively but that complete randomization of the ethyl hydrogens has occurred in the transfer process. This may be taken to indicate either that such a cyclic transition state is not applicable or that randomization of the ethyl hydrogens has occurred prior to formation of the intermediate. With regard to the latter possibility, it might be noted that for the ethyl esters a rather simple rearrangement of the parent ion (reaction [4]) could lead to essentially complete randomization of the hydrogens in reaction [2].

[4]

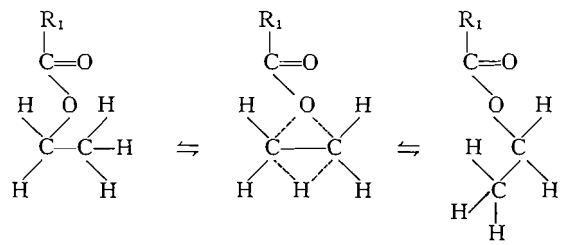

Such a rearrangement would be less likely for the isopropyl esters since it would involve shifting of the oxygen linkage from a secondary to a primary carbon rather than the symmetrical shift shown above. The above suggestion is clearly speculative since no other evidence can be found in the spectra of the ethyl esters to support such a rearrangement.

Can. J. Chem. Downloaded from www.nrcresearchpress.com by 210.87.254.105 on 09/05/12
For personal use only.

Can. J. Chem. Downloaded from www.nrcresearchpress.com by 210.87.254.105 on 09/05/12
For personal use only.

For reaction [3] it has been suggested (7) that the first hydrogen transfer also may occur by the cyclic intermediate I. It is not surprising therefore that the ethyl esters show extensive randomization of the ethyl hydrogens in reaction [3] as well as in reaction [2]. The results for the isopropyl esters are in accord with this suggestion while the results for the butyl (11) and pentyl (12) acetates suggest a selective transfer of the first hydrogen but through an intermediate of larger ring size. The major difference in the results for the isopropyl esters as compared to the butyl and pentyl esters is that transfer of the second hydrogen in the isopropyl esters appears to be specifically one of the terminal methyl hydrogens while for the other esters randomization of all the hydrogen has occurred.

A possible reason for this selectivity in the isopropyl case may be surmised from an examination of the energetics of formation of $R_1C(OH)_2^+$. The relevant data are summarized in Table V. The heats of formation of the neutral esters necessary for the thermochemical calculations were taken from Brion and Dunning (19) while the heats of formation of other neutral species were taken from the compilation of Bernecker and Long (20).

TABLE V

Energetics of formation of $R_1C(OH)_2^+$ from R_1COOR_2 (all data in eV)

	$R_2 = C_2H_5$		$R_2 = CH(CH_3)_2$	
R_1	$A(R_1C(OH)_2^+)$	$\Delta H_f(R_1C(OH)_2^+)$	$A(R_1C(OH)_2^+)$	$\Delta H_f(R_1C(OH)_2^+)$
CH_3	10.80±0.1* 10.75† 10.95‡ 11.0±0.2§	3.42	10.42±0.1* 10.72±0.03‖	4.24
CH_3			10.48±0.07‖ (R_2 = *n*-propyl)	4.28
C_2H_5	10.77‡ 10.67±0.1*	2.91	10.40±0.1*	3.74

*This work.
†Reference 20.
‡Reference 8.
§Sharkey, Hickam, and Friedel, private communication to ref. 8.
‖Reference 19.

The average $A(CH_3C(OH)_2^+)$ from ethyl acetate leads to $\Delta H_f(CH_3C(OH)_2^+) = 3.42$ eV assuming C_2H_3 (vinyl) as the neutral fragment. On the other hand, $A(CH_3C(OH)_2^+)$ from isopropyl acetate leads to $\Delta H_f(CH_3C(OH)_2^+) = 4.24$ eV assuming C_3H_5 (allyl) as the neutral fragment. This higher heat of formation is also obtained from the appearance potential of $CH_3C(OH)_2^+$ in *n*-propyl acetate. This difference in the calculated heats of formation for $R_1C(OH)_2^+$ from the ethyl and isopropyl esters is also found in the propionates and it is clear that the neutral fragment (or fragments) for the isopropyl esters cannot be the allyl radical.

One may reverse the calculations and use $\Delta H_f(R_1C(OH)_2^+)$ derived from the ethyl esters in the thermochemical cycle for the isopropyl esters to calculate $\Delta H_f(C_3H_5) = 2.15 \pm 0.2$ eV. Although the heat of formation of the cyclopropyl radical is not known accurately it is probably about 2.4 eV and it is therefore possible that the C_3H_5 formed from the isopropyl esters in reaction [3] has the cyclopropyl structure. For the isopropyl esters transfer of one hydrogen from each methyl group in reaction [3] would permit the formation of the cyclopropyl radical without further hydrogen rearrangement and would also explain the selective transfer of the hydrogens in the rearrangement reaction.

The mass spectra obtained for the deuterium-labelled molecules provide information on some of the other fragmentation processes, particularly for the butyrate esters, and deserve some comment.

Formation of Mass 73 in Butyrate Esters

Both the ethyl and isopropyl butyrates show a significant ion current at mass 73. For the isopropyl ester a metastable at 60.6 indicates the decomposition

[5] $$C_3H_7COOH^+ \rightarrow CH_2CH_2COOH^+ + CH_3.$$

This is supported by the observation that the fragment ion moves to mass 74 and the metastable to 61.5 in the labelled ester since the precursor ion has become $C_3H_7COOD^+$. A similar fragmentation is observed in the spectrum of butyric acid.

For the ethyl-d_2 butyrate the major contribution remains at mass 73 with smaller contributions at masses 74 and 75. The contributions at 73 and 74 presumably arise by reaction [5] although no metastable was observed. That portion occurring at mass 75 must incorporate both deuteriums and probably originates by loss of methyl from the $CH_2{=}C(OH)OCD_2CH_3^+$ ion.

Formation of Mass 70 in Ethyl Butyrate

The ion current at mass 70 in ethyl butyrate has the empirical formula $C_4H_6O^+$ (2). In the d_2 compound approximately one-half of this intensity moves to mass 72 indicating retention of both deuteriums. The most probable reaction is the loss of H_2O from the mass 90 intermediate.

[6] $$CH_2{=}C(OH)OCD_2CH_3^+ \rightarrow CH{\equiv}COCD_2CH_3^+ + H_2O.$$

The remainder of the ion current is found at masses 70 and 71 and the mechanism of formation is not clear.

Formation of Masses 60 and 61 in Butyrate Esters

The mass spectrum of ethyl butyrate shows a mass 61 ion current which is considerably more intense than that observed for isopropyl butyrate. The precursor ion is undoubtedly the $CH_2{=}C(OH)OCH_2CH_3^+$ ion and the rearrangement is therefore similar to that occurring in the spectrum of ethyl acetate. The relative intensities at masses 63, 62, and 61 in the d_2 compound are in agreement with complete scrambling of the ethoxy hydrogens in the rearrangement process. A similar rearrangement might be expected from the enol form of the isopropyl acetate ion (mass 102), however, the intensity of the precursor ion is much lower.

Both the ethyl and isopropyl esters show large ion currents at mass 60. In the isopropyl-d_6 butyrate this peak moves to mass 61 indicating retention of one deuterium and suggesting reaction [7] similar to that observed in butyric acid, although one cannot eliminate a concerted mechanism proceeding from the parent ester ion.

[7] $$C_3H_7COOH^+ \rightarrow CH_2{=}C(OH)_2^+ + C_2H_4.$$

A similar reaction in ethyl butyrate will account for the observed results.

Formation of R_1^+ and R_2^+ from R_1COOR_2

For ethyl propionate and isopropyl butyrate R_1^+ and R_2^+ occur at the same mass for the unlabelled esters. The spectra of the labelled esters allows an estimate of the relative contributions. For ethyl-d_2 propionate approximately 50% of the mass 29 moves to mass 31 indicating that $C_2H_5^+$ is formed equally from both ends of the ester molecule. For the

Can. J. Chem. Downloaded from www.nrcresearchpress.com by 210.87.254.105 on 09/05/12
For personal use only.

isopropyl-d_6 butyrate approximately 66% of the mass 43 of the unlabelled ester is found at mass 49 in the labelled ester indicating the relative contributions $R_1^+:R_2^+ = 1:2$.

ACKNOWLEDGMENTS

We are indebted to Mr. D. Van Raalte for measurement of some of the appearance potentials. The financial support of the National Research Council of Canada and the Alfred P. Sloan Foundation is gratefully acknowledged.

REFERENCES

1. A. G. SHARKEY, J. L. SHULTZ, and R. A. FRIEDEL. Anal. Chem. **31**, 87 (1959).
2. J. H. BEYNON, R. A. SAUNDERS, and A. E. WILLIAMS. Anal. Chem. **33**, 221 (1961).
3. T. E. DICKELMAN. M.S. Thesis, Massachusetts Institute of Technology. 1962. *Quoted by* K. Biemann. *In* Mass spectrometry. McGraw-Hill, New York. 1962.
4. E. STENHAGEN. Z. Anal. Chem. **181**, 462 (1961).
5. NG. DINH-NGOGEN, R. RYHAGE, S. STALLBERG-STENHAGEN, and E. STENHAGEN. Arkiv. Kemi, **18**, 393 (1961).
6. D. H. WILLIAMS, H. BUDZIKIEWICZ, and C. DJERRASSI. J. Am. Chem. Soc. **86**, 284 (1964).
7. F. W. MCLAFFERTY. Mass spectrometry of organic ions. Academic Press, New York. 1963. Chap. 7; Anal. Chem. **31**, 82 (1959).
8. E. W. GODBOLE and P. KEBARLE. Trans. Faraday Soc. **58**, 1897 (1962).
9. D. VAN RAALTE and A. G. HARRISON. Can. J. Chem. **41**, 2054 (1963).
10. F. W. MCLAFFERTY and M. C. HAMMING. Chem. Ind. London, 1366 (1958).
11. D. R. BLACK, W. H. MCFADDEN, and J. W. CORSE. J. Phys. Chem. **68**, 1237 (1964).
12. W. BENZ and K. BIEMANN. J. Am. Chem. Soc. **86**, 2375 (1964).
13. A. G. HARRISON and T. W. SHANNON. Can. J. Chem. **40**, 1730 (1962).
14. A. I. VOGEL. J. Chem. Soc. 629 (1948).
15. R. H. BAKER and F. G. BORDWELL. Org. Syn. **24**, 18 (1944).
16. D. VAN RAALTE and A. G. HARRISON. Can. J. Chem. **41**, 3118 (1963).
17. R. R. BERNECKER. Ph.D. Thesis, Cornell University. 1961.
18. K. BIEMANN. Mass spectrometry. McGraw-Hill, New York. 1962.
19. C. E. BRION and W. J. DUNNING. Trans. Faraday Soc. **59**, 647 (1963).
20. R. R. BERNECKER and F. A. LONG. J. Phys. Chem. **65**, 1565 (1961).

Can. J. Chem. Downloaded from www.nrcresearchpress.com by 210.87.254.105 on 09/05/12
For personal use only.

Can. J. Chem. Downloaded from www.nrcresearchpress.com by 210.87.254.5 on 09/05/12
For personal use only.

THE USE OF POLYACRYLAMIDE GELS FOR CHROMATOGRAPHY OF PROTEINS

K. SUN[1] AND A. H. SEHON
Department of Chemistry, McGill University, Montreal, Quebec
Received October 29, 1964

ABSTRACT

Sixteen copolymers of acrylamide and N,N′-methylene bisacrylamide were synthesized using ammonium persulfate and dimethylaminopropionitrile as initiators. The water regain values of these gels were found to increase with decreasing total monomer concentration and with decreasing N,N′-methylene bisacrylamide / acrylamide ratio. The partition coefficients (K_d) of a variety of compounds of molecular weights between 104 and 580 000 were determined by normal elution column chromatography for three gels. The K_d values for a given solute using different gels were found to increase with decreasing total monomer concentration of the gel and with decreasing N,N′-methylene bisacrylamide / acrylamide ratio. For various solutes through the same column, the K_d values varied linearly with the logarithms of the corresponding molecular weights over the K_d range of 0.1 to 0.6. However, a number of compounds showed deviations from this relationship.

INTRODUCTION

In recent years, the use of cross-linked natural and synthetic polymers for column chromatography has proved to be a very versatile tool for the fractionation of macromolecules according to molecular size. Starch (1), dextran (2), polystyrene (3, 4), agar (5), polyacrylamide (6, 7), and agarose (8, 9) gels have all been used. Of these compounds, polystyrene is hydrophobic and, therefore, not suitable for the fractionation of most biological materials, which are hydrophilic. The use of starch columns for the chromatographic separation of proteins from polypeptides, or from other small molecules was shown to be effective (1). However, starch is not too useful for the separation of macromolecules.

Commercially available cross-linked dextrans (known as Sephadex and supplied by A. B. Pharmacia, Uppsala, Sweden) have been widely and successfully used. Similarly, polyacrylamide gels have been shown to be effective in the separation of proteins (6, 7, 10, 11) and agarose gels have been used for the fractionation of large aggregates, such as cells, mitochondria, and microsomes (8). The R_f values of solutes on polyacrylamide gels were found to increase with their molecular weights (10), and there was a linear relationship between the R_f values for a given macromolecule and the total concentrations of the monomers used in the polymerization procedure. From a recent abstract (12), it appears that the partition coefficients of 17 test substances with molecular weights ranging from 193 to 3 500 000 have been determined by upward elution chromatography on polyacrylamide gels.

The present study constitutes an extension of the work done in this laboratory on the preparation of a number of synthetic gels from well-defined vinyl and divinyl water-soluble monomers (6). A series of gels was synthesized from acrylamide and N,N′-methylene bisacrylamide by varying the concentration of the reagents. The water regain for each of these gels was determined and the partition coefficients of a group of 18 compounds with molecular weights ranging from 104 to 580 000 were established. As

[1]*This work will be incorporated into a thesis to be submitted to McGill University in partial fulfillment for the requirements of the Ph.D. degree.*

will be illustrated for two gels, the partition coefficients (in the range of 0.1 to 0.6) were shown to be directly proportional to the logarithms of the molecular weights of the solutes.

MATERIALS AND METHODS

Acrylamide, N,N′-methylene bisacrylamide, ammonium persulfate, and β-dimethylaminopropionitrile were generously supplied by Cyanamid Co. of Canada Ltd. Chlorogenic acid and caffeic acid were purchased from Aldrich Chemical Co. Inc., Milwaukee, Wisconsin. Histamine, 5-hydroxyindole-3-acetic acid and sodium chloride were Fisher Scientific Co. (Montreal) reagent grade chemicals. Bovine gamma globulin and lysozyme were purchased from Pentex Inc., Kankakee, Illinois. Bovine fibrinogen, bovine haemoglobin, bovine serum albumin, pepsin, ovomucoid, trypsin, and ribonuclease were purchased from Nutritional Biochemicals Corp., Cleveland, Ohio. Conjugates of bovine serum albumin with chlorogenic acid,[2] caffeic acid,[2] 5-hydroxyindole-3-acetic acid[3], and histamine[3] were prepared in this laboratory.

(i) Preparation of Polymers

Sixteen different cross-linked polymers were prepared by varying the relative and absolute concentrations of acrylamide and N,N′-methylene bisacrylamide. For the sake of brevity, the different polymers will be identified by a code consisting of two numbers; the first number denotes the number of grams of acrylamide in 100 ml of the reacting solution and the second number denotes the number of grams of the cross-linking agent, N,N′-methylene bisacrylamide, used with every 100 g of acrylamide. Below is given a detailed description of the preparation of polymer "5-5".

Acrylamide (25.0 g) and N,N′-methylene bisacrylamide (1.25 g) were dissolved at room temperature in boiled distilled water. The solution was filtered, diluted to 500 ml with boiled distilled water, and deareated by a water pump for approximately 5 min, and then β-dimethylaminopropionitrile (0.5 ml) and ammonium persulfate (0.5 g) were cautiously added with gentle stirring. The reaction vessel was then placed into a thermostated water bath at 50 °C. Polymerization started in a few minutes and was practically complete in 2 h. The gel formed was cut into small pieces and washed exhaustively with distilled water to remove any unreacted monomers. It was then freeze dried, pulverized in a mortar, and separated into batches of uniform granular size by passage through a series of standard sieves. The fraction of 100 to 200 mesh was used for packing the chromatography columns.

(ii) Determination of Water Regain Values

A method similar to that of Pepper *et al.* was used (13). The polymer granules were allowed to swell in water for at least 24 h. About 15 ml of the gel was then transferred into a weighed Lusteroid tube (100 × 16 mm), the bottom of which was perforated and covered with glass wool. The tube was suspended inside a glass centrifuge tube (120 × 35 mm), which was provided with a constriction (at about 30 mm from the bottom) so that the lower part acted as a reservoir for the filtered liquid. The water in the interstitial space of the gel was removed by centrifugation at 300 – 1 000 g for about 20 min at 5 °C. The Lusteroid tube containing the gel was weighed and then dried to constant weight in a vacuum desiccator at room temperature. From the difference of the two weights,[4] the water regain (denoted as W_r) was calculated as grams of water imbibed per gram of dry gel.

(iii) Chromatography and Analyses

Packing of the columns and sample application were performed according to the method described by Flodin (14). Usually a column of 425 × 25 mm was used and the eluant was 0.9% saline (w/v). In general, 1 ml samples, consisting of artificial mixtures of 2–4 components of the substances listed in Table I, were applied. Experiments were usually performed at 5 °C in a cold room.

Effluent fractions of 3 or 5 ml were collected with an LKB Radi Rac fraction collector[5] and their optical densities recorded with an LKB Uvicord Spectrophotometer[5] or with a Beckman DU Spectrophotometer. In addition, bovine gamma globulin, bovine serum albumin, and lysozyme were qualitatively identified by the "ring" test with the appropriate homologous rabbit antisera, by paper electrophoresis, and by sedimentation velocity experiments. The identities of haemoglobin and of the various protein–hapten conjugates were established by comparing their spectra over the range of 200–600 mμ with those of the pure compounds. The concentrations of these substances were determined spectrophotometrically at 490 and 280 mμ, respectively. Trypsin, ovomucoid, and pepsin were identified by their mobility on paper electrophoresis. Chlorogenic acid, caffeic acid, 5-hydroxyindole-3-acetic acid, histamine, and tryptophane were measured spectrophotometrically at 280 mμ and compared with the spectra of the pure compounds in the ultraviolet spectral region.

The peak volume, V_e, of each compound was estimated to the nearest ml from the recordings of the Uvicord. The void volume for a given gel, V_0, was determined by the elution of a sample of dilute India ink.

[2]*Our thanks are due to Mrs. S. Tenenhouse for these compounds.*
[3]*Our thanks are due to Mr. N. S. Ranadive for these compounds.*
[4]*Appropriate correction for the water absorbed by the glass wool and the Lusteroid tube was made.*
[5]*Purchased from Fisher Scientific Co., Ltd., Montreal.*

Can. J. Chem. Downloaded from www.nrcresearchpress.com by 210.87.254.5 on 09/05/12
For personal use only.

TABLE I

Elution volumes (V_e) and partition coefficients (K_d) of various solutes through 25 × 425 mm columns of polyacrylamide gels using 0.9% saline (w/v) as eluant. V_i and V_0 are the imbibed and void volumes, respectively

Solute	Log (mol. wt.)	Gel 5-5 (V_0 = 68 ml, V_i = 134 ml)		Gel 5-20 (V_0 = 107 ml, V_i = 97 ml)		Gel 15-15 (V_0 = 91 ml, V_i = 109 ml)	
		V_e	K_d	V_e	K_d	V_e	K_d
Fibrinogen (bovine)	5.763	68	0.000	107	0.000	91	0.000
Gamma globulin (bovine)	5.164	80	0.089	118	0.113	91	0.000
BSA–hapten conjugates	4.840	—	—	—	—	91	0.000
Serum albumin (bovine)	4.840	98	0.224	122	0.155	91	0.000
Haemoglobin (bovine)	4.833	109	0.306	131	0.248	94	0.028
Pepsin	4.591	118	0.373	140	0.340	95	0.037
Ovomucoid	4.464	126	0.433	143	0.371	96	0.046
Trypsin	4.373	133	0.485	153	0.475	122	0.285
Lysozyme	4.230	158	0.671	188	0.835	180	0.726
Ribonuclease	4.104	150	0.614	166	0.609	134	0.394
Caffeic acid	2.255	—	—	—	—	194	0.946
Tryptophane	2.307	185	0.876	217	1.134	205	1.045
Histamine	2.017	—	—	—	—	211	1.102
Chlorogenic acid	2.549	—	—	—	—	232	1.295
5-Hydroxyindole-3-acetic acid	2.243	—	—	—	—	251	1.470

The imbibed volume of a given column, V_i, was calculated by multiplying the number of grams of the gel used for packing (denoted by a) by the water regain of that particular gel, i.e. $V_i = aW_r$. For calibration purposes, the elution volume of each compound was established by passing the compound on its own through the chromatographic column. The partition coefficients of the various compounds eluted were calculated for each gel using the expression (15)

$$K_d = \frac{V_e - V_0}{V_i} = \frac{V_e - V_0}{aW_r}.$$

RESULTS AND DISCUSSION

The rigidity of the gels was found to increase with increasing concentrations of both mono- and di-vinyl monomers used in the copolymerization process and to depend particularly markedly on the degree of cross-linking. In experiments with the relatively more rigid gels (20-20, 20-15, 20-10, 20-5, 15-20, 15-15, 15-10, 15-5, 10-20, 10-15, and 10-10), flow rates were regulated to ca. 20 ml/h by adjusting the hydrostatic head or with the use of an adjustable screw clamp at the outlet of the column. In the case of the softer gels (10-5, 5-20, 5-15, 5-10, and 5-5), only much slower flow rates of the order of 2–7 ml/h could be obtained and often the columns were clogged and needed repacking. Uniformity of the size and shape of the granules is another important factor controlling flow rates and affecting the void volume of a given gel; it is obvious that for a better characterization of the gels, it would be advantageous to use granules prepared by the bead-polymerization procedure.[6]

The water regain may be taken as a good indication of the degree of porosity of a gel. In Fig. 1 are given the water regain values of 16 gels prepared at different concentrations of monomers. It is evident that the amount of water accommodated within the gels depends on the concentration of both mono- and di-vinyl monomers; it increases with the decreasing concentrations of reagents, this effect being enhanced by a decrease of the concentration of the cross-linking divinyl monomer at a constant concentration of

[6]*During preparation of this paper, the availability of different grades of bead-polymerized polyacrylamide gels was announced by Calbiochem., Los Angeles, California.*

Can. J. Chem. Downloaded from www.nrcresearchpress.com by 210.87.254.5 on 09/05/12
For personal use only.

acrylamide. As would be expected, these results demonstrate that on decreasing the ratio of methylene bisacrylamide to acrylamide, the resulting three-dimensional network becomes more loosely bound and more easily accessible to water clusters. One arrives at a similar conclusion from a consideration of the peak elution volumes for compounds of different molecular weights (see Table I). Thus, from the partition coefficients (K_d) for gels 15-15, 5-20, and 5-5 listed in Table I, for a series of compounds of molecular weights varying from 104 to 580 000, it can be inferred that the more cross-linked gel 5-20 is less easily permeable than gel 5-5 to all solutes except those that show adsorption properties to the gel bed, i.e. lysozyme and tryptophane.

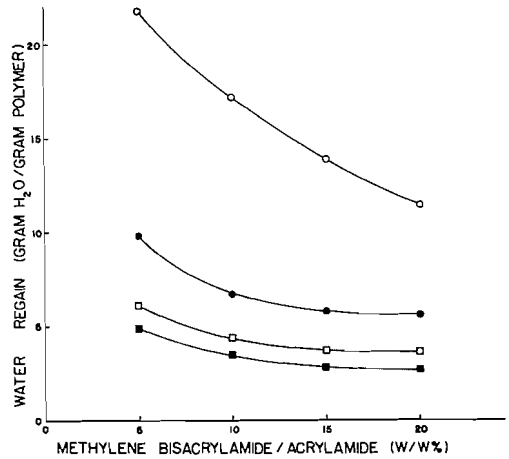

FIG. 1. Water regain values of polyacrylamide gels as a function of acrylamide concentration (○ 5%, ● 10%, □ 15%, ■ 20%) and of the relative concentrations of methylene bisacrylamide and acrylamide.

Although the values of the partition coefficients of many solutes listed in Table I are distinctly different, in practice, perfect separation could not be accomplished unless the partition coefficients of the two solutes differed by 0.3 or more. The reason is that the solutes were eluted in rather diffuse peaks, often spreading through 20–70 ml, increasing with increasing elution volume. A possible remedy for this situation is to employ an upward elution technique which may provide sharper elution zones. To illustrate the degree of separation, a chromatogram of the fractionation of bovine gamma globulin, bovine haemoglobin, ovomucoid, and tryptophane with a 5-5 column is shown in Fig. 2. As can be seen from Table I and Fig. 2, these gels were found useful for the separation of protein–hapten conjugates from the haptens themselves (e.g. BSA – chlorogenic acid conjugate from chlorogenic acid with a 15-15 column) and of high molecular weight proteins from smaller ones (e.g. bovine gamma globulin from lysozyme with a 15-15 column and bovine gamma globulin from ovomucoid, trypsin, or lysozyme with a 5-5 column). According to experimental data, the recovery in all cases is almost 100%. If a low yield of a pure component can be tolerated, even compounds of close molecular weights (e.g. bovine gamma globulin and bovine serum albumin, or bovine gamma globulin and bovine haemoglobin) can be separated with one or two repeated runs, each time recovering only the peak eluate.

The peak volumes in Table I were obtained from single component runs. In a multi-component system, interaction of the solutes may alter the degree of separation and the elution volume, which would be reflected in a change in the partition coefficients. However,

Can. J. Chem. Downloaded from www.nrcresearchpress.com by 210.87.254.5 on 09/05/12
For personal use only.

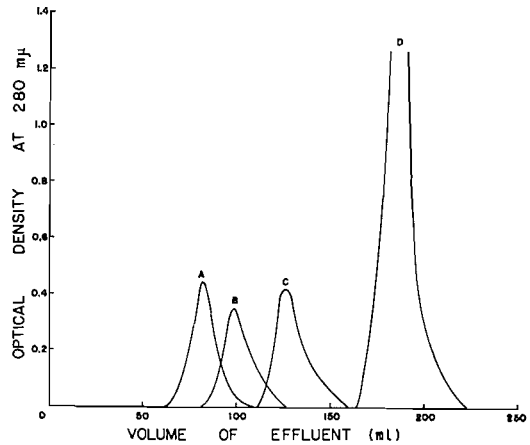

FIG. 2. Fractionation of bovine gamma globulin (A) mol. wt. 150 000, bovine haemoglobin (B) mol. wt. 68 000, ovomucoid (C) mol. wt. 29 000, and tryptophane (D) mol. wt. 203; with a 25 × 425 mm column of gel 5-5 and 0.9% saline (w/v) as eluant.

for the systems used, interaction between solutes was not too serious and peak volumes in single and multiple component runs were quite close (±3 ml) and reproducible. In Figs. 3 and 4 are given the chromatograms for the separation of bovine serum albumin from lysozyme and from ribonuclease, respectively and for the pure components.

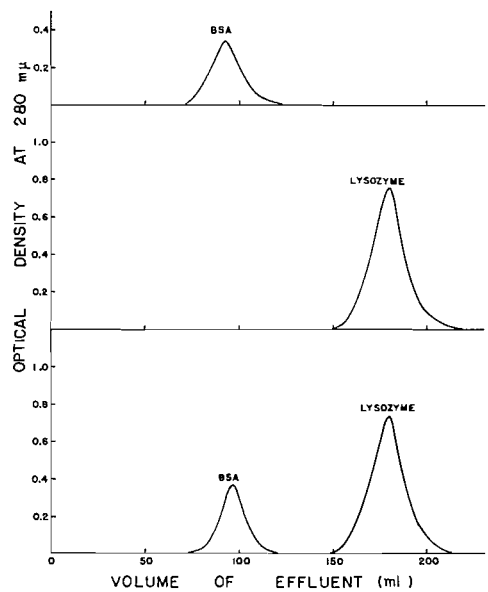

FIG. 3. Chromatograms of single and multiple component runs of bovine serum albumin and lysozyme through a 25 × 425 mm column of gel 15-15 using 0.9% saline (w/v) as eluant.

It should be noted that the gel was under different stress in experiments designed to determine the water regain and during chromatography. In the former case, it was under a strong centrifugal force, whereas in the latter it was only subjected to 1 or 2 ft of hydrostatic pressure, the effect of which is conceivably much smaller. The calculated imbibed

Can. J. Chem. Downloaded from www.nrcresearchpress.com by 210.87.254.5 on 09/05/12
For personal use only.

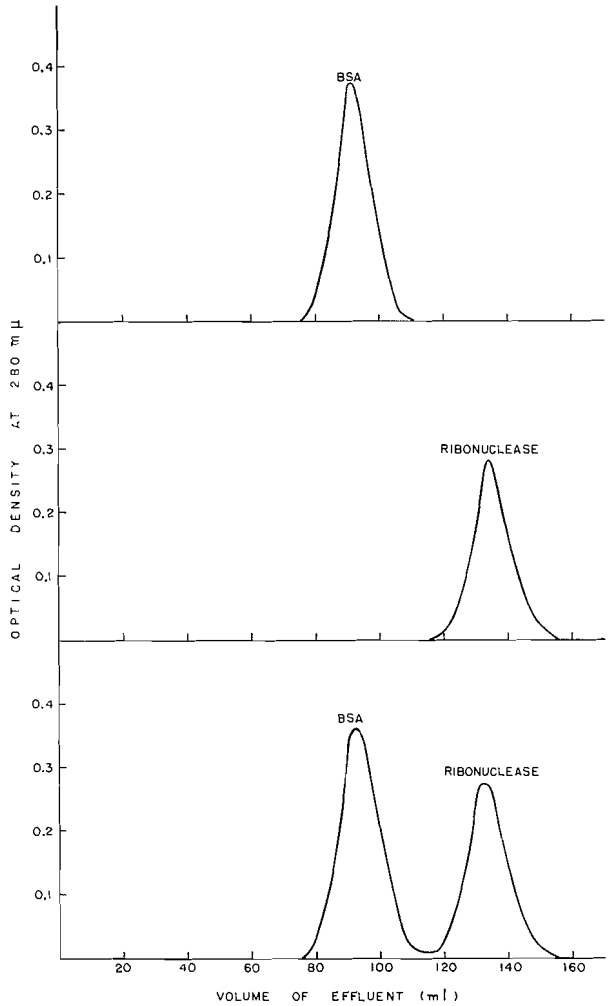

FIG. 4. Chromatogram of single and multiple component runs of bovine serum albumin and ribonuclease through a 25 × 425 mm column of gel 15-15 using 0.9% saline as eluant.

volumes can, therefore, be slightly lower and the calculated partition coefficients consequently slightly higher than the real values, but probably by a constant factor and hence still correct on a relative scale. An additional error may have been introduced by neglecting the effect of ionic strength on the water regain values. In retrospect, it would seem advisable to establish the water regain for a given gel with each eluant.

From the plot of the partition coefficients of eight proteins (bovine gamma globulin, bovine serum albumin, bovine haemoglobin, pepsin, ovomucoid, trypsin, lysozyme, and ribonuclease) in gel 5-20 and gel 5-5 versus the corresponding logarithms of molecular weights (Fig. 5), it is evident that a simple linear relationship exists between these two parameters. A similar relationship was observed with Sephadex (16) and agar gels (17). Further, as can be seen in Fig. 5, bovine haemoglobin and lysozyme have much bigger K_d values than those expected from their molecular weights. These discrepancies may be due to the molecular weight dependence of haemoglobin on concentration (17, 18) and

Can. J. Chem. Downloaded from www.nrcresearchpress.com by 210.87.254.5 on 09/05/12
For personal use only.

on the known adsorptive properties of lysozyme on polyacrylamide (12) and other columns. Also in Fig. 5, one can see that the K_d value of bovine gamma globulin is slightly larger for gel 5-20 than for gel 5-5. However, this difference of 0.014 would correspond to an error of approximately 1 ml in the elution volume and this is considered to be within the limit of accuracy obtainable with the present method.

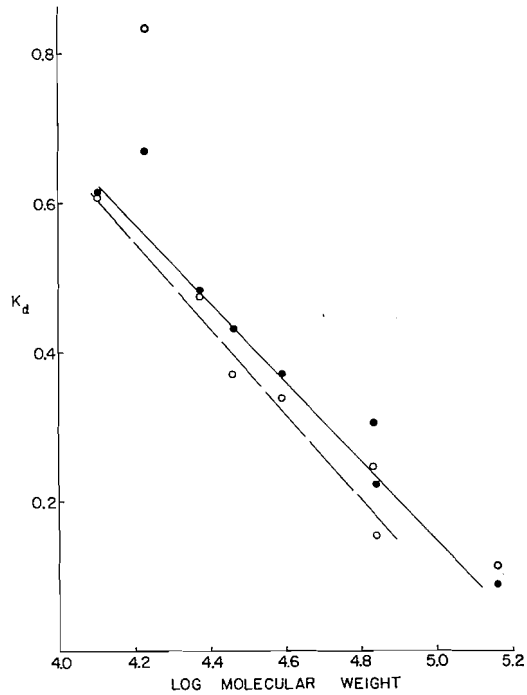

FIG. 5. Plot of the partition coefficients of the solutes versus the logarithms of their molecular weights in gels (●) 5-5 and (○) 5-20.

The relationship between the partition coefficients and molecular weights outside the K_d range of 0.1 to 0.6 are not shown. In the case when $K_d < 0.1$, the molecules are only partially admitted or completely excluded by the gel matrix. When $K_d > 0.6$, the molecules are so small that their molecular dimensions are not appreciably different to be separated by the molecular sieve mechanism alone. The fact that some of the K_d values exceed 1.0 clearly indicates that other mechanisms, e.g. adsorption, are also present. The small molecules used all contained an aromatic ring and it was shown that such substances exhibit adsorptive properties to beds of Sephadex (19). Perhaps this is also the case with polyacrylamide gel.

Although the various commercially available Sephadex grades have proved to be very useful in the fractionation of biopolymers, polyacrylamide gels seem to offer some advantages which make them worthy of further consideration: 1, the starting materials are cheaper and more readily available; 2, the lack of ionizable groups in the polymer chain minimizes possible complications due to adsorption and ion-exchange properties; 3, the stability of this gel network in the presence of acids is expected to be higher than that of the dextrans since the former contains only carbon–carbon bonds and no glycosidic linkages as in the case of the latter (15); 4, the similarity in chemical structure between

Can. J. Chem. Downloaded from www.nrcresearchpress.com by 210.87.254.5 on 09/05/12
For personal use only.

acrylamide and N,N′-methylene bisacrylamide and the well-defined nature of these monomers make these gels more amenable to a systematic study of their physical properties.

ACKNOWLEDGMENTS

This study was supported by grants from the National Research Council of Canada, Ottawa, and the National Institute of Allergy and Infectious Diseases, National Institutes of Health (E-2085), Bethesda, Md.

REFERENCES

1. G. H. LATHE and C. R. J. RUTHVEN. Biochem. J. **62**, 665 (1956).
2. J. PORATH and P. FLODIN. Nature, **183**, 1657 (1959).
3. M. F. VAUGHAN. Nature, **188**, 55 (1960).
4. J. C. MOORE. J. Polymer Sci. Part A, **2**, 835 (1964).
5. A. POLSON. Biochim. Biophys. Acta, **50**, 565 (1961).
6. D. J. LEA and A. H. SEHON. Can. J. Chem. **40**, 159 (1961).
7. S. HJERTEN and R. MOSBACK. Anal. Biochem. **3**, 109 (1962).
8. S. HJERTEN. Arch. Biochem. Biophys. **99**, 466 (1962).
9. S. HJERTEN. Biochim. Biophys. Acta, **79**, 393 (1964).
10. S. HJERTEN. Arch. Biochem. Biophys. Suppl. 1, 147 (1962).
11. H. G. BOMAN and S. HJERTEN. Arch. Biochem. Biophys. Suppl. 1, 276 (1962).
12. J. S. FAWCETT and C. J. O. R. MORRIS. Abstract II-54, 16th International Congress of Biochemistry, New York. 1964.
13. K. W. PEPPER, D. REICHENBERG, and D. K. HALE. J. Chem. Soc. 3129 (1952).
14. P. FLODIN. J. Chromatog. **5**, 103 (1961).
15. P. FLODIN. Dextran gels and their application in gel filtration. Uppsala. Meijels Bokindustri, Halmstad. 1962.
16. K. A. GRANATH and P. FLODIN. Makromol. Chem. **48**, 160 (1961).
17. P. ANDREWS. Nature, **196**, 36 (1962).
18. H. GUTFREUND. Haemoglobin. *Edited by* F. J. W. Roughton and J. C. Kendrew. Butterworth, London. 1949.
19. B. GELOTTE. J. Chromatog. **3**, 330 (1960).

Can. J. Chem. Downloaded from www.nrcresearchpress.com by 210.87.254.5 on 09/05/12
For personal use only.

Can. J. Chem. Downloaded from www.nrcresearchpress.com by 210.87.254.6 on 09/05/12
For personal use only.

SYNTHESIS OF 4-ACETAMIDO-4-DEOXY-SUGARS

A. J. DICK[1] AND J. K. N. JONES
Department of Chemistry, Queen's University, Kingston, Ontario
Received October 26, 1964

ABSTRACT

The tri-*O*-methanesulfonate derivative (I) of methyl α-D-xylopyranoside has been prepared. This compound when heated with sodium azide in *N*,*N*-dimethylformamide yielded a 4-azido derivative with inversion at C_4. It (I) was thus converted to a methyl 4-azido-4-deoxy-β-L-arabinopyranoside (II) and thence by removal of methanesulfonate residues to a 2,3-anhydro-L-ribopyranoside derivative and further to methyl 4-amino-4-deoxy-β-L-xylopyranoside (V); 4-acetamido-4-deoxy-1,2;3,5-di-*O*-isopropylidene-L-xylose (IX), a sugar with nitrogen in the ring, was prepared from 4-acetamido-4-deoxy-L-xylose. Acetolysis of methyl 4-acetamido-4-deoxy-L-xylopyranoside yielded a pentacetate of unknown ring size (X or XI).

The synthesis of sugar derivatives containing nitrogen as the hetero atom in pyranose rings has been a subject of recent investigation (1). The first synthesis of a sugar derivative with nitrogen as the hetero atom in a five-membered ring, methyl 4-acetamido-4-deoxy-L-erythrofuranoside, was also achieved recently (2). These syntheses all involve replacement of the ring oxygen atom of sugars by the nitrogen atom of an *N*-acetyl group on a primary carbon atom.

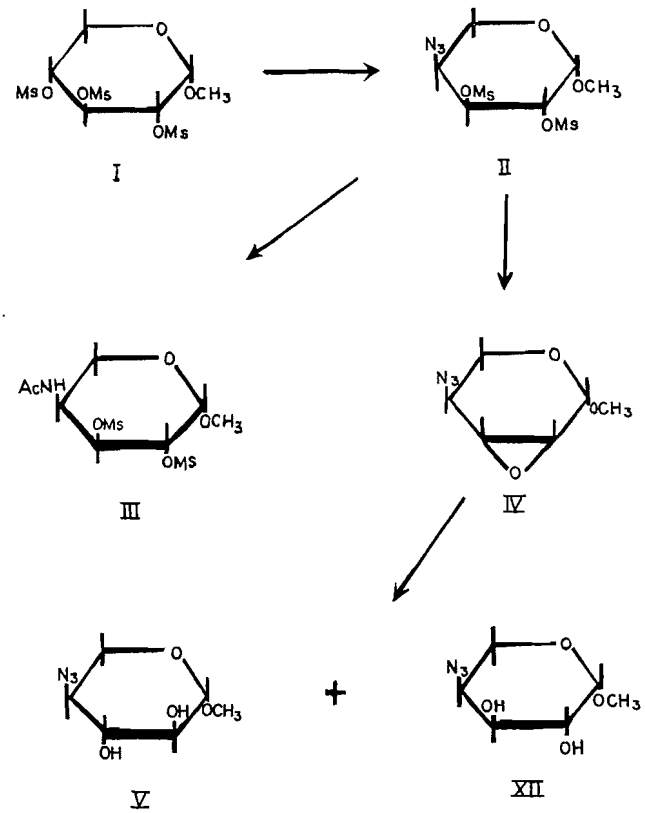

[1]*Present address: Department of Chemistry, University of Bristol, Bristol, England.*

Can. J. Chem. Downloaded from www.nrcresearchpress.com by 210.87.254.6 on 09/05/12
For personal use only.

The synthesis of derivatives of 4-amino-sugars with the nitrogen function on a secondary carbon atom is of interest in order to investigate the possible formation of a five-membered furanose ring containing nitrogen as the hetero atom. Methyl 4-amino-4-deoxy-α-D-glucopyranoside has been synthesized (3) via an S_N2 displacement of the 4-*O*-methanesulfonyl group of methyl 2,3,6-tri-*O*-benzoyl-4-*O*-methanesulfonyl-α-D-galactopyranoside by azide. Overend *et al.* (4) have synthesized methyl 4-amino-4-deoxy-α-D-lyxoside by the preferential cleavage of the epoxide ring of methyl 3,4-anhydro-β-L-riboside by ammonia.

The present communication reports a facile route to the synthesis of derivatives of 4-amino-4-deoxy-pentoses (5). The reaction of sodium azide with the 2,3,4-tri-*O*-methylsulfonyl derivative of methyl α-(I)D-xylopyranoside in dimethylformamide solution gave an azido-deoxy-di-*O*-methylsulfonyl derivative. The azide ion is considered to attack selectively at C-4 in an S_N2 displacement reaction to yield, methyl 2,3-di-*O*-methylsulfonyl-4-azido-4-deoxy-β-L-arabinopyranoside (II). Goodman *et al.* (6) have observed the selective replacement of the 4-*p*-tolysulfonyl group of methyl 2-*O*-benzoyl-3,4-di-*O*-*p*-tolysulfonyl-β-L-arabinopyranoside by azide which led to the synthesis of 4-acetamido-4-deoxy-D-ribose. An analogous situation exists for the reaction of the chlorosulfate ester derivatives of methyl α-D-glucopyranoside, methyl β-D-glucopyranoside, methyl α-D-galactopyranoside, and methyl β-D-galactopyranoside with pyridine hydrochloride. With an excess of pyridine hydrochloride, Jennings and Jones (7) have obtained 4,6-dichloro-dideoxy-substituted derivatives, with inversion of configuration occurring at C-4, in each of these cases, except with methyl 2,3,4,6-tetra-*O*-chlorosulfonyl-β-D-galactopyranoside, which gave a 3,4,6-trichloro-substituted compound as well as other products. It may be noted that reaction of methyl 2,3,4,6-tetra-*O*-methylsulfonyl-α-D-glucopyranoside (V) with an excess of sodium azide in *N*,*N*-dimethylformamide has been shown (8) to give a di-azido-deoxy derivative which is methyl 2,3-di-*O*-methylsulfonyl-4,6-di-azido-4,6-dideoxy-α-D-galactopyranoside.

Reduction of methyl 2,3-di-*O*-methylsulfonyl-4-azido-4-deoxy-β-L-arabinopyranoside (II) with Raney nickel in methanol followed by *N*-acetylation with acetic anhydride in *tert*-butyl alcohol – water gave methyl 2,3-di-*O*-methylsulfonyl-4-acetamido-4-deoxy-β-L-arabinopyranoside (III).

Reaction of methyl 2,3-di-*O*-methylsulfonyl-4-azido-4-deoxy-β-L-arabinopyranoside (II) with methanolic potassium hydroxide gave the 2,3-anhydro derivative (IV). Sorkin and Reichstein (9) report that the reaction of methyl 2,3-di-*O*-*p*-tolysulfonyl-4,6-*O*-benzylidene-α-D-galactopyranoside with sodium methoxide in methanol yields methyl 2,3-anhydro-4,6-*O*-benzylidene-α-D-gulopyranoside. By analogy, the anhydro sugar, (XII), is probably methyl 2,3-anhydro-4-azido-4-deoxy-β-L-lyxopyranoside* and (IV) not the corresponding ribopyranoside. Cleavage of this epoxide with aqueous potassium hydroxide gave a mixture containing predominantly methyl 4-azido-4-deoxy-β-L-xylopyranoside (V) with a low positive optical rotation, and in smaller yield methyl 4-azido-4-deoxy-β-L-arabinopyranoside (XII) with a high optical rotation. The mixture could be separated by fractional crystallization from chloroform–petrol.

Reduction of methyl 4-azido-4-deoxy-β-L-xylopyranoside (V) gave methyl 4-amino-4-deoxy-β-L-xylopyranoside (VI), isolated as the crystalline hydrochloride salt, which consumed 2 moles of periodate and liberated 1 mole of formic acid in unbuffered periodate. *N*-Acetylation of VI gave methyl 4-acetamido-4-deoxy-β-L-xylopyranoside (VII) which consumed 1 mole of periodate per mole. Hydrolysis of VII with Amberlite IR 120 cation

**Nuclear magnetic resonance studies and further chemical work have now shown XII to be the* L-*ribopyranoside derivative. Details will be given in a later publication.*

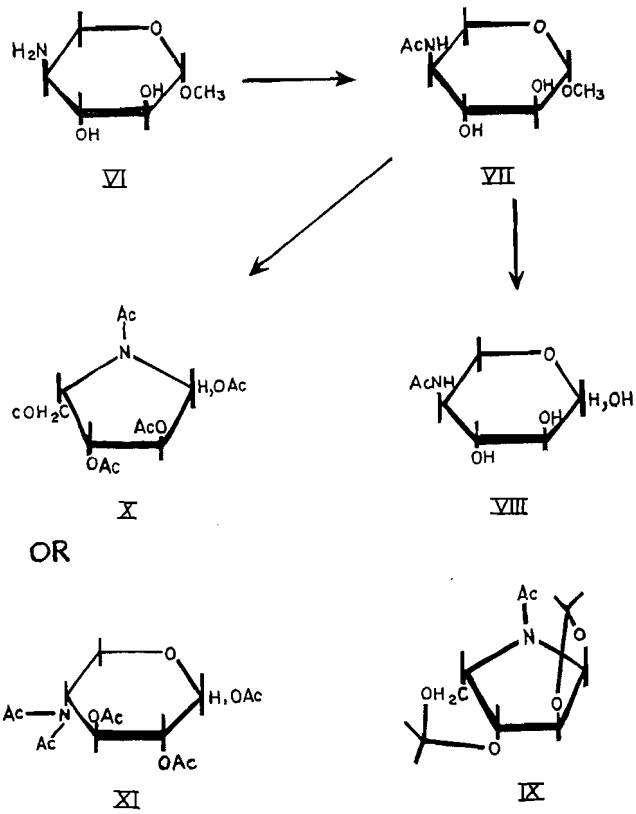

exchange resin (H^+ form) yielded a clear colorless syrup which was strongly reducing to Fehling's solution and which gave absorptions in the infrared corresponding to *OH*, *N—H*, and *N—Ac*. Paper chromatography of the syrup and the purified crystalline material showed only one component. The compound, on periodate oxidation in unbuffered aqueous solution consumed 2 moles of periodate and liberated 1 mole of formic acid; no overoxidation occurred and no formaldehyde was produced. Had the *N*-acetyl group been on C_2, overoxidation would have occurred. These results are consistent with the structure proposed for 4-acetamido-4-deoxy-L-xylopyranose and indicate that the six-membered oxygen ring is the highly favored ring form for the free sugar. The isopropylidene derivative of VIII was a colorless syrup, which crystallized after vacuum distillation. Its infrared spectrum showed absorptions corresponding to *N*—Ac and the isopropylidene group but no absorption attributable to *—OH* or *—NH*. The elemental analysis supports these results and is consistent with the structure 1,2;3,5-di-*O*-isopropylidine-4-acetamido-α-L-xylofuranose (IX). Molecular models indicate that a pyranose type structure is most unlikely.

Acetolysis of methyl 4-acetamido-4-deoxy-β-L-xylopyranoside (VII), gave a syrupy acetate which showed absorptions in the infrared corresponding to *—O—*Ac and *N—*Ac, but no absorption attributable to *—NH*. This compound is thus either 1,2,3,5-tetra-*O*-acetyl-4-acetamido-4-deoxy-L-xylofuranose (X) or 1,2,3-tri-*O*-acetyl-4-diacetamido-4-deoxy-L-xylopyranose (XI). Acetolysis of methyl 4-acetamido-4-deoxy-α-D-ribopyranoside was claimed to give 1,2,3,4-tetra-*O*-acetyl-4-acetamido-4-deoxy-D-ribofuranose (6) but no proof was given.

Can. J. Chem. Downloaded from www.nrcresearchpress.com by 210.87.254.6 on 09/05/12
For personal use only.

The investigation of the other monoazido-di-*O*-methylsulfonyl derivatives is being continued.

EXPERIMENTAL

Solutions were concentrated under reduced pressure below 40° with a rotating vacuum-type evaporator. Melting points were determined on a Fisher-Johns melting point apparatus and are uncorrected. Optical rotations were measured at 23 ± 3° with a Hilger Standard Polarimeter. Infrared spectra were measured with a Perkin–Elmer Model 21 spectrophotometer. Paper chromatography was carried out by the descending method at room temperature on Whatman No. 1 filter paper for qualitative purposes or on Whatman 3MM filter paper for preparative purposes in butan-1-ol : ethanol : water, 3:1:1. Sugars were detected on paper chromatograms by the following spray reagents: (i) alkaline silver nitrate (10); (ii) *p*-anisidine hydrochloride (11); (iii) sodium metaperiodate – potassium permanganate (12); (iv) sodium iodide and methyl red (epoxide spray (13)). Rates of movement of the sugars on paper chromatograms are given relative to that of rhamnose (R_{rh}).

Methyl 2,3,4-Tri-O-methylsulfonyl-α-D-xylopyranoside (I)

D-Xylose (technical) (100 g) was treated with methanolic hydrogen chloride according to the method of Hudson (14) and yielded crystalline methyl β-D-xylopyranoside (23 g). The residual syrups (75 g), $[\alpha]_D = +98°$ (*c*, 6.60 in water) containing approximately 50 g methyl α-D-xylopyranoside (calculated from the specific rotation) was dried thoroughly, dissolved in dry pyridine (400 ml), and treated with methanesulfonyl chloride (180 g) in the usual manner. The syrupy product was dissolved in hot ethyl acetate and the solution allowed to cool. Methyl 2,3,4-tri-*O*-methylsulfonyl-α-D-xylopyranoside crystallized slowly from this solution; 60 g were obtained from several crops. Three crystallizations from ethyl acetate gave colorless plates which melted at 130.5–131.5° and had $[\alpha]_D = +80°$ (*c*, 2.54 in chloroform).

Anal. Calcd. for $C_9H_{18}O_{11}S_3$: C, 27.1; H, 4.5; S, 24.1. Found: C, 27.0; H, 4.3; S, 24.3.

Reaction of Methanesulfonyl Derivatives with Sodium Azide

(*a*) Methyl 2,3,4-tri-*O*-methylsulfonyl-α-D-xylopyranoside (I) (12.0 g) was dissolved in *N*,*N*-dimethylformamide (150 ml) and a solution of sodium azide (2.35 g, 1.2 mole) and urea (0.4 g) in water (15 ml) was added. This solution was heated at 115° under a stream of nitrogen for 36 h. The black reaction mixture, containing precipitated sodium methanesulfonate, was cooled and poured into ice water (200 ml). The crystalline precipitate which formed was filtered off and the filtrate partitioned between chloroform and water. The chloroform layer was dried (Na_2SO_4), decolorized with charcoal, and filtered, and the filtrate evaporated to dryness. The residue crystallized on standing and was recrystallized from methanol to give methyl 2,3-di-*O*-methylsulfonyl-4-azido-4-deoxy-β-L-arabinopyranoside (II) as large, colorless needles (9.6 g, 92%) which melted at 128–128.5° and had $[\alpha]_D = +140°$ (*c*, 1.96 in chloroform).

Anal. Calcd. for $C_8H_{15}N_3O_8S_2$: C, 27.8; H, 4.35; N, 12.2; S, 18.5. Found: C, 27.6; H, 4.2; N, 12.2; S, 18.8.

When this reaction was carried out with I (4.0 g) dissolved in *N*,*N*-dimethylformamide (100 ml) containing excess sodium azide (2.3 g, 3.5 mole) and urea (0.15 g) in water (5 ml), under the same conditions as described above, the monoazido-deoxy-derivative (II) was again isolated in 50% yield. No other products were isolable.

The infrared spectrum of II in chloroform showed strong absorption at 2 140 cm^{-1} attributable to azide, and strong absorption at 1 370 cm^{-1} and 1 182 cm^{-1} attributable to sulfonate.

Methyl 2,3-Di-O-methylsulfonyl-4-acetamido-4-deoxy-β-L-arabinopyranoside (III)

Methyl 2,3-di-*O*-methanesulfonyl-4-azido-4-deoxy-β-L-arabinopyranoside (4.0 g) was reduced with Raney nickel in methanol. The Raney nickel was filtered off, the filtrate was evaporated to a pale-yellow syrup which was *N*-acetylated in *tert*-butyl alcohol – water (10.1) solution (100 ml) with acetic anhydride (2.0 ml). Evaporation of the solvent gave a glass which on crystallization from methanol gave XI (3.4 g, 81%) as colorless crystals which melted at 158–159° and had $[\alpha]_D = +117°$ (*c*, 2.06 in methanol). The infrared spectrum in chloroform showed absorption at 3 450 cm^{-1} and 1 513 cm^{-1} attributable to *N*—H, strong absorption at 1 683 cm^{-1} attributable to *N*—Ac, and strong absorption owing to the sulfonate groups.

Anal. Calcd. for $C_{10}H_{19}NO_9S_2$: C, 33.2; H, 5.3; N, 3.9; S, 17.7. Found: C, 33.0; H, 5.0; N, 4.2; S, 18.0.

Reaction of Methyl 2,3-Di-O-methylsulfonyl-4-azido-4-deoxy-β-L-arabinopyranoside (II) with Methanolic Potassium Hydroxide

To a solution of potassium hydroxide (10 g) in methanol–water (4:1) (200 ml) (II) (10.0 g) was added. This mixture was heated to boiling point which caused II to dissolve. The solution was refluxed for 2 h. The dark-brown reaction solution was diluted to 400 ml with water, concentrated to 200 ml, and extracted with ether (200 ml). The ether extract was washed with water, dried (Na_2SO_4), and filtered, and the filtrate was concentrated to a clear syrup (4.5 g) which crystallized on standing. Recrystallization of this material from petrol (35–60°) gave long, fine needles which melted at 54–55° and had $R_{rh} = 2.2$ (spray iv) and $[\alpha]_D = -14°$ (*c*, 1.54 in chloroform). This substance analyzed for the anhydro sugar, methyl 2,3-anhydro-4-azido-4-deoxy-β-L-ribopyranoside.

Can. J. Chem. Downloaded from www.nrcresearchpress.com by 210.87.254.6 on 09/05/12
For personal use only.

Can. J. Chem. Downloaded from www.nrcresearchpress.com by 210.87.254.6 on 09/05/12
For personal use only.

Anal. Calcd. for $C_6H_9O_3N_3$: C, 42.1; H, 5.3; N, 24.6. Found: C, 41.8; H, 5.5; N, 24.2.

The infrared spectrum in chloroform showed absorption at 2 120 cm^{-1} attributable to the azido groups and absorption at 1 270 cm^{-1} attributable to the epoxide ring.

Reaction of Methyl 2,3-Anhydro-4-azido-4-deoxy-β-L-ribopyranoside with Aqueous Potassium Hydroxide

To an aqueous solution (150 ml) of potassium hydroxide (5 g) IV (4.5 g) was added and the mixture was heated under reflux for 4 h. The dark-brown reaction solution was cooled and de-ionized by passing it through Amberlite IR 120 cation exchange resin (H^+ form). The elute was evaporated to a mobile syrup (3.8 g) which crystallized on standing. This material was dissolved in chloroform, and petrol (b.p. 60–80°) was added to incipient turbidity. Fine needles (0.55 g) were obtained which, after two recrystallizations from chloroform–petrol, melted at 108–108.5° and had R_{rh} = 2.2 (spray iii) and $[\alpha]_D$ = 141° (*c*, 0.56 in chloroform).

Anal. Calcd. for methyl 4-azido-4-deoxy-β-L-arabinopyranoside (XII), $C_6H_{11}O_4N_3$: C, 38.1; H, 5.8; N, 22.2. Found: C, 38.1; H, 6.1; N, 21.9.

The mother liquors were concentrated to a syrup which crystallized on standing. Recrystallization from chloroform–petrol (35–60°) gave fine needles (2.7 g) which melted at 81–83° and had R_{rh} = 1.7 (spray iii) and $[\alpha]_D$ = +31.3° (*c*, 1.64 in chloroform).

Anal. Calcd. for methyl 4-azido-4-deoxy-β-L-xylopyranoside (V), $C_6H_{11}O_4N_3$: C, 38.1; H, 5.8; N, 22.2. Found: C, 38.4; H, 6.0; N, 22.4.

Reduction of Methyl 4-Azido-4-deoxy-β-L-xylopyranoside (V)

The above compound V (1.1 g) was reduced with Raney nickel in methanol to yield a clear colorless syrup (0.84 g). The crystalline hydrochloride salt of VI was prepared by dissolving the crude amino sugar in acetone and adding concentrated hydrochloric acid. The hydrochloride salt was recrystallized from methanol–acetone and melted at 136–137° (decomp.) and had R_{rh} = 0.94 and $[\alpha]_D$ = +53° (*c*, 0.225 in water). Periodate oxidation of VI in unbuffered aqueous solution resulted in the consumption of 2 moles of periodate and the liberation of 1 mole of acid.

Anal. Calcd. for $C_6H_{14}O_4NCl$: C, 36.1; H, 7.0; N, 7.0; Cl, 17.8. Found: C, 36.0; H, 7.0; N, 7.2; Cl, 18.1.

Methyl 4-Acetamido-4-deoxy-β-L-xylopyranoside (VII)

Syrupy 4-amino-4-deoxy-β-L-xylopyranoside (VI, 0.84 g) was dissolved in water (20 ml) and acetic anhydride (2 ml) was added. This mixture was allowed to stand at room temperature with occasional shaking for 20 min. The solution was concentrated to a clear colorless syrup (1.05 g) which crystallized on standing. This material was crystallized from chloroform–petrol (60–80°) to give white needles of VII which melted at 157–158° and had R_{rh} = 1.48 (spray iii) and $[\alpha]_D$ = +52.7° (*c*, 2.22 in methanol). When oxidized in unbuffered aqueous solution, VII consumed 1 mole of periodate.

Anal. Calcd. for $C_8H_{15}O_5N$: C, 46.8; H, 7.3; N, 6.8. Found: C, 46.3; H, 7.7; N, 6.9.

Hydrolysis of Methyl 4-Acetamido-4-deoxy-β-L-xylopyranoside (VII)

Amberlite IR cation exchange resin (H^+ form) (2 g) was added to a solution of VII (0.65 g) in water (50 ml). This mixture was heated at a bath temperature of 90° with stirring for 4 h. The mixture was then cooled, the resin filtered off, and the filtrate concentrated to a colorless syrup (0.48 g) which was strongly reducing to Fehling's solution and which showed one spot on a paper chromatogram at R_{rh} = 0.81 (sprays i, ii, iii). The infrared spectrum (smear on NaCl) showed a broad absorption band at 3 550 – 3 220 cm^{-1} attributable to *OH* and *NH*, absorption at 1 640 cm^{-1} attributable to *N*—Ac, and strong absorption at 1 560 cm^{-1} attributable to *NH*. The syrup was caused to crystallize by treatment with ethyl acetate and was recrystallized from methanol–ether to give 4-acetamido-4-deoxy-L-xylopyranose (VIII), which melted at 157–158° and had $[\alpha]_D$ = −22°, mutarotating to −16° (*c*, 1.00 in water). When oxidized in unbuffered aqueous solution, VIII consumed 2 moles of periodate and liberated 1 mole of acid. No overoxidation occurred and no formaldehyde was produced.

Anal. Calcd. for $C_7H_{13}O_5N$: C, 43.93; H, 6.8; N, 7.3. Found: C, 44.0; H, 7.0; N, 7.2.

1,2;3,5-Di-O-isopropylidene-4-acetamido-4-deoxy-α-L-xylofuranose (IX)

Dry acetone (50 ml), anhydrous $CuSO_4$ (0.5 g), and a drop of concentrated sulfuric acid was added to syrupy VII (0.12 g). The mixture was shaken at room temperature for 40 h and was then filtered, the filtrate was neutralized with barium hydroxide and filtered, and the filtrate was concentrated. The syrupy residue was partitioned between ether and water and the ether layer dried (Na_2SO_4) and filtered, and the filtrate concentrated to a colorless syrup (0.055 g). The syrup was distilled under reduced pressure and the resultant syrup crystallized to give IX, m.p. 66–80°; $[\alpha]_D$ = +131 ± 3° (*c*, 2.30 in chloroform) and R_{rh} = 2.47 (spray ii). The infrared spectrum (smears on NaCl) showed strong absorption at 1 677 cm^{-1} attributable to *N*—Ac and a doublet at 1 392, 1 384 cm^{-1} attributable to the ispropylidene group but no absorption attributable to *OH* or *NH*.

Anal. Calcd. for $C_{13}H_{21}O_5N$: C, 57.6; H, 7.8; N, 5.2. Found: C, 57.8; H, 7.9; N, 5.33.

Acetolysis of Methyl 4-Acetamido-4-deoxy-β-L-xylopyranoside (VII)

The above compound VII (0.18 g) was acetolyzed according to the method of Hudson (14) in 10 ml

acetolysis solution. The reaction was followed polarimetrically and the optical rotation had become constant after 24 h. The solution was then poured into an excess of sodium bicarbonate in water and this solution was extracted with carbon tetrachloride. The carbon tetrachloride extract was washed with water and concentrated to a colorless syrup (0.065 g) which was distilled under vacuum. This material was homogeneous on thin-layer chromatography. The infrared spectrum (smear on NaCl) showed strong absorption at 1 755 cm^{-1} for *O*—Ac and at 1 686 cm^{-1} for *N*—Ac but no absorption owing to *N*—*H*. 1,2,3-Tri-*O*-acetyl-4-diacetamido-4-deoxy-L-xylopyranose (XI) (1,2,3,5-tetra-*O*-acetyl-4-acetamido-4-deoxy-L-xylofuranose (X)) had $[\alpha]_D = -23°$ (*c*, 0.95 in chloroform).

Anal. Calcd. for $C_{16}H_{21}O_9N$: C, 50.1; H, 5.9; N, 3.9; *O*-acetyl, 47.9; total acetyl (*O* + *N*), 59.9. Found: C, 48.8; H, 5.9; N, 4.0; *O*-acetyl, 54.4, 57.2; total acetyl (*O* + *N*), 61.1.

ACKNOWLEDGMENTS

The authors wish to thank the National Research Council for a grant (N.R.C. T-19) and for a scholarship (A. J. D.). They also wish to thank Dr. E. Buncel for his advice and assistance.

REFERENCES

1. J. K. N. Jones and J. C. Turner. J. Chem. Soc. 4699 (1962). J. K. N. Jones and W. A. Szarek. Can. J. Chem. **41**, 636 (1963). S. Hanessian and T. H. Haskell. Abstr. Papers Am. Chem. Soc. **144**, 19*c* (1963); J. Org. Chem. **28**, 2604 (1963. H. Paulsen. Agnew. Chem. **74**, 901 (1962).
2. W. A. Szarek and J. K. N. Jones. Can. J. Chem. **42**, 20 (1964).
3. E. J. Reist, R. R. Spencer, B. R. Baker, and L. Goodman. Chem. Ind. London, 1794 (1962).
4. W. G. Overend, A. C. White, and N. R. Williams. Chem. Ind. London, 1840 (1963).
5. W. A. Szarek and J. K. N. Jones. Preliminary communication. Abstr. Intern. Symp. Carbohydrate Chem., Munster. 1964. p. 33.
6. D. E. Gueffrog, E. J. Reist, and L. Goodman. Abstr. Papers Am. Chem. Soc. **148**, 2D (1964).
7. H. J. Jennings and J. K. N. Jones. Ph.D. Thesis, Queen's University. 1964.
8. A. J. Dick and J. K. N. Jones. Unpublished results. Cf. J. Hill, L. Hough, and A. C. Richardson. Proc. Chem. Soc. 346 (1963). K. Hess and H. Stenzel. Ber. **68**B, 981 (1935).
9. E. Sorkin and T. Reichstein. Helv. Chim. Acta, **28**, 1 (1945).
10. W. E. Trevelyan, D. P. Proctor, and J. S. Harrison. Nature, **166**, 444 (1950).
11. L. Hough, J. K. N. Jones, and W. H. Wadman. J. Chem. Soc. 1702 (1950).
12. R. U. Lemieux and H. F. Bauer. Anal. Chem. **26**, 920 (1954).
13. J. G. Buchanan and J. C. P. Schwartz. J. Chem. Soc. 4770 (1962).
14. C. S. Hudson. J. Am. Chem. Soc. **47**, 265 (1925).

Can. J. Chem. Downloaded from www.nrcresearchpress.com by 210.87.254.6 on 09/05/12
For personal use only.

Can. J. Chem. Downloaded from www.nrcresearchpress.com by 210.87.254.105 on 09/05/12
For personal use only.

NOTES

THE REACTION OF GALACTOSE WITH HYDRAZINE AT ELEVATED TEMPERATURE[1]

J. K. N. JONES, P. REID,[2] AND J. R. TURVEY[3]

An investigation (1) of the hydrazinolysis of the α_1-acid glycoprotein of human plasma is in progress in this laboratory. We wished to study the effects of hydrazine on the carbohydrate moiety of the glycoprotein and therefore investigated the effect of hydrazine on some model compounds. It has already been shown (1) that the optimum results are obtained with α_1-glycoprotein using a reaction time of 48 h and this time therefore was adopted for the present study of the effect of hydrazine on galactose. Yosizawa and Sato (2) treated reducing sugars in 10% (w/v) solution in anhydrous hydrazine at 100° for 10 h (in sealed tubes). Under these conditions they reported that 20.9% of galactose was destroyed with production of a pentose, a 2,5-anhydro-hexose, and other unidentified products. In contrast, Kaverzneva and Tsi De-Fan (3) concluded that mannose was not decomposed (appreciably) when treated with anhydrous hydrazine for 4 h at 100°. The results obtained by us with D-galactose are reported here.

When a 2% (w/v) solution of galactose in 95+% hydrazine was boiled under reflux for 48 h, the products contained little unchanged galactose. Paper chromatography of the products and use of the silver nitrate spray (4) indicated the presence of three major components and traces of others. One of these major products, compound A, was obtained crystalline from the crude reaction mixture after removal of excess hydrazine. Paper chromatographic separation of the residual syrup yielded the other major products, B and C.

Compound A, which was obtained in 33% yield, was identified as L-fucitol (*syn*-1-deoxy-D-galactitol) on the basis of its optical rotation, and that of the derived pentabenzoate and on the basis of the melting point and mixed melting point with authentic specimens of the alcohol and its pentabenzoate.

Compound B was obtained as a syrup contaminated with traces of a pentose and compound C. It was chromatographically identical with 3,4,5,6-tetrahydroxy-L-*lyxo*-hex-1-ene, prepared by the acid hydrolysis and subsequent reduction with sodium borohydride of methyl 5,6-didehydroxy-α-L-*arabino*-hexoside (5). Ozonolysis of compound B yielded D-lyxose, whereas ozonolysis of the synthetic tetrahydroxy-L-*lyxo*-hex-1-ene yielded L-lyxose. Compound B is thus probably 3,4,5,6-tetrahydroxy-D-*lyxo*-hex-1-ene.

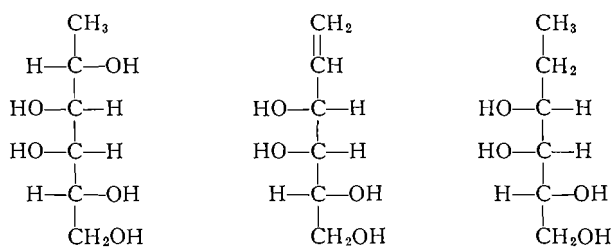

Compound A Compound B Compound C

[1]*Part of a paper presented at the Meeting of the American Chemical Society, Philadelphia, 1964.*
[2]*Present address: Chemistry Department, University of British Columbia, Vancouver 8, British Columbia.*
[3]*Present address: Chemistry Department, University College of North Wales, Bangor, Wales.*

Catalytic hydrogenation of 3,4,5,6-tetrahydroxy-L-*lyxo*-hex-1-ene and of compound B gave products which were chromatographically identical with compound C. This is, therefore, tentatively identified as 1,2-dideoxy-D-*lyxo*-hexose (*syn* 5,6-dideoxy-D-*arabino*-hexose).

The reaction of hydrazine with galactose to give these three products is complex. Initial hydrazone formation and subsequent Wolff–Kishner reduction of the hydrazone under the slightly basic conditions of the reaction would account for compound A. Similarly, compound C could arise from a reduction of the osazone but compound B must arise from an elimination reaction, the mechanism of which is obscure.

EXPERIMENTAL

For paper chromatography the solvent systems were (*a*) 1-butanol, ethanol, water (3:1:1, v/v), (*b*) ethyl acetate, acetic acid, water (6:3:2, v/v). Rates of migration on paper chromatograms are quoted relative to the rate of movements of the solvent front (R_F), to that of fucose (R_{Fucose}), and to that of galactose (R_{Gal}). All solutions were concentrated under diminished pressure.

Optical rotations were measured at 20 ± 2° in water unless otherwise stated.

Hydrazinolysis of Galactose

D-Galactose (2.057 g) in 95+% hydrazine (Eastman; 100 ml) was boiled under reflux for 48 h using a "Drierite" guard tube. Excess of hydrazine was removed by distillation and the last traces removed by drying *in vacuo* over concentrated sulfuric acid. Chromatographic examination of the residual syrup in solvent (*a*) (silver nitrate spray) indicated the presence of three major components with R_{Gal} values of 2.62, 3.82, and 4.6, together with minor components, R_{Gal} 4.73, and a component streaking behind R_{Gal} 2.62. The *p*-anisidine hydrochloride spray reagent (6) showed only traces of material resembling a pentose.

Isolation and Characterization of Compound A

The hydrazine-free syrup crystallized on being moistened with methanol and cooled. The crystals were filtered, washed with methanol at −15°, and dried (0.559 g), m.p. 153–156°. After two recrystallizations from methanol and one from acetone the melting point was 155–157°, mixed melting point with authentic L-fucitol 156–157; $[\alpha]_D$ +185° (*c*, 0.216 in a 4:1 (v/v) mixture of 5% ammonium molybdate and 1 *N* sulfuric acid). Richtmyer and Hudson (7) give $[\alpha]_D$ +196 for this compound and $[\alpha]_D$ −195° for D-fucitol in acidified ammonium molybdate solution. The benzoate of compound A was prepared and, after recrystallization had m.p. 150–151°; mixed melting point with authentic L-fucitol benzoate (m.p. 148–150°) was 148–150°; $[\alpha]_D$ −4.1 (*c*, 4.42 in chloroform); lit. values (8), m.p. 149–150°; $[\alpha]_D$ −5.96° (in chloroform).

Anal. Calcd. for $C_{41}H_{34}O_{10}$: C, 71.7; H, 4.95; molecular weight, 686. Found: C, 71.68, 71.49; H, 5.12, 5.2; molecular weight, 657 (determined on a 0.5% solution in chloroform using a Mechtrolab osmometer).

Isolation and Characterization of Compounds B and C

The syrup (0.96 g) remaining after crystallization of compound A was separated on sheets of Whatman 3 MM paper using multiple development in solvent (*b*). The compounds were located by spraying guide strips with the silver nitrate spray (4) and three compounds recovered by extraction of the appropriate zones with water. Compound A (0.12 g) yielded a benzoate with melting point and mixed melting point with authentic L-fucitol benzoate of 147–149°.

Compound B (0.193 g) was a syrup with R_F 0.50, R_{Fucose} 1.82 in solvent (*a*) and was contaminated with traces of a pentose and compound C. It reduced neutral permanganate solution and decolorized bromine water. Subsequently, it was shown to be chromatographically indistinguishable from 3,4,5,6-tetrahydroxy-L-*lyxo*-hex-1-ene, in the two solvent systems.

Compound C (0.293 g) was a syrup with R_F 0.57, R_{Fucose} 2.08 in solvent (*a*). It had $[\alpha]_D$ +2.6°. It was chromatographically indistinguishable from the products obtained by catalytic reduction of compound B and of 3,4,5,6-tetrahydroxy-L-*lyxo*-hex-1-ene in the two solvent systems.

Synthesis of 3,4,5,6-Tetrahydroxy-L-lyxo-hex-1-ene

Methyl 5,6-didehydroxy-α-L-*arabino*-hexoside (0.8 g), prepared by the method of Ball, Flood, and Jones (5), was hydrolyzed with *N* sulfuric acid at 100° for 1 h. The solution was cooled, neutralized with barium hydroxide, filtered, and then concentrated to 10 ml. Sodium borohydride (1 g) was then added and the solution left for 16 h. Acetic acid was added to pH 6 and the solution passed through a column of Amberlite IR 120 (H^+ form). After concentration of the eluate to dryness, boric acid was removed as methyl borate by distilling off portions (10 ml) of methanol. The product was then purified by chromatography on sheets of Whatman 3 MM paper as described previously (yield, 0.18 g).

Ozonolysis of 3,4,5,6-Tetrahydroxy-L-lyxo-hex-1-ene

The above compound (0.15 g) in methanol (25 ml) was ozonolyzed for 15 min with external cooling. The

Can. J. Chem. Downloaded from www.nrcresearchpress.com by 210.87.254.105 on 09/05/12
For personal use only.

solution was then boiled under reflux for a few minutes with zinc powder and filtered, and the filtrate concentrated to a syrup. Chromatographic examination in solvents (*a*) and (*b*) indicated that the main product was lyxose. This product was separated from impurities by chromatography on filter paper as described above and yielded syrupy L-lyxose, $[\alpha]_D$ +7.0°. The *p*-tolylsulfonylhydrazone derivative had m.p. 141–142° (lit. 141° (9)).

Ozonolysis of Compound B

Compound B (0.15 g) was ozonolyzed and the product separated as described above to yield D-lyxose (89 mg), $(\alpha)_D$ −10.0°. The *p*-tolylsulfonylhydrazine derivative had m.p. 141–142°, mixed melting point with the *p*-tolylsulfonylhydrazine derivative of authentic D-lyxose (m.p. 142–143°) 142–143°.

Reduction of 3,4,5,6-Tetrahydroxy-L-lyxo-hex-1-ene

This compound (0.405 g) in ethanol (100 ml) was reduced with hydrogen (5 atm) over 5% palladium on charcoal for 10 h. After being filtered, the solution was evaporated to a syrup (0.400 g). Paper chromatography showed the absence of starting material and production of a compound identical in R_F value with compound C.

Reduction of Compound B

Compound B (5 mg) was reduced as above to give a compound identical in chromatographic mobility with compound C.

ACKNOWLEDGMENTS

We wish to thank the National Research Council of Canada for financial assistance (N.R.C. T.19). One of us (J. R. T.) thanks the Royal Society and Nuffield Foundation for the award of a Commonwealth Bursary. We also thank Dr. M. B. Perry of the Division of Applied Biology, N.R.C. for the molecular weight determinations.

1. M. ALLEN, J. K. N. JONES, I. M. MACKIE, and P. REID. Meeting of the American Chemical Society, Philadelphia. April, 1964.
2. Z. YOSIZAWA and T. SATO. Tohoku J. Exptl. Med. **77**, 213 (1962).
3. E. D. KAVERZNEVA and TSI DE-FAN. Biokhimiya, **26**, 782 (1961).
4. W. E. TREVELYAN, D. P. PROCTER, and J. S. HARRISON. Nature, **166**, 444 (1950).
5. D. H. BALL, A. E. FLOOD, and J. K. N. JONES. Can. J. Chem. **37**, 1018 (1959).
6. L. HOUGH, J. K. N. JONES, and W. H. WADMAN. J. Chem. Soc. 1702 (1950).
7. N. K. RICHTMYER and C. S. HUDSON. J. Am. Chem. Soc. **73**, 2249 (1951).
8. A. T. NESS, R. M. HANN, and C. S. HUDSON. J. Am. Chem. Soc. **64**, 982 (1942).
9. D. G. EASTERLY, L. HOUGH, and J. K. N. JONES. J. Chem. Soc. 3416 (1951).

RECEIVED OCTOBER 20, 1964.
DEPARTMENT OF CHEMISTRY,
QUEEN'S UNIVERSITY,
KINGSTON, ONTARIO.

THE DIHYDROXYSTRYCHNINES

D. M. S. WHEELER,[1] MARY C. SMITH, ABBIE M. KNEECE, AND JAN B. MCMASTER

Edward (1) pointed out that reagents should attack the double bond of strychnine (I) (2) from the convex side of the molecule. He assigned structure II to 21,22-dihydroxydihydrostrychnine, which is obtained from strychnine by oxidation with potassium permanganate (3) or osmium tetroxide (4). Prelog and Kathriner (5) reported the preparation

[1]*Present address: Department of Chemistry, University of Nebraska, Lincoln, Nebraska, 68508.*

Can. J. Chem. Downloaded from www.nrcresearchpress.com by 210.87.254.105 on 09/05/12
For personal use only.

solution was then boiled under reflux for a few minutes with zinc powder and filtered, and the filtrate concentrated to a syrup. Chromatographic examination in solvents (*a*) and (*b*) indicated that the main product was lyxose. This product was separated from impurities by chromatography on filter paper as described above and yielded syrupy L-lyxose, $[\alpha]_D$ +7.0°. The *p*-tolylsulfonylhydrazone derivative had m.p. 141–142° (lit. 141° (9)).

Ozonolysis of Compound B

Compound B (0.15 g) was ozonolyzed and the product separated as described above to yield D-lyxose (89 mg), $(\alpha)_D$ −10.0°. The *p*-tolylsulfonylhydrazine derivative had m.p. 141–142°, mixed melting point with the *p*-tolylsulfonylhydrazine derivative of authentic D-lyxose (m.p. 142–143°) 142–143°.

Reduction of 3,4,5,6-Tetrahydroxy-L-lyxo-hex-1-ene

This compound (0.405 g) in ethanol (100 ml) was reduced with hydrogen (5 atm) over 5% palladium on charcoal for 10 h. After being filtered, the solution was evaporated to a syrup (0.400 g). Paper chromatography showed the absence of starting material and production of a compound identical in R_F value with compound C.

Reduction of Compound B

Compound B (5 mg) was reduced as above to give a compound identical in chromatographic mobility with compound C.

ACKNOWLEDGMENTS

We wish to thank the National Research Council of Canada for financial assistance (N.R.C. T.19). One of us (J. R. T.) thanks the Royal Society and Nuffield Foundation for the award of a Commonwealth Bursary. We also thank Dr. M. B. Perry of the Division of Applied Biology, N.R.C. for the molecular weight determinations.

1. M. ALLEN, J. K. N. JONES, I. M. MACKIE, and P. REID. Meeting of the American Chemical Society, Philadelphia. April, 1964.
2. Z. YOSIZAWA and T. SATO. Tohoku J. Exptl. Med. **77**, 213 (1962).
3. E. D. KAVERZNEVA and TSI DE-FAN. Biokhimiya, **26**, 782 (1961).
4. W. E. TREVELYAN, D. P. PROCTER, and J. S. HARRISON. Nature, **166**, 444 (1950).
5. D. H. BALL, A. E. FLOOD, and J. K. N. JONES. Can. J. Chem. **37**, 1018 (1959).
6. L. HOUGH, J. K. N. JONES, and W. H. WADMAN. J. Chem. Soc. 1702 (1950).
7. N. K. RICHTMYER and C. S. HUDSON. J. Am. Chem. Soc. **73**, 2249 (1951).
8. A. T. NESS, R. M. HANN, and C. S. HUDSON. J. Am. Chem. Soc. **64**, 982 (1942).
9. D. G. EASTERLY, L. HOUGH, and J. K. N. JONES. J. Chem. Soc. 3416 (1951).

RECEIVED OCTOBER 20, 1964.
DEPARTMENT OF CHEMISTRY,
QUEEN'S UNIVERSITY,
KINGSTON, ONTARIO.

THE DIHYDROXYSTRYCHNINES

D. M. S. WHEELER,[1] MARY C. SMITH, ABBIE M. KNEECE, AND JAN B. MCMASTER

Edward (1) pointed out that reagents should attack the double bond of strychnine (I) (2) from the convex side of the molecule. He assigned structure II to 21,22-dihydroxydihydrostrychnine, which is obtained from strychnine by oxidation with potassium permanganate (3) or osmium tetroxide (4). Prelog and Kathriner (5) reported the preparation

[1]*Present address: Department of Chemistry, University of Nebraska, Lincoln, Nebraska, 68508.*

Can. J. Chem. Downloaded from www.nrcresearchpress.com by 210.87.254.42 on 09/05/12
For personal use only.

of a dihydroxystrychnine by catalytic hydrogenation of the ketol III, which had been obtained from I by oxidation with weakly acidic permanganate. Prelog, apparently on the basis of the similarity in melting points, concluded that his dihydroxy compound was identical with Kotake's, and thus had structure II. This assignment is generally accepted (6).

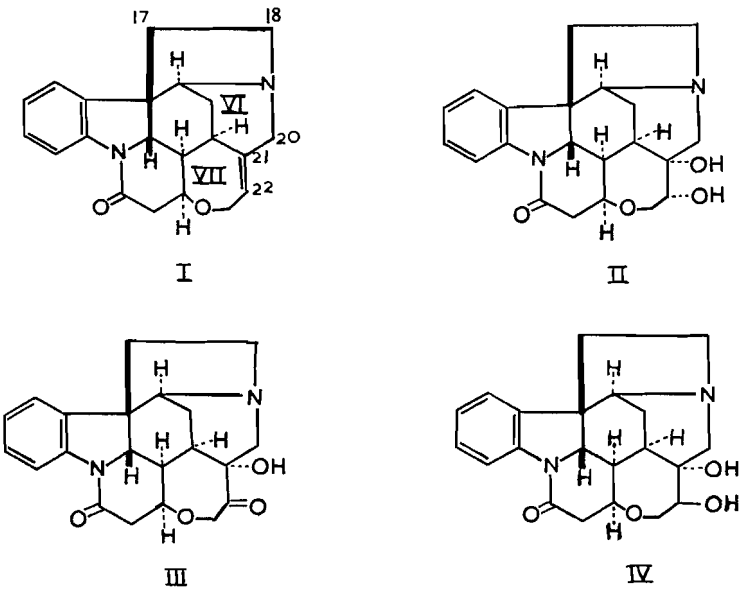

I II III IV

Consideration of models shows that the structure of Prelog's product depends on the conformation of ring VII in the ketol III. If this ring exists in a boat conformation (similar to the one which it is forced to adopt by the double bond in I), the hydrogen would be delivered from the convex face of the molecule, and the reduction product would have structure IV. If ring VII in III is a chair, the carbonyl group is turned in such a way that the delivery of hydrogen should lead to structure II. It is difficult to decide from models which of the conformations is favored. In the boat one, ring VI also exists as a boat and there is an interaction between the carbonyl group and two of the hydrogens on C_{17} and C_{18}; if ring VII exists in a chair conformation, ring VI is a chair and the main interactions would involve a hydrogen attached at C_{20}. Probably the chair conformation is the more stable one.

In the present work (started in connection with another problem) we prepared III (5). The spectra of this compound are in accord with the structure previously assigned. Catalytic reduction of III gave after crystallization of the crude product a compound which from physical properties and the tenacious way it held solvent was clearly the same as Prelog's material. This compound was (as Prelog had suggested (5)) identical with II prepared directly from I (4). In the later crops from the crystallizations of the hydrogenation product, we obtained a second material. A study of the mass spectra of II and the new compound shows that they are isomers, probably stereoisomers. On the basis of spectra and analysis, the new compound is assigned structure IV, and is therefore the previously unknown *trans* dihydroxy compound. These results indicate that ring VII in

Can. J. Chem. Downloaded from www.nrcresearchpress.com by 210.87.254.42 on 09/05/12
For personal use only.

III exists in both of the possible conformations; the relative yields of II and IV suggest that the chair conformation is favored.

EXPERIMENTAL

21-Hydroxy-22-ketodihydrostrychnine (III)

The ketol III, which was prepared by the method of Prelog and Kathriner (5), had m.p. 235–237° (from ethanol) (lit. 239–241°). $\nu_{max}^{CH_2Cl_2}$ 3 450, 2 870, 1 702, 1 673, 1 604, 1 484, 1 397, 1 332, 1 204, 1 135, 1 107, 1 089, 1 053, 1 020, 980, and 960 cm^{-1}; the nuclear magnetic resonnace (n.m.r.) spectrum does not have the vinyl absorption at 5.87 δ, which is present in strychnine.

cis-21,22-Dihydroxydihydrostrychnine (II)

The dihydroxy compound II was prepared by the method of Kogure and Kotake (4) except that dioxane with a trace of pyridine was used as a solvent for the reaction. The product after drying in vacuum for several days at 140° had m.p. 228° (lit. 228–230° (4), 240° (3), and 243–245° (5)). ν_{max}^{KBr} 3 350, 3 050, 2 905, 2 850, 1 665, 1 604, 1 490, 1 467, 1 425, 1 406, 1 370, 1 339, 1 292, 1 209, 1 157, 1 142, 1 095, 1 047, 1 030, 1 017, 992, 967, 942, 884, and 772 cm^{-1}; R_F (on Camag DF5 alumina using 1:1 acetone–water) = 0.57.

Reduction of the Ketol (III)

The ketol III (2.3 g) was hydrogenated following the method of Prelog and Kathriner (5). The crude product was purified by crystallization from ethanol – ethyl acetate mixtures. The earlier crops of crystals (1.1 g) had m.p. 97–99° and 144–145°. A portion of these on drying in high vacuum had m.p. 226–228° not depressed by addition of II; identity was confirmed by infrared and n.m.r. (in deuteropyridine) spectra and by thin-layer chromatography.

Later crops of crystals (350 mg) had m.p. (without vacuum drying) 248°, depressed by addition of II. ν_{max}^{KBr} 3 440, 2 920, 2 860, 1 643, 1 598, 1 488, 1 468, 1 416, 1 333, 1 318, 1 290, 1 280, 1 257, 1 226, 1 193, 1 168, 1 150, 1 136, 1 108, 1 088, 1 065, 1 028, 988, 968, 938, 818, and 765 cm^{-1}; R_F (on Camag DF5 alumina using 1:1 acetone–water) = 0.81. The n.m.r. spectrum of this compound in deuteropyridine differs from that of II. The compound is assigned structure IV.

Anal. Calcd. for $C_{21}H_{24}N_2O_4$: C, 68.46; H, 6.57; N, 7.60; O, 17.37. Found: C, 68.31; H, 6.72; N, 7.38; O, 17.40.

The mass spectra of II and IV were determined on a Hitachi RMU-6D single focussing mass spectrometer using a Micro-Tek inlet system and an ionizing voltage of 80 eV. The spectra were similar but showed some differences. Neither spectrum showed a molecular ion at m/e 368; both have peaks at 350, 332, and 303. They also show peaks at 130, 143, 167, and 220, which appear in the spectrum of strychnine (7).

ACKNOWLEDGMENTS

A. M. K. (High School Teacher Research Participant Summer 1960), J. B. M. (Undergraduate Research Participant 1959–1960) and M. C. S. (Undergraduate Research Participant Summer 1962) thank the National Science Foundation for support. D. M. S. W. thanks the Dupont Fund of the Department of Chemistry at the University of Nebraska for support during the summer of 1959. We are grateful to Mr. A. Struck of the Perkin–Elmer Corporation for the mass spectra. We thank Mrs. M. Wheeler for assistance.

1. J. T. Edward. Tetrahedron, **2**, 356 (1958).
2. A. F. Peerdeman. Acta Cryst. **9**, 824 (1956).
3. M. Kotake and T. Mitsuwa. Bull. Chem. Soc. Japan, **11**, 231 (1936).
4. A. Kogure and M. Kotake. J. Inst. Polytech. Osaka City Univ. Ser. C, **2**, 39 (1951).
5. V. Prelog and A. Kathriner. Helv. Chim. Acta, **31**, 505 (1948).
6. H.-G. Boit. Ergebnisse der alkaloid-Chemie bis 1960. Akademie-Verlag, Berlin. 1961. p. 605.
7. K. Biemann. Mass spectrometry. McGraw-Hill, New York. 1962. p. 332.

Received November 4, 1964.
Department of Chemistry,
University of Nebraska,
Lincoln, Nebraska,
and
Department of Chemistry,
University of South Carolina,
Columbia, South Carolina.

Can. J. Chem. Downloaded from www.nrcresearchpress.com by 210.87.254.42 on 09/05/12
For personal use only.

11α,12α-EPOXY-3,20-DIOXOPREGNANE

P. ZIEGLER

In the course of work on the preparation of steroids with a ruptured C-ring, 3,20-dioxo-Δ^{11}-pregnene was oxidized with chromic acid. The reaction was carried out at room temperature in aqueous acetic acid – sulfuric acid, using equimolar proportions of steroid and oxidizing agent to provide 60–70% of a crude, crystalline product. Spectrophotometric examination in the infrared region showed the absence of hydroxyl, acetoxyl, carboxyl, and aldehyde groups; there was, however, an indication of the presence of epoxide absorption as evidenced by two medium-sized bands at 805 cm^{-1} and 878 cm^{-1}. Elemental analyses of the purified compound agreed with the formula for 11,12-epoxy-3,20-dioxopregnane. The n.m.r. spectrum showed the presence of an AB type pattern in the region of 3 p.p.m., characteristic of steroidal 11,12-epoxides; the chemical shifts (δ, 2.98 and 3.14 p.p.m.) and coupling constants ($J_{11,12} = 4$, and $J_{9,11} = 0$ c.p.s.) are in excellent agreement with values reported (1) for 11α,12α-epoxides, but not for the corresponding β-epoxides. Reduction of the unknown with lithium aluminium hydride and subsequent oxidation of the product with chromic acid provided 70% of 3,12,20-trioxopregnane (2). This evidence gives further support for the α-configuration of the epoxide; it is known (3, 4) that the lithium aluminium hydride reduction of a steroidal 11α,12α-epoxide, such as 3β-acetoxy-11α,12α-epoxy-5α,22a-spirostane, yields the corresponding 12α-hydroxy compound, while 11β,12β-epoxides provide (5, 6) 11β-hydroxy steroids. These results agree with the concept (7) of axial attack on an epoxide by aluminiohydride ions via an S_N2 mechanism, the product having the hydroxyl group in the axial position. An exception to this rule seems to have been observed (5, 8) in the lithium aluminium hydride reduction of methyl 3α-acetoxy-11α,12α-epoxycholanate to 3α,11α,24-trihydroxycholane.*

The reaction of isolated double bonds with chromic acid is a complex one, but there are many indications that epoxides are formed as final or intermediary products. Chromic acid oxidations of 2,4,4-trimethylpent-1-ene (9), 2,4-dimethylpent-2-ene (10), and 1,1-diphenyl-2-methyl-prop-1-ene (11) gave good yields of the corresponding epoxides. In the steroid field, chromic acid oxidation of 5α-hydroxy-6β,16α-dimethyl-$\Delta^{6,7}$-pregnenolone 3-acetate yielded (12) the corresponding 6α,7α-epoxide, and $\Delta^{8,14}$-cholestenyl acetate (13) as well as $\Delta^{8,14}$-ergostenyl acetate (14) afforded a mixture of products including the 7-oxo- and 15-oxo-8α,14α-epoxides.

EXPERIMENTAL

11α,12α-Epoxy-3,20-dioxopregnane

A solution of chromic acid (1 g) in water (2 ml), acetic acid (25 ml), and sulfuric acid (1 ml) was added within 10 min to a solution of 3,20-dioxo-Δ^{11}-pregnene (3.15 g) in acetic acid (25 ml). During this addition, the mixture first turned cloudy, and then a green–black, gummy precipitate formed. As soon as all of the oxidizing solution had been added, the mixture was diluted with water (100 ml). This addition of water was made in several portions over a period of 10–15 minutes, and the gummy precipitate gradually dissolved to give a clear, green solution. A precipitate settled out shortly after the addition of water had been completed; after ½ h, the precipitate was filtered off, washed with water, and vacuum dried at 70° to provide 1.28 g of material, m.p. 142–152°. Dilution of the filtrate with more water (35 ml) yielded an additional

**A personal communication from Ciba Ltd., received since acceptance of this manuscript, states that an error was made in U.S. patent 2,599,481 and in corresponding patents issued in other countries, and that the lithium aluminium hydride reduction of methyl 3α-acetoxy-11α,12α-epoxycholanate actually yields 3α,12α,24-trihydroxycholane.*

Can. J. Chem. Downloaded from www.nrcresearchpress.com by 210.87.254.42 on 09/05/12
For personal use only.

0.82 g of solid, m.p. 147–153°. The two crops were combined and charcoal added. Recrystallization from ethyl acetate gave 1.47 g of crystals, m.p. 170–178°. Two further recrystallizations from this solvent raised the melting point to 182–185°; $[\alpha]_D^{25}$ +78.1° (*c*, 0.598, dioxane).

Anal. Calcd. for $C_{21}H_{30}O_3$: C, 76.32; H, 9.15; O, 14.53. Found: C, 76.50, 76.29; H, 9.18, 9.18; O, 14.68, 14.59.

3,12,20-Trioxopregnane

Lithium aluminium hydride (0.57 g) and 11α,12α-epoxy-3,20-dioxopregnane (1 g) were refluxed in ether (100 ml) for 4 h. An additional 0.75 g of reducing agent was then added, and refluxing was continued for 4 more hours. The cooled mixture was decomposed by dilute acetic acid and then poured into dilute hydrochloric acid, and the products were extracted with ether. After washing and evaporation of the solvent extract, the residue (0.9 g) was dissolved in acetic acid (20 ml) and water (2 ml). This solution was then treated dropwise, over a period of 15 min, with a solution of chromic acid (0.8 g) in water (10 ml), acetic acid (40 ml), and sulfuric acid (1 ml). After 15 h the mixture was poured into water, the products were extracted with ether – methylene chloride, and the solvent extract was worked up in the usual way. The residue (0.85 g) was crystallized from ether to give 0.67 g of material, m.p. 190–192°. Two further recrystallizations from ether and acetone gave pure 3,12,20-trioxopregnane, m.p. 198–201°, giving no depression on admixture melting point, and exhibiting an infrared spectrum which was superimposable on that of an authentic sample of this compound.

1. K. Tori, T. Komeno, and T. Nakagawa. J. Org. Chem. **29**, 1136 (1964).
2. T. Reichstein and E. von Arx. Helv. Chim. Acta, **23**, 747 (1940).
3. R. Hirschmann, C. S. Snoddy, Jr., C. F. Hiskey, and N. L. Wendler. J. Am. Chem. Soc. **76**, 4013 (1954).
4. J. Elks, G. H. Phillipps, D. A. H. Taylor, and L. J. Wyman. J. Chem. Soc. 1739 (1954).
5. P. Plattner. U.S. Patent No. 2,599,481 (June 3, 1952).
6. H. B. Henbest and T. I. Wrigley. J. Chem. Soc. 4596 (1957).
7. E. L. Eliel. *In* Steric effects in organic chemistry. *Edited by* M. S. Newman. John Wiley & Sons, Inc., New York. 1956. pp. 130–132.
8. N. G. Gaylord. Reduction with complex metal hydrides. Interscience Publishers, Inc., New York. 1956. pp. 665–666.
9. A. Byers and W. J. Hickinbottom. J. Chem. Soc. 1334 (1948).
10. W. J. Hickinbottom, D. Peters, and D. G. M. Wood. J. Chem. Soc. 1360 (1955).
11. W. J. Hickinbottom and G. E. M. Moussa. J. Chem. Soc. 4195 (1957).
12. J. Iriarte, J. N. Schoolery, and C. Djerassi. J. Org. Chem. **27**, 1139 (1962).
13. O. Wintersteiner and M. Moore. J. Am. Chem. Soc. **65**, 1513 (1943).
14. H. E. Stavely and G. N. Bollenback. J. Am. Chem. Soc. **65**, 1285 (1943).

Received September 15, 1964.
Research and Development Laboratories,
Canada Packers Limited,
Toronto, Ontario.

THE ALKALOIDS OF FUMARIACEOUS PLANTS. LII. A NEW ALKALOID, CULARICINE, AND ITS STRUCTURE

Richard H. F. Manske

The author (1) has described an investigation of the alkaloids of *Corydalis claviculata* (L.) DC. in which an amorphous phenolic fraction was obtained. At the time of publication it had not been possible to isolate pure individual bases from this fraction although it was shown to consist, to a large extent, of a base or bases which on O-methylation generated cularine. It has now been possible to isolate two phenolic bases and to determine the structure of one of these, namely that of cularicine. The other base proved to be identical with cularidine which had already been obtained from *Dicentra cucullaria* (L.) Bernh. (2).

The empirical formula of cularicine, $C_{18}H_{17}O_4N$, suggests that it might be cularidine or an isomer in which two methoxyls have been replaced by a methylenedioxy group and

Can. J. Chem. Downloaded from www.nrcresearchpress.com by 210.87.254.42 on 09/05/12
For personal use only.

0.82 g of solid, m.p. 147–153°. The two crops were combined and charcoal added. Recrystallization from ethyl acetate gave 1.47 g of crystals, m.p. 170–178°. Two further recrystallizations from this solvent raised the melting point to 182–185°; $[\alpha]_D^{25}$ +78.1° (*c*, 0.598, dioxane).

Anal. Calcd. for $C_{21}H_{30}O_3$: C, 76.32; H, 9.15; O, 14.53. Found: C, 76.50, 76.29; H, 9.18, 9.18; O, 14.68, 14.59.

3,12,20-Trioxopregnane

Lithium aluminium hydride (0.57 g) and 11α,12α-epoxy-3,20-dioxopregnane (1 g) were refluxed in ether (100 ml) for 4 h. An additional 0.75 g of reducing agent was then added, and refluxing was continued for 4 more hours. The cooled mixture was decomposed by dilute acetic acid and then poured into dilute hydrochloric acid, and the products were extracted with ether. After washing and evaporation of the solvent extract, the residue (0.9 g) was dissolved in acetic acid (20 ml) and water (2 ml). This solution was then treated dropwise, over a period of 15 min, with a solution of chromic acid (0.8 g) in water (10 ml), acetic acid (40 ml), and sulfuric acid (1 ml). After 15 h the mixture was poured into water, the products were extracted with ether – methylene chloride, and the solvent extract was worked up in the usual way. The residue (0.85 g) was crystallized from ether to give 0.67 g of material, m.p. 190–192°. Two further recrystallizations from ether and acetone gave pure 3,12,20-trioxopregnane, m.p. 198–201°, giving no depression on admixture melting point, and exhibiting an infrared spectrum which was superimposable on that of an authentic sample of this compound.

1. K. Tori, T. Komeno, and T. Nakagawa. J. Org. Chem. **29**, 1136 (1964).
2. T. Reichstein and E. von Arx. Helv. Chim. Acta, **23**, 747 (1940).
3. R. Hirschmann, C. S. Snoddy, Jr., C. F. Hiskey, and N. L. Wendler. J. Am. Chem. Soc. **76**, 4013 (1954).
4. J. Elks, G. H. Phillipps, D. A. H. Taylor, and L. J. Wyman. J. Chem. Soc. 1739 (1954).
5. P. Plattner. U.S. Patent No. 2,599,481 (June 3, 1952).
6. H. B. Henbest and T. I. Wrigley. J. Chem. Soc. 4596 (1957).
7. E. L. Eliel. *In* Steric effects in organic chemistry. *Edited by* M. S. Newman. John Wiley & Sons, Inc., New York. 1956. pp. 130–132.
8. N. G. Gaylord. Reduction with complex metal hydrides. Interscience Publishers, Inc., New York. 1956. pp. 665–666.
9. A. Byers and W. J. Hickinbottom. J. Chem. Soc. 1334 (1948).
10. W. J. Hickinbottom, D. Peters, and D. G. M. Wood. J. Chem. Soc. 1360 (1955).
11. W. J. Hickinbottom and G. E. M. Moussa. J. Chem. Soc. 4195 (1957).
12. J. Iriarte, J. N. Schoolery, and C. Djerassi. J. Org. Chem. **27**, 1139 (1962).
13. O. Wintersteiner and M. Moore. J. Am. Chem. Soc. **65**, 1513 (1943).
14. H. E. Stavely and G. N. Bollenback. J. Am. Chem. Soc. **65**, 1285 (1943).

Received September 15, 1964.
Research and Development Laboratories,
Canada Packers Limited,
Toronto, Ontario.

THE ALKALOIDS OF FUMARIACEOUS PLANTS. LII. A NEW ALKALOID, CULARICINE, AND ITS STRUCTURE

Richard H. F. Manske

The author (1) has described an investigation of the alkaloids of *Corydalis claviculata* (L.) DC. in which an amorphous phenolic fraction was obtained. At the time of publication it had not been possible to isolate pure individual bases from this fraction although it was shown to consist, to a large extent, of a base or bases which on O-methylation generated cularine. It has now been possible to isolate two phenolic bases and to determine the structure of one of these, namely that of cularicine. The other base proved to be identical with cularidine which had already been obtained from *Dicentra cucullaria* (L.) Bernh. (2).

The empirical formula of cularicine, $C_{18}H_{17}O_4N$, suggests that it might be cularidine or an isomer in which two methoxyls have been replaced by a methylenedioxy group and

Can. J. Chem. Downloaded from www.nrcresearchpress.com by 210.87.254.6 on 09/05/12
For personal use only.

the absence of methoxyl (Zeisel) lends further support to such a hypothesis. It has been possible to convert cularicine to cularine by well-known reactions. Its O-methyl ether when heated with phloroglucinol and sulfuric acid (3) generated a vicinal dihydroxy compound and this on reacting with diazomethane yielded cularine. The structure of cularicine is therefore that shown below.

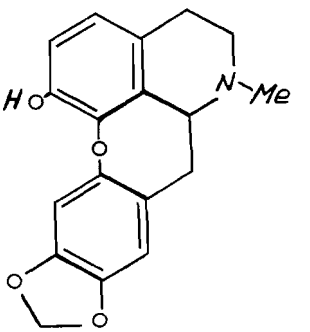

EXPERIMENTAL

Though it was possible to achieve a fair degree of separation by passing a chloroform solution of the total phenolic alkaloids through a column of neutral alumina it was later discovered that cularidine formed a very sparingly soluble perchlorate whereas that of cularicine was readily soluble.

Cularidine

A hot methanolic solution of the phenolic bases was treated with perchloric acid until the mixture was just acid to Congo test paper. Even while hot the sparingly soluble perchlorate of cularidine separated in virtually colorless prisms. It was separated from the cooled mixture, washed with methanol, and recrystallized from a large volume of boiling methanol. It then melted at 297°* with slight gas evolution but little darkening. Cularidine was liberated from this salt by shaking with chloroform and aqueous ammonia. The washed chloroform extract was evaporated to a resin and the latter dissolved in a small volume of methanol. Seeding with a crystal of cularidine induced immediate crystallization. When recrystallized from methanol the cularidine thus obtained melted at 156° either alone or in admixture with a specimen from *D. cucullaria*. The ultraviolet and infrared spectra of the bases from the two sources were superimposable respectively; $[\alpha]_D^{22}$ +292° and +295° (c = 0.99, $CHCl_3$). Five kilograms of dried plant material yielded 10 g of cularidine perchlorate.

Cularicine

The methanolic filtrate from the cularidine perchlorate was concentrated somewhat, diluted with aqueous ammonia to incipient turbidity, and shaken with a large volume of ether. The ether extract was washed with water and the solvent removed. The residue from the latter was dried, dissolved in dry chloroform, and passed through a long column of neutral alumina. The eluate consisted of a small amount of cularidine isolated as its perchlorate. The column was then eluated with chloroform–methanol (100–4) and the eluate evaporated to a resin. The latter when dissolved in a small volume of methanol readily yielded a crop of colorless stout prisms of cularicine melting at 183–184° which when recrystallized from methanol melted at 185°; $[\alpha]_D^{22}$ +295° (c = 0.96, $CHCl_3$). The yield was ca. 2.0 g from 5 kg of plant material.

Anal. Calcd. for $C_{18}H_{17}O_4N$: C, 69.45; H, 5.47; N, 4.50. Found: C, 69.92, 69.87; H, 5.42, 5.48; N, 4.70.

Conversion of Cularicine to Cularine

A solution of 0.25 g of cularicine in methanol was left overnight with an excess of an ethereal solution of diazomethane. The resulting non-phenolic base isolated in the usual way was obtained only as a colorless non-crystalline resin. It yielded a hydrochloride which crystallized readily from methanol and then melted with only slight decomposition at 267° when placed in the bath at 250°.

Anal. Calcd. for $C_{19}H_{19}O_4N.HCl$: C, 63.08; H, 5.53; N, 3.87; 1OMe, 6.97. Found: C, 63.06; H, 6.04; N, 3.60; OMe, 8.69.

The high methoxyl value could be still further increased by further digestion in the Zeisel apparatus and is undoubtedly due in part at least to the elimination of methyl iodide from the N-methyl group.

**All melting points are corrected.*

Can. J. Chem. Downloaded from www.nrcresearchpress.com by 210.87.254.6 on 09/05/12
For personal use only.

The above O-methylcularicine (0.22 g) was brought to the boiling point in a solution containing 0.5 g phloroglucinol in 8 cc of a solution of sulfuric acid prepared from 21 cc of concentrated acid and 25 cc water. Boiling was continued for 2 min and the mixture was then heated on a steam bath for 4 h. The diluted and cooled mixture was filtered to remove the phloroglucide and then extracted with three successive portions (200 cc) of ether. The aqueous solution was then rendered just alkaline with ammonia and extracted with three successive portions (150 cc) of ether. The combined ether extract was evaporated to dryness and the brittle colorless resin (0.09 g) dissolved in methanol, treated with an ethereal solution of diazomethane, and allowed to remain overnight.

The non-phenolic base (0.075 g) isolated in the usual way from the above reaction mixture was dissolved in hexane containing a small amount of dry ether. Seeding of this solution with a crystal of cularine caused immediate crystallization and the base thus obtained melted sharply at 115° either alone or in admixture with cularine. The acid oxalate prepared from this in methanol was washed with the same solvent and then melted at 245° either alone or in admixture with an authentic specimen of cularine oxalate.

Cularicine O-Ethyl Ether

The O-ethylation of cularicine with diazoethane in methanol–ether proceeded readily and the resulting non-phenolic base yielded a hydrochloride which was virtually insoluble in acetone but could be crystallized from hot methanol. It was obtained in colorless prisms which melted with only little decomposition at 275°.

Anal. Calcd. for $C_{20}H_{21}O_4N.HCl$: C, 63.91; H, 5.86; 1OEt, 11.98. Found: C, 64.17; H, 5.99; OEt, 12.58.

The free base, O-ethylcularicine, regenerated from this hydrochloride was crystallized from ether–hexane and consisted of stout prisms melting at 114°.

Anal. Calcd. for $C_{20}H_{21}O_4N$: C, 70.80; H, 6.20; N, 4.13. Found: C, 70.83, 70.87; H, 6.19, 6.21; N, 4.20.

1. R. H. F. Manske. Can. J. Research **B**, **18**, 97 (1940).
2. R. H. F. Manske. Can. J. Research **B**, **16**, 81 (1938).
3. E. Späth and H. Holter. Ber. **60**, 1891 (1927).

Received November 30, 1964.
Research Laboratory,
Dominion Rubber Co. Ltd.,
Guelph, Ontario.

AN IMPROVED SYNTHESIS OF ε-*N*-ACETYL-L-LYSINE AND SIMILAR COMPOUNDS

Leo Benoiton and Jean Leclerc

Enzymic experiments in our laboratory have required us to prepare large amounts of ε-*N*-acetyl-L-lysine. We have found that use of the original procedure (1), or a modification of it (2), for its synthesis, leads to material which is free of lysine only after several recrystallizations which are accompanied by a considerable loss of material. Final yields were usually in the 20–35% range. To overcome this, various ion-exchange resin systems have been used to purify the compound (3, 4). These are adequate but their use renders the procedure laborious. We have sought and found a procedure which is simpler and which gives better yields of pure ε-*N*-acetyl-L-lysine.

The usual synthesis consists in the acylation of the copper salt of the amino acid with acetic anhydride (1, 2). However, the reaction is far from being complete; and since the solubility of the unreacted starting material is similar to that of the product, purification by recrystallization is not efficient. We have overcome the difficulty by using a different acylating agent, namely, *p*-nitrophenyl acetate. Nitrophenyl esters are used routinely as acylating or peptide bond forming agents in peptide chemistry (5). In the presence of an excess of *p*-nitrophenyl acetate, no unsubstituted amino acid remained in a solution of the copper salt of lysine after 12 h. Moreover, most of the product had precipitated out of

Can. J. Chem. Downloaded from www.nrcresearchpress.com by 210.87.254.6 on 09/05/12
For personal use only.

The above O-methylcularicine (0.22 g) was brought to the boiling point in a solution containing 0.5 g phloroglucinol in 8 cc of a solution of sulfuric acid prepared from 21 cc of concentrated acid and 25 cc water. Boiling was continued for 2 min and the mixture was then heated on a steam bath for 4 h. The diluted and cooled mixture was filtered to remove the phloroglucide and then extracted with three successive portions (200 cc) of ether. The aqueous solution was then rendered just alkaline with ammonia and extracted with three successive portions (150 cc) of ether. The combined ether extract was evaporated to dryness and the brittle colorless resin (0.09 g) dissolved in methanol, treated with an ethereal solution of diazomethane, and allowed to remain overnight.

The non-phenolic base (0.075 g) isolated in the usual way from the above reaction mixture was dissolved in hexane containing a small amount of dry ether. Seeding of this solution with a crystal of cularine caused immediate crystallization and the base thus obtained melted sharply at 115° either alone or in admixture with cularine. The acid oxalate prepared from this in methanol was washed with the same solvent and then melted at 245° either alone or in admixture with an authentic specimen of cularine oxalate.

Cularicine O-Ethyl Ether

The O-ethylation of cularicine with diazoethane in methanol–ether proceeded readily and the resulting non-phenolic base yielded a hydrochloride which was virtually insoluble in acetone but could be crystallized from hot methanol. It was obtained in colorless prisms which melted with only little decomposition at 275°.

Anal. Calcd. for $C_{20}H_{21}O_4N.HCl$: C, 63.91; H, 5.86; 1OEt, 11.98. Found: C, 64.17; H, 5.99; OEt, 12.58.

The free base, O-ethylcularicine, regenerated from this hydrochloride was crystallized from ether–hexane and consisted of stout prisms melting at 114°.

Anal. Calcd. for $C_{20}H_{21}O_4N$: C, 70.80; H, 6.20; N, 4.13. Found: C, 70.83, 70.87; H, 6.19, 6.21; N, 4.20.

1. R. H. F. MANSKE. Can. J. Research **B**, **18**, 97 (1940).
2. R. H. F. MANSKE. Can. J. Research **B**, **16**, 81 (1938).
3. E. SPÄTH and H. HOLTER. Ber. **60**, 1891 (1927).

RECEIVED NOVEMBER 30, 1964.
RESEARCH LABORATORY,
DOMINION RUBBER CO. LTD.,
GUELPH, ONTARIO.

AN IMPROVED SYNTHESIS OF ε-*N*-ACETYL-L-LYSINE AND SIMILAR COMPOUNDS

LEO BENOITON AND JEAN LECLERC

Enzymic experiments in our laboratory have required us to prepare large amounts of ε-*N*-acetyl-L-lysine. We have found that use of the original procedure (1), or a modification of it (2), for its synthesis, leads to material which is free of lysine only after several recrystallizations which are accompanied by a considerable loss of material. Final yields were usually in the 20–35% range. To overcome this, various ion-exchange resin systems have been used to purify the compound (3, 4). These are adequate but their use renders the procedure laborious. We have sought and found a procedure which is simpler and which gives better yields of pure ε-*N*-acetyl-L-lysine.

The usual synthesis consists in the acylation of the copper salt of the amino acid with acetic anhydride (1, 2). However, the reaction is far from being complete; and since the solubility of the unreacted starting material is similar to that of the product, purification by recrystallization is not efficient. We have overcome the difficulty by using a different acylating agent, namely, *p*-nitrophenyl acetate. Nitrophenyl esters are used routinely as acylating or peptide bond forming agents in peptide chemistry (5). In the presence of an excess of *p*-nitrophenyl acetate, no unsubstituted amino acid remained in a solution of the copper salt of lysine after 12 h. Moreover, most of the product had precipitated out of

Can. J. Chem. Downloaded from www.nrcresearchpress.com by 210.87.254.5 on 09/05/12
For personal use only.

solution, rendering the purification very simple. The copper was removed from the salt with hydrogen sulfide without the usual addition of acid, and the product crystallized after evaporating the solution. Two other ω-*N*-substituted diamino acids were also prepared by the same technique.

TABLE I

Compounds	Yield (%)	Analyses					
		Calculated (%)			Found (%)		
		C	H	N	C	H	N
ϵ-*N*-Acetyl-L-lysine*	65–75	51.0	8.6	14.9	51.0	8.6	14.9
δ-*N*-Acetyl-L-ornithine	60	—	—	16.1	—	—	16.0
γ-*N*-Acetyl-L-diaminobutyric acid†	65	45.0	7.6	17.5	44.8	7.6	17.5

*$[\alpha]_D^{23}$ +22.1 (1 in 5 *N* HCl).
†New compound, $[\alpha]_D^{23}$ +42.8 (0.6 in 5 *N* HCl).

The results of the experiments are summarized in Table I. Optical rotation measurements indicated that no racemization had occurred. Assay of a sample of ϵ-*N*-acetyl-L-lysine for its L-lysine content using lysine decarboxylase from *Bacterium cadaveris* (6) indicated a contamination not exceeding 0.2%.

The copper salt of γ-*N*-acetyl-L-diaminobutyric acid did not precipitate out of the reaction mixture. Consequently, the product was isolated using an ion-exchange resin. In two preparations, ϵ-*N*-acetyl-L-lysine was also isolated in this manner without previously filtering off the copper salt. Material of the same purity with no increase in yield was obtained.

EXPERIMENTAL

p-Nitrophenyl acetate, crystallized from 95% ethanol, m.p. 78°, was prepared from acetyl chloride and the sodium salt of *p*-nitrophenol as described for the chloracetyl ester (7). It has been prepared using acetic anhydride (8), and is commercially available (Eastman Co., Rochester, N.Y.).

General Procedure

Excess cupric carbonate was added to a boiling solution of the amino acid (0.01 mole) and the mixture was filtered. To the filtrate, at room temperature, was added sodium bicarbonate (0.03 mole), *p*-nitrophenyl acetate (0.02 mole), and a few milliliters of ethyl acetate to keep the ester in solution. The mixture was stirred vigorously for 15 h after which time the precipitated copper salt was filtered off and washed with cold water and ethyl acetate. The material was suspended in warm water, freed of copper with H_2S followed by charcoal treatment, and the resulting solution evaporated to dryness. The residue was recrystallized from water-ethanol.

Isolation Using Dowex 50

After the reaction had been completed, the mixture was acidified to litmus with HCl (enough to dissolve the precipitate if one was present), and extracted twice with ether. The mixture was freed of copper with H_2S, and stirred in the presence of 80 ml of Dowex 50 (H^+ form) for 1 h. The resin was filtered off, washed with copious amounts of water, and then stirred in 3 *N* ammonium hydroxide for $\frac{1}{4}$ h. The resin was removed by filtration, the filtrate evaporated to dryness, and the residue crystallized from water.

ACKNOWLEDGMENT

Financial support of this work by the Medical Research Council and the Department of Education of the Province of Quebec (a bursary to J. L.) is gratefully acknowledged.

1. A. NEUBERGER and F. SANGER. Biochem. J. **37**, 515 (1943).
2. J. P. GREENSTEIN and M. WINITZ. Chemistry of the amino acids. Vol. 3. J. Wiley & Sons, Inc., New York, N.Y. 1961. p. 2117.

Can. J. Chem. Downloaded from www.nrcresearchpress.com by 210.87.254.5 on 09/05/12
For personal use only.

3. W. K. Paik and L. Benoiton. Can. J. Biochem. Physiol. **41**, 1643 (1963).
4. M. Koivusala, C. Elorriaga, Y. Kaziro, and S. Ochoa. J. Biol. Chem. **238**, 1038 (1963).
5. M. Bodansky. Ann. N.Y. Acad. Sci. **88**, 655 (1960).
6. W. K. Paik, L. Bloch-Frankenthal, S. M. Birnbaum, M. Winitz, and J. P. Greenstein. Arch. Biochem. Biophys. **69**, 56 (1957).
7. L. Benoiton. J. Chem. Soc. 763 (1961).
8. F. D. Chattaway. J. Chem. Soc. 2495 (1931).

Received November 20, 1964.
Department of Biochemistry,
Faculty of Medicine,
University of Ottawa,
Ottawa, Canada.

Can. J. Chem. Downloaded from www.nrcresearchpress.com by 210.87.254.5 on 09/05/12
For personal use only.

ERRATUM: AMINO ACIDS AND PEPTIDES. II. SYNTHESIS OF ε-*N*-METHYL-L-LYSINE AND RELATED COMPOUNDS

Leo Benoiton

(Ref. Can. J. Chem. 42, 2043 (1964))

On page 2047, the last line of the text should read $C_9H_{22}Cl_2N_2O_2$ (261.2) requires C, 41.4; H, 8.5; N, 10.7%.

Reference 13 should read Arch. Biochem. Biophys. **69**, 56 (1957).

Department of Biochemistry,
Faculty of medicine,
University of Ottawa,
Ottawa, Canada.

Canadian Journal of Chemistry. Volume 43 (1965)

ERRATUM: EFFECTS OF pH IN THE γ-RADIOLYSIS OF AQUEOUS SOLUTIONS OF CYSTEINE AND METHYL MERCAPTAN

D. A. Armstrong and V. G. Wilkening

(Ref. Can. J. Chem. 42, 2631 (1964))

On page 2632, reaction [8] should be

[8] $$e_{aq}^- + H^+ \rightarrow H.$$

On page 2635, in the second sentence of the note added in proof, k_7 should be substituted for k_8.

Chemistry Department,
University of Alberta,
Calgary, Alberta.

Canadian Journal of Chemistry. Volume 43 (1965)

p 995-2452

Canadian Journal of Chemistry

Issued by THE NATIONAL RESEARCH COUNCIL OF CANADA

VOLUME 43 MAY 1965 NUMBER 5

REACTIONS OF AMIDES AND RELATED COMPOUNDS

II. NUCLEAR MAGNETIC RESONANCE INVESTIGATION OF ADDUCTS OF *N*-METHYLFORMAMIDE WITH HCl AND HBr AND *N,N*-DIMETHYLFORMAMIDE WITH PROTONATING ACIDS AND SILVER SALTS[1]

STEPHEN J. KUHN AND JOHN S. MCINTYRE

Exploratory Research Laboratory, Dow Chemical of Canada, Limited, Sarnia, Ontario

Received October 1, 1964

ABSTRACT

The proton magnetic resonance spectra of dimethylformamide – proton acid and dimethylformamide – silver salt complexes in 2-nitropropane solution as well as *N*-methylformamide·HCl and HBr adducts in tetramethylene sulfone solution have been investigated. The results indicate that the protonation takes place on the carbonyl oxygen. For most of the acids investigated, the acid strength correlates with shifts of both the methyl proton and the proton complexed at the carbonyl oxygen. The dimethylformamide – silver salt complexes have a structure similar to the DMF – Lewis acid or protonating acid adducts.

INTRODUCTION

The structure of the adducts formed when amides are dissolved in protonating acids has been the subject of many investigations during recent years. A geat deal of the previous work has been discussed by Jones and Katritzky (1) and the present authors (2) who conclude that amides predominantly interact with protonating acids, Lewis acids, and alkylhalides at the oxygen atom.

In the n.m.r. spectra of liquid dimethylformamide two peaks of equal area have been found for the *N*-methyl groups. Fraenkel and Niemann (3) have shown that these two peaks remain unchanged in aqueous strong acid solution and in 100% H_2SO_4 and D_2SO_4. They point out that in the *O*-protonated form, restricted rotation around the C—N bond would still exist, while in *N*-protonated amides this restriction would be eliminated. No definite peak could be assigned to the O—H proton because of the fast exchange of protons. Gillespie and Birchall (4) recorded the proton resonance spectra of acetamide, formamide, dimethylacetamide, and dimethylformamide in fluorosulfonic acid at low temperature and were able to observe for the first time the signal from the captured proton and determine with certainty the site of protonation.

We have reported an n.m.r. study of the Lewis acid adducts of dimethylformamide and concluded that the interaction is on the carbonyl oxygen of the molecule (2). In the present investigation, salts of dimethylformamide from different protonating acids have been prepared and the proton resonance spectra of these compounds have been recorded. The *N*-methylformamide·HCl and HBr salts, DMF·$AgBF_4$, and DMF·$AgClO_4$ are also

[1]*Contribution No. 117.*

Can. J. Chem. Downloaded from www.nrcresearchpress.com by 210.87.254.5 on 09/05/12
For personal use only.

included. All of our investigations have been carried out at room temperature with the exception of the DMF·HCl salt which was also studied at −57 °C.

EXPERIMENTAL

(1) Preparation of DMF – Proton Acid Adducts

(*a*) DMF (0.2 mole) was dissolved in 100 ml of ether and the solution was saturated with HCl or HBr. The precipitated solid was filtered, washed three times with 25 ml of ether, and pumped dry, and 0.1 mole of product was dissolved in 80 g of 2-nitropropane.

(*b*) The $ClSO_3H$, CH_3SO_3H, CCl_3COOH, CF_3COOH, $CHCl_2COOH$, $CH_2ClCOOH$, picric acid, benzoic acid, and CH_3COOH adducts were made by carefully measuring 0.1 mole of DMF and 0.1 mole of acid into 80 g of 2-nitropropane. The n.m.r. spectra of these solutions were recorded without isolating the compounds.

(2) Preparation of N-Methylformamide·HCl and HBr Salts

N-Methylformamide (0.2 mole) was dissolved in 100 ml of ether and the solution was saturated with either HCl or HBr gas at 0 °C. The solid product was filtered, washed with ether, and pumped dry. The salts were dissolved in tetramethylene sulfone and their n.m.r. spectra were recorded at room temperature.

(3) Preparation of DMF·$AgBF_4$ and DMF·$AgClO_4$ Salts

Anhydrous silver salt (0.1 mole) was dissolved in 80 g of 2-nitropropane, and 0.1 mole of DMF was added dropwise to the solution which was kept around 0 °C during the addition.

Nuclear Magnetic Resoance

The nuclear magnetic resonance spectra were recorded on a Varian A-60 spectrometer. All spectra were obtained at room temperature; the DMF·HCl complex was also measured at −57 °C.

Chemical shifts of the methyl protons were measured relative to the second band of the 2-nitropropane septuplet on a 100 cycle sweep width. The aldehyde, the amine, and the protonated oxygen peaks were measured relative to internal tetramethylsilane. For the *N*-methylformamide·HCl and HBr adducts, the peaks are relative to external tetramethylsilane.

RESULTS AND DISCUSSION

N-Methylformamide·HCl and HBr Salts

The n.m.r. spectra of solutions of *N*-methylformamide·HCl and HBr adducts in tetramethylene sulfone contain three signals below the methyl region; assignments were made as in Table I. The presence of three peaks at low field immediately shows that the protonation takes place on the carbonyl oxygen. The relative areas of the peaks are approximately 1:1:1. If the *N*-atom of the molecule is protonated, one less proton signal should be present and the ratio of areas should be 2:1. The spectra for *N*-methylformamide and the *N*-methylformamide·HBr complex are shown in Fig. 1 and Fig. 2 respectively. The adducts were recovered unchanged by diluting the solution with ether.

TABLE I

Proton shifts of *N*-methylformamide·HCl and HBr complexes in tetramethylene sulfone*

Adduct	Formyl	NH	OH
N-Methylformamide	512(1.1)	438(0.9)	
N-Methylformamide·HCl	528(1.1)	581(1.0)	953(0.9)
N-Methylformamide·HBr	538(1.1)	612(0.9)	890(1.0)

*Shifts are in c.p.s. downfield from tetramethylsilane; areas of the peaks are shown in parentheses.

N,N-Dimethylformamide Salts

The results in Table II show that there are considerable shifts in the proton peaks of DMF – proton acid adducts. In all of the spectra a new peak appears which is assigned to the proton captured by the carbonyl oxygen. The presence of two methyl peaks

423611

Can. J. Chem. Downloaded from www.nrcresearchpress.com by 210.87.254.5 on 09/05/12
For personal use only.

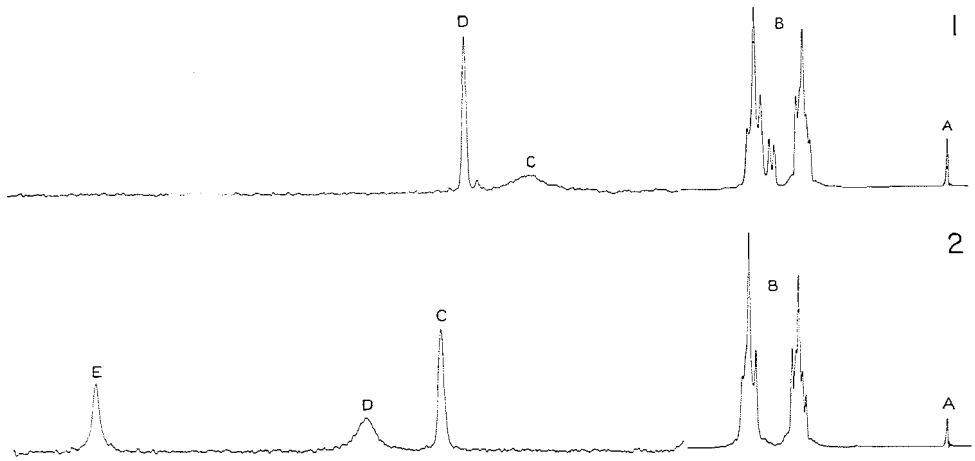

FIG. 1. *N*-Methylformamide in tetramethylene sulfone: A, external tetramethylsilane; B, tetramethylene sulfone; C, NH; D, formyl proton.
FIG. 2. *N*-Methylformamide·HBr in tetramethylene sulfone: A, external tetramethylsilane; B, tetramethylene sulfone; C, formyl proton; D, NH; E, OH.

indicates the retention of the conjugated structure of DMF in these complexes. The two methyl proton signals are doublets for most of the compounds and in the others appear as broad peaks. In all cases including a solution of DMF·HCl in chloroform at −57° only a singlet was observed for the OH and CH proton.

TABLE II

Proton shifts of DMF – protonating acid and silver salt adducts in 2-nitropropane

Adduct	*cis* Methyl*	*trans* Methyl*	Aldehyde†	OH†
DMF	102	94	474	—
DMF·$ClSO_3H$	73	62	508	827
DMF·HBr	78	65	524	822
DMF·HCl	84	72	506	832
DMF·CH_3SO_3H	87	77	497	874
DMF·CF_3COOH	91	82	488	828
DMF·CCl_3COOH	91	82	488	806
DMF·$CHCl_2COOH$	94	85	485	695
DMF·Picric acid	97	87	478	686
DMF·$CH_2ClCOOH$	96	87	484	667
DMF·Benzoic acid	96	89	—	635
DMF·CH_3COOH	98	90	481	591
DMF·$AgBF_4$	94	87	488	—
DMF·$AgClO_4$	96	90	490	—

*Shifts in c.p.s. upfield from second peak in nitropropane septuplet. The *cis* or *trans* is with respect to the aldehyde proton.
†Shifts in c.p.s. downfield from internal tetramethylsilane.

In an earlier study a correlation between the Lewis acid strength and the methyl proton shift has been found (2). It was expected that a similar correlation between the proton shifts of the DMF – proton acid adduct and the acid strength would be obtained. The relative order of acid strength of protonating acids measured by the ionization constant in water solution at 25 °C (5) is compared below with the relative order of acid strength obtained by comparing the n.m.r. spectra of DMF – protonating acid adducts.

Can. J. Chem. Downloaded from www.nrcresearchpress.com by 210.87.254.5 on 09/05/12
For personal use only.

$-\log k$	Methyl proton shifts in DMF·HX adducts	Position of OH-proton in DMF·HX adducts
Trifluoroacetic acid	Trifluoroacetic acid	Trifluoroacetic acid
Picric acid (0.38)	Trichloroacetic acid	Trichloroacetic acid
Trichloroacetic acid (0.89)	Dichloroacetic acid	Dichloroacetic acid
Dichloroacetic acid (1.30)	Picric acid	Picric acid
Chloroacetic acid (2.86)	Chloroacetic acid	Chloroacetic acid
Benzoic acid (4.20)	Benzoic acid	Benzoic acid
Acetic acid (4.76)	Acetic acid	Acetic acid

It can be seen that the results obtained by the two methods agree well with the exception of picric acid.

DMF·AgX Adducts

Adducts (1:1) of DMF with $AgBF_4$ and $AgClO_4$ have also been prepared in solution and the proton resonance spectra of these compounds have been recorded. Their spectra show close similarity to those of the DMF – Lewis acid and DMF – protonating acid complexes (Table II). The coordination has taken place again on the carbonyl oxygen as indicated by the preservation of the conjugated structure of the DMF. The proton shifts in these salts are comparable to those of DMF – weak Lewis acid or protonating acid complexes.

REFERENCES

1. R. A. Y. Jones and A. R. Katritzky. Chem. Ind. London, 722 (1961).
2. S. J. Kuhn and J. S. McIntyre. Can. J. Chem. **43**, 375 (1965).
3. G. Fraenkel and C. Niemann. Proc. Natl. Acad. Sci. U.S. **44**, 688 (1958).
4. R. J. Gillespie and T. Birchall. Can. J. Chem. **41**, 148 (1963).
5. N. A. Lange. Handbook of chemistry. 10th ed. McGraw-Hill Book Co., Inc., Toronto. 1961.

Can. J. Chem. Downloaded from www.nrcresearchpress.com by 210.87.254.5 on 09/05/12
For personal use only.

Can. J. Chem. Downloaded from www.nrcresearchpress.com by 210.87.254.40 on 09/05/12
For personal use only.

CADMIUM SPECIES IN BASIC SOLUTION

D. E. RYAN, J. R. DEAN, AND R. M. CASSIDY
Department of Chemistry, Dalhousie University, Halifax, Nova Scotia

Received October 30, 1964

ABSTRACT

The principal cadmium-containing species in basic solutions varies with the concentration of hydroxide ion such that the solubility of cadmium hydroxide can be satisfactorily expressed, in solutions of high ionic strength, in terms of $[Cd(OH)^+] = 3.0 \times 10^{-9}[OH^-]^{-1}$, $[Cd(OH)_2]_{soln} = 1.0 \times 10^{-6}$, $[Cd(OH)_3^-] = 1.2 \times 10^{-6}[OH^-]$, and $[Cd(OH)_4^{2-}] = 3.1 \times 10^{-6}[OH^-]^2$. Since the solubility varies from 10^{-4} to 10^{-6} *M*, the predominant species at high concentrations of hydroxide ion is $Cd(OH)_4^{2-}$; at low concentrations of hydroxide ion $Cd(OH)^+$ is the principal cadmium-containing ion in solution. There is little free cadmium ion in solutions whose hydroxide ion concentration is greater than 10^{-4} *M*.

Cadmium hydroxide is precipitated as stable β-$Cd(OH)_2$ on the addition of an excess amount of alkali to a solution of a cadmium salt (1). Unlike zinc hydroxide, its solubility is not greatly increased by the presence of excess hydroxide ion. Nevertheless, the existence of hydroxo complexes is indisputable. Casey (2), in discussing the cadmium electrode of the nickel:cadmium battery, stated that the conversion of cadmium to cadmium hydroxide involves an intermediate complex that must be considered. Lake and Goodings (3) concluded from polarographic studies that the cadmium, in concentrated hydroxide solutions, exists in finite concentrations as the tetrahydroxocadmate ion, $Cd(OH)_4^{2-}$. In dilute solutions no appreciable amounts of cadmate ion are formed (4) but solid compounds corresponding to $Na_2Cd(OH)_4$ have been prepared in saturated sodium hydroxide (5). Marcus (6) found no evidence for the existence of polynuclear species and stated that slight hydrolysis, corresponding to the reaction $Cd^{2+} + H_2O \rightleftarrows Cd(OH)^+ + H^+$, was observed. Dryssen (7) has recently shown, through solvent extraction studies using long-chained amines in benzene, that Cd^{2+} forms four mononuclear hydroxo complexes in the rather narrow pH range 9–13 and reported a pK_4 value, at an ionic strength = 3, of 12.0.

Other workers (8, 9, 10) have reported results on solubility and complex formation but failure to consider ionic strength variations makes it difficult, in practical work, to use the values reported. Since a knowledge of the cadmium-containing species in 7 *N* alkali was required, this paper records the results of an investigation into the change in solubility of cadmium hydroxide with changing hydroxide ion concentration; from the data obtained the amounts of Cd^{2+}, $CdOH^+$, $Cd(OH)_2$, $Cd(OH)_3^-$ and $Cd(OH)_4^{2-}$ present in basic solution can be calculated.

METHOD

The overall method involved the equilibration of freshly prepared cadmium hydroxide with solutions containing various concentrations of hydroxide ion and determination of the total cadmium content in the equilibrated solution. A colorimetric method using cadion (11) was first used to determine the cadmium at an ionic strength of 1; however, at higher ionic strengths potassium perchlorate was precipitated through reaction of the reagent solution (cadion in potassium hydroxide) with the perchlorate used to maintain constant ionic strength, and development of another procedure for the determination of small differences in cadmium concentration was necessary. A method, based on measurement of the fluorescence developed when 8-hydroxyquinoline-5-sulfonic acid reacts with cadmium ion (12), proved satisfactory for determining 0.1 p.p.m. cadmium with a precision better than 5%; a detailed account of the factors influencing the method will be published shortly.

Cadmium hydroxide preparation.—The white precipitate of cadmium hydroxide was prepared by the dropwise addition, with stirring, of 1.5 *N* carbonate-free sodium hydroxide to 0.64 *N* cadmium nitrate solution. The base was added at a rate of about 60 drops/min and the entire precipitation process was carried out under a nitrogen gas atmosphere. The precipitate was washed with doubly distilled water and tested to ensure complete removal of excess hydroxide ions. Since aging could have a marked effect on the solubility, the precipitation process was the same for each run and the precipitate was allowed to stand in water for approximately 12 h before filtration.

Equilibrium procedure.—Sodium perchlorate was used to maintain a constant ionic strength and the freshly prepared cadmium hydroxide was agitated, in contact with sodium hydroxide solutions, in a constant temperature bath and shaker. The agitation period was from 10 to 14 d at a bath temperature of 24.5 ± 0.5 °C. All precautions were taken to avoid contact of the solutions with the air. The Nalgene tubes and contents were flushed with nitrogen, capped, and then sealed with wax to ensure tightness. After the agitation period the tubes were centrifuged and the supernatant liquid was decanted through a sintered glass funnel; an aliquot of this solution was made up to a volume to be analyzed.

RESULTS

The solubility of cadmium hydroxide at various equilibrium hydroxide concentrations is given in Table I; at least three replicate samples were studied. Initial concentrations of hydroxide ion are recorded for $[OH^-]$ greater than 10^{-3} *M*; here the differences between beginning and equilibrium concentrations are negligible. Lower concentrations of hydroxide ion at ionic strength = 1 were calculated from measured pH_a values made with a combination glass electrode; we assumed an activity coefficient of 0.809 for hydrogen ion and a K_w of 1.69×10^{-14} (13). The solubilities are uncertain by about $\pm 1 \times 10^{-6}$ *M*.

TABLE I

Solubility of cadmium hydroxide

Ionic strength = 7		Ionic strength = 1	
$[OH^-]$, *M*	Solubility × 10^5, *M*	$[OH^-]$, *M*	Solubility × 10^5, *M*
7.0	16.0	0.93	0.4_8
6.0	11.0	0.54	0.2
5.0	7.6	0.47	0.1
4.0	4.9	0.26	0.2
3.0	2.5	0.047	0.2
2.0	1.2	6.3×10^{-4}	0.6
1.0	0.5_3	4.1×10^{-4}	0.8
0.75	0.3	1.7×10^{-4}	2.2
0.10	0.2	0.68×10^{-4}	4.8
0.05	0.2	0.55×10^{-4}	5.5
0.01	0.3		
0.005	0.4		

INTERPRETATION OF RESULTS

Solid cadmium hydroxide can go into solution through the following processes.

(*a*) $$Cd(OH)_2\downarrow \rightleftarrows Cd(OH)_{2\ soln}$$

(*b*) $$Cd(OH)_2\downarrow \rightleftarrows CdOH^+ + OH^- \quad \Updownarrow \quad Cd^{2+} + OH^-$$

(*c*) $$Cd(OH)_2\downarrow + OH^- \rightleftarrows Cd(OH)_3^- \quad \uparrow\downarrow \ OH^- \quad Cd(OH)_4^{2-}$$

As the concentration of hydroxide increases from 0.55×10^{-4} *M*, the solubility decreases until a minimum solubility of 0.1×10^{-5} is approached. The only reaction which will give a decreasing cadmium concentration with increasing hydroxide concentration is reaction (*b*); as the concentration of hydroxide ion increases, the amount of cadmium

Can. J. Chem. Downloaded from www.nrcresearchpress.com by 210.87.254.40 on 09/05/12
For personal use only.

hydroxide dissolving by reaction (*b*) must decrease (the $[Cd^{2+}]$ and $[Cd(OH)^+]$ in solution decreases) and the solubility becomes smaller. At the minimum solubility it seems reasonable to assume that the cadmium concentration in solution is the result of reaction (*a*) and that the undissociated species, $Cd(OH)_2$, predominates. Beyond this minimum, since the solubility now begins to increase with increasing hydroxide concentration, reaction (*c*) becomes significant and higher hydroxo complexes $Cd(OH)_3^-$ and $Cd(OH)_4^{2-}$ are formed.

If the following reactions are assumed,

$$Cd^{2+} + OH^- \rightleftarrows CdOH^+$$
$$CdOH^+ + OH^- \rightleftarrows Cd(OH)_{2\ soln}$$
$$Cd(OH)_{2\ soln} + OH^- \rightleftarrows Cd(OH)_3^-$$
$$Cd(OH)_3^- + OH^- \rightleftarrows Cd(OH)_4^{2-},$$

and since $[Cd^{2+}][OH^-]^2 = K_{sp}$, the amounts of cadmium-containing species in solution are given by the following expressions,

$$[CdOH^+] = K_1K_{sp}[OH^-]^{-1}$$
$$[Cd(OH)_2]_{soln} = K_2K_{sp}$$
$$[Cd(OH)_3^-] = K_3K_{sp}[OH^-]$$
$$[Cd(OH)_4^{2-}] = K_4K_{sp}[OH^-]^2,$$

where K_1, K_2, K_3, and K_4 are the overall formation constants for $Cd(OH)^+$, $Cd(OH)_2$, $Cd(OH)_3^-$, and $Cd(OH)_4^{2-}$ respectively.

If the possibility of the presence of all entities Cd^{2+}, $CdOH^+$, $Cd(OH)_{2\ soln}$, $Cd(OH)_3^-$, and $Cd(OH)_4^{2-}$ is assumed, it follows that the measured cadmium concentration is composed of a fraction of each. Therefore:

$$[Cd]_{tot} = \text{solubility}$$
$$= [Cd^{2+}] + [CdOH^+] + [Cd(OH)_2]_{soln} + [Cd(OH)_3^-] + [Cd(OH)_4^{2-}]$$
$$= K_{sp}[OH^-]^{-2} + K_1K_{sp}[OH^-]^{-1} + K_2K_{sp} + K_3K_{sp}[OH^-] + K_4K_{sp}[OH^-]^2.$$

At low concentrations of hydroxide ion, where cadmate complexes are not present, the $[Cd]_{tot}$ can be expressed in terms of K_{sp}, K_1, K_2, and the $[OH^-]$; similarly at high hydroxide ion concentrations the solubility is dependent upon the formation of cadmate complexes and the $[Cd]_{tot}$ is correctly expressed in terms of K_{sp}, K_3, K_4, and $[OH^-]$. For example, if it is assumed that only the tetrahydroxo species is present at high concentrations of hydroxide ion, the calculated value for K_4K_{sp} is $(3.1 \pm 0.1) \times 10^{-6}$ in 2–7 *N* base; the constancy of the calculated value shows the assumption to be a valid one and the concentration of $Cd(OH)_4^{2-}$ in solution at any hydroxide ion concentration is given by $3.1 \times 10^{-6}[OH^-]^2$. A similar calculation for solutions 1 *M* in hydroxide ion gives 5.3×10^{-6} for K_4K_{sp} and lower complexes must make a significant contribution to the solubility here. Since a minimum solubility of 1.0×10^{-6} is approached, the intrinsic solubility of cadmium hydroxide may be taken as equal to this value and K_2K_{sp} would be 1.0×10^{-6}. The calculated value for K_3K_{sp}, therefore, from the solubility determined in 1 *M* hydroxide solution, is 1.2×10^{-6} when the contributions of $Cd(OH)_4^{2-}$ and $Cd(OH)_2$ are considered.

Calculated solubilities, using the equation

$$[Cd]_{tot} = 1.0 \times 10^{-6} + 1.2 \times 10^{-6}[OH^-] + 3.1 \times 10^{-6}[OH^-]^2,$$

Can. J. Chem. Downloaded from www.nrcresearchpress.com by 210.87.254.40 on 09/05/12
For personal use only.

agree satisfactorily with the experimental results at hydroxide ion concentrations greater than the minimum solubility value. The minimum solubility occurs experimentally between 0.5 and 0.05 M OH^- where measured solubilities were (0.1–0.2) $\times 10^{-5}$ M; all calculations for constants were made outside these limits for cases where significant solubility changes were observed. The results show that the predominant species at high basicities is the tetrahydroxo complex and that significant solubility changes with increasing hydroxide ion concentration are due to the formation of $Cd(OH)_4^{2-}$.

From solubility measurements at lower concentrations of hydroxide ion K_1K_{sp} can be calculated. Because of the high sodium ion content meaningful measurements of low concentrations of hydroxide ion were not obtained at an ionic strength of 7; however, cadmium hydroxide showed the same solubility at an ionic strength of 1 for similar concentrations of hydroxide ion (Table I), and the calculated constants should apply equally well at high ionic strengths. Since at low concentrations of hydroxide ion

$$[Cd]_{tot} = K_{sp}[OH^-]^2 + K_1K_{sp}[OH^-]^{-1} + K_2K_{sp},$$

the calculated value for K_1K_{sp} is $(3.0 \pm 0.1) \times 10^{-9}$ from hydroxide ion concentrations 6.3×10^{-4} and 4.1×10^{-4} M. (The recorded values of K_{sp} are between 10^{-14} and 10^{-15} (1) and $K_{sp}[OH^-]^{-2}$ makes a negligible contribution here.) The amount of $CdOH^+$ in solution is therefore given by $3.0 \times 10^{-9}[OH^-]$; calculated solubilities at lower hydroxide ion concentrations are within 10% of the experimentally determined solubilities. The value $10^{-14}[OH^-]^{-2}$ calculated for the concentration of free cadmium ion in solution, although unreliable since it varied by $\pm 10^{-1}$, shows that there is little free cadmium ion in solutions with hydroxide ion concentrations greater than 10^{-4} M.

A comparison of the results calculated from

$$[Cd]_{tot} = 3.0 \times 10^{-9}[OH^-]^{-1} + 1 \times 10^{-6} + 1.2 \times 10^{-6}[OH^-] + 3.1 \times 10^{-6}[OH^-]^2$$

with the experimentally determined solubilities is shown in Table II.

TABLE II

Calculated and determined solubilities

	Solubility $\times 10^5$, M	
$[OH^-]$, M	Calculated	Measured
7	16.1	16.0
6	12.0	11.0
5	8.3	7.6
4	5.4	4.9
3	3.0	2.5
2	1.5	1.2
1	0.5_3	0.5_3
0.93	0.5	0.5
0.75	0.4	0.3
0.54	0.3	0.2
0.47	0.2	0.1
0.25	0.2	0.2
0.10	0.1	0.2
0.047	0.1	0.2
6.3×10^{-4}	0.6	0.6
4.1×10^{-4}	0.8	0.8
1.7×10^{-4}	1.9	2.2
0.68×10^{-4}	4.5	4.8
0.55×10^{-4}	5.6	5.5

Can. J. Chem. Downloaded from www.nrcresearchpress.com by 210.87.254.40 on 09/05/12
For personal use only.

The results show that, at the ionic strengths considered, a satisfactory estimate of the solubility of cadmium hydroxide in hydroxide solutions can be calculated from the above equation. The equilibration procedure used to obtain these results is an attractive one in its simplicity and its general applicability to complex formation involving a common ion of a slightly soluble substance; however, accurate measurements of small changes in solubility are necessary and are often difficult experimentally.

ACKNOWLEDGMENT

This work was supported by a grant from the Defence Research Board of Canada.

REFERENCES

1. W. FEITKNECHT and P. SCHINDLER. Pure Appl. Chem. **6**, No. 2, 180 (1963).
2. E. J. CASEY. Chem. Can. **12**, 10 (1960).
3. P. E. LAKE and J. M. GOODINGS. Can. J. Chem. **36**, 1089 (1958).
4. W. M. LATIMER. Oxidation potentials. 2nd ed. Prentice-Hall Inc., New York, N.Y., 1952. p. 172.
5. V. R. SCHOLDER and E. STAUFENBIEL. Z. Anorg. Chem. **247**, 259 (1941).
6. Y. MARCUS. Acta Chem. Scand. **11**, 690 (1957).
7. D. DRYSSEN. Rept. of Seventh Intern. Conf. on Co-ordination Chem. Stockholm, Sweden. 1962.
8. K. H. GAYER and L. WOONTNER. J. Phys. Chem. **61**, 364 (1957).
9. T. MOELLER and P. W. RHYMER. J. Phys. Chem. **46**, 477 (1942).
10. J. PIATER. Z. Anorg. Chem. **174**, 321 (1928).
11. P. CHAVANNE and C. GERONIMI. Anal. Chim. Acta, **19**, 377 (1958).
12. J. A. BISHOP. Anal. Chim. Acta, **29**, 172 (1963).
13. H. S. HARNED and B. B. OWEN. The physical chemistry of electrolytic solutions. 3rd ed. Reinhold Publ. Corp., New York. 1958.

Can. J. Chem. Downloaded from www.nrcresearchpress.com by 210.87.254.40 on 09/05/12
For personal use only.

Can. J. Chem. Downloaded from www.nrcresearchpress.com by 210.87.254.40 on 09/05/12
For personal use only.

HEATS OF MIXING AND HEAT CAPACITIES IN THE SYSTEM: ACETIC ACID – CHLOROFORM – WATER, AT 25°

A. N. CAMPBELL AND J. M. T. M. GIESKES[1]
Department of Chemistry, University of Manitoba, Winnipeg, Manitoba
Received November 19, 1964

ABSTRACT

The heats of mixing, H^E, and heat capacities, at 25 °C, have been determined both for the ternary system: acetic acid – chloroform – water, and for the component binary systems: acetic acid – chloroform and acetic acid – water. The results are discussed in their bearing on the equilibria existing in these systems.

This paper is a continuation of previous work on the thermodynamic properties of the system: acetic acid – chloroform – water (1). The heat of mixing can be readily obtained from direct calorimetric measurements and is, therefore, not subject to the inaccuracies which are involved when the quantity is obtained from the temperature variation of the excess free energy.

The heat of mixing is a direct measure of non-ideality. It can be represented, for a binary solution, by equations such as those suggested by Redlich and Kister (2) of the form

$$H^E = x(1 - x)[A + B(2x - 1) + C(2x - 1)^2 + \ldots],$$

whence the partial molal enthalpies of mixing can be calculated from the following equations:

$$H_1^E = (1 - x)^2[A + B(4x - 1) + C(2x - 1)(6x - 1) + D(2x - 1)^2(8x - 1)],$$

$$H_2^E = x^2[A + B(4x - 3) + C(2x - 1)(6x - 5) + D(2x - 1)^2(8x - 7)],$$

where x is the mole fraction of component 1. The variation of H^E with temperature or the excess heat capacity at constant pressure is another important quantity in the theory of solutions.

The International Critical Tables report some values for the heats of solution of chloroform and of acetic acid in water, but there is some doubt about their reliability: no recent data could be found in the literature. Timofeev (3) gives the heats of solution of acetic acid in chloroform and of chloroform in acetic acid, presumably at infinite dilution, as −502 and −581 cal per mole of solute, respectively. Faucon (4) studied the heats of mixing of acetic acid and water, over the complete range of concentration, at 7°. Pickering (5) studied dilute solutions of acetic acid at 18.6°.

The specific heat of chloroform has been obtained with a reasonable degree of accuracy by a number of authors and their values are reported in the International Critical Tables. The most recent values are those obtained by Staveley, Tupman, and Hart (6) who report the value of C_p over the temperature range 10–56 °C. The specific heats of acetic acid and acetic acid – water mixtures have been investigated by Neumann (7) who reports data for 23.9, 42.0, 59.5, and 80.5 °C. No work has been done on mixtures of acetic acid and chloroform, or on the ternary mixtures of acetic acid, chloroform, and water.

[1]*Holder of Canadian Industries Limited Fellowship, 1963–1964.*

Can. J. Chem. Downloaded from www.nrcresearchpress.com by 210.87.254.40 on 09/05/12
For personal use only.

EXPERIMENTAL

Purification of the Materials

Acetic acid.—The water content of acetic acid obtained from Canadian Industries Limited was determined from the observed freezing point. After addition of a calculated amount of acetic anhydride, the acetic acid was boiled under reflux for about 12 h. After distillation the acetic acid was further purified by means of fractional crystallization until a freezing point of 16.58 °C was obtained.

Chloroform.—Fisher Certified chloroform (A.C.S.) was treated with concentrated sulfuric acid to remove possible traces of alcohol. After extraction of the sulfuric acid with water, the chloroform was dried over anhydrous calcium chloride and finally distilled from anhydrous phosphorus pentoxide. Chloroform had to be purified every 2 weeks because of decomposition of chloroform after several weeks.

Water.—Distilled water was obtained by means of the distillation of water in a Barnstead still, yielding water with a specific conductivity of 5×10^{-6} mho/cm at 25 °C.

1. Heats of Mixing

The calorimeter was similar to that used by Campbell, Kartzmark, and Friesen (8). As a check of the reliability of the apparatus, we determined the heats of mixing of the system: methanol–benzene; this system has been studied by Scatchard *et al.* (9), who give a Redlich and Kister type of equation to reproduce the heat of mixing for any given mole fraction. For five mixtures extending over the complete range of concentration, our results differed by +2 to −4.5 cal from the calculated values, on a total of from 62 to 159 cal. We estimate the overall accuracy of the measured heats of mixing to be of the order of ±3%.

2. Heat Capacities

These were determined by a method essentially the same as that of Campbell and Nagarajan (10). The accuracy of the measurements is ±0.5%.

RESULTS

1. Heats of Mixing

(a) The system: acetic acid – water.—The results are given in Table I. These results when plotted on a smoothed curve gave values which were used for the establishment of an equation of the Redlich and Kister form (2), where $A = 296$, $B = 166$, $C = 19$, $D = 321$, and x is the mole fraction of acetic acid.

TABLE I

Heats of mixing in the binary system: acetic acid – water

Mole fraction HAc	H^E, cal/mole		Temp., °C
	Obsd.	Calcd.	
0.059	−4.7	−3.1	23.0
0.102	0.0	+1.0	25.0
0.214	30	25	23.8
0.218	24.5	26	23.9
0.233	29	27	23.9
0.327	50.5	50	23.8
0.330	55	50.5	24.0
0.426	67.5	66	24.0
0.462	72	70	24.1
0.543	77	77	23.8
0.552	76	78	23.7
0.561	76	78	24.0
0.669	81	81	24.1
0.713	82	81	24.5
0.713	80	80	24.1
0.771	78	80	24.1
0.779	78	78	24.6
0.839	69	70	24.3
0.892	57.5	57	23.8
0.895	51	56	24.4
0.903	54	53	24.5

(b) The system: acetic acid – chloroform.—Similar data are reported in Table II. Here the Redlich and Kister equation now has the constants $A = -574$, $B = -71$, $C = 78$, and x is the mole fraction acetic acid.

TABLE II

Heats of mixing in the system: acetic acid – chloroform

Mole fraction HAc	H^E, cal/mole		Temp., ° C
	Obsd.	Calcd.	
0.167	68	68	22.9
0.196	88	79	23.7
0.207	87	83	24.2
0.214	82	85	24.3
0.291	119	109	23.5
0.330	122	120	24.6
0.404	136	134	24.6
0.429	138	138	24.8
0.526	139	144	23.2
0.540	144	144	23.8
0.546	145	144	23.6
0.552	142	143	24.3
0.555	147	144	24.1
0.647	137	134	24.4
0.666	131	131	24.4
0.673	130	130	24.4
0.696	122	125	24.2
0.771	102	104	24.3
0.773	105	104	24.4
0.781	102	101	24.4
0.785	95	99	24.6
0.794	106	96	24.4
0.822	90	86	24.1
0.840	78	79	24.0
0.846	82	76	24.8
0.871	67	66	25.0
0.876	63	63	24.8
0.882	63	61	24.4
0.908	52	48	24.8
0.909	47	48	24.3
0.911	47	47	24.1
0.912	40	47	24.3
0.921	35	42	24.6
0.941	27	32	24.5
0.954	21	25	24.3

(c) The system: acetic acid – chloroform – water.—The results of heat of mixing are reproduced in Table III and graphically in Fig. 1, where lines of equal heat of mixing, deduced from binary and ternary data, are drawn, including that of zero heat of mixing. Campbell and Kartzmark (8) have proposed to call these lines "idemcals".

We have been able to calculate, using four measured points, a slightly modified Redlich–Kister equation for the ternary heats of mixing data. This equation has the form:

$$H^E = x_1x_2[296 + 166(x_1 - x_2) + 19(x_1 - x_2)^2 + 321(x_1 - x_2)^3] + x_1x_3[-574 - 71(x_1 - x_3) + 78(x_1 - x_3)^2] + x_2x_3[395 - 730(x_2 - x_3) + 2\,138(x_2 - x_3)^2] + 1\,507x_1x_2x_3,$$

where x_1 = mole fraction HAc, x_2 = mole fraction H_2O, x_3 = mole fraction $CHCl_3$, and the units of H^E are cal per mole of mixture. Heats of mixing calculated by this equation are also shown in Table III.

The first three parts of the equation are due to the binary systems HAc–H_2O, HAc–$CHCl_3$, and H_2O–$CHCl_3$, respectively. In other words, this equation yields, for the

Can. J. Chem. Downloaded from www.nrcresearchpress.com by 210.87.254.40 on 09/05/12
For personal use only.

TABLE III

Heats of mixing in the system: acetic acid – chloroform – water

Mole fraction HAc	Mole fraction $CHCl_3$	H^E, cal/mole		Temp., °C
		Obsd.	Calcd.	
0.463	0.099	79	81	24.0
0.444	0.135	79	79	24.0
0.436	0.151	78	78	24.6
0.417	0.188	75	75	24.1
0.650	0.193	18	11	23.3
0.564	0.300	−3	−11	23.9
0.675	0.163	23.5	20	24.6
0.507	0.370	−7	−19	23.6
0.735	0.088	48	43	23.4
0.520	0.235	44	40	24.1
0.606	0.109	64	62	23.9
0.447	0.344	31	29	23.0
0.414	0.391	29	29	23.7
0.402	0.410	29	29	24.1
0.578	0.342	−43	−53	23.4
0.467	0.468	−52	−61	24.8
0.726	0.174	−12	−12	25.2
0.781	0.110	18	12	23.5
0.476	0.215	63	58	24.4
0.558	0.079	77	76	25.0
0.392	0.354	49	49	23.5
0.387	0.153	81	83	25.0
0.429	0.060	82	82	25.4
0.364	0.091	82.5	85	26.4
0.379	0.052	78	79	25.0

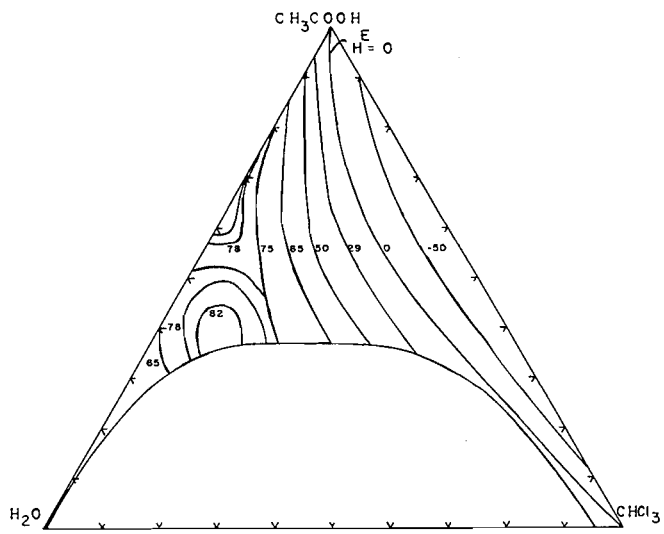

FIG. 1. Heats of mixing for the system acetic acid – chloroform – water.

Can. J. Chem. Downloaded from www.nrcresearchpress.com by 210.87.254.40 on 09/05/12
For personal use only.

binary system H_2O–$CHCl_3$ at 25 °C, an equation which could not be obtained experimentally because of the immiscibility. The last part of the equation is a ternary correction term.

The heat of mixing for the system H_2O–$CHCl_3$ can therefore be represented by the equation:

$$H^E = x_2x_3[395 - 730(x_2 - x_3) + 2\,138(x_2 - x_3)^2],$$

where x_2 = mole fraction H_2O and x_3 = mole fraction $CHCl_3$. Hence the heat of mixing is positive over the entire region of concentration for which miscibility is possible.

2. Heat Capacities

The results obtained for the binary system: acetic acid – chloroform and for the ternary system: acetic acid – chloroform – water are reported in Table IV. In Fig. 2 the excess heat capacity, calculated from the heat capacities of the pure components, is represented as a function of concentration for the binary system: acetic acid – chloroform. In Fig. 3 some lines of equal excess heat capacity for the ternary system, deduced from the data of Table IV, are represented.

TABLE IV

Heat capacities and excess heat capacities of the system: acetic acid – chloroform – water at 25.5 ± 0.5 °C

Mole % HAc	Mole % $CHCl_3$	Mole % H_2O	C_p, cal deg^{-1} g^{-1}	C_p^E, cal deg^{-1} mole^{-1}
79.2	20.8	—	0.406	0.39
58.1	41.9	—	0.342	0.55
68.5	31.5	—	0.369	0.35
64.0	29.5	6.5	0.384	0.73
59.4	27.3	13.3	0.400	1.08
52.7	24.3	23.0	0.425	1.29
44.9	20.6	34.5	0.459	1.54
57.7	42.3	—	0.341	0.58
51.2	37.6	11.2	0.367	1.16
44.3	32.5	23.2	0.406	2.22
43.5	56.5	—	0.307	0.50
38.9	50.6	10.5	0.331	1.24
81.8	18.2	—	0.414	0.31
69.5	15.4	15.1	0.448	0.79
66.2	14.9	18.9	0.453	0.66
60.6	13.5	25.9	0.474	0.93
50.6	11.2	38.2	0.514	1.22
23.7	76.3	—	0.267	0.31
100.0	—	—	0.490	—

DISCUSSION OF RESULTS

1. Heats of Mixing

(a) The System: Acetic Acid – Water

In this system there occurs a change of sign in the heat of mixing. The heat of mixing is negative only in the concentration range 0–0.1 mole fraction acetic acid. The fact that the heat of mixing is positive over a large range of concentration (heat absorbed) can be explained in accordance with the ideas of Joerges and Nikuradse (11). In the pure state both water and acetic acid are strongly associated. On mixing, the acetic acid dimer forms an open chain dimer and acetic acid monomers, both of which associate with water molecules. Energy is required for the dissociation of the associated complexes, but

Can. J. Chem. Downloaded from www.nrcresearchpress.com by 210.87.254.40 on 09/05/12
For personal use only.

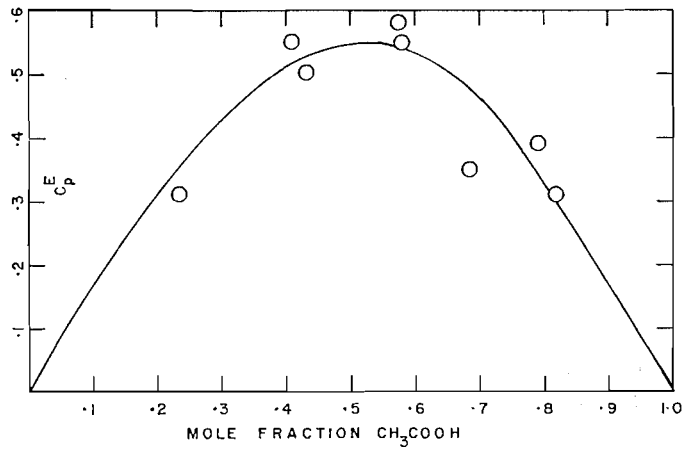

FIG. 2. Excess heat capacity for the system acetic acid – chloroform.

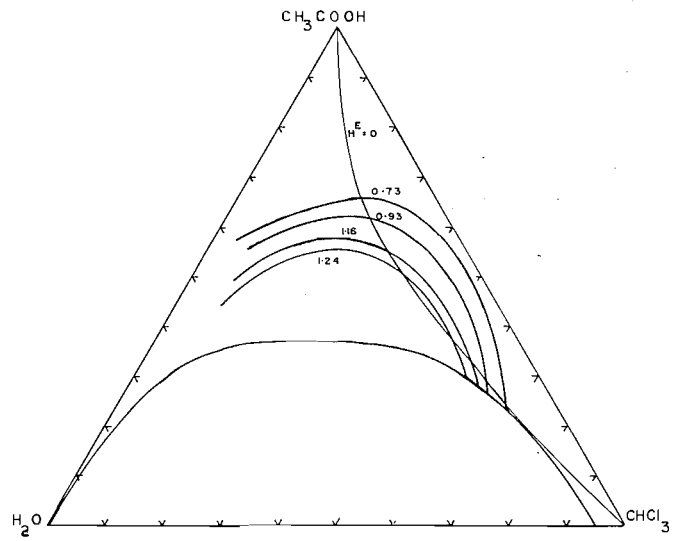

FIG. 3. Lines of equal excess heat capacity for the system acetic acid – chloroform – water.

energy is liberated by the formation of the mixed complexes. The number of mixed associated complexes cannot be larger, and is usually smaller, than the total number of dissociation products. This means that, even if

$$H_{\text{diss}}(\text{I}) + H_{\text{diss}}(\text{II}) < H_{\text{ass}}$$

where the H's represent the heats of dissociation or association per mole of acetic acid, of water, and of mixed complexes, respectively, a positive ΔH of mixing can result; in other words, the energy required to break up the individual associates may be larger than the energy set free by the formation of the mixed complexes. This is clearly what happens with mixtures of water and acetic acid. In the dilute region, ionic hydration energies will play an increasingly important role and this may be one of the factors leading to a negative value of the heat of mixing.

Can. J. Chem. Downloaded from www.nrcresearchpress.com by 210.87.254.40 on 09/05/12
For personal use only.

The Redlich and Kister equation represents the data within the limits of accuracy, as can be seen from Table I.

(b) The System: Acetic Acid – Chloroform

In this system the heat of mixing is negative over the complete range of concentration, i.e. heat is set free on mixing.

The Redlich and Kister formula can be applied successfully, and from Table II it follows that this formula represents the results within limits of accuracy.

In this system, only acetic acid is associated in the pure state. On mixing with chloroform, two processes can occur. The acetic acid dimers can break up to give monomers which in turn will associate with chloroform molecules. The ring dimer may also persist and associate with chloroform in an antiparallel dipole arrangement, and this latter process will be accompanied by a negative heat effect. The negative value of H^E and also the evidence reported in our paper on the dielectric behavior of this system (12) (in particular, the extrapolated value of 216 for the Debye polarization) suggest that both processes may occur but that the latter process is dominant.

(c) The System: Acetic Acid – Chloroform – Water

In this system (disregarding the solutions with very high concentration of water) there are two distinct regions, one of positive heat of mixing and one of negative heat of mixing. The region of negative heat of mixing is relatively small, which indicates that the interaction between water and acetic acid and between water and chloroform is more important than that between chloroform and acetic acid. Furthermore, the interaction between chloroform and water also leads to a positive heat of mixing. From Fig. 1 it can be seen that in the ternary system there occurs a maximum heat of mixing, which is larger than any in the contiguous binary systems. This maximum is mainly due to the chloroform–water interaction.

Of particular interest is the line of zero heat of mixing. This line coincides with the line of zero volume of mixing, as found by Campbell, Kartzmark, and Gieskes (13). In the ternary system, therefore, there appears to be a series of solutions where pseudo-ideality exists, i.e., the opposing interactions are such that the effects of these interactions on the values of the excess functions are balanced to give ideal values of the excess functions. Nevertheless, we consider that the coincidence of the $H^E = 0$ and $V^E = 0$ line is purely accidental. It does not mean that $G^E = 0$ and $C_p{}^E = 0$ for these concentrations, and all the evidence seems to point to $G^E > 0$ over the entire region of concentration. Hence, the pseudoideality is at best partial.

2. Heat Capacities

From the measurements by Neumann (7) and by ourselves, it seems that the value of the excess heat capacity is positive over the entire region of concentration of the ternary system. The error involved in the determination of specific heat is usually less than 0.5% but this has a large effect on the calculated value of the excess heat capacity. Nevertheless, from Fig. 2 it can be seen that the curve of the excess heat capacity ($C_p{}^E[x]$) is approximately symmetrical. The lines of equal excess heat capacity, as represented in Fig. 3, are of an approximate nature. There is no doubt, however, that the lines will follow the pattern of those in Fig. 3. The consequence of the positive value of $C_p{}^E$ is that both H^E and S^E will increase in value with increasing temperature over the entire range of concentration. The line of zero heat of mixing will shift to the side of the binary system: acetic acid – chloroform, with increasing temperature.

Can. J. Chem. Downloaded from www.nrcresearchpress.com by 210.87.254.40 on 09/05/12
For personal use only.

REFERENCES

1. A. N. CAMPBELL *et al.* Can. J. Chem. **41**, 407 (1963); **41**, 1088 (1963); **42**, 186 (1964); **42**, 1379 (1964).
2. O. REDLICH and A. T. KISTER. Ind. Eng. Chem. **40**, 345 (1948).
3. W. TIMOFEEV. Chem. Zentr. (II), **76**, 429 (1905).
4. A. FAUCON. Ann. Chim. Phys. **19**, 70 (1910).
5. S. U. PICKERING. J. Chem. Soc. **67**, 664 (1895).
6. L. A. K. STAVELEY, W. I. TUPMAN, and K. B. HART. Trans. Faraday Soc. **51**, 323 (1955).
7. M. B. NEUMANN. Z. Phys. Chem. A, **158**, 258 (1932).
8. A. N. CAMPBELL, E. M. KARTZMARK, and H. FRIESEN. Can. J. Chem. **39**, 735 (1961).
9. G. SCATCHARD *et al.* J. Am. Chem. Soc. **74**, 3721 (1952).
10. A. N. CAMPBELL and M. K. NAGARAJAN. Can. J. Chem. **42**, 1616 (1964).
11. M. JOERGES and A. NIKURADSE. Z. Naturforsch. **5a**, 259 (1950).
12. A. N. CAMPBELL and J. M. T. M. GIESKES. Can. J. Chem. **42**, 1379 (1964).
13. A. N. CAMPBELL, E. M. KARTZMARK, and J. M. T. M. GIESKES. Can. J. Chem. **41**, 407 (1963).

Can. J. Chem. Downloaded from www.nrcresearchpress.com by 210.87.254.40 on 09/05/12
For personal use only.

Can. J. Chem. Downloaded from www.nrcresearchpress.com by 210.87.254.40 on 09/05/12
For personal use only.

ELECTRON SPIN RESONANCE SPECTRA OF ^{15}N-CENTERED RADICALS AT LOW TEMPERATURES

I. THE RADICAL NH_3^+ TRAPPED IN NH_4ClO_4[1]

M. FUJIMOTO[2] AND J. R. MORTON

Division of Applied Chemistry, National Research Council, Ottawa, Canada

Received October 8, 1964

ABSTRACT

The electron spin resonance spectrum of NH_3^+ trapped in ammonium perchlorate (95% ^{15}N) was examined at 300 °K, 77 °K, and 4 °K. The spectra are interpreted in terms of π-radical theory, and demonstrate the different stages in the freezing-out of the rotational motion of the ion.

INTRODUCTION

Interesting changes (1, 2) in the electron spin resonance (e.s.r.) spectra of the trapped radicals $NH_2^+SO_3^-$ and $NHSO_3^-$ on cooling the host crystals to 77 °K prompted this reexamination of the spectra (3, 4) of NH_3^+ trapped in NH_4ClO_4. It was anticipated that changes in the hyperfine interactions of the protons and the nitrogen nucleus on cooling to 77 °K and 4 °K would elucidate the different stages (4) in the freezing-out of the rotational motion of the ion.

EXPERIMENTAL

In order to obtain improved resolution ammonium perchlorate enriched in $^{15}NH_4ClO_4$ to 95% was purchased from Merck, Sharp, and Dohme Co. Ltd., Montreal. Single crystals of this material, grown by slow evaporation of aqueous solutions, were irradiated with 1.3 MeV ^{60}Co γ-rays in order to generate in them the $^{15}NH_3^+$ radicals. The latter are stable indefinitely at room temperature (4), but before taking low-temperature spectra it was necessary to monitor the decay (3) of the ClO_3 radicals, also formed on irradiation.

Crystals of ammonium perchlorate are orthorhombic (5), and the unit cell, which contains four molecules of NH_4ClO_4, has dimensions $a = 9.20$ Å, $b = 5.82$ Å, $c = 7.45$ Å in the space-group *Pnma*. The unit-cell directions of the crystals were identified with a polarizing microscope, and correlated with the above axes by means of X-ray diffraction photographs. The crystals usually formed hexagonal tablets on {001}, and were elongated along [010].

Electron spin resonance spectra of the irradiated crystals were obtained with a Varian V-4502 spectrometer and V-4012A magnet system. Magnetic field measurements were carried out with the aid of a Varian F-8A proton fluxmeter and a Computer Measurements Company model 707B frequency counter. Low temperature spectra were obtained with Dewar vessels fitting into the V-4532 cavity. The liquid nitrogen Dewar was a quartz vessel of conventional design; the liquid helium Dewar was similar to that described (6) by Hornig and Hyde.

RESULTS

The spectra of NH_3^+ trapped in NH_4ClO_4 crystals at 300 °K have already been described by Cole (3), who advances convincing evidence for the planarity of the radical. The three protons are equivalent for all orientations of the crystal in the magnetic field, and their hyperfine tensors are diagonal in the crystallographic *abc* axis system, as is that of the nitrogen nucleus. The spectrum for the orientation H_0 parallel to the *a*-axis is shown in Fig. 1*a*. The ^{15}N nucleus has spin 1/2 and a higher magnetogyric ratio ($\gamma_{15} = 4.315$) than the normal isotope (^{14}N, spin 1, $\gamma_{14} = 3.076$) and so the spectra of $^{15}NH_3^+$ are somewhat simpler than those of $^{14}NH_3^+$. The principal values of the proton and ^{15}N tensors are given in Table I.

[1]*N.R.C. No. 8314.*

[2]*Visiting scientist, on leave from Department of Physics, University of Manitoba, Winnipeg, Manitoba.*

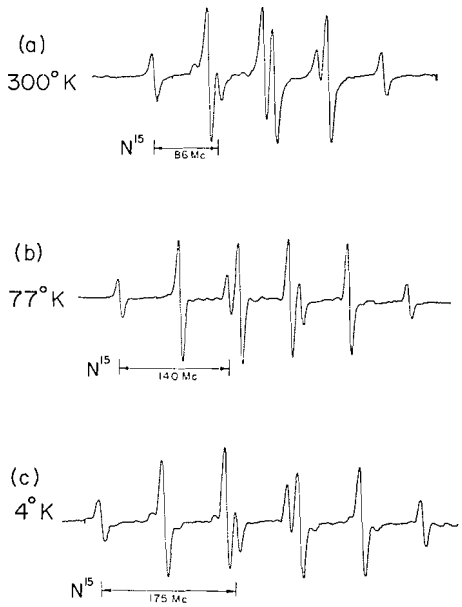

FIG. 1. First derivative electron spin resonance spectra of $^{15}NH_3^+$ in γ-irradiated ammonium perchlorate, H_0 parallel to a-axis, at (*a*) 300 °K, (*b*) 77 °K, and (*c*) 4 °K.

As will be apparent from Fig. 1*b* the spectra obtained at 77 °K differed in some respects from those obtained at room temperature. A large increase in the ^{15}N hyperfine interaction for H_0 parallel to the a-axis was accompanied by a decrease in its value for H_0 parallel to b or c. Moreover, two magnetically distinguishable sites for the radical were apparent when H_0 explored the ac plane. The three protons in the radical remained equivalent at all orientations, however.

TABLE I

Hyperfine tensors for $^{15}NH_3^+$ at 300 °K

Nucleus	Tensor	Principal values*	Principal directions†
Protons	73.3 0.0 0.0 0.0 73.2 0.0 0.0 0.0 69.6	73.3 73.2 69.6	(1.000, 0.000, 0.000) (0.000, 1.000, 0.000) (0.000, 0.000, 1.000)
^{15}N	85.7 0.0 0.0 0.0 73.2 0.0 0.0 0.0 69.6	85.7 73.2 69.6	(1.000, 0.000, 0.000) (0.000, 1.000, 0.000) (0.000, 0.000, 1.000)

*Units of all tensors are Mc/s.
†Direction cosines refer to the *abc* axis system.

At 4 °K the spectra were much more difficult to interpret, because the $^{15}NH_3^+$ radical was no longer rapidly rotating in the crystal. Hyperfine interactions with four non-equivalent spin 1/2 nuclei were apparent, and, in addition, two sites could be distinguished as H_0 explored the ac and bc planes. The spectrum for H_0 parallel to the a-axis is shown in Fig. 1*c*, and it will be seen that ^{15}N hyperfine interaction has increased still further, to 175 Mc/s. At this orientation, which is almost (Fig. 2) perpendicular to the radical plane,

Can. J. Chem. Downloaded from www.nrcresearchpress.com by 210.87.254.40 on 09/05/12
For personal use only.

the inequivalence of the three protons is not resolvable. It was quite impossible to determine the off-diagonal elements α_{ac} and α_{bc} ($\alpha_{ab} = 0$) for the three proton and the ^{15}N hyperfine tensors. Instead, Table III shows the diagonal elements only, that is, the parameters obtained for the orientations H_0 parallel to a, b, and c. Even here some difficulty was experienced, particularly for the orientation H_0 parallel to b. An ^{15}N interaction of approximately 15 Mc/s, together with the normal line-width of 10 Mc/s, led to an ill-resolved spectrum and errors of ± 5 Mc/s in the hyperfine constants. In assigning to the various nuclei the eight hyperfine constants obtained for the orientations H_0 parallel to b and c, use was made of the assumption that the three proton interactions should have the same diagonal sum (within experimental error).

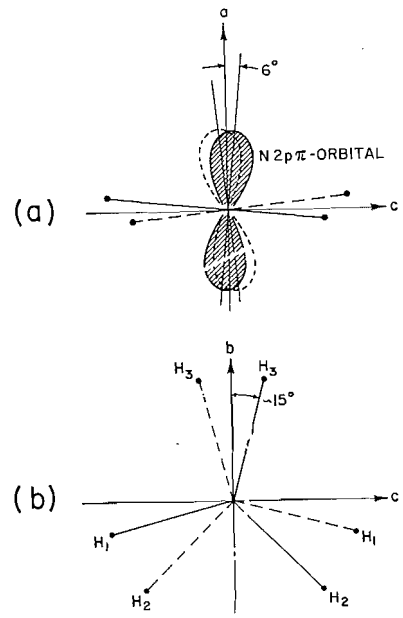

FIG. 2. Orientation of NH_3^+ radical in ammonium perchlorate crystal, projection along (*a*) *b*-axis, (*b*) *a*-axis.

DISCUSSION

Interest in the radical NH_3^+ arises from the fact that NH_3^+ and the isoelectronic methyl radical are the prototypes of a large number of π-electron radicals. The methyl radical has been found to be "planar or very nearly planar" (7), although this had not been anticipated theoretically (8, 9). Radicals derived from methyl, including (10, 11) $CH_2(CO_2H)$ and $CH(CO_2H)_2$ and many others (12), have been trapped in single crystal matrices and studied by e.s.r. The proton and ^{13}C hyperfine interactions are consistent (13, 14) with a planar configuration for these radicals. The radical NH_3^+ was first studied in 1961 (3), and since then detailed calculations (15) of the *isotropic* nitrogen and proton hyperfine interactions have confirmed its planar configuration. It will be shown that the present determination of the *anisotropic* proton interaction in NH_3^+ at 4 °K is consistent with theoretical predictions (2, 13).

It was clear from the results of previous workers (3, 4) that the NH_3^+ radical in NH_4ClO_4 was "tumbling" in the lattice at room temperature, there being only a slight preference for the crystallographic *a*-axis as an axis of rotation. At 77 °K the present

Can. J. Chem. Downloaded from www.nrcresearchpress.com by 210.87.254.40 on 09/05/12
For personal use only.

TABLE II

Hyperfine tensors for $^{15}NH_3^+$ at 77 °K

Nucleus	Tensor	Principal values	Principal directions
Protons	78.4 0.0 ±1.4 0.0 70.4 0.0 ±1.4 0.0 69.3	78.6 70.4 69.1	(∓0.989, 0.000, 0.149) (0.000, 1.000, 0.000) (±0.149, 0.000, 0.989)
^{15}N	140.0 0.0 ±10.0 0.0 48.0 0.0 ±10.0 0.0 40.2	141.0 48.0 39.2	(∓0.995, 0.000, 0.099) (0.000, 1.000, 0.000) (±0.099, 0.000, 0.995)

TABLE III

Hyperfine tensor components for $^{15}NH_3^+$ at 4 °K

Nucleus	Magnetic field parallel to: *a*	*b*	*c*
H_1	81.5±0.5	120±5	25±2
H_2	81.5±0.5	70±5	71±2
H_3	81.5±0.5	20±5	129±2
^{15}N	175.0±0.5	15±5	41±2

results indicate that the motion is largely restricted to rotation about an axis perpendicular to the proton plane (in *ac*, ±6° from *a*), the rotation rate being rapid compared to anisotropic electron–proton hyperfine interactions of about 10^8 s^{-1}. The spectra obtained at 4 °K clearly demonstrated that at this temperature the rotation rate about the axis perpendicular to the proton plane had slowed to very much less than 10^8 s^{-1}.

The principal values of the proton tensors cannot be obtained from Table III. However, it will be seen that the proton interaction parameters for H_0 parallel to *b* are almost equal to those for H_0 parallel to *c*. This must mean that, within the overall experimental error, the radical is symmetrically oriented with respect to the *b* and *c* axes, as, for example, in Fig. 2*b*. The smallest (numerically) principal value of an α-proton tensor in a π-electron radical is (11) parallel to the X—H bond, and the largest (numerically) is perpendicular to the X—H bond but in the radical plane. Neglecting the fact that the perpendicular to the radical plane is 6° from *a*, and assuming that the radical is planar, the largest and smallest principal values of the H_1 and H_3 tensors can be estimated from the data of Table III by a 15° rotation of axes about the *a*-axis. The "principal values" so obtained were 127 and 18 Mc/s for H_1, 137 and 12 Mc/s for H_3. The reasonable agreement obtained suggests the following principal values for the proton tensors in NH_3^+: (−)15 ± 5 Mc/s parallel to the N—H bond; (−)83 ± 2 Mc/s perpendicular to the radical plane; and (−)132 ± 5 Mc/s perpendicular to the N—H bond in the radical plane. The negative sign given these parameters was not determined experimentally but is required theoretically (11, 13). The isotropic proton interaction is therefore (−)77 ± 7 Mc/s and the anisotropic (traceless) tensor has principal values +61, −6, and −55 Mc/s, corresponding to the above principal directions. The anisotropic proton interactions in NH_3^+ are thus considerably larger than those expected (12) from protons attached to a carbon-centered π-radical. However, this has been predicted theoretically (2, 13) and, for example, with a bond length of 1.0 Å, and effective nuclear charge 3.7, the calculated (2) principal values for the corresponding principal directions are +63, −11, and −53 Mc/s.

Can. J. Chem. Downloaded from www.nrcresearchpress.com by 210.87.254.40 on 09/05/12
For personal use only.

The ^{15}N hyperfine interaction in $^{15}NH_3^+$ is similar to that reported (2) for other nitrogen-centered π-radicals, when the conversion factor $\gamma_{15}/\gamma_{14} = 1.403$ is applied. The very large principal value for H_0 perpendicular to the radical plane is typical (2), and the apparent deviation from axial symmetry is due, in part, to this large principal value, which has a component along c but not along b.

ACKNOWLEDGMENT

The authors are grateful to Dr. L. D. Calvert for checking the unit-cell dimensions of the crystals by means of X-ray diffraction photographs.

REFERENCES

1. J. R. Rowlands and D. H. Whiffen. Nature, **193**, 61 (1962).
2. J. R. Rowlands. Mol. Phys. **5**, 565 (1962).
3. T. Cole. J. Chem. Phys. **35**, 1169 (1961).
4. J. S. Hyde and E. S. Freeman. J. Phys. Chem. **65**, 1636 (1961).
5. C. Gottfried and C. Schusterius. Z. Krist. **84**, 65 (1932).
6. A. W. Hornig and J. S. Hyde. Mol. Phys. **6**, 33 (1963).
7. G. Herzberg. Proc. Roy. Soc. London, Ser. A, **262**, 291 (1961).
8. A. D. Walsh. J. Chem. Soc. 2296 (1953).
9. J. W. Linnett and A. J. Poë. Trans. Faraday Soc. **47**, 1039 (1951).
10. A. Horsfield, J. R. Morton, and D. H. Whiffen. Mol. Phys. **4**, 327 (1961).
11. H. M. McConnell, C. Heller, T. Cole, and R. W. Fessenden. J. Am. Chem. Soc. **82**, 766 (1960).
12. J. R. Morton. Chem. Rev. **64**, 453 (1964).
13. H. M. McConnell and J. Strathdee. Mol. Phys. **2**, 129 (1959).
14. G. K. Fraenkel. Pure Appl. Chem. **4**, 143 (1962).
15. G. Giacometti and P. L. Nordio. Mol. Phys. **6**, 301 (1963).

Can. J. Chem. Downloaded from www.nrcresearchpress.com by 210.87.254.40 on 09/05/12
For personal use only.

Can. J. Chem. Downloaded from www.nrcresearchpress.com by 210.87.254.105 on 09/05/12
For personal use only.

GAS–LIQUID CHROMATOGRAPHY OF TERPENES

PART XIII. THE VOLATILE OIL OF THE LEAVES OF JUNIPERUS HORIZONTALIS MOENCH[1]

F. M. COUCHMAN[2] AND E. VON RUDLOFF

National Research Council of Canada, Prairie Regional Laboratory, Saskatoon, Saskatchewan

Received November 25, 1964

ABSTRACT

The neutral leaf oil of the creeping juniper from the Prairies was analyzed by gas–liquid chromatography. *d*-Sabinene (36.5%) was found to be the major constituent, and smaller amounts of *d*-limonene (17.5%), *p*-cymene (3.0%), *d*-α-pinene (1.6%), γ-terpinene (0.4%), *d*-terpinen-4-ol (4.6%), linalool (0.8%), citronellol (0.8%), γ-cadinene (1.3%), *l*-elemol (3.8%), α-cadinol or γ-eudesmol (1.6%), and impure α-cyperone (3.9%) were isolated. α-Thujene (3.0%), camphene (0.2%), β-pinene (0.3%), myrcene (3.0%), β-phellandrene (0.2%), terpinolene (0.1%), 2,4-(8)-*p*-menthadiene (0.1%), methyl citronellate (0.4%), and geraniol (0.2%) were tentatively identified. The composition of this oil closely resembles that of Rocky Mountain juniper leaves. A small amount of the oil from a hybrid of these two species was analyzed and the possibility of detecting hybridization by analysis of the leaf oil is discussed.

The creeping juniper (*Juniperus horizontalis* Moench) is widely distributed in Canada, being found from coast to coast. It is ordinarily distinguished by its low creeping habit of growth and radiating branches. Like the Rocky Mountain juniper, it has no commercial value except for ornamental planting and numerous forms have been developed. In Parts IX and XI of this series (1, 2) the analysis of the volatile oils of the leaves of savin juniper (*J. sabina* L.) and Rocky Mountain juniper (*J. scopulorum* Sarg.), respectively, were described. This publication deals with a similar analysis of the leaf oil of the creeping juniper. No reference in the chemical literature dealing with this oil could be found.

A large batch of leaves of mature plants found near Saskatoon, Saskatchewan, was steam distilled to give a pale-yellow oil (0.89% yield) having n_D^{30} 1.4763 and $[\alpha]_D^{30}$ +36.76°. The oil was prefractionated into hydrocarbons and oxygenated compounds by elution chromatography on modified silicic acid as described previously (2). These fractions were subdivided into mono- and sesqui-terpenes, by preparative gas–liquid chromatography (g.l.c.) on short columns. The four fractions thus obtained were fractionated further into single components by preparative g.l.c. All major and some minor constituents were isolated and characterized by their physical properties. Several trace components were tentatively identified by their relative retention times (r.r.t.). The percentage composition (Table I, column A) was determined by measurement of the area under the peaks (triangulation method, average of duplicate) as recorded in linear temperature-programmed runs (Fig. 1A). The components identified by r.r.t. only are shown in parentheses. The error of the method was discussed before (2). The numbering of peaks is the same as used for the oil from Rocky Mountain juniper (2).

Whereas it is accepted that some of the chemical components of conifer wood can be used for taxonomic correlations (3–7), it has only recently been demonstrated that the same may hold for the components of conifer leaf oils (1, 8). Comparison of the composition of the leaf oils from Savin (1), Rocky Mountain (2), and creeping juniper shows that all three contain *d*-sabinene as a major component. Also, common to all three junipers

[1]*Issued as N.R.C. No. 8345.*

[2]*National Research Council of Canada Postdoctorate Fellow, 1963–1965.*

TABLE I

Percentage composition of the volatile leaf oil of creeping juniper

Peak No.	Compound	r.r.t.	% A	% B
2*a*	(α-Thujene)	0.29	3.0	4.5
b	*d*-α-Pinene	0.29	1.6	
3	(Camphene)	0.42	0.2	0.2
4*a*	(β-Pinene)	0.55	0.3	38.5
b	*d*-Sabinene	0.62	36.5	
5	(Car-3-ene)	0.73	1.2	0.5
6	(Myrcene)	0.82	3.0	1.5
8*a*	*d*-Limonene	1.00	17.5	12.5
b	(β-Phellandrene)	1.06	0.2	
9	γ-Terpinene	1.40	0.4	0.5
10	*p*-Cymene	1.63	3.0	2.2
11*a*	(Terpinolene)	1.79	0.1	0.2
b	(*p*-Menth-2,4(8)-diene)	1.85	0.1	
A	Unidentified	—	0.4	0.1
B	Unidentified	—	0.3	0.1
12	(Thujone)	0.64	0.8	0.2
13	(Isothujone)	0.68	0.7	1.7
14	Linalool	1.02	0.8	3.3
C	Unidentified	—	0.4	0.5
15	(Methyl citronellate)	1.20	0.4	—
16*a*	*d*-Terpinen-4-ol	1.40	4.6	3.3
b	(*l*-Elemene)	1.42	?	?
17	Unidentified	1.60	0.6	0.2
X	Unidentified	—	—	0.2
18*a*	(Sabinyl acetate)	1.90	0.3	0.1
b	C_{15} Hydrocarbon	—	0.3	
19*a*	C_{15} Hydrocarbon	—	0.8	0.3
b	(Sabinol)	2.20	0.2	0.2
20	Cadinene I	2.46	1.6	0.5
22*a*	γ-Cadinene	3.30	1.3	2.6
b	*d*-Citronellol	3.30	0.8	
23	C_{15} Hydrocarbon	—	0.5	1.1
24*a*	C_{15} Hydrocarbon	—	0.2	0.2
b	C_{15} Hydrocarbon	—	0.8	—
25	(Geraniol)	5.00	0.2	0.3
D	Unidentified	—	0.2	0.3
26	Unidentified	—	0.8	0.4
27	Unidentified	—	0.2	—
28	Unidentified	—	0.4	—
29	Unidentified	0.64	0.1	1.2
30	Unidentified	—	—	0.3
31	Unidentified	—	—	3.9
32	Unidentified	—	0.3	—
33	*l*-Elemol	0.84	3.8	6.9
34	(Acetate I)	—	0.2	?
35	Unidentified	—	0.2	0.4
36	α-Cadinol or γ-eudesmol	1.18	1.6	0.8
37	Unidentified	—	1.9	0.4
38	α-Cyperone + (δ-cadinol)	1.25	3.9	2.1
E	Unidentified	—	0.4	0.4
F	Unidentified	—	0.2	0.1
39	Unidentified	—	0.2	0.7
40	Unidentified	—	0.8	?
41	Acetate II	—	0.5	6.0
42	Unidentified	—	1.2	0.6
Y	Unidentified	—	—	1.6
Z	Unidentified	—	—	0.6

are nearly all monoterpene hydrocarbons and methyl citronellate, terpinen-4-ol, citronellol, geraniol, the isomeric cadinenes, elemol, and α-cadinol or γ-eudesmol. However, the oil of creeping juniper has a noticeably higher content of limonene and *p*-cymene and contains α-cyperone which was not found in the other two oils. The many similarities confirm a close correlation between chemical composition (qualitative) and botanical relationship, all three junipers belonging to the subgenus Sabina (9). Furthermore, the lack of sabinyl acetate (the major constituent of the oil of Savin) in the leaf oils of creeping and Rocky Mountain junipers indicates a close genetic relationship between these two species. The absence of safrole from the oil of creeping juniper in contrast to the presence of 1.5 to 4% in that of the Savin juniper is noteworthy.

The creeping juniper is known to hybridize extensively with Rocky Mountain juniper in the Banff area (10). Since it was found that the oil of Rocky Mountain juniper plants from different localities (2) did not differ qualitatively nor to any marked extent quantitatively, it was of interest to determine if the oil from a hybrid would show any specific chemical differences. A small amount of the oil from a creeping juniper with considerable Rocky Mountain juniper character (the plant selected was a 2 ft high mature female) was analyzed by linear temperature-programmed runs (see Fig. 1B and Table I, column B). Comparison shows that the oil from the hybrid contains all components except the trace peaks *A*, 15, 24*b*, and 32. Also, peaks *B*, 12, 24, and 25 were recorded in trace amounts only, whereas these were present in somewhat larger amounts in the oil of creeping juniper

Can. J. Chem. Downloaded from www.nrcresearchpress.com by 210.87.254.105 on 09/05/12
For personal use only.

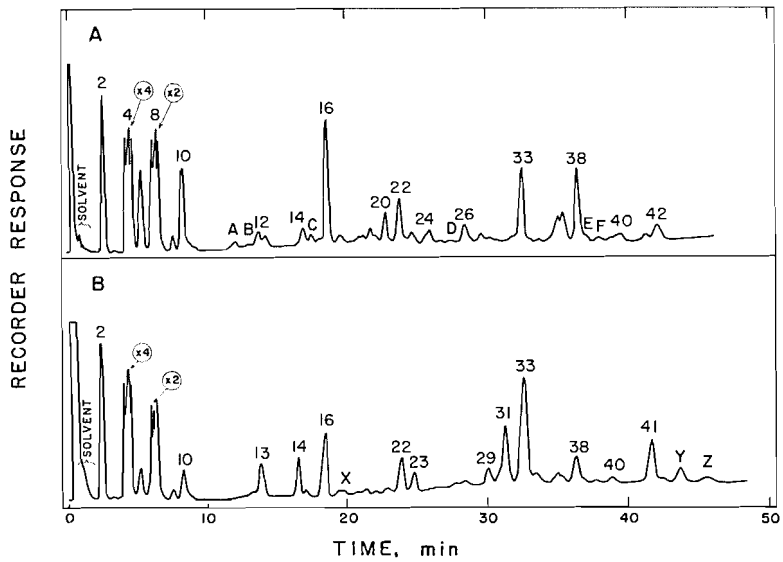

FIG. 1. Gas chromatogram of the volatile oil of (A) creeping juniper and (B) hybrid leaves (6 ft × 3/16 in. o.d. polyethylene glycol 20M column, temperature programmed from 65 to 210 °C at 4° per min).

and peak 25 was recorded in 1.8 to 4.3% amount in the oil of Rocky Mountain juniper. Three new components, *X*, *Y*, and *Z*, were recorded and components 13 (isothujone), 14 (linalool), 23 (unidentified C_{15} hydrocarbon), 29 (unidentified), and especially 31 (unidentified) and 41 (acetate II) were present in considerably larger amounts. The reversal of the relative amounts of components 41 and 42 may be significant since Rocky Mountain juniper leaves contained about 5% of component 41 and only about 1% of component 42. These differences indicate that a direct comparison of chromatograms of the leaf oils of junipers, and perhaps also other conifers, may be helpful in taxonomic classifications. However, many individual hybrids as well as parent plants will have to be investigated to substantiate this observation.

EXPERIMENTAL

The g.l.c. techniques used have already been described in detail (1, 5). An F & M model 500 chromatograph (F & M Scientific Corp.) was used for analytical runs using linear temperature-programming (2), and preparative runs were carried out with an Aerograph "Autoprep" model 700. Optical rotations were measured on solutions in chloroform (1 to 5%) at room temperature. Infrared spectra were recorded on a Perkin–Elmer model 21 double-beam spectrophotometer as liquid films between sodium chloride plates. Individual components were identified by comparison of their infrared spectra and relative retention times.

Materials

The foliage of the creeping juniper was obtained from mature plants growing near the South Saskatchewan River approximately 10 miles south of Saskatoon. Woody branches and berries were removed and the residual leaves (6.56 kg) were steam distilled for 3 h. The distillate was taken up in ether, washed with saturated $NaHCO_3$ solution and water, and dried (Na_2SO_4), and the ether evaporated. The residual oil (58.5 g, 0.89%) had n_D^{30} 1.4763, $[\alpha]_D^{30}$ +36.76° (*c*, 2.57). Reference compounds were those obtained previously (1, 5). The liquid phases used in g.l.c. columns were commercial products. The foliage (32 g) of the hydrid juniper was obtained on the south slope of the eastern portion of Tunnel Mountain, Banff, Alberta. Steam distillation gave a light-yellow oil (0.35 g), n_D^{25} 1.4775, $[\alpha]_D^{25}$ +38.2°.

Analytical Chromatograms

Linear temperature-programmed chromatograms were obtained with 2–3 μl aliquots of oil using 6 ft × 3/16 in. o.d. polyethylene glycol (PEG 20M) (Fig. 1) or Apiezon N (A-N) columns. The percentage composition was determined by measurement of the area under each peak (triangulation method) on duplicate

Can. J. Chem. Downloaded from www.nrcresearchpress.com by 210.87.254.105 on 09/05/12
For personal use only.

chromatograms obtained on the PEG 20M column (see Table I). The values for those components which were unresolved on this column (e.g. α-thujene and α-pinene) were obtained from runs on other columns (1, 2).

The r.r.t. values and purity of isolated components were determined on PEG 20M, A-N, polyethylene glycol adipate polyester (APEG), rapeseed oil (RO), and ethylene glycol bis-(propionitrile) (EGPN) columns under the conditions (isothermal) described previously (1, 11). The r.r.t. values of monoterpenes were measured relative to limonene, oxygenated monoterpenes and sesquiterpenes relative to camphor, and oxygenated sesquiterpenes relative to cedrol (see Table I).

Prefractionation

Silicic acid was impregnated with polyethylene glycol (Carbowax 20M) as described by Kugler and Kovats (12).

Creeping juniper leaf oil (22.02 g) was dissolved in petrol (Skellysolve B, b.p. 60–80 °C) (50 ml) and poured onto a previously prepared column of deactivated silicic acid (200 g). Elution with Skellysolve B (1 000 ml) gave a hydrocarbon fraction (14.61 g), while elution with methanol (1 000 ml) yielded oxygenated terpenes (9.85 g). Aliquots (500 μl) of the hydrocarbon mixture were injected onto a 3 ft $\times$ 3/8 in. o.d. SE-30 silicone polymer (25% on Chromosorb W, 40–60 mesh) column, which was nonlinearly programmed from 80 to 150 °C in 20 min. The monoterpenes were eluted within 11 min and collected as a single fraction in an ice-cooled collection flask. The sesquiterpenes were collected similarly as a second, unresolved fraction. Aliquots (100 μl) of the oxygenated terpenes were fractionated in the same manner into mono- and sesqui-terpenes, programming the same column from 120 to 200 °C in 20 min.

Monoterpene Hydrocarbons

Preparative g.l.c. of the monoterpene hydrocarbon fraction (repeated injections of 100 μl aliquots) on a 20 ft $\times$ 3/8 in. PEG 20M column programmed from 100 to 170 °C in 40 min resulted in the isolation of components 2, 4, 8, 9, and 10. Component 2 was found to be a mixture of α-pinene and tentatively identified α-thujene (r.r.t. 0.35 and 0.31 on the A-N and EGPN columns respectively). Component 4 was found to be sabinene, n_D^{26} 1.4656, $[\alpha]_D^{26}$ +90.84° (*c*, 2.6), containing a small amount of β-pinene (r.r.t. = 0.57 on EGPN column). The r.r.t. values and spectral properties showed component 8*a* to be *d*-limonene, n_D^{26} 1.4698, $[\alpha]_D^{26}$ +95.59° (*c*, 2.4); component 9 to be γ-terpinene, n_D^{26} 1.4713; and component 10 to be *p*-cymene, n_D^{26} 1.4820. Components 6, 8*b*, 11*a*, and 11*b* were obtained only impure, but the r.r.t. values showed them to correspond to myrcene, β-phellandrene, terpinolene, and 2,4-(8)-*p*-menthadiene respectively.

Oxygenated Monoterpenes

Aliquots (100 μl) of the mixture of oxygenated monoterpenes were chromatographed on a 6 ft $\times$ 3/8 in. PEG 20M column (100 to 210 °C in 35 min). Components 16*a* and 22*b* were isolated almost pure and were found to correspond to terpinen-4-ol, n_D^{27} 1.4747, $[\alpha]_D^{28}$ +14.81° (*c*, 4.57), and citronellol, n_D^{27} 1.4593, $[\alpha]_D^{28}$ +11.47° (*c*, 1.57), respectively. Component 14, n_D^{27} 1.4588, $[\alpha]_D^{27}$ +44.09° (*c*, 0.98), corresponded to linalool with a carbonyl impurity. The remaining oxygenated monoterpenes could not be identified.

Sesquiterpene Hydrocarbons

Preparative g.l.c. on the 20 ft $\times$ 3/8 in. o.d. PEG 20M column (30 μl aliquots, 150 to 205 °C in 50 min) gave component 22*a* in a fairly pure state. The infrared spectrum of this component corresponded to γ-cadinene; n_D^{26} 1.5068. Components 18*b*, 19*a*, 23, and 24 were not obtained in sufficient amount to permit characterization. Component 20 had an infrared spectrum similar to cadinene I of the oil of *J. scopulorum*.

Oxygenated Sesquiterpenes

Aliquots (50 μl) of the last fraction were chromatographed on the 6 ft $\times$ 3/8 in. o.d. PEG 20M column (160 to 220 °C in 30 min) and components 33, 36, and 38 were isolated in a fairly pure state. Component 33 corresponded to *l*-elemol, n_D^{28} 1.4955, $[\alpha]_D^{24}$ −14.00° (*c*, 0.60). Component 36 had the r.r.t. of α-cadinol and γ-eudesmol, but since these two alcohols cannot be distinguished by their infrared spectra (13), the identification is uncertain. Component 38 had n_D^{26} 1.5109, $[\alpha]_D^{24}$ +36.66° (*c*, 0.06) and its infrared spectrum was very similar to that of α-cyperone, although it contained an alcoholic impurity. Since δ-cadinol has the same r.r.t. on the PEG 20M column it could be the contaminant. Component 41 appeared to be the same as acetate II from the oil of Rocky Mountain juniper, but the presence of relatively large amounts of component 42, which may be an isomer, prevented isolation in the pure state.

ACKNOWLEDGMENTS

We wish to thank Mr. M. Granat for technical assistance and Mr. W. C. Haid for recording the infrared spectra.

REFERENCES

1. E. VON RUDLOFF. Can. J. Chem. **41**, 2876 (1963).
2. E. VON RUDLOFF and F. M. COUCHMAN. Can. J. Chem. **42**, 1890 (1964).

Can. J. Chem. Downloaded from www.nrcresearchpress.com by 210.87.254.105 on 09/05/12
For personal use only.

3. H. ERDTMAN. *In* Perspectives in organic chemistry. *Edited by* A. Todd. Interscience Publishers, Inc., New York. 1956. p. 453.
4. R. D. GIBBS. *In* Chemical plant taxonomy. *Edited by* T. Swain. Academic Press, New York. 1963. p. 41.
5. E. C. BATE-SMITH. *In* Chemical plant taxonomy. *Edited by* T. Swain. Academic Press, New York. 1963. p. 127.
6. N. T. MIROV and R. G. STANLEY. Ann. Rev. Plant Physiol. **10**, 223 (1959).
7. N. T. MIROV. J. Am. Pharm. Assoc. Sci. Ed. **47**, 410 (1958).
8. E. VON RUDLOFF. Can. J. Chem. **42**, 1057 (1964).
9. P. A. RYDBERG. *In* Flora of the prairies and plains of central North America. New York Botanical Gardens. 1932. p. 18.
10. R. T. OGILVIE. Personal communication. N. C. FASSETT. Bull. Torrey Botan. Club, **71**, 40, 475 (1944); **72**, 42, 379 (1945).
11. E. VON RUDLOFF. Can. J. Chem. **41**, 1737 (1963).
12. E. KUGLER and E. SZ. KÖVATS. Helv. Chim. Acta, **46**, 1480 (1963).
13. E. VON RUDLOFF and G. V. NAIR. Can. J. Chem. **42**, 421 (1964).

Can. J. Chem. Downloaded from www.nrcresearchpress.com by 210.87.254.105 on 09/05/12
For personal use only.

Can. J. Chem. Downloaded from www.nrcresearchpress.com by 210.87.254.105 on 09/05/12
For personal use only.

THE Hg 6($^3P_1$) PHOTOSENSITIZATION OF CHLORODIFLUOROMETHANE

M. G. Bellas, O. P. Strausz, and H. E. Gunning
Department of Chemistry, University of Alberta, Edmonton, Alberta

Received December 7, 1964

ABSTRACT

The reaction was studied in a circulatory apparatus under a variety of conditions. The sole primary process occurring is C—Cl bond scission. The Cl atoms formed in the primary step, through an abstractive attack on the substrate, generate chlorodifluoromethyl radicals ($CF_2Cl\cdot$). All principal reaction products, CF_2H_2, CF_2Cl_2, CF_2ClCF_2Cl, CF_2HCF_2H, and CF_2HCF_2Cl, can be accounted for by the combination–disproportionation reactions of the $CF_2H\cdot$ and $CF_2Cl\cdot$ radicals. The observed strong dependence of the primary quantum yields on the incident light intensities has been ascribed to a rapid substrate-reforming step.

INTRODUCTION

In mercury photosensitization only methyl chloride has been investigated (1, 2) in detail among the alkyl chlorides. With the higher homologs, only the primary processes have been examined by the monoisotopic sensitization technique (2). At room temperature the sole primary step occurring with methyl chloride, and probably with the higher homologs as well, is the scission of the C—Cl bond with a quantum efficiency of unity.

Our interest in the present study was to establish the mode of primary decomposition of the chlorodifluoromethane molecule. Probable primary routes are: (*a*) C—Cl bond rupture, as with the alkyl chlorides, giving rise to difluoromethyl radicals and (*b*) a molecular split, to form difluorocarbene and HCl. In either case the system could serve as a useful source of the corresponding radicals, and in addition provide information on the effect of fluorine substitution on the primary alkyl chloride reactions.

EXPERIMENTAL

Because of the difficulties associated with calomel formation in the reactions of Hg 6($^3P_1$) atoms with chlorinated hydrocarbons, this reaction was studied in a circulating system, described elsewhere (3), at cell temperatures of 120° and above. Since, under these conditions, calomel does not deposit on the cell face, a constant light intensity was ensured during the entire illumination period.

Two mercury resonance lamps were utilized in all experiments described in the present study. The first source of Hg 2 537 Å resonance radiation was a Hanovia SC-2537 quartz discharge tube of helical shape, and the second was a Hanovia No. 87A45 U-shaped discharge tube, fashioned of Vycor 7910. A Vycor 7910 filter for the first source, and the envelope of the lamp itself for the second, served to remove the 1 849 Å resonance line. The lamps were thermostated at 25.1 ± 0.1 °C. The warm-up period was always at least 90 min. Lamp intensities were determined using propane actinometry, and the nitrous oxide – paraffin system. The values obtained by the two different actinometers agreed within 1%.

The reactant was circulated for 5 min prior to irradiation to allow mercury vapor–liquid equilibration. At the conclusion of the irradiation the fractions volatile at −183 °C were analyzed by gas chromatography (g.c.) on a 28 ft di-*n*-butyl maleate column (I). The following compounds could be resolved: difluoromethane, dichlorodifluoromethane, 1,2-dichlorotetrafluoroethane, *sym*-tetrafluoroethane, 1-chloro-1,1,2,2-tetrafluoroethane, 1,3-dichlorohexafluoropropane, 1,1,2,2,3,3-hexafluoropropane, and 1-chloro-1,1,2,2,3,3-hexafluoropropane, as well as the substrate, chlorodifluoromethane. In the experiments with added HCl, the procedure was similar to that described above.

In the experiments with added methanethiol products noncondensable at −138.7 °C were removed by means of a Toepler pump and analyzed on column I. This fraction consisted of CF_2H_2, CF_2HCl, CF_2Cl_2, CF_2HCF_2H, CF_2HCF_2Cl, and CF_2ClCF_2Cl. The material condensed at −138.7 °C was analyzed by g.c. using an 8 ft tri-*o*-tolyl phosphate column at room temperature. CH_3SH, CF_2HSCH_3, and CH_3SSCH_3 could be resolved. In the flow experiments with added nitric oxide, carried out in a single-pass system (4), the fraction condensable at −117.0 °C was trapped and analyzed by g.c. using a 10 ft polyethylene glycol column with temperature programming. It consisted of nitrosodifluoromethane and difluoroformaldeoxime.

The products were identified by their g.c. retention times, as well as by mass spectrometric analysis of the isolated peaks. In the case of CF_2HNO and $CF_2{=}NOH$ infrared absorption spectra were also obtained. The gas chromatograph was calibrated using pure samples.

The gases were obtained from Matheson of Canada. The chlorodifluoromethane, with a stated purity of 99.9% minimum, was further purified by preparative g.c. on two different columns, a 22 ft dimethyl sulfolane column, and column I, both operated at 0 °C, after which no impurities could be detected. The nitric oxide, 99.0% minimum purity, was triply distilled through liquid oxygen prior to use. Mass spectrometric analysis showed it to be at least 99.9% pure. The methanethiol and the hydrogen chloride, both with a stated purity of 99.0% minimum were purified by low temperature distillation. Mass spectrometric analysis revealed no detectable impurities.

RESULTS AND DISCUSSION

CF_2HNO and $CF_2{=}NOH$ were the only products found in single-pass flow experiments, carried out at room temperature, using 12 Torr substrate pressure with 2 mole % added nitric oxide. These results, coupled with the fact that hydrogen and hydrogen chloride were not detected as products in the uninhibited runs, indicate that C—Cl bond scission is the only primary process occurring in the reaction. Only two modes involving a C—Cl split can be written.

[1*a*] $$Hg^* + CF_2HCl \rightarrow CF_2H + Cl + Hg$$

[1*b*] $$Hg^* + CF_2HCl \rightarrow CF_2H + HgCl.$$

The quantum yield of [1*b*] has been shown to be $\leqslant 0.13$ mole/einstein (5), while the combined quantum yield for [1*a*] and [1*b*] will be shown later in this paper to have a value $\geqslant 0.94$.

The main products of the uninhibited reaction were CF_2H_2, CF_2Cl_2, CF_2ClCF_2Cl, CF_2HCF_2H, CF_2HCF_2Cl, and calomel which could not be measured under the experimental arrangements. Consequently, to account for the CF_2Cl-containing products, reactions must be considered which lead to CF_2Cl radicals since these species are not formed in the primary process. The only possibilities are

[2] $$CF_2H + CF_2HCl \rightarrow CF_2H_2 + CF_2Cl$$

[3] $$Cl + CF_2HCl \rightarrow HCl + CF_2Cl,$$

the latter being the more important since abstraction by Cl atoms have been shown to be more rapid than abstraction by radicals (6). Thus the E_a for H-atom abstraction from CH_3Cl by Cl atoms is 3.1 kcal/mole (6, 7), whereas for abstraction by CH_3 radicals it is 9.4 kcal/mole (8). The observation that $\Phi(CF_2H_2) \ll \Phi(CF_2Cl)$ (cf. Table II) indicates that reaction [3] rather than [2] is the predominant source of CF_2Cl radicals. The C_2 products can be accounted for by the following combinations:

[4] $$CF_2H + CF_2H \rightarrow CF_2HCF_2H$$

[5] $$CF_2Cl + CF_2Cl \rightarrow CF_2ClCF_2Cl$$

[6] $$CF_2H + CF_2Cl \rightarrow CF_2HCF_2Cl.$$

Although arguments have been presented for the occurrence of reaction [3], no measurable amount of HCl could be found. It appears that if HCl is formed it is consumed rapidly in the system. This is expected since methyl radicals are known to react rapidly with HCl (9), with $E_a = 5$ kcal/mole and $\log A = 9.0$ (l mole s) (7). The rate for difluoromethyl radicals should not be greatly different.

The data appearing in Fig. 1 support this conclusion. The increase in $\Phi(CF_2H_2)$ with time indicates that some of the CF_2H_2 product is formed in a secondary reaction such as

[7] $$CF_2H + HCl \rightarrow CF_2H_2 + Cl.$$

**Small quantities of* HCl *are extremely difficult to detect; consequently they could have been lost in the analysis.*

Can. J. Chem. Downloaded from www.nrcresearchpress.com by 210.87.254.105 on 09/05/12
For personal use only.

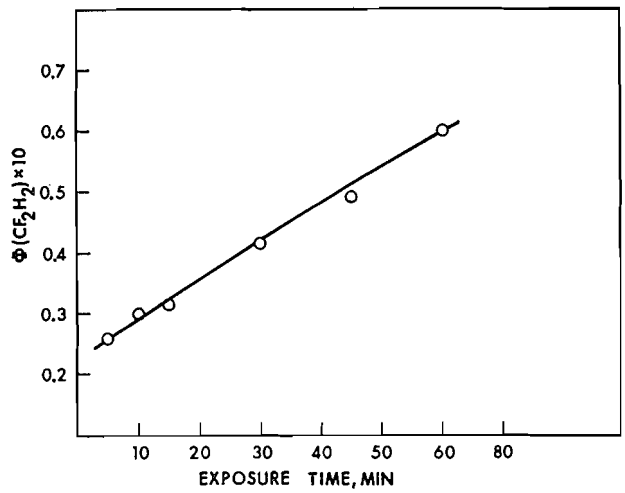

FIG. 1. Quantum yield of difluoromethane as a function of exposure time $P(CF_2HCl) = 25$ Torr. $T = 120$ °C.

Further support for this argument comes from experiments performed with added HCl, for which the data are summarized in Table I. It is seen that with increasing amounts of added HCl, $\Phi(CF_2H_2)$ increases and $\Phi(C_2F_4H_2)$ simultaneously decreases, owing to the more efficient competition of [7] with the recombination step [4].

TABLE I

Quantum yields* of products as a function of mole % added HCl in the decomposition of chlorodifluoromethane

	Φ,† mole/einstein		
Product	0 mole % HCl	0.72 mole % HCl	4.15 mole % HCl
CF_2H_2	0.038	0.091	0.30
CF_2Cl_2	0.022	0.024	0.039
CF_2ClCF_2Cl	0.047	0.055	0.12
CF_2HCF_2H	0.22	0.15	0.067
CF_2HCF_2Cl	0.18	0.18	0.19
$CF_2H\cdot$‡	0.66	0.57	0.62

*Corrected for competitive quenching.
†Substrate pressure = 27.7 Torr; exposure time = 5 min; cell temperature = 120 °C; light intensity = 3.16×10^{15} quanta/s.
‡The contribution of the C_3 products was neglected (see text).

To examine the effect of incident light intensities on the reaction, three runs were performed at different intensities, covering a tenfold range. The data in Table II show a large change in the overall quantum yield. Thus $\Phi(CF_2H)$ and $\Phi(CF_2Cl)$ increased from 0.33 and 0.19 at 8.9×10^{15} quanta/s to 0.74 and 0.32 at 9.8×10^{14} quanta/s, respectively. This intensity effect can be attributed largely to an efficient back reaction of Cl atoms with difluoromethyl radicals.

[8] $$CF_2H + Cl \rightarrow CF_2HCl.$$

This indicates that although [3] is faster than [2], it is still not sufficiently rapid to suppress [8], even when assisted by Cl-atom scavenging by mercury atoms:

[9] $$Hg + Cl + M \rightarrow HgCl + M.$$

Can. J. Chem. Downloaded from www.nrcresearchpress.com by 210.87.254.105 on 09/05/12
For personal use only.

Alternatively, the cause of the intensity effect could be a decrease in light absorption in the cell at high intensities, owing to the depletion of mercury vapor through [9] and [16]. In the runs with added HCl, there was an increase in the Cl-atom concentration because of the increased importance of reaction [7]. Despite this there was no significant change in the total yield of CF_2H-containing products. From the data in Table I, with pure substrate, $\Phi(CF_2H) = 0.66$ while with 4.15 mole % added HCl (where $\Phi(CF_2H_2)$ increased tenfold), $\Phi(CF_2H) = 0.62$. This indicates that reaction [8] is the predominant factor in the effect of light intensity.

TABLE II

Quantum yields of products as a function of light intensity in the decomposition of chlorodifluoromethane

	Φ,* mole/einstein		
Product	1†	2‡	3§
CF_2H_2	0.06	0.07	0.03
CF_2Cl_2	0.02	0.02	0.01
CF_2ClCF_2Cl	0.05	0.05	0.03
CF_2HCF_2H	0.22	0.15	0.08
CF_2HCF_2Cl	0.18	0.18	0.11
Calomel	0.46	0.35	0.16
$CF_2H\cdot$‖	0.74	0.62	0.33
CF_2Cl¶	0.32	0.32	0.19
$\frac{k_6}{(k_4k_5)^{1/2}}$	1.8	2.1	2.2

*Substrate pressure = 26 Torr; cell temperature = 145 °C.
†I_a (quanta/s × 10^{14}) = 9.8; exposure time (min) = 16.2.
‡I_a (quanta/s × 10^{14}) = 33; exposure time (min) = 28.2.
§I_a (quanta/s × 10^{14}) = 89; exposure time (min) = 10.0.
‖Obtained from the following relation, on the assumption that CF_2H_2 arises from the disproportionation reaction of the CF_2H radical (see text), $\Phi(CF_2H) = \Phi(C_2F_4HCl) + 2\Phi(C_2F_4H_2) + 2\Phi(CF_2H_2)$.
¶Obtained from the following relation, on the assumption that CF_2Cl_2 arises from the disproportionation reaction of the CF_2Cl radical (see text), $\Phi(CF_2Cl) = \Phi(C_2F_4HCl) + 2\Phi(CF_2Cl_2) + 2\Phi(C_2F_4Cl_2)$.

The yield of calomel could be estimated roughly, neglecting the minor C_3 products of the reaction (*vide infra*), from the following equation:

$$\Phi(\text{calomel}) = \Phi(CF_2H) + \Phi(CF_2H_2) - \Phi(CF_2Cl) - \Phi(CF_2Cl_2).$$

The Φ(calomel) values in Table II were calculated on this basis.

The values for the rate constant ratio, $k_6/(k_4k_5)^{1/2}$, appearing in the last row of the table were obtained from the product yield ratios and are reasonably close to two, as expected for reactions without activation energy (10).

TABLE III

Quantum yields of products as a function of substrate pressure in the decomposition of chlorodifluoromethane

	Φ,* mole/einstein			
Product	P (Torr) = 76.5	P (Torr) = 127	P (Torr) = 204	P (Torr) = 313
CF_2H_2	0.053	0.060	0.062	0.063
CF_2Cl_2	0.010	0.012	0.013	0.013
CF_2ClCF_2Cl	0.034	0.038	0.042	0.041
CF_2HCF_2H	0.049	0.054	0.058	0.053
CF_2HCF_2Cl	0.089	0.10	0.12	0.11
$\frac{k_6}{(k_4k_5)^{1/2}}$	2.2	2.2	2.5	2.4

*Exposure time = 60 min; cell temperature = 145 °C; light intensity = 8.9 × 10^{15} quanta/s.

Can. J. Chem. Downloaded from www.nrcresearchpress.com by 210.87.254.105 on 09/05/12
For personal use only.

The reaction was also examined as a function of substrate pressure in the range, 76 to 313 Torr. From the data given in Table III only a very small dependence on pressure appears. If the back reaction of chlorine atoms with difluoromethyl radicals is truly represented by step [8] the overall quantum yield should rise with increasing substrate pressure. This discrepancy dictates a third body restriction on the recombination step and instead of [8] we should write

[10] $$CF_2H + Cl + M \rightarrow CF_2HCl + M.$$

Additional evidence for the importance of reaction [10] comes from the results of experiments with added CH_3SH which are presented in Table IV. It is seen that upon addition of 4.98 mole % mercaptan, $\Phi(CF_2H_2)$ increases from 0.04 to 0.63. Under these conditions the primary quantum efficiency rises to 0.94. The mercaptan provides an easily abstractable H atom ($D(CH_3S—H)$ = 77 kcal (11)) leading to the rapid reaction:

[11] $$CF_2H + CH_3SH \rightarrow CF_2H_2 + CH_3S.$$

The methanethiol is also an efficient scavenger for Cl atoms and, at relatively low concentrations, completely suppresses secondary calomel formation (5).

TABLE IV

Quantum yields* of products as a function of mole % added methanethiol in the decomposition of chlorodifluoromethane

	Φ,† mole/einstein		
Product	0 mole % CH_3SH	1.74 mole % CH_3SH	4.98 mole % CH_3SH
CF_2H_2	0.04	0.38	0.63
CF_2HCF_2H	0.22	0.12	0.05
CF_2HSCH_3	—	0.26	0.21
CF_2H	0.66‡	0.88	0.94

*Corrected for competitive quenching.
†Substrate pressure = 27.2 Torr; exposure time = 5 min; cell temperature = 120 °C; light intensity = 3.16×10^{15} quanta/s.
‡The additional contribution from CF_2HCF_2Cl must be included. Here $\Phi(CF_2HCF_2Cl) = 0.18$.

The effect of temperature on the reaction was examined in three runs performed at 140, 180, and 230°. The results are given in Table V. With rising temperature $\Phi(CF_2H)$ increases slightly from 0.30 at 140 °C to 0.47 at 230 °C, but $\Phi(CF_2H_2)$ increases nearly threefold. These increases are evidently due to the higher efficiency of the abstraction reactions [2] and [3] at elevated temperatures.

It should be noted that the rate constant ratios, $k_6/(k_4k_5)^{1/2}$, for the present system show no temperature effect, as was reported for the cross recombination reactions of methyl and trifluoromethyl radicals (12). However, from our data a small pressure effect is evident. Thus at 25 Torr pressure these ratios have a mean value of 1.9 (cf. Tables II and VI), but at the higher pressures, 200–313 Torr, their mean value is 2.4 (cf. Tables III and V). It is unlikely that this pressure trend is due to a secondary mercury photosensitized decomposition of the products, in view of the reported quenching efficiency of these compounds.*

In addition to the products already mentioned, $CF_2HCF_2CF_2H$, $CF_2HCF_2CF_2Cl$, and $CF_2ClCF_2CF_2Cl$ are also formed and account for approximately 10% of the product yield. They appeared as very broad peaks under the g.c. column conditions used, and were difficult to measure in short runs. Sufficient quantities of the first two were produced in

*The pertinent quenching cross section values are CF_2HCl = 19.1 Å²; C_2F_4HCl = 14.7 Å²; $C_2F_4Cl_2$ = 23.6 Å²; and $C_2F_4H_2$ estimated to be negligibly small (13).

Can. J. Chem. Downloaded from www.nrcresearchpress.com by 210.87.254.105 on 09/05/12
For personal use only.

TABLE V

Quantum yields of products as a function of temperature in the decomposition of chlorodifluoromethane

Product	Φ,* mole/einstein		
	1†	2‡	3§
CF_2H_2	0.062	0.10	0.17
CF_2Cl_2	0.013	0.019	0.023
CF_2ClCF_2Cl	0.042	0.065	0.091
CF_2HCF_2H	0.058	0.077	0.060
CF_2HCF_2Cl	0.12	0.17	0.18
CF_2H	0.30	0.42	0.47
$\frac{k_6}{(k_4k_5)^{1/2}}$	2.4	2.4	2.4

*Substrate pressure = 204 Torr; exposure time = 60 min.
†Temperature = 140 °C; I_a (quanta/s × 10^{15}) = 8.9.
‡Temperature = 180 °C; I_a (quanta/s × 10^{15}) = 7.2.
§Temperature = 230 °C; I_a (quanta/s × 10^{15}) = 7.2.

high conversion experiments to permit their identification by mass spectrometry. This was not feasible in the case of 1,3-dichlorohexafluoropropane since its yield was small. However, there was only one unidentified peak on the chromatogram and it had a retention time that one would expect for $C_3F_6Cl_2$. Unfortunately, standard samples were not available to check the retention times of these C_3 products.

It is unlikely that these C_3 compounds are formed in secondary quenching reactions at the pressures and conversions used. Since the products formed in largest yield are those arising from radical–radical recombination reactions, it is reasonable to suppose that radical–radical disproportionation reactions might be the source of the C_3 products. A scheme analogous to that proposed by Bowles, Majer, and Robb (14) would certainly explain the experimental findings.

[12] $$2CF_2H \rightarrow CF_2H_2 + CF_2$$

[13] $$2CF_2Cl \rightarrow CF_2Cl_2 + CF_2$$

[14] $$CF_2H + CF_2Cl \rightarrow CF_2HCl + CF_2$$

[15] $$CF_2 + CF_2H \rightarrow C_2F_4H$$

[16] $$CF_2 + CF_2Cl \rightarrow C_2F_4Cl$$

[17] $$C_2F_4H + CF_2H \rightarrow CF_2HCF_2CF_2H$$

[18] $$C_2F_4H + CF_2Cl \rightarrow CF_2HCF_2CF_2Cl$$

[19] $$C_2F_4Cl + CF_2H \rightarrow CF_2HCF_2CF_2Cl$$

[20] $$C_2F_4Cl + CF_2Cl \rightarrow CF_2ClCF_2CF_2Cl$$

It is now evident why a quantum efficiency of unity is never observed for the primary reaction. The importance of a substrate-reforming step [10] has already been discussed. Reaction [14] also reforms substrate. Lastly, CF_2H contributions from the C_3's formed were not considered. Consequently, it is not unreasonable to suggest that the primary step proceeds with perfect quantum efficiency.

From runs performed at very low conversions (reported in Table VI) where the occurrence of reaction [7] can be neglected, a value of about 0.19 can be deduced for the rate of disproportionation to recombination, k_d/k_r, for CF_2H radicals. (The values for C_2H_5 and n-C_3H_7 radicals are, respectively: 0.14 and 0.16 (10).) A similar estimate for CF_2Cl radicals is not feasible since the contribution of

[21] $$CF_2Cl + Cl + M \rightarrow CF_2Cl_2 + M$$

Can. J. Chem. Downloaded from www.nrcresearchpress.com by 210.87.254.105 on 09/05/12
For personal use only.

TABLE VI

Quantum yields of products in experiments performed at very low conversions in the decomposition of chlorodifluoromethane

Product	Φ, mole/einstein		
	1*	2†	3‡
CF_2H_2	0.038	0.049	0.049
CF_2Cl_2	0.022	0.018	0.018
CF_2ClCF_2Cl	0.047	0.051	0.044
CF_2HCF_2H	0.22	0.26	0.25
CF_2HCF_2Cl	0.18	0.19	0.18
CF_2H	0.70	0.81	0.78
$\frac{k_d}{k_r}(CF_2H)$	0.17	0.19	0.20
$\frac{k_6}{(k_4k_5)^{1/2}}$	1.8	1.8	1.7

*Pressure (Torr) = 27.6; cell temperature = 119 °C; exposure time (min) = 5; I_a (quanta/s × 10^{14}) = 31.6.
†Pressure (Torr) = 25.4; cell temperature = 117 °C; exposure time (min) = 16.2; I_a (quanta/s × 10^{14}) = 9.8.
‡Pressure (Torr) = 25.3; cell temperature = 75 °C; exposure time (min) = 16.2; I_a (quanta/s × 10^{14}) = 9.8.

is not known. This reaction must occur to some extent since, as has been shown above, reaction [10] is important. Nonetheless, an upper limit of 0.5 for k_d/k_r for CF_2Cl radicals may be estimated.

The radicals, C_2F_4H and C_2F_4Cl formed in [15] and [16] respectively, owing to their high C—H bond energies, may undergo hydrogen-abstraction reactions with HCl. This would have a slight influence on the $k_6/(k_4k_5)^{1/2}$ ratio. But even the possible occurrence of these reactions would not explain the observed pressure dependence of the rate constant ratios. Thus it would appear that at 25 Torr pressure the recombination reactions [4], [5], and [6] become third body dependent, although this might be spurious owing to the complexity of the overall mechanism.

CONCLUSION

The primary step in the mercury photosensitization of chlorodifluoremethane is C—Cl bond cleavage with a probable quantum efficiency of unity. The CF_2H radicals formed in the primary process and the CF_2Cl radicals formed in the subsequent abstraction by Cl-atoms undergo disproportionation and recombination reactions. The ratio $k_{AB}/(k_{AA}k_{BB})^{1/2}$ for the recombination rate constants of CF_2H and CF_2Cl radicals is 2.4 and the rate constant ratio for the disproportionation to recombination of the CF_2H radicals is 0.19. For the CF_2Cl radicals only an upper limit of ca. 0.5 could be derived for the disproportionation–recombination ratio. The disproportionation reactions of both radicals presumably yield difluorocarbene, which through combination reaction with the monoradicals present gives rise to C_3 products.

ACKNOWLEDGMENTS

The authors wish to express their appreciation to Mr. G. N. C. Woodall for performing the flow experiments with added nitric oxide. The financial support of the National Research Council of Canada is gratefully acknowledged.

Can. J. Chem. Downloaded from www.nrcresearchpress.com by 210.87.254.105 on 09/05/12
For personal use only.

REFERENCES

1. G. L. LEE and D. J. LEROY. Can. J. Research B, **28**, 500 (1950). C. R. MASSON and E. W. R. STEACIE. J. Chem. Phys. **19**, 183 (1951).
2. J. K. S. WAN, O. P. STRAUSZ, W. F. ALLEN, and H. E. GUNNING. Can. J. Chem. **42**, 2056 (1964).
3. M. G. BELLAS, J. K. S. WAN, W. F. ALLEN, O. P. STRAUSZ, and H. E. GUNNING. J. Phys. Chem. **68**, 2170 (1964).
4. G. N. C. WOODALL and H. E. GUNNING. Bull. Soc. Chim. Belges, **71**, 725 (1962).
5. T. DINGLE. Ph.D. Thesis, University of Alberta. 1965. H. E. GUNNING and O. P. STRAUSZ. Advances in photochemistry. Vol. 1. *Edited by* W. A. Noyes, Jr., G. S. Hammond, and J. N. Pitts. Interscience Publishers, New York. 1963.
6. J. H. KNOX. Trans. Faraday Soc. **58**, 275 (1962).
7. G. CHILTZ, P. GOLDFINGER, G. HUYBRECHTS, G. MARTENS, and G. VERBEKE. Chem. Rev. **63**, 355 (1963).
8. F. A. RAAL and E. W. R. STEACIE. J. Chem. Phys. **20**, 578 (1952).
9. R. J. CVETANOVIC and E. W. R. STEACIE. Can. J. Chem. **31**, 158 (1953).
10. A. F. TROTMAN-DICKENSON. Progress in reaction kinetics. Vol. I. *Edited by* G. Porter. Pergamon Press, New York. 1961.
11. T. L. COTTRELL. The strengths of chemical bonds. Butterworth and Co., Ltd., Toronto. 1958.
12. G. O. PRITCHARD and J. R. DACEY. Can. J. Chem. **38**, 182 (1960). G. O. PRITCHARD, Y. P. HSIA, and G. H. MILLER. J. Am. Chem. Soc. **85**, 1568 (1963).
13. M. G. BELLAS, Y. ROUSSEAU, O. P. STRAUSZ, and H. E. GUNNING. J. Chem. Phys. **41**, 768 (1964).
14. R. BOWLES, J. R. MAJER, and J. C. ROBB. Trans. Faraday Soc. **58**, 541 (1962).

Can. J. Chem. Downloaded from www.nrcresearchpress.com by 210.87.254.105 on 09/05/12
For personal use only.

Can. J. Chem. Downloaded from www.nrcresearchpress.com by 210.87.254.5 on 09/05/12
For personal use only.

HYDROGENOLYSIS BY $AlCl_3$–$LiAlH_4$ OF ETHER SOLUTIONS OF *cis* AND *trans* ISOMERS OF 2,4-DISUBSTITUTED-1,3-DIOXOLANES[1]

B. E. LEGGETTER AND R. K. BROWN
Department of Chemistry, University of Alberta, Edmonton, Alberta

Received November 30, 1964

ABSTRACT

Hydrogenolysis by $LiAlH_4$–$AlCl_3$ of ether solutions of the *cis* and *trans* isomers of both 2,4-dimethyl-1,3-dioxolane and 2-ethyl-4-methyl-1,3-dioxolane have been carried out.

The *cis* isomers are hydrogenolyzed respectively about 6.8 times and 10 times faster than are the corresponding *trans* isomers. The ratio of C_2—O_1 to C_2—O_3 bond cleavage in the *cis* isomers is at least 15 to 1 while that for the *trans* isomers is about 1 to 2. Isomerization during the aluminium chloride catalyzed hydrogenolysis is not detectable for the *trans* isomers. Slight indications of isomerization are discerned for the *cis* isomers.

INTRODUCTION

It has been found (1) that electron donor substituents on C_4 of the 1,3-dioxolane ring system cause hydrogenolysis, by a mixture of $LiAlH_4$ and $AlCl_3$ in ether, to occur predominantly at the C_2—O bond remote from the C_4 position (eq. [*a*]). However, it was noted that with the 2,4-disubstituted-1,3-dioxolanes, which are capable of *cis–trans* isomerism, the extent of C_2—O_1 vs. C_2—O_3 cleavage depended upon the proportion of *cis* and *trans* isomers present in the mixture subjected to hydrogenolysis.

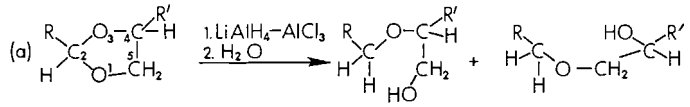

I. R = R′ = CH_3
(*a*) *cis* isomer
(*b*) *trans* isomer
(Preferred if R′ = alkyl.)

II. R = ethyl, R′ = methyl
(*a*) *cis* isomer
(*b*) *trans* isomer

III. (*a*) R = R′ = methyl
(*b*) R = ethyl
R′ = methyl

IV. (*a*) R = R′ = methyl
(*b*) R = ethyl
R′ = methyl

This paper describes the results of a study of the reductive cleavage by $LiAlH_4$–$AlCl_3$ of ether solutions of the *cis* and *trans* isomers of both 2,4-dimethyl-1,3-dioxolane (I*a*, *b*) and 2-ethyl-4-methyl-1,3-dioxolane (II*a*, *b*).

RESULTS AND DISCUSSION

A configurational assignment for the isomeric 2,4-dimethyl-1,3-dioxolanes has been made by Barker *et al.* (2) by taking advantage of the similarity of the geometry of 2,4-dimethyl-1,3-dioxolane to that of 1,3-dimethylcyclopentane. Since the 1,3-dimethylcyclopentane isomer which has both the higher boiling point and greater density has been assigned the *trans* configuration, the isomeric 2,4-dimethyl-1,3-dioxolane which also has the higher boiling point as well as greater density was considered to be the *trans* isomer. We have accepted this reasonable configurational assignment in the work discussed below.

[1]*Taken from the thesis of B. E. Leggetter, submitted to the Graduate School, University of Alberta, Edmonton, Alberta, in partial fulfillment of the requirements for the degree of Doctor of Philosophy.*

Preferred Direction of Ring Cleavage of cis and trans Isomers

Equimolar quantities (0.1 mole each) of lithium aluminium hydride, aluminium chloride, and the dioxolane in ether solution were allowed to react for 1 h, a time sufficient to ensure complete hydrogenolysis to the hydroxy ethers (III or IV). Reductions were carried out identically for each of *cis*- and *trans*-2,4-dimethyl-1,3-dioxolane (I*a* and *b*) and *cis*- and *trans*-2-ethyl-4-methyl-1,3-dioxolane (II*a* and *b*). As well reductions were carried out on 0.1 *M* amounts of the equilibrium mixtures of *cis*- and *trans*-2,4-dimethyl-1,3-dioxolane (63%:37% respectively) and of *cis*- and *trans*-2-ethyl-4-methyl-1,3-dioxolane (68%:32% respectively). Results of these experiments (Table I) show that the ratio of C_2—O_1 to C_2—O_3 cleavage in the *cis* isomers is at least 15 to 1 while for the *trans* isomers this ratio is about 1 to 2.

TABLE I

Hydrogenolysis of *cis* and *trans* isomers of 2,4-disubstituted-1,3-dioxolanes by lithium aluminium hydride and aluminium chloride*

Expt. No.	Dioxolane	Reduction products	Amount of each constituent in total reduction product, %
1	*cis*-2,4-Dimethyl-1,3-dioxolane	1-Ethoxy-2-propanol	4
		2-Ethoxy-1-propanol	96
2	*trans*-2,4-Dimethyl-1,3-dioxolane	1-Ethoxy-2-propanol	65
		2-Ethoxy-1-propanol	35
3	*cis* and *trans*-2,4-Dimethyl-1,3-dioxolane (equilibrium mixture 63%:37%)	1-Ethoxy-2-propanol	24
		2-Ethoxy-1-propanol	76
4	*cis*-2-Ethyl-4-methyl-1,3-dioxolane	1-*n*-Propoxy-2-propanol	6
		2-*n*-Propoxy-1-propanol	94
5	*trans*-2-Ethyl-4-methyl-1,3-dioxolane	1-*n*-Propoxy-2-propanol	67
		2-*n*-Propoxy-1-propanol	33
6	*cis*- and trans-2-Ethyl-4-methyl-1,3-dioxolane (equilibrium mixture 68%:32%)	1-*n*-Propoxy-2-propanol	32
		2-*n*-Propoxy-1-propanol	68

*Each hydrogenolysis was carried out in ether solution and allowed to proceed for 60 min.

The Possibility of Isomerization during Hydrogenolysis

We have found that *cis*-2,4-dimethyl-1,3-dioxolane, left at room temperature in ether solution in contact with a catalytic amount of aluminium chloride, in a few hours reaches an equilibrium composition of 63% *cis* and 37% *trans* very much like the equilibrium ratio of 65:35 found for this material by Barker *et al.* (2). The occurrence of isomerization simultaneously with reductive cleavage would give a false impression of the extent of preferential C_2—O bond cleavage of the *cis* and *trans* isomers. To discover whether isomerization does in fact occur during hydrogenolysis, partial reductions were carried out on both *cis*- and *trans*-2,4-dimethyl-1,3-dioxolane. The product from these separate reductions was then analyzed by gas–liquid chromatography (g.l.c.) for the expected reduction products and for the unreduced dioxolane. The latter would reveal the occurrence of any isomerization since the *cis* and *trans* isomers have different retention times. Table II contains the results of these experiments.

It is seen that over the limited ranges of reduction (controlled by the addition of limited amounts of $LiAlH_4$ and $AlCl_3$) the *trans* isomer shows no evidence of conversion to the *cis* isomer. The *cis* isomer isomerizes to the *trans* very slightly, but this occurs only when the molar proportion of aluminium chloride approaches that of the lithium aluminium

Can. J. Chem. Downloaded from www.nrcresearchpress.com by 210.87.254.5 on 09/05/12
For personal use only.

TABLE II

Partial reductions of *cis* and *trans* isomers of 2,4-dimethyl-1,3-dioxolane*

Expt. No.	Dioxolane, moles	$LiAlH_4$, moles	$AlCl_3$, moles	Ratio of reduction products, %†		Amount of other isomer present
				IIIa	IVa	
trans-2,4-Dimethyl-1,3-dioxolane						
1	0.05	0.01	0.005	37	63	None
2	0.05	0.01	0.01	33	67	None
3	0.05	0.025	0.02	33	67	None
cis-2,4-Dimethyl-1,3-dioxolane						
4	0.05	0.01	0.005	96	4	None
5	0.05	0.02	0.005	96	4	None
6	0.05	0.025	0.02	96	4	Trace
7	0.05	0.035	0.03	96	4	Trace (plus)

*The total reaction time was 30 min in all cases. Total recovery was of the order of 80% in all cases. The extent of reduction was limited by a deficiency in both the $LiAlH_4$ *and* $AlCl_3$.
†IIIa is 2-ethoxy-1-propanol; IVa is 1-ethoxy-2-propanol.

hydride. Since isomerization must occur by C_2—O bond breaking, a step which is considered to be rate determining in the hydrogenolysis reaction (1), the above observations might be interpreted as indicating that the irreversible reduction step is much faster than the isomerization step and as long as the hydride is in excess, little or no isomerization takes place. The detection of some conversion of *cis* to *trans* but none of *trans* to *cis* could be due to a greater rate of hydrogenolysis of the *cis* than of the *trans* isomer. Thus the *cis* isomer would reduce as quickly as it was formed, while the *trans* isomer would survive to some extent. Evidence that the *cis* isomer does hydrogenolyze faster than the *trans* isomer is shown in the following work.

Relative Rate of Hydrogenolysis of cis- and trans-2,4-Dialkyl-1,3-dioxolanes

Absolute rates of hydrogenolysis have not yet been obtained due to the failure to find a satisfactory method of following this heterogeneous reaction. However, an approximate value for the *relative rate* of reduction of the *cis* and *trans* isomers was found by use of a competitive reduction of mixtures of these isomers, with the amount of reducing agent limited so as to permit only 10 to 15% reduction. The more reactive isomer should be consumed to a greater extent and yield a greater quantity of its particular proportion of the two isomeric hydroxy ethers. From Table I it is seen that *cis*-2,4-dimethyl-1,3-dioxolane gives a reduction product which has the composition 96% of 2-ethoxy-1-propanol and 4% of 1-ethoxy-2-propanol while the product from the reduction of *trans*-2,4-dimethyl-1,3-dioxolane is composed of 35% of 2-ethoxy-1-propanol and 65% of 1-ethoxy-2-propanol. Since little or no isomerization occurs, then in a competitive and very limited reduction of a mixture of *cis* and *trans* isomers, if X moles of *cis* isomer is reduced for every mole of *trans* isomer, the ratio of 2-ethoxy-1-propanol to 1-ethoxy-2-propanol obtained is $(96X + 35):(4X + 65)$. From a knowledge of the initial amounts of isomers subjected to reduction and a measurement of the relative amounts of the two alcohols in the reduction product, both X and the relative rate of reduction of the isomers can be calculated. The results, shown in Table III, reveal that the *cis* isomer is reduced about 6.8 times faster than is the *trans* isomer. This observation is confirmed by noting that following a partial reduction of an equimolar mixture of the two isomers, the amount of *cis* isomer in the remaining unchanged dioxolanes was diminished to a far greater extent than was the *trans* isomer. Similar studies on the relative rate of hydrogenolysis of the *cis* and *trans* isomers of 2-ethyl-4-methyl-1,3-dioxolane showed the *cis* isomer to be reduced approximately 10 times faster than the *trans*.

Can. J. Chem. Downloaded from www.nrcresearchpress.com by 210.87.254.5 on 09/05/12
For personal use only.

TABLE III

The relative rates of hydrogenolysis of the *cis* and *trans* isomers of 2,6-dimethyl-1,3-dioxolane with lithium aluminium hydride and aluminium chloride

Expt. No.	Rates of *cis* to *trans* in starting material	Composition of reduction product, %	Rates of *cis* to *trans* isomer reduced	Relative rate of reduction of *cis* isomer (*trans* = 1)
1	50:50	1-Ethoxy-2-propanol, 11 2-Ethoxy-1-propanol, 89	7.7	7.7
2	50:50	1-Ethoxy-2-propanol, 12 2-Ethoxy-1-propanol, 88	6.6	6.6
3	65:35	1-Ethoxy-2-propanol, 9 2-Ethoxy-1-propanol, 91	11.2	6.1
4	35:65	1-Ethoxy-2-propanol, 17 2-Ethoxy-1-propanol, 83	3.7	6.9
			Average	6.8

In view of the fact that acid-catalyzed equilibration of *cis*- and *trans*-2,4-dimethyl-1,3-dioxolane results in a ratio of *cis* to *trans* of about 65:35, the observation that the *cis* isomer is reduced faster than the *trans* is surprising. However, our results agree with the finding by Salomaa (3) that acid-catalyzed hydrolysis of *cis*-2,4-dimethyl-1,3-dioxolane is about 4 times faster than that of *trans*-2,4-dimethyl-1,3-dioxolane. Any plausible explanation of these results must account for (*1*) the different proportions of products obtained on hydrogenolysis of the *cis* and *trans* isomers, (*2*) the enhanced rate of Lewis acid catalyzed hydrogenolysis and also acid-catalyzed hydrolysis of the *cis* isomer with respect to the *trans* isomer, (*3*) the acid-catalyzed 65:35 equilibration ratio of *cis* to *trans* isomers.

It is noteworthy that the 96:4 ratio of C_2—O_1 to C_2—O_3 bond cleavage obtained in the hydrogenolysis of *cis*-2,4-dimethyl-1,3-dioxolane (Table I) is comparable with that of other 1,3-dioxolanes containing an electron donor alkyl group at C_4 (Table I in ref. 1). For example 2,2,4-trimethyl-1,3-dioxolane, 2,4,4-trimethyl-1,3-dioxolane, 4-methyl-1,3-dioxolane, and 4,4-dimethyl-1,3-dioxolane gave respectively 82%, 90%, 93%, and 92% of C_2—O_1 bond cleavage. One might then consider that C_2—O_1 bond cleavage is the "normal" or expected course and that the *cis* isomer then follows the expected preferential C_2—O_1 bond breakage. Thus C_2—O_1 bond breakage in the *trans* isomer can then be considered as retarded, permitting more of C_2—O_3 bond cleavage. No explanation for such a retardation of C_2—O_1 bond cleavage in the *trans* isomer is apparent to us. Relevant to this is the finding that 2,2,4,4-tetramethyl-1,3-dioxolane cleaves "abnormally" to yield 1-isopropoxy-2-methyl-2-propanol (94%) and only 6% of the expected compound 2-isopropoxy-2-methyl-1-propanol (4).

Of interest also is our observation that in parallel reductions of 2,4,4-trimethyl-1,3-dioxolane using either boron trifluoride or aluminium chloride as the Lewis acid but with otherwise identical reaction conditions, no difference could be observed in the proportion of C_2—O_1 to C_2—O_3 bond cleavage. This ratio in each case was 82:18. If approach of the Lewis acid to the dioxolane were influenced by steric factors, and if this were part of the rate-controlling step, then one should expect differences in the proportion of C_2—O_1 to C_2—O_3 bond cleavage due to these two Lewis acids. The inference from these results is that steric effects are not significant in the attack of the Lewis acids upon the *cis* and *trans* isomers during the hydrogenolysis reactions. It should be pointed out, however, that since the exact structure of these Lewis acids in ether solution is not known, boron

Can. J. Chem. Downloaded from www.nrcresearchpress.com by 210.87.254.5 on 09/05/12
For personal use only.

trifluoride may still be "large" enough to produce closely similar steric effects to these shown by aluminium chloride. Hence one cannot be certain that steric effects do not play an important role in this reaction.

EXPERIMENTAL

All boiling points are uncorrected.

Gas–liquid chromatography analyses were done with a Burrell K-2 Kromo-Tog apparatus using a 2 m column packed with 25% of carbowax 20 M on Gas-Chrom P. Helium at a flow rate of about 80 ml/min was the carrier gas. The column temperature employed was dependent upon the boiling point of the compounds analyzed. All compounds were identified by comparison of their g.l.c. retention times, as well as by their isolation and comparison of the infrared and nuclear magnetic resonance (n.m.r.) spectra and boiling points with those of authentic compounds. Quantitative analyses were made by measuring peak areas and comparison of these with the areas obtained by use of carefully measured amounts of the known compounds. Infrared spectra were recorded on a Perkin–Elmer Model 221 instrument. Nuclear magnetic resonance spectra were obtained with a Varian Associates A-60 spectrometer.

Preparation of Compounds

2,4-Dimethyl-1,3-dioxolane was prepared by the following modification of Fischer and Pfahler's procedure (5). Acetaldehyde (100 g, 2.3 mole) was added portionwise to a stirred mixture of 1,2-propanediol (152 g, 2.0 mole), anhydrous magnesium sulfate (60 g), and *p*-toluenesulfonic acid (1 g). The temperature of the reaction mixture was maintained below 20° by ice cooling during the addition. After complete addition of the reagents the reaction mixture stood at 0° for 16 h, and was then filtered free of the magnesium sulfate. The product was distilled to give 121 g (59%) of material boiling at 88–89°. Lit. b.p. 92.8° (6). Analysis of this material by g.l.c. showed it to be a mixture of two components, the *cis* and *trans* isomers of 2,4-dimethyl-1,3-dioxolane in the ratio of 63% to 37% (cf. 65%:35% obtained by Barker *et al.* (2)). Separation of these isomers was effected by several fractional distillations through a 1 m column packed with stainless steel saddles. The course of the distillation was followed by g.l.c. analyses. The isomers so obtained were finally distilled from sodium hydroxide pellets. The lower boiling *cis* isomer distilled at 87° and 700 mm. Lit. b.p. 89.7(2). The higher boiling *trans* isomer distilled at 89–90° and 700 mm. Lit. b.p. 93.5°(2).

2-Ethyl-4-methyl-1,3-dioxolane was prepared by a procedure similar to that employed for the preparation of 2,4-dimethyl-1,3-dioxolane, starting with propionaldehyde and 1,2-propanediol. Boiling point of the mixture of *cis* and *trans* isomers, 114–117° at 700 mm. Lit. b.p. 113–118°(7). The two isomers in the equilibrium ratio of 68:32 were separated by several distillations through a spinning band column. The pure isomers were stored over sodium hydroxide pellets. Boiling point of *trans* isomer, 117° at 700 mm. Boiling point of *cis* isomer, 115° at 700 mm. Configurational assignment was made on the same bases as used for the assignment of the configurations to the low and high boiling isomeric *cis*- and *trans*-2,4-dimethyl-1,3-dioxolanes (2).

1-n-Propoxy-2-propanol was made by a modification of a literature procedure (8). 1,2-Epoxypropane (Eastman Kodak Company) (15 g, 0.26 mole) was added dropwise to a solution of sodium *n*-propoxide (from 2 g of sodium in 70 ml of 1-propanol). The resulting solution was allowed to stand at 25° for 16 h and then poured into cold water. The organic layer was separated, washed with water, and then dried ($MgSO_4$). After removal of the solvent, the remaining oil was distilled under reduced pressure to yield 22.0 g (72%) of material boiling at 73° and 45 mm. Lit. b.p. 148.5–149° at 730 mm (9).

1-Ethoxy-2-propanol was prepared by the same method used to make 1-*n*-propoxy-2-propanol starting with 1,2-epoxypropane and sodium ethoxide in ethanol. Boiling point 130° at 700 mm. Lit. b.p. 130–130.8° (8).

2-Ethoxy-1-propanol was made by a standard literature procedure (10) involving lithium aluminium hydride reduction of the corresponding ester or acid as described below. The precursor, *ethyl α-ethoxypropionate* was prepared in 64% yield from sodium ethoxide and ethyl α-bromopropionate (Eastman Kodak Company) according to the procedure advocated by Nieman *et al.* (11) for the preparation of methyl α-methoxypropionate. Boiling point 70° at 30 mm. Lit. b.p. 66–68° at 27 mm (12). Ethyl α-ethoxypropionate (28.0 g, 0.19 mole) was added dropwise to a stirred suspension of lithium aluminium hydride (7.7 g, 0.2 mole) in 200 ml of dry ether. After complete addition of the reagents, the reaction mixture was stirred for 1 h and then cold water cautiously added to decompose any excess hydride and aluminium salts. After removal of the inorganic solid by filtration, the ether solution was separated and dried over anhydrous magnesium sulfate. Removal of the ether afforded an oil which was purified by distillation to give 16.1 g (81%) of 2-ethoxy-1-propanol boiling at 143° and 700 mm. Lit. b.p. 137.5–138° (8).

2-n-Propoxy-1-propanol.—A mixture of α-chloropropionic acid (Fischer Scientific Co.) (1.0 mole), 1-propanol (400 ml), and concentrated sulfuric acid (20 ml) was refluxed for 3 h, then cooled and poured into aqueous sodium carbonate. The organic layer was separated, dried over anhydrous sodium carbonate, and then distilled to give a 70% yield of *n-propyl α-chloropropionate* boiling at 68° and 23 mm. Lit. b.p. 57° at 12 mm (13). *n-Propyl α-n-propoxypropionate* was made in 79% yield from sodium *n*-propoxide and *n*-propyl α-chloropropionate in 1-propanol as solvent according to the general procedure of Nieman *et al.* (11). Boiling

Can. J. Chem. Downloaded from www.nrcresearchpress.com by 210.87.254.5 on 09/05/12
For personal use only.

point 85° at 16 mm. Lit. b.p. 187–188° (14). Reduction of *n*-propyl α-*n*-propoxypropionate by lithium aluminium hydride according to the same procedure employed above for the preparation of 2-ethoxy-1-propanol gave 2-*n*-propoxy-1-propanol in 58% yield. Boiling point 154–155° at 700 mm. Lit. b.p. 150.5–151° at 730 mm (9).

Determination of the Relative Rates of Reductions of the Dioxolanes

The following description of the competitive partial reduction of *cis*- and *trans*-2-ethyl-4-methyl-1,3-dioxolane is typical of the general procedure used to obtain *relative rates* of hydrogenolysis of the 1,3-dioxolanes. The hydroxy ethers obtained were found to be stable under the reaction conditions, hence their relative amounts in the product can be considered as an indication of the relative rates of formation via hydrogenolysis.

A solution of *cis*-2-ethyl-4-methyl-1,3-dioxolane (2.9 g, 0.025 mole) and *trans*-2-ethyl-4-methyl-1,3-dioxolane (2.9 g, 0.025 mole) in 50 ml of dry ether was stirred whilst lithium aluminium hydride (0.95 g, 0.025 mole) was added. Then a solution of aluminium chloride (0.7 g, 0.005 mole) in ether (10 ml) was added dropwise over a period of 3 min. The reaction mixture was stirred for 30 min and then water was cautiously added to decompose the hydride and aluminium complexes. The inorganic solid was removed by filtration and the ethereal filtrate dried over anhydrous sodium carbonate. Removal of the ether afforded 5.4 g (92%) of material which was analyzed by g.l.c. to determine the composition of the product of reduction. Of the reduced product, 89% was 2-*n*-propoxy-1-propanol and 11% was 1-*n*-propoxy-2-propanol. Of the unreacted dioxolanes, 62% was the *trans* isomer and 38% the *cis* isomer, showing that more of the *cis* than the *trans* isomer had been reduced. Results for similar reductions of a mixture of *cis* and *trans* isomers of 2,4-dimethyl-1,3-dioxolane are given in Table III.

Typical Procedure for Hydrogenolysis of 1,3-Dioxolanes

The dioxolane (0.1 mole) was added to a stirred suspension of lithium aluminium hydride (0.1 mole) in 300 ml of dry ether. The resulting mixture was stirred whilst an ether solution of aluminium chloride (0.1 mole) was added dropwise over about a 10 min period. The reaction mixture was stirred for 1 h after complete addition of the chloride, then cautiously treated with cold water to decompose the aluminium complexes and the excess hydride. The inorganic material was removed by filtration and the ethereal filtrate dried over anhydrous magnesium sulfate. Removal of the ether afforded an oil which was analyzed by g.l.c. Results of these reactions are shown in Table I.

Partial Reductions of cis- and of trans-2,4-Dialkylated-1,3-dioxolanes

These reductions were carried out in a manner identical to that described immediately above, but with a limited amount of reducing agent and aluminium chloride present. A 30 min reaction time was allowed in each case. Amounts of reagents and results of each experiment are shown in Table II.

ACKNOWLEDGMENT

The authors wish to thank the National Research Council of Canada for their financial support for much of this work.

REFERENCES

1. B. E. Leggetter and R. K. Brown. Can. J. Chem. **42**, 990 (1964).
2. S. A. Barker, E. J. Bourne, R. M. Pinkard, M. Stacey, and D. H. Whiffen. J. Chem. Soc. 3232 (1958).
3. P. Salomaa. Ann. Univ. Turku. Ser. A, **46**, 15 (1961); Chem. Abstr. **55**, 12387 (1961).
4. B. E. Leggetter and R. K. Brown. Can. J. Chem. **42**, 1005 (1964).
5. E. Fischer and E. Pfahler. Ber. **53**, 1606 (1920).
6. H. J. Lucas and M. S. Guthrie. J. Am. Chem. Soc. **72**, 5490 (1950).
7. P. Mastagli and C. de Fournas. Compt. Rend. **250**, 3336 (1960); Chem. Abstr. **54**, 24791 (1960).
8. H. C. Chitwood and B. T. Freure. J. Am. Chem. Soc. **68**, 680 (1946).
9. H. L. Cos, W. L. Nelson, and L. H. Cretcher. J. Am. Chem. Soc. **49**, 1081 (1927).
10. W. G. Brown. Organic reactions. Vol. VI. John Wiley and Sons, Inc., New York. p. 469.
11. C. Nieman, A. A. Benson, and J. F. Mead. J. Org. Chem. **8**, 397 (1943).
12. D. Bardon. Bull. Soc. Chim. France, **49**, 1426 (1931).
13. J. W. Walker. J. Chem. Soc. 919 (1895).
14. T. Purdie and D. G. Lander. J. Chem. Soc. 871 (1898).

Can. J. Chem. Downloaded from www.nrcresearchpress.com by 210.87.254.5 on 09/05/12
For personal use only.

Can. J. Chem. Downloaded from www.nrcresearchpress.com by 210.87.254.105 on 09/05/12
For personal use only.

SUBSOLUTIONS IN MULTICOMPONENT SYSTEMS: APPLICATIONS TO SOME TERNARY AQUEOUS ACID SULFATE SYSTEMS AT UNIVARIANCE

A. J. SUKAVA
Department of Chemistry, University of Western Ontario, London, Ontario
Received January 20, 1964

ABSTRACT

A method is described by which univariant composition data for multicomponent solutions may be tested for consistency or accuracy, and used to estimate or verify invariant points, by reference to the vapor pressure data for an appropriate binary subsolution derived from the system. A subsolution is defined as any homogeneous part of a multicomponent solution, such that it is composed of a smaller number of the components than the total but in which the relative masses of these components are the same as in the parent solution.

Published data for ternary systems containing sulfuric acid, water, and the metal sulfates $MnSO_4$, $FeSO_4$, $ZnSO_4$, $BeSO_4$, Na_2SO_4, and $CuSO_4$ are examined. Some new data for the $CuSO_4$ system are also presented. The subsolution in each case is the binary H_2SO_4–H_2O solution, for which adequate vapor pressure data are available.

INTRODUCTION

The composition of any multicomponent solution can be expressed in terms of the relative masses of the various components that are present, and therefore any array of mass ratios can be written as a function of the independent state variables as shown by

$$[1] \qquad m_2/m_1,\ m_3/m_1,\ \ldots,\ m_c/m_1 = f(x, y, \ldots)$$

where the m's are the masses of the different components 1, 2, . . . c and x, y, . . . are the state variables that determine the composition. The number of these variables is the variance, or number of degrees of freedom, of the system.

If a mixture of components is considered such that it consists of any smaller number of the components than the total present in a given multicomponent solution, but with the restriction that the relative masses of these fewer components must be the same as in the parent solution, then it is a consequence of eq. [1] that the composition of such a *part mixture* is also a function of the same independent variables. This can be shown for any choice of part mixture by writing

$$[2] \qquad \begin{aligned} m_2/m_1 &= g(x, y, \ldots), \\ m_3/m_1,\ m_5/m_1 &= h(x, y, \ldots), \text{ etc.} \end{aligned}$$

It can happen of course that a part mixture derived in this way could constitute a solution at the prevailing values of x, y, ... Such a *subsolution** might be unsaturated or supersaturated in practice, depending upon the substances present, but in any case its particular state will be determined by these variables.

SUBSOLUTIONS AT UNIVARIANCE

One consequence of eqs. [1] and [2] offers some practical advantages. If a multicomponent solution is univariant, then the properties of any subsolution derived from it will vary in a regular manner as single-valued functions of the one independent state variable. Since the subsolution will be univariant too by reason of the restriction on its composition, it

**The term "subsolution" is adopted as sufficiently appropriate to describe the physical consequence of eqs. [1] and [2] in the case of any homogeneous part mixture derived from a multicomponent parent solution in the manner shown. The geometric term "projection" might also be used since the functions in [2] are projections of the array in [1].*

would follow, for example, that its vapor pressure might show a dependence on temperature somewhat like any typical Clausius–Clapeyron log P vs. $1/T$ relation for a (univariant) pure liquid or for a solution at constant composition. This possibility is examined in this paper, with emphasis on two main practical applications, (i) detection of errors in original multicomponent composition data and (ii) estimation of invariant points.

The vapor pressure of a binary subsolution can be related very simply to the composition of the multicomponent parent. If components 1 and 2 of a multicomponent solution constitute a subsolution, then

$$P_1 = P_1^0 \gamma_1 X_1, \qquad [3]$$

where P_1^0 is the vapor pressure of pure 1 and P_1, X_1, and γ_1 are the vapor pressure, mole fraction, and activity coefficient of 1 in the subsolution. Since the ratio of the mole numbers (n) of components 1 and 2 is the same in the subsolution and multicomponent parent, one can write

$$X_1 = \frac{n_1}{n_1 + n_2} = \frac{n_1'}{n_1' + n_2'} = \frac{X_1'}{X_1' + X_2'}, \qquad [4]$$

where the unprimed quantities are those for the subsolution and the primes identify corresponding quantities in the parent. Equation [4] is obviously valid for any number of components in the multicomponent solution.

Under univariant conditions the vapor pressure can be considered a function of temperature and composition, with the composition also a function of temperature. Thus, to get the log P vs. $1/T$ relation, the dependence of P_1 on temperature and composition can be written as

$$\log P_1 = f(1/T, X_1)$$

to give the desired derivative

$$\frac{\mathrm{d} \log P_1}{\mathrm{d}(1/T)} = \left(\frac{\partial \log P_1}{\partial(1/T)}\right)_{X_1} + \left(\frac{\partial \log P_1}{\partial X_1}\right)_{1/T} \left(\frac{\mathrm{d}X_1}{\mathrm{d}(1/T)}\right). \qquad [5]$$

The first term on the right in eq. [5] can be obtained by differentiating [3] with respect to $1/T$, giving

$$\left(\frac{\partial \log P_1}{\partial(1/T)}\right)_{X_1} = \frac{\mathrm{d} \log P_1^0}{\mathrm{d}(1/T)} + \left(\frac{\partial \log a_1}{\partial(1/T)}\right)_{X_1} \qquad [6]$$

where a_1 is the activity. Since the first term on the right in [6] is the Clausius–Clapeyron slope for pure 1, and since the second term can be easily shown to be

$$\left(\frac{\partial \log a_1}{\partial(1/T)}\right)_{X_1} = \frac{\bar{H}_1 - H_1^0}{2.3R},$$

where H_1^0 and $\bar{H}_1$ are the molal enthalpy of pure 1 and the partial molal enthalpy of 1 in the subsolution, eq. [6] becomes the simple Clausius–Clapeyron expression for component 1 in a binary solution at constant composition:

$$\left(\frac{\partial \log P_1}{\partial(1/T)}\right)_{X_1} = \frac{-(H_1^{\mathrm{v}} - \bar{H}_1)}{2.3R},$$

where H_1^{v} is the molal enthalpy of the equilibrium vapor. When the major component in the subsolution is 1, the value of $\bar{H}_1$ does not differ greatly from H_1^0. Under these conditions

Can. J. Chem. Downloaded from www.nrcresearchpress.com by 210.87.254.105 on 09/05/12
For personal use only.

the second term in eq. [5] can be interpreted as the difference in slope between the log P vs. $1/T$ curve for the subsolution and the log P vs. $1/T$ curve for pure 1.

Adequate vapor pressure data are available for binary mixtures of sulfuric acid and water (1). Multicomponent systems containing these two components can therefore be readily tested for the log P vs. $1/T$ behavior of the H_2SO_4–H_2O subsolution provided the univariant compositions are available for the same phase equilibrium for at least three different temperatures. These conditions are met by published data for the ternary systems composed of sulfuric acid, water, and the metal sulfates $MnSO_4$ (2, 3), $FeSO_4$ (4–8), $ZnSO_4$ (9, 10), $BeSO_4$ (11), Na_2SO_4 (12, 13, 14), and $CuSO_4$ (12, 15, 16). The compositions of the subsolutions were calculated and the vapor pressures were found by graphical interpolation from the literature values (1), with the results shown in Figs. 1 to 6. It is evident that the downwardly concave log P vs. $1/T$ curves are in many cases almost linear over wide ranges of temperature, especially when the sulfuric acid concentration of the subsolution is low. Greater non-linearity tends to occur with the higher concentrations of acid.

Examination of other univariant data shows that the near linearity of the log P vs. $1/T$ curves is a general property of subsolutions. A good example is a univariant equilibrium in the quaternary system $(NH_4)_2SO_4$–Li_2SO_4–C_2H_5OH–H_2O (17). The log P vs. $1/T$ curve for the ethanol–water subsolution derived from the upper quaternary liquid layer is nearly linear whether P is the partial pressure of the ethanol or of the water. Easier empirical plots such as log X_1 or X_2/X_1 vs. temperature are considerably more curved, in general.

ACCURACY OF UNIVARIANT MULTICOMPONENT COMPOSITION DATA

If the composition of a subsolution is abstracted from the data for some multicomponent solution at univariance, and if the vapor pressure of the subsolution is plotted against the temperature, then the plotted points must lie on a smooth curve if the multicomponent data are accurate or at least self-consistent. Scatter of the points for a given phase equilibrium will indicate error or inconsistency, provided of course that the computation of vapor pressures for the subsolution does not also introduce error in significant amount. The near linearity of the log P vs. $1/T$ curves for the subsolutions offers an advantage in detecting such errors, and specific errors can be found if the multicomponent composition data are sufficient to establish the trend of the log P vs. $1/T$ relation with the necessary certainty. Numerous examples are given in the diagrams.

BINARY TRANSITION POINTS FROM UNIVARIANT TERNARY DATA

Any univariant ternary acid sulfate system in which there are two different hydrates of a normal metal sulfate in equilibrium with a liquid and a vapor phase reduces to the invariant binary system with the same two solids when the concentration of sulfuric acid in the liquid phase becomes zero with rise in temperature. (One of the equilibrium solids can of course be the normal anhydrous salt.) Therefore, for any such univariant normal-sulfate equilibrium, the log P vs. $1/T$ curve for the H_2SO_4–H_2O subsolution ends at the log P vs. $1/T$ curve for pure water as temperature rises. The point at which the two curves meet then corresponds to the invariant binary transition temperature for the particular hydrate mixture in the equilibrium.

Figures 1 to 6 include the log P vs. $1/T$ curve for pure water, the uppermost curve in each diagram, to allow estimation or verification of binary transition points in this way. This method provides an obvious advantage if the curves are sufficiently linear and if the

Can. J. Chem. Downloaded from www.nrcresearchpress.com by 210.87.254.105 on 09/05/12
For personal use only.

angle of intersection is sufficiently large. In the most favorable cases simple geometrical calculation could give the transition point more precisely from the appropriate ternary composition and binary vapor pressure data. Extrapolating the sulfuric acid concentration of the univariant ternary solution to zero provides a more obvious method of locating a binary transition point in sulfate systems, but this has the disadvantage of greater and uncertain curvature.

TERNARY QUINTUPLE POINTS FROM UNIVARIANT DATA

An invariant quintuple point in any ternary aqueous acid–sulfate system involves three solid phases in equilibrium with one liquid, and the associated univariant equilibria can in theory involve any two of these solids. It follows that the quintuple point can be found as the point of intersection of either two or three log P vs. $1/T$ curves for the univariant H_2SO_4–H_2O subsolutions, the number depending on which solid phases form the experimentally stable pairs at the different temperatures near the quintuple point. Various circumstances shown in the diagrams illustrate both of these possibilities. As before, the advantage lies in the near linearity of many of the curves.

TREATMENT OF PUBLISHED DATA

The System $MnSO_4$–H_2SO_4–H_2O

Some univariant compositions for the system $MnSO_4$–H_2SO_4–H_2O, reported by Taylor (2), are represented in Fig. 1 by log P vs. $1/T$ plots for the H_2SO_4–H_2O subsolutions, with each different equilibrium designated by letter. Equilibrium A involves the normal salt only, B normal and acid salts, and C and D acid salts only. In A, the necessary third point for the graphical plot is provided by the limiting binary equilibrium at 24.5°, credited to Krepelka and Rejha (3).

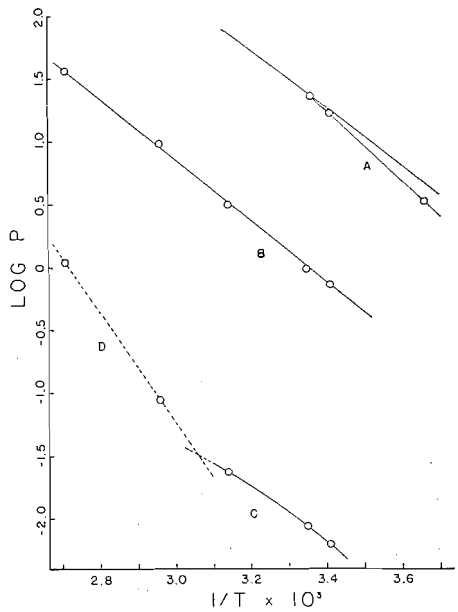

FIG. 1. Log P vs. $1/T$ relations for H_2SO_4–H_2O subsolutions in the system $MnSO_4$–H_2SO_4–H_2O at univariance (2, 3): (A) $MnSO_4 \cdot 5H_2O$ – $MnSO_4 \cdot H_2O$ – solution – vapor, (B) $MnSO_4 \cdot H_2O$ – $MnSO_4 \cdot H_2SO_4 \cdot H_2O$ – solution – vapor, (C) $MnSO_4 \cdot H_2SO_4 \cdot H_2O$ – $MnSO_4 \cdot 3H_2SO_4$ – solution – vapor, (D) $MnSO_4 \cdot H_2SO_4 \cdot H_2O$ – $MnSO_4 \cdot H_2SO_4$ – solution – vapor.

Can. J. Chem. Downloaded from www.nrcresearchpress.com by 210.87.254.105 on 09/05/12
For personal use only.

The three points for equilibrium A appear to lie on a reasonably good straight line. The five points for B, despite some irregularity, show the same trend. The scatter is an indication of experimental or computational error, or both. Curve C, which shows marked downward concavity, is based on somewhat uncertain graphically estimated small vapor pressure values. It may not be correct as drawn. Curve D, for lack of sufficient data, cannot be established with certainty. The broken line in the diagram is included merely to provide a rough estimate of the invariant quintuple-point temperature for the ternary equilibrium

$$MnSO_4 \cdot H_2SO_4 \cdot H_2O - MnSO_4 \cdot H_2SO_4 - MnSO_4 \cdot 3H_2SO_4 - \text{ternary solution} - \text{vapor}.$$

If curves C and D are at least approximately correct, their intersection places this quintuple point at about 55°.

The System $FeSO_4$–H_2SO_4–H_2O

Univariant data for the system $FeSO_4$–H_2SO_4–H_2O are represented in Figs. 2*a* and 2*b*. These were obtained from several sources (4–8), one reason for the wide interest being that the waste "pickle liquor" of the steel industry is primarily an acid iron(II) sulfate solution. The symbols used for the individual plots identify the source of the original data.

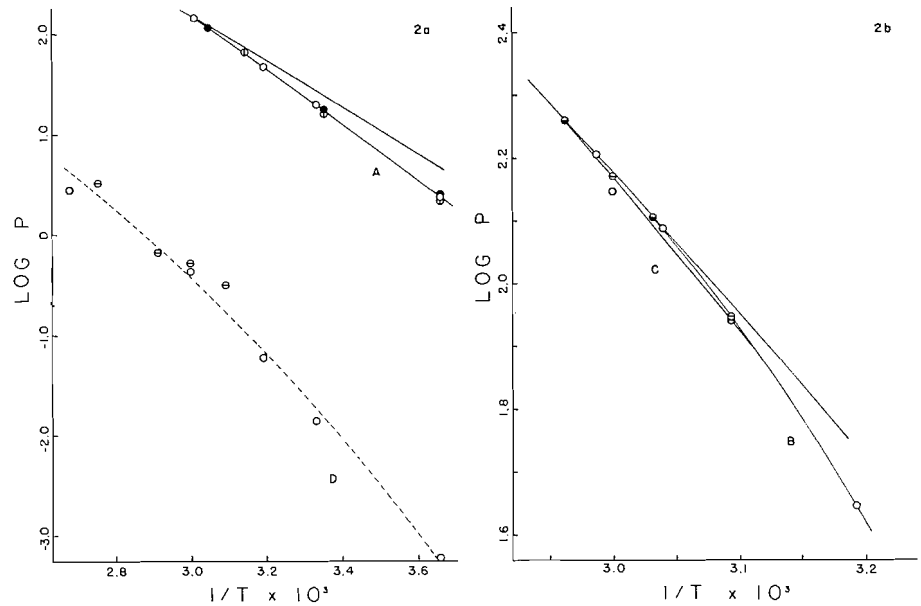

FIG. 2. Log P vs. $1/T$ relations for H_2SO_4–H_2O subsolutions in the system $FeSO_4$–H_2SO_4–H_2O at univariance: (A) $FeSO_4 \cdot 7H_2O$ – $FeSO_4 \cdot H_2O$ – solution – vapor, (B) $FeSO_4 \cdot 7H_2O$ – $FeSO_4 \cdot 4H_2O$ – solution – vapor, (C) $FeSO_4 \cdot 4H_2O$ – $FeSO_4 \cdot H_2O$ – solution – vapor, (D) $FeSO_4 \cdot H_2O$ – $FeSO_4$ – solution – vapor. ⦶ Bullough *et al.* (5), ● Cameron (6), ○ Kobe and Fredrickson (8), ⊖ Belopol'skii and Shpunt (4), ◒ Fraenckel (7).

Curve A in Fig. 2*a* is best represented as slightly concave downward. Except for some disagreement at 0° and at 25°, the data from the different sources seem to be in reasonable accord. The Kobe and Fredrickson value for the invariant heptahydrate–monohydrate transition point, given as 59.0° (8), appears to be verified.

Curve B in Fig. 2*b* is also concave downward. No definite conclusion can be drawn about the better accuracy of one or the other of the two values reported for the heptahydrate–tetrahydrate transition point, 56.6° (7) and 56.0° (8), except that both values, in good agreement anyway, are obviously reasonable.

Can. J. Chem. Downloaded from www.nrcresearchpress.com by 210.87.254.105 on 09/05/12
For personal use only.

The two sets of data for equilibrium C (Fig. 2*b*) reported by Belopol'skii and Shpunt (4) produce a good straight line with the Fraenckel value for the tetrahydrate–monohydrate transition temperature, given as 64.4° (7). The extrapolated Kobe and Fredrickson value of 61.7° (8) for this point appears to be too low. The Kobe and Fredrickson data for the univariant ternary tetrahydrate–monohydrate equilibrium at 60° (8) are definitely in error.

Despite the small angle between curves B and C, their point of intersection can be estimated at about 49°. This is then the approximate quintuple point for the equilibrium

$$FeSO_4 \cdot 7H_2O - FeSO_4 \cdot 4H_2O - FeSO_4 \cdot H_2O - \text{ternary solution} - \text{vapor}.$$

Because of the solids present, curve A in Fig. 2*a* must also pass through this point, and it may be noted that equilibria A and B occur experimentally both above and below this temperature while equilibrium C has been found above it only.

At least some of the data for equilibrium D, as represented in Fig. 2*a*, must be quite inaccurate. The broken curve shows the approximate trend only.

The System $ZnSO_4$–H_2SO_4–H_2O

Data for some univariant and invariant equilibria in the system $ZnSO_4$–H_2SO_4–H_2O, reported by Copeland and Short (9) and by Joshi and Devadatta (10), are represented in Fig. 3. Some of the data for equilibrium A appear to be slightly inaccurate, while all points for B indicate good accuracy. The heptahydrate–hexahydrate transition at 39° and the ternary quintuple point at 21° are both consistent with the univariant data.

The Joshi and Devadatta data for equilibrium C are in poor agreement with those of Copeland and Short. The latter appear to be self-consistent, but the curve cannot be taken as evidence of accuracy for the two highest points. The 60° value for the hexahydrate-monohydrate transition seems to be too high. Lorimer has pointed out recently (18) that extrapolating the curve obtained by plotting the sulfuric acid concentration of the ternary solution against reciprocal temperature gives a value of 52.5° for this transition. It is also worth noting that the four lower Copeland and Short points for equilibrium C, including the quintuple point, all lie on a nearly linear curve that meets the water curve at 51°. This is shown by the alternative (broken) curve in the diagram.

The System $BeSO_4$–H_2SO_4–H_2O

Data for one univariant equilibrium in the system $BeSO_4$–H_2SO_4–H_2O, reported by Campbell and co-workers (11), are represented in Fig. 4. The overall trend of the log P vs. $1/T$ curve indicates only very slight downward concavity. The data may be judged accurate, except perhaps at 75°. The tetrahydrate–dihydrate transition point is verified at about 89°.

The System Na_2SO_4–H_2SO_4–H_2O

Figure 5 shows some univariant data for the more complicated system Na_2SO_4–H_2SO_4–H_2O. These were compiled from papers by Foote (12), Faust and Esselmann (13), and Luk'yanova (14). To make the diagram as complete as possible, some univariant data which were not found in the literature were estimated by extrapolating the ternary bivariant data. No great precision can be claimed for these extrapolations, and the diagram in such respects should be taken only as a very rough approximation.

For lack of sufficient data, only three of the curves in Fig. 5 can be established with any certainty. These are B, D, and E. The first is nearly linear and the other two are markedly concave downward. The curves for the other three equilibria, A, C, and F, are shown as broken lines to suggest approximation only. These enable rough estimates of the quintuple

Can. J. Chem. Downloaded from www.nrcresearchpress.com by 210.87.254.105 on 09/05/12
For personal use only.

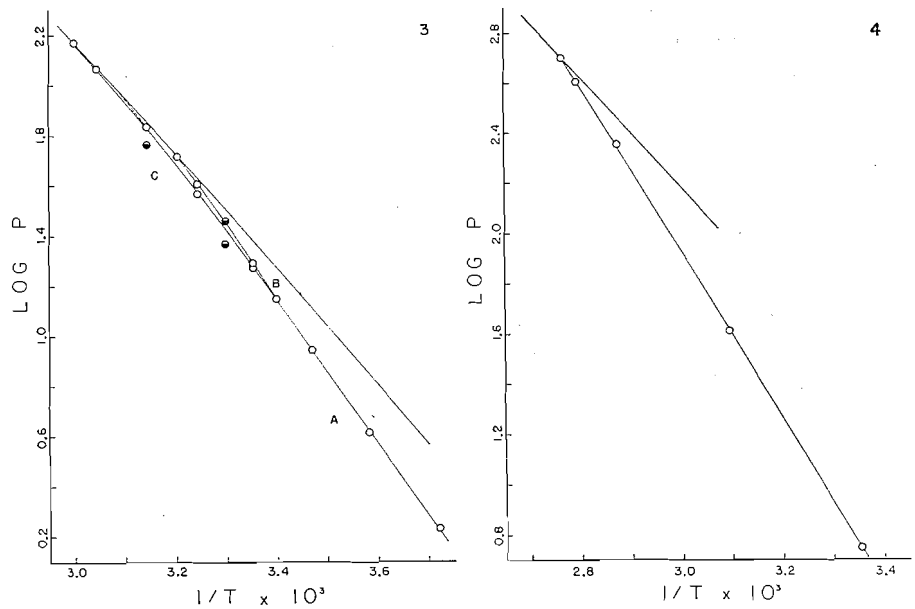

FIG. 3. Log P vs. $1/T$ relations for H_2SO_4–H_2O subsolutions in the system $ZnSO_4$–H_2SO_4–H_2O at univariance: (A) $ZnSO_4 \cdot 7H_2O$ – $ZnSO_4 \cdot H_2O$ – solution – vapor, (B) $ZnSO_4 \cdot 7H_2O$ – $ZnSO_4 \cdot 6H_2O$ – solution – vapor, (C) $ZnSO_4 \cdot 6H_2O$ – $ZnSO_4 \cdot H_2O$ – solution – vapor. ○ Copeland and Short (9), ● Joshi and Devadatta (10).

FIG. 4. Log P vs. $1/T$ relation for H_2SO_4–H_2O subsolution in the system $BeSO_4$–H_2SO_4–H_2O at univariance (11). Equilibrium phases: $BeSO_4 \cdot 4H_2O$ – $BeSO_4 \cdot 2H_2O$ – solution – vapor.

point temperatures, one of which may be taken as reasonably correct. This point, the intersection of curves A, B, and C, shows the quintuple point for the equilibrium

$$Na_2SO_4 \cdot 10H_2O - Na_2SO_4 - Na_3H(SO_4)_2 - \text{ternary solution} - \text{vapor}$$

to be about 16°.

The System $CuSO_4$–H_2SO_4–H_2O

The curves in Fig. 6 represent univariant equilibria in the system $CuSO_4$–H_2SO_4–H_2O. Ternary data from Foote (12), Crockford and Warrick (15), and Posnjak and Tunell (16) are included together with the results of some new analyses shown in Table I.* The three equilibria are identified by letter in both table and diagram.

Equilibration in this system is a very slow process, especially at low temperatures and high concentrations of acid. It is therefore not surprising that the data show rather poor agreement. The differences in color and rates of settling of the solid phases nevertheless favor establishment of the univariant conditions experimentally. This is done by careful adjustment of the sulfuric acid concentration of the equilibrium liquid to give visual evidence of the simultaneous presence of two solids.

All three log P vs. $1/T$ curves show only slight downward concavity. Some of the older data for the pentahydrate–trihydrate equilibrium at the lower temperatures (curve A) are obviously in error. The new data for the higher temperatures are reasonably consistent with the known binary transition point, 95.9° (19).

The data for equilibrium B are not sufficient to allow accurate extrapolation to the

Credit for the new data goes to the following students: R. G. Benbow, L. B. Bezeau, M. A. Clarke, and G. W. Gray.

Can. J. Chem. Downloaded from www.nrcresearchpress.com by 210.87.254.105 on 09/05/12
For personal use only.

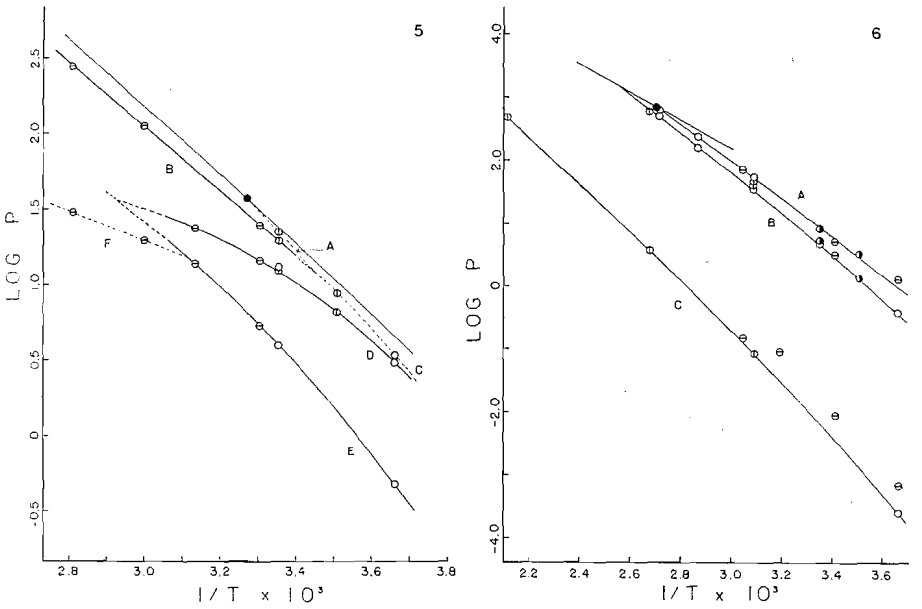

FIG. 5. Log P vs. $1/T$ relations for H_2SO_4–H_2O subsolutions in the system Na_2SO_4–H_2SO_4–H_2O at univariance. (A) $Na_2SO_4 \cdot 10H_2O$ – Na_2SO_4 – solution – vapor, (B) Na_2SO_4 – $Na_3H(SO_4)_2$ – solution – vapor, (C) $Na_2SO_4 \cdot 10H_2O$ – $Na_3H(SO_4)_2$ – solution – vapor, (D) $Na_3H(SO_4)_2$ – $NaHSO_4 \cdot H_2O$ – solution – vapor, (E) $NaHSO_4 \cdot H_2O$ – $NaHSO_4$ – solution – vapor, (F) $Na_3H(SO_4)_2$ – $NaHSO_4$ – solution – vapor. ◑ Foote (12), ⊖ Faust and Esselmann (13), ○ Luk'yanova (14), ● Known transition point for $Na_2SO_4 \cdot 10H_2O \rightleftharpoons Na_2SO_4$ + saturated binary solution.

FIG. 6. Log P vs. $1/T$ relations for H_2SO_4–H_2O subsolutions in the system $CuSO_4$–H_2SO_4–H_2O at univariance. (A) $CuSO_4 \cdot 5H_2O$ – $CuSO_4 \cdot 3H_2O$ – solution – vapor, (B) $CuSO_4 \cdot 3H_2O$ – $CuSO_4 \cdot H_2O$ – solution – vapor, (C) $CuSO_4 \cdot H_2O$ – $CuSO_4$ – solution – vapor. ◑ Foote (12), ⊖ Crockford and Warrick (15), ◑ Posnjak and Tunell (16), ● Miles and Menzies (19), ○ new data.

TABLE I

Univariant data for the system $CuSO_4$–H_2SO_4–H_2O

		Ternary liquid	
Equilibrium	Temp. (°C)	$CuSO_4$ (%)	H_2SO_4 (%)
A	50	8.42	37.31
A	75	22.83	21.05
A	95	37.92	3.95
B	0	0.25	64.82
B	25	2.07	56.47
B	50	5.39	48.00
B	75	13.92	36.69
B	95	25.71	22.56
C	0	0.39	91.57

water curve. The average trend gives a value of about 120° for the trihydrate–monohydrate transition. The new data alone give 115°.

In view of the general downward concavity of the log P vs. $1/T$ curves, the one new point for equilibrium C seems to agree with the Posnjak and Tunell data (16). This suggests that the three lowest-temperature Crockford and Warrick points are in error. If the curve is reasonably correct as shown, the monohydrate–anhydrous transition lies in the supercritical region.

Can. J. Chem. Downloaded from www.nrcresearchpress.com by 210.87.254.105 on 09/05/12
For personal use only.

ACKNOWLEDGMENTS

Many helpful discussions with Dr. J. W. Lorimer are gratefully acknowledged. This work received financial assistance from the National Research Council of Canada.

REFERENCES

1. International critical tables. Vol. III. 1928. p. 303.
2. D. TAYLOR. J. Chem. Soc. 2370 (1952).
3. J. H. KREPELKA and B. REJHA. Collection Czech. Chem. Commun. **5**, 67 (1933).
4. A. P. BELOPOL'SKII and S. YA. SHPUNT. J. Appl. Chem. USSR English Transl. **14**, 716 (1941).
5. W. BULLOUGH, T. A. CANNING, and M. I. STRAWBRIDGE. J. Appl. Chem. London, **2**, 703 (1952).
6. F. K. CAMERON. J. Phys. Chem. **34**, 692 (1930).
7. F. FRAENCKEL. Z. Anorg. Chem. **55**, 223 (1907).
8. K. A. KOBE and R. E. FREDRICKSON. Chemical and engineering data series. Vol. I, No. 1. American Chemical Society, Washington, D.C. 1956. p. 13.
9. L. C. COPELAND and O. A. SHORT. J. Am. Chem. Soc. **62**, 3285 (1940).
10. N. K. JOSHI and S. C. DEVADATTA. Proc. Indian Acad. Sci. A, **7**, 131 (1938).
11. A. N. CAMPBELL, A. J. SUKAVA, and J. KOOP. J. Am. Chem. Soc. **73**, 2831 (1951).
12. H. W. FOOTE. J. Ind. Eng. Chem. **11**, 629 (1919).
13. O. FAUST and P. ESSELMANN. Z. Anorg. Allgem. Chem. **157**, 290 (1926).
14. E. I. LUK'YANOVA. Sbornik Statei Obshchei Khim. Akad. Nauk S.S.S.R. **1**, 106 (1953).
15. H. D. CROCKFORD and L. E. WARRICK. J. Phys. Chem. **34**, 1064 (1930).
16. E. POSNJAK and G. TUNELL. Am. J. Sci. Ser. 5, **18**, 1 (1929).
17. F. A. H. SCHREINEMAKERS. Z. Physik. Chem. **59**, 641 (1907).
18. J. W. LORIMER. Can. J. Chem. **42**, 2215 (1964).
19. F. T. MILES and A. W. C. MENZIES. J. Am. Chem. Soc. **59**, 2392 (1937).

Can. J. Chem. Downloaded from www.nrcresearchpress.com by 210.87.254.105 on 09/05/12
For personal use only.

Can. J. Chem. Downloaded from www.nrcresearchpress.com by 210.87.254.6 on 09/05/12
For personal use only.

NUCLEAR MAGNETIC RESONANCE STUDIES OF THE PROTONATION OF WEAK BASES IN FLUOROSULFURIC ACID

V. KETONES, CARBOXYLIC ACIDS, AND SOME OTHER OXYGEN BASES

T. BIRCHALL AND R. J. GILLESPIE
Department of Chemistry, McMaster University, Hamilton, Ontario
Received October 19, 1964

ABSTRACT

The proton n.m.r. spectra of the conjugate acids of some ketones and carboxylic acids, and of ethyl acetate, nitromesitylene, and ethyl alcohol have been observed. A correlation has been found between the chemical shift of the C=OH^+ proton of the conjugate acids of some para-substituted acetophenones and their pK_{BH^+} and σ^+ values. The rates of proton loss from these conjugate acids have been obtained.

INTRODUCTION

The proton n.m.r. spectra of the conjugate acids of acetone, ethyl alcohol, and water were first observed in solutions of the bases in anhydrous hydrogen fluoride saturated with boron trifluoride at −75° (1). The successful observation of the C=OH^+ resonances in the n.m.r. spectra of the conjugate acids of amides and related compounds in solution in fluorosulfuric acid at low temperatures (2) has led us to the examination of the low-temperature spectra of some other oxygen bases in this solvent.

RESULTS AND DISCUSSIONS

Ketones

The n.m.r. spectra of a series of para-substituted acetophenones in fluorosulfuric acid were recorded at various temperatures. It is possible to observe the spectrum of the conjugate acid in all cases, although in the case of para-nitroacetophenone it is not possible to completely stop exchange with the solvent even at −88°. The chemical shifts are recorded in Table I. No spin–spin coupling is observed between the captured proton and the protons of the methyl group.

TABLE I

Chemical shifts of the conjugate acids of some ketones

	Temp., °C	$-\delta$, p.p.m. from external tetramethylsilane			
		=OH^+	Phenyl	$OC\cdot CH_3$	CH_3
p-Nitroacetophenone	−84	15.33	8.87*	3.66	
p-Chloroacetophenone	−79	13.52	8.67, 8.53, 7.95, 7.82	3.42	
Acetophenone†	−82	13.46	8.49, 8.36, 7.78, 7.65	3.17	
p-Fluoroacetophenone	−71	13.34	8.77, 7.76, 7.63, 7.51	3.44	
p-Methylacetophenone	−46	12.85	8.63, 8.49, 7.83, 7.70	3.37	2.74
p-Methoxyacetophenone	−81	12.46	8.85, 8.72, 7.61, 7.48	3.34	4.38
Acetone‡	25	14.45		3.25	

*Phenyl spectrum not resolved.
†Only the chemical shifts of the most prominent phenyl peaks are recorded.
‡Spectrum in SbF_5/HSO_3F.

A notable feature of these spectra is the very large chemical shift, from tetramethylsilane, of the captured proton. We note that the C=OH^+ resonance shifts to lower field as

the para-substituent becomes more electron attracting. Figure 1 shows that there is a very satisfactory linear correlation between the chemical shift of the captured proton and the pK_{BH^+} values. Since a linear relation has been found between pK_{BH^+} and the substituent constant σ^+ (3) there is also a good correlation between the chemical shift and σ^+ (Fig. 2).

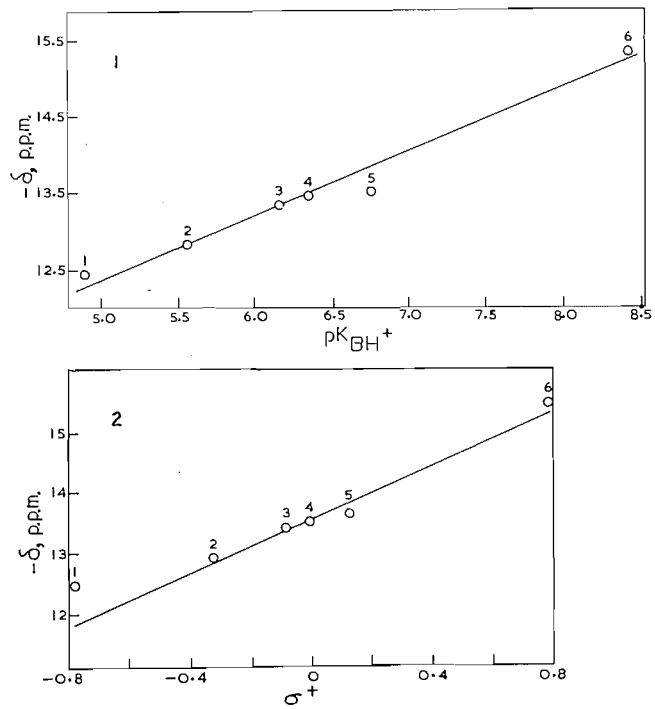

FIG. 1. Chemical shift of the $=OH^+$ proton of the conjugate acids of some para-substituted acetophenones vs. pK_{BH^+}: (1) p-OCH_3, (2) p-CH_3, (3) p-F, (4) p-H, (5) p-Cl, (6) p-NO_2.

FIG. 2. Chemical shift of the $=OH^+$ proton of the conjugate acids of some para-substituted acetophenones versus σ^+: (1) p-OCH_3, (2) p-CH_3, (3) p-F, (4) p-H, (5) p-Cl, (6) p-NO_2.

The ring portion of the spectra of the protonated acetophenones would be expected to be of the A_2B_2 type. Presumably because cross-ring coupling is weak, the actual spectra approximate to $(AB)_2$ spectra (Fig. 3). As the electron-withdrawing character of the para-substituent is increased from OCH_3 to NO_2, the chemical shift between the A and B protons decreases until in the latter case it becomes very small indicating that the electron-withdrawing powers of the NO_2 and $HO^+{=}C\cdot CH_3$ groups are very similar.

The n.m.r. spectrum of the conjugate acid of acetone, obtained in an SbF_5/HSO_3F solution, consists of two peaks, one due to the proton on the carbonyl oxygen and the other due to the methyl protons: the shifts are given in Table I.

Carboxylic Acids

Stewart and Yates (4) have found a close correlation between the basicities of a number of substituted benzoic acids and their acetophenone analogues and they conclude that the site of protonation in benzoic acid and its derivatives is the carbonyl oxygen. In an attempt to obtain confirmation of their conclusion, carboxylic acids have been examined in SbF_5/HSO_3F solution. The chemical shifts are given in Table II.

Can. J. Chem. Downloaded from www.nrcresearchpress.com by 210.87.254.6 on 09/05/12
For personal use only.

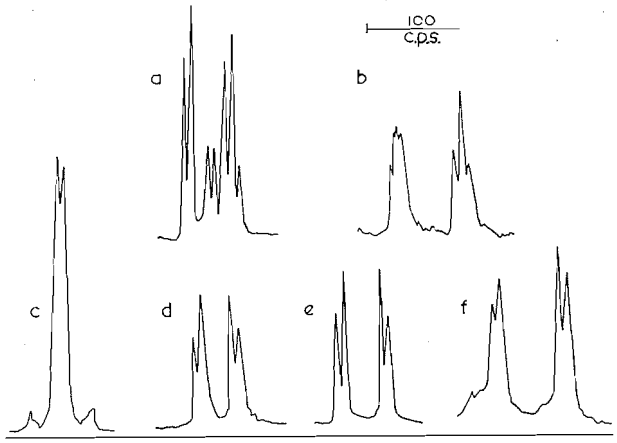

FIG. 3. Aromatic proton spectra for solutions of acetophenones in fluorosulfuric acid: (*a*) *p*-H, (*b*) *p*-F, (*c*) *p*-NO_2, (*d*) *p*-Cl, (*e*) *p*-Me, (*f*) *p*-OMe.

TABLE II

Chemical shifts of the conjugate acids of some carboxylic acids and ethyl acetate in HSO_3F/SbF_5

Base	Temp., °C	−δ, p.p.m. from external tetramethylsilane			
		OH	Phenyl	CH_2	CH_3
Acetic acid	−75	12.89, 12.28			3.12
	−25	12.56			3.12
Propionic acid	−77	12.62, 12.39		3.40	1.67
Benzoic acid	−84.5	12.10	8.42, 8.32, 7.95, 7.82		
Ethyl acetate	−75	12.75		5.14	2.97, 1.82

The n.m.r. spectrum of benzoic acid in SbF_5/HSO_3F solution shows, in addition to peaks arising from the phenyl protons, another peak with a chemical shift similar to that observed for the $=OH^+$ peak of protonated ketones. That this low-field peak is the result of protonation is confirmed by the measurement of the relative areas of the peaks which were found to be 1.89:5.0. One cannot on the basis of this evidence decide between structures I and II for the conjugate acid provided that there is free rotation about the $C—OH_2^+$ bond in II.

I II

The conjugate acid of acetic acid in SbF_5/HSO_3F shows, at low temperature, two peaks at low field and a peak due to the methyl protons; the relative areas of the peaks were found to be 1.08:0.96:3.0. Raising the temperature results in broadening of the low-field peaks which eventually collapse together and merge with the solvent. Similar results were obtained for the conjugate acid of propionic acid (Table II). Unlike protonated benzoic acid, where both OH protons appear equivalent, the OH protons of the conjugate acids

Can. J. Chem. Downloaded from www.nrcresearchpress.com by 210.87.254.6 on 09/05/12
For personal use only.

of these aliphatic acids are non-equivalent, presumably because of the formation of a very strong hydrogen bond between one of the hydrogens and the oxygen atom to which it is not directly attached (III).

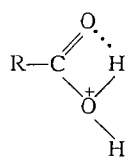

IIIa

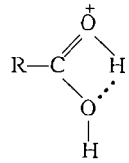

IIIb

Again, it is not possible to distinguish between IIIa and IIIb. Consideration of the donor and acceptor properties of oxygen would lead one to conclude that hydrogen bonding would be considerably stronger in IIIa than in IIIb and that IIIa might therefore be favored. However no spin–spin coupling between the non-equivalent hydrogens is observed.

Ethyl Acetate

In the n.m.r. spectrum of the conjugate acid of ethyl acetate, a new peak is observed at low temperature in addition to peaks due to the CH_3 and CH_2 protons of the ethyl group and the single sharp peak due to the CH_3 protons of the acetate group. One might expect that protonation of the ether oxygen would result in a change in the CH_2 quartet due to additional spin–spin coupling with the captured proton only three bonds removed. No change in the pattern is observed, even at very low temperatures, and the signal from the captured proton remains a single sharp line. It is concluded that protonation takes place on the carbonyl oxygen, and by analogy we might conclude that the conjugate acids of acetic and propionic acids have structure IIIb rather than IIIa.

Nitromesitylene

The n.m.r. spectrum of nitromesitylene in CCl_4 consists of a single line A, due to the phenyl protons and two overlapping lines, B and C, due to the ortho and para methyl groups. In a strongly acidic solution at low temperatures peaks A, B, and C are again observed and in addition a new peak, D, appears at −14.86 p.p.m. from tetramethylsilane (Fig. 4): the relative areas were found to be D:A:B+C:: 0.93:1.85:9.0. The chemical shift (Table III) between the non-equivalent methyl groups increases from 0.05 p.p.m. in CCl_4 to 0.24 p.p.m. in acid solution. The absence of any peaks in the "methylene" region of the spectrum which would result from protonation of the aromatic ring (5, 6), the area measurements, and the fact that the new peak has a chemical shift characteristic of an $=OH^+$ proton, indicate that protonation takes place on one of the oxygen atoms of the nitro group.

It is interesting to compare the structure of the conjugate acid of nitromesitylene with the structure IV proposed by Oláh (7) for the compound formed by the reaction of trifluoromethylbenzene, NO_2F, and BF_3.

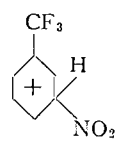

IV

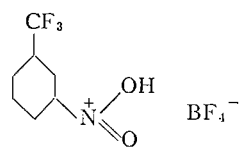

V

In the light of our n.m.r. evidence V appears to be a more likely structure than IV.

Can. J. Chem. Downloaded from www.nrcresearchpress.com by 210.87.254.6 on 09/05/12
For personal use only.

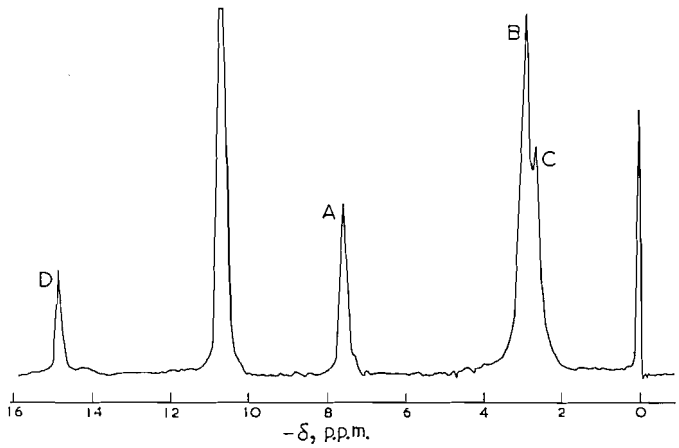

FIG. 4. The n.m.r. spectrum of a solution of nitromesitylene in SbF_5/HSO_3F at −84.5°.

TABLE III

Chemical shifts of some oxygen bases in various solvents

Base	Solvent	Temp., °C	−δ, p.p.m. from external tetramethylsilane				
			OH	Solvent	Phenyl	CH_2	CH_3
Nitromesitylene	HSO_3F/SbF_5	−84.5	14.86		7.66		2.97, 2.73
Ethyl alcohol	$CDCl_3$	25	2.58			3.70	1.22
	HSO_3F	25	—	10.92		4.95	1.83
	HSO_3F	−82	10.35	11.65		4.83	1.72
	HSO_3F	−95	9.89	11.78(32)*		4.85	1.74
Water		25	5.20				
	HSO_3F/SbF_5	−80	—	11.24(14)			
	HSO_3F/SbF_5	−90	—	11.30(136)			

*Figures in brackets denote line width in cycles/s.

Ethyl Alcohol and Water

The chemical shifts obtained for solutions of ethyl alcohol and water in fluorosulfuric acid are given in Table III. In the case of ethyl alcohol only the CH_2 and CH_3 peaks are visible at room temperature but on cooling the solution a new peak appears, as was found by MacLean and Mackor in HF/BF_3 solution (1). However, we were unable to observe any fine structure in the new peak. At −95° the relative areas of the three peaks were found to be 1.74:1.89:3.0 which agrees reasonably well with the values 2.0:2.0:3.0 expected for $H_2O^+ \cdot CH_2 \cdot CH_3$.

Only a single peak was observed in the spectra of solutions of water in fluorosulfuric acid or in SbF_5/HSO_3F solutions even at low temperatures. MacLean and Mackor (1) have found that the peak due to H_3O^+ in hydrogen fluoride occurs 0.52 p.p.m. to lower field than the H_2O^+ signal from protonated ethyl alcohol, and it is very likely therefore that the H_3O^+ peak in HSO_3F solutions is very close to the solvent. Since the solvent line is quite broad at these low temperatures, it is not unreasonable to suppose that the peak due to H_3O^+ is overlapped by the solvent peak and is therefore not observable.

Rates of Proton Exchange and Activation Energies

Raising the temperature of solutions of these bases in HSO_3F results in a broadening of the OH^+ peak due to a decrease in the lifetime of the conjugate acid. Since there is no overlapping of the OH^+ and solvent peaks, the conditions for slow exchange may be applied

Can. J. Chem. Downloaded from www.nrcresearchpress.com by 210.87.254.6 on 09/05/12
For personal use only.

and the rates of proton exchange calculated. If $1/T_2'$ is the measured line width at any particular temperature, $1/T_2$ is the line width in the absence of exchange, and $1/\tau$ is the lifetime of the conjugate acid, then

$$1/T_2' = 1/T_2 + 1/\tau.$$

The first-order rate constant for proton loss by the conjugate acid is given by

$$k = \tau^{-1}$$

and the dependence of the rate of deprotonation on the temperature can be expressed by the Arrhenius equation

$$k = k_0 \, e^{-E/RT}.$$

Rate data for the substituted acetophenones is given in Table IV. In the case of *p*-nitroacetophenone it was not possible to stop the exchange process completely and hence $1/T_2$ could not be measured. In this case a value for $1/T_2$ was estimated from the results for the other ketones. Plots of log k against $1/T$ (Fig. 5) for these acetophenones give straight lines from which the activation energies were obtained. Except for the *p*-nitro compound the activation energies fall in the range 11–12 kcal. Whether or not the large deviation from this value in the case of *p*-nitroacetophenone is real, or is due to the choice of an incorrect value for T_2, could perhaps be answered by carrying out a comparable investigation in a more acidic solvent than HSO_3F so that proton exchange by the conjugate acid of *p*-nitroacetophenone could be stopped completely.

TABLE IV

Rate data for solutions of acetophenones in fluorosulfuric acid

Base	Conc., mole %	E, kcal/mole	Log k_0	Log k ($-60°$)	$-pK_{BH^+}$
p-Nitroacetophenone	3.28	7.6	10.89	3.10	8.43
p-Chloroacetophenone	2.93	11.4	12.89	1.17	6.77
Acetophenone	3.36	11.1	12.64	1.49	6.36
p-Fluoroacetophenone	2.94	12.9	14.14	0.90	6.29
p-Methylacetophenone	3.22	11.4	12.57	0.87	5.57
p-Methoxyacetophenone	3.10	11.6	12.97	1.08	4.91

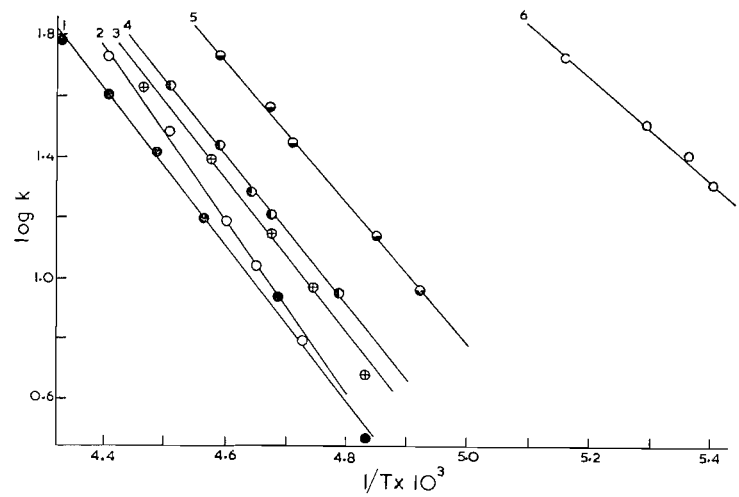

FIG. 5. Log k against $1/T$ for solutions of acetophenones in fluorosulfuric acid: (1) *p*-CH_3, (2) *p*-F, (3) *p*-OCH_3, (4) *p*-Cl, (5) *p*-H, (6) *p*-NO_2.

Can. J. Chem. Downloaded from www.nrcresearchpress.com by 210.87.254.6 on 09/05/12
For personal use only.

There is no obvious correlation between the rate of proton loss and pK_{BH^+} or σ^+. Although *p*-nitroacetophenone exchanges more rapidly than the other acetopheones, *p*-methoxyacetophenone does not exchange as slowly as might be expected. It is possible, however, that in this latter case the calculated rate may not be correct, as the $=OH^+$ peak is much closer to the solvent peak than for the other bases studied, and when exchange becomes appreciable some merging of the $=OH^+$ and solvent peaks is apparent, and therefore the conditions for slow exchange may not apply.

EXPERIMENTAL

The bases were commercial samples; solid samples were recrystallized from suitable solvents, while the liquids were dried and then distilled. All samples were prepared in the manner reported previously (2).

The spectra were recorded on a Varian HR60 n.m.r. spectrometer equipped with a low-temperature probe and integrator.

ACKNOWLEDGMENT

We thank the Petroleum Research Fund of the American Chemical Society for financial support of this work.

REFERENCES

1. C. MacLean and E. L. Mackor. J. Chem. Phys. **34**, 2207 (1961).
2. T. Birchall and R. J. Gillespie. Can. J. Chem. **41**, 148, 2642 (1963).
3. R. Stewart and K. Yates. J. Am. Chem. Soc. **80**, 6355 (1958). K. Yates and B. F. Scott. Can. J. Chem. **41**, 2320 (1963).
4. R. Stewart and K. Yates. J. Am. Chem. Soc. **82**, 4059 (1960).
5. C. MacLean and E. L. Mackor. J. Chem. Phys. **34**, 2208 (1961).
6. T. Birchall and R. J. Gillespie. Can. J. Chem. **42**, 502 (1964).
7. G. Oláh, L. Noszkó, and A. Paváth. Nature, **179**, 146 (1957).

Can. J. Chem. Downloaded from www.nrcresearchpress.com by 210.87.254.6 on 09/05/12
For personal use only.

Can. J. Chem. Downloaded from www.nrcresearchpress.com by 210.87.254.42 on 09/05/12
For personal use only.

ELECTROCRYSTALLIZATION

I. SURFACE DIFFUSION

S. K. RANGARAJAN
Central Electrochemical Research Institute, Karaikudi, India

Received October 19, 1964

ABSTRACT

A solution of the boundary value problem posed by Fleischmann and Thirsk is presented here for a generalized time dependence of $\eta(t)$, the overpotential. The results for various techniques have been derived. Expressions for the transients have also been obtained. The formulations reported earlier for the potentiostatic, the faradaic impedance, and the galvanostatic techniques are deduced as special cases. It has also been shown that in the 'potential step method' a relatively simple relationship exists between the first and the second overpotentials.

Recent investigations* have suggested that two important paths to be reckoned with in the discussion of the kinetics of electrocrystallization can formally be idealized as follows:

(*a*) The ions (or the reactive species) are discharged (or transferred) from the solution so as to form the so-called adions (or adatoms). This stage is the one involving electrochemical reactions. Adatoms, then, diffuse over the surface to the sites where the lattice formation is facilitated and accomplished.

(*b*) The reactive species is first to be transferred to the pre-electrode layer before the electrochemical reaction can occur. The discharge takes place at the sites where the lattice building takes place.

Formally (*a*) and (*b*) can be termed "surface diffusion" and "direct deposition" models respectively—implying that these are the probable rate-controlling steps in the sequence of events characterizing the two paths. It is to be noted that the stages characterizing (*a*) and (*b*) are not to be considered mutually exclusive. Usually the point of interest is to determine which of these eclipses the other in any particular study. It must be emphasized again that (*a*) and (*b*) themselves are "simplified versions" and the actual physical situation may be too complicated to elude both of these cleverly (1, 2). Attempts have been made to interpret the experimental results in terms of the models (*a*) and (*b*). Interpretations based on simplified versions of (*a*) have been put forward (1, 3, 4, 5) and, obviously, are limited in scope. A rigorous approach may have to take into account simultaneously (i) the mass transfer processes in the solution (not neglecting the double layer structure), (ii) the details of the reaction mechanisms (homogeneous chemical reactions following or preceding, adsorption etc.), (iii) surface diffusion of adatoms (whose 'ionic nature' (6) also is to be detailed), (iv) a description of the surface dislocations and their dependence on the applied field, the effect of the nature of the surface, the interference of impurities in the step motion etc. (2, 7, 8)—to mention a few. It is obvious that such a theory is very difficult, if not impossible. Nevertheless, quantitative formulations worked out for well defined models can themselves be of significant value in interpreting the results. The most systematic attempt available as regards the model (*a*) is by Fleischmann and Thirsk (1*b*) who have, besides formulating the problem that is solved in this paper, worked out an exact solution for the potentiostatic case and a

**For a critical discussion of this problem and comprehensive bibliography see refs. 1a, 1b.*

formulation for the faradaic impedance when the amplitude of the sinusoidal wave is sufficiently small. Fleischmann and Thirsk (1*b*) have also suggested some possible experiments. The diffusion process of the adatoms over the surface as assumed in this model (1*b*) is as follows.

The steps are spaced at a distance $2l$ and at the steps the density of Kossel kinks is high and the mean displacement of the adsorbed species on the surface is much greater than the mean distance between the kinks so as to maintain an equilibrium for the 'exchange *at* the kinks' and consequently to ensure a uniform concentration along these. This enables one to consider a step as 'a continuous line-sink' (cf. p. 304 of ref. 7). The mass transfer process in the solution does not interact or influence this.

Under these assumptions, a mathematical representation of the diffusion phenomenon becomes considerably simplified. If the steps are represented as $x = 0$, $x = 2l$, and the concentration of the adatoms at any position x and any instant t is $C(x, t)$, we have

$$\frac{\partial C}{\partial t} = D\frac{\partial^2 C}{\partial x^2} + k_1(t) - k_2(t)C. \qquad [1]$$

Herein, $k_1(t)$, the rate of deposition, is equal to $i_0(zF)^{-1}\exp[\alpha zF\eta(t)/RT]$, $k_2(t)$, the rate of removal, is equal to $i_0C(zFC_0)^{-1}\exp[(\alpha - 1)zF\eta(t)/RT]$, where $\eta(t)$ is the overpotential and C_0 is the concentration at $\eta = 0$.

The initial condition is

$$C(x, t) = C_0 \text{ when } t = 0, \qquad [2]$$

and the boundary conditions are

$$C(x, t) = C_0,\ x = 0,\ t \geqslant 0; \qquad [3]$$

$$\partial C(x, t)/\partial x = 0,\ x = l,\ t \geqslant 0. \qquad [4]$$

In this paper, we solve eq. [1] with [2–4] for *any* given functional form of $\eta(t)$ and all values of α (Section 1). The limitations of the solutions, if any, are then those of the model. We also present explicit dependence of the current on time t for the following techniques, besides rederiving the results of Fleischmann (1) for the potentiostatic conditions (Section 2).

A. Potentiodynamic (or potentiokinetic) (Section 3),

$$\eta(t) = \eta_0 + \omega t. \qquad [5]$$

B. Potential step method ((Section 4), wherein

$$\eta(t) = \eta_0',\ 0 < t < t_1;\ \eta(t) = \eta_0,\ t_1 \leqslant t. \qquad [6]$$

C. Faradaic impedance (Section 5),

D. Faradaic rectification (Section 6),

$$\eta(t) = \eta_0 + v_0\cos\omega t. \qquad [7]$$

Cases A and B have been solved exactly. In the case of C and D, v_0 is assumed to be small but the results can be expected to be valid over a wider range than that allowed for the known linearization model (1*b*). The significance of the approximation made earlier (1*b*) is discussed. The expressions for the transients in all these cases have been explicitly stated so as to be useful in the experiments dealing with transients. Besides

Can. J. Chem. Downloaded from www.nrcresearchpress.com by 210.87.254.42 on 09/05/12
For personal use only.

the analysis with reference to the mathematical significance of the general solutions and the degeneracy of these into special cases, a brief discussion of the results of Fleischmann (1*b*) and Gerischer and Tischer (9) with reference to the potential step method is presented. It is indeed shown that eq. 40 of ref. 1*b* can be simplified resulting in an elegant relationship between the two overpotentials, η_0' and η_0 of eq. [6].

As the galvanostatic experiments (3, 4) are usually confined to small excursions of the current i and time t from their zero values, a simple, trivial expression relating $i(t)$ and $\eta(t)$ is given for various functional forms of $i(t)$ which, we hope, would be valid for sufficiently small t. Though this expression might be useful for such experiments in transients with $i(t)$ as any *known function* of time, the limitations are many and one has to be aware of them before applying the expression. Of course, an exact inversion of $\eta(t)$ for *any* given $i(t)$ remains a tricky and laborious question. Aside from rederiving the earlier results (1, 6, 7), we do not present in this paper any important results concerning the galvanostatic experiments (Section 7).

Lastly it may be mentioned here that the results for various techniques have been presented more as illustrations—with emphasis on the 'mathematical completeness'—than as suggestions for further experimentation. This paper confines itself to theoretical derivations and no comparison is made with experimental results. The discussion of models and numerical representation of some of the expressions derived here will be communicated later.

1. General Solution

The differential equation [1] is solved with the initial and boundary conditions [2–4] and the concentration distribution of adatoms $C(x, t)$ is found to be (cf. Appendix I),

$$C(x, t) = C_0 + \frac{C^*(x, t) - \mathscr{K}(t)}{K(t)}, \qquad [8]$$

where

$$C^*(x, t) = C_0 - \frac{D}{l}\frac{\partial}{\partial x}\left\{\int_0^t [C_0 - \mathscr{K}(t)]\theta_1\left[\frac{l-x}{2l}, \frac{\pi D(t-\tau)}{l^2}\right] d\tau\right\} \qquad [9]$$

$$C(x, t) = C_0 - \frac{D}{K(t)}\frac{\partial}{\partial x}\left\{\int_0^t [C_0 - \mathscr{K}(t)]\theta_1\left[\frac{l-x}{2l}, \frac{\pi D(t-\tau)}{l^2}\right] d\tau\right\} + \frac{1}{K(t)}\int_0^t [k_1(\tau) - k_2(\tau)C_0]K(\tau)\, d\tau \qquad [10]$$

$$K(t) = \exp\left[\int_0^t k_2(\tau)\, d\tau\right] \qquad [11]$$

$$\mathscr{K}(t) = C_0K(t) - \int_0^t k_1(\tau)K(\tau)\, d\tau$$

$$= C_0 - \int_0^t [k_1(\tau) - k_2(\tau)C_0]K(\tau)\, d\tau \qquad [12]$$

$$\theta_1(v, t) = 2\sum_0^\infty (-1)^{n+1} \exp[-\pi(n + \tfrac{1}{2})^2 t] \sin[(2n + 1)\pi v] \qquad [13]$$

is the theta function.

Can. J. Chem. Downloaded from www.nrcresearchpress.com by 210.87.254.42 on 09/05/12
For personal use only.

Can. J. Chem. Downloaded from www.nrcresearchpress.com by 210.87.254.42 on 09/05/12
For personal use only.

The current $i(t)$ is given by

$$[14] \qquad i(t) = zFl^{-1} \int_0^l [k_1 - k_2 C(x, t)]\, dx.$$

We give below three alternate forms for $i(t)$ which would prove to be useful under appropriate conditions:

$$[15] \qquad i(t) = zF \frac{d}{dt}\left[\frac{1}{K(t)} \int_0^t [k_1(\tau) - k_2(\tau)C_0]K(\tau)\, d\tau\right] + \frac{2ZFDk_2(t)}{K(t)l^2} \sum_{n=0}^{\infty} \exp\left[-\frac{\pi^2 Dt}{4l^2}(2n+1)^2\right] \cdot \left\{\int_0^t [C_0 - \mathscr{K}(\tau)] \exp\left[\frac{\pi^2 D\tau}{4l^2}(2n+1)^2\right] d\tau\right.$$

(cf. Appendix, A.22),

$$[16] \qquad \frac{i(t)}{zF} = [k_1(t) - k_2(t)C_0] - \frac{8}{\pi^2} \sum \frac{k_2(t)}{(2n+1)^2} \exp\left[-\left(\frac{\pi^2 Dt}{4l^2}(2n+1)^2 + \int_0^t k_2(\tau)\, d\tau\right)\right] \cdot \left\{\int_0^t [k_1(\tau) - k_2(\tau)C_0] \exp\left[\frac{\pi^2 D\tau}{4l^2}(2n+1)^2 + \int_0^\tau k_2(z)\, dz\right] d\tau\right\}$$

(cf. Appendix, A.24),

$$[17] \qquad \frac{i(t)}{zF} = [k_1(t) - k_2(t)C_0] - \frac{32l^2}{\pi^2} k_2(t) \sum \frac{k_1(t) - k_2(t)C_0}{[4l^2 k_2(t) + \pi^2 D(2n+1)^2](2n+1)^2} + \frac{32l^2}{\pi^2} k_2(t) \sum \frac{k_1(+0) - k_2(+0)C_0}{[4l^2 k_2(+0) + \pi^2 D(2n+1)^2](2n+1)^2} \cdot \exp\left[-\left[\frac{\pi^2 Dt(2n+1)^2}{4l^2} + \int_0^t k_2(\tau)\, d\tau\right]\right] + \frac{32l^2}{\pi^2} k_2(t) \sum \exp\left[-\left[\frac{\pi^2 Dt(2n+1)^2}{4l^2} + \int_0^t k_2(\tau)\, d\tau\right]\right] / (2n+1)^2 \left\{\int_0^t \frac{d}{d\tau}\left[\frac{k_1(\tau) - k_2(\tau)C_0}{4l^2 k_2(\tau) + \pi^2 D(2n+1)^2}\right] \exp\left[\frac{\pi^2 D\tau(2n+1)^2}{4l^2} + \int_0^\tau k_2(z)\, dz\right] d\tau\right\}$$

(cf. Appendix, A.25). It can be shown (cf. Appendix I) that eqs. [15], [16], and [17] are equivalent. Equation [15] is particularly useful in approximations involving $t \to 0$ (cf. Section 7), eq. [16] is more easily integrable than [15] and can be used with advantage for $t \to \infty$, while [17] suggests how successive approximations can be adopted in problems involving a complicated dependence of $\eta(t)$ on time t (also cf. Section 4). If $\alpha = 1$, the expressions are considerably simplified since $k_2(t) = i_0/(zFC_0)$, a constant, and $K(t) = \exp[i_0 t/(zFC_0)]$. The resulting expression under these conditions can be seen to be identical with that given earlier (2)*.

*The sign of one of the terms will have to be corrected in eq. 21, p. 154 of ref. 1a.

(i) As $\pi Dt/l^2$ tends to zero, one approximates [1] as

$$\partial C/\partial t = k_1(t) - k_2(t)C \qquad [18]$$

with the conditions [2–4]. It is easily seen that

$$i(t) = \frac{zF}{l}\int_0^t [k_1(t) - k_2(t)C(x,t)]\,dx = \frac{d}{dt}\left\{\frac{1}{K(t)}\int_0^t [k_1(\tau) - k_2(\tau)C_0]K(\tau)\,d\tau\right\}. \qquad [19]$$

(ii) As t tends to infinity and

$$\int_0^t k_2(\tau)\,d\tau \ll \pi^2 D\tau(4l^2)^{-1}, \qquad [20]$$

eq. [16] gives

$$i(t) \rightarrow [k_1(t) - k_2(t)C_0]. \qquad [21]$$

When $zF\eta(t)/RT$ is a constant, δ_0 say, eq. [21] results as a steady state if

$$k_2{}^0 = (i_0/zFC_0)\exp[(\alpha - 1)\delta_0] \ll \pi^2 D(4l^2)^{-1}.$$

(iii) As t tends to infinity (steady state), i.e.,

$$\pi^2 Dt(4l^2)^{-1}, \quad \int_0^t k_2(z)\,dz \rightarrow \infty.$$

Then,

$$i(t) \simeq [k_1(t) - k_2(t)C_0] - \frac{32l^2}{\pi^2}k_2(t)\sum\left[\frac{k_1(t) - k_2(t)C_0}{[4l^2k_2(t) + \pi^2 D(2n+1)^2](2n+1)^2} - \frac{1}{(2n+1)^2}\frac{1}{k_2(t) + \pi^2 D(4l^2)^{-1}(2n+1)^2}\frac{d}{dt}\left\{\frac{k_1(t) - k_2(t)C_0}{4l^2k_2(t) + \pi^2 D(2n+1)^2}\right\}\right]. \qquad [22]$$

For the sake of brevity, a discussion on the magnitude of the approximations expressed through eqs. [19], [21], and [22] is not given.

2. Potentiostatic Case

If

$$zF\eta(t)/RT = \delta_0, \text{ a constant}, \qquad [23]$$

$$k_1(t) = i_0/(zF)\exp(\alpha\delta_0) = k_1{}^0, \qquad [24]$$

and

$$k_2(t) = i_0/(zFC_0)\exp[(\alpha - 1)\delta_0] = k_2{}^0, \text{ say} \qquad [25]$$

$$K(t) = \exp(k_2{}^0 t). \qquad [26]$$

When eqs. [23–26] are substituted in [16], one obtains,

$$\frac{i(t)}{zF} = (k_1{}^0 - k_2{}^0C_0) - \frac{8k_2{}^0}{\pi^2}(k_1{}^0 - k_2{}^0C_0)\cdot\sum\frac{1 - \exp[-(\pi^2 Dt(4l^2)^{-1} + k_2{}^0 t)]}{(2n+1)^2[\pi^2 D(2n+1)^2(4l^2)^{-1} + k_2{}^0]}. \qquad [27]$$

Can. J. Chem. Downloaded from www.nrcresearchpress.com by 210.87.254.42 on 09/05/12
For personal use only.

Can. J. Chem. Downloaded from www.nrcresearchpress.com by 210.87.254.42 on 09/05/12
For personal use only.

Observing that

$$\sum \frac{1}{(2n+1)^2[A(2n+1)^2+B]} = \frac{1}{B}\left[\sum \frac{1}{(2n+1)^2} - \sum \frac{A}{A(2n+1)^2+B}\right]$$

$$= \frac{\pi^2}{8B}\left[1 - \sum \frac{2}{\pi^2(2n+1)^2/4 + \pi^2 B/4A}\right]$$

$$= \frac{\pi_2}{8B}\left[1 - \frac{\tanh(\pi/2\sqrt{B/A})}{\pi/2\sqrt{B/A}}\right], \quad [28]$$

eq. [27] becomes

$$\frac{i(t)}{zF} = (k_1^0 - k_2^0 C_0)\frac{\tanh(\sqrt{k_2^0/D}\cdot l)}{\sqrt{k_2^0/D}\cdot l} + 32(k_1^0 - k_2^0 C_0)k_2^0 l^2 \sum \frac{\exp[-(\pi^2 D(2n+1)^2(4l^2)^{-1} + k_2^0 t)]}{(2n+1)^2[4l^2 k_2^0 + \pi^2 D(2n+1)^2]} \quad [29]$$

a result identical with that derived earlier (1*b*). Except for the derivation of [29] as a special case of [16], no discussion is presented since this has been dealt with in detail by Fleischmann and Thirsk (1).

3. Potentiokinetic Technique

We consider here the derivation of the faradaic current $i(t)$ when the applied potential varies linearly with time. It is of interest to note here that lately this technique has assumed important significance in the studies of electrode kinetics. (For a review see refs. 10 and 11.)

Writing $zF\eta(t)/RT = \delta_0 + \delta_1 t$,

$$k_1(t) = k_1^0 \exp(\alpha\delta_1 t) \quad [30]$$

$$k_2(t) = k_2^0 \exp[(\alpha - 1)\delta_1 t] \quad [31]$$

and

$$K(t) = \exp(k_2^0(\alpha-1)^{-1}\{\exp[(\alpha-1)\delta_1 t] - 1\}). \quad [32]$$

With [30–32] made use of in [16], an expression for $i(t)$ is derived (cf. Appendix II). The steady state of $i(t)$ is

$$i_{st}(t) = zF[k_1(t) - k_2(t)C_0] - \frac{8zFk_2(t)}{\pi^2}\sum\left\{\frac{k_1(t)}{(2n+1)^2}\frac{\Phi(1, A_n+1; k_2(t)/(1-\alpha)\delta_1)}{[\pi^2 D(4l^2)^{-1}(2n+1)^2 + \alpha\delta_1]} - \frac{k_2(t)C_0}{(2n+1)^2}\frac{\Phi(1, A_n+1+(1-\alpha)^{-1}; k_2(t)/(1-\alpha)\delta_1)}{[\pi^2 D(4l^2)^{-1}(2n+1)^2 + (\alpha-1)\delta_1]}\right\}, \quad [33]$$

while the transient is

$$i_{tr}(t) = \frac{8zFk_2(t)}{\pi^2}\exp\left[\frac{k_2(t) - k_2^0}{(1-\alpha)\delta_1}\right]\sum\{\exp[-\pi^2 D(4l^2)^{-1}(2n+1)^2 t]\}/(2n+1)^2 \cdot \left\{\frac{k_1^0\Phi[1, A_n+1; k_2^0/(1-\alpha)\delta_1]}{\pi^2 D(4l^2)^{-1}(2n+1)^2 + \alpha\delta_1} - \frac{k_2^0 C_0\Phi[1, A_n+1+(1-\alpha)^{-1}; k_2^0/(1-\alpha)\delta_1]}{\pi^2 D(4l^2)^{-1}(2n+1)^2 + (\alpha-1)\delta_1}\right\}. \quad [34]$$

The instantaneous faradaic current $i(t)$ is then $i_{st}(t) + i_{tr}(t)$ where the steady state and the transient currents are given through equations [33–34]. In [33–34], $\Phi(a, c; x)$ represents the confluent hypergeometric function defined by

$$\Phi(a, c; x) = 1 + \frac{a}{c}x + \frac{a(a+1)}{c(c+1)}\frac{x^2}{2!} + \ldots \qquad [35]$$

and

$$A_n = -\left[\frac{\pi^2 D(2n+1)^2}{4l^2(1-\alpha)\delta_1} + \frac{\alpha}{1-\alpha}\right]. \qquad [36]$$

Equations [33–34] can as well be expressed in terms of incomplete gamma functions (cf. Appendix II).

An Approximate Expression for $i(t)$

Considering the time dependence of $\eta(t)$ on t as a perturbation so that $(\delta_1 t)$ is assumed to be quite small, we approximate,

$$K(t) = \exp\left[\frac{k_2^0}{(\alpha-1)\delta_1}\{\exp[(\alpha-1)\delta_1 t] - 1\}\right] \simeq \exp(k_2^0 t). \qquad [37]$$

With the approximation implicit in [37], the result [16] then takes a particularly simple form:

$$\frac{i(t)}{zF} = [k_1(t) - k_2(t)C_0] - \frac{8}{\pi^2}\sum \frac{k_2(t)}{(2n+1)^2}\exp\left[-\frac{\pi^2 Dt(2n+1)^2}{4l^2} + \frac{k_2^0 - k_2(t)}{(1-\alpha)\delta_1}\right] \cdot\left\{\int_0^t [k_1(\tau) - k_2(\tau)C_0]\exp\left[\frac{\pi^2 D\tau(2n+1)^2}{4l^2} + k_2^0\tau\right]d\tau\right\} = i_{st}(t) + i_{tr}(t); \qquad [38]$$

with

$$i_{st}(t) = zF[k_1(t) - k_2(t)C_0] - \frac{8zF}{\pi^2}k_2(t)\sum\left\{\frac{k_1(t)}{[\pi^2 D(4l^2)^{-1}(2n+1)^2 + k_2^0 + \alpha\delta_1](2n+1)^2} - \frac{k_2(t)C_0}{[\pi^2 D(2n+1)^2(4l^2)^{-1} + k_2^0 + (\alpha-1)\delta_1](2n+1)^2}\right\}; \qquad [39]$$

and

$$i_{tr}(t) = \frac{8zF}{\pi^2}k_2(t)\exp\left[\frac{k_2(t) - k_2^0}{(1-\alpha)\delta_1}\right] \sum \frac{\exp(-\pi^2 Dt(4l^2)^{-1}(2n+1)^2)}{(2n+1)^2}\left\{\frac{k_1^0}{\pi^2 D(4l^2)^{-1}(2n+1)^2 + k_2^0 + \alpha\delta_1} - \frac{k_2^0 C_0}{\pi^2 D(4l^2)^{-1}(2n+1)^2 + k_2^0 + (\alpha-1)\delta_1}\right\}. \qquad [40]$$

With the help of [28], eq. [39] is rewritten as

$$i_{st}(t) = zF[k_1(t) - k_2(t)C_0] - \frac{zFk_1(t)k_2(t)}{k_2^0 + \alpha\delta_1}\left[1 - \frac{\tanh\sqrt{(k_2^0 + \alpha\delta_1)/D}\cdot l}{\sqrt{(k_2^0 + \alpha\delta_1)/D}\cdot l}\right] + \frac{zFk_2(t)^2 C_0}{k_2^0 + (\alpha-1)\delta_1}\left[1 - \frac{\tanh\sqrt{[k_2^0 + (\alpha-1)\delta_1]/D}\cdot l}{\sqrt{[k_2^0 + (\alpha-1)\delta_1]/D}\cdot l}\right]. \qquad [41]$$

Can. J. Chem. Downloaded from www.nrcresearchpress.com by 210.87.254.42 on 09/05/12
For personal use only.

Equations [39] and [41] become identical with the corresponding expressions for the potentiostatic case (cf. eq. [29]) by making $\delta_1 = 0$.

Some Particular Cases

(i)

[42] $$k_2(t) \ll \pi^2 D/(4l^2).$$

(ii)

[43] $$k_2(t) \gg \pi^2 D/(4l^2).$$

(iii)

$$k_2{}^0/[(1-\alpha)\delta_1] \to \infty, \quad \pi^2 D/[4l^2(1-\alpha)\delta_1] \to \infty \quad \text{while the ratio is finite.}$$

(iv)

$$\delta_1 \to 0 \text{ (potentiostatic case).}$$

(v)

$$\delta_1 \text{ is small (perturbation expressions [40–41]).}$$

(Note: a direct substitution of $\delta_1 = 0$ in the general equations [33–34] presents difficulties since both the parameters A_n and argument $k_2(t)/(1-\alpha)\delta_1$ of the hypergeometric function tend to infinity.)

For case (i), $k_2(t) \ll \pi^2 D/(4l^2)$, as

[44] $$\Phi(a, c; x) \to 1, \qquad \text{if } x/c \to 0 \ (a \text{ bounded}),$$

eq. [33] gives

[45] $$i_{st}(t) \to zF[k_1(t) - k_2(t)C_0] - zFk_2(t)\left\{\frac{k_1(t)}{\alpha\delta_1}\left[1 - \frac{\tanh\sqrt{\alpha\delta_1/D}\cdot l}{\sqrt{\alpha\delta_1/D}\cdot l}\right] - \frac{k_2(t)C_0}{(\alpha-1)\delta_1}\left[1 - \frac{\tanh\sqrt{(\alpha-1)\delta_1/D}\cdot l}{\sqrt{(\alpha-1)\delta_1/D}\cdot l}\right]\right\}.$$

Cases (ii–v) are all deduced by making use of the representation of $i(t)$ in terms of incomplete gamma function and making use of the asymptotic representation of these functions given by Tricomi (12).

Noting that the asymptotic behavior of gamma function is

[46] $$\gamma(1+\alpha, x+y) - \gamma(1+\alpha, x) \simeq \exp(-x)\cdot x^{1+\alpha}(x-\alpha)^{-1} - \exp[-(x+y)]\cdot(x+y)^{1+\alpha}(x+y-\alpha)^{-1},$$

if the parameter $z = \alpha^{1/2}/(x-\alpha)$ is small, the parameter

$$z^2 = \alpha/(x-\alpha)^2 = \frac{\pi^2 D(4l^2)^{-1}(1-\alpha)\delta_1}{[k_2(t) + \pi^2 D(4l^2)^{-1} + \alpha\delta_1]^2} \ll 1,$$

if (i) $\delta_1 \to 0$ and $k_2(t), \pi^2 D/4l^2 \gg \delta_1$

or (ii) $k_2(t) \gg \pi^2 D(4l^2)^{-1}(1-\alpha)\delta_1$.

Can. J. Chem. Downloaded from www.nrcresearchpress.com by 210.87.254.42 on 09/05/12
For personal use only.

Condition (i) allows us to attain the limit corresponding to the potentiostatic condition ($\delta_1 = 0$) whatever be the relative magnitudes of $k_2(t)$ and $\pi^2 D/4l^2$. An approximate result for small δ_1 can also be derived under these conditions.

If $k_2(t) \gg \pi^2/4l^2$ and $k_2^0 \gtrsim \delta_1$, the same asymptotic approximation can be used. Thus one arrives at the same limiting expression under varied conditions depending upon the parameters of interest. Thus,

$$\left[\frac{k_2^0}{(1-\alpha)\delta_1}\right]^{-A_n}\left[\frac{1}{(1-\alpha)\delta_1}\right]\left\{\gamma\left[A_n, \frac{k_2^0}{(1-\alpha)\delta_1}\right] - \gamma\left[A_n, \frac{k_2(t)}{(1-\alpha)\delta_1}\right]\right\}$$

and

$$\left[\frac{k_2^0}{(1-\alpha)\delta_1}\right]^{-(A_n+(1-\alpha)^{-1}}\left[\frac{1}{(1-\alpha)\delta_1}\right]\left\{\gamma\left[A_n + \frac{1}{1-\alpha}, \frac{k_2^0}{(1-\alpha)\delta_1}\right] - \gamma\left[A_n, \frac{k_2(t)}{(1-\alpha)\delta_1}\right]\right\}$$

are approximated with the help of [22] and it can be proved that [B.11] then becomes

$$[47]\quad \frac{i(t)}{zF} = [k_1(t) - k_2(t)C_0]$$
$$- \frac{8}{\pi^2}k_2(t)\left\{\sum \frac{1}{(2n+1)^2}\left[\frac{k_1(t)}{k_2(t) + \pi^2 D(4l^2)^{-1}(2n+1)^2 + \alpha\delta_1}\right]\right.$$
$$\left. - \sum \frac{1}{(2n+1)^2}\left[\frac{k_2(t)C_0}{k_2(t) + \pi^2 D(4l^2)^{-1}(2n+1)^2 + (\alpha-1)\delta_1}\right]\right\}$$
$$+ \frac{8}{\pi^2}k_2(t)\exp\left[\frac{k_2(t) - k_2^0}{(1-\alpha)\delta_1}\right]\left\{\sum \frac{k_1^0 \exp[-\pi^2 D(4l^2)^{-1}(2n+1)^2 t]}{(2n+1)^2[k_2^0 + \pi^2 D(4l^2)^{-1}(2n+1)^2 + \alpha\delta_1]}\right.$$
$$\left. - \sum \frac{k_2^0 C_0 \exp[-\pi^2 D(4l^2)^{-1}(2n+1)^2 t]}{(2n+1)^2[k_2^0 + \pi^2 D(4l^2)^{-1}(2n+1)^2 + (\alpha-1)\delta_1]}\right\}.$$

It may be observed here that the approximate treatment made earlier (cf. eqs. [39] and [41] gives a result identical with [47] if the approximations made in deriving the former are properly introduced in [47].

4. Potential Step Method

Let us assume that

$$[48]\quad \eta(t) = \eta_0' \qquad 0 < t < t_1 \text{ and}$$
$$= \eta_0 \qquad t_1 \leqslant t$$

so that

$$[49]\quad k_1(t) = k_1^{0\prime} \qquad 0 < t < t_1 \text{ and}$$
$$= k_1^0 \qquad t_1 \leqslant t$$

and

$$[50]\quad k_2(t) = k_2' \qquad 0 < t < t_1 \text{ and}$$
$$= k_2^0 \qquad t_1 \leqslant t.$$

Obviously,

$$\frac{k_1(t) - k_2(t)C_0}{4l^2 k_2(t) + \pi^2 D(2n+1)^2}$$

Can. J. Chem. Downloaded from www.nrcresearchpress.com by 210.87.254.42 on 09/05/12
For personal use only.

has a discontinuity (a jump) of magnitude

$$\frac{k_1^0 - k_2^0 C_0}{4l^2 k_2^0 + \pi^2 D(2n+1)^2} - \frac{k_1^{0\prime} - k_2^{0\prime} C_0}{4l^2 k_2^{0\prime} + \pi^2 D(2n+1)^2}$$

at $t = t_1$.
Consequently

$$\frac{\mathrm{d}}{\mathrm{d}t}\left\{\frac{k_1(t) - k_2(t)C_0}{4l^2 k_2(t) + \pi^2 D(2n+1)^2}\right\}$$

can be represented as

[51] $$\left\{\frac{k_1^0 - k_2^0 C_0}{4l^2 k_2^0 + \pi^2 D(2n+1)^2} - \frac{k_1^{0\prime} - k_2^{0\prime} C_0}{4l^2 k_2^{0\prime} + \pi^2 D(2n+1)^2}\right\} \cdot \delta(t - t_1),$$

where $\delta(t)$ is Dirac's delta function. Also it is well known that

[52] $$\int_0^t \delta(\tau - t_1) f(\tau)\, \mathrm{d}\tau = f(t_1), \quad t > t_1.$$

Equation [17] then gives

[53] $$\frac{i(t)}{zF} = (k_1^0 - k_2^0 C_0)\frac{\tanh\sqrt{k_2^0/D}\cdot l}{\sqrt{k_2^0/D}\cdot l} + \frac{32l^2}{\pi^2} k_2^0 [k_1^{0\prime} - k_2^{0\prime} C_0] \sum \frac{\exp\{-[\pi^2 Dt(4l^2)^{-1}(2n+1)^2 + k_2^{0\prime} t_1 + k_2^0(t - t_1)]\}}{[4l^2 k_2^0 + \pi^2 D(2n+1)^2](2n+1)^2}$$
$$+ \frac{32l^2}{\pi^2} k_2^0 \sum \left[\frac{k_1^0 - k_2^0 C_0}{[4l^2 k_2^0 + \pi^2 D(2n+1)^2](2n+1)^2} - \frac{k_1^{0\prime} - k_2^{0\prime} C_0}{[4l^2 k_2^{0\prime} + \pi^2 D(2n+1)^2](2n+1)^2}\right] \cdot \exp\left\{-\left[\frac{\pi^2 D(t - t_1)}{4l^2}(2n+1)^2 + k_2^0(t - t_1)\right]\right\}.$$

The first term of [53] is the steady state value, viz.,

$$(k_1^0 - k_2^0 C_0)\frac{\tanh\sqrt{k_2^0/D}\cdot l}{\sqrt{k_2^0/D}\cdot l}$$

caused by the second overpotential. The other terms are transients. If the η_0 is applied only after the steady state due to the first η_0' has been attained, a limiting expression of [53] can be obtained by allowing $t, t_1 \to \infty$ while $t - t_1 = T$ remains finite. Under these conditions,

[54] $$\frac{i(t)}{zF} = [k_1^0 - k_2^0 C_0]\frac{\tanh\sqrt{k_2^0/D}\cdot l}{\sqrt{k_2^0/D}\cdot l} + \frac{32l^2}{\pi^2} k_2^0 [k_1^0 - k_2^0 C_0] \cdot \sum \frac{\exp[-(\pi^2 DT(4l^2)^{-1}(2n+1)^2 + k_2^0 T)]}{[4l^2 k_2^0 + \pi^2 D(2n+1)^2](2n+1)^2} - \frac{32l^2}{\pi^2} k_2^0 [k_1^{0\prime} - k_2^{0\prime} C_0] \cdot \sum \frac{\exp[-(\pi^2 DT(4l^2)^{-1}(2n+1)^2 + k_2^{0\prime} T)]}{[4l^2 k_2^{0\prime} + \pi^2 D(2n+1)^2](2n+1)^2}.$$

Can. J. Chem. Downloaded from www.nrcresearchpress.com by 210.87.254.42 on 09/05/12
For personal use only.

The first two terms in [54] are identical with the response after a time T due to the application of the overpotential η_0 at $T = 0$. The last one is a 'cross term'.

The equation derived by Fleischmann and Thirsk (1*b*) for the problem corresponding to the solution [54] differs from that obtained here. After proper modifications (Appendix III) the two are shown to be identical.

It has been suggested by Gerischer (9) that the excess concentration polarization (that remaining after the corrections due to the mass transfer polarization in the solution) is to be accounted for by the concentration polarization of the adatoms. For the model discussed in this paper, one would write

$$[55] \qquad i(t_1 + 0) = zFl^{-1} \int_0^l [k_1^0 - k_2^0 C_1^*(x)]\, dx,$$

where $C_1^*(x)$ is the steady state concentration attained due to the application of η_0'.

$$[56] \qquad C_1^*(x) = C_0 + \frac{k_1^{0\prime} - k_2^{0\prime} C_0}{k_2^{0\prime}} \left[1 - \frac{\cosh \sqrt{k_2^{0\prime}/D} \cdot (l - x)}{\cosh \sqrt{k_2^{0\prime}/D} \cdot l}\right].$$

If η_0' has been so chosen as to make $i(t_1 + 0) = 0$,

$$[57] \qquad \frac{k_1^0}{k_2^0} = C_0 \exp\left[\frac{zF\eta_0}{RT}\right] = \frac{1}{l} \int_0^l C^*(x)\, dx = C_0 + \frac{k_1^{0\prime} - k_2^{0\prime} C_0}{k_2^{0\prime}} \left[1 - \frac{\tanh \sqrt{k_2^{0\prime}/D} \cdot l}{\sqrt{k_2^{0\prime}/D} \cdot l}\right].$$

Equation [57] demonstrates the dependence of the second overpotential on the average steady state concentration due to the first potential. The similarity with Nernst equation is too obvious.

In contrast to what has been stated earlier (1*a*, 1*b*) a relatively simple relationship* exists between the two overpotentials η_0' and η_0. As a matter of fact

$$[58] \qquad \exp\left(\frac{zF\eta_0}{RT}\right) = \exp\left(\frac{zF\eta_0'}{RT}\right) - \frac{\tanh \sqrt{k_2^0/D} \cdot l}{\sqrt{k_2^0/D} \cdot l} \left[1 - \exp\left(\frac{zF\eta_0'}{RT}\right)\right].$$

If the second overpotential has the equilibrium values, then $k_1^0 - k_2^0 C_0 = 0$, and one has

$$[59] \qquad i(t) = \frac{8i_0}{\pi^2} \left[1 - \exp\left(\frac{zF\eta_0'}{RT}\right)\right] \cdot \sum \frac{\exp\left[-(\pi^2 Dt(4l^2)^{-1}(2n+1)^2 + k_2^{0\prime} t)\right]}{[1 + \pi^2 D(4l^2 k_2^{0\prime})^{-1}(2n+1)^2](2n+1)^2}.$$

It has been suggested (2) that, if the second overpotential is chosen to be the reversible one, a study of the transient would provide a method of estimating i_0/C_0. But the dependence of [59] on t shows that the interpretation is not simple enough in the general case.

5. Faradaic Impedance

It is well known that superimposing a sinusoidal perturbation on a 'base value' and studying the alternating component of the response offers a wide scope in the interpretation of the kinetic processes.

**The same relationship results from eq. [40] of ref. 2 by using the identity given by eq. [28] of this paper.*

Can. J. Chem. Downloaded from www.nrcresearchpress.com by 210.87.254.42 on 09/05/12
For personal use only.

Can. J. Chem. Downloaded from www.nrcresearchpress.com by 210.87.254.42 on 09/05/12
For personal use only.

We assume that

[60] $$zF\eta(t)/RT = \delta_0 + \delta_1 \cos \omega t \qquad (\omega = \text{angular frequency})$$

Since the $i - \eta$ characteristics are fundamentally nonlinear, $i(t)$ contains the higher harmonic terms besides a transient and a 'fundamental response'. From the relationship [16] between $i(t)$ and $\eta(t)$ it is easy to see that $i(t)$ can be expressed as

[61] $$i_{st} + \sum_{n=1}^{\infty} i_n \cos (n\omega t - \phi_n) + i_{tr}(t)$$

($i_{tr}(t)$ tends to zero as t tends to infinity). As one would expect, i_n, ϕ_n, and i_{st} are complicated functions of the parameters.

As regards the magnitude of δ_1, the basic approximation made in the treatment reported here is contained in the assumption:

$$K(t) = \exp\left(\int_0^t k_2(\tau)\, d\tau \right)$$

$$\simeq \exp [\{k_2{}^0 I_0[1 - \alpha)\delta_1]t\} - 2k_2{}^0\omega^{-1} I_1[(1 - \alpha)\delta_1] \sin \omega t].$$

The explicit expressions for i_1 and ϕ_1 are (cf. Appendix IV)

[62] $$i_1 \cos (\omega t - \phi_1) = 2zF[k_1{}^0 I_1(\alpha\delta_1) - k_2{}^0 I_1(\alpha\delta_1 - \delta_1)] \cos \omega t$$

$$- \frac{zFA_1[k_1{}^0 I_0(A_2) - k_2{}^0 C_0 I_0(A_2')]}{I_0(\alpha\delta_1 - \delta_1)} \left[1 - \frac{\tanh [\sqrt{k_2{}^0 I_0(\alpha\delta_1 - \delta_1)/D} \cdot l]}{\sqrt{k_2{}^0 I_0(\alpha\delta_1 - \delta_1)/D} \cdot l} \right] \cos (\omega t + \chi_1)$$

$$- 2zFI_0 \left[\frac{2k_2{}^0}{\omega} I_1(\alpha\delta_1 - \delta_1) \right] . E'[k_1{}^0 I_1(A_2) \cos (\omega t - \chi_2 - \lambda')$$

$$- k_2{}^0 C_0 I_1(A_2') \cos (\omega t - \chi_2' - \lambda')].$$

(By simple manipulations, it is possible to reduce further the right hand side of [62] to the form $K \cos (\omega t - \kappa)$. But as the resulting expressions for K and κ would be more involved, this is not attempted.) In [62], $I_0(z)$ and $I_1(z)$ are the modified Bessel functions of argument z and orders zero and one respectively. In particular, $I_0[2k_2{}^0\omega^{-1} I_1(\alpha\delta_1 - \delta_1)]$ is the Bessel function of order zero and argument $2k_2{}^0\omega^{-1} I_1(\alpha\delta_1 - \delta_1)$. (Here the argument itself involves the Bessel functions).

[63] $$A_1{}^2 = [2I_0(\alpha\delta_1 - \delta_1) I_1\{2k_2{}^0\omega^{-1} I_1(\alpha\delta_1 - \delta_1)\}]^2$$

$$+ [2I_1(\alpha\delta_1 - \delta_1) I_0\{2k_2{}^0\omega^{-1} I_1(\alpha\delta_1 - \delta_1)\}]^2;$$

[64] $$\tan \chi_1 = \frac{I_0(\alpha\delta_1 - \delta_1) I_1[2k_2{}^0\omega^{-1} I_1(\alpha\delta_1 - \delta_1)]}{I_1(\alpha\delta_1 - \delta_1) I_0[2k_2{}^0\omega^{-1} I_1(\alpha\delta_1 - \delta_1)]}$$

[65] $$A_2{}^2 = \alpha^2\delta_1{}^2 + [2k_2{}^0\omega^{-1} I_1(\alpha\delta_1 - \delta_1)]^2$$

[66] $$A_2{}'^2 = (\alpha - 1)^2\delta_1{}^2 + [2k_2{}^0\omega^{-1} I_1(\alpha\delta_1 - \delta_1)]^2$$

[67] $$\tan \chi_2 = \frac{2k_2{}^0 I_1(\alpha\delta_1 - \delta_1)}{\alpha\delta_1\omega}$$

[68] $$\tan \chi_2' = \frac{2k_2{}^0 I_1(\alpha\delta_1 - \delta_1)}{(\alpha - 1)\delta_1\omega}$$

$$[69] \quad E' \exp(-i\lambda') = \frac{k_2{}^0 I_0(\alpha\delta_1 - \delta_1)}{k_2{}^0 I_0(\alpha\delta_1 - \delta_1) + i\omega}\left\{1 - \frac{\tanh\sqrt{[k_2{}^0 I_0(\alpha\delta_1 - \delta_1) + i\omega]/D}\cdot l}{\sqrt{[k_2{}^0 I_0(\alpha\delta_1 - \delta_1) + i\omega]/D}\cdot l}\right\}.$$

(Note: The relationship between E' and λ' defined here and E and λ of p. 40 of ref. 1*b* is $E'\exp(-i\lambda') = 1 - E\exp(-i\lambda)$ *provided* one substitutes $k_2{}^0 I_0(\alpha\delta_1 - \delta_1)$ for k_2 in eqs. [71–77] of ref. 1*b*.)

Considering δ_1 to be small such that quantities like $\delta_1{}^2$ and $[k_2{}^0(\alpha - 1)\delta_1\omega^{-1}]^2$ are neglected, one obtains the following limits for the parameters,

$$[70] \quad A_1 \rightarrow A_2'$$

$$[71] \quad \chi_1 \rightarrow \chi_2'$$

$$[72] \quad A_2{}^2 \rightarrow \alpha^2\delta_1{}^2 + [k_2{}^0(\alpha - 1)\delta_1\omega^{-1}]^2$$

$$[73] \quad A_2{}'^2 \rightarrow (\alpha - 1)^2\delta_1{}^2 + [k_2{}^0(\alpha - 1)\delta_1\omega^{-1}]^2$$

$$[74] \quad \tan\chi_2 \rightarrow k_2{}^0\omega^{-1}(\alpha - 1)\alpha^{-1}$$

$$[75] \quad \tan\chi_2' \rightarrow k_2{}^0\omega^{-1} = \tan\theta \text{ (say)}$$

$$[76] \quad E' \exp(-i\lambda') \rightarrow \frac{k_2{}^0}{k_2{}^2 + i\omega}\left[1 - \frac{\tanh\sqrt{(k_2{}^0 + i\omega)/D}\cdot l}{\sqrt{(k_2{}^0 + i\omega)/D}\cdot l}\right]$$

$$= 1 - E\exp(-i\lambda)$$

(E and λ are identical with those given in ref. 1).

$$[77] \quad I_0(A_2),\ I_0(A_2') \rightarrow 1$$

$$[78] \quad 2I_1(A_2) \rightarrow A_2;\quad 2I_1(\alpha\delta_1) \rightarrow \alpha\delta_1;\quad 2I_1(\alpha\delta_1 - \delta_1) \rightarrow (\alpha - 1)\delta_1;$$

$$[79] \quad 2I_1(A_2') \rightarrow A_2'.$$

The corresponding limiting expression for [62] is

$$[80] \quad i_1\cos(\omega t - \phi_1) = zF\delta_1\Big[[\alpha k_1{}^0 - (\alpha - 1)k_2{}^0 C_0]\cos\omega t$$

$$- [k_1{}^0 - k_2{}^0 C_0]\left[(\alpha - 1)\cos\omega t - \frac{k_2(\alpha - 1)}{\omega}\sin\omega t\right]\left(1 - \frac{\tanh\sqrt{k_2{}^0/D}\cdot l}{\sqrt{k_2{}^0/D}\cdot l}\right)$$

$$- E'[k_1{}^0\alpha - k_2{}^0 C_0(\alpha - 1)]\cos(\omega t - \lambda')$$

$$+ E'\frac{k_2{}^0(\alpha - 1)}{\omega}(k_1{}^0 - k_2{}^0 C_0)\sin(\omega t - \lambda')\Big]$$

$$[81] \quad = \delta_1\Big[[\alpha k_1{}^0 - (\alpha - 1)k_2{}^0 C_0]E\cos(\omega t - \lambda)$$

$$- (\alpha - 1)(k_1{}^0 - k_2{}^0 C_0)\left[\left\{1 - \frac{\tanh\sqrt{k_2{}^0/D}\cdot l}{\sqrt{k_2{}^0/D}\cdot l}\right\}\cos\omega t\right.$$

$$\left.+ \frac{k_2{}^0}{\omega}\frac{\tanh\sqrt{k_2{}^0/D}\cdot l}{\sqrt{k_2{}^0/D}\cdot l}\sin\omega t - \frac{k_2{}^0}{\omega}E\sin(\omega t - \lambda)\right]\Big]$$

Can. J. Chem. Downloaded from www.nrcresearchpress.com by 210.87.254.42 on 09/05/12
For personal use only.

If the superimposition of the alternating component is on the reversible potential, $\delta_0 = 0$ and $k_1^0 = k_2^0 C_0 = i_0/zF$; Hence,

$$[82] \qquad i_1 \cos(\omega t - \phi_1) \rightarrow i_0 \delta_1 (zF)^{-1} E \cos(\omega t - \lambda),$$

as derived by Fleischmann (1).

The above result [82] shows that expressions derived earlier (1) have assumed implicitly that δ_1^2 and $[k_2^0(\alpha - 1)\delta_1 \omega^{-1}]^2$ are to be neglected. This limitation should be taken note of especially when one is interested in the limiting case $k_2^0 \omega^{-1} \rightarrow \infty$ (very low frequencies). (For example, to apply eq. [82], under the conditions defined by $k_2^0 = i_0/zFC_0 \simeq 10^5\ s^{-1}$, $|\eta| = 1$ mV, one should have $\omega \gg 100$ cycles/s). Equation [62] can be expected to be valid over a wider range* of values of δ_1 (or $|\eta|$) in view of less stringent conditions imposed upon the parameters.

A detailed discussion of [62] and its implications will be given later.

6. Faradaic Rectification

Doss and Agarwal discovered that for small amplitudes of an alternating current a rectified component in the potential results in the steady state. They also pointed out how this phenomenon can be exploited in the study of the kinetic parameters.

Since then, many interesting techniques† have been developed based on this concept. We present here a derivation of an expression for $i_{st}(t)$ which is defined through the equation,

$$i(t) = i_{st}(t) + \sum i_n \cos(n\omega t - \phi_n) + i_{tr}(t).$$

Herein, $i_{st}(t) + i_{tr}(t)$ is the 'nonperiodic' part and $i_{tr}(t)$ is that which decays to zero with $t \rightarrow \infty$. As has been proved in Appendix IV,

$$\begin{aligned}[83] \quad i_{st}(t) = {} & [k_1^0 I_0(\alpha\delta_1) - k_2^0 C_0 I_0(\alpha\delta_1 - \delta_1] \\ & - I_0[2k_2^0 \omega^{-1} I_1(\alpha\delta_1 - \delta_1)][k_1^0 I_0(A_2) - k_2^0 C_0 I_0(A_2')] \\ & \qquad \left\{1 - \frac{\tanh\sqrt{k_2^0 I_0(\alpha\delta_1 - \delta_1)/D}\cdot l}{\sqrt{k_2^0 I_0(\alpha\delta_1 - \delta_1)/D}\cdot l}\right\} \\ & - I_0[2k_2^0 \omega^{-1} I_1(\alpha\delta_1 - \delta_1)] A_1 E' \{k_1^0 I_1(A_2) \cos(\lambda' + \chi_1 + \chi_2) \\ & \qquad - k_2^0 C_0 I_1(A_2') \cos(\lambda' + \chi_1 + \chi_2')\}.\end{aligned}$$

(For the definition of constants, refer to eqs. [63–69].) We hasten to remark here that the steady state direct component as given by eq. [83] is not entirely due to the superimposition of the sinusoidal overpotential, $RT(zF)^{-1}\delta_1 \cos\omega t$; it includes the contribution of the base potential $RT(zF)^{-1}\delta_0$ as well. The latter is given by, cf. eq. [29],

$$[84] \qquad i_{\eta_0}(t \rightarrow \infty) = (k_1^0 - k_2^0 C_0) \frac{\tanh\sqrt{k_2^0/D}\cdot l}{\sqrt{k_2^0/D}\cdot l}.$$

It may be noted from [83] that

$$[85] \qquad i(t) \rightarrow (k_1^0 - k_2^0 C_0) \frac{\tanh\sqrt{k_2^0/D}\cdot l}{\sqrt{k_2^0/D}\cdot l}$$

*That an earlier derivation of an expression for redoxokinetic potential (cf. J. Electroanal. Chem. 1, 396 (1960) is valid for a wider range of amplitudes than the limiting solution, has been shown by Oldham (Proc. Natl. Inst. Sci., Seminar on Electrochemistry, 1961. In press. 1964.)

†For a review see Chap. 3 of ref. 10b.

Can. J. Chem. Downloaded from www.nrcresearchpress.com by 210.87.254.42 on 09/05/12
For personal use only.

as $\delta_1 \to 0$. Again for small values of δ_1,

$$I_0(\alpha\delta_1) \simeq 1 + (\alpha^2\delta_1^2/4),$$

$$I_0(\alpha\delta_1 - \delta_1) \simeq 1 + [(\alpha - 1)^2\delta_1^2/4],$$

$$I_0[2k_2^0 I_1(\alpha\delta_1 - \delta_1)/\omega] \simeq 1 + [k_2^0(2\omega)^{-1}(\alpha - 1)\delta_1]^2,$$

$$k_1^0 I_0(A_2) - k_2^0 C_0 I_0(A_2') \simeq (k_1^0 - k_2^0 C_0) + [k_1^0\alpha^2 - k_2^0 C_0(\alpha - 1)^2]\cdot\delta_1^2/4 + (k_1^0 - k_2^0 C_0)[k_2^0(2\omega)^{-1}(\alpha - 1)\delta_1]^2,$$

[86] $$1 - \frac{\tanh\sqrt{k_2^0 I_0(\alpha\delta_1 - \delta_1)/D}\cdot l}{\sqrt{k_2^0 I_0(\alpha\delta_1 - \delta_1)/D}\cdot l} \simeq \left[1 - \frac{\tanh\sqrt{k_2^0/D}\cdot l}{\sqrt{k_2^0/D}\cdot l}\right] \cdot \frac{\delta_1^2(\alpha - 1)^2}{8}\left[\operatorname{sech}^2(\sqrt{k_2^0/D}\cdot l) - \frac{\tanh\sqrt{k_2^0/D}\cdot l}{\sqrt{k_2^0/D}\cdot l}\right].$$

Therefore in the limiting case, $\omega \to \infty$, we write

[87] $$i_{st}(\omega \to \infty) - i_{\eta_0} = \frac{\delta_1^2}{4}[k_1^0\alpha^2 - k_2^0 C_0(\alpha - 1)^2]\frac{\tanh\sqrt{k_2^0/D}\cdot l}{\sqrt{k_2^0/D}\cdot l} + (k_1^0 - k_2^0 C_0)\frac{\delta_1^2(\alpha - 1)^2}{8}\left[\operatorname{sech}^2(\sqrt{k_2^0/D}\cdot l) - \frac{\tanh\sqrt{k_2^0/D}\cdot l}{\sqrt{k_2^0/D}\cdot l}\right].$$

(i) If $k_1^0 = k_2^0 C_0 = i_0/zF$; $\delta_0 = 0$,

[88] $$I_0(\omega \to \infty) \to i_0\left(\frac{zF\eta_1}{RT}\right)^2 \frac{(2\alpha - 1)}{4}\frac{\tanh(\sqrt{k_2^0/D}\cdot l)}{\sqrt{k_2^0/D}\cdot l}.$$

For sufficiently small values of l such that

[89] $$I_0(\omega \to \infty) \to i_0\left(\frac{zF\eta_1}{RT}\right)^2 \frac{(2\alpha - 1)^2}{4}$$

—a simple result that would result from

$$i(t) = zFl^{-1}\int_0^l (k_1^0 - k_2 C)\,dx$$

if one neglects the concentration polarization of the adatoms, i.e., if $C(x) = C_0$—a valid assumption for $\eta_0 = 0$, $l \to 0$ and $\omega \to \infty$.

The behavior of I_0 and the redoxokinetic potential χ with the frequency ω, δ_0 and a discussion of the various types of control will be presented later.

7. Galvanostatic Technique

Gerischer (3) and, independently, Bockris and Mehl (4) studied the kinetics under galvanostatic conditions assuming that surface diffusion is a significant step. A simple theory was suggested by these authors and this was later critically analyzed by Fleischmann and Thirsk (1*a*). It has been shown (1) that for $t \to 0$,

[90] $$zF(RT)^{-1}\eta(t) \simeq a + bt$$

where $a = i/i_0$ and $b = i/zFC_0$.

Can. J. Chem. Downloaded from www.nrcresearchpress.com by 210.87.254.42 on 09/05/12
For personal use only.

Confining oneself to conditions where $\pi Dtl^{-2} \rightarrow 0$ but greater than τ_1, the relaxation time for the charging of the double layer, an approximate expression for $\eta(t)$ can be attempted under current-controlled conditions. Then, as $\pi Dtl^{-2} \rightarrow 0$,

$$[91] \qquad \frac{i(t)}{zF} = \frac{\mathrm{d}}{\mathrm{d}t}\left\{\frac{1}{K(t)} \int_0^t [k_1(\tau) - k_2(\tau)C_0]K(\tau)\,\mathrm{d}\tau\right\}$$

or

$$[92] \qquad \frac{q(t)}{zF}K(t) = \int_0^t [k_1(\tau) - k_2(\tau)C_0]K(\tau)\,\mathrm{d}\tau$$

$$[93] \qquad zF\left[k_1(t) - k_2(t)C_0\left(1 + \frac{q(t)}{zFC_0}\right)\right] = i(t)$$

$$[94] \qquad q(t) = \int_0^t i(\tau)\,\mathrm{d}\tau.$$

Equation [93] enables one to evaluate $\eta(t)$ for any given $i(t)$ as $t \rightarrow 0$.

In particular, let $i(t) = i$, a constant. Then $q(t) = it$ so that

$$[95] \qquad \frac{i}{i_0(1 + it/zFC_0)} = \exp\left[\frac{\alpha zF\eta(t)}{RT}\right] - \exp\left[\frac{(\alpha - 1)zF\eta(t)}{RT}\right].$$

Let us substitute $zF\eta(t)/RT = a + bt + \phi(t^2)$,
With a^2, $(bt)^2 \ll 1$, one deduces that,

$$[96] \qquad a = i/i_0 \quad \text{and} \quad b = i/zFC_0$$

as reported earlier (1*a*).

If $zF\eta(t)(RT)^{-1} = \delta$ is so small that δ^2 and higher powers can be neglected, a limiting expression for $\eta(t \rightarrow 0)$ can be derived for all $t \rightarrow 0$, relaxing the usual assumption, viz. $t \gg \tau_1$. It is easily proved that

$$[97] \qquad \eta(t) = \frac{q(t)}{C_a} + \left(\frac{1}{C_i} - \frac{1}{C_a}\right) \int_0^t \exp\left[-\left(\frac{t - \tau}{\tau_m}\right)\right] i(\tau)\,\mathrm{d}\tau$$

$$[98] \qquad \tau_m = \left[\frac{zF}{RT}\frac{i_0}{C_i} + \frac{i_0}{zFC_0}\right]^{-1}$$

and

$$[99] \qquad C_a = C_i\left(\frac{zFC_0}{i_0\tau_m}\right)$$

Three particular cases follow.

(*a*) If $i(t) = i$, a constant,

$$[100] \qquad \eta(t) = \frac{it}{C_a} + \left(\frac{1}{C_i} - \frac{1}{C_a}\right)\left[1 - \exp\left(-\frac{t}{\tau_m}\right)\right]$$

with

$$\frac{zF}{RTC_i} \gg \frac{i_0}{zFC_0}, \quad \frac{RT}{z^2F^2}\frac{C_i}{C_0} \ll 1,$$

Can. J. Chem. Downloaded from www.nrcresearchpress.com by 210.87.254.42 on 09/05/12
For personal use only.

and

$$t \gg \frac{RTC_l}{zFi_0} = \tau_1,$$

$$\frac{zF\eta(t)}{RT} \rightarrow \frac{it}{zFC_0} + \frac{i}{i_0} \qquad [101]$$

as has been proved above (cf. eq. [96]).
(*b*) If $i(t) = i_1$, $t < t_1$ and $= i_2$, $t_1 \leqslant t$;

$$[102] \quad \eta(t) = \frac{1}{C_l}[(i_1 - i_2)t_1 + i_2 t] + \tau_m\left(\frac{1}{C_l} - \frac{1}{C_a}\right)\left[(i_1 - i_2)\exp\left[-\left(\frac{t - t_1}{\tau_m}\right)\right] - i_1 \exp\left(-\frac{t}{\tau_m}\right) + i_2\right].$$

If $i_2 = 0$ in [102],

$$[103] \quad \eta(t) = \frac{1}{C_a}(i_1 t_i) + i_1\tau_m\left(\frac{1}{C_l} - \frac{1}{C_a}\right)\left[\exp\left[-\left(\frac{t - t_1}{\tau_m}\right)\right] - \exp\left(-\frac{t}{\tau_m}\right)\right].$$

(*c*) If $i(t) = Q\delta(t)$, where $\delta(t)$ is Dirac's delta function,

$$\eta(t) = \frac{Q}{C_a} + Q\left(\frac{1}{C_l} - \frac{1}{C_a}\right)\exp(-t/\tau_m). \qquad [104]$$

This can also be deduced from [103] by taking the limit when $t_1 \rightarrow 0$ and $i_1 \rightarrow \infty$ so that $i_1 t_1 = Q$.

APPENDIX I

DERIVATION OF THE GENERAL SOLUTION

The differential equation to be solved is

$$D\partial^2 C/\partial x^2 + k_1(t) - k_2(t)C = \partial C/\partial t. \qquad [A.1]$$

The initial and boundary conditions are

$$[A.2] \quad \begin{cases} C = C_0, & x = 0, \quad t > 0; \\ \partial C/\partial x = 0, & x = l, \quad t > 0; \\ C = C_0, & x > 0, \quad t = 0; \end{cases}$$

$$k_1(t) = (i_0/zF)\exp[\alpha zF\eta(t)/RT] \qquad [A.3]$$

and

$$k_2(t) = (i_0/zFC_0)\exp[(\alpha - 1)zF\eta(t)/RT]. \qquad [A.4]$$

The solution of [A.1] is accomplished by reducing [A.1] to a homogeneous form by the substitution,

$$C^* = C(x, t)K(t) - \int_0^t k_1(t)K(t)\,dt. \qquad [A.5]$$

Herein,

$$K(t) = \exp\left[\int_0^t k_2(t)\,dt\right].$$

Can. J. Chem. Downloaded from www.nrcresearchpress.com by 210.87.254.42 on 09/05/12
For personal use only.

Can. J. Chem. Downloaded from www.nrcresearchpress.com by 210.87.254.42 on 09/05/12
For personal use only.

Consequently, [A.1] transforms into

$$D\partial^2 C^*/\partial x^2 = \partial C^*/\partial x, \tag{A.6}$$

since

$$\partial C^*/\partial t = K(t)[\partial C/\partial t + k_2(t)C - k_1(t)] \tag{A.7}$$

and

$$\partial C^*/\partial x = K(t)\partial C/\partial x. \tag{A.8}$$

Also [A.2] now becomes

$$\begin{cases} (a)\ C^* = C_0K(t) - \int_0^t k_1(t)K(t)\,\mathrm{d}t,\ x = 0,\ t > 0; \\ (b)\ \partial C^*/\partial x = 0,\ x = l,\ t > 0; \\ (c)\ C^* = C_0,\ x > 0,\ t = 0. \end{cases} \tag{A.9}$$

Defining the Laplace transform of $f(t)$ as

$$L[f(t)] = \overline{f(p)} = p\int_0^\infty f(t)\exp(-pt)\,\mathrm{d}t, \tag{A.10}$$

we write [A.6] in the form,

$$D\partial^2\bar{C}^*/\partial x^2 - p\bar{C}^* = -pC_0; \tag{A.11}$$

Also,

$$\begin{aligned} \bar{C}^*(0,p) &= L[C_0K(t) - \int_0^t k_1(t)K(t)\,\mathrm{d}t] \\ &= L\left[C_0 - \int_0^t [k_1(t) - k_2(t)C_0]K(t)\,\mathrm{d}t\right] \\ &= L[\mathscr{K}(t)],\ \text{say.} \end{aligned} \tag{A.12}$$

$$\partial C^*/\partial x = 0,\ x = l,\ t > 0;$$

The solution of [A.11] with [A.12] is

$$\bar{C}^*(x,p) = C_0 + A(p)\cosh[\sqrt{p/D}(l-x)],$$

where

$$A(p) = L[\mathscr{K}(t) - C_0]\,\mathrm{sech}\,[\sqrt{p/D}\cdot l]$$

or

$$\bar{C}^*(x,p) - C_0 = L[\mathscr{K}(t) - C_0]\frac{\cosh[\sqrt{p/D}(l-x)]}{\cosh[\sqrt{p/D}\cdot l]}. \tag{A.13}$$

Observing that

$$L\left[\frac{\partial\theta_1(v,t)}{\partial v}\right] = -2\pi p\frac{\cosh(2v\sqrt{\pi p})}{\cosh(\sqrt{\pi p})} \tag{A.14}$$

and

$$L[f(\lambda t)] = \overline{f(p/\lambda)}, \tag{A.15}$$

we write

$$[A.16] \qquad \frac{D}{l} L\left\{\frac{\partial\theta_1[(l-x)/2l,\ \pi Dt/l^2]}{\partial x}\right\} = p\,\frac{\cosh\,[\sqrt{p/D}(l-x)]}{\cosh\,(\sqrt{p/D}\cdot l)}.$$

The theta function $\theta_1(v, t)$ in [A.14] is defined by

$$[A.17] \qquad \theta_1(v,t) = \sum_{-\infty}^{\infty} \exp\,[-\pi(n-\tfrac{1}{2})^2 t + 2\pi i(n-\tfrac{1}{2})(v+\tfrac{1}{2})]$$

$$= -t^{-1/2}\sum_{-\infty}^{\infty}(-1)^n \exp\,[-\pi(n+v+\tfrac{1}{2})^2/t]$$

$$= -2q^{1/4}\sum_{n=0}^{\infty}(-1)^n q^{n(n+1)} \sin\,[(2n+1)\pi v],$$

with $q = \exp\,(-\pi t)$.

Thus,

$$[A.18] \qquad C^*(x,t) = C_0 - \frac{D}{l}\frac{\partial}{\partial x}\left\{\int_0^t [C_0 - \mathscr{K}(t)]\theta_1\left[\frac{l-x}{2l}, \frac{\pi D(t-\tau)}{l^2}\right] d\tau\right\}$$

and

$$[A.19] \qquad C(x,t) = C_0 + [C^*(x,t) - \mathscr{K}(t)]/K(t)$$

with $C^*(x, t)$ completely determined by [A.18].

Equations [A.18] and [A.19] are the same as those given in equations [9] and [10] of the text. Again,

$$[A.20] \quad i = zFl^{-1}\int_0^l [k_1(t) - k_2(t)C(x,t)]\,dx$$

$$= zF[k_1(t) - k_2(t)C_0] - zFl^{-1}k_2(t)\int_0^l [C(x,t) - C_0]\,dx$$

$$= zF[k_1(t) - k_2(t)C_0] - \frac{zFk_2(t)}{K(t)}[C_0 - \mathscr{K}(t)]$$

$$- \frac{zFk_2(t)}{K(t)l}\int_0^l [C^*(x,t) - C_0]\,dx$$

$$[A.21] \quad = zF\frac{d}{dt}\left\{\frac{1}{K(t)}\int_0^t [k_1(\tau) - k_2(\tau)C_0]K(\tau)\,d\tau\right\}$$

$$- \frac{zFDk_2(t)}{K(t)l^2}\int_0^t [C_0 - \mathscr{K}(\tau)]\theta_1\left[\frac{1}{2}, \frac{\pi D(t-\tau)}{l^2}\right] d\tau$$

$$[A.22] \quad = zF\frac{d}{dt}\left\{\frac{1}{K(t)}\int_0^t [k_1(t) - k_2(t)C_0]\,dt\right\}$$

$$+ \frac{2zFDk_2(t)}{K(t)l^2}\sum \exp\,[-\pi^2 Dt(n+\tfrac{1}{2})^2/l^2]$$

$$\cdot\left\{\int_0^t [C_0 - \mathscr{K}(t)]\exp\,[\pi^2 D\tau(n+\tfrac{1}{2})^2/l^2]\,d\tau\right\}.$$

Can. J. Chem. Downloaded from www.nrcresearchpress.com by 210.87.254.42 on 09/05/12
For personal use only.

(cf. eq. [15] of the text). Since

$$[A.23]\quad \int_0^t [C_0 - \mathscr{K}(\tau)] \exp\,[\pi^2 D\tau(n+\tfrac{1}{2})^2/l^2]\,d\tau = \frac{4l^2}{\pi^2 D(2n+1)^2}[C_0 - \mathscr{K}(\tau)] \exp\,[\pi^2 D\tau(2n+1)^2/4l^2] - \frac{4l^2}{\pi^2 D(2n+1)^2}\int_0^t [k_1(\tau) - k_2(\tau)C_0] \cdot \exp\left[\int_0^\tau k_2(t)\,dt + \pi^2 D\tau(2n+1)^2/4l^2\right] d\tau$$

and

$$\sum_{n=0}^{\infty} \frac{1}{(2n+1)^2} = \frac{\pi^2}{8},$$

eq. [A.22] becomes

$$[A.24]\quad \frac{i(t)}{zF} = [k_1(t) - k_2(t)C_0] - \frac{8}{\pi^2}\sum \frac{k_2(t)}{(2n+1)^2} \exp\left\{-\left[\int_0^t k_2(t)\,dt + \pi^2 D(2n+1)^2/4l^2\right]\right\} \int_0^t [k_1(\tau) - k_2(\tau)C_0] \exp\left[\int_0^\tau k_2(t)\,dt + \pi^2 D\tau(2n+1)^2/4l^2\right] d\tau.$$

Again, by integrating by parts, [A.24] can be written as

$$[A.25]\quad \frac{i(t)}{zF} = [k_1(t) - k_2(t)C_0] - \frac{32l^2}{\pi^2}k_2(t)\sum \frac{k_1(t) - k_2(t)C_0}{[4l^2k_2(t) + \pi^2 D(2n+1)^2](2n+1)^2} + \frac{32l^2k_2(t)}{\pi^2}\sum \frac{k_1(+0) - k_2(+0)C_0}{[4l^2k_2(+0) + \pi^2 D(2n+1)^2](2n+1)^2} \cdot \exp\left\{-\left[\int_0^t k_2(t)\,dt + \pi^2 Dt(2n+1)^2/4l^2\right]\right\} + \frac{32l^2k_2(t)}{\pi^2}\sum \exp\left[-\left\{\int_0^t k_2(t)\,dt + Dt(2n+1)^2/4l^2\right\}\right] \int_0^t \frac{d}{d\tau}\left\{\frac{k_1(\tau) - k_2(\tau)C_0}{k_2(\tau) + [(\pi^2 D)/(4l^2)](2n+1)^2}\right\} \exp\left[\left\{\int_0^\tau k_2(t)\,dt + \pi^2 D\tau(2n+1)^2/4l^2\right\}\right] d\tau.$$

APPENDIX II
POTENTIOKINETIC METHOD

Since

$$[B.1]\quad zF\eta(t)/RT = \delta_0 + \delta_1 t,$$

we have

$$[B.2]\quad k_1(t) = (i_0/zF) \exp\,[\alpha(\delta_0 + \delta_1 t)] = k_1^0 \exp\,(\alpha\delta_1 t),$$

$$[B.3]\quad k_2(t) = k_2^0 \exp\,[(\alpha - 1)\delta_1 t],$$

Can. J. Chem. Downloaded from www.nrcresearchpress.com by 210.87.254.42 on 09/05/12
For personal use only.

Can. J. Chem. Downloaded from www.nrcresearchpress.com by 210.87.254.42 on 09/05/12
For personal use only.

[B.4] $$\int_0^t k_2(t)\,dt = k_2^0[1 - \exp\{(\alpha - 1)\delta_1 t\}]/(1 - \alpha)\delta_1,$$

[B.5] $$\int_0^t [k_1(\tau) - k_2(\tau)\,C_0] \exp\left[\int_0^\tau k_2(z)\,dz + \pi^2 D(2n+1)^2\tau/4l^2\right] d\tau$$

$$= \exp[k_2^0/(\alpha - 1)\delta_1]\; k_1^0 \int_0^t \exp\left[\frac{k_2 \exp[(\alpha - 1)\delta_1\tau]}{(\alpha - 1)\delta_1} + \left(\frac{\pi^2 D(2n+1)^2}{4l^2} + \alpha\delta_1\right)\tau\right] d\tau$$

$$- k_2^0 C_0 \int_0^t \exp\left\{\left[\frac{k_2^0 \exp[(\alpha - 1)\delta_1\tau]}{(\alpha - 1)\delta_1} + \left(\frac{\pi^2 D(2n+1)^2}{4l^2} + (\alpha - 1)\delta_1\right)\tau\right\} d\tau,$$

[B.6] $$= \frac{1}{(1 - \alpha)\delta_1} \exp\left\{\frac{k_2^0}{(1 - \alpha)\delta_1}\right\} \left\{k_1^0\left[\frac{k_2^0}{(1 - \alpha)\delta_1}\right]^{-A_n}\left[\gamma\left(A_n, \frac{k_2^0}{(1 - \alpha)\delta_1}\right]\right.\right.$$

$$\left. - \gamma\left(A_n, \frac{k_2^0 \exp[(\alpha - 1)\delta_1 t]}{(1 - \alpha)\delta_1}\right)\right]$$

$$\left. - k_2^0 C_0 \left\{\frac{k_2^0}{(1 - \alpha)\delta_1}\right\}^{-(A_n + (1/1-\alpha))}\left[\gamma\left(A_n + \frac{1}{1 - \alpha}, \frac{k_2^0}{(1 - \alpha)\delta_1}\right)\right.\right.$$

$$\left.\left. - \gamma\left(A_n + \frac{1}{1 - \alpha}, \frac{k_2^0 \exp[(\alpha - 1)\delta_1 t]}{(1 - \alpha)\delta_1}\right)\right]\right\}.$$

In [B.1] to [B.6],

$$k_1^0 = (i_0/zF) \exp(\alpha\delta_0),$$

$$k_2^0 = (i_0/zFC_0) \exp[(\alpha - 1)\delta_0],$$

and $\gamma(\alpha, x)$ is the incomplete gamma function defined as

$$\int_0^x t^{\alpha-1} \exp(-t)\,dt$$

or through

[B.7] $$\gamma(\alpha, x) = \sum_0^\infty \frac{(-1)^n x^{\alpha+n}}{n!(\alpha + n)}, \alpha \neq 0, -1, -2, \ldots$$

(Note: if $A_n \to -m$, a negative integer, the limit of [B.6], which exists, is to be taken) and,

[B.8] $$A_n = -\left(\frac{\pi^2 D(2n+1)^2}{4l^2(1 - \alpha)\delta_1} + \frac{\alpha}{1 - \alpha}\right).$$

An alternate form for [B.6] which is more convenient for deriving an expression for the steady state is obtained through a relationship between the incomplete gamma function $\gamma(\alpha, x)$ and the confluent hypergeometric function $\Phi(1, 1 + \alpha; x)$, viz.,

[B.9] $$\gamma(\alpha, x) = \exp(-x)\, x^\alpha \Phi(1, 1 + \alpha; x)/\alpha$$

[B.10] $$\Phi(a, c; x) = 1 + \frac{a}{c}x + \frac{a(a+1)}{c(c+1)}\frac{x^2}{2!} + \ldots.$$

Can. J. Chem. Downloaded from www.nrcresearchpress.com by 210.87.254.42 on 09/05/12
For personal use only.

Since,

$$\frac{i(t)}{zF} = [k_1(t) - k_2(t)C_0] - \frac{8}{\pi^2}\sum \frac{k_2(t)}{(2n+1)^2}\exp\left[-\left\{\int_0^t k_2(t)\,dt + \pi^2 D(2n+1)^2 t/4l^2\right\}\right] \cdot \int_0^t [k_1(t) - k_2(t)C_0]\exp\left[\int_0^t k_2(t)\,dt + \pi^2 D(2n+1)^2 t/4l^2\right],$$

[B.11]
$$\frac{i(t)}{zF} - [k_1(t) - k_2(t)C_0] = -\frac{8}{\pi^2}\frac{k_2(t)}{(1-\alpha)\delta_1}\sum \frac{1}{(2n+1)^2}\exp\left\{-\left(A_n + \frac{\alpha}{1-\alpha}\right)(\alpha-1)\delta_1 t + \frac{k_2{}^0}{(1-\alpha)\delta_1}\exp[(\alpha-1)\delta_1 t]\right\} \cdot\left[\left\{\frac{k_2{}^0}{(1-\alpha)\delta_1}\right\}^{-A_n} k_1{}^0 \cdot\left\{\gamma\left(A_n, \frac{k_2{}^0}{(1-\alpha)\delta_1}\right) - \gamma\left(A_n, \frac{k_2{}^0\exp[(\alpha-1)\delta_1 t]}{(1-\alpha)\delta_1}\right)\right\} - \left\{\frac{k_2{}^0}{(1-\alpha)\delta_1}\right\}^{-(A_n+(1/1-\alpha))} k_2{}^0 C_0\left\{\gamma\left(A_n + \frac{1}{1-\alpha}, \frac{k_2{}^0}{(1-\alpha)\delta_1}\right) - \gamma\left(A_n + \frac{1}{1-\alpha}, \frac{k_2{}^0\exp[(\alpha-1)\delta_1 t]}{(1-\alpha)\delta_1}\right)\right\}\right]$$

[B.12]
$$= \frac{8k_2(t)}{\pi^2(1-\alpha)\delta_1}\sum\left[\frac{k_1(t)}{A_n(2n+1)^2}\Phi\left(1, A_n+1; \frac{k_2(t)}{(1-\alpha)\delta_1}\right) - \frac{k_2(t)C_0}{\left(A_n + \frac{1}{1-\alpha}\right)(2n+1)^2}\Phi\left(1, A_n+1+\frac{1}{1-\alpha}; \frac{k_2(t)}{(1-\alpha)\delta_1}\right)\right] - \frac{8k_2(t)}{\pi^2(1-\alpha)\delta_1}\sum\left[\frac{k_1(t)}{(2n+1)^2 A_n}\{\exp[(1-\alpha)\delta_1 t]\}^{A_n}\Phi\left(1, A_n+1; \frac{k_2{}^0}{(1-\alpha)\delta_1}\right) - \frac{k_2(t)C_0}{(2n+1)^2\left(A_n + \frac{1}{1-\alpha}\right)}[\exp(1-\alpha)\delta_1 t]^{A_n+(1/1-\alpha)} \cdot\Phi\left(1, A_n+1+\frac{1}{1-\alpha}; \frac{k_2{}^0}{(1-\alpha)\delta_1}\right)\right].$$

The confluent hypergeometric function $\Phi(a, c; x) \to 1$ as $x \to 0$ and hence, in the steady state,

[B.13]
$$\frac{i(t)}{zF} - [k_1(t) - k_2(t)C_0] \to -\frac{8k_2(t)}{\pi^2(1-\alpha)\delta_1}\left[\sum \frac{k_2(t)C_0}{(2n+1)^2(A_n + (1-\alpha)^{-1})} - \sum \frac{k_1(t)}{(2n+1)^2 A_n}\right].$$

Using eq. [28],

$$[B.14] \qquad i(t) = [k_1(t) - k_2(t)C_0] + k_2(t)\left[\frac{k_1(t)}{\alpha\delta_1}\left(\frac{\tanh l\sqrt{\alpha\delta_1/D}}{l\sqrt{\alpha\delta_1/D}} - 1\right) - \frac{k_2(t)C_0}{(\alpha-1)\delta_1}\left(\frac{\tanh l\sqrt{(\alpha-1)\delta_1/D}}{l\sqrt{(\alpha-1)\delta_1/D}} - 1\right)\right].$$

The steady state solution given by [B.14] is valid under the condition $t \to \infty$ *and*

$$[B.15] \qquad k_2(t) \ll \pi^2 D/4l^2.$$

In deriving [B.13] and [B.14], $zF\eta(t)/RT$ has been assumed to be equal to $\delta_0 + \delta_1 t$; hence, one may expect to deduce from these, expressions for the current under constant potential conditions by allowing $\delta_1 \to 0$; obviously [B.14] gives the corresponding steady state when $k_2^0 \ll \pi^2 D/4l^2$; [B.14] gives,

$$[B.16] \qquad i(t) = (k_1^0 - k_2^0 C_0)(1 + k_2^0 l^2/3D) \simeq (k_1^0 - k_2^0 C_0)\frac{\tanh(\sqrt{k_2^0/D}\cdot l)}{(\sqrt{k_2^0/D}\ l\cdot)},$$

as has been derived elsewhere (2) (cf. eq. [29] in this paper).

APPENDIX III

POTENTIAL STEP METHOD

The differential equation [1] or [A.1] is to be solved under the following boundary conditions,

$$[C.1] \qquad C(x,t) = \frac{k_1'}{k_2'} - \frac{k_1' - k_2'C_0}{k_2'}\frac{\cosh[\sqrt{k_2'/D}\cdot(l-x)]}{\cosh(\sqrt{k_2'/D}\cdot l)}$$

at $t = 0$, instead of eq. [3] of the text.

$$[C.2] \qquad D(\partial C/\partial x)_{x=l} = 0, \quad \text{and} \quad C(x,t) = C_0,\ x = 0.$$

As in Appendix I, we transform $C(x, t)$ to $C^*(x, t)$ through

$$[C.3] \qquad C^*(x,t) = C(x,t)K(t) - \int_0^t k_1(\tau)\,K(\tau)\,d\tau.$$

Conditions [A.9*a*] and [A.9*b*] remain valid while for [A.9*c*] we have, now,

$$[C.4] \qquad C^*(x,t) = C_0 + \frac{k_1' - k_2'C_0}{k_2'}\left[1 - \frac{\cosh[\sqrt{k_2'/D}\cdot(l-x)]}{\cosh\sqrt{k_2'/D}\cdot l}\right].$$

Consequently, we derive

$$[C.5] \qquad C^*(x,p) = C_0 + L[\mathscr{K}(t) - C_0]\cdot\frac{\cosh[\sqrt{p/D}\cdot(l-x)]}{\cosh(\sqrt{p/D})\cdot l} + \frac{k_1' - k_2'C_0}{k_2'}\left[1 - \frac{\cosh[\sqrt{k_2'/D}(l-x)]}{\cosh(\sqrt{k_2'/D}\cdot l)}\cdot\frac{p}{p-k_2'}\right] + \frac{k_1' - k_2'C_0}{p-k_2'}\cdot\frac{\cosh[\sqrt{p/D}\cdot(l-x)]}{\cosh(\sqrt{p/D}\cdot l)}.$$

Can. J. Chem. Downloaded from www.nrcresearchpress.com by 210.87.254.42 on 09/05/12
For personal use only.

(*Apparently* eq. [C.5] suggests that a pole for $\bar{C}^*(x, p)$ exists at $p = k_2'$. Actually the residue can be proved to be zero at $p = k_2'$).

Inverting [C.5] and substituting in the expression for $i(t)$ one evaluates $i(t)$ as

$$i(t) = -I_1(t) + I_2(t),$$

where $I_1(t)$ is the transient due to the concentration polarization caused by the first pulse and equals

$$[C.6] \quad I_1(t) = \frac{8}{\pi^2} \frac{zFDk_2(t)}{k(t)} (k_1' - k_2'C_0) \cdot \sum \frac{\exp[-(\pi^2 Dt(4l^2)^{-1}(2n+1)^2)]}{(2n+1)^2 k_2' + \pi^2 D(4l^2)^{-1}(2n+1)^2}.$$

The quantity $I_2(t)$ is the current that would have been observed in the absence of the first pulse and is given by the eq. [29] of the text.

Thus eq. [40] of ref. (1*b*) will have to be modified as [C.6].

APPENDIX IV

Assuming $zF\eta(t)/RT = \delta_0 + \delta_1 \cos \omega t$,

$$[D.1] \quad k_1(t) = k_1^0 \exp(\alpha\delta_1 \cos \omega t)$$
$$= k_1^0[I_0(\alpha\delta_1) + 2I_1(\alpha\delta_1) \cos \omega t + 2I_2(\alpha\delta_1) \cos 2\omega t + \ldots].$$

Similarly,

$$[D.2] \quad k_2(t) = k_2^0 \exp[(\alpha - 1)\delta_1 \cos \omega t]$$
$$= k_2^0\{I_0[(\alpha-1)\delta_1] + 2I_1[(\alpha-1)\delta_1] \cos \omega t + 2I_2[(\alpha-1)\delta_1] \cos 2\omega t + \ldots\}.$$

$$[D.3] \quad \int_0^t k_2(z)\, dz = k_2^0 \left\{ I_0[(\alpha-1)\delta_1]t + 2I_1[(\alpha-1)\delta_1] \frac{\sin \omega t}{\omega} + 2I_2[(\alpha-1)\delta_1] \frac{\sin 2\omega t}{2\omega} + \ldots \right\}.$$

$$\frac{k_2(t)}{K(t)} = k_2(t) \exp\left[-\int_0^t k_2(z)\, dz \right]$$
$$= \frac{d}{dt}\left[-\exp\left\{ -\int_0^t k_2(z)\, dz \right\} \right]$$
$$= -\frac{d}{dt}\left[\exp\left\{ -k_2^0 \left(I_0[(\alpha-1)\delta_1]t + 2I_1[(\alpha-1)\delta_1] \frac{\sin \omega t}{\omega} + 2I_2[(\alpha-1)\delta_1] \frac{\sin 2\omega t}{2\omega} + \ldots \right) \right\} \right]$$

$$[D.4] \quad \simeq \exp(-k_2^0 I_0[(\alpha-1)\delta_1]t) \left[k_2^0 I_0[(\alpha-1)\delta_1] + 2k_2^0 I_1[(\alpha-1)\delta_1] \cos \omega t \right] \left[I_0\left\{ \frac{2k_2^0 I_1[(\alpha-1)\delta_1]}{\omega} \right\} - 2I_1\left\{ \frac{2k_2^0 I_1[(\alpha-1)\delta_1]}{\omega} \right\} \sin \omega t \right]$$

$$[D.5] \quad \simeq k_2^0 \exp\{-k_2^0 I_0[(\alpha-1)\delta_1]\} \left[I_0[(\alpha-1)\delta_1] I_0\left\{ \frac{2k_2^0 I_1[(\alpha-1)\delta_1]}{\omega} \right\} + A_1 \cos(\omega t + \chi_1) \right],$$

Can. J. Chem. Downloaded from www.nrcresearchpress.com by 210.87.254.42 on 09/05/12
For personal use only.

where

$$[D.6] \qquad A_1^2 = \left[2I_0(\alpha\delta_1 - \delta_1)I_1\left\{\frac{2k_2^0 I_1(\alpha\delta_1 - \delta_1)}{\omega}\right\}\right]^2 + \left[2I_1(\alpha\delta_1 - \delta_1)I_0\left\{\frac{2k_2^0 I_1(\alpha\delta_1 - \delta_1)}{\omega}\right\}\right]^2;$$

and

$$[D.7] \qquad \tan\chi_1 = \frac{I_0(\alpha\delta_1 - \delta_1)}{I_1(\alpha\delta_1 - \delta_1)} \cdot \frac{I_1(2k_2^0 I_1(\alpha\delta_1 - \delta_1)\omega^{-1})}{I_0(2k_2^0 I_1(\alpha\delta_1 - \delta_1)\omega^{-1})}.$$

Also,

$$[D.8] \qquad \int_0^t k_1(\tau)\exp\left[\int_0^\tau k_2(z)\,dz + \frac{\pi^2 D(2n+1)^2\tau}{4l^2}\right]d\tau$$
$$\simeq k_1^0\int_0^t \exp\left[\frac{\pi^2 D\tau}{4l^2}(2n+1)^2 + k_2^0 I_0(\alpha\delta_1 - \delta_1)\tau\right]$$
$$[I_0(A_2) + 2I_1(A_2)\cos(\omega\tau - \chi_2)]\,d\tau.$$

$$[D.9] \qquad = k_1^0\left[\exp\left\{\frac{\pi^2 D(2n+1)^2 t}{4l^2} + k_2^0 t I_0(\alpha\delta_1 - \delta_1)\right\}\right]$$
$$\left\{\frac{I_0(A_2)}{\pi^2 D(2n+1)^2(4l^2)^{-1} + k_2^0 I_0(\alpha\delta_1 - \delta_1)} + \text{real part of } \frac{2I_1(A_2)\exp[i(\omega t - \chi_2)]}{B_n}\right\}$$
$$- k_1^0\left\{\frac{I_0(A_2)}{\pi^2 D(2n+1)^2(4l^2)^{-1} + k_2^0 I_0(\alpha\delta_1 - \delta_1)} + \text{real part of } \frac{2I_1(A_2)\exp(-i\chi_2)}{B_n}\right\},$$

where

$$[D.10] \qquad A_2^2 = \alpha^2\delta_1^2 + [2k_2^0 I_1(\alpha\delta_1 - \delta_1)\omega^{-1}]^2,$$

$$[D.11] \qquad \tan\chi_2 = \frac{2k_2^0 I_1(\alpha\delta_1 - \delta_1)}{\omega\alpha\delta_1},$$

and

$$[D.12] \qquad B_n = [\pi^2 D(4l^2)^{-1}(2n+1)^2 + k_2^0 I_0(\alpha\delta_1 - \delta_1)] + i\omega.$$

Similarly,

$$[D.13] \qquad \int_0^t k_2(\tau)\exp\left(\int_0^\tau k_2(z)\,dz + \frac{\pi^2 D(2n+1)^2\tau}{4l^2}\right)d\tau$$
$$= k_2^0\exp\left[\frac{\pi^2 D(2n+1)^2 t}{4l^2} + k_2^0 t I_0(\alpha\delta_1 - \delta_1)\right]$$
$$\left\{\frac{I_0(A_2')}{\pi^2 D(4l^2)^{-1}(2n+1)^2 + k_2^0 I_0(\alpha\delta_1 - \delta_1)}\right.$$

Can. J. Chem. Downloaded from www.nrcresearchpress.com by 210.87.254.42 on 09/05/12
For personal use only.

$$+ \text{ real part of } \frac{2I_1(A_2')\exp[i(\omega t - \chi_2)]}{B_n}$$

$$- k_2{}^0\left[\frac{I_0(A_2')}{\pi^2 D(2n+1)^2(4l^2)^{-1} + k_2{}^0 I_0(\alpha\delta_1 - \delta_1)} + \text{ real part of } \frac{2I_1(A_2')\exp(-i\chi_2')}{B_n}\right]\Bigg\}.$$

with

[D.14] $$A_2'^2 = (\alpha - 1)^2\delta_1{}^2 + \left[\frac{2k_2{}^0 I_1(\alpha\delta_1 - \delta_1)}{\omega}\right]^2,$$

[D.15] $$\tan\chi_2' = \frac{2k_2{}^0 I_1(\alpha\delta_1 - \delta_1)}{\omega(\alpha - 1)\delta_1},$$

and B_n as defined by [D.12].

Thus $i(t)$ is obtained by using eq. [16] of the text and substituting the expressions derived above. Writing,

[D.16] $$i(t) = i_{st}(t) + \sum_{n=1}^{\infty} i_n \cos(n\omega t - \phi_n) + i_{tr}(t),$$

and equating the Fourier coefficients, one obtains, formally, i_n and ϕ_n, $n = 1, 2, \ldots$; $i_{st}(t)$ is the steady state constant value attained by $i(t)$ whereas $i_{tr}(t)$ is the transient part of $i(t)$ tending to zero as t tends to infinity, For example, i_1 is found as follows:

The right hand side of eq. [16] is

[D.17] $$[k_1{}^0 I_0(\alpha\delta_1) - k_2{}^0 C_0 I_0(\alpha\delta_1 - \delta_1)] + 2[k_1{}^0 I_1(\alpha\delta_1) - k_2{}^0 C_0 I_1(\alpha\delta_1 - \delta_1)]\cos\omega t$$

$$+ \text{ terms in higher harmonics } - \frac{8}{\pi^2}k_2{}^0\left[I_0(\alpha\delta_1 - \delta_1)I_0\left(\frac{2k_2{}^0 I_1(\alpha\delta_1 - \delta_1)}{\omega}\right) + A_1\cos(\omega t + \chi_1)\right]\cdot\sum\frac{1}{(2n+1)^2}\left[\frac{k_1{}^0 I_0(A_2) - k_2{}^0 C_0 I_0(A_2')}{\pi^2 D(4l^2)^{-1}(2n+1)^2 + k_2{}^0 I_0(\alpha\delta_1 - \delta_1)}\right]$$

$$+ \sum\frac{1}{(2n+1)^2}\left[\text{real part of }\left\{\frac{2k_1{}^0 I_1(A_2)\exp[i(\omega t - \chi_2)]}{B_n} - \frac{k_2{}^0 C_0 I_1(A_2')\exp[i(\omega t - \chi_2')]}{B_n}\right\}\right] + \text{a transient } i_{tr}(t).$$

Also,

[D.18] $$\frac{8}{\pi^2}\sum\frac{k_2{}^0 I_0(\alpha\delta_1 - \delta_1)}{(2n+1)^2 B_n}$$

$$= \frac{8}{\pi^2}\sum\frac{1}{(2n+1)^2[\pi^2 D(2n+1)^2(4l^2)^{-1} + k_2{}^0 I_0(\alpha\delta_1 - \delta_1) + i\omega]}$$

$$= \frac{k_2{}^0 I_0(\alpha\delta_1 - \delta_1)}{k_2{}^0 I_0(\alpha\delta_1 - \delta_1) + i\omega}\left[1 - \frac{\tanh\sqrt{[k_2{}^0 I_0(\alpha\delta_1 - \delta_1) + i\omega]/D}\cdot l}{\sqrt{[k_2{}^0 I_0(\alpha\delta_1 - \delta_1) + i\omega]/D}\cdot l}\right]$$

$$= E'\exp(-i\lambda'), \text{ say.}^*$$

**The symbols E' and λ' are used in [D.17] to draw attention to the relationship between (E', λ') and (E, λ) used in ref. 1b; as a matter of fact, if one substitutes $k_2{}^0 I_0(\alpha\delta_1 - \delta_1)$ for $k_2{}^0$ in eqs. 71–77 of ref. 1b, $E'\exp(-i\lambda')$ and $[1 - E\exp(-i\lambda)]$ will be identical.*

Can. J. Chem. Downloaded from www.nrcresearchpress.com by 210.87.254.42 on 09/05/12
For personal use only.

In view of [D.16], eq. [D.17] becomes

$$i(t) = i_{st}(t) + \sum i_n \cos(n\omega t + \phi_n) + i_{tr}(t),$$

with

$$[D.19]\quad \frac{i_{st}(t)}{zF} = [k_1^0 I_0(\alpha\delta_1) - k_2^0 C_0 I_0(\alpha\delta_1 - \delta_1)] - I_0\left[\frac{2k_2^0 I_1(\alpha\delta_1 - \delta_1)}{\omega}\right][k_1^0 I_0(A_2) - k_2^0 C_0 I_0(A_2')] \cdot \left[1 - \frac{\tanh\sqrt{k_2^0 I_0(\alpha\delta_1 - \delta_1)/D}\cdot l}{\sqrt{k_2^0 I_0(\alpha\delta_1 - \delta_1)/D}\cdot l}\right] - I_0\left(\frac{2k_2^0 I_1(\alpha\delta_1 - \delta_1)}{\omega}\right) A_1 \cdot E'[k_1^0 I_1(A_2)\cos(\lambda' + \chi_1 + \chi_2) - k_2^0 C_0 I_1(A_2')\cos(\lambda' + \chi_1 + \chi_2)].$$

$$[D.20]\quad i_1 \cos(\omega t - \phi_1) = 2zF[k_1^0 I_1(\alpha\delta_1) - k_2^0 C_0 I_1(\alpha\delta_1 - \delta_1)]\cos\omega t - zF[k_1^0 I_0(A_2) - k_2^0 C_0 I_0(A_2')] \cdot \frac{A_1}{I_0(\alpha\delta_1 - \delta_1)}\left[1 - \frac{\tanh\sqrt{k_2^0 I_0(\alpha\delta_1 - \delta_1)/D}\cdot l}{\sqrt{k_2^0 I_0(\alpha\delta_1 - \delta_1)/D}\cdot l}\right] \cdot\cos(\omega t + \chi_1) - 2zFI_0\left[\frac{2k_2^0 I_1(\alpha\delta_1 - \delta_1)}{\omega}\right] E'[k_1^0 I_1(A_2)\cos(\omega t - \lambda' - \chi_2) - k_2^0 C_0 I_1(A_2')\cos(\omega t - \lambda' - \chi_2')],$$

and

$$[D.21]\quad i_{tr}(t) = \frac{8zF}{\pi^2} k_2^0 \left\{ I_0(\alpha\delta_1 - \delta_1) I_0\left(\frac{2k_2^0}{\omega} I_1(\alpha\delta_1 - \delta_1)\right)\right\} \sum \frac{1}{(2n+1)^2}\exp\left[-(\pi^2 Dt(2n+1)^2(4l^2)^{-1} + k_2^0 I_0(\alpha\delta_1 - \delta_1)t)\right] \left[\frac{k_1^0 I_0(A_2) - k_2^0 C_0 I_0(A_2')}{\pi^2 D(4l^2)^{-1}(2n+1)^2 + k_2^0 I_0(\alpha\delta_1 - \delta_1)} + 2[k_1^0 I_1(A_2)\cos(\omega t - \chi_2 - b_n) - k_2^0 C_0 I_1(A_2')\cos(\omega t - \chi_2' - b_n)]|B_n|^{-1}\right]$$

where

$$|B_n|^2 = [\pi^2 Dt(4l^2)^{-1}(2n+1)^2 + k_2^0 I_0(\alpha\delta_1 - \delta_1)]^2 + \omega^2,$$

$$b_n = \tan^{-1}[\omega/[\pi^2 Dt(4l^2)^{-1}(2n+1)^2 + k_2^0 I_0(\alpha\delta_1 - \delta_1)]].$$

ACKNOWLEDGMENT

The author thanks Professor K. S. G. Doss, Director, Central Electrochemical Research Institute, Karaikudi, for his kind encouragement and valuable discussions.

Can. J. Chem. Downloaded from www.nrcresearchpress.com by 210.87.254.42 on 09/05/12
For personal use only.

REFERENCES

1. (*a*) M. FLEISCHMANN and H. R. THIRSK. *In* Advances in electrochemistry and electrochemical engineering. Vol. 3. *Edited by* P. Delahay. Interscience, New York. 1963. Chap. 3.
(*b*) M. FLEISCHMANN and H. R. THIRSK. Electrochim. Acta, **2**, 22 (1960).
2. D. A. VERMILYEA. *In* Advances in electrochemistry and electrochemical engineering. Vol. 3. *Edited by* P. Delahay. Interscience, New York. 1963. Chap. 3.
3. H. GERISCHER. Z. Electrochem. **62**, 259 (1958).
4. J. O'M. BOCKRIS and W. MEHL. Can. J. Chem. **37**, 190 (1959).
5. W. LORENZ. Z. Physik. Chem. Frankfurt, **17**, 136 (1958); **19**, 377 (1959).
6. J. O'M. BOCKRIS and B. E. CONWAY. Proc. Roy. Soc. London, Ser. A, **248**, 394 (1958).
7. W. K. BURTON, N. CABRERA, and C. F. FRANK. Phil. Trans. Roy. Soc. London, Ser. A, **123**, 299 (1951).
8. D. A. VERMILYEA. J. Chem. Phys. **25**, 1254 (1956).
9. H. GERISCHER and R. P. TISCHER. Z. Elctrochem. **61**, 1159 (1957).
10. (*a*) P. DELAHAY. New instrumental methods in electrochemistry. Interscience, New York. 1954.
(*b*) P. DELAHAY. Advances in electrochemistry and electrochemical engineering. Vol. 1. Interscience, New York. 1961.
11. R. S. NICHOLSON and I. SHAIN. Anal. Chem. **36**, 706 (1964).
12. A. ERDELYI *et al.* Higher transcendental functions. Vol. 2. McGraw-Hill Book Co., Inc., New York. 1953. p. 140

Can. J. Chem. Downloaded from www.nrcresearchpress.com by 210.87.254.42 on 09/05/12
For personal use only.

Can. J. Chem. Downloaded from www.nrcresearchpress.com by 210.87.254.6 on 09/05/12
For personal use only.

CHARGE TRANSFER AND ELECTRON CAPTURE IN THE RADIOLYSIS OF ALIPHATIC HYDROCARBONS[1]

P. J. DYNE
Research Chemistry Branch, Atomic Energy of Canada Limited, Chalk River, Ontario
Received January 4, 1965

ABSTRACT

A mechanism is suggested for the radiolysis of hydrocarbons. Both ions and excited molecules are produced in the initial excitation. Ion–electron recombination leads to the formation of excited molecules which have similar properties to those formed initially; all subsequent decomposition proceeds through these excited molecules. In mixtures of hydrocarbons, ions and molecules may undergo positive charge exchange and additives reduce the hydrogen yield by capturing electrons or reacting with the positive ion. The mechanism provides a rationalization for a variety of observations.

This paper presents a mechanism for part of the radiolytic decomposition of hydrocarbons in which electron capture and charge exchange play a dominant role. There is no novelty in postulating these reactions as mechanistic steps. The significance of electron capture has been discussed on many occasions by Hamill and his colleagues (see, for instance, refs. 1, 2, 3). Charge exchange was proposed by Hardwick (4) as a mechanism for the reactivity transfer observed in mixtures of aliphatic hydrocarbons and has also been suggested by Hamill. The crux of this proposed mechanism lies in the combination of two hypotheses, first, that the initial act of excitation leads to the formation of both ions and excited molecules and secondly, that, in pure hydrocarbons, the recapture of the electron by the positive ion also leads to the formation of excited molecules which are, for practical purposes, identical to these formed in the initial excitation. The mechanism provides an explanation for a variety of phenomena; viz., the rapid inhibition of part but not all of the hydrogen yield by solutes, reactivity transfer in mixtures of aliphatic and alicyclic hydrocarbons, and the effects of additives on the isotopic composition of radiolytic hydrogen produced from mixtures containing deuterated hydrocarbons.

The Mechanism

(*1*) Radiolysis of a hydrocarbon A produces, initially, positive ions, an equivalent number of electrons, and excited, un-ionized molecules A*.

[1*a*] [1*b*]
$$A \rightsquigarrow \begin{cases} A^+ + e^- \\ A^* \end{cases}$$

The yields of ions and excited molecules are comparable and probably $\sim 3/100$ eV absorbed.

(*2*) The recapture of the electron by the positive ion produces an excited species which is, for the purposes of the present discussion, identical with A* produced in [1*b*].

[2]
$$A^+ + e^- \rightarrow A^*$$

(*3*) In mixtures of hydrocarbons, A and B, charge exchange may occur.

[3*a*]
$$A^+ + B \rightarrow B^+ + A$$

[3*b*]
$$B^+ + A \rightarrow A^+ + B$$

[1]*Issued as AECL No. 2174.*

The ionization potentials of the hydrocarbons will determine the preferred direction of charge exchange, that is, whether [3*a*] or [3*b*] is preferred.

(*4*) Solutes S may react rapidly with electrons formed in [1*a*] to give negative ions.

[4] $$S + e^- \rightarrow S^-$$

(*5*) When reaction [4] occurs electron capture [2] is replaced by electron transfer which does not lead to the excited species A*.

[5*a*] $$S^- + A^+ \rightarrow S + \text{not-A}^*$$

It is also possible that solutes S react with the positive ions A^+. In this process and the subsequent electron capture, products other than A* are formed.

[5*b*] $$S + A^+ \text{ (and later, } + e^-) \rightarrow \text{not-A}^*$$

(*6*) In a pure hydrocarbon the intermediate A* is therefore the precursor of all subsequent reactions. In the experiments we are discussing we shall be interested almost exclusively in the decompositions which give hydrogen gas. For this decomposition, we postulate that A* can decompose in two ways: (i) to give a reactive intermediate X_H which reacts further with other hydrocarbon molecules to give H_2, or (ii) to give hydrogen by molecular detachment.

[6*a*] $$A^* \nearrow X_H + \text{products}$$

[6*b*] $$A^* \searrow H_2 + \text{products}$$

[7] $$X_H + A \rightarrow H_2 + \text{products}$$

In a mixture of deuterated and non-deuterated hydrocarbons HD can only be formed through reactions [6*a*] and [7] and, for dilute solutions of the deuterated hydrocarbon, D_2 is only formed by [6*b*].

The number of excited states formed initially is, of course, large. This initial spectrum of excitation is, however, rapidly changed by processes of internal conversion to a more restricted spectrum of states which can decompose in relatively few ways. In studying hydrogen yields we observe only those excited states which decompose to give molecular hydrogen or its precursors. It happens that all these excited states appear alike, and we describe the spectrum as consisting of only one state, A*. Other experiments might, very well, resolve A* into a number of components.

Formal Structure of the Mechanism

It is useful to note the logical structure of this mechanism without identifying species as ions, electrons, or excited molecules, etc. Radiolytic decomposition of a hydrocarbon proceeds via two precursors A′ and A″.

[I*a*] [I*b*] $$A \rightsquigarrow \begin{cases} A' \\ A'' \end{cases}$$

A′ can relatively slowly be converted to A″.

[II] $$A' \rightarrow A''$$

In mixtures of hydrocarbons change of identity reactions can occur.

[III*a*] $$A' + B \rightarrow B' + A$$

or

[III*b*] $$B' + A \rightarrow A' + B$$

Solutes may react with A′.

[IV] $$S + A' \rightarrow \text{not-A}''$$

Can. J. Chem. Downloaded from www.nrcresearchpress.com by 210.87.254.6 on 09/05/12
For personal use only.

A″ is the precursor of all subsequent reactions. Our mechanism makes the identification $A' \equiv A^+ + e^-$, $A'' \equiv A^*$. Any other species having the properties required by reactions [I] to [IV] above would provide satisfactory rationalizations of experiment.

Discussion of the Mechanism

We will now point out the features of hydrocarbon radiolysis which are rationalized by this mechanism. While some new experimental results are reported most of the data are already published.

1. Ions and Electrons in Liquids and Solids

The key hypothesis in the mechanism is firstly, that the yields of ions in a condensed phase is an appreciable fraction of the total product yield and, secondly, that the recombination of electron and positive ion may be slow compared to the rate of electron capture by solutes and to the rate of charge exchange processes. The major support for this comes from the work of Hamill and his colleagues on the radiolysis of organic glasses at liquid nitrogen temperature (3). They found that electrons can be captured by solutes in these glasses to give known anions. The maximum yield of anions, ~ 3, is equated to the yield of electrons. In some materials (methyl tetrahydrofuran, methyl pentene, and ethanol) the glass itself captures ("traps") electrons. Although trapped electrons are not observed in any significant yield in pure alkanes, solute anions can be observed in them (5). The non-appearance of trapped electrons in alkanes is, consequently, attributed to the absence of traps rather than to the absence of electrons.

Measurements of the conductivity of irradiated alkanes show a much lower yield (0.1–0.3) of electrons (6, 7). In these measurements an electric field is applied to the system to extract ions and electrons. These measurements only detect the fraction of electrons which escape recombination in the parent spur. It is assumed in the mechanism discussed here that efficient electron scavenging, at high concentrations of solute, takes place in the spur volume itself so that electrons undetected in conductivity measurements may, nevertheless, take part in reactions with electron scavengers.

2. Processes Which Reduce the Hydrogen Yield

Small concentrations of many substances reduce the yield of hydrogen and other products from aliphatic hydrocarbons. This effect has been intensively studied and we will first summarize the principal observations.

(*a*) A small concentration ($\sim 1\%$) of an additive produces a sharp decrease of the hydrogen yield; at a greater concentration ($\sim 3\%$), where the product yield is about half that in the pure material, the decrease in product yield with increasing concentration is much slower. This effect of concentration, which is found in so many systems that it seems to be a universal observation, is generally interpreted in terms of two decomposition modes, one of which is inhibited by the solute; the other is unaffected. We have called these modes respectively the inhibited and the residual yields (8). While these two modes have been identified in a variety of ways (8) there has been no clear demonstration from a product analysis in the radiolysis of a single aliphatic hydrocarbon that the decomposition paths of the two modes lead to different products; on the contrary, isotopic experiments showed that the decomposition paths were identical (9).

(*b*) Isotopic experiments (10) have also shown conclusively that, in many cases, the additive interacts by a physical mechanism (like energy transfer or charge transfer) on an intermediate which is the precursor of both molecular detachment processes and of bimolecular processes for the formation of molecular hydrogen. The clearest evidence that this physical process may be electron capture comes from the work of Scholes and

Can. J. Chem. Downloaded from www.nrcresearchpress.com by 210.87.254.6 on 09/05/12
For personal use only.

Simic (11) who have shown that nitrous oxide, a good electron scavenger, reduces $G(H_2)$ from cyclohexane. The rate constant for reaction of nitrous oxide with electrons is $\sim 10^5$ greater than that for reactions with hydrogen atoms (12, 13). Solutions of nitrous oxide in cyclohexane showed a reduced hydrogen yield and a yield of nitrogen which is somewhat greater than the reduction in hydrogen yield. They further found that in solutions of nitrous oxide with either carbon tetrachloride or benzene, the nitrogen yields were consistent with a further competition for electrons between nitrous oxide and the other solutes. The ratio of the electron affinities of N_2O:CCl_4:C_6H_6 was in accord with other measurements.

These conclusions are in accord with several experimental studies performed in these laboratories. Detailed product analyses in the cyclohexane–benzene (14) and cyclohexane – carbon tetrachloride (15) systems have shown that the primary interactions in reactions giving hydrogen gas are physical and not chemical, i.e. they do not involve the making or breaking of a chemical bond. For carbon tetrachloride, electron capture was one of the possible physical interactions which was suggested by direct chemical evidence (the yield of Cl^-). There is, therefore, a considerable body of interlocking evidence supporting the hypothesis that electron capture is, for several solutes, a significant mode of interaction. If this is accepted then most of the other steps in this mechanism are logically required by the experimental evidence.

The yield of hydrogen occupies a crucial position in this mechanism as we suppose that its formation is directly related to the formation of the excited state A*. While it appears that many solutes inhibit the formation of hydrogen it does not follow that all other decompositions are inhibited. On the contrary, reactions following electron capture may lead to a net increase in decomposition (as is shown in the detailed product analysis of the C_6H_{12}–CCl_4 system (15)) even though the yields of some products, hydrogen in particular, may be reduced. The two decomposition modes are now interpreted as being due to the formation of ions and electrons (the inhibited yield) and to the formation of excited molecules (the residual yield). Since, however, the whole decomposition proceeds after electron–ion recombination through the same excited species, there is no essential difference in products in the two regimes.

The formation of ions and excited species should be a general phenomenon, not restricted to hydrocarbons. The separation of the yields into two parts should therefore be observable in other systems. This has indeed been found by Lee and Armstrong in the radiolysis of HCl and HBr (16). Part of the hydrogen yield was produced via the reaction of electrons with positive ions; this was inhibited by electron scavengers such as bromine or sulfur hexafluoride. The rest of the yield proceeds via decompositions which do not involve thermal electrons. Our proposed mechanism for hydrocarbons has several features in common with those suggested by Armstrong for hydrogen halides.

While we are emphasizing in this paper the role of electron capture processes in the radiolysis of hydrocarbons, it should be noted that the positive ion is also an intermediate which may have a high reactivity. As pointed out, reaction [5*b*], a reaction with the positive ion would also prevent the formation of A* and lead to many effects which, in simple experiments such as measurements of the hydrogen yield, would be indistinguishable from those produced by electron capture.

3. Electron Scavenging and Spur Reactions

In organic glasses the electron, formed in the initial ionizing step, is trapped at a small distance, 100 Å or less, from the positive ion. If this distance is appropriate to liquid hydrocarbons then the process of electron capture by a solute is competing with the

Can. J. Chem. Downloaded from www.nrcresearchpress.com by 210.87.254.6 on 09/05/12
For personal use only.

recombination of ions and electrons in a spur, or in the geminate recombination of an ion–electron pair. The competition is kinetically equivalent to the reactions of radical scavengers in the radiolysis of water where the scavenger competes for free radicals (H, e_{aq}^-, or OH) preventing their recombination in spurs to give molecular products H_2 and H_2O_2. We shall now show that the hydrogen yield in benzene–cyclohexane mixtures is predicted by the theories of diffusion-controlled kinetics which have been worked out for water.

Schwarz (17) found empirically that for a large number of solutes in water, the values of G/G_0 (where G_0 is the yield at infinitely low concentration of the additive and G the yield at concentration C) fall on a universal curve when plotted against log kC. The constant k is proportional to the rate constant for the reaction between the solute and the free radical. Schwarz also made a theoretical calculation where the constant k is found to be equal to BT where B is the rate constant for the solute – free radical reaction and T is a time related to (and defining) the initial size of the spur. This theoretical curve is shown in Fig. 1 with $BT = 0.1$. The experimental values of G/G_0 for the hydrogen yield in benzene-cyclohexane mixtures are in good agreement with the theoretical predictions.

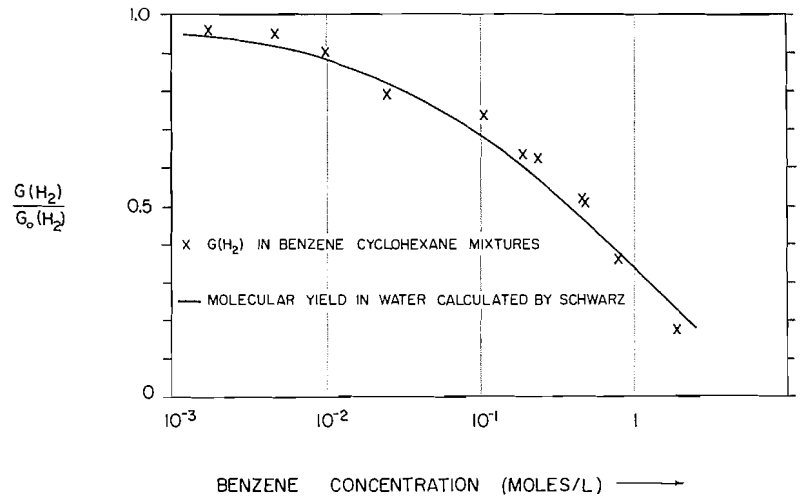

FIG. 1. Hydrogen yields from benzene–cyclohexane mixtures. The calculated curve is taken from Schwarz (17) with a correction to the concentration scale described in the text.

This agreement does not, however, mean that spur sizes and diffusion constants appropriate to water are equally relevant to the reactions of ions and electrons in organic systems. A rigorous treatment for the reactions we are postulating must include, amongst other things, the effect of Coulomb attraction in ion–electron recombination and the effect of electron energy, the rate of electron thermalization, and the energy dependence of the electron capture cross section on the probability of electron capture by a solute. The data in Fig. 1 indicate that inclusion of these effects has not made a large difference to the shape of the yield curve. This is, perhaps, to be expected when it is noted, from Kuppermann's review (18), that the shape of this yield curve is not markedly altered by quite drastic changes in the parameters of the model.

These conclusions are very similar to those proposed by Ffrancon Williams (19) to explain the kinetics of the formation of HD from solutions of ND_3 in cyclohexane. At

Can. J. Chem. Downloaded from www.nrcresearchpress.com by 210.87.254.6 on 09/05/12
For personal use only.

low concentrations of ND_3 ($< 10^{-3}$ M) ammonia reacts with positive ions which have not undergone recombination. At high concentrations, ND_3 competes in a spur reaction with the recombination of positive ions and electrons in spurs. The yield of HD, plotted against log [ND_3] is similar in shape to our figure except that G(HD) increases with scavenger concentration where, in our experiments $G(H_2)$ decreases. One curve is, as it were, the complement of the other. This interpretation implies that the distinction between the yields of ions and the yields of excited molecules is, in part, artificial; some ion–electron pairs have such a high probability of recombining that, except at very high scavenger concentrations, they, for all practical purposes, contribute to the yield of excited molecules and not to the ionic yield. The rigorous kinetic separation of the two yields is also made difficult by Freeman's observations (20) that there are other weak interactions observable at high additive concentrations which can be attributed to another energy transfer process. This corresponds, in our mechanism, to an interaction between A* and S.

The effects of solutes on yields in hydrocarbon systems have, hitherto, been calculated on the assumption that the reactions occurred homogeneously. While the experimental data do follow the predictions of many homogeneous mechanisms over a limited concentration range it is now clear that this agreement is fortuitous. Typical of these predictions is the 'scavenger plot' which states that $1/(G_0(H_2) - G(H_2)) \equiv 1/\Delta G(H_2)$ is a linear function of $1/c$ where $G_0(H_2)$ is the yield in the pure hydrocarbon and $G(H_2)$ is the yield at the concentration c (21). Klots, Raef, and Johnsen (22) have, however, recently shown that this function is not accurately obeyed over a wide concentration range. It is easy to verify that theoretical curves of the type calculated by Schwarz have all the numerical properties of the yield curves (G vs. concentration) found in organic systems, and for instance give linear plots of $1/\Delta G$ vs. $1/c$ over certain concentration ranges with a second segment at low concentrations as observed by Stone and Dyne (14).

4. Charge Exchange Processes

In the radiolysis of a hydrocarbon containing a small amount of a deuterated hydrocarbon the decomposition of the deuterated component is readily seen from the isotopic composition of the radiolytic hydrogen. Such experiments show a very large variation in the reactivity of cyclohexane-d_{12} and methyl-cyclohexane-d_{14} when mixed with other aliphatic and alicyclic hydrocarbons (23, 24). Recent experiments in this laboratory have shown that similar effects are found in mixtures of butane-d_{10}, propane-d_8, or ethane-d_6 with other aliphatic hydrocarbons (25). This reactivity transfer is not therefore restricted to cyclohexane or its derivatives.

From these experiments it appears that excitation produced in one component of a hydrocarbon mixture may be transferred to the second component. With the knowledge that electron capture processes can occur in hydrocarbons it is natural to suggest that this excitation transfer occurs by positive charge exchange. In a hydrocarbon mixture where components A and B are of comparable molecular weight then the ions A^+ and B^+ will be initially formed in a ratio close to that given by the mole ratio (or electron fraction). The number of ions A^+ and B^+ which decompose after charge transfer may be very different from this if one of the processes [3*a*] or [3*b*] is much more efficient than the other.

This charge transfer mechanism was first proposed by Hardwick (4) for these isotopic experiments and for others in which the total hydrogen yield in hydrocarbon mixtures was measured. Hardwick pointed out a general correlation: solvents with a higher ionization potential than the detector molecule (C_6D_{12} in our experiments) activated the detector molecule; solvents with a lower ionization potential deactivated it giving lower yields than for C_6D_{12} in C_6H_{12}. This correlation is also observed in the results obtained

Can. J. Chem. Downloaded from www.nrcresearchpress.com by 210.87.254.6 on 09/05/12
For personal use only.

by Stone and Quirt (25) using butane-d_{10}, propane-d_8, and ethane-d_6. A correlation of this nature is reasonable since charge transfer can only go in the exothermic direction.

5. The Effects of Additives on the Charge Transfer Process

The role of excited molecules in the radiolysis of hydrocarbons is seen most clearly in the effects of additives on hydrocarbon mixtures in which there is considerable activation of one component by charge transfer. These effects were discussed in some detail by Dyne, Denhartog, and Smith (10) and this discussion elaborates some of the ideas presented in that paper.

We will first show that a mechanism involving reactions of positive ions alone (the independent formation of A* by reaction [1*b*] being omitted) is inadequate. Since charge transfer and electron capture are independent processes charge transfer will continue until the solute anion S^- reacts with the positive ion. If ions were the only precursors of decomposition then the effects of charge transfer would still be apparent in the presence of solutes even though the total hydrogen yield is reduced. Put another way; in an isotopic mixture positive charge transfer to the deuterated hydrocarbon can lead to high percentage of D_2 and HD in the radiolytic gas. An electron scavenger would inhibit the production of hydrogen but the percentages of D_2 and HD in the gas would be the same as without the scavenger. This, however, is not what is observed; in activating solvents the yields of $G_1(D)$ and $g(HD)$[2] are reduced more rapidly than the yields of hydrogen (the percentage of D_2 and HD decreases). This is shown in Fig. 2 for the effects of CCl_4 on solutions of C_6D_{12} in *n*-hexane. (Figure 3 of ref. (10) is an example of similar data for the addition of benzoquinone to *c*-C_6D_{12} – *n*-hexane mixtures.) In solvents which are deactivating (i.e. in which the D_2 and HD yields are considerably lower than for solutions of *c*-C_6D_{12} in *c*-C_6H_{12}) the converse is observed; the D_2 and HD yields are reduced less rapidly than the total hydrogen yield (Fig. 3). The solvent here is decalin.

The solution to this difficulty is most clearly seen through Stone's detailed study of products in mixtures of cyclohexane with cyclopentane (26). Cyclopentane is an activating

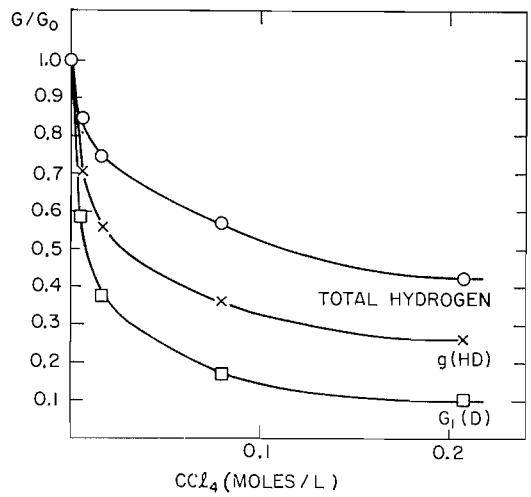

FIG. 2. Normalized yields of total hydrogen, $G_1(D)$, $g(HD)$ for additions of CCl_4 to cyclohexane-d_{12} – *n*-hexane mixtures. These data appear, in a different form, in ref. (10). The values of the normalizing constants G_0 are $G_0(H_2) = 5.1$, $G_1(D) = 2.6$, $g(HD) = 10.5$.

[2]*G_1(D) and g(HD) are, respectively, the yields of* D_2 *and* HD *per unit electron fraction of the deuterated hydrocarbon.*

Can. J. Chem. Downloaded from www.nrcresearchpress.com by 210.87.254.6 on 09/05/12
For personal use only.

solvent and so at low concentrations of cyclohexane the liquid products derived from cyclohexane, in particular cyclohexene, show enhanced yields. In the presence of solutes (iodine and carbon tetrachloride) no activation is observed; the yields of products derived from the two components are regular and follow the "mixture law."

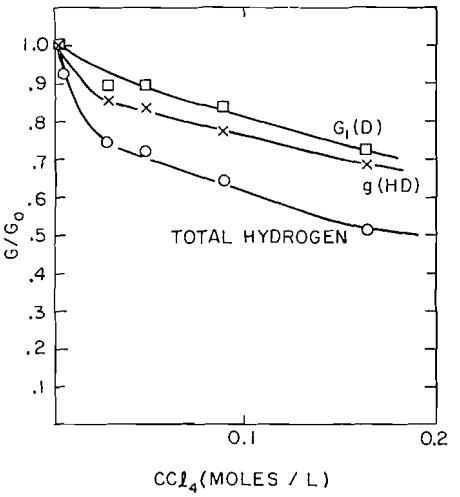

FIG. 3. Normalized yields of total hydrogen, $G_1(D)$, $g(HD)$ for additions of CCl_4 to cyclohexane-d_{12}–decalin mixtures. The values of the normalizing constants G_0 are G(total hydrogen) = 4.7, $g(HD)$ = 3.1, $G_1(D)$ = 0.15.

These observations lead us to postulate the existence of another precursor, other than the positive ion, which could not undergo a transfer reaction. This is the excited state A*. We shall now show that this mechanism predicts the effects of additives on the yields of D_2, HD, and D_2 for both activating and deactivating solvents. Suppose that the number of excited states and ions formed from the solvent are E_S and I_S and the numbers formed from the detector molecule (C_6D_{12}) are E_D and I_D. The yield of hydrogen from the pure solvent is then proportional to $(E_S + I_S)$, and

$$G_0(H_2) \simeq k(E_S + I_S).$$

In the presence of an electron scavenger which prevents the decomposition of some fraction of the ions the yield will be

$$G(H_2) \simeq k(E_S + \beta I_S)$$

when β is the fraction of ions unaffected by the solute. The reduction in the total yield, relative to the initial yield G_0 is

$$G(H_2)/G_0(H_2) \simeq (E_S + \beta I_S)/(E_S + I_S).$$

In the absence of charge transfer the same relation will apply to the detector molecule and the reduction in the D_2 yield, relative to $G_0(D_2)$, will be

$$\frac{G(D_2)}{G_0(D_2)} \simeq \frac{E_D + \beta I_D}{E_D + I_D}.$$

In an activating solvent the number of ions of the detector molecule will be increased by charge transfer by a number T.

$$G_0(D_2) \simeq k(E_D + I_D + T).$$

Can. J. Chem. Downloaded from www.nrcresearchpress.com by 210.87.254.6 on 09/05/12
For personal use only.

Can. J. Chem. Downloaded from www.nrcresearchpress.com by 210.87.254.6 on 09/05/12
For personal use only.

If the concentration of the detector molecule is small then the effect of charge transfer on the number of solvent ions is negligible and I_S is effectively unaltered (i.e. $I_S - T \simeq I_S$). Since the quenched part of the D_2 yield ($I_D + T$) is a larger part of the yield the D_2 yield will be reduced more rapidly than the hydrogen yield, i.e.

$$\frac{E_S + \beta I_S}{E_S + I_S} > \frac{E_D + \beta(I_D + T)}{E_D + I_D + T} \quad \text{or} \quad \frac{G(H_2)}{G_0(H_2)} > \frac{G(D_2)}{G_0(D_2)}.$$

If the solvent is deactivating the converse applies. The reduction in the D_2 yield will be

$$\frac{G(D_2)}{G_0(D_2)} \simeq \frac{E_D + \beta(I_D - T)}{E_D + I_D - T},$$

which is now greater than $G(H_2)/G_0(H_2)$. The D_2 yield will be reduced less rapidly than the hydrogen yield.

The effect of an additive on the yield of HD will be intermediate between its effect on D_2 and H_2. Neglecting isotope effects we can expect that approximately equal amounts of HD come from the reaction $X_D + RH \rightarrow HD + ----$ and from $X_H + RD \rightarrow HD + ----$ (RH and RD are respectively the "light" solvent and deuterated detector). The yield of X_D is affected by the charge transfer process but, again in dilute solutions of the detector the yield of X_H is unaffected. In an activating solvent that part of the HD yield formed via X_D will be rapidly reduced to the same extent as the D_2 yield; the part formed via X_H will only be reduced as the H_2 yield. The normalized HD yield will therefore fall more rapidly than H_2 but less rapidly than D_2. These effects for activating and deactivating solvents are shown in Figs. 2 and 3.

Nitrous oxide and sulfur hexafluoride show the same qualitative effects when added to solutions of *c*-C_6D_{12} in *n*-hexane as do carbon tetrachloride (Figs. 4 and 5).

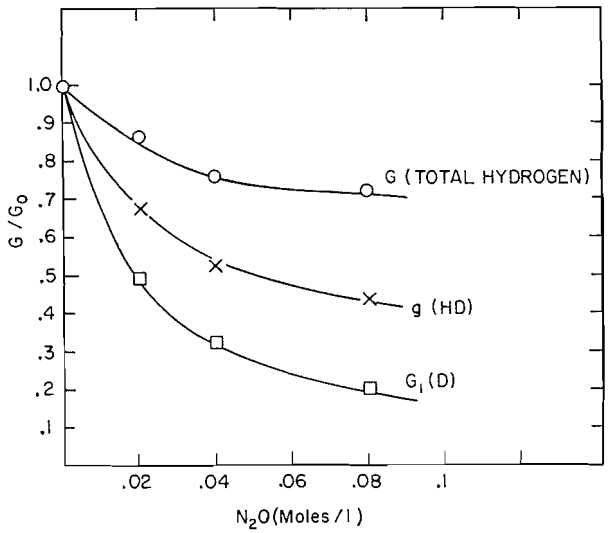

FIG. 4. Normalized yields of total hydrogen, $G_1(D)$ and $g(HD)$ for additions of nitrous oxide to cyclohexane-d_{12} – *n*-hexane mixtures. The normalizing constants are as for Fig. 2.

The simple theory presented here would predict a unique relation between G(total hydrogen) and $G_1(D)$; one is proportional to $E_S + \beta I_S$, the other is proportional to $E_D + \beta(I_D + T)$. Accordingly G(total hydrogen) and $G_1(D)$ should lie on a universal

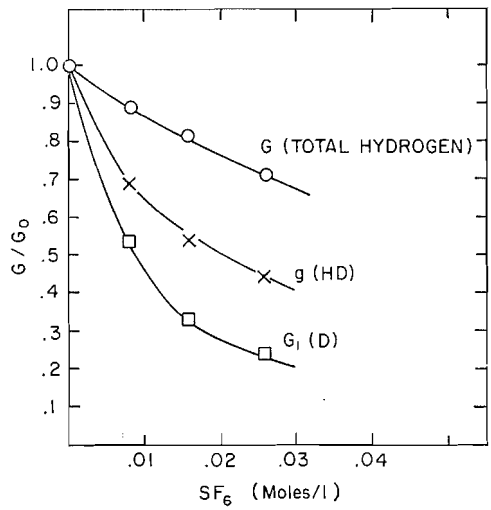

FIG. 5. Normalized yields of total hydrogen, G_1(D) and g(HD) for additions of sulfur hexafluoride to cyclohexane-d_{12} – n-hexane mixtures. The normalizing constants are as for Fig. 2.

curve for all solutes. This correlation was observed empirically in ref. (8). The data presented there are also shown in Fig. 6 with additional data for sulfur hexafluoride and nitrous oxide. This correlation is observed to a fairly high approximation. The data shown in Figs. 4 to 6 provide a link between our isotopic experiments for which we have hitherto presented a formal "physical" mechanism and the evidence for the electron capture step shown by the effects produced by N_2O and SF_6. As suggested by Toma and Hamill (3) some of the other additives we have studied, in particular cyclohexene and benzene, may undergo positive charge transfer with the positive ion ($C_6D_{12}^+$). The reaction [5*b*] would have, qualitatively, the same effect as electron capture in these isotopic experiments.

6. The Effect of Hydrogen Halides on the Radiolysis of Hydrocarbons

The yield of hydrogen from cyclohexane (and other aliphatic hydrocarbons) increases by about 1 G unit on the addition of hydrogen halides. Nash and Hamill (27) studied the isotopic composition of the hydrogen evolved from solutions of HI in C_6D_{12}. They suggested that the increase in yield arose from a competition between

$$C_6D_{12}^+ + e \rightarrow C_6D_{10} + D_2,$$
$$HI + e \rightarrow H + I^-,$$
$$I^- + C_6D_{12}^+ \rightarrow C_6D_{12} + I.$$

Electron capture by HI produces H atoms with a greater efficiency than the production of D_2 by neutralization of $C_6D_{12}^+$. The recombination of I^- and $C_6D_{12}^+$ produces no hydrogen. We would write Hamill's mechanism as follows (for HCl, the solute used in experiments carried out in this laboratory by J. Denhartog and M. G. Bailey).

$$C_6D_{12}^+ + e \rightarrow C_6D_{12}^* \begin{cases} \nearrow D_2 + \text{---} \\ \searrow X_D + \text{---} \end{cases}$$

[8] $$HCl + e \rightarrow Y_H + Cl^-, \; Y_H + C_6D_{12} \rightarrow HD$$

[9] $$Cl^- + C_6D_{12}^+ \rightarrow \text{not-}C_6D_{12}^*$$

Can. J. Chem. Downloaded from www.nrcresearchpress.com by 210.87.254.6 on 09/05/12
For personal use only.

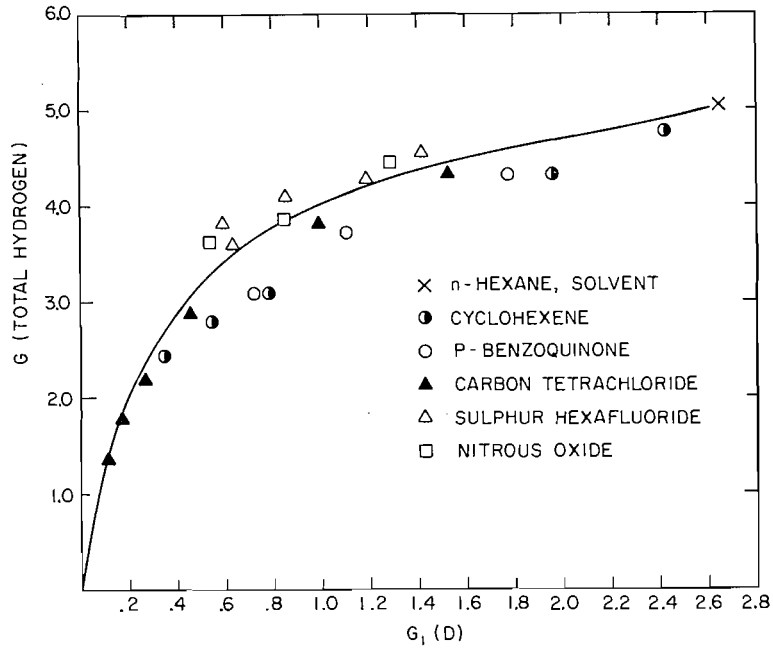

FIG. 6. Values of G(total hydrogen) from mixtures of C_6D_{12} in n-hexane plotted against G_1(D), the deuterium yield per unit mole fraction C_6D_{12}. The data for sulfur hexafluoride and nitrous oxide are new; other data were presented in ref. (10), Fig. 6.

We will now examine the effects of HCl on solutions of C_6D_{12} in an activating solvent, n-hexane. Using the notation of the previous section the yield of D_2 and HD will be proportional to $E_D + I_D + T$ and the yield of hydrogen will be proportional to $E_S + I_S$. If sufficient HCl is added to scavenge all electrons and prevent the reactions of all ions, then the D_2 yield will be reduced and will be proportional to E_D. The yield of ions $(I_D + T)$ is replaced by a somewhat larger yield $\gamma(I_D + T)$ of the intermediate Y_H where γ is the ratio of the efficiencies of processes [2] and [8], and the yield of ions I_S is replaced by a yield of $Y_H = \gamma(I_S)$. The yield of D_2 will be drastically reduced even though the total hydrogen yield is increased. This is observed experimentally (Fig. 7). The yield of HD will not be reduced as much for the following reasons. In the absence of HCl, HD is produced by the reaction of X_D on the light hydrocarbon and by the action X_H on the deuterated hydrocarbon. The presence of HCl suppresses the yield of X_D from decomposition of excited molecules. At the same time the yield of species Y_H (which will react to give HD as did X_H) will be increased in two ways. In the absence of HCl the ions $C_6H_{12}^+$ decompose after electron capture to give H_2 and X_H; i.e., only a fraction of the ions gave X_H. In the presence of HCl all ions give Y_H and in addition the efficiency of production of Y_H is greater than the total production of H_2 and X_H. There will, therefore, be a much larger yield of HD through the reactions of Y_H. The net effect will be a reduction of the yield of HD which is not as drastic as that for D_2.

This mechanism depends on the possibility that the efficiency of dissociative electron attachment (molecules decomposed / electrons captured) is greater for one molecule (HCl) than for the ion $C_6H_{12}^+$. There is evidence from other systems that dissociative electron attachment is less efficient for $C_6H_{12}^+$ than it is for other ions. Scholes and Simic (11) find that the yields of N_2 in solutions of N_2O in cyclohexane are greater than the

Can. J. Chem. Downloaded from www.nrcresearchpress.com by 210.87.254.6 on 09/05/12
For personal use only.

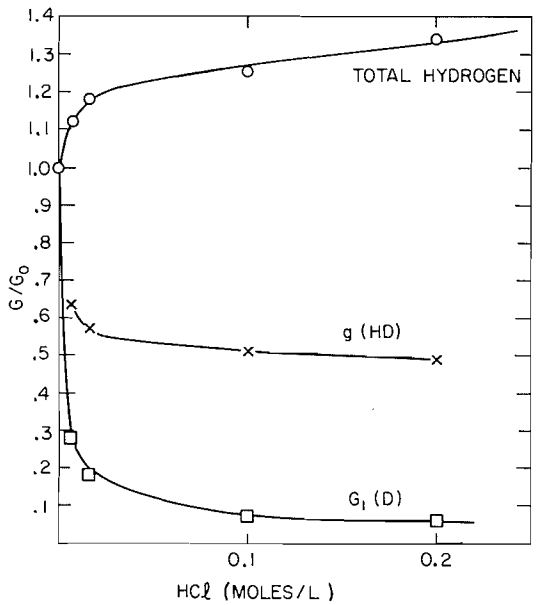

FIG. 7. Normalized yields of total hydrogen, $G_1(D)$, $g(HD)$ for additions of hydrogen chloride to cyclohexane-d_{12} – n-hexane mixtures. The normalizing constants are as for Fig. 2.

decrease in hydrogen yield and suggest that "N_2O can scavenge some electrons which do not normally lead to hydrogen gas." Stone and Dyne (15) found that, in solutions of CCl_4 in C_6H_{12}, the yield of HCl was greater than the decrease in hydrogen yield by as much as 1 G unit and that this was correlated with a larger number of cyclohexyl residues in the products. In their words "carbon tetrachloride enhances radiolytic action."

7. Problems Raised by this Mechanism

The main uncertainties in this mechanism stem from our ignorance of the rates or efficiences of ionic and electron capture reactions in liquids. In addition, as we believe that these reactions occur in spurs we have also to cope with the problems of non-homogeneous kinetics. Because of these difficulties we have so far only developed this mechanism qualitatively; much work has to be done before such a mechanism can be treated quantitatively. In this section we will review some of the problems which have to be treated in a quantitative theory.

Firstly, let us consider the efficiency of the charge transfer step. As can be seen from the following argument this efficiency is not very high in alkane mixtures. This efficiency can be estimated by comparing the sum of the yields of D_2 and HD in mixtures of c-C_6D_{12} in cyclohexane and n-hexane respectively. For a 5.5 mole % solution of c-C_6D_{12} the sum $G(D_2)$ and $G(HD)$ is 0.26 for cyclohexane as solvent and 0.7 for n-hexane as a solvent. The difference, 0.44 G units, is approximately the number of ions of C_6D_{12} formed by charge transfer from n-hexane ions. This is about one-tenth the total number of ions formed in the mixture if $G(e^-)$ is taken to be ~ 3. By contrast, Stone (28) finds very efficient charge transfer in solid mixtures of alkanes with krypton. In dilute mixtures of the hydrocarbon (~ 5 mole %) it appears that virtually all the krypton ions undergo charge transfer with neighboring hydrocarbon molecules since $G(H_2)$ in these mixtures is ~ 3. Although the efficiency of charge transfer is small in alkane mixtures the process must be fast compared to charge neutralization.

Can. J. Chem. Downloaded from www.nrcresearchpress.com by 210.87.254.6 on 09/05/12
For personal use only.

Charge transfer is exothermic and could presumably go to completion. What then limits the efficiency of the process? If it is limited by the time for charge neutralization then one would expect that more charge transfer might be observed in the presence of an electron-capturing solute since the negative ion will have a lower mobility than the free electron and would take longer to return to the positive ion. The efficiences of charge transfer processes in vapors are a related problem. We have shown that the activation processes observed in liquid mixtures are absent in the gas phase (10). According to this mechanism, therefore, charge transfer can occur in liquids but not in vapors. We have to conclude that charge transfer occurs slowly relative to the duration of a gas phase collision but can occur when the molecule and ion are held together in a solvent cage.

The kinetics of electron capture processes raises the perennial question of how far the electron gets away from the positive ion before it is thermalized and can be recaptured. When an electron-capturing solute is present, it must be remembered that the cross section for electron capture is energy dependent. With some solutes, electrons may more easily be captured before they are thermalized. For this reason it could be argued that, at certain concentrations, electron capture by a solute could even reduce the time for positive ion neutralization.

ACKNOWLEDGMENTS

The new experimental data on solutions containing N_2O and SF_6 were obtained by Mr. J. Denhartog. It is a pleasure to acknowledge his experimental work, and, in addition, the many entertaining and enlightening discussions I had with Dr. J. A. Stone on the substance of this paper.

REFERENCES

1. L. J. Forrestal and W. H. Hamill. J. Am. Chem. Soc. **83**, 1535 (1961).
2. M. R. Ronayne, J. P. Guarino, and W. H. Hamill. J. Am. Chem. Soc. **84**, 4230 (1962).
3. S. Z. Toma and W. H. Hamill. J. Am. Chem. Soc. **86**, 1478 (1964).
4. T. J. Hardwick. J. Phys. Chem. **66**, 2132 (1962).
5. J. P. Guarino and W. H. Hamill. J. Am. Chem. Soc. **86**, 777 (1964).
6. A. O. Allen and A. Hummel. Discussions Faraday Soc. **36**, 95 (1963).
7. G. R. Freeman. J. Chem. Phys. **39**, 988 (1963).
8. P. J. Dyne, D. R. Smith, and J. A. Stone. Ann. Rev. Phys. Chem. **14**, 313 (1963).
9. P. J. Dyne and W. M. Jenkinson. Can. J. Chem. **39**, 2163 (1961).
10. P. J. Dyne, J. Denhartog, and D. R. Smith. Discussions Faraday Soc. **36**, 135 (1964).
11. G. Scholes and M. Simic. Nature, **202**, 895 (1964).
12. S. Gordon, E. J. Hart, M. Matheson, J. Rabani, and J. K. Thomas. Discussions Faraday Soc. **36**, 214 (1963).
13. F. S. Dainton and D. B. Peterson. Proc. Roy. Soc. London Ser. A, **267**, 443 (1962).
14. J. A. Stone and P. J. Dyne. Radiation Res. **17**, 353 (1962).
15. J. A. Stone and P. J. Dyne. Can. J. Chem. **42**, 669 (1964).
16. R. A. Lee and D. A. Armstrong. Nature, **200**, 552 (1963).
17. H. A. Schwarz. J. Am. Chem. Soc. **77**, 4960 (1955).
18. A. Kuppermann. *In* The chemical and biological action of radiations. *Edited by* M. Haissinsky. Masson et Cie. 1961.
19. Ffrancon Williams. J. Am. Chem. Soc. **86**, 3954 (1964).
20. G. R. Freeman. J. Chem. Phys. **33**, 71 (1960).
21. G. E. Adams, J. H. Baxendale, and R. D. Sedgwick. J. Phys. Chem. **63**, 854 (1959).
22. C. E. Klots, Y. Raef, and R. H. Johnsen. J. Phys. Chem. **68**, 2040 (1964).
23. P. J. Dyne and J. Denhartog. Can. J. Chem. **40**, 1616 (1962).
24. P. J. Dyne and J. Denhartog. Can. J. Chem. **41**, 1794 (1963).
25. J. A. Stone and A. Quirt. Private communications.
26. J. A. Stone. Can. J. Chem. **42**, 2872 (1964).
27. J. R. Nash and W. H. Hamill. J. Phys. Chem. **66**, 1097 (1962).
28. J. A. Stone. Can. J. Chem. **43**, 809 (1965).

Can. J. Chem. Downloaded from www.nrcresearchpress.com by 210.87.254.6 on 09/05/12
For personal use only.

Can. J. Chem. Downloaded from www.nrcresearchpress.com by 210.87.254.42 on 09/05/12
For personal use only.

THE STRUCTURE OF HOMOCHASMANINE[1]

O. ACHMATOWICZ, JR.[2] AND LÉO MARION
Division of Pure Chemistry, National Research Council, Ottawa, Canada

Received January 6, 1965

ABSTRACT

The structure of homochasmanine, a new alkaloid isolated from *Aconitum chasmanthum* Stapf, has been determined. Its empirical formula is $C_{26}H_{43}O_6N$ and the spectroscopic evidence shows that the base contains five methoxyl and one hydroxyl group. The presence of the hydroxyl group is confirmed by the formation of a monoacetyl derivative. That homochasmanine is 8-*O*-methylchasmanine has been shown by the synthesis of this substance from the previously known diacetylchasmanine.

Five alkaloids have been reported as occurring in *Aconitum chasmanthum* Stapf (1). The structure of four, i.e., indaconitine (2), chasmaconitine (1), chasmanthinine (1), and chasmanine (3) have already been determined. The fifth alkaloid, obtained from the fraction containing the strong bases, was initially identified as base A. It is now proposed to name it homochasmanine.

Homochasmanine has the empirical formula $C_{26}H_{43}O_6N$, m.p. 105–107°, $[\alpha]_D^{25}$ +19.2°. It is not stable and gradually decomposes on standing. Its infrared spectrum contains a band at 3 420 cm^{-1} indicative of a hydroxyl group, but no carbonyl absorption. The nuclear magnetic resonance (n.m.r.) spectrum shows five methoxyl signals (δ 3.36, 3.32, 3 30, 3.24, 3.23) and a triplet centered at δ 1.07 characteristic of an imino-ethyl group. The five methoxyl groups and one hydroxyl account for all the oxygen present in the molecule. The presence of a hydroxyl indicated by the infrared spectrum is confirmed by acetylation of the base to a monoacetate that could not be induced to crystallize, but was homogeneous in thin layer chromatography. In the infrared the monoacetate showed a carbonyl absorption band at 1 725 cm^{-1}, while its n.m.r. spectrum contained signals for five methoxyl groups, δ 3.32 (6H), 3.30 (3H), 3.22 (6H), a signal at δ 2.03 attributable to the three protons of the acetyl group, a triplet centered at δ 1.07 due to the imino-ethyl, and a poorly resolved triplet at δ 4.77 that will be referred to later.

The empirical formula of homochasmanine ($C_{26}H_{43}O_6N$) differs from that of chasmanine ($C_{25}H_{41}O_6N$) in that it contains an additional CH_2. Whereas chasmanine contains two hydroxyl and four methoxyl groups, homochasmanine contains one hydroxyl and five methoxyl groups. It was therefore assumed, as a working hypothesis, that homochasmanine was an *O*-methylchasmanine. From the structure of chasmanine I, it is obvious that the additional methyl group in homochasmanine can be linked to the oxygen only

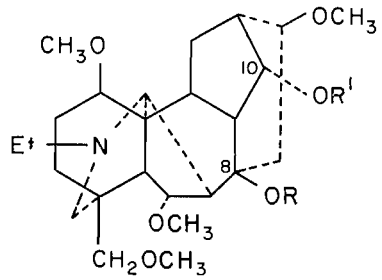

I, R = R' = H
II, R = CH_3, R' = H
III, R = R' = Ac

[1]*Issued as N.R.C. No. 8360.*
[2]*National Research Council of Canada Postdoctorate Fellow.*

at C-8 or C-10. In the light of the assumption of the structure of homochasmanine, the poorly resolved triplet at δ 4.77 in the n.m.r. spectrum of monoacetylhomochasmanine would be attributable by analogy with many other cases (4) to a proton located on the carbon carrying the ester group. This carbon must be flanked by two neighboring protons to account for the splitting of the signal into a triplet. Of the two hydroxyls present in chasmanine only that at C-10 fills these conditions and hence it must be the C-8 position that carries a methoxyl so that homochasmanine should be 8-*O*-methylchasmanine II.

In order to confirm or disprove this conclusion we made use of the reaction whereby the acetoxy group at C-8 in aconitine (5) or in delphinine (6) is replaced by a methoxyl when the base is heated under pressure with methanol. Diacetylchasmanine III prepared from chasmanine (3) and heated in a sealed tube with methanol gave rise to an amorphous product which after saponification crystallized readily, m.p. 105–107°, $[\alpha]_D^{25}$ +19.4°. This base was identical in every respect with homochasmanine.

Homochasmanine, therefore, is 8-*O*-methylchasmanine and is represented by structure II. This is the first reported natural occurrence of a highly oxygenated diterpenoid alkaloid containing an *O*-methyl group in the C-8 position. It is conceivable that homochasmanine might be an artifact formed during the extraction of the alkaloids. It should be pointed out, however, that chasmanine itself was not methylated under the conditions in which diacetylchasmanine was converted into monoacetylhomochasmanine and also that no alkaloid corresponding to an ester of chasmanine was found in the plant.

EXPERIMENTAL

The infrared spectra were taken in Nujol mulls on a Perkin–Elmer double beam Model 21B spectrometer. The n.m.r. spectra were measured in chloroform solution containing tetramethylsilane as an internal reference on a Varian A-60 instrument. For column chromatography Woelm Grade IV neutral alumina was used, and for thin layer chromatography the adsorbent was Merck silica gel G, the developing solvent cyclohexane–chloroform–diethylamine. Melting points were taken on a Kofler hot stage and were not corrected.

Homochasmanine

The alkaloid was isolated from the crude basic extract of *Aconitum chasmanthum* Stapf as reported previously (1). It was purified by repeated crystallization in *n*-hexane from which it separated as clumps of colorless prisms, m.p. 105–107°, $[\alpha]_D^{25}$ +19.2° (*c*, 2.4 in EtOH). The base is unstable and decomposes gradually at room temperature. Found: C, 67.32; H, 9.07; N, 2.96. Calcd. for $C_{26}H_{43}O_6N$: C, 67.06; H, 9.31; N, 3.01%. Infrared: ν_{max} 3 420 cm^{-1} (OH), 1 110, 1 093 cm^{-1} (OCH_3). In the n.m.r. spectrum: singlets at δ 3.36 (3H), 3.32 (3H), 3.30 (3H), 3.24 (3H), 3.23 (3H), triplet centered at δ 1.07 (3H).

Acetylhomochasmanine

Homochasmanine (25 mg) and *p*-toluenesulfonic acid (20 mg) in acetic anhydride (2 ml) were heated for 1 h on a steambath. The reaction mixture, worked up as usual, gave a gummy monoacetate (21 mg). Infrared: ν_{max} 1 725 cm^{-1} (CO). In the n.m.r. spectrum: singlets at δ 3.32 (6H), 3.30 (3H), 3.22 (6H), 2.03 (3H), triplet at δ 1.07 (3H), and a poorly resolved triplet at δ 4.77.

Partial Synthesis of Homochasmanine

Diacetylchasmanine (52 mg), prepared as described previously (3), dissolved in methanol (5 ml) was heated in a sealed tube at 120–130° for 1 h. The solvent was evaporated and the residue, dissolved in *n*-hexane, was chromatographed on alumina. Elution first with *n*-hexane and then with *n*-hexane – benzene (1:1) produced a homogeneous gum (42 mg), the infrared spectrum of which contained a band at 1 725 cm^{-1}. In thin layer chromatography, it had the same mobility as the monoacetate described above. The product was refluxed for 30 min with 2% methanolic potassium hydroxide (5 ml), the solvent evaporated, and the residue dissolved in water. Extraction of the aqueous solution with chloroform and evaporation of the extract yielded a gum (31 mg) that solidified when triturated with *n*-hexane. The gum was dissolved in *n*-hexane, chromatographed on alumina, and eluted with the same solvent. The eluate on evaporation left a residue that crystallized from *n*-hexane as clumps of colorless prisms, m.p. 105–107°, $[\alpha]_D^{25}$ +19.4° (EtOH). This basic product proved to be identical with homochasmanine in every respect (melting point, mixture melting point, and infrared absorption spectra).

Can. J. Chem. Downloaded from www.nrcresearchpress.com by 210.87.254.42 on 09/05/12
For personal use only.

ACKNOWLEDGMENTS

We acknowledge with thanks our indebtedness to Mr. R. Lauzon who measured the infrared spectra and to Mr. M. Lesage for the n.m.r. spectra.

REFERENCES

1. O. ACHMATOWICZ, JR. and L. MARION. Can. J. Chem. **42**, 154 (1964).
2. R. GILMAN and L. MARION. Tetrahedron Letters, No. 20, 923 (1962); Can. J. Chem. **42**, 2700 (1964).
3. O. ACHMATOWICZ, JR., Y. TSUDA, L. MARION, T. OKAMOTO, M. NATSUME, H. S. CHANG, and K. KAJIMA. Can. J. Chem. **43**, 825 (1965).
4. Y. TSUDA and L. MARION. Can. J. Chem. **41**, 1634 (1963).
5. H. SCHULZE. Arch. Pharm. **244**, 165 (1906).
6. W. A. JACOBS and L. C. CRAIG. J. Biol. Chem. **128**, 431 (1939).

Can. J. Chem. Downloaded from www.nrcresearchpress.com by 210.87.254.42 on 09/05/12
For personal use only.

Can. J. Chem. Downloaded from www.nrcresearchpress.com by 210.87.254.5 on 09/05/12
For personal use only.

CATION EXCHANGE IN ANHYDROUS ETHYLENEDIAMINE

WALTER R. HEUMANN, ONIL DIONNE, AND GILLES TREMBLAY
Département de Chimie, Université de Montréal, Montreal, Quebec

Received October 16, 1964

ABSTRACT

The swelling of the strongly acid cation exchangers Dowex 50W of various degrees of cross-linking is markedly less in ethylenediamine than in water. However, it is sufficient for exchange reactions to occur. In contrast with aqueous solutions, electrolytes dissolved in ethylenediamine cause the swelling to increase, which is attributed to the low degree of dissociation attainable in this solvent. This explanation is supported by the observation that in water slightly dissociated electrolytes also produce a slight increase in swelling. Exchange reactions were carried out successfully with the slightly cross-linked resin Dowex 50W-X2. The bromide, ethoxide, aminoethoxide, and 2-aminoethylamide of lithium exchanged the latter cation with other alkali metals or tetrabutylammonium easily.

INTRODUCTION

Little is known on the behavior of ion exchange resins in strongly basic anhydrous solvents. Keenan and McDowell (1) reported briefly on the possibility of exchanging potassium and ammonium in anhydrous liquid ammonia. For ion exchange to take place between a resin and an electrolyte in solution, the solvent must be capable of penetration into the resin, and thus to cause swelling of the resin network. For a given exchange resin the maximum swelling in a particular solvent depends largely on the solvent's polarity as expressed by its dielectric constant ϵ, the degree of swelling being high with highly polar solvents and nil with nonpolar solvents. Ethylenediamine is only moderately polar, its dielectric constant being about 12.5 at 25 °C. Ion exchange resins could, therefore, not be expected to swell very much in this solvent, and it was by no means certain that ion exchange reactions would be easy to accomplish in this medium. It was the purpose of the present investigation to establish whether and under what conditions cation exchange in ethylenediamine could be possible.

The exchangers studied were the strongly acid cation exchangers Dowex 50W (sulfonated polystyrene divinylbenzene copolymers) of various degrees of cross-linking. All exchangers used had either lithium, a small inorganic ion, or tetrabutylammonium, a large organic ion, as their counterions. The extent of swelling of all samples in pure anhydrous ethylenediamine and its variation with the degree of cross-linking were determined. For the purpose of comparison, the swelling of identical samples was also determined in water, a highly polar solvent (ϵ = 78.5 at 25 °C), and in anhydrous methanol, a solvent of intermediate polarity (ϵ = 32.6 at 25 °C). To some extent, the influence of solutes in the ethylenediamine phase on the swelling was also investigated. Finally, several exchange reactions between the ions lithium, sodium, potassium, and tetrabutylammonium were carried out. These ions were present in the liquid phase either as alkoxides or amides.

EXPERIMENTAL

Exchangers

The exchangers used were the commercial resins Dowex 50W of 30–50 mesh/in. size of the dry material, having cross-linking degrees corresponding to 1, 2, 4, and 8% divinylbenzene (DVB) content respectively, and being labelled accordingly X1, X2, etc. The resins were thoroughly washed with deionized water, converted into either the lithium or tetrabutylammonium form, dehydrated by drying for at least 20 h at 115–120 °C, and weighed. Exchange capacities were determined by alkalimetric titration of the hydrogen form as described by Kunin (2).

Can. J. Chem. Downloaded from www.nrcresearchpress.com by 210.87.254.5 on 09/05/12
For personal use only.

Ethylenediamine

Anhydrous ethylenediamine was prepared from commercial material of at least 98% purity by first drying for several days with porous barium oxide (Barium and Chemicals, Inc., Willoghby, Ohio). The liquid was decanted into a vacuum distilling apparatus equipped with Teflon-sleeved ground glass joints and Teflon stopcocks. Liquid potassium–sodium alloy containing 78% potassium was added from a separatory funnel in successive portions until a persistent dark-blue coloration of the solution was obtained. This liquid alloy offers the advantage of dissolving much faster than either one of the two solid metals. It is easily prepared by mixing small pieces of the two metals in a separatory funnel under a high-boiling hydrocarbon having a density of less than 0.84, such as *n*-decane or *n*-dodecane. Vacuum distillation of the blue ethylenediamine solution at a temperature not exceeding 40 °C in presence of an excess of alkali metal finally gave the pure anhydrous solvent. Boiling at higher temperatures in presence of potassium can cause loss by polymerization (formation of dark-brown residues).

Lithium 2-Aminoethoxide $LiOC_2H_4NH_2$

A 0.5 *M* solution in ethylenediamine was prepared by first dissolving under anhydrous conditions 700 mg of pure lithium metal in 80–100 ml of liquid ammonia kept well below its boiling point in an ethanol – dry ice bath. After complete dissolution of the metal, which was attained after several minutes, anhydrous 2-aminoethanol (approximately 6 ml) was added slowly from a burette until the dark-blue solution became colorless. The reaction was complete within 15 min. The ammonia was allowed to evaporate from this solution of lithium 2-aminoethoxide and was gradually replaced by ethylenediamine until a volume of 200–220 ml was reached. The solution was transferred to a glove box containing dry nitrogen and filtered over a rapid filtering folded paper such as Whatman No. 40 or 541. This filtration removed any lithium hydroxide which could have formed, since it was found to be insoluble in ethylenediamine, forming a gelatinous precipitate.

Note. Pure alkali 2-aminoethoxides cannot be prepared by direct reaction of the metals with the amino-alcohol, as a side reaction takes place by which volatile decomposition products are formed.

Lithium 2-Aminoethylamide $LiNHC_2H_4NH_2$

The commercially available product of 97–98% purity (Foote Mineral Co., Exton, Pennsylvania) was used to prepare its ethylenediamine solution, which is dark-blue to violet. Its composition and purity were checked by decomposing a weighed sample with an excess of water and titrating the resulting aqueous solution conductometrically with standard hydrochloric acid. Three distinct equivalence points, corresponding to lithium hydroxide and the two basic functions of ethylenediamine respectively, could easily be established. The lithium content was determined by flame photometrical analysis of the aqueous solution.

Swelling Measurements

All experiments with both ethylenediamine and methanol were carried out in a glove box in an atmosphere of dry nitrogen. To determine volumes of swollen resins, weighed samples of anhydrous resins were placed in glass-stoppered graduated cylinders, mixed with solvent, and shaken from time to time until constant volumes were attained. The volumes of the resin layers as read by the cylinder graduation were taken as the volumes of the resin phase. These somewhat arbitrary measurements were considered satisfactory for the purpose of this investigation, although the true volumes of the resin were slightly smaller.

Exchange Columns

For the ion exchange reactions which were likewise carried out in a glove box, a glass column of 14 × 240 mm was used, fitted at the top with a 100 ml ampoule connected by a tapered joint with Teflon sleeve. The flow rate was controlled by a "Lab-Crest" Teflon needle valve (Fischer & Porter Co., Warminster, Pa.). All connections between glass tubes were of thin-walled Teflon tubing. This column was adequate for work with 25–30 milliequivalents (meq) of exchanger. Exchange reactions were carried out between this amount of exchanger and 2–5 meq of electrolyte in 0.1–0.3 *M* solutions in ethylenediamine with flow rates between 0.1 and 0.3 ml/min.

Analyses

The composition of both the resin samples and ethylenediamine solutions could always be found by flame photometric determination of one or two alkali metals, since in all experiments at least one alkali metal ion was involved. The resin samples to be analyzed were first digested in a Kjeldahl flask by boiling with a mixture of 4–5 volumes concentrated sulfuric acid and 1 volume concentrated nitric acid. Fresh portions of the latter were added several times until all organic matter was completely oxidized. The acids were then eliminated by evaporation, the residue taken up with water, and this solution analyzed with a Zeiss-PMQII spectrophotometer with flame attachment. Samples of the ethylenediamine solutions were diluted with water to five times their volume and analyzed directly. The presence of the organic solvent had the advantage of enhancing the sensitivity of the measurements.

RESULTS AND DISCUSSION

Swelling

The absorption of ethylenediamine by the exchangers is rather slow. The various samples took up to about 2 days to reach maximum swelling, whereas with water not

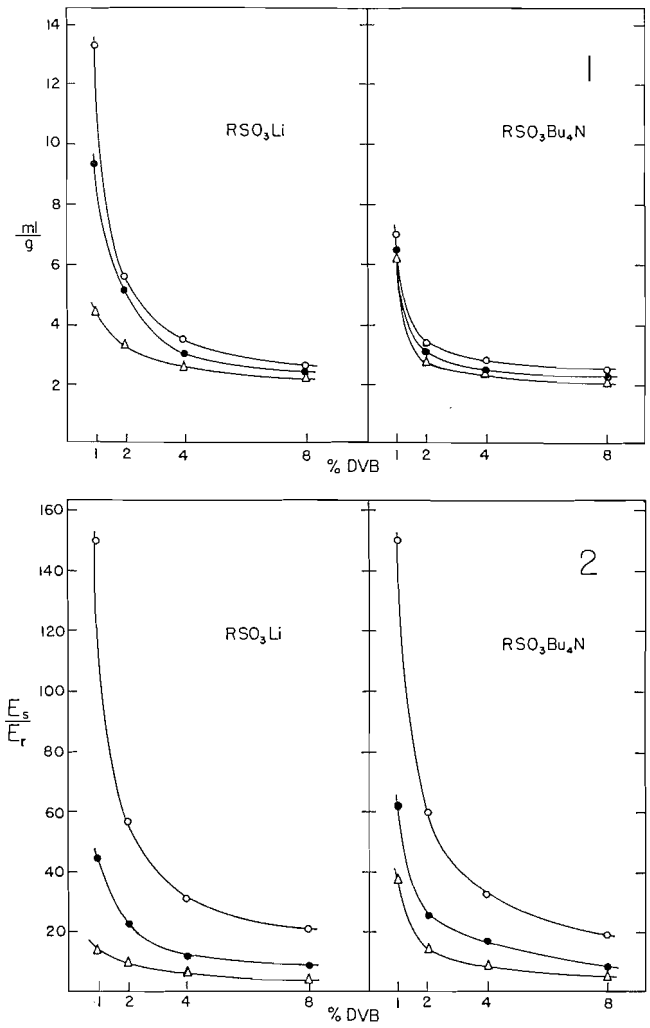

FIG. 1. Swelling of cation exchange resins Dowex 50W in various solvents as a function of cross-linking degree. Swelling expressed in ml of swollen resin obtained from 1 g of dry resin. Key: ○, water; ●, methanol; △, ethylenediamine; Bu, butyl; DVB, divinylbenzene; R, resin polymer network.

FIG. 2. Same data as in Fig. 1, but swelling expressed in moles of solvent (E_s) absorbed per 1 equivalent of resin (E_r).

more than a few minutes are usually required. Figure 1 shows the results obtained with both the lithium and the tetrabutylammonium forms in water, methanol, and ethylenediamine respectively. Swelling is expressed as is usual, i.e. in ml of swollen resin obtained from 1 g of dry resin. The variation of swelling as a function of the degree of cross-linking (% DVB) of the polymer is shown. As to be expected swelling is greatest in water and smallest in ethylenediamine. The tetrabutylammonium form seems to swell less than the lithium form in water and methanol, whereas in ethylenediamine the former tends to be more swollen. However, this presentation of the data does not take into account the equivalent weights of the two resin forms which are rather different, namely 190–200 for the lithium form and 430–440 for the other form. It would, therefore, appear more meaningful to express the swelling in moles of solvent absorbed by 1 mole of

Can. J. Chem. Downloaded from www.nrcresearchpress.com by 210.87.254.5 on 09/05/12
For personal use only.

exchanger as is shown in Fig. 2. This "equivalent swelling" appears to be practically the same for both cation forms in water, whereas in the organic solvents the tetrabutylammonium form swells more strongly. This seems to indicate that the cation tetrabutylammonium, having a pronounced organic character, is more solvated in the organic solvents than is lithium. For the more cross-linked resins X4 and X8, however, this difference between the two cationic forms is rather small. An explanation for this was found in the fact that these more cross-linked resins cannot be converted completely into the tetrabutylammonium form. Table I gives the results obtained when the lithium forms were treated with 1 *M* solutions of tetrabutylammonium bromide in either water or ethylenediamine. In water only the little cross-linked resins are able to exchange all the lithium ions, while this capacity is reduced to 61% when cross-linking reaches a degree of X8. In ethylenediamine, where swelling is less than in water, even the slightly cross-linked resins cannot exchange completely, and the more cross-linked ones do not exchange at all. Therefore, it must be said that the swelling data given in Figs. 1 and 2 for the tetrabutylammonium forms of the resins X4 and X8 have been obtained with mixed resins containing a minor equivalent portion of lithium form. This limited capacity for large ions, which has already been reported for other tetraalkylammonium ions (3), seems to support the opinion that in commercial exchange resins there is considerable variation in pore size.

TABLE I

Exchange capacities of the exchangers Dowex 50W for the tetrabutylammonium ion $(C_4H_9)_4N^+$

Degree of cross-linking	Exchange capacity in % of total capacity	
% divinylbenzene	In water	In ethylenediamine
1	100	86
2	100	77
4	88	0
8	61	0

Some interesting observations were made of the effect solutes have on the swelling in ethylenediamine. When an exchange resin is swollen in pure water, swelling decreases upon contact with an electrolyte solution, whereas in ethylenediamine the reverse takes place. Table II shows the changes of swelling obtained with Dowex 50W-X2 both in water and ethylenediamine, when the pure solvent is changed to a 0.5 *M* solution of the bromide of the exchanger's counterion. It can be seen that the increase of swelling in ethylenediamine is as pronounced as the decrease in water. The explanation of this paradox lies probably in the fact that these electrolytes are present mainly as associated ion-pairs because of the ethylenediamine's low polarity. Schaap and co-workers (4) have determined the ion-pair association constants in ethylenediamine of several halides of alkali metals and of tetrabutylammonium, and all were found to have values between 1.5 and 6×10^3. That means that in the present experiments the degree of dissociation of the bromides of lithium and tetrabutylammonium could not be more than 2–3%. In water the penetration of nonexchanging strong electrolytes into the resin phase is subject to a Donnan equilibrium, which allows but a small fraction of the electrolytes to enter the resin. Weak electrolytes, however, behave more or less like nonelectrolytes and, therefore, are absorbed in considerable amounts. This has been reported for phenol, and a number of carboxylic acids and organic bases (5, 6), and could be explained, in part at least,

Can. J. Chem. Downloaded from www.nrcresearchpress.com by 210.87.254.5 on 09/05/12
For personal use only.

TABLE II

Influence of solutes on the swelling of the cation exchanger Dowex 50W-X2 in water and ethylenediamine

Cation form of exchanger	Solute	Solute concn. (*M*)	Change of volume %	
			In water	In ethylenediamine
Li	LiBr	0.5	−19.6	+17.6
$(C_4H_9)_4N$	$(C_4H_9)_4NBr$	0.5	−12.0	+10.4
H	CH_3COOH	0.5	+0.7	
H	CH_3COOH	1.0	+2.1	
H	C_6H_5OH	0.5	+1.7	
H	C_6H_5OH	1.0	+4.2	

by the common-ion effect of the resin's counterion, which will cause the weak electrolyte to be virtually undissociated in the resin phase. Such free absorption of the solute could be, if not the exclusive cause, at least a factor contributing to the increase of swelling in ethylenediamine. If this were so, then weak electrolytes in water should likewise cause the swelling to increase. As can be seen from Table II, this is indeed the case with acetic acid and phenol, each inducing a slight increase in swelling of the resin's hydrogen form.

Ion Exchange Applications

Since it was found that the exchange capacity of medium cross-linked resins for larger ions in ethylenediamine is limited, all reactions were carried out with the slightly cross-linked resin Dowex 50W-X2. Table III summarizes the reactions attempted of which only Nos. 1 through 3 were successful. In each of these cases the alkali cation originally present in the solution was removed quantitatively and could subsequently be eluted from the resin by drying and washing with 3 *M* hydrochloric acid. The solutions resulting from these exchanges were used to titrate potentiometrically ethylenediamine solutions of phenol as described by one of us earlier (7). In all three cases the titration curves were similar to those described in that report for a titrant solution of tetrabutylammonium ethoxide. No attempt was made to isolate these rather delicate reaction products, which are easily decomposed by both humidity and atmospheric carbonic acid. The flame photometric analyses of both the solution and the resin together with the potentiometrical titration were taken as satisfactory proof that the cations had been exchanged without any other chemical reaction. The three experiments lead thus to pure solutions of tetrabutylammonium ethoxide, potassium 2-aminoethoxide, and tetrabutylammonium 2-aminoethoxide respectively. None of these solutions or solutes seem to have been prepared hitherto, and earlier attempts by us at their preparation by other methods had failed. Only the preparation of tetrabutylammonium ethoxide by a precipitation reaction in a mixed benzene–ethylenediamine medium has been reported (7), but this method does not give pure solutions since the precipitation reaction is not quantitative.

The preparation of the potassium 2-aminoethylamide solution according to reaction

TABLE III

Cation exchange reactions in ethylenediamine

1.	$Bu_4N^+RSO_3^- + K^+C_2H_5O^-$	$\rightarrow K^+RSO_3^- + Bu_4N^+C_2H_5O^-$
2.	$K^+RSO_3^- + Li^+NH_2C_2H_4O^-$	$\rightarrow Li^+RSO_3^- + K^+NH_2C_2H_4O^-$
3.	$Bu_4N^+RSO_3^- + Li^+NH_2C_2H_4O^-$	$\rightarrow Li^+RSO_3^- + Bu_4N^+NH_2C_2H_4O^-$
4.	$K^+RSO_3^- + Li^+NH_2C_2H_4NH^-$	$\rightarrow Li^+RSO_3^- + K^+NH_2C_2H_4NH^-$

NOTE: Bu = C_4H_9; R = resin polymer network.

Can. J. Chem. Downloaded from www.nrcresearchpress.com by 210.87.254.5 on 09/05/12
For personal use only.

4 in Table III did not succeed, and that of the analogous sodium amide was only partly successful. When 50 ml of a 0.1 *M* solution of lithium 2-aminoethylamide in ethylenediamine (5 meq) was percolated through 29.2 meq of Dowex 50W-X2 in the potassium form at a rate of 0.3 ml/min, 45% of the lithium (2.25 meq) disappeared from the liquid phase without being replaced by potassium. However, this lithium fraction was recovered completely together with all the potassium from the dried resin by eluting it with 3 *M* aqueous hydrochloric acid. This seems to indicate that the exchange between lithium and potassium took place, but that the reaction product potassium 2-aminoethylamide is insoluble in ethylenediamine and precipitated in the resin. This precipitate will block certain exchange sites and thus prevent the reaction from becoming complete.

Since lithium 2-aminoethylamide is quite soluble in ethylenediamine, it seemed probable that the corresponding sodium amide should have an intermediate solubility. When 20 ml of a 0.258 *M* solution of the lithium amide (5.16 meq) was passed through 28.8 meq of the exchanger's sodium form at 0.1 ml/min, 65% of the lithium (3.36 meq) left the solution, whereas 16% of the total amount of lithium (0.83 meq) was replaced by sodium. In another experiment, where 90 ml of a 0.0272 *M* solution of the lithium amide (2.45 meq) was passed through the same column in the sodium form, 93.5% of the lithium (2.29 meq) left the solution, but only 4.5% of the total amount of lithium (0.110 meq) was replaced by sodium. In both these experiments the balance of both lithium and sodium was recovered from the dried resin by elution with hydrochloric acid. It was concluded that the sodium 2-aminoethylamide must be somewhat soluble in ethylenediamine, but no further attempt was made to determine its solubility. No explanation can be offered for the apparent difference in solubility in the two experiments. That the exchange between the three alkali metals potassium, sodium, and lithium is in principle possible was established by passing 0.05 *M* ethylenediamine solutions of sodium bromide through either the potassium or the lithium form of the exchanger and in both instances complete exchange was obtained. Here all three alkali bromides involved are sufficiently soluble in ethylenediamine.

ACKNOWLEDGMENT

We are grateful to the National Research Council for financial support of this work.

REFERENCES

1. C. W. KEENAN and W. J. MCDOWELL. J. Am. Chem. Soc. **75**, 6348 (1953).
2. R. KUNIN. Ion exchange resins. 2nd ed. John Wiley and Sons, New York. 1958. p. 341.
3. D. K. HALE, D. I. PACKHAM, and K. W. PEPPER. J. Chem. Soc. 844 (1953).
4. W. B. SCHAAP *et al.* Record Chem. Progr. Kresge-Hooker Sci. Lib. **22**, 197 (1961).
5. C. W. DAVIES and G. THOMAS. J. Chem. Soc. 2624 (1951).
6. D. REICHENBERG and W. F. WALL. J. Chem. Soc. 3364 (1956).
7. W. R. HEUMANN. *In* Titrimetric methods. *Edited by* D. Jackson. Plenum Press, New York. 1961. p. 121.

Can. J. Chem. Downloaded from www.nrcresearchpress.com by 210.87.254.5 on 09/05/12
For personal use only.

Can. J. Chem. Downloaded from www.nrcresearchpress.com by 210.87.254.5 on 09/05/12
For personal use only.

REACTIONS OF THE ETHYL RADICAL

VI. ADDITION TO CONJUGATED DIENES

A. C. R. BROWN[1] AND D. G. L. JAMES

Department of Chemistry, The University of British Columbia, Vancouver, British Columbia

Received December 7, 1964

ABSTRACT

Arrhenius parameters have been measured for the addition of the ethyl radical to the conjugated diene system in three representative molecular environments. Significant differences are found among the values of the energy of activation for addition, which are: 4.5 ± 0.2 kcal/mole for 2,3-dimethylbutadiene-1,3, 5.2 ± 0.3 kcal/mole for cyclohexadiene-1,3, and 6.6 ± 0.3 kcal/mole for 2,5-dimethylhexadiene-2,4. The increase in the energy of activation in this series is paralleled by an increase in the degree of shielding of the terminal carbon atoms of the conjugated system by substituent groups. The energy of activation for metathesis is significantly lower for cyclohexadiene-1,3 (5.4 ± 0.5 kcal/mole) than for 2,5-dimethylhexadiene-2,4 (7.6 ± 0.4 kcal/mole); the activated hydrogen atoms of the former are all secondary, whereas those of the latter are all primary. The ratio of the rate constants for addition and metathesis at 60° indicate that the radical homopolymerization of cyclohexadiene-1,3 and 2,5-dimethylhexadiene-2,4 should be subject to extensive degradative chain transfer.

INTRODUCTION

The reactivity of the conjugated diene system towards the addition of free radicals is likely to be profoundly influenced by its molecular environment. The aim of this investigation is to find a pattern of reactivity among substituted butadienes by measuring the Arrhenius parameters for the addition of the ethyl radical in the gas phase. These substituted butadienes were chosen so that the reactivity of the conjugated system could be studied in three characteristic molecular environments: extending the full length of the carbon chain (2,3-dimethylbutadiene-1,3); doubly substituted at each end by methyl groups (2,5-dimethylhexadiene-2,4); and as part of a six-membered carbon ring (cyclohexadiene-1,3).

The relative methyl affinity is the only systematic measure of reactivity towards the addition of free radicals which has included all three butadienes (1, 2). At 65 °C the methyl affinity is 2 230 for 2,3-dimethylbutadiene-1,3, 21.3 for 2,5-dimethylhexadiene-2,4, and 665 for cyclohexadiene-1,3. The reactivity of these dienes has also been demonstrated less comprehensively in relation to the addition of trichloromethyl (3) and thiyl (4, 5) radicals, and in homopolymerization (6–9) and copolymerization (10, 11, 12).

The high reactivity of 2,3-dimethylbutadiene-1,3 and cyclohexadiene-1,3 in radical copolymerization is conveyed by the Q values of the Alfrey–Price parameters, which are $Q = 5.86$ and $e = -1.81$ for 2,3-dimethylbutadiene-1,3 (13) and $Q = 1.76$ and $e = -1.18$ for cyclohexadiene-1,3 (12); the electron-donating nature of each monomer is evident from the negative values of e. The radical homopolymerization of 2,3-dimethylbutadiene-1,3 has been reviewed recently by Morton and Gibbs, who have measured the propagation constant, $k_p = 8.9 \times 10^7 \exp(-9\,000/RT)$ l mole^{-1} s^{-1} (6); the radical homopolymerization of cyclohexadiene-1,3 is kinetically complex (7, 8), and the propagation constant has not been measured (9). The structure of 2,5-dimethylhexadiene-2,4 is sterically unfavorable to the propagation reaction of radical polymerization, but its reactivity towards the methyl and thiyl radicals indicates that it should be included in this study as an example of complete substitution at the reactive sites for addition.

[1]*Present address: Petrochemical and Polymer Laboratory, Imperial Chemical Industries Ltd., Runcorn, Cheshire, England.*

Can. J. Chem. Downloaded from www.nrcresearchpress.com by 210.87.254.5 on 09/05/12
For personal use only.

EXPERIMENTAL PROCEDURE

Ethyl radicals were generated in the presence of each olefin by the illumination of a gaseous mixture of diethyl ketone and the olefin with 3 130 Å radiation. To simplify the kinetics, the reaction conditions were controlled so that the ethyl radical was always present in great excess over all other radicals.

The apparatus and general method have been described previously (14). The reagents were of the purest grade commonly obtainable commercially; each was further purified by the Beckman Megachrom preparative gas chromatograph, and the purity of the selected fraction was then examined on the Perkin-Elmer Vapour Fractometer, model 154C. The only evidence of residual impurities was found for cyclohexadiene-1,3, which still contained 1% of benzene. Benzene was found to be unreactive towards the ethyl radical, but its presence among the reactants prevented the direct measurement of the rate of formation of benzene in the cyclohexadiene-1,3 system. A procedure which was devised to estimate this rate indirectly is described in the next section.

The analysis of the products followed the pattern of separation and measurement of CO, $C_2H_4 + C_2H_6$, and C_4H_{10} fractions. The purity of the fractions was established, and the composition of the C_2 fraction determined, by means of the Perkin-Elmer gas chromatograph.

THE KINETIC ANALYSIS

Under the experimental conditions of this investigation, the photolysis of diethyl ketone conforms to the following simple mechanism (14–19).

[1] $$CH_3CH_2COCH_2CH_3 + h\nu \rightarrow 2CH_3CH_2\cdot + CO$$

[2] $$2CH_3CH_2\cdot \rightarrow C_4H_{10}$$

[3] $$2CH_3CH_2\cdot \rightarrow C_2H_6 + C_2H_4$$

[4] $$CH_3CH_2\cdot + CH_3CH_2COCH_2CH_3 \rightarrow CH_3CH_3 + CH_3\dot{C}HCOCH_2CH_3$$

[5] $$CH_3CH_2\cdot + CH_3\dot{C}HCOCH_2CH_3 \rightarrow CH_3CH(CH_2CH_3)COCH_2CH_3$$

If a gaseous mixture of diethyl ketone and an olefin is illuminated, the ethyl radicals formed will also react with the olefin, and both addition and metathesis should be observed. If the olefin is cyclohexadiene-1,3 and the ethyl radical is present in great excess over all other radicals, then the following additional reactions may be expected.

[6] $CH_3CH_2^{\bullet}$ + → CH_3CH_3 +

[6c] $CH_3CH_2^{\bullet}$ + → (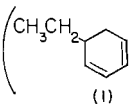 and 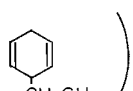)

(I) (II)

[6d] → CH_3CH_3 +

[6e] → $CH_2{=}CH_2$ + (and)

[7] $CH_3CH_2^{\bullet}$ + → 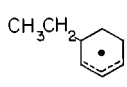

[7c] $CH_3CH_2^{\bullet}$ + → (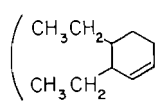 and 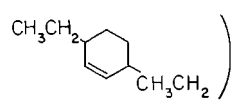)

(VI) (VII)

[7d] $\longrightarrow CH_3CH_3 +$ 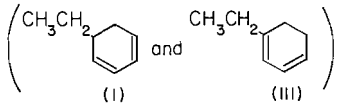 (I) and (III)

[7e] $\longrightarrow CH_2{=}CH_2 +$ 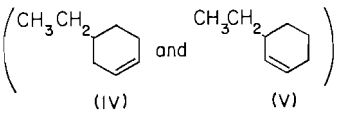 (IV) and (V)

The cyclohexadienyl radical is formed by reaction [6], and the reactions of this radical with the ethyl radical are known from a study of the photolysis of a gaseous mixture of diethyl ketone and cyclohexadiene-1,4 (14). It was found that $k_{6d}/k_{6c} = 0.38 \pm 0.03$, and $k_{6e}/k_{6c} = 0$. The latter value is perhaps surprising, but it has been indirectly confirmed by the study of the photolysis of a gaseous mixture of diisopropyl ketone and cyclohexadiene-1,4; the value of the corresponding ratio was also found to be zero (20). Reaction [6*e*] should therefore be negligible in the present system, and this is confirmed by the absence of cyclohexadiene-1,4 from the products, especially as it could have been detected in trace quantity. We shall assume that the disproportionation reactions [7*d*] and [7*e*] can be neglected, so that the adduct radical, $C_8H_{13}^{\cdot}$, is consumed solely by combination with the ethyl radical. A parallel but more detailed study of the interaction of the isopropyl radical with cyclohexadiene-1,3, in which disproportionation reactions should be relatively more important, has shown that the neglect of the corresponding disproportionation reactions of the adduct radical has a negligible effect upon the values of the rate constants and the Arrhenius parameters (21). The significant reactions for the cyclohexadiene-1,3 system are therefore: [1–5, 6, 6*c*, 6*d*, 7, and 7*c*]. Ethane is formed only in reactions [3, 4, 6, and 6*d*], and therefore the rate constants may be calculated from the equations:

$$\frac{k_6}{k_2^{1/2}} = \frac{R(C_2H_6) - R(C_2H_4) - R(C_6H_6)}{[B]R(C_4H_{10})^{1/2}} - \frac{[D]}{[B]}\frac{k_4}{k_2^{1/2}}$$

$$= \left\{\frac{R(C_2H_6) - R(C_2H_4)}{[B]R(C_4H_{10})^{1/2}} - \frac{[D]}{[B]}\frac{k_4}{k_2^{1/2}}\right\} \Big/ \left(1 + \frac{k_{6d}}{k_{6c} + k_{6d}}\right) \qquad [I]$$

$$\frac{k_7}{k_2^{1/2}} = \frac{R(CO) + R(C_6H_6) - R(C_2H_6) - R(C_4H_{10})}{[B]R(C_4H_{10})^{1/2}}$$

$$= \left\{\frac{R(CO) - R(C_2H_6) - R(C_4H_{10})}{[B]R(C_4H_{10})^{1/2}}\right\} + \frac{k_{6d}}{k_{6c} + k_{6d}}\frac{k_6}{k_2^{1/2}}, \qquad [II]$$

where $R(Z)$ is the rate of formation of product Z, [D] and [B] are the concentrations of diethyl ketone and the olefin, respectively, and $k_4/k_2^{1/2}$ is known from previous work. Since $k_{6d}/k_{6c} = 0.38 \pm 0.03$ (14), $k_{6d}/(k_{6c} + k_{6d}) = 0.275$, and this value was used uniformly in equations [I] and [II]. The mechanisms proposed for the interaction of the ethyl radical with the other olefins of this study parallel the mechanism given above for cyclohexadiene-1,3 with the single difference that reaction [6*d*] is considered to be negligible for these other olefins. The validity of neglecting reaction [6*d*] has been discussed previously (14) with special reference to cyclooctadiene-1,5; it was concluded that reaction [6*d*] could be neglected except where it was particularly favored energetically by the formation of a highly stabilized product, as in the formation of benzene from the cyclohexadienyl radical in the cyclohexadiene systems. The significant reactions for the 2,3-dimethylbutadiene-1,3, 2,5-dimethylhexadiene-2,4, and octene-1 systems are therefore

Can. J. Chem. Downloaded from www.nrcresearchpress.com by 210.87.254.5 on 09/05/12
For personal use only.

[1–5, 6, 6*c*, 7, and 7*c*]. Equations I and II may be used to calculate the rate constants by placing $k_{6d} = 0$, and the expression in curly brackets is then obtained in each case.

Rate constants for both addition and metathesis were obtained for each of the four olefins except 2,3-dimethylbutadiene-1,3; addition to this diene was too rapid to allow measurement of the rate of metathesis.

In the mechanism proposed for the reactions of the ethyl radical with the three dienes we have assumed that the ethyl radical will add to either of the terminal carbon atoms of the conjugated system. This assumption does not affect the validity of the kinetic analysis, but it does form the basis of our discussion of the influence of structure upon reactivity, and so we shall present below the evidence for addition at the terminal atoms of the conjugated systems in closely related reactions.

The mechanism of the addition of free radicals to substituted butadiene systems has been clarified recently by the analysis of the products of addition of bromotrichloromethane (3) and certain thiols (4, 5) to 2,3-dimethylbutadiene-1,3 and to 2,5-dimethylhexadiene-2,4.

The addition of bromotrichloromethane to 2,3-dimethylbutadiene-1,3 yields exclusively an equimolar adduct by a 1,4 addition process (3); exactly parallel results were obtained for the addition of diethyldithiophosphoric acid (5). The 1,4 addition patterns indicate initial attack of a trichloromethyl (or thiyl) radical at either terminal carbon atom (which we shall call $C_{(1)}$) of the conjugated chain; this point of addition yields the most stable adduct radical and is therefore favored energetically. The adduct radical then abstracts a bromine (or hydrogen) atom from a molecule of the addendum at either the $C_{(2)}$ or $C_{(4)}$ atom of the conjugated chain. Attachment to the primary $C_{(4)}$ atom is energetically much more favorable than attachment to the tertiary $C_{(2)}$ atom, and accordingly an exclusively 1,4 pattern of addition emerges.

Successive substitution of methyl groups at the terminal atoms of the conjugated diene chain increasingly favors the 1,2 pattern of addition over the 1,4. The single terminal methyl group of piperylene raises the proportion of the 1,2 adduct of diethyl dithiophosphoric acid to 50%, and the four terminal methyl groups of 2,5-dimethylhexadiene-2,4 raise the proportion of the 1,2 adduct to 85%, the remainder being the 1,4 adduct (5). A 1,2 pattern of addition to 2,5-dimethylhexadiene-2,4 is consistent with a mechanism of initial radical attack at the terminal atom $C_{(1)}$ of the conjugated system, and is supported by the energetics of the two successive steps of addition. Initial attack at $C_{(1)}$ is favored because it forms the more stable allylic radical. The $C_{(2)}$ atom of the resultant adduct is then secondary, whereas the $C_{(4)}$ atom is tertiary, so that hydrogen atom transfer to the $C_{(2)}$ site is favored energetically, causing the 1,2 pattern of addition to predominate. However, if the initial adduct radical were to engage in a bond-forming reaction of negligible activation energy, then the difference in the strengths of the bonds formed at the $C_{(2)}$ and $C_{(4)}$ atoms would be irrelevant to the kinetics; and if an exclusively 1,4 addition mechanism emerged in such a system, then the theory that the initial attack is at the terminal atom of the conjugated system would be vindicated. The low temperature co-oxidation of aromatic thiols and 2,5-dimethylhexadiene-2,4 by molecular oxygen conforms to a 1,4 pattern of addition (4). Crystalline 2,5-dimethyl-2-arylmercapto-hex-3-en-5-yl hydroperoxides were isolated; these products clearly indicate an initial addition of the thiyl radical at $C_{(1)}$, followed by addition of the oxygen molecule at $C_{(4)}$.

On the basis of the evidence given above we conclude that the addition of the ethyl radical to 2,3-dimethylbutadiene-1,3, 2,5-dimethylhexadiene-2,4, and cyclohexadiene-1,3 will occur at one of the terminal atoms of the conjugated system.

Can. J. Chem. Downloaded from www.nrcresearchpress.com by 210.87.254.5 on 09/05/12
For personal use only.

Can. J. Chem. Downloaded from www.nrcresearchpress.com by 210.87.254.5 on 09/05/12
For personal use only.

TABLE I*a*

Addition of the ethyl radical*

Substrate	No. of expts.	Range of temp. (°C)	C	B	$13 + \log A_7/A_2^{1/2}$	$E_7 - \frac{1}{2}E_2$ (kcal/mole)	$13 + \log k_7/k_2^{1/2}$ at 100 °C	$\frac{R(C_2H_4)}{R(C_4H_{10})}$
Octene-1	11	66–152	5.485	1.664	5.5±0.1	7.6±0.2	1.03±0.03	0.137±0.006
2,5-Dimethylhexadiene-2,4	9	55–147	5.164	1.435	5.2±0.2	6.6±0.3	1.32±0.04	0.120±0.006
Cyclohexadiene-1,3	14	49–116	5.552	1.145	5.5±0.2	5.2±0.3	2.48±0.04	0.120±0.010
2,3-Dimethylbutadiene-1,3	27	45–141	5.643	0.991	5.6±0.1	4.5±0.2	2.99±0.06	0.121±0.006

TABLE I*b*

Metathesis with the ethyl radical*

Substrate	No. of expts.	Range of temp. (°C)	C	B	$13 + \log A_6/A_2^{1/2}$	$E_6 - \frac{1}{2}E_2$ (kcal/mole)	$13 + \log k_6/k_2^{1/2}$ at 100 °C	k_7/k_6 at 60 °C
Octene-1	12	66–152	5.053	1.641	5.0±0.3	7.5±0.5	0.66±0.07	2.3
2,5-Dimethylhexadiene-2,4	10	53–147	5.532	1.658	5.5±0.2	7.6±0.4	1.09±0.06	2.0
Cyclohexadiene-1,3	17	43–154	4.967	1.175	5.0±0.3	5.4±0.5	1.82±0.11	4.7

*The quantities B and C are the coefficients of the straight lines $13 + \log k_r/k_2^{1/2} = C - 10^3B/T$ fitted to the experimental results (r represents 7 for addition and 6 for metathesis). The units of k are cm^3 $molecule^{-1}$ s^{-1}; the limits of error are calculated at the 5% probability level.

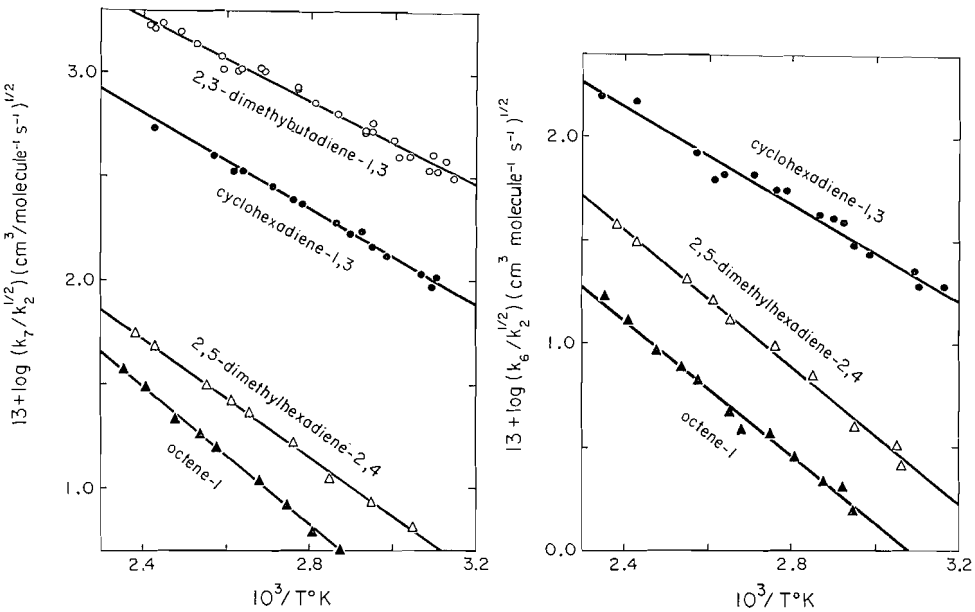

FIG. 1. Addition of the ethyl radical. Values for $E_7 - \frac{1}{2}E_2$ are: 2,3-dimethylbutadiene-1,3 = 4.5 ± 0.2 kcal/mole; cyclohexadiene-1,3 = 5.2 ± 0.3 kcal/mole; 2,5-dimethylhexadiene-2,4 = 6.6 ± 0.3 kcal/mole; octene-1 = 7.6 ± 0.2 kcal/mole.

FIG. 2. Metathesis with the ethyl radical. Values for $E_6 - \frac{1}{2}E_2$ are: cyclohexadiene-1,3 = 5.4 ± 0.5 kcal/mole; 2,5-dimethylhexadiene-2,4 = 7.6 ± 0.4 kcal/mole; octene-1 = 7.5 ± 0.5 kcal/mole.

RESULTS AND DISCUSSION

I. The Addition Reaction

The order of reactivity of the four hydrocarbons towards the addition of the ethyl radical is clear from the results of Table I*a* and Fig. 1:

2,3-dimethylbutadiene-1,3 > cyclohexadiene-1,3 > 2,5-dimethylhexadiene-2,4 > octene-1.

Moreover, each member of the series is significantly more reactive than its successor, whether the criterion of reactivity is the energy of activation ($E_7 - \frac{1}{2}E_2$) or the rate constant (given in the form $13 + \log k_7/k_2^{1/2}$ in Table I*a*). The dienes thus show the same order of reactivity towards the ethyl radical as towards the addition of the methyl radical at 65 °C (1, 2). Conjugation raises the reactivity of each of the dienes significantly above that of octene-1, although the terminal vinyl group of the latter is much less shielded from attack than the reactive position of 2,5-dimethylhexadiene-2,4. The terminal carbon atom of a conjugated diene system is normally the favored position for addition, as the allylic adduct is then the radical of lowest possible energy. The reactivity of the dienes decreases as the shielding of the terminal carbon atom of the conjugated system increases from two hydrogen atoms through a methylene group to two methyl groups. The effect of an increase in shielding upon the kinetics of the addition reaction is expressed mainly by an increase in the value of the energy of activation, but, furthermore, the pre-exponential factor for 2,5-dimethylhexadiene-2,4 is significantly lower than for the other dienes. The carbon atoms of the delocalized systems of cyclohexadiene-1,3 and of its adduct, the ethylcyclohexenyl radical, form part of a six-membered ring. It is probable that these carbon atoms are either coplanar or able to become coplanar very

Can. J. Chem. Downloaded from www.nrcresearchpress.com by 210.87.254.5 on 09/05/12
For personal use only.

easily, and therefore that the energy of activation for addition to cyclohexadiene-1,3 does not include an appreciable contribution from the release of strain in the carbon ring.

Butadiene-1,3 and isoprene were not included in this investigation, but their reactivities towards the addition of the ethyl radical may be estimated from the results obtained for 2,3-dimethylbutadiene-1,3. Substituent methyl groups at the $C_{(2)}$ and $C_{(3)}$ atoms of the conjugated system increase the electron density at the terminal carbon atoms (22), but this appears to have little effect upon the reactivity of the diene system towards hydrocarbon radical addition. Thus, butadiene-1,3, isoprene, and 2,3-dimethylbutadiene-1,3 possess very similar methyl affinities (2 015 ± 30, 2 090 ± 50, and 2 230 ± 70, respectively, at 65 °C (1)), propagation rate constants (100, 50, and 120 l mole^{-1} s^{-1}, respectively, at 60 °C (6)) and propagation activation energies (9.3, 9.8, and 9 kcal/mole, respectively (6)). We conclude that the reactivity of these three butadienes towards the addition of the ethyl radical should be similar in magnitude and should stand in the same order as the methyl affinity.

The energy of activation for the addition of the ethyl radical to 2,3-dimethylbutadiene-1,3 lies over 4 kcal/mole below the energy of activation for the propagation of the radical polymerization of this diene. Such a difference is consistent with the difference in reactivity of an *n*-alkyl and a substituted allyl radical towards a common substrate.

II. The Metathetical Reaction

The order of reactivity towards metathesis with the ethyl radical is clear from the rate constants given in Table I*b* and Fig. 2:

cyclohexadiene-1,3 > 2,5-dimethylhexadiene-2,4 > octene-1.

Moreover, the value of $13 + \log k_6/k_2^{1/2}$ for each member of the series is significantly greater than for its successor. Cyclohexadiene-1,3 has a significantly lower energy of activation than the other olefins, but it alone possesses secondary hydrogen atoms activated by a conjugated system. The activation of the methylene groups is probably not reduced by the cyclic structure of cyclohexadiene-1,3, because the four carbon atoms of the conjugated system are not likely to deviate much from coplanarity and the carbon atoms of the cyclohexadienyl radical are known to be coplanar (23). The pre-exponential factor for 2,5-dimethylhexadiene-2,4 is significantly higher than for the other olefins when limits of error are assessed at the 10% probability level. If n denotes the number of equivalent hydrogen atoms, then $13 + \log (A_6/A_2^{1/2} n)$ takes the value of 4.4 for both 2,5-dimethylhexadiene-2,4 and for cyclohexadiene-1,3.

The Arrhenius parameters given in Table I for addition and metathesis between the ethyl radical and octene-1 differ from the previous values (24). In the earlier study the C_2 fraction was not analyzed, but $R(C_2H_4)$ was obtained from $R(C_4H_{10})$ by applying a uniform value of 0.136 for $R(C_2H_4)/R(C_4H_{10})$ to the results of each experiment. In the present study this ratio was found to be 0.137 ± 0.006, confirming the earlier value. Now if the rate constants are calculated from the values of $R(CO)$, $R(C_2)$, and $R(C_4H_{10})$ obtained in the present study using the original method, then the corresponding Arrhenius parameters are in agreement with the original values. However, if each rate constant is calculated using the known composition of the C_2 fraction, then the parameters of Table I are obtained. These revised parameters should be used in the comparative arguments of this discussion, as the Arrhenius parameters of all the other substrates have been calculated using the actual composition of the C_2 fraction of each experiment.

Chain transfer controls the course of the free radical homopolymerization of alkenes (25) and of cyclohexadiene-1,3 (7). The degree of polymerization is accordingly low;

Can. J. Chem. Downloaded from www.nrcresearchpress.com by 210.87.254.5 on 09/05/12
For personal use only.

typical values are 7 for butene-1 at 130 °C and 20 000 p.s.i. (25), and 10–12 for cyclohexadiene-1,3 (9). Such behavior could be predicted from the values of the ratio k_7/k_6 listed for octene-1 and cyclohexadiene-1,3 in Table I*b*, assuming that this ratio gives a measure of k_p/k_t, the ratio of the rate constants for propagation and degradative chain transfer. On this basis we suggest that the radical homopolymerization of 2,5-dimethylhexadiene-2,4 should be subject to extensive chain transfer, and that as $E_7 - E_6 \approx 0$ for cyclohexadiene-1,3 and for octene-1, the corresponding degrees of polymerization should be relatively insensitive to temperature.

ACKNOWLEDGMENT

We wish to thank the National Research Council for the financial support of this work and for a studentship to A. C. R. B.

REFERENCES

1. A. RAJBENBACH and M. SZWARC. J. Am. Chem. Soc. **79**, 6343 (1957).
2. J. GRESSER, A. RAJBENBACH, and M. SZWARC. J. Am. Chem. Soc. **83**, 3005 (1961).
3. C. S. HSIA CHEN and E. F. HOSTERMAN. J. Org. Chem. **28**, 1585 (1963).
4. A. A. OSWALD, B. E. HUDSON, JR., G. RODGERS, and F. NOEL. J. Org. Chem. **27**, 2439 (1962).
5. A. A. OSWALD, K. GRIESBAUM, and B. E. HUDSON, JR. J. Org. Chem. **28**, 1262 (1963).
6. M. MORTON and W. E. GIBBS. J. Polymer Sci. A, **1**, 2679 (1963).
7. P. S. SHANTAROVICH and I. A. SHLYAPNIKOVA. Vysokomolekul. Soedin. **3**, 1364 (1961).
8. B. V. EROFEEV, S. F. NAUMOVA, and L. G. TSYKALO. Dokl. Akad. Nauk SSSR, **147**, 106 (1962).
9. G. LEFEBVRE and F. DAWANS. J. Polymer Sci. A, **2**, 3277 (1964).
10. R. J. ORR AND H. L. WILLIAMS. Can. J. Chem. **30**, 108 (1952).
11. F. DAWANS. J. Polymer Sci. A, **2**, 3297 (1964).
12. E. S. FERDINANDI, W. P. GARBY, and D. G. L. JAMES. Can. J. Chem. **42**, 2568 (1964).
13. L. J. YOUNG. J. Polymer Sci. **54**, 411 (1961).
14. A. C. R. BROWN and D. G. L. JAMES. Can. J. Chem. **43**, 660 (1965).
15. L. M. DORFMANN and Z. D. SHELDON. J. Chem. Phys. **17**, 511 (1949).
16. K. O. KUTSCHKE, M. H. J. WIJNEN, and E. W. R. STEACIE. J. Am. Chem. Soc. **74**, 714 (1952).
17. R. K. BRINTON and E. W. R. STEACIE. Can. J. Chem. **33**, 1840 (1955).
18. D. S. WEIR. J. Am. Chem. Soc. **83**, 2629 (1961).
19. L. C. FISCHER and G. J. MAINS. J. Phys. Chem. **68**, 188 (1964).
20. D. G. L. JAMES and R. D. SUART. J. Am. Chem. Soc. **86**, 5424 (1964).
21. D. G. L. JAMES and R. D. SUART. Unpublished results.
22. M. SHIMA, J. SMID, and M. SZWARC. J. Polymer Sci. B, **2**, 735 (1964).
23. R. W. FESSENDEN and R. H. SCHULER. J. Chem. Phys. **38**, 773 (1963).
24. D. G. L. JAMES and E. W. R. STEACIE. Proc. Roy. Soc. London, Ser. A, **244**, 289 (1958).
25. G. A. MORTIMER and LL. C. ARNOLD. J. Polymer Sci. A, **2**, 4247 (1964).

Can. J. Chem. Downloaded from www.nrcresearchpress.com by 210.87.254.5 on 09/05/12
For personal use only.

Can. J. Chem. Downloaded from www.nrcresearchpress.com by 210.87.254.105 on 09/05/12
For personal use only.

THE REACTIVITY OF THE CYCLIC POLYENES TOWARDS FREE RADICALS

III. ADDITION OF THE ETHYL RADICAL

A. C. R. BROWN[1] AND D. G. L. JAMES

Department of Chemistry, University of British Columbia, Vancouver, British Columbia

Received December 7, 1964

ABSTRACT

Arrhenius parameters have been measured for the addition of the ethyl radical to cycloheptatriene-1,3,5 and to bicyclo[2.2.1]heptadiene-2,5 in the gas phase; the values for the energy of activation are distinct at 6.4 ± 0.2 and 7.0 ± 0.1 kcal/mole respectively. The addition of the ethyl radical to benzene, cyclohexadiene-1,4, and cyclooctadiene-1,5 proceeds too slowly to be detected. The significance of these results is considered in conjunction with those obtained previously for cyclohexadiene-1,3 and cyclooctatetraene, and the possibility of interpreting the reactivity of the cyclic polyenes in terms of molecular structure is discussed.

INTRODUCTION

A kinetic study of the addition of the ethyl radical to cycloheptatriene, bicycloheptadiene, cyclohexadiene-1,4, cyclooctadiene,1-5, and benzene completes our preliminary survey of the reactivity of the cyclic polyenes towards the ethyl radical. Arrhenius parameters could be measured for cycloheptatriene and bicycloheptadiene only, but, in conjunction with the corresponding results obtained previously for cyclohexadiene-1,3 (1) and cyclooctatetraene (2), they provide a quantitative basis for a discussion of the influence of structure upon the reactivity of the cyclic polyenes.

The most comprehensive study of the addition of a free radical to this group of compounds was limited to the measurement of the relative rate constant for the addition of the methyl radical in isooctane solution at 65 °C, but nevertheless a clear pattern of reactivity emerged (3). A kinetic study of the addition of the polyacrylonitrile radical to the four more reactive of the cyclic polyenes revealed that polar effects may dominate the pattern of reactivity for the addition of a highly electrophilic radical (4). Accordingly the polarographic half-wave potential has been measured for the cyclic polyenes wherever possible, and the results have been considered in relation to the enhanced reactivity of cyclooctatetraene towards the addition of the ethyl radical (2).

Under the experimental conditions of this investigation, the photolysis of diethyl ketone conforms to the following simple mechanism (2).

[1] $$CH_3CH_2COCH_2CH_3 + h\nu \rightarrow 2CH_3CH_2\cdot + CO$$

[2] $$2CH_3CH_2\cdot \rightarrow C_4H_{10}$$

[3] $$2CH_3CH_2\cdot \rightarrow C_2H_6 + C_2H_4$$

[4] $$CH_3CH_2\cdot + CH_3CH_2COCH_2CH_3 \rightarrow CH_3CH_3 + CH_3\dot{C}HCOCH_2CH_3$$

[5] $$CH_3CH_2\cdot + CH_3\dot{C}HCOCH_2CH_3 \rightarrow CH_3CH(CH_2CH_3)COCH_2CH_3$$

If a gaseous mixture of diethyl ketone and cycloheptatriene is illuminated with 3 130 Å light, and the ethyl radical is present in great excess over all other radicals, then the following additional reactions should be significant.

[1]*Present address: Petrochemical and Polymer Laboratory, Imperial Chemical Industries, Ltd., Runcorn, Cheshire, England.*

[6] $CH_3CH_2\cdot + C_7H_8 \rightarrow CH_3CH_3 + C_7H_7\cdot$

[6c] $CH_3CH_2\cdot + C_7H_7\cdot \rightarrow C_7H_7CH_2CH_3$

[7] $CH_3CH_2\cdot + C_7H_8 \rightarrow C_9H_{13}\cdot$

[7c] $CH_3CH_2\cdot + C_9H_{13}\cdot \rightarrow C_{11}H_{18}$

A similar set of reactions may be expected to describe the photolysis of a gaseous mixture of diethyl ketone and bicycloheptadiene under similar conditions, with the reservation that reaction [6] proceeds too slowly to be detected. Rate constants may be calculated from the equations:

[I] $$\frac{k_6}{k_2^{1/2}} = \frac{R(C_2H_6) - R(C_2H_4)}{[B]R(C_4H_{10})^{1/2}} - \frac{[D]}{[B]}\frac{k_4}{k_2^{1/2}}$$

[II] $$\frac{k_7}{k_2^{1/2}} = \frac{R(CO) - R(C_2H_6) - R(C_4H_{10})}{[B]R(C_4H_{10})^{1/2}},$$

where $R(Z)$ is the rate of formation of the product Z, [D] and [B] are the concentrations of diethyl ketone and the olefin respectively, and $k_4/k_2^{1/2}$ is known from previous work (5) to be given by

$$k_4/k_2^{1/2} = 10^{(-7.5\pm0.1)} \exp(-7\,800 \pm 200)/RT \quad (\text{cm}^3 \text{ molecule}^{-1} \text{ s}^{-1})^{1/2}.$$

EXPERIMENTAL PROCEDURE

Ethyl radicals were generated in the presence of each olefin by the illumination of a gaseous mixture of diethyl ketone and the olefin with 3 130 Å radiation. To ensure that the kinetics should conform to the simple mechanism given above, the reaction conditions were controlled so that the ethyl radical was always present in great excess over all other radicals. The apparatus and procedure for purification of the reactants, conduct of the photolysis, and analysis of the products are given in Part II of this series (2).

Polarographic half-wave potentials were measured for the reduction of certain unsaturated compounds at the dropping mercury electrode, using a Sargent model XXI d-c. polarograph. Solutions, 1.0 mM, were prepared in acetonitrile containing 0.1 M tetrabutylammonium iodide as a supporting electrolyte. The acetonitrile and the tetrabutyl ammonium iodide were respectively of the Spectro and the White Label grade of the Eastman Chemical Company, and the mercury was freshly distilled before use. Each solution was held at 25 °C in a thermostat and deoxygenated by bubbling purified nitrogen through it for 20 min before making a measurement. The half-wave potentials were measured relative to the potential of the mercury pool. In certain systems the supporting electrolyte began to decompose before the completion of the polarographic step. To obtain an approximate result, a blank run was made first, and then the reduction of a 5 mM solution was recorded on the same chart; the difference of the two traces was evaluated.

RESULTS AND DISCUSSION

The Arrhenius parameters and rate constants for the addition of the ethyl radical to cycloheptatriene and bicycloheptadiene are given in Table I and Fig. 1; corresponding results obtained for cyclohexadiene-1,3 (1), cyclooctatetraene (2), and octene-1 (1) are included for reference. The principal aim of this section is to enquire whether the kinetic results reveal any general pattern of reactivity among the cyclic polyenes. Figure 2 reveals a satisfactory correlation between the relative methyl affinity and the rate constant for the addition of the ethyl radical; the scatter about the reference line of unit gradient is small. In a few cases the comparison has been made between the values for two closely related substrates; details are given in Table II.

In addition to the five olefins mentioned above, cyclohexadiene-1,4, cyclooctadiene-1,5, and benzene were examined but were found to be unreactive towards the addition of the ethyl radical. The monocyclic polyenes will be considered as a group first; the special problem of the reactivity of bicycloheptadiene then forms a natural sequel.

Can. J. Chem. Downloaded from www.nrcresearchpress.com by 210.87.254.105 on 09/05/12
For personal use only.

Can. J. Chem. Downloaded from www.nrcresearchpress.com by 210.87.254.105 on 09/05/12
For personal use only.

TABLE I

Addition of the ethyl radical to cyclic polyenes*

Substrate	No. of expts.	Range of temp. (°C)	C	B	$13 + \log (A_7/A_2^{1/2})$	$E_7 - \frac{1}{2}E_2$ (kcal/mole)	$13 + \log (k_7/k_2^{1/2})$ at 100 °C	k_7/k_6 at 60 °C	$R(C_2H_4)/R(C_4H_{10})$
Cyclohexadiene-1,3	14	49–116	5.552	1.145	5.5±0.2	5.2±0.3	2.48±0.04	4.7	0.120±0.010
Cycloheptatriene	11	50–133	5.857	1.391	5.9±0.1	6.4±0.2	2.13±0.04	4.3	0.119±0.005
Cyclooctatetraene	12	51–119	5.271	1.216	5.3±0.4	5.6±0.6	2.01±0.07	17	0.123±0.006
Bicycloheptadiene	9	50–131	5.811	1.526	5.8±0.1	7.0±0.1	1.72±0.17	High	0.132±0.002
Octene-1	11	66–152	5.485	1.664	5.5±0.1	7.6±0.2	1.03±0.03	2.3	0.137±0.006

*The quantities B and C are the coefficients of the straight line $13 + \log k_7/k_2^{1/2} = C - 10^3B/T$ fitted to the results; the units of k are cm^3 molecule^{-1} s^{-1}; the limits of error are calculated at the 5% probability level.

TABLE II

Correlation of the rate constant for the addition of the ethyl radical to the substrate B with the methyl affinity of the identical or closely related substrate B′, each at 65 °C

Substrate B	$13 + \log (k_7/k_2^{1/2})$	Log (methyl affinity)	Substrate B′
Octene-1 (1)	0.56	1.14	Heptene-1 (9)
2-Methylpentene-1 (6)	0.79	1.56	Isobutene (9)
Vinyl acetate (7)	0.91	1.57	Vinyl acetate (10)
2,5-Dimethylhexadiene-2,4 (1)	0.92	1.33	2,5-Dimethylhexadiene-2,4 (11)
Bicycloheptadiene	1.30	2.06	Bicycloheptadiene (3)
cis-Crotononitrile (8)	1.38	1.87	Mixed crotononitriles (12)
trans-Crotononitrile (8)	1.55	1.87	Mixed crotononitriles (12)
Methyl *trans*-crotonate (6)	1.61	1.83	Methyl crotonate (95% *trans*) (12)
Cyclooctatetraene (2)	1.67	1.91	Cyclooctatetraene (3)
Cycloheptatriene	1.88	2.19	Cycloheptatriene (3)
Cyclohexadiene-1,3 (1)	2.16	2.82	Cyclohexadiene-1,3 (3)
Styrene (7)	2.30	2.91	Styrene (10)
Methyl methacrylate (6)	2.55	3.16	Methyl methacrylate (12)
Methyl acrylate (6)	2.57	3.02	Methyl acrylate (12)
2,3-Dimethylbutadiene-1,3 (1)	2.71	3.35	2,3-Dimethylbutadiene-1,3 (11)
Methacrylonitrile (8)	2.76	3.33	Methacrylonitrile (12)
Acrylonitrile (7)	2.94	3.24	Acrylonitrile (10, 12)

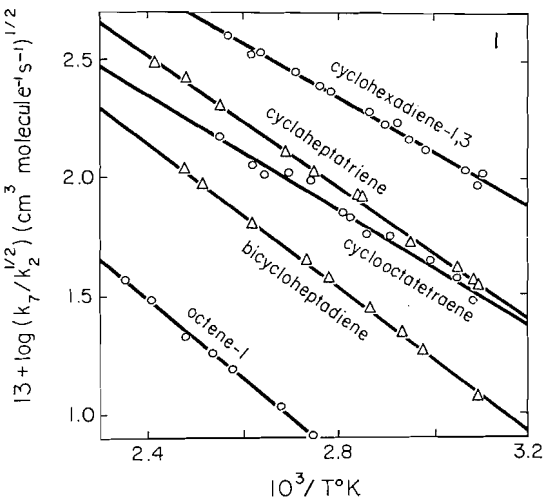

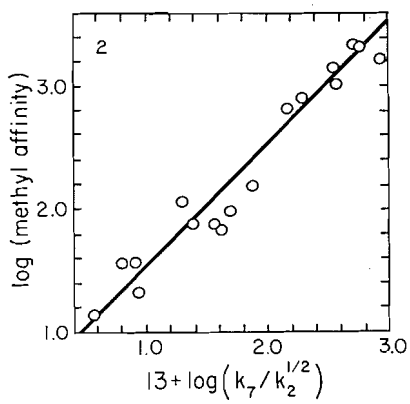

FIG. 1. Addition of the ethyl radical to cyclic polyenes. Values of $E_7 - \frac{1}{2}E_2$ are: cyclohexadiene-1,3, 5.2 ± 0.3 kcal/mole; cycloheptatriene, 6.4 ± 0.2 kcal/mole; cyclooctatetraene, 5.6 ± 0.6 kcal/mole; bicycloheptadiene, 7.0 ± 0.1 kcal/mole; octene-1, 7.6 ± 0.2 kcal/mole.

FIG. 2. Correlation of the rate constant for addition of the ethyl radical in the gas phase with the methyl affinity in solution, each at 65 °C. The values of the rate constants are listed in Table II. The reference line has unit gradient.

THE MONOCYCLIC POLYENES

Cyclohexadiene-1,3 is significantly more reactive than cycloheptatriene-1,3,5 with respect to both the energy of activation and the rate constant at 100 °C. The diene system of cyclohexadiene-1,3 is probably almost coplanar and fully delocalized. The triene system of cycloheptatriene is characterized by a dihedral angle of 40.5°, but even so a quite high degree of delocalization is indicated by the particularly short C—C single bonds of the conjugated system (13). Reactivity should therefore be high for both cycloheptatriene and cyclohexadiene-1,3, but higher for the latter, as it is more completely

Can. J. Chem. Downloaded from www.nrcresearchpress.com by 210.87.254.105 on 09/05/12
For personal use only.

delocalized. Both molecules should show reactivity toward addition at the two terminal atoms of the conjugated system; furthermore cycloheptatriene may also be reactive at the medial atoms $C_{(3)}$ and $C_{(4)}$, as the adduct should then possess allylic stability. This is suggested by the values of the pre-exponential factor, which is twice as great for cycloheptatriene as for cyclohexadiene-1,3, and is supported by a study of the free radical arylation of cycloheptatriene, where medial addition appears to be important (14). The latter evidence should be treated with reserve, however, as an intramolecular 1,5-transannular hydrogen shift occurs readily in cycloheptatriene and its monophenyl derivatives between 100 and 140 °C, accompanied by a complementary migration of double bonds (15, 16).

The rate constants for addition to cycloheptatriene and cyclooctatetraene do not differ greatly over the temperature range of our experiments, but the energies of activation are significantly different at 6.37 ± 0.22 and 5.56 ± 0.58 kcal/mole respectively. These results should be considered in conjunction with Trætteberg's critical assessment (13) of the significance of the molecular parameters of the conjugated systems of butadiene-1,3, cycloheptatriene, and cyclooctatetraene obtained by electron diffraction studies in the gas phase. The relevant values are listed in order for butadiene-1,3, cycloheptatriene, and cyclooctatetraene:

single bond length, 1.483, 1.446, and 1.462 Å;
double bond length, 1.337, 1.356, and 1.334 Å;
dihedral angle, 0, 40.5, and 42.3°.

Comparison of the bond distances indicates a higher degree of delocalization in the cycloheptatriene molecule than in cyclooctatetraene molecule. On the other hand, the π-electron system of the cyclooctatetraene molecule extends around the entire molecule, whereas the π-electron system of the cycloheptatriene molecule is interrupted by the methylene group, which separates the $C_{(1)}$ and $C_{(6)}$ atoms by 2.511 Å. Perhaps a mutual compensation of these two effects leads to the similarity in the rate constants for cycloheptatriene and cyclooctatetraene. However, anomalies in the values of the molecular parameters above compel us to regard the question as open until the bond lengths of butadiene-1,3 and cyclooctatetraene have been confirmed or revised (13).

The energy of activation for the addition of the ethyl radical to cyclooctatetraene is sufficiently low to suggest that an explanation should be sought in terms of those properties of cyclooctatetraene which set it apart from the other cyclic polyenes. Electron affinity is such a property, and relative values may be obtained from the polarographic half-wave reduction potentials. Half-wave potentials relative to the mercury pool were measured for cyclooctatetraene and a variety of other unsaturated compounds in acetonitrile, and are listed in Table III with some corresponding literature values obtained under comparable conditions (17–19). The electron affinity of cyclooctatetraene is remarkably high for a non-aromatic hydrocarbon, and high in comparison with acrylonitrile. The electron spin resonance spectrum of the cyclooctatetrenyl radical-anion indicates that the electron spin density is the same at each of the eight carbon atoms of the ring (20). A planar conformation for the radical anion is consistent with the spectral parameters, with the position of the disproportionation equilibrium, and with the rates of the electron exchange reactions (20). The radical-anion resembles the dianion in conformation, but differs from cyclooctatetraene, which has D_{2d} symmetry with dihedral angles of 42.3° (21). However, a study of the rapid interconversion of the single and double bonds of cyclooctatetraene indicates that the molecule must very frequently

Can. J. Chem. Downloaded from www.nrcresearchpress.com by 210.87.254.105 on 09/05/12
For personal use only.

assume the planar configuration of the transition state, having a compression energy of 13.7 kcal/mole, a strain energy of 20–30 kcal/mole, and a resonance energy of 5–15 kcal/mole (22). A possibly more accurate estimate of 21 kcal/mole for the compression energy was obtained from the polarographic results (18, 20).

In view of the properties of cyclooctatetraene and its radical-anion, it seems reasonable to propose that the high electron affinity of cyclooctatetraene, in conjunction with the ionization potential of 8.78 V for the ethyl radical (23), may introduce an appreciable and favorable polar effect into the addition reaction, and so contribute to the lowering of the activation energy for addition to cyclooctatetraene.

Addition of the ethyl radical to cyclooctatetraene is likely to follow a 1,4 pattern yielding 1,4-diethylcyclooctatriene-2,5,7. Certainly the α-cyanoisopropyl radical adds to cyclooctatetraene in solution at 80° yielding 1,4-bis(α-cyanoisopropyl)cyclooctatriene-2,5,7 without producing coloration, ring contraction, or polymerization (24). The ethyl radical should react more rapidly than the α-cyanoisopropyl radical with cyclooctatetraene, as the latter is both less reactive and subject to an unfavorable polar effect; ring contraction is therefore unlikely to accompany the addition of the ethyl radical to cyclooctatetraene.

TABLE III

Polarographic half-wave potentials relative to the mercury pool, measured for 1.0 mM solutions in acetonitrile containing 0.1 M tetrabutylammonium iodide at 25 °C

Compound	Half-wave potential (volts)	
	This work	Literature value
Cyclooctatetraene	−1.28	−1.12 in 96% dioxane–water (19)
Cycloheptatriene	−1.96	—
Styrene	−1.98	−1.96 in dimethyl formamide (20)
Acrylonitrile	−1.67	—
cis-Crotononitrile	−1.94	—
trans-Crotononitrile	−1.95	—
Anthracene	−1.47	−1.48 in acetonitrile (20)
2,3-Dimethylbutadiene-1,3	−2.35*	—
2,5-Dimethylhexadiene-2,4	−2.35*	—
Cyclohexadiene-1,3	No wave	—
Bicycloheptadiene	No wave	—

*This value is approximate as the reduction wave was incomplete.

The addition of the ethyl radical to benzene, to cyclohexadiene-1,4, and to cyclooctadiene-1,5 proceeded too slowly to be detected by the methods of this investigation. Indeed, benzene appears to be generally unreactive towards the ethyl radical in the gas phase, as neither metathesis nor addition could be detected. However, an estimate can be made, for each experiment performed, of the maximum value (U_7) that the addition rate constant could have while addition remained undetectable. As

$$M = [R(C_2H_6) + R(C_4H_{10})]/R(CO) = 1.005 \pm 0.005$$

for the photolysis of pure gaseous diethyl ketone, it seems reasonable to assume that the rate of addition should be detectable if:

$$\frac{k_7}{k_2^{1/2}} > \frac{0.02R(CO)}{[B]R(C_4H_{10})^{1/2}} = U_7.$$

Each value of U_7 was compared with the value (V_7) of $k_7/k_2^{1/2}$ for octene-1 at the same temperature, obtained from the observed results by interpolation. Table IV shows that

Can. J. Chem. Downloaded from www.nrcresearchpress.com by 210.87.254.105 on 09/05/12
For personal use only.

the ratio U_7/V_7 may be as low as 0.006. Similarly we can estimate the maximum value (U_6) that the metathetical rate constant could have while metathesis remained undetectable in a given experiment. It was assumed that metathesis should be detectable if:

$$\frac{k_6}{k_2^{1/2}} > \frac{[D]k_4}{10[B]k_2^{1/2}} = U_6.$$

Each value of U_6 was compared with the value (V_6) of $k_6/k_2^{1/2}$ for octene-1 at the same temperature, obtained from the observed results by interpolation. Table IV shows that the ratio U_6/V_6 may be as low as 0.02. The radical displacement reaction:

$$CH_3CH_2\cdot + C_6H_6 \rightarrow CH_3CH_2C_6H_5 + H\cdot$$

may be ruled out as no hydrogen was found among the products. We conclude that benzene is generally unreactive towards the ethyl radical in the gas phase.

The low reactivity of benzene towards alkyl radicals is evident from the behavior of a mixture of benzene and ethylene under conditions which lead to the radical polymerization of ethlyene. In the presence of di-*tert*-butyl peroxide at 20 000 p.s.i. and 130 °C, polymer was formed containing a small but definite amount of benzene, but kinetic analysis showed that the benzene was incorporated entirely by chain transfer. Copolymerization failed because the polyethylene radical would not add to benzene; as this is the most reactive of the polymer radicals, it is unlikely that conventional methods will bring about the free radical copolymerization of benzene (25).

TABLE IV

Comparison of the reactivity of benzene and octene-1 towards the ethyl radical with respect to both addition and metathesis

Temp. (°C)	Addition			Metathesis		
	$U_7(C_6H_6)$	$V_7(C_8H_{16})$	U_7/V_7	$U_6(C_6H_6)$	$V_6(C_8H_{16})$	U_6/V_6
101	0.101	10.8	0.0093	0.082	4.6	0.018
104	0.111	11.8	0.0094	0.080	5.0	0.016
113	0.103	14.9	0.0069	0.111	6.3	0.018
130	0.130	22.7	0.0057	0.202	9.6	0.021

*The quantities U_i and V_i represent respectively an estimated upper limit and an actual value of $k_i/k_2^{1/2}$ for the species named, where $i = 7$ for addition and $i = 6$ for metathesis.

Metathesis with the ethyl radical is rapid for both cyclohexadiene-1,4 and cyclooctadiene-1,5. This raises the accessible lower limit of U_7 to relatively high values, as only those conditions which give accurate values of $k_6/k_2^{1/2}$, and thereby confirm that the simple mechanism remains valid, may be used for the calculation of U_7. Accordingly the values of U_7 may be many times greater than the corresponding values of $k_7/k_2^{1/2}$. With bicycloheptadiene as the reference substance, the values of U_7/V_7 for cyclohexadiene-1,4 included 0.13, 0.19, 0.16, and 0.17 at 74, 95, 118, and 133 °C respectively; for cyclooctadiene-1,5 the values included 0.11, 0.08, 0.07, 0.12, and 0.08 at 77, 99, 100, 111, and 129 °C respectively. Clearly, both cyclohexadiene-1,4 and cyclooctadiene-1,5 are significantly less reactive than bicycloheptadiene towards the addition of the ethyl radical.

In contrast, the radicals $CCl_3\cdot$, $CH_3CO\cdot$ and $(CH_3)_3CNHCO\cdot$ all add readily to cyclooctadiene-1,5 in solution. The adduct radicals isomerize by cycloaddition to a bicyclic structure, and derivatives of bicyclo[3.3.0]octane have been isolated (26). It is perhaps significant that all the radicals which add readily to cyclooctadiene-1,5 are markedly electrophilic. Conjugation between the double bonds of cyclooctadiene-1,5 is most

Can. J. Chem. Downloaded from www.nrcresearchpress.com by 210.87.254.105 on 09/05/12
For personal use only.

unlikely, but the *cis–cis* conformation appears to promote intramolecular cycloaddition. The bicyclocopolymerization of sulfur dioxide with cyclooctadiene-1,5 is a related radical addition reaction; the copolymer repeating unit contains two molecules of sulfur dioxide per molecule of cyclooctadiene-1,5, and includes a 1,5 transannular sulfur dioxide bridge indicating intramolecular cyclization (27). Intramolecular cyclization also occurs in the radical copolymerization of sulfur dioxide with bicycloheptadiene, leading to nortricyclyl units in the polymer (28). Indeed, intramolecular cyclization commonly accompanies radical addition to bicycloheptadiene, and will be discussed in the next section.

BICYCLO[2.2.1]HEPTADIENE-2,5

Bicycloheptadiene is significantly more reactive than octene-1 towards the addition of the ethyl radical. Table I shows that bicycloheptadiene has a significantly greater value for the energy of activation, the pre-exponential factor, and the rate constant at 100 °C; if the last value is divided by 4 on statistical grounds, the quotient is still greater than the corresponding rate constant for octene-1. Bicycloheptadiene is also significantly more reactive than cyclohexene (29) and cyclohexadiene-1,4 towards the addition of the ethyl radical.

Each of these cyclic olefins possesses formally isolated double bonds which form part of a six-membered ring. The pre-eminence of bicycloheptadiene is therefore remarkable, and it is paralleled in other systems, notably in the addition of methyl (3), thiyl (30, 31), acyl, and trichloromethyl radicals (31), and in the easy radical homopolymerization (32, 33) and copolymerization (4, 28, 33, 34) of bicycloheptadiene. The bicyclic structure of bicycloheptadiene is strained, and maintains the carbon atoms of the double bonds in greater continuous proximity than is possible in the molecule of cyclohexadiene-1,4. These two aspects of the molecular geometry provide the basis for two interpretations of the high reactivity of bicycloheptadiene towards radical addition: release of I-strain on the formation of the new bond, or stabilization of the adduct by the assumption of a non-classical mesomeric homoallylic structure. The second explanation is made plausible by the formation of both norbornenyl and nortricyclyl aryl thioethers on the addition of thiocresol (30) or thiophenol (31) to bicycloheptadiene under free radical conditions. However, kinetic studies indicate that a non-classical radical adduct is unlikely to be the common precursor of the nortricyclyl and norbornenyl isomers. First, the ratio of the isomers was not independent of the concentration of the reactants, but decreased substantially as the thiol concentration was increased (30). This is consistent with the slow isomerization of the initial radical adduct from a norbornenyl structure to a nortricyclyl structure. Secondly, the ratio of the rate constants for addition to bicyclo[2.2.1]-heptadiene-2,5 and to bicyclo[2.2.1]heptene-2 is 2.3 for the methyl radical (3) and 2.06 for the trichloromethyl radical (31). Homoallylic stabilization of the adduct cannot occur with bicycloheptene, and therefore cannot be important with bicycloheptadiene, and the effect of the second double bond upon the reactivity must be almost entirely additive. The release of I-strain upon the formation of the adduct remains as a plausible common basis for the reactivity of both bicyclic olefins (3). The absence of homoconjugative stabilization in the molecule of bicycloheptadiene has been confirmed by wave-mechanical calculations based upon the models of Pariser and Parr, and of Longuet-Higgins. Each method predicted that the ground state is the classical Kekulé structure with a delocalization energy of zero, and also predicted the wavelength of maximum absorption in the ultraviolet almost quantitatively (35). Heats of hydrogenation also give no indication of homoconjugative stabilization in bicycloheptadiene (36).

Can. J. Chem. Downloaded from www.nrcresearchpress.com by 210.87.254.105 on 09/05/12
For personal use only.

We conclude that the addition of the ethyl radical to bicycloheptadiene will form initially the 2-ethylbicyclohept-5-en-3-yl radical, which will slowly isomerize to the 2-ethyl-3-nortricycl-6-yl radical. At the relatively high ethyl radical concentrations used, the initial adduct is probably consumed by the addition of a second ethyl radical before much isomerization has occurred, so that the principal product should be 2,3-diethylbicycloheptene-5.

Metathesis between the ethyl radical and bicycloheptadiene proceeds too slowly to be detected in our systems (2); this is not unexpected, as metathesis is very slow with both the methyl radical (3) and the trichloromethyl radical (31). The ratio k_7/k_6 is therefore high for bicycloheptadiene, and this is consistent with the ready formation of high polymer from this monomer with little chain transfer under free radical conditions (32, 33).

CONCLUSION

The observed reactivity of each of the cyclic polyenes may be rationalized in terms of its molecular structure, and a broad pattern of reactivity then emerges which includes each of the polyenes studied. However, this interpretation has a piecemeal character, and it would be more satisfactory to relate the energy of activation for addition to some clearly defined, calculable parameter, such as the maximum free valence or the localization energy at the reaction center. The latter appears to be the more reliable measure of the reactivity of unsaturated compounds towards the addition of alkyl radicals and hydrogen atoms. The energy of activation for the addition of the hydrogen atom to a group of olefins shows an approximately linear correlation with the localization energy but not with the free valence (37). In this type of correlation the logarithm of the rate constant at a given temperature may replace the energy of activation if the compounds examined have a common value for the pre-exponential factor, and therefore the success of the correlation of the methyl affinity of terminal olefins with the localization energy is meaningful (38), but its general significance is diminished. Preliminary calculations (39) of localization energy and free valence for the unsaturated molecules of this and parallel investigations are currently being revised and extended, and the degree of success attained in each of the possible correlations will be discussed elsewhere (40).

ACKNOWLEDGMENT

We wish to thank the National Research Council for the financial support of this work, and for a studentship to A. C. R. B.

REFERENCES

1. A. C. R. Brown and D. G. L. James. Can. J. Chem. In press. 1965.
2. A. C. R. Brown and D. G. L. James. Part II of this series. Can. J. Chem. **43**, 660 (1965).
3. J. Gresser, A. Rajbenbach, and M. Szwarc. J. Am. Chem. Soc. **83**, 3005 (1961).
4. E. S. Ferdinandi, W. P. Garby, and D. G. L. James. Part I of this series. Can. J. Chem. **42**, 2568 (1964).
5. D. G. L. James and E. W. R. Steacie. Proc. Roy. Soc. London, Ser. A, **244**, 289 (1958).
6. D. G. L. James and S. M. Kambanis. Unpublished results.
7. D. G. L. James and D. MacCallum. Can. J. Chem. **43**, 633 (1965).
8. D. G. L. James and T. Ogawa. Can. J. Chem. **43**, 640 (1965).
9. R. P. Buckley and M. Szwarc. Proc. Roy. Soc. London, Ser. A, **240**, 396 (1957).
10. M. Szwarc. J. Polymer Sci. **16**, 367 (1955).
11. A. Rajbenbach and M. Szwarc. J. Am. Chem. Soc. **79**, 6343 (1957).
12. L. Herk, A. Stefani, and M. Szwarc. J. Am. Chem. Soc. **83**, 3008 (1961).
13. M. Traetteberg. J. Am. Chem. Soc. **86**, 4265 (1964).
14. R. Weiss and M. Lalande. J. Am. Chem. Soc. **82**, 3117 (1960).
15. A. P. ter Borg, H. Kloosterziel, and N. van Meurs. Rec. Trav. Chim. **82**, 717 (1963).
16. A. P. ter Borg and H. Kloosterziel. Rec. Trav. Chim. **82**, 741 (1963).

Can. J. Chem. Downloaded from www.nrcresearchpress.com by 210.87.254.105 on 09/05/12
For personal use only.

17. P. H. GIVEN and M. E. PEOVER. Advan. Polarography, **3**, 948 (1960).
18. T. J. KATZ, W. H. REINMUTH, and D. E. SMITH. J. Am. Chem. Soc. **84**, 802 (1962).
19. S. WAWZONEK, E. W. BLAHA, R. BERKEY, and M. E. RUNNER. J. Electrochem. Soc. **102**, 235 (1955).
20. H. L. STRAUSS, T. J. KATZ, and G. K. FRAENKEL. J. Am. Chem. Soc. **85**, 2360 (1963).
21. O. BASTIANSEN, L. HEDBERG, and K. HEDBERG. J. Chem. Phys. **27**, 1311 (1957).
22. F. A. L. ANET. J. Am. Chem. Soc. **84**, 671 (1962).
23. J. B. FARMER and F. P. LOSSING. Can. J. Chem. **33**, 861 (1955).
24. J. L. KICE and T. S. CANTRELL. J. Am. Chem. Soc. **85**, 2298 (1963).
25. G. A. MORTIMER and LL. C. ARNOLD. J. Am. Chem. Soc. **84**, 4986 (1962).
26. R. DOWBENKO. J. Am. Chem. Soc. **86**, 946 (1964).
27. A. H. FRAZER and W. P. O'NEILL. J. Am. Chem. Soc. **85**, 2613 (1963).
28. R. J. ALEXANDER and J. R. DOYLE. J. Polymer Sci. B, **1**, 625 (1963).
29. D. G. L. JAMES and E. W. R. STEACIE. Proc. Roy. Soc. London, Ser. A, **244**, 297 (1958).
30. S. J. CRISTOL, G. D. BRINDELL, and J. A. REEDER. J. Am. Chem. Soc. **80**, 635 (1958).
31. D. J. TRECKER and J. P. HENRY. J. Am. Chem. Soc. **85**, 3204 (1963).
32. R. H. WILEY, W. H. RIVERA, T. H. CRAWFORD, and N. F. BRAY. J. Polymer Sci. **61**, S40 (1962).
33. J. PELLON, R. L. KUGEL, R. MARCUS, and R. RABINOWITZ. J. Polymer Sci. A, **2**, 4105 (1964).
34. N. ZUTTY. J. Polymer Sci. A, **1**, 2231 (1963).
35. C. F. WILCOX, JR., S. WINSTEIN, and W. G. MCMILLAN. J. Am. Chem. Soc. **82**, 5450 (1960).
36. R. B. TURNER, W. R. MEADOR, and R. E. WINKLER. J. Am. Chem. Soc. **79**, 4116 (1957).
37. K. YANG. J. Am. Chem. Soc. **84**, 3795 (1962).
38. J. H. BINKS and M. SZWARC. J. Chem. Phys. **30**, 1494 (1959).
39. A. C. R. BROWN. Doctoral Thesis, The University of British Columbia. October 1962.
40. J. E. BLOOR, A. C. R. BROWN, and D. G. L. JAMES. Unpublished results.

Can. J. Chem. Downloaded from www.nrcresearchpress.com by 210.87.254.105 on 09/05/12
For personal use only.

Can. J. Chem. Downloaded from www.nrcresearchpress.com by 210.87.254.42 on 09/05/12
For personal use only.

LA PYROLYSE DU PROPANE ET DE L'ISOPENTANE

INFLUENCE DE TRACES D'OXYGÈNE ET EFFETS DE PAROIS[1]

M. NICLAUSE, R. MARTIN, A. COMBES ET M. DZIERZYNSKI
Laboratoire de Chimie Générale, Université de Nancy, Nancy, France

Reçu le 16 novembre 1964

ABSTRACT

Results obtained in an analytical and kinetic study of propane or isopentane pyrolysis, either pure or in presence of trace amounts of oxygen, are reported. It is shown particularly, that oxygen accelerates or inhibits the reaction, depending upon wall conditions; an interpretation of this dual effect is proposed. The fact that the pyrolysis of these hydrocarbons can be inhibited almost completely under given conditions proves that any molecular mechanism of decomposition is negligible as compared to the chain reaction.

INTRODUCTION

Il a été montré (1) que des traces d'oxygène accélèrent fortement la pyrolyse de divers hydrocarbures saturés, du moins dans un réacteur "vide" en pyrex dont le rapport surface/volume (en abrégé: rapport s/v) est voisin de 1 cm^{-1}. Mais, dans ces travaux préliminaires, on n'a pas recherché si les parois du réacteur jouent ou non un rôle dans cette réaction, ni si la présence de traces d'oxygène modifie la composition des produits de pyrolyse de l'hydrocarbure; l'influence cinétique des pressions initiales de l'oxygène et de l'hydrocarbure n'a pas été étudiée non plus.

Aussi avons-nous entrepris, en 1959, une nouvelle étude comparée de la décomposition thermique d'hydrocarbures saturés, purs ou additionnés de traces d'oxygène. Nos premières observations et conclusions (relatives au propane) ont été présentées entre 1961 et 1964 (2).

Nous présentons ci-dessous les principaux résultats obtenus dans les cas du propane et de l'isopentane.

Ces réactions ont été examinées à faible avancement (inférieur à 10%) à l'aide d'un montage statique à volume constant. Pour suivre la réaction en fonction du temps, nous avons employé la technique de la chromatographie gazeuse et la méthode manométrique (manomètre différentiel à phtalate de butyle). La pyrolyse du propane a été étudiée dans des réacteurs en pyrex ou en silice, celle de l'isopentane seulement dans des réacteurs en pyrex.

PYROLYSE DU PROPANE PUR OU DE L'ISOPENTANE PUR

(1) Nous avons tout d'abord analysé, par chromatographie gazeuse, les produits de pyrolyse de ces hydrocarbures à faible avancement.

Dans le cas du propane, la réaction peut être essentiellement représentée par les deux équations stoechiométriques suivantes:

$$C_3H_8 = H_2 + C_3H_6$$
$$C_3H_8 = CH_4 + C_2H_4$$

qui, à moins de 5% d'avancement, ont des importances sensiblement égales vers 550 °C (2).

[1]*Communication présentée au symposium: The kinetics of pyrolytic reactions, qui s'est tenu à l'Université d'Ottawa, Canada, 9–11 septembre 1964.*

A 480 °C, les produits principaux de pyrolyse de l'isopentane (P_0 = 25 mm Hg) sont les suivants: hydrogène, méthane, éthane, propane, éthylène, propylène, butènes (isobutène, butène-1, butènes-2 *cis* et *trans*) et isopentènes. La réaction peut être essentiellement représentée par les cinq équations stoechiométriques suivantes, dont les importances relatives, vers 2% d'avancement, sont indiquées entre parenthèses:

$$i\text{-}C_5H_{12} = CH_4 + \text{butènes} \quad (73.2\%)$$

$$i\text{-}C_5H_{12} = H_2 + C_2H_4 + C_3H_6 \quad (14.4\%)$$

$$i\text{-}C_5H_{12} = C_2H_6 + C_3H_6 \quad (9.8\%)$$

$$i\text{-}C_5H_{12} = C_3H_8 + C_2H_4 \quad (2\%)$$

$$i\text{-}C_5H_{12} = H_2 + \text{isopentènes}. \quad (0.6\%)$$

Ces résultats analytiques vers 2% d'avancement (et à 480 °C) sont notablement différents de ceux observés récemment par Bryce et Chrysochoos (3) à 42% d'avancement (et à 510 °C).

(2) Nous avons ensuite cherché à voir si les parois du réacteur ont, ou non, une influence sur la vitesse de pyrolyse du propane pur ou de l'isopentane pur.

Voevodsky (4) signalait que la vitesse initiale de pyrolyse du propane (T = 610 °C; P_0 = 25 mm Hg) diminue fortement lorsqu'on augmente le rapport s/v d'un réacteur en silice (Fig. 1, courbe 2). Au contraire, Laidler, Sagert et Wojciechowski (5) observaient seulement de légers effets des parois en silice ($530 < T$ (°C) < 620; $30 < P_0$ (mm Hg) < 600).

Nos résultats expérimentaux montrent que la vitesse initiale de pyrolyse du propane ($525 < T$ (°C) < 600; $10 < P_0$ (mm Hg) < 150) est pratiquement indépendante du rapport s/v ($0.7 < s/v$ (cm^{-1}) < 16) du réacteur en pyrex ou en silice (Fig. 1, courbe 1, et Fig. 2) (les vitesses initiales V_0 portées dans les figures ont subi la correction d'espace mort).

De plus, la vitesse est pratiquement la même, que les parois aient été ou non traitées à l'acide fluorhydrique ou recouvertes de KCl ou de PbO (2).

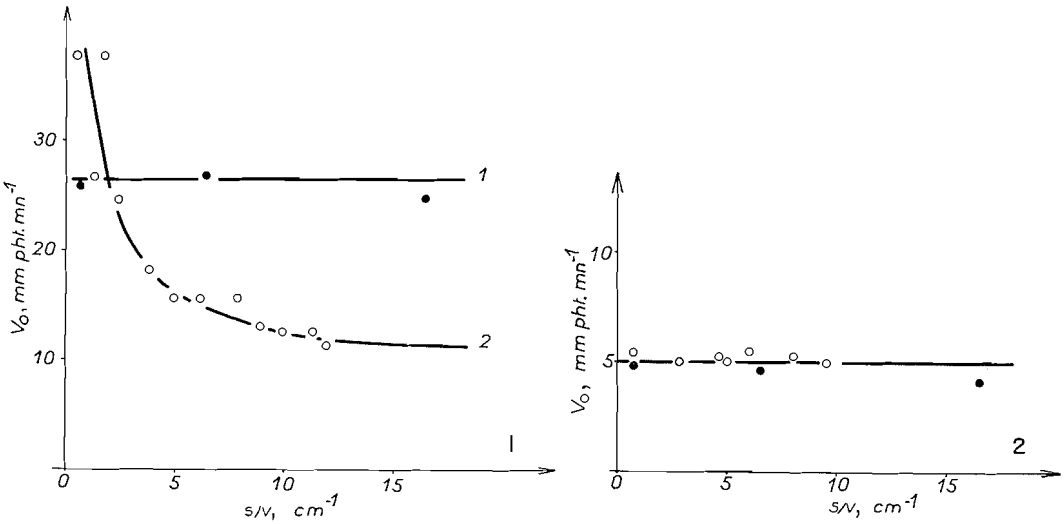

FIG. 1. Pyrolyse du propane (P_0 = 25 mm Hg), vitesse initiale en fonction du rapport surface/volume du réacteur en silice: (1) d'après nos expériences à 600 °C; (2) d'après Voevosdky (1959) à 610 °C.

FIG. 2. Pyrolyse du propane (P_0 = 25 mm Hg, T = 546 °C), vitesse initiale en fonction du rapport surface/volume du réacteur: ○ pyrex; ● silice.

Can. J. Chem. Downloaded from www.nrcresearchpress.com by 210.87.254.42 on 09/05/12
For personal use only.

De même, la vitesse initiale de pyrolyse de l'isopentane dans des réacteurs en pyrex (T = 480 °C; P_0 = 25 mm Hg) est pratiquement indépendante du rapport s/v ($0.8 < s/v$ (cm^{-1}) < 12), contrairement à ce qui a été observé récemment par Bryce et Chrysochoos (3) dans des réacteurs en silice. Le dépôt de KCl ou de PbO sur les parois n'affecte pratiquement pas, non plus, la vitesse initiale de pyrolyse de l'isopentane (Fig. 3).

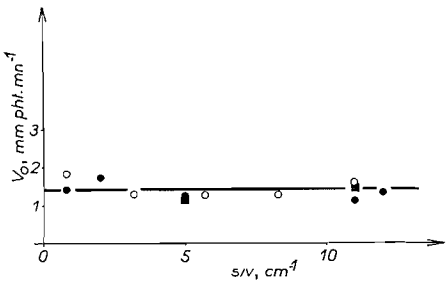

FIG. 3. Pyrolyse de l'isopentane (P_0 = 25 mm Hg, T = 480 °C), vitesse initiale en fonction du rapport surface/volume du réacteur: ○ pyrex; ■ pyrex traité à KCl; ● pyrex traité à PbO.

Il convient de noter que, dans certains cas, nous avons observé un léger abaissement de la vitesse de pyrolyse du propane ou de l'isopentane après introduction, dans le réacteur, d'un remplissage non spécialement nettoyé. Mais ce phénomène disparaissait après lavage du réacteur et de son remplissage au mélange sulfo-chromique ou, plus difficilement, après séjour d'oxygène (à la pression atmosphérique) dans le réacteur, à la température de l'expérience.

(3) Contrairement à l'opinion de Voevodsky (4), mais en accord avec celle émise en 1962 par Laidler, Sagert et Wojciechowski (5), nous pensons donc que la pyrolyse du propane pur est une réaction essentiellement homogène (du moins dans des réacteurs en silice, en pyrex et en pyrex traité à HF ou recouvert de KCl ou de PbO), comme la décomposition thermique du butane-*n* pur (dans des réacteurs en pyrex et en pyrex traité à HF ou recouvert de KCl) étudiée par Purnell et Quinn (6). Nous pensons qu'il en est de même de la pyrolyse de l'isopentane pur (dans des réacteurs en pyrex et en pyrex recouvert de KCl ou de PbO).

Comme l'ont fait remarquer Wojciechowski et Laidler (7) en 1963, l'éventualité de la participation à l'initiation et à la terminaison des chaînes, de processus hétérogènes, ne peut pas être totalement éliminée; mais elle nous paraît peu probable dans nos conditions expérimentales, car il faudrait alors que les divers traitements de parois envisagés modifient dans un même rapport les vitesses d'initiation et de terminaison.

Quant au désaccord entre les résultats de Voevodsky (4) et les nôtres relatifs au propane, nous allons voir qu'il pourrait s'expliquer par la présence de traces d'oxygène dans les expériences de Voevodsky.

PYROLYSE DU PROPANE OU DE L'ISOPENTANE EN PRÉSENCE DE TRACES D'OXYGÈNE

(1) Nous avons tout d'abord mis en évidence les faits suivants, à propos de la décomposition thermique du propane ou de l'isopentane ($480 < T$ (°C) < 550; $20 < P_0$ (mm Hg) < 100) en présence de traces d'oxygène (0.5 à 2%).

Dans un réacteur de faible rapport s/v, l'oxygène accélère considérablement la pyrolyse du propane ou de l'isopentane à ses débuts, mais cet effet accélérateur n'est observé que pendant un temps très court (Fig. 4 et 5, courbes 1). Lorsque le rapport s/v augmente,

Can. J. Chem. Downloaded from www.nrcresearchpress.com by 210.87.254.42 on 09/05/12
For personal use only.

l'effet accélérateur de l'oxygène diminue (Fig. 4 et 5). Dans le cas du propane, il finit même, à de fortes valeurs du rapport s/v, par se transformer en un effet inhibiteur croissant, qui persiste alors pendant un certain temps (Fig. 4, courbes 2 et 2').

Autrement dit, la vitesse initiale de pyrolyse du propane ou de l'isopentane additionné de traces d'oxygène décroît très fortement lorsque le rapport s/v augmente, tandis qu'en l'absence d'oxygène, la variation de vitesse avec s/v est négligeable (Fig. 6 et 7).

L'allure des courbes 1 des Fig. 4 et 5 montre qu'il est très difficile—voire impossible—de mesurer la vitesse initiale réelle V_0 de la réaction, lorsque celle-ci est fortement accélérée

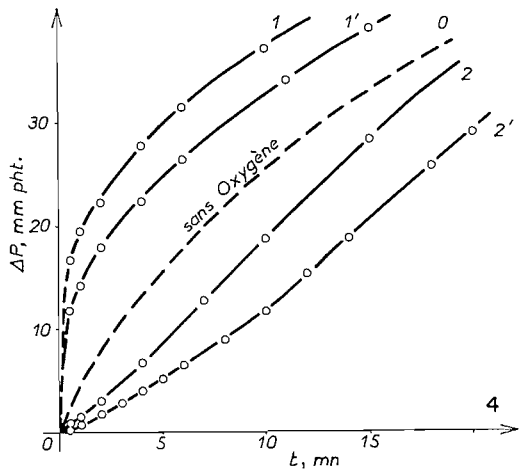

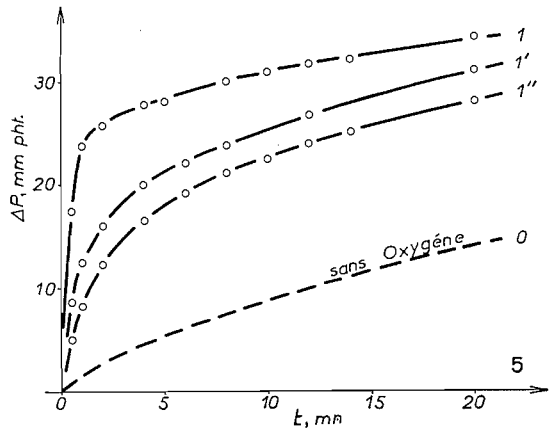

FIG. 4. Pyrolyse du propane (P_0 = 25 mm Hg, T = 546 °C) en présence de traces d'oxygène (0.5%); augmentation de pression en fonction du temps dans un réacteur en pyrex: (1) s/v = 0.7 cm^{-1}; (1') s/v = 5 cm^{-1}; (2) s/v = 8 cm^{-1}; (2') s/v = 9.5 cm^{-1}.

FIG. 5. Pyrolyse de l'isopentane (P_0 = 25 mm Hg, T = 480 °C) en présence de traces d'oxygène (1%); augmentation de pression en fonction du temps dans un réacteur en pyrex: (1) s/v = 0.8 cm^{-1}; (1') s/v = 5.7 cm^{-1}; (1'') s/v = 12 cm^{-1}.

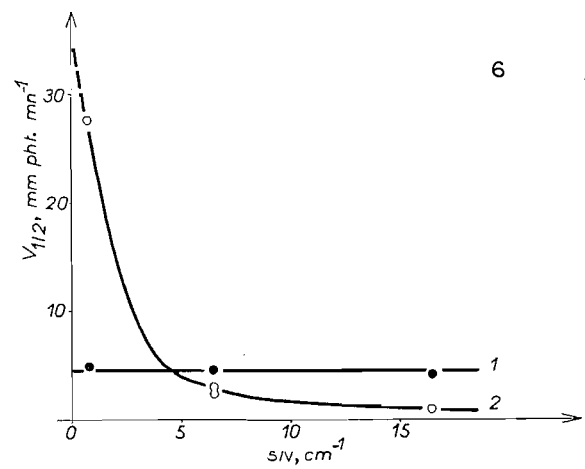

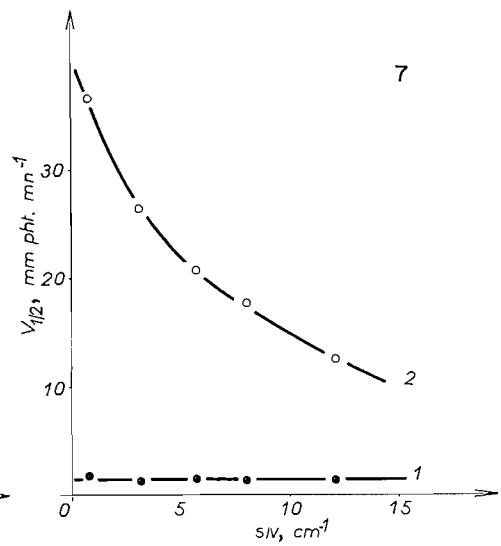

FIG. 6. Pyrolyse du propane (P_0 = 25 mm Hg, T = 546 °C); vitesse "initiale" $V_{1/2}$ en fonction du rapport surface/volume du réacteur en silice: (1) sans oxygène; (2) avec 0.5% d'oxygène.

FIG. 7. Pyrolyse de l'isopentane (P_0 = 25 mm Hg, T = 480 °C); vitesse "initiale" $V_{1/2}$ en fonction du rapport surface/volume du réacteur en pyrex: (1) sans oxygène; (2) avec 1% d'oxygène.

Can. J. Chem. Downloaded from www.nrcresearchpress.com by 210.87.254.42 on 09/05/12
For personal use only.

par l'oxygène; en effet, la vitesse est alors initialement très grande et elle décroît très rapidement. Aussi avons-nous convenu (cf. Fig. 6 et 7) de déterminer la vitesse moyenne pendant les 30 premières secondes (1/2 mn):

$$V_{1/2} = \frac{\Delta P_{1/2}}{1/2} \text{ mm phtalate mn}^{-1}.$$

Cette vitesse "initiale" $V_{1/2}$ représente une valeur approchée par défaut de la vitesse initiale réelle V_0 de pyrolyse, lorsque celle-ci est accélérée par des traces d'oxygène; au contraire, $V_{1/2}$ représente une valeur légèrement approchée par excès de la vitesse initiale réelle V_0 de pyrolyse, lorsque celle-ci est inhibée par l'oxygène. Enfin, $V_{1/2}$ représente avec une bonne approximation la vitesse initiale réelle V_0 de pyrolyse de l'hydrocarbure pur (cf. réf. 2*d*).

Il convient de remarquer que la décroissance de la vitesse initiale de pyrolyse du propane signalée par Voevodsky (4) lorsque le rapport s/v augmente (Fig. 1, courbe 2) est analogue à celle que nous observons en présence de traces d'oxygène (Fig. 6, courbe 2). Le désaccord entre les résultats de Voevodsky (Fig. 1, courbe 2) et les nôtres relatifs au propane pur (Fig. 1, courbe 1) pourrait donc s'expliquer par la présence de traces d'oxygène (moins de 0.1%) dans les expériences de Voevodsky. De même, il est vraisemblable que la pyrolyse très rapide du propane observée par cet auteur en présence de parois recouvertes de perchlorate de magnésium (4), est due à l'oxygène provenant de la décomposition thermique de ce sel.

Par ailleurs, la vitesse de pyrolyse du propane ou de l'isopentane en présence de traces d'oxygène est très sensible à la nature et à l'état des parois du réacteur.

Par exemple, la réaction est plus rapide après lavage d'un réacteur en pyrex au mélange sulfo-chromique (2).

Au contraire, la réaction est plus lente après dépôt de KCl ou de PbO sur les parois d'un réacteur (2).

L'inhibition de la réaction peut même devenir quasi-complète, pendant un certain temps, dans un réacteur de fort rapport s/v traité à PbO (Figs. 8 et 9). Ce fait expérimental nouveau prouve clairement que tout processus moléculaire de décomposition est négligeable devant la réaction en chaînes.

(2) On note, par chromatographie gazeuse, que les parois ont également une influence inhibitrice sur la vitesse de consommation de l'oxygène. C'est ainsi que lorsqu'il accélère la pyrolyse du propane, l'oxygène est très rapidement consommé (l'effet accélérateur n'est alors observé que pendant un temps très court); au contraire, lorsqu'il inhibe la réaction, l'oxygène n'est consommé que lentement (l'effet inhibiteur persiste alors pendant un temps notable) (2).

Par ailleurs, l'étude analytique, par chromatographie gazeuse, montre que la nature des produits principaux de pyrolyse du propane ou de l'isopentane n'est pas modifiée par la présence de traces d'oxygène, que celui-ci soit accélérateur ou inhibiteur. Mais la présence de traces d'oxygène introduit une stoechiométrie d'oxydation de l'hydrocarbure et modifie les importances relatives des cinq équations stoechiométriques principales de décomposition de l'isopentane en début de réaction.

(3) Nous venons de montrer que, selon les conditions expérimentales, la vitesse initiale de pyrolyse du propane ou de l'isopentane est augmentée ou diminuée (parfois considérablement) par des traces d'oxygène.

Nous pensons que ce rôle double (accélérateur et inhibiteur) de l'oxygène moléculaire

Can. J. Chem. Downloaded from www.nrcresearchpress.com by 210.87.254.42 on 09/05/12
For personal use only.

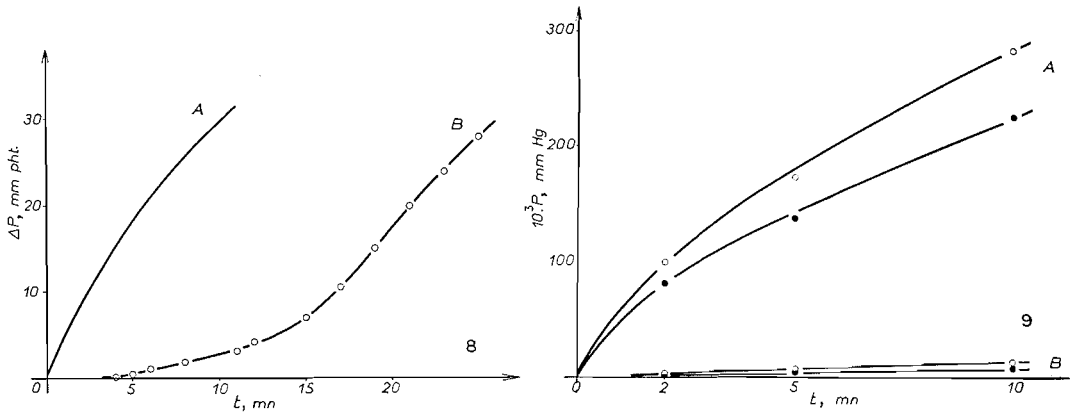

FIG. 8. Pyrolyse du propane (P_0 = 27 mm Hg, T = 551 °C); augmentation de pression en fonction du temps: (A) sans oxygène; (B) avec 1.8% d'oxygène dans un réacteur en pyrex (s/v = 4.6 cm^{-1}) traité à PbO.

FIG. 9. Pyrolyse de l'isopentane (P_0 = 25 mm Hg, T = 480 °C, pression d'échantillon = 10 mm Hg): ○ $P = C_2H_4 + C_3H_6$ + butènes: ● $P = CH_4 + C_2H_6 + C_3H_8$. (A) Sans oxygène dans un réacteur en pyrex (s/v = 0.8 cm^{-1}); (B) avec 1% d'oxygène dans un réacteur en pyrex (s/v = 11 cm^{-1}) traité à PbO.

peut s'expliquer comme suit, en partant de considérations relatives à la concurrence entre mécanismes en chaînes ayant un porteur de chaînes commun dans la réaction complexe entre l'oxygène et une substance organique (8).

(*a*) Par réaction avec l'hydrocarbure M, l'oxygène provoque l'apparition d'un processus d'induction, du type:

$$M + O_2 \rightarrow \text{radicaux libres};$$

ce nouveau processus d'initiation s'ajoutant au processus d'initiation normale:

$$M \rightarrow \text{radicaux libres}$$

l'oxygène tend à *accélérer* la pyrolyse de l'hydrocarbure.

(*b*) En l'absence d'oxygène, les radicaux libres hydrocarbonés R· ne peuvent propager que la décomposition en chaînes de l'hydrocarbure M. Mais, en présence d'oxygène, ils peuvent également s'oxyder en donnant naissance à d'autres radicaux libres R′·, oxygénés (par exemple: HO_2· et ·OH). Il se propage alors simultanément, dans le milieu, deux types de chaînes: une chaîne de décomposition et une chaîne d'oxydation de l'hydrocarbure M. La "chaîne globale complexe" qui en résulte comporte donc un certain nombre de "maillons" représentatifs de chacun des deux types de chaînes et il apparaît de nouveaux processus de terminaison des chaînes (disparition de radicaux libres oxygénés R′·). Du fait que la réaction de décomposition et celle d'oxydation ont des porteurs de chaînes communs (R·), ces deux réactions se font mutuellement concurrence et, par suite, l'oxygène peut aussi *inhiber* la pyrolyse de l'hydrocarbure M.

Rappelons que nos résultats expérimentaux mettent en évidence une influence inhibitrice des parois sur la réaction globale complexe (décomposition et oxydation) du propane ou de l'isopentane additionné de petites quantités d'oxygène. Ces faits indiquent que:

(*a*) le nouveau processus d'initiation provoqué par l'oxygène est essentiellement homogène;

(*b*) au contraire, les nouveaux processus de terminaison (qui apparaissent en présence d'oxygène) sont, en partie au moins, hétérogènes (aux parois).

Can. J. Chem. Downloaded from www.nrcresearchpress.com by 210.87.254.42 on 09/05/12
For personal use only.

Notre interprétation de la pyrolyse de l'hydrocarbure M, à l'instant initial, peut être schématisée comme indiqué ci-dessous, R· pouvant être un radical R_β· ou un radical R_μ· dans la terminologie de Goldfinger, Letort et Niclause (9).

Processus de pyrolyse de l'hydrocarbure pur.—

[1] Initiation: $M \rightarrow$ radicaux libres

[2] Propagation: $R_\mu\cdot\ (+X) \rightarrow R_\beta\cdot + P_1\ (+X)$

[3] $R_\beta\cdot + M \rightarrow R_\mu\cdot + P_2$

[4] Terminaison: $2R\cdot \rightarrow$ produits

Processus apparaissant en présence d'oxygène.—

[5] Terminaison: $R\cdot + R'\cdot \rightarrow$ produits

[6] $2R'\cdot \rightarrow$ produits

[7] $R'\cdot \xrightarrow{\text{parois}}$ produits

[8] Propagation: $R\cdot + O_2 \rightarrow R'\cdot\ (+P'_1)$

[9] $R'\cdot + M \rightarrow R_\mu\cdot + P'_2$

[10] Initiation: $M + O_2 \rightarrow$ radicaux libres

Cette représentation n'est que schématique, puisque les symboles R_β·, R_μ· et R'· peuvent, chacun, désigner plusieurs radicaux différents, étant donné que plusieurs équations stoechiométriques sont nécessaires pour représenter la réaction de décomposition du propane ou de l'isopentane.

La pyrolyse du propane ou de l'isopentane en présence d'oxygène serait donc une coréaction impliquant deux types de chaînes à interactions mutuelles, comme diverses autres réactions de décomposition, de polymérisation ou de chloration en présence d'oxygène (2*e*, 8) et comme la pyrolyse du butane-*n* en présence de propylène (10); mais, dans ce dernier cas, le propylène ne ferait pas apparaître de processus de terminaison aux parcis, ni de processus d'initiation appréciable.

A partir du schéma précédent, on peut calculer le rapport $(V_0)_{M,O_2}/(V_0)_M$ des vitesses initiales de pyrolyse de l'hydrocarbure M additionné ou non d'oxygène (toutes autres choses égales par ailleurs) dans le cas limite où l'on opérerait en l'absence de parois; que R· représente un radical R_β· ou un radical R_μ·, on trouve finalement:

$$\frac{(V_0)_{M,O_2}}{(V_0)_M} \simeq \left[\frac{1+\dfrac{k_{10}(O_2)_0}{k_1}}{1+\dfrac{k_5}{k_4}\dfrac{k_8(O_2)_0}{k_9(M)_0}+\dfrac{k_6}{k_4}\dfrac{k_8^2(O_2)_0^2}{k_9^2(M)_0^2}}\right]^{1/2}.$$

On voit que l'oxygène a non seulement une influence *accélératrice*, mais encore une influence *inhibitrice*, même en l'absence de parois.

Le rôle inhibiteur de l'oxygène est accentué par la présence de parois, puisque celles-ci font apparaître un processus hétérogène (processus 7) de terminaison des chaînes. Par conséquent, en présence de parois, on a:

$$0 < \frac{(V_0)_{M,O_2}}{(V_0)_M} < \left[\frac{1+\dfrac{k_{10}(O_2)_0}{k_1}}{1+\dfrac{k_5}{k_4}\dfrac{k_8(O_2)_0}{k_9(M)_0}+\dfrac{k_6}{k_4}\dfrac{k_8^2(O_2)_0^2}{k_9^2(M)_0^2}}\right]^{1/2};$$

Can. J. Chem. Downloaded from www.nrcresearchpress.com by 210.87.254.42 on 09/05/12
For personal use only.

en outre, la vitesse initiale de consommation de l'oxygène est elle-même plus faible qu'en l'absence de parois.

Notre représentation permet donc de concevoir que l'oxygène moléculaire joue un double rôle dans la pyrolyse du propane ou de l'isopentane—il est à la fois accélérateur et inhibiteur—et que l'importance relative de ces deux influences opposées et la nature de l'effet global qui en résulte (accélération ou inhibition) dépendent des conditions expérimentales.

(*a*) On comprend, en particulier, que la vitesse initiale de décomposition de l'hydrocarbure, en présence de traces d'oxygène, diminue lorsque le rapport s/v du réacteur augmente. Le dépôt de KCl ou de PbO sur les parois doit augmenter l'efficacité de ces parois vis-à-vis du processus hétérogène de terminaison, puisque l'influence inhibitrice de l'oxygène est accrue par de tels traitements des parois.

Remarquons que l'influence inhibitrice des parois mise en évidence ici pour la réaction globale complexe (décomposition et oxydation) du propane ou de l'isopentane, additionné de petites quantités d'oxygène, est analogue à celle observée dans les réactions d'oxydation proprement dite (en présence d'une concentration notable d'oxygène) de l'hydrogène et de divers hydrocarbures (cf. par exemple réf. 11).

(*b*) A partir de notre schéma de pyrolyse en présence d'oxygène, on peut prévoir les allures des variations de la vitesse initiale de décomposition, avec les concentrations initiales d'oxygène et d'hydrocarbure M (Fig. 10). Ce sont effectivement des allures de ce genre que l'on observe expérimentalement avec le propane (2) et avec l'isopentane.

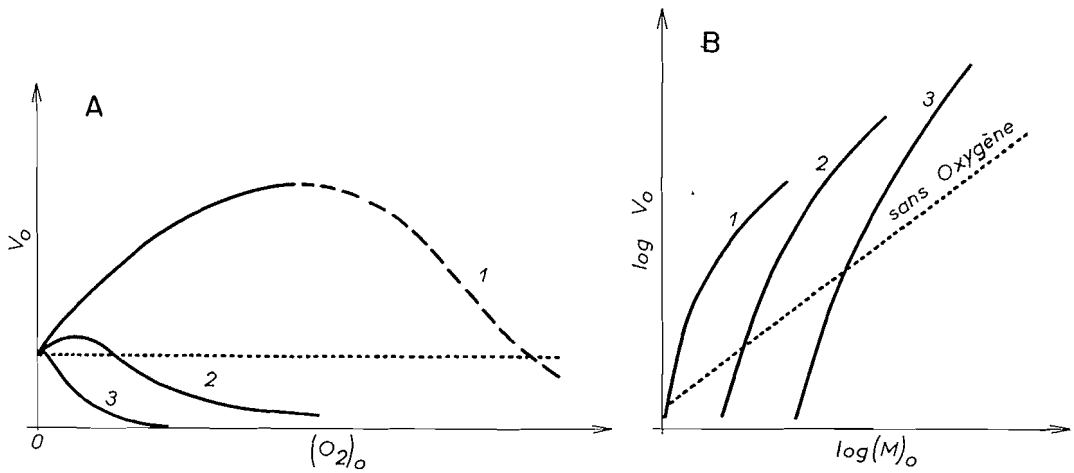

FIG. 10. Influence des concentrations initiales d'oxygène (A), dans le cas où $(M)_0 > k_1k_5k_8/k_{10}k_4k_9$, et d'hydrocarbure (B) sur la vitesse initiale V_0 de pyrolyse de l'hydrocarbure M en présence d'oxygène (représentation schématique d'après la théorie). (1) En l'absence de parois, (2) en présence de parois "moyennement efficaces", (3) en présence de parois "très efficaces" vis-à-vis du processus [7].

Remarque.—La Fig. 11 montre comment varie la vitesse instantanée V de pyrolyse du propane au cours d'une expérience: (*a*) dans le cas du propane pur, la réaction est très fortement auto-inhibée: l'ordre n au cours du temps [environ 17] est très supérieur à l'ordre initial n_0 [environ 1.25 (5)]; (*b*) en présence de traces d'oxygène (0.5%), on note, en début de réaction, une importante inhibition ou une très forte accélération de la pyrolyse selon les conditions de parois; mais la vitesse de la réaction en présence d'oxygène finit par devenir égale à celle de pyrolyse du propane pur (à même avancement). On observe des phénomènes semblables dans le cas de l'isopentane.

Can. J. Chem. Downloaded from www.nrcresearchpress.com by 210.87.254.42 on 09/05/12
For personal use only.

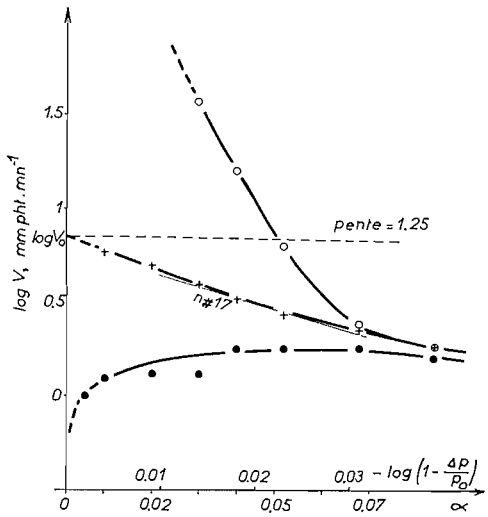

FIG. 11. Pyrolyse du propane (P_0 = 26 mm Hg, T = 547 °C, réacteur en pyrex); variations de la vitesse instantanée V au cours d'une expérience: × $(O_2)_0$ = 0% et s/v = 9.5 cm^{-1}; ● $(O_2)_0$ = 0.5% et s/v = 9.5 cm^{-1}; ○ $(O_2)_0$ = 0.5% et s/v = 0.7 cm^{-1}.

Etant donné, d'une part que la pyrolyse du propane ou de l'isopentane est une réaction très fortement auto-inhibée, d'autre part que sa vitesse initiale est très sensible aux traces d'oxygène et qu'en présence de telles traces elle dépend beaucoup des conditions de parois, il nous a paru très difficile de déterminer, avec précision, les caractéristiques cinétiques (ordre et énergie d'activation), à l'instant initial, de la pyrolyse homogène de ces hydrocarbures purs. C'est pourquoi nous n'avons pas étudié systématiquement cette question. De nos résultats expérimentaux, on peut toutefois déduire les caractéristiques cinétiques approximatives, dans certaines conditions, de la pyrolyse du propane ou de l'isopentane. En particulier, l'ordre initial n_0 est compris entre 1 et 3/2, en accord avec les observations de Laidler et coll. (5) relatives au propane. Nos résultats expérimentaux ne mettent toutefois pas en évidence des variations de n_0 si prononcées que celles observées par Laidler et coll. (5) dans le cas de la pyrolyse du propane dans un réacteur vide en silice. D'ailleurs, de brusques changements d'ordre n_0 (avec la pression initiale d'hydrocarbure) nous sembleraient difficiles à interpréter uniquement: soit par des variations des importances relatives des processus de terminaison des chaînes; soit par le fait que la décomposition d'un radical $R_\mu\cdot$, d'ordre 2 à basse pression, devient d'ordre 1 à haute pression.

CONCLUSIONS

La pyrolyse du propane pur est une réaction essentiellement homogène, du moins dans des réacteurs en silice, en pyrex et en pyrex traité à HF ou recouvert de KCl ou de PbO. Il en est de même de la pyrolyse de l'isopentane pur dans des réacteurs en pyrex et en pyrex recouvert de KCl ou de PbO.

Nous avons montré expérimentalement qu'il est possible d'inhiber de façon pratiquement complète la pyrolyse du propane ou de l'isopentane; ceci prouve que tout processus moléculaire de décomposition est négligeable devant le mécanisme en chaînes.

Il avait déjà été signalé que des traces d'oxygène accélèrent certaines réactions, tandis qu'elles en inhibent d'autres. Mais nous avons montré, avec le propane et l'isopentane, que, selon les conditions expérimentales, l'effet inhibiteur de l'oxygène sur la pyrolyse d'une

Can. J. Chem. Downloaded from www.nrcresearchpress.com by 210.87.254.42 on 09/05/12
For personal use only.

substance organique peut l'emporter ou non sur son effet accélérateur. Nous avons proposé une interprétation de cette double influence de l'oxygène. Elle postule que la pyrolyse du propane ou de l'isopentane en présence de petites quantités d'oxygène est une co-réaction impliquant deux types de chaînes à interactions mutuelles et que l'oxygène fait apparaître un nouveau processus d'initiation essentiellement homogène (qui traduit le rôle accélérateur de O_2) et de nouveaux processus de terminaison, en partie au moins hétérogènes (qui traduisent le rôle inhibiteur de O_2).

Nos expériences attirent l'attention sur le fait qu'il est très difficile de déterminer, avec précision, les caractéristiques cinétiques, à l'instant initial, de la pyrolyse homogène de ces hydrocarbures purs.

Nous poursuivons actuellement l'étude de ces phénomènes avec d'autres hydrocarbures saturés.

REMERCIEMENTS

Les auteurs remercient très sincèrement le Centre d'Etudes et Recherches des Charbonnages de France et la Société Progil de l'aide matérielle apportée dans l'exécution du présent travail.

BIBLIOGRAPHIE

1. J. ENGEL, A. COMBE, M. LETORT et M. NICLAUSE. Bull. Soc. Chim. France, 1202 (1954); Rev. Inst. Franc. Pétrole Ann. Combust. Liquides, **12**, 627 (1957).
2. (*a*) R. MARTIN. Bull. Soc. Chim. France, 1262 (1961). (*b*) R. MARTIN, M. NICLAUSE et M. DZIERZYNSKI. Compt. Rend. **254**, 1786 (1962). (*c*) R. MARTIN. Thèse de Doctorat, Nancy. 1962. (*d*) R. MARTIN, M. DZIERZYNSKI et M. NICLAUSE. J. Chim. Phys. **61**, 286, 790 (1964). (*e*) R. MARTIN et M. NICLAUSE. J. Chim. Phys. **61**, 802 (1964).
3. W. A. BRYCE et J. CHRYSOCHOOS. Trans. Faraday Soc. **59**, 1842 (1963).
4. V. V. VOEVODSKY. Trans. Faraday Soc. **55**, 65 (1959).
5. K. J. LAIDLER, N. H. SAGERT et B. W. WOJCIECHOWSKI. Proc. Roy. Soc. London, Ser. A, **270**, 242 (1962).
6. J. H. PURNELL et C. P. QUINN. J. Chem. Soc. 4128 (1961).
7. B. W. WOJCIECHOWSKI et K. J. LAIDLER. Trans. Faraday Soc. **59**, 369 (1963).
8. M. NICLAUSE, A. COMBE et M. LETORT. J. Chim. Phys. **49**, 605 (1952). M. NICLAUSE. Thèse de Doctorat, Nancy. 1953; Publ. Sci. Tech. Min. Air, France, No. 292 (1954). M. NICLAUSE. Ind. Chim. Belge, **23**, 1197 (1958).
9. P. GOLDFINGER, M. LETORT et M. NICLAUSE. Volume Commémoratif Victor Henri: Contribution à l'étude de la structure moléculaire. Desoer, Liège. 1947–1948. p. 283.
10. C. P. QUINN. Communication D au symposium: The kinetics of pyrolytic reactions. Université d'Ottawa, Canada. 9–11 septembre 1964.
11. K. J. LAIDLER. Chemical kinetics. McGraw-Hill, New York et Londres. 1950. B. LEWIS et G. VON ELBE. Combustion, flames and explosions of gases. 2ème éd. Acad. Press, New York. 1961.

Can. J. Chem. Downloaded from www.nrcresearchpress.com by 210.87.254.42 on 09/05/12
For personal use only.

Can. J. Chem. Downloaded from www.nrcresearchpress.com by 210.87.254.40 on 09/05/12
For personal use only.

PROTON SPIN RELAXATION BY PARAMAGNETIC MOLECULAR OXYGEN

M. E. MIRHEJ[1]

Institute of Oceanography, University of British Columbia, Vancouver, British Columbia

Received October 22, 1964

ABSTRACT

The proton spin–lattice relaxation time, T_1, was measured for oxygen solutions of water, methanol, and acetone at different temperatures and resonance frequencies of 10.8, 20.0, and 29.8 Mc/s. The contribution of O_2 to the relaxation was assumed to be due to the dipole–dipole and hyperfine interaction between the proton spins and the unpaired spins of the O_2 molecule. The correlation times of the two interactions were related to the motion and the size of the polymeric cluster of the solvent. Activation energies for the two correlation times were obtained for the oxygen–water system from the dependence of the relaxation time on the resonance frequency. No separation of the two terms was possible for either the oxygen–methanol or oxygen–acetone systems because of their independence of magnetic field variations. The correlation time of the hyperfine term was postulated to be a measure of the extent of solvent–oxygen hydrogen bond strength in all the measured systems.

INTRODUCTION

Earlier studies on the influence of paramagnetic substances on the proton spin–lattice relaxation time, T_1, in water solutions, were interpreted assuming that the relaxation was due to dipole–dipole interactions between electron and nuclear spins, where fluctuations in such interactions are governed by viscosity and diffusion. Bloembergen *et al.* (1) found the addition of paramagnetic ions to water to decrease both the spin–lattice and the spin–spin relaxation time, T_1 and T_2 respectively. The additional contribution to the relaxation rates was found to be proportional to the concentration of the paramagnetic ions concentrations. Later, Conger (2) and Morgan *et al.* (3) concluded from measurements of relaxation times in water–glycerol solutions of several aquated ions that the observed changes were not entirely attributable to the change in viscosity according to the early theory. It was suggested that the difference observed might well provide an insight into the nature of molecular interactions in those and similar solutions. Bloembergen (4), on the other hand, followed with comparison of the ratio of T_1 to T_2 in paramagnetic ion solutions and found a deviation from unity for most ions to as high as 7.1 for Mn^{++}. The interpretation advanced emphasized that a spin exchange interaction was contributing to the relaxation due to the formation of a hydrated complex between the paramagnetic ions and water molecules. This was extended by Bloembergen and Morgan (5) to interpret the different effect on relaxation between various paramagnetic ions and the role played by the electron spins of the ions.

The influence of paramagnetic but nonionic substances in water was studied by Guilotto (6). By measuring T_1 of water in the presence and absence of oxygen, he demonstrated the change in T_1 at 20 °C and the linear dependence of the reciprocal of the spin–lattice relaxation time on the concentration of oxygen. Recently, Gutowsky and Tai (7) investigated the solvent–proton and fluorine nuclear relaxation mechanisms in solutions of organic free radicals. Their findings confirmed further the presence of a spin exchange or a hyperfine relaxation mechanism between electron and nuclear spin in these systems.

It was attempted in this work to investigate the existence of any hyperfine interaction between the two unpaired electrons of dissolved molecular oxygen and the protons of

[1]*Present address: Research and Development Division, Polymer Corporation Limited, Sarnia, Ontario, Canada.*

different liquid solvents. For this purpose, T_1 was measured for oxygen solutions of water, methanol, and acetone at different temperatures and three different resonance frequencies. Employing the Solomon–Bloembergen equation (5), the experimental results were fitted to its various forms as deemed by the dependence of the relaxation times on the variation of resonance frequency.

EXPERIMENTAL

A. Apparatus

(i) Nuclear Magnetic Resonance Free Induction Technique

The apparatus used was a conventional pulsed n.m.r. instrument (8), operated at the proton Larmor precession frequencies of 29.8, 20.0, and 10.8 Mc/s.

(ii) Thermostated Induction Coil Chamber

A copper coil 1/4 in. in diameter was helically shaped to a height of 6 cm and an o.d. of 3 cm. It was insulated with aluminium foil on the outside and placed in a wooden sample holder block leaving a small opening at the top for the sample entrance. The induction coil was fitted between the copper coil and the sample tube. The ends of the copper coil were joined to a circulating water bath with a temperature range of 1 to 90 °C and a temperature control of 0.1 °C. A thermocouple was placed inside the induction coil to determine the temperature. The measured temperatures fluctuated by an amount of the order of 0.5 °C at low temperatures and 1.0 °C at high temperatures during the course of the measurements.

(iii) Degassing Instrument

A 1 l bulb with two openings was joined to a high-vacuum line at one end, and to the sample tube at the other. The bulb contained a Teflon-covered bar magnet and was placed over a magnetic stirrer.

(iv) Sample Tubes

These were of pyrex glass 0.6 cm i.d. and about 8 cm in length. Two designs of tubes were used. One, for oxygen-free solvent, which was sealed off from the degassing bulb and used permanently, and the second for oxygenated solvents. The latter contained two small openings, one for the introduction of air or oxygen and the other for its escape.

B. Reagents

(*i*) Double distilled water.

(*ii*) Compressed air. The 'Liquid Air' cylinder contained 21% oxygen. The remaining gases were the same as atmospheric gas content.

(*iii*) Compressed oxygen. The 'Liquid Air' cylinder contained 99.5% oxygen and 0.5% nitrogen.

(*iv*) Acetone. Fisher 'Spectranalyzed' reagent grade.

(*v*) Methanol absolute. This was prepared in the laboratory from the reaction of methylphthalate and sodium hydroxide (9) and was kept in a dry box until used.

C. Procedures

(i) Degassing Method

Approximately 100 ml of water, methanol or, acetone was placed in the degassing bulb. The stopcock to the high vacuum line was opened and the magnetic stirrer started. Degassing was carried out normally from 1/2 to 1 h depending on the rate of solvent evaporation. The stopcock was closed, and the bulb was tilted until 4 or 5 ml of liquid solvent entered the sample tube at the other side. The sample tube content was frozen with liquid nitrogen and the tube sealed off. Sample tubes prepared in this manner were used for relaxation time measurements of oxygen-free solvents.

(ii) Oxygen Concentration Method

Two oxygen concentrations were employed for water and only one concentration for acetone and methanol. The solvent was saturated at a particular temperature with either air containing 21% oxygen, or with oxygen under 1 atm pressure. The degassed sample tubes were placed in the circulating water bath with the open tubes, each containing 5 or 6 ml of the solvent, after the thermoregulator has been adjusted for the desired temperature. A polyethylene tube, 0.2 cm o.d. was connected to one of the gas cylinders through a series of drying and carbon dioxide absorbing tubes. The polyethylene tube was inserted in the open sample tube until it reached the bottom, and then either air or oxygen was bubbled slowly through allowing the solvent to come to equilibrium with the ambient temperature and the gas saturation point at the same time. At the end of 10–15 min the polyethylene tube was withdrawn, and the sample tube stoppered, dried carefully, and placed quickly in the induction coil chamber, which was then at the same temperature, for relaxation time measurements.

The oxygen concentrations were checked occasionally on water samples by the micro-gasometric technique of Scholander *et al.* (10). The results were 2.5% of the theoretical concentration at any particular temperature. This is of the same order of magnitude as the usual error in estimating oxygen concentration by this method.

Can. J. Chem. Downloaded from www.nrcresearchpress.com by 210.87.254.40 on 09/05/12
For personal use only.

(iii) Measurement of Spin–Lattice Relaxation Time, T_1

While the three sample tubes were being brought to the desired temperature and pressure, a glycerine sample tube was placed in the induction coil chamber, and the Larmor frequency of the protons was adjusted to an optimum height signal. The glycerine tube was then replaced by a sample tube, and T_1 was determined. Using a $\pi/2$–$\pi/2$ pulse sequence, the amplitude of the first pulse signal or that of the echo, A, was read at $A(\infty)$ and at various $A(t)$'s. T_1 was deduced from the usual relation:

$$A(t) = A(\infty)\ [1 - \exp\ (-t/T_1)],$$

where $A(\infty)$ is the value of $A(t)$ for $t \gg T_1$.

THEORETICAL CONSIDERATION

The Solomon–Bloembergen equation (5) for the proton spin–lattice relaxation time, T_1, in the presence of molecular oxygen in a protonic solvent, may be written as:

$$[1] \qquad \frac{1}{T_1} = \frac{4}{15}\frac{Ng^2\beta^2\gamma_I{}^2N_h}{N_p r^6}\left[3\tau_c + \frac{7\tau_c}{1+\omega_S{}^2\tau_c{}^2}\right] + \frac{4}{3}\left(\frac{A}{\hbar}\right)^2\frac{NN_h}{N_p}\frac{\tau_e}{1+\omega_S{}^2\tau_e{}^2}.$$

Where ω_S refers to the electron Larmor precessional frequency; γ_I, the nuclear gyromagnetic ratio; g, the electron spectroscopic splitting factor; β, the Bohr magneton; N, the molar concentration of paramagnetic ions; N_h, the number of protons in the hydration sphere; N_p, the molar concentration of protons in solution; A, the spin exchange constant; τ_c and τ_e, the correlation times for dipoles and spin exchange interactions respectively; and r, the effective separation between the nucleus and the electron. The correlation time τ_c is related to the dipole–dipole interaction which depends on the vector $\boldsymbol{r}$ joining the proton–O_2 pair, while τ_e is a function of the scalar $\boldsymbol{I.S}$. interaction and is independent of the orientation of the pair. The spin-lattice relaxation time

$$[2] \qquad \frac{1}{T_1} = \frac{1}{T_1(O_2)} - \frac{1}{T_1(\text{pure})},$$

where T_1(pure) indicates the spin–lattice relaxation in oxygen-free solvent, and $T_1(O_2)$ the spin–lattice relaxation in the presence of oxygen.

Equation [1] contains three approximations: (*a*) $\omega_S \gg \omega_I$, i.e. $\omega_S \pm \omega_I \approx \omega_S$; (*b*) $\omega_I{}^2\tau_c{}^2 \ll 1$; and (*c*) the spin temperature of the S system of the electrons is taken to be the same as the lattice temperature; where ω_I is the proton Larmor precessional frequency.

If the electron spins of the dissolved paramagnetic substance are relaxed in a time τ_s, the electron spin relaxation time, then the values of τ_c and τ_e are as follows:

$$[3] \qquad \frac{1}{\tau_c} = \frac{1}{\tau_r} + \frac{1}{\tau_s},$$

$$[4] \qquad \frac{1}{\tau_e} = \frac{1}{\tau_h} + \frac{1}{\tau_s}.$$

In general τ_s is a function of temperature and magnetic field, while τ_r and τ_h are functions of temperature only (5).

For the oxygen molecule, however, it is assumed that τ_s is much larger than either τ_r or τ_h for all the investigated systems and that τ_c is mainly dependent on τ_r, and τ_e on τ_h. This assumption is supported by the knowledge that electron relaxation times of free radicals are generally much longer than those of paramagnetic ions (7). Therefore, at magnetic field strengths of 2 540, 4 700, and 7 000 gauss (G), ω_S is 0.45×10^{11},

Can. J. Chem. Downloaded from www.nrcresearchpress.com by 210.87.254.40 on 09/05/12
For personal use only.

0.83×10^{11}, and 1.24×10^{11} s^{-1}, respectively. τ_c is considered to be less than 10^{-11} s and τ_e of the order of 10^{-11} s for the water–oxygen system but much smaller than 10^{-11} s for either the methanol– or the acetone–oxygen system.

For the situation where τ_c is determined mainly by τ_r, and τ_c by τ_h, an exponential temperature dependence may be written after the fashion of Bloembergen and Morgan (5) as:

$$\tau_c = \tau_c^0 \exp (E_c/RT), \quad [5]$$

$$\tau_e = \tau_e^0 \exp (E_e/RT). \quad [6]$$

E_c is considered a measure of the activation energy of the tumbling of the oxygen-solvent complex, and E_e a measure of the hydration or solvation of molecular oxygen.

RESULTS AND DISCUSSION

A. Water–Oxygen System

(i) Determination of T_1

The spin–lattice relaxation time was measured in oxygen-free double distilled water and in gas-saturated water under 1 atm of air and 1 atm of oxygen. The range of temperature employed was 10 to 75 °C. Three different proton resonance frequencies were used, 10.8, 20.0, and 29.8 Mc/s. At least three separate runs were made for each temperature at any resonance frequency. Figure 1 shows the actual scatter of the points at 20.0 Mc/s, while Fig. 2 represents all the obtained data at the three frequencies and three oxygen concentrations based on a similar treatment of the data. There was essentially no change in the value of oxygen-free water when the frequency was varied at any particular temperature; however, a marked change in T_1 values resulted from frequency

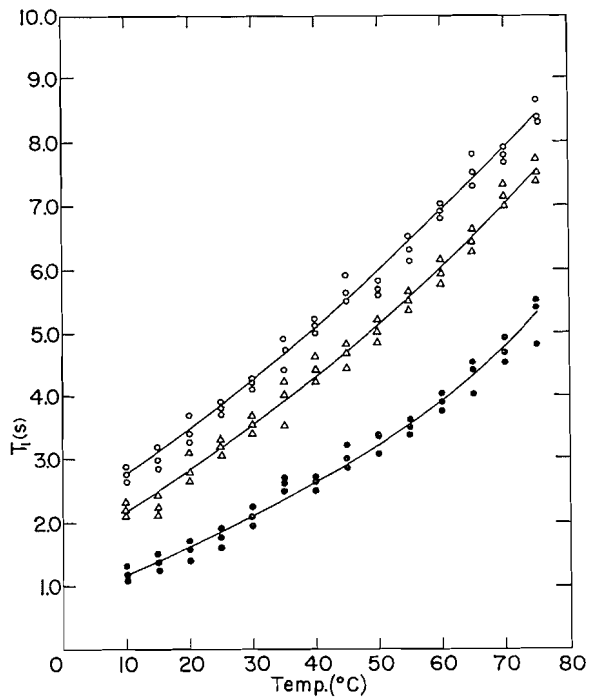

FIG. 1. Values of T_1 in water at 20.0 Mc/s in oxygen free, ○; under 1 atm of air, △; and under 1 atm of oxygen, ●.

Can. J. Chem. Downloaded from www.nrcresearchpress.com by 210.87.254.40 on 09/05/12
For personal use only.

alteration for any of the oxygen-containing samples. T_1 decreased with increase of oxygen concentration, but increased with the increase of frequency at constant concentration of oxygen.

The estimated maximum error for T_1 data for the smoothed curves was of the order of $\pm 5\%$. Comparison of T_1 values for oxygen-free water was made with those of Simpson and Carr (11), who measured T_1 and the diffusion coefficient D of proton in water at temperatures between 0 and 100 °C. The agreement above 40 °C was very apparent and of the order of 1–2%. At lower temperatures, the difference was more pronounced. Simpson and Carr's T_1 values were lower by 19% at 10 °C, 13% at 20 °C, and 10% at 30 °C. Better agreement at lower temperature was obtained with Guilotto's (6) value, where the two T_1's were of the order of 1% at 20 °C.

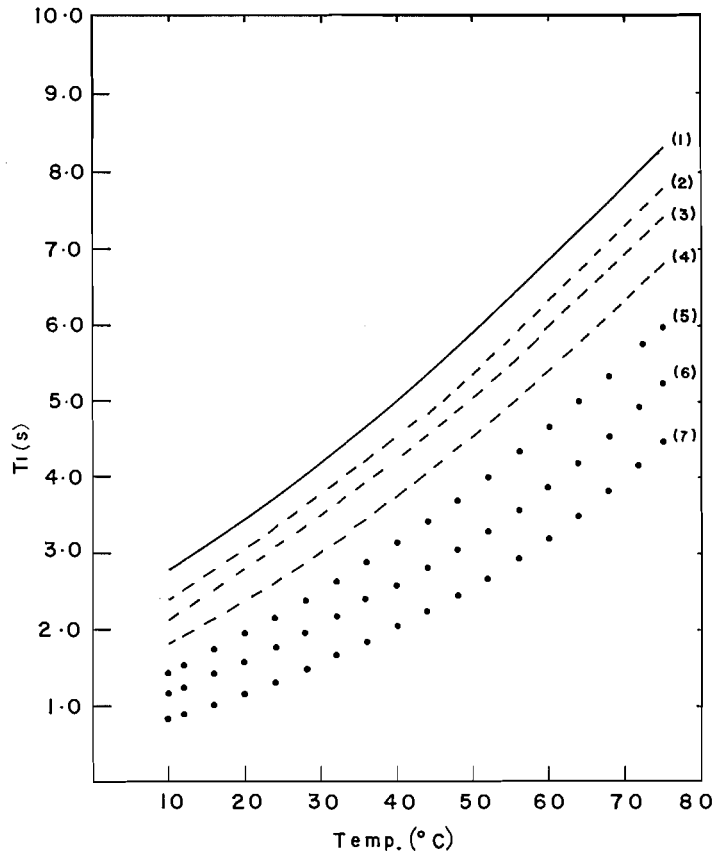

FIG. 2. Values of T_1 in water at 10.8 Mc/s ((1), (4), and (7)), 20.0 Mc/s ((1), (3), and (6)), and 29.8 Mc/s ((1), (2), and (5)) in oxygen free (—); under 1 atm of air (- - -); and under 1 atm of oxygen (●).

The inability of obtaining constant oxygen concentrations at different temperatures warranted the use of an indirect approach whereby $1/T_1$ was plotted vs. dissolved oxygen concentration at the various temperatures (6). The slopes of the line between zero and 10^{-3} mole/l were computed for $1/T_1N$ at each temperature of measurement and for the three resonance frequencies and listed in Table I.*

**The solubility values of oxygen in distilled water were obtained from the 'Handbook of physics and chemistry', 1960, p. 1706.*

Can. J. Chem. Downloaded from www.nrcresearchpress.com by 210.87.254.40 on 09/05/12
For personal use only.

TABLE I

Values of $R = 1/T_1N$ for the oxygen solution of water

Temp. (°C)	R_1 (mole^{-1} s^{-1}) at H^1 frequency of 10.8 Mc/s	R_2 (mole^{-1} s^{-1}) at H^1 frequency of 20.0 Mc/s	R_3 (mole^{-1} s^{-1}) at H^1 frequency of 29.8 Mc/s	$R_1 - R_2$ (mole^{-1} s^{-1})	$R_2 - R_3$ (mole^{-1} s^{-1})
10	540	300	200	240	100
15	490	270	180	220	90
20	450	250	160	200	90
25	410	230	150	180	80
30	380	220	140	160	80
35	350	200	130	150	70
40	320	190	120	130	70
45	290	180	110	110	70
50	260	170	110	90	60
55	245	160	100	85	60
60	220	150	100	70	50
65	210	145	100	55	45
70	195	140	100	55	40
75	190	140	100	50	40

(ii) Relaxation Terms

It was shown that $1/T_1N$ for dissolved oxygen in water varies with the magnetic field strength, H_0. This is related in turn to the dependence of the electron precession frequency, ω_S, on H_0. The best fit for the experimental results obeyed the relationship.

[7] $$R = 1/T_1N = \alpha\tau_c + B\tau_e/(1 + \omega_S{}^2\tau_e{}^2)$$

where

$$\alpha \text{ is } \frac{40}{15}\frac{g^2\beta^2\gamma_I{}^2N_h}{N_p r^6}$$

and

$$B \text{ is } \frac{4}{3}\left(\frac{A}{\hbar}\right)^2\frac{N_h}{N_p}$$

at any particular temperature and $\omega_S{}^2\tau_c{}^2 \ll 1$.

The magnitude sequence of the three correlation times, τ_h, τ_s, and τ_r, which are related to τ_c and τ_e by eqs. [3] and [4], for the protons in presence of paramagnetic molecular oxygen, should differ from their sequence in paramagnetic ions solutions. Whereas in the latter they follow the order $\tau_h \geqslant \tau_s \gg \tau_r$ (5), they should possess, in the former, a new order of magnitude, $\tau_s \gg \tau_h \geqslant \tau_r$. This is based on two considerations. 1. Because τ_s for a free radical is usually much larger than that of a paramagnetic ion (7). 2. Because the O_2 molecule is nonpolar and thus is incapable of forming a hydration layer of the same strength as a charged ion in solution. Furthermore, paramagnetic, nonionic molecules may participate in the relaxation mechanism without disruption of the normal cluster arrangement of the solvent. On this basis, eq. [7] was solved at three different magnetic field strengths from the plot of $R = 1/T_1N$ vs. temperature, using the relationship:

[8] $$\frac{R_1 - R_2}{R_2 - R_3} = \frac{(\omega_{S2}{}^2 - \omega_{S1}{}^2)}{(\omega_{S3}{}^2 - \omega_{S2}{}^2)}\frac{(1 + \omega_{S3}{}^2\tau_e{}^2)}{(1 + \omega_{S1}{}^2\tau_e{}^2)}.$$

The square of the correlation time, $\tau_e{}^2$ and hence τ_e were evaluated. An average value for $B\tau_e$ was obtained from both $(R_1 - R_2)$ and $(R_2 - R_3)$ and was used to determine $\alpha\tau_c$ (average), at the three different frequencies. The values are shown in Table II.

Can. J. Chem. Downloaded from www.nrcresearchpress.com by 210.87.254.40 on 09/05/12
For personal use only.

TABLE II

Evaluation of the correlation times

Temp. (°C)	$\tau_c \times 10^{11}$ (s)	$\beta\tau_c$ (mole^{-1} s^{-1})	$\alpha\tau_c$ (mole^{-1} s^{-1})
10	2.0	830	100
15	2.1	750	90
20	1.9	690	60
25	1.9	620	50
30	1.7	540	45
35	1.7	490	40
40	1.5	440	30
45	1.4	390	28
50	1.3	350	23
55	1.2	320	20
60	1.2	280	15
65	1.2	260	12
70	1.1	230	8
75	1.0	220	5

Due to the presence of the 3/7 term in the dipole–dipole interaction expression, it is reasonable to expect that if the hyperfine term did not contribute to T_1, i.e. if $<A>$ was zero, the proper expression could be written as follows:

[9] $$\frac{1}{NT_1} = \frac{3}{10}\alpha\tau_c + \frac{(7/10)\alpha\tau_c}{1 + \omega_S^2\tau_c^2}.$$

However, neither this consideration nor the reversal of the assumption that $\omega_s^2\tau_c^2 \ll 1$ was found to be capable of suitable correlation with the data. In accordance with such findings it was discovered that the variation in τ_c^2 values were only of the order of 30%.

(iii) Activation Energies

It was assumed that $\tau_s \gg \tau_e$ or τ_c, as postulated earlier, and the exponential temperature dependence for the two latter correlation times follow eqs. [5] and [6]. The two activation energies E_e and E_c were obtained as 6.5 kcal mole^{-1} and 2.5 kcal mole^{-1} respectively. Furthermore, the validity for the assumption that $\tau_c < 10^{-11}$ s in water may be reasoned as follows: τ_c is proportional to τ_D where $\tau_D = 4\pi\eta a^3/kT$. From data of dielectric relaxation (12), neutron diffraction (13), and diffusion and viscosity (14), τ_D or its equivalent was estimated to be not more than 10^{-11} s at 0 °C. Also τ_D was found to be equal to $3\tau_c$ (15) and both τ_D and τ_c to decrease with increase in temperature.

Both τ_D and τ_c should vary proportionally with η/T of water. This relation is demonstrated by the linear variation of $\alpha\tau_c$ with η/T. Accordingly, it is believed that τ_c is principally a measure of the hydrogen bond breaking between water molecules in the process of the cluster tumbling in the body of the solvent.

The energy of activation E_c being 6.5 kcal mole^{-1}, is viewed as the energy required for one hydrogen bond breaking between two water molecules, within the accumulated experimental error of 30–40%. Comparison of this value with various other experimental values of hydrogen bond breaking in water at temperatures between −65 and 100 °C shows a similar order of magnitude with those of Scatchard (16), 3.4 kcal mole^{-1}, Rowlinson (17), 4.4 kcal mole^{-1}, and Lambert (18), 5.7 kcal mole^{-1}. Also, the activation energy for dielectric absorption in ice was found by Auty and Cole (19) to be 13.2 kcal mole^{-1} and was interpreted as the breaking of three hydrogen bonds each being 4.5 kcal mole^{-1}. The activation energy of hydration or solvation, E_e, on the other hand, is believed to be due to solvent–solute bond breaking between water and oxygen molecules. This was found to have the value of 2.5 kcal mole^{-1} for the range of temperature from 10 to 75 °C.

Can. J. Chem. Downloaded from www.nrcresearchpress.com by 210.87.254.40 on 09/05/12
For personal use only.

B. The Methanol– and Acetone–Oxygen Systems

(i) Measurement of T_1

The spin–lattice relaxation time measurements of the methanol– and acetone–oxygen systems were carried out in the same manner as that for water–oxygen except for two variations. 1. Only two magnetic field strengths of 7 000, and 2 540 G were used since no apparent change in the value of T_1 was found within the experimental error to necessitate the use of a third field strength. 2. One concentration of oxygen under 1 atm of air was employed. Figures 3 and 4 show the influence of temperature variation between 0 and 50 °C on T_1 for the oxygen-free and oxygen-containing acetone and methanol respectively. The inverse value of $1/T_1N$ was again obtained from the slope of $1/T_1$ vs. O_2 concentration. The concentration of dissolved oxygen in acetone was obtained from Horiuti (20) and in methanol from Seidell (21) as the Ostwald coefficient, γ, and were converted to moles of O_2 per liter of solvent.

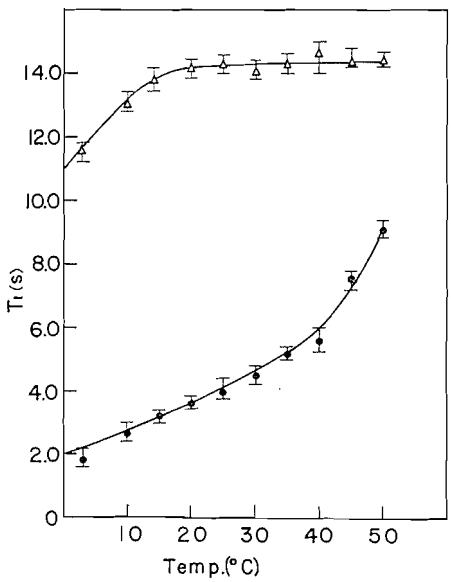

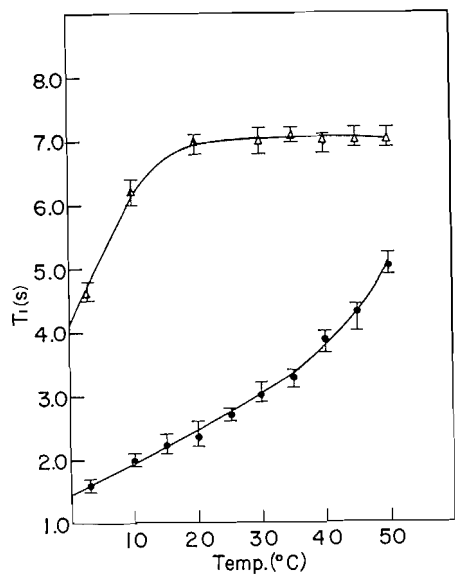

FIG. 3 (left). Values of T_1 in acetone at 29.8 Mc/s and 10.8 Mc/s in oxygen free, △ and under 1 atm of air, ●.

FIG. 4 (right). Values of T_1 in methanol at 29.8 Mc/s and 10.8 Mc/s in oxygen free, △ and under 1 atm of air, ●.

(ii) Relaxation Terms and Activation Energies

The independence of $1/T_1N$ of magnetic field variations in acetone and methanol, in contrast to that of water, indicates that either $AI.S.$ is zero or that both $\omega_S^2\tau_c^2$ and $\omega_S^2\tau_e^2$ are much less than unity. To verify either of these indications $1/T_1N$ was plotted vs. η/T. (Viscosity data, as for water, were obtained from the International critical tables (22).) If $1/T_1N$ is only a function of τ_e then a linear relationship should exist between the two quantities. The non-linear behavior, however, for both systems led to the conclusion that in all probability, $1/T_1N = \alpha\tau_c + B\tau_e$. The magnitude of τ_e and the extent of its variation were nevertheless expected to be small.

The large values of τ_e point to strong solvation or hydration and a large E_e, while small values ultimately involve a smaller activation energy. Since the oxygen molecule is nonpolar, but polarizable nevertheless, the contribution to hydrogen bond strength

Can. J. Chem. Downloaded from www.nrcresearchpress.com by 210.87.254.40 on 09/05/12
For personal use only.

between the solvent and solute will depend chiefly on the polarity of the solvent cluster at any particular temperature. The decrease in the solvent cluster size should reduce the resultant polarity of the cluster and thus the hydrogen bond strength between solvent and solute.

CONCLUSION

It is concluded that the solvation of paramagnetic molecular oxygen in protonic solvents decreases the spin–lattice relaxation time by two mechanisms, a dipole–dipole and a hyperfine interaction. The extent of each depends on the capacity of polymeric cluster formation and the strength of the O_2–solvent hydrogen bond. In solvents where hydrogen-bonding potential is small, the dipole–dipole mechanism predominates, while the converse is true in solvents of higher hydrogen-bonding capacity. Because of the nonionic nature of the oxygen molecule, no disruption of solvent cluster formation is expected, and the dipole–dipole interaction is considered to be independent of the molecular oxygen size contribution.

ACKNOWLEDGMENTS

The author wishes to thank Professor M. Bloom for his generous contribution of time and equipment towards this study as well as for his many helpful suggestions and criticisms. Thanks is also extended to Mr. I. M. Kristensen for his assistance in the evaluation of the variability of τ_e^2.

REFERENCES

1. N. Bloembergen, E. M. Purcell, and R. V. Pound. Phys. Rev. **73**, 679 (1948).
2. R. L. Conger. J. Chem. Phys. **21**, 937 (1953).
3. L. O. Morgan, A. W. Nolle, R. L. Hull, and J. Murphy. J. Chem. Phys. **25**, 206 (1956).
4. N. Bloembergen. J. Chem. Phys. **27**, 572 (1957).
5. N. Bloembergen and L. O. Morgan. J. Chem. Phys. **34**, 842 (1961).
6. L. Guilotto. Arch. Sci. (Facicule Speciale) **9**, 212 (1956).
7. H. S. Gutowsky and Julia Chow Tai. J. Chem. Phys. **39**, 208 (1963).
8. E. L. Hahn. Phys. Rev. **80**, 980 (1950).
9. A. I. Vogel. A textbook of practical organic chemistry. 3rd ed. Wiley, New York. 1956. p. 168.
10. D. L. Scholander, L. van Dam, C. L. Claff, and J. W. Kanwisher. Biol. Bull. **109**, 328 (1955).
11. J. H. Simpson and H. Y. Carr. Phys. Rev. **111**, 1201 (1958).
12. M. Eigen and L. De Maeyer. Proc. Roy. Soc. London Ser. A, **247**, 505 (1958).
13. B. N. Brockhouse. Nuovo Cimento Suppl. Ser. 10, **9**, 45 (1958).
14. J. H. Wang, C. V. Robinson, and I. S. Edelman. J. Am. Chem. Soc. **76**, 466 (1953).
15. N. Bloembergen. Nuclear magnetic resonance. W. A. Benjamin, Inc., New York. 1961.
16. G. Scatchard, G. M. Kavanagh, and L. B. Ticknor. J. Am. Chem. Soc. **74**, 3715, 3724 (1952).
17. J. S. Rowlinson. Trans. Faraday Soc. **45**, 974 (1949).
18. J. D. Lambert. Discussions Faraday Soc. **15**, 226 (1953).
19. R. P. Auty and R. H. Cole. J. Chem. Phys. **20**, 1309 (1952).
20. J. Horiuti. Sci. Papers Inst. Phys. Chem. Res. Tokyo, **17**, 125 (1931).
21. A. Seidell. Solubilities of inorganic and metal organic compounds. Vol. **1**, suppl. to 3rd ed. D. van Nostrand Co., Inc., New York. 1940. p. 497.
22. International Critical Tables. Vol. V, p. 10; Vol. V, p. 11; Vol. VII, p. 215. McGraw-Hill Publ. Co. 1929.

Can. J. Chem. Downloaded from www.nrcresearchpress.com by 210.87.254.40 on 09/05/12
For personal use only.

REFINEMENT OF THE CRYSTAL STRUCTURE OF β-$Mg_2P_2O_7$

CRISPIN CALVO
Department of Chemistry, McMaster University, Hamilton, Ontario
Received September 14, 1964

The crystal structure of $Mg_2P_2O_7$ reported by Lukaszewicz has been refined by least squares analysis. Data of the *hkl* type with $0 \leqslant k \leqslant 6$ have been used to obtain improved atomic parameters. The central oxygen atom of the $P_2O_7^{-4}$ is found to have enhanced thermal motion in the plane perpendicular to the P—P vector. Thus the P—O—P bond angle appears to be linear in this phase because of a thermal averaging of the position of the central oxygen atom. This conclusion is in agreement with that obtained by Lazarev from infrared studies.

INTRODUCTION

β-$Mg_2P_2O_7$ is one of a series of chemically and crystallographically related pyrophosphate compounds. Included in this series are $Mn_2P_2O_7$, $Cu_2P_2O_7$, $Mg_2P_2O_7$, and $Zn_2P_2O_7$. Each of these pyrophosphates except that of Mn^{++} shows a phase transition. $Zn_2P_2O_7$ has a first order phase transition at 132 °C featuring an increase in symmetry from I*c* or I2/*c* and roughly a halving and a thirding of the *c*- and *a*-axes respectively (1). A further gradual phase transition was found at 155 °C and proposed to be of second order. No substantial change occurred in the lattice parameters across this transition but the crystal symmetry increased to *C*2/*m* beyond 155 °C. A phase transformation in $Cu_2P_2O_7$ is found at $\sim$72 °C with the space group changing from *C*2/*c* to *C*2/*m* (2). Here the *c*-axis is halved in passing through the transition.

An apparent first order phase transition was noted near 68 °C in $Mg_2P_2O_7$. The crystal parameters seemed to change discontinuously (3) and an enthalpy change of 729 cal/mole at the transition has been found (4). However, a detailed examination of the powder pattern suggested that a gradual phase transition occurs as did the fact that the specific heat anomaly was spread over more than 20° in temperature. Thus the true thermodynamic nature of the transition remains uncertain. The space group transition is from $B2_1/c$ (5) at room temperature to *C*2/*m* above the transition with a simultaneous having of the *a*- and *c*-axes.

Lazarev (6) has investigated the infrared absorption of $Mg_2P_2O_7$ from −150 to 150 °C. He found that the anion in the low temperatures phase showed a symmetry no greater than C_s or C_2 and suggested that the P—O—P bond angle was no larger than 160°. Further he concluded that in the high temperature form the central oxygen atom vibrates across a potential surface containing at least a double minima.

Because of the multiplicity of related phases, this system of pyrophosphates should be important in any attempt to "read" chemical bonding information from the geometry of the $P_2O_7^{-4}$. A correlation between these bond lengths and the $p\pi$–$d\pi$ bond order has been proposed by Cruickshank (7). He investigated the overlap possibilities of the available oxygen and phosphorus orbitals for the cases of a linear and nearly 120° P—O—P bond angle. Further delocalization to the cations was ignored. The two strongly coupled π-bonding systems that can occur in an isolated PO_4 group are found to differ in their ability to extend throughout the $P_2O_7^{-4}$. This ability is determined by the central bond angle. On a simple valence bond picture Cruickshank proposes that the outer P—O bond should have a bond order of 1.60 and the inner P—O bond a bond order 1.20

Can. J. Chem. Downloaded from www.nrcresearchpress.com by 210.87.254.105 on 09/05/12
For personal use only.

in the case of a nearly 120° bond angle. In the linear case, these values are 1.53 and 1.40 respectively. From an assumed linear relationship of bond order to bond length one can predict bond lengths from bond order estimations and vice versa.

Lazarev (8) has proposed that the force constants obtained from molecular vibration studies are a more sensitive measure of the actual bond character. Based upon these constants he concludes that the magnitude of the central angle in pyro compounds should be a measure of the $p\pi$–$d\pi$ bonding. The influence of the cations on this bonding and, therefore, on the angle arises from the degree of covalency of the bond between the cation and the oxygen atoms. The greater the basic character of the cation, the smaller should be the covalency of the M—O bond which, in turn, favors a decrease in the X—O—X bond order and, therefore, a decrease in the bond angle. The influence of the cation on the nature of the bonding in the pyrophosphate anion can be monitored in a study of crystallography of the pyrophosphate compounds.

Lukaszewicz has shown the β-$Mg_2P_2O_7$ at 80 °C is isostructural with thortveitite (9) ($Sc_2Si_2O_7$). Unfortunately the rather large residual suggests an incomplete refinement. Further suggestive evidence has been provided by the resolution of the crystal structure of β-$Zn_2P_2O_7$ (10) where the central oxygen atom undergoes considerable enhanced motion. The resolution of the detail structure of β-$Mg_2P_2O_7$ is desirable because the low scattering power of the cation would permit the most reliable determination of the "true" shape of the $P_2O_7^{-4}$ in these high temperature phases.

EXPERIMENTAL

Crystals of $Mg_2P_2O_7$ doped with either Mn^{++} or Cu^{++}, for concurrent electron paramagnetic resonance (e.p.r.) work, were prepared by slow cooling of the melt obtained from the decomposition of precipitated $MgNH_4PO_4$ (11). These crystals consisted of thin plates of diamond cross section. The twofold axis lies parallel to the small diagonal and the plate face has a Miller index of (001).

The crystal chosen for study was Cu^{++} doped and had dimensions of 0.08 mm × 0.12 mm × 0.15 mm. Mo K_α radiation was used to minimize absorption effects. This crystal was also used in obtaining data on the α-phase whose crystal structure is presently being resolved. The lattice parameters were determined from films calibrated with TiO_2 lines (a = 4.594 Å, c = 2.959 Å) (12). The parameters obtained at ~ 95 °C were a = 6.494 ± 0.007 Å, b = 8.28 ± 0.01 Å, c = 4.522 ± 0.005 Å, β = 103.8 ± 0.1°, and z = 2. These values vary slightly from those reported by Lukazewicz. The X-ray extinctions of β-$Mg_2P_2O_7$ (I_{hkl} = 0 if $h + k$ = odd) restrict the space group choice to among $C2$, Cm, or $C2/m$. Electron paramagnetic resonance experiments with $Mg_2P_2O_7$:Mn^{++} (13) have shown only one active site above 64 °C and this result has been interpreted as indicating a space group symmetry of $C2/m$. The arguments supporting this are the same as were used in the discussion of the e.p.r. of $Zn_2P_2O_7$ (1). Supporting evidence for the e.p.r. method of establishing the space group has been provided by a recent complete investigation of the spectra of α-$Mg_2P_2O_7$:Mn^{++} (13). In this case the space group symmetry $B2_1/c$ is uniquely determined by the pattern of the scattered X-rays. This suggests that the e.p.r. spectra should show four Mn^{++} sites related in pairs by the mirror operation associated with the glide plane.

The crystal was heated to 95 ± 5 °C with a hair dryer inserted along the axis of the Weissenberg camera and photographs of the first seven layer lines about the b-axis were recorded using Mo K_α radiation. Photographs of the [100] and [001] zones were obtained with the precession camera. The intensities of these reflections, visually estimated, were corrected for Lorentz and polarization effects and converted into scaled structure factors. These data were directly inserted into a modified Busing, Martin, and Levy (14) least squares program with the atomic parameters obtained from two least square refinement cycles on the $h0l$ and $hk0$ data of Lukaszewicz. The value of the residual for these data had decreased from the reported value of 0.26 to 0.15 when the calculated structure factors were adjusted for anisotropic thermal vibrations of the atoms. The new data were substituted for those of Lukaszewicz and the refinement carried through until no further significant shifts in the atomic parameters were obtained. The weights were assigned by the method of Ibers (15). At this point the residual was 0.108 for the 340 observed reflections and 0.15 if the 148 unobserved reflections were included. The large number of unobserved reflections are due to the use of Mo K_α radiation combined with short exposure times (4 h). The electron density of the final structure projected onto the y = 0 plane is shown in Fig. 1.

The calculated and observed structure factors are compared in Table I. In Table II the positional parameters obtained in this study are compared with those obtained by Lukaszewicz. The largest change is seen to be a shift of about 0.2 Å in the position of O_{II}; significant shifts, however, are found for all other

Can. J. Chem. Downloaded from www.nrcresearchpress.com by 210.87.254.105 on 09/05/12
For personal use only.

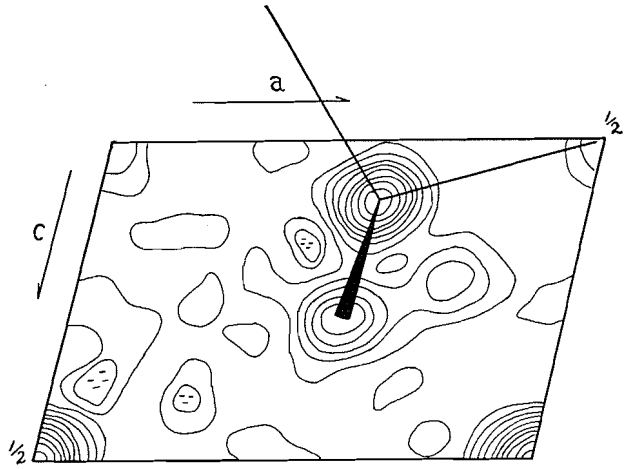

FIG. 1. Electron density projected onto the $y = 0$ plane. The electron density of β-$Mg_2P_2O_7$ is shown projected onto the $y = 0$ plane. The contours are at equal intervals and the regions of negative electron density are depicted with negative signs. The projected position of half of the anion is shown. O_I is at the origin and O_{II} falls outside of the cell boundary.

atoms (except O_I, of course). The new nonthermally adjusted bond distances are collected in Table III and the thermal parameters in the form of mean square displacements in Table IV. The magnitudes of these quantities clearly show the enhanced thermal activity of O_I. The direction of this thermal motion is in the plane perpendicular to the P—P vector with the major component along the *b*-direction. The motion of the other oxygen atoms are modest and restricted primarily to the *a*–*c* plane. These "raw" temperature parameters yield nonpositive definite values for some of the minors of the thermal matrix for every one of the atoms. This means that the effective thermal motion cannot be represented as an ellipsoid and this, in turn, may result from an absorption effect or from the nonharmonic nature of the thermal motion. That is, if we have a double well potential energy minima, we are attempting to represent a function of the form

$$\tfrac{1}{2}f_j\, e^{-\mathbf{H}\cdot B\cdot \mathbf{H}}\, e^{2\pi i \mathbf{H}\cdot(\mathbf{r}_j+\Delta\mathbf{r}_j)} + \tfrac{1}{2}f_j\, e^{-\mathbf{H}\cdot B\cdot \mathbf{H}}\, e^{2\pi i \mathbf{H}\cdot(\mathbf{r}_j-\Delta\mathbf{r}_j)}$$

by a function

$$f_j\, e^{2\pi i \mathbf{H}\cdot\mathbf{r}_j}\, e^{-\mathbf{H}\cdot B'\cdot \mathbf{H}},$$

where $\mathbf{H}$ is a reciprocal lattice vector, B is the thermal motion dyadic for the atom in the potential well and displaced from the average position by $\pm\Delta\mathbf{r}_j$, and B' the thermal parameter when the nature of the potential surface is ignored. Equating the two expressions permits us to relate B and B' as in

$$\mathbf{H}\cdot B'\cdot\mathbf{H} = \mathbf{H}\cdot B\cdot\mathbf{H} - \log\cos 2\pi\mathbf{H}\cdot\Delta\mathbf{r}_j.$$

Clearly the value of B' will not represent B very well. In the light of this discussion, it is clear that these thermal parameters have only qualitative significance if the thermal motion is a disordering. This would be consistent with the fact that the hyperfine lines of Mn^{++} are not resolved in $Mg_2P_2O_7$ until a temperature of 174 °C is reached (13).

The fact that so many of the U_{22} values are significantly negative might be suggestive of erroneous space group choice. In this regard an attempt was made to establish the space group by the more traditional means of seeking a solution within one of the subgroups of $C2/m$. Since the anion in α-$Mg_2P_2O_7$ nearly possesses a twofold axis, a refinement was sought in the $C2$ space group where the anion necessarily lies on the twofold axis. Trial parameters were manufactured from the atomic parameters obtained from the partially refined α-$Mg_2P_2O_7$ structure. The minimum residual obtained was 0.27.

PHASE TRANSITION

The temperature of the phase transition was determined by recording oscillation photographs while heating the crystal. In addition, by this experiment we hoped to determine whether the gradual phase transition reported by Roy *et al.* for a powdered sample

Can. J. Chem. Downloaded from www.nrcresearchpress.com by 210.87.254.105 on 09/05/12
For personal use only.

Can. J. Chem. Downloaded from www.nrcresearchpress.com by 210.87.254.105 on 09/05/12
For personal use only.

TABLE I

Observed and calculated structure factors

H	K	L	F(O)	F(C)	H	K	L	F(O)	F(C)	H	K	L	F(O)	F(C)	H	K	L	F(O)	F(C)
2	0	0	17.5	-19.6	3	1	2	18.9	-18.3	7	3	2	<4.2	0.2	1	5	1	24.1	23.0
4	0	0	27.0	30.8	5	1	2	<4.6	3.1	9	3	2	10.0	8.7	3	5	1	5.4	-8.1
6	0	0	4.5	3.7	7	1	2	<6.5	-1.2	9	3	-3	<7.9	-0.7	5	5	1	27.2	27.2
8	0	0	9.2	9.6	9	1	2	<8.7	0.5	7	3	-3	7.2	5.8	7	5	1	<4.9	-2.0
10	0	0	9.4	10.7	9	1	-3	<7.1	5.9	5	3	-3	21.0	-20.0	9	5	1	8.5	8.2
12	0	0	<8.4	-4.0	7	1	-3	8.2	9.0	3	3	-3	8.9	-9.3	11	5	1	<6.2	-0.6
0	0	1	7.8	7.7	5	1	-3	<4.3	0.3	1	3	-3	36.0	-36.8	11	5	-2	9.3	-8.2
2	0	1	<3.8	-1.3	3	1	-3	8.9	8.6	1	3	3	18.3	19.1	9	5	-2	7.2	6.4
4	0	1	16.5	-16.5	1	1	-3	<3.6	-2.7	3	3	3	24.1	-20.3	7	5	-2	6.8	-7.5
6	0	1	<6.1	-1.4	1	1	3	26.3	23.2	5	3	3	5.7	-4.9	5	5	-2	10.9	-13.0
8	0	1	12.7	-13.9	3	1	3	<4.4	-1.1	7	3	3	6.4	-3.7	3	5	-2	4.4	-3.1
10	0	1	9.9	9.4	5	1	3	<6.2	4.1	9	3	3	<4.4	-5.3	1	5	-2	19.0	-17.9
12	0	1	8.4	-7.7	7	1	3	<7.2	2.1	11	3	3	<9.3	4.9	1	5	2	7.4	7.1
2	0	-1	46.7	-49.5	9	1	3	<8.5	1.5	11	3	-4	<9.2	2.9	3	5	2	22.3	-27.9
4	0	-1	11.2	11.2	9	1	-4	<8.3	-4.4	9	3	-4	<8.1	-3.6	5	5	2	<4.4	0.5
-6	0	1	19.7	-17.3	7	1	-4	8.4	8.2	7	3	-4	13.9	15.6	7	5	2	7.1	-6.2
-8	0	1	7.2	6.1	5	1	-4	8.5	-8.3	5	3	-4	<5.8	-1.9	9	5	2	<9.6	-1.6
10	0	-1	6.7	-5.4	3	1	-4	9.0	-3.9	3	3	-4	18.4	19.9	11	5	2	<10.4	-1.3
0	0	2	<3.0	0.2	1	1	-4	21.5	-22.6	1	3	-4	<3.3	-3.3	9	5	-3	<5.5	6.0
2	0	2	31.0	32.1	1	1	4	10.9	10.0	1	3	4	9.5	10.6	7	5	-3	8.4	10.8
4	0	2	7.0	7.8	3	1	4	<9.6	-3.9	3	3	4	21.0	15.8	5	5	-3	<3.7	-0.1
6	0	2	18.6	17.9	5	1	4	<6.6	-1.1	5	3	4	14.6	-1.1	3	5	-3	16.1	15.6
8	0	2	6.8	-5.4	7	1	4	<7.8	-0.3	7	3	4	11.1	9.9	1	5	-3	3.8	-3.1
10	0	2	9.0	11.2	9	1	4	<9.5	-6.6	9	3	4	<5.2	-4.7	1	5	3	26.3	27.2
-2	0	2	17.8	19.1	7	1	-5	10.7	11.4	11	3	4	9.2	10.8	3	5	3	3.5	2.3
-4	0	2	26.8	26.3	5	1	-5	8.5	-8.8	9	3	-5	8.5	-7.9	5	5	3	5.7	5.5
6	0	-2	5.5	4.2	3	1	-5	21.2	19.9	7	3	-5	<7.6	2.3	7	5	3	6.7	5.5
8	0	-2	13.7	12.8	1	1	-5	6.0	-6.1	5	3	-5	9.7	-8.4	9	5	3	<7.1	2.0
0	0	3	12.3	-10.3	1	1	5	<6.3	1.3	3	3	-5	<6.8	3.1	9	5	-4	7.5	-7.7
2	0	3	13.3	-14.3	3	1	5	8.7	7.7	1	3	-5	7.3	-7.3	7	5	-4	6.1	5.4
4	0	3	8.8	-9.6	5	1	5	<8.2	-2.0	1	3	5	12.4	-12.1	5	5	-4	11.9	-12.1
6	0	3	<7.0	4.1	7	1	5	11.5	9.9	3	3	5	<4.5	0.7	3	5	-4	5.0	5.8
2	0	-3	11.1	-10.5	7	1	-6	<7.9	6.5	5	3	5	<7.4	-6.6	1	5	-4	23.0	-23.4
-4	0	3	4.9	5.0	5	1	-6	9.0	-9.1	7	3	5	<5.7	2.1	1	5	4	<3.8	0.8
-6	0	3	16.4	-16.2	3	1	-6	<7.1	2.8	9	3	5	7.7	-9.6	3	5	4	6.0	-4.9
-8	0	3	3.7	4.1	1	1	-6	<7.1	5.8	9	3	-6	<8.8	-2.6	5	5	4	7.8	-6.3
0	0	4	11.6	11.8	1	1	6	9.6	-11.4	7	3	-6	10.1	8.8	7	5	4	<6.0	-2.6
2	0	4	16.0	15.1	3	1	6	8.7	5.8	5	3	-6	8.1	-6.1	9	5	4	9.5	-8.5
4	0	4	6.6	-5.7	5	1	6	8.5	-9.6	3	3	-6	10.7	12.1	7	5	-5	10.2	10.5
6	0	4	15.3	17.7	5	1	-7	<7.8	-0.6	1	3	-6	5.0	5.1	5	5	-5	5.9	-5.0
-2	0	4	13.1	11.6	3	1	-7	<7.2	-4.5	1	3	6	<8.0	2.9	3	5	-5	19.6	19.2
4	0	-4	15.1	15.0	1	1	-7	12.4	10.9	3	3	6	<8.5	3.9	1	5	-5	<7.7	-1.9
6	0	-4	5.5	-6.1	1	1	7	<7.9	-3.6	5	3	6	<8.4	0.7	1	5	5	5.7	4.0
8	0	-4	13.8	16.9	3	1	7	<8.3	6.4	7	3	6	9.5	10.1	3	5	5	9.1	8.6
0	0	5	20.8	-19.7	5	1	7	<8.6	-6.1	9	3	6	<9.1	-1.5	5	5	5	<5.9	2.4
2	0	5	12.4	13.5	10	2	-1	<8.4	2.2	7	3	-7	<8.8	6.6	7	5	5	10.4	9.7
4	0	5	21.6	-20.9	8	2	-1	9.2	10.7	5	3	-7	<8.8	-8.3	5	5	-6	11.0	-11.9
-2	0	5	6.0	6.2	6	2	-1	<5.9	3.5	3	3	-7	<8.6	-4.3	3	5	-6	<5.1	1.7
-4	0	5	15.1	-14.4	4	2	-1	22.5	24.0	1	3	-7	<8.5	3.2	1	5	-6	<5.2	0.6
-6	0	5	4.1	-1.7	2	2	-1	14.9	-13.5	1	3	7	7.7	-7.4	1	5	6	9.6	-11.4
0	0	6	8.1	-7.8	0	2	1	42.2	41.8	3	3	7	<5.4	3.5	3	5	6	<5.8	1.1
2	0	6	14.3	16.1	2	2	1	14.2	11.7	5	3	7	10.6	-13.1	5	5	6	10.1	-10.7
4	0	6	7.4	3.5	4	2	1	14.8	15.4	7	3	7	<9.0	4.8	5	5	-7	<5.9	-0.7
6	0	6	<8.6	-1.0	6	2	1	5.9	5.1	7	3	-8	<5.6	3.6	3	5	-7	<5.9	-2.7
8	0	6	8.5	6.3	8	2	1	<7.6	-0.6	5	3	-8	11.8	7.6	1	5	7	<6.1	-2.7
2	0	-6	16.5	16.3	10	2	1	11.1	12.6	3	3	-8	8.3	-8.7	1	5	-7	11.0	12.4
4	0	-6	7.5	-7.6	10	2	-2	9.5	-7.2	1	3	-8	10.7	11.4	3	5	7	<6.1	9.6
6	0	-6	16.6	15.6	8	2	-2	<7.3	6.1	1	3	8	<5.4	-5.6	5	5	7	<6.2	-6.5
0	0	7	8.5	-7.6	6	2	-2	13.7	-15.9	3	3	8	12.6	13.3	5	5	-8	<6.2	2.9
2	0	7	7.6	-6.0	4	2	-2	21.0	19.0	5	3	8	<9.0	-5.1	3	5	-8	10.4	-10.3
2	0	-7	<6.6	1.7	2	2	-2	32.6	-30.8	8	4	-1	<7.4	4.8	1	5	-8	<6.2	2.5

Can. J. Chem. Downloaded from www.nrcresearchpress.com by 210.87.254.105 on 09/05/12
For personal use only.

1	1	0	3.3	-2.5	0	2	2	<5.0	-2.2	6	4	-1	<6.1	-1.5	1	5	8	<10.4	-5.8
3	1	0	14.6	-11.7	2	2	2	7.2	-8.5	4	4	-1	10.7	10.6	3	5	8	<6.2	4.0
5	1	0	22.2	20.2	4	2	2	5.4	-5.1	2	4	-1	23.4	-21.9	5	5	8	<5.8	-6.5
7	1	0	18.6	-17.3	6	2	2	6.8	3.6	0	4	1	21.6	23.1	10	6	-1	<7.0	-5.9
9	1	0	8.0	8.2	8	2	2	13.9	-14.5	2	4	1	4.7	-5.9	8	6	-1	7.7	5.6
0	2	0	18.4	22.3	10	2	2	<9.4	6.5	4	4	1	6.8	8.5	6	6	-1	10.1	-14.1
2	2	0	18.4	-18.3	8	2	-3	13.5	13.8	6	4	1	<6.4	-3.5	4	6	-1	8.8	9.4
4	2	0	9.2	-5.8	6	2	-3	7.9	-8.5	8	4	1	<4.7	-3.5	2	6	-1	37.5	-32.6
6	2	0	8.0	-7.4	4	2	-3	24.9	22.5	8	4	-2	9.6	8.7	0	6	-1	6.2	4.3
8	2	0	<3.9	-1.0	2	2	-3	13.7	12.4	6	4	-2	11.7	-12.2	2	6	1	6.1	-5.5
10	2	0	<9.6	4.3	0	2	3	<3.7	2.1	4	4	-2	26.9	27.0	4	6	1	8.7	-10.6
1	3	0	12.0	12.2	2	2	3	14.4	15.7	2	4	-2	24.5	-24.2	6	6	1	<5.1	-10.8
3	3	0	18.1	18.4	4	2	3	5.2	-3.8	0	4	-2	14.7	11.4	8	6	1	12.2	-12.5
5	3	0	20.9	22.5	6	2	3	18.9	20.9	2	4	2	<3.9	-2.2	10	6	1	11.0	9.3
7	3	0	3.7	-2.3	8	2	3	7.4	-6.9	4	4	2	<4.8	1.8	10	6	-2	<7.1	-3.6
9	3	0	9.4	9.3	6	2	-4	9.9	-9.9	6	4	2	7.9	8.7	8	6	-2	8.0	8.3
11	3	0	<9.4	0.5	4	2	-4	6.3	-7.1	8	4	2	12.8	-12.3	6	6	-2	<6.0	-1.2
0	4	0	21.9	17.8	2	2	-4	5.7	6.8	10	4	2	9.0	9.2	4	6	-2	15.7	16.1
2	4	0	2.6	-2.6	0	2	4	10.8	-14.4	8	4	-3	10.7	10.7	2	6	-2	4.3	4.1
4	4	0	<3.1	0.5	2	2	4	6.3	5.5	6	4	-3	14.2	-14.5	0	6	2	3.4	-0.5
6	4	0	<2.9	-1.8	4	2	4	16.9	-19.2	4	4	-3	14.9	14.5	2	6	2	20.9	17.9
8	4	0	<7.3	2.6	6	2	4	8.7	7.7	2	4	-3	4.0	3.6	4	6	2	4.1	1.6
10	4	0	<9.7	5.5	8	2	-5	7.3	5.8	0	4	-3	8.6	-10.0	6	6	2	11.2	13.5
1	5	0	15.9	-15.3	4	2	-5	<6.8	-3.9	2	4	3	8.8	10.4	8	6	2	9.2	-8.1
3	5	0	19.1	-16.5	2	2	-5	12.8	12.5	4	4	3	12.1	-12.9	10	6	2	11.2	9.2
5	5	0	9.5	8.5	0	2	5	<5.8	-0.7	6	4	3	15.9	17.4	8	6	-3	<6.2	3.3
7	5	0	20.2	-19.1	2	2	5	15.3	16.2	8	4	3	13.3	-10.8	6	6	-3	11.1	-14.8
9	5	0	<5.5	3.5	4	2	5	8.0	-4.9	8	4	-4	9.7	8.8	4	6	-3	6.3	5.6
11	5	0	<6.1	-6.4	6	2	5	<8.4	4.4	6	4	-4	6.7	-5.2	2	6	-3	8.2	-7.3
0	6	0	48.7	48.8	6	2	-6	8.1	6.2	4	4	-4	6.0	-4.7	0	6	3	10.3	-8.2
2	6	0	15.0	-15.2	4	2	-6	11.3	-9.0	2	4	-4	12.0	14.4	2	6	3	8.1	-8.4
4	6	0	19.1	18.5	2	2	-6	<7.1	2.7	0	4	4	8.0	-9.5	4	6	3	7.5	-7.6
6	6	0	<2.8	-1.4	0	2	6	12.4	-12.5	2	4	4	10.4	10.9	6	6	3	<6.0	5.1
8	6	0	8.5	6.4	2	2	6	8.1	6.7	4	4	4	11.6	-13.3	8	6	3	11.1	-9.1
10	6	0	<7.1	7.7	4	2	6	9.1	-4.5	6	4	4	<9.6	9.6	8	6	-4	13.5	13.5
12	6	0	<7.7	-5.8	6	2	6	<9.5	-4.9	4	4	4	<9.9	-0.8	6	6	-4	9.1	-8.6
1	7	0	8.3	6.0	2	2	-7	11.4	11.7	8	4	-5	<8.1	6.0	4	6	-4	7.9	9.0
3	7	0	6.3	-5.4	0	2	7	<8.7	-7.5	6	4	-5	<7.5	2.5	2	6	-4	7.1	7.0
5	7	0	24.2	23.4	2	2	7	<9.1	5.8	4	4	-5	8.7	-7.3	0	6	4	7.3	5.8
0	8	0	10.1	10.4	4	2	7	<9.3	5.5	2	4	-5	6.2	5.4	2	6	4	11.6	9.7
2	8	0	20.8	-24.5	11	3	-1	6.8	-6.1	0	4	5	<6.8	-3.0	4	6	4	7.4	-7.6
4	8	0	5.3	-5.2	9	3	-1	6.3	1.2	2	4	5	8.6	8.6	6	6	4	14.1	14.3
1	9	0	2.9	1.9	7	3	-1	19.5	-19.8	4	4	5	<7.4	-7.0	8	6	4	<7.6	-0.7
3	9	0	<2.3	1.7	5	3	-1	3.5	3.4	6	4	5	<9.0	0.2	6	6	-5	9.5	-1.3
0	10	0	16.7	17.1	3	3	-1	19.7	-17.6	8	4	5	<8.3	2.5	4	6	-5	8.5	-12.6
2	10	0	2.6	2.9	1	3	-1	8.5	7.4	6	4	-6	7.3	6.8	2	6	-5	19.3	-15.9
1	1	-1	12.2	14.0	1	3	1	26.4	-25.5	4	4	-6	<7.4	-5.1	0	6	5	14.6	13.8
1	1	-1	6.1	-7.3	3	3	1	19.7	-20.8	2	4	-6	<7.2	4.6	4	6	5	17.7	-19.0
1	1	-1	6.6	8.4	5	3	1	5.5	6.5	2	4	6	12.5	0.	6	6	5	<7.4	2.9
3	1	-1	25.4	27.3	7	3	1	10.7	-11.8	4	4	6	9.0	-3.2	6	6	-6	13.6	13.4
1	1	-1	3.4	-3.4	9	3	1	<5.0	1.2	6	4	6	9.6	-1.0	4	6	-6	9.9	-8.8
1	1	1	32.6	31.9	11	3	1	<5.4	-5.6	4	4	-7	8.5	-6.7	2	6	-6	12.9	13.0
3	1	1	22.1	-18.4	13	2	-2	8.0	5.1	2	4	-7	11.0	10.8	0	6	6	8.3	-9.7
5	1	1	32.4	26.4	11	3	-2	<5.1	-4.7	0	4	7	12.5	-12.1	2	6	6	16.2	14.6
7	1	1	<5.3	-3.8	9	3	-2	15.5	16.5	2	4	7	<9.2	4.9	4	6	6	<7.4	1.5
9	1	1	8.3	6.4	7	3	-2	<3.8	0.7	4	4	7	<9.6	2.3	6	6	6	<7.7	-2.1
9	1	-2	8.0	8.9	5	3	-2	8.8	7.7	11	5	-1	<7.1	-1.8	0	6	6	9.1	-9.0
7	1	-2	<4.9	-1.7	3	3	-2	21.8	18.5	9	5	-1	13.5	13.9	2	6	6	12.3	10.8
5	1	-2	10.1	-9.8	1	3	-2	10.5	7.1	7	5	-1	6.0	-5.5					
3	1	-2	7.5	6.7	1	3	2	39.7	43.3	5	5	-1	14.0	12.7					
1	1	-2	5.7	-5.4	3	3	2	14.8	-15.6	3	5	-1	20.8	19.6					
1	1	2	16.0	14.0	5	3	2	22.4	23.5	1	5	-1	17.9	10.5					

TABLE II

Atomic coordinates

	x	y	z
Results of Lukaszewicz			
Mg	0	0.306	0.5
P	0.217	0	0.895
O_I	0	0	0
O_{II}	0.405	0	0.222
O_{III}	0.233	0.155	0.710
Present study (with standard errors $\times 10^4$)			
Mg	0	0.3124 (5)	0.5
P	0.2162 (3)	0	0.9078 (4)
O_I	0	0	0
O_{II}	0.3997 (9)	0	0.2152 (9)
O_{III}	0.2217 (9)	0.1549 (7)	0.7206 (11)

TABLE III

Interatomic distances and angles

	Distances, Å			Angles,°	
$Mg—O_6$ group					
$Mg—O_{II}$	2.05				
$Mg—O_{III}$	2.02				
$Mg—O_{III}'$	2.15				
P_2O_7 group (e.s.d.* $\times 10^4$ in brackets and values for $\beta Zn_2P_2O_7$ in parenthesis)					
$P—O_I$	1.557 [2]	(1.569)	$P—O_I—P$	180	(180)
$P—O_{II}$	1.534 [10]	(1.556)	$O_I—P—O_{II}$	103.3	(102.1)
$P—O_{III}$	1.542 [9]	(1.554)	$O_I—P—O_{III}$	106.8	(110.0)
$O_I—O_{II}$	2.424	(2.430)	$O_{II}—P—O_{III}$	113.3	(110.9)
$O_I—O_{III}$	2.487	(2.558)	$O_{III}—P—O_{III}'$	112.6	(112.6)
$O_{II}—O_{III}$	2.569	(2.561)			
$O_{III}—O_{III}'$	2.570	(2.586)			

*Estimated standard deviation = e.s.d.

TABLE IV

Mean square atomic displacements in $Å^2$ units (e.s.d. $\times 10^3$ in parenthesis)

	U_{11}	U_{22}	U_{33}	$2U_{12} = 2U_{21}$	$2U_{13} = 2U_{31}$	$2U_{23} = 2U_{32}$
Mg	0.010	−0.008 (8)	0.017 (3)		−0.005 (1)	
P	0.001 (1)	−0.006 (4)	0.000 (1)		−0.000 (1)	
O_I	−0.002 (3)	0.148 (7)	0.062 (2)		−0.012 (5)	
O_{II}	0.005 (2)	−0.013 (4)	−0.003 (4)		−0.001 (2)	
O_{III}	0.027 (3)	−0.009 (4)	0.013 (3)	0.006 (2)	−0.002 (2)	0.009 (3)

could be seen in a single crystal pattern. Again the same crystal used in the structure analysis was used for this study. Hour-long exposures were recorded at various temperatures with the camera slightly displaced between exposures. By this technique a transition was found to occur abruptly at 62 ± 1 °C. At 63.5 ± 1 °C, however, two patterns were found superimposed on, in particular, a $h2l$ type photograph. One pattern had lattice parameters similar to those of the β-phase whereas the second appeared contracted along the $(10\bar{1})$ direction. However, a one to one correlation existed between reflections of the two patterns. The coexisting phases reported by Hummel *et al.* (3) appears to involve two β-like phases with a much suppressed range of coexistence for our crystal.

Can. J. Chem. Downloaded from www.nrcresearchpress.com by 210.87.254.105 on 09/05/12
For personal use only.

Weissenberg photographs of the α- and β-phases for the [010] zone were superimposed on a single film. These showed the contraction of the β-angle with small changes in the lengths of the $\mathbf{b}_1$ and $\mathbf{b}_3$ axes. The major change was clearly seen to be a contraction along the $\mathbf{b}_1 + \mathbf{b}_3$ direction and an expansion along the $\mathbf{b}_1 - \mathbf{b}_3$ direction in reciprocal space. Further comments on the details of the phase transition will soon be published together with the crystal structure of α-$Mg_2P_2O_7$ and the e.p.r. study of the phase transition of $Mg_2P_2O_7$:Mn^{++}.

DISCUSSION

Since β-$Mg_2P_2O_7$ is an isostructure of $Sc_2Si_2O_7$ and β-$Zn_2P_2O_7$ and both of these structures have previously been discussed in some detail we will only comment on the relevant points of comparison. Again as in β-$Zn_2P_2O_7$ the central oxygen atom manifests enhanced thermal activity in the plane perpendicular to the P—P vector of the anion. Any reasonable correction for the effects of this motion will result in a substantially enlarged central P—O bond and thus lead to a significant difference between the terminal and inner P—O bond distance. Good agreement is found among the anion bond distances obtained for the refined structures of $Mn_2P_2O_7$ (16, 17), β-$Mg_2P_2O_7$, and β-$Zn_2P_2O_7$. The bond distances of β-$Zn_2P_2O_7$ are compared with those reported here in Table III.

The cation environment is an irregular octahedral arrangement of the oxygen atoms. The major distortions from a perfect octahedron arise from a rotational displacement of $\sim 30°$ of the O_{III}—O_{III}' pair from the ideal octahedral position and an elongation of the Mg—O_{III}' bond as compared to the other cation oxygen bond distances. The mean positions of O_{II} and O_{III} are found to lie very nearly in the same plane as the two cations and phosphorus to which it is ligated. This suggests the possibility of sp^2 hydribization of the oxygen atoms with a lone p_z orbital available for π-bonding to the cation. Such a contribution would of course change the amount of $p\pi$–$d\pi$ bonding within the anion. This structural feature, which is common to these β-phase pyrophosphates, implies that electron delocalization between the cation and the anion can play a significant role in the detailed properties of the individual compounds. The only crystallographic suggestion of such a possibility lies in the fact that the average nonthermally corrected average P—O bond distance exceed the predicted value of 1.54 Å for an isolated anion. This value, when corrected for thermal motion, would probably lie significantly outside the range of error.

It appears that the phase transformations are triggered or at least paralleled by an enhanced disorder for the central oxygen atom. Whether this is actually a time disordering or a positional disorder is at present immaterial. The wide dispersion found in the transition temperatures of the four phases together with the similar but unique low temperature phases implies that indeed the cations play a role in the bonding beyond what is generally implied in terms of their effective size and charge. Unfortunately questions like the nature of the disordering, thermal corrections, and a more definitive manifestation of the role of the environment must await the resolution of the α-structures in this series.

ACKNOWLEDGMENT

This work was supported by the National Research Council of Canada.

REFERENCES

1. J. G. Chambers, W. R. Datars, and C. Calvo. J. Chem. Phys. **41**, 806 (1964).
2. B. E. Robertson. Master's Thesis, McMaster University. 1964.
3. R. Roy, E. T. Middleswarth, and F. A. Hummel. Am. Mineralogist, **33**, 458 (1948).

Can. J. Chem. Downloaded from www.nrcresearchpress.com by 210.87.254.105 on 09/05/12
For personal use only.

4. F. L. OETTING and R. A. MCDONALD. J. Phys. Chem. **67**, 2757 (1963).
5. C. CALVO. This issue.
6. A. N. LAZAREV. Izv. Akad. Nauk Kaz. SSR Ser. Khim. 242 (1964).
7. D. W. J. CRUICKSHANK. J. Chem. Soc. 5486 (1961).
8. A. N. LAZAREV. Izv. Akad. Nauk Kaz. SSR Ser. Khim. 235 (1964).
9. K. LUKASZEWICZ. Roczniki Chem. **35**, 31 (1961).
10. C. CALVO. Can. J. Chem. To be published.
11. W. RIEMAN, J. D. NEUSS, and B. NAIMAN. Quantitative analysis. McGraw-Hill Book Co. 1942.
12. W. H. BAUR. Acta Cryst. **9**, 515 (1956).
13. C. CALVO, J. S. LEUNG, and W. R. DATARS. To be published.
14. W. R. BUSING, K. O. MARTIN, and H. A. LEVY. ORNL-TM-305. 1962.
15. J. A. IBERS. Acta Cryst. **9**, 652 (1956).
16. K. LUKASZEWICZ and R. SMAJIEWICZ. Roczniki Chem. **35**, 741 (1961).
17. B. E. ROBERTSON and C. CALVO. Canadian Assoc. of Physicists' Congress, Dalhousie University, June 10–13, 1964.

Can. J. Chem. Downloaded from www.nrcresearchpress.com by 210.87.254.105 on 09/05/12
For personal use only.

THE CRYSTAL STRUCTURE AND PHASE TRANSITIONS OF β-$Zn_2P_2O_7$

CRISPIN CALVO
Department of Chemistry, McMaster University, Hamilton, Ontario
Received August 13, 1964

ABSTRACT

β-$Zn_2P_2O_7$ crystallizes in the $C2/m$ space group with lattice parameters $a = 6.61 \pm 0.01$ Å, $b = 8.29 \pm 0.01$ Å, $c = 4.51 \pm 0.01$ Å, $\beta = 105.4° \pm 0.2°$ and $z = 2$. The anion, $P_2O_7^{-4}$, is centered with its mirror plane coinciding with the mirror plane of the space group. The central oxygen atom, however, shows high anisotropic thermal motion and thus it appears that the P—O—P bond angle is linear only as a result of thermal averaging. The cations are found on twofold axes in irregular sixfold coordination and these ZnO_6 groups share three edges with neighboring cations. This cation coordination is, therefore, consistent with that predicted from the red emission of β-$Zn_2P_2O_7$:Mn^{++}.

INTRODUCTION

An investigation of the structures of the α- (low temperature) and the β-forms (high temperature) of $Zn_2P_2O_7$ was undertaken (*a*) to determine whether the correlation found between the cation coordination and the luminescence of the Mn^{++}-activated zinc orthophosphate (1, 2) could be extended to zinc pyrophosphate and (*b*) to determine the structural nature of the reported phase transition between the α- and β-phases (3). Additional impetus for this study has been provided by Cruickshank's study of the relationship of the P—O bond length and the π-bonding through the 3d orbitals of the phosphorus (4). In this paper, we will deal primarily with the crystal structure of β-$Zn_2P_2O_7$ although some comment on related phases will be necessary.

The pyrophosphate of Zn, Mg (5), Cu (6), and Mn (7) have isostructural high temperature forms and save for $Mn_2P_2O_7$ related but distinct low temperature structures. No phase transition has been found in this latter compound above −60 °C. Qualitatively the *c*-axes of the unit cells of the low temperature phases of Zn, Mg, and Cu are twice that of the high temperature structure and the *a*-axes are thrice; twice and the same length as found for the β-cells, respectively. The lengths of the *b*-axes and the β-angles remain substantially the same through the transition. The space group symmetry is lowered from $C2/m$ to Ic (8), $B2_1/c$ (9), and $C2/c$ (6) respectively for unit cell axes chosen parallel to those of the high temperature cells. In addition to the reversible first order phase transition at 132° in $Zn_2P_2O_7$ a gradual (in temperature) transition has been identified near 155 °C by electron paramagnetic resonance (e.p.r.) studies (10). In $Mg_2P_2O_7$ a gradual phase transition near 68 °C was reported by Roy, Middleswarth, and Hummel (11) and recently confirmed by the specific heat measurements of Oetting and McDonald (12). However, the changes in the unit cell symmetries of $Mg_2P_2O_7$ do not readily support the type of phenomena reported in $Zn_2P_2O_7$. Larazev (13–16) has extensively studied the infrared adsorption of pyrocompounds and has proposed a thermal excitation across a double well potential barrier to explain the phase transition in $Mg_2P_2O_7$. No such study has been reported for $Zn_2P_2O_7$. Further comment on the relevance of these studies to the results reported here will be presented below.

Previous crystallographic studies of pyrophosphate structures have indicated that the geometric configuration of the $P_2O_7^{-4}$ ion is not independent of the environment in which it appears. For example, the P—O—P bond is 133.6° in $Na_4P_2O_7.10H_2O$ (17) with inner and average outer P—O bond lengths of 1.61 Å and 1.51 Å respectively. In ZrP_2O_7

Can. J. Chem. Downloaded from www.nrcresearchpress.com by 210.87.254.6 on 09/05/12
For personal use only.

(18, 19) the P—O—P bond angle appears to be fixed by the crystal symmetry at 180°; the inner P—O bond length is 1.56 Å and the outer 1.52 Å. Studies by Larazev (13), however, indicated a phase transition in this compound near 300 °K and thus a further crystallographic examination is indicated. The structure of β-$Zn_2P_2O_7$, to be discussed here, appears to have a linear P—O—P bond fixed by the crystal symmetry. A similar result has been obtained in the partial resolution of the crystal structures of β-$Mg_2P_2O_7$ (5) and $Mn_2P_2O_7$ (7). It will be shown that the enhanced thermal motion of the central oxygen atom suggests that the bond is, in fact, bent, but appears linear as a result of the thermal motion.

EXPERIMENTAL

Crystals of $Zn_2P_2O_7$ were prepared by crystallization from a melt obtained from the decomposition of precipitated zinc ammonium phosphate. These crystals had their (110), (001), and (10$\bar{1}$) faces sufficiently developed to permit optical alignment. Photographs of both the α- and β-forms were obtained with the Weissenberg camera using Cu K_α and Mo K_α radiation. To obtain photographs from the β-form, the crystals were heated by a soldering iron placed on the axis of the camera at a distance of about 2 mm from the crystal. In later experiments, the crystals were heated by the air flow from a pair of hair dryers arranged in series. The temperatures were estimated from e.m.f. readings from a thermocouple attached to the collimator and placed near the crystal. Temperature stabilities of the order of ±2 °C in an hour could easily be maintained with this hair dryer technique.

The lattice parameters for the β-phase were obtained from photographic films calibrated with reflections from the identical crystal in the α-phase. The parameters for the α-phase, $a = 19.59$ Å, $b = 8.28$ Å, $c = 9.103$ Å and $\beta = 100.17°$, have been obtained by deWolff (20) from powder data. Note that on the basis of this cell the α-space group would be face centered rather than body centered as indicated above. The lattice parameters obtained for the β-phase are, $a = 6.61 \pm 0.01$ Å, $b = 8.30 \pm 0.01$ Å and $c = 4.51 \pm 0.01$ Å and $\beta = 105.4°$. From the measured density for the α-phase, 4.1 g/cm^3, it was concluded that the β-phase had two molecules per unit cell. Only those reflections labelled by hkl with $h + k =$ odd were systematically absent and thus the space group must lie among the choices $C2$, Cm, or $C2/m$. The centric space group was chosen on the basis of e.p.r. experiments (10). In this space group the cation, the phosphorus atom, and at least 6 of the 14 oxygen atoms must be located in special positions. The special position for the cation is on the twofold axis and, in addition, all the cations are either translationally equivalent or related by the inversion operation. The magnetic moment tensor is invariant to these operations and thus only one e.p.r.-active site should be seen in the spectrum. Such was the case for $Zn_2P_2O_7$ above $\sim$ 155 °C. This method of establishing the space group is to be contrasted with the traditional crystallographic method. Customarily, one attempts a refinement of the crystal structure separately in each of the possible space groups. Ideally, all these refinements should ultimately lead to the same "correct" structure. Such a precedure was applied to $Sc_2Si_2O_7$ (21), an isostructure of β-$Zn_2P_2O_7$, with the result that chemical considerations ultimately were necessary for the resolution of the space group symmetry.

Historically, work was first begun on the structure of α-$Zn_2P_2O_7$. The Patterson functions prepared from the $h0l$ data and $hk0$ data strongly suggested the existence of a superstructure. Once the lattice parameters and space group had been established for the β-$Zn_2P_2O_7$ phase, these Patterson functions were interpreted for a trial structure for the β-phase. This trial structure consisted of cations on the twofold axis, related in pairs by the mirror plane, in an octahedral environment of oxygen atoms. Each of these ZnO_6 groups shares three edges with three neighboring cations. These cations are related to it by the mirror plane and the C-centering and this arrangement extends as sheets along the x- and y-directions. These ZnO_6 groups form a hexagonal network similar to that found in $CdCl_3$ (see Wells (22), Fig. 51 (*iii*)). Adjacent sheets are held by the $P_2O_7^{-4}$ groups. The anion, of course, consists of a pair of corner-shared PO_4 groups. As a trial arrangement these $P_2O_7^{-4}$ groups were placed on the mirror plane with the central oxygen atom at the origin in a manner which proved to be analogous to the thortveitite structure. This trial structure, seen in Fig. 1, was used in subsequent refinements.

The crystals selected for intensity measurements had dimensions of the order of 0.1 mm × 0.1 mm × 0.15 mm. Data of the type hnl with $n = 0$, 1, and 2 were recorded with Cu K_α and Mo K_α radiation. In addition, data indexed as $hk0$, $0kl$, and hhl were also recorded with Mo K_α radiation. The temperature of the crystal was not monitored while the intensity photographs were taken. However, the heating elements were arranged in a manner that yielded temperatures well above 160 °C in previous experiments. These reflections were visually estimated and these data, suitably corrected for Lorentz and polarization effects, were used in a detailed refinement of the crystal structure. Early refinements used only Fourier and difference Fourier techniques. Recently an IBM-7040 (20K) became available and thus the final refinements were carried out on this unit with a modified Busing, Martin, and Levy least squares program (23). Weights were assigned to the structure factors according to the criterion suggested by Ibers (24). In this procedure

Can. J. Chem. Downloaded from www.nrcresearchpress.com by 210.87.254.6 on 09/05/12
For personal use only.

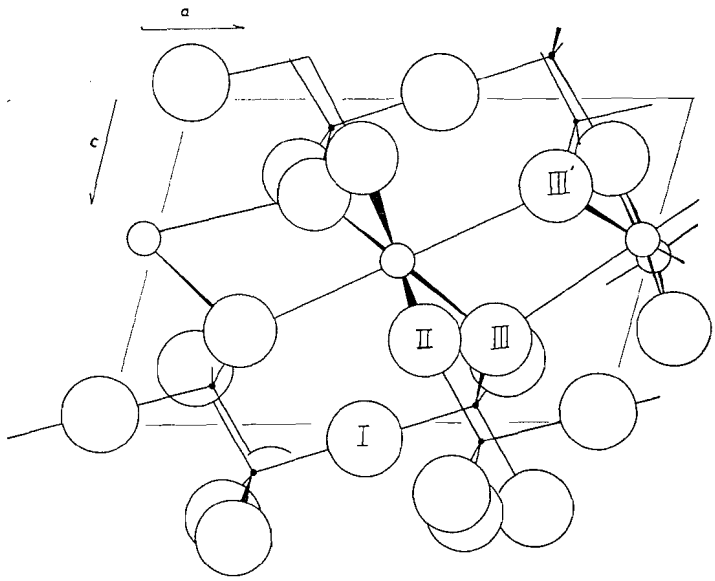

FIG. 1. A view of structure of β-$Zn_2P_2O_7$. The large circles represent the oxygen atoms, the full circles the phosphorus atoms, and the small open circles the cations. No attempt has been made to represent the motion of O_I. The axial directions are represented on the figure.

weights are assigned according to values determined from a curve of the standard deviation versus F_{obs} for multiply observed reflections. Least squares refinements were also carried through with unit weights and weights as suggested by Hughes (25). Some of the results of these refinements will be discussed below. The final R-factor for all 217 unique reflections is 0.137 and for the observed reflections only, it is 0.098. The observed and calculated structure factors are compared in Table I. The atomic parameters, including both positional and thermal coordinates are collected in Table II.

Crystals of $Zn_2P_2O_7$ were studied through the range of temperatures corresponding to the two reported phase transitions. Oscillation photographs were taken with a crystal rotating about the [110] axis near 132 °C to ascertain whether the halving of the c-axis and the thirding of the a-axis occurred simultaneously. Both changes occurred at 132 ± 1 °C. The transition near 155 °C was more difficult to detect since the unit cell dimension and extinctions remain the same. Two 180° oscillation photographs were superimposed on the same film with the camera displaced translationally by 2 mm between exposures. These exposures were of equal duration (4 h); the first was taken with the temperature maintained between 135 and 145 °C and the second with the temperature above 160 °C. The crystal was disaligned by about 2° to prevent the reflections from superimposing on the photograph. The intensities from the crystal at the lower temperatures were found to be more diffuse and, except for the stronger intensities, this set was found to be of consistently weaker intensity.

DISCUSSION

The cations in this structure are coordinated irregularly to six oxygen atoms. Although the Zn^{++} lies on the twofold axis they are not at the center of the oxygen atom environment. In fact, the Zn^{++} lies displaced by about 0.3 Å from a line joining $O_{III'}$ to its mate generated by the twofold axis. This, no doubt, results from the fact that the y-parameter for $O_{III'}$ is fixed by the requirements of the bonding to the phosphorus atom and the existence of the mirror plane. The $O_{III'} - O_{III''}$ separation is 2.59 Å, a distance of approach too small for neighboring Zn^{++}. The distance actually found between the cations along the b-axis is 3.17 Å, a somewhat shorter distance than that found between cations related by C-centering (3.44 Å). The cation–oxygen atom bond lengths are 2.06 Å, 2.00 Å, and 2.27 Å for the cation to $O_{II'}$ O_{III}, and $O_{III'}$ displacements respectively with no correction applied for correlated thermal motion. The oxygen atom environment

Can. J. Chem. Downloaded from www.nrcresearchpress.com by 210.87.254.6 on 09/05/12
For personal use only.

Can. J. Chem. Downloaded from www.nrcresearchpress.com by 210.87.254.6 on 09/05/12
For personal use only.

TABLE I

Observed and calculated structure factors

H	K	L	F(O)	F(C)	H	K	L	F(O)	F(C)	H	K	L	F(O)	F(C)	H	K	L	F(O)	F(C)
0	0	1	26.4	-27.9	0	4	0	20.1	19.5	5	9	0	7.1	6.6	6	2	1	17.1	16.0
0	0	2	29.1	29.7	0	6	0	48.5	49.7	2	10	0	8.6	9.9	8	2	1	7.2	1.7
0	0	3	34.8	-34.2	0	8	0	5.5	-5.7	-9	1	1	11.7	11.5	10	2	1	11.2	9.2
0	0	4	21.9	23.0	0	10	0	12.9	12.9	-7	1	1	4.9	-4.7	-8	2	2	< 6.9	0.8
0	0	5	26.5	-27.6	0	2	1	77.0	63.5	-5	1	1	11.2	12.8	-6	2	2	19.8	-21.9
0	0	6	6.2	7.2	0	4	1	15.3	17.3	-3	1	1	43.7	34.6	-4	2	2	6.7	7.5
0	0	7	11.7	-11.1	0	6	1	7.6	-6.9	-1	1	1	7.9	8.2	-2	2	2	54.8	-46.4
2	0	0	11.5	11.3	0	8	1	23.9	27.2	1	1	1	43.0	42.9	2	2	2	27.2	-22.9
2	0	1	33.7	-31.2	0	10	1	3.1	-3.1	3	1	1	6.3	-8.2	4	2	2	18.7	-21.5
2	0	2	55.4	53.5	0	2	2	22.9	-23.4	5	1	1	27.0	26.3	6	2	2	< 6.6	-3.6
2	0	3	27.8	-27.8	0	4	2	14.9	12.0	7	1	1	< 4.7	-0.4	8	2	2	12.8	-13.3
2	0	4	27.2	30.6	0	6	2	9.7	8.8	-7	1	2	< 4.3	-5.7	-8	2	3	17.1	13.7
2	0	5	< 7.9	-8.4	0	8	2	16.2	-16.1	-5	1	2	9.9	-12.7	-6	2	3	< 5.9	-3.8
2	0	6	20.4	16.1	0	10	2	14.7	14.2	-3	1	2	< 2.9	-3.2	-4	2	3	25.8	29.5
2	0	-1	70.3	-77.3	0	2	3	15.6	16.8	-1	1	2	17.2	-15.2	2	2	3	22.3	26.4
2	0	-2	42.9	44.0	0	4	3	9.6	-9.8	1	1	2	3.5	3.3	2	2	3	30.6	29.7
2	0	-3	32.4	-30.5	0	6	3	10.8	-13.1	3	1	2	23.5	-22.8	4	2	3	7.4	6.9
-2	0	4	23.7	26.3	0	8	3	10.7	11.2	5	1	2	5.2	-3.0	6	2	3	24.2	18.7
-2	0	5	< 7.3	-6.9	0	2	4	21.8	-25.0	7	1	2	< 5.0	-3.6	8	2	3	< 10.5	2.1
2	0	-6	18.0	18.7	0	4	4	6.1	-5.8	-9	1	3	7.1	6.9	-8	2	4	< 8.9	4.6
4	0	0	49.1	48.5	0	6	4	8.6	7.7	-7	1	3	6.6	7.1	-6	2	4	17.1	-13.4
4	0	1	37.5	-36.2	0	8	4	13.0	-14.8	-5	1	3	4.9	5.2	-4	2	4	12.4	-14.9
4	0	2	20.0	20.7	0	2	5	7.2	7.3	-3	1	3	9.7	12.7	-2	2	4	< 5.6	-5.6
4	0	3	28.7	-27.5	0	2	6	13.8	-14.6	-1	1	3	5.5	3.8	2	2	4	6.3	-7.3
4	0	4	7.2	10.5	1	1	0	12.0	-13.7	1	1	3	29.5	25.8	4	2	4	17.1	-20.0
4	0	5	19.4	-18.6	3	1	0	19.7	-21.0	3	1	3	5.6	6.3	6	2	4	< 7.9	-4.6
4	0	6	9.2	11.3	5	1	0	12.4	12.4	5	1	3	6.9	6.1	8	2	4	< 11.9	-6.2
4	0	-1	8.9	-9.8	7	1	0	18.8	-17.2	-7	1	4	5.4	4.4	-6	2	5	< 7.0	7.5
4	0	-2	40.7	40.3	2	2	0	38.7	-37.4	-5	1	4	9.0	-10.4	-4	2	5	< 6.6	2.3
4	0	-3	7.7	-7.9	4	2	0	18.9	-20.8	-3	1	4	6.2	6.4	-2	2	5	18.1	17.7
4	0	-4	18.9	22.8	6	2	0	11.6	-11.9	-1	1	4	27.3	-23.0	2	2	5	16.4	18.6
4	0	-5	24.3	-21.4	8	2	0	< 7.1	-8.6	1	1	4	< 4.4	-2.1	4	2	5	8.2	6.8
6	0	0	17.3	16.0	1	3	0	31.0	39.1	3	1	4	5.8	-6.3	2	2	6	8.1	-6.1
6	0	1	10.5	-10.3	3	3	0	34.0	34.5	5	1	4	< 5.7	-8.1	-2	2	7	11.0	10.2
6	0	2	25.7	26.0	5	3	0	31.7	31.7	-7	1	5	8.9	9.4	-3	3	5	< 14.9	-5.7
6	0	3	7.8	-7.7	7	3	0	4.1	4.5	-5	1	5	7.6	-5.8	3	3	-4	29.2	25.5
6	0	4	19.2	16.7	2	4	0	2.9	3.1	-3	1	5	18.4	17.3	3	3	-3	< 11.7	-4.5
6	0	-1	22.8	-25.5	4	4	0	< 3.4	1.4	-1	1	5	5.9	2.4	3	3	-2	30.4	33.3
6	0	-2	15.6	14.2	6	4	0	< 3.6	3.3	1	1	5	5.2	4.4	3	3	-1	40.6	-36.8
6	0	-3	24.9	-24.8	1	5	0	28.5	-31.2	3	1	5	10.4	10.1	3	3	1	30.7	-36.4
-6	0	4	< 7.8	-2.7	3	5	0	28.8	-30.7	5	1	5	< 6.2	0.2	3	3	2	< 11.8	7.7
-6	0	5	< 7.8	-5.2	5	5	0	3.8	-3.0	7	1	5	9.2	6.5	3	3	3	31.3	-27.1
8	0	0	9.6	9.6	7	5	0	23.1	-18.8	-5	1	6	7.7	-8.4	3	3	4	15.5	20.8
8	0	1	13.7	-17.8	2	6	0	4.9	-2.4	-3	1	6	< 5.6	-2.2	3	3	5	< 17.0	-8.7
8	0	2	< 8.9	2.7	4	6	0	22.3	20.7	-1	1	6	5.6	-0.2	4	4	-1	< 11.4	8.1
8	0	3	10.5	-12.0	6	6	0	4.9	4.8	1	1	6	9.8	-9.9	4	4	-2	32.1	27.3
8	0	4	< 9.2	6.9	1	7	0	16.2	14.1	3	1	6	< 6.2	0.1	4	4	-3	16.8	10.1
-8	0	1	< 7.7	-2.9	3	7	0	7.1	3.2	5	1	6	7.4	-6.9	-4	4	4	< 14.0	-3.5
8	0	-2	10.3	11.9	5	7	0	23.3	19.7	-1	1	7	8.2	7.9	5	5	-1	23.4	21.4
-8	0	3	< 7.8	-1.1	7	7	0	5.2	-4.9	-8	2	1	11.1	9.2	5	5	-2	18.1	-17.7
8	0	-4	18.2	19.3	2	8	0	25.7	-24.7	-6	2	1	11.5	11.6	-5	5	3	< 14.2	8.7
10	0	0	7.8	10.5	4	8	0	12.3	-10.6	-4	2	1	33.6	35.8	5	5	-4	19.8	-14.2
10	0	1	< 7.8	1.9	6	8	0	8.7	-9.0	-2	2	1	6.5	7.2					
10	0	2	8.7	8.8	1	9	0	2.8	2.6	2	2	1	29.1	31.9					
0	2	0	3.4	-3.1	3	9	0	< 3.6	1.8	4	2	1	26.3	24.5					

TABLE II

Atomic coordinates

	A. Positional (error × 10^4 in parenthesis)		
	x/a	y/b	z/c
Zn	0	.3092(4)	1/2
P	.2104(7)	0	.9014(11)
O_I	0	0	0
O_{II}	.3781(20)	0	.2167(34)
O_{III}	.2262(18)	.1559(12)	.7181(31)

	B. Thermal (mean square displacements, Å² with e.s.d. × 10^4 in parenthesis)					
	U_{11}	U_{22}	U_{33}	$2U_{12}$	$2U_{13}$	$2U_{23}$
Zn	0.029(2)	0.023(3)	0.013(1)	—	−0.007(1)	—
P	0.008(2)	0.021(4)	0.013(2)	—	0.006(1)	—
O_1	0.027(13)	0.069(28)	0.073(15)	—	0.024(13)	—
O_2	0.032(5)	0.016(8)	0.034(8)	—	0.031(8)	—
O_3	0.034(5)	0.004(6)	0.044(7)	0.008(5)	0.026(6)	−0.007(7)

about the cation deviates substantially from that of a perfect octahedron. The major component of these distortions arises from a rotation of the O_{III}—O_{III}''' edge from its ideal position by $\sim 30°$ about the twofold axis. Such a distortion arises from the constraints placed upon the positions of the oxygen atoms by the requirements of its bonding to the phosphorus atom.

TABLE III

Bond distances and angles

Bond distances, Å		Bond angles, °	
ZnO_6 group			
Zn—O_{II}	2.061		
Zn—O_{III}	2.001		
Zn—O_{III}'	2.275		
P_2O_7 group			
P—O_I	1.569	O_I—P—O_{II}	102.1
P—O_{II}	1.556	O_I—P—O_{III}	110.0
P—O_{III}	1.554	O_{II}—P—O_{III}	110.9
O_I—O_{II}	2.430	O_{III}—P—O_{III}'	112.6
O_I—O_{III}	2.558		
O_{II}—O_{III}	2.561		
O_{III}—O_{III}'	2.586		

The pyrophosphate ion is also quite irregular. The three unique uncorrected P—O bond lengths are P—O_I = 1.569 Å, P—O_{II} = 1.557 Å, and P—O_{III} = 1.554 Å with estimated standard deviation (e.s.d.) of 0.005 Å, 0.019 Å, 0.013 Å, respectively. See Table III. These distances cannot be used directly to estimate $p\pi$–$d\pi$ bond character since the thermal motions of the atoms are high and probably highly correlated. The large values of thermal parameters for the central oxygen atom in the plane perpendicular to the P—P vector indicates that the P—O—P bond is essentially non-linear. It is not at all clear whether the motion is real or represents a statistical disordering in the order–disorder sense, and if real whether it represents vibrational or rotational motion.

For any of the proposed sources of the high thermal parameters of the central oxygen

Can. J. Chem. Downloaded from www.nrcresearchpress.com by 210.87.254.6 on 09/05/12
For personal use only.

atom, the apparent P—O_I bond length will be significantly shorter than the true internuclear distance. The effect of the apparent thermal motion on the other P—O bonds will be much smaller. The structure thus appears to manifest different distances for the inner and outer P—O bonds. However, the difference is not as large as found in $Na_4P_2O_7.10H_2O$.

The value obtained for the P—O_{II} bond distance is very sensitive to the details of the weighting used. If constant weights are used the value is 1.48 Å whereas with weights assigned as suggested by Hughes a value of 1.51 Å is obtained. In general, except for the position of O_{II} all the atoms lie within the range determined from the sum of the e.s.d. These latter quantities are about 50% higher than the values shown in Table II for these two weighting schemes.

A detailed analysis of the effect of the thermal motion on the "true" bond lengths is not feasible without a better knowledge of the molecular source of this motion. It may be that β-$Zn_2P_2O_7$ features a disordering of the central oxygen atom across a double well potential as has been suggested for the phase transition in $Mg_2P_2O_7$ (15). In this latter case the specific heat anomaly, according to Tisza (26) is suggestive of an entropy-driven anomaly. The transition of the second kind found at 155 °C in $Zn_2P_2O_7$ together with the line broadening (10) would be consistent with the requirement of continuity for this type of transition (27) arising from a positional disordering of a bent $P_2O_7^{-4}$ ion. A better representation for the structure would then be a split central oxygen atom, the details of which would be determined by the anion configuration found for the α-$Zn_2P_2O_7$ phase. It seems prudent to postpone any attempt to analyze the $p\pi$–$d\pi$ bond character in the anion, the role of the environment together with the nature of the disorder until the low temperature structure is resolved.

This investigation further substantiates the correlation between the red emission of Mn^{++} and the octahedrally coordinated site in phosphate systems. In this case e.p.r. evidence proves that the Mn^{++} substitutes directly for the cation. Hummel and Katnack (28) have determined the emission intensity versus wavelength for α-$Zn_2P_2O_7$. This emission peaks at 6 900 Å but the emission curve appears to be composed of at least two major peaks. In the case of β-$Zn_2P_2O_7$:Mn the emission is definitely red under X-ray bombardment but no details of the curve shapes are available.

ACKNOWLEDGMENTS

The author wishes to acknowledge the financial support of the National Research Council. Special thanks are to be extended to Casimir J. Rosa for his aid with the translations of some of the pertinent literature.

REFERENCES

1. C. Calvo. J. Phys. Chem. Solids, **24**, 141 (1963).
2. C. Calvo. Can. J. Chem. **43**, 436 (1965).
3. F. L. Katnack and F. A. Hummel. J. Electrochem. Soc. **105**, 125 (1958).
4. D. W. J. Cruickshank. J. Chem. Soc. 5486 (1961).
5. K. Lukaszewicz. Roczniki Chem. **35**, 31 (1961).
6. B. E. Robertson. Master's Thesis, McMaster University. 1964.
7. L. Lukaszewicz and R. Smajkiewicz. Roczniki Chem. **35**, 741 (1961).
8. C. Calvo. To be published.
9. C. Calvo. To be published.
10. J. G. Chambers, W. R. Datars, and C. Calvo. J. Chem. Phys. **41**, 806 (1964).
11. R. Roy, E. T. Middleswarth, and F. A. Hummel. Am. Mineralogist, **33**, 458 (1948).
12. F. L. Oetling and R. A. McDonald. J. Phys. Chem. **67**, 2737 (1963).
13. A. N. Larazev. Izv. Akad. Nauk SSSR, Otd. Khim. Nauk, 1314 (1962).
14. A. N. Larazev. Izv. Akad. Nauk Kaz. SSR Ser. Khim. (2) 235 (1964).
15. A. N. Larazev. Izv. Akad. Nauk Kaz. SSR Ser. Khim. (2) 242 (1964).

Can. J. Chem. Downloaded from www.nrcresearchpress.com by 210.87.254.6 on 09/05/12
For personal use only.

16. A. N. LARAZEV and T. F. TENISHEVA. Izv. Akad. Nauk Kaz. SSR Ser. Khim. (3) 403 (1964).
17. D. W. S. CRUICKSHANK. Acta Cryst. **17**, 672 (1964).
18. G. R. LEVI and G. PEYRONEL. Z. Krist. **92**, 190 (1935).
19. H. MCGEACHIN. Acta Cryst. **14**, 1286 (1961).
20. P. M. DEWOLFF. X-ray Powder Data File, A.S.T.M. 1958. Card 8-238/239.
21. D. W. J. CRUICKSHANK, H. LYNTON, and G. A. BARCLAY. Acta Cryst. **15**, 491 (1962).
22. A. F. WELLS. Structural inorganic chemistry. Oxford University Press. 1962.
23. W. R. BUSING, K. O. MARTIN, and H. A. LEVY. ORNL-TM-305. 1962.
24. J. A. IBERS. Acta Cryst. **9**, 652 (1956).
25. E. W. HUGHES. J. Am. Chem. Soc. **63**, 1737 (1941).
26. L. TISZA. Phase transformations in solids. *Edited by* Smoluchowski. Mayer and Weyl. Wiley. 1951. Chap. 1.
27. L. LANDAU and E. LIFSHITZ. Statistical physics. Addison-Wesley. 1958. p. 432.
28. F. A. HUMMEL and F. L. KATNACK. J. Electrochem. Soc. **105**, 525 (1958).

Can. J. Chem. Downloaded from www.nrcresearchpress.com by 210.87.254.6 on 09/05/12
For personal use only.

Can. J. Chem. Downloaded from www.nrcresearchpress.com by 210.87.254.42 on 09/05/12
For personal use only.

SPECTRES INFRAROUGES DE COMPOSÉS RICHES EN AZOTE

MÉÜDE TREMBLAY
Centre Canadien de Recherches et Perfectionnement des Armes, Québec, Québec
Reçu le 3 décembre 1964

RÉSUMÉ

L'étude des spectres infrarouges des dérivés de la guanidine et du tétrazole obtenus par synthèse a permis de vérifier leur structure. Les sels suivants de diazotétrazole, contenant de 72 à 86% d'azote, ont été préparés; le sel d'aminoguanidine, de triaminoguanidine, de cyanoguanidine, d'aminotétrazole et de diaminotétrazole.

INTRODUCTION

Les substances qui contiennent un haut pourcentage d'azote sont habituellement très instables et difficiles à caractériser. Les groupes azotés présents peuvent pour la plupart être déterminés par spectrophotometrie infrarouge permettant d'établir la structure des composés qui les contiennent.

Au cours du présent travail nous avons tenté la synthèse de diazocyanures (—N=N—CN). Le guanidinyldiazocyanure (NH_2—C(=NH)—NH—N=N—CN) a été synthétisé à partir de l'azide d'amidine (1). Nous avons essayé de synthétiser le cyanoguanidinyl diazocyanure et le nitroguanidinyl diazocyanure. Nous croyions pouvoir former le dérivé cyano à partir de l'azide de cyanamidine (2) et de l'acide cyanhydrique. D'autre part le dérivé nitro aurait dû se former à partir de l'azide de nitroamidine (3) et l'acide cyanhydrique. Le dérivé cyano n'a pas été isolé et la structure du 5-cyanamidotétrazote formé à été étudiée à l'aide de son spectre infrarouge. Le produit obtenu à partir du dérivé nitro a été identifié comme étant du 5-nitroaminotétrazole.

Nous avons synthétisé une autre série de composés à partir du sel de potassium du diazotétrazole et de substances riches en azote tels que l'aminoguanidine, la triaminoguanidine, la cyanoguanidine, le 5-aminotétrazole et le 1,5-diaminotétrazole.

SPECTRES INFRAROUGES

Nous avons déterminé les spectres infrarouges du diazocyanure de guanidine et du bis-diazoguanidinyl diazotétrazole. Le spectre de diazocyanure de guanidine est donné dans la littérature (4) mais le spectre de son dérivé, le bis-diazoguanidinyl-diazotétrazole n'est pas décrit. Le premier spectre fut déterminé dans un but d'identification et aussi dans l'intention de le comparer à nos dérivés diazocyanures. Le dérivé bis-diazoguanidinyl-diazotétrazole d'autre part a été comparé à nos sels de diazotetrazole. Nous avons aussi déterminé le spectre du produit isolé à partir de l'azide de cyanamidine et de l'acide cyanhydrique, les spectres du 1,5-diaminotétrazole et des sels de diazotétrazole. Nous voulions ainsi confirmer leur structure et éventuellement les caractériser.

Notre attention s'est porté plus particulièrement sur la région de 3 800 à 500 cm^{-1}, où apparaissent les bandes dues aux groupement azotés. D'après la littérature (4, 5) le groupe imino (C=NH), la double liaison azote (—N=N—) et l'anneau du tétrazole (—CN_4H) ont des bandes d'absorption infrarouges caractéristiques. Une bande relativement forte entre 1 620 et 1 650 cm^{-1} est attribuée au groupe imino, des bandes très fortes et très étroites dans la région de 1 575 à 1 630 cm^{-1} caractérisent la double liaison azote–azote, et trois bandes d'à peu près la mêne intensité entre 975 et 1 150 cm^{-1} sont carac-

téristiques de l'anneau tétrazolique. Les bandes caractéristiques observées chez les produits étudiés sont données dans le Tableau I.

TABLEAU I

Frequences d'absorption (en cm^{-1}) des composés étudiés

Composés	N—H	C≡N	C=NH	NH_2	N=N	Tétrazole
Guanidinyl diazocyanide (4)	3 325, —	2 300	1 655	1 640	1 575	
5-Cyanamidotétrazole	3 325, —	2 300				— , 1 065, 1 030, 980
1,5-Diaminotétrazole	3 325, 3 325			1 640		1 110, 1 075, 1 000, —
Bis-diazoguanidinyl-diazotétrazole	3 325, —		1 680	1 640	1 570	1 095, 1 045, — —
Sel de diazotétrazole						
Aminoguanidine	3 450, 3 125		1 667		1 600	1 120, 1 065, 1 010, —
Triaminoguanidine	3 325, 3 225		1 680	1 640	1 600	— , 1 035, 1 010, 1 000
Diaminotétrazole	3 325, 3 125			1 640	1 587	1 115, 1 085, 1 010, —

Le produit de la réaction de l'azide de cyanamidine et de l'acide cyanhydrique donne un spectre infrarouge possédant une bande de forte intensité à 2 300 cm^{-1} attribuable à un groupe CN, et trois bandes de même intensité à 980 et 1 030 et 1 065 cm^{-1} qui indiqueraient la présence d'un anneau tétrazolique. Au surplus la bande située à 3 325 cm^{-1} serait dûe aux vibrations du groupe NH. L'étude spectrographique, la méthode de synthèse et l'analyse élémentaire nous porte à croire que ce composé est le 5-cyanamidotétrazole formé par cyclisation de l'azide de cyanamidine.

Le spectre obtenu du 1,5-diaminotétrazole se caractérise par une bande double à 3 225 et 3 325 cm^{-1}, attribuable aux vibrations NH, une autre bande à 1 640 cm^{-1} dûe aux groupes amino et trois petits pics 1 000, 1 075 et 1 110 cm^{-1} caractéristiques de l'anneau tétrazolique. Sa méthode de formation à partir du 1-benzalamino-5-aminotétrazole et son analyse spectrale sont en accord avec la structure proposée.

Tous les sels de diazotétrazole étudiés dans l'infrarouge ont donné des spectres possédant une forte bande entre 1 570 et 1 600 cm^{-1} attribuable au groupe diazo venant du diazotétrazole. Les bandes à 3 450 et 1 667 cm^{-1} du spectre du sel d'aminoguanidine étaient caractéristiques des groupements NH_2 et C=NH respectivement. Le spectre du sel de triaminoguanidine possède des bandes à 3 325, 1 680 et 1 640 cm^{-1} caractéristiques de la triaminoguanidine. De même le spectre du sel de diaminotétrazole révèle des bandes à 3 325, 3 125 et 1 640 cm^{-1} dûes aux groupements amino. L'analyse des spectres des sels de diazotétrazole, la solubilité de ces produits dans l'eau et l'analyse élémentaire des composés isolés nous porte à croire que nous sommes en présence de sels formés par double échange du potassium avec les dérivés de la guanidine ou du tétrazole selon le cas. Par exemple le chlorohydrate de triaminoguanidine et le sel de potassium du diazotétrazole donne le bis-triaminoguanidinium-5,5′-diazotétrazole sans perte de groupement fonctionnel, au contraire du composé suivant qui pendant la réaction perd un groupe cyano.

Le spectre du bis-diazoguanidinyl diazotétrazole préparé d'après la méthode de Thiele (6, 7) a été étudié dans le but de déterminer si dans ce cas nous sommes en présence d'un sel de diazotétrazole. Nous remarquons dans ce spectre l'absence de la bande à 2 300 cm^{-1}, ce qui indiquerait la disparition du groupe C≡N dans le diazocyanure de guanidine de départ.

Une comparaison de ce spectre avec celui du diazocyanure de guanidine décrit dans

Can. J. Chem. Downloaded from www.nrcresearchpress.com by 210.87.254.42 on 09/05/12
For personal use only.

la littérature (4) indique la présence du diazotétrazole en plus de l'absence du groupe C≡N. D'après l'analyse élémentaire, la nature non-ionique du produit et l'insolubilité dans l'eau, nous croyons que le radical diazoguanyl s'est substitué sur l'anneau de tétrazole par élimination de KCN et formation du composé suivant:

$$NH_2—C(=NH)—NH—N=N—N_4C—N=N—CN_4—N=N—NH—C(=NH)NH_2$$

le 1,1′-diazoguanyl-5,5′-diazotétrazole, tout comme l'avait supposé Thiele (1).

PARTIE EXPÉRIMENTALE

Technique générale

Les points de fusion ont été déterminés sur le "Melt-Pointer Vanderkamp" (Scientific Glass Apparatus Co., Inc.) et ne sont pas corrigés.

Les analyses élémentaires ont été faites par le Dr. C. Daessle, 5757 ave Decelles Montreal, Canada.

Les produits de départs excepté le sel de potassium du diazotétrazole et le 1,5-diaminotétrazole sont vendu dans le commerce. Le sel de potassium fut obtenu d'après la méthode de Thiele (6, 7) et le 1,5-diaminotétrazole connu sous forme de dérivé benzal (8) a été isolé comme amine libre par hydrazinolyse. Le contenu en azote des sels de diazotétrazole formés variait entre 72 et 86%.

Les spectres infrarouges ont été déterminés à l'aide du spectrographe Perkin–Elmer, Modèle 21, en pulvérisant des échantillons de 10 à 30 mg dans l'huile Nujol. Il n'a pas toujours été possible d'obtenir des échantillons très finement pulvérisés, en raison de la sensibilité de certains sel à la friction, mais en variant la concentration de l'échantillon il a été possible de minimiser l'effet de dispersion de la lumière et de choisir les meilleures courbes.

5-Cyanamidotétrazole

(a) On ajoute goutte à goutte une solution d'azide de cyanamidine (28.5 g, 0.25 mole) dans l'acide chlorhydrique dilué (25 g d'HCl dans 100 ml d'eau) et refroidi à 0 °C à une solution de KCN (16.2 g dans 50 ml d'eau). Lorsque le mélange est complété à température de la pièce, on extrait trois fois à l'éther. Par refroidissement de la solution aqueuse, on obtient 7.2 g de solide qu'on recrystallise de l'eau. Rendement 25.2%; p.f. = 147 °C.

Anal. Calc. pour $C_2H_2N_6$: C, 21.8; H, 1.8; N, 76.3. Trouvé: C, 22.0; H, 2.06; N, 75.9

(b) On dissout l'azide de cyanamidine (10 g, 0.09 mole) dans l'éther, dans laquelle on fait barboter l'acide cyanhydrique gazeux (27 g, 0.09 mole). Après évaporation de l'éther et crystallization de l'eau, 8 g de solide fondant à 147 °C sont obtenus. Rendement 80%.

Anal. Calc. pour $C_2H_2N_6$: C, 21.8; H. 1.82; N, 76.3. Trouvé: C, 22.5; H, 2.06; N, 75.6.

1,5-Diaminotétrazole

On dissout le 1-benzalamino-5-aminotétrazole (2.0 g) préparé d'après la méthode de la littérature (6) dans l'alcool éthylique absolu (25 ml). Après l'addition d'hydrazine anhydre (95%+, 1 g) on chauffe à reflux pendant 24 h. Le mélange après concentration et refroidissement donne, une fois recrystallisé, 0.7 g de solide (rendement de 80%); p.f. = 187–188 °C.

Anal. Calc. pour CH_4N_6: C, 12.0; H, 4.03; N, 83.9. Trouvé: C, 11.9; H, 3.81; N, 84.3.

Sel d'aminoguanidine du 5,5′-diazotétrazole

On ajoute une solution du sel de potassium du diazotétrazole pentahydraté (3.32 g, 0.01 mole) dans l'eau (10 ml) à une solution aqueuse de nitrate d'aminoguanidine (2.74 g, 0.02 mole). Le solide jaune obtenu est crystallisé de l'eau jusqu'à ce que la solution mère soit libre de nitrate; p.f. = 209 °C.

Anal. Calc. pour $C_4H_{14}N_{18}$: C, 15.3; H, 4.49; N, 80.2. Trouvé: C, 16.7; H, 5.0; N, 78.7.

Sel de triaminoguanidine du 5,5′-diazotétrazole

On mélange une solution de sel de potassium du diazotétrazole pentahydraté (3.32 g, 0.01 mole) dans l'eau (10 ml) à une solution aqueuse (10 ml) du chlorhydrate de triaminoguanidine (2.88 g, 0.02 mole) préparé d'après une méthode connue (9). Après plusieurs cyrstallisations de l'eau et élimination complète du chlorure, le solide obtenu, légèrement jaune, fond à 190 °C.

Anal. Calc. pour $C_4H_{18}N_{22}$: C, 12.9; H, 4.85; N, 82.3. Trouvé: C, 12.6; H, 4.5; N, 82.6.

Sel de cyanoguanidine du 5,5′-diazotétrazole

On mélange une solution de cyanoguanidine (1.68 g, 0.02 mole) dans 50 ml d'eau à une solution de sel de potassium du diazotétrazole pentahydraté (3.32 g, 0.01 mole). Le mélange est acidulé par addition d'acide chlorhydrique (1.7 cc d'HCl conc.). Par refroidissement un solide crystallise; p.f. = 195 °C avec décomposition. Le mélange de ce composé avec le bis-diazoguanyl-5,5′-diazotétrazole fondant à la même température et préparé par Thiele (1) fondait à 179 °C.

Anal. Calc. pour $C_6H_{10}N_{18}$: C, 21.5; H, 3.01; N, 75.4. Trouvé: C, 21.5; H, 3.8; N, 74.8.

Can. J. Chem. Downloaded from www.nrcresearchpress.com by 210.87.254.42 on 09/05/12
For personal use only.

Sel de 5-aminotétrazole du 5,5'-diazotétrazole

On mélange les solutions aqueuses du sel de potassium du diazotétrazole (3.32 g, 0.01 mole) et du chlorhydrate d'aminotétrazole (2.4 g, 0.02 mole). Le solide obtenu crystallise de l'eau; p.f. = 150 °C avec décomposition.

Anal. Calc. pour $C_4H_8N_{20}$: C, 14.2; H, 2.39; N, 83.3. Trouvé: C, 14.6; H, 2.9; N, 83.2.

Sel de 1,5-diaminotétrazole du 5,5'-diazotétrazole

On mélange une solution de sel de potassium du diazotétrazole (0.83 g) dans l'eau à une solution de 1,5-diaminotétrazole (0.59 g) dans HCl dilué (0.5 ml HCl dans 25 ml d'eau). Le solide obtenu crystallise de l'eau; p.f. = 176 °C.

Anal. Calc. pour $C_4H_{10}N_{22}$: C, 13.1; H, 2.61; N, 84.6. Trouvé: C, 13.0; H, 2.7; N, 85.0.

BIBLIOGRAPHIE

1. J. THIELE et W. OSBORNE. Ann. **305**, 69 (1899).
2. C. V. HART. J. Am. Chem. Soc. **50**, 1922 (1928).
3. E. LIEBER, E. SHERMAN, R. A. HENRY et J. COHEN. J. Am. Chem. Soc. **73**, 2328 (1951).
4. E. LIEBER, D. R. LEVERING et L. J. PATTERSON. Anal. Chem. **23**, 1594 (1951).
5. H. M. RANDALL, R. C. FOWLER, N. FUSON et J. R. DANGL. Infrared determination of organic structures. D. Van Nostrand Co., New York. 1949. L. J. BELLAMY. The infra-red spectra of complex molecules. John Wiley and Sons, Inc., New York. 1958. C. N. R. RAO. Chemical applications of infrared spectroscopy. Academic Press. 1963. A. R. KATRITZKY. Physical methods in heterocyclic chemistry. Vol. II. Academic Press. 1963.
6. J. THIELE. Ann. **270**, 46 (1893).
7. J. THIELE. Ann. **303**, 61 (1898).
8. J. VON STOLLE et E. GAERTNER. J. Prakt. Chem. **132**, 209 (1931).
9. T. E. O'CONNOR, K. HORGAN et J. REILLY. J. Appl. Chem. **1**, 91 (1951).

Can. J. Chem. Downloaded from www.nrcresearchpress.com by 210.87.254.42 on 09/05/12
For personal use only.

Can. J. Chem. Downloaded from www.nrcresearchpress.com by 210.87.254.6 on 09/05/12
For personal use only.

APPLICATION OF THE EXTENDED HAMMETT RELATIONSHIP TO THE IONIZATION CONSTANTS OF SUBSTITUTED ANTHRANILIC ACIDS[1]

P. LEGGATE[2] AND G. E. DUNN
Department of Chemistry, University of Manitoba, Winnipeg, Manitoba

Received November 30, 1964

ABSTRACT

The overlapping ionization constants of the carboxyl and amino groups in 14 substituted anthranilic acids have been determined by a spectrophotometric method. The results have been fitted to the extended Hammett relationship $\log K_1K_2/K_1^0K_2^0 = \rho_1\sigma_A + \rho_2\sigma_B$, where A and B refer to ionization of the carboxyl and amino group, respectively. The values of ρ_1 and ρ_2 so obtained have been used to estimate K_Z^0, the equilibrium constant for ionization of neutral anthranilic acid to zwitterion.

An earlier paper (1) described an investigation of the rates of decarboxylation of 4- and 5-substituted anthranilic acids in nitrobenzene. Recently a parallel study of the decarboxylation of substituted salicylic acids in nonaqueous solvents has been performed (2). The extension of this work to the decarboxylation of anthranilic acids in water requires, as a first step, the determination of the two overlapping ionization constants of the acids. The complex character of the ionization equilibria of such acids in aqueous solution provides the opportunity for a somewhat unusual application of a linear free energy relationship.

THE HAMMETT EQUATIONS

In aqueous solutions of anthranilic acids there are assumed to exist four ionic and molecular species in equilibria (3, 4). These are shown in the diagram below with the accompanying hydronium ions omitted.

[1]

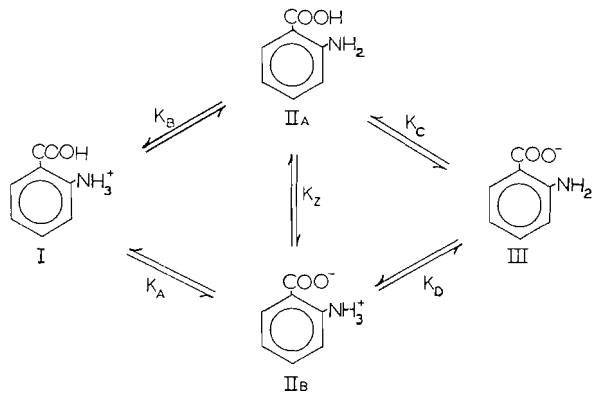

The ionization constants K_1 and K_2, which are obtained experimentally, define the equilibria:

[2] $$RH_2^+ \overset{K_1}{\rightleftarrows} RH + H^+,$$

[3] $$RH \overset{K_2}{\rightleftarrows} R^- + H^+.$$

[1]*Presented at the 1962 Chemical Institute of Canada Conference, Edmonton, Alberta.*
[2]*N.R.C. Postdoctorate Fellow, 1960–1962.*

RH_2^+ and R^- are the species I and III, respectively, of eq. [1], RH is a mixture of zwitterion, $RH^{\pm}$ (II*B*), and 'non-zwitterion', RH^0 (II*A*). However, in the equilibria of eqs. [2] and [3], RH can be treated as a single species since the ratio of $RH^{\pm}$ to RH^0 is independent of pH.

The experimental ionization constants K_1 and K_2 are related to the 'true' constants K_A, K_B, K_C, and K_D by the equations:

$$K_1 = K_A + K_B, \quad [4]$$

$$1/K_2 = 1/K_C + 1/K_D, \quad [5]$$

$$K_1K_2 = K_AK_D = K_BK_C. \quad [6]$$

Furthermore,

$$K_Z = \frac{K_A}{K_B} = \frac{K_C}{K_D}, \quad [7]$$

where

$$K_Z = \frac{[RH^{\pm}]}{[RH^0]}.$$

For a series of substituted anthranilic acids, each of the ionization constants K_A, K_B, K_C, and K_D should obey a Hammett relationship. If, however, there is strong hydrogen bonding between the amino and carboxyl groups, then two electronic pathways are available for transmitting the substituent effect. The extension of the Hammett equation to reaction series of this type has been discussed by Jaffe (5) who proposes the use of an equation of the form:

$$\log \frac{K}{K^0} = \rho_1\sigma_1 + \rho_2\sigma_2. \quad [8]$$

This equation provides the means of estimating the relative importance of the two possible electronic paths in reactions in which, either two side chains react with one another, or the site of reaction is linked to the benzene ring at two points. The ionization of ortho-substituted benzoic acids represents a special case of the latter type. In this special case a hydrogen bond provides one of the two electronic pathways and a distinction can be made between a 'direct' substituent effect and an 'indirect' (and presumably less potent) effect exerted through the hydrogen bond. Jaffe showed (5) that, among the acids so far investigated, only the *o*-(hydroxymethyl)-benzoic acids provide evidence of a significant 'indirect' effect. However, as there is almost certainly a strong interaction between the amino and carboxyl groups of anthranilic acids, the possibility of indirect effects must be taken into account.

If we consider as an example the ionization constant K_A, a substituent in, say, the 4-position will behave as if para to the reaction site in exerting a direct effect on the ionization of the —COOH group and as if meta in exerting an indirect effect via the $-NH_3^+$ group. The Hammett equation* is:

$$\log \frac{K_A}{K_A^0} = {}_D\rho_A\sigma_A + {}_I\rho_A\sigma_B. \quad [9a]$$

**In this and subsequent equations ρ_A and ρ_B are the Hammett constants for a given substituent considered in relation to the —COOH (or —COO^-) and the $-NH_3^+$ (or $-NH_2$) groups, respectively. Reaction constants are defined by a suffix (A, B, C, or D) referring to the constants K_A, K_B, K_C, and K_D of eq. [1], and a prefix (I or D) indicating whether a direct or indirect effect is involved. In other cases where it is necessary to distinguish between two or more ρ or σ values, numerical suffixes are used.*

Can. J. Chem. Downloaded from www.nrcresearchpress.com by 210.87.254.6 on 09/05/12
For personal use only.

The corresponding equations for K_B, K_C, and K_D are:

$$[9b] \qquad \log \frac{K_B}{K_B^0} = {}_I\rho_B\sigma_A + {}_D\rho_B\sigma_B$$

$$[9c] \qquad \log \frac{K_C}{K_C^0} = {}_D\rho_C\sigma_A + {}_I\rho_C\sigma_B$$

$$[9d] \qquad \log \frac{K_D}{K_D^0} = {}_I\rho_D\sigma_A + {}_D\rho_D\sigma_B.$$

Equation [9*a*] can be rewritten as:

$$[10] \qquad K_A = K_A^0 10^{({}_D\rho_A\sigma_A + {}_I\rho_A\sigma_B)},$$

and K_B, K_C, and K_D can be redefined in a similar manner. Substitution of these expressions for K_A, K_B, K_C, and K_D in eqs. [4] and [5] enables K_1 and K_2 to be expressed in terms of Hammett parameters:

$$[11a] \qquad K_1 = K_A^0 10^{({}_D\rho_A\sigma_A + {}_I\rho_A\sigma_B)} + K_B^0 10^{({}_I\rho_B\sigma_A + {}_D\rho_B\sigma_B)},$$

$$[11b] \qquad \frac{1}{K_2} = \frac{1}{K_C^0} 10^{-({}_D\rho_C\sigma_A + {}_I\rho_C\sigma_B)} + \frac{1}{K_D^0} 10^{-({}_I\rho_D\sigma_A + {}_D\rho_D\sigma_B)}.$$

These equations are obviously too complex to be fitted to the ionization constants, but fortunately a very much simpler Hammett equation is available. Thus, from eq. [6] there may be obtained the logarithmic relationships:

$$[12] \qquad \log \frac{K_1K_2}{K_1^0K_2^0} = \log \frac{K_AK_D}{K_A^0K_D^0} = \log \frac{K_BK_C}{K_B^0K_C^0}.$$

Combining eqs. [12], [9*a*], and [9*d*] gives:

$$[13] \qquad \log \frac{K_1K_2}{K_1^0K_2^0} = \sigma_A({}_D\rho_A + {}_I\rho_D) + \sigma_B({}_I\rho_A + {}_D\rho_D).$$

Similarly, from eqs. [12], [9*b*], and [9*c*]:

$$[14] \qquad \log \frac{K_1K_2}{K_1^0K_2^0} = \sigma_A({}_I\rho_B + {}_D\rho_C) + \sigma_B({}_D\rho_B + {}_I\rho_C).$$

However, if two or more sets of experimental data are available, a linear equation of general form:

$$\log \frac{K_1K_2}{K_1^0K_2^0} = A\sigma_A + B\sigma_B,$$

in which A and B are constants, must have a unique solution providing σ_A and σ_B are not themselves linearly related. Equations [13] and [14] can therefore be rewritten as a single equation.

$$[15] \qquad \log \frac{K_1K_2}{K_1^0K_2^0} = \rho_1\sigma_A + \rho_2\sigma_B,$$

where

$$[16a] \qquad \rho_1 = {}_D\rho_A + {}_I\rho_D = {}_I\rho_B + {}_D\rho_C,$$

$$[16b] \qquad \rho_2 = {}_I\rho_A + {}_D\rho_D = {}_D\rho_B + {}_I\rho_C.$$

Can. J. Chem. Downloaded from www.nrcresearchpress.com by 210.87.254.6 on 09/05/12
For personal use only.

Equation [15] defines a simple relationship between the experimental ionization constants and the Hammett parameters and it is, therefore, of importance that the chemical significance of this equation be defined. For this purpose it is convenient to consider the 'specific' case in which the postulated indirect substituent effects are assumed to be negligible. (Henceforth the 'general' case is that in which the indirect effects are taken into account and the 'specific' case is that in which indirect effects are assumed to be negligible.)

In the specific case the identities [16*a*] and [16*b*] simplify to:

[17*a*] $$\rho_1 = {}_D\rho_A = {}_D\rho_C,$$

[17*b*] $$\rho_2 = {}_D\rho_B = {}_D\rho_D.$$

(For the remainder of this paper only ρ_A and ρ_B are referred to; the argument could equally well be pursued in terms of ρ_C and ρ_D.)

The identity [17*a*] implies that the effect of a substituent on the ionization of the —COOH is the same whether an NH_2 or NH_3^+ group occupies the ortho position and the identity [17*b*] carries the same implication for the ionization of the $-NH_3^+$ group. These conclusions are related to the principle, proposed by Jaffe (6), that the effect of a substituent is independent of a second substituent in an ortho position relative to the reacting side chain, provided that this ortho substituent does not participate in the reaction. The independence of the reaction constant on the nature of an ortho substituent should include the case where there is no ortho substituent. It follows, therefore, that within the limits of experimental error, ${}_D\rho_A$ should have the value 1.00 which is by definition the ρ-value for benzoic acid. Similarly, the value of ${}_D\rho_B$ should show reasonable agreement with the experimentally determined value (7) of 2.889 for the Hammett reaction constant of the anilinium ion. From the identities [17*a*] and [17*b*] it follows that in the specific case eq. [15] becomes:

[18] $$\log \frac{K_1K_2}{K_1^0K_2^0} = {}_D\rho_A\sigma_A + {}_D\rho_B\sigma_B.$$

This equation is mathematically identical to the eq. [8], proposed by Jaffe (5), for reactions in which the substituent effect can be transmitted by two electronic pathways. Equation [18], however, possesses a very different chemical significance. As implied by eq. [12], this equation provides a Hammett relationship for both the experimental constants K_1 and K_2 and the true constants K_A and K_D (or K_B and K_C). When expressed in the latter terms it is seen as an application of the Hammett equation to two successive equilibria which are not readily distinguished by experimental means. The two equilibria may be represented (for example) by the lower half of eq. [1] which may be rewritten in an abbreviated form:

$$\text{I} \overset{K_A}{\rightleftarrows} \text{II}B \overset{K_D}{\rightleftarrows} \text{III}.$$

The character of the system requires that a substituent para (or meta) to the reaction center (the carboxyl group) in I is meta (or para) to the reaction center (the anilinium group) in II*B*. The above interpretation can be extended to the general case represented by eq. [15]; this is an abbreviated form of eq. [13] which contains four Hammett reaction constants and represents the application of the Hammett relationship to a system of two successive equilibria, in each of which both indirect and direct substituent effects are assumed to operate. Whether or not the indirect effects are significant, eq. [15] enables

Can. J. Chem. Downloaded from www.nrcresearchpress.com by 210.87.254.6 on 09/05/12
For personal use only.

the product of the two experimental ionization constants to be fitted to a Hammett equation which can be solved for ρ_1 and ρ_2. Relationships between the individual constants (K_1 or K_2) and the Hammett parameters are provided by eqs. [11] in the general case or in the specific case, by the equations

$$K_1 = K_A^0 10^{\rho_A\sigma_A} + K_B^0 10^{\rho_B\sigma_B}, \qquad [19a]$$

$$\frac{1}{K_2} = \frac{1}{K_C^0} 10^{-\rho_A\sigma_A} + \frac{1}{K_D^0} 10^{-\rho_B\sigma_B}. \qquad [19b]$$

Thus, if a significant fit of the experimental data to eq. [15] is obtained, then the values of ρ_1 and ρ_2 required by this equation can be used to solve eqs. [11] or [19] for the true ionization constants K_A^0, K_B^0, K_C^0, and K_D^0 of anthranilic acid. Finally, by use of eq. [7] the zwitterion constant K_Z^0 and therefore the zwitterion content can be obtained. Providing that there is a statistically significant agreement between experimental data and the theoretical equations then we have a most unusual method for determining the zwitterion content of an aromatic amino acid. Furthermore, the fit of the experimental data to eqs. [11] or [19] could provide a criterion as to whether or not the indirect substituent effects are significant. However, this criterion must be used with caution as the extended computational sequence will greatly magnify errors in both the experimental data and the Hammett substituent constants. Lack of agreement between experiment and theory may well be due to these errors rather than indicative of indirect substituent effects.

In the above discussion the possible application of the Hammett equation to the zwitterion constant K_Z has been ignored. Actual K_Z values are difficult to determine and any such relationship could not be easily verified experimentally. Nevertheless, this equilibrium is of interest in that it involves the interaction of two side chains and is therefore subject to two 'direct' substituent effects. In this respect it is closely analogous to the intramolecular reaction of the *o*-nitroazides.

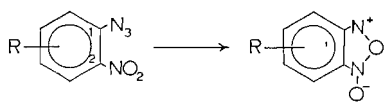

Andersen *et al.* (8) have recently correlated the rate constants for a series of substituted *o*-nitroazides by the use of a two-parameter Hammett equation of the type proposed by Jaffe (5):

$$\log \frac{K}{K^0} = \rho_1\sigma_1 + \rho_2\sigma_2. \qquad [8]$$

The σ_1 and σ_2 terms are the substituent constants of R relative to positions 1 and 2, the points of attachment of the nitro and azido groups. Anderson found that ρ_1 is positive and ρ_2 negative in agreement with the rule that ρ-values are negative when a high electron density favors the reaction. Similarly, the tautomeric equilibrium defined by K_Z involves simultaneously the release of a proton from the —COOH group (favored by low electron density) and the acceptance of a proton by the —NH_2 group (favored by high electron density). The expected Hammett equation would be:

$$\log \frac{K_Z}{K_Z^0} = \rho_1\sigma_A + \rho_2\sigma_B,$$

Can. J. Chem. Downloaded from www.nrcresearchpress.com by 210.87.254.6 on 09/05/12
For personal use only.

where ρ_1 is positive and ρ_2 negative. In the specific case in which the indirect substituent effects on the other equilibrium constants are ignored, ρ_1 and ρ_2 can be identified with the reaction constants ρ_A and ρ_B. Thus

$$[20] \qquad \log \frac{K_Z}{K_Z^0} = \rho_A\sigma_A - \rho_B\sigma_B.$$

Both ρ_A and ρ_B are assumed to be positive as they are defined for reactions which are favored by a low electron density—the ionizations of the —COOH and $-NH_3^+$ groups respectively. Equation [20] can also be deduced directly from eq. [7] on the assumption that K_A, K_B, K_C, and K_D each obey a simple Hammett relationship.

Equation [15] is crucial to the present work in that it provides the simplest experimentally verifiable Hammett relationship for the system. However, in deducing this and other relationships, it has been assumed that eq. [1] is a valid representation of the equilibria existing in aqueous solutions of an anthranilic acid. The possibility must be considered that there are alternatives to this hypothesis. The only chemically reasonable alternative assumption is that the interactions between —COOH (or $-COO^-$) and $-NH_2$ (or NH_3^+) groups are so strong that it is impossible either to consider the zwitterion (II*B*) and non-zwitterion (II*A*) as separate species or to distinguish between ionizations from the —COOH and $-NH_3^+$ groups. In such circumstances the ionic equilibria could be represented as:

[21] 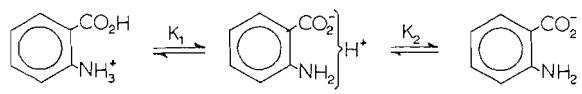

Experimental and true ionization constants are now identical. The substituent effects will be somewhat similar to those found in reactions of the nitroazides, two 'direct' effects at a single reaction center. The Hammett equations would be:

$$[22] \qquad \log \frac{K_1}{K_1^0} = \rho_1\sigma_A + \rho_2\sigma_B,$$

$$[23] \qquad \log \frac{K_2}{K_2^0} = \rho_3\sigma_A + \rho_4\sigma_B.$$

A combination of eqs. [22] and [23] gives an equation which is mathematically identical to eq. [15]. This equation is therefore still valid even if the existing equilibria are represented by eq. [21]. However, if eq. [21] rather than eq. [1] represents the equilibria existing in aqueous solutions of anthranilic acids, then the data should fit eqs. [22] and [23] individually as well as eq. [15].

DETERMINATION OF IONIZATION CONSTANTS

A spectrophotometric method for the determination of the overlapping ionization constants of dibasic acids was first described by Thamer and Voigt (9). This method was modified by Kok-Peng Ang (10) and, in this latter form, has been applied to aromatic amino acids by Bryson and Matthews (11). In the present work some further modifications were made, particularly as regards the method of computation.

The extinction coefficient, ϵ, of an aqueous solution of a dibasic acid at any given wavelength is related to the hydrogen ion activity, α, by the equation:

$$\alpha^2(\epsilon - \epsilon_1) + \alpha K_1(\epsilon - \epsilon_2) + K_1K_2(\epsilon - \epsilon_3) = 0.$$

Can. J. Chem. Downloaded from www.nrcresearchpress.com by 210.87.254.6 on 09/05/12
For personal use only.

In the present case ϵ_1, ϵ_2, and ϵ_3 are the extinction coefficients of RH_2^+, RH, and R^- respectively, and K_1 and K_2 are the first and second ionization constants as defined in eqs. [2] and [3]. ϵ_1 and ϵ_3 can be determined directly by measurements in acid or alkaline solutions, but ϵ_2 is not directly available. In the present work all the solutions used in the determination of K_1 and K_2 for any particular acid were of the same concentration and it is therefore convenient to use D, the optical density, in place of ϵ in describing the method and carrying out the calculations. The above equation can therefore be rewritten:

$$[24] \qquad \alpha^2(D - D_1) + \alpha K_1(D - D_2) + K_1K_2(D - D_3) = 0.$$

Kok-Peng Ang's solution of this equation for K_1 and K_2 requires that some wavelength be found for which the variation of D with pH exhibits a maximum or minimum (Fig. 1). Any value of D corresponding to the 'steep' portion of the curve will then define two values (α_1, α_2) of α and thus provide two simultaneous equations of the form of eq. [24]. Combining these equations gives

$$[25] \qquad D = D_2 + K_2P,$$

where

$$P = \frac{(D_3 - D)(\alpha_1 + \alpha_2)}{\alpha_1\alpha_2}$$

and

$$[26] \qquad D = D_1 + K_1Q,$$

where

$$Q = \frac{D_2 - D}{\alpha_1 + \alpha_2}.$$

A plot of D against P is linear with slope K_2 and intercept D_2. The value of D_2 is inserted into eq. [26] and D is plotted against Q to give K_1.

In the present work an IBM 1620 computer was available and computational labor

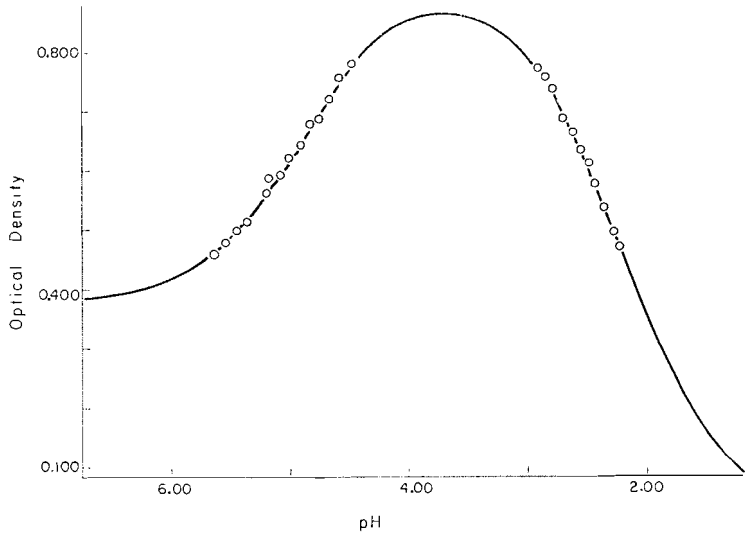

FIG. 1. Variation of optical density with pH at $\lambda = 345$ mμ for anthranilic acid. Circles represent the experimental points of Table I and the line is calculated from eq. [24] using the parameters of Table II.

Can. J. Chem. Downloaded from www.nrcresearchpress.com by 210.87.254.6 on 09/05/12
For personal use only.

was not an important consideration. It was therefore possible to eliminate the following, otherwise unavoidable, weaknesses in the method of computation.

(*i*) The value of K_2 is highly dependent upon D_3, the optical density of an alkaline solution, which must therefore be determined with extreme accuracy to avoid undetectable, systematic error in K_2.

(*ii*) Similarly, and as previously pointed out by Bryson and Matthews (11), an error in the computed value of D_2 introduces a systematic error into the calculation of K_1.

(*iii*) The usual 'least squares' procedure for determining the slope and intercept of a line assumes that only $y(= D)$ is in error and that $x(= P$ or $Q)$ is inerrant; this is clearly not true in the present case.

For the computation used in the present work eqs. [25] and [26] are rearranged;

[27] $$D = \frac{D_2 + K_2D_3A}{1 + K_2A} \quad \text{from [25]},$$

where $$A = 1/\alpha_1 + 1/\alpha_2;$$

[28] $$D = \frac{D_1 + K_1D_2A^1}{1 + K_1A^1} \quad \text{from [26]},$$

where $$A^1 = 1/(\alpha_1 + \alpha_2).$$

Equations [27] and [28] were solved on the computer by Dolittle's least squares method (12, 13) which takes into account errors in both D and α and thus provides more reliable estimates of the standard errors of the parameters. By this method independent values for K_1 and K_2 are obtained without the necessity of determining either D_1 or D_3. Furthermore two independent estimates of D_2 are available as a test of the consistency of the calculations.

The method of obtaining the values of D, α_1, and α_2 for use in the computation of K_1K_2 was also modified. Kok-Peng Ang's procedure required that a continuous curve be constructed through the experimental points (pH, D). The values of α_1 and α_2 are then read *from the curve*. However, the responsibility of drawing a 'true' curve can be avoided. Thus, in the present work, using the determination of K_2 as the example, the values of D and α_2 which are used in the calculation are the actual experimental points. To obtain the corresponding values of α_1 it is still necessary to draw a curve through the experimental points on the low pH side of the maximum. However, in eq. [27] the terms α_1 and α_2 appear only in the function $A = 1/\alpha_1 + 1/\alpha_2$. For most values $1/\alpha_2 \gg 1/\alpha_1$, and errors in α_1 due to inaccurate curve construction have a negligible effect on the accuracy of the overall calculation.

Similarly for K_1, D and α_1 are experimental points and α_2 is obtained from a constructed curve.

EXPERIMENTAL

(A) Preparation of the Substituted Anthranilic Acids

The 5-chloro, 5-hydroxy, and 5-methyl anthranilic acids, and anthranilic acid itself, were commercial products. The 5-bromo, 4-chloro, 4-nitro, and 5-nitro acids were prepared as described by Dunn and Prysiazniuk (1). The compound described in that paper as the 4-bromoanthranilic acid was found to be the 5-bromo isomer; an unambiguous synthesis of the 4-bromo acid is described in the present paper.

All the anthranilic acids were purified by one or more recrystallizations from aqueous ethanol in the presence of animal charcoal. The melting points given are for the recrystallized acids. All melting points were determined with a Hershberg melting point apparatus (14) using Anschutz thermometers and are expressed in °C.

'Analar' acetone was purified for use in the permanganate oxidations by distillation from solid potassium permanganate.

Can. J. Chem. Downloaded from www.nrcresearchpress.com by 210.87.254.6 on 09/05/12
For personal use only.

4-Methylanthranilic Acid

4-Methyl-2-nitrobenzoic acid was prepared by the procedure described by Grob (15). 4-Methyl-2-nitroaniline was diazotized and the diazonium solution treated with cuprous cyanide to yield the 4-methyl-2-nitrobenzonitrile, which was hydrolyzed to the 4-methyl-2-nitrobenzoic acid. The crude nitro acid (10 g) in ethanol (75 ml) was hydrogenated during 20 min at 3 atm pressure in the presence of 10% palladium-on-charcoal (1.0 g). 4-Methylanthranilic acid (6.0 g, 65%) was recovered from the reaction mixture and, after recrystallization from aqueous ethanol, had m.p. 181–182° (lit. (15) 178–180°).

4-Methoxyanthranilic Acid

4-Methoxy-2-nitrobenzoic acid, m.p. 192–193°, was prepared from 4-methoxy-2-nitroaniline by the procedure of Steven *et al.* (16) who give m.p. 195–196°. The nitro acid was hydrogenated under conditions already described (for the 4-methyl-2-nitro acid) to give a 73% yield of 4-methoxyanthranilic acid, m.p. 180–181° (lit. (16) 180–181°).

5-Methoxyanthranilic Acid

4-Methoxy-2-methylaniline (93 g) was dissolved in 0.4 *N* hydrochloric acid (1.7 l) to give a dark-brown solution which was stirred with animal charcoal and filtered. To this filtrate at 50° were added acetic anhydride (82 ml) and then sodium acetate trihydrate (109 g). The solution was cooled to 15° to precipitate the 4-methoxy-2-methylacetanilide (100 g, 82%) which had m.p. 135–136° (lit. (17) 132–134°). The anilide (10.00 g) in acetone (500 ml) was treated with potassium permanganate (27.0 g) and magnesium sulfate during 48 h at room temperature. Sodium sulfite was then added to destroy excess permanganate and the reaction mixture was filtered. The filtrate was evaporated to 100 ml, diluted with water, and extracted with chloroform to remove unreacted starting material. Acidification yielded N-acetyl-5-methoxyanthranilic acid (3.9 g, 85% of reacted material), m.p. 165–166° (lit. (18) 165–166°). Hydrolysis of the acetylanthranilic acid (7.6 g) was accomplished by warming for 30 min with 6 *N* sodium hydroxide solution. Acidification of the alkaline solution precipitated 5-methoxyanthranilic acid (2.5 g, 42%), m.p. 151–152° (lit. (19) 151°).

4-Fluoroanthranilic Acid

The preparation of this acid from 5-fluoro-2-methylaniline followed the published procedure of Steck and Fletcher (20). The 4-fluoroanthranilic acid so prepared had m.p. 198–199° (lit. (20) 192.5–193.0°).

5-Fluoroanthranilic Acid

The 5-fluoro acid was obtained from 4-fluoro-2-methylaniline by the successive acetylation, oxidation, and hydrolysis steps which are described in detail for the preparation of 5-methoxyanthranilic acid. Acetylation of the aniline gave an 87% yield of 4-fluoro-2-methylacetanilide, m.p. 110–112° (lit. (21) 113°), which was oxidized in 43% yield to 5-fluoro-N-acetylanthranilic acid, m.p. 178°. Hydrolysis of this compound gave a 91% yield of the 4-fluoroanthranilic acid, m.p. 183–184° (lit. (22) 180°).

5-Phenoxyanthranilic Acid

2-Nitro-5-chlorobenzoic acid (25 g) was reacted with potassium phenoxide in nitrobenzene solution as described by Süs and Möller (23) to give 5-phenoxy-2-nitrobenzoic acid (14 g, 65%), m.p. 154–155° (lit. (23) 157°). Hydrogenation of the crude nitro acid (14 g) under conditions already described in the present paper gave 5-phenoxyanthranilic acid (9 g, 70%), m.p. 148–149° (lit. (23) 148°). Attempts to apply the same method to the preparation of the 4-phenoxyanthranilic acid were unsuccessful, even though the more reactive 2-nitro-4-bromobenzoic acid was used in place of the 4-chloro compound. This failure is to be expected in the absence of an activating nitro group para to the halogen atom.

4-Bromoanthranilic Acid

4-Bromo-2-nitrobenzoic acid was prepared from *o*-nitroaniline by the three stage procedure of Erickson *et al.* (24). Bromination of the *o*-nitroaniline gave an 84% yield of 4-bromo-2-nitroaniline, m.p. 105–106° (lit. (24) 111–112°), which was then diazotized and the diazonium solution treated with cuprous cyanide to give 4-bromo-2-nitrobenzonitrile in 67% yield. The nitrile was hydrolyzed to 4-bromo-2-nitrobenzoic acid, m.p. 161–162° (lit. (24) 164–165°). The nitroacid (10.8 g) was dissolved in ammonium hydroxide solution and treated with ferrous ammonium sulfate hexahydrate (100 g) in water (200 ml). The reaction mixture was boiled briefly, cooled, and filtered. Acidification of the filtrate gave 4-bromoanthranilic acid (7.0 g, 83%), m.p. 225° (lit. (25) 222°). A melting point depression was observed on mixing with 5-bromoanthranilic acid (m.p. 215–216°).

A small quantity of the 4-bromo compound was converted by a diazotization procedure to 4-bromosalicylic acid, m.p. 203–204° (lit. (26) 214°). This compound was readily distinguished both by melting point and mixed melting point from the 5-bromo isomer which has m.p. 169°. It is of interest that in one recent paper (27) a melting point of 164–165° is quoted for 4-bromosalicyclic acid; it is almost certain that this was in fact the 5-isomer.

(B) pK_a Determinations

All measurements were made on solutions of ionic strength $\mu = 0.10$ since for the stronger acids it was necessary to measure optical densities at pH's as low as 1. Consequently, only apparent pK values are reported. These are adequate for the present purpose since the Hammett relationships always concern differences between the pK's of substituted and unsubstituted aromatic acids where the activity coefficients will be very similar and cancel.

Can. J. Chem. Downloaded from www.nrcresearchpress.com by 210.87.254.6 on 09/05/12
For personal use only.

Experimental Procedure

Stock solutions of each acid were prepared by dissolving the appropriate weight of the acid in a slight excess of sodium hydroxide (0.1 *N*) and then diluting to 1 l with distilled water containing sufficient potassium chloride to give an ionic strength of 0.10. Aliquots (10 ml) of this stock solution, delivered from an automatic burette, were diluted to 50 ml with the appropriate buffer to give the solutions on which pH and optical density (*D*) determinations were made. Preliminary experiments were performed on solutions of each acid in 10 to 12 buffers spanning the range 1.0–5.5. The absorption spectra of these solutions in the range 2 750 – 4 500 Å were recorded. These spectra indicated the optimum wavelength for a pK_a determination, the required concentration of the stock solution, and the approximate pH ranges of the 'steep' portions of pH/*D* curve at the chosen wavelength. In the actual pK_a determinations the buffers were chosen so as to concentrate the experimental points in these steep portions.

Solutions of all the acids eventually became colored on standing, but in the case of the 5-methoxy, 5-hydroxy, and 5-bromo acids and in particular the 5-phenoxy acid, discoloration was observed within a few hours and anomalous optical density readings resulted. Stock solutions of these acids were therefore prepared in oxygen-free water and stored in opaque bottles under nitrogen. Under these conditions no significant variations in optical density were observed during the course of the pK_a determination.

Buffer Solutions

Hydrochloric acid (pH 1.0–1.8), chloroacetate (1.9–3.6), acetate (3.7–5.4), and phosphate (5.7, 6.0, 6.8) buffers were used. All buffers were adjusted to ionic strength 0.10 by addition of potassium chloride. In some initial experiments citrate buffers were used. It was found, however, that the optical density of an acid in a citrate buffer was significantly higher than that in hydrochloric acid or acetate buffers of the same pH and it was assumed that some degree of complex formation was occurring.

pH Measurements

These were made with a Radiometer Model 4C pH meter with shielded glass and silver chloride electrodes in a water bath thermostatically controlled at 25.0 ± 0.1°. The instrument was standardized at pH's 1.68, 4.01, and 6.80 with potassium tetroxalate (0.1 *N*), potassium hydrogen phthalate (0.1 *N*), and sodium hydrogen phosphate – potassium hydrogen phosphate (0.25 *N*) buffers prepared from the corresponding National Bureau of Standards pH standards.

Optical Density Measurements

A Beckman DK1 spectrophotometer was used with matched cells contained in a thermostated cell holder at 25.0 ± 1.0°. The appropriate buffer solution was used as a standard in the reference cell. In making a pK_a determination the instrument was set at the predetermined optimum wavelength throughout the determination. For each solution a record was made of the optical density over a period of several minutes during which the temperature of the cell oscillated between 24° and 26° several times. This temperature variation produced changes in the optical density of not more than 0.001 absorbance units, except in the case of strongly acid solutions of the nitro acids, in which slightly larger variations were observed.

RESULTS

Table I details the experimental data for anthranilic acid itself. Solutions Nos. 1–11 define the steep portion of the curve on the low pH side of the maximum and solutions Nos. 12–25 the steep portion on the high pH side. These data were used to solve eqs. [27] and [28] by the methods already described.

The values of pK_1 and pK_2 (and K_1 and K_2) calculated from these data are given in Table II, row 1, which also shows the excellent agreement between the two values obtained for D_2, and between the computed value for D_3 and an experimental value. The values of K_1 and K_2 from a second, independent experiment using a different concentration of anthranilic acid are also given in Table II. The mean values of K_1 and K_2 from the two experiments are seen to be in agreement with previously published values.

Figure 1 compares the experimental data of Table I with a pH vs. *D* curve defined by eq. [24], using the computed values for the parameters K_1, K_2, D_1, D_2, and D_3. (The mean of the two computed values of D_2 was used.) A test of the degree of coincidence between experimental data and theoretical equation is given by the value of s(ext.), the external estimate of error.* This is 0.005 for both equation [27] which gives K_2 and eq. [28] which

**Throughout this paper, for any set of experimentally derived data, $y, x_1, x_2, \ldots$, which are used to determine the constant parameters $a_1, a_2, \ldots$ of an equation $y = f(x_1, x_2 \ldots a_1, a_2 \ldots)$, the "external estimate of error" is defined as $s^2(\text{ext.}) = \sum (y - \tilde{y})^2/(\text{degrees of freedom})$, where $\tilde{y}$ is the value of y calculated by inserting the computed values of $a_1, a_2, \ldots$ into the equation.*

Can. J. Chem. Downloaded from www.nrcresearchpress.com by 210.87.254.6 on 09/05/12
For personal use only.

TABLE I

Optical densities of 3.34×10^{-4} M solutions of anthranilic acid at $\lambda = 345$ mμ and $\mu = 0.10$

Soln. No.	pH	Optical density	Soln. No.	pH	Optical density
1	2.879	0.769	12	4.458	0.779
2	2.820	0.753	13	4.557	0.775
3	2.756	0.735	14	4.647	0.718
4	2.667	0.684	15	4.723	0.687
5	2.582	0.666	16	4.813	0.678
6	2.523	0.629	17	4.897	0.643
7	2.458	0.608	18	4.982	0.620
8	2.408	0.573	19	5.074	0.592
9	2.339	0.533	20	5.182	0.562
10	2.268	0.492	21	5.266	0.541
11	2.206	0.467	22	5.350	0.515
			23	5.444	0.499
			24	5.533	0.480
			25	5.634	0.460
			26	0.1 N NaOH	0.390

gives K_1. The actual experimental uncertainty in the optical density, D, (i.e., the internal estimate of error) is about 0.005.

Ionization constants were obtained for 15 substituted anthranilic acids. Values of K_1, K_2, and D_2 are given in Table III, including duplicate determinations which were made for four of the acids. For these acids the weighted mean of the duplicate values of K_1 and K_2 were used in the calculations of the Hammett relationships described in the next section. No value of K_1 is given for the 5-nitro acid, which exhibited a very broad maximum at a very low pH. The determination of K_1 would have required the use of very strongly acidic solutions for which sufficiently accurate pH data were unobtainable.

The third ionization constant of 5-hydroxyanthranilic acid, involving ionization of the hydroxyl group, was readily accessible from our data so it was calculated although it was not needed for the purposes of this paper.

$$K_3 = \frac{[A^{=}][H^{+}]}{[A^{-}]}.$$

On the assumption that there is no significant overlapping of the second and third ionization constants, K_3 may be determined approximately by use of the relationship:

$$K_3 = \frac{(D - D_3)a}{D_4 - D},$$

where D_3 and D_4 are optical densities of solutions of the same concentration containing only A^- and $A^=$ respectively. D is the optical density at hydrogen ion concentration a. A value of D_3 has already been computed in the calculation of K_2; D_4 was obtained by measurement of a solution in 0.10 N sodium hydroxide. Using $D_3 = 0.154$, $D_4 = 0.929$, $D = 0.414$ at pH = 9.069, the values $K_3 = 4.31 \times 10^{-10}$, $pK_3 = 9.36$ were obtained.

DISCUSSION

Equation [15] can be written in the form:

$$[15] \qquad \log K_1K_2 = \rho_1\sigma_A + \rho_2\sigma_B + \log K_1^0K_2^0.$$

Can. J. Chem. Downloaded from www.nrcresearchpress.com by 210.87.254.6 on 09/05/12
For personal use only.

Can. J. Chem. Downloaded from www.nrcresearchpress.com by 210.87.254.6 on 09/05/12
For personal use only.

TABLE II

Apparent ionization constants of anthranilic acid at 25 °C and $\mu = 0.10$

	$K_1 \times 10^3$	$K_2 \times 10^5$	pK_1	pK_2	D_2 (From K_1)	D_2 (From K_2)	D_3 (Calcd.)	D_3 (Expt.)
Experiment 1*	6.97±1.20	1.46±0.14	2.16±0.07	4.84±0.04	0.935±0.016	0.944±0.018	0.387	0.387
Experiment 2*	6.72±0.37	1.40±0.10	2.17±0.02	4.85±0.03	0.912±0.008	0.919±0.010	0.383	0.381
Weighted Mean*	6.74±0.36	1.42±0.08	2.17±0.02	4.85±0.03				
Liquori and Ripamonti (28)†	7.32	1.60	2.14	4.80				
Kilpe and Harjanne (29)‡	9.34	1.05	2.05	4.95				

*The uncertainties shown are standard deviations.
†Extrapolated to $\mu = 0$.
‡$\mu = 0.012$ for pK_1 and $\mu = 0.108$ for pK_2.

TABLE III

Ionization constants K_1 and K_2

Substituent	λ, mμ	Concn. × 10^1 M	D_2 From K_1	D_2 From K_2	$K_1 \times 10^3$	$K_2 \times 10^5$
5-OMe	307 (min.)	3.54	0.158±0.008	0.177±0.008	4.25± 0.34	0.300±0.032
5-Me	290 (min.)	4.06	0.201±0.013	0.230±0.019	4.35± 0.34	0.252±0.057
5-F	288 (min.)	9.02	0.200±0.020	0.225±0.005	9.32± 0.49	1.56 ±0.05
5-Br	360 (max.)	6.12	1.184±0.034	1.038±0.018	19.9 ± 2.7	3.89 ±0.31
		5.14			27.3 ± 1.7	
5-Cl	355 (max.)	3.84	0.861±0.014	0.852±0.009	20.6 ± 4.1	4.50 ±0.28
5-OH	308 (max.)	8.54	0.442±0.004	0.454±0.004	1.91± 0.11	0.432±0.023
None	345 (max.)	6.68	0.935±0.016	0.944±0.018	6.97± 1.20	1.46 ±0.14
		6.59	0.912±0.008	0.919±0.010	6.72± 0.37	1.40 ±0.10
4-OMe	340 (max.)	3.42	0.572±0.011	0.571±0.007	8.74± 0.94	1.33 ±0.07
4-Me	347 (max.)	7.42	0.951±0.033	0.945±0.014	4.51± 1.01	0.845±0.057
4-F	325 (max.)	5.42	1.053±0.020	0.993±0.010	38.4 ± 5.3	2.50±0.14
4-Br	340 (max.)	2.64	1.033±0.008	1.027±0.013	57.5 ± 4.3	4.30 ±0.25
4-Cl	340 (max.)	2.94	1.015±0.016	0.963±0.057	59.5 ± 9.0	3.29 ±0.80
		2.94	0.995±0.015	0.994±0.007	66.1 ±13.6	3.64 ±0.16
4-NO_2	408 (max.)	3.92	0.921±0.009	0.931±0.007	222. ±43.	20.6 ±2.6
		3.86				18.8 ±3.1
5-OPh	302 (min.)	5.06	0.345±0.010	0.339±0.018	4.55± 0.31	1.65 ±0.17
5-NO_2	345 (max.)	0.63				12.3 ±0.1

This equation was solved for the constant terms ρ_1, ρ_2, and log $K_1^0K_2^0$ by application of Dolittle's least squares procedure (12, 13) to the experimental data for 13 of the 14 acids for which both K_1 and K_2 had been determined. Data for the 5-phenoxy acid were rejected for reasons given below. The σ-values which were used are listed in Table IV and are those given by McDaniel and Brown (30) with the exception of the σ_B values for the 5-fluoro and 5-nitro acids. The values reported by Biggs and Robinson (7) are used for these two σ_B's which define the effect of a *p*-fluoro and of a *p*-nitro substituent, respectively, on the amino group. Statistical weights were calculated from an assumed standard deviation (30) of 0.020 for all the σ's, and from standard deviations of log K_1K_2 values which were calculated from the standard deviations given in Table III for each of the individual ionization constants.

TABLE IV

Comparison of experimental and calculated values of log K_1K_2

Substituent	σ_A	σ_B	Log K_1K_2 Experimental	Log K_1K_2 Calculated
5-OMe	0.115	−0.268	7.91±0.05	7.79
5-Me	−0.069	−0.170	7.61±0.04	7.62
5-F	0.337	−0.026	6.84±0.03	6.87
5-Br	0.391	0.232	6.01±0.09	6.02
5-Cl	0.373	0.227	6.03±0.09	6.05
5-OH	0.121	−0.370	8.08±0.03	8.10
None	0.000	0.000	7.02±0.03	7.04
4-OMe	−0.268	0.115	6.93±0.05	6.88
4-Me	−0.170	−0.069	7.42±0.10	7.38
4-F	0.062	0.337	6.02±0.07	5.94
4-Br	0.232	0.391	5.61±0.04	5.65
4-Cl	0.227	0.373	5.65±0.06	5.71
4-NO_2	0.778	0.710	4.35±0.10	4.25
5-OPh	0.252	−0.320	7.12±0.05	(7.85)

Can. J. Chem. Downloaded from www.nrcresearchpress.com by 210.87.254.6 on 09/05/12
For personal use only.

Solution of eq. [15] gave $\rho_1 = 0.751$, $\rho_2 = 3.111$, and $\log K_1^0K_2^0 = -7.039$. These calculated constants were inserted into eq. [15] to obtain calculated values ($\tilde{y}$) of $\log K_1K_2$ which are listed, together with the corresponding experimental values (y), in Table IV.

When data for all 14 acids were fitted to eq. [15] the difference, $y - \tilde{y}$, between the experimental and the calculated values for the 5-phenoxy acid was several times larger than the corresponding value for any other acid and also its own standard deviation. The K_1 and K_2 constants for this acid were, therefore, not used in subsequent calculations. This large discrepancy between observed and calculated values of $\log K_1K_2$ for 5-phenoxyanthranilic acid is shown in Table IV where the Hammett parameters defined by the other 13 acids have been used to calculate $\log K_1K_2$ for the 5-phenoxy acid.

The data for the same 13 acids were also fitted to the four other equations following.

[22] $$\log K_1 = \rho_1\sigma_A + \rho_2\sigma_B + \log K_1^0,$$

[23] $$\log K_2 = \rho_1\sigma_A + \rho_2\sigma_B + \log K_2^0,$$

[29] $$\log K_1K_2 = \rho_1\sigma_A + \log K_1^0K_2^0,$$

[30] $$\log K_1K_2 = \rho_1\sigma_B + \log K_1^0K_2^0.$$

Table V gives the calculated parameters for these equations. Equations [22] and [23] are valid only if the existing equilibria can be represented by eq. [21] rather than the generally accepted eq. [1]. Equations [29] and [30] have no obvious physical significance; they are included only for purposes of comparison in estimating the significance of the fit of the data to eq. [15].

TABLE V

Comparison of Hammett equations

Eq.	ρ_1	ρ_2	s^2(ext.)*	s^2(int.)†	R‡	F§	F′‖
[15]	0.751±.084	3.111±.071	0.0039	0.0057	0.997	1 560	73
[22]	0.491±.146	1.727±.114	0.0091	0.0024	0.981	255	
[23]	0.426±.144	1.254±.130	0.0113	0.0009	0.949	93	
[29]	2.086±.121		0.640	0.0057	0.481		
[30]	3.331±.019		0.0419	0.0057	0.983		

*s^2(ext.) $= \Sigma (y - \tilde{y})^2/(n - 3)$, where the numerator is the sum of the squares of the deviations from the estimated regression equation and the denominator is the degrees of freedom.
†s^2(int.) $= \Sigma$ (observed standard error of $y)^2/(n - 3)$.
‡R = multiple correlation coefficient.
§F is the variance ratio comparing the equation in question with a completely random distribution and tests the hypothesis $\rho_1 = 0$, $\rho_2 = 0$.
‖F' is the variance ratio between the three-parameter eq. [15] and the two-parameter eq. [30] and indicates whether the former gives a significantly better fit to the data.

The statistics of Table V, which describe the significance of the fit of the data to each equation, amply demonstrate the superiority of eq. [15] as an accurate interpretation of the experimental results. Only for this equation is s^2(int.), calculated from the known experimental uncertainties, greater than s^2(ext.) which is calculated from the fit of the data to the theoretical equation. The data give a considerably less significant fit to eqs. [22] and [23], indicating that the zwitterion and neutral acid cannot be treated as a single species.

The multiple correlation coefficient and the F-test show eq. [15] to be significant within the 99% confidence limit. Jaffe (5) has pointed out that equations of the same mathematical form as eq. [15] may give an excellent but entirely fallacious fit of the data if σ_A and σ_B are highly correlated. He has proposed that equations of this type should only be considered to give a meaningful interpretation of the data if $r_{AB} < 0.9$, where r_{AB} is

Can. J. Chem. Downloaded from www.nrcresearchpress.com by 210.87.254.6 on 09/05/12
For personal use only.

TABLE VI

Comparison of experimental and calculated values of pK_1 and pK_2

Substituent	pK_1			pK_2		
	Expt.	From eq. [11*a*]	From eq. [19*a*]	Expt.	From eq. [11*b*]	From eq. [19*b*]
5-OMe	2.37±.03	2.38	2.54	5.57±.06	5.45	5.38
5-Me	2.48±.03	2.43	2.54	5.13±.01	5.20	5.16
5-F	2.03±.02	2.03	2.17	4.82±.01	4.86	4.76
5-Br	1.60±.03	1.66	1.61	4.41±.03	4.34	4.39
5-Cl	1.69±.08	1.68	1.63	4.35±.03	4.36	4.40
5-OH	2.72±.02	2.42	2.58	5.37±.02	5.72	5.67
None	2.17±.03	2.18	2.23	4.85±.05	4.85	4.83
4-OMe	2.06±.05	1.98	1.99	4.88±.02	4.85	4.86
4-Me	2.35±.10	2.35	2.42	5.07±.03	5.02	5.00
4-F	1.42±.07	1.45	1.34	4.60±.02	4.44	4.55
4-Br	1.24±.03	1.33	1.17	4.37±.03	4.27	4.42
4-Cl	1.21±.07	1.37	1.22	4.44±.03	4.29	4.43
4-NO_2	0.65±.08	0.56	0.19	3.70±.06	3.63	3.99
5-OPh	2.34±.08	(2.28)	(2.48)	4.88±.04	(5.58)	(5.53)
s^2(ext.)		0.125	0.282		0.196	0.207

the correlation coefficient between σ_A and σ_B. The value of $r_{AB} = 0.590$ for our substituents amply fulfills this condition and, indeed, is lower than in any of the cases discussed by Jaffe.

It was pointed out earlier that in the specific case, where indirect effects are negligible, $\rho_1 = {}_D\rho_A$ and $\rho_2 = {}_D\rho_B$. Furthermore, ${}_D\rho_A$ and ${}_D\rho_B$ should, in theory, be approximately equal to 1.00 and 2.89, respectively. These theoretical values are outside the standard deviations of $\rho_1(= 0.751 \pm 0.084)$ and $\rho_2(= 3.111 \pm 0.071)$ shown in Table V. This might be considered evidence for the existence of an indirect effect, although the differences between theoretical and experimental values are no greater than some reported by Jaffe (6) for ortho-substituted systems where chelation is impossible. However, it may be worthwhile to explore the possibility of indirect effects as an explanation for the discrepancy. In that case eq. [16] would give

$$\rho_1 = {}_D\rho_A + {}_I\rho_D = 0.751,$$

$$\rho_2 = {}_I\rho_A + {}_D\rho_D = 3.111.$$

If ${}_D\rho_A$ and ${}_D\rho_D$ were given their theoretical values of 1.000 and 2.889, respectively, the indirect effects would become ${}_I\rho_D = -0.249$ and ${}_I\rho_A = +0.222$. Since the former of these represents the indirect effect of substituents via chelation upon the ionization of a NH_3^+ group, it would be expected to be positive. It seems unlikely, therefore, that the deviation from the theoretical values is really the result of an indirect effect. This conclusion is reinforced by the fact that no indirect effect is observed in the similar but simpler system of salicylic acids (5, 31).

A further test of the indirect effect would be to compare the fit of the experimental K_1's and K_2's to eqs. [11*a*] and [11*b*] which include the indirect effect, with the fit of the same data, to [19*a*] and [19*b*] which do not. This was attempted using ${}_D\rho_A = 1.000$, ${}_I\rho_A = 0.222$, ${}_D\rho_D = 2.889$, and ${}_I\rho_D = -0.249$ for eqs. [11], or $\rho_A = 0.751$ and $\rho_B = 3.111$ for eqs. [19], and weighting the K's inversely as the squares of their standard deviations. Table VI compares the observed pK_1's and pK_2's with those calculated by the two methods. It is seen that, while the pK_1's fit eq. [11] somewhat better than eq. [19], there is little to choose between [11] and [19] as methods for calculating pK_2. Since for both

Can. J. Chem. Downloaded from www.nrcresearchpress.com by 210.87.254.6 on 09/05/12
For personal use only.

series s^2(ext.) is at least double s^2(int.), the better fit to eq. [11] can hardly be taken as evidence for an indirect effect.

TABLE VII

Calculated ionization constants for eq. [1]

Eq.	$K_A^0 \times 10^3$	$K_B^0 \times 10^3$	$(K_A^0 + K_B^0) \times 10^3$	Experimental $K_1^0 \times 10^3$	K_Z^0
[11*a*]	3.2±.3	3.4±.6	6.6±.8	6.7±.4	1.0±.3
[19*a*]	1.9±.2	3.9±.6	5.9±.8	6.7±.4	0.5±.1
Eq.	$K_C^0 \times 10^5$	$K_D^0 \times 10^5$	$(1/K_C^0 + 1/K_D^0) \times 10^{-5}$	Experimental $1/K_2^0 \times 10^{-5}$	K_Z^0
[11*b*]	3.2±.4	2.5±.2	0.71±.04	0.70±.04	1.2±.3
[19*b*]	2.7±.1	3.2±.3	0.68±.04	0.70±.04	0.9±.1

In fitting the K_1's and K_2's to eqs. [11] and [19] the data for 5-phenoxyanthranilic acid were omitted, as indicated previously, because of their poor fit to eq. [15]. The values of K_A^0, K_B^0, K_C^0, and K_D^0 obtained from the remaining 13 acids were used to calculate pK_1 and pK_2 for the 5-phenoxy acid and these are shown in parentheses in Table VI. It is seen that the calculated pK_1 agrees reasonably well with experiment but that pK_2 is widely out. Examination of eq. [19*b*] shows that the calculated value of K_2 for this acid is largely determined by the second term of the equation, which depends upon σ for the para-phenoxy group. It appears, therefore, that either the experimental value of K_2 is grossly in error or σ_{para} is incorrect. In order to fit the experimental K_2 into eqs. [15] and [19*b*] a value of $\sigma = -0.088$ would be required for the *p*-phenoxy group, and it is interesting to note that this is in good agreement with the σ_p reported by Jaffe (6) for reactions other than ionization constants of benzoic acids. However, our data ought, in principle, to correlate with the ionization constants of benzoic acids, and the 5-phenoxy acid is particularly susceptible to oxidative side reactions, so that it is probably not safe to attach any particular significance to our apparent σ-value.

Table VII shows the values for K_A^0, K_B^0, K_C^0, and K_D^0 obtained from eqs. [11] and [19] and for the values of K_Z^0 derived from these by means of eq. [7]. The extended series of computations from the original data causes an accumulation of uncertainties in the quantities presented in Table VII but it is seen that they are consistent within their standard deviations. For example, eq. [4], which requires that $K_A^0 + K_B^0 = K_1^0$, and eq. [5], which requires that $1/K_C^0 + 1/K_D^0 = 1/K_2^0$, are both satisfied. The uncertainty in K_Z^0 is correspondingly large, but K_Z^0 evidently lies in the region 0.4–1.5, with the theoretically preferable eq. [19*a*] giving a range of 0.4–1.0, equivalent to 30–50% zwitterion.

Previous calculations giving $K_Z^0 = 0.2$, or 17% zwitterion, have been based on the assumption that K_A^0 may be equated to the ionization constant of the methyl ester of anthranilic acid, p$K_E = 2.09$ (3). This assumption, as applied to *p*-aminobenzoic acid, has been criticized by Bryson and Matthews (11) on the grounds that the various alkyl esters have different ionization constants and that among these the methyl ester is out of line. The assumption may be particularly questionable when applied to anthranilic acid esters because of the known acid-strengthening effect of bulky ortho substituents in anilinium ions (32). The reported ionization constant of the ester, $K_E = 8.13 \times 10^{-3}$, is indeed larger than our K_A^0, whether one considers its most probable value of 1.9×10^{-3} or the maximum value of 3.5×10^{-3} obtained by inclusion of indirect substituent effects

Can. J. Chem. Downloaded from www.nrcresearchpress.com by 210.87.254.6 on 09/05/12
For personal use only.

via eq. [11*a*]. In fact, Table II shows that the ionization constant of the ester is larger than most modern estimates of K_1^0, which, since $K_1^0 = K_A^0 + K_B^0$, makes the assumption that $K_E = K_A^0$ untenable.

Finally, it may be pointed out that, although the equilibrium constant for zwitterion formation by anthranilic acid is still not known with great precision, the relative equilibrium constants for zwitterion formation by substituted anthranilic acids may be calculated from eq. [20] with considerable certainty. If K_Z^0 is assumed to be 1.0, then among our acids K_Z varies from 17.5 (95% zwitterion) for 5-hydroxy to 0.019 (2% zwitterion) for 4-nitroanthranilic acid.

SUMMARY

The ionization constants of substituted anthranilic acids give an excellent fit to the two-parameter Hammett eq. [15], showing that these acids at the isoelectric point are better represented as a mixture of zwitterion and neutral acid than as a single hybrid species; previous estimates of the % zwitterion are low because of the erroneous assumption that the ionization of the amino group is the same in anthranilic acid as in its methyl ester; and indirect transmission of substituent effects via chelation is very improbable since in some cases it would have to act in the sense opposite to that predicted by theory.

ACKNOWLEDGMENT

The authors are grateful to Mr. Immo E. Scheffler for assistance with the experimental work,

REFERENCES

1. G. E. Dunn and R. Prysiazniuk. Can. J. Chem. **39**, 285 (1961).
2. G. E. Dunn and W. Rodewald. Unpublished work.
3. E. J. Cohn and J. T. Edsall. Proteins, amino acids and peptides. Reinhold Publ. Co., New York. 1943. pp. 99, 128.
4. N. Bjerrum. Z. Physik. Chem. **104**, 147 (1923).
5. H. H. Jaffe. J. Am. Chem. Soc. **76**, 4261 (1954).
6. H. H. Jaffe. Chem. Rev. **53**, 191 (1953).
7. A. I. Biggs and R. A. Robinson. J. Chem. Soc. 388 (1961).
8. E. Andersen, E. A. Birkheimer, and T. A. Bak. Acta Chem. Scand. **14**, 1899 (1960).
9. B. J. Thamer and A. F. Voigt. J. Phys. Chem. **56**, 225 (1952).
10. Kok-Peng Ang. J. Phys. Chem. **62**, 1109 (1958).
11. A. Bryson and R. W. Matthews. Australian J. Chem. **14**, 237 (1961).
12. W. E. Deming. Statistical adjustment of data. J. Wiley and Sons, Inc., New York. 1944.
13. B. Ostle. Statistics in research. Iowa State College Press. Ames, Iowa. 1954.
14. E. B. Hershberg. Ind. Eng. Chem. Anal. Ed. **8**, 312 (1936).
15. C. A. Grob. Helv. Chim. Acta, **33**, 1787 (1950).
16. J. M. L. Steven, I. M. Tonkin, and J. Walker. J. Chem. Soc. 1034 (1947).
17. O. Yu Magidson and A. I. Travin. J. Gen. Chem. USSR Eng. Transl. **11**, 243 (1941); Chem. Abstr. **35**, 7965 (1941).
18. A. Morrison and T. P. C. Mulholland. J. Chem. Soc. 2702 (1958).
19. G. B. Bachman and G. M. Picha. J. Am. Chem. Soc. **68**, 1599 (1946).
20. E. A. Steck and L. T. Fletcher. J. Am. Chem. Soc. **70**, 439 (1948).
21. A. Ostaszynski. Bull. Soc. Sci. Lettres Lodz Classe III. **3**, No. 15 (1952); Chem. Abstr. **49**, 203 (1955).
22. B. E. Volcani, S. Sicher, E. D. Bergmann, and H. Bendas. J. Biol. Chem. **207**, 411 (1954).
23. O. Sus and K. Möller. Ann. **593**, 91 (1955).
24. J. L. E. Erickson, J. M. Dechary, and T. R. Pullig. J. Am. Chem. Soc. **74**, 5621 (1952).
25. P. Friedlander, S. Bruckner, and G. Deutsch. Ann. **388**, 23 (1912).
26. H. H. Hodgson and T. A. Jenkinson. J. Chem. Soc. 3041 (1927).
27. L. A. Yanovskaya, A. P. Terent'ev, and L. I. Belen'kiu. Zh. Obshch. Khim. **22**, 1594 (1952).
28. A. M. Liquori and A. Ripamonti. Gazz. Chim. Ital. **85**, 578 (1955).
29. S. Kilpi and D. Harjanne. Suomen Kemistilehti B, **21**, 14 (1948); Chem. Abstr. **42**, 8051 (1948).
30. D. H. McDaniel and H. C. Brown. J. Org. Chem. **23**, 420 (1958).
31. G. E. Dunn and Fei-Lin Kung. Unpublished work.
32. H. C. Brown, D. H. McDaniel, and O. Hafliger. *In* Determination of organic structures by physical methods. Vol. I. *Edited by* E. A. Braude and F. C. Nachod. Academic Press, Inc., New York. 1955. p. 611.

Can. J. Chem. Downloaded from www.nrcresearchpress.com by 210.87.254.6 on 09/05/12
For personal use only.

Can. J. Chem. Downloaded from www.nrcresearchpress.com by 210.87.254.105 on 09/05/12
For personal use only.

SPECTRAL PROPERTIES OF *p*-SUBSTITUTED BENZOYLTRIPHENYLSILANES

A. G. Brook, Ryan Kivisikk, and G. E. LeGrow[1]
Department of Chemistry, University of Toronto, Toronto, Ontario
Received October 26, 1964

ABSTRACT

A series of *p*-substituted benzoylsilanes have been synthesized and their infrared and ultraviolet spectra determined. Correlations of both the infrared carbonyl stretching frequency and the n–π^* ultraviolet absorption with Hammett substituent constants have been found. Benzoylsilanes are generally unstable in ethanol undergoing light-catalyzed decomposition. Benzoyldiphenylphosphine was found to give spectra similar to those of benzoylsilanes.

The yellow color and general spectral properties of benzoylsilanes are of some interest since the analogous carbon compounds are colorless and since the benzoylsilanes represent the only known group of colored silicon-containing compounds in which the silicon atom is obviously acting as part of the chromophoric system (1–4). As part of our continuing investigation of the behavior of silyl ketones we were led to synthesize a number of substituted benzoyltriphenylsilanes, where substituents were present either on the para position of the benzoyl group or on the para positions of all three phenyl groups attached to silicon. All of the substituted silanes were varying shades of yellow. The infrared and ultraviolet spectral data are given in Tables I and II.

TABLE I

Infrared carbonyl stretching frequency

For Ph_3SiCO–C$_6$H$_4$–X		For (Y–C$_6$H$_4$–)$_3$SiCOPh	
X	cm^{-1}	Y	cm^{-1}
H	1 617	H	1 617
NO_2	1 624	Cl	1 617
Br	1 618	CF_3	1 617
Cl	1 618		
F	1 617.5		
OCH_3	1 616		
$C(CH_3)_3$	1 616		

The carbonyl infrared stretching frequency for all ketones occurred near 1 617 cm^{-1} (6.18 μ). An approximately linear correlation between the stretching frequency and σ, the Hammett substituent constant, was found for the *p*-substituted benzoyltriphenylsilanes (Fig. 1), as had been observed previously for the corresponding acetophenones (5) except that in the present case the σ^- value for the *p*-nitro group fitted the data better. Since the frequencies for all compounds occurred over a range of only 8 cm^{-1} a more precise correlation could not be expected.

One difference noted between the acetophenones and the benzoylsilanes was in the slope of the ν vs. σ plot; in the acetophenones the slope $\Delta\nu/\Delta\sigma$ was 16.6, whereas in the benzoylsilanes the slope was 5.4, indicating considerably less sensitivity of the carbonyl

[1]*Dow Corning Silicones of Canada Predoctorate Fellow, 1962–1964.*

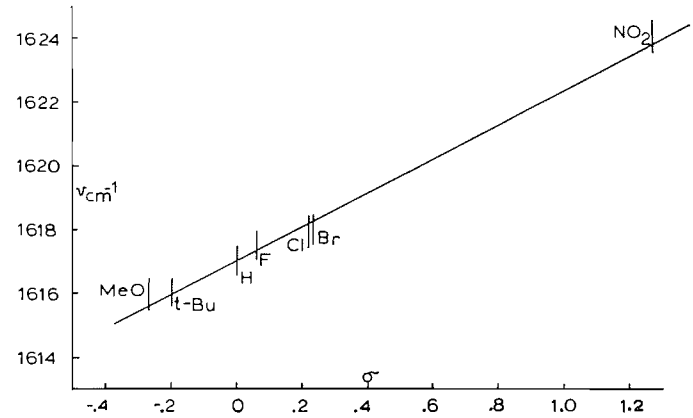

FIG. 1. Infrared carbonyl stretching frequency vs. Hammett σ (or σ^-) constant for *p*-substituted benzoylsilanes.

group in the latter compounds to inductive and mesomeric effects of the *p*-substituent. This is to be expected because of the significant degree of single bond or polar character present in the carbonyl group of these compounds. The carbonyl stretching frequencies of the tris-*p*-substituted phenylbenzoylsilanes occurred in the same position as the unsubstituted compound within experimental error. The insensitivity of the stretching frequency to the nature of the group attached to silicon has been observed before, triphenyl- and trimethyl-benzoylsilanes, as well as mixed methylphenylbenzoylsilanes, absorbing at the same frequency (2).

In the ultraviolet and visible region benzoylsilanes have two absorptions, one in the region of 260 mμ assigned as a π–π^* transition and the other occurring at about 420 mμ ascribed as an n–π^* transition of the carbonyl group involving interaction with the silicon d-orbitals (3, 4). The high intensity π–π^* band occurs in essentially the same position as that of its carbon analog β-benzpinacolone (2), while the n–π^* transition is, of course, at much longer wavelength. Comparing the absorption data with that of the related acetophenones (6), we found, with the exception of the *p*-nitrobenzoylsilane, where the shift in wavelength is rather smaller, that the π–π^* absorption maxima of *p*-substituted benzoylsilanes occurs at 17–18 mμ longer wavelength than that of the corresponding acetophenones, suggesting that the silicon atom adjacent to the carbonyl group is not significantly involved in the π–π^* transition, and that the *p*-substituents are acting in their normal manner as far as their effects on the position of absorption maxima are concerned. The extinction coefficients of benzoylsilanes are, however, slightly larger than those of the corresponding acetophenones. On the other hand, the n–π^* absorption band of the benzoylsilanes occurs at approximately 100 mμ longer wavelength, and with a considerably greater extinction coefficient than the n–π^* band for the corresponding acetophenones. Unfortunately, the position of this band in acetophenones has not always been reported, but from the available data (7), the minor changes in wavelength caused by *p*-substituents appear to vary in the same way with both benzoylsilanes and acetophenones.

An interesting correlation between the wavelength of the most intense n–π^* band and σ, the Hammett substituent constant, was noted (Fig. 2). Although it is recognized that ultraviolet data, which involve both ground and excited states, cannot normally be

Can. J. Chem. Downloaded from www.nrcresearchpress.com by 210.87.254.105 on 09/05/12
For personal use only.

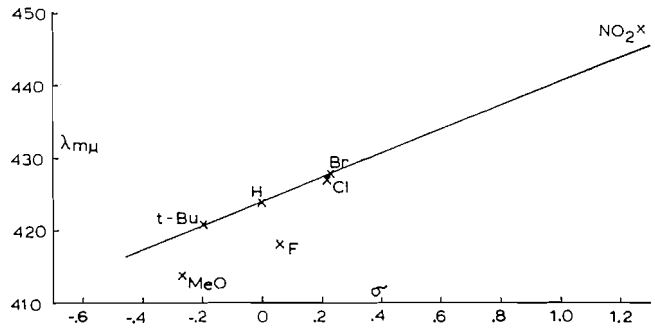

FIG. 2. n–π^* Carbonyl absorption wavelength vs. Hammett σ (or σ^-) constant for *p*-substituted benzoylsilanes.

related to Hammett substituent effects, which involve ground states only, the apparent correlation appears worthy of comment. A linear correlation of wavelength with σ was found for benzoyltriphenylsilane and its *p-tert*-butyl, *p*-chloro, and *p*-bromo derivatives. The *p*-nitro, *p*-fluoro, and *p*-methoxy compounds deviate significantly from this correlation: in other cases involving Hammett correlations of kinetic data, compounds with these same substituents have been observed to deviate in the same direction. Thus *p*-nitro compounds fitted the data better here, and in Eaborn's work (8) if σ^- values were used, and in both base-catalyzed hydrolyses of benzylsilanes (9) and in base-catalyzed isomerizations of α-silylcarbinols (10), the *p*-fluoro and *p*-methoxy compounds required, as here, more negative σ values than those normally employed to fit the correlation. Further data seems desirable, before the significance of the correlation and the deviations from it can be assessed. We believe that this deviation is a real and significant effect and will be discussed in more detail in a future publication.

The ultraviolet data reported in Table II were measured in cyclohexane, and in some cases, in ethanol as well. In ethanol, the solvent employed in previous studies (2), the 420 mμ band appears as one peak, with shoulders on each side, whereas in cyclohexane all the ketones showed three clearly resolved bands as well as a shoulder on the short wavelength side of the shortest wavelength band. This fine structure, previously observed with simple carbonyl compounds in nonpolar solvents (11), is presumably associated with various vibrational levels of the n–π^* excitation. A comparison of the data in cyclohexane and ethanol showed small changes in wavelength of both absorption bands. The n–π^* transition occurred at 5–10 mμ shorter wavelength in ethanol than in cyclohexane (blue shift) whereas the π–π^* transition generally occurred at 1–2 mμ longer wavelength in changing to the more polar solvent (red shift). These changes follow the pattern usually observed in carbonyl compounds in changing from nonpolar to polar solvents and hence substantiate the assignment of the spectroscopic transitions as π–π^* and n–π^* (12).

Apart from the enhanced resolution of the n–π^* band an additional reason for changing the solvent from ethanol to cyclohexane was the observation that some of the ketones appeared to be unstable in ethanol; different extinction coefficients were found for new and aged solutions, and in extreme cases, the yellow color of the solutions faded rapidly to colorless. It was shown that this decomposition was light catalyzed. Thus several grams of benzoyltriphenylsilane in methanol were irradiated with a lamp rich in near ultraviolet radiation and in 1–2 h the yellow color was entirely bleached. Distillation of

Can. J. Chem. Downloaded from www.nrcresearchpress.com by 210.87.254.105 on 09/05/12
For personal use only.

TABLE II

Ultraviolet spectra

	X	Cyclohexane (λ(ϵ))	Ethanol (λ(ϵ))
Of Ph_3SiCO—C$_6$H$_4$—X			
	H	257(16 200) 388(s)(118), 405(222) 424(292), 440(177)	258(15 500) 403(264), 417(300)
	NO_2	266(17 800) 411(s)(132), 434(192) 448(192), 478(89)	267(15 600) 430(215)
	Br	271(21 700) 390(s)(117), 407(216) 428(271), 448(158)	271(21 300) 410(266), 421(288) 442(165)
	Cl	268(18 400) 391(s)(117), 407.5(217) 427(273), 448 (159)	*
	F	260(13 700) 384(s)(119), 400(223) 418.5(290), 440(188)	*
	OCH_3	290(20 800), 298(s)(17 400) 380(s)(132), 396(246) 414(335), 434(232)	†
	$C(CH_3)_3$	269(19 800) 386(s)(120), 403(227) 421(305), 442(200).	*
Of (X—C$_6$H$_4$—)$_3$SiCOPh			
	Cl	228.5(38 400), 257(s)(19 600) 387(s)(149), 403(277) 422(363), 442(230)	259(17 400) 400(288), 411(325) 425(218)
	CF_3	266(17 250) 384(s)133, 401(239) 418(314), 438(201)	†
	CH_3	263 404, 423, 446	263 405(s), 417, ‡
Of Ph_2P—COPh		*	265(12 000) 377(247), 390(270) 404(175)

Abbreviation: s = shoulder.
*Spectrum not determined.
†Unstable in ethanol.
‡Compound not pure so extinction coefficient unknown.

the solution gave triphenylmethoxysilane in high yield, a small amount of benzaldehyde and a much larger yield of benzaldehydedimethylacetal, identified by its infrared and nuclear magnetic resonance (n.m.r.) spectra, and physical properties.

$$Ph_3SiCOPh \xrightarrow[MeOH]{h\nu} Ph_3SiOMe + PhCH(OMe)_2$$

This decomposition occurs much more slowly, if at all, in the dark in methanol and is completely avoided in nonpolar solvents such as cyclohexane.

It has been reported in the literature that benzoyldiphenylphosphine is a yellow solid although no spectral data is reported (13). Because of the obvious analogy between benzoylsilanes and benzoylphosphines the synthesis was repeated and a yellow solid was obtained. The material could not be entirely freed of benzaldehyde, and the compound was found to be rather less stable than the original literature suggested. In air, it decomposed yielding benzoic acid and diphenylphosphonic acid. As expected the yellow (impure)

Can. J. Chem. Downloaded from www.nrcresearchpress.com by 210.87.254.105 on 09/05/12
For personal use only.

material, freshly distilled, showed a low frequency carbonyl stretching band (1 645 cm^{-1}) although the frequency was higher than that of benzoylsilanes, and the ultraviolet spectra showed π–π^* absorption at 265 mμ, and n–π^* absorption centered about 390 mμ, rather lower than that of a benzoylsilane. It seems clear in view of the similar spectra that benzoylsilanes and benzoylphosphines are closely related species subject to the same sort of group interactions.

It now seems quite clear that the abnormally low infrared carbonyl stretching frequency in benzoylsilanes is a result of significant single bond character in the carbonyl group caused by inductive release of electrons by the adjacent silicon atom. In accord with this Yates and Agolini (14) have established that benzoyltriphenylsilane is significantly more basic than benzoyltriphenylmethane. Also, Brook and Pierce (3) have shown that β- but not γ-silyl ketones absorb at a lower frequency than their carbon analogs, a result consistent with inductive electron release acting through a single intervening methylene group. Thus in the ground state benzoylsilanes must have a significant negative charge associated with the carbonyl-oxygen atom. Back bonding of this charge from oxygen into the available d orbitals on silicon forming n–d π-bonding seems inconsistent with the basicity studies, but cannot be excluded on the present available data. As noted before, the π–π^* transition is little affected in ketones by replacement of carbon by silicon, wherease the n–τ^* is significantly affected by this change. West has explained these effects as due to a general lowering of both the π and π^* levels, relative to the n energy level in silyl ketones (4) which implies stabilization of the excited state by contributions from structures such as

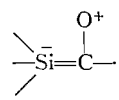

through charge delocalization from carbon into the adjacent unoccupied silicon d orbitals. At the same time, it seems probable that the n level is raised relative to the π^* level, by virtue of the strong inductive electron release of the adjacent silicon atom, as characterized by the infrared stretching frequency. These two effects in concert result in π–π^* transitions at about the same wavelength for ketones and benzoylsilanes, while at the same time the n–π^* wavelength is raised significantly. Superimposed on these two effects are the general effects of para substituents (6) which appear to influence both transitions in the same way and to about the same extent in both ketones and benzoylsilanes.

The new ketones employed in this study were all prepared from the appropriately substituted benzylsilane by dibromination with N-bromosuccinimide followed by hydrolysis in aqueous organic solvent mixtures employing either silver acetate (1) or silver trifluoroacetate (3), the latter effecting hydrolysis much more rapidly. The triphenylbenzylsilanes were prepared by one of several general routes; viz. (*a*) coupling of a *p*-substituted benzyl Grignard reagent with triphenylchlorosilane (X = *p*-*tert*-butyl, *p*-methoxy), (*b*) reaction of a *p*-substituted benzyl Grignard reagent with silicon tetrachloride, followed by coupling of the benzyltrichlorosilane with 3 mole equivalents of phenyl Grignard reagent (X = *p*-fluoro, *p*-chloro), (*c*) bromination of benzyltrichlorosilane, followed by coupling with phenyl Grignard reagent (X = *p*-bromo), (*d*) nitration of benzyltriphenylsilane (X = *p*-nitro). The properties of these compounds and of their intermediates are given in Table III.

The tris-*p*-substituted phenylbenzylsilanes were synthesized by similar routes; viz. (*a*) coupling of the appropriately tris-*p*-substituted phenylchloro- or bromo-silane with

Can. J. Chem. Downloaded from www.nrcresearchpress.com by 210.87.254.105 on 09/05/12
For personal use only.

TABLE III

p-Substituted benzyltriphenylsilanes and their derivatives

Compound	Reagents	Yield (%)	Melting point (°C)
p-$BrC_6H_4CH_2SiPh_3$	*p*-$BrC_6H_4CH_2SiCl_3$ + PhLi (15)	96	133–135[a]
p-$BrC_6H_4CBr_2SiPh_3$	NBS	85	144–146[b]
p-$BrC_6H_4COSiPh_3$	$AgOOCCF_3$	94	116–117[c]
o-$NO_2C_6H_4CH_2SiPh_3$	$PhCH_2SiPh_3$ + HNO_3[d]	54	155–156[e]
o-$NO_2C_6H_4CHBrSiPh_3$	NBS[f]	91	148–149[g]
p-$NO_2C_6H_4CH_2SiPh_3$	$PhCH_2SiPh_3$ + HNO_3[d]	28	114.5–116.5[h]
p-$NO_2C_6H_4CBr_2SiPh_3$	NBS	77	112–120[i]
p-$NO_2C_6H_4COSiPh_3$	$AgOOCCF_3$	72	155–157[j]
p-$CH_3CONHC_6H_4CH_2SiPh_3$	*p*-$NO_2C_6H_4CH_2SiPh_3$, H_2, Pt, Ac_2O	86	207–208[k]
p-$MeOC_6H_4CH_2SiPh_3$	*p*-$MeOC_6H_4CH_2MgCl$ + Ph_3SiCl	80	107–108[l]
p-$MeOC_6H_4COSiPh_3$	NBS; AgOAc	44	131.5–132.5[m]
p-$ClC_6H_4CH_2SiPh_3$	*p*-$ClC_6H_4CH_2MgCl$ + Ph_3SiCl	3	106–108[n]
p-$ClC_6H_4CH_2SiPh_3$	*p*-$ClC_6H_4CH_2SiCl_3$ + PhLi	83	111–112[n]
p-$ClC_6H_4CBr_2SiPh_3$	NBS	83	134.5–135.5[o]
p-$ClC_6H_4COSiPh_3$	AgOAc	89	93–95[p]
p-$FC_6H_4CH_2SiPh_3$	*p*-$FC_6H_4CH_2SiCl_3$ + PhLi	79	98–99[q]
p-$FC_6H_4CBr_2SiPh_3$	NBS	76	107–108[r]
p-$FC_6H_4COSiPh_3$	AgOAc	83	116–118[s]
p-*t*-$BuC_6H_4CH_2SiPh_3$	*p*-*t*-$BuC_6H_4CH_2MgCl$ + Ph_3SiCl	89	125–126[t]
p-*t*-$BuC_6H_4CBr_2SiPh_3$	NBS	92	138.5–139.5[u]
p-*t*-$BuC_6H_4COSiPh_3$	AgOAc	78	151–152[v]

Recrystallization solvent shown in parenthesis prior to analytical data.
[a](EtOH) Calcd. for $C_{25}H_{21}SiBr$: C, 69.9; H, 4.93. Found: C, 69.7; H, 4.90.
[b](1:1 EtOH–EtOAc.)
[c](EtOH) Calcd. for $C_{25}H_{19}SiOBr$: C, 67.7; H, 4.32. Found: C, 67.1; H, 4.22.
[d]Mixture of ortho and para isomers obtained, separated by crystallization.
[e](1:1 EtOH–EtOAc) Calcd. for $C_{25}H_{21}SiNO_2$: C, 75.9; H, 5.35; N, 3.56. Found: C, 75.1; H, 5.36; N, 3.56.
[f]Conditions favoring dibromination gave only monobromide.
[g](1:1 EtOH–EtOAc) Calcd. for $C_{25}H_{20}SiBrNO_2$: C, 63.3; H, 4.25; N, 2.95. Found: C, 62.6; H, 4.39; N, 3.07.
[h](EtOH) Calcd. for $C_{25}H_{21}SiNO_2$: C, 75.9; H, 5.35; N, 3.56. Found: C, 75.8; H, 5.35; N, 3.78.
[i]Not further purified (EtOH–EtOAc).
[j](EtOH) Calcd. for $C_{25}H_{19}SiNO_3$: C, 73.3; H, 4.68; N, 3.42. Found: C, 72.8; H, 4.56; N, 3.60.
[k](MeOH) Calcd. for $C_{27}H_{25}SiNO$: C, 79.5; H, 6.18; N, 3.44. Found: C, 77.0; H, 6.23; N, 3.48.
[l](1:1 EtOH–hexane) Calcd. for $C_{26}H_{24}SiO$: C, 82.0; H, 6.36. Found: C, 81.5; H, 6.35.
[m]Intermediate dibromide not isolated. (EtOH) Calcd. for $C_{26}H_{22}SiO_2$: C, 79.1; H, 5.62. Found: C, 78.7; H, 5.81.
[n]Literature m.p. 114° (16). (EtOH) Calcd. for $C_{25}H_{21}SiCl$: C, 77.9; H, 5.50. Found: C, 77.8; H, 5.47.
[o](EtOH) Calcd. for $C_{25}H_{19}SiBr_2Cl$: C, 55.3; H, 3.43. Found: C, 55.6; H, 3.65.
[p](EtOH) Calcd. for $C_{25}H_{19}SiOCl$: C, 75.3; H, 4.80. Found: C, 75.6; H, 4.98.
[q](EtOH) Calcd. for $C_{25}H_{21}SiF$: C, 81.5; H, 5.75. Found: C, 81.5; H, 5.66.
[r](EtOH) Calcd. for $C_{25}H_{19}SiBr_2F$: C, 57.1; H, 3.64. Found: C, 57.6; H, 3.63.
[s](EtOH) Calcd. for $C_{25}H_{19}SiOF$: C, 78.5; H, 5.01. Found: C, 78.6; H, 5.12.
[t](EtOH – 90–100° petroleum ether) Calcd. for $C_{29}H_{30}Si$: C, 85.7; H, 7.44. Found: C, 85.1; H, 7.32.
[u](EtOH – 90–100° petroleum ether) Calcd. for $C_{29}H_{28}SiBr_2$: C, 61.7; H, 5.00. Found: C, 62.0; H, 4.90.
[v](EtOH) Calcd. for $C_{29}H_{28}SiO$: C, 82.8; H, 6.71. Found: C, 82.4; H, 6.62.

benzyl magnesium chloride (X = *p*-Me_2N, *p*-Me, *p*-Cl,), or (*b*) of the methoxysilane with benzyl magnesium chloride (X = *p*-CF_3), (*c*) coupling of benzyltrichlorosilane with 3 equivalents of the appropriate *p*-substituted phenyl Grignard reagent (X = *p*-Me). The benzylsilanes were converted in the ordinary way to the ketones. In the case of tri-*p*-tolylbenzylsilane bromination probably occurred both on the methylene hydrogens and also on the methyl group. The dibromide isolated was crystallized to give an apparently pure product which analyzed correctly, but hydrolysis gave a yellow oil with the characteristic spectrum of a benzoylsilane but which was contaminated with unhydrolyzable bromine-containing material and acetate esters from which it could not be separated by crystallization or chromatography. Properties of the compounds are given in Table IV.

EXPERIMENTAL

All reactions involving organometallic reagents were carried out under an atmosphere of nitrogen.

Infrared spectra were obtained on a Perkin–Elmer 221 instrument run at very slow speed using carbon tetrachloride as solvent and are probably accurate to 1–2 cm^{-1}. Ultraviolet spectra were determined in ethanol on a Beckmann DK 1 instrument or in cyclohexane on a Perkin–Elmer 350 instrument.

Can. J. Chem. Downloaded from www.nrcresearchpress.com by 210.87.254.105 on 09/05/12
For personal use only.

TABLE IV

Tris(*p*-substituted phenyl)benzylsilanes and their derivatives

Compound	Reagents	Yield (%)	Melting point (°C)
$(p\text{-}Me_2NC_6H_4)_3SiCH_2Ph$	$(p\text{-}Me_2NC_6H_4)_3SiCl$[a] + $PhCH_2MgCl$	11	163–165[b]
$(p\text{-}ClC_6H_4)_3SiCH_2Ph$	$(p\text{-}ClC_6H_4)_3SiBr$[c] + $PhCH_2MgCl$	44	148–150[d]
$(p\text{-}ClC_6H_4)_3SiCOPh$	NBS[e]; $AgOOCCF_3$	62	111–111.5[f]
$(p\text{-}CF_3C_6H_4)_3SiCH_2Ph$	$(p\text{-}CF_3C_6H_4)_3SiOMe$[g] + $PhCH_2MgCl$	53	138.5–140[h]
$(p\text{-}CF_3C_6H_4)_3SiCOPh$	NBS[e]; $AgOOCCF_3$	63	79–80[i]
$(p\text{-}CH_3C_6H_4)_3SiCH_2Ph$	$PhCH_2SiCl_3$ + $p\text{-}CH_3C_6H_4Li$	97	102–103.5[j]
	$(p\text{-}CH_3C_6H_4)_3SiCl$ + $PhCH_2MgCl$	58	102–103.5[j]
	$(p\text{-}CH_3C_6H_4)_3SiBr$[k] + $PhCH_2MgCl$	94	102–103.5[j]
$(p\text{-}CH_3C_6H_4)_3SiCBr_2Ph$	NBS[e]	62	131–134[m]
$(p\text{-}CH_3C_6H_4)_3SiCOPh$	AgOAc		Oil[n]

Recrystallization solvent given in parenthesis prior to analytical data.
[a]See reference 17.
[b](EtOH–benzene) Calcd. for $C_{31}H_{37}SiN_3$: C, 77.6; H, 7.70; N, 8.80. Found: C, 77.5; H, 8.04; N, 8.93.
[c]From tris-*p*-chlorophenylsilane (18) and NBS, m.p. 86–91° crude.
[d](EtOH) Calcd. for $C_{25}H_{19}SiCl_3$: C, 66.1; H, 4.22. Found: C, 65.5; H, 3.99.
[e]Intermediate dibromide not isolated.
[f](EtOH) Calcd. for $C_{25}H_{17}SiOCl_3$: C, 64.2; H, 3.66. Found: C, 64.7; H, 3.48.
[g]See Experimental.
[h](Hexane) Calcd. for $C_{28}H_{19}SiF_9$: C, 60.6; H, 3.45. Found: C, 61.0; H, 3.45.
[i](Pentane) Calcd. for $C_{28}H_{17}SiOF_9$: C, 59.2; H, 3.01. Found: C, 59.4; H, 3.48.
[j](EtOH) Calcd. for $C_{28}H_{28}Si$: C, 85.7; H, 7.19. Found: C, 85.9; H, 7.19.
[k]From tri-*p*-tolylsilane (18) + NBS.
[l]Both methylene and methyl groups probably brominated.
[m](EtOH–benzene) Calcd. for $C_{28}H_{26}SiBr_2$: C, 61.1; H, 4.76. Found: C, 61.6; H, 4.90.
[n]Yellow oil obtained, contaminated with acetate esters (infrared, 5.8 μ) and brominated products which could not be removed.

Reagents

p-Bromobenzyltrichlorosilane was prepared by bromination of benzyltrichlorosilane (15).

p-Fluorobenzyltrichlorosilane, b.p. 56° at 0.13 mm, was prepared in 56% yield by reaction of silicon tetrachloride in 1:5 ether–hexane at 0° with the Grignard reagent of *p*-fluorobenzyl bromide in ether.

Anal. Calcd. for $C_7H_6SiCl_3F$: Cl (titratable), 43.5. Found: Cl, 43.5.

The *p*-fluorobenzyl bromide was prepared in 63% yield by treatment of *p*-fluorotoluene with 1 equivalent of N-bromosuccinimide in CCl_4, b.p. 29.3–31° at 0.035 mm, n_D^{22} 1.5480. *p*-Chlorobenzyltrichlorosilane was similarly prepared from the Grignard reagent of *p*-chlorobenzylchloride and silicon tetrachloride in 64% yield, b.p. 80° at 0.10 mm.

Anal. Calcd. for $C_7H_6SiCl_4$: Cl (titratable), 40.4. Found: Cl, 41.3.

Tri-(p-trifluoromethylphenyl)-methoxysilane

A solution of *p*-trifluoromethylphenylmagnesium bromide, prepared from 60.8 g (0.27 mole) of *p*-bromobenzotrifluoride and 6.55 g (0.27 g-atom) of magnesium in 250 ml of dry ether, was added over 1 h to 10.0 g (0.074 mole) of trichlorosilane in 50 ml of dry ether. There was immediate evolution of heat. After 4 h reflux, the reaction mixture was cooled and drowned in ice water and dilute acid, and was ether extracted. Bubbles of gas were evolved during the extraction. The organic phase was dried over anhydrous sodium sulfate and then distilled to give 18.3 g of product, b.p. 136–146° at 0.15 mm. The infrared spectrum had a strong band at 2.7 μ (SiO—H) but no band at 4.7 μ (Si—H). Crystallization from methanol gave 18.8 g (51.5%) of tri-(*p*-trifluoromethylphenyl)-methoxysilane, m.p. 123°, which was raised to 130–131° by further recrystallization. Evidently, the silanol reacted with the methanol since the product had no SiO—H peak at 2.7 μ but a new peak at 3.5 μ (CH_3O) had appeared.

Anal. Calcd. for $C_{22}H_{15}SiOF$: C, 53.4; H, 3.06. Found: C, 53.4; H, 3.16.

Synthesis of Benzyl- and Benzoyl-silanes

Typical procedures for the synthesis of the benzyl- and benzoyl-silanes are described below.

Method A. Coupling of p-Methoxybenzylmagnesium Chloride with Triphenylchlorosilane

To 11.8 g (0.040 mole) of triphenylchlorosilane in 150 ml of tetrahydrofuran was added over 45 min 160 ml of 0.25 *N* *p*-methoxybenzylmagnesium chloride (0.04 mole) prepared by the method of Van Campen *et al.* (19) except that tetrahydrofuran was employed as solvent. The reaction was refluxed for 1 h and then stirred overnight. After hydrolysis with dilute acid the organic phase was water washed, dried, and evaporated to dryness. Addition of ethanol gave 12.2 g (80%) of *p*-methoxybenzyltriphenylsilane, m.p. 107–108° after recrystallization from 1:1 ethanol–hexane.

Method B

To 2.73 g (0.011 mole) of *p*-fluorobenzyltrichlorosilane in ether was added slowly at 0° 3 equivalents of phenyllithium in ether. A negative color test was obtained at the end of the addition. After hydrolysis with

Can. J. Chem. Downloaded from www.nrcresearchpress.com by 210.87.254.105 on 09/05/12
For personal use only.

dilute acid and work-up 3.30 g (79%) of *p*-fluorobenzyltriphenylsilane was obtained, m.p. 98–99° after recrystallization from absolute ethanol.

Method C. Nitration of Benzyltriphenylsilane

To a solution of 15.2 g (0.043 mole) of benzyltriphenylsilane in 150 ml of acetic anhydride was added over 45 min 5 g of red fuming nitric acid, specific gravity 1.59. The reaction became warm. After cooling to room temperature the reaction was poured into ice water and concentrated ammonium hydroxide. The crude product was filtered and crystallized from 1:1 ethanol – ethyl acetate to yield 9.40 g (55%) of *o*-nitrobenzyltriphenylsilane, m.p. 155–156°. This material was shown to be the ortho-nitro compound as follows.* A mixture of 4.0 g (0.01 mole) of the nitro compound, m.p. 155–156°, in 50 ml of a solution prepared from 1 volume of 50% aqueous sodium hydroxide and 7 volumes of ethanol was refluxed for 30 h. After addition of water and ether extraction, the dried ether layers were concentrated and then distilled to yield 1.0 g (73%) of *o*-nitrotoluene, b.p. 50° at 1 mm, identified by the identity of its infrared and n.m.r. spectra with those of an authentic sample. The filtrate from which the ortho-nitro compound was isolated was evaporated to dryness leaving an oil which crystallized from absolute ethanol to give 4.75 g (28%) of *p*-nitrobenzyltriphenylsilane, m.p. 105–115°. Several recrystallizations raised the m.p. to 114.5–116.5°.

p-(N-Acetylamino)-benzyltriphenylsilane.—A suspension of 3.75 g (0.0075 mole) of *p*-nitrobenzyltriphenylsilane in 120 ml of glacial acetic acid and 20 ml of acetic anhydride was shaken under 30 p.s.i. of hydrogen in the presence of PtO_2 for 24 h. Work-up gave 3.35 g of crude water-insoluble product which after recrystallization from methanol gave white *p*-(N-acetylamino)-benzyltriphenylsilane, m.p. 207–208°. Attempted reduction under the same conditions but using glacial acetic acid or ethanol as solvents failed.

Halogenation of Benzylsilanes

p-tert-Butyl-αα-dibromobenzyltriphenylsilane

A mixture of 12.2 g (0.030 mole) of *p-tert*-butyl benzyltriphenylsilane, 10.7 g (0.060 mole) of N-bromosuccinimide and 200 ml of carbon tetrachloride was refluxed for 3 h. A trace of benzoyl peroxide was added to initiate the reaction. On cooling 6.7 g (107%) of succinimide was filtered off, the filtrate was evaporated to dryness under reduced pressure, and the residue on crystallization from ethanol–petroleum ether (90–100°) gave 14.95 g (92%) of product, m.p. 138.5–139.5°.

Other benzylsilanes were similarly halogenated. *o*-Nitrobenzyltriphenylsilane gave only a monobromide even when refluxed for prolonged periods, presumably due to steric hindrance.

Hydrolysis of αα-Dibromobenzylsilanes

Hydrolyses with silver acetate or silver trifluoroacetate were carried out in benzene–acetone–water or ethanol–water media according to previously described techniques (1, 3). Silver trifluoroacetate, prepared by reaction of trifluoroacetic acid with a slurry of silver oxide in benzene, appeared to react more rapidly with dibromides than did silver acetate.

Light-catalyzed Decomposition of Benzoyltriphenylsilane

A solution of 2.5 g (0.0069 mole) of benzoyltriphenylsilane in 50 ml of dry reagent grade methanol was exposed for 4 h to radiation from a General Electric "Bonus Line Mercury Reflector Spot" lamp, by which time the solution was entirely colorless. The excess methanol was removed under reduced pressure, and the residue (a mushy solid below room temperature) was distilled. Two main fractions were obtained. (*a*) Benzaldehyde dimethylacetal, 0.5 g (48%), b.p. 82° at 14 mm, n.m.r. 3.21 δ, singlet (CH_3—O), 5.35 δ, singlet (C—H), and 7.2-7.6 δ, multiplet (C—H aromatic), areas 5.7:1:5.5 (calcd. 6:1:5). The materialw as slightly contaminated with benzaldehyde, as judged by odor, and the presence of weak infrared absorption peaks at 3.65 and 5.85 μ (CH + C=O). (*b*) Triphenylmethoxysilane, 1.7 g (85%), b.p. 165–175° at 0.5 mm, m.p. 56–57°, identified by mixed melting point with an authentic sample.

Benzoyldiphenylphosphine

The compound was prepared as described in the literature (13) and the yellow product was twice distilled to give a 20% yield of material, m.p. 71–80°, b.p. 162–164° at 0.12 mm. An odor of benzaldehyde was noted after distillation, and was observable in the infrared spectrum as bands at 3.65 and 5.85 μ. When air was bubbled through 0.65 g of benzoyldiphenylphosphine in carbon tetrachloride for 15 min, 0.35 g (71%) of white solid, shown by mixed melting point to be diphenylphosphonic acid, m.p. 185°, precipitated. The filtrate was evaporated to dryness and was recrystallized from boiling water to yield 0.10 g (37%) of benzoic acid, m.p. 118–120°, identified by mixed melting point.

ACKNOWLEDGMENTS

This research was supported by Dow Corning Silicones of Canada in the form of a Fellowship to G. E. L. and by the National Research Council of Canada.

**This experiment was performed by D. MacRae.*

Can. J. Chem. Downloaded from www.nrcresearchpress.com by 210.87.254.105 on 09/05/12
For personal use only.

REFERENCES

1. A. G. BROOK. J. Am. Chem. Soc. **79**, 4373 (1957).
2. A. G. BROOK, M. A. QUIGLEY, G. J. D. PEDDLE, N. V. SCHWARTZ, and C. M. WARNER. J. Am. Chem. Soc. **82**, 5102 (1960).
3. A. G. BROOK and J. B. PIERCE. Can. J. Chem. **42**, 298 (1964).
4. D. F. HARNISH and R. WEST. Inorg. Chem. **2**, 1082 (1963).
5. R. N. JONES, W. F. FORBES, and W. A. MUELLER. Can. J. Chem. **35**, 504 (1957).
6. W. F. FORBES and W. A. MUELLER. Can. J. Chem. **35**, 488 (1957).
7. J. TARAKA, S. NAGAKURA, and M. KABAYASHI. J. Chem. Phys. **24**, 311 (1956).
8. C. EABORN and S. H. PARKER. J. Chem. Soc. 126 (1955).
9. R. W. BOTT, C. EABORN, and T. W. SWADDLE. J. Chem. Soc. 2342 (1963).
10. A. G. BROOK and G. E. LEGROW. Unpublished results.
11. C. N. R. RAO, G. K. GOLDMAN, and A. BALASIBRAMANIAN. Can. J. Chem. **38**, 2508 (1960).
12. H. H. JAFFE and M. ORCHIN. Theory and applications of ultraviolet spectra. J. Wiley and Sons, New York, N.Y. 1962. p. 186.
13. K. ISSLEILS and E. PRUBE. Chem. Ber. **92**, 3183 (1959).
14. K. YATES and F. AGOLINI. 1964 Annual Conference of the Chemical Institute of Canada, Kingston, Ontario. June, 1964.
15. A. D. PETROV, E. A. CHERNYSHEV, and N. F. TALSTIKOVA. Dokl. Akad. Nauk SSSR **118**, 957 (1958); Chem. Abstr. **52**, 12787 (1958).
16. H. R. ALLCOCK. Can. J. Chem. **41**, 954 (1963).
17. H. GILMAN, M. A. PLUNKETT, and G. E. DUNN. J. Am. Chem. Soc. **73**, 1686 (1951).
18. R. A. BENKESER and F. J. RIEL. J. Am. Chem. Soc. **73**, 3472 (1951).
19. M. G. VAN CAMPEN, D. F. MEISNER, and S. M. PARMERTER. J. Am. Chem. Soc. **70**, 2296 (1948).

Can. J. Chem. Downloaded from www.nrcresearchpress.com by 210.87.254.105 on 09/05/12
For personal use only.

Can. J. Chem. Downloaded from www.nrcresearchpress.com by 210.87.254.40 on 09/05/12
For personal use only.

CYCLOHEXENE-3,3,6,6-d_4

A USEFUL COMPOUND FOR THE STUDY OF MECHANISM AND STRUCTURE[1]

SAUL WOLFE AND P. G. C. CAMPBELL[2]
Department of Organic Chemistry, Gordon Hall, Queen's University, Kingston, Ontario
Received November 17, 1964

ABSTRACT

The title compound (I) was prepared by Diels–Alder reaction of butadiene-1,1,4,4-d_4 with ethylene. The considerations which led to the synthesis of I are presented and some examples are then given of how use of I can simplify the study of, and provide new information about, a number of different kinds of problems. In the proton magnetic resonance (n.m.r.) spectra of the products of additions to I, the tertiary protons usually appear as clearly defined quartets. Since $|J_{AB}|$ can be read directly from these spectra, both the stereochemistry of the additions and the conformations of the products can be deduced. Thus, oxymercuration of I is clearly a *trans* addition and Na/Hg reduction of the mercury takes place with retention of configuration. When the second step is performed in D_2O, the oxymercuration–reduction sequence represents a convenient route for the *trans* addition of DOH to a double bond. Deuteroboration provided an example of *cis* addition of DOH to I. Acid-catalyzed hydration of I resulted in scrambling of the deuterium atoms. The value of $G_{Hg/OH}$ is small; $G_{Br/OH}$ is 600 cal/mole. The position of the double bond in a product resulting from allylic substitution of I is determined by integration of the n.m.r. spectrum. Relative to I, the possibilities are no rearrangement, 50% rearrangement, and 100% rearrangement of the double bond. The first product of allylic substitution by *N*-bromosuccinimide shows no rearrangement; therefore, this reaction does not require a "free" radical intermediate. The structure of an adduct formed during allylic acetoxylation of I by mercuric acetate (the Treibs reaction) has been determined.

INTRODUCTION

This is Part I of a series which will deal with the use of selectively deuterated cyclohexenes in the study of mechanism and structure. The purpose of this paper is to present the considerations which led to the synthesis of cyclohexene-3,3,6,6-d_4 (I) along with some of the ways in which the compound seems to be useful. Subsequent papers in this series will be concerned with detailed consideration of specific reactions.

APPLICATION OF I TO THE STUDY OF ALLYLIC SUBSTITUTION

The replacement of a hydrogen allylic to a double bond by oxygen or halogen represents an established method for the introduction of additional functionality into an organic compound; however, it is often observed that substitution is accompanied by rearrangement of the allylic system. Though rearrangements of allylic compounds are well known and have been the subject of numerous investigations (1), it is perhaps less well appreciated that varying amounts of rearrangement can also occur during the initial substitution, with the result that the product may have the new substituent at one end of the original double bond. In fact, we do not know of any reaction which will lead to allylic substitution of an olefin without rearrangement. Among the more common reagents which can effect allylic substitution, *t*-butylperesters[3] (2), lead tetraacetate[4] (7), unsensitized photooxygenation (10), *N*-bromosuccinimide (11), and chromium trioxide (12) are reported to

[1]*Presented in part at the 47th Annual Conference of the Chemical Institute of Canada, Kingston, June 1964.*
[2]*Holder of a Woodrow Wilson Fellowship, 1963–1964, and of a National Research Council Studentship, 1964–1965.*
[3]*The original reports (3, 4) suggested that t-butylperesters gave substitution without rearrangement and a rather elaborate mechanism had to be proposed (3); this mechanism was subsequently made invalid by the finding that products of rearrangement are present in the reaction mixtures (5, 6).*
[4]*Oxidation of α-pinene was reported by Criegee (7, 8) to give trans-verbenol acetate (i), the unrearranged product;*

give partial rearrangement; sensitized photooxygenation (13) and mercuric acetate (14, 15) afford mainly rearranged products.

Though some workers have utilized rather ingenious methods to move a new substituent from the synthetically less desirable end of an allylic system[5] (16), on the whole it is difficult to predict the position of the new substituent or to know which reaction will best suit a given synthetic requirement.

From the foregoing it would appear that the synthetic utility of allylic substitution might be improved if the timing of rearrangement or the relationship between substrate structure and the position of the new substituent could be determined. Compound I should be useful for the study of these problems for two reasons: first, the extent of rearrangement during allylic substitution of this compound can be easily determined by nuclear magnetic resonance spectroscopy (n.m.r.); secondly, if rearrangement does occur, it can be predicted that either 50% or 100% rearrangement will be observed. The rationale is shown in Chart 1. A priori, five different mechanisms can be considered: *A*, a carbonium ion mechanism in which the reagent, acting as an electrophile (17), removes a deuteride ion from the allylic position. The resulting carbonium ion should be mesomeric (18) and, unless the deuterium atoms exert an unusually large secondary isotope effect, the substituent, Z, will then be found with equal probability at positions *a* and *b*. This corresponds to 50% rearrangement. In fact, it has been found (*vide infra*) that the deuterium atoms do not display an observable isotope effect. In mechanism *B*, the reagent can remove a deuterium atom; the resulting radical should be mesomeric and, as with mechanism *A*, the product will correspond to 50% rearrangement. In mechanism *C*, the reagent, Z, attacks the double bond; concerted rearrangement of the resulting π-complex will then lead to 100% rearrangement, with the new substituent exclusively at position *a*. It would be anticipated that processes *A*–*C* would be more important than *D*, the direct replacement of allylic deuterium. Finally, as shown in *E*, substitution might be the result of addition of the reagent YZ, followed by elimination of DY or DZ. Mechanism *E* would lead to 100% rearrangement but should be distinguishable from *C* if the intermediate can be detected.

subsequent work (9), however, suggests that the initial product is actually cis-2-acetoxypin-3-ene (ii), the rearranged compound, and that (ii) is converted to (i) upon distillation.

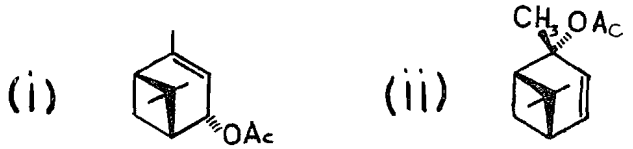

[5]*In their total synthesis of dl-atisine, Nagata et al. (16) accomplished the transformation as follows:*

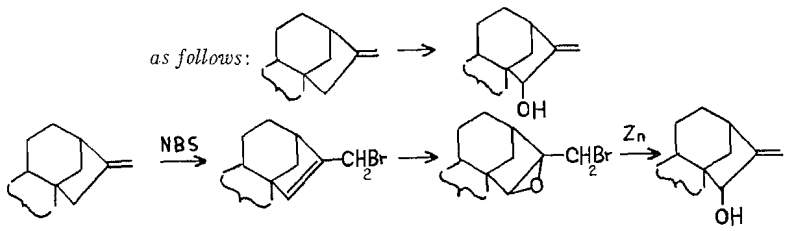

Can. J. Chem. Downloaded from www.nrcresearchpress.com by 210.87.254.40 on 09/05/12
For personal use only.

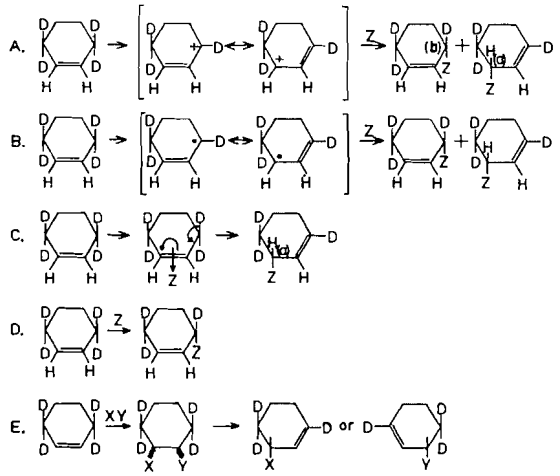

CHART 1. The various possible mechanisms for allylic substitution of I: *A*, carbonium ion mechanism; *B*, free radical mechanism; *C*, π-complex mechanism; *D*, direct displacement mechanism; *E*, addition–elimination mechanism.

With compound I as the substrate, determination of the extent of rearrangement in any given reaction can be performed by integration of the n.m.r. spectrum. Products formed without rearrangement will have two vinyl protons and no allylic protons; products of 50% rearrangement will show a vinyl:allyl proton ratio of 3; and products of 100% rearrangement will show a vinyl:allyl proton ratio of 1.

APPLICATION OF I TO THE STUDY OF ELECTROPHILIC ADDITIONS TO A DOUBLE BOND

The use of n.m.r. spectroscopy to determine configuration and conformation is based on experimental (19) and theoretical equations (20) relating vicinal coupling constants to dihedral angle. Although no single equation can be applied to all organic compounds (21), for substituted cyclohexanes it is well established that $|J_{aa}|$ is of the order of 10–11 c/s, and $|J_{ee}|$ ($\cong |J_{ea}|$) is 2.5–3.5 c/s (22). Therefore, if $|J_{AB}|$ could be determined for the product of addition of XY to the double bond of cyclohexene (where H_A and H_B are the protons geminal to X and Y respectively in the product), then it should be possible to deduce the stereochemistry of the addition. However, since H_A and H_B are also coupled to protons at C_3 and C_6, in practice the experimental determination of $|J_{AB}|$ is too difficult. Several methods have been developed to overcome this problem. The spectra can be simplified by the use of lower temperatures (23); structural information can be obtained by measurement of the widths of the unresolved multiplets (24, 25). But clearly the most useful simplification that could be introduced would be the removal of the factors which complicate the AB pattern in the n.m.r. spectra, i.e., the removal of the protons at C_3 and C_6.

Thus it would seem that I should be a useful compound for the study of additions to a double bond. The rationale for a number of different situations is shown in Chart 2. If an unsymmetrical reagent XY adds *cis* to the double bond of I, then, regardless of the position of the conformational equilibrium, $|J_{AB}|$ will be 2.5–3.5 c/s.[6] On the other hand,

[6]*Unless the molecule adopts a true boat conformation. However, it is now recognized that the boat is disfavored relative to the twist conformation (26, 27) and in this conformation the dihedral angle (33°) between* H_A *and* H_B *would lead to a* $|J_{AB}|$ *of 6–7 c/s.*

Can. J. Chem. Downloaded from www.nrcresearchpress.com by 210.87.254.40 on 09/05/12
For personal use only.

the observed $|J_{AB}|$ for *trans* addition of XY will depend on the position of the conformational equilibrium between the ee and aa isomers; if X and Y are axial, then $|J_{AB}|$ will be 2.5–3.5 c/s; if X and Y are equatorial, $|J_{AB}|$ should be 10–11 c/s. It would be anticipated that only rarely should the conformational situation make the interpretation of $|J_{AB}|$ ambiguous (e.g., *trans* addition and substituents diaxial or *cis* addition and the ring in a twist conformation), but for these cases determination of $|J_{AB}|$ at various temperatures should remove the ambiguity. A corollary of these considerations is that once the stereochemistry of the addition of XY to cyclohexene is known, then the magnitude of $|J_{AB}|$ can be used to obtain information concerning the conformational equilibria.

For *trans* addition of X_2 to I, H_A and H_B are equivalent and do not couple. One would expect a single peak at room temperature (corresponding to the averaged chemical shift of the aa and ee conformers) splitting into two peaks at lower temperatures as the rate of the aa $\rightleftarrows$ ee interconversion is slowed down. For *cis* addition of X_2 to I, one would expect a single peak at room temperature, splitting to a quartet at lower temperatures because of the different chemical shifts of the equatorial and axial protons (28, 29).

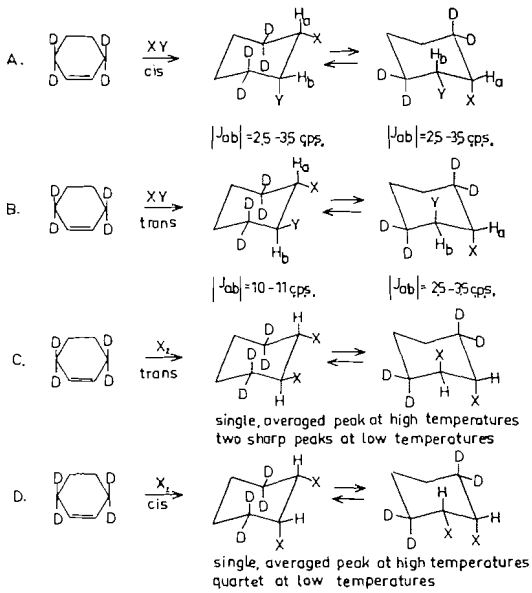

CHART 2. The various possibilities for electrophilic additions of XY and X_2 to the double bond of I; *A*, *cis* addition of XY; *B*, *trans* addition of XY; *C*, *trans* addition of X_2; *D*, *cis* addition of X_2.

RESULTS AND DISCUSSION

The preparation of cyclohexene from butadiene and ethylene was reported a number of years ago (30), but the Diels–Alder reaction as a route to deuterated cyclohexenes does not seem to have been tried. For the synthesis of cyclohexene-3,3,6,6-d_4 the required reagents are ethylene and butadiene-1,1,4,4-d_4. Since the latter compound is now available through the elegant procedure of Cope and co-workers (31), it was anticipated that the preparation of I would be straightforward. Because we do not have the equipment which is required for the Diels–Alder reaction, we asked Merck, Sharp and Dohme of Canada to undertake the synthesis of I. The product which we received had the n.m.r. spectrum shown in Fig. 1; the spectrum of ordinary cyclohexene is also shown in Fig. 1. The integrated intensities of the two peaks of the deuterated compound were 1:2, as required

Can. J. Chem. Downloaded from www.nrcresearchpress.com by 210.87.254.40 on 09/05/12
For personal use only.

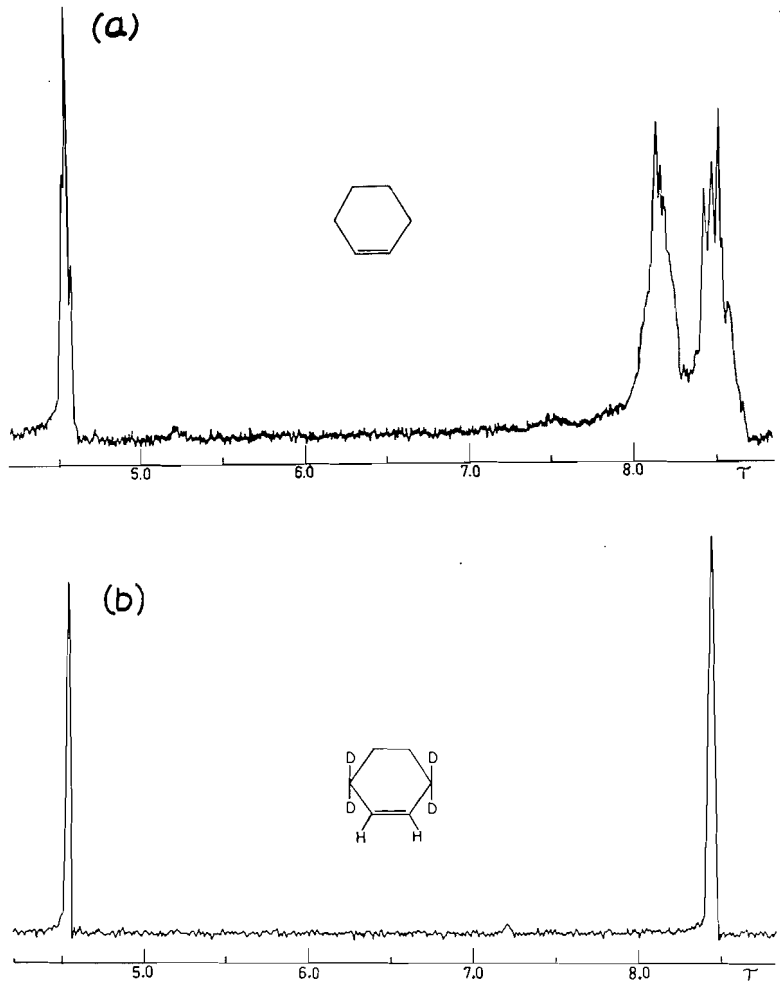

FIG. 1. (*a*) Nuclear magnetic resonance spectrum of cyclohexene in CCl_4; (*b*) n.m.r. spectrum of I in CCl_4.

for cyclohexene-3,3,6,6-d_4. It is clear that the Diels–Alder reaction took place without scrambling of the deuterium atoms.[7]

The n.m.r. spectrum of 2-deuteroxycyclohexylmercuric acetate, prepared by treatment of cyclohexene with mercuric acetate in D_2O, is shown in Fig. 2*a*; the proton geminal to the —OD appears as an unresolved multiplet at τ 5.85; the proton geminal to mercury is the sextet centered at τ 7.1. First order analysis of this sextet indicates that this proton is coupled (ca. 10 c/s) large to two other protons and small (ca. 3 c/s) to a third. The product of oxymercuration of I gives the much simpler spectrum shown in Fig. 2*b*. The AB quartet shows a coupling constant of 10.3 c/s.[8] The magnitude of this coupling constant is near the maximum expected for two vicinal axial protons; therefore, the reaction of mercuric acetate with cyclohexene in D_2O proceeds by *trans* addition (33, 34).

[7]*Compound I is available from Merck at a cost of about $42 per gram.*

[8]*The spectrum of Fig. 2a is apparently identical with one described by Anderson and Henry (32). These authors concluded that the oxymercuration of cyclohexene is trans. While we are in agreement with Anderson and Henry, it should be recognized that their interpretation is qualitative only since $|J_{AB}|$ cannot be obtained from the spacings of the sextet.*

Can. J. Chem. Downloaded from www.nrcresearchpress.com by 210.87.254.40 on 09/05/12
For personal use only.

Can. J. Chem. Downloaded from www.nrcresearchpress.com by 210.87.254.40 on 09/05/12
For personal use only.

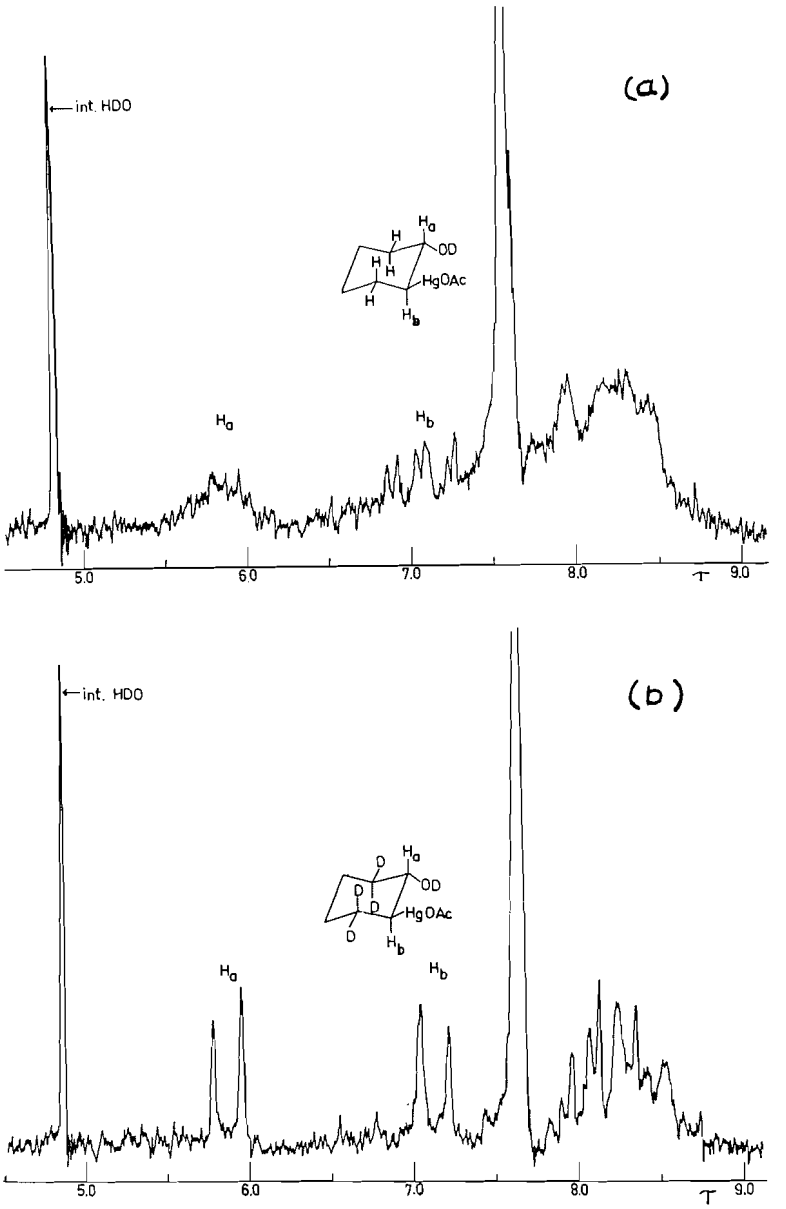
(a)
←int. HDO
H
H
H
H
H
H
OD
HgOAc
H
H
H
H
H
H

TABLE I

Oxymercuration of cyclohexene-3,3,6,6-d_4

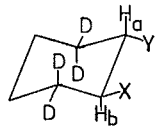

X	Y	Solvent	$\|J_{AB}\|$, c/s
HgOAc	OD	D_2O	10.3
HgCl	OD	Pyridine	10.0
HgOAc	OCH_3	$CDCl_3$	10.1
HgCl	OCH_3	$CDCl_3$	10.1

Jensen has reported (35) that the A-value ($F_{(axial)} - F_{(equatorial)}$) for the chloromercuric grouping is zero. Assuming 90% of the diequatorial conformation for the product of oxymercuration of I, we have, at 40°,

$$\Delta F = -2.303RT \log 90/10 = 1\,400 \text{ cal/mole} = A_{Hg} + A_{OH} - G_{Hg/OH},$$

where G is the parameter introduced by Lemieux and Lown (19) to estimate *gauche* interactions. Using our experimental value of 1 400 cal for ΔF, Jensen's value of 0 for A_{Hg}, and Anet's value of 1 250 cal/mole for A_{OH} in D_2O (36), we conclude that the G-value for the hydroxyl–mercury interaction is approximately 0.

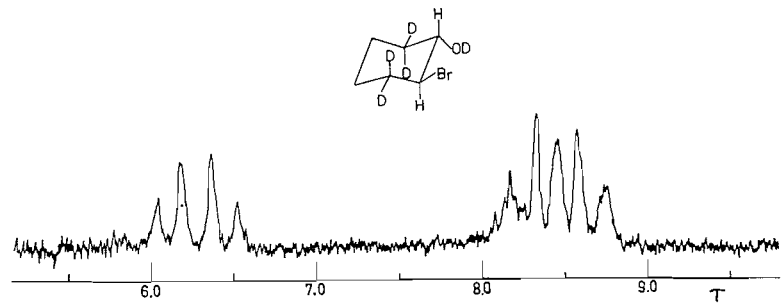

FIG. 3. Nuclear magnetic resonance spectrum of *trans*-2-deuteroxycyclohexyl bromide-3,3,6,6-d_4 in CCl_4.

Figure 3 shows the n.m.r. spectrum in CCl_4 of the *trans*-2-deuteroxycyclohexyl bromide prepared by treatment of I with N-bromosuccinimide in D_2O (37). Here $|J_{AB}|$ is 9.0 c/s; this means that the ratio of ee to aa conformers is approximately 85/15. Using the values A_{Br} = 600 cal/mole (38) and A_{OH} = 1 000 cal/mole (CCl_4), we estimate that $G_{Br/OH}$ is ca. 600 cal/mole. Clearly it is possible to extend this method of estimation of G-values to many pairs of groups. Studies of this nature are underway.

Various methods have been reported for the replacement of mercury by hydrogen. These include Na/Hg in water (39) and sodium borohydride (40). We were unable to convert *trans*-2-hydroxycyclohexylmercuric acetate or the derived mercuric chloride to cyclohexanol with either sodium borohydride or lithium aluminium hydride. Instead, under all conditions tried, reductive *elimination* to cyclohexene was observed (41). We had hoped, using the corresponding deuterohydrides, to determine the stereochemistry of the reduction. However, the oxymercuration products were smoothly converted to cyclohexanol by shaking with Na/Hg in water. Figure 4 shows the n.m.r. spectrum in carbon tetrachloride of the product obtained by treatment with Na/Hg in D_2O of the

Can. J. Chem. Downloaded from www.nrcresearchpress.com by 210.87.254.40 on 09/05/12
For personal use only.

trans-2-deuteroxycyclohexylmercuric acetate derived from I. The doublet at τ 6.55 represents the proton geminal to the deuteroxy grouping, and the coupling constant (9.5 c/s) is just that expected *if the replacement of mercury by deuterium occurred with retention of configuration.* This may be calculated as follows: from the A-value for hydroxyl of 1 000 cal (36), the proportions of equatorial and axial hydroxyl are 88:12; therefore, the hydrogen geminal to deuteroxyl in the hexadeuterocyclohexanol formed by *trans* addition of D_2O to I should show a coupling constant of $0.88 \times 10.5 + 0.12 \times 3.5 = 9.7$ c/s, a value which is in good agreement with the above, observed value.[9]

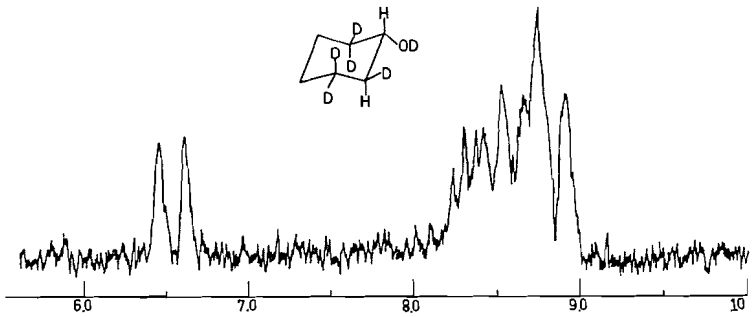

FIG. 4. Nuclear magnetic resonance spectrum in CCl_4 of cyclohexanol-2,3,3,6,6-d_5 from the Na/Hg reduction.

Although it has been pointed out by others (42) that the combination of oxymercuration followed by reductive displacement of mercury represents a useful and experimentally easy method for the addition of HOR to a double bond, the above results provide the further information that the overall addition is *trans*. Clearly, it is now possible by *trans* addition of DOR onto a double bond to effect stereospecific deuterium labelling and thus provide compounds which may be useful for further work.

The hydroboration reaction has been reported to proceed by *cis* addition of HOH to a double bond (43, 44). The n.m.r. spectrum shown in Fig. 5 is that of the 2,3,3,6,6-pentadeuterocyclohexanol obtained by treatment of I with lithium aluminium deuteride and boron trifluoride etherate, followed by oxidation with alkaline hydrogen peroxide (44). The hydrogen geminal to hydroxyl shows the doublet with $|J| = 3.8$ c/s at τ 6.55. The doublet shows considerable line broadening due to coupling of this proton with the adjacent deuterium atoms. Confirmation of this was obtained by a deuterium decoupling experiment[10] which led to the sharp doublet, $|J| = 3.8$ c/s, also shown in Fig. 5. The magnitude of this coupling constant is in agreement with expectation (part A of Chart 2).[11]

Since the two pentadeuterocyclohexanols resulting from *cis* and *trans* addition of DOH to I were available, it seemed that it was now possible to study the stereochemistry of acid-catalyzed hydration of cyclohexene. The conversion of ordinary cyclohexene to cyclohexanol could be performed by shaking cyclohexene for 1 h at 50° with a mixture

[9]*No mechanistic significance should be attached to this conclusion. Though retention of configuration is commonly observed in the cleavage of organomercury compounds (35),* Na/Hg *reduction is a heterogeneous reaction. Traylor and Baker (34) found retention in the* Na/Hg *reduction of exo-cis-3-hydroxy-2-norbornylmercuric chloride; in this case retention would be sterically favored.*

[10]*We thank Professor F. A. L. Anet for assistance with this experiment.*

[11]*Actually, the cis addition of* DOH *observed here is the result of two reactions: reaction of I with* B_2D_6 *to form a trialkylborane, followed by oxidation of the borane to cyclohexanol. An overall cis addition could occur by a (generally accepted) route involving cis addition of* B_2D_6 *and retention of configuration during the oxidation, or by trans addition of* B_2D_6 *followed by inversion of configuration during the oxidation.*

Can. J. Chem. Downloaded from www.nrcresearchpress.com by 210.87.254.40 on 09/05/12
For personal use only.

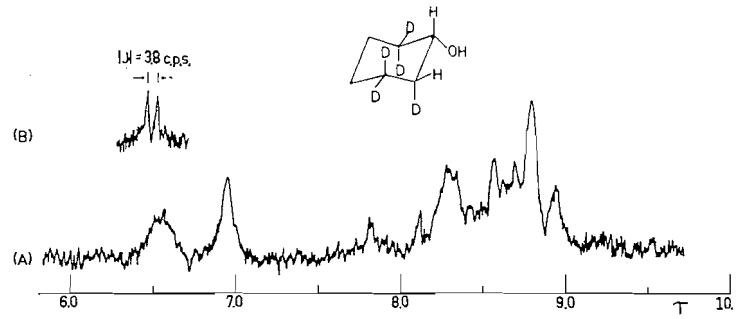

FIG. 5. Nuclear magnetic resonance spectrum in CCl_4 of cyclohexanol-2,3,3,6,6-d_5 from deuteroboration of I.

of 75% H_2SO_4 and CCl_4. However, repetition of the experiment with I and D_2SO_4/CCl_4 gave a cyclohexanol whose n.m.r. spectrum, after deuterium decoupling,[10] showed that considerable scrambling of deuterium had occurred. This reaction is presently being examined in more detail.

The results described above show that useful information can be obtained from studies of additions of unsymmetrical reagents onto the double bond of I. We now turn to some results obtained from allylic substitution experiments. Figure 6*a* shows the n.m.r. spectrum of the CCl_4 reaction mixture obtained by treatment of a 1% w/v solution of I with *N*-bromosuccinimide under the usual conditions for allylic bromination (45); Fig 6*b* shows the spectrum obtained upon concentration or further warming of this solution. The spectrum of an authentic sample of 3-bromocyclohexene is shown in Fig. 7; the

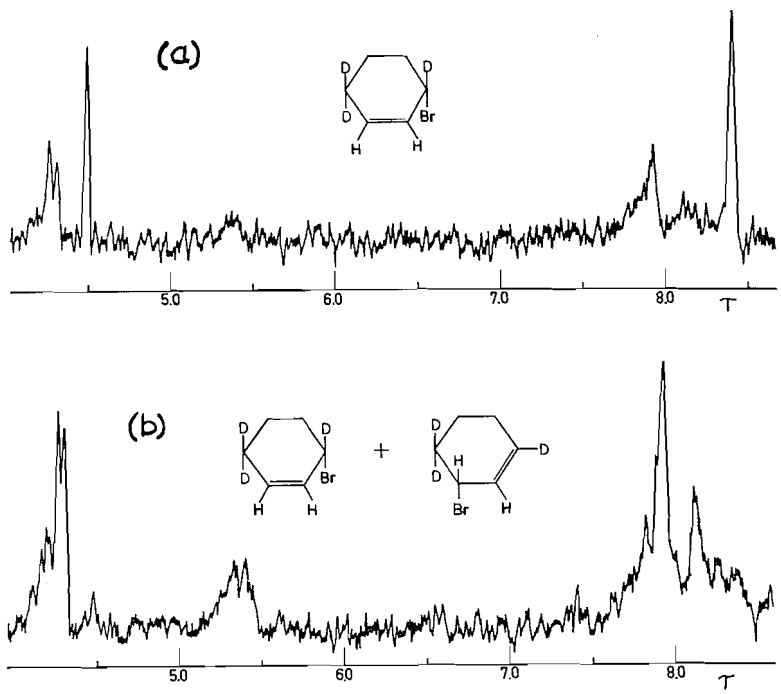

FIG. 6. (*a*) Nuclear magnetic resonance spectrum of the mixture obtained from the reaction of I with *N*-bromosuccinimide in CCl_4; (*b*) n.m.r. spectrum obtained upon concentration of the solution of Fig. 6*a*.

Can. J. Chem. Downloaded from www.nrcresearchpress.com by 210.87.254.40 on 09/05/12
For personal use only.

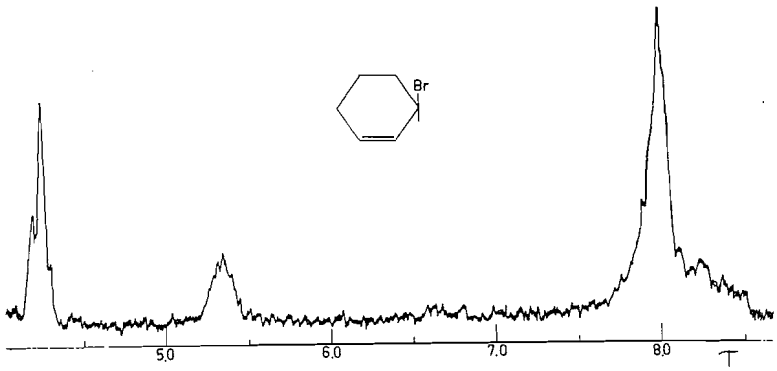

FIG. 7. Nuclear magnetic resonance spectrum of 3-bromocyclohexene in CCl_4.

multiplet (2H) at τ 4.25 represents the vinyl protons and the multiplet (1H) at τ 5.35 is the proton geminal to the allylic bromine. Figure 6*a* shows some unreacted I, as well as absorption at τ 4.25 and weak absorption at τ 5.35. *The integral at τ 5.35 is considerably less than one-third of the integral at τ 4.25.* This experiment has been repeated many times, with essentially the same result. Differences between experiments seemed to be related to the time interval between the end of the reaction and the taking of the n.m.r. spectrum. This result means that the initial product of the *N*-bromosuccinimide reaction contained less than 50% of II. On the other hand, the integrated intensities (3:1) of the peaks at τ 4.25 and τ 5.35 in the spectrum of Fig. 6*b* is just that expected for a 1:1 mixture

II: 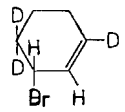 III: 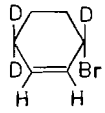

of II and III. Gas chromatography confirmed that the mixture which gave the spectrum in Fig. 6*a* contained only I and 3-bromocyclohexene. Thus the primary product of allylic bromination of I with *N*-bromosuccinimide is III, which subsequently rearranges to a mixture containing equal amounts of II and III. Three conclusions may therefore be drawn. (i) The formation of 3-bromocyclohexene is not the result of a "free" radical reaction; (ii) the rearrangement of the primary product does proceed via a symmetrical intermediate; (iii) the deuterium atoms do not affect the expected 1:1 product distribution when a mesomeric intermediate is formed. Several interpretations of this result can be suggested, but it appears to us that the most reasonable explanation is that the radical chain reaction which is known to lead to allylic bromination (46, 47, 48), *occurs on the surface of the N-bromosuccinimide* (45). Detailed discussion of this point and the results of other experiments which we have carried out to test this explanation will be presented separately.

The demonstration that oxymercuration of I is a *trans* addition is in accord with the view that the reaction proceeds via a π-complex (IV) which collapses to a mercurinium ion (V) (34, 49). We felt that the Treibs reaction (14) should also involve the intervention of these initial steps. In water or alcohol the mercurinium ion then opens to give the product of *trans* addition while in hot acetic acid a different series of steps starting with IV or V leads to cyclohexenyl acetate.

Can. J. Chem. Downloaded from www.nrcresearchpress.com by 210.87.254.40 on 09/05/12
For personal use only.

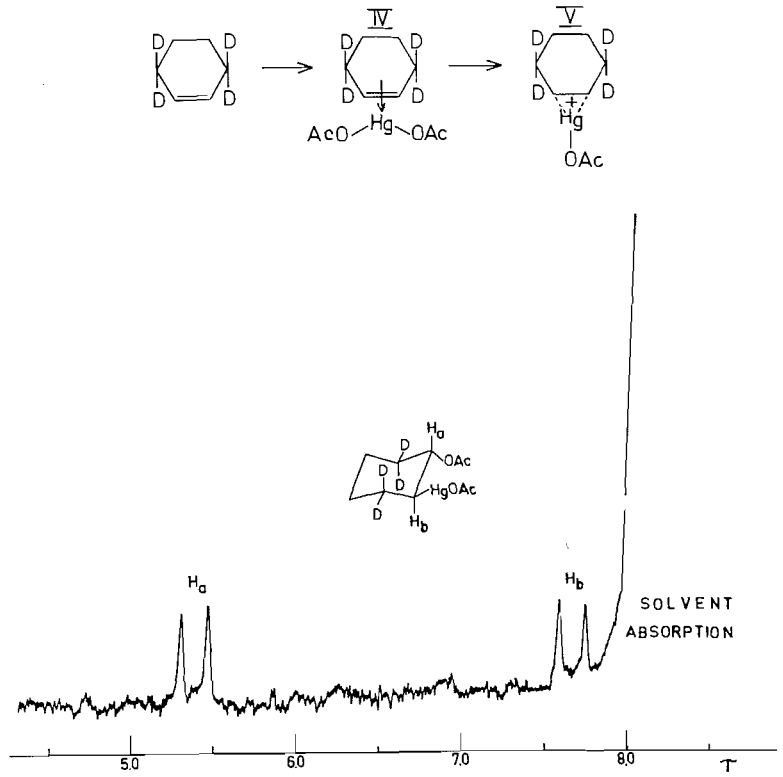

FIG. 8. Nuclear magnetic resonance spectrum of the mixture obtained upon treatment of I with $Hg(OAc)_2$ in glacial acetic acid at 70°.

Treatment of I with mercuric acetate in acetic acid at 65° resulted in the immediate and complete disappearance of the vinyl protons from the n.m.r. spectrum and the concomitant appearance of a new series of peaks; the spectrum is shown in Fig. 8. There was no further change in this spectrum during the next 20 h. Though the reaction mixture at this stage apparently contained no unreacted olefin, attempted isolation of the product gave mainly cyclohexene with less than 10% of 3-acetoxycyclohexene. This result along with the n.m.r. spectrum suggested that either VI or VII was formed during the Treibs reaction.

VI VII

Either VI or VII could show the observed AB quartet in the n.m.r. spectrum with the indicated chemical shifts for the A and B protons. The reversion of VI to cyclohexene could then occur as shown (50).

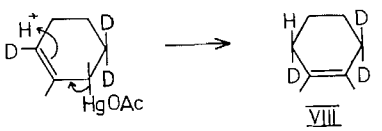

VIII

Can. J. Chem. Downloaded from www.nrcresearchpress.com by 210.87.254.40 on 09/05/12
For personal use only.

On the other hand, solvolysis of VI would give 3-acetoxycyclohexene (51).

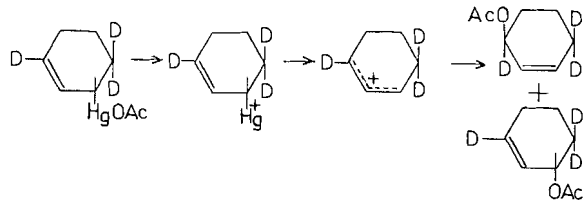

Conversion of VII to cyclohexene is the usual acid-catalyzed demercuration reaction (52); decomposition of VII to 3-acetoxycyclohexene could occur in several ways (15).

That the compound formed during the Treibs reaction is VII was established by a study of the n.m.r. spectrum of the recovered deuterated cyclohexene. As indicated above, reversion of VI to cyclohexene gives VIII, while demercuration of VII gives I. In practice, the conversion of the intermediate to cyclohexene was best accomplished by warming the mercuric acetate – cyclohexene – acetic acid reaction mixture with zinc dust; under these conditions quantitative reversion to cyclohexene occurred. The cyclohexene thus obtained was identical with I. If VI had been the intermediate, reaction with zinc in ordinary acetic acid could not have restored the deuterium atom lost in the formation of VI. Therefore, the Treibs reaction involves the quantitative formation of an *adduct*. The mechanism by which the mercuric acetate – olefin adduct decomposes to give an allylic acetate is presently being studied. It is not yet known whether the adduct is a necessary intermediate or is formed reversibly from a mercurinium ion which can also decompose irreversibly to allylic acetate.[12]

EXPERIMENTAL

The n.m.r. spectra were obtained on a Varian A-60 spectrometer, with tetramethylsilane (10% in chloroform) as an external standard. The deuterium decoupling experiment on cyclohexanol-2,3,3,6,6-d_5 was performed by Professor F. A. L. Anet on a 40 Mc instrument at the University of Ottawa. The solvents for n.m.r. samples were dried by conventional means. Gas chromatographic separations were made on a GC-2 instrument; the column packing was 1% SE-30 on Embacel.

Reaction of I with Mercuric Acetate in Deuterium Oxide

To 70 mg (0.82 mmole) of I in a 1 ml vial were added 270 mg (0.85 mmole) of mercuric acetate and 1 ml of deuterium oxide. The vial was then capped and shaken vigorously for 20 min, whereupon the solution became clear. The solution was allowed to stand for 70 min with occasional shaking. The reaction mixture then gave the n.m.r. spectrum shown in Fig. 2*b*. To the above solution of *trans*-1-deuteroxy-2-acetoxymercuricyclohexane-3,3,6,6-d_4 was added a solution of 0.65 g of sodium chloride in 4 ml of water. A copious

[12]*From the reaction of allylbenzene with mercuric acetate the adduct IX can be isolated in 90% yield. Heating this compound in refluxing acetic acid leads to quantitative precipitation of mercury and formation of X in 80–90% yield. Deuterium-labelling experiments show that the secondary acetate group is lost during the transformation of IX to X (53).*

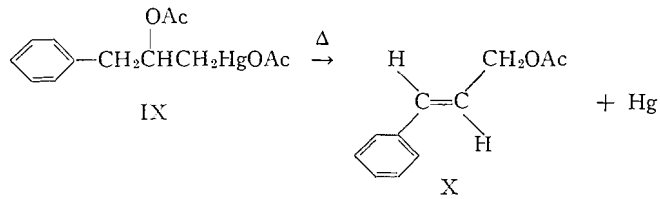

After this paper was submitted for publication, a paper by Wiberg and Nielsen appeared (54) with some additional observations on the Treibs reaction. These workers observed 50% rearrangement in the conversion of cyclohexene-1,2-^{13}C to cyclohexenyl acetate; this result means that a mesomeric intermediate is formed during the reaction. Wiberg and Nielsen suggest that a mercurinium ion partitions itself between addition of acetate to form an adduct and loss of a proton to give an allylmercuriacetate. The mesomeric intermediate is then formed during the solvolysis of the latter.

Can. J. Chem. Downloaded from www.nrcresearchpress.com by 210.87.254.40 on 09/05/12
For personal use only.

white precipitate formed immediately. The mixture was cooled to 0°; the precipitate was collected and dried *in vacuo* at 80°. The yield of *trans*-1-hydroxy-2-chloromercuricyclohexane-3,3,6,6-d_4 was 238 mg (85%). This product was dissolved in 0.7 ml of dry pyridine for determination of the n.m.r. spectrum.

Reaction of I with Mercuric Acetate in Methanol

A solution was prepared containing 60 mg (0.70 mmole) of I in 2.5 ml of absolute methanol. To this solution was added 233 mg (0.73 mmole) of mercuric acetate. The resulting solution was stirred at room temperature for 1 h. The solvent was then completely removed *in vacuo*, and the resulting viscous oil was dissolved in 0.7 ml of deuterochloroform and the n.m.r. spectrum was obtained. The deuterochloroform was then removed *in vacuo*. To the residue was added a solution of 0.56 g of sodium chloride in 5 ml water. The resulting mixture was shaken for 5 min and was then cooled to 0°. The precipitate which formed was collected and dried. The yield of *trans*-1-methoxy-2-chloromercuricyclohexane-3,3,6,6-d_4 was 241 mg (96%). This product was dissolved in 0.8 ml of deuterochloroform for determination of the n.m.r. spectrum.

Reaction of I with N-Bromosuccinimide in Deuterium Oxide

A mixture of I (60 mg, 0.7 mmole), *N*-bromosuccinimide (130 mg, 0.7 mmole) and deuterium oxide (1 ml) was shaken for 20 min, by which time the *N*-bromosuccinimide had dissolved. Carbon tetrachloride (1 ml) was added and the organic layer, after drying, gave the n.m.r. spectrum shown in Fig. 3.

Reduction of trans-1-Hydroxy-2-chloromercuricyclohexane-3,3,6,6-d_4 with Sodium Amalgam in Deuterium Oxide

Freshly prepared *trans*-1-hydroxy-2-chloromercuricyclohexane-3,3,6,6-d_4 (270 mg) was stirred in 1 ml of water with 50 mg of sodium bicarbonate to remove traces of the acetic acid produced during the oxymercuration. The mixture was cooled in an ice bath and the precipitate was collected. After drying *in vacuo* at 80° the yield was 226 mg. This relatively large loss was due in part to the partial conversion of the water-insoluble chloromercuricyclohexane to the water-soluble hydroxymercuricyclohexane. The 226 mg (0.67 mmole) of *trans*-1-hydroxy-2-chloromercuricyclohexane-3,3,6,6-d_4 were transferred to a 5 ml volumetric flask. Into this flask were weighed 7.5 g of 2% sodium amalgam and 1.45 g of deuterium oxide. The flask was securely stoppered and was then shaken at room temperature for 6 h. The deuterium oxide layer was decanted and was then extracted with 2 ml of carbon tetrachloride. The carbon tetrachloride extract was dried by filtration through a column of anhydrous sodium sulfate. The n.m.r. spectrum of the filtrate is shown in Fig. 4.

Deuteroboration of I

A solution of 100 mg (1.16 mmole) of I in 3 ml of diethyl ether (freshly distilled from $LiAlH_4$) was placed in a three-necked 25 ml flask. This flask was fitted with a stirrer, a dropping tube, and a condenser with a nitrogen inlet. The reaction flask was maintained at 0°. A solution of 178 mg (1.25 mmole) boron trifluoride etherate in 2 ml of dry diethyl ether was added to the ether solution of I. Then a suspension of 94 mg (2.45 mmole) of lithium aluminium deuteride in 5 ml of dry diethyl ether was gradually added with vigorous stirring. The addition required 1 h. The ice bath was then removed, and the reaction mixture was stirred for an additional 2 h. The mixture was then cooled again to 0°, and 0.75 ml of acetone was added to destroy any excess lithium aluminium deuteride. Saturated sodium sulfate (2 ml) was then added followed by 1.5 g of solid sodium sulfate. The solution was decanted from the precipitated inorganic salts and the solvent was removed *in vacuo*. The residual oil was dissolved in 3 ml of 90% ethanol and 100 mg of sodium hydroxide were added, followed by six 0.2 ml portions of 30% hydrogen peroxide, the solution being warmed at 70° for 5 min between each addition. The mixture was diluted with 9 ml of water and extracted with three 10 ml portions of diethyl ether. The combined ether extracts were washed with water, dried over anhydrous sodium sulfate, and concentrated *in vacuo*. The oil remaining after the complete removal of the diethyl ether was dissolved in 0.7 ml of carbon tetrachloride. This solution gave the n.m.r. spectrum shown in Fig. 5.

Reaction of I with N-Bromosuccinimide in Carbon Tetrachloride

To a solution of I (60 mg, 0.7 mmole) in carbon tetrachloride (5 ml) were added *N*-bromosuccinimide (130 mg, 0.7 mmole) and benzoyl peroxide (2 mg). The mixture was then heated to reflux temperature and the heat source was removed while the mixture was illuminated with a 100 W Photoflood No. 2 lamp. The illumination was stopped after 6 min. Filtration of the reaction mixture then gave a solution whose n.m.r. spectrum is shown in Fig. 6*a*; concentration of this solution to 1 ml led to the n.m.r. spectrum shown in Fig. 6*b*.

Reaction of I with Mercuric Acetate in Glacial Acetic Acid

A solution was prepared containing 60 mg (0.70 mmole) of I in 0.85 ml of glacial acetic acid. The n.m.r. spectrum of this solution showed the characteristic strong unsplit absorption of the olefinic protons in I at τ 4.5. The solution was then decanted from the n.m.r. tube and 230 mg (0.70 mmole) of mercuric acetate were added. The mixture was warmed to aid solution of the mercuric acetate, and was then returned to the n.m.r. tube. The n.m.r. spectrum (70 s after mixing) now showed no olefinic absorption, but did show two new doublets at τ 5.4 and τ 7.6 forming a quartet with $|J_{AB}|$ 10.0 c.p.s. This spectrum is shown in Fig. 8. The reaction mixture was kept at 65 °C for 20 h and there was no further change in the n.m.r. spectrum. Then 140 mg (2.14 mmole) of zinc dust and 1 drop of water were added. This mixture was warmed for 12 h

Can. J. Chem. Downloaded from www.nrcresearchpress.com by 210.87.254.40 on 09/05/12
For personal use only.

at about 35 °C in a sealed vial, with occasional shaking. The clear supernatant liquid was decanted into a n.m.r. tube. The n.m.r. spectrum showed the olefinic absorption of I at τ 4.5; on a 50 cycle sweep width there was no observable splitting of the peak. The remainder of the spectrum was largely overrun by the acetic acid solvent. This solution was then diluted with an equal volume (0.8 ml) of carbon tetrachloride, and the resulting solution was distilled from a water bath, the bath temperature being slowly raised from 50 to 90°. The distillate (0.75 ml) was condensed at 0°, washed with a solution of 150 mg of sodium bicarbonate in 1 ml of water, and dried over anhydrous sodium sulfate. The n.m.r. spectrum of this solution was identical with that of I (Fig. 1*b*). Repetition of the above experiment using deuteroacetic acid (AcOD) as the solvent and 1 drop of deuterium oxide in the zinc dust treatment gave the same results.

Acid-Catalyzed Hydration of Cyclohexene

To a solution of 150 mg (1.83 mmole) of cyclohexene in 0.5 ml of carbon tetrachloride was added 0.3 ml of a 75% (by weight) solution of sulfuric acid in water. The reaction flask was stoppered and shaken at 50 °C for 90 min. Dilution with 2 ml of water, followed by saturation with sodium chloride and steam distillation, gave a distillate which was then saturated with sodium chloride and extracted with carbon tetrachloride. The carbon tetrachloride extract was dried over anhydrous sodium sulfate and concentrated *in vacuo* to a pale-yellow oil. The infrared and n.m.r. spectra of this oil were identical with those of an authentic sample of cyclohexanol. When the above procedure was repeated using I and a 75% solution of deuterosulfuric acid in deuterium oxide, a pale-yellow oil was again obtained. The n.m.r. spectrum of a carbon tetrachloride solution of this oil was correct for a cyclohexanol, but not for cyclohexanol-2,3,3,6,6-d_5, the expected product of simple addition. Deuterium decoupling indicated that considerable scrambling of deuterium had occurred.

ACKNOWLEDGMENTS

The authors thank the National Research Council of Canada, the Research Council of Ontario, and the McLaughlin Science Fund of Queen's University for financial support of this work, and Bristol Laboratories for a generous gift.

REFERENCES

1. P. B. D. DE LA MARE. Molecular rearrangements. *Edited by* P. de Mayo. John Wiley and Sons, Inc., New York. 1963. p. 27.
2. M. S. KHARASCH and G. SOSNOVSKY. J. Am. Chem. Soc. **80**, 756 (1958).
3. D. B. DENNEY, D. Z. DENNEY, and G. FEIG. Tetrahedron Letters, 19 (1959).
4. M. S. KHARASCH, G. SOSNOVSKY, and N. C. YANG. J. Am. Chem. Soc. **81**, 5819 (1959).
5. J. K. KOCHI. J. Am. Chem. Soc. **84**, 774 (1962).
6. H. L. GOERING and U. MAYER. J. Am. Chem. Soc. **86**, 3753 (1964).
7. R. CRIEGEE. Newer methods of preparative organic chemistry. Vol. II. *Edited by* W. Foerst. Academic Press, New York. 1963. p. 367.
8. C. WEIS. Ph.D. Dissertation. Technische Hochschule, Karlsruhe, 1953.
9. G. H. WHITHAM. J. Chem. Soc. 2232 (1961).
10. E. H. FARMER, H. P. KOCH, and D. SUTTON. J. Chem. Soc. 541 (1943).
11. C. DJERASSI. Chem. Rev. **43**, 271 (1948).
12. L. F. FIESER, M. FIESER, and R. N. CHAKRAVARTI. J. Am. Chem. Soc. **71**, 2226 (1949).
13. A. NICKON and J. F. BAGLI. J. Am. Chem. Soc. **81**, 6330 (1959).
14. W. TREIBS, G. LUCIUS, H. KOGLER, and H. BRESLAUER. Ann. **581**, 59 (1953).
15. D. H. R. BARTON and W. J. ROSENFELDER. J. Chem. Soc. 2381 (1951).
16. W. NAGATA, T. SUGASAWA, M. NARISADA, T. WAKABAYASHI, and Y. HAYASE. J. Am. Chem. Soc. **85**, 2342 (1963).
17. L. S. LEVITT. J. Org. Chem. **20**, 1297 (1955).
18. P. B. D. DE LA MARE. Molecular rearrangements. *Edited by* P. de Mayo. John Wiley and Sons, Inc., New York. 1963. p. 29.
19. R. U. LEMIEUX and J. W. LOWN. Can. J. Chem. **42**, 893 (1964).
20. M. KARPLUS. J. Chem. Phys. **30**, 11 (1959); J. Phys. Chem. **64**, 1793 (1960).
21. M. KARPLUS. J. Am. Chem. Soc. **85**, 2871 (1963).
22. A. C. HUITRIC, J. B. CARR, W. F. TRAGER, and B. J. NIST. Tetrahedron, **19**, 2145 (1963).
23. L. W. REEVES and K. O. STROMME. Trans. Faraday Soc. **57**, 390 (1961).
24. S. BROWNSTEIN and R. MILLER. J. Org. Chem. **24**, 1886 (1959).
25. A. HASSNER and C. C. HEATHCOCK. Tetrahedron Letters, 1125 (1964).
26. J. L. MARGRAVE, M. A. FRISCH, R. G. BAUTISTA, R. L. CLARKE, and W. S. JOHNSON. J. Am. Chem. Soc. **85**, 547 (1963).
27. J. B. HENDRICKSON. J. Org. Chem. **29**, 991 (1964).
28. R. U. LEMIEUX, R. K. KULLNIG, H. J. BERNSTEIN, and W. G. SCHNEIDER. J. Am. Chem. Soc. **80**, 6098 (1958).
29. E. L. ELIEL, M. H. GIANNI, TH. H. WILLIAMS, and J. B. STOTHERS. Tetrahedron Letters, 741 (1962).
30. L. M. JOSHEL and L. W. BUTZ. J. Am. Chem. Soc. **63**, 3350 (1941).
31. A. C. COPE, G. A. BERCHTOLD, and D. L. ROSS. J. Am. Chem. Soc. **83**, 3859 (1961).

Can. J. Chem. Downloaded from www.nrcresearchpress.com by 210.87.254.40 on 09/05/12
For personal use only.

32. M. M. ANDERSON and P. M. HENRY. Chem. Ind. London, 2053 (1961).
33. M. J. ABERCROMBIE, A. RODGMAN, K. R. BHARUCHA, and G. F WRIGHT. Can. J. Chem. **37**, 1328 (1959).
34. T. G. TRAYLOR and A. W. BAKER. J. Am. Chem. Soc. **85**, 2746 (1963).
35. F. R. JENSEN and L. W. GALE. J. Am. Chem. Soc. **81**, 6337 (1959); J. Am. Chem. Soc. **81**, 1261 (1959).
36. F. A. L. ANET. J. Am. Chem. Soc. **84**, 1053 (1962).
37. C. O. GUSS and R. ROSENTHAL. J. Am. Chem. Soc. **77**, 2549 (1955).
38. E. L. ELIEL and R. G. HABER. J. Am. Chem. Soc. **81**, 1249 (1959).
39. J. SAND and F. SINGER. Ber. **35**, 3170 (1902).
40. J. H. ROBSON and G. F WRIGHT. Can. J. Chem. **38**, 21 (1960).
41. J. F. KING and R. G. PEWS. Can. J. Chem. **42**, 1294 (1964).
42. H. B. HENBEST and B. NICHOLLS. J. Chem. Soc. 227 (1959).
43. H. C. BROWN and K. J. MURRAY. J. Org. Chem. **26**, 633 (1961).
44. S. WOLFE, M. NUSSIM, Y. MAZUR, and F. SONDHEIMER. J. Org. Chem. **24**, 1034 (1959).
45. L. HORNER and E. H. WINKELMAN. Angew. Chem. **71**, 349 (1959).
46. C. WALLING, A. L. RIEGER, and D. D. TANNER. J. Am. Chem. Soc. **85**, 3129 (1963).
47. G. A. RUSSELL and K. M. DESMOND. J. Am. Chem. Soc. **85**, 3139 (1963).
48. R. E. PEARSON and J. C. MARTIN. J. Am. Chem. Soc. **85**, 3142 (1963).
49. H. J. LUCAS, F. R. HEPNER, and S. WINSTEIN. J. Am. Chem. Soc. **61**, 3102 (1939).
50. P. D. SLEEZER, W. G. YOUNG, and S. WINSTEIN. J. Am. Chem. Soc. **85**, 1890 (1963).
51. F. R. JENSEN and R. J. OUELLETTE. J. Am. Chem. Soc. **83**, 4477 (1961).
52. J. CHATT. Chem. Rev. **48**, 7 (1951).
53. S. WOLFE and G. H. PALMER. Unpublished results.
54. K. B. WIBERG and S. D. NIELSEN. J. Org. Chem. **29**, 3353 (1964).

Can. J. Chem. Downloaded from www.nrcresearchpress.com by 210.87.254.40 on 09/05/12
For personal use only.

Can. J. Chem. Downloaded from www.nrcresearchpress.com by 210.87.254.105 on 09/05/12
For personal use only.

ON THE FORMATION OF "Ag_2O_3" ON SILVER ELECTRODES[1]

E. J. Casey and W. J. Moroz
Defence Chemical, Biological, and Radiation Laboratories, Defence Research Board, Ottawa, Canada

Received November 20, 1964

ABSTRACT

"Ag_2O_3" was examined electrochemically in eutectic KOH–H_2O at −40 °C by coulombic measurements of quantities formed, open circuit potential decays, variation of potential as a function of anodic current density, and temperature coefficients of decomposition rates. It can be formed directly from Ag_2O on Ag at current density (c.d.) > 15 $\mu A/cm^2$, with a maximum thickness during the first oxidation cycle (25 layers, assuming a surface roughness factor of one) occurring at 65 $\mu A/cm^2$. Potential decay ($-\partial E/\partial \log t \equiv b$) curves have protracted linear regions where $0.045 < b < 0.078$, sometimes higher. One-tenth of a layer of adsorbed species superimposed on the higher oxide exists on the surface during O_2 evolution. Reduction curves show a minimum in the potential decay of the higher oxide preceding the formation of Ag_2O. The "Ag_2O_3" decomposes in approximately 1 h at −40 °C to either AgO or Ag_2O. The activation energy for its thermal decomposition is 12.0 ± 2.0 kcal/mole. Under most experimental conditions studied the results indicated that the material is not true Ag_2O_3 but it is probably better described as $Ag_2O[O]$ where [O] is trapped oxygen.

The evidence does point to the probable existence of a thin layer, which may be true Ag_2O_3, on the surface in a steady state which is maintained at high anodic current density (> 100 $\mu A/cm^2$ at −40°).

INTRODUCTION

About 100 papers have been published in which the existence of higher oxides of silver (i.e. Ag^{+3}) are discussed, implied, or claimed. The papers fall into two groups. In one there is a definite claim or implication that the compound studied was Ag_2O_3; in the other there is concern over the proximity of the oxygen electrode, the presence of peroxides on the surface, and the influence which foreign ions such as nitrate and sulfate have on the crystal structure and stability of a material which behaves like a higher oxide of silver. However, the question of whether a pure phase of trivalent silver oxide exists still remains. This question is not only of intrinsic interest but is also a practical one, as it concerns charge acceptance in the zinc – silver oxide battery, and the use of silver oxide catalyzed oxygen electrodes in fuel cells. Sections of three excellent reviews discuss Ag_2O_3 (1, 2, 3).

The present investigation was undertaken at low temperature (−40 °C), where the rate of decay of "Ag_2O_3" is slow enough to permit study over an hour or two. We use the symbol "Ag_2O_3" to indicate the uncertainty about the chemical composition and structure of the material under study. We use the symbol 'Ag_2O_3' when the experimental indications are such that the material may be in fact the stoichiometric compound Ag_2O_3.

EXPERIMENTAL METHODS

The test cell consisted of a test electrode, a counter electrode, and a reference electrode (Hg/HgO) with a luggin capillary, immmersed in eutectic KOH–H_2O in a cylindrical glass vessel equipped with a Teflon covered magnetic stirrer. The cell contained 125 ml of electrolyte made from deionized water. The carbonate content of the electrolyte was of the order of 0.5%.

The silver electrodes were cut from rolled sheet 0.005 in. thick and 99.99% pure, and measured 1.27 × 2.54 cm. The apparent surface area exposed to the electrolyte was 6.46 cm^2. Before use, all electrodes were degreased in hot acetone, and then etched in dilute nitric acid or scraped with glass. A silver wire mounted in a glass capillary tube was forge welded to a tab at the top of the test electrode. The tab, wire, and capillary tube were then sealed off from the electrolyte with stop-off lacquer. The counter electrode was a commercially available porous silver electrode of large area. Formed into the shape of a cylindrical tube, it completely

[1]*Issued as DCBRL Report No. 454.*

surrounded the test electrode. During the course of the experiments the counter electrode was always kept at or near the potential of the AgO/Ag_2O electrode by periodic oxidation.

Some experiments were carried out with porous silver test electrodes for purposes of comparison with data obtained using the planar or sheet electrodes.

Temperature control was $\pm 1°$ at $-40°$ in a Tenney two-stage freon low temperature cabinet, with the cell temperature cycling at $\pm 0.2°$. Potential measurements were made on a General Radio DC Amplifier, type 1230-A, used with an Esterline-Angus Model AW, continuous recording DC Milliammeter. The input resistance of the G.R. amplifier was set at 10^{10} ohms. The ammeters used were calibrated against our own secondary standard. All oxidations and reductions were carried out using constant current techniques, with manual control, direct current being supplied from a 6 V storage battery through the appropriate resistors. Amounts of materials formed on or removed from the surface were thus easily determined.

RESULTS AND DISCUSSION

Anodic Oxidation at −40°

The oxidation curve of voltage vs. time for a planar or a porous silver electrode can take one of two shapes depending upon the rate of oxidation. If the oxidation current density is below a critical value, the peak which generally precedes AgO formation is evident and the oxidation curve can be considered normal. However, if the oxidation current density is above the critical value, the electrode potential rises quickly through the peak without inflection (4) (there is no evidence of the usual AgO plateau) and continues to rise until oxygen evolution commences.

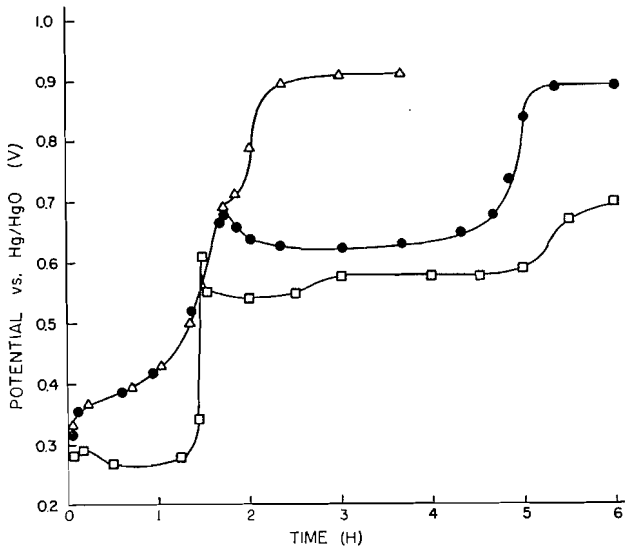

FIG. 1. Anodic oxidation curves of planar silver electrodes illustrating Ag_2O_3 and AgO formation △, ●, oxidation at c.d. of 15 $\mu A/cm^2$ at $-40°$; □, oxidation at 75 $\mu A/cm^2$ at 25 °.

In Fig. 1 are shown the two types of curves. The critical current densities were found to be 15 $\mu A/cm^2$ for the planar electrode and $\sim 10^3$ $\mu A/cm^2$ for the porous electrode (apparent areas). Electrolytic reduction following a charge shows the presence of AgO, as would be expected after a normal charge, but no evidence of AgO following oxidation at higher than critical current densities. In the latter case the usual mechanism by which Ag_2O is oxidized to AgO is obviously missing or altered as evidenced by the absence of the peak, and also of any AgO potential plateaus during forced or open circuit (o.c.) potential decays. The presence of a new, well-defined voltage plateau at approximately 725 mV with respect to (w.r.t.) Hg/HgO/KOH reference electrode during oxidation, and

Can. J. Chem. Downloaded from www.nrcresearchpress.com by 210.87.254.105 on 09/05/12
For personal use only.

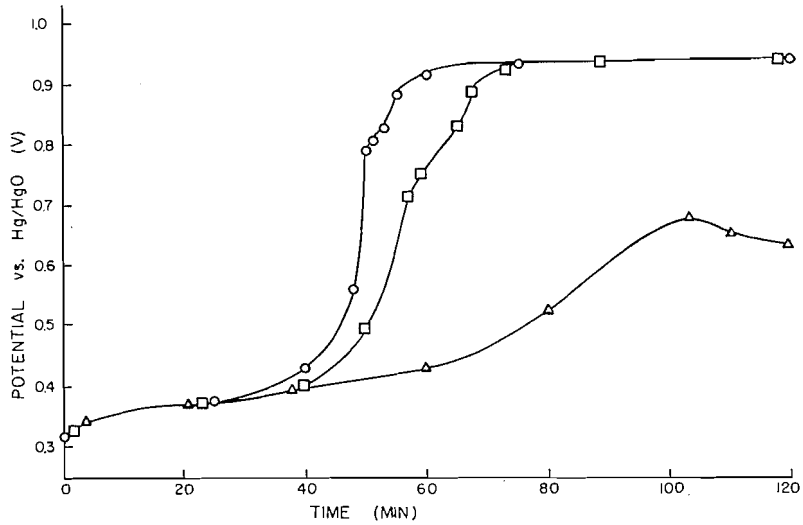

FIG. 2*a*. Consecutive anodic oxidations of a *planar* silver electrode at −40° showing transition from Ag_2O_3 to AgO formation. Oxidation c.d. was 15 $\mu A/cm^2$.

a similar well-defined potential arrest both on forced and o.c. decay in the 800–600 mV region, lead one to suspect that a new intermediate stage may be occurring in this potential region.

Three successive oxidation curves on a planar electrode are shown in Fig. 2*a*. The electrode was alternately oxidized and reduced (to O_2 evolution and Ag, respectively) at the critical current density of 15 $\mu A/cm^2$. As can be seen, both types of oxidation curves were obtained and the transition from the one type to the other is clearly evident. Successive oxidations at higher current densities produced changes of degree, but not of kind, in the shape of the oxidation curve. Generally speaking the result of repetitive oxidation–reduction cycles on planar electrodes is to increase the depth of the oxidation layer and increase the area of the electrode surface. At the apparent critical current density used above, this was equivalent to reducing the actual current density by the third cycle to somewhat below the critical value. The necessary conditions for higher oxide formation were not sustained, and the formation of AgO resulted.

Fig. 2*b* shows tracings of potential during two successive oxidations of a *porous* silver electrode at its critical current density at −40°. The fine structure in the vicinity of the peak is much better developed than in the case of the planar electrode.

The Oxygen Precursor

The decay of o.c. potential at −40° of an anodically polarized planar electrode which has been evolving O_2 for some time is linear with the logarithm of time from about the fifth second to the time (up to as long as an hour or so later) when it falls to the next potential plateau (Fig. 3). However, within the first 5 s, curvature of the E vs. log t plot occurs, concave upward. If the linear plot is extrapolated back to very small values of time, and the extrapolated values are subtracted from the measured ones, a set of potential differences ΔE at the different times can be obtained. These values can be considered to refer to an oxygen precursor superimposed on the higher oxide, and can be described by a diffusion-controlled model of O_2 liberation. Thus, if one assumes that the activity of the reduced form (OH^-?) is constant in the double layer, that the decay is governed by

Can. J. Chem. Downloaded from www.nrcresearchpress.com by 210.87.254.105 on 09/05/12
For personal use only.

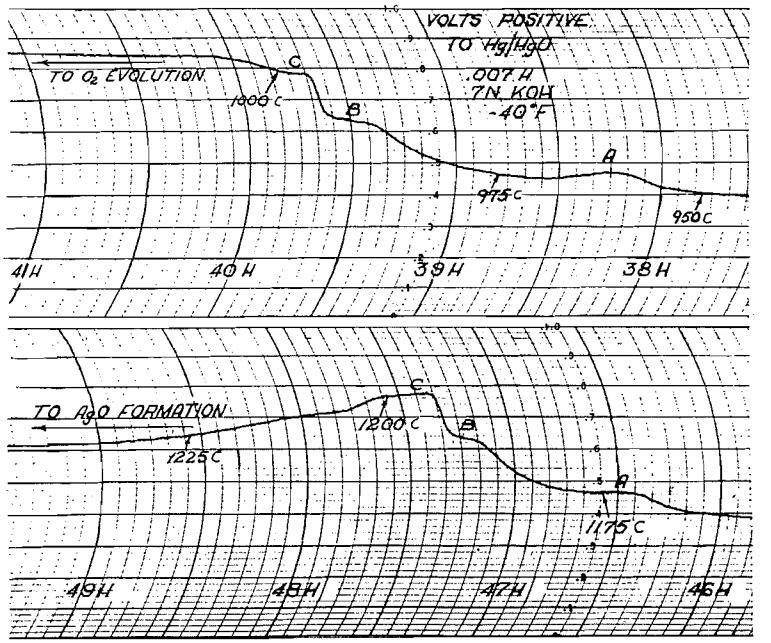

FIG. 2*b*. Consecutive anodic oxidations of a *porous* silver electrode at −40° showing transition from Ag_2O_3 to AgO formation. Oxidation current density was 227 $\mu A/cm^2$.

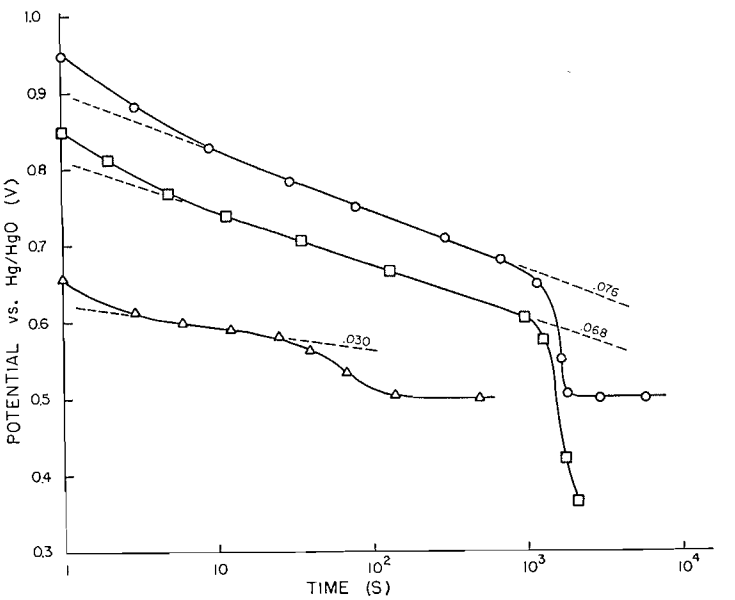

FIG. 3. Open circuit potential decays of Ag_2O_3; ○, decay at −40° to AgO; □, decay at −40° to Ag_2O; △, decay at +25 °C to AgO.

Fick's second law of diffusion, that the Nernst equation holds, and that the boundary conditions must be consistent with a source on a plane diffusing normal to the plane; the potential E decays as the sum of two terms, $1/t + C \log t$. It was found that ΔE vs.

Can. J. Chem. Downloaded from www.nrcresearchpress.com by 210.87.254.105 on 09/05/12
For personal use only.

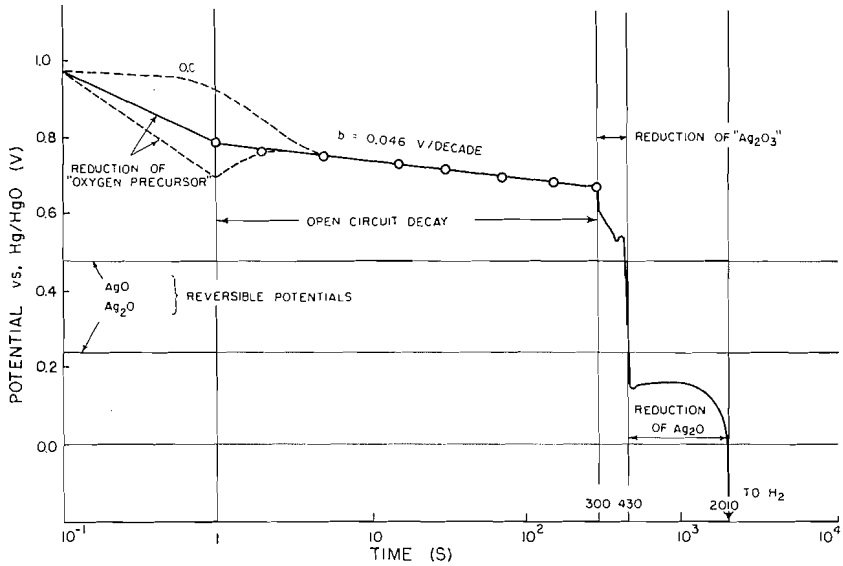

FIG. 4. Coulombic measurements of oxygen precursor, Ag_2O_3 and Ag_2O, following anodic oxidation at $-40°$ at a c.d. of 30 $\mu A/cm^2$.

$1/t$ was linear for planar electrodes over the first two or three cycles. Hence qualitatively the early stages of potential decay, during the first few cycles of a planar electrode, can be interpreted as being diffusion controlled.

By rapid reduction immediately following anodic oxidation to O_2 evolution, it was possible to obtain a rough estimate ($\pm 25\%$) of the amount of oxygen precursor that had been present in the steady state of current flow. The value of the reduction current was chosen so that in a 1 s reduction the potential was lowered to that value obtained by extrapolating, back to $t = 1$ s, the E vs. log t decay which exists beyond 5 s. In this way it was found that 0.1–0.3 of the passivated electrode surface had been covered with oxygen precursor. This measurement is illustrated on the left half of Fig. 4. Note that if the number of coulombs required to reduce the oxygen precursor have been exceeded, the potential on subsequent o.c. decay will recover to that of the higher oxide. The right half of Fig. 4 deals with coulombic measurements, to be discussed later. For the present simply note the little "hitch", or potential minimum, in the reduction curve of Ag_2O_3, between 300 and 430 s.

Open Circuit and Cathodic Potential Decays

In Fig. 5 are shown a group of o.c. potential decays (Fig. 5*b*) taken from a planar electrode at $-40°$. Each decay curve followed anodic polarization at c.d. 780 $\mu A/cm^2$ to a preselected potential value, (Fig. 5*a*). Then after approximately 100 s of o.c. decay a cathodic current was used to reduce any of the oxides on the electrode to silver. The potential values selected (points 1 to 12 on Fig. 5*a*) were taken over a period of time from just after the start of anodic polarization to a time when the electrode was vigorously evolving O_2.

These curves clearly show the absence of AgO on the electrode. There is no potential arrest evident at or near the usual AgO/Ag_2O potential of 0.49 V (see Fig. 5*b*). The buildup of the higher oxide can be traced stepwise with the help of the o.c. decay curves.

Can. J. Chem. Downloaded from www.nrcresearchpress.com by 210.87.254.105 on 09/05/12
For personal use only.

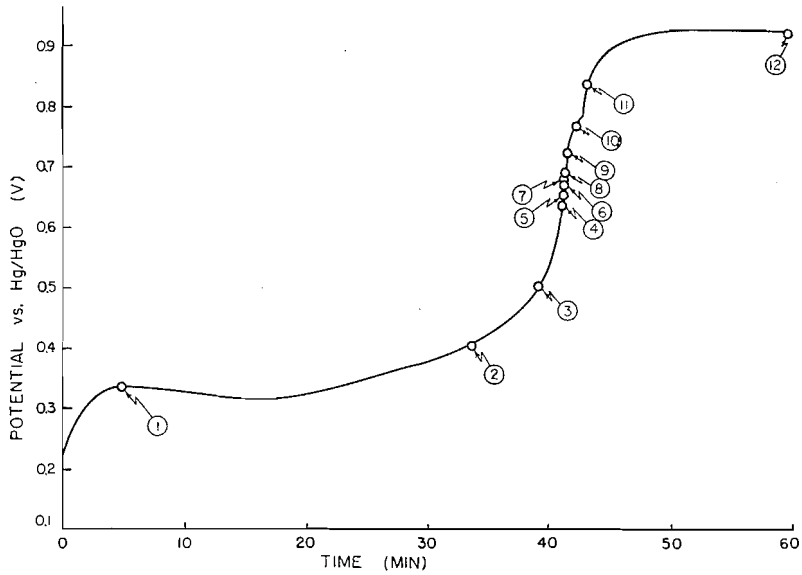

FIG. 5*a*. Anodic oxidation curve of a planar silver electrode at −40° at a c.d. of 780 μA/cm². Numbers (1 to 12) indicate the potential values at which o.c. decays (Fig. 5*b*) were taken.

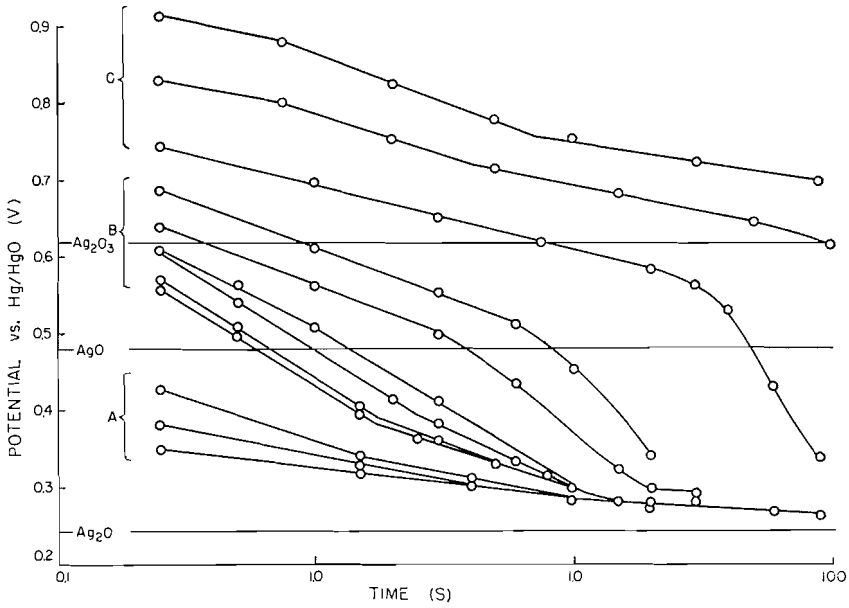

FIG. 5*b*. Open circuit potential decays of a planar silver electrode, showing buildup of Ag_2O_3 with anodic oxidation to increasingly positive potentials. Group A shows no higher oxide is present. Group C shows the existence of a higher oxide with an o.c. decay life in excess of 100 s. Group B represents the transition from A to C.

The lower group (A) shows no higher oxide is present. The top group (C) shows the existence of a higher oxide with an o.c. decay life in excess of 100 s. The middle group (B) represents the transition from A to C.

Can. J. Chem. Downloaded from www.nrcresearchpress.com by 210.87.254.105 on 09/05/12
For personal use only.

From many other o.c. decay curves obtained during the course of the experiments it was found that the decay of the higher oxide could take any one of the following paths: (i) Decay to Ag_2O from the Ag_2O_3/AgO potential level (calculated as 0.64 V w.r.t. Hg/HgO) (4, 5, 6). (ii) Decay to Ag_2O from the Ag_2O_3/Ag_2O potential level (calculated as 0.56 V w.r.t. Hg/HgO) (5, 6). (iii) Decay to Ag_2O from the Ag_2O_3/Ag_2O potential level, but with the presence of a "hitch". (iv) Decay to AgO from either the Ag_2O_3/AgO or Ag_2O_3/Ag_2O potential levels.

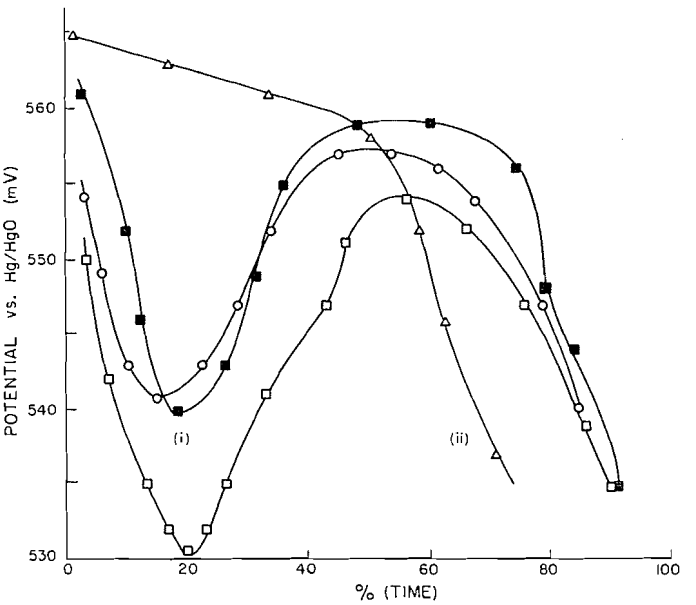

FIG. 6. Normalized curves showing details of potential minimum (i) during cathodic reduction of a planar silver electrode at −40°. Hitch does not occur (ii) if sufficiently large quantities of Ag_2O_3, Ag_2O, or nuclei of AgO are present.

Details of the "hitch" which occurs during discharge of the higher oxide, or under certain conditions on o.c. decay, can be seen on an expanded scale of the decay of potential vs. time in Fig. 6. The time scale has been normalized (100% being the time required for the potential to fall during cathodic reduction to 480 mV) so that several reduction curves which referred to different amounts of "Ag_2O_3" could be compared directly. At times no minimum occurred, and the decay curve was then of the type represented by curve (ii) in Fig. 6.

Generally it was found that this minimum in the potential–time curve did not occur if the quantities of "Ag_2O_3" and Ag_2O on the electrode were large, or if AgO was present. The hitch did occur during the cathodic reduction of small quantities of "Ag_2O_3", or even on o.c. decay if the amount of "Ag_2O_3" on the surface was small. In most cases the total amount of coulombs passed to the bottom of the minimum (assuming a surface roughness factor of one) amounted to 3–5 layers of higher oxide being reduced on the electrode surface. From the potential region in which the minimum occurs ($\sim$ 560 mV, Ag_2O_3/Ag_2O rev. pot.) and from the magnitude of the potential drop, $\sim$ 30 mV, one is inclined to believe that first the higher oxide is reduced to Ag_2O (high specific resistance) which then either breaks regularly or is reduced further to Ag as further charge is passed. From

Can. J. Chem. Downloaded from www.nrcresearchpress.com by 210.87.254.105 on 09/05/12
For personal use only.

the minimum value the potential rises again to a maximum before decaying precipitously to the Ag_2O/Ag potential as the higher oxide becomes exhausted. The discharge might be represented by

$$Ag_2O_3 + 2H_2O + 4e^- \rightarrow Ag_2O + 4OH^-.$$

When the coherent Ag_2O film breaks or is otherwise removed, the depleted oxygen content of the surface layer is restored from underneath (7), and the potential rises from the minimum towards the maximum of the hitch. In those cases in which the hitch is not present, the rapid formation of the coherent, passivating layer of Ag_2O is in some manner prevented. The presence of large quantities of Ag_2O, "Ag_2O_3", or the presence of AgO were found to discourage the formation of this passivating surface layer. Large quantities of "Ag_2O_3" (> 50 layers), perhaps approaching in stoichiometry the formula Ag_2O_3, when present on the electrode, due to very favorable forming conditions, probably exhibit a different, more stable crystal structure in which oxygen atoms are more tightly bound to the crystal lattices on the surface and the solid phase remains during reduction.

In those cases in which AgO was present on the electrode in sufficient quantities to show its presence during discharge, no evidence of a hitch in the decay curve was observed which would accompany the formation of a coherent surface layer of Ag_2O. It appears therefore that in the presence of nuclei of AgO the higher oxide discharges preferentially to AgO.

$$Ag_2O_3 + H_2O + 2e^- = 2AgO + 2OH^-.$$

Hence, the discharge of "Ag_2O_3" can proceed to either AgO or Ag_2O.

Coulombic Measurements

A composite measurement of the amounts of oxygen precursor, higher oxide and Ag_2O, as well as the o.c. "*b*" value are shown following the first oxidation of a planar electrode in Fig. 4. The results on this first cycle are typical of the behavior of this electrode at $-40°$ and are listed in Table I. The number of layers of silver which oxidized to form

TABLE I

Quantities of oxides formed anodically (30 $\mu A/cm^2$) during the first cycle on a planar silver electrode at $-40°$ in eutectic KOH–H_2O

Measured capacity on reduction (C/cm^2)	Region	Layers of Ag oxidized (calcd.)
2.6×10^{-5}	O_2 precursor	0.1
3.6×10^{-3}	Ag_2O_3	13
Nil	AgO	Nil
4.2×10^{-2}*	Ag_2O	156

*4.3×10^{-2} on oxidation.

Ag_2O and the higher oxide were calculated from the measured coulombic capacity, the silver radius 1.26 Å (8) and a surface roughness arbitrarily chosen as unity. If the ratio of real area to apparent area is taken even as high as 10, as Hickling did (4), then the thickness of the higher oxide would still be at least a monolayer thick on the surface of the Ag_2O oxide layer.

The amounts of "Ag_2O_3" and Ag_2O formed at $-40°$ vary with the oxidation c.d. (Figs. 7 and 8) and are dependent on the state of the electrode surface prior to oxidation. The formation of maximum amounts of "Ag_2O_3" (Fig. 7) and Ag_2O (Fig. 8) occur at different

Can. J. Chem. Downloaded from www.nrcresearchpress.com by 210.87.254.105 on 09/05/12
For personal use only.

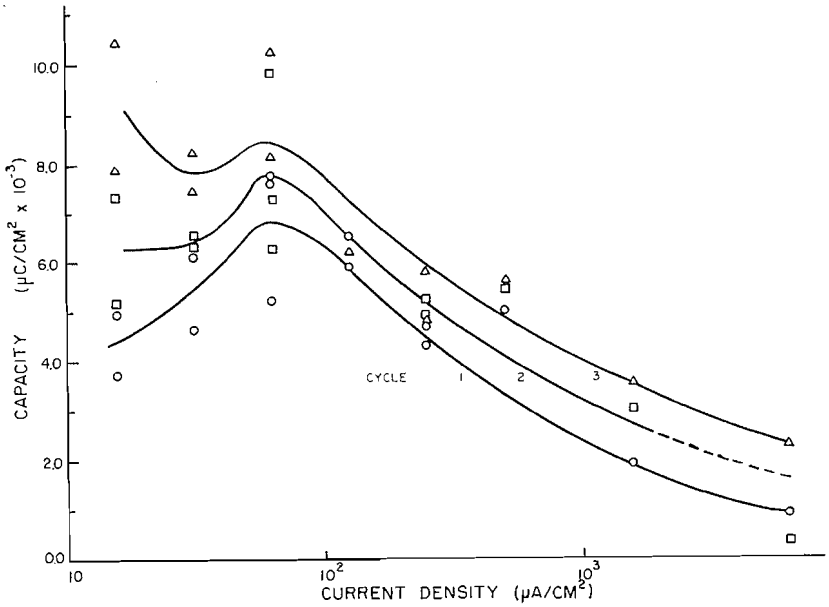

FIG. 7. Ag_2O_3 capacity at −40° as a function of the current density of anodic oxidation, and the effect of cycling on this capacity.

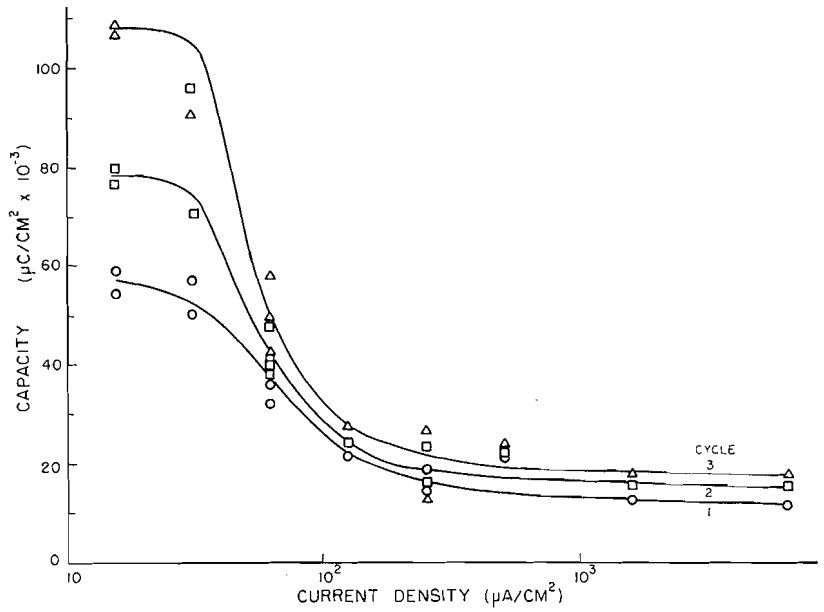

FIG. 8. Ag_2O capacity at −40° as a function of the current density of anodic oxidation and the effect of cycling on this capacity.

current densities. From data collected on 13 fresh planar electrodes, over the range of current densities shown, it was found that maximum amounts of "Ag_2O_3" and Ag_2O were formed at c.d.'s of 62 $\mu A/cm^2$ and below about 30 $\mu A/cm^2$, respectively. During the first cycle on a fresh electrode, maximum amounts of 25 layers of Ag oxidized to "Ag_2O_3", and

Can. J. Chem. Downloaded from www.nrcresearchpress.com by 210.87.254.105 on 09/05/12
For personal use only.

215 layers (if the surface roughness factor is taken as unity) of Ag oxidized to Ag_2O were found. The quantity of Ag_2O formed decreases very quickly at c.d. greater than 30 $\mu A/cm^2$. Repeated cycling had the effect of increasing the amounts of "Ag_2O_3" and Ag_2O formed per cycle by about 15 and 25% respectively, from the first to the third cycle. This held true for all current densities studied.

Let us now introduce a conceptually significant quantity, the ratio of the amounts (equivalents) of "Ag_2O_3" and Ag_2O formed under different conditions. This ratio, C_r, is the amount of "Ag_2O_3" formed per unit amount of underlying Ag_2O substrate. The results plotted in Fig. 9 show that above the critical current density for AgO formation (15 $\mu A/cm^2$) C_r increases *linearly* with log anodic c.d. up to $\sim$ 140 $\mu A/cm^2$, and then decreases, *again linearly*, with further increase in c.d., at least up to 6 200 $\mu A/cm^2$. Thus the amount of "Ag_2O_3" formed per unit of underlying Ag_2O has a maximum value at what we shall call the *transition current density of formation*; and this maximum is determined by two competing processes one of which increases linearly and one of which decreases linearly with increasing log c.d.

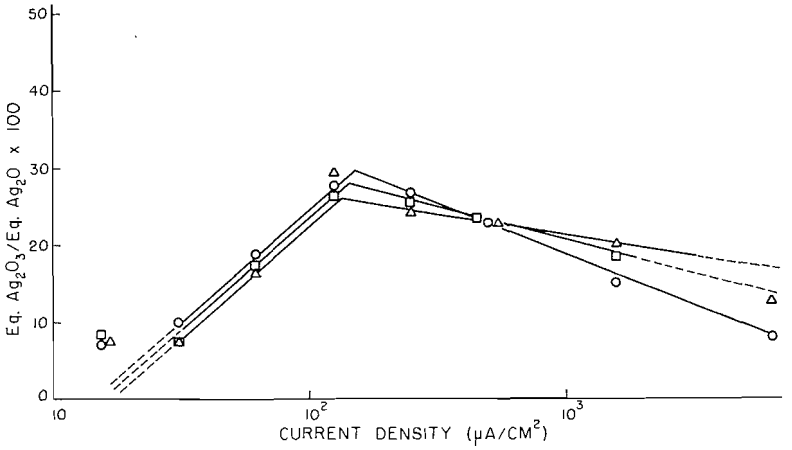

FIG. 9. The effect of anodic current density on the ratio (C_r) of the equivalents of Ag_2O_3:Ag_2O formed on a planar silver electrode at −40° during the first three cycles (○, cycle 1; □, cycle 2; △, cycle 3).

Unfortunately, so far we have been unable to account quantitatively for the linearities in the plot of C_r vs. log t. Not surprisingly, the overpotential for oxygen evolution shows a discontinuity just preceding this same maximum value of C_r (Fig. 10), indicating a change in the mechanism by which O_2 is evolved. Thus above C_r the Tafel slope was found to be 100 mV/decade; below C_r it was 160 mV/decade. At c.d.'s > 10^4 $\mu A/cm^2$, the curve deviates from linearity and the potential values begin to rise very rapidly until, beyond 10^6 $\mu A/cm^2$ the slope of the curve is almost infinite. At these very high current densities the processes become diffusion controlled.

Three other facts complete the basis for an interpretation.

1. At the current density of 60 $\mu A/cm^2$, which forms the lower end of the discontinuity and is the beginning of the transition between the two oxygen evolution processes, prolonged (18 h) anodic oxidation results in the formation of some AgO. By contrast no AgO was formed during prolonged oxidation at current densities of 30 and 15 $\mu A/cm^2$.

2. *Both E and C_r increase* linearly with log c.d. below the c.d. of maximum C_r. Above this value E increases while C_r *decreases* with increasing log c.d. (See Fig. 9.)

Can. J. Chem. Downloaded from www.nrcresearchpress.com by 210.87.254.105 on 09/05/12
For personal use only.

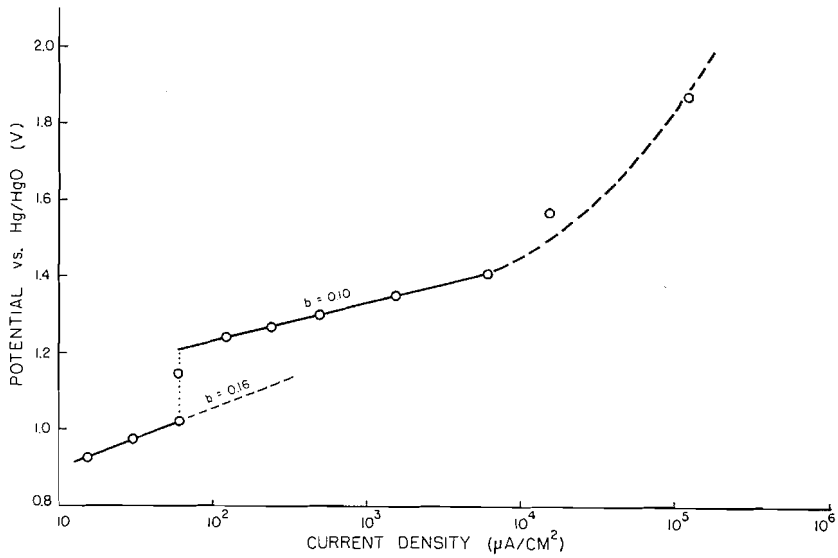

FIG. 10. The end of charge potential for oxygen evolution as a function of the anodic current density (Tafel curve) for planar silver electrodes at −40°.

3. Whatever the value of the reversible oxygen potential at −40°, it is obvious from Fig. 10 that the exchange current for the high current process of oxygen evolution must be lower than the exchange current for the low current process. In other words, whatever the high current process is, once it is instituted it can be maintained at lower c.d. than can the low current process. This is perhaps due to the formation of a "blanket" of an oxygen-precursor species (Ag_2O_3?) which is tightly bound during anodic oxidation, and which also gives rise to hysteresis behavior to be discussed later.

From these facts one can picture O_2 being evolved *primarily* off Ag_2O[O] sites at c.d.'s below 60 μA/cm^2, and *primarily* off filled Ag_2O_3 sites at c.d.'s above 120 μA/cm^2; that below this lower value the "Ag_2O_3" is substantially Ag_2O plus trapped oxygen; above the higher value the crystal form has shifted more towards true Ag_2O_3. In the current density region between 60 and 120 μA/cm^2 the process of crystal deformation is continuously occurring, and results, whenever the configuration is favorable, in an alternative crystalline transition to AgO. Above this transitional region the mass is protected by the blanket of what *may be* true Ag_2O_3 but which we shall call 'Ag_2O_3'. Below the transitional region the Ag_2O lattice does not become strained enough to form true Ag_2O_3. Above this region the 'Ag_2O_3' is so thermally unstable at −40° that more oxygen forced in at the interface causes less to be retained in the thin, coherent blanket in the steady state, while below it, more [O] can be stored by the Ag_2O the higher the steady state current.

If these inferences are correct, it would follow that the true crystalline phase Ag_2O_3 is likely face-centered cubic, like Ag_2O, and not monoclinic like AgO (9). Indeed the structures of the nitrate- and sulfate-stabilized higher oxides, Ag_7NO_{11} and Ag_7SO_{12}, and often confused with Ag_2O_3, are close to that of Ag_2O (7, 8).

Tafel Slopes

Fully charged *porous* electrodes at room temperature show two limiting slopes in the overpotential vs. log current plots, viz. 0.05 and 0.25 V per decade (Fig. 11). The hysteresis introduced in the previous section of this paper was observed during Tafel

Can. J. Chem. Downloaded from www.nrcresearchpress.com by 210.87.254.105 on 09/05/12
For personal use only.

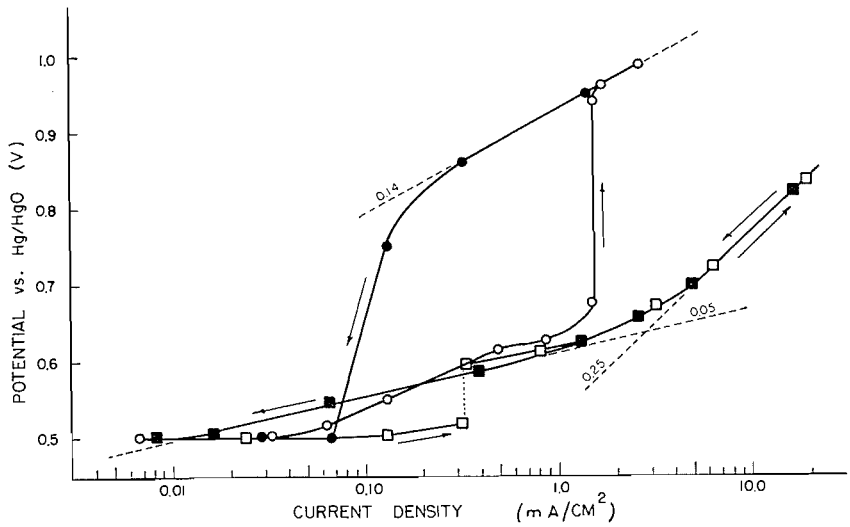

FIG. 11. Tafel curves on a porous silver electrode at 25° and −40° (○, ●, −40°; □, ■, +25 °C).

measurements, when the current was being reduced from large to smaller values. The hysteresis is much larger at −40°. As mentioned already, this behavior is taken as evidence for the formation of a protective blanket ('Ag_2O_3'?) which is relatively slow to form, but once formed is relatively slow to decay. It seems to decay rapidly when present in a small quantity, but much more slowly if it has been formed gradually and has had an opportunity to form well-defined crystallites.

Planar electrodes oxidized at current densities below the critical value (AgO forms) show hysteresis at −40° (Fig. 12*a*), and have high *b* values. If no AgO forms (Fig. 12*b*),

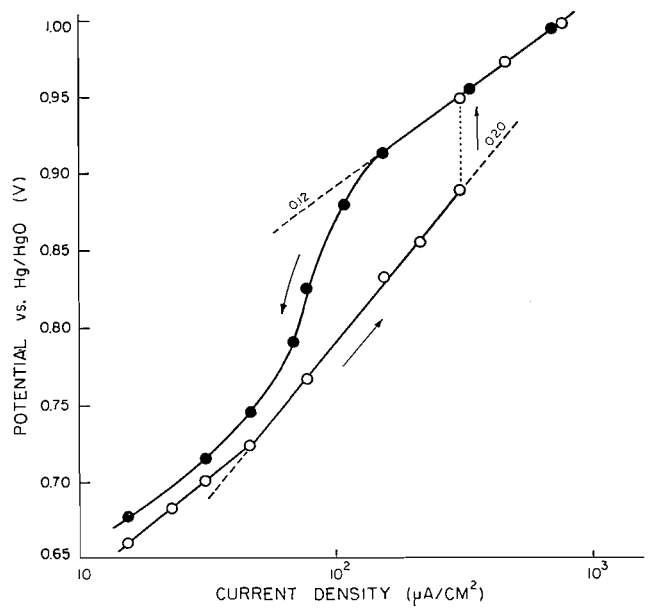

FIG. 12*a*. Tafel curve on a planar silver electrode at −40°; AgO present on the electrode.

Can. J. Chem. Downloaded from www.nrcresearchpress.com by 210.87.254.105 on 09/05/12
For personal use only.

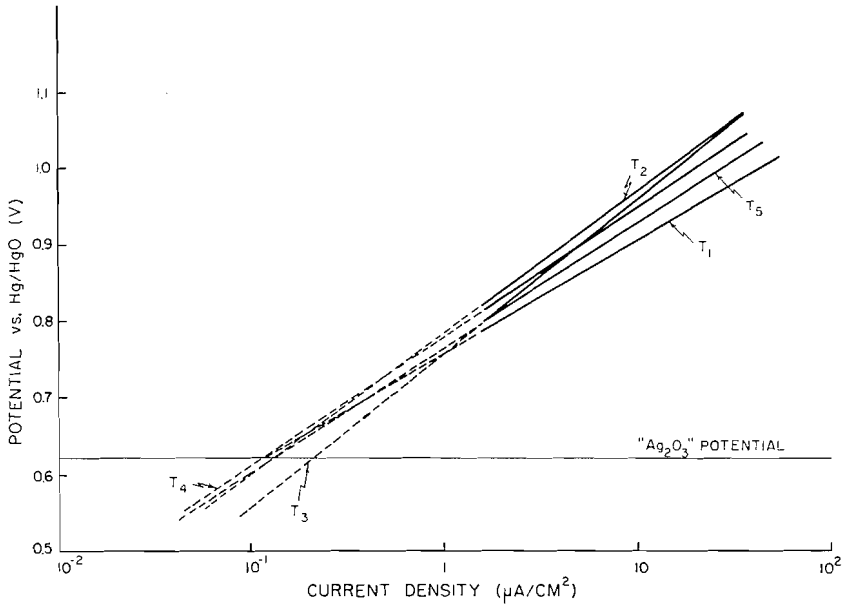

FIG. 12*b*. Tafel curves on a planar silver electrode at −40°; no AgO present on the electrode. T_1, T_2, etc. refer to the order in which the Tafel curves were taken.

hysteresis may not occur. The curves of Fig. 12*b* show that both the slope and the intercept at 0.62 V change unpredictably with time. This is one indication that the area from which oxygen is being electrochemically evolved is changing with time during the experiment. However if it were only a change in the *area* of the oxygen precursor, the *b* values, at least, should remain constant. Since they are not constant, then the rate of thermal decomposition of the higher oxide must also be changing in an uncontrollable and unpredictable manner or perhaps decomposing by parallel but different paths. Since these trends on oxide electrodes are well known at room temperature, it is not likely that the −40° temperature in itself makes much difference; and whether or not these trends lead to steady values of current after prolonged periods is of little importance. The important point is that the changes that do occur are unpredictable, uncontrollable, and very slow. These facts are taken as further evidence that there may be a great many (perhaps an infinite gradation of) metastable, intermediate states represented by $Ag_2O[O]$.

Temperature Coefficient of Decomposition Rate

If the higher oxide is decomposing thermally, then the current required to maintain the electrode at any selected potential in the higher oxide region should be a measure of the rate of its thermal decomposition. From the shape of the potential vs. time curves for oxidation, reduction, and open circuit decay in the higher oxide region, the average potential of the higher oxide was estimated to be about 0.62 V vs. Hg/HgO or 130 mV positive to the AgO electrode. The temperature coefficient of current needed to maintain the potential at 0.62 V was easily obtained on porous electrodes (Fig. 13) and was found to be 12.0 ± 2.0 kcal/mole from −40 to +10 °C. The course of the experiment is indicated by the arrows in the figure. Note that the current required to maintain a potential was much lower early in the experiment, but that after AgO had formed at +10° or thereabouts the current required to maintain the higher oxide on top of AgO was much higher.

Can. J. Chem. Downloaded from www.nrcresearchpress.com by 210.87.254.105 on 09/05/12
For personal use only.

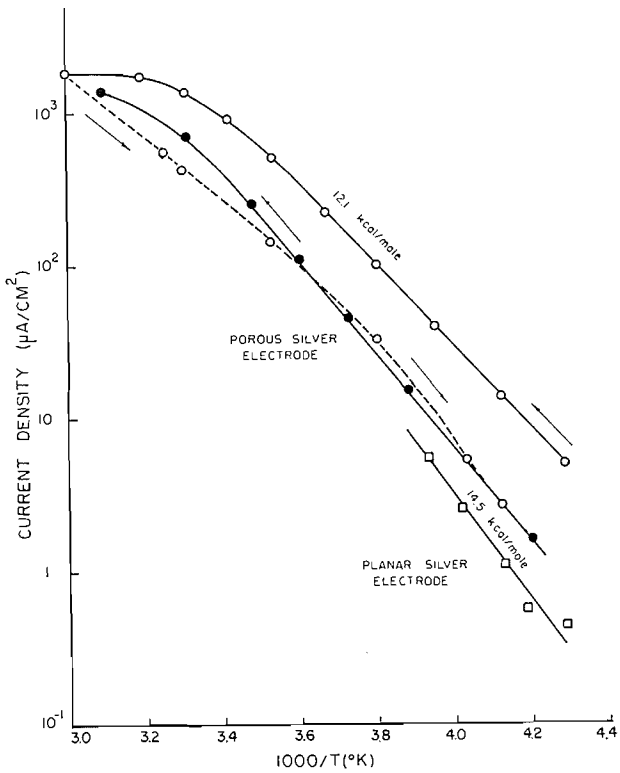

FIG. 13. Temperature coefficient of current required to maintain the electrode at a steady state at 0.62 V vs. Hg/HgO ($\sim Ag_2O_3$ reversible potential).

The same measurement on a planar sheet was difficult to make, probably for two reasons. First of all, the electrode surface was all free to the electrolyte and the area of the precursor (as interpreted by wanderings of the current required to maintain a constant potential) was changing by as much as a factor of 10 over a period of a week before settling to a steady value. Secondly, the thicknesses of Ag_2O and "Ag_2O_3" were small and probably subject to mechanical strains related to conductivity, porosity, and repair. In any case, perseverance yielded five points between -40 and -17.8 °C which gave an activation energy of about 14 kcal/mole, in the same range as found on the porous electrode.

It was thought that if the higher oxide was simply chemisorbed oxygen, then a higher potential should correspond to a greater surface coverage by adsorbate, which would be more weakly held to the surface. However a determination of activation energy on a planar electrode at a potential of 0.72 V still resulted in an activation energy of about 12 kcal/mole for the same temperature range. Thus the evidence seems to point again toward a higher oxide, a new phase.

More rapid activation energy measurements on the same planar electrode taken over a temperature range of -40 to -50 °C gave values of 8 to 9.5 kcal/mole at a potential of 0.72 V. The implication here is that when the temperature is low enough that modification and repair of the surface is slow, the outer layers of adsorbate are less tightly bound. Conversely, it would follow that the less tightly bound oxygen (chemisorbed?)

Can. J. Chem. Downloaded from www.nrcresearchpress.com by 210.87.254.105 on 09/05/12
For personal use only.

contributes little to the potential. In other words, it is electrochemically relatively inactive, or has a very low exchange current, perhaps because of some barrier to electron transfer right at the site of adsorption.

SEMICONDUCTOR ELECTRODES

The higher oxides of silver seem to belong to a class of materials in which both electrons and ions can move, and in which oxygen-containing species can be trapped into or onto the base material. During the anodic formation of "Ag_2O_3" on Ag_2O at low temperatures, extra oxygen, perhaps in the form of O atoms (12), penetrates the Ag_2O mass, either interstitially or at grain boundaries. The stability of the higher oxide should be dependent upon the energy with which the extra oxygen is bound into the Ag_2O lattice. Although this value does not seem to vary with experimental conditions (constant E^*), apparently the number of paths by which the trapped oxygen can escape does vary (varying rate of decay), as does also the contribution of parallel electrochemical paths (varying b value) through more than one oxygen-containing species (O, OH, HO_2). The time and space distribution of these species in the crystal defines the semiconduction paths which are essential to the electrochemical processes.

The class contains also the oxy-hydroxides of manganese, nickel, vanadium, iron, cobalt, and possibly lead. Further knowledge of the complex fundamental physical and electrochemical processes of one would doubtless contribute rapidly to a better understanding of the whole class.

SUMMARY

In eutectic KOH–H_2O at $-40°$, the higher oxide formed anodically on silver decomposes slowly, and some properties of this oxide, called for convenience, "Ag_2O_3", can be measured.

1. At $-40°$, Ag_2O forms readily on Ag. If the c.d. is $> 15\ \mu A/cm^2$, AgO does not form readily and the electrode passes immediately from Ag_2O formation to O_2 evolution. Two intermediate states are indicated, one that can be attributed to be "Ag_2O_3", the other to an oxygen precursor, possibly adsorbed HO_2.

2. Decay of o.c. potential through the Ag_2O_3 region is slow ($\sim$ 1 h) and electrochemical reduction completed within 5 min of anodic oxidation shows the stored capacity of the higher oxide to be up to $\sim 9 \times 10^3\ \mu C/cm^2$ if formed within the first three cycles. The largest number of layers of silver which were formed to higher oxide on rolled, etched, or polished silver sheet, after much cycling was 70 (assuming a surface roughness factor of one).

3. Similar measurements, less accurate, however, because of the much faster decay at the oxygen precursor potential, indicated that about one-tenth of a layer of an adsorbed species (HO_2, O, OH?) exists on the surface during O_2 evolution.

4. The temperature coefficient of the current required to maintain the potential of a porous electrode at 130 mV above the AgO/Ag_2O potential (that is, in the region of the Ag_2O_3 reversible potential) was 12.0 ± 2.0 kcal/mole. This value can be considered to be the energy by which oxygen atoms are bound in the higher oxide. Activation energy measurements on planar electrodes [although more difficult to make] were about the same at both 130 and 230 mV above the AgO/Ag_2O potential, i.e. 14.0 ± 2.0 kcal/mole.

5. Tafel slopes and intercepts were measured and recorded, but they are difficult to interpret since they change unpredictably with time. However, they do underline the complex nature and the time variance of the reactions taking place on the electrode surface.

Can. J. Chem. Downloaded from www.nrcresearchpress.com by 210.87.254.105 on 09/05/12
For personal use only.

6. Open circuit potential decay curves, with their protracted linear regions of $\partial E/\partial \log t$, have many slopes and potential regions which seem to be typical of the non-stoichiometric type of oxide.

7. The evidence for a higher oxide phase can be summed up by the following: (i) the presence of voltage plateaus in oxidation and reduction curves in a region well above the AgO potential; (ii) the recovery of the potential if reduction is interrupted in the higher oxide region; (iii) the substantial electrochemical capacity of this phase and its thickness on the surface of the electrode; and (iv) the activation energy of 12 kcal/mole, not a function of the potential in the higher oxide region.

8. The variation of the amount of "Ag_2O_3" formed per unit amount of Ag_2O substrate under various experimental conditions suggests that as the material $Ag_2O[O]$ becomes filled up with oxygen atoms to form stoichiometric Ag_2O_3, an abrupt change occurs in the structure of the higher oxide which results in an abrupt change in the mechanism of oxygen evolution.

REFERENCES

1. J. A. McMillan. Chem. Rev. **62**, 65 (1962).
2. P. Ray and D. Sen. Chemistry of bi- and tripositive silver. Natl. Sci. Inst. India, 1960.
3. M. E. Bedwell. Bibliography of subjects relating to the zinc – silver oxide cell. Report No. Chem. 511, Royal Aircraft Establishment, England. June 1957.
4. A. Hickling and D. Taylor. Discussions Faraday Soc. **1**, 277 (1947).
5. R. Luther and F. Pokorny. Z. Anorg. Chem. **57**, 290 (1908).
6. W. M. Latimer. Oxidation potentials. 2nd ed. Prentice-Hall, Inc., New York. 1953.
7. T. P. Dirkse. J. Electrochem. Soc. **107**, 725 (1960).
8. Handbook of chemistry and physics. 44th ed. Chemical Rubber Publishing Co., Cleveland. 1963. p. 3507.
9. V. Scatturin, P. Bellon, and A. J. Salkind. J. Electrochem. Soc. **108**, 819 (1961).
10. H. Braekken. Kgl. Norske Videnskab. Selskabs Forh. **7**, 143 (1935).
11. W. S. Graff and H. H. Stadelmeier. J. Electrochem. Soc. **105**, 446 (1958).
12. P. Jones, H. R. Thirsk, and W. F. K. Wynne-Jones. Trans. Faraday Soc. **52**, 1003 (1956).

Can. J. Chem. Downloaded from www.nrcresearchpress.com by 210.87.254.105 on 09/05/12
For personal use only.

THE ELECTRICAL CONDUCTIVITIES OF SOME TETRA-*n*-ALKYLAMMONIUM SALTS IN ACETONITRILE[1]

A. C. HARKNESS AND H. M. DAGGETT, JR.
Department of Chemistry, The University of British Columbia, Vancouver, British Columbia
Received October 28, 1964

ABSTRACT

The conductances of a number of tetra-*n*-alkylammonium bromides and iodides have been measured in acetonitrile. Limiting equivalent conductances and dissociation constants have been evaluated by two methods. Limiting equivalent ionic conductances have been evaluated from these results. Correlations have been made of the effect of ion size on the ionic conductances and on the relative order of magnitude of the dissociation constants. In an appendix the limiting ionic conductances of a number of other ions have been collected from the existing literature.

INTRODUCTION

There has been no systematic study made of the effect of ion size on the conductance of salts in acetonitrile. The few investigations that have been carried out deal with the conductances of a variety of salts, but the data are such that no correlations can be made regarding the effect of ion size. It is the purpose of this paper to report on some measurements made on solutions of the tetra-*n*-alkylammonium bromides and iodides from methyl to *n*-amyl. From the results of these measurements the limiting equivalent conductances and dissociation constants have been evaluated using the Shedlovsky method (1). Ionic conductances have been evaluated using the method suggested by Coplan and Fuoss (2). Using these results a correlation is made of the effect of ion size on conductances and dissociation constants in the solvent acetonitrile.

EXPERIMENTAL

Solvent

Acetonitrile (Carbide and Carbon Chemicals Co.) was purified as follows. The middle two thirds of the product obtained by a preliminary distillation from silver nitrate was collected over freshly activated alumina. After standing for 2 d, this product was distilled from activated alumina. The product from this distillation had a specific conductance of $0.8–1.0 \times 10^{-8}$ mhos as compared to $10^{-6}–10^{-5}$ mhos for the starting material. The boiling point of the solvent was 81.5–82.0 °C. Its density was determined to be 0.7768 g/ml at 25 °C, in satisfactory agreement with the literature (3). The dielectric constant was taken to be 36.1 (the average of values reported in refs. 4–8) and the viscosity was taken to be 0.3442 cP (the average of values reported in refs. 4–7).

Salts

Tetra-*n*-alkylammonium bromides and iodides were prepared by allowing equivalent amounts of redistilled tertiary amine and of alkyl halide to react at room temperature until the mixture solidified. The product was then repeatedly recrystallized from appropriate solvents until the conductance results from successive recrystallizations were in agreement. The recrystallization solvents and the melting points of the various salts are listed in Table I.

Procedure

Conductivity cells of the flask type described by Kraus and Fuoss (9) were used. The electrodes were lightly platinized. They were intercompared and finally standardized against aqueous solutions of purified potassium chloride. The specific conductivities of the solutions were calculated from the concentrations by means of the empirical Shedlovksy equation (10) corrected to the Jones and Bradshaw standard (11). A correction was made for the conductivity of the water used.

[1]*Based on a thesis submitted by A. C. Harkness in partial fulfillment of the requirements for the degree of Master of Science in the Faculty of Graduate Studies of the University of British Columbia.*

TABLE I

Recrystallization solvents and melting points

Salt*	Recrystallization solvent	m.p. (°C)†
Me_4NI	60% Ethanol/water	375–380 d.
Et_4NI	Ethanol	275–276 d.
Pr_4NI	Ethanol	291 d.
Bu_4NI	Ethanol ppt. with ether	145–146
Am_4NI	Ethanol ppt. with ether	134–135
Me_4NBr	60% Ethanol/water	351–353 d.
Et_4NBr	Ethanol	276 d.
Pr_4NBr	Ethanol	261–262 d.
Bu_4NBr	Benzene	116–117
Am_4NBr	Benzene	99–101

*The following abbreviations are used in this paper: Me = methyl, Et = ethyl, Pr = *n*-propyl, Bu = *n*-butyl, Am = *n*-amyl.
†Melting points are uncorrected.

Measurements of cell resistances were made using a precision a-c. resistance bridge constructed in this laboratory. Polarization effects were eliminated by making measurements at several frequencies and extrapolating to infinite frequency. All measurements were made at 25.000 ± 0.002 °C; an oil thermostat was used to achieve a constant temperature.

Measurements were carried out by the dilution method, all dilutions being made by weight. In calculating concentrations the densities of the solutions were assumed to be the same as that of the solvent. All measured specific conductivities were corrected by subtracting the specific conductivity of the pure solvent from those of the solutions.

RESULTS

The results are tabulated in Tables II and III and are shown graphically in Figs. 1 and 2. It should be noted that the phoreograms are all catabatic.

These results were analyzed in two different ways. In the first, the data were treated by the method of least squares using the relationship:

$$\Lambda = \Lambda_0 - \mathscr{S}\sqrt{C}$$

where Λ is the equivalent conductance at a concentration of C g equiv/l, Λ_0 is the limiting equivalent conductance, and $\mathscr{S}$ is the slope of the $\Lambda - \sqrt{C}$ plot. From this treatment Λ_0 and $\mathscr{S}$ were evaluated. In the second method used in dealing with the data the results were treated by the Shedlovsky method (1) yielding Λ_0 and the dissociation constant K. In these calculations the dielectric constant was taken to be 36.1 and the viscosity 0.3442 cP. An IBM 1620 computer was used to facilitate these calculations. The results of these calculations are given in Table IV.

DISCUSSION

Consistency of the Results

To test the consistency of the results, Kohlrausch's law of independent migration of ions was applied to the Λ_0-values tabulated in Table IV. Taking the differences $\Lambda_0(R_4NI) - \Lambda_0(R_4NBr)$, the average value of the differences was found to be 1.7 ± 0.5 Λ-units when the Λ_0-values based on the $\Lambda - \sqrt{C}$ plot were used and 2.0 ± 0.5 Λ-units when the Shedlovsky values were used. Thus the Λ_0-values are consistent to within about 0.3%.

The values of Λ_0 for Et_4NI was 0.43 Λ-units lower than that found by Kortüm (8) and by Walden (12). The values of Λ_0 for Me_4NBr, Me_4NI, Et_4NBr, Et_4NI, and Pr_4NI were from 1.24 to 5.07 Λ-units higher than those found by other investigators (12, 13, 14,). Data for the other salts do not appear in the literature.

TABLE II

The conductances of tetra-*n*-alkylammonium bromides*

Me_4NBr		Et_4NBr		Pr_4NBr		Bu_4NBr		Am_4NBr	
$C \times 10^4$	Λ	$C \times 10^4$	Λ	$C \times 10^4$	Λ	$C \times 10^4$	Λ	$C \times 10^4$	Λ
61.97	147.0	53.52	155.5	27.03	150.5	32.90	141.9	19.88	140.6
35.89	158.5	17.80	167.6	8.462	159.2	13.54	149.1	6.628	147.2
12.17	174.7	5.076	176.2	2.958	164.2	5.247	154.3	2.212	151.3
5.129	182.8	2.189	179.5	1.156	167.1	2.104	157.5	0.7845	153.6
1.986	188.0	0.7965	181.9	33.87	148.1	1.054	159.1	0.2791	155.1
42.07	156.0	37.35	160.2	14.89	155.3	12.78	149.4	18.23	141.4
12.84	174.5	16.07	168.7	6.722	160.4	4.409	154.8	7.292	146.6
3.157	186.1	5.356	175.8	1.838	165.5	1.600	158.0	3.586	149.6
1.558	189.6	2.684	178.7	0.6710	168.7	0.7908	159.7	1.566	151.9
		1.053	181.2						

*Concentrations are given in g equiv l^{-1} and conductances in ohm^{-1} cm^2. See also first footnote to Table I.

TABLE III

The conductances of tetra-*n*-alkylammonium iodides*

Me_4NI		Et_4NI		Pr_4NI		Bu_4NI		Am_4NI	
$C \times 10^4$	Λ	$C \times 10^4$	Λ	$C \times 10^4$	Λ	$C \times 10^4$	Λ	$C \times 10^4$	Λ
46.20	163.6	43.62	160.6	41.21	149.2	25.12	146.0	15.68	143.9
30.73	169.8	16.16	170.6	18.57	156.7	14.58	150.2	8.199	147.7
10.53	181.9	5.348	177.7	7.738	162.4	7.936	154.0	3.274	151.6
2.788	190.5	1.540	182.0	2.845	166.4	3.179	157.9	1.556	153.7
0.8960	194.0	0.5824	183.7	1.267	169.0	1.293	160.3	0.7247	155.1
0.3051	195.7	0.1364	184.8	36.76	150.5	31.68	143.7	28.28	139.4
15.99	178.2	54.91	157.8	8.478	162.1	17.42	148.9	10.10	146.8
8.060	184.2	21.36	168.2	2.614	167.0	5.925	155.4	4.419	151.0
2.936	189.9	6.232	176.8	0.8579	170.1	1.380	160.4	1.412	154.5
1.569	192.2	1.434	182.5	0.3625	171.3	0.3763	162.9	12.86	145.5
								8.777	147.3
								3.800	151.1
								1.929	153.3
								0.7102	155.4

*See first footnote to Table II.

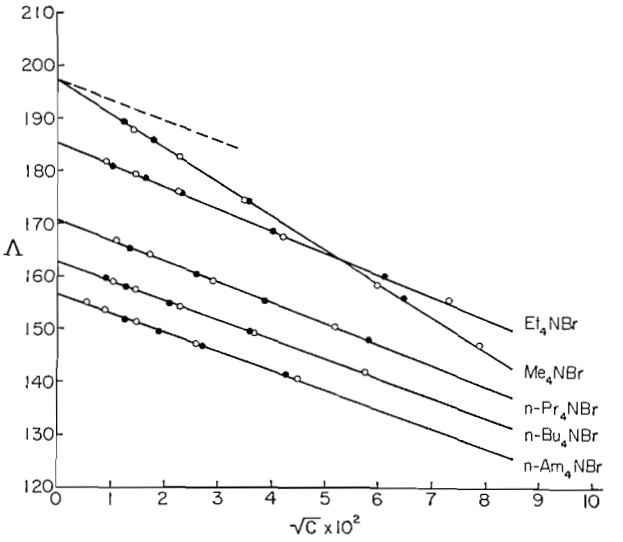

FIG. 1. Phoreograms of some tetra-*n*-alkylammonium bromides in acetonitrile at 25 °C. The dotted line represents the theoretical Onsager slope for tetramethylammonium bromide.

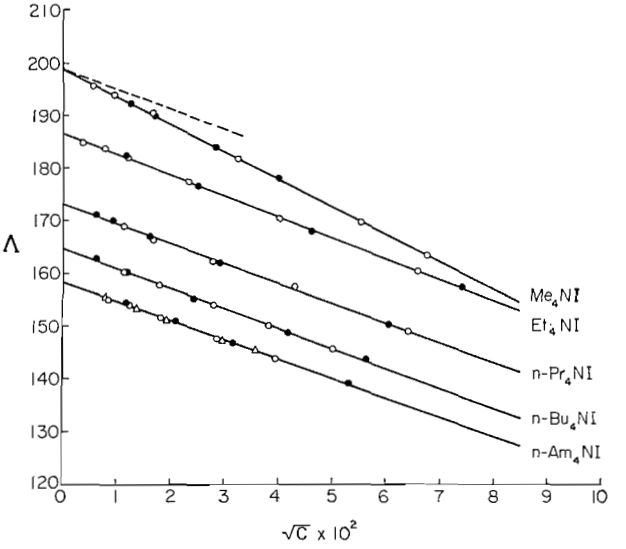

FIG. 2. Phoreograms of some tetra-*n*-alkylammonium iodides in acetonitrile at 25 °C. The dotted line represents the theoretical Onsager slope for tetramethylammonium iodide.

Experimental Slopes

All of the experimental slopes of the $\Lambda - \sqrt{C}$ plots were greater than theoretical, the ratios $\mathcal{S}_{exp}/\mathcal{S}_{th}$ varying from 1.699 to 1.038 (i.e. the phoreograms are all catabatic). This indicates a substantial degree of association of the ions, the degree of association being greatest with the methyl salts and least with the amyl salts. This trend is to be expected, for the electrical field around the small Me_4N^+ ion would be greater than that around the larger Am_4N^+ ion and hence there would be a greater degree of association with the counterions Br^- and I^- with Me_4N^+. The ratio $\mathcal{S}_{exp}/\mathcal{S}_{th}$ is unexpectedly high for Bu_4NI. There seems to be no logical explanation for this.

TABLE IV

Results of the analysis of the conductance data

$\Lambda - \sqrt{C}$ method		Shedlovsky method	
Salt*	Λ_0	Λ_0	K
Me_4NBr	197.29±0.18	195.16±0.26	0.0190±0.0003
Et_4NBr	185.45±0.12	185.13±0.07	0.069 ±0.001
Pr_4NBr	170.94±0.22	170.61±0.17	0.072 ±0.005
Bu_4NBr	162.75±0.12	162.66±0.08	0.094 ±0.005
Am_4NBr	156.67±0.15	156.55±0.12	0.10 ±0.01
Me_4NI	198.83±0.11	197.73±0.09	0.0348±0.0005
Et_4NI	186.69±0.16	186.61±0.11	0.088 ±0.003
Pr_4NI	173.20±0.17	173.10±0.13	0.095 ±0.006
Bu_4NI	164.77±0.14	164.59±0.11	0.084 ±0.005
Am_4NI	158.30±0.14	158.23±0.10	0.101 ±0.009

*See first footnote to Table I.

Dissociation Constants

The dissociation constants obtained by application of the Shedlovsky method to the data vary in the manner predicted in the previous section. The *dissociation* constants for the methyl salts are the lowest (indicating a high degree of association of the ions), while those for the other salts increase regularly to amyl. The only exception to this trend is Bu_4NI, where the dissociation constant is unexpectedly low (as was indicated in the previous section).

It is also of interest to compare the dissociation constants for the bromide series with those for the iodide series. The values of K for the bromide series are lower than those for the iodide series (the exception again being Bu_4NI). These trends are easily interpreted on the basis of the higher electrical field around Br^- due to its smaller size. This higher field would cause more interaction between R_4N^+ and Br^- than between R_4N^+ and I^-, leading to a greater degree of association and hence a lower value of K for the bromide series.

Ionic Conductances

Ionic conductances were evaluated by the method suggested by Coplan and Fuoss (2). In this method tri-*i*-amyl-*n*-butylammonium tetraphenylboride is taken as the standard. The limiting ionic conductances for $(i\text{-Am})_3BuN^+$ and Ph_4B^- are each assumed to be one half of the limiting conductance for the salt. The argument is based on the fact that the ionic radii of the two ions are nearly the same and hence should have the same values for the limiting ionic conductance, for they would meet with the same resistance in passing through the solution. We have adopted the value of 116.1 ± 0.1 Λ-units for the limiting equivalent conductance for the salt (15). Thus the value of Λ_0^+ for the tri-*i*-amyl-*n*-butylammonium ion is 58.0 Λ-units which is the same as that for the tetraphenylboride ion. Using these Λ_0-values, we have determined the Λ_0^+-values for the tetra-*n*-alkylammonium ions and for the Br^- and I^- ions in acetonitrile, using the results of Fuoss and coworkers (4, 5, 6) for Bu_4NPh_4B. The results (based on Shedlovsky Λ_0-values) are presented in Table V.

It is to be noted from Table V that the Λ_0^--value for Br^- is smaller than that for I^- in spite of the fact that the Br^- ion is smaller and so should have the greater ionic conductance. This apparent discrepancy is easily explained by the fact that the Br^- ion will have a higher electrical field around it (because of its smaller size) and so will interact more strongly with the polar solvent leading to a greater hydrodynamic radius. Thus its

TABLE V

Limiting ionic conductances based on $\Lambda_0^+(Bu_4N^+) = 61.3 \pm 0.1$*

Ion	Λ_0 value
Br^-	101.3±0.1
I^-	103.3±0.1
Me_4N^+	94.2±0.3
Et_4N^+	83.6±0.2
Pr_4N^+	69.6±0.3
Bu_4N^+	61.3±0.1
Am_4N^+	55.1±0.1

*See first footnote to Table I.

conductance will be smaller than that of the I^- ion where the interaction with the solvent will not be as great.

The trend of Λ_0^+-values for the R_4N^+ ions is in line with the change in ionic radius—the smaller the radius the greater will be the conductance of the ion.

APPENDIX I

The ionic conductances reported in Table V enable us to evaluate ionic conductances for a large number of ions from results reported in the literature. To effect this evaluation all conductance data were reprocessed by the Shedlovsky function to gain consistent values for the limiting equivalent conductance of the various salts in acetonitrile. The results are reported in Table VI.

TABLE VI

Limiting ionic conductances in acetonitrile*

Cations			Anions		
Ion	Ref.	Λ_0^+	Ion	Ref.	Λ_0^-
Me_4N^+	16	94.2±0.3	Cl^-	17	94.0±0.3¶
Et_4N^+	8, 12, 16	83.7±0.4	Br^-	16	101.3±0.1
Pr_4N^+	16	69.6±0.3	I^-	15, 16	102.9±0.4
Bu_4N^+	4, 5, 6	61.3±0.1	I_3^-	13	97.6±0.6
$(i\text{-Am})_3Bu_4N^+$	15	58.0±0.1	I_5^-	13	97.3±1.0
Am_4N^+	16	55.1±0.1	I_7^-	13	99.2±0.5
$EtNH_3^+$	12	91.7±0.7	IBr_2^-	14	98.9±0.6
$Et_2NH_2^+$	12	90.2±0.5	$IBrCl^-$	14	103.2±0.4
Et_3NH^+	12	81.0±0.8	NO_3^-	12, 22	106.1±0.9
$i\text{-}BuNH_3^+$	12	82.6±0.8	ClO_4^-	12	103.0±0.4
$n\text{-Cetyl-}NH_3^+$	12	35.1±0.6	HSO_4^-	21	90.7±2.3
Bz_3NH^+	7	46.4±0.6	PF_6^-	23	102.9±0.5
Ph_4As^+	17, 18	58.6±0.3	Ph_4B^-	5, 15	58.0±0.1
Li^+	20	79.9±0.6†	Pi^-	7	80.1±0.6**
Na^+	17	76.9±0.2‡	Tricyanovinyl-alcoholate$^-$	24	97.5±0.5
K^+	12, 19	83.4±0.2§	1,1,2,3,3-Penta-cyanopropenide$^-$	24, 25	85.3±0.4
Rb^+	20	97.6±0.9	1,1,2,6,6,7-Hexacyano-1,3,5-heptatrienide$^-$	24	62.0±0.4
Cs^+	20	101.0±0.7‖	Bis(tricyanovinyl)-amine anion$^-$	24	72.8±0.4
Ag^+	12	82.6±2.3	1,1,2,4,5,5-Hexacyano-3-azapentadienide$^-$	25	72.4±0.5
H^+	21	81.3±0.6			

*See first footnote to Table I. Also, Bz = benzyl, Ph = phenyl, Pi = picrate.
†Walden and Birr (12) yields 53.0 ± 1.6.
‡Minc and Werblan (20) yields 88.1 ± 0.6 and Walden and Birr (12) yields 64.0 ± 0.5.
§Minc and Werblan (20) yields 104.0 ± 0.9.
‖Popov and Skelly (14) yields 88.4 ± 0.3.
¶Popov and Skelly (14) yields 99.3 ± 0.6 and Walden and Birr (12) yields 90.8 ± 0.6.
**Walden and Birr (12) and Coplan and Fuoss (15) yield 77.0 ± 0.6.

ACKNOWLEDGMENTS

We wish to thank the Research Corporation and the National Research Council of Canada for grants in aid of this research. One of us (A. C. H.) is indebted to the British Columbia Sugar Refining Co. Ltd. for the award of a scholarship. We also wish to thank the staff of the Computing Center of the University of British Columbia for their help in setting up the computer programs used in the analysis of the results.

REFERENCES

1. T. SHEDLOVSKY. J. Franklin Inst. **225**, 739 (1938). R. M. FUOSS and T. SHEDLOVSKY. J. Am. Chem. Soc. **71**, 1496 (1949).
2. M. A. COPLAN and R. M. FUOSS. J. Phys. Chem. **68**, 1177 (1964).
3. A. WEISSBERGER, E. PROSKAUER, J. A. RIDDICK, and E. E. TOOP. Organic solvents. 2nd ed. Interscience Publishers Inc., New York, 1955. p. 224.
4. F. ACCASCINA, S. PETRUCCI, and R. M. FUOSS. J. Am. Chem. Soc. **81**, 1301 (1959).
5. D. S. BERNS and R. M. FUOSS. J. Am. Chem. Soc. **82**, 5585 (1960).
6. A. M. BROWN and R. M. FUOSS. J. Phys. Chem. **64**, 1341 (1960).
7. C. M. FRENCH and D. F. MUGGLETON. J. Chem. Soc. 2131 (1957).
8. G. KORTÜM, S. D. GOKHALE, and H. WILSKI. Z. Physik. Chem. Frankfurt, **4**, 286 (1955).
9. C. A. KRAUS and R. M. FUOSS. J. Am. Chem. Soc. **55**, 21 (1933).
10. T. SHEDLOVSKY. J. Am. Chem. Soc. **54**, 1411 (1932).
11. G. JONES and B. C. BRADSHAW. J. Am. Chem. Soc. **55**, 1780 (1933).
12. P. WALDEN and E. J. BIRR. Z. Physik. Chem. A, **144**, 269 (1929).
13. A. I. POPOV, R. H. RYGG, and N. E. SKELLY. J. Am. Chem. Soc. **78**, 5740 (1956).
14. A. I. POPOV and N. E. SKELLY. J. Am. Chem. Soc. **76**, 5309 (1954).
15. M. A. COPLAN and R. M. FUOSS. J. Phys. Chem. **68**, 1181 (1964).
16. This work.
17. R. E. HUMPHREY. Thesis, Iowa State University. 1958. Dissertation Abstr. **19**, 455 (1958).
18. A. I. POPOV and R. E. HUMPHREY. J. Am. Chem. Soc. **81**, 2043 (1959).
19. A. E. MARKINKOWSKY. Thesis, Rensselaer Polytechnic Institute. 1961. Dissertation Abstr. **22**, 97 (1961).
20. S. MINC and L. WERBLAN. Electrochim. Acta, **7**, 257 (1962).
21. J. F. COETZEE and I. M. KOLTHOFF. J. Am. Chem. Soc. **79**, 6110 (1957).
22. D. S. BERNS and R. M. FUOSS. J. Am. Chem. Soc. **83**, 1321 (1961).
23. J. ELIASSAF, R. M. FUOSS, and J. E. LIND, JR. J. Phys. Chem. **67**, 1941 (1963).
24. R. H. BOYD. J. Phys. Chem. **65**, 1834 (1961).
25. J. E. LIND, JR. and R. M. FUOSS. J. Am. Chem. Soc. **83**, 1828 (1961).

Can. J. Chem. Downloaded from www.nrcresearchpress.com by 210.87.254.105 on 09/05/12
For personal use only.

NOTES

A COMPARISON OF THE RAMAN CRYSTAL AND SOLUTION SPECTRA OF THE HEXANIOBATE AND HEXATANTALATE IONS

R. STUART TOBIAS

INTRODUCTION

About a decade ago, Lindqvist, in reviewing methods for studying inorganic polyions in aqueous solution (1), noted that efforts to explain the relatively complicated Raman spectra of solutions of polyanions had not been very successful. On the positive side, he commented that "the most important result is the confirmation, in some cases, of the identity of the ions in crystals and in solution." He also noted that such measurements "may give valuable information about the ions in solution if the interpretation of the spectra can be related to the known structure of the ions in the solid state."

During the past ten years, few Raman studies of polycondensed inorganic species have been made in spite of the availability now of more crystallographic information and of commercial Raman equipment with double-grating monochromators and photoelectric detection. These permit accurate recording of the rather weak scattering from inorganic oxyanions in solution as well as the determination of the spectra of powdered crystalline samples. While it would not be expected that the spectra would show appreciable changes with small variations in the degree of polymerization of, for example, a large polyphosphate, they should be sensitive to significant changes in the species symmetry. That this much is true seems to be supported by the recent observations of Aveston, Anacker, and Johnson (2) on the Raman spectra of different polymolybdates.

On the basis of light scattering and ultracentrifugation, it has been suggested recently that solutions prepared by dissolving $K_{14}Nb_{12}O_{37}\cdot 27H_2O$ (3) and $K_8Ta_6O_{19}\cdot 16H_2O$ (4, 5) contain polyanions with the same degree of polymerization, $[M_6O_{19}^{-8}]$, M = Nb(V), Ta(V). In the case of the niobate, the conclusion is supported by the e.m.f. measurements of Neumann (6). Single crystal X-ray studies on the niobate (7) and tantalate (8) indicate that the crystals contain isostructural anions $[M_6O_{19}^{-8}]$ with cubic symmetry. The Raman spectrum of the tantalate has been published (9), and this note reports a comparison of the niobate and tantalate solution and crystal spectra made to ascertain whether the same structural unit exists in the niobate and tantalate crystals and solutions.

EXPERIMENTAL

Materials

The preparations and analyses of the $K_8Ta_6O_{19}\cdot 16H_2O$ and $K_{14}Nb_{12}O_{37}\cdot 27H_2O$ have been described earlier (3, 4). Solutions of the niobate and tantalate were prepared by saturating carbonate-free KOH solution with the salt.

Raman Spectra

The Raman spectra were recorded photoelectrically with a Cary Model 81 spectrophotometer. The general procedure has been described elsewhere (10). Crystal spectra were measured using a conical cell patterned after that described by Busey and Keller (11), for this was found far superior to straight cells. All spectra were excited with the 4 358 Å mercury line.

RESULTS AND DISCUSSION

Figure 1 illustrates the Raman spectra for 1 *M* KOH saturated with $K_{14}Nb_{12}O_{37}\cdot 27H_2O$ and with $K_8Ta_6O_{19}\cdot 16H_2O$. In Fig. 2 are given the corresponding crystal spectra. Our

tantalate spectra are virtually identical with those given earlier by Aveston and Johnson and are shown only for comparison. One exception arises from the use of 1 *M* KOH as the solvent in this work. Its use leads to an increase in intensity of the 450 cm^{-1} librational mode of water, and this tends to obscure this region in our spectra. Values of the frequencies and the state of polarization are tablulated in Table I. The 260 cm^{-1} line in our tantalate crystal spectra was so weak that it was only identified by comparison with Aveston and Johnson's spectrum. The pronounced similarity of all of the spectra make it seem very likely that the isostructural niobate and tantalate anions found in the crystals are also present in the solutions.

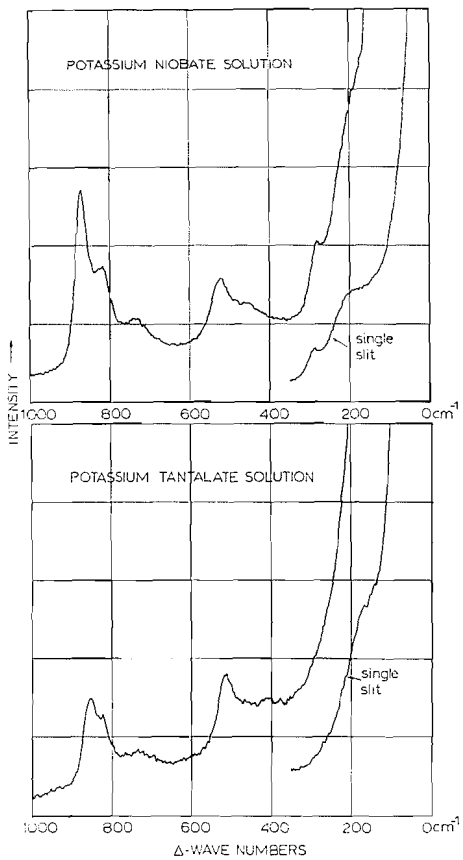

FIG. 1. Niobate and tantalate solution spectra.

Because of the complexity of the anions (there are 69 vibrational degrees of freedom) it is not possible to discuss any detailed assignments. If one assumes the structure suggested by Lindqvist (7, 8) to be correct, the representation of the normal coordinates can be obtained using the relations given by Herzberg (12) as

$$\Gamma_{vib} = 3A_{1g} + A_{2g} + A_{2u} + 4E_g + E_u + 3F_{1g} + 7F_{1u} + 4F_{2g} + 4F_{2u}.$$

On this basis, as noted by Aveston and Johnson (9), 11 Raman active and 7 infrared active normal modes would be predicted. Fewer lines might appear because of accidental degeneracy resulting from the very heavy metal atoms and because many of the bending

Can. J. Chem. Downloaded from www.nrcresearchpress.com by 210.87.254.105 on 09/05/12
For personal use only.

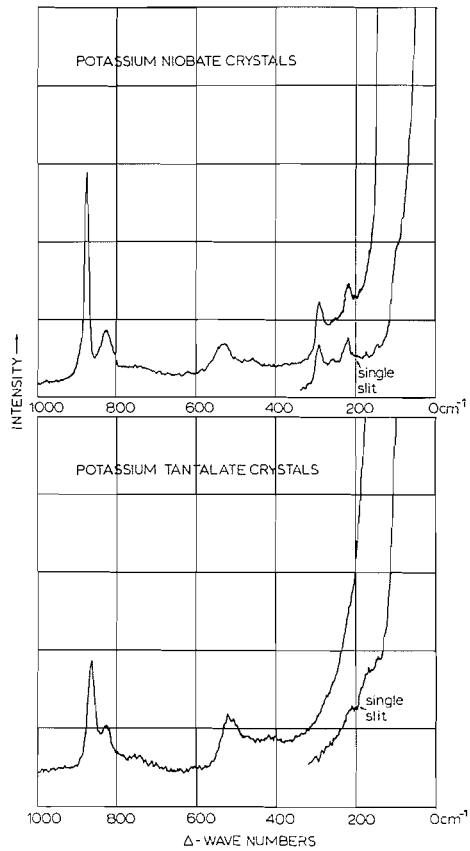

FIG. 2. Niobate and tantalate crystal spectra.

TABLE I

Raman shifts (cm^{-1}) for potassium niobate and potassium tantalate

Crystalline $K_{14}Nb_{12}O_{37}\cdot 27H_2O$	Aqueous $K_{14}Nb_{12}O_{37}\cdot 27H_2O$	Crystalline $K_8Ta_6O_{19}\cdot 16H_2O$	Aqueous $K_8Ta_6O_{19}\cdot 16H_2O$
877	878 p	862	853
823	823 dp	823	825
750	733 dp	740	740
528	533 dp	514	515
475	475 dp (?)	464	—*
435	450 dp (?)	413	415
291	290 p	260	—
219	215	208	200

Abbreviations: p, polarized; dp, depolarized.
*A line was observed by Aveston and Johnson at 466 cm^{-1}.

modes would be expected at very low frequencies, and no more than three polarized lines should be observed. In these spectra, two lines were polarized. In addition for a cubic point group where the polarizability ellipsoid reduces to a sphere, the A_{1g} modes should be completely polarized, i.e., $\rho = 0$. Under these conditions the Rayleigh scattering should also be completely polarized, and it was noted earlier that no depolarization was detected (3). Unfortunately it is very difficult to make precise measurement of the degree of

Can. J. Chem. Downloaded from www.nrcresearchpress.com by 210.87.254.105 on 09/05/12
For personal use only.

depolarization for either Rayleigh or Raman scattering. The depolarization ratio for the 878 cm^{-1} line of the niobate solution, $\rho = 0.23$, was comparable to the values obtained for other ions belonging to cubic point groups using similar experimental conditions.

The polarized niobate and tantalate lines at 878 and 853 cm^{-1}, respectively, in solution can be assigned to an A_{1g} mode. While no precise description of the normal mode can be given, it would be expected to consist of symmetrical metal–oxygen bond stretching involving mainly the six unshared peripheral oxygens. The very similar frequencies for the niobate and tantalate are to be expected if one considers the similarity in the frequencies of the breathing modes, ν_1, of the tetrahedral $MoO_{4(aq)}^{-2}$ and $WO_{4(aq)}^{-2}$ anions which appear at 894 and 928 cm^{-1} (13). The fact that these niobate and tantalate lines arise from relatively straightforward bond stretching is supported by similarity of the frequencies to the value for the breathing mode of VO_4^{-3}, 870 cm^{-1} (13).

It might be expected that the metal–oxygen stretching force constants would be considerably smaller with the octahedrally coordinated niobium(V) and tantalum(V) than with tetrahedrally coordinated molybdenum(VI) and tungsten(VI) or technetium(VII) and rhenium(VII). There does not seem to be a pronounced effect, for only a rather regular trend with the metal oxidation state is observed for the highest frequency totally symmetrical mode: $Nb_6O_{19(aq)}^{-8}$, 878 cm^{-1}; $MoO_{4(aq)}^{-2}$, 894 cm^{-1} (13); $TcO_{4(aq)}^{-}$, 912 cm^{-1} (11); and $Ta_6O_{19(aq)}^{-8}$, 853 cm^{-1}; $WO_{4(aq)}^{-2}$, 928 cm^{-1} (13); $ReO_{4(aq)}^{-}$, 971 cm^{-1} (11).

ACKNOWLEDGMENT

The support of the United States National Science Foundation through grants G14173 and GP-653 is gratefully acknowledged.

1. I. Lindqvist. Symposium on Structure and Properties of Heteropoly Anions, 130th National Meeting, American Chemical Society, Atlantic City, New Jersey. September 1956. p. 20.
2. J. Aveston, E. W. Anacker, and J. S. Johnson. Inorg. Chem. **3**, 735 (1964).
3. W. H. Nelson and R. S. Tobias. Can. J. Chem. **42**, 731 (1964).
4. W. H. Nelson and R. S. Tobias. Inorg. Chem. **2**, 985 (1963).
5. W. H. Nelson and R. S. Tobias. Inorg. Chem. **3**, 653 (1964).
6. G. Neumann. Acta Chem. Scand. **18**, 278 (1964).
7. I. Lindqvist. Arkiv Kemi, **5**, 247 (1952).
8. I. Lindqvist and B. Aronsson. Arkiv Kemi, **7**, 49 (1954).
9. J. Aveston and J. S. Johnson. Inorg. Chem. **3**, 1051 (1964).
10. M. M. McGrady and R. S. Tobias. Inorg. Chem. **3**, 1157 (1964).
11. R. H. Busey and O. L. Keller, Jr. J. Chem. Phys. **41**, 215 (1964).
12. G. Herzberg. Infrared and raman spectra of polyatomic molecules. D. Van Nostrand, Princeton. 1945. p. 139.
13. H. Siebert. Z. Anorg. Allgem. Chem. **275**, 225 (1954).

Received November 5, 1964.
Department of Chemistry,
University of Minnesota,
Minneapolis, Minnesota.

THE ACIDITY OF SOME SUBSTITUTED ACETONITRILES[1]

Ross Stewart, J. P. O'Donnell, and Keith Bowden

In connection with the establishment of an acidity scale for strongly basic solutions (1–4) several nitriles have been examined as possible indicators.

$$RCH_2CN + OH^- \rightarrow RCHCN^- + H_2O.$$

[1]*Part VI of the series "Strongly Basic Systems".*

Can. J. Chem. Downloaded from www.nrcresearchpress.com by 210.87.254.105 on 09/05/12
For personal use only.

depolarization for either Rayleigh or Raman scattering. The depolarization ratio for the 878 cm^{-1} line of the niobate solution, $\rho = 0.23$, was comparable to the values obtained for other ions belonging to cubic point groups using similar experimental conditions.

The polarized niobate and tantalate lines at 878 and 853 cm^{-1}, respectively, in solution can be assigned to an A_{1g} mode. While no precise description of the normal mode can be given, it would be expected to consist of symmetrical metal–oxygen bond stretching involving mainly the six unshared peripheral oxygens. The very similar frequencies for the niobate and tantalate are to be expected if one considers the similarity in the frequencies of the breathing modes, ν_1, of the tetrahedral $MoO_{4(aq)}^{-2}$ and $WO_{4(aq)}^{-2}$ anions which appear at 894 and 928 cm^{-1} (13). The fact that these niobate and tantalate lines arise from relatively straightforward bond stretching is supported by similarity of the frequencies to the value for the breathing mode of VO_4^{-3}, 870 cm^{-1} (13).

It might be expected that the metal–oxygen stretching force constants would be considerably smaller with the octahedrally coordinated niobium(V) and tantalum(V) than with tetrahedrally coordinated molybdenum(VI) and tungsten(VI) or technetium(VII) and rhenium(VII). There does not seem to be a pronounced effect, for only a rather regular trend with the metal oxidation state is observed for the highest frequency totally symmetrical mode: $Nb_6O_{19(aq)}^{-8}$, 878 cm^{-1}; $MoO_{4(aq)}^{-2}$, 894 cm^{-1} (13); $TcO_{4(aq)}^{-}$, 912 cm^{-1} (11); and $Ta_6O_{19(aq)}^{-8}$, 853 cm^{-1}; $WO_{4(aq)}^{-2}$, 928 cm^{-1} (13); $ReO_{4(aq)}^{-}$, 971 cm^{-1} (11).

ACKNOWLEDGMENT

The support of the United States National Science Foundation through grants G14173 and GP-653 is gratefully acknowledged.

1. I. Lindqvist. Symposium on Structure and Properties of Heteropoly Anions, 130th National Meeting, American Chemical Society, Atlantic City, New Jersey. September 1956. p. 20.
2. J. Aveston, E. W. Anacker, and J. S. Johnson. Inorg. Chem. **3**, 735 (1964).
3. W. H. Nelson and R. S. Tobias. Can. J. Chem. **42**, 731 (1964).
4. W. H. Nelson and R. S. Tobias. Inorg. Chem. **2**, 985 (1963).
5. W. H. Nelson and R. S. Tobias. Inorg. Chem. **3**, 653 (1964).
6. G. Neumann. Acta Chem. Scand. **18**, 278 (1964).
7. I. Lindqvist. Arkiv Kemi, **5**, 247 (1952).
8. I. Lindqvist and B. Aronsson. Arkiv Kemi, **7**, 49 (1954).
9. J. Aveston and J. S. Johnson. Inorg. Chem. **3**, 1051 (1964).
10. M. M. McGrady and R. S. Tobias. Inorg. Chem. **3**, 1157 (1964).
11. R. H. Busey and O. L. Keller, Jr. J. Chem. Phys. **41**, 215 (1964).
12. G. Herzberg. Infrared and raman spectra of polyatomic molecules. D. Van Nostrand, Princeton. 1945. p. 139.
13. H. Siebert. Z. Anorg. Allgem. Chem. **275**, 225 (1954).

Received November 5, 1964.
Department of Chemistry,
University of Minnesota,
Minneapolis, Minnesota.

THE ACIDITY OF SOME SUBSTITUTED ACETONITRILES[1]

Ross Stewart, J. P. O'Donnell, and Keith Bowden

In connection with the establishment of an acidity scale for strongly basic solutions (1–4) several nitriles have been examined as possible indicators.

$$RCH_2CN + OH^- \rightarrow RCHCN^- + H_2O.$$

[1]*Part VI of the series "Strongly Basic Systems".*

Can. J. Chem. Downloaded from www.nrcresearchpress.com by 210.87.254.5 on 09/05/12
For personal use only.

One of these, *p*-nitrobenzyl cyanide has been frequently used as an indicator in mixed solvent systems in the critical area spanning the completely aqueous and partly aqueous regions. We have found this compound to be an unreliable indicator because of the complicated spectral changes that accompany its ionization. These are shown in Figs. 1 and 2. The behavior of this carbon acid is in marked contrast to that of the other nitriles reported herein and the nitrogen acids reported earlier. In all these cases a simple ionization process (proton loss) was indicated by the spectral changes.

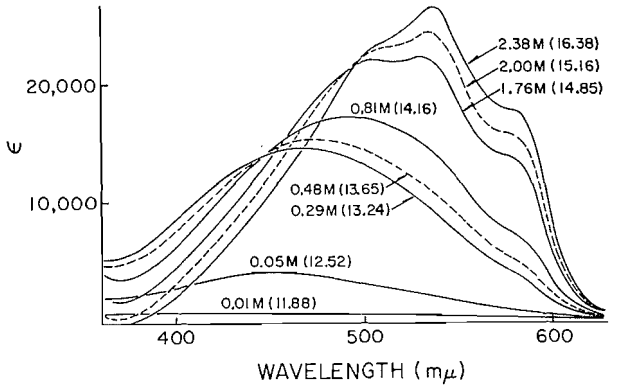

FIG. 1. The spectrum of *p*-nitrobenzyl cyanide in various concentrations of aqueous benzyltrimethylammonium hydroxide.

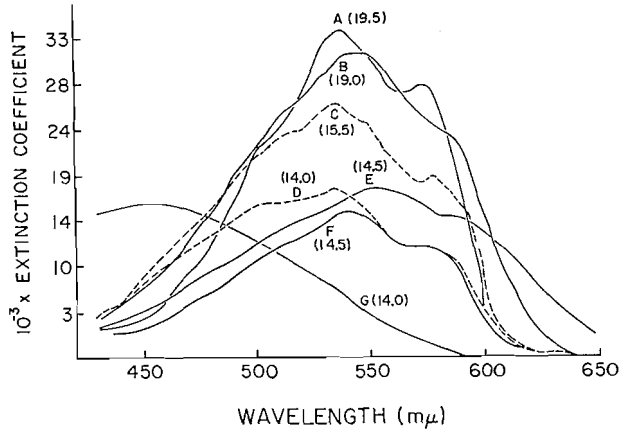

FIG. 2. The spectrum of *p*-nitrobenzyl cyanide in various solvent systems. The bracketed quantity is the H_- value of the system. A. 95 mole % sulfolane in water containing 0.11 *M* tetramethylammonium hydroxide. B. 30 mole % pyridine in water containing 1.19 *M* benzyltrimethylammonium hydroxide. C. 73.2% hydrazine in water. D. 45.3% hydrazine in water. E. 1.0 *M* aqueous phenyltrimethylammonium hydroxide. F. Anhydrous ethanolamine. G. 1.0 *M* aqueous sodium hydroxide.

Figure 1 shows the spectral changes that occur as the concentration of benzyltrimethylammonium hydroxide is increased and Fig. 2 the changes that occur when the solvent is altered. Each of these curves is labelled with the H_- value of the solution (3) and it is clear that the spectrum continues to change over the H_- region from 12 to 20. Schaal has suggested that two successive ionizations occur (5) to give, finally, the ion $p\text{-}NO_2C_6H_4CCN^{=}$. Although the loss of the second proton may occur in strongly basic solution the variety of spectra that can be obtained in moderately basic solution show that this is not the sole answer.

Can. J. Chem. Downloaded from www.nrcresearchpress.com by 210.87.254.5 on 09/05/12
For personal use only.

O'Ferrall and Ridd (6) have shown that *p*-nitrobenzyl cyanide reacts in different ways with aqueous and methanolic base. None of the nitrogen acids used in the development of the H_- scale (1–4) nor the other nitriles reported herein behave in this way and we suspect that nucleophilic addition to the aromatic ring (7, 8) must be competing with proton removal in this case. The other nitriles lack the nitro substituent and nucleophilic addition to the ring does not occur.

TABLE I

Ionization data for cyano compounds

Compound	pK_a	Anion absorption maxima λ_{max} (mμ)	ϵ	Solvent
Malononitrile	11.14 (4)	226	20 800	Ethanol
9-Cyanofluorene	11.41 (4)	410	2 220	Ethanol
3-Chlorobenzyl cyanide	18.18	348	18 200	Ethanol–DMSO*
	18.10	346	18 500	Water–DMSO*

*Dimethyl sulfoxide.

Table I lists the ionization data for the other nitriles. In addition to these, diphenylacetonitrile was examined but this compound decomposes rapidly in basic aqueous dimethyl sulfoxide after the appearance of a transient yellow color that is due, presumably, to the carbanion.

EXPERIMENTAL

The compounds used were commercially available or were prepared by standard methods, as described elsewhere (4). The pK determinations were made as previously described (3).

1. R. Stewart and J. P. O'Donnell. J. Am. Chem. Soc. **84**, 493 (1962).
2. R. Stewart, J. P. O'Donnell, D. J. Cram, and B. Rickborn. Tetrahedron, **18**, 917 (1962).
3. R. Stewart and J. P. O'Donnell. Can. J. Chem. **42**, 1681, 1694 (1964).
4. K. Bowden and R. Stewart. Tetrahedron. **21**, 261 (1965).
5. R. Schaal. J. Chim. Phys. **52**, 784, 796 (1955).
6. R. A. M. O'Ferrall and J. H. Ridd. J. Chem. Soc. 5030 (1963).
7. R. J. Pollitt and B. C. Saunders. J. Chem. Soc. 1132 (1964).
8. V. Gold and C. H. Rochester. J. Chem. Soc. 1727 (1964); references therein. J. M. Miller and H. Pobiner. Anal. Chem. **36**, 238 (1964).

Received November 12, 1964.
Department of Chemistry,
University of British Columbia,
Vancouver, British Columbia.

POTENTIAL ANTICANCER AGENTS. I. URETHANE-TYPE NITROGEN MUSTARDS OF SOME SYNTHETIC ESTROGENS

E. Grant and I. Niculescu-Duvăz

As early as 1959 the grafting of urethane-type nitrogen mustards on biologically active molecules was attempted on amino acids (2) or hexoses (11) giving rise to low toxicity products whose serine derivative proved to be active against Walker 256 carcinosarcoma. To obtain a selective transport of nitrogen mustards to hormone-dependent tumors, a

Can. J. Chem. Downloaded from www.nrcresearchpress.com by 210.87.254.5 on 09/05/12
For personal use only.

O'Ferrall and Ridd (6) have shown that *p*-nitrobenzyl cyanide reacts in different ways with aqueous and methanolic base. None of the nitrogen acids used in the development of the H_- scale (1–4) nor the other nitriles reported herein behave in this way and we suspect that nucleophilic addition to the aromatic ring (7, 8) must be competing with proton removal in this case. The other nitriles lack the nitro substituent and nucleophilic addition to the ring does not occur.

TABLE I

Ionization data for cyano compounds

Compound	pK_a	Anion absorption maxima λ_{max} (mμ)	ϵ	Solvent
Malononitrile	11.14 (4)	226	20 800	Ethanol
9-Cyanofluorene	11.41 (4)	410	2 220	Ethanol
3-Chlorobenzyl cyanide	18.18	348	18 200	Ethanol–DMSO*
	18.10	346	18 500	Water–DMSO*

*Dimethyl sulfoxide.

Table I lists the ionization data for the other nitriles. In addition to these, diphenylacetonitrile was examined but this compound decomposes rapidly in basic aqueous dimethyl sulfoxide after the appearance of a transient yellow color that is due, presumably, to the carbanion.

EXPERIMENTAL

The compounds used were commercially available or were prepared by standard methods, as described elsewhere (4). The pK determinations were made as previously described (3).

1. R. Stewart and J. P. O'Donnell. J. Am. Chem. Soc. **84**, 493 (1962).
2. R. Stewart, J. P. O'Donnell, D. J. Cram, and B. Rickborn. Tetrahedron, **18**, 917 (1962).
3. R. Stewart and J. P. O'Donnell. Can. J. Chem. **42**, 1681, 1694 (1964).
4. K. Bowden and R. Stewart. Tetrahedron. **21**, 261 (1965).
5. R. Schaal. J. Chim. Phys. **52**, 784, 796 (1955).
6. R. A. M. O'Ferrall and J. H. Ridd. J. Chem. Soc. 5030 (1963).
7. R. J. Pollitt and B. C. Saunders. J. Chem. Soc. 1132 (1964).
8. V. Gold and C. H. Rochester. J. Chem. Soc. 1727 (1964); references therein. J. M. Miller and H. Pobiner. Anal. Chem. **36**, 238 (1964).

Received November 12, 1964.
Department of Chemistry,
University of British Columbia,
Vancouver, British Columbia.

POTENTIAL ANTICANCER AGENTS. I. URETHANE-TYPE NITROGEN MUSTARDS OF SOME SYNTHETIC ESTROGENS

E. Grant and I. Niculescu-Duvăz

As early as 1959 the grafting of urethane-type nitrogen mustards on biologically active molecules was attempted on amino acids (2) or hexoses (11) giving rise to low toxicity products whose serine derivative proved to be active against Walker 256 carcinosarcoma. To obtain a selective transport of nitrogen mustards to hormone-dependent tumors, a

Can. J. Chem. Downloaded from www.nrcresearchpress.com by 210.87.254.40 on 09/05/12
For personal use only.

series of derivatives of that type have been synthesized, starting from natural or synthetic estrogenic hormones, estrone (10), stilbestrol (I) (1, 5, 10), and hexestrol (1, 5, 10).

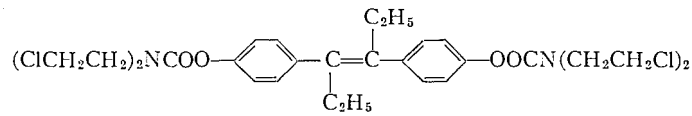

(I)

Danielli showed that tumors treated with urethanes with cytostatic properties became urethane resistant owing to the appearance of an enzyme in the tumor tissue which hydrolyzed and inactivated the urethanes (6). Urethane-type nitrogen mustards remain active since they are hydrolyzed by the enzyme previously formed inside the tumor tissue (5, 6). In the case of urethanes derived from estrogenic hormones (natural or synthetic) such a hydrolysis might also set free in the tumor the base estrogen, e.g. in the case of compound I the diethylstilbestrol, known to have cytostatic properties for some hormone-dependent tumors. There is no proof that this mechanism is responsible for the anticancerous effect observed on urethane-nitrogen mustards of the stilbestrol and hexestrol type. If the hypothesis of enzymatic hydrolysis is correct, there might exist a direct relationship between the anticancer activity of urethane-type nitrogen mustards and the estrogenic activity of the initial *p,p'*-dihydroxydiaryl derivatives.

To elucidate the point a study was undertaken on the anticancer activity of some urethane-type nitrogen mustards, derived from compounds of the *p,p'*-dihydroxydiaryl derivatives class with various estrogenic effects but with similar structures (II) (see Table I).

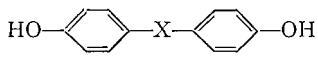

(II)

The following new urethane-type nitrogen mustards of the symmetrical *p,p'*-dihydroxydiaryl derivatives were therefore synthesized (see Table II).

TABLE I

Estrogenic activity of *p,p'*-dihydroxydiaryl derivatives

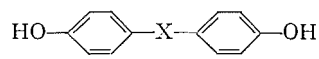

No.	X	m.p. (°C)	Estrogenic* activity	Reference list
1	CH=CH *trans*	284	++	7,9,12,13
2	CO—CO	249	++	12,13
3	CH_2	161–162	+	3
4	$CH(CCl_3)$	204.5–205.3	+	8
5	—	272–272.5	+	13
6	N=N	214–215	+	13
7	O	163	+	7
8	S	150	+	13
9	SO_2	246–247	—	13
10	CH=CH—CO—CH=CH	229–232	—	13
11	SO	200–201	?	?
12	CO	212–212.5	?	?
13	$\begin{matrix} C \\ \| \\ CCl_2 \end{matrix}$	216.5	?	?

*Estrogenic activity: (+++) under 1 mg/kg body weight (rat); (++) 1–100 mg/kg body weight; (+) 100–1 000 mg/kg body weight; (—) over 1 000 mg/kg body weight.

Can. J. Chem. Downloaded from www.nrcresearchpress.com by 210.87.254.40 on 09/05/12
For personal use only.

Can. J. Chem. Downloaded from www.nrcresearchpress.com by 210.87.254.40 on 09/05/12
For personal use only.

TABLE II

Urethane-type nitrogen mustards

$(ClCH_2CH_2)_2NCOO$—C$_6$H$_4$—X—C$_6$H$_4$—$OOCN(CH_2CH_2Cl)_2$

No.	X	m.p. (°C) (corrected)	Elemental analysis: Calcd. C	Calcd. H	Calcd. N	Found C	Found H	Found N	ν_{max}* carbamate group (cm^{-1})	Reaction time (days)	Yield (%)
1	CH=CH (*trans*)	137–138	52.57	4.72	5.10	52.50	4.70	5.12	1 717	7	79
2	CO—CO	119–119.5	49.78	4.15	4.84	49.60	4.30	4.85	1 720	4	81
3	CH_2	43–45	51.49	4.85	5.26	51.58	4.91	5.30	1 720	4	54
4	$CH(CCl_3)$	98	44.01	3.83	4.29	44.32	3.85	4.27	1 730	4	72
5	—	153–153.5	50.55	4.59	5.36	50.19	4.55	5.21	1 714	4	85
6	N=N	129	48.00	4.36	10.18	48.36	4.34	10.16	1 714	4	80
7	O	89–90	49.07	4.46	5.20	49.12	4.55	5.19	1 714	4	95
8	S	63–63.5	47.70	4.33	5.06	47.30	4.37	5.05	1 714	7	93
9	SO_2	116–116.5	45.05	4.09	4.77	45.10	4.12	4.69	1 714	5	80
10	CH=CH—CO—CH=CH	107–107.5	53.82	4.53	4.65	53.60	4.59	4.57	1 715	—†	45
11	SO	105	46.31	4.21	4.91	46.64	4.32	4.82	1 716	5	91
12	CO	94–94.5	50.18	4.36	5.09	50.68	4.59	5.10	1 725	6	69
13	C(=CCl_2)	99–100	46.67	3.89	4.54	46.30	3.84	4.52	1 723	6	78

*Spectra were carried out by pastillation in KBr, on a spectrophotometer URIO Zeiss-Jena–RDG.
†Two hours at reflux.

To obtain nitrogen mustard carbamates, the condensation of the above *p,p'*-dihydroxydiarylic derivatives with nitrogen mustard chloroformate, prepared according to Childs *et al.* (4), was used. The condensation was carried out in pyridine (10) and has the advantage of directly and efficiently yielding easily crystallized products.

Infrared spectra from the synthesized products present a characteristic peak in the range of 1 740 – 1 710 cm^{-1} corresponding to the carbamate function. The synthesis was performed according to Nogrady's method (10). For some products the reaction lasted up to 6–7 days (see Table II).

The carbamates were recrystallized from anhydrous methanol or ligroin.

SUMMARY

This work was carried out to study the relationship between the estrogenic activity of *p,p'*-dihydroxydiaryl derivatives and the possible anticancer activity of their tetrakis N,N,N',N'-(2 chlorethyl)urethanes. New nitrogen mustard-type urethanes were synthesized from: 4,4'-dihydroxystilbene (*trans*); 4,4'-dihydroxydibenzil; 4,4'-dihydroxydiphenylmethane; 4,4-dihydroxy-1,1-diphenyl-2,2,2,-trichlorethane; 4,4'-dihydroxydiphenyl; 4,4'-dihydroxyazobenzene; 4,4'-dihydroxydiphenyl ether; 4,4'-dihydroxydiphenyl sulfide; 4,4'-dihydroxydiphenyl sulfone; 4,4'-dihydroxydibenzeliden acetone; 4,4'-dihydroxydiphenyl sulfoxide; 4,4'-dihhydroxybenzophenone; and 4,4'-dihydroxy-1,1-diphenyl-2,2-dichloroethylene. Infrared spectra were obtained. Substances are under biological tests.

1. J. F. Benner. University Microfilms. Order **63**, 1710. Ann Arbor, Mich. 1963.
2. F. Bergel and R. Wade. J. Chem. Soc. 941 (1959).
3. N. R. Campbell. Proc. Roy. Soc. London Ser. B, **129**, 528 (1940).
4. A. F. Childs, L. J. Goldworthy, C. F. Harding, F. E. King, A. W. Nineham, W. L. Norris, S. G. Plant, B. Selton, and A. L. C. Tompsett. J. Chem. Soc. 2174 (1948).
5. E. Ciorănescu and D. Raileanu. Acad. Rep. Populare Romine, Studii Cercetari Chim. **10** (3–4), 295 (1962).
6. J. F. Danielli. Ciba Found. Symp. Leukaemia Res. 263 (1954); Brit. Empire Cancer Campaign Ann. Rept. **34**, 448 (1956).
7. C. W. Emmens. J. Endocrinol. **2**, 444 (1941).
8. A. L. Fischer, A. H. Keastling, and F. W. Schneler. Proc. Soc. Exptl. Biol. Med. **81**, 439 (1952).
9. R. D. Jaap. Endocrinology, **37**, 369 (1945).
10. T. Nogrady, M. K. Vagi, and V. W. Adamkiewicz. Can. J. Chem. **40**, 2126 (1962).
11. T. F. Nogrady. J. Org. Chem. **26**, 4117 (1961).
12. D. Salmony. Biochem. J. **62**, 411 (1956).
13. D. Schmahl. Arzneimittel-Forsch. **7**, 211 (1957).

Received October 9, 1964.
Department of Organic Synthesis and Physical Chemistry,
Oncological Institute,
Bucharest, Romania.

SYNTHESIS OF SOME TETRAZOLE SALTS

Méude Tremblay

INTRODUCTION

The objective of the synthesis work was to prepare solid organic compounds consisting mainly of nitrogen and hydrogen, and containing the smallest amount of carbon and oxygen.

Three 5-nitroaminotetrazole salts were prepared by the reaction of nitroguanylazide or potassium 5-nitroaminotetrazole with the mineral salts of guanidine derivatives or

Can. J. Chem. Downloaded from www.nrcresearchpress.com by 210.87.254.40 on 09/05/12
For personal use only.

To obtain nitrogen mustard carbamates, the condensation of the above *p,p'*-dihydroxydiarylic derivatives with nitrogen mustard chloroformate, prepared according to Childs *et al.* (4), was used. The condensation was carried out in pyridine (10) and has the advantage of directly and efficiently yielding easily crystallized products.

Infrared spectra from the synthesized products present a characteristic peak in the range of 1 740 – 1 710 cm^{-1} corresponding to the carbamate function. The synthesis was performed according to Nogrady's method (10). For some products the reaction lasted up to 6–7 days (see Table II).

The carbamates were recrystallized from anhydrous methanol or ligroin.

SUMMARY

This work was carried out to study the relationship between the estrogenic activity of *p,p'*-dihydroxydiaryl derivatives and the possible anticancer activity of their tetrakis N,N,N',N'-(2 chlorethyl)urethanes. New nitrogen mustard-type urethanes were synthesized from: 4,4'-dihydroxystilbene (*trans*); 4,4'-dihydroxydibenzil; 4,4'-dihydroxydiphenylmethane; 4,4-dihydroxy-1,1-diphenyl-2,2,2,-trichlorethane; 4,4'-dihydroxydiphenyl; 4,4'-dihydroxyazobenzene; 4,4'-dihydroxydiphenyl ether; 4,4'-dihydroxydiphenyl sulfide; 4,4'-dihydroxydiphenyl sulfone; 4,4'-dihydroxydibenzeliden acetone; 4,4'-dihydroxydiphenyl sulfoxide; 4,4'-dihhydroxybenzophenone; and 4,4'-dihydroxy-1,1-diphenyl-2,2-dichloroethylene. Infrared spectra were obtained. Substances are under biological tests.

1. J. F. Benner. University Microfilms. Order **63**, 1710. Ann Arbor, Mich. 1963.
2. F. Bergel and R. Wade. J. Chem. Soc. 941 (1959).
3. N. R. Campbell. Proc. Roy. Soc. London Ser. B, **129**, 528 (1940).
4. A. F. Childs, L. J. Goldworthy, C. F. Harding, F. E. King, A. W. Nineham, W. L. Norris, S. G. Plant, B. Selton, and A. L. C. Tompsett. J. Chem. Soc. 2174 (1948).
5. E. Ciorănescu and D. Raileanu. Acad. Rep. Populare Romine, Studii Cercetari Chim. **10** (3–4), 295 (1962).
6. J. F. Danielli. Ciba Found. Symp. Leukaemia Res. 263 (1954); Brit. Empire Cancer Campaign Ann. Rept. **34**, 448 (1956).
7. C. W. Emmens. J. Endocrinol. **2**, 444 (1941).
8. A. L. Fischer, A. H. Keastling, and F. W. Schneler. Proc. Soc. Exptl. Biol. Med. **81**, 439 (1952).
9. R. D. Jaap. Endocrinology, **37**, 369 (1945).
10. T. Nogrady, M. K. Vagi, and V. W. Adamkiewicz. Can. J. Chem. **40**, 2126 (1962).
11. T. F. Nogrady. J. Org. Chem. **26**, 4117 (1961).
12. D. Salmony. Biochem. J. **62**, 411 (1956).
13. D. Schmahl. Arzneimittel-Forsch. **7**, 211 (1957).

Received October 9, 1964.
Department of Organic Synthesis and Physical Chemistry,
Oncological Institute,
Bucharest, Romania.

SYNTHESIS OF SOME TETRAZOLE SALTS

Méude Tremblay

INTRODUCTION

The objective of the synthesis work was to prepare solid organic compounds consisting mainly of nitrogen and hydrogen, and containing the smallest amount of carbon and oxygen.

Three 5-nitroaminotetrazole salts were prepared by the reaction of nitroguanylazide or potassium 5-nitroaminotetrazole with the mineral salts of guanidine derivatives or

Can. J. Chem. Downloaded from www.nrcresearchpress.com by 210.87.254.40 on 09/05/12
For personal use only.

5-aminotetrazole. The guanidium 5-nitroaminotetrazole, formed by the condensation of guanidine carbonate and nitroguanylazide, is described in the literature (1). This compound contains 4.5 moles of nitrogen per mole of carbon or oxygen. By a similar method, other salts of 5-nitroaminotetrazole containing higher percentages of nitrogen were synthesized. Aminoguanidinium 5-nitroaminotetrazole was formed from aminoguanidine bicarbonate and nitroguanylazide. Triaminoguanidinium 5-nitroaminotetrazole was obtained by the condensation of triaminoguanidine nitrate and potassium 5-nitroaminotetrazole. 5-Aminotetrazolyl-5′-nitroaminotetrazole was also obtained from 5-aminotetrazole nitrate and potassium 5-nitroaminotetrazole. The compounds obtained formed monobasic salts that display slightly acidic properties as in the case of guanidinium 5-nitroaminotetrazole (1, 2). Most starting materials were available except nitroguanylazide (3) and triaminoguanidine (4). These salts contained between 68 and 73% nitrogen, and by decomposition, liberated large volumes of hydrogen, nitrogen, and carbon monoxide. Upon combustion a large amount of heat is also evolved, owing to the positive heat of formation of these salts, i.e. +26.59 kcal/mole for guanidinium 5-nitroaminotetrazole (5).

The shock sensitivity of 5-nitroaminotetrazole salts was determined on the Bruceton impact machine with a 2 kg weight. It is given as the minimum height (cm) at which the hammer should fall to give 50% detonation. Their shock sensitivity varied from 30 cm / 2 kg for aminoguanidinium 5-nitroaminotetrazole to 8 cm / 2 kg for triaminoguanidinium 5-nitroaminotetrazole. The infrared absorption spectra of tetrazole derivatives were determined in Nujol emulsion and absorption bands were obtained which were assigned on the basis of data published in the literature (6). The spectra of nitroaminotetrazole salts of aminoguanidine, triaminoguanidine, and aminotetrazole have shown the presence of tetrazole rings together with the functional groups present in the individual guanidines.

EXPERIMENTAL

The elemental analyses for carbon, hydrogen, and nitrogen were made by C. Daessle, Micro Analyses, Montreal. In some instances explosions occurred upon combustion.

Aminoguanidinium 5-Nitroaminotetrazole

To aminoguanidine bicarbonate (3.4 g, 0.025 mole) dissolved in water (25 ml) and ethanol (40 ml) was added nitroguanylazide (3.3 g, 0.025 mole). There was an evolution of CO_2 with formation of a salt which was insoluble in the alcoholic solution. After recrystallization from water, m.p. 214–215 °C.

Anal. Calcd. for $C_2H_8N_{10}O_2$: C, 11.7; H, 3.94; N, 68.6. Found: C, 11.4; H, 3.73; N, 67.6.

Triaminoguanidinium 5-Nitroaminotetrazole

To the potassium salt of 5-nitroaminotetrazole (2.3 g, 0.0137 mole) dissolved in water (25 ml) was added triaminoguanidinium nitrate (2.3 g, 0.0137 mole), and the mixture heated. Upon cooling a white solid (melting at 184–186 °C) was obtained.

Anal. Calcd. for $C_2H_{10}N_{12}O_2$: C, 10.2; H, 4.3; N, 71.8. Found: C, 9.3; H, 4.7; N, 71.0.

5-Aminotetrazolyl-5′-nitroaminotetrazole

(*a*) To nitroguanylazide (1.5 g, 0.0115 mole) dissolved in ethanol (25 ml) was added aminotetrazole monohydrate (1.2 g, 0.0115 mole). The mixture was warmed, filtered, and upon cooling a solid melting at 171 °C (explodes) was obtained. Several recrystallizations from water yielded a compound melting at 178 °C (decomp.).

Anal. Calcd. for $C_2H_5N_{11}O_2$: C, 11.1; H, 2.34; N, 71.6. Found: C, 11.0; H, 2.10; N, 71.1.

(*b*) To 5-aminotetrazole nitrate (1.48 g, 0.01 mole), prepared by the literature method (7), dissolved in water (25 ml). An aqueous solution was added to potassium salt of 5-nitroaminotetrazole (1.68 g, 0.01 mole, 25 ml). The 5-aminotetrazole-5′-nitroaminotetrazole precipitated. Yield, 1.5 g (70%). After recrystallization from water, m.p. 178 °C (decomp.). An admixture with the previous compound did not depress the melting point.

Can. J. Chem. Downloaded from www.nrcresearchpress.com by 210.87.254.40 on 09/05/12
For personal use only.

Triaminoguanidinium 5-Nitroaminotetrazole from Aminoguanidinium 5-Nitroaminotetrazole

To a solution of aminoguanidinium 5-nitroaminotetrazole (2.04 g, 0.01 mole) in water (50 ml), anhydrous hydrazine (95%, 0.6 g, 0.02 mole) was added. The mixture was heated under reflux in a water bath for 2 h, partially evaporated, cooled, and filtered. The solid obtained melted at 184–186 °C. A mixed melting point with authentic triaminoguanidinium 5-nitroaminotetrazole was not depressed.

1. E. Lieber, E. Sherman, R. A. Henry, and J. Cohen. J. Am. Chem. Soc. **73**, 2327 (1951).
2. E. Lieber, E. Sherman, and S. H. Patinkin. J. Am. Chem. Soc. **73**, 2329 (1951).
3. T. E. O'Connor, G. Fleming, and J. Reilly. J. Soc. Chem. Ind. London, **68**, 309 (1949).
4. T. E. O'Connor, K. Horgan, and J. Reilly. J. Appl. Chem. **1**, 91 (1951).
5. W. S. McEwan and M. W. Rigg. J. Am. Chem. Soc. **73**, 4725 (1951).
6. E. Lieber, R. D. Levering, and L. J. Patterson. Anal. Chem. **23**, 1954 (1951).
7. R. M. Herbst and J. A. Garrison. J. Org. Chem. **18**, 941 (1953).

Received November 4, 1964.
Canadian Armament Research and Development Establishment,
Valcartier, Quebec.

SYNTHESIS OF α-ALKYL-SUBSTITUTED AMINO ACIDS AND DERIVATIVES

C. J. Abshire and L. Berlinguet

The interesting biological properties of some α-substituted amino acids (1–5) made their preparation and pharmacological study of interest to us. We describe two such preparations starting from the available ketones.

α-(2-Furyl)-alanine was prepared from 2-furyl methyl ketone via the corresponding hydantoin 5-(2′-furyl)-5-methylhydantoin.* This new amino acid is an isomer of β-(2-furyl) alanine, β-(3-furyl) alanine, and β-(2-furyl)-β-alanine, all of which have been previously reported (8–10). The amino acid was characterized by its N-phenylcarbamyl derivative which was converted to the 3-phenylhydantoin by treatment with boiling glacial acetic acid. Although stable toward alkali each of these three compounds were decomposed by mineral acids, owing presumably to the lability of the furan nucleus. This instability resulted in the failure of the attempted cyclization of the N-phenylcarbamyl derivative to the 3-phenylhydantoin by hydrochloric acid.

α-Ethylserine has been prepared previously from 2-amino-2-hydroxymethyl-1-butanol (11, 12), from α-aminobutyric acid by the action of formaldehyde (13), and by a long route from ethyl α-acetylbutyrate (14). We report the convenient synthesis of this amino acid from 1-acetoxy-2-butanone via the hydantoin in an overall yield of 38%. α-Ethylserine was characterized by its cupric salt. Probably because of its high solubility, the hydantoin could not be isolated as an intermediate but was obtained from the pure amino acid. Reaction of α-ethylserine with phenyl isocyanate yielded N-phenylcarbamyl-α-ethylserine which in turn was cyclized to 3-phenyl-5-ethyl-5-hydroxymethylhydantoin.

Biological Evaluation

The amino acids and their carbamyl derivatives were nontoxic to rats on intraperitoneal injection and had no effect on Walker-cancer bearing rats. The amino acids had no effect on growth curves when fed to rats at a 1% concentration in the diet. The hydantoins (as their sodium salts) had no visible effects on metrazole-induced epileptic fits in rats.

**This hydantoin has been previously reported in two patents (6, 7).*

Can. J. Chem. Downloaded from www.nrcresearchpress.com by 210.87.254.40 on 09/05/12
For personal use only.

Triaminoguanidinium 5-Nitroaminotetrazole from Aminoguanidinium 5-Nitroaminotetrazole

To a solution of aminoguanidinium 5-nitroaminotetrazole (2.04 g, 0.01 mole) in water (50 ml), anhydrous hydrazine (95%, 0.6 g, 0.02 mole) was added. The mixture was heated under reflux in a water bath for 2 h, partially evaporated, cooled, and filtered. The solid obtained melted at 184–186 °C. A mixed melting point with authentic triaminoguanidinium 5-nitroaminotetrazole was not depressed.

1. E. Lieber, E. Sherman, R. A. Henry, and J. Cohen. J. Am. Chem. Soc. **73**, 2327 (1951).
2. E. Lieber, E. Sherman, and S. H. Patinkin. J. Am. Chem. Soc. **73**, 2329 (1951).
3. T. E. O'Connor, G. Fleming, and J. Reilly. J. Soc. Chem. Ind. London, **68**, 309 (1949).
4. T. E. O'Connor, K. Horgan, and J. Reilly. J. Appl. Chem. **1**, 91 (1951).
5. W. S. McEwan and M. W. Rigg. J. Am. Chem. Soc. **73**, 4725 (1951).
6. E. Lieber, R. D. Levering, and L. J. Patterson. Anal. Chem. **23**, 1954 (1951).
7. R. M. Herbst and J. A. Garrison. J. Org. Chem. **18**, 941 (1953).

Received November 4, 1964.
Canadian Armament Research and Development Establishment,
Valcartier, Quebec.

SYNTHESIS OF α-ALKYL-SUBSTITUTED AMINO ACIDS AND DERIVATIVES

C. J. Abshire and L. Berlinguet

The interesting biological properties of some α-substituted amino acids (1–5) made their preparation and pharmacological study of interest to us. We describe two such preparations starting from the available ketones.

α-(2-Furyl)-alanine was prepared from 2-furyl methyl ketone via the corresponding hydantoin 5-(2′-furyl)-5-methylhydantoin.* This new amino acid is an isomer of β-(2-furyl) alanine, β-(3-furyl) alanine, and β-(2-furyl)-β-alanine, all of which have been previously reported (8–10). The amino acid was characterized by its N-phenylcarbamyl derivative which was converted to the 3-phenylhydantoin by treatment with boiling glacial acetic acid. Although stable toward alkali each of these three compounds were decomposed by mineral acids, owing presumably to the lability of the furan nucleus. This instability resulted in the failure of the attempted cyclization of the N-phenylcarbamyl derivative to the 3-phenylhydantoin by hydrochloric acid.

α-Ethylserine has been prepared previously from 2-amino-2-hydroxymethyl-1-butanol (11, 12), from α-aminobutyric acid by the action of formaldehyde (13), and by a long route from ethyl α-acetylbutyrate (14). We report the convenient synthesis of this amino acid from 1-acetoxy-2-butanone via the hydantoin in an overall yield of 38%. α-Ethylserine was characterized by its cupric salt. Probably because of its high solubility, the hydantoin could not be isolated as an intermediate but was obtained from the pure amino acid. Reaction of α-ethylserine with phenyl isocyanate yielded N-phenylcarbamyl-α-ethylserine which in turn was cyclized to 3-phenyl-5-ethyl-5-hydroxymethylhydantoin.

Biological Evaluation

The amino acids and their carbamyl derivatives were nontoxic to rats on intraperitoneal injection and had no effect on Walker-cancer bearing rats. The amino acids had no effect on growth curves when fed to rats at a 1% concentration in the diet. The hydantoins (as their sodium salts) had no visible effects on metrazole-induced epileptic fits in rats.

**This hydantoin has been previously reported in two patents (6, 7).*

Can. J. Chem. Downloaded from www.nrcresearchpress.com by 210.87.254.5 on 09/05/12
For personal use only.

Can. J. Chem. Downloaded from www.nrcresearchpress.com by 210.87.254.5 on 09/05/12
For personal use only.

EXPERIMENTAL

5-(2'-Furyl)-5-methylhydantoin

The use of ammonium chloride with potassium cyanide in this preparation is a departure from the patent procedures (6, 7). To a stirred solution of 13.75 g of 2-furyl methyl ketone and 10 g of ammonium chloride in 200 ml of ethanol–water (1:1) was added a solution of 12.2 g of potassium cyanide in 20 ml of water; this was stirred at room temperature for 3 h. Then a mixture of 48 g of ammonium carbonate and 100 ml of water was added during 1 h; the resulting mixture was stirred overnight at 50–70°. Excess ammonium carbonate was decomposed by heating and the solution was concentrated *in vacuo* until a precipitate began to form. The cooled solution afforded 17 g (75%) of white crystals, m.p. 178–180° (lit. (6) 176–178°).

Anal. Calcd. for $C_8H_8N_2O_3$: N, 15.55. Found: N, 15.63.

α-(2-Furyl) Alanine

A mixture of 7 g of 5-(2'-furyl)-5-methylhydantoin and 14.2 g of barium hydroxide in 150 ml water was boiled under reflux in a stainless steel flask overnight. Addition of 2.4 ml of concentrated sulfuric acid precipitated barium sulfate which was removed by filtration. The filtrate was concentrated to a yellow gum, which crystallized after trituration with acetone. A 4.9 g yield (82%) of white solid melting at 194–200° was obtained; the crystals began to darken and decompose slowly at 174°. The amino acid gave the usual purple color with ninhydrin. A circular paper chromatogram developed in pyridine–water (4:1) gave an R_f of 0.71 for the compound.

Anal. Calcd. for $C_7H_9NO_3$: N, 9.14. Found: N, 9.15.

N-Phenylcarbamyl-α-(2-furyl) Alanine

α-(2-Furyl) alanine (1.55 g, 0.01 mole) in an equivalent of 4% sodium hydroxide was shaken for 1/2 h with a slight excess of phenyl isocyanate (1.55 g, 0.014 mole). The reaction mixture was filtered, the filtrate acidified with concentrated hydrochloric acid, and the white precipitate collected and washed with water. Crystallization from ethanol–water afforded 1.55 g (57%) of pure product, m.p. 159–161°; neutralization equivalent, found 276 (calcd. 274).

Anal. Calcd. for $C_{14}H_{14}N_2O_4$: N, 10.21. Found: N, 10.26.

3-Phenyl-5-(2'-furyl)-5-methylhydantoin

A solution of 6 g of N-phenylcarbamyl-α-(2-furyl) alanine in 50 ml glacial acetic acid was refluxed for 10 min then quickly cooled; if heating is continued for a longer period of time some darkening of the solution occurs probably due to decomposition of the furan ring. Excess water was added; the precipitate was filtered and recrystallized from ethanol–water. Yields in the range of 27 to 36% of a product melting at 170–172° were obtained. Cyclization had taken place because the product is now neutral in alcohol solution to bromothymol blue, whereas the starting material requires 1 equivalent of base for neutrality.

Anal. Calcd. for $C_{14}H_{12}N_2O_3$: N, 10.93. Found: N, 10.67.

α-Ethylserine and Its Copper Salt

Potassium cyanide (65 g, 1 mole) was added, with stirring, to a solution of 1-acetoxy-2-butanone (87 g, 0.67 mole) and ammonium chloride (53.5 g, 1 mole) in a 1:1 ethanol–water mixture (600 ml). The resulting mixture was stirred at room temperature for 3 h; then ammonium carbonate (300 g) was added and the mixture was stirred overnight at 50–70°. Residual ammonium carbonate was decomposed by refluxing 3 h, following which the solution was concentrated *in vacuo* to a brown oil; this was triturated with hot acetone and filtered, the filtrate being subsequently concentrated again. The residue, presumably a hydantoin, consisted of 152.8 g of a brown oil. Numerous attempts to crystallize it failed, so 87.6 g of it was hydrolyzed; this was added to a solution of 165.8 g of barium hydroxide in 500 ml of water and the solution was refluxed overnight in a steel vessel. Excess ammonium carbonate was added; the solution was refluxed 3 h and filtered, and concentrated to an oil *in vacuo*. This was subsequently dissolved in 171 ml of water and divided into two parts: 57 ml to make the copper salt, and 114 ml to isolate the free amino acid.

The 114 ml of solution above were added to 700 ml of acetone and allowed to crystallize slowly. The large white crystals were filtered and recrystallized from ethanol–water to yield 12 g (38%) of α-ethylserine melting at 257–259°. In electrophoresis using a buffer of pH 8.6, the product remained at the point of origin. A circular paper chromatogram employing pyridine–water (4:1) as solvent gave an R_f of 0.63 for the amino acid.

Anal. Calcd. for $C_5H_{11}NO_3$: N, 10.52. Found: N, 10.75.

The remaining 57 ml of the above solution was boiled for 15 min with excess cupric carbonate, then filtered. The copper salt was precipitated by the addition of acetone–ethanol and an 8.5 g yield (41%) was obtained. The compound does not melt below 300°; it turns from blue to brown gradually upon heating at about 194°. The product was dried at 100° for 2 h, then analyzed.

Anal. Calcd. for $C_{10}H_{20}N_2O_6Cu$: N, 8.55. Found: N, 8.75.

5-Ethyl-5-hydroxymethylhydantoin

A solution of α-ethylserine (2 g, 0.015 mole) and potassium cyanate (1.22 g, 0.015 mole) in 14 ml of water was stirred at 60–70° for 2 h. Then 14 ml of concentrated hydrochloric acid was added and the solution was

refluxed for 1 h, following which the solvent was removed by vacuum leaving a clear oily residue. This was triturated with hot alcohol; the inorganic salts were filtered and the filtrate again concentrated to an oil which crystallized on standing. An 800 mg yield (34%) of the hydantoin melting at 165–168° was obtained.

Anal. Calcd. for $C_6H_{10}N_2O_3$: N, 17.71. Found: N, 17.23.

N-Phenylcarbamyl-α-ethylserine

α-Ethylserine (1 g, 0.00752 mole) was dissolved in an equivalent of 10% aqueous sodium hydroxide (3 ml) and about 20 ml of water. To this was added a slight excess of phenyl isocyanate (1.07 g, 0.01 mole). The mixture was shaken vigorously for 1/2 h and then filtered. Acidification of the filtrate with concentrated hydrochloric acid precipitated a white solid which was filtered, washed with water, recrystallized from ethanol–water, and dried. A 1.3 g (69%) yield of pure material melting at 150–152° was obtained. The compound is acidic and requires 1 mole of sodium hydroxide for neutralization; neutralization equivalent, found 264 (calcd. 252).

Anal. Calcd. for $C_{12}H_{16}N_2O_4$: N, 11.11. Found: N, 10.64.

3-Phenyl-5-ethyl-5-hydroxymethylhydantoin

A solution of 350 mg of N-phenylcarbamyl-α-ethylserine in 20 ml of 6 *N* hydrochloric acid was refluxed 1 h, then concentrated *in vacuo* until a precipitate began to form. A small amount of water (10 ml) was added; the mixture was cooled and filtered, and the precipitate was dried. A 220 mg yield (68%) of a product melting at 155–156° was obtained. Cyclization had occurred because the product is now neutral.

Anal. Calcd. for $C_{12}H_{14}N_2O_3$: N, 11.96. Found: N, 11.62.

ACKNOWLEDGMENTS

The authors thank the Medical Research Council of Canada and the National Cancer Institute of Canada for financial support.

1. G. A. Stein, H. A. Bronner, and K. Pfister, III. J. Am. Chem. Soc. **77**, 700 (1955).
2. T. L. Sourkes. Arch. Biochem. Biophys. **51**, 444 (1954).
3. L. I. Goldberg, F. M. Da Costa, and M. Ozaki. Nature, **188**, 509 (1960).
4. J. A. Oates, L. Gillespie, S. Udenfriend, and A. Sjoerdsma. Science, **131**, 1890 (1960).
5. E. Westermann, H. Balzer, and J. Knell. Arch. Exptl. Pathol. Pharmakol. **234**, 194 (1958).
6. Fr. Patent No. 780,461; Chem. Abstr. **29**, 5995[5] (1935).
7. Swiss Patent No. 179,693; Chem. Abstr. **30**, 3592[3] (1936).
8. A. Ahmed, P. B. Marshall, and D. M. Shepherd. J. Pharm. Pharmacol. **10**, 672 (1958).
9. D. A. Clark and K. Dittmer. J. Biol. Chem. **173**, 313 (1948).
10. K. Dittmer. Ann. N.Y. Acad. Sci. **52**, 1274 (1950).
11. J. H. Billman and E. E. Parker. J. Am. Chem. Soc. **67**, 1069 (1945).
12. J. H. Billman and E. E. Parker. U.S. Patent No. 2,556,791; Chem. Abstr. **46**, 525*g* (1952).
13. T. T. Otani and M. Winitz. Arch. Biochem. Biophys. **90**, 254 (1960).
14. S. Mejer. Roczniki Chem. **36** (6), 115 (1962); Chem. Abstr. **59**, 1747*e* (1963).

Received November 12, 1964.
Department of Biochemistry,
Faculty of Medicine,
Laval University,
Quebec, Quebec.

STUDIES OF SODIUM CUPRATE(III) STABILITY

J. S. Magee, Jr.[1] and R. H. Wood

We have recently completed a study of the stability of sodium dioxocuprate(III) in various alkali bases at several different base strengths. In no case did we find that the salt was stable in solution and, in fact, the half-life of the CuO_2^- ion was estimated to be only 25 s. Thus, it appears that tervalent copper can be present in aqueous solution only in the presence of large stabilizing anions such as periodate or tellurate (1–3) or in the presence of large concentrations of hypobromite (4).

[1]*Present address: W. R. Grace & Co., Washington Research Center, Clarksville, Maryland.*

Can. J. Chem. Downloaded from www.nrcresearchpress.com by 210.87.254.5 on 09/05/12
For personal use only.

refluxed for 1 h, following which the solvent was removed by vacuum leaving a clear oily residue. This was triturated with hot alcohol; the inorganic salts were filtered and the filtrate again concentrated to an oil which crystallized on standing. An 800 mg yield (34%) of the hydantoin melting at 165–168° was obtained.

Anal. Calcd. for $C_6H_{10}N_2O_3$: N, 17.71. Found: N, 17.23.

N-Phenylcarbamyl-α-ethylserine

α-Ethylserine (1 g, 0.00752 mole) was dissolved in an equivalent of 10% aqueous sodium hydroxide (3 ml) and about 20 ml of water. To this was added a slight excess of phenyl isocyanate (1.07 g, 0.01 mole). The mixture was shaken vigorously for 1/2 h and then filtered. Acidification of the filtrate with concentrated hydrochloric acid precipitated a white solid which was filtered, washed with water, recrystallized from ethanol–water, and dried. A 1.3 g (69%) yield of pure material melting at 150–152° was obtained. The compound is acidic and requires 1 mole of sodium hydroxide for neutralization; neutralization equivalent, found 264 (calcd. 252).

Anal. Calcd. for $C_{12}H_{16}N_2O_4$: N, 11.11. Found: N, 10.64.

3-Phenyl-5-ethyl-5-hydroxymethylhydantoin

A solution of 350 mg of N-phenylcarbamyl-α-ethylserine in 20 ml of 6 *N* hydrochloric acid was refluxed 1 h, then concentrated *in vacuo* until a precipitate began to form. A small amount of water (10 ml) was added; the mixture was cooled and filtered, and the precipitate was dried. A 220 mg yield (68%) of a product melting at 155–156° was obtained. Cyclization had occurred because the product is now neutral.

Anal. Calcd. for $C_{12}H_{14}N_2O_3$: N, 11.96. Found: N, 11.62.

ACKNOWLEDGMENTS

The authors thank the Medical Research Council of Canada and the National Cancer Institute of Canada for financial support.

1. G. A. Stein, H. A. Bronner, and K. Pfister, III. J. Am. Chem. Soc. **77**, 700 (1955).
2. T. L. Sourkes. Arch. Biochem. Biophys. **51**, 444 (1954).
3. L. I. Goldberg, F. M. Da Costa, and M. Ozaki. Nature, **188**, 509 (1960).
4. J. A. Oates, L. Gillespie, S. Udenfriend, and A. Sjoerdsma. Science, **131**, 1890 (1960).
5. E. Westermann, H. Balzer, and J. Knell. Arch. Exptl. Pathol. Pharmakol. **234**, 194 (1958).
6. Fr. Patent No. 780,461; Chem. Abstr. **29**, 5995[5] (1935).
7. Swiss Patent No. 179,693; Chem. Abstr. **30**, 3592[3] (1936).
8. A. Ahmed, P. B. Marshall, and D. M. Shepherd. J. Pharm. Pharmacol. **10**, 672 (1958).
9. D. A. Clark and K. Dittmer. J. Biol. Chem. **173**, 313 (1948).
10. K. Dittmer. Ann. N.Y. Acad. Sci. **52**, 1274 (1950).
11. J. H. Billman and E. E. Parker. J. Am. Chem. Soc. **67**, 1069 (1945).
12. J. H. Billman and E. E. Parker. U.S. Patent No. 2,556,791; Chem. Abstr. **46**, 525*g* (1952).
13. T. T. Otani and M. Winitz. Arch. Biochem. Biophys. **90**, 254 (1960).
14. S. Mejer. Roczniki Chem. **36** (6), 115 (1962); Chem. Abstr. **59**, 1747*e* (1963).

Received November 12, 1964.
Department of Biochemistry,
Faculty of Medicine,
Laval University,
Quebec, Quebec.

STUDIES OF SODIUM CUPRATE(III) STABILITY

J. S. Magee, Jr.[1] and R. H. Wood

We have recently completed a study of the stability of sodium dioxocuprate(III) in various alkali bases at several different base strengths. In no case did we find that the salt was stable in solution and, in fact, the half-life of the CuO_2^- ion was estimated to be only 25 s. Thus, it appears that tervalent copper can be present in aqueous solution only in the presence of large stabilizing anions such as periodate or tellurate (1–3) or in the presence of large concentrations of hypobromite (4).

[1]*Present address: W. R. Grace & Co., Washington Research Center, Clarksville, Maryland.*

Can. J. Chem. Downloaded from www.nrcresearchpress.com by 210.87.254.40 on 09/05/12
For personal use only.

Can. J. Chem. Downloaded from www.nrcresearchpress.com by 210.87.254.40 on 09/05/12
For personal use only.

EXPERIMENTAL

One of the methods reported by Scholder and Voelskow (4) for preparing $NaCuO_2$ was modified and used throughout this study. This procedure involves oxidation of copper(II) hydroxide with sodium hypobromite in strong base, the sodium cuprate(III) precipitating as a reddish-brown precipitate.

All reagents used were C.P grade. The sodium hypobromite and microcrystalline copper(II) hydroxide used were prepared according to the procedure of Scholder and Voelskow (4).

The analytical procedure used was a modification of Park's (5) method for determining Cu(II) in the presence of As(III). An ice-cold mixture of 30 ml of 3.3 *N* NaOH and 15.00 ml of standard 0.2 *N* arsenic(III) solution was added to a sample of about 0.15 g solid sodium cuprate(III). The mixture, which contained a fine precipitate of copper(II) oxide was diluted with 90 ml of ice-cold water and acidified with 15 ml of cold 12 *N* sulfuric acid. Excess arsenic(III) was determined by titration with standard cerium(IV) solution using ferrous orthophenanthroline as the indicator and osmium tetraoxide as catalyst (meq Cu(III) = meq As(III) − meq Ce(IV)). Three grams of potassium acid phthalate was added to the solution and the pH was adjusted to 3.5 with concentrated ammonium hydroxide (28% NH_3). Ten grams of potassium iodide, dissolved in a minimum quantity of water, was added and the solution was titrated with standard sodium thiosulfate to a light-orange end point. Starch solution was used as the indicator. The number of equivalents of sodium thiosulfate used equalled the number of moles of copper.

The decomposition of sodium cuprate(III) may be represented by the following equation:

$$4NaCuO_2 + 2H_2O \rightarrow 4NaOH + 4CuO + O_2.$$

In this study, we followed the rate of decomposition of solid sodium cuprate(III) in the presence of base using a Warburg apparatus (6). A small sample of $NaCuO_2$ was placed in a glass vial which was inserted in a Warburg flask containing a known volume of base. After the flask had come to equilibrium in a constant temperature bath, the contents of the vial were mixed with the base and the mixture was shaken vigorously until an equilibrium pressure reading was obtained. Oxygen pressure readings were taken as a function of time during the decomposition. When decomposition was complete the solution of base and copper(II) was acidified and the amount of copper(II) was determined iodometrically. Decomposition of sodium cuprate(III) in 1 *N* NaOH by this technique was used to check the analytical method given above.

RESULTS AND DISCUSSION

Products prepared by the above procedure contained 95 to 99% of the copper as copper(III). As a check on the accuracy of the arsenic(III) method of analysis, duplicate analyses of the same sample of sodium cuprate(III) gave a ratio of copper(III) to total copper of 0.796 and 0.800 by the gas volume method and 0.796 by the arsenic(III) method. As a check on possible air oxidation of the arsenic(III) solutions a series of blank runs were performed. Under the conditions of the analysis dissolved copper(II) is an excellent catalyst for the air oxidation of arsenic(III). However, solid copper(II) oxide and decomposed sodium cuprate(III) produced a maximum of 0.5 mole % oxidation in 1 h.

Scholder and Voelskow report that moist sodium cuprate(III) decomposes slowly. Analysis of a sample prepared by the method previously given showed 10% decomposition when stored for 8 days at room temperature. A portion of the same sample stored at 5 °C showed only 1% decomposition in the same period. In an effort to both dry and purify the sodium cuprate(III), samples were leached with various solvents. With freshly dried ethyl alcohol, dioxane, and acetone extensive decomposition occurred. Ethyl ether caused a slight decomposition (about 6%) but did not remove any moisture from the solid. Sodium cuprate(III) samples dried in a vacuum desiccator using either $Mg(ClO_4)_2$ or silica gel showed partial decomposition (20 to 35%). However, once dried the sodium cuprate(III) did not show further decomposition when stored in a desiccator over silica gel for 2 months at room temperature. These results are consistent both with the results of Scholder and Voelskow, who report a partial decomposition on drying the solid, and with those of Klemm and Wahl (7), who report that dry solid potassium dioxocuprate(III) is stable.

The results of the study of the decomposition of sodium cuprate(III) in the presence

of base are given in Table I. Inspection of Table I shows that sodium cuprate(III) decomposes more rapidly when in contact with KOH than NaOH and that the extent of decomposition increases as base strength decreases. Further, as may be expected, decomposition is more rapid at room temperature than at 0 °C.

TABLE I

Decomposition rate of sodium cuprate(III) in base*

	0.0 °C decompositions		25.2 °C decompositions	
Base	meq Cu present	Time (min) for 50% decomposition	meq Cu present	Time (min) for 50% decomposition
Satd. KOH	0.630	None in 40	0.510	25
10 *M* KOH	0.664	14	0.685	1.5
7.5 *M* KOH	0.619	7	0.452	1.0
0.5 *M* KOH	0.878	5	—	—
0.01 *M* KOH	0.633	4	—	—
Satd. NaOH	0.773	None in 150	0.736	50
10 *M* NaOH	0.595	None in 150	0.448	47
5 *M* NaOH	1.00	100	0.529	10
Satd. LiOH	0.633	40	0.597	15

*In all cases 20.0 ml base was used.

Except in the case of decompositions in lithium hydroxide, the rate of O_2 evaluation appears reasonably linear. In 10 *M* and saturated NaOH however, we observed a 10 min period in which essentially no decomposition occurs followed by a constant rate of O_2 evolution to the equilibrium pressure reading. In saturated LiOH at 25.2 °C, the rate of O_2 evolution is equivalent to that observed in 5 *M* NaOH up to a point corresponding to about 45% of the equilibrium O_2 pressure reading. The O_2 evolution rate then becomes progressively smaller so that complete decomposition in saturated LiOH requires 60 min compared to 20 min in 5 *M* NaOH.

Qualitative observations of the precipitates indicated that the decomposition rate was primarily influenced by the rate of solution. This observation is confirmed by the fact that saturated potassium hydroxide at both 0 °C and 25 °C in which $NaCuO_2$ was dissolving and decomposing gave no indication of Cu(III) in solution when we titrated a rapidly filtered portion of the $NaCuO_2$–base mixture with a known amount of excess As(III) followed by standard Ce(IV). More than 0.02 meq of copper(III) in solution with a solid sample containing 0.60 meq of copper(III) would have been detected. These results show that the cuprate(III) ion is so unstable in basic solutions that it can not have a half-life of more than a fraction of a minute.

Lister's study (3) of the rate of oxygen evolution in a copper(III) hypochlorite solution at 20 °C can be used to give a lower limit to the half-life of a copper(III) solution assuming that 4 moles of copper(III) give 1 mole of oxygen and that no hypochlorite complexes are present. At 20 °C Lister finds a rate of oxygen evolution of 0.25 ml of oxygen per minute for 2.77×10^{-5} moles of copper. This represents a half-life of about 25 s. This result is approximately the upper limit given by our experiments and would fix the half-life of cuprate(III) ion at about 25 s. However, Lister's results can also be explained by assuming that only a small fraction of the copper is present as copper(III), and that the rest of the copper is present as a hypochlorite complex.

Scholder and Voelskow have shown that solutions of copper(III) are stable in the presence of both excess base and excess hypobromite. This indicates that the hypobromite is either stabilizing the cuprate(III) ion by forming a complex ion or the rate of oxidation of copper(II) by hypobromite is greater than the rate of copper(III) decomposition.

Can. J. Chem. Downloaded from www.nrcresearchpress.com by 210.87.254.40 on 09/05/12
For personal use only.

1. L. JENSOVSKY. Chem. Listy, **50**, 1103 (1956); Z. Anorg. Allgem. Chem. **307**, 208, 219 (1961).
2. Z. KOVATS. Chem. Abstr. **54**, 11666 (1960).
3. M. W. LISTER. Can. J. Chem. **31**, 638 (1953).
4. R. SCHOLDER and U. VOELSKOW. Z. Anorg. Allgem. Chem. **266**, 256 (1951).
5. B. PARK. Ind. Eng. Chem. Anal. Ed. **3**, 77 (1931).
6. W. W. UMBREIT, R. H. BURRIS, and J. F. STAUFFER. Manometric techniques and tissue metabolism. Burgess, Minneapolis. 1949.
7. W. KLEMM and K. WAHL. Z. Anorg. Allgem. Chem. **270**, 69 (1952).

RECEIVED OCTOBER 16, 1964.
DEPARTMENT OF CHEMISTRY,
UNIVERSITY OF DELAWARE,
NEWARK, DELAWARE.

Can. J. Chem. Downloaded from www.nrcresearchpress.com by 210.87.254.40 on 09/05/12
For personal use only.

A PROTON MAGNETIC RESONANCE STUDY OF SODIUM 3,5,5-TRIMETHYL HEXANOATE

T. J. R. CYR AND B. A. DUNELL

Continuing with an investigation of molecular motion of fatty acids and their salts, we have examined the broad line nuclear magnetic resonance (n.m.r.) spectra of the sodium salt of 3,5,5-thrimethyl hexanoic acid. A commercial sample of the acid was distilled at 1 atm. Most of the acid distilled over between 226 and 228 °C and a portion of this central cut was taken for neutralization with an alcoholic solution of reagent grade sodium hydroxide. The solvent was partially evaporated and the precipitated soap was filtered and dried for some 24 h under vacuum. The precipitate was crushed to a powder, packed into pyrex sample tubes, and heated in the tubes for a further 24 h at 200° under vacuum before the tubes were sealed off.

Spectra were obtained on a Varian dual purpose spectrometer mainly at 60 Mc/s, although a few were run at 40 Mc. The depth of modulation varied from 0.14 gauss (G) to approximately 1 G, but most spectra were run at 0.14, 0.24, or 0.38 G modulation. Line shape and width were not observed to depend on the depth of modulation, and more specifically they were independent of modulation depth over the range 0.14 to 1 G at liquid nitrogen temperature and at 154 °K. This fact provides evidence that the narrowing of the absorption signal between 100 and 160 °K is not a spurious effect caused by the presence of an impurity whose absorption signal narrows at this temperature and obscures the still broad absorption of the main substance. Increasing the depth of modulation to 1 G from 0.14 G should produce at least some change in line shape at 154 °K if there is a broad as well as a narrow component of absorption actually present in the spectrum (1). The temperature of the sample was controlled by passing heated air or tank nitrogen cooled by passage through a cryostatic bath over the sample which was held in a dewar vessel within the n.m.r. probe. The temperature was measured by thermocouples placed in the airflow both upstream and downstream from the sample.

Typical spectra are presented in Fig. 1, and line width and second moment are shown as a function of temperature in Fig. 2. Three steps are distinguishable in the decrease of each of these parameters. The first and most obvious step begins immediately above liquid oxygen temperature and continues to about 160 °K. The second step is marked by a clear decrease in line width between 450 and 470 °K and a levelling off of the second moment at approximately 1.2 G^2 at 470 °K after a gradual decrease from some 4.5 G^2 at 350 °K. At temperatures above the third step, which occurs sharply at 538 °K, the line width is determined by depth of modulation and field homogeneity, and the second

1. L. JENSOVSKY. Chem. Listy, **50**, 1103 (1956); Z. Anorg. Allgem. Chem. **307**, 208, 219 (1961).
2. Z. KOVATS. Chem. Abstr. **54**, 11666 (1960).
3. M. W. LISTER. Can. J. Chem. **31**, 638 (1953).
4. R. SCHOLDER and U. VOELSKOW. Z. Anorg. Allgem. Chem. **266**, 256 (1951).
5. B. PARK. Ind. Eng. Chem. Anal. Ed. **3**, 77 (1931).
6. W. W. UMBREIT, R. H. BURRIS, and J. F. STAUFFER. Manometric techniques and tissue metabolism. Burgess, Minneapolis. 1949.
7. W. KLEMM and K. WAHL. Z. Anorg. Allgem. Chem. **270**, 69 (1952).

RECEIVED OCTOBER 16, 1964.
DEPARTMENT OF CHEMISTRY,
UNIVERSITY OF DELAWARE,
NEWARK, DELAWARE.

Can. J. Chem. Downloaded from www.nrcresearchpress.com by 210.87.254.105 on 09/05/12
For personal use only.

A PROTON MAGNETIC RESONANCE STUDY OF SODIUM 3,5,5-TRIMETHYL HEXANOATE

T. J. R. CYR AND B. A. DUNELL

Continuing with an investigation of molecular motion of fatty acids and their salts, we have examined the broad line nuclear magnetic resonance (n.m.r.) spectra of the sodium salt of 3,5,5-thrimethyl hexanoic acid. A commercial sample of the acid was distilled at 1 atm. Most of the acid distilled over between 226 and 228 °C and a portion of this central cut was taken for neutralization with an alcoholic solution of reagent grade sodium hydroxide. The solvent was partially evaporated and the precipitated soap was filtered and dried for some 24 h under vacuum. The precipitate was crushed to a powder, packed into pyrex sample tubes, and heated in the tubes for a further 24 h at 200° under vacuum before the tubes were sealed off.

Spectra were obtained on a Varian dual purpose spectrometer mainly at 60 Mc/s, although a few were run at 40 Mc. The depth of modulation varied from 0.14 gauss (G) to approximately 1 G, but most spectra were run at 0.14, 0.24, or 0.38 G modulation. Line shape and width were not observed to depend on the depth of modulation, and more specifically they were independent of modulation depth over the range 0.14 to 1 G at liquid nitrogen temperature and at 154 °K. This fact provides evidence that the narrowing of the absorption signal between 100 and 160 °K is not a spurious effect caused by the presence of an impurity whose absorption signal narrows at this temperature and obscures the still broad absorption of the main substance. Increasing the depth of modulation to 1 G from 0.14 G should produce at least some change in line shape at 154 °K if there is a broad as well as a narrow component of absorption actually present in the spectrum (1). The temperature of the sample was controlled by passing heated air or tank nitrogen cooled by passage through a cryostatic bath over the sample which was held in a dewar vessel within the n.m.r. probe. The temperature was measured by thermocouples placed in the airflow both upstream and downstream from the sample.

Typical spectra are presented in Fig. 1, and line width and second moment are shown as a function of temperature in Fig. 2. Three steps are distinguishable in the decrease of each of these parameters. The first and most obvious step begins immediately above liquid oxygen temperature and continues to about 160 °K. The second step is marked by a clear decrease in line width between 450 and 470 °K and a levelling off of the second moment at approximately 1.2 G^2 at 470 °K after a gradual decrease from some 4.5 G^2 at 350 °K. At temperatures above the third step, which occurs sharply at 538 °K, the line width is determined by depth of modulation and field homogeneity, and the second

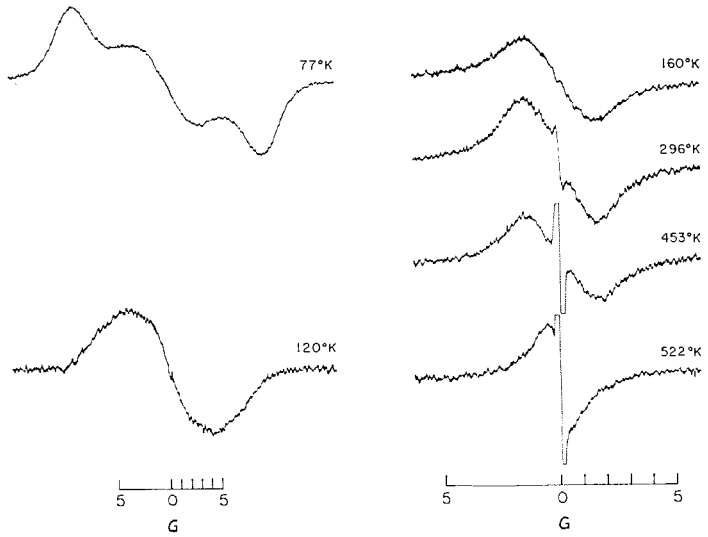

FIG. 1. Typical spectra of sodium 3,5,5-trimethyl hexanoate at various temperatures.

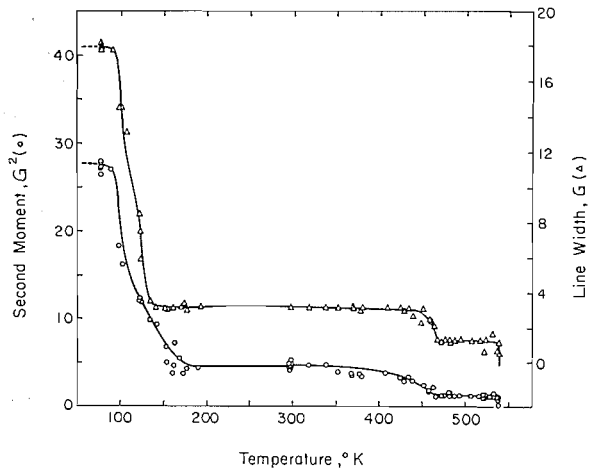

FIG. 2. Variation of line width and second moment of sodium 3,5,5-trimethyl hexanoate with temperature.

moment becomes vanishingly small. The final melting point was measured on a hot stage microscope as approximately 580 °K.

The intramolecular contribution to the rigid lattice second moment was calculated from proton positions, which were determined on the assumption that all bond angles were tetrahedral, that C—C bond lengths were 1.54 Å, and that C—H bond lengths were 1.10 Å. In the *t*-butyl group, one C—H bond of each CH_3 was assumed to be parallel to the C_4—C_5 bond direction. For interproton distances less than 5 Å, the intramolecular contribution was found to be 24.7 G^2. The magnitude of the intermolecular contribution is a matter for speculation since no crystallographic data were known for this salt. For potassium caprate to caproate the intermolecular contribution, from known crystal structure, is some 6.3 G^2 (2), and for sodium stearate it is estimated to be 9.4 G^2 (3).

Can. J. Chem. Downloaded from www.nrcresearchpress.com by 210.87.254.105 on 09/05/12
For personal use only.

It would be reasonable to assume that the intermolecular contribution in this compound is 7.5 ± 2 G^2. One might therefore estimate the total second moment to be 32 ± 3 G^2. The experimental value at 77 °K is 27 ± 1 G^2, and the difference between this and the theoretical value is 5 ± 4 G^2. The internal contribution of a methyl group to the second moment is 3.76 G^2 if it is rigid and 0.94 G^2 if it rotates. It is thus reasonable (2) to consider that the theoretical rigid lattice second moment is decreased by 3.5 G^2 for each methyl group which rotates. Construction of the molecule from Fisher–Hirschfelder atom models shows that free reorientation of all the methyl groups simultaneously is sterically impossible. In some conformations two methyl groups are strongly hindered and two rotate easily. If two methyl groups are rotating at 77 °K the difference between experimental and theoretical second moments should be 7 G^2, a value which is consistent with the estimated difference 5 ± 4 G^2. Until information is available concerning the crystal structure of this salt, the n.m.r. results cannot distinguish between one and two methyl groups rotating at liquid nitrogen temperature. The second moment does indicate, however, that it is improbable that no methyl groups rotate, and very improbable that more than two rotate. Alternatively, limited reorientation of all the methyl groups and of the whole *t*-butyl group, in which the possibility of motion of one group is dependent on reorientation of another, cannot be excluded as an interpretation of the results. Reorientation of the whole acid anion about the axis joining the carboxyl carbon and the central carbon atom of the *t*-butyl group reduces the intramolecular second moment to 5.5 G^2 if no other motion is considered. Addition of 0.6 of the estimated rigid lattice intermolecular contribution gives a total second moment of 10 ± 1 G^2 for rotation of the whole hydrocarbon chain. Simultaneous, limited reorientation of methyl groups would lower the second moment further, bringing it into the vicinity of the value of 4.5 G^2, which is observed experimentally over the temperature range of 180 to 340 °K. Molecular motion continues to increase above 340 °K, until by about 470 °K the experimental second moment of 1.2 G^2 indicates that only diffusional motion is not yet taking place at a frequency sufficient to influence the n.m.r. line, i.e. at about 10^4 s^{-1} (4). At approximately 537 °K line width and second moment approach zero, and we may assume that diffusion becomes significant above this sharply defined transition temperature, which is still some 40° below the melting point as it can be observed visibly with a hot stage microscope. It is, of course, also understood that the rate of rotational reorientation increases with increasing temperature over a wide temperature range, passing through the frequency range which is critical for n.m.r. line narrowing, viz., the order of the line width expressed as frequency (some 10^4 to 10^5 s^{-1}), in the temperature region in which line narrowing is observed.

The subsidiary maximum and minimum in the derivative curves at liquid nitrogen temperature may be attributed to a comparatively large contribution to the total signal from three-proton groups, broadened by large interactions from beyond the groups (5). It is established that increasing molecular motion with rise in temperature smooths out even this residual structural detail in the line shape of the three-proton system (5), and this is indeed observed in our spectra. A very narrow component of the spectrum appears at room temperature and increases in intensity as the temperature rises. We attribute this, as in other fatty acids and their salts (6), to premelting or to an abnormally early occurrence of the transition which is observed at 537 °K. The fact that the intensity of this narrow component does not increase especially rapidly with rise in temperature after its appearance at 300 °K may be taken as supporting evidence that the sample has a good degree of purity.

Can. J. Chem. Downloaded from www.nrcresearchpress.com by 210.87.254.105 on 09/05/12
For personal use only.

ACKNOWLEDGMENT

The authors thank the National Research Council of Canada for a grant in aid of this research.

1. F. A. RUSHWORTH. J. Chem. Phys. **20**, 920 (1952).
2. W. R. JANZEN and B. A. DUNELL. Trans. Faraday Soc. **59**, 1260 (1963).
3. R. F. GRANT and B. A. DUNELL. Can. J. Chem. **38**, 2395 (1960).
4. E. R. ANDREW. Nuclear magnetic resonance. Cambridge University Press. 1955. p. 173.
5. J. G. POWLES and H. S. GUTOWSKY. J. Chem. Phys. **21**, 1695 (1953).
6. M. R. BARR, B. A. DUNELL, and R. F. GRANT. Can. J. Chem. **41**, 1188 (1963).

RECEIVED DECEMBER 9, 1964.
CHEMISTRY DEPARTMENT,
UNIVERSITY OF BRITISH COLUMBIA,
VANCOUVER, BRITISH COLUMBIA.

Can. J. Chem. Downloaded from www.nrcresearchpress.com by 210.87.254.105 on 09/05/12
For personal use only.

MAGNETIC STUDIES ON COPPER(II) TRIFLUOROACETATE

R. C. THOMPSON AND D. B. W. YAWNEY

Magnetically dilute copper(II) compounds have magnetic moments essentially temperature independent and in the range 1.8–2.0 Bohr magnetons (B.M.) (1). Most of the alkyl- and aryl-carboxylates of copper(II), however, have abnormally low magnetic moments which vary with temperature in a manner indicative of the presence of antiferromagnetic interactions in these compounds (2–4). Extensive magnetic and structural studies have shown that one of the major factors affecting the magnetic properties is whether the compound has a binuclear structure, as has copper(II) acetate monohydrate, or a polymeric structure, as has copper(II) formate tetrahydrate. In carboxylate compounds of copper(II) which have the binuclear configuration, the magnetic interaction is relatively large as it arises through overlap of atomic orbitals on pairs of copper ions held in close proximity by four bridging carboxylate groups. Magnetic moments at room temperature for this type of compound range from approximately 1.4 B.M. observed for copper(II) acetate and the higher homologous alkanoates to 1.0 B.M. observed for copper(II) formate hemidioxane (5). In the group of compounds with polymeric configurations the magnetic interaction is much weaker since it occurs, not from direct metal–metal bonding but via the bridging carboxylate groups by a super-exchange mechanism. Room temperature moments observed here range from the value 1.61 B.M. for the power-blue form of copper(II) formate to 1.90 B.M. for the royal-blue form of the same compound (3).

In a review article on copper(II) complexes with subnormal magnetic moments, Kato, Jonassen, and Fanning (6), referring to unpublished work, report copper(II) trifluoroacetate to have a room temperature moment of 1.9 B.M. No further details were given. The magnetic properties of this compound have now been studied over the temperature range 90–300 °K. The criterion that carboxylates of copper(II) which have a binuclear configuration will exhibit magnetic interactions of a magnitude at least of the order of that observed in copper(II) acetate, or possibly larger, has been used to deduce structural information on copper(II) trifluoroacetate.

ACKNOWLEDGMENT

The authors thank the National Research Council of Canada for a grant in aid of this research.

1. F. A. RUSHWORTH. J. Chem. Phys. **20**, 920 (1952).
2. W. R. JANZEN and B. A. DUNELL. Trans. Faraday Soc. **59**, 1260 (1963).
3. R. F. GRANT and B. A. DUNELL. Can. J. Chem. **38**, 2395 (1960).
4. E. R. ANDREW. Nuclear magnetic resonance. Cambridge University Press. 1955. p. 173.
5. J. G. POWLES and H. S. GUTOWSKY. J. Chem. Phys. **21**, 1695 (1953).
6. M. R. BARR, B. A. DUNELL, and R. F. GRANT. Can. J. Chem. **41**, 1188 (1963).

RECEIVED DECEMBER 9, 1964.
CHEMISTRY DEPARTMENT,
UNIVERSITY OF BRITISH COLUMBIA,
VANCOUVER, BRITISH COLUMBIA.

Can. J. Chem. Downloaded from www.nrcresearchpress.com by 210.87.254.105 on 09/05/12
For personal use only.

MAGNETIC STUDIES ON COPPER(II) TRIFLUOROACETATE

R. C. THOMPSON AND D. B. W. YAWNEY

Magnetically dilute copper(II) compounds have magnetic moments essentially temperature independent and in the range 1.8–2.0 Bohr magnetons (B.M.) (1). Most of the alkyl- and aryl-carboxylates of copper(II), however, have abnormally low magnetic moments which vary with temperature in a manner indicative of the presence of antiferromagnetic interactions in these compounds (2–4). Extensive magnetic and structural studies have shown that one of the major factors affecting the magnetic properties is whether the compound has a binuclear structure, as has copper(II) acetate monohydrate, or a polymeric structure, as has copper(II) formate tetrahydrate. In carboxylate compounds of copper(II) which have the binuclear configuration, the magnetic interaction is relatively large as it arises through overlap of atomic orbitals on pairs of copper ions held in close proximity by four bridging carboxylate groups. Magnetic moments at room temperature for this type of compound range from approximately 1.4 B.M. observed for copper(II) acetate and the higher homologous alkanoates to 1.0 B.M. observed for copper(II) formate hemidioxane (5). In the group of compounds with polymeric configurations the magnetic interaction is much weaker since it occurs, not from direct metal–metal bonding but via the bridging carboxylate groups by a super-exchange mechanism. Room temperature moments observed here range from the value 1.61 B.M. for the power-blue form of copper(II) formate to 1.90 B.M. for the royal-blue form of the same compound (3).

In a review article on copper(II) complexes with subnormal magnetic moments, Kato, Jonassen, and Fanning (6), referring to unpublished work, report copper(II) trifluoroacetate to have a room temperature moment of 1.9 B.M. No further details were given. The magnetic properties of this compound have now been studied over the temperature range 90–300 °K. The criterion that carboxylates of copper(II) which have a binuclear configuration will exhibit magnetic interactions of a magnitude at least of the order of that observed in copper(II) acetate, or possibly larger, has been used to deduce structural information on copper(II) trifluoroacetate.

Can. J. Chem. Downloaded from www.nrcresearchpress.com by 210.87.254.105 on 09/05/12
For personal use only.

EXPERIMENTAL

Copper(II) trifluoroacetate was prepared by mixing copper(II) carbonate with a slight excess of trifluoroacetic acid in the form of a concentrated aqueous solution. The resulting blue solution, when placed in a desiccator containing phosphoric oxide, was reduced to a blue glassy residue and further dehydration under vacuum yielded anhydrous copper(II) trifluoroacetate, a pale-green, exceptionally hygroscopic solid.

Anal. Calcd. for $CuC_4F_6O_4$: Cu, 21.94; C, 16.59; F, 39.36; H, 0.0. Found: Cu, 21.6; C, 16.46; F, 39.37; H, 0.25.

Magnetic susceptibilities were determined by the Gouy method using an apparatus described previously (7). Calibration was achieved using a gravimetrically analyzed nickel(II) chloride solution (8). Measurements made at field strengths of approximately 8 500, 7 000, and 4 500 G gave no evidence for the dependence of the susceptibility of copper(II) trifluoroacetate upon the strength of the magnetic field. The diamagnetic contribution to the magnetic susceptibility of copper(II) trifluoroacetate was estimated from Pascal's constants (9) to be 89×10^{-6} c.g.s., e.m.u. Infrared spectra in Nujol were obtained using a Perkin–Elmer model 137 spectrophotometer.

DISCUSSION

The magnetic susceptibility data are given in Table I. A plot of reciprocal molar susceptibility versus temperature yields a straight line which intercepts the temperature abscissa at -42 °K. A slight curvature in the plot is noticeable at high temperatures, a type of behavior which has been observed in other copper(II) compounds and explained by the presence of a temperature-independent paramagnetic contribution to the susceptibility (1). The compound, therefore, obeys Curie–Weiss law of the form $\chi_M \alpha (T - \theta)^{-1}$ with a Weiss constant, θ, of $-42°$. The magnetic moment at 24 °C, calculated using the formula $\mu = 2.84[(\chi_M - 60)T]^{1/2}$ which includes a temperature-independent paramagnetic correction for copper(II) of 60×10^{-6} c.g.s., e.m.u., is 1.81 B.M.

TABLE I

Experimental gram and molar susceptibilities (c.g.s., e.m.u.) at various absolute temperatures

Temp. (°K)	$10^6\chi_g$	$10^6\chi_M$
296.8	4.64	1 430
291.1	4.73	1 460
233.2	5.45	1 670
223.7	5.64	1 720
208.7	6.11	1 860
189.7	6.57	1 990
180.0	6.83	2 070
151.3	7.97	2 400
122.3	9.33	2 790
94.5	11.45	3 400

The small, negative θ value observed for copper(II) trifluoroacetate probably arises through weak antiferromagnetic interactions, a result which strongly suggests that this compound does not have the binuclear configuration but may have a polymeric structure.

On comparing the infrared spectra of several copper(II) carboxylates with those of the corresponding sodium salts it has been observed that, where the copper salt has a binuclear configuration, the COO^- antisymmetric stretching frequencies, ν_a, are higher for the copper compounds than for the sodium compounds (6). The value of ν_a for copper(II) trifluoroacetate (1 650 cm^{-1}) is lower than the value (1 680 cm^{-1}) observed for sodium trifluoroacetate (10), a result supporting the conclusion reached by the magnetic studies that copper(II) trifluoroacetate does not adopt the binuclear configuration.

The fact that copper(II) trifluoroacetate is not binuclear while copper(II) acetate is lends strong support to the ideas of Martin and Waterman concerning the effect of the

donor properties of the ligands on the structures of copper(II) carboxylates (3). These authors suggest that one of the factors determining whether or not a copper(II) carboxylate adopts the binuclear configuration is the residual charge left on the copper ions after bonding with the carboxylate ligand. The separation of the two copper ions in the binuclear unit is small compared to the copper–copper distances in the polymeric configuration and hence a large residual charge on the metal ions may result in a repulsion between them which is strong enough to render the binuclear configuration unstable with respect to the polymeric configuration. The trifluoroacetate group is similar in size to the acetate group; however, due to the large inductive effect of the fluorine atoms, the former is a much weaker base. Hence the residual charge left on the copper ions is greater for copper(II) trifluoroacetate than for copper(II) acetate and the binuclear configuration is expected to be less stable for the former compound.

ACKNOWLEDGMENT

Financial assistance for this work was obtained from the National Research Council of Canada.

1. B. N. Figgis and C. M. Harris. J. Chem. Soc. 855 (1959).
2. R. L. Martin and H. Waterman. J. Chem. Soc. 2545 (1957).
3. R. L. Martin and H. Waterman. J. Chem. Soc. 1359 (1959).
4. J. Lewis and R. C. Thompson. Nature, **200**, 468 (1963).
5. R. L. Martin and H. Waterman. J. Chem. Soc. 2960 (1959).
6. M. Kato, H. B. Jonassen, and J. C. Fanning. Chem. Rev. **64**, 99 (1964).
7. H. C. Clark and R. J. O'Brien. Can. J. Chem. **39**, 1030 (1961).
8. H. R. Nettleton and S. Sugden. Proc. Roy. Soc. London, Ser. A, **173**, 313 (1939).
9. B. N. Figgis and J. Lewis. *In* Modern coordination chemistry. *Edited by* J. Lewis and R. G. Wilkins. Interscience, New York. 1960. p. 403.
10. W. Klemperer and G. C. Pimentel. J. Chem. Phys. **22**, 1399 (1954).

Received December 28, 1964.
Department of Chemistry,
University of British Columbia,
Vancouver, British Columbia.

STRUCTURAL DETERMINATIONS BY NUCLEAR MAGNETIC RESONANCE. 3-SUBSTITUTED PROPIONYL CHLORIDES

George H. Schmid and Larry S. J. Weiler

The possibility that 3-substituted propionyl chlorides might exist in a cyclic form or in equilibrium with a cylic form has been previously considered (1–8). In particular, succinyl dichloride (I*a*) and levulinyl chloride (I*c*) have received considerable attention (1, 2).

Various physical measurements have indicated that succinyl dichloride exists predominantly in the open chain form I*a*. These measurements have included infrared spectroscopy (1), refractivity (4), molecular volume (5), parachor (6), and dipole moments (7).

The structure of levulinyl chloride has been the subject of considerable work which has not firmly established its structure. Various workers have concluded that levulinyl chloride exists in the open chain form (4) while others concluded that the structure was cyclic (8). The nuclear magnetic resonance (n.m.r.) spectra of succinyl dichloride, levulinyl chloride, and 3-carbomethoxypropionyl chloride were taken in an attempt to provide

Can. J. Chem. Downloaded from www.nrcresearchpress.com by 210.87.254.105 on 09/05/12
For personal use only.

donor properties of the ligands on the structures of copper(II) carboxylates (3). These authors suggest that one of the factors determining whether or not a copper(II) carboxylate adopts the binuclear configuration is the residual charge left on the copper ions after bonding with the carboxylate ligand. The separation of the two copper ions in the binuclear unit is small compared to the copper–copper distances in the polymeric configuration and hence a large residual charge on the metal ions may result in a repulsion between them which is strong enough to render the binuclear configuration unstable with respect to the polymeric configuration. The trifluoroacetate group is similar in size to the acetate group; however, due to the large inductive effect of the fluorine atoms, the former is a much weaker base. Hence the residual charge left on the copper ions is greater for copper(II) trifluoroacetate than for copper(II) acetate and the binuclear configuration is expected to be less stable for the former compound.

ACKNOWLEDGMENT

Financial assistance for this work was obtained from the National Research Council of Canada.

1. B. N. Figgis and C. M. Harris. J. Chem. Soc. 855 (1959).
2. R. L. Martin and H. Waterman. J. Chem. Soc. 2545 (1957).
3. R. L. Martin and H. Waterman. J. Chem. Soc. 1359 (1959).
4. J. Lewis and R. C. Thompson. Nature, **200**, 468 (1963).
5. R. L. Martin and H. Waterman. J. Chem. Soc. 2960 (1959).
6. M. Kato, H. B. Jonassen, and J. C. Fanning. Chem. Rev. **64**, 99 (1964).
7. H. C. Clark and R. J. O'Brien. Can. J. Chem. **39**, 1030 (1961).
8. H. R. Nettleton and S. Sugden. Proc. Roy. Soc. London, Ser. A, **173**, 313 (1939).
9. B. N. Figgis and J. Lewis. *In* Modern coordination chemistry. *Edited by* J. Lewis and R. G. Wilkins. Interscience, New York. 1960. p. 403.
10. W. Klemperer and G. C. Pimentel. J. Chem. Phys. **22**, 1399 (1954).

Received December 28, 1964.
Department of Chemistry,
University of British Columbia,
Vancouver, British Columbia.

STRUCTURAL DETERMINATIONS BY NUCLEAR MAGNETIC RESONANCE. 3-SUBSTITUTED PROPIONYL CHLORIDES

George H. Schmid and Larry S. J. Weiler

The possibility that 3-substituted propionyl chlorides might exist in a cyclic form or in equilibrium with a cylic form has been previously considered (1–8). In particular, succinyl dichloride (I*a*) and levulinyl chloride (I*c*) have received considerable attention (1, 2).

Various physical measurements have indicated that succinyl dichloride exists predominantly in the open chain form I*a*. These measurements have included infrared spectroscopy (1), refractivity (4), molecular volume (5), parachor (6), and dipole moments (7).

The structure of levulinyl chloride has been the subject of considerable work which has not firmly established its structure. Various workers have concluded that levulinyl chloride exists in the open chain form (4) while others concluded that the structure was cyclic (8). The nuclear magnetic resonance (n.m.r.) spectra of succinyl dichloride, levulinyl chloride, and 3-carbomethoxypropionyl chloride were taken in an attempt to provide

Can. J. Chem. Downloaded from www.nrcresearchpress.com by 210.87.254.42 on 09/05/12
For personal use only.

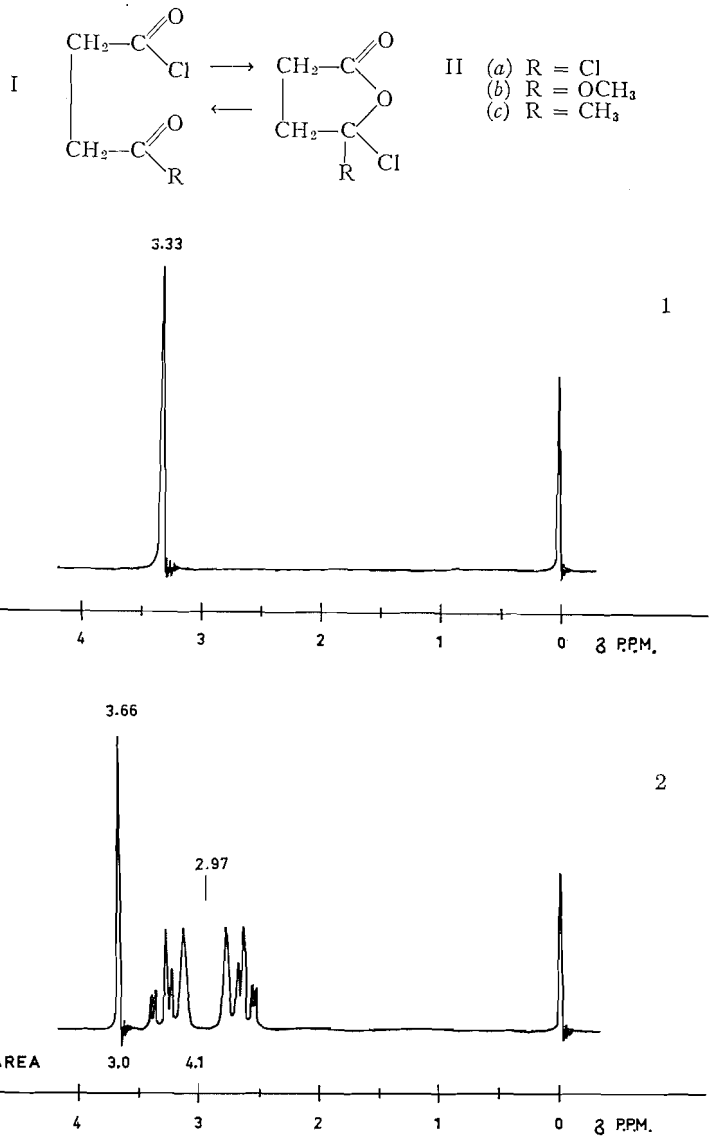

FIGS. 1 and 2. Nuclear magnetic resonance spectrum of succinyl dichloride and 3-carbomethoxypropionyl chloride.

further evidence for the structure of these compounds. The evidence from nuclear magnetic resonance spectra for a cyclic or an acyclic structure for the 3-substituted propionyl chlorides rests on the following two points: (*i*) the methylene splitting pattern for a cyclic structure should be an asymmetric ABCD type and (*ii*) there should be a difference between the chemical shift of the methylene, methyl, and methoxy protons in a cyclic as compared with an acyclic structure. The nuclear magnetic resonance spectra of succinyl dichloride, 3-carbomethoxypropionyl chloride, and levulinyl chloride are shown in Figs. 1, 2, and 3 respectively. Figures 4 and 5 show the nuclear magnetic resonance spectra of the pseudo-ester (III), prepared from levulinyl chloride by the method of Langlois

Can. J. Chem. Downloaded from www.nrcresearchpress.com by 210.87.254.42 on 09/05/12
For personal use only.

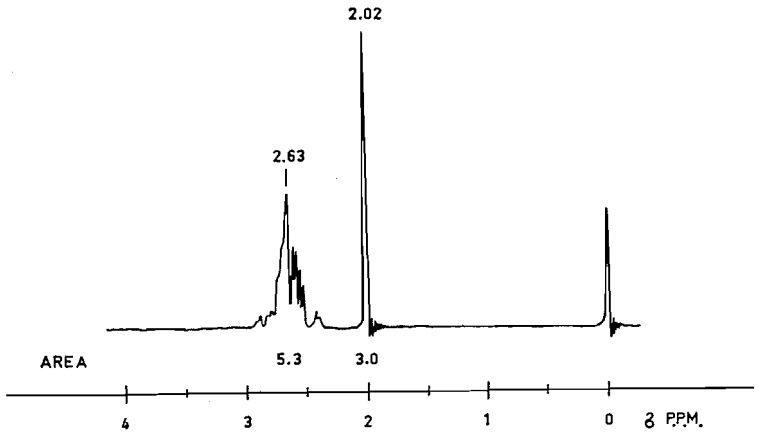

FIG. 3. Nuclear magnetic resonance spectrum of levulinyl chloride.

and Wolff (2), and the normal ester (IV), prepared from levulinic acid by the method of Frank (9).

III

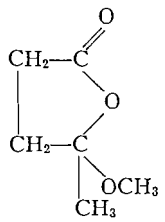

IV

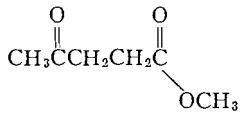

Figures 4 and 5 show clearly the different splitting pattern of the methylene protons in the pseudo-ester (III), as compared to the acyclic normal ester (IV). A comparison of the chemical shifts of the protons in (III) and (IV) shows that the methylene, methyl, and methoxy protons of the cyclic pseudo-ester (III) are all further upfield than those in (IV). This indicates that the protons in (III) are more shielded, which is consistent with a cyclic structure. Thus the structure of the pseudo-ester (III) derived from levulinyl chloride is clearly cyclic while the structure of methyl levulinate (IV) derived from levulinic acid is acyclic. The asymmetric methylene proton pattern in Fig. 3 leads to the conclusion that levulinyl chloride exists predominantly in the cyclic form. The replacement of a methoxy group by a chlorine atom (compare Figs. 3 and 4) leads to a downfield shift of the methyl group and a decrease in the spread of the methylene proton pattern, indicating that chlorine is less shielding than a methoxy group. While the methylene proton splitting pattern is consistent with a cyclic structure, the ratio of the integrated areas of methyl to methylene protons is in poor agreement with the theoretical ratio of 4:3. There is the possibility that an appreciable concentration of the acyclic form is present in the neat liquid. The methyl and the methylene protons of the acyclic form would be found approximately 0.3 p.p.m. to 0.6 p.p.m. downfield from the cyclic methyl and methylene proton peaks. This would place them in the region of the cyclic methylene protons and could account for the discrepancy in the ratio of the integrated areas. If it is assumed that only the cyclic and the acyclic forms are present, this indicates that 15.5% of levulinyl chloride may exist in the open chain form.

The nuclear magnetic resonance spectrum of 3-carbomethoxypropionyl chloride (Fig. 2)

Can. J. Chem. Downloaded from www.nrcresearchpress.com by 210.87.254.42 on 09/05/12
For personal use only.

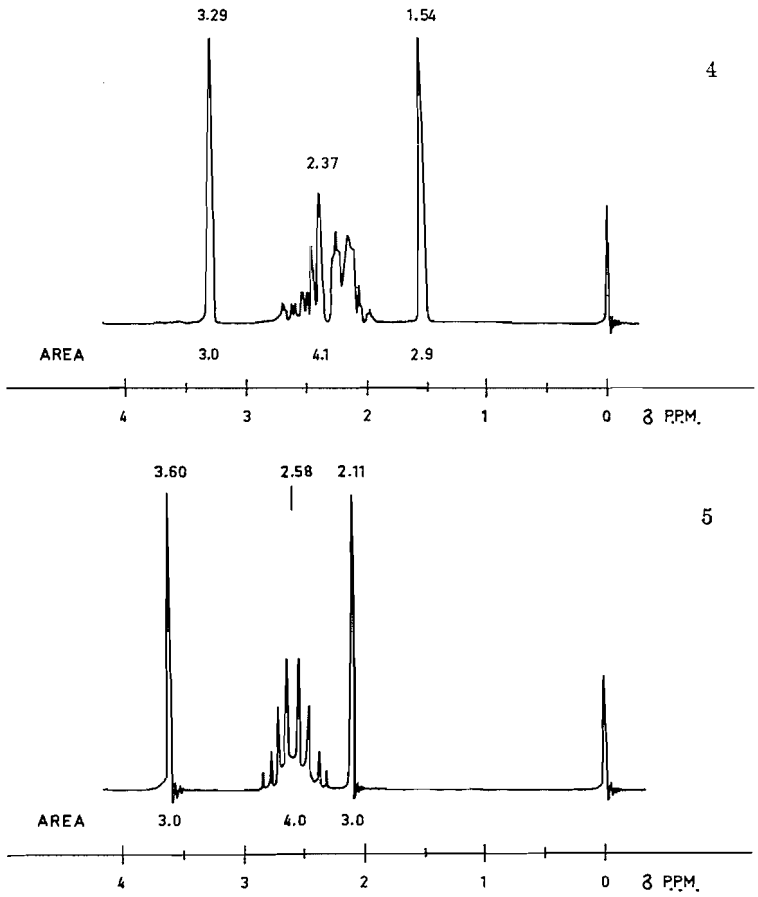

FIGS. 4 and 5. Nuclear magnetic resonance spectrum of pseudo-methyl ester of levulinic acid and methyl levulinate.

is in accord with an acyclic structure for this compound. The excellent agreement between the theoretical ratio and the ratio of the integrated areas of the methylene and methoxy protons tends to rule out the presence of an appreciable concentration of the cyclic form whose methoxy and methylene protons would be hidden by the acyclic methylene protons. Furthermore the chemical shift of the methoxy protons are in the positions expected for an open chain structure. Thus the methoxy protons are found at 3.66 p.p.m., a position similar to that of the methoxy group in methyl levulinate.

The nuclear magnetic resonance spectrum of succinyl dichloride (Fig. 1) shows only a singlet at 3.33 p.p.m. in accord with an open chain structure for this compound. The possibility exists that the complex multiplet of a small amount of the cyclic form might be hidden under the singlet. Such a possibility cannot be ruled out until the pure cyclic form is prepared and its spectrum determined. However, the sharpness of the singlet indicates that succinyl dichloride exists predominantly in the acyclic form.

The use of nuclear magnetic resonance has not conclusively established that an equilibrium exists between an open and a cyclic form of 3-substituted propionyl chlorides since in no case has it been possible to detect proton signals from both forms simultaneously. It is interesting to notice that the structure of the 3-substituted propionyl chloride is

Can. J. Chem. Downloaded from www.nrcresearchpress.com by 210.87.254.42 on 09/05/12
For personal use only.

dependent upon the substituent R. When R is methoxy or chlorine the structure is predominantly acyclic while when R is methyl the structure is largely cyclic. This can be explained on the basis of the electronegativity of the substituent. The more electronegative the substituent, the greater the decrease in the stability of the cyclic form relative to the open chain form resulting in the observed structures.

EXPERIMENTAL

All melting and boiling points are uncorrected. Nuclear magnetic resonance spectra were taken on a Varian A-60 Spectrometer on the neat compounds unless otherwise stated with tetramethylsilane as internal standard. Vapor phase chromatography (v.p.c.) was performed on a F and M Model 500 Gas Chromatograph using helium as a carrier gas.

Succinyl dichloride (Ia) was prepared by the method of Cason and Reist (1) in 77% yield. Boiling point 65–66° at 2 mm; lit. b.p. 65° at 5 mm.

Levulinyl chloride (IIc) was prepared by the method of Cason and Reist (1) in 95% yield. Since this acid chloride is very sensitive to heat, it was not distilled. Excess thionyl chloride was removed at reduced pressure below 50°. The last traces of thionyl chloride were removed by an azeotrope with benzene at reduced pressure. The nuclear magnetic resonance was taken of the yellow residual acid chloride.

Pseudo-methyl levulinate (III) was prepared by the method of Langlois and Wolff (2) in 27% yield. Boiling point 83° at 2 mm; lit. b.p. 90–92° at 15 mm. Vapor phase chromatographic analysis showed the product to be contaminated by a small amount of the normal ester. The pure pseudo-ester for spectral studies was obtained by isolation from v.p.c. on an 8 ft diisodecyl phthalate column at 120°. The nuclear magnetic resonance spectrum was taken in carbon tetrachloride.

β-Carbomethoxypropionyl chloride (Ib) was prepared according to the method of Cason (10) in 92% yield. Boiling point 44–45° at 0.5 mm; lit. b.p. 58–59° at 2.5 mm.

Methyl levulinate (IV) was prepared by the method of Frank *et al.* (11) in 16% yield. Boiling point 82–85° at 8 mm; lit. b.p. 89–91° at 15 mm (2).

ACKNOWLEDGMENT

The authors are grateful to the National Research Council of Canada for financial aid.

1. J. Cason and E. J. Reist. J. Org. Chem. **23**, 1492 (1958); references cited therein.
2. D. P. Langlois and H. Wolff. J. Am. Chem. Soc. **70**, 2624 (1948).
3. B. H. Chase and D. H. Hey. J. Chem. Soc. 553 (1952).
4. K. V. Auwers and M. Schmidt. Ber. **46**, 457 (1913).
5. G. F. Morrell. J. Chem. Soc. **105**, 1733 (1914).
6. F. B. Garner and S. Sugden. J. Chem. Soc. 2877 (1927).
7. G. T. O. Martin and J. R. Partington. J. Chem. Soc. 1178 (1936).
8. J. H. Hilberger. Ann. **522**, 269 (1936).
9. R. L. Frank, R. G. Arvan, J. W. Richter, and C. R. Vanneman. J. Am. Chem. Soc. **66**, 4 (1944).
10. J. Cason. *In* Organic syntheses. Collective Vol. III. John Wiley and Sons, Inc., New York. 1955. p. 170.

Received November 30, 1964.
Department of Chemistry,
University of Toronto,
Toronto, Ontario.

CARBONYL AND THIOCARBONYL COMPOUNDS. IX. SYNTHESIS OF BENZOXANTHENE ETHERS BY THE ACTION OF TETRAHALO-*o*-BENZOQUINONES[1]

N. Latif and I. Fathy

Recently, it has been shown that methylene ethers derived from xanthene can be directly obtained by the action of tetrahalo-*o*-benzoquinones on ketohydrazones (1). In the present study, the 1,2-benzoxanthene ethers I*a* and I*b* are similarly produced by the interaction of 1,2-benzoxanthone hydrazone with tetrachloro- and tetrabromo-*o*-benzoquinones, respectively, in dry ether at room temperature. It is believed that the reaction

[1]*Abstracted from the Ph.D. thesis of I. Fathy, December 1963.*

Can. J. Chem. Downloaded from www.nrcresearchpress.com by 210.87.254.42 on 09/05/12
For personal use only.

dependent upon the substituent R. When R is methoxy or chlorine the structure is predominantly acyclic while when R is methyl the structure is largely cyclic. This can be explained on the basis of the electronegativity of the substituent. The more electronegative the substituent, the greater the decrease in the stability of the cyclic form relative to the open chain form resulting in the observed structures.

EXPERIMENTAL

All melting and boiling points are uncorrected. Nuclear magnetic resonance spectra were taken on a Varian A-60 Spectrometer on the neat compounds unless otherwise stated with tetramethylsilane as internal standard. Vapor phase chromatography (v.p.c.) was performed on a F and M Model 500 Gas Chromatograph using helium as a carrier gas.

Succinyl dichloride (Ia) was prepared by the method of Cason and Reist (1) in 77% yield. Boiling point 65–66° at 2 mm; lit. b.p. 65° at 5 mm.

Levulinyl chloride (IIc) was prepared by the method of Cason and Reist (1) in 95% yield. Since this acid chloride is very sensitive to heat, it was not distilled. Excess thionyl chloride was removed at reduced pressure below 50°. The last traces of thionyl chloride were removed by an azeotrope with benzene at reduced pressure. The nuclear magnetic resonance was taken of the yellow residual acid chloride.

Pseudo-methyl levulinate (III) was prepared by the method of Langlois and Wolff (2) in 27% yield. Boiling point 83° at 2 mm; lit. b.p. 90–92° at 15 mm. Vapor phase chromatographic analysis showed the product to be contaminated by a small amount of the normal ester. The pure pseudo-ester for spectral studies was obtained by isolation from v.p.c. on an 8 ft diisodecyl phthalate column at 120°. The nuclear magnetic resonance spectrum was taken in carbon tetrachloride.

β-Carbomethoxypropionyl chloride (Ib) was prepared according to the method of Cason (10) in 92% yield. Boiling point 44–45° at 0.5 mm; lit. b.p. 58–59° at 2.5 mm.

Methyl levulinate (IV) was prepared by the method of Frank *et al.* (11) in 16% yield. Boiling point 82–85° at 8 mm; lit. b.p. 89–91° at 15 mm (2).

ACKNOWLEDGMENT

The authors are grateful to the National Research Council of Canada for financial aid.

1. J. Cason and E. J. Reist. J. Org. Chem. **23**, 1492 (1958); references cited therein.
2. D. P. Langlois and H. Wolff. J. Am. Chem. Soc. **70**, 2624 (1948).
3. B. H. Chase and D. H. Hey. J. Chem. Soc. 553 (1952).
4. K. V. Auwers and M. Schmidt. Ber. **46**, 457 (1913).
5. G. F. Morrell. J. Chem. Soc. **105**, 1733 (1914).
6. F. B. Garner and S. Sugden. J. Chem. Soc. 2877 (1927).
7. G. T. O. Martin and J. R. Partington. J. Chem. Soc. 1178 (1936).
8. J. H. Hilberger. Ann. **522**, 269 (1936).
9. R. L. Frank, R. G. Arvan, J. W. Richter, and C. R. Vanneman. J. Am. Chem. Soc. **66**, 4 (1944).
10. J. Cason. *In* Organic syntheses. Collective Vol. III. John Wiley and Sons, Inc., New York. 1955. p. 170.

Received November 30, 1964.
Department of Chemistry,
University of Toronto,
Toronto, Ontario.

CARBONYL AND THIOCARBONYL COMPOUNDS. IX. SYNTHESIS OF BENZOXANTHENE ETHERS BY THE ACTION OF TETRAHALO-*o*-BENZOQUINONES[1]

N. Latif and I. Fathy

Recently, it has been shown that methylene ethers derived from xanthene can be directly obtained by the action of tetrahalo-*o*-benzoquinones on ketohydrazones (1). In the present study, the 1,2-benzoxanthene ethers I*a* and I*b* are similarly produced by the interaction of 1,2-benzoxanthone hydrazone with tetrachloro- and tetrabromo-*o*-benzoquinones, respectively, in dry ether at room temperature. It is believed that the reaction

[1]*Abstracted from the Ph.D. thesis of I. Fathy, December 1963.*

Can. J. Chem. Downloaded from www.nrcresearchpress.com by 210.87.254.42 on 09/05/12
For personal use only.

proceeds through the intermediate formation of an unstable 9-diazo-1,2-benzoxanthene, which reacts with the tetrahaloquinone to give the methylene ether. The production of the corresponding tetrahalocatechol in this reaction together with the evolution of gas supports this suggestion. Constitution of the products is based on analogy (2, 3), analytical data and lack of color, and on the fact that they could be produced by condensing 9,9-dichloro-1,2-benzoxanthene with the corresponding tetrahalocatechol.

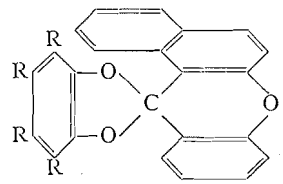

I*a*; R = Cl
I*b*; R = Br

1,2-Benzoxanthone hydrazone is prepared by the action of hydrazine hydrate on 1,2-benzoxanthione, which is obtained readily by the action of phosphorus pentasulfide on 1,2-benzoxanthone. The latter is synthesized by condensing salicylic acid with β-naphthol in presence of polyphosphoric acid. The product obtained by Desai *et al.* (4) from a similar experiment and described by them as 2,3-benzoxanthone is shown, in the present investigation, to be actually the 1,2-analogue. It is identical with the product obtained by von Dilthey *et al.* (5) from *o*-iodobenzoyl-β-naphthol, and different from 2,3-benzoxanthone (5, 6).

The benzoxanthene ethers exhibit remarkable chemical reactivity towards different nucleophiles resulting in cleavage of the dioxole ring. Thus, I*a* undergoes, quite readily, reductive cleavage by lithium aluminium hydride in boiling ether yielding 1,2-benzoxanthene and tetrachlorocatechol. The ease of cleavage, compared with the parent xanthene analogues (7), might be rationalized by assuming that the carbonium ion intermediate is stabilized by resonance with the ethereal oxygen and the conjugated naphthalene nucleus (cf. II). Delocalization of charge via π-orbitals is enhanced by the fused 1,2-benzenoid ring and this promotes stability of the carbonium ion formed.

The dioxole ring of the benzoxanthene ethers is also readily cleaved by active hydrogen compounds furnishing the corresponding 1,2-benzoxanthylenes. Thus, I*a* and I*b* react with hydrazines in boiling ethanol to give the corresponding hydrazones. In the case of hydrazine itself, 1,2-benzoxanthone azine is found among the products formed presumably through the action of a part of the hydrazone first formed on the cyclic ether. With malononitrile and ethyl cyanoacetate, the unsaturated nitriles III*a* and III*b* are readily produced. It is believed that cleavage proceeds, for example in the case of hydrazine, through the intermediate formation of IV which gives directly the hydrazone together with tetrachlorocatechol by a β-elimination process (8). Authentic samples of the

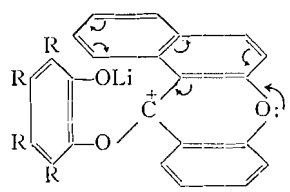

II

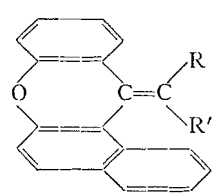

III*a*; R = R′ = CN
III*b*; R = $COOC_2H_5$, R′ = CN

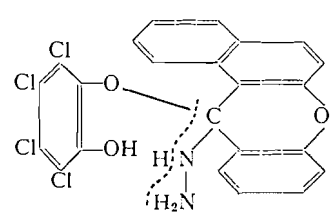

IV

Can. J. Chem. Downloaded from www.nrcresearchpress.com by 210.87.254.42 on 09/05/12
For personal use only.

benzoxanthylenes are prepared by two established procedures: (*a*) by condensing 1,2-benzoxanthione with malononitrile or ethyl cyanoacetate in presence of a desulfurizing agent, or (*b*) by the reaction of 1,2-benzoxanthone dichloride with the cyanocompounds. The fused 1,2-benzenoid ring seems to have no retarding steric effect on the reactivity of the benzoxanthene analogues as compared with the parent xanthene ethers.

EXPERIMENTAL

Microanalyses were performed by A. Bernhardt, Germany, and the Microanalysis Unit, National Research Center, Cairo.

Preparation of 1,2-Benzoxanthone

A mixture of salicyclic acid (12 g), β-naphthol (12 g), and polyphosphoric acid (from 50 ml orthophosphoric acid and 80 g phosphorus pentaoxide) was heated at 140–145 °C (oil bath) for 6 h with occasional shaking. The reaction mixture was left to cool, poured onto crushed ice, then strongly stirred. The separated solid was filtered off, and washed with water several times. It was then heated with 10% sodium hydroxide solution for 15 min in a boiling water bath, left to cool, and filtered off. The solid obtained was washed with hot water till free from alkali, dried, and crystallized from ethanol to give 1,2-benzoxanthone (4.5 g) as colorless crystals m.p. 142 °C (undepressed when admixed with an authentic sample prepared according to von Dilthey *et al.* (5)).

Preparation of 1,2-Benzoxanthione

A finely powdered mixture of 1,2-benzoxanthone (2 g) and phosphorus pentasulfide (2.5 g) was heated at 120 °C for 1 h. The reaction mixture was left to cool, and extracted with hot benzene. The extract was filtered, concentrated, and left to cool. The separated solid (1.4 g) was recrystallized from benzene to give 1,2-benzoxanthione as dark-green crystals m.p. 145 °C (undepressed when admixed with an authentic sample (9)).

Anal. Calcd. for $C_{17}H_{10}OS$: C, 77.86; H, 3.81; S, 12.21. Found: C, 78.12; H, 3.95; S, 11.98.

Preparation of Benzoxanthone Hydrazone

To a boiling solution of 1,2-benzoxanthione (2 g) in absolute alcohol (50 ml), hydrazine hydrate (80%, 0.5 ml) was added. The solution was refluxed for 1 h, filtered, concentrated, and left to cool. The separated solid (1.5 g) was recrystallized from ethanol to give 1,2-benzoxanthone hydrazone as pale-yellow crystals m.p. 146 °C.

Anal. Calcd. for $C_{17}H_{12}ON_2$: N, 10.76. Found: N, 10.29.

Preparation of 9,9-(Tetrachloro-o-phenylenedioxy)1,2-benzoxanthene (Ia)

Tetrachlorocatechol (2 g) and 9,9-dichloro-1,2-benzoxanthene (from 2 g 1,2-benzoxanthone and thionyl chloride) were heated together, for 1 h, in a round bottom flask protected from moisture at 120 °C (oil bath). The reaction mixture was left to cool, washed with acetone several times, and recrystallized from xylene to give I*a* as colorless crystals m.p. 333–334 °C.

Anal. Calcd. for $C_{23}H_{10}O_3Cl_4$: C, 57.98; H, 2.10; Cl, 29.81. Found: C, 58.15; H, 2.53; Cl, 29.74.

Reaction of Tetrachloro-o-benzoquinone with 1,2-Benzoxanthone Hydrazone

To a dry ethereal solution of the quinone (2 g), the hydrazone (1 g) was added in portions at room temperature. After each addition a vigorous reaction with evolution of gas occurred. When all the hydrazone had been added, a colorless crystalline product separated out. This was filtered off, and recrystallized from xylene to give I*a* as colorless crystals m.p. 333–334 °C (undepressed when admixed with an authentic sample prepared as above). The ethereal mother liquor was evaporated to dryness, extracted with methanol, and the extract poured onto ice and acidified with hydrochloric acid. The separated solid was shown to be tetrachlorocatechol as before.

Reaction of Tetrabromo-o-benzoquinone with 1,2-Benzoxanthone Hydrazone

The reaction was carried out as in the case of the chloro analogue. The separated product was filtered off and recrystallized from benzene to give I*b* as colorless crystals which decompose at 344 °C.

Anal. Calcd. for $C_{23}H_{10}O_3Br_4$: C, 42.20; H, 1.52; Br, 48.92. Found: C, 42.12; H, 1.42; Br, 48.24.

Tetrabromocatechol was isolated from the ethereal mother liquor as described in the case of the chloro analogue, and was identified as its diacetate (melting point and mixed melting point).

Reaction of Ia with Lithium Aluminium Hydride

The reaction was carried out as in the case of the parent xanthene ether (7). The reaction mixture was decomposed with ethanol, then with dilute hydrochloric acid, and extracted several times with ether. The combined ethereal extracts were dried over anhydrous sodium sulfate and then filtered, and the ether was driven off. The solid which separated was recrystallized from methanol to give 1,2-benzoxanthene (0.26 g) as colorless crystals m.p. 92–93 °C (undepressed when admixed with an authentic sample (9)). The alcoholic

Can. J. Chem. Downloaded from www.nrcresearchpress.com by 210.87.254.42 on 09/05/12
For personal use only.

mother liquor was poured onto ice-cold water and acidified with hydrochloric acid. The precipitate formed was shown to be tetrachlorocatechol as before.

Preparation of 1,2-Benzoxanthone Azine

A solution of 1,2-benzoxanthone hydrazone (1 g) in benzene (20 ml) was refluxed with yellow mercuric oxide (1 g) for 1 h. The reaction mixture was filtered while hot, concentrated, and cooled. The product obtained was crystallized from benzene to give the azine as orange-yellow crystals m.p. 314 °C.

Anal. Calcd. for $C_{34}H_{20}O_2N_2$: C, 83.60; H, 4.10; N, 5.73. Found: C, 83.49; H, 4.35; N, 6.03.

Reaction of Ia with Hydrazine Hydrate

I*a* (0.2 g) and hydrazine hydrate (99–100%, 0.2 ml) in absolute alcohol (20 ml) were refluxed together for 3 h. The reaction mixture was filtered while hot, and the solid obtained (0.02 g) was shown to be 1,2-benzoxanthone azine (melting point and mixed melting point). The filtrate was concentrated and left to cool; a yellow crystalline solid separated (0.07 g) and proved to be 1,2-benzoxanthone hydrazone (melting point and mixed melting point). Tetrachlorocatechol was identified in the main alcoholic mother liquor as above.

Reaction of Ia with Benzoylhydrazine

The reaction was carried out as above using 1 g of I*a* and ½ g of benzoylhydrazine. The solution was filtered, concentrated, and left to cool. The separated product (0.45 g) was recrystallized from methanol to give 1,2-benzoxanthone benzoylhydrazone as pale-yellow crystals m.p. 164 °C.

Anal. Calcd. for $C_{24}H_{16}O_2N_2$: C, 79.10; H, 4.39; N, 7.69. Found: C, 78.93; H, 4.36; N, 8.44.

Reaction of Ia with Phenylhydrazine

The reaction was carried out as above when 1,2-benzoxanthone phenylhydrazone was obtained as yellow crystals (from methanol) m.p. 124 °C (decomp.).

Anal. Calcd. for $C_{23}H_{16}ON_2$: N, 8.33. Found: N, 7.70.

Preparation of Δ^9,α-1,2-Benzoxanthenemalononitrile (IIIa)

Method A.—A mixture of 9,9-dichloro-1,2-benzoxanthene (from 1 g 1,2-benzoxanthone) and malononitrile (0.5 g) was heated at 120 °C (oil bath) for 3 h in absence of moisture. The reaction mixture was left to cool, washed with methanol, and extracted with boiling benzene. The benzene extract was concentrated and cooled when III*a* (0.9 g) was obtained as yellow crystals m.p. 224–225 °C.

Anal. Calcd. for $C_{20}H_{10}ON_2$: C, 81.63; H, 3.40; N, 9.53. Found: C, 81.41; H, 3.58; N, 9.76.

Method B.—A suspension of 1,2-benzoxanthione (0.5 g), malononitrile (0.5 g), and yellow mercuric oxide (1 g) in dry benzene (20 ml) was heated under reflux for 5 h. The reaction mixture was filtered while hot, concentrated, and left to cool. The separated yellow crystals (0.26 g) proved to be III*a* (melting point and mixed melting point).

Preparation of Δ^9,α-1,2-Benzoxantheneacetic Acid, α-Cyanoethyl Ester (IIIb)

9,9-Dichloro-1,2-benzoxanthene (from 2 g 1,2-benzoxanthone) and ethyl cyanoacetate (1 ml) were allowed to react together as above. The reaction mixture was extracted with methanol, and the alcoholic extract was concentrated and cooled. The separated solid was recrystallized from acetone to give III*b* (1.2 g) as yellow crystals m.p. 118–120 °C.

Anal. Calcd. for $C_{22}H_{15}O_3N$: C, 77.41; H, 4.39; N, 4.10. Found: C, 77.30; H, 4.64; N, 3.77.

III*b* could be also obtained by the reaction between 1,2-benzoxanthione and ethyl cyanoacetate.

Reaction of Ia with Malononitrile

Malononitrile (0.2 g) and I*a* (0.4 g) in absolute alcohol (30 ml) were refluxed together for 6 h. The reaction mixture was filtered, concentrated, and cooled. The separated yellow crystals (0.1 g) proved to be III*a* (melting point and mixed melting point). Tetrachlorocatechol was identified in the main alcoholic mother liquor as usual.

When the reaction was carried out using ethyl cyanoacetate, instead of malononitrile, III*b* was similarly produced.

1. N. Latif, I. Fathy, and N. Mishriky. J. Org. Chem. **24**, 1883 (1959).
2. N. Latif and I. Fathy. Can. J. Chem. **37**, 863 (1959).
3. N. Latif, I. Fathy, N. Mishriky, and A. Atallah. J. Org. Chem. **25**, 1618 (1960).
4. B. Desai, P. Desai, and R. Desai. J. Indian Chem. Soc. **37**, 53 (1960).
5. W. von Dilthey, F. Quint, and F. Dahm. J. Prakt. Chem. **141**, 65 (1934).
6. A. El-Abbady, S. Ayoub, and F. Baddar. J. Chem. Soc. 2556 (1960).
7. N. Latif and N. Mishriky. J. Org. Chem. **27**, 846 (1962).
8. N. Latif, I. Fathy, and N. Mishriky. Can. J. Chem. **42**, 1736 (1964).
9. A. Mustafa and M. Hilmy. J. Chem. Soc. 1343 (1952).

Received May 27, 1964.
Organic Chemistry Department,
National Research Center,
Dokki, Cairo, U.A.R.

Can. J. Chem. Downloaded from www.nrcresearchpress.com by 210.87.254.42 on 09/05/12
For personal use only.

HETEROCYCLONIUMYL ZWITTERIONS. PART I. THE ALKALI-CATALYZED CLEAVAGE OF 2-HYDROXYMETHYL- AND 2-FORMYL-PYRIDINIUM CATIONS

S. GOLDING AND A. R. KATRITZKY

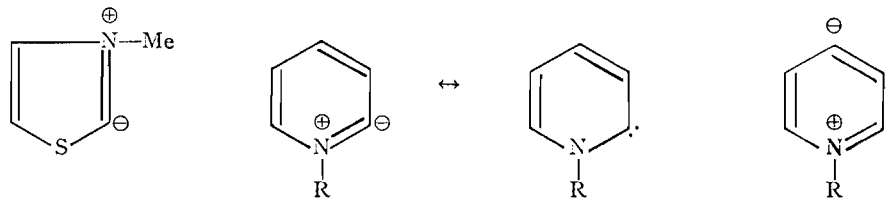

I II III

Heterocycloniumyl zwitterions of type I are well known to be of importance in the biological activity of thiamine (1), and recently azolonium zwitterion intermediates have received attention (2). Certain pyridinium derivatives have been shown to exchange α-hydrogen atoms by way of zwitterions of type II (3). We have now shown that the relative stability of such species facilitates the reaction sequences (IV $\rightarrow$ VI) and (VII $\rightarrow$ VI).

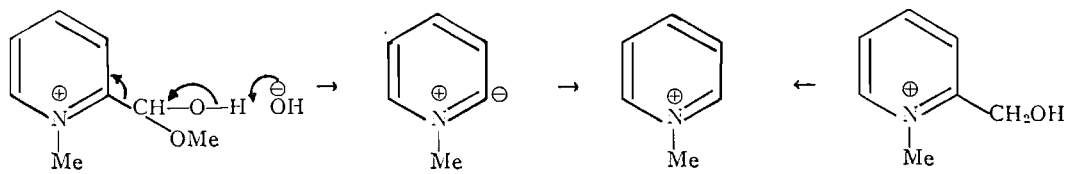

IV V VI VII

1-Methyl-2-formylpyridinium iodide has been previously reported as an oil (4), or as a solid of m.p. 174° (5) or 178–179° (6), but in none of these references is there mention of any analytical data. 1-Methyl-4-formylpyridinium iodide was reported (5) as a "low melting solid", but was apparently not characterized. Repetition of these procedures gave ill-defined products. Attempted preparation of the aldehyde methiodides in methanol solution gave crystalline derivatives which were shown by analysis and spectroscopy to be the corresponding methyl hemi-acetals.

2-Hydroxymethyl-1-methylpyridinium iodide, and the 2-acetoxymethyl analogue, cleaved readily to yield the 1-methylpyridinium ion (isolated as the sodium double picrate (7)) on refluxing with aqueous sodium hydroxide, or with an aqueous buffer of pH 9.6. 2-Formylpyridinium methiodide, in the form of its hemi-acetal, behaved similarly. However, the cleavage reaction did not occur in neutral or acidic solution, and moreover, the corresponding derivatives of the 4-pyridyl series were stable under those conditions which cleaved the 2-derivatives, indicating the lower stability of zwitterions of type III than those of type II.

The present results rationalize the formation (8) of the stilbazole derivative (VIII) on reaction of the hydroxymethyl compound (IX), and the 2-formyl analogue, with dimethylaminobenzaldehyde. In addition to proposing the mechanism favored by us,

Can. J. Chem. Downloaded from www.nrcresearchpress.com by 210.87.254.42 on 09/05/12
For personal use only.

HETEROCYCLONIUMYL ZWITTERIONS. PART I. THE ALKALI-CATALYZED CLEAVAGE OF 2-HYDROXYMETHYL- AND 2-FORMYL-PYRIDINIUM CATIONS

S. GOLDING AND A. R. KATRITZKY

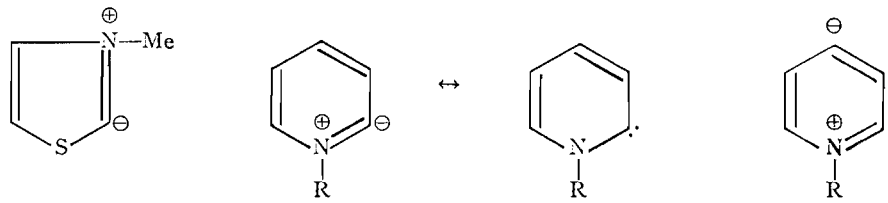

I II III

Heterocycloniumyl zwitterions of type I are well known to be of importance in the biological activity of thiamine (1), and recently azolonium zwitterion intermediates have received attention (2). Certain pyridinium derivatives have been shown to exchange α-hydrogen atoms by way of zwitterions of type II (3). We have now shown that the relative stability of such species facilitates the reaction sequences (IV $\rightarrow$ VI) and (VII $\rightarrow$ VI).

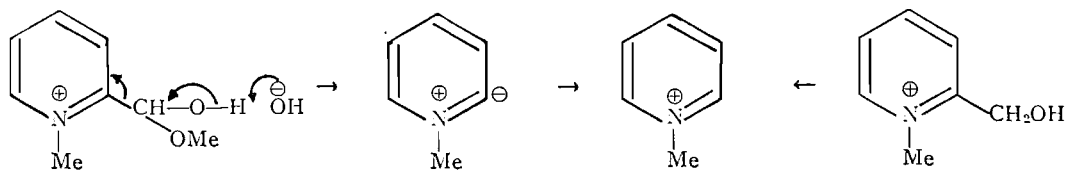

IV V VI VII

1-Methyl-2-formylpyridinium iodide has been previously reported as an oil (4), or as a solid of m.p. 174° (5) or 178–179° (6), but in none of these references is there mention of any analytical data. 1-Methyl-4-formylpyridinium iodide was reported (5) as a "low melting solid", but was apparently not characterized. Repetition of these procedures gave ill-defined products. Attempted preparation of the aldehyde methiodides in methanol solution gave crystalline derivatives which were shown by analysis and spectroscopy to be the corresponding methyl hemi-acetals.

2-Hydroxymethyl-1-methylpyridinium iodide, and the 2-acetoxymethyl analogue, cleaved readily to yield the 1-methylpyridinium ion (isolated as the sodium double picrate (7)) on refluxing with aqueous sodium hydroxide, or with an aqueous buffer of pH 9.6. 2-Formylpyridinium methiodide, in the form of its hemi-acetal, behaved similarly. However, the cleavage reaction did not occur in neutral or acidic solution, and moreover, the corresponding derivatives of the 4-pyridyl series were stable under those conditions which cleaved the 2-derivatives, indicating the lower stability of zwitterions of type III than those of type II.

The present results rationalize the formation (8) of the stilbazole derivative (VIII) on reaction of the hydroxymethyl compound (IX), and the 2-formyl analogue, with dimethylaminobenzaldehyde. In addition to proposing the mechanism favored by us,

Can. J. Chem. Downloaded from www.nrcresearchpress.com by 210.87.254.5 on 09/05/12
For personal use only.

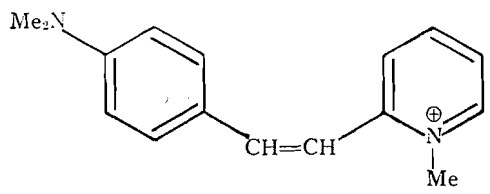

VIII

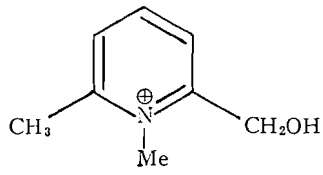

IX

the previous authors suggested an alternative which involved participation of the dimethylamino group to facilitate protonation. Previous work (9, 10) by one of us, makes this alternative very unlikely.

EXPERIMENTAL

2-Acetoxymethyl-1-methylpyridinium Iodide

2-Acetoxymethylpyridine (1 g) was refluxed with methyl iodide (1ml) in methanol (2 ml) for 6 h. Addition of ether to the cooled mixture gave the methiodide which formed colorless plates, m.p. 154–155°, from ethanol–ether. Calc. for $C_9H_{12}INO_2$: C, 36.9; H, 4.1; N, 4.8. Found: C, 36.8; H, 4.1; N, 4.8.[1]

The following were similarly prepared: 2-hydroxymethyl-1-methylpyridinium iodide, m.p. 153.5–154.5° (lit. (11) m.p. 153°). Calc. for $C_7H_{10}INO$: C, 33.4; H, 4.0; N, 5.6. Found: C, 33.5; H, 4.0; N, 5.5. 4-hydroxymethyl-1-methylpyridinium iodide, m.p. 97–98° (lit. (12) m.p. 94°).

2-Acetoxymethyl-1-methylpyridinium picrate formed yellow needles, m.p. 101–102°, from ethanol. Calc. for $C_{15}H_{14}N_4O_9$: C, 45.7; H, 3.6; N, 14.2. Found: C, 45.7; H, 3.7; N, 14.4.

2-Hydroxymethyl-1-methylpyridinium picrate formed yellow needles, m.p. 121–122°, from ethanol. Calc. for $C_{13}H_{12}N_4O_8$: C, 44.3; H, 3.4; N, 15.9. Found: C, 44.3; H, 3.6; N, 16.1.

Hemi-methyl Acetals of 2- and 4-Formyl-1-methylpyridinium Iodide

2-Pyridine aldehyde on treatment as above gave the hemi-methyl acetal methiodide, m.p. 101–105°, as plates which decomposed on attempted recrystallization. Calc. for $C_8H_{12}INO_2$: C, 34.2; H, 4.3; N, 5.0. Found: C, 34.4; H, 4.5; N, 5.8. The infrared spectrum (Nujol) showed strong bands at 3 240 (bonded OH), 1 640 (pyridinium ring), and 1 100 cm^{-1} (ether). The nuclear magnetic resonance (n.m.r.) spectrum showed a multiplet at 1.35–2.35 (4 aromatic protons), and singlets at 3.7 (CH), 5.8 (O—Me), and 6.9 τ (N—Me).

The hemi-acetal methiodide from 4-pyridine aldehyde formed plates, m.p. 75–78°, which decomposed on attempted recrystallization. Found: C, 33.7; H, 4.9; N, 5.6. The infrared spectrum (Nujol) showed strong bands at 3 250 (bonded OH), 1 650 (pyridinium ring), and 1 080 cm^{-1} (ether). The n.m.r. spectrum showed doublets at 1.4 and 2.1 (4 aromatic protons), and singlets at 4.0 (CH), 5.7 (OMe), and 6.9 τ (NMe).

Cleavage Reaction Procedure

The cleavage reaction was carried out by heating the compound (0.5 g) with sodium hydroxide or sodium carbonate buffer (50 ml) on a water bath for 6 h. Sodium 1-methylpyridinium dipicrate was isolated by the addition of 10% ethanolic picric acid (10 ml); on cooling, it separated as yellow needles, m.p. 215–216°. The double picrate was synthesized independently by dissolving pyridine methiodide (0.25 g) in *N* sodium hydroxide (25 ml) and adding 10% ethanolic picric acid (5 ml). On cooling the double picrate (0.35 g, 100%) was obtained as yellow needles, m.p. 215–216° (reported, 215–220° (7)), after recrystallization from ethanol. The double picrates from the cleavage reactions were identical with those directly synthesized, as was shown by mixed melting points and infrared spectra.

ACKNOWLEDGMENT

This work was carried out during the tenure (by S. G.) of a D.S.I.R. Advanced Course Studentship.

1. R. Breslow. J. Am. Chem. Soc. **79**, 1762 (1957).
2. H. A. Staab, M.-Th. Wu, A. Mannschreck, and G. Schwalbach. Tetrahedron Letters, **15**, 845 (1964). R. A. Olofson, W. R. Thompson, and J. S. Michelman. J. Am. Chem. Soc. **86**, 1865 (1964).
3. A. San Pietro. J. Biol. Chem. **217**, 589 (1955).
4. G. Lennart. Ann. **410**, 95 (1915).
5. S. Ginsberg and I. B. Wilson. J. Am. Chem. Soc. **79**, 481 (1957).

[1]*This compound has recently been recorded by K. Augustinsson and H. Hasselquist, Acta Chem. Scand. 18, 1006 (1964), as having m.p. 160–161°.*

Can. J. Chem. Downloaded from www.nrcresearchpress.com by 210.87.254.5 on 09/05/12
For personal use only.

6. R. I. ELLIN and A. A. KONDRITZER. Anal. Chem. **31**, 200 (1959).
7. F. G. MANN and F. C. BAKER. J. Chem. Soc. 3845 (1961).
8. R. A. BARNES and A. ASZALOS. J. Am. Chem. Soc. **86**, 523 (1964).
9. A. R. KATRITZKY, A. J. BOULTON, and D. J. SHORT. J. Chem. Soc. 2954 (1960).
10. A. R. KATRITZKY and B. J. RIDGEWELL. J. Chem. Soc. 3753 (1963).
11. M. FERLES and M. PRYSTAŠ. Collection Czech. Chem. Commun. **24**, 3326 (1959).
12. J. YOUATT. Australian J. Chem. **14**, 308 (1961).

RECEIVED NOVEMBER 30, 1964.
SCHOOL OF CHEMICAL SCIENCES,
UNIVERSITY OF EAST ANGLIA,
NORWICH, ENGLAND.

Can. J. Chem. Downloaded from www.nrcresearchpress.com by 210.87.254.5 on 09/05/12
For personal use only.

THE INFRARED SPECTRUM OF AMMONIA ADSORBED ON CABOSIL SILICA POWDER

N. W. CANT AND L. H. LITTLE

Measurements of length changes and infrared spectra of Vycor porous silica glass during the adsorption of ammonia led Folman and Yates (1, 2) to propose that two types of adsorption sites existed on the surface. They showed that free surface hydroxyl groups constitute one of these sites while surface silicon or oxygen atoms were assumed to be the other. Recently (3), using thinner samples of porous glass, we showed that ammonia adsorbed on the free hydroxyl groups and gave bands at 3 400 cm^{-1} and 3 320 cm^{-1} due to the asymmetric and symmetric NH-stretching vibrations. These bands disappeared on room-temperature evacuation of gas phase ammonia. In addition, we were able to distinguish bands at 3 365 cm^{-1} and 3 280 cm^{-1} that were unaffected by room-temperature evacuation. From comparison with the spectrum of the Lewis acid–base complex $F_3B{:}NH_3$, we proposed that these bands were due to ammonia strongly held to surface Lewis acid sites, possibly boron or aluminium atoms. Roev, Filiminov, and Terenin (4) observed similar bands for residual ammonia adsorbed on a silica–alumina catalyst and attributed them to ammonia molecules chemisorbed to surface aluminium atoms.

In view of these results it was decided to study the infrared spectrum of ammonia adsorbed on Cabosil silica powder as had been suggested to us by Professor Fripiat (5). This material is extremely pure and does not contain boria, alumina, and other oxides, which occur in Vycor silica glass and which are considered to be active sites for chemisorption of ammonia (3). If the above assignments (3) are correct, only the absorption bands at 3 400 cm^{-1} and 3 320 cm^{-1}, due to ammonia molecules hydrogen bonded to surface hydroxyl groups, should appear for adsorption onto Cabosil. No evidence for chemisorption should appear.

In the infrared spectra of both types of silica sample, absorption bands appear due to surface hydroxyl groups, some of which are free and others hydrogen bonded among themselves. The former are responsible for a band at 3 747 cm^{-1}, the latter for a shoulder at 3 670 cm^{-1}. Very recently Yates (6) quoted optical densities for the free hydroxyl absorption band, before and after the adsorption of ammonia, but no ammonia frequencies or spectra were given.

EXPERIMENTAL

Cabosil powder (from Godrey L. Cabot Inc.) was compressed into thin self-supporting discs under a pressure of 10 tons/sq. in. The quantity of material in the infrared beam was approximately 12 mg/cm^2.

6. R. I. ELLIN and A. A. KONDRITZER. Anal. Chem. **31**, 200 (1959).
7. F. G. MANN and F. C. BAKER. J. Chem. Soc. 3845 (1961).
8. R. A. BARNES and A. ASZALOS. J. Am. Chem. Soc. **86**, 523 (1964).
9. A. R. KATRITZKY, A. J. BOULTON, and D. J. SHORT. J. Chem. Soc. 2954 (1960).
10. A. R. KATRITZKY and B. J. RIDGEWELL. J. Chem. Soc. 3753 (1963).
11. M. FERLES and M. PRYSTAŠ. Collection Czech. Chem. Commun. **24**, 3326 (1959).
12. J. YOUATT. Australian J. Chem. **14**, 308 (1961).

RECEIVED NOVEMBER 30, 1964.
SCHOOL OF CHEMICAL SCIENCES,
UNIVERSITY OF EAST ANGLIA,
NORWICH, ENGLAND.

Can. J. Chem. Downloaded from www.nrcresearchpress.com by 210.87.254.105 on 09/05/12
For personal use only.

THE INFRARED SPECTRUM OF AMMONIA ADSORBED ON CABOSIL SILICA POWDER

N. W. CANT AND L. H. LITTLE

Measurements of length changes and infrared spectra of Vycor porous silica glass during the adsorption of ammonia led Folman and Yates (1, 2) to propose that two types of adsorption sites existed on the surface. They showed that free surface hydroxyl groups constitute one of these sites while surface silicon or oxygen atoms were assumed to be the other. Recently (3), using thinner samples of porous glass, we showed that ammonia adsorbed on the free hydroxyl groups and gave bands at 3 400 cm^{-1} and 3 320 cm^{-1} due to the asymmetric and symmetric NH-stretching vibrations. These bands disappeared on room-temperature evacuation of gas phase ammonia. In addition, we were able to distinguish bands at 3 365 cm^{-1} and 3 280 cm^{-1} that were unaffected by room-temperature evacuation. From comparison with the spectrum of the Lewis acid–base complex $F_3B{:}NH_3$, we proposed that these bands were due to ammonia strongly held to surface Lewis acid sites, possibly boron or aluminium atoms. Roev, Filiminov, and Terenin (4) observed similar bands for residual ammonia adsorbed on a silica–alumina catalyst and attributed them to ammonia molecules chemisorbed to surface aluminium atoms.

In view of these results it was decided to study the infrared spectrum of ammonia adsorbed on Cabosil silica powder as had been suggested to us by Professor Fripiat (5). This material is extremely pure and does not contain boria, alumina, and other oxides, which occur in Vycor silica glass and which are considered to be active sites for chemisorption of ammonia (3). If the above assignments (3) are correct, only the absorption bands at 3 400 cm^{-1} and 3 320 cm^{-1}, due to ammonia molecules hydrogen bonded to surface hydroxyl groups, should appear for adsorption onto Cabosil. No evidence for chemisorption should appear.

In the infrared spectra of both types of silica sample, absorption bands appear due to surface hydroxyl groups, some of which are free and others hydrogen bonded among themselves. The former are responsible for a band at 3 747 cm^{-1}, the latter for a shoulder at 3 670 cm^{-1}. Very recently Yates (6) quoted optical densities for the free hydroxyl absorption band, before and after the adsorption of ammonia, but no ammonia frequencies or spectra were given.

EXPERIMENTAL

Cabosil powder (from Godrey L. Cabot Inc.) was compressed into thin self-supporting discs under a pressure of 10 tons/sq. in. The quantity of material in the infrared beam was approximately 12 mg/cm^2.

The discs were evacuated for 3 h at 400–450 °C before recording the initial spectrum. The spectra shown in Fig. 1 were recorded with a Perkin–Elmer Model 521 spectrometer for which the spectral slit width was about 5 cm^{-1} at 3 800 cm^{-1}. The disc was enclosed in an evacuated silica test tube cell of approximately 1 cm internal diameter. This cell absorbed slightly near 3 670 cm^{-1}, for which a correction was made. The deuteration experiments quoted in the text were carried out with a Perkin–Elmer Model 137G spectrometer. A 1 cm path length cell, consisting of magnesium oxide windows attached to a Pyrex tube with epoxy resin, was used in this work. In both cases the ammonia gas band at 3 337 cm^{-1} was used for calibration.

RESULTS AND DISCUSSION

Figure 1*a* shows the spectrum of the Cabosil disc after evacuation for 3 h at 450 °C; the 3 747 cm^{-1} band being due to free surface hydroxyl groups and a shoulder at about 3 670 cm^{-1}, not clearly discernible in spectrum (*a*), to adjacent hydroxyl groups hydrogen bonded together. The spectrum is similar to that recorded by McDonald (7). Spectrum 1*b* was obtained 1 h after 6 cm pressure of ammonia had been admitted to the cell at room temperature. No changes were observed after further standing. The circles in this figure represent optical densities after evacuation of ammonia for 15 min at room temperature.

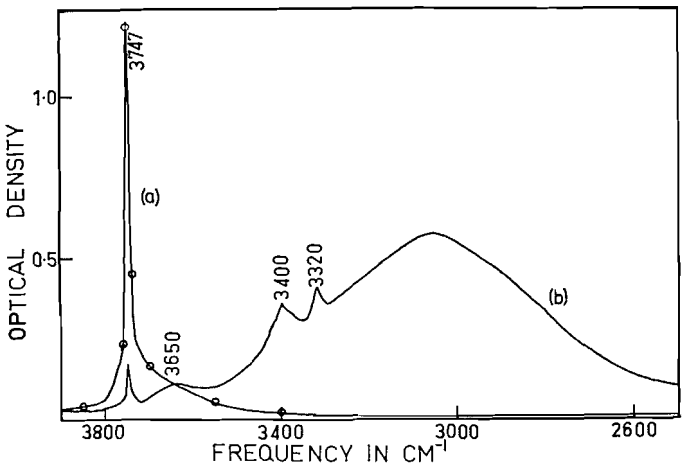

FIG. 1. (*a*) The infrared spectrum of Cabosil from 3 900 cm^{-1} to 2 500 cm^{-1} after evacuation for 3 h at 450 °C. (*b*) The spectrum 1 h after admission of 6 cm of ammonia at room temperature. The circles represent the resulting optical densities after evacuation at room temperature for 1 h. A shoulder appears at 3 670 cm^{-1} in spectrum (*a*). After adsorption of ammonia the shoulder is displaced to 3 650 cm^{-1} (spectrum (*b*)).

The great reduction in the intensity of the free hydroxyl band and the appearance of a very broad, intense band at 3 050 cm^{-1} after admission of ammonia to the cell show that adsorption has occurred by hydrogen bonding to free surface hydroxyl groups. This is confirmed by the appearance of bands at 3 400 cm^{-1} and 3 320 cm^{-1}, due to NH-stretching vibrations of ammonia. The absence of bands after room-temperature evacuation of the ammonia shows that Cabosil contains no adsorption sites of the second type found on Vycor.

As can be seen from Fig. 1*a* and 1*b* the adsorption of ammonia greatly reduced the intensity of the free hydroxyl band without appreciably affecting the intensity of the hydrogen-bonded one. When the pressure of ammonia in the cell was raised to 12 cm the free hydroxyl band was indistinguishable from background noise. This indicates that all free hydroxyl groups are able to interact with ammonia molecules and are therefore surface groups. Similar results were obtained for the free hydroxyls on Vycor glass.

Can. J. Chem. Downloaded from www.nrcresearchpress.com by 210.87.254.105 on 09/05/12
For personal use only.

Fripiat and Uytterhoeven (8) concluded that after evacuation of Degussa Aerosil (which is made by an identical process to the Cabosil used here) at 400 °C, only 30% of the total hydroxyl content was on the surface. If it is assumed, as Fripiat did, that the absorption coefficients of both types of surface hydroxyl groups are identical, then it is possible to estimate roughly the ratio of free to hydrogen-bonded groups from the relative areas beneath the bands of Fig. 1*a*. Using this method we found that the free hydroxyl groups, which all reside on the surface, represent at least 50% of the total hydroxyl content of our silica after 450 °C evacuation. It is likely that the absorption coefficient of the hydrogen-bonded hydroxyls is considerably greater than that of the free groups (9). On this basis the free surface hydroxyl content should greatly exceed 50% of the total. Although ammonia does not interact by hydrogen bonding to the hydroxyls responsible for the 3 670 cm^{-1} band of either Cabosil (Fig. 1) or Vycor (3), it can be established that a considerable proportion of these hydroxyl groups are also on the surface.

Fripiat, Gastuche, and Brichard (10) showed that both types of hydroxyl groups of Degussa Aerosil can be converted to deuteroxyl groups by room-temperature treatment with D_2O vapor. We have been able to show that these deuteroxyl groups (both free and bonded) can be reconverted to hydroxyl groups by exchange with ammonia at room temperature. These reactions are only possible if an appreciable proportion of the bonded hydroxyls (or deuteroxyls) exist on the surface. On this basis it is estimated that approximately 80% of the total hydroxyl content of the Cabosil silica resides on the surface of the particles.

ACKNOWLEDGMENTS

One of us (N. W. C.) gratefully acknowledges financial assistance in the form of a Commonwealth Scientific and Industrial Research Organization Senior Studentship. The authors express gratitude to the Australian Institute of Nuclear Science and Engineering for a grant towards the purchase of the spectrometer.

1. M. Folman and D. J. C. Yates. Proc. Roy. Soc. London, Ser. A, **246**, 32 (1958).
2. M. Folman and D. J. C. Yates. J. Phys. Chem. **63**, 183 (1959).
3. N. W. Cant and L. H. Little. Can. J. Chem. **42**, 802 (1964).
4. L. M. Roev, V. N. Filiminov, and A. N. Terenin. Opt. i Spektroskopiya, **4**, 328 (1958).
5. J. J. Fripiat. Private communication.
6. D. J. C. Yates. J. Chem. Phys. **40**, 1157 (1964).
7. R. S. McDonald. J. Phys. Chem. **62**, 1168 (1958).
8. J. J. Fripiat and J. Uytterhoeven. J. Phys. Chem. **66**, 800 (1962).
9. G. C. Pimentel and A. L. McClellan. The hydrogen bond. W. H. Freeman & Co., San Francisco and London. 1960.
10. J. J. Fripiat, M. C. Gastuche, and R. Brichard. J. Phys. Chem. **66**, 805 (1962).

Received August 10, 1964.
Department of Chemistry,
University of Western Australia,
Nedlands, Western Australia.

Can. J. Chem. Downloaded from www.nrcresearchpress.com by 210.87.254.105 on 09/05/12
For personal use only.

Can. J. Chem. Downloaded from www.nrcresearchpress.com by 210.87.254.40 on 09/05/12
For personal use only.

ISOPIMARIC ACID[1]

W. ANTKOWIAK,[2] O. E. EDWARDS, AND R. HOWE[2]
Division of Pure Chemistry, National Research Council, Ottawa, Canada

AND

J. W. APSIMON[2]
Department of Chemistry, Carleton University, Ottawa, Canada

Received November 18, 1964

Dedicated to Professor R. B. Sandin on the Occasion of his Sixty-Eighth Birthday

ABSTRACT

Evidence is presented for the epimeric character of the C-13 substituents in pimaric and isopimaric acids and for the nuclear double bond location in isopimaric acid. This work, coupled with recent synthetic work and rotatory dispersion evidence, permits assignment of the structure and stereochemistry IV to isopimaric acid. Hydroboration and selenium dioxide oxidation of the acid are described.

In 1948 Harris and Sanderson suggested structures for two diterpenoid constituents of pine oleoresin, pimaric and isopimaric acids (1). Extensive chemical work (2–6) appeared to confirm their assignments. In combination with arguments based on optical rotation (7) and optical rotatory dispersion (8), this led to general acceptance of the structure and stereochemistry shown in I for pimaric acid and in II for isopimaric acid. Another isomer, sandaracopimaric acid, was assigned configuration III (9). The elegant

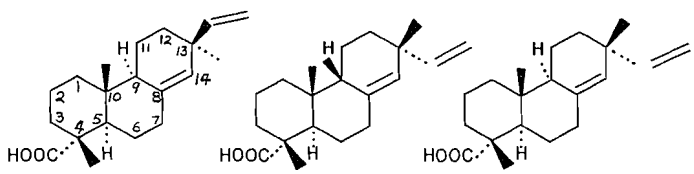

total synthesis by Ireland and Schiess of *dl*-pimaradiene and *dl*-sandaracopimaradiene confirmed the structure of the corresponding acids (10). With reasonable assumptions regarding the steric course of the reactions, supplemented by evidence from ultraviolet absorption spectra and relative adsorption, this work provided strong support for the stereochemistry shown in I and III. Further confirmation of the structure and absolute configuration was given by Milne and Smith, who transformed a steroid degradation product into pimar-8-ene (11).[3] Finally, transformation of testosterone into sandaracopimaradiene by Bose and Harrison (12) and of 3β-hydroxyandrost-5-ene-17-one into the same diene by Fetizon and Golfier (12*a*) established beyond question the configuration at C-13 for all three acids. Thus, pimaric and sandaracopimaric acids are correctly represented in every detail by I and III.

[1]*Issued as N.R.C. No. 8297.*
[2]*National Research Council Postdoctorate Fellow.*
[3]*It seems logical to use the phenanthrene numbering system for the pimaric acids. However, because of the widespread familiarity with the steroid numbering system, most North American groups have applied this to the resin acids. For this reason we also use the latter in this paper.*

Can. J. Chem. Downloaded from www.nrcresearchpress.com by 210.87.254.40 on 09/05/12
For personal use only.

The chemistry and optical rotatory dispersion (2, 8) of isopimaric acid seemed perfectly consistent with the structure and stereochemistry denoted by II. However, Church and Ireland synthesized the corresponding pimaradiene (13) and found it to be different from isopimaradiene. This observation proved that the double bond of isopimaric acid was not in the 8,14 position. They pointed out that, since the nuclear vinyl hydrogen signal for isopimaric acid (14) was a broadened doublet, it must be coupled with adjacent hydrogens. Since the double bond migrates easily to the 8,9 position, the most logical location for it, on this and biogenetic grounds, was the 7,8 position. They hence postulated that isopimaric acid had the structure and stereochemistry illustrated in IV. This expression was also consistent with all the previous evidence except that of Harris and Sanderson.

We now amplify our preliminary report on work which interrelated pimaric and isopimaric acids and proved that they are epimeric at C-13 (6), and on the experiments which proved Church and Ireland's structure IV to be correct for the latter (15).

A direct and unequivocal way of interrelating the acids and settling whether or not they were isomeric at C-13 proved to be the conversion of both to the 13,13-dimethyl compounds (6). Pimaric acid reacted with 1 mole of osmium tetroxide in dry ether to give an osmate which was decomposed by alkaline mannitol solution. A diol acid V was obtained in poor yield.[4]

This was cleaved in aqueous dioxane solution by periodic acid to a rather sensitive aldehydo acid VI. Wolff–Kishner reduction of VI (preforming the hydrazone) gave the 13,13-dimethyl acid VII. This could be quantitatively isomerized by hydrogen chloride in chloroform to the Δ^8 acid VIII.

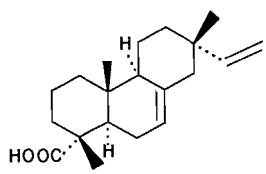

IV

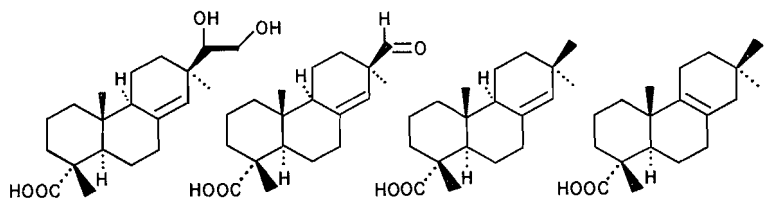

V VI VII VIII

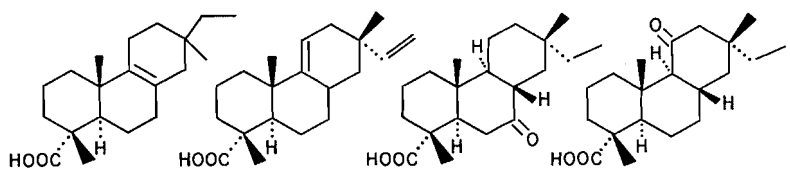

IX X XI XII

[4]*This diol acid does not correspond to either of the acids previously described as arising by permanganate oxidation of pimaric acid (16).*

Can. J. Chem. Downloaded from www.nrcresearchpress.com by 210.87.254.40 on 09/05/12
For personal use only.

Hydroxylation of isopimaric acid in the same way gave a mixture of sparingly soluble products. Two isomeric diol acids and a triol acid were separated by fractional crystallization. The major diol acid gave an aldehydo acid when treated with periodic acid. Wolff–Kishner reduction of this gave a 13,13-dimethyl acid distinct from the one from pimaric acid. When exposed to dry HCl in $CHCl_3$ this acid was isomerized to the $\Delta^{8,9}$ isomer, which proved identical with VIII derived from pimaric acid. This confirmed the earlier conclusion (2–5) that pimaric and isopimaric acids had identical skeletons and stereochemistry at C-4, C-5, and C-10. Since the $\Delta^{8,9}$ acids (IX) derived from dihydro pimaric and isopimaric acids were different, it followed that the parent acids were epimeric at C-13.

Although structure IV for isopimaric acid seemed the most plausible one on biogenetic grounds, the chemical evidence did not exclude the $\Delta^{9,11}$ isomer X from consideration. We hence sought experiments which would clearly distinguish between these. One possibility was that of converting the acid via the keto acids XI or XII to 1,7,9- or 1,5,7-trimethyl phenanthrene or to the phenols 1,7-dimethyl-9-phenanthrol or 1,7-dimethyl-5-phenanthrol. Hydroboration of the double bond of dihydroisopimaric acid gave a mixture of alcohols[5] which on oxidation with Jones's reagent (17) have one keto acid. Since this was stable to base, the ring fusion at this point was in its most stable configuration. The nuclear magnetic resonance (n.m.r.) spectrum of the keto acid had signals between τ 7.5 and τ 8.2 corresponding to three hydrogens alpha to the ketone carbonyl. This was consistent with either XI or XII. An indication that the carbonyl was at C-7 (XI) was given by the facile formation of a 2,4-dinitrophenylhydrazone. An 11-ketone as in XII should (if the ring fusion were *trans*–anti–*trans*) be inert to the reagent by analogy to the behavior of 11-keto steroids.

The keto acid was treated with methyl magnesium iodide to give the methyl carbinol (probably configuration XIII if structure XI is correct). This, however, gave only small amounts of phenanthrenes which could not be purified when it or its sodium salt was heated with selenium. Dehydrogenation of the keto acid (XI or XII) did give a phenolic product very similar to 1,7-dimethyl-9-phenanthrol, but identity could not be rigorously established.

The second approach to location of the double bond of isopimaric acid proved more definitive. It had already been shown that photolysis of the azide of dihydropimaric acid gave a mixture of the corresponding isocyanate and the γ-lactam XIV (18). It appeared likely that the same course would be followed with isopimaric acid, and experiment confirmed this expectation. A 9% yield of γ-lactam ($\nu_{max}^{CHCl_3}$ 1 685 cm^{-1}) was produced when the azide was photolyzed in hexane solution. On the basis of structure IV this should be XV, while structure X would give rise to XVI. Only in structure XV is the amide nitrogen allylic to the double bond. Inspection of the geometry of this structure (see XVII) indicated that the 6-hydrogen should be weakly coupled, if at all, to the 7-hydrogen ($\phi \simeq 90°$) and hence should give a fairly clean doublet in the n.m.r. spectrum of the compound. In contrast, the 6-hydrogen in XVI and XVIII should give rise to a complex signal, since it should be coupled with the 5-hydrogen and the two on C-7 (see XVIII). In fact, the 6-hydrogen of the lactam from pimaric acid XVIII gave a very broad and complex signal between τ 5.95 and 6.65. The corresponding signal for the γ-lactam from isopimaric acid was a doublet centered at τ 6.17 (J = 10 c.p.s.). This observation excludes structure XV from consideration and proves that isopimaric acid has the sekeleton shown in IV.

[5]*In most experiments the carboxyl group was partially reduced by the diborane simultaneously with hydroboration of the double bond.*

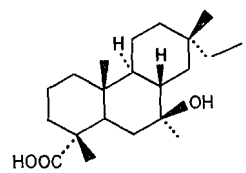

XIII

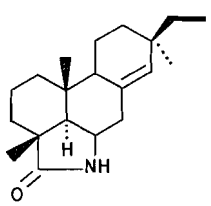

XIV

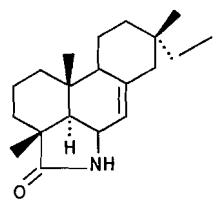

XV

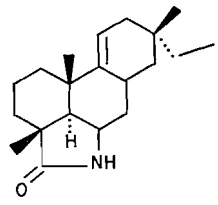

XVI

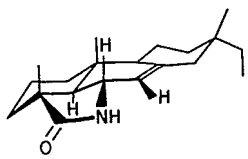

XVII

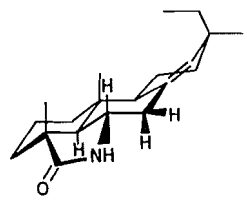

XVIII

The stereochemistry of isopimaric acid can be deduced on the following grounds. C-13: The configuration at C-13 has been shown above to be epimeric to that of pimaric acid (I) whose stereochemistry is established by the syntheses of Ireland (10), Smith (11), and Bose (12). C-9: If dihydropimaric acid had a 9-α-hydrogen, it is clear from the orientation shown in XIX that its rotatory dispersion curve should be very similar to

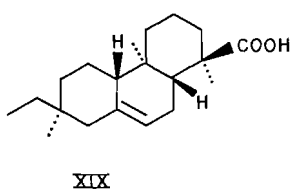

XIX

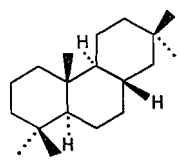

XX

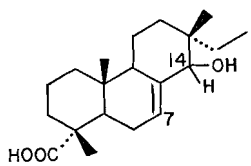

XXI

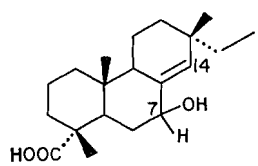

XXII

that of cholest-5-ene. The O.R.D. curve for dihydroisopimaric acid is plain and negative (8), almost identical with that of the steroid (19); hence this is the correct stereochemistry.

Proof of this configuration was also provided by Ireland and Newbould (20). They converted pimaradiene to the pentamethyl *trans*–anti–*trans* perhydrophenanthrene XX.

Can. J. Chem. Downloaded from www.nrcresearchpress.com by 210.87.254.40 on 09/05/12
For personal use only.

By a similar sequence which left the asymmetry at C-9 untouched, they converted isopimaric acid to the same hydrocarbon, proving that it has a 9-α-hydrogen. Thus, no doubt is left that the structure and absolute stereochemistry of isopimaric acid is that shown in IV.

Ukita's acid, for which a $\Delta^{7,8}$ structure was suggested (2), has since proved to be a mixture of isopimaric and sandaracopimaric acids (21). Our interest in Ukita's report that the dihydro compound derived from this mixture gave a 7-hydroxy-$\Delta^{8,9}$ derivative on oxidation with selenium dioxide led us to examine the reaction of methyl dihydroisopimarate with this reagent. In ethanol at room temperature a very complex mixture of products resulted. These appeared to be mainly dienes ($\lambda\lambda_{max}$ 235, 244, and 253 mμ). However, careful chromatography on alumina enabled isolation of small quantities of two alcohols. These appeared to be allylic, since in each case manganese dioxide oxidized them to α–β unsaturated ketones (λ_{max} 242 mμ). The n.m.r. spectrum of the first, which melted at 84°, contained a vinyl hydrogen signal as a very broad doublet (J = 4 c.p.s.) centered at τ 4.42. This appeared identical with the 7-hydrogen signal of isopimaric acid (14). A second hydrogen resonating at τ 6.44 was a singlet. These observations accord with structure XXI, the second deshielded hydrogen being the one on C-14.

The second alcohol, m.p. 92°, had a n.m.r. signal at τ 4.55 (one hydrogen, half band width 4 c.p.s.). This is consistent with structure XXII.

EXPERIMENTAL

Rotations were of solution in absolute ethanol. Infrared spectra were determined on a Perkin–Elmer model 21 spectrometer and were of Nujol mulls unless otherwise stated. Nuclear magnetic resonance spectra were obtained with Varian HR-60 and A-60 spectrometers, in chloroform or deuterochloroform with tetramethylsilane as internal standard. Melting points were determined on a Kofler hot stage unless otherwise stated.

Diol V from Pimaric Acid

Pure pimaric acid (9.17 mg, m.p. 211–214°, $[\alpha]_D$ +79°) was suspended in 5 ml of dry ether. A solution of 876 mg of osmium tetroxide in 5 ml of ether was added followed by 5 ml of ether washings. The mixture was shaken for 10 min to dissolve the pimaric acid. The dark solution was left at 5 °C for 65 h. The black precipitate recovered by filtration weighed 1.53 g. Evaporation of the filtrate gave 450 mg of dark residue. The precipitate was heated on the steam bath for 1 h with a mixture of 1 g of sodium hydroxide and 5 g of mannitol in 15 ml of water. The solution was then cooled, acidified with acetic acid, and the precipitate collected by filtration. The solid was dissolved in chloroform, the solution was washed with water, and the water layer back-extracted with chloroform. The chloroform solution was combined with a chloroform extract of the aqueous filtrate from the reaction, dried, and distilled, giving 842 mg of solid. The ether-soluble osmate, when treated similarly, gave 268 mg of solid acid. These were fractionally crystallized separately from ether, giving in each case unchanged pimaric acid, crude diol, and a small quantity of prisms, m.p. 252–257°, which gave analytic figures between those of a diol and a monohydroxy acid.

The crude diol (m.p. up to 165°) was purified by chromatography on a 20-fold ratio of silica gel, from which the main component was eluted with 50% benzene–ether mixture. After three recrystallizations from ether this had m.p. 160–163°, $[\alpha]_D^{23}$ +3 ± 2° (c, 1.11), ν_{max} 1 681 cm^{-1} (COOH) and 821 cm^{-1} (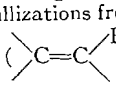). Yield was approximately 17%.

Anal. Found: C, 71.56; H, 9.50. Calcd. for $C_{20}H_{32}O_4$: C, 71.39; H, 9.59.

Aldehydo Acid VI

Diol acid V (70 mg) was dissolved in 5 ml of pure dioxane. A solution of 108 mg of paraperiodic acid in 1 ml of water was added, and the solution left at room temperature in the dark for 1 h. The bulk of the solvent was then removed under reduced pressure, water added, and the product extracted into methylene chloride. The organic layer was back-washed with water, dried, and distilled, giving 70 mg of crystalline residue, m.p. 195–204°. After four recrystallizations from ether this melted at 215–217° (evacuated capillary) and had $[\alpha]_D^{23}$ +119° (c, 1.60); ν_{max} 2 700, 1 720 cm^{-1} (—CHO), 1 693 cm^{-1} (COOH), 824 cm^{-1} (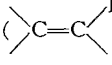). A form melting at 174–177° (evacuated capillary) was obtained once.

Anal. Found: C, 75.09; H, 9.10. Calcd. for $C_{19}H_{28}O_3$: C, 74.96; H, 9.27.

Can. J. Chem. Downloaded from www.nrcresearchpress.com by 210.87.254.40 on 09/05/12
For personal use only.

13,13-Dimethyl Acid VII

A solution of 55 mg of the aldehydo acid VI in 2 ml of triethylene glycol containing 0.5 ml of 95% hydrazine was heated on the steam bath for 30 min, then at 140° for 30 min. After cautious addition of 0.64 g of potassium hydroxide the bath temperature was raised slowly to 205° under a slow nitrogen stream, then maintained at this temperature for 3 h. The mixture was cooled, diluted with water, and extracted with methylene chloride. The organic layer was back-washed with dilute alkali. The combined aqueous layers were acidified with sulfuric acid, and extracted with methylene chloride. The 54 mg of acid recovered crystallized spontaneously, m.p. 228–235°. After several recrystallizations from methanol it melted at 232–238° and had $[\alpha]_D^{22}$ +17 ± 2° (*c*, 1.0), ν_{max} 1 692 and 823 cm^{-1}.

Anal. Found: C, 78.41; H, 10.10. Calcd. for $C_{19}H_{30}O_2$: C, 78.57; H, 10.41.

Δ^8-13,13-Dimethyl Acid VIII

The 13,13-dimethyl acid VII (26 mg) was dissolved in 5 ml of dry ethanol-free chloroform and the solution cooled to 0°. Dry hydrogen chloride was then bubbled into the solution for 3.5 h. The hydrogen chloride was then removed from the chloroform by a water wash. An attempt to extract the acid into dilute sodium hydroxide failed, since the sodium salt was more soluble in moist chloroform than in water. The free acid (23 mg) crystallized from aqueous methanol as thick hexagonal plates, m.p. 156.5° after preliminary sintering at 147°, $[\alpha]_D^{24}$ +67 ± 4° (*c*, 0.725), ν_{max} 1 693 cm^{-1} (COOH).

Osmylation of Isopimaric Acid

A solution of 1.21 g of isopimaric acid (m.p. 160–163°, $[\alpha]_D$ 0° (*c*, 2.1)) in 10 ml of dry ether containing 1.0 g of osmium tetroxide quickly turned dark and deposited a precipitate. After 17 h at 5 °C the suspension was filtered and the solid washed with ether, leaving 2.28 g. This was suspended in 15 ml of water containing 1 g of sodium hydroxide and 5 g of mannitol; then the mixture was heated on a steam bath for 1 h. After cooling, the solution was acidified with acetic acid. The solid which separated was collected by filtration, and then washed with hot methylene chloride. The insoluble residue weighed 1.17 g, while the methylene chloride dissolved 14 mg.

The solid was recrystallized from absolute ethanol, giving 407 mg of diol 1, m.p. 205–223°. After four more recrystallizations this melted at 222–228° and had $[\alpha]_D^{22}$ +1° (*c*, 1.14); ν_{max} 3 420, 3 160, 2 520 cm^{-1} (OH's), 1 695 cm^{-1} (C=O), and 825 cm^{-1} (vinyl hydrogen).

Anal. Found: C, 71.66; H, 9.59. Calcd. for $C_{20}H_{32}O_4$: C, 71.39; H, 9.59.

The main mother liquor crystallized slowly, giving blades, m.p. 205–218°, and soft feathery crystals, which were mechanically separated. After two recrystallizations from methanol the blades melted at 208–218°, markedly depressed on admixture with the above diol. Found: C, 71.75; H, 9.56. Hence, this is a second diol acid. The feathery crystals from the mother liquor were separated by crystallization into diol 1 and a new compound. The latter, when recrystallized from methanol, melted at 283°.

Anal. Found: C, 68.33; H, 8.92. Calcd. for $C_{20}H_{32}O_5$: C, 68.15; H, 9.15. This appears to be a triol acid.

Aldehydo Acid from Diol 1 (from Pimaric Acid)

To a solution of 80 mg of diol 1 in 5 ml of pure dioxane was added a solution of 122 mg of paraperiodic acid in 2 ml of water. After 1.5 h in the dark the solution was concentrated to ca. 1 ml *in vacuo*, diluted with water, and extracted with methylene chloride. The organic layer was washed with sodium thiosulfate solution, dried, and distilled, giving 78 mg of nearly pure aldehydo acid. An ether solution of this was diluted with hexane, clarified by filtration, and then concentrated. The aldehydo acid crystallized and had m.p. 145–185° on a hot stage, 166–168° in an evacuated capillary. One recrystallization from ether–hexane raised the melting point to 168–169° (evacuated capillary); $[\alpha]_D^{24}$ −3° (*c*, 1.97); ν_{max} 2 725, 1 721 cm^{-1} (CHO), 1 693 cm^{-1} (COOH), and 825 cm^{-1} (vinyl hydrogen).

Anal. Found: C, 74.85; H, 9.23. Calcd. for $C_{19}H_{28}O_3$: C, 74.96; H, 9.27.

13,13-Dimethyl Acid (from Isopimaric Acid)

Pure aldehydo acid (69 mg) was dissolved in 2 ml of triethylene glycol containing 0.5 ml of 95% hydrazine. This was left overnight at room temperature, and then heated to 150°. After cautious addition of 0.6 g of potassium hydroxide the bath temperature was raised to 200 ± 5° and held there for 4.5 h. The mixture was cooled, diluted with water, acidified, and extracted with methylene chloride. The 80 mg of material from the methylene chloride crystallized spontaneously. After three recrystallizations from aqueous methanol the product melted at 149–154° and had $[\alpha]_D^{24}$ −7° (*c*, 1.38); ν_{max} 2 820, 1 695 cm^{-1} (COOH), and 824 cm^{-1} (vinyl hydrogen).

Anal. Found: C, 78.55; H, 10.24. Calcd. for $C_{19}H_{30}O_2$: C, 78.57; H, 10.41.

Isomerization of the 13,13-Dimethyl Acid (from Isopimaric Acid)

Dry hydrogen chloride was bubbled through an ice-cold solution of 25 mg of the dimethyl acid in 5 ml of dry ethanol-free chloroform for 4 h. The solution was then extracted twice with cold water, dried, and distilled. The residue was dissolved in hexane and the acid extracted into dilute sodium hydroxide solution. The aqueous solution was acidified and the liberated acid extracted into methylene chloride, giving 26 mg

Can. J. Chem. Downloaded from www.nrcresearchpress.com by 210.87.254.40 on 09/05/12
For personal use only.

of product. This was recrystallized twice from aqueous methanol, giving 14 mg of flat needles, m.p. 146–156°, $[\alpha]_D$ +69° (*c*, 0.83). This did not depress the melting point of the Δ^8-13,13-dimethyl acid from pimaric acid, and the mull spectra of the two acids were identical.

Anal. Found: C, 78.59; H, 10.29. Calcd. for $C_{19}H_{30}O_2$: C, 78.57; H, 10.41.

Photolysis of the Azide of Dihydroisopimaric Acid

This azide was prepared as described previously (18). The hydrazide formed prisms from aqueous methanol, m.p. 153°; $[\alpha]_D$ +3° (*c*, 0.97); ν_{max} 3 380 cm^{-1} (>NH), 1 620 cm^{-1} and 1 590 cm^{-1} (amide).

Anal. Found: C, 75.29; H, 10.67; N, 8.73. Calcd. for $C_{20}H_{34}N_2O$: C, 75.42; H, 10.76; N, 8.80.

A hexane solution of the acyl azide prepared from this hydrazide (800 mg), which showed infrared absorption at 2 125 cm^{-1} and 1 700 cm^{-1}, was photolyzed as described previously (18). After 16 h all the azide absorption in the infrared spectrum had disappeared, and the solution was then evaporated to dryness and chromatographed on alumina (grade IV). Hexane eluted the isocyanate (510 mg) as a colorless oil showing infrared absorption at 2 245 cm^{-1}. Elution with benzene yielded a crystalline product (66 mg, 9%) which was purified by sublimation (160° at 10^{-4} mm pressure), yielding small prisms, m.p. 178°, $[\alpha]_D$ 32° (*c*, 0.75).

Anal. Found: C, 79.91; H, 10.17; N, 4.52. Calcd. for $C_{20}H_{31}NO$: C, 79.67; H, 10.37; N, 4.65.

Infrared spectrum: ν_{max} 3 250 cm^{-1} (>NH), 1 690 and 1 645 cm^{-1} (γ-lactam), or 1 685 cm^{-1} (γ-lactam in chloroform). Nuclear magnetic resonance spectrum: τ 1.73, one-hydrogen singlet (NH); τ 4.20, broad one-hydrogen signal, half band width 6 c.p.s. (vinyl hydrogen); τ 6.17, one-hydrogen doublet with J = 10 c.p.s. and half band width for each branch of 6 c.p.s. (hydrogen on C-6). Dihydroisopimaric acid (300 mg) in hexane (100 ml) was unchanged after photolysis for 24 h.

Hydroboration of Methyl Dihydroisopimarate

Freshly distilled boron trifluoride etherate (5 ml) in tetrahydrofuran (70 ml) was treated with sodium borohydride (5.9 g) during 10 min and the mixture was stirred overnight at room temperature before being filtered through glass wool. The diborane solution was made up to 100 ml and used as a standard solution for hydroboration. A solution of methyl dihydroisopimarate (1.5 g) in tetrahydrofuran (50 ml) at 0° under nitrogen was treated with 30 ml of the above diborane solution with vigorous stirring for 3 h. Water (20 ml) was added to the reaction mixture and the mixture evaporated under reduced pressure to about 10 ml. Ethanol (30 ml of 95%), containing sodium hydroxide (1 g), and hydrogen peroxide (2.5 ml of 10%) were added, and the mixture was heated on a steam bath for 15 min and then evaporated to dryness under reduced pressure. The residue was extracted with ether and the ether layer washed with water, dried, and evaporated to yield a colorless oil (1.6 g) which was oxidized directly with Jones's reagent (17). The oxidation product obtained by dilution of the reaction mixture with water and ether extraction was chromatographed on alumina (grade IV). Ether–benzene (1:3) eluted a crystalline solid (600 mg), m.p. 79–80°, raised to 83° on crystallization from aqueous methanol. An analytical sample was sublimed at 120° under 10^{-3} mm pressure, giving colorless prisms, m.p. 83°, $[\alpha]_D$ +10.0° (*c*, 0.37).

Anal. Found: C, 75.62; H, 10.16. Calcd. for $C_{21}H_{34}O_3$: C, 75.40; H, 10.25.

Its infrared spectrum had a broad peak at 1 720 cm^{-1} (—COOMe and >C=O) and its n.m.r. spectrum contained complex signals integrating for three hydrogens between τ 7.5 and 8.2. The keto ester reacted immediately with 2,4-dinitrophenyl hydrazine at room temperature. The product formed orange needles from ethyl acetate – methanol, m.p. 193°.

Equilibrium of Keto Ester XI with Base

The keto ester XI (30 mg) in methanol (10 ml) was refluxed with 20% aqueous potassium hydroxide (2 ml) for 3 h. The mixture was cooled, acidified, and ether extracted. Evaporation of the dried extract yielded an acid (25 mg) which crystallized from benzene–hexane as prisms, m.p. 238–240°, $[\alpha]_D$ +2° (*c*, 1.0).

Anal. Found: C, 74.85; H, 9.80. Calcd. for $C_{20}H_{32}O_3$: C, 74.96; H, 10.06.

Infrared spectrum: ν_{max} at 3 150 cm^{-1} and 1 690 cm^{-1} (—COOH) and 1 725 cm^{-1} (>C=O). Nuclear magnetic resonance spectrum: three-hydrogen signals between τ 7.5 and 8.1. Methylation of this acid with ethereal diazomethane gave the same keto ester, m.p. and mixed m.p. 83°, $[\alpha]_D$ +10°, with its infrared spectrum and thin-layer mobility identical with those of the original ester described above.

Dehydrogenation of the Keto Ester

The keto ester (500 mg) and selenium (2 g) were intimately mixed and heated at 300° for 14 h. The mixture was cooled and the black solid was extracted several times with boiling benzene. The benzene extract was refluxed with freshly precipitated silver for 1 h, filtered, and refluxed again with fresh silver. The benzene extract was washed 4 times with 5-ml portions of 2 *N* sodium hydroxide. The aqueous solution was acidified and extracted with ether. The ether extract was dried and evaporated to yield a yellow oil

Can. J. Chem. Downloaded from www.nrcresearchpress.com by 210.87.254.40 on 09/05/12
For personal use only.

(15 mg) which showed phenanthrene-like absorption in its ultraviolet spectrum. Methylation of the crude product with dimethyl sulfate and potassium carbonate in boiling acetone yielded a neutral product which gave one spot on a thin-layer chromatogram after purification by chromatography on alumina. Despite the fact that its ultraviolet spectrum and R_f in two solvents were identical with those of authentic 1,7-dimethyl-9-methoxyphenanthrene,[6] it would not crystallize when seeded with this. The infrared spectrum of the oil was nearly superimposable on that of the authentic sample.

Methyl Carbinol XIII

A solution of 400 mg of keto acid X in 40 ml of dry ether was added slowly to methyl Grignard reagent prepared from methyl iodide and 300 mg of magnesium in 10 ml of ether. The mixture was stirred overnight at room temperature, and then poured into 40 g of ice and 20 ml of 4 *N* sulfuric acid. The ether layer was washed with sodium hydrogen sulfite solution, dried, and distilled, giving 440 mg of residue. The residue was adsorbed on a column of silica gel (20 g). Hexane eluted 123 mg, but the main product (301 mg) was eluted by 30% ether in benzene. The strongly adsorbed material was converted to its methyl ester, which was distilled over a short path at 110–120°, 2×10^{-3} mm pressure. It then melted at 100–103°. After purification by chromatography on alumina the methyl ester of XIII melted at 105° and had $[\alpha]_D$ +6° (*c*, 3.0).

Anal. Found: C, 75.53; H, 10.76. Calcd. for $C_{22}H_{38}O_3$: C, 75.38; H, 10.93.

Dehydrogenation of XIII and Its Salt

A mixture of XIII (500 mg) and 2 g of selenium was heated at 300° for 17 h. The product extractable into benzene was refluxed in this solvent with freshly precipitated silver for 1 h. The filtrate gave a product showing phenanthrene-like ultraviolet absorption, but no pure product was obtained.

An intimate mixture of 800 mg of the sodium salt of XIII with selenium was covered with more selenium (total 8 g) and heated at 260° for 16 h and at 300° for 7 h. Extraction of the reaction mixture as described above did not give any pure products.

Selenium Dioxide Oxidation of Methyl Dihydroisopimarate

To a solution of methyl dihydroisopimarate (500 mg) in ethanol (20 ml) was added freshly sublimed selenium dioxide (200 mg) in ethanol (10 ml) and water (2 ml). The solution was stirred at room temperature for 8 h, after which the yellow solution was filtered to remove precipitated selenium. The solution on evaporation left a yellow oil (510 mg) which was redissolved in ethanol and filtered through active charcoal (Darco G 60). Evaporation gave a colorless oil (470 mg) showing hydroxyl absorption in its infrared spectrum. Thin-layer chromatography indicated the presence of at least seven components. The oxidation product was chromatographed on alumina (Woelm grade III). Benzene eluted a crystalline compound (40 mg) which, on rapid crystallization from the minimum amount of pentane at 0 °C, yielded colorless prisms, m.p. 84°.

Anal. Found: C, 75.16; H, 10.00. Calcd. for $C_{21}H_{34}O_3$: C, 75.40; H, 10.25.

Infrared spectrum: ν_{max} at 3 510 cm^{-1} (hydroxyl), 1 710 cm^{-1} (ester), and 830 cm^{-1} (trisubstituted double bond). Nuclear magnetic resonance spectrum: a broad one-hydrogen doublet at τ 4.42, J = 4 c.p.s. (vinyl hydrogen), a three-hydrogen singlet at τ 6.36 (carbomethoxyl), and a one-hydrogen singlet at τ 6.44 (carbinol hydrogen). Chloroform eluted a further crystalline product (57 mg) which on sublimation furnished colorless prisms, m.p. 92°.

Anal. Found: C, 75.51; H, 10.13. Calcd. for $C_{21}H_{34}O_3$: C, 75.40; H, 10.25.

Infrared spectrum: ν_{max} at 3 650 cm^{-1} (hydroxyl), 1 725 cm^{-1} (ester), and 820 cm^{-1} (trisubstituted double bond). Nuclear magnetic resonance spectrum: 4.55 τ (one-hydrogen singlet, half-band width 4 c.p.s., vinyl hydrogen), 5.94 τ (one-hydrogen broadened singlet, half-band width 7 c.p.s., carbinol hydrogen), 6.36 τ (three-hydrogen singlet, carbomethoxyl).

The other components of the reaction mixture could not be obtained pure but appeared to be other allylic alcohols and dienes (based upon spectra).

Oxidation of the two alcohols by manganese dioxide in chloroform yielded, in both cases, products with ultraviolet absorption at λ_{max} 242 mμ, log ϵ 3.5 (assuming molecular weight of 300) and infrared absorption at 1 665 cm^{-1}. These products could not be purified nor were derivatives obtained. Dehydration experiments with hydrochloric acid in ethanol on the allylic alcohols gave an inseparable mixture of dienes.

ACKNOWLEDGMENTS

We thank Mr. A. Knoll (N.R.C.) and Mrs. I. Lemke (Carleton University) for technical assistance. We are indebted to Mr. H. Séguin for the analyses, to Mr. R. Lauzon for the infrared spectra, and to Mr. J. Nicholson for the n.m.r. spectra. One of us (J. W. A.) thanks the National Research Council for financial support for the work carried out at Carleton University.

[6]*Kindly supplied by Professor W. B. Whalley, whom we cordially thank.*

Can. J. Chem. Downloaded from www.nrcresearchpress.com by 210.87.254.40 on 09/05/12
For personal use only.

REFERENCES

1. G. C. HARRIS and T. F. SANDERSON. J. Am. Chem. Soc. **70**, 2081 (1948).
2. O. E. EDWARDS and R. HOWE. Chem. Ind. London, 629 (1958). O. E. EDWARDS and R. HOWE. Can. J. Chem. **37**, 760 (1959).
3. E. WENKERT and J. W. CHAMBERLIN. J. Am. Chem. Soc. **80**, 2912 (1958).
4. B. GREEN, A. HARRIS, and W. B. WHALLEY. J. Chem. Soc. 4715 (1958).
5. LE VAN THOI. Compt. Rend. **247**, 1343 (1958).
6. O. E. EDWARDS and R. HOWE. Chem. Ind. London, 537 (1959).
7. A. K. BOSE. Chem. Ind. London, 1104 (1960).
8. A. K. BOSE and W. A. STRUCK. Chem. Ind. London, 1628 (1959).
9. O. E. EDWARDS, A. NICOLSON, and M. N. ROGER. Can. J. Chem. **38**, 663 (1960).
10. R. E. IRELAND and P. W. SCHIESS. J. Org. Chem. **28**, 6 (1963).
11. G. W. A. MILNE and H. SMITH. Chem. Ind. London, 1307 (1961).
12. A. K. BOSE and S. HARRISON. Chem. Ind. London, 254 (1963).

12(*a*). M. FETIZON and M. GOLFIER. Bull. Soc. Chim. France, 167 (1963).

13. R. F. CHURCH and R. E. IRELAND. J. Org. Chem. **28**, 17 (1963).
14. E. WENKERT and P. BEAK. J. Am. Chem. Soc. **83**, 998 (1961).
15. W. ANTKOWIAK, J. W. APSIMON, and O. E. EDWARDS. J. Org. Chem. **27**, 1930 (1962).
16. L. RUZICKA and F. BALAS. Ann. **460**, 202 (1928). P. LEVY. Ber. **61**, 616 (1928).
17. K. BOWDEN, I. M. HEILBRON, E. R. H. JONES, and B. C. L. WEEDON. J. Chem. Soc. 39 (1946). C. DJERASSI, R. R. ENGLE, and A. BOWERS. J. Org. Chem. **21**, 1547 (1956).
18. J. W. APSIMON and O. E. EDWARDS. Can. J. Chem. **40**, 896 (1962).
19. C. DJERASSI, W. CLOSSEN, and A. E. LIPMAN. J. Am. Chem. Soc. **78**, 3163 (1956).
20. R. E. IRELAND and J. NEWBOULD. J. Org. Chem. **28**, 23 (1963).
21. A. TAHARA, O. HOSHINO, and N. IKEKAWA. Chem. Pharm. Bull. Tokyo, **10**, 995 (1962).

Can. J. Chem. Downloaded from www.nrcresearchpress.com by 210.87.254.40 on 09/05/12
For personal use only.

Can. J. Chem. Downloaded from www.nrcresearchpress.com by 210.87.254.6 on 09/05/12
For personal use only.

REACTION OF DIHYDROPYRAN WITH ETHYL AZIDOFORMATE[1,2]

I. BROWN[3] AND O. E. EDWARDS
Division of Pure Chemistry, National Research Council, Ottawa, Canada
Received November 18, 1964

Dedicated to Professor R. B. Sandin on the Occasion of his Sixty-Eighth Birthday

ABSTRACT

Photochemical reaction of ethyl azidoformate with dihydropyran gave a good yield of the very reactive aziridine III. The thermal reaction between the two compounds took a completely different course, via triazoline XI to 2-hydroxy-2-ethoxycarbonamidotetrahydropyran XIII.

Interest in new and reactive ring systems, in the synthesis of analogues of 2-amino-2-deoxy sugars, and in the mechanism of acyl azide reactions led us to study the photochemical and thermal reactions of ethyl azidoformate with dihydropyran.

Recent work has shown that ethyl azidoformate reacts under ultraviolet irradiation with cyclohexene (1) and with benzene (2). The products from reaction with cyclohexene were mainly the aziridine I and urethane II in the ratio 4.5:1. It was hoped that in the case of dihydropyran a reactive N-ethoxycarbonyl aziridine would be formed in good yield by attack on the double bond.

Irradiation, with ultraviolet light, of a solution of ethyl azidoformate in dihydropyran resulted in nitrogen evolution and gradual disappearance of the characteristic azide bands (ν_{max} 2 120, 2 170 cm^{-1}) in its infrared spectrum (3). The product, after removal of the bulk of the excess dihydropyran under reduced pressure, was a mobile oil, with infrared absorption at 1 710 cm^{-1}. This could be distilled over a short path at 80° under 5×10^{-4} mm, but a large high-boiling residue remained. The distilled material reacted rapidly with water or methanol to give a hydroxyurethane ($\nu_{max}^{CHCl_3}$ 1 710 cm^{-1}) or ethoxy urethane respectively. The former analyzed correctly for structure III, and its nuclear magnetic resonance (n.m.r.) spectrum[4] (see structure) was in harmony with this assignment. Attempts to obtain the pure methoxy urethane IV always resulted in partial hydrolysis to III. The vicinal nature of the hydroxyl and urethane groups in III was proved by heating the compound with 2,4-dinitrophenylhydrazine hydrochloride solution. The osazone V was formed and identified by comparison with an authentic specimen (4, 5).

Finally, the hydroxyurethane III could be oxidized to a lactone VI that retained the urethane group, thus confirming the location of the nitrogen in III and IV. We hence conclude that the reactive product from the photochemical reaction is the desired aziridine VII.

The direction of hydrolytic opening of the aziridine ring and its reactivity are normal when viewed either as attack of solvent on the zwitter ion VIII (S_N1 process) or S_N2 displacement at the most electron-deficient carbon (see IX). The nonvolatile residue produced on heating the product was probably of the type X, the polymerization being initiated by traces of III resulting from reaction with minute amounts of water. If the

[1]*Presented in part at the Symposium on Reactive Intermediates, Laval University, Quebec, August 27–29, 1964.*
[2]*Issued as N.R.C. No. 8283.*
[3]*N.R.C. Postdoctorate Fellow.*
[4]*All chemical shifts are given as τ values (G. D. Tiers, J. Phys. Chem. 62, 1151 (1958)).*

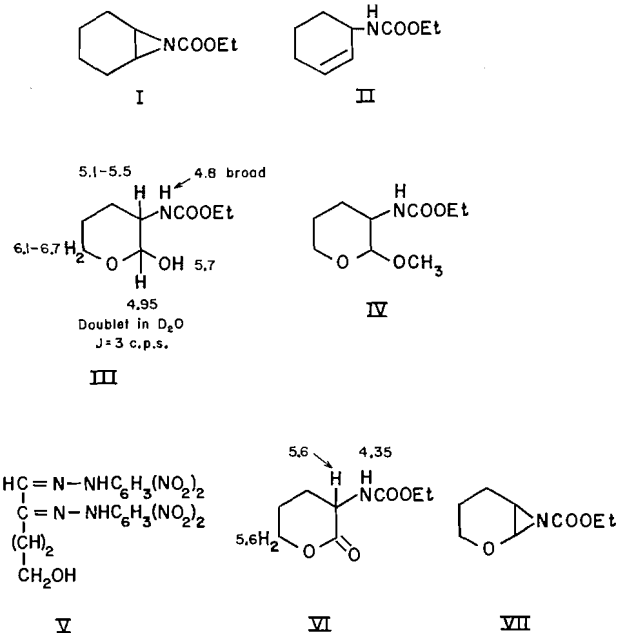

photolysis was conducted in the presence of water (as a second phase), the product was III in excellent yield. The only significant products besides those derived from VII were produced from photolysis of dihydropyran itself (ca. 0.3 g from 100 ml in blank runs for 5 h). These have not been characterized.

The notable selectivity of attack on the double bond suggests one of two things: (*a*) that the reaction is one involving an excited azide, giving an excited triazoline which spontaneously loses nitrogen, or (*b*) that an electrophilic singlet nitrene is the reacting entity, so that attack on the polarized double bond overshadows insertion into C—H bonds.

To examine possibility (*a*) we hoped to prepare and photolyze the triazoline XI. If the product was *not* the aziridine VII, then there would be some indication that the triazoline was not an intermediate in the photolysis of the mixture of dihydropyran and ethyl azidoformate.[5] In fact, the triazoline could not be obtained, since dihydropyran reacted at temperatures from ambient to 80° with ethyl azidoformate, with simultaneous nitrogen evolution. That the triazoline was an intermediate in the thermal reaction, however, was evident, since the rate of reaction at 80° (measured by nitrogen evolution) was 20 times the rate of decomposition of ethyl azidoformate in dioxane at the same temperature. The formal 1,3-dipolar addition seems likely to proceed via the intermediate XII.

The major product from the thermal reaction followed by exposure to water at room temperature was a crystalline solid analyzing for $C_8H_{15}NO_4$. Its infrared spectrum (Nujol mull) had peaks at 1 765 cm^{-1} (urethane) and 3 265 and 3 200 cm^{-1} (OH and (or) NH). In chloroform solution, however, two carbonyl peaks at 1 760 and 1 705 cm^{-1} were evident, in addition to a broad band at 3 400 cm^{-1}. Its n.m.r. spectrum ($CDCl_3$) had signals at 1.7 (NH) and 7.3 (OH) which disappeared when D_2O was added. An ethoxy group

[5]*This involves the assumption that the excited states from the two routes would be comparable in their chemical reactivity.*

Can. J. Chem. Downloaded from www.nrcresearchpress.com by 210.87.254.6 on 09/05/12
For personal use only.

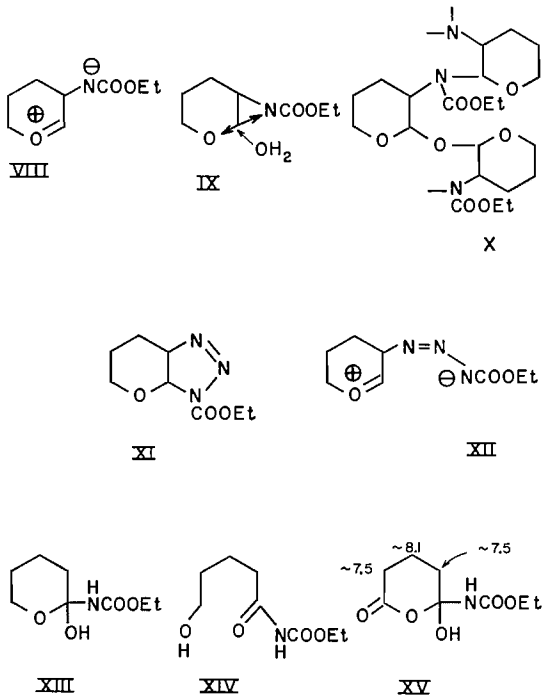

was indicated by a triplet at 8.7 and a quartet at 5.8. Two broad two-hydrogen signals at 6.4 and 7.3 corresponded to CH_2—O— and —CH_2—C(=O)— groups respectively. The hydroxyl hydrogen gave rise to a triplet centered at 5.7 in dimethyl sulfoxide; hence, it was a primary alcohol (6). On the basis of the above evidence and mechanistic considerations, structure XIII seemed plausible for the compound in the solid state, and XIV for it in solution. To test this, the compound was oxidized with Jones reagent. The product analyzed for $C_8H_{13}NO_5$ (loss of two hydrogens and addition of one oxygen). Its infrared spectrum (Nujol) showed the presence of two carbonyl groups (ν_{max} 1 760 and 1 720 cm^{-1}) and OH and (or) NH groups (ν_{max} 3 265 and 3 200 cm^{-1}). This and its n.m.r. spectrum in D_2O (see assignment on the structure) are consistent with structure XV. Finally, hydrolysis of the oxidation product gave glutaric acid, confirming the structures XIII through XV. The formation of XIII can be rationalized as shown in Reaction Scheme 1.

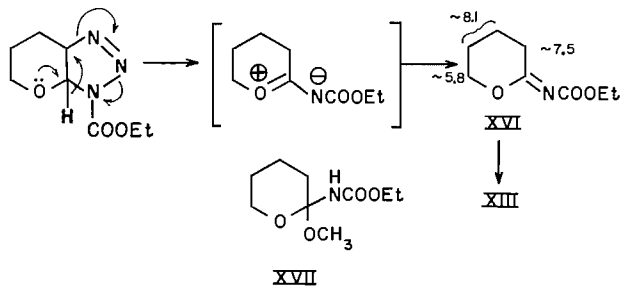

REACTION SCHEME 1.

Can. J. Chem. Downloaded from www.nrcresearchpress.com by 210.87.254.6 on 09/05/12
For personal use only.

The n.m.r. spectrum of the product before addition of water contained no vinyl hydrogen, as expected if it contained the intermediate XVI. Addition of methanol, rather than water, to the reaction mixture gave a new product with R_f 0.8 in a thin-layer chromatogram, compared to R_f 0.2 for XIII. A spot at R_f 0.2, however, was also present. When the component with R_f 0.8 was recovered from a preparative plate, only the hydroxy compound XIII was obtained. It seems that the methoxy compound XVII had been formed by addition of methanol to intermediate XVI, but that it was hydrolyzed fairly rapidly on the silica gel surface to XIII. The imino intermediate itself must react almost instantly with water in the silica gel, since the initial reaction mixture gave a main spot at R_f 0.2 identical with that of XIII. These observations support the suggestion that XVI is the primary product of the thermal reaction.

When a sample of aziridine VII was heated at 80° in dihydropyran, the dihydropyran removed under reduced pressure, and the residue treated with water, III was present among the products but there was no evidence of XIII on a thin-layer chromatogram. We conclude that VII is not an intermediate in the formation of XVI.

A search for tetrahydrofurfural, which might have been formed in the thermal reaction by the sequence given in Reaction Scheme 2 (cf. ref. 7), was fruitless.

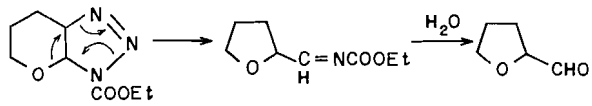

REACTION SCHEME 2.

The contrast between the thermal and photochemical reactions described above seems at first sight to discount the triazoline as a possible intermediate in the photochemical process. However, it seems dangerous to extrapolate from the reaction of a vibrationally excited ground state in the thermal reaction to that of the probably vibrationally and electronically excited intermediate in the irradiation. This caution is reinforced by the observation that irradiation of the corresponding triazoline XVIII from norbornylene *does* give the same products as light-induced reaction of norbornylene and ethyl azidoformate.[6] We hence reserve judgment about the nature of the intermediates in the photochemical reaction.

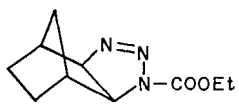

XVIII

The apparent cyclol character of XIII and XV in the solid state has analogy in the observations of other groups on hydroxy-N-acyl lactams (8–10). Although the two compounds appear to be acyclic in solution, they only show end absorption in the ultraviolet, as contrasted with the maxima near 220 mμ reported for N-acyl lactams. A referee has suggested that this difference is due to less conjugation in N-acylcarbamates such as XIII and XV than in the N-acyl lactams. Since the excited state probably

[6] *Unpublished observations by O. E. Edwards, J. Elder, and M. Lesage.*

Can. J. Chem. Downloaded from www.nrcresearchpress.com by 210.87.254.6 on 09/05/12
For personal use only.

resembles $^{\delta-}O\cdots C\cdots \overset{+}{N}(H)\cdots C\cdots O^{\delta-}$, the higher electrical symmetry of the N-acyl lactams should lower the energy of their excited states relative to those of the carbamates.

The hydroxyurethane III is a derivative of a 2-amino-2,3,4-trideoxyaldopentose. The more oxygenated analogues of the aziridine VII, if they can be prepared from the glycals, would provide valuable precursors for the 2-amino-2-deoxy sugars and their polymers.

EXPERIMENTAL

Melting points were measured on a Kofler hot stage; ultraviolet spectra were determined in 95% ethanol, and n.m.r. spectra in deuterochloroform with tetramethylsilane as internal standard, unless otherwise stated.

Dihydropyran was purified by distillation at atmospheric pressure, irradiation with a 100-W low-pressure mercury lamp in an immersion cell with water cooling and quartz filter, drying, and distilling twice. In this way photochemically active impurities in the dihydropyran were removed.

A solution of ethyl azidoformate (11) (4 g) in purified dihydropyran (100 ml) exhibited a split azide band at 2 120 and 2 170 cm^{-1} and a carbonyl absorption at 1 730 cm^{-1}. The solution was irradiated for 5 h with agitation by a stream of dry nitrogen, after which time the azide absorption had been replaced by a band at 1 710 cm^{-1}. The excess dihydropyran was removed under reduced pressure at 50° and the residual mobile oil (5.6 g) was immediately distilled at 5×10^{-4} mm and a bath temperature of 80°. A colorless oil (1.91 g) distilled, leaving a brown high-boiling residue. The distillate was dissolved in dioxane and excess water added. After the solution had stood for 30 minutes at room temperature, the solvent was removed on a rotating evaporator at 50°. The oily product crystallized on scratching and was recrystallized from acetone to give colorless needles (0.63 g) of III, m.p. 115–117°.

Anal. Found: C, 50.73; H. 7.78; N, 7.53. Calcd. for $C_8H_{15}NO_4$: C, 50.78; H, 7.99; N, 7.40.

Photolysis in the Presence of Water

Ethyl azidoformate (6.8 g) in dihydropyran (100 ml) and water (10 ml) was irradiated as above for 5 h. The mixture was then diluted with an equal volume of methylene dichloride and dried over anhydrous sodium sulfate. The organic solvent was taken to dryness at 50° under reduced pressure and the residual oil crystallized from acetone to give colorless needles (9.5 g) of III, m.p. 115–117°.

Osazone V

The hydroxyurethane, m.p. 117°, was dissolved in a methanolic solution of 2,4-dinitrophenylhydrazine hydrochloride, and then boiled for 1 h. The orange needles which separated melted at 241° and did not depress the melting point of the derivative of 5-hydroxy-2-ketopentanal (4, 5).

Oxidation of III with Sodium Dichromate

To the hydroxyurethane III (0.50 g) dissolved in glacial acetic acid (15 ml) was added sodium dichromate (0.577 g; 1.1 mole). The mixture was swirled to effect solution and allowed to stand for 20 h. Thin-layer chromatography in silica gel with ether as developing solvent indicated disappearance of starting material and the formation of two new components. Benzene (50 ml) was added to the acetic acid solution followed by excess powdered sodium carbonate. The slurry of sodium acetate and sodium carbonate was filtered off and washed with benzene. The combined filtrates were washed with sodium bicarbonate solution, then water, and dried. Evaporation of the solvent left a yellow oil (0.217 g). A portion of this oil (0.125 g) was separated into its two components by preparative thin-layer chromatography on silica gel with ether as developing solvent, the bands being located by iodine vapor. The absorbed iodine was allowed to evaporate; the silica gel was scraped off, mixed with an equal quantity of "Celite", and eluted in a column with chloroform–methanol. The eluate was taken to dryness; the filtrate was taken up in chloroform, filtered, and the solvent evaporated off. The main component (R_f 0.4, 0.072 g) was distilled over a short path at 95°, 3×10^{-3} mm, to give a colorless oil (0.068 g) which showed only end absorption in the ultraviolet and had infrared absorption at 1 750 cm^{-1} and 1 710 cm^{-1} ($CHCl_3$ solution).

Anal. Found: C, 51.52; H, 7.18. Calcd. for $C_8H_{13}NO_4$: C, 51.33; H, 7.00.

Thermal Reaction

Ethyl azidoformate (0.57 g) in purified dihydropyran was refluxed for 10 h, after which time no more nitrogen was evolved. The excess dihydropyran was removed at 50° under reduced pressure, and the residual oil was dissolved in aqueous dioxane and allowed to stand 24 h. The solvent was evaporated. The residual oil (0.80 g) crystallized on scratching. It was recrystallized from benzene to give XIII as needles (0.60 g), m.p. 68.5–70°. It had only strong end absorption below 210 mμ.

Anal. Found: C, 50.74; H, 7.79; N, 7.68. Calcd. for $C_8H_{15}NO_4$: C, 50.78; H, 7.99; N, 7.40.

Can. J. Chem. Downloaded from www.nrcresearchpress.com by 210.87.254.6 on 09/05/12
For personal use only.

Thermal Reaction of Aziridine VII

A sample of aziridine VII was dissolved in dihydropyran and the solution boiled for 16 h. After removal of the dihydropyran under reduced pressure, the residue was dissolved in cold aqueous dioxane and left for 1 h. A thin-layer chromatogram of the product showed three spots, one of which had an R_f identical with that of III. No spot was present with the same R_f as XIII.

Oxidation of XIII with Jones Reagent

The compound (0.86 g) dissolved in 15 ml acetone was titrated with Jones reagent (12) with magnetic stirring at 20°. A color end point was observed after 1.8 moles of reagent had been added. A further 0.3 moles of reagent was added, the slurry stirred for 5 min, and then excess reagent destroyed by addition of a few drops of ethanol. The chromium salts were filtered from the acetone solution and the filtrate taken to dryness. The solid residue was taken up in benzene, filtered through charcoal, and then recrystallized first from benzene – *n*-hexane and subsequently from chloroform to give needles of XV (0.62 g), m.p. 136.5–139.5°. It had strong end absorption below 210 mμ.

Anal. Found: C, 47.36; H, 6.44; N, 6.90. Calcd. for $C_8H_{13}NO_5$: C, 47.29; H, 6.45; N, 6.89.

HBr in Acetic Acid Hydrolysis of XV to Glutaric Acid

The lactone (0.043 g) was heated on the steam bath with a mixture of glacial acetic acid (2 ml) and 47% hydrobromic acid (2 ml) for 1 h. The solution was then taken to dryness at 70° on the water pump and the solid residue was extracted with acetone to give, after recrystallization from benzene, plates (m.p. 95–99.5°) identical (infrared, mixed melting point) with authentic glutaric acid.

ACKNOWLEDGMENTS

We are indebted to Mr. M. Lesage for determination of n.m.r. spectra and Mr. H. Seguin for the analyses.

REFERENCES

1. W. Lwowski, T. J. Maricich, and T. W. Mattingly. J. Am. Chem. Soc. **85**, 1200 (1963).
2. K. Hafner and C. Koenig. Angew. Chem. **75**, 89 (1963).
3. E. Lieber, C. N. R. Rao, A. E. Thomas, E. Oftedahl, R. Minnis, and C. V. N. Nambury. Spectrochim. Acta, **19**, 1135 (1963).
4. C. D. Hurd and C. D. Kelso. J. Am. Chem. Soc. **70**, 1484 (1948).
5. C. D. Hurd and O. E. Edwards. J. Org. Chem. **14**, 680 (1949).
6. O. L. Chapman and R. W. King. J. Am. Chem. Soc. **86**, 1256 (1964).
7. C. D. Hurd and O. E. Edwards. J. Org. Chem. **19**, 1319 (1954).
8. R. G. Griot and A. J. Frey. Tetrahedron, **19**, 1661 (1963).
9. V. K. Antonov, A. M. Shkrob, and M. M. Shemyakin. Tetrahedron Letters, 439 (1963).
10. G. L. Glover and H. Rapoport. J. Am. Chem. Soc. **86**, 3397 (1964).
11. M. O. Foster and H. E. Fierz. J. Chem. Soc. **93**, 72 (1908).
12. K. Bowden, I. M. Heilbron, E. R. H. Jones, and B. C. L. Weedon. J. Chem. Soc. 39 (1946). C. Djerassi, R. R. Engle, and A. Bowers. J. Org. Chem. **21**, 1547 (1956).

Can. J. Chem. Downloaded from www.nrcresearchpress.com by 210.87.254.6 on 09/05/12
For personal use only.

Can. J. Chem. Downloaded from www.nrcresearchpress.com by 210.87.254.40 on 09/05/12
For personal use only.

COMPLEXES OF STANNIC IODIDE WITH AROMATIC HYDROCARBONS

J. F. MURPHY[1] AND D. E. BAKER[2]
University of Idaho, Moscow, Idaho
Received November 13, 1964

Dedicated to Professor R. B. Sandin on the Occasion of his Sixty-Eighth Birthday

ABSTRACT

Spectrophotometric measurements on solutions of stannic iodide were found to provide evidence for complex formation with aromatic hydrocarbons. Calculations, based on spectra for mixed solutions of benzene and stannic iodide in carbon tetrachloride, yield values of 0.26 for the equilibrium constant (mole fraction), 28 400 l/mole cm for the molar extinction coefficient of the benzene – stannic iodide complex. Kinetic evidence indicates that the order of decreasing complex stabilities is from xylene to toluene to benzene. The formation of stannic iodide – aromatic hydrocarbon complexes provides an explanation for the discrepancy between measured solubilities of stannic iodide in benzene, toluene, and xylene, and the solubilities predicted by the Hildebrand theory of regular solutions.

INTRODUCTION

The Hildebrand theory of regular solutions has been very successful in predicting solubilities. In a few cases, however, unexpected discrepancies have appeared. For example, the solubility of iodine in benzene, toluene, and xylene was found to be in reverse order to the order of the solubilities calculated from regular solution theory. The early spectrophotometric study of iodine in aromatic hydrocarbons by Benesi and Hildebrand (1) showed that complexes were formed. Since then many other systems have been studied (2). Benesi and Hildebrand considered the complexes as examples of acceptor–donor combinations in the Lewis acid–base sense. The order of stability of the complexes, as calculated from spectrophotometric data, was such as to explain satisfactorily the disagreement between the observed order of solubility and that predicted from the theory of regular solutions. A similar disagreement of predicted and observed solubility order has been noted by Hildebrand and Scott (3) for solutions of stannic iodide. Regular solution theory predicts a decrease in solubility as the internal pressure of the solvent decreases from benzene through toluene to xylene, whereas the observed solubilities increase from benzene to toluene.

The work described in this paper was undertaken to determine whether complex formation could account for these discrepancies between theory and observation.

EXPERIMENTAL

Stannic iodide was prepared by the method of Dorfman and Hildebrand (4). Reagent grade solvents were used without further purification. Spectrophotometric measurements were made at 25 ± 2 °C with a Beckmann spectrophotometer, model DU.

RESULTS

General Nature of Spectra

Preliminary measurements were made on solutions of stannic iodide in dioxane, carbon tetrachloride, hexane, petroleum ether, benzene, toluene, and *m*-xylene (Table I). The

[1]*Present address: Metals Research Laboratory, Olin Mathieson Chemical Corporation, New Haven, Connecticut.*
[2]*Present address: General Electric Company, Hanford, Washington.*

TABLE I

Wavelengths of absorption maxima and molar extinction coefficients for stannic iodide in various solvents

Solvent	SnI_4 concn. range $\times 10^5$	λ_1	ϵ_1	λ_2	ϵ_2
Carbon tetrachloride	4.4–9.7	365	8 500	285	4 600
Petroleum ether	1.6–7.9	365	8 300	285	4 600
Hexane	8.1	365	8 000	285	4 400
1,4-Dioxane	2.6–5.2	454	1 760	264	9 200
Benzene	5.0–10.9	365	8 500	297	8 500
Toluene	8.7–9.7	365	9 540	(300)	—
m-Xylene	4.6	365	10 100	(300)	—

molar extinction coefficient curves showed maxima at 285 and 365 mμ for carbon tetrachloride, hexane, and petroleum ether. Extinction coefficient curves for stannic iodide in these three solvents are identical. Solutions of stannic iodide in dioxane exhibited absorption maxima at 264 and 454 mμ. Solutions in benzene showed maxima at 297 and 365 while toluene and xylene solutions showed only one clearly defined maximum at 365 mμ. Representative spectra for solutions of stannic iodide in carbon tetrachloride, benzene, and toluene are shown in Fig. 1. There is an obvious difference between the spectra in carbon tetrachloride and in the aromatic compounds in the 285–300 mμ region.

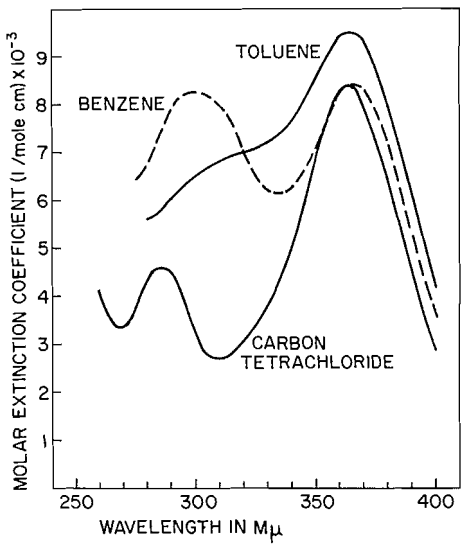

FIG. 1. Molar extinction coefficients vs. wavelength for stannic iodide. Temperature 25 ± 2 °C; concentration range 8.5–9.5 × 10^{-5} *M*.

Solutions of stannic iodide in benzene, toluene, and xylene exhibited a marked color change on standing in air while exposed to sunlight or artificial light. Figure 2 illustrates the effect of a 3 h exposure to sunlight on the spectrum of a solution of SnI_4 in benzene open to the air. A molar extinction curve for iodine in benzene is also shown for comparison. For these solutions the change in color was more rapid in sunlight than in artificial light. For the same exposure to light, the rate of color change was found to

Can. J. Chem. Downloaded from www.nrcresearchpress.com by 210.87.254.40 on 09/05/12
For personal use only.

increase in the order: benzene, toluene, and xylene. Spectrophotometric measurements of the iodine produced by illumination of solutions of stannic iodide in benzene showed that the color change was due to a photochemically accelerated reaction of oxygen with stannic iodide to form iodine (see Fig. 2). When the reaction was allowed to go to completion, the iodine formed was equivalent to complete decomposition of the stannic iodide. Removal of oxygen by bubbling deoxygenated nitrogen through the solution decreased the rate of reaction to the point that no iodine could be detected in solutions exposed to artificial light for 5 h. Therefore, all further measurements were made on deoxygenated solutions.

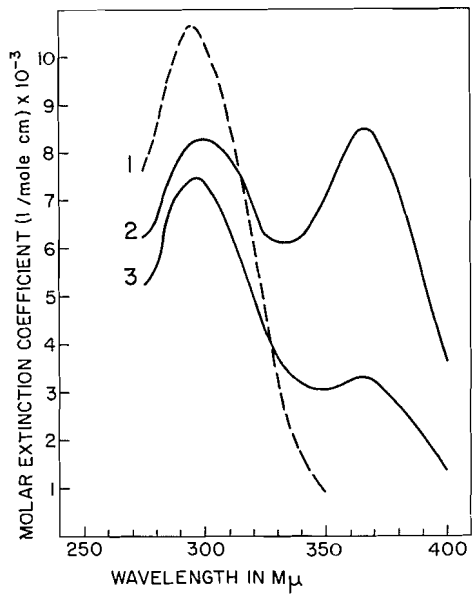

FIG. 2. Photochemical oxidation of stannic iodide in benzene at 25 ± 2 °C. Curve 1, iodine in benzene; curve 2, stannic iodide in deaerated benzene-fresh solution; curve 3, stannic iodide in benzene after 3 h exposure to sunlight.

Assignment of Absorption Peaks for Benzene Solutions

Both iodine and stannic iodide in benzene have an absorption maximum at 297 mμ (Fig. 2) and stannic iodide decomposes to form iodine. Therefore, it is important to eliminate the possibility that the peak observed for stannic iodide solutions is due to the presence of iodine from decomposition of the stannic iodide. To eliminate this possibility we were careful to use data for solutions in which the stannic iodide 365 mμ peak height was correct for the concentration of stannic iodide used.

We also considered the possibility that one or both of the peaks were due to, or modified by, an "acid–base" reaction between stannic iodide and iodine (produced by decomposition of a part of the stannic iodide). This possibility was tested by examining the spectra of solutions containing various ratios of iodine to stannic iodide at a constant total concentration of 1×10^{-4} moles/l in carbon tetrachloride. No absorption maximum was observed at 297 mμ in these solutions. Further, the extinction coefficients for iodine at 517 mμ and for stannic iodide at 365 and 285 mμ were equal to the values obtained for simple solutions of iodine and stannic iodide in carbon tetrachloride. Therefore, the

Can. J. Chem. Downloaded from www.nrcresearchpress.com by 210.87.254.40 on 09/05/12
For personal use only.

absorption maxima at 365 mμ were attributed to free stannic iodide and the enhancement and shift of the 285 mμ peak to the formation of a benzene – stannic iodide complex.

Properties of the Benzene – Stannic Iodide Complex

When benzene was added in small concentrations to a solution of stannic iodide in carbon tetrachloride, a progressive shift of the lower wavelength absorption maximum from 285 to 297 mμ was observed. The apparent extinction coefficient was found to increase as the benzene concentration was increased. Table II lists data for mixed solutions of benzene and iodine in carbon tetrachloride. The increase in extinction coefficient with benzene concentration indicates that there is interaction between the stannic iodide and the benzene.

TABLE II

Variation of apparent extinction coefficient and absorbance with mole fraction of benzene in carbon tetrachloride

Benzene mole fraction, C_D	Apparent molar ext. coeff., $\lambda = 297$	Absorbance, $A = \log I_0/I$	$A - A^0$	$\frac{C_{SI} \times 10^4}{A - A^0}$	$1/C_D$
0	3 800	0.332	—	—	—
0.171	5 000	0.420	0.088	9.90	5.85
0.213	5 100	0.441	0.109	7.98	4.79
0.290	5 800	0.487	0.155	5.62	3.45
0.405	6 300	0.538	0.206	4.19	2.46
0.540	6 900	0.600	0.248	3.51	1.85
0.621	7 100	0.615	0.283	3.07	1.61
0.698	7 200	0.636	0.304	2.86	1.43
0.813	8 000	0.700	0.368	2.37	1.23
1.00	8 500	0.771	0.439	1.98	1.00

If we assume the formation of a complex according to eq. [1], we may calculate the equilibrium constant for the formation of the complex by eq. [2].

[1] $$D + SI \rightleftarrows DSI$$

[2] $$K_C = \frac{[C_C]}{[C_D - C_C][C_{SI} - C_C]}.$$

In these equations C_C is the concentration of the complex DSI at equilibrium; C_D is the initial concentration of the donor (benzene); and C_{SI} is the initial concentration of stannic iodide. Rose and Drago (5) have shown that, in the general case, K_C is related to experimental parameters as shown in eq. [3].

[3] $$K^{-1} = \frac{A - A^0}{\epsilon_C - \epsilon_{SI}} - C_{SI} - C_D + \frac{C_D C_{SI}(\epsilon_C - \epsilon_{SI})}{A - A^0},$$

where ϵ_C and ϵ_{SI} are the molar extinction coefficients for the complex and the stannic iodide, respectively, while the absorbances A^0 and A are given by:

[4] $$A^0 = \epsilon_{SI} C_{SI}$$

and

[5] $$A = \epsilon_C C_C + \epsilon_{SI}(C_{SI} - C_C).$$

Can. J. Chem. Downloaded from www.nrcresearchpress.com by 210.87.254.40 on 09/05/12
For personal use only.

When experimental conditions are such that the first two terms on the right side of eq. [3] are negligible compared to the last two terms, eq. [3] can be simplified.

$$[6] \qquad \frac{C_{SI}}{(A - A^0)} = \frac{1}{K_X(\epsilon_C - \epsilon_{SI})} \cdot \frac{1}{C_D} + \frac{1}{(\epsilon_C - \epsilon_{SI})}.$$

Equation [6] is a form of the equation derived by Ketelaar (6) for cases in which the absorption bands of the solute and complex overlap as they do in the case of stannic iodide in benzene. If C_D is expressed as a mole fraction, then the dimensionless constant, K_X, rather than K_C is used.

Experimental conditions in the present work were chosen so that eq. [6] could be used. This equation is of the form $Y = ABX + B$ where $Y = C_{SI}(A - A^0)^{-1}$, $X = (C_D)^{-1}$, $A = K_X^{-1}$, and $B = (\epsilon_C - \epsilon_{SI})^{-1}$. Therefore a plot of $C_{SI}(A - A^0)^{-1}$ against $(C_D)^{-1}$ should give a straight line with an intercept of $(\epsilon_C - \epsilon_{SI})^{-1}$ and slope of $K_X^{-1}(\epsilon_C - \epsilon_{SI})^{-1}$. Assuming that A^0 and ϵ_{SI} are equal to the absorbance and the molar extinction coefficient of stannic iodide in carbon tetrachloride, it is possible to determine K_X, the complex formation constant, and ϵ_C, the extinction coefficient of the complex. The absorbance A is calculated from the spectrum of stannic iodide in benzene.

The data shown in the last two columns of Table II give a straight line plot. A least-squares analysis of the data yields the equation

$$[7] \qquad \frac{C_{SI}}{(A - A^0)} = \frac{1.592 \times 10^{-4}}{C_D} + 0.42 \times 10^{-4}.$$

From the slope and intercept we calculate values of the dimensionless equilibrium constant based on mole fractions, $K_X = 0.264$, and the molar extinction coefficient for the complex, $\epsilon_C = 28\,400$ l/mole cm. The fit of this equation to the data may be judged to be very good on the basis of correlation coefficient of 0.955. The student "t" test on the Z score for a correlation coefficient of 0.955 (9 data points) shows significance at the 95% confidence level ($0.955\sqrt{n-1} = 2.70 > 2.306$). These results support the assumption of a 1:1 complex between stannic iodide and benzene.

DISCUSSION

In an extensive discussion of methods for the spectroscopic determination of equilibrium constants of benzene complexes, Rose and Drago (5) point out that the value of K_X in pure benzene is much more dependent on the accuracy of ϵ_C than those in dilute solution. We can assume that uncomplexed stannic iodide has the same molar extinction coefficient in benzene as in carbon tetrachloride at 297 mμ, and that the higher total absorbance of stannic iodide in benzene is due to the contribution by the complex. If $K_X = 0.26$ and $C_D = 1$ for pure benzene, then C_C and $(C_{SI} - C_C)$ may be calculated. Using $\epsilon_C = 2.84 \times 10^4$ l/mole cm, $\epsilon_{SI} = 3\,800$ l/mole cm, in eq. [5], we calculate an absorbance of 0.78, in agreement with the measured value of 0.77. This agreement indicates that the calculated K_X and ϵ_C values are correct in pure benzene as well as in carbon tetrachloride – benzene mixtures.

The values for K_X and ϵ_C for benzene – stannic iodide may be compared with those for other complexes. Benesi and Hildebrand (1) found $K_X = 1.73$ and $\epsilon_C = 15\,400$ l/mole cm for the benzene–iodine complex. Andrews and Keefer (7) found $K_X = 5.8$ and $\epsilon_C = 8\,100$ l/mole cm for iodine monochloride – benzene. Thus K_X is lower and the ϵ_C is higher for the stannic iodide complex than for related benzene complexes. If we assume that the bonding in the complex depends on two iodine atoms of the stannic iodide

Can. J. Chem. Downloaded from www.nrcresearchpress.com by 210.87.254.40 on 09/05/12
For personal use only.

molecule acting in absorption like a diatomic iodine molecule, the low K_X and high ϵ_C are to be expected. The most probable structure for the benzene – stannic iodide complex is discussed below.

Structure of the Complex

Both iodine–benzene (1) and stannic iodide – benzene have absorption maxima at 297 mμ. Iodine–toluene solutions show an absorption maximum at 306 mμ (1) and the spectrum of stannic iodide – toluene solutions show a levelling off in the same region (Fig. 1). The stannic iodide molecule should exhibit some of the characteristics of the iodine molecule. It seems reasonable, therefore, that interpretation of the spectrum of stannic iodide in benzene should be similar to interpretation of the spectrum of iodine in benzene.

On the basis of quantum mechanical considerations, Mulliken (8) chose for the iodine–benzene complex a model in which the iodine molecule rests on the benzene molecule with its axis parallel to the plane of the benzene and its center on the sixfold axis of the benzene. A similar model for the stannic iodide – benzene complex would place two of the peripheral iodine atoms on the benzene ring with the line joining the centers of iodine atoms parallel to the plane of the benzene. Pringsheim (9) has noted that the iodine atoms in stannic iodide are tetrahedrally arranged around the tin atom. At high temperatures the amplitude of oscillation becomes sufficiently great that the two iodine atoms can approach each other so closely that they can be separated in a single act from the parent molecule as an excited iodine molecule (9). Measurements on the fluorescence of stannic iodide vapor have indicated that in the 215 to 245 mμ region the molecule decomposes photochemically to stannous iodide and iodine (10). Terenin and Tshubarov concluded that photodissociation is simultaneous with union of iodine atom sbefore they leave the molecule with the liberated iodine molecule in an excited state as evidenced by fluorescence (10). The similarity of the spectra of benzene solutions of iodine and stannic iodide may, therefore, be due to a strengthening of the residual bond between iodine atoms in stannic iodide by the formation of the complex with benzene. The observation that the rate of photochemical oxidation of stannic iodide increases in the order of increasing solvent basicity for benzene, toluene, and xylene also supports the contention that complex formation strengthens the iodine–iodine bond and weakens the iodine–tin bond. Also, if the complex bond depends on the iodine–iodine bond, then K should be lower for stannic iodide than for iodine. The evidence appears to support a model of the complex in which two of the peripheral iodine atoms in stannic iodide are involved in the bond with the aromatic hydrocarbon. Mulliken's resting model for the iodine – aromatic hydrocarbon complex is also indirectly supported.

Solutions in Toluene and Xylene

The low wavelength absorption maxima for stannic iodide in toluene and xylene were not well enough defined in our measurements to allow an evaluation of the stability and extinction coefficient of the complex. However, the order of the rates of the photochemical reaction between stannic iodide and these solvents indicates that the stability of the stannic iodide in the complexes decreases in the order: benzene, toluene, xylene (least stable). In the aromatic solvents, the formation of the complex probably increases the rate of oxidation by air to form free iodine and stannic oxide. An increased strength of bond between the iodine portion of the stannic iodide and the aromatic solvent should lead to a lowering of the activation energy for the reaction of the stannic ion with oxygen. An increase in solubility due to increased strength of complexing in the order benzene,

Can. J. Chem. Downloaded from www.nrcresearchpress.com by 210.87.254.40 on 09/05/12
For personal use only.

toluene, xylene, would also seem to provide an adequate explanation for the discrepancies between observed and theoretically predicted solubilities (3).

REFERENCES

1. H. A. BENESI and J. H. HILDEBRAND. J. Am. Chem. Soc. **71**, 2703 (1949).
2. L. S. ANDREWS. Chem. Rev. **54**, 714 (1954).
3. J. H. HILDEBRAND and R. L. SCOTT. The solubility of nonelectrolytes. Reinhold Publishing Co., New York. 1950. p. 277.
4. M. E. DORFMAN and J. H. HILDEBRAND. J. Am. Chem. Soc. **49**, 729 (1927).
5. N. J. ROSE and R. S. DRAGO. J. Am. Chem. Soc. **81**, 6138 (1959).
6. J. A. A. KETELAAR *et al.* Rec. Trav. Chim. **71**, 1104 (1952).
7. L. J. ANDREWS and R. M. KEEFER. J. Am. Chem. Soc. **74**, 4500 (1952).
8. R. S. MULLIKEN. J. Am. Chem. Soc. **72**, 811 (1952).
9. P. PRINGSHEIM. Fluorescence and phosphorescence. Interscience Publishers, Inc., New York. 1949. p. 278.
10. A. TERENIN and R. TSHUBAROV. Acta Physicochim. U.R.S.S. **7**, 1 (1937).

Can. J. Chem. Downloaded from www.nrcresearchpress.com by 210.87.254.40 on 09/05/12
For personal use only.

Can. J. Chem. Downloaded from www.nrcresearchpress.com by 210.87.254.40 on 09/05/12
For personal use only.

LABELLING OF NUCLEOSIDES WITH TRITIUM

G. A. LePage and Irene G. Junga
Life Sciences Research, Stanford Research Institute, Menlo Park, California
Received November 13, 1964

Dedicated to Professor R. B. Sandin on the Occasion of his Sixty-Eighth Birthday

ABSTRACT

The synthesis of 9-(α,β-D-2′-deoxyribofuranosyl)-2-amino-6-mercaptopurine with tritium labelling in both base and sugar was attempted. At the step where a mercury salt of the base and the blocked chlorosugar were coupled in benzene, the tritium labelling was lost, apparently by an exchange with the protons of the solvent. This appeared to be catalyzed by the mercuric chloride. It was demonstrated that unlabelled nucleoside could be tritium labelled by refluxing it in benzene-T or toluene-T with mercuric chloride. By this exchange process, both base and sugar were tritiated, but a larger amount of tritium appeared in the base. Because of the availability of benzene-T and toluene-T of high specific radioactivity, this appears to be a practical means of synthesis of the labelled nucleoside. This exchange reaction may be useful for the study of carbon–hydrogen bond stabilities.

Biological investigations with the fraudulent nucleoside, 9-(β-D-2′-deoxyribofuranosyl)-2-amino-6-mercaptopurine, have shown that it has carcinostatic activity, and that its activity was also evident in several lines of experimental cancers that were resistant to 2-amino-6-mercaptopurine (1). Moreover, the unexpected result that the α-anomer of the fraudulent nucleoside had carcinostatic activity, with very low host toxicity, was obtained. When 9-(α-D-2′-deoxyribofuranosyl)-2-amino-6-mercaptopurine was labelled in the purine base with radiocarbon and administered to tumor-bearing mice, the radiocarbon appeared in the deoxyribonucleic acids of tumor cells which could not so incorporate labelled 2-amino-6-mercaptopurine. It thus became important to synthesize the α-anomer of this nucleoside with tracer labelling in both the purine base and the sugar to establish whether this α-anomer was incorporated into nucleic acids without cleavage.

The cost of the necessary radiocarbon-labelled starting materials would be prohibitive. Labelling with tritium by the Wilzbach method (2), or by commercially available catalytic methods, would be expected to involve extensive decomposition of this labile nucleoside. We therefore planned the synthesis with tritium-labelled guanine (guanine-8-T) and tritium-labelled glucose (glucose-6-T) as starting materials. These two materials were purchased from the Nuclear-Chicago Corporation. A 100-millicurie batch of D-glucose-6-T was diluted, with D-glucose monohydrate, to 1.0 millicurie/millimole. The resulting 19.8-g quantity was converted, by the procedure of Diehl and Fletcher (3), to 2-deoxyribose-5-T in approximately 5% yield. The 2-deoxyribose anilide melted at 180 °C. A 25-mcurie batch of guanine-8-T was converted to 2-amino-6-mercaptopurine-8-T, as described by LePage (4), in 65% yield and diluted to approximately 1.0 mcurie/mmole with unlabelled material. The 2.66 g of purinethiol was converted to 2-amino-6-chloropurine-8-T by the method of Davis *et al.* (5) in 50% yield, and to the 2-acetamido-6-chloro-9-Hg-purine salt by the method of Iwamoto *et al.* (6) in 31% yield. The 2-deoxyribose-5-T was converted to 1-chloro-3′,5′-di-O-*p*-toluyl-2′-deoxyribose-5-T (6). At this stage approximately 2.2 mmoles of the mercury salt of the purine derivative and an equivalent amount of the chlorosugar were available. Measurements with a Nuclear-Chicago scintillation counting system established that each derivative contained approximately 1.0 mcurie/mmole of tritium. The two labelled derivatives were refluxed together in benzene for the coupling reaction, as described by Iwamoto *et al.* (6). The resulting

blocked nucleoside was isolated and separated into α- and β-anomers. Both were found to contain negligible amounts of radioactivity. The tritium on the labelled derivatives appeared to have exchanged with the hydrogens of the solvent, which was then distilled off. The other product of the reaction, mercuric chloride, was suspected of catalyzing this exchange.

It seemed imperative to determine whether the above conclusion was correct, and whether the tritium exchange could be reversed by the use of a tritium-labelled solvent. No tritiated benzene was immediately available, but a standard solution of toluene-T at 1.09 μcuries/ml (2.39×10^6 counts per minute per milliliter) was on hand. To a 50-mg batch of 2-acetamido-6-chloro-9-(2′-deoxy-3′,5′-di-O-*p*-toluyl-D-ribofuranosyl)-9-H-purine was added 50 mg mercuric chloride and 5.0 ml of the toluene-T. These were refluxed together for 30 minutes in a 20-ml flask and cooled, and the solvent removed *in vacuo*. Addition of unlabelled solvent and removal *in vacuo* were carried out to assure removal of any labile tritium. The residue was taken up in chloroform and the mercuric chloride removed by washing twice with a 30% solution of potassium iodide, then with water. The blocked nucleoside was crystallized from chloroform and found to have the same melting point as the starting material (184 °C). Scintillation counting in a toluene system was carried out, with standards to determine any quenching. The blocked nucleoside was found to contain 650 c/min mg. A 50-mg sample of 9-(β-D-2′-deoxyribofuranosyl)-2-amino-6-mercaptopurine was refluxed 30 minutes with 5.0 ml of toluene-T and 50 mg of mercuric chloride. The solvent was removed *in vacuo*. Unlabelled solvent was added and evaporated off as before, with water used once as solvent. Scintillation counting carried out in a polar solvent system (6% efficiency), identical with that described by Bray (7), demonstrated that the mercury salt of the nucleoside contained 11 000 c/min mg. The nucleoside would therefore contain approximately 18 700 c/min mg. Removal of the mercury as sulfide led to a very low yield of nucleoside (4%), presumably because of adsorption on the mercuric sulfide.

Benzene-T was obtained commercially and found to have 0.54 mcuries/ml (1.2×10^9 c/min ml). A reaction mixture containing 195 mg of 2-acetamido-6-chloro-9-(2′-deoxy-3′,5′-di-O-*p*-toluyl-D-ribofuranosyl)-9-H-purine, 195 mg of mercuric chloride, and 10 ml of benzene-T was refluxed for 30 minutes and cooled, and the solvent removed *in vacuo*. Unlabelled solvent was added and evaporated as before. Purification was carried out as described earlier. The melting point and optical rotation indicated that the properties of the product were unchanged from those of the starting material. Scintillation counting showed that the blocked nucleoside contained 1.4×10^5 c/min mg. Removal of the blocking groups and conversion to the 9-(β-D-2′-deoxyribofuranosyl)-2-amino-6-mercaptopurine were carried out as described by Iwamoto *et al.* (6). This product was found to contain 1.4×10^4 c/min mg.

An 8.8-mg batch of the above nucleoside was suspended in 2.6 ml of 1.0 *M* perchloric acid and heated for 10 minutes at 100 °C to cleave the sugar from the base. The solution was chilled and neutralized to pH 7 with potassium hydroxide, and the potassium perchlorate removed. The solution was passed onto a Dowex-1-formate column, 5×45 mm. This would retain the base and allow passage of the sugar. The resin was washed with several portions of water. Then the base was eluted with two portions of 1.0 *M* formic acid. The eluates were analyzed for the base (by extinction at 345 mμ), and scintillation counting was carried out. The first acid eluate contained about 75% of the base, the second one about 25%. The water eluates contained no material absorbing at 345 mμ. Counts present in the two acid eluates correlated with base content, as indicated by ultraviolet absorption. The sample used contained radioactivity measured as 1.23×10^5

Can. J. Chem. Downloaded from www.nrcresearchpress.com by 210.87.254.40 on 09/05/12
For personal use only.

c/min. That recovered in the base was found to be 1.04×10^5 c/min, and for the water eluate (sugar) 1.96×10^4 c/min. Thus the tritium was distributed 84% in the base and 16% in the sugar moiety. Initially, a large fraction of the radioactivity was in the blocking groups.

A limited study was made of the progress of the tritium exchange with time. The experiment with the blocked nucleoside and mercuric chloride in refluxing benzene-T was repeated, and at intervals samples were withdrawn through the condenser with a capillary pipette. This indicated that radioactivity in the blocked nucleoside increased only from 1 032 c/min mg after 20 minutes of refluxing to 1 440 c/min mg after 150 minutes.

Another purine nucleoside, arabinosyl adenine, was refluxed with toluene-T and mercuric chloride. The mercuric chloride was removed by extraction in methanol. The nucleoside was found to have a significant level of radioactivity.

DISCUSSION

The results of our tritium-exchange experiments support the conclusion that a catalytic exchange of tritium can occur between an aromatic solvent and the protons of a purine base or a sugar. Although more potential exchange sites were available on the sugar than on the base (7 vs. 1), the exchange was more active on the base. The higher temperature for the reaction in toluene appeared to produce a more active exchange than occurred in benzene. The difference evidenced in the stability of the protons of purine and sugar may indicate a utility of this reaction for studies of the stability of carbon–hydrogen bonds in various materials. The sensitivity of scintillation counting and the present availability of inexpensive tritiated solvents would encourage use of this as an investigative tool.

Determination of optimum conditions for this tritium exchange will require much more extensive studies, which we have initiated. The labelling of nucleosides seems to be proportional to the level of radioactivity in the solvent, and solvents such as benzene-T and toluene-T are available at relatively low price and high specific radioactivity (250 mcuries/mmole). The synthesis of the nucleosides we require, with tritium in both base and sugar, thus appears practical.

It will be important to determine the general applicability of this reaction and whether superior catalysts can be found. If it does have general applicability to tritium labelling of organic compounds, there would be a distinct advantage to the mild conditions used, since the Wilzbach (2) technique is destructive to labile materials.

ACKNOWLEDGMENTS

This work was supported by contract No. SA-43-ph-3068 with the Cancer Chemotherapy National Service Center, National Cancer Institute, National Institutes of Health.

We thank Dr. Leon Goodman and his colleagues, of Stanford Research Institute, for supplies of nucleoside derivatives, and for rotational analyses of the products obtained in this study.

REFERENCES

1. G. A. LEPAGE, I. G. JUNGA, and B. BOWMAN. Cancer Res. **24**, 835 (1964).
2. K. E. WILZBACH. J. Am. Chem. Soc. **79**, 1013 (1957).
3. H. W. DIEHL and H. G. FLETCHER, JR. Biochemical preparations. John Wiley and Sons, Inc., New York. 1961. p. 49.
4. G. A. LEPAGE. Cancer Res. **20**, 403 (1960).
5. G. D. DAVIS, JR., C. W. NOELL, R. R. ROBINS, H. C. KOPPEL, and A. G. BEAMAN. J. Am. Chem. Soc. **82**, 2633 (1960).
6. R. H. IWAMOTO, E. M. ACTON, and L. GOODMAN. J. Med. Pharm. Chem. **6**, 684 (1963).
7. G. A. BRAY. Anal. Biochem. **1**, 279 (1960).

Can. J. Chem. Downloaded from www.nrcresearchpress.com by 210.87.254.40 on 09/05/12
For personal use only.

Can. J. Chem. Downloaded from www.nrcresearchpress.com by 210.87.254.105 on 09/05/12
For personal use only.

ELECTRONIC EFFECTS IN E2 REACTIONS

II. *t*-BUTOXIDE-INDUCED ELIMINATIONS OF 2-METHYL-3-PENTYL ARENESULFONATES[1,2]

ALLAN K. COLTER AND DONALD R. MCKELVEY
Department of Chemistry, Carnegie Institute of Technology, Pittsburgh, Pennsylvania

Received November 13, 1964

Dedicated to Professor R. B. Sandin on the Occasion of his Sixty-Eighth Birthday

ABSTRACT

As part of a study of the influence of electronic effects imposed by the leaving group on orientation in E2 reactions, a study of elimination in a series of 2-methyl-3-pentyl arenesulfonates (I) has been carried out. The compositions of the olefin mixtures resulting from reaction of selected members of this series with potassium *t*-butoxide in *t*-butanol (I*a*, I*d*), 50% (by volume) *t*-butanol – dioxane (I*a*–I*g*), 25% (by volume) *t*-butanol – dioxane (I*d*–I*f*), and 25% (by volume) *t*-butanol – dimethyl sulfoxide (I*a*, I*d*, I*f*, I*g*), at 50 °C, have been determined using vapor phase chromatography. Second-order rate constants were measured for these reactions in *t*-butanol (I*e*), and 50% *t*-butanol – dioxane (I*a*, I*c*–I*g*) at 50 °C and in 25% *t*-butanol – dimethyl sulfoxide (I*a*, I*d*, I*e*) at 25 °C.

The compositions of the olefin mixtures vary in a fairly regular way with changes in the electronic nature of the leaving group, the fraction of 2-methyl-2-pentene and ratio of *trans*- to *cis*-4-methyl-2-pentene for the most part increasing with increasing electron withdrawal. The E2 reactions in 25% *t*-butanol – dimethyl sulfoxide produce *trans*- and *cis*-4-methyl-2-pentene in ratios (20 to 35) considerably higher than those in an equilibrium mixture (ca. 6).

The results are discussed in terms of recent views on the E2 transition state.

INTRODUCTION

In recent years, the concept of a continuous spectrum of transition states for the E2 reaction (Fig. 1), differing in the extent to which the C_β—H and C_α—X bonds are broken, has become widely accepted (1–13). Factors expected to influence the position of an

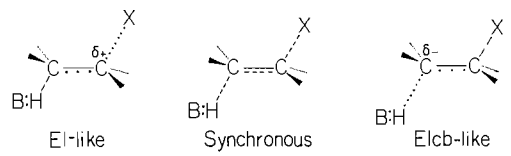

FIG. 1. Spectrum of E2 transition states.

elimination among the spectrum of transition states and methods of assessing the quality of the transition state have recently been discussed by Bunnett (12). In E2 reactions in alkyl systems having two or more constitutionally nonequivalent β-hydrogens, it is generally agreed that transition states in the E1*cb*-like region favor abstraction of the most acidic hydrogen, thereby leading to predominant amounts of the product having the smallest number of alkyl groups attached to the olefinic function (Hofmann pattern). Transition states in the synchronous to E1-like regions favor formation of the most highly alkylated olefin (Saytzeff pattern).

In this and previous work (13) we have been concerned with evaluating the importance of electronic effects imposed by the leaving group in determining orientation in E2

[1]*Part I in this series: A. K. Colter and R. D. Johnson, J. Am. Chem. Soc. 84, 3289 (1962).*
[2]*Abstracted from a thesis submitted by Donald R. McKelvey in partial fulfillment of the requirements for the degree of Doctor of Philosophy at the Carnegie Institute of Technology, June, 1964.*

Can. J. Chem. Downloaded from www.nrcresearchpress.com by 210.87.254.105 on 09/05/12
For personal use only.

reactions. Our approach has been to examine the olefin mixtures produced from E2 reactions of a series of alkyl arenesulfonates differing only in a substituent in the meta or para position of the benzene ring in the leaving group. In this way, steric influences (14) are constant throughout the series.

Applied to a series of alkyl arenesulfonates, the model of the E2 transition state discussed by Bunnett does not lead to a clear-cut prediction about how direction of elimination should change with leaving group. Whereas a change to a leaving group of greater electron-attracting character, by increasing the acidity of the β-hydrogens, is predicted to result in a shift toward the E1*cb*-like extreme, such a change in a series of arenesulfonates, by increasing the ease of heterolysis of the C—O bond, could also produce a shift toward the E1-like extreme (12). Thus, a study of this kind allows some evaluation of the relative importance of these two effects in determining orientation.

In the first paper in this series we reported the results of a study of the reactions of a series of 2-pentyl arenesulfonates with ethanolic sodium ethoxide. There appeared to be a very small but regular increase in the percentage of 2-pentene and in the ratio of *trans*- to *cis*-2-pentene with increasing electron withdrawal in the leaving group. However, this conclusion was clouded somewhat by the fact that, under the conditions studied, observed olefin compositions had to be corrected for competing first-order elimination. The corrections were based on two assumptions (13), neither of which could be rigorously justified.

In the present work, our aim was to minimize competition by first-order elimination by appropriate choice of base–solvent system. The compounds studied were the series of 2-methyl-3-pentyl arenesulfonates (I). This system offers an advantage over the 2-pentyl system in that E1 elimination in the solvents studied produces 15–20% of the

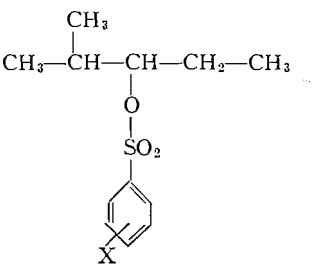

I*a*, X = *p*-$N(CH_3)_2$
I*b*, X = *p*-NH_2
I*c*, X = *p*-OCH_3
I*d*, X = *p*-CH_3
I*e*, X = *p*-Br
I*f*, X = 3,4-di-Cl
I*g*, X = *p*-NO_2

rearranged olefin 2-methyl-1-pentene. The presence or absence of this olefin therefore provides a test for competing first-order elimination and a non-kinetic method for correcting for competing first-order elimination, if necessary.

RESULTS

Synthesis of Starting Materials

The desired arenesulfonates were synthesized by conventional methods. All except the *p*-aminobenzenesulfonate I*b* were prepared by treatment of 2-methyl-3-pentanol with the appropriate arenesulfonyl chloride in dry pyridine. The *p*-aminobenzenesulfonate was prepared by reaction of *p*-aminobenzenesulfonyl fluoride with sodium 2-methyl-3-pentoxide.

Product Studies

Product studies were carried out in the four solvents: *t*-butanol, 50% (by volume)

t-butanol – dioxane, 25% (by volume) *t*-butanol – dioxane, and 25% (by volume) *t*-butanol – dimethyl sulfoxide. All product studies, except when stated otherwise, were carried out at 50 °C. Potassium *t*-butoxide was the base employed in all the E2 reactions. The olefinic products were separated from the reaction mixtures by distillation and were analyzed by vapor phase chromatography.

Table I summarizes the results of the E1 product studies. The formation of the rearranged olefin 2-methyl-1-pentene indicates that at least part of the reaction involves a carbonium ion or ion pair intermediate. Direct analysis of the reaction mixture from solvolysis of I*d* in *t*-butanol showed, by the absence of any detectable *t*-butyl 2-methyl-3-pentyl ether, that at least 95% of the first-order reaction leads to olefinic products.

TABLE I

Products of E1 reactions of 2-methyl-3-pentyl arenesulfonates

Ester	Solvent	% 2-methyl-2-pentene	% *cis*-4-methyl-2-pentene	% *trans*-4-methyl-2-pentene	% 2-methyl-1-pentene
p-CH_3*	*t*-Butanol	77.2	0	7.0	15.8
p-$N(CH_3)_2$*†	50% *t*-butanol – dioxane	65.5	1.9	15.5	17.0
p-Br‡	50% *t*-butanol – dioxane	71.4±0.4	0.9±0.1	8.3±0.1	19.4±0.3

*Single run; estimated uncertainties ±0.4%.
†Temperature = 100.0°.
‡Average of three runs listed with average deviations.

The results of the E2 product studies are shown in Table II. Corrections for competing first-order elimination were made whenever 2-methyl-1-pentene was present in the olefinic products. In such cases, two sets of values are listed; the values in parentheses are uncorrected percentages based on the E2 products alone.

TABLE II

Products of E2 reactions of 2-methyl-3-pentyl arenesulfonates at 50 °C*†

Ester	[Ester], *M*	[Base], *M*	% 2-methyl-2-pentene	% *cis*-4-methyl-2-pentene	% *trans*-4-methyl-2-pentene	No. runs
t-Butanol						
p-$N(CH_3)_2$	0.08	0.48	53.3±0.2	10.8±0.1	35.9±0.2	3
p-CH_3	0.11	0.48	51.1(52.6)±0.3	16.3(15.6)±0.1	32.6(31.8)±0.2	2
50% *t*-butanol – dioxane						
p-$N(CH_3)_2$	0.10	0.47	51.9±0.3	13.4±0.1	34.7±0.2	3
p-NH_2	0.10	0.43	54.0±0.0	14.9±0.1	31.1±0.2	2
p-OCH_3	0.10	0.46	48.9±0.2	20.6±0.2	30.4±0.1	3
p-CH_3	0.10	0.46, 0.48	50.4±0.2	19.3±0.2	30.2±0.1	5
p-Br	0.10	0.45	51.1(51.8)±0.0	17.8(17.5)±0.0	31.1(30.7)±0.1	3
3,4-di-Cl	0.10	0.48	51.1(52.5)±0.2	16.1(15.9)±0.2	31.8(31.6)±0.3	3
p-NO_2	0.12, 0.09 0.10, 0.07	0.50, 0.67, 0.41	59.3(61.1)±0.6	9.7(9.1)±0.2	31.1(29.8)±0.6	6
25% *t*-butanol – dioxane						
p-CH_3	0.10	0.19	50.8±0.2	19.0±0.1	30.2±0.1	3
p-Br	0.10	0.19	52.5±0.1	17.0±0.0	30.5±0.1	3
3,4-di-Cl	0.10	0.23	52.3±0.4	15.8±0.2	31.9±0.2	3
25% *t*-butanol – dimethyl sulfoxide						
p-$N(CH_3)_2$	0.08, 0.10	0.18, 0.25	47.9±0.2	2.4±0.2	49.7±0.2	2
p-CH_3	0.10	0.30	50.2±0.4	1.9±0.1	47.9±0.3	3
3,4-di-Cl	0.07, 0.09	0.28, 0.18	53.5±0.2	1.3±0.3	45.2±0.1	2
p-NO_2‡	0.10	0.20	61(67)±3	3(3)±1	36(31)±3	1

*Values listed with average deviations.
†Values in parentheses uncorrected for competing first-order elimination.
‡Analysis made difficult by exceptionally low olefin yield (see also ref. 15).

Can. J. Chem. Downloaded from www.nrcresearchpress.com by 210.87.254.105 on 09/05/12
For personal use only.

In correcting E2 product mixtures for E1 reaction, the fraction of the total olefin product arising from first-order elimination was taken as a fraction of 2-methyl-1-pentene in the mixture divided by the fraction of 2-methyl-1-pentene in the E1 product. The olefin composition from the E1 reaction of I*e* in 50% *t*-butanol – dioxane was used in making all corrections, with the single exception of the E2 reaction of I*d* in *t*-butanol, in which case the E1 product of the same compound in *t*-butanol was used. The use of a single E1 product composition cannot lead to any significant error, since the E1 product mixtures are expected to be quite insensitive to leaving group and the corrections are very small.

The method of correcting for first-order elimination is based on the assumption that the carbonium ion intermediate leads to the same product mixture in the presence of base as in the absence of base. While this assumption is unlikely to be completely valid, the corrections are probably approximately correct for the following reason. In the basic media a carbonium ion is expected to yield an olefin mixture which is intermediate in composition between the E1 and E2 mixtures. Thus, while the fraction of 2-methyl-1-pentene in the basic reaction product would then underestimate the amount of competing E1 reaction, the E1 product composition used in the correction tends to make the correction too large. Most important, the corrections in all cases are much too small to change the general trends in product composition. The correction procedure is described in detail, with an example, in the Experimental section.

With the exception of the two *p*-amino esters, I*a* and I*b*, in *t*-butanol and 50% *t*-butanol – dioxane, the percentage of 2-methyl-2-pentene and the ratio of *trans*- to *cis*-4-methyl-2-pentene increase in a regular way with increasing electron withdrawal in the leaving group. The changes are substantial, the percentage of Saytzeff elimination increasing from 48.9% (*p*-OCH_3) to 59.3% (*p*-NO_2) in 50% *t*-butanol – dioxane and from 47.9% (*p*-$N(CH_3)_2$) to 61% (*p*-NO_2) in 25% *t*-butanol – dimethyl sulfoxide. The *trans* to *cis* ratio in the Hofmann olefins increases from 1.48 (*p*-OCH_3) to 3.20 (*p*-NO_2) in 50% *t*-butanol – dioxane and from 20.7 (*p*-$N(CH_3)_2$) to 34.8 (3,4-di-Cl) in 25% *t*-butanol – dimethyl sulfoxide. Aside from elimination of competing E1 reaction, replacement of *t*-butanol by dioxane mixtures has almost no effect on the E2 products. However, whereas the E2 reactions in 25% *t*-butanol – dimethyl sulfoxide yield a similar fraction of 2-methyl-2-pentene as the reactions in *t*-butanol and the *t*-butanol – dioxane mixtures, the ratio of *trans*- to *cis*-4-methyl-2-pentene is dramatically increased.

Rate Studies

Substituent and solvent effects on rates of elimination could provide information about the extent of C—O bond fission and charge separation in the transition states. Consequently, second-order rate constants for reaction of selected esters with potassium *t*-butoxide were measured in *t*-butanol and 50% *t*-butanol – dioxane at 50° and in 25% *t*-butanol – dimethyl sulfoxide at 25°. The results are listed in Table III. Although certain of these reactions are known from the product studies to be accompanied by first-order reaction, no observable regular trend in calculated second-order rate constants was observed in any instance. Order of magnitude corrections for competing first-order elimination can be made where complementary product studies have been carried out. It seems safe to assume that no appreciable substitution occurs in either the first- or second-order reaction, since it was demonstrated that at least 95% of the reaction of I*d* in *t*-butanol at 50° leads to olefin (see above). Therefore, the fraction of the total reaction occurring via a first-order process under the conditions of the product runs can be

Can. J. Chem. Downloaded from www.nrcresearchpress.com by 210.87.254.105 on 09/05/12
For personal use only.

TABLE III

Second-order rate constants for reaction of 2-methyl-3-pentyl arenesulfonates with potassium *t*-butoxide

Ester	k_2, l mole^{-1} s^{-1} *
t-Butanol, 50.06±0.02 °C	
p-Br	$9.13\pm0.29 \times 10^{-5}$ †
50% *t*-butanol – dioxane, 50.06±0.02 °C	
p-N(CH$_3$)$_2$	$5.36\pm0.10 \times 10^{-6}$
p-OCH$_3$	$1.86\pm0.08 \times 10^{-5}$
p-CH$_3$	$2.81\pm0.20 \times 10^{-5}$
p-Br‡	$6.76\pm0.19 \times 10^{-5}$
3,4-di-Cl§	$2.18\pm0.07 \times 10^{-4}$
p-NO$_2$‖	$1.07\pm0.10 \times 10^{-3}$
25% *t*-butanol – dimethyl sulfoxide, 25.00±0.02 °C	
p-N(CH$_3$)$_2$	$1.01\pm0.06 \times 10^{-3}$
p-CH$_3$	$1.24\pm0.05 \times 10^{-2}$
p-Br	$1.00\pm0.04 \times 10^{-1}$

*Rate constants listed with average deviations.
†First-order correction would reduce this value by ca. 0.27 × 10^{-5} l mole^{-1} s^{-1}.
‡First-order correction ca. 0.36 × 10^{-5} l mole^{-1} s^{-1}.
§First-order correction ca. 0.06 × 10^{-4} l mole^{-1} s^{-1}.
‖First-order correction ca. 0.15 × 10^{-3} l mole^{-1} s^{-1}.

estimated as already described. This value can then be used to estimate the relative magnitudes of the first- and second-order rate constant (k_1/k_2) under the conditions of the product run (13) and, if one assumes that the same ratio prevails under the conditions of the rate measurements, an approximate correction can then be applied to the observed second-order rate constant.[3] Corrections for the rate constants in 50% *t*-butanol – dioxane estimated in this way are listed as footnotes to Table III. The correction for the single E2 rate in *t*-butanol was estimated as described in ref. 13 by using an approximate first-order rate constant in *t*-butanol (see below).

The rate measurements were carried out at moderately high (0.15–0.38 *M*) base concentrations to approximate the conditions of the product runs. The extent of aggregation of the base will, of course, be concentration dependent. Second-order behavior was assumed; however, an appreciable fraction of the reaction could depend on a higher-than-first power of the base concentration without producing noticeable trends in calculated second-order rate constants. An increase in base concentration from 0.145 *M* to 0.352 *M* produced an increase of about 20% in the second-order rate constant for the *p*-N(CH$_3$)$_2$ ester (the one listed corresponds to 0.145 *M* base). This increase could be a result of elimination induced by higher aggregates of base, complex formation between the potassium ion and the amino group (see Discussion), or less specific salt effects. Further studies of the effect of base concentration on rates and products of elimination in these systems are in progress; at present, a measure of the effect of base concentration on the rates of elimination of the other arenesulfonates is not available. It is clear, however, that such effects are not large enough to affect the general nature of the results reported, and are unlikely to change appreciably the slopes of the Hammett plots (see below).

[3]*Such corrections are only very approximate for two reasons. First, the method assumes that the ratio (k_1/k_2) is unaffected by the base concentration. Secondly, we must assume that the fraction of 2-methyl-1-pentene gives an accurate measure of the fraction of the reaction proceeding by first-order reaction.*

Can. J. Chem. Downloaded from www.nrcresearchpress.com by 210.87.254.105 on 09/05/12
For personal use only.

Hammett plots[4] for the E2 rates in 50% *t*-butanol – dioxane at 50 °C and 25% *t*-butanol – dimethyl sulfoxide at 25 °C are shown in Figs. 2 and 3. The range of log *k* shown graphically for each point includes the uncertainty introduced by the competing first-order reaction. A least squares fit of the plot shown in Fig. 1 gives $\rho = 1.51$, a value not too different from that (1.35) obtained for the E2 reactions of 2-pentyl arenesulfonates in ethanolic sodium ethoxide at 50 °C (13). In contrast, the E2 rates in 25% *t*-butanol – dimethyl sulfoxide show an unusual sensitivity to substitution in the leaving group, ρ here being 2.40. The reactivity of the *p*-bromobenzenesulfonate relative to the *p*-toluenesulfonate in this system (8.1) is, to our knowledge, the largest ever reported in any substitution or elimination reaction of arenesulfonates (16, 17).

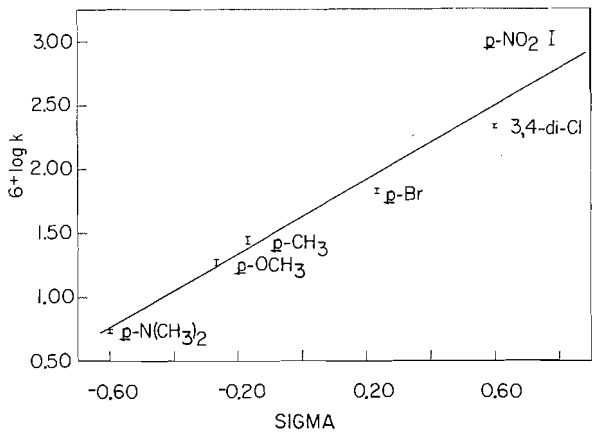

FIG. 2. Hammett plot for E2 rates in 50% *t*-butanol – dioxane.

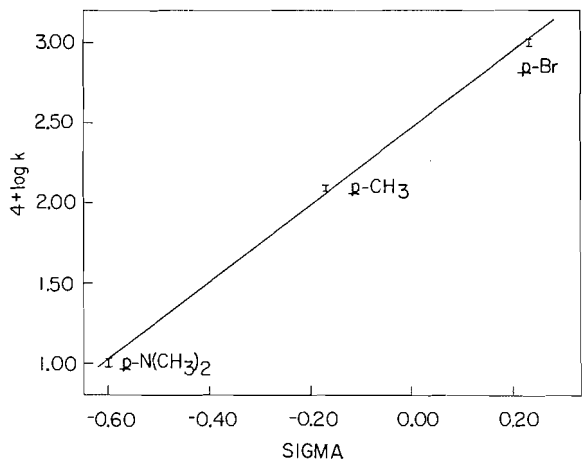

FIG. 3. Hammett plot for E2 rates in 25% *t*-butanol – dimethyl sulfoxide.

For purposes of comparison, it would be instructive to have a measure of solvent and substituent effects for the E1 reactions of compounds I in the solvents studied. For this reason, several first-order rates were run in *t*-butanol and 50% *t*-butanol – dioxane (18). However, accurate determination of first-order rate constants was made very difficult

[4]*Hammett sigma values are taken from H. H. Jaffé, Chem. Rev. 53, 191 (1953).*

Can. J. Chem. Downloaded from www.nrcresearchpress.com by 210.87.254.105 on 09/05/12
For personal use only.

by the enormous salt effects in these nonpolar solvents (19), especially in 50% *t*-butanol – dioxane, so that first-order rate constants increase sharply with extent of reaction. From the measurements made, it can be estimated that first-order rates in *t*-butanol are faster than those in 50% *t*-butanol – dioxane by a factor of about 10. This is to be compared with a factor of 1.35 for the E2 reaction of the *p*-bromobenzenesulfonate.

Control Experiments

The stability of the olefin mixtures under the conditions of the product studies was demonstrated for all reaction media. The absence of any significant fractionation of olefins accompanying their distillation from the reaction medium was demonstrated by showing that identical olefin compositions were obtained by direct analysis of a product mixture without separation of olefins and by a method involving separation of olefins by toluene extraction. The E2 product from reaction of I*d* with potassium *t*-butoxide in 50% *t*-butanol – dioxane was unaffected by 0.52 *M* aniline. (See Discussion for the significance of this control.) The possibility that an appreciable portion of the E2 products in 25% *t*-butanol – dimethyl sulfoxide arises through a prior displacement of the leaving group by dimethyl sulfoxide can be ruled out on the basis of our E2 rates and rates of dimethyl sulfoxide displacements reported by Smith and Winstein (20).

DISCUSSION

With the exception of the *p*-amino esters I*a* and I*b* in *t*-butanol and 50% *t*-butanol – dioxane, the E2 product compositions show two important trends. First, as substitution in the leaving group is made increasingly electron withdrawing, the fraction of 2-methyl-2-pentene increases. Second, paralleling this increase in the proportion of Saytzeff elimination is an increase in the ratio of *trans*- to *cis*-4-methyl-2-pentene. Both trends are consistent with the suggestion (13) that increasing the ease of heterolysis of the C—O bond should result in a shift in the character of the transition state toward the E1-like extreme (Fig. 1). Consequently, it appears that, in the systems studied in this work, electronic influences on the ease of heterolysis of the C—O bond have a greater effect on the character of the transition state than changes in the acidities of the β-hydrogens. It must be emphasized, however, that this picture is oversimplified, since we have neglected a dimension in the spectrum of transition states. Thus, one can visualize a spectrum of synchronous transition states, for example, with little C_β—H and C_α—X bond stretching at one extreme to nearly complete bond fission at the other.

It is, of course, also possible to explain the trends in product composition in terms of changing proportions of elimination arising from two competing processes. Two such processes could be, for example, one involving a fairly synchronous E2 transition state and one involving reaction of base with an ion pair which, to account for the second-order rate law, returns to covalent ester more often that it reacts with base. The latter mechanism does not seem unreasonable for E2 reactions of secondary arenesulfonates in ethanol, *t*-butanol, or *t*-butanol – dioxane mixtures. Since competing E1 reaction occurs in most of these solvents, it seems logical to assume that the E2 transition states lean toward the E1-like extreme (11, 21).

Two features of the results deserve particular comment. The first is the dramatic difference in the character of the E2 product in 25% *t*-butanol – dimethyl sulfoxide from that in the other solvents. Although the proportion of Saytzeff elimination is similar in all solvents, elimination in the dimethyl sulfoxide containing solvent leads to remarkably high (21:1 to 35:1) ratios of *trans*- to *cis*-4-methyl-2-pentene. Equilibration of a

Can. J. Chem. Downloaded from www.nrcresearchpress.com by 210.87.254.105 on 09/05/12
For personal use only.

mixture containing the two olefins with potassium *t*-butoxide in dimethyl sulfoxide at 55 °C leads to a *trans* to *cis* ratio of about 6:1 (22). Thus, if one assumes a similar ratio in 25% *t*-butanol – dimethyl sulfoxide at 50 °C, the difference in the standard free energies of the activated complexes leading to *cis*- and *trans*-4-methyl-2-pentene is greater than the difference in the standard free energies of the olefins themselves. It is apparent, then, that the simple view that the proportion of Saytzeff elimination and the *trans* to *cis* ratio are both simple functions of the amount of double bond character in the transition state is incorrect, or at least not the whole story.

Several possible reasons for the abnormally high *trans* to *cis* ratio come to mind. One possibility is that the assumption of *trans* elimination through a pure symmetrical staggered transition state is incorrect. This problem is being investigated further. Whatever the reason, this result is not a general characteristic of E2 reactions in dimethyl sulfoxide. Hofmann *et al.* (23) report that reaction of 2-chlorobutane with potassium *t*-butoxide yields *trans*- and *cis*-2-butene in a ratio of 3.46:1, which is close to the equilibrium value.

The reason for the "anomalous" behavior of the *p*-amino compounds in *t*-butanol – dioxane is not known, but some of the possible causes have been eliminated by control experiments. The amino groups, through more effective solvation of the potassium cation, could conceivably alter the nature of the base enough to throw the product composition out of line. This possibility was eliminated, however, by showing that the E2 product composition from I*d* in 50% *t*-butanol – dioxane in the presence of 0.52 *M* aniline is identical with that obtained in the absence of added aniline. It was also considered that a unimolecular *cis* elimination (24, 25) could be occurring in competition with the E2 reaction. To account for the anomalous E2 products, however, such a process would have to be comparable in rate to the E2 reaction. Since the absence of 2-methyl-1-pentene in the base-induced reaction product indicates that the normal E1 process does not compete with the E2 reaction, the cyclic process would have to be much faster than the normal E1 process. However, the E1 product for I*a* in 50% *t*-butanol – dioxane at 100° (Table I) is normal in every respect; hence, no other type of unimolecular reaction can be important under E2 conditions. A third possible reason for the irregular behavior of the *p*-amino esters is complex formation between the *p*-amino or *p*-dimethylamino group and the potassium cation. This explanation could account for the "normal" behavior of I*a* in 25% *t*-butanol – dimethyl sulfoxide, because complex formation should occur to a much smaller extent in this solvent, since dimethyl sulfoxide is an effective cation-solvating solvent (26). If a small fraction of the substrate, say 1%, were complexed in this way and the complexed leaving group were more reactive by a factor of 100, the observed rate constant would be approximately doubled, while about 50% of the product would arise through the complexed leaving group. The E2 rate constant for I*a* in 50% *t*-butanol – dioxane did indeed show a substantial increase with an increase in base concentration (see Results), but this may simply be a normal salt effect. A more complete study of the effect of base concentration on the E2 products is needed to answer this question. Such a study is in progress. Finally, it is possible that changes in the character of the E2 transition state brought about by substitution in a series of benzenesulfonates may be more complex than those predicted on the basis of our simple model.

EXPERIMENTAL

Preparation of Esters

2-Methyl-3-pentanol was prepared from 2-bromopropane and propionaldehyde by a procedure similar

Can. J. Chem. Downloaded from www.nrcresearchpress.com by 210.87.254.105 on 09/05/12
For personal use only.

to that of Krollpfeiffer and Seebaum (27). The crude material was fractionated and the portion boiling at 127.1 °C (at 734 mm pressure) collected. Analysis by gas chromatography showed this material to be greater than 99% pure.

Commercially available *p*-methyl-, *p*-bromo-, and *p*-nitro-benzenesulfonyl chlorides were purified as previously described (13). *p*-Aminobenzenesulfonyl fluoride and *p*-methoxybenzenesulfonyl chloride were prepared as previously described (13). Commercially available 3,4-dichlorobenzenesulfonyl chloride was purified by two fractional freezings.

p-N,N-Dimethylaminobenzenesulfonyl chloride was prepared by reaction of phosphorus pentachloride with sodium N,N-dimethylsulfanilate (28) in refluxing toluene. Dry recrystallized sodium N,N-dimethylsulfanilate (0.1 mole) and phosphorus pentachloride (0.1 mole) were refluxed in 150 ml of reagent grade toluene until the theoretical amount of hydrogen chloride was liberated (4–6 h). The reaction mixture was filtered and the filtrate washed thoroughly with aqueous sodium carbonate and water. After it was dried over magnesium sulfate, the toluene was evaporated under reduced pressure and crystallization induced by addition of pentane. The yellow crystals (70% yield) melted at 109–110 °C (lit. (29), 110°) and were not purified further.

With the exception of 2-methyl-3-pentyl *p*-aminobenzenesulfonate, the esters were prepared by reaction of the appropriate acid chloride with a stoichiometric amount of 2-methyl-3-pentanol in enough dry pyridine to effect solution. In preparing the 3,4-dichloro and *p*-nitro esters it was necessary to moderate the reaction by addition of an equal volume of dry benzene. The tightly stoppered reaction flask was left overnight in the refrigerator, after which the ester was extracted into ether and washed twice with dilute hydrochloric acid, twice with dilute aqueous sodium hydroxide, and twice with water. After it was dried over magnesium sulfate and treated with Norite A, the ether was evaporated under reduced pressure. The *p*-methyl-, *p*-bromo-, *p*-methoxy-, and 3,4-dichloro-benzenesulfonates are liquids at room temperature. The *p*-nitrobenzenesulfonate first appeared as a yellow oil but crystallized upon addition of a small amount of *n*-pentane. This ester had m.p. 51–52 °C and decomposed within a few hours at room temperature. The *p*-N,N-dimethylbenzenesulfonate was obtained as a white solid, m.p. 84–86 °C.

2-Methyl-3-pentyl *p*-aminobenzenesulfonate was prepared by reaction of *p*-aminobenzenesulfonyl fluoride with sodium 2-methyl-3-pentoxide in ether as previously described (13) for the corresponding 2-pentyl ester. The product was obtained as white plates, m.p. 99–100 °C.

Anal. Calcd. for $C_{14}H_{23}NO_3S$ (I*a*): C, 58.92; H, 8.12. Found: C, 58.93; H, 8.07. Calcd. for $C_{12}H_{19}NO_3S$ (I*b*): C, 56.00; H, 7.44. Found: C, 56.12; H, 7.10. Calcd. for $C_{13}H_{20}O_4S$ (I*c*): C, 57.32; H, 7.40. Found: C, 57.02; H, 7.20. Calcd. for $C_{13}H_{20}O_3S$ (I*d*): C, 60.90; H, 7.86; S, 12.51. Found: C, 60.87; H, 8.17; S, 12.13. Calcd. for $C_{12}H_{17}BrO_3S$ (I*e*): C, 44.86; H, 5.34. Found: C, 44.71; H, 5.26. Calcd. for $C_{12}H_{16}SO_3Cl_2$ (I*f*): C, 46.31; H, 5.18. Found: C, 44.59; H, 5.18.

The *p*-nitrobenzenesulfonate (I*g*) was very unstable and, for this reason, it was not possible to obtain an elemental analysis. The infrared spectrum showed strong absorption at 6.52 μ, 7.41 μ, and 11.68 μ (characteristic of aromatic nitro) and at 7.32 μ and 8.45 μ (characteristic of sulfonates (30)).

Reaction Media

t-Butanol (Fisher certified reagent grade) was distilled twice over sodium. Dimethyl sulfoxide (Fisher certified reagent grade) was distilled over calcium hydride under reduced pressure, b.p. 50 °C at 3 mm pressure, and was freshly prepared for each experiment. Dioxane was purified by Fieser's method (31). The reaction media were prepared by first dissolving, under nitrogen, clean potassium metal in an accurately known volume of *t*-butanol and then adding an accurately known volume of either dioxane or dimethyl sulfoxide. An aliquot of this mixture was then titrated with standard hydrochloric acid to determine, in moles per liter, the concentration of potassium *t*-butoxide and, hence, the amount of *t*-butanol consumed by reaction with potassium. The appropriate weight of *t*-butanol was then added to an accurately known volume of the mixture to obtain an accurately known volume ratio of the two solvents.

Product Studies

A weighed portion of ester was dissolved in 100 ml of the reaction medium in a 200-ml round-bottomed flask. The flask was swept out with nitrogen, sealed, and immersed in a constant temperature bath maintained at 50.06 ± 0.02 °C. In cases where the rate of reaction was very rapid, i.e. all reactions involving the 3,4-dichloro- and *p*-nitro-benzenesulfonates and all reactions in 25% *t*-butanol – dimethyl sulfoxide, the reaction medium was preheated to 50.06° before addition of the ester. After the reaction was calculated to be at least 99% complete, the mixture was transferred to a 500-ml round-bottomed flask containing about 350 ml of water. The olefinic materials were then concentrated by careful distillation through an 18-inch tantalum-wire spiral column fitted with an ice condenser. The methylpentenes were chased through the column with a small volume of *t*-butanol – water azeotrope (b.p. 80°). Everything distilling up to 80 °C was collected.

The olefins were analyzed by vapor phase chromatography at room temperature, using helium carrier gas at a pressure of 20 p.s.i.g. and a 35-ft column packed with tricresyl phosphate (Burrell Corp., catalogue No. 341-139). The individual methylpentenes were identified by comparison of retention times with those of authentic samples.

The E2 reactions in *t*-butanol and *t*-butanol – dioxane mixtures were accompanied by precipitation of

Can. J. Chem. Downloaded from www.nrcresearchpress.com by 210.87.254.105 on 09/05/12
For personal use only.

potassium arenesulfonate. Rate measurements showed, however, that no appreciable coprecipitation of base occurs and that no appreciable reaction occurs at the surface of the precipitate. E1 product runs always contained an excess of 2,6-lutidine to neutralize the arenesulfonic acid formed.

Correction of E2 Product Compositions

The E2 reaction of I*e* in 50% *t*-butanol – dioxane will serve to illustrate the procedure for correction for competing E1 reaction. The analysis gave four peaks of area listed in the second column in Table IV. Since the pure E1 process yields 19.4% 2-methyl-1-pentene (Table I), 1.7 cm^2 represents 19.4% of all the E1 products and 1.7/0.194 = 8.76 cm^2 represents 100% of all the E1 products. The area of the *cis*-4-methyl-2-pentene peak should then be corrected by 0.009 × 8.76 = 0.1 cm^2, the area of the *trans*-4-methyl-2-pentene peak by 0.083 × 8.76 = 0.7 cm^2, and the area of the 2-methyl-2-pentene peak by 0.714 × 8.76 = 6.3 cm^2. The uncorrected and corrected areas and percentages are listed in Table IV.

TABLE IV

Correction of E2 product from I*e* in 50% *t*-butanol – dioxane

Olefin	Uncorrected area, cm^2	Uncorrected %*	Corrected area, cm^2	Corrected %
cis-2-Methyl-2-pentene	64.8	17.5	64.7	17.8
trans-2-Methyl-2-pentene	113.6	30.7	112.9	31.1
2-Methyl-2-pentene	191.2	51.8	184.9	51.0
2-Methyl-1-pentene	1.7	—	0.0	—

*Based on the E2 products alone.

Kinetic Studies

In *t*-butanol and 50% *t*-butanol – dioxane, 5-ml samples of the reaction mixture were sealed in monax glass ampoules under a nitrogen atmosphere and immersed in a constant temperature bath at 50.06 ± 0.02 °C. After thermal equilibrium, 2–3 tubes were withdrawn for the initial (zero) point. At appropriate time intervals additional tubes were withdrawn, leaving two for infinity measurements. Upon withdrawal from the bath the tubes were quenched by plunging in ice water and broken open, and the contents quantitatively transferred to a flask containing crushed ice. The mixture was then titrated with standard aqueous HCl to a phenolphthalein end point. Initial ester and base concentrations were, respectively: I*e* in *t*-butanol, 0.076 *M*, 0.223 *M*; in 50% *t*-butanol – dioxane: I*a*, 0.131 *M*, 0.145 *M*; I*c*, 0.202 *M*, 0.323 *M*; I*d*, 0.100 *M*, 0.158 *M*; I*e*, 0.103 *M*, 0.236 *M*; I*f*, 0.314 *M*, 0.380 *M*; and I*g*, 0.20 *M*, 0.34 *M*.

In 25% *t*-butanol – dimethyl sulfoxide, a weighed quantity of ester was dissolved in the reaction medium in a volumetric flask already immersed in a constant temperature bath maintained at 25.00 ± 0.02 °C. By using a 5-ml pipette, aliquots were transferred at appropriate time intervals to flasks containing cracked ice. The mixtures were then titrated with standard aqueous HCl using phenolphthalein indicator. Initial ester and base concentrations were, respectively: I*a*, 0.100 *M*, 0.162 *M*; I*d*, 0.095 *M*, 0.162 *M*; and I*e*, 0.106 *M*, 0.162 *M*.

Rate constants were calculated using the integrated second-order rate expression

$$k_2t = [1/(b - a)] \ln[a(b - x)/b(a - x)],$$

where a and b are initial ester and base concentrations, respectively, and $(a - x)$ and $(b - x)$ are the ester and base concentrations at time t.

Control Experiments

The stability of the olefin mixtures in 50% *t*-butanol – dioxane – 0.47 *M* potassium *t*-butoxide at 50 °C was demonstrated by reaction of I*a* for periods ranging from 33 to 90 days. Product compositions were identical within experimental uncertainty.

A 1-ml sample of olefin consisting of 90.4% *cis*-4-methyl-2-pentene and 9.6% *trans*-4-methyl-2-pentene was added to 50 ml of 25% *t*-butanol – dimethyl sulfoxide, 0.20 *M* in potassium *t*-butoxide. After 96 min at 50 °C (twice the longest reaction time for this medium), the olefin mixture was analyzed by the usual procedure. The composition was unchanged.

A sample of the reaction mixture from solvolysis of I*d* in *t*-butanol was analyzed by injecting it directly into the gas chromatograph. The analysis gave the same results, within experimental error, as those obtained by first concentrating the olefins via distillation. The spectrum showed no detectable (estimated less than 5%) *t*-butyl 2-methyl-3-pentyl ether.

In the E2 reaction of I*b* in 50% *t*-butanol – dioxane, the olefins were separated from the reaction mixture by the usual distillation procedure and also by extraction with toluene. The reaction mixture from one run (100 ml) was washed three times with 10-ml portions of toluene. The toluene extract was washed

Can. J. Chem. Downloaded from www.nrcresearchpress.com by 210.87.254.105 on 09/05/12
For personal use only.

twice with 10-ml portions of 2 *N* HCl. The olefins were then concentrated by distillation. Analysis of the two olefin samples gave identical results.

The runs carried out in the presence of aniline were carried out in the usual manner, except that aniline was added to the reaction medium before addition of the ester.

ACKNOWLEDGMENT

This work was supported in part by the U.S. Army Research Office (Durham).

REFERENCES

1. D. J. CRAM, F. D. GREENE, and C. H. DEPUY. J. Am. Chem. Soc. **78**, 790 (1956).
2. W. H. SAUNDERS, JR. and R. A. WILLIAMS. J. Am. Chem. Soc. **79**, 3712 (1957).
3. W. H. SAUNDERS, JR. and D. H. EDISON. J. Am. Chem. Soc. **82**, 138 (1960).
4. C. H. DEPUY and C. A. BISHOP. J. Am. Chem. Soc. **82**, 2532, 2535 (1960).
5. S. J. CRISTOL and R. S. BLY, JR. J. Am. Chem. Soc. **82**, 142 (1960).
6. S. AŠPERGER, N. ILAKOVAC, and D. PAVLOVIĆ. J. Am. Chem. Soc. **83**, 5032 (1961).
7. J. F. BUNNETT, G. T. DAVIS, and H. TANIDA. J. Am. Chem. Soc. **84**, 1606 (1962).
8. W. B. SMITH and W. H. WATSON, JR. J. Am. Chem. Soc. **84**, 3174 (1962).
9. G. AYREY, A. N. BOURNS, and V. A. VYAS. Can. J. Chem. **41**, 1759 (1963).
10. L. J. STEFFA and E. R. THORNTON. J. Am. Chem. Soc. **85**, 2680 (1963).
11. C. K. INGOLD. Proc. Chem. Soc. 265 (1962).
12. J. F. BUNNETT. Angew. Chem. Intern. Ed. Engl. **1**, 225 (1962).
13. A. K. COLTER and R. D. JOHNSON. J. Am. Chem. Soc. **84**, 3289 (1962).
14. H. C. BROWN and I. MORITANI. J. Am. Chem. Soc. **78**, 2203 (1956).
15. C. H. SNYDER and A. R. SOTO. J. Org. Chem. **29**, 742 (1964).
16. A. STREITWIESER, JR. Solvolytic displacement reactions. McGraw-Hill Book Co., Inc., New York. 1962. p. 82.
17. R. E. ROBERTSON. Can. J. Chem. **31**, 589 (1953).
18. D. R. MCKELVEY. Unpublished results.
19. S. WINSTEIN, S. SMITH, and D. DARWISH. J. Am. Chem. Soc. **81**, 5511 (1959).
20. S. G. SMITH and S. WINSTEIN. Tetrahedron, **3**, 317 (1958).
21. E. D. HUGHES and J. WILBY. J. Chem. Soc. 4094 (1960).
22. A. SCHRIESHEIM and C. A. ROWE, JR. J. Am. Chem. Soc. **84**, 3160 (1962).
23. J. E. HOFMANN, T. J. WALLACE, and A. SCHRIESHEIM. J. Am. Chem. Soc. **86**, 1561 (1964).
24. P. S. SKELL and W. L. HALL. J. Am. Chem. Soc. **85**, 2851 (1963).
25. H. R. NACE. Chem. Ind. London, 1631 (1958).
26. A. J. PARKER. Quart. Rev. London, 163 (1962).
27. F. KROLLPFEIFFER and H. SEEBAUM. J. Prakt. Chem. **119**, 141 (1928).
28. H. E. FIERZ-DAVID and L. BLANGEY. Helv. Chim. Acta, **23**, 213 (1940).
29. J. HOUBEN and TH. WEYL. Methoden der organischen Chemie. Vol. 9. G. Thieme Verlag, Stuttgart. 1955. p. 570.
30. L. J. BELLAMY. The infrared spectra of complex molecules. 2nd ed. John Wiley and Sons, Inc., New York. 1958.
31. L. F. FIESER. Experiments in organic chemistry. 3rd ed. D. C. Heath and Co., Boston. 1957. p. 284.

Can. J. Chem. Downloaded from www.nrcresearchpress.com by 210.87.254.105 on 09/05/12
For personal use only.

Can. J. Chem. Downloaded from www.nrcresearchpress.com by 210.87.254.105 on 09/05/12
For personal use only.

THE PREPARATION OF 3-ALKYLTHIOINDOLES[1]

R. V. JARDINE[2] AND R. K. BROWN
Department of Chemistry, University of Alberta, Edmonton, Alberta
Received November 13, 1964

Dedicated to Professor R. B. Sandin on the Occasion of his Sixty-Eighth Birthday

ABSTRACT

3-Ethylthioindole has been prepared by Fischer cyclization of the condensation product of phenylhydrazine and ethylthioacetaldehyde diethyl acetal, and also by a route involving the reaction of ethyl iodide with the sodium borohydride reduction product of 1,2-dithiolo[4,3-*b*]indole-3-(4H)-thione. The last-named compound was obtained by reaction of 2-carbethoxyindoxyl with phosphorus pentasulfide.

INTRODUCTION

The need for a quantity of 3-indolylthioacetic acid evoked interest in the general problem of preparing 3-alkylthioindoles. Information in the literature concerning such compounds is meager. Several attempts have been made to prepare 3-mercaptoindole, from which, via a Williamson ether synthesis, the requisite 3-alkylthioindole might then be made. When indole magnesium bromide was treated with sulfur, 3,3′-diindolyl sulfide was obtained rather than the expected 3-mercaptoindole (1). Oddo and Mingoia (2) have recorded the preparation of 3- as well as some 2-benzoylthioindole when the indole Grignard reagent was allowed to react successively with sulfur and then benzoyl chloride. Hydrolysis of the resulting thiol esters led to 3- and 2-mercaptoindole.

The formation of thioethers from 3-mercaptoindole does not appear to be straightforward. Grant and Snyder (3), upon hydride reduction of 3,3′-diindolyl disulfide followed by addition of 2,4-dinitrochlorobenzene, quite readily obtained 3-(2,4-dinitrophenylthio)-indole, but when ethyl bromoacetate was used instead of the dinitrochlorobenzene there was obtained mainly unchanged 3,3′-diindolyl disulfide with only a trace of the expected 3-indolylthioacetic acid. These same authors were unable to isolate 3-mercaptoindole from hydride reduction of the disulfide, presumably because of the remarkably easy oxidation of 3-mercaptoindole back to the disulfide. Grant and Snyder, furthermore, have pointed out the similarity of the melting point of their 3,3′-diindolyl disulfide (m.p. 217–218°) to that of the reported (2) 3-mercaptoindole (235°). The 3,3′-diindolyl disulfide prepared by Woodbridge and Dougherty (4) is reported to melt at 227–229.5°. Hence, a doubt exists that 3-mercaptoindole (2) has actually been obtained. The 2-mercaptoindole, however, seems to be more readily isolated, since the compound reported by Oddo and Mingoia (2) melted at 148–150°, very close to that found for 2-mercaptoindole (m.p. 145°) easily prepared in 70% yield by treatment of oxindole with phosphorus pentasulfide (5).

Two reports of the preparation of 3-substituted 2-methylthioindoles have appeared (6, 7), but to our knowledge there is no account, other than those mentioned above, of the synthesis of 3-alkylthioindoles.

[1]*Taken from the thesis of R. V. Jardine, submitted to the Faculty of Graduate Studies, University of Alberta, Edmonton, Alberta, in partial fulfillment of the requirements for the degree of Doctor of Philosophy.*
[2]*Present address: General Aniline and Film Corporation, Dyestuff and Chemical Division, P.O. Box 12, Linden, New Jersey, U.S.A.*

RESULTS AND DISCUSSION

3-Alkylthioindoles via the Fischer Indole Synthesis

When ethylthioacetaldehyde diethyl acetal (8) was condensed with phenylhydrazine in acetic acid in the presence of boron trifluoride etherate catalyst, a smooth exothermic reaction occurred (eq. [*a*]) and yielded 3-ethylthioindole (~60%). Elemental analysis,

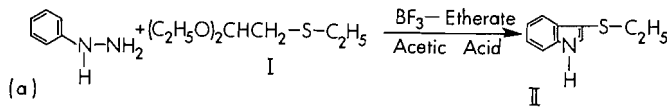

molecular weight (by mass spectrometry), and infrared and nuclear magnetic resonance (n.m.r.) spectra, as well as the method of synthesis, showed conclusively that the product was 3-ethylthioindole (II).

Attempts to form the N-acetyl derivative with either acetic anhydride in benzene or acetyl chloride in pyridine gave only unchanged thioether. This agrees with a similar resistance to N-acylation shown by 3,3′-diindolyl sulfide (1). When II was treated with an alcoholic solution of mercuric chloride, a precipitate of ethylthiomercuric chloride (9) was obtained, a reaction characteristic of a number of alkyl aryl and aryl aralkyl thioethers (10).

The utility of this reaction in preparing 3-alkylthioindoles is obviously dependent upon the availability of the appropriate alkylthioacetaldehyde diethyl acetal (I).

3-Alkylthioindoles via Reaction of P_2S_5 with 2-Carbethoxyindoxyl

Since the reaction of oxindole with phosphorus pentasulfide is known to produce 2-mercaptoindole (5), 2-carbethoxyindoxyl was treated with phosphorus pentasulfide in boiling xylene (eq. [*b*]). From the reaction mixture was isolated in 11% yield the compound 1,2-dithiolo[4,3-*b*]indole-3(4H)-thione (IV).*

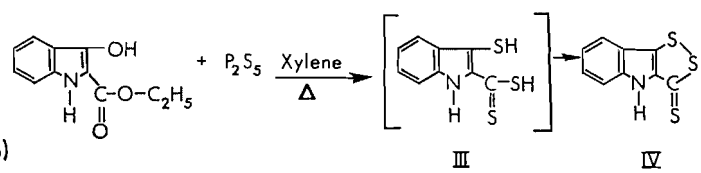

The isolation of IV (the oxidized form of III) rather than the 3-mercaptoindole (III) is analogous to the reported isolation of 3,3′-diindolyl disulfide rather than the expected 3-mercaptoindole upon reduction of this disulfide (3). Elemental analysis, molecular weight, and infrared and nuclear magnetic resonance spectra, as well as a negative Ehrlich test (11, 12), supported structure IV for this product. In addition, Raney nickel desulfurization (13) of IV afforded a compound whose infrared spectrum was identical with that of authentic 2-methylindole (14).

Reduction of IV, with sodium borohydride in ethanol, followed by reaction of the product with ethyl iodide (eq. [*c*]) gave an 84% yield of ethyl 3-ethylthio-2-indoledithiocarboxylate (V), whose structure was corroborated by elemental analysis and infrared and

**The reaction of β-ketoesters (N. Lozac'h and L. Legrand, Compt. Rend. 234, 1291 (1952); A. Luttringhaus, H. Trefzger, and U. Schmidt, Angew. Chem. 67, 274 (1955)) and of aromatic o-hydroxycarboxylic acids (L. Katz, W. Schroeder, and M. Cohen, J. Org. Chem. 19, 711 (1954)) with P_2S_5 has been shown to produce the stable 1,2-dithiolo-3-thione structure found in compound IV.*

Can. J. Chem. Downloaded from www.nrcresearchpress.com by 210.87.254.105 on 09/05/12
For personal use only.

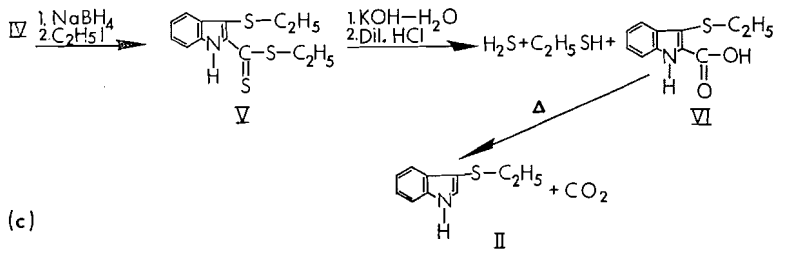

nuclear magnetic resonance spectra. Hydrolysis of V gave hydrogen sulfide, ethyl mercaptan, and 3-ethylthioindole-2-carboxylic acid (VI). Compound VI readily decarboxylated and distilled when heated under vacuum, producing 3-ethylthioindole (II), identical with that prepared by the Fischer reaction.

EXPERIMENTAL

Infrared spectra were obtained with Perkin–Elmer instruments, models 21, 221G, and 421. Nuclear magnetic resonance spectra were provided by a Varian Associates instrument, model A-60. Mass spectra were obtained with a MS2-H Metropolitan-Vickers instrument. Gas–liquid chromatography was carried out on a Burrell K-2 Kromo-Tog using a 2½-m column containing a packing of 20% Apiezon L on Kromat F.B. (30–60 mesh) and employing helium as carrier gas.

3-Ethylthioindole (II) by Fischer Cyclization

A mixture of 17.8 g (0.1 mole) of ethylthioacetaldehyde diethyl acetal (8) and 10.8 g (0.1 mole) of phenylhydrazine was added to 100 ml of glacial acetic acid at room temperature. A slightly exothermic reaction took place. Addition of 15.1 g (0.1 mole) of boron trifluoride etherate caused a rise in temperature to 90°. The mixture was maintained at this temperature for 1 h, then poured into 1 l of cold water, and extracted with ether (3 × 200 ml). The combined ether extracts were neutralized with sodium bicarbonate and then washed successively with water (1 × 300 ml), 1 *N* HCl (3 × 300 ml), and water (3 × 300 ml). The dried ethereal solution ($MgSO_4$) was freed from solvent and afforded 12 g (67.5%) of red oil which was shown by gas–liquid chromatography to be reasonably pure 3-ethylthioindole.

An analytical sample was prepared by passing a portion of the oil through a column of neutral alumina (activity grade 1)* using benzene as eluant. The benzene eluate was freed from solvent and the residual oil distilled at 95° at 1.5 mm pressure. Much decomposition accompanied distillation but the product came over as a light yellow oil, η_D^{24} 1.6285.

Anal. Calcd. for $C_{10}H_{11}NS$: C, 67.8; H, 6.26; N, 7.95; S, 18.07. Found: C, 67.54; H, 6.19; N, 7.74; S, 18.27.

Infrared absorption (neat) at 3 405 cm^{-1} indicated N—H stretching characteristic of indoles (15). Aliphatic C—H absorption occurred at 2 885, 2 910, and 2 985 cm^{-1}. The n.m.r. spectrum obtained in deuterochloroform showed a triplet centered at 8.80 τ (J = 7 c.p.s.) and a quartet centered at 7.3 τ (J = 7 c.p.s.), both characteristic of an ethyl group. Signals at 2.0–3.0 τ were attributed to aromatic protons and, according to the integrated area, also included the C_2 proton signal shifted downfield from its normal position at about 2.9–3.4 τ (16, 17) as a result of the combined inductive effects of the nitrogen and the C_3 sulfur substituent. Analysis of the compound by mass spectrometry gave a molecular weight of 177. The empirical formula calculated from mass spectrometric data by the method of Silverstein and Bassler (18) was $C_{10}H_{11}NS$.

Acetylation of 3-ethylthioindole with either acetic anhydride in benzene or acetyl chloride in pyridine failed. Only unchanged 3-ethylthioindole was recovered.

Treatment of 3-ethylthioindole with an ethanolic solution of picric acid gave an amorphous precipitate; attempts at crystallization failed to improve this precipitate. The substance melted over the range −10 to 0°.

When 55 mg (2.55 × 10^{-4} mole) of pure 3-ethylthioindole was treated with 69 mg (2.55 × 10^{-4} mole) of mercuric chloride in 1 ml of 95% ethanol and the solution allowed to stand overnight at room temperature, 50 mg of ethylthiomercuric chloride was deposited. This gave an infrared spectrum in Nujol identical with that of an authentic specimen (9). Thin-layer chromatography of the remaining ethanolic solution showed spots, developed by Ehrlich's reagent (11, 12), whose R_f values were identical with those of authentic samples of indole and 3-ethoxyindole (19, 20).

3-Ethylthioindole via Reaction of P_2S_5 with 2-Carbethoxyindoxyl

1,2-Dithiolo[4,3-b]indole-3(4H)-thione (IV)

To 10 g (0.028 mole) of 2-carbethoxyindoxyl (20) in 150 ml of practical grade xylene was added 20 g (0.09 mole) of phosphorus pentasulfide and the resulting mixture heated to reflux for 2.5 h. The solution was

**Alupharm Chemicals, P.O. Box 755, New Orleans, Louisiana, U.S.A.*

Can. J. Chem. Downloaded from www.nrcresearchpress.com by 210.87.254.105 on 09/05/12
For personal use only.

then filtered hot, and the filtrate reduced in volume to 50 ml and chromatographed on a column of neutral alumina (activity grade 1) using ether as eluant. Removal of the ether from the eluate deposited deep orange crystals which were recrystallized from toluene. Yield, 1.2 g (11%); m.p. 208° (decomp.). Molecular weight by Rast, 231; by mass spectrometry, 223.

Anal. Calcd. for $C_9H_5NS_3$: C, 48.40; H, 2.24; N, 6.28; S, 43.10. Found: C, 48.53; H, 2.35; N, 6.42; S, 43.07.

The infrared spectrum showed absorption at 3 310 cm^{-1} (indolic NH) (14) but no carbonyl absorption between 1 600 and 1 735 cm^{-1} (21). No absorption bands could be clearly discerned as being due to $\diagup C{=}S$, usually found at 1 050 – 1 200 cm^{-1} (15, p. 357). The n.m.r. spectrum in dimethyl sulfoxide showed a N—H signal at $-2.34\ \tau$ and aromatic absorption at 1.83–3.0 τ, while in pyridine a signal at $-2.79\ \tau$ occurred for N—H, and between 2 and 3 τ for aromatic absorption, but no signals were found above 3.0 τ.

Compound IV gave a negative Ehrlich test, indicating that both C_2 and C_3 positions of the indole ring were blocked by substituents (11, 12).

A solution of 300 mg (0.0013 mole) of 1,2-dithiolo[4,3-*b*]indole-3(4H)-thione in 200 ml of 95% ethyl alcohol, containing 40 g of active Raney nickel (13), was refluxed for 24 h. The hot solution was separated from the nickel by filtration and the sludge extracted with hot alcohol (3 × 100 ml). The combined alcohol solutions were freed from solvent, giving 10 mg of a compound whose infrared spectrum was identical with that of authentic 2-methylindole (14).

Ethyl 3-(Ethylthio)-2-indoledithiocarboxylate (V)

A solution of IV (0.445 g, 0.0021 mole) in 12.5 ml of 95% ethyl alcohol and 2.5 ml of water containing 0.2 g of sodium carbonate was treated with 0.25 g (0.0066 mole) of sodium borohydride under an atmosphere of nitrogen. The mixture was then heated to reflux for 30 min and cooled. To this ice-cold solution was then added 1 ml of ethyl iodide and the resulting mixture brought to reflux for an additional 30 min. The originally dark red solution became light orange. The reaction mixture was then filtered free from solid, and the filtrate diluted with water and extracted with ether (2 × 50 ml). The ether extract was washed with water and dried ($MgSO_4$). Upon removal of the ether the residue was taken up in hexane and the solution chromatographed on 20 g of neutral alumina. Elution with a benzene–hexane mixture (1:1) gave 440 mg of a red-orange oil upon removal of the solvent. On standing, it solidified. Recrystallization was best accomplished from a minimum amount of toluene (2 ml) diluted with *n*-pentane (25 ml). Upon standing overnight at −20°, the solution deposited fine orange needles melting at 49–50°. Yield, 0.356 g (61%).

Anal. Calcd. for $C_{13}H_{15}NS_3$: C, 55.50; H, 5.34; N, 4.98; S, 34.15. Found: C, 55.66; H, 5.15; N, 4.86; S, 34.50.

The infrared spectrum (Nujol) showed a band at 3 340 cm^{-1} for indolic N—H (15). The signals and integrated area of the n.m.r. spectrum in deuterochloroform were consistent with structure V, showing two triplets centered at 8.58 τ (J = 7.5 c.p.s.) and 8.8. τ (J = 7.5 c.p.s.) and two quartets centered at 6.6 τ (J = 7.5 c.p.s.) and 7.1 τ (J = 7.5 c.p.s.) respectively, thereby indicating two differently located ethyl groups. Aromatic proton absorption occurred at 2–3 τ.

Hydrolysis of V to 3-Ethylthioindole-2-carboxylic Acid (VI)

To a solution of ethyl 3-(ethylthio)-2-indoledithiocarboxylate (V) (0.362 g) in 10 ml of 95% ethanol was added 1 ml of water containing 1 g of potassium hydroxide. The mixture was stirred and refluxed for 7 h under an atmosphere of nitrogen. Ethyl mercaptan was evolved and could be detected by the white precipitate which occcurred when it was passed through a solution of mercuric chloride. The reaction mixture was then cooled, diluted with a small amount of water, and then filtered to remove suspended particles. The cooled filtrate (ice) was acidified with 4 ml of 6 *N* hydrochloric acid. Hydrogen sulfide was liberated. After the solution had stood for an hour, 245 mg (86%) of crude yellow material, m.p. 97–100°, was deposited. Solution of this material in 5 ml of benzene followed by addition of hexane (35 ml) and cooling of the resulting solution gave dark yellow needles melting at 105–106°. Yield, 185 mg (65%). The solid was soluble in dilute aqueous sodium hydroxide. A 10-mg sample required 9.9 ml of 0.00441 *N* sodium hydroxide, giving a neutral equivalent of 229 (theoretical, 221).

An infrared spectrum in Nujol showed indolic N—H absorption at 3 310 cm^{-1} and carbonyl absorption at 1 710 cm^{-1}.

Anal. Calcd. for $C_{11}H_{11}O_2NS$: C, 59.72; H, 5.01; N, 6.33. Found: C, 59.51; H, 5.26; N, 6.47.

3-Ethylthioindole (II)

3-Ethylthioindole-2-carboxylic acid (380 mg) was heated at 150° at 6 mm pressure. A gas was evolved (CO_2) and a liquid was distilled under these conditions, giving 85 mg (26.6%) of pure 3-ethylthioindole identical in boiling point and infrared and n.m.r. spectra with those of an authentic sample prepared by Fischer cyclization.

ACKNOWLEDGMENTS

The authors are grateful to the National Research Council of Canada for generous financial support during the course of this investigation. They thank Mr. Brian Brownlee

Can. J. Chem. Downloaded from www.nrcresearchpress.com by 210.87.254.105 on 09/05/12
For personal use only.

for his assistance in the preparation of a quantity of some of the intermediates and Dr. U. G. Nayak for his purification and characterization of the carboxylic acid VI.

REFERENCES

1. W. MADELUNG and M. TENCER. Ber. **48**, 949 (1915).
2. B. ODDO and Q. MINGOIA. Gazz. Chim. Ital. **62**, 299 (1932); Chem. Abstr. **26**, 4603 (1932).
3. M. S. GRANT and H. R. SNYDER. J. Am. Chem. Soc. **82**, 2742 (1960).
4. R. G. WOODBRIDGE and G. DOUGHERTY. J. Am. Chem. Soc. **72**, 4320 (1950).
5. S. SUGASAWA, I. SATODA, and J. YAMAGISAWA. J. Pharm. Soc. Japan, **58**, 139 (1938); Chem. Abstr. **32**, 4161 (1938).
6. H. WUYTS and A. LACOURT. Bull. Classe Sci. Acad. Roy. Belg. **21**, 736 (1935); Chem. Abstr. **29**, 7952 (1935).
7. T. WIELAND, O. WEIBERG, E. FISCHER, and G. HORLEIN. Ann. **587**, 146 (1954).
8. L. BIRKOFER and I. STORCH. Ber. **87**, 571 (1954).
9. F. CHALLENGER and A. A. RAWLINGS. J. Chem. Soc. 868 (1937).
10. D. C. GREGG, H. A. IDDLES, and P. W. STEARNS. J. Org. Chem. **16**, 246 (1951).
11. M. FREUND and G. LEBACH. Ber. **38**, 2640 (1905).
12. W. VON DOBENEK and G. MARESCH. Z. Physiol. Chem. **289**, 271 (1951); Chem. Abstr. **49**, 11620 (1955).
13. G. R. PETTIT and E. E. VAN TAMELN. Organic reactions. Vol. 12. John Wiley and Sons, Inc., New York. 1962. p. 356.
14. E. FISCHER. Ber. **19**, 1563 (1886).
15. R. J. BELLAMY. The infrared spectra of complex molecules. John Wiley and Sons, Inc., New York. 1958. p. 251.
16. L. A. COHEN, J. W. DALEY, H. KNY, and B. WITKOP. J. Am. Chem. Soc. **82**, 2184 (1960).
17. R. V. JARDINE and R. K. BROWN. Can. J. Chem. **41**, 2067 (1963).
18. R. W. SILVERSTEIN and G. C. BASSLER. J. Chem. Educ. **39**, 546 (1962).
19. A. BAYER. Ber. **14**, 1741 (1881).
20. A. ETIENNE. Bull. Soc. Chim. France, 651 (1948).
21. A. D. CROSS. Introduction to practical infrared spectroscopy. Butterworth Scientific Publications, London. 1960. p. 64.

Can. J. Chem. Downloaded from www.nrcresearchpress.com by 210.87.254.105 on 09/05/12
For personal use only.

Can. J. Chem. Downloaded from www.nrcresearchpress.com by 210.87.254.42 on 09/05/12
For personal use only.

ANOMALOUS REACTIONS IN ATTEMPTS TO PREPARE 3-ALKYLTHIOINDOLES[1]

R. V. JARDINE[2] AND R. K. BROWN
Department of Chemistry, University of Alberta, Edmonton, Alberta
Received November 13, 1964

Dedicated to Professor R. B. Sandin on the Occasion of his Sixty-Eighth Birthday

ABSTRACT

Indole magnesium bromide reacting with ethanesulfenyl chloride produces ethyl mercaptan, diethyl disulfide, indole, 3-ethylindole, 3-ethylthioindole, and 3,3′-diindolyl sulfide, along with at least three compounds not yet identified.

The reaction of ethyl mercaptan with N-benzoyl-3-bromoindole in dimethylformamide containing potassium carbonate produces indole, 3-bromoindole, ethyl thiolobenzoate, 3-ethylindole, diethyl disulfide, and 3-ethylthioindole.

In both of these reactions a substance (or substances) which caused strong allergenic reactions in persons exposed to the reaction mixtures was produced. 3,3′-Diindolyl disulfide was found to be allergenic in minute amounts.

INTRODUCTION

A recent publication (1) has described two routes for the preparation of 3-alkylthioindoles, one involving initially the reaction of phosphorus pentasulfide with carbethoxyindoxyl while the other and preferred method employed the Fischer indole synthesis. This paper reports the results from attempts to obtain 3-ethylthioindole from the reaction between indole magnesium bromide and ethanesulfenyl chloride on the one hand and of ethyl mercaptide with N-benzoyl-3-bromoindole on the other. Although neither scheme was suitable for the thioether preparation, the anomalous product formation was interesting.

RESULTS AND DISCUSSION

Reaction between Indole Magnesium Bromide and Ethanesulfenyl Chloride

The reaction between sulfenyl halides and Grignard reagents is known to yield thioethers (2–5). In view of this, ethanesulfenyl chloride was added slowly to an ethereal solution of indole magnesium bromide at $-10°$ and the reaction worked up as described in the Experimental section. A number of compounds, at least three of which still remain unknown, were formed, as shown by gas–liquid chromatography (g.l.c.) and thin-layer chromatography (t.l.c.). Actually isolated by precipitation were ethyl mercaptan (as the silver salt) and 3,3′-diindolyl sulfide, while by distillation of the mother liquor were obtained both indole and 3-ethylindole. The same ethylindole was obtained as its picrate by treatment of the ether extract of the reaction mixture, before distillation, with picric acid; hence, it was an actual product of the original reaction and not a result of pyrolysis during distillation.

Gas–liquid chromatography of the ether extract of the original mixture, first freed from mercaptan, showed the presence of indole and 3-ethylindole as well as diethyl disulfide

[1]*Taken from the thesis of R. V. Jardine, submitted to the Faculty of Graduate Studies, University of Alberta, Edmonton, Alberta, in partial fulfillment of the requirements for the degree of Doctor of Philosophy.*

[2]*Present address: General Aniline and Film Corporation, Dyestuff and Chemical Division, P.O. Box 12, Linden, New Jersey, U.S.A.*

Can. J. Chem. Downloaded from www.nrcresearchpress.com by 210.87.254.42 on 09/05/12
For personal use only.

and 3-ethylthioindole. Attempts to isolate 3-ethylthioindole failed, but further evidence for its presence was obtained by precipitation of ethylthiomercuric chloride when an ether extract of the reaction mixture, freed from ethyl mercaptan, was treated with ethanolic mercuric chloride. This reagent is known to react readily with unsymmetrical thioethers to produce the characteristic alkyl or arylthiomercuric chlorides (6). In trial runs under our room temperature conditions, no visible reaction occurred between ethanolic mercuric chloride and diethyl disulfide (a compound found in our reaction mixture), although such a reaction has been reported (7). The same precipitate was obtained when ethanolic mercuric chloride was added to the traces of 3-ethylthioindole collected by g.l.c. Thin-layer chromatography also indicated the presence of 3-ethylthioindole as well as 3,3′-diindolyl.

Identification of the isolated compounds was made by comparing infrared spectra, nuclear magnetic resonance (n.m.r.) spectra, melting points, or boiling points with those of authentic samples, while those compounds not isolated were identified by their retention times or R_f values compared with those of known compounds. The 3,3′-diindolyl (8) could be readily identified by its R_f value (t.l.c.) and by its characteristic strong blue-white fluorescence, first noted by Gabriel *et al.* (9).

3-Ethylthioindole occurs, no doubt, via the known reaction (5, 10, 11) indicated by

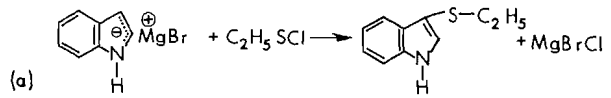

eq. [*a*]. Indole and diethyl disulfide could arise from hydrolysis of unreacted indole magnesium bromide and ethanesulfenyl chloride. The latter compound is known to hydrolyze to a mixture of products, one of which is diethyl disulfide (12, 13).

A possible source of 3,3′-diindolyl was indicated by the next experiment. Chromatographically pure indole was converted to indole magnesium bromide and the ethereal solution stirred for several hours without precaution for exclusion of air. When the mixture was treated with water and worked up as usual, indole was found to be the main product as expected. However, in addition, there was obtained evidence by t.l.c. for 3,3′-diindolyl and at least nine other unidentified compounds, each giving a positive Ehrlich test for the 2- and (or) 3-unsubstituted indole nucleus (14).

The formation of ethyl mercaptan, 3-ethylindole, or 3,3′-diindolyl sulfide is not at all clear. The possibility that indole magesium bromide and ethanesulfenyl chloride will

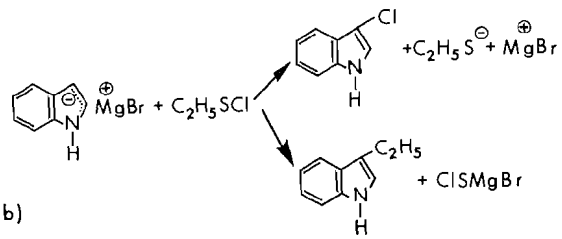

react to form 3-ethylindole or 3-chloroindole (eq. [*b*]) is unlikely, since in our hands phenyl magnesium bromide and ethanesulfenyl chloride gave only ethyl phenyl sulfide and no indication of ethylbenzene or chlorobenzene.

Can. J. Chem. Downloaded from www.nrcresearchpress.com by 210.87.254.42 on 09/05/12
For personal use only.

It is reported that Grignard reagents are capable of cleaving thioethers, but this occurs usually at higher temperatures (15). When 3-ethylthioindole was treated with indole magnesium bromide at room temperature or below (our conditions), only unchanged starting materials were found in the product. Furthermore, although it is known that phenyl magnesium bromide reacts with diphenyl disulfide to produce diphenyl sulfide (10) and that disulfides are cleaved by nucleophilic species (5, 16), our attempts to produce a similar reaction between indole magnesium bromide and 3,3′-diindolyl disulfide resulted in nearly complete recovery of starting material. The possibility that 3,3′-diindolyl disulfide might have been formed, even though this highly insoluble and readily isolable substance was not in fact obtained, was entertained because of pronounced and characteristic allergic effects experienced during experiments involving the reaction of indole magnesium bromide with ethanesulfenyl chloride.* Of the available pure compounds tested for this allergenic reaction, only 3,3′-diindolyl disulfide was found to be active and, even in minute amounts, gave rise to acute allergic symptoms. Because of these undesirable physiological effects, further work on this reaction was discontinued.

Reaction between Ethyl Mercaptide and N-Benzoyl-3-bromoindole

The high nucleophilicity of the alkali salts of mercaptans (17) and the reported facile reaction of alkyl halides with 6-mercaptopurines in dimethylformamide containing potassium carbonate (18) suggested the possibility of a similar reaction between 3-bromoindole and ethyl mercaptan to form 3-ethylthioindole.

To avoid the spontaneous decomposition and polymerization which 3-bromoindole undergoes during its isolation and purification if conditions are not carefully controlled (19), N-benzoyl-3-bromoindole was employed. It was hoped that the presence of the N-benzoyl group might result in increased nucleophilic attack at C_3 of the indole ring.

A mixture of equimolar amounts of N-benzoyl-3-bromoindole, dry powdered potassium carbonate, and ethyl mercaptan was heated in previously distilled dimethylformamide at reflux (150°) for 12 h. This high temperature was chosen because preliminary experiments revealed that one of the products was 3-bromoindole, which, because of its characteristic decomposition, complicated the isolation procedure. It had also been found that, when 3-bromoindole was heated at 150° in dimethyl formamide containing potassium carbonate, all of it was converted smoothly to indole and bromide ion, neither of which presented any problem during isolation.

An ether extract of the reaction mixture, which was first washed with aqueous silver nitrate to remove unreacted mercaptan, then dried, and freed of solvent, gave, upon distillation, ethyl thiolobenzoate (48%), indole (28%), and 3-ethylindole (25%) plus a tarry residue. No 3-ethylthioindole was obtained, but this is not unexpected, since this thioether does tend to decompose upon distillation even when it is reasonably pure (1). When an ether extract from a second reaction was first freed from mercaptan as above, then reduced in volume, and subjected to gas–liquid chromatography using either a column packed with Apiezon L on Kromat B or silicone rubber on Kromat B, several peaks were noted. Identified by comparison of retention times with those of authentic samples were diethyl disulfide, 3-ethylindole, indole, ethyl thiolobenzoate, and 3-ethylthioindole. At least three other unidentified peaks were present. The detection of 3-ethylindole in this case showed that it was an actual product of the original reaction.

If the mixture of equimolar quantities of N-benzoyl-3-bromoindole, ethyl mercaptan,

Exposure to this substance caused urticaria, edema, and finally a serious case of serum sickness. Other persons in the same room, when in contact with equipment contaminated by this substance, also developed mild symptoms.

and potassium carbonate in dimethylformamide was heated for 2 h at 60° rather than 150° and if the ether extract, purified as above, was reduced in volume with simultaneous addition of benzene to displace the ether, followed by chromatography of this solution on neutral alumina (activity grade 1), indole and 3-bromoindole were eluted initially, using pentane. Further elution with additional pentane gave oils which could not be crystallized. Subsequent elution with benzene gave an oil which reacted with mercuric chloride in ethyl alcohol to give ethylthiomercuric chloride, indicative of 3-ethylthioindole.

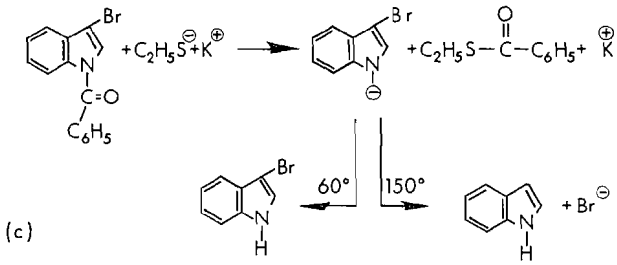

(c)

The formation of ethyl thiolobenzoate (20) by reaction of ethyl mercaptide occurs, no doubt, by the expected reaction (eq. [*c*]). Diethyl disulfide could arise via oxidation of ethyl mercaptan (21). The origin of 3-ethylindole is unknown. Although 3-ethylindole is obtained from the reaction of indole with ethyl alcohol in the presence of acid or base and at a temperature of 180–200° (22), we found no 3-ethylindole when indole, ethyl mercaptan, and potassium carbonate were heated in dimethylformamide to 150° for 6 h. Furthermore, when ethyl thiolobenzoate was distilled with 3-bromoindole, there was obtained only unchanged ester and dark greenish product as a result of decomposition of 3-bromoindole.

Further experiments designed to clarify this reaction were discontinued when allergic reactions, similar to those noted previously, developed from exposure to some factor(s) in the products of this reaction.

EXPERIMENTAL

All melting points and boiling points are uncorrected.

Gas–liquid chromatography was accomplished with a Burrell K-2 Kromo-Tog using a 2.5-m column packed with 20% Apiezon L on Kromat F.B. (30–60 mesh) and a similar column packed with 20% silicone rubber on Kromat F.B. (30–60 mesh). The column temperatures employed depended upon the boiling point of the compounds analyzed. The carrier gas was helium.

Compounds were identified by comparison of their retention times with those of authentic samples. In several cases compounds were also isolated and identified according to usual procedures.

Analyses were also made via thin-layer chromatography using aluminium oxide as the adsorbant and Ehrlich's reagent (14) to detect the position of indole compounds.

Infrared spectra were obtained with Perkin–Elmer instruments, models 21, 221G, and 421. Nuclear magnetic resonance spectra were made with a Varian Associates model A-60 spectrometer. X-ray diffraction patterns were obtained with a Philips Electronics Inc. X-ray diffraction unit, type No. 12045.

Source or Preparation of Reagents

N-Benzoyl-3-bromoindole

N-Benzoylindole was prepared by a modification of the method of Weissgerber (23). A mixture of indole (117 g, 1 mole) and 23 g (1 g-atom) of sodium in 1.5 l of purified dry dioxane (24) was refluxed for 48 h. To the cooled solution, freed from unreacted sodium, was slowly added 140.5 g (1 mole) of benzoyl chloride. The resulting mixture was refluxed for an additional 12 h and then poured into 4 l of water. The precipitated crude N-benzoylindole was collected and extracted with pentane to remove unreacted indole. Crystallization of the crude amide from ethyl alcohol gave the pure product in 55% yield, m.p. 67–68° (lit. m.p. 67–68° (23)).

N-Benzoylindole was converted to N-benzoyl-3-bromoindole according to published directions (23). Yield, 82%; m.p. 97–98° (lit. m.p. 97–98°).

3-Bromoindole was prepared from N-benzoyl-3-bromoindole by the method of Weissgerber, or preferably by direct bromination of indole with pyridinium bromide perbromide (19).

Can. J. Chem. Downloaded from www.nrcresearchpress.com by 210.87.254.42 on 09/05/12
For personal use only.

Ethyl thiolobenzoate was prepared by a modification of a literature synthesis (20). A solution of 6.2 g (0.1 mole) of ethyl mercaptan in 50 ml of anhydrous dimethylformamide (24) containing 13.8 g (0.1 mole) of anhydrous potassium carbonate was treated with 14.0 g (0.1 mole) of benzoyl chloride. The resulting mixture was refluxed for 2 h and then poured into 200 ml of water. The aqueous mixture was extracted with ether (3 × 100 ml) and the combined extracts dried over magnesium sulfate. The ether was removed under reduced pressure and the remaining oil distilled, b.p. 146° at 31 mm pressure (lit. b.p. 146° at 31 mm pressure (20)).

Ethylthiomercuric chloride was prepared by the method of Challenger and Rawlings (7).

2-Ethylindole was prepared according to published directions (25).

3-Ethylindole

The published procedure (26) was modified as follows. N-Butyraldehyde (14.4 g, 0.2 mole) was treated with 21.6 g (0.2 mole) of phenylhydrazine in 200 ml of glacial acetic acid. The resulting solution was warmed to 50° and stirred at this temperature for 2 h. The reaction mixture was allowed to cool to room temperature and 30.2 g (0.2 mole) of boron trifluoride etherate added carefully. When the ensuing exothermic reaction had subsided, the mixture was stirred for an additional half hour and then poured into 1 l of water, and the whole extracted with ether (3 × 100 ml). The combined ethereal extracts were neutralized with sodium bicarbonate, washed with water (2 × 100 ml), and dried ($MgSO_4$). The ether was removed on a rotary evaporator and the residual oil distilled at 175° at 6 mm pressure (lit. b.p. 282–284 (26)). The picrate (from ethanol) melted at 143° (lit. m.p. 143° (26)).

3,3′-Diindolyl disulfide was prepared according to published directions (27). Yield, 23%; m.p. from toluene 227–229° (lit. m.p. 217–218° (28), 227–229.5° (27)).

Diethyl disulfide and sulfuryl chloride were obtained from Eastman Kodak Co.

Ethanesulfenyl Chloride

This was prepared by a modification of literature directions (29). Diethyl disulfide (60 g, 0.41 mole), in a 1-l flask protected with a calcium chloride tube, was cooled to −70° in a dry ice – acetone mixture. To the flask was added dropwise 55 g (0.41 mole) of sulfuryl chloride. The solution became orange immediately upon addition of the first portion of the sulfuryl chloride. During the addition, the solution was allowed to warm slowly to room temperature, thus preventing precipitation of solutes. Upon completion of the addition, the reaction mixture was heated on a steam bath for 20 min to remove dissolved sulfur dioxide, and then distilled. Yield, 70% of material boiling at 51° at 74 mm pressure (lit. b.p. 51° at 74 mm pressure (29)).

3,3′-Diindolyl was prepared according to known directions (8), m.p. (from toluene followed by drying for 20 h at 25° at 0.2 mm pressure) 284–286° (lit. m.p. 286–287° (9), 284–286° (8)).

3,3′-Diindolyl sulfide was prepared according to published directions (30), m.p. (from toluene) 232°.

3-Ethylthioindole was prepared as described previously (1).

Attempted Reaction of N-Sodio-3-bromoindole with Sodium Ethyl Mercaptide

3-Bromoindole (5.0 g, 0.025 mole) in 50 ml of anhydrous dioxane (24) was treated with 0.6 g (0.026 g-atom) of sodium to form N-sodio-3-bromoindole. To the reaction mixture was added a solution of sodium ethyl mercaptide (0.6 g, 0.026 g-atom of sodium in 10 ml of anhydrous ethanol followed by addition of ethyl mercaptan to the cooled sodium ethoxide). The resulting dioxane – ethyl alcohol mixture was heated at 60° for 2 h and then poured into 250 ml of cold water. 3-Bromoindole was recovered in 86.5% yield. No indication of 3-ethylthioindole was found.

Decomposition of 3-Bromoindole in Dimethylformamide Containing Potassium Carbonate

3-Bromoindole (5.0 g, 0.025 mole) and 3.52 g (0.025 mole) of dry powdered potassium carbonate in 100 ml of anhydrous dimethylformamide (24) were heated at 150° for 12 h, during which time carbon dioxide was evolved. The mixture was then poured into 500 ml of cold water and the resulting mass was extracted with ether (3 × 100 ml). The dried ($MgSO_4$) ethereal extract was freed from solvent. Crystallization of the residue from pentane gave 2.6 g (87.4%) of indole, m.p. 52°. Addition of excess aqueous silver nitrate (1 *N*) to the acidified (HNO_3) aqueous phase gave 4.65 g of silver bromide, accounting for 97.5% of the theoretical amount of bromine in this 3-bromoindole.

When the above experiment was repeated, but at the reaction temperature of 60° rather than 150°, only 17.5% of the 3-bromoindole had decomposed, as indicated by the amount of silver bromide precipitated from the aqueous phase after ether extraction. The 3-bromoindole and indole could be recovered from the ether if care was taken in its isolation (see latter portion of the next experiment).

Reaction of N-Benzoyl-3-bromoindole with Ethyl Mercaptan in Dimethylformamide at 150° Containing Potassium Carbonate

A mixture of N-benzoyl-3-bromoindole (10 g, 0.035 mole) in 150 ml of anhydrous dimethylformamide (24), containing 4.8 g (0.035 mole) of anhydrous potassium carbonate and 2.17 g (0.035 mole) of ethyl mercaptan, was heated at 150° for 12 h. The cooled solution was extracted with peroxide-free ether (2 × 200 ml), and the combined ethereal extracts were washed with 0.2 *N* aqueous silver nitrate (2 × 100 ml) to remove unreacted mercaptan, then washed with water (2 × 200 ml), and finally dried ($MgSO_4$).

Can. J. Chem. Downloaded from www.nrcresearchpress.com by 210.87.254.42 on 09/05/12
For personal use only.

Can. J. Chem. Downloaded from www.nrcresearchpress.com by 210.87.254.42 on 09/05/12
For personal use only.

A small part of this dried ethereal extract was subjected to gas–liquid chromatography (g.l.c.) using a column packed with 20% Apiezon L on Kromat F.B. (30–60 mesh). Peaks with retention times identical with those of diethyl disulfide, indole, ethylthiolobenzoate, 3-ethylindole, and 3-ethylthioindole were observed. At least three other unidentified compounds were indicated.

A 10-ml portion of the ethereal extract was treated with 2 ml of ethyl alcohol saturated with mercuric chloride and gave a precipitate of ethylthiomercuric chloride, identified by its characteristic infrared spectrum and its X-ray diffraction pattern.

The remainder of the above ethereal extract was freed from solvent and the residue distilled under vacuum. There was obtained 1.6 g of indole (24% based upon the N-benzoyl-3-bromoindole used), b.p. 105° at 5 mm pressure; 2.6 g of ethyl thiolobenzoate (48%), b.p. 108–110° at 5 mm pressure; and 1.23 g of 3-ethylindole (24%), b.p. 138–140° at 1.5 mm pressure. Considerable decomposition occurred during the distillation. The indole and 3-ethylindole were identified by melting point, mixed melting point, and comparative infrared spectra of the respective picrates with those of authentic compounds. That the ethylindole was actually 3-ethylindole and not the 2-isomer was verified by synthesis of both 3-ethylindole (26) and 2-ethylindole (25).

The reaction of N-benzoyl-3-bromoindole with ethyl mercaptan in dimethylformamide containing potassium carbonate was repeated, but at 60° rather than 150°, and a portion of the ether extract was reduced in volume. A spontaneous exothermic reaction occurred, yielding hydrogen bromide and a green amorphous material—a reaction characteristic of the behavior of 3-bromoindole under these circumstances, thus indicating that 3-bromoindole had been formed during this reaction. When the solvent was removed from the remainder of the ether extract, but with simultaneous addition of benzene to replace most of the ether, this decomposition of the 3-bromoindole could be avoided. Chromatography of the benzene solution on neutral alumina (activity grade 1*), with pentane as eluant, removed first the indole and then 3-bromoindole from the column. The indole and 3-bromoindole could be obtained from the separate fractions and were crystallized from pentane and *n*-heptane respectively (19). The remaining fractions obtained with the eluant pentane were oils which could not be induced to crystallize. Subsequent elution with benzene gave an oil which yielded ethylthiomercuric chloride when treated with ethanolic mercuric chloride (7), indicative of the presence of 3-ethylthioindole.

Attempted Reaction of Indole with Ethyl Mercaptan in Dimethylformamide

A mixture of indole (6.9 g, 0.059 mole), 3.64 g (0.059 mole) of ethyl mercaptan, and 8.1 g (0.059 mole) of anhydrous potassium carbonate in 100 ml of anhydrous dimethylformamide (24) was refluxed for 6 h at 150°. The cooled reaction products were poured into 1 l of cold water. The aqueous mixture was extracted with ether (2 × 200 ml), and the combined ethereal extracts were washed with 0.2 *N* aqueous silver nitrate (3 × 100 ml) and then dried ($MgSO_4$). Gas–liquid and thin-layer chromatography of this solution indicated only unreacted indole, with no evidence of ethylindole.

Attempted Reaction between 3-Bromoindole and Ethylthiolobenzoate

A mixture of 3-bromoindole (5 g, 0.029 mole) and ethyl thiolobenzoate (5 g, 0.03 mole) was distilled at 146° at 31 mm pressure. Much decomposition occurred, attributed to 3-bromoindole. The distillate contained only ethylthiolobenzoate as shown by infrared spectroscopy, with no evidence of 3-ethylindole.

Attempted Reaction between Ethylthiolobenzoate or Diethyl Disulfide and Mercuric Chloride

A sample (1 g) of each of ethylthiolobenzoate and diethyl disulfide was added to separate 10-ml quantities of saturated ethanolic mercuric chloride. On standing for 48 h, the solutions deposited no ethylthiomercuric chloride.

Reaction of Indole Magnesium Bromide with Ethanesulfenyl Chloride

Ethyl bromide (26.1 g, 0.26 mole) in 600 ml of anhydrous ether was treated with 6 g (0.25 mole) of magnesium turnings. When the reaction was complete 27 g (0.23 mole) of indole in 50 ml of dry ether was added as quickly as refluxing permitted and the solution then gently refluxed for 10 min. To the resulting indole magnesium bromide (now cooled to −15°) was added dropwise 23.1 g (0.26 mole) of ethanesulfenyl chloride in 50 ml of anhydrous ether so that the temperature of the reaction was maintained at −10°. The mixture slowly became deep red. When the addition of the halide was completed, the vessel and contents were allowed to attain room temperature and then the solution was refluxed for 3 h. The mixture was cooled and poured into 2 l of water, and the pH adjusted to 7 with acetic acid. The ether layer was separated and the aqueous layer extracted with ether (2 × 200 ml). The volume of the combined ethereal solutions was reduced to about 400 ml. This solution was extracted with water (3 × 200 ml) and washed with 0.2 *N* aqueous silver nitrate (2 × 100 ml), from which was obtained 1.5 g of silver ethyl mercaptide whose infrared spectrum (halo oil mull) was identical with that of a sample prepared from aqueous ethyl mercaptan and silver nitrate. The remaining ether filtrate was freed from solvent and the brown oil, when taken up in ethyl alcohol and kept overnight at −20°, afforded 5.1 g of 3,3′-diindolyl sulfide. One recrystallization from toluene gave a melting point of 232° (lit. m.p. 232° (30)).

Anal. Calcd. for $C_{16}H_{12}N_2S$: C, 72.73; H, 4.65; N, 9.44; S, 12.12. Found: C, 72.76; H, 4.61; N, 9.47; S, 11.94.

**Alupharm Chemicals, P.O. Box 755, New Orleans, Louisiana, U.S.A.*

The filtrate obtained after removal of the 3,3′-diindolyl sulfide was freed of solvent and the resulting oil divided into two equal portions. One portion was subjected to vacuum distillation and gave 2.1 g of indole, b.p. 110° at 6 mm pressure, and 3.8 g of 3-ethylindole, b.p. 170° at 3 mm pressure. These compounds were identified by melting points of their respective picrates as well as by comparative infrared spectra with those of authentic samples. Portions of the remaining half of the above filtrate were analyzed by gas–liquid chromatography. Peaks with retention times identical with those of authentic indole, 3-ethylindole, 3-ethylthioindole, and diethyl disulfide appeared. At least three other unidentified compounds were indicated by peaks in the gas–liquid chromatography. A portion of this filtrate, treated with saturated ethanolic mercuric chloride, precipitated ethylthiomercuric chloride (7). Thin-layer chromatography yielded similar results but showed, in addition, the presence of 3,3′-diindolyl, identified by its R_f value and the characteristic blue-white fluorescence (9).

Attempted Reaction of Indole Magnesium Bromide with 3-Ethylthioindole

Magnesium turnings (1.2 g, 0.05 mole) in 50 ml of dry ether were treated at 5° with 5.5 g (0.05 mole) of ethyl bromide in 10 ml of dry ether. On completion of the reaction, 6 g (0.05 mole) of indole in 25 ml of dry ether was added as quickly as the reaction permitted. When the evolution of ethane had ceased (about 0.5 h later) the mixture was cooled to 0° and 8.55 g (0.05 mole) of 3-ethylthioindole (1) in 10 ml of anhydrous ether was added dropwise so that the reaction temperature remained between 0–5°. The solution was then warmed to reflux and maintained at this temperature for 3 h. It was then worked up in the same manner as in the reaction of indole magnesium bromide with ethanesulfenyl chloride to the point of silver nitrate wash. It was dried ($MgSO_4$) and reduced in volume. Gas–liquid chromatography indicated the presence of only two products whose retention times were identical with those of indole and 3-ethylthioindole. The ether was removed and the oil taken up in ethanol, from which products could not be induced to crystallize.

A repetition of this experiment, using enough magnesium and ethyl bromide to form indole dimagnesium bromide, gave the same results.

Air Oxidation of Indole Magnesium Bromide

An ether solution of indole magnesium bromide, prepared as described above, was stirred at room temperature for 26 h, in a flask equipped with a drying tube but with no precaution taken for the exclusion of dry air. The mixture was then treated with ice and water, followed by sufficient acetic acid to convert the solution to a pH of 7. The solution was washed with water, dried ($MgSO_4$), and freed from ether. Thin-layer chromatography indicated that the main product was indole. It was also accompanied by a small amount of 3,3′-diindolyl, as shown by the strong blue-white fluorescence (9), a positive Ehrlich test (14), and comparison of its R_f value with that of an authentic specimen (8). Also, at least nine other indole compounds were indicated by the Ehrlich spray on the thin-layer chromatogram.

Reaction of Phenyl Magnesium Bromide with Ethanesulfenyl Chloride

Magnesium turnings (1.2 g, 0.05 mole) in 50 ml of dry ether at 5° were treated with 8 g (0.05 mole) of bromobenzene in 10 ml of ether. When the reaction was completed, the solution was cooled to 0° and 4.8 g (0.05 mole) of ethanesulfenyl chloride in 10 ml of dry ether was added dropwise so that the temperature remained between 0 and 5°. The solution was then refluxed for 2 h, cooled, and worked up as described for the reaction of indole magnesium bromide with ethanesulfenyl chloride to the point of silver nitrate and subsequent water wash. The dried ($MgSO_4$) solution was reduced in volume and subjected to g.l.c. analysis. Only benzene and ethyl phenyl sulfide were present, identified by comparison of the retention times with those of authentic samples. There was no evidence of ethyl benzene or chlorobenzene.

Attempted Reaction of Indole Magnesium Bromide with 3,3′-Diindolyl Disulfide

Magnesium turnings (1 g, 0.0416 mole) in 50 ml of dry ether were treated with 6.16 g (0.0395 mole) of ethyl iodide in 10 ml of dry ether. On completion of the reaction, 4.68 g (0.06 mole) of indole in 10 ml of dry ether was added dropwise. Twenty minutes after the addition of the indole, 4.0 g (0.00135 mole) of 3,3′-diindolyl disulfide (27) in 10 ml of dry tetrahydrofuran was added dropwise. The resulting mixture was refluxed for 2 h, then poured into 400 ml of ice water, and filtered. The filtrate, dried ($MgSO_4$) and extracted in a Soxhlet extractor with pentane, gave a recovery of 3.75 g of the 3,3′-diindolyl disulfide. No 3,3′-diindolyl sulfide was detected.

ACKNOWLEDGMENTS

The authors are grateful to the National Research Council of Canada for their generous financial support during the course of this work.

Grateful acknowledgment is also made to Dr. T. H. Aaron of the Baker Clinic, Edmonton, for his generous medical assistance when allergic reactions developed, and for his cooperation in conducting tests on potential allergenic substances.

Can. J. Chem. Downloaded from www.nrcresearchpress.com by 210.87.254.42 on 09/05/12
For personal use only.

REFERENCES

1. R. V. JARDINE and R. K. BROWN. Can. J. Chem. This issue.
2. H. LECHER. Ber. **58**, 409 (1925).
3. G. E. HILBERT and J. B. JOHNSON. J. Am. Chem. Soc. **51**, 1926 (1929).
4. G. SANNA and S. STEPHEN. Gazz. Chim. Ital. **72**, 305 (1942); Chem. Abstr. **38**, 3953 (1944).
5. N. KHARASCH (*Editor*). Organic sulfur compounds. Vol. 1. Pergamon Press, New York. 1961. Chap. 30.
6. D. C. GREGG, H. A. IDDLES, and P. W. STEARNS. J. Org. Chem. **16**, 246 (1951).
7. F. CHALLENGER and A. A. RAWLINGS. J. Chem. Soc. 868 (1937).
8. W. CARPENTER, M. S. GRANT, and H. R. SNYDER. J. Am. Chem. Soc. **82**, 2739 (1960).
9. S. GABRIEL, W. GERHARD, and R. WALTER. Ber. **56**, 1024 (1923).
10. H. WUYTS. Bull. Soc. Chim. [3] **35**, 166 (1906).
11. H. BRINTZINGER and H. SCHMAHL. Ber. **87**, 314 (1954).
12. A. SCHOBERL and A. WAGNER. Methoden der organischen Chemie. Houben-Weyl. Vol. 9. Georg Thieme Verlag, Stuttgart. 1955. p. 276.
13. N. KHARASCH, W. KING, and T. C. BRUCE. J. Am. Chem. Soc. **77**, 931 (1955).
14. W. C. SUMPTER and F. M. MILLER. Heterocyclic compounds with indole and carbazole systems. Interscience Publishers, Inc., New York. 1954. p. 49.
15. D. S. TARBELL and D. P. HARNISH. J. Am. Chem. Soc. **54**, 4100 (1932).
16. A. J. PARKER and N. KHARASCH. J. Am. Chem. Soc. **82**, 3071 (1960).
17. J. F. BUNNETT. J. Am. Chem. Soc. **79**, 5969 (1957).
18. T. P. JOHNSTON, L. B. HOLUM, and J. A. MONTGOMERY. J. Am. Chem. Soc. **80**, 6265 (1958).
19. K. PIERS, C. MEIMAROGLOU, R. V. JARDINE, and R. K. BROWN. Can. J. Chem. **41**, 2399 (1963).
20. A. HANTZSCH and E. SCHARF. Ber. **46**, 3582 (1913).
21. H. BOTTGER. Ann. **223**, 248 (1884).
22. H. E. JOHNSTON and D. G. CROSBY. J. Org. Chem. **28**, 1246 (1963).
23. R. WEISSGERBER. Ber. **46**, 651 (1913).
24. L. F. FIESER. Experiments in organic chemistry. 3rd ed., revised. D. C. Heath and Co., Boston, Mass. 1957. p. 284.
25. A. VERLEY and J. BEDURVÉ. Bull. Soc. Chim. France, [IV] **37**, 189 (1925).
26. A. KORCZYNSKI, W. BRYDORWNA, and L. KIERZEK. Gazz. Chim. Ital. **56**, 905 (1926); Chem. Abstr. **21**, 1262 (1927).
27. R. G. WOODBRIDGE and G. DOUGHERTY. J. Am. Chem. Soc. **72**, 4320 (1950).
28. M. S. GRANT and H. R. SNYDER. J. Am. Chem. Soc. **82**, 2742, (1960).
29. H. BRENTZINGER, M. LANGHECK, and H. ELLWANGER. Ber. **87**, 320 (1954).
30. W. MADELUNG and M. TENCER. Ber. **48**, 949 (1915).

Can. J. Chem. Downloaded from www.nrcresearchpress.com by 210.87.254.42 on 09/05/12
For personal use only.

Can. J. Chem. Downloaded from www.nrcresearchpress.com by 210.87.254.40 on 09/05/12
For personal use only.

AUTOXIDATION REACTIONS CATALYZED BY COBALT ACETATE BROMIDE

ALLAN S. HAY AND HARRY S. BLANCHARD
General Electric Research Laboratory, Schenectady, New York

Received November 13, 1964

Dedicated to Professor R. B. Sandin on the Occasion of his Sixty-Eighth Birthday

ABSTRACT

Cobalt acetate bromide in acetic acid solution is an extraordinarily active catalyst for the autoxidation of hydrocarbons. Carboxylic acids and ketones are readily prepared in high yields at moderate temperatures and at atmospheric pressure. In addition, benzylic and allylic groups can be converted to esters of the corresponding alcohols, and the oxidation of tetralin can be controlled to give either α-tetralone or 1,2-dihydronaphthalene as the major product. A mechanism for these reactions is postulated.

INTRODUCTION

The autoxidation of aralkyl hydrocarbons has received considerable attention in recent years, and the mechanism (eqs. [1]–[5]) is now well understood (1).

[1] $$\text{Initiator} \xrightarrow{k_i} 2R'\cdot$$

[2] $$R'\cdot + O_2 \rightarrow R'OO\cdot$$

[3] $$R'OO\cdot + RH \rightarrow R'OOH + R\cdot$$

[4] $$R\cdot + O_2 \rightarrow ROO\cdot$$

$$ROO\cdot + RH \xrightarrow{k_p} ROOH + R\cdot$$

[5] $$2ROO\cdot \xrightarrow{k_t} \text{nonradical products}$$

In the presence of heavy metal salts this reaction sequence is modified principally by reactions [6] and [7], which increase the rate of free radical production (2) and have a profound effect on the products of the reaction.

[6] $$Co^{+2} + ROOH \rightarrow Co^{+3} + RO\cdot + OH^-$$

[7] $$Co^{+3} + ROOH \rightarrow Co^{+2} + ROO\cdot + H^+$$

For compounds having a methyl group on an aromatic ring, these degradation reactions eventually result in a carboxyl group, and this is the basis of some commercial processes for the production of such acids.

In a previous report (3) we described the ozone-initiated cobalt-catalyzed autoxidation of aralkyl hydrocarbons. Ozone oxidizes cobalt(II) to cobalt(III) and thus serves to initiate the cyclic sequence in eqs. [6] and [7]. As soon as oxidation of the aralkyl hydrocarbon begins, the ozone may be stopped since the peroxy intermediates will reoxidize cobalt(II) efficiently. Thus, ozone serves the same function as acetaldehyde and methyl ethyl ketone in the processes described by Hull (4) and Brill (5).

In this system, *p*-xylene and *m*-xylene are readily oxidized to the corresponding toluic acids. Continued oxidation results in high yields of corresponding dibasic acids. However, when *o*-xylene is subjected to this system, the principal product is *o*-toluic acid, and

o-phthalic acid is formed only in amounts equivalent to the cobalt ion in solution. Apparently *o*-phthalic deactivates the catalyst, since the reaction proceeds only very slowly.

We hypothesized that *o*-phthalic acid was influencing the oxidation potential of the Co(II)–Co(III) couple by chelation with cobalt ions. If so, the propagation reactions (eqs. [6] and [7]) would be affected and the rates decreased. To circumvent this retardation by *o*-phthalic acid, we decided to run the reaction in the presence of acids stronger than acetic and *o*-phthalic. Among the many acids tried, α-bromoacetic acid was unique in that it allowed *o*-xylene to be rapidly oxidized in high yield to *o*-phthalic acid. The reaction mixture became deep blue and the effect was soon found to be due to a bromine ion presumably formed via reaction with cobalt acetate.

[8] $$BrCH_2CO_2H + Co(Ac)_2 \rightarrow CoAcBr + AcOCH_2CO_2H$$

No ozone was necessary in this reaction.

This paper describes the scope of cobalt acetate bromide (CAB) catalyzed autoxidations and the results of our study on the mechanism of the reaction. The effect of bromine on metal-catalyzed autoxidations, principally as a route to the phthalic acids, has been the subject of intensive work in other laboratories (6), and a comparison with these results is made.

DISCUSSION AND RESULTS

The addition of an equimolar amount of hydrogen bromide to cobalt(II) acetate in acetic acid solution gives a catalyst that is extraordinarily active for the autoxidation of methylene or methyl groups adjacent to an aromatic ring to ketones or carboxylic acids, respectively (7). Thus, *p*-xylene can be readily oxidized to terephthalic acid at atmospheric pressures and at temperatures as low as 60–100 °C. Tetralin is oxidized rapidly at room temperature to α-tetralone. Phenacyl esters can be prepared from the corresponding β-phenethyl esters and oxidation of methylphenyl acetate yields methylphenyl glycoxylate. Further examples are described in the Experimental section. All of these reactions are performed at atmospheric pressure and moderate temperatures (25–120 °C) and thus are readily adaptable to conventional equipment in the laboratory.

Most metal-catalyzed autoxidation reactions require only trace amounts of catalyst and, in fact, the catalytic effect reaches a maximum value at relatively low concentrations (8). In the CAB system, concentrations of catalyst of at least 0.1 *M* are necessary for optimum reaction rates. Below this concentration the rates drop off rapidly. This can be qualitatively demonstrated by oxidizing *p*-xylene at various catalyst concentrations and observing the point at which terephthalic acid, which is insoluble in the reaction mixture, first precipitates (Fig. 1).

In most metal ion autoxidation systems, the anion associated with the metal ion is of minor importance in determining the activity of the metal ion as a catalyst. Obviously, the anion can play a role in aiding solubility of the salt or in increasing or decreasing the oxidation–reduction potential of the metal ions. In general, however, these effects are small. Bromine, however, is unique in that, when used in conjunction with cobalt(II) ion, it yields a catalyst of increased activity. Other metal ions such as manganese and cerium also show this effect, but to a more limited extent. Moreover, we discovered that the ratio of the atoms of bromine to the atoms of cobalt in the catalyst system and the molar concentration of the catalyst have a profound and unexpected effect on the low-temperature oxidation reaction. Therefore, we have devoted considerable study to defining the scope of the reaction and to elucidating the mechanism of the reaction.

Can. J. Chem. Downloaded from www.nrcresearchpress.com by 210.87.254.40 on 09/05/12
For personal use only.

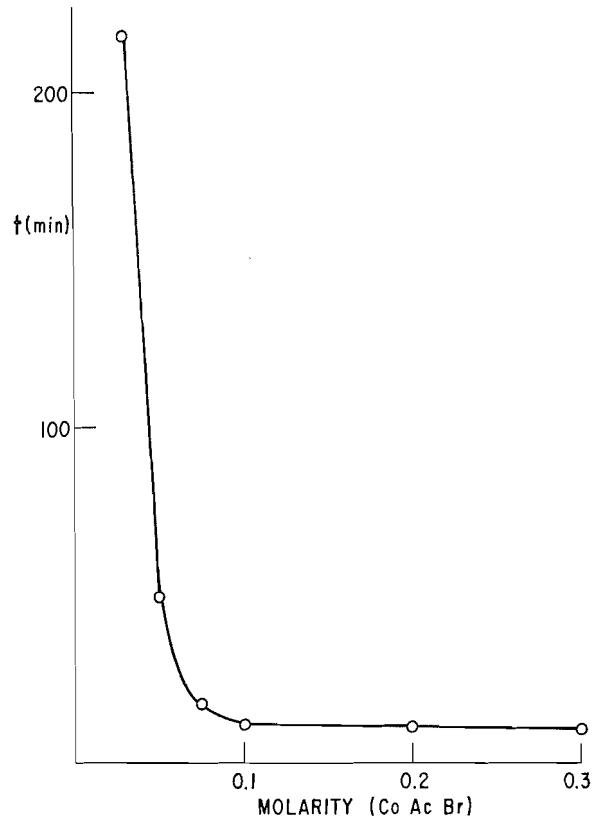

FIG. 1. Oxidation of *p*-xylene (0.4 *M*) at 90 °C in acetic acid. [CoAcBr] = 0.1 *M*; *t* = time in minutes for the appearance of terephthalic acid.

Any explanation devised to account for the uniqueness of the CAB system must account for the following facts. (i) The rates of autoxidation are greatly enhanced by the presence of the bromine, much more so than if the metal ions were present alone. (ii) The nature of the products in a given autoxidation can be profoundly altered. Thus, for example, *p*-xylene is converted easily and at temperatures as low as 60 °C to terephthalic acid. (iii) Bromine is unique in its effect. None of the other halogens or their compounds approach it in activity.

Since bromine has such a profound effect on autoxidations it seemed important to establish unequivocally that the free-radical nature of the reaction was preserved in the presence of the bromine-containing catalyst. It might be imagined, for example, that the addition of bromine had completely changed the reaction to such an extent that we were no longer dealing with a free-radical chain reaction. Indeed, in the early phases of the investigation, it was found that hydrocarbons such as toluene, xylene, and cumene could be autoxidized in the presence of CAB without the addition of the usual free-radical initiator. However, when highly purified hydrocarbons were treated in this manner, induction periods were observed which were apparently dependent on the degree of purity. Moreover, these induction periods could be removed by (*a*) exposing the purified hydrocarbons to air and light before the oxidation or (*b*) adding hydroperoxides or α,α-azo-bisisobutyronitrile (AIBN) as an initiator. Further, and significantly, it was found

Can. J. Chem. Downloaded from www.nrcresearchpress.com by 210.87.254.40 on 09/05/12
For personal use only.

that addition of such a typical free-radical chain inhibitor as 2,6-di-*t*-butyl-*p*-cresol (DBPC) inhibited the oxidations. These findings offer strong support to the idea that the autoxidations in the presence of CAB follow the typical free-radical chain mechanism operative in normal initiated autoxidations.

Since the mechanism for initiated autoxidations is composed of three distinct parts, namely, initiation, propagation, and termination, it is conceivable that CAB could have an effect on any or all of these steps. To determine its effect on the initiation step, we have studied rates of initiation in the AIBN-initiated autoxidation of cumene in the presence and in the absence of CAB. The results of this phase of the investigation, which was carried out as described in ref. 9 for cobalt(II) ions themselves, are presented in Table I.

TABLE I

Inhibited oxidations of cumene (1.03 *M*) in acetic acid initiated by azo-bisisobutyronitrile (0.097 *M*) at 60 °C

$[Co^{++}]$ (mole l^{-1}) $\times 10^3$	$[Br^-]$ (mole l^{-1}) $\times 10^3$	[DBPC]* (mole l^{-1}) $\times 10^3$	Time of inhibition (min)	Rate† (mole l^{-1} s^{-1}) $\times 10^6$
—	—	—	2	4.89
8.0	—	—	2	5.72
16.0	—	—	2	6.96
—	—	1.77	48	4.89
—	—	3.54	93	4.89
8.0	8.0	1.77	48	38.6
16.0	16.0	1.77	48	76.0
16.0	16.0	3.54	93	76.0
14.0‡	14.0‡	1.77	47	5.30

*Initial concentration of 2,6-di-*t*-butyl-*p*-cresol.
†Rate following the inhibition period.
‡Initial concentration of cobaltous acetate chloride.

As is evident from the data in Table I, the lengths of the inhibition periods in the presence and in the absence of CAB are identical within experimental error. From this fact, the important conclusion can be drawn that the rate of free-radical production is the same in the presence as it is in the absence of the added CAB, and therefore the CAB has no effect on the initiation reaction. Stated somewhat differently, it can be concluded that there is no direct reaction between CAB, oxygen, and hydrocarbon which leads directly to free-radical production, and therefore an enhanced rate of oxidation (10). It follows that the explanation for the bromine effect must be sought either in the propagation reaction and (or) the termination reaction.

First, let us consider the possibility that the main function of the CAB is to enhance the rate of autoxidation by speeding up the propagation reaction. As shown in Table I, the rates of oxidation in the presence of CAB are substantially faster than those in the absence of CAB. Moreover, this rate enhancement must be intimately bound up with the bromine since, as shown by the data in Table I, those runs containing cobalt(II) ions with no bromine show only a slight rate enhancement. Moreover, as shown by the last experiment in Table I, cobaltous acetate chloride shows virtually no rate enhancement. Based on the earlier work of Vaughan, Rust, and their co-workers (11) we were led to consider the possibility that bromine could enhance the rate of autoxidations independent of the metal ion. To this end we studied the effect of anhydrous hydrogen bromide on the initiated oxidation of cumene. The results of this phase of the study are presented in Fig. 2.

As shown in Fig. 2, anhydrous hydrogen bromide enhances the rate of oxidation of cumene markedly. Indeed, in the initial stages of oxygen absorption the rates are increased

Can. J. Chem. Downloaded from www.nrcresearchpress.com by 210.87.254.40 on 09/05/12
For personal use only.

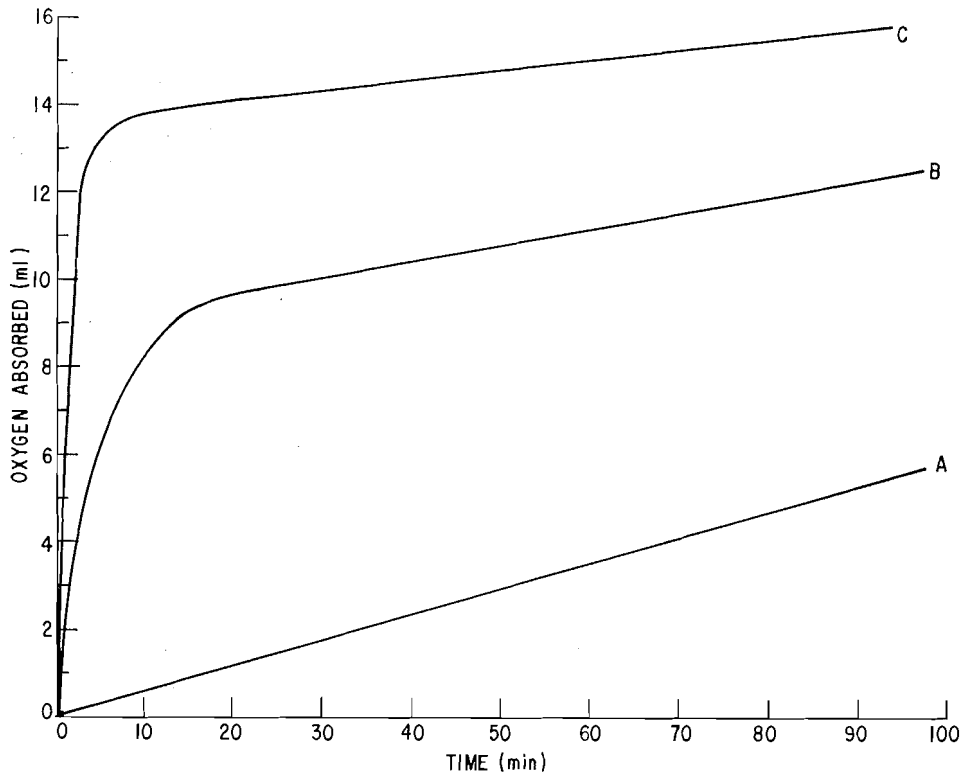

FIG. 2. The effect of hydrogen bromide on the AIBN-initiated oxidation of cumene. Curve A, AIBN-initiated rate, no HBr; curve B, AIBN plus 0.022 *M* HBr; curve C, AIBN plus 0.04 *M* HBr.

by 3–4 orders of magnitude. This rate enhancement is best explained on the basis of eqs. [9], [10], and [11] as postulated by Vaughan, Rust, and co-workers.

[9] $$ROO\cdot + HBr \rightarrow ROOH + Br\cdot$$

[10] $$Br\cdot + RH \rightarrow HBr + R\cdot$$

[11] $$R\cdot + O_2 \rightarrow ROO\cdot$$

Moreover, reaction [9] would not be expected to be important in the case of anhydrous hydrogen chloride since the bond energy for this substance is some 15 kcal/mole higher than that for anhydrous hydrogen bromide (12). Obviously, hydrogen iodide possesses a low enough bond energy to participate in the propagation step. However, because of the facile oxidation of iodide ion to molecular iodine, a well-known scavenger of free radicals, this substance actually functions as an inhibitor. Thus, the oxidation curves presented in Fig. 2 show that the rates of oxygen absorption can be greatly enhanced quite independently of the cobalt(II) ions.

As shown in Fig. 2, the initially fast rates continue only for a relatively short time and ultimately approach a value which is, in fact, slower than the AIBN-initiated rate of oxidation of cumene. This is due, at least in part, to the production of phenolic inhibitors, apparently arising from the heterolytic rearrangement of cumene hydroperoxide (eq. [12]). As pointed out earlier, the reaction is a free-radical chain process and, hence, is subject to inhibition by phenolic-type inhibitors. However, this is not the whole story, because even

Can. J. Chem. Downloaded from www.nrcresearchpress.com by 210.87.254.40 on 09/05/12
For personal use only.

[12] 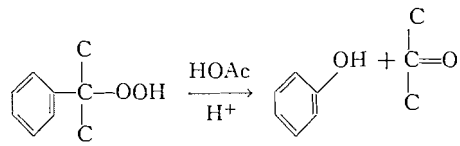

triptane shows this same kind of behavior and the products of the acid-catalyzed rearrangement of triptane hydroperoxide (*tert*-butyl alcohol and acetone, eq. [13]) are not oxidation inhibitors. Rather, what appears to be the case is that the bromine is actually consumed, causing the reaction to "run downhill."

[13] 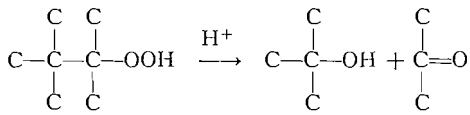

Support for this idea is gained by the fact that addition of more hydrogen bromide to a triptane oxidation where the rate has fallen off to a very low value causes a resumption in the rate. Thus, a solution of triptane (1.03 *M*) in benzene containing anhydrous hydrogen bromide (0.06 *M*) and AIBN (0.097 *M*) absorbs approximately 15 ml of oxygen in 10 min, after which oxidation virtually ceases. If, at this point, the solution is again made 0.06 *M* with respect to anhydrous hydrogen bromide, oxidation can be resumed and an additional 15 ml of oxygen will be absorbed in 10 min time. This cycle can be repeated several times. To account for this behavior, we suggest the following reactions.

[14] $$Br\cdot + Br\cdot \rightarrow Br_2$$

[15] $$R\cdot + Br_2 \rightarrow RBr + Br\cdot$$

Each time reaction [15] takes place, bromine will be "lost" as a catalyst and, providing those reactions are efficient enough, all of the bromine can be used up in reactions of this kind.

More recently, McIntyre and Ravens (13) have oxidized aralkyl hydrocarbons to carboxylic acids in high yield in aqueous hydrogen bromide with oxygen in the temperature range 180–200 °C. These reactions, in all probability, proceed by the same mechanism as those described by Rust and Vaughan. The intermediate hydroperoxides formed in both cases would be thermally decomposed to the aldehyde and alcohol. Lorand and Edwards (14) have, for example, prepared *p*-methylbenzyl hydroperoxide and find it rapidly decomposes above 130 °C. In reactions studied by Rust and Vaughan, a significant side reaction is the formation of the benzyl bromide; however, in the aqueous system, as pointed out by McIntyre and Ravens (13), any bromides formed would be rapidly hydrolyzed to the alcohol and subsequently oxidized to the acid under the reaction conditions.

From the results described, it appears that the rate enhancement can be explained on the basis that the rate of the propagation reaction is greatly increased by the presence of bromine atoms. It remains, however, to assign a role to the metal ions. From the nature of the products (phthalic acid from xylene, acetophenone from ethyl benzene, etc.) it is clear that reactions [6] and [7] are operative in this system and one function of the metal ions is to degrade the intermediate hydroperoxides. This will, of course, lead to rate enhancement since the rate of free-radical production is increased. However, as shown previously (9) for cobalt(II) ions, this rate enhancement is not strikingly large. We feel that the major function of the metal ions in this system can best be explained on the basis of equilibrium [16]. As shown, this equilibrium is shifted well to the right and thus one

Can. J. Chem. Downloaded from www.nrcresearchpress.com by 210.87.254.40 on 09/05/12
For personal use only.

function of the cobalt(II) ions is to keep the concentration of free hydrogen bromide at a

[16] $$Co(OAc)_2 + HBr \rightleftharpoons Co\begin{matrix}OAc\\ \diagup\\ \\ \diagdown\\ Br\end{matrix} + HOAc$$

very low value, thus preventing any heterolytic rearrangement of hydroperoxides to phenol.

It is interesting to note that in the oxidation of benzyl *n*-butyl ether an appreciable by-product is benzaldehyde. Increasing the concentration of bromide ion (and hence increasing the acidity of the reaction mixture) increases the amount of benzaldehyde formed. The intermediate hydroperoxide,

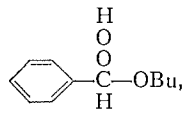

which has an acetal structure, would be expected to be readily cleaved by acid to benzaldehyde in competition with the cobalt-catalyzed decomposition to butyl benzoate. Secondly, cobalt(II) must also have the ability of preventing bromine from being consumed by reactions such as [14] and [15]. Since the above equilibrium is shifted to the right, the concentration of free hydrogen bromide will be low and, thus, the concentration of bromine atoms will be low. This situation will make the recombination reaction [14] slow. Addition of cobalt(II) acetate to a warm solution of benzyl bromide in acetic acid immediately generates the intense blue color caused by cobalt acetate bromide. Thus, the cobalt acetate is able to reconvert benzylic bromide back to ionic bromine and keep the catalyst active.

[17] $$Co(OAc)_2 + \phi CH_2Br \rightarrow CoAcBr + \phi CH_2OAc$$

Interestingly, it was observed that when these reactions became too anhydrous the catalyst rapidly lost its activity, as evidenced by the change in color of the solution from blue to pink and the presence of lachymatory materials in the reaction mixture, presumably benzyl bromides. Also, if the reactions were deliberately performed under anhydrous conditions with sodium acetate added, the blue color of the reactions was maintained and a major product was the allylic or benzylic ester, e.g.

[18] 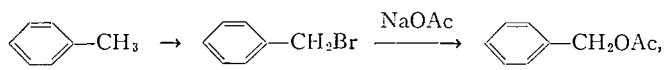

[19] 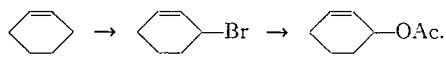

A useful method for the preparation of allylic and benzylic esters in moderate yields using inexpensive reagents is thus afforded.

The oxidation of tetralin is of particular interest. This oxidation takes place rapidly at room temperature to give α-tetralone as the major product. However, on distillation of the product the fraction containing unreacted tetralin also contained appreciable amounts of 1,2-dihydronaphthalene and naphthalene. The intermediate α-tetralyl radical can react in either of the following ways.

Can. J. Chem. Downloaded from www.nrcresearchpress.com by 210.87.254.40 on 09/05/12
For personal use only.

[20] 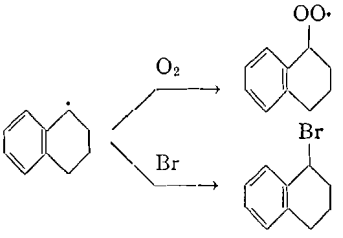

[21]

The reaction with oxygen eventually gives α-tetralone; however, under the present reaction conditions the bromotetralin would dehydrohalogenate to 1,2-dihydronaphthalene. Subsequent oxidation of 1,2-dihydronaphthalene could give, in the same manner, naphthalene or α-naphthol. The latter would inhibit the oxidation and consume bromine, and indeed in the latter stages of the reaction the blue color of the active catalyst is invariably lost. When the oxidation is starved for oxygen the major product then becomes 1,2-dihydronaphthalene. Presumably, if the reaction were performed at higher oxygen pressures, this side reaction could be eliminated.

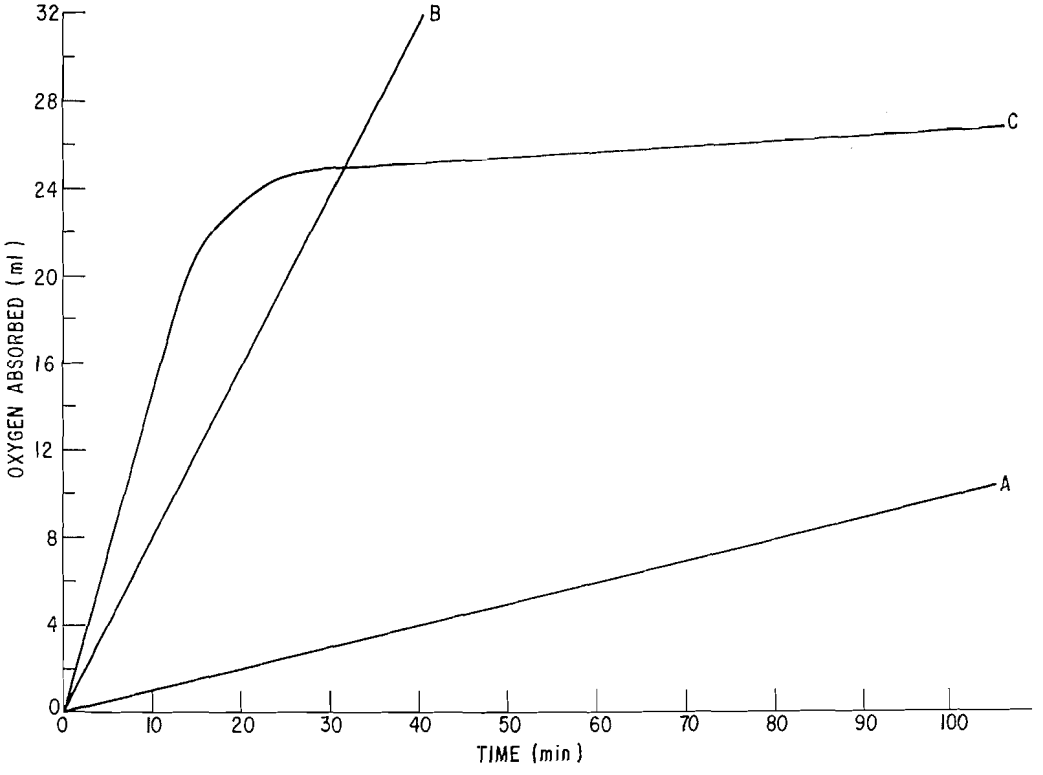

FIG. 3. Oxidation of cumene. (A) AIBN-initiated oxidation; (B) AIBN plus CAB; (C) AIBN plus cobalt(II) bromide.

If the equilibrium situtation depicted in eq. [16] actually prevails, it should follow that increases in the bromine to cobalt ratio should cause increases in the rates of oxygen absorption. As shown by the typical oxidation curves in Fig. 3, this prediction is borne out. Thus, curve A shows the AIBN-initiated rate of oxidation of cumene in the absence of

Can. J. Chem. Downloaded from www.nrcresearchpress.com by 210.87.254.40 on 09/05/12
For personal use only.

cobalt(II) acetate bromide. Curve B shows the marked rate enhancement observed in the presence of cobalt(II) acetate bromide (prepared from equimolar amounts of cobalt(II) acetate and anhydrous hydrogen bromide). Finally, curve C shows the even greater enhancement observed in the *initial* rate of oxygen absorption caused by cobalt(II) bromide. However, as shown in Fig. 3, the initially rapid oxidation observed in the presence of cobalt(II) bromide is sustained for only a very short period and quickly falls to a value lower than the AIBN-initiated rate of oxidation itself. We interpret this result to mean that the concentration of hydrogen bromide present in the equilibrium depicted in eq. [15] has now increased to such an extent that phenolic inhibitors are formed and the oxidation will not proceed to completion. By way of comparison, it should be noted that curve B shows no evidence of departure from linearity and, in fact, oxidations in the presence of equimolar amounts of cobalt(II) acetate and hydrogen bromide proceed readily to completion. Thus, from a practical standpoint, when the reaction is run below 120 °C the optimum catalyst is obtained when quantities of cobalt(II) acetate and hydrogen bromide are in the range encompassing equimolar amounts.

EXPERIMENTAL

Most of the reactions described represent only one experiment and no attempt has been made to optimize the reactions.

The general reaction conditions employed are illustrated by the oxidation of *o*-bromotoluene to *o*-bromobenzoic acid.

The reaction flask consisted of a 1-l round-bottomed flask equipped with an oxygen inlet tube and thermometer and a condenser which also served as a gas exit tube. Efficient oxygen–liquid mixing was obtained with a Vibromixer stirrer. Flowmeters were attached to the inlet and exit tubes to measure the oxygen consumption to indicate when the reactions were completed.

Oxidation of R—CH_3 to R—COOH

To the reaction flask was added 25 g (0.1 mole) of cobalt(II) acetate, 27 g (0.1 mole) of 30% hydrogen bromide in acetic acid, 500 ml of acetic acid, and 86.5 g (0.5 mole) of *o*-bromotoluene. Oxygen (600 ml/min) was bubbled through the vigorously stirred reaction mixture, which was initially heated to 90°, at which point the reaction became exothermic and kept the reaction at the temperature of reflux. The reaction was continued for 2 h, during which time the temperature rose to a maximum of 112°. At the end of this period, oxygen was no longer being absorbed. The reaction mixture was cooled and made up to 1 l with ice water. From the solution, *o*-bromobenzoic acid (90.5 g, 91% yield) separated, m.p. 146.5–148°. There was no depression in a mixed melting point with an authentic sample. In a similar fashion the carboxylic acids in Table II were prepared.

TABLE II

Oxidation of 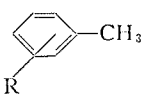

R	Product	Yield	m.p.	N.E.
H-	Benzoic acid	86	121	
p-Cl-	*p*-Chlorobenzoic acid	88	240	
o-Cl-	*o*-Chlorobenzoic acid	86	141	
p-Me-	Terephthalic acid	71.5*	>300	86.3
p-Me 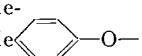	Oxydibenzoic acid	87*	>300	131.2
p-Me 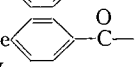	Benzophenone dicarboxylic acid	76*	>300	132.2
m-Me-	Isophthalic acid	67*	>300	86.5
p-Et-	4-Acetylbenzoic acid	78		157

*The dibasic acid is insoluble in the reaction mixture. By dilution of the filtrate with water the monocarboxylic acid is obtained.

Can. J. Chem. Downloaded from www.nrcresearchpress.com by 210.87.254.40 on 09/05/12
For personal use only.

Phenacyl Benzoate

To a 250-ml flask was added 5 g (0.02 mole) of cobalt acetate, 4 ml (0.02 mole) of 30% hydrogen bromide in acetic acid, 22.6 g (0.1 mole) of β-phenethylbenzoate, and 100 ml of acetic acid. Oxygen (600 ml/min) was passed through the vigorously stirred solution for 75 min, during which time the temperature of the reaction mixture was raised from 60 °C to 80 °C. The reaction mixture was poured into 1 l of ice water and the solid removed by filtration. The solid was dissolved in ether and washed with potassium carbonate solution to remove benzoic acid. The ether layer was dried and evaporated to yield 17.0 g (0.071 mole, 71% yield) of phenacyl benzoate, m.p. 121 °C.

n-Butyl Benzoate

Oxygen (600 ml/min) was passed through a vigorously stirred solution of 5 g (0.02 mole) of cobalt acetate, 4 ml (0.02 mole) of 30% hydrogen bromide in acetic acid, and 32.8 g (0.2 mole) of benzyl-*n*-butyl ether in 100 ml of acetic acid. Over a period of 11 min, the temperature rose from 30 to 100 °C. The reaction was continued for a further 50 min and then poured into 1.5 l ice water and extracted with ether. The ether was washed with potassium carbonate solution and then dried, evaporated, and distilled to yield 21.5 g (0.12 mole, 60% yield) of *n*-butyl benzoate, b.p. 60° at 0.5 mm, n_D^{20} 1.4975. From the potassium carbonate layer after acidification there was obtained 7.5 g (0.61 mole, 31% yield) of benzoic acid.

A series of three reactions were run in a similar fashion except that the temperature was kept below 45 °C and at different bromine to cobalt ratios, and the neutral portion of the product was examined by vapor phase chromatography for benzaldehyde.

Br/Co	Benzaldehyde, % yield
1	13.7
1.5	15.2
1.9	28.5

n-Hexyl Caproate

To a 500-ml flask equipped as previously described with the addition of a Dean–Stark trap was added 150 g (1.47 moles) of *n*-hexanol, 50 g of benzene, 5 g (0.02 mole) of cobalt acetate, and 3.27 g (0.01 mole) of cobalt bromide. Oxygen (1 000 ml/min) was passed through the vigorously stirred solution at reflux and water was collected in the Dean–Stark trap. Over a 2-h period the temperature of the reaction mixture rose from 89 to 143 °C and a total of 24 ml of water was collected. The reaction mixture was cooled and dissolved in 300 ml of ether, then washed with cold dilute hydrochloric acid to remove the cobalt salts. The ether layer was washed with cold dilute potassium carbonate solution, then dried, and distilled to yield 14.9 g (0.15 mole) of *n*-hexanol and 56.9 g (0.28 mole) of *n*-hexyl caproate. The potassium carbonate layer was acidified and after distillation there was obtained 26.7 g (0.23 mole) of caproic acid.

Methylphenylglyoxylate

To a 1-l flask was added 600 ml of acetic acid, 10 g (0.04 mole) of cobalt(II) acetate, 2.6 g (0.008 mole) of cobalt(II) bromide, and 75 g (0.5 mole) of methylphenylacetate. Oxygen (800 ml/min) was bubbled through the vigorously stirred reaction mixture at the temperature of reflux for 80 min. The reaction mixture was flooded with ice water and extracted with ether. The ether layer was washed with cold potassium carbonate solution, dried ($MgSO_4$), and distilled. There was obtained 46.5 g (0.31 mole) of methylphenylacetate, b.p. 77° at 6 mm, and 12.7 g (0.08 mole, 41% yield) of methylphenylglyoxylate, b.p. 102.5–106° at 6.5 mm, DNP m.p. 175.5–176° (lit. (15) 174°).

Benzyl Acetate

To a 1-l three-necked round-bottomed flask equipped with gas inlet tube, Vibromixer stirrer, thermometer, and water condenser which also served as a gas exit was added 20 g (0.08 mole) of cobalt(II) acetate, 8 g (0.08 mole) of sodium bromide, 3.3 g (0.04 mole) of sodium acetate, 200 ml of acetic acid, 186 g (1.82 moles) of acetic anhydride, and 138 g (1.5 moles) of toluene. Oxygen was bubbled through the vigorously stirred solution. The temperature was raised and, when the reaction mixture reached about 70°, it became exothermic and rose rapidly to 109°, and oxygen was absorbed by the solution at a rate of 600 ml/min. The reaction was continued for 65 min and then poured into ice water and extracted with ether. The ether layer was washed with sodium bicarbonate solution to remove acetic acid (and any benzoic acid present), then dried over anhydrous magnesium sulfate, and filtered. The ether was distilled off on the steam bath and 158.9 g of a light yellow oil remained. This was examined quantitatively by vapor phase chromatography (v.p.c.) using known solutions for calibration. The product contained 97.2 g of unreacted toluene, 30 g of benzyl acetate (44.7% yield), 10.1 g of benzaldehyde (21.5%), and 15.6% of an unidentified product. The remainder (19.2%) probably is principally benzoic acid which was not isolated.

p-Methylbenzyl Acetate

In a similar fashion 160 g (1.5 moles) of *p*-xylene was oxidized for 160 min to yield 185.4 g of a yellow oil containing 102 g (0.96 mole) of *p*-xylene, 23 g of *p*-tolualdehyde (0.21 mole, 39%), and 52 g (0.31 mole, 57%) of *p*-methylbenzyl acetate.

Can. J. Chem. Downloaded from www.nrcresearchpress.com by 210.87.254.40 on 09/05/12
For personal use only.

α-Methylbenzyl Acetate

Oxidation of ethylbenzene (159 g, 1.5 moles) gave 35 g (0.33 mole) of ethyl benzene, 35 g (0.29 mole, 25% yield) of acetophenone, and 25 g (0.15 mole, 13% yield) of α-methylbenzyl acetate. The products isolated by v.p.c. were identified by comparison of their infrared spectra with those of the known compounds.

3-Acetoxycyclohexene

To a 500-ml three-necked round-bottomed flask equipped with thermometer, Vibromixer stirrer, and water condenser which also served as a gas exit was added 200 g (0.08 mole) of colbalt(II) acetate, 8 g (0.08 mole) of sodium bromide, 26.5 g of sodium acetate, 200 ml of acetic acid, 186 g of acetic anhydride, and 123 g (1.5 moles) of cyclohexene. Oxygen was bubbled through the vigorously stirred solution (600 ml/min) at reflux temperature. Over a period of 5 h the pot temperature rose from 80 to 111 °C.

The reaction mixture was flooded with water and extracted with ether. The ether layer was washed with sodium bicarbonate solution, then dried over magnesium sulfate, filtered, and evaporated. There was obtained 96.0 g of a sweet-smelling oil which was distilled to yield 23 g of 3-acetoxycyclohexene, b.p. 53 °C at 6 mm, n_D^{20} 1.4618 (literature n_D^{20} 1.4609). Vapor phase chromatography showed it was a pure material.

α-Acetoxymethylstyrene

Oxidation of α-methylstyrene (177 g, 1.5 moles) gave by v.p.c. 98 g (0.83 mole) of α-methylstyrene, 54 g (0.45 mole, 62% yield) of acetophenone (identified by comparison of infrared spectrum), and 28 g (0.16 mole, 24% yield) of α-acetoxymethylstyrene. A sample was isolated for anlysis; n_D^{20} 1.5329 (lit. 1.5281).

Anal. Calcd. for $C_{11}H_{12}O_2$: C, 74.97; H, 6.86. Found: C, 74.75, 74.61; H, 6.61, 7.04.

α-Tetralone

To a 2-l round-bottomed flask equipped as described previously was added 750 ml of acetic acid, 25 g (0.1 mole) of cobalt(II) acetate tetrahydrate, and 30 g (0.092 mole) of cobalt(II) bromide hexahydrate. Oxygen in excess was kept passing through the vigorously stirred solution maintained at 40° with an ice bath and "jackomatic". Over a 30-min period was added 330 g (2.5 moles) of tetralin dissolved in 255 g of acetic anhydride. The reaction was very exothermic and up to 1 200 ml/min of oxygen was absorbed during this period. The reaction was continued for 30 min,* then flooded with ice water, and extracted with ether. The ether layer was washed with cold sodium carbonate solution, then dried ($MgSO_4$), and distilled. A fraction (86 g), b.p. 40–50 °C at 0.5 mm, and 168 g (1.15 moles), b.p. 90–95 °C at 0.5 mm, were obtained. The latter fraction was α-tetralone, m.p. 6.5 °C.

A number of smaller scale runs were performed and analyzed by vapor phase chromatography (Perkin–Elmer K column). In all cases, in addition to α-tetralone and unreacted tetralin, naphthalene (0.5–3%) and 1,2-dihydronaphthalene (10–15%) were identified. The latter was isolated by preparative vapor phase chromatography, b.p. 63 °C at 3.2 mm, n_D^{20} 1.5829, m.p. −8 °C.

Oxidation of Tetralin to 1,2-Dihydronaphthalene

To a 500-ml wide-mouthed Erlenmeyer flask equipped with a gas inlet tube, thermometer, and a Vibromixer was added 10 g (0.04 mole) of cobalt(II) acetate tetrahydrate, 10.8 g (0.04 mole) of 30% hydrogen bromide in acetic acid, 250 ml of propionic acid, and 66 g (0.05 mole) of tetralin. Air (50 ml/min) was bubbled through the stirred reaction mixture for 16 h. The reaction mixture was then flooded with water, extracted with ether, washed with cold sodium bicarbonate solution, and dried ($MgSO_4$), and the ether removed on the steam bath to leave 67 g of a light orange oil.

The oil was analyzed by vapor phase chromatography and contained tetralin, 67%; 1,2-dihydronaphthalene, 21%; naphthalene, 5%; and α-tetralone, 5%. This is a 71% yield of 1,2-dihydronaphthalene based on the tetralin consumed.

Rate and Inhibition Studies

The rate and inhibition studies were carried out exactly as described in ref. 10.

ACKNOWLEDGMENTS

Distillations and vapor phase chromatographic analyses were performed by Mr. E. M. Hadsell. It is a pleasure to acknowledge the capable assistance of Mr. R. J. Flatley.

REFERENCES

1. J. L. BOLLAND. Quart. Rev. London, **3**, 1 (1949). L. BATEMAN. Quart. Rev. London, **8**, 147 (1954). G. A. RUSSELL. J. Am. Chem. Soc. **79**, 3781 (1957); **77**, 4583 (1955); **78**, 1047 (1956). H. S. BLANCHARD. J. Am. Chem. Soc. **81**, 4548 (1959).
2. A. E. WOODWARD and R. B. MESROBIAN. J. Am. Chem. Soc. **75**, 6189 (1953).
3. A. S. HAY, J. W. EUSTANCE, and H. S. BLANCHARD. J. Org. Chem. **25**, 616 (1960).

**When reactions are continued longer the blue color of the catalyst is lost, indicating that consumption of the bromide ion and considerably larger amounts of high-boiling residue are obtained in the reaction.*

Can. J. Chem. Downloaded from www.nrcresearchpress.com by 210.87.254.40 on 09/05/12
For personal use only.

4. D. C. HULL. U.S. Patent No. 2,673,217 (March 23, 1954).
5. W. F. BRILL. Ind. Eng. Chem. **52**, 837 (1960).
6. D. A. S. RAVENS. Trans. Faraday Soc. 1768 (1959). R. S. BARKER and A. SAFFER. U.S. Patent No. 2,833,816 (May 6, 1958).
7. A. S. HAY. Canadian Patents Nos. 642,668 (June 12, 1962); 620,356 (May 16, 1961); 620,360 (May 16, 1961); 619,149 (April 25, 1961); 616,727 (March 21, 1961).
8. A. V. TOBOLSKY, D. J. METZ, and R. B. MESROBIAN. J. Am. Chem. Soc. **72**, 1942 (1950). Y. KOMIYA, S. BEATON, A. LAFORTUNE, and K. U. INGOLD. Can. J. Chem. **42**, 2020 (1964).
9. H. S. BLANCHARD. J. Am. Chem. Soc. **81**, 4548 (1959).
10. N. URI. Nature, **177**, 1177 (1956). F. L. HEATON and N. URI. J. Lipid Res. **2**, 152 (1961).
11. F. F. RUST and W. E. VAUGHAN. Ind. Eng. Chem. **41**, 2595 (1949).
12. T. L. COTTRELL. The strengths of chemical bonds. Butterworths Scientific Publications, London. 1954. pp. 273–274.
13. J. E. MCINTYRE and D. A. S. RAVENS. J. Chem. Soc. 4082 (1961).
14. E. J. LORAND and E. I. EDWARDS. J. Am. Chem. Soc. **77**, 4035 (1955).
15. A. H. SCHLUSACH and V. FRANZEN. Ann. **578**, 220 (1952).

Can. J. Chem. Downloaded from www.nrcresearchpress.com by 210.87.254.40 on 09/05/12
For personal use only.

Can. J. Chem. Downloaded from www.nrcresearchpress.com by 210.87.254.6 on 09/05/12
For personal use only.

SYNTHESIS OF ANHYDRODIDEOXYHEXITOLS RELATED TO ANHYDRODEOXYHEXITOLS FROM OXO REACTION OF 3,4-DI-*O*-ACETYL-D-XYLAL

ALEX ROSENTHAL AND D. ABSON
Department of Chemistry, University of British Columbia, Vancouver, British Columbia
Received November 13, 1964

Dedicated to Professor R. B. Sandin on the Occasion of his Sixty-Eighth Birthday

ABSTRACT

2,3-Di-*O*-acetyl-1,5-anhydro-4,6-dideoxy-D-*arabino*-hexitol (VI) and 2,3-di-*O*-acetyl-1,5-anhydro-4,6-dideoxy-L-*xylo*-hexitol (VII) were prepared by reaction of methyl magnesium bromide with 3,4-di-*O*-acetyl-D-*xylo*-pyranosyl chloride. An independent synthesis of compounds (VI) and (VII) was also achieved from the 6-*O*-tosyl derivatives of the oxo products from 3,4-di-*O*-acetyl-D-xylal, thus confirming that the configuration of the secondary hydroxyls of glycals is not inverted during the oxo reaction.

Part II of this series (1) showed that application of the oxo reaction to 3,4-di-*O*-acetyl-D-xylal, followed by deacetylation, gave 1,5-anhydro-4-deoxy-D-*arabino*-hexitol (I) and 1,5-anhydro-4-deoxy-L-*xylo*-hexitol (II). The L-configuration of C-5 of (II) was established by correlation with C-4 of 1,4-anhydro-5-deoxy-D-*arabino*-hexitol; the C-5 configuration of (I) must therefore be D, as this anhydrodeoxyhexitol, on cleavage of the α-glycol bond and reduction, formed a triol ether which was the mirror image of that derived from (II). The remaining asymmetric centers of (I) and (II), at C-2 and C-3, were assumed to be unchanged in configuration from the parent polyol.

Von Rudloff *et al.* (2) carried out the hydrogenolysis of methyl-α-D-glucopyranoside at 240° to give 1,5-anhydro-4-deoxy-hexitol along with other products. Gorin (3) subsequently showed that the hexitol consisted of two 1,5-anhydro-4-deoxy-D-hexitols. On the bases of comparative rates of lead tetracetate oxidation and comparison of observed specific rotations with those calculated from application of the principle of optical superposition, these hexitols were postulated to have structures (I) and (III) (1,5-anhydro-4-deoxy-D-*lyxo*-hexitol). The compound to which they assigned the D-*arabino* configuration ($[\alpha]_D$ +19°; tris-*p*-nitrobenzoate, m.p. 115–119°, $[\alpha]_D$ +59°) is clearly different from our compound (I) ($[\alpha]_D$ −13°; tris-*p*-nitrobenzoate, m.p. 215°, $[\alpha]_D$ −50°). We have accordingly carried out a series of reactions correlating the secondary hydroxyl configurations of (I) and (II) with those of D-xylal, thereby confirming our assignments of structures (I) and (II).

Bonner (4) has shown that the hemiacetal halogen of polyacetylglycosyl halides undergoes a metathetical reaction with Grignard reagent when the latter is present in sufficient excess, and has, moreover, provided adequate experimental proof to show that decomposition of the Grignard adduct to the ester group does not involve rupture of asymmetric bonds, and therefore no change of configuration takes place during reaction with the Grignard reagent. Using the Grignard synthesis we have been successful in preparing the diacetates of the two 6-deoxy analogues of (I) and (II), namely 2,3-di-*O*-acetyl-1,5-anhydro-4,6-dideoxy-D-*arabino*-hexitol (VI) and 2,3-di-*O*-acetyl-1,5-anhydro-4,6-dideoxy-L-*xylo*-hexitol (VII).

Hydrogen chloride readily adds across the double bond of 3,4-di-*O*-acetyl-D-xylal (cf. ref. 5), as was evidenced by complete disappearance of the characteristic C=C

stretching vibration at ca. 1 640 cm^{-1} in the infrared spectrum. The unstable product, 3,4-di-*O*-acetyl-2-deoxy-D-*xylo*-pyranosyl chloride (IV), was immediately caused to react

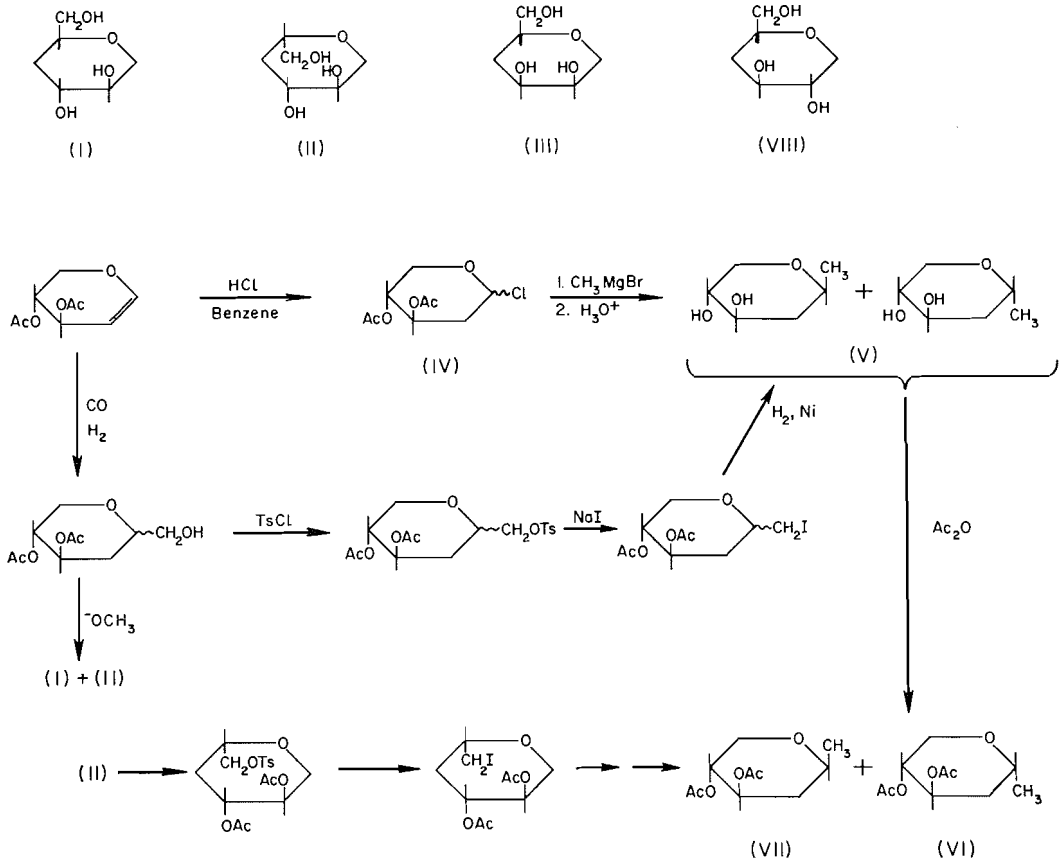

with about 10 molar equivalents of methyl magnesium bromide, according to the general procedure outlined by Bonner (4), except that the product was isolated in the deacetylated form since it was hoped to effect a separation by paper chromatography. However, only one zone was detected on spraying of the samples with sodium periodate – Schiff reagent (6), although a variety of solvent systems was tried. Nevertheless, the sirupy product isolated from the Grignard reaction and purified by preparative paper chromatography undoubtedly consisted of a mixture of the two anhydrodideoxyhexitols (V), as was clear from the proton nuclear magnetic resonance (n.m.r.) spectrum, which showed a pair of overlapping "*C*"-methyl doublets (J = 6 c.p.s.) at δ = 1.14 p.p.m. and δ = 1.17 p.p.m. By acetylation and gas–liquid partition chromatography (g.l.p.c.), the two components of the mixture could be separated in sufficient amounts for characterization. The faster-moving component (relative retention time 1.00), $[\alpha]_D$ −21°, was identified as 2,3-di-*O*-acetyl-1,5-anhydro-4,6-dideoxy-L-*xylo*-hexitol (VII) by preparation of (VII) from 1,5-anhydro-4-deoxy-L-*xylo*-hexitol (II) as described in the Experimental section. The slower-moving component (relative retention time 1.10), $[\alpha]_D$ −82°, was therefore 2,3-di-*O*-acetyl-1,5-anhydro-4,6-dideoxy-D-*arabino*-hexitol.

3,4-Di-*O*-acetyl-D-xylal was caused to react with carbon monoxide and hydrogen as

Can. J. Chem. Downloaded from www.nrcresearchpress.com by 210.87.254.6 on 09/05/12
For personal use only.

described previously (1). After removal of the catalyst, a portion of the sirupy product was deacetylated, and separated by paper chromatography into fractions (I) and (II). A further portion of the catalyst-free product was treated with *p*-toluenesulfonyl chloride in pyridine to give a mixture of 2,3-di-*O*-acetyl-6-*O*-tosyl derivatives of (I) and (II), which without purification was heated with sodium iodide in acetone solution, whereby the tosyloxy groups were replaced by iodine. The crude mixture of 2,3-di-*O*-acetyl-1,5-anhydro-4,6-dideoxy-6-iodo-hexitols was then shaken in basic solution with hydrogen in the presence of Raney nickel (7), effecting simultaneous reduction of $-CH_2I$ to CH_3, and deacetylation. Paper chromatography of the product showed only one zone identical in R_f value with that of the mixture of 1,5-anhydro-4,6-dideoxyhexitols (V) obtained by the action of methyl magnesium bromide on (IV). Confirmation that the product was a mixture of 1,5-anhydro-4,6-dideoxy-D-*arabino*- and -L-*xylo*-hexitols was obtained on acetylating the mixture and separating it by g.l.p.c. into two pure components, identical with (VI) and (VII) by virtue of their relative retention times, optical rotations, and nuclear magnetic resonance and infrared spectra.

The D-*arabino* and L-*xylo* configurations of the anhydrodeoxyhexitols (I) and (II) are thus confirmed unambiguously; consequently, the polyol of R_{Rh} 1.3* (denotes distance moved on paper relative to rhamnose in 1-butanol – ethanol – water (40:11:19 v/v/v) solvent) isolated by Gorin (3) from the hydrogenolysis products of methyl-α-D-glucopyranoside is not 1,5-anhydro-4-deoxy-D-*arabino*-hexitol. Both this and the other polyol of R_{Rh} 1.1 are known to be of the D series, as they gave 2-deoxy-3-*O*-(2-hydroxyethyl)-L-*glycero*-tetritol on oxidative cleavage followed by reduction with sodium borohydride (1). Furthermore, as the rate of oxidation by lead tetracetate indicated a *trans*-α-glycol group in the faster-moving polyol (3), we concluded that this compound was probably 1,5-anhydro-4-deoxy-D-*xylo*-hexitol (VIII). This was confirmed on examination of a sample of the compound kindly made available by Dr. P. A. J. Gorin, which proved to be enantiomeric with (II). Thus, the n.m.r. spectra were identical, the specific rotations were equal and opposite, and the compound formed a crystalline tri-*O*-acetyl derivative enantiomeric with 2,3,6-tri-*O*-acetyl-1,5-anhydro-4-deoxy-L-*xylo*-hexitol (1).

Comparison of a sample of the crystalline anhydrodeoxyhexitol of R_{Rh} 1.1, also furnished by Dr. Gorin, with 1,5-anhydro-4-deoxy-D-*lxyo*-hexitol (III), one of the products obtained by the oxo reaction of 3,4-di-*O*-acetyl-D-arabinal (8), confirmed the identity of the two compounds.

EXPERIMENTAL

General Considerations

Gas–liquid partition chromatography separations were carried out on an Aerograph "Autoprep" model A-700 employing a column (10 ft × 1/4 in.) of 20% Silicone GE-SF-96 on firebrick at a temperature of 180°, with helium as the carrier gas at a flow rate of 40 ml/min. Samples (3–4 mg in chloroform solution) were injected directly onto the column using a 6-in. needle. Conditions for paper chromatographic separations, isolation and deacetylation of oxo products, and measurement of infrared spectra have been described (1). The n.m.r. spectra of the acetates were obtained on a Varian A-60 instrument using tetramethylsilane as the internal standard (set at $\delta = 0$).

Microanalyses were carried out by Dr. A. Bernhardt, Mülheim (Ruhr), West Germany.

Preparation of 2,3-Di-O-acetyl-1,5-anhydro-4,6-dideoxy-D-arabino-hexitol (VI) and 2,3-Di-O-acetyl-1,5-anhydro-4,6-dideoxy-L-xylo-hexitol (VII)

(a) By Reaction of 3,4-Di-O-acetyl-D-xylopyranosyl Chloride with Methyl Magnesium Bromide

A cooled solution of 3,4-di-*O*-acetyl-D-xylal (2.5 g) in dry benzene (5 ml) was saturated with dry hydrogen chloride. After 1 h, the solvent was removed under reduced pressure at 30° to give a colorless oil. An infrared spectrum of the product showed no absorption at ca. 1 640 cm^{-1}. The product loses hydrogen chloride on standing and must be used immediately.

Can. J. Chem. Downloaded from www.nrcresearchpress.com by 210.87.254.6 on 09/05/12
For personal use only.

Can. J. Chem. Downloaded from www.nrcresearchpress.com by 210.87.254.6 on 09/05/12
For personal use only.

To a stirred solution of methyl magnesium bromide in dry ether, prepared by the slow addition of methyl bromide gas to a stirred suspension of magnesium (3.2 g) in dry ether (50 ml) under an atmosphere of dry nitrogen, was added dropwise over 45 min a solution of 3,4-di-*O*-acetyl-2-deoxy-D-*xylo*-pyranosyl chloride (prepared from the 2.5 g of 3,4-di-*O*-acetyl-D-xylal as described above) in dry ether (30 ml). After it had been heated under reflux for 5 h, the solution was cooled and added slowly to a large volume of ice water containing 5 ml of acetic acid. The aqueous phase was filtered through Celite, neutralized with 2 *N* sodium hydroxide, and evaporated to a white solid. The reaction product was separated from inorganic material by repeated extraction, filtration, and evaporation with ethanol (and subsequently with acetone) to yield a yellow sirup (0.95 g). Paper chromatography (water-saturated 1-butanol containing 5% ethanol, v/v) showed one zone, $R_f = 0.69$, on spraying of the samples with sodium periodate–Schiff reagent (6). A portion of the product (0.33 g) was purified by chromatography on paper to yield a sirup (0.22 g); n.m.r. spectrum (D_2O solution, relative areas in parentheses): complex multiplet 3.0–4.2 p.p.m. (5); pair of overlapping doublets ($J = 6$ c.p.s.) centered at 1.14 and 1.17 p.p.m. (3) caused by C—CH_3.

A portion of the purified mixture of 1,5-anhydro-4,6-dideoxy-D-*arabino*- and -L-*xylo*-hexitols (100 mg) was acetylated with acetic anhydride (1 ml) and anhydrous pyridine (1 ml) overnight. The mixture was poured into ice water, and after 30 min stirring, the resulting homogeneous solution was extracted three times with chloroform. The combined chloroform extracts were washed successively with sodium hydrogen sulfate solution, sodium hydrogen carbonate solution, and water, and dried over anhydrous magnesium sulfate. Under reduced pressure the extracts were evaporated to a sirup (110 mg) which, when fractionated by g.l.p.c., yielded two pure components (VI) and (VII), the latter identified as 2,3-di-*O*-acetyl-1,5-anhydro-4,6-dideoxy-L-*xylo*-hexitol by independent synthesis from 1,5-anhydro-4-deoxy-L-*xylo*-hexitol (II) as described below.

*Fraction (VI) (2,3-di-O-acetyl-1,5-anhydro-4,6-dideoxy-*D*-arabino-hexitol).*—Relative retention time 1.10; a colorless liquid of $[\alpha]_D^{24}$ −82° (*c*, 1.0, chloroform). N.m.r. spectrum (CCl_4 solution): multiplets at 4.75–5.00 p.p.m. (2), 4.4–4.65 p.p.m. (1), and 3.35–3.9 p.p.m. (3); two sharp signals at 2.02 p.p.m. (3) and 2.06 p.p.m. (3) caused by acetyl hydrogens; multiplet at 1.5–1.85 p.p.m. (2) caused by C—CH_2—C; doublet ($J = 6$ c.p.s.) centered at 1.13 p.p.m. (3) caused by C—CH_3.

Anal. Calcd. for $C_{10}H_{16}O_5$: C, 55.54; H, 7.46. Found: C, 55.61; H, 7.55.

*Fraction (VII) (2,3-di-O-acetyl-1,5-anhydro-4,6-dideoxy-*L*-xylo-hexitol.*—Relative retention time 1.00; a colorless liquid of $[\alpha]_D^{24}$ −21° (*c*, 0.9, chloroform). N.m.r. spectrum (CCl_4 solution): multiplets at 4.65–5.00 p.p.m. (2), 3.8–4.2 p.p.m. (1), and 3.0–3.65 p.p.m. (3); sharp signal at 1.97 p.p.m. (6) caused by acetyl hydrogens, superimposed on multiplet (2) caused by C—CH_2—C; doublet ($J = 6$ c.p.s.) centered at 1.20 p.p.m. (3) caused by C—CH_3.

Anal. Calcd. for $C_{10}H_{16}O_5$: C, 55.54; H, 7.46. Found: C, 55.47; H, 7.42.

*2,3-Di-O-acetyl-1,5-anhydro-4,6-dideoxy-*L*-xylo-hexitol (VII) from 1,5-anhydro-4-deoxy-*L*-xylo-hexitol (II).*—To an ice-cold solution of anhydrodeoxyhexitol (II) (70 mg) in anhydrous pyridine (0.5 ml) was added over 20 min a solution of *p*-toluenesulfonyl chloride (105 mg, 1.1 molar equivalents) in anhydrous pyridine (1.0 ml). After the mixture had been allowed to stand at 5° for 18 h, acetic anhydride (1.0 ml) was added and the mixture was kept at room temperature for 12 h. Isolation of the product by an isolation procedure identical with that described above gave a sirup (140 mg) which contained approximately 80% of 2,3-di-*O*-acetyl-1,5-anhydro-4-deoxy-6-*O*-tosyl-L-*xylo*-hexitol, as judged by the amount of sodium *p*-toluenesulfonate liberated therefrom. The crude product in acetone (2 ml) was heated with sodium iodide (140 mg) in a sealed tube at 140° for 3 h. After cooling, sodium *p*-toluenesulfonate (58 mg) was removed by filtration and the solution was evaporated to dryness. Extraction with refluxing ether and evaporation of solvent gave a sirup (125 mg). The crude 6-deoxy-6-iodo derivative was dissolved in methanol (10 ml) containing 0.5 ml 5 *N* sodium hydroxide, and shaken with hydrogen in the presence of Raney nickel (15 mg) for 30 min. Filtration, neutralization with carbon dioxide, and evaporation gave a white solid, which was acetylated by being heated at 100° for 3 h with acetic anhydride (2 ml) and anhydrous sodium acetate (0.4 g). Isolation of the product in the usual way gave a brown sirup (50 mg). Gas–liquid partition chromatography of the product showed one zone whose retention time was identical with that of fraction (VII). The infrared spectrum of a portion of the product purified by g.l.p.c. was identical with that of fraction (VII).

*(b) From Oxo Products Obtained by Reaction of 3,4-Di-O-acetyl-*D*-xylal with Carbon Monoxide and Hydrogen*

3,4-Di-*O*-acetyl-D-xylal was converted into a mixture of 2,3-di-*O*-acetyl-1,5-anhydro-4-deoxy-D-*arabino*-hexitol and 2,3-di-*O*-acetyl-1,5-anhydro-4-deoxy-L-*xylo*-hexitol by the method previously described (1). To a portion of this oxo product (1.5 g) in anhydrous pyridine (6 ml) was added *p*-toluenesulfonyl chloride (1.8 g). After the mixture had been allowed to stand at room temperature for 18 h, water (5 ml) was added in small portions over a period of 20 min, with cooling in ice. The mixture was then poured into ice water and the product was isolated by extraction with chloroform. The combined chloroform extracts were washed successively with sodium bisulfate solution, water, sodium bicarbonate solution, and again with water, and dried over anhydrous magnesium sulfate. Evaporation under reduced pressure gave a sirup (1.6 g) whose n.m.r. spectrum indicated approximately 75% of 2,3-di-*O*-acetyl-1,5-anhydro-4-deoxy-6-*O*-tosyl-hexitols to be present. This mixture was converted into a mixture of 1,5-anhydro-4,6-dideoxy-L-*xylo*- and -D-*arabino*-hexitols by the procedure described in the preceding section, and then purified by preparative paper chromatography. A portion of the purified product (110 mg) was acetylated to yield a syrup (140 mg) which was

fractionated by g.l.p.c. into (VI) and (VII), identical with the two fractions isolated as described in Section *a* on the basis of retention times, specific rotations ($[\alpha]_D^{24}$ −81° and −23° (*c*, 1.2, chloroform) respectively), and n.m.r. and infrared spectra.

Identification of Anhydrodeoxyhexitol of R_{Rh} 1.3 from Hydrogenation of Methyl α-D-Glucopyranoside (3)

The tris-*p*-nitrobenzoate of this compound (170 mg), kindly supplied by Dr. P. A. J. Gorin, was debenzoylated by heating it under reflux with 0.1 *N* methanolic sodium methoxide for 1 h. Isolation of the product in the usual way gave a colorless sirup (38 mg), $[\alpha]_D^{22}$ +40° (*c*, 2.0, chloroform), whose n.m.r. spectrum was identical with that of the levorotatory L-isomer (II) (1), and which formed a tri-*O*-acetyl derivative, m.p. 80–82°; $[\alpha]_D^{22}$ +40° (*c*, 2.0, chloroform), whose infrared spectrum was identical with that of 2,3,6-tri-*O*-acetyl-1,5-anhydro-4-deoxy-L-*xylo*-hexitol (1).

ACKNOWLEDGMENTS

The authors gratefully acknowledge the financial assistance of the National Research Council and the University of British Columbia Research Grant. One of us (D. A.) gratefully acknowledges the Standard Oil Fellowship and the University of British Columbia Research Fellowship.

The authors thank Dr. P. A. J. Gorin for making available samples of his two anhydrodeoxyhexitols.

REFERENCES

1. A. Rosenthal and D. Abson. Can. J. Chem. **42**, 1811 (1964).
2. E. von Rudloff, H. F. Bauer, and D. E. Stuetz. Can. J. Chem. **35**, 315 (1957).
3. P. A. J. Gorin. Can. J. Chem. **38**, 641 (1960).
4. W. A. Bonner. Methods in carbohydrate chemistry. Vol. II. *Edited by* R. L. Whistler and M. L. Wolfrom. Academic Press, Inc., New York, N.Y. 1963. p. 465.
5. J. Davoll. J. Chem. Soc. 2526 (1949).
6. J. Baddiley, J. G. Buchanan, R. E. Handschumacher, and J. F. Prescolt. J. Chem. Soc. 2818 (1956).
7. O. Th. Schmidt. Methods in carbohydrate chemistry. Vol. I. *Edited by* R. L. Whistler and M. L. Wolfrom. Academic Press, Inc., New York, N.Y. 1962. p. 191.
8. A. Rosenthal and H. J. Koch. Can. J. Chem. **42**, 2025 (1964).

Can. J. Chem. Downloaded from www.nrcresearchpress.com by 210.87.254.6 on 09/05/12
For personal use only.

Can. J. Chem. Downloaded from www.nrcresearchpress.com by 210.87.254.105 on 09/05/12
For personal use only.

SYNTHESIS OF 8-AZA-D-HOMO-18-NORESTRONE METHYL ETHER

NORMAN A. NELSON[1] AND YASUMITSU TAMURA
Department of Chemistry, Massachusetts Institute of Technology, Cambridge, Massachusetts
Received November 13, 1964

Dedicated to Professor R. B. Sandin on the Occasion of his Sixty-Eighth Birthday

ABSTRACT

Alkylation of the potassium salt of 1,4-dihydro-2,6-dimethoxybenzene with 2-(2-bromoethyl)piperidine yielded the bis-enol ether I, which, on acid hydrolysis, afforded the crystalline vinylogous amide II. Lithium aluminium hydride reduction of II gave two isomers of 1,2,3,4,4*a*,5,6,6*a*,8,9,10,10*a*-dodecahydro-7H-benzo[*c*]quinolizin-7-one (III). A similar series of reactions starting with 1-(2-chloroethyl)-6-methoxy-1,2,3,4-tetrahydroisoquinoline hydrochloride (V) gave two isomers of 2,3,4,4*a*,6,7,11*b*,12,13,13*a*-decahydro-9-methoxy-1H-dibenzo[*a*,*f*]quinolizin-1-one (8-aza-D-homo-18-norestrone methyl ether) (IX).

In an earlier report (1) we described some nitrogen-containing tricyclic analogues of 18-nor-D-homoestrone having anti-inflammatory activity. This pharmacological finding prompted us to prepare some of the corresponding tetracyclic analogues. The preparation of two isomers of 2,3,4,4*a*,6,7,11*b*,12,13,13*a*-decahydro-9-methoxy-1H-dibenzo[*a*,*f*]-quinolizin-1-one (8-aza-D-homo-18-norestrone methyl ether) (IX) is the subject of this paper.

A number of years ago we (2) prepared 1-(2-hydroxyethyl)-6-methoxy-1,2,3,4-tetrahydroisoquinoline (IV) in anticipation of utilizing it as an intermediate in the preparation of IX. At the outset of the present work we utilized the more readily available 2-(2-hydroxyethyl)piperidine (3) as a model of IV in our effort to elaborate two additional rings corresponding to the C and D rings of a steroid.

2-(2-Hydroxyethyl)piperidine was converted to 2-(2-bromoethyl)piperidine hydrobromide in 83% yield using hot 48% hydrobromic acid. Conversion of 2-(2-hydroxyethyl)piperidine hydrobromide to the corresponding 2-bromoethyl derivative was also effected using phosphorus tribromide (29% yield) or thionyl bromide (69% yield).

Alkylation of the potassium salt of 1,4-dihydro-2,6-dimethoxybenzene (4) with 2-(2-bromoethyl)piperidine in liquid ammonia proceeded smoothly, giving 2-[2-(1,4-dihydro-2,5-dimethoxyphenyl)ethyl]piperidine (I). Hydrolysis of the bis-enol ether was accompanied by cyclization of the intermediate diketone, yielding the tricyclic vinylogous amide II in 71% yield. Treatment of II with lithium aluminium hydride resulted in a net reduction of the carbon–carbon double bond, thereby giving a crystalline isomer (isomer A) of III in 44% yield and a liquid believed to represent a second isomer (isomer B) of III in 36% yield. The two isomers were characterized as their picrates. Lithium aluminium hydride reduction of vinylogous amides may lead to loss of the carbonyl oxygen (5, 6) or to the production of aminoalcohols or aminoketones (7–9).

The conversion of II to III can be pictured as a 1,4-reduction or a 1,2-reduction followed by hydrolysis of the enamine to a 3-hydroxycyclohexenone, elimination of water, and finally a Michael addition of the nitrogen to the intermediate 2-substituted cyclohexenone. On the basis of a closely related example (9), the 1,4-reduction mechanism is to be preferred.

[1]*To whom inquiries should be addressed. Present address: Department of Chemistry, The Upjohn Company, Kalamazoo, Michigan.*

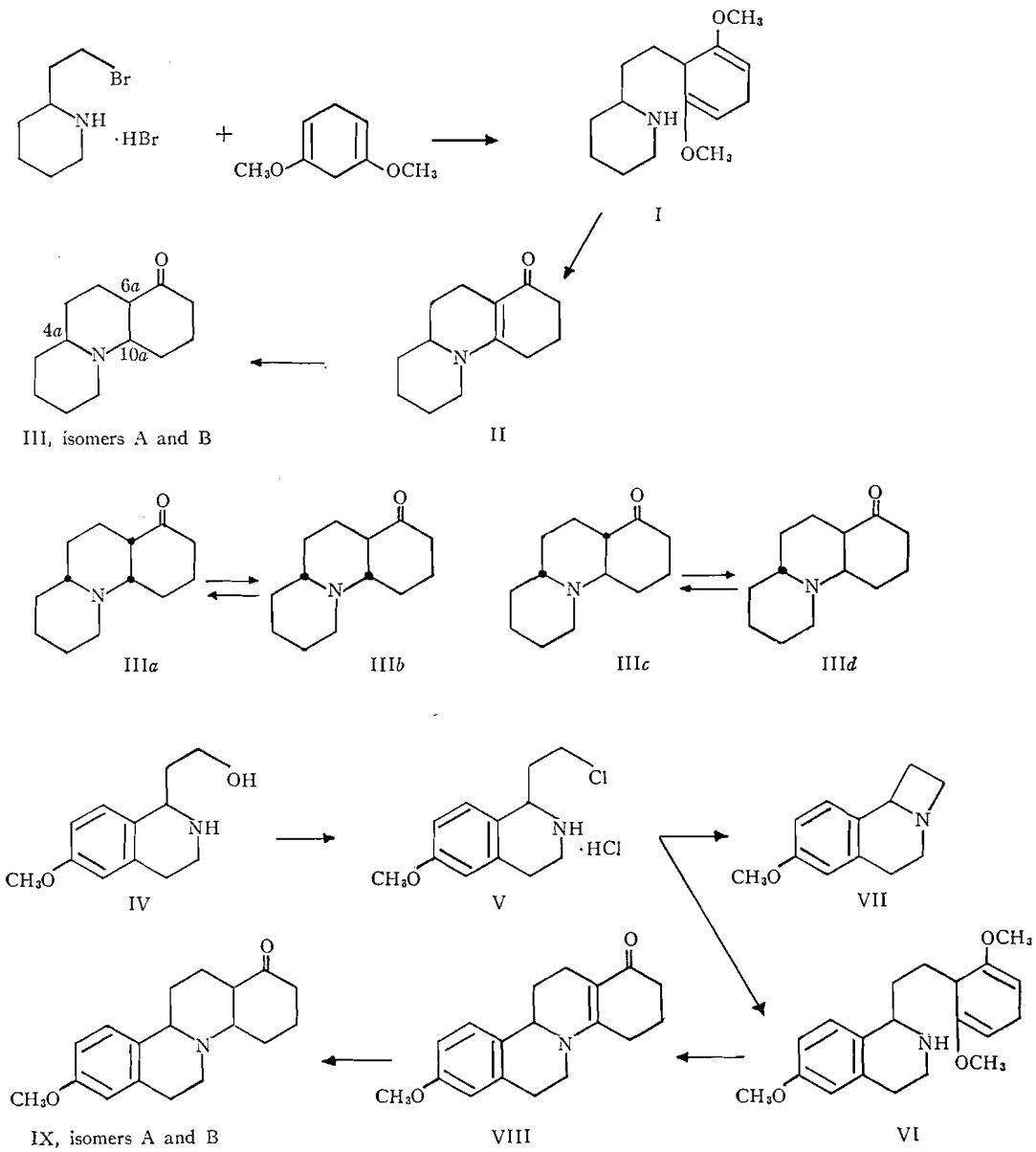

The crystalline isomer A of III, on treatment with ethanolic sodium ethoxide, was isomerized to the corresponding oily isomer B. The infrared spectra of the two isomers of III both exhibit infrared absorption bands at 2 790 and 2 754 cm^{-1}. Such bands have been attributed to amines which have at least two α-hydrogens *trans*-diaxial to the unshared electron pair of the nitrogen (10–12). On this basis, it would appear that the two isomers of III exist in carbon tetrachloride solution as *trans*-fused quinolizidines (at least to a considerable extent). The various conformations that are possible for III and which have a *cis*-fused quinolizidine system have only one α-hydrogen *trans*-diaxial to the unshared electron pair on nitrogen.

Can. J. Chem. Downloaded from www.nrcresearchpress.com by 210.87.254.105 on 09/05/12
For personal use only.

Can. J. Chem. Downloaded from www.nrcresearchpress.com by 210.87.254.105 on 09/05/12
For personal use only.

The isomers of III are believed to be epimeric at the asymmetric center alpha to the carbonyl function. If such is the case, isomer A should be III*a* or III*c*, while isomer B should be III*b* or III*d* respectively. The prediction of stabilities of the various conformations of III is based on the known stabilities of the corresponding perhydrophenanthrenes (13) and the similar stereochemical requirements of tetrahedral carbon and nitrogen (see refs. 14 and 15 for recent papers regarding the steric requirements of the lone electron pair on nitrogen). The possibility that isomers III*c* and III*d* could also be isomerized to III*b* (through the substituted cyclohexenone formed by β-elimination of nitrogen) cannot be ruled out.

1-(2-Hydroxyethyl)-6-methoxy-1,2,3,4-tetrahydroisoquinoline was converted to 1-(2-chloroethyl)-6-methoxy-1,2,3,4-tetrahydroisoquinoline hydrochloride (V) in 93% yield using thionyl chloride. Treatment of V with an excess of the potassium salt of 1,4-dihydro-2,6-dimethoxybenzene in liquid ammonia yielded the bis-enol ether VI, in addition to a small amount of material having properties consistent with 1,4,5,9*b*-tetrahydro-7-methoxy-2H-azeto[2,1-*a*]isoquinoline (VII). The formation of VII is analogous to the formation of conidine from 2-(2-chloroethyl)piperidine (3).

Acid hydrolysis of VI and cyclization of the intermediate gave the tetracyclic vinylogous amide VIII. Lithium aluminium hydride reduction of VIII yielded two crystalline isomers of IX which were separated by chromatography on Florisil. The isomer with m.p. 158.5–160° (isomer A) was isomerized in the presence of methanolic sodium methoxide to isomer B (m.p. 143.5–144°). As in the model series, these isomers are believed to be epimeric at the asymmetric center alpha to the carbonyl group. The isomers exhibit infrared absorption bands characteristic of *trans*-quinolizidine systems; however, it is not possible to say whether or not one of the isomers of IX (8-aza-D-homo-18-norestrone methyl ether) corresponds in configuration with naturally occurring estrone.

Recently, the hydrobromide salt of an isomer of IX was described (16), but unfortunately it was not possible to relate it with our isomers because the supplies of the various compounds had been exhausted. Since this work was completed, the synthesis of 8-aza-estrone (17) and other 8-azasteroids (18) has appeared.

EXPERIMENTAL

Infrared spectra were determined with a Baird model B spectrophotometer fitted with a sodium chloride prism unless otherwise specified. Ultraviolet spectra were determined in 95% ethanol with a Cary recording spectrophotometer (model 11 MS). The microanalyses were performed by Dr. S. M. Nagy and his associates. Melting points are uncorrected.

2-(2-Bromoethyl)piperidine Hydrobromide

A solution of 38.7 g of 2-(2-hydroxyethyl)piperidine (3) in 120 ml of 48% hydrobromic acid was refluxed for 1 h before 70 ml of distillate was collected. An additional 100 ml of 48% hydrobromic acid was added to the residue and the resulting solution was refluxed for 6 h before the excess acid was removed *in vacuo*. The residue was washed with ethyl acetate and recrystallized from ethanol, giving 59 g (72%) of product, m.p. 167–168°, and 9.2 g (11%) of material with m.p. 166–167°. The analytical sample had m.p. 167–167.2°.

Anal. Calcd. for $C_7H_{15}Br_2N$: C, 30.77; H, 5.49; Br, 58.61. Found: C, 30.77; H, 5.49; Br, 58.39.

Initial attempts to prepare 2-(2-bromoethyl)piperidine hydrobromide using phosphorus tribromide gave a 29% yield of product, while thionyl bromide gave a 69% yield.

2-[2-(1,4-Dihydro-2,5-dimethoxyphenyl)ethyl]piperidine (I)

Potassium amide was prepared from 8 g of the metal, 700 ml of liquid ammonia, and a trace of ferric chloride. To this mixture was added with stirring 21 g of 2,5-dihydro-1,3-dimethoxybenzene (4) and 7 ml of ether (rinse solution). The resulting red solution was stirred for 10 min before 24.9 g of powdered 2-(2-bromoethyl)piperidine hydrobromide was added over a period of 17 min to discharge the red color. Most of the ammonia was evaporated, 200 ml of water was added, and the product was extracted with ether. The ether extract was washed with water and saturated sodium chloride solution, dried, and concentrated. Distillation of the residue gave 18.8 g of product, b.p. 138–140° at 5.0 mm pressure. The analytical sample

had b.p. 105° at 0.25 mm pressure, α_D^{26} 1.5104, and infrared absorption bands (in CCl_4) at 1 694 and 1 662 cm^{-1} (unconjugated enol ether double bonds).

Anal. Calcd. for $C_{15}H_{25}NO_2$: C, 71.71; H, 9.96; N, 5.58. Found: C, 71.44; H, 9.96; N, 5.61.

1,2,3,4,4a,5,6,8,9,10-Decahydro-7H-benzo[c]quinolizin-7-one (II)

A solution of 12.5 g of 2-[2-(1,4-dihydro-2,5-dimethoxyphenyl)ethyl]piperidine in 40 ml of 2 *N* hydrochloric acid was heated to 60° for 30 min, cooled, and neutralized with 2 *N* sodium hydroxide solution. The water was removed from the reaction mixture by azeotropic distillation with benzene–ethanol. The product was separated from sodium chloride by trituration of the residue with cold ethanol. Evaporation of the ethanol gave a residue which, after crystallization from ether and then ether–hexane (3:4), gave 7.4 g (71%) of product, m.p. 76.5–77.5°. The ultraviolet spectrum has a maximum absorption at 316 mμ (ϵ 31 900). The infrared spectrum shows a strong maxima at 1 620 and 1 580 cm^{-1} associated with the conjugated ketone–enamine grouping.

Anal. Calcd. for $C_{13}H_{19}NO$: C, 76.05; H, 9.33; N, 6.82. Found: C, 75.89; H, 9.43; N, 6.69.

1,2,3,4,4a,5,6,8,9,10-Decahydro-7H-benzo[c]quinolizin-7-one Picrate

This was prepared in the usual way and recrystallized from ethanol, m.p. 153.5–154°.

Anal. Calcd. for $C_{19}H_{22}N_4O_8$: C, 52.53; H, 5.10; N, 12.90. Found: C, 52.60; H, 5.20; N, 13.03.

1,2,3,4,4a,5,6,6a,8,9,10,10a-Dodecahydro-7H-benzo[c]quinolizin-7-one (III); Isomers A and B

To a mixture of 170 mg of lithium aluminium hydride in 5 ml of dry tetrahydrofuran was added with stirring 410 mg of 1,2,3,4,4*a*,5,6,8,9,10-decahydro-7H-benzo[*c*]quinolizin-7-one (II) in 2.5 ml of tetrahydrofuran. The mixture was refluxed under a nitrogen atmosphere for 4.5 h and cooled, and 1 ml of ethyl acetate was added before the mixture was poured into 20 ml of dilute sodium hydroxide solution. The mixture was extracted with ether, and the ether extract was dried and then concentrated. Trituration of the residue with ether and recrystallization of the solid several times from hexane gave 280 mg (44%) of an isomer (isomer A) of III, m.p. 124–125°, and infrared absorption peaks (in CCl_4) at 1 709 (C=O) and 1 060 cm^{-1} (characteristic of this isomer). The infrared spectrum (using a CaF_2 prism) shows peaks at 2 790 and 2 754 cm^{-1} (characteristic of a *trans*-quinolizidine system).

Anal. Calcd. for $C_{13}H_{21}NO$: C, 75.31; H, 10.21; N, 6.76. Found: C, 75.32; H, 10.33; N, 6.80.

The *picrate* of III (isomer A) was crystallized from ethanol, m.p. 154° (decomp.).

Anal. Calcd. for $C_{19}H_{24}N_4O_8$: C, 52.29; H, 5.54; N, 12.84. Found: C, 52.29; H, 5.53; N, 12.84.

The filtrate from the trituration of the crystalline isomer A of III above yielded an additional small amount of isomer A and 150 mg (36%) of an oily residue (presumably an isomer B of III) whose infrared spectrum (carbonyl absorption at 1 712 cm^{-1} and 2 790 and 2 754 cm^{-1} using a CaF_2 prism) was different from that of isomer A and which was converted to a different *picrate* derivative of III, crystallized from ethanol, m.p. 185° (decomp.).

Anal. Calcd. for $C_{19}H_{24}N_4O_8$: C, 52.29; H, 5.54; N, 12.84. Found: C, 52.33; H, 5.56; N, 12.78.

Chromatographic purification of the oily isomer B on Florisil did not yield any additional isomers and indicated that it was probably a single substance.

Isomerization of Isomer A of 1,2,3,4,4a,5,6,6a,8,9,10,10a-Dodecahydro-7H-benzo[c]quinolizin-7-one (III)

To a solution prepared from 25 mg of sodium and 5 ml of absolute ethanol was added 100 mg of the crystalline isomer A of III and the mixture was refluxed in a nitrogen atmosphere for 1 h. The mixture was diluted with 20 ml of water, most of the alcohol was removed *in vacuo*, and the product was extracted with ether. Concentration of the dried ether extract *in vacuo* gave 90 mg of an oil whose infrared spectrum was essentially identical with the liquid isomer B described above.

In a similar isomerization experiment involving 150 mg of the liquid isomer B of III, only unchanged starting material was recovered.

1-(2-Chloroethyl)-6-methoxy-1,2,3,4-tetrahydroisoquinoline Hydrochloride (V)

A solution of 10.4 g of 1-(2-hydroxyethyl)-6-methoxy-1,2,3,4-tetrahydroisoquinoline in 40 ml of chloroform was cooled in a water bath while it was saturated with hydrogen chloride. To the mixture at 0° was added 8.3 g of thionyl chloride. The mixture was allowed to stand at room temperature for 30 min before it was refluxed for 105 min. The reaction mixture was cooled, diluted with 5 ml of water, and concentrated *in vacuo*. The residual solid was recrystallized from ethanol, giving 12.2 g (93%) of product, m.p. 165–166.5°.

Anal. Calcd. for $C_{12}H_{17}Cl_2NO$: C, 55.00; H, 6.50; Cl, 27.06; N, 5.35. Found: C, 55.02; H, 6.72; Cl, 26.69; N, 5.14.

1-[2-(1,4-Dihydro-2,5-dimethoxyphenyl)ethyl]-6-methoxy-1,2,3,4-tetrahydroisoquinoline (VI) and 1,4,5,9b-Tetrahydro-7-methoxy-2H-azeto[2,1-a]isoquinoline (VII)

To a mixture of potassium amide (prepared from 7.8 g of the metal) in 1 l of liquid ammonia was added 28 g of 2,5-dihydro-1,3-dimethoxybenzene and, after the resultant red solution was stirred for 10 min, 10.4 g of 1-(2-chloroethyl)-6-methoxy-1,2,3,4-tetrahydroisoquinoline hydrochloride was added over a period of 30 min. The mixture was stirred for 50 min, most of the ammonia was evaporated, and the residue

Can. J. Chem. Downloaded from www.nrcresearchpress.com by 210.87.254.105 on 09/05/12
For personal use only.

was shaken with ether and water. The residue obtained from the washed and dried ether layer was distilled *in vacuo*. The fraction with b.p. 88–90° at 0.02 mm pressure amounted to 2.5 g and is presumably VII. The infrared spectrum (in CCl_4) has the characteristic aromatic (C=C) absorption bands at 1 610, 1 575, and 1 500 cm^{-1}.

Anal. Calcd. for $C_{12}H_{15}NO$: C, 76.15; H, 7.99; N, 7.40. Found: C, 76.14; H, 7.93; N, 7.51.

Treatment of VII with picric acid in the usual way gave a *picrate derivative*, recrystallized from ethanol, m.p. 133.5–134.5°.

Anal. Calcd. for $C_{18}H_{18}N_4O_8$: C, 51.67; H, 4.34; N, 13.39. Found: C, 51.72; H, 4.38; N, 13.54.

The residue from the above distillation amounted to 6.6 g and was largely the desired product VI. An analytical sample of 1-[2-(1,4-dihydro-2,5-dimethoxyphenyl)ethyl]-6-methoxy-1,2,3,4-tetrahydroisoquinoline (VI) was prepared by evaporative distillation at 0.006 mm pressure and a bath temperature of 150°.

Anal. Calcd. for $C_{20}H_{27}NO_3$: C, 72.92; H, 8.26; N, 4.25. Found: C, 72.63; H, 8.04; N, 4.42.

9-Methoxy-2,3,4,6,7,11b,12,13-octahydro-1H-dibenzo[a,f]quinolizin-1-one (VIII)

A mixture of 6.0 g of 1-[2-(1,4-dihydro-2,5-dimethoxyphenyl)ethyl]-6-methoxy-1,2,3,4-tetrahydroisoquinoline (VI), 20 ml of 2 *N* hydrochloric acid, and 10 ml of water was warmed to 50° for 15 min with occasional stirring. The mixture was cooled, neutralized with 20 ml of 2 *N* sodium hydroxide solution, and extracted with chloroform. The chloroform extract was washed, dried, and concentrated to give 6.2 g of a brown oil. A portion of this oil was purified for analysis by evaporative distillation at a bath temperature of 180° and at 0.003 mm pressure. The ultraviolet spectrum of a different sample has an inflection at 286 mμ (ε 7 100) and a maximum at 316 mμ (ε 21 000).

Anal. Calcd. for $C_{18}H_{21}NO_2$: C, 76.29; H, 7.47; N, 4.94. Found: C, 76.05; H, 7.65; N, 4.84.

The *picrate of 9-methoxy-2,3,4,6,7,11b,12,13-octahydro-1H-dibenzo[a,f]quinolizin-1-one (VIII)* was crystallized from ethanol, m.p. 174–175° (decomp.).

Anal. Calcd. for $C_{24}H_{24}N_4O_9$: C, 56.25; H, 4.72; N, 10.93. Found: C, 56.34; H, 4.72; N, 10.79.

2,3,4,4a,6,7,11b,12,13,13a-Decahydro-9-methoxy-1H-dibenzo[a,f]quinolizin-1-one (IX); Isomers A and B

A solution of 5.6 g of crude 9-methoxy-2,3,4,6,7,11*b*,12,13-octahydro-1H-dibenzo[*a*,*f*]quinolizin-1-one (VIII) in 35 ml of dry tetrahydrofuran was added dropwise with stirring to a mixture of 4.2 g of lithium aluminium hydride in 60 ml of tetrahydrofuran. The mixture was refluxed for 4 h, cooled, treated dropwise with 10 ml of ethyl acetate, and then poured into 600 ml of cold 1% potassium hydroxide solution. The mixture was extracted with benzene–ether (5:1) and the extract was washed with water, dried, and concentrated to give 4.5 g of a brown oil. Chromatographic purification of the oil on 100 g of Florisil with benzene as the eluent gave, as the first band, 960 mg of a white solid. Several recrystallizations of this material from ether–benzene (3:1) gave 170 mg of isomer A of IX, m.p. 158.5–160°. The infrared absorption spectrum (in $CHCl_3$) shows bands at 2 780 and 2 700 cm^{-1} (characteristic of a *trans*-fused quinolizidine) and 1 708 cm^{-1} (C=O).

Anal. Calcd. for $C_{18}H_{23}NO_2$: C, 75.75; H, 8.12; N, 4.91. Found: C, 75.73; H, 8.20; N, 5.03.

Further elution of the column gave a mixture of substances followed by a second band of 850 mg of a solid. Recrystallization of this material from benzene–ether (3:1) gave 110 mg of isomer B of IX, m.p. 143.5–144°. The infrared spectrum (in $CHCl_3$) shows a peak at 1 705 cm^{-1} (C=O) and 2 790 cm^{-1} (poor resolution).

Anal. Calcd. for $C_{18}H_{23}NO_2$: C, 75.75; H, 8.12; N, 4.91. Found: C, 75.72; H, 7.90; N, 5.01.

Isomerization of 2,3,4,4a,6,7,11b,12,13,13a-Decahydro-9-methoxy-1H-dibenzo[a,f]quinolizin-1-one (IX); Isomer A to Isomer B

A solution of 28 mg of isomer A (m.p. 156–160°) in 5 ml of sodium methoxide solution (prepared from 25 mg of sodium and 5 ml of methanol) was refluxed under a nitrogen atmosphere for 2 h. The mixture was cooled and diluted with water, and the product extracted with ether. The ether extract was dried and concentrated, giving white crystals which were recrystallized from ether to give 17 mg of isomer B, m.p. 135–139° (mixed m.p. with isomer A, 125–130°, and mixed m.p. with pure isomer B, 136–140°).

ACKNOWLEDGMENT

This investigation was supported in part by research grants CY-2999 (C2 and C3) from the National Cancer Institute, Public Health Service.

REFERENCES

1. N. A. Nelson, R. S. P. Hsi, J. M. Schuck, and L. D. Kahn. J. Am. Chem. Soc. **82**, 2573 (1960).
2. N. A. Nelson, K. O. Gelotte, Y. Tamura, H. B. Sinclair, J. M. Schuck, V. J. Bauer, and R. W. White. J. Org. Chem. **26**, 2599 (1961).
3. E. R. Lavagnino, R. R. Chauvette, W. N. Cannon, and E. C. Kornfeld. J. Am. Chem. Soc. **82**, 2609 (1960).
4. A. J. Birch. J. Chem. Soc. 1551 (1950).

Can. J. Chem. Downloaded from www.nrcresearchpress.com by 210.87.254.105 on 09/05/12
For personal use only.

5. N. G. GAYLORD. Experientia, **10**, 166 (1954).
6. C. F. KOELSCH and D. L. OSTERCAMP. J. Org. Chem. **26**, 1104 (1961).
7. J. M. OSBOND. J. Chem. Soc. 4711 (1961).
8. K. T. POTTS and D. R. LILJERGREN. J. Org. Chem. **28**, 3202 (1963).
9. G. DESTEVENS and A. HALAMANDARIS. J. Org. Chem. **26**, 1614 (1961).
10. F. BOHLMANN. Chem. Ber. **91**, 2157 (1958).
11. T. M. MOYNEHAN, K. SCHOFIELD, R. A. Y. JONES, and A. R. KATRITZKY. J. Chem. Soc. 2637 (1962).
12. A. I. MEYERS and N. K. RALHAN. J. Org. Chem. **28**, 2950 (1963).
13. W. S. JOHNSON. Experientia, **7**, 315 (1951).
14. R. J. BISHOP, L. E. SUTTON, D. DINEEN, R. A. Y. JONES, and A. R. KATRITZKY. Proc. Chem. Soc. 257 (1964).
15. K. BROWN, A. R. KATRITZKY, and A. J. WARING. Proc. Chem. Soc. 257 (1964).
16. Belgium Patent No. 642,060 (February 7, 1964).
17. R. I. MELTZER, D. M. LUSTGARTEN, R. J. STANABACK, and R. E. BROWN. Tetrahedron Letters, 1581 (1963).
18. R. E. BROWN, D. M. LUSTGARTEN, R. J. STANABACK, M. E. OSBORNE, and R. I. MELTZER. J. Med. Pharm. Chem. **7**, 232 (1964).

Can. J. Chem. Downloaded from www.nrcresearchpress.com by 210.87.254.105 on 09/05/12
For personal use only.

Can. J. Chem. Downloaded from www.nrcresearchpress.com by 210.87.254.40 on 09/05/12
For personal use only.

THE Hg 6($^3P_1$) PHOTOSENSITIZED DECOMPOSITION OF CYCLOHEXENE VAPOR

G. R. De Maré, O. P. Strausz, and H. E. Gunning
Department of Chemistry, University of Alberta, Edmonton, Alberta

Received November 13, 1964

Dedicated to Professor R. B. Sandin on the Occasion of his Sixty-Eighth Birthday

ABSTRACT

The reaction follows the pattern established for the triplet state reactions of olefins in general. The major products, ethylene, 1,3-butadiene, vinylcyclobutane, cyclohexane, various C_{12}-compounds, and polymer, can best be accounted for by the allylic C—H and C—C bond cleavage of the primary triplet biradicals and the ring closure and fragmentation reactions of the resulting open chain biradicals. At least three types of triplet state species must be involved in the mechanism. The rate equations, developed on the assumed mechanism, satisfactorily describe the observed product distribution and kinetic features of the system and permit the estimation of the elementary rate constant values and the lifetimes of the various transient biradicals involved. Preliminary experiments with cycloheptene indicate that vinylcyclopentane is an important product.

INTRODUCTION

It is well established that the interaction of triplet mercury atoms with olefinic hydrocarbons, through a π–π transition, results in the formation of a vibrationally excited triplet biradical. The main features of these processes along with the variety of reactions which these excited species may undergo have recently been reviewed by Cvetanović (1). Previous studies on monoolefins were mainly concerned with open chain molecules and among the cyclic structures only cyclopentene has been dealt with briefly (2). The basic differences in behavior between the linear and cyclic olefins arise from the fact that in the latter case the characteristic allylic C—C bond cleavage leads to an allylic-type biradical with widely separated free spins which, according to indications (2), exhibits some unique reactivity. To test the generality of the ring contraction reaction found for cyclopentene (2) and to get a deeper insight in its mechanism a detailed study was made of the cyclohexene reaction and a brief examination of the cycloheptene system.

EXPERIMENTAL

The static reaction system consisted of a cylindrical quartz cell, 2 cm long and 5 cm in diameter, connected to a differential manometer. A mercury float valve isolated the reaction system from a conventional high vacuum apparatus. The mercury resonance radiation source was a Hanovia 87A45 low-pressure Hg-lamp. The use of such a short reaction cell was necessitated by the gas chromatographic (g.c.) technique employed.* The absorption of the incident radiation was incomplete in this cell and furthermore it varied with gas pressure, owing to Lorentz broadening of the Hg-resonance line. It therefore became necessary to determine the amount of light absorbed in the cell as a function of substrate gas pressure. To this end a 1P28 photomultiplier tube, powered by a 225 V battery, and equipped with a 2 537 Å interference filter was placed behind the reaction cell at a distance of 3.8 cm. The light inlet to the photomultiplier was 1.3 cm in diameter.

The total response (T) of the photomultiplier was measured by freezing all mercury out of the cell with liquid nitrogen. The response (R) with Hg or with Hg + added gas was measured after time was allowed for equilibration. The difference ($T - R$) divided by T was then taken as a measure of the fractional absorption in the cell. Plots of $(1 - (R/T))$ vs. added gas pressure are given for propane and cyclohexene in Figs. 1 and 2 respectively. All the data reported here, unless otherwise stated, are corrected on this basis.

Light intensities, 3.0×10^{16} and 1.7×10^{15} quanta/s were determined by propane actinometry. A.P.I. cyclohexene, standard sample 522-5S, with a stated maximum impurity level of 0.023 ± 0.020 mole % was stored at -196 °C and used without further purification. Airco Assayed Reagent CO_2 was degassed

**Good resolution of the vinylcyclobutane, cyclohexane, and cyclohexene peaks could be obtained only with limited quantities of substrate.*

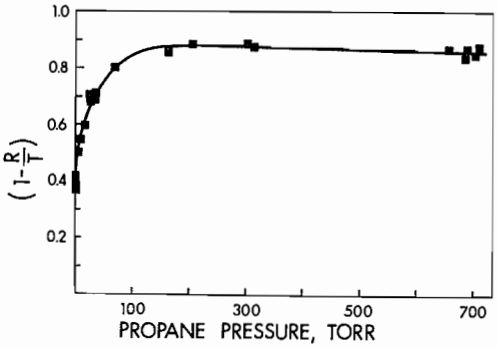

FIG. 1. Plot of fractional absorption, $(1 - (R/T))$, vs. propane pressure.

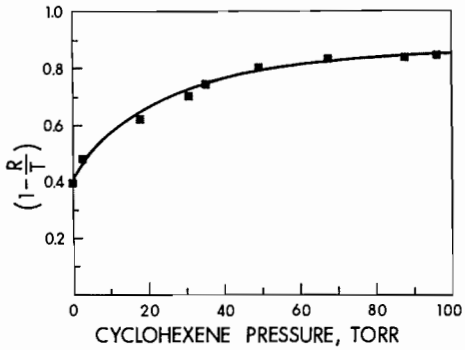

FIG. 2. Plot of fractional absorption, $(1 - (R/T))$, vs. cyclohexene pressure.

before use. Nitric oxide (Matheson C.P.) was purified by triple distillation from liquid oxygen. Ethane-d_6 (Merck) was thoroughly degassed by trap-to-trap distillation. Mass spectral analysis indicated the presence of ca. 2.5% C_2D_5H, but no other impurity could be detected by g.c. analysis on a silica gel column.

At the conclusion of irradiation the noncondensable products were removed at liquid nitrogen temperature by a Toepler pump, measured in a gas buret and subsequently analyzed by mass spectrometry for H_2 and C_2H_4. The remaining products and substrate were transferred to a g.c. unit for analysis. Good resolution of the C_2H_4, C_4H_6, vinylcyclobutane (VCB) and cyclohexane products, and the substrate was achieved on a 10 ft column of 20% diisodecyl phthalate on 60/80 Ultraport (A.W.). After each experiment the reaction vessel was cleaned by flaming.

With added CO_2 and C_2D_6, the addend and products noncondensable at -130 °C were removed and analyzed only for butadiene by g.c. as above. (C_2H_4 could not be separated from the large excess of added gas.) With the exception of VCB, the C_2 to C_6 products were identified by comparison of their mass spectra and g.c. retention value with those of authentic samples.

The characterization of VCB was made on the basis of mass spectrometric, infrared, and n.m.r. analysis.* The mass spectrum confirmed the molecular weight and the cracking pattern discounted the 1,5-hexadiene structure. The absence of allylcyclopropane was concluded from g.c. retention time measurements. The vapor phase infrared spectrum indicated the absence of methyl groups (1 385 ± 10 cm^{-1}) and the presence of a terminal vinyl group (1 820, 1 638, 1 420 – 1 440, 990, 910, etc. cm^{-1}). Strong methylene absorption was indicated by the broad bands at 2 880 and 2 975 cm^{-1}. The characteristic ν_{CH_2} ring vibration band at 900–950 cm^{-1} (3) was indicated by the absorption at 915 cm^{-1}, which, however, coincides with the δ_{CH} absorption of the terminal vinyl group at 910 cm^{-1}. The spectrum was entirely consistent with those obtained with an A.P.I. certified sample of vinylcylopentane, and reported for vinylcyclopropane (4). Now the presence of a double bond, the absence of methyl groups, and a molecular weight of 82, taken in conjunction with the mass spectral cracking pattern data, allow only two structural possibilities: vinylcyclobutane and methylene cyclopentane with a strong preference for the former.

The n.m.r. spectrum of this product determined in CS_2 using TMS as an internal standard was found to be consistent with the vinylcyclobutane structure but not with methylene cyclopentane. Thus the spectrum showed four multiplet resonances: a heptet centered at τ-value of 4.2 for the vinyl proton, two complex

**The synthesis of VCB has been reported by C. G. Overberger et al. J. Polymer Sci. Part A, 2, 755 (1964). The infrared and n.m.r. spectra are in good agreement with those reported here.*

Can. J. Chem. Downloaded from www.nrcresearchpress.com by 210.87.254.40 on 09/05/12
For personal use only.

doublets of the terminal vinyl protons centered at $\tau = 5.1$, while the complex multiplets of the ring bridgehead proton and the ring methylene protons appeared at $\tau = 7.1$ and 8.1 respectively. Also the integrated peak areas were in the right proportions, that is 1:2:1:6.

Bicyclohexyl and the other C_{12} products were tentatively identified by g.c. retention time comparisons. Product determinations were obtained from calibrated g.c. peak areas with the exception of VCB in which case the detector response was based on cyclohexene. The vinylcyclopentane formed in the decomposition of cycloheptene was identified by comparison of its mass spectrum, infrared and n.m.r. spectra with those of vinylcyclopentane (A.P.I.). All runs reported were performed at 26 ± 2 °C.

RESULTS

The products of the reaction were hydrogen, acetylene, ethylene, 1,3-butadiene, VCB, cyclohexane, and bicyclohexyl. Traces of 1,3-cyclohexadiene were also detected. Two additional isomers of butadiene, in minor yields, as well as a heavy oil, mainly C_{12} compounds, were also found. A specific search for methane and ethane in the fraction noncondensable at −160° proved the absence of these materials. It is not possible to state with certainty that no C_6 isomers other than VCB were formed in the reaction since some of these isomers could have eluted from the g.c. column with the substrate which was always present in large excess. However, the fact that no inconsistency was observed in the results on successive reuse of the substrate recovered by g.c. would argue against this possibility. For a number of the possible C_6 isomers, the g.c. retention time values were specifically checked, and as a result their absence in the reaction mixture can be regarded as proved. These were: 1,3-, 1,5-, and 2,4-hexadiene; allylcyclopropane; bicyclo[2.1.1]-hexane; 1-methylcyclopentene; 1-hexyne; 2,3-dimethyl-1,3-butadiene; 2-ethyl-1,3-butadiene; and bicyclo[3.1.0]hexane. In all runs reported the ethylene yield includes a small amount of acetylene and the butadiene yield some C_4-isomers. However, ethylene and butadiene comprised over 95% of their respective fractions.

Five main series of experiments were carried out.

I. Product yields were studied as a function of substrate pressure at an incident light intensity of 3.0×10^{16} quanta/s. The results are shown in Fig. 3. At substrate pressures exceeding 20 Torr, the exposure time was 10 min while at the lower pressures it was proportionally shorter. As can be seen from the figure, the yield of ethylene equals that of butadiene except at pressures below ca. 10 Torr where a deficiency in the butadiene yield appears. The suppressing effect of pressure on the ethylene-, butadiene-, and VCB-forming reactions is evident from the data. The yield of cyclohexane on the other hand shows no pressure dependency above ca. 5 Torr.

II. The quantum yields of ethylene, butadiene, VCB, and cyclohexane at a substrate pressure of 26 Torr were examined as a function of exposure time. According to the data

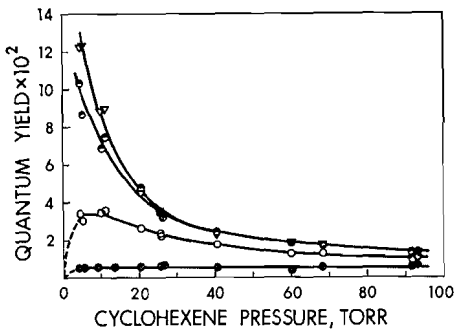

FIG. 3. Quantum yield for ethylene ▽, butadiene ◓, vinylcyclobutane ○, and cyclohexane ● formation as a function of cyclohexene pressure. $I_a = 3.0 \times 10^{16}$ quanta/s.

Can. J. Chem. Downloaded from www.nrcresearchpress.com by 210.87.254.40 on 09/05/12
For personal use only.

appearing in Fig. 4 all of these species are primary reaction products. The quantum yield of cyclohexene disappearance, as determined directly from substrate consumption, was ca. 0.2. The difference between yields of substrate consumption and the combined yields of product formation was largely due to the formation of the oily polymer, bicyclohexyl, and other C_{12}-compounds, which were not determined quantitatively.

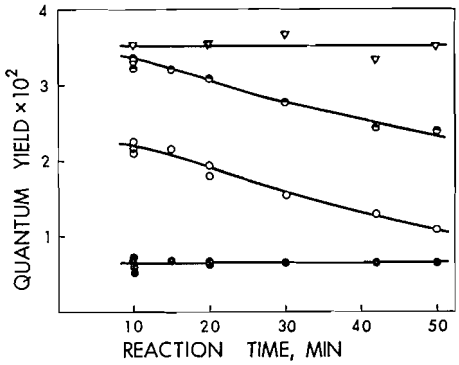

FIG. 4. Quantum yield for ethylene ▽, butadiene ◓, vinylcyclobutane ○, and cyclohexane ● formation as a function of exposure time.

III. To extend the range of pressure study which was limited by the low vapor pressure of the substrate, two series of experiments were performed with varying amounts of added inert gas at a constant pressure of cyclohexene. The data obtained with carbon dioxide as inert gas are presented in Fig. 5. and those with C_2D_6 in Fig. 6. For both cases a pressure effect similar to that found for cyclohexene itself is evident. The order of effectiveness in collisional deactivation for the three molecules is cyclohexene > C_2D_6 > CO_2.

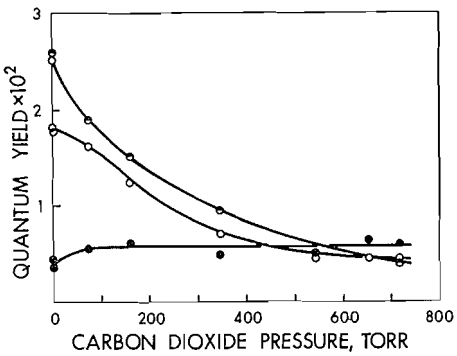

FIG. 5. Quantum yield of butadiene ◓, vinylcyclobutane ○, and cyclohexane ● formation as a function of added carbon dioxide pressure. P(cyclohexene) = 26 Torr. Uncorrected for incomplete absorption.

IV. To examine the effect of light intensity on the reaction, the pressure study with the pure substrate was repeated at the lower intensity of 1.7×10^{15} quanta/s. The results are plotted in Fig. 7. The reaction time was 100 min in experiments at pressures above 17 Torr, and 50 min at lower pressures.

V. Finally, a few experiments were done with a small amount of added nitric oxide. While cyclohexane formation was completely suppressed, the yields of butadiene and VCB were not affected by nitric oxide. In separate experiments carried out in a single pass

Can. J. Chem. Downloaded from www.nrcresearchpress.com by 210.87.254.40 on 09/05/12
For personal use only.

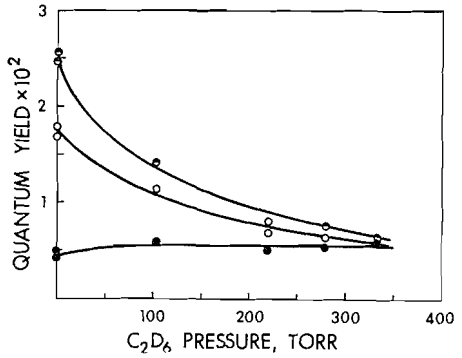

FIG. 6. Quantum yield of butadiene ◓, vinylcyclobutane ○, and cyclohexane ● formation as a function of added ethane-d_6 pressure. P(cyclohexene) = 26 Torr. Uncorrected for incomplete absorption.

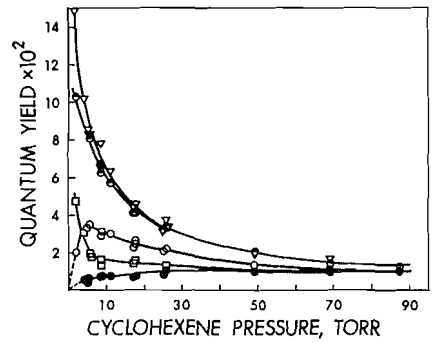

FIG. 7. Quantum yield for ethylene ▽, butadiene ◓, vinylcyclobutane ○, cyclohexane ●, and hydrogen □ formation as a function of cyclohexene pressure. $I_a = 1.7 \times 10^{15}$ quanta/s.

system, a white solid product deposited on the walls, which by infrared and n.m.r. analyses was found to be mainly cyclohexenone oxime.

DISCUSSION

The nature of the products, the lack of an inhibiting effect by nitric oxide on butadiene and VCB formation, and the kinetic characteristics of the reaction dictate that the primary reaction between triplet mercury atoms and cyclohexene molecules leads to a long-lived excited cyclohexene molecule, which on the basis of the generally accepted view on olefin reactions, is assumed to be a vibrationally excited triplet biradical. Also the pressure independence of the hydrogen and cyclohexane yields above ca. 30 Torr (cf. Figs. 3, 5, 6, and 7) suggests a minor paraffinic C—H scission by direct quenching at the methylene groups of the molecule. Thus the primary steps of the reaction may be represented by the sequence

[1a] $\quad Hg^* + \bigcirc \rightarrow Hg + \dot{\bigcirc}$

[1b] $\quad Hg^* + \bigcirc \rightarrow Hg + H +$ cyclo-$C_6H_9\cdot$

where cyclo-$C_6H_9\cdot$ represents a cyclohexenyl radical with the odd electron at the α- or β-position. It has been shown that paraffinic quenching reactions exhibit a large H/D kinetic isotope effect, but the olefinic reactions do not (5). Now if step [1b] is operative,

Can. J. Chem. Downloaded from www.nrcresearchpress.com by 210.87.254.40 on 09/05/12
For personal use only.

the quenching cross section of cyclo-C_6H_{10} should be somewhat larger than that of cyclo-C_6D_{10}. This was indeed borne out by experiment: $*\sigma_Q^2$(cyclo-C_6H_{10}) = 48.2 and σ_Q^2(cyclo-C_6D_{10}) = 42.9 Å^2 (6).

The following further reactions of the species formed in [1*a*] may be envisaged.

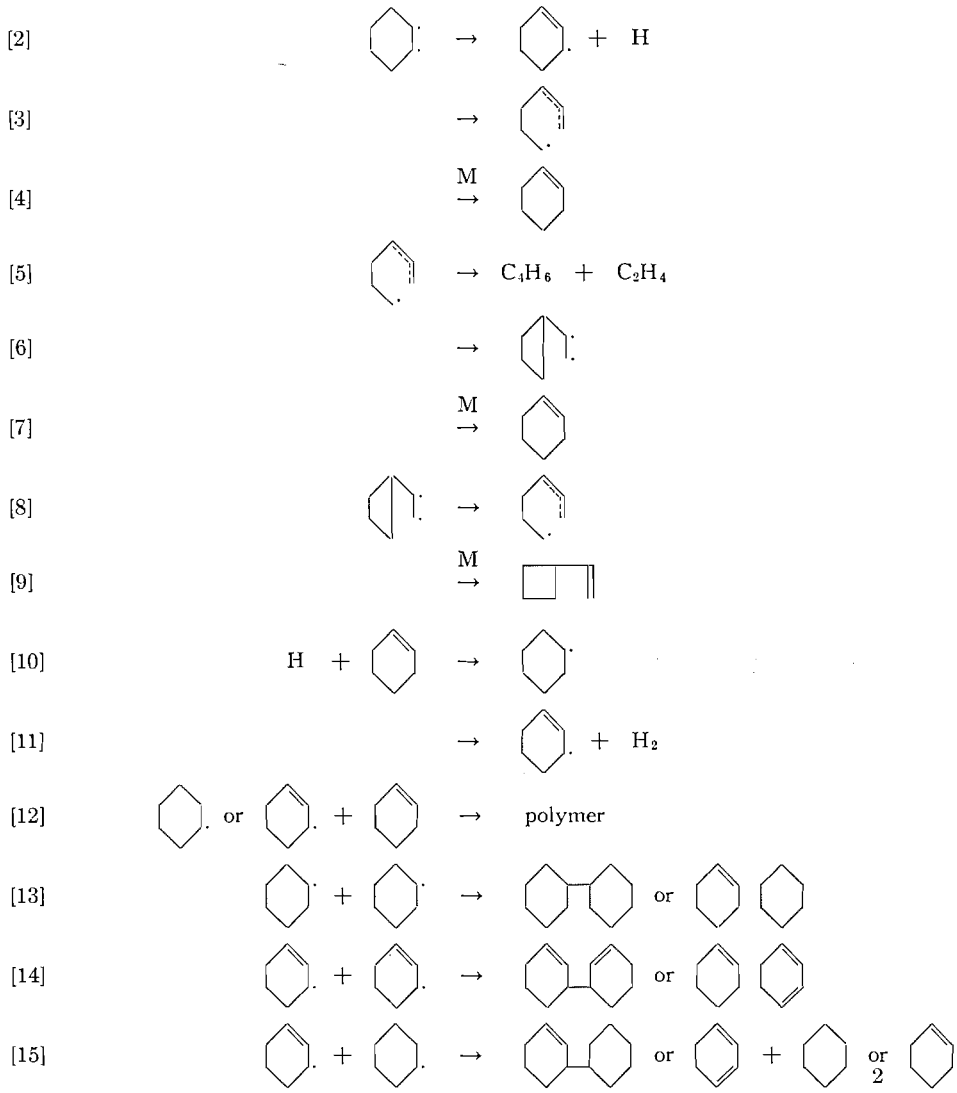

Step [2] is the familiar allylic C—H and [3] is the C—C bond cleavage which latter in the present case results in an open chain biradical with widely separated free spins. This open chain, resonance-stabilized biradical has an appreciable lifetime and may undergo unimolecular C—C bond cleavage yielding ethylene and butadiene, [5], or unimolecular isomerization to a triplet vinylcyclobutane, [6]. The mode of cleavage of the allylic biradical in step [5] was confirmed in studies on methyl-labelled cyclohexenes, currently in progress. Thus 4-methylcyclohexene and 3-methyl cyclohexene gave propylene + 1,3-butadiene, and ethylene + 1,3-pentadiene, respectively, in the corresponding reactions.

**For the lower olefins where the* Hg*—(C—H) *interaction is presumably negligible the following* σ_Q^2 *values were obtained:* C_2H_4 *(26.0 Å^2),* C_2D_4 *(25.5 Å^2),* C_3H_6 *(29.8 Å^2), and* C_3D_6 *(28.7 Å^2) (7, 5).*

Can. J. Chem. Downloaded from www.nrcresearchpress.com by 210.87.254.40 on 09/05/12
For personal use only.

The overall reaction to $C_2H_4 + C_4H_6 - 1,3$ is exothermic to about 71 kcal (8) and since the lowest triplet state for butadiene has been estimated to lie 60 kcal above the ground state (9) it is possible that the observed deficiency in butadiene yield at low pressures is due to some triplet state reaction.

The fate of the triplet vinylcyclobutane biradical is either reversal to the open chain biradical, [8], or alternatively as with the other excited species present, collisional deactivation to the ground state [9]. Other modes of decomposition of the excited VCB may also be operative leading to some additional products which could have been lost in the analysis. Without product evidences, such reactions would be speculative and are therefore omitted from the mechanism. The appearance of hydrogen, cyclohexane, and the C_{12} compounds in the products as well as the formation of polymer would probably be adequately accounted for by steps [10] to [15].

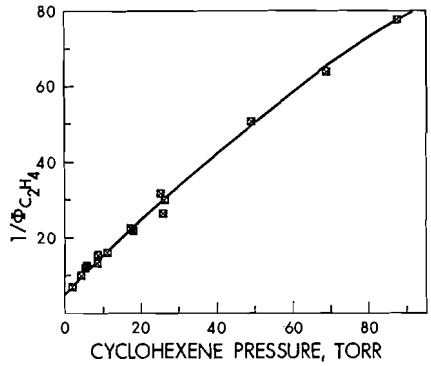

FIG. 8. Plot of $1/\Phi(C_2H_4)$ vs. cyclohexene pressure.

On the basis of a steady-state treatment of the above mechanism it can be shown that the plot of $1/\Phi(C_2H_4)$ vs. P, (Fig. 8), on extrapolation to $P = 0$, gives the expression:

$$[I] \qquad 1/\Phi(C_2H_4)_{at\ P=0} = 1 + \frac{k_2}{k_3},$$

from which $k_2/k_3 = 4.0$.

If the above mechanism is correct the following relation should also hold:

$$[II] \qquad P.\frac{R(C_2H_4)}{R(VCB)} = \frac{k_5k_8}{k_6k_9} + \frac{k_5}{k_6}.P,$$

where P is the substrate pressure.

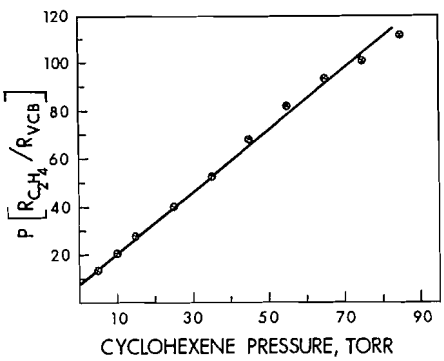

FIG. 9. Plot of $P[R(C_2H_4)/R(VCB)]$ vs. cyclohexene pressure.

Can. J. Chem. Downloaded from www.nrcresearchpress.com by 210.87.254.40 on 09/05/12
For personal use only.

In Fig. 9 the L.H.S. of eq. [II] is plotted against pressure and a good linear relation is obtained. Rearranging [II] we obtain

$$[III] \qquad \frac{R(C_2H_4)}{R(VCB)} = \frac{k_5k_8}{k_6k_9}P^{-1} + \frac{k_5}{k_6}.$$

From the slopes of [II] and [III] (which can be obtained with better accuracy than the ordinate intersections) from a least-mean-squares calculation we obtain: $k_5k_8/k_6k_9 = 6.7_5$ Torr and $k_5/k_6 = 1.2_5$. Assuming perfect collision efficiency for all deactivation reactions and taking $k_4 = k_7 = k_9 = 1.0 \times 10^{-10}$ cc molecule^{-1} s^{-1}, k_8 equals 1.7×10^7 s^{-1} and the lifetime of the excited VCB molecule is 5.8×10^{-8} s. It should be pointed out that this value of k_8 includes the rate constant values of other modes of decomposition if operative.

For the yield of ethylene formation, (Φ), the steady-state treatment results in the following equation:

$$[IV] \qquad Ak_3k_5 - Bk_5 - Ck_3 - \alpha^2 = 0,$$

where $\alpha = k_4P = k_7P = k_9P$; $A = (\Phi)^{-1} - 5 - [4\alpha/(k_8 + \alpha)]$; $B = \alpha[0.80\alpha/(k_8 + \alpha) + 1]$; $C = 5\alpha$. Equation [IV] cannot be solved explicitly, but only by approximation, because the rate constant values, k_3 and k_5, exhibit a small pressure trend. In the pressure interval of 10 to 80 Torr, k_3 and k_5 have nearly equal values which monotonously increase with pressure from about 3×10^7 s^{-1} at 10 Torr to about 5×10^7 s^{-1} at 80 Torr. Taking the mean value we obtain $4 \pm 1 \times 10^7$ s^{-1}. (The approximation method would in actual fact tolerate a variation in the ratio k_5/k_3 from 1 to 4.) Thus the lifetimes of the vibrationally excited triplet cyclic biradicals formed in [1*a*] and the open chain allylic biradicals formed in [3] are 0.5×10^{-8} and 1.4×10^{-8} s, respectively, which values are close to that obtained for the excited vinyl cyclobutane molecule, 5.8×10^{-8} s. The reason for the apparent small pressure trend in k_3 and k_5 is not clear but in addition to a systematic experimental error the following possibilities should be considered: *a*) in the estimation of $\Phi(C_2H_4)$ step [1*b*] was neglected which introduces a small systematic error in the calculation; *b*) the calibration of g.c. detector response for VCB was based on cyclohexene; *c*) the assumption that $k_4 = k_7 = k_9$ may not be valid and also their numerical value was chosen arbitrarily; *d*) some other reactions not considered in the mechanism may be operative; *e*) finally, the exposure time dependence of some of the products could not properly be taken into consideration.

Substituting the values of k_5 and k_3 in the ratios $k_5/k_6 = 1.2_5$ and $k_2/k_3 = 4.0$, we obtain $k_6 = 3.2 \times 10^7$ s^{-1} and $k_2 = 1.6 \times 10^8$ s^{-1} and for the lifetimes, $\tau_6 = 3.1 \times 10^{-8}$ and $\tau_2 = 6.3 \times 10^{-9}$ s. If we consider the rate constant values per bond we conclude that C—H cleavage is twice as fast as C—C cleavage, in spite of the fact that the C—C bond is the weaker. This indicates a higher frequency factor for the hydrogen-scission reaction.

It may be instructive now to compare the lifetimes for the various excited species obtained here to those available in the literature for 1-butene (10) and 2-butene (11). The relevant data are summarized in Table I. The species listed have equal total excitation energies (electronic + vibration) of 112.7 kcal, the electronic energy of Hg $6(^3P_1)$ atom, and all lifetimes were obtained on the generally accepted, but experimentally yet unverified, assumption that every collision of the excited species leads to deactivation, i.e. complete loss of reactivity. If we take τ to be inversely proportional to the number of available allylic bonds in the radical and take τ(C—C)/τ(C—H) = 2, we obtain a 'normalized' lifetime value for the triplet molecules which is taken as the reciprocal of the ratio of rate constants for the allylic C—C cleavage to the number of allylic C—C

Can. J. Chem. Downloaded from www.nrcresearchpress.com by 210.87.254.40 on 09/05/12
For personal use only.

TABLE I

Lifetime values for excited triplet olefins

Process	τ (s $\times 10^9$)	τ(normalized) (s $\times 10^9$)
C_2H_5—$\dot{C}H$—$\dot{C}H_2$ → decomposition	6.3	32
CH_3—$\dot{C}H$—$\dot{C}H$—CH_3 → decomposition	3.3	40
→ decomposition	5.0	50(100)*
→ decomposition	58	232

*This value was obtained by taking $k_3 = 2.0 \times 10^7$ and $k_5 = 8.0 \times 10^7$ s^{-1}.

bonds in the molecule. It is seen from the table that these normalized τ-values are nearly equal for the two butenes, 1.3 to 3 times larger for cyclohexene and still higher for VCB. The higher values for the latter two can be explained by the increased number of bonds present. However, it is not clear why the normalized lifetime of VCB is so much larger than that of cyclohexene.

A preliminary study on cycloheptene has indicated that this reaction is considerably more complicated than with the smaller ring homologs. The reaction products are more numerous and there are at least four isomeric C_7H_{12} compounds formed in comparable yields, one of which is vinylcyclopentane.

Combining the results of the present study with those obtained earlier on the cyclopentene reaction it may be concluded that ring contraction is a general, characteristic reaction of cyclic monoolefins, and that the mechanism of this reaction involves an allylic-type, open-chain triplet biradical with widely separated free spins.

ACKNOWLEDGMENT

The authors are grateful to the National Research Council for financial support.

REFERENCES

1. R. J. Cvetanović. *In* Recent advances in reaction kinetics. *Edited by* G. Porter. Pergamon Press. 1964.
2. W. A. Gibbons, W. F. Allen, and H. E. Gunning. Can. J. Chem. **40**, 568 (1962).
3. K. Nakanishi. Infrared absorption spectroscopy. Holden-Day, Inc., San Francisco. 1964.
4. R. Van Volkenburgh, K. W. Greenlee, I. M. Derfer, and C. E. Boord. J. Am. Chem. Soc. **71**, 3595 (1949).
5. Y. Rousseau and H. E. Gunning. Can. J. Chem. **41**, 465 (1963). Y. Rousseau, O. P. Strausz, and H. E. Gunning. J. Chem. Phys. **39**, 962 (1963).
6. M. G. Bellas, Y. Rousseau, O. P. Strausz, and H. E. Gunning. J. Chem. Phys. **41**, 768 (1964).
7. A. J. Yarwood, O. P. Strausz, and H. E. Gunning. J. Chem. Phys. **41**, 768 (1964). Unpublished data.
8. M. B. Epstein, K. S. Pitzer, and F. D. Rossini. J. Res. Natl. Bur. Std. **42**, 379 (1949).
9. D. F. Evans. J. Chem. Soc. 1735 (1960).
10. R. J. Cvetanović and L. C. Doyle. J. Chem. Phys. **37**, 543 (1962).
11. R. B. Cundall and T. F. Palmer. Trans. Faraday Soc. **56**, 1211 (1960).

Can. J. Chem. Downloaded from www.nrcresearchpress.com by 210.87.254.40 on 09/05/12
For personal use only.

Can. J. Chem. Downloaded from www.nrcresearchpress.com by 210.87.254.6 on 09/05/12
For personal use only.

PREPARATION AND PROPERTIES OF DIETHYL(DIPHENYLPHOSPHINYL)ALUMINIUM[1]

A. WILLIAM JOHNSON,[2] WILLARD D. LARSON,[3] AND GERD H. DAHL[4]
Chemistry Department, University of North Dakota, Grand Forks, North Dakota
Received November 13, 1964

Dedicated to Professor R. B. Sandin on the Occasion of his Sixty-Eighth Birthday

ABSTRACT

Two methods of preparing diethyl(diphenylphosphinyl)aluminium have been investigated. This compound exists as a dimer which can be cleaved to monomeric complexes by a variety of Lewis bases. The structure of the dimer and its chemical transformations are discussed.

INTRODUCTION

Considerable effort has been expended examining the chemistry of inorganic molecules which are isoelectronic with olefins. These studies have involved the formation of compounds by the bonding of an atom from group III with one from group V of the periodic table, both atoms often carrying organic substituents. Interest has centered on the chemical and physical properties of such systems but it has focused especially on the nature of the bonding between the group III and group V atoms. The major efforts in this area have involved studies of the B—N system (mainly trimeric) (1) and the B—P system (mainly trimeric) (2). Less is known about the Al—N system (3, 4). No "double bonding" has been observed to date.

When our work was started only three reports could be found on the chemistry of compounds containing aluminium–phosphorus bonds. Davidson and Brown (5) observed that trimethylphosphine and trimethylaluminium formed a stable adduct which eliminated methane, but only at high temperatures, to form dimethyl(dimethylphosphinyl)-aluminium, $Me_2Al—PMe_2$.[5] This compound was reported to be trimeric and not subject to cleavage by trimethylamine or dimethyl ether. In 1960 Burg and Mödritzer (6) attempted to prepare dimethylphosphinylalane, $Me_2P—AlH_2$, by a variety of methods but failed. Fritz and Trenczek (7) found that treatment of aluminium chloride with lithium diethylphosphide afforded dichloro(diethylphosphinyl)aluminium. They reported that this substance existed as a trimer but it must be noted that this conclusion was based on cryoscopy in phosphorus oxychloride, a solvent with which the compound in question reacted, albeit slowly.

Our purposes in studying the chemistry of aluminium–phosphorus compounds were: 1, to develop useful and general methods of synthesis of the compounds; 2, to investigate the nature of the bonding in these systems; and 3, to study the chemical behavior of aluminium–phosphorus compounds. Since the ultimate goal of most of the work in this field has been to detect the presence or absence of double bonding in the inorganic systems,

[1]*Presented in part at the 148th meeting of the American Chemical Society, Chicago, September 1964.*
[2]*To whom inquiries should be addressed.*
[3]*From the dissertation submitted to the Graduate School of the University of North Dakota in partial fulfillment of the requirements for the degree of Doctor of Philosophy, June 1964. Present address: Dow Corning Corporation, Midland, Michigan.*
[4]*Present address: Pennsalt Chemical Company, King of Prussia, Pennsylvania.*
[5]*Abbreviations used: Me = methyl, Et = ethyl, Ph = phenyl, THF = tetrahydrofuran.*

that became one of our goals as well. There was virtually no information available about the chemical properties of the aluminium–phosphorus compounds. In fact, most compounds reported were, at best, poorly characterized and nothing was known of their reactions.

RESULTS

In our study of the chemistry of aluminium–phosphorus compounds we decided to use diethyl(diphenylphosphinyl)aluminium (I), $Et_2Al—P(Ph)_2$, as our model compound. This choice was dictated primarily by the availability of starting materials but it was thought its chemistry would be typical nonetheless.

Lithium diphenylphosphide was required for one of our synthetic approaches to I. The only previous reports regarding the preparation of lithium diphenylphosphide involved either the cleavage of triphenylphosphine with metallic lithium (8) or the reaction of phenyllithium with diphenylphosphine (9). The former method has the distinct disadvantage of cost and the presence of phenyllithium. The latter method is tedious since the diphenylphosphine usually has to be prepared from the metal phosphide or from diphenylphosphinous chloride (8, 10). Methods are known for the preparation of sodium or potassium diphenylphosphide directly from the diphenylphosphinous chloride (11, 12) but these involved the use of the molten metals.

It was found that metallic lithium would react with diphenylphosphinous chloride in tetrahydrofuran solution to afford lithium diphenylphosphide. This reaction appeared to be rather specific in that it would not occur in diethyl ether or in dioxane solution. A convenient method of assaying for the phosphide was to react an aliquot with methyl iodide and isolate the diphenyldimethylphosphonium iodide. By this method, it was determined that the yield of the phosphide was normally 95%. The diphenylphosphinous chloride was shown not to react under these conditions. The solution of phosphide was stable for several hours and gave no indication of reacting with the solvent (13).

Diphenylphosphine at first was prepared according to literature procedures by the reduction of diphenylphosphinous chloride with lithium aluminium hydride (10). However, this reduction took place in only 47–67% yields. We found that conversion of the chloride into lithium diphenylphosphide followed by treatment of the latter with gaseous hydrogen chloride until the color of the phosphide was discharged led to the formation of diphenylphosphine in 83% overall yield. No attempt was made to maximize this yield. These methods developed for the synthesis of diphenylphosphine and lithium diphenylphosphide are much simpler, experimentally, than those presently in the literature (14). In addition, the yields are high and the products uncontaminated. They appear to be the methods of choice.

Reaction of lithium diphenylphosphide with diethylaluminium bromide (15) gave lithium bromide (91%) and an amorphous tetrahydrofuran etherate of I. Reaction of the potassium diphenylphosphide with diethylaluminium bromide initially afforded uncomplexed I but crystallization from ether gave an etherate of I. Issleib and Deylig (12) first carried out this reaction and obtained the etherate directly. Microanalytical data indicated that the etherate was converted to its uncomplexed dimer before analysis. However, ethane analysis and cryoscopy in benzene confirmed the monomeric etherate structure.

[1] $$Ph_2P^-Li^+ + Et_2AlBr \rightarrow Ph_2P—AlEt_2 + LiBr.$$

Mixing diphenylphosphine and triethylaluminium either neat or in a solvent led to

Can. J. Chem. Downloaded from www.nrcresearchpress.com by 210.87.254.6 on 09/05/12
For personal use only.

the instantaneous evolution of ethane and the formation of dimeric diethyl(diphenylphosphinyl) aluminium (eq. [2]). The dimer gave satisfactory aluminium and phosphorus analyses but the carbon and hydrogen values were consistently low, probably due to hydrolysis. The compound also gave satisfactory ethane analyses and cryoscopy in benzene confirmed the dimeric structure.

[2] $$Et_3Al + Ph_2PH \rightarrow [Et_3\bar{A}l—\overset{+}{P}HPh_2] \rightarrow Et_2Al—PPh_2 + EtH.$$

The dimer of I was very sensitive to moisture. Protolysis with ethanol then water led to the evolution of ethane and the formation of diphenylphosphine. The latter was not isolated as such but was permitted to oxidize during the work-up to diphenylphosphinic acid. The yield of this acid could be increased by the addition of dilute hydrogen peroxide to the hydrolysis mixture prior to work-up. The dimeric structure could be cleaved by the action of a variety of Lewis bases. Simple crystallization of the dimer from diethyl ether at low temperatures led to the isolation of the diethyl etherate of monomeric I. This sample was identical to one prepared directly from diethylaluminium chloride and potassium diphenylphosphide (12).

In a similar manner the dimer (I) reacted with acridine to form a 1:1 complex between the acridine and the monomeric aluminium–phosphorus compound. This complex was an amorphous material but after purification it gave satisfactory phosphorus, aluminium, and ethane analyses. The dimer appeared to form complexes with a variety of amines but most were not crystalline. Evidence was obtained for some reaction between the dimer and trimethylamine in the form of a color change but only unreacted dimer could be isolated from the reaction mixture.

The dimer (I) was cleaved readily by *n*-butyllithium to *n*-butyldiethylaluminium and lithium diphenylphosphide. The presence of the latter was confirmed by trapping it in a reaction with iodobenzene to form triphenylphosphine (eq. [3]). Authentic lithium diphenylphosphide was shown to afford triphenylphosphine upon reaction with iodobenzene. The dimer was shown not to react with iodobenzene.

[3] $$\underset{\text{I}}{Et_2Al—P(Ph)_2} + C_4H_9Li \rightarrow Et_2AlC_4H_9 + (Ph)_2P^-Li^+ \xrightarrow{Ph—I} (Ph)_3P$$

Diethyl(diphenylphosphinyl)aluminium (I) also was shown to react with methyl iodide and the resulting diphenyldimethylphosphonium iodide was isolated in 90% yield. No attempt was made to isolate the aluminium-containing product.

DISCUSSION

When we began our work on the aluminium–phosphorus system the only known compounds of this type, $Me_2Al—P(Me)_2$ (5) and $Cl_2Al—P(Et)_2$ (7), had been reported to be trimeric. These observations appeared somewhat anomalous in view of Gillespie's arguments that valency-angle deformation from the tetrahedral (109°) hybridization to a square (90°) hybridization should occur rather readily with elements of the second and lower periods (16). Nonetheless, only trimeric aluminium–phosphorus compounds had been reported, those presumably having a six-membered ring structure.

Since our work was undertaken there have been three publications, including this one, reporting studies on aluminium–phosphorus compounds. Interestingly, all three of these independent reports indicated that the substances under study existed as *dimers* rather than trimers as had been reported earlier. Issleib and Deylig (12) prepared $Et_2Al—P(Et)_2$, Coates and Graham (17) prepared $Me_2Al—P(Ph)_2$, and we have prepared $Et_2Al—P(Ph)_2$.

Can. J. Chem. Downloaded from www.nrcresearchpress.com by 210.87.254.6 on 09/05/12
For personal use only.

It should be noted that Issleib and Deylig (12) earlier had failed to obtain the dimer of $Et_2Al—P(Ph)_2$ and had reported only the monomeric etherate. It would appear that the recent trend in the aluminium–phosphorus compounds is in accord with Gillespie's arguments (16) favoring the dimeric structures as the most common.

The aluminium atom in the dialkyl(disubstitutedphosphinyl)aluminium compounds obviously is very acidic and tends to be complexed by a Lewis base. In spite of the presence of an adjacent phosphorus atom with an unshared pair of electrons potentially available for sharing with the vacant orbital of aluminium, thereby satisfying the electron demand of the aluminium, there has been no evidence provided for the existence of a free monomeric structure (III). In other words, there is no evidence to indicate that multiple bonding exists in the aluminium–phosphorus series.

$$R_2Al—\ddot{P}R_2 \leftrightarrow R_2\bar{A}l=\overset{+}{P}R_2$$

III

Instead, the compounds dimerize (e.g. IV) and a phosphorus atom acts as a Lewis base to complex with the aluminium atom of another molecule, both atoms probably being tetrahedrally hybridized. This apparent lack of double bonding is in spite of the fact that the size relationship of the two atoms, phosphorus and aluminium, should be favorable for overlap and double bonding. Lack of appreciable overlap may be due to the hybridization of the two atoms being incompatible with pi bonding.

We have been able to demonstrate that the dimer of I is readily converted into the monomeric etherate. It appears that the ether is sufficiently nucleophilic to displace the diphenyl(diethylaluminio)phosphine molecule as a complexing group for the other aluminium atom (eq. [4]). Such was not the case for the tetraethyl analog of IV, $(Et_2Al—PEt_2)_2$, since Issleib and Deylig (12) reported obtaining only the dimer with no mention made of a monomeric etherate. This is to be expected since the diethylphosphorus group in the latter case should be a stronger nucleophile than the diphenylphosphorus group in IV and more difficult to displace with ether.

[4] $$\underset{\text{IV}}{\begin{matrix}Et_2Al—P(Ph)_2\\ \diagdown\ \diagup\\ (Ph)_2P—Al(Et)_2\end{matrix}} \xrightarrow{Et_2O} \left[\begin{matrix}Et_2Al—P(Ph)_2\\ \diagdown\\ (Ph)_2P—Al(Et)_2\\ \uparrow\\ Et—O—Et\end{matrix}\right] \xrightarrow{Et_2O} 2\ \begin{matrix}Et_2Al—P(Ph)_2\\ \diagdown\\ Et—O—Et\end{matrix}$$

It was somewhat surprising to find that our dimer (IV) appeared to react only slightly with trimethylamine, a stronger nucleophile than ether. Under no conditions could a stable complex be isolated. In contrast, Coates and Graham (17) reported that $Me_2Al—P(Ph)_2$ would complex with trimethylamine (stable to 65°) but there was no indication of the stoichiometry of the product. We did find, however, that acridine would cleave the dimeric form of I and form a stable complex with the monomeric form. It may be that the steric requirements of a trimethylamine complex were too large and that acridine, while even less basic, does have a lower steric requirement.

Very little work has been published on the reactions undergone by aluminium–phosphorus compounds. We have found that diethyl(diphenylphosphinyl)aluminium (I) is very sensitive to moisture. Hydrolysis of I led to the initial cleavage of the aluminium–carbon bonds and then to the cleavage of the aluminium–phosphorus bond, resulting in the formation of ethane and diphenylphosphine. In view of our observations on the hydrolytic instability of I it is interesting to note that Fritz and Trenczek (18) recently reported, in a communication devoid of experimental data, that $H_2Al—P(Et)_2$, thought

Can. J. Chem. Downloaded from www.nrcresearchpress.com by 210.87.254.6 on 09/05/12
For personal use only.

to exist as a trimer, was stable in the atmosphere. This is particularly surprising since the indications from all previous work on aluminium–phosphorus compounds are that all of these compounds are very moisture sensitive.

We have found that I is subject to cleavage by other nucleophiles, especially organolithium reagents. Reaction of I with *n*-butyllithium apparently proceeded by nucleophilic attack of the butyl carbanion on the aluminium atom resulting in the formation of *n*-butyldiethylaluminium and lithium diphenylphosphide (eq. [3]). Since the solution containing the colorless dimer acquired the orange coloration typical of the diphenylphosphide anion immediately upon the addition of *n*-butyllithium and it exhibited reactions characteristic of that anion (reaction with iodobenzene to form triphenylphosphine), it appears unlikely that an intermediate of the type V had an appreciable lifetime. This observation is somewhat surprising in view of the acidity of the aluminium atom. However, credence was lent to our observation by the recent report that $Et_3Ge—P(Ph)_2$ reacted similarly, affording *n*-butyltriethylgermane and the diphenylphosphide ion (19).

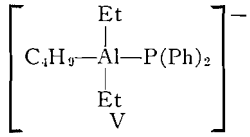

In accord with the observation initially made by Issleib and Deylig (12) we have confirmed that the aluminium–phosphorus bond is cleaved readily by methyl iodide, compound I forming diphenyldimethylphosphonium iodide and, presumably, diethyliodoaluminium. Again the reaction is not unique for the aluminium–phosphorus system since $Et_3Ge—P(Ph)_2$ was cleaved in an analogous manner (19). These cleavages most likely occurred by initial quaternization of the phosphorus atom followed by nucleophilic attack of the iodide on the aluminium or germanium atom (eq. [5]).

[5] $$Et_2Al—P(Ph)_2 + MeI \rightarrow [Et_2Al—\overset{+}{P}(Me)(Ph)_2\ I^-] \rightarrow Et_2Al—I + MeP(Ph)_2,$$
$$MeP(Ph)_2 + MeI \rightarrow Me_2\overset{+}{P}(Ph)_2\ I^-.$$

EXPERIMENTAL

General Manipulative Methods

All operations were carried out under a blanket of oxygen-free nitrogen. Mechanical manipulations were done in a nitrogen-filled plastic "dry bag" (available from I²R, Inc., Cheltenham, Penna.). All solvents were meticulously purified and dried by standard procedures. Molecular weights were determined cryoscopically in benzene. It was necessary to degas the solvent thoroughly before use. Samples for elemental analysis were first oxidized with sodium peroxide in a Parr bomb. The oxidation solution was acidified with nitric acid, then an aliquot was analyzed for phosphorus essentially as described by Bachofer and Wagner (20). A second aliquot was analyzed for aluminium using the 8-hydroxyquinoline reagent in a standard manner. Ethane analyses were carried out by treating the compounds with *n*-butyl alcohol then 6 *N* hydrochloric acid and determining the volume of the liberated ethane.

Aluminium Starting Materials

Ethylaluminium sesquibromide was obtained by the procedure of Grosse and Mavity (15) in 73% yield as a colorless liquid, b.p. 140° (10 mm).

Using the procedure of the same authors we obtained diethylaluminium bromide in 75% yield as a colorless liquid, b.p. 64° (1.0 mm).

Anal. Calcd. for $C_4H_{10}AlBr$: Al, 16.35; Br, 48.5; ethane, 35.7. Found: Al, 15.65; Br, 48.0; ethane, 34.9.

Triethylaluminium was at first prepared by treatment of diethylaluminium bromide with sodium (15) but was later purchased from Texas Alkyls, Inc. It was redistilled as a colorless liquid, b.p. 54° (0.5 mm).

Anal. Calcd. for $C_6H_{15}Al$: ethane, 83.6. Found: ethane, 83.4.

Lithium Diphenylphosphide

To a stirred slurry of 2.0 g (0.29 g-atoms) of finely divided lithium metal in 250 ml of dry tetrahydrofuran was added 25 g (0.11 mole) of diphenylphosphinous chloride over a period of 30 min. After heating under

Can. J. Chem. Downloaded from www.nrcresearchpress.com by 210.87.254.6 on 09/05/12
For personal use only.

reflux for 30–45 min the solution was siphoned away from the excess lithium and stored under nitrogen until needed. To 1.0 ml of the above orange solution was added excess methyl iodide in 2 ml of THF. The color rapidly disappeared and a colorless precipitate appeared simultaneously. After the mixture was warmed for a few minutes under a hot water tap the precipitate was filtered and dried. The yield of diphenyldimethyl phosphonium iodide was 0.135 g (95%) and it crystallized from ethanol–water as colorless needles, m.p. 240° (lit. (21) m.p. 241°).

Diphenylphosphine

To the stored solution of lithium diphenylphosphide prepared exactly as described above was added gaseous hydrogen chloride through a straight bore adapter until the orange color of the phosphide had just disappeared. A distillation head was then attached to the flask and the THF was removed. Distillation under vacuum afforded 17.5 g (83%) of diphenylphosphine as a colorless liquid, b.p. 84–86° (0.5 mm), n_D^{20} 1.6279, λ_{max} 4.5 μ (lit. (21) b.p. 280°).

Diethyl(diphenylphosphinyl)aluminium (I)

A solution of lithium diphenylphosphide was prepared as described above from 20.9 g (0.095 mole) of diphenylphosphinous chloride and 3.8 g (0.55 g-atom) of lithium. To this stirred solution was gradually added 15.6 g (0.095 mole) of diethylaluminium bromide, during which time the color faded to a golden yellow. The solvent was evaporated and replaced by benzene then the lithium bromide (7.5 g, 91%) was removed by filtration. Evaporation of the benzene left an oily residue which was taken up in ether. After 24 h a precipitate appeared which could not be recrystallized and which did not afford a satisfactory melting point.

Anal. Calcd. for $C_{16}H_{20}AlP \cdot C_4H_8O$: Al, 7.9; P, 9.06. Found: Al, 7.76; P, 8.1.

To a cold solution of 8.25 g (0.05 mole) of diethylaluminium bromide in 120 ml of diethyl ether was added slowly 20 g (0.05 mole) of $(Ph)_2PK \cdot (dioxane)_2$ (9). After the mixture was stirred for 2 h the potassium bromide was removed by filtration and the ether filtrate evaporated, leaving 8.0 g (60%) of crude diethyl-(diphenylphosphinyl)aluminium (I), m.p. 121–122°. The solid crystallized from diethyl ether at −70° as colorless needles of the monomeric diethyl etherate of I, m.p. 148° (lit. (12) m.p. 151°).

Anal. Calcd. for $C_{16}H_{20}AlP \cdot (C_2H_5)_2O$: P, 9.02; Al, 7.85; mol. wt. 344; ethane, 16.8. Found: P, 11.31; Al, 9.66; mol. wt. 340, 358, 340, 345; ethane, 16.6.

To 15.1 g (0 081 mole) of diphenylphosphine cooled to 0° was added, with stirring, 9.27 g (0.081 mole) of triethylaluminium over a period of 30 min. Some gas was evolved but the rate of evolution increased when the temperature was raised to 90°. After 2 h at this temperature the oily mass solidified. The crude solid (21 g, 96%) was taken up in warm benzene, then the dimer of diethyl(diphenylphosphinyl)aluminium (I) was crystallized as colorless needles upon the addition of petroleum ether, m.p. 124–126°.

Anal. Calcd. for $(C_{16}H_{20}AlP)_2$: C, 71.2; H, 7.42; P, 11.5; Al, 10.0; mol. wt. 540; ethane, 21.5. Found: C, 66.6; H, 6.74; P, 11.39; Al, 9.96; mol. wt. 540, 550, 555; ethane, 20.9.

Dimeric I was dissolved in a minimum of warm diethyl ether. After cooling for 1 day the monomeric etherate of I crystallized as colorless needles, m.p. 148–150°, shown to be identical to the sample prepared above by admixture melting point and a comparison of the infrared spectra.

To a solution of 5.0 g of the dimer (I) in 25 ml of benzene was added 3.4 g of freshly sublimed acridine. The solution became a green-brown but it was warmed gently until all of the acridine had dissolved. After the solution stood overnight at room temperature the benzene was evaporated *in vacuo* and the residue was washed with a benzene – petroleum ether solution to remove unreacted acridine. Additional unreacted acridine was removed by heating the residue to 120° *in vacuo*. The presumed complex of monomeric I and acridine remained as a black porous solid, m.p. 130–145°.

Anal. Calcd. for $C_{29}H_{29}AlPN$: Al, 6.03; P, 6.91; ethane, 12.92. Found: Al, 5.95; P, 6.67; ethane, 13.0.

Hydrolysis of I

A solution of 3.0 g of I in 5 ml of benzene was treated with 10 ml of ethanol then 20 ml of water. A very strong phosphine odor was evident. The solvent mixture was replaced with pure benzene and this solution was extracted with dilute sodium hydroxide. Acidification of the aqueous layer afforded 0.4 g (20%) of crude diphenylphosphinic acid, m.p. 175–190°. The acid crystallized from ethanol–water as colorless needles, m.p. 190–193° (lit. (21) m.p. 195°). The yield of acid was increased to 43% when the additon of water was followed by the addition of 10% aqueous hydrogen peroxide.

Reaction of I with Methyl Iodide

To a solution of 5.0 g (9.3 mmoles) of dimeric I in 10 ml of cold benzene was added 11.5 g of methyl iodide. No visible reaction occurred but upon allowing the mixture to warm to room temperature and stand overnight a mass of colorless needles precipitated. When the supernatant liquid was treated with ethanol or dilute hydrochloric acid a gas was evolved. The precipitate was filtered, affording 7.0 g (90%) of crude diphenyldimethylphosphonium iodide, m.p. 235–239° (lit. (21) m.p. 241°).

Reaction of I with n-Butyllithium

To a solution of 6.0 g (0.22 mole) of I in 10 ml of benzene was added 0.07 mole of *n*-butyllithium in 20 ml of hexane. The solution immediately became yellow and the color darkened to orange with gentle warming.

Can. J. Chem. Downloaded from www.nrcresearchpress.com by 210.87.254.6 on 09/05/12
For personal use only.

A 10 ml aliquot of this solution was treated with excess iodobenzene whereupon the orange color gradually disappeared. The addition of ethanol and then water led to the evolution of a gas. The organic layer was separated, the aqueous layer extracted with benzene, and the combined organic layers were chromatographed on alumina to afford 0.7 g (38%) of crude triphenylphosphine, m.p. 65–72°. The phosphine crystallized from benzene–ethanol as colorless plates, m.p. 77–78°. It was identified by admixture melting point with an authentic sample, a comparison of its infrared spectrum with that of an authentic sample, and oxidation to triphenylphosphine oxide, m.p. 151–152°.

ACKNOWLEDGMENTS

We gratefully acknowledge the financial support of the Olin Mathieson Chemical Corporation throughout this work. We would like to thank the Victor Chemical Division of the Stauffer Chemical Co. for generous gifts of diphenylphosphinous chloride. The senior author acknowledges his personal debt to an inspiring teacher, Reuben B. Sandin.

REFERENCES

1. F. G. A. STONE. *In* Advances in inorganic chemistry and radiochemistry. Vol. 2. *Edited by* H. J. Emeleus and A. G. Sharpe. Academic Press, Inc., New York, N.Y. 1960. p. 285. E. K. MELLON, JR. and J. J. LAGOWSKI. *In* Advances in inorganic chemistry and radiochemistry. Vol. 5. *Edited by* H. J. Emeleus and A. G. Sharpe. Academic Press, Inc., New York, N.Y. 1963. p. 259.
2. F. G. A. STONE. *In* Advances in inorganic chemistry and radiochemistry. Vol. 2. *Edited by* H. J. Emeleus and A. G. Sharpe. Academic Press, Inc., New York, N.Y. 1960. p. 294.
3. A. W. LAUBENGAYER, K. WADE, and G. LENGNICK. Inorg. Chem. **1**, 632 (1962).
4. T. R. R. MCDONALD and W. S. MCDONALD. Proc. Chem. Soc. 382 (1963).
5. N. DAVIDSON and H. C. BROWN. J. Am. Chem. Soc. **64**, 316 (1942).
6. A. B. BURG and K. MÖDRITZER. J. Inorg. Nucl. Chem. **13**, 318 (1960).
7. G. FRITZ and G. TRENCZEK. Z. Anorg. Allgem. Chem. **313**, 236 (1961).
8. D. WITTENBERG and H. GILMAN. J. Org. Chem. **23**, 1063 (1958).
9. K. ISSLEIB and A. TZSCHACH. Chem. Ber. **92**, 1118 (1959).
10. W. KUCHEN and H. BUCHWALD. Chem. Ber. **91**, 2871 (1958).
11. W. KUCHEN and H. BUCHWALD. Angew. Chem. **69**, 307 (1957).
12. K. ISSLEIB and H. J. DEYLIG. Z. Naturforsch. **17b**, 198 (1962).
13. A. Y. GARNER and A. A. TEDESCHI. J. Am. Chem. Soc. **84**, 4734 (1962). K. B. MALLION and F. G. MANN. Chem. Ind. London, 654 (1963).
14. L. MAIER. *In* Progress in inorganic chemistry. Vol. 5. *Edited by* F. A. Cotton. Interscience Publishers. 1963.
15. A. V. GROSSE and J. M. MAVITY. J. Org. Chem. **5**, 106 (1940).
16. R. J. GILLESPIE. J. Am. Chem. Soc. **82**, 5978 (1960).
17. G. E. COATES and J. GRAHAM. J. Chem. Soc. 233 (1963).
18. G. FRITZ and G. TRENCZEK. Angew. Chem. **75**, 723 (1963).
19. F. GLOCKLING and K. A. HOOTON. Proc. Chem. Soc. 146 (1963).
20. M. D. BACHOFER and E. C. WAGNER. Ind. Eng. Chem. Anal. Ed. **15**, 601 (1943).
21. G. M. KOSOLAPOFF. Organophosphorus compounds. John Wiley and Sons, Inc., New York, N.Y. 1950.

Can. J. Chem. Downloaded from www.nrcresearchpress.com by 210.87.254.6 on 09/05/12
For personal use only.

Can. J. Chem. Downloaded from www.nrcresearchpress.com by 210.87.254.5 on 09/05/12
For personal use only.

PHOTOCHEMICAL TRANSFORMATIONS OF SOME 4′-AMINO-2-STYRYLPYRIDINES AND THEIR SALTS

J. L. R. Williams, J. M. Carlson, R. E. Adel, and G. A. Reynolds
Research Laboratories, Eastman Kodak Company, Rochester, New York

Received November 13, 1964

Dedicated to Professor R. B. Sandin on the Occasion of his Sixty-Eighth Birthday

ABSTRACT

The photochemical behavior of 4′-amino-, 4′-dimethylamino-, 4′-diethylamino-, and 4′-di-*n*-propylamino-substituted *trans*-2-styrylpyridine were studied. Ultraviolet irradiation of aqueous solutions of the bishydrochlorides and methiodide–hydrochlorides for moderate periods of time produced mixtures of the corresponding *cis* and *trans* isomers. Long irradiation times produced the corresponding dimers in all cases except that of *trans*-4′-di-*n*-propylamino-2-styrylpyridine. The *cis* isomers of the free bases and methiodides were isolated from the *cis–trans* mixtures. The *trans*-methiodides are not photochemically labile. The spectra of each pair of isomers were determined in water and in 50% methanol–water, with the exception of the 4′-di-*n*-propylamino derivative, which is not sufficiently water soluble. In addition, the spectra of the corresponding methiodides, hydrochlorides, bishydrochlorides, and methiodide–hydrochlorides were determined. The basic strengths of the nitrogens in the *cis–trans* isomer pairs of the free bases and methiodides have been determined spectroscopically in water and in 50% methanol–water.

INTRODUCTION

Earlier papers (1, 2) discussed the photoisomerization and photodimerization of some substituted styrylpyridines. When dimethylamino groups were placed in the 4′-position (4-position in the phenyl group), dimerization of *trans*-2-styrylpyridine methiodide (I*a*) in the solid state did not take place.

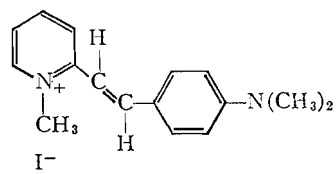

I*a*

This effect appearing in the solid state was attributed to improper spacing of the double bonds in the crystal lattice. The corresponding bismethosulfate (XII) did, however, photodimerize in the solid state.

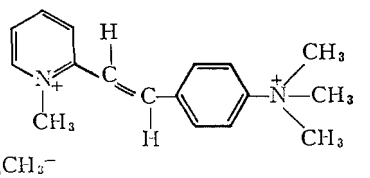

$SO_4CH_3^-$ XII

Furthermore, dimerization and photoisomerization of *trans*-4′-dimethylamino-2-styrylpyridine methiodide (I*a*) and *trans*-5-ethyl-4′-dimethylamino-2-styrylpyridine (XI) failed to occur in aqueous solution. On the other hand, the 4′-methyl- and 4′-methoxyl-substituted *trans*-2-styrylpyridine methiodides gave *cis–trans* mixtures and dimers when irradiated in water solution. The photochemical behaviors of the hydrochlorides of the

monobasic styrylpyridines were analogous to those of the monoquaternary salts (2). Tables I and II summarize the symbols which represent the various derivatives studied in the present work.

DISCUSSION

The fact that I*a*, II*a*, and III*a* do not photoisomerize in solution suggests that extreme structures in which the ethylenic double bonds do not exist as such contribute greatly to the ground state of the molecules. One such example would be:

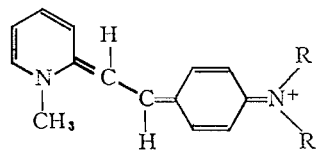

I⁻

I*a*–III*a*.

The lack of double-bond character at the ethylenic bond could be responsible for the failure of I*a*, II*a*, and III*a* to undergo photochemical change.

In the present work the spectra and photochemical behavior of 4′-dimethylamino-2-styrylpyridine (I), 4′-diethylamino-2-styrylpyridine (II), 4′-(di-*n*-propyl)-2-styrylpyridine (III), 4′-amino-2-styrylpyridine (IV), and their salts were studied. A second purpose was to study the base strengths of the *cis* and *trans* isomers prepared during the work. Base strengths were determined by the method of Hammett (3), as modified for difunctional compounds by Rosenblatt (4). The use of the Rosenblatt scheme was necessary, since during determinations of base strength the monohydrochlorides I*b* to IX*b* never exist in their pure form. The wavelengths of λ_{max} and molecular extinction coefficients of these monohydrochlorides were obtained from the ultraviolet absorption curves measured at various values of pH and by calculation. Both the spectra and the base strength values were determined in water and in 50:50 methanol–water, since III is not water soluble. Table I summarizes the ultraviolet absorption data of the *trans* forms of the free bases and salts of I, II, III, and IV. The free bases (I–IV) show wavelengths of λ_{max} in the range of 337–380 mμ, whereas the *trans*-methiodides (I*a*–IV*a*) and *trans*-monohydrochlorides (I*b*–IV*b*) show corresponding absorptions in the range of 385–470 mμ. Under the same conditions, the *trans*-bishydrochlorides (I*c*–IV*c*) and the *trans*-methiodide–hydrochlorides (I*d*–IV*d*) show wavelengths of λ_{max} in the range of 324–328 mμ. Thus, it appears that the ethylenic linkage in the *trans* free bases (I–IV), the *trans*-bishydrochlorides (I*c*–IV*c*), and the *trans*-methiodide–hydrochlorides (I*d*–IV*d*) possesses greater double-bond character than in the *trans*-methiodides (I*a*–IV*a*) and monohydrochlorides (I*b*–IV*b*). As a result, photochemical change takes place when compounds I–IV, I*c*–IV*c*, and I*d*–IV*d* are irradiated. The unsubstituted salt, *trans*-2-styrylpyridine methiodide (V*a*), absorbs at a wavelength of λ_{max} of 340 mμ. In all the other cases we have examined, including 4′-CH_3–, 4′-OCH_3–, 4′-chloro-, and 4′-nitro-substituted *trans*-2-styrylpyridine methiodides, a bathochromic shift of the wavelength of λ_{max} occurred upon introduction of a substituent into the 4′-position of *trans*-2-styrylpyridine methiodide (V*a*). The charged group —$\overset{+}{H}N(CH_3)_2Cl^-$ caused the reverse effect, a hypsochromic shift due to the high electrophilicity of the positive group. A similar difference was noted by Phillips (5) between the spectra of the bismethiodide of *trans*-4′-dimethylamino-2-styrylpyridine (I), I, and I*a*.

The values of the red shifts produced in the *trans*-methiodides (I*a*–IV*a*) when the

Can. J. Chem. Downloaded from www.nrcresearchpress.com by 210.87.254.5 on 09/05/12
For personal use only.

TABLE I

Absorption spectra of *trans*-4′-amino-substituted 2-styrylpyridines

		In water		In 50% methanol–water	
		λ_{max} (mμ)	ϵ	λ_{max} (mμ)	ϵ
I	*trans*-4′-Dimethylamino-2-styrylpyridine	348	26 200	359	27 700
I*a*	Methiodide	437	26 400	453	33 200
I*b*	Monohydrochloride	425	17 900*	442	32 200*
I*c*	Bishydrochloride	324	31 600	325	31 600
I*d*	Methiodide–hydrochloride	326	27 400	327	28 200
II	*trans*-4′-Diethylamino-2-styrylpyridine	368	22 800	376	32 400
II*a*	Methiodide	456	33 300	469	39 400
II*b*	Monohydrochloride	446	17 900*	455	28 200*
II*c*	Bishydrochloride	326	32 500	327	32 600
II*d*	Methiodide–hydrochloride	325	28 100	328	28 400
III	*trans*-(4′-Di-*n*-propylamino)-2-styrylpyridine			380	34 400
III*a*	Methiodide	459	37 100	470	41 700
III*b*	Monohydrochloride			458	37 000*
III*c*	Bishydrochloride			326	32 000
III*d*	Methiodide–hydrochloride	327	29 100	328	29 200
IV	*trans*-4′-Amino-2-styrylpyridine	337	30 100	339	29 500
IV*a*	Methiodide	392	25 300		
IV*b*	Monohydrochloride	385	32 100*	398	27 800*
IV*c*	Bishydrochloride	328	30 700	328	30 400
IV*d*	Methiodide–hydrochloride	327	25 600		
V	*trans*-2-Styrylpyridine	309	26 300	310	26 300
V*a*	Methiodide	340	28 000		
V*b*	Hydrochloride	334	27 900		

*Calculated. The monohydrochlorides do not exist as such in dilute acid solution, since they are in equilibrium with free base and bishydrochloride. Their complete ultraviolet absorption curves cannot be determined but the values of λ_{max} and their corresponding molecular extinction coefficients can be determined by calculation.

alkyl group of the amino group was changed from hydrogen to methyl, ethyl, and propyl are 45 mμ, 64 mμ, and 67 mμ. Thus, there seems to be very little steric interference of the dialkylamino groups with the phenyl ring, and coplanarity of the dialkylamino groups and the phenyl ring is possible. The molecular extinction coefficients increase in the same order. On the basis of absorption spectra, the methyl group appears to be less effective in promoting the release of electrons into the conjugated system via the amino nitrogen than does ethyl or propyl.

Furthermore, there is little or no solvent shift when the spectra of I*c*–IV*c* and I*d*–IV*d* are determined in water or in 50% methanol–water. The localized electron pairs of the amino groups of I–IV, I*a*–IV*a*, and I*b*–IV*b* do participate in solvent interactions, as evidenced by the shifts of wavelengths of λ_{max}. These species, I*a*–IV*a* and I*b*–IV*b*, undergo photochemical change only after extremely long irradiation times. Since the species I–IV,

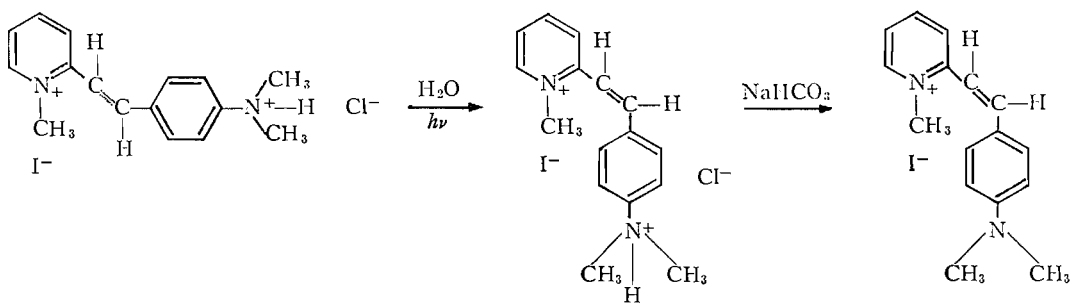

REACTION SCHEME 1.

Can. J. Chem. Downloaded from www.nrcresearchpress.com by 210.87.254.5 on 09/05/12
For personal use only.

I*c*–IV*c*, and I*d*–IV*d* do undergo rapid photoisomerization, the *cis* isomers were prepared by solution irradiation according to the sequence shown in Reaction Scheme 1. The scheme involving bishydrochlorides, I*c*–IV*c*, was analogous.

Difficulty was at first encountered during the isolation of the *cis* isomers. Since the *cis* isomers are readily thermally isomerized to their *trans* forms, all operations were carried out at room temperature or below. At the same time, it was necessary to carry out manipulations under dark conditions to avoid photoequilibration of the products. Table II summarizes the absorption spectra data of the *cis* isomers. In general, the changes

TABLE II

Absorption spectra of *cis*-4′-amino-substituted 2-styrylpyridines

		In water		In 50% methanol–water	
		λ_{max} (mμ)	ϵ	λ_{max} (mμ)	ϵ
VI	*cis*-4′-Dimethylamino-2-styrylpyridine	323	10 900	323	12 800
VI*a*	Methiodide	403	8 400	403	8 400
VI*b*	Hydrochloride	410	8 000*	428	7 950*
VI*c*	Bishydrochloride	310	9 920	308	9 380
VI*d*	Methiodide–hydrochloride	308	11 000		
VII	*cis*-4′-Diethylamino-2-styrylpyridine	328	10 900	353	11 440
				333	11 380
VII*a*	Methiodide	434	10 000		
VII*b*	Hydrochloride	435	3 600*	446	9 000*
VII*c*	Bishydrochloride	307	9 920	308	10 400
VII*d*	Methiodide–hydrochloride	309	6 800		
VIII	*cis*-(4′-Di-*n*-propylamino)-2-styrylpyridine			356	12 970
				335	12 600
VIII*a*	Methiodide	440	11 150		
VIII*b*	Hydrochloride			449	8 800
VIII*c*	Bishydrochloride	309	11 000	309	10 880
VIII*d*	Methiodide–hydrochloride	310	10 720		
IX	*cis*-4′-Amino-2-styrylpyridine	313	12 800	319	12 800
IX*a*	Methiodide	374	9 020		
IX*b*	Hydrochloride	378	10 320*	388	12 200*
IX*c*	Bishydrochloride	317	12 680	318	12 500
IX*d*	Methiodide–hydrochloride	313	11 000		
X	*cis*-2-Styrylpyridine	288	9 500	288	10 200
X*a*	Methiodide	325	14 600		
X*b*	Hydrochloride	317	12 680	318	9 700

*Calculated. The monohydrochlorides do not exist as such in dilute acid solution, since they are in equilibrium with free base and bishydrochloride. Their complete ultraviolet absorption curves cannot be determined but the values of λ_{max} and their corresponding molecular extinction coefficients can be determined by calculation.

of wavelengths of λ_{max} of the *cis* isomers with substitution on the nitrogens and acidity conditions follow those of the *trans* forms. However, the *cis* forms consistently show wavelengths of λ_{max} at shorter wavelengths than do the *trans* isomers.

Each pair of *cis* isomers of the free bases (VI–IX) required a different method of separation because of the changes in physical properties resulting from the variation of substituents on the amino nitrogen. The methods used were cold extraction, column chromatography, and fractional crystallization. The *cis*-methiodide salts (VI*a*–IX*a*) were even more sensitive to heat and light than VI–IX and thus their melting points were of no use in characterization. Further irradiation of the methiodide–hydrochloride photoequilibrium mixtures did not produce dimers. However, when the irradiations of the bishydrochloride photoequilibrium mixtures were continued, the dimers of I*c*, II*c*, and IV*c* were produced and were subsequently treated with base to give the dimers of I, II, and IV. Long irradiation of III*c* gave several unidentified products but no dimers.

Can. J. Chem. Downloaded from www.nrcresearchpress.com by 210.87.254.5 on 09/05/12
For personal use only.

The base strengths of the various 4′-amino substituents are influenced by the conjugated 2-styrylpyridyl group. At the same time, the base strengths of the pyridine nitrogens are interdependent with those of the 4′-amino nitrogen through the conjugated system. Both nitrogens can therefore alter their base strength by the interaction of their lone-pair electrons in the π-system. In all cases examined, the 4′-amino nitrogens possessed lower basic strengths than aniline, indicating donation of the electron pairs from the 4′-amino group into the π-system of the 2-styrylpyridyl group. Table III demonstrates that,

TABLE III

Base strengths of 4′-amino-substituted 2-styrylpyridine methiodides

R	In water	
	trans, pK_{a_2}	*cis*, pK_{a_2}
NH_2	2.83	3.20
$N(CH_3)_2$	3.10	3.44
$N(C_2H_5)_2$	4.48	4.83
$N(n\text{-}C_3H_7)_2$	4.67	4.42

when the lone pair of the pyridine nitrogen is tied up by quaternization to form the methiodide, the difference between the base strength values of the 4′-amino nitrogen of the *cis* isomers and *trans* isomers of 4′-dimethylamino- (I*a* and VI*a*), 4′-diethylamino- (II*a* and VIII*a*), 4′-amino- (IV*a* and IX*a*), and 4′-di-*n*-propylamino- (III*a* and VIII*a*) 2-styrylpyridines is a constant value of 0.35 ± 0.02 pH unit. The basic strengths of the amino groups are in the same relative order as reported (6) in the aniline–dialkylaniline series:

$$N(C_2H_5)_2 > N(C_3H_7)_2 > N(CH_3)_2 > NH_2.$$

Furthermore, in the methiodide series, the 4′-amino nitrogens of the *cis* isomers (VI*a*, VII*a*, VIII*a*, and IX*a*) have higher base strengths than those of the corresponding *trans* isomers (I*a*, II*a*, III*a*, and IV*a*), indicating reduced interaction between the pyridinium and phenyl rings via the double bond. Jaffé and Orchin (7) attributed the reduced interaction between the two phenyl rings of *cis*-stilbene to steric interference and resulting noncoplanarity of the rings. The same effect can operate in the case of the *cis*- and *trans*-methiodides (V*a*–IX*a* and I*a*–IV*a*) to cause changes in the basicity of the amino nitrogens. This effect was noted earlier in the differences of absorption spectra between the *cis* isomers (V*a*–IX*a*) and the *trans* isomers (I*a*–IV*a*).

The base strength value of the pyridine nitrogen in *trans*-2-styrylpyridine (V), pK_a 5.23, is slightly larger than that of pyridine, pK_a 5.15. This indicates that the unpaired electrons of the pyridine nitrogen in V are not donated to the styryl system and that, in fact, a shift in the reverse direction occurs. The pK_a value for the nitrogen in *cis*-2-styrylpyridine is 5.20. Table IV summarizes the base strength figures determined for the *cis* and *trans* free bases (I–IX).

The contribution of the electron pair from the pyridine nitrogen via the conjugated system can reduce the value of pK_a of the amino nitrogen. The value of pK_a of the 4′-amino group in *trans*-4′-amino-2-styrylpyridine (IV) is 2.92, compared to 4.58 for aniline. The pK_a value of the pyridine nitrogen in IV is 5.72, compared to 5.23 for V and 5.15 for pyridine. Replacement of the amino-group hydrogens by alkyl groups which donate electron character increases the base strength of the 4′-amino and pyridine

Can. J. Chem. Downloaded from www.nrcresearchpress.com by 210.87.254.5 on 09/05/12
For personal use only.

TABLE IV

Base strengths* of 4′-amino-substituted 2-styrylpyridines

	In water				In 50% methanol–water			
	trans		*cis*		*trans*		*cis*	
R	pK_{a_1}	pK_{a_2}	pK_{a_1}	pK_{a_2}	pK_{a_1}	pK_{a_2}	pK_{a_1}	pK_{a_2}
H	5.23		5.20		4.25		4.10	
NH_2	5.72	2.92	5.78	2.99	5.11	2.40	4.84	2.50
$N(CH_3)_2$	6.40	3.54	5.52	3.70	5.28	2.25	4.96	2.64
$N(C_2H_5)_2$	6.11	4.55	6.18	4.50	5.59	3.31	5.55	3.42
$N(n\text{-}C_3H_7)_2$	—	—	—	—	5.52	2.94	5.31	3.06

*pK_{a_1} corresponds to the pyridine nitrogen and pK_{a_2} to the 4′-amino nitrogen.

nitrogens by a factor similar to that seen for the base strengths in the aniline–dialkylaniline series (6). Methyl groups are generally accepted to be superior in their electron-donating ability to ethyl or propyl groups because of hyperconjugation effects (8).

In the present work, the superior release of electron character by the methyl group is evident when the relative base strengths of the 4′-amino groups in the methiodide series or the free bases are compared in water and in 50% methanol–water solution (Table IV). Quaternization causes the pyridine nitrogen to become very electron attracting. Since the methyl groups donate electron character, there is a greater decrease in the base strength of the 4-dimethylamino group in the methiodide salt (I*a*), compared to the free base (I), than occurs in the other pairs of 4′-amino-substituted derivatives (II*a* and II, III*a* and III). A similar situation exists when the base strengths of the free bases (I, II, III, and IV) are compared in water and in 50% methanol–water. The base strengths of all free amino groups are dependent on the number of hydrated ($—N \overset{+}{\rightarrow} HOH$) bonds associated with the nitrogen (9). In aqueous solution, the pyridine nitrogen is preferentially ionized and stabilized by solvation. Such solvation causes the nitrogen to act as an electron-withdrawing group similar to that of the quaternary methiodide group. The fact that the 4′-dimethylamino group is the superior electron-releasing group explains the fact that the pyridine nitrogen in I has the highest base strength (pK_a 6.40) of any amino group in the present series of compounds. In 50% methanol–water the solvation effects are much reduced, causing all the nitrogen atoms to have lower base strengths than in water.

As already pointed out, solvation effects are seen in the absorption spectra. By changing the system from 50% methanol–water to water, more hydrogen bonding can occur. Accordingly, the wavelengths of λ_{max} of the free bases (I–IV) and of the monohydrochlorides (I*b*–IV*b*) shift to shorter wavelengths. The greatest shift occurs with I and I*b*. The shift of both is equal and corresponds to an energy increase of approximately 2.6 kcal/mole. This value represents the energy necessary to break the hydrogen bond so that a nonbonding electron of the amino group or molecule can be raised to the first excited state. Therefore, hydrogen bonding cannot be maintained in the excited state (10).

In 50% methanol–water solution, the absence of large solvation effects changes the order of magnitude of the effect of the groups that contribute the most electron character to the conjugated system. The absence of strong solvation effects involving the pyridine nitrogen of the *trans* free bases (I) lowers its electron-attracting power, and electron character is not drawn to the conjugated system as readily from the 4′-amino group.

Can. J. Chem. Downloaded from www.nrcresearchpress.com by 210.87.254.5 on 09/05/12
For personal use only.

Therefore, the base strength of the pyridine nitrogens of I–IV becomes directly proportional to the base strength or electronegativity of the 4′-amino groups.

The base strength of the nitrogens becomes weaker in all cases when the solvent is changed from water to 50% methanol–water. The largest change occurs in I, the smallest in IV.

CONCLUSIONS

The *trans*-methiodides, I*a*–IV*a*, are not photochemically isomerized in solution to the *cis* isomers (V*a*–IX*a*) because of the lack of double-bond character at the ethylenic bond. The corresponding bishydrochlorides (I*c*–IV*c*) and methiodide–hydrochlorides (I*d*–IV*d*) absorb light at wavelengths shorter than those of I*a*–IV*a* or even the corresponding free bases I–IV and can be photoisomerized and photodimerized. The photochemical susceptibility is due to the tying-up of the lone-pair electrons on the positively charged nitrogens, thereby imparting sufficient double-bond character to the ethylenic bonds. The molecules under these conditions become more stilbene-like. Under highly acid conditions, existence of the bishydrochloride (I*c*–IV*c*) and methiodide–hydrochloride (I*d*–IV*d*) species would promote $\pi \rightarrow \pi^*$ transitions at the ethylenic bonds. The excited molecule can then rotate about the ethylenic bond. The excitation of the monohydrochlorides (I*b*–IV*b*) and the methiodides (I*a*–IV*a*) would not involve promotion of an electron at the same site in the molecule, making rotation about the ethylenic bond impossible. Currently, we are undertaking measurements of basic strengths, in their excited states, of the nitrogens in these compounds to provide a truer picture of the role of the lone-pair electrons in the excited state. The solvent shifts (between water and 50% methanol–water) of wavelengths of λ_{max} indicate that electrons are available on the amino groups for hydrogen bonding. Comparison of the double-salts series (I*c*–IX*c*, I*d*–IX*d*) (no solvent shift) with the free bases (I–IX) and the monosalts (I*a*–IX*a*, I*b*–IX*b*), which do show a solvent shift, illustrates this fact.

Interaction of the lone-pair electrons of the two nitrogens via the conjugated system in both isomers is indicated by the fact that the free bases of both *cis* and *trans* isomers (I–IX) absorb at longer wavelengths than do the double salts (I*c*–IX*c*, I*d*–IX*d*). This effect is also illustrated by the interdependent changes of value of base strength of the two nitrogens in the free bases (I–IX). However, release of electron character to the conjugated system by the amino group is more striking in the case of the methiodide salts (I*a*–IX*a*). The values of pK_a of the amino nitrogen of the methiodide *cis* isomers (VI*a*–IX*a*) are all greater than those of the *trans* isomers (I*a*–IV*a*) by 0.35 ± 0.02 pH unit.

EXPERIMENTAL

Determination of the Basic Strength of cis- and trans-4′-Amino-substituted 2-Styrylpyridines

A 5×10^{-4} *M* stock solution in dilute hydrochloric acid of each compound was prepared. Such stock solutions were diluted further, to 2.5×10^{-5} *M* for the *trans* compounds or to 5×10^{-5} *M* for the *cis* compounds in a solution of the desired pH made by the addition of hydrochloric acid or sodium hydroxide solutions. The total ion concentrations were kept low and did not exceed 5×10^{-3} *M*, except for the measurements made in strong acids. The pH measurements were made by using a Beckman pH meter equipped with a calomel reference cell and a glass electrode. The absorption spectra were measured at several pH values ranging between 1 and 10. All measurements involving the *cis* compounds were obtained in red safelight illumination because of the sensitivity of the co-derivatives to yellow light.

From such data a plot of absorption of the different λ_{max} vs. pH was drawn. For a monobase, the pK_a can be determined by finding the point on such a curve halfway between the free base value and the value for 100% salt. However, when a dibase of which the ΔpK_a is less than 4 is considered, this method does not give a true pK_a value. The incorrect pK_a value results from the fact that the molecule will never

Can. J. Chem. Downloaded from www.nrcresearchpress.com by 210.87.254.5 on 09/05/12
For personal use only.

exist as a 100% monosalt. Therefore, the absorption spectra of the monosalts remain unknown. By extrapolation of the straight-line portions of absorbance vs. pH curves, a better approximation of the pK_a value is found. For a more accurate determination, the pK_a's of the compounds were also calculated using the method described by Rosenblatt (4). The absorption of all three species (free dibase, monosalt, and disalt) and the two equilibrium constants can be calculated by setting up five simultaneous equations using measurements at five different pH values. The general form of the equations is as follows:

$$a_n\epsilon_n\left(\frac{1}{K_2}\right) + \frac{\epsilon_n}{a_n}(K_1) - a_n\frac{(\epsilon_\alpha)}{K_2} - \frac{1}{a_n}(\epsilon_\gamma K_1) - \epsilon_\beta = -\epsilon_n,$$

where a_n = hydrogen activity, ϵ_n = extinction coefficient at the measured pH, K_2 = second equilibrium constant, K_1 = first equilibrium constant (Note: K_1 and K_2 are interchanged from Rosenblatt's equation since his applied to dibasic acids rather than to bases), ϵ_α = extinction coefficient of double salt, ϵ_γ = extinction coefficient of free base, and ϵ_β = extinction coefficient of monosalt.

Since points were found at which addition of more acid did not change the absorption spectra of the double salt or the addition of base did not change the absorption spectra of the free base, the extinction coefficients were thereby determined. These constants can then be placed in the equation, which can be simplified to the following:

$$a_n(\epsilon_n - \epsilon_\alpha)\frac{1}{K_2} + \frac{(\epsilon_n - \epsilon_\gamma)}{a_n}K_1 - \epsilon_\beta = -\epsilon_n.$$

Since the total concentration and the same cell path length were used for all measurements, these two values will cancel out. $\epsilon = A/Cl$, where A = absorption, ϵ = excitation coefficient, C = concentration, and l = cell thickness. Thus, the absorption value can be used rather than the extinction coefficient. The equation then becomes

$$a_n(A_n - A_\alpha)\frac{1}{K_2} + \frac{(A_n - A_\gamma)}{a_n}K_1 - A_\beta = -A_n,$$

where a_n = hydrogen activity, A_n = absorption of solution at a_n, A_α = absorption of double salt, A_γ = absorption of free base, and A_β = absorption of monosalt.

For the present calculation, $[H^+]$ was used rather than a_n, but the error introduced is small, since the calculations were carried out using values obtained for solutions where the ion concentrations would be about 10^{-3} M. Thus, the activity coefficients would be very close to unity. The fact that the ultraviolet absorption curves all passed through isosbestic points at these ion concentrations is further evidence of the insignificant effect of ion concentration. Therefore, the equation was further modified to

$$[H^+](A_n - A_\alpha)\frac{1}{K_2} + \frac{(A_n - A_\gamma)}{[H^+]}K_1 - A_\beta = -A_n.$$

The values were calculated at the three wavelengths corresponding to the absorption maxima of each form and using three different pH values for each calculation.

trans-4'-Dimethylamino-2-styrylpyridine (I)

This was prepared as described previously (11).

trans-4'-Diethylamino-2-styrylpyridine (II)

A mixture of 56 g (0.6 mole) of 2-picoline, 106 g (0.6 mole) of 4-diethylaminobenzaldehyde, and 2 g of anhydrous $ZnCl_2$ was placed in an autoclave and heated at 200 °C for 16 h. The cooled reaction mixture was poured into ether and stirred at room temperature for a short time. The solid was collected by filtration and crystallized from ethanol to yield 74 g (50.3%) of a yellow solid (II), m.p. 319–141°.

Anal. Calcd. for $C_{17}H_{20}N_2$: C, 81.0; H, 8.0; N, 11.1. Found: C, 81.4; H, 7.9; N, 10.8.

trans-4'-Di-n-propylamino-2-styrylpyridine (III)

A mixture of 56 g (0.6 mole) of 2-picoline, 82 g (0.4 mole) of 4-dipropylaminobenzaldehyde, and 2 g of anhydrous $ZnCl_2$ was placed in an autoclave and heated at 200 °C for 16 h. The reaction mixture was then distilled using a pot temperature of 142–167°/8 μ to give 70.5 g (63%) of a red oil (III) which could not be crystallized.

Anal. Calcd. for $C_{19}H_{24}N_2$: C, 81.4; H, 8.6; N, 10.0 Found: C, 81.1; H, 8.6; N, 10.1.

trans-2-(4'-Aminostyryl)pyridine (IV)

The following procedure is an adaptation of that used for the preparation of 4-(4'-aminostyryl)pyridine (12).

A solution of 22.6 g (0.1 mole) of 2-(4'-nitrostyryl)pyridine in 200 ml of hot 5% hydrochloric acid was added over a 10-min period to a stirred solution of 60 g of stannous chloride in 100 ml of concentrated

Can. J. Chem. Downloaded from www.nrcresearchpress.com by 210.87.254.5 on 09/05/12
For personal use only.

hydrochloric acid while the solution was heated on a steam bath. The heating and stirring were continued and hydrogen chloride was passed through the reaction mixture for 1 h. The mixture was cooled and 20% sodium hydroxide solution was added until the mixture was strongly basic. The solid was collected, washed with water, dried, and extracted with acetone in a Soxhlet extractor. The extract was cooled to room temperature and filtered, and the filtrate was diluted with water and chilled to yield 16 g of crude product which was recrystallized from toluene to give IV, 15.1 g (77%), m.p. 137–138° (lit. (13) m.p. 138–139°).

Anal. Calcd. for $C_{13}H_{12}N_2$: C, 79.6; H, 6.1; N, 14.3. Found: C, 79.8; H, 6.3; N, 14.1.

trans-4′-Dimethylamino-2-styrylpyridine Methiodide (Ia)

This was prepared as previously described (11).

trans-4′-Diethylamino-2-styrylpyridinium Methiodide (IIa)

A mixture of 23.5 g (0.1 mole) of 2-picoline methiodide, 35.4 g (0.2 mole) of 4-diethylaminobenzaldehyde, 150 ml of methanol, and 5 ml of piperidine was refluxed on a steam bath for 1 h. The reaction mixture was chilled and the product isolated by filtration. The solid was crystallized from acetonitrile to yield IIa, 33 g (84.5%), m.p. 242–245° (lit. (5) m.p. 246–247°).

Anal. Calcd. for $C_{18}H_{23}IN_2$: C, 54.8; H, 5.9; I, 32.2; N, 7.1. Found: C, 54.7; H, 5.7; I, 32.4; N, 7.0.

trans-4′-Di-n-propylamino-2-styrylpyridine Methiodide (IIIa)

A mixture of 11.8 g (0.05 mole) of 2-picoline methiodide, 11.3 g (0.055 mole) of 4-dipropylaminobenzaldehyde, 50 ml of methanol, and 2.5 ml of piperidine was refluxed on the steam bath for 1 h. The reaction mixture was chilled, and the product isolated by filtration and then crystallized from ethanol to yield IIIa, 3.9 g (66%), m.p. 209–211°.

Anal. Calcd. for $C_{20}H_{27}IN_2$: C, 57.0; H, 6.5; I, 30.1; N, 6.6. Found: C, 56.8; H, 6.2; I, 30.4; N, 6.4.

4′-Amino-2-styrylpyridine Methiodide (IVa)

A mixture of 7.4 g (0.02 mole) of 4′-nitro-2-styrylpyridine methiodide, 14 g of stannous chloride, and 50 ml of concentrated hydrochloric acid was heated on the steam bath, with stirring, for 1 h. The mixture was cooled and the solid collected. The solid was added to 250 ml of water and 10 ml of concentrated hydrochloric acid. Hydrogen sulfide was passed through the mixture, with heating, until no further tin sulfide was precipitated. The hot mixture was filtered and the filtrate was neutralized with solid sodium bicarbonate to yield 4.1 g (61%) of IVa, m.p. 260°.

Anal. Calcd. for $C_{14}H_{15}IN_2$: C, 49.7; H, 4.4; N, 8.3. Found: C, 49.5; H, 4.3; N, 8.2.

Purification of cis Isomers

The irradiation mixtures containing primarily the *cis* isomer were subjected to column chromatography or fractional crystallization. The various fractions from elution of the column or from crystallization were analyzed by determination of their ultraviolet absorption spectra. The fractions which contained material exhibiting the shortest wavelength of λ_{max} were selected as the pure *cis* fractions. We have found that the accuracy of infrared spectroscopy for determining the present *cis–trans* ratios is less than that of ultraviolet absorption spectroscopy methods. Further evidence of the purity of the *cis* isomers is found when their ultraviolet absorption spectra are determined at several values of pH (14). When such a series of ultraviolet absorption spectra are plotted, a precise isosbestic point is obtained only if the free base and the conjugate acid of a single species are present. The presence of *trans* isomer in *cis* isomer would cause the junction of the series of curves to scatter and give a number of scattered isosbestic points. The *cis* isomers isolated and purified as reported below gave precise isosbestic points when subjected to the above method.

cis-4′-Dimethylamino-2-styrylpyridine (VI)

A solution of 5 g (0.0223 mole) of *trans*-4′-dimethylamino-2-styrylpyridine (I) in 2 l of 1 *N* hydrochloric acid was placed in an irradiation flask equipped with a nitrogen inlet tube at the bottom. A 450-W medium-pressure Hanovia mercury arc lamp equipped with a Pyrex glass water jacket was then immersed in the solution. The solution was stirred by a Teflon-covered stirring bar, driven magnetically through the bottom of the flask. Nitrogen was bubbled through the solution while the irradiation was conducted for 25 min, with stirring. The irradiated solution was made alkaline with potassium carbonate and was extracted with three 250-ml portions of chloroform. The chloroform solutions were dried over anhydrous potassium carbonate. The dried chloroform extracts from five such irradiations were combined and the chloroform evaporated at room temperature and reduced pressure, using a rotary evaporator and an ice-chilled collection flask. The residue was triturated with 400 ml of cold petroleum ether (b.p. 66–75°) for 30 min, after which time the solids were removed by filtration. The solid weighed 5.0 g, and consisted principally of I. The petroleum ether extract was evaporated at room temperature and reduced pressure to give 19.5 g *cis*-4′-dimethylamino-2-styrylpyridine (VI): λ_{max} (MeOH) 348 mμ, ϵ 9 100; λ_{max} (1 *N* hydrochloric acid) 308 mμ, ϵ 7 920.

This material was further purified by column chromatography by means of an activated alumina column with ethyl acetate as the solvent and eluent. The ultraviolet absorption spectra of each fraction were determined and the fractions containing material having λ_{max} of 347 mμ were combined. The ethyl acetate

Can. J. Chem. Downloaded from www.nrcresearchpress.com by 210.87.254.5 on 09/05/12
For personal use only.

was evaporated at room temperature and reduced pressure to give VI, a pale yellow liquid, λ_{max} (MeOH) 347 mμ, ϵ 10 300.

Anal. Calcd. for $C_{15}H_{16}N_2$: C, 80.3; H, 7.2; N, 12.5. Found: C, 80.5; H, 7.3; N, 12.4.

cis-4′-Diethylamino-2-styrylpyridine (VII)

The procedure used was the same as that used for VI. Five runs using 5.72 g of II yield 22.4 g (78%) of VII, λ_{max} 359 mμ, ϵ 13 100. A 5-g sample was further purified by column chromatography, as described for VI, to give 2.6 g of VII, a yellow oil, λ_{max} (MeOH) 359 mμ, ϵ 13 500.

Anal. Calcd. for $C_{17}H_{20}N_2$: C, 80.9; H, 8.0; N, 11.1. Found: C, 80.9; H, 8.3; N, 11.4.

cis-4′-Di-n-propylamino-2-styrylpyridine (VIII)

Three 5-g portions of III were irradiated and combined as described for VI. The residue from the combined chloroform extract was dissolved in 400 ml of ethyl acetate. The solution was then passed through an activated alumina column, as described for VI. Eluate samples of approximately 20 ml were taken and the one containing a sample of VIII, which showed the shortest wavelength of λ_{max}, was selected. Its characteristics were λ_{max} (ethyl acetate) 355 mμ; λ_{max} (CH_3OH) 359 mμ, ϵ 14 400, and 330 mμ, ϵ 12 000.

Anal. Calcd. for $C_{19}H_{24}N_2$: C, 81.5; H, 8.5; N, 9.7. Found: C, 81.2; H, 8.4; N, 9.7.

By combination and evaporation *in vacuo* of the eluates containing VIII of wavelength λ_{max} 355–360 mμ (ethyl acetate), there was obtained 4.0 g of VIII showing λ_{max} (CH_3OH) 362 mμ, ϵ 14 400; 330 mμ, ϵ 11 000, which corresponded to 95% *cis* isomer (VIII). The remaining elates, which were the first to traverse the column, were combined to give 0.5 g of essentially *trans* isomer (III), λ_{max} (ethyl acetate) 362–372 mμ.

cis-4′-Aminostyrylpyridine (IX)

Three 5-g portions of IV were irradiated and the product was extracted as described for the preparation of VI. The residue from the combined, dried, and evaporated chloroform extracts was triturated with 400 ml of cold cyclohexane. The volume of the cyclohexane solution was reduced at room temperature *in vacuo* to 40 ml and chilled to 1 °C. The yellow crystals (IX) which separated and were collected weighed 0.06 g, m.p. 80–83°, λ_{max} (CH_3OH) 330 mμ, ϵ 12 350. The residue from the cyclohexane trituration was triturated with 250 ml of cold diethyl ether. The undissolved material which was collected and dried weighed 5.2 g, m.p. 113–135°, and consisted principally of *trans* isomer (IV). The diethyl ether solution was cooled at 1 °C to give 0.2 g of a dimer – *trans* isomer mixture which melted at 169–188°. On longer storage, two crops of essentially *cis* isomer (IX) separated: m.p. 78–82°, 0.7 g, λ_{max} (CH_3OH) 332 mμ, ϵ 7 140; and m.p. 79–81°, 0.1 g, λ_{max} (CH_3OH) 342 mμ, ϵ 12 100. The diethyl ether solution was then evaporated to dryness and the residue dissolved in 90 ml of 50:50 benzene–heptane. After the solution had cooled to 1 °C, the oil which separated crystallized to give 4 g of IX melting at 73–80°, λ_{max} (CH_3OH) 337 mμ, ϵ 13 500. On evaporation, the mother liquors yielded 1.5 g of IX, m.p. 71–85°, λ_{max} (CH_3OH) 330 mμ, ϵ 11 750. The 4-g sample of IX was dissolved in 50 ml of diethyl ether. When the solution was cooled to 1 °C, 1.9 g of IX, m.p. 80–100°, λ_{max} (CH_3OH) 337 mμ, ϵ 13 500, was collected. The diethyl ether was evaporated, leaving 2.0 g of IX, m.p. 70–75°, λ_{max} (CH_3OH) 333 mμ, ϵ 12 200.

Anal. Calcd. for $C_{13}H_{12}N_2$: C, 79.6; H, 6.1; N, 14.2. Found: C, 79.2; H, 6.2; N, 13.9.

The yield of combined fractions containing greater than 97% *cis* isomer (XI) was 4.1 g.

cis-4′-Dimethylamino-2-styrylpyridine Methiodide (VIa)

A solution of 10 g (0.0274 mole) of *trans*-4′-dimethyl-amino-2-styrylpyridine methiodide in 2 l of 0.5 *N* hydrochloric acid was placed in a Pyrex glass irradiation flask. The solution was irradiated during 2 h in the same manner as already described for the preparation of *cis*-4′-dimethylamino-2-styrylpyridine (VI). The solution was concentrated to 500 ml at room temperature and reduced pressure and made alkaline with sodium bicarbonate. The resulting solution was warmed gently to dissolve all material and then cooled to room temperature. The first crop of crystals collected was principally *trans* isomer (I*a*), weighing 4.0 g, m.p. 253–264°, λ_{max} (H_2O) 437 mμ, ϵ 25 100. The second crop consisted of red prism-like crystals weighing 2.6 g and was *cis*-4′-dimethylamino-2-styrylpyridine methiodide (VI*a*), λ_{max} (H_2O) 404 mμ, ϵ 8 400. The sample of VI*a* melted at 268–270°, since, when it was heated, it reverted to the *trans* isomer (I*a*). This was confirmed by ultraviolet absorption data.

Anal. Calcd. for $C_{16}H_{19}IN_2$: C, 52.4; H, 5.2; I, 34.7; N, 7.7. Found: C, 52.1; H, 5.2; I, 34.9; N, 7.5.

The remaining material in the mother liquors was the *trans* isomer (I*a*).

cis-4′-Diethylamino-2-styrylpyridine Methiodide (VIIa)

A solution of 10.0 *g* of *trans*-4′-diethylamino-2-styrylpyridine methiodide (II*a*) in 2 l of 1 *N* hydrochloric acid was irradiated for 1 h. The irradiation conditions and product isolation were carried out as described for VI*a*. However, the first material which crystallized from aqueous solution consisted of 75% inorganic salts. The expected product (VIII*a*) did not crystallize from water. Therefore, the inorganic salts and mother liquors were extracted with chloroform. The chloroform extract was concentrated at room temperature and reduced pressure until the solid began to crystallize. The crops of crystals collected were the *trans* isomer (II*a*). The solubility of the *cis* isomer was so high in chloroform that it was necessary to add diethyl ether to cause crystallization. In this manner, a yield of 4.8 g of *cis*-4′-diethylamino-2-styrylpyridine methiodide, m.p. 238–241°, λ_{max} (H_2O) 437 mμ, ϵ 10 100, was obtained.

Anal. Calcd. for $C_{18}H_{23}IN_2$: C, 54.9; H, 5.8; I, 32.2; N, 7.1. Found: C, 54.5; H, 5.4; I, 31.9; N, 6.9.

Can. J. Chem. Downloaded from www.nrcresearchpress.com by 210.87.254.5 on 09/05/12
For personal use only.

cis-4'-Di-n-propylamino-2-styrylpyridinium Methiodide (VIIIa)

A single 5-g sample of IIIa was irradiated as described for VIIa. The aqueous solution was made basic with sodium bicarbonate and concentrated at reduced pressure and room temperature to 600 ml. The aqueous solution was extracted with 60 ml of chloroform (extract A). The aqueous solution was then extracted with three 60-ml portions of chloroform, which were then combined and evaporated to 80 ml (extract B). To both extracts there was added 100 ml of diethyl ether. When both solutions were cooled to 1 °C, *trans* isomer (IIIa) separated from them: A, 1.3 g, B, 0.6 g. On addition of 80 ml of diethyl ether to solution B, an additional 0.3 g of IIIa was obtained. Both solution A and solution B were then evaporated to dryness at room temperature and reduced pressure. The residues were held *in vacuo* for several hours at 0.3 mm pressure. Sample A weighed 1.0 g, λ_{max} (H_2O) 440 mμ, ϵ 11 100.

Anal. Calcd. for $C_{20}H_{27}N_2$: C, 57.0; H, 6.4; N, 6.6. Found: C, 56.7; H, 6.6; N, 6.4.

Sample B weighed 1.5 g, λ_{max} 448 mμ, ϵ 8 320.

cis-4'-Amino-2-styrylpyridine Methiodide (IXa)

A solution of 2.5 g of IVa in 1 l of 1 *N* hydrochloric acid was irradiated for 1 h as described earlier for VIa. The irradiated solution was made alkaline with sodium bicarbonate and evaporated to dryness at room temperature and reduced pressure.

The residue was triturated at room temperature with three portions of acetone: 150 ml, 400 ml, and 250 ml. The acetone solutions were successively concentrated and cooled to yield fractions of crystalline materials consisting of *cis-* and *trans*-isomer mixtures. The fractions containing IXa, which exhibited λ_{max} (H_2O) 374 mμ, ϵ 9 000, and which totaled 1.4 g, were selected to be essentially pure IXa.

Anal. Calcd. for $C_{14}H_{15}IN_2$: C, 49.7; H, 4.4; I, 37.6; N, 8.3. Found: C, 49.6; H, 4.4; I, 37.3; N, 8.0.

Dimerization of trans-4'-Dimethylamino-2-styrylpyridine (I)

A solution of 5 g of I in 1 l of 1 *N* hydrochloric acid was irradiated for 27 h in the manner described for the preparation of VI. The irradiation solution was made basic with potassium carbonate and extracted with two 200-ml portions of benzene and one 200-ml portion of diethyl ether. The combined extracts were dried over anhydrous potassium carbonate and evaporated at room temperature and reduced pressure. The residue was stirred with 40 ml of cold diethyl ether for 20 min. The crude dimer which was isolated by filtration weighed 1.7 g, m.p. 246–253°. Recrystallization from 50 ml of benzene gave 1.2 g of dimer, m.p. 255–257°. An earlier sample (see ref. 2) melted at 248–250°. The ultraviolet spectra of the two samples of dimer I were identical. The combined mother liquors were evaporated to give 3.3 g of a mixture of I and VI.

Dimerization of 4'-Diethylamino-2-styrylpyridine (II)

A solution of 5.0 g of II in 1 l of 1 *N* hydrochloric acid was irradiated during 30 h as described for VII. The solution was made basic with potassium carbonate and extracted with four 125-ml portions of chloroform. The extracts were combined and dried over anhydrous potassium carbonate. The chloroform solution was evaporated at room temperature and reduced pressure and the residue was triturated with 200 ml of cold low-boiling petroleum ether. The material not soluble in the petroleum ether was separated by filtration (1.5 g) and recrystallized from 40 ml of a 50:50 mixture of diethyl ether and methanol. Thus, 0.9 g of dimer, m.p. 184–185°, λ_{max} 268 mμ (methanol), ϵ 40 400, was obtained.

Anal. Calcd. for $C_{34}H_{30}N_4$: C, 80.9; H, 8.0; N, 11.1; mol. wt., 504. Found: C, 80.6; H, 8.1; N, 11.5; mol. wt., 510.

The petroleum ether mother liquor was evaporated at room temperature and reduced pressure, leaving 3.3 g of a mixture of II and VIII, λ_{max} (MeOH) 363 mμ, ϵ 8 000.

Dimerization of 4'-Amino-2-styrylpyridine (IV)

A solution of 5.0 g of IV in 2 l of 1 *N* hydrochloric acid was irradiated during 43 h in the manner described for VI. The solution was made basic and the solids were separated by filtration. The crude product was dried *in vacuo* and melted at 160–187°; yield, 4.3 g. The solid was recrystallized from a 100 ml 50:50 benzene–chloroform solution. The first crop of crystals, which melted at 207–209° and weighed 2.5 g, λ_{max} (MeOH) 243 mμ, ϵ 23 200, was recrystallized from benzene to give 2.2 g of dimer IV, m.p. 213–214°, λ_{max} (methanol) 243 mμ, ϵ 24 800.

Anal. Calcd.: C, 79.6; H, 6.1; N, 14.3; mol. wt., 392. Found: C, 80.1; H, 6.4; N, 13.8; mol. wt., 428.

The mother liquors were evaporated and 1.8 g of a mixture of *cis-* and *trans*-4'-amino-2-styrylpyridine was obtained, λ_{max} 342 mμ, ϵ 7 160.

Attempted Photoisomerization of Ia–IVa

For irradiation purposes a 1-cm quartz spectrophotometer cell was filled with a 2.5×10^{-5} *M* aqueous solution of the *trans* isomer of the compound to be studied. The absorption spectrum of the starting solution was first determined. The cell was then irradiated sequentially using the light sources tabulated below. After each irradiation (A and D) the ultraviolet absorption spectra were determined.

A. The sample cell was placed at a distance of 10 cm from a 500-W Hanovia water-cooled medium-pressure mercury arc lamp. A Kodak Wratten 18A filter was interposed between the sample cell and the light source. (The 18A filter transmits light of wavelengths 310–390 mμ.)

B. The sample cell was placed at a distance of 10 cm from the source used in A. The 18A filter was not used.

Can. J. Chem. Downloaded from www.nrcresearchpress.com by 210.87.254.5 on 09/05/12
For personal use only.

C. The sample cell was placed at a distance of 10 cm from the source used in A. A Kodak Wratten 2A filter was interposed between the sample cell and the source. (The 2A filter transmits all wavelengths of light longer than 410 mμ.)

D. The sample cell was placed at a distance of 10 cm from a 100-W (80 W at 253°) Hanovia mercury resonance lamp.

Prolonged irradiation of solutions of I*a*–IV*a* with any of the above sources failed to produce significant changes in their ultraviolet absorption spectra. Thus, I*a*–IV*a* were considered to be photochemically stable in dilute aqueous solution.

REFERENCES

1. J. L. R. Williams, S. K. Webster, and J. A. VanAllan. J. Org. Chem. **26**, 4893 (1961).
2. J. L. R. Williams, J. M. Carlson, G. A. Reynolds, and R. E. Adel. J. Org. Chem. **28**, 1317 (1963).
3. L. A. Flexser, L. P. Hammett, and A. Dingwall. J. Am. Chem. Soc. **57**, 2103 (1935).
4. D. H. Rosenblatt. J. Phys. Chem. **58**, 40 (1954).
5. A. P. Phillips. J. Org. Chem. **12**, 333 (1947).
6. H. C. Brown and A. Cahn. J. Am. Chem. Soc. **72**, 2939 (1950).
7. H. H. Jaffé and M. Orchin. Theory and application of ultraviolet spectroscopy. John Wiley and Sons, Inc., New York, N.Y. 1962. p. 424.
8. J. W. Baker and W. S. Nathan. J. Chem. Soc. 1844 (1935).
9. E. Folkers and O. Rundequist. J. Am. Chem. Soc. **86**, 830 (1964).
10. H. H. Jaffé and M. Orchin. Theory and application of ultraviolet spectroscopy. John Wiley and Sons, Inc., New York, N.Y. 1962. p. 187.
11. J. L. R. Williams, R. E. Adel, J. M. Carlson, G. A. Reynolds, D. G. Borden, and J. A. Ford, Jr. J. Org. Chem. **28**, 387 (1963).
12. R. Royer. J. Chem. Soc. 560 (1947).
13. R. Baumert. Ber. **39**, 2972 (1906).
14. H. H. Jaffé and M. Orchin. Theory and application of ultraviolet spectroscopy. John Wiley and Sons, Inc., New York, N.Y. 1962. p. 561.

Can. J. Chem. Downloaded from www.nrcresearchpress.com by 210.87.254.5 on 09/05/12
For personal use only.

Can. J. Chem. Downloaded from www.nrcresearchpress.com by 210.87.254.6 on 09/05/12
For personal use only.

TERPENOIDS

VIII. THE IMMEDIATE PRECURSORS OF HELMINTHOSPORAL AND HELMINTHOSPOROL

P. DE MAYO AND R. E. WILLIAMS
Department of Chemistry, University of Western Ontario, London, Ontario

AND

E. Y. SPENCER
Research Institute,[1] Canada Department of Agriculture, London, Ontario

Received November 13, 1964

Dedicated to Professor R. B. Sandin on the Occasion of his Sixty-Eighth Birthday

ABSTRACT

An earlier investigation had shown that helminthosporal, the toxin isolated from growths of *Helminthosporium sativum*, does not exist as such in the culture, but is formed from a precursor on subsequent mild treatment with acid, base, or heat. What is believed to be the immediate precursor of helminthosporal has now been isolated, as the acetal (IV), from an aged fungus extract. The corresponding precursor of helminthosporol, also as the acetal (V), accompanied it. Hydrolysis of the latter gave prehelminthosporol (also isolated from fresh extracts), which was converted into helminthosporol. Hydrolysis of the acetal of prehelminthosporal gave helminthosporal directly.

Although prehelminthosporol exists in the fresh extracts, it appears that more exists, together with prehelminthosporal, in the form of unstable complexes, possibly dimeric hemiacetals, which break down under very mild conditions. One of these has been obtained in moderately pure condition.

Previous investigations from these laboratories (1, 3) have established that helminthosporal, the toxin produced by *Helminthosporium sativum* (4), has the structure and stereochemistry shown in (I). This structure has recently been confirmed by a synthesis which has provided the absolute stereochemistry (5). This substance, which along with the fungus is responsible for seedling blight, foot and root rot, and leaf spot of cereals, has similar growth-inhibiting activity possessed by the crude extract, but as has been pointed out (1) the unpurified toxin does not show the characteristic carbonyl absorption of the dialdehyde. These bands (at 1 715 and 1 685 cm^{-1}) only appear on heat treatment of the extract, as in distillation, or on treatment with acid or base. More recently we have demonstrated, by thin-layer chromatography (t.l.c.), the total absence of helminthosporal (I) and of helminthosporol (II) (2) from the extracts.

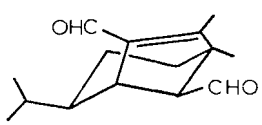

(I)

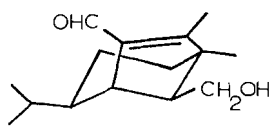

(II)

It was surmised that the precursors present in the extract, in view of their ready conversion to (I) and (II), were probably present as some form of hemiacetal.

There was available to us, from an early isolation, a chloroform extract of the active

[1]*University Sub Post Office, London, Ontario.*

material (1) which had been standing for several months. Careful evaporation of the solvent from this material, and examination of the residual oil by thin-layer chromatography, showed the absence of (I) and (II) and the presence of two fast-running main components. These substances were isolated in pure form by a combination of chromatography in liquid and vapor phases.

One of these, designated acetal A, was crystalline and gave analytical figures compatible with the empirical formula $C_{19}H_{32}O_3$. In agreement, the molecular weight (M), determined by mass spectrometry, was 307 ± 1. Since some relationship to helminthosporal was required, a surplus of four carbon atoms remained. Alkoxyl estimation indicated that they should be attributed to two ethoxyl groups.

The mass spectrum also showed peaks at (M-45) and (M-73). These would be compatible with the loss of ethoxyl and the loss of ethoxyl + ethyl, as would be expected from the breakdown of an acetal (III) as indicated below.

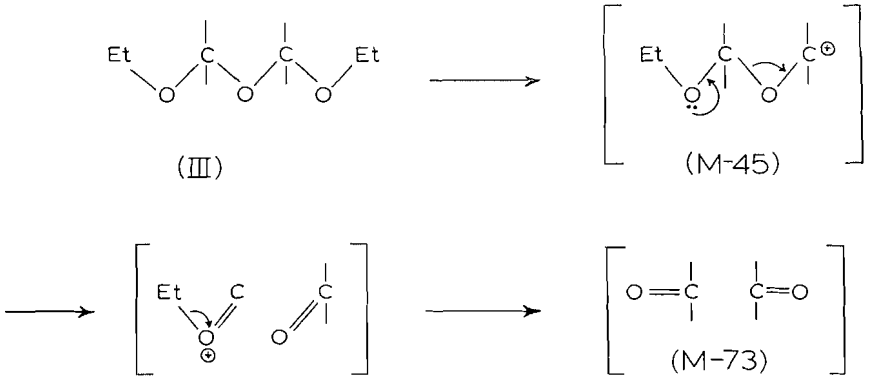

The infrared spectrum of acetal A, while indicating the absence of carbonyl functions, showed, by absorption at 3 060, 1 657, and 885 cm^{-1}, the probable presence of an exocyclic methylene group. This led to the consideration of (IV) as a representation of acetal A.

The nuclear magnetic resonance (n.m.r.) spectrum of acetal A was informative (Fig. 1). The two low-field protons (at τ 5.32 and 5.16), very weakly coupled together, provided added confirmation of the presence of the exocyclic methylene group. In addition, there could be discerned a singlet methyl, two partly superimposed doublets for the isopropyl group, and the methyls of two ethoxyl groups. Two doublets, at τ 5.38 and 5.63, were attributed to the acetal methine protons. That at τ 5.63 was coupled to the allylic proton at τ 7.48, as shown by double irradiation, whereas that at τ 5.38 was coupled with an unresolved proton near τ 9.0. The bridgehead proton at τ 7.02, normally found at such low-field positions in helminthosporal derivatives, was coupled to an unresolved proton near τ 8.9. The pattern was complicated by the four protons of the ethoxyl methylene groups. In these the methylene protons were not equivalent, because of the attachment of the oxygen atom to an asymmetric center (6) resulting in the production of a large number of lines.

As would be expected from this formulation, acetal A on treatment with aqueous acid was converted into helminthosporal, further characterized as the bis-oxime (1). In the absence of acid, acetal A was stable under conditions which would convert the sought-for precursor of helminthosporal to helminthosporal.

It thus appeared that acetal A was an artifact produced from the precursor of helminthosporal during the prolonged standing in solution. The method of isolation (1) involved

Can. J. Chem. Downloaded from www.nrcresearchpress.com by 210.87.254.6 on 09/05/12
For personal use only.

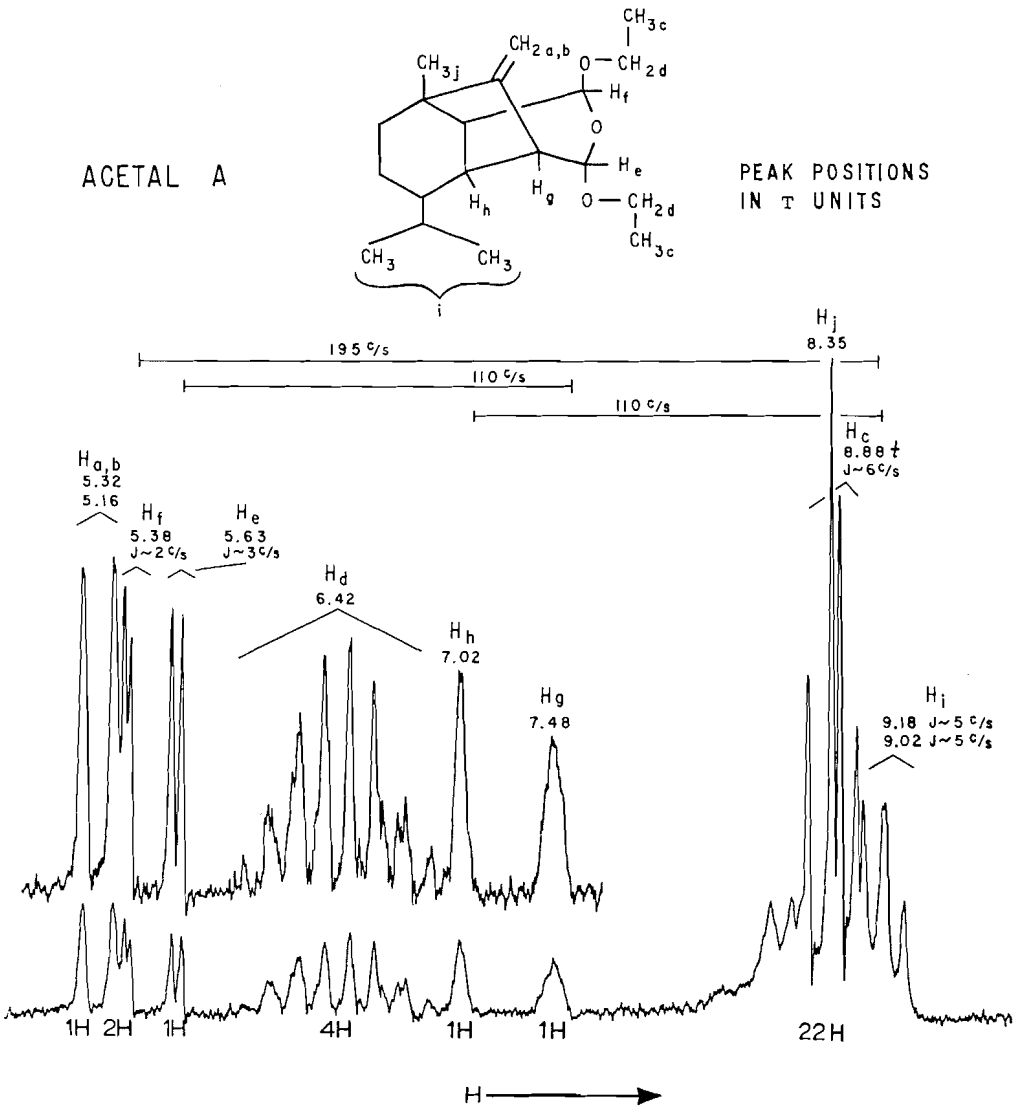

FIG. 1.

washing the charcoal cake, on which the toxin was adsorbed, with ethanol before extraction with chloroform. The chloroform extract would, therefore, contain significant amounts of ethanol.

The second substance, acetal B, isolated from the aged chloroform extract had an analysis compatible with the empirical formula $C_{17}H_{28}O_2$, containing a surplus of two carbon atoms over that required for a sesquiterpenoid. These were contained in an ethoxyl group as was shown by alkoxyl determination and the lack of a methoxyl signal in the n.m.r. spectrum.

In view of the structure of acetal A it was presumed that acetal B would have some relationship to helminthosporol. The presence of an exocyclic methylene group was signalled by appropriate absorption in the infrared spectrum, and by the presence in the

Can. J. Chem. Downloaded from www.nrcresearchpress.com by 210.87.254.6 on 09/05/12
For personal use only.

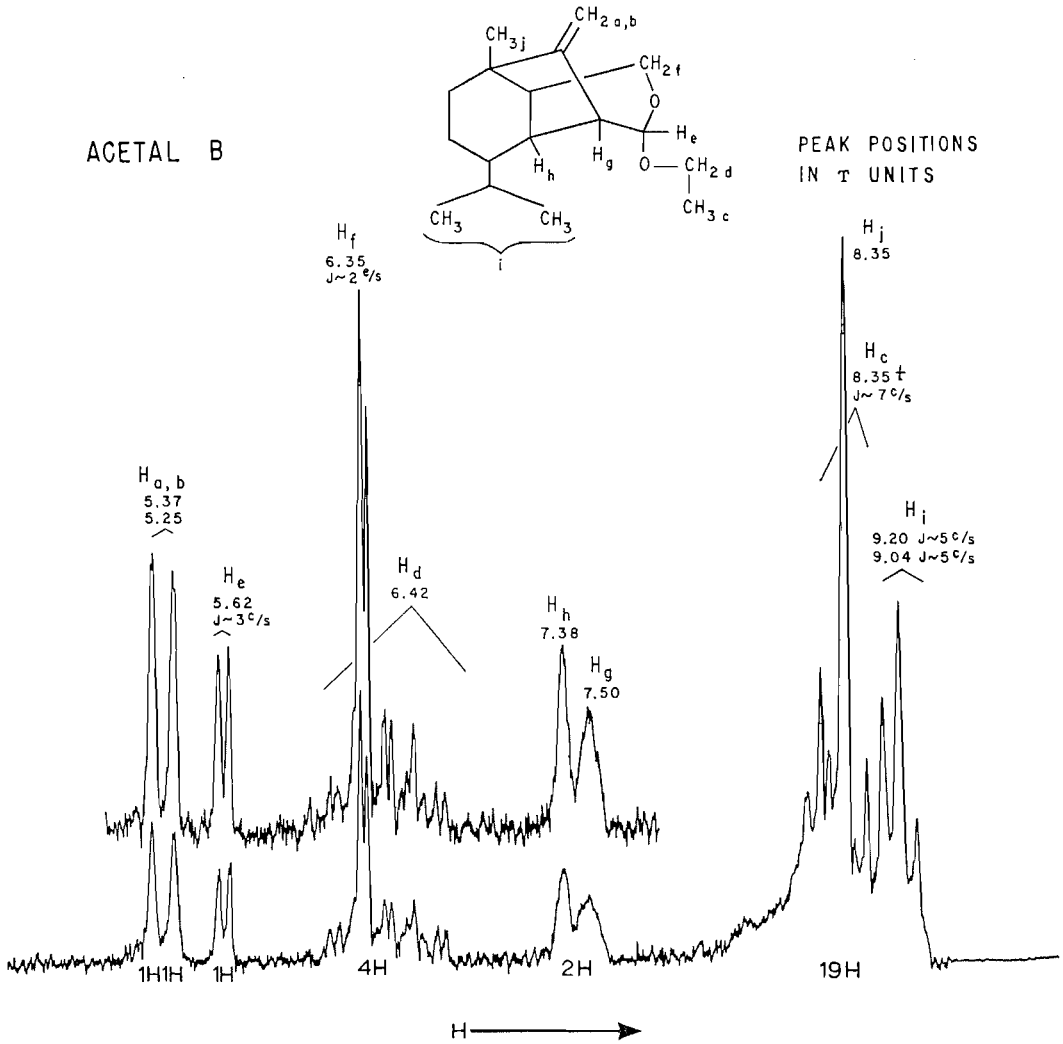

FIG. 2.

n.m.r. spectrum (Fig. 2) of two singlets at τ 5.37 and 5.25. Signals caused by only one acetal methine proton (at τ 5.62) could be observed, and the presence of four protons in the τ 6.0–6.5 region required that there be an oxymethylene group (in addition to that of the ethoxyl) present in the molecule. Acetal B could thus be provisionally formulated

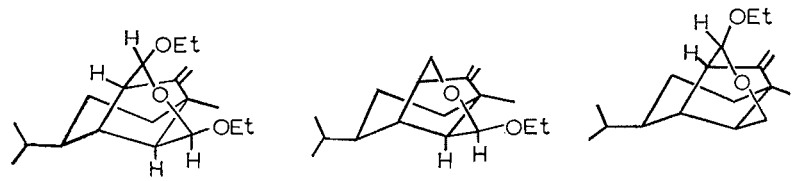

(IV) (VI) (V)

Can. J. Chem. Downloaded from www.nrcresearchpress.com by 210.87.254.6 on 09/05/12
For personal use only.

as (V) or (VI). Of these (V) would be favored since the acetal methine proton (τ 5.62) corresponds closely in signal position with the corresponding proton (at τ 5.63) in (IV).

Treatment of acetal B with aqueous acid resulted in hydrolysis of the acetal to the hemiacetal and no further change. Two formulations, corresponding to (V) and (VI), were possible for the hemiacetal; however, it was possible to discriminate between them by the sequence of reactions shown below.

Oxidation of the hemiacetal, now formulated as (VII), gave a δ-lactone (ν_{max} 1 754 cm^{-1}) (VIII). The signals in the n.m.r. spectrum at τ 5.24 and 4.90 were attributed to the exocyclic methylene group (attested to also by absorption at 3 060, 1 680, and 860 cm^{-1}), whereas those at τ 7.63 and 6.83 were attributed to the bridgehead and allylic protons respectively. The methylene group of the lactone appeared as two superimposed non-equivalence quartets between τ 5.59–6.08.

Ozonolysis of the lactone (VIII) gave the keto-lactone (IX) showing absorption at 1 773 and 1 742 cm^{-1}. The higher value for the δ-lactone is attributed to the adjacent carbonyl function. A similar observation was made in the case of the keto-lactone (X) (3) which absorbed at 1 802 and 1 767 cm^{-1}.

Alkaline hydrolysis of the keto-lactone, with opening of the lactone, resulted in spontaneous decarboxylation to give the ketol (XI). The ketone carbonyl now absorbed in the normal position at 1 739 cm^{-1}. The carbonyl of the lactone in (VIII), and therefore the acetal function in (V), is thus required to be β to the trigonal carbon atom; (VI) is thus excluded as an adequate formulation.

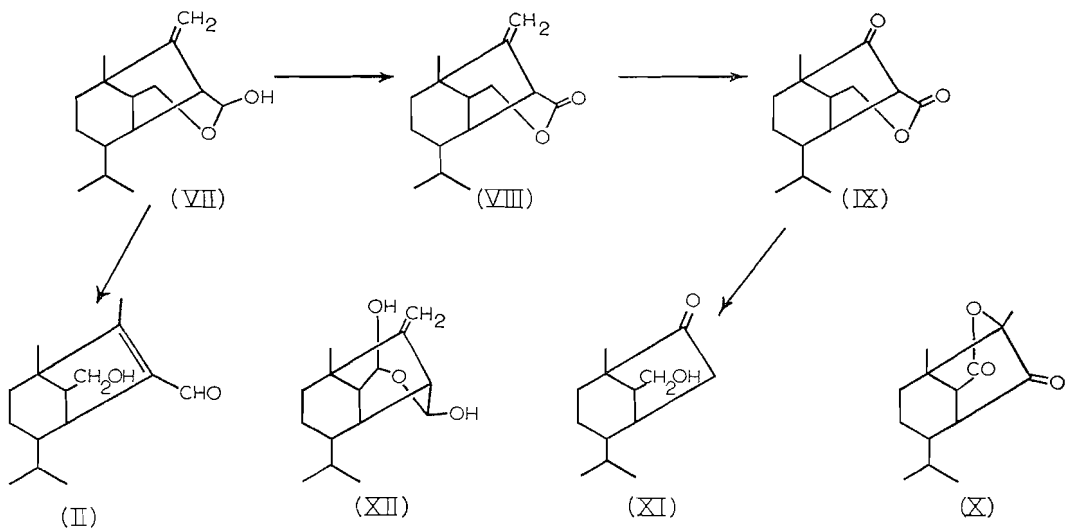

The above considerations rendered the correctness of the structure (V) for acetal B a matter of considerable probability as regards the functional groups and their relationship, but direct evidence about the nature of the carbon skeleton was lacking. This was obtained by the direct conversion of (VII) to helminthosporol (II) by the action of triethylamine. The helminthosporol so obtained was identical in every way with a specimen obtained from Professor Tamura* (Tokyo) which has, in turn, been correlated with helminthosporal.

The serendipitous isolation of the two acetals suggested that the immediate precursors

*We are glad to express our thanks to Professor Tamura for this specimen.

Can. J. Chem. Downloaded from www.nrcresearchpress.com by 210.87.254.6 on 09/05/12
For personal use only.

of helminthosporal and helminthosporol were (XII) and (VII) respectively, and in sanguine expectancy these substances were termed prehelminthosporal and prehelminthosporol respectively.

Attention was now directed to fresh chloroform extracts of the toxin in which the ethanol wash had been omitted. Thin-layer chromatography revealed, as expected, the absence of helminthosporal and helminthosporol and also of acetals A and B. Prehelminthosporol was present and could be isolated directly, but, even though (XII) would be expected to run more slowly than (VII) on the plate, it appeared to be absent. The main bulk of the material was present as material running considerably ahead of (VII). This material appeared to be unstable and attempts at purification led to the appearance of carbonyl absorption. By preparative thin-layer chromatography a small amount of one of the materials was isolated in almost pure form.

Although insufficient data are available to permit the ascribing of specific structures to these substances, the following observations are pertinent.

First, at least four of these compounds appear to be present; yet, after passage through alumina (an effective mode of disrupture) only helminthosporal, prehelminthosporol, and traces of helminthosporol can be detected. A hemiacetal such as (XII) would be expected to be dehydrated under these conditions. Secondly, the n.m.r. spectrum of the purified material was roughly compatible with that of the addition of the spectrum of (VII) to what would be expected for the spectrum of (XII). The infrared spectrum, while indicating hydroxyl absorption, did not have absorption in the 3 600 cm^{-1} region of the intensity to be expected by comparison with that of (VII). This was borne out by the high R_f on thin-layer chromatography.

In view of the mildness of the conditions required to disrupt the complexes some form of acetal between (VII) and (XII) seemed likely. Determination of the molecular weight of the purified complex by the method of isothermal distillation gave, with appropriate controls, values somewhat less than dimeric.

It thus appears that, while prehelminthosporol is the immediate precursor of helminthosporol and prehelminthosporal may be the immediate precursor of helminthosporal, these substances, at least in the chloroform extracts obtained, are present as loose complexes.

We suggested previously (7) that helminthosporal was derived from a tricyclic precursor (XIII) by oxidative cleavage, and have provided some evidence for this view. The structures of the presently described immediate precursors are compatible with this concept, since the ethylenic linkage occupies the biogenetically prescribed position.

In our search for earlier presursors of helminthosporal the culture medium was examined at daily intervals up to the 5 days normally necessary for optimum production. The composition of the extract showed little change, after the appearance of activity as determined by the inhibition of germination of *Monilinia fructicola*, although the total amount of material increased. The results are tabulated in the Experimental section.

From the extract of the first day's growth a small amount of a crystalline solid was

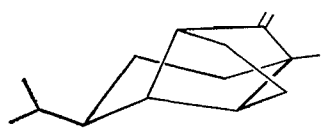

(XIII)

Can. J. Chem. Downloaded from www.nrcresearchpress.com by 210.87.254.6 on 09/05/12
For personal use only.

isolated. This was present—a trace—in the extract from the second day's growth, but not subsequently. By examination of its absorption and mass spectra it was identified as anthraquinone, and its identity confirmed by melting point and mixed melting point with an authentic specimen. Anthraquinone has previously been isolated from *Penicillium islandicum* (8).

EXPERIMENTAL*

Isolation of Acetal A (IV) and Acetal B (V)

A chloroform extract, obtained during the normal isolation procedure for helminthosporal by washing the charcoal cake on which the active agents were adsorbed (1), was allowed to stand for about 9 months before use. It was then evaporated under reduced pressure at 40° to give 25 g residual oil.

The oil (4 g) was chromatographed on alumina (Woelm, neutral, grade I; 300 g) and the fractions eluted with light petroleum, combined, and evaporated. Partial crystallization occurred and the crystals (ca. 0.5 g) were collected and recrystallized from light petroleum to give prehelminthosporal diethyl diacetal (acetal A), m.p. 60.5–61.5°; $[\alpha]_D$ −68° (*c*, 0.86); $\nu_{max}^{CCl_4}$ 3 060, 1 657, 885 cm^{-1}; n.m.r. spectrum: Fig. 1.

Anal. Calcd. for $C_{19}H_{32}O_3$: C, 73.98; H, 10.46; OEt (2), 29.2. Found: C, 74.01; H, 10.22; OEt, 29.3.

The fractions (0.7 g) eluted with benzene were combined with the mother liquors from the crystallization of acetal A and separated by g.l.c. on Carbowax 20M (20% on Chromosorb P, 190°) into two fractions. The second g.l.c. fraction crystallized to give a further 0.5 g acetal A. The first g.l.c. fraction was further purified by g.l.c. on the column indicated above to give prehelminthosporol ethyl acetal (acetal B) as an oil, $[\alpha]_D$ +1° (*c*, 2.56); $\nu_{max}^{CCl_4}$ 3 068, 1 657, 886 cm^{-1}; n.m.r. spectrum: Fig. 2.

Anal. Calcd. for $C_{17}H_{28}O_2$: C, 77.22; H, 10.67; OEt, 17.0. Found: C, 76.98; H, 10.40; OEt, 14.8.

Prehelminthosporol

(*a*) A sterile infusion (100 l), prepared using 22 g dehydrated potatoes and 100 g sucrose per liter, was directly inoculated with spores of *Helminthosporium sativum* obtained by washing moist sterile barley seed which had been inoculated with spores and then incubated at 22–24° for 14 days. The infusion growth was allowed to proceed for 6 days. The active materials were adsorbed on 400 g charcoal, as previously, and the main portion (300 g) of the charcoal was extracted with chloroform (but without ethanol washing as previously (1)). The extract was evaporated below 40° under reduced pressure to give an oil (16 g).

The extract (660 mg) was chromatographed on alumina (Woelm, neutral, grade IV; 30 g). The fractions eluted with benzene (160 mg) were combined and separated by t.l.c. on silica gel. The prehelminthosporol obtained (10 mg) was identified by comparison of its infrared spectrum with that of an authentic specimen (see below) and by its conversion with triethylamine into helminthosporol, m.p. 91–92°.

(*b*) Acetal B (58.2 mg) was dissolved in hydrochloric acid – dioxane – water (1:36:18; 10 ml) and heated at 70° under nitrogen for 45 min. After neutralization with 5% aqueous sodium bicarbonate the product was isolated with ether (51.3 mg). This was separated by preparative t.l.c. on silica gel to give prehelminthosporol (30 mg), $[\alpha]_D$ −91° (*c*, 1.31); $\nu_{max}^{CCl_4}$ 3 608, 3 067, 1 656, 884 cm^{-1}; n.m.r. spectrum: 9.10 (6H, two superimposed doublets, $J \sim 5$ c.p.s.), 8.85 (3H, singlet), 7.52 (1H, multiplet), 7.36 (1H, multiplet), 6.23 (2H, multiplet), 6.02 (1H, multiplet), 5.37 (1H singlet), 5.23 (1H, singlet), 5.16 (1H, doublet, $J \sim 2$ c.p.s.).

Anal. Calcd. for $C_{15}H_{24}O_2$: C, 76.22; H, 10.24. Found: C, 76.26; H, 10.41.

The Prehelminthosporal Complex

The extract described in the previous section (*a*) (3.5 g) was applied to silica gel (B.D.H.; 110 g) in light petroleum solution. The fraction (2.3 g) eluted with benzene–ether (17:3) was collected. On thin-layer chromatography this showed the presence of prehelminthosporol (R_f 0.4), but most of the material was contained in a number of spots (R_f 0.6–0.8) running ahead of the prehelminthosporol. Further, the presence of acetal A and B (R_f 1.0) and substantial amounts of material running behind the prehelminthosporol could not be detected. A 1.8-g quantity of this material was separated repeatedly by preparative thin-layer chromatography. During the separation, decomposition occurred with the formation of helminthosporal and prehelminthosporol. The product was an apparently homogeneous oil (75 g) whose R_f (0.7) on the thin-layer plate (benzene–ether 4:1) was different from that of acetals A and B (R_f 1.0) and that of prehelminthosporol (R_f 0.4), $\nu_{max}^{CCl_4}$ 3 608 (w), 3 065, 1 659, 1 075, 922, 885 cm^{-1}; n.m.r. spectrum: 9.14 (6H, doublet, $J \sim 5$ c.p.s.); 9.07 (6H, doublet, $J \sim 5$ c.p.s.); 8.87 (3H, singlet); 8.84 (3H, singlet); 7.45 (4H, complex); 7.09 (2H, complex); 6.33 (2H, broad); 5.33 (2H, broad singlet); 5.18 (2H, broad singlet); 4.96 (2H, complex). Mol. wt. 457 ± 46 (isopiestic method using acetal A as reference).

The complex (11.4 mg) was applied to a column of alumina (Woelm, neutral, grade I; 1 g) in light petroleum solution and allowed to remain on the column for 4 h. The column was then washed with ether and the eluate separated by t.l.c. on silica gel using benzene–ether (4:1) as developing solvent. Unreacted starting material (1.9 mg, R_f 0.7), helminthosporal (1.9 mg, R_f 0.5, identified by R_f and infrared spectrum),

**For general directions, see Part IV (3).*

Can. J. Chem. Downloaded from www.nrcresearchpress.com by 210.87.254.6 on 09/05/12
For personal use only.

and a mixture (2.1 mg) of prehelminthosporol (R_f 0.4) and helminthosporol (R_f 0.1) (identified by comparison of R_f and infrared spectra) were obtained.

The Conversion of Prehelminthosporol to Helminthosporol

Prehelminthosporol (8.5 mg) was heated under reflux (nitrogen atmosphere) in triethylamine (2 ml) for 7½ h. The triethylamine was removed under reduced pressure and the residue separated by t.l.c. on silica gel to give helminthosporol (2.8 mg), m.p. 93–93.5°, undepressed on admixture with an authentic specimen. The infrared spectra were also identical.

Conversion of Acetal A to Helminthosporal

Acetal A (54.8 mg) was dissolved in dioxane (3 ml) containing 2% (v/v) sulfuric acid and the mixture allowed to stand (nitrogen atmosphere) at room temperature overnight. After dilution with water and neutralization with 5% aqueous sodium bicarbonate the product (47 mg) was isolated with ether and separated by t.l.c. on silica gel using ether–benzene (1:4) as developing solvent. Two fractions were obtained. One (16.7 mg) was identified as helminthosporal, $[\alpha]_D$ −43° (*c*, 1.23), by comparison with an authentic specimen (infrared spectrum) and by conversion to the bis-oxime, m.p. 167–169°, undepressed on admixture with an authentic specimen.

The other fraction (12.5 mg) was a product derived from helminthosporal and ethylene glycol (5) (a contaminant of the dioxane), as was shown by the appropriate control experiments. It was not further investigated.

Oxidation of Prehelminthosporol

The alcohol (11.4 mg) and chromium trioxide (85 mg) in pyridine (1 ml) were shaken at room temperature for 3½ hours. The slurry was warmed briefly to 80° and poured into cold dilute aqueous sodium bisulfite solution. After acidification the product was isolated with ether to give the δ-lactone (VIII), m.p. 78.5–79.0°; $[\alpha]_D$ −119° (*c*, 1.09); $\nu_{max}^{CCl_4}$ 3 060, 1 754, 1 680, 860 cm^{-1}; n.m.r. spectrum: 9.13 (3H, doublet, $J \sim 5$ c.p.s.); 9.03 (3H, doublet, $J \sim 5$ c.p.s.); 8.78 (3H, singlet); 7.60 (1H, multiplet); 6.73 (1H, multiplet); 5.83 (1H, AB system, $\delta_B-\delta_A = 14.9$ c.p.s., $J_{AB} = 10$ c.p.s.); 5.80 (1H, AB system, $\delta_B-\delta_A = 7.1$ c.p.s., $J_{AB} = 11.5$ c.p.s.); 5.20 (1H, singlet); 4.87 (1H, singlet).

Anal. Calcd. for $C_{15}H_{22}O_2$: C, 76.88; H, 9.46. Found: C, 76.77; H, 9.43.

Ozonolysis of Prehelminthosporol δ-Lactone (VIII) (with Dr. R. W. White)

The lactone (60 mg) was dissolved in ethyl acetate and a stream of ozonized oxygen passed through at −70° for 20 min. After evaporation of the solvent, water (5 ml) was added and the solution boiled briefly. Removal of the water under reduced pressure gave a partially crystalline gum which was chromatographed on silica gel (5 g). The fraction eluted with benzene gave, after crystallization from ether – light petroleum, the nor δ-lactone (IX), m.p. 100–101.5°; $[\alpha]_D$ −4° (*c*, 0.99); $\nu_{max}^{CCl_4}$ 1 773, 1 742 cm^{-1}.

Anal. Calcd. for $C_{14}H_{20}O_3$: C, 71.16; H, 8.53. Found: C, 70.93 ;H, 8.14.

Decarboxylation of the Nor δ-Lactone (XI) (with Dr. R. W. White)

The keto-lactone (IX) (51 mg) was added to aqueous sodium hydroxide (10%; 10 ml) and the mixture refluxed for 30 min. After acidification the product was isolated with ether and chromatographed on silica gel (5 g). The fraction eluted with benzene–ether (9:1) was sublimed (120°; 2 torr) to give the ketol (XI) (22 mg), m.p. 56–58°; $[\alpha]_D$ +35° (*c*, 1.18); $\nu_{max}^{CCl_4}$ 3 610, 1 739, 1 410 cm^{-1}; n.m.r. spectrum: 9.12 (3H, doublet, $J \sim 5$ c.p.s.); 9.08 (3H, singlet); 9.04 (3H, doublet, $J \sim 5$ c.p.s.); 8.7–7.79 (9H, complex); 7.42 (1H, complex); 7.04 (1H, singlet); 6.46 (2H, complex).

Anal. Calcd. for $C_{13}H_{22}O_2$: C, 74.24; H, 10.54. Found: C, 74.55; H, 10.48.

Isolation of Anthraquinone

A sterile infusion (100 l) was prepared and inoculated with *Helminthosporium sativum* as described above. Samples of the infusion were taken after 24, 48, 72, 96, and 120 h and worked up as described previously (Table I). The evaporated chloroform extracts were examined by t.l.c. on silica gel, but showed relatively little variation in composition of the extract after the appearance of toxicity as determined by inhibition of germination of *Monilinia fructicola* (Table II).

TABLE I

h after inoculation	Sample volume, l	Weight evaporated chloroform extract, g
24	20	1.27
48	20	1.68
72	20	2.30
96	20	7.75
120	28	8.47

Can. J. Chem. Downloaded from www.nrcresearchpress.com by 210.87.254.6 on 09/05/12
For personal use only.

TABLE II

h after inoculation	% inhibition					
	Culture filtrate dilution:					
	1:2	1:4	1:8	1:16	1:32	1:64
24	0	0	0	0	—	—
48	100	100	68	11	—	—
72	100	100	91	33	—	—
96	100	100	100	63	20	0
120	100	100	100	52	20	0

After they had been allowed to stand overnight at 4°, both the evaporated chloroform extracts obtained after 24 and 48 h of growth contained small amounts (ca. 15 and ca. 1 mg respectively) of a crystalline material. None was present in any of the later extracts. This crystalline material was identified as anthraquinone, m.p. 280–282° (sealed capillary), undepressed on admixture with an authentic sample, by its infrared and mass spectra.

ACKNOWLEDGMENTS

The authors thank Mr. C. H. Unwin and Mr. M. Ktenas for technical assistance, Mr. R. E. Klinck for the n.m.r. spectra, and Mr. J. Aberhart for the double-irradiation n.m.r. spectrum. They are indebted to Dr. R. W. White for the experiments indicated. Two of us (P. de M. and R. E. W.) thank the National Institutes of Health for financial support under grant No. EF-AI-00419-01, Division of Environmental Engineering and Food Protection.

REFERENCES

1. P. DE MAYO, E. Y. SPENCER, and R. W. WHITE. Can. J. Chem. **39**, 1608 (1961).
2. S. TAMURA, A. SAKURAI, K. KAINUMA, and M. TAKAI. Agr. Biol. Chem. Tokyo, **27**, 738 (1963).
3. P. DE MAYO, E. Y. SPENCER, and R. W. WHITE. Can. J. Chem. **41**, 2996 (1963).
4. R. A. LUDWIG. Can. J. Botany, **35**, 291 (1957).
5. E. J. COREY and S. NOZOE. J. Am. Chem. Soc. **85**, 3527 (1963).
6. F. KAPLAN and J. D. ROBERTS. J. Am. Chem. Soc. **83**, 4666 (1961).
7. P. DE MAYO, J. R. ROBINSON, E. Y. SPENCER, and R. W. WHITE. Experientia, **18**, 359 (1962).
8. M. KIKUCHI, Y. OKAMOTO, and K. HAYASHI. Botan. Mag. Tokyo, **73**, 195 (1960); Chem. Abstr. **55**, 6601 (1961).

Can. J. Chem. Downloaded from www.nrcresearchpress.com by 210.87.254.6 on 09/05/12
For personal use only.

Can. J. Chem. Downloaded from www.nrcresearchpress.com by 210.87.254.42 on 09/05/12
For personal use only.

THE SOLVOLYSIS OF ARENESULFINATES, SULFUR–OXYGEN VERSUS CARBON–OXYGEN BOND FISSION[1,2]

DAVID DARWISH AND JOHN NOREYKO
Department of Chemistry, University of Alberta, Edmonton, Alberta
Received November 13, 1964

Dedicated to Professor R. B. Sandin on the Occasion of his Sixty-Eighth Birthday

ABSTRACT

The base-catalyzed solvolysis of *p*-methoxyneophyl benzenesulfinate and the corresponding 2,6-dimethyl-, 2-methyl-, 4-methyl-, and 2-chloro-benzenesulfinates has been studied in ethanol and aqueous ethanol. The reactions involve sulfur–oxygen bond fission. The rate of sulfur–oxygen bond fission is decreased by the introduction of two methyl groups ortho to the sulfur. The rate decrease may be partly due to steric hindrance to nucleophilic attack on the sulfinate sulfur, but this effect is very small compared to the effect in carboxylate ester hydrolysis. The reactions are catalyzed by ethoxide, acetate, and pyridine. Reaction is very slow in the presence of 2,6-lutidine. With certain arenesulfinate esters one can control the reaction to give sulfur–oxygen or carbon–oxygen bond fission by choice of an appropriate base.

INTRODUCTION

The solvolysis of arenesulfinates can involve either sulfur–oxygen or carbon–oxygen bond fission. Kenyon and co-workers (1, 2) have shown that (−)-α-phenylethyl *dl*-*p*-toluenesulfinate yields α-phenylethyl alcohol of retained configuration on hydrolysis and ethanolysis, indicating that sulfur–oxygen bond cleavage has taken place. The ethoxide ion catalyzed ethanolysis of the diasterioisomeric (−)-menthyl (+)-*p*-iodobenzenesulfinate and (−)-menthyl (−)-*p*-iodobenzenesulfinate both yield (−)-menthol in a concentration equivalent to the amount of ester originally present, indicating essentially exclusive sulfur–oxygen bond cleavage (3). Methyl *p*-toluenesulfinate undergoes a slow neutral hydrolysis as well as a rapid reaction in alkaline solution and an acid-catalyzed hydrolysis in dioxane–water mixtures. The base- and acid-catalyzed reactions have been shown (4) by the use of ^{18}O tracers to involve sulfur–oxygen bond fission. Similarly, the sulfur–oxygen bond is broken on alkaline hydrolysis of diphenylmethyl *p*-toluenesulfinate (5). The formation of sulfones and substitution products on solvolysis of arenesulfinates (6, 7, 8) indicates that under certain conditions carbon–oxygen bond fission must occur.

Our interest in the reaction of arenesulfinates centered mainly on reactions involving carbon–oxygen bond fission (8, 9). However, it was necessary to investigate the sulfur–oxygen bond cleavage reactions to choose conditions under which sulfur–oxygen bond fission would not take place as an undesirable side reaction. Two general approaches were followed. First, an examination of the effect of substituents upon the rate of sulfur–oxygen bond fission was made. Secondly, the effect of various nucleophiles upon the rate of reaction was investigated.

Different products are obtained from alcoholysis of arenesulfinates involving sulfur–oxygen and carbon–oxygen bond fission. Sulfur–oxygen bond fission gives rise to ester interchange and yields a new arenesulfinate ester as shown in eq. [1]. Carbon–oxygen

[1]*Presented in part at the Fifth Biennial Organic Symposium of the Chemical Institute of Canada, Hamilton, Ontario, August 30, 1962.*
[2]*Abstracted in part from the M.Sc. Thesis of John Noreyko, University of Alberta, 1963.*

Can. J. Chem. Downloaded from www.nrcresearchpress.com by 210.87.254.42 on 09/05/12
For personal use only.

[1] $$R{-}O{-}\overset{\overset{O}{\uparrow}}{S}{-}Ar + R'OH \rightarrow R'{-}O{-}\overset{\overset{O}{\uparrow}}{S}{-}Ar + ROH$$

[2] $$R{-}O{-}\overset{\overset{O}{\uparrow}}{S}{-}Ar + R'OH \rightarrow ArSO_2H + ROR' \ (+ \text{olefin})$$

bond fission gives rise to an arenesulfinic acid and solvolysis products as shown in eq. [2]. Thus, product analysis provides information on the type of bond cleavage. If water is the substituting agent, a sulfinic acid and an alcohol are produced by both sulfur–oxygen and carbon–oxygen bond fission. One must then use other criteria to determine the type of bond fission which has occurred.

The systems chosen for this study were arenesulfinate esters of *p*-methoxyneophyl alcohol. Since these esters have a neophyl type of structure, one can rule out direct nucleophilic displacement on the primary carbon as a major route for carbon–oxygen bond fission. If carbon–oxygen bond fission were to occur, the reaction should involve neighboring *p*-anisyl participation (10), giving rise to products from the rearranged carbonium ion as shown in eq. [3]. Sulfur–oxygen bond fission would yield the unrearranged alcohol, *p*-methoxyneophyl alcohol. Therefore, with this system one can distinguish between carbon–oxygen and sulfur–oxygen bond fission by product analysis, even with water as the nucleophile.

[3] $$H_3C{-}\overset{\overset{An}{|}}{\underset{\underset{CH_3}{|}}{C}}{-}CH_2{-}O{-}\overset{\overset{O}{\uparrow}}{S}{-}Ar \rightarrow CH_3{-}\overset{\overset{+}{|}}{\underset{\underset{CH_3}{|}}{C}}{-}CH_2{-}An + ArSO_2^- \rightarrow \text{products}$$

RESULTS

Preparation of Esters

The 2,6-dimethyl-, *o*-chloro-, and *o*-methyl-benzenesulfinic acids were prepared by a method described by Hanke (11) which involved diazotization of the corresponding substituted aniline and treatment of the solution with sulfur dioxide in the presence of copper powder. Benzene- and *p*-toluene-sulfinic acids were prepared by reduction of the corresponding sulfonyl chlorides with zinc powder.

The arenesulfinic acids were treated with thionyl chloride in pentane to obtain the corresponding acid chlorides. The acid chlorides were dissolved in pyridine and treated with the appropriate alcohol to yield the arenesulfinate esters after work-up.

Rate Measurements

A summary of the rate constants for the reaction of a number of *p*-methoxyneophyl arenesulfinates is presented in Table I. In most cases the reactions were followed by measuring the increase in absorption of the band at ca. 11.35 μ where the corresponding ethyl arenesulfinates have an intense absorption band. These reactions were therefore studied by measuring the rate of formation of the product of sulfur–oxygen bond fission. In the cases where the solvent was an ethanol–water mixture the disappearance of absorption at ca. 10.4 μ, associated with the *p*-methoxyneophyl arenesulfinate, was measured.

In every case first-order rate constants were calculated within any run. Good first-order rate constants were obtained with ethoxide or acetate as the added base, except for the reactions of *p*-methoxyneophyl 2,6-dimethylbenzenesulfinate in the presence of acetate ion. These rate constants showed a marked upward drift as the reaction progressed. The initial rate constants reported for these reactions are obtained from the slope of the curve obtained by plotting log $(a - x)$ versus time. When 2,6-lutidine and pyridine were

TABLE I

Summary of solvolysis rate constants of *p*-methoxyneophyl arenesulfinates

p-Methoxyneophyl arenesulfinate	Solvent	Temp. (°C)	Ester (10^2 *M*)	Added base	Base (10^2 *M*)	$10^5 k_1$ (s^{-1})	$10^3 k_1$/base (l $mole^{-1}$ s^{-1})
Benzenesulfinate	EtOH	90.0	2.56	KOAc	1.59	10.7	6.7
	EtOH	90.0	2.53	KOAc	3.18	19.6	6.2
	EtOH	90.0	2.50	KOAc	4.78	27.8	5.8
	EtOH	90.0	2.50	KOAc	7.96	48.1	6.0
	EtOH	90.0	2.42	2,6-Lutidine	5.04	0.008	
	EtOH	90.0	2.46	Pyridine	5.42	0.12	
2-Chlorobenzene-sulfinate	EtOH	90.0	2.50	KOAc	1.95	18.9	9.7
	EtOH	90.0	2.50	KOAc	3.89	32.5	8.4
	EtOH	90.0	2.49	KOAc	4.78	40.5	8.5
	EtOH	90.0	2.49	KOAc	7.96	65.5	8.2
2-Methylbenzene-sulfinate	EtOH	90.0	2.57	KOAc	4.78	11.9	2.5
	EtOH	90.0	2.41	KOAc	7.79	16.8	2.2
4-Methylbenzene-sulfinate	EtOH	90.0	2.46	KOAc	4.78	16.0	3.4
	EtOH	90.0	2.51	KOAc	7.79	31.3	4.0
2,6-Dimethylbenzene-sulfinate	EtOH	25.0	2.54	NaOEt	2.60	32.4	12.5
	EtOH	25.0	2.42	NaOEt	4.86	60.9	12.5
	80% EtOH	25.0	2.42	NaOEt	1.37	6.7	4.9
	80% EtOH	25.0	2.42	NaOEt	2.81	16.2	5.7
	80% EtOH	25.0	2.42	NaOEt	5.12	24.8	5.5
	80% EtOH	25.0	2.42	NaOEt	9.73	55.1	5.7
	EtOH	90.0	2.41	KOAc	3.18	0.60	0.19
	EtOH	90.0	2.42	KOAc	4.78	0.75	0.16
	EtOH	90.0	2.47	KOAc	7.76	0.87	0.15
	EtOH	90.0	2.41	Pyridine	5.12	0.013	
	EtOH	90.0	2.47	2,6-Lutidine	5.05	0.0006	
	60% EtOH	90.0	2.53	KOAc	5.73	0.047	
	60% EtOH	90.0	2.49	2,6-Lutidine	6.04	0.007	

the added bases the reactions were very slow, and again only initial rate constants were estimated. The rate constants estimated for the reaction of the 2,6-dimethylbenzenesulfinate in the presence of added acetate ion and for all the reactions with added pyridine and 2,6-lutidine are very crude. These rate constants may be in error by as much as a factor of two. As shown in Table I the reactions were second order: first order in ester and first order in added ethoxide or acetate. The order of the reaction with respect to added pyridine and lutidine was not determined.

Titrations for acid were also carried out at each point in the rate determinations when ethoxide or acetate was the base. In the reactions involving anhydrous ethanol as solvent, acid production would indicate reaction via carbon–oxygen bond fission. No change in acid titer was detected in the course of the reactions in solvent ethanol. Therefore, only sulfur–oxygen bond fission occurred.

Reaction Products

In solvent ethanol the reaction product was the corresponding ethyl arenesulfinate as shown by the kinetic studies. A product run was carried out on the reaction of methoxyneophyl 2,6-dimethylbenzenesulfinate in 60% ethanol–water with 2,6-lutidine as added base. The reaction mixture was heated for 46 days at 90.0°, corresponding to ca. 20% reaction. The reaction mixture was separated into ester and alcohol fractions by chromatography. The ester was unreacted *p*-methoxyneophyl 2,6-dimethylbenzenesulfinate and the alcohol was *p*-methoxyneophyl alcohol as shown by infrared spectroscopy.

Can. J. Chem. Downloaded from www.nrcresearchpress.com by 210.87.254.42 on 09/05/12
For personal use only.

Can. J. Chem. Downloaded from www.nrcresearchpress.com by 210.87.254.42 on 09/05/12
For personal use only.

DISCUSSION

The displacement reaction must involve sulfur–oxygen bond fission as shown by the reaction products.

The reaction is second order: first order with respect to the ester and first order with respect to the base when ethoxide or acetate is the added base. The order of the reactions with respect to pyridine and 2,6-lutidine has not been determined.

There are four types of mechanisms which are consistent with the data. These four mechanisms can be divided into two categories. (i) Catalysis, which involves a nucleophilic displacement on sulfur by the base to yield a substitution product. In the case of ethoxide ion the substitution product would be the product ethyl arenesulfinate. In the case of acetate ion a mixed anhydride would be formed. The mixed anhydride would be converted rapidly to the ethyl arenesulfinate by reaction with the solvent. (ii) General base catalysis, which involves attack by the solvent on the ester concerted with transfer of a proton to the added base. The ethyl arenesulfinate would be produced directly regardless of the nature of the base.

Within each of the mechanistic schemes described above a further subdivision can be made. Substitution could involve concerted bond-making and bond-breaking to yield the substitution product in a manner analogous to that for a nucleophilic displacement on saturated carbon. Alternatively, displacement could occur in a stepwise fashion involving, first, addition of the nucleophile to sulfur followed, in a second step, by loss of the leaving group. In the hydrolysis of cyclic sulfite esters Bunton *et al.* (12) have reported that ^{18}O exchange with the solvent does not occur in significant competition with hydrolysis. Davis (14) suggested that the small amount of exchange observed by Bunton (12) indicated that there was evidence for an intermediate. However, de la Mare *et al.* (13) have indicated that the exchange may represent experimental error.

The data here reported cannot distinguish between these four alternative mechanisms. For the amines, one can exclude mechanisms in which the lyate ion of the solvent is formed in a rapid preequilibrium step by reaction with the added base followed by a slow reaction of the lyate ion with the substrate as shown in eqs. [4] and [5].

$$\text{B:} + \text{C}_2\text{H}_5\text{OH} \overset{K}{\rightleftarrows} \text{C}_2\text{H}_5\text{O}^{\ominus} + \text{BH}^{\oplus} \qquad [4]$$

$$\text{C}_2\text{H}_5\text{O}^{\ominus} + \text{RO}_2\text{SAr} \overset{k}{\rightarrow} \text{C}_2\text{H}_5\text{O}_2\text{SAr} + \text{RO}^{\ominus} \qquad [5]$$

The latter alternative is ruled out as follows. 2,6-Lutidine is a stronger base than pyridine. If reaction occurred by the above scheme, then the reaction should be faster in the presence of 2,6-lutidine than in the presence of pyridine. The opposite result is observed and, therefore, this alternative can be excluded.

Within the framework of the four mechanisms the effects of substituents, solvents, and bases are consistent and are discussed below.

Substituent Effects

A summary of the relative rates of ethanolysis of a number of arenesulfinates is presented in Table II. It is instructive to compare these relative rates with the relative rates of base-catalyzed hydrolysis of the correspondingly substituted ethyl benzoates in 85% aqueous ethanol (25). One ortho substituent has a small and roughly equivalent effect on both reactions. Two ortho methyl groups have a much smaller effect on the rate of reaction of the arenesulfinate ester than on the rate of hydrolysis of the benzoate ester.

TABLE II

Relative rates of reaction of various *p*-methoxyneophyl arenesulfinates at 90° in anhydrous ethanol with potassium acetate as added base

Benzenesulfinate	Ester (*M*)	Base (*M*)	$10^4 k$ (s^{-1})	Relative rates
2-Chloro	0.02486	0.0478	4.05	1.45
4-Methyl	0.02465	0.0478	1.60	0.58
2-Methyl	0.02510	0.0478	1.15	0.41
Unsubstituted	0.02502	0.0478	2.78	1.0
2,6-Dimethyl	0.02422	0.0478	0.075	0.028

If the decrease in rate on changing from the benzenesulfinate to the 2-methybenzenesulfinate is ascribed entirely to an electronic effect and if it is assumed that the electronic effect of a second ortho methyl group would reduce the rate by a similar amount, then the 2,6-dimethylbenzenesulfinate reacts at a rate which is ca. 1/6 of the anticipated value. This extra rate decrease may be associated with steric hindrance to attack on the sulfinate sulfur. Even if all of the rate reduction observed in comparing the benzenesulfinate and 2,6-dimethylbenzenesulfinate is ascribed to a steric effect, the difference in rates is less than a factor of 40. In contrast, the hydrolysis of ethyl benzoate is nearly five powers of 10 faster than the hydrolysis of ethyl 2,6-dimethylbenzoate.

Any increase in non-bonded interactions at the transition state relative to the ground state must be very small for the arenesulfinate esters as compared to the large effect for the carboxylate esters. The carbon–sulfur bond in the arenesulfinates is longer (ca. 1.8 Å) than the carbon–carbon bond of the Ar—C=O system (1.5 Å). Therefore, the region of greatest size of the transition state may effectively be removed further from the ortho methyl groups in the arenesulfinate than in the benzoate ester reactions and may account for much of the difference in behavior of the two systems.

The arenesulfinate esters appear to be more nearly analogous in behavior to the sulfonate esters than to the benzoate esters. Thus, Bunnett and Bassett (15) have observed that there is no detectable steric hindrance on the rate of sulfur–oxygen bond fission of a number of arenesulfonate esters.

Solvent Effects

The change of solvent from anhydrous ethanol to 80% ethanol and 60% ethanol reduced the rate constant for 2,6-dimethylbenzenesulfinate ester disappearance with ethoxide and acetate ion, respectively, as added bases. The reaction in the presence of 2,6-lutidine was faster in 60% ethanol–water than in anhydrous ethanol. These observations are consistent with all four mechanisms. The reaction of the negatively charged bases with the ester must involve charge dispersal at the transition state and, hence, increasing the polarity of the medium should hinder reaction (16). The reaction of neutral bases with the ester must involve charge formation at the transition state and will be facilitated by increasing the polarity of the solvent.

The above discussion of solvent effects must be qualified, since it considers only changes in charge distribution and solvent polarity. Other factors, such as the extent of ion pairing of the salts, and the change from ethoxide to hydroxide ion as the water content of the solvent is increased, may also be of importance. Bunton and co-workers (5) have reported that the hydroxide ion catalyzed hydrolysis of methyl *p*-toluenesulfinate is 40 times faster in 40% dioxane–water than in 60% dioxane–water. This reaction would

Can. J. Chem. Downloaded from www.nrcresearchpress.com by 210.87.254.42 on 09/05/12
For personal use only.

be expected to be faster in 60% dioxane–water than 40% dioxane–water, if only the effect of solvent polarity on changes in charge distribution were important.

Effect of the Base

The rate of sulfur–oxygen bond fission varies enormously with the nature of the added base. The esters are particularly susceptible to attack by the strongly basic ethoxide ion; the nitrogen bases 2,6-lutidine and pyridine are much less effective than acetate ion at facilitating the reaction. Edwards and Pearson (17) have suggested that basicity is of prime importance for nucleophilic character towards tetrahedral sulfur. On this basis, if the reactions of the arenesulfinates involved nucleophilic attack on sulfur by the added base, then one would predict the observed reactivity order. Similarly, if the reactions of the esters involved general base catalysis, the observed order of reactivity would be anticipated. The fact that pyridine is a more effective catalyst than 2,6-lutidine would, in the first case, reflect the steric hindrance of the methyl groups to attack on sulfur by the nitrogen base. In the latter, it would be required that steric hindrance to general base catalysis be invoked to explain the greater effectiveness of pyridine than 2,6-lutidine. Westheimer and co-workers (18, 19) have reported a number of examples of reactions which exhibit steric hindrance in general base catalysis.

The difference in rates for ethanolysis of the arenesulfinates with pyridine and 2,6-lutidine as added bases may be larger than it appears from an examination of the data in Table I. The 2,6-lutidine used in these experiments contained a small amount of a methylpyridine. The observed reaction may have involved catalysis by the impurity and not by the 2,6-lutidine. If the reaction in the presence of pure 2,6-lutidine were significantly slower than the value reported, it would tend to suggest that the reactions of the other bases involve a nucleophilic substitution on sulfur by the added base.

The most important result of these experiments is the demonstration that one can greatly reduce the rate of sulfur–oxygen bond fission in arenesulfinate esters by the use of weak bases. In systems which can undergo facile carbon–oxygen as well as sulfur–oxygen bond fission, it is possible to control the type of bond cleavage by choosing the appropriate base. A remarkable illustration of this behavior is found in the ethanolysis of allyl 2,6-dimethylbenzenesulfinate (20). In anhydrous ethanol at 90.0° with acetate ion as the added base, allyl 2,6-dimethylbenzenesulfinate yielded ethyl 2,6-dimethylbenzenesulfinate plus a trace of allyl 2,6-dimethylphenylsulfone. Under the same conditions but with 2,6-lutidine as the added base, the reaction was slower and allyl 2,6-dimethylphenyl sulfone was the only detectable reaction product.

EXPERIMENTAL

α,α-Dimethyl-p-methoxybenzyl Cyanide

This compound was prepared by the method of Heyningen (21, 10) from *p*-methoxybenzyl cyanide (22). The yield of product, b.p. 110–113° at 2 mm pressure, η_D^{25} 1.5142 (reported (10), b.p. 110° at 3 mm pressure, η_D^{25} 1.5143), was 50%.

p-Anisyldimethylacetic Acid

α,α-Dimethyl-*p*-methoxybenzyl cyanide was hydrolyzed by the method described by Heyningen (21). The acid, recrystallized from aqueous methanol, melted at 88–89.5° (reported (10), 88–89.5°).

p-Methoxyneophyl Alcohol

Lithium aluminium hydride reduction of the above acid produced *p*-methoxyneophyl alcohol, m.p. 46.5–48.5° (reported (10), m.p. 45–46.5°) after recrystallization from Skellysolve B.

Arenesulfinic Acids

Benzene- and *p*-toluene-sulfinic acids were prepared by reduction of the corresponding sulfonyl chlorides with zinc dust by the method described by Vogel (23).

Can. J. Chem. Downloaded from www.nrcresearchpress.com by 210.87.254.42 on 09/05/12
For personal use only.

Can. J. Chem. Downloaded from www.nrcresearchpress.com by 210.87.254.42 on 09/05/12
For personal use only.

TABLE III

Properties and analyses of some arenesulfinates

Ester	η_D^{25}	Formula	Analyses (%) Calcd. C	Calcd. H	Calcd. S	Found C	Found H	Found S	Infrared absorption§ (cm^{-1})
2,6-$(CH_3)_2C_6H_3SO_2R$*	57.2–57.9†	$C_{19}H_{24}O_3S$	68.84	7.28	9.65	69.08	7.31	9.81	1142, 980
2-$CH_3C_6H_4SO_2R$	1.5638	$C_{18}H_{22}O_3S$	67.89	6.97	10.07	67.82	6.64	10.42	1128
4-$CH_3C_6H_4SO_2R$	51.2–52.0†	$C_{18}H_{22}O_3S$	67.89	6.97	10.07	67.78	7.03	9.98	1130
$C_6H_5SO_2R$	1.5676	$C_{17}H_{20}O_3S$	67.07	6.62	10.54	67.31	6.55	10.4	1135
2-$ClC_6H_4SO_2R$	46.1–46.8†	$C_{17}H_{19}O_3SCl$	60.27	5.61	9.46	60.40	5.52	9.34	1137
2,6-$(CH_3)_2C_6H_3SO_2C_2H_5$	47.3–48.6†	$C_{10}H_{14}O_2S$	60.56	7.12	16.17	60.74	6.91	16.43	1132, 882
2-$CH_3C_6H_4SO_2C_2H_5$	1.5338	$C_9H_{12}O_2S$	58.67	6.57	17.40	58.84	6.60	17.47	1133, 880
4-$CH_3C_6H_4SO_2C_2H_5$	1.5307	$C_{19}H_{12}O_2S$	58.67	6.5	17.40	58.54	6.63	17.31	1135, 880
$C_6H_5SO_2C_2H_5$	1.5317	$C_8H_{10}O_2S$	56.45	5.92	18.84	56.50	5.97	18.63	1135, 880
2-$ClC_6H_4SO_2C_2H_5$‡	1.5486	$C_8H_9O_2SCl$	46.94	4.43	15.67	47.07	3.96	15.91	1137, 882

*R represents *p*-methoxyneophyl.
†Melting point (°C).
‡% Cl: found, 17.24; calcd. 17.32.
§The bands at lower frequency, where recorded, were used in the rate determinations.

The 2,6-dimethyl-, 2-chloro-, and 2-methyl-benzenesulfinic acids were prepared by the method described by Hanke (11) from the correspondingly substituted anilines. In a typical experiment 31 g of 2,6-dimethylaniline yielded 32.6 g of 2,6-dimethylbenzenesulfinic acid, m.p. 95–98°.

Arenesulfinates

All the arensulfinates were prepared by the same general procedure. In a typical preparation 4.6 g of 2,6-dimethylbenzenesulfinic acid was treated with 15 ml of thionyl chloride in 50 ml of pentane. After vigorous reaction had subsided, the solution was filtered through a glass wool filter. The solution was warmed on a steam bath to remove the pentane. The thionyl chloride was removed by pumping under vacuum overnight. The residual 2,6-dimethylbenzenesulfinyl chloride, an oil, was dissolved in 15 ml of anhydrous pyridine and cooled in a dry ice – acetone bath. A solution of 5 g of *p*-methoxyneophyl alcohol in 25 ml of pyridine was added. The reaction mixture was then allowed to warm up to room temperature. The mixture was poured into a mixture of ice and 35 ml of concentrated hydrochloric acid and extracted with ether. The ether extract was washed 3 times with water, then with dilute hydrochloric acid, again with water, and then 6–8 times with 10% sodium carbonate solution or until no yellow color appeared in the aqueous layer. After the extract was dried over magnesium sulfate, the ether was removed by warming the solution on a steam bath. The residue was recrystallized from 10% ether–pentane to yield 4.5 g of *p*-methoxyneophyl 2,6-dimethylbenzenesulfinate, m.p. 57–58.5°.

Analyses and physical properties of the arenesulfinates are summarized in Table III. The nuclear magnetic resonance spectra of these and other arenesulfinates are of interest and will be described in a subsequent paper.

Solvents

Ethanol was dried by treatment with magnesium ethoxide as described by Fieser (24).

Ethanol–water (80% by volume) was prepared by mixing 8 volumes of anhydrous ethanol to which the appropriate amount of base had been added and 2 volumes of boiled distilled water which had previously been equilibrated at 25°.

Ethanol–water (60% by volume) was prepared by mixing 6 volumes of ethanol to which the appropriate amount of base had been added and 4 volumes of boiled distilled water which had previously been equilibrated at 25°.

Kinetic Measurements

A sample of ester was accurately weighed into a 100-ml volumetric flask. A stock solution of the solvent containing the appropriate base was added and the solution was made up to the mark with the solvent. For rates at 90° the sealed ampoule technique was employed. Ampoules were removed from the constant temperature bath controlled to ±0.03° and quenched in ice water. The ampoules were equilibrated to 25° and a 5-ml aliquot was removed by means of a calibrated 5-ml automatic pipette. The 5-ml aliquots were delivered into a 60-ml separatory funnel containing 25 ml of pentane and 10 ml of water. The pentane layer was washed 4 times with 10 ml of water. The pentane layer was dried over anhydrous granular potassium carbonate. The combined water washings were titrated with standard hydrochloric acid (for reactions in which ethoxide was the base) or standard sodium methoxide in methanol using phenolphtholein as the indicator. The residual oil, obtained by removal of the pentane from the dried pentane solution, was diluted with two 1-ml aliquots of carbon disulfide using a 1-ml automatic pipette. The infrared spectrum of the

TABLE IV

Rate of ethanolysis of *p*-methoxyneophyl 2-methylbenzenesulfinate (0.02571 *M*) in anhydrous ethanol with potassium acetate (0.04776 *M*) as base

Time (s)	Base*	Absorbance	$10^4 k_1$ (s^{-1})
0	0.055		
960	0.053	0.0792	1.22
2 700	0.052	0.198	1.20
3 600	0.056	0.250	1.19
4 500	0.051	0.318	(1.31)
5 460	0.057	0.332	1.14
7 200	0.060	0.332	(0.86)
10 800	0.051	0.509	1.14
12 720	0.051	0.572	1.25
18 840	0.055	0.641	1.19
25.5 h	0.045	0.717	
Average			1.19 ± 0.03

*Milliliters of 0.0347 *M* sodium methoxide in methanol required to neutralize the aqueous extracts.

Can. J. Chem. Downloaded from www.nrcresearchpress.com by 210.87.254.42 on 09/05/12
For personal use only.

solution was recorded in the region from 10 to 12 μ with the 20 cm per micron scale using a Perkin–Elmer model 21 infrared spectrophotomer. The reference cell containing carbon disulfide was of the variable spacer type. The values of log (I_0/I) were measured using the base line technique. For rates at 25° the volumetric flask was immersed in the constant temperature bath. Aliquots were removed using a 5-ml automatic pipette and quenched by transferring to a 60-ml separatory funnel containing 25 ml of pentane and 10 ml of water. The rest of the procedure was as described for reactions at 90°.

Controls were run on all the esters to ensure that a linear relationship between absorbance and concentration was obeyed after the extraction procedure had been carried out. A sample rate run is presented in Table IV.

Product Run

A 0.844-g quantity of *p*-methoxyneophyl 2,6-dimethylbenzenesulfinate and 0.447 g of 2,6-lutidine were dissolved in 100 ml of ethanol (60% by volume) and transferred to a 250-ml flask having a constricted neck. The flask was sealed and placed in the 90° constant temperature bath for 46 days. The cooled reaction mixture was poured onto ice containing 1 ml of 6 *N* hydrochloric acid. The mixture was extracted twice with ether. The combined ether extracts were washed twice with saturated aqueous sodium bicarbonate and dried over magnesium sulfate. The ether was removed by careful distillation through a Vigreux column. The residue was separated into ester and alcohol fractions by chromatography on 30 g of alumina. The infrared spectrum of the ester fraction (0.72 g, 85%) showed it to be the starting material, *p*-methoxyneophyl 2,6-dimethylbenzenesulfinate. The infrared spectrum of the alcohol (25 mg, 6%) corresponded to the spectrum of authentic *p*-methoxyneophyl alcohol. The presence of less than 5% of ethyl 2,6-dimethylbenzenesulfinate or 1-*p*-anisyl-2-methyl-2-propanol in the ester and alcohol fractions respectively would not have been detected.

ACKNOWLEDGMENT

The authors gratefully acknowledge the financial assistance given by the National Research Council.

REFERENCES

1. M. P. Balfe, J. Kenyon, and A. Tarnoky. J. Chem. Soc. 446 (1943).
2. J. Kenyon, H. Phillips, and F. M. H. Taylor. J. Chem. Soc. 173 (1933).
3. H. F. Herbrandson and C. M. Cusano. J. Am. Chem. Soc. **83**, 2124 (1961).
4. C. A. Bunton and B. N. Hendy. J. Chem. Soc. 2562 (1962).
5. C. A. Bunton and B. N. Hendy. J. Chem. Soc. 627 (1963).
6. C. L. Arcus, M. P. Balfe, and J. Kenyon. J. Chem. Soc. 485 (1938).
7. A. H. Wragg, J. S. McFadyen, and T. S. Stevens. J. Chem. Soc. 3603 (1958).
8. D. Darwish and R. A. McLaren. Tetrahedron Letters, No. 26, 1231 (1962).
9. D. Darwish and E. A. Preston. Tetrahedron Letters, No. 2, 113 (1964).
10. R. Heck and S. Winstein. J. Am. Chem. Soc. **78**, 4801 (1956).
11. M. E. Hanke. J. Am. Chem. Soc. **45**, 1325 (1923).
12. C. A. Bunton, P. B. D. de la Mare, P. M. Greaseley, D. R. Llewellyn, N. H. Pratt, and J. G. Tillet. J. Chem. Soc. 4751 (1958).
13. P. B. D. de la Mare, J. G. Tillet, and H. F. von Woerden. J. Chem. Soc. 4888 (1962).
14. R. E. Davis. J. Am. Chem. Soc. **84**, 599 (1962).
15. J. F. Bunnett and J. Y. Bassett, Jr. J. Org. Chem. **27**, 2345 (1962).
16. C. K. Ingold. Structure and mechanism in organic chemistry. Cornell University Press, Ithica, N.Y. 1953. p. 347.
17. J. O. Edwards and R. G. Pearson. J. Am. Chem. Soc. **84**, 16 (1962).
18. G. O. Dudek and F. H. Westheimer. J. Am. Chem. Soc. **81**, 2641 (1959).
19. F. Covitz and F. H. Westheimer. J. Am. Chem. Soc. **85**, 1773 (1963).
20. S. Braverman. Unpublished results.
21. E. Heyningen. J. Am. Chem. Soc. **74**, 4862 (1952).
22. K. Rorig, J. D. Johnson, R. W. Hamilton, and T. J. Telinski. Organic syntheses. Vol. 36. John Wiley and Sons, Inc., New York, N.Y. 1956. p. 50.
23. A. I. Vogel. A textbook of practical organic chemistry. 3rd ed. Longmans, Green and Co. 1955. p. 898.
24. L. F. Fieser. Experiments in organic chemistry. 3rd ed. D. C. Heath and Co., Boston, Mass. 1957. p. 286.
25. C. K. Ingold. Structure and mechanism in organic chemistry. Cornell University Press, Ithaca, N.Y. 1953. p. 759.

Can. J. Chem. Downloaded from www.nrcresearchpress.com by 210.87.254.42 on 09/05/12
For personal use only.

Can. J. Chem. Downloaded from www.nrcresearchpress.com by 210.87.254.42 on 09/05/12
For personal use only.

THE REACTION OF UNSATURATED CARBOHYDRATES WITH CARBON MONOXIDE AND HYDROGEN

V. ABSOLUTE STEREOCHEMISTRY OF ANHYDRODEOXYHEPTITOLS FROM 3,4,6-TRI-*O*-ACETYL-D-GLUCAL. STEREOCHEMISTRY OF HYDROFORMYLATION. CONFORMATIONAL ANALYSIS

ALEX ROSENTHAL AND HANS J. KOCH
Department of Chemistry, University of British Columbia, Vancouver, British Columbia
Received November 13, 1964

Dedicated to Professor R. B. Sandin on the Occasion of his Sixty-Eighth Birthday

ABSTRACT

3,4,6-Tri-*O*-acetyl-D-glucal reacted with carbon monoxide and hydrogen in the presence of dicobalt octacarbonyl to yield a mixture of two epimeric anhydrodeoxyheptitols, namely, 4,5,7-tri-*O*-acetyl-2,6-anhydro-3-deoxy-D-*manno*-heptitol (I) and 4,5,7-tri-*O*-acetyl-2,6-anhydro-3-deoxy-D-*gluco*-heptitol (II). De-*O*-acetylation of the mixture, followed by chromatographic separation, yielded crystalline 2,6-anhydro-3-deoxy-D-*manno*-heptitol (III) and 2,6-anhydro-3-deoxy-D-*gluco*-heptitol (IV). Reaction of the mixture of heptitols (I) and (II) with *p*-bromobenzenesulfonyl chloride, followed by fractional crystallization of the brosylates, gave pure 4,5,7-tri-*O*-acetyl-2,6-anhydro-1-*O*-(*p*-bromophenylsulfonyl)-3-deoxy-D-*gluco*-heptitol (VII). The absolute configuration of (VII) has been previously established by X-ray crystallographic analysis. The absolute configuration of (III) was established by correlation with that of (VII). The conversion of compound (II) into various derivatives is described.

Reaction of 3,4,6-tri-*O*-acetyl-D-glucal with carbon monoxide and deuterium afforded 2,6-anhydro-3-deoxy-D-*manno*-heptitol-1,1,3-$^2H_3$ (XIII) and 2,6-anhydro-3-deoxy-D-*gluco*-heptitol-1,1,3-$^2H_3$ (XIV). Examination of the nuclear magnetic resonance (n.m.r.) spectra of the normal and deuterated anhydrodeoxyheptitols confirmed the structural assignments and showed that *cis* addition to the double bond took place to give (XIV).

Comparison of the exchange reaction of sodium iodide with 4,5,7-tri-*O*-acetyl-2,6-anhydro-3-deoxy-1-*O*-tosyl-D-*gluco*-heptitol (VIII) and with 4,5,7-tri-*O*-acetyl-2,6-anhydro-3-deoxy-1-*O*-tosyl-D-*manno*-heptitol (XV) revealed that the equatorial primary tosyloxy group of (VIII) was exchanged by iodine twice as readily as the axial primary tosyloxy group of (XV).

Preceding papers in this series (1, 2) have reported that pentals react preferentially at C-1 with carbon monoxide and hydrogen to yield epimeric anhydrodeoxyhexitols. This paper deals with the extension of the oxo reaction to 3,4,6-tri-*O*-acetyl-D-glucal. A preliminary report of part of this work has already appeared (3).

When 3,4,6-tri-*O*-acetyl-D-glucal was subjected to the oxo reaction at a temperature of about 130°, an almost quantitative yield of a mixture of 4,5,7-tri-*O*-acetyl-2,6-anhydro-3-deoxy-D-*manno*-heptitol (I) and 4,5,7-tri-*O*-acetyl-2,6-anhydro-3-deoxy-D-*gluco*-heptitol (II) was obtained. De-*O*-acetylation of this mixture with methanolic sodium methoxide afforded the crystalline parent anhydrodeoxyheptitols (III) and (IV) which were readily separated by paper chromatography or cellulose column chromatography. Both heptitols were also converted into crystalline acetates.

Alternatively, the oxo product mixture was separated in the following ways. Tosylation of the mixture of (I) and (II) yielded the monotosylate esters (VIII) and (XV), which, on fractional crystallization, afforded pure crystalline 4,5,7-tri-*O*-acetyl-2,6-anhydro-3-deoxy-1-*O*-tosyl-D-*gluco*-heptitol (VIII). Chromatographic separation of the monotosylates by thin-layer chromatography (t.l.c.) gave both epimers. Similarly, treatment of (I) and (II) with *p*-bromobenzenesulfonyl bromide, followed by fractional crystallization of the

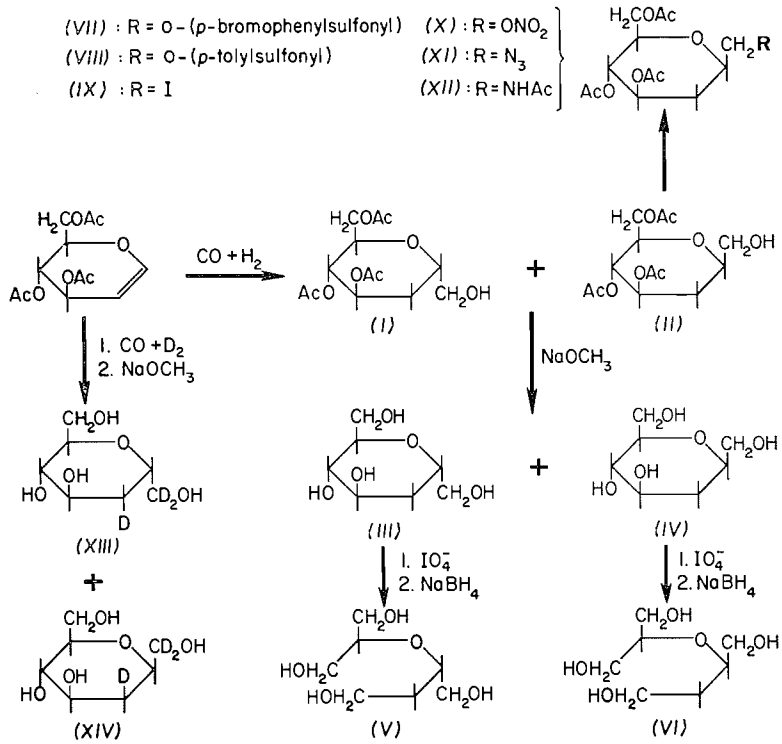

brosylates, produced pure 4,5,7-tri-*O*-acetyl-2,6-anhydro-1-*O*-(*p*-bromobenzenesulfonyl)-3-deoxy-D-*gluco*-heptitol (VII). The purity of the tosylate and brosylate esters was established by their conversion into 4,5,7-tri-*O*-acetyl-2,6-anhydro-1,3-dideoxy-1-iodo-D-*gluco*-heptitol (IX), which, on treatment with silver nitrate, yielded the 1-*O*-nitro derivative (X). Reduction of the latter substance with hydrogen over palladium, followed by de-*O*-acetylation, gave the crystalline anhydrodeoxyheptitol (IV).

In order that the point of attachment of the hydroxymethyl group to the glycal might be ascertained, the heptitols (III) and (IV) were first oxidized with periodate (1 mole consumed by each) and the resulting dialdehydes were then reduced with sodium borohydride. The fact that enantiomeric tetrol ethers (V) and (VI) were produced established that the heptitols (III) and (IV) are epimers which differ in the configuration of C-2. This assignment of structure was confirmed by analysis of the n.m.r. spectra of the heptitols. The spectra of both heptitols (see Fig. 1, *a* and *c*) exhibit a multiplet of peaks at $\delta = 1.5$ to 2 having an area which corresponds to the two methylenic hydrogens on C-3.

The configuration of C-2 of both epimeric 2,6-anhydro-3-deoxyheptitols was then readily established by application of n.m.r. spectroscopy, as previously described (1), to the 3-deoxy-3-deuterioanhydroheptitols (XIII) and (XIV) which were produced when 3,4,6-tri-*O*-acetyl-D-glucal was caused to react with carbon monoxide and deuterium. Thus, as shown in Fig. 1, *b*, the chemical shift and quartet structure (width of 17.7 c.p.s.) of the signal of intensity one at around $\delta = 1.7$ require the C-3 proton to be in an axial orientation and coupled with the C-4 axial and C-2 equatorial hydrogens. On the other hand, as depicted in Fig. 1, *d*, the corresponding narrower quartet of signals (width 7.3 c.p.s.) of intensity one at the lower field ($\delta = 1.94$) necessitates that the C-3 proton of compound (XIV) is in an equatorial orientation and coupled with the C-4 and C-2 axial hydrogens.

Can. J. Chem. Downloaded from www.nrcresearchpress.com by 210.87.254.42 on 09/05/12
For personal use only.

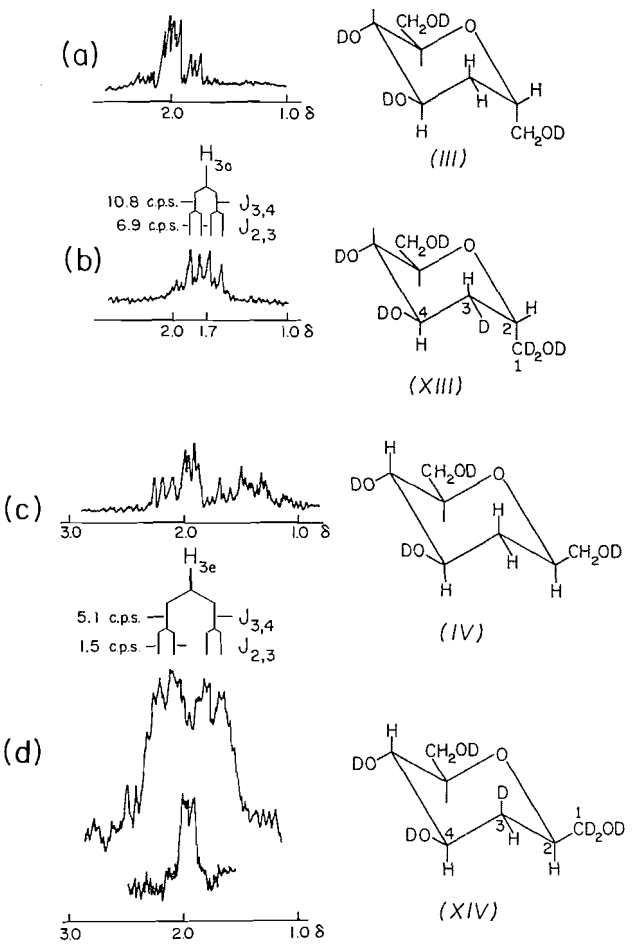

FIG. 1. Proton n.m.r. spectra in D_2O solution at 60 Mc/s with chemical shifts given in p.p.m. from tetramethylsilane as zero: (*a*) 2,6-anhydro-3-deoxy-D-*manno*-heptitol; (*b*) 2,6-anhydro-3-deoxy-D-*manno*-heptitol-1,1,3-$^2H_3$; (*c*) 2,6-anhydro-3-deoxy-D-*gluco*-heptitol; (*d*) 2,6-anhydro-3-deoxy-D-*gluco*-heptitol-1,1,3-$^2H_3$. (Only signals of protons attached to C-4 are shown.)

Therefore, compounds (XIII) and (XIV) are 2,6-anhydro-3-deoxy-D-*manno*-heptitol-1,1,3-$^2H_3$ (*cis*) and 2,6-anhydro-3-deoxy-D-*gluco*-heptitol-1,1,3-$^2H_3$ (*cis*), respectively. Evidently, the deuterated heptitols (XIII) and (XIV) must have been formed by a *cis* addition of the hydroxymethyl group and of the deuterium to the 1,2-unsaturated bond of 3,4,6-tri-*O*-acetyl-D-glucal. Unequivocal confirmation of the structures of the heptitols was provided by carrying out an independent X-ray crystallographic analysis (4) of a derivative of compound (II), namely, 4,5,7-tri-*O*-acetyl-2,6-anhydro-1-*O*-(*p*-bromobenzenesulfonyl)-3-deoxy-D-*gluco*-heptitol (VII).

The utility of the monotosylate ester (VIII) in synthesis was demonstrated by its conversion into the 1-amino derivative. Treatment of compound (VIII) with ammonia in methanol afforded the 1-amino derivative, which was isolated in the fully acetylated form (XII). Attempts to convert the tosylate ester (VIII) into the amino derivative via the monoiodo derivative (IX), thence into the azido derivative, followed by catalytic reduction of the azido compound to (XII), were not successful and were abandoned.

Can. J. Chem. Downloaded from www.nrcresearchpress.com by 210.87.254.42 on 09/05/12
For personal use only.

Can. J. Chem. Downloaded from www.nrcresearchpress.com by 210.87.254.42 on 09/05/12
For personal use only.

Very little work has been reported (5) on correlating the reactivity of primary hydroxyl groups of carbohydrates with their orientation. From this work, which has dealt mainly with the polyol bicyclic acetal derivatives, it has been adduced that the axially oriented tosyloxy group reacts with sodium iodide with greater ease than the equatorial group when both groups are in similar environments (5). Preferential reaction at the axial tosyloxy group would not be expected in a reaction that seems to be (6) rather strongly retarded by an increase in the size of substituents in the vicinity of tosyloxy groups.

Since an acetal ring is known to greatly reduce the chemical reactivity of adjacent tosyloxy groups (7–9), we believed that carbohydrates possessing the pyran ring and only one tosyloxy group would be suitable model substances for correlating chemical reactivity of the tosyloxy group and its orientation. The mono-1-*O*-tosylate derivative of 4,5,7-tri-*O*-acetyl-2,6-anhydro-3-deoxy-D-*gluco*-heptitol and of 4,5,7-tri-*O*-acetyl-2,6-anhydro-3-deoxy-D-*manno*-heptitol appeared to be ideal model compounds because these epimers differ in one aspect only, namely, one possesses an equatorial tosyloxy group whereas the other has an axial tosyloxy group. X-ray crystallographic studies have definitely established that 4,5,7-tri-*O*-acetyl-2,6-anhydro-3-deoxy-1-*O*-tosyl-D-*gluco*-heptitol (VIII) exists in the chair conformation with all groups in equatorial positions (4). On the bases of the facts that 4,5,7-tri-*O*-acetyl-2,6-anhydro-3-deoxy-1-*O*-tosyl-D-*manno*-heptitol (XV) was prepared by tosylation of 4,5,7-tri-*O*-acetyl-2,6-anhydro-3-deoxy-D-*manno*-heptitol following the same procedure as utilized in the preparation of its epimer, and the n.m.r. spectra of the two tosylates were similar, the tosyl group was assumed to be on C-1. If there had been acetyl migration before the tosylation, then the tosyl group would have been on a secondary hydroxyl group. Because replacements by iodide of a tosyloxy group on a secondary hydroxy under the conditions used in our work are not known to occur (10), the assumption that compound (XV) had its tosylate group on C-1 appears to be valid.

Samples of 4,5,7-tri-*O*-acetyl-2,6-anhydro-3-deoxy-1-*O*-tosyl-D-*gluco*-heptitol (VIII) and of 4,5,7-tri-*O*-acetyl-2,6-anhydro-3-deoxy-1-*O*-tosyl-D-*manno*-heptitol (XV) were allowed to react with sodium iodide in acetone at 100° in closed tubes for varying periods of time as shown in the Experimental section. The solutions were equimolecular with respect to each other. The extent of the exchange reaction was determined by weighing the sodium *p*-toluenesulfonate precipitated. In the figures quoted in the Experimental section, the solubility of sodium *p*-toluenesulfonate in a solution of acetone and sodium iodide was taken into account. The results clearly show that the equatorial tosyloxy group at C-1 of (VIII) was replaced at about double the rate by iodine than was the axial tosyloxy group at C-1 of (XV).

When a 0.01-mole mixture of 4,5,7-tri-*O*-acetyl-2,6-anhydro-3-deoxy-D-*manno*-heptitol (I) and 4,5,7-tri-*O*-acetyl-2,6-anhydro-3-deoxy-D-*gluco*-heptitol (II) was allowed to react with 0.011 mole of *p*-toluenesulfonyl chloride at room temperature for 22 h, all of compound (II) was tosylated, whereas only a trace of compound (I) was converted into the tosylate (XV).

EXPERIMENTAL

General Considerations

General conditions for chromatographic separations have been described previously (1). Preparation of *p*-nitrobenzoyl derivatives was carried out by a procedure similar to that described by Gorin (11).

Reaction of 3,4,6-Tri-O-acetyl-D-glucal with Carbon Monoxide and Hydrogen to Yield 2,6-Anhydro-3-deoxy-D-manno-heptitol (III) and 2,6-Anhydro-3-deoxy-D-gluco-heptitol (IV)

3,4,6-Tri-*O*-acetyl-D-glucal (12) was caused to react with carbon monoxide and hydrogen in the presence of preformed dicobalt octacarbonyl according to a procedure previously described (1). The product was de-*O*-acetylated with sodium methoxide to yield a mixture of compounds (III) and (IV). Fractionation of

the mixture of anhydrodeoxyheptitols was carried out by preparative paper chromatography or by cellulose column chromatography at 37°.

The ratio of (I) and (II) depended on the temperature of the reaction. At 130° it was almost equimolar.

Characterization of Fractions (III) and (IV)

*Fraction (III) (2,6-anhydro-3-deoxy-*D*-manno-heptitol).*—This fraction was crystallized from methanol – isopropyl ether; m.p. 152–153°, $[\alpha]_D^{20}$ +60° (*c*, 1.4, water), R_F = 0.21.

Anal. Calcd. for $C_7H_{14}O_5$: C, 47.18; H, 7.92. Found: C, 47.30; H, 7.82.

*1,4,5,7-Tetra-O-acetyl-2,6-anhydro-3-deoxy-*D*-manno-heptitol.*—Fraction (III) was acetylated with acetic anhydride in the presence of sodium acetate to yield a tetra-*O*-acetyl derivative which was first purified by chromatography on silica gel using 2.5% methanol in benzene as developer and then crystallized from ether – light petroleum ether; m.p. 123–124°, $[\alpha]_D^{20}$ +28° (*c*, 0.5, acetone).

Anal. Calcd. for $C_{15}H_{22}O_9$: C, 52.02; H, 6.40. Found: C, 52.53; H, 6.55.

*Fraction (IV) (2,6-anhydro-3-deoxy-*D*-gluco-heptitol).*—This fraction was crystallized from methanol – isopropyl ether; m.p. 137–138°, $[\alpha]_D^{20}$ −1° (*c*, 3.5, water), R_F = 0.30.

Anal. Calcd. for $C_7H_{14}O_5$: C, 47.18; H, 7.92. Found: C, 47.19; H, 7.63.

*1,4,5,7-Tetra-O-acetyl-2,6-anhydro-3-deoxy-*D*-gluco-heptitol.*—Fraction (IV) was acetylated and purified in the same way as described above to yield a tetra-*O*-acetyl derivative; m.p. 79–80°, $[\alpha]_D^{21}$ +2° (*c*, 0.5, acetone).

Anal. Calcd. for $C_{15}H_{22}O_9$: C, 52.02; H, 6.40. Found: C, 52.48; H, 6.50.

Structure and Stereochemistry of Compounds (III) and (IV)

*2-Deoxy-3-O-(1,3-dihydroxy-2-propyl)-*D*-glycero-tetritol (V) from 2,6-Anhydro-3-deoxy-*D*-manno-heptitol (III)*

Oxidation of 2,6-anhydro-3-deoxy-D-*manno*-heptitol with 0.1 *M* periodic acid (1 mole consumed), followed by reduction of the resulting dialdehyde with sodium borohydride in water according to the procedure described by Gorin (11), gave the tetrol ether (V) as a sirup; $[\alpha]_D^{19}$ −25° (*c*, 0.7, methanol). This sirup was converted into a tetra-*O*-(*p*-nitrobenzoyl) derivative; m.p. 149–150.5°, $[\alpha]_D^{22}$ −22° (*c*, 1.5, chloroform).

Anal. Calcd. for $C_{35}H_{28}O_{17}N_4$: C, 54.13; H, 3.63; N, 7.21. Found: C, 54.55; H, 3.71; N, 7.30.

*2-Deoxy-3-O-(1,3-dihydroxy-2-propyl)-*L*-glycero-tetritol (VI) from 2,6-Anhydro-3-deoxy-*D*-gluco-heptitol (IV)*

Periodate oxidation and sodium borohydride reduction of the dialdehyde from (IV) under similar conditions to those described above gave the tetrol ether (VI); $[\alpha]_D^{22}$ +26° (*c*, 2.9, water). This formed a tetra-*O*-(*p*-nitrobenzoyl) derivative which was recrystallized from ethyl acetate – petroleum ether; m.p. 151–152°; $[\alpha]_D^{21}$ +22° (*c*, 1.2, chloroform).

Anal. Calcd. for $C_{35}H_{28}O_{17}N_4$: C, 54.13; H, 3.63; N, 7.21. Found: C, 54.50; H, 3.94; N, 7.50.

The infrared spectra of the tetra-*O*-(*p*-nitrobenzoyl) derivatives of the tetrol ethers (V) and (VI) were identical.

Alternative Methods of Separation of the Heptitols (I) and (II) by Conversion to 1-O-Sulfonate Esters (VII) and (VIII)

*A. 4,5,7-Tri-O-acetyl-2,6-anhydro-1-O-(p-bromophenylsulfonyl)-3-deoxy-*D*-gluco-heptitol (VII)*

p-Bromobenzenesulfonyl bromide (2.6 g) was added to 2 g of an ice-cold anhydrous mixture of oxo product (I) and (II) dissolved in anhydrous pyridine (15 ml). After the mixture was left at room temperature for 30 h, 20 ml of water was added and the mixture left to stand for 24 h. The solution was then extracted with three portions of chloroform. The combined chloroform extracts were washed with water and then dried over anhydrous sodium sulfate. Evaporation of the chloroform left a residue which was twice recrystallized from methanol, and then from methanol–water; yield 1.01 g; m.p. 104°; $[\alpha]_D^{22}$ −10° (*c*, 3, chloroform).

Anal. Calcd. for $C_{19}H_{23}O_{10}SBr$: C, 43.58; H, 4.43; S, 6.13; Br, 15.27. Found: C, 43.57; H, 4.47; S, 6.32; Br, 15.26.

The proof of structure of compound (VII) by X-ray crystallographic studies has been described previously (4).

*B. 4,5,7-Tri-O-acetyl-2,6-anhydro-3-deoxy-1-O-tosyl-*D*-gluco-heptitol (VIII)*

The tosylate ester (VIII) was prepared by tosylation of the mixture of compounds (I) and (II) following the same procedure as used in the preparation of the brosylate ester (VII). Fractional crystallization of the tosylates gave compound (VIII) in pure form; m.p. 117–118°, $[\alpha]_D^{20}$ −5° (*c*, 0.5, chloroform); n.m.r. (given in δ units; spectra obtained in deuterated chloroform): 2.0 (acetyl and CH_2, area = 11H), 2.37 (CH_3, area = 3H), 3.55 (area = 2H), 3.95 (multiplet, area = 4H), 4.85 (area = 2H), 7.17 (doublet, area = 2H), 7.61 (doublet, area = 2H).

Anal. Calcd. for $C_{20}H_{26}O_{10}S$: C, 52.50; H, 5.52. Found: C, 52.20; H, 5.51.

*4,5,7-Tri-O-acetyl-2,6-anhydro-3-deoxy-1-O-tosyl-*D*-manno-heptitol (XV)*

An amount of 4.8 g of the oxo products (I) and (II) was allowed to react with 6.0 g of *p*-toluenesulfonyl chloride in 125 ml of anhydrous pyridine at room temperature for 12 h and then heated at 100° for 1 h. Work-up of the product in the usual way gave 5.06 g of a mixture of compounds (VIII) and (XV). Thin-layer chromatographic separation of this mixture (0.45 g) on silica gel using toluene–ether (2:1, v:v), or isopropyl

Can. J. Chem. Downloaded from www.nrcresearchpress.com by 210.87.254.42 on 09/05/12
For personal use only.

ether, as developer afforded 0.30 g of (VIII) and 0.08 g of (XV). The tosylates were detected by spraying the samples with diphenylamine in methanol (1% solution) and viewing them under ultraviolet light.

4,5,7-Tri-*O*-acetyl-2,6-anhydro-3-deoxy-1-*O*-tosyl-D-*manno*-heptitol (XV) was obtained as an oil; $[\alpha]_D^{23}$ +30° (*c*, 1.7, chloroform); n.m.r.: 2.0 (11H), 2.40 (3H), 3.55 (2H), 4.00 (multiplet, 4H), 4.90 (multiplet, 2H), 7.17 (2H), 7.65 (2H).

Anal. Calcd. for $C_{20}H_{26}O_{10}S$: C, 52.50; H, 5.52. Found: C, 52.36; H, 6.18.

Comparative Rate of Tosylation of Oxo Products (I) and (II)

An amount of 0.010 mole of oxo product mixture (70% of 4,5,7-tri-*O*-acetyl-2,6-anhydro-3-deoxy-D-*manno*-heptitol (I) and 30% of 4,5,7-tri-*O*-acetyl-2,6-anhydro-3-deoxy-D-*gluco*-heptitol (II)) was allowed to react with 0.011 mole of *p*-toluenesulfonyl chloride (0.011 mole) at room temperature for varying periods of time and the product analyzed by t.l.c. on silica gel using isopropyl ether as developer. Compound (II) was completely tosylated after 22 h whereas only a trace of compound (I) was converted into the tosylate (XV) during the same time.

4,5,7-Tri-O-acetyl-2,6-anhydro-1,3-dideoxy-1-iodo-D-gluco-heptitol (IX)

4,5,7-Tri-*O*-acetyl-2,6-anhydro-3-deoxy-1-*O*-tosyl-D-*gluco*-heptitol was allowed to react with sodium iodide in acetone in a closed tube at 100° for 6 h to afford 4,5,7-tri-*O*-acetyl-2,6-anhydro-1,3-dideoxy-1-iodo-D-*gluco*-heptitol; m.p. 100°, $[\alpha]_D^{22}$ −13° (*c*, 0.1, chloroform).

Anal. Calcd. for $C_{13}H_{19}O_7I$: C, 37.69; H, 4.62; I, 30.64. Found: C, 37.58; H, 4.35; I, 30.58.

Treatment of the brosylate (VII) with sodium iodide in acetone also yielded compound (IX).

4,5,7-Tri-O-acetyl-2,6-anhydro-3-deoxy-1-O-nitro-D-gluco-heptitol (X)

4,5,7-Tri-*O*-acetyl-2,6-anhydro-1,3-dideoxy-1-iodo-D-*gluco*-heptitol dissolved in acetonitrile was caused to react with silver nitrate according to a procedure previously described (10). The product (X) was recrystallized from ether – light petroleum ether; m.p. 79°, $[\alpha]_D^{22}$ −8° (*c*, 0.7, acetone).

Anal. Calcd. for $C_{13}H_{19}O_{10}N$: C, 44.71; H, 5.48; N, 4.08. Found: C, 44.58; H, 5.12; N, 4.06.

Conversion of 4,5,7-Tri-O-acetyl-2,6-anhydro-3-deoxy-1-O-nitro-D-gluco-heptitol (X) into 2,6-Anhydro-3-deoxy-D-gluco-heptitol (IV)

An amount of 30 mg of compound (X) dissolved in anhydrous methanol (10 ml) was hydrogenated over palladium black (3 mg) at atmospheric pressure and room temperature for 75 min. After removal of the catalyst, the solvent was evaporated under vacuum and the product then dried. De-*O*-acetylation of the residual sirup with methanolic sodium methoxide gave a compound having a melting point, R_F value, and infrared spectrum identical with those of authentic 2,6-anhydro-3-deoxy-D-*gluco*-heptitol (IV).

1-Acetamido-4,5,7-tri-O-acetyl-2,6-anhydro-1,3-dideoxy-D-gluco-heptitol (XII)

An amount of 0.148 g of 4,5,7-tri-*O*-acetyl-2,6-anhydro-3-deoxy-1-*O*-tosyl-D-*gluco*-heptitol was added to an ammonia-saturated solution of methanol (12 ml). The reactants were heated in a sealed tube at 100° for 65 h. After the ammonia evaporated, the methanol was removed under reduced pressure and the product then dried. Acetylation of the product with 4 ml of acetic anhydride and 4 ml of pyridine in the usual way gave the fully acetylated amino compound (XII). Purification of (XII) was achieved by column chromatography on silica gel using benzene–methanol (96:4, v:v) as developer. Recrystallization of the product (0.065 g) from acetone – isopropyl ether – heptane gave pure (XII); m.p. 136–137°, $[\alpha]_D^{22}$ −3° (*c*, 1.8, chloroform); n.m.r.: 2.05 (multiplet, area = 14H), 3.5 (multiplet, area = 4H), 4.1 (multiplet, area = 2H), 4.82 (multiplet, 2H), 5.75 (broad, area = 1H).

Anal. Calcd. for $C_{15}H_{23}O_8N$: C, 52.17; H, 6.71; N, 4.06. Found: C, 51.94; H, 7.01; N, 3.94.

Attempt to Prepare 1-Acetamido-2,6-anhydro-1,3-dideoxy-D-gluco-heptitol from Compound (IX)

An amount of 0.24 g of 4,5,7-tri-*O*-acetyl-2,6-anhydro-1,3-dideoxy-1-iodo-D-*gluco*-heptitol (IX) was caused to react with sodium azide (0.5 g) in acetone (3 ml) and water (2 ml) for 10 h at a temperature of 110–120 °C in a sealed tube. After the tube was opened, 5 ml of ether was added. The ether layer was washed with water, dried over an anhydrous sodium sulfate, and then evaporated. The resulting azido compound (XI), dissolved in acetone, was decolorized by passage through a short column of charcoal; yield 0.083 g. Compound (XI) showed an azide peak at 2 120 cm^{-1} in the infrared spectrum. After it was dissolved in ethanol (20 ml), it was hydrogenated at atmospheric pressure for 6 h over platinum oxide (0.022 g) according to a procedure previously described (13). After removal of the catalyst, the solvent was evaporated under reduced pressure. The product was then acetylated in the usual way using acetic anhydride and pyridine. Addition of water to the reaction product gave a trace of crystalline product which was removed by filtration. After removal of the volatile components, the product was analyzed by thin-layer chromatography and shown to contain a trace of compound (XII).

Reaction of 3,4,6-Tri-O-acetyl-D-glucal with Carbon Monoxide and Deuterium to Yield 2,6-Anhydro-3-deoxy-D-manno-heptitol-1,1,3-$^2H_3$ (cis) (XIII) and 2,6-Anhydro-3-deoxy-D-gluco-heptitol-1,1,3-$^2H_3$ (cis) (XIV)

3,4,6-Tri-*O*-acetyl-D-glucal was caused to react with carbon monoxide and deuterium at 130°, under

Can. J. Chem. Downloaded from www.nrcresearchpress.com by 210.87.254.42 on 09/05/12
For personal use only.

conditions similar to those used in the preparation of the normal anhydrodeoxyheptitols, to yield the above-mentioned deuterated heptitols (XIII) and (XIV). The stereochemisty of the deuterium atom on C-3 of both heptitols was determined by proton n.m.r. analysis (see Discussion).

Comparative Iodine Exchange Experiments of Tosylates (VIII) and (XV)

In each experiment each Carius tube contained 9.1 mg of the tosylate, 9.1 mg of sodium iodide, and 1.4 ml of acetone. After the tubes were cooled in solid carbon dioxide, they were sealed and then heated at 100° (±0.1) for varying periods of time. The amount of sodium *p*-toluenesulfonate was collected in a sintered-glass crucible, washed with 2 ml dry acetone, and dried under reduced pressure before they were weighed. A correction of 0.20 mg of sodium *p*-toluenesulfonate was added to each weight as this amount dissolved in the acetone at room temperature. The results are as follows: % exchange of tosylate by iodine of compound (VIII) 14 (5 min), 18 (10 min), 41 (23 min), 46 (41 min), 51 (60 min), 59 (90 min), 93 (162 min); % exchange of tosylate by iodine of compound (XV) 20 (30 min), 32 (60 min), 41 (120 min), 47 (300 min), 56 (420 min), 73 (630 min).

ACKNOWLEDGMENTS

The authors gratefully acknowledge the financial assistance of the National Cancer Institute of Canada, the National Research Council of Canada, the University of British Columbia Research Grant, and the Petroleum Research Fund administered by the American Chemical Society for support of this work.

Part of the preliminary experimental work was done by Mr. T. Field and Mr. R. Bolster.

The senior author (A. R.) expresses his gratitude to University Chemical Laboratory, University of Cambridge, for use of its facilities during the writing of this manuscript.

REFERENCES

1. A. ROSENTHAL and D. ABSON. Can. J. Chem. **42**, 1811 (1964).
2. A. ROSENTHAL and H. J. KOCH. Can. J. Chem. **42**, 2025 (1964).
3. A. ROSENTHAL and D. READ. Methods in carbohydrate chemistry. Vol. II. *Edited by* R. L. Whistler and M. L. Wolfrom. Academic Press, New York, N.Y. 1963. p. 457.
4. A. CAMERMAN, J. TROTTER, H. J. KOCH, and A. ROSENTHAL. Can. J. Chem. **42**, 2630 (1964).
5. J. A. MILLS. Advan. Carbohydrate Chem. **10**, 39 (1955).
6. R. S. TIPSON. Advan. Carbohydrate Chem. **8**, 107 (1953).
7. A. B. FOSTER, W. G. OVEREND, M. STACEY, and L. F. WIGGINS. J. Chem. Soc. 2542 (1949).
8. M. L. WOLFROM, W. J. BURKE, and E. A. METCALF. J. Am. Chem. Soc. **69**, 1667 (1947).
9. A. J. NESS, R. M. HANN, and C. S. HUDSON. J. Am. Chem. Soc. **75**, 132 (1953).
10. J. W. OLDHAM and J. K. RUTHERFORD. J. Am. Chem. Soc. **54**, 366 (1932).
11. P. A. GORIN. Can. J. Chem. **38**, 641 (1960).
12. B. HELFERICH, E. N. MULCAHY, and H. ZIEGLER. Ber. **87**, 233 (1954).
13. R. W. JEANLOZ and A. M. C. RAPIN. J. Org. Chem. **28**, 2978 (1963).

Can. J. Chem. Downloaded from www.nrcresearchpress.com by 210.87.254.42 on 09/05/12
For personal use only.

Can. J. Chem. Downloaded from www.nrcresearchpress.com by 210.87.254.40 on 09/05/12
For personal use only.

SOME TRANSFORMATIONS OF TETRACYCLINE AT THE 4-POSITION[1]

ROBERT K. BLACKWOOD AND CHARLES R. STEPHENS
Medical Research Laboratories, Chas. Pfizer and Co., Inc., Groton, Connecticut
Received November 13, 1964

Dedicated to Professor R. B. Sandin on the Occasion of his Sixty-Eighth Birthday

ABSTRACT

Reactions leading to the replacement of the 4-dimethylamino group of tetracycline by keto, hydroxy, hydroxyimino, hydrozono, and amino groups are reported.

INTRODUCTION

Only a limited number of transformations of tetracycline at C-4 have been previously reported: 4-dedimethylaminotetracyclines (3, 4), 4-epitetracyclines (5), and tetracycline methiodides (4, 6). An extension of earlier halogenation studies (7) has provided an entrée to further modification at this position. The chemistry investigated should be adaptable to the preparation of a broad variety of related derivatives.

DISCUSSION

The reaction of *amphoteric* tetracycline (I) with N-chlorosuccinimide in aqueous solvents to yield 11*a*-chlorotetracycline-6,12-hemiketal (II) has been described (7). A less-than-drastic change in reaction conditions—treatment of tetracycline *hydrochloride* with N-chlorosuccinimide in water—leads to rapid precipitation of a very different product, which we have characterized as 4-oxo-4-dedimethylaminotetracycline-4,6-hemiketal (III). Carbonyl absorption at 5.7 μ and ultraviolet absorption in acid (8-hydroxytetralone and unmodified A-ring chromophores) at first suggested possible close structural analogy to 11*a*-substituted tetracyclines (e.g. XV, cf. ref. 7). However, in excess methanolic sodium hydroxide, the ultraviolet absorption indicated that III is enolic, suggesting alternative analogy to 12*a*-epi-4-dedimethylamino-5-hydroxytetracycline (XVI, cf. refs. 6 and 8), which is isolated in the completely ketonic form, but is also enolized under basic conditions. Analyses on III confirmed suspected loss of the dimethylamine, and, further, showed that it contains additional oxygen, *but no chlorine*. The chemical properties of III, detailed below, demonstrate the presence, or potential presence, of a ketone group at C-4 and retention of the *cis* A- to B-ring juncture. No additional infrared absorption beyond that seen with compounds such as XV and XVI is noted in the carbonyl region. This and the unmodified A-ring ultraviolet chromophore in acid lead to the conclusion that the C-4 ketone is not free. By employment of the now firmly established stereochemistry of tetracycline (I, cf. ref. 9), model studies clearly indicate that the only reasonable structure which will account for all of the facts is that depicted in structure III, which results from formation of an internal hemiketal between the 6-hydroxyl and the newly formed 4-oxo group.

The same reaction has been applied successfully to 11*a*-chlorotetracycline-6,12-hemiketal (II) to provide the 11*a*-chloro-4-oxo analogue (V). Structural assignment is based

[1]*Much of the work described herein has been the subject of a preliminary communication (1). Similar independent studies employing 6-demethyltetracyclines have been reported by a group at Lederle Laboratories (2).*

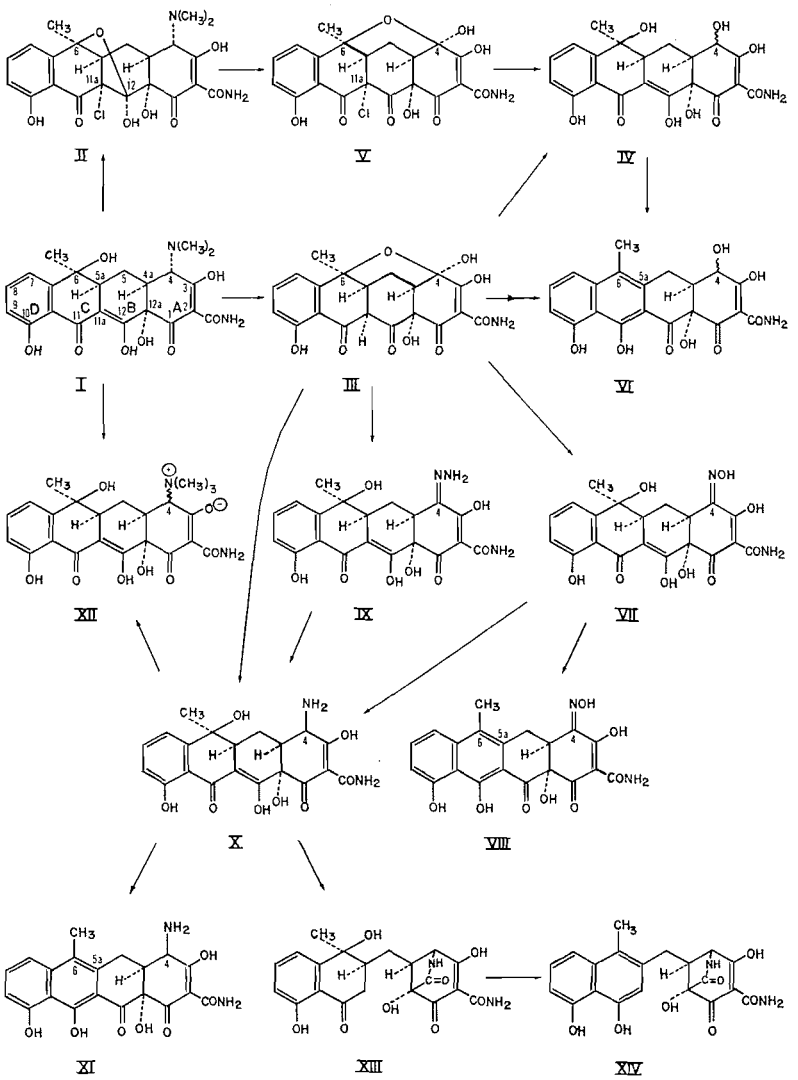

on ultraviolet absorption in methanol – hydrochloric acid (virtually identical with that of the precursor, II), infrared absorption in the carbonyl region (closely analogous to those of III, XV, and XVI), and catalytic reduction to the alcohol (IV) with uptake of 2 equivalents of hydrogen.

The reaction which leads to formation of the 4-oxotetracyclines (III and V) appears to be of a novel type insofar as ketone formation is concerned, although aldehydes have been reported as products in prior studies on the interaction of tertiary amines with N-bromosuccinimide (10) and with hypochlorous acid (11). In the case of the N-bromosuccinimide reaction, initial bromination on carbon adjacent to nitrogen has been indicated (13). We would, therefore, suggest that, in the case of tetracycline, formation of the 4-oxo derivative occurs as shown in Reaction Scheme 1. Esse *et al.* (2), on the basis of additional evidence, have also proposed an imine intermediate in connection with their analogous studies on 6-demethyltetracyclines.

Can. J. Chem. Downloaded from www.nrcresearchpress.com by 210.87.254.40 on 09/05/12
For personal use only.

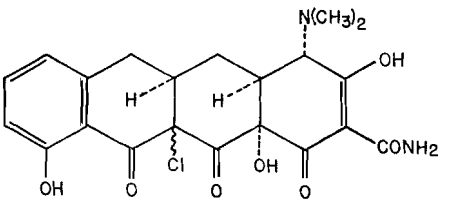

XV

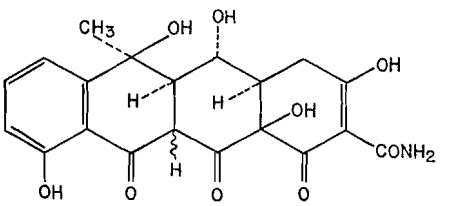

XVI

4-Dedimethylamino-4-oxotetracycline-4,6-hemiketal (III) is readily reduced to the alcohol (IV, e.g. by sodium hydrosulfite, zinc combination, or catalytic hydrogenation). The latter shows the typical ultraviolet chromophores of tetracycline and no infrared carbonyl bands below 6 μ. The alcohol in turn is converted by acid degradation to its 5a,6-anhydro derivative (VI). Preliminary evidence indicates that the same anhydro alcohol is obtained by degradation of the 4,6-hemiketal in anhydrous hydrogen fluoride followed by reduction.

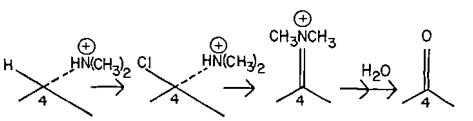

REACTION SCHEME 1.

Reaction of hydrazine and of hydroxylamine with the 4-oxo derivative (III) produces hydrazone (IX) and oxime (VII) respectively. The C,D-β-diketone system in these compounds is enolic, with the now more highly conjugated A-ring ultraviolet chromophores shifted to longer wavelengths. Both compounds are readily reduced to 4-epi-N^4,N^4-didemethyltetracycline (X). Under the conditions which we have employed (sodium hydrosulfite, zinc – acetic acid, or catalytic hydrogenation), it appears that the primary sight of reduction is the N—N or the N—O bond, rather than the C=N double bond. Thus, we have seen no evidence of intermediate hydrazines or hydroxylamines in these reactions. Furthermore, a major by-product in the case of sodium hydrosulfite reduction of VII or IX in aqueous solvents is the 4-hydroxy derivative (IV). Since there is no apparent hydrolysis in the absence of the reducing agent, it is proposed that there is initial reduction to an imine, part of which is reduced to amine and part of which is hydrolyzed to ketone (III) and then reduced to alcohol (IV). The amine (X) may also be obtained directly from the 4-ketone by reductive amination.[2]

[2]*Esse et al. (2) have reported extensively on reductive amination of the 6-demethyl analogue of III. They employed a variety of primary amines, although they did not describe use of ammonia. They have also assigned the 4-epi configuration to their alkylamino products and have shown them to contain the normal more active epimer as a minor component.*

Can. J. Chem. Downloaded from www.nrcresearchpress.com by 210.87.254.40 on 09/05/12
For personal use only.

Can. J. Chem. Downloaded from www.nrcresearchpress.com by 210.87.254.40 on 09/05/12
For personal use only.

Assignment of stereochemistry at C-4*a* in the 4-amino derivative (X) and its precursors is based on smooth conversion of X to tetracycline methyl betaine (XII) by reaction with methyl iodide, in the presence of excess propylene oxide as an acid scavenger.[3] Tentative assignment of stereochemistry at C-4 was earlier (1) deduced from the short wavelength ultraviolet absorption (almost identical with that of 4-epitetracycline) and from the presence of a minor more antibacterial substance in all preparations of the amine.[2] Unequivocal assignment of stereochemistry at C-4 in compound X derives from degradation studies in hot aqueous bicarbonate, which followed earlier studies by Korst and Butler (12) using an N^4-demethyltetracycline prepared by an unrelated reaction sequence. Under these conditions, the normal epimer persists, and can be readily separated from the degradation product, which has been characterized as the lactam, XIII. This non-basic compound is isomeric with its precursor and possesses 8-hydroxytetralone—A-ring ultraviolet chromophores and infrared absorption at 5.7 μ. It is degraded in acid to compound XIV, which displays ultraviolet absorption typical of 1,8-dihydroxynaphthalene and A-ring chromophores as well as retention of lactam carbonyl absorption. Formation of the lactam (XIII) from X undoubtedly occurs by transannular attack of the 4-amino group on the 12-carbonyl. Such an interaction requires that the amine be *trans* to C-4*a*-hydrogen (4-epi configuration). The undegraded minor component, which was not isolated in analytical pure form, shows the ultraviolet absorption characteristics of tetracycline, and, like the latter, is epimerized at C-4 in pyridine – acetic acid.

EXPERIMENTAL

4-Oxo-4-dedimethylaminotetracycline-4,6-hemiketal (III)

Tetracycline hydrochloride (10 g) was dissolved in 500 ml of water containing 2 ml of concentrated hydrochloric acid. (Initial experiments without added hydrochloric acid gave somewhat lower yields of crude product contaminated by greater amounts of tetracycline.) To the solution, with stirring at room temperature, was added 7 g of powdered N-chlorosuccinimide. The crude product began to precipitate within a few minutes. It was recovered by filtration, with water wash, after 30 min reaction time. Partial purification of the crude air-dried product (6.7 g) was achieved by distributing it between 150 ml of water and 400 ml of ether. The aqueous phase and five 40-ml water washes of the ether phase were discarded. The ether phase was stripped to dryness, the residue treated with water, and the product recovered by filtration. The yield of partially purified product, suitable for further transformations, was 5.6 g (65% overall).

For analysis, partially purified product (1 g) was dissolved in 4 ml of methanol, treated with Darco G-60, and filtered. The product crystallized as the monopotassium salt upon the addition of 0.40 ml of 5 *N* potassium hydroxide. The yield of material, dried *in vacuo* at 50° for 48 h, was 0.50 g (46%). It showed λ_{max}^{KBr} 5.7 μ; $\lambda_{max}^{MeOH\ -\ 0.01\ N\ HCl}$ 268 and 346 mμ (log ϵ 4.40 and 3.72); in MeOH – 0.01 *N* NaOH the compound is very unstable—a rapidly determined spectrum includes $\lambda_{max} \sim 370$ mμ (log $\epsilon \sim 4.4$).

Anal. Calcd. for $C_{20}H_{16}O_9NK \cdot 0.5H_2O$: C, 52.0; H, 3.7; N, 3.0; Cl, 0.0; K, 8.4; H_2O, 1.9. Found: C, 52.0; H, 3.8; N, 3.2; Cl, 0.0; K, 8.2; H_2O, 1.7.

Compcund III shows the typical acid instability of tetracyclines having a hydroxyl group at C-6 and unblocked at C-11*a*. For example, when the potassium salt of III was dissolved in liquid hydrogen fluoride, allowed to stand for 1.5 h, and then evaporated to dryness, it gave a crude product, presumed to be 5*a*,6-anhydro-4-oxotetracycline, possessing the expected ultraviolet spectral properties. The latter, on reduction with sodium hydrosulfite, is indicated by spectral and paper chromatographic evidence to yield the same anhydro–hydroxy derivative (VI) obtained by the alternative reduction–dehydration sequence.

4-Hydroxy-4-dedimethylaminotetracycline (IV)

Crude 4-oxo-4-dedimethylaminotetracycline-4,6-hemiketal (III, 25 g) was dissolved in 300 ml of methanol. A solution of sodium hydrosulfite (10 g) in 200 ml of water was added. The temperature rose from 25 °C to 35 °C during this process. The mixture was stirred for 40 min at room temperature. Water (250 ml) was added and the solution extracted twice with 1.25-l portions of ether. The combined ether layers were

[3]*Under these conditions tetracycline and 4-epitetracycline yield the same betaine. Without the acid scavenger, the reaction of X with methyl iodide ceases with uptake of 1 equivalent of the reagent to produce a mixture which is indicated by paper chromatography to include appreciable amounts of starting material, presumed 4-epi-N^4-demethyltetracycline, and 4-epitetracycline, as well as a minor quantity of tetracycline.*

back washed with five 50-ml portions of water, dried over anhydrous sodium sulfate, filtered, and evaporated to dryness in a rotating evaporator. The residue was treated with ca. 250 ml of water and the amorphous product (19.1 g) recovered by filtration. The product was crystallized from hot ethylene dichloride (recovery in three crops, 10.7 g, 33% overall from tetracycline). It shows λ_{max}^{KBr}, no carbonyl bands below 6 μ; $\lambda_{max}^{MeOH - 0.01\,N\,HCl}$ 257 mμ and 362 mμ (log ϵ 4.42 and 3.68); $\lambda_{max}^{MeOH - 0.01\,N\,NaOH}$ 246, 264, and 378 mμ (log ϵ 4.26, 4.23, and 4.28).

Anal. Calcd. for $C_{20}H_{19}NO_9$: C, 57.6; H, 4.6; N, 3.3. Found: C, 57.3; H, 4.6; N, 3.2.

The same 4-hydroxy compound (IV) is also obtained by sodium hydrosulfite reduction of partially purified, or the potassium salt of, 4-oxo-4-dedimethylaminotetracycline. Alternatively, it may be obtained by zinc dust reduction (e.g. in 50% aqueous acetic acid with excess zinc, with stirring for 30 min at room temperature) or catalytic hydrogenation (e.g. H_2, Pd/C in methanol at atmospheric pressure and room temperature) of either IV or the corresponding 11*a*-chloro derivative (V).

11a-Chloro-4-oxo-4-dedimethylaminotetracycline-4,6-hemiketal (V)

11*a*-Chlorotetracycline-6,12-hemiketal (II, ref. 2, 2.3 g) was slurried in 110 ml water containing 0.7 ml of concentrated hydrochloric acid. Powdered N-chlorosuccinimide (1.6 g) was added and the mixture stirred for 1 h at room temperature. The crude product was isolated by filtration with water wash. It crystallized on trituration with methanol. The yield was 11 g. For analysis, 1 g was dissolved in excess ether and filtered. The filtrate was washed with dilute hydrochloric acid and water, dried over anhydrous sodium sulfate, filtered, and finally stripped to dryness, and the residue triturated with methanol. The material, dried *in vacuo*, showed λ_{max}^{BKr} 5.77 μ; $\lambda_{max}^{MeOH - 0.01\,N\,HCl}$ 258 and 343 mμ (log ϵ 4.42 and 3.68).

Anal. Calcd. for $C_{20}H_{16}O_9NCl$: C, 53.4; H, 3.6; N, 3.1; Cl, 7.9. Found: C, 53.0; H, 3.7; N, 2.8; Cl, 8.0.

5a,6-Anhydro-4-hydroxy-4-dedimethylaminotetracycline (VI)

A solution of 4-hydroxy-4-dedimethylaminotetracycline (V, 0.5 g) was boiled in 5 ml of acetone containing 1.0 g of *p*-toluene sulfonic acid until the volume was reduced to ca. 1.5 ml. The product crystallized when the solution was cooled. It was recovered by filtration and dried *in vacuo* for analysis. It showed $\lambda_{max}^{MeOH - 0.01\,N\,HCl}$ 222, 262, 310, and 423 mμ (log ϵ 4.46, 4.70, 3.68, and 4.01).

Anal. Calcd. for $C_{20}H_{17}O_4N$: C, 60.1; H, 4.3; N, 3.5. Found: C, 59.8; H, 4.5; N, 3.3.

4-Hydroxyimino-4-dedimethylaminotetracycline (VII)

Partially purified 4-oxo-4-dedimethylaminotetracycline-4,6-hemiketal (III, 7.5 g) was dissolved in 30 ml of methanol. Potassium bicarbonate (15 g) and hydroxylamine hydrochloride (3.13 g) were added and the slurry stirred for 15 min. The mixture was filtered. Water (120 ml) was added to the mother liquor and the pH was adjusted to 2.0. The partially precipitated product was extracted into excess ether and recovered by evaporation dryness. The residue was slurried with 100 ml of benzene and the insoluble product (4.7 g, 60%) recovered by filtration. The crude product (2.1 g) was recrystallized by dissolving it in 6.3 ml of toluene and 4.2 ml of isopropyl alcohol, filtering it, adding 5.0 ml toluene to the mother liquor, and allowing the mixture to stand at room temperature overnight. The yield of product recovered by filtration and dried *in vacuo* at 50 °C was 1.0 g (48%). It showed $\lambda_{max}^{MeOH - 0.01\,N\,HCl}$ 222, 276, 308, and 359 mμ (log ϵ 4.25, 4.07, 4.23, and 4.19); $\lambda_{inf}^{MeOH - 0.01\,N\,HCl}$ 237 and 268 mμ (log ϵ 4.17 and 4.06); $\lambda_{max}^{MeOH - 0.01\,N\,NaOH}$ 235, 245, and 373 mμ (log ϵ 4.25, 4.24, and 4.28); $\lambda_{inf}^{MeOH - 0.01\,N\,NaOH}$ 256 and 325 mμ (log ϵ 4.21 and 4.16).

Anal. Calcd. for $C_{20}H_{18}O_9N_2$: C, 55.8; H, 4.2; N, 6.5. Found: C, 55.7; H, 4.4; N, 6.2.

5a,6-Anhydro-4-hydroxyimino-4-dedimethylaminotetracycline (VIII)

4-Hydroxyimino-4-dedimethylaminotetracycline (VII, 500 mg) was dissolved in 3 ml of 4% methanolic hydrogen chloride. The solution was boiled about 3 min and left to crystallize overnight at room temperature. The product (240 mg, 51%) was recovered by filtration with methanol wash and dried *in vacuo* at room temperature. It showed $\lambda_{max}^{MeOH - 0.01\,N\,HCl}$ 225, 263, 302, and 422 mμ (log ϵ 4.48, 4.64, 4.26, and 4.07).

Anal. Calcd. for $C_{20}H_{16}O_8N_2 \cdot 0.5CH_3OH$: C, 57.6; H, 4.2; N, 6.6. Found: C, 57.7; H, 4.1; N, 6.8.

4-Hydrazono-4-dedimethylaminotetracycline (IX)

Partially purified 4-oxotetracycline (III, 11.5 g), dissolved in 80 ml of 95% ethanol, was added to a solution of 1.7 ml of hydrazine hydrate in 80 ml of the same solvent. The mixture, which began to precipitate immediately, was stirred for 1 h and then left to stand overnight. The product was recovered by filtration and the crude air-dried product reslurried in an additional 100 ml of 95% ethanol for 1 h at room temperature. The yield of crystalline product, air-dried at room temperature, was 6.0 g (37%). For analysis, a sample was recrystallized from tetrahydrofuran–water. It showed $\lambda_{max}^{MeOH - 0.01\,N\,HCl}$ 264 and 335 mμ (log ϵ 4.16 and 4.53); $\lambda_{max}^{MeOH - 0.01\,N\,NaOH}$ 261, 323, and 373 mμ (log ϵ 4.33, 4.25, and 4.29).

Anal. Calcd. for $C_{20}H_{19}O_8N_3 \cdot H_2O$: C, 53.6; H, 4.7; N, 9.4. Found: C, 53.8; H, 4.6; N, 9.0.

4-Epi-N^4,N^4-didemethyltetracycline (X)

4-Hydrazono-4-dedimethylaminotetracycline (8.7 g) was dissolved in 350 ml of acetone. Water (260 ml) and then 17.4 g of sodium hydrosulfite were added to the stirred solution. The temperature rose from 25 °C to 32 °C. After it was stirred for an additional 30 min at room temperature, the now heterogeneous mixture was treated with charcoal and filtered through a Supercel pad with 1:1 acetone–water wash. The mother

Can. J. Chem. Downloaded from www.nrcresearchpress.com by 210.87.254.40 on 09/05/12
For personal use only.

liquor was stripped of acetone. The pH was adjusted to 4.5 and nonamphoteric by-products, including very considerable presumed 4-hydroxy-4-dedimethylaminotetracycline, were removed from the aqueous phase by thorough extraction with ethyl acetate. The desired product was then extracted into butanol (four times with 100-ml portions). The butanol was dried over anhydrous sodium sulfate, filtered, and evaporated to dryness *in vacuo* in a rotating evaporator. The residue was slurried with and filtered from 33 ml of ethyl acetate. The yield of crude air-dried product was 2.6 g. This crude product was dissolved in 100 ml of dimethylformamide. The solution was clarified and 35 ml of water added to the mother liquor. When the solution was stirred slowly for 2 h, the product crystallized. The yield of vacuum-dried 4-epi-N^4,N^4-didemethyltetracycline, solvated with dimethylformamide, was 2.1 g (20%). It shows $\lambda_{max}^{MeOH - 0.01\ N\ HCl}$ 260 and 360 mμ (log ϵ 4.25 and 4.17); $\lambda_{max}^{MeOH - 0.01\ N\ NaOH}$ 246, 266, and 375 mμ (log ϵ 4.23, 4.22, and 4.25). Paper chromatography – bioautography indicate the product to contain a minor, slightly less polar material which is much more active against *Klebsiella pneumonia*.

Anal. Calcd. for $C_{20}H_{20}O_8N_2 \cdot 1.5(CH_3)_2NCHO$: C, 55.9; H, 5.8; N, 9.3. Found: C, 55.8; H, 5.9; N, 9.2.

The same compound (X) may also be obtained by analogous sodium hydrosulfite reduction of the oxime (VII). Alternatively, the hydrozane and the oxime (3 g) in 50% aqueous acetic acid (100 ml) were reduced by stirring for 30 min at room temperature with 3 g of zinc dust. Excess zinc was removed by filtration and the mother liquor evaporated to low volume. Water (100 ml) was added and the pH adjusted to 7.0 with sodium hydroxide. Crude zinc complex of X (3.9 g) was isolated by filtration and air dried. The product was characterized by ultraviolet absorption, paper chromatography, and conversion to the analytically pure 5*a*,6-anhydro derivative.

Compound X was obtained directly from 4-oxotetracycline-4,6-hemiketal by reductive amination. The partially purified hemiketal (III, 2.5 g) and 1.2 g of magnesium chloride hexahydrate were added to a slurry of platinum oxide (300 mg) prereduced in a mixture of 24 ml of dimethyl formamide and 3 ml of 28% ammonium hydroxide. Approximately 5 mmoles of hydrogen was taken up in 2.5 h at room temperature and atmospheric pressure. The catalyst was removed by filtration and crude product precipitated by addition of the mother liquor to 700 ml of ether that was being stirred. The crude magnesium complex (3.1 g) was characterized by ultraviolet absorption, paper chromatography, and conversion to the 5*a*,6-anhydro derivative.

5a,6-Anhydro-4-epi-N^4,N^4-didemethyltetracycline (XI)

The 5*a*,6-anhydro derivative (XI) was readily obtained from crude zinc complex of compound X (2.5 g) by dissolving in 15 ml of tetrahydrofuran and 1.5 ml of conc. hydrochloric acid. The filtered solution was allowed to stand at room temperature for 8 days. The tetrahydrofuran solvated product, which crystallized slowly, was recovered by filtration and dried *in vacuo* at 50 °C for 48 h. The yields were 0.7 g (30% overall from oxime) and 1.2 g (55% overall from hydrazone). It showed $\lambda_{max}^{MeOH - 0.01\ N\ HCl}$ 223, 272, and 423 mμ (log ϵ 4.45, 4.79, and 3.93); $\lambda_{max}^{MeOH - 0.01\ N\ NaOH}$ 229, 271, 338, and 428 mμ (log ϵ 4.39, 4.57, 3.73, and 4.09).

Anal. Calcd. for $C_{20}H_{18}O_7N_2 \cdot (CH_2)_4O \cdot HCl$: C, 56.8; H, 5.4; N, 5.5; Cl^-, 7.0; NH_2, 3.4. Found: C, 56.7, 56.6; H, 5.4, 5.0; H, 5.6, 5.5; Cl^-, 7.1, 7.1; NH_2, 3.2.

The volatile portion was only 3.7% when the compound was dried overnight *in vacuo* at 100 °C. When the compound was dried for 48 h at 100 °C, the analysis was consistent with loss of only part of the tetrahydrofuran.

Anal. Calcd. for $C_{20}H_{18}O_7N_2 \cdot 0.25(CH_2)_4O \cdot HCl$: C, 55.8; H, 4.7; Cl^-, 8.0. Found: C, 55.6; H, 5.0; Cl^-, 7.5.

Identical product was obtained by analogous acid degradation of either the purified 4-amino compound (X, dimethylformamide solvate) or the crude magnesium complex.

Tetracycline Methyl Betaine (XII)

The 4-amino derivative (X, dimethylformamide solvate, 100 mg) was refluxed overnight in a mixture of 2 ml acetone, 0.5 ml propylene oxide, and 0.5 ml methyl iodide. When the mixture was cooled, pure crystalline N^4-methyltetracycline betaine (70 mg, 79%) was recovered by filtration. The same product is obtained by use of this process with either tetracycline or 4-epitetracycline (87% and 84% yield respectively). They show identical behavior on paper chromatography and identical infrared absorption (KBr); $\lambda_{max}^{MeOH - 0.01\ N\ HCl}$ 271 and 358 mμ (log ϵ 4.24 and 4.17).

Anal. Calcd. for $C_{23}H_{26}O_8N_2 \cdot H_2O$: C, 58.0; H, 5.9; N, 5.9. Found: C, 58.0; H, 6.0; N, 5.6.

Tetracycline methyl betaine has been previously reported as a methanol solvate (4).

Degradation of 4-Epi-N^4,N^4-didemethyltetracycline

A solution of the amino compound (X, dimethylformamide solvate, 2.0 g) in 50 ml of 40% aqueous sodium bicarbonate was heated on a steam bath under nitrogen for 30 min. The solution was cooled to room temperature, transferred to a beaker, layered with 50 ml of ethyl acetate, and carefully acidified to pH 2.0 with 5% hydrochloric acid. The aqueous phase was further extracted with six 50-ml portions of ethyl acetate. After drying over anhydrous sodium sulfate, the combined ethyl acetate extracts were evaporated to dryness *in vacuo* to yield 1.34 g of crude lactam degradation product (XIII). To free the product of traces of the 4-amino derivative (principally the normal epimer), the crude product was taken up in

Can. J. Chem. Downloaded from www.nrcresearchpress.com by 210.87.254.40 on 09/05/12
For personal use only.

1.9 l of ether and reevaporated to dryness. The recovery was 1.14 g. For analysis, the lactam was recrystallized from hot acetone–water. The recovery in two crops, dried *in vacuo*, was 0.87 g (51%). It shows $\lambda_{max}^{MeOH - 0.01\ N\ HCl}$ 258 and 335 mμ (log ϵ 4.38 and 3.73); $\lambda_{max}^{MeOH - 0.01\ N\ NaOH}$ 249, 262, and 335 mμ (log ϵ 4.22, 4.17, and 3.71); $\lambda_{max}^{dioxane}$ 5.72 and 6.07 μ.

Anal. Calcd. for $C_{20}H_{20}O_8N_2 \cdot 2H_2O$: C, 5.31; H, 5.3; N, 6.2. Found: C, 53.2; H, 5.4; N, 6.5.

In a separate experiment 200 mg of compound X was similarly degraded in bicarbonate. The pH was adjusted to 2.0 and the mixture filtered (insoluble, 10 mg). The mother liquor was extracted with eight 15-ml portions of butanol. The combined butanol extracts were evaporated to dryness. The residue (150 mg) was taken up in 20 ml water and 20 ml of ethyl acetate. The aqueous phase, after three further extractions with ethyl acetate, was freeze dried to yield 21 mg of crude N^4,N^4-didemethyltetracycline which paper chromatography indicated to be virtually free of the 4-epi compound. It showed $\lambda_{max}^{MeOH - 0.01\ N\ HCl}$ 268 and 362 mμ, and was readily epimerized (e.g. in acetic acid – pyridine) to compound X (paper chromatographic evidence).

The lactam (XIII) was degraded to the 1,8-dihydroxynaphthalene derivative (XIV) by refluxing the former (300 mg) in 10 ml of 1:6 conc. hydrochloric acid – methanol. The solution was cooled, clarified, and evaporated to dryness. The residue was taken up in excess ether and the ether washed with several small portions of water, dried over anhydrous sodium sulfate, and evaporated to dryness, and the amorphous product dried *in vacuo* for analysis. The yield of compound XIV was 250 mg (92%). It showed $\lambda_{max}^{MeOH - 0.01\ N\ HCl}$ 232, 257, 310, 325, and 339 mμ (log ϵ 4.43, 3.94, 3.48, 3.56, and 3.59); $\lambda_{max}^{dioxane}$ 5.73 and 6.05 μ.

Anal. Calcd. for $C_{20}H_{18}O_7N_2 \cdot 0.5H_2O$: C, 59.0; H, 4.7; N, 6.9. Found: C, 59.1; H, 5.1; N, 6.4.

ACKNOWLEDGMENTS

The authors thank Prof. R. B. Woodward, Dr. L. H. Conover, and Prof. H. Muxfeldt for stimulating discussions concerning this work. They are also grateful to Mr. T. J. Toolan and his associates for physical measurements and microanalyses, Mr. P. J. DeMuria and his associates for paper chromatographic studies, and Mr. J. A. Aimetti for technical assistance.

REFERENCES

1. R. K. Blackwood and C. R. Stephens. J. Am. Chem. Soc. **86**, 2736 (1964).
2. R. C. Esse, J. A. Lowery, C. R. Tamorria, and G. M. Sieger. J. Am. Chem. Soc. **86**, 3874, 3875 (1964). R. C. Esse and G. M. Sieger. South African Patent Application 63/4791.
3. F. A. Hochstein, C. R. Stephens, L. H. Conover, P. P. Regna, R. Pasternack, P. N. Gordon, F. J. Pilgrim, K. J. Brunings, and R. B. Woodward. J. Am. Chem. Soc. **75**, 5455 (1953).
4. J. H. Boothe, G. E. Bonvicino, C. W. Waller, J. P. Petisi, R. W. Wilkinson, and R. B. Broschard. J. Am. Chem. Soc. **80**, 1654 (1958).
5. C. R. Stephens, L. H. Conover, P. N. Gordon, F. C. Pennington, R. L. Wagner, K. J. Brunings, and F. J. Pilgrim. J. Am. Chem. Soc. **78**, 1515 (1956). A. P. Doerschuk, B. A. Bitler, and J. R. D. McCormick. J. Am. Chem. Soc. **77**, 4687 (1955).
6. L. H. Conover. Special Publication No. 5. The Chemical Society, London. 1956.
7. R. K. Blackwood, J. J. Beereboom, H. H. Rennhard, M. Schach von Wittenau, and C. R. Stephens. J. Am. Chem. Soc. **83**, 2773 (1961); **85**, 3943 (1963).
8. M. Schach von Wittenau, L. H. Conover, R. K. Blackwood, R. Glauert, and R. B. Woodward. J. Am. Chem. Soc. **87**, 134 (1965).
9. J. Donohue, J. D. Dunitz, K. N. Trueblood, and M. S. Webster. J. Am. Chem. Soc. **85**, 851 (1963).
10. R. Fuller. Chem. Rev. **63**, 21 (1963).
11. A. J. Ellis and F. G. Soper. J. Chem. Soc. 1750 (1954).
12. J. J. Korst and K. Butler. Manuscript in preparation.
13. L. Horner, E. Winkelmann, K. H. Knapp, and W. Ludwig. Chem. Ber. **92**, 288 (1959).

Can. J. Chem. Downloaded from www.nrcresearchpress.com by 210.87.254.40 on 09/05/12
For personal use only.

Can. J. Chem. Downloaded from www.nrcresearchpress.com by 210.87.254.105 on 09/05/12
For personal use only.

PYRAZOLINES

IV. REARRANGEMENT OF ALKYL GROUPS DURING THE PYROLYSIS OF 4,4-DIALKYL-3-CYANO-3-CARBOMETHOXY-Δ^1-PYRAZOLINES

DONALD E. MCGREER, ROBERT S. MCDANIEL, AND MAGNUS G. VINJE
Department of Chemistry, University of British Columbia, Vancouver, British Columbia
Received November 13, 1964

Dedicated to Professor R. B. Sandin on the Occasion of his Sixty-Eighth Birthday

ABSTRACT

A number of 4,4-dialkyl-3-cyano-3-carbomethoxy-Δ^1-pyrazolines have been synthesized. Pyrolysis of these pyrazolines yielded cyclopropane and olefin products. The formation of olefin products by rearrangement of an alkyl group from C_4 to C_5 of the pyrazoline system suggests that positive charge is developed on C_5 in the transition state. Ionic character in the transition state was also indicated by the fact that the rate of pyrolysis is faster in polar than in nonpolar solvents.

A mechanism which has been considered by a number of workers for the pyrolysis of 3-carbalkoxy-Δ^1-pyrazolines (I) and related systems has followed a form similar to the scheme shown in eq. [*a*] (1, 2). The products consist of cyclopropane derivatives and α,β- and β,γ-unsaturated olefins. The ring-opened intermediate II has been considered, since rotation around the bonds in II would explain the experimental fact (2) that cyclopropane products in which the stereochemistry in the cyclopropane is different from that in the pyrazoline are formed. As a starting point for further study we have therefore assumed II to closely represent the intermediate or transition state for this reaction. In this paper and the next paper in this series (3) we have looked for rearrangements which are characteristic of ionic compounds and which might be expected for intermediates with the ionic character shown in II.

Structure II suggests that positive charge is built up at C_5 of the pyrazoline system in the transition state. If this is the case, then rearrangements characteristic of carbonium ions should be possible for this system. Wagner–Meerwein rearrangements and related reactions clearly demonstrate that alkyl groups can readily migrate to a positive center. However, the migration of alkyl groups to a radical center or an anion center are predicted to be especially unfavorable (4). The occurrence of alkyl migration would be diagnostic of positive charge at C_5 in the transition state for the pyrolysis reaction.

In the pyrolysis of the many pyrazolines to date, there has been no observation of rearrangement of an alkyl or aryl group from C_4 of the pyrazoline ring to C_5 (see eq. [*b*]). This has been due, presumably, to the facile competitive migration of hydrogen in those pyrazolines analogous to compound III. To observe alkyl migration we therefore need two alkyl groups at C_4.

The pyrazoline from mesityl oxide is known (5, 6); however, heating this Δ^2-pyrazoline does not give an identifiable product. Attempts in this laboratory to prepare the corresponding methyl ester by reaction of diazomethane and methyl senecioate were unsuccessful. The presence of the two β-methyl groups on the acrylate system sterically hinders the system to such an extent that no reaction occurred when the reaction was carried out in a sealed tube for several days.

Successful preparation of a series of 4,4-dialkyl-Δ^1-pyrazolines was achieved by the

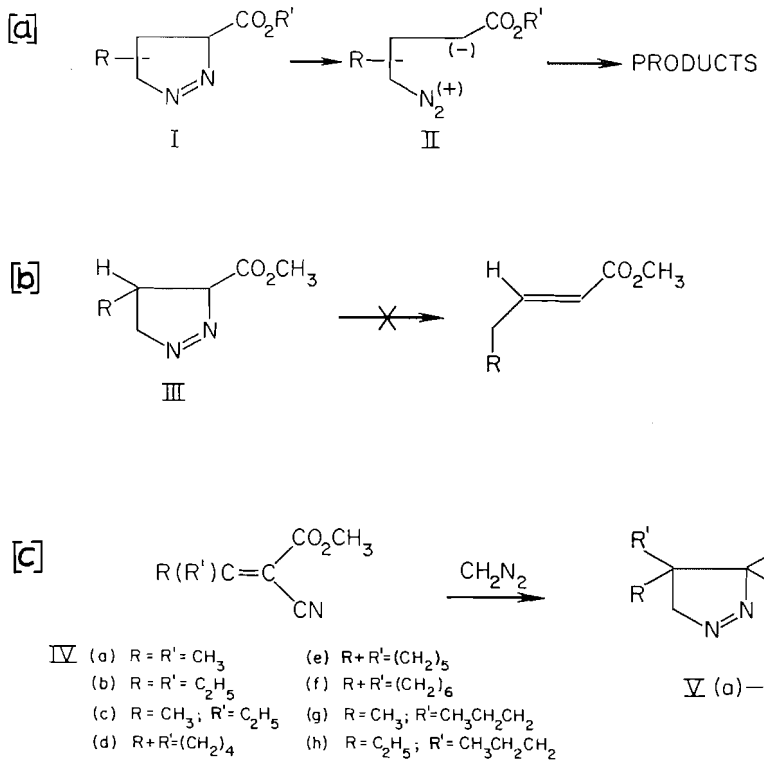

reaction of diazomethane with a number of methyl alkylidenecyanoacetates (IV*a*–IV*e*) (see eq. [*c*]). The required alkylidenecyanoacetates (IV) were readily prepared by the procedure of Cope (7) with modifications as developed by Widequist (8). Nuclear magnetic resonance (n.m.r.) was useful for the assignment of stereochemistry to compounds IV*c* and IV*g*. The assignments are based on the fact that the isopropylidene derivative (IV*a*) shows different peak positions for the two β-methyl groups (7.61 and 7.71 τ). In methyl *cis*- and *trans*-crotonate the β-methyls are found at 7.86 and 8.12 τ respectively (9), and in *cis*- and *trans*-crotonitrile the β-methyls are found at 8.05 and 8.20 τ respectively (10). The downfield shift is greater in the *cis* isomers and is greater for the *cis* ester than the *cis* nitrile. We therefore have assigned the β-methyl at 7.61 τ in IV*a* to that group *cis* to the carbomethoxy group and the β-methyl at 7.71 τ to that group *cis* to the nitrile.

The alkylidene derivatives IV*c*, IV*g*, and IV*h* for which R ≠ R′ are mixtures of two isomers. For IV*c* and IV*g* these mixtures contain one isomer with a β-methyl *cis* to the carbomethoxy group and one with a β-methyl *trans* to the carbomethoxy group. These compounds as isolated from the Cope reaction showed the β-methyls at 7.62 and 7.72 τ for IV*c* and 7.63 and 7.72 τ for IV*g* with intensities which indicated mixtures of about 50:50 composition. The isomers with the lower-field β-methyl were assigned the structure having the β-methyl *cis* to the carbomethoxy group and in this paper are referred to as IV*c* (methyl *cis*) and IV*g* (methyl *cis*).

Addition of diazomethane to methyl isopropylidenecyanoacetate (IV*a*) in ether at room temperature gave a solution which contained 4,4-dimethyl-3-cyano-3-carbomethoxy-Δ^1-pyrazoline (V*a*). Evaporation of the ether at 0° gave an oil which, when warmed to room temperature, decomposed exothermally to yield nitrogen and pyrolysis products.

Can. J. Chem. Downloaded from www.nrcresearchpress.com by 210.87.254.105 on 09/05/12
For personal use only.

The oil was more stable in solvents and was identified as pyrazoline (V*a*) by its n.m.r. spectrum.

Similarly, pyrazolines V*b* and V*c* were obtained from the alkylidenecyanoacetates IV*b* and IV*c*. The pyrazoline V*d* obtained from IV*d* was sufficiently less stable than the other pyrazolines that pyrolysis occurred during its preparation. A discussion of its structure is reserved until after the pyrolysis reaction has been discussed.

Pyrolysis of 4,4-dimethyl-3-cyano-3-carbomethoxy-Δ^1-pyrazoline (V*a*) gave a mixture of three products (see eq. [*d*]). Vapor chromatographic separation (v.p.c.) gave 2,2-dimethyl-1-cyano-1-carbomethoxycyclopropane (VI) and a mixture of the two isomeric methyl 1-methylpropylidenecyanoacetates (IV*c* (methyl *cis*) and IV*c* (ethyl *cis*)). This latter mixture could not be separated and was analyzed by n.m.r. The product analysis for pyrolysis of V*a* neat and in two solvents is given in Table I.

TABLE I

Product compositions for the pyrolysis of 4,4-dimethyl-3-cyano-3-carbomethoxy-Δ^1-pyrazoline V*a*

Solvent	VI	IV*c* (methyl *cis*)	IV*c* (ethyl *cis*)
Neat	39	39	22
Benzene	38	28	34
Tetrachloroethylene	57	5	38

Pyrolysis of the 4,4-diethylpyrazoline V*b* and the 4-ethyl-4-methylpyrazoline V*c* gave similar results with the formation of both cyclopropane and olefin products (see eqs. [*e*] and [*f*]). The olefins IV*b* and IV*g* were identical with authentic samples and IV*h* was

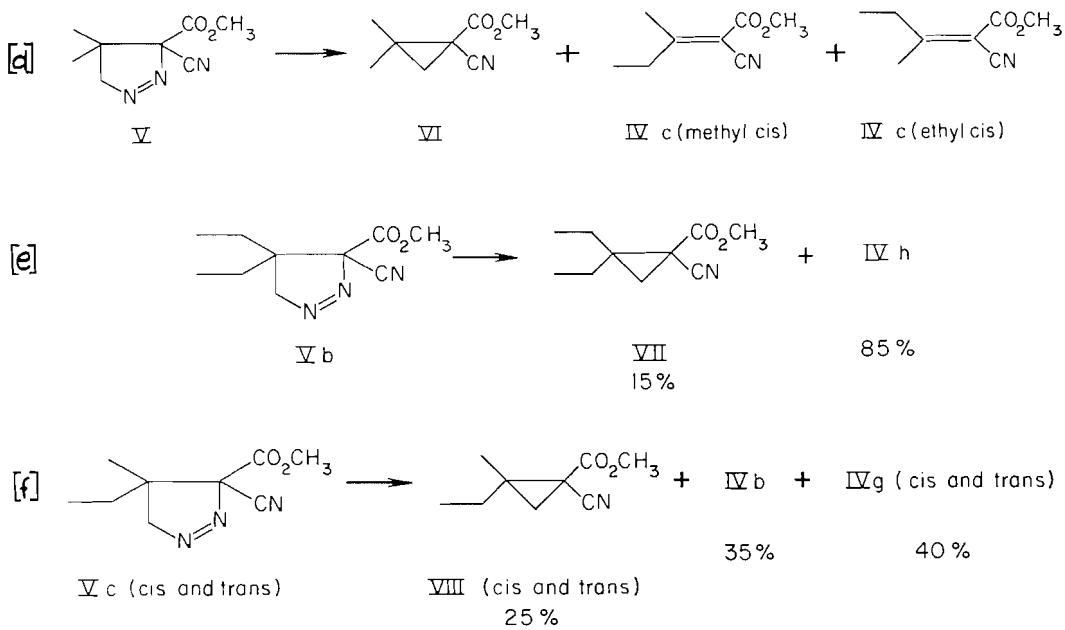

suggested by its analysis and n.m.r. spectrum. The cyclopropane VIII was characterized by its physical data and particularly by the absence of unsaturation as shown by n.m.r. and infrared. The cyclopropane VII could not be isolated. Instead, when attempts were

Can. J. Chem. Downloaded from www.nrcresearchpress.com by 210.87.254.105 on 09/05/12
For personal use only.

made to isolate it, only a rearranged product which was indicated to be methyl 2-cyano-4-ethyl-4-hexenoate by its n.m.r. spectrum could be obtained. This rearrangement product was expected, since at the higher temperature needed for separation it was found that the related cyclopropanes VI and VIII were also rearranged (12). Thus, VI gave pure methyl 2-cyano-4-methyl-4-pentenoate (IX) when heated to 200° (see eq. [*g*]). The cyclopropane VII is therefore undoubtedly formed as a product from pyrazoline V*b*. The product compositions were determined for neat pyrolysis by vapor chromatography and are included in the equations for the reaction.

As mentioned above, the preparation of the pyrazoline from methyl cyclopentylidenecyanoacetate (IV*d*) was complicated by concurrent pyrolysis. Thus, methyl cyclohexylidenecyanoacetate (IV*e*), an expected product, was being formed during the reaction and also was reacting with the excess diazomethane. This reaction was readily followed by n.m.r. as shown by Fig. 1. At early stages of the reaction, removal of the ether gave an oil which showed peaks (Fig. 1A) in the n.m.r. caused by ether and methyl cyclopentylidenecyanoacetate (IV*d*) at 6.19 and 7.10 τ (ester methyl and β-methylenes respectively), and the pyrazoline V*d* at 5.12 and 5.59 τ (AB system, J = 17.8 c.p.s., for the hydrogens on C_5) and 6.11 τ (ester methyl), in addition to the ring hydrogens of IV*d* and V*d* at 8.25 τ. At later stages in the reaction (Fig. 1B) a similar sample showed peaks caused by

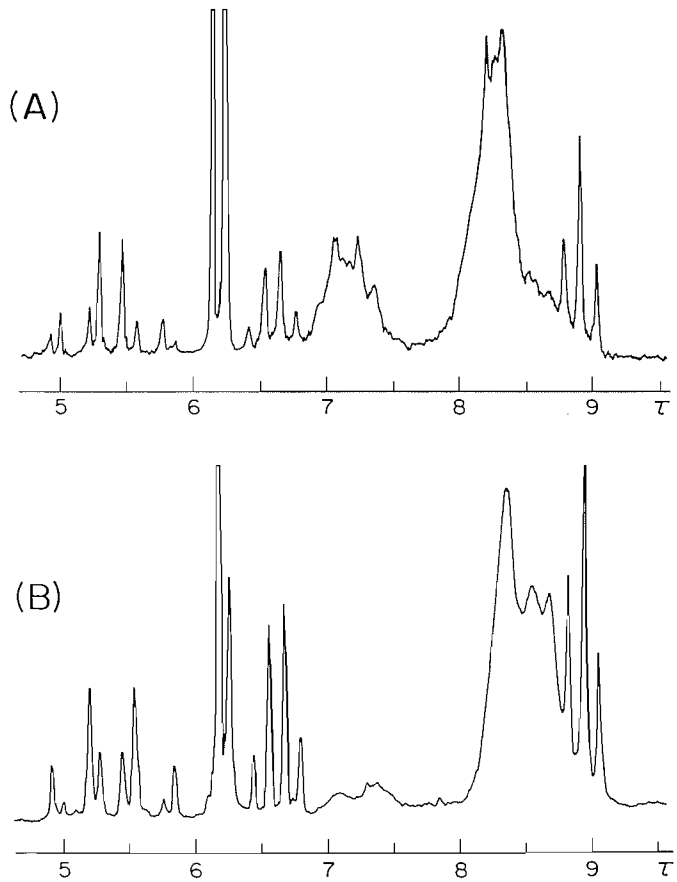

FIG. 1. A, product from reaction of IV*d* with diazomethane for 2 h at 22°; B, product for reaction time of 4 h.

Can. J. Chem. Downloaded from www.nrcresearchpress.com by 210.87.254.105 on 09/05/12
For personal use only.

ether and methyl cyclohexylidenecyanoacetate IV*e* at 6.21 τ (ester methyl) and 7.06 and 7.31 τ (two broad bands for the β-methylenes), and pyrazoline V*e* at 5.04 and 5.68 τ (AB system, $J = 17.6$ c.p.s., for the hydrogens on C_5) and 6.13 τ (ester methyl), in addition to the ring hydrogens of IV*e* and V*e* at 8.3 τ. Thus, although the individual pyrazolines V*d* and V*e* were not isolated, their presence was inferred by the n.m.r. spectra in Fig. 1 and the products isolated from pyrolysis. Vapor chromatography of the pyrolysis mixtures gave the alkylidenecyanoacetates IV*d*–IV*f*. In addition, there was obtained a small fraction, which represented less than 5% of the product and for which the n.m.r. spectrum indicated the structure methyl 2-cyano-3-(1-cyclopentenyl)propanoate (XI). Again, pyrolysis of the anticipated cyclopropane product, 5-cyano-5-carbomethoxyspiro[4.2]-heptane (X), during isolation, would be expected to yield XI (12) (see eq. [*h*]).

[g]

VI IX

[h]

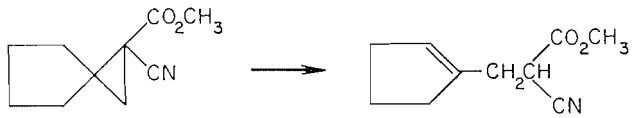

X XI

[i]

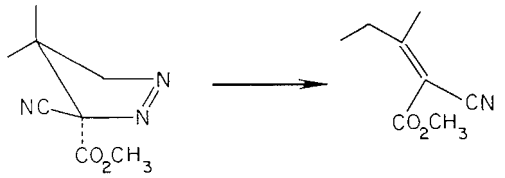

XII IVc (ethyl cis)

In the pyrolysis of pyrazolines V*a* to V*e* we have observed alkyl migration from C_4 to C_5 of the pyrazoline system to give α,β-unsaturated esters. Such migration is diagnostic of the development of positive charge at C_5 of the pyrazoline ring (4) and is suggested by structure II. In addition, we have done some preliminary studies on the rate of pyrolysis of pyrazolines V*a* and V*d* (mixed with V*e*) in a variety of solvents. (13). Typical results are shown in Table II where the half-lives of V*a* and V*d* are estimated from the slope of the first-order plots of nitrogen evolution during pyrolysis. The kinetic data reported here are from a relatively simple and crude setup (the gas burette was not jacketed, the thermometer was not calibrated, and the solution was agitated but not stirred), but the results were reproducible to better than 5% and show the trends we might expect when measurements can be made more accurately. These results suggest a transition state for pyrolysis which is more polar than the starting material, as is also suggested by structure II, since the rate is greater in the more polar solvents.

On the other hand structure II, through rotation around the single bonds, would be

Can. J. Chem. Downloaded from www.nrcresearchpress.com by 210.87.254.105 on 09/05/12
For personal use only.

TABLE II

Calculated half-lives for pyrazolines V*a* and V*d* (mixed with V*e*) (13)

Solvent	$t_{\frac{1}{2}}$ at 53° for V*a* (min)	$t_{\frac{1}{2}}$ at 20° for V*d* (min)
Butyl ether	23	98
Tetralin	16	—
Benzene	—	65
Nitrobenzene	13	19
Formamide	≠	0.5*

*Extrapolated from 3.5° by measuring the relative rate in nitrobenzene and formamide at 3.5° and the rate in nitrobenzene at 20°. ≠, the rate in formamide was sufficiently faster than that in nitrobenzene so that the two could not be run at the same temperature.

anticipated to give a nearly 50:50 mixture of the olefins because of the migration of the groups on C_4. The data in Table I show, however, that pyrolysis of V*a* in tetrachloroethylene yielded an 8:1 mixture of the two possible olefins. In addition, this ratio was found to be solvent dependent. Also, although the results in Table II support the postulation of an ionic intermediate, the variation in the rate with solvent does not correlate with other polar reactions in nonpolar media (14). Particularly, the increase in rate in changing from the solvent nitrobenzene to formamide is not expected.

We feel that the product analysis results of Table I can best be explained by assuming that the methyl group migrates concerted with nitrogen loss. This would make the reaction analogous to that proposed for the pyrolysis of 3,5-dimethyl-3-carbomethoxy-Δ^1-pyrazolines (11), for which it was suggested that hydrogen on C_4 migrates concerted with nitrogen loss. Thus, for the pyrolysis of V*a* in the tetrachloroethylene the methyl *cis* to the carbomethoxy group appears to be in the better position for migration. This is illustrated by structure XII → IV*c* (ethyl *cis*) (see eq. [*i*]). Just how the reaction parameters are influenced by the steric and electronic factors in the pyrazoline and by the solvent to give this stereospecificity is not clear. A study is now underway to determine the importance of these individual factors on the reaction.

The rearrangements observed in this paper and the effects of solvent on the reaction discussed show many similarities to the reactions of ketones with diazomethane (15). It is hoped that further work on this reaction will help us decide whether a betaine structure is an intermediate in the reactions of ketones with diazomethane as has been proposed.

EXPERIMENTAL

The apparatus and methods are as described in Part V (3).

Methyl Alkylidenecyanoacetates (IV)

These compounds were prepared by the procedure of Cope (7) as modified by Widequist (8).

Methyl isopropylidenecyanoacetate (IV*a*), b.p. 103–105° at 8 mm, n_D^{25} 1.4720 (lit. (7), b.p. 99–101° at 9 mm, n_D^{25} 1.4696), showed peaks in the n.m.r. spectrum at 6.21, 7.61, and 7.71 τ. The peak at 7.61 τ was assigned to the methyl *cis* to the ester group, that at 7.71 τ to the methyl *trans* to the ester group, and that at 6.21 τ to the methyl of the ester group (see the text).

Methyl 1-ethylpropylidenecyanoacetate (IV*b*), b.p. 110° at 8 mm, n_D^{25} 1.4699 (lit. (7), b.p. 112–114° at 9 mm, n_D^{25} 1.4708), showed peaks in the n.m.r. spectrum at 6.13 τ, 7.18 τ (quartet, J = 7.3 c.p.s.), 7.39 τ (quartet, J = 7.6 c.p.s.), 8.77 τ (triplet, J = 7.3 c.p.s.), and 8.85 τ (triplet, J = 7.8 c.p.s.). By analogy with IV*a* it is anticipated that the 7.18 τ peak is *cis* to the carbomethoxy group.

Methyl 1-methylpropylidenecyanoacetate (IV*c*), b.p. 129–130° at 28 mm, n_D^{25} 1.4705 (lit. (7), b.p. 105–106° at 9 mm, n_D^{25} 1.4705), showed n.m.r. peaks at 6.17 τ, 7.19 τ (quartet, J = 7.6 c.p.s.), 7.40 τ (quartet, J = 7.6 c.p.s.), 7.62 τ, 7.72 τ, and 8.80 τ (triplet, J = 7.5 c.p.s.), and 8.87 τ (triplet, J = 7.6 c.p.s.). By analogy with IV*a* and because of the relative peak intensities, peaks at 6.17, 7.40, 7.62, and 8.80 τ were

Can. J. Chem. Downloaded from www.nrcresearchpress.com by 210.87.254.105 on 09/05/12
For personal use only.

assigned to the isomer in which the β-methyl is *cis* to the carbomethoxy group (IV*c*, methyl *cis*). The ratio of IV*c* (methyl *cis*) to IV*c* (ethyl *cis*) was estimated to be 53:47 on the basis of the integral of the 7.62 and 7.72 τ peaks respectively.

Methyl cyclopentylidenecyanoacetate (IV*d*) (Aldrich) showed n.m.r. peaks at 6.18 τ, 7.12 τ (broad band,) and 8.12 τ (broad band) for the ester methyl, the β-methylenes, and the γ-methylenes respectively.

Methyl cyclohexylidenecyanoacetate (IV*e*), b.p. 93–95° at 0.1 mm, n_D^{25} 1.5033 (lit. (7), b.p. 146–147° at 9 mm, n_D^{25} 1.5035), showed n.m.r. peaks at 6.19 τ (ester methyl), 7.03 and 7.36 τ (two broad bands for the β-methylenes), and 8.28 τ (broad band for the γ- and δ-methylenes).

Methyl cycloheptylidenecyanoacetate (IV*f*), b.p. 122–123° at 0.1 mm, n_D^{25} 1.5088, showed n.m.r. peaks at 6.20 τ (ester methyl), 6.96, 7.06, 7.17, and 7.28 τ (group of four peaks for the β-methylenes), and 8.38 τ (broad band for the γ- and δ-methylenes).

Anal. Calcd. for $C_{11}H_{15}O_2N$: C, 68.37; H, 7.82; N, 7.25. Found: C, 68.26; H, 7.83; N, 7.40.

Methyl 1-methylbutylidenecyanoacetate (IV*g*), b.p. 139–140° at 28 mm., n_D^{25} 1.4700 (lit. (7), b.p. 116–118° at 9 mm, n_D^{25} 1.4700), showed n.m.r. peaks at 6.19 τ and 7.22 τ (complex group of bands), 7.63 τ, 7.72 τ, and 8.44 τ (complex group of bands), 8.98 τ (triplet, J = 6.6 c.p.s.), and 9.00 τ (triplet, J = 6.6 c.p.s.). Two isomers were indicated by the singlets at 7.63 and 7.72 τ for the β-methyl groups of the two compounds. By analogy with IV*a* the peak at 7.63 τ was assigned to the isomer IV*g* (methyl *cis*). The ratio of the peaks at 7.63 and 7.72 τ was 54:46 respectively.

Preparation of Pyrazolines Va to Vd

Pyrazolines V*a* to V*d* were prepared by reacting an excess of diazomethane (prepared from nitrosomethylurea) in ether with the appropriate methyl alkylidenecyanoacetate (IV*a* to IV*d*) at room temperature. The excess diazomethane was either evaporated from the solution or reacted with acetic acid. Evaporation of the solution on a rotary evaporator at 0° gave a satisfactory sample for n.m.r. analysis. No other physical data were obtained as a result of the instability of the pyrazolines.

4,4-Dimethyl-3-cyano-3-carbomethoxy-Δ¹-pyrazoline (V*a*) showed n.m.r. peaks at 5.24 and 5.63 τ (AB group with J = 17.3 c.p.s.) and 6.13 τ, 8.80 τ, and 8.88 τ, in addition to minor peaks caused by ether and pyrolysis products. The peaks at 5.24 and 5.63 τ were assigned to the hydrogens on C_5, the peaks at 8.80 and 8.88 τ to the methyls on C_4, and the peak at 6.13 τ to the ester methyl.

4,4-Diethyl-3-cyano-3-carbomethoxy-Δ¹-pyrazoline (V*b*) showed n.m.r. peaks at 5.19 and 5.80 τ (AB group with J = 17.4 c.p.s.), 6.08 τ and 8.38 τ (quartet, J = 7.2 c.p.s.), 8.48 τ (quartet, J = 6.6 c.p.s.), 9.03 τ (triplet, J = 6.8 c.p.s.), and 9.21 τ (triplet, J = 7.1 c.p.s.). The presence of the AB group at 5.19 and 5.80 τ and the presence of two ethyl groups confirmed the structure as V*b*.

4-Ethyl-4-methyl-3-cyano-3-carbomethoxy-Δ¹-pyrazoline (V*c*) showed n.m.r. peaks at 5.24, 5.27, and 5.72 τ (two AB groups which overlap for which J = 17.7 c.p.s.), 6.09 τ and 8.50 τ (group of peaks not fully resolved), 8.89 and 8.95 τ (two singlets), and 9.16 τ (group of peaks not fully resolved). The presence of the two AB groups at 5.24 and 5.72 τ, and at 5.27 and 5.72 τ, for the hydrogens on C_5 was anticipated, since there would be a mixture of isomers present. Similarly, the peaks at 8.89 and 8.95 τ (intensity ratio of 51:49) would be for the methyls on C_4 for the two isomers. The ethyl groups of the two isomers were sufficiently overlapped that the spectra were not resolved; however, the assignment was clearly that for structure V*c*.

The pyrazoline V*d* from methyl cyclopentylidenecyanoacetate decomposed during its formation, and thus the n.m.r. spectrum contained considerable amounts of other products as shown in Fig. 1. The composition of the mixture is discussed in the text.

Pyrolysis of the Pyrazolines

For product analysis the pyrazolines were pyrolyzed neat at temperatures near room temperature. The products were separated using an Apiezon J column in an Aerograph A 90-P. Analytical studies were made using a 150-ft Golay column in a Perkin–Elmer 226 chromatograph.

Pyrolysis of the 4,4-dimethylpyrazoline V*a* gave a mixture which was separated by v.p.c. into two components. The first component, isolated with a column temperature of 173°, was 2,2-dimethyl-1-cyano-1-carbomethoxycyclopropane (VI), n_D^{25} 1.4479, with n.m.r. peaks at 6.21 τ, 8.26 and 8.62 τ (AB system with J = 4.8 c.p.s.), 8.53 τ, and 8.71 τ.

Anal. Calcd. for $C_8H_{11}O_2N$: C, 62.72; H, 7.24; N, 9.14. Found: C, 62.73; H, 6.91; N, 9.19.

The n.m.r. was consistent with the assigned structure with peaks at 8.53 and 8.71 τ assigned to the methyls at C_2, the peak at 6.21 τ assigned to the ester methyl, and the peaks at 8.26 and 8.62 τ assigned to the ring hydrogens. The low value of the geminal coupling constant was normal for a cyclopropane derivative (16).

The second component, n_D^{25} 1.4701, gave infrared and n.m.r. spectra identical with those found for methyl 1-methylpropylidenecyanoacetate (IV*c*). The relative proportions of the *cis* and *trans* isomers, as estimated by the 7.62 and 7.72 τ peaks respectively, depended on the solvent used for the pyrolysis, and these results are recorded in Table I.

Pyrolysis of the 4,4-diethylpyrazoline V*b* gave a mixture which was separated by v.p.c., at 240°, into two components. The first component showed n.m.r. peaks at 4.60 τ (quartet, J = 6.9 c.p.s.), 6.21 τ and 6.43 τ (four lines for one hydrogen coupled unequally to two hydrogens with J = 8.1 c.p.s. and 6.8 c.p.s.), 7.40 τ (poorly resolved group of lines), 7.91 τ (quartet, J = 7.5 c.p.s.), 8.36 τ (doublet, J = 6.9 c.p.s.), and

Can. J. Chem. Downloaded from www.nrcresearchpress.com by 210.87.254.105 on 09/05/12
For personal use only.

9.03 τ (triplet, J = 7.5 c.p.s.). This spectrum is consistent with that expected for methyl 2-cyano-4-ethyl-4-hexenoate. It would be anticipated (12) from pyrolysis of 2,2-diethyl-1-cyano-1-carbomethoxycyclopropane (VII) under the conditions of separation (see pyrolysis of VI below). The peaks were assigned as follows: 4.60 τ (hydrogen on C_5), 6.21 τ (ester methyl), 6.43 τ (hydrogen on C_2), 7.40 τ (hydrogens on C_3), 7.91 and 9.03 τ (ethyl on C_4), and 8.36 τ (hydrogens on C_6).

The second component, n_D^{25} 1.4682, was identified by its n.m.r. and infrared spectra to be methyl 1-ethylbutylidenecyanoacetate (IV*h*).

Anal. Calcd. for $C_{10}H_{15}NO_2$: C, 66.27; H, 8.34; N, 7.73. Found: C, 66.37; H, 8.46; N, 8.12.

The n.m.r. spectrum showed three complex regions at 7.32, 8.36, and 8.90 τ in addition to the ester methyl at 6.16 τ. Integration gave values of 4.2:2.0:6.7:3.0 for the four regions, which corresponds to a hydrogen ratio of 4:2:6:3 in IV*h*.

Pyrolysis of the 4-methyl-4-ethylpyrazoline V*c* gave a mixture which was separated by v.p.c., at 173°, into two components. The first component, n_D^{25} 1.4525, gave a complex n.m.r. spectrum with no signals below 8.0 τ other than the ester methyl at 6.18 τ. Two strong singlets appeared at 8.55 and 8.76 τ.

Anal. Calcd. for $C_9H_{13}O_2N$: C, 64.65; H, 7.84; N, 8.38. Found: C, 64.15; H, 7.90; N, 8.78.

The absence of olefin stretching vibrations in the infrared and the absence of signals below 8.0 τ in the n.m.r. spectrum confirm that this compound is a cyclopropane derivative. It was assigned the structure 2-ethyl-2-methyl-1-cyano-1-carbomethoxycyclopropane (VIII) on the basis of its mode of synthesis. The complexity of the n.m.r. spectrum is partly caused by the presence of *cis–trans* isomers, which are indicated by the signals at 8.55 and 8.76 τ assigned to the methyls on C_2 in the two isomers. The relative amounts of the two isomers were about 50:50; however, overlap of some peaks prevented accurate estimation of the distribution.

The second component, which by analytical v.p.c. showed two peaks corresponding to alkylidene derivatives IV*b* and IV*g*, showed peaks in the n.m.r. attributable to all of the peaks of IV*b* and IV*g*. The proportions of VIII, IV*b*, and IV*g* in the product from the neat pyrolysis were 25:35:40 respectively.

Pyrolysis of the pyrazoline mixtures obtained from the reaction of diazomethane with methyl cyclopentylidenecyanoacetate gave the following products by vapor chromatography at 240°. The first component showed n.m.r. peaks at 4.38 τ (broad singlet), 6.18 τ and 6.31 τ (triplet, J = 7.0 c.p.s.), 7.29 τ (doublet, J = 7.0 c.p.s.), and 7.55 to 8.40 τ (complex group of peaks). The n.m.r. spectrum and the mode of synthesis and isolation suggested that this compound was methyl 2-cyano-3-(1-cyclopentenyl)propanoate (XI) (see the text). The n.m.r. peaks at 6.31 τ were very similar to the signals found in other α-cyano-γ,δ-unsaturated esters for the α-hydrogen. The peak at 4.38 τ was assigned to the vinyl hydrogen, that at 7.29 τ to the β-hydrogens, and those from 7.55 to 8.40 τ to the ring hydrogens.

The remaining three components were isolated and identified by their retention times and n.m.r. and infrared spectra to be methyl cyclopentylidenecyanoacetate (IV*d*), methyl cyclohexylidenecyanoacetate (IV*e*), and methyl cycloheptylidenecyanoacetate (IV*f*).

Pyrolysis of 2,2-Dimethyl-1-cyano-1-carbomethoxycyclopropane (VI) (12)

The cyclopropane VI, when heated above 200°, rearranged to form a new isomer with a slightly longer retention time (7.32 min vs. 7.08 min for VI) as determined at 166° on the P-E 226. The new isomer, n_D^{25} 1.4454, showed n.m.r. peaks at 5.08 τ, 6.20 τ, and 6.28 τ (four lines with J = 8.0 and 6.8 c.p.s.), 7.36 τ (doublet, J = 7.4 c.p.s.), and 8.20 τ (broad singlet).

Anal. Calcd. for $C_8H_{11}O_2N$: C, 62.72; H, 7.24; N, 9.14. Found: C, 62.92; H, 6.92; N, 9.27.

The n.m.r. suggested that the new isomer was methyl 2-cyano-4-methyl-4-pentenoate (IX) with the vinyl hydrogens at 5.08 τ, the ester methyl at 6.20 τ, the α-hydrogen at 6.28 τ, the β-hydrogens at 7.36 τ, and the γ-methyl at 8.20 τ.

ACKNOWLEDGMENTS

The authors gratefully appreciate the support received for this work from the National Research Council and from the Committee on Research of the University of British Columbia.

Thanks are also extended to Mrs. Jenkins for the microanalyses and to Mrs. A. Brewster for the n.m.r. spectra.

REFERENCES

1. W. G. Young, L. J. Andrews, S. L. Lindenbaum, and S. J. Cristol. J. Am. Chem. Soc. **66**, 810 (1944).
2. T. V. Van Auken and K. L. Rinehart, Jr. J. Am. Chem. Soc. **84**, 3736 (1962).
3. D. E. McGreer, N. W. K. Chiu, and M. G. Vinje. Can. J. Chem. This issue.
4. H. E. Zimmerman. *In* Molecular rearrangements. Part I. *Edited by* P. de Mayo. Interscience, New York, N.Y. 1963. p. 395.
5. H. O. House, E. J. Grubbs, and W. F. Gannon. J. Am. Chem. Soc. **82**, 4099 (1960).

Can. J. Chem. Downloaded from www.nrcresearchpress.com by 210.87.254.105 on 09/05/12
For personal use only.

6. D. W. ADAMSON and J. W. KENNER. J. Chem. Soc. 1551 (1937).
7. A. C. COPE. J. Am. Chem. Soc. **59**, 2327 (1937).
8. S. WIDEQUIST. Acta Chem. Scand. **3**, 303 (1949).
9. R. R. FRASER and D. E. McGREER. Can. J. Chem. **39**, 505 (1961).
10. G. S. REDDY, J. H. GOLDSTEIN, and L. MANDELL. J. Am. Chem. Soc. **83**, 1300 (1961).
11. D. E. McGREER, N. W. K. CHIU, M. G. VINJE, and K. C. K. WONG. Can. J. Chem. This issue.
12. D. E. McGREER, N. W. K. CHIU, and R. S. McDANIEL. Proc. Chem. Soc. 415 (1964).
13. D. E. McGREER and N. W. K. CHIU. Unpublished results.
14. R. E. PINCOCK. J. Am. Chem. Soc. **86**, 1820 (1964).
15. C. D. GUTSCHE. *In* Organic reactions. Vol. VIII. John Wiley and Sons, New York, N.Y. 1954. p. 364.
16. D. J. PATEL, M. E. H. HOWDEN, and J. D. ROBERTS. J. Am. Chem. Soc. **85**, 3218 (1963).

Can. J. Chem. Downloaded from www.nrcresearchpress.com by 210.87.254.105 on 09/05/12
For personal use only.

Can. J. Chem. Downloaded from www.nrcresearchpress.com by 210.87.254.42 on 09/05/12
For personal use only.

PYRAZOLINES[1]

V. RING CLOSURE TO OXYGEN IN THE PYROLYSIS OF 3-ACETYL-Δ^1-PYRAZOLINES

DONALD E. MCGREER, NORMAN W. K. CHIU, AND MAGNUS G. VINJE
Department of Chemistry, University of British Columbia, Vancouver, British Columbia
Received November 13, 1964

Dedicated to Professor R. B. Sandin on the Occasion of his Sixty-Eighth Birthday

ABSTRACT

The pyrolysis of 3-methyl-3-acetyl-Δ^1-pyrazoline (IV) and *cis*- and *trans*-3,5-dimethyl-3-acetyl-Δ^1-pyrazoline (V and VI) has been studied. Pyrolysis of IV gave 2,3-dimethyl-4,5-dihydrofuran (XI) as a minor product, indicating some ring closure to oxygen in these reactions. Pyrolysis of V gave 2,3,5-trimethyl-4,5-dihydrofuran (XVII) as 23% of the product, whereas VI yielded only a trace of XVII. This fact and other differences in the product analysis from isomers V and VI are discussed in terms of the possible mechanism for the pyrolysis reaction.

In Part IV of this series (1) we reported a rearrangement in the pyrolysis of a series of pyrazolines which supports a mechanism involving ionic intermediates (I → III) and specifically the development of a positive charge on C_5 of the pyrazoline system during reaction. If we illustrate this effect by means of structure II, we see that there is also built up in the molecule a negative charge at C_3 which is presumably delocalized into the electron-withdrawing groups attached to C_3.

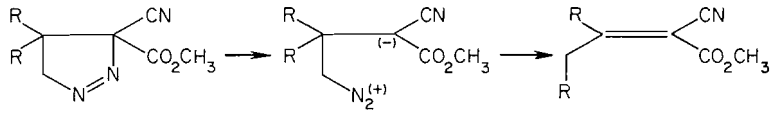

I II III

Major products from the pyrolysis of many pyrazolines are cyclopropane derivatives. It has been proposed (2) that such products arise by ring closure of an intermediate like II in a manner analogous to the many classical anionic cyclopropane-forming reactions. For example, the preparation of cyclopropyl cyanide is believed to follow the mechanism (3) illustrated in eq. [*a*].

When the acetyl group is the electron-withdrawing group in a cyclopropane ring closure, there is often also ring closure to the oxygen of the acetyl group. This was first noted by Perkin (4) in the application of the Perkin ring closure reaction to acetoacetic ester (see eq. [*b*]). More recently, related reactions have been used to synthesize dihydrofurans (5, 6). When trimethylene bromide was used by Perkin the major product was a dihydropyran caused by ring closure to oxygen (7).

We have prepared three 3-acetyl-Δ^1-pyrazolines to see if in their pyrolysis there may also be ring closure to oxygen and in the hope that such studies will help to elucidate the mechanism of this reaction.

3-Methyl-3-acetyl-Δ^1-pyrazoline (IV) and *cis*- and *trans*-3,5-dimethyl-3-acetyl-Δ^1-pyrazoline (V and VI) were prepared by the addition of diazomethane and diazoethane to isopropenyl methyl ketone. The latter reaction gave a mixture of two pyrazolines which

[1]*Taken in part from the M.Sc. Thesis of N. W. K. Chiu and the B.Sc. Thesis of M. G. Vinje, University of British Columbia, 1964.*

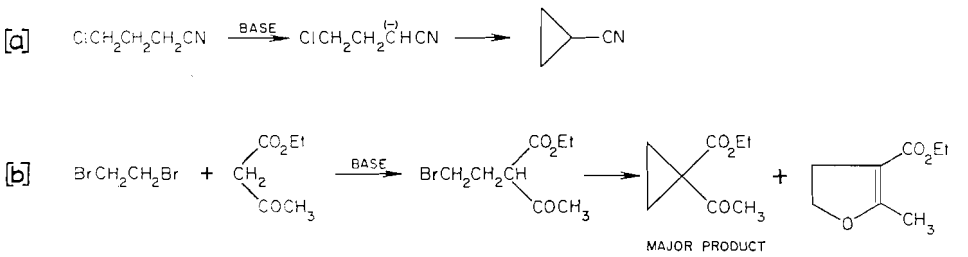

were partially separated by fractional distillation using a spinning-band column. The lower-boiling isomer, which was assigned the *cis* structure V, was obtained up to 81% pure and the higher-boiling isomer, which was assigned the *trans* structure VI, was obtained up to 87% pure. These mixtures were readily analyzed by nuclear magnetic resonance (n.m.r.), for the acetyl resonance of V occurs 0.13 p.p.m. above that of VI.

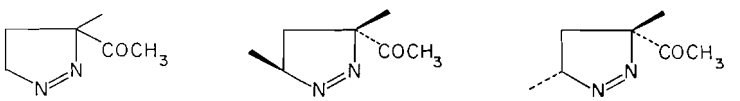

IV V VI

Assignment of structure to these isomers is of particular importance for the discussion of the mechanism of pyrolysis given in Part VI (8). Although the above assignment is not unequivocal, it is based on the following three points which all suggest the same stereochemistry.

(*i*) The higher-boiling isomer is predominant (60:40 ratio) in the product from the reaction of diazoethane with isopropenyl methyl ketone. Since this reaction is quite sensitive to steric effects (9) and since the methyl group would be expected to have a larger steric requirement than the acetyl group (it is assumed that the acetyl group would have a steric requirement similar to that of the carbethoxyl group, which has been shown to have a smaller steric requirement than methyl as a substituent on the cyclohexane ring (10)), this ratio would suggest that the higher-boiling isomer is the *trans* isomer VI.

(*ii*) Photolysis of the higher-boiling isomer yielded predominantly *trans*-1,2-dimethyl-1-acetylcyclopropane in the cyclopropane portion of the product (*trans* to *cis* ratio was 3.5:1). This conversion in a previous example was found to be highly stereospecific (11) and, thus, a greater stereospecificity is expected in the photolysis than in the pyrolysis of pyrazolines.

(*iii*) The peak positions in the n.m.r. spectrum for the C_4 hydrogens in the higher-boiling isomer are at about 8.53 τ. The hydrogen *cis* to the acetyl group would be expected to appear at lower field than that *trans* to the acetyl group, since such stereochemical effects are present in olefins (see ref. 12 and see compounds VIII, IX, XIV, and XV below) and some ring compounds (13, 14, for reference to some cyclopropane systems see ref. 8). This effect is apparently offset by the anisotropy of the —N=N— group which affects the C_4 hydrogens unequally as a result of folding of the five-membered ring. The hydrogen *cis* to the acetyl would be expected to be folded towards and above the —N=N— group, giving it a greater shielding than the hydrogen remaining in the plane of the ring. This situation is closely analogous to the situation of the C_6 hydrogens in the bicycloheptene systems described by Fraser (13) for which unequivocal assignment could be made.

For the lower-boiling isomer the C_4 hydrogens appear at 7.57 τ and 9.30 τ. Thus the shift caused by the acetyl group and the —N=N— group are not counterbalanced, with the

Can. J. Chem. Downloaded from www.nrcresearchpress.com by 210.87.254.42 on 09/05/12
For personal use only.

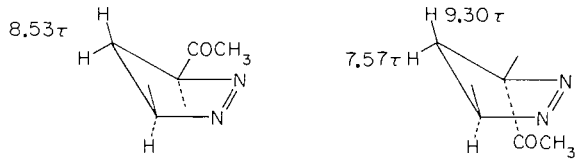

Free valences represent methyls.

result that the hydrogen *trans* to the acetyl group has been shifted up to 9.30 τ by the —N=N— group and that *cis* to the acetyl group has been shifted down to 7.57 τ by the acetyl group.

It is interesting that the formation of a dihydrofuran product from the lower-boiling isomer and not from the higher-boiling isomer, which is reported below, also corroborates these assignments.

Pyrolysis of 3-methyl-3-acetyl-Δ^1-pyrazoline gave a mixture of five isomeric products which were separated by vapor chromatography and identified on the basis of their physical data (see eq. [*c*]). The products were 1-methyl-1-acetylcyclopropane (VII), *trans*-3-methyl-3-penten-2-one (VIII), *cis*-3-methyl-3-penten-2-one (IX), 3-methyl-4-penten-2-one (X), and 2,3-dimethyl-4,5-dihydrofuran (XI). Compounds VII and XI were synthesized by independent routes for proof of structure. The variation of the product composition with the conditions used for the pyrolysis of IV are given in Table I.

TABLE I

Product compositions for the pyrolysis of 3-methyl-3-acetyl-Δ^1-pyrazoline (IV)

Reaction conditions	Δ VII	*trans* VIII	*cis* IX	β,γ X	XI
Neat at 120°	65	14	14	4	3
Ester neat* at 120°	65	15	15	5	
Vapor phase at 125°	78	8	5	5	4
125° in cyclohexane	69	3	13	2	13
125° in ether	69	4	13	4	10
125° in methylene chloride	71	17	7	3	2
125° in acetonitrile	64	17	14	5	0

*These figures are from the pyrolysis of 3-methyl-3-carbomethoxy-Δ^1-pyrazoline (22).

Pyrolysis of *cis*- and *trans*-3,5-dimethyl-3-acetyl-Δ^1-pyrazoline (V and VI) gave a mixture which contained up to six isomeric products (see eq. [*d*]). These products have

[c] 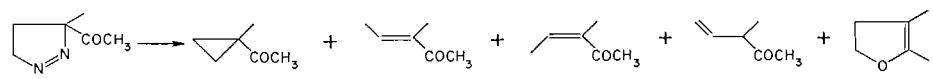

IV VII VIII IX X XI

[d] 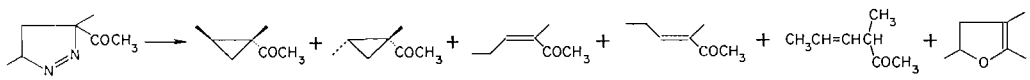

V cis, VI trans XII XIII XIV XV XVI XVII

been isolated and identified on the basis of their physical data. They are *cis*- and *trans*-1,2-dimethyl-1-acetylcyclopropane (XII and XIII), *cis*- and *trans*-3-methyl-3-hexen-2-one (XIV and XV), 3-methyl-4-hexen-2-one (XVI), and 2,3,5-trimethyl-4,5-dihydrofuran

Can. J. Chem. Downloaded from www.nrcresearchpress.com by 210.87.254.42 on 09/05/12
For personal use only.

(XVII). 3-Methyl-3-hexen-2-one has been reported in the literature (15), but a comparison of the properties with those of our samples would indicate that the earlier prepared compound was *cis–trans* mixture. The dihydrofuran derivative XVII has also been reported in the literature (16), but our evidence for its structure and that of the other products is based mainly on the physical properties and spectral data. The stereochemical assignment to cyclopropanes XII and XIII is based on the fact that XIII, when heated 9 h at 220°, rearranged to 3-methyl-5-hexen-2-one, while XII was unchanged after 14 h at 220°. An analogous rearrangement of the related esters has been reported (17). The variation of the product composition with the conditions used for the pyrolysis of V and VI is given in Table II. These data have been corrected to represent reaction of pure V and VI.

TABLE II

Product compositions for the pyrolysis of *cis*- and *trans*-3,5-dimethyl-3-acetyl-Δ^1-pyrazoline (V and VI)

		Δ		α,β			
Sample	Reaction conditions	*cis* XII	*trans* XIII	*cis* XIV	*trans* XV	β,γ XVI	XVII
V (*cis*)	Neat at 100°	16	24	35	0	2	32
	Vapor phase at 125°	27	48	7	3	2	13
	125° in cyclohexane	17	29	18	0	2	34
	Ether with BF_3	10	1	44	42	2	1
VI (*trans*)	Neat at 100°	61	17	0	18	4	0
	Vapor phase at 125°	67	19	2	7	2	3
	125° in cyclohexane	72	20	0	5	2	1
	Ether with BF_3	2	15	0	81	2	0

The formation of dihydrofuran derivatives from these pyrazolines can be explained if we assume an intermediate is formed with negative charge built up on C_3 of the pyrazoline system. As this negative charge is delocalized into the carbonyl oxygen, the oxygen will be able to participate in a ring closure reaction.

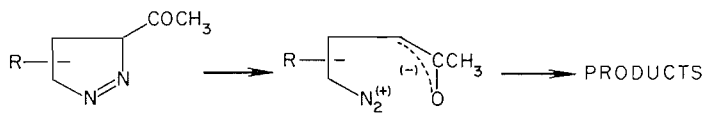

XIX

The results presented in Table II for pyrolysis of the isomeric 3,5-dimethyl-3-acetyl-Δ^1-pyrazolines are particularly interesting for, in general, the *cis* isomer V yields the dihydrofuran product while the *trans* isomer VI yields little or no dihydrofuran product. For such to be the case, the intermediate XIX cannot have free rotation around the C_3—C_4 bond. Restriction of this rotation infers that there is some bonding (either ionic or partially covalent) between C_3 and N in the transition state. With rotation restricted around the C_3—C_4 bond, the reaction of an intermediate like XIX will still be influenced by steric factors present in the original pyrazoline. Thus, V, which has the methyl substituents *cis*, would twist in such a way that the carbonyl group would be forced under the ring towards C_5 and in a position favorable for ring closure to oxygen. On the other hand, the *trans* isomer would twist to force the carbonyl group away from the C_5 carbon. This argument also gives further support to the original geometric assignments made for the isomeric 3,5-dimethyl-3-acetyl-Δ^1-pyrazolines V and VI.

The medium in which the pyrolysis of these pyrazolines is carried out also influences the

Can. J. Chem. Downloaded from www.nrcresearchpress.com by 210.87.254.42 on 09/05/12
For personal use only.

amount of dihydrofuran derivative formed. The percentage of this derivative is highest in the nonpolar solvent cyclohexane and is very low in more polar solvents like acetonitrile. Pyrolysis in the vapor phase tends to give results analogous to those in a nonpolar solvent but does not give the extreme situation that one might expect. The solvent effect suggests that the structure of the transition state (or states) is sensitive to the polarity of the solvent and the product composition is altered as a result. Competing reactions through similar transition states might also explain this variation in product composition with solvent.

A similar trend has been found in the effect of solvents on the proportion of cyclopropane products to olefins. The cyclopropane formation and dihydrofuran formation appear to be very closely related. This can be illustrated by the ratio of *cis* to *trans* cyclopropane derivatives from V and VI and from their corresponding esters (8). In general, the product analysis from the ketopyrazolines correlates well with that from the ester pyrazolines. (For example, see the neat pyrolysis of the 3-methyl-3-carbomethoxy-Δ^1-pyrazoline included in Table I for comparison with the neat pyrolysis of IV.) The neat pyrolysis of VI from Table II gives a ratio of *cis* to *trans* cyclopropanes of 60:17 and no dihydrofuran, corresponding to 60:15 for the ester (8). The neat pyrolysis of V from Table II gives a ratio of *cis* to *trans* cyclopropanes of 16:24 and 23% dihydrofuran, to be compared with 18:48 for the ester (8). The dihydrofuran percentage, if added to the *trans* cyclopropane percentage, would alter the ratio from V to 16:47 and thus would give a better correspondence. This suggests that the dihydrofuran is being formed at the expense of cyclopropane products and mainly at the expense of the *trans* derivative. A further discussion of the product ratios listed in Table II is given in Part VI of this series (8).

Nominé and Bertin (18) have found that the rate of nitrogen loss from a 3-keto-Δ^1-pyrazoline is greatly enhanced by the addition of boron trifluoride. In addition, boron trifluoride catalysis appeared to increase the proportion of the cyclopropane product in their reaction.

The effect of boron trifluoride on the pyrolysis of V and VI is given in Table II. The reaction occurs readily at 5°, indicating the catalytic effect of the boron trifluoride. 3-Carbomethoxy-Δ^1-pyrazolines, on the other hand, simply precipitate as the amine–boron trifluoride salt without pyrolysis. The catalytic effect of boron trifluoride is therefore probably due to coordination with the carbonyl of the acetyl group, resulting in stabilization of the negative charge developing at C_3. In this way, this reaction is analogous to the 3-cyano-3-carbomethoxy pyrazolines (1) which also pyrolyze at low temperatures.

The catalyzed reaction does not give a greater proportion of cyclopropane derivatives, as observed by Nominé and Bertin. It does, however, considerably alter the product composition and, although the results are not readily explained, they still show that differences are present in the reactions of the isomers V and VI. The products were stable to similar treatment by boron trifluoride and thus, even under these conditions, the intermediates from V and VI must be structurally different. This conclusion is also supported by the fact that recovered pyrazoline VI, after 50% reaction, showed none of isomeric V to be present. The presence of both α,β-unsaturated olefins from the *cis*-pyrazoline and not the *trans*-pyrazoline may reflect a larger effective bulk for the acetyl group coordinated to the boron trifluoride than for the acetyl group alone, thus causing a flattening of the molecule and a change in the availability of the C_4 hydrogens for migration (8).

A reaction in the literature which may well be formally analogous to the pyrolysis of 3-acetylpyrazolines is the reaction of diazoketones with ketenes. In this reaction the product is mainly a result of ring closure to oxygen, although the intermediacy of a pyrazolone has not been demonstrated (19, 20).

Can. J. Chem. Downloaded from www.nrcresearchpress.com by 210.87.254.42 on 09/05/12
For personal use only.

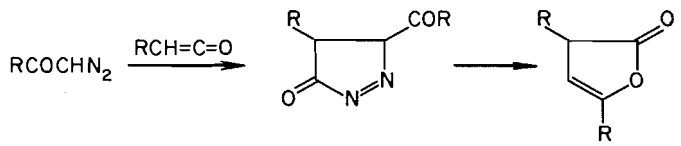

EXPERIMENTAL

Melting points and boiling points are uncorrected. Boiling points were determined by the micro inverted capillary method.

Infrared spectra were measured with a Perkin–Elmer model 137 infracord. The n.m.r. spectra were recorded on a Varian A60 instrument with internal tetramethylsilane as the standard. Samples were run as 30% solutions in carbon tetrachloride and the area integration fits the assigned structure unless otherwise noted. The vapor chromatograms were obtained with an Aerograph A-90-P and a Perkin–Elmer model 226. Percentage compositions were determined by area measurements and are estimated to be accurate to ±2%. The reproducibility was generally found to give values to ±4% from different runs under the same conditions.

The pyrolyses in low-boiling solvents at 125° were carried out on 1% solutions in a sealed tube and, in work-up, the solvent was partially distilled before chromatographic analysis. The vapor pyrolysis was carried out on 3-μl samples in a 1-l flask at 1 mm pressure.

3-Methyl-3-acetyl-Δ¹-pyrazoline (IV)

Methyl isopropenyl ketone (K and K), after purification by precipitation of polymeric impurities with ether, filtration, and distillation (b.p. 95°), was reacted with a solution of diazomethane in ether prepared from nitrosomethyl urea. After distillation of the ether, the product was distilled to give 3-methyl-3-acetyl-Δ¹-pyrazoline (IV), b.p. 45° at 0.3 mm, n_D^{20} 1.4610.

Anal. Calcd. for $C_6H_{10}ON_2$: C, 57.11; H, 7.99; N, 22.20. Found: C, 57.10; H, 7.94; N, 22.30.

An infrared band at 1 720 cm^{-1} and n.m.r. peaks at 5.53 τ (triplet with splitting of 8 c.p.s. for the hydrogens on C_5), 7.73 τ (acetyl methyl), 8.57 τ (methyl on C_3), and a group of peaks from 8.0 to 8.8 τ for the non-equivalent hydrogens on C_4 were consistent with the assigned structure.

Pyrolysis of 3-Methyl-3-acetyl-Δ¹-pyrazoline (IV)

The product analysis on mixtures obtained by pyrolysis of IV under a variety of conditions are listed in Table I. The individual components were isolated by chromatographic separation using a 10-ft didecyl phthalate column of 0.25 inch diameter at 128° with a head pressure of 40 p.s.i. The properties recorded for each component are boiling point, refractive index, retention time, pertinent infrared bands, and n.m.r. peak positions.

3-Methyl-4-penten-2-one (X): b.p. 112°; retention time 10.6 min; infrared bands at 3 030, 1 725, and 1 630 cm^{-1}; n.m.r. peaks at 4.0 to 5.0 τ (group of peaks assigned to the olefin hydrogens), 6.88 τ (pentet with splitting of 7 c.p.s. for the hydrogen on C_3), 7.93 τ (hydrogens on C_1), and 8.81 τ (doublet with J = 6.9 c.p.s. for the methyl on C_3). An analysis was carried out on a mixture (approximately 50:50) of this component and the 2,3-dimethyl-4,5-dihydrofuran component.

Anal. Calcd. for $C_6H_{10}O$: C, 73.43; H, 10.27. Found: C, 73.70; H, 10.50.

2,3-Dimethyl-4,5-dihydrofuran (XI): b.p. 111°; retention time 11.5 min; infrared bands at 1 695, 1 432, and 1 375 cm^{-1}; n.m.r. peaks at 5.92 τ (triplet with splitting of 9.3 c.p.s. for the hydrogens on C_5), 7.54 τ (broadened triplet with splitting of 9.3 c.p.s. for the hydrogens on C_4), and 8.42 τ (broadened singlet for the methyls on C_2 and C_3). This sample was identical in all respects with a sample prepared by an independent route reported below.

cis-3-Methyl-3-pentene-2-one (IX): b.p. 124°; retention time 16.0 min; infrared bands at 1 685 and 1 618 cm^{-1}; n.m.r. peaks at 4.23 τ (multiplet for the hydrogen on C_4), 7.84 τ (hydrogens on C_1), 8.15 τ (methyl on C_3), and 8.19 τ (doublet with J = 7.0 c.p.s. for the hydrogens on C_5). The *cis* assignment is based on the fact that the hydrogen on C_4 appears to higher field than that in the *trans* isomer (12).

Anal. Calcd. for $C_6H_{10}O$: C, 73.43; H, 10.27. Found: C, 73.40; H, 10.14.

1-Methyl-1-acetylcyclopropane (VII): b.p. 128°; n_D^{20} 1.4332 (lit. (21), b.p. 126°; n_D^{20} 1.4330); retention time 17.3 min. This compound was identical with a sample prepared by the procedure of Julia (21) using 5-chloro-3-methyl-2-pentanone and powdered potassium hydroxide. Vapor chromatographic analysis showed less than 1.5% of 2,3-dimethyl-4-5-dihydrofuran in the latter product.

trans-3-Methyl-3-penten-2-one (VIII): b.p. 147°; n_D^{20} 1.4496; retention time 23.6 min; infrared bands at 1 668 and 1 642 cm^{-1}; n.m.r. peaks at 3.36 τ (quartet with J = 7 c.p.s. for the hydrogen on C_4), 7.82 τ (hydrogens on C_1), 8.27 τ (methyl on C_3), and 8.18 τ (doublet with J = 7 c.p.s. for the hydrogens on C_5).

Anal. Calcd. for $C_6H_{10}O$: C, 73.43; H, 10.27. Found: C, 73.59; H, 10.43.

2,3-Dimethyl-4,5-dihydrofuran

α-Methyl-α-acetylbutyrolactone, b.p. 62° at 0.04 mm, n_D^{20} 1.4561 (lit. (21), b.p. 128° at 20 mm, n_D^{20} 1.4560), was prepared by the procedure of Julia (21) from α-acetylbutyrolactone (Aldrich).

Can. J. Chem. Downloaded from www.nrcresearchpress.com by 210.87.254.42 on 09/05/12
For personal use only.

Can. J. Chem. Downloaded from www.nrcresearchpress.com by 210.87.254.42 on 09/05/12
For personal use only.

α-Methyl-α-acetylbutyrolactone (30 g) was hydrolyzed in 100 ml of 5% hydrochloric acid until the solution became homogeneous (30 min). The solution was made basic with potassium hydroxide and saturated with potassium carbonate to give 19.8 g of product which was dried over potassium carbonate and distilled to give 17.8 g (71%) of 3-methyl-2-pentanon-5-ol, b.p. 89° at 18 mm, n_D^{20} 1.4391.

Anal. Calcd. for $C_6H_{12}O_2$: C, 62.03; H, 10.41. Found: C, 61.84; H, 10.40.

3-Methyl-2-pentanon-5-ol (6.8 g) was placed in a 8-ml pear-shaped flask fitted with a short column (4 inches) and a condenser for distillation. A trace of orthophosphoric acid was added and the flask was heated in an oil bath. At a bath temperature of 140° distillation began and was steady at 155° with a head temperature of 94°. Water was removed from the distillate during distillation with a pipette. The organic layer was immediately redistilled to give 4.5 g of 2,3-dimethyl-4,5-dihydrofuran, b.p. 108–110°, n_D^{20} 1.4410.

Anal. Calcd. for $C_6H_{10}O$: C, 73.43; H, 10.27. Found: C, 73.36; H, 10.35.

cis- and trans-3,5-Dimethyl-3-acetyl-Δ¹-pyrazoline (V and VI)

A solution of diazoethane in ether was prepared from nitrosoethyl urea and 40% potassium hydroxide. Isopropenyl methyl ketone was added to this solution until the orange color disappeared and the mixture was distilled to give the pyrazoline mixture, b.p. 56–57° at 1.2 mm.

Anal. Calcd. for $C_7H_{12}NO$: C, 59.97; H, 8.63; N, 19.99. Found: C, 59.60; H, 8.22; N, 20.27.

The n.m.r. spectrum, based on the acetyl resonances, showed this to be 40% of the lower-boiling isomer and 60% of the higher-boiling isomer.

The *cis*- and *trans*-pyrazoline mixture was separated by distillation through a Nester and Faust 45-cm by 6-mm spinning-band column at 0.2 to 0.3 mm with the still pot immersed in an oil bath maintained at 65–70°. Of the various fractions obtained, the best separation gave the lower-boiling fraction 81% pure and the higher-boiling fraction 87% pure as determined by the proportion of the acetyl resonances in the n.m.r. spectra at 7.78 and 7.65 τ respectively. The lower-boiling isomer was assigned the *cis* structure V and the higher-boiling isomer the *trans* structure VI for reasons described in the text. The n.m.r. spectrum of *cis*-3,5-dimethyl-3-acetyl-Δ¹-pyrazoline (V) had peaks at 5.66 τ (sextet with splitting of 7.5 c.p.s. for the C_5 hydrogens), 7.57 τ (two doublets with J_{gem} = 13.0 c.p.s. and J_{vic} = 8.7 c.p.s. for one of the C_4 hydrogens), 7.78 τ (acetyl methyl), 8.40 τ (C_3 methyl), 8.52 τ (doublet with J = 7.0 c.p.s. for the C_5 methyl), and 9.30 τ (two doublets with J_{gem} = 12.9 c.p.s. and J_{vic} = 7.7 c.p.s. for the other C_4 hydrogens). The n.m.r. spectrum of *trans*-3,5-dimethyl-3-acetyl-Δ¹-pyrazoline (VI) had peaks at 5.67 τ (sextet with splitting of 7.4 c.p.s.), 7.65 τ (acetyl methyl), 8.48 τ (doublet with J = 6.0 c.p.s. for the C_5 methyl), 8.53 τ (multiplet for the unresolved C_4 hydrogens), and 8.63 τ (C_3 methyl).

Pyrolysis of cis- and trans-3,5-Dimethyl-3-acetyl-Δ¹-pyrazoline (V and VI)

The product analysis on mixtures obtained by pyrolysis of samples of V and VI of 81 and 87% purity have been corrected to represent compositions from pure V and VI and are recorded in Table II. The individual components were separated using a 10-ft didecyl phthalate column of 0.25 inch diameter at 140° with a head pressure of 48 p.s.i. Compounds XIII and XVI were not separted under these conditions. The combined sample was analyzed by analytical vapor phase chromatography (P-E 226) and n.m.r.

2,3,5-Trimethyl-4,5-dihydrofuran (XVII): b.p. 119–120°; n_D^{24} 1.4305 (lit. (16), b.p. 118.3–118.6° at 746 mm; n_D^{24} 1.4390); retention time 6.2 min; infrared band at 1 698 cm^{-1}; n.m.r. peaks at 5.59 τ (sextet for the hydrogen on C_5), 7.40 τ (two doublets) and 7.98 τ (two doublets) for the hydrogens on C_4, 8.43 τ (broadened singlet for the methyls on C_2 and C_3), and 8.79 τ (doublet with J = 6.1 c.p.s. for the methyl on C_5). The hydrogens on C_4 form the AB part of an $ABXM_3$ system from which the following constants are calculated without second-order corrections: Δ_{AX} = 144.5 c.p.s., Δ_{BX} = 109 c.p.s., Δ_{AB} = 35.5 c.p.s., J_{AB} = 14.5 c.p.s., J_{AX} = 8.0 c.p.s., and J_{BX} = 9.5 c.p.s.

trans-1,2-Dimethyl-1-acetylcyclopropane (XIII): b.p. 137°; n_D^{24} 1.4275; retention time 10.5 min; C=O band at 1 694 cm^{-1}; n.m.r. peaks at 7.86 τ (acetyl methyl), 8.62 τ (C_1 methyl), 9.03 τ (broad peak for the C_2 methyl), and two sets of multiplets in the region from 8.75 to 9.60 τ for the ring hydrogens. A sample (500 μl) of XIII was heated at 220° for 9 h in a sealed tube. Vapor chromatography of the product at 130° showed two peaks at 12.9 min and 21.9 min in the ratio of 85:15 respectively. The components were collected and the latter proved to be identical with *trans*-3-methyl-3-hexen-2-one (XV), while the former was a new compound which on the basis of its n.m.r. spectrum was assigned (17) the structure 3-methyl-5-hexen-2-one, b.p. 138°; n_D^{22} 1.4225; C=O band at 1 710 cm^{-1} and C=C band at 1 643 cm^{-1}; n.m.r. peaks at 4.45 τ (group of peaks from 4.1 to 4.8 τ for the hydrogen on C_5), 5.12 τ (two broadened peaks for the hydrogens on C_6 with separation of 13 c.p.s.), the hydrogens on C_3 and C_4 were not resolved and gave a group of peaks between 7.25 and 8.10 τ, 7.98 τ (singlet for the hydrogens on C_1), and 8.96 τ (doublet with J = 6.7 c.p.s. for the methyl on C_3).

Anal. Calcd. for $C_7H_{12}O$: C, 74.95; H, 10.78. Found: C, 74.97; H, 10.78.

The chromatographic separation of *trans*-1,2-dimethyl-1-acetylcyclopropane (XIII) and 3-methyl-4-hexen-2-one (XVI) could only be accomplished on the analytical P-E 226 instrument. Microanalysis was carried out on the mixture of XIII and XVI.

Anal. Calcd. for $C_7H_{12}O$: C, 74.95; H, 10.78. Found: C, 74.87; H, 10.91.

For the above data on XIII the mixture was treated with bromine in carbon tetrachloride and then separated by v.p.c. to give pure XIII. The n.m.r. spectrum of the mixture of XVI and XIII established the

structure of XVI to be 3-methyl-4-hexen-2-one through the presence of peaks at 4.57 τ (multiplet for the two vinyl hydrogens on C_4 and C_5), 7.97 τ (hydrogens on C_1), 8.32 τ (doublet with J = 4.8 c.p.s. for the hydrogens on C_6), and 8.92 τ (doublet with J = 7.0 c.p.s. for the methyl on C_3).

cis-3-Methyl-3-hexen-2-one (XIV): b.p. 145° (lit. (15), b.p. 151° for 3-methyl-3-hexen-2-one); n_D^{24} 1.4370; retention time 12.2 min; infrared bands at 1 692 and 1 620 cm^{-1}; n.m.r. peaks at 4.44 τ (broadened triplet with J = 7.2 c.p.s. for the hydrogen on C_4), 7.73 τ (multiplet for the hydrogens on C_5), 7.86 τ (hydrogens on C_1), 8.12 τ (broadened singlet for the methyl on C_3), and 9.02 τ (triplet with J = 7.3 c.p.s. for the hydrogens on C_6). The higher position of the vinyl hydrogen (4.44 τ) compared to the *trans* isomer (3.52 τ) is the basis for the *cis* assignment to this isomer (12).

Anal. Calcd. for $C_7H_{12}O$: C, 74.95; H, 10.78. Found: C, 75.02; H, 10.77.

cis-1,2-Dimethyl-1-acetylcyclopropane (XII): b.p. 152°; n_D^{24} 1.4376; retention time 15.7 min; C=O at 1 680 cm^{-1}; n.m.r. peaks at 8.00 τ (acetyl methyl), 8.72 τ (methyl on C_1), 8.88 τ (distorted doublet for the methyl on C_2), and two of the ring hydrogens centered around 8.68 τ and one centered around 9.74 τ. (See assignment under the *trans* isomer XIII.)

Anal. Calcd. for $C_7H_{12}O$: C, 74.95; H, 10.78. Found: C, 74.85; H, 10.95.

trans-3-Methyl-3-hexen-2-one (XV): b.p. 157°; n_D^{23} 1.4481; retention time 17.7 min; infrared bands at 1 680 and 1 650 cm^{-1}; n.m.r. peaks at 3.52 τ (broadened triplet with J = 7.6 c.p.s. for the hydrogen on C_4), 7.76 τ (multiplet for the hydrogens on C_5), 7.81 τ (hydrogens on C_1), 8.39 τ (broadened singlet for the methyl on C_3), and 8.93 τ (triplet with J = 7.5 c.p.s. for the hydrogens on C_5). (See assignment under the *cis* isomer XIV.)

Anal. Calcd. for $C_7H_{12}O$: C, 74.95; H, 10.78. Found: C, 75.03; H, 10.81.

Boron Trifluoride Catalyzed Pyrolysis of V and VI

A solution of 0.2 ml (0.0015 mole) of the pyrazoline in 10 ml of anhydrous ether was cooled to 15°. To this solution was added with stirring 0.21g (0.0015 mole) of boron trifluoride etherate (b.p. 126°) in 1 ml of ether. Decomposition was complete in 25 min. The ether solution was washed with ice-cold water until neutral, dried with sodium sulfate, and analyzed by chromatography. The results are reported in Table II.

The above procedure was followed with 0.5 ml of *trans*-pyrazoline VI (99% pure) and 0.5 g of boron trifluoride etherate in 5 ml of ether at 0 °C. After 50% (35 ml) of the theoretical volume of nitrogen had been evolved, the reaction was worked up as above. Removal of all of the ether and pyrolysis products on a vacuum line left a pyrazoline sample which showed no evidence of the *cis* isomer in its n.m.r. spectrum.

Photolysis of Pyrazolines IV, V, and VI

Photolyses were carried out on 5% solutions in refluxing ether in a pyrex vessel by irradiation with a 450-W Hanovia medium-pressure mercury lamp No. 79A36. The product obtained from IV contained VII, VIII, IX, X, and XI in the ratio of 78:4:3:1:14. The products obtained from V and VI, as corrected to 100% pure samples, contained XII, XIII, XIV, XV, XVI, and XVII in the ratios of 59:28:1:0:6:6 and 21:70:2:1:4:2 respectively. The products were stable to photolysis under the reaction conditions. Not more than 1% of methyl isopropenyl ketone was formed from IV, V, or VI.

ACKNOWLEDGMENTS

The authors gratefully appreciate the support received for this work from the National Research Council of Canada and from the Committee on Research of the University of British Columbia.

Thanks are also extended to Mrs. A. Aldrich for some microanalyses and to Mrs. E. Brion and Mr. P. Horn for some of the n.m.r. spectra.

REFERENCES

1. D. E. McGREER, R. S. McDANIEL, and M. G. VINJE. Can. J. Chem. This issue.
2. W. G. YOUNG, L. J. ANDREWS, S. L. LINDENBAUM, and S. J. CRISTOL. J. Am. Chem. Soc. **66**, 810 (1944).
3. J. B. CLOKE, R. J. ANDERSON, J. LACHMANN, and G. E. SMITH. J. Am. Chem. Soc. **53**, 2791 (1931).
4. T. H. MARSHALL and W. H. PERKIN, JR. J. Chem. Soc. 853 (1891).
5. H. W. BERSCH, R. MEYER, A. V. MLETZKO, and K. H. FISCHER. Arch. Pharm. **291**, 82 (1958).
6. A. S. SOPOVA, V. V. PEREKALIN, and YA. S. BOBOVICH. Zh. Obshch. Khim. **31**, 1528 (1961).
7. W. H. PERKIN, JR. J. Chem. Soc. 792 (1887).
8. D. E. McGREER, N. W. K. CHIU, M. G. VINJE, and K. C. K. WONG. Can. J. Chem. This issue.
9. R. HUISGEN, H. STANGL, H. J. STURM, and H. WAGENHOFER. Angew. Chem. **73**, 170 (1961).
10. E. L. ELIEL, H. HAUBENSTOCK, and R. V. ACHARYA. J. Am. Chem. Soc. **83**, 235 (1961).
11. T. V. VAN AUKEN and K. L. RINEHART, JR. J. Am. Chem. Soc. **84**, 3736 (1962).
12. L. M. JACKMAN and R. H. WILEY. J. Chem. Soc. 2881 (1960).
13. R. FRASER. Can. J. Chem. **40**, 78 (1962).
14. K. L. WILLIAMSON. J. Am. Chem. Soc. **85**, 517 (1963).
15. E. ROHRMAN and H. G. SHOULE. J. Am. Chem. Soc. **66**, 1519 (1944).

Can. J. Chem. Downloaded from www.nrcresearchpress.com by 210.87.254.42 on 09/05/12
For personal use only.

16. YU. K. YUR'EV and E. G. ROSANTSEV. Vestn. Mosk. Univ. Ser. Mat. Mekhan. Astron. Fiz. i Khim. No. 6, 171 (1959); Chem. Abstr. **54**, 19637*f* (1960).
17. D. E. MCGREER, N. W. K. CHIU, and R. S. MCDANIEL. Proc. Chem. Soc. 415 (1964).
18. G. NOMINÉ and D. BERTIN. Bull. Soc. Chim. France, 550 (1960).
19. K. B. WIBERG and T. H. HUTTON. J. Am. Chem. Soc. **76**, 5367 (1954).
20. P. YATES and T. J. CLARK. Tetrahedron Letters, 435 (1961).
21. M. JULIA, S. JULIA, and Y. NOEL. Bull. Soc. Chim. France, 1708 (1960).
22. D. E. MCGREER, W. WAI, and G. CARMICHAEL. Can. J. Chem. **38**, 2410 (1960).

Can. J. Chem. Downloaded from www.nrcresearchpress.com by 210.87.254.42 on 09/05/12
For personal use only.

Can. J. Chem. Downloaded from www.nrcresearchpress.com by 210.87.254.6 on 09/05/12
For personal use only.

PYRAZOLINES

VI. THE STEREOCHEMISTRY IN THE PYROLYSIS OF PYRAZOLINES FOR THE C_3 AND C_5 POSITIONS OF THE PYRAZOLINE MOLECULE[1,2]

DONALD E. MCGREER, NORMAN W. K. CHIU,
MAGNUS G. VINJE, AND KEN C. K. WONG
Department of Chemistry, University of British Columbia, Vancouver, British Columbia
Received November 13, 1964

Dedicated to Professor R. B. Sandin on the Occasion of his Sixty-Eighth Birthday

ABSTRACT

cis- and *trans*-3,5-Dimethyl-3-carbomethoxy-Δ^1-pyrazoline (IV and V) have been separated, and product analysis for the pyrolysis and photolysis of these compounds has been completed. The cyclopropane products are formed with some change in the relative configuration of the *cis–trans* groups in both reactions. The α,β-unsaturated olefin product is formed stereospecifically with IV, yielding methyl 2-methyl-*cis*-2-pentenoate (XI), and with V, yielding methyl 2-methyl-*trans*-2-pentenoate (X). The results of the pyrolysis and photolysis of *cis,trans*-3,4,5-trimethyl-3-carbomethoxy-Δ^1-pyrazoline are also described. The product studies and some kinetic studies are the basis of a new mechanism proposed for the pyrolysis of pyrazolines.

Recent studies on the pyrolysis of pyrazolines have reopened the question regarding the stereochemistry of the conversion of pyrazolines into cyclopropanes (1–3). This reaction was reported by von Auwers (4) to be essentially stereospecific and this was the accepted view on the reaction for many years (stereospecific here is used to mean that the substituents on the cyclopropane ring have the same *cis–trans* relationship as on the initial pyrazoline). Van Auken and Rinehart (1) showed that the pyrolysis of a pair of isomeric pyrazolines with methyls *cis* and *trans* on C_3 and C_4 (compounds I and II) gave cyclopropanes with effective randomization of this *cis–trans* relationship. On the other hand, Overberger and Anselme (2) have found that the pyrolysis of *trans*-3,5-diphenyl-Δ^1-pyrazoline (III) gave stereospecifically the *trans*-1,2-diphenylcyclopropane, and thus the stereochemistry of this reaction is not clear.

We have prepared some new pyrazolines, which show a *cis–trans* relationship at positions C_3 and C_5, in an effort to find out more about the pyrolysis reaction. The preparation of a *cis–trans* mixture of 3,5-dimethyl-3-carbomethoxy-Δ^1-pyrazoline and its pyrolysis was reported earlier (5). This mixture has now been separated by distillation through a spinning-band column at a temperature slightly below the pyrolysis temperature. The lower-boiling isomer has been assigned the structure with the methyl groups *cis* (IV) and the higher-boiling isomer that with the methyl groups *trans* (V). The preparation and

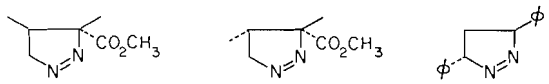

I II III

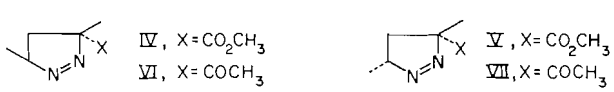

[1]*Presented in part at the 148th Meeting of the American Chemical Society, Chicago, Illinois, September, 1964.*
[2]*Taken in part from the M.Sc. Thesis of N. W. K. Chiu and the B.Sc. Thesis of M. G. Vinje.*

pyrolysis of a related pair of isomers having an acetyl group in place of the carbomethoxy group (VI and VII) have also been studied in this laboratory (6).

The stereochemical assignment to the pyrazolines has been discussed in detail earlier (6) and similar arguments are applicable to compounds IV and V. The predominant formation of the higher-boiling isomer (3:2) ratio suggests that it has the methyl groups *trans*. The fact that photolysis of the lower-boiling isomer gives predominantly (3:1) (see Table III) the cyclopropane with the methyls *cis*, and conversely the higher-boiling isomer gives predominantly (3:1) the cyclopropane with the methyls *trans*, suggests also that the higher-boiling isomer has the methyls *trans*, since the photolysis reaction has been found in an earlier case to be more stereospecific than the pyrolysis reaction (1). The nuclear magnetic resonance (n.m.r.) spectrum of the higher-boiling isomer shows the C_3 hydrogens at 8.28 and 8.56 τ, consistent with the suggestion made earlier (6) that the hydrogen *cis* to the carbomethoxy group is shielded by the —N=N— group and deshielded by the carbomethoxy group, with the result that its chemical shift remains close to the other C_4 hydrogen. In the other isomer, the C_4 hydrogens appear at 7.68 and 9.14 τ, consistent with deshielding of the hydrogen *cis* to the carbomethoxy group by the carbomethoxy group to give a chemical shift of 7.68 τ and with shielding of the hydrogen *trans* to the carbomethoxy group by the —N=N—. Folding of the molecule to make such differential shielding is illustrated in structures XX and XXI.

The n.m.r. spectra of mixtures of pyrazolines IV and V can readily be used to estimate the composition of these mixtures, since the ester methyl peak of V is 0.06 p.p.m. downfield from the ester methyl peak of IV. The samples of IV and V used for the product study were 83% and 100% pure respectively. The results reported in Tables I and II on material of 83% purity have been corrected for the 17% of V present.

The products from the pyrolysis of pyrazolines IV and V have been reported earlier (5). It has now been possible to confirm by n.m.r. the *cis–trans* relationship of the methyl 2-methyl-2-pentenoates to be as reported therein (see eq. [a]). The product composition has been found to be sensitive to the pyrazoline used and the conditions of pyrolysis. The results from a number of runs are given in Table I.

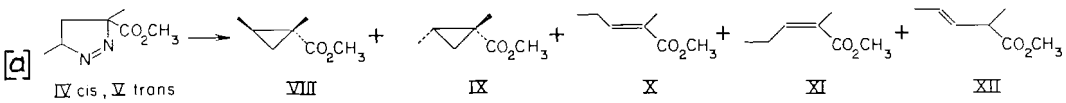

There are two striking features in this data. First, α,β-olefin formation is essentially stereospecific with the *cis* olefin XI being formed from the *cis*-pyrazoline IV and the *trans* olefin X being formed from the *trans*-pyrazoline V. Even the small amounts of X formed from IV could be due to errors in the estimation of the products for 100% pure IV. Second, the cyclopropane with the methyls *trans* (IX) is the predominant cyclopropane from the *cis*-pyrazoline IV and the cyclopropane with the methyls *cis* (VIII) is the predominant cyclopropane from the *trans*-pyrazoline V. The cyclopropane-forming reaction, however, does not have the high stereospecificity that the olefin-forming reaction has and *requires* inversion at *either* C_3 or C_5 during cyclopropane formation.

The effect of solvent on the reaction has been to raise the proportion of the olefins in the product as the dielectric constant of the solvent is increased. At the same time there has been little change in the stereospecificity of the reaction. In an earlier study we found (7) that the rate of pyrolysis of a 4,4-dialkyl-3-cyano-3-carbomethoxy-Δ^1-pyrazoline (XIII) was faster in polar solvents than in nonpolar solvents. For comparison we have

Can. J. Chem. Downloaded from www.nrcresearchpress.com by 210.87.254.6 on 09/05/12
For personal use only.

TABLE I

Product compositions for the pyrolysis of *cis*- and *trans*-3,5-dimethyl-3-carbomethoxy-Δ^1-pyrazolines (IV and V)

Sample	Reaction conditions	Dielectric constant (D)	Δ		α,β		β,γ
			cis VIII	*trans* IX	*trans* X	*cis* XI	XII
IV (*cis*)	Neat liquid at 100°		18	48	0	32	2
	Gas phase at 125°		23	65	2	5	5
	125° in cyclohexane	2	30	55	3	11	1
	125° in ether	4.5	25	56	2	16	1
	125° in methanol	31.5	21	38	4	35	2
	125° in acetonitrile	37	21	42	4	31	2
	125° in formamide	109	19	33	2	44	2
	81° in cyclohexane		25	62	0	12	1
V (*trans*)	Neat liquid at 100°		60	15	22	0	3
	Gas phase at 125°		76	15	3	1	5
	125° in cyclohexane	2	72	20	6	0	2
	125° in ether	4.5	66	18	13	0	3
	125° in methanol	31.5	48	6	44	0	3
	125° in acetonitrile	37	67	6	25	0	2
	125° in formamide	109	31	12	52	0	5
	81° in cyclohexane		79	14	6	0	1

TABLE II

Kinetics for the pyrolysis of a sample of 40% IV and 60% V

Solvent	Dielectric* constant (D)	$t_{\frac{1}{2}}$ (min^{-1})
n-Butyl ether	3.06 at 25°	26.2
Tetralin	2.78 at 20°	29
Nitrobenzene	34.8 at 20°	43.6
Formamide	109 at 20°	83.1

*A. C. Maryott and E. R. Smith, Table of dielectric constants of pure liquids, National Bureau of Standards Circular No. 514, 1951.

determined the kinetics of the pyrolysis of a mixture of IV and V in four solvents. The results of these runs at 100° in butyl ether, tetralin, nitrobenzene, and formamide are given in Table II. The polarity of the solvent has little effect on the rate and one must conclude that for pyrazolines related to IV and V there is no increase and possibly some decrease in the polarity of the transition state over the starting material.

The mechanism proposed for the pyrolysis of pyrazolines related to IV and V suggests that the initial step of the reaction is the breaking of the N_2—C_3 bond (1). Immediately

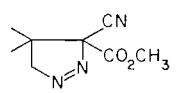

XIII

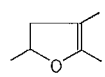

XVI

XIV XV

Can. J. Chem. Downloaded from www.nrcresearchpress.com by 210.87.254.6 on 09/05/12
For personal use only.

one anticipates free rotation around the single bonds of XV and such has been suggested (1). If the lifetime of XV is sufficiently long to permit rotations, then we would expect (A) reversal of step 1 would give some pyrazoline with inversion of geometry at C_3, and (B) the product analysis from any pair of pyrazolines isomeric at C_3 should be independent of the starting material since, because of rapid inversion of C_3 in XV or because of its planar nature (8), the intermediate from the two pyrazoline isomers would be identical.

These conditions are not satisfied. We have carried out the pyrolysis of *trans*-pyrazoline V to 50% reaction and the recovered pyrazoline was pure *trans* as determined by n.m.r. under conditions which would have detected 1% of the *cis* isomer IV. Similar results have been obtained by van Auken and Rinehart (1) on I. The product analyses from IV and V show many differences (Table I). Even in the pyrolysis of pyrazolines I and II where the cyclopropane products are formed with randomization at C_3, there is a major difference in the proportion of olefin to cyclopropane product corresponding to 3.97:1.70 and 1.31:2.22 respectively. We have repeated this reaction in the gas phase and find that this difference is still present.

The product analyses for the pyrolysis of the isomeric 3-acetylpyrazolines VI and VII also show differences which cannot be explained by an intermediate like XV (6). 2,3,5-Trimethyl-4,5-dihydrofuran (XVI) was formed from VI and not from VII. It is interesting that a comparison of the products from the 3-carbomethoxy derivatives (IV and V) and the 3-acetyl derivatives (VI and VII) has been found to suggest that the dihydrofuran (XVI) is being formed at the expense of the *trans*-cyclopropane (6).

Pertinent to the question of bond breaking in the transition state are the recent results of Seltzer on acyclic azo compounds. Kinetic studies on the pyrolysis of azo-bis-α-phenylethane (XVII) (9), α-phenylethylazo-2-propane (XVIII) (10), α-phenylethylazomethane (XIX) (11), and their α-deuterium derivatives have shown that for XVII both C—N bonds are breaking equally in the transition state, for XVIII the C—N bonds are both breaking but to a different degree, and for XIX only the C—N bond with the α-phenyl substitution is breaking in the transition state.

A similar spectrum of situations may also be present in the cyclic azo systems where symmetric pyrazolines like III would have both C—N bonds breaking equally in the transition state. Pyrazolines like I, II, IV, and V would have unequal breaking of the bonds, but would still retain some bonding for both C—N bonds in the transition state. A study on the kinetics of the pyrolysis of a number of pyrazolines related to I–VII (12) has found that substitution of H by CH_3 at C_5 causes a sevenfold increase in rate. This effect and similar substitution factors at C_3 also suggest that both C—N bonds are being broken in the transition state. For pyrazolines related to XIII the transition state is highly polar, and yet the product suggests some bonding of N_2 to C_3 in the transition state (7). This could be caused by an intermediate like XV having a short lifetime with respect to rotation.

The conformation of the pyrazolines will be controlled by the large groups present (two methyls and a carbomethoxy group), since the gauche interactions of hydrogens have little effect in locking a cyclopentene ring into a specific conformation (13). The coupling constants for the C_5 hydrogen with each of the C_4 hydrogens are almost the same (8.6 c.p.s. for the *cis* and 8.3 c.p.s. for the *trans* pair in IV and 8.0 c.p.s. for both pairs in V). If we assume a projected angle of 120° for the geminal C_4 hydrogens and that the Karplus equation (14) is applicable, with a possible upward displacement of the curve because of substituent effects (15), then equal coupling constants predict dihedral angles of 25 and 145° (calculated values of J for 25° and 145° (14) are 6.5 and 6.2 c.p.s. respectively). From the calculations of Abraham and McLauchlan (16) on a C_5 cyclopentane

Can. J. Chem. Downloaded from www.nrcresearchpress.com by 210.87.254.6 on 09/05/12
For personal use only.

structure, this will correspond to a folding of the pyrazoline ring to the extent that the plane of atoms 3, 4, and 5 would make an angle of slightly less than 25° with the plane of atoms 5, 1, 2, and 3 in agreement with models of this system. Because of the assumptions made here, this is only an approximate result but confirms the folding of the ring assumed earlier. If results on studies on the cyclopentene system (13) can be applied to this system, we can further assume that variations from this mean by tens of degrees can occur with little increase in the potential energy.

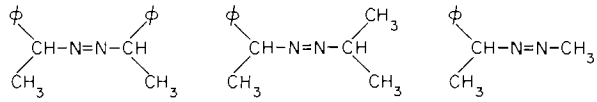

XVII XVIII XIX

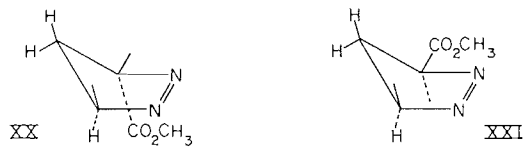

XX XXI

Free volences represent methyls.

An explanation of the stereochemistry of the olefin-forming reaction is therefore possible, if we assume that hydrogen migration is concerted with nitrogen elimination. Hydrogen migration concerted with bond breaking has been suggested in other pyrolysis reactions (17, 18). As a result of the nonplanar conformation of the pyrazoline ring in IV and V, one of the C_4 hydrogens is in a better position to migrate to C_5 than the other as it is *trans* to the nitrogen (the C_4 hydrogen *cis* to the carbomethoxy group in XX and that *trans* to the carbomethoxy group XXI). It is just these hydrogens which must migrate to give the α,β-unsaturated systems with the geometry found experimentally. Similarly, the migration of the same hydrogen to C_3 would give, in both cases, the β,γ-unsaturated system with the *trans* geometry. It is therefore significant that the *trans* β,γ-ester is formed and none of the *cis* ester has been detected in the pyrolysis of IV and V. The relative proportion of α,β- to β,γ-unsaturated product should therefore be a measure of the relative migrational aptitude of hydrogen as a hydride or a proton. An examination of the few studies (earlier work from this laboratory primarily) which have measured both α,β- and β,γ-unsaturated products shows this ratio to be around 10:1. The charge delocalization of the anion or cation center may, however, be important in determining this ratio.

The cyclopropane-forming reaction gives such a variety of stereochemical results that a simple explanation does not present itself. The fact that the product composition changes with the conditions of the reaction suggests that the cyclopropane products are formed through a slightly different transition state (and presumably less polar) than the olefins. This transition state may well be a diradical or dipolar structure along the lines of XV, which could be expected to give the retention and inversion found for this reaction. To obtain predominant inversion at one of C_3 or C_5, one can simply require that nitrogen is lost stepwise (3) and that the second step is backside displacement.

The ring-opened intermediate as drawn in XV would be expected to be more polar and have quite a different energy from that expected for the transition state envisioned for the olefin-forming step. For these reasons and since pyrolysis gives no methyl

Can. J. Chem. Downloaded from www.nrcresearchpress.com by 210.87.254.6 on 09/05/12
For personal use only.

methacrylate (a product which should be formed by a low-energy process from a ring-opened intermediate), we favor a process which is concerted.

To obtain inversion by a concerted process, let us consider two extremes for nitrogen elimination.

(*i*) Loss of nitrogen by a stretching vibration in the plane of atoms 3, 4, and 5 would be accompanied by formation of two p-orbitals at C_3 and C_5 which, because of their orientation towards each other, would couple to give product of retained configuration.

(*ii*) Loss of nitrogen by a stretching vibration perpendicular to the plane of atoms 3, 4, and 5 would be expected to give two p-orbitals at C_3 and C_5 parallel to each other. However, the substituents on C_3 and C_5 would be sufficiently close that the parallel orientation could only be approximated. To accommodate this steric factor a greater stretching of one C—N bond in the transition state would permit a twisting of the molecule and stacking of the groups which interact sterically. Such stacking would lead to p-orbitals at C_3 and C_5 in a position to give inversion at one center.

Whether *i* or *ii* is concerted or not depends on whether the developing p-orbitals on C_3 and C_5 overlap in the transition state or not. Process *i*, if concerted, would then be identical with the process proposed for the photochemical reaction by van Auken and Rinehart (1). Process *ii*, if not concerted, simply adds a geometrical restriction to the dipolar intermediate earlier proposed.

In the actual reaction a situation between *i* and *ii* is expected, and thus both inversion and retention are anticipated, with the proportion depending on the conformations available for reaction and the substituents present. Further work on the stereochemistry of this reaction is therefore justified.

In a further pyrazoline which we have studied, we wished to examine the stereochemistry at both C_3 and C_5 relative to an independent center (at C_4) and not just relative to each other. The results are somewhat clouded by the fact that the pyrazoline used was a mixture, but the results are still informative and are described below.

Addition of diazoethane to methyl tiglate gave a pyrazoline product which by n.m.r. appeared to be a 90:10 mixture. It was assumed, on the grounds that steric effects will be important and that the geometry at C_3 and C_4 for both isomers will be that of methyl tiglate (1), that the major pyrazoline was XXII and the minor one was XXIII (see eq. [*b*]).

Pyrolysis of this pyrazoline mixture gave three products identified as methyl *cis,trans*-1,2,3-trimethyl-1-cyclopropanecarboxylate (XXIV), methyl *cis,cis*-1,2,3-trimethyl-1-cyclopropanecarboxylate (XXV), and methyl 2,3-dimethyl-2-pentenoate (XXVI) (see eq. [*c*]). Von Auwers and Konig (4) have reported that the pyrolysis of the same pyrazoline gave XXIV and XXVI in the proportion of 86:14 as estimated by bromine titration.

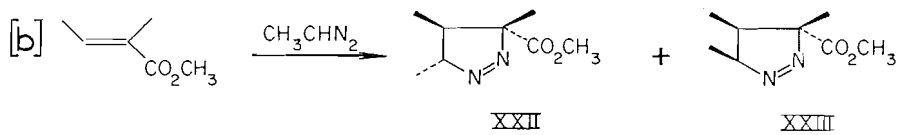

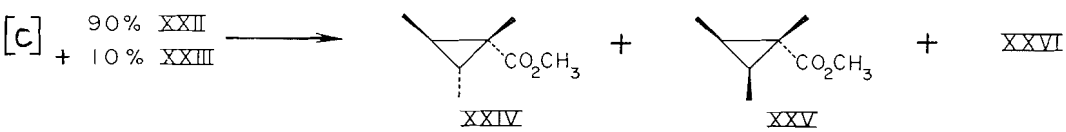

	XXIV	XXV	XXVI
pyrolysis	61%	32%	6%
photolysis	88%	10%	—

Can. J. Chem. Downloaded from www.nrcresearchpress.com by 210.87.254.6 on 09/05/12
For personal use only.

The n.m.r. spectrum of XXIV was used for its structural assignment. Peaks for three ring methyl groups appear at 8.80 τ (C_1 methyl) and 8.91 and 8.94 τ (doublets). The methyl at 8.91 τ is split by a hydrogen at 9.37 τ and the methyl at 8.94 τ is split by a hydrogen at 8.67 τ. Only structure XXIV satisfies non-equivalence of the methyls and the hydrogens on C_2 and C_3. The chemical shift separation between the ring hydrogens is undoubtably due to the anisotropy of the carbonyl of the ester group, which by comparison with other cyclopropanecarboxylic acid esters (19) and cyclopropanecarboxylic acids (19–22) would be expected to deshield the hydrogen *cis* to it.

The n.m.r. spectrum of XXV shows, in addition to the C_1 methyl at 8.96 τ, a doublet at 9.07 τ for the two equivalent methyls on C_2 and C_3 and a multiplet at 8.59 τ for the two ring hydrogens. The low-field position of the ring hydrogens suggests that they are *cis* to the carbomethoxy group. This assignment would also follow if the cyclopropane formation in the photolysis reaction were assumed to be stereospecific (1).

Formation of cyclopropane XXIV requires retention at C_5 from at least 55% of XXII and formation of XXV requires inversion at C_5 from at least 25% of XXII in the pyrolysis reaction. Total inversion at C_5 therefore need not be a mechanistic requirement of the pyrolysis reaction.

Photolysis of Pyrazolines

The products from the photolysis of the *cis–trans* pair of pyrazolines IV and V under a number of conditions were analyzed and the results are recorded in Table III. When

TABLE III

Product compositions for the photolysis of *cis*- and *trans*-3,5-dimethyl-3-carbomethoxy-Δ^1-pyrazoline

		Δ		α,β			X*
Sample	Reaction conditions	*cis* VIII	*trans* IX	*trans* X	*cis* XI	β,γ XII	
IV (*cis*)	81° in cyclohexane	42	46	1	6	1	4
	35° in ether	61	23	2	6	2	6
	23° in formamide	53	21	6	9	1	10
V (*trans*)	81° in cyclohexane	45	46	3	1	1	4
	35° in ether	22	65	5	0	2	6
	−55° in ether	25	53	10	1	4	7
	23° in formamide	15	58	16	2	3	6

*Methyl methacrylate.

the photolysis products are compared to the products from pyrolysis, we find a higher percentage of cyclopropane derivatives present, the formation of an additional product from cleavage of the molecule at the N_2—C_3 and C_4—C_5 bonds, and a different stereochemical result. Even when the photolysis is carried out at the same temperature and in the same solvent as the pyrolysis reaction we find that these differences are still present. In refluxing cyclohexane the rate of nitrogen evolution during photolysis was 3 times the rate of nitrogen evolution during pyrolysis only, and thus both reactions can be studied under these conditions (Tables I and III). Photolysis at −55° in ether gives essentially the same product ratio as the photolysis in refluxing ether.

Van Auken and Rinehart (1) have also observed significant differences between the pyrolysis and photolysis of I and II. They found the cyclopropanes formed by photolysis to be formed stereospecifically and suggested a molecular mechanism with bonding between C_3 and C_5 taking place concerted with nitrogen elimination.

Can. J. Chem. Downloaded from www.nrcresearchpress.com by 210.87.254.6 on 09/05/12
For personal use only.

It seems unlikely that the electronically excited molecule would decompose more readily than the ground-state molecule. Thus, photodecomposition probably results from regeneration of the ground-state molecule with excess vibrational and rotational energy. The amount of this excess energy is probably more than enough for decomposition (this is suggested by the appearance of a new mode of decomposition to give methyl methacrylate), and thus small factors like conformational preferences would have less control on this reaction. The higher energy of the reacting molecules might lead to a more nearly planar (mean conformation) transition state with a result closer to mechanism *i* than for the pyrolysis reaction. This explanation is preferred to one invoking a completely new mechanism for the photolysis reaction, since the effect of solvent and the stereospecificity in olefin formation are still present but not to the same degree as in the pyrolysis reaction.

EXPERIMENTAL

The apparatus and procedures used were the same as reported earlier (6).

cis- and trans-3,5-Dimethyl-3-carbomethoxy-Δ^1-pyrazoline (IV and V)

This pyrazoline was prepared as reported earlier (5) and fractionally distilled with a Nester and Faust 45 cm by 6 mm spinning-band still at a pressure of 1 mm and with the still pot in an oil bath held between 80 and 90°. The head temperature varied from 55 to 65° but was not an accurate measure of the boiling point, as pyrolysis occurred, to some extent, simultaneous with distillation and thus the head pressure fluctuated during distillation. The lower-boiling fraction was not obtained pure and contained 13% of the higher-boiling fraction as determined by n.m.r. The n.m.r. peaks attributable to the lower-boiling fraction were at 5.42 τ (sextet with splitting of about 7.5 c.p.s. for the hydrogen on C_5), 6.33 τ (ester methyl), 7.68 τ (two doublets with J_{gem} = 12.9 c.p.s. and J_{vic} = 8.6 c.p.s. for one of the C_4 hydrogens), 8.38 τ (methyl on C_3), 8.51 τ (doublet with J = 7.0 c.p.s. for the methyl on C_5), and 9.14 τ (two doublets with J_{gem} = 12.8 c.p.s. and J_{vic} = 8.3 c.p.s. for the second hydrogen on C_4). This isomer was assigned the structure IV with the methyls *cis* (see the text).

The higher-boiling fraction was obtained essentially pure and showed peaks in the n.m.r. at 5.43 τ (sextet with splitting of about 7.5 c.p.s. for the hydrogen on C_5), 6.27 τ (ester methyl), 8.28 τ (two doublets with J_{gem} = 12.8 c.p.s. and J_{vic} = 8.0 c.p.s. for one of the C_4 hydrogens), 8.55 τ (doublet with J = 7.0 c.p.s. for the methyl on C_5), 8.56 τ (two doublets with J_{gem} = 12.6 c.p.s. and J_{vic} = 8.0 c.p.s. for the second hydrogen on C_4), and 8.63 τ (methyl on C_3). This isomer was assigned the structure V with the methyls *trans* (see the text).

Pyrolysis and Photolysis of IV and V

Pyrolysis in the vapor phase was carried out on a 3-μl sample placed in a 1-l flask. The flask was evacuated to 1 mm with the sample cooled in a side arm in liquid nitrogen. The flask was closed with a stopcock and placed in an oven at 125°. The sample completely vaporized before its pyrolysis temperature was reached.

Pyrolyses in solvents were carried out at 125° on 200-μl samples of IV or V in 25 ml of solvent in a sealed tube. For low-boiling solvents the solvent was distilled through a spinning-band column and the concentrated solution was analyzed by vapor chromatography. For formamide the volatile products were removed from the solvent on a vacuum line.

The photolysis was carried out by placing a Hanovia 450-W medium-pressure mercury arc 6 inches from a flask containing the sample and by allowing the solvent to reflux. For the run at −55° the sample flask was cooled by an external coolant flowing through a jacket around the flask and insulated by another air jacket. Ethanol was used as the coolant and was cooled to −55° before it was pumped through the cooling jacket.

The products from the pyrolysis and photolysis of pyrazolines IV and V are listed in Tables I and III. The individual products have been previously identified. A n.m.r. spectrum has now been obtained on methyl *cis*-2-methyl-2-pentenoate and showed peaks at 4.16 τ (broadened quartet with J = 7.2 c.p.s. for the hydrogen on C_3), 6.34 τ (ester methyl), 7.55 τ (multiplet for the hydrogens on C_4), 8.15 τ (broadened singlet for the methyl on C_2), and 9.02 τ (triplet with J = 7.4 c.p.s. for the hydrogens on C_5). The higher field position (23) for the hydrogen on C_3 compared to that in the *trans* isomer (3.48 τ (5)) confirms the assignment of geometry given to these isomers earlier (5).

Kinetics of the Pyrolysis of IV and V

The apparatus used consisted of a flask heated in a constant temperature bath held at 100.5 ± 0.5°. The solvent (6 ml) was preheated in the bath and a 250-μl sample (40% IV and 60% V) was added with thorough mixing. The flask was connected to a 100-ml burette and the time for generation of each 2-ml sample was recorded until 60–80% reaction. The infinity point (≃ 40 ml) was determined by raising the

Can. J. Chem. Downloaded from www.nrcresearchpress.com by 210.87.254.6 on 09/05/12
For personal use only.

temperature of the reaction to complete the reaction and cooling it to 100°. Plots of $\log -(V_\infty/(V_\infty - V_t))$ vs. t gave straight lines except for *n*-butyl ether which gave some divergence above 70% reaction. The $t_{\frac{1}{2}}$ values from runs in *n*-butyl ether, tetralin, nitrobenzene, and formamide are recorded in Table II.

3,4,5-Trimethyl-3-carbomethoxy-Δ¹-pyrazoline

Tiglic acid (Aldrich) was esterified with diazomethane and the methyl tiglate was distilled. To 15 g of methyl tiglate was added three portions of diazoethane in ether (prepared from 25 g of nitrosoethylurea) over a 1-week period. After the reaction was complete the mixture was distilled to give 4 g of pyrazoline, b.p. 50° at 0.005 mm, n_D^{25} 1.4536 (lit. (24), b.p. 88° at 3 mm, $n_{H_2O}^{20}$ 1.453). The n.m.r. spectrum fitted a pyrazoline structure with peaks at 6.12 τ (multiplet for the C_5 hydrogen), 6.33 τ (ester methyl), 8.30 τ (multiplet for the C_4 hydrogen), 8.62 τ (doublet with J = 7 c.p.s. for the C_5 methyl), 8.92 τ (C_3 methyl), and 9.09 τ (doublet with J = 6.5 c.p.s. for the C_4 methyl). The assignments of the methyl groups are based on the fact that the peaks of the doublet at 8.62 τ are more nearly equal in intensity and therefore coupled to a hydrogen further downfield than the doublet at 9.09 τ. There is evidence for a second pyrazoline as a result of peaks at 6.42 τ (singlet), 7.71 τ (multiplet), and 9.34 τ (doublet). By comparison of the intensity of the peaks of these two pyrazolines it is possible to estimate this to be a 90:10 mixture. The major component was assigned the structure *cis,trans*-3,4,5-trimethyl-3-carbomethoxy-Δ¹-pyrazoline (XXII) and the minor component the *cis,cis* structure (XXIII) (see the text).

Pyrolysis of 3,4,5-Trimethyl-3-carbomethoxy-Δ¹-pyrazoline

The pyrazoline was pyrolyzed by heating a sample in an oil bath at 120° and the products were separated by chromatography.

Methyl *cis,trans*-1,2,3-trimethyl-1-cyclopropanecarboxylate (XXIV): b.p. 151°; n_D^{25} 1.4308; infrared band of C=O at 1 710 cm^{-1}; n.m.r. peaks at 6.39 τ (ester methyl), 8.67 τ (quartet with J = 6 c.p.s.), 8.80 τ (methyl on C_1), 8.91 and 8.94 τ (doublets with J = 6 c.p.s.), and 9.37 τ (quartet with J = 6 c.p.s.). The assignments of the peaks are given in the text.

Anal. Calcd. for $C_8H_{14}O_2$: C, 67.57; H, 9.93. Found: C, 67.36; H, 10.15.

Methyl 2,3-dimethyl-2-pentenoate (?) (XXVI): b.p. 163°; infrared band of C=O at 1 715 cm^{-1}; n.m.r. peaks at 6.38 τ (ester methyl), 7.68 τ (quartet with J = 7.6 c.p.s. for hydrogens on C_4), 8.23 τ (methyls on C_2 and C_3 unresolved), and 9.0 τ (triplet with J = 7.6 c.p.s. for the hydrogens on C_5). Application of the mechanism herein described would predict this olefin to have the methyls *cis*.

Anal. Calcd. for $C_8H_{14}O_2$: C, 67.57; H, 9.93. Found: C, 66.99; H, 10.27.

Methyl *cis,cis*-1,2,3-trimethyl-1-cyclopropanecarboxylate (XXV): b.p. 166°; n_D^{25} 1.4410; infrared band of C=O at 1 725 cm^{-1}; n.m.r. peaks at 6.44 τ (ester methyl), 8.59 τ (multiplet for the two ring hydrogens), 8.96 τ (methyl on C_1), and 9.07 τ (doublet with J = 5.5 c.p.s. for the methyls on C_2 and C_3). The assignments of these peaks are discussed in the text.

Anal. Calcd. for $C_8H_{14}O_2$: C, 67.57; H, 9.93. Found: C, 67.38; H, 10.12.

ACKNOWLEDGMENTS

The authors gratefully appreciate the support received for this work from the National Research Council of Canada and from the Committee on Research of the University of British Columbia.

Thanks are also extended to Mrs. A. Aldrich for determining the microanalyses and to Mrs. E. Brion for determining the n.m.r. spectra.

REFERENCES

1. T. V. VAN AUKEN and K. L. RINEHART, JR. J. Am. Chem. Soc. **84**, 3736 (1962).
2. C. G. OVERBERGER and J.-P. ANSELME. J. Am. Chem. Soc. **86**, 658 (1964).
3. H. M. WALBORSKY and C. G. PITT. J. Am. Chem. Soc. **84**, 4831 (1962).
4. K. VON AUWERS and F. KONIG. Ann. **496**, 252 (1932).
5. D. E. MCGREER, P. MORRIS, and G. CARMICHAEL. Can. J. Chem. **41**, 726 (1963).
6. D. E. MCGREER, N. W. K. CHIU, and M. G. VINJE. Can. J. Chem. This issue.
7. D. E. MCGREER, R. S. MCDANIEL, and M. G. VINJE. Can. J. Chem. This issue.
8. D. J. CRAM, C. A. KINGSBURY, and B. RICKBORN. J. Am. Chem. Soc. **83**, 3688 (1961).
9. S. SELTZER. J. Am. Chem. Soc. **83**, 2625 (1961).
10. S. SELTZER. J. Am. Chem. Soc. **85**, 14 (1963).
11. S. SELTZER. Abstracts, 146th Meeting of the American Chemical Society, January, 1964. p. 4*c*.
12. H. R. SNYDER. Dissertation Abstr. **19**, 2481 (1959).
13. E. L. JAMES. Ph.D. Thesis, University of Pennsylvania. 1963. p. 28.
14. M. KARPLUS. J. Chem. Phys. **30**, 11 (1959).
15. R. U. LEMIEUX, J. D. STEVENS, and R. R. FRASER. Can. J. Chem. **40**, 1955 (1962).

Can. J. Chem. Downloaded from www.nrcresearchpress.com by 210.87.254.6 on 09/05/12
For personal use only.

16. R. J. ABRAHAM and K. A. MCLAUCHLAN. Mol. Phys. **5**, 513 (1962).
17. C. STEEL, R. ZAND, P. HURWITZ, and S. G. COHEN. J. Am. Chem. Soc. **86**, 679 (1964).
18. D. W. SETSER and B. S. RABINOVITCH. J. Am. Chem. Soc. **86**, 564 (1964); References therein.
19. D. J. PATEL, M. E. H. HOWDEN, and J. D. ROBERTS. J. Am. Chem. Soc. **85**, 3218 (1963).
20. H. M. HUTTON and T. SCHAEFFER. Can. J. Chem. **40**, 875 (1962).
21. K. B. WIBERG and B. J. NIST. J. Am. Chem. Soc. **85**, 2722 (1963).
22. K. L. WILLIAMSON, C. A. LANGFORD, and C. R. NICHOLSON. J. Am. Chem. Soc. **86**, 762 (1964).
23. L. M. JACKMAN and R. H. WILEY. J. Chem. Soc. 2881 (1960).
24. K. VON AUWERS and F. KONIG. Ann. **496**, 27 (1932).

Can. J. Chem. Downloaded from www.nrcresearchpress.com by 210.87.254.6 on 09/05/12
For personal use only.

Can. J. Chem. Downloaded from www.nrcresearchpress.com by 210.87.254.105 on 09/05/12
For personal use only.

PHOTOREARRANGEMENT OF 2,3-DIMETHYL-4,5-DIHYDROFURAN AND 2-METHYL-4,5-DIHYDROFURAN

DONALD E. MCGREER, MAGNUS G. VINJE, AND ROBERT S. MCDANIEL
Department of Chemistry, University of British Columbia, Vancouver, British Columbia
Received November 13, 1964

Dedicated to Professor R. B. Sandin on the Occasion of his Sixty-Eighth Birthday

ABSTRACT

Irradiation of an ether solution of the title compounds with a medium-pressure mercury arc gave in each case a rearrangement reaction, with formation of an acetyl cyclopropane isomer as the major product. This reaction is similar to that induced thermally at 450°.

2-Methyl-4,5-dihydrofurans are formed as minor products in the pyrolysis and photolysis of 3-acetyl-Δ^1-pyrazolines (1). These derivatives were found to be stable to light filtered by a pyrex vessel; however, in a silica-glass flask they were rearranged under irradiation by a mercury lamp to cyclopropane derivatives.

When 2,3-dimethyl-4,5-dihydrofuran (I) (λ_{max} = 218 mμ) was irradiated in an ether solution, the work-up of the reaction after 86% of I had reacted gave a mixture which contained 1-methyl-1-acetylcyclopropane (II) as the major component. Other products identified only by their retention times in the vapor chromatogram were *trans*-3-methyl-3-buten-2-one (III), *cis*-3-methyl-3-buten-2-one (IV), and 3-methyl-4-buten-2-one (V) (see eq. [*a*]). Similarly, photolysis of 2-methyl-4,5-dihydrofuran (λ_{max} = 210 mμ) gave methyl cyclopropyl ketone. This latter reaction is complicated by extensive polymerization.

The photorearrangement of dihydrofurans is analogous to the thermally induced rearrangement (2–4). For example, 2-methyl-4,5-dihydrofuran, when heated to 450° in a flow system, is converted to methyl cyclopropyl ketone and 3-buten-2-one (2, 3).

It is of interest that the product ratio for compounds II–V in the photorearrangement of I (90:5:3:2 respectively) is close to that obtained for the photolysis of 3-acetyl-3-methyl-Δ^1-pyrazoline (88:6:3:3 respectively) (1). Although this may be fortuitous, it may mean that a similar intermediate is involved in the two reactions.

The photolysis of vinyl ethers in the gas phase has been found to give two primary processes, the first caused by cleavage of the alkyl group – oxygen bond and the second caused by rearrangement and fragmentation to give an aldehyde and ethylene (5) (see eq. [*b*]). In the dihydrofuran system analogous cleavage would give a diradical intermediate which, in a dipolar form, is similar to that proposed for the pyrolysis of pyrazolines (6) (see eq. [*c*]). However, the possibility of a molecular mechanism must also be considered, since stereochemical results in the pyrolysis and photolysis of pyrazolines suggested a molecular mechanism is possible (7).

Boykin and Lutz (8) have observed that the photorearrangement of 2,3,5,5-tetraphenyl-4,5-dihydrofuran gives the valence tautomer 1-benzoyl-1,2,2-triphenylcyclopropane (these results were published while the present paper was in press). Their system is interesting in that the dihydrofuran can be reformed from the cyclopropane by treatment with acid, and more drastic conditions are needed to give ring-opened products. This might suggest also that ring opening is not involved in the dihydrofuran–cyclopropane tautomerism.

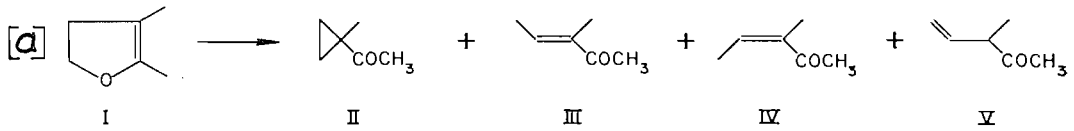

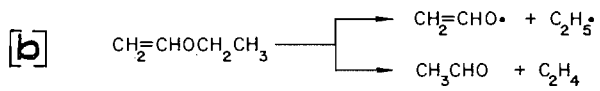

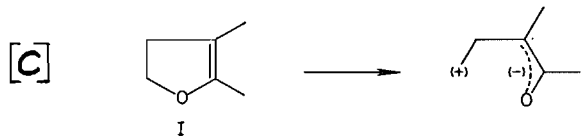

EXPERIMENTAL

Photolysis of 2,3-Dimethyl-4,5-dihydrofuran (I)

A solution of 0.5 ml of I (1) in 25 ml of ether was placed in a silica-glass flask fitted with a reflux condenser. The solution was irradiated with a Hanovia 450-W medium-pressure lamp No. 79A36 placed 3 inches from the flask. After 4 h of irradiation the solution was concentrated and analyzed by vapor chromatography (Aerograph A-90-P using a 10-ft dinonyl phthalate column at 122°). The chromatogram showed that 14% of the mixture (by areas) was I (retention time 12.2 min). Other components identifiable by their retention times as compared with those of authentic samples (1) were 3-methyl-4-buten-2-one (V) (1%, 11.3 min), *cis*-3-methyl-3-buten-2-one (IV) (1%, 17.3 min), 1-methyl-1-acetylcyclopropane (II) (74%, 19.2 min), and *trans*-3-methyl-3-buten-2-one (III) (4%, 25.1 min). The 1-methyl-1-acetylcyclopropane (II) was isolated and found to have a nuclear magnetic resonance (n.m.r.) spectrum identical with that of an authentic sample (1). II was stable under the reaction conditions.

Photolysis of 2-Methyl-4,5-dihydrofuran

The 2-methyl-4,5-dihydrofuran (Columbia Organic Chemicals) was distilled before use, b.p. 78.5–79.5°, n_D^{25} 1.4289 (lit. (9), b.p. 78.9°, n_D^{25} 1.4289). A solution of 5 ml of 2-methyl-4,5-dihydrofuran in 15 ml of ether was irradiated as above. The progress of the reaction was followed by vapor chromatography and at 25 h 10% of the volatile fraction (excluding solvent) was starting material. The product was distilled to give 0.4 ml, b.p. 80–150°. The residue (3 ml) was polymeric in nature. Vapor chromatography (P-E 226 using a 150-ft Golay polyglycol column at 103°) of the distillate showed one major component at 1.3 min in addition to starting material at 0.6 min. The 1.3-min component was collected (Aerograph A-90-P) and identified as methyl cyclopropyl ketone, b.p.111.0–111.2°, n_D^{20} 1.4241 (lit. (2), b.p. 110.2–110.4°, n_D^{20} 1.4250). The n.m.r. spectrum agreed with that of the assigned structure. The 2,4-dinitrophenylhydrazone was prepared by the procedure of Shine (10), m.p. 154–156° (lit. (3), m.p. 147.8–149.2°).

ACKNOWLEDGMENT

The authors acknowledge financial support from the National Research Council of Canada.

REFERENCES

1. D. E. McGreer, N. W. K. Chiu, and M. G. Vinje. Can. J. Chem. This issue.
2. N. I. Shuikin, I. P. Bel-Skii, and R. A. Karakjanov. Dokl. Akad. Nauk SSSR, **125**, 1051 (1959).
3. D. M. A. Armitage and C. L. Wilson. J. Am. Chem. Soc. **81**, 2437 (1959).
4. C. L. Wilson. J. Am. Chem. Soc. **69**, 3002 (1947).
5. E. Murad. J. Am. Chem. Soc. **83**, 1327 (1961).
6. W. G. Young, L. J. Andrews, S. L. Lindenbaum, and S. J. Cristol. J. Am. Chem. Soc. **66**, 810 (1944).
7. D. E. McGreer, N. W. K. Chiu, M. G. Vinje, and K. C. K. Wong. Can. J. Chem. This issue.
8. D. W. Boykin, Jr. and R. E. Lutz. J. Am. Chem. Soc. **86**, 5046 (1964).
9. S. Swadish, S. Smith, and A. P. Dunlop. J. Org. Chem. **16**, 476 (1951).
10. H. J. Shine. J. Org. Chem. **24**, 252 (1959).

Can. J. Chem. Downloaded from www.nrcresearchpress.com by 210.87.254.105 on 09/05/12
For personal use only.

Can. J. Chem. Downloaded from www.nrcresearchpress.com by 210.87.254.40 on 09/05/12
For personal use only.

REACTIVITY AND GEOMETRY IN ALLYLIC SYSTEMS

III. PHOTOSENSITIZED OXYGENATION OF CHOLEST-4-ENE, A STEROID OLEFIN WITH A CONFORMATIONALLY FLEXIBLE RING[1,2]

A. NICKON[3] AND W. L. MENDELSON
Department of Chemistry, The Johns Hopkins University, Baltimore, Maryland
Received November 13, 1964

Dedicated to Professor R. B. Sandin on the Occasion of his Sixty-Eighth Birthday

ABSTRACT

Photosensitized oxygenation of cholest-4-ene with hematoporphyrin in pyridine followed by reduction of the derived hydroperoxides gave five allylic alcohols in these relative amounts: cholest-4-en-3α-ol (V*a*, 37%); cholest-4-en-3β-ol (IV*a*, 7.5%); 5α-cholest-3-en-5-ol (VIII*a*, 29%); 5β-cholest-3-en-5-ol (VI*a*, 2%); and cholest-5-en-4β-ol (X*a*, 8.5%). A by-product from breakdown of the hydroperoxides was cholest-4-en-3-one (III, 6.5%). The Δ^4-stenols are not primary products from the photosensitized process but arose by gradual isomerization of the initially derived 5-hydroperoxycholest-3-enes. When the original hydroperoxide mixture was allowed to stand in chloroform, the rearrangement went to completion and no isolable amounts of the Δ^3-stenols remained. After rearrangement, V*a* and IV*a* were present in a ratio of about 8:1, and this sequence affords a convenient new route to cholest-4-en-3α-ol. The photooxidation products and their relative proportions are readily understood if oxygen can attack both half-chair conformations of ring A in cholest-4-ene and can cyclically abstract a quasi-axial (or an axial) allylic hydrogen. Conclusions are drawn on the importance of steric hindrance and of ring inversion on the photosensitized oxygenation reaction.

INTRODUCTION

Photosensitized oxygenation of monoolefins gives allylic hydroperoxides with a rearranged double bond (1). Work with steroids showed that the bonds formed and broken (C—O and C—H respectively) are *cis* to each other and led to the suggestion of a cyclic mechanism, with no implication about the timing of the events or the extent of participation by the sensitizer (2, 3). Geometric considerations indicate that in a half-chair cyclohexenoid ring a quasi-axial (*a'*) hydrogen is better suited than a quasi-equatorial

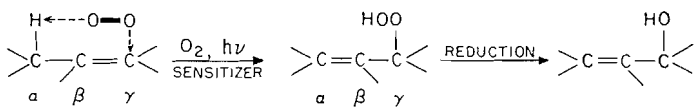

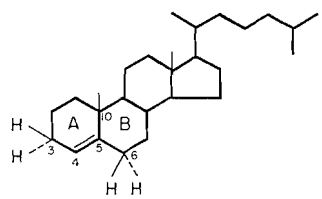

I

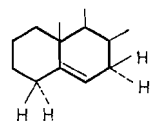

II

(*e'*) hydrogen for cyclic abstraction. All results so far are interpretable on this basis and no definitive examples have been found of *e'* hydrogen abstraction in a rigid ring system.

[1]*For Part II see ref. 15a.*
[2]*Taken from the Ph.D. Dissertation of W. L. Mendelson, Johns Hopkins University, 1963.*
[3]*Alfred P. Sloan Foundation Fellow, 1957–61.*

In those cases where the preferred ring conformation is different for the starting olefin and product, ring inversion or distortion must occur at some stage, but in one test case studied (5β-cholest-3-ene) it was shown that this factor by itself was insufficient to stop the reaction, though it may have slowed it (4). Results with steroids and simpler olefins indicate that the reaction is subject to steric hindrance. In particular, an axial alkyl group in a 1,3-relationship both to the developing C—O bond and to the allylic C—H bond inhibits the oxygenation markedly (2–5).[4] Which of these two 1,3-interactions is the more important emerges from the present study and from work to be described elsewhere (4, 5).

Although several monocyclic olefins have been photooxygenated with sensitizers (1), the only studies involving complete product analysis have been by Kenney and Fisher (6, 7) and by Schenck *et al.* (8). The former workers examined (+)-carvomenthene, and the latter group investigated (+)-carvomenthene and (+)-limonene. Both research groups satisfactorily accounted for their products on the basis of the cyclic *cis* mechanism.[5] To find out the effect of conformational flexibility in a condensed ring system we examined the photosensitized oxygenation of cholest-4-ene (I). The double-bond environment in this substrate is similar to that in Δ^5-steroids (part of structure II) but, unlike these ring B olefins, cholest-4-ene can exist in two interconvertible half-chair conformations; hence, it was of interest to learn if products could be derived from each. Furthermore, the behavior of the cholest-4-ene system would help assess other steric features of the reaction.

RESULTS

Cholest-4-ene was prepared from cholest-4-en-3β-ol acetate (or benzoate) and also from cholest-4-en-3-one (III) by reported methods (9, 10). To facilitate identification and assay of oxygenation products we separately synthesized the five allylic alcohols IV*a*, V*a*, VI*a*, VIII*a*, and X*a*, and some of their esters as follows.

Cholest-4-en-3β-ol (IV*a*) was obtained by reduction of III with lithium aluminium hydride and then separation of the epimers with digitonin. In a simplified route sodium borohydride reduction produced the 3β-ol in such preponderance that this epimer could be isolated directly by crystallization without resort to digitonide formation. Reduction of III with aluminium isopropoxide (11) gave the 1:1 complex of the epimers IV*a* and V*a*. After removal of the 3β-epimer with digitonin we obtained cholest-4-en-3α-ol (V*a*). An improved route to V*a* arose from the photooxygenation of I and will be described in the sequel. The reduction of 4β,5-epoxy-5β-cholestan-3-one with hydrazine gave us 5β-cholest-3-en-5-ol (VI*a*) as reported (24), and we applied the same reduction to 4α,5-epoxy-5α-cholestan-3-one (VII) and obtained the new allylic alcohol 5α-cholest-3-en-5-ol (VIII*a*). As expected (12) the molecular rotation increment of VIII*a* relative to 5α-cholest-3-ene for introduction of the OH group at C-5 is strongly negative. The synthesis of 4β-acetoxycholest-5-ene (X*c*) by a reported method proved unsuitable; hence, we developed a two-step procedure which involved conversion of cholest-4-ene to the diol monoacetate IX by treatment with hydrogen peroxide in acetic acid – acetic anhydride, followed by dehydration to X*c*.

We photooxygenated cholest-4-ene (I) in dilute pyridine solution (ca. 0.03 *M*) at

[4]*The formation of relatively little cis-carveol (5%) among the photosensitized oxygenation products of (+)-limonene can be rationalized on a similar basis, although alternate explanations are possible (8).*

[5]*Kenney and Fisher originally favored a concerted process for the cyclic mechanism (6) but have reinterpreted their results (7) in terms of Schenck's stepwise mechanism (1) in which* C—O *bond formation creates an intermediate diradical and precedes* C—H *cleavage.*

Can. J. Chem. Downloaded from www.nrcresearchpress.com by 210.87.254.40 on 09/05/12
For personal use only.

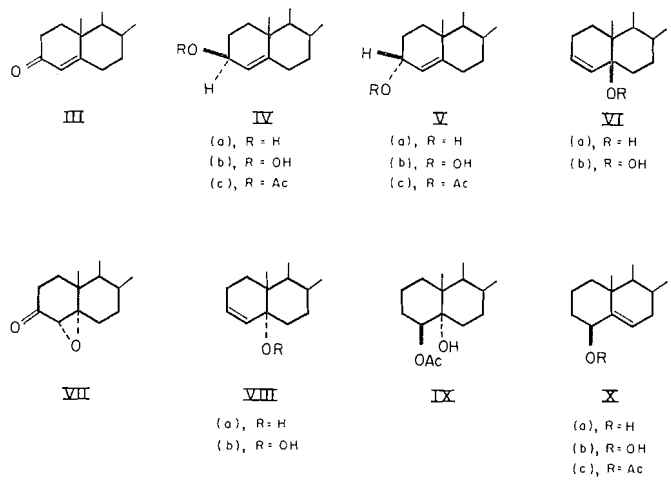

about 35–40° with hematoporphyrin (ca. 2×10^{-4} *M*) as sensitizer. In a typical run it underwent about 90% conversion in 25 h,[6] and the crude product (after correction for unchanged olefin) contained 6.5% cholest-4-en-3-one (III, assayed by its ultraviolet absorption at 240 mμ) and 83% mixed hydroperoxides (assayed by quantitative hydrogenation of an aliquot). The total product was reduced with sodium iodide and chromatographed on alumina. In addition to starting olefin (ca. 11%) and cholest-4-en-3-one (III) we identified five allylic alcohols IV*a*, V*a*, VI*a*, VIII*a*, and X*a*. Table I lists the alcohols, in order of elution, and their approximate relative yields after correction for recovered olefin. The compounds were identified by infrared spectroscopic comparison and, except for VI*a*, also by appropriate melting point and mixture melting point comparisons of the alcohol (or one of its esters) with the genuine samples from synthesis. In a control photooxygenation conducted in the same way except that the sensitizer was omitted, no detectable hydroperoxidic material was produced and the starting olefin was recovered entirely. When a free-radical initiator (*t*-butyl hydroperoxide) was added in nearly equivalent amount, a control run in the absence of sensitizer gave about 5% oxidation. These results reasonably exclude a radical-chain pathway as a significant source of oxygenation products.

TABLE I*

	Relative %
5α-Cholest-3-en-5-ol (VIII*a*)	29
Cholest-5-en-4β-ol (X*a*)	8.5
5β-Cholest-3-en-5-ol (VI*a*)	2
Cholest-4-en-3α-ol (V*a*)	37
Cholest-4-en-3β-ol (IV*a*)	7.5

*The total recovery from chromatography was 95%, which included about 9.5% of unidentified mixtures.

DISCUSSION

Because photosensitized oxygenation is invariably accompanied by a shift of the double bond (1), the hydroperoxides IV*b* and V*b* (corresponding to the alcohols IV*a* and V*a*)

[6]*Longer reaction times encouraged breakdown of the hydroperoxides, as evidenced from diminished infrared intensities in the* OH *region and increased intensities in the carbonyl region.*

Can. J. Chem. Downloaded from www.nrcresearchpress.com by 210.87.254.40 on 09/05/12
For personal use only.

Can. J. Chem. Downloaded from www.nrcresearchpress.com by 210.87.254.40 on 09/05/12
For personal use only.

cannot be primary products of the sensitized process. That they can arise by subsequent allylic rearrangement of the expected 5-hydroperoxycholest-3-enes in the original solution or during the iodide reduction was indicated when a chloroform solution of the crude hydroperoxidic mixture was found to mutarotate during polarimetric readings. When rearrangement in the chloforom solution was allowed to go to completion (48 h), the mixture was reduced with sodium iodide and chromatographed as before. The two cholest-3-en-5-ols (VI*a* and VIII*a*) were no longer present, and the epimeric cholest-4-en-3-ols (V*a* and IV*a*) were obtained in higher yields and in a ratio greater than 8:1 (cf. original ratio of 5:1 from Table I). These allylic rearrangements of tertiary hydroperoxides to secondary hydroperoxides have analogy,[7] and, because of the favorable final proportion of the α-epimer V*a*, we recommend photosensitized oxygenation of cholest-4-ene followed by allylic rearrangement of the hydroperoxidic mixture in chloroform as a convenient route to cholest-4-en-3α-ol (V*a*). From the *cis* stereochemistry required both for the oxygenation step (2, 3) and for the subsequent allylic rearrangement of the tertiary hydroperoxides (13, 14) it follows that the combined yield (66%) of V*a* and VIII*a* represents the total abstraction of the α-hydrogen at C-3; similarly, the combined yield (9.5%) of IV*a* and VI*a* represents the net abstraction of the β-hydrogen at C-3. The fifth alcohol X*a* (obtained in 8.5% yield) arises from removal of the β-hydrogen at C-6. These are the first cases where β-attack has been observed in photosensitized oxygenation of a steroid monoolefin. The relative ease of hydrogen abstraction for $3\alpha/3\beta/6\beta$ lies between 8.5/1.1/1 and 7.8/1.9/1.[8] The following conformational analysis satisfactorily accounts for these results and leads to some new conclusions about the oxygenation reaction.

In cholest-4-ene, ring A can adopt two half-chair conformations depicted in XI and XII. We shall first consider attack by oxygen[9] at C-5 and abstraction of hydrogen from C-3. In half-chair XI, α-attack by oxygen meets no serious steric hindrance and the 3α-hydrogen is quasi-axial (a'). Consequently, circumstances are favorable for production of hydroperoxide XIII by a cyclic mechanism. Importantly, this hydroperoxide can adopt only one half-chair conformation (shown in XIII) and no ring inversion is involved when the double bond shifts from Δ^4 (in XI) to Δ^3 (in XIII). The C—O bond in XIII is a' and therefore well disposed sterically and stereoelectronically for intramolecular allylic rearrangement to XV, which can ultimately equilibrate with its alternate half-chair conformation, XVII.

Beta attack by oxygen cannot be consummated from half-chair XI because the 3β-hydrogen is quasi-equatorial (e') and therefore relatively inaccessible for cyclic transfer.[10] The situation changes in half-chair XII, because now the C—H bonds in ring A have reversed their conformational character. The 3α-hydrogen is e' and precludes hydroperoxidation from the α-side.[11] On the other hand, the 3β-hydrogen is a' and the overall steric situation for β-attack is now similar to that noted above for α-attack on half-chair

[7]*Schenck et al. (13) and Lythgoe and Trippett (14) first observed this type of isomerization with 5-hydroperoxy-5α-cholest-6-en-3β-ol, which rearranged to 7α-hydroperoxycholest-5-en-3β-ol. Schenck's mechanistic studies showed that the isomerization is both intramolecular and stereospecifically cis.*

[8]*The uncertainty in these ratios arises because a portion of the 3α- and 3β-hydroperoxides breaks down to cholest-4-en-3-one, and presently we have no way to estimate how much of the ketone is derived from each hydroperoxide. The first set of figures applies if the ketone (6.5%) arose exclusively from Vb; the second set applies if the ketone came entirely from IVb. The true figures probably lie between these extremes.*

[9]*The photochemical aspects of sensitized reactions have been discussed elsewhere (see refs. 1, 3, and 15 for leading references).*

[10]*Note also that the angular methyl group at* C-10 *would present an almost eclipsed 1,2-interaction to an incipient beta* C—O *bond at* C-5 *and might further impede β-attack.*

[11]*An added feature that could impede α-attack on XII is the* C_9—C_{10} *bond, which would eclipse a* C—O *bond being created at* C-5.

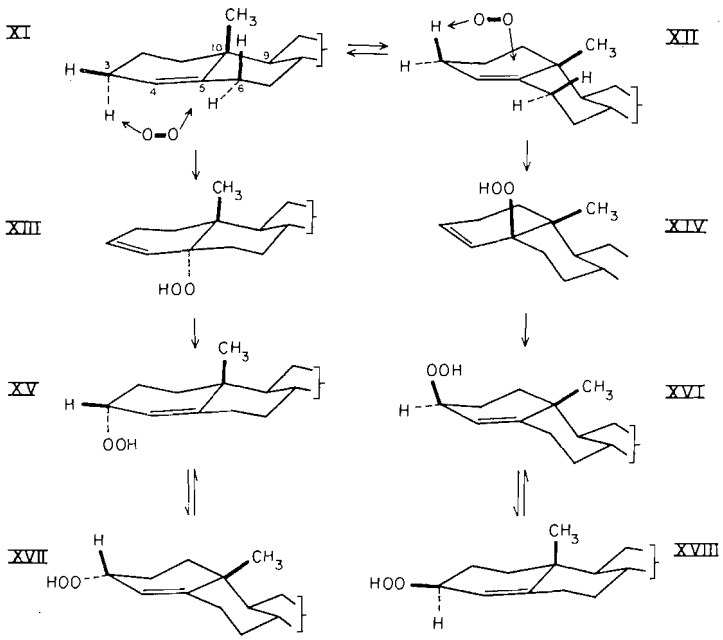

XI. On this basis, hydroperoxide XIV should arise from half-chair XII about as readily as XIII did from half-chair XI. Once formed, XIV has its hydroperoxy group suitably poised (*a'* to ring A) for allylic rearrangement to XVI. Ring inversion plays no role in the formation of XIV or in its isomerization to XVI but enters only in the final equilibration of XVI with its alternate half-chair form XVIII. The yields in Table I reveal that the fraction of XIV that rearranged (0.83 ∓ 0.04)[8] is higher than that (0.58 ± 0.02)[8] of XIII. The A/B *cis* ring fusion in XIV is probably less stable than the A/B *trans* fusion in XIII, and the drive to release strain may be correspondingly greater in the former system.

We now turn our attention to oxygenation at C-4 accompanied by hydrogen abstraction from C-6. Alpha attack is not fruitful from either half-chair XI or half-chair XII, because the 6α-hydrogen is equatorial (*e*) to ring B and unsuitably oriented with respect to the olefinic bond. Beta attack on XI is sterically blocked by the methyl group at C-10, which is axial to ring B and quasi-axial to ring A and which presents diaxial-type 1:3-interactions to a developing C—O bond at C-4 and also to the 6β-hydrogen. Other examples that attest to the difficulty of hydroperoxidation in molecules with comparable steric situations are available (2–8). In half-chair XII the offending methyl group is *e'* to ring A and no longer confronts an incipient beta C—O bond at C-4 with serious hindrance. Consequently, the cholest-5-en-4β-ol (X*a*) is most reasonably derived from half-chair XII and, concomitant with the double-bond shift from Δ^4 to Δ^5, ring A must either undergo conformational inversion or develop initially into a twist boat form. Another example where the ring-inversion factor has failed to block oxygenation has been observed with 5β-cholest-3-ene (4).

Half-chair XII contains a geometric feature not exemplified so far. The angular methyl group is quasi-equatorial to ring A but is axial to ring B and presents a diaxial 1:3-interaction to the 6β-hydrogen but not to a developing beta C—O bond at C-4. Therefore, unless X*a* is formed by some abnormal mechanism, this case illustrates that a diaxial 1:3-relationship between an alkyl group and an allylic hydrogen is insufficient by itself to block

Can. J. Chem. Downloaded from www.nrcresearchpress.com by 210.87.254.40 on 09/05/12
For personal use only.

the reaction. Insofar as these hindrance effects can be separately evaluated, steric interactions with the developing C—O bond rather than with the allylic hydrogen appear to be of greater importance. The formation of X*a* from cholest-4-ene is of additional interest, because the double bond is initially exo to ring B and finally exo to ring A. Schuller and Lawrence have implied that a structural change of this type would involve a prohibitive amount of strain as the transition state is approached and would lead to nonreactivity (16).

EXPERIMENTAL

General

Melting points are corrected. Optical rotations refer to the sodium D-line and were taken at room temperature in chloroform. Ultraviolet spectra were taken in 95% ethanol on a Beckmann DK-2 or a Cary model 11 M recording instrument. Infrared spectra were taken in carbon disulfide solution with a Perkin–Elmer model 21 double-beam spectrophotometer. In color tests for hydroperoxide 1 drop of a saturated solution of sodium iodide in isopropyl alcohol was added to the unknown (0.002–0.003 g) dissolved in glacial acetic acid. Authentic steroid hydroperoxides were used as controls.

To assay for total hydroperoxide in a crude product we used quantitative hydrogenation with Raney nickel catalyst (17), in pyridine (13, 18). The hydrogen uptake was usually complete within 20–30 min with pre-blanked catalyst and was reproduced in a duplicate run to within 3–4%. For the determinations we used 0.015–0.030 g of the hydroperoxide and ca. 0.5 g of the ethanol-moistened Raney nickel.

Reductions of hydroperoxides with sodium iodide were conducted as soon as possible after work-up of the oxygenation. In a typical reduction, sodium iodide (ca. 0.6 g) was dissolved in a solution containing the crude hydroperoxide (0.15 g) in absolute methanol (10 ml), anhydrous ether (2 ml), and glacial acetic acid (3–4 drops). After 12 h most of the solvent was removed, an excess of ether was added, and the solution was washed with sodium thiosulfate (until the ether was clear) and then with water. The ether was dried over sodium sulfate, which was the drying agent throughout this work, and evaporation gave the allylic alcohol.

Sterols were acetylated and benzoylated by conventional procedures (3).

Photosensitized oxygenations were conducted in a vertical pyrex tube (30 cm) irradiated along its length by two standard fluorescent desk lamps (each containing two 15-W fluorescent tubes, each about 17 inches long) mounted about 1 inch away. A long glass tube with a fritted glass plate at the end was used to admit oxygen at the bottom of the solution, slowly and without interruption. The lamps kept the temperature of the solution between 35–40°. Hematoporphyrin (Mann Research Laboratories) and reagent grade pyridine were used in all of the photosensitized oxygenations. A typical work-up procedure for a 20-ml aliquot was as follows. After evaporation of the solvent under reduced pressure at 35–45°, anhydrous ether (15 ml) and charcoal (ca. 0.02 g) were added; the mixture was warmed briefly and filtered, and the filtrate was evaporated under vacuum at a temperature not exceeding 40°.

Cholest-4-en-3-one (III)

This compound, prepared as described (19), had m.p. 79–81°, $[\alpha]$ +90°, λ 241 (ϵ 16 600). Reported m.p. 79.5–80.5° (19), λ 240.5 (ϵ 18 000) (20).

*Cholest-4-en-3β-ol (IV*a*)*

(i) By Reduction with Lithium Aluminium Hydride

Reduction of cholest-4-en-3-one (III) with lithium aluminium hydride yielded a white solid, usual m.p. 125–127°. The optical rotations (three runs) ranged from +55° to +65°, which indicated about a 4:1 ratio of cholest-4-en-3β-ol to cholest-4-en-3α-ol (V*a*). Recrystallization from aqueous ethanol or methanol–acetone raised the m.p. to 129–130°. In contrast to a literature report (21*a*), the 1:1 molecular compound of IV*a* and V*a* (m.p. 141°, $[\alpha]$ +85°) could not be obtained by us this way (cf. 21*b*). However, we obtained pure IV*a* (m.p. 132–133°, $[\alpha]$ +46°) by treatment of the reaction product with digitonin as reported (21). We could not isolate cholest-4-en-3α-ol (V*a*) from the digitonide mother liquors, presumably because it was present only in small amounts.

(ii) By Reduction with Sodium Borohydride

A suspension of sodium borohydride (1.2 g) in a small volume of methanol was added to the enone (4.1 g) in methanol (300 ml) and the mixture was stirred at room temperature for 24 h, was poured into water (300 ml), and was extracted with ether, which was dried and evaporated. The product was crystallized once from ethyl acetate – methanol, m.p. 126–127° (3.5 g), $[\alpha]$ +51°. Pure cholest-4-en-3β-ol (IV*a*, m.p. 130–132°, $[\alpha]$ +46°) was obtained by one or two further recrystallizations (ca. 75% recovery) from ethyl acetate – methanol or from aqueous ethanol. Reported m.p. 131–132°, $[\alpha]$ +44° in benzene (21).

Acetylation of IV*a* gave cholest-4-en-3β-ol acetate IV*c*, m.p. 84–86°, $[\alpha]$ +6°. Reported m.p. 87–88°, $[\alpha]$ +8° (22). Benzoylation of IV*a* gave cholest-4-en-3β-ol benzoate, m.p. 125–126°, $[\alpha]$ +1°. Reported m.p. 125–128°, $[\alpha]$ ±0° (9).

Can. J. Chem. Downloaded from www.nrcresearchpress.com by 210.87.254.40 on 09/05/12
For personal use only.

Can. J. Chem. Downloaded from www.nrcresearchpress.com by 210.87.254.40 on 09/05/12
For personal use only.

Cholest-4-en-3α-ol (Va)

Reduction of enone III with aluminium isopropoxide (11) gave us the 1:1 complex of IV*a* and V*a* with m.p. 141–142°, [α] +84°. Separation of this complex with digitonin (21*a*) gave cholest-4-en-3α-ol (V*a*) as a hardened oil ([α] +121°). Two crystallizations from acetone–water gave solid with m.p. 78–82°. Reported m.p. 84°, [α] +120.8° in benzene (21).

Acetylation of V*a* (oil) gave cholest-4-en-3α-ol acetate V*c*, m.p. 83–84°, [α] +175°. Reported m.p. 82–83°, [α] +177° (22).

Cholest-4-ene (I)

Method A

This method involved the lithium–ethylamine reduction of the allylic acetate (IV*c*) (or benzoate) as reported (9). The product was purified by chromatography on alumina and then by one crystallization from ethyl acetate – methanol, m.p. 81–82°, [α] +73°. Reported m.p. 82–83.5°, [α] +76°, for olefin purified through the dibromide (20). The infrared spectrum (potassium bromide disc) of our product had bands at 1 655 and 810 cm^{-1} in agreement with those reported by Bladon *et al.* (20). The reduction proceeded equally well (yields 35–40%) with either the acetate or benzoate. In one run we carried out the reaction on a mixture (ca. 1:2) of cholest-4-en-3α-ol and -3β-ol acetates and obtained cholest-4-ene of the same purity.

Method B

This method was useful for larger scale preparations of the olefin (2.5 g); however, the product was not as pure as that from method A. This procedure involved treatment of an ether solution of the cholest-4-en-3-one (II) with aluminium chloride and lithium aluminium hydride as reported by Wheeler and Mateos (10). They reported m.p. 65°, [α] +56°, for material obtained after chromatography of the crude product and indicated that the product was a mixture of cholest-4-ene (80%) and cholestane (20%). Our product, after chromatography, had m.p. 65–70°, [α] +56°. Two crystallizations from ethyl acetate – methanol gave cholest-4-ene (25%, m.p. 78–80°, [α] +70°), whose infrared spectrum (potassium bromide) was identical in all essential respects with that of the olefin produced by method A.

4β,5-Epoxy-5β-cholestan-3-one

This synthesis was carried out by modification of the procedure of Plattner *et al.* (23). A solution of cholest-4-en-3-one (2.0 g) in 95% ethanol (500 ml, at room temperature) was treated simultaneously and dropwise with 30% hydrogen peroxide (12 ml) and 5 *N* sodium hydroxide (12 ml). After the solution had stood at 0° for 24 h, water (100 ml) was added and most of the solvent was removed in a rotary evaporator. The resulting pasty solution was extracted with methylene chloride, and the organic layer was washed several times with water and dried over sodium sulfate. Evaporation of the solvent gave a solid, which crystallized in needles from acetone–methanol, 1.3 g, m.p. 118–119°, [α] +128°. Reported m.p. 116–117°, [α] +136° (23).

5β-Cholest-3-en-5-ol (VIa)

This compound was obtained by treatment of 4β,5-epoxy-5β-cholestan-3-one with hydrazine hydrate as reported (24). The crude product (oil, 0.25 g) was chromatographed on alumina (9 g). Elution with benzene – petroleum ether yielded a clear oil (0.15 g, [α] +94°) which hardened to a semisolid. Reported m.p. 93–94.5°, [α] +98°. The infrared spectrum of our product had bands at 3 600, 3 550, 1 015, 1 000, 975, 925, 740, 720, and 625 cm^{-1}.

4α,5-Epoxy-5α-cholestan-3-one (VII)

This epoxyketone was prepared by the photosensitized oxygenation of cholest-4-en-3β-ol IV*a* as reported previously (15*a*). After chromatography on deactivated alumina and crystallization, it had m.p. 121–122°, [α] −39°. Reported m.p. 120–121°, [α] −42.5° (26).

5α-Cholest-3-en-5-ol (VIIIa)

This new allylic alcohol was prepared by treatment of 4α,5-epoxy-5α-cholestan-3-one (VII) with hydrazine hydrate (24) followed by chromatography on alumina. Elution with benzene – petroleum ether (1:1) gave a solid, m.p. 72–74°, with infrared bands at 3 600, 955, 930, 918, 895, 725, and 688 cm^{-1}. One crystallization from methanol gave crystals, m.p. 74–75°, [α] −14°. (For analysis, the material from the oxygenation of cholest-4-ene was purified (see below).)

4β-Acetoxy-cholest-5-ene (Xb)

The following procedure was found to be superior to a reported method (25). A solution of cholest-4-ene (0.5 g) in benzene (1 ml) was treated with acetic anhydride (3 ml) and acetic acid (8 ml). The reaction mixture was stirred rapidly at 40–45° while 30% hydrogen peroxide (3 ml) was added over a 2.5-h period. Stirring was continued for 14 h at 40–50°, after which several milliliters of the solution was distilled. When the solution was cool, an excess of ether was added, and the solution was washed successively with water, with 5% sodium bicarbonate (until the washings were neutral), and with saturated sodium chloride, and then dried. Removal of the ether under reduced pressure gave an oil, which was dissolved in hexane and

chromatographed on alumina (15 g). Elution with benzene–hexane (1:1) gave 4β-acetoxy-5α-cholestan-5-ol (IX) as a crystalline solid. Crystallization from methanol gave plates, m.p. 177–178°. Reported m.p. 175–176°, [α] +38° (25). This diol monoacetate was converted to 4β-acetoxy-cholest-5-ene (X*c*) by a published method (reported m.p. 108°, [α] −70° (25)). After chromatography and crystallization from acetone–methanol, we obtained X*c* with m.p. 111.5–112°, [α] −71° (20–25% overall yield from cholest-4-ene).

Photosensitized Oxygenation of Cholest-4-ene (I)

Exploratory oxygenations revealed that conversion was largely complete after 24 h. Longer reaction (e.g. 48 h, 72 h) led to diminution of hydroperoxidic infrared bands and gradual increase in the intensities of bands attributable to ketonic breakdown products (e.g. 1 710, 1 660 cm^{-1}); consequently, shorter reaction times were chosen for the definitive runs described below.

Run 1

A solution of cholest-4-ene (1.00 g, m.p. 77–79°) and hematoporphyrin (0.008 g) in pyridine (75 ml) was oxygenated and irradiated for 25 h. After normal work-up, the product contained 6% α,β-unsaturated ketone (ultraviolet intensity at 240 mμ), and quantitative hydrogenation of an aliquot indicated a hydroperoxide content of 74% (based on a molecular weight of 402). The specific rotation (+28°) of another aliquot in chloroform gradually increased with time and reached +64° after 48 h, with no further change after an additional 12 h. A portion of the original crude product (0.70 g) was reduced with sodium iodide and the resulting oil ([α] +48°) was dissolved in hexane and chromatographed on alumina (25 g). Elution with benzene–hexane (1:10) gave a clear oil (0.114 g) whose infrared spectrum indicated it was largely (at least two-thirds) cholest-4-ene, with some contamination by unidentified material having bands at 1 095, 1 080, 895, and 710 cm^{-1}.

Elution with benzene–hexane (1:4) gave crystalline fractions (0.167 g, m.p. 65–74°) shown to be 5α-cholest-3-en-5-ol (VIII*a*) from the infrared spectra. Crystallization from methanol gave m.p. 72–74° ([α] −15°) which was not depressed by VIII*a* (m.p. 74–75°) prepared as described earlier. The analytical sample (m.p. 75–76°) was obtained by rechromatography on alumina and elution with hexane. Thin-layer chromatography on silica gel gave only one spot.

Anal. Calcd. for $C_{27}H_{46}O$ (386.64): C, 83.87; H, 11.99. Found: C, 83.87; H, 11.74.

Benzene–hexane (1:2) eluted a pasty solid (0.068 g) whose infrared spectrum indicated it was a mixture of VIII*a* and cholest-5-en-4β-ol (X*a*), roughly in the ratio 1:4, along with a small amount of ketonic material. A separate photooxygenation (see run 3) was conducted to isolate and identify X*a*. Continued elution gave fractions (0.014 g) identified as 5β-cholest-3-en-5-ol (VI*a*) by infrared comparison with authentic material, followed by fractions of a clear oil (0.231 g), which was largely cholest-4-en-3α-ol (V*a*) according to its infrared spectrum. For confirmation, a portion of the clear oil was acetylated and the acetate was crystallized from acetone–methanol, m.p. 82–83°, [α] +170°. The melting point was not depressed by the authentic acetate V*c*. A second portion of the clear oil was treated with Girard's reagent (27) to remove ketonic impurity and, after chromatography on alumina, gave V*a* whose infrared spectrum was the same as that of authentic material.

Methylene chloride containing increasing proportions of acetone eluted crude crystalline cholest-4-en-3β-ol (IV*a*, 0.046 g, m.p. 113–120°) identified by infrared comparison. A portion was benzoylated and gave, after crystallization from methanol, pure cholest-4-en-3β-ol benzoate identical in all respects (melting point, mixture melting point, and infrared spectrum) with an authentic sample.

Final elution with acetone gave unidentified oily mixtures (0.024 g) containing hydroxyl and carbonyl absorption in their infrared spectra. The total recovery from the column was 0.664 g (95%). Cholest-4-en-3-one (III) was not separately isolated in this run but its presence in several of the fractions was evident from the infrared spectra.

Run 2

This photooxygenation of cholest-4-ene (0.880 g) and hematoporphyrin (0.008 g) in pyridine (75 ml) was conducted for 24 h in a cold room that maintained the solution at about 15°. The crude hydroperoxidic product had an infrared spectrum similar to those from the other runs except that carbonyl absorption was absent, an indication that the hydroperoxides underwent less breakdown at the lower temperature. However, when the product was reduced with sodium iodide, appreciable cholest-4-en-3-one was produced (ultraviolet spectrum). We believe that the inadvertent use of too much acetic acid in the reduction promoted decomposition of the hydroperoxides. Chromatography gave the same products as in run 1. In addition, cholest-4-en-3-one (III) was identified (by infrared and ultraviolet spectra) in several of the fractions eluted with benzene–hexane (1:2).

Run 3

*Identification of cholest-5-en-4β-ol (X*a*).*—Cholest-4-ene (0.350 g) was photooxygenated for 24 h as in run 1. The product was reduced with sodium iodide and then treated with Girard's reagent (27) to remove ketonic material. Chromatography on alumina gave, in some of the fractions eluted with benzene–hexane, a white solid (0.027 g) whose infrared spectrum corresponded to that of authentic X*a*. Acetylation gave cholest-5-en-4β-ol acetate (X*c*), with m.p. 108° after recrystallization from acetone–methanol. Mixture melting point and infrared determinations established its identity with authentic X*c*.

Can. J. Chem. Downloaded from www.nrcresearchpress.com by 210.87.254.40 on 09/05/12
For personal use only.

Photooxygenation and rearrangement of hydroperoxides.—A solution of cholest-4-ene (1.0 g) and hematoporphyrin (0.006 g) in pyridine was irradiated and oxygenated for 24 h. The crude product (0.950 g), which contained ca. 6% of enone (ultraviolet analysis), was dissolved in chloroform (100 ml) and allowed to stand in the dark at room temperature until the optical rotation attained a constant value (48 h). The chloroform was removed with a rotary evaporator and the residue was reduced with sodium iodide.

A portion of the reduced product (0.350 g) was treated with Girard's reagent (27) to remove the ketonic component, and the non-ketonic material was chromatographed on alumina (9 g). All fractions that contained cholest-4-en-3α-ol (V*a*) and cholest-4-en-3β-ol (IV*a*) were combined (0.170 g, eluted with benzene–hexane from 1:4 to 1:1). Infrared inspection showed that the 3β-alcohol IV*a* was only a minor component of the mixture. Neither of the cholest-3-en-5-ols (VI*a* or VII*a*) was detected during the chromatography.

A second portion of the reduced product was acetylated and 0.242 g of the derived acetate was chromatographed on alumina (12 g). Elution with petroleum ether gave 0.180 g of fractions containing only the two cholest-4-en-3-ol acetates V*c* and IV*c*. Semiquantitative assay of the epimeric ratio was obtained by comparison of the infrared spectrum with authentic mixtures of the two acetates and indicated a V*c*:IV*c* ratio greater than 8:1. No 5α- or 5β-cholestan-3-en-5-ols were detected in the chromatography.

Attempted photooxygenations without sensitizer.—(A) A solution of cholest-4-ene (0.450 g, m.p. 80.5–81.5°) in pyridine (35 ml) was irradiated and oxygenated for 26 h in the absence of sensitizer. The olefin (m.p. 79–80°) was recovered virtually quantitatively and its identity with starting material was confirmed by melting point, mixture melting point, and infrared inspection. (B) A solution of cholest-4-ene (202 mg, containing 1.6% of cholesta-3,5-diene, based on ultraviolet absorption in isooctane at 228, 235, and 244 mμ (28)) in pyridine (15 ml) was photooxygenated 25 h without sensitizer. During this period a solution of 0.9 equivalent of *t*-butyl hydroperoxide in pyridine (1 ml) was added portionwise (0.1 ml initially and every 2 hours, the remainder after 8 h). Normal work-up left a solid (quantitative yield), which gave a positive hydroperoxide test and whose infrared spectrum showed very weak absorption at 3 540 and 1 680 cm^{-1}, but which otherwise appeared identical with that of starting material. The ultraviolet absorption (isooctane) at 232 mμ indicated ca. 3.5% cholest-4-en-3-one. The product was allowed to stand for 2 days in chloroform and then was reduced with potassium iodide in the usual way. Finally, it was oxidized with manganese dioxide, after which the enone content (λ 232) was 4.3–6.8%. The range arises because of the diene, whose presence was indicated by an inflection at 244 mμ but whose contribution to the 232-mμ peak cannot be accurately evaluated.

ACKNOWLEDGMENTS

This work was supported by the National Institutes of Health (grant GM 09693), and an early phase of it was aided by the Alfred P. Sloan Foundation, and by a grant-in-aid from the Hynson, Westcott and Dunning fund of The Johns Hopkins University. We are grateful to Messrs. Richard Maffezzoli, Anthony Baum, and Maurice Brookhart for valuable assistance in the preparative work, to Mr. J. Walter for the elemental analyses, and to Drs. J. B. DiGiorgio, P. J. L. Daniels, N. Schwartz, and D. Widdowson for helpful contributions.

REFERENCES

1. G. O. Schenck. Angew. Chem. **69**, 579 (1957).
2. A. Nickon and J. F. Bagli. J. Am. Chem. Soc. **81**, 6330 (1959).
3. A. Nickon and J. F. Bagli. J. Am. Chem. Soc. **83**, 1498 (1961).
4. N. Schwartz. Ph.D. Dissertation, The Johns Hopkins University. 1962. Results to be published in J. Org. Chem. (in press).
5. J. B. DiGiorgio and P. J. L. Daniels. To be published.
6. R. L. Kenney and G. S. Fisher. Abstracts, 138th Meeting of the American Chemical Society, New York, N.Y. September, 1960. p. 79P.
7. R. L. Kenney and G. S. Fisher. J. Org. Chem. **28**, 3509 (1963).
8. G. O. Schenck, K. Gollnick, G. Buchwald, S. Schroeter, and G. Ohloff. Ann. **674**, 93 (1964); references cited there.
9. A. S. Hallsworth, H. B. Henbest, and T. I. Wrigley. J. Chem. Soc. 1969 (1957).
10. O. H. Wheeler and J. L. Mateos. Can. J. Chem. **36**, 1430 (1958).
11. R. Schoenheimer and E. A. Evans. J. Biol. Chem. **114**, 567 (1936).
12. J. A. Mills. J. Chem. Soc. 4976 (1952).
13. G. O. Schenck, O. A. Neumuller, and W. Eisfeld. Ann. **618**, 202 (1958).
14. B. Lythgoe and S. Trippett. J. Chem. Soc. 471 (1959).
15. (*a*) A. Nickon and W. L. Mendelson. J. Am. Chem. Soc. **85**, 1894 (1963).
    (*b*) C. S. Foote and S. Wexler. J. Am. Chem. Soc. **86**, 3879, 3880 (1964). E. J. Corey and W. C. Taylor. J. Am. Chem. Soc. **86**, 3881 (1964).
16. W. H. Schuller and R. V. Lawrence. J. Am. Chem. Soc. **83**, 2563 (1961).
17. H. R. Billica and H. Adkins. Organic syntheses. Vol. 29. John Wiley and Sons, Inc., New York, N.Y. 1949. p. 24 (note 3, p. 28).

Can. J. Chem. Downloaded from www.nrcresearchpress.com by 210.87.254.40 on 09/05/12
For personal use only.

18. G. O. SCHENCK and K. SCHULTE-ELTE. Ann. **618**, 185 (1958).
19. J. F. EASTHAM and R. TERANISHI. Organic syntheses. Vol. 35. John Wiley and Sons, Inc., New York, N.Y. 1955. p. 39.
20. P. BLADON, J. FABIAN, H. B. HENBEST, H. P. KOCH, and G. W. WOOD. J. Chem. Soc. 2402 (1951).
21. (*a*) H. MCKENNIS and G. W. GAFFNEY. J. Biol. Chem. **175**, 217 (1948).
(*b*) W. G. DAUBEN, R. A. MICHELI, and J. F. EASTHAM. J. Am. Chem. Soc. **74**, 3852 (1952).
22. C. W. SHOPPEE, B. D. AGASHE, and G. H. R. SUMMERS. J. Chem. Soc. 3107 (1957).
23. P. A. PLATTNER, A. FURST, F. KOLLER, and W. LANG. Helv. Chim. Acta, **31**, 1455 (1948). P. A. PLATTNER, H. HEUSSER, and A. B. KULKARNI. Helv. Chim. Acta, **31**, 1822 (1948).
24. P. S. WHARTON and D. H. BOHLEN. J. Org. Chem. **26**, 3615 (1961).
25. D. N. JONES, J. R. LEWIS, C. W. SHOPPEE, and G. H. R. SUMMERS. J. Chem. Soc. 2876 (1955).
26. E. P. OLIVETO, G. GEROLD, and E. B. HERSHBERG. J. Am. Chem. Soc. **79**, 3596 (1957).
27. L. F. FIESER. Experiments in organic chemistry. D. C. Heath and Co., Boston, Mass. 1955. p. 88.
28. K. STICH, G. ROTZLER, and T. REICHSTEIN. Helv. Chim. Acta, **42**, 1480 (1959).

Can. J. Chem. Downloaded from www.nrcresearchpress.com by 210.87.254.40 on 09/05/12
For personal use only.

Can. J. Chem. Downloaded from www.nrcresearchpress.com by 210.87.254.105 on 09/05/12
For personal use only.

THE OXIDATION OF METHYL FUMAROPIMARATE WITH LEAD TETRAACETATE

W. A. Ayer and C. E. McDonald
Chemistry Department, University of Alberta, Edmonton, Alberta

Received November 13, 1964

Dedicated to Professor R. B. Sandin on the Occasion of his Sixty-Eighth Birthday

ABSTRACT

The oxidation of methyl fumaropimarate (VII) with lead tetraacetate has been found to lead to four different products, two of which have rather novel structures. The results which led to the elucidation of the structures of these products are presented, along with speculation on their mode of formation.

In connection with our studies aimed at the chemical correlation of the resin acids with the diterpene alkaloids of the atisine type (1), we became interested in the Diels–Alder adducts formed between levopimaric acid (I) and various dienophiles as intermediates in the construction of the bicyclo[2.2.2]octane ring system present in compounds such as atisine. The use of this approach for the synthesis of the hydrocarbon III has been

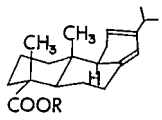

I R=H
II R=CH_3

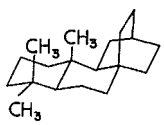

III

reported (1, 2) and the correlation of III with a degradation product of atisine has been achieved (1).

The most readily accessible Diels–Alder adduct of levopimaric acid is the commercially available[1] maleopimaric acid (the adduct with maleic anhydride), which has been shown to possess structure IV (3–6). Since one of the problems encountered in the Diels–Alder

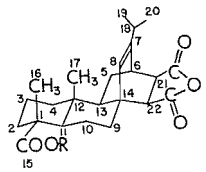

IV R=H
V R=CH_3

approach to a bicyclo[2.2.2]octane system using maleic anhydride or fumaric acid as the dienophile involves the removal of the two vicinal carboxyl groups (or anhydride function), we decided to use the readily available methyl maleopimarate (V) as a model compound for investigating methods for removal of the unwanted functional groups.

In 1952 Doering and co-workers (7) discovered that 1,2-dicarboxylic acids (and anhydrides) could be converted to olefins, albeit in low yield, by the action of lead dioxide.

[1]*Distillation Products Industries, Rochester, N.Y.*

In 1958, Grob *et al.* (8, 9) showed that the yields in this oxidative bisdecarboxylation sequence could be greatly improved by the use of lead tetraacetate in benzene or acetonitrile in the presence of an organic base. A further modification (10) involves the use of pyridine as the solvent for the lead tetraacetate oxidation. When subjected to these various conditions, methyl maleopimarate (V) was recovered unchanged. This is perhaps not surprising, however, since the anhydride ring in V is very stable (it is impossible to isolate the corresponding dicarboxylic acid) and presumably does not undergo facile mixed-ester formation by exchange with lead tetraacetate, a step which is necessary to initiate the reaction (8, 11). We therefore turned our attention to the C-15 monomethyl

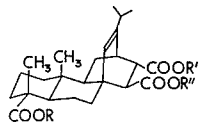

VI R = R' = R'' = H

VII R = CH_3, R' = R'' = H

ester (VII) of fumaropimaric acid (VI) (12) in which the anhydride function has been replaced by a *trans*-1,2-dicarboxylic acid system. Fumaropimaric acid (VI) is the product of the reaction of levopimaric acid or rosin with fumaric acid (12), but may also be obtained from maleopimaric acid (IV) by the action of hot methanolic potassium hydroxide (3). The configuration of the carboxyls at C-21 and C-22 as shown in VI was first assigned (3) on the basis of a result to be discussed in detail below and has since been corroborated by two other groups (13, 14). The monomethyl ester VII, which will be referred to as methyl fumaropimarate, was prepared by treatment of methyl maleopimarate (V) with methanolic sodium hydroxide followed by acidification or, more conveniently, by addition of fumaric acid to either methyl levopimarate (II) or methyl abietate.

When a pyridine solution of methyl fumaropimarate was treated with a slight molar excess of lead tetraacetate at room temperature, a reaction rapidly set in as evidenced by a rise in temperature and the evolution of a gas, and a total of four different products was isolated from the reaction mixture. Three of these, separated by chromatography over silica gel, were neutral compounds, and the fourth, separated from unreacted starting material by crystallization and chromatography, was an acid. Since a knowledge of the structure of the acidic product was useful in assigning the stereochemistry at C-21 and C-22 in methyl fumaropimarate, it will be discussed first.

The acidic product (obtained in 6% yield) crystallized from benzene as a hemisolvate ($C_{25}H_{34}O_6 \cdot \frac{1}{2}C_6H_6$) and was further characterized as its methyl ester ($C_{26}H_{36}O_6$). An examination of the spectral properties of the acid and its ester led to the assignment of structure VIII. The infrared spectrum of the acid showed bands at 1 771 (γ-lactone), 1 725 (ester), 1 717 (acid), and 1 675 cm^{-1} (carbon–carbon double bond). The n.m.r. spectrum showed signals at τ 9.29 (3H, singlet, methyl at C-12 shielded by C-7, C-18 double bond (3)), τ 8.84 (3H, singlet, methyl at C-1 (3)), τ 8.20 (6H, singlet, isopropylidene methyls), τ 6.33 (3H, singlet, carbomethoxyl protons), τ 4.97 (1H, singlet, proton at C-8), and τ 2.61 (3H, singlet, benzene of solvation). The formation of the lactone acid VIII (R = H) establishes that the carboxyl at C-22 in fumaropimaric acid (VI) is *endo* to the unsaturated ring. Since the double bond in VI is extremely hindered, we feel that the formation of the lactone VIII probably does not involve direct attack by lead tetraacetate on the double bond (15), but instead involves intramolecular electrophilic attack by the C-22 carboxyl as illustrated in IX (arrows *a*, *b*, and *c*). The preparation of the

Can. J. Chem. Downloaded from www.nrcresearchpress.com by 210.87.254.105 on 09/05/12
For personal use only.

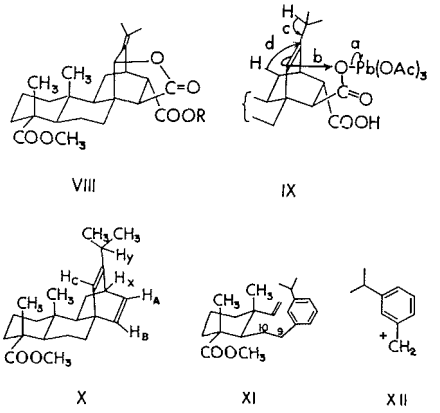

ester VIII by oxidation of fumaropimaric acid with alkaline permanganate followed by esterification has recently been described (14).

The neutral products of the oxidation, as mentioned earlier, were separated by chromatography over silica gel. The first substance eluted was a compound $C_{23}H_{34}O_2$, obtained in 10% yield, which showed the properties expected of the diene X, the product of straightforward oxidative bisdecarboxylation of diacid VII. The infrared spectrum showed olefinic C—H stretching at 3 040 cm^{-1} and ester carbonyl absorption at 1 732 cm^{-1}. Evidence for the unrearranged bicyclo[2.2.2]octadiene structure X was provided by the n.m.r. spectrum, which showed the shielded C-12 methyl (τ 9.38) (3), the isopropyl group as a pair of doublets at τ 8.93 and 9.00, and the C-1 methyl as a singlet at τ 8.88. The chemical shifts and coupling constants for the protons designated by letter in X are given in Table I. The assignments, which are consistent[2] with the proposed structure, were

TABLE I

Signals for lettered protons in diene X

Proton	Chemical shift (τ)	Multiplicity
H_A	3.84	Quartet, J_{AB} 7 c.p.s., J_{AX} 6 c.p.s.
H_B	4.05	Quartet, J_{AB} 7 c.p.s., J_{BX} 1.5 c.p.s.
H_C	4.59	Triplet, J_{CY} 1.7 c.p.s., $J_{CX} \approx 1$ c.p.s.
H_X	6.75	Multiplet, not completely resolved
H_Y	7.70	Multiplet, not completely resolved

verified by appropriate decoupling experiments. Thus, irradiation of the signal at τ 6.75 greatly simplified the olefinic region, the signals for H_A and H_B then appearing as a simple AB quartet (J = 7 c.p.s.) and H_C appearing as a doublet (splitting 1.7 c.p.s.). When the signal at τ 7.70 was irradiated, H_C appeared as a poorly resolved doublet of splitting about 1 c.p.s. Simultaneous irradiation of *both* the τ 6.75 and the τ 7.70 signal caused H_C to collapse to a singlet. The diene X was thermally unstable and was transformed in part to an aromatic compound on attempted distillation. A sample of X which had been heated at 180° for 30 min showed strong signals in its n.m.r. spectrum at τ 3.0–3.3 (aromatic protons) and its ultraviolet spectrum displayed typical benzenoid absorption. We believe this to be indicative of an aromatization process similar to the thermal transformation of bicyclo[2.2.2]octadiene to benzene and ethylene (17), leading in this

[2]*For a summary of and references to recent work on the n.m.r. spectra of bridged ring compounds, see ref. 16.*

Can. J. Chem. Downloaded from www.nrcresearchpress.com by 210.87.254.105 on 09/05/12
For personal use only.

Can. J. Chem. Downloaded from www.nrcresearchpress.com by 210.87.254.105 on 09/05/12
For personal use only.

case to compound XI. The mass spectrum of the diene X provided further evidence for the facility of this aromatization process, the most intense peak in the spectrum appearing at m/e 133 corresponding to the cleavage of the C-9 to C-10 bond in an ion of structure XI with the formation of the benzylic ion XII (or its tropylium ion counterpart (18)). Hydrogenation of the diene X at atmospheric pressure yielded a dihydro derivative in which the 21,22 double bond had been reduced as revealed by the n.m.r. spectrum, which showed a single olefinic proton (τ 4.60) and a high-field methyl signal (τ 9.42) that is due to the shielded methyl group at C-12 (3).

The diene X was eluted from the silica gel column with benzene. Elution with benzene–ether yielded first a compound $C_{24}H_{34}O_4$ (lactone A) followed by a compound $C_{26}H_{36}O_6$ (lactone B). Lactone A was isolated in 7% yield and lactone B in 3% yield. When the reaction was carried out in acetic acid, in the presence of sodium acetate, lactone A was not isolated but lactone B was obtained in 11% yield.

To lactone B was assigned structure XIII on the basis of the following observations. The infrared spectrum showed absorption at 1 784 cm^{-1} (γ-lactone), 1 740 cm^{-1} (acetoxyl), and 1 722 cm^{-1} (carbomethoxyl). The n.m.r. spectrum confirmed the presence of the carbomethoxyl group (three-proton singlet at τ 6.31) and the acetoxyl group (three-proton singlet at τ 7.90) and indicated the presence of four methyl groups attached to saturated carbon. Two of these appeared as sharp singlets at τ 8.79 (methyl at C-1 (3)) and 9.05 (C-12 methyl (3)), while the other two appeared as a pair of doublets at τ 8.94 (splitting 7 c.p.s.) and 9.16 (splitting 7 c.p.s.). These latter signals are attributed to the methyls of the isopropyl group, made non-equivalent by the asymmetry of their environment (19). Both these doublets collapsed to singlets when the region τ 8.12 (isopropyl methine) was simultaneously irradiated. A one-proton singlet at τ 5.19 is attributed to the lactonic hydrogen at C-8 and a doublet at τ 4.85 (splitting 5 c.p.s.) to the proton on the acetoxyl-bearing C-21.

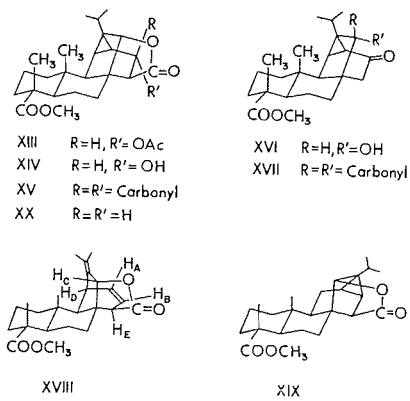

Methanolysis of lactone B provided the hydroxylactone XIV. The infrared spectrum of XIV exhibited, besides the lactone and ester absorption, a band at 3 610 cm^{-1} indicative of a nonhydrogen-bonded hydroxyl group. The n.m.r. spectrum of XIV was very similar to that of lactone B (XIII) except that the doublet at τ 4.85 (C*H*OAc) and the singlet at 7.90 (OCOC*H*$_3$) has been replaced by a poorly resolved peak at τ 5.80 (C*H*OH) and a concentration-dependent peak at about 7.2 (O*H*). Oxidation of XIV with chromic acid yielded the ketolactone XV, which showed carbonyl absorption at 1 790 cm^{-1} (γ-lactone), 1 725 cm^{-1} (ester), and 1 715 cm^{-1} (ketone) in the infrared. In agreement with the

formulation of XV as a cyclopropyl ketone, the ultraviolet spectrum measured in isooctane showed a maximum at 199 mμ (ε 2 400) (20). Compound XV is also a β-keto lactone and as such would be expected to be sensitive to base. In fact it was found that, when XV was heated under reflux with methanolic sodium methoxide, it underwent a reverse Claisen reaction and methanolysis to give the hydroxyketone XVI, the infrared spectrum of which showed nonbonded hydroxyl (3 610 cm^{-1}), ester (1 727 cm^{-1}), and ketone (1 687 cm^{-1}) absorption. The C-8 proton now appeared at τ 5.58 (singlet) in the n.m.r. spectrum. Oxidation of XVI with chromic acid yielded the diketone XVII, which showed a maximum at 202 mμ (ε 6 500) in the ultraviolet.

To test further the validity of structure XIII for lactone B, it was treated with *p*-toluenesulfonic acid in hot benzene in the hope that cleavage of the C_{21}–oxygen or C_8–oxygen bond would occur with concomitant opening of the cyclopropane ring in a manner analogous to that observed for the transformation of cyclopropylcarbinyl derivatives into allylcarbinyl derivatives (21). The product, formed in 90% yield, was a diene to which structure XVIII is assigned on the basis of the following information. The infrared spectrum showed absorption at 3 042 cm^{-1} (olefinic C—H), 1 765 cm^{-1} (γ-lactone), 1 720 cm^{-1} (ester), and 1 630 cm^{-1} (carbon–carbon double bond(s)). Pertinent details of the n.m.r. spectrum, including results obtained or confirmed by spin-decoupling experiments, are presented in Table II. The presence of a *cis*-disubstituted double bond is revealed by the appearance of the two strongly coupled (8.8 c.p.s.) olefinic protons. The fact that each of these protons is involved in a further large coupling (6.7 and 4.8 c.p.s.) suggests the presence of the grouping CH—CH=CH—CH. The fact that H_A is further split but H_B is not is explained by the fact that H_A and H_E fulfill the steric requirements for maximum allylic coupling (22) while H_B and H_D do not. The further splitting of H_E is attributed to long-range "tail-to-tail" coupling (22) with H_C and this has been confirmed by double-irradiation experiments. The presence of an isopropylidene

TABLE II

Details of n.m.r. spectrum of diene XVIII

Proton(s)	Chemical shift (τ)	Multiplicity
H_A	3.56	Septet, J_{AB} 8.8 c.p.s., J_{AD} 6.7 c.p.s., J_{AE} 1.7 c.p.s.
H_B	4.48	Quartet, J_{AB} 8.8 c.p.s., J_{BE} 4.8 c.p.s.
H_C	4.93	Broadened singlet
H_D	6.99	Poorly resolved doublet
H_E	7.06	Sextet, J_{BE} 4.8 c.p.s., J_{AE} 1.7 c.p.s., J_{CE} 1.7 c.p.s.
$COOCH_3$	6.33	Singlet
C-19, C-20	8.23, 8.32	Broadened singlets
C-16	8.81	Singlet
C-17	9.25	Singlet

group in the diene is indicated by the methyl signals at τ 8.23 and 8.32. The fact that the C-17 protons (τ 9.25) are somewhat more shielded than in the starting material is consistent with the location of an unsaturated function near the quaternary methyl group (3) as in structure XVIII. The diene XVIII readily formed a dihydro derivative when subjected to catalytic hydrogenation. The n.m.r. spectrum of the dihydro compound showed the isopropylidene methyls at τ 8.26 and 8.32 but no olefinic protons, clearly indicating that the unhindered (from the underside) *endocyclic* double bond had been reduced. The formation of XVIII (via the homoallylic cation formed by loss of the C-21 acetoxyl group with participation of the C-6, C-7 bond) provides evidence for the C-5 to C-7 bond in lactone B (XIII).

Can. J. Chem. Downloaded from www.nrcresearchpress.com by 210.87.254.105 on 09/05/12
For personal use only.

Can. J. Chem. Downloaded from www.nrcresearchpress.com by 210.87.254.105 on 09/05/12
For personal use only.

The acetoxyl group at C-21 in lactone B (XIII) was assigned the *exo* configuration (*trans* to the lactone group), since the infrared spectrum of the corresponding alcohol (XIV) showed no intramolecular hydrogen bonding and since the n.m.r. spectrum of XIII displayed a doublet whose splitting (5 c.p.s.) is compatible only with a *trans* arrangement of the protons on C-21 and C-22 (3).

One possible mode of formation of lactone B (XIII) is illustrated by arrows *a*, *b*, and *d* in IX. This process, which finds analogy in the lead tetraacetate induced transformation of norbornene into 3-acetoxynortricyclene (23), is either preceded by or followed by oxidative replacement of the C-21 carboxyl by acetoxyl (see below).

The third neutral product of the oxidation, lactone A, is assigned structure XIX. The presence of the γ-lactone is suggested by infrared absorption at 1 780 cm^{-1} and by a one-proton signal at τ 5.30 (—C*H*—OCO—) in the n.m.r. spectrum. The other two oxygens of lactone A are accounted for by the carbomethoxyl group, which gives rise to absorption at 1 720 cm^{-1} in the infrared and at τ 6.33 (3H, singlet) in the n.m.r. spectrum. As was the case with lactone B, the isopropyl methyls were markedly non-equivalent, giving rise to doublets at τ 8.96 (splitting 7.5 c.p.s.) and 9.24 (splitting 7.5 c.p.s.). The possibility that lactone A was 21-desacetoxylactone B (XX) was excluded when it was shown that compound XX, prepared by transformation of ketone XV to the corresponding thioketal and desulfurization, was not identical with lactone A.

Lactone A was transformed to the corresponding hydroxydiester XXI by the action

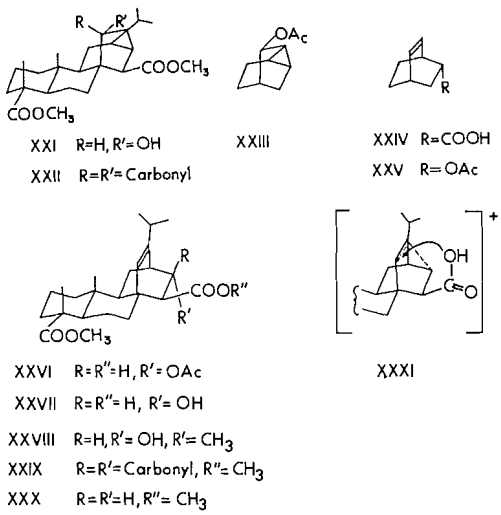

XXI R=H, R'=OH
XXII R=R'=Carbonyl
XXIII
XXIV R=COOH
XXV R=OAc
XXVI R=R"=H, R'=OAc
XXVII R=R"=H, R'=OH
XXVIII R=H, R'=OH, R'=CH_3
XXIX R=R'=Carbonyl, R"=CH_3
XXX R=R'=H, R"=CH_3
XXXI

of methanolic sodium hydroxide followed by diazomethane. Oxidation of XXI with chromic acid in acetic acid afforded the ketone XXII, which absorbed at 1 729 and 1 718 cm^{-1} in the infrared and at 202 mμ (ϵ 4 000) (cyclopropyl ketone (20)) in the ultraviolet. The formation of lactone A (XIX) from methyl fumaropimarate (VII) is closely analogous to the formation of tricyclo[2.2.2.$0^{2,6}$]octan-3-yl acetate (XXIII) from *exo*-5-carboxybicyclo[2.2.2]oct-2-ene (XXIV), which is brought about by the action of lead tetraacetate in acetic acid in the presence of potassium acetate (24). The fact that the tricyclic compound XXIII was transformed by the action of acid into *exo*-bicyclo-[2.2.2]oct-5-en-2-yl acetate (XXV) led us to attempt a similar reaction on lactone A. It was found that lactone A (XIX) was extremely sensitive to hot acetic acid and was converted in less than 20 min to an oily three-component mixture (as determined by thin-layer

chromatography (t.l.c.)), which, from n.m.r. analysis, was judged to contain ca. 80% of the acetoxy acid XXVI. Thus, restoration of the bicyclo[2.2.2]octene system was indicated by an olefinic proton at τ 4.63 (0.8H relative to the carbomethoxyl signal) and a shielded C-methyl group signal at 9.38 (2.4H). Attempts to isolate XXVI were unsuccessful. However, methanolysis of the crude solvolysis product led to the isolation of the major component in the form of the hydroxy acid (XXVII). Esterification of XXVII with diazomethane gave the corresponding ester XXVIII, which exhibited the expected infrared and n.m.r. spectral behavior. The most intense peak in the mass spectrum of XXVIII occurred at m/e 316 and is attributable to an ion of structure II formed by "retro-Diels–Alder" fragmentation of the molecular ion, a process shown previously to be important in bicyclo[2.2.2]octene derivatives (1). Oxidation of XXVIII with chromic acid yielded the corresponding ketone XXIX, which absorbed at 1 722 cm^{-1} (esters) and 1 705 cm^{-1} (ketone) in the infrared and at 296 mμ (ϵ = 139, enhanced $n \rightarrow \pi^*$ absorption of a β,γ-unsaturated ketone (25)) in the ultraviolet. In agreement with the generalized Octant rule (26) and its application to β,γ-unsaturated ketones (26, 27) the ketone XXIX displayed a strongly negative Cotton effect.

The ketone XXIX was transformed, via the thioketal and desulfurization, into the diester XXX, which was shown to be identical with the diester of the Diels–Alder adduct of levopimaric acid and acrylic acid. Since the structure of this adduct has been established as XXX (13), this result rigorously establishes the structure of the solvolysis product XXVI and thus provides further support for the structure of lactone A (XIX). The formation of lactone A is presumed to involve lactonization of the homoallylic cation XXXI, which is formed by oxidative loss of the C-21 carboxyl group (11, 24). As mentioned earlier, lactone A is not detected when the reaction is carried out in acetic acid – sodium acetate but the yield of lactone B is increased, indicating that in acetic acid XXXI reacts with acetate ion rather than undergoing lactonization. Further oxidation of the acetoxy acid XXVI could lead to lactone B (XIII).

The results obtained in this model series clearly indicated that the presence of a double bond in the bicyclo[2.2.2]octane system was undesirable when one is attempting oxidative bisdecarboxylations. This knowledge was useful in planning the preparation of the hydrocarbon III (1).

EXPERIMENTAL

Nuclear magnetic resonance spectra were measured on 5–10% (w/v) solutions in deuterochloroform (unless otherwise noted), using either a Varian A-60 or HR 100 spectrometer. Tetramethylsilane was used as an internal standard. Spin-decoupling experiments were carried out with the HR 100 spectrometer using the method described by Johnson (28). Unless otherwise noted, infrared spectra were determined in carbon tetrachloride solution using a Perkin–Elmer model 421 spectrophotometer. Ultraviolet spectra of the cyclopropyl ketones were obtained, through the courtesy of Dr. K. H. Palmer, on a Unicam SP 700 spectrophotometer. The mass spectra were determined on an AEI MS2-H mass spectrometer. Samples were introduced through a heated inlet system kept at 200°. Skellysolve B refers to Skelly Oil Company light petroleum, b.p. 62–70°. Melting points are uncorrected. Kiliani's reagent was prepared from sodium dichromate (60 g) in water (270 ml) to which concentrated sulfuric acid (80 g) was added. Microanalyses are by Pascher Mikroanalytisches Laboratorium, Bonn, West Germany, and C. Daessle, Montreal, Quebec.

Fumaropimaric Acid from Maleopimaric Acid

Maleopimaric acid (IV, 10 g) was dissolved in a solution of potassium hydroxide (16 g) in aqueous methanol (200 ml, 1:10 water–methanol) and the resulting solution heated under reflux for 1½ h. Most of the methanol was then removed at the pump, dilute hydrochloric acid was added, and the resulting precipitate filtered off and recrystallized from acetic acid. The fumaropimaric acid (4 g, 38% yield) thus obtained melted at 193–195°, and analyzed as a monohydrate after it was dried at 110° *in vacuo*.

Anal. Calcd. for $C_{24}H_{34}O_6 \cdot H_2O$: C, 66.03; H, 8.310 O, 25.65. Found: C, 66.14; H, 8.05; O, 25.90.

A sample recrystallized from aqueous ethanol melted at 244–248°. The reported melting points are 280–282° (sample dried at 152° *in vacuo* (12)) and 249–252° (hydrated form from dioxane (29)). A sample of

Can. J. Chem. Downloaded from www.nrcresearchpress.com by 210.87.254.105 on 09/05/12
For personal use only.

fumaropimaric acid prepared by Diels–Alder addition of fumaric acid to rosin (12) showed identical properties.

Methyl Fumaropimarate (VII)

A. From Methyl Maleopimarate

Methyl maleopimarate (60 g) was dissolved in methanol (600 ml) containing sodium hydroxide (36 g) and the solution refluxed for 45 min; then 2 *N* aqueous sodium hydroxide (400 ml) was added and heating continued for a further 100 min. The solution was then neutralized with hydrochloric acid, most of the methanol removed at the pump, and the residue made strongly acidic with 2 *N* hydrochloric acid. The precipitate which separated was collected by filtration, washed first with water and then with benzene, and recrystallized from acetic acid to yield methyl fumaropimarate (15 g), m.p. 269–279°. The analytical sample, m.p. 274–279°, was prepared by further recrystallization from ethanol.

Anal. Calcd. for $C_{25}H_{36}O_6$: C, 69.40; H, 8.39; O, 22.20; OCH_3, 5.69. Found: C, 69.49; H, 8.35; O, 22.10; OCH_3, 4.98.

Infrared spectrum: ν_{max}^{Nujol} 3 200 (broad), 1 725, 1 705 cm^{-1}.

B. From Methyl Abietate

Crude methyl abietate (860 g, prepared by esterification of rosin) was stirred under nitrogen with fumaric acid (500 g) at 170–185° for 18 h. The mixture was then transferred to a large Erlenmeyer flask and washed with benzene (2 l, in portions). The benzene-insoluble residue was then suspended successively in 3-, 2-, and 1-l portions of hot water, the insoluble portion being collected each time by filtration. In this way methyl fumaropimarate (202 g), m.p. 269–279°, identical with that prepared above, was obtained. Further purification could be effected by recrystallization from ethanol.

Lead Tetraacetate Oxidations

A. In Pyridine

Methyl fumaropimarate (VII, 21 g, 0.049 mole) was dissolved in pyridine (250 ml) at 30° and lead tetraacetate (31 g, 0.07 mole) added. After a few minutes the temperature rose to 45° and a gas was evolved. The solution was cooled to 30° and allowed to stand at room temperature for 12 h. Excess reagent was destroyed by the addition of ethylene glycol, the solvent evaporated on the steam bath under reduced pressure, and the residue washed with four 125-ml portions of ether. The combined ether solutions were washed with water, dilute hydrochloric acid, and extracted with dilute sodium hydroxide (extract A). Evaporation of the ether yielded an oil (6.0 g) which was subjected to chromatography over silica gel (400 g). Fractions 2–4, eluted with benzene (1.5 l), gave the diene X as a colorless oil (1.7 g) which showed a single spot on thin-layer chromatography. For analysis, a sample was dried *in vacuo* at 50° for 48 h.

Anal. Calcd. for $C_{23}H_{34}O_2$: C, 80.65; H, 10.00. Found: C, 80.77; H, 9.80.

Infrared spectrum: ν_{max} 3 040, 1 732 cm^{-1}. Mass spectrum: *m/e* 342 (molecular ion), 133 (base peak). See Table I for details of n.m.r. spectrum.

Fractions 7 and 8, eluted with benzene–ether (1 l of 7:1) afforded lactone A (XIX) (1.4 g) as colorless needles which melted, after recrystallization from benzene – Skellysolve B, at 176–180°.

Anal. Calcd. for $C_{24}H_{34}O_4$: C, 74.57; H, 8.87; O, 16.56. Found: C, 74.48; H, 8.74; O, 16.56.

Infrared spectrum: ν_{max} 1 780, 1 720 cm^{-1}. Nuclear magnetic resonance spectrum: τ 9.25 (3H, doublet, J = 7.5 c.p.s.), 9.17 (3H), 8.96 (3H, doublet, J = 7.5 c.p.s), 8.85 (3H), 7.61 (1H), 6.33 (3H, singlet), and 5.30 (1H).

Fractions 10–12, also eluted with benzene–ether (7:1, 1.5 l), gave lactone B (XIII) (0.6 g) as colorless needles which melted at 194–195° after recrystallization from benzene – Skellysolve B and then methanol.

Anal. Calcd. for $C_{26}H_{36}O_6$: C, 70.25; H, 8.16; O, 21.60. Found: C, 70.35; H, 7.88; O, 21.58.

Infrared spectrum: ν_{max} 1 784, 1 740, 1 722, 1 242 cm^{-1}.

The acidic components were present both in the free form (extract A) and as lead salts (residue from ether trituration). The latter portion was dissolved in acetic acid and hydrogen chloride bubbled in until no more precipitate formed. The precipitated lead chloride was filtered off and the filtrate concentrated under reduced pressure. Benzene was added to the partially crystalline residue and the insoluble portion (0.7 g) collected by filtration. This portion was identified by its melting point and infrared spectrum as unreacted starting material. The benzene filtrate was combined with the acids liberated by acidification of extract A and the residue (12 g) obtained by removal of the solvents was subjected to chromatography over silica gel (700 g). Elution with benzene provided only trace amounts of unidentified material. Elution with benzene–ether (3:1) provided the lactone acid VIII (R = H) which crystallized in solvated form from benzene, m.p. 189–190°.

Anal. Calcd. for $C_{25}H_{34}O_6 \cdot \frac{1}{2}C_6H_6$: C, 71.60; H, 7.95; O, 20.44; OCH_3, 6.61. Found: C, 71.21; H, 7.95; 20.60; OCH_3, 6.75.

Infrared spectrum: $\nu_{max}^{CHCl_3}$ 1 771, 1 725, 1 717, 1 675 (w) cm^{-1}. The methyl ester VIII (R = CH_3), prepared by reaction of the above acid with diazomethane, melted at 180–181° after recrystallization from methanol.

Anal. Calcd. for $C_{26}H_{36}O_6$: C, 70.25; H, 8.18; O, 21.59; OCH_3, 13.96. Found: C, 70.10; H, 8.38; O, 21.51; OCH_3, 14.48.

Can. J. Chem. Downloaded from www.nrcresearchpress.com by 210.87.254.105 on 09/05/12
For personal use only.

Infrared spectrum: $\nu_{max}^{CHCl_3}$ 1 770, 1 733, 1 725, 1 674 (w) cm^{-1}.

The later fractions from the chromatogram yielded further unchanged starting material.

B. In Acetic Acid

Methyl fumaropimarate (VII, 10 g, 0.023 mole) was suspended in hot (steam bath) acetic acid (100 ml) containing acetic anhydride (2 ml) and lead tetraacetate (12 g, 0.027 mole). The reaction mixture was kept at 90° for 10 min with no evidence of reaction. The addition of sodium acetate (3.0 g, 0.037 mole) resulted in the immediate evolution of gas and the dissolution of the suspended solids. After 7 min, additional lead tetraacetate (16 g, 0.036 mole) was added and the heating continued for 30 min. The cooled solution was diluted with a large volume of water and extracted several times with chloroform. The residue left after evaporation of the chloroform was chromatographed over acid-washed alumina (150 g). Elution with benzene gave a small amount of impure diene X, and elution with benzene–ether and ether yielded lactone B (XIII) (1.12 g) but no lactone A. Further elution (chloroform, chloroform – acetic acid) yielded acidic material which was not investigated further.

Reactions of Diene X

A. Hydrogenation

The diene X (260 mg) was dissolved in methanol (6 ml) and stirred in an atmosphere of hydrogen in the presence of finely divided platinum (from 14 mg of Adams catalyst) for 22 h. Removal of the catalyst and concentration of the filtrate yielded the dihydro derivative (220 mg) as a colorless oil, which absorbed at 1 720 cm^{-1} in the infrared. The nuclear magnetic resonance spectrum showed absorption at τ 9.42 (3H), 9.02 (6H, doublet, J = 6 c.p.s.), 8.91 (3H), 6.37 (3H), and 4.60 (1H).

B. Thermal Decomposition

The diene X (100 mg) was heated at 180° for 25 min and then distilled under vacuum. The n.m.r. spectrum of the oily distillate (80 mg) showed very little absorption at τ 9.38 (0.4H as compared to the carbomethoxyl peak taken as 3H) but strong absorption (2.5H) in the aromatic region. The ultraviolet spectrum of the distillate showed typical aromatic absorption at 254, 262, 270, and 274 mμ.

Methanolysis of Lactone B

Lactone B (XIII, 0.31 g) was dissolved in methanolic sodium methoxide (0.01 g sodium in 10 ml methanol) and kept at room temperature for 9 h. Water (100 ml) was then added and the aqueous solution extracted twice with methylene chloride. Evaporation of the methylene chloride and crystallization of the residue from benzene–Skellysolve gave the hydroxylactone XIV (0.245 g), m.p. 189–190°.

Anal. Calcd. for $C_{24}H_{34}O_5$: C, 71.61; H, 8.52; O, 19.87. Found: C, 72.25; H, 8.31; O, 19.60.

Infrared spectrum: ν_{max} 3 610, 3 480, (concentration dependent, absent in dilute solution), 1 782, 1 729 cm^{-1}. Nuclear magnetic resonance spectrum: τ 9.15 (3H, doublet, J = 7 c.p.s.), 9.06 (3H), 8.94 (3H, doublet, J = 6.5 c.p.s.), 8.80 (3H), 7.22 (concentration dependent, O*H*), 5.78 (1H), 5.24 (1H).

Ketolactone XV

The hydroxy lactone XIV (0.34 g) was dissolved in acetic acid (25 ml) and Kiliani's reagent (0.45 ml) added. The solution was left at room temperature for 60 min, then diluted with water (100 ml), and extracted 4 times with benzene. The combined benzene extracts were washed several times with water, dried, and evaporated to give an off-white foam which crystallized from benzene – Skellysolve B as fine colorless needles (0.30 g) which melted at 179–180°, then resolidified and remelted at 184–185°.

Anal. Calcd. for $C_{24}H_{32}O_5$: C, 71.96; H, 8.07; O, 19.97. Found: C, 71.80; H, 8.01; O, 20.18.

Infrared spectrum: $\nu_{max}^{CHCl_3}$ 1 790, 1 725, 1 715 cm^{-1}. Nuclear magnetic resonance spectrum: τ 9.11 (3H, doublet, J = 7 c.p.s.), 8.98 (3H), 8.88 (3H, doublet, J = 6.5 c.p.s.), 8.78 (3H), 6.35 (3H), 4.97 (1H). Ultraviolet spectrum: λ_{max}^{EtOH} 286 mμ (ϵ 82), $\lambda_{max}^{isooctane}$ 199 mμ (ϵ 2 400). Rotatory dispersion in methanol (c, 0.33): α_{589} +92°, α_{500} +210°, α_{400} +494°, α_{350} +930°, α_{318} +2060° (inflection), α_{308} +2370° (peak), α_{285} ± 0°, α_{270} −745°, α_{260} −550°.

Hydroxyketone XVI

Ketolactone XV (0.30 g) was dissolved in methanol (150 ml) in which sodium (2.1 g) was dissolved and the solution was heated under reflux for 18 h. The solution was concentrated, diluted with dilute aqueous hydrochloric acid, and extracted 3 times with chloroform. Evaporation of the chloroform left the crystalline hydroxyketone XVI (0.29 g), which, after recrystallization from benzene and then methanol, melted at 228–229°.

Anal. Calcd. for $C_{23}H_{34}O_4$: C, 73.74; H, 9.16; O, 17.09. Found: C, 74.04; H, 8.93; O, 17.06.

Infrared spectrum: $\nu_{max}^{CHCl_3}$ 3 610, 3 450, 1 727, 1 687 cm^{-1}. Nuclear magnetic resonance spectrum: τ 9.05 (3H, doublet, J = 8 c.p.s.), 8.98 (3H), 8.92 (3H, doublet, J = 7 c.p.s.), 8.80 (3H), 6.32 (3H), 5.58 (1H). Ultraviolet spectrum: λ_{max}^{EtOH} 275 mμ (ϵ 50).

Diketone XVII

The hydroxyketone XVI (0.09 g) was dissolved in acetic acid (4 ml) and Kiliani's reagent (0.15 ml) added. After 60 min, excess solvent was destroyed with methanol, most of the solvent removed at the pump, and water added. Chloroform extraction provided the diketone XVII (0.07 g), m.p. 178–179° (from ethanol).

Can. J. Chem. Downloaded from www.nrcresearchpress.com by 210.87.254.105 on 09/05/12
For personal use only.

Anal. Calcd. for $C_{23}H_{32}O_4$: C, 74.15; H, 8.67; O, 17.18; molecular weight 372. Found: C, 73.99; H, 8.74; O, 17.10; molecular weight (mass spectrometry) 370 ± 2.

Infrared spectrum: ν_{max} 1 742 (sh), 1 727, 1 715 cm^{-1}. Ultraviolet spectrum: λ_{max}^{MeOH} 202 mμ (ε 6 500), 273–287 mμ (ε 90).

Thioketal of Ketolactone XV

The ketolactone XV (0.2 g, 0.5 mmole) was dissolved in freshly distilled boron trifluoride etherate (3 ml) containing ethanedithiol (0.53 g, 5.6 mmoles) and left at room temperature for 45 min. Benzene (50 ml) was then added and the solution washed several times with water and then evaporated. One crystallization of the residue from ethyl acetate afforded 0.12 g of crude thioketal, m.p. 225–236°. The analytical sample, prepared by recrystallization from ethyl acetate and then from benzene – Skellysolve B, melted at 238–239°.

Anal. Calcd. for $C_{26}H_{36}O_4S_2$: C, 65.52; H, 7.62; S, 13.45. Found: C, 65.57; H, 7.60; S, 13.61.

Infrared spectrum: $\nu_{max}^{CHCl_3}$ 1 765, 1 712 cm^{-1}. The nuclear magnetic resonance spectrum showed a four-proton multiplet at τ 6.60 assigned to the —S—CH_2—CH_2—S— protons.

Desulfurization of the Thioketal

The crude thioketal (0.17 g) prepared above was dissolved in acetone (30 ml), W2 Raney nickel (4 g) added, and the mixture heated under reflux for 8½ h. The nickel was then filtered off and washed with acetone and the filtrate evaporated. The crude deoxylactone XX (0.11 g) crystallized on trituration with methanol and was recrystallized from methanol, m.p. 135–137°.

Anal. Calcd. for $C_{24}H_{34}O_4$: C, 74.57; H, 8.87; O, 16.56. Found: C, 74.75; H, 8.79; O, 16.97.

Infrared spectrum: ν_{max} 1 775, 1 723 cm^{-1}. Nuclear magnetic resonance spectrum: τ 9.14 (3H, doublet, J = 7 c.p.s.), 9.03 (3H), 8.87 (3H, doublet, J = 7 c.p.s.), 8.81 (3H), 6.36 (3H), 5.29 (1H).

Preparation of Diene XVIII

Lactone B (XIII, 1.74 g) was dissolved in benzene (80 ml) containing *p*-toluenesulfonic acid (0.5 g) and the solution heated under reflux for 12 h. The cooled solution was filtered through alumina (20 g) and the alumina washed with benzene–ether (200 ml of 20:1). Evaporation of the solvents and crystallization of the residue from Skellysolve B provided 1.34 g of the crude diene XVIII, m.p. 167–170°. Recrystallization from methanol and then Skellysolve gave the analytical sample, m.p. 171–172°.

Anal. Calcd. for $C_{24}H_{32}O_4$: C, 74.96; H, 8.40. Found: C, 74.72; H, 8.20.

Infrared spectrum: ν_{max} 3 042(w), 1 765, 1 720, 1 630(w) cm^{-1}. Details of the n.m.r. spectrum are presented in Table II.

Hydrogenation of Diene XVIII

Diene XVIII (0.46 g) was dissolved in ethyl acetate (50 ml) and hydrogenated over platinum (from 55 mg of Adams catalyst) at atmospheric pressure. Hydrogen uptake (1 mole) was complete in 30 min. The dihydro compound was crystallized from ethyl acetate and then from benzene – Skellysolve B and melted at 184–185.5°.

Anal. Calcd. for $C_{24}H_{34}O_4$: C, 74.56; H, 8.89; O, 16.56. Found: C, 74.62; H, 8.92; O, 16.41.

Infrared spectrum: ν_{max} 1 765, 1 722, 1 632(w) cm^{-1}. Nuclear magnetic resonance spectrum: τ 9.29 (3H), 8.82 (3H), 8.26 (6H), 6.32 (3H), 5.00 (1H).

Methanolysis of Lactone A

Lactone A (XIX, 0.21 g) was dissolved in a solution of sodium methoxide (0.26 g) in methanol – dimethyl sulfoxide (8 ml of 1:3). Solution was effected by warming the mixture on the steam bath and the solution was then left at room temperature for 7 days, after which time benzene was added. The resulting solution was washed several times with water and the combined aqueous extracts acidified with concentrated hydrochloric acid. Chloroform extraction yielded the crude hydroxy acid (0.20 g), which was recrystallized to constant melting point (212–215°) from methanol – ethyl acetate. Infrared spectrum: ν_{max} 3 480 (broad) 3 300 – 2 400, 1 710 cm^{-1}. Esterification with diazomethane yielded the hydroxy ester XXI, m.p. 140–141° (from benzene – Skellysolve B).

Anal. Calcd. for $C_{25}H_{38}O_5$: C, 71.73; H, 9.15; O, 19.11. Found: C, 71.84; H, 9.06; O, 19.50.

Infrared spectrum: ν_{max} 3 460 (concentration independent, hydrogen-bonded hydroxyl) 1 715 cm^{-1}. Nuclear magnetic resonance spectrum: τ 9.27 (3H, doublet, J = 7 c.p.s.), 9.03 (3H), 8.95 (3H, doublet, J = 7 c.p.s.), 8.89 (3H), 6.49 (1H, doublet, J = 12 c.p.s., CHO*H*), 6.41 (3H), 6.35 (3H), 6.00 (1H, doublet, J = 12 c.p.s., C*H*OH).

Ketoester XXII

The hydroxy ester XXI (95 mg, 0.23 mmole) was dissolved in acetic acid (5 ml) and oxidized for 1 h with Kiliani's reagent (0.15 ml, 0.22 mmole H_2CrO_4) at room temperature. Excess oxidant was destroyed with methanol and the solution then diluted with water and extracted with chloroform. Evaporation of the chloroform and recrystallization of the residue from Skellysolve B and then methanol provided the ketoester XXII, m.p. 122–123°. Infrared spectrum: ν_{max} 1 729 (sh), 1 718 cm^{-1}. Nuclear magnetic resonance spectrum: τ 9.27 (3H), 9.06 (3H, doublet, J = 7 c.p.s.), 8.96 (3H, doublet, J = 7 c.p.s.), 8.88 (3H), 6.37 (6H). Ultraviolet spectrum: $\lambda_{max}^{isooctane}$ 202 mμ (ε 4 000), 288 mμ (ε 70). Rotatory dispersion in methanol (c 0.204): α_D −39°, α_{400} +34°, α_{303} +2 580°, α_{288} 0°, α_{268} −3 320°, α_{250} −2 500°.

Can. J. Chem. Downloaded from www.nrcresearchpress.com by 210.87.254.105 on 09/05/12
For personal use only.

Solvolysis of Lactone A in Acetic Acid

Lactone A (XIX, 1.26 g) was dissolved in acetic acid (50 ml) and the solution heated on the steam bath for 20 min, then diluted with a large volume of water, and extracted 4 times with benzene. Removal of the solvents left an oily residue (1.3 g) shown by t.l.c. to consist of one major and two minor components. The infrared spectrum of the mixture showed absorption at 2 500–3 300, 1 715, and 1 695 cm^{-1}. The n.m.r. spectrum showed peaks at τ 9.38 (2.4H using the carbomethoxyl signal (3H) at 6.40 as an internal standard), 8.95 (doublet, $J = 6.5$ c.p.s.), 8.89, 8.00 (3H, —OCOCH_3), 5.50 (0.8H, C*H*OAc), 4.63 (0.8H, olefinic proton). Attempts to crystallize the free acid or the derived cyclohexylamine salts were unsuccessful. The reaction product was therefore deacetylated by allowing it to stand for 10 h in methanol (25 ml) containing sodium methoxide (0.23 g), then adding dilute hydrochloric acid, and extracting the mixture with benzene. Trituration of the oily residue with Skellysolve B and seeding (seed prepared in a separate experiment via the cyclohexylamine salt) provide the crude hydroxy acid XXVII (0.55 g), which, after recrystallization from benzene–Skellysolve, melted at 161–162°. Esterification with diazomethane followed by recrystallization from benzene – Skellysolve B provided the hydroxyester XXVIII, m.p. 135–136°.

Anal. Calcd. for $C_{25}H_{38}O_5$: C, 71.73; H, 9.15. Found: C, 71.56; H, 9.20.

Infrared spectrum: ν_{max} 3 610, 1 715 cm^{-1}. Nuclear magnetic resonance spectrum: τ 9.37 (3H), 8.95 (6H, doublet, $J = 7.5$ c.p.s.), 8.87 (3H), 6.40 (3H), 6.31 (3H), 6.24 (1H, C*H*OH), 4.64 (1H, olefinic.) The mass spectrum showed a weak parent peak at m/e 418 and the base peak at m/e 316.

Ketodiester XXIX

The hydroxydiester XXVIII (58 mg, 0.14 mmole) was dissolved in acetic acid (5 ml), Kiliani's reagent (0.12 ml, 0.18 mmole H_2CrO_4) added, and the solution kept at room temperature for 70 min. Excess oxidant was destroyed with methanol, and the reaction mixture was diluted with water and extracted several times with chloroform. Evaporation of the chloroform and recrystallization of the residue from methanol and then Skellysolve B provided the pure ketodiester XXIX, m.p. 160.5–161.5°.

Anal. Calcd. for $C_{25}H_{36}O_5$: C, 72.07; H, 8.72; O, 19.21. Found: C, 72.16; H, 8.46; O, 19.28.

Infrared spectrum: $\nu_{max}^{CHCl_3}$ 1 722, 1 705 cm^{-1}. Nuclear magnetic resonance spectrum: τ 9.32 (3H), 8.95 (6H, $J = 7$ c.p.s.), 8.84 (3H), 6.38 (3H), 6.34 (3H), 4.29 (1H). Ultraviolet spectrum: $\lambda_{max}^{isooctane}$ 282 (ϵ 120), 296 (ϵ 139), 305 (ϵ 122), 318 mμ (ϵ 61). Rotatory dispersion in isooctane: α_D −120°, α_{400} −595°, α_{317} −5 620°, α_{311} −4 400°, α_{307} −4 800°, α_{300} −1 440°, α_{295} 0°, α_{280} +5 450°.

Diester XXX

The ketodiester XXIX (0.40 g) was dissolved in anhydrous chloroform (15 ml), the solution saturated with hydrogen chloride, and ethanedithiol (2.5 ml) added. After 4 days at room temperature the solution was diluted with benzene (150 ml), washed with aqueous carbonate solution, then with water, and evaporated. The oily residue was dissolved in ethanol (50 ml) and heated under reflux with W2 Raney nickel (4 g) for 10½ h. After removal of the nickel by filtration and evaporation of the solvent, the residue was triturated with methylene chloride and the soluble portion (0.33 g) subjected to chromatography over neutral alumina (10 g). Elution with Skellysolve B (200 ml) and benzene–Skellysolve B 1:20 (100 ml) and 1:10 (200 ml) provided traces of uncharacterized oils. Elution with benzene – Skellysolve B 1:3 (250 ml) and 1:1 (400 ml) and benzene (150 ml) provided the crystalline deoxy diester XXX (0.11 g), m.p. 69–69.5 (from methanol–water), identical (melting point, mixed melting point, infrared spectrum, n.m.r. spectrum) with an authentic sample of the diester of the levopimaric acid – acrylic acid adduct (13) kindly provided by R. V. Lawrence.

ACKNOWLEDGMENTS

We thank Dr. R. V. Lawrence for a sample of the levopimaric acid – acrylic acid adduct and for a gift of levopimaric acid. Thanks are also due to Messrs. R. N. Swindlehurst and G. Bigam and their associates for the determination of most of the infrared and nuclear magnetic resonance spectra, and to the National Research Council for financial support.

REFERENCES

1. W. A. AYER, C. E. McDONALD, and G. G. IVERACH. Tetrahedron Letters, No. 17, 1095 (1963).
2. L. H. ZALKOW and N. N. GIROTRA. J. Org. Chem. **28**, 2037 (1963).
3. W. A. AYER, C. E. McDONALD, and J. B. STOTHERS. Can. J. Chem. **41**, 1113 (1963).
4. W. D. LLOYD and G. W. HEDRICK. J. Org. Chem. **26**, 2029 (1961).
5. W. L. MEYER and R. W. HUFFMAN. Tetrahedron Letters, No. 16, 691 (1962).
6. L. H. ZALKOW, R. A. FORD, and J. P. KUTNEY. J. Org. Chem. **27**, 3535 (1962).
7. W. VON E. DOERING, M. FARBER, and A. SAYIGH. J. Am. Chem. Soc. **74**, 4370 (1952).
8. C. A. GROB, M. OHTA, and A. WEISS. Angew. Chem. **70**, 343 (1958).
9. C. A. GROB, M. OHTA, E. RENK, and A. WEISS. Helv. Chim. Acta, **41**, 1191 (1958).
10. E. GROVENSTEIN, D. V. RAO, and J. W. TAYLOR. J. Am. Chem. Soc. **83**, 1705 (1961).

Can. J. Chem. Downloaded from www.nrcresearchpress.com by 210.87.254.105 on 09/05/12
For personal use only.

11. E. J. COREY and J. CASANOVA, JR. J. Am. Chem. Soc. **85**, 165 (1963).
12. N. J. HALBROOK and R. V. LAWRENCE. J. Am. Chem. Soc. **80**, 368 (1958).
13. N. J. HALBROOK, R. V. LAWRENCE, R. L. DRESSLER, R. C. BLACKSTONE, and W. HERZ. J. Org. Chem. **29**, 1017 (1964).
14. L. H. ZALKOW and D. R. BRANNON. J. Org. Chem. **29**, 1296 (1964).
15. R. CRIEGIE. *In* Neure Methoden der praparativen organischen Chemie. Band II. Verlag Chemie. 1960. p. 252.
16. P. LASZLO and P. VON R. SCHLEYER. J. Am. Chem. Soc. **86**, 1171 (1964).
17. C. A. GROB, H. KNY, and A. GAGNEUX. Helv. Chim. Acta, **40**, 130 (1957).
18. K. BIEMANN. Mass spectrometry. Organic chemical applications. McGraw-Hill. New York. 1962. p. 84.
19. L. M. JACKMAN. Applications of nuclear magnetic resonance spectroscopy in organic chemistry. Pergamon Press, New York. 1959. pp. 99–103.
20. A. I. SCOTT. Interpretation of the ultraviolet spectra of natural products. Pergamon Press, New York. 1964. p. 28.
21. J. D. ROBERTS and Y. MAZUR. J. Am. Chem. Soc. **73**, 2509, 3542 (1952).
22. S. STERNHELL. Rev. Pure Appl. Chem. **14**, 15 (1964).
23. K. ALDER, F. H. FLOCK, and H. WIRTZ. Chem. Ber. **91**, 609 (1958).
24. N. A. LEBEL and J. E. HUBER. J. Am. Chem. Soc. **85**, 3193 (1963).
25. R. C. COOKSON and N. S. WARYIAR. J. Chem. Soc. 2302 (1956).
26. A. MOSCOWITZ, K. MISLOW, M. A. W. GLASS, and C. DJERASSI. J. Am. Chem. Soc. **84**, 1945 (1962).
27. K. MISLOW and J. G. BERGER. J. Am. Chem. Soc. **84**, 1956 (1962).
28. L. F. JOHNSON. Varian Associates Technical Bulletin. No. 87-100-082. 1962.
29. M. ABO. Bull. Chem. Soc. Japan, **33**, 798 (1960).

Can. J. Chem. Downloaded from www.nrcresearchpress.com by 210.87.254.105 on 09/05/12
For personal use only.

Can. J. Chem. Downloaded from www.nrcresearchpress.com by 210.87.254.5 on 09/05/12
For personal use only.

SUBSTITUENT EFFECTS IN THE FLUORENE SERIES

I. SYNTHESIS AND ACETOLYSIS OF SOME DINITRO-9-FLUORENYL *p*-TOLUENESULFONATES

FREDERICK F. GUZIK AND ALLAN K. COLTER
Department of Chemistry, Carnegie Institute of Technology, Pittsburgh, Pennsylvania
Received November 13, 1964

Dedicated to Professor R. B. Sandin on the Occasion of his Sixty-Eighth Birthday

ABSTRACT

2,4-, 2,5-, and 2,7-Dinitrofluorenones (I*a*, I*b*, and I*c*) were converted to 2,4-, 2,5-, and 2,7-dinitro-9-fluorenyl *p*-toluenesulfonates (IV*a*, IV*b*, and IV*c*) through the corresponding 9-diazo compounds (III*a*, III*b*, and III*c*). These diazo compounds were converted directly to the three dinitro-9-fluorenols (VI*a*, VI*b*, and VI*c*) and 9-fluorenyl acetates (V*a*, V*b*, and V*c*).

Rates of acetolysis of the three *p*-toluenesulfonates (IV*a*, IV*b*, and IV*c*) were measured in glacial acetic acid at 50.17° and 70.07°. The results are discussed.

INTRODUCTION

As part of a comprehensive study of charge-transfer complexes in solvolysis reactions (1, 2), 2,4-, 2,5-, and 2,7-dinitro-9-fluorenyl *p*-toluenesulfonates (IV*a*, IV*b*, and IV*c*) were desired. These compounds are also of interest in connection with a study of substituent effects in the fluorene series. The 2-, 4-, 5-, and 7-positions may be thought of as pseudo-meta positions with respect to the 9-position. Hence, introduction of a substituent at the 2- (or 7-) position is expected, as a first approximation, to have a similar effect on rates or equilibria involving reaction at the 9-position as introduction of the same substituent at the 4- (or 5-) position. However, no quantitative comparison of substituent effects at the two types of positions is presently available. Further, it is of interest to compare the effects of disubstitution involving two of the benzene rings in the fluorene ring system with equivalent substitution involving a single benzene ring. One might anticipate a special kind of "saturation effect" (3), possibly important in structure–reactivity correlations in polynuclear aromatic systems, whereby multiple substitution in a single benzene ring has a smaller influence than multiple substitution in more than one ring. Again, quantitative comparisons are lacking. Finally, the sequence ketone → hydrazone → diazo compound → alcohol represents a potentially useful method for selective reduction of base-sensitive carbonyl compounds (4). The present work was aimed at further defining the scope of this method.

RESULTS AND DISCUSSION

The synthetic sequence (Reaction Scheme 1) starts with the known dinitrofluorenones (I). Structures were characterized by infrared and analytical data (Table I), as well as by acetolysis of the *p*-toluenesulfonates (IV*a*, IV*b*, and IV*c*) to the corresponding acetates (V*a*, V*b*, and V*c*) and oxidation of the alcohols (VI*a*, VI*b*, and VI*c*) to the corresponding ketones. Schmidt and Bauer (5) have described the synthesis of V*c* and VI*c* by an indirect procedure starting from 2,7-dinitro-9,10-phenanthrenequinone. There is little basis for comparison of their results with those of the present work, except the reported melting points, which are in approximate agreement. These authors also reported the preparation of 4,5-dinitro-9-fluorenol and 4,5-dinitro-9-fluorenyl acetate by the same route, starting

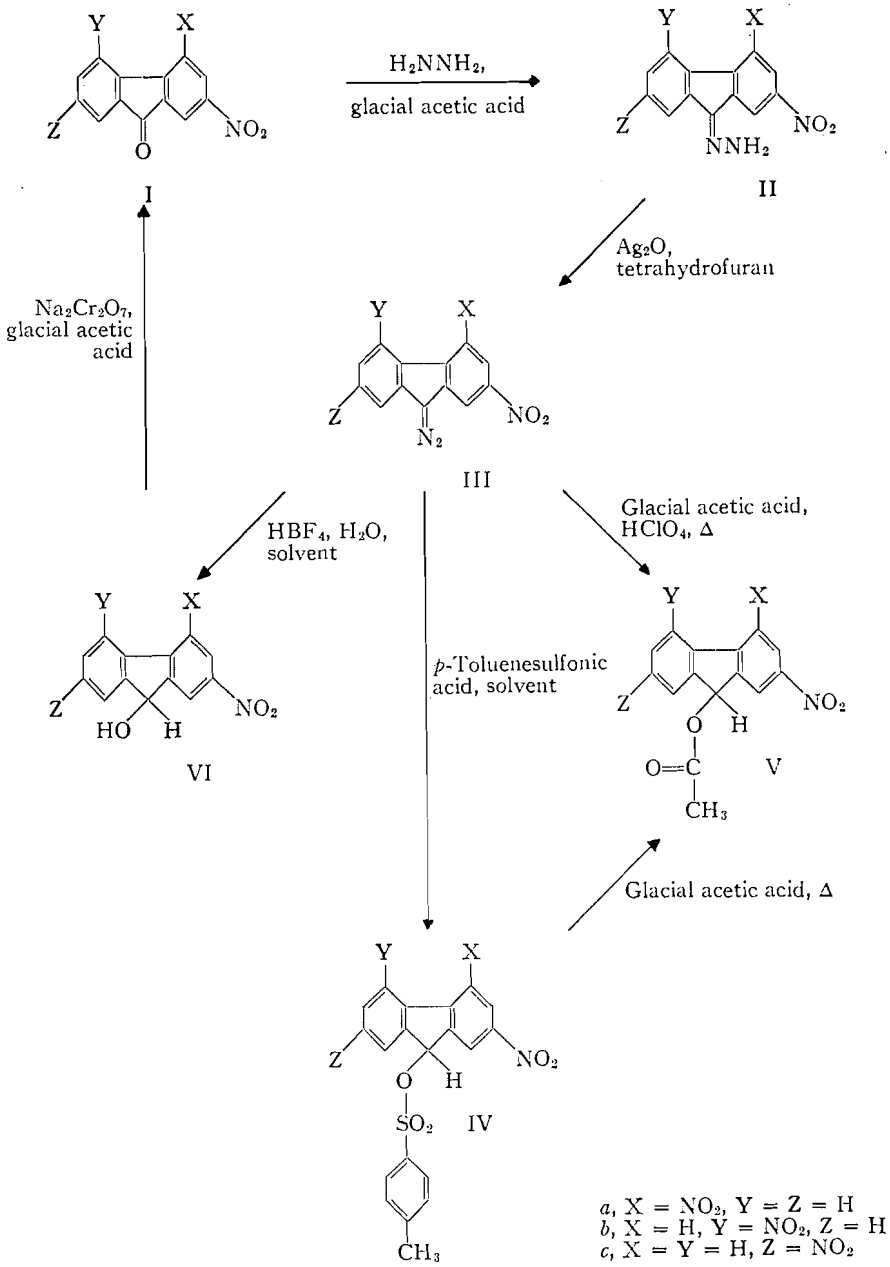

REACTION SCHEME 1.

with 4,5-dinitro-9,10-phenanthrenequinone. However, the alleged 4,5-dinitro-9,10-phenanthrenequinone was subsequently shown to be the 2,5-isomer (see, for example, refs. 6 and 7); hence, it is likely that Schmidt and Bauer actually prepared V*b* and VI*b* (6). If the "4,5-dinitro compounds" are assumed to be the 2,5-isomers, the earlier results are inconsistent with those reported here in only one important respect. The precurser of the "4,5-dinitro-9-fluorenyl acetate", a dinitro-9-hydroxy-9-fluorenecarboxylic acid, was

Can. J. Chem. Downloaded from www.nrcresearchpress.com by 210.87.254.5 on 09/05/12
For personal use only.

converted, by heating it in acetic anhydride in an air stream, to "4,5-dinitrofluorenone". The C, H, and N analyses for this compound were consistent with a dinitrofluorenone, but its melting point (>350°) was much higher than that reported (8) for 2,5-dinitrofluorenone.

TABLE I

Summary of analytical and spectral data for derivatives of 2,4-, 2,5-, and 2,7-dinitrofluorenes

Compound	m.p., °C		Analytical data, % C	H	N	Infrared data Found	Assignment
II*a*	255–256	Calcd.	54.97	2.84	19.75	2.89 μ (w)	
	(decomp.)	Found	54.77	2.98	19.46	2.98 μ (w)	N—H stretching*
						3.05 μ (w)	
III*a*	192–192.5	Calcd.	55.36	2.14	19.85	4.81 μ (s)	N=N stretching,
	(decomp.)	Found	55.29	2.22	19.77		diazo group†
IV*a*	164–166	Calcd.	56.33	3.31	6.57	7.37 μ (s)	
		Found	56.49	3.51	6.32	8.53 μ (m)	Sulfonate ester group‡
						8.58 μ (s)	
V*a*	178–180	Calcd.	57.32	3.21	8.91	5.81 μ (s)	C=O stretching§
		Found	57.03	3.17	8.86	8.20 μ (s)	Acyl C—O stretching‖
						9.70 μ (m)	Alkyl C—O stretching‖
VI*a*	154–156	Calcd.	57.36	2.96	10.29	2.99 μ (m)	O—H stretching¶
		Found	57.18	3.01	10.06		
II*b*	264–266	Calcd.	54.97	2.84	19.75	2.89 μ (w)	
	(decomp.)	Found	54.66	3.18	20.01	2.98 μ (w)	N—H stretching
						3.06 μ (w)	
III*b*	208	Calcd.	55.36	2.14	19.85	4.79 μ (s)	N=N stretching,
	(decomp.)	Found	55.34	2.32	19.67		diazo group
IV*b*	178–179	Calcd.	56.33	3.31	6.57	7.35 μ (s)	
		Found	56.41	3.60	6.29	8.43 μ (m)	Sulfonate ester group
						8.53 μ (s)	
V*b*	213–216	Calcd.	57.32	3.21	8.91	5.76 μ (s)	C=O stretching
		Found	57.58	3.32	8.67	8.24 μ (s)	Acyl C—O stretching
						9.75 μ (m)	Alkyl C—O stretching
VI*b*	181–184	Calcd.	57.36	2.96	10.29	2.86 μ (m)	O—H stretching
		Found	57.63	3.27	10.40		
II*c*	275–278	Calcd.	54.97	2.84	19.75	2.86 μ (w)	
	(decomp.)	Found	54.88	3.08	19.69	2.95 μ (w)	N—H stretching
						3.06 μ (w)	
III*c*	196–199	Calcd.	55.36	2.14	19.85	4.77 μ (s)	N—N stretching,
	(decomp.)	Found	55.63	2.44	19.84		diazo group
IV*c*	208–210	Calcd.	56.33	3.31	6.57	7.33 μ (s)	
		Found	56.55	3.59	6.32	8.42 μ (m)	Sulfonate ester group
						8.52 μ (s)	
V*c*	244–245	Calcd.	57.32	3.21	8.91	5.73 μ (s)	C=O stretching
		Found	57.54	3.35	8.92	8.22 μ (s)	Acyl C—O stretching
						9.67 μ (m)	Alkyl C—O stretching
VI*c*	210–213	Calcd.	57.36	2.96	10.29	2.89 μ (m)	O—H stretching
		Found	57.16	3.16	10.02		

*Ref. 9, p. 249.
†Ref. 10.
‡Ref. 9, p. 364.
§Ref. 9, p. 179.
‖Ref. 9, p. 189.
¶Ref. 9, p. 96.

Rates of acetolysis of IV*a*, IV*b*, and IV*c* at 50.17 °C and 70.07 °C are listed, together with activation parameters at 50.17 °C, in Table II. Comparison of the rates of acetolysis of the 2,5- and 2,7-dinitro-*p*-toluenesulfonates (IV*b* and IV*c*) reveals that a nitro group in the 7-position has a larger deactivating effect than a nitro group in the 5-position. Two factors may be responsible for the difference. First, the distribution of charge in the 9-fluorenyl cation (and hence in the transition state leading to the cation) may be such that its stability is less sensitive to substitution at the 4- (or 5-) position than the 2- (or 7-) position. Calculations designed to provide a measure of this factor are underway;

Can. J. Chem. Downloaded from www.nrcresearchpress.com by 210.87.254.5 on 09/05/12
For personal use only.

TABLE II

Rates of acetolysis of 2,4-, 2,5-, and 2,7-dinitro-9-fluorenyl *p*-toluenesulfonates

Compound	k_1, s^{-1}* 50.17 °C	k_1, s^{-1}* 70.07 °C	$\Delta H^{\neq}$, kcal $mole^{-1}$† (50.17 °C)	$\Delta S^{\neq}$, e.u. $mole^{-1}$‡ (50.17 °C)
IV*a*	$6.31 \pm 0.06 \times 10^{-6}$	$6.31 \pm 0.03 \times 10^{-5}$	24.9	−5.54
IV*b*	$1.88 \pm 0.02 \times 10^{-6}$	$1.89 \pm 0.02 \times 10^{-5}$	24.9	−7.77
IV*c*	$5.58 \pm 0.02 \times 10^{-7}$	$5.59 \pm 0.08 \times 10^{-6}$	24.9	−10.3

*Rate constants listed with average deviations.
†Estimated experimental uncertainty ±0.2 kcal $mole^{-1}$.
‡Estimated experimental uncertainty ±0.47 e.u. $mole^{-1}$.

a full discussion of this point is properly postponed until more experimental data are available. A second factor to be considered is steric interference between a nitro group at the 4- (or 5-) position and a hydrogen at the 5- (or 4-) position. Calculations show that complete coplanarity would require an O—H distance of ca. 1.5 Å, considerably less than the sum of the van der Waals radii of oxygen and hydrogen (ca. 2.6 Å).

Comparison of the rates of acetolysis of the 2,4- and 2,5-dinitro-*p*-toluenesulfonates (IV*a* and IV*b*) shows that two nitro groups on a single benzene ring result in a smaller deactivating effect than equivalent substitution in two benzene rings. This result is in line with the expectation that successive substitution of strongly electron-withdrawing groups, because of a successive decrease in the polarizability of the pi electrons, should result in successively smaller substituent effects. In the fluorene ring system, such an effect can be rationalized by a simple argument involving resonance structures. For a nitro group in either the 2- or the 4-position, contributing structures having a positive charge at the 1-, 3-, 4*a*-, 5-, 7-, and 8*a*-positions (starred positions in VII*a*) can be written. A nitro group in the 5- or 7-position should produce the greatest electron deficiency at the 2-, 4-, 4*b*-, 6-, 8-, and 9*a*-positions (starred positions in VII*b*). Hence, the 5-nitro group in the 2,5-dinitro system should exert a greater influence than the 4-nitro group in the 2,4-system. Alternatively, the "saturation effect" observed here may not depend on

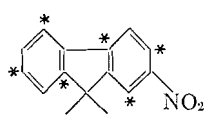

VII*a*

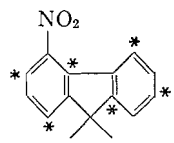

VII*b*

conjugation between the two rings. For this reason, we plan to look for effects of this kind in systems containing isolated and insulated benzene rings and in completely alternant systems.

EXPERIMENTAL[1]

2,4-Dinitrofluorenone (Ia)

This compound was prepared by the method of Ullman and Broido (11), m.p. 194–195° (reported (11), m.p. 197°).

2,5-Dinitrofluorenone (Ib)

This compound was prepared by oxidation of 2,5-dinitrofluorene with sodium dichromate in glacial acetic acid, m.p. 237–239° (reported (8), m.p. 241°). 2,5-Dinotrofluorene was prepared as described by Courtot (12).

[1]*Melting points are uncorrected. Microanalyses were performed by Galbraith Microanalytical Laboratories, Knoxville, Tenn. Infrared spectra were measured in* KBr *pellets with a Perkin–Elmer model 137B spectrophotometer.*

Can. J. Chem. Downloaded from www.nrcresearchpress.com by 210.87.254.5 on 09/05/12
For personal use only.

2,7-Dinitrofluorenone (Ic)

This compound was prepared by oxidation of 2,7-dinitrofluorene (12) with sodium dichromate in glacial acetic acid, m.p. 289–290° (reported (8), m.p. 290°).

2,4-Dinitrofluorenone Hydrazone (IIa)

A 22-g quantity of I*a* was dissolved in 500 ml of boiling glacial acetic acid and a solution of 20 ml of 100% hydrazine hydrate in 50 ml of glacial acetic acid was slowly added with stirring. In about 5 min an orange precipitate began to appear. After it was heated for an additional 15 min, the mixture was allowed to cool to room temperature and suction filtered, and the product washed several times with 95% ethanol. After it was air-dried, the product weighed 17.5 g (76%) and had m.p. 255–256° (decomp.). Recrystallization from glacial acetic acid left the melting point unchanged.

Anal. Calcd. for $C_{13}H_8N_4O_4$: C, 54.97; H, 2.84; N, 19.75. Found: C, 54.77; H, 2.98; N, 19.46.

2,5-Dinitrofluorenone Hydrazone (IIb)

A 20-g quantity of I*b* was dissolved in 1 500 ml of boiling glacial acetic acid and a solution of 20 ml of 100% hydrazine hydrate in 50 ml of glacial acetic acid was slowly added with stirring. An orange precipitate began to appear in about 10 min. Heating was continued for an additional 5 min. The solution was cooled and filtered, and the product washed thoroughly with water and 95% ethanol. The dried product, 20.4 g (97%), had m.p. 260–265° (decomp.). Crystallization from glacial acetic acid yielded material of m.p. 264–266° (decomp.).

Anal. Calcd. for $C_{13}H_8N_4O_4$: C, 54.97; H, 2.84; N, 19.75. Found: C, 54.66; H, 3.18; N, 20.01.

2,7-Dinitrofluorenone Hydrazone (IIc)

A 16-g quantity of I*c* was dissolved in boiling glacial acetic acid and a solution of 16 ml of 100% hydrazine hydrate in 30 ml of glacial acetic acid was slowly added with stirring. The mixture was heated for 16 min (orange precipitate after 5 min) and the cooled solution filtered, washed with water, and dried under vacuum. The crude product weighed 15 g (89%) and had m.p. 275–278° (decomp.).

Anal. Calcd. for $C_{13}H_8N_4O_4$: C, 54.97; H, 2.84; N, 19.75. Found: C, 54.88; H, 3.08; N, 19.69.

9-Diazo-2,4-dinitrofluorene (IIIa)

In a three-necked flask equipped with an efficient power-driven stirrer and a condenser, 17.5 g of II*a* was dissolved in 1 500 ml of refluxing technical tetrahydrofuran. A 21-g quantity of powdered silver oxide was introduced in small portions over a period of 15 min. Refluxing was continued for 3 h with vigorous stirring. The silver residue was filtered while the solution was warm. The orange crystals which formed when the solution was cooled were filtered and washed thoroughly with 95% ethanol. The remainder of the product was obtained by evaporating the solution to dryness. The dried product weighed 11 g (63%). Recrystallization from nitromethane yielded reddish-orange needles, m.p. 192–192.5° (decomp.).

Anal. Calcd. for $C_{13}H_6N_4O_4$: C, 55.36; H, 2.14; N, 19.85. Found: C, 55.29; H, 2.22; N, 19.77.

9-Diazo-2,5-dinitrofluorene (IIIb)

The procedure was similar to that for III*a*. A suspension of 9 g of II*b* in 1 500 ml of technical tetrahydrofuran was oxidized with 12 g of powdered silver oxide. After it was refluxed for 4 h the mixture was filtered while warm, cooled, and diluted with an equal volume of water. The product was filtered, washed with 95% ethanol, and dried. The crude product weighed 5.7 g (64%), m.p. 207–209° (decomp.). Recrystallization from nitromethane (1 g in 250 ml) yielded orange crystals, m.p. 208° (decomp.).

Anal. Calcd. for $C_{13}H_6N_4O_4$: C, 55.36; H, 2.14; N, 19.85. Found: C, 55.34; H, 2.32; N, 19.67.

9-Diazo-2,7-dinitrofluorene (IIIc)

The procedure was similar to that for III*a*. A suspension of 15 g of II*c* in 1 800 ml of technical tetrahydrofuran was oxidized with 23 g of powdered silver oxide. After it was refluxed for 5 h the warm solution was filtered and evaporated to one-third of its original volume. The brownish-orange material which separated was filtered and washed with 95% ethanol. Additional product was obtained by diluting the filtrate with water. The crude product weighed 10 g (67%), m.p. 196–199° (decomp.).

Anal. Calcd. for $C_{13}H_6N_4O_4$: C, 55.36; H, 2.14; N, 19.85. Found: C, 55.63; H, 2.44; N, 19.84.

2,4-Dinitro-9-fluorenyl p-Toluenesulfonate (IVa)

To a warm solution (70–75°) of 10 g of *p*-toluenesulfonic acid in 500 ml of acetonitrile, 10 g of crude III*a* was slowly added with stirring. After it was heated for an additional 10 min the solution was filtered while warm. The filtrate was cooled to −25 °C for several hours, during which time the product crystallized. The peach-colored solid was filtered and washed with ether. The dried product weighed 11.5 g (76%), m.p. 106–164°. Recrystallization from acetonitrile raised the melting point to 164–166°.

Anal. Calcd. for $C_{20}H_{14}N_2O_7S$: C, 56.33; H, 3.31; N, 6.57. Found: C, 56.49; H, 3.51; N, 6.32.

2,5-Dinitro-9-fluorenyl p-Toluenesulfonate (IVb)

To a warm solution (70–75°) of 1.6 g of *p*-toluenesulfonic acid in 100 ml of acetonitrile, 1.6 g of crude III*b* was slowly added with stirring. After it was heated for an additional 5 min the reaction mixture was

Can. J. Chem. Downloaded from www.nrcresearchpress.com by 210.87.254.5 on 09/05/12
For personal use only.

cooled and filtered. The filtrate was evaporated to about 5 ml and filtered, and the solid product washed thoroughly with ether. The crude product weighed 1.3 g (54%). Crystallization from acetonitrile gave orange crystals, m.p. 178–179°.

Anal. Calcd. for $C_{20}H_{14}N_2O_7S$: C, 56.33; H, 3.31; N, 6.57. Found: C, 56.41; H, 3.60; N, 6.29.

2,7-Dinitro-9-fluorenyl p-Toluenesulfonate (IVc)

A 2-g quantity of III*c* was added to a warm solution (90–95°) of 2 g of *p*-toluenesulfonic acid in 100 ml of nitromethane. After it was heated for an additional 5 min the reaction mixture was filtered and cooled at −25° for several hours. The crude product was filtered and washed thoroughly with ether. Additional product was obtained by evaporation of the filtrate to one-third of its original volume. The crude product weighed 1.85 g (61%). Crystallization from nitromethane afforded tan crystals, m.p. 208–210° (decomp.).

Anal. Calcd. for $C_{20}H_{14}N_2O_7S$: C, 56.33; H, 3.31; N, 6.57 Found: C, 56.55; H, 3.59; N, 6.32.

2,4-Dinitro-9-fluorenyl Acetate (Va)

A mixture of 1.0 g of III*a*, 100 ml of glacial acetic acid, and 1.5 ml of 70–72% perchloric acid was refluxed for 2 h. After the solution was cooled to room temperature, the product was precipitated by addition of 200 ml of water. Filtration and drying led to 1.0 g (90%) of crude product. Crystallization from glacial acetic acid gave orange crystals, m.p. 178–180°.

Anal. Calcd. for $C_{15}H_{10}N_2O_6$: C, 57.32; H, 3.21; N, 8.91. Found: C, 57.03; H, 3.17; N, 8.86.

2,5-Dinitro-9-fluorenyl Acetate (Vb)

To a hot solution (100–110°) of 50 ml of glacial acetic acid and 1 ml of 70–72% perchloric acid, 0.30 g of crude III*b* was slowly added with stirring. After it was heated for an additional 5 min the mixture was filtered and cooled, and the product precipitated by addition of an equal volume of water. After it was filtered, washed with water, and dried, the crude product weighed 0.30 g (90%). Crystallization from glacial acetic acid yielded material of m.p. 213–216° (reported (5), m.p. 220–221°).

Anal. Calcd. for $C_{15}H_{10}N_2O_6$: C, 57.32; H, 3.21; N, 8.91. Found: C, 57.58; H, 3.32; N, 8.67.

2,7-Dinitro-9-fluorenyl Acetate (Vc)

To a hot solution (100–110°) of 50 ml of glacial acetic acid and 1 ml of 70–72% perchloric acid, 0.75 g of III*c* was slowly added with stirring. After it was heated for an additional 5 min the solution was filtered and evaporated under reduced pressure to one-half of its original volume. The crystalline product which separated was filtered and washed with ether. Additional product was obtained by diluting the filtrate with an equal volume of water, giving a total of 0.65 g (78%) of crude product. Crystallization from glacial acetic acid gave light brown crystals, m.p. 205–208°. Several recrystallizations yielded material of m.p. 244–245° (reported (5), 244, 247 (decomp.)).

Anal. Calcd. for $C_{15}H_{10}N_2O_6$: C, 57.32; H, 3.21; N, 8.91. Found: C, 57.54; H, 3.35; N, 8.92.

2,4-Dinitro-9-fluorenol (VIa)

A 1.5-g quantity of III*a* was slowly added to a warm solution (70–75°) of 2 ml 42–45% fluoboric acid, 3 ml of water, and 60 ml of acetonitrile. After it was cooled and filtered, the solution was evaporated almost to dryness under reduced pressure. The product was filtered and washed with 95% ethanol, yielding 1.2 g (83%) of dried crude product. Crystallization from acetonitrile yielded beige crystals, m.p. 154–156°.

Anal. Calcd. for $C_{13}H_8N_2O_5$: C, 57.36; H, 2.96; N, 10.29. Found: C, 57.18; H, 3.01; N, 10.06.

2,5-Dinitro-9-fluorenol (VIb)

A mixture of 0.70 g of III*b*, 5 ml of water, 5 ml of 42–45% fluoboric acid, and 50 ml of acetonitrile was refluxed for 72 h. The mixture was cooled and filtered, and the filtrate diluted with an equal volume of water. The beige precipitate was filtered and dried, yielding 0.35 g (52%) of crude product. Crystallization from acetonitrile–water gave beige crystals of m.p. 181–184° (reported (5), m.p. 201–202°).

Anal. Calcd. for $C_{13}H_8N_2O_5$: C, 57.36; H, 2.96; N, 10.29. Found: C, 57.63; H, 3.27; N, 10.40.

2,7-Dinitro-9-fluorenol (VIc)

To a warm solution (70–75°) of 3.5 ml of water, 2.5 ml of 42–45% fluoboric acid, and 75 ml of acetonitrile, 1.5 g of crude III*c* was slowly added with stirring. The reaction was heated for an additional 5 min, filtered while warm, and kept at −25° for several hours. The tan precipitate was filtered and dried, yielding 0.9 g (62%) of crude product. Crystallization from nitromethane gave tan crystals of m.p. 210–213° (reported (5), m.p. 212°).

Anal. Calcd. for $C_{13}H_8N_2O_5$: C, 57.36; H, 2.96; N, 10.29. Found: C, 57.16; H, 3.16; N, 10.02.

Acetolysis of IVa, IVb, and IVc

Acetolysis of the *p*-toluenesulfonate esters IVa, IV*b*, and IV*c* was carried out by refluxing for 8–24 h in glacial acetic acid (ca. 100 ml per g of ester). The acetates were isolated by cooling and evaporation and filtration. In all cases, high yields (up to 95%) of acetates, shown by infrared spectra and mixed melting points to be identical with the acetate prepared from the 9-diazo compounds III*a*, III*b*, and III*c*, were obtained.

Can. J. Chem. Downloaded from www.nrcresearchpress.com by 210.87.254.5 on 09/05/12
For personal use only.

Oxidation of VIa, VIb, and VIc

The alcohols were oxidized by refluxing for 1–2 h in glacial acetic acid (100–200 ml per g of alcohol) plus sodium dichromate dihydrate (1–3 g per g of alcohol). The ketones were isolated by cooling or addition of water, followed by filtration. In all cases, high yields (up to 90%) of ketones, shown by infrared spectra and mixed melting points to be identical with authentic I*a*, I*b*, or I*c*, were obtained.

Kinetic Measurements

Rates of acetolysis were measured as previously described (2). Ester concentrations were close to 2×10^{-3} *M*.

ACKNOWLEDGMENT

We thank the National Science Foundation for a grant in support of this research.

REFERENCES

1. A. K. COLTER and S. S. WANG. J. Am. Chem. Soc. **85**, 114 (1963).
2. A. K. COLTER, S. S. WANG, G. H. MEGERLE, and P. S. OSSIP. J. Am. Chem. Soc. **86**, 3106 (1964).
3. H. VAN BEKKUM, P. E. VERKADE, and B. M. WEPSTER. Rec. Trav. Chim. **78**, 815 (1959).
4. A. K. COLTER and S. S. WANG. J. Org. Chem. **27**, 1517 (1962).
5. J. SCHMIDT and K. BAUER. Ber. **38**, 3737 (1905).
6. Elsevier's encyclopedia of organic chemistry. Elsevier Publishing Co., Inc., New York and Amsterdam. 1946. Vol. 13.
7. R. KUHN and G. ALBRECHT. Ann. **455**, 272 (1927).
8. G. MORGAN and R. THOMASON. J. Chem. Soc. 2691 (1926).
9. L. J. BELLAMY. The infrared spectra of complex molecules. John Wiley and Sons, Inc., New York. 1958. p. 249.
10. P. YATES, B. L. SHAPIRO, N. YODA, and J. FUGGER. J. Am. Chem. Soc. **79**, 5756 (1957).
11. F. ULLMANN and J. BROIDO. Ber. **39**, 360 (1906).
12. CH. COURTOT. Ann. Chim. **14**, 5 (1930).

Can. J. Chem. Downloaded from www.nrcresearchpress.com by 210.87.254.5 on 09/05/12
For personal use only.

Can. J. Chem. Downloaded from www.nrcresearchpress.com by 210.87.254.40 on 09/05/12
For personal use only.

SUBSTITUTED QUINODIMETHANS

VIII. SALTS DERIVED FROM THE 7,7,8,8-TETRACYANOQUINODIMETHAN ANION–RADICAL AND BENZOLOGUES OF QUATERNARY PYRAZINIUM CATIONS[1,2]

L. Russell Melby

Central Research Department, Experimental Station, E. I. du Pont de Nemours and Co., Inc., Wilmington, Delaware

Received November 13, 1964

Dedicated to Professor R. B. Sandin on the Occasion of his Sixty-Eighth Birthday

ABSTRACT

Our continued study of derivatives of the 7,7,8,8-tetracyanoquinodimethan anion–radical ($TCNQ^{-}\cdot$) has shown that the simple N-methylphenazinium salt (II*a*) exhibits a volume electrical resistivity of 7×10^{-3} Ω cm and thus is the most highly electrically conductive organic compound known. In contrast, the N-ethyl analogue has a resistivity of 10^{9} Ω cm. Electrical properties of pyrazinium, quinoxalinium, and phenazinium analogues, including phenazine-derived cation–radical salts of $TCNQ^{-}\cdot$, are discussed. Qualitative observations are made concerning the electron paramagnetic resonance of the N,N′-dimethyldihydrophenazinylium cation–radical.

In a previous publication (1) we discussed the electrical properties of salts of the anion–radical derived from 7,7,8,8-tetracyanoquinodimethan (TCNQ, I). Those derivatives included the simple salts comprising one cation and one $TCNQ^{-}\cdot$ anion–radical (e.g. $Li^{+}TCNQ^{-}\cdot$), and the complex salts wherein the unit composition requires inclusion of a formally neutral molecule of TCNQ (e.g. the triethylammonium complex salt formulated conveniently as $Et_3NH^{+}\ (TCNQ)_2^{-}\cdot$). In general the simple $TCNQ^{-}\cdot$ salts exhibit electrical resistivities in the range 10^{5} to 10^{8} Ω cm, while the more highly conducting complexes have resistivities falling in the range 10^{-2} to 10^{2} Ω cm (1).

Pursuing an inquiry into the electrical effect of the cation portion of these $TCNQ^{-}\cdot$ salts and complexes, we have examined analogues of the pyrazine ring system, including quaternized quinoxaline, acridine, phenazine, and phenazine-derived cation–radicals.

Electrical Properties

Most of the simple $TCNQ^{-}\cdot$ salts listed in Table I exhibited electrical resistivities similar to those of previously described analogues. However, the N-methylphenazinium salt II*a* exhibited the unusually low value of 7×10^{-3} Ω cm measured on single crystals in the long needle axis direction. This is the most highly electrically conductive organic compound known. In marked contrast, the N-ethyl compound II*b* had a single crystal resistivity of 10^{9} Ω cm.

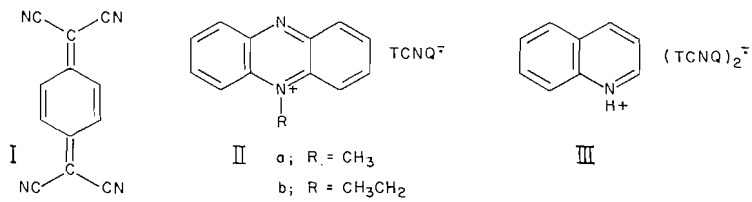

[1]*For paper VII in this series, see J. Diekmann, W. R. Hertler, and R. E. Benson. J. Org. Chem. 28, 2719 (1963).*

[2]*Contribution No. 1025 of the Central Research Department.*

Can. J. Chem. Downloaded from www.nrcresearchpress.com by 210.87.254.40 on 09/05/12
For personal use only.

TABLE I

Pyrazinium benzologue simple salts of the 7,7,8,8-tetracyanoquinodimethan anion-radical

Cation	Yield, %	Decomp. point, °C	Analyses						$\epsilon_{842\,m\mu}$*	Volume electrical resistivity, Ω cm†	Density
			% C		% H		% N				
			Calcd.	Found	Calcd.	Found	Calcd.	Found			
	71	ca. 200	68.1	68.0	3.8	3.8	28.1	28.2	42 000	3.4×10^{7}	1.33
	89	195–197	72.2	72.0	3.7	4.2	24.1	24.4	Unstable	126	1.36 and 1.33
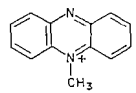	93	192–193	75.3	75.0	3.8	3.9	21.1	21.2	44 000	0.007‡ 0.5	1.44
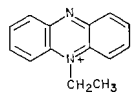	50	204–207	75.5	75.8	4.2	4.4	20.3	20.5	43 400	10^{9}‡ 10^{11}	1.33
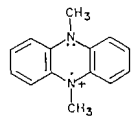	90	204–207	75.3	75.1	4.4	4.4	20.2	20.0	See text	6×10^{4}	—
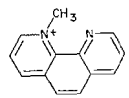	86	250–252	75.3	75.1	3.8	4.0	21.1	21.0	43 000	8×10^{5}	1.36
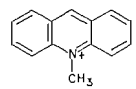	89	225–230	78.3	78.4	4.3	4.7	17.9	17.6	Unstable	4.7×10^{4}	1.33

*Compared with $Li^{+}TCNQ^{-}\cdot$ for which $\epsilon_{842\,m\mu}$ = 43 000 in acetonitrile (see ref. 1).
†Determined on polycrystalline compaction unless otherwise noted.
‡Determined on single crystal.

Preliminary X-ray measurements by Dr. C. J. Fritchie of this laboratory have shown that in the N-methyl salt the $TCNQ^{-}\cdot$ units are stacked one above the other. Furthermore, the compound has a remarkably high density (1.44). These observations suggest that the low steric requirement of the N-methyl group in the cation allows very efficient packing of the $TCNQ^{-}\cdot$ units which presumably mediate the electronic conduction. On the other hand, the N-ethyl derivative has a density of 1.33; the bulky N-ethyl group apparently disrupts the packing, resulting in an appreciable barrier to electron movement. Previously, the most conductive compound we have prepared is the complex quinolinium salt III. It had a single crystal resistivity of 0.01 Ω cm and a density of 1.36. However, in this case, the complex anion $(TCNQ)_2^{-}\cdot$ is thought to be the principal conducting moiety and it is apparently relatively less disturbed by cation spatial effects. In Table II are listed a number of complex salts related to the simple salts of Table I; the resistivities of the complex salts were all in the expected range.

Attention is drawn to the apparently high conductivity of the simple salt N-methylquinoxalinium $TCNQ^{-}\cdot$ (126 Ω cm). The result is believed to be specious since, although elemental analytical data were satisfactory, density measurements indicated a mixture, perhaps, of simple and complex salts. The complex component in the solid state would increase the conductivity. This was the only compound listed which was not shown convincingly to be pure by our standard criteria.

Synthesis and Spectral Data

The simple salts of $TCNQ^{-}\cdot$ were prepared by metathesis of an appropriate quaternary compound with $Li^{+}TCNQ^{-}\cdot$ as previously described (1) (illustrated in eq. [1] for the N-methylpyrazinium salt, IV). The compounds prepared in this way are listed in Table I. These salts are stable in the solid state, and most were purified by recrystallization from acetonitrile in air. Under these conditions, however, the N-methylacridinium compound (V) was completely converted to the complex salt (VI), presumably by air oxidation of a portion of the anion–radical (eq. [2]). A similar transformation apparently occurs to some extent when the N-methylquinoxalinium simple salt is recrystallized. The stability in solution of compound IV and, particularly, of the N-alkylphenazinium compounds II*a* and II*b* suggests a protecting effect on the anion by the associated cations. It is tempting to postulate some sort of ion pairing to account for this solution stability, but visible absorption spectral data point to complete dissociation of II and IV in acetonitrile solution. Thus, the pyrazinium and phenazinium compounds, and also N-methyl-1,10-phenanthrolinium $TCNQ^{-}\cdot$, showed molar extinction coefficients, $\epsilon_{842\,m\mu} \simeq 43\,000$, characteristic of the $TCNQ^{-}\cdot$ anion (reference compound $Li^{+}TCNQ^{-}\cdot$). The N-methylquinoxalinium and N-methylacridinium compounds were so unstable in solution that spectral measurement was precluded.

The corresponding complex salts were prepared by recrystallizing the simple salts from acetonitrile containing a molar equivalent of neutral tetracyanoquinodimethan (see ref. 1).

The previously unknown cation–radical salt N,N′-dimethyldihydrophenazinylium iodide (VIII) was prepared by iodine oxidation of the free base VII in acetonitrile (eq. [3]). By metathesis, the salt VIII was converted to the simple $TCNQ^{-}\cdot$ salt IX. The spectrum of this derivative showed considerable absorption attributed to neutral TCNQ and attenuation of absorption by the cation–radical, indicating an equilibrium between ion–radical and uncharged species (eq. [4]). The extinctions are given in Table III. The data indicate an equilibrium comprising about 30–40% neutral species. In the solid state this compound may more properly be represented as a π-complex rather than an ion–radical salt.*

**Similar spectral behavior was observed for the π-complex derived from N,N,N′,N′-tetramethyl-p-phenylenediamine and TCNQ (see ref. 1).*

Can. J. Chem. Downloaded from www.nrcresearchpress.com by 210.87.254.40 on 09/05/12
For personal use only.

Can. J. Chem. Downloaded from www.nrcresearchpress.com by 210.87.254.40 on 09/05/12
For personal use only.

TABLE II

Pyrazinium benzologue complex salts of $(TCNQ)_2^-$·

Cation	Yield, %	Decomp. point, °C	Analyses % C Calcd.	% C Found	% H Calcd.	% H Found	% N Calcd.	% N Found	$\epsilon_{842\,m\mu}$*	Volume electrical resistivity, Ω cm†
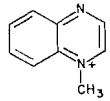	63	205–206	71.6	71.0 71.5	3.1	3.7 4.0	25.3	25.8 24.6	Unstable	62
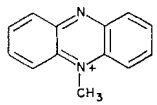	85	207–208	73.6	73.4	3.2	3.5	23.2	23.2	44 700	1.4
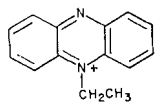	70	220–225	73.9	73.9	3.4	3.6	22.7	22.7	44 200	1.2
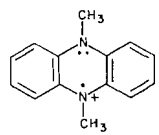	97	ca. 203	73.8	74.2	3.6	3.8			See text	2.2
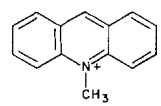	41‡ 34§	ca. 273	75.7	75.5 75.5	3.3	3.7 3.7	21.0	21.7 21.0	39 800 39 600	14 5.3

*See Table I.
†See Table I.
‡By air oxidation of simple salt.
§By addition of neutral TCNQ to simple salt.

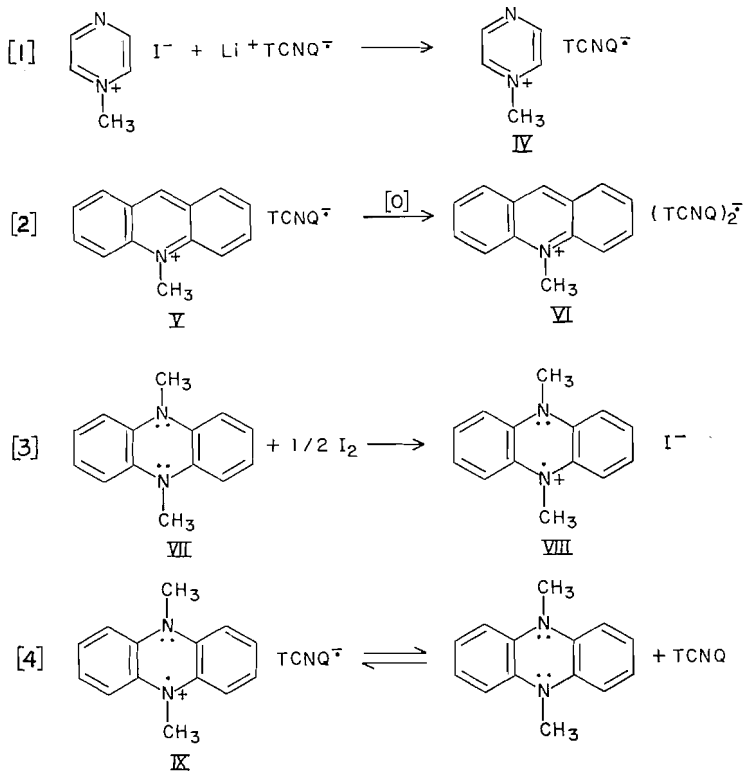

TABLE III

Absorption spectrum of dimethyldihydrophenazinylium $TCNQ^{-}\cdot$ (IX) in acetonitrile

λ_{max} (mμ)	ϵ
842	26 000*
394	43 000†
258	58 000†

*Compare $Li^{+}TCNQ^{-}\cdot$ $\epsilon_{842\ m\mu}$ = 43 300.
†Neutral TCNQ ϵ_{391} = 64 400; $Li^{+}TCNQ^{-}\cdot$ ϵ_{391} = 21 500.
‡Compound VIII ϵ_{258} = 84 000.

Treatment of the base VII with 2 equiv. of TCNQ afforded the corresponding complex salt. In this transformation the neutral base presumably donates one electron to a molecule of TCNQ to form the anion–radical; the ionic species then precipitates with a neutral TCNQ molecule to form the complex salt. The absorption spectrum showed characteristics similar to that of the simple salt.

The electron paramagnetic resonance (e.p.r.) spectrum of the cation–radical VIII is of some interest. At a concentration of 10^{-2} *M* in ethylene glycol, this compound showed an 11-line spectrum attributed to hyperfine splitting of the electron resonance by both nitrogen nuclei and methyl-group protons. When the solution was diluted to 5×10^{-4} *M* the spectrum was resolved into over 65 lines as a result of splitting by the benzo-ring protons. These observations are similar to those of Hausser *et al.* (2) and Matsunaga and McDowell (3) on the e.p.r. of the unmethylated analogue.

Can. J. Chem. Downloaded from www.nrcresearchpress.com by 210.87.254.40 on 09/05/12
For personal use only.

In the Experimental section there is recorded a convenient preparation of the water-soluble dimethyldihydrophenazinylium chloride.

EXPERIMENTAL

Quaternary Salts

o-Phenanthroline methiodide and pyrazine methiodide were prepared by allowing concentrated ether solutions of the bases and excess methyl iodide to stand at room temperature for several days. The salts separated as yellow crystalline solids. N-Methylacridinium and N-methylphenazinium methyl sulfate were prepared by heating the respective bases and excess dimethyl sulfate in benzene at 70° for several hours. N-Ethylphenazinium ethyl sulfate was formed by heating equal weights of the base and diethyl sulfate in nitrobenzene at 120–125° for 2 h, cooling to 60°, and adding ether to precipitate the quaternary salt.

N,N'-Dimethyldihydrophenazinylium Iodide

In 10 ml of warm acetonitrile was dissolved 0.21 g (1 mmole) of dimethyldihydrophenazine (4), and a warm solution of 0.13 g (1 g-atom equiv.) of iodine in 10 ml of acetonitrile was added. The green solution was cooled in wet ice – acetone, and the black needles were collected and washed with ether. The yield of analytically pure material was 0.28 g (83%), m.p. 204–206° (decomp.).

Anal. Calcd. for $C_{14}H_{14}N_2I$: C, 50.0; H, 4.2. Found: C, 50.0; H, 4.3.

N,N'-Dimethyldihydrophenazinylium Chloride Monohydrate

In 75 ml of chloroform was dissolved 2.1 g (10 mmoles) of dimethyldihydrophenazine, and 0.25 ml of liquid chlorine was allowed to evaporate over the surface of the stirred solution. The green-black solid was collected on a filter and washed with chloroform. It was recrystallized from 100 ml of 95% ethanol to obtain 1.85 g of shiny black needles, m.p. 142–145° (decomp.).

Anal. Calcd. for $C_{14}H_{14}N_2Cl \cdot H_2O$: C, 63.8; H, 6.1; Cl, 13.4. Found: C, 64.0; H, 6.1; Cl, 13.4.

The infrared spectrum showed a strong band at 3 300 cm^{-1} attributed to water of hydration. Reduction with zinc in ethanol afforded authentic dimethyldihydrophenazine.

Preparation of Simple $TCNQ^-\cdot$ Salts (Table I)

The compounds listed in Table I were prepared by treatment of the respective quaternary iodides or methyl sulfates in hot absolute alcohol (about 0.1 *M*) with a boiling solution of 1 equiv. of LiTCNQ (1) in absolute ethanol (about 0.05 *M*). After the solution was cooled to room temperature, the products were collected on a filter and were recrystallized from acetonitrile.

Preparation of the Complex $(TCNQ)_2^-\cdot$ Salts (Table II)

One millimole of simple salt was dissolved in a boiling solution of 25 ml of acetonitrile containing 1 mmole of neutral TCNQ; the solution was filtered hot and then cooled to precipitate the product.

N,N'-Dimethyldihydrophenazinylium $(TCNQ)_2^-\cdot$

A hot filtered solution of 0.10 g (0.5 mmole) of N,N'-dimethyldihydrophenazine in 10 ml of acetonitrile was added to a hot filtered solution of 0.2 g (1 mmole) of TCNQ in 15 ml of acetonitrile. Black needles separated almost immediately. The mixture stood at room temperature for 30 min, and the product was collected on a filter and washed with acetonitrile and ether.

ACKNOWLEDGMENTS

The author thanks Dr. W. E. Mochel for helpful discussions and Drs. R. G. Kepler, H. G. Hoeve, and P. Arthur, respectively, for the electrical, electron paramagnetic resonance, and density measurements.

REFERENCES

1. L. R. Melby, R. J. Harder, W. R. Hertler, W. Mahler, R. E. Benson, and W. E. Mochel. J. Am. Chem. Soc. **84**, 3374 (1962).
2. K. H. Hausser, A. Häbich, and V. Franzen. Z. Naturforsch. **16a**, 836 (1961).
3. Y. Matsunaga and C. A. McDowell. Proc. Chem. Soc. London, 175 (1960).
4. H. Gilman and J. J. Dietrich. J. Am. Chem. Soc. **79**, 6178 (1957).

Can. J. Chem. Downloaded from www.nrcresearchpress.com by 210.87.254.40 on 09/05/12
For personal use only.

SYNTHESIS OF DERIVATIVES OF 1,2-DICHLORO-4-BENZENESULFONAMIDO-5-NITROBENZENE AND THEIR USE IN THE CHEMOTHERAPY OF SPONTANEOUS CANCERS

D. W. Woolley and T. Van Der Hoeven
The Rockefeller Institute, New York, New York
Received November 13, 1964

Dedicated to Professor R. B. Sandin on the Occasion of his Sixty-Eighth Birthday

ABSTRACT

A series of compounds related to 1,2-dichloro-4-benzenesulfonamido-5-nitrobenzene has been synthesized. These included derivatives in which ionizable groups had been placed in the para position of the benzenesulfonamido portion to confer on the compounds water solubility at physiological pH. Thus, carboxyl and quaternary ammonium groupings were introduced in this position. Water solubility was also conferred by introduction at the same position of non-ionizable groups such as polyhydroxyalkylamido groups. Additional relatives of the parent compound in which the chlorine atoms were replaced by methyl groups, and in which para-substituted benzenesulfonamido groups replaced those in the 4 and 5 positions, were synthesized. These compounds were tested for their ability to cure permanently the spontaneous mammary cancers of two strains of mice. All compounds were tested in combination with 1,2-dimethyl-4-(*p*-carboxyphenylazo)-5-hydroxybenzene. The most active substance found was 1,2-dichloro-4-(*p*-carboxybenzenesulfonamido)-5-nitrobenzene.

INTRODUCTION

Woolley and Stewart (1) showed that some spontaneous mammary cancers of mice could be cured permanently when the animals were given a mixture of two antimetabolites of 1,2-dimethyl-4,5-diaminobenzene. The two antimetabolites were 1,2-dimethyl-4-(*p*-carboxyphenylazo)-5-hydroxybenzene and 1,2-dichloro-4-benzenesulfonamido-5-nitrobenzene (I). These compounds were noteworthy not only because they actually cured spontaneous cancers but also because they were not very toxic to the animals themselves. They destroyed the cancers but did not at the same time poison the hosts. They apparently were able to do this because of their ability to inhibit the biosynthesis of vitamin B_{12}, and because this vitamin is synthesized by the spontaneous cancers but not by the hosts (2–6).

Certain shortcomings and anomalies in the actions of these two substances were, however, pointed out by Woolley and Stewart. In the first place, the compounds were not able to cure all of the cancerous mice. At most, only 35% were permanently cured, and a further 33% experienced only a transient regression of their cancers, after which the disease progressed. Thus, 32% of the cancers were not affected detectably by the compounds.

In the second place, the dose–response curve was unusual. Small doses produced no cures, and larger ones gave greater and greater numbers of cures up to a certain point. Beyond this point no additional numbers of cures could be produced by further increases in the dose of the antimetabolites.

The purpose of the work to be described in this paper was to synthesize derivatives of 1,2-dichloro-4-benzenesulfonamido-5-nitrobenzene which might prove to be more potent than the parent compound, and might be able, in conjunction with 1,2-dimethyl-4-(*p*-carboxyphenylazo)-5-hydroxybenzene, to cure all of the mammary cancers in a group of mice.

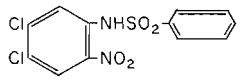

I

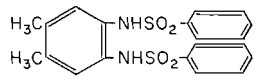

II

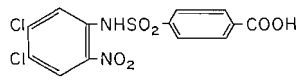

IV

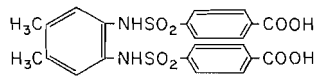

XII

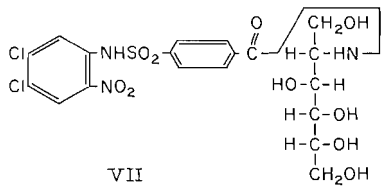

VII

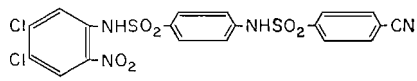

X

The strategy followed was to introduce chemical groups into 1,2-dichloro-4-benzenesulfonamido-5-nitrobenzene which would increase its water solubility. At the pH of animal tissues this parent compound was only very slightly ionized, and was consequently rather insoluble. It was felt that if its water solubility could be increased without sacrifice of its oncolytic activity a more potent substance might result.

The ways which were explored to achieve this end were, first, to introduce carboxyl groups to solubilize the compound as an anion at pH 7.5 or cationic groups of sufficient basic strength that the cations (or their zwitterions with the acidic sulfonamide group) would exist at physiological pH. It was recognized that the conversion of the drug to an ionized derivative might destroy its chemotherapeutic potency either because the derivative might be excreted too rapidly or because it might fail to penetrate into cells.

If achievement of solubility by introduction of ionizable groups were found to lead to biologically inactive compounds, it was planned to leave the ionizability of the parent compound untouched, but instead, to introduce polyhydroxyalkyl groups to achieve the desired solubility.

The proposed structural alterations could be introduced at many different points in the molecule. However, it was thought best to make all of the modifications in the benzenesulfonamide portion, and to leave untouched the "business end" of the molecule, viz. the part which gives it its structural analogy to dimethyldiaminobenzene. This plan was followed. In addition, some derivatives of another antimetabolite of this series were also prepared and tested. These were derivatives of 1,2-dimethyl-4,5-bis-(benzenesulfonamido)-benzene (II). This compound (1) had been found to exhibit some ability to cure spontaneous mammary cancers, but suffered from the same shortcomings as did 1,2-dichloro-4-benzenesulfonamido-5-nitrobenzene. The idea pursued again in designing the derivatives was to introduce solubilizing groups into the benzenesulfonamido portions.

EXPERIMENTAL

All compounds were recrystallized to constant melting point from the solvents indicated in the text.

1,2-Dichloro-4-(p-carboxybenzenesulfonamido)-benzene, Compound III

A solution of 53 g of 3,4-dichloroaniline in 180 ml of pyridine was cooled to 0°, stirred, and slowly treated with 76 g of *p*-cyanobenzenesulfonyl chloride, prepared as described by Remsen *et al.* (7). When the addition was complete, the solution was allowed to stand at room temperature for 20 h. Without isolation of the nitrile derivative, the reaction mixture was then treated with 56 g of NaOH in 1 l of water. The resulting solution was refluxed for 2 h to hydrolyze the nitrile. The hydrolysate was diluted with 8 l of water, treated with 10 g of Norit, filtered, and acidified to pH 2 with HCl. It was necessary to have a large volume at the time of the acidification. Otherwise, an intractable gel was formed. The crystalline precipitate which formed was collected, washed with water, and recrystallized to constant melting point (255°) from 1 l hot acetone by addition of 0.5 l of water; yield 97 g.

Anal. Calcd. for $C_{13}H_9Cl_2NO_4S$: C, 45.1; H, 2.9; N, 4.0. Found: C, 45.4; H, 2.7; N, 3.9.

1,2-Dichloro-4-(p-carboxybenzenesulfonamido)-5-nitrobenzene, Compound IV

Yellow fuming nitric acid, specific gravity 1.48 (950 ml), was cooled to 20° and stirred, and 95 g of dry powdered 1,2-dichloro-4-(*p*-carboxybenzenesulfonamido)-benzene was added to it at such a rate that the temperature did not rise above 25°. A clear solution was soon produced. When the nitration was attempted at lower temperatures, the starting material was found to be so insoluble in the nitric acid that incomplete reaction occurred. The reaction mixture was held for 0.5 h at 20°, and was then poured slowly with much stirring into 6 l of ice and water. The crystalline precipitate which formed was collected, washed with water, and recrystallized to constant melting point from 1.5 l butanol, or from acetone by addition of benzene. The yield was 54.5 g; m.p. 225° (decomp.).

The position of the nitro group was inferred from the similar preparation of 1,2-dichloro-4-benzenesulfonamido-5-nitrobenzene (8), in which case the position of the group was proved by alternate synthesis.

Anal. Calcd. for $C_{13}H_8Cl_2N_2O_6S$: C, 39.9; H, 2.0; N, 7.2. Found: C, 38.7; H, 2.0; N, 7.1.

1,2-Dichloro-4-(p-carboxamidobenzenesulfonamido)-5-nitrobenzene, Compound V

The preceding compound IV (19.5 g) was dried at 100°, powdered, and suspended in 250 ml of anhydrous ether, and 11.5 g of PCl_5 was added to it. The suspension was stirred at room temperature until a clear solution was obtained. The reaction mixture was concentrated under reduced pressure to dryness, and the crystalline acid chloride was triturated with dry petroleum ether to remove $POCl_3$. The acid chloride was then dissolved in 175 ml of acetone, and the solution was added dropwise during 30 min to 100 ml of concentrated aqueous ammonia which was being stirred and cooled to 0°. The resulting solution was held at room temperature overnight and then was concentrated under reduced pressure to 100 ml and acidified to pH 6.0 with HCl. The precipitate which formed was collected, washed with water, and recrystallized from 200 ml of ethanol. The yield was 19.0 g; m.p. 222° (decomp.).

Anal. Calcd. for $C_{13}H_9Cl_2N_3O_5S$: C, 40.0; H, 2.3; N, 10.8. Found: C, 40.4; H, 2.4; N, 10.5.

1,2-Dichloro-4-[p-(N-glucosaminocarbonyl)-benzenesulfonamido]-5-nitrobenzene, Compound VI

The acid chloride of compound IV was prepared as described in the preceding section from 19.5 g of the acid and dissolved in 175 ml of acetone. This solution was then added dropwise with stirring to a freshly prepared suspension of MgO (10 g) and D-glucosamine hydrochloride (10.8 g) in 250 ml of cold (0°) water. After the reaction of the acid chloride had proceeded for 2 h at 0 °C, and overnight at room temperature, the unused MgO was filtered off and washed thoroughly with water. The filtrate was concentrated under reduced pressure to about 100 ml. This concentrated solution was then acidified to pH 4 with concentrated HCl. The desired product, which crystallized out, was collected and washed with small amounts of water. It was then dried to constant weight *in vacuo* and triturated with 250 ml of acetone to remove any unchanged compound IV. If the material had not been thoroughly dried before treatment with acetone, it became dark and gummy and some of it dissolved in the acetone, but thorough drying prevented these problems. The acetone-insoluble material (28 g) was recrystallized from water. The yield was 20 g; m.p. 170° (decomp.), with sintering from 160 °C. In boiling water it was soluble at 2 mg per ml and at 0.6 mg per ml in cold water. Crystals contained 1 mole of water which was lost at 78 °C *in vacuo*.

Anal. Calcd. for $C_{19}H_{19}Cl_2N_3O_{10}S$: C, 41.3; H, 3.5; N, 7.6. Found: C, 41.2; H, 3.5; N, 7.3.

Reaction of Compound VI with 1,2-Dimethyl-4-(p-carboxyphenylazo)-5-hydroxybenzene

It was proposed to test compound VI in combination with 1,2-dimethyl-4-(*p*-carboxyphenylazo)-5-hydroxybenzene for chemotherapeutic action against cancers. Quite unexpectedly, however, it was found that these two compounds reacted with each other in aqueous solutions. When the aqueous solutions at pH 8 were mixed at room temperature, a brownish-red precipitate slowly separated. The chemical nature of this precipitate was not established, but it was plain that the aldehydo group in compound VI was necessary for the reaction. This was shown by the fact that the corresponding compound (compound VII, see below) in which the aldehydo group had been reduced to $—CH_2OH$ did not produce a color change or a precipitate when aqueous solutions of it were added to neutral aqueous solutions of 1,2-dimethyl-4-(*p*-carboxyphenylazo)-5-hydroxybenzene.

1,2-Dichloro-4-[p-(2'-desoxy-2'-glucitolaminocarbonyl)-benzenesulfonamido]-5-nitrobenzene, Compound VII

A solution of 30 g of compound VI in 550 ml of water and 5.5 g of $NaHCO_3$, which had stood at room temperature for 2 h to allow complete mutarotation, was mixed all at once with a freshly prepared solution of sodium borohydride (6 g in 140 ml of water) (cf. ref. 9). After the mixture had stood for 2 h at room temperature it was acidified below pH 6 with acetic acid, and the precipitate which formed was collected and washed 3 times with 150 ml of water. This precipitate was dissolved in aqueous $NaHCO_3$, treated with Norit, filtered, and reprecipitated by acidification. It was then recrystallized from 0.02 *N* aqueous HCl. The yield was 15 g; m.p. 138° (decomp.). The compound was soluble in boiling water at 8 mg per ml and in cold water to the extent of 1 mg per ml.

Anal. Calcd. for $C_{19}H_{21}Cl_2N_3O_{10}S$: C, 41.2; H, 3.8; N, 7.6. Found: C, 40.7; H, 3.7; N, 7.5.

1,2-Dichloro-4-(p-cyanobenzenesulfonamido)-5-nitrobenzene, Compound VIII

A solution of 21.5 g of 3,4-dichloro-6-nitroaniline, prepared according to the directions of Beilstein and Kurbatow (10) in 75 ml of pyridine, was treated with 21 g of *p*-cyanobenzenesulfonyl chloride prepared as described by Remsen *et al.* (7). The mixture was held at room temperature in a stoppered flask for 24 h and was then poured into 1 l of ice water. The gummy precipitate which formed crystallized after several hours, was collected, and was well washed with water. Unchanged dichloronitroaniline was removed from it by trituration with 1 l of water containing 11 g Na_2CO_3 and 4 g NaOH, and by filtration. The recovered dichloronitroaniline weighed 12 g. The filtrate was immediately acidified with acetic acid, and the precipitate which formed was collected, washed with water, and recrystallized from acetic acid by the addition of water. The yield was 7.3 g; m.p. 199–201°.

Anal. Calcd. for $C_{13}H_7Cl_2N_3O_4S$: C, 41.9; H, 1.9; N, 11.3. Found: C, 41.7; H, 2.1; N, 11.0.

1,2-Dichloro-4-(p-trimethylaminobenzenesulfonamido)-5-nitrobenzene, Compound IX

The methyl betaine of sulfanilic acid was prepared by rearrangement of methyl *p*-dimethylaminobenzenesulfonate as suggested by Kuhn and Ruelius (11). The rearrangement was best carried out by heating the ester at 100° for 3 h without solvent.

The betaine was converted to its acid chloride by heating under reflux a suspension of 17 g of the betaine with 100 ml of CCl_4 and 29 g of PCl_5 for 24 h. The acid chloride which remained insoluble as its hydrochloride was filtered off and washed with CCl_4. It was then added to a solution of 3,4-dichloro-6-nitroaniline (12.4 g) (10) in 50 ml of pyridine. The mixture was held at 50° and stirred for 24 h. It was then concentrated under reduced pressure to dryness. Unchanged dichloronitroaniline and pyridine hydrochloride were removed by extraction with chloroform (200 ml). The compound IX, because it was a zwitterion, was not soluble in this solvent. All attempts to remove the dichloronitroaniline by recrystallization failed until this method was found. The chloroform-insoluble material (12 g) was then recrystallized from boiling water, or from glacial acetic acid.

Compound IX was (for an ionized salt) surprisingly insoluble in water. At 100° the solubility was approximately 0.5 mg per ml. It was also rather insoluble in acetic acid or ethanol. It was no more soluble in aqueous 1 *N* HCl or 1 *N* NaOH than it was in water. The melting point (235–238°) was a decomposition point which, in contrast to that for other compounds of this series, was of little value as a criterion of purity.

Anal. Calcd. for $C_{15}H_{15}Cl_2N_3O_4S$: C, 44.6; H, 3.7; N, 10.4. Found: C, 44.5; H, 3.6; N, 10.2.

1,2-Dichloro-4-[p-(p'-cyanobenzenesulfonamido)-benzenesulfonamido]-5-nitrobenzene, Compound X

Compound V (3.8 g) was converted to the corresponding amine (viz. 1,2-dichloro-4-(*p*-aminobenzenesulfonamido)-5-nitrobenzene) by a standard Hofmann degradation with NaOCl. The product was isolated from the alkaline aqueous reaction mixture by acidification to pH 4. The amine was weak enough that it did not form a hydrochloride at that pH and readily crystallized. The amine was then dried, dissolved in pyridine, and acylated with *p*-cyanobenzenesulfonyl chloride (10) by use of the conditions described for other acylations in this paper. The product was recrystallized from acetic acid; m.p. 136° after sintering from 115°.

Anal. Calcd. for $C_{19}H_{12}Cl_2N_4O_6S_2$: C, 43.3; H, 2.3; N, 10.6. Found: C, 43.3; H, 2.4; N, 10.3.

1,2-Dimethyl-4,5-bis-(p-cyanobenzenesulfonamido)-benzene, Compound XI

A cooled and stirred solution of 14 g of 1,2-dimethyl-4,5-diaminobenzene in 50 ml of pyridine was slowly treated with 44 g of *p*-cyanobenzenesulfonyl chloride (10), and allowed to stand at room temperature for 1 h. The reaction mixture was then poured into 1 l of ice water, and the precipitate which formed was collected, washed with water, dried, and recrystallized from 200 ml of boiling glacial acetic acid with addition of 200 ml of water. The yield was 38.5 g; m.p. 207–209°.

Anal. Calcd. for $C_{22}H_{18}N_4O_4S_2$: C, 56.7; H, 3.9; N, 12.0. Found: C, 56.7; H, 3.8; N, 11.7.

1,2-Dimethyl-4,5-bis-(p-carboxybenzenesulfonamido)-benzene, Compound XII

The dinitrile, compound XI (9.3 g), was dissolved in 200 ml of aqueous 1 *M* NaOH, and the solution was refluxed for 2 h. It was then cooled, diluted with 500 ml of water, decolorized with Norit, and acidified to pH 2 with HCl. The precipitate which formed was collected, washed, and recrystallized by suspension in 100 ml of hot glacial acetic acid and addition of 250 ml of water. The yield was 9.8 g; m.p. 255° (decomp.).

Anal. Calcd. for $C_{22}H_{20}N_2O_8S_2$: C, 52.4; H, 4.0; N, 5.6. Found: C, 52.2; H, 3.8; N, 5.6.

TABLE I

Effect of compounds on spontaneous mammary cancers of mice (all animals received 6 g 1,2-dimethyl-4-(*p*-carboxyphenylazo)-5-hydroxybenzene per kg rations in addition to the compounds listed)

		Oral dose (g per kg ration)	I.P. dose (mg per mouse per day)	SPFS mice			C3H mice		
				No. mice	Transient suppression	Permanent cures	No. mice	Transient suppression	Permanent cures
1,2-Dichlorobenzenes									
	None	0	0	33	2	2	58	1	0
I	4-Benzene sulfonamido-5-nitro-	0.5	0	36	14	11	17	10	0
		1.0	0	14	7	3	0	0	0
IV	4-(*p*-Carboxybenzenesulfonamido)-5-nitro-	1.0	0	11	6	1	4	0	0
		2.0	10	21	5	6	8	0	0
		3.0	0	6	0	1	9	0	0
		3.0*	2	12	3	3	6	0	0
V	4-(*p*-Carboxamidobenzenesulfonamido)-5-nitro-	2.0	0	6	0	0	0	0	0
VI	4-*p*-(N-Glucosaminocarbonyl)-benzenesulfonamido-5-nitro-	2.0	10	11	3	0	6	0	0
VII	4-*p*-(2′-Desoxy-2′-glucitolaminocarbonyl)-benzenesulfonamido-5-nitro-	2.0	5	3	0	1	4	0	0
IX	4-(*p*-Trimethylaminobenzenesulfonamido)-5-nitro-	1.0	2.5	6	1	0	12	0	0
1,2-Dimethylbenzenes									
XII	4,5-Bis-(*p*-carboxybenzenesulfonamido)-	3.0	5	6	1	0	0	0	0
		3.0*	5	6	1	2	6	0	0
XIII	4,5-Bis-(*p*-amidinobenzenesulfonamido)-	0*	1	6	0	0	5	0	0

*These mice received no 1,2-dimethyl-4-(*p*-carboxyphenylazo)-5-hydroxybenzene.

1,2-Dimethyl-4,5-bis-(p-amidinobenzenesulfonamido)-benzene Dihydrochloride, Compound XIII

The dinitrile, compound XI (28.5 g), was dissolved in 50 ml of acetone and 200 ml of dry chloroform and mixed with 22 ml of 10 *M* alcoholic hydrogen chloride. The mixture was allowed to stand at room temperature for 24 h. It was then concentrated under reduced pressure to dryness at 25°, and freed of acetone by addition of anhydrous ether and reconcentration. The residue was dissolved in 100 ml of absolute ethanol at 0°, and immediately mixed with 250 ml of ethanol previously saturated with NH_3. The solution which resulted was held at room temperature for 3 days, and was then concentrated under reduced pressure to dryness at 25°. The residue was triturated with 1 l of boiling chloroform, and the insoluble portion was dried and triturated with ethanol which was then diluted with water. The desired amidine remained in the water-soluble portion along with the impurities (fraction A). The water-insoluble portion was a mixture of several compounds, one of which appeared to be the cyclic amidine formed by reaction of the two bis-imino-ether groups with 1 molecule of NH_3. It was purified by suspension in ethanol, addition of chloroform, and concentration under reduced pressure to remove most of the ethanol. It melted at 187°.

Anal. Calcd. for $C_{22}H_{21}O_4N_5S_2$: C, 54.6; H, 4.3; N, 14.5. Found: C, 54.5; H, 4.5; N, 14.0.

The desired diamidine was obtained from the water-soluble fraction A by conversion to the dihydrochloride by addition of ethanolic hydrogen chloride. The dihydrochloride (3 g) crystallized from this mixture, m.p. 276° (decomp.).

Anal. Calcd. for $C_{22}H_{26}Cl_2N_6O_4S_2$: C, 46.1; H, 4.5; N, 14.7. Found: C, 45.4; H, 4.3; N, 14.3.

Effects on Spontaneous Mammary Cancers of Mice

Most of the compounds were tested for their ability to cure the spontaneous mammary cancers of two strains of mice, viz. the SPFS and C3H strains. The methods of testing, and the criteria of cure or regression were those described in the preceding paper (1). The compounds were administered both orally (mixed with the food) as well as by daily intraperitoneal injections. All compounds were tested in combination with 1,2-dimethyl-4-(*p*-carboxyphenylazo)-5-hydroxybenzene, but some were also tested without this compound.

It is important to note that the compounds were tested against spontaneous cancers, not against transplants. The importance of this distinction has been discussed in preceding papers (1, 12).

Because mice with spontaneous mammary cancers are rare, each test group contained limited numbers of animals, usually six. Any compound which showed promising potency was then retested with larger numbers of animals. In this way, the best use could be made of the limited numbers of rare animals. The precise relative potencies were thus not determined with accuracy, but this was of only secondary interest. The assay was adequate to reveal any compound which would cure *all* of the cancers. Other compounds of less potency were of less interest.

The results of the chemotherapeutic experiments are summarized in Table I. It can be seen that the most active new compound was IV. Only the SPFS cancers were susceptible to these compounds. The C3H strain showed no permanent cures with any one of them. This difficulty in causing an effect in the C3H strain accorded with the previous experience with the parent compound (1).

REFERENCES

1. D. W. Woolley and J. M. Stewart. Biochem. Pharmacol. **11**, 1163 (1962).
2. D. W. Woolley. J. Exptl. Med. **93**, 13 (1951).
3. D. W. Woolley. Proc. Soc. Exptl. Biol. Med. **75**, 745 (1950).
4. D. W. Woolley. J. Am. Chem. Soc. **74**, 5450 (1952).
5. D. W. Woolley. Proc. Natl. Acad. Sci. U.S. **39**, 6 (1953).
6. D. W. Woolley. Proc. Natl. Acad. Sci. U.S. **41**, 111 (1955).
7. I. Remsen, R. N. Hartman, and A. M. Muckenfuss. Am. Chem. J. **18**, 150 (1896).
8. D. W. Woolley and J. M. Stewart. J. Med. Chem. **6**, 599 (1963).
9. A. B. Foster, D. Horton, N. Salim, M. Stacey, and J. M. Webber. J. Chem. Soc. 2587 (1960).
10. F. Beilstein and U. Kurbatow. Ann. Chem. **196**, 214 (1879).
11. R. Kuhn and H. Ruelius. Chem. Ber. **83**, 420 (1950).
12. D. W. Woolley and G. Schaffner. Cancer Res. **14**, 802 (1954).

Can. J. Chem. Downloaded from www.nrcresearchpress.com by 210.87.254.105 on 09/05/12
For personal use only.

THE MECHANISMS OF THE HALOGENATIONS AND HALOGENOMETHOXYLATIONS OF D-GLUCAL TRIACETATE, D-GALACTAL TRIACETATE, AND 3,4-DIHYDROPYRAN[1]

R. U. LEMIEUX AND B. FRASER-REID
Department of Chemistry, University of Alberta, Edmonton, Alberta
Received November 13, 1964

Dedicated to Professor R. B. Sandin on the Occasion of his Sixty-Eighth Birthday

ABSTRACT

The stereochemical routes of the reactions showed trends, when the halogen, the olefin, and the solvent were changed, which can be accounted for on the basis of (*a*) the relative stabilities of the halonium and oxocarbonium ions formed as intermediates, (*b*) the effect of ring conformation on the ease of formation of oxocarbonium ions involving the ring-oxygen of the pyranose ring, (*c*) the role of the anomeric effect in determining the stability of the transition state, and (*d*) the influence on the route of reaction of whether or not the intermediate cations are solvated by a nucleophile as they are formed. Proton magnetic resonance spectroscopy was extensively used to determine the compositions of products and the configurations and conformations of the compounds obtained.

The stereochemical routes of the bromination and halogenomethoxylations of D-glucal triacetate were reported in an earlier communication (1). The product of the chlorination has now been established and the reactions were extended to D-galactal triacetate (2) and 3,4-dihydropyran. The halogenations were performed at 0° in carbon tetrachloride and the halogenomethoxylations at 0° in methanol containing silver acetate. The yields and configurations of the products formed in each of the reactions are given in Table I. The bases for these conclusions are presented in the Experimental section of this paper and in the previous communications (1).

The results appear to shed light on the nature of the intermediates formed in halogenation reactions and on the stereoelectronic requirements for ring-oxygen participation in reactions at the anomeric center of sugar derivatives. This becomes apparent when the results (Table I) are considered and one keeps in mind the probable effect of the electronegativity of the halogen on the relative stabilities of the intermediates B to E, the effect of the nature and concentration of the nucleophile Y in the reactions of these intermediates, and the stereoelectronic demands for the transformations involved in the conversion of the cyclic vinyl ethers (A) to the products (L to O).

In theory, four diastereoisomeric products (L to O) can be expected to form, if the nucleophilic attack in the second stage of the reaction is restricted to the anomeric center. This route of reaction must be expected, since it allows the ring-oxygen to help delocalize positive charge at the anomeric center. That is, the intermediates B to E are expected, as shown, to possess oxocarbonium-ion character and, therefore, to undergo nucleophilic attack most readily at the anomeric center. All the results of the halogenomethoxylations are in accord with this expectation.

The exact nature of the halogenating agent is not known. Nevertheless, it suffices for the present purposes to assume that it is a form of complexed cationic halogen and that the initial interaction is with the pi-orbitals of the six-membered cyclic vinyl ethers

[1]*This research was part of a thesis submitted by B. F.-R. in partial fulfillment of the requirements for the degree of Doctor of Philosophy, University of Alberta, 1964.*

Can. J. Chem. Downloaded from www.nrcresearchpress.com by 210.87.254.105 on 09/05/12
For personal use only.

TABLE I

Stereochemical routes of reaction

Reactant (A)	Reaction	% yield and configuration of products			
		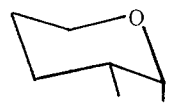 L X Y	M X	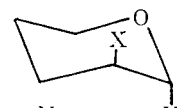 N Y	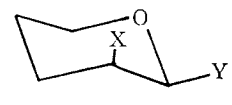 O
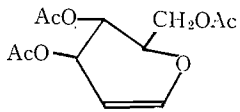 D-Glucal triacetate (I)	Chlorination	>80 (II)	—	—	—
	Bromination*	60	—	30	—
	Chloromethoxylation*	8	41 (III)	51	—
	Bromomethoxylation*	—	33	66	—
	Iodomethoxylation*	—	33	66	—
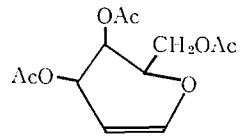 D-Galactal triacetate (IV)	Chlorination	>80 (V)	—	—	—
	Bromination	50 (X)	—	50 (IX)	—
	Chloromethoxylation	39 (VII)	53 (VI)	8 (VIII)	—
	Bromomethoxylation	11 (XV)	37 (XII)	52 (XI)	—
	Iodomethoxylation	—	19 (XVI)	81 (XVII)	—
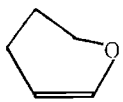 3,4-Dihydropyran† (XVIII)	Chlorination	50 (XIX)	—	50 (XX)	—
	Bromination	11 (XXIV)	—	89 (XXIII)	—
	Chloromethoxylation	25 (XXI)	—	75 (XXII)	—
	Bromomethoxylation	13 (XXVI)	—	87 (XXV)	—
	Iodomethoxylation	—		100 (XXVII)	—

* Ref. 1.

† Products L and O are indistinguishable, as are products M and N, and both are formed as racemates. The yields are listed under the more stable conformation for these compounds.

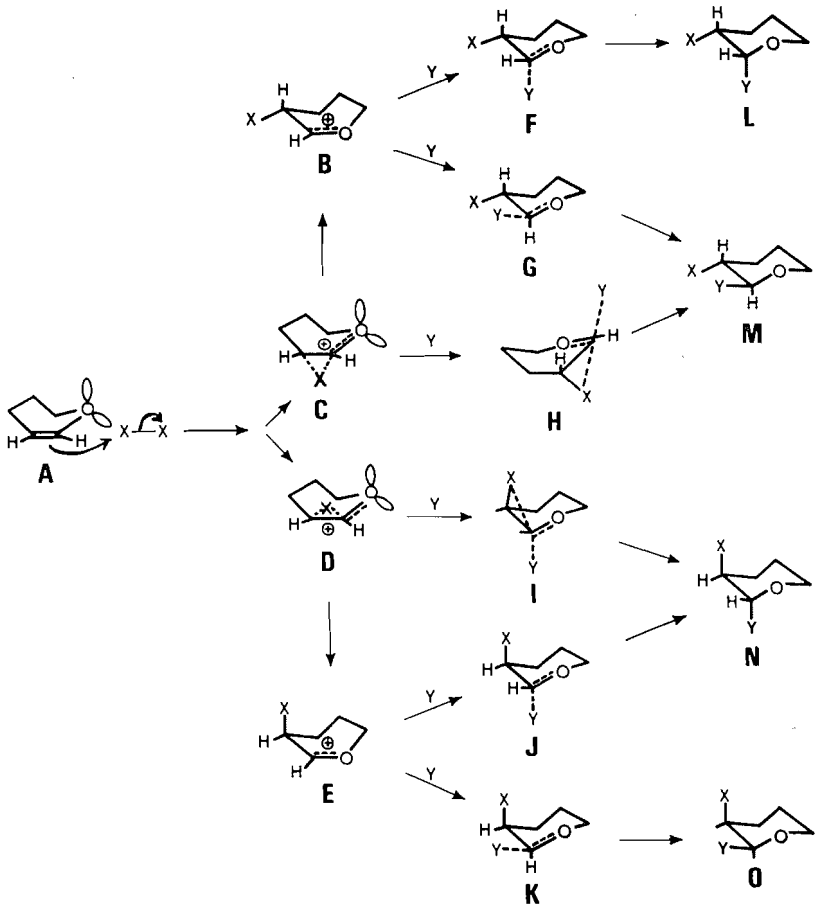

[A (I, IV, and XVIII)] used as reactants to form cations akin to C and D. The structures of these cations can be expected to vary greatly with the nature of the halogen (X). That is, the actual structure can be expected to be a resonance hybrid of the following canonical structures.

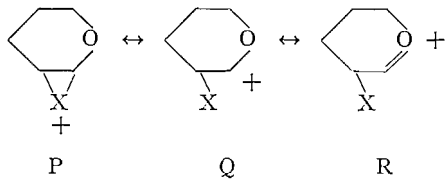

P Q R

In view of the strong anchimeric assistance provided by the participation of iodine (3), it can be expected that structure P will contribute most strongly when X = I. On the other hand, structure P must be expected (4–6) to be of little, if any, importance when X = Cl. The cations with X = Br should be of intermediate structure and stability. De la Mare *et al.* (7) have demonstrated the migration of iodine and bromine in the reactions of hypochlorous acid with allyl iodide and allyl bromide, respectively, and pointed out that this is consistent with the facts established concerning the relative efficiency of iodine, bromine, and chlorine in neighboring group participation. Although

Can. J. Chem. Downloaded from www.nrcresearchpress.com by 210.87.254.105 on 09/05/12
For personal use only.

Can. J. Chem. Downloaded from www.nrcresearchpress.com by 210.87.254.105 on 09/05/12
For personal use only.

the methanolysis of tri-*O*-acetyl-2-bromo-2-deoxy-α-D-mannopyranosyl bromide proceeded without evidence for 2-bromine participation (1), the methanolysis of tri-*O*-acetyl-2-bromo-2-deoxy-α-D-talopyranosyl bromide (IX) proceeded with equal amounts of retention and inversion of the anomeric center. It is possible that the reaction proceeded, in part, with 2-bromine participation in the case of IX because formation of the 1,2-bromonium ion released the non-bonded interaction between the axial 2-bromine and the opposing axial 4-acetoxy group. Methanolysis of *trans*-2,3-dibromotetrahydropyran also appeared to proceed with extensive (50–60%) participation of the 3-bromine. Certainly, the indication is apparent that with X = Br the structure R makes an important contribution. In the absence of a contribution by structure P, the structure of the cation corresponds to Q ↔ R. The formulas for the cations B and E are considered to represent this type of ion, often referred to as an oxocarbonium ion.

The classical route for the halogenation of alkenes is to provide the *trans* adduct (8, 9), and this route is usually considered to involve cyclic halonium ions as intermediates. In cyclic systems, the diaxial adduct is *normally* formed most readily but *may* rearrange to the more stable diequatorial form (10). These aspects of the reaction have received much attention and appear to be rather well understood. Heterolytic *cis* addition of halogen to an olefin must presumably either involve the formation of an open carbonium ion as an intermediate or else proceed by way of a four-centered transition state.

The most outstanding result contained in Table I is the lack of the formation of products corresponding to structure O. The hindrance to this course of reaction cannot simply be attributed to problems inherent to *cis* addition, since *cis* addition to form the diastereoisomeric structure L was prevalent in several of the reactions. The lack of products corresponding to O must arise because either the formation of the ion E or the transition state K for its reaction with a nucleophile (or both) is unfavorable as compared to the alternate routes of reaction. That this should be the case can be appreciated on stereoelectronic grounds. Clearly, the p-orbitals of the ring-oxygen are not as well oriented for charge delocalization in ion D as in ion C. Therefore, the energy barrier should be less for the formation of ion B than that for ion E. In the absence of axial substituents at the 3- or 5-positions, an ion of structure E would be expected to react by way of transition state J rather than K, since axial approach of the nucleophile avoids interaction with the axial 2-substituent. Thus, the absence of structures corresponding to O is understandable. Structures corresponding to O were formed in the methanolysis of both the tri-*O*-acetyl-2-bromo-2-deoxy-α-D-mannopyranosyl (1) and tri-*O*-acetyl-2-bromo-2-deoxy-α-D-talopyranosyl (IX) bromides. Likely, these reactions with methanol as the solvent proceeded by way of the following transition state.

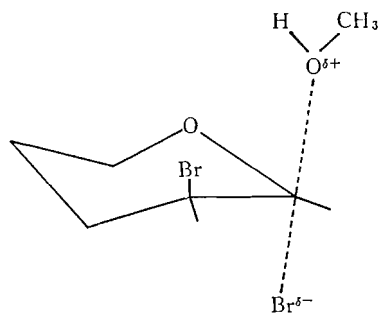

That is, in the presence of the very high concentration of methanol, some bonding of the anomeric center with methanol was established before the bromide ion had time to

depart (11). This shielding by a departing group is not present in the halogenomethoxylation reactions.

In view of the above-mentioned facts, the chlorination reactions should proceed directly to the oxocarbonium ions B and E. The ion B should form more readily and tend to accept the chloride ion by way of transition state F rather than G to form the *cis* adduct L for two reasons: (*a*) because of the anomeric effect (12), L is more stable than the anomer M and, with a negative entering group (halide ion), this effect should be felt in the transition state; and (*b*) the chloride ion most likely was formed from the chlorine molecule which made the electrophilic attack and, therefore, because of the absence of other nucleophiles in the environment, *cis* addition, by way of a process approaching a four-centered transition state, can be expected. In fact, the only products detectable in appreciable concentration (>80%) from the chlorination of both D-glucal triacetate (I) and D-galactal triacetate (IV) were those (II and V) corresponding to structure L. That the β-anomers corresponding to structure M were not first formed and rapidly anomerized seems definite, in view of the observation that tetra-*O*-acetyl-β-D-glucopyranosyl chloride was not anomerized to a detectable extent when subjected to the conditions of chlorination. Anomerization could not be detected in the bromination of D-glucal triacetate (1). The *cis* addition of nitrosyl chloride to acetylated glycals to form products corresponding to structure L has been demonstrated (13). The chlorination of 3,4-dihydropyran (XVIII) gave equal amounts of the *cis* and *trans* adducts. The course of reaction leading to the *trans* product may have resulted from a tendency of the presumably first-formed ion B to undergo conformational change before accepting the chloride ion. The energy barrier to the conformational change must be very small and, although the ion E has the chlorine in axial orientation, the charge separation (between the chlorine and the ring-oxygen) is less in E than in B. Therefore, although B must be expected to form more readily than E, the difference in stability between E and B in carbon tetrachloride solution may be small. It is possible, on the other hand, that the *trans* isomer (XX) was formed by anomerization of first-formed *cis* adduct (XIX). Unfortunately, this possibility was not examined. That the *trans* isomer is, in fact, the more stable compound was established by showing an increase in the concentration of this isomer both when the reaction mixture was heated before isolation and when the product in acetonitrile was treated with tetraethylammonium chloride. The formation of the *cis* adduct (XIX) in a concentration greater than its presence in equilibrium mixture (XIX $\rightleftarrows$ XX) suggests that, as found for the chlorinations of the acetylated glycals, the ion corresponding to B was formed more readily than that represented by E. That is, it is improbable that the less stable isomer (XIX) would have formed to an extent greater than its presence in the equilibrium mixture, had its cationic intermediate (*B*) not formed more readily.

The anomeric effect (12) favors the conformations for XIX and XX wherein the 2-chlorine is in axial orientation. In view of this effect and the conformational properties of *trans*-1,2-dichlorocyclohexane (14), it was not surprising to find (n.m.r. evidence) that the compounds in fact possessed these conformations.

A greater tendency for *trans* addition can be expected to occur in brominations than in chlorinations both for steric reasons (greater non-bonding interactions between the gauche halogens) and the established greater favorability of cyclic bromonium ions (corresponding to structures C and D). The results of the bromination reactions agree with this expectation. Thus, it is seen that, for the brominations, the rates of *trans* addition to products of structure N are close to those of *cis* addition to products corresponding to

Can. J. Chem. Downloaded from www.nrcresearchpress.com by 210.87.254.105 on 09/05/12
For personal use only.

L. Unless the cyclic bromonium ion corresponding to C is considerably more stable than the oxocarbonium ion B, reaction initiated by formation of C would be expected to proceed by way of B to give the *cis* adduct corresponding to L. This would follow for the reasons outlined above with regard to the routes of the chlorination reactions and the fact that *trans* addition of the bromine by way of the transition state H represents a sterically unfavorable route of reaction. It is probably for these reasons that *cis* addition, to provide the products corresponding to L, occurred. However, in contrast to the chlorinations, substantial yields of the diaxial *trans* dibromides were formed in the brominations. These results suggest that, for bromine, cyclic bromonium ion intermediates are formed and, in view of the favorability of the transition state I, this route of reaction is about as favorable as that by way of ion B. The formation of these products by way of oxocarbonium ions corresponding to E seems unlikely, in view of the absence of products corresponding to O in all of the reactions studied. It must be admitted, however, that there is little basis for distinguishing between the transition states I and J.

Except for the chloromethoxylations, the halogenomethoxylation reactions using methanol as solvent must lead directly to strongly solvated (complexed) intermediate cations which can be represented by structures F to K with Y = CH_3OH. Since the formation of these complexes is expected to begin with the attack on the double bond by the halogen, the products of *trans* addition should form most readily, and this was in fact observed in all cases; *cis* addition was extensive only in special cases, namely, chloromethoxylations and the bromomethoxylation of D-galactal triacetate. That *cis* addition was prevalent in the chloromethoxylations can, of course, be attributed to the instability of chloronium ions and the consequent tendency for the reactions to proceed directly by way of oxocarbonium ions. Reactions by way of ion B should be more important, as was observed, in the chloromethoxylation of D-galactal triacetate than for D-glucal triacetate, since in the former case the oxocarbonium ion E has the axial chlorine opposing the axial acetoxy group at the 4-position. This situation would also influence the bromomethoxylations of these compounds and promote *cis* addition to D-galactal triacetate.

The formation of appreciable amounts of the diequatorial products corresponding to structure M in the halogenomethoxylations is in sharp contrast to their absence in the products of the halogenations. As already mentioned, solvation of the ion as it is forming is probably mainly responsible for this result. It should be noted, however, that the intermediates F and G must differ less in stability with Y = CH_3OH than with Y = X^-, since in the former case the oxygen in Y must possess a partial positive charge and, therefore, stabilization of F over G through the anomeric effect is precluded.

The tendency to form *trans* adducts by way of the intermediates H and I should increase with increasing stability for the cyclic halonium ion and, therefore, increase as the halogen is changed from chlorine to bromine and from bromine to iodine. The results are seen to agree with this expectation. The formation of the *trans* adducts only in the iodomethoxylations is not surprising in view of the stability of the cyclic iodonium ions, and presumably these reactions proceeded exclusively by way of the intermediates H and I. For reasons already discussed, the preference for the route leading to the diaxial product is not surprising. The slightly greater preference for this route of reaction found in the iodomethoxylation of D-galactal triacetate over that observed for D-glucal triacetate likely is due to a shielding by the axial 4-acetoxy group in D-galactal triacetate of the approach by methanol to form the intermediate H. The result could, of course, also be rationalized by assuming a stabilization of the iodonium ion of structure D by

Can. J. Chem. Downloaded from www.nrcresearchpress.com by 210.87.254.105 on 09/05/12
For personal use only.

Coulombic interaction of the positive iodine with the axial 4-acetoxy group in the case of the reaction with D-galactal triacetate. This interpretation appears less attractive in view of the results obtained in the bromomethoxylations. The iodomethoxylation of 3,4-dihydropyran gave the *trans* adduct exclusively. Of course, there was no possibility of distinguishing between the products corresponding to M and N since, in this case, these products are merely conformers.

In conclusion, although the results of this study cannot be interpreted with precision, it is seen that the stereochemical routes of the reactions studied showed trends, when the halogen, the olefin, and the solvent were changed, which can be rationalized by taking into account (*a*) the expected relative stabilities for iodonium, bromonium, and chloronium ions, (*b*) the expectation that the axially oriented p-orbital of the ring-oxygen is more favorably disposed for participation in delocalization of developing charge at the anomeric center than is the equatorially oriented p-orbital, (*c*) the expectation that axial attack at the anomeric center is more favorable for reasons of the anomeric effect by a negative ion than by a neutral molecule, and (*d*) the expectation that the route of the reaction is influenced by whether or not the intermediate cations can be solvated (complexed) by a nucleophile as they are formed. The display of the stereoelectronic demands for ring-oxygen participation is of obvious importance to an understanding of reactions at the anomeric center of glycosidic structures.

EXPERIMENTAL

Halogenations

A stirred solution of 26 mmoles of the acetylated glycal in 50 ml of carbon tetrachloride was cooled in an ice bath and protected from light. Bromine was added dropwise, or chlorine was bubbled in, until a color caused by excess halogen was present. After the solution had stood for a further 15 min, air was bubbled into the solution to remove the excess halogen, and the solvent was evaporated *in vacuo* at 40°. In all cases yields were better than 95% and samples were checked by nuclear magnetic resonance spectroscopy (n.m.r.) before work-up to ensure that the isolation procedures had not changed the product.

Tetra-*O*-acetyl-β-D-glucopyranosyl chloride (17) was recovered unchanged when subjected to chlorination under these conditions.

Methanolysis of the Acetylated 2-Deoxy-2-halogenoglycosyl Halides

The dihalide (41 mmoles) was dissolved in 50 ml of dry methanol and, after the addition of dry freshly prepared silver carbonate (0.2 mole), the mixture was stirred until a portion of the filtered reaction mixture failed to give a precipitate with ethanolic silver nitrate—usually 1 to 1.5 h. The silver salts were removed by filtration through Celite and the filter cake was thoroughly washed before the filtrate was evaporated to dryness. Decolorization of an ethanolic solution with charcoal was usually necessary and, finally, a chloroform solution of the product was eluted through a short column of silicic acid. Samples of the product so obtained were analyzed by n.m.r. before purification of the components was attempted.

Halogenomethoxylations

The acetylated glycal (37 mmoles) was dissolved in 250 ml of dry methanol containing 8.76 g (52 mmoles) of silver acetate. The mixture was cooled to 0° and 52 mmoles of bromine or iodine was added over a period of 10 min with stirring. Chlorine was bubbled into the reaction mixture until a starch–iodide paper test on the effluent gases indicated an excess. After an additional 20 min, the silver salts were removed by filtration and washed with methanol. The filtrate was evaporated *in vacuo* to a residue which was taken up in chloroform. The chloroform solution was washed with aqueous sodium bicarbonate and sodium thiosulfate solutions, and dried by passage through chloroform-wetted filter paper. Evaporation then produced clear syrups or oils, usually in better than 90% yield, and in each case a portion of the material was reserved for n.m.r. analysis before isolation or characterization of the components was attempted.

Chlorination of D-Glucal Triacetate (I)

A 92% yield of a colorless syrup, $[\alpha]_D$ +152.7° (*c*, 1.64, in chloroform), of nearly pure tri-*O*-acetyl-2-chloro-2-deoxy-α-D-glucopyranosyl chloride (II) was obtained. The n.m.r. spectrum of the syrup (which resisted crystallization for over 1 year) recovered from an ether solution which had been left at room temperature for 1 week was the same as that of the freshly prepared material (Fig. 1). The crystalline product melted at 96–97°, $[\alpha]_D$ +218° (*c*, 2, in chloroform), in good agreement with the constants reported by Fischer *et al.* (17) for their crystalline "triacetyl glucal dichloride", m.p. 92–94°, $[\alpha]_D$ +173.6° (acetylene tetrachloride). A comparison of the spectra in Fig. 1 suggested that the chlorination gave II in 80–90% yield.

Can. J. Chem. Downloaded from www.nrcresearchpress.com by 210.87.254.105 on 09/05/12
For personal use only.

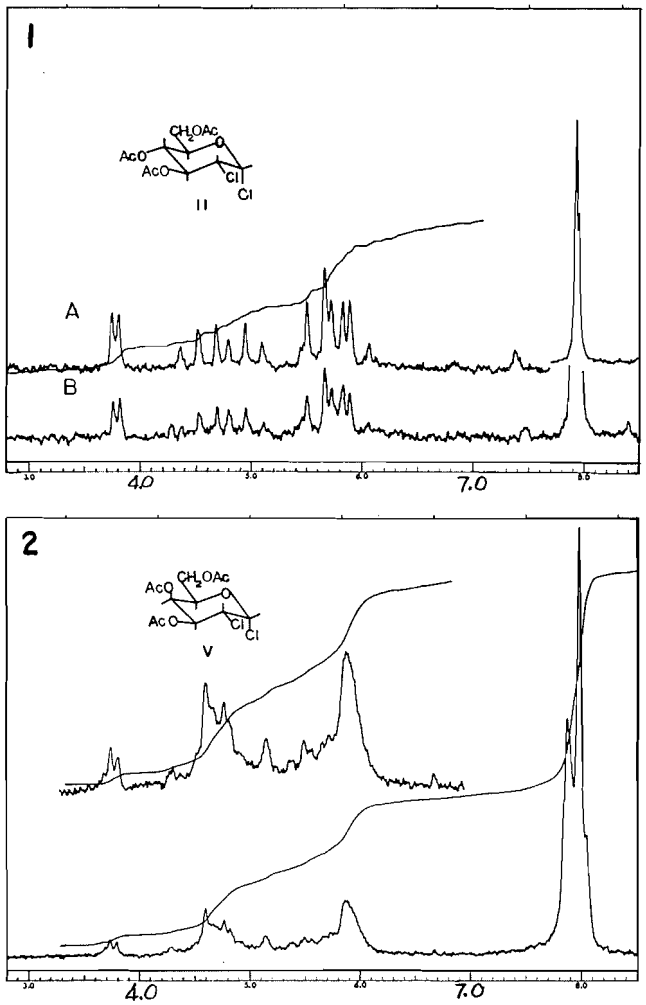

FIG. 1. The n.m.r. spectrum (B) at 60 Mc.p.s. of the product of the chlorination of D-glucal triacetate (I) in carbon tetrachloride. Spectrum A is that of pure tri-*O*-acetyl-2-chloro-2-deoxy-α-D-glucopyranosyl chloride (II).

FIG. 2. The n.m.r. spectrum at 60 Mc.p.s. of the product (V) of the chlorination of D-galactal triacetate (IV) in carbon tetrachloride.

Methyl 2-Chloro-2-deoxy-β-D-glucopyranoside Triacetate (III) (1)

Methanolysis of the syrupy dichloride (II) yielded a syrup in 86% yield. The n.m.r. spectrum indicated the formation of only one methyl glycoside. Crystalline material was readily deposited from ethanol and was characterized by mixed melting point determination with an authentic sample (1).

Reactions of D-Galactal Triacetate (IV)

(a) Chlorination.—A 96% yield of a colorless syrup which resisted crystallization was obtained, $[\alpha]_D$ +71.5° (*c*, 3.6, in chloroform). The n.m.r. spectrum (Fig. 2) required the product to be at least 80% pure tri-*O*-acetyl-2-chloro-2-deoxy-α-D-galactopyranosyl chloride (V).

Methanolysis of the dichloride (V) gave a near quantitative yield of a crystalline product, which was purified by recrystallization from ethanol, m.p. 127–129°, $[\alpha]_D$ +33.3° (*c*, 1.5, in chloroform).

Anal. Calcd. for $C_{13}H_{19}O_8Cl$: C, 46.15; H, 5.62. Found: C, 46.02; H, 5.38.

The n.m.r. spectrum of the compound (Fig. 3) required it to be methyl tri-*O*-acetyl-2-chloro-2-deoxy-β-D-galactopyranoside (VI). Deacetylation with 5% triethylamine in 50% aqueous methanol gave methyl 2-chloro-2-deoxy-β-D-galactopyranoside, m.p. 143.5–144.5°, $[\alpha]_D$ +11.0° (*c*, 1.06, in methanol).

Can. J. Chem. Downloaded from www.nrcresearchpress.com by 210.87.254.105 on 09/05/12
For personal use only.

Can. J. Chem. Downloaded from www.nrcresearchpress.com by 210.87.254.105 on 09/05/12
For personal use only.

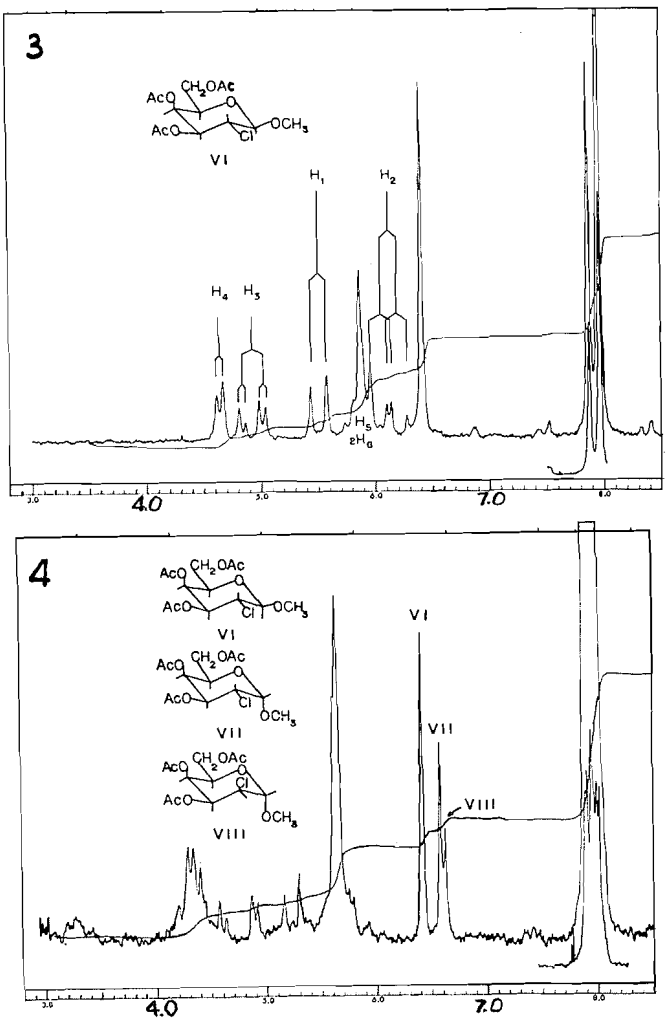

FIG. 3. The n.m.r. spectrum at 60 Mc.p.s. of methyl tri-*O*-acetyl-2-chloro-2-deoxy-β-D-galactopyranoside (VI) in chloroform.

FIG. 4. The n.m.r. spectrum in pyridine at 60 Mc.p.s. of the product of the chloromethoxylation of D-galactal triacetate.

(b) Chloromethoxylation.—The n.m.r. spectrum (Fig. 4) of the syrupy product indicated the presence of three methyl glycosides, in view of the signals for methoxy-group protons at τ 6.42, 6.58, and 6.62. The relative intensities of these signals were 53:39:8, respectively.

The syrup was dissolved in ethanol and, on standing overnight at 4°, the solution deposited 1.75 g (14% yield) of methyl tri-*O*-acetyl-2-chloro-2-deoxy-β-D-galactopyranoside (VI), identified by direct comparison.

The mother liquor from the above crystallization was evaporated to a syrup, 3.0 g of which was preparatively chromatographed on six 46 cm × 57 cm sheets of Whatman 3MM paper impregnated with dimethyl sulfoxide (18) and eluted with Skellysolve B for 7 h. Although separation was not complete, the fastest-moving zone provided 0.64 g of a syrup, the n.m.r. spectrum of which was devoid of methoxy-group signal at τ 6.42. When an ether – Skellysolve B solution of the material was refrigerated for several months, crystals were deposited, m.p. 86–88°, $[\alpha]_D$ +73.8° (*c*, 1.5, in chloroform).

Anal. Calcd. for $C_{13}H_{19}O_8Cl$: C, 46.15; H, 5.62. Found: C, 46.56; H, 5.65.

The n.m.r. spectrum of the compound showed absorption for the anomeric proton at τ 4.90 and methoxy-group protons at τ 6.58. The substance was methyl tri-*O*-acetyl-2-chloro-2-deoxy-α-D-galactopyranoside (VII), since these signals were present in the syrupy product obtained when the β-anomer was treated with

Can. J. Chem. Downloaded from www.nrcresearchpress.com by 210.87.254.105 on 09/05/12
For personal use only.

titanium tetrachloride in chloroform under the conditions previously described (1). The extent of anomerization achieved was 37%, based on the n.m.r. spectrum of the product.

Deacetylation of VII gave a crystalline product, methyl 2-chloro-2-deoxy-α-D-galactopyranoside, m.p. 145–147°, $[\alpha]_D$ +75.4° (*c*, 0.52, in methanol).

Examination of the syrupy residue from the isolation of VII by n.m.r. spectroscopy showed the substance to be a 1:1 mixture of VII and the methyl glycoside which produced the signal for methoxy-group protons at τ 6.62 in the original reaction product. The n.m.r. spectrum of the mixture in chloroform at 100 Mc.p.s. showed two doublet signals in the region characteristic for anomeric protons of methyl glycosides. The doublet at τ 4.90 with a spacing of 3.8 c.p.s. arose from VII. The doublet of equal intensity at τ 4.88 with a spacing of 1.1 c.p.s. must, therefore, have arisen either from methyl tri-*O*-acetyl-2-chloro-2-deoxy-α-D-talopyranoside (VIII) or the β-anomer. The α-configuration was assigned to this product of the chloromethoxylation in view of the position of the signal for the methoxy group and the high specific rotation of the syrup, +67.8° (*c*, 2.22, in chloroform). Since VII has a rotation of 73.8°, the other isomer in the 1:1 mixture must have a rotation of 61.8°. This rotation agrees well with that expected on the basis of the rotation of α-D-talopyranose pentaacetate, +70.2 (*c*, 4, in chloroform) (19). Also, the rotation agrees well with that reported below for methyl tri-*O*-acetyl-2-bromo-2-deoxy-α-D-talopyranoside (XI).

(c) Bromination.—An 88% yield of colorless syrupy product was obtained. Integration of the signals for anomeric protons in the n.m.r. spectrum of a solution in deuterochloroform at τ 3.20 and 3.46 with spacings of less than 1 and of 4.0 c.p.s., respectively, required the formation of two isomers in equal amounts. In view of the chemical shifts and spacings for these signals and the expectation that for both isomers the bromine at the 1-position is axially oriented, the compounds are assigned the α-D-*talo* (IX) and α-D-*galacto* (X) configurations, respectively.

Methanolysis of the mixture of dibromides gave a 90% yield of syrup which had signals for three different methoxy groups in the n.m.r. spectrum measured in chloroform solution at 100 Mc.p.s. The signals were at τ 6.39, 6.42, and 6.58 and their relative intensities were 23:50:27, respectively. A 3.0-g portion of the syrup was chromatographed on six 46 cm × 57 cm Whatman 3MM paper impregnated with dimethyl sulfoxide (18) and the chromatograms were developed with Skellysolve B for 7 h. Two overlapped zones were located by spraying side and center cuts with alkaline silver nitrate in the usual manner. The region of overlap was discarded and the remaining strips were extracted with chloroform. The chloroform solution was washed with water and percolated through a short column of silicic acid to remove dimethyl sulfoxide. Evaporation of the extract of the faster-moving zone gave a colorless syrup, $[\alpha]_D$ +65.6° (*c*, 1.8, in chloroform), which failed to crystallize. The n.m.r. spectrum shown in Fig. 5 requires the substance (XI) to be a virtually pure compound. A portion of the substance dissolved in a 10:9:1 mixture of methanol–water–triethylamine, respectively, and was hydrogenolyzed at room temperature and atmospheric pressure using 5% palladium-on-charcoal as catalyst. The product (XIV) resisted crystallization and was identified by paper chromatographic comparison with an authentic sample of methyl 2-deoxy-α-D-galactopyranoside prepared in the following manner. Crystalline methyl 4,6-*O*-benzylidene-2-deoxy-α-D-galactopyranoside, m.p. 177–178°, $[\alpha]_D$ +122° (*c*, 1.05, in chloroform), was prepared following the procedure described by Tamm and Reichstein (20). Hydrogenolysis in ethanol using 5% palladium-on-charcoal gave a syrup with the specific rotation, +69.5° in methanol, expected (21) for methyl 2-deoxy-α-D-galactopyranoside. The R_f value on Whatman No. 1 paper, using the *n*-butanol – water – ethanol (5:4:1) system, was 0.46. Treatment of D-galactal with 3% methanolic hydrogen chloride (21) gave a product with two components, the R_f values of which were 0.39 and 0.46. Hydrogenolysis of crystalline methyl 2-bromo-2-deoxy-β-D-galactopyranoside (XII), under the conditions described for the hydrogenolysis of XI, gave a product, methyl 2-deoxy-β-D-galactopyranoside, with a R_f value of 0.39. Therefore, compound XIV is methyl 2-deoxy-α-D-galactopyranoside.

The signal for the anomeric proton in the n.m.r. spectrum of XI (Fig. 5) has a spacing of 1.5 c.p.s. This spacing is incompatible with the α-*galacto* configuration, since a spacing of 3.5–4 c.p.s. is expected for this configuration. Furthermore, treatment of methyl tri-*O*-acetyl-2-bromo-2-deoxy-β-D-galactopyranoside (XII) with titanium tetrachloride in chloroform as previously described (1) gave rise to the α-anomer (XV) of XII, and this compound (XV) had the signal for its methoxy group at τ 6.54 in contrast to the position of τ 6.58 for the methoxy-group signal of XI. This small chemical shift was readily established by examining the compounds (XI and XV) together at 100 Mc.p.s. Therefore, compound XI is methyl tri-*O*-acetyl-2-bromo-2-deoxy-α-D-talopyranoside.

The slower-moving zone in the above-mentioned preparative paper chromatogram provided a syrup, 1.69 g, which deposited, from ethanol, 0.62 g of a crystalline compound. After two recrystallizations from ethanol, the melting point was 134–135°, $[\alpha]_D$ +33.2° (*c*, 1.37, in chloroform).

Anal. Calcd. for $C_{13}H_{19}O_8Br$: C, 40.73; H, 4.97. Found: C, 40.98; H, 4.88.

The n.m.r. spectrum of the compound in chloroform was completely first order at 100 Mc.p.s., and the signals for the 1-, 2-, 3-, and 4-protons were definitely assigned through double irradiation experiments. The coupling constants, $J_{1,2}$ = 8.5 c.p.s. and $J_{2,3}$ = 10.3 c.p.s., are consistent only with the structure of methyl tri-*O*-acetyl-2-bromo-2-deoxy-β-D-galactopyranoside (XII). The position of the methoxy-group signal was τ 6.42.

Hydrogenolysis, as described above, of the syrup in the mother liquor from the isolation of XII gave

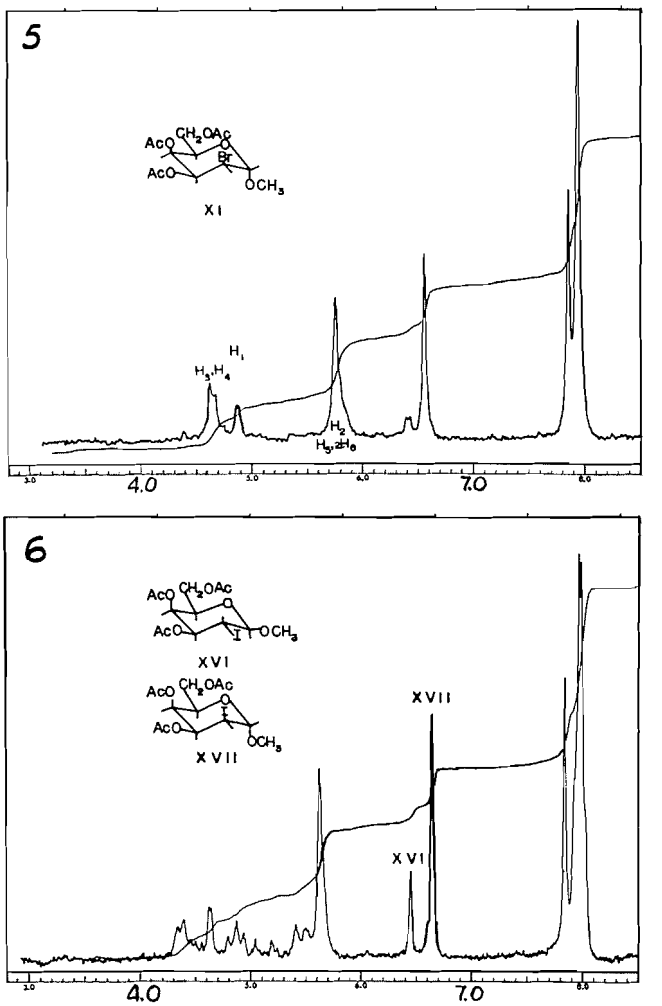

FIG. 5. The n.m.r. spectrum at 60 Mc.p.s. of syrupy methyl tri-*O*-acetyl-2-bromo-2-deoxy-α-D-talopyranoside (XI) in chloroform.

FIG. 6. The n.m.r. spectrum at 60 Mc.p.s. of a chloroform solution of the product formed on the iodomethoxylation of D-galactal triacetate (IV).

only methyl 2-deoxy-β-D-galactopyranoside, as judged by paper chromatographic examination of the product as described above. This observation, together with the chemical shift of the methoxy group, τ 6.39, for the third isomer formed in the methanolysis, requires the compound to be methyl tri-*O*-acetyl-2-bromo-2-deoxy-β-D-talopyranoside (XIII).

The assignments of the *talo* configuration to compounds XI and XIII agree with the abundance of these compounds expected in the product from the amount of IX in the dibromide mixture.

(d) Bromomethoxylation.—A 90% yield of a colorless syrupy product was obtained. The n.m.r. spectrum in chloroform solution, measured at 100 Mc.p.s., showed the presence of three methyl glycosides with the signals for the methoxy groups at τ 6.41, 6.54, and 6.58. The relative intensities were 37:11:52, respectively. It was concluded, therefore, that the product was a mixture of compounds XII, XV, and XI in the amounts indicated above, respectively. In agreement with this conclusion, deacetylation of the product for chromatography on a cellulose column (22) using *n*-butanol as irrigant followed by reacetylation of the fractions obtained provided pure samples of compounds XI and XII. Deacetylation of the product of the bromomethoxylation and paper chromatography using *n*-butanol – water – ethanol (5:4:1) (23) gave three spots with R_f values of 0.63, 0.83, and 0.89. The deacetylated forms of X and XI were shown to give spots with R_f values of 0.63 and 0.89. The deacetylated product of the titanium tetrachloride catalyzed anomerization

Can. J. Chem. Downloaded from www.nrcresearchpress.com by 210.87.254.105 on 09/05/12
For personal use only.

of XI gave spots with R_f values of 0.63 and 0.83. Thus, the assignments of structure based on the n.m.r. spectra were confirmed.

(e) Iodomethoxylation.—A quantitative yield of a syrupy product was obtained. The n.m.r. spectrum is shown in Fig. 6. The relative intensities of the methoxy-group signals at τ 6.42 and τ 6.75 established a 19:81 ratio for the two components in the product. The compounds were readily separated by preparative paper chromatography as described above using dimethylsulfoxide-impregnated Whatman 3MM paper. The well-separated zones were readily detected by exposure to ultraviolet light. Chromatography of 2.0 g of the reaction product gave 0.21 g of the slower-moving component and 0.97 g of the more mobile substance.

The minor component of the reaction mixture crystallized from ethanol and, after two recrystallizations from ethanol, melted at 125–126°, $[\alpha]_D$ +14° (*c*, 4.1, in chloroform).

Anal. Calcd. for $C_{13}H_{19}O_8I$: C, 36.28; H, 4.42. Found: C, 36.16; H, 4.54.

The n.m.r. spectrum of the compound in chloroform gave the signal for the anomeric proton at τ 5.40, spacing 8.5 c.p.s. The methoxy-group signal was at τ 6.42. The spectrum was very similar to that of the *β-galacto* bromide XII and was therefore assigned the structure of methyl tri-*O*-acetyl-2-deoxy-2-iodo-β-D-galactopyranoside (XVI). Deacetylation gave a syrup, $[\alpha]_D$ +34.6° (*c*, 0.47, in methanol), and hydrogenolysis in the usual manner gave methyl 2-deoxy-β-D-galactopyranoside.

The major component of the iodomethoxylation failed to crystallize. However, the n.m.r. spectrum shown in Fig. 7 required the syrup to be a pure compound, $[\alpha]_D$ +27.7° (*c*, 3.13, in chloroform). The n.m.r. spectrum at 100 Mc.p.s. was first order for the ring protons and provided the following parameters: H_1, τ 4.77, $J_{1,2}$ = 1.1 c.p.s.; H_2, τ 5.80, $J_{2,3}$ = 5.3 c.p.s.; H_3, τ 5.13, $J_{3,4}$ = 3.9 c.p.s.; H_4, τ 4.61, $J_{4,5}$ = 1.1 c.p.s.; CH_3O, τ 6.75. Deacetylation gave a syrup, $[\alpha]_D$ +57.0° (*c*, 2.4, in methanol), and hydrogenolysis provided methyl 2-deoxy-α-D-galactopyranoside In view of these data, the compound was assigned the structure of methyl tri-*O*-acetyl-2-deoxy-2-iodo-α-D-talopyranoside (XVII).

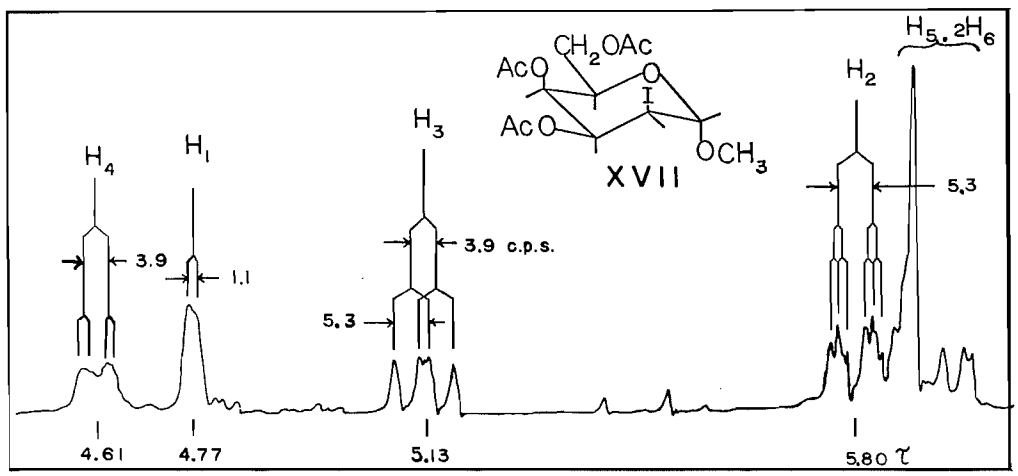

FIG. 7. The n.m.r. spectrum at 100 Mc.p.s. of syrupy methyl tri-*O*-acetyl-2-deoxy-2-iodo-α-D-talopyranoside (XVII).

Reactions of 3,4-Dihydropyran (XVIII)

(a) Chlorination (24, 25).—A product, b.p. 37° at 38 mm, n_D^{23} = 1.4935, was obtained in near quantitative yield. The n.m.r. spectrum is shown in Fig. 8A. The spectrum at 100 Mc.p.s. showed the signal at τ 3.97 to be a multiplet which could not have arisen from a single kind of anomeric proton. The product (5 g) was diluted with 5 ml of dry acetonitrile saturated with tetraethylammonium chloride. The material was isolated after 1.5 h. Prolonged treatment caused the appearance of a new signal at τ 3.4, probably as a result of dehydrochlorination. The n.m.r. spectrum of the product resulting from this treatment is shown in Fig. 8B. As expected, the structure of the signal for anomeric proton was changed, and the simpler spectrum suggested that the signal now closely represented a single kind of anomeric proton. It could therefore be concluded that the chlorination produced about equal amounts of the *cis* and *trans* adducts (XIX and XX). Both Crombie and Harper (24) and Paul (25) assumed that their preparations using ether as solvent contained only the *trans* isomer. When their preparations were repeated, it was found that the same mixture was formed as when carbon tetrachloride was the solvent. When a solution of 3,4-dihydropyran in carbon tetrachloride was saturated at 0° with chlorine and the mixture then kept at 78° for 4 h in a sealed tube (26), the product obtained was identical (n.m.r. spectra) with that resulting from the equilibration using

Can. J. Chem. Downloaded from www.nrcresearchpress.com by 210.87.254.105 on 09/05/12
For personal use only.

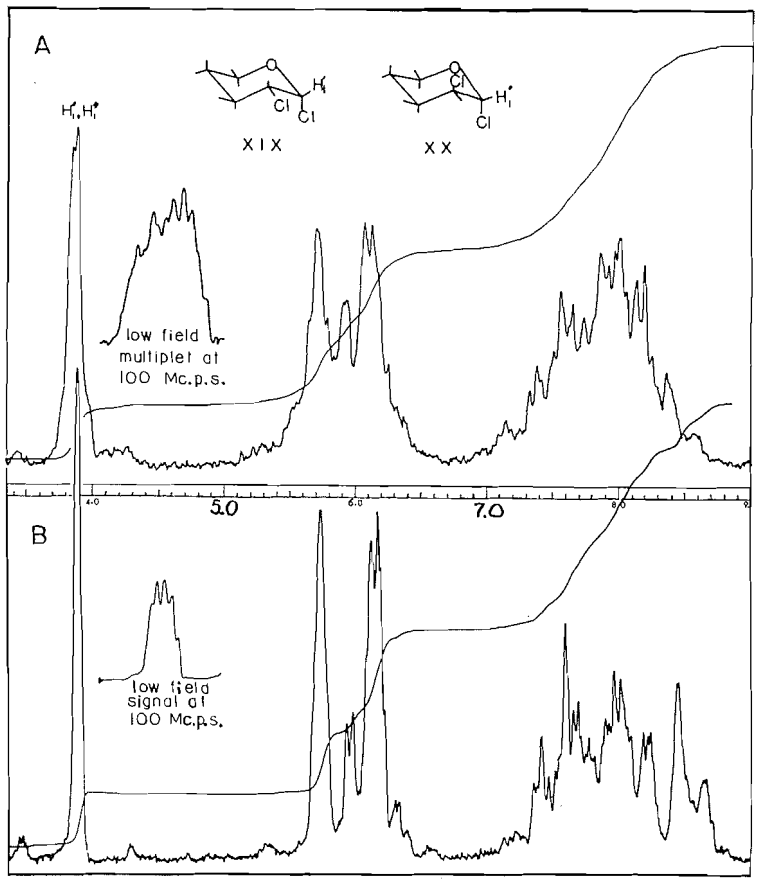

FIG. 8. The n.m.r. spectra of mixtures of the *cis* (XIX) and *trans* (XX) isomers for 2,3-dichlorotetrahydropyran. The 60 Mc.p.s. spectra were measured on the neat liquids. The 100 Mc.p.s. spectra were determined using solutions in deuterochloroform. A. The product formed on chlorination of 3,4-dihydropyran in carbon tetrachloride at 0°. B. The equilibrated mixture of compounds XIX and XX.

tetraethylammonium chloride. It should be noted that the rules for naming heterocyclic structures require that the anomeric proton in these derivatives of tetrahydropyran be designated the 2-proton.

Reaction of the product of the chlorination of 3,4-dihydropyran (XVIII) (25) with methanol gave a product with the n.m.r. spectrum shown in Fig. 9. The spectrum required the product to be a mixture of the *cis*- and *trans*-3-chloro-2-methoxytetrahydropyrans (XXI and XXII, respectively), and the relative intensities of the signals at τ 5.42 and 5.57, which must arise from anomeric 2-protons, required the isomers to be present in the same relative amounts (1:1) as the dichlorides in the starting material. It seemed probable, therefore, that both of the 2,3-dichlorides underwent methanolysis, with inversion or retention of configuration. In view of the routes followed in the methanolyses of compounds II and V, inversion was expected and was established by an examination of the route of the methanolysis of the mixture of dichlorides obtained in the anomerization reaction. That the predominant dichloride in this product possessed the 2,3-*trans* configuration (XX) was established by n.m.r. investigation of a chloroform solution at 100 Mc.p.s. with double irradiation to determine the magnitudes of the $J_{2,3}$, $J_{3,4}$, and $J_{3,4'}$ coupling constants. Irradiation at τ 1.67 upfield from the anomeric signal at τ 3.97 resulted in a collapse of the signal from a closely spaced quintet to a triplet. Therefore, the signal at τ 5.64 arose from the proton at the 3-position and the coupling constant was about 1.5 c.p.s. Therefore, H_2 and H_3 were in gauche relationship and, from the magnitude of the coupling constant, most likely (14) in the *trans*-diequatorial conformation. In view of the anomeric effect (12), the 2-hydrogen must be equatorial. That the 3-hydrogen is also equatorial was established by the magnitudes of $J_{3,4}$ and $J_{3,4'}$. Irradiation at both τ 1.57 and 1.97 upfield from the signal for the 3-proton at τ 5.64 caused collapse of the latter signal, and it could be concluded, therefore, that the signals for the 4-axial and 4'-equatorial protons were at τ 7.21 and 7.61, respectively. The changes in the structure of the

Can. J. Chem. Downloaded from www.nrcresearchpress.com by 210.87.254.105 on 09/05/12
For personal use only.

3-proton signal in these double irradiation experiments required both protons at the 4-position to be coupled to an extent of about 3.2 c.p.s. with the 3-proton. Therefore, the thermodynamically more stable 2,3-dichlorotetrahydropyran has the 1,2-*trans* configuration (XX) and prefers the conformation wherein both chlorines are axial.

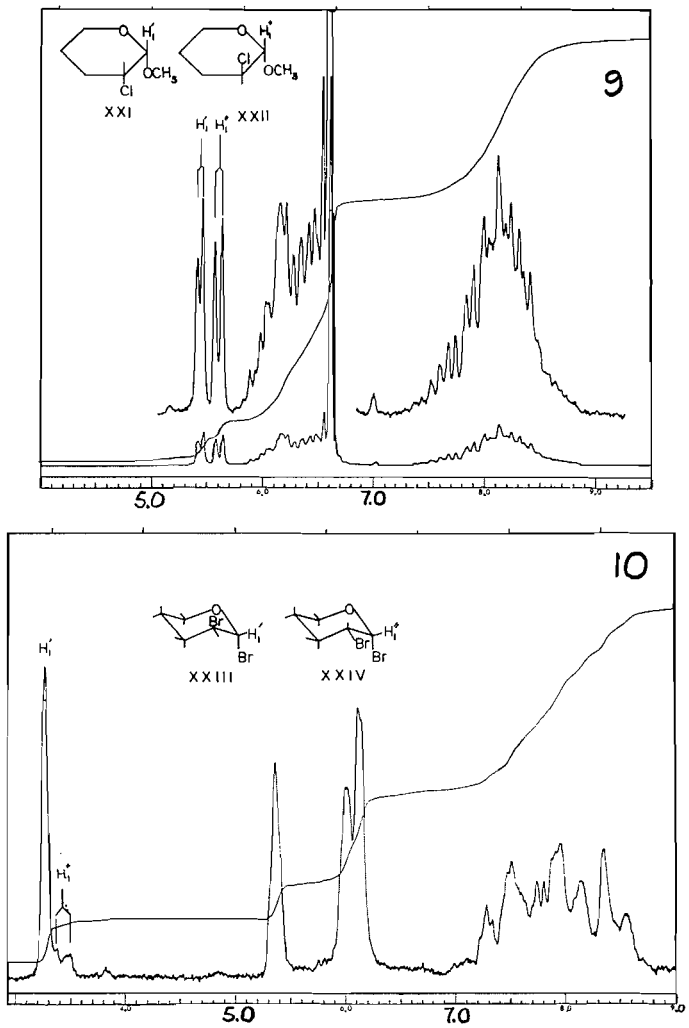

FIG. 9. The n.m.r. spectrum at 60 Mc.p.s. of the product (no solvent) formed on methanolysis of a 1:1 mixture of *cis*- and *trans*-2,3-dichlorotetrahydropyran (XIX and XX, respectively).

FIG. 10. The n.m.r. spectrum at 60 Mc.p.s. of the product (no solvent) formed on the bromination of 3,4-dihydropyran (XVIII).

Methanolysis of the equilibrated mixture of dichlorides gave a 7:3 mixture of the *cis* (XXI) and *trans* (XXII) isomers of 3-chloro-2-methoxytetrahydropyran, if one judges from the relative intensities of the signals for anomeric protons at τ 5.42 and 5.57 with spacings of 3.0 and 4.0 c.p.s., respectively. If one assumes inversion of the anomeric center in the methanolysis, the product would contain 70% of the *cis*-3-chloro-2-methoxytetrahydropyran (XXI), and the equilibrated mixture of dichlorides was therefore a 70% pure preparation of the 2,3-*trans* isomer (XX).

On this basis, the 2,3-*cis* protons are coupled to an extent of about 3.0 c.p.s. The larger coupling constant, 4.0 c.p.s., would then be associated with the 2,3-*trans* isomer and presumably arose from contributions by the compound in both the diaxial and diequatorial conformations. This conclusion is in agreement with the n.m.r. properties of the *trans*-3-bromo-2-methoxy (XXV) and *trans*-3-iodo-2-methoxy (XXVII) derivatives of tetrahydropyran to be described later on.

Can. J. Chem. Downloaded from www.nrcresearchpress.com by 210.87.254.105 on 09/05/12
For personal use only.

(b) Chloromethoxylation.—The reaction gave a 93% yield of a 1:3 mixture of the *cis* (XXI) and *trans* (XXII) isomers of 3-chloro-2-methoxytetrahydropyran, respectively, as indicated by the relative intensities of the methoxy-group signals in the n.m.r. spectrum.

(c) Bromination (27).—A quantitative yield was obtained of a product, b.p. 86° at 10 mm, $n_D^{23} = 1.4642$, with the n.m.r. spectrum shown in Fig. 10. The relative intensities of the signals for anomeric protons at τ 3.24 and 3.45 required the isomer with $J_{2,3}$ less than 1 c.p.s. to be formed in 89% yield. The structure of the rather sharp signal at τ 5.36 for the 3-proton of this isomer required that the 3-proton be weakly coupled with both protons at the 4-position. Therefore, the 3-proton is in equatorial orientation and, since the 2-proton is undoubtedly also in equatorial orientation (anomeric effect), the main product of the reaction was the 2,3-*trans* isomer (XXIII). The spacing of 3.0 c.p.s. for the signal of the anomeric proton of the second isomer is that expected for the 2,3-*cis* isomer (XXIV).

Methanolysis of the mixture of dibromides proceeded in 86% yield to a product, b.p. 161° at 723 mm, 78° at 10 mm; $n_D^{23} = 1.4841$. The relative intensities of the two signals for anomeric proton (Fig. 11) at τ 5.45 (spacing 2.7 c.p.s.) and τ 5.54 (spacing 3.9 c.p.s.) required the product to consist of a 2:3 mixture of the isomeric 3-bromo-2-methoxytetrahydropyrans. The n.m.r. spectrum of the mixture in acetonitrile saturated with tetra-*n*-butylammonium bromide showed spacings of 2.7 and 5.0 c.p.s. for the signals of the anomeric protons (see Fig. 11). The change in the spacing of the signal for the anomeric proton of the major component of the mixture required it to be the 2,3-*trans* isomer (XXIII). If one assumes that the 1,2-*cis*-dibromide (XXIV) reacted completely with inversion, it followed that the 1,2-*trans*-dibromide (XXIII) reacted to an extent of 50–60% with retention of configuration.

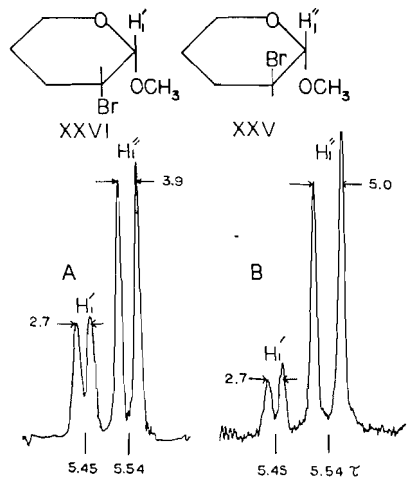

FIG. 11. The n.m.r. signals at 100 Mc.p.s. for the anomeric protons of the mixture of 3-bromo-2-methoxytetrahydropyrans formed on the methanolysis of a 9:1 mixture of the *trans* (XXIII) and *cis* (XXIV) 2,3-dibromotetrahydropyrans, respectively. A. In deuterochloroform. B. In acetonitrile saturated with tetra-*n*-butylammonium bromide.

(d) Bromomethoxylation.—A near-quantitative yield was obtained of an oily product with the physical constants reported above for the mixture of 3-bromo-2-methoxytetrahydropyrans. The n.m.r. spectrum of the mixture (100 Mc.p.s.) showed the presence of a 9:1 mixture of the *trans* (XXV) and *cis* isomers (XXVI), respectively.

(e) Iodomethoxylation.—A product which was distilled under vacuum, b.p. 84° at 9 mm, $n_D^{23} = 1.5177$, was obtained in 90% yield. The material contained a single component whose n.m.r. signal for the 2-hydrogen at τ 5.48 was a doublet with spacing 5.0 c.p.s. and, because of this spacing, it was judged to be *trans*-3-iodo-2-methoxytetrahydropyran (XXVII).

ACKNOWLEDGMENTS

The 60 Mc.p.s. nuclear magnetic resonance spectra were determined by R. M. Swindlehurst and Mrs. G. B. Conway, those at 100 Mc.p.s. by G. Bigam. The research was supported by National Research Council of Canada Studentships to B. F.-R., and National Research Council of Canada grants-in-aid of research (T-172) to R. U. L.

Can. J. Chem. Downloaded from www.nrcresearchpress.com by 210.87.254.105 on 09/05/12
For personal use only.

REFERENCES

1. R. U. LEMIEUX and B. FRASER-REID. Can. J. Chem. **42**, 532 (1964).
2. P. A. LEVENE and R. S. TIPSON. J. Biol. Chem. **93**, 631 (1931).
3. S. WINSTEIN, E. GRUNWALD, and L. INGRAHAM. J. Am. Chem. Soc. **70**, 821 (1948).
4. S. WINSTEIN, E. GRUNWALD, R. E. BUCKLES, and C. HANSON. J. Am. Chem. Soc. **70**, 816 (1948).
5. S. WINSTEIN and E. GRUNWALD. J. Am. Chem. Soc. **70**, 828, 841, 846 (1948).
6. E. GRUNWALD. J. Am. Chem. Soc. **73**, 5458 (1951).
7. P. B. D. DE LA MARE, P. G. NAYLOR, and D. L. H. WILLIAMS. J. Chem. Soc. 443 (1962); 3429 (1963).
8. I. ROBERTS and G. E. KIMBALL. J. Am. Chem. Soc. **59**, 947 (1937).
9. D. S. TARBELL and P. D. BARTLETT. J. Am. Chem. Soc. **59**, 407 (1937).
10. D. H. R. BARTON and R. C. COOKSON. Quart. Rev. London, **10**, 44 (1956).
11. A. J. RHIND-TUTT and C. A. VERNON. J. Chem. Soc. 4637 (1960).
12. R. U. LEMIEUX. *In* Molecular rearrangements. Part 2. *Edited by* Paul de Mayo. Interscience Publishers, Inc., New York. 1963. pp. 735–743.
13. R. U. LEMIEUX, T. L. NAGABHUSHAN, and I. K. O'NEILL. Tetrahedron Letters, No. 29, 1909 (1964).
14. R. U. LEMIEUX and J. W. LOWN. Can. J. Chem. **42**, 893 (1964).
15. R. U. LEMIEUX and S. LEVINE. Can. J. Chem. **42**, 1473 (1964).
16. W. KORYTNYK and J. A. MILLS. J. Chem. Soc. 636 (1959).
17. E. FISCHER, M. BERGMANN, and H. SCHOTTE. Ber. **53**, 509 (1920).
18. B. WICKBERG. Acta Chem. Scand. **12**, 615 (1958).
19. W. W. PIGMAN and H. S. ISBELL. J. Res. Natl. Bur. Std. **19**, 189 (1937).
20. C. TAMM and T. REICHSTEIN. Helv. Chim. Acta, **31**, 1630 (1948).
21. W. G. OVEREND, F. SHAFIZADEH, and M. STACEY. J. Chem. Soc. 671 (1950).
22. L. HOUGH, J. K. N. JONES, and W. H. WADMAN. J. Chem. Soc. 2511 (1949).
23. E. L. HIRST and J. K. N. JONES. Discussions Faraday Soc. **7**, 268 (1949).
24. L. CROMBIE and S. H. HARPER. J. Chem. Soc. 873 (1950).
25. R. PAUL. Compt. Rend. **218**, 122 (1944).
26. C. ALTONA, C. ROMERS, and E. HAVINGA. Tetrahedron Letters, No. 10, 16 (1959).
27. G. F. WOODS and H. SANDERS. J. Am. Chem. Soc. **68**, 2483 (1946).

Can. J. Chem. Downloaded from www.nrcresearchpress.com by 210.87.254.105 on 09/05/12
For personal use only.

Can. J. Chem. Downloaded from www.nrcresearchpress.com by 210.87.254.5 on 09/05/12
For personal use only.

EFFECT OF ELECTROLYTE ENVIRONMENT ON DIVALENT TARTRATE ION MOBILITY[1]

JAMES C. NICHOL, DUANE G. HEIKKINEN[2], AND GARY E. GLASS[3]
Department of Chemistry, University of Minnesota, Duluth, Minnesota
Received November 13, 1964

Dedicated to Professor R. B. Sandin on the Occasion of his Sixty-Eighth Birthday

ABSTRACT

The variation of the electrophoretic mobility, u_T, of divalent tartrate ion with changing electrolyte environment has been studied. Mobilities were determined from boundary velocity measurements at 1.00 °C in the Tiselius electrophoresis apparatus. The solutions used, which were adjusted to pH 8.3–8.5, were principally either 0.04667 *M* C_2T or 0.01 *M* C_2T – 0.11 *M* CA, where C^+, $T^=$, and A^- are, respectively, a univalent cation, divalent tartrate ion, and a univalent anion. Relative viscosities, η_{rel}, of a number of these solutions were also obtained. For a given anion environment, the variation of u_T with changing cation is characterized by a minimum at sodium and a maximum at tetramethylammonium for a series of six alkali metal and tetraalkylammonium ions. For the alkali metal cations and for tetrapropylammonium ion, u_T undergoes a distinct decrease when the solution is changed from 0.04667 *M* C_2T to 0.01 *M* C_2T – 0.11 *M* CCl. For all solutions containing an anion A^-, u_T decreases with increasing hydrocarbon content of A^- for a given cation. Possible ion association, obstruction, and ion–solvent interaction effects are considered.

INTRODUCTION

In Dole's development of the steady state moving boundary theory for strong electrolytes (1), it is assumed that the mobilities of the ions in solutions of electrolytes vary by the same proportional factor with change in composition, that is, the relative mobilities are constant. This assumption makes possible an elegant mathematical treatment for the general case of *n* ions. Only the relative mobilities appear in the equations, since the ion mobilities themselves always occur in the fundamental moving boundary relationship as ratios. Thus, the much poorer assumption of constant ion mobilities is avoided. The assumed constancy of relative mobilities is justified to the extent that the final results of a moving boundary experiment (boundary velocities and refractive index gradients), predicted from the initial conditions by the Dole theory, have been found to agree to within 1% or less of the observed values for uni-univalent electrolytes (2). Also, for simple systems involving weak electrolytes, the application of moving boundary theory, which includes the assumption that the relative mobilities of the ionic subspecies are constant, yields predictions in accord with observed results to within about 1% (3). Nevertheless, especially in experiments with strong electrolyte solutions containing more highly charged ions, pronounced mobility changes can occur. For example, we have observed (Table III) that the decrease of divalent tartrate ion mobility with increasing ionic strength varies markedly with the nature of the solutions in which it is measured. The value in 0.04667 *M* disodium tartrate is about 4% lower than that in 0.03333 *M* disodium tartrate, while in a mixture of 0.11 *M* sodium acetate and 0.01 *M* disodium tartrate, the decrease is about 13%, although the change in ionic strength, 0.04 units, is the same in both cases. These

[1]*This investigation was supported by Public Health Service Research Grant GM-10841 from the Division of General Medical Sciences, National Institutes of Health, and by Grants G16272 and G21720 from the National Science Foundation. Presented in part at the 147th National Meeting of the American Chemical Society, Philadelphia, Pa., April 1964.*
[2]*National Science Foundation Undergraduate Research Participant, 1962–1963.*
[3]*National Science Foundation Undergraduate Research Participant, 1961–1962.*

results led us to suspect a significant deviation of the relative mobility from constancy, a suspicion which was confirmed by the determination of the sodium ion mobility, u_{Na} in each of the three solutions, and the calculation of tartrate relative mobilities, r_T, therefrom on the basis of $r_{Na} = 1$ (Table III). That good agreement of moving boundary theory with experiment is obtained for such systems (4) may simply reflect an insensitivity of the predicted concentrations and boundary velocities to the values chosen for relative mobilities, rather than constancy of the latter.

To obtain an idea of how general such pronounced effects of electrolyte environment upon mobility might be, a survey of the mobility of divalent tartrate ion in a variety of electrolyte solutions was undertaken, using the Tiselius free electrophoresis method. The presentation and discussion of the results of this study is the objective of this paper. To avoid complications arising from variations in concentration and charge type, most of the experiments were performed using either 0.04667 M C_2T (in transference number type experiments, with an appropriate indicator electrolyte), or 0.01 M C_2T plus 0.11 M CA (analogous to the electrophoresis of a single protein in a buffer), where C^+, $T^=$, and A^- are, respectively, a univalent cation, divalent tartrate ion, and a univalent anion. (See experimental section for details.) In many cases, electrolyte viscosities were also determined. The determination of mobilities in a study of electrolyte behavior has the obvious advantage of singling out a property of the individual ion, rather than obtaining measurements on the solution as a whole, as in the case of conductance or viscosity determinations alone.

The Tiselius instrument, despite its limitations of accuracy (in comparison with the conventional moving boundary apparatus for transference number determinations) and of concentration range, is well suited for a survey of the type undertaken here, in which the variations being studied are large, and in which solutions containing more than one electrolyte are used. It possesses the advantage of recording accurately, both with schlieren and Rayleigh interference fringe optical systems, the diffuse boundaries frequently observed. Small convective effects, which would render a particular experimental arrangement unsatisfactory, are detected readily, and there is considerable flexibility in redesigning the experiment to produce a stable system. The sources of error and the reproducibility and accuracy of the mobility measurements are discussed in detail in the following section.

EXPERIMENTAL

All moving boundary experiments were performed at 1.00 °C with a Spinco Model H electrophoresis apparatus. Mobilities were calculated using the equation $u_T = Al\kappa/it$, where u_T is the electrophoretic mobility of divalent tartrate ion in a solution of specific conductance κ, A is the cross-sectional area of the cell limb, and l is the distance moved by the boundary with respect to the cell in time t if the electric current is i. One limb only of an 11 ml quartz Tiselius cell, equipped with reference paths, was used for all experiments. The mean cross-sectional area of the limb was 0.7654 ± 0.0002 cm², this value being determined from measurements at 5 mm intervals using a Gaertner Model M2001P comparator. The magnification factor from cell to photographic plate was 1.0000 ± 0.0007. Simultaneous schlieren (Wolter phase plate) and Rayleigh integral fringe photographs were taken at about 30 min intervals on Kodak metallographic plates. Exposures were of 15 s duration, as timed with a calibrated stopwatch. The overall error in the time intervals was estimated to be ±0.02%. Boundary displacements, l, were usually determined from the schlieren patterns as described previously (3). In some experiments, the change in field strength across the boundary was slight, so that the latter was very diffuse and failed to attain a steady state in the time required for it to move the length of the cell. In such cases, corrected fringe displacements from the Rayleigh integral fringe photographs were used (3). In all determinations, the gradients were sufficiently symmetrical that the maximum ordinate could be considered to establish the boundary position without significant error (5). Boundary velocities calculated in this manner from the five or six successive displacements which were photographed in each experiment were observed to be constant. Furthermore, in two instances, the velocities calculated from the displacements of the first moment axis were determined and found to be identical with those obtained using the maximum ordinate. The current source was one of the power supplies provided with the instrument.

Can. J. Chem. Downloaded from www.nrcresearchpress.com by 210.87.254.5 on 09/05/12
For personal use only.

Can. J. Chem. Downloaded from www.nrcresearchpress.com by 210.87.254.5 on 09/05/12
For personal use only.

The current was adjusted from run to run to give a field strength of 2 to 3 V cm^{-1}, and ranged from 4 to 10 mA. (A few test runs at as high as 16 mA and 5 V cm^{-1} yielded mobilities within the limits of reproducibility of those obtained at the lower field strengths.) Several checks on the current were made during every run by measuring the voltage drop across a calibrated 100 Ω resistance with a Rubicon Model 2780 potentiometer. When the power supply was operating properly the current was found to stay constant to within ±0.03%. Only experiments for which the electrical leakage from bath to cell was less than 0.05% of the total current at the start and finish were used for mobility determinations. It was observed that the leak remained at or below this value if not more than one experiment was done per day, and if the cell sections were rinsed thoroughly with absolute ethanol after the regular cleanup.

Solutions were prepared either from reagent grade salts or by neutralization of the acids with carbon dioxide free base. All solutions, including both leading and indicator electrolytes, were adjusted to pH 8.3–8.5, in order that hydrogen tartrate ion should not be present or formed in significant concentration. The pH values of the leading and following solutions were checked at the end of several moving boundary experiments, and were found to agree with the original values to within 0.1–0.2 pH units in all cases. Since pK_2 for tartaric acid has been determined to be 4.1 at 1.00 °C and 0.1 ionic strength (4), it is evident that an insignificant amount of hydrogen tartrate ion would be present. All mobility experiments were performed at least in duplicate, with fresh solutions being used for each run. For each system, preliminary experiments were carried out in order to establish that the proposed arrangement was stable, and to ensure that the initial following solution was within about 5% of the adjusted indicator concentration behind the boundary (6, 7), with the experiment designed so that the solution of lower density was on top. The initial boundary was compensated into view in these trial runs. Boundaries were ascending or descending, as density considerations dictated. The indicator electrolytes for transference number type experiments (all descending) were the acetate salts of the cations concerned (i.e. COAc). In experiments with Li^+, Na^+, K^+, TMA^+, and TEA^+ (see Fig. 1 for definitions of symbols), for which the COAc densities increase with increasing concentration, the proper initial COAc concentrations were found to lie in the range 0.072–0.075 *M* (i.e., about 5% lower than those of the adjusted COAc solutions generated immediately above the descending tartrate boundaries in the course of the experiments). Since the density of TPAOAc decreases with increasing concentration, a top solution concentration of 0.085 *M* (a few percent *higher* than the adjusted TPAOAc solution) was used. For the experiments analogous to the electrophoresis of a single protein in a buffer, the tartrate boundaries were descending except in those cases for which the "buffers" were the chlorides of Li^+, Na^+, K^+, TMA^+, and TEA^+ and the iodate of Na^+. The top solutions in the descending boundary experiments consisted of the "buffer" salts in the concentration range 0.11–0.12 *M*, except for TPACl (0.140 *M*) and TPAOAc (0.135 *M*), which again for density reasons had to have a higher concentration than that of the adjusted solution, and except for the sodium iodide and sodium bromate experiments. In these, to prevent density inversions, it was found necessary to use 0.1370 *M* NaI and 0.1367 *M* $NaBrO_3$ as leading solutions, behind which were generated 0.01 *M* Na_2T – 0.11 *M* NaI and 0.01 *M* Na_2T – 0.11 *M* $NaBrO_3$, respectively. The initial top solutions were 0.0095 *M* Na_2T – 0.1045 *M* NaI and 0.00996 *M* Na_2T – 0.1096 *M* $NaBrO_3$. In these experiments, the moving boundary was allowed to migrate completely out of the cell center section, in order to make possible the isolation and removal of the adjusted phases for conductance measurements needed in calculating mobilities. A similar procedure, with similar ranges of concentration to the above, was found necessary in all the ascending boundary experiments except for the one involving iodate, in which the leading (top) solution required for conductance was the original solution. For the sodium ion mobilities of Table III, lithium ion was used as the following ion in descending boundary experiments, while the mobility of acetate ion was obtained in a 0.11 *M* NaOAc – 0.01 *M* Na_2T solution generated behind 0.076 *M* Na_2T in a descending experiment.

Electrode volume corrections were made in the usual manner (6). Partial molal volumes for solutions appearing between the moving boundary and closed electrode were calculated from density measurements using Weld pycnometers, where literature values were unavailable. Bearman (8) has pointed out that if appreciable volume changes occur at the liquid junctions the electrode volume correction is suspect. A consideration of the known partial molal volume data for the electrolytes involved in the various junctions indicated that such effects were not significant in the present experiments. Furthermore, substitution of tetramethylammonium chloride for sodium chloride as the electrode electrolyte in some runs did not affect the corrected mobility values.

Conductances were measured at 0 °C, using a Jones conductance bridge and a cell of the Jones and Bollinger type. Hence, the computed mobility is the value at 0 °C, rather than 1 °C, if the transference number of the ion does not change significantly with the change in temperature (9). The best transference data available indicate that this is true to within 0.1% or better at low concentrations of simple salts (10). The reproducibility of the mobilities calculated from the several photographs taken during a single run averaged ±0.05%. However, the average agreement of values from separate identical runs was ±0.13%, which is slightly larger than the maximum error calculated from the error estimates in the individual quantities. This probably reflects the difficulty in performing experiments reproducibly, particularly as regards greasing of the rather large cell and standard taper surfaces.

Relative viscosities, η_{rel}, were determined in duplicate at 0.30 °C, using Ostwald viscometers for which the flow times were about 200 s, and for which the constants were determined in the usual manner. It was found

possible to maintain this temperature conveniently over an extended period by vigorous stirring of crushed ice and water in a large glass container. Values of η_{rel} determined with separate viscometers were found to agree to within $\pm 0.17\%$. As in the case of the transference number, an examination of the temperature dependence of η_{rel} of electrolyte solutions indicated that it should undergo no significant change between 0 °C and the bath temperature.

RESULTS AND DISCUSSION

In Table I are listed all the divalent tartrate ion mobilities, u_T, obtained in solutions of 0.04667 *M* C_2T and of 0.01 *M* C_2T plus 0.11 *M* CA. (It should be noted that the ionic strength is always 0.14, but that the cation concentration is 0.09334 *M* in the former type of solution and 0.13 *M* in the latter.) Also included are relative viscosity values, η_{rel}, and the corresponding mobility–viscosity products, $u_T\eta_{rel}$. A number of η_{rel} values for 0.11 *M* CA solutions (the "solvent") are included which show that for the most part omission of C_2T (at least at 0.01 *M* concentration) has only a small effect upon η_{rel}. In Fig. 1 the mobilities of Table I are plotted in order to show clearly the variation of u_T with changing

TABLE I

Principal mobility and viscosity data

Solution type		$-u_T \times 10^5$ ($cm^2\ s^{-1}\ V^{-1}$)	η_{rel}	$-u_T\eta_{rel} \times 10^5$ ($cm^2\ s^{-1}\ V^{-1}$)	η_{rel} (0.11 *M* CCl)	η_{rel} (0.11 *M* NaX)
Cation, C^+						
0.04667 *M* C_2T*	Li^+	21.47	1.030	22.12		
	Na^+	21.34	1.018	21.71		
	K^+	21.69	1.002	21.72		
	TMA^+	22.42	1.020	22.87		
	TEA^+	21.99				
	TPA^+	21.41				
Cation, C^+						
0.01 *M* C_2T	Li^+	20.85	1.013	21.12	1.019	
+	Na	20.26	0.997	20.20	1.002	
0.11 *M* CCl	K^+	20.86	0.990	20.65	0.990	
	TMA^+	22.43	1.020	22.88	1.013	
	TEA^+	22.04	1.071	23.61	1.064	
	TPA^+	20.91	1.172	24.51	1.141	
Cation, C^+						
0.01 *M* C_2T	Li^+	19.42	1.054	20.46		
+	Na^+	19.29	1.042	20.10		
0.11 *M* COAc	K^+	20.32	1.024	20.80		
	TMA^+	21.19				
	TEA^+	20.38				
	TPA^+	19.59				
Anion, X^-						
0.01 *M* NA_2T	I^-	20.43				
+	Cl^-	20.26	0.997	20.20		1.002
0.11 *M* NaX	BrO_3^-	20.26				
	IO_3^-	20.20				
	$Form^-$	19.75	1.021	20.16		1.016
	OAc^-	19.29	1.042	20.10		1.038
	$Prop^-$	19.11	1.058	20.22		1.052
	But^-	18.76	1.070	20.07		1.069
	$Glyc^-$	19.55	1.033	20.19		1.028

*See legend of Fig. 1 for description of symbols.

electrolyte environment. Consideration was given to plotting the mobility as a function of the ionic radius of the cation. However, since the significance of the crystal radius as a factor directly affecting the mobility in aqueous solution is not clear, and since reported values for hydrated radii vary so widely that their relative magnitudes change depending on which ones are chosen, it was decided simply to space the mobilities corresponding to solutions of the various cations at equal distances in order of increasing cation formula

Can. J. Chem. Downloaded from www.nrcresearchpress.com by 210.87.254.5 on 09/05/12
For personal use only.

weight. This also turns out to be the order of increasing crystal radii for the cations we have used (11). No particular significance is to be attached to the three sets of lines joining the points. They are intended to serve as an aid in distinguishing mobility trends for the three main types of solutions.

Several distinct trends are apparent upon inspection of Tables I and II and Fig. 1.

TABLE II

Effect of concentration on divalent tartrate ion mobility

C_2T concentration (mole l^{-1})	Ionic strength	$-u_T \times 10^5$ ($cm^2\ s^{-1}\ V^{-1}$)		
		$C^+ = Li^+$	$C^+ = Na^+$	$C^+ = K^+$
0.02334	0.07	23.26	23.18	23.35
0.04667	0.14	21.47	21.34	21.69
0.07	0.21	20.17	19.78	20.37

1. For a *constant* anion environment, the qualitative variation of u_T with changing cation is the same regardless of whether the solution contains only tartrate ion, a mixture of tartrate and chloride ions, or a mixture of tartrate and acetate ions (connected points in Fig. 1). In each case, there is a minimum value for u_T when the cation is sodium. Furthermore, for solutions containing only tartrate ion, the minimum becomes more pronounced with increasing concentration (Table II). This is in contrast to the frequently observed steady progression of a physical property with atomic weight and radius in the alkali metal series. The values of η_{rel}, on the other hand, decrease regularly from lithium to potassium. Also, in each case the highest mobility of u_T is observed when the cation is tetramethylammonium, and there is a steady drop in u_T with increasing size of the tetraalkylammonium ion. It will be observed in Table I that the increase in η_{rel} more than offsets the decrease in u_T in the tetraalkylammonium series, so that $u_T\eta_{rel}$ rises with increasing size of the tetraalkylammonium ions, and that the $u_T\eta_{rel}$ values as a group are distinctly higher than those for the alkali metal ions.

2. *Change* of the anion environment in the sequence pure tartrate, tartrate–chloride, tartrate–acetate results in significant variations in u_T (Fig. 1). In the case of the alkali metal cations, u_T decreases regularly in the order tartrate > tartrate–chloride > tartrate–acetate. For tetramethylammonium and tetraethylammonium ions the u_T values are essentially the same in pure tartrate and in tartrate–chloride, while for tetrapropylammonium u_T is somewhat lower in tartrate–chloride. For all three tetraalkylammonium cations, u_T is much lower in tartrate–acetate than in the other two anion environments.

3. In C_2T–CA solutions in which sodium is the cation, the nature of the anion, A^-, has a pronounced effect (Fig. 1). The tartrate mobilities in solutions containing iodide, bromate, chloride, and iodate comprise a fairly compact group, while those in the series of solutions containing formate, acetate, propionate, and butyrate decrease regularly with increasing size of the anion. Introduction of a hydroxyl group, by substitution of glycolate for acetate ion, results in an increase in u_T. The constancy of $u_T\eta_{rel}$ in the fatty acid anion series of solutions (Table I) is in marked contrast to its steady increase with increasing size of the tetraalkylammonium cations, in solutions of constant anion (tartrate–chloride) environment.

In attempting to account for these observations, we are faced with the problem of sorting out a variety of influences which may simultaneously affect the behavior of the tartrate ion. The situation is very complex, since the ion is present in electrolyte solutions, the

Can. J. Chem. Downloaded from www.nrcresearchpress.com by 210.87.254.5 on 09/05/12
For personal use only.

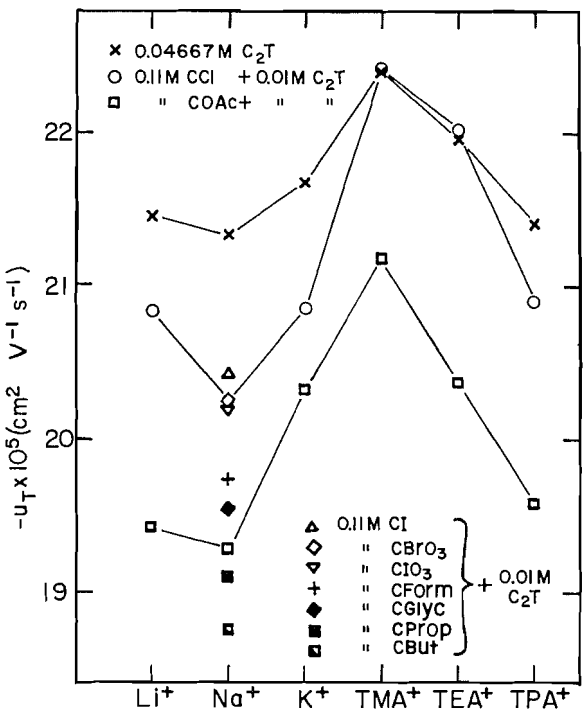

FIG. 1. Effect of ionic environment upon the mobility, u_T, of divalent tartrate ion. Symbols: $T^=$, divalent tartrate; C^+, univalent cation shown on abscissa; $Form^-$, formate; OAc^-, acetate; $Prop^-$, propionate; But^-, butyrate; $Glyc^-$, glycolate; TMA^+, TEA^+, and TPA^+, tetramethylammonium, tetraethylammonium, and tetrapropylammonium, respectively. The other symbols have their usual chemical significance.

total concentrations of which are far from infinite dilution. Therefore, the most we can hope to do is to point out some of the factors which may be involved in establishing the major trends. Among the possibilities which appear to be worth considering are ion association and the effect of the properties of the other ions present, such as size and tendency to interact with the solvent, on the forces impeding the movement of the tartrate ion.

Results reported by a number of workers indicate that the alkali metal cations form weak complexes, CT^-, with tartrate (12) and with related ions such as malate (13, 14). In the present experiments, if the concentrations of cations and tartrate should change in such a way as to increase the extent of association, then u_T would drop, since it would be a constituent mobility, related to the ion mobilities $u_{T^=}$ and u_{CT^-} and to the molar concentrations $c_{T^=}$ and c_{CT^-} by the equation

$$u_T = \frac{u_{T^=}c_{T^=} + u_{CT^-}c_{CT^-}}{c_{T^=} + c_{CT^-}} .$$

This may explain in part the decrease in u_T in going from pure tartrate to tartrate–chloride solutions of the alkali metal cations. The metal ion concentration increases from 0.09334 M to 0.13 M, while that of the tartrate ion decreases from 0.04667 M to 0.01 M. For the sodium ion, Wu and Hsu (12) report an association constant of 3.66 at 25 °C and 0.2 ionic strength. If calculations are carried out on the assumption that K_{assoc} lies somewhere between 2 and 6 under the conditions existing in our experiments, a decrease of from 3 to 6% in u_T is obtained for the concentration change under consideration. The

Can. J. Chem. Downloaded from www.nrcresearchpress.com by 210.87.254.5 on 09/05/12
For personal use only.

observed drop for the sodium ion case is about 7%. It will be noted that there is very little change in u_T in going from pure tartrate to tartrate–chloride when the cation is tetramethylammonium or tetraethylammonium. This would be reasonable on the basis that if ion association is playing a role, its effect should be significantly less for the large tetraalkylammonium ions with their low charge density, than for the alkali metal ions used in this study. However, the decrease of u_T in the tetrapropylammonium case is almost as great as that when lithium is the cation. Therefore, an explanation of the above mobility changes based only upon the one effect is undoubtedly an oversimplification.

TABLE III

Mobilities and relative mobilities in various solutions

Concentration (mole l^{-1})		Ionic strength	Mobility $\times 10^5$ ($cm^2\ s^{-1}\ V^{-1}$)			Relative mobility		
Na_2T	NaOAc		u_{Na}	$-u_T$	$-u_{OAc}$	r_{Na}	$-r_T$	$-r_{OAc}$
0.03333	0	0.10	20.25	22.22		1	1.093	
0.00714	0.0785	0.10		20.41				
0.04667	0	0.14	19.24	21.34		1	1.109	
0.03	0.05	0.14		20.08				
0.01	0.11	0.14	20.80	19.29	16.44	1	0.928	0.791

With regard to effects arising from variations in ion size and ion–solvent interactions, the regular decrease of u_T with increasing amount of the hydrocarbon portion of the ions of both the fatty acid anion series and the three tetraalkylammonium cation series appears to be significant. Only a rough connection between mobility, as measured by conductance or diffusion, and the bulk viscosity can be expected, since the viscosity measured by capillary flow can be considered as the resultant of strongly varying local viscous effects (15). Nevertheless, the fact that η_{rel} rises as u_T decreases in all experiments for which data were obtained in the above series, suggests that at least there is an effect on the mobility connected with the change in viscosity. Robinson and Stokes have suggested that, where large increases in bulk viscosity occur in solutions containing big, approximately spherical ions (large viscosity B-coefficients in the Jones and Dole equation (16)), they are mainly the result of the distortion of the stream-lines (17). The ions are considered to behave hydrodynamically as though they were rigid spherical obstructions. Robinson and Stokes also draw attention to and elaborate on Wang's suggestion (18) that the increased viscosity and decreased conductance represent two parallel effects of a common cause, the obstructive action of the solute. These effects are considered to be the distortion of the stream-lines by the solute molecules or ions in viscous flow and the lengthening of the effective paths of the moving particles in conductance and diffusion. This picture accounts qualitatively for the above results on the basis that the obstructive effect increases regularly with ion size, and that the tetraalkylammonium and fatty acid ions approximate spheres, However, ion–solvent interactions, such as the postulated tightening or immobilization of the surrounding water structure by tetraalkylammonium cations and fatty acid anions (19, 20, 21), may also play a role, and it is impossible on the basis of the present experiments to distinguish between the two effects. The same uncertainties are involved in attempting to account for the consistently and distinctly higher u_T values and the lower η_{rel} values in chloride–tartrate solutions as compared to acetate–tartrate (Fig. 1). The chloride ion is both smaller than acetate and, like iodide, bromate, and iodate (in the solutions of which the u_T values are about the same), is considered to be a structure

Can. J. Chem. Downloaded from www.nrcresearchpress.com by 210.87.254.5 on 09/05/12
For personal use only.

breaker (22). The increase in u_T and decrease in η_{rel} when glycolate is substituted for acetate recalls a solvent structure effect discussed by Frank (23) in connection with the viscosity and apparent molal heat capacity of tetraethanolammonium bromide. He regards introduction of the hydroxyl group as making the ion more water-like, so that the surrounding water is more nearly able to retain its normal, less rigid structure.

It is difficult to say whether the constancy of the $u_T\eta_{rel}$ products for the fatty acid anion series and the steady increase for the tetraalkylammonium series has any special significance. For large ions in water–sucrose mixtures, constancy is approached (24), but tartrate is not very large compared to the fatty acid anions used, and there is the added complication of the medium being an electrolyte solution. Somewhat comparable data are provided by tracer-diffusion coefficient determinations of iodide ion in aqueous alkali chloride solutions (25). At concentrations of about 0.1 M the $D\eta_{rel}$ values are much more nearly equal to one another than the D-values themselves, but, at higher concentrations, multiplication by η_{rel} overcorrects badly.

The occurrence of a minimum in u_T at sodium ion for the series in which the cation is varied again probably reflects a combination of factors such as those discussed above, rather than any single effect. Since the minimum is observed in three different types of anion environment, it would appear to be definitely related to the specific nature of the cations.

ACKNOWLEDGMENTS

The authors gratefully acknowledge helpful discussions with Dr. L. C. Thompson, and the assistance of Mrs. G. Stromme and Mr. S. Ji in carrying out a number of the experiments.

REFERENCES

1. V. P. Dole. J. Am. Chem. Soc. **67**, 1119 (1945).
2. L. G. Longsworth. J. Am. Chem. Soc. **67**, 1109 (1945).
3. J. C. Nichol, E. B. Dismukes, and R. A. Alberty. J. Am. Chem. Soc. **80**, 2610 (1958).
4. L. B. Friedman and J. C. Nichol. J. Phys. Chem. **67**, 1716 (1963).
5. L. G. Longsworth. J. Am. Chem. Soc. **65**, 1755 (1943).
6. D. A. McInnes. The principles of electrochemistry. Reinhold Publishing Corp., New York. 1939. pp. 80 ff.
7. A. R. Gordon and R. L. Kay. J. Chem. Phys. **21**, 131 (1953).
8. R. J. Bearman. J. Chem. Phys. **36**, 2432 (1962).
9. L. G. Longsworth. *In* Electrophoresis. *Edited by* M. Bier. Academic Press, Inc. 1959. p. 160.
10. H. S. Harned and B. B. Owen. The physical chemistry of electrolytic solutions. 3rd ed. Reinhold Publishing Corp., New York. 1958. pp. 233 ff.
11. R. A. Robinson and R. H. Stokes. Electrolyte solutions. Butterworth Scientific Publications, London. 1959. pp. 125 and 461.
12. C. K. Wu and K. H. Hsu. Hua Hsueh Hsueh Pao, **29**, 173 (1963); Chem. Abstr. **59**, 9388*f* (1963).
13. L. E. Erickson and J. A. Denbo. J. Phys. Chem. **67**, 707 (1963).
14. G. A. Rechnitz and S. B. Zamochnik. Talanta, **11**, 1061 (1964).
15. S. Broersma. J. Chem. Phys. **24**, 659 (1956).
16. G. Jones and M. Dole. J. Am. Chem. Soc. **51**, 2950 (1929).
17. R. A. Robinson and R. H. Stokes. Electrolyte solutions. Butterworth Scientific Publications, London. 1959. p. 307.
18. J. H. Wang. J. Am. Chem. Soc. **76**, 4755 (1954).
19. R. M. Diamond. J. Phys. Chem. **67**, 2513 (1963).
20. W. Y. Wen and S. Saito. J. Phys. Chem. **68**, 2639 (1964).
21. S. S. Danyluk and E. S. Gore. Nature, **203**, 748 (1964).
22. J. L. Kavanau. Water and solute–water interactions. Holden-Day, Inc., San Francisco. 1964. p. 59.
23. H. S. Frank. Reprint of paper presented at the International Symposium on Solvation Phenomena, Calgary, Alberta. August, 1963. p. 6.
24. B. J. Steel, J. M. Stokes, and R. H. Stokes. J. Phys. Chem. **62**, 1514 (1958).
25. R. H. Stokes, L. A. Woolf, and R. Mills. J. Phys. Chem. **61**, 1634 (1957).

Can. J. Chem. Downloaded from www.nrcresearchpress.com by 210.87.254.5 on 09/05/12
For personal use only.

Can. J. Chem. Downloaded from www.nrcresearchpress.com by 210.87.254.6 on 09/05/12
For personal use only.

THE RADIOLYSIS OF ETHANOL

IV. DEUTERATED ETHANOLS IN THE LIQUID AND GAS PHASES

J. J. J. Myron and G. R. Freeman
Chemistry Department, University of Alberta, Edmonton, Alberta

Received November 13, 1964

Dedicated to Professor R. B. Sandin on the Occasion of his Sixty-Eighth Birthday

ABSTRACT

The value of $G(-\text{ethanol})$ in the vapor phase is nearly double that in the liquid phase. Part of the difference appears to be due to the recombination of radicals in liquid cages. Ethanol molecules, on the average, break into smaller fragments in the gas than in the liquid phase radiolysis. The isotopic compositions of the hydrogen produced from various deuterated ethanols are consistent with the suggestion that the reaction

$$CH_3CH_2OH^+ + CH_3CH_2OH \rightarrow CH_3CH_2OH_2^+ + CH_3CH_2O$$

occurs to a significant extent in the liquid but not in the gas phase. This reaction probably involves the shift of a hydrogen atom along a hydrogen bond. The reaction

$$C_2H_5OH_2^+ + e_{solv}^- \rightarrow C_2H_5O + H_2$$

does not occur to an appreciable extent in the liquid phase. In the liquid phase the relative contributions of the three different groups in the ethanol molecule to hydrogen production are in the order $CH_2 > OH \gg CH_3$. A similar trend occurs in the gas, although the contributions of the three groups are more nearly equal in this phase. Isotope effects, in the range $k_H/k_D = 2.2$–3.9 per bond, occur in the methane formation mechanism. The isotope effects are somewhat smaller in the liquid than in the vapor phase and somewhat smaller in the inhibited than in the uninhibited systems. A comparison of product distributions in the liquid and gas radiolyses of several compounds by γ-rays and by α-particles indicates that L.E.T. effects can also occur in the gas phase.

INTRODUCTION

It has been suggested that the reaction

[1] $$CH_3CH_2OH^+ + CH_3CH_2OH \rightarrow CH_3CH_2OH_2^+ + CH_3CH_2O$$

occurs in the liquid phase radiolysis of ethanol (1). Since this reaction merely involves the shift of a hydrogen atom along a hydrogen bond, it should occur to a smaller extent in the vapor than in the liquid phase. This hypothesis can be tested by irradiating C_2H_5OD and C_2D_5OH in the liquid and vapor states to determine the contributions of the hydroxyl hydrogen to the product hydrogen in the two phases. It is expected that the contribution of the hydroxyl hydrogen will be greater in the liquid phase. The present paper reports the results of this test. To increase the confidence that may be placed in the results and their interpretation, the isotopic composition of the product hydrogen from CH_3CD_2OH, CD_3CH_2OH, and C_2D_5OD is also reported.

Ryan *et al.* (2) have recently observed that reaction [1] does not occur to an appreciable extent in a mass spectrometer, but that the reaction

[2] $$CH_3CHOH^+ + C_2H_5OH \rightarrow CH_3CHO + C_2H_5OH_2^+$$

occurs very readily. However, all of the reactions [3]–[5] occurred readily under the same conditions as those used for the ethanol study, so the situation is not clear.

[3] $$CH_3OH^+ + CH_3OH \rightarrow CH_3OH_2^+ + CH_3O$$

[4] $$\rightarrow CH_3OH_2^+ + CH_2OH$$

[5] $$CH_2OH^+ + CH_3OH \rightarrow CHO_3H_2^+ + CH_2O$$

Since the above-mentioned experiments involved a comparison of results of the γ-radiolyses of the liquid and vapor phases of expensive deutero-ethanols, it was necessary first to compare the γ-radiolyses of the two phases using ordinary ethanol. In addition to the above, isotope effects were observed in the methane yields and are reported herein.

EXPERIMENTAL

Part of the experimental procedure has been described elsewhere (1). Only additional procedures will be reported here.

Materials

The isotopic purities of the deutero-ethanols (Merck, Sharp and Dohme, Ltd.) were measured with a Varian Associates Model A-60 Analytical NMR Spectrometer (see Table I). Phillips Research Grade ethylene was used.

TABLE I

Isotopic analysis of deuterated alcohols

Alcohol	Group	Isotopic purity (%)
C_2H_5OD	OD	>99
C_2D_5OH	CD_2	99.0
	CD_3	99.4
CH_3CD_2OH	CD_2	96.3
CD_3CH_2OH	CD_3	>99
C_2D_5OD	OD	99.5
	CD_2	99.6
	CD_3	99.6

Sample Preparation and Irradiation

The alcohols and 1,3-pentadiene were thoroughly degassed at −112°. Before introducing C_2H_5OD or C_2D_5OD into the sample preparation system, all surfaces with which the alcohol would come in contact were equilibrated with D_2O vapor. The D_2O remained in the system for 20 min, then was pumped away and the system was baked out. The process was then repeated. The nuclear magnetic resonance (n.m.r.) analyses reported in Table I were done on samples that had passed through the sample filling system. When an "OH" alcohol was used after an 'OD' compound, the system was preequilibrated with H_2O and baked out. The amount of deuterated alcohol in each sample was determined from liquid volume measurements, assuming that the density ratio for deuterated to 'light' ethanol was equal to the molecular weight ratio. This assumption is correct to within 0.3% for heavy and light water at 25°,* to within 0.1% for C_2H_5OD and C_2H_5OH at 0° (3), and would be even closer to exact for the other deuterated ethanols.

Gas phase samples were contained in 500 ml bulbs. The bulbs were placed in a heating mantle during radiolysis. Ethanol and its solutions were irradiated at a temperature of 105 ± 3° and a pressure of about 800 Torr. Ethylene, at 32° and about 900 Torr, served as the gas phase dosimeter and $G(H_2) = 1.28$ (4) was used. A stopping power correction, to convert the dosimetry from ethylene to ethanol, was calculated from the Bethe equation (5); this amounted to 1%. Liquid phase dosimetry was done with the Fricke dosimeter, using $G(Fe^{3+}) = 15.5$ and $\epsilon(Fe^{3+}, 304\ m\mu, 25°) = 2\ 225$. The liquid ethanol samples were irradiated at 28°. The dose rate in the Gammacell-220 was about 6×10^{19} eV/g h for both liquid and gas samples.

Product Analysis

The products that were volatile at −196° were separated from the sample by distillation under vacuum. The gas mixture was analyzed with a Metropolitan-Vickers MS-2 mass spectrometer.

RESULTS

The high cost of the deutero-alcohols prevented a complete study of the radiolysis of these compounds. Each alcohol was irradiated to a dose of 3.8 ± 0.4 (10^{20} eV/g) in the presence and absence of an electron fraction of 1,3-pentadiene equal to 0.20 ± 0.01. This concentration of pentadiene suppresses, essentially completely, the contributions of

*D_2O *was obtained from Bio-Rad Laboratories and the density of* D_2O *was given on the label as 1.105 g/ml at 25 °C.*

Can. J. Chem. Downloaded from www.nrcresearchpress.com by 210.87.254.6 on 09/05/12
For personal use only.

free radicals and e_{solv}^- to the yields of hydrogen and methane (1). The isotopic composition of the product hydrogen from each of the samples is listed in Tables II and III. The ratios of the various methanes produced from the different ethanols are also given in Table II. Only the methanes mentioned in the table were formed in detectable amounts.

TABLE II

Isotopic composition of hydrogen and methane

Alcohol	Phase	ϵ_p*	% H_2	% HD	% D_2	$\frac{G(CH_3D)}{G(CH_4)}$	$\frac{G(CHD_3)}{G(CD_4)}$†
C_2H_5OH	Liquid	0.0	100	0	0	0.00	—
C_2D_5OD	Liquid	0.0	1	4	95	—	0.08
C_2H_5OD	Liquid	0.0	31	67	2	0.17	—
C_2D_5OH	Liquid	0.0	13	66	21	—	0.6
CH_3CD_2OH	Liquid	0.0	30	59	11	0.8	—
CD_3CH_2OH	Liquid	0.0	87	12	1	—	24.
C_2H_5OH	Liquid	0.2	100	0	0	0.00	—
C_2D_5OD	Liquid	0.2	11	19	70	—	0.2
C_2H_5OD	Liquid	0.2	76	23	1	0.25	—
C_2D_5OH	Liquid	0.2	27	52	21	—	0.8
CH_3CD_2OH	Liquid	0.2	48	44	9	0.8	—
CD_3CH_2OH	Liquid	0.2	79	18	2	—	11.
C_2H_5OH	Gas	0.0	100	0	0	0.00	—
C_2D_5OD	Gas	0.0	1	5	94	—	0.09
C_2H_5OD	Gas	0.0	60	37	3	0.10	—
C_2D_5OH	Gas	0.0	6	40	54	—	0.7
CH_3CD_2OH	Gas	0.0	22	51	27	0.7	—
CD_3CH_2OH	Gas	0.0	77	19	3	—	44.
C_2H_5OH	Gas	0.2	100	0	0	0.00	—
C_2D_5OD	Gas	0.2	12	13	75	—	0.3
C_2H_5OD	Gas	0.2	75	25	1	0.23	—
C_2D_5OH	Gas	0.2	25	30	46	—	0.7
CH_3CD_2OH	Gas	0.2	54	32	14	0.7	—
CD_3CH_2OH	Gas	0.2	68	21	11	—	24.

*ϵ_p = electron fraction of 1,3-pentadiene.
†Small amounts of CH_2D_2 were produced from the CD_3 ethanols.

TABLE III

Percentage of D in the radiolytic hydrogen from deuterated ethanols and ethanol – 1,3-pentadiene mixtures

Alcohol	Pure liquid	Pure gas	Inhibited liquid	Inhibited gas
C_2H_5OD	35 (34)*	21	13	13
C_2D_5OH	54	74	47	61
CH_3CD_2OH	41 (42)	53	30	31
CD_3CH_2OH	7 (4)	13	12	22
CD_3CD_2OD	97 (94)	96	81	82

*The numbers in parenthesis are the values of Burr, ref. 12.

A moderately complete product analysis in the gas phase γ-radiolysis of light ethanol was made so that the product yields could be compared with those from the α-radiolysis (6). The results, listed in Table IV, are the averages from two experiments.

DISCUSSION

Comparison of the γ-Radiolyses of Ethanol in the Liquid and Gas Phases

One great difference between the results of the γ-radiolyses of liquid and gaseous ethanol is that in the liquid $G(-\text{ethanol}) = 7.5$, while in the gas phase $G(-\text{ethanol}) = 13.9$. These values refer to doses greater than 10^{20} eV/g. The value of $G(-\text{ethanol})$ increases at lower doses but the difference between the values for the two phases persists,

Can. J. Chem. Downloaded from www.nrcresearchpress.com by 210.87.254.6 on 09/05/12
For personal use only.

TABLE IV

Yields of some of the products of the radiolysis of ethanol

	G (product)				
	Liquid (present work)		Gas (present work)		Gas (ref. 6)
	$\epsilon_p = 0$*	$\epsilon_p = 0.20$†	$\epsilon_p = 0$	$\epsilon_p = 0.20$†	$\epsilon_p = 0$
Product					
Hydrogen	4.2	1.1	7.5	1.8	7.6
Methane	0.5	0.10	2.3	0.28	1.7
Carbon Monoxide	0.04	0.04	0.6	0.36	1.1
Ethane	0.21	0.06	0.2	0.01	0.2
Ethylene	0.13	0.11	1.2	1.1	0.7
Acetylene	0.01	0.02	0.09	0.35	0.03
Acetaldehyde	1.8	1.9	3.5	1.8	4.5
1,2-Propanediol	0.12	0.0	0.9	0.0	0.15
2,3-Butanediol	2.4	0.0	3.1	0.0	1.2
Radiation	^{60}Co γ		^{60}Co γ		^{210}Po α
Dose (10^{20} eV/g)	4		4		6
Dose rate (10^{19} eV/g h)	6		6		1
Temperature (°C)	28		105		108

*ϵ_p = electron fraction of 1,3-pentadiene in the sample.
†The numbers in these columns are $G_{observed}/0.80$, i.e. they refer to the energy absorbed initially by the ethanol. The 1,3-pentadiene contributes $G(H_2) \approx 0.04$ and 0.1 to the liquid and gas phase yields, respectively.

judging from the hydrogen yields (1, 6). Larger values of $G(-\text{substrate})$ in the gas than in the liquid phase have been observed in several systems (6–9). Part of the increase might be due to the higher temperature used in most of the gas phase studies ($\sim 100°$, refs. 6, 8, 9, compared to $\sim 25°$ in the liquids). However, methanol radiolyses in the two phases at room temperature also showed greater decomposition in the vapor than in the liquid state (7). Part of this difference is probably due to the decomposition in the gas of some of the activated species that are deactivated in the liquid (this includes back reactions in liquid cages). Part might also be due to the formation of different activated states in the two phases.

Assuming that each observable C—C bond break eventually gives rise to a molecule of methane, i.e. neglecting reactions such as

[6] $$CH_3 + R \rightarrow CH_3R,$$

the ratio of $G(CH_4)/G(H_2)$ reflects the ratio of primary C—C bond breakage to the C—H and O—H breakages, i.e. (C—C)/(C—H + O—H). The values of this ratio corrected by a statistical factor of six (the ratio of the number of bonds to hydrogen to the number of C—C bonds in the molecule) are 0.7 for the liquid and 1.9 for the gas radiolysis. These figures indicate that in the radiolysis of the liquid, a large amount of C—C bond rupture may be masked by cage effects (cage recombination). Methyl radicals are more susceptible than hydrogen atoms to cage recombination because the former are larger and less mobile than the latter. The nearly twofold increase in the extent of decomposition on going from the liquid to the gas is reflected to varying degrees in the yields of each of the observed products.

The ethylene yield is an order of magnitude greater in the gas phase, while the ethane yield is unchanged. These facts are probably due to the active species having a greater amount of time to decompose before being deactivated by collisions, e.g.

[7] $$C_2H_5OH^* \rightarrow C_2H_4 + H_2O,$$

[8] $$C_2H_5^* \rightarrow C_2H_4 + H.$$

Can. J. Chem. Downloaded from www.nrcresearchpress.com by 210.87.254.6 on 09/05/12
For personal use only.

Ethylene formation is not appreciably inhibited by 1,3-pentadiene in either phase. Ethane formation is inhibited in both phases, probably by the scavenging of ethyl radicals.

While the acetaldehyde yield is greater in the gas than in the liquid, the unscavengeable yields of this compound are the same in the two phases. The scavengeable acetaldehyde is probably formed by the disproportionation reactions of CH_3CHOH and CH_3CH_2O radicals. It has been suggested (1) that a large part of the unscavengeable acetaldehyde in the liquid phase was formed by the reactions

[9] $$C_2H_5OH \longrightarrow CH_3CHOH^+ + H + e^-,$$

[2] $$CH_3CHOH^+ + C_2H_5OH \rightarrow CH_3CHO + C_2H_5OH_2^+.$$

It is doubtful that reaction [9] would occur with the same G value in the two phases, so the agreement between the unscavengeable acetaldehyde yields is probably fortuitous. The unscavengeable yield of hydrogen equals that of acetaldehyde in the gas phase, but the former is smaller than the latter in the liquid. Thus the reaction

[10] $$C_2H_5OH^* \rightarrow CH_3CHO + H_2$$

might be more important in the gas than in the liquid phase.

The yield of 2,3-butanediol increased by about a third while that of 1,2-propanediol increased sevenfold on going from the liquid to the gas. This is another illustration of the enhanced C—C bond cleavage in the gas phase.

Hydrogen Formation

In the uninhibited systems, the percentage of D in the product hydrogen from C_2H_5OD and the percentage of H in the hydrogen from the 'OH' alcohols decreased on going from the liquid to the gas phase radiolysis (see Table III). These results are consistent with the suggestion that reaction [1] occurs to a significant extent in the liquid but not in the vapor state (see Introduction).

[1] $$C_2H_5OH^+ + C_2H_5OH \rightarrow C_2H_5OH_2^+ + C_2H_5O$$

The reaction would be facilitated by the hydrogen bonding in the liquid.

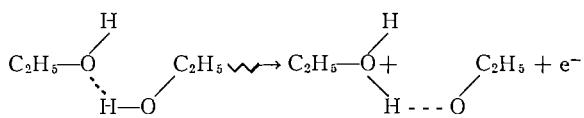

Reaction [1] would be followed by reactions [11] and [12].

[11] $$C_2H_5OH_2^+ + e_{solv}^- \rightarrow H + nC_2H_5OH$$

[12] $$H + C_2H_5OH \rightarrow H_2 + CH_3CHOH$$

Reaction [11] probably occurs in the spurs (1). The hydrogen atoms in reaction [12] also abstract from the methyl and to a very small extent from the hydroxyl but the main portion of the abstraction is from the methylene group. This is in agreement with the findings of other workers (10, 11) and is consistent with the relative bond strengths in the molecule. The amount of D_2 in the products from C_2H_5OD was very small (Table II), so the reaction

[13] $$C_2H_5OH_2^+ + e_{solv}^- \rightarrow C_2H_5O + H_2$$

does not occur to an appreciable extent in the liquid phase. If reaction [2] is the only source of $C_2H_5OH_2^+$ in the vapor phase, reaction [13] is also unimportant in the vapor (the

Can. J. Chem. Downloaded from www.nrcresearchpress.com by 210.87.254.6 on 09/05/12
For personal use only.

electron is probably not 'solvated' in the vapor, although the probability of formation of negative clusters is not known).

In the inhibited systems, the % D in the product hydrogen is the same for liquid and gaseous C_2H_5OD (Table III). This is in contrast to the results from the uninhibited systems and is consistent with the proposed mechanism because the hydrogen atom that results from reactions [1] and [11] is scavengeable.

[14] $$H + C_5H_8 \rightarrow C_5H_9\cdot$$

The % D in the product hydrogen from the three alcohols that were deuterated at only one of the three different groups in the molecule indicate the relative contributions of each of the groups to hydrogen formation. In the pure liquid the relative contributions from the three sites are in the order methylene > hydroxyl $\gg$ methyl. This is consistent with the results of other measurements of the isotopic composition of the hydrogen produced by the radiolysis of various deutero-alcohols (12–14) and with the fact that CH_3CHOH is the main radical observed in irradiated solid ethanol at 77 °K (15, 16).

A similar trend was observed in the pure gas phase, although the relative importance of the methyl group doubled, that of the methylene group increased by 30% and that of the hydroxyl group decreased by 40% from those in the liquid phase (see Table III). In both phases, the % D in the hydrogen from the CD_3CH_2OH–pentadiene solutions was greater than that in the hydrogen from pure CD_3CH_2OH. For all the other deutero-alcohols, the % D in the hydrogen from the pentadiene solution was smaller than that in the hydrogen from the corresponding pure alcohol. Thus the methyl group is relatively more important in the formation of unscavengeable hydrogen than it is in the formation of scavengeable hydrogen. This is consistent with the idea that the unscavengeable hydrogen is formed from a very reactive species that reacts with less selectivity than do those which form the scavengeable hydrogen (e_{solv}^- and thermal H).

Methane Formation

The methane results were sufficiently simple (Table II) that certain rate constant ratios and isotope effects could be calculated from the present data. For simplicity, both the scavengeable and the unscavengeable methane yields will be considered to be produced by the following reactions.

[15] $$CH_3 + CH_3CH_2OH \rightarrow CH_4 + CH_3CHOH$$

[16] $$\rightarrow CH_4 + CH_3CH_2O$$

[17] $$\rightarrow CH_4 + CH_2CH_2OH$$

If the unscavengeable methane were produced by the unimolecular decomposition of activated ethanol species or by the disproportionation reactions of radicals in spurs, the rate constant ratios and isotope effects reported here could be readily transferred to these types of reaction.

Values of k_{15}/k_{16}, k_{15}/k_{17}, and of the kinetic isotope effect k_H/k_D can be calculated from the isotopic compositions of the methanes obtained from the various deutero-ethanols (Table II). For example, values of k_{15}/k_{16} and k_H/k_D in the liquid phase were calculated as follows.

[15′] $$CH_3 + CH_3CD_2OH \rightarrow CH_3D + CH_3CDOH$$

[16′] $$\rightarrow CH_4 + CH_3CD_2O$$

[15″] $$CH_3 + C_2H_5OD \rightarrow CH_4 + CH_3CHOD$$

[16″] $$\rightarrow CH_3D + C_2H_5O$$

Can. J. Chem. Downloaded from www.nrcresearchpress.com by 210.87.254.6 on 09/05/12
For personal use only.

From the data in Table II, $k_{15'}/k_{16'} = 0.8$ and $k_{15''}/k_{16''} = 6.0$. The isotope effects in reactions [15] and [16] are assumed to be about the same. Thus, $k_{15}/k_{16} = (0.8 \times 6.0)^{1/2} = 2.2$ and $k_H/k_D = (6.0/0.8)^{1/2} = 2.7$. These values would not be appreciably changed by including reaction [17] in the calculations because the contributions of the corresponding reactions [17'] and [17''] would tend to cancel each other. The unscavengeable yield of methane is only 12% of the total methane yield in the gas phase and 20% in the liquid phase radiolysis of ethanol (Table IV), so little error is introduced into the calculation of the kinetic parameters by using the total methane yields in calculating the values for the scavengeable reactions.

TABLE V

Some kinetic parameters of the methane formation reactions

Radical	Phase	Methane type	k_{15}/k_{16}	k_{15}/k_{17}	k_H/k_D*
CH_3	Liquid, 28°	Scavengeable	2.2	—	2.7
CH_3	Liquid, 28°	Unscavengeable	1.8	—	2.2
CD_3	Liquid, 28°	Scavengeable	—	6.2	2.7†
CD_3	Liquid, 28°	Unscavengeable	—	3.2	2.2†
CH_3	Gas, 105°	Scavengeable	2.7	—	3.9
CH_3	Gas, 105°	Unscavengeable	1.8	—	2.5
CD_3	Gas, 105°	Scavengeable	—	8.0	3.9†
CD_3	Gas, 105°	Unscavengeable	—	6.4	2.5†

*k_H/k_D is the isotope effect per bond.
†Assumed.

The values of k_{15}/k_{16}, k_{15}/k_{17}, and k_H/k_D for liquid ethanol at 28° and gaseous ethanol at 105° are recorded in Table V. The isotope effect is smaller for the unscavengeable processes than for the scavengeable processes in both phases. This indicates that the former processes involve more energetic reactants than the latter. The results in Table II also allow calculation of the ratio $(k_H/k_D)(k_{15}/k_{16})$ when CD_3 radicals replace the free CH_3 radicals in reactions [15] and [16]. For the scavengeable and the unscavengeable methane in both the liquid and the gas phases, the results indicate that

$$\left(\frac{k_H}{k_D} \cdot \frac{k_{15}}{k_{16}}\right)^{\frac{1}{2}}_{CH_3} = 2\left(\frac{k_H}{k_D} \cdot \frac{k_{15}}{k_{16}}\right)_{CD_3}.$$

The conclusions of earlier photolytic studies in methanol (17, 18) cast some doubt upon the suggestion that the scavengeable methane is formed by methyl radical reactions during the radiolysis of ethanol. Shannon and Harrison (17) studied reactions [18] and [19] in the gas phase.

[18] $$CH_3 + CH_3OH \rightarrow CH_4 + CH_2OH$$

[19] $$\rightarrow CH_4 + CH_3O$$

Extrapolation of their results to 105° gives $k_{18}/k_{19} = 0.66$, which lies between the values $k_{15}/k_{16} = 2.7$ and $k_{17}/k_{16} = 0.34$ as would be expected. However, their results yield $k_H/k_D = 7.4$ at 105°, which is significantly larger than the present value of 3.9. Furthermore, Cher (18) studied reactions [18] and [19] in the liquid phase at 30° using CD_3 rather than CH_3 radicals. He found $k_{18}/k_{19} = 45 \pm 12$ and $k_H/k_D = 8.7 \pm 2.8$. These values are much larger than the $k_{15}/k_{16} = 2.2$, $k_{17}/k_{16} = 0.35$, and $k_H/k_D = 2.7$ found in the liquid phase radiolysis at 28°. More work is required to prove or disprove the occurrence of reactions [15]–[17] during the radiolysis of ethanol.

Can. J. Chem. Downloaded from www.nrcresearchpress.com by 210.87.254.6 on 09/05/12
For personal use only.

Comparison of the γ- and α-Radiolyses of Ethanol

The most striking difference between the α- and γ-radiolyses of ethanol vapor (Table IV) is the acetaldehyde/2,3-butanediol ratio; the value of the ratio is 1.1 for γ's and 3.8 for α's. The conditions (pressure, temperature, dose rate, surface/volume ratio of sample container) in the two studies were similar and could not account for the widely different ratios, so the difference must be attributed to the nature of the radiation. The same trend can be noted in other systems. The acetaldehyde/2,3-butanediol ratio from liquid ethanol has the value of 0.9 for γ's (1) and 2.1 for α's (19); the formaldehyde / ethylene glycol ratio from liquid methanol is 0.43 for γ's and 1.0 for α's (20).

The difference in the aldehyde/glycol ratios in the liquid systems are due to L.E.T. effects. For example, the yield of 'free ions' is very probably much smaller for α- than for γ-radiolysis. Thus reactions such as [20] and [21],

[20] $$CH_3CHO + e_{solv}^- \rightarrow CH_3CHO^-$$

[21] $$CH_3CHO^- + C_2H_5OH_2^+ \rightarrow CH_3CHOH + C_2H_5OH,$$

which destroy aldehydes, occur to a smaller extent in the α- than in the γ-radiolysis. At the doses used to measure the yields of these products reaction [20] is the main fate of the 'free' solvated electrons in liquid ethanol (1). This effect would tend to make the aldehyde/glycol ratio larger in the α- than in the γ-radiolytic systems. The relative amounts of the various free radicals produced are probably also affected by L.E.T. because the glycol yields, which are nearly unaffected by reactions [20] and [21], are different for the different radiations (1, 19, 20). It thus appears that L.E.T. effects can also occur in gas phase radiolyses. Differences in product distributions have also been noted between the α- and X-radiolyses of hydrocarbon vapors (21).

There are many possible reasons for these differences, some of which are (*a*) different states might be formed in different abundances in the two systems; (*b*) space charge along the α-particle track might cause a larger amount of local charge neutralization to occur during the α-radiolysis than would occur during γ-radiolysis; (*c*) a significant amount of charge neutralization might occur on the reaction vessel wall under the usual conditions of γ-radiolysis. The following observation leaves some doubt about reason (*a*). An extrapolation of mass spectrometric results from fast electrons (22) and protons (23) to α-particles as an ionization source indicates that the primary species formed during the α- and γ-radiolyses of the compounds would be quite similar. However, caution should be used in extrapolating conclusions from mass spectrometry to the interpretation of radiolysis systems. The above reason (*b*) is a sort of local dose rate effect. Both (*b*) and (*c*) could be checked by doing γ- or fast electron radiolyses at very high dose rates in the vapor phase.

ACKNOWLEDGMENT

The authors are grateful to the National Research Council for financial assistance of this work.

REFERENCES

1. J. J. J. Myron and G. R. Freeman. Can. J. Chem. **43**, 381 (1965).
2. K. R. Ryan, L. W. Sieck, and J. H. Futrell. J. Chem. Phys. **41**, 111 (1964).
3. I. B. Rabinovich, V. G. Golov, N. A. Efimova, and S. M. Rustzmov. Acad. Sci. USSR Proceedings, Phys. Chem. Section, **114**, 339 (1957).
4. R. A. Back, T. W. Woodward, and K. A. McLauchlan. Can. J. Chem. **40**, 1380 (1962).
5. G. J. Hine and G. L. Brownell. Radiation dosimetry. Academic Press, Inc., New York. 1956.
6. J. M. Ramaradhya and G. R. Freeman. Can. J. Chem. **39**, 1836 (1961).

Can. J. Chem. Downloaded from www.nrcresearchpress.com by 210.87.254.6 on 09/05/12
For personal use only.

7. J. H. BAXENDALE and R. D. SEDGWICK. Trans. Faraday Soc. **57**, 2157 (1961). J. H. BAXENDALE and F. W. MELLOWS. J. Am. Chem. Soc. **83**, 4720 (1961).
8. R. F. FIRESTONE. J. Am. Chem. Soc. **79**, 5593 (1957).
9. J. M. RAMARADHYA and G. R. FREEMAN. J. Chem. Phys. **34**, 1726 (1961).
10. C. LIFSHITZ and G. STEIN. J. Chem. Soc. 3706 (1962).
11. P. RIESZ and B. E. BURR. Radiation Res. **16**, 661 (1962).
12. J. G. BURR. J. Am. Chem. Soc. **79**, 751 (1957).
13. J. G. BURR. J. Phys. Chem. **61**, 1477 (1957).
14. I. A. TAUB and L. M. DORFMAN. J. Am. Chem. Soc. **84**, 4053 (1962).
15. R. LIVINGSTONE. J. Chem. Educ. **36**, 349 (1959).
16. J. R. ROWLANDS and D. H. WHIFFEN. 2nd International Congress of Radiation Research, Harrogate, England. 1962.
17. T. W. SHANNON and A. G. HARRISON. Can. J. Chem. **41**, 2455 (1963).
18. M. CHER. J. Phys. Chem. **67**, 605 (1963).
19. A. S. NEWTON and W. R. MCDONELL. J. Am. Chem. Soc. **78**, 4554 (1956).
20. W. R. MCDONELL and S. GORDON. J. Chem. Phys. **23**, 208 (1955).
21. R. A. BACK and N. MILLER. Trans. Faraday Soc. **55**, 911 (1959).
22. P. KEBARLE and E. W. GODBOLE. J. Chem. Phys. **36**, 302 (1962).
23. S. WEXLER. J. Chem. Phys. **41**, 2781 (1964).

Can. J. Chem. Downloaded from www.nrcresearchpress.com by 210.87.254.6 on 09/05/12
For personal use only.

Can. J. Chem. Downloaded from www.nrcresearchpress.com by 210.87.254.42 on 09/05/12
For personal use only.

THE METHYLATION OF THE RESORCINOLATE DIANION

I. THE EFFECTS OF SOLVENT AND BASE AND THE ALKYLATION SEQUENCE

ALLAN R. STEIN[1]

Noyes Laboratory of Chemistry, University of Illinois, Urbana, Illinois

Received November 13, 1964

Dedicated to Professor R. B. Sandin on the Occasion of his Sixty-Eighth Birthday

ABSTRACT

The alkylation of the di-alkali metal salts of resorcinol with methyl iodide under various conditions was examined. Solvent and cation effects on the mode and position of resorcinolate anion methylation are discussed. By examination of the neutral and phenolic fractions and comparison with the alkylation of methoxyphenols and mesorcinol, the principal methylation sequences are determined. The intermediacy of the various hydroxydienones, for example, 2,4,6,6-tetra- and 2,6,6-tri-methyl-1-hydroxycyclohexa-1,4-dien-3-one, in the formation of the principal product, 2,2,4,6,6-pentamethylcyclohex-4-en-1,3-dione, from the methylation of the resorcinolate dianion in nonpolar solvents or water is established by the isolation of such intermediates. The 2,2,4,6,6-pentamethylcyclohex-4-en-1,3-dione itself will be discussed in detail in the second paper in this series.

INTRODUCTION

Substituent effects on the alkylation of enolates (1), of oxime salts (2, 3), and of thiophenolates (4) have been examined, but the only study of the effect of substituents on the alkylation of phenoxides is that reported by Curtin *et al.* (5), who examined only the sodium salts of phenol and its 4-methyl and 4-bromo derivatives. An examination of the methylation of resorcinol was undertaken after a cursory examination of substituent effects confirmed an expectation that a meta-methoxyl group ($\sigma_{meta} = 0.115$; $\sigma_{para} = -0.268$) on phenol greatly enhanced carbon alkylation over that observed with phenol and, especially, with *p*-methoxyphenol.

The alkylation of polyhydroxylic benzene salts has been studied. Herzig and Zeisel (7), contrary to a report by Will (8), found that treatment of phloroglucinol with ethyl iodide in alcoholic alkali solution gave a pentaethylphloroglucinol which they considered to be 2,2,4,4,6-pentaethylcyclohexan-1,3,5-trione (I). Margulies (9) and Herzig and Erthal (10) both report the isolation of II from the methylation of phloroglucinol in methanolic potassium hydroxide solution. Di- and tri-methylated phloroglucinols were also obtained and were assumed to be carbon-alkylation products (9).

A hexamethylphloroglucinol to which was assigned the structure 2,2,4,4,6,6-hexamethylcyclohexan-1,3,5-trione (III) was first reported by Kaufler (11) and later by Herzig and Erthal (10). This material was later found to be identical with the compound formed by the base-catalyzed trimerization of dimethylketene (12). Under the reaction conditions employed, II was not further methylated to give III, nor were the usual carbonyl derivatives of either species obtained (10). Grignard reagents, however, did add to II to give IV.

Kaufler (11) obtained hexa-, penta-, and tetra-methylphloroglucinols by using methyl iodide, carefully dried phloroglucinol, and alkaline absolute methanol. In addition, he reported the monomethyl ethers of penta- and tetra-methylphloroglucinols. In aqueous solution, only assorted ethers were obtained and, in methanolic solution, varying the amount of base varied the product composition. Ethyl, *n*-propyl, and isopropyl iodide behaved similarly, but as the alkyl group increased in size, Kaufler found the amount of carbon methylation was reduced. To explain the fact that with benzyl chloride he obtained

[1]*Current address: Central Research Laboratories, Dominion Tar and Chemical Company, Ltd., Senneville, Quebec.*

almost exclusively the mono-, di-, and tri-benzyl ethers of phloroglucinol, he stated that phloroglucinol acts as a ketone towards methylation but as a phenol towards benzylation. It is, perhaps, of interest that the dianion of phloroglucinol has recently been shown to exist principally in the ketonic cross-conjugated dienone form (13).

An attempt to characterize the tetra-, penta-, and hexa-methylphloroglucinols (V, II, and III respectively) was made by Spitzer (14). In an attempt to establish the origin of the 2,2,4,4,6,6-hexamethylcyclohexan-1,3,5-trione (III), Herzig and Erthal (15) found that a mixture of II and III was formed when V was methylated with methyl iodide in 10% aqueous potassium hydroxide.

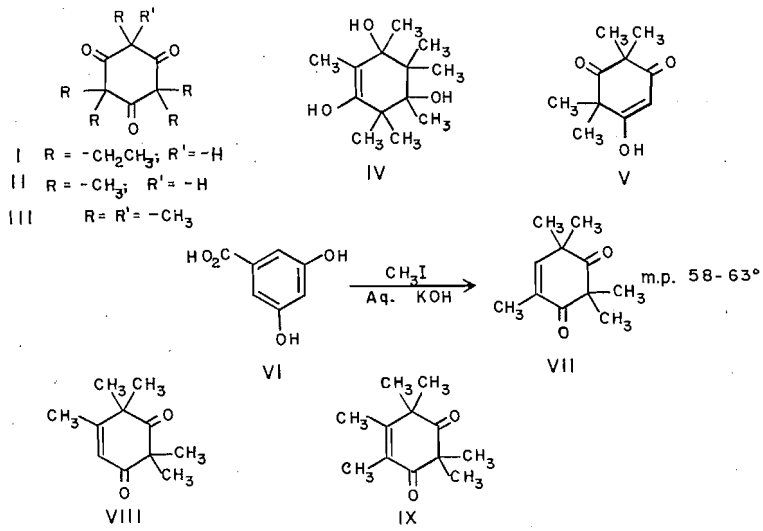

The first reported study of a resorcinolate alkylation is that of Kurzweil (16). Using orcinol carboxylic acid (VI) and methyl iodide in basic aqueous solution, he obtained, among assorted methyl ethers and esters, a compound $C_{11}H_{16}O_2$ to which he erroneously assigned the structure 2,2,4,6,6-pentamethylcyclohex-4-en-1,3-dione (VII).

Herzig and Wenzel (17) studied the methylation of orcinol (i.e. 5-methylresorcinol) in basic solutions with diazomethane, dimethylsulfate, and methyl iodide. Only the last gave carbon- as well as oxygen-methylated products. Herzig and Wenzel stressed the fact that minor variations in temperature, concentration, thoroughness of drying the orcinol, or the order in which the reagents were added greatly affected the product distribution. Even supposedly identical runs gave varying product distributions.

Herzig and Wenzel (18) attempted to identify their tetra- and penta-methylorcinols but met with dubious success. The tetramethylorcinol was brominated and then treated with aqueous potassium hydroxide to give fumaric acid (12%), diisopropylketone (11%), and an acid $C_{11}H_{16}O_4$ (67%), which they failed to identify. With similar treatment, the pentamethylorcinol gave only an acid $C_{12}H_{18}O_3$ (73%), again unidentified. These results are inconsistent with the proposed structures for the tetra- and penta-methylorcinol (VIII and IX respectively). Compound VIII was not further methylated by methyl iodide in 10% aqueous potassium hydroxide, conditions under which orcinol gave a mixture of VIII and IX in 10% yield (15).

In 1911, Herzig and Wenzel (18) proposed the mechanism shown in Reaction Scheme 1 for the carbon methylations observed. Applying this mechanism repetitively, they suggested a stepwise methylation for the formation of VIII and IX. Resorcinol and orcinol

Can. J. Chem. Downloaded from www.nrcresearchpress.com by 210.87.254.42 on 09/05/12
For personal use only.

were reported to behave similarly, but resorcinol was methylated somewhat less readily (15).

While reports of the alkylation and acylation of resorcinol and phloroglucinol under acid conditions (i.e. using alcohols, olefins or alkyl halides, or acid anhydrides or acyl halides and assorted protonic or Lewis acids as catalysts) are very numerous, the only recent reports of the alkylation of resorcinolates have both used allylic halides. Monroe (19) used allyl chloride in a sodium dihydrophosphate buffered solution (pH 5–7) near room temperature to obtain a diallylresorcinol, and Fitton and Ramage (20) obtained the monobenzyl ether by treating resorcinol with benzyl chloride and potassium carbonate in dry acetone.

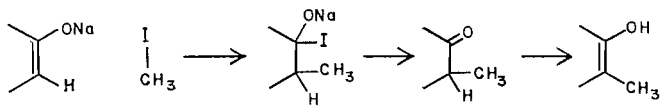

REACTION SCHEME 1.

RESULTS AND DISCUSSION

Studies of the alkylation of the resorcinolate dianion present several difficulties. For many of the products, it is impossible to distinguish between ortho and para alkylation and it is impossible to discern which species is alkylated. More important, however, is the multiplicity of possible products. As many as 23 of the 40 possible products summarized in Table I were observed in a single product mixture from the methylation of the resorcinolate dianion with methyl iodide, and examples of each class of product were isolated and identified.

Some of the overlapping effects or factors operative in alkylations of the resorcinolate dianion will be discussed. These will be followed by a more complete examination of the neutral fraction and phenolic fraction, together with some mechanistic interpretations of these results.

Cation Effects

As is general for the alkylation of phenoxides (5, 6, 21), the sodium salts of resorcinol gave far less carbon methylation than did the lithium salts. Thus, in tetrahydrofuran the sodium salt gave a carbon-to-oxygen methylation ratio of less than 0.2 while the lithium salt gave a ratio of over 2.0. In methanolic solution where a more ionic reaction is probably occurring, little difference between the two cations was noted. Both gave a carbon-to-oxygen alkylation ratio of about 0.8–1.0.

Solvent Effects

An appreciation of the complexity of solvent effects on the alkylation of ambient anions can be gained by an examination of the tabulation of the variation of the composition of the neutral fraction with the mole % of water in tetrahydrofuran used as a solvent for the methylations of the lithium salt (Table II). Four equivalents were found to be sufficient base to convert essentially all (97–99%) of the resorcinol to neutral fraction (except in pure water where only 80% conversion was attained), so that 4 moles of lithium hydride were used for each mole of resorcinol. None of the phenolic fractions examined contained any resorcinol but were made up mainly of high-boiling tars.

It should be noted in examining the results represented in Table II that, with the concentration range employed, only 3.2 mole % of water was sufficient to convert all of the excess lithium hydride to lithium hydroxide. This change of base, together with the anticipated "solvent sorting" (22), whereby the water would collect about the ionic charge centers, could account for the drastic changes in product composition observed when

Can. J. Chem. Downloaded from www.nrcresearchpress.com by 210.87.254.42 on 09/05/12
For personal use only.

TABLE I

Possible methylation products from resorcinol

Classification	Basic structure(s)	No. C-methyls	No. possible structures
Neutral species			
m-Dimethoxybenzenes	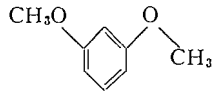	0–3	6
Methoxydienones	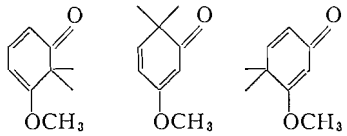	2–4	9
"Enediones"	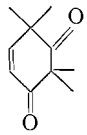	4–5	2
Acidic species			
Methoxyphenols	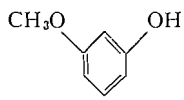	0–3	8
Resorcinols	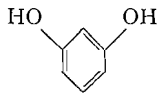	0–3	6
Hydroxydienones*	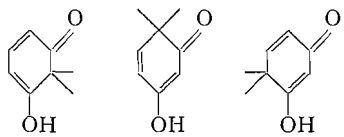	2–4	9
Total			40

*Possible tautomers are not included, e.g.

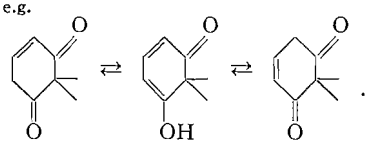

small amounts of water were present. A mechanistic change is indicated, however, as the reaction solvent is changed from tetrahydrofuran to water. A similar mechanism change was indicated by the cation effects mentioned above. This will be discussed in more detail below.

Extrapolation from the moderately nonpolar tetrahydrofuran to even less polar solvents like hexane or toluene would be expected to give far more carbon methylation. Because it was impossible to form the resorcinol salts with the metal hydrides in these solvents, they were formed in a small quantity of tetrahydrofuran, and toluene or hexane was then added. As indicated in Table III, in 16.5% (by volume) tetrahydrofuran in toluene, methyl iodide alkylations of the lithium salt gave a 68% yield of a mixture of 2,2,4,6,6-pentamethylcyclohex-4-en-1,3-dione (VII) and 2,2,6,6-tetramethylcyclohex-4-en-1,3-dione (X). The former, enedione VII, is the major topic of the second paper in this series (23).

Can. J. Chem. Downloaded from www.nrcresearchpress.com by 210.87.254.42 on 09/05/12
For personal use only.

Can. J. Chem. Downloaded from www.nrcresearchpress.com by 210.87.254.42 on 09/05/12
For personal use only.

TABLE II

The neutral fraction from the methylation of lithium resorcinolates in aqueous tetrahydrofuran

Mole % water	% neutral fraction	C/O* ratio	Product composition (% yield)†						
			Enedione	*m*-DiMeO-benzene	2,6-DiMeO-toluene	2,4-DiMeO-toluene	2,4-DiMeO-xylene	4,6-DiMeO-xylene	DiMeO-mesitylene
0.00‡	99	1.5	23.6	3.6	41.4	8.8	17.8	2.6	1.7
2.96‡	99	1.0	16.0	10.0	39.7	11.2	18.4	3.8	0.0
5.78‡	99	0.5	5.0	32.8	22.8	21.8	11.6	7.1	0.0
15.5‡	99	0.3	0.9	53.9	12.8	18.3	4.4	3.8	0.8
24.3‡	99	0.3	1.2	54.0	14.7	21.8	5.3	3.0	<1.0
33.5‡	98	0.6	4.8	33.4	15.9	20.5	13.3	8.4	3.6
47.5	98	0.9	11.0	26.5	11.1	15.4	16.9	8.0	9.8
62.1	97	1.1	18.0	26.2	8.3	12.9	13.8	6.2	14.6
83.8	97	1.9	35.1	26.4	6.2	10.1	6.7	3.6	8.4
100.0	79	3.5	42.3	18.2	3.9	7.3	3.0	2.5	2.1

*The ratio of the total area of the carbon methyl protons to that of the methoxy protons in the nuclear magnetic resonance spectrum of the neutral fraction.
†The percentage of the total integrated signal area in the vapor phase chromatographic spectrum of the neutral fraction.
‡Solid phase present throughout the reaction.

TABLE III

Methylation of lithium phenoxides

Starting phenol	Solvent used	% neutral fraction	% product composition				
			Enedione* mixture	*m*-DiMeO-benzene	DiMeO-toluenes	DiMeO-xylenes	DiMeO-mesitylene
m-MeOphenol	THF	99	0.0	89	11	<0.5	<0.5
	H_2O	99	0.0	92	7	<0.5	<0.5
	21% THF – toluene	15	0.0	11	4	<1.0	<0.5
Resorcinol	THF	99	24	4	50†	20‡	2
	H_2O	79	42	18	11§	6‖	2
	16.5% THF – toluene	69	68	Negl.	Negl.	Negl.	<2
	30% THF – toluene	92	30	Negl.	13¶	38**	12
	30% THF – hexane	93	30	Negl.	13¶	28††	13
	DMSO	98	1.4	64	30	4.7	Negl.
	DMF	97	0.1	78	21	1.6	Negl.

*2,2,4,6,6-Penta- and 2,2,6,6-tetra-methylcyclohex-4-en-1,3-diones, VII and X respectively (25).
†41.4% 2,6- and 8.8% 2,4-dimethoxytoluene.
‡17.8% 2,4- and 4.6% 4,6-dimethoxy-1,3-xylene.
§3.9% 2,6- and 7.3% 2,4-dimethoxytoluene.
‖3.0% 2,4- and 2.5% 4,6-dimethoxy-1,3-xylene.
¶10.0% 2,6- and 3.0% 2,4-dimethoxytoluene.
**33% 2,4- and 5% 4,6-dimethoxy-1,3-xylene.
††23% 2,4- and 5% 4,6-dimethoxy-1,3-xylene.

Can. J. Chem. Downloaded from www.nrcresearchpress.com by 210.87.254.42 on 09/05/12
For personal use only.

Kornblum and his co-workers have attempted to break similar solvent effects, observed in other phenoxide alkylations, into some of their component parts, i.e. hydrogen bonding (24) and dielectric constant effects. Too few solvents were tested to attempt such correlations with this system, but several of the interrelated factors are apparent from the results presented here. Thus, comparison of the relative amounts of 2,4- and 2,6-dimethoxytoluenes reported in Table II shows that, in tetrahydrofuran (THF) solution, four or five times as much 2- as 4-methylation occurs —a relative rate difference of more than eightfold when the two equivalent 4-positions are considered. This is confirmed by the relative amounts of the 2,4- and 2,6-dimethoxy-1,3-xylenes. As water is added, methylation at the 4-position becomes more and more competitive until the two relative rates are approximately equal, that is, about twice as much 4- as 2-dimethoxytoluene was formed. This product change indicates that, as water strongly solvates the two negatively charged oxygens, the di-ortho 2-position between them becomes sterically blocked to attack and the normally less favored attack at the ortho–para 4-carbons can compete on a more equal basis. Tying up oxygen with water of solvation would promote carbon attack over oxygen attack (23, 24), and hence explain the increase in the carbon-to-oxygen alkylation ratio and, thus, the amount of per-methylated products, the enediones (25), at the higher concentrations of water. To compare more meaningfully the results for the methylation of the lithium salts of resorcinol in nonpolar aprotic and in polar hydroxylic solvents, resorcinol, with 4 equiv. of lithium hydride present, was methylated with methyl iodide in several polar aprotic solvents. The analyses of the neutral fractions from methylation at 66° in dimethylsulfoxide (DMSO) and in N,N-dimethylformamide (DMF) are reported in Table III.

The comparatively small yield of carbon methylation products was anticipated, since both solvents are excellent cation-solvating solvents but are poor at solvating anions (27). The more electronegative oxygen would then be expected to be the major point of attack in methylation (26). One definite objection to working in either of these two solvents is that they apparently react with alkyl halides (28, 29) and are apparently reduced by the lithium hydride. In dimethylsulfoxide in particular, considerable quantities of iodine and of the sulfide and mercaptan reduction products of dimethylsulfoxide were liberated. In dimethylformamide, less iodine formed but reduction products of dimethylformamide were formed in quantities readily detectable by their amine odor.

Similarly, the relative amounts of carbon alkylation of the sodium salt in tetrahydrofuran and in methanol can be attributed to the greater hydrogen-bonding ability of the latter, enabling it to "tie up" the oxygens. It is interesting to note that methanol apparently was not a potent enough hydrogen-bonding solvent to cause such effects in other systems studied (24), and that such specific solvation must overcome the effect of increased resorcinolate ionization, which always favors oxygen alkylation in phenoxide systems (5, 26).

The Anionic Species

Thus far it has been assumed that the major amount of carbon methylation occurs on the dianion. That this is indeed so can be inferred from the data in Table III by comparing the amounts of the C-methylated products obtained from resorcinol and *m*-methoxyphenol under the same conditions. Under similar conditions in tetrahydrofuran solution, lithium 3,5-dimethoxyphenoxide gave 39% of 1,3,5-trimethoxybenzene, 43% of 2,4,6-trimethoxytoluene, 9% of 2,4,6-trimethoxyxylene, and only 9% of carbonyl-containing materials. (Little or no para methylation must have occurred as noted by the complete absence of trimethoxymesitylene in the product.) Thus, even the 3,5-dimethoxyphenoxide is less readily methylated than is the resorcinolate.

Since hydroxy and methoxy groups have similar Hammett "σ" constants and since electron donor substituents ortho to the alkylation site are found to greatly favor carbon alkylation (6), similar results would be expected from *m*-methoxyphenoxide and *m*-hydroxyphenoxide or the resorcinol dianion which could readily be mono-oxygen methylated to the *m*-methoxyphenoxide ion. *m*-Dimethoxybenzene and its carbon-methylated analogues are inert under the reaction conditions so that, by a process of elimination, we are left only with the resorcinolate dianion as the alkylated species. An ortho-"oxide" substituent should have a large negative "σ" value and, hence, would give much more carbon alkylation than a methoxy substituent.

Methylation Sequence

Since it is apparent that virtually all of the carbon methylation must occur before the methylation of the first "oxide", the analyses of the neutral fractions can yield some indication of the main order or sequence of the methylation, if it is assumed that the ease of oxygen methylation and particular carbon methylation are relatively independent of the carbon methylation or vary smoothly with additional carbon methylation. Thus, from the results presented in Table II, in tetrahydrofuran solution, nearly five times as much 2,6- as 2,4-dimethoxytoluene was obtained. This represents a difference in relative rate of a factor of about nine. In water, the relative rates are about equal, while in 30% tetrahydrofuran–toluene solution, the relative rate for 2-methylation is again about eight times that for 4- (or 6-) methylation. While relative rates for further methylation are more difficult to estimate, it appears that in the nonpolar solvents 2-methylation is still favored, while in water 2- and 4- (or 6-) methylation proceed at approximately the same rates.

While the examination of the neutral fraction allows some generalizations to be made concerning the sequence of the methylation of the resorcinolate dianion to the enediones, VII and X, only an examination of the acid or phenolic fraction as the reaction proceeds can lead to definite conclusions concerning the pathway of, and intermediates in, their formation. Because the methylation reaction is heterogeneous in nonpolar solvents, it was not possible to simply analyze aliquots of a single reaction. To minimize the extensive analysis requirement, only a single solvent (20% (by volume) tetrahydrofuran in toluene) at a single temperature (66.1°) with constant initial concentrations of resorcinol, methyl iodide, and lithium hydride (mole ratio of 1:12:2) was used, with reaction times varying from 5 to 1 440 min. The analysis of the phenolic fraction is reported in Table IV. The composition of the neutral fraction obtained varied randomly about that for 16.5% THF–toluene reported in Table III.

An estimate of the relative rates of the various steps indicated in Reaction Scheme 2 can be drawn from the results in Table IV. Thus, it appears that k_1 is about twice k_2 (four times k_2 if the statistical factor is included), that k_3 is approximately equal to $k_4 + k_5$ (or $(k_4 + k_5)/2$ if the statistical factor is included), and so on. Over six half-lives, the disappearance of resorcinol was first order in resorcinol with a rate constant of 1.67×10^{-3} s^{-1}. Unfortunately, when an analogue computer was used in an attempt to determine the relative rate constants and, hence, their absolute magnitude using the resorcinol disappearance as a calibration point, it was found to be impossible to get self-consistent values for k_1 and k_2, let alone for the subsequent rate constants. Apparently, other factors, such as those dependent upon heterogeneous reactions with base, rates of solution of the solid salt, or side reactions, could not be considered.

From the data presented, the sequence of the methylation in the formation of the two enedione products (VII and X) given in Reaction Scheme 2 seems quite well established. That this picture was still far from complete was apparent when mesorcinol (dihydroxymesitylene) itself was methylated under the conditions used for the resorcinol acid fraction

Can. J. Chem. Downloaded from www.nrcresearchpress.com by 210.87.254.42 on 09/05/12
For personal use only.

TABLE IV

Composition of the acid fraction from the methylation of resorcinol as a function of time

Reaction time	% acid fraction	Acid fraction composition (% yield)					
		Resorcinol	2-Methyl-resorcinol	4-Methyl-resorcinol*	2,4-DiMe-resorcinol	4,6-DiMe-resorcinol	Mesorcinol
0 min	100	100	0.0	0.0	0.0	0.0	0.0
5 min	100	57.5	23.6	18.2	0.7	0.0	0.0
15 min	100	32.0	37.1	20.8	5.6	0.4	0.0
30 min	98	5.3	22.4	29.0	22.4	11.6	1.2
1 h	96	1.8	17.8	16.2	34.9	11.4	4.0
2 h	88	0.0	4.9	3.0	27.0	12.4	21.6
4 h	75	0.0	0.6	4.3	15.8	9.8	20.8
11 h	62	0.0	0.0	3.3	1.7	9.7	28.1
24 h	56	0.0	0.0	4.2	1.2	9.0	19.1
65 h†	45	0.0	0.0	—	—	—	21.1

*In the later stages of the reaction an unidentified component with the same retention time appeared. The correct amount of 4-methylresorcinol was thus less than that reported.

†3-Methoxymesitol, identified by its nuclear magnetic resonance spectrum, was present in 12.1%. Whether it was also present in the other reaction products was not checked.

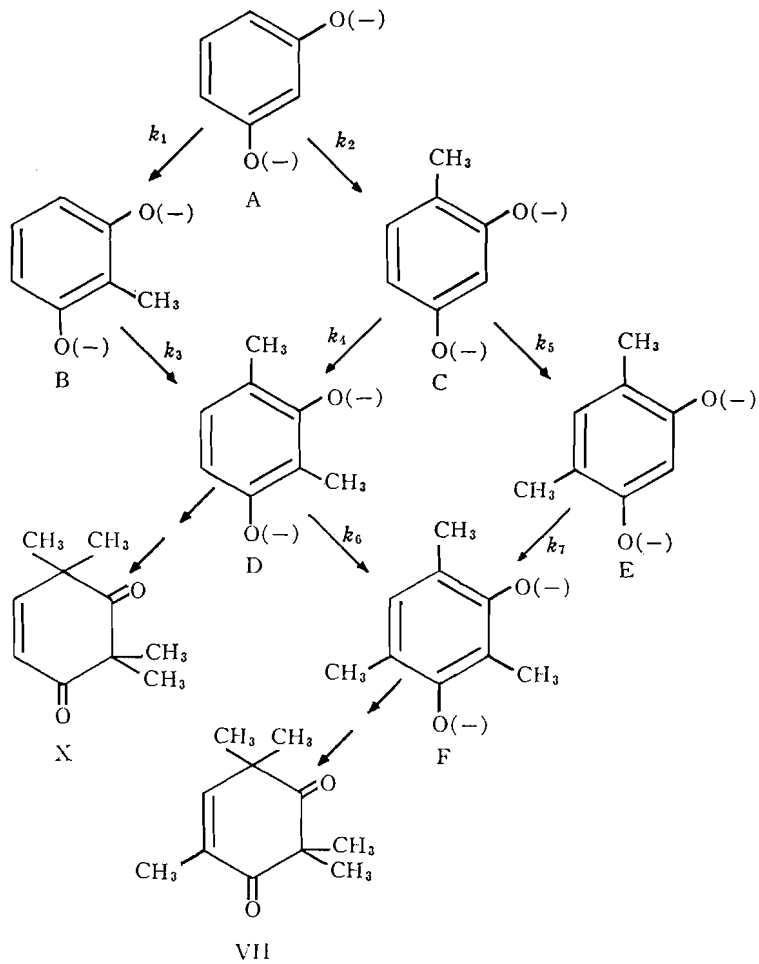

REACTION SCHEME 2. Apparent sequence of resorcinol dianion carbon methylation.

Can. J. Chem. Downloaded from www.nrcresearchpress.com by 210.87.254.42 on 09/05/12
For personal use only.

study. Comparison of the neutral fraction analyses of the methylation of resorcinol in tetrahydrofuran–toluene solution with those obtained for the methylation of mesorcinol reported in Table V shows that the enediones have another source, or a far larger portion of the product would have been dimethoxymesitylene.

TABLE V

Neutral fractions from the methylation of resorcinol and mesorcinol*

Phenol used	Equiv. LiH	Reaction time (h)	% neutral	Neutral fraction composition (%)		
				Enedione	DiMeOmesitylene	Others
Resorcinol	4	11	38	87‡	2.4	11
Resorcinol	4	24	44	86§	1.8	12
Resorcinol	6	24	47	99‖	0.0	<1
Mesorcinol	4	23	99	59¶	38	2.7
Mesorcinol†	1	8	37	50¶	44	6

*66° in 20% (by volume) tetrahydrofuran–toluene.
†The acid fraction was 58% 3-methoxymesitol.
‡Composition not checked.
§Contained about 85% VII and 15% X.
‖Contained about 94% VII and 6% X.
¶Contained only VII.

The first indication of what alternative paths could be operating in the methylation of the resorcinol dianion was the observation that some of the early fractions from the vapor phase chromatograph of the phenolic or acid fraction, which could not be sufficiently resolved for individual collection, exhibited nuclear magnetic resonance signals in the region of the geminal dimethyls in the enedione products (i.e. between 8.5 and 9.1 τ and between 7.8 and 8.2 τ) (25). By double collection on the vapor phase chromatograph, first from an Apiezon-1 and then from a polar Ucon column, it was possible to separate two components in 19 and 8% yields respectively from the acid fraction of a resorcinol methylation in 20% (by volume) tetrahydrofuran–toluene solution at 66° for 13.5 h with 6 equiv. of lithium hydride.

The nuclear magnetic resonance spectrum of the first component shows a single hydroxylic proton at 2.00 τ, a quartet (J = 1.5 c.p.s.) of area one at 3.65 τ, a doublet ($J \simeq 1.5$ c.p.s.) of area three at 8.12 τ overlapping a singlet of area three at 8.14 τ, and a sharp singlet of area six at 8.69 τ. The infrared spectrum shows a hydroxylic absorption as well as the three strong bands at 1 730, 1 675, and 1 605 cm^{-1} which are characteristic of the cyclohex-2,5-diene-1-one system. The geminal dimethyl doublets at 1 375 and 1 364, and 1 180 and 1 145 cm^{-1}, were also present. The ultraviolet spectrum showed a maximum at 236 mμ ($\epsilon = 4.1 \times 10^3$). From this spectral evidence the structure XI was assigned to the material.

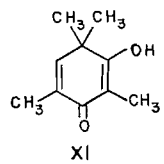

XI

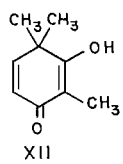

XII

The second component was assigned structure XII on the basis of its nuclear magnetic resonance spectrum, which showed a hydroxylic proton at 2.10 τ, two doublets (J = 10.0 c.p.s.) each of area one at 3.50 and 3.72 τ, and sharp singlets of areas three and six at 8.13 and 8.69 τ. Its infrared spectrum showed a hydroxylic proton and the same geminal dimethyl doublets as did that of XIX. In the double-bond region, strong absorptions occurred at 1 735, 1 690 (shoulder), and 1 662 and a broad band at 1 590 cm^{-1}. In the ultraviolet region a maximum at 221 mμ ($\epsilon = 4.5 \times 10^3$) was present.

Can. J. Chem. Downloaded from www.nrcresearchpress.com by 210.87.254.42 on 09/05/12
For personal use only.

To establish that the components XI and XII are indeed intermediates in the formation of the enedione products, a portion of the acid fraction from which the two tentative intermediates were isolated was further methylated in tetrahydrofuran solution and found to be quickly converted in over 97% yield to neutral material with VII as the major constituent. Also, the fact that no hydroxydienone product was observed in the methylation of mesorcinol and 1 equiv. of lithium hydride established that the hydroxydienone intermediate must indeed be much more readily methylated at carbon than at oxygen and than mesorcinol or *m*-methoxymesitol is at either oxygen or carbon.

Since intermediates XI and XII occur in the methylation of resorcinol dianion, it is probable that the other intermediates of this type (i.e. hydroxydienones) can also occur to a greater or lesser extent. Thus, Reaction Scheme 2 should be extended to include these other intermediates, as is done in Reaction Scheme 3. Little evidence about the relative importance of the various routes to the enedione products has been obtained, but the large amount of dimethoxymesitylene formed in the methylation of the mesorcinol dianion suggests that, at least in the 20% (by volume) tetrahydrofuran–toluene solution, the route through mesorcinol is of minor importance.

Phloroglucinol Methylations

For purposes of comparison, several methylations of phloroglucinol in the presence of 6 equiv. of lithium hydride at 66° were performed. In tetrahydrofuran solution, more than 85% of neutral fraction, which was made up of yields of 49% 2,2,4,4,6,6-hexamethylcyclohexan-1,3,5-trione III, 14% 2,2,4,4-tetramethyl-5-methoxycyclohex-5-en-1,3-dione, 8% 2,4,6-trimethoxyxylene, and 2% trimethoxymesitylene, was obtained. An additional three neutral components (total yield 12%) were unassigned. In aqueous solution under similar conditions, only a 19% yield of neutral fraction was obtained. It was made up of yields of 15% of the hexamethyltrione and 4% of the tetramethylenedione. The acid fractions were not sufficiently volatile for vapor phase chromatographic analysis and consequently were not examined in detail.

In tetrahydrofuran solution, the phloroglucinol trianion was even more readily carbon methylated than was the resorcinol dianion. Just why so little neutral fraction was obtained from the aqueous methylation of phloroglucinol is not clear and perhaps warrants more study. Unfortunately, the nonvolatility of the acid fraction would necessitate the use of separation and analytical techniques other than vapor phase chromatography.

EXPERIMENTAL

The phenols employed throughout the following experiments were reagent grade materials which were doubly sublimed and stored in the dark. They melted over less than a 1° range and showed no or minuscule impurities on the vapor phase chromatograph. All organic solvents, except the alcohols, were dried over, and freshly distilled from, $LiAlH_4$. Methyl iodide was freshly distilled from calcium hydride. All manipulation of lithium and sodium hydrides was done in a nitrogen-purged dry box and reactions were run under a nitrogen atmosphere in carefully dried equipment. Water used as a reaction solvent was deionized water which was distilled, degassed under vacuum, and saturated with nitrogen before transfer. Reaction times were measured from the start of methyl iodide addition.

Cation Effects

Into a 500-ml Morton (creased) flask equipped with a reflux condenser, an equilibrating addition funnel, and a high-speed stirrer were placed 0.118 ± 0.002 mole of metal hydride (LiH or NaH) and 3.22 ± 0.05 g (0.0292 ± 0.0005 mole) of resorcinol, and 150 or 175 ml of tetrahydrofuran was slowly added. The white slurry was slowly brought to gentle reflux and 25 ml (57 g, 0.400 mole) of methyl iodide was added over several hours with vigorous high-speed stirring. After 30 ± 5 h, the reaction was stopped, the solvents were removed on a rotary evaporator, and the residue was taken up in 100 ml each of diethyl ether and 1:1 aqueous Claisen's alkali.* The ethereal layer was extracted with additional 50-ml portions of the alkali

*KOH *(350 g) and 250 ml of water made up to 1 l with methanol.*

Can. J. Chem. Downloaded from www.nrcresearchpress.com by 210.87.254.42 on 09/05/12
For personal use only.

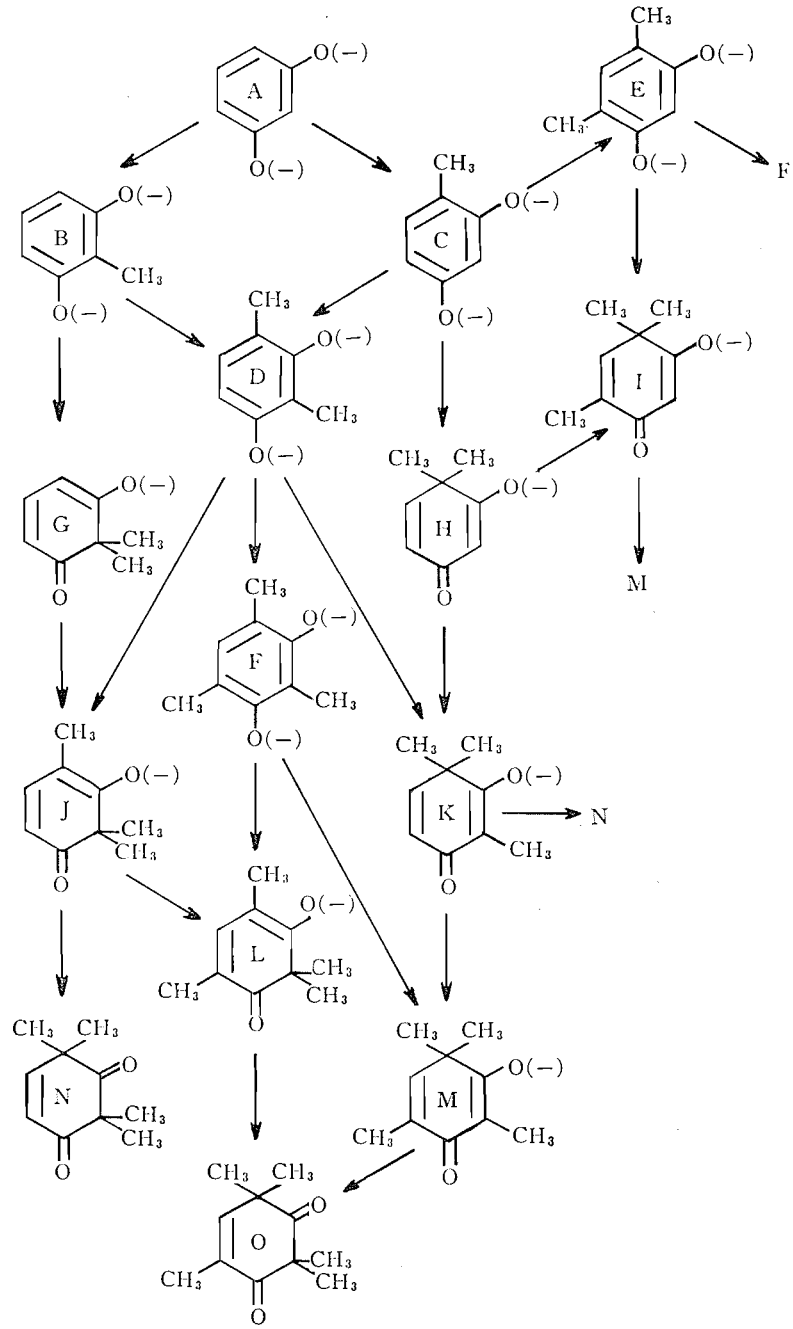

REACTION SCHEME 3. Sequence of resorcinol dianion carbon methylation including hydroxydienone intermediates.

until the extract was colorless. The combined alkaline fractions were extracted with several 50-ml portions of ether. The combined ethereal layers were dried and the ether was removed to leave the neutral fraction. The alkaline layers were acidified with hydrochloric acid and the acid or phenolic fraction was recovered by three or four extractions with ether. The ethereal extract was dried and the ether removed to leave the phenolic fraction.

Vapor phase chromatographic analysis (v.p.c.) of the two fractions for the lithium and for the sodium salts

Can. J. Chem. Downloaded from www.nrcresearchpress.com by 210.87.254.42 on 09/05/12
For personal use only.

respectively are: neutral fraction, 99%, 82%; enedione mixture, 24%, <2%; *m*-dimethoxybenzene, 4%, 55%; 2,6- and 2,4-dimethoxytoluene, 41% and 9%, 18% (total); 2,4-dimethoxy-1,3-xylene, 18%, 3%; 4,6-dimethoxy-1,3-xylene, 5%, 2%; and dimethoxymesitylene, 2%, <1%. The yields from the 18% of acid fraction in the case of the sodium salt were 11% *m*-methoxyphenol, 4% resorcinol, and at least five other components.

Solvent Effects

Aqueous Tetrahydrofuran

Into the Morton flask of the apparatus previously described was placed 0.97 ± 0.14 g (0.092–0.120 mole, 4 equiv.) of lithium hydride, and 10–25 ml of tetrahydrofuran was added (except in the pure aqueous reaction). In the addition funnel, 3.00 ± 0.45 g (0.023–0.031 mole, 2 equiv.) of resorcinol was dissolved in 25–40 ml of tetrahydrofuran (100 ml of water in the aqueous reaction) and slowly added to the lithium hydride with gentle stirring. After hydrogen evolution ceased, the remaining quantities of tetrahydrofuran and water were added to give a total of 150 ml of solvent, and then heating and vigorous stirring commenced. At reflux, 25 ml (57.0 g, 0.400 mole, >13 equiv.) of methyl iodide was added dropwise over 1–2 h.

The reaction was gently refluxed with vigorous stirring for about 10 h and without stirring for another 12 h before it was worked up by the extractive procedure presented above. The v.p.c. analyses of the neutral fractions on a polar Ucon column are presented in Table II. Except in pure water, the neutral fraction accounted for 97–100% of the resorcinol. In water, it was 80%. The resinous acid fractions were not examined in detail but no resorcinol was present and, at most, there were only small amounts of *m*-methoxyphenol present.

Other Solvents

For the other solvents presented in Table III, the quantities of lithium hydride, resorcinol, and methyl iodide were very similar to those for the aqueous tetrahydrofuran reactions. In the case of the nonpolar solvents such as hexane and toluene, the resorcinol was taken up in 25–50 ml of tetrahydrofuran and added to the lithium hydride in the Morton flask so that the resorcinol salt was formed before the addition of the nonpolar solvent. In the case of methanol, dimethylsulfoxide, and dimethylformamide, the resorcinol was dissolved in a portion of the solvent and added normally. The reaction and work-up were performed as before and the analyses of the neutral fractions are reported in Table III.

Methylation of m-Methoxyphenoxide

Into the Morton flask was placed 0.95 ± 0.08 g (0.017 ± 0.009 mole, 2 equiv.) of lithium hydride, and 5.9 g (0.050 mole, 1 equiv.) of *m*-methoxyphenol dissolved in 25 ml of the solvent employed (tetrahydrofuran or water) was slowly added with gentle stirring. After hydrogen evolution ceased, the remaining solvent (water, tetrahydrofuran, or toluene) was added to give 150 ml, and gentle reflux and vigorous stirring commenced. Over a period of 2 h, 25 ml (57 g, 0.400 mole) of methyl iodide was added. After the 30-h reaction period, the reaction mixture was worked up like the resorcinol methylations. Product analysis is reported in Table III.

Methylation of 3,5-Dimethoxyphenoxide

Following the procedure of Pratt and Robinson (30), 3,5-dimethoxyphenol was synthesized from phloroglucinol and methanol with hydrogen chloride catalysis. To 1.040 g (0.118 mole) of lithium hydride and 10 ml of tetrahydrofuran in the Morton flask, 3.820 g (0.0207 mole) of 3,5-dimethoxyphenol (b.p. 132° at 0.9 mm, m.p. 39–40°) in 40 ml of tetrahydrofuran was slowly added. After hydrogen evolution ceased, an additional 100 ml of tetrahydrofuran was added, and at gentle reflux with vigorous stirring 25 ml (57 g, 0.400 mole) of methyl iodide was added over a period of 1 h. After 24 h, the reaction was worked up by the usual extractive procedure to give 4.47 g of neutral and 0.01 g of acid fraction. Vapor phase chromatographic analysis on a polar Ucon column showed the neutral fraction to be 39% 1,3,5-trimethoxybenzene, 43% 2,4,6-trimethoxytoluene, and 9% 2,4,6-trimethoxyxylene. The remaining two unidentified fractions, in 6 and 3% yields, showed geminal dimethyl proton signals in their nuclear magnetic resonance spectrum at 7.95–8.05 τ and carbonyl absorption in the infrared, indicating that they were dienone products.

The Phenolic Fraction

The phenolic fraction from the methylation of resorcinol in tetrahydrofuran–toluene solution with 4 equiv. of lithium hydride and excess methyl iodide was examined at 66° for various times of reaction. To 1.102–1.312 g (0.125–0.148 mole) of lithium hydride in the Morton flask, 3.446–4.073 g (0.0312–0.0370 mole) of resorcinol in 25 ml of tetrahydrofuran was slowly added with gentle stirring. After hydrogen evolution had ceased, 100 ml of toluene was added, the flask was lowered into the 66° constant temperature bath, and vigorous high-speed stirring commenced. After equilibration for ¾–1 h, 25 ml (57 g, 0.400 mole) of methyl iodide was rapidly added. The reaction time was measured from the start of the methyl iodide addition to the removal of the flask from the oil bath. After the desired interval, stirring was stopped, the methyl iodide and other solvents were quickly removed on the rotary evaporator, and the reaction was worked up by the usual extraction method to give the neutral and phenolic or acid fractions.

The exact quantities of reagents used and weights of neutral and acid fractions are reported in Table VI. The compositions of the acid fractions are reported in Table IV. Structural assignment of the components of the acid fraction was by nuclear magnetic resonance and infrared spectra obtained on the materials collected from a 10-ft Apiezon-1 column of the v.p.c. and by comparison of spectra and retention times with those of knowns of all compounds identified except the two dimethylresorcinols (see Table IV). The components of the neutral fraction were also collected from a 16-ft Ucon 50-HB-5000 and identified by spectral

Can. J. Chem. Downloaded from www.nrcresearchpress.com by 210.87.254.42 on 09/05/12
For personal use only.

TABLE VI

Methylation of resorcinol in tetrahydrofuran–toluene* solution for various time intervals at 66°

Reaction time	Moles LiH	Moles resorcinol	Product weights		% acid fraction
			Acid	Neutral	
5 min	0.125	0.0312	2.67	0.0	100
15 min	0.138	0.0346	3.64	0.0	100
30 min	0.126	0.0317	3.61	0.05	98
1 h	0.141	0.0355	4.42	0.18	96
2 h	0.148	0.0370	4.85	0.65	88
4 h	0.135	0.0338	3.80	1.31	75
11 h†	0.134	0.0335	3.55	2.20	62
24 h†	0.135	0.0338	3.08	2.44	56
65 h†	0.138	0.0348	2.63	3.18	45

*Tetrahydrofuran (25 ml) and 100 ml of toluene.
†No excess LiH was evident in the work-up.

methods, but the only trend noted was a small decrease in the amounts of the intermediately methylated toluenes, xylenes, and mesitylene compared to the enediones as the reaction proceeded. The analyses of the acid fractions are reported in Table IV.

Preparation of Mesorcinol

Attempts to prepare mesorcinol (dihydroxymesitylene or 2,4,6-trimethylresorcinol) from mesitol (2,4,6-trimethylphenol) by first nitrating or sulfonating were unsuccessful because of oxidation and decomposition of the mesitol. (Judson and Kilpatrick were also unable to prepare *m*-nitromesitol directly (31).) The preparation reported by Cornforth *et al.* (32) for mesorcinol by methylation of resorcinol with sodium methoxide and methanol could not be repeated. Friedel and Crafts reactions with zinc chloride or boron trifluoride and methyl iodide in a variety of solvents were also singularly ineffective. Attempts to diazotize diaminomesitylene with sodium nitrite in hydrochloric acid or sulfuric acid solutions, either stepwise or both amine groups at once, and to decompose the diazonium salts formed gave little hydroxyl-containing material. (Morgan and Davies were able to couple both the mono- and the di-diazonium salt of diaminomesitylene with β-naphthol but no yields and few details are given (33).) Equally unsuccessful were the attempts to exchange the amino groups for hydroxyl groups in diaminomesitylene by use of the Bucherer reaction (34).

The procedure finally used for the preparation of dihydroxymesitylene was essentially that employed by Knecht (35).

Dinitromesitylene

To 350 ml of red fuming nitric acid cooled in an ice bath to 0°, 140 ml (121 g, 1.0 mole) of mesitylene (b.p. 164–165°) was very slowly added, drop by drop, with magnetic stirring. After the addition was complete (4–5 h) the reaction mixture was stirred at room temperature for 2 h and then poured onto ice (about 700 g). Water (1 000 ml) was added and the cake of dinitromesitylene was broken into small pieces before the flask was placed in a refrigerator overnight.

The aqueous acid was decanted and the solid washed with several liters of water. The solid was then taken up in hot absolute ethanol (about 700 ml) and recrystallized to give beautiful pale yellow needles. The 204.1 g of dinitromesitylene (m.p. 84.5–85.0°, lit. 86° (36)) obtained corresponds to a 96.5% yield.

Nitromesidine

In a 3-l three-necked flask, 100 g (0.485 mole) of dinitromesitylene was dissolved in 750 ml of absolute ethanol and 85 ml of concentrated aqueous ammonia was added. The solution was gently refluxed on a steam bath while hydrogen sulfide gas was slowly bubbled through it. Every few hours, the solution was saturated with ammonia. After 50 h, the hydrogen sulfide gas flow was stopped and the reaction cooled to 0° for 4–6 h to precipitate the sulfur, which was then removed by filtration. The yield of 43.3 g (0.135 mole) of monoclinic sulfur (m.p. 119.5–120.5°) corresponds to 96% of theoretical yield.

The ethanol was removed from the filtrate on the steam bath to leave a yellow-brown oil which solidified on cooling. The crude nitromesidine was purified by dissolving it in 500 ml of toluene and by precipitating the amine as the hydrochloride salt by bubbling hydrogen chloride through the solution. The amine hydrochloride was removed by filtration and the filtrate was treated with more hydrogen chloride to recover any remaining amine. The salt was washed with copious quantities of toluene and air dried (m.p. 219° (decomp.)). The nitromesidine was recovered by treating the hydrochloride salt with aqueous ammonia and by recovering the liberated amine with several 150-ml ether extractions. Removal of the ether gave 81.5 g (95%, m.p. 71–72.5°, lit. 75°) of a yellow solid. Either the hydrochloride salt or the free amine could be used in the next step.

m-Nitromesitol

To the hot solution formed by adding 50 ml of concentrated sulfuric acid to 250 ml of water, 50 g (0.277 mole) of nitromesidine was added. After all the amine went into solution, 250 ml of water was added together with about 500 g of ice. By vigorous stirring with a stirring rod, the solid amine salt was kept finely divided.

Can. J. Chem. Downloaded from www.nrcresearchpress.com by 210.87.254.42 on 09/05/12
For personal use only.

With external cooling and occasional addition of ice, 19.70 g (0.281 mole) of sodium nitrite in 90 ml of water was slowly added while the solution was stirred and swirled. Small portions of solid sodium nitrite were added until the solution still gave a positive starch–iodide paper nitrous acid test after it had stood for 10–15 min. Several grams of urea were then added to remove the excess nitrous acid.

After it had stood for several hours at room temperature, the solution was heated on a steam bath for several hours. The nitromesitol was removed from the by-products by steam distillation. By acidifying the distillate with 5–10 ml of concentrated hydrochloric acid per liter of distillate, 41.35 g (82%) of crude nitromesitol was recovered from the 24–35 l of distillate by ether extraction. The nitromesitol was purified by extraction of an ethereal solution with 1:1 aqueous Claisen's alkali, which was then washed with several portions of ether. The alkaline material was acidified and re-extracted with ether to give 30.1 g (60%) of nitromesitol (m.p. 63–64.5° after recrystallization from toluene).

Anal. Calcd. for $C_9H_{11}NO_3$: C, 59.66; H, 6.12; N, 7.73. Found: C, 59.43; H, 6.19; N, 7.60.

Mesorcinol

Reductions of nitromesitol with lithium aluminium hydride exploded two out of three times; thus, this reduction was performed with tin and hydrochloric acid.

On a steam bath 50 g (0.277 mole) of nitromesitol was heated for several hours in 175 ml of concentrated hydrochloric acid and 65 g (0.548 mole) of granulated tin, and swirled frequently. The reaction mixture was poured into 1.5 l of water and heated on a steam bath while hydrogen sulfide was bubbled through the solution to decompose the tin salts. After the tin sulfide was removed by filtration, the filtrate was evaporated to dryness on the steam bath.

The salt was taken up in 350 ml of water and 70 ml of sulfuric acid, and the solution was cooled to 0° before 19.0 g (0.272 mole) of sodium nitrite in 90 ml of water was slowly added with stirring. After it was stirred for several hours at room temperature, the solution was heated for 3 h on the steam bath, cooled, and extracted with a number of 100-ml portions of ether. From the black tarry mess left after ether removal, 19.9 g (48%) of crude mesorcinol was obtained after two sublimations. After two recrystallizations from toluene, 9.8 g (23%) of mesorcinol (m.p. 152–153.5°, lit. 149–150°) was obtained in 12% overall yield.

Anal. Calcd. for $C_9H_{12}O_2$: C, 71.02; H, 7.95. Found: C, 70.85; H, 7.93.

Methylation of Mesorcinol

Two methylations of mesorcinol were performed in tetrahydrofuran–toluene solution, the first with 4 equiv. and the second with 1 equiv. of lithium hydride. The procedures were parallel and, where different, the quantities of reagents or products indicated refer to the first and second reaction respectively.

To 1.25 g (0.142 mole) or 0.238 g (0.0273 mole) of lithium hydride placed in the Morton flask, 5.217 g (0.0342 mole) or 4.142 g (0.0272 mole) of mesorcinol in 25 ml of tetrahydrofuran was slowly added. After hydrogen evolution had ceased, the flask was lowered into the 66° oil bath and vigorous stirring was commenced. After equilibration for $\frac{3}{4}$–1 h, 25 ml (57 g, 0.400 mole) of methyl iodide was added over several hours.

The reaction was allowed to proceed for 23 or 8 h before being worked up by the usual extractive procedure to give 5.965 g or 1.673 g of neutral fraction and 0.065 g or 2.801 g of phenolic fraction. The analyses of the neutral fractions are reported in Table V. Of the two phenolic fractions, only the second was examined and found to be exclusively *m*-methoxymesitol and mesorcinol, representing a 36.4% yield and a 26.2% recovery respectively. The products accounted for over 97 or 99% of the starting mesorcinol.

Isolation of Hydroxydienones

Hydroxydienone intermediates were isolated from several methylations of resorcinol with 6 equiv. of lithium hydride in tetrahydrofuran–toluene solution. Thus, to 2.450 g (0.277 mole) of lithium hydride in the Morton flask, 5.073 g (0.0461 mole) of resorcinol in 25 ml of tetrahydrofuran was cautiously added. After hydrogen evolution ceased, 100 ml of toluene was added, the mixture was allowed to equilibrate at 66°, and, with vigorous stirring, 25 ml (57 g, 0.400 mole) of methyl iodide was run in. After 13.5 h, the usual work-up gave 3.940 g of neutral and 4.034 g of acid fraction. The neutral fraction contained enediones (40% yield) and another three components (10% yield). Vapor phase chromatographic analysis of the acid fraction showed it to contain, in addition to peaks assigned to the usual methylated resorcinols (each in 0.5–3.7% yield), a large unsymmetrical peak (32% overall yield) with an Apiezon-1 column. Re-separation of the collected fraction on a polar Ucon column showed it to be made up of two components in the ratio of 5:2 (i.e. in 19 and 8% yields on 39 and 16% of the acid fraction, respectively). The two components were assigned structures XI and XII, principally on the basis of spectral evidence presented above.

Intermediacy of the Hydroxydienones

To establish that the two hydroxydienones XI and XII were potential intermediates, 1.772 g of the acid fraction, containing a total of 55% of the two hydroxydienones, and 1.33 g (0.151 mole) of lithium hydride were treated in 100 ml of tetrahydrofuran at reflux with 25 ml (57 g, 0.400 mole) of methyl iodide for 25 h. (The yellow complex which immediately forms when methyl iodide comes in contact with lithium resorcinolates and which persists as long as any of the salt remains faded within 1 h to the off-white color that indicates no resorcinolates remain.) Normal work-up gave 1.868 g of neutral and 0.054 g of acid fraction. The neutral fraction was 37% 2,2,4,6,6-pentamethylcyclohex-4-en-1,3-dione (VII), 19% dimethoxymesitylene, 12% dimethoxytoluenes and xylenes, and the rest unidentified products.

Methylation of Phloroglucinol in THF

To 2.194 g (0.249 mole) of lithium hydride in the Morton flask, 4.8023 g (0.0380 mole) of phloroglucinol dissolved in 125 ml of tetrahydrofuran was slowly added. Little hydrogen evolution was noted. The flask was

Can. J. Chem. Downloaded from www.nrcresearchpress.com by 210.87.254.42 on 09/05/12
For personal use only.

lowered into the 66° bath and allowed to equilibrate for 1.5 h with vigorous stirring before 25 ml (57 g, 0.400 mole) of methyl iodide was added over a period of 1 h. The reaction was run for 30 h with stirring throughout. The solution was heterogeneous throughout and considerable lithium hydride was present at the end.

The usual extraction work-up gave 6.83 g of neutral and 1.31 g of acid fraction. The acid fraction was not sufficiently volatile to be analyzed on the v.p.c. The 85.4% by weight of neutral fraction had the following composition: 48.5% 2,2,4,4,6,6-hexamethylcyclohexan-1,3,5-trione (m.p. 80.0–81.0°, lit. 80–81° (12)), 14.1% 2,2,4,4-tetramethyl-5-methoxycyclohex-5-en-1,3-dione (m.p. 58.5–60.5°), 7.9% 2,4,6-trimethoxyxylene, and 2.0% trimethoxymesitylene. In addition, peaks of 9.2%, 2.7%, and 0.3% of the total area were unassigned.

Methylation of Phloroglucinol in Water

To 1.2610 g (0.143 mole) of lithium hydride in the Morton flask, 3.489 g (0.0276 mole) of phloroglucinol in 125 ml of water was cautiously added. After the reaction subsided, the flask was lowered into the 66° oil bath and allowed to equilibrate for 1 h with vigorous stirring before the slow addition of 25 ml (57 g, 0.400 mole) of methyl iodide was started. After 28 h the reaction mixture, which was heterogeneous only with respect to the methyl iodide phase, was worked up in the usual manner. The reaction gave 0.937 g of neutral fraction (a low-melting solid) and 4.042 g of acid fraction.

The neutral fraction (19%) consisted of yields of 14.8% of 2,2,4,4,6,6-hexamethylcyclohexan-1,3,5-trione and 4% of 2,2,4,4-tetramethyl-5-methoxycyclohex-5-en-1,3-dione. The acid fraction could not be analyzed by v.p.c.

ACKNOWLEDGMENTS

The author expresses his appreciation to Dr. R. B. Sandin for his personal interest and encouragement. The author also thanks Dr. D. Y. Curtin for his guidance, aid, and encouragement throughout the study and for reading this manuscript, and the University of Illinois and the Firestone Tire and Rubber Company for financial support while this research was undertaken.

REFERENCES

1. H. D. Zook and W. L. Rellahan. J. Am. Chem. Soc. **79**, 881 (1957).
2. P. A. S. Smith and J. E. Robertson. J. Am. Chem. Soc. **84**, 1197 (1962).
3. O. L. Brady and N. M. Chokshi. J. Chem. Soc. 2271 (1929).
4. R. F. Hudson and G. Klopman. J. Chem. Soc. 1062 (1962).
5. D. Y. Curtin, R. J. Crawford, and M. Wilhelm. J. Am. Chem. Soc. **80**, 1391 (1958).
6. A. R. Stein. Ph.D. Dissertation, University of Illinois, Urbana, Illinois. 1964.
7. J. Herzig and S. Zeisel. Monatsh. **9**, 217, 882 (1882); **11**, 291, 311 (1890).
8. W. Will. Chem. Ber. **21**, 602 (1888).
9. O. Margulies. Monatsh. **9**, 1045 (1888).
10. J. Herzig and Br. Erthal. Monatsh. **32**, 505 (1911).
11. F. Kaufler. Monatsh. **21**, 993 (1900).
12. G. F. Pregaglia and M. Binaghi. J. Org. Chem. **28**, 1152 (1963). J. L. E. Erickson and G. C. Kitchens. J. Org. Chem. **27**, 460 (1962).
13. R. J. Highet and T. J. Batterham. J. Org. Chem. **29**, 475 (1964).
14. A. Spitzer. Monatsh. **11**, 104, 287 (1890).
15. J. Herzig and Br. Erthal. Monatsh. **32**, 491 (1911).
16. P. Kurzweil. Monatsh. **24**, 910 (1903).
17. J. Herzig and F. Wenzel. Monatsh. **27**, 781 (1906).
18. J. Herzig and F. Wenzel. Monatsh. **32**, 461 (1911).
19. K. P. Monroe. U.S. Patent No. 2,459,835; Chem. Abstr. **43**, 3037*f* (1949).
20. A. O. Fitton and G. R. Ramage. J. Chem. Soc. 4870 (1962).
21. R. R. Fraser. Ph.D. Dissertation, University of Illinois, Urbana, Illinois. 1958.
22. J. B. Hyne. J. Am. Chem. Soc. **82**, 5129 (1960). J. F. Eastham and G. W. Gibson. J. Am. Chem. Soc. **85**, 2171 (1963).
23. A. R. Stein. Can. J. Chem. This issue.
24. N. Kornblum, P. J. Berrigan, and W. J. LeNoble. J. Am. Chem. Soc. **85**, 1141 (1963); **82**, 1257 (1960).
25. N. Kornblum, R. Seltzer, and P. Haberfield. J. Am. Chem. Soc. **85**, 1148 (1963).
26. E. A. Gould. Mechanism and structure in organic chemistry. Henry Holt and Co., New York, N.Y. 1959. p. 298.
27. A. J. Parker. Quart. Rev. London, **16**, 163 (1962).
28. H. R. Nace and J. J. Monagle. J. Org. Chem. **24**, 1792 (1959).
29. G. M. Coppinger. J. Am. Chem. Soc. **76**, 1372 (1954).
30. D. D. Pratt and R. Robinson. J. Chem. Soc. **125**, 188 (1924).
31. C. M. Judson and M. Kilpatrick. J. Am. Chem. Soc. **71**, 3110 (1949).
32. J. W. Cornforth, R. K. Cornforth, and Sir R. Robinson. J. Chem. Soc. 682 (1942).
33. G. T. Morgan and G. R. Davies. J. Chem. Soc. **123**, 228 (1923).
34. N. L. Drake. Organic reactions. Vol. I. John Wiley and Sons, Inc., New York, N.Y. 1942. p. 105.
35. E. Knecht. Ann. **215**, 97 (1882).
36. R. Fittig. Ann. **141**, 133 (1867).

Can. J. Chem. Downloaded from www.nrcresearchpress.com by 210.87.254.42 on 09/05/12
For personal use only.

Can. J. Chem. Downloaded from www.nrcresearchpress.com by 210.87.254.42 on 09/05/12
For personal use only.

THE METHYLATION OF THE RESORCINOLATE DIANION

II. PER-METHYLATED RESORCINOL: 2,2,4,6,6-PENTAMETHYLCYCLOHEX-4-EN-1,3-DIONE

ALLAN R. STEIN[1]

Noyes Laboratory of Chemistry, University of Illinois, Urbana, Illinois

Received November 13, 1964

Dedicated to Professor R. B. Sandin on the Occasion of his Sixty-Eighth Birthday

ABSTRACT

Structural evidence for the enedione products, 2,2,4,6,6-pentamethylcyclohex-4-en-1,3-dione and 2,2,6,6-tetramethylcyclohex-4-en-1,3-dione, which are the principal products from the methyl iodide alkylation of the dilithium resorcinol salt in nonpolar aprotic or very polar hydroxylic solvents, is presented. The diimide and lithium aluminium hydride reduction products are presented and, together with the decarboxylated hydrolysis product, 2,4,6-trimethylcyclohex-2-en-5-one, constitute proof of the structure of the 2,2,4,6,6-pentamethylcyclohex-4-en-1,3-dione. Some of the synthesis potential of resorcinolate alkylations is indicated.

INTRODUCTION

Earlier studies in this laboratory on the nuclear alkylation of phenoxides, and, in particular, those studies on 2,6-disubstituted phenoxides, led to the study of the alkylation of polyhydroxylic benzenes under basic conditions. Curtin *et al.* (1) first observed that the sealed-tube methylation of lithium 2,6-dimethylphenoxide with methyl iodide leads to the formation of 2,6-dimethylanisole and a carbonyl-containing species to which was assigned structure I. Some of the many factors which influence the relative amounts of carbon and oxygen alkylation have been discussed by Curtin *et al.* (1), Curtin and Fraser (2), Curtin and Dybvig (3), Kornblum and Lurie (4), Kornblum and Seltzer (5), Kornblum *et al.* (6), Kornblum *et al.* (7), and Barner and Schmid (8). A brief review of the alkylation of analogous systems (e.g. enolates, oxime salts, and thiophenolates) is given in the recent paper by Curtin and Dybvig (3).

By analogy to the phenoxide methylations, the various alkylated *m*-dimethoxybenzenes and, possibly, the dienone analogues II and III would be among the expected neutral products from the methylation of the dilithium salt of resorcinol. It is conceivable that even the higher methylation products IV and V might be formed. It is the last of these, the 2,2,4,6,6-pentamethylcyclohex-4-en-1,3-dione (V), with which this paper deals.

The only previous report of the synthesis of V is the questionable work of Kurzweil in 1903 (9). The 5-methyl substituted compound, however, was reported by Herzig and Wenzel in 1906 (10) as a minor product from the methyl iodide methylation of orcinol (5-methylresorcinol). Herzig and Zeisel (11) have reported that the methylation of phloroglucinol gives 2,2,4,4,6,6-hexamethylcyclohexan-1,3,5-trione (VI), a structure which has recently been confirmed by the independent synthesis of Erickson and Kitchens (12).

This paper deals with the synthesis and structure of 2,2,4,6,6-pentamethylcyclohex-4-en-1,3-dione, VI, and some of its properties and reactions.

RESULTS AND DISCUSSION

Methyl iodide methylations of resorcinol in the presence of excess base in solvents of intermediate polarity (e.g. methanol, ethanol, and tetrahydrofuran) give, among the

[1]*Current address: Central Research Laboratories, Dominion Tar and Chemical Co., Ltd., Senneville, Quebec.*

neutral products, a small carbonyl-containing fraction and all seven of the possible 1,3-dimethoxybenzenes—methylation meta to the oxygens was never observed in the products. By use of the less polar solvent mixture of 16% tetrahydrofuran in toluene, it was possible to raise the yield of the carbonyl compounds to about 70%, based upon starting resorcinol, or to about 93–98% of the neutral fraction.

Comparison of the infrared, nuclear magnetic resonance, and ultraviolet spectra of the carbonyl fraction to those of 2,6,6-trimethylcyclohexa-2,4-dienone (I) suggested a similar structure. Thus, the carbonyl fraction collected on the vapor phase chromatograph had carbonyl bands in the infrared at 1 717 and 1 676 cm^{-1} and a geminal dimethyl doublet at 1 382 and 1 362 cm^{-1} compared to those at 1 720 and 1 680 cm^{-1} and at 1 385 and 1 363 cm^{-1} for the Diels–Alder dimer of I (14). In its nuclear magnetic resonance spectrum, the carbonyl fraction had signals at 8.74 and a narrow doublet at 8.16 τ compared to those at 8.80 and 8.13 τ in I. Even the coupling constant giving rise to the doublet was about 1.45 c.p.s. for both species. The ultraviolet absorbance maxima at 231 mμ (ϵ = 8 450) and at 305 mμ ($\epsilon \simeq 57$) suggest that the fraction contains both a conjugated and non-conjugated carbonyl. This conclusion is confirmed by the infrared carbonyl absorption frequencies quoted above.

A molecular weight and elemental analysis determination gave the molecular formula $C_{11}H_{16.5}O_{2.05}$ for one carbonyl fraction. The nuclear magnetic resonance spectrum of this particular fraction showed the aforementioned signals at 8.74 τ (area = 12.97, a singlet), at 8.16 τ (area = 3.05, a doublet, $J \simeq 1.5$ c.p.s.), and at 3.47 τ (area = 1.00, a quartet, $J \simeq 1.5$ c.p.s.) and two pairs of doublets at 3.98 and 3.21 τ (area 0.09, $J \simeq 10.5$ c.p.s.). The relative intensities of the olefinic quartet and pair of doublets varied from reaction to reaction, so that they must be caused by two separate components. Indeed, the spectrum of the carbonyl fraction collected on the vapor phase chromatograph from the methylation of mesorcinol (dihydroxymesitylene) was completely free of the olefinic doublets. It showed only the signals at 3.47, 8.16, and 8.74 τ (relative areas, 1:3:12) and analyzed for $C_{11}H_{16}O_2$.

Nuclear magnetic resonance spin-decoupling studies confirmed that the pairs of olefinic doublets were coupled to each other and that the olefinic quartet at 3.47 τ and the doublet at 8.16 τ were spin coupled. Upon expansion, the 8.74 τ signal was found to be a narrow jagged doublet with separation of about 0.8 c.p.s. The signal was unaffected by temperature variations between −35° and 65°.

From the spectral evidence discussed above, it was concluded that the carbonyl-containing fraction from the methylation of resorcinolate dianion must be a mixture of IV and V. The percentage of IV present varied from 8 to 30%, with the higher end of the range occurring in the reactions with lower conversions of resorcinol to the enediones, as would be expected from the data presented in Part I of this series (13).

While attempts to make the usual derivatives of the double bond or carbonyls in V were unsuccessful, additional evidence for the structure of the enedione (V) is found in some of its reactions. By using pure V derived from the methylation of mesorcinol under conditions identical with those used in the methylation of resorcinol, a diimide reduction of the carbon–carbon double bond was performed by the procedure of van Tamelen *et al.* (15). The reduced material, 2,2,4,4,6-pentamethylcyclohexan-1,3-dione, VII, showed carbonyl absorption frequency shifts from 1 727 and 1 683 cm^{-1} to 1 695 and 1 724 cm^{-1} and disappearance of the 900 cm^{-1} vinyl proton bending frequency. In its nuclear magnetic resonance spectrum, VII showed a pair of overlapping multiplets (J = 6.5 c.p.s.) centered at 7.28 and 7.49 τ of total area one, a narrow doublet (J = 1.5 c.p.s.) at 8.15 τ

Can. J. Chem. Downloaded from www.nrcresearchpress.com by 210.87.254.42 on 09/05/12
For personal use only.

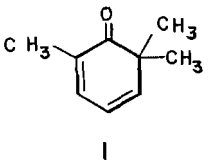

I

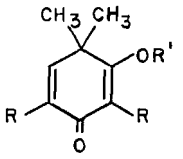

R = H or CH_3
R' = H or CH_3

II

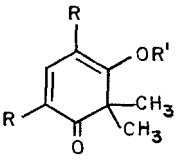

R = H or CH_3
R' = H or CH_3

III

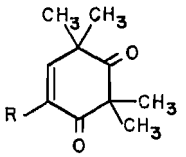

IV R = H
V R = CH_3

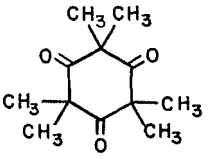

VI

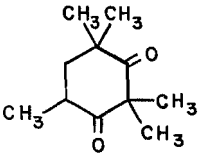

VII

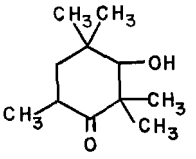

VIII

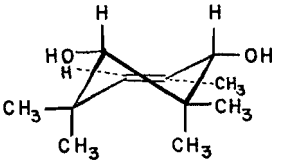

IX

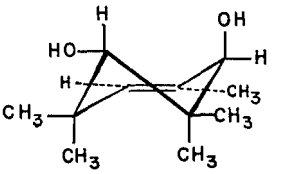

X

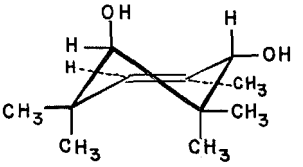

XI

of area one, a doublet (J = 6.5 c.p.s.) at 8.30 τ of area one, and an unsymmetrical quartet at 8.84 τ of area 15. Spin-decoupling studies confirmed that the downfield multiplets were coupled both to the protons at 8.15 and 8.30 τ and to the methyl protons at 8.84 τ. The protons at 8.15 τ were also coupled with the methyl protons. Further confirmation of the structure of VII was found in its ultraviolet spectrum, which showed absorption maxima at 290 mμ (ϵ = 47) and at 214 mμ (ϵ = 725).

Lithium aluminium hydride reduction of V gave three fractions upon vapor phase chromatographic separation. The minor constituent (11% of the product) showed infrared absorptions attributed to hydroxyl and to carbonyl (1 709 cm^{-1}). No olefinic proton signal appeared on the nuclear magnetic resonance spectrum and, in the ultraviolet, maxima appeared at 280 mμ (ϵ = 44) and at 235 mμ (ϵ = 143) as a shoulder on end absorption. This spectral evidence is consistent with structure VIII, arising from V by the 1,4- or Michael addition of the hydride to the conjugated carbonyl (16) and simple reduction of the other carbonyl.

Can. J. Chem. Downloaded from www.nrcresearchpress.com by 210.87.254.42 on 09/05/12
For personal use only.

The infrared spectra of the two remaining fractions, IX and (X + XI), showed no carbonyl absorption but did show very weak carbon–carbon double bond absorption at about 1 650 cm^{-1} and very strong broad hydroxyl absorption. The ultraviolet spectra showed only weak absorptions at about 230 mμ with $\epsilon \simeq 53$ and 38, respectively, for the major (52% yield) and final (37% yield) fractions. Nuclear magnetic resonance and spin-decoupling results are summarized in Table I.

TABLE I

The products of $LiAlH_4$ reduction of the enedione V: n.m.r. and spin-decoupling studies

Compound	Signal	Chemical shift (τ)	Relative area	Multiplicity	J (c.p.s.)	Double resonance
VII	A	6.85	1.2	Multiplet	—	—
	B	7.41	1.8	Multiplet	—	—
	C	8.35	2.0	Multiplet	—	—
	D	9.0	15.0	Multiplet	—	—
IX	A	4.87	0.9	Quartet	1.0	At F gave a singlet
	B	5.54	1.8	Doublet	7.0	" E " " "
	C	5.72		Doublet	7.0	" D " " "
	D	6.56	2.1	Doublet	7.0	" C " " "
	E	6.72		Doublet	7.0	" B " " "
	F	8.30	2.7	Doublet	1.0	" A " " "
	G	9.1	12.0	Unsym. triplet		Unaffected
X + XI	A	4.87	0.6	Multiplet	—	At E gave a narrow doublet
	B	5.51	1.4	Overlapping	7.5	Indeterminable
	C	5.55		doublets	6.0	At D gave a singlet
	D	6.92	0.8	Doublet	6.0	" C " " "
	E	8.37	2.0	Multiplet	—	" A " " narrow doublet
	F	9.1	12.0	Unsym. quintet		Unaffected

After IX had stood in d_6-dimethylsulfoxide for several weeks, or after a small amount of water had been added and the mixture had stood for a few minutes, the nuclear magnetic resonance spectrum of IX was simplified. The pair of doublets at 5.54 and 5.72 τ became a broad singlet, while the doublets at 6.56 and 6.72 τ became two singlets. The rest of the spectrum was unchanged. The low-field doublets then are caused by the hydroxylic protons, and their spin coupling to the protons on the hydroxylic carbon is confirmed.

On the basis of this evidence, the major fraction was assigned structure IX. Because of the marked similarity of the spectra of the major and final fractions, it was concluded that they were isomeric. That the third fraction was about an equal-part mixture of the two possible isomers of IX was inferred from the nuclear magnetic resonance spectrum and especially from the fact that, in the spin-decoupling studies, a narrow "doublet" was obtained from several signals, while the corresponding signals in IX decoupled to a sharp singlet. Structures X and XI were assigned to the components of this mixture.

Aqueous base cleavage of V did not give reverse aldol cleavage at the double bond but did give a quantitative yield of a sharp-melting solid with the molecular formula $C_{11}H_{18}O_3$, corresponding to the addition of the elements of water to the enedione. The infrared spectrum contained the characteristic very broad carboxylic acid hydroxyl absorption between 3 600 and 2 400 cm^{-1}. The ultraviolet spectrum showed only a strong maximum at 233 mμ ($\epsilon = 2.7 \times 10^3$).

Heating the acid above 150° resulted in decarboxylation to give $C_{10}H_{18}O$. The decarboxylated material showed a single sharp carbonyl absorption at 1 720 cm^{-1}, which is

Can. J. Chem. Downloaded from www.nrcresearchpress.com by 210.87.254.42 on 09/05/12
For personal use only.

in the region of non-conjugated carbonyl groups. At 845 cm^{-1}, a band characteristic of C—H bending in trisubstituted ethylenes was present. In the ultraviolet region absorption maxima were present at 293 mμ (ϵ = 220) and at 212 mμ ($\epsilon = 3.2 \times 10^3$). The nuclear magnetic resonance signals and the results of spin decoupling for the decarboxylated compound are summarized in Table II.

TABLE II

Nuclear magnetic resonance and double resonance studies on 2,4,6-trimethylhept-2-en-5-one (XII)

Signal	τ value	Area ratio	Multiplicity	J (c.p.s.)	Double resonance
A	5.02	1	Pair of heptets	10.0 and 1.3	At B gave a single heptet (J = 1.3) " D " " " doublet (J = 10.0)
B	6.53	1	Pair of overlapping quartets	10.0 and 7.0	" A " " " quartet (J = 7.0) " E–F " " " doublet (J = 10.0)
C	7.34	1	Heptet	7.0	" E–F " " singlet
D	8.28	6	Narrow doublet	1.3	" A " " "
E	8.98	6	Pair of overlapping doublets	7.0	" B " an unsymmetrical triplet
F	9.02	3		6.9	" C " " " "

From this spectral evidence, the decarboxylated material was assigned structure XII. This 2,4,6-trimethylcyclohex-2-en-5-one can arise by decarboxylation of either or both of the acids derived from attack of the hydroxide ion at the 1-carbonyl in V, that is, from either XIII or XIV.

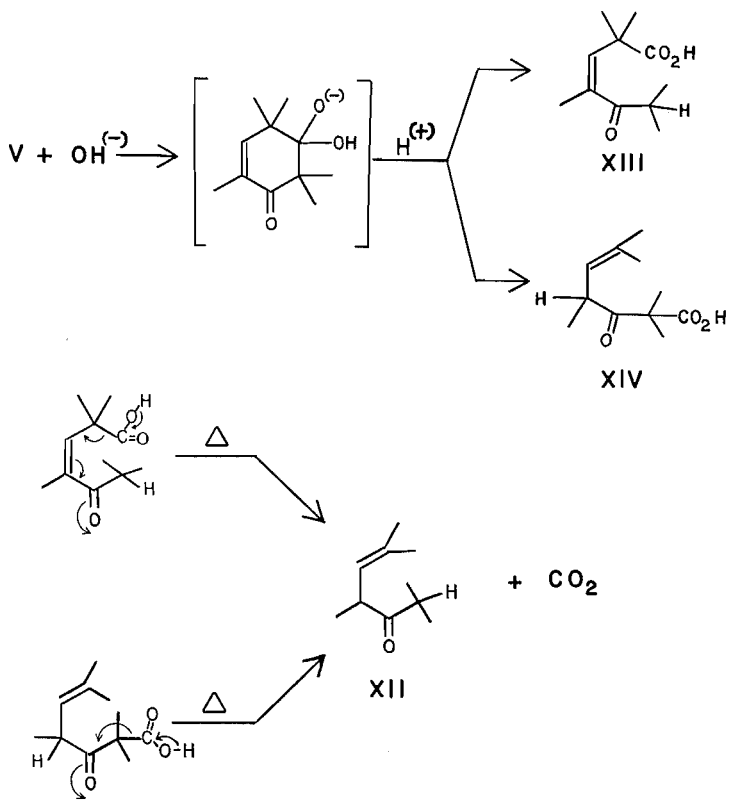

Can. J. Chem. Downloaded from www.nrcresearchpress.com by 210.87.254.42 on 09/05/12
For personal use only.

Nuclear magnetic resonance spectroscopy should readily distinguish between the two acids, XIII and XIV. Unfortunately, even the sharp-melting (88.5–88.8°) analytical sample of the acid gave a spectrum which could be either of, or more likely a mixture of, the two acids. The ultraviolet maximum at 233 mμ ($\epsilon = 2.7 \times 10^3$), corresponding to that at 231 mμ ($\epsilon = 8.5 \times 10^3$) for V, suggests that approximately 30–35% of the "enone" chromophore is present in the acid mixture. This approximately 1:2 composition of XIII and XIV is consistent with the nuclear magnetic resonance spectrum of the acids.

Analogies for the ring cleavage by aqueous base treatment are to be found in a study by Stetter (17) of the formation of δ-ketocarboxylic acids by the treatment of 1,3-cyclohexandiones with aqueous base.

All of the physical data presented for the major product from the methylation of resorcinol in basic nonpolar solution, 2,2,4,6,6-pentamethylcyclohex-4-en-1,3-dione, and some of its reaction products are consistent only with the structure proposed. Potential synthetic uses for the enedione or its analogues produced by substituting other alkyl halides for the methyl iodide at any point along the alkylation sequence, as presented in the previous paper (13), are numerous and varied.

EXPERIMENTAL

Infrared spectra reported were obtained for the most part with a Perkin–Elmer model 21 on 10% solutions in carbon tetrachloride. Nuclear magnetic resonance spectra were obtained with a Varian A-60 on 10–30% solutions in carbon tetrachloride or deuterochloroform, except in those cases (IX, X, and XI) where the sample was not soluble. d_6-Dimethylsulfoxide was then used. Spin-decoupling studies were performed on a Varian HR-60 with side-band double resonance. Ultraviolet spectra were obtained in ethanolic solution on a Bausch and Lomb Spectronic 505 spectrophotometer.

Preparation of 2,2,4,6,6-Pentamethylcyclohex-4-en-1,3-dione (Enedione)

Into a 500-ml Morton (creased) flask continually purged with dry nitrogen, 6.568 g (0.0596 mole) of resorcinol in 25 ml of tetrahydrofuran, which had been freshly distilled from lithium aluminium hydride, was very slowly added to 3.162 g (0.358 mole) of lithium hydride powder while the mixture was gently stirred. In the violent evolution of hydrogen, considerable tetrahydrofuran vapors were entrained. After hydrogen evolution had ceased, 125 ml of toluene, which had been freshly distilled from lithium aluminium hydride, was added, and heating and vigorous high-speed stirring commenced. At gentle reflux, 50 ml (114 g, 0.800 mole) of methyl iodide, which had been freshly distilled from calcium hydride, was dropped in over an 8-h period. The milky-white slurry turns brilliant yellow with the first drops of methyl iodide.

After it was refluxed and stirred for 24–30 h, the solution was allowed to settle and cool before the supernatant liquid was poured off and concentrated on a rotary evaporator. The residue from both the flask and the solvents was taken up in 100 ml each of ether and 1:1 aqueous Claisen's alkali (13). Extraction and re-extraction of each of the ethereal layers until the fresh alkali extracts were colorless, and drying and removal of the ether, gave 6.18 g of neutral fraction. Vapor phase chromatographic analysis on a 16-ft 20% liquid-phase Ucon 50-HB-2000 column at 188° showed the neutral fraction to be 98% enediones and 2% dimethoxymesitylene.

The enedione fraction collected from the vapor phase chromatograph was found to be 93% V and 7% IV. The oil (b.p. 75–82° at 2.3 mm and 62–66° at 0.9 mm) had an average molecular weight of 178.

Anal. Calcd. for $C_{11}H_{16}O_2$: C, 73.30; H, 8.95. Calcd. for $C_{10}H_{14}O_2$: C, 71.65; H, 8.44. Found: C, 72.91; H, 8.78.

Attempted Preparation of Derivatives of the Enedione V

2,4-Dinitrophenylhydrazone

The procedure of Shriner *et al.* (18) was followed, but the small amount of solid obtained after it had stood at 3° for 5 days melted over a 50° range, even after six recrystallizations from ethanol.

Semicarbazone

The procedure of Shriner *et al.* (19) was followed, but even after 2 months in the refrigerator no precipitate had formed.

Bromine Addition

Bromine failed to add to the double bond with carbon tetrachloride or acetic acid solutions of bromine or pure bromine. Aqueous bromine solution gave some paste-like material which failed to crystallize in 15 months.

Can. J. Chem. Downloaded from www.nrcresearchpress.com by 210.87.254.42 on 09/05/12
For personal use only.

Diimide Reduction of the Enedione

By the procedure of Thiele (20), 20 g (0.172 mole) of azodicarboxamide was hydrolyzed with 50 ml of carbon dioxide free 50% aqueous potassium hydroxide at 0° under a nitrogen blanket in a 1-l beaker. The dipotassium azodicarboxylate was vacuum-filtered in a chilled Büchner funnel, again under a blanket of nitrogen. The salt was promptly dissolved in water (100 ml) at 0° and filtered through a chilled sintered-glass funnel into 400 ml of cold absolute ethanol, where the salt again precipitated as a fine bright yellow powder. The product was recovered from the ethanolic solution by filtration and was thoroughly washed with three 400-ml portions of absolute methanol at 0° and under a nitrogen blanket. The yellow salt was transferred to a vacuum desiccator and dried overnight to yield 27.2 g or 83% of the theoretical amount of dipotassium diazodicarboxylate.

Following the general procedure of van Tamelen *et al.* (15), 3.50 g (0.021 mole) of the enedione was added to 75 ml of methanol containing 10.0 g (0.0515 mole) of dipotassium diazodicarboxylate. With magnetic stirring at 0°, 11 ml (11 g, 0.18 mole) of glacial acetic acid in 30 ml of methanol was very slowly added under a nitrogen atmosphere. After several hours at 0°, the solution was allowed to warm slowly to room temperature, where it was stirred for 6 h.

The methanol was removed on a rotary evaporator and the slurry was taken up in ether and water. The ether layer was washed twice with 50-ml portions of 1:1 aqueous Claisen's alkali to remove the excess acetic acid and then washed with water before being dried by an extraction with saturated aqueous sodium chloride and filtration through a cone of sodium sulfate.

Vapor phase chromatographic analysis showed the enedione to be only 15% reduced, so that the reduction procedure was repeated three additional times to give an overall yield of 3.35 g (90%) of a material which was 3.4% enedione, 3.4% miscellaneous products, and 93.4% 2,2,4,6,6-pentamethylcyclohexan-1,3-dione. Analysis of a fraction of VII collected on the vapor phase chromatograph follows.

Anal. Calcd. for $C_{11}H_{18}O_2$: C, 72.49; H, 9.95. Found: C, 72.33; H, 9.90.

Lithium Aluminium Hydride Reduction of the Enedione

Under an atmosphere of dry nitrogen, 1.00 g (0.006 mole) of the enedione was dissolved in 75 ml of reagent grade ether, and 0.696 g (0.0183 mole) of lithium aluminium hydride was added.

After the solution was refluxed for 20 h with magnetic stirring, 1.5 ml of water was cautiously added to destroy the excess hydride and the solution was stirred overnight, before the precipitated salt was removed by filtration and washed with several portions of ether. The ethereal solution was dried with sodium sulfate and the ether removed to leave 0.95 g of white solid (m.p. 106–122°). The three components which were separated on the vapor phase chromatograph were assigned the structures 2,2,4,4,6-pentamethylcyclohexan-3-ol-1-one, VIII (10.6%), 1,3,3,5,5-pentamethylcyclohex-1-en-4*e*,6*e*-diol, IX (52.0%), and the two stereoisomers with pseudo-axial and equatorial hydroxyl groups, X and XI (37.4%).

Treatment of the Enedione with Refluxing Aqueous Potassium Hydroxide

Under a slight positive pressure of nitrogen, 1.05 g of V (b.p. 59° at 0.75 mm, m.p. 5–8°) was refluxed for 2 h in 50 ml of 10% aqueous potassium hydroxide made with freshly opened reagent grade potassium hydroxide and degassed distilled demineralized water. Still under nitrogen, the flask was allowed to cool to room temperature. The solution was extracted with two 75-ml portions of ether which were, in turn, washed with water and dried, and the ether removed to give 0.009 g of neutral fraction, all of which was recovered enedione.

The alkaline solution was acidified with hydrochloric acid and the white solid which separated was recovered with two 50-ml ether extractions. The ethereal layers were washed once with 10 ml of water and dried as usual before the ether was removed on a rotary evaporator. From the $C_{11}H_{18}O_3$ formula calculated from the analysis of a recrystallized portion of the white solid, the 1.127 g of acid fraction obtained corresponds to a 97.8% yield.

Recrystallization of 100 mg of the product from 2 ml of hexane gave 75 mg of very fluffy solid carboxylic acid mixture (m.p. 88.5–88.8°).

Anal. Calcd. for $C_{11}H_{18}O_3$: C, 66.63; H, 9.15. Found: C, 66.67; H, 9.09.

Either collection of the material which passes through the v.p.c. or heating the acid or mixture of acids above 150° for several minutes results in decarboxylation to give a colorless liquid, XII.

Anal. Calcd. for $C_{10}H_{18}O$: C, 77.84; H, 11.77. Found: C, 77.54; H, 11.74.

ACKNOWLEDGMENTS

The author expresses his appreciation to Dr. R. B. Sandin for his personal interest and encouragement. The author also thanks Dr. D. Y. Curtin for his guidance, aid, and encouragement throughout the study, and for reading the manuscript, and the University of Illinois and the Firestone Tire and Rubber Company for financial support while this research was undertaken.

Can. J. Chem. Downloaded from www.nrcresearchpress.com by 210.87.254.42 on 09/05/12
For personal use only.

REFERENCES

1. D. Y. CURTIN, R. J. CRAWFORD, and M. WILHELM. J. Am. Chem. Soc. **80**, 1391 (1958).
2. D. Y. CURTIN and R. FRASER. J. Am. Chem. Soc. **80**, 6016 (1958).
3. D. Y. CURTIN and D. H. DYBVIG. J. Am. Chem. Soc. **84**, 225 (1962).
4. N. KORNBLUM and A. P. LURIE. J. Am. Chem. Soc. **81**, 2705 (1959).
5. N. KORNBLUM and R. SELTZER. J. Am. Chem. Soc. **83**, 3668 (1961).
6. N. KORNBLUM, P. J. BERRIGAN, and W. J. LE NOBLE. J. Am. Chem. Soc. **85**, 1141 (1963).
7. N. KORNBLUM, R. SELTZER, and P. HABERFIELD. J. Am. Chem. Soc. **85**, 1148 (1963).
8. R. BARNER and H. SCHMID. Helv. Chim. Acta, **43**, 1393 (1960).
9. P. KURZWEIL. Monatsh. **24**, 910 (1903).
10. J. HERZIG and F. WENZEL. Monatsh. **27**, 781 (1906).
11. J. HERZIG and S. ZEISEL. Monatsh. **9**, 217, 882 (1882); **11**, 219, 311 (1890).
12. J. L. E. ERICKSON and G. C. KITCHENS. J. Org. Chem. **27**, 460 (1962).
13. A. R. STEIN. Can. J. Chem. This issue.
14. T. L. BROWN, D. Y. CURTIN, and R. FRASER. J. Am. Chem. Soc. **80**, 4339 (1958).
15. E. E. VAN TAMELEN, R. S. DEWEY, and R. J. TIMMONS. J. Am. Chem. Soc. **83**, 3725 (1961).
16. N. G. GAYLORD. Reductions with complex metal hydrides. Interscience Publishers, Inc., New York. 1956. p. 956.
17. H. STETTER. Angew. Chem. **67**, 769 (1955).
18. R. L. SHRINER, R. C. FUSON, and D. Y. CURTIN. Systematic identification of organic compounds. 4th ed. John Wiley and Sons, Inc., New York. 1956. p. 219.
19. R. L. SHRINER, R. C. FUSON, and D. Y. CURTIN. Systematic identification of organic compounds. 4th ed. John Wiley and Sons, Inc., New York. 1956. p. 218.
20. J. THIELE. Ann. **271**, 127 (1892).

Can. J. Chem. Downloaded from www.nrcresearchpress.com by 210.87.254.42 on 09/05/12
For personal use only.

Can. J. Chem. Downloaded from www.nrcresearchpress.com by 210.87.254.42 on 09/05/12
For personal use only.

KETO–ENOL TAUTOMERISM IN β-DICARBONYLS STUDIED BY NUCLEAR MAGNETIC RESONANCE SPECTROSCOPY

II. SOLVENT EFFECTS ON PROTON CHEMICAL SHIFTS AND ON EQUILIBRIUM CONSTANTS

MAX T. ROGERS AND JANE L. BURDETT
Department of Chemistry, Michigan State University, East Lansing, Michigan
Received November 13, 1964

Dedicated to Professor R. B. Sandin on the Occasion of his Sixty-Eighth Birthday

ABSTRACT

The effect of various solvents on the proton chemical shifts of a number of acyclic β-diketones and β-ketoesters has been observed by nuclear magnetic resonance spectroscopy. These shifts are discussed in terms of the dissociation of intramolecular and intermolecular hydrogen bonds on dilution. A complex of benzene with the enol tautomer of the β-dicarbonyl molecule is proposed. The effect of solvents on the position of the tautomeric equilibrium is discussed.

INTRODUCTION

Proton chemical shifts and equilibrium constants for pure β-dicarbonyls are given in the first paper of this series (1). Reeves (2), Reeves and Schneider (3), Schneider and Reeves (4), and Balta-Calleja (5) have investigated solvent effects on acetylacetone by nuclear magnetic resonance (n.m.r.), and Giessner-Prettre (6) has observed the effect of solvents on the n.m.r. spectrum of ethyl acetoacetate. The present study involves a series of β-diketones and β-ketoesters with various substituents and has been extended to include additional solvents. The effects of solvents on proton chemical shifts and on the position of equilibrium have been determined.

EXPERIMENTAL

Instrumental

Proton magnetic resonance spectra were obtained on the Varian A-60 spectrometer. Chemical shift and equilibrium constant measurements have been made at 33 ± 2 °C. Chemical shift values are reported in c.p.s. from internal tetramethylsilane to within ±1 c.p.s. Dilution chemical shifts are reported in c.p.s. relative to the pure compound. A positive shift of a resonance peak is one which occurs at a higher applied magnetic field than the corresponding peak of the pure compound. Equilibrium constants have been obtained by integration of the areas of certain keto and enol resonance peaks. At least six integrations have been performed, and reported percentages of enol tautomer are accurate to within ±2%.

Solvent Purification

Benzene, chloroform, acetic acid, and dioxane were purified according to Vogel (7). Other solvents were dried and fractionally distilled.

Sample Preparation

Solutions were weighed on an analytical balance to ±0.1 mg, and mole fractions were determined to within ±0.001. Tetramethylsilane was added as an internal reference to each solution; the quantity added was the same in each case and did not affect the calculated mole fraction to within 0.001. Spectra made with samples in unsealed tubes were compared with those for samples sealed *in vacuo*, and usually no difference in line width or shape was found. For acetic acid solutions and those using acetylacetone, tubes were evacuated and sealed, but for the other solutions unsealed sample tubes were used.

Compound Preparation and Purification

Synthesis and purification of the β-dicarbonyls used in this study have been described in the first paper of this series (1).

Can. J. Chem. Downloaded from www.nrcresearchpress.com by 210.87.254.42 on 09/05/12
For personal use only.

RESULTS AND DISCUSSION

Chemical shifts at infinite dilution for various proton groups of both the enol and keto tautomers of β-diketones and β-ketoesters are listed in Table I for carbon tetrachloride, benzene, chloroform, and hexane. Similar data are given in Table II for acetylacetone and ethyl acetoacetate in 13 different solvents. The values represent the changes in chemical shifts for given proton groups between pure compound and an infinitely dilute solution in the given solvent, measured in c.p.s., and are positive when the solution shift is at higher magnetic field. In a few cases (m = masked) the values could not be measured because of overlapping of resonances. Where hydrogen bonding occurs only a single proton resonance is seen, and its chemical shift is an average of the shifts for bonded and non-bonded protons.

Inert Solvents

There is very little effect on most of the chemical shifts on dilution in carbon tetrachloride, hexane, carbon disulfide, dioxane, or ether, and we call these solvents inert for that reason. The α-protons of the keto isomer usually move to high field by 10–15 c.p.s. This was explained by Giessner-Prettre (6) as resulting from the breaking up of intermolecularly hydrogen-bonded polymers on dilution. Variable temperature studies confirm the dissociation of intermolecular hydrogen bonds, since the α-proton resonances occur at higher applied fields at increased temperatures (8).

The α-protons of the enol tautomers also move to higher field by 2–12 c.p.s. on dilution, but the most marked effect is on the hydroxyl protons, which are shifted to higher magnetic field by about 6–21 c.p.s. These chemical shifts are illustrated in Fig. 1 where the chemical

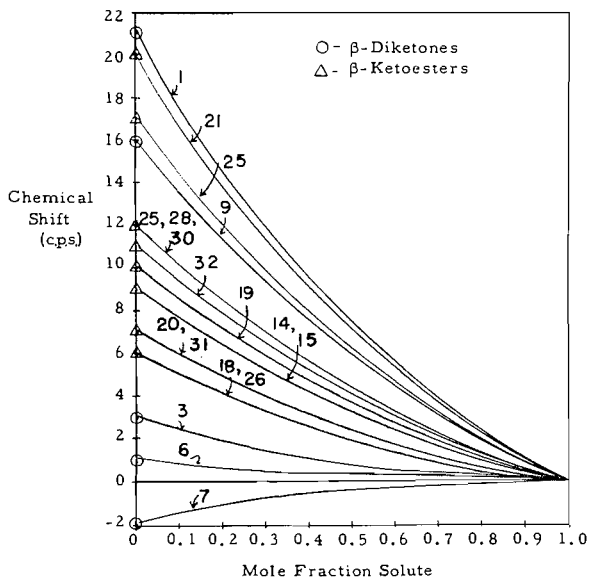

FIG. 1. Chemical shift relative to pure solute of the OH proton in β-dicarbonyls in carbon tetrachloride vs. mole fraction of solute (code numbers refer to compounds of Table I).

shift of the OH proton is plotted as a function of concentration in carbon tetrachloride solution for all the β-dicarbonyls studied. These shifts can be attributed to the breaking up on dilution of the intramolecularly hydrogen-bonded species of the enol tautomer.

Can. J. Chem. Downloaded from www.nrcresearchpress.com by 210.87.254.42 on 09/05/12
For personal use only.

TABLE I

Chemical shifts of the proton groups of β-diketones and β-ketoesters in various solvents at infinite dilution*

Code	Compound	Ethyl		Acetyl					Alkyl α-group	Other
		CH_3	CH_2	CH_3[e]	CH_3[k]	α-H[k]	α-H[e]	OH[e]		
Benzene solutions										
1	Acetylacetone	—	—	25	33	50	39	−45	—	—
3	α-Chloroacetylacetone	—	—	25	29	39	—	−29	—	—
6	Hexafluoroacetylacetone	—	—	—	—	—	40	+37	—	—
7	Trifluoroacetylacetone	—	—	57	54	—	46	+27	—	—
9	α-Methylacetylacetone	—	—	24	29	47	—	−34	20[k] 32[e]	—
14	Butyl acetoacetate	—	—	23	29	28	5	−36	—	8(bu CH_2)
15	*t*-Butyl acetoacetate	—	—	22	29	25	2	−37	—	8[e]($(CH_3)_3$) 5[k]($(CH_3)_3$)
18	Ethyl acetoacetate	19[k] 21[e]	16[k] 14[e]	25	31	35	8	−35	—	—
19	Ethyl α-allylacetoacetate	22	17	15	20	19	—	−34	−1, 4, 5	—
20	Ethyl α-isoamylacetoacetate	18	14	m	15	13	—	−38	5, 5, −2	—
21	Ethyl benzoylacetate	14[k] 14[e]	12[k] 14[e]	—	—	24	3	−22	—	—
24	Ethyl α-isobutylacetoacetate	20	16	m	16	9	—	−38	−2, 7, 8	—
25	Ethyl α-*n*-butylacetoacetate	20	16	m	17	13	—	−31	m	—
26	Ethyl α-chloroacetoacetate	30[k] 27[e]	30[k] 26[e]	21	32	43	—	−25	—	—
28	Ethyl α-ethylacetoacetate	21	15	m	19	20	—	−36	6, 0	—
29	Ethyl α-fluoroacetoacetate	28	29	—	28	44	—	—	—	—
30	Ethyl trifluoroacetoacetate	30[k] 32[e]	31[k] 33[e]	—	—	47	24	−10	—	—
31	Ethyl α-methylacetoacetate	23	18	—	24	28	—	−39	8	—
32	Ethyl α-isopropylacetoacetate	18	15	19	28	11	—	−33	(7, 3, −1)[k] (16, 6)[e]	—
34	Methyl acetoacetate	—	—	—	38	34	—	—	—	23(OCH_3)
Carbon tetrachloride solutions										
1	Acetylacetone	—	—	2	1	10	12	21	—	—
3	α-Chloroacetylacetone	—	—	−2	0	18	—	3	—	—
6	Hexafluoroacetylacetone	—	—	—	—	—	0	1	—	—
7	Trifluoroacetylacetone	—	—	2	—	—	9	−2	—	—
9	α-Methylacetylacetone	—	—	0	3	18	—	16	0[k] (CH_3) 0[e] (CH_3)	

Can. J. Chem. Downloaded from www.nrcresearchpress.com by 210.87.254.42 on 09/05/12
For personal use only.

TABLE I (*Concluded*)

Code	Compound	Ethyl		Acetyl					Alkyl	Other
		CH_3	CH_2	CH_3[e]	CH_3[k]	α-H[k]	α-H[e]	OH[e]	α-group	
14	Butyl acetoacetate	—	—	−1	−1	9	7	9	—	−1(bu CH_2)
15	*t*-Butyl acetoacetate	—	—	0	0	6	2	9	—	−1[e,k] ($(CH_3)_3$)
18	Ethyl acetoacetate	−3	1	1	1	13	8	6	—	—
19	Ethyl α-allylacetoacetate	−3	0	1	1	13	—	10	1, 0, 2	—
20	Ethyl α-isoamylacetoacetate	−2	0	m	1	10	—	7	−1, −2, 0	—
21	Ethyl benzoylacetate	−5[k] −5[e]	2[k] 2[e]	—	—	11	9	20	—	—
24	Ethyl α-isobutylacetoacetate	−3	0	m	1	13	—	12	−1, 0, 2	—
25	Ethyl α-*n*-butylacetoacetate	−3	1	m	1	13	—	17	−3, 3[m]	—
26	Ethyl α-chloroacetoacetate	0[k] −1[e]	2	1	2	8	—	6	—	—
28	Ethyl α-ethylacetoacetate	−1	1	m	3	15	—	12	—	—
29	Ethyl α-fluoroacetoacetate	−2	5	—	1	29	—	—	—	—
30	Ethyl trifluoroacetoacetate	−1[k] 1[e]	0[k] 3[e]	—	—	6	7	12	—	—
31	Ethyl α-methylacetoacetate	−1	0	4	2	12	—	7	2	—
32	Ethyl α-isopropylacetoacetate	0	1	0	2	13	—	11	0, 2	—
34	Methyl acetoacetate	—	—	—	0	9	—	—	—	0 (OCH_3)
Chloroform solutions										
1	Acetylacetone	—	—	−4	−5	0	2	20	—	—
7	Trifluoroacetylacetone	—	—	−2	−2	4	2	31	—	—
15	*t*-Butylacetoacetate	—	—	3	5	—	−4	0	—	3 ($(CH_3)_3$)
18	Ethyl acetoacetate	−4	−5	0	−3	3	3	2	—	—
21	Ethyl benzoylacetate	−10[k] −5[e]	−9[k] −6[e]	—	—	−2	−1	22	—	—
26	Ethyl α-chloroacetoacetate	−2[k] −2[e]	−3	−2	−3	15	—	−3	—	—
31	Ethyl α-methylacetoacetate	−6	−6	m	4	2	—	−2	−5	
Hexane solutions										
1	Acetylacetone	—	—	8	7	17	16	6	—	—
18	Ethyl acetoacetate	0	1	8	7	17	10	−3	—	—
26	Ethyl α-chloroacetoacetate	m	5	3	5	28	—	3	—	—
31	Ethyl α-methylacetoacetate	m	1	2	7	17	—	3	—	—
34	Methyl acetoacetate	—	—	—	5	15	—	—	—	5 (OCH_3)

*Chemical shifts are in c.p.s. relative to the pure compound. k = keto, e = enol, and m = masked.

Trifluoroacetylacetone and hexafluoroacetylacetone are exceptions. In this case the electronegative substituents may lead to the formation of stronger hydrogen bonds not appreciably broken up at the lowest dilutions used here (~0.03 mole fraction solute). However, the intramolecular hydrogen bond of these compounds is particularly sensitive to heat, and increased temperatures result in marked shifts of the hydroxyl proton to high fields (8). The small downfield shift of the hydroxyl proton of the enol tautomer of ethyl acetoacetate on dilution in ether and hexane is also an exception to the above generalizations.

Hydrogen-Bonding Solvents

When the solvent molecules are able to form hydrogen bonds with the α-protons of the keto tautomer, or with the hydroxyl proton of the enol tautomer, the chemical shifts of these protons do not tend to change much on going from pure liquid to solution. This behavior is noted, in general, for the solvents chloroform, acetonitrile, acetic acid, and ethanol, and may be the result of the simultaneous breaking up of solute–solute intermolecular hydrogen bonds and the re-forming of solute–solvent intermolecular hydrogen bonds. We might expect a shift of the α-proton to lower magnetic field on dilution if the hydrogen bond to solvent molecules were stronger than that to the carbonyl group of the β-dicarbonyl itself. Such downfield shifts are observed (Table II) particularly for acetylacetone and ethyl acetoacetate in dimethylsulfoxide and in methanol.

TABLE II

Chemical shifts for the proton groups in acetylacetone and ethyl acetoacetate in various solvents at infinite dilution*

		Ethyl		Acetyl		α-Proton		
Code	Solvent	CH_3	CH_2	CH_3[e]	CH_3[k]	CH_2[k]	CH[e]	OH[e]
Acetylacetone								
9	Acetic acid	—	—	−1	−1	−2	0	32[b]
13	Acetonitrile	—	—	−1	0	0	−4	−10
5	Benzene	—	—	25	33	50	39	−41
3	Carbon disulfide	—	—	3	4	14	13	16
2	Carbon tetrachloride	—	—	2	1	10	12	21
6	Chloroform	—	—	−4	−5	0	2	20
12	Dimethylsulfoxide	—	—	−2	3	−5	−8	68[b]
8	Dioxane	—	—	1	2	m	2	38
7	Absolute ethanol	—	—	−1	−1	m	−1	595
10	95% ethanol	—	—	−3	−4	m	−4	605
4	Ether	—	—	3	4	m	7	21
1	Hexane	—	—	8	7	17	16	6
11	Methanol	—	—	−2	−3	−4	−3	625
Ethyl acetoacetate								
9	Acetic acid	−3	−3	1	−2	−4	2	4
13	Acetonitrile	0	0	m	1	−1	0	1
5	Benzene	19[k] 17[e]	15[k] 13[e]	26	32	36	9	−33
3	Carbon disulfide	1	4[k,e]	4	5	13	9	8
2	Carbon tetrachloride	−2	0	2	2	14	9	6
6	Chloroform	−4	−5	0	−3	3	3	2
12	Dimethylsulfoxide	1	2	0	2	−6	−5	6
8	Dioxane	−1	1	2	3	3	2	2
7	Absolute ethanol	−2	−1	1	−1	−1	2	1
10	95% ethanol	−1	−2	−1	−3	−3	0	2
4	Ether	0	0	4	4	11	6	−3
1	Hexane	0	1	8	7	17	10	−3
11	Methanol	−1	−2	1	−1	−3	−1	1

*Chemical shifts are in c.p.s. relative to the pure compound. k = keto, e = enol, m = masked, and b = broad.

Can. J. Chem. Downloaded from www.nrcresearchpress.com by 210.87.254.42 on 09/05/12
For personal use only.

On the other hand, the enol hydroxyl proton chemical shifts for acetylacetone are quite variable. In going from pure acetylacetone to acetic acid or chloroform solution this proton resonance shifts upfield by 32 c.p.s. or 20 c.p.s., respectively, suggesting that the chemical shift of the hydroxyl proton is at higher field when involved in an intermolecular hydrogen bond than in an intramolecular hydrogen bond (chelated structure). Exceptions are benzene (discussed below) and acetonitrile, where there may be a particularly important long-range diamagnetic anisotropy correction. No specific conclusions can be drawn from the data for alcohol solutions of acetylacetone, since the OH peaks of solvent and solute are coalesced (whereas they are distinct in acetic acid solutions).

The enol hydroxyl proton resonance for ethyl acetoacetate is very nearly unchanged (±6 c.p.s.) in going from pure solute to solution in a hydrogen-bonding solvent. The same is true for the β-ketoesters in going to chloroform solution (with the exception of ethyl benzoyl acetate). The hydroxyl peak for the alcohol solvents is now distinct from the enol peak.

In the case of chloroform the effect of the β-dicarbonyls, considered as solvents, on the chemical shift of the chloroform proton resonance may be observed (Fig. 2). It is seen

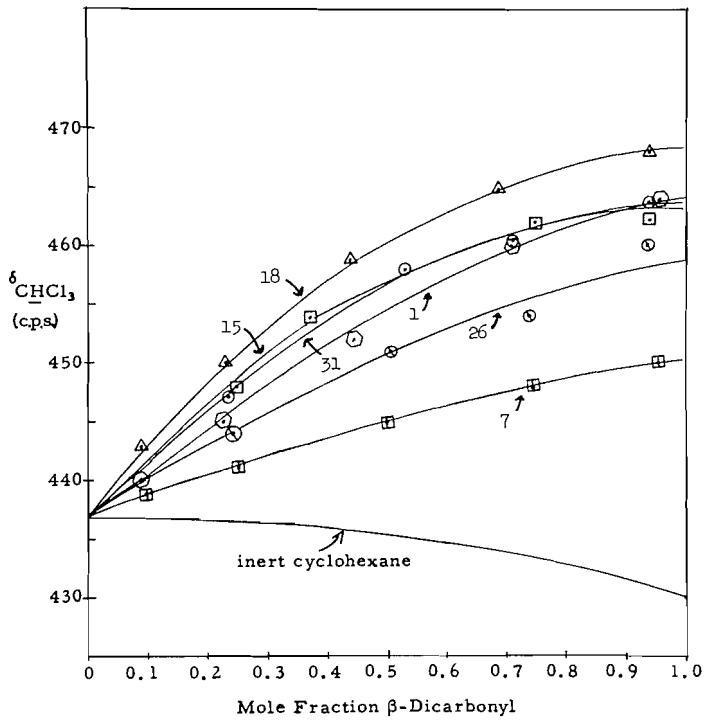

FIG. 2. Chemical shift of the chloroform proton in β-dicarbonyls as solvents (code numbers refer to compounds of Table 1).

that this resonance is shifted to higher field by 10–30 c.p.s. Korinek and Schneider (9) related this shift to the "donor strength" of the solvent molecule, and on this basis ethyl acetoacetate would be the best donor and trifluoroacetylacetone the poorest. It should be noted that the largest upfield shift of the hydroxyl proton resonance on dilution in chloroform is 31 c.p.s. for trifluoroacetylacetone and the smallest shift (nearly zero) is for

Can. J. Chem. Downloaded from www.nrcresearchpress.com by 210.87.254.42 on 09/05/12
For personal use only.

the β-ketoesters, so that trifluoroacetylacetone would also be the poorest donor on this basis.

Benzene

Chemical shifts of the various proton groups of β-dicarbonyls in benzene are given in Table I for infinitely dilute solutions (relative to pure liquid). Most of the proton resonances (alkoxy and acetyl groups and α-protons) are at higher magnetic field in benzene. However, the hydroxyl protons of the enol tautomer are shifted to lower magnetic field, while the protons of alkyl α-substituents tend to be almost unchanged (±8 c.p.s.). It seems probable that these unusual chemical shifts arise from ring current effects in a solute–solvent complex, as has been observed for a number of solutes in benzene (10, 11, 12), although no single structure for the collisional complex seems to account for all the data in this case. If the molecules are placed roughly parallel as in Fig. 3, with the benzene

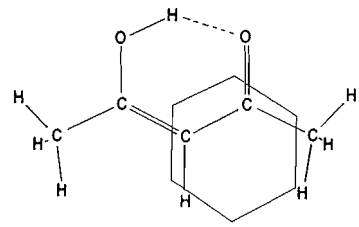

FIG. 3. Proposed complex of acetylacetone with benzene.

rings over a region of large positive charge density of the enol molecule, the high-field shifts of the methyl protons and the α-protons may be semiquantitatively accounted for by the tables of Johnson and Bovey (13). However, to obtain the observed low-field shift of the enol proton by this mechanism the rings would have to be tipped down by the methyl groups, putting the enol proton roughly in the same plane as the benzene ring and so in a paramagnetic region.

Trifluoroacetylacetone and hexafluoroacetylacetone, where there is a large negative charge density on the end groups of the enol molecules, evidently do not form this type of complex, since the hydroxyl proton and the α-proton are both now shifted to higher field, as would be expected for a complex in which the benzene ring and the six-membered ring of the enol were parallel.

Basic Solvents

In triethylamine solution the β-ketoesters tend to show peaks for only the keto tautomer and the β-diketones peaks for only the enol tautomer (2, 3). For *t*-butyl acetoacetate and ethyl α-allylacetoacetate both tautomers may be detected, but the peaks tend to be broad. Chemical shifts from pure solute to solution are generally small, but the enol hydroxyl proton of acetylacetone is shifted to higher field on dilution.

In diethylamine solutions of the β-ketoesters only the keto tautomer is detected. The esters, with the exception of methyl acetoacetate, tend to react with the amine. Acetylacetone is present only as the enol tautomer, which has been shown previously to form a complex with solvent molecules (2, 3).

Solvent Effects on Keto–Enol Equilibria

Equilibrium constants (K_e) for the equilibrium, keto $\rightleftharpoons$ enol, of acetylacetone and ethyl acetoacetate in various solvents are given in Table III. Since both enol and keto molecules may form hydrogen bonds with the solvent, the relative stability of the tautomers is

Can. J. Chem. Downloaded from www.nrcresearchpress.com by 210.87.254.42 on 09/05/12
For personal use only.

TABLE III

Equilibrium constants for tautomerization of acetylacetone and ethyl acetoacetate in various solvents at 0.1 mole fraction of solute

Solvent	Acetylacetone		Acetylacetone†		Ethyl acetoacetate	
	% enol	K_e*	% enol	K_e*	% enol	K_e*
Hexane	95	19	93.6	14.7	39	0.64
Carbon tetrachloride	96	24	92.8	12.9	28	0.39
Ether	95	19	90.4	9.4	22	0.29
Carbon disulfide	94	16	91.2	10.3	20	0.25
Benzene	89	8.1	87.2	6.7	16	0.19
Chloroform	87	6.7	85.0	5.6	7.5	0.081
Dioxane	82	4.6	79.4	3.9	11	0.12
Absolute ethanol	82	4.6	81.6	4.4	10	0.11
Pure solute	81	4.3	—	—	7.5	0.081
95% ethanol	77	3.4	78.0	3.6	7.2	0.078
Methanol	74	2.8	74.0	2.8	5.8	0.062
Acetic acid	67	2.0	78.0	3.5	1.9	0.019
Acetonitrile	62	1.6	67.2	2.1	4.9	0.052
Dimethylsulfoxide	62	1.6	76.0	3.2	2.2	0.023

*K_e = [enol]/[keto], and measurements are at 33 ± 2 °C.
†Measurements at 0.3 mole fraction of solute.

often solvent dependent. For comparison purposes all values of Table III have been derived from the spectra of solutions 0.1 or 0.3 mole fraction in solute at 33 °C. Figure 4 shows the percentage of enol tautomer throughout the concentration range for ethyl acetoacetate in various solvents, and similar results have been obtained for acetylacetone.

The β-diketones are principally in the enol form and the "inert" solvents favor this form, since the internally hydrogen-bonded enol molecule is less polar than the keto molecule. In polar solvents the fraction of keto molecules increases. The electrostatic repulsion between carbonyl groups of the keto form is reduced in a polar solvent. Also, the solvation energy of keto molecules is presumably greater than for enol molecules in polar solvents (14) and the solubility of the keto tautomer is greater in these solvents (15); hence, one might expect the equilibrium to shift toward the keto tautomer on dilution in polar solvents.

The β-ketoesters are principally in the keto form and the fraction of keto tautomer increases on dilution in polar solvents for the reasons mentioned above. In hydrogen-bonding solvents this effect is particularly marked and the enol tautomer becomes difficult to detect in acetic acid or dimethylsulfoxide solution.

Values for the fraction of enol tautomer reported here for acetylacetone and ethyl acetoacetate agree reasonably well, where they may be compared, with those of Meyer (16), Kabachnik *et al.* (17, 18), and Murthy *et al.* (19), but less well with the values of Conant and Thompson (20). Since many of the previous results were based on bromine titration, where errors may be large, close agreement with the n.m.r. data would not be expected.

Powling and Bernstein (21) showed that the enthalpy, and also the free energy, of tautomerization for several systems was a linear function of the solvent quantity $[(\epsilon - 1)/(2\epsilon + 1)]\rho/M$. This latter quantity, when multiplied by the difference between the squares of the dipole moments of the tautomers, gives the difference between the enthalpy of the tautomerization in dilute solution and in the gas phase. Although our measurements (Table III) are for moderately concentrated solutions, we have plotted ΔF vs.

Can. J. Chem. Downloaded from www.nrcresearchpress.com by 210.87.254.42 on 09/05/12
For personal use only.

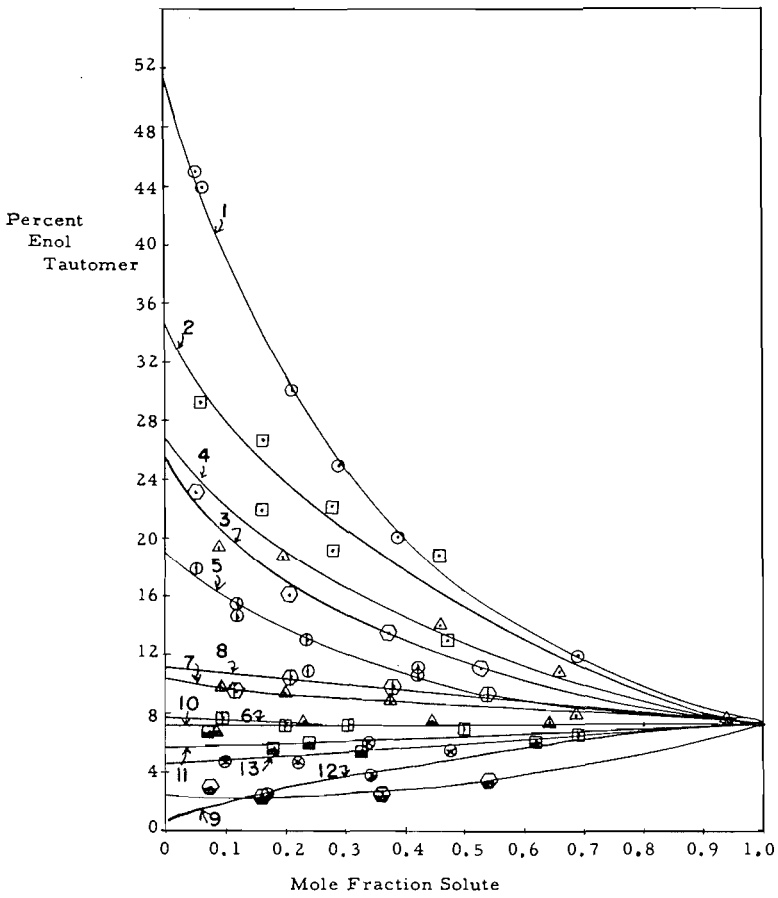

FIG. 4. Percentage of enol tautomer for ethyl acetoacetate in various solvents (code numbers refer to solvents of Table II).

$[(\epsilon - 1)/(2\epsilon + 1)]\rho/M$ for acetylacetone (Fig. 5) and ethyl acetoacetate (Fig. 6); in the former case the values for solute mole fraction 0.3 were used, since the probable error in ΔF becomes very large in the more dilute solutions where the fraction of keto isomer is low.

For ethyl acetoacetate a straight line drawn according to the method of least squares (omitting the alcohols) has an intercept at $\Delta F = 0.16$ kcal/mole, somewhat above the gas phase value of 0. The points for solvents where important specific intermolecular interactions might be expected (acetic acid, chloroform, and perhaps benzene) are scattered rather widely, but the points for a group of 'inert' solvents (hexane, carbon tetrachloride, ether, carbon disulfide, and acetonitrile) do fall close to a line extrapolating to $\Delta F = 0$.

For acetylacetone the plot (Fig. 5) is less informative. The least-squares line (omitting the points for the alcohols) has an intercept $\Delta F = -1.79$ kcal/mole, considerably higher than the gas phase value of -1.5 kcal/mole. Indeed, for two 'inert' solvents, hexane and carbon disulfide, ΔF is more negative for the solutions than for the gas phase—an unexplained anomaly previously found for several tautomeric systems (21).

Can. J. Chem. Downloaded from www.nrcresearchpress.com by 210.87.254.42 on 09/05/12
For personal use only.

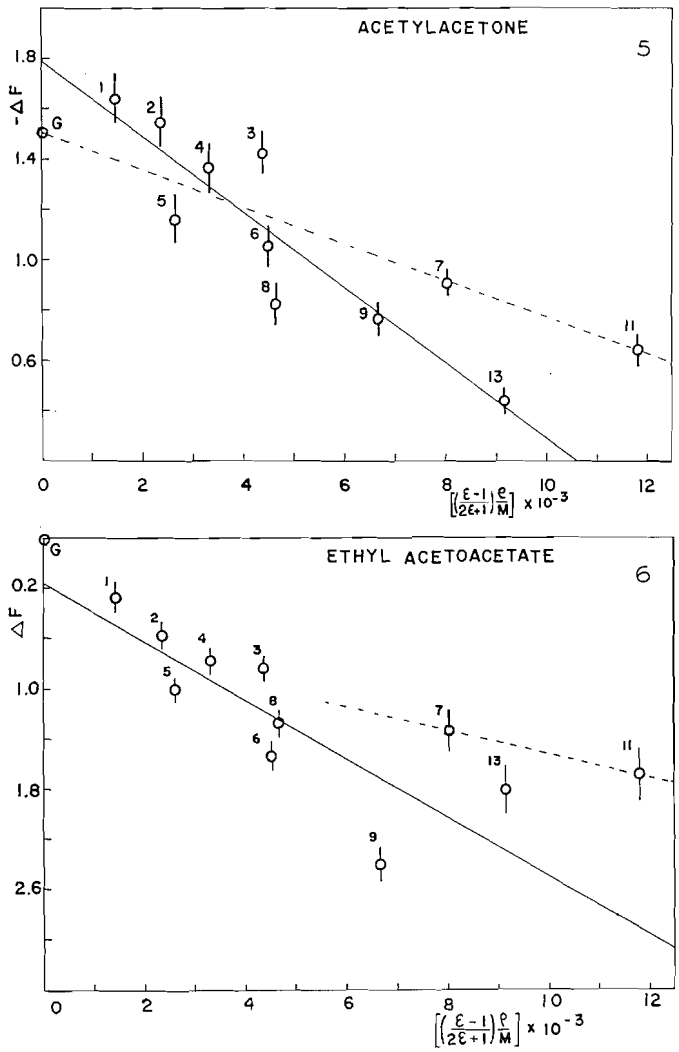

FIG. 5. Free energy of tautomerization for acetylacetone vs. solvent property (code numbers refer to solvents of Table II).

FIG. 6. Free energy of tautomerization for ethyl acetoacetate vs. solvent property (code numbers refer to solvents of Table II). The point G is the value reported for the gas phase.

It is interesting to note that the points for methyl and ethyl alcohol appear to fall on lines of different slope; in the case of acetylacetone this line extrapolates almost exactly to the gas phase value of ΔF as was observed by Powling and Bernstein (21).

The scatter of points in these graphs is perhaps not too surprising in view of the rather concentrated solutions used, the specific interactions expected in hydrogen-bonding solvents, the possible substantial entropy effects in these systems (8), and the errors at present associated with the n.m.r. method for determining K_e when the amount of one tautomer is below about 10%; further research will be required for a more complete understanding of the factors influencing tautomeric equilibria.

Can. J. Chem. Downloaded from www.nrcresearchpress.com by 210.87.254.42 on 09/05/12
For personal use only.

ACKNOWLEDGMENT

This research was supported through a contract with the Atomic Energy Commission and a grant from the National Science Foundation. We also thank Varian Associates for the use of their equipment at the Varian Applications Laboratory in Pittsburgh.

REFERENCES

1. J. L. BURDETT and M. T. ROGERS. J. Am. Chem. Soc. **86**, 2105 (1964). J. L. BURDETT. Ph.D. Thesis Michigan State University, East Lansing, Michigan. 1963.
2. L. W. REEVES. Can. J. Chem. **35**, 1351 (1957).
3. L. W. REEVES and W. G. SCHNEIDER. Can. J. Chem. **36**, 793 (1958).
4. W. G. SCHNEIDER and L. W. REEVES. Ann. N.Y. Acad. Sci. **70**, 858 (1958).
5. F. J. BALTA-CALLEJA. Compt. Rend. **249**, 1102 (1959).
6. C. GIESSNER-PRETTRE. Compt. Rend. **250**, 2547 (1960).
7. A. I. VOGEL. Practical organic chemistry. John Wiley & Sons, Inc., New York. 1956.
8. J. L. BURDETT and M. T. ROGERS. Unpublished data.
9. G. J. KORINEK and W. G. SCHNEIDER. Can. J. Chem. **35**, 1157 (1957).
10. J. V. HATTON and R. E. RICHARDS. Mol. Phys. **3**, 253 (1960).
11. W. G. SCHNEIDER. J. Phys. Chem. **66**, 2653 (1962).
12. L. LAPLANCHE and M. T. ROGERS. J. Am. Chem. Soc. **85**, 3728 (1963); **86**, 337 (1964).
13. C. E. JOHNSON, JR. and F. A. BOVEY. J. Chem. Phys. **29**, 1012 (1958).
14. M. J. S. DEWAR. Electronic theory of organic chemistry. Clarendon Press, Oxford. 1949.
15. G. W. WHELAND. Advanced organic chemistry. 3rd ed. John Wiley & Sons, Inc., New York. 1960.
16. K. H. MEYER. Chem. Ber. **45**, 2843 (1912).
17. M. I. KABACHNIK, S. T. YOFFE, and K. V. VATSURO. Tetrahedron, **1**, 317 (1957).
18. M. I. KABACHNIK, S. T. YOFFE, and K. V. VATSURO. Tetrahedron, **12**, 76 (1961).
19. A. S. N. MURTHY, A. BALASUBRAMANIAN, and C. N. R. RAO. Can. J. Chem. **40**, 2267 (1962).
20. J. B. CONANT and A. F. THOMPSON, JR. J. Am. Chem. Soc. **54**, 4039 (1932).
21. J. J. POWLING and H. J. BERNSTEIN. J. Am. Chem. Soc. **73**, 4353 (1951).

Can. J. Chem. Downloaded from www.nrcresearchpress.com by 210.87.254.42 on 09/05/12
For personal use only.

Can. J. Chem. Downloaded from www.nrcresearchpress.com by 210.87.254.6 on 09/05/12
For personal use only.

AZASTEROIDAL HORMONE ANALOGUES RELATED TO DOISYNOLIC ACID[1]

NORMAN A. NELSON[2] AND JAMES M. SCHUCK
Department of Chemistry, Massachusetts Institute of Technology, Cambridge, Massachusetts
Received November 13, 1964

Dedicated to Professor R. B. Sandin on the Occasion of his Sixty-Eighth Birthday

ABSTRACT

Condensation of β-*m*-methoxyphenethylamine with methyl coumalate followed by saponification of the ester gave N-(*m*-methoxyphenethyl)-5-carboxy-2-pyridone (I). Cyclization of the pyridone using phosphorus oxychloride gave 3-carboxy-6,7-dihydro-9-methoxybenzo[*a*]-quinolizinium chloride (II*e*), which, on catalytic reduction, afforded the two possible racemic 3-carboxy-1,3,4,6,7,11*b*-hexahydro-9-methoxy-2H-benzo[*a*]quinolizines (III*b* and IV*b*). The corresponding ethyl esters were prepared in an analogous manner and their stereochemistry was assigned on the basis of equilibration experiments. Mercuric acetate oxidation of the racemic esters gave 3-carbethoxy-1,2,3,4,6,7-hexahydro-9-methoxybenzo[*a*]quinolizinium perchlorate (V).

In continuing our work on the preparation of amino acid analogues of artificial estrogens (1), we became interested in incorporating a nitrogen atom into the skeleton of compounds related to doisynolic acid. Several isomers of the latter compound are known to be potent estrogens (2). This paper describes the preparation of some polyhydrobenzo[*a*]quinolizines (III–V) which represent 8-aza analogues of doisynolic acid.

By the method of Wiley, Smith, and Knabeschuh (3), treatment of methyl coumalate (4) with an excess of *m*-methoxyphenethylamine and saponification of the crude product gave N-(*m*-methoxyphenethyl)-5-carboxy-2-pyridone (I) in 82% yield. Cyclization of this pyridone using phosphorus oxychloride in xylene (3) followed by treatment of the intermediate acid chloride with absolute ethanol gave 3-carbethoxy-6,7-dihydro-9-methoxybenzo[*a*]quinolizinium chloride (II*a*) in 72% yield. Treatment of the crude reaction mixture with potassium iodide gave the corresponding iodide (II*b*). Hydrolysis of the intermediate acid chloride gave the quinolizinium acid salts II*d* and II*e*.

A number of attempted cyclizations of pyridones to produce substituted quinolizinium compounds have yielded simply the corresponding pyridinium salts (ref. 5 and references therein). That N-(*m*-methoxyphenethyl)-5-carboxy-2-pyridone did undergo cyclization to the quinolizinium ring system is evidenced by the fact that the products II*a*–II*e* have ultraviolet absorption spectra characteristic of this ring system (3), but different from what would be expected from a composite of the isolated *m*-methoxyphenyl and carboxychloropyridinium chromophores had cyclization not occurred. It is generally found that Bischler-Napieralski reactions of N-*m*-methoxyphenethylamides and lactams occur preferentially with cyclization para to the methoxyl group (6–8). That a para ring closure occurred in the present work is indicated by spectral means, and will be discussed later under the preparation of III*a*.

Catalytic hydrogenation of the quinolizinium ester salts II*a*–II*c* using Adams catalyst resulted in the isolation of the two possible racemic forms of the free amino ester. The best results were obtained when the chloride salt II*a* was used because of its greater

[1]*From part of the thesis presented by J. M. S. in partial fulfillment of the requirements for the Ph.D. degree, 1960.*
[2]*Author to whom inquiries should be addressed: Department of Chemistry, The Upjohn Company, Kalamazoo, Michigan.*

solubility as compared with the iodide and perchlorate salts II*b* and II*c*. Thus, when 3-carbethoxy-6,7-dihydro-9-methoxybenzo[*a*]quinolizinium chloride (II*a*) was reduced catalytically using Adams catalyst and a solvent mixture composed of 2 parts ethanol, 2 parts water, and 1 part acetic acid, 3 molecular equivalents of hydrogen were absorbed, and the product obtained in 76% yield was the hydrochloride of 3-carbethoxy-1,3,4,6,7,11*b*-hexahydro-9-methoxy-2H-benzo[*a*]quinolizine IV*a* in which the relationship of the hydrogen atoms attached to C-3 and C-11*b* is *trans*. The basis for this assignment will be given below. Also isolated from this reduction was 16% of a lower-melting hydrochloride salt which was a mixture of the two racemic forms. That the reduction took place in the pyridinium ring rather than the benzene ring is shown by the ultraviolet absorption spectrum. The hydrochloride of compound IV*a* has maxima at 277 (ϵ 1 750) and 284 mμ (ϵ 1 720) while 6-methoxy-1,2,3,4-tetrahydroisoquinoline hydrochloride has maxima at 278 (ϵ 1 960) and 285 mμ (ϵ 1 840).

Treatment of the hydrochloride of IV*a* with dilute sodium hydroxide liberated *trans*-3-carbethoxy-1,3,4,6,7,11*b*-hexahydro-9-methoxy-2H-benzo[*a*]quinolizine IV*a* in 95% yield.

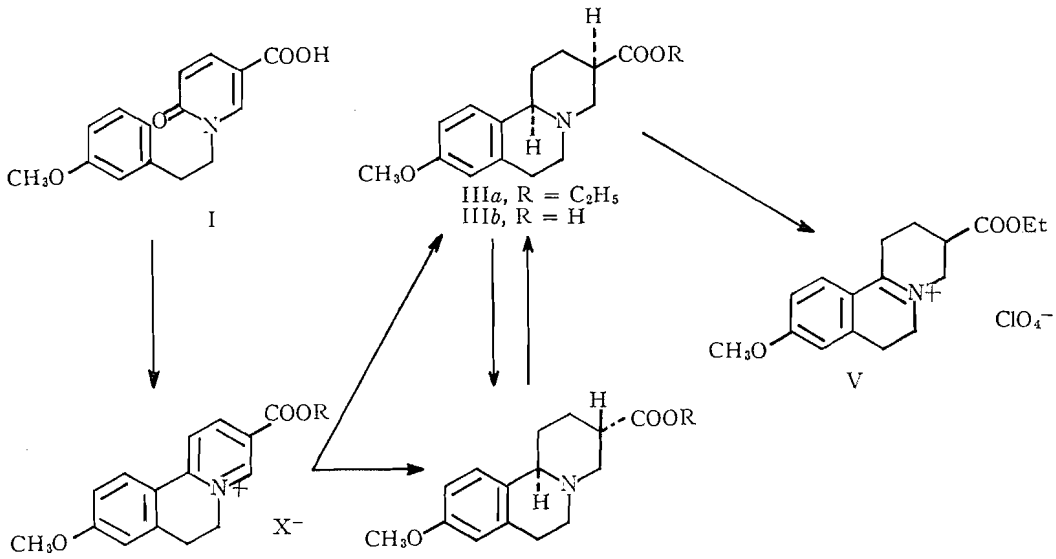

II*a*, R = C_2H_5, X = Cl
II*b*, R = C_2H_5, X = I
II*c*, R = C_2H_5, X = ClO_4
II*d*, R = H, X = ClO_4
II*e*, R = H, X = Cl

IV*a*, R = C_2H_5
IV*b*, R = H

On the other hand, catalytic reduction of II*a* using Adams catalyst in glacial acetic acid again resulted in an uptake of 3 molecular equivalents of hydrogen. After evaporation of the reduction mixture, treatment of the crude oil with dilute ammonium hydroxide resulted in the isolation of 86% of the isomeric *cis* ester III*a*. The ultraviolet spectra of compounds III*a* and IV*a* are consistent with the presence of a 6-methoxy-1,2,3,4-tetrahydroisoquinoline chromophore and are inconsistent with an 8-methoxy-1,2,3,4-tetrahydroisoquinoline chromophore (7). This rules out the possibility that cyclization of I occurred at the less favorable position ortho to the methoxy group. Further conformation for the para ring closure of I can be found in the n.m.r. spectrum of III*a*. The aromatic region of the curve is typical of a 1,2,4-trisubstituted benzene of the estrone type (cf. ref. 8).

Can. J. Chem. Downloaded from www.nrcresearchpress.com by 210.87.254.6 on 09/05/12
For personal use only.

Can. J. Chem. Downloaded from www.nrcresearchpress.com by 210.87.254.6 on 09/05/12
For personal use only.

Equilibration studies on the isomeric esters III*a* and IV*a* indicated that III*a* is the less stable isomer and that the equilibrium position lies approximately 80% on the side of IV*a*. The isomer IV*a* was therefore assigned the thermodynamically more stable configuration in which the carbethoxy group is equatorial. Treatment of both esters with mercuric acetate in aqueous acetic acid followed by the addition of perchloric acid (6) resulted in the formation of the same dehydro product, 3-carbethoxy-1,2,3,4,6,7-hexahydro-9-methoxybenzo[*a*]quinolizinium perchlorate (V), in about 90% yield. Catalytic hydrogenation of V using Adams catalyst in glacial acetic acid gave a mixture of the two esters III*a* and IV*a* with the more stable isomer IV*a* predominating in about the same ratio as found in the equilibration of the amino ester.

The ease with which the mercuric acetate oxidation proceeds under the mild conditions used for both esters is indicative of a *trans* quinolizine system having an axial hydrogen at the bridgehead (9). Further evidence for the *trans* ring juncture is given by the fact that infrared spectra of both esters show four characteristic peaks in the carbon–hydrogen stretching region when a calcium fluoride prism is used: the major band at 2 940 cm^{-1} and three peaks of medium intensity at 2 850, 2 815, and 2 780 cm^{-1}. Such bands appear to be associated with tertiary amines which have two or more adjacent hydrogens *trans* diaxial to the electron pair of the nitrogen (refs. 10, 11; see, however, ref. 12 for possible exceptions).

On the basis of the above evidence for *trans*-fused rings, and the results of the equilibration studies, the more stable low-melting material is assigned structure IV*a* with the carbethoxy group equatorial. The isomeric ester is assigned the configuration with an axial carbethoxy and is represented by III*a*. After this work had been completed, Ohki and Noike (13) published independently the structural assignment of the isomeric 3-carbethoxyquinolizidines, in which essentially the same methods of elucidation were employed.

Once the configuration of the amino esters had been determined, the preparation of the corresponding amino acids was investigated. Hydrogenation of 3-carboxy-6,7-dihydro-9-methoxybenzo[*a*]quinolizinium chloride (II*a*), using Adams catalyst in glacial acetic acid and in aqueous acetic acid solution, resulted in the formation of mixtures of amino acids as their hydrochlorides. Separation of the isomeric compounds by fractional crystallization from absolute ethanol gave 46% of the less soluble higher-melting isomer later shown to be the hydrochloride of IV*b*. The filtrate gave the lower-melting hydrochloride of III*b* in 50% yield. The homogeneity of the different isomers was shown by paper chromatography.

Treatment of the hydrochloride of IV*b* with exactly 1 equivalent of sodium hydroxide afforded the amino acid IV*b* in 94% yield. The relationship of this amino acid and therefore of its antecedent hydrochloride to the amino esters was determined by treating an ethanolic solution of the free amino acid with ethereal diazoethane. The amino acid IV*b* was converted to the amino ester IV*a* (equatorial carbethoxy) in a 93% yield.

In the same manner as above, the hydrochloride of III*b* was converted to the free amino acid III*b* in 89% yield and this in turn was transformed into the amino ester III*a* (axial carbethoxy) in 72% yield by treatment with ethereal diazoethane.

The infrared spectra of these isomeric acids are of interest, in that III*b* with its axial carboxyl group can form an intramolecular hydrogen bond while the isomeric amino acid IV*b* cannot form such a bond unless the nitrogen atom undergoes inversion to give the less favorable cisoid ring juncture with the electron pair on nitrogen oriented equatorially and the N-alkyl group oriented axially. Spectra of the amino acids in potassium

bromide pellets show that III*b* (axial carboxyl) has absorption peaks at 2 860 cm^{-1} (m, C—H stretching), 2 740–2 580 cm^{-1} (w, broad, characteristic of amine salts), and two peaks associated with carboxyl absorption: 1 675 cm^{-1} (s, broad, hydrogen-bonded associated carboxyl) and 1 590 cm^{-1} (m, ionized carboxyl).

The isomeric amino acid IV*b* shows essentially the same peaks but there are significant differences in intensity and exact location. The 2 860 cm^{-1} peak is almost nonexistent and the absorption at 2 720–2 580 cm^{-1} is more intense than in III*b*. The carboxyl absorption, however, shows the greatest change. The free-carboxyl absorption has shifted to 1 650 cm^{-1} and is present only as a shoulder. The ionized carboxyl at 1 590 cm^{-1} has increased greatly in intensity and is the most intense band in the spectrum.

Paper chromatography of the two amino acid preparations indicated that the preparations were homogeneous. The more soluble *cis* material III*b* moved faster under the conditions employed and a mixture of the two isomers was separated without difficulty.

EXPERIMENTAL

Infrared spectra were determined with a Perkin–Elmer (model 21) spectrophotometer fitted with a sodium chloride prism unless otherwise specified. Ultraviolet spectra were determined in 95% ethanol with a Cary recording spectrophotometer (model 11 MS). The microanalyses were performed by Dr. S. M. Nagy and his associates. Melting points are uncorrected.

N-(m-Methoxyphenethyl)-5-carboxy-2-pyridone (I)

A mixture of 2.0 g of methyl coumalate (4) and 5 ml of *m*-methoxyphenethylamine was converted to 3.0 g (82%) of crude product, m.p. 179–181°, by the method of Wiley *et al.* (3). Recrystallization of the material twice from 95% ethanol gave white crystals of I, m.p. 180.5–181°. The ultraviolet spectrum showed peaks at 261 mμ (ϵ 16 100) and 303 mμ (ϵ 5 310). The infrared spectrum (KBr pellet) showed carbonyl peaks at 1 700 and 1 640 cm^{-1}.

Anal. Calcd. for $C_{15}H_{15}NO_4$: C, 65.92; H, 5.55; N, 5.13. Found: C, 65.62; H, 5.54; N, 5.08.

3-Carbethoxy-6,7-dihydro-9-methoxybenzo[a]quinolizinium Iodide (IIb)

Following a known method (3), we converted 1.4 g of N-(*m*-methoxyphenethyl)-5-carboxy-2-pyridone to 1.8 g of II*b*, m.p. 215–219° (decomp.) (recrystallized from ethanol–ether). The ultraviolet spectrum showed maxima at 220 (ϵ 23 800), 291 (ϵ 6 620), and 364 mμ (ϵ 27 320) and a shoulder at 258 mμ (ϵ 5 090). The infrared spectrum showed a carbonyl peak at 1 725 cm^{-1}.

Anal. Calcd. for $C_{17}H_{18}INO_3$: C, 49.65; H, 4.41; N, 3.41. Found: C, 49.72; H, 4.37; N, 3.51.

3-Carbethoxy-6,7-dihydro-9-methoxybenzo[a]quinolizinium Chloride (IIa) and Perchlorate (IIc)

Cyclization of 5.0 g of I using phosphorus oxychloride (3) gave a product which was recrystallized from 25 ml of water to give 4.2 g (72%) of II*a*, m.p. 200–201°, raised to 208–209° after recrystallization from ethanol–ether. The ultraviolet and infrared spectra showed essentially the same characteristics as described above for the corresponding iodide salt (II*b*).

The filtrates from the above crystallizations were combined and treated with 2 ml of 72% perchloric acid to give 1.9 g (27%) of the perchlorate salt II*c*, m.p. 210–212°. An analytical sample recrystallized from aqueous methanol had m.p. 209–210° and suitable infrared and ultraviolet spectra.

Anal. Calcd. for $C_{17}H_{18}ClNO_7$: C, 53.20; H, 4.74; N, 3.65. Found: C, 53.32; H, 4.64; N, 3.50.

3-Carboxy-6,7-dihydro-9-methoxybenzo[a]quinolizinium Perchlorate (IIa)

N-(*m*-Methoxyphenethyl)-5-carboxy-2-pyridone (1.9 g) was cyclized as described above in the preparation of II*b*; however, water (20 ml) rather than ethanol was used in the reaction with the intermediate acid chloride. The aqueous mixture was allowed to stand at room temperature for 10 min, then 70 ml of water was added to dissolve the precipitate. To the solution was added 2.0 g of sodium perchlorate, a precipitate forming immediately. The suspension was cooled at 5° overnight and then filtered. Recrystallization of the precipitate from ethanol–water gave 2.0 g (81%) of product, m.p. 270° (decomp.). The ultraviolet spectrum has maxima at 220 (ϵ 23 800), 284 (ϵ 6 650), and 355 mμ (ϵ 23 400) and a shoulder at 254 mμ (ϵ 4 900).

Anal. Calcd. for $C_{15}H_{14}ClNO_7$: C, 50.80; H, 3.97; N, 3.95. Found: C, 50.78; H, 4.01; N, 3.88.

3-Carboxy-6,7-dihydro-9-methoxybenzo[a]quinolizinium Chloride (IIe)

To 5.0 g of N-(*m*-methoxyphenethyl)-5-carboxy-2-pyridone was added 25 ml of phosphorus oxychloride and 25 ml of xylene. After the mixture was heated gently under reflux for 2 h, the volatile material was removed under reduced pressure. The residue was dissolved in 125 ml of water and allowed to cool slowly.

Can. J. Chem. Downloaded from www.nrcresearchpress.com by 210.87.254.6 on 09/05/12
For personal use only.

Filtration gave 5.3 g (98%) of product, m.p. 265–266°. Maxima in the ultraviolet spectrum occur at 220 (ε 9 600), 283 (ε 7 460), and 355 mμ (ε 24 200) and a shoulder at 254 mμ (ε 5 520).

Anal. Calcd. for $C_{15}H_{14}ClNO_3$: C, 61.75; H, 4.84; N, 4.81. Found: C, 61.71; H, 4.96; N, 4.58.

trans-3-Carbethoxy-1,3,4,6,7,11b-hexahydro-9-methoxy-2H-benzo[a]quinolizine (IVa) Hydrochloride

To a solution of 3.0 g of II*a* dissolved in a mixture of 24 ml of acetic acid, 50 ml of ethanol, and 50 ml of water was added 500 mg of Adams catalyst. Hydrogen was introduced at atmospheric pressure and the suspension was stirred vigorously. After the hydrogen uptake ceased (8 h), the suspension was filtered and the filtrate was evaporated to dryness. The oil was dissolved in 15 ml of absolute ethanol, treated with Norit, and filtered. The product was crystallized from absolute ethanol–ether giving 2.3 g (76%) of IV*a* hydrochloride, m.p. 194–197°, raised to 201–202.5° after recrystallization. The ultraviolet spectrum shows maxima at 227 (ε 8 630), 277 (ε 1 755), and 284 mμ (ε 1 720).

Anal. Calcd. for $C_{17}H_{24}ClNO_3$: C, 62.66; H, 7.42; N, 4.30. Found: C, 62.55; H, 7.40; N, 4.10.

The filtrate yielded an additional 500 mg of material, m.p. 115–170°, which appeared to be a mixture of the two isomeric hydrochlorides.

trans-3-Carbethoxy-1,3,4,6,7,11b-hexahydro-9-methoxy-2H-benzo[a]quinolizine (IVa)

Treatment of a solution of 5.3 g of IV*a* hydrochloride in 25 ml of water with a slight excess of dilute sodium hydroxide solution and recrystallization of the crude product from ethanol–water gave 4.5 g (96%) of IV*a*, m.p. 47–50°, raised to 51–52.5° after one recrystallization. The ultraviolet spectrum of IV*a* has maxima at 220 (ε 9 275), 278 (ε 1 890), and 286 mμ (ε 1 840). The infrared spectrum (in CCl_4, calcium fluoride prism) shows maxima at 2 850, 2 815, 2 780, and 2 760 cm^{-1} (C—H stretching of transoid-ring system) and (with sodium chloride prism) 1 730 cm^{-1} (ester C=O) and two peaks at 1 110 and 990 cm^{-1} (characteristic of this *trans* isomer).

Anal. Calcd. for $C_{17}H_{23}NO_3$: C, 70.56; H, 8.01; N, 4.84. Found: C, 70.54; H, 7.96; N, 4.75.

cis-3-Carbethoxy-1,3,4,6,7,11b-hexahydro-9-methoxy-2H-benzo[a]quinolizine (IIIa)

A mixture of 2.5 g of II*a*, 100 ml of glacial acetic acid, and 200 mg of Adams catalyst was shaken in the presence of hydrogen at atmospheric pressure until the theoretical amount of hydrogen was absorbed (7 h). The suspension was filtered and evaporated to dryness. The residue was dissolved in 50 ml of water to which dilute ammonium hydroxide was added until the mixture was alkaline. The aqueous suspension was extracted with ether and the ether extract was washed with water until neutral. The solvent was removed under reduced pressure and the oil was crystallized from aqueous methanol yielding 1.85 g (86%) of product III*a*, m.p. 83–86°, raised to 85–86° on recrystallization from aqueous ethanol. The ultraviolet spectrum of III*a* has maxima at 220 (ε 9 720), 278 (ε 1 925), and 286 mμ (ε 1 850). The infrared spectrum (in CCl_4, calcium fluoride prism) shows maxima at 2 850, 2 815, and 2 780 cm^{-1} (C—H stretching of transoid-ring system) and (with sodium chloride prism) 1 735 cm^{-1} (ester C=O) and two peaks at 1 100 and 1 076 cm^{-1} (characteristic of this *cis* isomer). The n.m.r. spectrum of III*a* in $CDCl_3$ shows signals centered at about 6.64, 6.74, and 7.12 p.p.m. (tetramethylsilane = 0) for the 8-, 10-, and 11-hydrogens, respectively.

Anal. Calcd. for $C_{17}H_{23}NO_3$: C, 70.56; H, 8.01; N, 4.84. Found: C, 70.67; H, 7.93; N, 4.80.

The hydrochloride salt of III*a* was prepared by passing hydrogen chloride into an ethereal solution of pure III*a*. The product was recrystallized from ethanol–ether, m.p. 210–211°, and gave normal ultraviolet and infrared spectra.

Equilibration Studies of the cis and trans Isomers of 3-Carbethoxy-1,3,4,6,7,11b-hexahydro-9-methoxy-2H-benzo[a]quinolizine

Standard curves of optical density vs. concentration were prepared from infrared data of synthetic mixtures (10% solutions in CCl_4) of III*a* and IV*a* using the 987 cm^{-1} peak and 1 076 cm^{-1} peak of the *trans* and *cis* isomers respectively.

(A) To 500 mg of IV*a* (m.p. 50.5–51.5°) was added 10 ml of sodium ethoxide solution prepared from 500 mg of sodium in 50 ml of absolute ethanol. The solution was kept under a nitrogen atmosphere at room temperature for 48 h. The solution was poured into 100 ml of ice water which was then extracted with ether. The ether extract was washed until neutral and evaporated to give 450 mg of mixed amino esters. The oil was dried for 24 h at 50° *in vacuo*. An infrared spectrum of the mixture and utilization of the standard curves indicated the presence of 86% of IV*a* and 17% of III*a*. Normalization gives the equilibrium position as 83.5% IV*a* and 16.5% III*a*.

(B) To 250 mg of III*a* (m.p. 85–85.4°) was added 5.0 ml of sodium ethoxide prepared from 500 mg of sodium and 50 ml of absolute ethanol. The solution was kept under a nitrogen atmosphere at room temperature for 48 h. The solution was worked up in the same manner as above to give 240 mg of mixed amino esters. The oil was dried for 24 h at 50° *in vacuo*. From the infrared spectrum of the mixture and utilization of the standard curves the mixture appeared to consist of 86% of IV*a* and 28% III*a*. Normalization gives the equilibrium position as 75.5% IV*a* and 24.5% III*a*.

3-Carbethoxy-1,2,3,4,6,7-hexahydro-9-methoxybenzo[a]quinolizinium Perchlorate (V)

Both III*a* and IV*a* gave the same quinolizinium perchlorate after mercuric acetate oxidation. The procedure used for each isomer was exactly the same and it is described below for the equatorial isomer IV*a*.

Can. J. Chem. Downloaded from www.nrcresearchpress.com by 210.87.254.6 on 09/05/12
For personal use only.

To a solution of 4.5 g of mercuric acetate in 25 ml of 5% acetic acid was added 1.0 g of *trans* ester IV*a*. Mercurous acetate began precipitating within 3 min as the temperature of the mixture was raised to 60° and kept there for 2 h. Filtration gave 1.7 g (95%) of mercurous acetate. The filtrate was saturated with hydrogen sulfide and the suspension filtered through Celite. The solution was concentrated under reduced pressure to 10 ml, at which point it was diluted to 50 ml with absolute ethanol. The solution was again concentrated to a volume of 10 ml under reduced pressure and 15 ml of absolute ethanol containing 0.5 ml of 70% perchloric acid was added. The solution was diluted with ether giving 1.1 g of V, m.p. 131.5–132.5°, and 90 mg, m.p. 129–131°. The sample melting at 131.5–132.5° was analytically pure. The ultraviolet spectrum of V has maxima at 230 (ϵ 5 890), 237 (ϵ 7 400), and 323 mμ (ϵ 18 900) and a shoulder at 244 mμ (ϵ 5 680).

Anal. Calcd. for $C_{17}H_{22}ClNO_7$: C, 52.65; H, 5.72; N, 3.62. Found: C, 52.52; H, 5.76; N, 3.64.

The *cis* amino ester gave 90% yield of V, m.p. 131.0–132.0°. The infrared spectra of the products obtained from the isomeric esters are superimposable and mixed melting point determination showed no depression.

Reduction of 3-Carbethoxy-1,2,3,4,6,7-hexahydro-9-methoxybenzo[a]quinolizinium Perchlorate (V)

To a suspension of 1.1 g of V in 50 ml of glacial acetic acid was added 100 mg of Adams catalyst. Hydrogen was introduced at atmospheric pressure and the uptake was completed in 6 h. The suspension was filtered and the filtrate evaporated to dryness. The oil was dissolved in 50 ml of water and dilute ammonium hydroxide was added until the mixture was basic. The suspension was extracted with ether. The ether extract was washed with water to neutrality. The ether was evaporated to give an oil which was a mixture of the amino esters III*a* and IV*a*. The oil was dissolved in a methanol–water solution and 110 mg of III*a*, m.p. 80.5–83°, precipitated. Addition of water to the filtrate followed by slow cooling precipitated 300 mg of IV*a*, m.p. 46–48°.

Hydrochlorides of cis- and trans-3-Carboxy-1,3,4,6,7,11b-hexahydro-9-methoxy-2H-benzo[a]quinolizines (IIIb and IVb)

A mixture of 4.5 g of 3-carboxy-6,7-dihydro-9-methoxybenzo[*a*]quinolizinium chloride (II*e*), 400 ml of acetic acid, and 400 mg of Adams catalyst was shaken in a hydrogen atmosphere at atmospheric pressure until the theoretical uptake of hydrogen had occurred (12 h). The catalyst was removed and the filtrate evaporated to dryness. The residue was leached with 30 ml of boiling absolute ethanol. The insoluble material amounted to 2.1 g (46%) of the *trans* isomer IV*b*, m.p. 274–280°, raised to 287–288° after two recrystallizations from 95% ethanol.

Anal. Calcd. for $C_{15}H_{20}ClNO_3$: C, 60.50; H, 6.77; N, 4.70. Found: C, 60.34; H, 6.79; N, 4.71.

The ethanol leach solution above was diluted to a volume of 100 ml with ether giving 1.75 g (38%) of the *cis* isomer III*b*, m.p. 231–235°, raised to 235–239° on recrystallization from aqueous ethanol–ether.

Anal. Calcd. for $C_{15}H_{20}ClNO_3$: C, 60.50; H, 6.77; N, 4.70. Found: C, 60.58; H, 6.88; N, 4.75.

Paper chromatography of the isomeric amino acid hydrochlorides indicated that the above materials were homogeneous as far as was indicated by the development techniques used. From a spot of 100 γ of each material was obtained a single spot. A mixture of 50 γ of each was separated into two spots. The mobile phase for these experiments was methyl ethyl ketone to which 1% methanol was added. Whatman No. 1 paper was used and the spots were developed by passing the dried paper strip through a solution of iodine in carbon tetrachloride. The compounds showed up as yellow spots.

cis-3-Carboxy-1,3,4,6,7,11b-hexahydro-9-methoxy-2H-benzo[a]quinolizine (IIIb)

A solution of 1.1 g of the hydrochloride of III*b* in 10 ml of water was neutralized to pH 7 with dilute sodium hydroxide. The solution was evaporated to dryness under reduced pressure and the residue was triturated with 50 ml of absolute ethanol. The suspension was diluted to a volume of 100 ml with ether and then filtered, giving 859 mg (89%) of III*b*, m.p. 219–224°, raised to 224–225° (with sintering at 218°). The ultraviolet spectrum of III*b* has maxima at 227 (ϵ 9 110), 277 (ϵ 1 720), and 285 mμ (ϵ 1 680). The infrared spectrum (KBr pellet) exhibits a strong band at 1 675 cm^{-1} (hydrogen-bonded carboxyl) and a medium band at 1 590 cm^{-1} (ionized carboxyl).

Anal. Calcd. for $C_{15}H_{19}NO_3$: C, 68.95; H, 7.32; N, 5.36. Found: C, 68.98; H, 7.37; N, 5.41.

Paper chromatography of the material melting at 224–225° with the same system used for the hydrochloride indicated that the material was homogeneous. The *cis* isomer moves more rapidly than the *trans* isomer (described below) and a mixture of the two isomers is separated.

trans-3-Carboxy-1,3,4,6,7,11b-hexahydro-9-methoxy-2H-benzo[a]quinolizine (IVb)

Conversion of 500 mg of the hydrochloride of IV*b* by essentially the same process as described above for the preparation of III*b* gave 410 mg (93%) of IV*b*, m.p. 231–240°, raised to 240–242° on recrystallization from aqueous ethanol. The ultraviolet spectrum of IV*b* has maxima at 227 (ϵ 9 200), 277 (ϵ 1 790), and 285 mμ (ϵ 1 730). The infrared spectrum (KBr pellet) exhibits a shoulder at 1 650 cm^{-1} (hydrogen-bonded carboxyl) and a strong band at 1 590 cm^{-1} (ionized carboxyl).

Anal. Calcd. for $C_{15}H_{19}NO_3$: C, 68.95; H, 7.32; N, 5.36. Found: C, 69.10; H, 7.39; N, 5.42.

Paper chromatography of a sample of IV*b* melting at 240–242° indicated that it was homogeneous.

Mixtures of the isomeric amino acids III*b* and IV*b* could be separated effectively by leaching them with

Can. J. Chem. Downloaded from www.nrcresearchpress.com by 210.87.254.6 on 09/05/12
For personal use only.

anhydrous benzene. The axial isomer III*b* is much more soluble in benzene and it was removed completely from the mixture. Concentration of the benzene followed by slow cooling gave III*b* in well-defined crystals.

Correlation of the Amino Acids IIIb and IVb with the Corresponding Axial and Equatorial Esters. Treatment with Diazoethane

(A) To a solution of 150 mg of IV*b* in 15 ml of 95% ethanol was added an excess of ethereal diazoethane solution (14). The solution was stirred at room temperature for 2 h and then evaporated to dryness. The residue was dissolved in 50 ml of anhydrous ether, filtered, and evaporated to dryness to give 160 mg (97.5%) of crude product. An infrared spectrum indicated that the material was the equatorial ester. Recrystallization of the oil from ethanol–water gave 145 mg (88%) of the equatorial amino ester IV*a*, m.p. 49–50°. The amino acid IV*b* and the corresponding hydrochloride therefore have equatorial carboxyl groups.

(B) To a solution of 150 mg of III*b* (softening 210°, m.p. 219–222°) in 15 ml of an ethanol–water mixture was added an excess of ethereal diazoethane. The solution was stirred for 2 h and then evaporated to dryness. The residue was dissolved in 50 ml of anhydrous ether, filtered, and evaporated to dryness to give 155 mg (93.5%) of crude product. Comparison of the infrared spectrum to that of the pure axial ester indicated that there was a small amount of the low-melting equatorial isomer present. The oil was crystallized from an ethanol–water mixture to give 119 mg (72%) of the axial ester III*a*, m.p. 83–84°. The amino acid III*b* and its corresponding hydrochloride therefore have axial carboxyl groups.

ACKNOWLEDGMENT

This investigation was supported in part by a research grant, CY-2999 (C3), from the National Cancer Institute, Public Health Service.

REFERENCES

1. N. A. Nelson and H. B. Sinclair. J. Am. Chem. Soc. **82**, 2577 (1960).
2. L. F. Fieser and M. Fieser. Steroids. Reinhold Publishing Corp., New York. 1959. p. 494; references contained therein.
3. R. H. Wiley, N. R. Smith, and L. H. Knabeschuh. J. Am. Chem. Soc. **75**, 4482 (1953).
4. R. H. Wiley and L. H. Knabeschuh. J. Am. Chem. Soc. **77**, 1615 (1955).
5. L. A. Paquette and N. A. Nelson. J. Org. Chem. **27**, 1085 (1962).
6. W. M. Whaley and T. R. Govindachari. Organic reactions. Vol. 6. John Wiley and Sons, Inc., New York. 1951. p. 74.
7. N. A. Nelson, K. O. Gelotte, Y. Tamura, H. B. Sinclair, J. M. Schuck, V. J. Bauer, and R. W. White. J. Org. Chem. **26**, 2599 (1961).
8. R. I. Meltzer, D. M. Lustgarten, R. J. Stanaback, and R. E. Brown. Tetrahedron Letters, 1581 (1963).
9. F. L. Weisenborn and P. A. Diassi. J. Am. Chem. Soc. **78**, 2022 (1956).
10. F. Bohlmann *et al.* Angew. Chem. **69**, 641 (1957); Chem. Ber. **90**, 653 (1957); Chem. Ber. **91**, 2157, 2167 (1958).
11. E. Wenkert and D. K. Roychaudhuri. J. Am. Chem. Soc. **78**, 6417 (1956).
12. W. E. Rosen. Tetrahedron Letters, 481 (1961).
13. S. Ohki and Y. Noike. Chem. Pharm. Bull. Tokyo, **7**, 708 (1959).
14. D. W. Adamson and J. Kenner. J. Chem. Soc. 1551 (1937).

Can. J. Chem. Downloaded from www.nrcresearchpress.com by 210.87.254.6 on 09/05/12
For personal use only.

Can. J. Chem. Downloaded from www.nrcresearchpress.com by 210.87.254.40 on 09/05/12
For personal use only.

THE CONVERSION OF META- AND PARA-SUBSTITUTED BENZALDOXIME ARENESULFONATES TO NITRILES

ROBERT J. CRAWFORD AND CHARLES WOO[1]
Department of Chemistry, University of Alberta, Edmonton, Alberta
Received November 13, 1964

Dedicated to Professor R. B. Sandin on the Occasion of his Sixty-Eighth Birthday

ABSTRACT

The meta- and para-substituted *syn*-benzaldoxime arenesulfonates were prepared from the reaction between the sodium salt of the oxime and the acid chloride in absolute ether. These oxime esters reacted in aqueous alcohol readily to yield the corresponding nitriles exclusively. The reaction rates can be correlated by a Hammett plot with a slope of −0.77. Several para-substituents tended to deviate from the line. Isotope study gives a k_H/k_D ratio of 4.51. The rate was found to be sensitive to the change in the ionizing power of the solvent, and to the change in the strength of the esterifying acid. The addition of lithium perchlorate gives rise to a normal salt effect. Sodium acetate brings about a basic elimination having a Hammett ρ value of +0.44. A mechanism is proposed in the light of these results.

INTRODUCTION

Since Beckmann (1) reported the conversion of oximes to the corresponding amides in acid media, numerous publications have appeared in an attempt to elucidate the mechanism of the transformation. Several authors, Blatt (2), Jones (3), Heldt (4), and Smith (5), have reviewed the Beckmann rearrangement up to 1963. The generally accepted view of the rearrangement involves migration of the hydrocarbon residue *anti* to the leaving group, followed by a rapid tautomerization of the intermediate. The transition state for such a reaction has been described as a pseudo three-membered ring, and the process was viewed as "an internal nucleophilic displacement, and may be described as ionization by rearrangement" (5). Although extensive work has been done on the subject of the

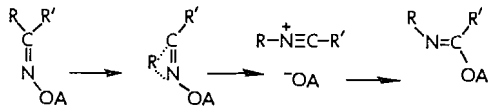

Beckmann rearrangement of ketoximes, the aldoximes have been less frequently investigated. Aldoximes and their derivatives usually undergo fragmentation to nitriles, under the conditions of the Beckmann rearrangement, so readily that examples of normal rearrangement to give amides are quite rare (4). For example, in the presence of phosphorus pentachloride and ether, *syn**-2-chloro-5-nitro-benzaldoxime gave rise to 2-chloro-5-nitrobenzonitrile (6); *syn*-2,6-dichloro-3-nitrobenzaldoxime yielded 2,6-dichloro-3-nitrobenzonitrile (7); and *syn*-α-bromocinnamaldoxime gave α-bromocinnamonitrile (8).

It would appear that aldoximes generally react by a different mode than do ketoximes; thus, "ionization by rearrangement" may not be operative for aldoximes. This paper initiates a general investigation about the difference of aldoxime and ketoxime esters under Beckmann conditions.

[1]*National Research Council of Canada Scholarship holder 1964–65.*

**The use of syn and anti with aldoximes is different from the common convention with ketoximes and refers to cis and trans to the hydrogen, respectively. See ref. 4a, p. 3; 4b, p. 321.*

Can. J. Chem. Downloaded from www.nrcresearchpress.com by 210.87.254.40 on 09/05/12
For personal use only.

RESULTS AND DISCUSSION

Aldoxime esters react in aqueous alcohol to give rise to the corresponding nitriles as the sole product. The reaction rates were measured spectrophotometrically by following

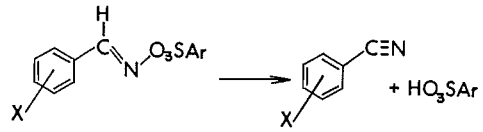

the disappearance of the band at the wavelength of maximum absorption of the corresponding aldoxime ester. The products, the nitrile and the acid, have only a small absorption at this wavelength. A correction in the rate expression was made to accommodate this product absorption, and the first-order rate equation becomes

$$\log \frac{(A_0 - A_\infty)}{(A_{obs} - A_\infty)} = \frac{kt}{2.303},$$

where A_0 represents the optical density at the beginning of the reaction, A_{obs} is the observed optical density at time t, and A_∞ is the optical density caused by the products at the end of the reaction. The reaction was found to follow first-order kinetics in aldoxime ester to greater than 90% completion. The first-order rate constants were obtained graphically by plotting $\log (A_0 - A_\infty)/(A_{obs} - A_\infty)$ versus t, and are summarized in Tables I, II, and III. The experimental uncertainty was calculated by the method of average, and found to be ±2.3%. A sample run is given in the Experimental section.

TABLE I

Rate constants for the reaction of substituted *syn*-benzaldoxime *p*-toluenesulfonates at 50.00 ± 0.02 °C in 80% methanol

Run No.	Substituent	$10^5 k$, s^{-1}	Run No.	Substituent	$10^5 k$, s^{-1}
1	*p*-OCH_3	93.5	7	*p*-Cl	10.3
2	*m*-OCH_3	16.3	8	*m*-Cl	10.6
3	*p*-CH_3	27.7	9	*p*-F	12.4
4	*m*-CH_3	25.7	10	*m*-F	10.2
5	—H	20.5	11	*p*-NO_2	7.90
6	*m*-Br	9.74	12	*m*-NO_2	6.33

TABLE II

Rate constants for the reaction of para-substituted *syn*-benzaldoxime *p*-toluenesulfonates at 50.00 ± 0.02 °C in 95% ethanol in the presence of 0.08 *M* sodium acetate

Run No.	Substituent	$10^3 k_2$, $l\ m^{-1}\ s^{-1}$
13	—NO_2	76.9
14	—Cl	26.6
15	—F	24.9
16	—H	23.1
17	—CH_3	19.2
18	—OCH_3	16.2

An examination of the rates in Table III reveals several characteristics of the reaction. First of all, runs 1, 19, and 20 show that the rate is sensitive to solvent change. Varying the solvent from 100% methanol to 60% methanol–water increases the rate by a factor

TABLE III

Rate constants for the reaction of *p*-methoxybenzaldoxime esters under varying conditions

Run No.	Ester	Solvent	Temp., ±0.02 °C	[Added salt]	$10^5 k$, s^{-1}
19	*syn*-*p*-Toluenesulfonate	100% MeOH	50.00	—	23.4
1	"	80% MeOH	"	—	93.5
20	"	60% MeOH	"	—	259
21	"	95% EtOH	"	—	23.5
22	"	"	"	0.20 *M* $LiClO_4$	29.0
23	"	"	"	0.50 *M* "	34.5
24	"	"	"	0.80 *M* "	43.1
25	"	"	"	0.20 *M* HOTs	26.8
26	*syn*-Benzenesulfonate	"	"	—	34.1
27	*syn*-*p*-Bromobenzene-sulfonate	"	"	—	92.9
28	*syn*-Acetate	"	141	—	22.9
29	*anti*-Acetate	"	50.00	—	8.11
30	"	"	60.00	—	16.1
31	"	"	70.00	—	34.3
32	"	"	141	—	1 490*

*Extrapolated rate constant.

of 11.3. This effect can be correlated by the equation proposed by Winstein and coworkers (9), using the scale of solvent-ionizing power derived from ionization of *p*-methoxyneophyl *p*-toluenesulfonate:

$$\log k_r = a \log k_1 + b,$$

where k_r is the rate constant for the reaction being examined, k_1 is the rate constant for the ionization of *p*-methoxyneophyl *p*-toluenesulfonate, and a is a measure of relative sensitivity of the reaction to the ionizing power of the solvent. The a values for several rearrangements have been calculated (9) from data available in the literature, being 0.690 for the ionic rearrangement of 9-decalyl perbenzoate; 0.569 for the allylic rearrangement of 1-phenylallyl 3,4,5-tribromobenzoate; and 0.119 for the Curtius rearrangement of benzoyl azide. In the latter, sensitivity to solvent change is low. Figure 1 shows a

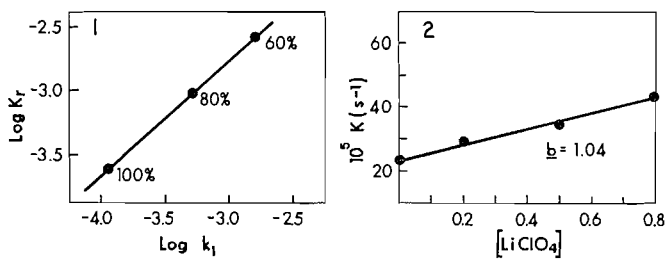

FIG. 1. Plot of log k_r for reaction of *syn*-*p*-methoxybenzaldoxime *p*-toluenesulfonate vs. log k_1 for solvolysis of *p*-methoxyneophyl *p*-toluenesulfonate in methanol at 50 °C.

FIG. 2. Plot of rate constant vs. lithium perchlorate concentration in the reaction of *syn*-*p*-methoxybenzaldoxime *p*-toluenesulfonate in 95% ethanol at 50 °C.

plot of log k_r versus log k_1 in methanol at 50°. The relatively high a value (0.950) indicates that the reaction is sensitive to changes in solvent-ionizing power in a manner similar to that for known ionization reactions.

Secondly, the addition of lithium perchlorate over a range of concentrations up to

Can. J. Chem. Downloaded from www.nrcresearchpress.com by 210.87.254.40 on 09/05/12
For personal use only.

0.80 M gives rise to a normal salt effect. This can be described by a linear relation (10) between the rate constant and the molar concentration of lithium perchlorate:

$$k_r = k_0(1 + b[LiClO_4]),$$

where k_r is the observed rate constant, k_0 represents the rate constant at zero salt concentration, and b is the slope of the linear plot representing the % increase in rate constant over k_0 per 0.01 M increment of lithium perchlorate. Figure 2, from runs 21 to 24, shows the linear plot of rate constant versus lithium perchlorate concentration in 95% ethanol at 50°, with a b value of 1.04. The salt effect is quite small, but is that expected in ionizing solvents such as alcohols.

Finally, runs 21, 26, and 27 indicate that the reaction is sensitive to variation of the leaving group. Changing the leaving group from *p*-toluenesulfonate to *p*-bromobenzenesulfonate increases the rate by a factor of 3.9. A comparison of relative rates of the reactions of isopropyl arenesulfonates and *syn*-*p*-methoxybenzaldoxime arenesulfonates in aqueous ethanol at 50° is tabulated in Table IV. Using the three arenesulfonates as

TABLE IV

Comparison of the rates of isopropyl arenesulfonates (11) and *syn*-*p*-methoxybenzaldoxime arenesulfonates

Arenesulfonate	Isopropyl in 50% EtOH at 50°	*syn*-*p*-Methoxybenzaldoxime in 95% EtOH at 50°
p-Toluene	0.63	0.65
Benzene	1.00	1.00
p-Bromobenzene	2.92	2.72

the leaving group, the reaction of the *syn*-aldoxime arenesulfonates varies in the same direction and by approximately the same magnitude as the ionization of isopropyl arenesulfonates.

An inspection of the rate constants from Table I clearly shows that electron-donating groups accelerate the reaction rate and that electron-withdrawing substituents retard it. The effect of meta- and para-substitution on the rate constant can be correlated by the Hammett equation (12)

$$\log k/k_0 = \rho\sigma,$$

where k is the rate constant of the substituted *syn*-aldoxime *p*-toluenesulfonates, k_0 is the rate constant of the unsubstituted compound, ρ is the reaction constant, and σ is the substituent constant. Figure 3 shows a plot of log k/k_0 versus σ, and a ρ value of -0.77 was obtained when only meta-derivatives (σ^n) were considered, as suggested by van Bekkum *et al.* (13). The *p*-OCH_3 substituent deviates significantly from this line (a Hammett σ value of -0.856 would be required to bring it on the line, which means that the σ^+ value of -0.77 would not fit) and a mesomeric para-interaction energy difference ($\Delta\Delta F_p$) of -0.78 kcal mole^{-1} is obtained from the equation

$$-\Delta\Delta F_p = (\sigma - \sigma^n) \times 2.303RT,$$

where ρ is the value derived from the meta-substituents (-0.77), σ is the -0.856 value required to place the point on the line, and σ^n is the value -0.175 suggested by van Bekkum *et al.* (13) for a para-methoxy substituent from the detailed examination of substituent effects.

Can. J. Chem. Downloaded from www.nrcresearchpress.com by 210.87.254.40 on 09/05/12
For personal use only.

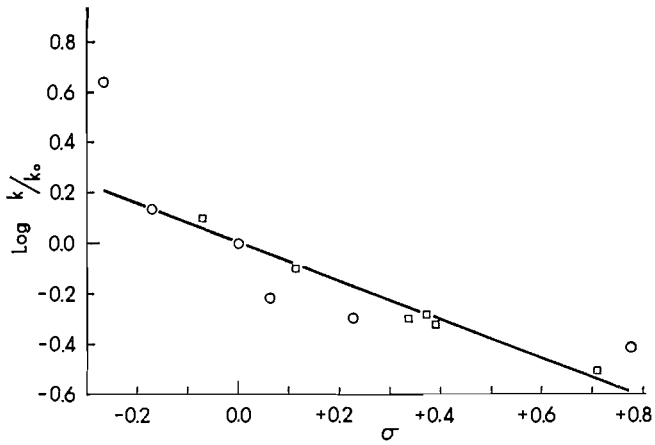

FIG. 3. Plot of log k/k_0 vs. σ for the reaction of meta- (□) and para- (○) substituted *syn*-benzaldoxime *p*-toluenesulfonates in 80% methanol at 50 °C.

It is difficult to envisage a direct resonance interaction between the substituent and the N—O bond in I that is being broken, as it would be expected to be in the nodal plane of the aromatic π orbitals. Thus, ionization to an imidonium species II would not be expected to give rise to a very negative ρ value, nor could we expect a significant resonance interaction with the ring.

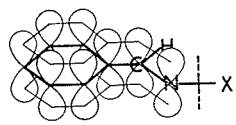

I

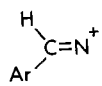

II

It should be noted, however, that *p*-methoxybenzonitrile, the product, gains additional stabilization from a resonance structure such as III.

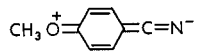

III

If the elimination has progressed to the point that the transition state is beginning to resemble the product, then the *p*-methoxy substituent would be expected to stabilize the transition state and thus react at an enhanced rate.

If, indeed, the transition state does resemble the product nitrile, we would expect a considerable amount of C—H bond breaking. In order that we may ascertain the degree of C—H bond breaking in the reaction, the deuterated aldoxime *p*-toluenesulfonate IV was prepared. A rate constant of 1.36×10^{-5} s^{-1} was obtained in 95% ethanol at 50° for the deuterated compound, as compared with 6.16×10^{-5} s^{-1} for the undeuterated ester under the same conditions. This gives rise to a k_H/k_D value of 4.51 at 50°.

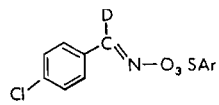

IV

Can. J. Chem. Downloaded from www.nrcresearchpress.com by 210.87.254.40 on 09/05/12
For personal use only.

Can. J. Chem. Downloaded from www.nrcresearchpress.com by 210.87.254.40 on 09/05/12
For personal use only.

An approximation of the theoretical isotope effect was calculated by the following expression (14) (this was necessary because of the sp^2 nature of the C—H bond being broken, a type of rupture not commonly observed):

$$k_D/k_H = \exp \frac{hc}{2kT}(\nu_D - \nu_H),$$

where k_D is the rate constant for the labelled compound, k_H is the rate constant for the unlabelled isomer, h is Planck's constant, c is the velocity of light, k is Boltzmann's constant, T is absolute temperature, and ν_D and ν_H represent the vibrational frequencies associated with a C—D and C—H bond, respectively. From the infrared spectra, the measured vibrational frequency of the C—D bond in *p*-chlorobenzaldoxime *p*-toluenesulfonate is 2 240 cm^{-1}, and that for the C—H bond is 3 030 cm^{-1}. Substituting these values into the above equation gives a theoretical k_H/k_D ratio of 5.81. The observed value of k_H/k_D of 4.51 suggests that the rate-determining step must involve the breaking of the C—H bond.

Run 25 in Table III indicates that the reaction is not acid catalyzed. The addition of 0.20 *M* *p*-toluenesulfonic acid had no appreciable effect on the rate. But the rates were observed to be greatly increased by the addition of sodium acetate. The second-order rate constants are calculated by the following equation:

$$k_2 = \frac{k_{obs} - k_1}{[OAc^-]},$$

where k_2 represents the second-order rate constant, k_{obs} is the observed pseudo first-order rate constant, and k_1 is the rate constant in the absence of sodium acetate. The second-order rate constants in the presence of 0.08 *M* sodium acetate are tabulated in Table II. It is interesting to note that the order of reactivity is completely reversed, with a ρ value of +0.44. This is similar to the base-catalyzed dehydrohalogenation of ald-chlorimines (15). A resemblance to this mild base-catalyzed process may also be responsible for the deviation of the *p*-nitro substituent in the uncatalyzed reaction (Fig. 3).

The possibility that the *syn*-aldoxime esters are being isomerized to the corresponding *anti*-ester followed by a *trans*-elimination must also be considered. Thus, in Scheme I,

SCHEME I

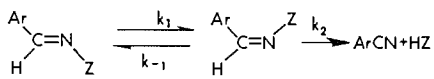

the reaction may be represented kinetically by the expression

$$-\frac{d[syn]}{dt} = \frac{k_1 k_2 [syn]}{k_{-1} + k_2}.$$

If k_1 and $k_{-1} > k_2$, then the expression reduces to

$$-\frac{d[syn]}{dt} = k_2 K [syn],$$

where $K = k_1/k_{-1}$, and we would thus obtain the same rate constant for either the *syn*- or the *anti*-ester. As may be seen in Table III, runs 28 to 32, the *anti*-isomer is 65 times faster than the *syn*-isomer. If, however, k_1 is slow and rate determining, we would

not expect to observe a kinetic isotope effect on replacing the oximino hydrogen by deuterium. The intermediate case where $k_{-1} \cong k_2$ reduces the above expression to

$$-\frac{d[syn]}{dt} = \frac{1}{2}k_1[syn]$$

and again no kinetic isotope effect would be observed. The observation of a 65-fold difference in rate between the *syn*- and *anti*-pair, and of a kinetic isotope effect of the magnitude of 4.51, allows us to exclude any possible isomerization mechanism.

A pyrolysis type of mechanism for the arenesulfonate esters may also be ruled out on the basis of the solvent sensitivity and the salt effect. The negative $\Delta S^{\ddagger}$ values in Table V

TABLE V

Determination of activation parameters of substituted *syn*-benzaldoxime *p*-toluenesulfonates in 80% methanol

Run No.	Substituent	Temp., ±0.02 °C	$10^5 k$, s^{-1}	$\Delta H^{\ddagger}$, kcal m^{-1}	$\Delta S^{\ddagger}$, e.u.$m.^{-1}$
33	*m*-CH_3	60.07	64.2		
4	*m*-CH_3	50.00	25.7	20.4	−12.0
34	*m*-CH_3	40.04	9.12		
35	—H	60.07	52.0		
5	—H	50.00	20.5	21.0	−10.6
36	—H	40.04	6.99		
37	*m*-Cl	60.07	27.3		
8	*m*-Cl	50.00	10.6	20.3	−14.1
38	*m*-Cl	40.04	3.92		

could readily arise from increased solvent constriction in the transition state and is consistent with ionization processes.

Solvent sensitivity, salt effect, and the dependence of the rate constant upon the leaving group suggest that the reaction is ionic in character. The effect of substituents suggests that a small positive charge may be developed on the conjugated system. The result of isotopic substitution shows that the C—H bond is also considerably stretched. This evidence supports a concerted *cis*-elimination mechanism, and the transition state involving varying degrees of rupture of the N—Z and C—H bonds (V).

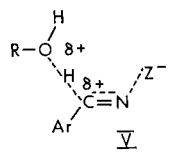

V

It is possible that the N—Z bond has been completely broken, and we are measuring the proton loss from species such as II. This suggests the possibility of an ion-pair mechanism (Scheme II) which would involve ionization to the ion pair VI followed by proton abstraction by the gegen ion.

SCHEME II

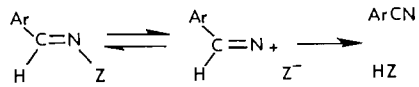

VI

Can. J. Chem. Downloaded from www.nrcresearchpress.com by 210.87.254.40 on 09/05/12
For personal use only.

This suffers from a possible handicap since, to accommodate the kinetic isotope effect, the last step would have to be rate determining and this would suggest that the stronger the arenesulfonate ion as a base the faster the reaction, which is the reverse of that observed in Table IV. This could be overcome by a large change in the prior equilibrium effectively increasing the steady-state concentration of the ion pair, and cannot be rigorously excluded. We are at this time, however, unable to cite any experiment which can satisfactorily differentiate whether the gegen ion or the solvent molecule is acting as base as in V.

EXPERIMENTAL

Preparation of Materials

p-Chlorobenzaldehyde-d

A solution of 40 g (0.37 mole) of N-methyl aniline in 250 ml of benzene was added slowly, with stirring, to a cooled solution of 60 g (0.34 mole) of *p*-chlorobenzoyl chloride in 250 ml of benzene. The mixture was refluxed for 2 h, cooled, and then washed with 250 ml of water, 250 ml of 5% hydrochloric acid, 250 ml of 5% sodium hydroxide, and 250 ml of water, respectively. The benzene solution was dried, the solvent evaporated, and the residue distilled at reduced pressure. The distillate solidified upon cooling in an ice bath. The yield of the pure N-methyl *p*-chlorobenzanilide was 56 g (60%), m.p. 54–56°.

Anal. Calcd. for $C_{14}H_{12}ClNO$: C, 68.5; H, 4.90; N, 5.71. Found: C, 68.1; H, 5.01; N, 5.58.

N-Methyl *p*-chlorobenzanilide (20 g (0.082 mole)) was dissolved in 200 ml of tetrahydrofuran which was redistilled over sodium just before use. The solution was cooled to 4° and 0.89 g (0.022 mole) of lithium aluminium deuteride was added and the mixture stirred at 4° for 15 h, whereupon 400 ml of 7% hydrochloric acid was added. The tetrahydrofuran was evaporated and the residue steam-distilled. The distillate was extracted with ether. The ethereal solution was dried, the solvent evaporated, and the residue distilled at diminished pressure. The distillate solidified on cooling in an ice bath. The yield of *p*-chlorobenzaldehyde-*d* was 7 g (58%), m.p. 47°. The infrared spectrum in chloroform shows that the vibrational frequency of the C—H bond at 2 837 cm^{-1} has been shifted to 2 112 cm^{-1} in the deuterated compound. The n.m.r. spectrum in deuterochloroform shows no absorption at τ 0.30 attributable to aldehydic C—H.

Oximes

All the *syn*-oximes were prepared by the following general procedure.

A 5-g quantity of hydroxylamine hydrochloride was dissolved in 30 ml of water and 20 ml of 10% sodium hydroxide, and 5 g of the aldehyde was then added. Sufficient 95% ethanol was added to the mixture to obtain a homogeneous solution. The mixture was refluxed for 15 min and cooled, and 100 g of crushed ice was added with shaking. If the oxime separated as a solid, the precipitate was filtered and pressed dry. The crude product was recrystallized from a mixture of skelly B and benzene. If the oxime separated as an oil, the oil was extracted with ether. The ethereal solution was dried, the solvent evaporated, and the residue distilled under reduced pressure. The distillate solidified on standing in the freezer. The yield of the pure oximes was in the range of 75–90%. Infrared spectra of the oximes in chloroform show a strong band at 3 580 cm^{-1} caused by O—H absorption (16). The melting point of the oximes together with the reported value (16) are *syn-p*-methoxybenzaldoxime, m.p. 64, reported 64; *syn-m*-methoxybenzaldoxime, m.p. 40, reported 40; *syn-p*-methylbenzaldoxime, m.p. 79, reported 79; *syn-m*-methylbenzaldoxime, m.p. 60, reported 60; *syn*-benzaldoxime, m.p. 35, reported 35; *syn-p*-fluorobenzaldoxime, m.p. 86, reported 86 (17); *syn-m*-fluorobenzaldoxime, m.p. 68, reported 63 (17); *syn-p*-chlorobenzaldoxime, m.p. 110, reported 106; *syn-m*-chlorobenzaldoxime, m.p. 71, reported 70; *syn-p*-chlorobenzaldoxime-*d*, m.p. 109; *syn-m*-bromobenzaldoxime, m.p. 75, reported 72; *syn-p*-nitrobenzaldoxime, m.p. 131, reported 129; *syn-m*-nitrobenzaldoxime, m.p. 124, reported 120; *anti-p*-methoxybenzaldoxime, m.p. 132–133°, reported 133° (18).

Oxime Acetates

A 0.5-g (3.3 mmoles) quantity of *syn-p*-methoxybenzaldoxime was dissolved in 0.5 ml of acetic anhydride. After 10 min, 5 ml of ether and 5 ml of hexane were added. The mixture was cooled and the precipitate was filtered. The yield of *syn-p*-methoxybenzaldoxime acetate was 0.47 g (74%), m.p. 48–49°, after recrystallization from a 50:50 mixture of ether and hexane. Reported m.p. 48–49° (18). The infrared spectrum in chloroform shows a strong band at 1 755 cm^{-1}.

anti-p-Methoxybenzaldoxime acetate was prepared by the same method as that for the *syn*-isomer. Yield 0.52 g (82%), m.p. 64–65°. Reported m.p. 64–65° (18). The infrared spectrum in chloroform shows a strong band at 1 760 cm^{-1}.

Oxime Arenesulfonates

The following general procedure was used for the preparation of the *syn*-aldoxime arenesulfonates except the nitro-substituted compounds.

To a rapidly stirred solution of 3 mmoles of the oxime in 20 ml of absolute ether, 3.1 mmoles of powdered sodium amide was added and the mixture was stirred for about 5 h. The mixture was filtered and the precipitate washed several times with ether.

Can. J. Chem. Downloaded from www.nrcresearchpress.com by 210.87.254.40 on 09/05/12
For personal use only.

p-Toluenesulfonyl chloride (0.36 g (2.5 mmoles) in 5 ml of ether) was slowly added to a rapidly stirred slurry of the sodium salt of the oxime in 5 ml of ether. The salt produced was removed by filtration and 10 ml of hexane was added to the filtrate. Upon cooling of the mixture, the oxime arenesulfonate crystallized. Recrystallization from a 50:50 mixture of ether and hexane generally gives a pure sample. Yield 50–60%. The infrared spectra in chloroform show strong bands at 1 380 and 1 170 cm^{-1}, characteristic of sulfonate esters (16).

Since the meta- and para-substituted *syn*-nitrobenzaldoximes gave a mixture of the original oxime and the corresponding nitrile when the above method was followed, the procedure was modified. The sodium salt of the oximes was prepared as previously. The salt was dissolved in 5 ml of 50% acetone–water and added slowly with stirring to a cooled solution of *p*-toluenesulfonyl chloride in 2 ml of acetone. The oxime ester separated was collected, washed with 50% acetone, and recrystallized as before. The yield was about 45%.

The relevant data for these *syn*-aldoxime arenesulfonates are summarized in Table VI.

TABLE VI

Summary of data for X—C_6H_4—CH=N—O—SO_2—C_6H_4—Y—*p*

	m.p.,* °C	Max., mμ	Molecular formula	Anal. calcd. C	H	N	Anal. found C	H	N
Y = CH_3									
X =									
p-OCH_3	99–100	274.5	$C_{15}H_{15}NO_4S$	59.0	4.91	4.59	59.1	5.02	4.50
p-CH_3	100–102	261.0	$C_{15}H_{15}NO_3S$	62.3	5.19	4.84	62.5	5.50	4.91
—H	85–86	255.0	$C_{14}H_{13}NO_3S$	61.1	4.41	5.08	61.3	4.56	5.03
p-F	98–99	253.5	$C_{14}H_{12}FNO_3S$	57.4	4.10	4.78	57.4	4.33	4.73
p-Cl	102–103	260.5	$C_{14}H_{12}ClNO_3S$	54.4	3.90	4.52	54.4	4.40	4.44
p-Cl-*d*	105–107	260.0	$C_{14}H_{11}DClNO_3S$						
p-NO_2	111–112	276.0	$C_{14}H_{12}N_2O_5S$	52.5	3.77	8.74	52.5	3.83	8.50
m-OCH_3	85–86	257.5	$C_{15}H_{15}NO_4S$	59.0	4.91	4.59	58.9	4.86	4.39
m-CH_3	83–84	256.0	$C_{15}H_{15}NO_3S$	62.3	5.19	4.84	62.4	5.13	4.71
m-F	95–96	252.0	$C_{14}H_{12}FNO_3S$	57.4	4.10	4.78	57.4	4.51	4.54
m-Cl	94–95	252.5	$C_{14}H_{12}ClNO_3S$	54.4	3.90	4.52	54.3	4.44	4.61
m-Br	106–107	254.5	$C_{14}H_{12}BrNO_3S$	47.4	3.39	3.96	47.2	3.58	4.07
m-NO_2	110–111	228.5	$C_{14}H_{12}N_2O_5S$	52.5	3.77	8.74	52.5	4.14	8.52
Y = H									
X = OCH_3	99–100	272.5	$C_{14}H_{13}NO_4S$	57.7	4.47	4.81	57.4	4.63	4.67
Y = Br									
X = OCH_3	104–105	274.0	$C_{14}H_{12}BrNO_4S$	54.5	3.25	3.78	54.5	3.59	3.70

*Melted with decomposition.

Product Analysis

syn-p-Chlorobenzaldoxime *p*-toluenesulfonate (0.50 g (1.6 mmoles)) was suspended in 10 ml of 95% ethanol at 50°. The suspension dissolved within 12 h, and the mixture was kept at 50° for an additional 24 h, whereupon 20 g of crushed ice was added. The solid separated was filtered and recrystallized from skelly B. The yield of *p*-chlorobenzonitrile was 0.13 g (80%), m.p. 92–93°. Reported m.p. 94–96° (17). The infrared spectrum in chloroform shows a strong band at 2 230 cm^{-1} caused by C≡N absorption (16). *p*-Methoxybenzonitrile, m.p. 61–62°, reported 61–62° (17), was similarly isolated from *syn-p*-methoxybenzaldoxime *p*-toluenesulfonate in 87% yield.

Kinetic Measurements

Absorption curves of the *syn*-aldoxime esters in the ultraviolet region were obtained on a Cary recording spectrophotometer model 14M. Kinetic measurements were taken from a Beckman model DU spectrophotometer at the wavelength of maximum absorption of the corresponding oxime ester. The spectrophotometer is equipped with a double set of thermospacers connected to a circulating constant temperature bath, thermostated within ±0.02° of the particular temperature. All kinetic runs were extrapolated back to zero time, and the small absorption caused by the products of the reaction was corrected in the rate expression. Good first-order curves were observed in every case. As an example, the reaction of the unsubstituted compound is recorded in Table VII, and the results are plotted in Fig. 4.

Reaction of *syn-p*-methoxybenzaldoxime acetate was carried out by the sealed-tube technique. A standard solution of the acetate (2 mg per 100 ml of the solvent) was made up. Samples of approximately 5 ml volume were sealed in ampoules and placed in the temperature bath. The reaction was followed by withdrawing and cooling ampoules at intervals of time, and the optical density was measured.

Can. J. Chem. Downloaded from www.nrcresearchpress.com by 210.87.254.40 on 09/05/12
For personal use only.

TABLE VII

Reaction of *syn*-benzaldoxime *p*-toluenesulfonate in 80% methanol at 50.0° and 255.0 mμ

Time, min	A_{obs}	$\frac{A_0 - A_\infty}{A_{obs} - A_\infty}$	$\log \frac{A_0 - A_\infty}{A_{obs} - A_\infty}$	$10^5 k$, s^{-1}
0	1.140	1.09/1.09	0.000	—
10	1.025	1.09/0.973	0.0493	18.6
20	0.905	1.09/0.853	0.106	20.3
30	0.815	1.09/0.763	0.154	19.7
40	0.722	1.09/0.670	0.211	20.3
50	0.647	1.09/0.595	0.263	20.2
60	0.580	1.09/0.548	0.300	19.3
98	0.328	1.09/0.330	0.519	20.3
125	0.288	1.09/0.235	0.666	20.4
144	0.237	1.09/0.185	0.747	20.0
∞	0.052			

NOTE: Average $k = 19.9 \pm 0.05 \times 10^{-5}$ s^{-1}.

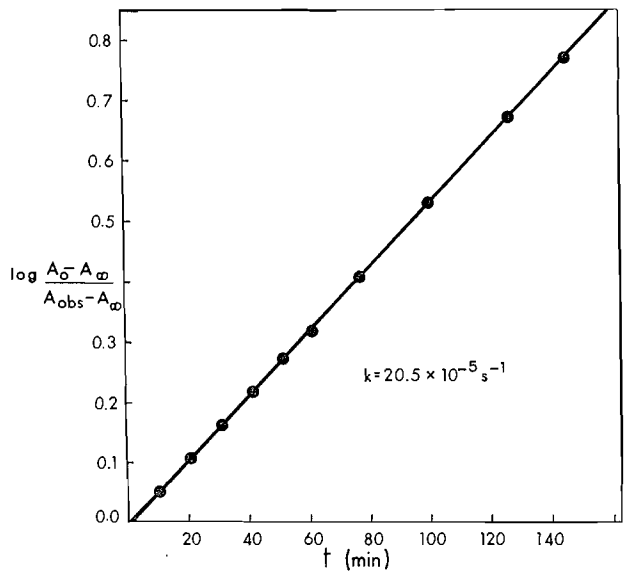

FIG. 4. Plot of log $(A_0 - A_\infty)/(A_{obs} - A_\infty)$ vs. t for the reaction of *syn*-benzaldoxime *p*-toluenesulfonate in 80% methanol at 50° and 255.0 mμ.

Infrared Spectra

The infrared spectra of *p*-chlorobenzaldoxime *p*-toluenesulfonate and the deutero-derivative were measured at 1% concentration in carbon tetrachloride solution using the same cells in each case. The spectrum of the deuterated compound has a C—D stretching band at 2 240 cm^{-1} that was not in the spectrum of the undeuterated ester. It also lacked a band at 3 030 cm^{-1}, which is present in the spectrum of the undeuterated aldoxime ester.

ACKNOWLEDGMENTS

The research described herein was supported by the National Research Council of Canada through a grant-in-aid to R. J. C. The n.m.r. and infrared spectra were measured by R. N. Swindlehurst and Mrs. Gail B. Conway; and the microanalyses were performed by Miss Darlene Roberts of this department.

Can. J. Chem. Downloaded from www.nrcresearchpress.com by 210.87.254.40 on 09/05/12
For personal use only.

REFERENCES

1. E. BECKMANN. Ber. **20**, 1507 (1887).
2. A. H. BLATT. Chem. Rev. **12**, 215 (1933).
3. B. JONES. Chem. Rev. **35**, 335 (1944).
4. (*a*) W. Z. HELDT and L. G. DONARUMA. Org. Reactions, **11**, Chap. I (1960).
   (*b*) E. L. ELIEL. Stereochemistry of carbon compounds. McGraw-Hill Book Co., New York, N.Y. 1962.
5. P. DE MAYO. Molecular rearrangements. John Wiley and Sons, Inc., N.Y. 1963. p. 483.
6. J. MEISENHEIMER, P. ZIMMERMANN, and O. VON KUMMER. Ann. **446**, 205 (1926).
7. J. MEISENHEIMER, W. THEILACKER, and O. BEISSWENGER. Ann. **495**, 249 (1932).
8. K. VON AUWERS and M. SEYFRIED. Ann. **484**, 178 (1930).
9. S. G. SMITH, A. H. FAINBERG, and S. WINSTEIN. J. Am. Chem. Soc. **83**, 618 (1961).
10. A. H. FAINBERG and S. WINSTEIN. J. Am. Chem. Soc. **78**, 2763 (1958).
11. R. E. ROBERTSON. Can. J. Chem. **31**, 589 (1953).
12. L. P. HAMMETT. Physical organic chemistry. McGraw-Hill Book Co., N.Y. 1940.
13. H. VAN BEKKUM, P. E. VERKADE, and B. M. WEPSTER. Rec. Trav. Chim. **78**, 815 (1958).
14. L. MELANDER. Isotope effects on reaction rates. Ronald Press Co., N.Y. 1960. p. 67.
15. C. R. HAUSER, J. W. LEMAISTRE, and A. E. RAINFORD. J. Am. Chem. Soc. **57**, 1056 (1935).
16. R. L. SHRINER, R. C. FUSON, and D. Y. CURTIN. The systematic identification of organic compounds. John Wiley and Sons, Inc., N.Y. 1956. pp. 172 and 283–284.
17. I. HEILBRON and H. M. BUNBURY. Dictionary of organic compounds. Eyre and Spottiswoode Ltd., London. 1953.
18. O. L. BRADY and H. A. M. SHARAWY. J. Chem. Soc. 4083 (1953).

Can. J. Chem. Downloaded from www.nrcresearchpress.com by 210.87.254.40 on 09/05/12
For personal use only.

Can. J. Chem. Downloaded from www.nrcresearchpress.com by 210.87.254.6 on 09/05/12
For personal use only.

SOME ASPECTS OF THE CHEMISTRY OF CATHARANTHINE AND CLEAVAMINE

JAMES P. KUTNEY, RICHARD T. BROWN, AND EDWARD PIERS
Department of Chemistry, University of British Columbia, Vancouver, British Columbia
Received November 13, 1964

Dedicated to Professor R. B. Sandin on the Occasion of his Sixty-Eighth Birthday

ABSTRACT

Chemical and spectroscopic evidence is presented for an interesting acid-catalyzed rearrangement of the alkaloid catharanthine. Four reaction products (descarbomethoxycatharanthine and cleavamine and its two dihydro derivatives) were isolated, and their formation is rationalized by a mechanism involving ring-opened intermediates. Evidence is presented in support of the proposed mechanism and, in particular, a novel transannular cyclization leading to the *Iboga* alkaloid skeleton is shown in support of the steps postulated for the formation of descarbomethoxycatharanthine.

The X-ray analysis of cleavamine methiodide established the absolute configuration of the lone asymmetric center present in the molecule and, from these results, the absolute configuration of the *Iboga* alkaloids can be derived.

During investigations by the Lilly group (1) on the dimeric *Vinca* alkaloids (vincaleukoblastine (VLB), leurosine, and leurocristine), it was found that each was cleaved by concentrated hydrochloric acid to an indole compound and vindoline derivative. The vindoline derivative of VLB and leurosine was desacetylvindoline (I), whereas leurocristine gave des-$N_{(a)}$-methyl-desacetylvindoline (II). Both VLB and leurocristine afforded the same indole derivative, velbanamine, $C_{19}H_{26}N_2O$, but the corresponding compound with leurosine was called cleavamine, $C_{19}H_{24}N_2$.

In the same communication it was also reported that the known alkaloid catharanthine (III (2)), when subjected to the same acid treatment, also provided cleavamine as one of the reaction products. The suggestion that cleavamine possessed a tetracyclic structure similar to the known *Aspidosperma* alkaloid quebrachamine (3) stimulated further research in our laboratory to establish conclusively the structure and stereochemistry of this substance. At the outset we felt that this investigation might not only provide indirect evidence for the presence of a catharanthine-like unit in the biologically important VLB molecule, but also illustrate a novel acid-catalyzed rearrangement in the *Iboga* alkaloid series. Furthermore, if the absolute configuration of the asymmetric center in the molecule could be established, it would provide indisputable evidence for the absolute configuration of the *Iboga* alkaloids.

With this view in mind, we initiated a detailed study of the catharanthine–cleavamine transformation and some of our results concerning the structure of cleavamine have already been published (4). Fortunately, the X-ray analysis of cleavamine methiodide established the structure and absolute configuration at C-2[1] as depicted in IV. We now wish to discuss these results in some detail and to present more recent evidence which is relevant to the mechanism of this interesting transformation.

Before considering mechanism, we wish to discuss briefly the stereochemistry of the *Iboga* alkaloids, since, in conjunction with the results of other workers and the evidence presented herein, it is possible to assign the absolute configuration for this series of

[1]*The numbering system used here is that of the Iboga alkaloids (see ref. 7).*

alkaloids. It is obvious that the absolute configuration of C-2 in IV immediately reveals the absolute configuration of this carbon atom in the catharanthine molecule, since there is little reason to suspect that any configurational change would occur in the catharanthine–cleavamine conversion. However, even this vague possibility has been eliminated in our recent transannular cyclization studies (5) wherein a cleavamine derivative has been converted to dihydrocatharanthine and the *Iboga* alkaloid, coronaridine. These results establish that the same stereochemistry at C-2 prevails in the rigid *Iboga* structure as in the relatively nonrigid cleavamine molecule. Since a previous X-ray study on ibogaine hydrobromide (6) had already established a *cis* relationship between the ethyl group at C-4 and the $\rangle$N—C-19 bridge, it is clear that the absolute configuration at C-4 and, in turn, for the entire *Iboga* alkaloid system is now established as shown in V for ibogamine.

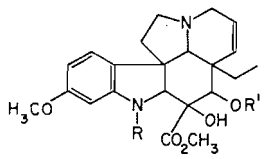

(I) R = CH_3; R' = H

(II) R = H; R' = H

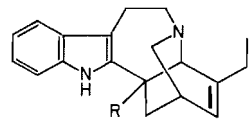

(III) R = $COOCH_3$

(VI) R = H

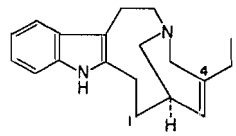

(IV)

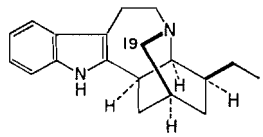

(V)

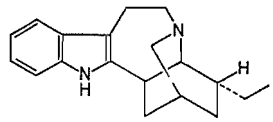

(VII)

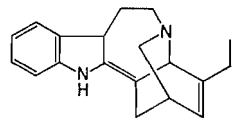

(VIII)

It should be noted that in their elegant work on the alkaloids of *Tabernanthe iboga*, the Ciba group (7) had previously postulated that the ethyl group at C-4 was *trans* to the $\rangle$N—C-19 bridge. Furthermore, these workers had compared the optical rotatory dispersion curve for one of their bicyclic degradation products with a decalin derivative of established configuration and on this basis suggested an absolute stereochemistry for this group of alkaloids. It is pleasing to note that, with the exception of the incorrect assignment at C-4, the remaining stereochemical centers were proposed as in V. Consequently, in this instance, the optical comparison of a piperidone ring with a cyclohexanone system has now been proved as valid, although some reservations about this point were understandably expressed at that time.

Turning to the mechanistic interpretation of the acid-catalyzed rearrangement of catharanthine, we felt that we should carry out a more detailed investigation of this reaction in an attempt to isolate as many products as possible, since these may provide evidence as to the nature of this rearrangement. Apart from the isolation of cleavamine, another product, descarbomethoxycatharanthine (VI), had been previously obtained from this reaction (8) but, since the combined yield of these two products constituted only about 20% of the total reaction mixture, we decided to examine this mixture more closely.

Can. J. Chem. Downloaded from www.nrcresearchpress.com by 210.87.254.6 on 09/05/12
For personal use only.

The cleavamine mother liquors and several cleavamine-containing fractions were combined and subjected to several very careful column chromatographic separations. Apart from the many fractions containing intractable gums and resins, one fraction which could be well characterized was obtained. It is appropriate to discuss this in some detail, since additional evidence which was germane to any mechanistic interpretation was furnished.

This fraction, designated as B9, was a mixture of two compounds, as shown by thin-layer chromatography, but numerous attempts to completely separate these compounds by various techniques failed. Consequently, we will discuss the spectral data obtained on B9 and show how the results led to the characterization of these two compounds as the two possible dihydrocleavamines epimeric at C-4. No olefinic protons were apparent in the nuclear magnetic resonance spectrum of B9, and the methyl triplet normally present at 8.96 τ in cleavamine had shifted to 9.13 τ. The mass spectrum showed a molecular ion at *m/e* 282, and other significant peaks at *m/e* 156, 143, 138, and 124 could be attributed to the following fragments, which are given by 4β-dihydrocleavamine (4, 10).[2]

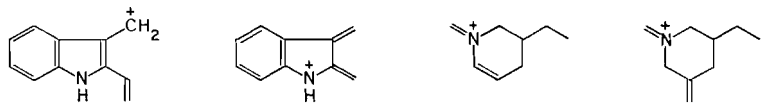

In general, the mass spectrum of B9 was practically superimposable on that of 4β-dihydrocleavamine, and also the infrared spectra were similar. The leading spot of the mixture had the same R_f value as 4β-dihydrocleavamine on thin-layer chromatography, and the second spot was thought to be due to a dihydrocleavamine epimeric at C-4, which we designated as 4α-dihydrocleavamine. Fortunately, from other studies at the Lilly laboratories, a C-4 epimer of 4β-dihydrocleavamine had been isolated and we were able to demonstrate that this compound was identical with our sample of 4α-dihydrocleavamine. A synthetic mixture of the dihydrocleavamines duplicated the behavior of fraction B9 on thin-layer chromatography and gave an identical infrared spectrum.

Two dihydro derivatives epimeric at C-4 could, in theory, arise from an acid-catalyzed rearrangement of dihydrocatharanthine, formed by the reduction of catharanthine during the course of the reaction, or they could arise from the reduction of cleavamine itself. The former possibility is eliminated, since it is well known (8) that dihydrocatharanthine does not yield any tetracyclic products under the reaction conditions utilized above, whereas we have recently shown that cleavamine is not reduced to the dihydro derivatives under these conditions as well. This evidence indicates that these dihydro compounds arise from a ring-opened intermediate which can lead to cleavamine on the one hand and to dihydrocleavamines on the other.

Perhaps the most interesting aspect of the acid reaction on catharanthine comes forth from consideration of the formation of descarbomethoxycatharanthine. Some earlier work by the Lilly group (8) established that, although dihydrocatharanthine, like its relatives in the *Iboga* series (7, 11, 12), decarboxylated readily to yield the corresponding descarbomethoxy base, epi-ibogamine (VII), catharanthine did not undergo an analogous transformation under these conditions. Although this may seem somewhat puzzling,

[2]*In a related investigation to be reported later, we have shown by the X-ray analysis technique that dihydrocleavamine prepared by catalytic reduction of cleavamine has the ethyl group at C-4 in the β-configuration and is therefore referred to as 4β-dihydrocleavamine. The C-4 epimer obtained from decarbomethoxylation of carbomethoxydihydrocleavamine is therefore 4α-dihydrocleavamine.*

Can. J. Chem. Downloaded from www.nrcresearchpress.com by 210.87.254.6 on 09/05/12
For personal use only.

there is a very reasonable rationalization for this difference in reaction. Consideration of the accepted decarboxylation mechanisms (7, 12) for these compounds leads to the realization that in the case of catharanthine an intermediate of type VIII becomes necessary. Molecular models reveal that this intermediate would be very highly strained and there is serious doubt whether it can exist at all. On the other hand, the corresponding intermediate in the reduced series can form easily and it is felt that this accounts for the marked difference in reactivity toward the decarboxylation reaction. Therefore, the formation of descarbomethoxycatharanthine does not involve a simple decarboxylation but must be explained in some other manner.

In relation to some transannular cyclization studies in our laboratory, some of which have been recently published (5, 13, 14), it was extremely attractive to consider that the formation of all the products which have been isolated from the reaction of catharanthine with concentrated hydrochloric acid can be rationalized on the basis of the mechanism shown in Reaction Scheme 1.

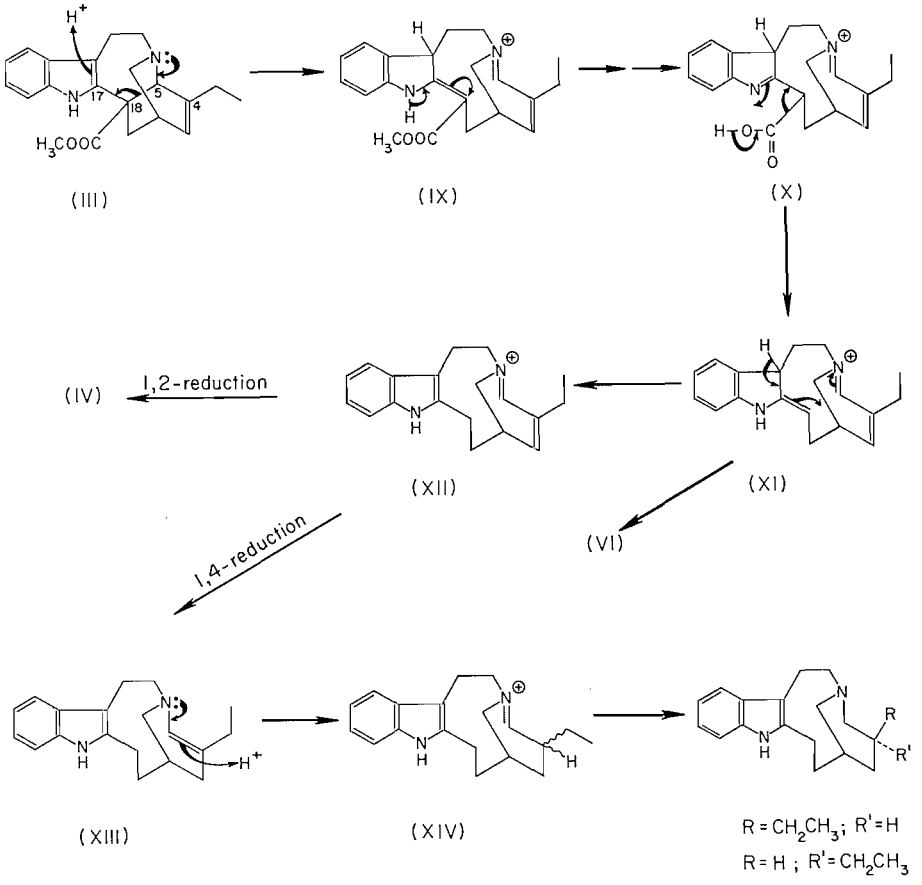

REACTION SCHEME 1.

The lone pair of electrons on $N_{(b)}$ in III can participate in a rearrangement to form an iminium ion, with concurrent ring cleavage and protonation at the β-position of the indole. The resulting ring-opened intermediate IX is stabilized by two factors: (i) the

Can. J. Chem. Downloaded from www.nrcresearchpress.com by 210.87.254.6 on 09/05/12
For personal use only.

conjugated nature of the iminium ion, and (ii) the conjugation of the newly generated double bond between C-17 and C-18 with both the ester and anilino functions. After acid hydrolysis of the ester, decarboxylation may occur via X in a manner analogous to the mechanism proposed for the *Iboga* alkaloids (7, 12). This ring-opened intermediate renders the molecule more flexible and the decarboxylated intermediate XI is obtained, whereas, as already mentioned above, the cyclic intermediate VIII necessary for decarboxylation of the rigid catharanthine molecule is highly strained.

The crucial intermediate XI may follow either of two reaction paths. If the original electron flow is reversed, then the C-5/C-18 bond is regenerated and the product is descarbomethoxycatharanthine (VI). But if the α-methylene indoline system in XI merely rearranges to the indole, the intermediate XII from which the ring-opened tetracyclic compounds must ultimately be formed is obtained. If one assumes that XII is the actual intermediate, 1,2-reduction of the iminium ion will give cleavamine directly. On the other hand, 1,4-reduction can also occur to afford an enamine, XIII, which rearranges in the well-known manner to the iminium compound XIV, with subsequent reduction to provide the two isomeric dihydrocleavamines. A mixture of 4α- and 4β-dihydrocleavamines is obtained, because the approach of the proton to C-4 in XIII can occur from above or below the plane of the ring with equal facility.

A mechanism involving tetracyclic intermediates has also been proposed by the Lilly group to explain some of their results (8), although their detailed mechanistic interpretation still remains to be published.[3]

We wish now to present additional evidence to the results already mentioned above, which we feel provide substantial support for the mechanistic speculations. One of the crucial steps in the mechanism implies a transannular cyclization of intermediate XI to provide a route to descarbomethoxycatharanthine. We have recently demonstrated (5) that this interesting reaction can indeed occur quite easily and does provide the *Iboga* alkaloid skeleton. These results can be summarized by the sequence shown in Reaction Scheme 2.

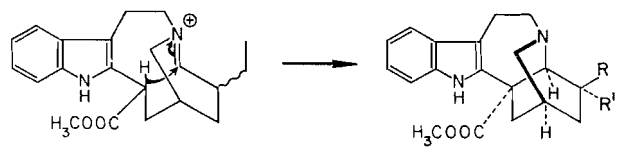

(XV) R = CH_2CH_3; R' = H

(XVI) R = H; R' = CH_2CH_3

REACTION SCHEME 2.

The isolation of coronaridine (XV) and dihydrocatharanthine (XVI) in this reaction (5) is of considerable interest to the mechanism postulated above. First of all, it provides reasonable evidence for the feasibility of the process XI → VI. Secondly, it also shows that epimerization at C-4, as suggested to explain the isolation of the two dihydrocleavamines, can and does proceed through an iminium–enamine equilibrium. We feel that these results add considerable strength to the postulates mentioned above.

We also wish to point out that it is not possible to ascertain, from the evidence presented herein, exactly when the loss of the ester group occurs, although the sequence

[3]*After our paper had been submitted for publication, a detailed account of this work appeared (9).*

Can. J. Chem. Downloaded from www.nrcresearchpress.com by 210.87.254.6 on 09/05/12
For personal use only.

suggested by IX → XI seems most reasonable at this time. It is pertinent to note that the recent isolation of carbomethoxydihydrocleavamine from the reduction of catharanthine with zinc in acetic acid (15) provides evidence that the reduction of the iminium system can occur before the loss of the ester group.

Finally, it is important to emphasize that the last steps of the above mechanism explain the formation of cleavamine and its dihydro derivatives when catharanthine is reacted with acid in the presence of a reducing agent (stannous chloride, mossy tin). Since it has been established (8) that cleavamine is also formed (although in lower yield) by the action of concentrated hydrochloric acid alone, one must account for its formation under these conditions. In the absence of an inorganic reducing agent, the reduction step possibly takes place via an intramolecular redox reaction wherein two molecules of the intermediate XII react to yield one molecule of cleavamine and one of a pyridinium compound XVII. The increase in yield of cleavamine in a reducing medium is thus explicable on the grounds that XII is reduced directly to cleavamine and no pyridinium compound is formed.

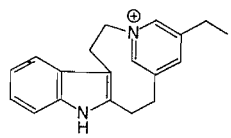

(XVII)

The acid-catalyzed rearrangement of catharanthine to the ring-opened intermediates is an interesting conversion both from a mechanistic and a biosynthetic standpoint. Some related aspects of this reaction are under study in our laboratory at present.

EXPERIMENTAL

Melting points were determined on a Kofler block and are uncorrected. Ultraviolet spectra were measured in methanol solution on a Cary 14 spectrophotometer and infrared spectra were taken on a Perkin–Elmer model 21 spectrophotometer. Nuclear magnetic resonance (n.m.r.) spectra were recorded at 60 Mc/s on a Varian A60 instrument. The line positions or centers of multiplets are given in the Tiers τ scale with reference to tetramethylsilane as the internal standard, with the multiplicity, integrated areas, and types of protons being indicated in parentheses. Silica gel G plates were used for thin-layer chromatography (t.l.c.) and were developed by ethyl acetate, or ethyl acetate – chloroform mixtures as given below. The alumina used for column chromatography was Shawinigan reagent, deactivated with 3% of 10% aqueous acetic acid unless otherwise stated. Analyses were performed by the Microanalytical Laboratory, University of British Columbia, and by Dr. A. Bernhardt and his associates, Mulheim (Ruhr), Germany. All molecular weights were determined by mass spectrometry on an Atlas CH4 spectrometer.

Reaction of Catharanthine with Concentrated Hydrochloric Acid

(a) Isolation of Cleavamine and Descarbomethoxycatharanthine

The procedure indicated here is somewhat modified from that originally developed in the Lilly Research Laboratories.

A mixture of catharanthine hydrochloride (40 g), stannous chloride (44 g), and mossy tin (4 g) in concentrated hydrochloric acid (520 ml) was heated under reflux in a nitrogen atmosphere for 75 min. By the end of this time an orange-red gum had formed in the reaction mixture. The acidic solution was decanted from the gum and washed with methylene chloride (3 × 100 ml). The washings were combined with the gum, and then methanol (50 ml) and methylene chloride (100 ml) were added so that a clear solution was obtained. This solution was shaken with 1 *N* aqueous sodium hydroxide (600 ml), separated, and washed with water (200 ml). The sodium hydroxide solution was washed with ether (2 × 100 ml) and the ethereal extract added to the methylene chloride solution. After it was dried over magnesium sulfate, the organic solution was evaporated to leave a reddish oil (32 g), which was taken up in benzene and chromatographed on alumina (1 200 g).

Can. J. Chem. Downloaded from www.nrcresearchpress.com by 210.87.254.6 on 09/05/12
For personal use only.

Cleavamine was eluted in the initial benzene – petroleum ether (b.p. 30–60°, 1:1) fractions and recrystallized from methanol to give needles (2.4 g), m.p. 117–119°; one spot of t.l.c. (ethyl acetate); $[\alpha]_D^{26}$ + 73° ($CHCl_3$); λ_{max} (log ϵ): 228 (4.60), 285 (3.87), 292 (3.86) mμ; ν_{max}^{Nujol}: 3 420 (NH), 2 800, 2 740, 2 700 cm^{-1} (Bohlmann bands) (16), no carbonyl absorption; n.m.r. signals (CD_3COCD_3): 0.87 (singlet, 1H, NH), 2.8 (multiplet, 4H, aromatic), 4.72 (doublet, 1H, olefinic), 8.96 τ (triplet, 3H, CH_2CH_3).

Anal. Found: C, 81.30; H, 8.54; N, 10.18; mol. wt. 280. Calcd. for $C_{19}H_{24}N_2$: C, 81.38; H, 8.63; N, 9.99; mol. wt. 280.

Cleavamine methiodide was formed by merely adding an excess of methyl iodide to a methanol solution of cleavamine and allowing the mixture to stand overnight in a refrigerator. The analytical sample was prepared by recrystallizing it from a mixture of methanol – ethyl ether – petroleum ether, m.p. 244–245° (decomp.). This derivative was used for the X-ray analysis (4).

Anal. Found: C, 56.83; H, 6.46; N, 6.63. Calcd. for $C_{20}H_{24}N_2I$: C, 56.87; H, 6.46; N, 6.45.

The sample of cleavamine was identical in every respect with an authentic sample kindly provided by Dr. M. Gorman, Eli Lilly and Company.

Benzene–chloroform (1:1) elution provided unreacted starting material (7 g) in the initial fractions and descarbomethoxycatharanthine (1.0 g) in the later fractions. The latter material was recrystallized twice from ether to yield needles, m.p. 103–104°.

Anal. Found: C, 81.70; H, 8.12; N, 10.10. Calcd. for $C_{19}H_{22}N_2$: C, 81.97; H, 7.97; N, 10.06.

This material was subsequently shown to be identical in every respect with an authentic sample of descarbomethoxycatharanthine kindly provided by Dr. M. Gorman, Eli Lilly and Company.

(b) Isolation of 4α- and 4β-Dihydrocleavamines (Fraction B9)

The later benzene – petroleum ether (1:1) fractions, after the major cleavamine-containing fractions had been removed in the above chromatography, displayed three spots on t.l.c. (ethyl acetate) with R_f values of 0.77, 0.53, and 0.27. The compound with a R_f value of 0.77 was found to correspond to cleavamine. These fractions were combined (5.4 g) and placed on another alumina column (450 g). Elution was begun with benzene – petroleum ether (1:2) and the first four fractions afforded cleavamine (1.4 g) after recrystallization from methanol. The later fractions contained progressively less cleavamine and more of the other two constituents. The last (B9, 55 mg) of the nine fractions obtained with this eluent contained no cleavamine and displayed only two spots on t.l.c. Recrystallization from aqueous ethanol gave light brown prisms, m.p. 127–132°; ν_{max}^{Nujol}: 3 410 (NH), 2 790, 2 740 cm^{-1} (Bohlmann bands); n.m.r. ($CDCl_3$): 2.8 (multiplet, 4H, aromatic), 9.13 τ (broad, 3H, CH_2CH_3), no olefinic proton signals.

Anal. Found: C, 80.56; H, 9.46; N, 10.04; mol. wt. 282. Calcd. for $C_{19}H_{26}N_2$: C, 80.80; H, 9.28; N, 9.92; mol. wt. 282.

Fraction B9 was shown to be a mixture of 4α- and 4β-dihydrocleavamines by comparison (t.l.c. and infrared and mass spectra) with authentic samples as prepared below.

4β-Dihydrocleavamine

Cleavamine (1.5 g) in ethyl acetate (20 ml) was hydrogenated over Adam's catalyst (150 mg). Uptake of hydrogen ceased after 50 min, at which time 1 mole of hydrogen had been absorbed. Filtration and evaporation of the solvent gave 4β-dihydrocleavamine, which recrystallized from methanol as prisms (1.2 g), m.p. 136–138°; one spot on t.l.c. (ethyl acetate); ν_{max}^{Nujol}: 3 410 (NH), 2 790, 2 750 cm^{-1} (Bohlmann bands); n.m.r. (CD_3COCD_3): 0.88 (singlet, 1H, NH), 2.8 (multiplet, 4H, aromatic), 9.17 τ (triplet, 3H, CH_2CH_3).

Anal. Found: C, 81.02; H, 9.59; N, 9.88; mol. wt. 282. Calcd. for $C_{19}H_{26}N_2$: C, 80.80; H, 9.28; N, 9.92; mol. wt. 282.

4α-Dihydrocleavamine

Carbomethoxydihydrocleavamine (15) (500 mg) in 5 *N* hydrochloric acid (30 ml) was heated on the water bath under a nitrogen atmosphere for 8 h. The solution was cooled in ice, made basic with aqueous ammonia, and extracted with methylene chloride (3 × 50 ml). The organic extract was dried, concentrated to a small volume, and filtered through alumina (10g). Evaporation of the solvent gave an amorphous powder (340 mg) which could not be induced to crystallize. In spite of its amorphous nature it showed only one spot on t.l.c. (ethyl acetate); ν_{max}^{Nujol}: 3 350 (NH), 2 750 cm^{-1}, no carbonyl absorption.

This material was subsequently shown to be identical (t.l.c. and infrared spectra) with an authentic sample of a 4-dihydrocleavamine isomer kindly supplied by Dr. M. Gorman, Eli Lilly and Company. We have now shown[2] that this isomer must have the ethyl group in the α-configuration, and therefore carbomethoxydihydrocleavamine is in the 4α series as well.

Mercuric Acetate Oxidation of Carbomethoxydihydrocleavamine

Carbomethoxydihydrocleavamine (4.5 g) and mercuric acetate (10.5 g) in glacial acetic acid (150 ml) were stirred under a nitrogen atmosphere for 40 h. The solution was then filtered from the precipitated mercurous acetate (8.2 g) and heated under reflux for 5 h. The solvent was removed as far as possible under vacuum, and the residue made basic with dilute ammonia (50 ml) and extracted with methylene chloride (3 × 50 ml).

After the solution was dried over sodium sulfate, the methylene chloride was removed, and the dark brown product chromatographed on alumina (200 g, deactivated with 0.6 ml of glacial acetic acid). The

Can. J. Chem. Downloaded from www.nrcresearchpress.com by 210.87.254.6 on 09/05/12
For personal use only.

initial benzene fractions afforded a vincadifformine-like product as a white powder (1.15 g). Although the structure of this material has been fully established (14), it bears no direct relevance to the present paper and a more detailed discussion of its chemistry will be presented in a later paper.

The later benzene fractions yielded an amorphous powder (450 mg); one spot on t.l.c. (ethyl acetate – chloroform, 1:9); λ_{max} 226, 285, 293 mμ; $\nu_{max}^{CCl_4}$: 3 400 (NH), 1 705 (C=O) cm^{-1}; n.m.r. ($CDCl_3$): 2.8 (multiplet, 4H, aromatic), 6.30 (singlet, 3H, CH_3O), 9.10 τ (triplet, 3H, CH_2CH_3). This compound was subsequently shown to be coronaridine by comparison with an authentic sample.

The amorphous material was taken up in anhydrous ether and the hydrochloride salt formed by passing in dry hydrogen chloride. Two recrystallizations from acetone–ether afforded the hydrochloride as needles, m.p. 221–223° (decomp.); ν_{max}^{Nujol}: 3 160 (NH), 2 530 (NH), 1 715 cm^{-1} (C=O). An authentic sample of coronaridine hydrochloride, m.p. 221–223° (decomp.), prepared from a sample of coronaridine, completely established the identity (mixed melting point, t.l.c., and infrared spectra).

Benzene–ether (1:1) eluted a compound (440 mg) which was recrystallized from petroleum ether (b.p., 60–80°) to afford prisms, m.p. 143–145.5°; $[\alpha]_D^{23}$ +49° ($CHCl_3$); λ_{max} 225, 286, 293 mμ; ν_{max}^{KBr}: 3 350 (NH), 1 700 cm^{-1} (C=O); n.m.r. ($CDCl_3$): 2.8 (multiplet, 4H, aromatic), 6.38 (singlet, 3H, CH_3O), 9.04 τ (triplet, 3H, CH_2CH_3). This material was identified as dihydrocatharanthine by comparison with an authentic sample which we prepared by hydrogenation of catharanthine.

Reaction of Cleavamine with Concentrated Hydrochloric Acid

A mixture of cleavamine (100 mg), stannous chloride (180 mg), and mossy tin (30 mg) in concentrated hydrochloric acid (3 ml) was heated under reflux in a nitrogen atmosphere for 75 min. The reaction mixture was then treated with dilute aqueous sodium hydroxide and extracted with chloroform. The chloroform extract was washed with water and then dried over anhydrous sodium sulfate. Removal of the solvent *in vacuo* provided 80 mg of a crude reaction product. This product was shown by thin-layer chromatography to consist mainly of cleavamine and a small amount of a very polar component, but *no* dihydrocleavamine. It should be emphasized that t.l.c. can readily detect even very minute amounts of any dihydrocleavamine, and so its absence is conclusively established.

ACKNOWLEDGMENTS

Financial aid from the National Cancer Institute of Canada, the National Research Council of Canada, and Eli Lilly and Company is very gratefully acknowledged. We express our sincere thanks to Drs. M. Gorman and N. Neuss, Eli Lilly and Company, for the generous samples of catharanthine hydrochloride, descarbomethoxycatharanthine, coronaridine, and 4α-dihydrocleavamine, and for their results on the chemistry of catharanthine before publication. We also express our gratitude to Professor Carl Djerassi for the mass spectrometric measurements. One of us (R. T. B.) is indebted to the Canadian Commonwealth Scholarship and Fellowship Committee for a scholarship.

REFERENCES

1. N. Neuss, M. Gorman, H. E. Boaz, and N. J. Cone. J. Am. Chem. Soc. **84**, 1509 (1962).
2. N. Neuss and M. Gorman. Tetrahedron Letters, 206 (1961).
3. K. Biemann and G. Spiteller. J. Am. Chem. Soc. **84**, 4578 (1962).
4. J. P. Kutney, J. Trotter, T. Tabata, A. Kerigan, and N. Camerman. Chem. Ind. London, 648 (1963).
5. J. P. Kutney, R. T. Brown, and E. Piers. J. Am. Chem. Soc. **86**, 2287 (1964).
6. G. Arai, J. Coppola, and G. A. Jeffrey. Acta Cryst. **13**, 553 (1960).
7. M. F. Bartlett, D. F. Dickel, and W. I. Taylor. J. Am. Chem. Soc. **80**, 126 (1958).
8. M. Gorman and N. Neuss. Abstracts, 144th American Chemical Society Meeting. 1963. p. 38M.
9. M. Gorman, N. Neuss, and N. J. Cone. J. Am. Chem. Soc. **87**, 93 (1965).
10. M. Gorman and N. Neuss. Ann. Chim. Rome, **53**, 43 (1963).
11. M. Gorman, N. Neuss, N. J. Cone, and J. A. Deyrup. J. Am. Chem. Soc. **82**, 1142 (1960).
12. U. Renner, D. A. Prins, and W. G. Stoll. Helv. Chim. Acta, **42**, 1572 (1959).
13. J. P. Kutney and E. Piers. J. Am. Chem. Soc. **86**, 953 (1964).
14. J. P. Kutney, R. T. Brown, and E. Piers. J. Am. Chem. Soc. **86**, 2286 (1964).
15. N. Neuss, M. Gorman, W. Hargrove, N. J. Cone, K. Biemann, G. Buchi, and R. E. Manning. J. Am. Chem. Soc. **86**, 1440 (1964).
16. F. Bohlmann. Ber. **91**, 2157 (1958); Angew. Chem. **69**, 641 (1959).

Can. J. Chem. Downloaded from www.nrcresearchpress.com by 210.87.254.6 on 09/05/12
For personal use only.

Can. J. Chem. Downloaded from www.nrcresearchpress.com by 210.87.254.6 on 09/05/12
For personal use only.

THE ELECTRON-SPIN RESONANCE SPECTRA OF SOME METHYLATED ANTHRASEMIQUINONES

EVIDENCE FOR RESTRICTED ROTATION[1]

R. M. ELOFSON, K. F. SCHULZ, B. E. GALBRAITH, AND R. NEWTON
Research Council of Alberta, Edmonton, Alberta

Received January 7, 1965

Dedicated to Professor R. B. Sandin on the Occasion of his Sixty-Eighth Birthday

ABSTRACT

The hyperfine electron-spin resonance spectra of a number of methyl-substituted 9,10-anthrasemiquinones have been determined. The spectra have been analyzed by computer techniques, and splitting constants have been assigned for all protons. The results indicate that, while the parent quinones are essentially free of steric hindrance, the methyl groups in the α position of the reduced quinones are not free to rotate. The methyl groups in the β position of the semiquinones show normal hyperconjugative behavior. These results are consistent with the different redox potentials of these compounds revealed in a previous study.

In a polarographic study of substituted 9,10-anthraquinones, Crawford *et al.* (1) showed that substitution of a methyl group for a β proton produced little change in the polarographic reduction potential. However, substitution of a methyl group for an α proton caused a considerable increase in the polarographic reduction potential or decrease in the oxidation potential. This was shown to be due to steric factors by judicious choice of suitably substituted anthraquinones. In particular, the steric factor was assumed to operate by causing a resistance to planarity in the reduced quinone compared with the quinone itself, which must be somewhat nonplanar (2). Gill and Stonehill (3) suggested that steric hindrance pushed both the =O and large α substituents out of the ring plane.

In this work an attempt is made to investigate the hyperconjugation (4) and restricted rotation by means of the electron-spin resonance (e.s.r.) hyperfine splitting constants of methylated anthrasemiquinones (5). The results are compared with preliminary observations on the nuclear magnetic resonance (n.m.r.) and infrared spectra of the corresponding quinones.

EXPERIMENTAL

The quinones used in this investigation, except those described below, were provided through the kindness of Dr. R. J. Crawford of the University of Alberta. They were prepared by known procedures and purified by careful recrystallization from isopropyl alcohol. The observed melting points were anthraquinone, 286–288°; 1-methylanthraquinone, 172–173°; 2-methylanthraquinone, 175–177°; 1,2-dimethylanthraquinone, 159–161°; 1,3-dimethylanthraquinone, 163–165°; 2,6-dimethylanthraquinone, 245–247°; 2,7-dimethylanthraquinone, 171–173°; and 1,4-dimethylanthraquinone, 141–142°.

2-CD_3-Anthraquinone

Toluene-CD_3, Merck, was allowed to react with phthalic anhydride in the presence of aluminium chloride. The resulting 4-CD_3-benzoylbenzoic acid was cyclized by treating it with fuming sulfuric acid. The resulting 2-CD_3-anthraquinone had a melting point of 172–174 °C, and no stretching vibration in the infrared caused by aliphatic CH bonds.

1-CD_3-Anthraquinone

Toluene-CD_3, Merck, was brominated in the presence of nitric acid (6). The product contained both *o*- and *p*-bromotoluene-CD_3 which were separated by preparative gas chromatography using a Wilken's Aerograph model 600 gas chromatograph with benzoquinoline on firebrick packing. *o*-Bromotoluene-CD_3

[1]*Research Council of Alberta contribution No. 286.*

was converted to the Grignard by magnesium in ether and treated with phthalic anhydride to produce 2-*o*-tolyl-CD_3 benzoic acid. This was converted by means of fuming sulfuric acid to 1-CD_3-anthraquinone, melting point 170–173°. This material showed no infrared absorption that was due to aliphatic CH bonds but did contain a small amount of 2-CD_3-anthraquinone.

Semiquinone Solution

Solutions of semiquinones were prepared by warming, in the absence of air, 10^{-3} M solutions of the quinones in isopropyl alcohol to which sodium or potassium had been added to produce 0.1 M solutions of the isopropoxide. Some solutions were subjected to irradiation with a mercury lamp instead of heat to produce the semiquinone but the resulting solutions had the same e.s.r. spectra. Solutions for e.s.r. studies were prepared in sealed Pyrex tubes, 0.4 mm o.d. The solutions were frozen, evacuated, and sealed. Occasionally, heating of the sealed solution for some time was required to remove traces of oxygen by oxidation of the semiquinone before a stable semiquinone solution was obtained.

Electron-spin resonance spectra were run on a Varian model 4500 spectrometer fitted with 100 kc modulation. Absolute splitting constants were obtained by using 1,4-benzosemiquinone, $a = 2.37$ oersted, as a standard (7).

Detailed analysis of the e.s.r. spectra was carried out using an IBM model 1620 computer by a technique that will be published elsewhere. This technique involves the numerical manipulations of the recorded spectrum, using only the assumption of symmetry with respect to each splitting constant of the spectrum to eliminate, in turn, each of these splitting constants. In Figs. 1 and 2 some typical spectra together with

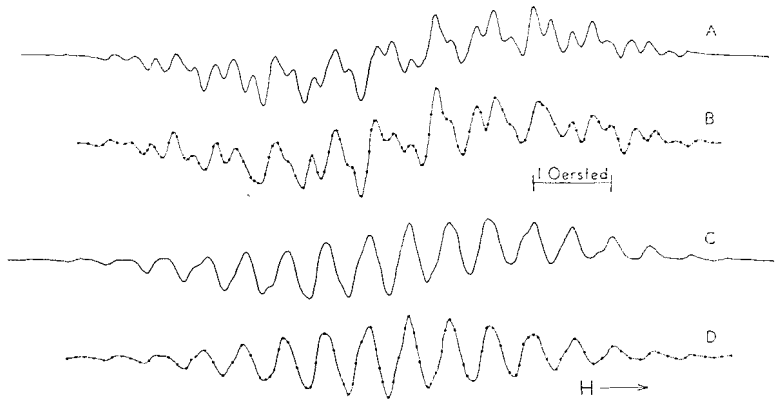

FIG. 1. (A) Experimental e.s.r. spectrum of 1-methylanthrasemiquinone; (B) calculated spectrum of 1-methylanthrasemiquinone; (C) experimental spectrum of 2-methylanthrasemiquinone; (D) calculated spectrum of 2-methylanthrasemiquinone.

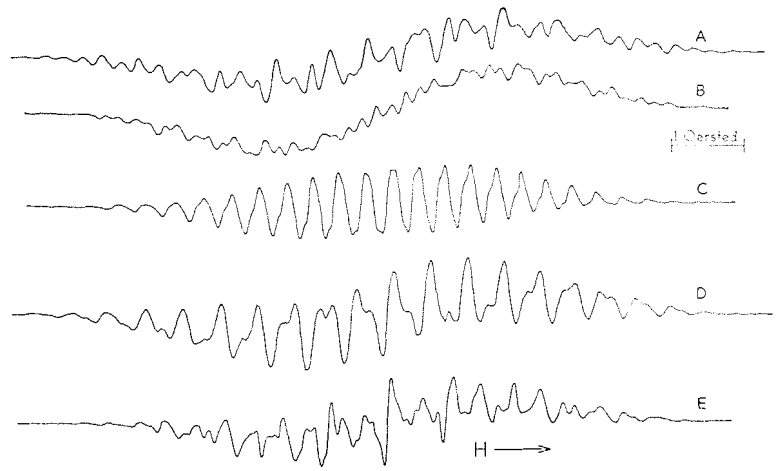

FIG. 2. Experimental e.s.r. spectra of 9,10-anthrasemiquinones: (A) 1,2-dimethyl; (B) 1,3-dimethyl; (C) 1,4-dimethyl; (D) 2,6-dimethyl; (E) 2,7-dimethyl.

Can. J. Chem. Downloaded from www.nrcresearchpress.com by 210.87.254.6 on 09/05/12
For personal use only.

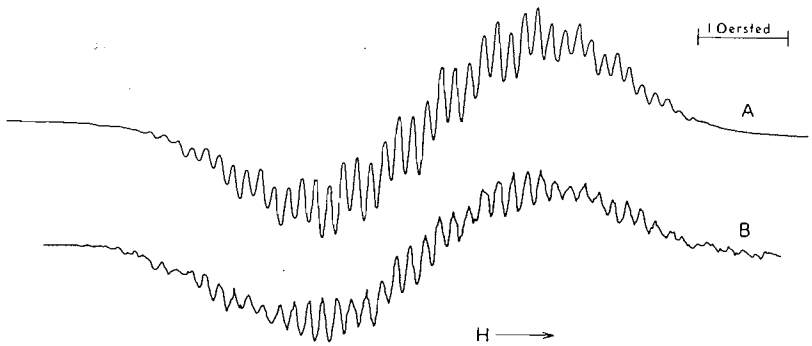

FIG. 3. Experimental e.s.r. spectra of 2-CD_3-anthrasemiquinone: (A) with potassium isopropoxide; (B) with sodium isopropoxide.

spectra reproduced from the numerical analyses are presented. These results are limited by the limitations of the current control to the magnet. However, some of the results might be improved if a Fieldial accessory were added to the present system, since this should improve the stability and linearity of field scan by a factor of 10.

Nuclear magnetic resonance spectra in chloroform solutions containing tetramethylsilane as an internal standard were run on a Varian model 1260 n.m.r. spectrometer.

Infrared spectra were run on a Perkin–Elmer model 221 prism-grating spectrometer.

While splittings due to sodium have not been observed previously in the e.s.r. spectra of alcohol solution of semiquinones, the high resolution obtained in these experiments and the small splitting constants observed in some of the compounds made it necessary to eliminate possible complications that were due to ion pairs (8). In Fig. 3 are shown spectra of 2-CD_3-anthrasemiquinone in sodium isopropoxide and potassium isopropoxide. It is seen that splittings due to the sodium of the order of 0.03 to 0.04 gauss are observed. Since splittings due to potassium are about one-fifth those of sodium, all spectra were finally run in potassium sopro poxide rather than sodium isopropoxide solutions. No splittings due to potassium were observed in his wo rk.

RESULTS

In Table I are summarized the results of the e.s.r. investigation. Since the quality, particularly the symmetry of the spectra, varied, the results have been obtained in differing detail. No attempt has been made to assign specific α or β constants to particular positions.

As previously mentioned, better results may be expected from the computation if spectra of higher symmetry can be obtained. The individual values assigned to splitting constants vary in accuracy but, in general, the smallest assigned splitting constant is known with the greatest accuracy. Since the largest splitting constants limit the width of the spectra, these are also known to a degree of accuracy approaching 10%. The intermediate constants are known with less accuracy. Since the argument developed in this paper is dependent on the value of the smallest and, to a lesser extent, the largest splitting constants, the present results are clearly acceptable even though technical improvements may modify some of the apparent values.

Anthrasemiquinone

In agreement with previous workers (9–11), we found that anthrasemiquinone has a 13-line spectrum which results from a coupling of four β protons with a splitting constant of 0.83 oersted (Oe) and four α protons with a splitting constant of 0.42 Oe, or almost exactly half the β value. The result is in good agreement with that of Adams *et al.* (9) of 0.46 and 0.92 Oe, but is considerably lower than those of Vincow and Fraenkel (10) and Brandon and Lucken (11).

Can. J. Chem. Downloaded from www.nrcresearchpress.com by 210.87.254.6 on 09/05/12
For personal use only.

TABLE I

Hyperfine splitting constants in semiquinone ions (values in oersteds)

Derivative of 9,10-anthrasemiquinone	β protons	α protons	Methyl protons
Unsubstituted	0.83 (4)*	0.41 (4)	
2-Methyl	0.81 (3)	0.38 (4)	0.91 (3)
2-CD_3			0.15‡ (3)
2,6-Dimethyl	0.71 (2)	0.47 (4)	0.87 (6)
2,7-Dimethyl	0.69 (2)	0.56 (2)	0.75 (6)
		0.31 (2)	
1-Methyl	0.69, 0.66	0.45 (2)	0.98 (2)
	0.62, 0.68	0.31 (1)	0.21 (1)
1-CD_3			0.17‡
1,2-Dimethyl	0.56 (2)	0.41	0.98 (2)
	0.43†	0.39	0.20
		0.36	0.85 (3)
1,3-Dimethyl	0.70 (3)	0.38 (3)	0.95 (2)
			0.20‡
			0.86 (3)
1,4-Dimethyl	0.68 (2)	0.33 (2)	0.99 (2)
	0.64 (2)		0.96 (2)
			0.05 (2)

*Numerals in parentheses represent the number of protons.
†Assignment arbitrary.
‡Smallest observed splitting constants.

2-Methylanthrasemiquinone

This compound has three groups of splitting constants and shows the normal effect of hyperconjugation of an unhindered methyl group. The four splitting constants of 0.38 Oe are plainly due to the four α protons. The three protons with splittings of 0.91 Oe and the three protons with 0.81 Oe are due to the three methyl protons and the three β protons respectively or vice versa. To distinguish between these two possibilities 2-CD_3-anthrasemiquinone was prepared. Its spectrum, illustrated in Fig. 3, had 46 lines with a spacing of 0.15 gauss arising from a final 7-line splitting that is due to the three deuterium atoms. Venkataraman and Fraenkel (12) found a value of 6.48 for the ratio of a_H/a_D. This strongly suggests that the three splitting constants of 0.91 gauss are due to the three methyl protons in 2-methylanthrasemiquinone.

2,6-Dimethylanthrasemiquinone

Analysis of this spectrum showed that the six methyl protons had large splitting constants, indicating that the electron concentration at the 2- and 6-carbon atoms were somewhat larger than at the 3 and 7 positions. No significant difference could be observed in the individual splitting constants for the α positions, although a more detailed analysis might be expected to yield some difference.

2,7-Dimethylanthrasemiquinone

For this compound the electron concentrations for all the β positions were nearly equal, as indicated by the values for the β positions and the methyl protons, while two distinct pairs were observed for the α positions. In other respects the assigned splitting constants are very close to what might be expected from the results for 2,6-dimethylanthrasemiquinone.

1-Methylanthrasemiquinone

The high degree of reproducibility of the experimental spectrum obtained by calculating back from the assigned values of the splitting constants attests to the uniqueness of the

Can. J. Chem. Downloaded from www.nrcresearchpress.com by 210.87.254.6 on 09/05/12
For personal use only.

solution and the interesting conclusions which follow. With high resolution the spectrum has yielded splitting constants that are due to all 10 protons, as shown in Table I. 1-CD_3-Anthrasemiquinone has the smallest detectable splitting constant of 0.17 Oe. This corresponds very closely to the ratio of 1:6.48 for the two large splitting constants at 0.98 Oe for the CH_3 derivative. Therefore, the two splittings of 0.98 Oe must be due to two of the protons on the methyl group. The smallest splitting constant of the 1-CH_3 derivative, 0.21 gauss, is assigned to the third proton of the methyl group, which must therefore occupy a position close to the plane of the ring (5). The rest of the values correspond to expected values for the β protons and the α protons. Under low resolution, i.e. a large modulation, nine protons produce an unevenly spaced spectrum of 12 lines which could arise from two protons with splittings of 0.98 Oe and seven protons with unequal splittings of about 0.60 Oe.

1,4-Anthrasemiquinone

The results for this compound substantiate the assignments made for 1-methylanthrasemiquinone. However, the minimum splitting constant assigned to the two protons of 0.05 gauss indicates that one proton of each methyl group must be still closer to the plane of the ring where the π electron density is nearly zero. The values for the other splitting constants are close to those of 1-methylanthrasemiquinone.

1,2-Dimethylanthrasemiquinone and 1,3-Dimethylanthrasemiquinone

The spectra of these compounds are complex and the precision of measured splitting constants is not high except for the smallest values of 0.20 and 0.22 Oe, each due to a single proton, which helps to confirm the assignment for 1-methylanthrasemiquinone. The differences in the minimum splitting constants are too small to really signify support for the crowding thesis enunciated in ref. 1 and supported by the polarographic data. The data do support the idea that, in 1,2-dimethylanthrasemiquinone, one proton is held closer to the plane of the ring than in the others, but the measured difference is too small to prove the point.

DISCUSSION

The results show clearly that in all compounds the protons on methyl groups in the β position in anthrasemiquinones show normal hyperconjugation behavior with equal splitting constants at least as large as for protons directly attached to the β positions. When a methyl group is in the α position, the splitting constants attributed to the methyl protons are always distributed as two large coupling constants and one small one. These results are best interpreted as occurring because the methyl groups do not rotate, with two protons being symmetrically distributed about the oxygen atom and well out of the ring plane and the third held near or in the plane of the ring.

The equality (near-equality for 1,4-dimethylanthrasemiquinone) of the two large splitting constants indicates that two protons are symmetrically disposed about the oxygen atom and out of the ring plane. If trigonal symmetry of the methyl protons is assumed, this requires the third proton to have an equilibrium position in the ring plane. The small value of the splitting constant assigned to this in-plane proton then becomes a measure of the amplitude of oscillation of the methyl group. This follows if we use the simplified form [1] of the original equation of Heller and McConnell (13) and shown by Stone and Maki (14) to be valid for small oscillations. In this equation, a_H is the splitting

$$a_H = B_2 \cos^2\theta \qquad [1]$$

Can. J. Chem. Downloaded from www.nrcresearchpress.com by 210.87.254.6 on 09/05/12
For personal use only.

constant due to a single proton, θ is the angle between the π orbital of the ring carbon and the CH bond both projected on a plane perpendicular to the CH_3—Ar bond, and B_2 is a constant differing for each compound but proportional to the unpaired electron concentration at the α position. Not unexpectedly, the methyl groups in 1,4-dimethylanthrasemiquinone are held in a much more rigid position than the compounds with only one methyl group in an α position. This pronounced difference was apparent in the polarographic reduction potentials of the quinones where the measured reduction potentials for 1-methyl-, 1,2-dimethyl-, 1,3-dimethyl-, and 1,4-dimethyl-anthrasemiquinone were respectively 0.48, 0.51, 0.50, and 0.53 V vs. S.C.E. compared with a value of 0.43 V vs. S.C.E. for anthraquinone.

Nuclear Magnetic Resonance

The methyl proton shifts of anthraquinones dissolved in chloroform were measured relative to tetramethylsilane. As expected, the methyl protons in the α position were shifted downfield (168 c.p.s.) compared to the shift of 150 c.p.s. for the β methyl protons. This larger shift on the 1-CH_3 is undoubtedly due to the anisotropy of the adjacent carbonyl (15). No evidence for hindered rotation in the form of resolved peaks or even increased line widths could be detected.

Infrared Spectra

In contrast to the n.m.r. results, evidence for some inhibition of rotation can be deduced from the infrared spectra of 1-methylanthraquinone compared with 2-methylanthraquinone. Examination of the symmetrical methyl bending vibration at 1 380 cm^{-1} in CS_2 solutions showed that, while the positions of the two vibrations were the same for both compounds, in 1-methylanthraquinone the shape was distinctly different and is shown in Fig. 4. The band is broader and flatter in 2-methylanthraquinone, suggesting free rotation about the carbon–carbon bond, whereas the band is very narrow, although intense, for 1-methylanthraquinone, suggesting inhibition of rotation (16). The band for 1,4-dimethylanthraquinone is also narrow compared to that of 2-methylanthraquinone.

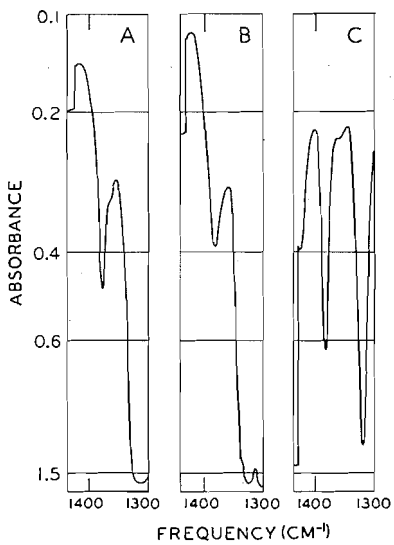

FIG. 4. Infrared spectra in CS_2 solutions of (A) 1-methyl-; (B) 2-methyl-; (C) 1,4-dimethyl-anthraquinone.

Can. J. Chem. Downloaded from www.nrcresearchpress.com by 210.87.254.6 on 09/05/12
For personal use only.

An explanation is required for the failure to detect restricted rotation by means of n.m.r. in the 1-methylanthraquinone, whereas there can be little doubt of its existence in the corresponding semiquinones as detected in the e.s.r. spectra. As previously suggested (1–3) the quinones may not be quite planar. If the carbonyl oxygens are not in the plane of the rings, the restricted rotation could be expected to be reduced in amount compared with that of the semiquinones, which, because of resonance and other considerations, must be planar. Possibly more important, and supported better by the X-ray data (2), is the fact that in anthraquinone and presumably in the other anthraquinones the C_9—C_{11} bond length is 1.478 Å or nearly that of a normal aliphatic C—C bond. In the completely planar and aromatic semiquinones the C_9—C_{11} bond length should approach that of the other aromatic C—C bonds, viz. 1.38 Å. This would be enough change to produce complete inhibition of rotation in the semiquinone but permit some rotation in the quinone.

Since n.m.r. relaxation times are much longer than those of e.s.r. or light spectroscopy, it is possible that the restriction of rotation observed in the infrared spectroscopy could be real but too small to detect by the longer time constants of n.m.r. spectroscopy. It would appear, therefore, that a small degree of restriction of rotation may occur in the quinone forms of 1-methyl derivatives and that this inhibition becomes complete in the corresponding semiquinones.

Finally, this decrease in entropy associated with the α methyl groups during reduction of the α-substituted quinones is consistent with the greater resistance of these quinones to reduction compared to the β-substituted quinones (1).

ACKNOWLEDGMENTS

Two of us, R. M. E. and B. E. G., acknowledge our great debt to Professor R. B. Sandin as an inspired teacher of chemistry and a true friend and confidant. All of us have worked with him and have been helped and inspired by his intuition. This paper, as previously noted, is a direct outgrowth of the work of R. J. Crawford, while he was a student under Professor Sandin. Thanks are extended to Mrs. F. F. Gadallah for preparation of the 1- and 2-CD_3-anthraquinones, and to Dr. Crawford of the University of Alberta for providing the remaining quinones and for many helpful discussions.

REFERENCES

1. R. J. Crawford, S. Levene, R. M. Elofson, and R. B. Sandin. J. Am. Chem. Soc. **79**, 3153 (1957).
2. B. V. R. Murty. Z. Krist. **113**, 445 (1960).
3. R. Gill and H. I. Stonehill. J. Chem. Soc. 1857 (1952).
4. R. Bersohn. J. Chem. Phys. **24**, 1066 (1956).
5. A. D. McLachlan. Mol. Phys. **1**, 233 (1958). A. H. Maki. J. Chem. Phys. **35**, 761 (1961). J. R. Bolton and A. Carrington. Mol. Phys. **5**, 161 (1962). A. Carrington. Mol. Phys. **5**, 425 (1962).
6. R. L. Datta and N. R. Chatterjee. J. Am. Chem. Soc. **38**, 2545 (1916).
7. B. Venkataraman, B. G. Segal, and G. K. Fraenkel. J. Chem. Phys. **30**, 1006 (1959).
8. N. Hirota. J. Chem. Phys. **37**, 1884 (1962).
9. M. Adams, M. S. Blois, and R. H. Sands. J. Chem. Phys. **28**, 774 (1958).
10. G. Vincow and G. K. Fraenkel. J. Chem. Phys. **34**, 1333 (1961).
11. R. W. Brandon and E. A. C. Lucken. J. Chem. Soc. 4273 (1961).
12. B. Venkataraman and G. K. Fraenkel. J. Chem. Phys. **24**, 737 (1956).
13. C. Heller and H. M. McConnell. J. Chem. Phys. **32**, 1535 (1960).
14. E. W. Stone and A. H. Maki. J. Chem. Phys. **37**, 1326 (1962).
15. J. A. Pople, W. G. Schneider, and H. J. Bernstein. High resolution nuclear magnetic resonance. McGraw-Hill, New York. 1959. p. 167 ff.
16. R. N. Jones and G. Sandorfy. *In* Techniques of organic chemistry. Vol. IX. *Edited by* A. Weissberger. Interscience, New York. 1956. p. 309.

Can. J. Chem. Downloaded from www.nrcresearchpress.com by 210.87.254.6 on 09/05/12
For personal use only.

Can. J. Chem. Downloaded from www.nrcresearchpress.com by 210.87.254.40 on 09/05/12
For personal use only.

SAMPLE INJECTION IN PROGRAMMED TEMPERATURE GAS CHROMATOGRAPHY AND ITS SIGNIFICANCE FOR TRACE ANALYSIS[1]

L. W. HOLLINGSHEAD[2] AND H. W. HABGOOD
Research Council of Alberta, Edmonton, Alberta
AND
W. E. HARRIS
Department of Chemistry, University of Alberta, Edmonton, Alberta
Received November 13, 1964

Dedicated to Professor R. B. Sandin on the Occasion of his Sixty-Eighth Birthday

ABSTRACT

The measurement of apparent plate heights resulting from various values of the total sample volume has been carried out for C_5 to C_8 *n*-alkanes on Apiezon L under both isothermal and p.t.g.c. conditions. Plug injection of samples was achieved through the use of a syringe plunger driven at constant speed by a motor. The time for injection of gas samples ranged from 1 to 300 s. All of the results, both isothermal and p.t.g.c., could be correlated to the same plot of H_{app}/H_o against $\sqrt{n}\Delta V_s/V_{T_0}$ where H_{app} is the observed plate height, H_o the limiting plate height at low sample volumes, n the true plate number, ΔV_s the sample volume, and V_{T_0} the isothermal retention volume at the initial temperature. The experimental values lie somewhat above the theoretical curve calculated by van Deemter *et al.* It is confirmed that sample volumes less than $V_{T_0}/2\sqrt{n}$ give negligible excess peak broadening. Applying these concepts to trace analysis, very large samples may be used in p.t.g.c. under such initial temperature conditions that the major component is only weakly retained, while traces of heavier components are concentrated into narrow bands and eluted as sharp peaks with the increased sensitivity provided by the large sample. As an example, chromatograms are presented for the p.t.g.c. analysis of natural gas on deactivated alumina, using sample volumes ranging from 2 to 500 ml.

INTRODUCTION

Early in the development of gas chromatography it was recognized by Glueckauf (1), van Deemter, Zuiderweg, and Klinkenberg (2), and by Porter, Deal, and Stross (3) that the volume occupied by the sample as injected into the gas stream at the column inlet should be maintained below a stipulated value in order to avoid any broadening in the outlet peaks beyond that produced by the chromatographic processes within the column. It has been suggested that the maximum sample size should be kept below a band width of one-quarter of the outlet band (1), or alternatively (2), that the sample volume should be less than $V/2\sqrt{n}$ where V is the retention volume for a component and n is the number of theoretical plates. In programmed temperature gas chromatography, p.t.g.c., Giddings (4) has pointed out that since most components are strongly retained at the initial temperature of the program, relatively large sample volumes in the inlet gas stream are equivalent to only narrow zones in the column. This initial-zone condensation has the effect of reducing the effective sample volume in the gas stream entering the column by the ratio V_{T_r}/V_{T_0} where V_{T_r} and V_{T_0} are the isothermal retention volumes (including column dead space) at the retention temperature and at the initial temperature, respectively. The degree of condensation depends upon the retention of an individual component; since the ratio V_{T_r}/V_{T_0} might easily have a value of 0.01 or less the use of p.t.g.c. would

[1]*RCA contribution No. 287.*
[2]*Permanent address: Southern Alberta Institute of Technology, Calgary, Alberta. Visiting Research Associate, Research Council of Alberta, summer 1964.*

permit sample volumes at least 100 times larger than those used for isothermal gas chromatography without loss of resolution.

The above reasoning assumes that the total amount of the sample components is kept below that which would overload the column. Application to trace analysis where particularly small amounts of material are dispersed through large volumes of sample would be an obvious development. The technique would be suited but not limited to trace components more strongly retained than the bulk of the sample material such as heavy impurities in air or higher hydrocarbons in natural gas. In such a case conditions may be chosen so that the bulk of the sample is only weakly retained and large samples can be used which, although yielding broadened major peaks, produce for the higher boiling trace components sharp narrow peaks. Thus maximum sensitivity and resolution are achieved. It is true that modern detectors have permitted great increases in the sensitivity of detection, but further increases in the detection limits through the use of larger samples are desirable.

The present work was initiated in order to determine the extent of initial-zone condensation in p.t.g.c., and to demonstrate the application to trace analysis of p.t.g.c. with large sample volumes. In addition, measurements have been obtained of the actual increase in isothermal and p.t.g.c. band widths as the result of excessively large samples; these are compared with measurements of van Deemter *et al.*, with a more recent report by Guiochon (5), and with various theoretical predictions.

THEORETICAL

Giddings (4) and Guiochon (5) have treated the sample volume in terms of a Gaussian distribution of the sample in the gas stream. The standard deviation of the sample distribution in the gas stream is converted to an equivalent standard deviation of the sample band on the column. In practice it may be convenient to use the base width of the entering sample peak which is equal to four standard deviations. The additional spreading due to chromatographic processes is then assumed to combine with this initial distribution by addition of variances. Consequently the total variance, σ^2, of the band when it reaches the end of the column is given by

$$\sigma^2 = \sigma_s^2 + \sigma_c^2, \qquad [1]$$

where σ_s^2 is the variance of the initial sample distribution and σ_c^2 that of the normal chromatographic processes in the column. The standard deviation of the band on the column must be converted to a peak standard deviation in the gas stream leaving the column, which may then be conveniently expressed in terms of an apparent plate height. If the sample volume is characterized by the base width of the sample distribution, designated as ΔV_s, then for isothermal chromatography the conclusions of Giddings and of Guiochon may be expressed in the form

$$H_{app} = \frac{L}{16}\left(\frac{W}{V}\right)^2 = \frac{L}{16}\left(\frac{W_c}{V}\right)^2 + \frac{L}{16}\left(\frac{\Delta V_s}{V}\right)^2 = H_c + \frac{L}{16}\left(\frac{\Delta V_s}{V}\right)^2, \qquad [2]$$

where H_{app} is the observed plate height calculated from the observed band width W, W_c is the limiting band width for small samples, and the second term is the contribution to H due to finite sample volume. For p.t.g.c. the effective sample volume becomes $\Delta V_s V_{Tr}/V_{T_0}$ (4) and the plate height relationship (6) takes the form

$$H_{app} = \frac{L}{16}\left(\frac{W}{V_{T_r}}\right)^2 = \frac{L}{16}\left(\frac{W_c}{V_{T_r}}\right)^2 + \frac{L}{16}\left(\frac{\Delta V_s}{V_{T_0}}\right)^2 = H_c + \frac{L}{16}\left(\frac{\Delta V_s}{V_{T_0}}\right)^2. \qquad [3]$$

Can. J. Chem. Downloaded from www.nrcresearchpress.com by 210.87.254.40 on 09/05/12
For personal use only.

According to this treatment the contribution to H due to finite sample volume is a different and constant value similar to an A term for each component and is added to the various chromatographic contributions.

We frequently are more interested in the relative increase in plate height, which may be expressed in the following forms:

$$[4] \qquad \frac{H_{app}}{H_c} = 1 + \left(\frac{\Delta V_s}{W_c}\frac{V_{Tr}}{V_{T_0}}\right)^2 = 1 + \left(\frac{\Delta V_s}{V_{T_0}}\right)^2 \frac{n}{16},$$

where n is the true plate number corresponding to W_c and V_{Tr} as obtained from small samples. This equation is expressed in general form; for isothermal chromatography V_{T_0} is identical with V_{Tr}.

An alternative treatment of large sample volumes has been presented in slightly different forms by Glueckauf (1, 7) and by van Deemter, Zuiderweg, and Klinkenberg (2). Their treatments are exact and detailed but are not readily amenable to simple theoretical development. They are developed for plug samples, i.e. injection in which the sample concentration is maintained constant over the total duration of the injection as opposed to the Gaussian distribution in concentration mentioned above (4, 5).

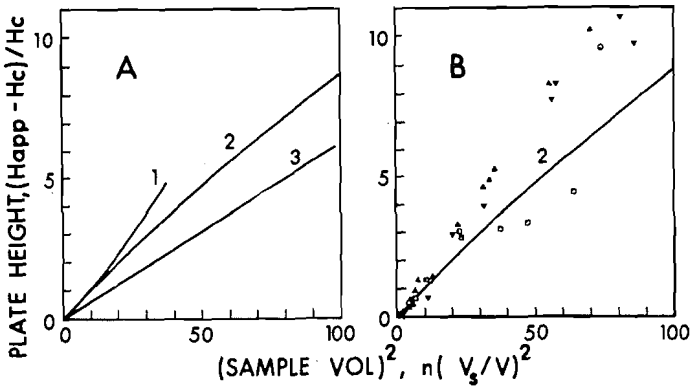

FIG. 1. Relative increase in plate height vs. square of the relative sample volume. A. Theoretical curves. 1. From Glueckauf (1, 7). Plug injection, H_{app} from width at h/e. 2. Derived from van Deemter, Zuiderweg, and Klinkenberg (2). Plug injection, H_{app} from base line intercept. 3. Gaussian injection, ΔV_s = base line intercept of injection. Compare Giddings (4) and Guiochon (5). B. Experimental points for 150 °C for pentane ○, hexane □, heptane ▽, and octane △ compared with curve 2.

The three treatments are compared in Fig. 1A as plots of the relative increase in apparent plate height against the square of the relative sample volume. The differences are largely, and perhaps almost entirely, due to the non-equivalence of the manners in which the plug and Gaussian peaks are described. The sample volume for a Gaussian sample distribution is taken as the base width, and for the plug profiles as the total plug volume. The peak shape of the outlet bands will be Gaussian in all cases for the Gaussian input, and will generally be intermediate between Gaussian and plug for the plug input. The van Deemter treatment is based on an apparent plate height calculated from the base line intercept of the tangents to the outlet peak, while the Glueckauf values are based on peak widths at h/e of the maximum peak height. Although these two widths (in their correct respective expressions) give the same apparent plate height for a Gaussian peak, the h/e width will give a relatively higher value for the flat-topped peaks observed with large plug samples. Thus the Glueckauf curve would be expected to lie above that of van Deemter and both would be expected to lie above that for Gaussian pulses.

Can. J. Chem. Downloaded from www.nrcresearchpress.com by 210.87.254.40 on 09/05/12
For personal use only.

Can. J. Chem. Downloaded from www.nrcresearchpress.com by 210.87.254.40 on 09/05/12
For personal use only.

EXPERIMENTAL

Systematic measurements of band width for various plug sample injections were made using a 4.3 m by 4 mm inside diameter glass column shaped into a 10 cm coil and packed with 20% Apiezon L on 45 to 60 mesh Chromosorb P. The total weight of stationary phase in the column was 5.6 g and the dead space volume was 41.7 ml. The column was heated in a bath of Dow Corning 550 Silicone oil contained in a 6 in. Dewar flask. A Gow-Mac thermal conductivity cell of pretzel geometry, for which the time constant is given as 1.5 s, was used as detector in conjunction with a Brown recorder of time constant 1 s.

Samples were injected by syringe through a Silicone rubber puncture seal immediately ahead of the column packing. A leak-tight 500 μl Hamilton 1 750 syringe with a Teflon-tipped plunger was used to inject gaseous samples. A special mechanical drive similar to that used by Reilley (8) was constructed to depress the syringe plunger at a controlled uniform rate. This apparatus consisted of a threaded shaft passing through a fixed nut, fitted with a pulley at one end and at the other with a Teflon tip pressing against the syringe plunger. The drive shaft through its fixed nut, a guide sleeve, and the syringe were clamped onto a small frame which could be raised or lowered to take and to inject samples. By using various pulley-belt combinations and a variable speed motor controlled by a GT-21 thyratron rectifier unit (G. K. Heller Co., Las Vegas, Nevada) a range of injection times from approximately one second to several hundred seconds could be obtained. A microswitch pressed by the descending pulley stopped the drive at the end of the injection and prevented damage to the syringe. The drive shaft could be retracted by a motor-reversing switch.

Gas samples included the normal alkanes pentane to octane. Samples were withdrawn from the vapor space above a mixture of the liquid hydrocarbons contained in a 100 ml conical flask closed with a puncture seal. A suitable mixture giving approximately equal amounts of the four components in air was made by injecting into the flask as liquids 5 ml *n*-octane, 1 ml *n*-heptane, 0.05 ml *n*-hexane, and 0.01 ml *n*-pentane. It was necessary to add more pentane when its peak became small. In a 0.5 ml sample convenient concentrations of all components were obtained if the sample flask was heated to about 40°. The syringe with its attached drive was then inserted through the puncture seal into the column. A heat lamp was used to keep the syringe warm during the injection. The column inlet pressure was as much as an atmosphere above atmospheric; this caused helium to flow back into the syringe and a waiting period of 2 min was allowed for the syringe contents to become uniform. The motor was switched on to start the injection and the time measured until the microswitch terminated the injection. By this procedure the earlier peaks from long injection periods were square and symmetrical, indicating uniform plug injection although without the 2 min waiting period the leading edge was distinctly rounded. The total sample appeared to be sufficiently small in all cases so that there was no column overloading.

Peak widths were measured as the base line intercepts of the tangents to the inflection points. Retention volumes were calculated from the midpoint of the injection period to the midpoint of the peak (half-way between the base line intercepts). Retention volumes were expressed at column temperature and mean column pressure; sample volumes at column temperature and inlet pressure. In calculation of the sample volumes, the 0.5 ml volume of the syringe was added to the volume corresponding to the injection time. All measurements were made with a flow rate, at atmospheric pressure and room temperature, of 55 ml per min. This was established in preliminary measurements as being distinctly above the minimum in the plate height – eluent gas velocity curve. For programmed temperature operation the oil bath was heated at $5.0 \pm 0.1°$ per min.

A series of trace analysis experiments was carried out with natural gas samples on a column of deactivated alumina in order to demonstrate the suitability of temperature programming for trace analysis. The column used was 22 g of 80 to 100 mesh alumina deactivated by treatment with 10% lithium chloride solution and packed into a 5 ft by $\frac{1}{4}$ in. copper tube. The copper tubing was wound tightly around an aluminium cylinder containing a cartridge heater and the whole assembly inserted into a Dewar vessel. With this apparatus the column could be cooled to −60° with dry ice and heated to 300° in an approximately linear program by small adjustments to the heater voltage. Gas flow rates and heating rates similar to those used with the gas–liquid column were used here.

For the trace analysis experiments a bypass sample injection system was employed with four different sample volumes ranging from 2.2 to 500 ml. The smaller ones were simply glass U tubes while the larger ones were constructed from round-bottomed flasks. Thus the smaller volumes approached plug injection while the larger ones were close to an exponential decay input pulse (3). The sample in all cases was natural gas from the laboratory supply taken at a pressure only slightly above atmospheric. Since the column inlet pressure was definitely above this, considerable disturbance in the flow occurred when the larger samples were switched in, but the effects of this had disappeared by the time the peaks of main interest emerged. Sample injection was at −60° and the heating was started after the major component, methane, was nearly all eluted. Variability in the minor components of the Edmonton gas supply meant that the samples used were not identical.

RESULTS AND DISCUSSION

Isothermal chromatograms of mixtures of the four hydrocarbons were obtained for a range of sample injection times at temperatures of 30°, 60°, 100°, 150°, and 210°. For

long injection times and wide sample bands mixtures of pentane–heptane and hexane–octane were run successively. Apparent plate heights were calculated from the observed band widths and retention volumes and the best limiting values were estimated by inspection. These are summarized in Table I, and the plate heights show relatively little variation except for the high values observed at 30°. It is assumed that these are due to high mass transfer resistances in the liquid phase resulting from the low liquid diffusivities at this temperature.

TABLE I

Retention volumes* and limiting plate heights

	30 °C	60 °C	100 °C	150 °C	210 °C
Pentane					
V(ml)	449	242	121	82.6	64.4
H(mm)	7.9	1.62	1.38	1.41	1.80
Hexane					
V(ml)	1 282	548	209	115	77.5
H(mm)	3.84	1.40	1.40	1.48	1.70
Heptane					
V(ml)	3 800	1 318	394	172	97.4
H(mm)	2.40	1.45	1.42	1.39	1.43
Octane					
V(ml)	—	3 250	769	272	127.3
H(mm)	—	1.23	1.19	1.40	1.46

*In milliliters at column temperature as measured from injection and corrected for pressure drop (including dead space volume of 41.7 ml).

The relative excess plate height is plotted in Fig. 1B against the square of the relative reduced sample volume as suggested by eq. [4]. The points shown were obtained at 150 °C and the data for other temperatures were in agreement. The experimental conditions correspond to those employed by van Deemter *et al.*; the theoretical line derived from their calculations is included in the figure. Although it is difficult to conclude whether the excess plate height is linear in the square of the sample volume, as would be expected by the simple treatment of the eq. [2], the experimental values lie distinctly above the theoretical curve. Van Deemter, Zuiderweg, and Klinkenberg reported measurements which fell closely on the calculated curve but did not describe their injection procedure nor their method of pressure-drop corrections in sufficient detail to permit a comparison with the methods used here. The present measurements indicate either apparent plate heights higher or relative sample volumes lower than would be expected from the theoretical curve.

Guiochon has reported a few measurements for peak broadening with samples injected by syringe (5). Although his values showed a wide scatter, he concluded that the injection time corresponded to six standard deviations in the sample distribution which would place his results on a curve much lower than ours. In fact they would lie well below curve 3 in Fig. 1A which is calculated for an injection time equal to four standard deviations. Bohemen and Purnell (9) and Purnell and Sawyer (10) have also reported measurements of band broadening with syringe injection of liquid samples. Their apparatus was constructed with one side of the thermal conductivity detector between the injection point and the column so that they were able to obtain a direct measurement of the sample pulse as injected. They did not describe the peak shapes they were working with but found that significant broadening occurred when the width of the sample pulse was more than one-quarter of the width of the eluted peak.

Can. J. Chem. Downloaded from www.nrcresearchpress.com by 210.87.254.40 on 09/05/12
For personal use only.

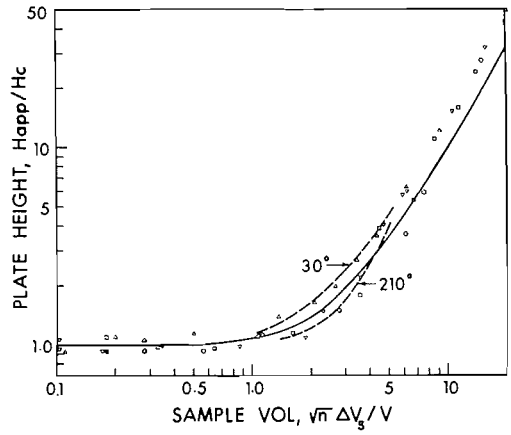

FIG. 2. Relative plate height at various relative sample volumes. Experimental points for 100°, symbols as in Fig. 1B. Best fit lines for measurements at 30° and 210° are also shown. Solid line is theoretical curve derived from van Deemter, Zuiderweg, and Klinkenberg (2).

A somewhat more satisfactory way of presenting the data over wide ranges of sample volume, and at the same time of showing the detailed behavior at the lower values, is by the log–log plot of Fig. 2. Here the relative plate height is plotted against the relative sample volume. The experimental points are given for the isothermal measurements at 100°; measurements at other temperatures showed slight deviations at lower values and the lines for the two extreme temperatures are indicated. Finally the theoretical curve derived from van Deemter, Zuiderweg, and Klinkenberg (2) is also included; the deviations appear to remain in constant proportion at high sample volumes. Glueckauf (1) suggested that the sample band width, considered as a plug, should be less than one-quarter the outlet band width as measured at a height h/e, i.e. $1/4\sqrt{2}$ times the outlet band width as measured by the base line intercept and this limit corresponds to an abscissa value in Fig. 2 of $1/\sqrt{2}$ or 0.7. The more commonly quoted criterion of van Deemter *et al.* that the sample volume should be less than $V/2\sqrt{n}$ corresponds to a feed plug one-eighth of the base width of the emergent band and to an abscissa value of 0.5. Here the increase in apparent plate height is only around 2%. If the sample volume were doubled beyond this point the effect would increase to approximately 10%. To cause a doubling of the apparent plate height the sample volume must be as much as $3V/\sqrt{n}$ or six times the van Deemter limit.

Programmed temperature chromatograms were obtained for the same sample and injection conditions with three different initial temperatures, 30°, 60°, and 100°. Representative chromatograms corresponding to relatively large sample volumes are shown in Fig. 3 for the three starting temperatures. The relative plate heights were plotted against the relative sample volumes as shown in Fig. 4. The points for the 60° initial temperature coincide closely with the line for the isothermal data at 60°. Since 60° was the starting temperature, the isothermal retention volumes at 60° must be used in calculating the relative sample volumes. The value of n, the plate number, is, of course, calculated from the limiting small sample values determined under the program conditions and is an average (11, 12) of the isothermal values over the temperature range of the program. Except for the high isothermal plate heights at 30° the variation of plate height for these conditions was small; even the 30° value contributed very little to the averages so that the variations with temperature in $\sqrt{n}$ were insignificant.

Can. J. Chem. Downloaded from www.nrcresearchpress.com by 210.87.254.40 on 09/05/12
For personal use only.

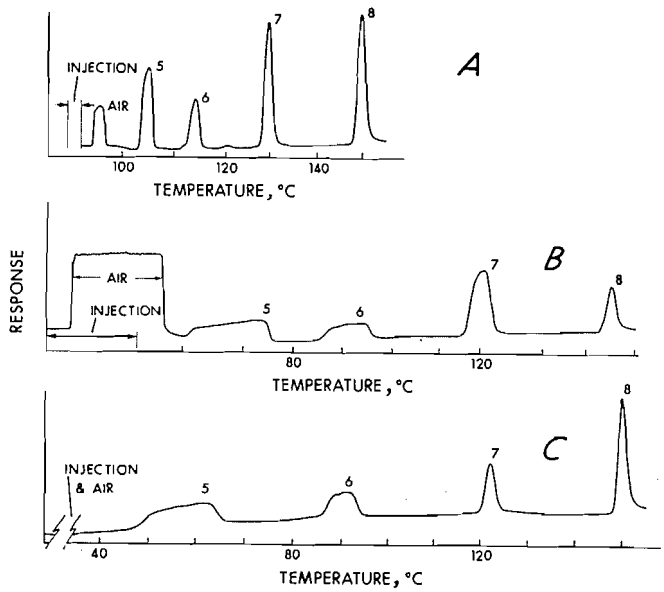

FIG. 3. Programmed temperature gas chromatography chromatograms for pentane, hexane, heptane, and octane. A. Initial temperature 30°, sample injection volume 160 ml. B. Initial temperature 60°, sample injection volume 119 ml. C. Initial temperature 100°, sample injection volume 17 ml.

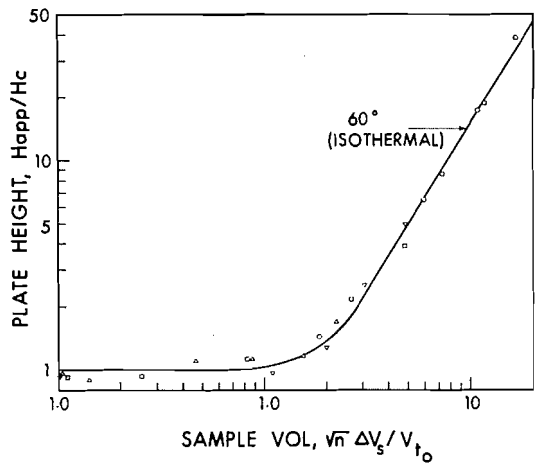

FIG. 4. Relative plate height as a function of relative sample volume for p.t.g.c., starting from an initial temperature of 60°. Symbols as in Fig. 1B, solid line from isothermal measurements at 60°.

The important conclusion from these measurements is that, *apart from differences in* $\sqrt{n}$ *between isothermal and programmed conditions*, the apparent plate height for large samples is the same for p.t.g.c. and for isothermal elution at the initial temperature. The advantage of p.t.g.c. is that it provides elution of all components under optimum or nearly optimum conditions, whereas isothermal elution would lead to such broad bands for the most strongly retained peaks that quantitative measurement or, sometimes, even detection would be impossible. Furthermore, as may be seen by a comparison of the three chromatograms in Fig. 3, larger samples may be accommodated without loss of resolution by simply lowering the initial temperature.

Can. J. Chem. Downloaded from www.nrcresearchpress.com by 210.87.254.40 on 09/05/12
For personal use only.

Many problems in trace analysis involve the determination of small amounts of relatively high-boiling impurities in a low-boiling material. The determination of most air pollutants is an example of this situation; another is the analysis of the heavy ends present in natural gas. Frequently these more condensable trace materials are trapped out of a large volume of the parent substance, e.g. air or natural gas, using either direct condensation or adsorption on cooled charcoal or other adsorbent. For example, Mackay, Lang, and Berdick (13) used a low temperature chromatographic precolumn. The concentrated impurities are then transferred to a chromatograph for analysis. The present results indicate that a more satisfactory alternative would be to inject the large volume of material to be analyzed directly onto the chromatographic column at a temperature sufficiently low to condense the trace impurities into narrow bands. Programmed temperature gas chromatography elution, while giving a broad main band, will yield sharp, easily measurable peaks for the trace components.

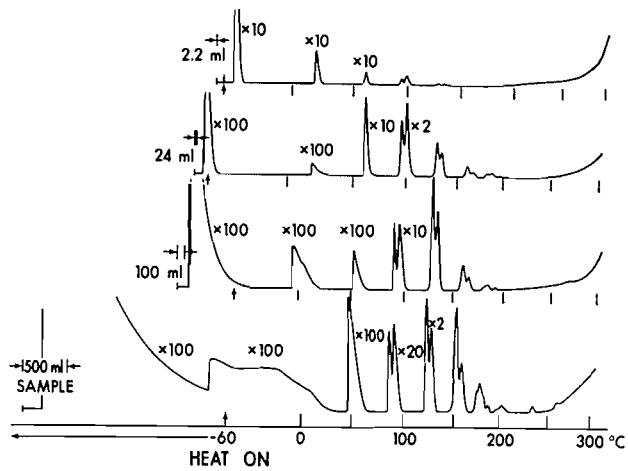

Fig. 5. Programmed temperature gas chromatography chromatograms of natural gas on a column of deactivated alumina using various sample volumes. Initial temperature −60°; heating was started at the time indicated by the arrow.

As an example of this application of p.t.g.c. to trace analysis, a number of experiments were carried out with natural gas from the city supply using a deactivated alumina column as described in the experimental section. Chromatograms obtained with sample volumes ranging from 2 to 500 ml are shown in Fig. 5. The choice of a solid adsorbent permitted lowering the initial temperature to −60°. Under these conditions methane was still only weakly retained, but the hydrocarbons, from butane up, were retained so strongly that even with the 500 ml sample there was no peak broadening. We did not extend this procedure to even higher sample volumes nor use it with a more sensitive detector; both of which would permit a much more comprehensive analysis of the trace components.

A number of advantages may be expected from the use of this technique as compared with the separate trapping out of the trace components. There is a gain in simplicity by the elimination of a separate trapping step. There is no uncertainty about the completeness of trapping, or worry about losses of material in the form of noncondensable fog. Frequently there is interest in compounds of intermediate volatiliy, which may be only partially collected in a conventional trap. In the p.t.g.c. technique, these compounds may give partially broadened bands which still provide useful information. For example, in

Can. J. Chem. Downloaded from www.nrcresearchpress.com by 210.87.254.40 on 09/05/12
For personal use only.

Fig. 5 the second peak (ethane) is measurable even though it exhibits pronounced broadening. Furthermore there is a suggestion of a small peak at the trailing edge which indicates the presence of an additional impurity of similar volatility.

These advantages derive from the greater flexibility inherent in programmed temperature as compared with isothermal operation. It is characteristic of p.t.g.c. that each component tends to be eluted under optimum conditions for detection and measurement and these may be further selected by choice of heating and flow rates. This paper has attempted to demonstrate that optimum sample injection conditions may be achieved by proper choice of initial temperature. In other words the operator has independent control of the injection conditions and of the retention characteristics.

ACKNOWLEDGMENTS

We wish to thank G. J. du Cloux for experimental assistance. M. P. Lee participated in preliminary work on trace analysis as did also a group of students under Mr. K. Glen from Victoria Composite High School.

REFERENCES

1. E. GLUECKAUF. Trans. Faraday Soc. **51**, 34 (1955).
2. J. J. VAN DEEMTER, F. J. ZUIDERWEG, and A. KLINKENBERG. Chem. Eng. Sci. **5**, 271 (1956).
3. P. E. PORTER, C. H. DEAL, and F. H. STROSS. J. Am. Chem. Soc. **78**, 2999 (1956).
4. J. C. GIDDINGS. Anal. Chem. **34**, 722 (1962).
5. G. GUIOCHON. Anal. Chem. **35**, 399 (1963).
6. H. W. HABGOOD and W. E. HARRIS. Anal. Chem. **32**, 450 (1960).
7. E. GLUECKAUF. Trans. Faraday Soc. **60**, 729 (1964).
8. C. M. REILLEY, G. P. HILDEBRAND, and J. W. ASHLEY. Anal. Chem. **34**, 1198 (1962).
9. J. BOHEMEN and J. H. PURNELL. J. Chem. Soc. 2630. 1961.
10. J. H. PURNELL and D. T. SAWYER. Anal. Chem. **36**, 668 (1964).
11. G. STEWART. Anal. Chem. **32**, 1205 (1960).
12. H. W. HABGOOD and W. E. HARRIS. Anal. Chem. **32**, 1206 (1960).
13. D. A. M. MACKAY, D. A. LANG, and M. BERDICK. Drug Cosmetic Ind. **86**, 46, 166 (1960).

Can. J. Chem. Downloaded from www.nrcresearchpress.com by 210.87.254.40 on 09/05/12
For personal use only.

Can. J. Chem. Downloaded from www.nrcresearchpress.com by 210.87.254.105 on 09/05/12
For personal use only.

SEMIEMPIRICAL SCF–LCAO–MO TREATMENT OF THIOPHENE, FURAN, AND PYRROLE[1]

N. SOLONY AND F. W. BIRSS
Department of Chemistry, University of Alberta, Edmonton, Alberta

AND

JOHN B. GREENSHIELDS
Department of Chemistry, Duquesne University, Pittsburgh, Pennsylvania

Received November 13, 1964

Dedicated to Professor R. B. Sandin on the Occasion of his Sixty-Eighth Birthday

ABSTRACT

The semiempirical SCF–LCAO–MO method of Pariser–Parr–Pople is utilized in the study of the π-electronic structures of thiophene, furan, and pyrrole. The core Hamiltonian expansion contains a U_Z^{++} term, the potential due to the ionized hetero-atom contributing two electrons to the π-system. The γ_{ZZ}, one-center coulomb repulsion integral for the hetero-atom is evaluated from the experimental spectroscopic data only. With the resonance integral β_{CZ}^{c} as the only variable parameter, the calculated π^*–π electronic transitions are in a satisfactory agreement with the experimental data.

INTRODUCTION

The semiempirical MO method of Pariser and Parr (1) has been used in a number of studies of π-electronic structures of the six-membered nitrogen-heterocyclic rings (1, 2) and the hetero-molecules containing carbonyl (3) and thiocarbonyl groups (4), with rather encouraging results. The same holds true for the five-membered heterocyclic rings: furan (5), thiophene (5, 7), and pyrrole (6), where each work has its own modifications to the method.

To further the study of π-electronic structures of the five-membered heterocyclic rings, the present work extends the semiempirical SCF–LCAO–MO method of Pariser–Parr and Pople (1, 8) to thiophene, furan, and pyrrole with several modifications for the treatment of the hetero-atoms. With the thought of making the method more general for such systems and to avoid any separate adjustments for each molecule, this work utilizes only one variable parameter β_{CZ}^{c}, fitted to give the best agreement with the experimental electronic spectra.

The main idea in any SCF calculation (9) is to obtain the best set of SCF–LCAO–π–MO functions from which the properties associated with π-electrons (the π^*–π transitions, the dipole moments, the reaction sites, etc.) can be calculated. The parameters necessary for the SCF calculations, α_i^{c}, β_{ij}^{c}, γ_{ii}, and γ_{ij}, defined by the expressions [1], [2], [3], and [4], are evaluated by recourse to the experimental data (10).

$$[1] \qquad \alpha_i^{c}(1) = \int \chi_i(1) H^{c}(1) \chi_i(1)\, d\nu(1),$$

$$[2] \qquad \beta_{ij}^{c}(1) = \int \chi_i(1) H^{c}(1) \chi_j(1)\, d\nu(1),$$

$$[3] \qquad \gamma_{ii} = \int \chi_i(1)\chi_i(1) 1/r_{12} \chi_i(2)\chi_i(2)\, d\nu(1)\, d\nu(2),$$

$$[4] \qquad \gamma_{ij} = \int \chi_i(1)\chi_i(1) 1/r_{12} \chi_j(2)\chi_j(2)\, d\nu(1)\, d\nu(2),$$

[1]*Part of this work is abstracted from the dissertation submitted by N. S. to the graduate school of Duquesne University in partial fulfillment of the requirement for the Ph.D. degree.*

where H^c stands for the core Hamiltonian (1). The exchange repulsion integrals vanish due to the zero differential overlap approximation. It is assumed that the orbital functions, χ_i, are real.

EVALUATION OF PARAMETERS

The five-membered rings are numbered in the usual manner (22), starting with the hetero-atom Z (Z = S, O, N) as number one. The values of the empirical parameter $\beta_{CZ}{}^c$ are given in Table I. The parameters $\beta_{CC}{}^c$ and the $\gamma_{C_iC_j}$, listed in Tables I and III respectively, are evaluated semiempirically from experimental spectroscopic data (10) following the method of Pariser and Parr (1).

TABLE I

Values of $\beta_{CZ}{}^c$ and $\beta_{CC}{}^c$, for interatomic distances in angstroms (11)

Center	$\beta_{CS}{}^c$ (eV) (thiophene)	$\beta_{CO}{}^c$ (eV) (furan)	$\beta_{CN}{}^c$ (eV) (pyrrole)
1–2, 1–5	−0.900	−1.800	−1.700
2–3, 4–5	−2.665	−2.903	−2.759
3–4	−2.006	−2.006	−1.905

The evaluation of γ_{CZ}, using the uniformly charged sphere approximation (1), requires γ_{ZZ}, the one-center coulomb repulsion integral. For the evaluation of this integral the following considerations are made. Because of the small C—Z—C angle (11), the orbitals on the O and S atoms in furan and thiophene, respectively, are assumed to be non-hybridized. The s orbital contains a lone pair of electrons which is not considered explicitly in this work but rather it is assumed to be included with the other σ and inner electrons in the core parameters.

The p_x and the p_y atomic orbitals (AO's) on the O and S atoms form σ bonds with the C atoms, and the p_z AO, perpendicular to the plane of the ring, contributes two electrons to the π-system.

In the case of pyrrole, the N atom is assumed to be in its sp^2 hybridization state and each sp^2 orbital forms a σ bond with the H and the C atoms, leaving the p_z AO fully occupied and participating in the π-bond formation.

In order to evaluate the integral γ_{ZZ}, it is postulated that on each Z center there exist two singly occupied χ^+ AO's which form an "ion-neutral atom pair".

$$[5] \qquad \underset{(-2W_2)}{2\chi^+(s^2xyz)} \xrightarrow{\Delta E} \underset{(0)}{\chi^{+2}(s^2xy)} + \chi(s^2xyz^2), \qquad (-2W_2 + \gamma_{ZZ} = -W_2 - W_1)$$

where W_2 and W_1 are the second and first ionization potentials, respectively, and $\gamma_{ZZ} = \Delta E = W_2 - W_1$ can be evaluated from the experimental values of W_2 and W_1. Table II gives the spectroscopic data necessary for the evaluation of γ_{ZZ}.

The integrals γ_{CZ} are defined by the expressions* [6], [7], [8], and [9]. Their numerical values are given in Table III.

$$[6] \qquad \gamma_{C_iC_j}\ (\text{eV}) = 11.08 + 0.2668r^2 - 2.9663r,$$

$$[7] \qquad \gamma_{CS}\ (\text{eV}) = 11.49 + 0.3057r^2 - 3.2181r,$$

$$[8] \qquad \gamma_{CO}\ (\text{eV}) = 15.165 + 0.6483r^2 - 5.4727r,$$

**Obtained by the uniformly charged sphere approximation (1) with an effective charge according to Slater (12).*

Can. J. Chem. Downloaded from www.nrcresearchpress.com by 210.87.254.105 on 09/05/12
For personal use only.

TABLE II

Changes in spectroscopic states (10)

Energy state	Energy state	ΔE (eV) Furan (Z = O)	Thiophene (Z = S)	Pyrrole
$Z^0(s^2p^4,{}^3P_2)$	$\rightarrow Z^+(s^2p^3,{}^4S)$	13.55*	10.36*	
$Z^0(s^2xyz^2,V_2)$	$\xrightarrow{W_1} Z^+(s^2xyz,V_3)$	14.69	10.98	
$Z^+(s^2p^3,{}^4S)$	$\rightarrow Z^{++}(s^2p^2,{}^3P)$	34.93*	23.40*	
$Z^+(s^2xyz,V_3)$	$\xrightarrow{W_2} Z^{++}(s^2xy,V_4)$	33.94	22.88	
	$W_2 - W_1 = \gamma_{ZZ}$	19.25	11.90	
$N^0(sp^4,{}^4S)$	$\rightarrow N^+(sp^3,{}^3P)$			14.48*
$N^0(sxyz^2,V_3)$	$\xrightarrow{W_1} N^+(sxyz,V_4)$			11.89
$N^+(sp^3,{}^3P)$	$\rightarrow N^{++}(sp^2,{}^2P)$			29.47*
$N^+(sxyz,V_4)$	$\xrightarrow{W_2} N^{++}(sxy,V_3)$			29.03
	$W_2 - W_1 = \gamma_{NN}$	17.14		

*Handbook of Chemistry and Physics, The Chemical Rubber Publishing Co., Cleveland, Ohio, 1961. p. 2586.

TABLE III

Values of $\gamma_{C_iC_j}$ in electron volts, for interatomic distances in angstroms (11)

Center	$\gamma_{C_iC_j}$ Thiophene	Furan	Pyrrole
1–2, 1–5	6.857	8.876	8.458
1–3, 1–4	5.248	6.166	6.065
2–3, 4–5	7.518	7.550	7.530
2–4, 3–5	5.651	5.795	5.751
2–5	5.382	5.851	5.754
3–4	7.398	7.406	7.388

[9] $$\gamma_{CN}\ (\text{eV}) = 14.11 + 0.5495r^2 - 4.8272r.$$

The integrals α_i^c, defined by eq. [1], are evaluated by expanding H^c according to Goeppert-Mayer and Sklar (13) with an additional hetero-atom term U_Z^{++}, i.e.,

[10] $$H^c(i) = -\tfrac{1}{2}\nabla^2(i) + U_Z^{++}(i) + \sum_{k=2}^{5} U_k^+(i),$$

where U_k^+ is the potential due to an ionized C atom in its sp^2 valence state, and is defined by

[11] $$U_k^+(i) = U_k^0(i) - \int \chi_k^2(j) 1/r_{12}\, dv(j),$$

U_k^0 being the potential due to a neutral C atom in its sp^2 valence state. The U_Z^{++} is the potential due to a doubly ionized hetero-atom, which has contributed two electrons from its p_Z AO; it is defined by

[12] $$U_Z^{++}(i) = U_Z^+(i) - \int [\chi_Z^+(j)]^2 1/r_{12}\, dv(j) - \int \chi_Z^2(j) 1/r_{12}\, dv(j),$$

Can. J. Chem. Downloaded from www.nrcresearchpress.com by 210.87.254.105 on 09/05/12
For personal use only.

where χ_Z^+ is a singly occupied hetero-atom AO, and U_Z^+ and U_Z^0 are the potentials due to a singly ionized and a neutral hetero-atom, respectively.

The α_2^c integral (for the C_2 atom) can be written as

$$[13]\quad \alpha_2^c(1) = \int \chi_2(1) H^c(1) \chi_2(1)\, dv(1)$$
$$= W_{1C_2} + \int U_1^0(1)\chi_2^2(1)\, dv(1) - \int \chi_2^2(1) 1/r_{12} \chi_1^2(2)\, dv(1)\, dv(2)$$
$$- \int \chi_2^2(1) 1/r_{12} [\chi_1^+(2)]^2\, dv(1)\, dv(2) + \int U_3^0(1)\chi_2^2(1)\, dv(1)$$
$$- \int \chi_2^2(1) 1/r_{12} \chi_3^2(2)\, dv(1)\, dv(2) + \int U_4^0(1)\chi_2^2(1)\, dv(1)$$
$$- \int \chi_2^2(1) 1/r_{12} \chi_4^2(2)\, dv(1)\, dv(2) + \int U_5^0(1)\chi_2^2(1)\, dv(1)$$
$$- \int \chi_2^2(1) 1/r_{12} \chi_5^2(2)\, dv(1)\, dv(2),$$

where W_{1C_2} is the first ionization potential of the C atom in its sp^2 valence state.

Neglecting the penetration integrals, represented by the positive terms in the expression [13], the general expression for a carbon α_i^c can be written as

$$[14]\quad \alpha_i^c = W_{1C} - \sum_{i \neq j} \gamma_{ij} - \sum_{i \neq Z^+} \gamma_{iZ^+}.$$

Similarly, α_Z^c for a hetero-atom can be written as

$$[15]\quad \alpha_Z^c(1) = \int \chi_Z^+(1) \left[-\tfrac{1}{2}\nabla^2(1) - U_Z^{++}(1) - \sum_{k=2}^{5} U_k^+(1) \right] \chi_Z^+(1)\, dv(1)$$
$$= W_{2Z} - \sum_{i \neq Z^+} \gamma_{iZ^+},$$

where W_{2Z} is the second ionization potential of a hetero-atom in its valence state.

TABLE IV

Values of γ_{CZ^+} in electron volts, for interatomic distances in angstroms (11)

Center	γ_{CS^+} (thiophene)	γ_{CO^+} (furan)	γ_{CN^+} (pyrrole)
1–2, 1–5	6.872	8.467	8.885
1–3, 1–4	5.263	6.007	6.175

The integrals γ_{iZ^+}, listed in Table IV, are evaluated from eqs. [16], [17], and [18], obtained using the uniformly charged sphere approximation (1) with effective charges determined by Slater's rules (12) for a particular doubly ionized Z^{++} hetero-atom:

$$[16]\quad \gamma_{CS^+}\ (\text{eV}) = 11.49 + 0.3057r^2 - 3.2181r,$$

$$[17]\quad \gamma_{CO^+}\ (\text{eV}) = 15.165 + 0.6463r^2 - 5.4643r,$$

$$[18]\quad \gamma_{CN^+}\ (\text{eV}) = 14.11 + 0.5488r^2 - 4.8206r.$$

The integrals α_i^c are listed in Table V.

RESULTS AND DISCUSSION

The method proposed above for the evaluation of the parameter γ_{ZZ} and the ionization potential of a hetero-atom utilizes the experimental spectroscopic data for a given molecular state of the hetero-atom, thus specifying the arrangement of the AO's on it

Can. J. Chem. Downloaded from www.nrcresearchpress.com by 210.87.254.105 on 09/05/12
For personal use only.

TABLE V

Values of α_i^c in electron volts, for interatomic distances in angstroms (11)

	α_i^c		
Center	Thiophene	Furan	Pyrrole
1	−47.150	−64.060	−58.118
2,5	−43.720	−48.497	−47.500
3,4	−42.618	−44.632	−44.351

and giving a somewhat clearer picture of how the hetero-atom could contribute two electrons to the π-system. This method avoids any further semiempirical adjustments of γ_{zz} (14) and the hetero-atom ionization potential (6).

The method differs in its approach from those previously applied to furan, pyrrole, and thiophene in the work of Pajol and Julg, Sappenfield and Kreevoy (5), and Hahl and Hansen (6). The latter two employ some aspect of the 'self-consistent electronegativity' method to obtain a single configuration function, followed by configuration interaction. Pajol and Julg have used a modified MO method in which the deformation of MO's is taken into account in the calculation of π-electron integrals. The present method is based upon obtaining self-consistency of the MO's, holding all integrals fixed within a single calculation and, between calculations, varying the β_{cz} parameters only. In this it most closely resembles the method due to Julg (5).

The ultraviolet spectra are the most widely used criteria for testing MO-type calculations performed on π-systems. In most cases the low-lying excited states are experimentally known and are assigned. In the case of the three heterocyclics considered in this work, the ultraviolet absorption spectra consists of the unassigned singlet absorption bands (see Table VI). For most of these bands the singlet absorption maxima and their intensities are known. The triplet states have not been reported, although a low-lying very weak band observed in thiophene is speculated to be due to a triplet state (15).

Most of the calculated electronic transitions given in Table VI show a good agreement with the experimentally observed absorption band maxima. The two low-lying overlapping bands in thiophene agree with Milazzo's observation (16). The third band which that author claims is due to the excitation of one electron left on the sulfur AO does not appear in our calculation; our formalism does not account for this situation. The calculated spectrum of thiophene is in better agreement with the work of Price and Walsh (17) who observed two bands from thiophene vapor. Our first two calculated transitions fall in the region of the first band, which extends from 5.16 to 5.90 eV. The third and fourth calculated transitions fall on the second observed band which extends from 6.59 to 8.85 eV.

Most of the transitions calculated agree with the calculations of Pajol and Julg (5), Dahl and Hansen (6), and Sappenfield and Kreevoy (5), although the assignments of Dahl and Hansen are different from ours, which agree with the assignments of Brown and Hefferman (6). The small discrepancies which exist between the observed and the calculated electronic transitions may not necessarily reflect the weakness of the method. It has been observed that the calculated electronic transitions are very sensitive to a relatively small change in the interatomic distances, and the use of rough and approximate dimensions may result in somewhat significant discrepancies between the calculated and the experimental results. For example, using three slightly different sets of interatomic

Can. J. Chem. Downloaded from www.nrcresearchpress.com by 210.87.254.105 on 09/05/12
For personal use only.

TABLE VI

Calculated π^*–π electronic transitions in electron volts

π^*–π	Sym.	Calcd. ΔE	Expt. ΔE	Expt. ΔE (16)	Expt. ΔE (25)	Other work
Thiophene						
$3 \rightarrow 4$	A_1^1	5.13	5.16–5.90 (17)	5.15		5.13 (5)
$3 \rightarrow 4$	A_1^3	4.18	3.89–3.96 (15)			
$2 \rightarrow 4$	B_1^1	5.42		5.33		
$2 \rightarrow 4$	B_1^3	3.42				
		—		5.62		5.71 (5)
$3 \rightarrow 5$	B_1^1	7.18	6.59–8.85 (17)	6.59–7.75		6.62 (5)
$3 \rightarrow 5$	B_1^3	6.79				
$2 \rightarrow 5$	A_1^1	7.47				
$2 \rightarrow 5$	A_1^3	5.54				
Pyrrole						
$3 \rightarrow 4$	B_1^1	5.98		5.88		
$3 \rightarrow 4$	B_1^3	4.10				
$2 \rightarrow 4$	A_1^1	6.56		6.77		
$2 \rightarrow 4$	A_1^3	4.26				
$2 \rightarrow 5$	B_1^1	7.19		7.21		
$2 \rightarrow 5$	B_1^3	6.02				
$3 \rightarrow 5$	A_1^1	7.64				
$3 \rightarrow 5$	A_1^3	5.74				
Furan						
$3 \rightarrow 4$	B_1^1	6.05			6.05	5.92, 5.80 (5)
$3 \rightarrow 4$	B_1^3	4.17				
$\Phi_{2\rightarrow4} - \Phi_{3\rightarrow5}$	A_1^1	6.80			6.48	6.49, 6.8 (5)
$\Phi_{2\rightarrow4} - \Phi_{3\rightarrow5}$	A_1^3	4.76				
$2 \rightarrow 4$	A_1^1	7.40			7.40	7.2 (5)
$2 \rightarrow 4$	A_1^3	5.25				
$3 \rightarrow 5$	A_1^1	7.96			7.80	7.5 (5)
$3 \rightarrow 5$	A_1^3	6.04				

TABLE VII

π^*–π Electronic transitions in electron volts for pyrrole, calculated for three sets of interatomic distances in angstroms ($\beta_{CN}^\circ = -1.80$ eV)

	Set 1 (24)	Set 2 (11)	Set 3 (11)
Dimensions			
N—C_2	1.42	1.382	1.391
C_2—C_3	1.35	1.371	1.364
C_3—C_4	1.44	1.429	1.428
$\angle$ C_5—N—C_2	108°	108° 56′	108° 08′
$\angle$ N—C_2—C_3	110°	108° 05′	108° 21′
$\angle$ C_2—C_3—C_4	108°	107° 27′	107° 35′
π^*–π			
B_1^1	6.42	5.91	6.05
A_1^1	6.73	6.35	6.65
B_1^1	7.17	6.95	7.19
A_1^1	7.95	7.53	7.65

dimensions reported for pyrrole, three different sets of electronic transitions (see Table VII) were calculated.

The calculated ionization potentials for thiophene, furan, and pyrrole, although too

Can. J. Chem. Downloaded from www.nrcresearchpress.com by 210.87.254.105 on 09/05/12
For personal use only.

high, (see Table VIII), follow the usual trend observed in the Pariser–Parr–Pople-type calculations which yield an ionization potential too high by about 1.5 to 2.5 eV (18). It was shown by Hoyland and Goodman (19) that this discrepancy could be removed by applying a correction for the σ-core contraction and the π-orbital deformation in the ionized state. This shows that in order to improve the ionization potential calculation a special treatment of the ionized state is required, and an open shell calculation will therefore be attempted in the near future.

TABLE VIII

SCF eigenvalues and eigenvectors

Φ_i	Sym.	C_1	C_2	C_3	E_i (eV)	Ion. pot. (eV)
Thiophene						
1	B_2	.35092	.42327	.50917	−13.8773	
2	A_2	.00000	−.57443	−.41234	−11.2160	
3	B_2	.91085	−.02816	−.29047	−11.1613	−8.91 (17)
4	B_2	.21722	−.56572	.39542	−0.2484	
5	A_2	.00000	.41234	−.57443	1.8757	
Furan						
1	B_2	.84120	.32894	.19490	−17.1194	
2	B_2	.47209	.27102	.56135	−12.8668	
3	A_2	.00000	−.58052	−.40371	−11.7382	−8.89 (25)
4	B_2	.26365	−.56422	.38327	0.2080	
5	A_2	.00000	.40371	−.58053	1.9371	
Pyrrole						
1	B_2	.68467	.41096	.31099	−15.5767	
2	B_2	−.64696	.14617	.51898	−12.0082	
3	A_2	.00000	−.58328	−.39973	−11.6475	−8.90 (16)
4	B_2	−.33565	.55653	−.36597	.1842	
5	A_2	.00000	.39972	−.58328	1.6866	

The experimental dipole moments have been reported as 1.8 D↑, 0.7 D↓, and 0.56 D↓ for pyrrole, furan, and thiophene, respectively. The above dipoles lie along the molecular axes and the negative end of the dipole for pyrrole is believed to point up toward the C_3—C_4 bond (20) as indicated by the arrow, and in thiophene and furan to point down toward the hetero-atom (11). The a priori calculation of the total dipole moment cannot be performed due to the uncertainty in the reported σ-moment values (21). The π-moments calculated from the SCF π-electron densities in the ground states (see Table VIII) are 0.87 D↑, 0.95 D↑, and 1.53 D↑ for thiophene, furan, and pyrrole, respectively. The calculated μ_π for thiophene agrees with the value reported by Bak, Christensen, Hansen-Nygard, and Rastrup-Andersen (11) and the μ_π for pyrrole is in agreement with the value given by Pauling (20).

TABLE IX

Ground state SCF π-electron densities q_i, free valency F_i, and π-bond orders P_{ij}

	Thiophene	Furan	Pyrrole
q_1	1.9056	1.8496	1.7747
q_2	1.0199	1.0401	1.0609
q_3	1.0273	1.0351	1.0517
F_1	1.9226	3.5840	2.5498
F_2	0.5652	0.5323	0.4848
F_3	0.4634	0.4506	0.4459
P_{12}	0.2457	0.2975	0.3736
P_{23}	0.9211	0.9012	0.8736
P_{34}	0.3472	0.3802	0.4125

Can. J. Chem. Downloaded from www.nrcresearchpress.com by 210.87.254.105 on 09/05/12
For personal use only.

It is known experimentally (22) that all three heterocyclics considered in this work undergo electrophilic substitution at the α-position. Pyrrole and furan exhibit slight basicity, and the oxygen in furan undergoes protonation in acidic media. The above chemical behavior can be best explained qualitatively by the free valency (F_i) distribution (23) shown in Table IX, which also gives the π-electron densities q_i, and the π-bond orders P_{ij}.

ACKNOWLEDGMENTS

The authors wish to express their thanks to the Department of Computing Science of the University of Alberta for their cooperation in permitting use of the IBM 1620 for these calculations. The support of the National Research Council is gratefully acknowledged.

REFERENCES

1. R. PARISER and R. G. PARR. J. Chem. Phys. **21**, 466, 767 (1953).
2. R. C. HIRT, F. HALVERSON, and R. G. SCHMITT. J. Chem. Phys. **22**, 1148 (1954). L. PAOLONI. J. Chem. Phys. **25**, 1277 (1956). M. J. S. DEWAR and L. PAOLONI. Trans. Faraday Soc. **53**, 261 (1957). T. ANNO. J. Chem. Phys. **29**, 1161 (1958).
3. R. G. PARR and R. PARISER. J. Chem. Phys. **23**, 711 (1955). T. ANNO, T. MATURBA, and A. SADO. Bull. Chem. Soc. Japan, **30**, 18 (1957). T. ANNO and A. SADO. Bull. Chem. Soc. Japan, **26**, 1756 (1957). J. W. SIDMAN. Bull. Chem. Soc. Japan, **27**, 429 (1957). M. SUARD, G. BERTHIER, and B. PULLMAN. Biochim. Biophys. Acta, **52**, 254 (1961). K. INUSUKA. Bull. Chem. Soc. Japan, **34**, 6 (1961).
4. H. HOYOYA, J. TANAKA, and S. NAGAKURA. Bull. Chem. Soc. Japan, **33**, 850 (1960).
5. M. K. ORLOFF and D. D. FITTS. J. Chem. Phys. **38**, 2334 (1963). L. PAJOL and A. JULG. Theoret. Chim. Acta, **2**, 125 (1964). D. S. SAPPENFIELD and M. KREEVOY. Tetrahedron, **19**, Suppl. 2, 157 (1963).
6. R. D. BROWN and M. L. HEFFERMAN. Australian J. Chem. **12**, 319 (1959). J. P. DAHL and A. E. HANSEN. Theoret. Chim. Acta, **1**, 199 (1963).
7. G. MILAZZO. Gazz. Chim. Ital. **89**, 2479 (1959). A. MANGINI and C. ZAULI. J. Chem. Soc. **22**, 2469 (1960).
8. J. A. POPLE. Trans. Faraday Soc. **49**, 1375 (1953).
9. C. C. J. ROOTHAAN. Rev. Mod. Phys. **23**, 69 (1951).
10. H. O. PRITCHARD and H. A. SKINNER. Trans. Faraday Soc. **49**, 1254 (1953).
11. B. BAK, D. CHRISTENSEN, L. HANSEN-NYGAARD, and J. RASTRUP-ANDERSEN. J. Mol. Spectry. **7**, 58 (1961); J. Chem. Phys. **24**, 720 (1956). B. BAK, L. HANSEN, and J. RASTRUP-ANDERSEN. Discussions Faraday Soc. **30**, 19 (1955).
12. J. C. SLATER. Phys. Rev. **36**, 57 (1930).
13. M. GOEPPERT-MAYER and A. L. SKLAR. J. Chem. Phys. **6**, 648 (1938).
14. L. PAOLONI. Nuovo Cimento, **4**, 410 (1956).
15. M. R. PADHYE and S. R. DESAI. Proc. Phys. Soc. London, **65**, 298 (1952).
16. G. MILAZZO. Spectrochim. Acta, **2**, 245 (1944); Gazz. Chim. Ital. **78**, 835 (1948); **83**, 392 (1953).
17. W. C. PRICE and A. D. WALSH. Quart. Rev. London, **2**, 73 (1948); Proc. Roy. Soc. London Ser. A, **179**, 201 (1941).
18. C. MOSER. J. Chim. Phys. **52**, 24 (1955).
19. J. R. HOYLAND and L. GOODMAN. J. Chem. Phys. **36**, 12 (1962).
20. H. KOFORD, L. E. SUTTON, and J. JACKSON. J. Chem. Soc. 1467 (1952).
21. C. A. COULSON. Trans. Faraday Soc. **38**, 433 (1942). R. DAUDEL, R. LEFEBVRE, and C. MOSER. Quantum chemistry. Interscience Publishers, Inc., New York. 1959. p. 206.
22. G. M. BADGER. The chemistry of heterocyclic compounds. Academic Press, New York. 1961.
23. W. E. MOFFITT. Trans. Faraday Soc. **45**, 373 (1949).
24. V. SCHOMAKER and L. PAULING. J. Am. Chem. Soc. **61**, 1769 (1939).
25. K. WATANABE and T. NAKAYAMA. J. Chem. Phys. **29**, 48 (1958).

Can. J. Chem. Downloaded from www.nrcresearchpress.com by 210.87.254.105 on 09/05/12
For personal use only.

Can. J. Chem. Downloaded from www.nrcresearchpress.com by 210.87.254.105 on 09/05/12
For personal use only.

MECHANISM OF ACTION OF UDPGal-4-EPIMERASE: ISOTOPE EFFECT STUDIES[1]

RARDON D. BEVILL III,[2] E. ALEXANDER HILL, F. SMITH, AND S. KIRKWOOD
Department of Biochemistry, Institute of Agriculture, University of Minnesota, St. Paul, and Department of Chemistry, University of Minnesota, Minneapolis, Minnesota

Received November 19, 1964

Dedicated to Professor R. B. Sandin on the Occasion of his Sixty-Eighth Birthday

ABSTRACT

The synthesis of uridine diphosphate glucose and uridine diphosphate galactose labeled with tritium in the 4-position permits the observation of the isotope effect associated with the UDPGal-4-epimerase reaction. This isotope effect has been measured for the reaction proceeding in both directions and the values of k_T/k_H fall in the range 1.5 to 3.0. This allows certain conclusions to be drawn concerning the mechanism of this important enzymatic catalysis. The direction and magnitude of the effect indicate that the 4-hydrogen is removed from the hexose in the course of the reaction. They also appear to dispose of several mechanisms that have been proposed for the epimerase. Specifically, mechanisms involving cleavage of the C—O or C—C bonds at carbon-4 of the hexose moiety, such as cleavage of the carbon chain, elimination and readdition of the carbon-4 hydroxyl as water, or ionization to form a carbonium ion, are not supported by the observed data. A mechanism consistent with all observations involves transfer of the hydrogen at carbon-4 to the enzyme in a step that is not rate determining. This is followed immediately by the rate-determining step, which may well be the reorganization of the enzyme–substrate complex to allow return of the hydrogen in the opposite configuration. The larger estimate of the isotope effect indicates a transfer of the carbon-4 hydrogen to a nitrogen atom located in the enzyme's structure; the smaller estimate is consistent with transfer to oxygen or carbon. Transfer to sulfur appears to be definitely eliminated.

During this work a degradative procedure that will permit the location and quantitation of the carbon-bound tritium in any hexose or pentose was developed.

INTRODUCTION

The biological interconversion of D-galactose and D-glucose has been shown to involve the uridine diphosphate hexoses (UDP-hexoses) rather than the free hexoses or hexose phosphates (1). Efforts to elucidate the mechanism of this important enzymatic reaction have shown that there is no incorporation of either hydrogen or oxygen from water during the epimerization (2–4). Purification of the enzyme involved, uridine diphosphate galactose-4-epimerase (UDPGal-4-epimerase), revealed that the coenzyme NAD^+ is required by the enzyme from both calf liver (5) and yeast (6). This suggests that the UDP-hexose is oxidized to the 4-keto derivative which is then reduced to yield the epimeric configuration at C-4 of the hexose moiety, the hydrogen acceptor and donor being NAD^+. However, there was no incorporation of tritium (T) from either NAD^+ or NADH which contained tritium in the 4-position, nor was it possible to detect a 4-keto intermediate (5). In addition, it has been demonstrated that there is no rearrangement of the carbon skeleton of the hexoses during the course of the reaction (7, 8). Bevill *et al.* (9) and Kohn *et al.* (10) have independently demonstrated that the carbon-bound hydrogen in position-4 of the hexoses is retained during the course of the reaction in vivo and in vitro. This establishes that the hydrogen at C-4 is either removed and reintroduced or remains attached to C-4 during the course of reaction.

[1]*Paper No. 5601, Scientific Journal Series, Minnesota Agricultural Experiment Station. This work was supported in part by a grant from the National Institutes of Health.*
[2]*Procter and Gamble Predoctorate Fellow, 1963–1964.*

To investigate this matter further we have studied the kinetic isotope effect observed when tritium is substituted in place of hydrogen at C-4 of the hexose moiety of the UDP-hexoses.

EXPERIMENTAL[3]

Preparation of Methyl α-D-Glucopyranoside-4-T (II)

D-Glucose-4-T (I) (11), 4.20 mg (23.4 μmoles), was dissolved in 100 ml of anhydrous methanol containing 1% HCl generated by the addition of 2.2 ml of acetyl chloride. The solution was refluxed for 3 h, neutralized with Ag_2CO_3, and filtered. To the filtrate was added 0.500 g of carrier methyl α-D-glucopyranoside and the solution concentrated to a sirup. It was taken up in absolute ethanol and crystallized. Yield: 0.3191 g, 63.8%; m.p. 169.0–169.5° (corrected).

Methyl α-D-glucopyranoside-4-T (II) was recrystallized twice from absolute ethanol and then purified through methyl 2,3,4,6-tetra-O-acetyl-α-D-glucopyranoside-4-T to insure chemical and radiochemical purity.

Preparation of Methyl 2,3,4,6-Tetra-O-acetyl-α-D-glucopyranoside-4-T

To a mixture of 3.0 ml of acetic anhydride (32 mmoles) and 3.0 ml of anhydrous pyridine was added 250 mg of methyl α-D-glucopyranoside-4-T (II) (1.30 mmoles). The reaction mixture was heated at 50° for 2 h, then cooled, and evaporated to a small volume (approximately 1 ml). This was dissolved in 15 ml of chloroform, and the solution washed with cold saturated sodium bicarbonate (15 ml) and then with water (15 ml). The chloroform layer was dried over $CaCl_2$ and concentrated *in vacuo* to a sirup which crystallized spontaneously. Recrystallization from absolute ethanol – petroleum ether gave methyl 2,3,4,6-tetra-O-acetyl-α-D-glucoside-4-T. Yield: 364.0 mg, 77%; m.p. 101–102.5° (corrected), mixed m.p. with an authentic sample 101.5–102.5°.

Deacetylation of Methyl 2,3,4,6-Tetra-O-acetyl-α-D-glucopyranoside-4-T

Methyl 2,3,4,6-tetra-O-acetyl-α-D-glucopyranoside-4-T, 360 mg (0.99 mmole), was dissolved in 5.0 ml of freshly prepared sodium methoxide solution (5.0 mg of Na^0 was dissolved in 100 ml of anhydrous methanol). The reaction mixture was allowed to stand overnight at room temperature and then concentrated *in vacuo* to dryness. The solid methyl α-D-glucopyranoside-4-T (II) was dissolved in hot absolute ethanol, filtered, and crystallized. Yield: 154.1 mg, 80%; m.p. 169–169.5°.

Periodic Acid Oxidation of Methyl α-D-Glucopyranoside-4-T (II) and Isolation of D′-Methoxy-D-hydroxymethyldiglycolic Aldehyde (III)

Methyl α-D-glucopyranoside-4-T (II), 0.150 g (0.774 mmole), was dissolved in 15 ml of water, and to this was added a solution containing 0.400 g of H_5IO_6 ((2 moles of periodic acid + 10% excess)/mole of glucoside) in 15 ml of water. This solution was allowed to stand *in the dark* for 4–6 h (it can be left overnight). The excess periodic acid was neutralized with $BaCO_3$ to pH 7.0 The solution was subsequently filtered to remove precipitated barium salts, the precipitate washed with H_2O, and the combined filtrate and washings concentrated to dryness *in vacuo* (bath temperature 40–45°). The white residue obtained was extracted with three 50-ml portions of absolute ethanol which were then filtered. The clear filtrate was evaporated *in vacuo* to yield D′-methoxy-D-hydroxymethyldiglycolic aldehyde (III) as a sirup.

Isolation of Carbon-3 as Ammonium Formate (Va)

The white residue from the ethanol extract, which is crude barium formate, was dissolved in water, filtered to remove any insoluble material, and passed over the cation exchange resin Amberlite IR-120 (H^+ form). The eluate containing formic acid was adjusted to pH 9 with 2 *N* ammonium hydroxide, concentrated to a small volume (3 ml), and transferred to a sublimation flask (5 ml), and the concentration continued to dryness. This solid residue of crude ammonium formate was further dried under vacuum (0.2 mm) for 2 h at room temperature to remove the final traces of moisture. After a cold finger had been inserted, the flask was heated in a water bath (35–40°) to sublime the ammonium formate. When the sublimation was complete, the cold finger was allowed to warm to room temperature and removed from the apparatus, and the sublimed ammonium formate collected. (Ammonium formate is very hydroscopic.) Yield: 47.0 mg, 96.5%; m.p. 112–114°.

Oxidation of the D′-Methoxy-D-hydroxymethyldiglycolic Aldehyde (III) to Strontium D′-Methoxy-D-hydroxymethyldiglycolate (IX)

A solution containing one-half (0.387 mmole) of the total dialdehyde (III) obtained was adjusted to a volume of 50 ml with H_2O. Strontium carbonate, 1.0 g, and Br_2, 0.20 ml, were added and the reaction mixture stirred at room temperature for 30 min, followed by aeration for 30 min. Silver carbonate, 0.50 g, was added and stirring continued for an additional 10 min (it can be left overnight at this point if necessary). The suspension was filtered, and the filtrate treated first with H_2S gas for 1.0 min and then aerated for 30 min.

[3]*The degradation of methyl α-D-glucopyranoside-4-T is given here in detail as an example of the method devised for the location of carbon-bound tritium in any hexose or pentose.*

Can. J. Chem. Downloaded from www.nrcresearchpress.com by 210.87.254.105 on 09/05/12
For personal use only.

The black solution was filtered through an ultrafine sintered-glass funnel and the clear filtrate was concentrated to a small volume (1–2 ml). Careful addition of warm methanol (6.0 ml) to the warm aqueous solution yielded strontium D′-methoxy-D-hydroxymethyldiglycolate (IX); 88.5 mg, 73.5%; $[\alpha]_D^{20} = -45.0°$, $c = 1.08$. The strontium D′-methoxy-D-hydroxymethyldiglycolate (IX), 80.0 mg (0.254 mmole), was dissolved in 2.0 ml of warm CO_2-free water and filtered while hot, and the funnel rinsed with an additional 1.0 ml of water. To this solution was added 5.0 ml of warm methanol and the clear solution allowed to stand at room temperature overnight. The fine needles of IX which separated were collected by filtration and washed with cold absolute methanol and then with cold anhydrous diethyl ether. Yield: 59.0 mg, 74%; $[\alpha]_D^{25} = -52.1°$, $c = 1.03$ (lit. value, $[\alpha]_D^{20} = -52.9°$, $c = 1$ (12, 13)).

Isolation and Degradation of D-*Glyceric Acid (XI)*

All of the strontium D′-methoxy-D-hydroxymethyldiglycolate from both crystallizations, 65.0 mg (0.206 mmole), was combined and dissolved in 5.0 ml of *N* HCl. The solution was heated on a steam bath for 2 h. Silver carbonate, 10.0 g, was added, the solution stirred for 15 min and filtered. The filtrate was passed over an Amberlite IR-120 exchange resin column (H^+ form) and the acidic effluent concentrated to dryness. Paper chromatography in solvent D for 12 h yielded D-glyceric acid in 91% of the theoretical amount as determined colorimetrically (14). The aqueous solution of D-glyceric acid eluted from the chromatogram was adjusted to pH 9.0 with $Ca(OH)_2$ and the solution evaporated to a small volume (1–2 ml). (A small volume of aqueous solution of calcium glycerate is very critical in the following procedure.) The solution was gently warmed and warm absolute ethanol added to the clouding point. The solution was allowed to crystallize at room temperature overnight, and the crystals of calcium glycerate collected by filtration. Yield: 25.4 mg, 90%; m.p. 137.5–138.0° (lit. m.p. 137–138° (15)). The calcium glycerate, 21.7 mg (0.077 mmole) was dissolved in 5.0 ml of H_2O and 0.077 mmole of H_2SO_4 added to precipitate the calcium ions as $CaSO_4$. The solution was filtered and to the filtrate was added H_5IO_6, 77 mg ((0.336 mmole − 2 moles + 10% excess)/mole of glyceric acid). The reaction mixture was allowed to stand overnight in the dark. It was neutralized to pH 6.6–6.9 with $BaCO_3$ and filtered, and dimedone reagent, 0.043 g (0.306 mmole), was added to the aqueous solution which was warmed gently for 5 min. The formaldehyde methone (XII), which readily crystallized from the reaction mixture, was collected by filtration and the filtrate (F) kept. Yield: 43.2 mg, 96.6%; m.p. 191–191.5°, mixed melting point with an authentic specimen 190–191° (16). The filtrate (F), which contains barium formate, was passed directly over a column of IR-120 (H^+ form) resin and the effluent adjusted with 2 *N* NH_4OH to pH 9.0. The ammonium formate was then sublimed as described previously. Yield: 9.5 mg, 98.1%; m.p. 112–113.5°.

Reduction of D′-*Methoxy-*D-*hydroxymethyldiglycolic Aldehyde (III)*

To a solution of $NaBH_4$ (0.280 g in 10 ml of H_2O) was added an aqueous solution containing one-half (0.387 mmole) of the D′-methoxy-D-hydroxymethyldiglycolic aldehyde (III) obtained. This was shaken to assure thorough mixing, and then allowed to stand 3–5 h. (It may be left overnight without harm.) The solution was neutralized with CO_2 to pH 7.0, and evaporated to dryness *in vacuo* (bath temperature 40–45°). The residue was extracted with absolute ethanol (3 × 50-ml portions) and filtered through an ultrafine sintered-glass funnel. The filtrate was concentrated to dryness, the extraction and filtration processes repeated, and the alcoholic solution concentrated to a clear sirup to give D′-methoxyhydroxymethyldiethylene glycol (IV). Yield: 65.7 mg, 103.0%.

Isolation of Glycolic Aldehyde Methone (VIII)

D′-Methoxyhydroxymethyldiethylene glycol (IV), 65.7 mg (0.387 mmole), was dissolved in 5.0 ml of *N* HCl, allowed to stand for 30 min, and neutralized to pH 6.4 with saturated $NaHCO_3$. To this aqueous solution containing glycolic aldehyde and glycerol was added 110 mg (0.774 mmole) of dimedone reagent and then absolute ethanol dropwise until the dimedone reagent just dissolved. This reaction mixture was allowed to stand overnight and then cooled to 0°, and the crystals of glycolic aldehyde methone (VIII) collected by filtration. The filtrate was concentrated *in vacuo* until a second crop of crystals was well formed and then cooled to 0°, and the crystals collected. This procedure was repeated a third time. The remaining filtrate, which contains glycerol, was evaporated to dryness and extracted first with chloroform (50 ml) to remove the last traces of methone, and then with absolute ethanol (80 ml) to extract the glycerol from the inorganic salts. The chloroform extract was concentrated to dryness and combined with the methone derivative already recovered, and the entire product recrystallized from the minimal amount of 50% ethanol. Yield: 116 mg, 92.8%; m.p. 232–233°, mixed melting point with an authentic specimen 231.5–232.5° (17).

Isolation of Glycerol Tris-O-p-nitrobenzoate (VII)

The ethanol extract containing the glycerol (0.382 mmole) was concentrated to dryness *in vacuo* and then dried under oil pump vacuum (0.2 mm) for 3 h to remove the final traces of ethanol. This dried sirup was dissolved in 5.0 ml of anhydrous pyridine and *p*-nitrobenzoyl chloride, 0.325 g (1.74 mmoles − 4.5 moles/mole of glycerol), was added to the solution. The reaction mixture was heated at 80–90° for 20 min, then cooled rapidly, and poured into 20 ml of saturated $NaHCO_3$ with vigorous stirring. An oil separated and solidified. The solid material was filtered off, washed with H_2O, and dissolved in 100 ml of chloroform. The chloroform

Can. J. Chem. Downloaded from www.nrcresearchpress.com by 210.87.254.105 on 09/05/12
For personal use only.

solution was dried over $CaCl_2$ and then concentrated to a small volume. Petroleum ether (b.p. 35–65°) was added slowly to the point of turbidity and the crystallization of glycerol tris-O-*p*-nitrobenzoate allowed to proceed. Recrystallization from chloroform – petroleum ether yielded 180 mg, 86%; m.p. 195.5–196.5°, mixed melting point 195–196.5° (18).

Preparation of Enzymes

(a) UDPGal-4-epimerase.—*Saccharomyces fragilis* cells, adapted to lactose, were grown as described by Maxwell and de Robichon-Szulmajster (6) with lactose instead of galactose as the carbon source. The cells were collected by centrifugation at 5 000 × *g* for 15 min, washed twice with distilled water, dried for 24 h at room temperature with the aid of a fan, and stored at −20°. All subsequent manipulations were performed at 0–5°. Dried yeast (10 g) was extracted with 24 ml of 2.2% $(NH_4)_2HPO_4$ for 24 h, the slurry being stirred with a magnetic stirrer. The extraction mixture was centrifuged for 20 min at 37 000 × *g*. The supernate (17.5 ml) was dialyzed against two changes, 2 l each, of distilled water containing 6.8×10^{-4} *M* 2-mercaptoethanol for 24 h. The dialyzate (18.0 ml) had 0.90 ml of 1.0 *M* $MnCl_2$ added to it to precipitate the nucleic acids. After it had been allowed to stand for 20 min, the solution was centrifuged at 37 000 × *g* for 15 min. The supernate (16.2 ml) was then fractionated as described by Maxwell and de Robichon-Szulmajster (6).

(b) UDPG dehydrogenase.—This was prepared through step 5 of the procedure of Strominger *et al.* (19).

Deionization, Concentration, Chromatography, and Detection of Sugar Compounds on Paper

All deionization steps used in this study were performed with either single or mixed bed resins in the form of a column. Amberlite IR-120 (H^+ form) was used as the cation exchanger and Amberlite IR-45 (OH^- form) as the anion exchanger. All sugar solutions were concentrated under reduced pressure at 40–45° (bath temperature) by means of a rotary evaporator. Descending chromatography was carried out at room temperature on either Whatman No. 1 or No. 3MM paper with the following solvent systems: (A) pyridine – ethyl acetate – water (2:5:7) using the organic phase (20); (B) isopropyl alcohol – ammonium hydroxide – water (7:1:2) (21); (C) ethyl alcohol – 1.0 *M* ammonium acetate, pH 7.5 (5:2) (22); (D) 1-butanol – acetic acid – water (2:1:1) (23). Free sugars were detected by the alkaline $AgNO_3$ method of Trevelyan *et al.* (24), sugar phosphates by the method of Hanes and Isherwood (25) as modified by Bandurski and Axelrod (26), and nucleotides by ultraviolet absorption.

Radioactivity Determinations

Carbon-14 and tritium were determined in a liquid scintillation counter, Nuclear-Chicago Corporation, model 724. Dual isotope counting (simultaneous determinations of tritium and carbon-14 in the same sample) was accomplished by the channels ratio method (27). Each counting sample contained 0.03 ml water, 2.0 ml of absolute ethanol, and 15.0 ml of scintillator fluid (4.0 g of 2,5-diphenyloxazole (PPO) and 0.050 g of 1,4-bis-2-(5-phenyloxazolyl)-benzene (POPOP) dissolved in 1.0 l of reagent grade toluene).

Preparation of Radioactive Nucleotide Hexoses

Radioactive hexoses (D-glucose-4-T, D-glucose-1-^{14}C, D-galactose-4-T, and D-galactose-1-^{14}C) were acetylated with anhydrous sodium acetate and acetic anhydride as previously described (28). Thus, D-galactose-4-T, 11.3 mg, was dissolved in 2.7 ml of acetic anhydride, and 200 mg of anhydrous sodium acetate was added. The reaction mixture was heated at 95–100° for 2 h and then washed into 50 ml of ice water. The aqueous solution was extracted with 2 × 25-ml portions of chloroform. The chloroform layer was dried over $CaCl_2$ and concentrated *in vacuo* to a sirup which did not crystallize. Yield of pentaacetate: 95% based on radioactivity in the chloroform extract. The β-pentaacetate so formed was phosphorylated by the method of MacDonald (29). Crystalline H_3PO_4, 36 mg, was melted at 50° in a 10-ml conical flask in which the β-pentaacetate above had previously been dried. The flask was tipped to insure mixing and then evacuated by an oil pump (0.2 mm) for 2 h at 50°. The dark brown residue was dissolved in 10 ml of dry tetrahydrofuran and added to 50 ml of ice-cold *N* LiOH. A white precipitate formed immediately and, after 12–16 h, the solution was centrifuged to remove the lithium phosphate. The remaining basic solution was passed over a column of IR-120 (H^+ form) resin, and the eluate neutralized with cyclohexylamine and evaporated to dryness. After it was washed with isopropyl alcohol to dissolve the cyclohexylammonium acetate, the residue was taken up in 50% ethanol and chromatographed in solvent B for 72 h. (The sugar phosphate has an R_{Pi} 1.5 (P_i = orthophosphate).) The D-galactose 1-phosphate-4-T was eluted and the solution concentrated to a sirup which did not crystallize. Yield: 42.1% based on radioactivity. Yields varied from 27% to 42% for the sugar phosphates. The preparation of uridine diphosphate hexoses was accomplished by the procedure of Roseman *et al.* (22). Thus, 12.8 μmoles of D-galactose 1-phosphate dicylcohexylammonium salt (6.0 mg) was converted into the bis-(tri-*n*-octylammonium) salt, and this product reacted with 12.8 μmoles of uridine-5′-phosphoromorpholidate in anhydrous pyridine (5.0 ml) for 5 days. The reaction mixture was treated as described (22) and the UDPGal isolated by paper chromatography in solvent C. Yield: 8.7 μmoles as assayed enzymatically with UDPGal-4-epimerase and UDPG dehydrogenase (5, 19), 68.1%. Average yields were 65–70%. Analytical data for the radioactive uridine diphosphate hexose nucleotides prepared are given in Table I. Reducing power was determined by the method of Park and Johnson (30), acid-labile inorganic phosphate by the procedure of Fiske and Subbarow (31), and total inorganic phosphate by the method of King (32).

Can. J. Chem. Downloaded from www.nrcresearchpress.com by 210.87.254.105 on 09/05/12
For personal use only.

TABLE I

Analytical data on prepared nucleotides

Run	UDPG dehydrogenase*	Reducing power after hydrolysis†	$A_{262\,m\mu}$‡	Inorganic phosphate	
				Acid-labile†	Total§
UDPG-4-T (I)	1.03	1.04	1.00	1.02	1.97
UDPG-4-T (II)	1.02	1.01	1.00	1.03	2.03
UDPG-1-^{14}C	0.98	0.97	1.00	0.95	1.95
UDPGal-4-T	1.01	0.96	1.00	0.98	2.06
UDPGal-1-^{14}C	0.97	1.15	1.00	1.17	2.16

*UDPG and UDPGal concentrations were determined by the enzymatic method of Maxwell (5) and Strominger (19).
†Reducing power (30) and acid-labile phosphate (31) were determined after hydrolysis in 0.01 *N* HCl, 100° for 10 min.
‡The concentration was obtained from the absorbance at 262 mμ, using 10 000 as the extinction coefficient. This was set equal to 1.0 for computing the above ratios.
§Total phosphate determined by King's method (32).

Determination of Isotope Effect

UDPGal-1-^{14}C and UDPGal-4-T were mixed together to give a T/^{14}C ratio of 10:1. Each reaction tube contained the following: UDPGal, 35 mμmoles, specific activity 71 500 c.p.m./μmole of T and 7 150 c.p.m./μmole of ^{14}C; glycine buffer, pH 8.7, 40 μmoles; and 36 units of purified yeast epimerase (1.2 μg of protein) in a final volume of 0.50 ml. The reaction mixtures were incubated at 24.8° for times sufficient to obtain 8 to 100% attainment of equilibrium. The reaction was stopped by addition of 10 *N* HCl to adjust the solution to pH 2 and then heated at 100° for 10 min. The hexose mixtures were deionized and chromatographed in solvent A for 36 h on Whatman No. 1 paper. By reference to glucose and galactose markers, the areas corresponding to glucose and galactose were cut out and eluted with water. The hexose solutions were concentrated to a final volume of 0.20 ml and the T/^{14}C ratios determined on suitable aliquots in duplicate.

RESULTS AND DISCUSSION

Degradation of Tritiated Sugars

During this investigation it was important to establish the position of tritium labeling in both glucose and galactose with complete certainty. This was necessary to check the location of T in the starting materials and in the products of enzymatic reaction. Many procedures are described in the literature for the determination of ^{14}C-distribution in sugars (see, for example, Abercrombie and Jones (33)), but only four of these afford a complete determination of the labeling on a millimolar scale (33–35, 12) and none allows the location of label in carbon-bound hydrogen. Consequently, it was necessary to devise a procedure for this purpose. The procedure described here is based on the reactions of Smith and Van Cleave (18) and of Jackson and Hudson (13). Boothroyd *et al.* (12) used the reactions of Jackson and Hudson to locate the position of ^{14}C in D-glucose, while Abercrombie and Jones (33) used the reactions of Smith and Van Cleave for the same purpose. A combination of the two reaction sequences, when properly modified, can be used to locate label in each of the carbon-bound hydrogens of any pentose or hexose. The reaction sequence is unambiguous, produces crystalline derivatives in high yields, and can be applied on a millimolar scale. The results of this degradation on the tritiated D-glucose (9) and the tritiated D-galactose (36) used in these experiments are shown in Table II. In addition, the location of tritium in D-glucose, which was prepared enzymatically from tritiated D-galactose, is presented. This is the first direct proof that 4-hydrogen of galactose remains in the 4-position of the glucose. Although this 4-hydrogen has previously been shown to remain throughout epimerization in vivo and in vitro (9, 10), its precise location in the product had not been determined.

Isotope Effect Studies

The usefulness of isotope effect data in interpreting chemical reaction mechanisms is well known (37–39). In this investigation we have made use of a method described by

Can. J. Chem. Downloaded from www.nrcresearchpress.com by 210.87.254.105 on 09/05/12
For personal use only.

TABLE II

Degradation of T-labeled methyl α-D-hexosides

Position of carbon-bound H atom	Glucose-4-T*		Galactose-4-T†		Glucose-4-T‡	
	c.p.m./ mmole	% total activity	c.p.m./ μmole	% total activity	c.p.m./ mmole	% total activity
All	71 000	100	1 265	100	29 300	100
1, 2	Nil	—	Nil	—	Nil	—
3	Nil	—	Nil	—	Nil	—
4, 5, 6	71 300	100.4	1 270	100	29 250	99.8
1, 5, 6	31 500	43.6	21.8	1.7	410	1.4
5	Nil	—	—	—	—	—
6	28 400	40.2	—	—	—	—

*Synthesized from methyl 2,3,6-tri-O-methyl-D-glucopyranoside (8).
†Synthesized from 2,3,5,6-diisopropylidene-D-glucose dimethylacetal (36).
‡Obtained by enzymatic epimerization of UDPGal-4-T prepared from the D-galactose-4-T described in (36).

Collins (38) for the study of the rates of competing reactions. UDP-hexose samples, labeled either in the 4-position with T or in the 1-position with ^{14}C, were prepared. These were mixed to give a predetermined T/^{14}C ratio and this mixed sample was submitted to the action of the enzyme. It is evident that the rate of appearance of ^{14}C in the product is a measure of the rate of reaction of the species with hydrogen in the 4-position, since any ^{14}C isotope effect should be negligible. The rate of appearance of T in the product is a measure of the rate of reaction of the species with T in the 4-position. At long reaction times, when equilibrium had been attained, the T/^{14}C ratio in the product was identical with that in the starting mixture. Therefore, there is no measurable equilibrium isotope effect. If A_{eq} is defined as the T/^{14}C ratio in the starting and equilibrium UDP-hexoses and A is defined as the ratio at any point in the reaction, the ratio A/A_{eq} can be determined experimentally at any point in the reaction. A plot of A/A_{eq} versus % attainment of equilibrium, when extrapolated to 0% attainment of equilibrium, gives an estimate of the isotope effect k_T/k_H. In view of the rather involved procedures necessary to separate the products and determine T/^{14}C ratios, the reaction was run in both directions over a range of 3–100% of attainment of equilibrium to assure that any systematic errors in the separation and analysis of the products were not affecting the results. The quantity A/A_{eq} was plotted against % attainment of equilibrium and the kinetic isotope effect, k_T/k_H, at 0% of equilibrium was obtained by extrapolation[4] (Fig. 1). It is probable that many systematic errors inherent in the methods used would affect the isotope effects determined for the forward and back reactions in an opposite sense. The reasonable agreement between the two values indicates that the separation procedures do not introduce any serious error. The value of k_T/k_H obtained from a study of the forward reaction (UDPGal → UDPG) was 3.2 and that from the back reaction (UDPG → UDPGal) was 2.9.

Another approach to the determination of the isotope effect requires a relationship between A/A_{eq} and G/G_{eq}, the latter being defined as the fractional approach to equilibrium corresponding to a given value of A/A_{eq}. A treatment somewhat similar to that of Stevens and Attree (41) predicts that a plot of log $(1 - (A/A_{eq} \times G/G_{eq}))$ vs. log $(1 - G/G_{eq})$ should give a straight line which passes through the origin and whose slope is the

[4]*Collins (40) has noted, in comparing the isotopic content of the first 3–6% of the reaction product with that of the initial reactant, that the first few % of reaction product often exhibit anomalous isotope content in comparison to samples removed at intervals during the entire reaction. Thus, there is the possibility of serious error in the evaluation of both the magnitude and direction of isotope effects determined solely on the basis of the isotopic composition of the initial fraction of the reaction product. The extrapolation procedure used here would appear to be greatly preferable.*

Can. J. Chem. Downloaded from www.nrcresearchpress.com by 210.87.254.105 on 09/05/12
For personal use only.

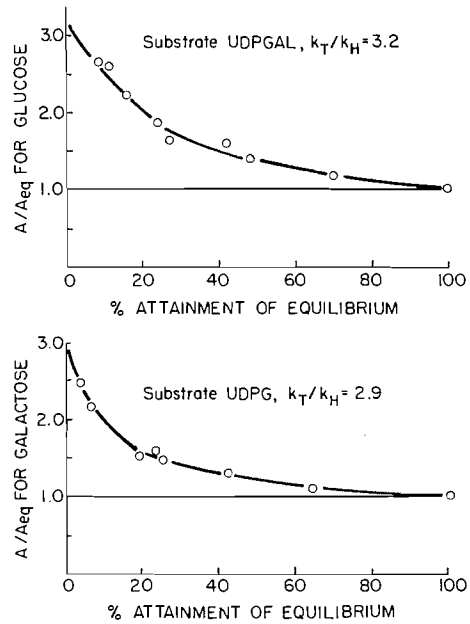

FIG. 1. The kinetic isotope effect: upper curve is A/A_{eq} obtained from glucose with the reaction run in the forward direction (UDPGal → UDPG); lower curve is A/A_{eq} obtained from galactose with the reaction run in the back direction (UDPG → UDPGal).

isotope effect k_T/k_H. The data obtained from reaction in the direction UDPG → UDPGal give a straight line plot at the lower values of log $(1 - G/G_{eq})$ which goes through the origin, but at higher values the plot develops a marked downward curvature. The slope of the straight line portion gives a value for the isotope effect of $k_T/k_H = 1.7$. The data obtained from the reaction in the direction UDPGal → UDPG give a considerable scatter of points, particularly at the higher values of log $(1 - G/G_{eq})$. The isotope effect determined from these points lies between 1.3 and 2.4, depending on the line drawn. It should be pointed out that the extrapolation procedure gives greater weight to the early points while the other procedure gives greater weight to the later points. These two sets of points are subject to a greater experimental error than the intermediate points. A possible explanation for the form of both types of plot would be that two mechanisms of reaction are involved, one of which has a large isotope effect (~3) which becomes unimportant as the reaction proceeds. Despite the element of uncertainty in the value of the isotope effect indicated by the two different methods of plotting, there can be no doubt that there is a "reverse" isotope effect and its magnitude lies somewhere between the values 1.5 and 3.0. Attempts are presently in progress to determine the value with greater precision.

Discussion of the Mechanism

The observations of an inverse isotope effect $k_T/k_H > 1.5$ allows certain conclusions to be drawn concerning the mechanism of the enzyme-catalyzed reaction. The direction and magnitude of the effect make it highly unlikely that this hydrogen is being transferred in the rate-determining step. In numerous cases sizeable normal isotope effects (k_D/k_H or $k_T/k_H < 1$) have been observed and their nature and magnitude have been discussed at length from the standpoint of theory (37–39). Primary deuterium isotope effects in the proton transfer step of the reaction:

$$\text{ethanol} + \text{NAD}^+ = \text{acetaldehyde} + \text{NADH} + \text{H}^+,$$

Can. J. Chem. Downloaded from www.nrcresearchpress.com by 210.87.254.105 on 09/05/12
For personal use only.

catalyzed by both yeast and liver alcohol dehydrogenase, have been found in the range $k_D/k_H = 0.57$ to 0.32 (42). This reaction is similar to one of the proposed mechanisms for UDPGal-4-epimerase (5). It is possible to obtain small or even inverse primary isotope effects if the hydrogen is bound more tightly in the transition state for its transfer than in the starting state (43, 44). Such a situation can occur in reactions of hydrogen atoms and in very exothermic proton transfers, but the present reaction seems to lack features that would lead to a sizeable inverse primary isotope effect explicable on this basis.

Several of the proposed mechanisms for the epimerase involve cleavage of the C—O or C—C bonds at C-4. Such reactions would involve a trigonal carbon at C-4 in the intermediate or transition state. In such cases it is to be expected that the normal compound would react 12–25% faster than the tritium-substituted compound—the commonly found α-hydrogen isotope effect (45). Specifically, the observed isotope effect would appear to eliminate cleavage of the carbon chain of the hexose as a possible mechanism, as proposed by Leloir (46), since this dictates that C-4 passes through a trigonal intermediate. Elimination and readdition of the carbon-4 hydroxyl as water, or ionization to a carbonium ion, also appear unlikely on the same basis. The assertion that these mechanisms are ruled out by the failure to observe exchange with either hydrogen or oxygen of water (2–4) is based on the assumption that the reaction site is freely available to the water in the reaction medium. If, as may well be the case, the reaction proceeds at a site from which water is excluded, then the exchange data have no bearing on the reaction mechanism. The isotope effect data, on the other hand, rule out these mechanisms regardless of the location of the active site. Small *inverse* secondary α-deuterium isotope effects have been observed for S_N2 reactions of some alkylarylsulfonates and halides (47–49). This reversal of the normal effect has been explained by steric restriction of the out-of-plane bending vibration of the hydrogen attached to the trigonal carbon in the transition state, as a result of repulsion of the entering and leaving groups. It is conceivable that an S_N2-like mechanism could explain a reverse isotope effect as large as 1.5, but a rather complex mechanism would then be required to account for the failure to exchange oxygen with the solvent. Until we have a clearer understanding of the nature of the binding to the enzyme, one cannot rule out this possible mechanism on the basis of the observed isotope effect alone.

The present results should be compared to those of Mahler *et al.* (42) obtained with alcohol dehydrogenase. As has been mentioned previously, the overall isotope effect in this reaction is normal. A more complete analysis of the kinetic data, based on postulated mechanisms, indicated that this isotope effect is not entirely associated with the proton transfer step. In particular, it appears that NADH with deuterium in the so-called α-position is preferentially bound to the enzyme. The isotope effect of the enzyme–coenzyme association is $K_D/K_H = 1.31$ for the liver alcohol dehydrogenase and about 1.4 for yeast alcohol dehydrogenase, indicating a greater constraint in the complex in both cases to the extent of 300–400 cm^{-1} increase in vibrational frequencies. Although the errors in these determinations are probably large, the isotope effects appear real. It is not clear what interactions are responsible for these isotope effects, but it does appear that binding to an enzyme molecule can produce considerable changes in vibrational frequencies.

The type of mechanism which appears to be most nearly consistent with the isotope effect we observe is one in which the carbon-4 hydrogen is transferred to some other atom in a reversible step preceding the rate-determining step. The observed effect is then the equilibrium isotope effect for this reversible step. An isotope effect of 1.6 corresponds to an increase of about 500 cm^{-1} in the total vibrational frequencies of the 4-hydrogen in the

Can. J. Chem. Downloaded from www.nrcresearchpress.com by 210.87.254.105 on 09/05/12
For personal use only.

transition state, while an isotope effect of 3.0 corresponds[5] to an increase of about 1 200 cm^{-1}. It is difficult to explain an isotope effect greater than 2.1 in the present reaction if vibrational frequencies of normal molecules are assumed to apply to enzyme-bound molecules.[6] However, the results of Mahler *et al.* suggest that larger isotope effects may be possible in enzymatic reactions. The larger estimate of our observed isotope effect might then be explained by transfer of the 4-hydrogen to a nitrogen. The lower estimate would be consistent with transfer either to oxygen or carbon, but transfer to sulfur seems definitely eliminated.

A mechanism consistent with all of the observations would be as follows:

$$E + SH \overset{K_1}{\rightleftarrows} ESH \overset{K_2}{\rightleftarrows} EH - S \underset{k_{-3}}{\overset{k_3}{\rightleftarrows}} EH - S' \overset{K_4}{\rightleftarrows} ES'H \overset{K_5}{\rightleftarrows} E + S'H.$$

Steps 2 and 4 are equilibrium hydrogen transfers to the enzyme; the rate-determining step 3 might be a reorganization of the enzyme–substrate complex which allows the hydrogen to return in the opposite configuration. The results could also be explained if the association of enzyme and substrate (K_1 and K_5) have large equilibrium isotope effects and the other steps occur with small isotope effects. Shiner *et al.* (56) have, however, observed no equilibrium isotope effect in the association of alcohol dehydrogenase with acetaldehyde bearing deuterium on the carbonyl carbon. Therefore, it is highly probable that steps 2 and 4, the equilibrium hydrogen transfers between enzyme and substrate, are associated with the reverse hydrogen isotope effect.

Recently, Wilson and Hogness (57) have reported on the UDPGal-4-epimerase from *E. coli*. This preparation has the highest specific activity yet reported for this enzyme. The difference spectrum between the enzyme plus substrate and the enzyme is very like that of NADH, but is slightly displaced toward the longer wavelengths. The data indicate that 19% of the enzyme-bound NAD is in the reduced form in the presence of the substrate. This provides evidence that, at least in the case of the *E. coli* enzyme, the mechanism involves the oxidation of the hexose to the 4-keto derivative followed by reduction to

[5]*The increase in total vibrational frequencies in the transition state was calculated from the expression (37):*

$$k_H/k_T = \exp 1/RT[(E_0^H - E_0^T) - (E_0^{H\pm} - E_0^{T\pm})],$$

where the E terms are the total zero point energies of the normal and tritiated ground and transition states. If fundamental constants are inserted, and it is assumed that

$$\nu_T \approx \sqrt{\mu_H/\mu_T}, \nu_H = \sqrt{1/2.65}\nu_H$$

for three fundamental frequencies involving the hydrogen in question, we obtain the expression

$$k_H/k_T = \exp 0.276/T\ (\sum\nu_H - \sum\nu_H^{\pm}).$$

Units of ν are cm^{-1}. The pre-exponential part of the isotope effect expression would change these calculations very slightly.

[6]*The sums of three vibrational frequencies associated with various types of hydrogen are tabulated, along with the isotope effect to be expected based on the lower frequency sum for* C—H *(tertiary). These are estimates derived from standard compilations of vibrational frequencies or from spectral analyses (50–53), and must be considered very approximate because of uncertainties resulting from the coupling of* X—H *bending modes with skeletal vibrational modes and of variations resulting from changes in structure or physical state. In particular, the tertiary* C—H *bend is uncertain. Results of this approximate calculation are in accord with available deuterium distribution data (54, 55).*

Bond	*Frequency sum*	k_T/k_H *(max)*
C—H *(tertiary)*	*5 000 – 5 600*	—
CH_2	*5 160*	*1.13*
OH *(alcohol)*	*5 100 – 5 330*	*1.32*
SH *(thiol)*	*4 100*	*0.42*
NH *(pyrrole)*	*5 110*	*1.08*
NH *(amine)*	*5 350 – 5 850*	*2.13*
NH *(ammonium)*	*5 350 – 5 570*	*1.63*

Can. J. Chem. Downloaded from www.nrcresearchpress.com by 210.87.254.105 on 09/05/12
For personal use only.

re-form the hydroxyl in the opposite configuration, NAD^+ being the hydrogen carrier involved. All previous attempts to demonstrate this type of function in the calf liver (5), yeast (6), and *L. bulgaricus* enzyme (2) led to negative results.

The higher estimate of k_T/k_H is not consistent with a transfer of the 4-hydrogen to NAD^+ as the first step of the reaction, since the transfer would be to a carbon atom and this would dictate a smaller isotope effect.[6] The lower estimate is still somewhat large for transfer to carbon, but it is possible that enzyme binding might increase the magnitude of the isotope effect. Certainly, the isotope effect data do not in any way preclude a function of NAD^+ in the sense postulated by Wilson and Hogness, since transfer of the 4-hydrogen to a nitrogen within the enzyme structure, with subsequent transfer to NAD^+, would be consistent with even the larger value of k_T/k_H. Since the enzyme catalyzes the reaction at a site on its surface that appears to exclude water, it is possible that it could transfer the equivalent of two hydrogen ions and two electrons from the substrate to form $NADH_2^+$, which would be stable in the absence of water. If the 4-hydrogen were specifically transferred to the nitrogen of NAD^+ by a mechanism of this type, then even the larger value of k_T/k_H could be accounted for by a direct transfer to NAD^+. A final possibility is, of course, that the *E. coli* enzyme utilizes a radically different mechanism than that used by the enzyme from *S. fragilis*.

REFERENCES

1. R. Caputto, L. F. Leloir, C. E. Cardini, and A. C. Palladini. J. Biol. Chem. **184**, 333 (1950); Nature, **165**, 191 (1950).
2. A. Kowalsky and D. E. Koshland, Jr. Biochim. Biophys. Acta, **22**, 575 (1956).
3. L. Anderson, A. M. Landel, and D. F. Diedrich. Biochim. Biophys. Acta, **22**, 573 (1956).
4. H. M. Kalckar and E. S. Maxwell. Biochim. Biophys. Acta, **22**, 588 (1956).
5. E. S. Maxwell. J. Biol. Chem. **229**, 139 (1957).
6. E. S. Maxwell and H. de Robichon-Szulmajster. J. Biol. Chem. **235**, 308 (1960).
7. P. M. L. Siu and H. G. Wood. J. Biol. Chem. **234**, 2223 (1959).
8. P. Kohn and B. L. Dmuchowski. Biochim. Biophys. Acta, **45**, 576 (1960).
9. R. D. Bevill, J. H. Nordin, F. Smith, and S. Kirkwood. Biochem. Biophys. Res. Commun. **12**, 152 (1963).
10. B. D. Kohn, R. C. Hoffmann, and P. Kohn. J. Biol. Chem. **238**, 1193 (1963).
11. R. D. Bevill. Ph.D. Thesis, University of Minnesota. 1964.
12. B. Boothroyd, S. A. Brown, J. A. Thorn, and A. C. Neish. Can. J. Biochem. Physiol. **33**, 62 (1955).
13. E. L. Jackson and C. S. Hudson. J. Am. Chem. Soc. **59**, 994 (1937).
14. G. R. Bartlett. J. Biol. Chem. **234**, 469 (1959).
15. E. Baer, J. M. Grosheintz, and H. O. L. Fischer. J. Am. Chem. Soc. **61**, 2607 (1939).
16. E. C. Horning and M. G. Horning. J. Org. Chem. **11**, 95 (1946).
17. W. E. Parham and H. E. Reiff. J. Am. Chem. Soc. **77**, 6391 (1955).
18. F. Smith and J. W. Van Cleave. J. Am. Chem. Soc. **77**, 3091 (1955).
19. J. L. Strominger, E. S. Maxwell, J. Axelrod, and H. M. Kalckar. J. Biol. Chem. **224**, 79 (1957).
20. E. F. McFarren, K. Brand, and H. Rutkowski. Anal. Chem. **23**, 1146 (1951).
21. D. M. Brown and A. R. Todd. J. Chem. Soc. 2040 (1953).
22. S. Roseman, J. J. Distler, J. G. Moffatt, and H. G. Khorana. J. Am. Chem. Soc. **83**, 659 (1961).
23. L. Hough, J. K. N. Jones, and W. H. Wadman. J. Chem. Soc. 1702 (1950).
24. W. E. Trevelyan, D. P. Proctor, and J. D. Harrison. Nature, **166**, 444 (1950).
25. C. S. Hanes and F. A. Isherwood. Nature, **164**, 1107 (1949).
26. R. S. Bandurski and B. Axelrod. J. Biol. Chem. **193**, 405 (1952).
27. R. W. Hendler. Dual isotope counting by channels ratio method. Preliminary Technical Bulletin, Nuclear-Chicago Corp., Des Plaines, Illinois. 1963.
28. C. S. Hudson and J. M. Johnson. J. Am. Chem. Soc. **38**, 1223 (1916).
29. D. L. MacDonald. J. Org. Chem. **27**, 1107 (1962).
30. J. T. Park and M. J. Johnson. J. Biol. Chem. **181**, 149 (1949).
31. C. H. Fiske and Y. Subbarow. J. Biol. Chem. **66**, 375 (1925).
32. E. J. King. Biochem. J. **26**, 292 (1932).
33. M. J. Abercrombie and J. K. N. Jones. Can. J. Chem. **38**, 1999 (1960).
34. I. C. Gunsalus and M. Gibbs. J. Biol. Chem. **194**, 871 (1952).
35. P. Kohn and B. L. Dmuchowski. J. Biol. Chem. **235**, 1867 (1960).
36. B. D. Kohn and P. Kohn. J. Org. Chem. **28**, 1037 (1963).
37. L. Melander. Isotope effects on reaction rates. The Ronald Press Co., New York. 1960.
38. C. J. Collins. *In* Advances in physical organic chemistry. Vol. 2. *Edited by* V. Gold. Academic Press, London and New York. 1964. p. 74.

Can. J. Chem. Downloaded from www.nrcresearchpress.com by 210.87.254.105 on 09/05/12
For personal use only.

39. N. GRELL (*Editor*). Pure Appl. Chem. **8**, 215 (1964).
40. V. F. RAAEN, T. K. DUNHAM, D. D. THOMPSON, and C. J. COLLINS. J. Am. Chem. Soc. **85**, 3497 (1963).
41. W. H. STEVENS and R. W. ATTREE. Can. J. Res. B, **27**, 807 (1949).
42. H. R. MAHLER, R. H. BAKER, JR., and V. J. SHINER, JR. Biochemistry, **1**, 47 (1962).
43. F. A. LONG and J. BIGELEISEN. Trans. Faraday Soc. **55**, 2077 (1959).
44. J. BIGELEISEN. J. Chem. Phys. **17**, 675 (1949).
45. A. STREITWIESER, R. H. JAGOW, R. C. FAHEY, and S. SUZUKI. J. Am. Chem. Soc. **80**, 2326 (1958).
46. L. F. LELOIR. *In* F. F. Nord. Advan. Enzymol. **14**, 193 (1953).
47. K. T. LEFFEK, J. A. LLEWELLYN, and R. E. ROBERTSON. J. Am. Chem. Soc. **82**, 6315 (1960).
48. J. A. LLEWELLYN, R. E. ROBERTSON, and J. M. W. SCOTT. Chem. Ind. London, 732 (1959).
49. R. R. JOHNSON and E. S. LEWIS. Proc. Chem. Soc. 52 (1958).
50. K. NAKANISHI. Infrared absorption spectroscopy. Holden-Day, Inc., San Francisco. 1962.
51. C. N. R. RAO. Chemical applications of infrared spectroscopy. Academic Press, New York. 1963.
52. L. J. BELLAMY. The infrared spectra of complex molecules. John Wiley and Sons, Inc., New York. 1958.
53. S. A. BARKER, E. J. BOURNE, M. STACEY, and D. H. WHIFFEN. J. Chem. Soc. 171 (1954).
54. V. GOLD and D. P. N. SATCHELL. Quart. Rev. London, **9**, 57 (1955).
55. C. G. SWAIN and M. M. LABES. J. Am. Chem. Soc. **79**, 1084 (1957).
56. V. J. SHINER, JR., H. R. MAHLER, R. H. BAKER, JR., and R. R. HIATT. Ann. N.Y. Acad. Sci. **84**, 583 (1960).
57. D. B. WILSON and D. S. HOGNESS. J. Biol. Chem. **239**, 2469 (1964).

Can. J. Chem. Downloaded from www.nrcresearchpress.com by 210.87.254.105 on 09/05/12
For personal use only.

Can. J. Chem. Downloaded from www.nrcresearchpress.com by 210.87.254.6 on 09/05/12
For personal use only.

CONFORMATIONAL STUDIES ON SYNTHETIC POLY-α-AMINO ACIDS: THE HELICAL SENSE OF POLY-L-TRYPTOPHAN: OPTICAL ROTATORY DISPERSION STUDIES[1]

GERALD D. FASMAN,[2] MARGARETE LANDSBERG, AND MANUEL BUCHWALD[3]
Graduate Department of Biochemistry,[4] Brandeis University, Waltham, Massachusetts
Received November 13, 1964

Dedicated to Professor R. B. Sandin on the Occasion of his Sixty-Eighth Birthday

ABSTRACT

The synthesis of high molecular weight (100 000 to 200 000) polymers and copolymers of L-tryptophan and γ-benzyl-L-glutamate is reported. The optical rotatory dispersion (o.r.d.) of these polypeptides is recorded in the wavelength range 540–320 mμ and the b_0 values of the Moffitt equation, using $\lambda_0 = 212$ mμ, are listed. Poly-L-tryptophan has a b_0 value of +570 in dimethylformamide (DMF). A linear relationship exists between this value, b_0 values of copolymers of various ratios of L-tryptophan and γ-benzyl-L-glutamate, and the value of −670 found for poly-γ-benzyl-L-glutamate. The o.r.d. curve of a poly-L-tryptophan film, in the 330–200 mμ wavelength range, reveals two positive Cotton effects in the 270–290 mμ region and a large negative Cotton effect at 233 mμ. Thus, despite the positive b_0 value, these data prove that poly-L-tryptophan, in DMF, has the right-handed helical conformation. Hypochromicity was found for the tryptophanyl residue in the helical polypeptide. The rotatory contribution of chromophores, such as tryptophan or coenzymes, when bound asymmetrically to a protein, can be very significant, and caution is advised in the interpretation of such o.r.d. curves.

Optical rotatory dispersion (o.r.d.) measurements have become extensively used to determine the conformation of proteins (1, 2, 3). The anomalous rotatory dispersion curves for many synthetic poly-α-amino acids and proteins in the helical conformation have been adequately interpreted by the Moffitt equation (4, 5) $[m']_\lambda = a_0\lambda_0^2/(\lambda^2 - \lambda_0^2) + b_0\lambda_0^4/(\lambda^2 - \lambda_0^2)^2$. Although it is acknowledged that this treatment of o.r.d. data is of a highly empirical nature, the constant b_0 in this equation has been successfully used as a measure of the helical content in polypeptides and proteins. The b_0 value of approximately −630 to −670 ($\lambda_0 = 212$ mμ) has been found for the 100% right-handed helical conformation (5, 6), while the random coil form has a b_0 value of zero (6). The sign of the b_0 has been taken to indicate the sense of helix, and has been corroborated by X-ray studies (7). Estimates of helical content derived from o.r.d. data (8, 9) agree remarkably well with X-ray data for myoglobin (10). More recently a modified Drude equation (11) has been proposed to estimate helical contents in polypeptides based on o.r.d. studies penetrating further into the ultraviolet region. However, this treatment is theoretically inadequate, as a new Cotton effect has since been discovered (Holzwarth and Doty (12) have shown that the 233 mμ Cotton effect is a composite of two such bands and that two circular dichroism bands are responsible for this Cotton effect, one caused by a $n \rightarrow \pi^*$ transition and the other caused by a $\pi \rightarrow \pi^*$ transition), which likewise places

[1]*This work was supported in part by research grants from the National Science Foundation (GB-428), the National Institutes of Health (AM-05852), and the American Heart Association (61F7E). A preliminary report of this work was presented at the Sixth International Congress of Biochemistry, New York, 1964.*
[2]*This work was done during the tenure of an Established Investigatorship of the American Heart Association. Inquiries regarding this article should be sent to G. D. F.*
[3]*Charles Revson Fellow.*
[4]*Contribution No. 348.*

this approach in the empirical category. Consequently, the Moffitt equation will be adhered to in this paper.

Positive b_0 values have been reported for a variety of polymers of D-amino acids and for poly-β-benzyl-L-aspartate (13), poly-L-tyrosine (14), and poly-L-tryptophan (15). Poly-β-benzyl-L-aspartate has been shown to exist as a left-handed helix by two research groups (16). However, poly-L-tyrosine was shown by o.r.d. studies (17, 18) and circular dichroism (19) studies to be a right-handed helix. Consequently, the positive b_0 value must be due to the contribution of the chromophoric side chains on the β-carbon which contributes to the rotation in the visible region of the spectrum.

Sela *et al.* (15) have reported a b_0 value of +410, in dimethylformamide (DMF), for poly-L-tryptophan. The study reported herein was undertaken to establish the sense of the helix of poly-L-tryptophan.

Poly-L-tryptophan was first prepared by Patchornik *et al.* (20). Polymers with average molecular weights of 17 000 (η_{sp}/c = 0.08, 0.2% in DMF) were obtained. As their method for the preparation of N-carboxy-L-tryptophan anhydride (L-tryptophan-NCA) did not readily yield pure anhydride, and since the reported molecular weights were low for definitive conformational studies, a new anhydride preparation is reported. The scheme of preparation is seen in Fig. 1. This method yields polymers with reduced specific vis-

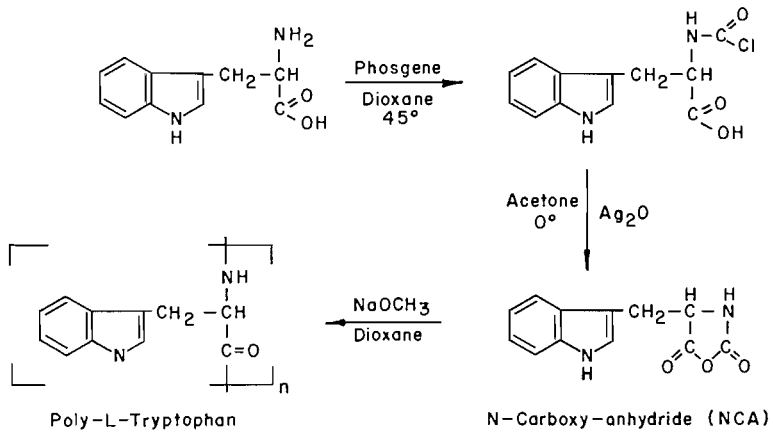

FIG. 1. Synthesis of poly-L-tryptophan.

cosities as high as 1.69 (0.2% in DMF) with weight average molecular weights estimated to be 123 000 (see below). Polymers of even greater molecular weights were completely insoluble in DMF. Poly-L-tryptophan was found to be extremely insoluble in most organic solvents. Dimethyl sulfoxide (DMSO) was found to be a suitable solvent; however, it appears to cause disruption of the secondary structure (see below).

In the following study the synthesis and the o.r.d. behavior of high molecular weight copolymers of various mole ratios of γ-benzyl-L-glutamate and L-tryptophan are reported to evaluate the sense of helix of poly-L-tryptophan, in the manner previously reported by Karlson *et al.* (16).

RESULTS

Poly-L-tryptophan was synthesized by the polymerization of L-tryptophan-NCA in dioxane (4%) by initiation with sodium methoxide (A/I = 50) (21). Poly-γ-benzyl-L-glutamate (PBLG) was prepared by the polymerization of γ-benzyl-L-glutamate-NCA

Can. J. Chem. Downloaded from www.nrcresearchpress.com by 210.87.254.6 on 09/05/12
For personal use only.

(21) in benzene, by initiation with $NaOCH_3$, A/I = 200. Copolymers of various mole ratios were prepared by dissolving each NCA in the solvent used for the synthesis of the homopolymer and mixing the two in the appropriate ratio. In Table I are listed some

TABLE I

Physical and optical properties of polymers and copolymers of L-tryptophan and γ-benzyl-L-glutamate

Polymer No.	Composition BLG*	Composition TRYP†	A/I‡	η_{sp}/c§	η_{sp}/c‖	Mol. wt.¶	b_0**	λ_c††
In dimethylformamide (DMF)								
GF-10-145-12	100	0	200	6.3	1.56	138 000	−670	
GF-11-179-16	90	10	25	0.83		98 000	−540	
GF-11-181-19	80	20	25	1.90	1.05	150 000	−390	
GF-11-213-17	50	50	10	1.09		107 500	0	
GF-11-207-17	20	80	10	1.69		127 500	+345	
GF-11-163-17	10	90	25	3.51	1.16	172 800	+475	
GF-11-65-16	0	100	50	1.69		123 000	+570	230
In dimethyl sulfoxide								
GF-11-65-16	0	100	50				0	190

*γ-Benzyl-L-glutamate.
†Tryptophan.
‡Anhydride/initiator ratio.
§Specific viscosity in DMF (0.2%).
‖Specific viscosity in DCA (0.2%). Specific viscosity of various PBLG samples in DMF and DCA (0.2%): 0.2, 0.23; 0.31, 0.27; 0.52, 0.51; 1.05, 0.72; 1.64, 0.92; 2.8, 1.1; 7.95, 1.74; 18.7, 2.55.
¶Weight average molecular weight.
**b_0 obtained from Moffitt–Yang plots, in the wavelength range 540–320 mμ, using λ_0 = 212 mμ, concentration 0.1 to 0.15% DMF in a 1-cm cell, at 24°.
††λ_c obtained from a Drude plot.

physical and optical properties of the polymers and copolymers, the conditions of polymerization, and their estimated weight average molecular weights. The viscosities of poly-L-tryptophan and the copolymers could not be determined with confidence in dichloroacetic acid (DCA) because of the immediate destruction of the indole moiety by this solvent, as indicated by gross discoloration of the solutions. Their viscosities were therefore determined in DMF and these values correlated with values obtained in DCA for a series of PBLG polymers of various molecular weights in both DMF and DCA. The weight average molecular weights of PBLG polymers, determined by viscosities in DCA, has previously been published (22). The molecular weights were estimated to be in the 100 000 to 172 000 range.

The o.r.d. of this set of polymers was determined in DMF, a helix-promoting solvent (1), over the wavelength range 350–540 mμ (Fig. 2). It can be seen that the dispersion changes from the negative curve for helical PBLG to an increasingly more positive one as the tryptophan mole ratio is increased. With these data, b_0 values were calculated using λ_0 = 212 mμ (Table I). The b_0 value for helical PBLG in DMF was found to be −670, agreeing with the value previously reported (5). The b_0 value for poly-L-tryptophan was found to be +570. The discrepancy with the value (+410) previously reported (15) may be due to the much larger molecular weight of the polymer used in this study (120 000 vs. the 18 000 in the previous study). The b_0 values vary linearly from +570 for poly-L-tryptophan to −670 for PBLG (Fig. 3). This indicates that the same helical sense is maintained in these copolymers, namely a right-handed helix. If poly-L-tryptophan and PBLG were helices of the opposite sense of twist, the b_0 value of their copolymers should change markedly over a relatively narrow range of copolymers, representing a region of transition from one helical sense to the other, as found for copolymers of β-benzyl-L-aspartate and γ-benzyl-L-glutamate (16). However, as seen here, this does not

Can. J. Chem. Downloaded from www.nrcresearchpress.com by 210.87.254.6 on 09/05/12
For personal use only.

Can. J. Chem. Downloaded from www.nrcresearchpress.com by 210.87.254.6 on 09/05/12
For personal use only.

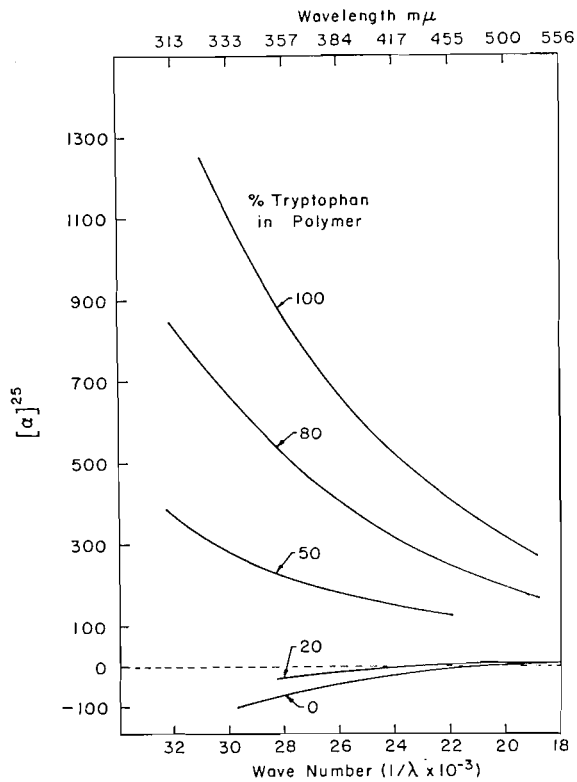

FIG. 2. Optical rotatory dispersion of copolymers of L-tryptophan and γ-benzyl-L-glutamate in dimethylformamide. Conditions given in Experimental section.

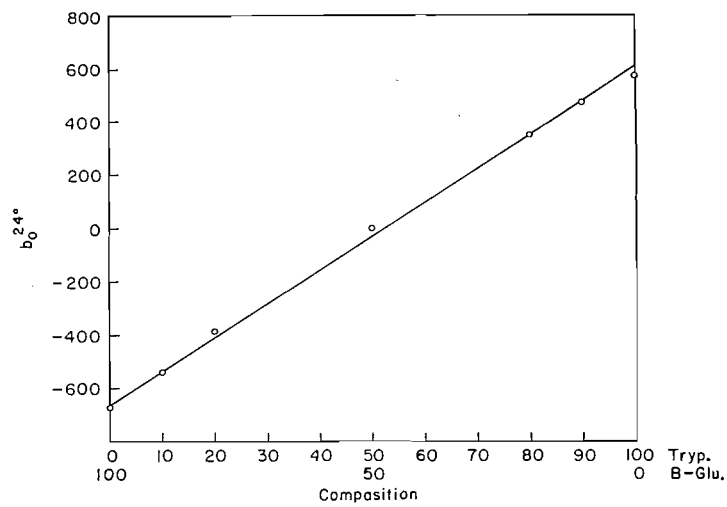

FIG. 3. b_0 values of polymers and copolymers of L-tryptophan and γ-benzyl-L-glutamate in dimethylformamide. Tryp = tryptophan; B-Glu = γ-benzyl-L-glutamate. The b_0 values obtained from the Moffitt equation, using $\lambda_0 = 212$ mμ. See Table I for conditions used.

occur, but rather a gradual b_0 change is seen, at any one point the b_0 being the sum of the mole ratio contribution of the two different b_0 values. Thus, the behavior of the tryptophan copolymers resembles that of the tyrosine copolymers (17). Both of these aromatic amino acids contain a strong chromophoric group on the β-carbon, in close proximity to the peptide bond chromophore, and it is this aromatic chromophore whose rotatory dispersion contribution predominates in the visible and is responsible for the positive b_0 values.

It was hoped that one could investigate the 233 mμ region, where a large negative Cotton effect was found by Simmons *et al.* (23) for the right-handed helical conformation of polypeptides. Such o.r.d. and circular dichroism studies of poly-L-tyrosine (18, 19) in aqueous media revealed this negative Cotton effect and circular dichroic band, further confirming the right-handed sense of the helix of this polymer. The optical rotation of solutions of poly-L-tryptophan in DMF could only be determined down to 300 mμ because of the absorbance of the solvent, and no other transparent helix-promoting solvent for this polymer could be found. In dimethyl sulfoxide, a more transparent solvent, the polymer had a b_0 value of zero, indicating a random conformation. However, films of poly-L-tryptophan could be investigated in the ultraviolet region.

L-Tryptophan was first examined in aqueous media, at pH 6.2, and the o.r.d. curve is seen in Fig. 4. A small positive Cotton effect, $[m'] = +186$, in the 290 mμ region is followed by a larger but yet small negative Cotton effect with its trough at approximately 276 mμ. The molar rotation of the latter trough is $-1\,600$, in comparison with the $-14\,000$ to $-18\,000$ value for a helical polymer at 233 mμ (23, 24). The optical rotation of poly-L-tryptophan at these lower wavelengths was measured on films on the optical face of quartz cells. These films were transparent throughout the whole range of the Bendix spectropolarimeter. The o.r.d. of such a film is seen in Fig. 5. When films were prepared so that at 300 mμ the direction of the rotation was the same as that of the DMF solution, a sharp negative trough was observed at approximately 233 mμ, similar in sign to those observed with solutions of PBLG in the helical conformation. It is significant that the trough in poly-L-tryptophan is at 233 mμ, while the monomer trough was found at 276 mμ. The $[m']_{233}$ is negative in the polymer and the wavelength of this trough is that found for the peptide helical conformation. This trough in the o.r.d. of the helical polymer is probably much larger than that of the monomer, and thus the latter trough is probably obliterated. The small trough at 276 mμ found in the monomer is due to the indole chromophore on the β-carbon atom next to the asymmetric center of the amino acid. Thus, the sign and the position of the Cotton effect in the polymer are what one would expect for a right-handed helix. The observed rotation, rather than the molar rotation, has been shown because the thickness of a film is difficult to calculate accurately. Also seen in Fig. 5 (the broken line) is the absorption spectrum of the film. One other notable feature of the o.r.d. curve is the multiple Cotton effect in the 270–300 mμ region. An expanded view of this region is seen in Fig. 6. The monomer shows only one Cotton effect in this region, with a peak at 296 mμ. The polymer has two peaks, at 296 mμ and 288 mμ. The absorption spectrum in this region shows several shoulders, indicating either more than one electronic transition or vibrational structure. The fact that several Cotton effects are observed in the helical conformation in both poly-L-tryptophan and poly-L-tyrosine may indicate interaction between residues in the helical conformation, thus bringing about either a resonance exciton interaction phenomenon or an enhancement of the contribution of the several vibrational states. Such interactions have been implicated to explain the excimer fluorescence bands found in helical poly-L-tyrosine (25).

Can. J. Chem. Downloaded from www.nrcresearchpress.com by 210.87.254.6 on 09/05/12
For personal use only.

Can. J. Chem. Downloaded from www.nrcresearchpress.com by 210.87.254.6 on 09/05/12
For personal use only.

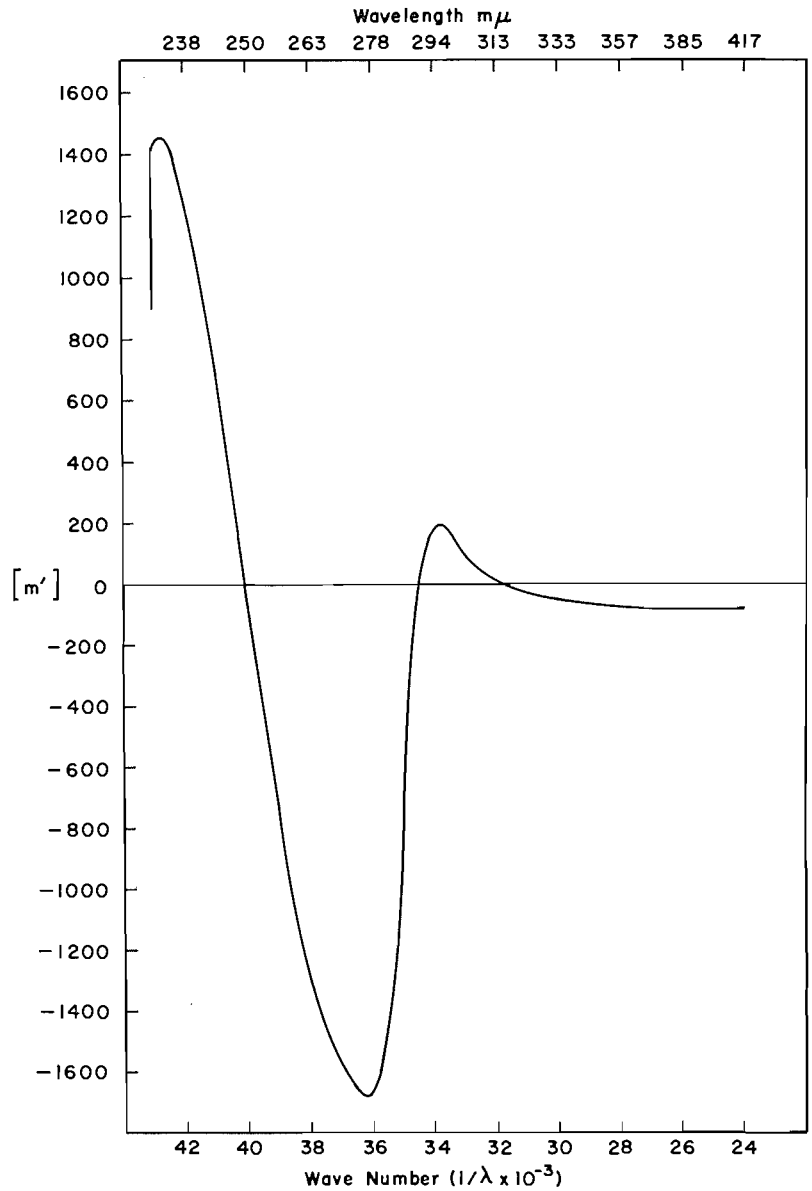

FIG. 4. The optical rotatory dispersion of L-tryptophan in H_2O at pH 6.2. [m'] is mean residue rotation. Concentration, ≃0.04%. Path length: 1 cm in 400–300 mμ range; 1 mm in 300–233 mμ range.

Another optical phenomenon frequently observed in interacting asymmetric systems is hypochromism. Thus, DNA has been found to be hypochromic in the helical conformation compared to the random state (26). In polycytidylic acid, hypochromism was observed in a double-stranded hydrogen-bonded helical structure, as well as in the single-stranded base-stacked helix (27). The extinction coefficient of the peptide absorption band at 190 mμ has also been shown to be conformation dependent (28). Thus, one might anticipate hypochromism in helical poly-L-tryptophan, and such is the case. In DMF the molar

Can. J. Chem. Downloaded from www.nrcresearchpress.com by 210.87.254.6 on 09/05/12
For personal use only.

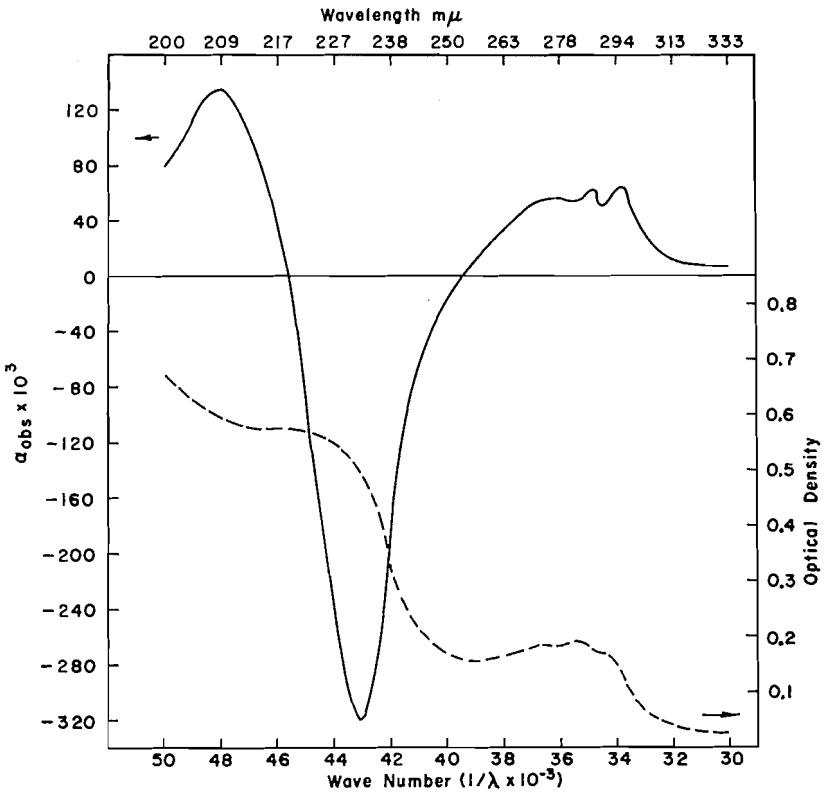

FIG. 5. The optical rotatory dispersion and ultraviolet absorption spectrum of a poly-L-tryptophan film. $\alpha_{observed}$ and optical density vs. wavelength.

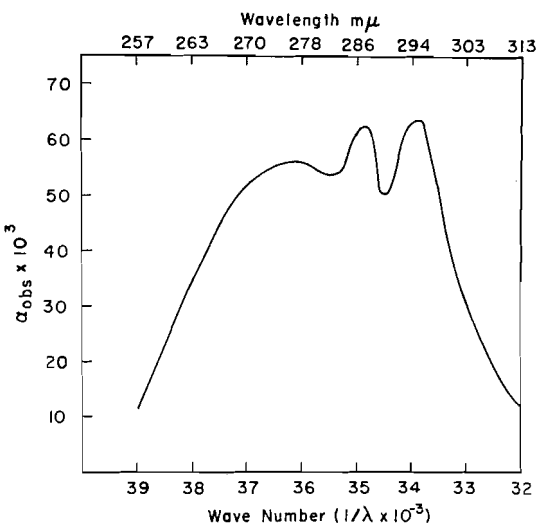

FIG. 6. The optical rotatory dispersion of a poly-L-tryptophan film. An expanded scale of wavelength range 313–257 mμ of film seen in Fig. 5.

extinction coefficient of the helical polymer is $5.58 \pm 0.025 \times 10^3$ at 283 mμ, while that of N-acetyl-L-tryptophan ethyl ester is $6.31 \pm 0.045 \times 10^3$ at 283 mμ. Thus, the hypochromism would further indicate indole–indole interactions. This interaction is also indicated by the low quantum fluorescence yield found for this polypeptide (29). In DMSO, where the polymer was thought to be random, the molar extinction coefficient was found to be 5.9×10^3 (288 mμ), while N-acetyl-L-tryptophan ethyl ester had a molar extinction coefficient of 6.2×10^3 (283 mμ). These values would indicate that the polymer exhibits hypochromicity in DMSO but not quite so large as found in DMF. This would imply that some secondary structure still persists in DMSO. These values for the molar extinction coefficient disagree with those published previously (30). However, as in the case of the b_0 value, the values were obtained with low molecular weight polymers that probably have an insufficient degree of polymerization to maintain a stable secondary structure.

A comment regarding the reported optical titration of poly-L-tryptophan in DMF with DCA (15) is in order. A sharp change in $[\alpha]_{546}^{20}$ occurred between 40–60% (by volume) DCA–DMF. A conformational transition was implied. However, the solvent properties of DMF–DCA (31) mixtures must be evaluated before the above conclusion can be accepted. In DMF–DCA mixtures the viscosity of the solutions increased as DCA was added to DMF until a DCA–DMF (75:25 v/v) composition was reached, and then the viscosity decreased again upon further addition of DCA. This maximum in the viscosity is consistent with the formation of complexes between the two components (32). Similar behavior has been reported for the systems water–dimethylacetamide (33) and DMF–H_2SO_4 (34). Thus, the solvents used in the optical titration are interacting and doubts can be raised concerning the interpretation of the changes in rotation.

SUMMARY

It has been shown that poly-L-tryptophan, despite its positive b_0 value, is a right-handed helix. This is concluded from the linear b_0 relationship of copolymers with γ-benzyl-L-glutamate and the observation of the negative 233 mμ Cotton effect usually found in right-handed helical polypeptides. The additional Cotton effect in the polymer in the 270–300 mμ region, compared to the monomer, and the hypochromism found, probably indicate a conformational-dependent interaction between indole residues, which probably stack in a helical array, or interact with the backbone peptide bonds.

This study also illustrates that great caution should be exercised in the interpretation of an altered b_0 value by the interaction of a chromophore, such as a coenzyme, with an asymmetric molecule, e.g. with an enzyme. A change in b_0 produced by the binding of a chromophore to an asymmetric region does not necessarily imply a conformational change and can be caused by conditions similar to the case studied herein. Such binding produces Cotton effects that may dominate the rotations far from the absorption maximum of the bound moiety and yield misleading b_0 values.

EXPERIMENTAL

Methods

Measurements of the optical rotation of the polymers in DMF* solutions were performed with two polarimeters. For copolymers with less than 20 mole % tryptophan a Rudolf high-precision photoelectric spectropolarimeter, model 800/200AS/759, equipped with a Beckman DU monochromator was used. The light source was a Hanovia (Newark, New Jersey) 150-W d-c. Xenon arc (No. 901C1), cooled by means of a water-jacketed housing. The symmetrical angle used was 3.5° and the wavelength range investigated was

**Reagent grade, Spectro quality, Matheson Coleman and Bell.*

Can. J. Chem. Downloaded from www.nrcresearchpress.com by 210.87.254.6 on 09/05/12
For personal use only.

365–589 mμ. Polarimeter tubes of 1 or 2 dm path length were used with concentrations of about 0.5% of the polymer. For copolymers containing more than 20 mole % tryptophan a Bendix–Ericcson Polarimatic-62 automatic spectropolarimeter* with a 150-W d-c. Xenon arc (No. 901C1 Hanovia) was used. The dispersions were performed with a slit of 1 mm. The recorder attachment employed was a Sargent recorder model SR. One-centimeter fused quartz cells were used, having been selected for minimal birefringence.† Concentrations used were in the range 0.10–0.15% and readings were taken in the range 500–300 mμ. Films were made by placing a drop of a dilute DMF polymer solution on the optical face of a 1-mm quartz cell and evaporating the solvent under reduced pressure. All measurements were made at 24°.

Calculation of Rotatory Data

In the spectral region 300–600 mμ, the coefficient, b_0, of the second term in the Moffitt equation (4)

$$[m']_\lambda = \frac{a_0\lambda_0^2}{\lambda^2 - \lambda_0^2} + \frac{b_0\lambda_0^4}{(\lambda^2 - \lambda_0^2)^2}$$

was derived from the slope of the plot $[m'][\lambda^2 - \lambda_0^2]$ vs. $[\lambda^2 - \lambda_0^2]^{-1}$ as suggested by Moffitt and Yang (5). The refractive index dispersion of DMF was obtained from tables (3). The value of $\lambda_0 = 212$ mμ was used. The o.r.d. data in Fig. 4 are expressed in terms of $[m']_\lambda$, the reduced mean residue rotation (1, 3), defined as

$$[m']_\lambda = [\alpha]_\lambda\left(\frac{\text{m.r.w.}}{100}\right)\left\{\frac{3}{n_\lambda^2 + 2}\right\},$$

where $[\alpha]_\lambda$ is the specific rotation at wavelength λ, m.r.w. is the mean residue weight, and n_λ is the refractive index of the solvent at wavelength λ.

Viscometry

Reduced specific viscosities were determined at a concentration of 0.2 g/100 cc in Cannon-Fenske Ostwald viscometers with flow time always exceeding 90 s. All measurements were made at 25 ± 0.1°.

Absorbance Measurements

Optical density measurements were made on a Cary model 14 recording spectrophotometer. For the determination of the molar extinction coefficients, concentrations of $\simeq 1.5 \times 10^{-4}$ *M* were used in a 1-cm cell.

L-*Tryptophan-N-carboxyanhydride*

Nitrogen was passed through dioxane‡ (500 ml) for 90 min in a three-necked 100-ml round-bottomed flask fitted with a thermometer, a gas inlet tube, and a reflux condenser with a gas outlet tube. L-Tryptophan (Calbiochem. grade A) (10 g, 0.049 mole) was added with stirring. Phosgene, first passed through H_2SO_4, was bubbled through the stirred solution, which was kept at 40°, for 90 min. The condenser was removed and dry nitrogen was passed through the clear colored solution (kept at 30 to 35°) until the solution was phosgene free. The solvent was removed on a rotatory evaporator at 40°. The resulting oil was dissolved in dry acetone§ (100 ml) and evaporated to dryness. The oil was dissolved in dry acetone (200 ml) Ag_2O (30 g), celite (15 g), and steel balls (2 doz) were added and the mixture rolled in a 2-l polyethylene bottle for 24 h at 4°. The solution was filtered through celite and the acetone was removed under reduced pressure (temperature maintained at 40°), yielding a thick oil. The oil was dissolved in dry ethyl acetate (400 ml), and *n*-hexane (1 600 ml) was added to the solution, causing heavy opalescence. The solution was then filtered through celite and the filtrate was placed at −20°. When the solution had cooled, *n*-hexane (100 ml) was added, causing crystallization. *n*-Hexane (1 200 ml) was added in several portions. The slightly colored crystals (6 g) were dissolved in ethyl acetate (240 ml), *n*-hexane (660 ml) was added to opalescence, the solution was filtered through celite, and *n*-hexane (2 000 ml) was added to the filtrate in several portions. L-Tryptophan-NCA crystallized out when the solution was allowed to stand at −20°. The crystals were filtered and dried *in vacuo* (1 mm Hg) at −20°, m.p. 145–146° (corrected). Yield: 4 g (35.2%). The supernatants yielded another 2.2 g of crystals. Total yield: 55%.

Anal. Calcd. for $C_{12}H_{10}O_3N_2$: C, 62.61; H, 4.38; N, 12.17. Found: C, 62.3; H, 4.3; N, 12.1.

*Poly-*L*-tryptophan*

L-Tryptophan-NCA (0.202 g, 8.70×10^{-4} mole) was dissolved in a dry dioxane (5 ml) by warming. Sodium methoxide (0.047 ml of 0.373 *N*, A/I = 50) was added with stirring, and the solution allowed to stand for 3 days, after which time the polymer had precipitated out of the viscous solution. The polymer was isolated by pouring the reaction mixture into anhydrous ether (25 ml), washed 3 times with anhydrous ether, and dried at 80° for 2 h *in vacuo* (1 mm Hg). Yield: 0.15 g (93%). $\eta_{sp}/c = 1.69$ ($c = 0.2\%$ in DMF).

**Manufactured by the Bendix–Ericcson U.K. Ltd. and distributed in the United States by the Bendix Corporation, Cincinnati Division, Cincinnati 8, Ohio.*

†*Optical Cell Co., Brentwood, Maryland.*

‡*Purified by the method described by Fieser (35).*

§*Purified by refluxing over* $KMnO_4$, *drying over anhydrous* K_2CO_3, *and distilling.*

Can. J. Chem. Downloaded from www.nrcresearchpress.com by 210.87.254.6 on 09/05/12
For personal use only.

Poly-L-tryptophan is insoluble in trifluoroethanol, methanol, acetonitrile, and dioxane. Higher molecular weight polymers were also insoluble in DMF.

Poly-γ-benzyl-L-glutamate

γ-Benzyl-L-glutamate-NCA (36) (0.6 g, 2.28×10^{-3} mole) was dissolved in dry benzene (1%) by warming. Sodium methoxide (0.355 ml, 0.355 *N*, A/I = 200) was added and the solution allowed to stand for 3 days. The polymer was isolated and treated in the same manner as poly-L-tryptophan. $\eta_{sp}/c = 6.3$ ($c = 0.2\%$ in DMF); $\eta_{sp}/c = 1.5$ ($c = 0.2\%$ DCA).

Copolymers of γ-Benzyl-L-glutamate and L-Tryptophan

Example: Copoly (γ-BLGlu:L-Tryp) (90:10). γ-Benzyl-L-glutamate-NCA (0.183 g, 6.95×10^{-4} mole), dissolved by warming in dry benzene (18 ml), was mixed with L-tryptophan-NCA (17.7 mg, 7.73×10^{-5} mole) and dissolved in dry dioxane (1.8 ml). The polymerization was initiated by the addition of sodium methoxide (0.09 ml, 0.345 *N*, A/I = 25) and the reaction mixture was allowed to stand for 2 days. The slightly viscous solution was slowly added to 5 times its volume of *n*-hexane with stirring. The polymer, which separated out as a fibrous material, was lyophilized from dioxane and dried under vacuum (1 mm Hg) at 80° for 2 h. Weight = 0.106 g; yield, 64%. $\eta_{sp}/c = 0.8$ ($c = 0.2\%$ DMF).

The other copolymers of γ-benzyl-L-glutamate and L-tryptophan were prepared in the same manner by varying the mole ratios of the two anhydrides. γ-Benzyl-L-glutamate-NCA (1% in benzene) and tryptophan-NCA (1% in dioxane) were mixed to yield the following compositions: 90:10, 80:20, 50:50, 20:80, 10:90. The copolymers (γ-benzyl-L-glutamate:L-tryptophan, 20:80 and 50:50) (both at A/I = 25) were not soluble in DMF ($c = 0.2\%$); so the A/I was decreased to 10. The conditions of polymerization, the viscosities, the estimated weight average molecular weights, and the optical properties are listed in Table I.

Poly-L-tryptophan Films

A few milligrams of polymer were dissolved in ca. 1 cc of DMF by heating the mixture on a steam bath for several hours. The solution was filtered through a sintered-glass funnel (medium porosity). A drop of the solution was placed on the outside optical surface of a 1-mm fused quartz cell and the cell placed in a vacuum desiccator which was evacuated on a water aspirator. The solution slowly evaporated, leaving a polymer film. The observed rotation varied according to the cell position. This was probably due to the uneven thickness of the film or to orientation of the film as it dried.

REFERENCES

1. P. URNES and P. DOTY. Advan. Protein Chem. **16**, 401 (1961).
2. E. R. BLOUT. *In* Optical rotatory dispersion. *Edited by* C. Djerassi. McGraw-Hill, New York. 1960. Chap. 17.
3. G. D. FASMAN. *In* Methods in enzymology. Vol. 6. *Edited by* S. P. Colowick and N. O. Kaplan. Academic Press, Inc., New York. 1963. p. 928.
4. W. MOFFITT. J. Chem. Phys. **25**, 467 (1956).
5. W. MOFFITT and J. T. YANG. Proc. Natl. Acad. Sci. U.S. **42**, 596 (1956). W. MOFFITT. Proc. Natl. Acad. Sci. U.S. **42**, 736 (1956).
6. J. T. YANG and P. DOTY. J. Am. Chem. Soc. **79**, 761 (1957).
7. A. ELLIOTT, W. E. HANBY, and B. R. MALCOLM. Nature, **180**, 1340 (1957).
8. P. URNES, K. IMAHORI, and P. DOTY. Proc. Natl. Acad. Sci. U.S. **47**, 1635 (1961).
9. S. BEYCHOK and E. R. BLOUT. J. Mol. Biol. **3**, 769 (1961).
10. J. C. KENDREW, H. C. WATSON, B. E. STRANDBERG, R. E. DICKERSON, D. C. PHILLIPS, and U. C. SHORE. Nature, **190**, 666 (1961).
11. E. SHECTOR and E. R. BLOUT. Proc. Natl. Acad. Sci. U.S. **51**, 695 (1964).
12. G. HOLZWARTH and P. DOTY. J. Am. Chem. Soc. **87**, 218 (1965).
13. E. R. BLOUT and R. H. KARLSON. J. Am. Chem. Soc. **80**, 1259 (1958).
14. A. ELLIOTT, W. E. HANBY, and B. R. MALCOLM. Nature, **180**, 1340 (1957). A. R. DOWNIE, A. ELLIOTT, and W. E. HANBY. Nature, **183**, 110 (1959). J. D. COOMBES, E. KATCHALSKI, and P. DOTY. Nature, **185**, 534 (1960).
15. M. SELA, I. Z. STEINBERG, and E. DANIEL. Biochim. Biophys. Acta, **46**, 433 (1961).
16. R. H. KARLSON, K. S. NORLAND, G. D. FASMAN, and E. R. BLOUT. J. Am. Chem. Soc. **82**, 2268 (1960). E. M. BRADBURY, A. R. DOWNIE, A. ELLIOTT, and W. E. HANBY. Proc. Roy. Soc. London Ser. A, **259**, 110 (1960).
17. G. FASMAN. Nature, **193**, 681 (1964).
18. G. D. FASMAN, E. BODENHEIMER, and C. LINDBLOW. Biochemistry, **3**, 1665 (1964).
19. S. BEYCHOK and G. D. FASMAN. Biochemistry, **3**, 1675 (1964).
20. A. PATCHORNIK, M. SELA, and E. KATCHALSKI. J. Am. Chem. Soc. **76**, 299 (1954).
21. E. R. BLOUT and R. H. KARLSON. J. Am. Chem. Soc. **78**, 941 (1956).
22. P. DOTY, J. H. BRADBURY, and A. M. HOLTZER. J. Am. Chem. Soc. **78**, 951 (1956).
23. N. S. SIMMONS, C. COHEN, A. G. SZENT-GYORGYI, D. B. WETLAUFER, and E. R. BLOUT. J. Am. Chem. Soc. **83**, 4766 (1961).
24. J. T. YANG and T. SAMEJIMA. J. Biol. Chem. **238**, 3262 (1963).
25. S. S. LEHRER and G. D. FASMAN. Biopolymers, **2**, 199 (1964).
26. J. MARMUR, R. ROWND, and C. L. SCHILDKRAUT. Progr. Nucleic Acid Res. **1**, 232 (1963).

Can. J. Chem. Downloaded from www.nrcresearchpress.com by 210.87.254.6 on 09/05/12
For personal use only.

27. G. D. FASMAN, C. LINDBLOW, and L. GROSSMAN. Biochemistry, **3**, 1015 (1964).
28. K. IMAHORI and J. TANAKA. J. Mol. Biol. **1**, 359 (1959). I. TINOCO, A. HALPERN, and W. T. SIMPSON. *In* Polyamino acids, polypeptides and proteins. *Edited by* M. Stahmann. University of Wisconsin Press. 1962. p. 147. K. ROSENHECK and P. DOTY. Proc. Natl. Acad. Sci. U.S. **47**, 1775 (1961).
29. G. D. FASMAN, E. BODENHEIMER, and A. PESCE. In preparation.
30. S. SHIFRIN. Nature, **192**, 751 (1961).
31. M. BUCHWALD and W. H. STOCKMAYER. Personal communication.
32. N. A. YAJNIK, M. D. BHALLA, R. C. TALWAR, and M. A. SOOFI. Z. Physik. Chem. **118**, 305 (1925).
33. R. C. PETERSON. J. Phys. Chem. **64**, 184 (1960).
34. G. FRANKEL and C. FRANCONI. J. Am. Chem. Soc. **82**, 4478 (1960).
35. L. F. FIESER. Experiments in organic chemistry. 2nd ed. D. C. Heath Co., Boston, Mass. 1941. p. 361.
36. E. R. BLOUT and R. H. KARLSON. J. Am. Chem. Soc. **78**, 497 (1956).

Can. J. Chem. Downloaded from www.nrcresearchpress.com by 210.87.254.6 on 09/05/12
For personal use only.

Can. J. Chem. Downloaded from www.nrcresearchpress.com by 210.87.254.40 on 09/05/12
For personal use only.

ISOBENZOFURANE,[1] A TRANSIENT INTERMEDIATE

LOUIS F. FIESER AND MAKHLUF J. HADDADIN
Chemical Laboratory, Harvard University, Cambridge, Massachusetts
Received November 13, 1964

Dedicated to Professor R. B. Sandin on the Occasion of his Sixty-Eighth Birthday

ABSTRACT

A study of Diels–Alder reactions of tetraphenylcyclopentadienone (II) coupled with development of two improved procedures for the generation of benzyne, one of which affords a practical route to the reactive dienophile 1,4-dihydronaphthalene-1,4-*endo*-oxide (I*a*), led to an investigation of the reaction of I*a* and II. At 80° these reactants combine readily to give the adduct III*a*, which is cleaved on pyrolysis to isobenzofurane VIII*a* and 1,2,3,4-tetraphenylbenzene (IX). The transient existence of isobenzofurane (VIII*a*) was established by trapping it with the 1,4-*endo*-oxide I*a* and isolation of the adducts X and XI. In confirmation of the interpretation, X and XI were obtained by independent synthesis from the adduct V*a* from I*a* and α-pyrone and thermal decomposition of V*a* in the presence of I*a* as trapping agent. Parallel experiments with 1,4-dimethyl-1,4-dihydronaphthalene-1,4-*endo*-oxide, as well as mixed additions, supported the interpretations advanced. Evidence is presented to show that isobenzofurane (VIII*a*) invariably adds *exo* to the bicyclic dienophile.

The background for this work was provided by the development of improved procedures suitable for use as student experiments (1). Diels–Alder reactions pertinent to the present discussion, and procedures for the preparation of intermediates, are recorded in the Experimental part and will be mentioned only briefly here. Tetraphenylcyclopentadienone is a particularly favorable diene for experimentation because termination of a reaction is evident from discharge of the intense purple color. Thus reaction of the dienone with dimethyl acetylenedicarboxylate with evolution of carbon monoxide is complete in 1–2 mins in refluxing *o*-dichlorobenzene, b.p. 179°. Reaction of the dienone with diphenylacetylene to form hexaphenylbenzene can be carried out satisfactorily without solvent (2) only on a small scale because the melting point of the hydrocarbon (455°) is somewhat above the temperature required for its formation. In this case a satisfactory solvent was found in benzophenone (b.p. 306°); the reaction is complete in about 45 min and addition of a little diphenyl ether prevents solidification of the solvent on cooling.

One of two procedures for generation of benzyne proved suitable for preparation of the dienophile required for the present work.

LeGoff (3) introduced diphenyliodonium-2-carboxylate as a benzyne precursor, and we were able to improve both the procedure for preparing the reagent (3, 4) and that for its reaction with tetraphenylcyclopentadienone to such an extent that a student can complete the synthesis of 1,2,3,4-tetraphenylnaphthalene in an afternoon. LeGoff conducted the reaction at a temperature of about 165° and had the task of separating the reaction product from the dienone by chromatography; we ran the reaction in a higher-boiling solvent, used enough benzyne precursor to combine with all the dienone, and so obtained pure 1,2,3,4-tetraphenylnaphthalene by simple crystallization. However, the method proved unsuitable for application to a low-boiling diene such as furane.

[1]*For reasons set forth in L. F. Fieser and M. Fieser, Style Guide for Chemists, L. F. F. strongly advocates this spelling. While he also advocates formula numbers set in boldface arabic type, this practice is inconsistent with the style of this journal. Preliminary communication: J. Am. Chem. Soc. 86, 2081 (1964).*

Can. J. Chem. Downloaded from www.nrcresearchpress.com by 210.87.254.40 on 09/05/12
For personal use only.

A new route to benzyne described by Friedman (5) consists in diazotization of anthranilic acid with isoamyl nitrite in an aprotic solvent in the presence of a diene; the benzenediazonium-2-carboxylate decomposes to benzyne as it is formed. We found that the reaction proceeds particularly well in 1,2-dimethoxyethane as solvent and developed a student preparation of triptycene (1), a second efficient synthesis of 1,2,3,4-tetraphenylnaphthalene, and a simple method for the reaction of benzyne with furane to produce 1,4-dihydronaphthalene-1,4-*endo*-oxide (I*a*, chart below), previously obtained by shaking a solution of *o*-fluorobromobenzene in furane with lithium amalgam for 4 days (6). Generation of benzyne in the presence of 2,5-dimethylfurane similarly afforded 1,4-dimethyl-1,4-dihydronaphthalene-1,4-*endo*-oxide (7).

It is evident that, with this background, we were interested in the report by Wolthuis (7) that 1,4-dihydronaphthalene-1,4-*endo*-oxide (I) is an effective dienophile for simple dienes and decided to investigate its reaction with tetraphenylcyclopentadienone (II). A solution of the reactants in diglyme was refluxed in the expectation that, at this temperature (165°), the adduct III would lose carbon monoxide and afford the tetrahydrotetraphenylanthracene-*endo*-9,10-oxide VI. A vigorous reaction ensued with gas evolution and with discharge of the color in 2 min. Dilution with water precipitated a colorless crystalline product, m.p. 190°, characterized by the n.m.r. spectrum as having only aromatic hydrogens and found by elemental analysis to be a hydrocarbon. The possibility that the product might be 1,2,3,4-tetraphenylanthracene was eliminated by synthesis of the latter (m.p. 295°) by aprotic diazotization of 3-amino-2-naphthoic acid in the presence of tetraphenylcyclopentadienone (II). Other ideas about the nature of the product were dismissed by the finding that 1,4-dimethyl-1,4-dihydronaphthalene-1,4-*endo*-oxide (I*b*) reacts with (II) to give the same aromatic hydrocarbon and this eventually was identified as 1,2,3,4-tetraphenylbenzene (IX) (8). Since this hydrocarbon must result from thermal decomposition of an intermediate, the reaction of I*a* with II was repeated in refluxing benzene. There resulted, in high yield, a colorless product melting at 182–184° (decomp.) and corresponding in analysis to the adduct III*a*. This structure is supported by the ultraviolet spectrum, which contains bands at 275 and 223 mμ (ϵ 11 400 and 35 000) characteristic of a *cis*-stilbene system, by infrared carbonyl absorption at 1 775 – 1 780 cm^{-1}, and by the n.m.r. spectrum: singlet at τ 4.72 (C_9 and C_{10} protons); singlet at τ 7.09 (C_{9a} and C_{10a} protons); multiplet at τ 2.6–2.9 (10 protons of the C_2 and C_3 phenyl groups and 4 protons of the *o*-disubstituted benzene ring); singlet at τ 3.17 (10 protons of the C_1 and C_4 phenyl groups). The fact that the C_9 and C_{9a} protons did not split each other furnishes evidence of an *exo* attack by II at the double bond of I*a* (9, 10).[2] There is no evidence of the configuration at C_1 and C_4, but the high melting point suggests that the carbonyl bridge is in the *exo* orientation to give the symmetrical structure formulated.

Adduct III*a* decomposed rapidly at the melting point with evolution of carbon monoxide and formation of tetraphenylbenzene (IX) as the only isolated product. We believe that elimination of carbon monoxide gives tetrahydrotetraphenylanthracene-*endo*-9,10-oxide (VI), and that this suffers retrogressive Diels–Alder reaction (11)[3] to isobenzofurane (VIII) and tetraphenylbenzene (IX).

Isobenzofurane (VIII) is unknown and all efforts to isolate it as a product of pyrolysis or to synthesize it thus far have proved fruitless. Nevertheless, its transient existence was

[2]*This conclusion is based on the dependence of the coupling constant for vicinal protons on the dihedral angle (9). For other examples see ref. 10.*

[3]*Comparable reactions are described (11) by Mackenzie and by Wittig and Härle.*

Can. J. Chem. Downloaded from www.nrcresearchpress.com by 210.87.254.40 on 09/05/12
For personal use only.

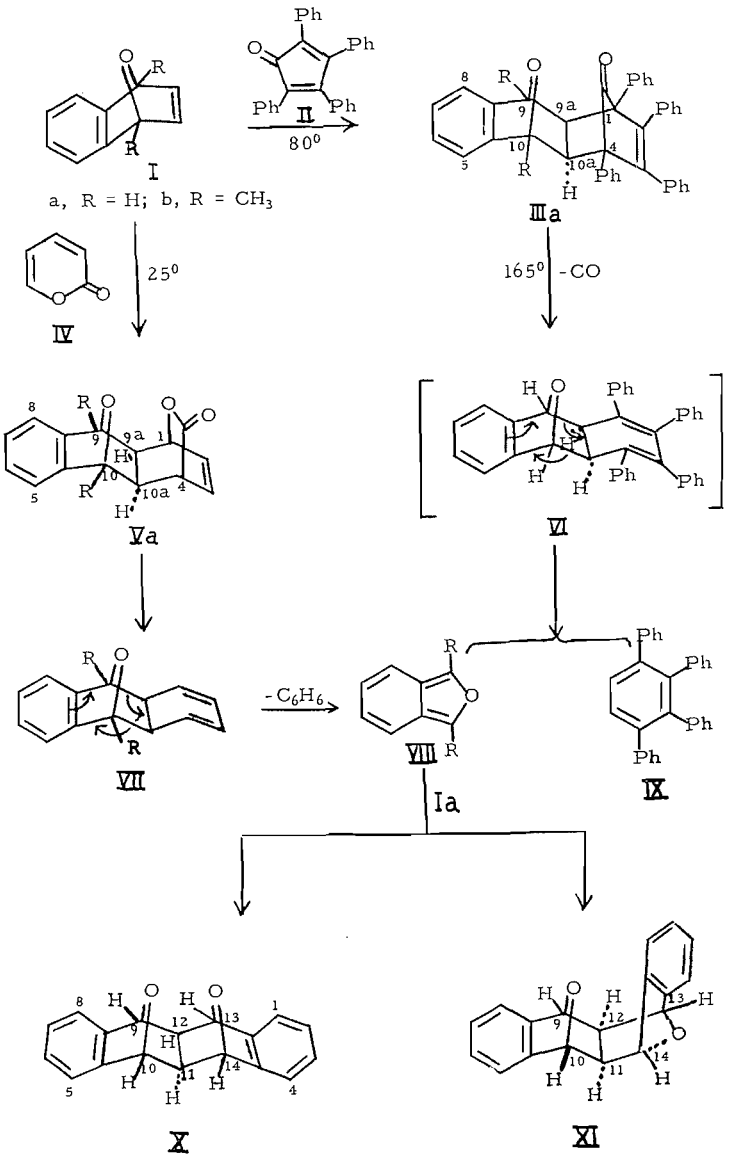

demonstrated by decomposing the adduct III*a* in refluxing diglyme in the presence of the *endo*-1,4-oxide I*a* as trapping agent and isolation of the *exo*, *exo*- and *exo*, *endo*-adducts X and XI, along with tetraphenylbenzene (IX). This hydrocarbon and the *exo*, *endo*-adduct XI are soluble in benzene, in which the *exo*, *exo*-adduct X is practically insoluble; IX and XI are separated easily by chromatography on neutral alumina. The total yield is 91% and the ratio of X to XI is 10:14.

Product X was characterized as follows: m.p. 264–265°; n.m.r.: singlets at τ 2.92 and 2.98 (eight aromatic protons); singlet at 4.59 (four allylic protons adjacent to oxygens); singlet at 8.02 (protons at C_{11} and C_{12}). The high melting point is consistent with the high symmetry of structure X. Product XI, m.p. 175–176°, was characterized as follows: singlets at τ 2.9 and 3.05 (eight aromatic protons); singlet at 5.48 (allylic protons at C_9

and C_{10} next to oxygen); unsymmetrical quartets at 4.85 and 7.35 (J = 2 c.p.s.), two protons each at C_{13}—C_{14} and at C_{11}—C_{12}, probably due to vicinal and long-range coupling (12). The fact that the n.m.r. spectrum of X shows no observable coupling between the protons at C_{10} (or C_{14}) and C_{11} (singlet), whereas that for XI shows coupling between the C_{11} and C_{14} protons but not between the C_{10} and C_{11} protons confirms the assignments *exo, exo* for X and *exo, endo* for XI (9, 10).

The structures assigned were confirmed by an independent synthesis from I and α-pyrone[4] (IV), a diene which is more reactive than II and which combines with I at room temperature to form the adduct V*a* in 95% yield. This adduct, m.p. 105–107°, which decolorizes permanganate and bromine solution, is characterized as follows. Infrared: 1 750 (carbonyl), 1 635 cm^{-1} (C=C); n.m.r.: singlet at τ 3 (four aromatic protons); triplet at 3.6 (two olefinic protons); multiplet at 4.62–5.06 (three allylic protons adjacent to oxygen); multiplet at 6.26–6.44 (C_4-proton); symmetrical quartets at 7.3–7.5 and at 7.73–7.92 (one proton each, probably those at C_{10a} and C_{9a}).

Adduct V*a* decomposes on recrystallization or on long standing at room temperature. When the adduct was added to a hot solution of the *endo*-1,4-oxide I*a* in diglyme and the solution kept at 130° for 2 min, bis-oxides X and XI were isolated in total yield of 81–85%, with carbon dioxide and benzene as by-products. The oxidolactone V*a* on being

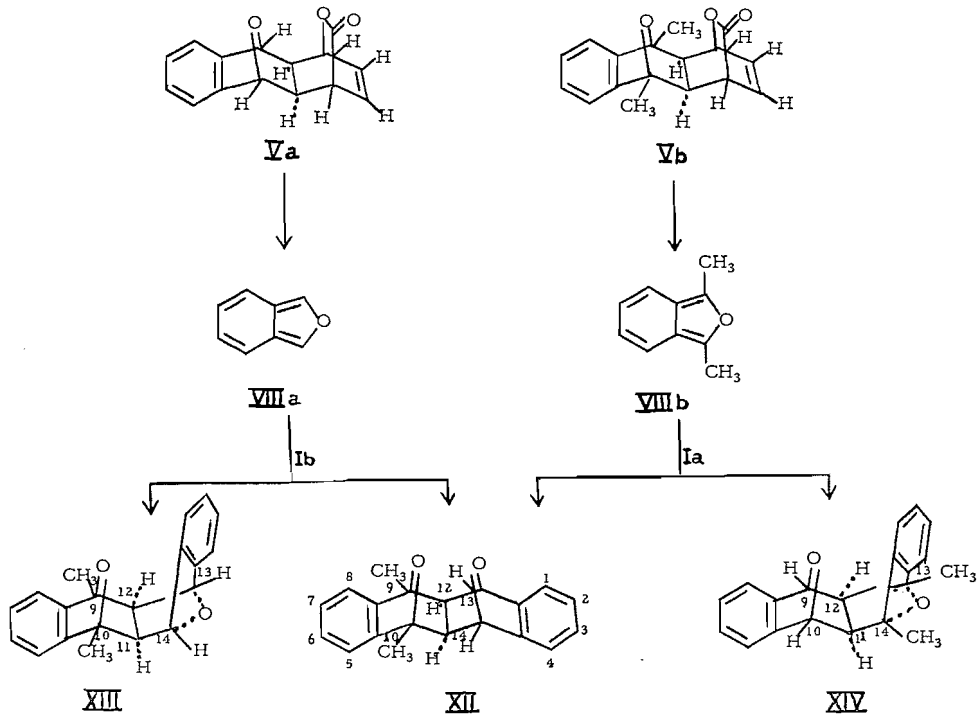

heated decomposes with evolution of carbon dioxide and, presumably, the unstable intermediate VII, which rearranges to yield benzene and isobenzofurane (VIII). The fact that X and XI result from two different reactions indicated a common intermediate, namely isobenzofurane (VIII). The n.m.r. data reported above for X show no splitting

[4]*Prepared by a procedure submitted to Org. Syn. by H. E. Zimmerman, G. L. Grunewald, and R. M. Paufler.*

Can. J. Chem. Downloaded from www.nrcresearchpress.com by 210.87.254.40 on 09/05/12
For personal use only.

between C_{11} and C_{10} or (and) C_{14} protons, which means that the addition of isobenzofurane (VIII*a*) must take place from the *exo* side of I*a* (9, 10). This argument does not hold in the case of XI because of the difficulty of identifying the portion of the molecule that belongs to the isobenzofurane substrate.

Analogous reactions starting with 1,4-dimethyl-1,4-dihydronaphthalene-1,4-*endo*-oxide (I*b*) are recorded in the Experimental part. Another set of experiments can be described as involving mixed additions, that is, generation of isobenzofurane (VIII*a*) in the presence of the 1,4-dimethyl-1,4-*endo*-oxide (I*b*), and generation of 1,3-dimethylisobenzofurane (VIII*b*) in the presence of the parent 1,4-*endo*-oxide (I*a*). As expected, each reaction gave a pair of products, one of which was common to both reactions. The product common to both reactions, the dihydrogen–dimethyl derivative XII, has a n.m.r. spectrum showing singlets for the C_{11} and C_{14} protons, which supports the evidence for *exo* attack of the double bond of I*b*. The n.m.r. of adduct XIII shows the same nonsplit pattern of the C_{11} and C_{14} protons as in adduct XI. For the isomeric adduct XIV, the n.m.r. evidence also is consistent with an *exo* addition of VIII*b* to I*a* (see Experimental section) (9, 10).

The substituent methyl groups of 1,3-dimethylisobenzofurane (VIII*a*) exert a control over the addition of this substance to the 1,4-dimethyl-1,4-*endo*-oxide (I*b*), for the sole product is the *exo, endo* adduct (the 13,14-dimethyl derivative of XIII). Inspection of models shows that the methyl groups exert substantial hindrance to an *exo, exo* approach.

This is the first report identifying isobenzofurane and 1,3-dimethylisobenzofurane as unisolated trapping agents. Wittig and Härle (11) reported the formation of polymeric isobenzofurane on heating XV at 180° with copper powder.

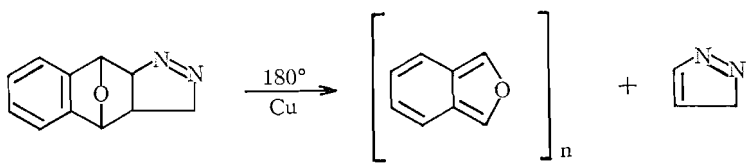

XV XVI XVII

EXPERIMENTAL[5]

Tetraphenylcyclopentadienone (L. F. F.)[6]

A mixture of 21 g of benzil, 21 g of dibenzyl ketone, and 100 ml of triethylene glycol was heated over a free flame to dissolve the solid, the temperature was adjusted to 100°, 10 ml of a 40% solution of benzyltrimethylammonium hydroxide was added, and the flask was swirled once for mixing and then let stand. Within 15–20 s the liquid set to a stiff paste of purple crystals and the temperature rose to 115°. When the temperature dropped to 80°, the mixture was cooled and thinned with 50 ml of methanol and the product was collected and washed with methanol; yield 35.5 g (93%), m.p. 219–220°. Recrystallization can be accomplished with 92% recovery by dissolving the ketone in triethylene glycol (10 ml per g) at 220°.

Dimethyl Tetraphenylphthalate (L. F. F.) (2)[7]

A mixture of 2 g of tetraphenylcyclopentadienone, 1 ml of dimethyl acetylenedicarboxylate, and 10 ml of *o*-dichlorobenzene was refluxed gently in a test tube until the color changed from purple to pale tan (about 5 min). The solution was cooled to 100°, 15 ml of 95% ethanol was stirred in, and the solution let stand for crystallization. The yield of colorless crystals, m.p. 257–258°, was 2.2 g (89%).

Hexaphenylbenzene (L. F. F.) (2)

A mixture of 8 g of tetraphenylcyclopentadienone, 8 g of diphenylacetylene, and 40 g of benzophenone was refluxed over a microburner so that it refluxed briskly but without flooding a short air condenser (liquid-phase temperature 301–303°). Carbon monoxide was evolved, the purple color began to fade in 15–20 min and changed to reddish brown in 25–30 min and then lightened slightly. After 45 min the burner was

[5]*Except as noted, the experiments were done by M. J. H. Nuclear magnetic resonance spectra were determined in deuterated chloroform with hexamethyldisiloxane as internal reference set at τ 9.91.*

[6]*Compare Org. Syn., Coll. Vol. 3, 806 (1955).*

[7]*Compare preparation of the anhydride, Org. Syn., Coll. Vol. 3, 807 (1955).*

Can. J. Chem. Downloaded from www.nrcresearchpress.com by 210.87.254.40 on 09/05/12
For personal use only.

removed, 8 ml of diphenyl ether was added, the mixture was reheated to dissolve crystals that separated, and the solution was let stand for crystallization at room temperature. The product, collected and washed free of brown mother liquor with benzene, was obtained as colorless plates, m.p. 454–456° (in a sealed capillary);[8] yield 9.4 g (85%). A satisfactory solvent for recrystallization is diphenyl ether (7 ml per g).

Diphenyliodonium Carboxylate (L. F. F. and M. J. H.) (3, 4)

A three-necked 2-l flask containing 20 g of *o*-iodobenzoic acid and 26 g of potassium persulfate was cooled in an ice bath, 80 ml of ice-cold concentrated sulfuric acid was added, and the mixture was swirled in the ice bath for 4–5 min to check the exothermal reaction and produce an even suspension. The time was noted and the flask removed and mounted in a pan of acetone, a stirrer with a curved Teflon blade was put in place and operated slowly, and a 250-ml dropping funnel was mounted to deliver into a side opening. Three flasks were put into an ice bath to cool: one containing 190 ml of distilled water, another 230 ml of 29% ammonium hydroxide, and another 400 ml of methylene chloride. After the oxidation had proceeded for 20 min, the cooling bath was brought to 10° by addition of crushed dry ice and the solution was stirred for 2–3 min before addition of 20 ml of thiophene-free benzene. Stirring at 10° was continued for 1 h to complete the reaction and the temperature of the cooling bath was kept at −15° while the chilled water was run in under efficient stirring; this precipitates the potassium salt of diphenyliodonium-2-carboxylic acid. The chilled methylene chloride was added for efficient extraction of the product as it is liberated on neutralization, and a 100° thermometer was mounted in a side opening. With efficient cooling (−15°) and stirring, the chilled ammonia solution was run in at an inner temperature of 15–25° in about 10 min. The aqueous layer should be alkaline to test paper (pH 9). The layers were separated and the aqueous layer extracted with two 100-ml portions of methylene chloride. Evaporation of the combined and dried extract afforded 23.3 g of crude material, m.p. 206–208° (decomp.). Crystallization from boiling water (275 ml), after clarification with Norit and cooling at 0°, gave 21.8 g (79%) of colorless prisms of diphenyliodonium-2-carboxylate monohydrate, m.p. 221–222° (decomp.).

Anal. Calcd. for $C_{13}H_9OI \cdot H_2O$ (342.13): C, 45.63; H, 3.24; I, 37.10. Found: C, 45.48; H, 3.19; I, 37.16.

1,2,3,4-Tetraphenylnaphthalene, Method A (L. F. F. and M. J. H.)

A 100-ml round-bottomed flask was charged with 10 g of tetraphenylcyclopentadienone, 11.8 g of diphenyliodonium-2-carboxylate monohydrate, and 60 ml of Eastman's *mp*-diethylbenzene (b.p. 175–181°), and fitted with an 11-cm water-cooled condenser designed as a bearing for a stirrer (Ace Glass 8244 Bearing 24/40). The flask was heated with the free flame of a microburner and the refluxing liquid let rise well into the condenser. When a cloudy zone of condensate appeared at the top, the moisture was removed with an applicator stick wrapped with absorbent cotton; by this technique the water of hydration (which does not appear to react with benzyne) was eliminated in 8–10 min. After 30 min considerable undissolved precursor could still be seen, under illumination, at the bottom of the flask. In another 5 min the color changed to transparent red, and in 1–2 min the solution became pale yellow. Refluxing was continued until the solid was all destroyed (5–10 min), and the flask was connected by means of an Ace Glass 5235 adapter to a condenser and 55 ml of liquid (solvent and iodobenzene) was removed by distillation. After it was cooled, the residue was dissolved in 25 ml of dioxane and the solution rinsed into an Erlenmeyer and diluted with 25 ml of 95% ethanol. The solution was then heated at the boiling point and water was added gradually (6–7 ml) until a few shiny prisms remained undissolved on boiling. Crystallization at room temperature and then for several hours at 0° afforded a product which melts initially in the range 196–199°, solidifies on cooling, and remelts sharply at 203–204°.[9] The yield is 10.3 g (91.6% based on the dienone), which represents 68.7% utilization of the benzyne precursor.

1,2,3,4-Tetraphenylnaphthalene, Method B

Solutions of 1.5 g of anthranilic acid and 2 ml of isoamyl nitrite, each in 15 ml of 1,2-dimethoxyethane, were added simultaneously by drops to a refluxing solution of 3.84 g of tetraphenylcyclopentadienone in 30 ml of 1,2-dimethoxyethane over a period of about 45 min. Evaporation of the solvent on the steam bath with evacuation at the water pump and trituration of the yellowish residue with methanol gave 4.05 g (93%) of white solid, m.p. 196–199°. Crystallization from dioxane–ethanol–water gave prisms of sharp remelt temperature 203–204°.

1,4-Dihydronaphthalene-1,4-endo-oxide

Solutions of 20 ml of isoamyl nitrite in 20 ml of 1,2-dimethoxyethane and of 13.7 g of anthranilic acid in 45 ml of 1,2-dimethoxyethane were added simultaneously by drops to a refluxing mixture of 50 ml of 1,2-dimethoxyethane and 50 ml of furane in a period of 1 hour. Refluxing was continued for 10 min and the brown solution was cooled, made basic with sodium hydroxide, and extracted with petroleum ether. The extract was washed thoroughly with water, clarified with Norit, dried, and evaporated to give an oil which

[8]*Determined with a Mel-Temp apparatus, Laboratory Devices, P. O. Box 68, Cambridge, Mass. 02139. The figure 456° is the average of two determinations of the temperature of melting; 454° is the average of two determinations of the point of solidification.*

[9]*The double melting point was observed also by Herwig, Metlesics, and Zeiss (13). The initial melting point varies with the state of subdivision and is not a reliable index of purity. Several recrystallizations did not change the melting behavior or the remelt temperature.*

Can. J. Chem. Downloaded from www.nrcresearchpress.com by 210.87.254.40 on 09/05/12
For personal use only.

solidified on cooling to give 7.4 g of crude, yellowish oxide (51% based on anthranilic acid). Crystallization from petroleum ether gave colorless, hard needles, m.p. 56° (53–54.5 (6); 56° (7)).

1,4-Dimethyl-1,4-dihydronaphthalene-1,4-endo-oxide

Diazotization of 13.7 g of anthranilic acid with isoamyl nitrite in 1,2-dimethoxyethane in the presence of 2,5-dimethylfurane was conducted by the same procedure and the product, a yellow liquid, distilled at 120° at 35 mm; yield 10.6 g (67.5%). The n.m.r. spectrum showed singlets at τ 8.66 (six methyl protons), and τ 3.43 (two olefinic protons), and a symmetrical multiplet at τ 3.13 (four aromatic protons).

1,2,3,4-Tetraphenylanthracene

Solutions of 1.9 g of 3-amino-2-naphthoic acid in 20 ml of 1,2-dimethoxyethane and of 3 ml of isoamyl nitrite in 20 ml of the same solvent were added simultaneously by drops to a refluxing solution of 3.84 g of tetraphenylcyclopentadienone in 50 ml of 1,2-dimethoxyethane. The solvent was evaporated at reduced pressure and the red residue was adsorbed from benzene on a column of 90 g of neutral alumina. Elution with 1:1 petroleum ether – benzene afforded 3.7 g of faintly yellow powder, m.p. 292–294° (evacuated capillary); 73% yield based on 3-amino-2-naphthoic acid. Elution with ether afforded 0.55 g of unreacted tetraphenylcyclopentadienone (yield based on the latter, 81.8%). Recrystallization from benzene–methanol gave shiny yellowish prisms, m.p. 293–295° (evacuated capillary), with 95% recovery.

Anal. Calcd. for $C_{38}H_{26}$ (482.58): C, 94.58; H, 5.42. Found: C, 94.51; H, 5.44.

1,2,3,4-Tetraphenyl-1,4-carbonyl-9,10-oxido-1,4,9,9a,10,10a-hexahydroanthracene (IIIa)

A solution of 1.92 g of tetraphenylcyclopentadienone and 1,4-dihydronaphthalene-1,4-*endo*-oxide in benzene was refluxed until the purple color disappeared (1.5 h) and the benzene was evaporated. Trituration of the residue with methanol gave a white solid which, when collected, washed with methanol, and dried, weighed 2.58 g (97.6%), m.p. 182–184° (decomp.). Crystallization from benzene–methanol raise dthe melting point to 184–185° (decomp.) (other physical constants already reported).

Anal. Calcd. for $C_{39}H_{28}O_2$ (528.61): C, 88.61; H, 5.34. Found: C, 88.68; H, 5.53.

Reaction of IIIa with Ia to give IX, X, and XI

A solution of 464 mg of III*a* and 144 mg of I*a* in 4 ml of diglyme was refluxed for 2 min, cooled, and diluted with water. The solid product was collected and dried and on crystallization from benzene afforded 100 mg of needles of X, m.p. 265°. On chromatography of the mother-liquor material on neutral alumina, 1:1 petroleum ether – benzene eluates gave 250 mg of 1,2,3,4-tetraphenylbenzene (IX) and 1:1 benzene–eluates gave 140 mg of XI, m.p. 175–176°. Recrystallization from methanol did not raise the melting point.

1,2,3,4-Tetraphenylbenzene (IX)

The hydrocarbon melted at 190° and corresponded to the known material (8).

Anal. Calcd. for $C_{30}H_{22}$ (382.48): C, 94.20; H, 5.80. Found: C, 94.30; H, 5.77.

Product X (exo, exo, m.p. 265°)

The spectral characteristics of this and other products are recorded in the theoretical part.

Anal. Calcd. for $C_{18}H_{14}O_2$ (262.29): C, 82.41; H, 5.38. Found: C, 82.23; H, 5.44.

Product XI (exo, endo, m.p. 176°)

Anal. Calcd. for $C_{18}H_{14}O_2$ (262.29): C, 82.41; H, 5.38. Found: C, 82.60; H, 5.40.

1,4-Carbonyloxy-9,10-oxido-1,4,9,9a,10,10a-hexahydroanthracene (Va)

1,4-Dihydronaphthalene-1,4-*endo*-oxide (2.88 g) was dissolved in α-pyrone (2 g) and the solution left to stand at room temperature for 4–5 days, during which time the adduct crystallized. Washing with chilled methanol gave 4.5 g (95%) of directly pure material, m.p. 105–107° (decomp.).

Anal. Calcd. for $C_{15}H_{12}O_3$ (240.25): C, 74.99; H, 5.03. Found: C, 74.92; H, 5.12.

Products X and XI from Va and Ia

A solution of 0.6 g of 1,4-dihydronaphthalene-1,4-*endo*-oxide (I*a*) in 10 ml of diglyme was adjusted to 130°, 1 g of V*a* was added in portions, and the solution was kept at 130° for 2 min and then cooled and diluted with water. The white solid which precipitated was collected, washed, and dried and amounted to 0.95 g (87.5%). Crystallization from benzene gave 300 mg of branch-like crystals melting at 264–265°, not depressed on admixture with XII. The mother liquor was poured onto a column of neutral alumina (prepared with benzene), and elution with benzene afforded 400 mg of product XI. Recrystallized from methanol, the substance formed prisms, m.p. 175–176°; a mixture with the product from I*a* and III*a* showed no melting point depression.

The reaction was also carried out by heating the components neat on the steam bath for 30 min; in this case the ratio of products was close to 1:1.

1,4-Carbonyloxy-9,10-oxido-9,10-dimethyl-1,4,9,9a,10,10a-hexahydroanthracene (Vb)

A solution of 1.72 g of 1,4-dimethyl-1,4-*endo*-oxide I*b* in 1 g of α-pyrone was left to stand a few days and when crystallization was delayed, rubbing or scratching was helpful. The yield of V*b*, m.p. 110–112° (decomp.), was 2.4 g (89%).

Can. J. Chem. Downloaded from www.nrcresearchpress.com by 210.87.254.40 on 09/05/12
For personal use only.

Anal. Calcd. for $C_{17}H_{16}O_3$ (268.30): C, 76.10; H, 6.01. Found: C, 76.31; H, 6.20.

The fluorescent product partially decomposes on recrystallization. It decolorized bromine in carbon tetrachloride and permanganate solution.

Infrared: 1 655 (C=O), 1 635 (C=C), 1 190, 1 170, 1 010, 975, 940, 865, 840, 800, 763 722 cm^{-1}; n.m.r.: singlet at τ 3.10 (four aromatic protons); quartet at 4.97 (allylic proton next to oxygen); multiplet at 6.5 (allylic proton next to carbonyl group); quartet at 7.91 (C_{10a} proton); singlet at 8.42 (six methyl protons).

1,2,3,4-Tetraphenyl-1,4-carbonyl-9,10-oxido-9,10-dimethyl-1,4,9,9a,10,10a-hexahydroanthracene (IIIb)

A solution of 1 g of tetraphenylcyclopentadienone in 4 ml of 1,4-dimethyl-1,4-dihydronaphthalene-1,4-*endo*-oxide was heated on the steam bath for 36 h and chromatographed on neutral alumina. The products isolated and identified were as follows: 1,2,3,4-tetraphenylbenzene (0.9 g), III*b* (100 mg), and the 13,14-dimethyl derivative of XIII (0.38 g).

Compound III*b*, m.p. 248–249° (decomp.), was characterized as follows: infrared, 1 780 cm^{-1} (C=O); ultraviolet, 275–250, 222 mμ (ϵ 6 550, 3 260).

Anal. Calcd. for $C_{41}H_{32}O_2$ (556.67): C, 88.46; H, 5.79. Found: C, 88.53; H, 5.64.

9,10-Dimethyl-9,10-exo-oxido-13,14-exo-oxido-9,10,11α,12α,13,14-hexahydronaphthacene (XII) and 9,10-Dimethyl-9,10-exo-oxido-13,14-endo-oxido-9,10,11α,12α,13,14-hexahydronaphthacene (XIII)

A refluxing solution of 0.6 g of 1,4-dihydronaphthalene-1,4-*endo*-oxide in 12 ml of diglyme was treated with 1.30 g of V*b* in portions; refluxing was continued for 2 min and the solution was cooled. Dilution with water precipitated a white product which was collected, washed with water, and dried (1.05 g, 87%). On chromatography on alumina, elution with petroleum ether gave 380 mg of product XIII, m.p. 157–159°, and 2:8 petroleum ether – benzene gave 420 mg of XII, m.p. 265–267°.

Product XIII crystallized from methanol in short needles, m.p. 159–160°.

Anal. Calcd. for $C_{20}H_{18}O_2$ (290.34): C, 82.73; H, 6.25. Found: C, 82.69; H, 6.38.

The n.m.r. spectrum showed singlets at τ 2.84, 2.9, and 3.09 (eight aromatic protons); unsymmetrical quartets at 4.9 (C_{13} and C_{14} protons) and 7.32 (C_{11} and C_{12} protons); singlet at 8.5 (six methyl protons).

Product XII crystallized from methanol in shiny flakes, m.p. 268–269°.

Anal. Calcd. for $C_{20}H_{18}O_2$ (240.34): C, 82.73; H, 6.25. Found: C, 82.68; H, 6.40.

The n.m.r. spectrum showed singlets at τ 3.07 (eight aromatic protons) and at 4.65 (C_{13} and C_{14} protons); singlets at 8.14–8.15 (six methyl protons and C_{11} and C_{12} protons).

13,14-Dimethyl-9,10-exo-oxido-13,14-endo-oxido-9,10,11α,12α,13,14-hexahydronaphthacene (XIV) and XII

A solution of 1.1 g of the 1,4-dimethyl-1,4-endo-oxide I*b* in 5 ml of diglyme was heated to boiling and treated with 1.8 g of V*a*, added in portions. On cooling, 0.67 g of product XII separated, m.p. 268–269°. Evaporation of the mother liquor and chromatography afforded 100 mg of product XIV, m.p. 144–146°, and 100 mg more of product XII. The n.m.r. spectrum showed singlets at 2.78 and 2.92 (eight aromatic protons), singlets at 5.45 (C_9 and C_{10} protons), at 7.49 (C_{11} and C_{12} protons), and at 8.25 (six methyl protons).

Anal. Calcd. for $C_{20}H_{18}O_2$ (290.34): C, 82.73; H, 6.25. Found: C. 82.62; H, 6.18.

13,14-Dimethyl Derivative of Product XIII

A solution of 80 mg of 1,4-dimethyl-1,4-dihydronaphthalene-1,4-*endo*-oxide in 1 ml of diglyme was heated to 155° and treated with 100 mg of V*b*. Dilution with water afforded 105 mg of product, which on crystallization from methanol, gave 80 mg (71%) of material, m.p. 202–203°.

Anal. Calcd. for $C_{22}H_{22}O_2$ (318.40): C, 82.98; H, 6.96. Found: C, 82.84; H, 6.90.

Infrared spectrum: 1 270, 1 200, 1 130, 1 070, 880, 860, 772, 754, 680 cm^{-1}; n.m.r. spectrum: singlets at τ 2.84, 3.05, 7.46, 8.3, 8.5.

ACKNOWLEDGMENT

We are indebted to the National Institutes of Health for grant CA-01696-12 in support of this work.

REFERENCES

1. L. F. FIESER. Organic experiments. D. C. Heath and Co. 1964.
2. W. DILTHEY and G. HURTIG. Ber. **67**, 2007 (1934).
3. E. LEGOFF. J. Am. Chem. Soc. **84**, 3786 (1962).
4. F. M. BERINGER and I. LILLIEN. J. Am. Chem. Soc. **82**, 725 (1960).
5. L. FRIEDMAN and F. M. LOGULLO. J. Am. Chem. Soc. **85**, 1549 (1963).
6. G. WITTIG and L. POHMER. Ber. **89**, 1334 (1956).
7. E. WOLTHUIS. J. Org. Chem. **26**, 2215 (1961).
8. W. DILTHEY, W. SCHOMMER, and O. TRÖSKEN. Ber. **66**, 1627 (1933).
9. M. KARPLUS. J. Chem. Phys. **30**, 11 (1959).
10. F. A. L. ANET. Can. J. Chem. **39**, 789 (1961). P. R. STORY. J. Am. Chem. Soc. **83**, 3347 (1961). W. R. MOORE, W. R. MOSER, and J. E. LAPRADE. J. Org. Chem. **28**, 2202 (1963).
11. K. MACKENZIE. J. Chem. Soc. 473 (1960). G. WITTIG and H. HÄRLE. Ann. **623**, 17 (1959).
12. J. MEINWALD and Y. C. MEINWALD. J. Am. Chem. Soc. **85**, 2514 (1963); references cited therein.
13. H. HERWIG, W. METLESICS, and H. ZEISS. J. Am. Chem. Soc. **81**, 6203 (1959).

Can. J. Chem. Downloaded from www.nrcresearchpress.com by 210.87.254.40 on 09/05/12
For personal use only.

Can. J. Chem. Downloaded from www.nrcresearchpress.com by 210.87.254.42 on 09/05/12
For personal use only.

ISOMERIC SYDNONES

I. THE REACTIONS OF 1- AND 2-BENZOYL-1-METHYLHYDRAZINES AND PHOSGENE

C. AINSWORTH
Chemical Research Division, The Lilly Research Laboratories, Indianapolis, Indiana
Received November 13, 1964

Dedicated to Professor R. B. Sandin on the Occasion of his Sixty-Eighth Birthday

ABSTRACT

The oxygen–carbonyl isomeric sydnone (V) has been synthesized from 1-benzoyl-1-methylhydrazine hydrochloride (VII) and phosgene. The isosydnone V itself reacts with phosgene to form 2-chloro-5-phenyl-1,3,4-oxadiazole (VI), a new substituted 1,3,4-oxadiazole. Thermal rearrangement of the salt VII takes place at 200° to give 1-benzoyl-2-methylhydrazine, which with phosgene forms the isomer XI. Some mechanistic pathways for these transformations are discussed.

INTRODUCTION

Sydnones I have been investigated extensively (1), but there is only one report (2*a*) on the preparation of the oxygen–carbonyl isomeric system[1] II. The non-mesoionic isomeric system III has not as yet been synthesized.[2] This paper reports the preparation and physical properties of an isosydnone II and an isomer IV.

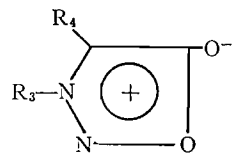

I

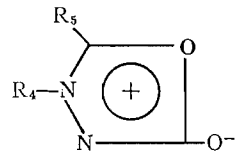

II

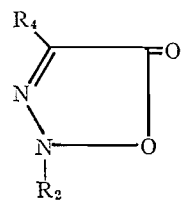

III

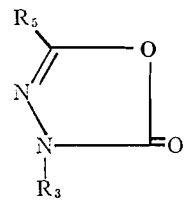

IV

4-Methyl-5-phenylisosydnone (V), together with 2-chloro-5-phenyl-1,3,4-oxadiazole (VI) and methyl chloride, was prepared in about 50% yield from the reaction of 1-benzoyl-1-methylhydrazine[3] hydrochloride (VII) (3) and excess phosgene heated in dioxane for 1 h. The structure of compound V is established by physical measurements and hydrolysis

[1]*Named ψ-2,4-dihydro-4,5-disubstituted 2-keto-1-oxa-3,4-diazole by M. Hashimoto and M. Ohta (2) and indexed in Chem. Abstr. as 5-hydroxy-2,3-disubstituted 1,3,4-oxadiazolium hydroxide, inner salt. For convenience this system will be called isosydnone throughout this paper.*

[2]*G. Sugarman (2b) called this type of compound isosydnone, but we prefer to reserve this name for the mesoionic system II.*

[3]*The n.m.r. spectrum of the free base in 10%* $CDCl_3$ *shows peaks at 2.60, 5.42, and 6.87* τ *in the ratio 5:2:3.*

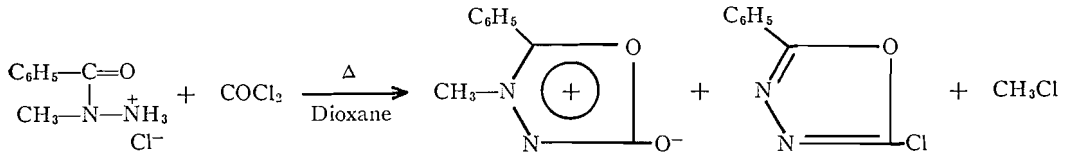

VII V VI

studies. The nuclear magnetic resonance (n.m.r.) spectrum in 10% deuterochloroform shows peaks at 2.30 and 6.05 τ in the ratio of 5:3. The dipole moment in benzene at 25° is 7.58 ± 0.06 D.[4] Mild hydrolysis of V with sodium hydroxide, followed by hydrochloric acid, gave the starting material VII, showing that no rearrangement had occurred.

Compound VI, isolated from the reaction of VII and phosgene, represents a type of substituted 1,3,4-oxadiazole not previously reported in the literature. The n.m.r. spectrum shows phenyl protons only at 2.0 and 2.4 τ in the ratio of 2:3, and other physical measurements are similar to those of 2-phenyl-1,3,4-oxadiazole (4). Compound VI was prepared by an independent synthesis in very low yield from 2-phenyl-1,3,4-oxadiazolin-5(4H)-one (VIII) and phosphorus pentachloride.

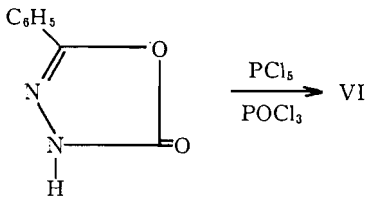

VIII

The following series of experiments (see Experimental) are related to the formation of the products V and VI. (*a*) Compound VII and phosgene heated in dioxane gave a residue that on thin-layer chromatography showed several spots in addition to those of V and VI. (*b*) Compound V and phosgene heated in dioxane gave VI, methyl chloride, and a residue that on thin-layer chromatography showed the same spots as in *a*. (*c*) The free base of VII added to ether containing phosgene very rapidly formed VII and the isosydnone V in high purity. (*d*) Compound VII and phosgene heated in toluene did not dissolve, and starting material only was recovered. (*e*) Reaction of VII and phosgene in dioxane containing pyridine gave the bis compound 1,5-dibenzoyl-1,5-dimethylcarbohydrazide[5] (IX). Compound IX heated in dioxane containing phosgene was recovered

$(C_6H_5CONCH_3NH)_2CO$

IX

unchanged. (*f*) The residue from reaction *a* when allowed to stand in a moist atmosphere gave a small yield of VIII. (*g*) Compound VIII was recovered unchanged when heated with phosgene in dioxane. (*h*) Compound V and hydrogen chloride heated in dioxane did not evolve methyl chloride.

Observations *a*, *b*, *c*, and *d* support the fact that VII in solution and phosgene form V and that V and excess phosgene give rise to the other products formed. Compound VII and phosgene probably form the intermediate X that is rapidly transformed to V. Phosgene may react with V (shown as one of the resonance structures) to form carbon dioxide

[4]*The average value for sydnones is 7–8.8 D (1a).*

[5]*The corresponding 1,5-dibenzoyl-1,5-diphenylcarbohydrazide was obtained by W. Baker et al. (5), by reaction of 1-benzoyl-1-phenylhydrazine hydrochloride and phosgene heated in toluene.*

Can. J. Chem. Downloaded from www.nrcresearchpress.com by 210.87.254.42 on 09/05/12
For personal use only.

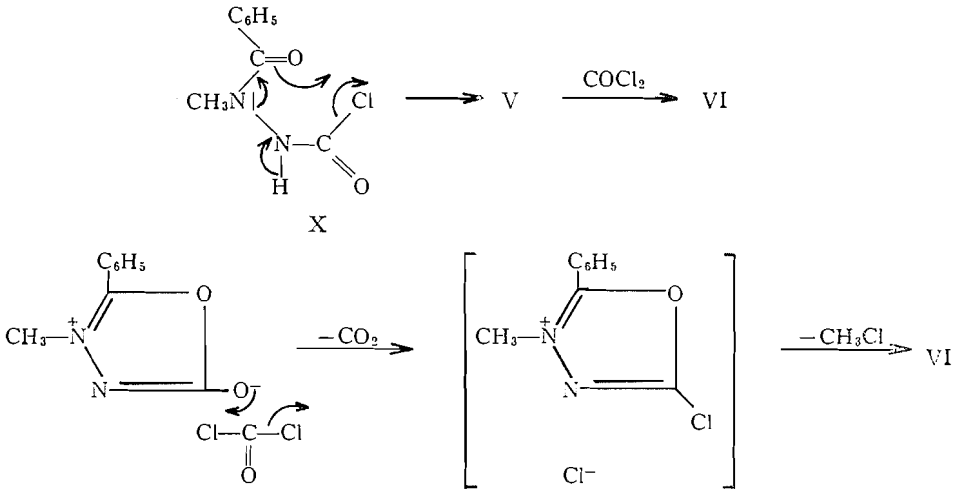

and the quaternary salt indicated. Such a salt would be expected to lose methyl chloride readily[6] and give VI.

Observation *e* shows that the bis compound IX is not an intermediate in the formation of V from VII. The findings *f*, *g*, and *h* eliminate the idea that V in acidic medium loses methyl chloride to form VIII, and also the possibility that VIII might be intermediate in the formation of VI.

Since the thermal stability of the starting hydrazide salt VII, at an early point in the study, seemed to be of importance, it was investigated. The salt was found to be stable at its melting point of 165°, but heated to 200° it decomposed, forming a clear melt. Nuclear magnetic resonance analysis of the melt showed that VII and its free base were absent, and 1-benzoyl-2-methylhydrazine and its hydrochloride were the products.

$$R{-}N(COC_6H_5)NH_2\cdot HCl \xrightarrow{\Delta} RNHNHCOC_6H_5 + HCl$$

When R is phenyl[7] in the above equation, the N_1 to N_2 rearrangement took place at 210° and gave a quantitative yield of the free base of 1-benzoyl-2-phenylhydrazine.[8]

The reaction would appear to be facilitated by hydrogen bonding in the starting salt and likely passes through the intramolecular intermediate indicated. The product where R is methyl is a base sufficiently strong to retain some of the hydrogen chloride, whereas when R is phenyl none is retained.

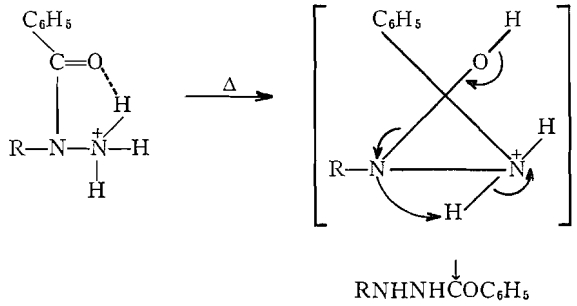

[6]*The thermal instability of quaternary pyrazoles is well documented (6).*

[7]*The free base of 1-benzoyl-1-phenylhydrazine is thermally stable to 260°, where it decomposes forming benzanilide and other products (7).*

[8]*Subsequent to our observations, T. Taguchi et al. (8) reported a similar N_1 to N_2 migration.*

Can. J. Chem. Downloaded from www.nrcresearchpress.com by 210.87.254.42 on 09/05/12
For personal use only.

Compound XI, isomeric with the isosydnone V, was prepared from 1-benzoyl-2-methylhydrazine hydrochloride and phosgene and also by alkylation of compound VIII.

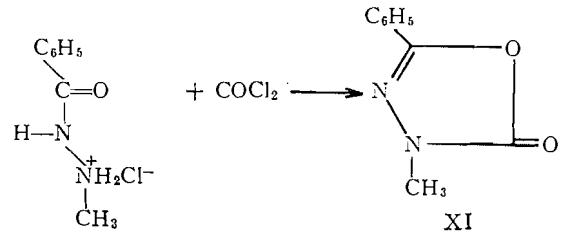

XI

The following reaction sequence was attempted in the hope of obtaining 1-benzoyl-2-methylhydrazine. Benzoic acid hydrazide and formaldehyde gave a product that analyzed for XII,[9] but physical measurements indicated that it was a polymer, most likely the

$$C_6H_5CONHNH_2 + CH_2O \rightarrow C_6H_5CONHN{=}CH_2$$
XII

trimer 1,3,5-tribenzamidohexahydro-*s*-triazine (XIII). The product was reduced catalytically in the presence of acetic acid and formed the desired 1-benzoyl-2-methylhydrazine that was prepared independently from methyl benzoate and methyl hydrazine (3).

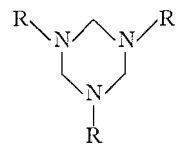

(where R is $NHCOC_6H_5$)

XIII

When benzoic acid hydrazide was treated with acetaldehyde, the ethylidene derivative was formed.

$$C_6H_5CONHNH_2 + CH_3CHO \rightarrow C_6H_5CONHN{=}CHCH_3$$

EXPERIMENTAL[10]

1-Benzoyl-1-methylhydrazine Hydrochloride (VII) (3)

Forty-six grams (1.0 mole) of methylhydrazine dissolved in 200 ml of water was held near 40° while 113 g (0.5 mole) of benzoic anhydride was added over a 1-h period. Stirring was continued for 0.5 h and then the solution was concentrated by heating under reduced pressure. Water was removed by adding 200 ml of ethanol and 200 ml of benzene and concentrating under reduced pressure. About 200 ml of ethanol near saturation with hydrogen chloride was added, followed by 1 l of dry ether. The salt that separated was collected and dissolved in 200 ml of water. Solid sodium carbonate was added until the solution was basic and the resulting mixture was extracted twice with 500 ml of ether. The ether extract was dried and then concentrated by heating on a steam bath. The residue was distilled under reduced pressure and 20 g of 1-benzoyl-1-methylhydrazine, b.p. 130° at 1 mm, was obtained. (For the n.m.r. spectrum see footnote 3.)

Anal. Calcd. for $C_8H_{10}N_2O$: C, 63.98; H, 6.71; N, 18.65. Found: C, 64.14; H, 6.91; N, 18.76.

The free base was treated with 100 ml of ethanol saturated with hydrogen chloride followed by about 300 ml of dry ether. The product that separated was recrystallized more slowly from about 100 ml of ethanol and gave approximately 23 g (20% yield) of compound VII, m.p. 165°.

Anal. Calcd. for $C_8H_{10}N_2O{\cdot}HCl$: C, 51.48; H, 5.94; N, 15.01. Found: C, 51.64; H, 6.06; N, 15.01.

A sample of compound VII was heated in an oil bath at 200° for 5 min. The crude product was shown by n.m.r. analysis to be a mixture of 1-benzoyl-2-methylhydrazine and its hydrochloride only. The n.m.r. spectrum of 1-benzoyl-2-methylhydrazine showed peaks at 0.9, 2.2, 2.6, 5.0, and 7.3 τ in the ratio 1:2:3:1:3.

[9]*R. L. Hinman (9) formulated the product as XII, and reported that it failed to reduce to 1-benzoyl-2-methylhydrazine using palladium-on-carbon in ethanol (3).*

[10]*Melting points were determined with a Fisher–Johns apparatus. The infrared spectra were obtained in chloroform unless otherwise indicated and the ultraviolet measurements were taken in ethanol. Nuclear magnetic resonance spectra were measured at 60 Mc with a Varian A60 spectrometer using 10–20% solution in deuterochloroform containing 1% tetramethylsilane as internal standard.*

Can. J. Chem. Downloaded from www.nrcresearchpress.com by 210.87.254.42 on 09/05/12
For personal use only.

(a) The Preparation of Compounds V and VI by Reaction of VII with Phosgene

A solution of 1.9 g (0.01 mole) of 1-benzoyl-1-methylhydrazine hydrochloride (VII) and 5 g of phosgene in 100 ml of dry dioxane was heated under reflux for 1 h. The effluent gas was bubbled into ether and methyl chloride was identified by gas chromatography. The mixture was concentrated to dryness by heating on a steam bath under reduced pressure. The residue was dissolved in 100 ml of ethyl acetate, concentrated to about 50 ml, and then allowed to cool. The solid that separated was recrystallized from 10 ml of dioxane and gave 0.8 g (46% yield) of 4-methyl-5-phenylisosydnone (V), m.p. 152° after drying at 100° under reduced pressure.

Anal. Calcd. for $C_9H_8N_2O_2$: C, 61.36; H, 4.58; N, 15.90; mol. wt. 176. Found: C, 61.64; H, 4.71; N, 16.07; mol. wt. Rast 179.

The ultraviolet absorption spectrum of compound V shows λ_{max} 294 mμ, log ϵ 4.05, and the infrared spectrum shows strong bands at 2 994, 1 754 (broad), 1 613, 1 499, 1 453, 1 420, 1 404, 1 284, 1 232 (broad), 1 011, and 688 cm^{-1}. (For other physical data see Introduction.)

The residue obtained after removal of V was dissolved in ethyl acetate and chromatographed using 28–200 mesh silica gel; 100 mg of compound VI (R_f 0.7) was obtained.

A 0.3-g sample of compound V was dissolved in 20 ml of 0.1 *N* sodium hydroxide and then treated with acetic acid. The solution was concentrated to dryness and ethanol – hydrogen chloride mixture was added followed by ether to give 0.1 g of compound VII, as shown by melting point, infrared, and n.m.r. measurements.

(b) The Reaction of Compound V with Phosgene

A solution of 1.5 g of compound V, 25 ml of dioxane, and 1.5 g of phosgene was heated under reflux for 1 h, during which time the effluent gas was collected and shown by comparison using gas chromatography to be methyl chloride. The solvent was removed by heating on a steam bath under reduced pressure and then the residue was extracted with 25 ml of ether. The ether-insoluble material weighed 0.3 g and was identified as V. The ether extract was concentrated and the residue was shown by thin-layer chromatography using a silica plate and ethyl acetate as solvent to be identical with the residue in expt. *a*. The residue was allowed to stand over water and a solid separated. It was recrystallized from water and gave 50 mg of 2-chloro-5-phenyl-1,3,4-oxadiazole (VI), m.p. 75°.

Anal. Calcd. for $C_8H_5ClN_2O$: C, 53.20; H, 2.79; Cl, 19.63; N, 15.51. Found: C, 53.77; H, 3.01; Cl, 19.37; N, 15.29.

The ultraviolet spectrum of compound VI shows λ_{max} 253 mμ, log ϵ 4.28, and the infrared spectrum has bands at 3 000 w, 1 607 w, 1 558 m, 1 526 s, 1 450 m, 1 193 s, 1 076 m, 1 064 s, 1 007 m, 707 m, and 685 cm^{-1} m. (The n.m.r. spectrum is given in the Introduction.)

(c) 1-Benzoyl-1-methylhydrazine and Phosgene

A solution of 2 g of 1-benzoyl-1-methylhydrazine free base was added to 100 ml of dry ether containing dissolved phosgene. A precipitate formed immediately and the mixture was quickly filtered. The filtrate was concentrated by heating at about 30° under reduced pressure. Water was added to the residue and a white solid separated. It was collected, air dried, and recrystallized from dioxane to give 0.3 g of compound V.

(d) Compound VII and Phosgene in Toluene

A mixture of 0.01 mole of compound VII and 100 ml of dry toluene containing 3 g of phosgene was heated under reflux for 1 h. The starting material VII was recovered in almost quantitative yield.

(e) The Preparation of Compound IX by Reaction of Compound VII and Phosgene in Pyridine

A solution of 3.8 g (0.02 mole) of compound VII in 25 ml of pyridine was treated with 1 g (0.01 mole) of phosgene contained in 25 ml of pyridine. After the solution was allowed to stand at room temperature for 1 h, about 100 ml of water was added and the solution was concentrated to dryness by heating under reduced pressure. The solid that formed was recrystallized from ethanol–water mixture and gave 1.5 g of compound IX, m.p. 195°.

Anal. Calcd. for $C_{17}H_{18}N_4O_3$: C, 62.56; H, 5.56; N, 17.17. Found: C, 62.57; H, 5.82; N, 17.05.

A sample of compound IX and phosgene heated in dioxane gave no isosydnone V, and IX was recovered.

(f) The Isolation of Compound VIII

The residue formed in reaction *a* after removal of V initially showed no spot for compound VIII on thin-layer chromatography. After it was allowed to stand in an open vessel for 2 weeks, the residue on recrystallization from benzene gave 50 mg of VIII identical with authentic material.[11]

(g) Compound VIII and Phosgene

A sample of compound VIII and dioxane containing phosgene and hydrogen chloride was heated under reflux for 1 h. The solution was concentrated to dryness by being heated under reduced pressure and compound VIII was recovered in almost quantitative yield.

[11]*Compound VIII was prepared from benzoic acid hydrazide and phosgene according to the method of B. Yasui and H. Uchida (10).*

Can. J. Chem. Downloaded from www.nrcresearchpress.com by 210.87.254.42 on 09/05/12
For personal use only.

(h) Compound V and Hydrogen Chloride

A sample of compound V dissolved in dioxane containing hydrogen chloride was heated under reflux while a slow stream of nitrogen was added. The effluent gas did not contain methyl chloride as shown by gas chromatography. The residue was placed on a thin-layer silica plate and compound V, but not VIII, was identified.

The Formation of Compound VI from Compound VIII

A mixture of 16.2 g (0.1 mole) of 2-phenyl-1,3,4-oxadiazolin-5(4H)-one[11] (VIII), 21 g of phosphorus pentachloride, and 50 ml of phosphorus oxychloride was heated under reflux for 45 min and then concentrated by being heated on a steam bath under reduced pressure. The residue was extracted with 100 ml of ether. The ether extract was distilled under reduced pressure and gave about 1 g of product, b.p. 140° at 10 mm. The material solidified and was recrystallized from water to give a small yield of compound VI as shown by comparison of the n.m.r. and infrared spectra with those of the material described earlier.

Rearrangement of 1-Benzoyl-1-phenylhydrazine Hydrochloride

A sample of 1-benzoyl-1-phenylhydrazine hydrochloride (11) was heated at 230° for 5 min. A near-quantitative yield of 1-benzoyl-2-phenylhydrazine, m.p. 165° (lit. (12), m.p. 168°), was obtained. The identity of the product was established by comparison of the n.m.r. spectrum with that of authentic material prepared according to the method of Fischer (12).

Preparation of Compound XIII and its Reduction to 1-Benzoyl-2-methylhydrazine

A solution of 21 g (0.15 mole) of benzoic acid hydrazide, 40 ml of ethanol, 12 ml (0.15 mole) of 37% aqueous formaldehyde, and 20 ml of water was heated on a steam bath for 5 min and crystals formed. The product XIII was insoluble in most solvents except dimethylsulfoxide and a sample recrystallized from dimethylsulfoxide–water melted near 170° (footnote 9, m.p. 169°).

Anal. Calcd. for $(C_8H_8N_2O)_3$: C, 64.85; H, 5.44; N, 18.91. Found: C, 64.37; H, 5.45; N, 18.68.

It was not possible to obtain an accurate molecular weight because of solubility problems. The n.m.r. spectrum obtained in dimethylsulfoxide was greatly different from benzoic acid ethylidenehydrazide and in agreement with compound XIII, τ = 2.2, 2.5, and 5.8 in the ratio 2:3:2. The ultraviolet absorption spectrum shows λ_{max} 224 mμ, log ϵ 3.95 (monomer), and the infrared spectrum obtained as a Nujol mull shows absorption peaks at 3 556 w, 3 195 w, 2 900 s, 1 686 s, 1 650 s, 1 481 m, 1 307 m, 939 m, 910 m, and 714 cm^{-1} s.

A mixture of 4.4 g (0.01 mole) of compound XIII, 0.5 g of 5% palladium-on-carbon, 100 ml of acetic acid, and hydrogen was shaken in a Paar apparatus for 2 h, during which time 0.03 mole of hydrogen was absorbed. The catalyst and solvent were removed, and the residue was suspended in 25 ml of 1 *N* sodium hydroxide solution and extracted with ethyl acetate. Evaporation of the dried ethyl acetate solution gave an oil that was dissolved in ethanol and treated with ether containing hydrogen chloride. The 1-benzoyl-2-methylhydrazine hydrochloride, 1.4 g (25% yield), was identical with that prepared from methylhydrazine and ethyl benzoate according to the procedure of Hinman (3).

Benzoic Acid Ethylidenehydrazide

A solution of 4 g of benzoic acid hydrazide, 1 ml of acetaldehyde, and 300 ml of benzene was evaporated on a steam bath and the residue was recrystallized from ether to give benzoic acid ethylidenehydrazide, m.p. 155° (lit. (13), m.p. 157°). The compound is a monomer as shown by physical measurements; mol. wt. calcd. 162, found 164 (micro osmometric); n.m.r. spectrum in $CDCl_3$ shows τ = 8.1 (three protons CH_3, J = 5), τ 2.2 and 2.6 (phenyl, with geminal olefinic proton at approximately same shift as ortho protons obscuring the character of each), τ = −0.9 (amide); infrared spectrum shows peaks at 3 333 vw, 3 215 w, 2 976 m, and 1 658 s, and 1 545, 1 512, 1 280, 1 262, 1 135, 865, 704, and 690 cm^{-1} all m.

3-Methyl-5-phenyl-2,3-dihydro-1,3,4-oxadiazol-2-one (XI)

(*i*) A solution of 1 g of 1-benzoyl-2-methylhydrazine hydrochloride, 1 g of phosgene, and 50 ml of dry dioxane was heated on a steam bath for 1 h and then concentrated at reduced pressure. The solid was recrystallized from ethanol and gave 0.2 g of compound XI, m.p. 105–107°.

Anal. Calcd. for $C_9H_8N_2O_2$: C, 61.36; H, 4.58; N, 15.90. Found: C, 61.29; H, 4.71; N, 15.64.

Compound XI displayed the following physical data: ultraviolet absorption spectrum shows λ_{max} 266 mμ, log ϵ 3.97; infrared spectrum shows strong peaks at 1 785, 1 358, 1 019, and 686 cm^{-1}; n.m.r. spectrum shows τ = 2.1, 2.5, and 6.5 in the ratio 2:3:3.

(*ii*) A solution of 4.8 g (0.03 mole) of 2-phenyl-1,3,4-oxadiazolin-5(4H)-one[11] (VIII), 1.6 g of sodium methylate, 4.3 g of methyl iodide, and 50 ml of methanol was stored at 40° overnight. About half the methanol was removed by evaporation and 100 ml of water was added. The solid that formed was recrystallized from ethanol and gave 2 g (38% yield) of XI identical with the material prepared in procedure *i*.

ACKNOWLEDGMENTS

The microanalyses were determined by W. L. Brown, H. L. Hunter, D. Cline, C. Ashbrook, and J. Gilliam; and the physical chemical measurements were made by H. Boaz,

Can. J. Chem. Downloaded from www.nrcresearchpress.com by 210.87.254.42 on 09/05/12
For personal use only.

G. M. Maciak, L. G. Tensmeyer, P. Landis, H. A. Rose, D. O. Woolf, Jr., L. Huckstep, Doris Stephens, J. Klemm, L. Spangler, and P. Unger of this laboratory. The dipole moment determination was supplied by Dr. L. E. Sutton, Oxford University, through the courtesy of Prof. W. David Ollis. After this work was completed, ref. 2*a* was kindly pointed out by Prof. Kevin T. Potts.

REFERENCES

1. (*a*) W. Baker and W. D. Ollis. Quart. Rev. London, **11**, 15 (1957).
   (*b*) F. H. C. Stewart. Chem. Rev. **64**, 129 (1964).
   (*c*) F. H. C. Stewart and N. Danieli. Chem. Ind. London, 1926 (1963).
   (*d*) K. D. Lawson, W. S. Brey, Jr., and L. B. Kier. J. Am. Chem. Soc. **86**, 463 (1964).
2. (*a*) M. Hashimoto and M. Ohta. Bull. Chem. Soc. Japan, **34**, 668 (1961); Chem. Abstr. **56**, 11580 (1962).
   (*b*) G. Sugarman. Dissertation Abstr. **24**, 526 (1963).
3. R. L. Hinman and D. Fulton. J. Am. Chem. Soc. **80**, 1895 (1958).
4. C. Ainsworth. J. Am. Chem. Soc. **77**, 1148 (1955).
5. W. Baker, W. D. Ollis, and V. D. Poole. J. Chem. Soc. 1542 (1950).
6. R. C. Elderfield. Heterocyclic compounds. Vol. 5. John Wiley and Sons, Inc., New York, N.Y. 1957. p. 93.
7. O. Silberrad. J. Chem. Soc. **77**, 1185 (1900).
8. T. Taguchi, J. Ishibashi, T. Matsuo, and M. Kojima. J. Org. Chem. **29**, 1097 (1964).
9. R. L. Hinman. J. Am. Chem. Soc. **79**, 414 (1957).
10. B. Yasui and H. Uchida. J. Pharm. Soc. Japan, **76**, 1300 (1956); Chem. Abstr. **51**, 6636 (1957).
11. G. Lockemann. Ber. **43**, 2223 (1910).
12. E. Fischer. Ann. **190**, 67, 125 (1878).
13. G. Klein and W. Fuchs. Biochem. Z. **213**, 40 (1929).

Can. J. Chem. Downloaded from www.nrcresearchpress.com by 210.87.254.42 on 09/05/12
For personal use only.

Can. J. Chem. Downloaded from www.nrcresearchpress.com by 210.87.254.105 on 09/05/12
For personal use only.

SYNTHESIS OF ISOTOPICALLY LABELLED OLEFINS VIA THE WITTIG REACTION

J. G. Atkinson, M. H. Fisher, D. Horley, A. T. Morse, R. S. Stuart, and E. Synnes
Isotopic Laboratories of Merck Sharp and Dohme of Canada, Ltd., Montreal, Quebec
Received January 6, 1965

Dedicated to Professor R. B. Sandin on the Occasion of his Sixty-Eighth Birthday

ABSTRACT

A new application of the Wittig reaction to the preparation of olefins of low molecular weight which allows selective labelling in the vinyl or allyl positions with isotopes of hydrogen and carbon has been developed. Using the modification of the Wittig reaction introduced by E. J. Corey, in which a solution of the methylsulfinyl carbanion in dimethyl sulfoxide serves as the base, a series of olefins from C_2 to C_8 were synthesized. The synthesis was applied to the preparation of the following labelled compounds: 5-methylene-^{14}C-bicyclo[2.2.1]hept-2-ene; propene-1-^{14}C; 1-butene-1-^{14}C; propene-1-d_1; 2-methylpropene-1,1-d_2; 2-methyl-d_3-propene-3,3,3-d_3; 2-methyl-2-butene-4,4,4-d_3; 2-methyl-d_3-2-butene-1,1,1-d_3; methylene-d_2-cyclohexane. For the synthesis of carbon-labelled olefins the reaction has few limitations since the intermediates and products are isotopically stable under the reaction conditions. Deuterium-labelled olefins can be obtained from deuterated formaldehyde or β-deuterated phosphonium salts, but α-deuteroketones and aldehydes and α-deuterophosphonium salts lose the isotope to the solvent.

In all the Wittig reactions, benzene was formed as a by-product in 10–15% yield. The mechanism of benzene formation is probably analogous to that proposed by Seyferth involving the decomposition of a pentacovalent phosphorous intermediate.

INTRODUCTION

The use of organic molecules specifically labelled with isotopes of carbon, hydrogen, oxygen, and nitrogen has become a classical method for the study of reaction mechanisms (2, 3). More recently, isotopically labelled molecules have proved to be invaluable sources of information in spectroscopic research. German workers (7) have recently made an extensive study of the infrared (i.r.) and Raman spectra of a number of selectively deuterated olefins. Studies of the dehydration of straight-chain alcohols, specifically labelled with deuterium, during mass spectral fragmentation have been carried out (5). Djerassi (6) has studied extensively the mass spectral cleavage patterns of numerous specifically deuterated steroid species. The mechanism of the retro Diels–Alder reaction of the maleic anhydride adduct of butadiene-1,1,4,4-d_4 has been investigated by Thornton (4). The unusually large H—H coupling constant of formaldehyde was obtained by Shapiro (1) using formaldehyde-d_1.

Carbon-13 labelled molecules have found use in electron-spin resonance (e.s.r.) spectroscopy. Rieker *et al.* (8) have studied the e.s.r. spectrum of the free radical from 2,4,6-tritertiarybutylphenol-1-^{13}C.

These uses have made it necessary to work out unequivocal syntheses for partially but specifically isotope-labelled organic molecules. The purpose of this paper is to report a new general synthesis of deuterated olefins which has been developed in these laboratories (9).

Olefins of low molecular weight, labelled either on the double-bond carbons or in the allylic positions, are widely used in gas-phase kinetics work and the study of hydrogen abstraction reactions. One of the attendant difficulties in the synthesis of such compounds

is allylic rearrangement, which leads to scrambling and (or) loss of the label. One approach which seemed particularly attractive was the Wittig reaction (10, 11).

The Wittig reaction has the advantage that, in general, the introduction of the double bond takes place under mild conditions without rearrangement. In addition, there are few side reactions and it seemed that it would be a straightforward matter to separate the volatile products from the main by-product, triphenylphosphine oxide.

RESULTS

Chemical Syntheses

This work began with the synthesis of 5-methylene-bicyclo[2.2.1]hept-2-ene(methylenenorbornene), II, from bicyclo[2.2.1]hept-2-en-5-one(dehydronorcamphor), I, and triphenylmethylphosphonium bromide.

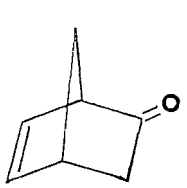

I

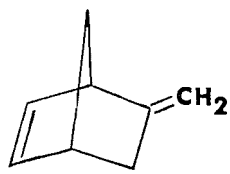

II

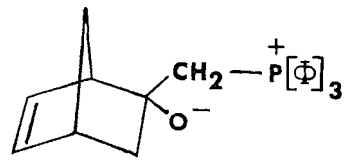

III

Dehydronorcamphor has been prepared from the Diels–Alder adduct between cyclopentadiene and α-acetoxyacrylonitrile (12) but this approach for introducing a ketone function is relatively unattractive because of the lack of a commercial source of the dienophile. Accordingly, dehydronorborneol was prepared by condensing cyclopentadiene with vinyl acetate followed by hydrolysis (13*a*). Oxidation of the mixture of epimers of dehydronorborneol with chromic acid under various conditions (13, 14) gave, in our hands, poor yields of a hydroxyl-containing ketone fraction. Apparently, under acidic conditions, further oxidation occurs readily and polyoxygenated products result.* The ketone was readily obtained, using Sarett's reagent (16) as described by Cristol and Freeman (17), in yields of 65–70% by modifications of the published procedure (17). A basic medium appears to be necessary for the successful oxidation of such sensitive alcohols to avoid electrophilic attack on the double bond. This is borne out by the successful oxidation of dehydronorborneol to dehydronorcamphor (17, 18) and the preparation of Δ^4-cholesten-3-one (19) by modifications of the Oppenauer oxidation.

Addition of the ketone I to an ethereal solution of triphenylphosphinemethylene and subsequent work-up yielded methylenenorbornene, II, in about 20% crude yield, contaminated with 10–15% of lower boiling impurities. It was not possible to improve the yield by prolonged refluxing of the reaction mixture. The slow decomposition of the initially formed betaine intermediate III (11*c*) is presumably due to the increase in ring strain accompanying the introduction of another trigonal carbon into the already strained bicycloheptene system. Accordingly, methylene-^{14}C-norbornene was prepared from triphenylmethyl-^{14}C-phosphonium iodide and purified by preparative vapor phase chromatography (v.p.c.).†

Because of difficulties encountered when ether was used as a solvent, it was decided to try the dimethyl sulfoxide – sodium hydride system which Corey has introduced as a

See, for example, the chromic acid oxidation of cholesterol (15).

†*The preparation of optically active methylenenorbornene from optically active dehydronorcamphor by the Wittig reaction has been reported (20).*

Can. J. Chem. Downloaded from www.nrcresearchpress.com by 210.87.254.105 on 09/05/12
For personal use only.

convenient modification of the Wittig reaction* (21) (eqs. [1] and [2]). Repetition of the preparation of methylenenorbornene using this reagent and examination of the volatile products by vapor phase chromatography showed it to be a mixture of methylenenorbornene, II, and a single lower boiling impurity in a ratio of 30:1; the yield of II was 59%. The lower boiling impurity was proved to be benzene and even careful exclusion of extraneous sources did not prevent its appearance in the product (see Discussion).

[1] $$CH_3{-}\overset{\overset{O}{\|}}{S}{-}CH_3 + NaH \rightarrow CH_3{-}\overset{\overset{O}{\|}}{S}{-}\overset{\ominus}{C}H_2\overset{\oplus}{N}a + H_2$$

IV

[2] $$\Phi_3\overset{\oplus}{P}{-}CH_3\overset{\ominus}{I} + CH_3{-}\overset{\overset{O}{\|}}{S}{-}CH_2Na \rightarrow \Phi_3P{=}CH_2 + CH_3{-}\overset{\overset{O}{\|}}{S}{-}CH_3 + NaI$$

[3] $$\Phi_3P{=}CH_2 + RR'C{=}O \rightarrow RR'C{=}CH_2 + \Phi_3P{=}O$$

A number of other gaseous and volatile hydrocarbons were then synthesized in this system using low molecular weight aldehydes and ketones; the results are shown in Table I.

The general procedure adopted was to prepare a solution of triphenylphosphine ylid in dry dimethyl sulfoxide (21), then to add the carbonyl compound as a solution in the same solvent or, in the case of formaldehyde, as anhydrous polyoxymethylene (eqs. [1–3]). Gaseous products were collected in a trap cooled to the necessary temperature and finally pulled off under vacuum into the trap cooled in liquid nitrogen. Liquid products were distilled into a liquid nitrogen cooled trap under vacuum after completion of the reaction. Purification of gaseous materials was accomplished by bulb-to-bulb distillation on a vacuum line, while liquids were purified by vapor phase chromatography. Identity was established in all cases by comparison of i.r. or n.m.r. spectra with those of authentic samples.

These are the first recorded syntheses of ethylene, propene, 1-butene, isobutene, and butadiene via the Wittig reaction and it is only recently that simple aliphatic aldehydes have been used as the carbonyl component in the Wittig reaction (22).

The last item in Table I records the attempted synthesis of ethyl vinyl ether by the reaction between triphenylphosphinemethylene and ethyl formate. However, the major volatile product was ethyl alcohol, which undoubtedly arises by an alternative decomposition of the betaine intermediate V.

$$\Phi_3P{=}CH_2 + H{-}\overset{\overset{O}{\|}}{C}{-}OC_2H_5 \rightarrow \Phi_3{-}\overset{\oplus}{P}{-}CH_2{-}\overset{\overset{O^{\ominus}}{|}}{\underset{\underset{H}{|}}{C}}{-}OC_2H_5$$

V

$$\Phi_3P{=}CH{-}CHO + C_2H_5OH \leftarrow \Phi_3{-}\overset{\oplus}{P}{-}CH_2{-}\overset{\overset{O}{\|}}{C}{-}H + \overset{\ominus}{O}C_2H_5$$

Isotopic Syntheses

After development of the chemical syntheses, several isotopically labelled compounds were synthesized and analyzed to determine the useful scope of the reaction for labelling with hydrogen and carbon isotopes. The results for deuterium and carbon-14 labelling are shown in Table II and Table III, respectively. Entries 7 to 11 in Table II record unsuccessful attempts to utilize α-deuterated carbonyl compounds and an α-deuterated phosphonium salt.

*We thank Professor L. F. Fieser for pointing out this modification during the early stages of this work.

Can. J. Chem. Downloaded from www.nrcresearchpress.com by 210.87.254.105 on 09/05/12
For personal use only.

Can. J. Chem. Downloaded from www.nrcresearchpress.com by 210.87.254.105 on 09/05/12
For personal use only.

TABLE I

Chemical synthesis of low molecular weight olefins via the Wittig reaction in dimethyl sulfoxide

Moles of phosphonium salt*		Moles of carbonyl component		Moles NaH	Product	Yield, %†	Purity, %‡
$[\Phi_3P—CH_3]Br$	0.10	$(CH_2O)_n$	0.13	0.13		40	98
$[\Phi_3P—CH_2CH_3]Br$	0.10	$(CH_2O)_n$	0.20	0.13		19	99.8
$[\Phi_3P—CH_3]Br$	0.16	CH_3CHO	0.14	0.15		21	99.5
$[\Phi_3P—CH(CH_3)_2]I$	0.10	$(CH_2O)_n$	0.15	0.10		20	99.0
$[\Phi_3P—CH_3]I$	0.04	CH_3CH_2CHO	0.060	0.036		50	99.0
$[\Phi_3P—CH_2CH=CH_2]Br$	0.15	$(CH_2O)_n$	0.10	0.17		43	97.5
$[\Phi_3P—CH_2CH_3]Br$	0.10	CH_3COCH_3	0.10	0.10		15	99.8
$[\Phi_3P—CH_3]Br$	0.11	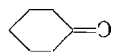	0.11	0.11		50	99.8
$[\Phi_3P—CH_3]I$	0.022		0.019	0.020		40	99.8
$[\Phi_3P—CH_3]Br$	0.10	$HCOOC_2H_5$	0.09	0.10	C_2H_5OH	74‡	—

*In contrast to the report of Collins and Hammond (27), no difficulty was experienced in the use of the iodide salts in the work described here.
†Yields of isolated and purified products.
‡Determined by vapor phase chromatography.

TABLE II

Deuterated olefins synthesized via the Wittig reaction*†

Phosphonium salt	Carbonyl component	Product	Analysis (mass spec.)
1. $[\Phi_3P—CH_2CH_3]Br$	$(CHDO)_n$	$CH_3CH{=}CHD$	97.8% -d_1 97.8 atom % D
2. $[\Phi_3P—CH(CH_3)_2]I$	$(CD_2O)_n$	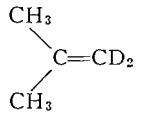	98.6% -d_2 99.3 atom % D 1.4% -d_1
3. $[\Phi_3P—CH(CD_3)_2]I$	$(CH_2O)_n$	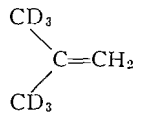	93.7% -d_6 99.0 atom % D 6.3% -d_5
4. $[\Phi_3P—CH_2CD_3]Br$	CH_3COCH_3	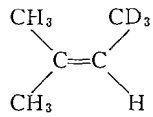	98.5% -d_3 99.5 atom % D 1.5% -d_2
5. $[\Phi_3P—CH(CD_3)_2]I$	CH_3CHO	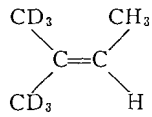	94.2% -d_6 99.0 atom % D 5.8% -d_5
6. $[\Phi_3P—CD_3]Br$	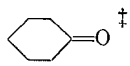 ‡	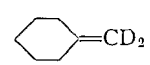	88.6% -d_2 94.3 atom % D 11.4% -d_1
7. $[\Phi_3P—CH_3]I$	CD_3CDO	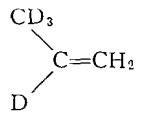	~25% -d_5 ~50% -d_4 ~25% -d_3
8. $[\Phi_3P—CH_3]I$	CD_3COCD_3	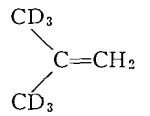	30% -d_6 22% -d_5 + d_4, d_7, d_8 species
9. $[\Phi_3P—CH_3]I$	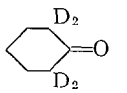	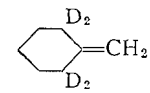	74% -d_4 15% -d_3 + others
10. $[\Phi_3P—CD_3]I$	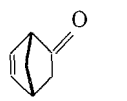	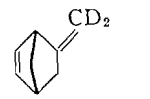	95.1% -d_0 4.8% -d_1
11. $[\Phi_3P—CD_3]I$	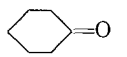	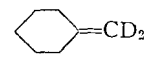	83.9% -d_1 15.5% -d_2

*Chemical yields are approximately as in Table I.
†All reactions were done in the dimethyl sulfoxide – sodium hydride system.
‡Run in ether using *n*-propyl lithium as the base.

It is apparent that the synthesis has wide application for the preparation of carbon-14 (and carbon-13) labelled olefins, which could, in turn, be converted to a number of other derivatives. Propene-1-^{14}C could conceivably have rearranged to give some propene-3-^{14}C, but the indirect evidence against this possibility is the complete absence of rearrangement in the preparation of 1-butene and methylenecyclohexane, both of which are less stable than their rearrangement products, 2-butene and 1-methylcyclohexene, neither of which was detected in these preparations.

Can. J. Chem. Downloaded from www.nrcresearchpress.com by 210.87.254.105 on 09/05/12
For personal use only.

TABLE III

Carbon-14 labelled olefins synthesized via the Wittig reaction

Phosphonium salt	Activity of phosphonium salt	Carbonyl component	Product	Yield
$[\Phi_3P—{}^{14}CH_3]I$	2 μc/mole			10%*
$[\Phi_3P—{}^{14}CH_3]I$	75 μc/mole	$CH_3—CHO$	$CH_3CH={}^{14}CH_2$	46%†
$[\Phi_3P—{}^{14}CH_3]I$	75 μc/mole	CH_3CH_2CHO	$CH_3CH_2CH={}^{14}CH_2$	50%†

*Run in ether using ethyl lithium as base.
†Run in dimethyl sulfoxide – sodium hydride system.
‡Activity 2.01 μc/mole.

The deuterium-labelled compounds were analyzed for isotopic content by mass spectrometry. The high isotopic content of the successful syntheses was also taken as indirect evidence for the position of the label. Had there been double-bond isomerization or equilibration, deuterium would also have been lost or diluted. The position of deuterium labelling was confirmed in the case of the two 2-methyl-2-butenes by a careful n.m.r. analysis (23), which showed that deuterium had completely replaced hydrogen in the positions indicated.

The deuterium-labelled isobutenes and 2-methyl-2-butenes are new compounds, but Italian workers (28) have reported the synthesis of several selectively deuterated propenes. Propene-1,1-d_2 was prepared by the sequence: 2-bromacetyl bromide → 2-bromo-1-propanol-1,1-d_2 → 1,2-dibromopropane-1,1-d_2 → propene-1,1-d_2. Both *cis*- and *trans*-propene-1-d_1 were obtained from the corresponding 1-bromopropene, via the vinyl lithium derivative, which was treated with heavy water, and propene-2-d_1 was synthesized by reduction of acetone with lithium aluminium deuteride and dehydration of the resulting alcohol.

DISCUSSION

The results obtained indicate the general usefulness of the Wittig reaction as a means of preparing a number of volatile hydrocarbons labelled in various positions. The products obtained are stable under the reaction conditions, both chemically and isotopically, which was anticipated on the basis of previous work with the Wittig reaction. Use of the dimethyl sulfoxide – sodium hydride system is particularly advantageous because the high-boiling solvent facilitates isolation of volatile products. The reaction is also very clean in comparison with the use of ether as solvent, the only volatile by-product being benzene.

For carbon labelling the present synthesis would seem to have few restrictions with regard to the structure of either the carbonyl component or the phosphonium salt and for stable products it should be widely applicable. For both carbon and hydrogen isotopes it provides a ready means to obtain allylic labelled compounds which are often difficult to prepare reliably by other means. Such compounds could be obtained by reduction of the appropriate α,β-unsaturated acid or ketone to the alcohol, conversion to the tosylate or bromide, and further reduction. But such intermediates and reactions are well known to lead to allylic rearrangements.

The last entries in Table II show that there are certain limitations to the synthesis of deuterium-labelled compounds. Thus, α-deuterated aldehydes and ketones undergo extensive loss of isotope before condensation with the ylid as evidenced by the low isotopic content of the products from acetaldehyde-d_4, acetone-d_6, and cyclohexanone-2,2,6,6-d_4.

Can. J. Chem. Downloaded from www.nrcresearchpress.com by 210.87.254.105 on 09/05/12
For personal use only.

The loss or scrambling of deuterium is probably due to enolization of the carbonyl compound with the ylid acting as the base according to the following scheme.

$$CD_3CDO + (C_6H_5)_3P{=}CH_2 \rightleftharpoons \overset{\ominus}{C}D_2CDO + (C_6H_5)_3\overset{\oplus}{P}{-}CH_2D \rightleftharpoons CD_2H{-}CDO + (C_6H_5)_3P{=}CHD$$

$$CD_2H{-}CDO + (C_6H_5)_3P{=}CH_2 \rightarrow CD_2H{-}CD{=}CH_2 \quad \text{(propene-}d_3\text{)}$$

$$CD_3{-}CDO + (C_6H_5)_3P{=}CH_2 \rightarrow CD_3{-}CD{=}CH_2 \quad \text{(propene-}d_4\text{)}$$

$$CD_3{-}CDO + (C_6H_5)_3P{=}CHD \rightarrow CD_3{-}CD{=}CHD \quad \text{(propene-}d_5\text{)}$$

It would seem to be possible to overcome these difficulties by reverting to the ether – alkyl lithium system for the reaction. One run (number 6, Table II) with cyclohexanone and triphenylmethyl-d_3-phosphonium iodide yielded methylene-d_2-cyclohexane, VI, of 94 atom % deuterium content in the methylene group. The slight (5%) loss of isotope is probably due to traces of water or hydroxide ion in the solvent, but the complete absence of any d_3 species in the mass spectrum indicates that there was no enolization of the ketone. Enolization would have produced some α-deuterated ketone, which, in turn, should lead to d_3 or higher species by condensation with doubly labelled ylid.

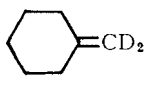

VI

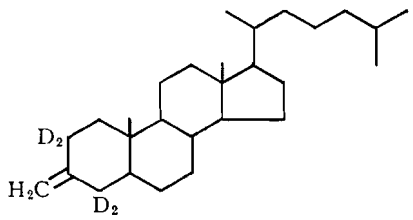

VII

The applicability of the conventional ether system to α-deuterated ketones is confirmed by Cookson's synthesis of 3-methylenecholestane-2,2,4,4-d_4, VII, from the exchanged ketone with good retention of deuterium (24).

During this work, an interesting side reaction which is worthy of comment was consistently observed. In every Wittig reaction run, whether in ether or dimethyl sulfoxide, benzene was formed as a by-product. In previous work (21), no observation of benzene was made, although Seyferth (25), in a careful investigation of the reactions between methyl lithium and triphenylmethylphosphonium bromide in ether, has shown that benzene is also formed under these conditions in 20–25% yields. In the present work a reaction between triphenylmethylphosphonium iodide and methylsulfinyl carbanion for 16 h yielded 7.5% of benzene by direct isolation. In another reaction, the yield of benzene was determined by isotope dilution using benzene-d_1 and was found to be 13.6%. Seyferth (25) postulated the decomposition of a pentacovalent phosphorous intermediate, VIII, as the source of benzene in his work. Attack of methylsulfinyl carbanion on triphenylmethylphosphonium iodide could lead to a similar structure, IX, which could decompose to yield benzene. Formation of a volatile by-product might be prevented by using a suitably substituted phosphine such as the tri-*p*-methoxyphenyl derivative and such a possibility is under investigation.

Entries 10 and 11 in Table II show that when triphenylmethyl-d_3-phosphonium iodide is used in the dimethyl sulfoxide system extensive loss of deuterium occurs. The most obvious explanation is a fast equilibrium between dimethyl sulfoxide and triphenylphosphinemethylene (eq. [4]). Such an equilibrium would effectively wash out the deuterium and lead to low isotopic content in the product.

Can. J. Chem. Downloaded from www.nrcresearchpress.com by 210.87.254.105 on 09/05/12
For personal use only.

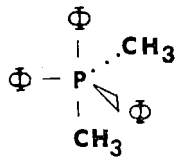

VIII

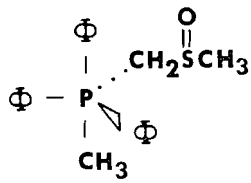

IX

However, such an equilibrium is made unlikely by the observation that the yield of benzene is unchanged with extended reaction time. If such an equilibrium were as fast as indicated by the loss of deuterium, then longer reaction times would give more opportunity for the formation of the pentacovalent intermediate IX and irreversible formation of benzene. Thus, another mechanism by which deuterium is lost from the phosphonium salt must be operative.

Equations 5 to 8 indicate the currently (11*e*) suggested path for the Wittig reaction. From a consideration of the various intermediates, betaine X is tentatively suggested as the source of deuterium exchange with the solvent (eq. [9]). The conjugate base XI of the betaine should be a stronger base than triphenylphosphinemethylene because it carries a net negative charge and hence should be more likely to remove a proton from a dimethyl sulfoxide molecule.

[4] $$\Phi_3P{=}CD_2 + CH_3{-}\overset{\overset{O}{\|}}{S}{-}CH_3 \rightleftharpoons \Phi_3\overset{\oplus}{P}{-}CD_2H + CH_3{-}\overset{\overset{O}{\|}}{S}{-}\overset{\ominus}{C}H_2$$
$$\Phi_3\overset{\oplus}{P}{-}CD_2H \rightleftharpoons \text{etc.}$$

[5] $$\Phi_3\overset{\oplus}{P}{-}CD_3 + CH_3{-}\overset{\overset{O}{\|}}{S}{-}\overset{\ominus}{C}H_2 \rightarrow \Phi_3P{=}CD_2 + CH_3{-}\overset{\overset{O}{\|}}{S}{-}CH_2D$$

[6] $$\Phi_3P{=}CD_2 + \rangle C{=}O \rightarrow \rangle C\begin{matrix}\diagup O^{\ominus}\\ \diagdown CD_2{-}\overset{\oplus}{P}\Phi_3\end{matrix}$$
X

[7] $$\rangle C\begin{matrix}\diagup O^{\ominus}\\ \diagdown CD_2{-}\overset{\oplus}{P}\Phi_3\end{matrix} \rightarrow \rangle C\begin{matrix}\diagup O\\ \diagdown CD_2\end{matrix}P\Phi_3$$

[8] $$\rangle C\begin{matrix}\diagup O\\ \diagdown CD_2\end{matrix}P\Phi_3 \rightarrow \rangle C{=}CD_2 + \Phi_3P{=}O$$

[9] $$\rangle C\begin{matrix}\diagup O^{\ominus}\\ \diagdown CD_2{-}\overset{\oplus}{P}\Phi_3\end{matrix} + CH_3{-}\overset{\overset{O}{\|}}{S}{-}\overset{\ominus}{C}H_2 \rightleftharpoons \rangle C\begin{matrix}\diagup O^{\ominus}\\ \diagdown CD{-}\overset{\oplus}{P}\Phi_3\\ \ominus\end{matrix} + CH_3{-}\overset{\overset{O}{\|}}{S}{-}CH_2D$$
$$\rangle C\begin{matrix}\diagup O^{\ominus}\\ \diagdown CD{-}\overset{\oplus}{P}\Phi_3\\ \ominus\end{matrix} \rightleftharpoons \text{etc.}$$

X XI

A firm decision about the mechanism of deuterium loss cannot be made at this time and the matter is under further investigation in these laboratories.

Can. J. Chem. Downloaded from www.nrcresearchpress.com by 210.87.254.105 on 09/05/12
For personal use only.

Can. J. Chem. Downloaded from www.nrcresearchpress.com by 210.87.254.105 on 09/05/12
For personal use only.

EXPERIMENTAL

Melting points were taken on a Fisher–Johns melting point block and are uncorrected; boiling points are uncorrected. Infrared spectra were run on a Perkin–Elmer model 21 spectrometer; gas samples were run in a 10-cm cell at about 100 mm pressure. N.m.r. spectra were obtained on a Varian A-60 spectrometer using neat liquids; mass analyses were done on an Associated Electrical Industries instrument, model MS-2.

Materials

The following isotopically labelled starting materials were commercially available (Merck Sharp and Dohme of Canada, Ltd.): methyl-d_3 bromide, methyl-d_3 iodide, 2-propyl-1,1,1,3,3,3-d_6 iodide, ethyl-2,2,2-d_3 bromide, acetaldehyde-d_4, acetone-d_6, cyclohexanone-2,2,6,6-d_4, benzene-d_1, methyl-^{14}C iodide, methyl-^{14}C bromide.

Preparation of Triphenylalkylphosphonium Salts

All the phosphonium salts were prepared by the reaction between triphenylphosphine and the appropriately labelled alkyl halide. Ether was found to be a more convenient solvent than benzene (26) for the preparation of the triphenylmethylphosphonium salts. The preparations are summarized as follows: mole ratio of triphenylphosphine to alkyl halide; concentration of alkyl halide; solvent; temperature and time of reaction; melting point; yield of phosphonium salt.

Triphenylmethyl-d_3-phosphonium bromide: 1.14; 0.5 *M*; ether; 25° for 7 days; 231–233°; 65%.

Triphenylmethyl-d_3-phosphonium iodide: 1.15; 0.4 *M*; ether; 25° for 4 days; 184–186°; 98%.

Triphenylethyl-2,2,2-d_3-phosphonium bromide: 1.05; 0.4 *M*; acetonitrile; reflux for 48 h; 205–208°; 97%.

Triphenyl-2-propyl-1,1,1,3,3,3-d_6-phosphonium iodide: 1.25; 0.4 *M*; acetonitrile; reflux for 4 days; 197–198°; 77%. Isopropyl bromide gave only 10% of phosphonium salt under the same conditions.

Triphenylallylphosphonium bromide: 0.85; 1.2 *M*; acetone; 30° for 24 h; 218–225° with softening at 214°; 92%.

Triphenylmethyl-^{14}C-phosphonium bromide: 1.0; 5 *M*; benzene; 25° for 3 days; 229–231°; 91%. Activity 2 μc/mmole.

Triphenylmethyl-^{14}C-phosphonium iodide: 1.1; 0.8 *M*; ether; 25° for 3 days; 187–189°; 100%. Activity 2 μc/mmole.

Procedure for Wittig Reactions in Dimethyl Sulfoxide

The preparation of butadiene is typical of the procedure used.

A 500-ml three-necked flask was fitted with a condenser and nitrogen inlet, thermometer, and magnetic stirring bar and flushed with nitrogen for 10 min. Reagent grade dimethyl sulfoxide (100 ml) was added to the flask and nitrogen passed over the surface of the vigorously stirred solvent for 30 min. Sodium hydride (50% dispersion, 7.7 g, 0.17 mole) was then added and the mixture heated at 65° under a positive pressure of nitrogen until all the hydride had dissolved (ca. 2 h).

To the cooled reaction mixture triphenylallylphosphonium bromide (57.5 g, 0.15 mole) was added in portions, over 15 min. The reaction was mildly exothermic, the temperature rising briefly to 40°. The dark red solution was stirred at room temperature for 1 h.

To the top of the condenser was attached a bubbler and dry ice cooled trap flushed with nitrogen. Polymeric formaldehyde (3.0 g, 0.1 mole) was added in one portion to the ylid solution stirred in a cold water bath. The temperature rose quickly to 50° and slowly dropped back. Heat was applied gently and the reaction was held at 65° for 1 h and at room temperature for 16 h. After the trap was cooled in liquid nitrogen, vacuum and gentle heating (~60°) were applied to pull volatile materials into the trap.

The volatile material was distilled bulb-to-bulb twice on a vacuum line to remove benzene and traces of dimethyl sulfoxide. It was finally passed slowly through a U-tube of Ascarite and Drierite to remove sulfur impurities and water and condensed into a steel cylinder. Vapor phase chromatography on activated silica gel at 90° showed less than 0.5% gaseous impurities and on polypropylene glycol at 25° it showed about 2.5% of a higher-boiling liquid, probably benzene. A gas phase i.r. spectrum was completely identical with that of an authentic sample of butadiene. Yield = 2.3 g, 0.043 mole (43%).

Conditions for the other syntheses are summarized in Table I and in the text. The product of the reaction between triphenylphosphinemethylene and ethyl formate was found to be a mixture of ethyl formate (1%), ethyl alcohol (85%), and benzene (15%).

Synthesis of isotopically labelled products was accomplished by the same general procedure. Usually the component containing the isotope was used in a slight deficiency unless the excess unlabelled material would have contaminated the product. The labelled compounds were all obtained with a chemical purity greater than 99%.

Benzene Formation

(i) To the reaction mixture of triphenylphosphinemethylene (0.1 mole) and cyclohexanone-2,2,6,6-d_4 (0.1 mole) was added 0.99 g of benzene-d_1 (98% d_1). A sample of the resulting benzene was separated from methylene-2,2,6,6-d_4-cyclohexane by v.p.c. and analyzed by mass spectroscopy. Found: 47.29% -d_1 and 52.70% -d_0, which corresponds to a 13.6% yield of benzene.

(ii) To a solution of 0.1 mole of methylsulfinyl carbanion in 150 ml of dimethyl sulfoxide was added 41 g (0.1 mole) of triphenylmethylphosphonium iodide over 5 min. The reaction was stirred at 25° for 16 h and

heated to 70° for 1 h, and the volatile materials removed under high vacuum. Bulb-to-bulb distillation afforded 0.6 g (0.008 mole, 8%) of pure benzene.

Dehydronorbornyl Acetate (13a)

The compound was prepared in 47% yield from cyclopentadiene and vinyl acetate at 165°; b.p. 85–88° at 19 mm; the infrared spectrum showed a very strong C=O absorption band at 1 725 cm^{-1}. If an excess of vinyl acetate was not used the product was impure and subsequently gave a low yield of dehydronorborneol.

*Dehydronorborneol**

To a cooled magnetically stirred solution of 72 g (1.8 moles) of sodium hydroxide in 1 000 ml of methanol was added 216 g (1.42 moles) of dehydronorbornyl acetate over 20 min. The reaction was protected with an Ascarite tube to exclude carbon dioxide and stirred at room temperature for 3 days. Most of the solvent was removed on a rotary evaporator, 1 500 ml of water added to the residue, and the aqueous phase extracted with 5 × 200 ml of ether. After the solution was dried over calcium chloride and the solvent evaporated, there was obtained 135 g (1.23 moles, 86%) of crude dehydronorborneol, m.p. 94–105°. Further extraction of the aqueous layer with ether yielded an additional 3 g of alcohol, bringing the yield to 88%. Crystallization from 200 ml of petroleum ether (35–60°) and concentration of the mother liquors gave 110 g (70%) of white crystalline product, m.p. 104.5–106°.

Dehydronorcamphor (17)*

A suspension of the chromium trioxide – pyridine complex was prepared by addition of 78.6 g (0.78 mole) of chromium trioxide to 780 ml of pyridine in a 3-l flask, with stirring and cooling to keep the temperature below 25° over 60 min. A further 120 ml of pyridine was then added to increase the fluidity of the reaction mixture. After 30 min of stirring at room temperature, a solution of 30 g (0.27 mole) of dehydronorborneol in 180 ml of pyridine was added over 30 min, the internal temperature being kept below 20°. The reaction mixture was stirred at room temperature for 17 h and filtered through a pad of celite, and the flask and filter pad washed thoroughly with 5 × 250 ml of ether. After dilution with 4 l of cold water, the filtrate was divided into two parts and each part extracted with 8 × 250 ml of ether. Each ether solution was washed with 15% sulfuric acid until the washings remained acidic (5 × 250 ml), 5% sodium bicarbonate (2 × 250 ml), and water (2 × 250 ml). The aqueous solutions were backwashed with ether and the combined ether solutions dried over calcium chloride, filtered, and distilled to yield 18.9 g (0.17 mole, 64% yield) of dehydronorcamphor, b.p. 55° at 15 mm. Analysis by vapor phase chromatography showed that the product had a purity greater than 98%, and the infrared spectrum contained a strong C=O band at 1 740 cm^{-1} and a very weak O—H band at 3 500 cm^{-1}. Several oxidations using 10-g quantities of alcohol gave yields of 65–70% consistently. In one run, half the usual molar amount of chromium trioxide was used but the product was found to contain large amounts of unreacted alcohol.

Methylene-^{14}C-norbornene

A solution of ethyl lithium in 150 ml of ether in a well-dried nitrogen-filled flask was prepared from 1.2 g (0.2 mole) of lithium shot and 13 g (0.12 mole) of ethyl bromide at −13°. To the solution of ethyl lithium, stirred in a bath at −5 to 0°, was added 41 g (0.10 mole) of triphenylmethyl-^{14}C-phosphonium iodide (2 μc per mmole) over 45 min. The ice bath was removed and after 1 h of further stirring a solution of 8 g (0.074 mole) of dehydronorcamphor in 60 ml of ether was added dropwise to the yellow solution of Wittig reagent over 1 h. A white solid formed immediately when each drop of ketone solution reached the solution of triphenylphosphinemethylene-^{14}C, presumably as a result of the rapid formation of the betaine III. The reaction mixture was then stirred and heated under reflux for 2 days, after which the solid was separated by filtration, washed well with ether, and suspended in 100 ml of water. Much of the solid dissolved in the water and the aqueous phase was extracted with 100 ml of ether, which was added to the original filtrate. The combined ether solutions were washed with cold water to neutrality and dried over anhydrous sodium sulfate. After filtration, the ether solution was carefully concentrated and the concentrate distilled through a small helices-packed column under nitrogen. The boiling point rose steadily from 80° to 120° with no sharp break. There was obtained about 3 g of water-white liquid having the characteristic odor of methylenenorbornene. The product was separated from benzene and other contaminants by preparative v.p.c. and finally purified by bulb-to-bulb distillation on a vacuum line. There was obtained 0.900 g (8.5 mmoles) of pure methylene-^{14}C-norbornene; yield, 11.5% based on dehydronorcamphor. Combustion and counting the barium carbonate obtained gave values of 1.90 and 2.12 μc/mmole; calculated: 2.0 μc/mmole.

ACKNOWLEDGMENTS

The infrared and vapor phase chromatographic analyses were performed under the supervision of Mr. Andrew Reich. Mass spectra were obtained through Professor J. Goodings of McGill University and the n.m.r. spectra were performed by Professor J. C. Richer through the cooperation of the Department of Chemistry of the University of Montreal.

**Experimental details are given because it was found that the modifications introduced resulted in higher yields and purer products.*

Can. J. Chem. Downloaded from www.nrcresearchpress.com by 210.87.254.105 on 09/05/12
For personal use only.

Can. J. Chem. Downloaded from www.nrcresearchpress.com by 210.87.254.105 on 09/05/12
For personal use only.

REFERENCES

1. B. L. SHAPIRO, R. M. KOPCHIK, and S. J. EBERSOLE. J. Chem. Phys. **39**, 3154 (1963).
2. G. J. KARABATSOS, C. E. ORZECH, JR., and S. MEYERSON. J. Am. Chem. Soc. **86**, 1994 (1964).
3. K. MISLOW, R. GRAEVE, A. J. GORDON, and G. H. WAHL, JR. J. Am. Chem. Soc. **86**, 1733 (1964).
4. S. J. WEININGER, V. T. MAI, and E. R. THORNTON. J. Am. Chem. Soc. **86**, 3732 (1964).
5. W. BENZ and K. BIEMANN. J. Am. Chem. Soc. **86**, 2375 (1964).
6. Z. PELAH, D. H. WILLIAMS, H. BUDZIKIEWICZ, and C. DJERASSI. J. Am. Chem. Soc. **86**, 3722 (1964).
7. H. W. SCHRÖTTER and E. G. HOFFMANN. Ann. **672**, 44 (1964).
8. A. RIEKER, K. SCHEFFLER, and E. MÜLLER. Ann. **670**, 23 (1963).
9. J. G. ATKINSON, M. H. FISHER, D. HORLEY, A. T. MORSE, and R. S. STUART. 145th Meeting of the American Chemical Society, New York, N.Y. Abstracts. September 8, 1963. p. 66Q.
10. G. WITTIG and U. SCHÖLLKOPF. Chem. Ber. **87**, 1318 (1954).
11. (*a*) J. LEVISALLES. Bull. Soc. Chim. France, 1021 (1958).
    (*b*) U. SCHÖLLKOPF. Angew. Chem. **71**, 260 (1959).
    (*c*) S. TRIPPETT. *In* Advances in organic chemistry. Vol. I. Interscience Publishers, Inc., New York. 1960. p. 83.
    (*d*) L. A. YANOVSKAYA. Usp. Khim. **30**, 813 (1961).
    (*e*) S. TRIPPETT. Quart. Rev. **17**, 406 (1963).
12. P. D. BARTLETT and B. E. TATE. J. Am. Chem. Soc. **78**, 2473 (1956).
13. (*a*) K. ALDER and H. F. RICHERT. Ann. **543**, 1 (1940).
    (*b*) J. D. ROBERTS, E. R. TRUMBULL, JR., W. BENNETT, and R. ARMSTRONG. J. Am. Chem. Soc. **72**, 3116 (1950).
14. H. C. BROWN and C. P. GARG. J. Am. Chem. Soc. **83**, 2952 (1961).
15. L. F. FIESER. J. Am. Chem. Soc. **75**, 4386 (1953).
16. G. I. POOS, G. E. ARTH, R. E. BEYLER, and L. H. SARETT. J. Am. Chem. Soc. **75**, 422 (1953).
17. S. J. CRISTOL and P. K. FREEMAN. J. Am. Chem. Soc. **83**, 4427 (1961).
18. N. J. TOIVONEN and J. KAILA. Suomen Kemistilehti B, **28**, 91 (1955); Chem. Abstr. **49**, 7529*a* (1955).
19. N. RABJOHN. Organic syntheses. Collective Vol. IV. John Wiley & Sons, Inc., New York. 1963. p. 192.
20. L. S. FORSTER, A. MOSCOWITZ, J. G. BERGER, and K. MISLOW. J. Am. Chem. Soc. **84**, 4353 (1962).
21. E. J. COREY and M. CHAYKOVSKY. J. Am. Chem. Soc. **84**, 866 (1962). R. GREENWALD, M. CHAYKOVSKY, and E. J. COREY. J. Org. Chem. **28**, 1128 (1963).
22. C. F. HAUSER, T. W. BROOKS, M. L. MILES, M. A. RAYMOND, and G. B. BUTLER. J. Org. Chem. **28**, 372 (1963).
23. J. G. ATKINSON, A. T. MORSE, and R. S. STUART. To be published.
24. R. C. COOKSON, D. P. G. HAMON, and R. E. PARKER. J. Chem. Soc. 5014 (1962).
25. D. SEYFERTH, J. K. HEEREN, and W. B. HUGHES, JR. J. Am. Chem. Soc. **84**, 1764 (1962).
26. M. NEWMAN. Organic syntheses. Vol. 40. John Wiley & Sons, Inc., New York. 1960. p. 66.
27. C. H. COLLINS and G. S. HAMMOND. J. Org. Chem. **25**, 1434 (1960).
28. M. FARINA and M. PERALDO. Gazz. Chim. Ital. **90**, 973 (1960); Chem. Abstr. **55**, 22088*h* (1961).

Can. J. Chem. Downloaded from www.nrcresearchpress.com by 210.87.254.40 on 09/05/12
For personal use only.

CHEMISTRY OF NYBOMYCIN

II. SYNTHESIS OF 4,5-DIMETHYL-2,7-DIOXO-1,2,7,8-TETRAHYDRO-1,8-DIAZAANTHRACENE[1]

GRAHAM LEADBETTER AND KENNETH L. RINEHART, JR.
Noyes Chemical Laboratory, University of Illinois, Urbana, Illinois

Received November 13, 1964

Dedicated to Professor R. B. Sandin on the Occasion of his Sixty-Eighth Birthday

ABSTRACT

4,5-Dimethyl-2,7-dioxo-1,2,7,8-tetrahydro-1,8-diazaanthracene, a compound previously obtained from phosphorus – hydrogen iodide reduction of deoxynybomycin, has been synthesized in eight steps from *m*-xylene, in 5% overall yield.

The water-insoluble antibiotic nybomycin (1, 2) was recently assigned (3) structure I (1-formyl-4-hydroxymethyl-5,8-dimethyl-2,7-dioxo-1,2,7,8-tetrahydro-1,8-diazaanthracene). In the assignment of structure I, a key degradation product was compound III (4,5-dimethyl-2,7-dioxo-1,2,7,8-tetrahydro-1,8-diazaanthracene), one of three products isolated from reduction of deoxynybomycin (II) with phosphorus – hydrogen iodide at 240° in a sealed tube.

Compound III was of particular significance in the structural studies on nybomycin, since it alone of the three reduction products (III, IV, and V) retained the basic ring system and fundamental chromophoric unit of nybomycin. Compound III was converted by treatment with dimethyl sulfate in base to its N,N′-dimethyl derivative (VI), which proved of prime importance in deduction of the ring system of nybomycin from nuclear magnetic resonance (n.m.r.) considerations. The present work reports the preparation of the two degradation compounds III and VI, both as confirmation of their structures and as an approach to the development of routes to more complex compounds containing the nybomycin ring system.[2]

In the present preparation *m*-xylene was treated with concentrated nitric and sulfuric acids at room temperature to give 4,6-dinitro-1,3-dimethylbenzene (VIII) (5) in 30% yield, together with the 2,4-dinitro isomer IX in 7% yield. Their previously assigned structures are confirmed by the n.m.r. coupling constants of the two isomers. In the spectrum of VIII, whose two aryl protons are para to one another, the singlets ($J < 1$ c.p.s.) expected (6) are found at τ 1.32 and τ 2.54 (Table I), while the ortho aryl protons of IX, at τ 1.76 and τ 2.36, have the expected (6) large coupling constant ($J = 9$ c.p.s.).

Oxidation of VIII to 4,6-dinitro-1,3-benzenedicarboxylic acid (X) was effected by chromium trioxide in concentrated sulfuric acid at approximately 15° (7). In addition to the dicarboxylic acid X, the monocarboxylic acid XI was always isolated. Chemical shift

[1]*For paper I in this series, see ref. 3.*
[2]*The unsubstituted ring system (VII) of compounds I, II, III, and VI had been prepared previously (4), but unfortunately before the widespread reporting of spectral data.*

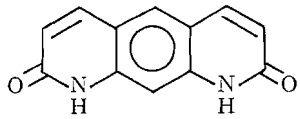

VII

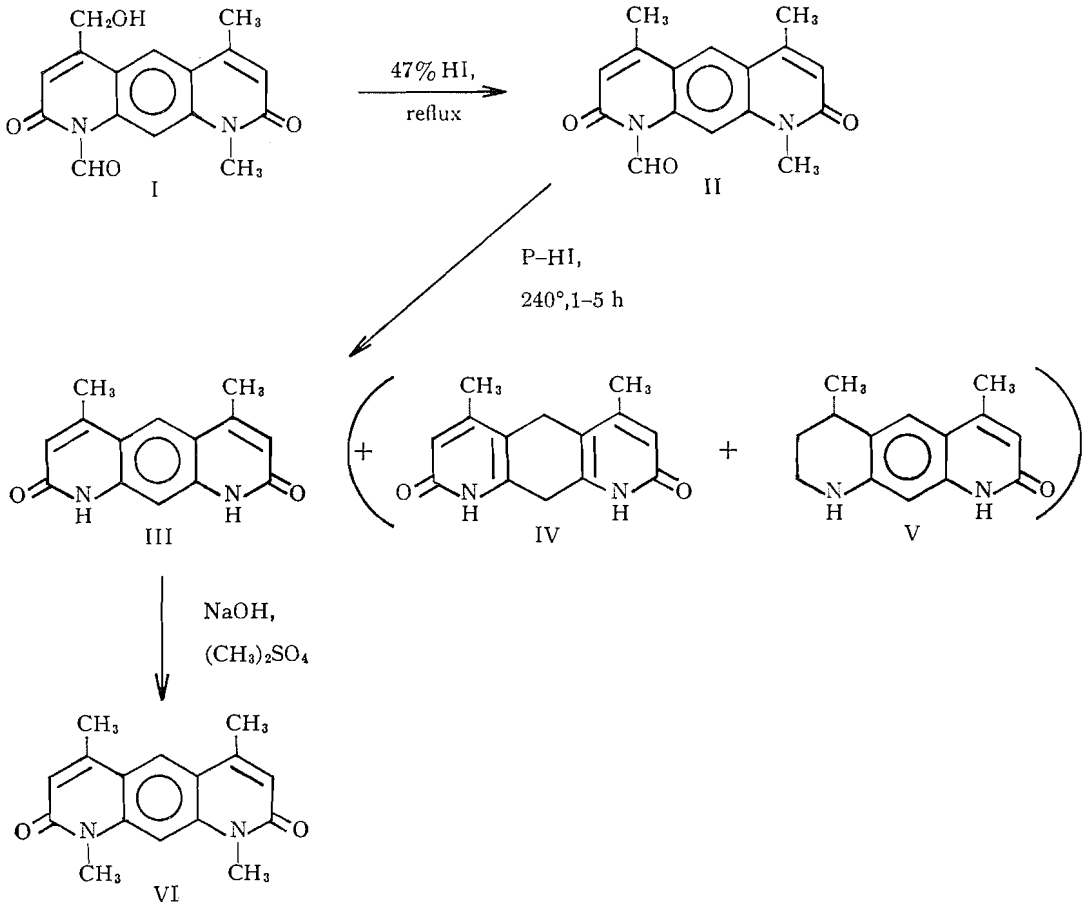

TABLE I

Chemical shift values (τ) for the protons of compounds having structure A*

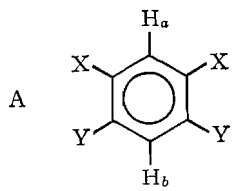

Compound	H_a	H_b	CH_3—	$=C(H)$—	Solvent
VIII (X = CH_3, Y = NO_2)	τ 2.54	τ 1.32	τ 7.30		$CDCl_3$
X (X = COOH, Y = NO_2)	1.80	1.34	—		D_2O
XIV (X = $COCH_3$, Y = NO_2)	2.46	1.10	7.40		CH_2Cl_2
	2.22	0.96	7.20		CF_3COOH
XVI (X = $COCH_3$, Y = NH_2)	1.00	2.80	7.10		CF_3COOH
XVII (X = $COCH_3$, Y = $NHCOCH_3$)	1.10	1.10	7.04, 7.50		CF_3COOH
III	1.80	1.16	7.08	2.76	CF_3COOH
VI	1.76	1.10	7.04, 5.70	2.60	CF_3COOH

*All peaks are singlets.

Can. J. Chem. Downloaded from www.nrcresearchpress.com by 210.87.254.40 on 09/05/12
For personal use only.

values for the dicarboxylic acid are reported in Table I; the monocarboxylic acid showed only singlets, at τ 1.30 (H-5), τ 2.12 (H-2), and τ 7.20 (aryl methyl).

Two routes were developed for conversion of the diacid X to 1,3-diacetyl-4,6-dinitrobenzene (XIV) via the known (7) diacid chloride XII. Conversion of XII to XIV by treatment of the former compound with diazomethane and subsequent reduction of the bis-diazoketone XIII with hydriodic acid gave XIV in yields as high as 59%. The yield of XIV by the alternative route, treatment of XII with diethyl magnesiomalonate, followed by concurrent hydrolysis and decarboxylation of the dimalonic ester XV, was approximately the same (53%). While the route via XV is somewhat longer and less convenient, it is preferred in view of the potential hazards of explosion and poisoning in working with large quantities of diazomethane and diazoketones.

The diacetyldinitrobenzene (XIV) was reduced by copper in sulfuric acid in 80% yield to 1,3-diacetyl-4,6-diaminobenzene (XVI)[3] and identified by melting point (7) and n.m.r. spectrum (Table I). Acetylation of XVI gave 94% of 1,3-diacetyl-4,6-diacetamidobenzene (XVII), characterized by its amide stretching absorption, elemental analyses, and n.m.r. spectrum (Table I).

Potassium *t*-butoxide catalyzed ring closure of XVII gave compound III in 69% yield. The overall yield of compound III from 4,6-dinitro-1,3-dimethylbenzene (VIII) was thus 15% by the diazomethane route and 14% by the magnesiomalonate route (5% and 4%, respectively, based on *m*-xylene).[4] Like nybomycin and related compounds, synthetic compound III did not melt below 350°. The infrared, ultraviolet, and n.m.r. (Table I) spectra of synthetic compound III matched those reported for the degradation product (8). As further proof of identity, synthetic compound III was converted by methylation to synthetic compound VI. For VI, too, n.m.r., ultraviolet, and infrared spectra (Fig. 1) were identical with those of the methylation product obtained in three steps from nybomycin (I → II → III → VI).

With completion of this synthesis, the heterocyclic skeleton of nybomycin is assured. Future efforts will be directed toward synthesis of derivatives of this ring system.

EXPERIMENTAL

Melting points were determined on a Kofler micro hot stage and are uncorrected. Nuclear magnetic resonance spectra and microanalyses were obtained at the University of Illinois by D. H. Johnson, J. Nemeth, and their associates. Infrared spectra were obtained with a Perkin–Elmer double-beam recording spectrophotometer, model 237, on chloroform solutions or Nujol mulls except as noted in the text. Nuclear magnetic resonance spectra were obtained with a Varian high-resolution n.m.r. spectrometer, model A-60, in the solvents noted in the text. Ultraviolet spectra were obtained with a Beckman recording ultraviolet spectrophotometer, model DB, on ethanolic solutions.

4,6-Dinitro-1,3-dimethylbenzene (VIII)

The procedure followed was that of Morgan (9). The crude product obtained from 200 ml of 70% nitric acid, 250 ml of 96% sulfuric acid, and 123 ml (ca. 106 g) of *m*-xylene weighed 150 g (76%). This was recrystallized repeatedly from 95% ethanol (5) until a constant melting product (59.5 g, 30%) was obtained. In five additional runs on a double scale the yields were 30–31%. 4,6-Dinitro-1,3-dimethylbenzene (VIII), m.p. 88–92° (lit. 89–93°) (5), was shown to be free of impurities by thin-layer chromatography over silica gel employing carbon tetrachloride solvent. The structure assigned was in accord with the compound's n.m.r. spectrum (Table I).

In addition to the desired 4,6-dinitro compound (VIII), 2,4-dinitro-1,3-dimethylbenzene (IX) could be isolated from the crude nitration product above by repeated recrystallization from chloroform (10). In

[3]*Ruggli and Reichwein (7) prepared XVI from XII via XIII, 4,6-dinitro-1,3-bischloracetylbenzene, and 4,6-diamino-1,3-bischloroacetylbenzene. Their yield of XVI from XII was approximately 44%, comparable to the present yields, but their route involved isolation of the intermediate bis-diazoketone (XIII) and one step more than either of the present routes.*

[4]*For comparison, the overall yield of compound VII from 4,6-dinitro-1,3-dimethylbenzene was approximately 10% (4).*

Can. J. Chem. Downloaded from www.nrcresearchpress.com by 210.87.254.40 on 09/05/12
For personal use only.

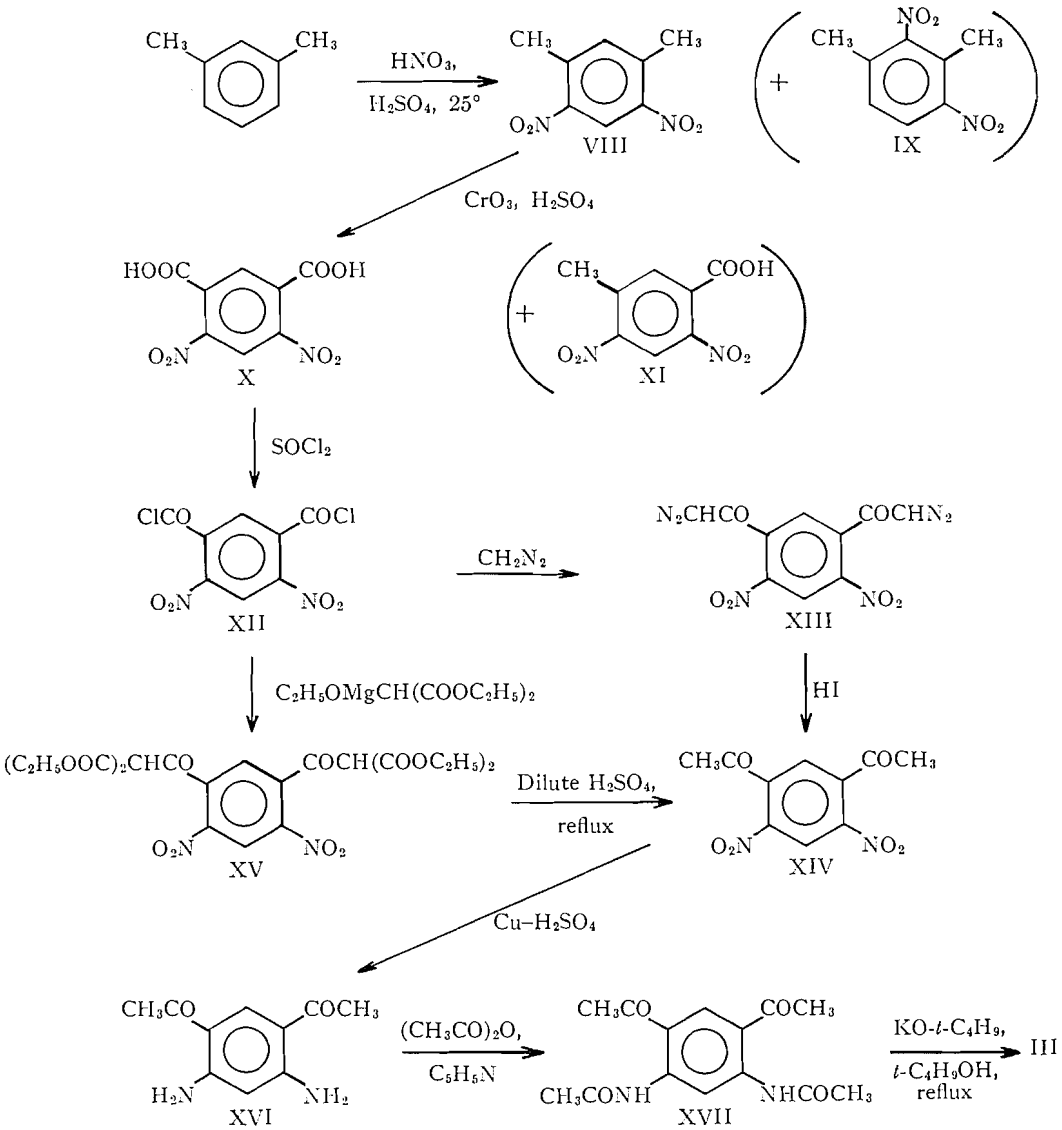

another run, from 135 g of mixed dinitroxylenes, the yield of crude 2,4-dinitro isomer (IX), shown to contain a small amount of the 4,6-dinitro isomer (VIII) by thin-layer chromatography, was 1.8 g (7%); the crude compound melted at 73–83° (lit. 82–83°) (10). Its n.m.r. spectrum (in deuterochloroform) contained a singlet at τ 7.54 (six protons, aryl methyl groups) and doublets (J = 9 c.p.s.) at τ 1.76 (one proton, H-5) and τ 2.36 (one proton, H-6).

4,6-Dinitro-1,3-benzenedicarboxylic Acid (X)

This compound was prepared exactly according to the oxidation procedure of Ruggli and Reichwein (7). From 20 g of 4,6-dinitro-1,3-dimethylbenzene (VIII), the yield of 4,6-dinitro-1,3-benzenedicarboxylic acid was 15.9 g (61%), m.p. 230–235° decomp. (lit. 234° decomp.) (7). Nuclear magnetic resonance data for the compound are presented in Table I. In 29 additional runs the yields varied from 29 to 51%.

The water-insoluble side product noted previously (7) was identified as a mixture of 4,6-dinitro-3-methylbenzoic acid (XI) and recovered starting material (VIII). A portion (1.2 g) of the material accumulated from several runs was separated into bicarbonate-soluble and -insoluble fractions. The base-soluble XI weighed 0.9 g and, after recrystallization from water, had m.p. 173–175° (lit. 171–171.5°) (11). Its infrared spectrum (Nujol) had a carbonyl band at 1 720 cm^{-1}; its n.m.r. spectrum (trifluoroacetic acid) contained only singlets, of area ratio 1:1:3 at τ 1.30 (H-5), τ 2.12 (H-2), and τ 7.20 (aryl methyl).

Can. J. Chem. Downloaded from www.nrcresearchpress.com by 210.87.254.40 on 09/05/12
For personal use only.

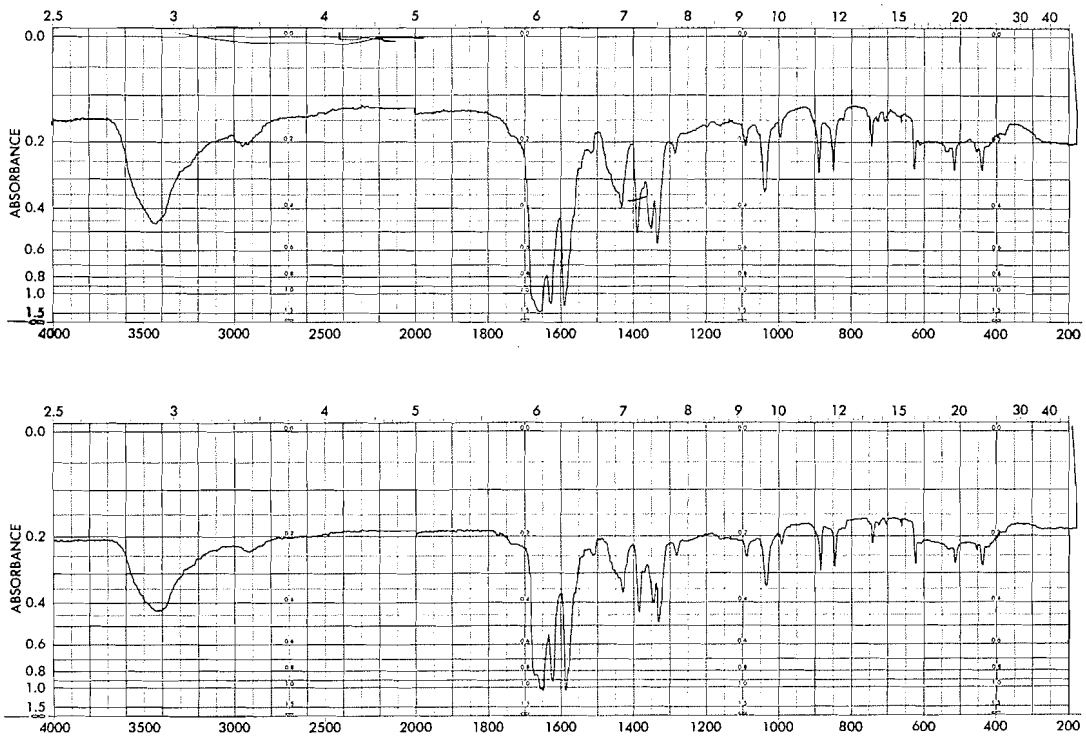

FIG. 1. Infrared spectra of 1,4,5,8-tetramethyl-2,7-dioxo-1,2,7,8-tetrahydro-1,8-diazaanthracene (VI), determined as potassium bromide pellets. Upper curve: sample obtained by methylation of 4,5-dimethyl-2,7-dioxo-1,2,7,8-tetrahydro-1,8-diazaanthracene (III) isolated from phosphorus – hydrogen iodide treatment of deoxynybomycin. Lower curve: sample obtained by methylation of synthetic compound III.

The bicarbonate-insoluble fraction weighed 95 mg and was identified as VIII, m.p. 86–88°.

Enhanced yields in the oxidation could be obtained by re-oxidizing the water-insoluble fraction. From each 20-g batch of material about 13 g of diacid was obtained. This would raise the yield of X by about 13% per run.

4,6-Dinitro-1,3-benzenedicarbonyl Chloride (XII)

The diacid chloride XII, m.p. 104–106° (lit. 106–108°) (7), was prepared in 82% yield by the exact procedure of Ruggli and Reichwein.

Preparation of 4,6-Dinitro-1,3-diacetylbenzene

A. Diethyl Malonate Procedure

The procedure followed was essentially that employed for the preparation of *o*-nitroacetophenone (12). From 27.1 g of magnesium turnings, 180.5 g of diethyl malonate, and 150 g of 4,6-dinitro-1,3-benzenedicarbonyl chloride (XII), the total yield of 4,6-dinitro-1,3-diacetylbenzene (XIV) was 71.2 g (53%). A single recrystallization from 95% ethanol gave the analytical sample, m.p. 137–138°.

Anal. Calcd. for $C_{10}H_8N_2O_6$: C, 47.62; H, 3.17; N, 11.11. Found: C, 47.31; H, 3.15; N, 11.12.

The infrared spectrum (chloroform) of the product contained a carbonyl band at 1 712 cm^{-1}. Its n.m.r. spectral data are found in Table I.

In a second run the yield was 52%.

B. Diazomethane Procedure

The procedure was essentially that of Wolfrom and Brown (11). A solution of 2.39 g (8.13 mmoles) of 4,6-dinitro-1,3-benzenedicarbonyl chloride (XII) in benzene was added dropwise to a stirred solution of 36.45 mmoles of diazomethane in ether (prepared from N-nitrosomethylurea and analyzed by decomposition with benzoic acid and titration with 0.2 *N* sodium hydroxide) (13). The yellow bis-diazoketone (XIII) precipitated and was filtered. It was then suspended in chloroform and stirred while 5 ml of 47% hydriodic acid was added; nitrogen was evolved and the mixture became deep purple. The chloroform solution was washed successively with water, sodium thiosulfate solution, sodium bicarbonate solution, and water; then

Can. J. Chem. Downloaded from www.nrcresearchpress.com by 210.87.254.40 on 09/05/12
For personal use only.

dried over magnesium sulfate; and finally evaporated to give 1.22 g (59%) of 4,6-dinitro-1,3-diacetylbenzene (XIV), m.p. 137–138° after two recrystallizations from 95% ethanol. The infrared spectrum and thin-layer chromatographic behavior (silica gel, chloroform solvent) of this sample were identical with those of the sample prepared by method A above. In four additional runs employing the diazomethane procedure, the yields of diacetyl compound (XIV) were 38–40%.

4,6-Diamino-1,3-diacetylbenzene (XVI)

From 948 mg of 4,6-dinitro-1,3-diacetylbenzene (XIV), the procedure of Ruggli and Reichwein gave 639 mg (80%) of 4,6-diamino-1,3-diacetylbenzene (XVI), m.p. 234–235° decomp. (lit. 235° decomp.) (7). An infrared spectrum (Nujol) of the product showed the expected two N—H stretching bands, at 3 500 and 3 320 cm^{-1}. Its n.m.r. values are found in Table I.

In a run on a 10-fold scale the yield was also 80%.

4,6-Diacetamido-1,3-diacetylbenzene (XVII)

The preparation followed a standard procedure (14). From 1.10 g of 4,6-diamino-1,3-diacetylbenzene (XVI) was obtained 1.51 g (94%) of 4,6-diacetamido-1,3-diacetylbenzene (XVII). Two recrystallizations from dimethylformamide gave the analytical sample, which did not melt below 350°.

Anal. Calcd. for $C_{14}H_{16}N_2O_4$: C, 60.86; H, 5.84; N, 10.14. Found: C, 60.78; H, 6.01; N, 10.43.

The infrared spectrum (Nujol) of the product contained amide bands at 3 250 cm^{-1} (N—H stretch) and 1 685 cm^{-1} (C=O stretch). Its n.m.r. spectral data are found in Table I.

4,5-Dimethyl-2,7-dioxo-1,2,7,8-tetrahydro-1,8-diazaanthracene (III)

The procedure was adapted from that of Camps (15). A mixture of potassium *t*-butoxide solution (prepared from 167 mg of potassium and 25 ml of dry *t*-butyl alcohol) and 500 mg of 4,6-diacetamido-1,3-diacetylbenzene (XVII) was heated under nitrogen for 1 h at reflux. Solid matter was filtered; weight, 244 mg. This was heated on the steam bath with 25 ml of 10% sodium hydroxide solution and then filtered hot. The filtrate was acidified with hydrochloric acid, and the resulting precipitate was filtered, washed with water, and dried; weight, 120 mg. Evaporation of the original *t*-butyl alcohol solution yielded further solid material, which was worked up with sodium hydroxide and acid as before to give an additional 179 mg of product. The total yield of compound III was thus 299 mg (69%); it did not melt below 350°. Its infrared (Nujol), ultraviolet, and n.m.r. (trifluoroacetic acid solution, see Table I) spectral data were the same as those of the product obtained from phosphorus – hydrogen iodide treatment of deoxynybomycin (8).

1,4,5,8-Tetramethyl-2,7-dioxo-1,2,7,8-tetrahydro-1,8-diazaanthracene (VI)

The dipyridone III (95 mg) dissolved in 25 ml of refluxing 10% sodium hydroxide solution. After addition of 2 ml of dimethyl sulfate a precipitate appeared; addition was continued until the solution was acidic to litmus. The precipitate was filtered, washed with water and acetone, and dried to give 62 mg (59%) of product (VI).

Anal. Calcd. for $C_{16}H_{16}N_2O_2$: C, 71.62; H, 6.01; N, 10.44. Found: C, 71.67; H, 6.13; N, 10.24.

The compound did not melt below 350°, but its infrared (Nujol or potassium bromide, see Fig. 1), ultraviolet, and n.m.r. (trifluoroacetic acid, see Table I) spectra were all identical with those of the material obtained (8) from methylation of the phosphorus – hydrogen iodide product of deoxynybomycin.

ACKNOWLEDGMENT

This investigation was supported by Public Health Research grant No. AI-01278 from the National Institute of Allergy and Infectious Diseases.

REFERENCES

1. F. Strelitz, H. Flon, and I. N. Asheshov. Proc. Natl. Acad. Sci. U.S. **41**, 620 (1955).
2. T. E. Eble, G. A. Boyack, C. M. Large, and W. H. Devries. Antibiot. Chemotherapy, **8**, 627 (1958).
3. K. L. Rinehart, Jr. and H. B. Renfroe. J. Am. Chem. Soc. **83**, 3729 (1961).
4. P. Ruggli, P. Hindermann, and H. Frey. Helv. Chim. Acta, **21**, 1066 (1938).
5. P. Ruggli, A. Zimmerman, and R. Thouvay. Helv. Chim. Acta, **14**, 1250 (1931).
6. L. M. Jackman. Applications of nuclear magnetic resonance spectroscopy in organic chemistry. Pergamon Press, New York. 1959.
7. P. Ruggli and H. Reichwein. Helv. Chim. Acta, **20**, 905 (1937).
8. H. B. Renfroe. Ph.D. Thesis, University of Illinois, Urbana, Illinois. 1961.
9. G. T. Morgan. J. Chem. Soc. **81**, 86 (1902).
10. R. Adams and A. S. Nagarkatti. J. Am. Chem. Soc. **72**, 1831 (1950).
11. M. L. Wolfrom and R. L. Brown. J. Am. Chem. Soc. **65**, 1516 (1943).
12. G. A. Reynolds and C. R. Hauser. Organic syntheses. Collective Vol. IV. John Wiley and Sons, New York. 1963. p. 708.
13. F. Arndt. Organic syntheses. Collective Vol. II. John Wiley and Sons, New York. 1943. p. 165.
14. N. D. Cheronis and J. B. Entrikin. Semimicro qualitative organic analysis; the systematic identification of organic compounds. 2nd ed. Interscience Publishers, Inc., New York. 1958. p. 410.
15. R. Camps. Arch. Pharm. **237**, 659 (1899).

Can. J. Chem. Downloaded from www.nrcresearchpress.com by 210.87.254.40 on 09/05/12
For personal use only.

Can. J. Chem. Downloaded from www.nrcresearchpress.com by 210.87.254.40 on 09/05/12
For personal use only.

Canadian Journal of Chemistry

Issued by THE NATIONAL RESEARCH COUNCIL OF CANADA

VOLUME 43 JUNE 1965 NUMBER 6

THE CHEMISTRY OF SINGLET AND TRIPLET METHYLENE

R. F. W. BADER[1]
Department of Chemistry, McMaster University, Hamilton, Ontario
AND
JOHN I. GENEROSA[2]
Department of Chemistry, University of Ottawa, Ottawa, Ontario

Received December 10, 1964

ABSTRACT

Results are reported for the photolysis of small, fixed amounts of diazomethane and *cis*-butene-2 in the presence of increasing pressures of the inert gases He, Ar, Xe, N_2, and CF_4. The variation in the percentage yield of the *trans*-dimethylcyclopropane as a function of the inert gas pressure indicates that two basic mechanisms, with opposite dependencies on the inert gas pressure, are responsible for its formation. An initial decrease in the percentage yield of this *trans* isomer with increasing pressure indicates that a source is an isomerization of energized molecules. These excited molecules result from the addition of methylene in a singlet state to *cis*-butene-2. A subsequent rise in the yield of the *trans* isomer with further increases in the pressure indicates that another mechanism, one whose rate is *increased* by an increase in pressure, must be present. This is attributed to a mechanism involving triplet methylene. The pressure regions for the observation of the singlet or triplet behavior of methylene are thus known and the modes of formation of the other C_5 products may be determined.

INTRODUCTION

Skell (1) introduced the idea of relating the stereospecificity (or lack of it) observed in the reaction of methylenes with *cis*-butene-2 to the singlet (or triplet) nature of the methylenic species. The reaction of a methylene molecule in a singlet state with *cis*-butene-2 could conceivably give the complete cyclopropane framework in a single three-center addition step with consequent retention of the *cis* geometry in the 1,2-dimethylcyclopropane product molecule.

[1] 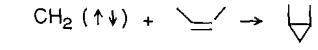

The addition of a triplet methylene to *cis*-butene-2 must, unless there is a simultaneous triplet to singlet transition, give rise to a triplet intermediate.

[2] 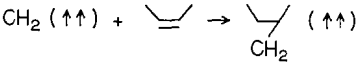

The triplet intermediate may be pictured as a structure with only two bonds of the ring system present or as some triplet excited state of the cyclopropane sigma bond structure.

[1] *Alfred P. Sloan Research Fellow.*
[2] *Abstracted from the thesis submitted by John I. Generosa in partial fulfillment of the requirements for the degree of Doctor of Philosophy.*

Either view leads to the prediction that the reaction need not necessarily lead to stereospecific products due to the weakening of the sigma bond framework. Thus the triplet intermediate can yield either *cis*- or *trans*-dimethylcyclopropane when the triplet to singlet transition does occur.

[3] 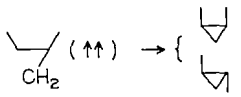

Skell (2) found an example of presumed triplet behavior by this method for diphenylmethylene. Cvetanović (3) also observed that the reaction of oxygen atoms in their ^3P ground state resulted in a mixture of the *cis* and *trans* epoxides. Skell *et al.* (1) have also found that the 1,2-dimethylcyclopropane formed from methylene itself and large excesses of *cis*- or *trans*-butene-2 in the gaseous or liquid phase is almost entirely the *cis* or *trans* isomer respectively. This provides an example of singlet behavior. Ideally, to firmly establish Skell's method of distinguishing singlet and triplet states, one should find a system in which a single species exhibits both kinds of behavior. This evidence has been provided in the case of methylene itself by Anet, Bader, and Van der Auwera (4). This latter experiment was instigated by the spectroscopic findings of Herzberg and Shoosmith (5, 6). Their results indicated that the flash photolysis of diazomethane yields methylene molecules in highly excited singlet states which are subsequently energetically degraded to the ground state, which is a triplet, through collisions with inert gas molecules. The most intense spectrum for the triplet state was obtained when a large excess of nitrogen was present. Thus Anet *et al.* (4) studied the products obtained from the photolysis of small partial pressures of diazomethane and *cis*-butene-2 in the presence of a large excess of nitrogen as the inert gas. They found that the stereospecificity of the reaction was entirely lost. Thus methylene is formed in a singlet state,

$$CH_2N_2 \xrightarrow{h\nu} CH_2(\uparrow\downarrow) + N_2;$$

it may react immediately in its singlet state in a stereospecific manner via eq. [1] as in Skell's original work or, if a large excess of an inert gas is present, it may be degraded to its electronic ground state,

[4] $$CH_2(\uparrow\downarrow) \xrightarrow[\text{frequent collisions}]{N_2} CH_2(\uparrow\uparrow),$$

which then may produce both geometrical isomers via reactions [2] and [3].

The *cis*-dimethylcyclopropane (hereafter referred to as *cis*-DMC) when initially formed by the addition of singlet methylene to an alkene contains a large amount of kinetic energy resulting from the decrease in potential energy on the formation of the two new covalent bonds (7). A large fraction of this energy resides in the vibrational degrees of freedom of the product molecule. The energized *cis*-DMC molecule has been shown to undergo both geometrical isomerization to *trans*-DMC and structural isomerization to *cis*- and *trans*-pentene-2, 2-methylbutene-2, and 2-methylbutene-1 (8, 9).

[5] 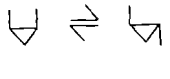

Can. J. Chem. Downloaded from www.nrcresearchpress.com by 210.87.254.40 on 09/05/12
For personal use only.

[6] 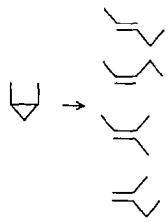

Thus all these C_5 hydrocarbons are obtained as products in the photolysis of diazomethane in the presence of *cis*-butene-2.

Frey (10) has criticized the work of Anet *et al.* on the grounds that the inert gas pressures employed by these workers (~560 mm Hg) were not sufficient to quench the geometrical isomerization of the highly energized *cis*-DMC molecule. Frey argued that Anet *et al.* had not observed triplet methylene and that their observed lack of stereospecificity in the cyclopropanes was due to the geometrical isomerization, reaction [5]. Frey (10) repeated the work of Anet *et al.* with inert gas pressures above 2 000 mm Hg and observed in the reaction the same lack of stereospecificity, which he attributed to the triplet species of methylene. Recently Benson and DeMore (11) have questioned the existence of triplet methylene even in Frey's experiments. They point out that dilution of the reaction mixture with nitrogen or argon in place of *cis*-butene-2 leads to a decreased deactivation efficiency and that the loss of stereospecificity observed by Frey could still be due to the geometrical isomerization reaction.

In this paper we present the results of experiments designed to determine whether or not it is indeed necessary to invoke the participation of triplet methylene in the photolysis of diazomethane, cis-butene-2, and inert gas mixtures, and if the presence of the triplet species is indicated, to determine the minimum pressure of inert gas necessary for the observation of the triplet behavior. The experiments consist of photolyzing mixtures of fixed, small amounts of diazomethane and *cis*-butene-2 held in a constant ratio of 2.5:1 in the presence of an increasing partial pressure of an inert gas.* The gases employed were He, Ar, Xe, N_2, and CF_4 in the pressure ranges of $0 \rightarrow 850$ mm Hg. The yield of *trans*-DMC expressed as a percentage of the total C_5 products is plotted vs. the pressure of the inert gas. This yield should be high at low pressures of the inert gas due to the geometrical isomerization of the energized *cis*-DMC, reaction [5]. As the pressure of inert gas is increased, the percentage yield of *trans*-DMC should decrease as the highly energized *cis*-DMC is deactivated by collision before isomerization can occur. Eventually, at some pressure of inert gas, the percentage yield of *trans*-DMC should begin to *increase* as there are now sufficient collisions with the inert gas molecules to permit the methylene to attain the triplet ground state before reacting with the butene. Only the formation of triplet methylene can cause the curve to rise since there is no other available mechanism for increasing the rate of formation of *trans*-DMC with increasing pressure. The graph of percentage yield of *trans*-DMC vs. inert gas pressure should be U shaped with the minimum in the curve indicating the pressure at which the rate of increase of *trans*-DMC formation from triplet methylene equals the rate of decrease of *trans*-DMC arising from the singlet species. Thus the participation of triplet methylene is proved for any pressure above the value at the minimum even though the absolute rate of formation of the *trans*-DMC from the geometrical isomerization reaction may still be the greater of the two.

**The partial pressures of diazomethane and cis-butene-2 employed in the experiments were 0.9 and 0.35 mm Hg respectively.*

Can. J. Chem. Downloaded from www.nrcresearchpress.com by 210.87.254.40 on 09/05/12
For personal use only.

Such a U-shaped curve is to be contrasted with the results obtained by Frey (9) for the photolysis of CH_2N_2 in the presence of increasing pressures of *cis*- or *trans*-butene-2 with no inert gas present. The discussion of these results will be given in terms of the variation in the percentage yields of *cis*-DMC rather than *trans*-DMC since his results for the reaction with *trans*-butene-2 cover a wider range of pressures than those with *cis*-butene-2. A plot of percentage yield of *cis*-DMC vs. increasing pressure showed the initial decrease as predicted due to the deactivation of the energized *trans*-DMC molecules by the *trans*-butene-2. However, the curve continues to decrease with increasing pressure of *trans*-butene-2 as little or no triplet methylene can be formed under these conditions. The rate of addition of methylene to an alkene is very rapid, being approximately 2.4 times smaller than the collision frequency (9). Consequently, with no inert species present, singlet CH_2 reacts before it is degraded to the triplet state. Thus the continued downward slope of the curve in Frey's work indicates a single source of *cis*-DMC, one which has an *inverse* pressure dependence. In the experiments reported here, any change in the sign of the slope must indicate the participation of a new source of *trans*-DMC, one whose rate increases with increasing pressures. The only reaction favoured by an increase in pressure is reaction [4], the conversion of singlet to triplet methylene.

Frey's criticism that pressures greater than 2 000 mm of Hg are necessary to unambiguously detect triplet participation can be checked immediately by noting the values of the pressure at the minima in the curves, and the very existence of a minimum will disprove the criticism of DeMore and Benson. Furthermore, the relative appearance of similar plots for the other C_5 product hydrocarbons will permit one to determine whether the product arises from the reaction of singlet or triplet methylene or both. Other things being equal, the relative efficiencies of the various inert gases in bringing about the singlet to triplet transition may be determined by noting the value of the pressure at which the minimum in the curve occurs and the slope of the line past this point. Also, their relative abilities in deactivating the energized *cis*-DMC molecules will be reflected in the initial slope of the curve before the minimum is reached.

RESULTS AND DISCUSSION

Figure 1 shows the amounts of *trans*-DMC formed at increasing pressures of inert gas expressed as a percentage of the total C_5 product yield. These yields are determined by the relative areas of gas–liquid chromatograms.* The predicted U-shaped curve is exhibited by the experiments with CF_4, N_2, Ar, and Xe while He has only a barely susceptible increase at the highest pressures used. The *relative* behavior of the downward and upward sloping portions of the curves finds a ready explanation in terms of a quenching of a geometrical isomerization and the intervention of triplet methylene respectively. The initial downward slopes should be a reflection of the relative efficiencies of the inert gases at deactivating the excited *cis*-DMC molecules which arise from singlet methylene. Since CF_4 has more internal degrees of freedom than does N_2 which in turn has more than He, one expects the deactivating ability of these species to decrease in the same order. This is precisely what is observed in Fig. 1 where the absolute values of the initial slopes

**Tables I—IX have been placed in*

The Depository of Unpublished Data,
National Science Library,
National Research Council,
Ottawa, Canada,

and photocopies may be obtained upon request to the Depository.

Can. J. Chem. Downloaded from www.nrcresearchpress.com by 210.87.254.40 on 09/05/12
For personal use only.

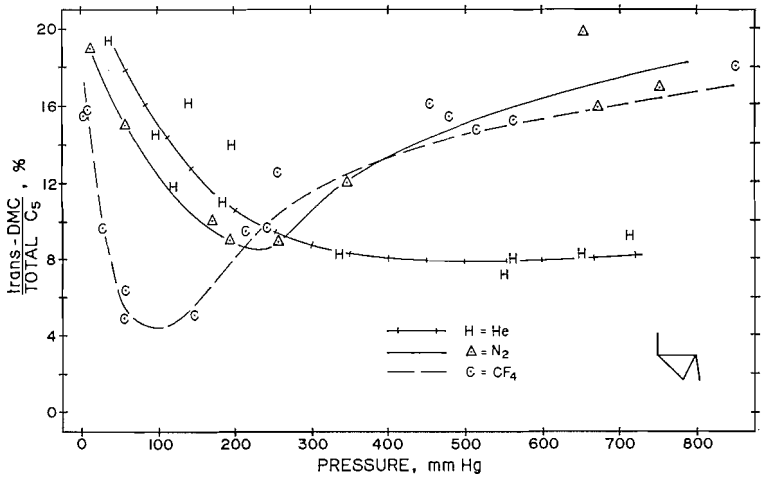

[FIG. 1. Percentage yield of *trans*-DMC vs. pressure for the inert gases He, N_2, and CF_4.

decrease in the order $CF_4 > N_2 > He$. The gases Xe and Ar have initial slopes experimentally indistinguishable from those for N_2. If the geometrical isomerization were the only source of *trans*-DMC these curves could only continue downwards with increasing pressures of inert gas. Rather, one observes a marked change in the sign of the slope which must be due to the appearance of a new source of the *trans*-DMC. This is ascribed to the reactions of triplet methylene whose relative concentration increases with increasing inert gas pressure. The methylene in this pressure region is energetically degraded to the triplet ground state by collisions with inert gas molecules before a reaction occurs, thus giving rise to the triplet intermediate and to the *trans*-DMC directly. In the highest pressure ranges investigated the gases CF_4, N_2, and Xe are experimentally indistinguishable in their yields of *trans*-DMC. All are superior in this respect to He, and Ar yields an intermediate value of 15% in the 700 mm pressure region. One cannot immediately conclude from this that CF_4, N_2, and Xe are all equally efficient at bringing about the singlet to triplet transition in methylene. There is still a contribution from singlet methylene in this high pressure region. Tetrafluoromethane must in fact be judged superior to the rest. The singlet contribution will be least in this case as CF_4 is the most efficient deactivator. Thus the contribution of the geometrical isomerization reaction at high pressures will be least for CF_4. The minimum in the curve for CF_4, which denotes the pressure at which the decrease in the rate of formation of *trans*-DMC equals the increase in its rate of formation due to triplet methylene, occurs in the region of 100 mm Hg. This is remarkably low. Nitrogen and xenon, both of which have distinct minima in their plots (at approximately 250 mm Hg) must have an almost equal ability at causing the singlet to triplet transition as their initial slopes are almost equal, but must be less efficient than CF_4 in this regard. Argon, which has approximately the same deactivating ability as N_2 and Xe, must be less efficient in causing the spin transition. Helium is the least effective both at deactivating and causing the spin conversion. The contribution of the geometrical isomerization reaction (at high pressures) must be greatest in the case of He but its percentage yield of *trans*-DMC is the smallest of all the gases in this region. This is an important observation as it indicates that at least 50% of the observed *trans*-DMC in this high pressure region for CF_4, Xe, and N_2 must arise from the triplet addition

Can. J. Chem. Downloaded from www.nrcresearchpress.com by 210.87.254.40 on 09/05/12
For personal use only.

reaction. This will be a lower estimate as the yield of *trans*-DMC in the He case is probably not due entirely to the geometrical isomerization. (The curve for He does level off, rather than undergo a continual decrease.)

Figure 2 presents other experimental results which further substantiate the above interpretation. These results are given in terms of the *trans*-DMC as a percentage of just the total cyclopropane yield to illustrate clearly the increase in one isomer at the expense of the other. The upper curve is the same set of standard runs for N_2 as presented in Fig. 1. The effect of increasing the *cis*-butene-2 to diazomethane ratio by a factor of 10 is illustrated in the second upper curve. This should result in a smaller fraction of methylene molecules reaching the triplet ground state and in a smaller yield of *trans*-DMC. This is observed. One of the lower curves is for a series of runs with no inert gas and increasing pressures of *cis*-butene-2. There is no U character to this curve within experimental error, the yield of the *trans*-DMC simply decreasing with increasing pressure of the butene as the geometrical isomerization is increasingly quenched. The remaining curve indicates the effect of added oxygen gas in the two pressure regions with the original *cis*-butene-2 : diazomethane ratio. The singlet region is almost unaffected, but the pressure region ascribed to the triplet state is radically changed. The curve never undergoes a change in the sign of its slope indicating that the second, high-pressure source of *trans*-DMC involving the triplet species is effectively quenched.

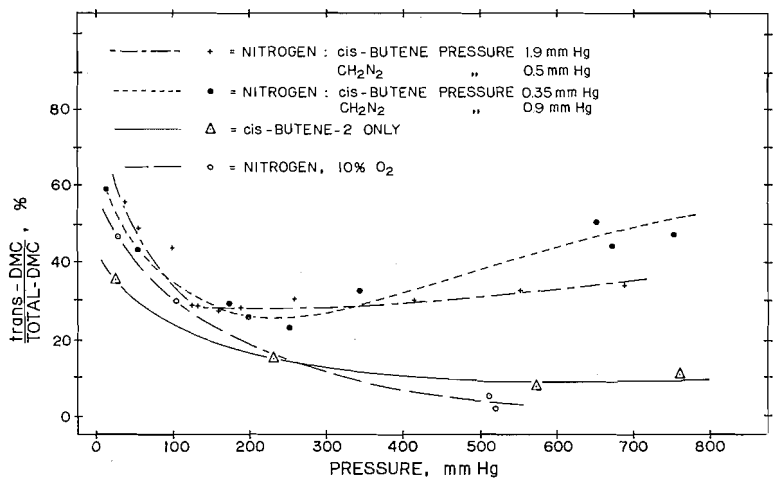

FIG. 2. Percentage yield of *trans*-DMC vs. pressure: ●, N_2 as inert gas; +, N_2 as inert gas with 10 times the *cis*-butene-2: diazomethane ratio; △, no inert gas present; ○, with added oxygen.

All the above data support the conclusion that the reactions observed in the pressure region below 100 mm Hg in the case of CF_4 and below 250 mm in the cases of N_2 and Xe are primarily due to singlet methylene, while for pressures above these values, they are due primarily to the triplet species. Thus whether the precursor of the other C_5 hydrocarbons is triplet or singlet, methylene is now determinable by noting the variation in the percentage yields of these products in the two pressure regions.

The variation in the yield of *cis*-DMC is plotted for CF_4 and He in Fig. 3 as a percentage yield of the total cyclopropanes to emphasize the variation in the *cis*:*trans* isomer ratio. The yield of *cis*-DMC increases initially due to the quenching of the geometrical isomerization to the *trans* isomer, the increase being greater in the case of CF_4

Can. J. Chem. Downloaded from www.nrcresearchpress.com by 210.87.254.40 on 09/05/12
For personal use only.

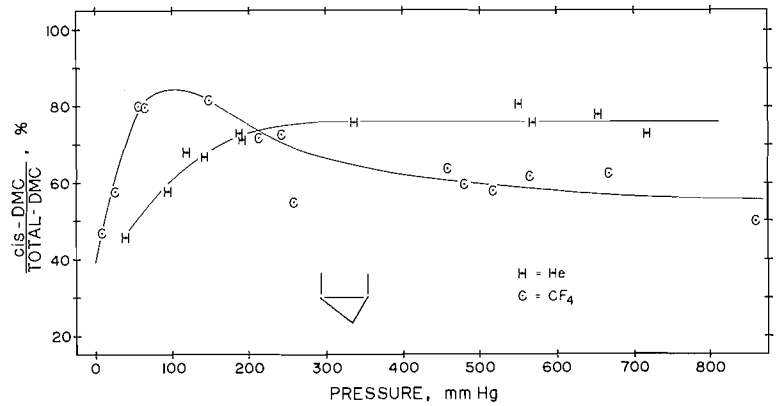

FIG. 3. Percentage yield of *cis*-DMC vs. pressure for the inert gases He and CF_4.

than with He. When the *trans*-DMC yield goes through a minimum, the *cis*-DMC exhibits a maximum, at 100 mm pressure in the case of CF_4. Beyond this point there is a steady decrease to some limiting value between 50 and 60%. This is a reflection of the fact that there are two reactions contributing to the formation of the *cis*-DMC, one which is inhibited by an increase in pressure and one which is made more pronounced. The yield of *cis*-DMC in the high-pressure region is greater for He than for CF_4 as He is less efficient at inducing the spin conversion. The yield with He in the low-pressure region is less since He is not as efficient as CF_4 at deactivation of the energized *cis*-DMC molecules.

Figure 4 shows the variation in the percentage yield of *cis*-pentene-2 with the inert gases CF_4 and He. The yield with CF_4 is seen to undergo a gradual decrease with increasing pressure of the inert gas. There are two modes of formation possible for *cis*-pentene-2. Methylene in its singlet state may insert into a C—H bond of the *cis*-butene-2 molecule to give the product directly, or it may arise from the isomerization of the energized cyclopropanes (12). The *cis*-pentene-2 resulting from the insertion reaction possesses sufficient internal kinetic energy to isomerize to the *trans* isomer. Stabilization of the product by increasing inert gas pressures should lead to an increase in the percentage yield. However, an increase in the inert gas pressure decreases the concentration of the singlet methylene necessary for the insertion reaction and stabilizes the energized DMC molecules. Thus the observed gradual decrease in the percentage yield of *cis*-pentene-2 does not allow one to determine which of the two modes of formation is the major source of this compound. We can obtain some indication of which of these processes is predominant by considering the related question of the variation in the percentage yield of the *trans* isomer. This is shown in Fig. 5. The initial decrease in the yield of *trans*-pentene-2 can be related to the increased collisional stabilization of the *cis* isomer. In the high-pressure region where the average percentage yield is greater, the *trans* isomer may also arise from the isomerization of the energized DMC resulting from the triplet addition reaction. It is reasonable to suppose that the DMC molecules will be more difficult to deactivate than the straight chain species as the structure of the cyclic species is a strained one. Thus the formation of *trans*-pentene-2 from the energized DMC should persist to high inert gas pressures, where its formation from the *cis* isomer is negligible. The addition of oxygen gas in the high-pressure region should reduce the yield of the *trans* isomer to almost zero by quenching the triplet addition reaction and leave as the only source of the *cis* isomer the singlet insertion reaction. The addition of oxygen gas was found to

Can. J. Chem. Downloaded from www.nrcresearchpress.com by 210.87.254.40 on 09/05/12
For personal use only.

reduce the percentage yield of the *trans* isomer to only trace amounts while that of the *cis* isomer was almost unchanged or at most slightly increased. These same observations have been reported by Frey (10).

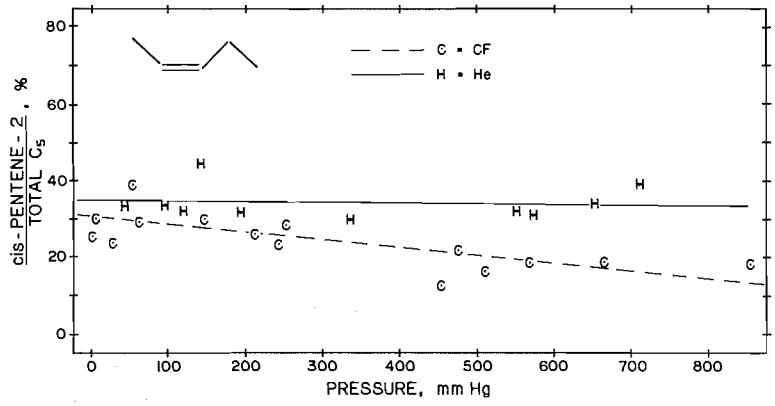

FIG. 4. Percentage yield of *cis*-pentene-2 vs. pressure for the inert gases He and CF_4.

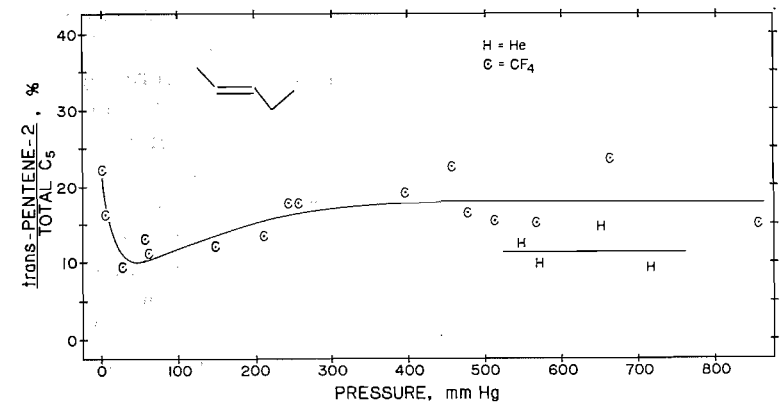

FIG. 5. Percentage yield of *trans*-pentene-2 vs. pressure for the inert gases He and CF_4.

These results are explicable if the principal source of the *trans* isomer is from the energized DMC molecules (or the triplet intermediate itself which should isomerize preferentially to the *trans*-pentene-2) which result from the triplet addition reaction. The *cis*-pentene-2 arises primarily from the singlet insertion reaction. The slight increase in the percentage yield of this isomer can be accounted for by the absolute decrease in the yields of the *trans* isomers on the addition of oxygen gas. The results with He as the inert gas bear out these interpretations. If the primary source of the *cis* isomer at high pressures is from the singlet insertion rather than from the isomerization of the energized DMC, the yield with He should be greater than the yield with CF_4 as the concentration of the singlet species is greater with He. The yield of the *trans* isomer is smaller with He than with CF_4, again reflecting the enhancement of the triplet addition reaction with the latter inert gas. If the major source of the *trans*-pentene-2 was from the isomerization of the energized *cis* isomer just the reverse behavior should have been observed.

Benson and DeMore (11) relate the vanishingly small yields of the *trans* isomers on

Can. J. Chem. Downloaded from www.nrcresearchpress.com by 210.87.254.40 on 09/05/12
For personal use only.

Can. J. Chem. Downloaded from www.nrcresearchpress.com by 210.87.254.40 on 09/05/12
For personal use only.

the addition of oxygen gas to an enhanced deactivating ability of this gas over that for N_2 or even *cis*-butene-2. This would explain the formation of the thermodynamically less favored product in a reaction in which the product distribution is determined by the quenching of a final adduct. Indeed, in the present experiments with increasing pressures of *cis*-butene-2 and no inert gas, the yield of *trans*-pentene-2 is again considerably decreased. Thus if one considers only the results with O_2 and *cis*-butene-2, one could conclude that all of the *trans*-pentene-2 arose from an isomerization of the energized *cis* isomers. However, if one compares two gases which may deactivate *without* at the same time reacting with the methylene and thus either prevent the formation of the triplet species, or rapidly remove it, then this argument is seen to be false. This is the case as seen from the results for CF_4 and He where not only does the percentage yield of *trans*-pentene-2 increase with increasing pressures, but does so more in the experiments with CF_4 than those with He. The small yields with O_2 and butene-2 are then explained by the absence of triplet methylene.

The variation in the percentage yield of 2-methylbutene-2 with increasing inert gas pressure is shown in Fig. 6. The form of this variation is readily accounted for by assuming that this isomer may arise either by direct insertion into the vinylic C—H bond of the *cis*-butene-2 or through the isomerization of the energized DMC molecules. The insertion reaction should decrease with increasing inert gas pressures as more of the singlet methylene is converted to the triplet form before reaction with the butene occurs. The deactivation of the energized DMC molecules by increasing concentrations of inert gas molecules should also lead to a decrease in this percentage yield. One would expect the percentage yield of 2-methylbutene-2 to be greater in the case of He than with CF_4 as He is less efficient as a deactivator and is also less efficient at causing the singlet to triplet transition. While singlet insertion must be invoked as the main source of *cis*-pentene-2, one could explain the entire form of the 2-methylbutene-2 curve without the insertion mechanism. That singlet methylene is a precursor of 2-methylbutene-2 is clearly illustrated by the continuous decrease in its percentage yield as the pressure of inert gas is increased.

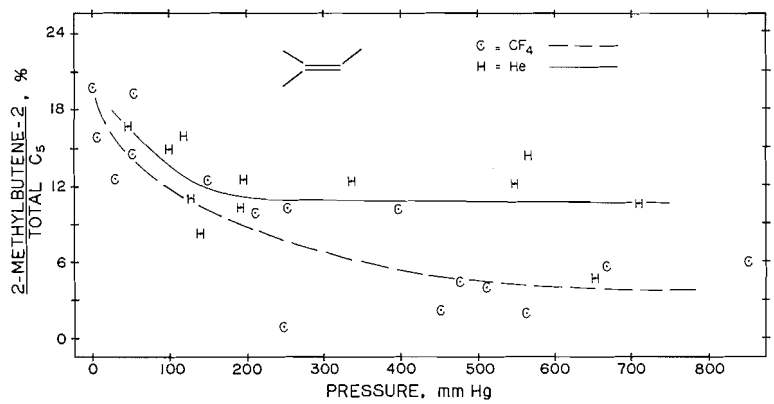

FIG. 6. Percentage yield of 2-methylbutene-2 vs. pressure for the inert gases He and CF_4.

The percentage yield of 3-methylbutene-1, Fig. 7, is seen to increase with increasing pressure of inert gas. This indicates that triplet methylene is a precursor of this isomer. The formation of this compound cannot be explained directly by any insertion mechanism. Nor is the *major source* due to the isomerization of the energized cyclopropanes since

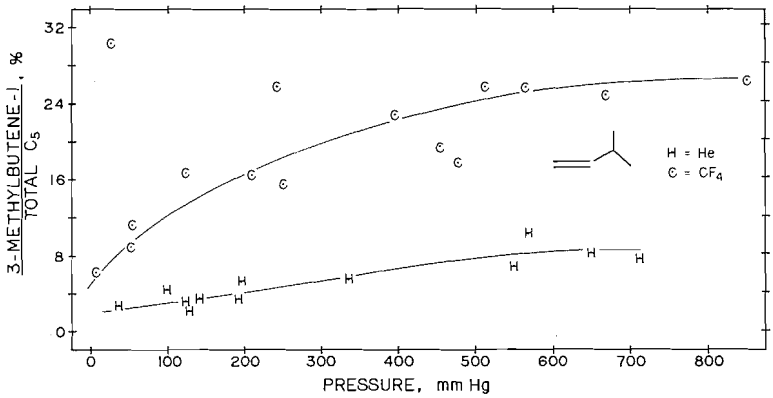

FIG. 7. Percentage yield of 3-methylbutene-1 vs. pressure for the inert gases He and CF_4.

this would decrease with increasing inert gas pressure and the yield with He should then be greater than that observed with CF_4. The opposite behavior is actually observed. The most direct explanation for the appearance of this compound and its dependence on triplet methylene is to propose that the triplet adduct may not only close to give both

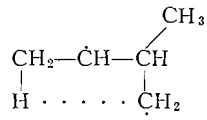

cis- and *trans*-DMC but may undergo an internal hydrogen abstraction through a five-membered cyclic intermediate to give the 3-methylbutene-1 directly. This mechanism was previously proposed by Duncan and Cvetanović (13) to account for the formation of this isomer in the photosensitized decomposition of ketene in the presence of *cis*-butene-2. Duncan and Cvetanović conclude, as did Frey (8) from his high-pressure work, that 3-methylbutene-1 can arise from the addition of triplet methylene to *cis*-butene-2. The yield of 3-methylbutene-1 is reduced to almost zero over the whole pressure range by the addition of oxygen gas. This again indicates the participation of triplet methylene. The same result was reported by Frey (8) for a single run in the high-pressure region. In the experiments with CF_4 and Xe, at pressures below 25 mm the yields of 3-methylbutene-1 are found to be high (see Fig. 7 for the CF_4 case) and to drop very rapidly with increasing pressure of inert gas. This effect did not appear in the experiments with N_2 where the lowest pressure employed was 14 mm. Setser and Rabinovitch (14) in studies on the pyrolysis of CH_2N_2 in the presence of *cis*-butene-2 detected a very rapid initial decrease in the percentage yield of 3-methylbutene-1. Thus there may be another mode of formation for the compound which has an inverse pressure dependence, and operates only at very low pressures. This can be explained by a similar type of migration in a highly energized singlet form of the intermediate postulated above, i.e., a bond in the cyclopropane ring structure is broken due to the large excess of vibrational energy giving the singlet form of the intermediate which may again give a 1,4 hydrogen shift to yield 3-methylbutene-1*. This mechanism has been proposed by DeMore and Benson

**There is considerable scatter in the plots for 3-methylbutene-1 in the* CF_4 *and* Xe *runs at these very low pressures, and the present results do not prove unambigously that there is a second mechanism operating at low pressures which gives this isomer. Flowers and Frey (15) in pyrolytic studies on cis-DMC found only minor amounts of 3-methylbutene-1 even at pressures as low as 6.5 mm. However, the cis-DMC molecules will be more efficient than* CF_4 *or* Xe *at cooling highly energized species.*

Can. J. Chem. Downloaded from www.nrcresearchpress.com by 210.87.254.40 on 09/05/12
For personal use only.

to explain the formation of 3-methylbutene-1 in all cases and they claim that the intervention of triplet methylene is not necessary to explain its appearance as claimed by Frey (10) and Duncan and Cvetanović (13). However, the present results prove that the principal source of 3-methylbutene-1 cannot be due to the rearrangement of a highly energetic species as its percentage yield increases with increasing inert gas pressure and the yield is greater with CF_4 than with He.

THE CONVERSION OF SINGLET TO TRIPLET METHYLENE

Jordan and Longuet-Higgins (16) have determined the relative energies of the lower electronic states of a number of hydride radicals. Their method is semiempirical, making use of observed spectroscopic and heat of formation data rather than attempting to calculate the electronic energies from approximate wave functions. This gives the method a quantitative basis. Their predictions regarding both the geometries and energies for these molecules are in excellent agreement with experiment. We have used their results for CH_2 to estimate the probability of the system crossing from a singlet to a triplet state due to a spin–orbit perturbation. The electronic configuration of the ground state of CH_2 is $(\sigma_g(1s))^2\ \sigma_g^2\ \sigma_u^2\ \pi_u^2$, which gives the following electronic molecular states in order of decreasing stability; $^3\Sigma_g^-$, $^1\Delta_g$, $^1\Sigma_g^+$. Thus if CH_2 is a linear molecule, the ground state should be a triplet. When the molecule is bent the degeneracy of the π_u orbital is lifted and a closed shell configuration can be written for the ground state, giving a singlet,

$$(a_1)^2\ (a_1)^2\ (b_2)^2\ (a_1)^2;\ ^1A_1.$$

Excited states of the bent molecule arise from single or double occupation of the second orbital, b_1, of the linear π_u set, i.e., $^3B_1$, $^1B_1$, and $^1A_1'$ states. Jordan and Longuet-Higgins have determined the relative energies of these states as a function of the bond angle. Their results are shown in Fig. 8. Their calculations predict that the $^3\Sigma_g^-$ state will be the most stable in agreement with the spectroscopic results of Herzberg and Shoosmith (5). The bent state is a singlet and is predicted to have an energy minimum at 107°. (The interaction of the two $^1A_1$ states was taken into account in the calculation.) The interesting feature of these calculations is the crossing of the potential curves for the $^1A_1$ and $^3B_1$ states with change in the bond angle. If the spin quantum numbers were "good" quantum numbers in the sense that the spin angular momentum was a completely independent quantity and always conserved, then no crossover from the singlet to the triplet curve could occur. However, the carbon atom Hamiltonian does have a small but finite spin–orbit interaction component, and thus conservation of spin angular momentum, while almost complete, is not a rigorous requirement in the system. We must ask two questions; will the spin–orbit perturbation indeed "mix" the $^1A_1$ and $^3B_1$ states and will this interaction lead to a kinetically significant rate for the singlet to triplet crossover?

The triplet state spin functions transform as the A_2, B_1, and B_2 irreducible representations of the C_{2v} point group and thus the overall symmetries (space and spin) of the wave function for the $^3B_1$ ground state are B_2, A_1, and A_2 (17). Since the perturbation will "mix" only those states which have identical symmetries, the $^1A_1$ state* may "mix" with the $^3B_1$ ground state. Following the method outlined by Sidman (18) and applying the perturbation at the point of intersection, one finds that the ± 1 spin components of the $^3B_1$ state (^+B and ^-B) mix with the $^1A_1$ state (^0A) giving

$$\psi_1 = \tfrac{1}{2}(^+B + {}^-B + \sqrt{2}\,{}^0A)$$

$$\psi_2 = \tfrac{1}{2}(^+B + {}^-B - \sqrt{2}\,{}^0A)$$

**The singlet spin function transforms as does the A_1 representation.*

Can. J. Chem. Downloaded from www.nrcresearchpress.com by 210.87.254.40 on 09/05/12
For personal use only.

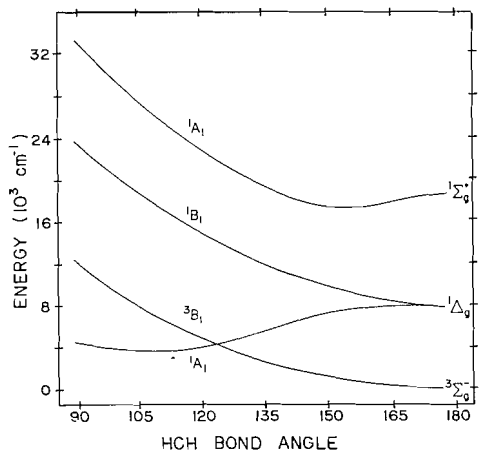

FIG. 8. Variation of the energy with bond angle for the lowest electronic states of methylene after Jordan and Longuet-Higgins (16).

with an energy splitting of $2\sqrt{2}\zeta$, where ζ is the spin–orbit coupling perturbation which we have considered to be determined completely by the carbon 2p orbitals and by an effective potential due to the carbon nucleus only, as suggested by Sidman (18). This yields a value for $\zeta = 14$ cm^{-1} compared to 16.4 cm^{-1} observed for an isolated carbon atom (19). Since these answers differ so little we have employed the value for the isolated carbon atom in our calculations giving $\langle V \rangle = 2\sqrt{2}\zeta = 46.2$ cm^{-1} or 9.18×10^{-15} erg. The probability of a transition from the singlet curve to the triplet curve during a double pass through the point of intersection (as occurs on every complete cycle of the bending vibration) is (20)

$$P_{3\leftarrow 1} = \frac{8\pi^2 \langle V \rangle^2}{h|F_2 - F_1|}\left(\frac{1}{v}\right),$$

where h is Planck's constant, $|F_2 - F_1|$ is the absolute value of the difference in the slopes of the two curves at their point of intersection, and v is the velocity with which the system approaches the crossing point. Dr. Jordan (21) has kindly supplied us with more recent, improved values for $E(^1A_1)$ and $E(^3B_1)$ vs. bond angle and we have used these values to determine a value of 2.80×10^{-12} erg/radian or 2.71×10^{-4} erg/cm for $|F_2 - F_1|$. The velocity of approach v is determined by the number of energy quanta possessed by the bending vibration, by its frequency and reduced mass, and by the C—H bond length. Jordan and Longuet-Higgins estimate the bending frequency ν_2 to be 1 180 cm^{-1}. This value of ν_2 gives a zero point energy which is not quite sufficient to enable the system to reach the point of intersection. (The system could still tunnel through the small remaining barrier of $\sim$175 cm^{-1}.) For the $n = 1$ level of ν_2, the average value of the kinetic energy at the point of intersection will be approximately 1 000 cm^{-1}*. From this value for the kinetic energy we calculate the classical velocity of the reduced mass point through the point of intersection to be 7.28×10^5 cm/s. Substitution of these values gives

$$P^1_{3\leftarrow 1} = 5.08 \times 10^{-3}.$$

**The quantum mechanical virial theorem when applied to a harmonic oscillator states that $\bar{T} = \bar{V} = \frac{1}{2}\bar{E}$, i.e., the average values of the kinetic ($\bar{T}$) and potential ($\bar{V}$) energies are equal for all values of the displacement. When viewed in this manner, rather than in the classical way given above, one calculates a slightly lower value for $\bar{T} = 885$ cm^{-1} for the $n = 1$ state.*

Can. J. Chem. Downloaded from www.nrcresearchpress.com by 210.87.254.40 on 09/05/12
For personal use only.

The superscript 1 is added to denote that $P_{3\leftarrow 1}$ depends on the vibrational quantum number through the velocity v. The first-order rate constant for singlet to triplet crossover is

$$k_{3\leftarrow 1} = P^1_{3\leftarrow 1} \times \nu_2 = 1.8 \times 10^{11}\ s^{-1}.$$

This frequency of crossover is approximately ten times greater than the number of collisions per second of an average sized molecule under standard conditions of temperature and pressure. The calculation thus predicts that the formation of triplet methylene from its $^1A_1$ state may compete favorably with the removal of the same singlet species by its reaction with *cis*-butene-2. The addition reaction occurs on almost every collision with the *cis*-butene-2 and if the concentration of the alkene is kept at a low value, as in the present experiments, the reactions of triplet methylene should be observed.

This calculation does not take into account the fact that the methylene molecule is not formed in the lowest of its singlet states (6). It must first, therefore, lose electronic energy either by a radiative process or by collision. Very little is known about the collisional transfer of electronic energy. However, these processes should be rapid compared to the rate of addition of singlet CH_2 to *cis*-butene-2 at the very low ratios of butene/inert gas ($= 5 \times 10^{-4}$) employed in the present experiments. Under these conditions a large percentage of the methylene must reach the $^1A_1$ ground state. Thus the competition will be between the addition reaction and the singlet to triplet crossover for the $^1A_1$ species.

The value of $P^n_{3\leftarrow 1}$ decreases with increasing velocity (large values of the vibrational quantum number n) through the point of intersection. The CH_2 molecule will still be vibrationally excited in the $^1A_1$ state and the rate of triplet formation should increase as the molecule is vibrationally deactivated, reaching a maximum for the $n = 0$ or 1 level. This would account for the enhanced efficiency of CF_4 in generating the triplet species: CF_4 will be the most efficient of the gases investigated here at removing the excess vibrational energy from CH_2. (Recall the very steep initial slope of the curve for CF_4 in Fig. 1 which is again a measure of its ability at removing excess vibrational energy through collisions.)

We have considered the mechanism of the crossover to be an intramolecular one and have not taken into account other magnetic perturbations which may arise through collisions with the inert gas molecules. If the magnetic perturbations induced by the collisions were of greater importance than the vibrational deactivation of the $^1A_1$ state discussed above, one might have expected Xe to be superior to N_2 and CF_4 in causing the singlet to triplet transition. Xenon, since it is the most polarizable of the three gases, should give rise to the greatest change in the electron distribution on collision. If the collision is strong enough to merit the writing of a single wave function for the combined system, CH_2 + inert gas, (i.e., electron exchange is important), one should expect the large spin–orbit forces present in Xe ($\zeta = 8\,250\ cm^{-1}$) to result in considerably higher yields of the triplet species than do N_2 or CF_4. Instead the abilities of Xe and N_2 in this regard are experimentally indistinguishable, and both are less efficient than CF_4. These observations are explicable on the grounds that it is necessary to remove excess vibrational energy in the singlet ground state to achieve appreciable rates of singlet to triplet crossovers. Specifically one wishes to remove vibrational energy from the bending mode of CH_2. Herzfeld and Litovitz (22) have demonstrated that molecules with vibrational frequencies close to the lowest frequency of the vibrationally excited molecule are particularly efficient at quenching, and CF_4 does in fact possess a mode with a frequency of 1 281 cm^{-1} (23), which is close to that predicted for the bending mode in methylene.

Can. J. Chem. Downloaded from www.nrcresearchpress.com by 210.87.254.40 on 09/05/12
For personal use only.

Can. J. Chem. Downloaded from www.nrcresearchpress.com by 210.87.254.40 on 09/05/12
For personal use only.

EXPERIMENTAL METHODS

A typical high-vacuum system was used for the transferring and purification, by bulb to bulb distillation, of all materials and for their introduction into a "seasoned" 2 l reaction bulb. All pressures were measured by Bourdon gauges (spoon type) to avoid contaminations with mercury vapor. The lamp employed in the photolyses was a medium-pressure mercury vapor lamp (G. E. H-4AB). Care was taken to maintain the reaction flask at 25 ± 5 °C by means of a 7 in. fan. The irradiation times were of 8 h duration.

Diazomethane was prepared by the method of Arndt and Amende (24) modified by extracting the product with decalin rather than diethyl ether. The diazomethane was stored at −196 °C. Before use it was alternately warmed to room temperature, refrozen, and pumped, this procedure being repeated a number of times to remove non-condensibles. The ethylene was removed by pumping for ½ h on the storage bulb, its temperature being maintained at −125 °C. This was followed by a distillation at −70 °C. The *cis*-butene-2 (Matheson, Canada) was degassed by alternate freezing and warming and was subjected to several trap to trap distillations at dry ice – acetone temperature. Nitrogen (Matheson, prepurified grade) specified to have less than 7 p.p.m. oxygen was used. Nitrogen was also treated by passing the gas through a powdered copper – kieselguhr column at 400 °C and then through a spiral trap immersed in liquid nitrogen. No detectable differences were found between runs with the nitrogen purified in this manner and runs with the Matheson lecture bottle grade. Helium, xenon, and argon were all of research grade (99.99% purity) and used without further purification. The carbon tetrafluoride was purified by low-temperature distillations and by passage through a large U tube filled with silica gel and maintained at a temperature of −135 °C. This latter step is to remove hydrocarbon contaminants. Gas – liquid phase chromatographic analysis of the purified CF_4 showed no hydrocarbon impurity.

Analysis of products were performed with g.l.c. The column consisted of an 8 m length of 23% by weight 2,5-hexanedione on 30–60 mesh Columnpax maintained at a temperature of 3 °C, followed by a Perkin-Elmer HX column (2 m, $AgNO_3$ – propylene glycol). Helium was used as the carrier gas. The products were identified by collecting the components as eluted from the g.l.c. in CS_2 cooled in a dry ice – acetone slurry. The solutions were then identified by infrared spectrophotometry. Retention times of the products were also compared with those of known samples.*

ACKNOWLEDGMENTS

We are grateful to Professor F. A. L. Anet, Dr. M. Back, and Mrs. Anne-Marie Van der Auwera for helpful discussions. We wish to thank the Ontario Research Foundation for a grant in aid of research.

REFERENCES

1. P. S. Skell and R. C. Woodworth. J. Am. Chem. Soc. **78**, 4496, 6427 (1956); **81**, 3383 (1959) and references therein.
2. R. M. Etter, H. S. Skovronek, and P. S. Skell. J. Am. Chem. Soc. **81**, 1008 (1959).
3. R. J. Cvetanović. Can. J. Chem. **36**, 623 (1958).
4. F. A. L. Anet, R. F. W. Bader, and Anne-Marie Van der Auwera. J. Am. Chem. Soc. **82**, 3217 (1960).
5. G. Herzberg and J. Shoosmith. Nature, **183**, 1801 (1959).
6. G. Herzberg. Proc. Roy. Soc. London, Ser. A, **262**, 291 (1961); Can. J. Phys. **39**, 1511 (1961).
7. J. N. Butler and G. B. Kistiakowsky. J. Am. Chem. Soc. **82**, 759 (1960); **83**, 1324 (1961).
8. H. M. Frey. J. Am. Chem. Soc. **80**, 5005 (1958).
9. H. M. Frey. Proc. Roy. Soc. London, Ser. A, **251**, 575 (1959).
10. H. M. Frey. J. Am. Chem. Soc. **82**, 5947 (1960).
11. W. B. DeMore and S. W. Benson. Advan. Photochem. **2**, 219 (1964).
12. H. M. Frey. Trans. Faraday Soc. **58**, 516 (1962).
13. F. J. Duncan and R. J. Cvetanović. J. Am. Chem. Soc. **84**, 3593 (1962).
14. D. Setser and B. Rabinovitch. Can. J. Chem. **40**, 1425 (1962).
15. M. C. Flowers and H. M. Frey. Proc. Roy. Soc. London, Ser. A, **260**, 424 (1961).
16. P. C. H. Jordan and H. C. Longuet-Higgins. Mol. Phys. **5**, 121 (1962).
17. D. S. McClure. J. Chem. Phys. **17**, 665 (1949).
18. J. W. Sidman. J. Chem. Phys. **29**, 644 (1958).
19. W. Kauzmann. Quantum chemistry. Academic Press Inc., New York. 1957.
20. L. D. Landau and E. M. Lifshitz. Quantum mechanics. Vol. 3. Addison-Wesley Pub. Co. Inc. Massachusetts. 1958.
21. P. C. H. Jordan. Private communication.
22. K. Herzfeld and T. Litovitz. Absorption and dispersion of ultrasonic waves. Academic Press, New York. 1959.
23. W. K. Winter, B. Curnutte, and S. E. Whitcomb. Spectrochim. Acta, **15**, 1085 (1959).
24. F. Arndt and J. Amende. Z. Angew. Chem. **43**, 444 (1930).

**The yield of 2-methylbutene-1 is always very low in the reaction of CH_2 with butene-2. Because of the extremely small amount of CH_2N_2 and cis-butene-2 employed in the present experiments, 2-methylbutene-1 was not detected.*

Can. J. Chem. Downloaded from www.nrcresearchpress.com by 210.87.254.40 on 09/05/12
For personal use only.

COMPLEXES OF BORON TRIFLUORIDE WITH FLUOBORATES[1]

S. BROWNSTEIN AND J. PAASIVIRTA[2]
Division of Applied Chemistry, National Research Council, Ottawa, Canada
Received December 23, 1964

ABSTRACT

The occurrence of complexes of boron trifluoride with some fluoborates has been established. Enthalpies of formation were determined for some of these complexes. Infrared and fluorine resonance spectra were obtained in an attempt to elucidate the structures of the complexes.

INTRODUCTION

Complexes of one molecule of boron trifluoride with one molecule of a Lewis base are well established. Only two cases have been reported where 2:1 complexes are stable in solution (1), and these have not been definitely confirmed by another technique (2). It was proposed that the second boron trifluoride in the 2:1 complexes was bound by a fluorine–boron–fluorine bridge. Although there are many examples of other bridging halogen atoms only a few cases have been established for fluorine (3–5). Investigations of Friedel-Crafts catalyzed isomerizations suggest that some reactive intermediates may contain two molecules of boron trifluoride for each molecule of Lewis base (6). It has been found that boron trifluoride at low temperatures forms complexes with alkyl fluorides (7). These results suggest that fluorine-bridged complexes may be of widespread occurrence and could be involved in Friedel-Crafts catalysis using nonmetal fluorides as catalyst. An attempt was made to investigate this phenomenon in extremely simple systems, fluoborate salts and boron trifluoride. Complexes were found but the dependence of stability upon cation shows that the situation is still rather complex.

EXPERIMENTAL

Most of the work was carried out with methylene chloride solutions. The solvent was prepared according to Eastham (8), and all solutions made under vacuum conditions. The $AgBF_4$ was prepared from AgF and BF_3 in nitromethane (9), and purified via its benzene complex (10). Tetra-*n*-butylammonium fluoborate was prepared by the reaction of aqueous alcoholic solutions of silver fluoborate and tetra-*n*-butylammonium iodide. The crude product was recrystallized from methanol–water and vacuum dried, m.p. 161.5 °C, lit. 161.8 °C (11).

Pressure measurements were obtained with a constant volume mercury manometer. The high vacuum system employed was so designed that a minimum quantity of gas was outside the thermostated container. Corrections were made for this volume. Fluorine resonance spectra were obtained at 56.4 and 94.1 Mc with a specially designed variable temperature probe (12). Infrared spectra were obtained with the samples incorporated in KBr pellets and as methylene chloride solutions.

RESULTS AND CONCLUSIONS

A typical plot of pressure vs. total BF_3 in the presence and absence of $AgBF_4$ is shown in Fig. 1. From the dimensions of the apparatus, and assuming gaseous BF_3 to behave idealy, it is possible to calculate the concentration of BF_3 in solution. For a BF_3 partial pressure of 100 mm the variation of solubility with temperature is shown in Fig. 2. If the differential heat of solution of BF_3 in a saturated solution of methylene chloride is constant, a straight line plot should be obtained in Fig. 2. Although there is deviation from

[1]*Issued as N.R.C. No. 8366.*
[2]*National Research Council of Canada Postdoctorate Fellow, 1963–1964. Present address: University of Oulu, Oulu, Finland.*

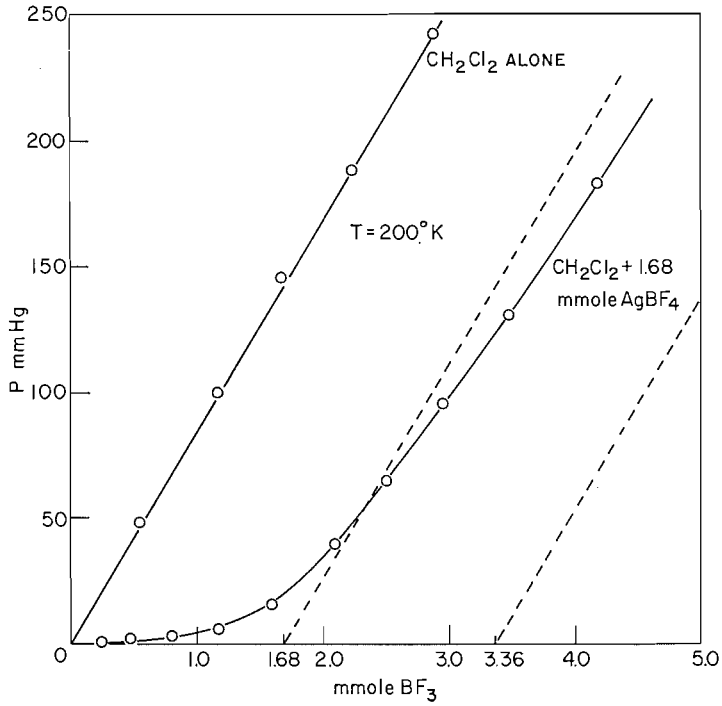

FIG. 1. Vapor pressure of BF_3 solutions at 200 °K.

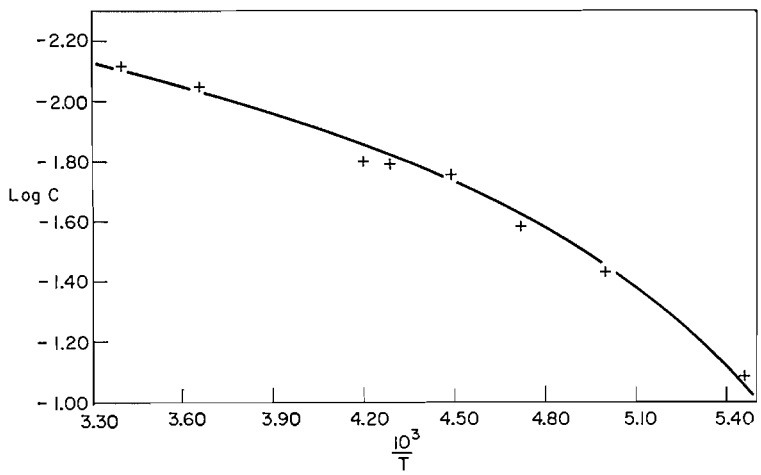

FIG. 2. Solubility of BF_3 in CH_2Cl_2. C is the concentration in mole/l.

ideal behavior, the average value of the heat of solution was calculated from the Clausius–Clapeyron equation and is listed in Table II.

Once the apparatus had been calibrated for solvent and BF_3, measurements were made with added fluoborate. If it is assumed that the partial pressure of BF_3 is a measure of the free BF_3 concentration in solution, the amount of complexed BF_3 may be calculated. Since the concentration of complex never exceeded 0.04 m this assumption appears

Can. J. Chem. Downloaded from www.nrcresearchpress.com by 210.87.254.40 on 09/05/12
For personal use only.

reasonable. It is then possible to calculate equilibrium constants for complex formation. Results and calculations for tetra-*n*-butylammonium fluoborate at 183 °K are shown in Table I.

TABLE I

Calculation of equilibrium constant for complex formation

BF_3 added*	P (mm Hg)	BF_3 (free)†	BF_3 (gas)‡	BF_3 (liquid)	$B_3F_{10}^-$§	$B_2F_7^-$	K_2‖
2.15	30.5	0.72	0.12	0.60	0.32	0.79	24
2.60	45.8	1.08	0.18	0.90	0.41	0.70	24
3.04	59.0	1.38	0.23	1.15	0.55	0.56	31
3.56	78.5	1.83	0.31	1.52	0.62	0.49	30
4.10	95.7	2.23	0.38	1.85	0.76	0.35	43
4.63	115.0	2.68	0.45	2.23	0.84	0.27	50

*Quantities are in mmoles; 1.11 mmoles of tetra-*n*-butylammonium fluoborate was placed in the apparatus.
†This value is obtained from the relationship between pressure and BF_3 in the absence of fluoborate.
‡This value is calculated from the pressure, temperature, and gas volume.
§Under these conditions there is complete formation of the 1:1 complex and the additional complexed BF_3 is present as the 2:1 complex.
‖This has been multiplied by 36.2 to express K for concentrations in molalities.

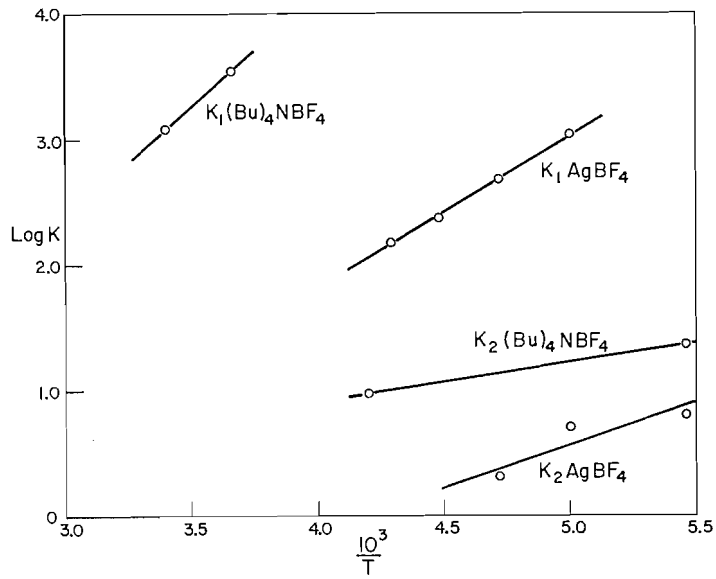

FIG. 3. Temperature dependence of complex formation.

The temperature dependence of the equilibrium constants for complex formation with silver fluoborate and tetra-*n*-butylammonium fluoborate is shown in Fig. 3. The equilibrium constants are given by the following expressions.

$$K_1 = \frac{[MB_2F_7]}{[BF_3][MBF_4]}$$

$$K_2 = \frac{[MB_3F_{10}]}{[BF_3][MB_2F_7]}$$

The nature of the cation has a marked effect on the stability of the complexes. It therefore seems likely that the various fluoborate complexes are present as ion pairs in methylene chloride solution. From the temperature dependence of the equilibrium constant the enthalpy and entropy of formation may be calculated. This is shown in Table II.

Can. J. Chem. Downloaded from www.nrcresearchpress.com by 210.87.254.40 on 09/05/12
For personal use only.

TABLE II

Some properties of fluoborate complexes

Compound	ΔH (kcal/mole)	ΔS (e.u.)*	δ_{CFCl_3} (p.p.m.)	K
BF_3	−2.8†		−125.3	
AgB_2F_7	−5.6±0.9	−14±4	−146.2	51±13 (−35°)
				240±30 (−50°)
				480±90 (−61°)
				1 110±70 (−73°)
AgB_3F_{10}	−2.8	−12	−140.2	2.1 (−61°)
				5.1 (−73°)
				6.5±0.8 (−90°)
$(Bu)_4NBF_4$			−149.5	
$(Bu)_4NB_2F_7$				2 400±300 (21°)
				3 500±200 (0°)
$(Bu)_4NB_3F_{10}$				9.8±0.3 (−35°)
				34±13 (−90°)

*For concentrations expressed as molalities. Errors are standard deviations.
†The differential heat of solution.

Fluorine resonance spectra of the fluoborate salts plus varying amounts of boron trifluoride were obtained from room temperature to the freezing points of the solutions at about 170 °K. Silver fluoborate is not sufficiently soluble to obtain a useful spectrum. However, in the presence of excess boron trifluoride it goes into solution as the complex fluoborate as the temperature is lowered. Under all circumstances only a single line was observed, suggesting rapid exchange between free and complexed boron fluoride and rapid exchange between non-equivalent fluorines within the complex fluoborate. Chemical shifts for the complexes were obtained from samples where composition and temperature were such that the complex was the predominant species in the sample. The fact that these shifts are not merely the average value for the boron fluoride and silver fluoborate is additional confirmation of the existence of complexes in the solution. For a sample with a sixfold excess of BF_3 over tetra-*n*-butylammonium fluoborate the signal from liquid BF_3 was clearly observed after the bulk of the solution had been frozen at 165 °K. This indicates that large amounts of complexes greater than 2:1 could not have been formed under these conditions. The upward drift of K_2 in Table I suggested the possibility of higher complex formation. This cannot be confirmed with these experimental techniques since lower temperatures and higher pressures might produce liquid boron trifluoride.

Infrared spectra of NH_4BF_4, $(Bu)_4NBF_4$, and $(Bu)_4NB_2F_7$ are shown in Fig. 4. The three bands between 1 000 and 1 200 cm^{-1} are characteristic of the fluoborate ion (5). Their replacement by a single very broad band in $(Bu)_4NBF_4$ suggests that there is considerable interaction between cation and anion for this compound. The $B_2F_7^-$ anion is iso-electronic with bis-trifluoromethyl ether, which has a bent structure (13). The infrared spectra of linear and bent molecules of this type have been measured and discussed (14, 15). A linear molecule will have three prominent bands while five are expected for a bent molecule. Since five bands at 8.2, 9.1, 9.5, 9.8, and 12.0 μ are observed for B—F bending and stretching in the spectrum of $(Bu)_4NB_2F_7$ this suggests the possibility that the structure of $B_2F_7^-$ might be as shown.

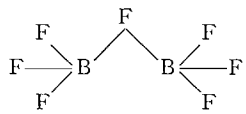

Other techniques would be required to establish its structure and that of $(Bu)_4NB_3F_{10}$.

Can. J. Chem. Downloaded from www.nrcresearchpress.com by 210.87.254.40 on 09/05/12
For personal use only.

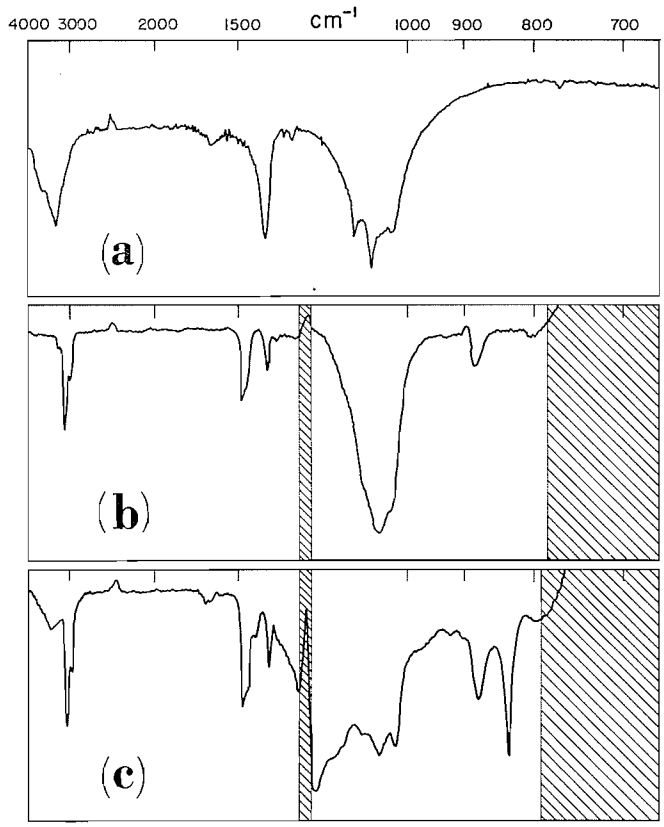

FIG. 4. Infrared spectra of fluoborates. (*a*) NH_4BF_4 in KBr disk. (*b*) $(Bu)_4NBF_4$ as a 0.1 *M* solution in CH_2Cl_2. The shaded areas are where the solvent is opaque. A similar spectrum was obtained in a KBr disk. (*c*) $(Bu)_4NB_2F_7$ as a 0.1 *M* solution in CH_2Cl_2.

REFERENCES

1. H. C. BROWN, P. F. STEHLE, and P. A. TIERNEY. J. Am. Chem. Soc. **79**, 2020 (1957).
2. S. BROWNSTEIN, A. M. EASTHAM, and G. A. LATREMOUILLE. J. Phys. Chem. **67**, 1028 (1963).
3. C. J. HOFFMAN, B. E. HOLDER, and W. L. JOLLY. J. Phys. Chem. **62**, 364 (1958).
4. A. J. EDWARDS, R. D. PEACOCK, and R. W. H. SMALL. J. Chem. Soc. 4486 (1962).
5. B. J. HATHAWAY and D. E. WEBSTER. Proc. Chem. Soc. 14 (1963).
6. J. M. CLAYTON and A. M. EASTHAM. Can. J. Chem. **39**, 138 (1961).
7. G. OLAH, S. KUHN, and J. OLAH. J. Chem. Soc. 2174 (1957).
8. A. M. EASTHAM. J. Am. Chem. Soc. **78**, 6040 (1956).
9. G. OLAH and H. W. QUINN. J. Inorg. Nucl. Chem. **14**, 295 (1960).
10. K. HEYRS and H. PAULSEN. Angew. Chem. **72**, 349 (1960).
11. C. R. WITSCHONKE and C. A. KRAUS. J. Am. Chem. Soc. **69**, 2473 (1947).
12. S. BROWNSTEIN and J. PAASIVIRTA. To be published.
13. A. DI GIACOMO and C. P. SMYTH. J. Am. Chem. Soc. **77**, 774 (1955).
14. H. W. THOMPSON. Trans. Faraday Soc. **37**, 38 (1941).
15. H. S. GUTOWSKY. J. Chem. Phys. **17**, 128 (1949).

Can. J. Chem. Downloaded from www.nrcresearchpress.com by 210.87.254.40 on 09/05/12
For personal use only.

Can. J. Chem. Downloaded from www.nrcresearchpress.com by 210.87.254.42 on 09/05/12
For personal use only.

LOCALIZATION OF THE C=Se VIBRATION IN THE INFRARED SPECTRA OF SELENOSEMICARBAZONES[1]

B. A. GINGRAS, T. SUPRUNCHUK, AND C. H. BAYLEY
Division of Applied Chemistry, National Research Council, Ottawa, Canada

Received January 4, 1965

ABSTRACT

Few organic compounds of selenium are known and, consequently, very little published data are available concerning the various vibrations around the selenium atom. The present paper discusses the C=Se vibration in selenosemicarbazones by comparing their infrared spectra with those of corresponding Se-benzyl derivatives in which the C=Se group has been replaced by a C—Se—Bz. On this basis, it can be seen that a band at 800–780 cm^{-1} in the spectra of selenosemicarbazones is absent in the spectra of the benzyl derivatives. This band is assigned to the C=Se vibration.

In recent years, a few organic compounds of selenium have been investigated with particular emphasis on the localization of the various infrared vibrations around the selenium atom, generally by comparison with infrared spectra of analogous sulfur compounds. For instance, a band at 942 cm^{-1} was attributed to the CSe_2^- ion of diselenocarboxylates by comparison with the spectra of dithiocarboxylates which lacked that band (1). In metal complexes of iso- and seleno-cyanates, the C—Se stretching vibration was found to be in the regions 650 cm^{-1} for $NCSe^-$, and 550 cm^{-1} for $SeCN^-$ (2, 3). In selenoesters of the type Ar—CSeOMe, the region 1 227 – 1 220 cm^{-1} was suggested by Collard-Charon and Renson (4) for the C=Se by comparison with the spectra of the corresponding thio and oxygen compounds, although these workers point out the great similarity between the spectra of sulfur and selenium compounds in this class as well as in all the other compounds of selenium and sulfur they have studied. Thus, in *n*-butyl-4-selenosemicarbazides a band at 1 045 cm^{-1} was assigned to the C=Se vibration while in the corresponding thio compound, a band at 1 055 cm^{-1} was suggested for the C=S, and at 1 070 cm^{-1} (C=Se) and 1 075 cm^{-1} (C=S) in *n*-butyl-4-methyl-2-seleno- and thio-semicarbazides (5). By the same method of comparison, bands at 1 080 cm^{-1} and 1 082 cm^{-1} were assigned to the C=S and C=Se respectively in thio- and seleno-ureas, and at 1 115 cm^{-1} (C=S) and 1 110 cm^{-1} (C=Se) in substituted ureas (6).

In view of the results recently reported from this laboratory on the localization of the C=S in thiosemicarbazones (7), it seemed appropriate to extend this study to selenosemicarbazones. Because of the great similarity between the spectra of thio and seleno compounds already mentioned and because this similarity was found to exist in the case of thio- and seleno-semicarbazones, it was felt that the method of comparison could lead to very misleading conclusions. Indeed, it was found by Jensen (8) that the spectra of thio- and seleno-amides, ureas, and semicarbazides were so much alike that it was impossible to discriminate between the various vibrations. Jensen even argues that all assignments of infrared bands to the C=S group of thioamides may have been erroneous since the same bands appear in spectra of selenoamides.

The present work describes a number of new selenosemicarbazones and their infrared spectra with particular emphasis on the C=Se vibration. Another purpose of this work

[1]*Issued as N.R.C. No. 8362.*

was to study the antifungal properties of selenosemicarbazones and their reaction with metals. Such studies were carried out earlier with thiosemicarbazones (7, 9, 10) and a relationship was found between antifungal activity and complex formation with copper.

The selenosemicarbazones investigated are listed in Table I, together with their melting points and analyses. The preparation of these compounds is complicated by the fact that the required starting material, selenosemicarbazide, is not readily available and cannot be obtained by the procedures used for the oxygen and sulfur analogs. Selenosemicarbazide was obtained accidentally and in low yields during the isomerization of a selenocyanate in the presence of butyraldehyde (11, 12). The possible methods of preparation of selenosemicarbazones were reviewed by Mautner (13) and later by Renson *et al.* (11), who arrived at the conclusion that the best method was one involving an exchange of carbonyl radicals starting from acetone selenosemicarbazone which can be obtained in fair yields. This method was used in the present work.

TABLE I

Selenosemicarbazones: R—C(H)=N—NH—C(=Se)—NH_2

No.	Carbonyl compounds	m.p. (°C)	Yield (%)	Formulae	Required (%)	Found (%)
1	*n*-Heptanal	70	75	$C_8H_{17}N_3Se$	C, 41.03 H, 7.26 N, 17.95	41.24 7.10 17.90
2	*n*-Octanal	99	53	$C_9H_{19}N_3Se$	C, 43.55 H, 7.66 N, 16.94	42.88 7.56 16.92
3	*n*-Nonanal	77	46	$C_{10}H_{21}N_3Se$	C, 45.80 H, 8.02 N, 16.03	46.26 7.97 16.18
4	*n*-Decanal	103	71	$C_{11}H_{23}N_3Se$	C, 47.83 H, 8.33 N, 15.22	47.87 8.37 15.22
5	*n*-Undecanal	80	60	$C_{12}H_{25}N_3Se$	C, 49.65 H, 8.62 N, 14.48	49.43 8.25 14.38
6	9-Undecenal	72	32	$C_{12}H_{23}N_3Se$	C, 50.00 H, 7.98 N, 14.58	50.12 8.15 14.58
7	*n*-Dodecanal	105	90	$C_{13}H_{27}N_3Se$	C, 51.31 H, 8.88 N, 13.82	51.53 9.16 13.94
8	Benzaldehyde	166*				

*Literature m.p. 167–168 (12, 17).

Due to the greater mass of the selenium atom, the C═Se vibration is expected to occur at somewhat lower frequencies than the C═S. The latter does not give rise to as characteristic a band as the C═O group due to the complication of interaction, particularly in the case of thiosemicarbazones where the NH rocking vibrations can interfere; however, the C═S vibration was reviewed recently for several compounds by Colthup (14) and was found to be in the range 1 200 – 1 050 cm^{-1}. Furthermore, in an earlier publication, we assigned a band at around 1 100 cm^{-1} to this vibration in the case of thiosemicarbazones (7). The region between 1 200 and 700 cm^{-1} is, therefore, the logical one for

Can. J. Chem. Downloaded from www.nrcresearchpress.com by 210.87.254.42 on 09/05/12
For personal use only.

the C═Se vibration to occur, at least in the case of selenosemicarbazones. This is substantiated by the value obtained for $\nu_{C=Se}$ using Gordy's rule and the harmonic oscillator equation.[2]

The method used previously (7) for the localization of the C═S vibration by comparing spectra of thiosemicarbazones with those of their copper complexes could not be used with reliability in the present case because of the difficulty in obtaining the copper complexes in sufficient degree of purity. Selenosemicarbazone–copper complexes can be prepared by the method described in a previous publication (10) but purification of the complexes, except in a few cases, resulted in partial decomposition and formation of colloidal selenium. However, benzyl derivatives of selenosemicarbazones, in which the benzyl radical is bonded to the selenium atom, are conveniently prepared and were found suitable for infrared studies, since the required change from C═Se to C—Se—Bz takes place.

Benzyl derivatives were then prepared from the series of selenosemicarbazones listed in Table I, and the new compounds are shown in Table II. Bands between 1 200 and 700 cm^{-1} in the spectra of selenosemicarbazones and their corresponding benzyl derivatives are shown in Table III.

It can be seen from Table III that the bands appear with a striking regularity in the

TABLE II

Benzylselenosemicarbazones: R—C(H)═N—N═C(Se—Bz)—NH_2

No.	Carbonyl compounds	m.p. (°C)	Yield (%)	Formulae	Required (%)	Found (%)
1*a*	*n*-Heptanal	58	59	$C_{15}H_{23}N_3Se$	C, 55.56 H, 7.10 N, 12.96	55.61 6.88 12.99
2*a*	*n*-Octanal	66	48	$C_{16}H_{25}N_3Se$	C, 56.80 H, 7.39 N, 12.43	56.86 7.20 12.51
3*a*	*n*-Nonanal	57	40	$C_{17}H_{27}N_3Se$	C, 57.95 H, 7.67 N, 11.93	58.13 7.79 11.65
4*a*	*n*-Decanal	68	30	$C_{18}H_{29}N_3Se$	C, 59.02 H, 7.92 N, 11.48	59.47 8.21 11.72
5*a*	*n*-Undecanal	67	47	$C_{19}H_{31}N_3Se$	C, 60.00 H, 8.16 N, 11.05	60.00 8.25 11.14
6*a*	9-Undecenal	53	40	$C_{19}H_{29}N_3Se$	C, 60.32 H, 7.67 N, 11.11	59.80 7.89 11.07
7*a*	*n*-Dodecanal	70	28	$C_{20}H_{33}N_3Se$	C, 60.91 H, 8.38 N, 10.66	61.03 8.60 10.88
8*a*	Benzaldehyde	158	75	$C_{15}H_{15}N_3Se$	C, 56.96 H, 4.75 N, 13.29	56.83 4.71 13.25

[2]*Professor R. A. Zingaro, Agricultural and Mechanical College of Texas, reviewed this paper, carried out the calculations, and suggested that they be included. Force constants are 2.7 and 5.9 × 10^5 dyn/cm for "isolated" pure* C—Se *bond and pure* C═Se *bond respectively. The corresponding values are* ν_{C-Se} = 685 cm^{-1}, $\nu_{C=Se}$ = 982 cm^{-1}.

Can. J. Chem. Downloaded from www.nrcresearchpress.com by 210.87.254.42 on 09/05/12
For personal use only.

TABLE III

Region 1 200 – 700 cm^{-1} for seleno- and benzylseleno-semicarbazones

1	1 105m	1 030m	975w	930m	885w	800w	770m	725m	
1*a*	1 125m	1 070w	975w	935w	870w	—	765s	725w	700s
		1 035w							
2	1 110m	1 045m	990w	935w	895w	780m	765w	725m	
2*a*	1 130m	1 070w	980w	945w	865w	—	765s	725w	700s
		1 030w							
3	1 110m	1 040m	990w	940w	890w	800w	770m	720m	
				925w			750w		
3*a*	1 130w	1 070w	980w	940w	865w	—	765s	725w	700s
		1 035w		915w					
4	1 110m	1 040w	1 020w	925w	865w	780m	765m	725m	
4*a*	1 125m	1 070w	1 005w	965m	825w	—	765s	725m	700s
		1 030w	990w	935m					
5	1 110m	1 045m	1 015w	925m	850w	800w	775m	725m	
5*a*	1 125m	1 070w	980w	935w	865w	—	765s	725w	700s
		1 030w	965w						
6	1 110m	1 040m	995w	920m	850w	790w	770m	725m	
6*a*	1 130m	1 070w	1 000w	945w	865w	—	765s	725w	700s
		1 035w	975w	920w					
7	1 105m	1 045w	980w	935w	865w	780m	765m	720m	
		1 025w		915w					
7*a*	1 125m	1 070w	970w	950w	865w	—	765m	725w	700s
		1 030w		935w					
8	1 100m	1 060m	1 035w	950m	865w	785m	765m		695s
8*a*	1 140m	1 075m	1 035m	950m	865m	—	765s		695s

spectra of seleno- and benzylseleno-semicarbazones. For instance, a band at 1 105 – 1 110 cm^{-1} in the spectra of the seleno compounds is shifted regularly by 15–20 cm^{-1} in the benzyl derivatives while a band at 1 030 – 1 045 cm^{-1} in the former is split into a doublet in the spectra of the latter. This regular pattern can be seen throughout the spectra. The spectra of selenosemicarbazones consistently show a group of two bands, of weak to medium intensity, at 800–780 cm^{-1} and at 775–765 cm^{-1}, while the spectra of benzyl derivatives show only one band at 765 cm^{-1}. The band at 800–780 cm^{-1} is therefore assigned to the C=Se vibration. It is realized that formation of benzyl derivatives not only replaces a C=Se by a C—Se—Bz, but also results in a change of configuration from =N—NH—C(Se)—NH_2 to =N—N=C(SeBz)—NH_2; hence, a loss of a hydrogen atom and replacement of a C—N bond by a C=N bond. The band at 800–780 cm^{-1} (C=Se) in the spectra of selenoisemicarbazones is too low to have resulted from a C—N stretching vibration since this is usually found in the 1 400 cm^{-1} region (15) or between 1 300 and 1 000 cm^{-1} in amines (16). It could be argued that N—H rocking vibration can be found at such a low frequency but there remains in the molecules of benzylselenosemicarbazones free NH_2 groups, so that any N—H rocking should still be detected. The new C=N bond in benzylseleno compounds is likely responsible for an extra band at 1 650 cm^{-1} in the spectra. The new band is at somewhat higher frequency than that normally associated with the aromatic ring. This was examined more closely by comparing the spectra of benzaldehyde selenosemicarbazone with its benzyl derivative. The former has a broad band at 1 600 cm^{-1}, probably due to overlapping of the C=N vibration of the benzilidene grouping with the double bond vibrations of the aromatic ring, while the benzyl derivative shows the same pattern at 1 600 cm^{-1} but has an extra band at 1 650 cm^{-1}. This band is attributed to the C=N of the selenocarbohydrazide residue since it is probable that the vibrations associated with the benzyl radical will overlap with those of the benzene ring in the benzaldehyde portion of the

Can. J. Chem. Downloaded from www.nrcresearchpress.com by 210.87.254.42 on 09/05/12
For personal use only.

molecule. The strong absorption at 700 cm^{-1} in the spectra of benzylselenosemicarbazones may be suggestive of a C—Se stretch but no definite assignment can be made since this band may be due to the aromatic ring. Thus, a similar band at 695 cm^{-1} is present in both compounds 8 and 8*a* (Table III) which are aromatic, benzaldehyde seleno- and benzaldehyde benzylseleno-semicarbazone.

In the N—H stretching region, the spectra of selenosemicarbazones are identical with those of corresponding thiosemicarbazones reported earlier (10); they show three bands of medium intensity at 3 420, 3 280, and 3 180 cm^{-1}.

It should be mentioned that, although the preparation of selenosemicarbazone–copper complexes was not generally satisfactory, some were obtained in a fair degree of purity; e.g. dodecanal, *m*-nitrobenzaldehyde, and decanal selenosemicarbazone – copper (I). As with the thiosemicarbazone–copper complexes, the infrared spectra of the seleno–copper complexes are not well resolved but it is interesting to note that the band at 800–780 cm^{-1} (C═Se) disappears while the one at 765 cm^{-1} remains.

The biological properties of selenosemicarbazones will be reported elsewhere but it should be mentioned that the compounds were found to be generally more active than the corresponding thiosemicarbazones against the two organisms studied, *Chaetomium globosum* and *Aspergillus niger*. Furthermore, the activity of thiosemicarbazones was limited to the aliphatic ones, while a number of aromatic selenosemicarbazones (benzaldehyde and *o*-hydroxy-, *o*-chloro-, and *p*-methoxy-benzaldehyde selenosemicarbazones) were found to be active at 10 p.p.m. against *C. globosum*.

EXPERIMENTAL

Selenosemicarbazones

The method used was described by Huls and Renson (17). The new aliphatic compounds are listed in Table I.

Benzylselenosemicarbazones

An alcoholic solution of equivalent amounts of a selenosemicarbazone (from Table I) and sodium was refluxed for 5 min and allowed to cool. An excess (10%) of benzyl chloride was then added and the resulting solution was stirred for 1 h at room temperature, followed by a 5 min refluxing period. After cooling, the sodium chloride was separated out by filtration and the resulting solution was evaporated to a gum which was taken up in benzene–hexane (1:1), and passed through a column of silica gel. Benzene eluted a small amount of a by-product which was found to be benzyl diselenide $(C_6H_5CH_2Se)_2$; m.p. 89, lit. m.p. 92–93 °C (18).

Anal. Calcd. for $C_{14}H_{14}Se_2$: C, 49.41; H, 4.12. Found: C, 50.08; H, 4.94.

The infrared spectrum of this compound supports the diselenide structure instead of the benzyl selenol, since it shows no band in the region where the Se—H vibration is known to occur, at 2 290 – 2 295 cm^{-1} in phenyl selenol and 2 300 – 2 315 cm^{-1} for *n*-butyl selenol (6). Benzene–ether (1:1) eluted the required benzylselenosemicarbazones, listed in Table II.

Selenosemicarbazonato–Copper

Three 1:1 complexes were obtained in a sufficiently pure form for identification: decanal, dodecanal, and *m*-nitrobenzaldehyde selenosemicarbazone–copper (I). They were prepared by adding equimolar amounts of cupric chloride in ethyl alcohol to a warm solution of the selenosemicarbazone in the same solvent. The mixture turned brown and, after cooling, the precipitated complex was collected by filtration. The analyses are given for C, H, N only, since the presence of selenium interferes with the determination of copper.

Decanal selenosemicarbazonato–copper(I), m.p. 104 °C. Required for $C_{11}H_{22}N_3SeCu$: C, 38.98; H, 6.50; N, 12.40%. Found: C, 36.34; H, 5.82; N, 12.11%.

Dodecanal selenosemicarbazonato–copper(I), m.p. 155 °C. Required for $C_{13}H_{26}N_3SeCu$: C, 42.6; H, 7.1; N, 11.45%. Found: C, 42.86; H, 6.5; N, 11.4%.

m-Nitrobenzaldehyde selenosemicarbazonato–copper(I), m.p. 214 °C. Required for $C_8H_7N_4O_2SeCu$: C, 28.8; H, 2.1; N, 16.8%. Found: C, 29.2; H, 2.6; N, 17.0%.

Infrared Spectra

Infrared spectra were taken on a Perkin–Elmer, Model 21, Double-Beam spectrophotometer using KBr pellets.

Can. J. Chem. Downloaded from www.nrcresearchpress.com by 210.87.254.42 on 09/05/12
For personal use only.

ACKNOWLEDGMENTS

We thank Mr. R. Ironside for the infrared spectra.

REFERENCES

1. K. A. JENSEN, J. B. CARLSEN, A. HOLM, and P. H. NIELSEN. Acta Chem. Scand. **17**, 550 (1963).
2. F. A. COTTON, D. M. L. GOODGAME, M. GOODGAME, and T. E. HAAS. Inorg. Chem. **1**, 565 (1962).
3. K. MICHELSEN. Acta Chem. Scand. **17**, 1811 (1963).
4. C. COLLARD-CHARON and M. RENSON. Bull. Soc. Chim. Belges, **71**, 563 (1962).
5. C. COLLARD-CHARON and M. RENSON. Bull. Soc. Chim. Belges, **72**, 291 (1963).
6. C. COLLARD-CHARON and M. RENSON. Bull. Soc. Chim. Belges, **72**, 149 (1963).
7. B. A. GINGRAS, R. L. SOMORJAI, and C. H. BAYLEY. Can. J. Chem. **39**, 973 (1961).
8. K. A. JENSEN. Acta Chem. Scand. **17**, 551 (1963).
9. B. G. BENNS, B. A. GINGRAS, and C. H. BAYLEY. Appl. Microbiol. **8**, 353 (1960).
10. B. A. GINGRAS, R. W. HORNAL, and C. H. BAYLEY. Can. J. Chem. **38**, 712 (1960).
11. R. HULS and M. RENSON. Bull. Soc. Chim. Belges, **65**, 511 (1956).
12. Belg. Patent No. 544031, Société des Laboratoires Labaz (1956).
13. H. G. MAUTNER and W. D. KUMLER. J. Am. Chem. Soc. **78**, 97 (1956).
14. N. B. COLTHUP, L. H. DALY, and S. E. WIBERLEY. Introduction to infrared and Raman spectroscopy. Academic Press, New York, London. 1964. p. 313.
15. L. G. BELLAMY. The infrared spectra of complex molecules. Methuen & Co., Ltd., London. 1954. p. 176.
16. L. G. BELLAMY. The infrared spectra of complex molecules. Methuen & Co., Ltd., London. 1954. p. 213.
17. R. HULS and M. RENSON. Bull. Soc. Chim. Belges, **65**, 684 (1956).
18. E. P. PAINTER, K. W. FRANKE, and R. AIKEN. J. Org. Chem. **5**, 579 (1940).

Can. J. Chem. Downloaded from www.nrcresearchpress.com by 210.87.254.42 on 09/05/12
For personal use only.

Can. J. Chem. Downloaded from www.nrcresearchpress.com by 210.87.254.5 on 09/05/12
For personal use only.

THE STEREOCHEMISTRY OF HALOGEN DISPLACEMENT BY NITRATE ION

RACEMIZATION AND RETENTION OF CONFIGURATION IN THE SYNTHESIS OF DINITRATE ESTERS

L. D. HAYWARD, M. JACKSON, AND I. G. CSIZMADIA

Department of Chemistry, University of British Columbia, Vancouver, British Columbia, and Institute of Physical Chemistry, Uppsala University, Sweden

Received December 15, 1964

ABSTRACT

The reaction of silver nitrate in dry acetonitrile with 2,5-dideoxy-2,5-diiodo-1,4;3,6-dianhydro-L-iditol resulted in formation of the dinitrate esters of the 1,4;3,6-dianhydrides of D-mannitol, D-glucitol, and L-iditol. Similarly both *endo-* and *exo*-nitrato groups were introduced in displacement of the *endo*-halogen in the 2-deoxy-2-iodo-5-*O*-acetyl and 2-deoxy-2-iodo-5-*O*-*p*-toluenesulfonyl derivatives of 1,4;3,6-dianhydro-L-iditol. Since both types of nitrato groups were stable to silver nitrate, the racemization occurred during the displacement and was attributed to formation of cyclic carbonium ion intermediates. The steric effect of the adjacent ring in the carbonium ions apparently suppressed the termolecular, ion-pair mechanism previously established for the metathesis of acyclic alkyl halides and caused preferential formation of the *exo*-nitrato derivatives.

The heterogeneous reaction of *meso*-dibromostilbene with silver nitrate in acetic acid or acetonitrile gave *meso*-dihydrobenzoin dinitrate with overall retention of configuration. This result could be most readily reconciled with the contrasting sequence of retention and inversion previously reported for *meso-* and *dl*-2,3-dibromobutane if participation of neighboring phenyl groups occurred in the second displacement step.

INTRODUCTION

The metathesis of primary and secondary alkyl halides with silver nitrate is generally more complex than other nucleophilic displacements at saturated carbon atoms (1) since it involves both S_N1 and S_N2 character, third-order kinetics (2), and autocatalysis by silver halide (3). A reaction mechanism [1]–[3] proposed by Hammond and co-workers (2) specified that both silver cation and nitrate ion participated in the rate-determining step [1] to give essentially an ion-pair; collapse of the ion-pair in organic solvents led to formation of nitrate ester [2], or of olefins or alkylated solvent products [3]. Kinetic evidence also indicated formation of a similar intermediate complex in aqueous solution where the organic product was the corresponding alcohol (4).

$$[1] \qquad NO_3^- + RHal + Ag^+ \xrightarrow{\text{slow}} NO_3^- R^+HalAg$$

$$[2] \qquad NO_3^- R^+HalAg \xrightarrow{\text{fast}} RONO_2 + AgHal$$

$$[3] \qquad NO_3^- R^+HalAg \xrightarrow{\text{fast}} HNO_3 + AgHal + \text{olefin or solvent alkylates}$$

Inversion of configuration occurred with optically active 2-octyl bromide either in acetonitrile or in suspension in ether (2, 5) and was consistent with formation of an intermediate, rigidly oriented ion-pair. On the other hand, in an ether suspension of silver nitrate optically active α-phenylethyl chloride reacted with *retention* of configuration although inversion occurred in acetonitrile solution (5). With the isomeric 2,3-dibromobutanes Fishbein (6) found that the first halogen was displaced with retention of configuration which was attributed to participation of the neighboring bromine (I and II)

while displacement of the second halogen occurred with inversion with little or no anchimeric assistance from the neighboring nitrato group (6, 7, 8).

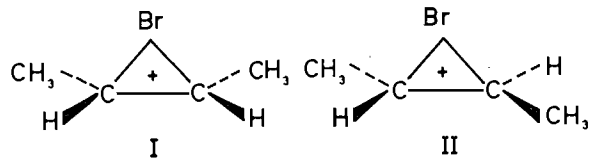

In contrast to these results we have observed both racemization and overall retention of configuration in the metathesis of alkyl dihalides during our study of the stereochemistry of nitrate esters (9, 10). Our results and their interpretation in terms of the above mechanisms are described here.

RESULTS AND DISCUSSION

In the three optically active deoxyiodo derivatives of 1,4;3,6-dianhydro-L-iditol (III–V) (11), the iodo groups are in the *exo*-position relative to the two *cis*-fused tetrahydrofuran rings, and, because of the restricted conformations of the V-shaped ring system, the carbon atoms to which they are attached, C-2 and C-5, are sterically hindered from backside attack (11–16). Treatment of the diiodo compound (III) with an excess of silver nitrate in boiling, anhydrous acetonitrile for 8 h gave the three diastereoisomeric

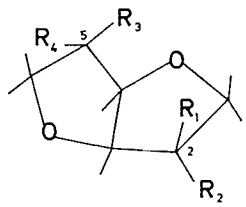

III $R_1 = R_3 = H$; $R_2 = R_4 = I$

IV $R_1 = R_3 = H$; $R_2 = I$; $R_4 = OCOCH_3$

V $R_1 = R_3 = H$; $R_2 = I$; $R_4 = OSO_2C_6H_4CH_3(p)$

VI $R_1 = R_3 = ONO_2$; $R_2 = R_4 = H$

VII $R_1 = R_4 = H$; $R_2 = R_3 = ONO_2$

VIII $R_1 = R_3 = H$; $R_2 = R_4 = ONO_2$

dinitrates (VI–VIII) (9) in yields of 3.7, 6.8, and 14.5% respectively, together with 70% of the theoretical amount of silver iodide (Table I). Compounds IV and V in similar conditions also yielded both *exo*- and *endo*-mononitrato derivatives which were detected chromatographically. The *exo*- and *endo*-nitrato groups were stable to the reaction conditions and hence the racemization occurred during the metathesis in this system thus indicating formation of a carbonium ion intermediate and inhibition of the termolecular S_N mechanism [1]–[3] by the molecular geometry. The slower reaction of compounds III–V (Table I) when compared to those of other alkyl halides (6) supported this conclusion since it indicated the absence of catalysis ("push" (6)) from nitrate ion or neighboring groups. The occurrence of a larger proportion of *exo*- as compared to *endo*-nitrato groups in the products was also consistent with a carbonium ion mechanism

Can. J. Chem. Downloaded from www.nrcresearchpress.com by 210.87.254.5 on 09/05/12
For personal use only.

and product formation under kinetic control, since the attacking anion could approach the carbonium ion with greater facility from the least hindered side resulting in preferential formation of the *exo*-derivative.

It would be of interest to compare the above results with those obtained with the corresponding *endo*-halo derivatives where the molecular geometry suggests that only *exo*-nitrato products would be formed in an S_N2 reaction. Unfortunately a synthetic method for the *endo*-halo derivatives in this series is not available at present.

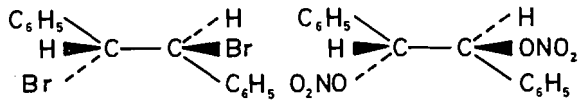

IX X

We also repeated the metathesis of *meso*-dibromostilbene (IX) first reported by von Walther and Wetzlich (17) in 1900, since the earlier workers had made no stereochemical assignment for their product which melted at 132°. In either 50% acetic acid or acetonitrile suspensions the only dinitrate product we obtained was the *meso*-isomer (X) (53% yield, m.p. 148.5–149.5°). The identity of compound X was confirmed both by catalytic hydrogenation to the parent *meso*-hydrobenzoin and through comparison with the dinitrate esters obtained by direct *O*-nitration of the *meso*- and *dl*-hydrobenzoins.

The result showed that the presence of the phenyl groups in the vicinal dihalide favored displacement of the halogens with *either* retention *or* inversion of configuration at both asymmetric carbons. The present evidence does not permit a final decision between these possibilities but the former appeared to us the more plausible when considered together with the facts reviewed earlier. It is most readily reconciled with the results of Fishbein with 2,3-dibromobutane (6) if it is assumed that the β-phenyl groups participate (18) in the displacement of the second halogen atom in a manner analogous to the participation of the neighboring bromine (I and II) in the displacement of the first halogen as proposed by Fishbein (6). Since β-phenyl participation was not possible in the reactions of α-phenylethyl chloride studied by Kornblum and Hardies (5), the retention of configuration observed in that case was possibly due to participation of the ether solvent in the intermediate complex.

TABLE I

Reaction of silver nitrate with deoxyiodo derivatives of 1,4;3,6-dianhydro-L-iditol

Compound	Temp. (°C)	Time (h)	Product yield (%) AgI	Product yield (%) Nitrate esters*
III	50	36	66	†
III	81	6	70	VI, 1.3; VII, 2.9; VIII, 4.4
III	81	8	70	VI, 3.7; VII, 6.8; VIII, 14.5
IV	81	6	94	R_f 0.34, 15,‡ R_f 0.19, 1‡
V	81	6	81	R_f 0.40 to 0.27, 55;‡ R_f 0.15, 2‡

*Products with the highest R_f values were assigned the *exo*-nitrato configuration (cf. ref. 21).
†Starting material (III, 17%) was recovered unchanged.
‡Based on area and intensity of spots on chromatograms (10).

The evidence for β-phenyl group participation in nucleophilic displacements seems clear but the mechanistic pathways apparently remain undecided between formation of a bridged phenonium ion and steric hindrance to attack at one side of a rapidly equili-

Can. J. Chem. Downloaded from www.nrcresearchpress.com by 210.87.254.5 on 09/05/12
For personal use only.

brating classical carbonium ion (18). A more detailed study of the dihalostilbene metathesis might help to clarify this picture since the nitrato group exerts little, if any, neighboring group effect in displacements at carbon, a property which has been used to good advantage in synthetic carbohydrate chemistry (19, 20). It should be noted, however, that the presence of a suitably oriented neighboring nitrato group retarded the E_{CO} reaction of nitrate esters, a result which was traced to interaction between the nitrato nitrogen and neighboring alkoxyl oxygen (10).

EXPERIMENTAL

Reaction of Silver Nitrate with Deoxyiodo Derivatives of 1,4;3,6-Dianhydro-L-iditol

The preparation of the crystalline deoxyiodo (III–V) and dinitrate ester (VI–VIII) derivatives of the 1,4;3,6-dianhydrohexitols has been previously described (9, 11). The reaction times, temperatures, and yields of the metathesis products are shown in Table I. A solution of the iodo compound and silver nitrate ("Baker Analyzed" Reagent) in mole proportions 1:2–3 (iodine:silver nitrate) in acetonitrile (dried successively over phosphorus pentoxide and calcium hydride) after being heated for a given time under anhydrous conditions, was cooled and filtered and the silver iodide washed with acetonitrile, dried at 50°, and weighed. The filtrate and washings were concentrated under reduced pressure, then diluted with water, and extracted with chloroform. The combined chloroform extracts were washed with sodium bicarbonate and sodium thiosulfate solutions and water, dried, and evaporated and the residual sirups were chromatographed on alumina columns eluted with ether – ethyl acetate mixtures (9). Eluate fractions were examined for nitrate esters by paper chromatography (21) and the crystalline dinitrates isolated by evaporation of appropriate fractions were weighed and identified by means of mixture melting points with authentic specimens (9). The mono-*O*-acetyl- and mono-*O*-*p*-toluenesulfonyl-nitrate esters of 1,4;3,6-dianhydro-L-iditol were similarly recovered in microgram quantities and identified on paper chromatograms through the photoreaction with diphenylamine (21, 22). The mononitrate isomers with highest R_f values (Table I) were assigned the *exo*-nitrato configuration since the order of the R_f values for the dinitrate esters was VIII > VII > VI (21); relative yields were estimated from the area and intensity of the spots on the chromatogram (10).

1,4;3,6-Dianhydro-D-glucitol-2,5-dinitrate (VII) (0.127 g) and silver nitrate (0.285 g) were dissolved in dry acetonitrile (24 ml) and the solution, after refluxing under a phosphorus pentoxide drying tube for 8 h, was worked up as described above to give 0.114 g (89.7%) of the original dinitrate. Thin layer chromatograms of the product (22) showed no trace of the isomeric dinitrates. Silver nitrate (0.28 g, 99%) was recovered from the aqueous solution on evaporation.

meso-Hydrobenzoin Dinitrate (X)

meso-Hydrobenzoin (21.0 g, m.p. 137.0–139.5°, lit. (23) 138.5°) was nitrated in a nitric acid – acetic acid – acetic anhydride mixture (9) and the crude dinitrate ester (32.3 g, 112%) was purified by chromatography on an alumina column (30 × 500 mm) with benzene – petroleum ether (b.p. 30–60°), followed by recrystallization from the same solvent until the melting point (148.5–149.5°) was not altered on further recrystallization. The infrared spectrum (KBr) showed the characteristic nitrate ester absorptions (10).

Anal. Calcd. for $C_{14}H_{12}N_2O_6$: C, 55.26; H, 3.98; N, 9.21. Found: C, 55.46; H, 3.91; N, 9.11.

Hydrogenation of 47.2 mg of the dinitrate in absolute ethanol (25 ml) over palladium–charcoal (48.6 mg) at 60 p.s.i. for 3.5 h produced *meso*-hydrobenzoin, m.p. 137–140°, with the correct infrared spectrum and R_f values on thin layer chromatograms.

dl-Hydrobenzoin Dinitrate

dl-Hydrobenzoin (24) (21.0 g, m.p. 122.5–124.5°, lit. (23) 119.5–120.5°) was nitrated as above and the crude dinitrate (25.5 g, 86%) after purification as for the *meso*-isomer melted at 105.5–107.5°. The infrared spectrum (KBr) showed the presence of nitrato groups.

Anal. Calcd. for $C_{14}H_{12}N_2O_6$: N, 9.21. Found: 9.17.

Hydrogenation of the dinitrate yielded *dl*-hydrobenzoin, m.p. 99–105°, which judging from the infrared spectrum and chromatograms, contained traces of unidentified impurities.

Reaction of Silver Nitrate with meso-Dibromostilbene

(*a*) *meso*-Dibromostilbene (24) (3.40 g, m.p. 251.0–252.5°, lit. (24) 238°) was suspended in acetic acid (100 ml) at the boiling point and silver nitrate (4.10 g) dissolved in 50% acetic acid (10 ml) was added dropwise with efficient stirring. The initially colorless suspension gradually became pale yellow and after 15 min was filtered and the filtrate was diluted with water (500 ml) and refrigerated. The crude dinitrate which precipitated (1.61 g, 52.6%) was recrystalized from petroleum ether (m.p. 139.5–142.0°) and then chromatographed on a 0.5 mm layer of silicic acid – calcium sulfate (22) with benzene – petroleum ether to give a product melting at 146–148°. The infrared spectrum (KBr) and R_f value agreed with those of authentic *meso*-hydrobenzoin dinitrate.

Can. J. Chem. Downloaded from www.nrcresearchpress.com by 210.87.254.5 on 09/05/12
For personal use only.

(*b*) *meso*-Dibromostilbene (3.40 g) suspended in boiling acetonitrile (50 ml) was similarly treated with a solution of silver nitrate (4.10 g) in acetonitrile (5 ml) and the filtrate was evaporated under reduced pressure. Extraction of the brown amorphous residue successively with hot petroleum ether (b.p. 65–110°) and hot methanol, and re-extraction of the residue from the methanol solution with petroleum ether, followed by evaporation of the combined petroleum ether extracts, gave 1.60 g (52.6%) of solid *meso*-hydrobenzoin dinitrate which melted at 145–147° after chromatography and recrystallization from petroleum ether (b.p. 30–60°), and had the correct infrared spectrum. *meso*-Hydrobenzoin, m.p. 137.0–139.5°, was recovered after hydrogenation of this product.

ACKNOWLEDGMENTS

This work was completed during tenure of a Guest Professorship by L. D. H. (1964–1965) at Uppsala University, Sweden. He wishes to thank Uppsala University for this appointment and particularly Professor Stig Claesson for his interest and the excellent facilities and hospitality provided at the Institute of Physical Chemistry. We thank the National Research Council of Canada for scholarships to M. J. and I. G. C. and the Defence Research Board of Canada for financial assistance.

REFERENCES

1. J. HINE. Physical organic chemistry. 2nd ed. McGraw-Hill Book Co. 1962. p. 123.
2. G. S. HAMMOND, M. F. HAWTHORNE, J. H. WATERS, and B. M. GRAYBILL. J. Am. Chem. Soc. **82**, 704 (1960).
3. M. MURAKAMI, S. OAE, and S. TAKEUCHI. Bull. Chem. Soc. Japan, **24**, 1 (1951); Chem. Abstr. **47**, 3220 (1953).
4. D. W. COLCLEUGH and E. A. MOELWYN-HUGHES. J. Chem. Soc. 2542 (1964).
5. N. KORNBLUM and D. E. HARDIES. Abstr. 130th American Chemical Society Meeting, Atlantic City. Sept. 1956. p. 2-0.
6. L. FISHBEIN. J. Am. Chem. Soc. **79**, 2959 (1957).
7. L. J. MORRIS. Chem. Ind. London, 1291 (1958).
8. S. J. CRISTOL and B. FRANZUS. J. Am. Chem. Soc. **79**, 2488 (1957).
9. M. JACKSON and L. D. HAYWARD. Can. J. Chem. **38**, 496 (1960).
10. L. D. HAYWARD and I. G. CSIZMADIA. Tetrahedron, **19**, 2111 (1963).
11. M. JACKSON and L. D. HAYWARD. Can. J. Chem. **37**, 1048 (1959).
12. L. F. WIGGINS. Advan. Carbohydrate Chem. **5**, 191 (1950).
13. A. C. COPE and T. Y. SHEN. J. Am. Chem. Soc. **78**, 3177 (1956).
14. R. U. LEMIEUX and A. G. MCINNES. Can. J. Chem. **38**, 136 (1960).
15. K. HEYNS, W. P. TRAUTWEIN, and H. PAULSEN. Chem. Ber. **96**, 3195 (1963).
16. L. D. HAYWARD and D. CONDER. Unpublished results.
17. R. VON WALTHER and A. WETZLICH. J. Prakt. Chem. **61**, 169 (1900).
18. B. CAPON. Quart. Rev. London, **18**, 45 (1964).
19. M. L. WOLFROM and I. C. GILLAM. J. Org. Chem. **26**, 3564 (1961).
20. C. P. J. GLAUDEMANS and H. G. FLETCHER, JR. J. Org. Chem. **29**, 3286 (1964).
21. M. JACKSON and L. D. HAYWARD. J. Chromatog. **5**, 166 (1961).
22. L. D. HAYWARD, R. A. KITCHEN, and D. J. LIVINGSTONE. Can. J. Chem. **40**, 434 (1962).
23. H. MEERWEIN and R. SCHMIDT. Ann. **44**, 221 (1925).
24. L. F. FIESER. Experiments in organic chemistry. 3rd ed. revised. D. C. Heath Co. 1957. Chaps. 31, 32.

Can. J. Chem. Downloaded from www.nrcresearchpress.com by 210.87.254.5 on 09/05/12
For personal use only.

X-RAY POWDER PATTERNS FOR THE IDENTIFICATION OF SOME *n*-ALKANONE SEMICARBAZONES

JACK RADELL, B. W. BRODMAN, AND KIMBALL KRAMER

Research and Development Group, Pitman-Dunn Institute for Research, Frankford Arsenal, Philadelphia, Pennsylvania

Received December 16, 1964

ABSTRACT

The interplanar spacings obtained from the X-ray powder patterns of a series of structurally related semicarbazones were used to unequivocally identify the ketones from which the derivatives were prepared. The advantages of the proposed over the currently used melting points to identify the compounds were cited. The method was found to be applicable to slightly contaminated mixtures of semicarbazones.

INTRODUCTION

The identification of organic compounds by crystalline derivatives is relatively old and well known. Semicarbazones are one of the many such derivatives for ketones. An examination of the literature reveals that different semicarbazones often have reported melting points that are the same or close to one another; e.g., the semicarbazones of 2-hexanone and 2-octanone both have a reported melting point of 122 °C (1).

Semicarbazones are very useful for the isolation of both synthetic and naturally occurring carbonyl compounds. Furthermore, the ease with which the crystalline semicarbazone can be prepared and parent ketone regenerated makes these derivatives especially useful. The value of these derivatives is enhanced by the greater amount of information which can be derived from the X-ray studies presented in this research for a series of similar compounds. This is especially desirable when the amounts of such material are small and insufficient for carrying out classical chemical tests for identification. This problem occurred in our research and led to the presently reported investigation after the use of melting points and mixed melting points were found to be highly unsatisfactory in the identification of the semicarbazones. Considerably smaller samples could be used with such mounting procedures as capillaries. This study was pursued in preference to preparing additional derivatives which would require more time and sample than was used in the X-ray studies. In this way we hoped to identify small quantities of unknown samples and to see how readily the interplanar spacing obtained could be used to distinguish a series of closely related derivatives. In addition, it was hoped that mixtures of derivatives could be used to characterize each of the constituents. An additional problem which makes the melting point identification of semicarbazones difficult is a frequent discrepancy in the reported melting point of a single semicarbazone by different investigators. For example, the melting point of the semicarbazone of 3-heptanone has been reported as 101, 103, and 152 °C (2). In addition the melting points of pure semicarbazones measured in this work differed from reported values (Table I). Although this could result from geometric isomers of the unsymmetrical ketone derivatives, it would not explain the symmetrical cases.

The semicarbazones of ketones studied were not intended to comprise an exhaustive catalogue of these derivatives but rather to show the feasibility of using this method in characterizing a series of closely related compounds. A similar study using 2,4-dinitrophenylhydrazones was reported by Calvert and Przybylska (3).

Can. J. Chem. Downloaded from www.nrcresearchpress.com by 210.87.254.6 on 09/05/12
For personal use only.

Can. J. Chem. Downloaded from www.nrcresearchpress.com by 210.87.254.6 on 09/05/12
For personal use only.

TABLE I

Semicarbazone of:		X-ray data									% C	% H	% N	Melting point (°C)	
2-Propanone	*d* (Å)	5.83	3.43	7.30	3.65	4.44	4.04	4.09	4.84	Found	41.58	7.77	36.25	Found	186–187
	*I**	100	60	58	29	19	11	10	7	Calcd.	41.73	7.82	36.50	Lit.†	190
2-Butanone	*d* (Å)	3.56	6.99	5.85	3.12	3.27	4.61	3.20	7.30	Found	46.45	8.78	32.16	Found	142–143
	I	100	9	8	4	4	4	3	3	Calcd.	46.49	8.55	32.61	Lit.	146, 135–136
2-Pentanone	*d* (Å)	10.49	4.11	3.49	5.24	3.41	3.74	3.83	2.83	Found	50.33	9.20	29.65	Found	104
	I	100	10	7	5	3	3	3	1	Calcd.	50.32	9.15	29.34	Lit.	112, 106
3-Pentanone	*d* (Å)	8.88	3.54	2.95	2.83	2.62	3.77	4.60	3.95	Found	50.46	9.23	29.32	Found	132–133
	I	100	21	8	7	7	7	6	4	Calcd.	50.32	9.15	29.34	Lit.	138–139
2-Hexanone	*d* (Å)	9.82	3.65	2.74	3.50	3.38	6.96	3.25	4.34	Found	53.35	9.77	26.60	Found	125–127
	I	100	100	9	9	7	7	5	5	Calcd.	53.47	9.62	26.75	Lit.	125
3-Hexanone	*d* (Å)	10.05	3.84	3.94	4.13	2.88	3.32	3.54	5.01	Found	53.66	9.65	26.46	Found	116–118
	I	100	19	12	10	9	7	7	6	Calcd.	53.47	9.62	26.75	Lit.	113
2-Heptanone	*d* (Å)	11.04	3.71	2.86	6.83	5.03	4.49	3.85	4.95	Found	56.38	10.27	24.67	Found	122–124
	I	100	63	8	7	6	5	5	2	Calcd.	56.11	10.01	24.54	Lit.	123, 127
3-Heptanone	*d* (Å)	10.57	2.83	3.74	10.00	4.15	4.07	3.97	3.26	Found	54.13	9.77	24.39	Found	99–100
	I	100	47	33	24	15	11	10	8	Calcd.	56.11	10.01	24.54	Lit.	
4-Heptanone	*d* (Å)	10.84	3.45	3.60	4.23	4.64	4.09	4.53	3.75	Found	56.08	10.15	24.67	Found	133–135
	I	100	16	8	7	6	5	5	4	Calcd.	56.11	10.01	24.54	Lit.	132
2-Octanone	*d* (Å)	3.70	12.73	3.57	2.84	6.80	2.96	4.62	4.77	Found	57.94	10.31	22.89	Found	117–118
	I	100	47	12	8	5	3	3	1	Calcd.	58.34	10.34	22.68	Lit.	122–123
3-Octanone	*d* (Å)	12.28	3.97	3.80	11.34	7.21	4.95	4.62	3.10	Found	58.33	10.35	22.95	Found	119–121
	I	100	60	27	23	11	10	10	14	Calcd.	58.34	10.34	22.68	Lit.	121–124
4-Nonanone	*d* (Å)	13.20	4.16	4.39	2.83	3.29	5.22	5.34	6.93	Found	60.38	10.52	20.96	Found	120–122
	I	100	12	9	7	5	4	4	3	Calcd.	60.26	10.62	21.08	Lit.	
5-Nonanone	*d* (Å)	10.89	3.84	4.44	4.15	4.21	2.89	7.37	5.34	Found	60.41	10.79	20.99	Found	87
	I	100	60	20	18	11	12	11	8	Calcd.	60.26	10.62	21.08	Lit.	90
2-Decanone	*d* (Å)	3.74	15.09	3.09	5.02	4.63	2.83	10.02	6.65	Found	61.93	11.13	19.75	Found	123–124
	I	100	90	10	7	6	6	5	5	Calcd.	61.93	10.87	19.70	Lit.	124–126
3-Decanone	*d* (Å)	3.78	9.28	4.22	5.95	3.51	4.90	4.31	3.18	Found	61.71	10.95	19.96	Found	94–95
	I	100	60	25	22	15	10	10	10	Calcd.	61.93	10.87	19.70	Lit.	
4-Decanone	*d* (Å)	9.98	3.65	3.32	4.99	2.83	5.39	3.97	4.53	Found	61.67	10.82	19.74	Found	67
	I	100	32	18	16	14	13	7	7	Calcd.	61.93	10.87	19.70	Lit.	148
2-Undecanone	*d* (Å)	3.75	16.54	3.15	4.71	5.45	6.60	3.34	5.73	Found	63.29	11.17	18.74	Found	125–126
	I	100	61	12	9	7	5	6	1	Calcd.	63.39	11.08	18.84	Lit.	122

*Relative intensity, 100 being the strongest.
†All melting points reported in ref. 2.

Can. J. Chem. Downloaded from www.nrcresearchpress.com by 210.87.254.6 on 09/05/12
For personal use only.

DISCUSSION

A number of ketones were converted to semicarbazones by a previously reported method (4). These semicarbazones were analyzed for carbon, hydrogen, and nitrogen. The analyses and melting points of the pure materials were determined and reported in Table I. The X-ray powder diffraction patterns were run and the eight most intense peaks are reported for the pure semicarbazones as well as for two sets of mixtures. The major spacings of all semicarbazones occurred between 3.56–13.20 Å. Usually the position of the most intense spacing was enough to identify the semicarbazone of the ketone. Only in four cases was it necessary to use the second most intense spacing for identification. All the semicarbazones could be positively identified by scanning from 6.8° to 25° (2θ) at a goniometer scanning speed of 2° per min. Thus it was possible to make a positive identification in 9 min or less. X-ray patterns of semicarbazide hydrochloride and sodium acetate were run to see if any of their characteristic spacings could be identified in the semicarbazones. None of these spacings appeared in the powder patterns of the semicarbazones reported. This observation was confirmed by the analysis reported in Table I. Since impurities of 2% or less did not effect the X-ray patterns, the unknown semicarbazone could be identified although not scrupulously pure. On the other hand, these impurities did affect the melting point. From runs with a silicon standard we were able to determine our error in measuring 2θ and the corresponding error in interplanar spacing (d) to be ± 0.02 Å at 8° (2θ) and ± 0.001 Å at 40° (2θ).

TABLE II

Mixture of semicarbazones of 2-hexanone (A) and 4-decanone (B)

d (Å)	I*	Spacing attributed to
3.65	100	A† and B‡
9.93	75	B
9.73	62	A
2.83	16	B
5.39	12	B
3.96	9	B
6.91	9	A
3.34	9	B
3.49	9	A
2.74	8	A
5.01	8	B

*Relative intensity, 100 being the strongest.
†Spacings attributed to 2-hexanone.
‡Spacings attributed to 4-decanone.

The intensities and interplanar spacings for each compound in Table I represents the average of four runs as described under Experimental. It was found that the four separate runs differed very little, if at all, in interplanar spacings or intensities.

To determine if components of mixtures could be identified equal weights of 2-hexanone and 4-decanone both with very similar X-ray diffraction patterns were mixed. Both compounds measured separately had a major spacing in common at 3.65 Å and another set in close proximity at 9.82 Å and 9.98 Å respectively. The X-ray diffraction pattern of the mixture showed the most intense spacings at 3.65 Å, 9.93 Å, and 9.73 Å. Although the latter two spacing are slightly shifted all the other spacings previously measured for each compound appeared in the mixture without change (Tables II and III). No spacings were present for the mixture which could not be attributed to one of the components.

TABLE III

Mixture of semicarbazones of 2-propanone (A) and 2-Butanone (B)

d (Å)	*I**	Spacing attributed to
3.56	100	A†
5.84	100	B‡
3.43	80	B
7.31	60	B
3.65	30	B
7.00	10	A
4.45	25	B
4.04	18	B
4.11	14	B
3.88	12	B

*Relative intensity, 100 being the strongest.
†Spacings attributed to semicarbazone of 2-propanone.
‡Spacings attributed to semicarbazone of 2-butanone.

EXPERIMENTAL

Semicarbazones

The semicarbazones were prepared by a previously described procedure (4).

Sample Preparation for X-Ray Measurements

Two portions of each semicarbazone were separately ground with a mortar and pestle. Each ground sample was packed into a $\frac{1}{2}$ in. diameter hole in a 1 mm thick microscope slide. The compounds were packed into the hole in the microscope slide by placing an intact microscope slide under the hole and tightly pressing the semicarbazone into the cavity with a spatula. A cover glass was glued over the packed cavity and the whole mount was inverted. The intact slide was slid out to give a finished mount. The mount with exposed sample side up was placed in the sample holder of the goniometer. Two sets of measurements were made for each mounting. After the first measurements were made the mount was rotated 90° for the second set of measurements. Since this procedure was followed for the two portions of each semicarbazone, a total of four runs were made for each sample. This was done in order to reduce the possibility of preferred orientation.

X-Ray Powder Diffraction Measurements

The X-ray measurements were made with a North American Phillips Co. X-Ray Diffractometer (Model 5001) which was equipped with a high angle goniometer. A proportional counter in conjunction with a pulse height analyzer was used for counting. Cu K_α radiation was obtained by operating the copper tube at 40 kV and 18 mA using a nickel filter and passing the radiation through 1° divergent and scattering slits, and a 0.003° receiving slit. The goniometer scanning speed was 2°/min.

CONCLUSIONS

The use of interplanar spacings from X-ray powder diffraction patterns was found to be preferable to the use of melting points for the identification of semicarbazones because (*a*) less sample is ultimately required, (*b*) the information obtained is unambiguous, (*c*) mixtures of semicarbazones can be identified, (*d*) small amounts of impurities do not interfere, and (*e*) the unaltered semicarbazone is recoverable.

ACKNOWLEDGMENT

The authors thank Mr. Dominic Stango of this laboratory for his assistance in the tabulation of the results.

REFERENCES

1. R. L. SHRINER and R. C. FUSON. The systematic identification of organic compounds. Wiley, N.Y. 1940. p. 221.
2. Tables for identification of organic compounds. Chemical Rubber Publishing Co., Cleveland. 1960.
3. L. D. CALVERT and M. PRZYBYLSKA. Appl. Spectry. **15**, 29 (1961).
4. R. L. SHRINER and R. C. FUSON. The systematic identification of organic compounds. Wiley, N.Y. 1940. p. 142.

Can. J. Chem. Downloaded from www.nrcresearchpress.com by 210.87.254.6 on 09/05/12
For personal use only.

Can. J. Chem. Downloaded from www.nrcresearchpress.com by 210.87.254.5 on 09/05/12
For personal use only.

EFFECTS OF THE ELECTRONIC BAND SHAPE OF PALLADIUM METAL ON THE PROTON MODEL FOR HYDROGEN ABSORPTION

J. W. Simons and Ted B. Flanagan
Department of Chemistry, University of Vermont, Burlington, Vermont
Received November 26, 1964

ABSTRACT

The statistical treatment of the proton model for hydrogen absorption by palladium is extended to include a variation of the electron donation energy with hydrogen content, as determined by a density of states function for the combined 4d- and 5s-bands for palladium. This improved model gives better agreement with the high pressure limiting solubility data and the observed critical composition than the original model, when both are fitted to the critical isotherm by the same method. An apparent anomaly in the variation of the isosteric enthalpy of absorption with content is explained by the improved model.

INTRODUCTION

The palladium–hydrogen system has been one of the most extensively studied and well characterized of the metal–hydrogen systems (1). The first statistical model for hydrogen in palladium metal was proposed by Lacher in 1937 (2). More recently, similar models which have a general applicability to interstitial compounds have been proposed by Anderson (3) and by Rees (4). Other quite different models, such as the anion model of Libowitz (5), have also been applied. All of these models have been successful in explaining the main features of the experimental pressure–composition–temperature relationships for hydrogen absorption by palladium.

In Lacher's model hydrogen atoms are considered to be absorbed as protons plus electrons; the electrons enter the lowest energy unfilled states in the electronic bands, primarily the 4d-band, of the palladium metal, and the protons enter a fixed number of energetically equivalent potential energy minima in the palladium lattice. The proton absorption sites have subsequently been shown to be the octahedral interstitial positions in the f.c.c. palladium lattice (6). Approximate theoretical calculations of the state of hydrogen in metals support the idea of hydrogen atoms in palladium existing as protons plus electrons (7, 8). A necessary postulate of the proton model is that nearest-neighbor protons interact attractively via their compensating atmospheres of electrons. This postulate was made, by analogy with Fowler's treatment of critical adsorption on surfaces (9), in order to account for the observed critical phenomenon in the Pd—H system; the P–C–T relationship exhibits a critical point below which two solid phases, α and β, coexist over a range of compositions and above which only a single phase exists. The nature of the attractive interaction between protons was unspecified by Lacher but has recently been discussed somewhat more specifically by Makrides (10).

From the above model Lacher derived the partition function for n absorbed and interacting protons (per Pd atom) distributed in n_s energetically equivalent absorption sites (per Pd atom). Fowler and Smithells (11) had shown previously, for a similar system, that the partition function for absorbed protons alone gives the same chemical potential as that for absorbed hydrogen atoms existing as absorbed protons plus donated electrons, provided that the energy of electron donation to a metal's bands of electronic states is included in the absorption energy for the protons. In Lacher's treatment a constant energy of electron donation is included implicitly in the constant interaction energy of a

proton with its site. The assumption of a constant energy of electron donation is not justified since it is well known that the electronic states in metals form bands and are distributed over a range of energies within each band. It is felt that a realistic proton absorption model, with electron donation to partially empty bands in the metal, must allow for a variable electron donation energy. The present treatment includes specifically the varying energy of electron donation as the unfilled states in the high density 4d-band and the overlapping low density 5s-band of palladium are filled with electrons from absorbed hydrogen atoms. It has been mentioned previously that the distribution of electronic states with energy in the d-band of palladium could affect the absorption of hydrogen (10), but a quantitative investigation has not been made to our knowledge of how this effect enters into a statistical model.

RESULTS AND DISCUSSION

Theory

The expression for the pressure of H_2 gas in equilibrium with absorbed hydrogen in Pd was derived from the above proton model with a variable energy of electron donation and is given by eq. [1].

$$[1] \qquad \ln P_{atm} = 2 \ln \frac{f^{1/2}}{Q(T)} + 2 \ln \frac{n/n_s}{1 - n/n_s} + \frac{2W_H}{RT} + \frac{X_d}{RT} + \frac{4W_{HH}n}{RTn_s} + \frac{2W_e(n)}{RT},$$

where f is the partition function for an H_2 molecule in the gas phase, $Q(T)$ is the partition function for the three degrees of freedom of an absorbed proton, n/n_s is the ratio of the number of absorbed protons to the number of absorption sites, W_H is the sum, relative to hydrogen atoms in the gas phase, of the energies per mole of the first absorbed proton and its donated electron, X_d is the dissociation energy per mole of a hydrogen molecule, W_{HH} is the average value per proton of the total proton–proton interaction energy per mole when all sites are filled, and $W_e(n)$ gives the variation of the energy of electron donation with n. The derivation of eq. [1] is identical to Lacher's derivation in which the effect of the H—H interaction on the distribution of protons among the sites was neglected, i.e., the Bragg–Williams approximation of random distribution was made; the only difference in the final expressions is an additional term, $2W_e(n)/RT$, in eq. [1]. The function, $W_e(n)$, can be evaluated directly from the variation of the density with energy, $N(W_e)$, of vacant electronic states in the combined 5s- and 4d-bands of palladium, assuming that the band shape is not altered appreciably as hydrogen enters interstitial positions in the lattice.

Hoare and co-workers (12) have determined, from the low temperature heat capacities of Ag/Pd alloys, an approximate dependence of $N(W_e)$ upon energy for palladium. This method assumes that each Ag atom donates one electron to the combined 5s- and 4d-bands of Pd which overlap, and the replacement of palladium by silver in the lattice does not alter the band shape of the palladium. Magnetic susceptibility measurements and other evidence support the former assumption but serious objections have arisen as to the validity of the latter, especially for alloys with large Ag contents. In any case, this band shape, as approximated in Fig. 1, can be used to explore the effect of including a variable band energy in the proton model on calculated P–C isotherms and thermodynamic quantities.

Evaluation of Parameters in Eq. [1]

The approximate curve in Fig. 1 for the density of states in the combined 5s- and 4d-bands is represented by the two linear relationships given in eqs. [2*a*], [2*b*].

Can. J. Chem. Downloaded from www.nrcresearchpress.com by 210.87.254.5 on 09/05/12
For personal use only.

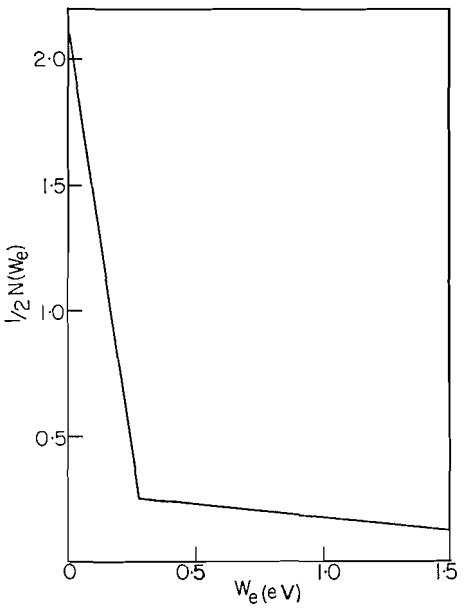

FIG. 1. An approximation to the curve derived by Hoare and co-workers (12) for the density of vacant states in the combined 4d- and 5s-bands of palladium.

[2a] $$N(W_e)_1 = -13.43W_e + 4.26, \qquad W_e \leqslant 0.28 \text{ eV};$$

[2b] $$N(W_e)_2 = -0.207W_e + 0.560, \qquad W_e \geqslant 0.28 \text{ eV}.$$

Since $N(W_e)$ is a decreasing function of W_e, the electrons can be assumed to enter the lowest energy vacant states. Thus the area under the $N(W_e)$ curve between zero and W_e represents the number of donated electrons per Pd atom necessary to increase the electron donation energy by W_e. The integral of $N(W_e)$ solved for W_e gives eqs. [3a], [3b] for the function, $W_e(n)$.

[3a] $$W_e(n)_1 = 7318 - 7318(1.0000 - 1.481n)^{1/2} \text{ cal/mole}, \quad n \leqslant 0.666;$$

[3b] $$W_e(n)_2 = 62404 - 80960(1.0000 - 0.7846n)^{1/2} \text{ cal/mole}, \quad n \geqslant 0.666.$$

The critical point conditions,

$$\left(\frac{\partial \ln P}{\partial n}\right)_T = 0 \text{ and } \left(\frac{\partial^2 \ln P}{\partial n^2}\right)_T = 0,$$

applied to eq. [1], with $W_e(n)$ replaced by $W_e(n)_1$, give eqs. [4] and [5] respectively.

[4] $$\frac{2}{n_c} + \frac{2}{n_s - n_c} + \frac{4W_{HH}}{RT_c n_s} + \frac{7318(1.481)}{RT_c(1.0000 - 1.481n)^{1/2}} = 0,$$

[5] $$-\frac{2}{n_c^2} + \frac{2}{(n_s - n_c)^2} + \frac{7318(1.481)^2}{2RT_c(1.0000 - 1.481n)^{3/2}} = 0.$$

The expression for $W_e(n)_1$ in eq. [3a] was substituted for $W_e(n)$ in eq. [1] since the critical composition, n_c, is known from experiment to be approximately 0.28 (13). An approximate value of $n_s(\sim 0.75)$ was calculated from eq. [5] using the experimental value of the critical

Can. J. Chem. Downloaded from www.nrcresearchpress.com by 210.87.254.5 on 09/05/12
For personal use only.

temperature, $T_c = 573$ °K, and $n_c \sim 0.28$. The critical temperature is accurately known but the value of n_c is uncertain (13). Unique values of the parameters n_c, n_s, and W_{HH} can be obtained which are solutions of both eqs. [4] and [5] and also give a fit of the low hydrogen content α-phase isotherm of Gillespie and Galstaun to eq. [1] at the critical temperature (13). In order to fit the α-phase data, eq. [1] was written in the form given in eq. [6], valid for the case of $n \ll 1$, in which the expression in eq. [3*a*] has been substituted for $W_e(n)$ and the term, $(1 - 1.481n)^{1/2}$, has been approximated by $1 - (1.481n/2)$.

$$[6] \qquad \ln P_{atm}\left(\frac{1 - n/0.75}{n}\right)^2 = 2 \ln \frac{f^{1/2}}{Q(T)} - 2 \ln n_s + \frac{2W_H + X_d}{RT} + \frac{[7318(1.481) + (4W_{HH}/n_s)]n}{RT}$$

The approximate value of $n_s(\sim 0.75)$, discussed above, was used for calculating the difference, $1 - n/n_s$, since for $n \ll 1$ any reasonable uncertainty in n_s will have a negligible effect on the value of this difference. The right-hand-side (r.h.s.) of eq. [6] is a linear function of n at a given temperature. It is seen from Fig. 2 that the α-phase data of

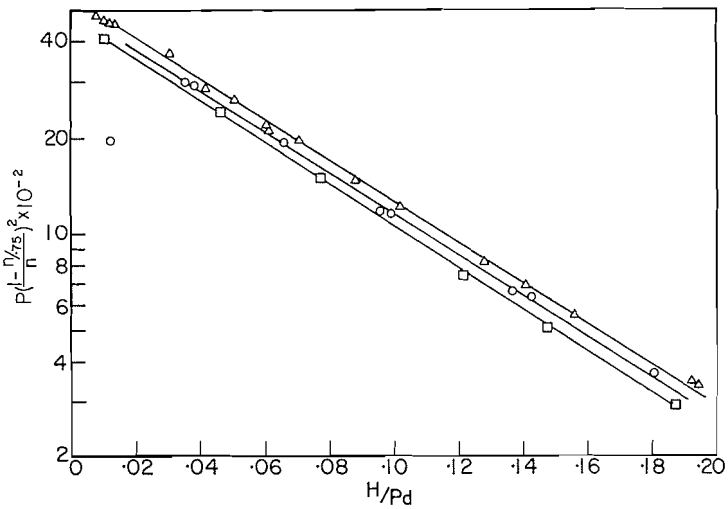

FIG. 2. The α-phase data of Gillespie and Galstaun (13) near the critical temperature plotted according to eq. [6]. (□) 290 °C data; (○) 300 °C data; (△) 310 °C data.

Gillespie and Galstaun at 290, 300, and 310 °C, plotted according to eq. [6], give the expected straight lines. The average slope of these three lines gives the relationship, $4W_{HH}/RT_c = -24.36n_s$. This result together with eqs. [4] and [5] determine the values of n_c, n_s, and W_{HH} given in the first row of Table I. The same treatment using Lacher's

TABLE I

Values of the critical composition, total number of sites, and the H—H interaction energy

	n_c	n_s	W_{HH} (cal/mole)
Equation [1], $W_e(n) = W_e(n)_1$	0.277	0.720	−4995
Equation [1], $W_e(n) = 0$	0.247	0.494	−2278

Can. J. Chem. Downloaded from www.nrcresearchpress.com by 210.87.254.5 on 09/05/12
For personal use only.

original expression, eq. [1] with $W_e(n) = 0$, gives the values in the second row of Table I. The value of n_c in Table I for $W_e(n) = W_e(n)_1$ is essentially the same as the approximate experimental value mentioned earlier, while the value determined with $W_e(n) = 0$ is probably near the limit of uncertainty in this experimental value. The magnitude of W_{HH} is very sensitive to the particular treatment of the data but, unfortunately, there seem to be no direct estimates of its expected magnitude. Both values of n_s in Table I are less than 1, but the value derived for $W_e(n)_1$ is larger than that for $W_e(n) = 0$, and thus is in better accord with observed maximum solubilities of hydrogen in palladium which approach $n \sim 1$ at high pressures (14). The interpretation of n_s as the number of octahedral positions per Pd atom in the f.c.c. Pd lattice, i.e., $n_s = 1$, is consistent with the model and the known location of H atoms in the lattice.

Enthalpy of Solution

The variation with hydrogen content of the isosteric partial molar enthalpy of solution,

$$\overline{\Delta H} = R\left(\frac{\partial \ln P}{\partial 1/T}\right)_{p,n},$$

of hydrogen in palladium clearly should depend on the electronic band shape for palladium, if this proton absorption model is valid. Lacher has shown that his original theory, in which a delta function band shape is implicitly assumed, predicts a continuous linear increase of $-\overline{\Delta H}$ with increasing n for each of the pure solid Pd—H phases (2). This result reflects the variation of the magnitude of the total H—H interaction energy term with n. The existing α-phase data give qualitative support to this predicted variation, but the paucity and irreproducibility by independent workers of the experimental α-phase results renders a quantitative comparison premature (13, 14*c*, 15, 16). Two recent experimental studies of the high content β-phase, one between 0 and 75 °C (14*c*) and another between 300 and 500 °C (14*b*), are in qualitative agreement with each other in as much as both yield decreasing values of $-\overline{\Delta H}$ with increasing n, which is the opposite behavior to that found in the α-phase and to that predicted by Lacher's original theory.

Equations. [7*a*], [7*b*] give the variation of $\overline{\Delta H}$ with n predicted by eq. [1] for the band shape given by eqs. [3*a*], [3*b*] and the value of n_s in the first row of Table I.

$$[7a] \qquad \Delta\overline{\Delta H}(n) = \frac{4W_{HH}n}{0.720} + 2(7318)[1 - (1.0000 - 1.481n)^{1/2}],\ n \leqslant 0.666,$$

$$[7b] \qquad \Delta\overline{\Delta H}(n) = \frac{4W_{HH}n}{0.720} - 2[62404 - 80960(1.0000 - 0.7846n)^{1/2}],\ n \geqslant 0.666,$$

where

$$\Delta\overline{\Delta H}(n) = \overline{\Delta H}(n) - \overline{\Delta H}(0).$$

A term,

$$\frac{4n}{0.72T}\left(\frac{\partial W_{HH}}{\partial 1/T}\right)_{p,n},$$

has been taken to be zero in eqs. [7*a*], [7*b*]. Although W_{HH} is undoubtedly temperature dependent (14*c*, 16, 17), the α-phase data, required to evaluate W_{HH} at various temperatures, is neither sufficiently extensive nor reproducible enough to unambiguously determine this temperature dependence. A plot of eqs. [7*a*], [7*b*] for the critical value of W_{HH} (first row of Table I), is shown in Fig. 3. It is seen from Fig. 3 that eqs. [7*a*], [7*b*] predict that $-\Delta H$ increases to a maximum value, then decreases as n goes from zero to n_s, which is qualitatively the same behavior exhibited by the experimental results. Any reasonable

Can. J. Chem. Downloaded from www.nrcresearchpress.com by 210.87.254.5 on 09/05/12
For personal use only.

temperature dependence of W_{HH} would probably not affect the qualitative features of Fig. 3.

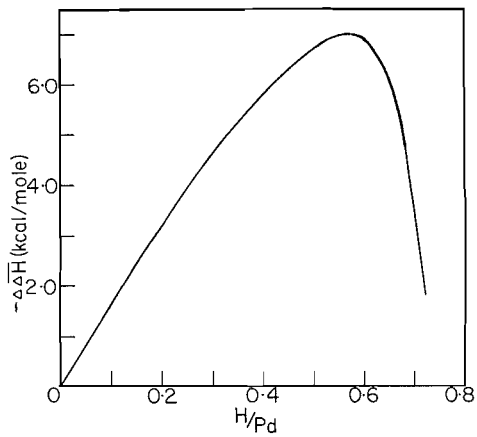

FIG. 3. Predicted variation of the isosteric enthalpy of solution with content.

CONCLUSION

The use of the α-phase data to evaluate theoretical parameters, instead of the two-phase region as in Lacher's original method, was first suggested by Everett and Nordon; they convincingly justify this procedure in a discussion of the hysteresis commonly observed in the two-phase region (16). The similar method employed in the present work uses the critical point in conjunction with the critical temperature α-phase data to determine all of the theoretical parameters shown in Table I. This has the advantages that the magnitude of n_s need not be assumed and the problems of nonequilibrium associated with hysteresis are circumvented. Some confusion exists in the literature as to whether n_s should be identified with the total number of vacancies in the 4d-band of electronic states for palladium, as originally defined, or with the total number of proton absorption sites in the palladium lattice. The high pressure limiting solubilities of hydrogen in palladium and the very nature of the statistical problem are convincing support, in the author's view, of the latter definition.

The results in Table I and Fig. 3 and the accompanying discussions indicate that the experimental band shape derived for Ag/Pd alloys incorporated into the proton statistical model gives generally better agreement with the various experimental observations cited than the original model with a delta function band shape. Quantitative agreement for n_s and the variation of $\overline{\Delta H}$ could probably be improved by using a slightly broader band, but such an attempt seemed unwarranted here in view of the neglected possible effects of lattice expansion during absorption on the band shape and theoretical energy parameters. The effect of lattice expansion on W_H and W_{HH} in Lacher's original theory has been treated by Harasima *et al.* (18). Their treatment leads to asymmetry in the calculated isotherms but does not predict a maximum in $-\overline{\Delta H}$ for values of $n < 1$. The inclusion of lattice expansion effects into the present treatment would be an interesting refinement but would not be expected to alter the above conclusions.

ACKNOWLEDGMENTS

Financial support for this work by U.S.A.E.C. contract AT(30-1)-3000 is gratefully acknowledged. We wish to thank Dr. F. L. Brooks for helpful discussions.

Can. J. Chem. Downloaded from www.nrcresearchpress.com by 210.87.254.5 on 09/05/12
For personal use only.

REFERENCES

1. D. P. SMITH. Hydrogen in metals. University of Chicago Press, Chicago. 1948.
2. J. R. LACHER. Proc. Roy. Soc. London Ser. A, **161**, 525 (1937).
3. J. S. ANDERSON. Proc. Roy. Soc. London Ser. A, **185**, 69 (1946).
4. A. L. G. REES. Trans. Faraday Soc. **50**, 335, 343 (1954).
5. G. G. LIBOWITZ. J. Appl. Phys. **33**, 399 (1962).
6. J. E. WORSHAM, JR., M. K. WILKINSON, and C. G. SHULL. J. Phys. Chem. Solids, **3**, 303 (1957).
7. I. ISENBERG. Phys. Rev. **79**, 736 (1950).
8. J. FRIEDEL. Phil. Mag. **43**, 153 (1952); Advan. Phys. **3**, 446 (1954).
9. H. H. FOWLER. Proc. Cambridge Phil. Soc. **32**, 144 (1936).
10. A. C. MAKRIDES. J. Phys. Chem. **68**, 2160 (1964).
11. R. H. FOWLER and C. J. SMITHELLS. Proc. Roy. Soc. London Ser. A, **160**, 37 (1937).
12. F. E. HOARE and B. YATES. Proc. Roy. Soc. London Ser. A, **240**, 42 (1957). F. E. HOARE, J. C. MATHEWS, and J. C. WALLING. Proc. Roy. Soc. London Ser. A, **216**, 502 (1953).
13. L. J. GILLESPIE and L. S. GALSTAUN. J. Am. Chem. Soc. **58**, 2565 (1936).
14. (*a*) P. S. PERMINOV, A. A. ORLOV, and A. N. FRUMKIN. Dokl. Acad. Nauk SSSR, **84**, 749 (1952).
(*b*) P. L. LEVINE and K. E. WEALE. Trans. Faraday Soc. **56**, 357 (1960).
(*c*) E. WICKE and G. H. NERNST. Z. Elektrochem. **68**, 224 (1964).
15. H. BRUNING and A. SIEVERTZ. Z. Physik. Chem. Leipzig A, **163**, 409 (1933).
16. D. H. EVERETT and P. NORDON. Proc. Roy. Soc. London Ser. A, **259**, 341 (1960).
17. K. A. MOON. J. Phys. Chem. **60**, 502 (1956).
18. A. HARASIMA, T. TANAKA, and K. SAKAOKU. J. Phys. Soc. Japan, **3**, 208 (1948).

Can. J. Chem. Downloaded from www.nrcresearchpress.com by 210.87.254.5 on 09/05/12
For personal use only.

Can. J. Chem. Downloaded from www.nrcresearchpress.com by 210.87.254.40 on 09/05/12
For personal use only.

NUCLEAR MAGNETIC RESONANCE SPECTROSCOPY OF SOME SELENIUM COMPOUNDS

T. BIRCHALL,[1] R. J. GILLESPIE, AND S. L. VEKRIS[2]
Department of Chemistry, McMaster University, Hamilton, Ontario
Received December 1, 1964

ABSTRACT

Selenium nuclear magnetic resonance spectra have been observed for a number of selenium compounds. Chemical shifts and coupling constants with hydrogen and fluorine have been obtained. Various systems involving selenium compounds have been studied. It was found that a mixture of $SeOF_2$ and $SeOCl_2$ contains SeOClF and that rapid selenium exchange occurs between $SeOCl_2$ and $SeOBr_2$ presumably via the intermediate SeOClBr. The reactions of selenium tetrahalides with sulfur and selenium trioxides and with boron trifluoride were studied. It was observed that antimony pentachloride, tin tetrachloride, arsenic trichloride, quinoline, and potassium chloride produce considerable shifts in the resonance of selenium oxychloride. These shifts can be interpreted in terms of the acid–base behavior of the solutes.

Although selenium-77 has a nuclear spin of $\frac{1}{2}$ and has a natural abundance of 8.3% there have only been two previous rather limited investigations of the selenium nuclear magnetic resonance and only a very few compounds were studied. Dharmatti and Weaver (1) measured the magnitude and sign of the selenium magnetic moment in a 12 *M* solution of selenous acid by reference to sodium-23. Walchli (2) measured the resonance frequencies of H_2Se, H_2SeO_3, and H_2SeO_4 with reference to D_2O and hence found the chemical shifts between the selenium compounds. The object of the present work was to measure the selenium chemical shifts and coupling constants with other nuclei for a number of selenium compounds and to attempt to use the data to obtain chemical and structural information on selenium compounds in the pure state and in systems with other components.

EXPERIMENTAL

Measurements were made with a Varian Associates DP60 spectrometer operating at 10.276 Mc/s. To make a preliminary observation of the selenium resonance the current control on the magnet power supply was first approximately calibrated by the relatively strong signals of ^{23}Na and ^{127}I. The approximate current required to obtain the selenium resonance was then calculated and the magnet current control adjusted accordingly. Because the selenium signal was expected to be relatively weak, the initial search for a selenium resonance was made using a concentrated aqueous solution of H_2SeO_3 in a non-spinning 15 cm o.d. sample tube and broad-line technique. However, the broad derivative signals obtained by this method were unsuitable for the accurate measurement of chemical shifts and the observation of fine structure due to spin–spin coupling. After a few resonances had been detected in this manner, a method of observing high-resolution spectra was devised. This was an audio side-band method which utilized the Varian V3521 Integrator operating at a modulation frequency of 2 034 c/s and gave a considerably enhanced signal-to-noise ratio (3).

The usual center-band operation employed for proton and fluorine spectra cannot be used for selenium resonance, since it is impossible to obtain the high modulation index ($\beta = 1.8$) required, owing to the much lower magnetogyric ratio of selenium,

$$\beta = \frac{\gamma H_m}{2\pi\nu_m},$$

where γ = magnetogyric ratio of nucleus, H_m = modulating field, and ν_m = frequency of modulating field. The integrator was therefore converted from center-band to side-band operation, the latter being feasible for modulation indices less than unity (3). The conversion was accomplished by inserting a 2 μF capacitor

[1]*Present address: Department of Chemistry, Latimer Hall, University of California, Berkeley, California.*
[2]*Present address: Research and Development Establishment, British-American Tobacco Co. Ltd., Regent's Park Road, Southampton.*

between the modulation output of the integrator and the sweep coils. This reduces the modulation index somewhat and also provides the 90° audio-phase change necessary for side-band operation (3). By suitable adjustment of both the r.f. phase and audio phase the centre band is eliminated and the signal observed in the first side band only. The spectrum therefore consists of two signals: the upper side band at +2 034 c/s and the lower side band at −2 034 c/s, and it is therefore automatically calibrated.

At normal r.f. power levels, side-band signals would be small, specifically $\beta/2$ times the usual absorption mode signal. However, under the conditions used in side-band operation, the saturation parameter is $\gamma^2(\frac{1}{2}\beta H_1)^2T_1T_2$ and the r.f. power can be increased to a relatively higher level. These conditions give a signal-to-noise ratio comparable to that which would be obtained from the usual absorption mode techniques, but eliminate the long-term noise which makes absorption mode spectra without modulation techniques impossible for selenium.

The field was swept at approximately 1 gauss/min. The modulation index was $\beta = 0.24$ in all cases. The r.f. field was approximately 5 milligauss, but the optimum power level varied from sample to sample. In a few cases adiabatic rapid passage was used. In this case H_1 was adjusted to be as large as possible without unbalancing the probe; approximately 70 milligauss was the maximum H_1 obtainable.

Samples were sealed in 15 mm o.d., 13 mm i.d. tubes except the very volatile SeF_6 and H_2Se, which were sealed in stronger 13 mm o.d., 8 mm i.d. tubes.

Shifts were measured by exchanging samples while sweeping the field. The reference used was either $SeOCl_2$, which gives a strong sharp signal, or 19 mole % aqueous H_2SeO_3. For some samples the spectrum occurred too close to the peaks of either of these reference compounds to enable the shifts to be obtained by the sample-changing technique. In such cases the less satisfactory H_2SeO_4, which gives a rather broad signal, was used as a secondary reference. Spectra were calibrated by the usual side-band technique using a Muirehead–Wigan decade audio oscillator or for large shifts by observing the upper and lower reference side bands, which are separated by twice the modulation frequency of 2 034 c/s.

Proton and fluorine signals were observed by the normal high-resolution technique at 60 Mc/s and at 56.4 Mc/s respectively.

All compounds except those below were the purest available commercial samples and were used without further purification.

Selenium Oxide Dibromide

Bromine (10 ml) was reacted with a mixture of 5 g red selenium and 6 g selenium dioxide in a dry atmosphere. Yellow crystals were obtained on vacuum sublimation at room temperature (4), m.p. 45° (lit. 41.7° (4)).

Selenium Oxide Dichloride

The commercial product was distilled at 1 mm to give a pale-yellow liquid.

Selenium Tetrachloride

Chlorine was passed over 5 g gray selenium and the sublimate was collected (5).

Selenium Oxide Difluoride

This was prepared by the reaction between SeO_2 and SeF_4 (6). Selenium tetrafluoride (20 g) was distilled in vacuum onto a small excess of selenium dioxide and the mixture was refluxed until no more SeO_2 dissolved. The product was vacuum distilled.

Selenium Trioxide

A mixture of phosphoric oxide and a slight excess of selenic acid was heated to 150° under vacuum and the resulting selenium trioxide was condensed onto a cold finger (7), m.p. 120° (lit. 118° (8)).

Anal. Calcd. for SeO_3: Se, 62.2. Found: Se, 63.8.

Selenic Acid

The commercial product was dehydrated by bubbling dry air through a sample of the acid at 2 mm and 150°.

Fluoroselenic Acid

A preparation carried out by the method of Bartels and Class (9), in which the two reactants were condensed together and excess HF was removed under vacuum at room temperature, gave a volatile product which was identified from its infrared spectrum as SeO_2F_2 (10) and a liquid residue which was shown from its Raman and n.m.r. spectra to contain a considerable amount of selenic acid. At 100° the decomposition

$$2HSeO_3F = SeO_2F_2 + H_2SeO_4$$

was found to be essentially complete. A purer product was obtained by carrying out the reaction in liquid SO_2. This gave the selenium resonance reported in Table I.

Chloroselenic Acid

Selenium trioxide was reacted with excess hydrogen chloride in solution in sulfur dioxide (11). After removing most of the excess HCl under vacuum, the mixture was sealed in an n.m.r. tube and kept cold.

Can. J. Chem. Downloaded from www.nrcresearchpress.com by 210.87.254.40 on 09/05/12
For personal use only.

It was warmed to room temperature just before the spectrum was run whereupon the mixture separated into two layers. The upper layer gave no selenium resonance, but the lower layer gave a resonance at 475.8 p.p.m. which we have attributed to chloroselenic acid and another very weak signal at 228.2 p.p.m. which was not assigned.

Selenium Dioxide Difluoride

Barium selenate (85 g) was treated with excess fluorosulfuric acid (500 g) at 150° (12). The product was condensed in a liquid air trap. A volatile yellow impurity was separated from the product by repeated vacuum distillation. The fact that the fluorine n.m.r. spectrum of the final product showed only one signal indicated that no fluorine-containing impurities were present in appreciable concentration.

Selenium Hexafluoride

The commercial product was vacuum distilled. The fluorine n.m.r. spectrum showed an extra peak due to an impurity at approximately 20 p.p.m. above, and approximately 5% the intensity of, the signal due to SeF_6.

Selenium Tetrafluoride

Fluorine diluted with nitrogen was passed over freshly sublimed selenium at 0° and the product vacuum distilled (13).

Anal. Calcd. for SeF_4: Se, 51.0. Found: Se, 50.2.

Hydrogen Selenide

Aluminium selenide was prepared by igniting a mixture of 25 g powdered selenium and 15 g powdered aluminium with burning magnesium. The product was treated with water, and the resulting gas was dried by passing it through calcium chloride and phophoric oxide and was finally trapped out in a trap cooled with solid carbon dioxide (14).

Trifluoromethylselenium Compounds

Bis(trifluoromethyl) selenide and bis(trifluoromethyl) diselenide were prepared by the reaction of trifluoromethyl iodide with selenium at 260 °C (15) and also by the reaction of silver trifluoroacetate with selenium at 280 °C (16). Bis(trifluoromethyl) diselenide was removed from the mixture by reaction with mercury; it formed bis(trifluoromethylseleno)mercury, from which it was regenerated with the stoichiometric quantity of iodine (15). Trifluoromethylselenomercuric chloride was obtained by evaporation of an ether solution of stoichiometric quantities of bis(trifluoromethylseleno)mercury and mercuric chloride (15). Bis(trifluoromethyl) selenide and bis(trifluoromethyl) diselenide were purified by vacuum distillation and bis(trifluoromethylseleno)mercury and trifluoromethylselenomercuric chloride were purified by vacuum sublimation at 50 and 70 °C respectively.

RESULTS AND DISCUSSION

Chemical Shifts and Coupling Constants

The selenium chemical shifts that were measured are given in Table I. Spin–spin coupling patterns were observed in a number of fluorine- and hydrogen-containing compounds, and the coupling constants obtained from the selenium, fluorine, and proton spectra are given in Table II. Isotope effects between the signal of fluorine on selenium-80 and fluorine attached to the other selenium isotopes were noted in a number of cases and have been discussed elsewhere (17).

We note that selenium(VI) compounds generally give a resonance to high field of selenium(IV) compounds. The very high-field shift of H_2Se is worthy of comment in view of the fact that PH_3 gives a ^{31}P resonance at very high field, H_2O gives a very high-field ^{17}O resonance, and NH_3 gives a very high-field ^{14}N resonance (18).

For selenium hexafluoride no signal could be detected by the audio side-band slow-passage method but five of the seven components of the spin–spin multiplet were observed by the adiabatic rapid-passage technique.

Selenium Tetrahalide Adducts

A solution of $SeCl_4$ in SO_3 gave a selenium resonance at +88.2 p.p.m., whereas $SeCl_4$ in dimethylformamide gave a resonance at +352 p.p.m. The large down-field shift of the selenium resonance is consistent with the formation of the complex $SeCl_4.SO_3$, which probably has the structure $SeCl_3^+SO_3Cl^-$ (19).

Can. J. Chem. Downloaded from www.nrcresearchpress.com by 210.87.254.40 on 09/05/12
For personal use only.

TABLE I
Chemical shifts

	Physical state	δ (p.p.m. from $SeOCl_2$)
$SeOBr_2$	Liquid	−80.3
$SeOCl_2$	Liquid	0
SeOFCl	$SeOF_2/SeOCl_2$ mixture	0.4
H_2SeCl_6	Aqueous solution	28.0
$SeOF_2$	Liquid	100.8
H_2SeO_3	Saturated solution in water	196.6
Se_2Cl_2	Liquid	204.5
Na_2SeO_3	Saturated solution in water	226.1
Se_2Br_2	Liquid	304.9
$SeCl_4$*	Saturated solution in dimethyl formamide	325.2
$SeF_4.BF_3$	Liquid (m.p. 46°)	356.8
SeF_4	Liquid	386.8
$SeF_4.SO_3$	Liquid (m.p. 70°)	421.8
K_2SeO_4	Saturated solution in water	454.8
$HSeO_3Cl$	Solution in SO_2	475.8
H_2SeO_4	Slightly aqueous	478.1
$HSeO_3F$	Impure liquid containing H_2SeO_4	478.0
SeO_3	Saturated solution in phosphorus oxychloride	521.8
SeO_2F_2	Liquid	531.2
SeO_3	Liquid (m.p. 120°)	535.3
$(CF_3)_2Se$	Liquid	784.6
SeF_6†	Liquid	868.7
$(CF_3Se)_2$	Liquid	950.9
$(CF_3Se)_2Hg$	Solution in methanol	1 145.2
$CF_3SeHgCl$†	Solution in methanol	1 214.7 1 246. ‡
H_2Se	Liquid	1 704.5

*The signal was very weak due to low solubility and could only be seen using the broad-line technique.
†The signal was weak and was observed by the rapid-passage technique.
‡Calculated value—see text.

TABLE II
Coupling constants

	J (c/s) from selenium spectrum	J (c/s) from fluorine or hydrogen spectrum
$SeOF_2$	837±2	837.1±0.6
$SeOF_2$ (mixture with $SeOCl_2$)	826±15	828.0±1.0
$SeOF_2$ (mixture with $SeOBr_2$)	818±10	—
SeOFCl	646	647.5±2.0
SeO_2F_2	1 577±20	1 583.9±0.6
SeF_6	1 432±25	1 420.9±0.5
$HSeO_3F$	1 445±2.5	1 453.6±0.7
H_2Se	62±1.5	63.4±0.5
$(CF_3)_2Se$	—	11.1±0.2
$(CF_3Se)_2$	—	6.4±0.2
$(CF_3Se)_2Hg$	39.2±1.0	39.5±0.6
$CF_3SeHgCl$	—	37.4±0.5 35.8±0.5*

*Calculated value—see text.

Selenium tetrafluoride forms compounds with SO_3 (6) and BF_3 (20), and the chemical shifts of these compounds in the molten state are given in Table I. The sample tube was heated to about 10° above the melting point of the compound, and the spectrum was observed before solidification occurred. As the shifts for the two compounds are different, one can conclude that both compounds cannot contain an identical SeF_3^+ ion. Other work in this laboratory indicates that $SeF_4.SO_3$ has the essentially covalent structure $SeF_3.SO_3F$ while $SeF_4.BF_3$ has the ionic structure $SeF_3^+.BF_4^-$ (21).

Can. J. Chem. Downloaded from www.nrcresearchpress.com by 210.87.254.40 on 09/05/12
For personal use only.

Selenium tetrafluoride was found to react readily with a small excess of selenium trioxide to give at room temperature a clear liquid which slowly deposits a white solid. The liquid gave a selenium spectrum of six peaks, three of which were identical with the three components of the SeO_2F_2 triplet (δ = 528.1 p.p.m. and J = 1 588 c/s); two of the remaining three peaks (δ = 439.7 and 582.3 p.p.m.) could possibly be attributed to the $SeF_4.SeO_3$ adduct, which would be expected to have the structure $SeF_3.SeO_3F$, and the other small peak at 512.4 p.p.m. could be attributed to the small excess of selenium trioxide. The deposition of the white solid and the formation of SeO_2F_2 may indicate that $SeF_4.SeO_3$ is unstable and decomposes slowly, possibly in the following manner:

$$SeF_3.SeO_3F \rightarrow SeOF_2 + SeO_2F_2$$

$$SeOF_2 + SeO_3 \rightarrow SeO_2 + SeO_2F_2.$$

An alternative interpretation of the results would be that the two peaks at 439.7 and 582.3 p.p.m. are a doublet arising from selenium coupled to a single fluorine, possibly in the molecule $Se_2O_5F_2$. The coupling constant J(Se–F) = 1 470 ± 22 c/s and the chemical shift 510.9 ± 4.8 p.p.m. are both consistent with the resonance being due to VI-valent selenium. The diselenyl fluoride could be formed by the reaction

$$SeO_2F_2 + SeO_3 = Se_2O_5F_2.$$

The remaining peaks may be assigned, as before, to excess SeO_3 and to SeO_2F_2.

Reaction occurs between $SeCl_4$ and SeO_3 in $POCl_3$ solution as evidenced by the dissolution of the $SeCl_4$ which only occurs upon the addition of SeO_3. This mixture is unstable at room temperature; a white solid is deposited and chlorine is evolved. An analogous mechanism to that put forward above would fit the experimental observations except that in this case SeO_2Cl_2 decomposes further to give SeO_2 and Cl_2.

Unfortunately, we were unable to obtain solutions of other $SeCl_4$ complexes such as $SeCl_4PCl_5$ and $SeCl_4AlCl_3$ that were concentrated enough to give a selenium signal.

Mixed Halides and Oxyhalides

An equimolecular mixture of $SeOF_2$ and $SeOCl_2$ gave three selenium resonances, a singlet, a doublet, and a triplet indicating the formation of a new compound. From their spin–spin coupling patterns and chemical shifts the singlet and the triplet can be unambiguously assigned to the two original components $SeOCl_2$ and $SeOF_2$. The third doublet peak can clearly be assigned to SeOFCl. As expected, the fluorine spectrum contained a new peak that could be assigned to SeOFCl in addition to the $SeOF_2$ peak. The SeF coupling constant in SeOFCl is appreciably smaller than in $SeOF_2$ (Table II). We note also that the coupling constant in this latter compound is somewhat solvent dependent. The coupling constants obtained from the fluorine spectra agree well with those obtained from the selenium spectra. A mixture of $SeOF_2$ and $SeOBr_2$ gave only two selenium resonances, but a mixture of $SeOBr_2$ and $SeOCl_2$ gave a single peak with a width of approximately 70 c/s lying between the resonances of the pure components. These observations indicate that there is rapid exchange presumably via the formation of the intermediate SeOBrCl.

Se_2Cl_2 is completely miscible with Se_2Br_2. The spectrum of the mixture showed only the two signals of the components except that each was rather broadened. On heating further broadening of the peaks occurred, which indicated that relatively slow exchange occurs between the two species.

Solutions of Selenium

Solutions of red selenium in CS_2, H_2SO_4, SO_3, SeF_4, and $SeOF_2$ were investigated, but

Can. J. Chem. Downloaded from www.nrcresearchpress.com by 210.87.254.40 on 09/05/12
For personal use only.

in no case could a signal from the dissolved selenium be detected. In most cases the solubility appears to be quite small.

Selenium dissolves readily in selenium oxychloride and it has been shown (22) that Se_2Cl_2 is formed, presumably according to the equation

$$Se + 2SeOCl_2 = SeO_2 + Se_2Cl_2.$$

In agreement with this the n.m.r. spectrum of the solution contained two signals: one at +15 p.p.m., which can reasonably be attributed to a solution of SeO_2 in $SeOCl_2$, and a broad signal at 205 p.p.m., which agrees well with the observed shift for pure liquid Se_2Cl_2 (Table I).

Trifluoromethylselenomercuric Chloride

The chemical shift of a solution trifluoromethylselenomercuric chloride in methanol was found to be 1 214.7 c/s and the coupling constant $J(^{77}Se–^{19}F) = 37.4$ c/s. However, it has been shown that disproportionation occurs, and the equilibrium constant for the reaction

$$(CF_3Se)_2Hg + HgCl_2 \rightleftharpoons 2CF_3SeHgCl$$

has been found to be 20 ± 2 in methanol at room temperature (23). Thus 69.1% of the CF_3Se groups are in the form $CF_3SeHgCl$ under these conditions. Since only one peak was observed in the ^{77}Se spectrum and one, with attendant ^{77}Se and ^{13}C satellites, in the ^{19}F spectrum, there must be rapid exchange of CF_3Se groups between $(CF_3Se)_2Hg$ and $CF_3SeHgCl$. This conclusion is supported by the absence of $^{199}Hg–^{19}F$ coupling in the ^{19}F spectrum, although a very small value for the coupling constant would produce the same result. From the ^{77}Se chemical shift, the $^{19}F–^{77}Se$ coupling constant for a solution of bis(trifluoromethylseleno)mercury, and the calculated composition of the equilibrium mixture formed by $CF_3SeHgCl$, approximate values for the hypothetical solution of pure trifluoromethylselenomercuric chloride were calculated. The values obtained are given in Tables I and II.

Solutions of Acids and Bases in Selenium Oxychloride

Conductivity and e.m.f. measurements (22) indicate that $SeOCl_2$ undergoes the self-ionization

$$SeOCl_2 = SeOCl^+ + Cl^-,$$

so that chloride ion acceptors may be regarded as acids

$$\text{e.g. } SbCl_5 + SeOCl_2 = SbCl_6^- + SeOCl^+,$$

and chloride ion donors or $SeOCl^+$ acceptors may be regarded as bases

$$\text{e.g. } C_5H_5N + SeOCl_2 = C_5H_5NSeOCl^+ + Cl^-.$$

We found that addition of $SbCl_5$ to selenium oxychloride gives a high-field shift that increases linearly with the mole ratio $SbCl_5/SeOCl_2$ (Table III and Fig. 1) which indicates that $SbCl_5$ is a strong acid of the selenium oxychloride solvent system since

$$\frac{\text{moles } SbCl_5}{\text{moles } SeOCl_2} = \frac{\text{moles } SeOCl^+}{\text{total moles } (SeOCl_2 + SeOCl^+)}.$$

Only very few measurements were made on other acids and they are summarized in Table IV. To facilitate comparison of these results it was assumed that the shift is proportional to the mole ratio acid/$SeOCl_2$, and shifts were calculated in each case for the mole ratio 1/3. The small shift for $AsCl_3$ and the apparent dependence of the calculated

Can. J. Chem. Downloaded from www.nrcresearchpress.com by 210.87.254.40 on 09/05/12
For personal use only.

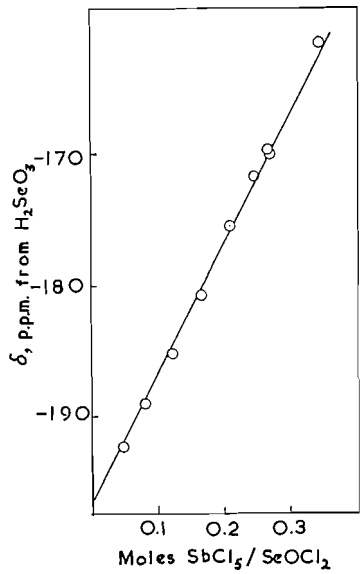

FIG. 1. Chemical shifts for solutions of $SbCl_5$ in $SeOCl_2$.

TABLE III

Chemical shifts for solutions of $SbCl_5$ in $SeOCl_2$

Moles $SeOCl_2$	Moles $SbCl_5$	Moles $SbCl_5$/moles $SeOCl_2$	δ (p.p.m. from H_2SeO_3)
0.07068	0.01941	0.2746	−170.1
0.07225	0.01972	0.2729	−169.7
0.07062	0.01758	0.2489	−171.8
0.07179	0.01538	0.2142	−175.6
0.07047	0.01186	0.1683	−180.8
0.07134	0.00890	0.1247	−185.3
0.07228	0.00587	0.0812	−189.1
0.07161	0.00338	0.0472	−172.4
0.074	0.026	0.35	−161.6

TABLE IV

Chemical shifts for some acids and bases in $SeOCl_2$

Acid	Moles acid/moles $SeOCl_2$	δ (p.p.m. from $SeOCl_2$)	δ calcd. for mole ratio = 1/3
$AsCl_3$	1:2	2.5	3.2
$AsCl_3$	1:1	7.0	2.3
$SnCl_4$	1:6	26.2	52.4
$SbCl_5$	1:2.9	35.0	33.6
Base	**Moles base/moles $SeOCl_2$**	**δ (p.p.m. from $SeOCl_2$)**	**δ calcd. for mole ratio = 1/3**
Quinoline	1:7	10.3	24.0
KCl	1:15	5.1	25.3

shift on the actual concentration used suggests that $AsCl_3$ is a weak acid. The large shift produced by $SnCl_4$ indicates that it is extensively if not completely ionized as a dibasic acid

$$SnCl_4 + 2SeOCl_2 = 2SeOCl^+ + SnCl_6^-.$$

Can. J. Chem. Downloaded from www.nrcresearchpress.com by 210.87.254.40 on 09/05/12
For personal use only.

The two bases quinoline and KCl give high-field shifts of the same order of magnitude as those produced by acids (Table IV). The relatively large shift produced by KCl is of interest as it indicates a strong interaction of the chloride ion with the solvent. This can be most simply expressed in terms of the formation of the complex ion $SeOCl_3^-$ so that the self-ionization of the solvent is perhaps better represented as a chloride ion transfer,

$$2SeOCl_2 = SeOCl^+ + SeOCl_3^-.$$

ACKNOWLEDGMENT

We thank the Directorate of Chemical Sciences of the United States Air Force of Scientific Research and the National Research Council for generous financial aid. We also thank Dr. K. C. Moss and Dr. H. J. Clase for help with the preparation of some of the compounds, Dr. W. A. Whitla for samples of $SeF_4.SO_3$ and $SeF_4.BF_3$, and Mr. J. Bacon for assistance with the development of the audio side-band method for observing the selenium signals.

REFERENCES

1. S. S. Dharmatti and H. E. Weaver. Phys. Rev. **86**, 259 (1952).
2. H. E. Walchli. Phys. Rev. **90**, 331 (1953).
3. W. A. Anderson. *In* N.m.r. and e.p.r. spectroscopy. Pergamon Press, New York. 1960. p. 180.
4. V. Lenher. J. Am. Chem. Soc. **44**, 1668 (1922).
5. H. G. Nowak and J. F. Suttle. Inorganic syntheses. Vol. 3. *Edited by* T. Moeller. McGraw-Hill Publishing Co. Inc., New York. 1957. p. 137.
6. R. D. Peacock. J. Chem. Soc. 3617 (1953).
7. F. Toul and K. Dostál. Collection Czech. Chem. Commun. **16**, 531 (1951).
8. H. A. Lehmann and G. Kruger. Z. Anorg. Chem. **267**, 324 (1952).
9. H. Bartels and E. Class. Helv. Chim. Acta, **45**, 179 (1962).
10. T. Birchall and R. J. Gillespie. Unpublished work.
11. M. Schmidt and I. Wilhelm. Chem. Ber. **97**, 876 (1964).
12. A. Engelbrecht and B. Stoll. Z. Anorg. Chem. **292**, 20 (1957).
13. E. E. Aynsley, R. D. Peacock, and P. L. Robinson. J. Chem. Soc. 1231 (1952).
14. G. R. Waitkins and R. Shutt. Inorganic Syntheses. Vol. II. *Edited by* W. C. Fernelius. McGraw-Hill Publishing Co. Inc., New York. 1946. p. 183.
15. J. W. Dale, H. J. Emeléus, and R. N. Haszeldine. J. Chem. Soc. 2939 (1958).
16. H. J. Emeléus and M. J. Dunn. J. Chem. Soc. In press.
17. T. Birchall, R. J. Gillespie, and S. L. Crossley. J. Chem. Phys. **41**, 2760 (1964).
18. P. C. Lauterbur. *In* Determination of organic structures by physical methods. Vol. 2. *Edited by* F. C. Nachod and W. D. Phillips. Academic Press, New York. 1962. p. 465.
19. H. Gerding. Rec. Trav. Chim. **75**, 589 (1956).
20. N. Bartlett and P. L. Robinson. Chem. Ind. London, 1351 (1956).
21. R. J. Gillespie and W. A. Whitla. Unpublished work.
22. L. F. Audrieth and J. Kleinberg. Non-aqueous solvents. John Wiley, New York. 1953. p. 234.
23. H. J. Clase and E. A. V. Ebsworth. J. Chem. Soc. In press.

Can. J. Chem. Downloaded from www.nrcresearchpress.com by 210.87.254.40 on 09/05/12
For personal use only.

Can. J. Chem. Downloaded from www.nrcresearchpress.com by 210.87.254.42 on 09/05/12
For personal use only.

SURFACE CHEMISTRY AND CATALYTIC PROPERTIES OF BORON PHOSPHATE

1. SURFACE AREA AND ACIDITY

J. B. MOFFAT AND H. L. GOLTZ
Department of Chemistry, University of Waterloo, Waterloo, Ontario

Received December 10, 1964

ABSTRACT

Surface properties of the dehydration catalyst, boron phosphate (BP), prepared by the reaction of triethyl borate and phosphoric acid, were investigated by the use of a microbalance system. During evacuation at elevated temperatures, weight changes of the BP were obtained. Nitrogen adsorption isotherms were measured after each treatment. Surface areas appear to increase, and reach a maximum in the range 200–300 °C. Weight changes are initially large but begin to level off as the temperature is increased. Ammonia isotherms were obtained at 25.00 °C on aliquots of the same BP sample after various pretreatments. Amounts of ammonia remaining adsorbed after evacuation overnight were taken as the quantity chemisorbed. An approximate value of 8.9 kcal/mole of ammonia was obtained for the heat of chemisorption of ammonia by measuring the pressure and weight change as the amount of chemisorbed ammonia is decreased on heating the BP to various temperatures in a closed system. Results are interpreted in terms of change of number of active sites with surface area and the deactivation of sites on loss of water.

INTRODUCTION

Much of the work done in an attempt to elucidate the mechanisms by which dehydration catalysts function has involved alumina. However, an examination of patent literature shows that at least one other material, namely boron phsophate, has a high prominence (in terms of numbers of patents devoted to it) as a potential dehydration catalyst. Remarkably little work has been done on the surface chemistry associated with its catalytic properties.

What work has been done on boron phosphate has been largely concerned with its bulk properties as opposed to its surface properties. The first important paper was that of Schulze (1) in 1934 on the crystal structure of boron phosphate. In 1950, Hummel and Kupinskii (2) reported on the vaporization of BPO_4. Cherbuliez and co-workers (3), in a paper published in 1953, worked on the preparation and properties of orthoboric esters. In so doing they experimented with the preparation of boron phosphate from phosphoric acid and triethyl borate. Gerrard and Griffey (4) discussed a novel preparation of boron phosphate from triethyl phosphate and boron trichloride. A number of papers (5, 6, 7) have been concerned with high-pressure forms of boron phosphate. V. F. Ross and co-workers (8) prepared boron phosphate for their n.m.r. studies on this phosphate and several borates.

Recently, several papers devoted exclusively to boron phosphate have appeared. Baccaredda (9) examined the reaction of alcohol and water with boron phosphate prepared by reacting boric acid with phosphoric acid. Friedlin and his co-workers (10) have studied the activity and stability of borophosphate catalysts in the dehydration of a mixture of pyrocatechol and methanol. After the work discussed in the present paper was completed, another paper (11) appeared from the Freidlin group in Russia. In this paper Freidlin discusses the effects of baking temperature and acidity on the dehydration of aliphatic alcohols. Their catalysts were prepared by reacting boric acid with phosphoric acid.

In view of the apparently widespread interest in boron phosphate for industrial use as a dehydration catalyst, it seemed worthwhile to examine the mechanism by which such dehydration takes place. Unfortunately, as has been mentioned, little work has been done on the properties of boron phosphate, especially those of its surface. Hence it appeared necessary and appropriate to initiate studies of the surface chemistry of boron phosphate prior to any attempts to study reactions on the surface.

Presumably the catalytic ability of boron phosphate will be related to (among other things) (1) the surface area, (2) the "acidity" of the sites available, (3) the number of such acid sites, (4) the "surface structure", that is, the inter-site separation on the surface. The surface area is presumably dependent on the prior treatment of the catalyst, such as heat treatment and evacuation. Indeed, the number of active sites may be related to such preliminary treatment, if one argues that the removal of a "sorbed" water molecule from a surface site may alter the activity of the site with respect to dehydration catalysis.

It therefore appeared to be of interest to examine the interdependence of amount of water lost on evacuation, temperature at which evacuation occurred, and surface area of the resulting solid. If one presumes that each acidic site will chemisorb a fixed number of ammonia molecules (most likely one per site) then the amount of ammonia chemisorbed should be directly related to the number of active sites. Further, one might expect that the "acidity" of the sites available will be related to the strength of binding of the ammonia molecules to such sites. Of course, the idea that the number and strength of acid sites might be related to catalytic activity in dehydration reactions is based on analogy with results of studies on silica–alumina catalysts.

Various methods have been suggested for the determination of the number and strength of acid sites on the surface of solids. Hammett indicators (12) have been employed for such purposes. More recently, ammonia chemisorption has found favor for such determinations. Webb (13) was one of the first to use such a method, but interest has been shown by a number of other workers (14–18).

EXPERIMENTAL

Materials

For the present work, samples of boron phosphate were prepared initially by three methods, (1) reaction of boric and phosphoric acids, (2) reaction of triethyl phosphate and boron trichloride, (3) reaction of triethyl borate (TEB) and phosphoric acid (PA). However, for most of the work to be described, samples prepared by method (3) were used. Various ratios of the reactants were tried in an attempt to determine the best method of preparation, and the ratio of 2:1 TEB:PA was ultimately chosen. The middle cut from a distillation of TEB was used for the preparation. Phosphoric acid, C.P. grade, was used without further treatment.

For the adsorption studies, nitrogen gas obtained commercially was passed through a trap filled with magnesium perchlorate and cooled in liquid nitrogen, and then was passed over heated copper filings contained in a copper tube, prior to passage into the vacuum system. Ammonia gas obtained commercially was subjected to a trap-to-trap distillation in the vacuum system before use.

Apparatus

A Cahn RG Electrobalance mounted in a glass bottle which was fitted with hang-down tubes for the sample and weights was employed for all of the present work. For other work, to be reported on later, a volumetric adsorption system fitted with both a manometer and thermistor gauge had been constructed. As a check against the gravimetric system a sample of finely divided titanium dioxide, kindly provided by Dr. R. W. Brickenkamp of National Lead Company, was used in the volumetric system.

The Cahn balance container was attached to a standard adsorption system consisting of a Veeco RG75 ionization gauge, Consolidated Vacuum Corp. triple-scale McLeod gauge, and a wide-bore mercury manometer. Mercury levels were read to ± 0.05 mm with a cathetometer. Appropriate bulbs and stopcocks were available for purifying and dispensing gases. Vacuum was obtained by the use of a Balzers DUO5 oil pump together with two mercury diffusion pumps in series, protected by large liquid nitrogen traps on both sides.

A Hoskin tube furnace, controlled by a de Khotinsky bimetallic strip regulator with a relay, was used to

Can. J. Chem. Downloaded from www.nrcresearchpress.com by 210.87.254.42 on 09/05/12
For personal use only.

heat and control the temperature of the sample contained in a quartz hemi-spherical pan which was suspended from the balance arm by a nichrome wire. The furnace was raised into position around the Pyrex hand-down tube by using two lab jacks. The same length of the hang-down tube was heated in each run. A thermocouple well protruded a distance of 3 cm into the hang-down tube from the bottom. With the quartz pan in weighing position, the bottom of the pan was held approximately $\frac{1}{4}$ in. above the top of the thermocouple well. Temperatures were read to ± 1 °C or better using an uncalibrated Chromel–Alumel thermocouple attached to a Varian G-11 recorder. For the studies of the chemisorption of ammonia, an oil bath outfitted with immersion heater, stirrer, mercury thermoregulator, and relay was used. Temperatures of this bath were checked against a National Bureau of Standards thermometer.

X-ray diffraction patterns were obtained by the capillary tube method using a Philips NRD899 camera. A copper tube and nickel filter were used to obtain diffraction patterns at 30 kV and 20 mA for various exposure times.

Method

The freshly prepared samples of boron phosphate were placed in screw cap bottles for storage. The sample which was used for most of the work was labelled BP6A and had been heated no higher than 100 °C in preparation. A sample of this boron phosphate was placed on the pan of the previously calibrated Cahn balance and pumped overnight at 25 °C. The weight of the sample was followed at the beginning and end of the pumping period on a Leeds and Northrup Speedomax G recorder which was attached to the electronic control of the microbalance. When constant weight (± 1 μg) had been obtained the system was closed from the pump, the sample tube was immersed in liquid nitrogen, and an adsorption isotherm of nitrogen on the sample was obtained. Several desorption points were also obtained for each isotherm. Normally a minimum of 10 points were obtained for each isotherm. On completion of the isotherm, the liquid nitrogen bath was removed and the sample was opened to the pump. At the beginning of the work, difficulties with "popping" of the sample occurred at pumping stages. This was eliminated by first opening the sample to a Cenco Pressovac pump until the weight was approximately constant, then opening the sample to the diffusion pumps, and finally isolating the sample from the Pressovac pump. No evidence of "popping" either visible or from balance readings was obtained with this method.

The furnace was then carefully raised around the sample tube and the sample was pumped at approximately 100 °C overnight. The procedure just described was then repeated. The whole operation was repeated until the previously selected maximum temperature had been obtained. Adsorption isotherms and weight losses were obtained after intervals of heating of approximately 50 deg or in some cases 100 deg.

When the preselected maximum temperature had been attained and the adsorption isotherm completed, pumping was again carried out overnight but this time at room temperature. Following this, the weight of ammonia adsorbed at various pressures was determined with the sample held at 25.00 °C. For each point on the ammonia isotherms times of 12 to 24 h were required to reach equilibrium. When an isotherm pressure of at least 15 to 20 cm Hg had been reached, the system was opened to the pump for a short time and the first desorption point was taken to be that obtained when the weight again became constant. This procedure was contained until four or five desorption points were obtained. Then the sample was opened to the pump and evacuation at 25.00 °C was continued overnight. The weight of the sample was again determined. This weight was taken to be the weight of the sample plus the amount of ammonia chemisorbed.

The sample system was then closed from the pump. The sample tube was heated to various temperatures, at each of which equilibrium was taken to have been reached when the weight of the sample became constant. Equilibrium pressures and sample weights were read for each temperature.

A fresh portion of the sample BP6A was selected for each of the runs previously described. Maximum temperatures from 25 to 450 °C were employed.

Corrections for buoyancy in the microbalance were obtained by employing a 110 mg sample of small diameter quartz rods. The apparent weight was obtained for various pressures up to 700 mm Hg while the quartz sample was held at a constant temperature of 100 $\pm$ 1 °C. This process was repeated for 25 °C and liquid nitrogen temperature.

RESULTS AND DISCUSSION

A Fortran II computer program was prepared for calculations associated with the adsorption isotherms. This program fitted the buoyancy correction data to a polynomial (of 10 terms), and used the equation for the polynomial to make the appropriate corrections to the weights of adsorbate. BET abscissae and BET ordinates were also obtained, together with the surface area by a least squares method. Finally, the number of moles adsorbed, number of molecules adsorbed, number of moles adsorbed per gram, and number of molecules adsorbed per gram were printed out for each pressure recorded. Input data consisted of equilibrium pressures, equilibrium weights adsorbed, buoyancy correction data, and weight of sample.

Can. J. Chem. Downloaded from www.nrcresearchpress.com by 210.87.254.42 on 09/05/12
For personal use only.

Figure 1 shows the change in the specific surface area with pretreatment temperature. It is interesting to note that in all cases the surface area initially increases on heating the sample above room temperature. No effort was made to prevent loss of surface area

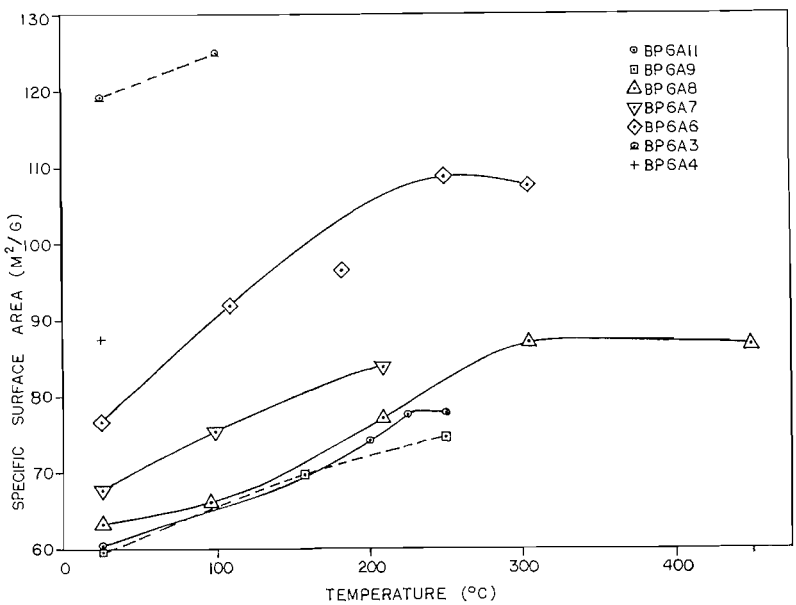

FIG. 1. Change in specific surface area with pretreatment temperature.

by the samples on standing at room temperature in screw cap bottles. Hence, although the initial (25 °C) values of surface area shown in Fig. 1 are all different, nevertheless each represents an aliquot from the same sample, BP6A. One notes that the sample of boron phosphate changed from approximately 120 m^2/g to approximately 55 m^2/g on standing in the sample bottles. Figure 1 also indicates that the surface area apparently reaches a maximum between 200 and 300 °C. It may be significant that many of the patented recipes recommend ultimate heating of the boron phosphate to about 300 °C before use.

It might have been expected that the specific surface area of the solid would decrease on heating, perhaps because of some type of sintering phenomena. However, it seems not unreasonable to presume that the unexpected increase in surface area may be due to the evolution of water from the bulk of the solid during the heating and evacuation process. The transfer of this water from the interior to the surface of the solid could lead to the production of additional porous structure. At some temperature between 200 and 300 °C, it is presumed that all the entrapped water has escaped and on further increase in temperature closing of some of the pores may occur, resulting in a decrease in surface area. This latter effect may become significant at much higher temperatures than were employed in the present work.

In Fig. 2, the weight of the catalyst after evacuation at various temperatures is shown. In general, the shape of the curves for each of the aliquots of BP6A is the same, which is of course to be expected. It should be noted that most of the change in weight (approximately 80% of the total change) has occurred in the temperature range below 250 to

Can. J. Chem. Downloaded from www.nrcresearchpress.com by 210.87.254.42 on 09/05/12
For personal use only.

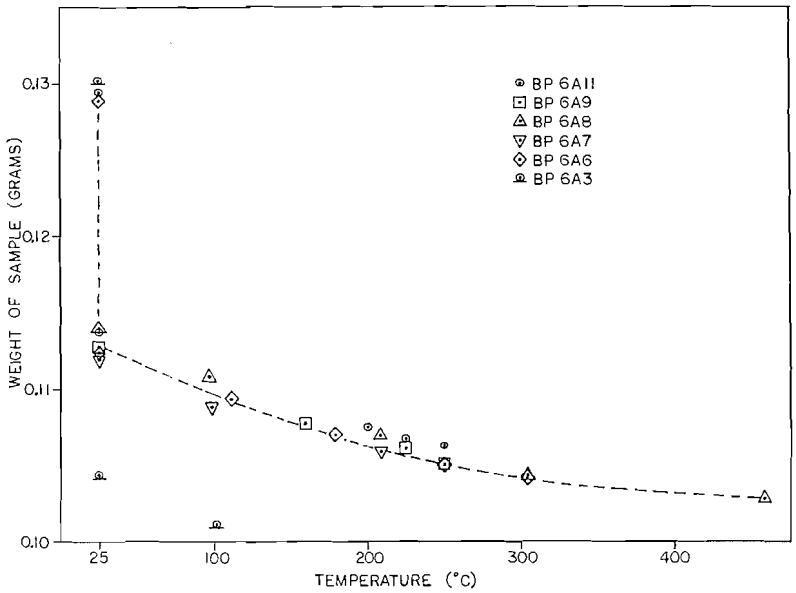

FIG. 2. Weight of catalyst after evacuation overnight at various temperatures.

300 °C. This appears to be consistent with the attainment of approximately constant surface areas in the same temperature region.

Presumably the change of weight which results on evacuation of the phosphate at various temperatures is due largely to loss of water from the surface and interior of the particles. Since, according to Hummel (2), the vaporization temperature is approximately 1 450 °C, it seems unlikely that much of the catalyst in the form of boron phosphate was lost on evacuation at the temperatures used in this experiment. For the same reason it is not expected that much boron or phosphorus in the form of boric oxide or phosphorus pentoxide, respectively, could have been lost from the solid. No attempt was made to determine the composition of the material which had been pumped off the boron phosphate. However, there was no evidence of any deposits on the portion of the vacuum line which was at room temperature, between the heated sample and the pumps.

Figure 3 shows the adsorption isotherms of nitrogen for one of the samples of boron phosphate at various stages in the heating process. No evidence of lack of reversibility was obtained from the desorption points on the isotherms for any of the samples at any of the temperatures employed.

In Fig. 4, isotherms for the adsorption of ammonia at 25.00 ± 0.05 °C are shown for typical samples in terms of milligrams of ammonia adsorbed per square meter of surface area.

The amount of ammonia remaining on the various samples after evacuation under high vacuum at 25 °C overnight is shown in Fig. 5 as a function of maximum pretreatment temperature for each of the aliquots. As has been mentioned previously, this is taken to be the amount of chemisorbed ammonia. The data in Fig. 5 scatter so badly that any positive conclusion may be questionable. However, if the 200 °C point is largely ignored, it then appears that the amount of ammonia chemisorbed is a continuously decreasing function of the temperature, at least up to about 450 °C. Unfortunately, no explanation can be offered for the discrepancy of the point at 200 °C.

Can. J. Chem. Downloaded from www.nrcresearchpress.com by 210.87.254.42 on 09/05/12
For personal use only.

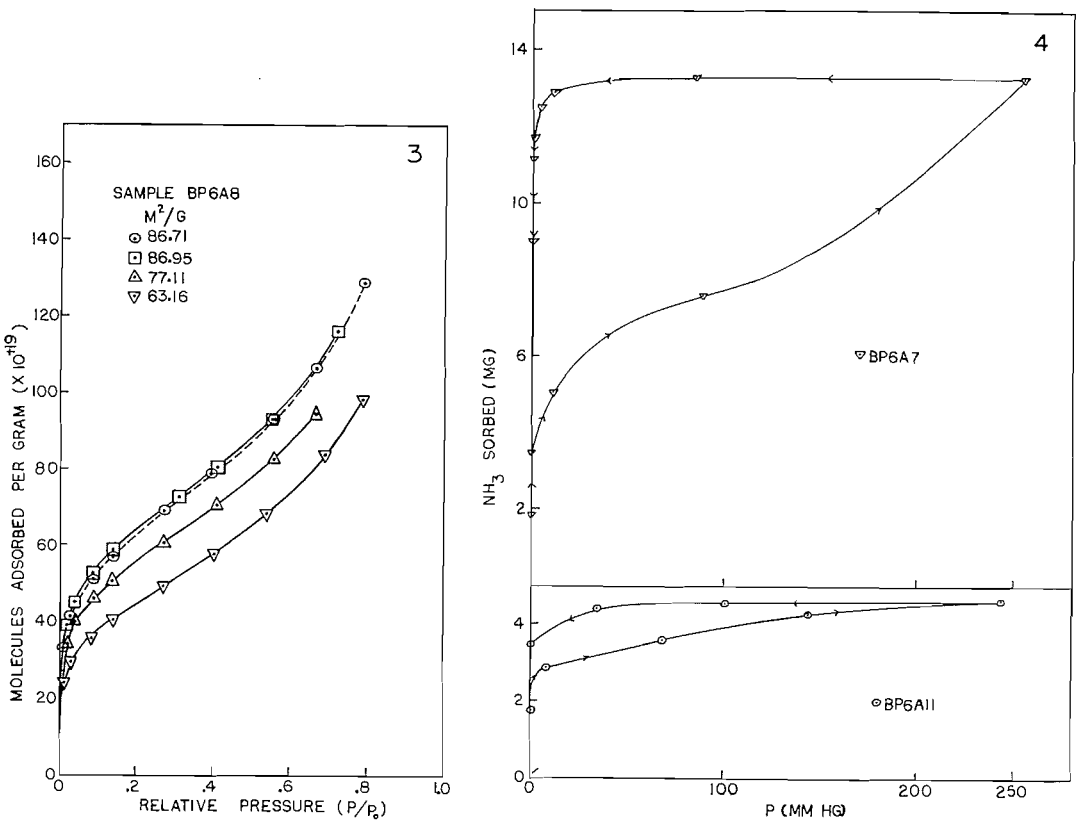

FIG. 3. Adsorption isotherms of nitrogen on a typical sample of boron phosphate at various stages in the pretreatment process.
FIG. 4. Typical adsorption isotherms for the adsorption of ammonia on boron phosphate at 25.00 °C.

To utilize the results obtained from the study of the increase of pressure of ammonia in the closed system with increase of temperature, the following reasoning was employed.

It is not unreasonable to presume that the equilibrium process involved can be represented by

$$BPO_4.NH_3(s) \leftrightarrows BPO_4(s) + NH_3(g)$$

for which an "equilibrium constant" can be defined as

$$K = \frac{N_e P_{NH_3}}{N_o},$$

where N_e = concentration of empty surface sites, N_o = concentration of occupied surface sites, and P_{NH_3} = pressure of ammonia.

It may be presumed that at the start of the run in which the pressure, weight, and temperature data were obtained, all chemisorption sites are occupied and the gas pressure is essentially zero. Hence the concentration of empty surface sites should be proportional to the pressure of ammonia, and the number of occupied surface sites should be given by

$$N_o = W_1 - W_t,$$

Can. J. Chem. Downloaded from www.nrcresearchpress.com by 210.87.254.42 on 09/05/12
For personal use only.

where W_i = initial weight of ammonia chemisorbed and W_t = weight of ammonia desorbed.

Since the pressure of ammonia should be proportional to the weight of ammonia desorbed, then

$$K = \frac{W_t^2}{W_i - W_t}.$$

A plot of the logarithm of this K against the reciprocal of the temperature in °K can then be related to the change in enthalpy or heat content ΔH^0 for the desorption process. It is presumed that this may be taken as a rough measure of the heat of chemisorption.

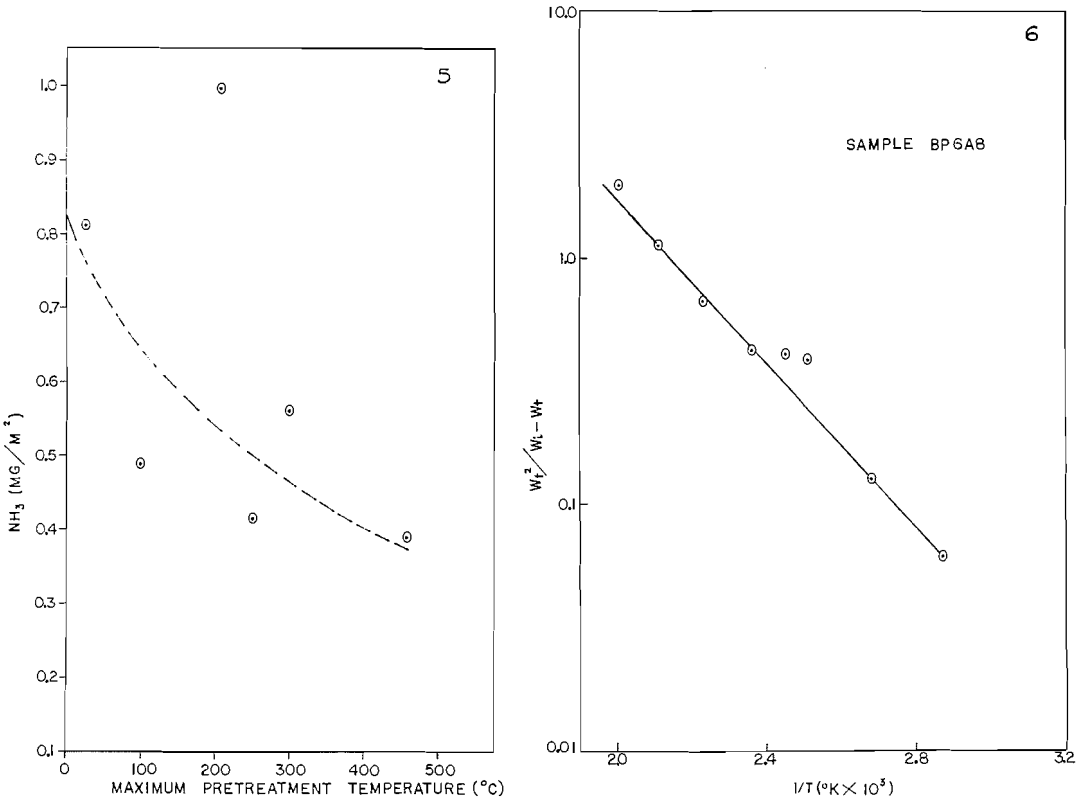

FIG. 5. Amount of chemisorbed ammonia per unit surface area after treatment at various maximum temperatures.

FIG. 6. Heat of chemisorption from the plot of logarithm of K vs. the reciprocal of absolute temperature.

A typical set of data are shown plotted in such fashion in Fig. 6. An average value of 8.9 ± 0.5 kcal/mole was obtained for the heat of chemisorption of ammonia for all the samples studied. This may be compared with the somewhat higher value of 11.5 kcal/mole obtained by Blyholder and Richardson (17) for ammonia on activated iron(III) oxide.

For X-ray powder diffraction measurements, other samples of BP in addition to those prepared in this laboratory were obtained for comparison purposes. Dr. V. Ross very kindly supplied samples from her n.m.r. work at Brown University. Stauffer Chemical Company kindly provided a sample. A sample was also obtained from Alpha Inorganics,

Can. J. Chem. Downloaded from www.nrcresearchpress.com by 210.87.254.42 on 09/05/12
For personal use only.

Inc. X-ray diffraction photographs were obtained on these samples and also on samples of BP6A which had been subjected to various pretreatments as mentioned in this paper. Line spacings on these photographs were essentially identical for each sample. However, the lines on those photographs obtained with sample BP6A prior to any kind of treatment were in general quite diffuse. In addition, so-called white radiation effects were apparent. These effects may be attributed to the finely divided nature of the solid.

Samples of BP6A which had been treated at various temperatures up to 450 °C yielded diffraction photographs in which the lines were only slightly sharper. Finally, a sample of BP6A was ignited at a temperature above 1000 °C for about 2 h. The X-ray diffraction pattern resulting from this ignited sample was virtually identical with those of the commercial and Brown samples.

What is perhaps the most disturbing aspect of the present results, at least to the author, is that encountered in a closer examination of the significance of the amounts of chemisorbed ammonia. If it be assumed, as has been done here, that all the ammonia remaining on the solid after pumping overnight is indeed chemisorbed, then one might naively expect that the number of chemisorbed molecules times the area covered per molecule would yield the total surface area.

If the cross-sectional area of the ammonia molecule is taken as 20 Å² (19), the calculated area for the sample containing the least amount of ammonia chemisorbed is approximately three times that obtained from nitrogen adsorption results. For the maximum amount of ammonia chemisorbed (~1 mg/m²), the calculated area corresponds to approximately seven times the measured area.

To calculate an area in agreement with the measured one, it is necessary to use a cross-sectional area for the ammonia molecule of about 3 Å², which corresponds to coverage of a square of approximately 1.4 Å in dimension. It is assumed that complete coverage of the surface occurs. It is interesting to note that Schulze (1) found the P—O distance to be 1.55 Å, and the B—O distance to be 1.44 Å.

The results discussed in this paper appear to indicate that the greater part of the change in surface area, in weight, and in number of acidic sites with change in temperature probably has occurred prior to 300 °C.

There may be some value, at least in terms of suggesting future work, in presenting even an admittedly grossly oversimplified mechanism. It is assumed that the surface of the boron phosphate particles consists in large part of oxygen atoms, so that a simple picture of the chemisorption of water may be as shown below.

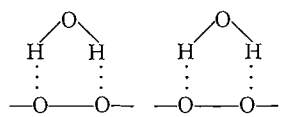

Within experimental error, the heat of chemisorption of ammonia is the same for all samples examined. This suggests that the number of sites for chemisorption of ammonia per unit surface area decreases with temperature, but that the strength of the sites remains fixed, at least over the range of temperature studied.

If it is postulated that most of the sites for chemisorption of ammonia are oxygen atoms, then it would appear that the number of sites should increase with pretreatment temperature. However, it may be that only those oxygen atoms which have a hydrogen atom attached are energetically favorable for chemisorption of ammonia. The removal of the water bound to the surface may expose oxygen atoms which are not energetically

Can. J. Chem. Downloaded from www.nrcresearchpress.com by 210.87.254.42 on 09/05/12
For personal use only.

favored. Further, the evidence that the degree of crystallinity increases with temperature may add support to this suggestion. Presumably, as the crystallinity increases, the forces operative between the species of the solid will increase, as the lattice takes shape. This may then lead to a reduction in the ability of the surface atoms to form chemisorption bonds.

It is tacitly assumed that the sites for chemisorption of ammonia are the same as those taking part in catalytic dehydration. If this is so, then it must be expected, on the basis of the present mechanism, that the catalytic ability of boron phosphate will decrease with the extent of the pretreatment heating and pumping. This has yet to be shown.

While the present results do not of course negate other mechanisms than the one suggested, nevertheless, qualitatively at least, the proposed mechanism appears to fit the experimental information. Further work is obviously necessary to substantiate the hypotheses. In particular, more direct information on the nature of the bond formed between ammonia and boron phosphate would be valuable. This aspect of the work is now being pursued in this laboratory.

ACKNOWLEDGMENTS

It is a pleasure to acknowledge the technical assistance of Mr. H. Goltz, who performed much of the experimental work reported. Translation of a paper from Italian to English was kindly supplied by Dr. M. Z. Cohn of the University of Waterloo. The author is indebted to Eleanor Moffat for preparation of all figures in the paper.

The generous provision of computer time by the Computation Center of the University of Waterloo is gratefully acknowledged. The author is indebted to the National Research Council for financial support, and to the University of Waterloo for the provision of the Cahn Electrobalance.

REFERENCES

1. G. E. R. Schulze. Z. Physik. Chem. B, **24**, 215 (1934).
2. F. A. Hummel and T. A. Kupinskii. J. Am. Chem. Soc. **72**, 5318 (1950).
3. E. Cherbuliez, J. P. Leber, and A. M. Ulrich. Helv. Chim. Acta, **36**, 910 (1953).
4. W. Gerrard and P. F. Griffey. Chem. Ind. London, 55 (1959).
5. J. D. Mackenzie, W. L. Roth, and R. H. Wentorf. Acta Cryst. **12**, 79 (1959).
6. F. Dachille and R. Roy. Z. Krist. **111**, 451 (1959).
7. F. Dachille and L. S. Dent Glasser. Acta Cryst. **12**, 820 (1959).
8. P. J. Bray, J. O. Edwards, J. G. O'Keefe, V. F. Ross, and I. Tatsuzaki. J. Chem. Phys. **35**, 435 (1961).
9. M. Baccaredda, G. F. Neucetti, and R. Tartarelli. Chim. Ind. Milan, **45**, 1483 (1963).
10. L. Kh. Freidlin, V. Z. Sharf, O. M. Kholmer, and L. L. Malkina. Kinetics Catalysis USSR, **2**, 228 (1961).
11. L. Kh. Freidlin, V. Z. Sharf, Z. T. Tukhtamuradov. Kinetics Catalysis USSR, **5**, 347 (1964).
12. H. A. Benesi. J. Am. Chem. Soc. **78**, 5490 (1956).
13. A. N. Webb. Ind. Eng. Chem. **49**, 261 (1957).
14. Y. Kubokawa. J. Phys. Chem. **67**, 769 (1963).
15. D. S. Maciver, H. H. Tobin, and R. T. Barth. J. Catalysis, **2**, 485 (1963).
16. A. Clark, V. C. F. Holm, and D. M. Blackburn. J. Catalysis, **1**, 244 (1962).
17. G. Blyholder and E. A. Richardson. J. Phys. Chem. **66**, 2597 (1962).
18. R. T. Barth and E. V. Ballou. Anal. Chem. **33**, 1080 (1961).
19. L. H. Reyerson and W. S. Hnojewyj. J. Phys. Chem. **67**, 1945 (1963).

Can. J. Chem. Downloaded from www.nrcresearchpress.com by 210.87.254.42 on 09/05/12
For personal use only.

Can. J. Chem. Downloaded from www.nrcresearchpress.com by 210.87.254.42 on 09/05/12
For personal use only.

ALIPHATIC VICINAL FLUOROBROMIDES

SOME PREPARATIONS AND REACTIONS[1]

F. L. M. PATTISON, D. A. V. PETERS, AND F. H. DEAN[2]
Department of Chemistry, University of Western Ontario, London, Ontario
Received November 16, 1964

ABSTRACT

The addition of "BrF", using *N*-bromoamides in anhydrous hydrogen fluoride, to a number of aliphatic alkenes has been studied. As expected, the bromine atom in the resultant vicinal fluorobromides exhibited relatively low reactivity in nucleophilic and hydrogenolytic reactions.

The bromine monofluoride addition reaction, first described by Bowers (2, 3, 4), has been employed mainly in the synthesis of fluorinated steroids. Its application to aliphatic alkenes was undertaken here partly to extend the scope of the reaction and partly to obtain the resultant vicinal fluorobromides as intermediates in other syntheses; of particular interest was their potential use in the synthesis of α-monofluoroalkanoic acids (5). While this work was in progress, parallel studies using perchloryl fluoride were continuing, with α-monofluoroalkanoic acids again as the main goal (5). The two methods are complementary, in that they permit the introduction of the fluorine atom at centers of low electron density (bromonium ion) and high electron density (carbanion) respectively. Prior to this work, the only common aliphatic vicinal fluorohalides were those derived from ethane. Of these, 1-bromo-2-fluoroethane had been reported by Schrader (6) to be formed by the direct addition of "BrF" (using a mixture of bromine and fluorine) to ethylene; the present work may thus be considered as a refinement of this original procedure.

$$RCH{=}CH_2 + CH_3C\overset{+}{O}NH_2Br \rightarrow RCH\underset{\diagdown\,+\,\diagup}{\overset{\diagup\ \ \diagdown}{}}\begin{matrix}Br\\ \\ CH_2\end{matrix} + CH_3CONH_2$$

I

$$RCH\underset{\diagdown\,+\,\diagup}{\overset{\diagup\ \ \diagdown}{}}\begin{matrix}Br\\ \\ CH_2\end{matrix} + HF \rightarrow RCHFCH_2Br + H^+$$

1-Alkenes of medium chain length on treatment with a molar quantity of *N*-bromoacetamide and excess anhydrous hydrogen fluoride in ether gave the expected products in good yield (70–80%), with small amounts of isomeric 2-bromo-1-fluoroalkanes. The structures of the major products were shown to be the 1-bromo-2-fluoroalkanes by nuclear magnetic resonance (n.m.r.) spectroscopy and by their conversion in high yield to the corresponding α-monofluoroalkanoic acids (5). The minor products were isolated in only a few instances (for example, in the addition to allyl bromide); they proved to be the anti-Markovnikov isomers. The minor product was usually not removed from the mixture, because it was destroyed or removed in many of the subsequent reactions. Yields are shown in Table I.

[1]*This paper was presented in part at the Second International Symposium on Fluorine Chemistry, Estes Park, Colorado, July 17–20, 1962 (1).*
[2]*Present address: Department of Chemistry, University of Delaware, Newark, Delaware.*

Can. J. Chem. Downloaded from www.nrcresearchpress.com by 210.87.254.42 on 09/05/12
For personal use only.

The most satisfactory general technique involved the addition of *N*-bromoacetamide and the alkene, alternately and in small portions, to a cooled (−80°) solution of anhydrous hydrogen fluoride in ether. Some variations were examined briefly. (*a*) *The nature of the bromine source.* Three reagents were tried, *N*-bromoacetamide (NBA), 1,3-dibromo-5,5-dimethylhydantoin (DBH), and 1-bromo-3,5,5-trimethylhydantoin (BTH). All gave approximately the same yields. However, the higher solubility of the hydantoins in the reaction medium permitted a simpler method of adding the reagents. (*b*) *The addition of reagents.* NBA was insoluble in the cold ether solution, but DBH and BTH were sufficiently soluble to be added in one portion prior to the dropwise addition of the alkene. The yields were comparable when the alkene was added in its entirety and the brominating agent was added in portions. Moreover, the yield was only slightly diminished when both the brominating agent and the alkene were added in one portion at the start of the reaction. In short, for maximum yield, alternate portionwise addition is recommended, whereas for maximum simplicity, addition of all reagents to the ether solution is preferred. (*c*) *Solvent.* Ether was found to be satisfactory in most instances. For ethylene, however, methylene dichloride, at a reaction temperature of −30°, proved to be the most effective solvent. 1-Butene gave the fluorobromide in chloroform or in ether–chloroform. In general, a mixture of solvents (such as an ether and a halogenoalkane) is likely to be most generally satisfactory.

The alkene component was varied in order to examine the versatility of the reaction. (*a*) Gases were found to react normally, but in lower yield; ethylene, propylene, and 1-butene thus gave the expected products in 25–50% yield. (*b*) Higher molecular weight alkenes could also be used; 1-decene gave a 78% yield of 1-bromo-2-fluorodecane. 1-Octadecene reacted more slowly, because of its low solubility in the reaction medium; the resultant mixture of product and starting material was used directly in subsequent steps. (*c*) Branched alkenes reacted in lower yield; for example, 2-ethyl-1-butene gave 1-bromo-2-fluoro-2-ethylbutane (56%). (*d*) The highly reactive alkene styrene gave a poor (25%) yield of the adduct by the usual process; much polymeric material was formed. When some pyridine was added to increase the concentration of fluoride ion, the yield of styrene fluorobromide was more than doubled. The designation of the product as 1-bromo-2-fluoro-2-phenylethane is consistent with the observations of Buckles and Knaack (7) on the mode of addition of iodine monochloride to styrene. Stilbene also reacted normally in low yield. (*e*) The presence of other functional groups seemed to have no effect on the addition reaction; for example, methyl 10-undecenoate gave methyl 11-bromo-10-fluoroundecanoate in 71% yield. The addition to acrylates, to allyl esters, and to bridged bicyclic systems (with concomitant Wagner–Meerwein rearrangement) will be described in later communications.

Allyl bromide was expected to form 1,3-dibromo-2-fluoropropane (II) as the predominant product by the usual Markovnikov addition mechanism. It was found, however, that the anti-Markovnikov adduct 1,2-dibromo-3-fluoropropane (III) was formed in 32% yield, while the yield of the Markovnikov adduct II was only 22%.

$BrCH_2CHFCH_2Br$ II

$BrCH_2CHBrCH_2F$ III

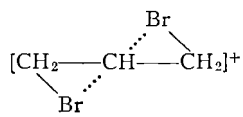

IV

Anomalous product ratios have been observed by de la Mare and co-workers in studies of the addition of hypochlorous acid to allyl halides (8, 9, 10). The products in the present

work may be explained by postulating that the reaction proceeds through the symmetrical bromonium ion IV (8). The major product would then arise from nucleophilic attack by fluoride ion on the more plentiful, exposed primary carbon atoms. Simple steric effects may also be involved.

Some side reactions were observed. Ether formation occurred in some reactions. For example, a bromoethoxyheptane was isolated from the addition reaction with 1-heptene; this is probably formed by partial hydrolysis of solvent ether to ethanol, which in turn reacts with the bromonium ion intermediate (I). Other side reactions included the addition of the elements of *N*-bromoacetamide to the double bond and proton elimination from the bromonium ion intermediate; both these reactions were observed principally in the addition to bridged bicyclic systems, and will be described in a later paper.

The aliphatic vicinal fluorobromides are colorless, mobile liquids possessing odors similar to those of the corresponding alkyl bromides. They are nontoxic, indicating that they are not metabolized to fluoroacetic acid; for example, both 1-iodo-2-fluorohexane and 2-fluoro-1-hexanol had $LD_{50} > 107$ mg/kg (intraperitoneal injection into mice). They boil at a higher temperature, have greater densities, and have lower refractive indices than the corresponding alkyl bromides (Table II). They normally exhibit a C—F band in the infrared at 1 010 – 1 016 cm^{-1}. Most of the vicinal fluorobromides are stable when stored in sealed glass ampoules at room temperature, but some, for example styrene fluorobromide and *trans*-1-bromo-2-fluorocyclohexane, showed a marked tendency to decompose; this could be due to autocatalysis by small amounts of hydrogen fluoride formed during the sealing process.

The reactivity of 1-bromo-2-fluoroalkanes towards nucleophilic reagents was expected to be less than that of *n*-alkyl bromides; thus, Hine (11, 12) has found that 1-bromo-2-fluoroethane reacts only one-eighth as rapidly as ethyl bromide with the thiophenoxide ion. In a series of scouting reactions, it was found that the 1-bromo-2-fluoroalkanes underwent nucleophilic substitutions under conditions which were more vigorous than those one might normally use for *n*-alkyl bromides. By this means one or more members (Table II) of the following classes of 2-fluoroalkyl derivatives were prepared (reagents in brackets): acetates (sodium acetate plus sodium iodide in dry dimethylformamide), azides (sodium azide in aqueous dimethylformamide), iodides (sodium iodide in acetone), formates (sodium formate plus sodium iodide in dry dimethylformamide), nitrates (silver nitrate in acetonitrile), thiocyanates (potassium thiocyanate in ethanol), *p*-nitrobenzoates (lithium *p*-nitrobenzoate in dry dimethylformamide), and tosylates (silver tosylate in acetonitrile). When treated with sodium cyanide in dimethyl sulfoxide, 1-bromo-2-fluorohexane gave 1,2-dicyanohexane rather than the expected 3-fluoroheptanonitrile; the analogous reaction of 1-bromo-2-fluoroethane to yield succinodinitrile has been reported by Mirosevic-Sorgo and Saunders (13). 1-Iodo-2-fluorohexane did not alkylate the dimethyl malonate anion. In a study of the reductive elimination of 1,2-dihalides with lithium aluminium hydride, King and Pews (14) have reported that *erythro*-1-bromo-2-fluoro-1,2-diphenylethane formed *trans*-stilbene in 86% yield, whereas *trans*-1-bromo-2-fluorocyclohexane (3) formed fluorocyclohexane in 45% yield.

The acetates (and, to a lesser extent, the nitrates and formates) were important intermediates in a general route to α-monofluoroalkanoic acids; this is probably the most valuable application of the work (5). The nitrates were readily hydrogenolyzed using platinum in ethanol to the corresponding 2-fluoro-1-alkanols, $RCHFCH_2OH$; this affords a convenient route to these hitherto inaccessible fluoroalcohols. (Most common procedures, such as opening of epoxides with hydrogen fluoride (15), yield the isomeric

Can. J. Chem. Downloaded from www.nrcresearchpress.com by 210.87.254.42 on 09/05/12
For personal use only.

Can. J. Chem. Downloaded from www.nrcresearchpress.com by 210.87.254.42 on 09/05/12
For personal use only.

TABLE I

Yields of vicinal fluorobromides

Alkene	Scale* (moles)	Solvent†	Molar ratio HF:alkene	% HF in solvent (w/w)	Product‡	Yield§ (%)
$CH_2{=}CH_2$	0.72	CH_2Cl_2	5.0	21	FCH_2CH_2Br	23‖
$CH_3CH{=}CH_2$	1.00*	CH_2Cl_2	5.0	18	CH_3CHFCH_2Br	38‖
$CH_3CH_2CH{=}CH_2$	0.35	$CHCl_3$ (68) – ether (32)	5.6	18	$CH_3CH_2CHFCH_2Br$	55‖
$CH_3(CH_2)_3CH{=}CH_2$	0.50	Et_2O	12.8	43	$CH_3(CH_2)_3CHFCH_2Br$	79
$CH_3(CH_2)_4CH{=}CH_2$	0.79	Et_2O	9.4	41	$CH_3(CH_2)_4CHFCH_2Br$	77
$CH_3(CH_2)_5CH{=}CH_2$	0.75	Et_2O	9.3	40	$CH_3(CH_2)_5CHFCH_2Br$	70
$CH_3(CH_2)_7CH{=}CH_2$	0.69	Et_2O	10.1	40	$CH_3(CH_2)_7CHFCH_2Br$	78
$CH_3(CH_2)_{15}CH{=}CH_2$	0.17	Et_2O (62) – dioxane (38)	33.6	12	$CH_3(CH_2)_{15}CHFCH_2Br$	—¶
$CH_3CH_2CEt{=}CH_2$	0.40	Et_2O	10.6	38	$CH_3CH_2CEtFCH_2Br$	56
$C_6H_5CH{=}CH_2$	0.21	Et_2O	22.7	40	$C_6H_5CHFCH_2Br$	25
$C_6H_5CH{=}CH_2$	0.42	Et_2O (79) – pyridine (21)**	13.4	20	$C_6H_5CHFCH_2Br$	68
$C_6H_5CH{=}CHC_6H_5$	0.02	THF	45.0	30	$C_6H_5CHFCHBrC_6H_5$	25
$CH_2{=}CHCH_2Br$	0.25	Et_2O	7.8	35	$BrCH_2CHFCH_2Br$ (II)	22
					$FCH_2CHBrCH_2Br$ (III)	32
$CH_2{=}CH(CH_2)_8COOMe$	0.35*	$CHCl_3$	7.2	14	$BrCH_2CHF(CH_2)_8COOMe$	72

*The figures shown are for the alkenes; the brominating agent was used in approximately equimolar quantities. *N*-Bromoacetamide was used in all reactions except those of propylene and methyl 10-undecenoate, when 1,3-dibromo-5,5-dimethylhydantoin was the bromine source.
†Ether was the most commonly used solvent, either alone or in combination.
‡The compound listed is the major product.
§The yield represents the total purified mixture of the two fluorobromide isomers; the minor (anti-Markovnikov) isomer amounted to some 3–8% of the total sample (g.l.c. analyses).
‖Yield is based on brominating agent.
¶Crude mixture of unreacted alkene and fluorobromide was used without purification.
**A total of 1.5 moles of pyridine was used (see Experimental).

Can. J. Chem. Downloaded from www.nrcresearchpress.com by 210.87.254.42 on 09/05/12
For personal use only.

1-fluoro-2-alkanols, $RCH(OH)CH_2F$.) An even simpler, direct procedure for converting the 1-bromo-2-fluoroalkanes to 2-fluoro-1-alkanols involved the use of sodium formate in hot aqueous dimethylformamide; thus, 2-fluoro-1-hexanol of high purity was obtained in 75% yield.

Because the crude 2-fluorooctadecyl acetate was a greasy, low-melting solid, a more satisfactory crystalline derivative was required for analysis and for conversion to 2-fluorooctadecanoic acid. The *p*-nitrobenzoate was therefore prepared in fair yield. Since nitrobenzoate esters are known to be resistant to acid hydrolysis (16), the *p*-aminobenzoate was prepared in excellent yield using Adams' catalyst.

Vicinal fluorobromides and fluoroiodides were entirely resistant to hydrogenolysis at room temperature and atmospheric pressure using platinum as catalyst; under the same conditions, vicinal dibromides were readily dehalogenated to the corresponding alkanes. For example, *trans*-1-bromo-2-fluorocyclohexane (3) failed to react under conditions that resulted in the ready conversion of *trans*-1,2-dibromocyclohexane to cyclohexane. This difference in reactivity was used to isolate pure 1,3-dibromo-2-fluoropropane (II) from its mixture with 1,2-dibromo-3-fluoropropane (III); the latter, containing a vicinal dibromide grouping, was destroyed by hydrogenation whereas the former was recovered unchanged. The facile hydrogenolysis of benzylic fluorides is well known; even the relatively stable *gem*-difluoro grouping may be reduced if it lies adjacent to a benzene ring (17). Consequently hydrogenolysis of 2-fluoro-2-phenylethyl nitrate yielded only 2-phenylethanol; similarly, styrene fluorobromide gave ethylbenzene. In this latter case, the β-fluorine atom cannot exert its "protecting" action over the bromine atom because, being labile itself, it is easily removed.

EXPERIMENTAL

Physical constants and analytical data for all new compounds are given in Table II. The preparations described below represent typical examples of each procedure; obvious variations for obtaining different members have not been included. Melting points (uncorrected) were determined on a Kofler hot stage, and densities with a Fisher-Davidson gravitometer. The nuclear magnetic resonance spectra were obtained with a Varian DP-60 spectrometer. Infrared spectra were obtained with Beckman IR-7 and IR-5 infrared spectrophotometers. Analyses were performed by the Schwarzkopf Microanalytical Laboratory, Woodside, 77, N.Y. Most of the alkenes were purchased from Humphrey-Wilkinson, Inc., Devine Street, North Haven, Conn. Other reactants were obtained from standard commercial sources. Fractionations were carried out using a 23-plate platinum-plated spinning-band column.

A. Preparation of Vicinal Fluorobromides

1-Bromo-2-fluorohexane

Anhydrous hydrogen fluoride (129.7 g, 6.49 moles) was condensed into a 500 ml polythene bottle cooled in dry ice. Cold (−80°) dry ether (240 ml) was added with magnetic stirring. *N*-Bromoacetamide (69.0 g, 0.50 mole) and 1-hexene (42.5 g, 0.505 mole) were added portionwise and alternately over 27 min, with cooling (−80°) and stirring. The NBA dissolved as it was added. The mixture was stirred for 2 h at −80° and then was allowed to stand overnight at this temperature. The resultant solution was neutralized by being poured slowly into a mixture of sodium carbonate (690 g), water (1 200 ml), ice (500 g), and ether (300 ml). The ether layer was separated and the aqueous layer was extracted with ether. The combined ether extracts were washed with water, treated with nitrous acid to destroy residual acetamide, and then washed with aqueous sodium carbonate and with water until neutral. After drying ($MgSO_4$) and removal of the ether, the resultant amber-colored liquid was fractionated to yield 71.8 g (79%) of 1-bromo-2-fluorohexane. Gas–liquid chromatography (g.l.c.) analysis (DEGS column, 158°) indicated 95 mole % of the main product and 5 mole % of 2-bromo-1-fluorohexane. The infrared spectrum ($CHCl_3$) showed a C—F band at 1 010 and 1 124 cm^{-1}. The n.m.r. spectrum (CCl_4) indicated a $—CH_2Br$ group (doublet of doublets centered at 3.39 p.p.m., J_{HF} 17.4 c/s, J_{HH} 5.6 c/s) and a −CHF group (two widely separated multiplets centered at 4.55 p.p.m., J_{HF} 46.8 c/s).

Variations in Procedure

1,3-Dibromo-5,5-dimethylhydantoin (DBH) and 1-bromo-3,5,5-trimethylhydantoin (BTH) gave results similar to those obtained with NBA. The three following variations in procedure (using DBH as the Br source) were simpler than the above portionwise addition, but gave lower yields.

Can. J. Chem. Downloaded from www.nrcresearchpress.com by 210.87.254.42 on 09/05/12
For personal use only.

TABLE II

Physical constants and analytical results

Compound	Formula	Boiling point (°C)	Boiling point (mm)	n_D^{25} or m.p.(°C)	d_4^{20}	MR_D Estimated	MR_D Found	Analytical results: C (%) Calcd.	C (%) Found	H (%) Calcd.	H (%) Found	Other (%) Calcd.	Other (%) Found
1. Fluorobromides													
1-Bromo-2-fluoroethane*	FCH_2CH_2Br	71.5	754	1.4227	1.668	18.94	19.35						
1-Bromo-2-fluoropropane	CH_3CHFCH_2Br	88.5	740	1.4213	1.506	23.59	23.73	25.56	25.71	4.29	4.11		
1-Bromo-2-fluorobutane	$CH_3CH_2CHFCH_2Br$	113	758	1.4288	1.410	28.24	28.40	30.99	30.97	5.20	5.17	Br, 51.55	Br, 51.43
1-Bromo-2-fluorohexane	$CH_3(CH_2)_3CHFCH_2Br$	62	18	1.4368	1.287	37.44	37.40	39.36	39.57	6.61	6.64		
1-Bromo-2-fluoroheptane	$CH_3(CH_2)_4CHFCH_2Br$	77	18	1.4395	1.238	42.05	42.09	42.65	42.89	7.16	7.15		
1-Bromo-2-fluorooctane	$CH_3(CH_2)_5CHFCH_2Br$	90	16	1.4423	1.198	46.75	46.80	45.51	45.72	7.64	7.66		
1-Bromo-2-fluorodecane	$CH_3(CH_2)_7CHFCH_2Br$	70	0.72	1.4467	1.136	56.19	56.44	50.22	50.36	8.43	8.48		
1-Bromo-2-fluoro-2-ethylbutane	$CH_3CH_2CEtFCH_2Br$	38	11	1.4391	1.293	37.44	37.40	39.36	39.52	6.61	6.71		
1-Bromo-2-fluoro-2-phenylethane	$C_6H_5CHFCH_2Br$	53	0.05	1.5411	1.468	43.64	43.60	47.32	47.45	3.97	3.98		
1-Bromo-2-fluoro-1,2-diphenylethane	$C_6H_5CHFCHBrC_6H_5$	—	—	106.5–107.5	—	—	—	60.23	60.44	4.33	4.53	Br, 28.63	Br, 28.65
1,3-Dibromo-2-fluoropropane(II)	$BrCH_2CHFCH_2Br$	96	74	1.5026	2.083	31.20	31.20	16.38	16.71	2.29	2.40		
1,2-Dibromo-3-fluoropropane(III)†	$FCH_2CHBrCH_2Br$	—	—	1.5097	—	—	—	16.38	16.64	2.29	2.40	Br, 72.68	Br, 72.44
Methyl 11-bromo-10-fluoroundecanoate	$BrCH_2CHF(CH_2)_8COOMe$	120	0.30	1.4587	1.217	67.01	66.88	48.49	48.57	7.46	7.35	Br, 26.89	Br, 26.73
2. Fluorinated products obtained from fluorobromides													
2-Fluoroethyl acetate‡	FCH_2CH_2OAc	118	745	1.3756	1.086	22.11	22.51						
2-Fluoropropyl acetate	CH_3CHFCH_2OAc	128.5	755	1.3806	1.029	26.76	27.07	49.99	50.22	7.55	7.51		
2-Fluorobutyl acetate	$CH_3CH_2CHFCH_2OAc$	147	761	1.3893	0.998	31.41	31.87	53.72	53.67	8.27	8.15		
2-Fluorohexyl acetate	$CH_3(CH_2)_3CHFCH_2OAc$	74	13	1.4034	0.970	40.51	41.02	59.24	59.46	9.32	9.21		
2-Fluoroheptyl acetate	$CH_3(CH_2)_4CHFCH_2OAc$	87	11	1.4086	0.958	45.20	45.63	61.33	61.51	9.73	9.64		
2-Fluorooctyl acetate	$CH_3(CH_2)_5CHFCH_2OAc$	99	11	1.4134	0.948	49.91	50.30	63.13	62.91	10.07	10.03		

Can. J. Chem. Downloaded from www.nrcresearchpress.com by 210.87.254.42 on 09/05/12
For personal use only.

TABLE II (*Concluded*)

Compound	Formula	Boiling point (°C)	Boiling point (mm)	n_D^{25} or m.p.(°C)	d_4^{20}	MR_D Estimated	MR_D Found	Analytical results: C (%) Calcd.	C (%) Found	H (%) Calcd.	H (%) Found	Other (%) Calcd.	Other (%) Found
2-Fluorodecyl acetate	$CH_3(CH_2)_7CHFCH_2OAc$	75	0.5	1.4210	0.932	59.55	59.65	66.02	66.15	10.62	10.78		
Methyl 11-acetoxy-10-fluoroundecanoate	$AcOCH_2CHF(CH_2)_8COOMe$	125	0.25	1.4383	1.029	70.19	70.40	60.85	61.01	9.12	9.24		
2-Fluoro-1-hexanol	$CH_3(CH_2)_3CHFCH_2OH$	66	14	1.4065	0.946	31.39	31.37	59.97	59.81	10.90	10.75		
2-Fluoro-1-heptanol	$CH_3(CH_2)_4CHFCH_2OH$	77	8	1.4135	0.932	36.04	36.10	62.65	62.90	11.27	11.28		
2-Fluorohexyl azide	$CH_3(CH_2)_3CHFCH_2N_3$	93	52	1.4248	0.984	37.40	37.88	49.63	49.92	8.27	8.34	N, 28.94	N, 28.80
2-Fluorohexyl iodide	$CH_3(CH_2)_3CHFCH_2I$	75	16	1.4788	1.531	42.62	42.65	31.32	31.56	5.26	5.22	I, 55.16	I, 55.47
2-Fluorodecyl iodide	$CH_3(CH_2)_7CHFCH_2I$	67	0.1	1.4754	1.323	61.12	61.32	41.97	42.00	7.05	6.93		
2-Fluorohexyl formate	$CH_3(CH_2)_3CHFCH_2OCHO$	81	27	1.4022	0.996	36.00	36.40	56.74	57.00	8.78	8.94		
2-Fluoroheptyl formate	$CH_3(CH_2)_4CHFCH_2OCHO$	78	9	1.4082	0.977	40.58	40.71	59.24	59.49	9.32	9.22		
2-Fluorohexyl nitrate	$CH_3(CH_2)_3CHFCH_2ONO_2$	83	14.5	1.4130	1.100	37.86	37.63	43.63	43.50	7.33	7.37	N, 8.48	N, 8.39
2-Fluoro-2-phenylethyl nitrate	$C_6H_6CHFCH_2ONO_2$	56	0.05	1.5030	1.263	43.80	43.50	51.89	52.10	4.35	4.57	N, 7.57	N, 7.60
2-Fluorohexyl thiocyanate§	$CH_3(CH_2)_3CHFCH_2SCN$	71	0.4	1.4563	1.040	42.19	42.32	52.14	52.28	7.50	7.41	N, 8.69	N, 8.83
2-Fluorooctadecyl *p*-nitrobenzoate	$CH_3(CH_2)_{16}CHFCH_2OCOC_6H_4NO_2$	—	—	68–70	—	—	—	68.62	68.70	9.21	9.35		
2-Fluorooctadecyl *p*-aminobenzoate	$CH_3(CH_2)_{16}CHFCH_2OCOC_6H_4NH_2$	—	—	87–89	—	—	—	73.66	73.63	10.39	10.39		
1,3-Bistosyloxy-2-fluoropropane‖	$TsOCH_2CHFCH_2OTs$	—	—	111–112	—	—	—	50.73	50.61	4.76	4.66	S, 15.93	S, 16.11
3. Miscellaneous compounds													
1,2-Dicyanohexane	$CH_3(CH_2)_3CH(CN)CH_2CN$	90	0.12	1.4380	0.925	39.13	38.78	70.54	70.45	8.88	8.74	N, 20.57	N, 20.57
1-Bromo-2-ethoxyheptane	$CH_3(CH_2)_4CH(OEt)CH_2Br$	38	0.17	1.4483	1.122	53.35	53.48	48.44	48.63	8.58	8.77		

*Pattison and Howell (20) report b.p. 70–71° at 745 mm, n_D^{25} 1.4236.
†Hoffmann (18) reports n_D^{23} 1.5092.
‡Millington and Pattison (21) report b.p. 116–117.5° at 740 mm, n_D^{25} 1.3784.
§Moderately toxic: LD_{50} 26.6 mg/kg (95% fiducial limits: 19.4–36.6 mg/kg) by intraperitoneal injection into mice.
‖Taylor and Kent (19) report m.p. 109°. The compound was shown to be nontoxic (LD_{50} > 100 mg/kg by intraperitoneal injection into mice).

(a) Alkene added dropwise.—Using 1-hexene (14.7 g, 0.175 mole), DBH (25.0 g, 0.0875 mole), hydrogen fluoride (45.0 g, 2.25 moles) in ether (50 ml), and carbon tetrachloride (50 ml), the alkene was added dropwise to the vigorously stirred mixture of the other components at −30° over 90 min. Yield: 64%.

(b) DBH added portionwise.—Using the same quantities as in (*a*), the DBH was added in 10 portions to the vigorously stirred mixture of the other components at −30° over 90 min. Yield: 66%.

(c) All reactants added together.—All the above reactants were mixed at the start of the reaction and were stirred for 4 h at −30°. Yield: 64%.

Variations in Alkene Component: Representative Procedures

(a) Ethylene.—Ethylene (20.2 g, 0.72 mole) was passed slowly through a stirred mixture of NBA (50.0 g, 0.36 mole), hydrogen fluoride (72.0 g, 3.6 moles), and methylene chloride (200 ml) at −40° to −20° for 5 h. The temperature should not rise above −20° before the neutralization step. Yield of 1-bromo-2-fluoroethane: 23%. Use of ether as solvent or too high a temperature before neutralization results in a negligible yield of product. A reaction using double quantities of reactants gave the same overall yield (23%).

(b) 1-Butene.—1-Butene (25.0 g, 0.45 mole) was passed into a stirred mixture of NBA (48.0 g, 0.35 mole), hydrogen fluoride (50.0 g, 2.5 moles) in chloroform (100 ml) and ether (100 ml) at −60° to −30° for 3.5 h. Yield of 1-bromo-2-fluorobutane: 55%.

(c) 1-Octadecene.—To anhydrous hydrogen fluoride (117 g, 5.85 moles), ether (725 ml), and dioxane (300 ml) in a half-gallon polythene bottle were added 1-octadecene (44 g, 0.174 mole) and NBA (23.1 g, 0.168 mole) alternately and in small portions over 15 min at −80°. The alkene solidified and floated on the surface; even at 0° it had not all dissolved. The tightly capped bottle was placed in a refrigerator for 17 h, at the end of which time the mixture was colorless and homogeneous. The usual isolation procedure gave the crude bromide as a greasy, pale-yellow solid (60.4 g) which was used directly without purification.

(d) 2-Ethyl-1-butene.—1-Bromo-2-fluoro-2-ethylbutane was prepared in the usual way from 2-ethyl-1-butene (34.0 g, 0.40 mole), NBA (57.5 g, 0.42 mole), anhydrous hydrogen fluoride (86.0 g, 4.30 moles) in ether (200 ml). The mixture was neutralized with potassium bicarbonate (208 g) and potassium carbonate (330 g) to minimize the risk of elimination from the tertiary fluoride. Treatment with nitrous acid removed traces of acetamide. Yield of fluorobromide: 56%.

(e) Styrene.—The usual method gave only 25% of the desired product; much polymeric material was formed. The following modified procedure gave a yield of 68%. In a half-gallon polythene bottle were placed anhydrous hydrogen fluoride (113 g, 5.65 moles) and ether (340 ml). With cooling (−80°) and magnetic stirring, a solution of pyridine (120.5 g, 1.5 moles) in ether (300 ml) was slowly added. The resultant pyridine hydrofluoride crystallized at −80° making magnetic stirring impossible. The mixture was stirred vigorously out of the cooling bath, and styrene (44 g, 0.42 mole) and NBA (59.5 g, 0.43 mole) were added alternately over 30 min. The mixture was cooled to −80° for 1 h and refrigerated at 8° overnight. Isolation and purification gave the required product (68%).

(f) trans-Stilbene.—The reaction was carried out in the usual way, using tetrahydrofuran as solvent. The product was isolated from the neutralized mixture by extraction with chloroform. Removal of the solvent and evaporation of the residue at 100° at 0.1 mm gave colorless needles. These were dissolved in benzene and chromatographed on silica gel. The first fraction on evaporation gave an oil which solidified. Recrystallization from 60–80° petroleum ether gave colorless needles of the pure product (25%); no C=C stretching vibration (ca. 1 600 cm^{-1}) or *trans* out-of-plane deformation (960 cm^{-1}) was observed in the infrared.

(g) Allyl bromide.—The reaction was carried out in the usual manner from 30.4 g (0.25 mole) of allyl bromide; reaction did not occur at −80° but was complete in 25 min at −20°. Further cooling and stirring, followed by isolation and fractionation gave 31.5 g of a colorless liquid of b.p. 69–73° at 3 mm. Gas–liquid chromatographic analysis on a Perkin–Elmer Vapor Fractometer (Model 134), using a polypropylene glycol 550 analytical column, showed that this liquid consisted of two major components (94% of total), both of which were shown to be dibromofluoropropanes by elemental analysis and molecular refractivity of the mixture (MR_D 31.38 cc/mole, estimated 31.20 cc/mole). Gas chromatography at 120°, with a flow rate of 80 ml/min of helium, gave retention times of 20 and 26 min and allowed collection of the pure components; to obtain satisfactory resolution, no more than 30 μl of liquid were injected at any one time. The pure components had n_D^{25} 1.5097 and n_D^{25} 1.5026 respectively, corresponding to 1,2-dibromo-3-fluoropropane (III) and 1,3-dibromo-2-fluoropropane (II); Hoffmann (18) reports n_D^{23} 1.5092 for III. Pure II was isolated in larger amounts by hydrogenolytic removal of III from the mixture of II and III, followed by fractionation (see below); the formation of the bis-tosyloxy derivative (q.v.) confirms the presence of II in the original mixture. The overall yields of II and III were 22% and 32% respectively.

(h) Methyl 10-undecenoate.—The ester (69.3 g, 0.35 mole) was added in portions over 10 min to a stirred mixture of DBH (50 g, 0.175 mole), anhydrous hydrogen fluoride (50 g, 2.5 moles), and chloroform (200 ml) at −55°. The mixture was stirred at −40° for a further 3 h. Isolation and fractionation gave the pure saturated ester (72%). An identical yield was obtained using NBA (49 g, 0.35 mole) in chloroform (200 ml) and ether (100 ml).

Side Reactions

The principal side reaction occurring in the addition to simple alkenes involved the formation of ethers (see Discussion). In the preparation of 1-bromo-2-fluoroheptane, a higher boiling fraction was obtained,

Can. J. Chem. Downloaded from www.nrcresearchpress.com by 210.87.254.42 on 09/05/12
For personal use only.

which was purified by preparative gas chromatography (Nester and Faust Prepko at 210° using a 1 in. × 6 ft column of 20% DEGS on 60/80 mesh firebrick with helium (600 ml/min) as carrier); the fraction (ca. 2 g) eluting in 1.7 min was distilled through a spinning-band column to give a bromoethoxyheptane. Its infrared spectrum (CCl_4) was very simple, the main feature being a strong band at 1 106 cm^{-1} (C—O stretch). The n.m.r. spectrum was too complex to permit an assignment of the location of the bromine and ethoxy groups.

B. Reactions of Vicinal Fluorobromides

2-Fluoro-1-hexanol

A mixture of 1-bromo-2-fluorohexane (8.0 g, 43.7 mmoles), sodium formate (5.0 g, 73.5 mmoles), dimethylformamide (50 ml), water (16.6 ml), and tetrahydrofuran (25 ml) was heated under reflux at 130° for 31 h. The cooled mixture was diluted with water (100 ml) and extracted with ether. The extracts were washed with water, with aqueous sodium bicarbonate, and with water again. The dried (Na_2SO_4) solvent-free product gave an infrared spectrum which showed the presence of some formate ester. Hence the product was hydrolyzed by refluxing at 105° for 19 h with water (8 g). Isolation in the usual way gave the pure fluoroalcohol (3.95 g, 75%).

2-Fluorohexyl Acetate

1-Bromo-2-fluorohexane (10.0 g, 54.6 mmoles) was stirred and refluxed with dry sodium acetate (7.0 g, 84.4 mmoles) and sodium iodide (10 g, 66.7 mmoles) in dry dimethylformamide (300 ml) at 130° for 25 h. The cooled mixture was diluted with water and extracted with ether. The extracts were washed, dried, and fractionated to give the pure acetate (6.22 g, 70%).

The following were prepared in essentially the same way (yields in brackets): *2-fluoroethyl acetate* (52%), *2-fluoropropyl acetate* (79%), *2-fluorobutyl acetate* (85%), *2-fluoroheptyl acetate* (78%), *2-fluorooctyl acetate* (71%), and *2-fluorodecyl acetate* (73%). Also prepared by the same method was *methyl 11-acetoxy-10-fluoroundecanoate* (74%) starting from methyl 11-bromo-10-fluoroundecanoate.

2-Fluorohexyl Azide

1-Bromo-2-fluorohexane (14.3 g, 78.2 mmoles) and sodium azide (7.1 g, 109 mmoles) were stirred and heated under reflux in 87% aqueous dimethylformamide (160 ml) for 23 h at 130°. Isolation by ether extraction and purification in the usual way gave the azide (9.52 g, 84%).

2-Fluorohexyl Iodide

1-Bromo-2-fluorohexane (10 g, 54.6 mmoles), sodium iodide (9.5 g, 63.2 mmoles), and acetone (50 ml) were heated under reflux for 22 h. Isolation and purification in the usual manner gave the iodide (10.8 g, 86%). Redistillation from mercury gave a stable liquid, which remained colorless on storing over clean, dry copper turnings in a brown bottle.

2-Fluorodecyl iodide was prepared by the same procedure in 72% yield.

2-Fluorohexyl Formate

1-Bromo-2-fluorohexane (10 g, 54.6 mmoles) was stirred with a suspension of dry sodium formate (6.8 g, 100 mmoles) and sodium iodide (9.0 g, 60 mmoles) in dimethylformamide (300 ml). The mixture, protected from atmospheric moisture, was heated under reflux at 103–105° for 48 h. Isolation and purification in the usual way gave the formate (5.4 g, 67%).

2-Fluoroheptyl formate was prepared in the same way in 77% yield.

Hydrolysis of 2-Fluoroheptyl Formate

2-Fluoroheptyl formate (7.76 g, 52.4 mmoles), 6 *N* hydrochloric acid (35 ml), and dioxane (40 ml) were stirred magnetically at room temperature. The mixture became homogeneous after 40 min, and g.l.c. analysis indicated that only 8% of the formate remained after 4 h. The stirring was continued for 6 h more, and the product was isolated in the usual way. The yield of 2-fluoro-1-heptanol was 5.66 g (81%). The hydrogen n.m.r. spectrum (30.7 w/v % in CCl_4) showed peaks at 0.91 and 1.35 p.p.m. due to the terminal methyl and to the methylene groups respectively; the OH appeared at 3.98 p.p.m. The CH_2OH appeared as a doublet of doublets centered at 3.57 p.p.m. with J_{HF} 24.1, J_{HH} 4.8 c.p.s. The CHF group appeared as a pair of multiplets centered at 4.43 p.p.m. (J_{HF} 51.6 c.p.s.).

2-Fluorohexyl Nitrate

1-Bromo-2-fluorohexane (10 g, 54.6 mmoles) and silver nitrate (12.3 g, 72.4 mmoles) were dissolved in acetonitrile (50 ml), and the solution was heated under reflux at 120° for 27 h. (After 5 h, only 72% of the theoretical amount of silver bromide had been formed.) Isolation and purification gave the pure nitrate (7.54 g, 84%).

2-Fluoro-2-phenylethyl nitrate was prepared in 76% yield from 1-bromo-2-fluoro-2-phenylethane by the same procedure; the first sample for analysis decomposed before reaching its destination, emphasizing its instability.

2-Fluorohexyl Thiocyanate

1-Bromo-2-fluorohexane (7.0 g, 38.2 mmoles), potassium thiocyanate (7.0 g, 72.0 mmoles), and 95% ethanol (25 ml) were heated under reflux at 110° for 20 h. Isolation and purification in the usual way gave

Can. J. Chem. Downloaded from www.nrcresearchpress.com by 210.87.254.42 on 09/05/12
For personal use only.

the thiocyanate (4.42 g, 72%). This compound is moderately toxic to mice by intraperitoneal injection; LD_{50} 26.63 (19.43–36.57) mg/kg.

2-Fluorooctadecyl p-Nitrobenzoate

Lithium *p*-nitrobenzoate was prepared from a suspension of the acid in methanol by neutralization with aqueous lithium hydroxide. Concentration to small bulk and addition of ether induced the salt to crystallize. Yield: 98%. Crude 1-bromo-2-fluorooctadecane (see above) (15.68 g, 44.7 mmoles), dry lithium *p*-nitrobenzoate (13.4 g, 77.4 mmoles), sodium iodide (8.0 g, 53.4 mmoles), and dimethylformamide (500 ml) were mixed, and *p*-nitrobenzoyl chloride (27.8 g, 149.5 mmoles) was added as a scavenger for water. The solution was refluxed with stirring at 115° for 40 h. A further 7.5 g (43.3 mmoles) of lithium *p*-nitrobenzoate was added, and the heating was continued for a further 31 h. Isolation by ether extraction, washing and drying of the extract, and removal of the solvent gave an oil which crystallized on desiccation at 0.5 mm over P_2O_5. Slow crystallization from ethanol–ligroin (35–60°) followed by recrystallization from 95% ethanol gave 10.6 g (55%) of the ester.

2-Fluorooctadecyl p-Aminobenzoate

2-Fluorooctadecyl *p*-nitrobenzoate (4.6 g, 10.5 mmoles) dissolved in 95% ethanol (100 ml) was hydrogenated at atmospheric pressure using platinum dioxide (200 mg). The theoretical hydrogen uptake was complete after about 5 h. The hydrogenation flask was purged with nitrogen, and conc. hydrochloric acid (20 ml) was added. The catalyst was removed by filtration and water (80 ml) was then added to the filtrate. Yield: 4.02 g (86%) of the hydrochloride salt. The hydrochloride salt was recrystallized three times from ethanol and was then heated at 61° for 4 h at 0.2 mm over P_2O_5 in an Abderhalden pistol, thus giving the free *p*-aminobenzoate (Cl^- negative). The infrared spectrum ($CHCl_3$) showed NH stretch at 3 370 cm^{-1} (w), C=O stretch at 1 711 cm^{-1} (s), and C=C (aromatic) at 1 622 and 1 607 cm^{-1}.

1,3-Bistosyloxy-2-fluoropropane

A mixture of 1,2-dibromo-3-fluoropropane and 1,3-dibromo-2-fluoropropane as prepared above (2.0 g, 9.1 mmoles) and silver *p*-toluenesulfonate (5.0 g, 17.9 mmoles) in acetonitrile (15 ml) was heated under reflux for 112 h, by which time 62% of the theoretical quantity of silver bromide had been formed. The silver salts were removed by filtration and were washed with acetonitrile. Ether was added to the mixture, followed by distilled water to dissolve the unchanged silver tosylate. The ether layer was separated, washed, and dried (Na_2SO_4). Removal of the ether and the acetonitrile at 100 mm gave a syrupy residue, which, on standing overnight in the refrigerator, gave 150 mg of crystals, m.p. 95–105°. Addition of ether to the viscous filtrate gave a further 480 mg, m.p. 108–110°. Total yield: 45%. Recrystallization twice from 95% ethanol gave fine, colorless needles, m.p. 111–112°. An authentic sample, prepared by tosylation of 2-deoxy-2-fluoroglycerol (19) and kindly provided by Dr. P. W. Kent, had m.p. 107–110°, mixed m.p. 108–111°. The toxicity of this fluorotosylate, by intraperitoneal injection into mice, was > 100 mg/kg.

1,2-Dicyanohexane

In an attempt to prepare 3-fluoroheptanonitrile, dried sodium cyanide (3.4 g, 69.5 mmoles) in dry dimethyl sulfoxide (30 ml) was warmed to 88°. 2-Fluorohexyl bromide (10.0 g, 54.7 mmoles) was then added dropwise to this suspension (10 min). The mixture was heated at 90° for a further 40 min. The thick, cooled mixture was diluted with ether (100 ml) and then washed with water. The washings were extracted with ether, and the combined ether extracts were dried (Na_2SO_4). Removal of the ether and distillation of the residue gave 2.63 g (56%) of 1,2-dicyanohexane.

C. Hydrogenations

Attempted Hydrogenolysis of 1-Iodo-2-fluorohexane, 1-Iodo-2-fluorodecane, and trans-1-Bromo-2-fluorocyclohexane

No hydrogenolysis occurred at atmospheric pressure using hydrogen and platinum dioxide in various solvents (methanol, ethanol, and glacial acetic acid). Even ultraviolet irradiation with a Hanovia low-pressure mercury lamp did not appear to promote hydrogenolysis. Under the same conditions (no irradiation), 1,2-dibromocyclohexane readily formed cyclohexane.

Hydrogenolysis of a Mixture of 1,2-Dibromo-3-fluoropropane (III) and 1,3-Dibromo-2-fluoropropane (II)

An approximately equal mixture of the above compounds (6.25 g, 28.4 mmoles) in 95% ethanol (30 ml) was hydrogenated at room temperature and atmospheric pressure, using platinum dioxide (300 mg) as catalyst. Hydrogen (720 ml) was absorbed over a 25 h period. Gas–liquid chromatography showed that the mixture now contained only 11% of III. Removal of the catalyst, isolation of the product, drying (Na_2SO_4), and purification by fractionation gave initially a mixture of the isomeric dibromofluoropropanes, followed by pure II. The latter was at least 98% pure by g.l.c. analysis.

Hydrogenolysis of 1-Bromo-2-fluoro-2-phenylethane

The fluorobromide (10.24 g, 50.5 mmoles) in 95% ethanol (40 ml) was hydrogenated as above, using platinum dioxide (150 mg). Hydrogen uptake (2 440 ml) was complete in about 10 h. Removal of the catalyst, isolation, drying, and purification by fractionation gave a mixture (4.02 g) consisting of 87 mole % of ethylbenzene and 13 mole % of ethylcyclohexane (g.l.c. at 155° on an Apiezon-L column). These two products were identified by comparison of their retention times with authentic samples.

Can. J. Chem. Downloaded from www.nrcresearchpress.com by 210.87.254.42 on 09/05/12
For personal use only.

Hydrogenolysis of 2-Fluorohexyl Nitrate

2-Fluorohexyl nitrate (5.05 g, 30.6 mmoles) was hydrogenated at atmospheric pressure using platinum dioxide (60 mg) in ethanol (50 ml) containing acetic acid (1.8 g, 30 mmoles). Hydrogen absorption began at once and was steady at about 10 ml/min. When about 90% had been taken up, absorption ceased. The catalyst was removed by filtration and was washed with methanol. The filtrate was diluted with ether (250 ml) and the solution was washed with water, with brine, and again with water. Drying (Na_2SO_4), removal of the ether, and distillation gave 2-fluoro-1-hexanol (2.47 g, 67%), identical in all respects with the material obtained by the hydrolysis of 1-bromo-2-fluorohexane (see above).

Hydrogenolysis of 2-Fluoro-2-phenylethyl Nitrate

The nitrate (1.12 g, 6.03 mmoles) was dissolved in 95% ethanol (20 ml) containing 6 *N* hydrochloric acid (2 ml). Platinum dioxide (65 mg) was added and the mixture was hydrogenated at room temperature and atmospheric pressure. After 7 h, 510 ml of hydrogen had been absorbed. The catalyst was removed by filtration, ether (100 ml) was added to the filtrate, and the ethereal solution was washed and dried (Na_2SO_4). Removal of the solvent gave a liquid which, by infrared spectroscopy, was shown to be 2-phenylethanol. Further confirmation of the identity of the product was obtained by gas chromatography on two different columns (Apiezon-L and DEGS), and comparison of the retention times with those of an authentic sample.

ACKNOWLEDGMENTS

We wish to express our indebtedness to the National Research Council for financial support, and to Canadian Industries Limited, Montreal, for the award of a Fellowship (F. H. D.). We wish to acknowledge with thanks the gift of a sample of 1,3-bistosyloxy-2-fluoropropane from Dr. P. W. Kent, Department of Biochemistry, University of Oxford, England. We are grateful to Dr. M. K. McPhail and Dr. C. A. deCandole, Suffield Experimental Station, Ralston, Alberta for determining the toxicities, Dr. J. Newton for preparing 1-bromo-2-fluoro-1,2-diphenylethane, and Dr. J. B. Stothers of this department for help with the nuclear magnetic resonance spectra.

REFERENCES

1. R. L. Buchanan, F. H. Dean, and F. L. M. Pattison. Preprints, Second International Symposium on Fluorine Chemistry, Estes Park, Colorado. 1962. p. 385.
2. A. Bowers. J. Am. Chem. Soc. **81**, 4107 (1959).
3. A. Bowers, L. C. Ibáñez, E. Denot, and R. Becerra. J. Am. Chem. Soc. **82**, 4001 (1960).
4. A. Bowers, E. Denot, and R. Becerra. J. Am. Chem. Soc. **82**, 4007 (1960).
5. F. L. M. Pattison, R. L. Buchanan, and F. H. Dean. Can. J. Chem. This issue.
6. G. Schrader. British Intelligence Objectives Subcommittee, Report No. 1808.
7. R. E. Buckles and D. F. Knaack. J. Chem. Ed. **37**, 298 (1960).
8. P. B. D. de la Mare and J. G. Pritchard. J. Chem. Soc. 3910 (1954).
9. P. B. D. de la Mare, P. G. Naylor, and D. L. H. Williams. J. Chem. Soc. 443 (1962).
10. P. B. D. de la Mare, P. G. Naylor, and D. L. H. Williams. J. Chem. Soc. 3429 (1963).
11. J. Hine and W. H. Brader, Jr. J. Am. Chem. Soc. **75**, 3964 (1953).
12. J. Hine. Physical organic chemistry. 2nd ed. McGraw-Hill Book Co., Inc., New York, N.Y. 1962. pp. 157–185.
13. P. Mirosevic-Sorgo and B. C. Saunders. Tetrahedron, **5**, 38 (1959).
14. J. F. King and R. G. Pews. Can. J. Chem. **42**, 1294 (1964).
15. I. L. Knunyants, O. V. Kil'disheva, and I. P. Petrov. J. Gen. Chem. USSR Eng. Transl. **19**, 87 (1949). I. L. Knunyants, O. V. Kil'disheva, and E. Bykhovskaya. J. Gen. Chem. USSR Eng. Transl. **19**, 93 (1949).
16. J. Hine. Physical organic chemistry. 1st ed. McGraw-Hill Book Co., Inc., New York, N.Y. 1956. pp. 266–282.
17. J. Bornstein and M. R. Borden. Chem. Ind. London, 441 (1958).
18. F. W. Hoffmann. J. Org. Chem. **14**, 105 (1949).
19. N. F. Taylor and P. W. Kent. J. Chem. Soc. 2150 (1956).
20. F. L. M. Pattison and W. C. Howell. J. Org. Chem. **21**, 748 (1956).
21. J. E. Millington and F. L. M. Pattison. Can. J. Chem. **34**, 1532 (1956).

Can. J. Chem. Downloaded from www.nrcresearchpress.com by 210.87.254.42 on 09/05/12
For personal use only.

Can. J. Chem. Downloaded from www.nrcresearchpress.com by 210.87.254.42 on 09/05/12
For personal use only.

THE SYNTHESIS OF α-MONOFLUOROALKANOIC ACIDS[1]

F. L. M. PATTISON, R. L. BUCHANAN,[2] AND F. H. DEAN[3]
Department of Chemistry, University of Western Ontario, London, Ontario
Received November 11, 1964

ABSTRACT

α-Monofluoroalkanoic acids are important intermediates in the synthesis of biologically active fluorine compounds. General methods of preparation have been examined, based on the three following reagents: (*a*) hydrogen fluoride + *N*-bromoacetamide; (*b*) diethyl monofluoromalonate; and (*c*) perchloryl fluoride. The first of these is the recommended procedure for simple unsubstituted α-fluoro acids; however, the fluoromalonate route is less vigorous, and is therefore the method of choice for those α-fluoro acids that contain labile functional groups.

INTRODUCTION

In our program directed towards the synthesis of biologically active fluorine compounds (fluorinated drugs, antimetabolites, amino acids, insecticides, etc.), frequent recourse must be made to α-monofluoroalkanoic acids as intermediates. A general study therefore was undertaken to develop new and improved means of obtaining this class of compound. The work is part of a more general project concerned with new methods of preparing aliphatic fluorine compounds.

A subsidiary motive in preparing these acids concerned their biological degradation. No toxicological data are available for α-monofluoroalkanoic acids higher than 2-fluoropropanoic acid. If acids of this type, containing four or more unbranched carbon atoms, were to undergo β-oxidation, all would be toxic irrespective of the length of the carbon chain, since the toxic fluoroacetyl coenzyme A would be produced in all cases. (The similarity in size of hydrogen and fluorine makes such a suggestion tenable.) However, as will be described later, both odd and even α-monofluoroalkanoic acids were found to be nontoxic, a fact implying inhibition of β-oxidation by the α-fluorine atom.

A survey of the literature indicated that there are no particularly satisfactory methods of preparation which are simple, mild, general, and inexpensive. Of the described procedures, the following are representative.

[*a*] $RCHXCOOR + KF \xrightarrow{\text{autoclave}} RCHFCOOR$ (2, 3)

[*b*] $RCHBrCOOEt + AgF(CaF_2) \rightarrow RCHFCOOEt$ (2, 4)

[*c*] $RBr + CH_2FCOOR \rightarrow RCHFCOOR$ (5)

[*d*] $RCHO + EtOOCCHFCOCOOEt \rightarrow RCH{=}CFCOOH + HOOCCOOEt + EtOH$ (6)

[*e*] $R_2CO + CHFICOOR \xrightarrow{Zn} R_2C(OH)CHFCOOR$ (7)

[*f*] $RCH(OTs)COOEt + KF \rightarrow RCHFCOOEt$ (8, 9)

[*g*] $RCH(OSO_2Ar)CN + KF \rightarrow RCHFCN \rightarrow RCHFCOOH$ (8, 10)

Several of the above methods have disadvantages. Reactions [*a*] and [*b*] require vigorous treatment and usually result in low or nonreproducible yields; moreover, reaction [*a*] is inconvenient in that a pressure autoclave is required. Reaction [*c*] gives rather low

[1]*This paper was presented in part at the Second International Symposium on Fluorine Chemistry, Estes Park, Colorado, July 17–20, 1962 (1).*
[2]*Present address: Department of Organic Chemistry, Bristol Laboratories, Syracuse, 1, N.Y.*
[3]*Present address: Department of Chemistry, University of Delaware, Newark, Delaware.*

yields and promotes undesirable side reactions in the presence of various functional groups. Reactions [*d*], [*e*], and [*f*] are all satisfactory procedures, but the essential intermediates (diethyl fluorooxalacetate, ethyl fluoroiodoacetate, and α-tosyloxyalkanoates respectively) are not easy or convenient to prepare. Reaction [*g*] is also satisfactory for the very low members, but the yields decrease markedly on ascent of the series (e.g. fluoroacetic acid: 60% dropping to 2-fluoropentanoic acid: 16%).

For these and other reasons, we examined a considerable number of procedures, from which the following were selected for more detailed investigation. The classification below is based on the key reagent:

(I) syntheses based on "BrF" addition (HF + $CH_3CONHBr$);

(II) syntheses based on diethyl fluoromalonate; and

(III) syntheses based on perchloryl fluoride.

The first of these permits the introduction of the fluorine atom at centers of low electron density (bromonium ion); the second utilizes a reagent in which the C—F bond has been preformed; and the third favors fluorination at centers of high electron density (carbanion).

RESULTS

I. Syntheses Based on "BrF" Addition

The "BrF" addition, using anhydrous hydrogen fluoride and *N*-bromoacetamide, is based on the work of Bowers (11). The application of the procedure to aliphatic alkenes has been described earlier (12). The vicinal fluorobromides so formed are somewhat resistant to nucleophilic attack (12); hence the routes shown below are time consuming but simple. For example, the formation of the fluoro acetate (12) requires 15 or more hours at 115° using sodium acetate and sodium iodide; the subsequent hydrolysis and oxidation using nitric acid and acetic acid at 50° is complete in about 20–40 h. Until this method had been developed, simple oxidation of the fluoroalcohols $RCHFCH_2OH$ had not been extensively examined, because these compounds are not easily obtained; most common procedures, such as opening of epoxides with hydrogen fluoride, yield the isomeric fluoroalcohols, $RCH(OH)CH_2F$. If these intermediate fluoroalcohols, $RCHFCH_2OH$, are required for other purposes, convenient preparative procedures include hydrogenolysis of the fluoronitrates or hydrolysis of the formates, as described earlier (12).

$$\text{RCH=CH}_2 \xrightarrow[\text{NBA}]{\text{HF}} \text{RCHFCH}_2\text{Br} \begin{cases} \xrightarrow[\text{AgNO}_3]{\text{route 1}} \text{RCHFCH}_2\text{ONO}_2 \xrightarrow[\text{HOAc}]{\text{HNO}_3} [\text{RCHFCH}_2\text{OH}] \rightarrow \text{RCHFCOOH} \\ \xrightarrow[\text{NaOAc}]{\text{route 2}} \text{RCHFCH}_2\text{OAc} \xrightarrow[\text{HOAc}]{\text{HNO}_3} [\text{RCHFCH}_2\text{OH}] \rightarrow \text{RCHFCOOH} \\ \xrightarrow[\text{HCOONa}]{\text{route 3}} \text{RCHFCH}_2\text{OCHO} \xrightarrow[\text{HOAc}]{\text{HNO}_3} [\text{RCHFCH}_2\text{OH}] \rightarrow \text{RCHFCOOH} \end{cases}$$

Some yields are shown in Table I. In the initial work with 1-bromo-2-fluorohexane, the acetate route gave a higher overall yield than that involving the nitrate or the formate; hence route 2 was used for examining the other members.

The above method is satisfactory for relatively low molecular weight unbranched alkenes, but certain variations in structure require special treatment. (*a*) *Styrene* gave the fluorobromide and the corresponding nitrate ($C_6H_5CHFCH_2ONO_2$) (12); attempts

Can. J. Chem. Downloaded from www.nrcresearchpress.com by 210.87.254.42 on 09/05/12
For personal use only.

TABLE I

Yields by the "BrF" route to α-monofluoroalkanoic acids

Alkene	Route to acid*	Overall yield of acid (%) based on alkene
$CH_2=CH_2$	2	6
$CH_3CH=CH_2$	2	17
$CH_3CH_2CH=CH_2$	2	27
$CH_3(CH_2)_3CH=CH_2$	1	40
	2	48
	3	36
$CH_3(CH_2)_4CH=CH_2$	2	51
$CH_3(CH_2)_5CH=CH_2$	2	43
$CH_3(CH_2)_7CH=CH_2$	2	47
$MeOOC(CH_2)_8CH=CH_2$	2	43

*The routes correspond to the equations shown above.

to prepare the acetate gave unsaturated products. The subsequent oxidation of the nitrate gave only benzoic and nitrobenzoic acids. This can be explained in terms of homolytic fission of the C—H bond, with resonance stabilization of the intermediate benzylic radical. It is therefore unlikely that α-phenyl-substituted acids can be prepared in good yield by this type of oxidative process. The required product, α-fluorophenylacetic acid, $C_6H_5CHFCOOH$ was accordingly obtained by an alternative procedure (see below). (*b*) *1-Alkenes branched at the 2-position* did not give satisfactory yields of the expected α-fluoroacids. For example, 2-ethyl-1-butene gave the fluorobromide but this was inert to such reagents as sodium iodide and silver nitrate. In an attempt to circumvent this difficulty, the corresponding fluoroiodide (crude) was prepared (12), using hydrogen fluoride and *N*-iodosuccinimide (11), which in turn gave, via the nitrate, an impure sample of 2-fluoro-2-ethylbutanoic acid in insignificant yield. This acid and its methyl ester were therefore obtained by another method (see below). (*c*) *1-Octadecene* gave rise, by the acetate route, to crude 2-fluorooctadecanoic acid; neither 2-fluorooctadecyl *p*-nitrobenzoate nor 2-fluorooctadecyl *p*-aminobenzoate were converted to 2-fluorooctadecanoic acid by the nitric acid treatment. Because of purification difficulties, this acid is more conveniently prepared by the fluoromalonate route, as described below.

When the nitric acid reaction is applied to alkyl acetates which do not contain a vicinal fluorine atom, pronounced chain degradation occurs, even when the concentration of the nitric acid in acetic acid is reduced from 1:1 to 1:3. For example, *n*-heptyl acetate gave heptanoic acid in only 50–60% yield, along with hexanoic and lower acids. Under conditions which favored the conversion of non-fluorinated acetates to acids, 2-fluorodecyl acetate gave 2-fluorodecanoic acid in only 1.3% yield with massive recovery of the starting material. Thus the vicinal fluorine atom, while reducing the reactivity of the acetate, gives rise to much less degradation of the resultant acid. In short, the procedure is mainly of value in the special type of application described in this paper.

II. Syntheses Based on Diethyl Fluoromalonate

$$RBr + CHF(COOEt)_2 \xrightarrow[DMF]{NaH} RCF(COOEt)_2 \rightarrow RCHFCOOH$$

Diethyl fluoromalonate was prepared in 28% yield by Bergmann's procedure (13) but with minor modifications (14). The method involves the reaction of ethyl chloroformate with the enolate of ethyl fluoroacetate in conventional glass apparatus; disadvantages include a low overall yield, a lengthy procedure, and the use of large quantities

Can. J. Chem. Downloaded from www.nrcresearchpress.com by 210.87.254.42 on 09/05/12
For personal use only.

Can. J. Chem. Downloaded from www.nrcresearchpress.com by 210.87.254.42 on 09/05/12
For personal use only.

of ethyl fluoroacetate (toxic and expensive). Gryszkiewicz-Trochimowski (3) has claimed a 40% yield by treating dimethyl chloromalonate with potassium fluoride in an autoclave. We have not been able to repeat this work, nor has Bergmann (13). The products which have been isolated from the autoclave reaction include dimethyl malonate and dimethyl difluoromalonate, both apparently formed by disproportionation, and tetramethyl ethenetetracarboxylate (see Table IV).

The alkylation step has not previously been reported. Fluoromalonate is more resistant to alkylation than malonate because its anion is a weaker base and therefore a weaker nucleophile. Initial experiments using sodium ethoxide in ethanol gave low yields, as did the more recent modification of first forming the fluoromalonate anion and then replacing the excess ethanol by diethyl carbonate (15). It soon became apparent, however, that the use of sodium hydride in the more polar solvent dimethylformamide gave good yields with no observable side reactions. The conditions for the alkylations varied considerably for the various members. The time of reaction ranged from 2 to 32 h at temperatures from 25 to 100°. The progress of the reactions was followed by pH changes; completion of the reaction was indicated by an acid pH or a levelling off to constant pH. The yields both in the alkylations and in the subsequent hydrolyses could undoubtedly be improved, because the figures shown (Table II) represent the result of one (or occasionally two) small-scale runs.

The hydrolyses were carried out until evolution of carbon dioxide ceased. Times ranged from 5 h (for 2,6-difluorohexanoic acid) to 70 h (for 2-fluorooctadecanoic acid). Dioxane was used as solvent in those cases where the reactants and products were insoluble in the aqueous medium. In some cases there were signs of acid-catalyzed removal of fluorine, as evidenced by etching of the reaction flasks; this is certainly one reason for the rather low yields obtained in many of the hydrolyses. The purity of the liquid acids was determined by preparing the methyl esters, using diazomethane, and examining these by vapor phase chromatography.

TABLE II

Yields by the fluoromalonate route to α-monofluoroalkanoic acids

Alkyl bromide (RBr)	Yield of $RCF(COOEt)_2$(%)	RCHFCOOH	
		Yield (%), based on $RCF(COOEt)_2$	Overall yield (%), based on $CHF(COOEt)_2$
CH_3CH_2-	77.8*	54.7	42.6
$CH_3(CH_2)_2$-	74.2	80.1	59.4
$(CH_3)_2CH$-	57.0	41.6	23.7
$CH_3(CH_2)_3$-	50.7†	82.8	42.0
$F(CH_2)_4$-‡	78.2	42.1	32.9
$EtOOC(CH_2)_4$-	57.9	39.5	22.9
$CH_3(CH_2)_{15}$-	81.4§	66.4	54.1
$C_6H_5CH_2$-‖	75.2	65.9	49.5

*The sodium ethoxide – diethyl carbonate route gave 53.3% yield.
†The sodium ethoxide – diethyl carbonate route gave 29.0% yield.
‡4-Fluorobutyl iodide was used.
§Crude yield of low-melting solid.
‖Benzyl chloride was used.

Allyl bromide formed diethyl allylfluoromalonate in 79.1% yield, but the hydrolysis and decarboxylation were unsuccessful because of side reactions with the double bond.

In related work, it was found that the fluoromalonate anion can cleave β-propiolactone to give α-fluoroglutaric acid on further treatment.

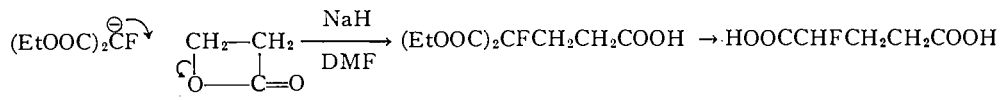

The less reactive γ-butyrolactone was recovered unchanged under the same conditions.

The application of diethyl fluoromalonate in the preparation of γ-fluoroglutamic acid by the Michael reaction has already been described (14). Its use in other routes to fluorinated amino acids will form the subject of a separate communication.

III. Syntheses Based on Perchloryl Fluoride

The general use of perchloryl fluoride is based on the pioneering work of the Pennsalt group (16). The application of this reagent in the preparation of monofluorosuccinic acid in this laboratory has already been described (17). The following additional reactions have been carried out.

[*a*] $CH_3CH(COOEt)_2 \xrightarrow[NaH/DMF]{ClO_3F} CH_3CF(COOEt)_2 \rightarrow CH_3CHFCOOH$

[*b*] $MeOOCCH_2CH_2CH(COOMe)_2 \xrightarrow[NaH/DMF]{ClO_3F} MeOOCCH_2CH_2CF(COOMe)_2 \rightarrow HOOCCH_2CH_2CHFCOOH$

[*c*] 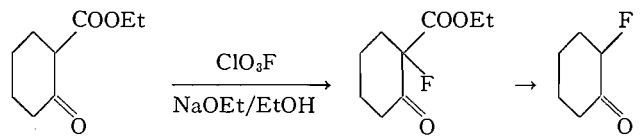

[*d*] $C_6H_5CH(COOEt)_2 \xrightarrow[NaH/DMF]{ClO_3F} C_6H_5CF(COOEt)_2 \rightarrow C_6H_5CHFCOOH$

[*e*] $O_2NCH(COOEt)_2 \xrightarrow[KOEt/dioxane]{ClO_3F} O_2NCF(COOEt)_2$

[*f*] $CH_3CH_2CHEtCHO \rightarrow CH_3CH_2CHEtCH(OCH_3)_2 \rightarrow CH_3CH_2CEt{=}CHOCH_3 \xrightarrow[pyridine]{ClO_3F} CH_3CH_2CEtFCOOCH_3 + CH_3CH_2CEtFCOOH$

Reactions [*d*] and [*f*] gave rise to two of the acids which could not readily be formed by the "BrF" method above. The chemistry of reactions [*a*], [*b*], [*c*], [*d*], and [*e*] is straightforward. Reaction [*f*] is the most interesting; a plausible mechanism is shown below. A small quantity of the free acid was produced directly, presumably by pyridine-catalyzed loss of methanol from the intermediate hemiacetal followed by oxidation of the resultant aldehyde. The identity of this acid was confirmed by the formation of its *p*-bromophenacyl derivative, using dimethylformamide as solvent. The isomeric 2-fluorohexanoic and 6-fluorohexanoic acids were also converted to their *p*-bromophenacyl derivatives by the same procedure.

DISCUSSION

Of the methods described above, we consider the perchloryl fluoride procedure to be least satisfactory, partly because of difficulties in separating the fluorinated from the non-fluorinated compounds, and partly because the overall yields are often rather low.

The recommended procedure for simple unsubstituted α-monofluoroalkanoic acids is, in our opinion, that utilizing "BrF" addition. Although time consuming, it involves

Can. J. Chem. Downloaded from www.nrcresearchpress.com by 210.87.254.42 on 09/05/12
For personal use only.

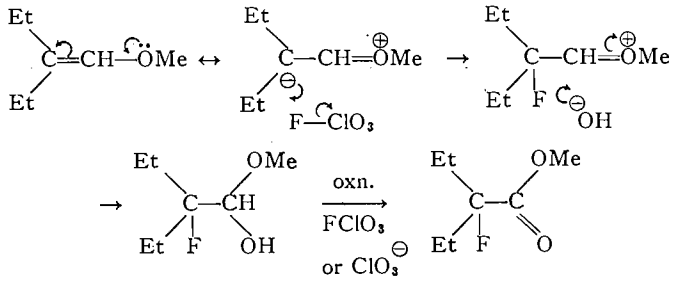

conventional apparatus and readily available intermediates, and is convenient and easy to carry out.

The fluoromalonate route is much milder, and is therefore the method of choice for those α-fluoro acids that contain labile functional groups. The only disadvantage of the method lies in the unsatisfactory preparation of the diethyl fluoromalonate itself as already mentioned; apart from this the alkylations and hydrolyses are very simple, and the procedure is applicable to a wide variety of halides. The fluoromalonate anion is apparently too weak a base appreciably to effect β-elimination from secondary bromides; thus isopropyl bromide alkylates diethyl fluoromalonate in 57% yield. The yields obtained by the fluoromalonate route are considerably better than those reported for the direct alkylation of ethyl fluoroacetate (5).

Many of the compounds described in this paper were submitted for toxicological testing. Results are shown in Table III.

TABLE III
Toxicities

Compound	LD_{50} (mice, I.P.) (mg/kg)	95% confidence limits (mg/kg)
1. α-Fluoromalonates		
$FCH(COOH)_2$	17	12.5–23.1
$FCH(COOEt)_2$	7.5	5.0–11.1
$O_2NCF(COOEt)_2$	>107	
$CH_3CH_2CF(COOEt)_2$	30	21.7–41.6
$CH_3(CH_2)_2CF(COOEt)_2$	57	46.0–72.9
$CH_3(CH_2)_3CF(COOEt)_2$	>107	
$CH_2{=}CHCH_2CF(COOEt)_2$	57	46.0–72.9
$C_6H_5CH_2CF(COOEt)_2$	>94	
$F(CH_2)_4CF(COOEt)_2$	18	13.7–23.4
$EtOOCCH_2CF(COOEt)_2$*	>107	
$MeOOC(CH_2)_2CF(COOMe)_2$	>107	
$EtOOC(CH_2)_4CF(COOEt)_2$	>94	
2. α-Fluoroalkanoic acids		
$CH_3CH_2CHFCOOH$	>100	
$CH_3(CH_2)_3CHFCOOH$	>107	
$CH_3(CH_2)_4CHFCOOH$	>100	
$CH_3(CH_2)_5CHFCOOH$	~25	
$CH_3(CH_2)_{15}CHFCOOH$	>100	
$F(CH_2)_4CHFCOOH$	>94	
$HOOCCH_2CH_2CHFCOOH$†	~90	
3. Miscellaneous		
$CH_3(CH_2)_3CHFCH_2OH$	>107	
HOOCCF=CFCOOH (*cis*)‡	>107	
HOOCCF=CHCOOH (*cis*)§	>107	
HOOCCF=CHCOOH (*trans*)‡	>107	

*Preparation described in ref. 17.
†Animals died in fluoroacetate-type convulsions.
‡Kindly supplied by Dr. M. S. Raasch.
§Fluoromaleic anhydride, kindly supplied by Dr. W. H. Sharkey, was hydrolyzed to the free acid (18).

Can. J. Chem. Downloaded from www.nrcresearchpress.com by 210.87.254.42 on 09/05/12
For personal use only.

Can. J. Chem. Downloaded from www.nrcresearchpress.com by 210.87.254.42 on 09/05/12
For personal use only.

TABLE IV

Physical constants and analytical results

Compound	Formula	Boiling point (°C)	Boiling point (mm)	n_D^{25} or m.p. (°C)	d_4^{20}	MR_D Estimated	MR_D Found	Analytical results: C (%) Calcd.	C (%) Found	H (%) Calcd.	H (%) Found
1. α-Fluoromalonates											
Diethyl fluoromalonate[a]	$FCH(COOEt)_2$	97–97.5	12	1.4056				47.19	46.82	6.22	6.46
Fluoromalonic acid[b]	$FCH(COOH)_2$			136–139				29.52	29.77	2.47	2.42
Diethyl ethylfluoromalonate	$CH_3CH_2CF(COOEt)_2$	96–99.5	13	1.4060	1.082	47.3	46.9	52.42	52.30	7.33	7.22
Diethyl *n*-propylfluoromalonate	$CH_3(CH_2)_2CF(COOEt)_2$	110–112	10	1.4101	1.073	52.0	51.0	54.53	54.56	7.78	7.69
Diethyl *n*-butylfluoromalonate	$CH_3(CH_2)_3CF(COOEt)_2$	54–55	0.07	1.4140				56.40	56.55	8.16	8.22
Diethyl isopropylfluoromalonate	$(CH_3)_2CHCF(COOEt)_2$	109–110.5	13	1.4136	1.064	51.6	51.7	54.53	54.72	7.78	8.03
Diethyl allylfluoromalonate	$CH_2{:}CHCH_2CF(COOEt)_2$	110–111	11	1.4194	1.088	51.3	51.0	55.04	54.79	6.93	6.79
Phenylfluoromalonic acid monohydrate	$C_6H_5CF(COOH)_2$, H_2O			113–116				50.01	50.37	4.20	4.07
Diethyl benzylfluoromalonate	$C_6H_5CH_2CF(COOEt)_2$	115–116	0.2	1.4769	1.138	67.1	66.7	62.67	62.87	6.39	6.54
Diethyl 4-fluorobutylfluoromalonate	$F(CH_2)_4CF(COOEt)_2$	71.5–73	0.005	1.4150	1.113	56.3	57.1	52.37	52.63	7.19	7.21
Dimethyl α-fluoro-α-carbomethoxyglutarate	$MeOOC(CH_2)_2CF(COOMe)_2$	94	0.07	1.4292	1.260	48.6	48.5	45.76	45.70	5.55	5.58
Diethyl 2-carboxyethylfluoromalonate	$HOOC(CH_2)_2CF(COOEt)_2$	103–104	0.17	1.4340				48.00	47.99	6.04	6.03
Diethyl α-fluoro-α-carbethoxypimelate	$EtOOC(CH_2)_4CF(COOEt)_2$	111–112	0.075	1.4313	1.097	72.8	72.6	54.89	54.90	7.57	7.76
Diethyl fluoronitromalonate[c,d]	$O_2NCF(COOEt)_2$	81–83	0.5	1.4078	1.231	44.5	44.9	37.67	37.89	4.52	4.70
2. α-Fluoroalkanoic acids											
Fluoroacetic acid[e]	FCH_2COOH	162–165	752	29							
2-Fluoropropanoic acid[f]	$CH_3CHFCOOH$	66	13	1.3839				39.13	39.26	5.47	5.50
2-Fluorobutanoic acid[g]	$CH_3CH_2CHFCOOH$	77–77.5	11	1.3940	1.132			45.28	45.03	6.65	6.85
2-Fluoropentanoic acid	$CH_3(CH_2)_2CHFCOOH$	90–90.5	12	1.4018				49.99	50.25	7.55	7.74
2-Fluorohexanoic acid[h]	$CH_3(CH_2)_3CHFCOOH$	106–106.5	11	1.4086				53.72	53.52	8.27	8.44
2-Fluoroheptanoic acid	$CH_3(CH_2)_4CHFCOOH$	62–63	0.15	34–35				56.74	56.67	8.78	8.97
2-Fluorooctanoic acid[i]	$CH_3(CH_2)_5CHFCOOH$			51–53				59.24	59.18	9.32	9.50
2-Fluorodecanoic acid	$CH_3(CH_2)_7CHFCOOH$			62–65				63.13	63.39	10.07	10.17
2-Fluorooctadecanoic acid[j]	$CH_3(CH_2)_{15}CHFCOOH$			88–90				71.47	71.72	11.66	11.85
2-Fluoro-3-methylbutanoic acid	$(CH_3)_2CHCHFCOOH$			35–40				49.99	49.92	7.55	7.64
α-Fluorophenylacetic acid	$C_6H_5CHFCOOH$			83–85				62.33	62.46	4.58	4.55
2-Fluoro-3-phenylpropanoic acid	$C_6H_5CH_2CHFCOOH$			71–74				64.28	64.41	5.39	5.45
Methyl 2-fluoro-2-ethylbutanoate	$CH_3CH_2CEtFCOOMe$	82	76	1.3960	0.988	35.8	36.0	56.74	56.93	8.84	8.90
2,6-Difluorohexanoic acid	$F(CH_2)_4CHFCOOH$			47.5–50				47.36	47.13	6.63	6.50

Can. J. Chem. Downloaded from www.nrcresearchpress.com by 210.87.254.42 on 09/05/12
For personal use only.

TABLE IV (*Concluded*)

Compound	Formula	Boiling point (°C)	Boiling point (mm)	n_D^{25} or m.p. (°C)	d_4^{20}	MR_D Estimated	MR_D Found	Analytical results: C (%) Calcd.	C (%) Found	H (%) Calcd.	H (%) Found
α-Fluoroglutaric acid	$HOOC(CH_2)_2CHFCOOH$			104–107				40.00	40.17	4.70	4.82
α-Fluoropimelic acid	$HOOC(CH_2)_4CHFCOOH$			122–123				47.19	47.45	6.22	6.23
2-Fluoroundecanedioic acid	$HOOC(CH_2)_8CHFCOOH$			116–116.5				56.39	56.61	8.17	8.30
2-Fluoro-2-carbethoxycyclohexanone	$(CH_2)_4$	66	0.35	1.4425	1.170	43.4	42.8	57.44	57.56	6.96	7.22
3. Miscellaneous											
Tetramethyl ethenetetracarboxylate[k]	$(MeOOC)_2C{:}C(COOMe)_2$			116–120				46.16	46.39	4.65	4.87
Dimethyl α-carbomethoxyglutarate	$MeOOC(CH_2)_2CH(COOMe)_2$	98.5	0.30	1.4362	1.176	48.4	48.8	49.54	49.77	6.47	6.57
1-Methoxy-2-ethyl-1-butene	$CH_3CH_2CEt{:}CHOMe$	75	135	1.4206	0.798			73.63	73.43	12.36	12.25
2-Fluorohexanoic acid, *p*-bromophenacyl derivative	$CH_3(CH_2)_3CHFCOOCH_2COC_6H_4Br$[l]			97–99				50.77	50.99	4.87	5.05
6-Fluorohexanoic acid, *p*-bromophenacyl derivative	$F(CH_2)_5COOCH_2COC_6H_4Br$[m]			50–52				50.77	50.53	4.87	4.81
2-Fluoro-2-ethylbutanoic acid, *p*-bromophenacyl derivative	$CH_3CH_2CEtFCOOCH_2COC_6H_4Br$[n]			56–59				50.77	50.71	4.87	4.86

[a] Bergmann *et al.* (13) report b.p. 121–122° at 30 mm, n_D^{27} 1.4040.
[b] LaZerte *et al.* (22) report m.p. 135.8–136.5°.
[c] Freeman (23) reports b.p. 52–54° at 0.5 mm, $n_D^{25.5}$ 1.4088.
[d] N (%): calcd. 6.28, found 6.31.
[e] Saunders and Stacey (2) report b.p. 167–168.5°, m.p. 31–32°; the product was further proved to be fluoroacetic acid by comparison of its ethyl ester with authentic ethyl fluoroacetate (g.l.c.).
[f] Gryszkiewicz-Trochimowski and Gryszkiewicz-Trochimowski (24) report b.p. 60–60.5° at 8 mm.
[g] Bockemüller (4) reports b.p. 90° at 13 mm.
[h] Melting point ca. 27–32°.
[i] Boiling point ca. 72–81° at 0.15 mm.
[j] The intermediate $CH_3(CH_2)_{15}CF(COOEt)_2$ was a low-melting solid which was not further purified.
[k] Corson *et al.* (25) report m.p. 119–120°; our sample on catalytic hydrogenation formed tetramethyl ethanetetracarboxylate, the melting point of which was undepressed on admixture with an authentic specimen.
[l] Br (%): calcd. 24.13; found 24.24.
[m] Br (%): calcd. 24.13; found 24.14.
[n] Br (%): calcd. 24.13; found 24.36.

Can. J. Chem. Downloaded from www.nrcresearchpress.com by 210.87.254.42 on 09/05/12
For personal use only.

Both fluoromalonic acid and its diethyl ester were found to be toxic. In an independent study, Bergmann and Shahak (19) made the same observation using the sodium salt, and reported that fluoroacetate-type symptoms were produced in mice, rats and guinea pigs with the characteristic accumulation of citrate in the kidneys. In short, the pattern is typical for fluoroacetate, which implies decarboxylation of the original fluoromalonate.

The substituted α-fluoromalonates do not show any particular trend, and are relatively innocuous. Diethyl 4-fluorobutylfluoromalonate was the most toxic member of the class, indicating, perhaps, some type of biochemical degradation to an ω-fluoro fragment containing an even number of carbon atoms. It is significant that alkylmalonic acids up to *n*-heptylmalonic acid are excreted unchanged, whereas *n*-octylmalonic and higher acids are metabolized completely by ω-oxidation (20).

The α-fluoroalkanoic acids are also nontoxic within the limits of biological variation. This can best be explained by inhibition of β-oxidation, as mentioned earlier. The most striking illustration of this is the lack of toxicity of 2,6-difluorohexanoic acid, $F(CH_2)_4CHFCOOH$. The corresponding monofluoro acid, 6-fluorohexanoic acid, $F(CH_2)_5COOH$ is very toxic (LD_{50} 1.35 mg/kg by intraperitoneal injection in mice), the biochemical explanation of which centers around β-oxidation to fluoroacetyl coenzyme A. Hence, the lack of toxicity of the difluoro acid must surely imply inhibition of the β-oxidation process by the α-fluorine atom.

The fluoroacetate-type convulsions observed with α-fluoroglutaric acid suggest that β-oxidation (at the non-fluorinated end of the molecule) has occurred, giving fluoromalonic acid, which in turn apparently decarboxylates to fluoroacetate, as outlined above. It has been reported recently (21) that α-fluoroglutaric acid is a competitive inhibitor of glutamate dehydrogenase, but is inactive against a variety of other enzymes including aconitase and the citrate-condensing enzyme.

The most interesting of the fluorinated unsaturated dibasic acids is monofluorofumaric acid, HOOCCF=CHCOOH (*trans*), in that it is a monofluorinated member of the tricarboxylic acid cycle. Its lack of toxicity indicates that it is not interfering with the normal operation of the cycle.

Infrared measurements on the *alkylated fluoromalonates* show that the α-fluorine atom causes a shift of about 25 cm^{-1} to higher frequency for the ester carbonyl band. The range is 1 754 – 1 757 cm^{-1} as compared with the ester carbonyl frequency of about 1 730 cm^{-1} for the non-fluorinated alkylated malonates. The C—F stretching band lies in the range 1 050 – 1 100 cm^{-1} and is of medium intensity. The fluorine in the *α-fluoroalkanoic acids* causes a similar shift in the acid carbonyl band. The range for the fluoro acids is 1 730 – 1 745 cm^{-1} as compared to 1 700 – 1 725 cm^{-1} for the non-fluorinated acids. The position of the C—F band (1 060 – 1 090 cm^{-1}) is very similar to that observed for the fluoromalonates and again is of medium intensity.

EXPERIMENTAL

Physical constants and analytical data for all new compounds are given in Table IV. The preparations described below represent typical examples of each procedure; obvious variations for obtaining different members have not been included. Purity of acids was checked by gas chromatography of their methyl esters. Melting points (uncorrected) were determined on a Kofler hot stage and densities with a Fisher-Davidson gravitometer. The nuclear magnetic resonance spectra were obtained with a Varian DP-60 spectrometer. Infrared spectra were obtained with Beckman IR-7 and IR-5 infrared spectrophotometers. Analyses were performed by the Schwarzkopf Microanalytical Laboratory, Woodside, 77, N.Y. The perchloryl fluoride was purchased from the Technical Division of Pennsalt Chemicals Corporation, Philadelphia 18, Pa. The sodium hydride dispersion (56.5%) in mineral oil was purchased from Metal Hydrides Incorporated, Beverly, Mass.

Can. J. Chem. Downloaded from www.nrcresearchpress.com by 210.87.254.42 on 09/05/12
For personal use only.

A. Syntheses Based on "BrF" Addition

2-Fluorohexanoic Acid

(a) From 2-fluorohexyl nitrate.—A mixture of 2-fluorohexyl nitrate (12) (8.8 g, 53.2 mmoles), glacial acetic acid (21 ml), and concentrated nitric acid (42 ml) was warmed in a 100 ml three-necked flask equipped with a reflux condenser at 40–42° for 52 h. The color changed from pale yellow to green and finally back to pale yellow. The mixture was then cooled, diluted with water (500 ml), and extracted five times with chloroform (50 ml portions). The chloroform extract was extracted with 5% aqueous sodium bicarbonate and the bicarbonate extract was acidified to methyl red with 6 *N* hydrochloric acid. The free acid was then extracted with ether. The ether extract was washed with water and dried over anhydrous sodium sulfate. Removal of the ether and distillation yielded the acid (4.40 g, 61.5%). It was subsequently found that the chloroform extraction and bicarbonate wash are unnecessary, as no neutral fraction remains after the oxidation procedure.

(b) From 2-fluorohexyl acetate.—A mixture of 2-fluorohexyl acetate (12) (5.36 g, 33.0 mmoles), glacial acetic acid (35 ml), and concentrated nitric acid (35 ml) was warmed at 48–51° for 20 or more hours. The mixture was cooled, diluted with water, and isolated by ether extraction. The extracts were washed with water and dried over anhydrous sodium sulfate. Removal of the ether, followed by fractionation through a spinning-band column, gave the acid (3.88 g, 87.5%).

(c) From 2-fluorohexyl formate.—A mixture of 2-fluorohexyl formate (12) (5.40 g, 36.4 mmoles), glacial acetic acid (35 ml), and concentrated nitric acid (35 ml) was warmed to 50°. No immediate reaction was apparent, but the mixture slowly turned yellow. After 90 min brown fumes were evolved and a vigorous exothermic reaction occurred. The flask was cooled in cold water, and the mixture was allowed to stand overnight, by which time it had turned green. It was left at room temperature for a further 100 h by which time the color had changed to pale yellow. The acid was isolated as under (*b*) above (3.34 g, 68.3%).

General Comments

(*a*) The color changes acted as a convenient internal indicator. During the reaction, samples were removed from time to time and extracted with chloroform; infrared analysis thereafter gave a measure of nitrate and acetate esters present. It was found that the end of the reaction coincided with the change from green to yellow. This conclusion was confirmed by gas chromatography.

(*b*) By the same procedure the following yields were obtained from the corresponding acetates (reaction times and yields in parentheses): *fluoroacetic acid* (44 h, 51%); *2-fluoropropanoic acid* (64 h, 55.5%); *2-fluorobutanoic acid* (21 h, 58%); *2-fluoroheptanoic acid* (25 h, 84%); *2-fluorooctanoic acid* (31 h, 86%); *2-fluorodecanoic acid* (46 h, 82%) (the last three acids were recrystallized from 35–60° petroleum ether); and *2-fluoroundecanedioic acid* (22 h, 81%), recrystallized from aqueous alcohol.

Special cases are discussed above (see Results).

B. Syntheses Based on Diethyl Fluoromalonate

Diethyl Fluoromalonate

This ester was prepared by the method of Bergmann, Cohen, and Shahak (13), with modifications; some of these have been described previously (14).

Sodium hydride dispersion (56.5%) in mineral oil (85 g, 2.0 moles) was added to anhydrous ether (400 ml) in an ice-cooled 2 l three-necked flask fitted with a stirrer, a reflux condenser with a drying tube, and an addition funnel. Ethyl fluoroacetate (212.2 g, 2.0 moles) in anhydrous ether (200 ml) was added dropwise with stirring over 19 h. No significant amount of hydrogen was evolved for about 4 h; then a slow steady evolution, which became vigorous after about 6 h, began. The mixture was allowed to warm to room temperature gradually over 24 h; it was then refluxed for 2 h to complete the formation of the enolate. Ethyl chloroformate (220.0 g, 2.03 moles) in anhydrous ether (100 ml) was then added over 20 min with stirring and cooling (ice bath). The ice bath was removed and the mixture was allowed to reflux spontaneously for 1.5 h, whereupon it was refluxed in warm water for a further 3 h. After stirring at room temperature for an additional 16 h, ice-cold water was added in sufficient amount to dissolve the sodium chloride present. The ether layer was separated and the aqueous layer was extracted with additional quantities of ether. The combined ether extracts were washed twice with 1% aqueous sodium bicarbonate solution and then with water, and were dried over anhydrous magnesium sulfate. The ether was removed by distillation, using anhydrous calcium sulfate as boiling stones; exclusion of moisture and acid is essential during distillation to avoid severe decomposition. Distillation through a 10 in. Vigreux column yielded recovered ethyl fluoroacetate (57.1 g) followed by crude diethyl fluoromalonate (72.1 g, 27.7%) of b.p. 86–94° at 9 mm, and n_D^{25} 1.4063. Redistillation through a platinum-plated spinning-band column gave the pure fluoroester (61.5 g, 23.6%).

Fluoromalonic Acid

This procedure is modified from that of Bergmann, Cohen, and Shahak (13).

Potassium hydroxide (3.86 g, 68.8 mmoles) was dissolved in absolute ethanol (30 ml) contained in a 50 ml three-necked flask fitted with a stirrer, a reflux condenser, and an addition funnel. Diethyl fluoromalonate (5.0 g, 28 mmoles) was added dropwise with stirring over 10 min. The initial reaction was exothermic; the white salt separated out and the mixture was stirred at room temperature for 7 h. The mixture was cooled and the salt was filtered. It was then dissolved in water and the solution was made distinctly acid

with concentrated hydrochloric acid. After extraction of the aqueous solution five times with ether, drying of the ether extracts over anhydrous magnesium sulfate, and removal the ether by evaporation, the fluoromalonic acid (1.64 g, 48%) was obtained as an off-white solid. Two recrystallizations from ether, the first using decolorizing charcoal, yielded the pure white crystalline acid.

Diethyl n-Propylfluoromalonate

Sodium hydride dispersion (56.5%) in mineral oil (2.38 g, 56 mmoles) was placed in a 100 ml three-necked flask fitted with a stirrer, a reflux condenser with drying tube, and an addition funnel; dry dimethylformamide (40 ml) was added. Diethyl fluoromalonate (10 g, 56 mmoles) was then added dropwise with stirring over 15 min, causing an exothermic reaction and a vigorous evolution of hydrogen. After 4.5 h, enolate formation was complete, as shown by a yellow solution and a lack of hydrogen evolution. *n*-Propyl bromide (6.90 g, 56 mmoles) was then added rapidly with stirring. The mixture was stirred and heated for 13 h at 70°, by which time the pH had levelled off at approximately 6.5; the acid pH indicated completion of the reaction. The reaction mixture was worked up by pouring it into water, extracting twice with ether, and washing the combined ether extracts 3 times with water to ensure removal of dimethylformamide. The ether solution was then dried over anhydrous magnesium sulfate and the ether was removed on a rotatory evaporator. The residual liquid was distilled through a small Vigreux column yielding diethyl *n*-propylfluoromalonate (9.16 g, 74.2%).

Other Alkylated Fluoromalonates

Other alkylated fluoromalonates were prepared in a similar manner (time of heating and temperature given in parentheses). Yields are listed in Table II. *Ethyl* (20 h, 55°), *isopropyl* (32 h, 70–80°), *n-butyl* (18 h, 60°), *4-fluorobutyl* (2 h, 70°), *4-carbethoxybutyl* (4 h, 80°), *hexadecyl* (11 h, 100°), *benzyl* (7 h, 80–85°), and *allyl* (12 h, 25°). Diethyl hexadecylfluoromalonate was not purified; it was hydrolyzed and decarboxylated directly to 2-fluorooctadecanoic acid.

2-Fluoropentanoic Acid

Diethyl *n*-propylfluoromalonate (9.0 g, 40.8 mmoles) and 6 *N* hydrochloric acid (60 ml) were heated under reflux for 23 h, i.e., until carbon dioxide was no longer evolved. The reaction mixture was then poured into water and extracted with ether. The ether extracts in turn were extracted with 5% sodium bicarbonate solution. The aqueous layer was acidified with dilute hydrochloric acid and extracted with ether. After drying of the extracts (anhydrous magnesium sulfate) and evaporation of the ether, vacuum distillation of the residual liquid through a spinning-band column yielded the pure acid (3.93 g, 80.1%). The purity of the acid was checked by vapor phase chromatography of its methyl ester.

Other α-Fluoroalkanoic Acids

Other α-fluoroalkanoic acids were prepared similarly from the corresponding alkylated malonates (time of reflux shown in parentheses): *2-fluorobutanoic* (23 h), *2-fluoro-3-methylbutanoic* (19 h), *2-fluorohexanoic* (17 h), *2,6-difluorohexanoic* (5 h), *α-fluoropimelic* (9 h), and *2-fluoro-3-phenylpropanoic* (8 h). The liquid members were purified by fractionation and the solid members by recrystallization from chloroform, benzene, or petroleum ether. Final purification of 2-fluoro-3-phenylpropanoic acid was achieved by sublimation (55° at 0.075 mm).

2-Fluorooctadecanoic Acid

Crude diethyl hexadecylfluoromalonate (17.3 g, 43.0 mmoles), 6 *N* hydrochloric acid (120 ml), and dioxane (200 ml) were refluxed for 70 h; at the end of this time, negligible evolution of carbon dioxide was observed. The mixture was poured into petroleum ether (b.p. 60–80°) and washed with water to remove the dioxane. An emulsion formed in the petroleum ether extract, and saturated brine solution was added to destroy it. A considerable amount of the sodium salt of the desired acid salted out at the interface and was filtered off. The petroleum ether layer was extracted twice with 10% aqueous potassium hydroxide solution. The sodium salt obtained above was added to the alkaline extract, and the combined mixture was acidified with concentrated hydrochloric acid. The organic acid was extracted with ether. The ether extracts were dried over anhydrous magnesium sulfate and the ether was evaporated on a rotatory evaporator, yielding the crude light-yellow α-fluorostearic acid (8.64 g, 66.4%). Recrystallization from petroleum ether (b.p. 35–60°) gave white crystals of the pure acid.

Diethyl 2-Carboxyethylfluoromalonate

The enolate of diethyl fluoromalonate was formed in the usual manner from diethyl fluoromalonate (5.0 g, 28.1 mmoles), 56.5% sodium hydride dispersion (1.20 g, 28.1 mmoles), and dry dimethylformamide (30 ml). β-Propiolactone (2.16 g, 30 mmoles) was then added rapidly with stirring. The reaction was stirred at room temperature for 1 h, then at 60–65° for 4 h; by this time the pH had levelled off at about 8.5, indicating that no further reaction was taking place. The mixture was poured into water and separated into neutral and acidic fractions in the usual manner. A small quantity of diethyl fluoromalonate (0.22 g) was recovered from the neutral extract. The acid fraction yielded the required product upon distillation (2.82 g, 41.8%).

α-Fluoroglutaric Acid

Crude diethyl 2-carboxyethylfluoromalonate (1.84 g, 7.3 mmole) was refluxed with 6 *N* hydrochloric acid (20 ml) in dioxane (50 ml) for 3.5 days, by which time carbon dioxide evolution had ceased. Most of the hydrochloric acid and solvents were distilled off under reduced pressure through a 10 in. Vigreux column.

Can. J. Chem. Downloaded from www.nrcresearchpress.com by 210.87.254.42 on 09/05/12
For personal use only.

The rest of the solvents were removed on a rotatory evaporator, leaving a brown syrup which gave a positive qualitative fluorine test but which would not crystallize. The syrup was thus taken up in ether and extracted with 5% sodium bicarbonate solution to separate the acid from any neutral materials present. The bicarbonate extract was acidified with dilute hydrochloric acid and extracted thoroughly with ether. (α-Fluoroglutaric acid is appreciably soluble in water.) After drying of the ether extracts over anhydrous magnesium sulfate and removal of the ether, 0.5 g of acidic material was obtained. Vapor phase chromatographic analysis of the methyl ester showed it to be only about 67% pure. Thus the yield of the hydrolysis is about 30%. The crude methyl ester was chromatographed through silica gel, the pure ester being eluted with 50:50 petroleum ether (30–60°) – benzene. The purified ester was then hydrolyzed by refluxing in dioxane with 6 *N* hydrochloric acid for 12 h. After removal of solvents the syrupy residue was dissolved in benzene from which white plates of α-fluoroglutaric acid separated, m.p. 105–112°; mixed with authentic sample (prepared by the PF route), m.p. 102–110°.

C. Syntheses Based on Perchloryl Fluoride

2-Fluoropropanoic Acid

Dry dimethylformamide (500 ml) and 56.5% sodium hydride dispersion in mineral oil (12.8 g, 299 mmoles) were placed in a three-necked flask fitted with a dropping funnel, a gas inlet tube, and a condenser. The flask was flushed with nitrogen, and diethyl methylmalonate (50 g, 295 mmoles) was added slowly over 1.5 h with stirring. Stirring was continued until effervescence ceased. The mixture was cooled in ice to 7° and perchloryl fluoride was introduced intermittently until a temperature increase was no longer observed and excess perchloryl fluoride had been added (31.2 g, 305 mmoles). The contents of the flask were flushed with nitrogen, and water (600 ml) was slowly added. The mixture was extracted with ether, and the extracts were washed with water, dried, and evaporated. The residue on fractional distillation gave crude diethyl methylfluoromalonate (30.05 g, 55%), b.p. 80–88° at 13 mm, n_D^{25} 1.4013. The impure ester (27.40 g, 143 mmoles) was heated under reflux with 6 *N* hydrochloric acid (500 ml) for 36 h, by which time a homogeneous solution was obtained. The solution was cooled, diluted with water, and extracted with ether. The extracts were washed with water, dried, and evaporated. The residue on fractional distillation gave impure 2-fluoropropanoic acid (6.74 g, 51%), b.p. 63–66° at 13 mm, n_D^{25} 1.3837. Further fractionation gave the pure acid.

α-Fluoroglutaric Acid

(a) Dimethyl α-carbomethoxyglutarate.—Sodium (2.3 g, 0.1 g-atom) was dissolved in methanol (200 ml) in a three-necked flask fitted with a reflux condenser, a dropping funnel, and a gas inlet tube. An atmosphere of nitrogen was maintained throughout, and the mixture was stirred magnetically. Dimethyl malonate (132.1 g, 1 mole) was added, followed by hydroquinone (200 mg). Methyl acrylate (43.0 g, 0.5 mole) was then added dropwise over a 30 min period to the refluxing solution. The mixture was refluxed for a further 23 h and then allowed to stand at room temperature for 2 days. Acidification (12 ml concentrated hydrochloric acid), filtration, and evaporation gave the crude ester. Chloroform was added, residual traces of sodium chloride were removed by filtration, the solvent was removed, and the residue was fractionated. The pure glutarate ester (83.9 g, 77%) was obtained after the excess dimethyl malonate (42.8% of original quantity) had been recovered.

(b) Dimethyl α-fluoro-α-carbomethoxyglutarate.—In a 500 ml three-necked flask carrying a drying tube, a dropping funnel, and a gas inlet tube was placed redistilled dimethylformamide (75 ml). Dry nitrogen was passed through and a 56.5% dispersion of sodium hydride in mineral oil (10.0 g, 235 mmoles) was introduced. The glutarate ester (50.0 g, 229 mmoles) was added dropwise over 1.5 h with stirring and cooling (ice bath). The dark mixture was stirred for a further 2.75 h at room temperature. Super-dry methanol (20 ml), to destroy the excess sodium hydride, and then dioxane (50 ml) were added. The flask was cooled in an ice bath and, when the temperature had fallen to 3.5°, perchloryl fluoride was introduced intermittently with stirring; the temperature was held in the range 3.5–16°. The addition required about 1.75 h. The end of the reaction was indicated by a fall in temperature on passing in perchloryl fluoride. After standing overnight, the mixture was diluted with water (800 ml) and the product extracted with ether. The extract was washed with water and the ether was removed. Benzene was used to azeotrope any residual water. The resulting residue was heterogeneous because of the presence of mineral oil. The latter (upper layer) was removed with a dropper prior to fractionation on the spinning-band column. After a forerun (6–7 g), the required fluoro ester (23.85 g, 44%) was obtained as a slightly turbid liquid. To obtain a clear, analytical sample, the ester was extracted three times with 60–80° petroleum ether and redistilled through a 23-plate platinum-plated spinning-band column.

(c) α-Fluoroglutaric acid.—The above ester (11.0 g, 46.5 mmoles) was hydrolyzed and decarboxylated by heating under reflux with 6 *N* hydrochloric acid (40 ml) at 115° for 6 h. The cooled hydrolysate was extracted with petroleum ether to remove any residual mineral oil or ester. The hydrochloric acid was distilled off under aspirator pressure. The crude acid was then distilled directly, using a simple distillation head attached to a vacuum adapter; the solid thus obtained (4.64 g, 66.6%), of b.p. 115–155° at 0.1–0.22 mm, was shown by infrared analysis to be the acid and not the anhydride (acetonitrile as solvent). The solid was recrystallized four times from 50:50 benzene–ether and dried at the temperature of refluxing chloroform at 0.5 mm for 3 h. No hydrate formation could be detected.

Can. J. Chem. Downloaded from www.nrcresearchpress.com by 210.87.254.42 on 09/05/12
For personal use only.

2-Fluoro-2-carbethoxycyclohexanone

Freshly cut sodium (8.25 g, 0.358 g-atom) was placed in a 1 l, three-necked flask fitted with a mercury-sealed stirrer, a reflux condenser with drying tube, and a dropping funnel. The flask was purged with dry nitrogen. Super-dry ethanol (700 ml) was added with cooling, and the mixture was stirred for 3 h. 2-Carbethoxycyclohexanone (26) (61.1 g, 0.358 mole) and then 0.05% bromthymol blue in alcohol (1 ml) were added. The flask was cooled, and perchloryl fluoride was introduced at such a rate as to maintain the temperature in the range 10–15°; 38.8 g of perchloryl fluoride was thus added over 85 min. The end of the reaction is marked by a color change from green to pale yellow. The flask was flushed with nitrogen, and the mixture was diluted with water (2 l) and extracted with ether. The extracts were washed with water, dried, and fractionated to yield 39.8 g (59%) of the fluoro ester.

The ester was converted to *2-fluorocyclohexanone* in 33.5% yield for other purposes (27) by treatment with aqueous sodium hydroxide at room temperature. Acidification, heating, extraction with ether, drying, and distillation yielded the fluoro ketone, b.p. 71° at 11 mm, n_D^{25} 1.4410, m.p. ca. 7° (lit. (28) b.p. 83–83.5° at 20 mm, n_D^{25} 1.4432); 2,4-dinitrophenylhydrazone, m.p. 138–140° (lit. (28) m.p. 139–140°).

α-Fluorophenylacetic Acid

(a) Diethyl phenylfluoromalonate.—In the usual apparatus and by the usual procedure, 56.5% sodium hydride in mineral oil (6.2 g, 145.6 mmoles) was added to dimethylformamide (250 ml); diethyl phenylmalonate (30 g, 126.8 mmoles) was then added dropwise. Excess sodium hydride was destroyed using dry ethanol (11 ml), and perchloryl fluoride (15.5 g, 151 mmoles) was passed in, the temperature being maintained in the range 7–23°. Bromthymol blue was used as indicator, the color changing from green to reddish brown at the conclusion of the reaction. Isolation in the usual way, followed by fractionation through the spinning-band column, gave the fluoro ester (25.15 g, 78.1%) (16).

(b) α-Fluorophenylacetic acid.—The above ester (5.0 g, 19.6 mmoles) was hydrolyzed and decarboxylated by refluxing at 115–120° with dioxane (30 ml) and 6 *N* hydrochloric acid (20 ml) for 18.5 h, by which time no further evolution of carbon dioxide could be observed. The dark solution was diluted with water (100 ml) and extracted with ether. The extract was washed with water, dried (sodium sulfate), filtered, and evaporated. The residue was placed in a vacuum desiccator (P_2O_5) at 10 mm for 12 h. The partly crystalline mass was then dissolved in benzene, and most of the solvent removed under aspirator pressure. This was repeated several times to ensure that the acid would be dry. Addition of petroleum ether and scratching induced crystallization. The crude material was redissolved by warming and adding a small amount of ether. Upon cooling in ice the acid crystallized as glistening platelets (1.93 g, 63.7%). A small amount was recrystallized from 60–80° petroleum ether – benzene, followed by sublimation at 65–68° at 0.1 mm over a 30 h period. Vapor phase chromatographic analysis (180°, DEGS column) of the methyl ester showed only one peak at 10.5 min (cf. methyl phenylacetate, 7.2 min). The acid is soluble in chloroform, benzene, and ether, but relatively insoluble in carbon tetrachloride and petroleum ether.

(c) Phenylfluoromalonic acid.—To a magnetically stirred solution of reagent grade potassium hydroxide (5.6 g, 100 mmoles) in absolute ethanol (100 ml) was added diethyl phenylfluoromalonate (5.0 g, 19.7 mmoles). Within a minute, the solution set to a white gel. The solid was filtered, washed with ether, and air dried (5.14 g, 95.2%). The salt was dissolved in water (240 ml) and acidified with 6 *N* hydrochloric acid (30 ml). The organic acid was thoroughly extracted with ether. The extracts were washed with water, dried (sodium sulfate), and evaporated under reduced pressure. The acid crystallized spontaneously. Yield: 1.87 g (48%). A small quantity was recrystallized from benzene–ether as the monohydrate; the melting point is unchanged even after standing in a P_2O_5 desiccator at 0.1 mm.

Diethyl Fluoronitromalonate

Diethyl nitromalonate (29) was converted to the fluoro nitro ester by the procedure subsequently described by Freeman (23). The infrared spectrum in carbon tetrachloride showed an ester C=O band at 1 785 cm^{-1} and a very strong C—F band at 1 083 cm^{-1}; also apparent were bands due to the —NO_2 group (1 605(s) and 1 280(s) cm^{-1}).

Methyl 2-Fluoro-2-ethylbutanoate

2-Ethylbutyraldehyde was converted (30) to 1,1-dimethoxy-2-ethylbutane in 82.5% yield using acetone dimethylketal; this in turn was treated with phthalic anhydride (31) to give *1-methoxy-2-ethyl-1-butene* in 80.7% yield. Into a 500 ml three-necked flask carrying a thermometer, a gas outlet tube, a gas inlet tube with a fritted-glass disc, and a stirring magnet was placed 1-methoxy-2-ethyl-1-butene (22.3 g, 195 mmoles), reagent grade pyridine (150 ml), and water (75 ml). Perchloryl fluoride (25.2 g, 246 mmoles) was admitted over 10.25 h with cooling (cold water). The mixture was allowed to stand overnight at room temperature. Five percent sodium bicarbonate (300 ml) was added and the neutral products were extracted with ether. This extract was washed with 6 *N* hydrochloric acid (to remove pyridine), water, sodium bicarbonate, and water. After drying (sodium sulfate) and removal of the ether, the residue was fractionated on the spinning-band column to give the fluoro ester (7.9 g, 34%). The infrared spectrum in $CHCl_3$ showed bands at 1 744 (C=O stretch) and 1 064 (C—F) cm^{-1}. The n.m.r. spectrum (19.3% in CCl_4) showed bands at 0.90 p.p.m. (triplet, J_{HH} 7.1 c.p.s.), at 1.79 p.p.m. (pair of overlapping quartets, J_{HF} 16.5 c.p.s., J_{HH} 7.1 c.p.s.), and at 3.73 p.p.m. (singlet due to OCH_3).

In order to recover the acid fraction, the bicarbonate solution was acidified and extracted with ether.

Can. J. Chem. Downloaded from www.nrcresearchpress.com by 210.87.254.42 on 09/05/12
For personal use only.

The extract, after it was washed, dried, and distilled, gave crude 2-fluoro-2-ethylbutanoic acid, b.p. 54–62° at 1 mm. This was converted to its *p-bromophenacyl derivative* by reaction of its dry potassium salt in dry dimethylformamide with *p*-bromophenacyl bromide at 75° for 10 h; removal of the dimethylformamide, addition of ether, filtration, and removal of the ether gave an oil which crystallized at 0°; recrystallization from 60–80° petroleum ether using Norit gave the pure material.

The *p-bromophenacyl derivatives of 2-fluorohexanoic and 6-fluorohexanoic acids* were prepared in the same way. Physical constants are given in Table IV.

ACKNOWLEDGMENTS

We wish to express our indebtedness to the National Research Council for financial support and for a studentship (R. L. B.), and to Canadian Industries Limited, Montreal, for the award of a fellowship (F. H. D.). We wish to acknowledge with thanks the gift of samples of difluoromaleic acid and monofluorofumaric acid from Dr. M. S. Raasch and of monofluoromaleic anhydride from Dr. W. H. Sharkey, Central Research Department, E. I. du Pont de Nemours and Co. Inc., Wilmington 98, Delaware. We are grateful to Dr. M. K. McPhail and Dr. C. A. deCandole, Suffield Experimental Station, Ralston, Alberta and Dr. C. W. Gowdey, University of Western Ontario for determining the toxicities; to Dr. D. A. V. Peters for preparing several of the fluoro acids and intermediates; to Dr. J. Newton for preparing 2-fluoropropanoic acid; to Mr. C. A. Gehrels for preparing diethyl fluoronitromalonate; and to Dr. J. B. Stothers of this department for help with the nuclear magnetic resonance spectra.

REFERENCES

1. R. L. Buchanan, F. H. Dean, and F. L. M. Pattison. Preprints, Second International Symposium on Fluorine Chemistry. 1962. p. 385.
2. B. C. Saunders and G. J. Stacey. J. Chem. Soc. 1773 (1948).
3. E. Gryszkiewicz-Trochimowski, A. Sporzynski, and J. Wnuk. Rec. Trav. Chim. **66**, 413 (1947).
4. W. Bockemüller. Ann. **506**, 20 (1933).
5. E. D. Bergmann and S. Szinai. J. Chem. Soc. 1521 (1956).
6. E. D. Bergmann and I. Shahak. J. Chem. Soc. 5261 (1960); 4033 (1961).
7. G. Schmidt and H. Jahn. Ann. **644**, 43 (1961).
8. E. D. Bergmann and I. Shahak. Chem. Ind. London, 157 (1958).
9. F. L. M. Pattison and J. E. Millington. Can. J. Chem. **34**, 757 (1956).
10. A. Ya. Yakubovich, T. G. Spiridonova, and P. O. Gitel. USSR Patent No. 122,744 (Oct. 10, 1959); Chem. Abstr. **54**, 7562*f* (1960).
11. A. Bowers. J. Am. Chem. Soc. **81**, 4107 (1959); subsequent papers.
12. F. L. M. Pattison, D. A. V. Peters, and F. H. Dean. Can. J. Chem. This issue.
13. E. D. Bergmann, S. Cohen, and I. Shahak. J. Chem. Soc. 3286 (1959).
14. R. L. Buchanan, F. H. Dean, and F. L. M. Pattison. Can. J. Chem. **40**, 1571 (1962).
15. V. H. Wallingford, M. A. Thorpe, and A. H. Homeyer. J. Am. Chem. Soc. **64**, 580 (1942).
16. C. E. Inman, R. E. Oesterling, and E. A. Tyczkowski. J. Am. Chem. Soc. **80**, 6533 (1958).
17. F. H. Dean and F. L. M. Pattison. Can. J. Chem. **41**, 1833 (1963).
18. M. S. Raasch, R. E. Miegel, and J. E. Castle. J. Am. Chem. Soc. **81**, 2678 (1959).
19. E. D. Bergmann and I. Shahak. Chem. Ind. London, 591 (1961).
20. K. Bernhard. Hoppe-Seyler's Z. Physiol. Chem. **269**, 135 (1941).
21. L. K. Gottwald, J. E. Ayling, and E. Kun. J. Biol. Chem. **239**, 435 (1964).
22. J. D. LaZerte, D. A. Rausch, R. J. Koshar, J. D. Park, W. H. Pearlson, and J. R. Lacher. J. Am. Chem. Soc. **78**, 5639 (1956).
23. J. P. Freeman. J. Am. Chem. Soc. **82**, 3869 (1960).
24. E. Gryszkiewicz-Trochimowski and O. Gryszkiewicz-Trochimowski. Bull. Soc. Chim. France, 928 (1949).
25. B. B. Corson, R. K. Hazen, and J. S. Thomas. J. Am. Chem. Soc. **50**, 913 (1928).
26. H. R. Snyder, L. A. Brooks, and S. H. Shapiro. Organic syntheses. Collective Vol. II. John Wiley and Sons, Inc., New York, N.Y. 1943. p. 531.
27. H. G. Ferguson, P. de Mayo, F. L. M. Pattison, and T. Tabata. Can. J. Chem. **41**, 2099 (1963).
28. S. Nakanishi, K-I. Morita, and E. V. Jensen. J. Am. Chem. Soc. **81**, 5259 (1959).
29. D. I. Weisblat and D. A. Lyttle. J. Am. Chem. Soc. **71**, 3079 (1949).
30. N. B. Lorette and W. L. Howard. J. Org. Chem. **25**, 521 (1960).
31. H. Scheibler and H. Baganz. Ann. **565**, 157 (1949).

Can. J. Chem. Downloaded from www.nrcresearchpress.com by 210.87.254.42 on 09/05/12
For personal use only.

Can. J. Chem. Downloaded from www.nrcresearchpress.com by 210.87.254.5 on 09/05/12
For personal use only.

CONDITIONS FOR THE PHOTOCHEMICAL NITRATION OF BENZENE

DAVID L. BUNBURY
Department of Chemistry, St. Francis Xavier University, Antigonish, Nova Scotia
Received February 4, 1964

ABSTRACT

The reaction of benzene and nitrogen dioxide to produce nitrobenzene has been studied in the liquid and gas phases, in the dark, and with irradiation by light of 439 mμ and of 366 mμ. The concentration of NO_2 in the liquid was varied from 0.08 to 1.6 moles/l and in the gas from 0.0035 to 0.053 moles/l. No nitrobenzene was produced under any conditions in the liquid phase. Nitrobenzene is produced in the gas phase at high NO_2 concentrations with irradiation by 366 mμ light. The quantum yield is 0.2. At 439 mμ the quantum yield is not more than 0.02. There is a very small dark reaction. As the concentration of NO_2 in the gas is reduced the yield of nitrobenzene falls off very rapidly and is zero at the lowest concentration used, both in dark and light.

INTRODUCTION

It is known that light of wavelength 365 mμ causes decomposition of nitrogen dioxide (1) and that of 436 mμ causes activation (2). It appeared to be interesting, then, to study the different types of reaction which might occur between benzene and NO_2 on using these two wavelengths to initiate the reaction, especially in view of the reported enhancement of the yield of nitrobenzene on irradiating mixtures of benzene and nitrogen dioxide with light (6, 9). The reactions of nitrogen dioxide with organic compounds have been reviewed by Riebsomer (3*a*), Gray and Yoffe (3*b*), Topchiev (3*c*), and Titov (3*d*). Table I summarizes the experimental results of the earlier workers who used conditions comparable to those used in this work.

EXPERIMENTAL

The nitrogen dioxide was obtained from the Matheson Company and purified further by fractional distillation, the middle third being kept. It was stored at dry-ice temperatures in a covered bulb and in all cases was pure white when frozen. It was measured either as a gas at room temperature or as a liquid at 0 °C using calibrated volumes. All calculations for obtaining NO_2 concentration from measured temperature and pressure and for NO_2/N_2O_4 ratios were based on the paper of Verhoek and Daniels (11). The benzene was Fisher certified grade and further purified by freezing. It was gas chromatographically pure on use and measured by pipette or Hamilton microsyringe. The benzene and nitrogen dioxide were handled on a conventional high vacuum system and were dried with P_2O_5 just before use, except where noted. The cells for the liquid phase runs had flat windows and were made of Pyrex glass (greater than 90% transmission in the regions of interest). In run 1 a cell of 30 ml was used, in the other liquid phase runs a cell of 10 ml was used. The gas phase runs were performed in either a liter flask or a 165 ml flask. Both had a small test tube attached with ground joint for freezing the reaction mixtures into the bulb and for removal after reaction. All cells were closed with a ground glass joint and stopcock, and samples degassed prior to use.

The light source was an HBO-109 high pressure mercury vapor lamp with fused quartz envelope, from George W. Gates and Co., Inc. This lamp has an arc of 0.3 mm × 0.3 mm. This arc was placed in the focal plane of a Pyrex lens. The 439 mμ line was isolated using a Farrand Interference Filter, half band width 13 mμ, while the 366 mμ line (actually 350–386) was isolated using a 7-83 filter from Corning Glass Works. Light intensity was measured using the potassium ferrioxalate actinometer of Hatchard and Parker (12). Complete absorption occurred in the liquid phase runs and practically complete absorption in the gas phase runs. After a run samples were usually washed with 10% $KHCO_3$ and then water, dried with Drierite, and analyzed on a Burrell K-1 Kromotog using either Ap-L or silicone columns and usually a thermal conductivity cell as dectector. In runs 23–29 where very small amounts of benzene were used (0.01–0.05 ml) 0.25 ml of benzene was added after the addition of $KHCO_3$. Following each injection of a sample a standard nitrobenzene solution was injected for comparison of retention times and of areas. Identification of the nitrobenzene product was made by trapping it at the exit of the column and comparing its infrared spectrum with that of an authentic sample. Amounts were calculated by the ratio of areas of the unknown and that

Can. J. Chem. Downloaded from www.nrcresearchpress.com by 210.87.254.5 on 09/05/12
For personal use only.

TABLE I

Summary of earlier work

	Conditions								Products		
Ref.	Temp. (°C)	Time	Hydrocarbons	ArH (moles)	ArH/NO_2 (moles)	Phase	Light used	Effect on yield of $ArNO_2$	$ArNO_2$ (%)	Poly-nitric	Phenolic (g)	Acidic
4	Low	Several days	C_6H_6	—	N_2O_3	Liquid	—	—	Some		Picric	Oxalic
5	80	6 h	C_6H_6(dry)	—	1 (N_2O_4)	Liquid	—	—	Low	Trinitro	Picric	Oxalic
5	Rm. temp.	—	C_6H_6	—		Liquid	—	—	No reaction	—	—	—
6	Rm. temp.	3 mo	C_6H_6(dry)	0.154	2.36(N_2O_4)	Liquid	—	—	3.8	—	—	—
6	Rm. temp.	3 mo	C_6H_6(dry)	0.128	2.36(NO_2)	Liquid	Sunlight	Increase	31.4	Dinitro	—	—
6	Rm. temp.	3 mo	$C_6H_5CH_3$	0.13	2.4(NO_2)	Liquid	—	—	—	—	—	Benzoic
6	55	4 h	$C_6H_6CH_3$(dry)	0.543	(NO_2)	Liquid	Hg quartz	None	—	—	—	—
6	Rm. temp.	6 h	$C_6H_6CH_3$(dry)	0.543	(NO_2)	Liquid	Hg quartz	None	—	—	—	Benzoic
7	Rm. temp.	35 days	C_6H_6	—	1.5	Liquid	—	—	30.	—	—	—
8	14–15	2 h	$C_6H_6CH_3$	0.435	0.02(NO_2)	Flow gas + CO_2	—	—	31.9	—	$C_6H_5CH_2NO_2$	—
8	14–15	2 h	$C_6H_5CH_3$	0.435	0.02(NO_2)	"	Hg quartz	Increase	45.3	—	$C_6H_5CH_2NO_2$	—
8	25–30	2 h	C_6H_6	0.513	0.024(NO_2)	"	—	—	27	—	—	—
8	25–30	2 h	C_6H_6	0.513	0.024(NO_2)	"	Hg quartz	Marginal	28.5	—	—	—
8	25–30	2 h	C_6H_6	0.513	0.05	"	—	—	27	—	—	—
8	25–30	2 h	C_6H_6	0.513	0.10		—	—	6	—	—	—
9	20	Several h	C_6H_6	—	0.82	Gas	—	—	2.18	—	—	—
9	20	Several h	C_6H_6	—	0.82	Gas	Visible	None	2.29	Some	—	—
9	20	Several h	C_6H_6	—	0.35	Gas	—	—	3.03	—	—	—
9	20	Several h	C_6H_6	—	0.35	Gas	Visible	None	3.03	—	—	—
9	Rm. temp.	5 h	C_6H_6	—	Sat. NO_2	Liquid	—	—	2.27	0.13	—	—
9	Rm. temp.	5 h	C_6H_6	—	Sat. NO_2	Liquid	7 000 – 2 000 Å	Decrease	1.49	1.56	—	—
9	Rm. temp.	5 h	C_6H_6	—	Sat. NO_2	Liquid	7 000 – 4 000 Å	Increase	3.43	1.21	—	—
9	Rm. temp.	5 h	C_6H_6	—	Sat. NO_2	Liquid	4 000 – 2 800 Å	Decrease	2.17	.72	—	—
10	20	4 mo	C_6H_6	2.25	1.08	Liquid	—	—	Combined 0.26 g	—	0.31	Oxalic
10	20	4 mo	C_6H_6	2.25	2.71	Liquid	—	—	0.87g	—	0.60	Oxalic
10	20	4 mo	C_6H_6	2.25	10.8	Liquid	—	—	2.6g	—	0.95	Oxalic

produced by the standard solution. To test the possibility of reaction of the nitrobenzene with the base or of adsorption on the drying agent, a 3.45×10^{-4} mole fraction solution of nitrobenzene was washed with 10% NaOH three times and then with water and allowed to stand over Drierite. There was no difference in the size of the nitrobenzene peak given by the washed and unwashed material. Runs 14, 15, 16, 17, and 19 were directly injected onto the column without any treatment.

The basic extract of runs 7 and 8 was acidified with HCl and extracted with 30 ml of benzene, and the benzene evaporated to dryness in a small container. The residue was ground together with a minimum amount of powdered KCl and an infrared spectrum taken of the disc. The only thing found was a small amount of some carboxylic acid which turned out to be in the reagent benzene itself.

RESULTS AND DISCUSSION

The results are summarized in Table II.

The lower limit for the detection of nitrobenzene was 3×10^{-5} mole fraction both for thermal conductivity and hydrogen flame detection. Much smaller samples had to be used with the hydrogen flame detector so the lower limit was no less than that with the thermal conductivity detector.

Reactions in the liquid phase at room temperature will be first considered. Yields in the dark reaction were: the present author 0.00% in 19 days; Wieland 0.00% (5); Gorislavetz 2.27% in 5 h (9); Bass and Johnson 3.8% in 3 months (6); Titov 0.69–6.9% in 4 months (10); and Schaarschmidt and Smolla > 30% in 35 days (7). Longer times with the last authors resulted in a decrease in the yield of nitro products. Ratios of reactants are not the same in any of these cases nor are reaction times, but in several pairs of experiments they are of the same order of magnitude (see Table I). Titov's solution with C_6H_6/NO_2 ratio of 10.8 (most comparable to the results here reported) had 0.0088 mole fraction nitrobenzene after 4 months. Assuming linearity of nitrobenzene production, after 19 days run 4 should have been 0.0014 mole fraction of nitrobenzene. This, however, is 40 to 50 times greater than the lower limit of detection. Also, according to Titov's results the yield of nitrobenzene should go up with an increase in the C_6H_6/NO_2 ratio; therefore, the yield in run 4, if anything, should have been higher. Titov varied the ratio by increasing the benzene, and the fact that the yield increased in almost direct proportion to the amount of benzene even though it was in an excess suggests that it was an impurity which was reacting. In the course of a study of molecular addition compounds of N_2O_4 and aromatic hydrocarbons, Addison and Sheldon (13) found no detectable reaction between benzene and dinitrogen tetroxide during a period of several hours at room temperature. In view of the negative results, the low yields when reaction did occur, and the fact that reaction with even a small amount of impurity would produce some nitric acid, the most probable conclusion is that there is no reaction between pure benzene and NO_2–N_2O_4 at room temperature.

For irradiated mixtures in the liquid phase the present author found no reaction after 3 h with unfiltered mercury light, light of 439 mμ, and light of 366 mμ. After 5 h Gorislavetz (9) found a decrease in yield from 2.27 to 1.49 with unfiltered light and increase to 3.43 (about double) with light of 700–400 mμ, and a small decrease to 2.17 with light of 400–280 mμ. Bass and Johnson (6) found an eightfold increase to 31.4% after irradiation with sunlight for 3 months. The amount of light absorbed in the last two examples is not stated. Under the conditions of the present work the quantum yield for nitrobenzene production is less than 0.01 at 439 mμ and less than 0.011 at 366 mμ. The calculation was based on the lower limit of detection of nitrobenzene and the volume of the sample.

Three runs were made on toluene with amounts and conditions approximately the same as runs 7, 8, and 9. No nitrotoluenes were found. Interestingly, Bass and Johnson (6) found no nitrotoluenes both in the dark and on irradiation with a mercury lamp.

Can. J. Chem. Downloaded from www.nrcresearchpress.com by 210.87.254.5 on 09/05/12
For personal use only.

Can. J. Chem. Downloaded from www.nrcresearchpress.com by 210.87.254.5 on 09/05/12
For personal use only.

TABLE II

Results of nitration runs

	Conditions								Products	
Run	Temp. (°C)	Time (h)	C_6H_6 (moles)	C_6H_6/NO_2 (molar ratio)	Concn. of NO_2* (moles/l × 10^2)	Phase	Light used (einsteins × 10^6)	Wavelength (mμ)	Nitrobenzene (moles × 10^6)	Other
1†	23	2	0.338	147	7.74	Liquid	—	Dark	None	—
4	25	19 days	0.1125	32.5	34.6	Liquid	—	Dark	None	—
5	27	2	0.1125	32.5	34.6	Liquid	—	Unfiltered Hg	None	—
7	25	3	0.1125	7.04	159.8	Liquid	370	439	None	—
8	25	3	0.1125	6.80	165.4	Liquid	300	366	None	None
9	25	3	0.1125	8.95	125.6	Liquid	—	Dark	None	None
13‡	25	2.58	0.1125	6.96	161.6	Liquid	314	439	None	—
14	25	3	0.00405	1.17	0.351	Gas	300	439	None	—
15	25	2.95	0.0045	1.3	0.351	Gas	200	366	None	—
19	25	1.5	0.0045	1.3	0.351	Gas	—	Dark	None	—
20	25	3	0.0045	1.3	0.351	Gas	200	366	None	—
21	100	1.6	0.00225	1.65	0.083	Gas	160	439	None	—
22	25	1.8	0.00225	Unknown§	Unknown	Liquid	180	439	None	—
23	26	2	112.5 × 10^6	0.016	4.32	Gas	—	Unfiltered Hg	85.8	—
24	21	2	506.4 × 10^6	0.070	4.28	Gas	—	Unfiltered Hg	141.9	—
25	21	2	112.5 × 10^6	0.075	0.886	Gas	—	Unfiltered Hg	14.3	—
26	23	17.5	112.5 × 10^6	0.0125	5.30	Gas	—	Dark	0.12	—
27	23	2	112.5 × 10^6	0.0136	4.87	Gas	200	439	2.78	—
28	25	2	112.5 × 10^6	0.0139	4.59	Gas	160	366	30.6	—
29	24	2	506.4 × 10^6	0.0786	0.62	Gas	—	Unfiltered Hg	0.37	—

*Recorded as if the NO_2–N_2O_4 mixture was all NO_2.
†Omitted runs were: runs with a lower light intensity under conditions where no reaction occurs, procedural checks, or involved toluene.
‡Benzene was half saturated with water.
§A mixture of nitrogen oxides was used.

Can. J. Chem. Downloaded from www.nrcresearchpress.com by 210.87.254.5 on 09/05/12
For personal use only.

Reaction to produce nitrobenzene does occur in the gas phase. The production of nitrobenzene is very dependent on irradiation, contrary to Schorigin and Toptschiew (8) and to Gorislavetz (9). The production of nitrobenzene is very dependent on the concentration of nitrogen dioxide, in agreement with the authors just mentioned. Comparing runs 23, 24, 25, and 29 and runs 20 and 28 (Table II) it is seen that as the concentration of nitrogen dioxide is reduced, the amount of nitrobenzene falls precipitously even though the nitrogen dioxide is in a large excess except in run 20. Comparing runs 23 and 24 it is seen that increasing the benzene/NO_2 ratio does not decrease the production of nitrobenzene. The fact that it increases is not surprising as about 76% of the benzene was nitrated in run 23. Light of wavelength 366 mμ with a quantum yield of 0.2 is more than 10 times as effective as that of 439 mμ. It may well be that the reaction apparent at 439 mμ is due to a few percent of 404.7 mμ (which can also dissociate NO_2, (14)) getting through the filter.

In a recent paper on the photolysis of NO_2, Pitts, Sharp, and Chan (14) propose a mechanism in which three reactive species are produced by the action of light, activated NO_2, O atoms, and NO_3. Since absorption is practically total at all concentrations here studied the amount of these reactive species produced should at least be of the same order of magnitude at all nitrogen oxide concentrations. Since light of 439 mμ is relatively ineffective, activated NO_2 is most probably not the species involved. Since the concentration of N_2O_4 falls more rapidly than the total oxide concentration (Table III), although not as rapidly as the production of nitrobenzene, it would appear that both N_2O_4 and O atoms or NO_3 are needed for the photochemical nitration of benzene at room temperature. Possibly the oxygen atoms combine with the N_2O_4 to make N_2O_5 which is quoted (3*d*) as being many times more effective than N_2O_4 as a nitrating agent. Titov, however, goes on to suggest that N_2O_5 is so effective because it dissociates to form NO_3 which of course would be present in the photolysis of NO_2 alone.

TABLE III

Actual concentrations of N_2O_4 and NO_2 as total oxide concentration changes calculated at 25°

Total oxide as NO_2 (moles/l $\times 10^2$)	Fraction N_2O_4 dissociated	N_2O_4 (moles/l $\times 10^2$)	NO_2 (moles/l $\times 10^2$)
4.28	0.216	1.68	0.924
0.886	0.421	0.256	0.392
0.62	0.487	0.159	0.302
0.35	0.584	0.073	0.205

No explanation can be offered for the lack of effect of light observed by the other workers. Schorigin and Toptschiew (8) do observe a substantial increase in yield of nitrotoluenes on irridation of toluene and NO_2 (Table I). With benzene and NO_2 they observe a variation in yield with temperature. At 10–12° it is 12.7%, at 25–30° it is 28.5%, at 55–60° it is 31.6%, and at 80–85° it is again 12.7%. Since at 1 atm N_2O_4 is 20% dissociated at 27°, 53% at 60°, and 90% at 100° (15), the variation that they observe might be explained by the requirement that both NO_2 and N_2O_4 be present for nitrobenzene to be formed.

ACKNOWLEDGMENTS

The writer gratefully acknowledges the support of the National Research Council for this work and thanks Miss J. M. Osyany for the translation of ref. 9 from Russian.

REFERENCES

1. W. A. NOYES, JR. and P. A. LEIGHTON. The photochemistry of gases. Reinhold Publishing Corp., New York. 1941. p. 400.
2. D. NEUBERGER and A. B. F. DUNCAN. J. Chem. Phys. **22**, 1693 (1956).
3. (*a*) J. L. RIEBSOMER. Chem. Rev. **36**, 157 (1945). (*b*) P. GRAY and A. D. YOFFE. Chem. Rev. **55**, 1099 (1955). (*c*) A. V. TOPCHIEV. Nitration of hydrocarbons and other compounds. Pergamon Press, Inc., New York. 1959. (*d*) A. I. TITOV. Tetrahedron, **19**, 557 (1963).
4. A. LEEDS. J. Am. Chem. Soc. **2**, 277 (1880).
5. H. WIELAND. Ber. **54**, 1776 (1921).
6. L. BASS and T. B. JOHNSON. J. Am. Chem. Soc. **46**, 456 (1924).
7. A. SCHAARSCHMIDT and E. SMOLLA. Ber. **57**, 32 (1924).
8. P. SCHORIGIN and A. TOPTSCHIEW. Ber. **67B**, 1362 (1924).
9. I. O. GORISLAVETS. J. Phys. Chem. USSR, **17**, 102 (1943).
10. A. I. TITOV. J. Gen. Chem. USSR Eng. Transl. **22**, 1373 (1952).
11. F. H. VERHOEK and F. DANIELS. J. Am. Chem. Soc. **53**, 1250 (1931).
12. C. G. HATCHARD and C. A. PARKER. Proc. Roy. Soc. London, Ser. A, **235** 518 (1956).
13. C. C. ADDISON and J. C. SHELDON. J. Chem. Soc. 1941 (1956).
14. J. N. PITTS, JR., J. H. SHARP, and S. I. CHAN. J. Chem. Phys. **42**, 3655 (1964).
15. N. V. SIDGWICK. The chemical elements and their compounds. Vol. 1. Oxford Univ. Press. 1950. p. 688.

Can. J. Chem. Downloaded from www.nrcresearchpress.com by 210.87.254.5 on 09/05/12
For personal use only.

Can. J. Chem. Downloaded from www.nrcresearchpress.com by 210.87.254.105 on 09/05/12
For personal use only.

TELLURATE COMPLEXES OF NICKEL, PALLADIUM, AND PLATINUM, AND A PERIODATE COMPOUND OF NICKEL

M. W. LISTER AND P. MCLEOD
Department of Chemistry, University of Toronto, Toronto, Ontario
Received October 19, 1964

ABSTRACT

The periodate or tellurate complexes of nickel, palladium, and platinum have been examined. The preparation of $NaNi_2IO_6.2H_2O$, $NaNi_4(H_3TeO_6)_3.6H_2O$, $Na_6Ni(H_3TeO_6)_3.H_2O$, $Na_9H_5Ni_2(TeO_6)_3$, $Na_5H_3Pd(TeO_6)_2.4H_2O$, and $Na_5H_3Pt(TeO_6)_2.2H_2O$ is described.

Periodate and tellurate ions are known to stabilize relatively high valency states of some transition metals, copper(III) and nickel(IV) in particular (1, 2, 3). Complex periodates and tellurates in general have been reviewed in ref. 4. The present work is concerned with these complexes of nickel, palladium, and platinum. The compounds $NaNiIO_6.H_2O$ and $KNiIO_6.H_2O$ from Ni(IV) have been prepared by Ray and Sarma (3) using somewhat acid conditions, and it was hoped that alkaline oxidation, for instance by hypochlorite ions, might yield different compounds. In fact no very unusual compounds turned up, but the following sections summarize what was found to be the behavior of the above three metals with tellurate or periodate ions.

Nickel

Attempts to prepare a complex periodate of nickel, with the nickel in a valency higher than two, by hypochlorite oxidation, were unsuccessful. Both sodium periodate and nickel hydroxide precipitated so readily that only mixed precipitates were obtained. Periodic acid alone in weakly acid solution did not oxidize divalent nickel ions, and the absorption spectrum of mixtures in solution on a pH from 2 to 4 gave no evidence of any complex ion being formed. When the pH was raised to 4.5 by adding sodium hydroxide, a green solid precipitated. This appeared to be of constant composition, and analyzed as follows: Na, 7.6; Ni, 29.3; I, 31.7; loss in weight at 150 °C (presumably water), 9.5; calcd. for $NaNi_2IO_6.2H_2O$: Na, 5.8; Ni, 29.4; I, 31.8; H_2O, 9.0%. The equivalent weight of the compound as an oxidizing agent (with acidified potassium iodide) agreed with a formula containing divalent nickel, and the green color supports this.

Nickel chloride solution and telluric acid were mixed in a molar ratio of 1 to 3 and addition of alkaline sodium hypochlorite gave a precipitate which was filtered off, washed, and dried. It was green in color, and had no oxidizing properties attributable to a nickel valency higher than two. It analyzed as follows: Na, 22.0; Ni, 11.8; Te, 38.6; calcd. for $Na_9H_5Ni_2(TeO_6)_3$: Na, 20.7; Ni, 11.7; Te, 38.2%. This is probably a genuine compound, since the Ni/Te ratio is quite different from what was put in, but it is so insoluble that no method was found for purifying it. On heating a mixture similar to that above, especially with a larger excess of sodium hypochlorite, a black precipitate resulted, which remained black if very cautiously dried. On heating it turned green. It analyzed as follows: Na, 17.0; Ni, 6.74; Te, 42.44; loss at 150 °C, 4.4; calcd. for $Na_6H_9Ni(TeO_6)_3.H_2O$: Na, 15.4; Ni, 6.56; Te, 42.79; H_2O, 2.0%. The compound turned green at 150 °C, so presumably decomposition as well as water loss had occurred. Its equivalent weight as an oxidizing agent (with excess acidified ferrous ammonium sulfate, and titration of the excess) corresponded to an apparent valency for nickel of 2.78. This is presumably

trivalent nickel, with some decomposition. The formula is probably more correctly written $Na_6Ni(H_3TeO_6)_3.H_2O$.

In acid solution (pH 1.4 to 5.4) nickel(II) perchlorate and telluric acid gave an absorption spectrum virtually the same as that of hydrated Ni^{++}, so there is no evidence of complexing in these solutions. If sodium hydroxide was added when the pH reached 6, an apple-green precipitate formed. A sample prepared from a solution containing equimolar amounts of nickel perchlorate and telluric acid analyzed as follows: Na, 2.1; Ni, 22.3; Te, 37.1; loss in weight at 150 °C, 9.9; calcd. for $NaH_9Ni_4(TeO_6)_3.6H_2O$: Na, 2.2; Ni, 22.45; Te, 36.6; H_2O, 10.3%. This unexpected ratio of ligand to metal is not unprecedented, as $Na_3Co_4(IO_6)_3.11H_2O$, and the corresponding potassium salt, have been prepared (5). The present compound is probably $NaNi_4(H_3TeO_6)_3.6H_2O$.

Palladium

Telluric acid and palladium(II) chloride were dissolved in water in the molar ratio of 3 to 1. The solution was warmed nearly to boiling and sodium hypochlorite (1.5 *M*) containing excess sodium hydroxide was added. An orange-yellow precipitate formed, but this slowly redissolved on continued heating to give a dark-orange solution. On cooling and standing, orange-yellow crystals formed. The compound analyzed as follows: Pd, 13.4; Te, 33.85; Na, 15.2; loss of weight on heating, 9.4; calcd. for $Na_5H_3Pd(TeO_6)_2.4H_2O$: Pd, 14.3; Te, 34.3; Na, 15.45; H_2O, 9.7%. The equivalent weight as an oxidizing agent with ferrous ammonium sulfate was 370; calculated for Pd(IV) to Pd(II), 372. The formula appears to require different numbers of hydrogens attached to the two tellurate groups, in an ion such as $Pd(HTeO_6)(H_2TeO_6)^{-5}$. However, since the compound formed from alkaline solution, it is possible that a hydroxide group is attached to the palladium, in an ion such as $Pd(OH)(H_2O)(H_2TeO_6)_2^{-5}$, differing from the previous ion by two water molecules. It was found that of the four waters formally present in the compound, two were lost easily, and two only at 150 °C. The compound was too insoluble to be investigated by pH titration in aqueous solution.

Platinum

Platinum(IV) chloride and telluric acid were dissolved in water in the molar ratio of 1 to 3. The mixture was made strongly alkaline with sodium hydroxide, and was kept at 95 °C for 2 h. On cooling and standing, bright-yellow crystals formed. The material was difficult to analyze, since reagents which precipitated tellurium also precipitated platinum, and in fact tellurium dust had been used earlier as a precipitant for platinum (6). The method of analysis eventually adopted was to dissolve the compound in 30 ml of concentrated hydrochloric acid, and then to add 50 ml of saturated aqueous sulfur dioxide and 15 ml of 15% aqueous hydrazine hydrochloride. The mixture was kept at 80 °C, and after standing overnight the precipitate of both tellurium and platinum was filtered off. On evaporating the filtrate, more precipitate usually formed, so the process was repeated until no further precipitate was produced. The precipitate was filtered off, transferred to a crucible, and heated in hydrogen at 700 °C for 2 h. This removed the tellurium (presumably as TeH_2) and the crucible was cooled in nitrogen and weighed. The heating in nitrogen was continued until the crucible reached constant weight. This gave the weight of platinum in the sample. The filtrate was evaporated to dryness with sulfuric acid, and the sodium was weighed as sodium sulfate. The tellurium was determined by the method of Gooch and Howland (7). A sample was mixed with 3 g of potassium bromide and 50 ml of 10% sulfuric acid. Bromine was liberated according to the equation

$$H_6TeO_6 + 6HBr \rightarrow TeBr_4 + Br_2 + 6H_2O$$

Can. J. Chem. Downloaded from www.nrcresearchpress.com by 210.87.254.105 on 09/05/12
For personal use only.

and this was swept out in a stream of nitrogen and caught in potassium iodide solution. The liberated iodine was titrated. The water was determined by the weight loss at 150 °C.

The result of the analysis was Pt, 22.5; Te, 33.9; Na, 13.1; loss on heating, 4.7; calcd. for $Na_5H_3Pt(TeO_6)_2.2H_2O$: Pt, 24.5; Te, 32.1; Na, 14.4; H_2O, 4.5. The compound did not reduce potassium permanganate, which was taken as evidence that it only contained Pt(IV) (see ref. 8). The compound formed rather slowly, even at 95 °C, as shown by progressive change in the spectrum of the solution. With 0.002 *M* platinum, and 0.006 *M* telluric acid, complex formation was half complete in about 1 h. The complex had a strong absorption band which extended just into the visible, but with a maximum at 256 mμ. It only dissolved in water to the extent of 0.05 g/l at 25 °C, though much more concentrated solutions existed briefly during its preparation.

DISCUSSION

Campbell and Nyman (9) have noted that, for similar compounds to those prepared above, the ratio ligand/metal is usually greater than one for complexes prepared from alkaline solution, and one or less from acid solution. The present compounds fit into this generalization: $NaNi_2IO_6.2H_2O$ and $NaNi_4(H_3TeO_6)_3.6H_2O$ were prepared in acid solution; $Na_6Ni(H_3TeO_6)_3H_2O$, $Na_9H_5Ni_2(TeO_6)_3$, $Na_5H_3Pd(TeO_6)_2.4H_2O$, and $Na_5H_3Pt(TeO_6)_2.2H_2O$ were prepared in alkaline solution. Campbell and Nyman suggest that the compounds formed in acid solution are polymers, but there is no evidence on this point for the present compounds.

The compounds $Na_5H_3Pd(TeO_6)_2.4H_2O$ and $Na_5H_3Pt(TeO_6).2H_2O$ are analogous to the compound of silver(III), $Na_6H_3Ag(TeO_6)_2.18H_2O$, prepared by Malatesta (10). This also was prepared from alkaline solution, so its apparently unsymmetrical formula may be due to the presence of a hydroxy group, as was suggested above for the palladium and platinum compounds.

REFERENCES

1. L. Malatesta. Gazz. Chim. Ital. **71**, 467 (1941).
2. L. Jensovsky. Z. Anorg. Allgem. Chem. **307**, 200 (1961).
3. P. Ray and B. Sarma. J. Indian Chem. Soc. **25**, 205 (1948).
4. M. W. Lister. Can. J. Chem. **39**, 2330 (1961).
5. L. Malaprade. Compt. Rend. **210**, 504 (1940); **204**, 979 (1937).
6. A. D. Westland and F. E. Beamish. Mikrochim. Acta, **5**, 625 (1957).
7. F. A. Gooch and J. Howland. Am. J. Sci. **48**, 375 (1894).
8. A. A. Grinberg, N. B. Karpenko, and E. H. Maksimyk. J. Appl. Chem. USSR English Transl. **26**, 1047 (1953).
9. M. J. M. Campbell and C. J. Nyman. Inorg. Chem. **1**, 842 (1962).
10. L. Malatesta. Gazz. Chim. Ital. **71**, 467, 580 (1941).

Can. J. Chem. Downloaded from www.nrcresearchpress.com by 210.87.254.105 on 09/05/12
For personal use only.

APPLICATION OF DIFFERENTIAL THERMAL ANALYSIS TO THE DISSOCIATION OF MnO_2 AND Mn_2O_3

T. MATSUSHIMA AND W. J. THOBURN
Department of Metallurgy and Materials Science, University of Toronto, Toronto, Ontario
Received November 4, 1964

ABSTRACT

The method of differential thermal analysis was employed to determine the oxygen pressures produced by the reactions

$$4MnO_2(s) = 2Mn_2O_3(s) + O_2(g)$$

and

$$6Mn_2O_3(s) = 4Mn_3O_4(s) + O_2(g)$$

in the temperature range 250–1 000 °C. The heats of reaction calculated from the slope of the van't Hoff curves are: $\Delta H_{835°K}^0 = 25.8 \pm 1.5$ and $\Delta H_{1200°K}^0 = 25.3 \pm 4.2$ kcal per mole of oxygen. These are in agreement with previously reported values based on equilibrium measurements, but are lower than those determined by calorimetry.

INTRODUCTION

Previous measurements of the oxygen pressures produced by the reactions

[1] $$4MnO_2(s) = 2Mn_2O_3(s) + O_2(g)$$

and

[2] $$6Mn_2O_3(s) = 4Mn_3O_4(s) + O_2(g)$$

present conflicting results, and in addition the corresponding thermodynamic data obtained are not in agreement with those based on calorimetric measurements. Part of the difficulty in static measurements is that the slow reaction rates involved render impractical the approach to equilibrium from both the dissociating and oxidizing sides. Thus, we measured the oxygen pressures by means of a dynamic technique, differential thermal analysis (d.t.a.), which appeared to be particularly suited to study these reactions.

EXPERIMENTAL

Preparation of MnO_2

The oxide was prepared according to the following steps. 1. Approximately 250 ml of Fisher's manganous nitrate solution was heated slowly on a hot plate to eliminate the water of crystallization according to $MnNO_3.6H_2O = Mn(NO_3)_2 + 6H_2O(g)$. 2. The resulting $Mn(NO_3)_2$ crystals were remelted and heated to 200 °C to drive off NO_2 according to $Mn(NO_3)_2 = MnO_2 + 2NO_2(g)$. 3. The resulting MnO_2 was crushed to −100 mesh and the powder was heated for 24 h at 400 °C in a closed alumina vessel and under a substantial flow of oxygen to prevent any dissociation of the MnO_2. 4. The resulting $MnO_2(s)$ was crushed to −200 mesh.

Apparatus

Samples were heated in a horizontal globar resistance furnace, with a 1 in. diameter alumina retort tube. The $MnO_2(s)$ powder and an alumina powder reference material were held in identical platinum crucibles, 1/2 in. in diameter and 1/2 in. deep. The crucibles were embedded symmetrically in alumina powder contained in a porcelain crucible to ensure that most heat absorbed or evolved during a reaction would affect the temperature of the sample.

The temperatures of the sample and alumina reference were measured with platinum – platinum 10% rhodium thermocouples. The diameter of the wires was 0.013 in. and the junctions were filed to a fine point to improve the thermal response of the measurements. Partial pressures of oxygen were maintained constant to within 0.1 mm Hg by means of a Cartesian diver-type manostat.

Experimental Procedure

The thermocouples were carefully centered in the sample and reference, and the boat was placed in the hot zone of the furnace. The furnace and gas system were sealed and evacuated. The temperature was

raised to 250 °C where degassing was allowed to continue for 1 h. Oxygen was then introduced and maintained at a desired pressure by means of the manostat. The temperature of the system was then raised at a uniform rate by increasing in small increments an auto-transformer which controlled the power input. It was found that a heating rate of 3 C°/min was optimum. The temperature of the sample and the temperature difference between the sample and reference, ΔT, were measured with a potentiometer and recorded at intervals from 1 to 2 min.

RESULTS

The differential curves shown in Fig. 1 are typical of these experiments. The components indicated by eqs. [1] and [2] were confirmed by X-ray diffraction analysis. It was assumed that the two sharp breaks in the curve (indicated by the arrows) correspond to the beginning of dissociation of the oxides, and also that the temperatures at these points correspond, within the limits of precision of the experiment, to the equilibrium temperatures for reactions [1] and [2] at the fixed oxygen pressure maintained in the system. These equilibrium temperatures were used to plot the results in the form of van't Hoff curves, as shown in Figs. 2 and 3.

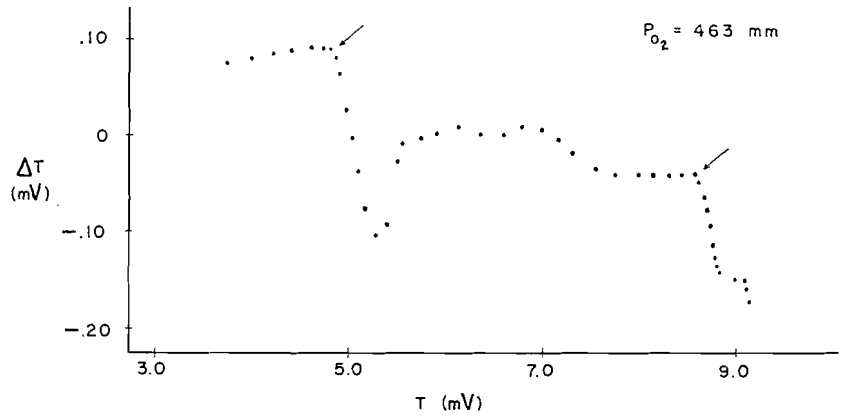

FIG. 1.

The analysis of the van't Hoff plots can be illustrated with reference to Fig. 2. There is first the possibility that the points can be represented by a single straight line. However, the correlation coefficient (r, which equals unity if all points fall on a perfect straight line) was too low (0.67) and the error limits (approximately ±20%) too high to validate such an assumption. A curve could be drawn through the points, indicating that the heat of reaction cannot be considered approximately constant over the temperature range of the experiments. This is not possible, however, as the change in slope over this range is too great to be explained by the effect of heat capacity.

It can be shown that the points fall along two distinct straight lines, the slopes of which were determined by the least squares method. Five pairs of correlation coefficients were determined for each of the two assumed lines by including (i) all of the five middle points with one group, (ii) four of the five middle points with one group, one with the other, etc. The slope and correlation coefficient of the lower temperature portion was affected only by the two higher temperature points of the central five. On the other hand the higher temperature line was appreciably affected only by the lowest temperature point in the central group. Thus, the points plotted in Fig. 2 can best be described as falling along two straight lines, of which the higher temperature part consists of the 10 highest temperature points and the lower temperature point consists of the remaining 7. This combination

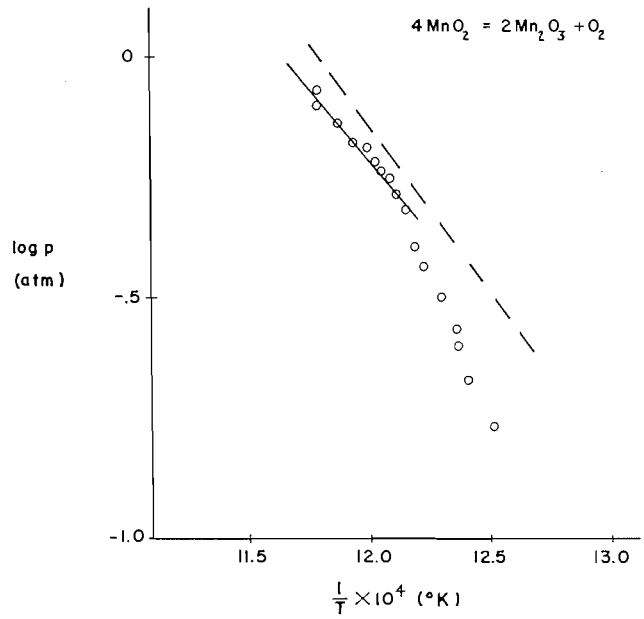

FIG. 2.

results in the maximum correlation coefficients for both lines (0.92 and 0.95 respectively). A similar analysis of the experimental points plotted in Fig. 3 shows that they can best be represented as lying along two straight lines with correlation coefficients of 0.93 and 0.90 respectively.

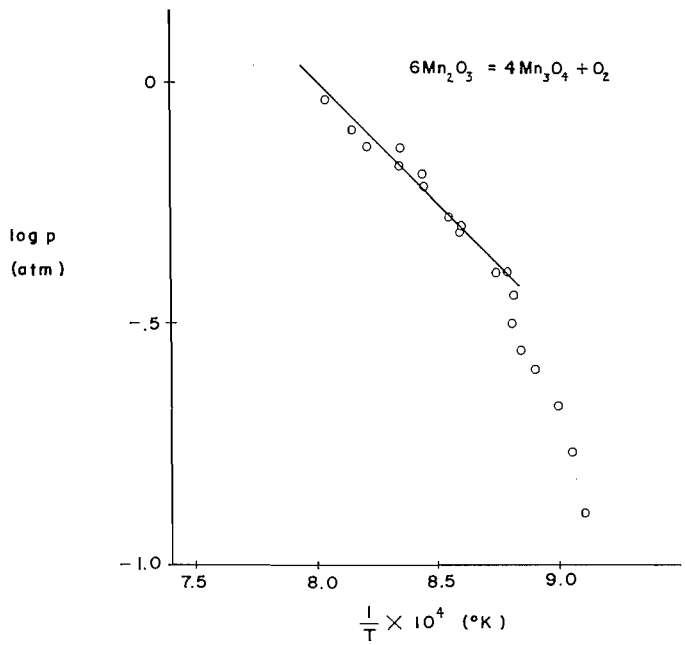

FIG. 3.

Validity of D.T.A. for Equilibrium Measurements

When employing d.t.a. for equilibrium determinations one must be certain that (*a*) the heat effect which causes a sharp break in a differential trace (for example, the break pointed to by the first arrow in Fig. 1) is actually due to the reaction assumed (reaction [1] in this case), and (*b*) at the temperature of this break the reaction is proceeding under reversible conditions within the limits of precision of the experiment.

(*a*) The components of each reaction were confirmed by X-ray analysis which showed, as in Fig. 1 for example, that the sharp breaks from a relatively linear ΔT vs. T trace (indicated by the arrows in Fig. 1) and the resulting peaks were due to the reactions assumed. The procedure consisted of heating MnO_2 under a fixed oxygen pressure to different temperatures and then quenching and analyzing the sample. For example, with respect to the first break at 4.90 mV (568 °C) and peak shown in Fig. 1, two separate runs were carried out heating the sample under identical conditions, with the exception that these runs were halted and the samples quenched when they had reached temperature levels of 4.82 mV (560 °C) and 5.50 mV (627 °C). X-ray analysis produced diffraction lines characteristic in the first case of MnO_2 only and in the latter of Mn_2O_3 only.

(*b*) Known thermodynamic data indicates that reactions [1] and [2] are thermodynamically reversible in the temperature and pressure ranges employed. That is, at a fixed oxygen pressure, MnO_2 is the stable oxide phase at lower temperatures, Mn_2O_3 becoming the stable phase at higher temperatures and Mn_3O_4 becoming the stable oxide phase at still higher temperatures.

The presence of kinetically reversible experimental conditions should also be considered. There is first the possibility that enough initial decomposition to cause a heat effect occurred (due to inhibition of the rate of the reverse reaction) before the equilibrium temperature was reached. This is unlikely as any decomposition substantial enough to cause a measurable heat effect would produce a fresh outer layer of oxide product with which the oxygen could react.

Similarly as the temperature of the sample increases just above the equilibrium temperature for the reaction (at the fixed oxygen pressure in the system) and the reaction begins to proceed, it is possible that at this point the rate of reaction is not high enough to produce a measurable heat effect. Such a slow rate could be due in part to the restriction of the forward reaction by the outer product layer. However, at some temperature significantly above the equilibrium temperature the rate of reaction may increase to such an extent so as to cause a measurable heat effect. For such oxide decomposition reactions as considered here such an increase could be due to either (i) the increase in rate of diffusion of oxygen to the surface of partially decomposed particles, (ii) the rupture of the outer product layer by the force of increased equilibrium oxygen pressure at the reactant–product interface, (iii) the increase in the rate of chemical decomposition as temperature rises, or (iv) a combination of two or all of the above.

With these points in mind reference should be made to the van't Hoff plots of Figs. 2 and 3. The differences in slope between the higher and lower temperature parts are much too large to be attributed to a phase change. Also the possibility that the occurrence of two competing reactions can explain the form of these curves must be discounted because (i) X-ray analysis showed that the heat effects associated with both parts of each van't Hoff curve were due to the same reaction, and (ii) extrapolation of the higher temperature line shows that it should be occurring at the lower temperatures while the lower temperature part should be occurring at the higher temperature.

The appearance of the two straight line portions can best be explained with reference to the rates of the forward reactions, which are sufficiently high to cause a measurable

temperature differential under conditions close to equilibrium only at temperatures above the breaks in the van't Hoff curves. In other words the slopes of the lower temperature lines are a function of the kinetics of the reaction as well as the equilibrium constants (these lines are not vertical indicating that the rates of the reactions are not solely a function of temperature, but also a function of the distance from equilibrium). Thus the points forming the higher temperature portions of the van't Hoff curves represent temperatures from the differential traces (such as those shown in Fig. 1) at which the observed initial decomposition at a fixed pressure (indicated by the arrows in Fig. 1) occurs under conditions close enough to equilibrium to be considered so within the limits of precision of the experiments.

The higher temperature lines in Figs. 2 and 3, representing equilibrium points, can be expressed by

$$\log p_{\text{atm}} = 7.29 - \frac{6250}{T} \quad [3]$$

and

$$\log p_{\text{atm}} = 4.00 - \frac{5000}{T} \quad [4]$$

for reactions [1] and [2] respectively. These lines formed the basis of the thermodynamic calculations outlined in the next section.

Thermodynamic Calculations

(1) MnO_2 Dissociation

The mean standard heat of reaction [1], as calculated from the slope of the van't Hoff curve is $\Delta H_{835^\circ K}^0 = 25.8 \pm 1.5$ kcal per mole of oxygen. The standard free energy change at the same temperature is $\Delta F_{835^\circ K}^0 = 0.763 \pm 0.03$ kcal per mole of oxygen. A third law calculation for the entropy change yields $\Delta S_{835^\circ K}^0 = 30.0 \pm 1.8$ entropy units (e.u.) per mole of oxygen.

(2) Mn_2O_3 Dissociation

The mean standard heat of reaction [2], as calculated from the slope of the van't Hoff curve is $\Delta H_{1200^\circ K}^0 = 25.3 \pm 4.2$ kcal per mole of oxygen. The standard free energy change at the same temperature is $\Delta F_{1200^\circ K}^0 = 0.90 \pm 0.07$ kcal per mole of oxygen. A third law calculation for the entropy change yields $\Delta S_{1200^\circ K}^0 = 20.3 \pm 3.6$ e.u. per mole of oxygen.

TABLE I

$4MnO_2(s) = 2Mn_2O_3(s) + O_2(g)$ (comparison of data)

Source	Method	$\Delta H_{835^\circ K}^0$	$\Delta F_{835^\circ K}^0$
Wicks and Block (3)	Calorimetric	39.2±5	8.8±5
Meyer and Rotgers (1)	Equilibrium	57.8	0
Kapustinsky and Bayushkina (2)	Equilibrium	31.5	0.32
Present work	Differential thermal analysis	25.8±1.5	0.76±.03

Comparison of Results

(1) MnO_2 Dissociation

The most reliable data for reaction [1] are summarized in Table I and are compared to those found by d.t.a. Uncertainty limits for the results of Meyer and Rotgers (1) and Kapustinsky and Bayushkina (2) are not available. For $\Delta H_{835^\circ K}^0$ the present work

is in reasonable agreement with that of the latter authors, while the $\Delta F_{835°K}^0$ values obtained by d.t.a. are in reasonable agreement with both static determinations. The dashed line in Fig. 2 represents the van't Hoff curve determined by Kapustinsky and Bayushkina (2).

TABLE II

$6Mn_2O_3(s) = 4Mn_3O_4(s) + O_2(g)$ (comparison of data)

Source	Method	$\Delta H_{1200°K}^0$	$\Delta F_{1200°K}^0$
Siemonsen (4)	Calorimetric	50.2±2	
Wicks and Block (3)	Calorimetric	—	−24.9±15.8
Meyer and Rotgers (1)	Equilibrium	33.3	3.2
Present work	Differential thermal analysis	25.3±4.2	0.90±.07

(2) Mn_2O_3 Dissociation

Table II indicates that the d.t.a. results are in agreement with the static measurements of Meyer and Rotgers.

For both reactions, thermodynamic values based on vapor pressure measurements are in reasonable agreement (with the exception of $\Delta H_{835°K}^0$ for reaction [1] reported by Meyer and Rotgers) and differ from those produced by calorimetric experiments. Inconsistencies in the data contained in the literature can also be illustrated by considering entropy changes. The value for the entropy change for reaction [1], as calculated from the difference between the entropy values of the components, is $\Delta S_{835°K}^0 = (\Delta H^0 - \Delta F^0)/T = 36.4 \pm 12$ e.u. Similarly, for reaction [2], the corresponding values are $\Delta S_{1200°K}^0 = 11.04 \pm 3$ e.u. and $\Delta S_{1200°K}^0 = 54.7 \pm 24.2$ e.u. The calculations are based on data presented by Wicks and Block (3).

CONCLUSIONS

Thermodynamic values for reactions [1] and [2] based on vapor pressure measurements are not in agreement with those produced by calorimetry. Entropy calculations indicate that some of this difference may be due to inaccurate heat capacity data. The discrepancies illustrate the value of determining thermodynamic functions by employing both equilibrium and calorimetric techniques.

REFERENCES

1. R. J. Meyer and K. Rotgers. Z. Anorg. Chem. **57**, 104 (1908).
2. A. F. Kapustinsky and K. S. Bayushkina. J. Phys. Chem. (U.S.S.R.) **11**, 77 (1938); Chem Abstr. **32**, 8252 (1938).
3. C. E. Wicks and F. E. Block. U.S. Bureau of Mines Bulletin 605. 1963.
4. H. Siemonsen. Z. Elektrochem. **45**, 637 (1937).

Can. J. Chem. Downloaded from www.nrcresearchpress.com by 210.87.254.105 on 09/05/12
For personal use only.

CONDUCTANCES AND SURFACE TENSIONS OF AQUEOUS SOLUTIONS OF SODIUM DECANOATE, SODIUM LAURATE, AND SODIUM MYRISTATE, AT 25° AND 35°

A. N. CAMPBELL AND G. R. LAKSHMINARAYANAN[1]
Chemistry Department, University of Manitoba, Winnipeg, Manitoba
Received December 11, 1964

ABSTRACT

The equivalent conductances of aqueous solutions of sodium decanoate, sodium laurate, and sodium myristate have been determined from the very dilute region up to saturation concentration, at 25° and 35°. The limiting conductances have been obtained from the measurements in the usual way. In addition and for the sake of completeness, the limiting equivalent conductances of sodium formate, sodium acetate, sodium propionate, and sodium butyrate have also been determined at 35°, since they were not known at this temperature.

The effect of increasing chain length on mobility is discussed. From a consideration of the experimental and the theoretical values of the slopes of the plots of equivalent conductance against the square root of the concentration, it is concluded that some sort of interaction, possibly a reversible dimerization of anions, occurs, even in the dilute region, and this could account for the lower experimental values of the slope. This phenomenon has been observed with other long chain electrolytes, however, and the hypothesis of dimerization is not the only possible one.

The critical micelle concentrations have been determined, and recent concepts of micelle formation are applied to interpret their structure. The surface tensions of the aqueous solutions have been measured at 25° and 50°.

The object of this work has been described in a previous publication (1). We have now extended our work to include the decanoate, laurate, and myristate ions (14 carbons, including the carboxyl group) and this is about as far as there is any point in going. In addition, however, to our interest in the limiting conductance of the anion, it was found that the slope of the conductance curve, in the very dilute region, is not that of the Onsager theory, when the number of carbon atoms exceeds six. This phenomenon has been observed by others and it points to peculiarities in the structure of solutions of these salts. Moreover, since the soap-like character of the solutions of these sodium salts is very marked, we were obliged to investigate other physical properties, notably the surface tension.

EXPERIMENTAL

Our method of determining conductances has been described previously (1). Densities were determined with Ostwald–Sprengel pycnometers, cap. 25 ml, and the usual precautions with respect to bouyancy, etc., were taken. The densities are correct to ±0.0001. Viscosities were determined with the Cannon and Fenske modification of the Ostwald viscometer. The stalagmometer method was used to determine surface tension. To obtain a sufficient degree of accuracy, it was necessary to count from 100 to 200 drops but, because these soap-like solutions are sometimes very viscous, this laborious operation could occupy as much as 3 h. An automatic system was therefore desired. Each drop as it fell from the stalagmometer fell into a glass cone, having platinum plates on opposite sides: these plates were connected to an electronic glow counter. The glow counter was enclosed in a Faraday cage to eliminate signal pickup. The apparatus was frequently checked with benzene; the agreement was excellent. Practically any liquid has sufficient conductance to operate the counter when a drop falls into the platinum cone. Because of this high sensitivity, precautions (such as the Faraday cage) against stray currents are necessary. With approximately 200 drops falling in 3 h, the time of formation of a drop is slightly less than 1 min.

[1]*Financed by the National Research Council.*

RESULTS

The limiting equivalent conductances of sodium decanoate, sodium laurate, and sodium myristate were determined by the extrapolation technique of Kohlrausch. Before plotting, the equivalent conductances were corrected for hydrolysis by the method of Campbell and Bock (2). The results are expressed graphically in Figs. 1, 2, and 3. The viscosities are not reproduced, since neither the plot of viscosity nor of fluidity, against either molar or weight concentration, reveals a distinct break at the critical micelle concentration. The surface tensions of aqueous solutions of sodium octanoate, sodium decanoate, sodium laurate, and sodium myristate are reproduced, as functions of the common logarithm of the concentration, in Fig. 4.

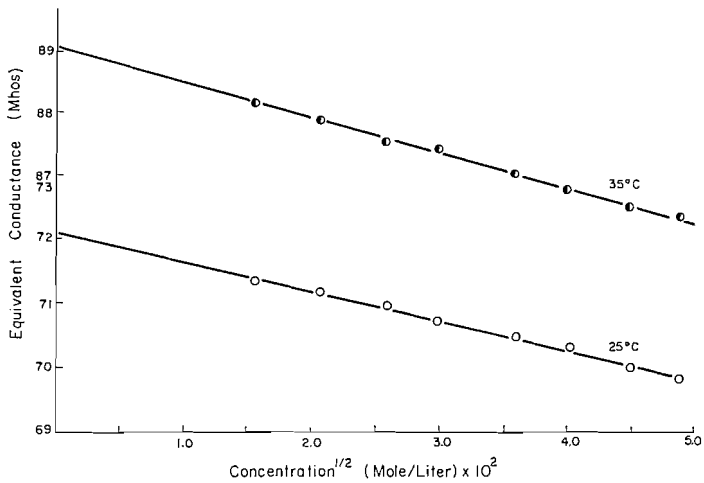

FIG. 1. Equivalent conductance vs. square root of concentration of sodium decanoate by the Kohlrausch method.

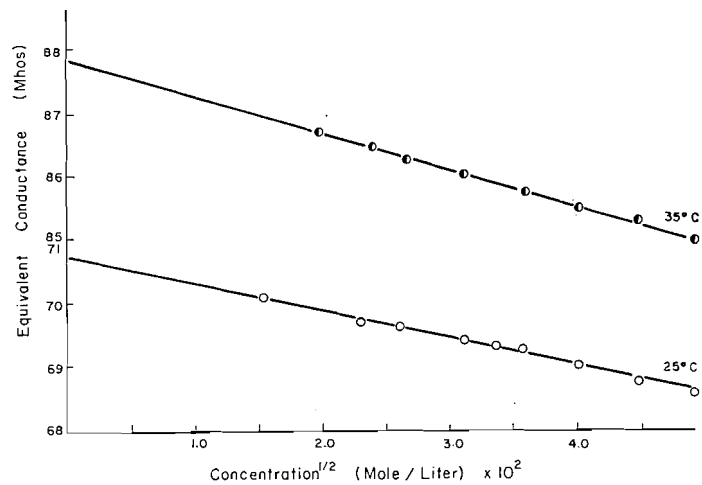

FIG. 2. Equivalent conductance vs. square root of concentration of sodium laurate by the Kohlrausch method.

Can. J. Chem. Downloaded from www.nrcresearchpress.com by 210.87.254.105 on 09/05/12
For personal use only.

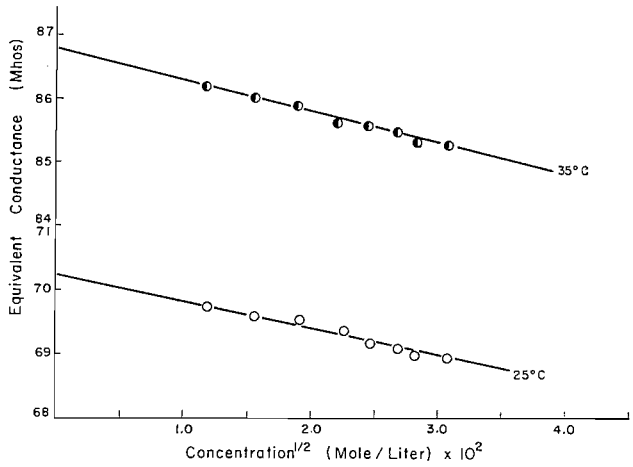

FIG. 3. Equivalent conductance vs. square root of concentration of sodium myristate by the Kohlrausch method.

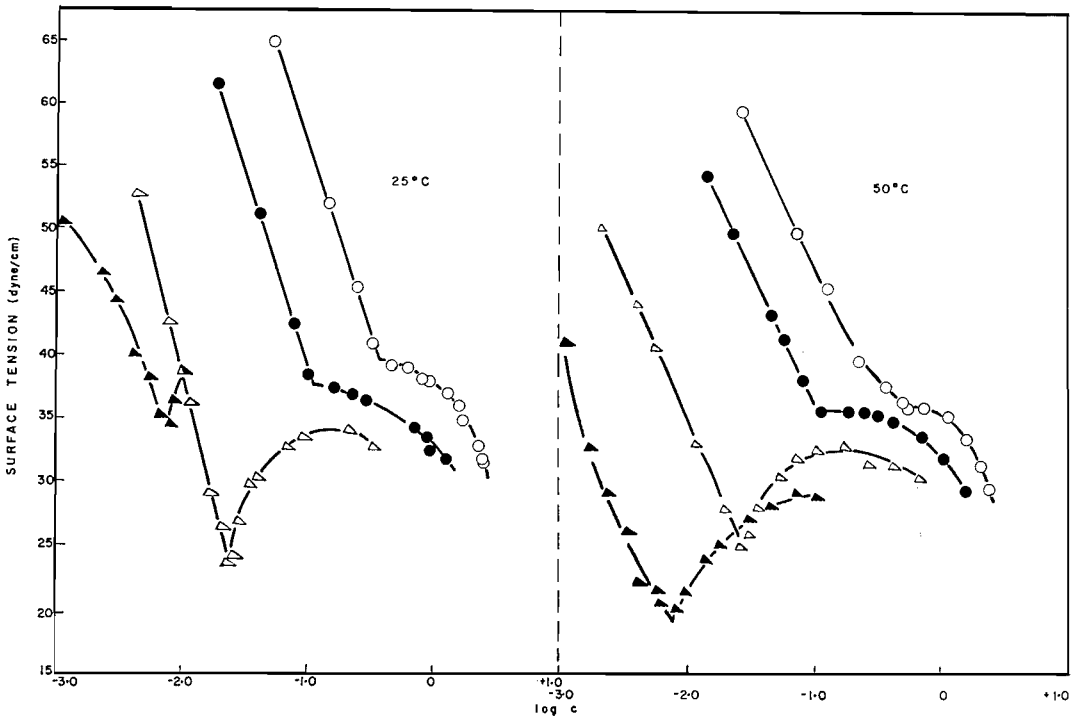

FIG. 4. Surface tension vs. log c: ○ sodium octanoate, ● sodium decanoate, △ sodium laurate, ▲ sodium myristate.

DISCUSSION AND RESULTS

The limiting equivalent conductances, obtained from the plots of equivalent conductance against the square root of the concentration, in the dilute regions, are tabulated in Table I. The limiting equivalent conductances of sodium formate, sodium acetate,

Can. J. Chem. Downloaded from www.nrcresearchpress.com by 210.87.254.105 on 09/05/12
For personal use only.

sodium propionate, and sodium butyrate, at 35°, were also determined, since no reliable data were available at this temperature. The limiting ionic conductances of the fatty acid anions, at 25° and at 35°, are summarized in Table II.

TABLE I

Limiting equivalent conductances of sodium salts of fatty acids at 25 and 35 °C

Salt	Temperature (°C)	Λ_0
Hexanoate	25	77.47
Hexanoate	35	96.23
Octanoate	25	73.18
Octanoate	35	90.63
Decanoate	25	72.11
Decanoate	35	89.10
Laurate	25	70.76
Laurate	35	87.86
Myristate	25	70.21
Myristate	35	86.77

TABLE II

Limiting equivalent conductances of fatty acid anions at 25 and 35 °C

		Temperature	
Anion*	Cation	25 °C	35 °C
Formate (C_1)		54.59 (3)	67.69
Acetate (C_2)		40.90 (4)	50.71
Propionate (C_3)		35.80 (5)	44.42
Butyrate (C_4)		32.60 (5)	40.29
Hexanoate (C_6)		27.37 (6)	34.69
Octanoate (C_8)		23.08 (1)	29.09 (1)
Decanoate (C_{10})		22.01	27.56
Laurate (C_{12})		20.66	26.32
Myristate (C_{14})		20.11	25.23
	Na^+	50.10 (7)	61.54 (7)

*C_1, C_2, C_3, etc. indicates the number of carbon atoms in the chain.

When the limiting equivalent conductances are plotted vs. the number of carbon atoms, it becomes obvious that in the lower members of the series the difference in the mobilities of successive anions is fairly high, but from octanoate onwards the decrement becomes smaller and smaller, so that the curve tends to become horizontal. The effect is observed at both temperatures. In other words, after decanoate ion (10 carbon atoms) the mobility of the anion approaches constancy. Similar results for the mobilities of sodium alkyl sulfates, with increasing number of carbon atoms, were obtained by Flockhart (8).

In the state of high dilution the motion of an ion is limited solely by its interaction with the surrounding solvent molecules, there being no other ions within a finite distance. As Edward (9) points out, the carboxyl group binds an inner sheath of water molecules and causes breakdown in the outer zone. Ions of smaller size, such as Na^+, Li^+, F^-, acquire by ion–solvent interaction, a permanent hydration sheath which must be assumed to be larger, the lower the mobility; with carboxylic ions the hydrophobic part increases with increase in number of carbon atoms and hence the hydration effect is correspondingly less. Since, however, the mobility is observed to decrease with increase in the number of

Can. J. Chem. Downloaded from www.nrcresearchpress.com by 210.87.254.105 on 09/05/12
For personal use only.

carbon atoms, this effect must be overbalanced by the absolute increase in ion size. The constant mobility finally attained is not so easily explained. It is probably not justifiable, however, to treat ions of this size as spheres and, if the large fatty acid anions are envisaged as coiled springs with one end oriented in the direction of motion, then it is obvious that the resistance to motion is approximately constant.

The temperature effect on the limiting equivalent conductances of the sodium salts is almost the same for all salts, the ratio varying between 1.236 for decanoate to 1.242 for hexanoate and laurate: the fluidity ratio of water between these temperature limits is 1.237.

It is well known that the equivalent conductances of uni-univalent electrolytes follows Onsager's theoretical equation in the dilute region (concentration $<0.001\ N$), well within the experimental error. In other words, the theoretical slope agrees well with the experimental slope. When, however, the experimental slopes (conductance vs. the square root of the concentration) of sodium octanoate, decanoate, laurate, and myristate are compared with the theoretical slope obtained from Onsager's equations, the experimental slopes are 40–45% lower than the theoretical, except for sodium octanoate, where the deviation is less. The experimental conductivities are higher than the theoretical and hence the slopes are smaller. The higher values can be explained in different ways, e.g., if there are present more ions than the simple uni-univalent sodium and fatty acid anions: i.e., if there is some sort of interaction between the simple ions, even in dilute solution, to form highly conducting ions.

Kraus and co-workers (10, 11, 12) have shown from their study of the conductances of alkyl trimethyl quaternary salts, in dilute solution, that dimerization of cations is responsible for the observed deviations from theory. Recently, Mukerjee and Mysels (13, 14, 15) have suggested that lauryl sulfate ions dimerizes reversibly to a certain extent in dilute solution, to form LS^- ions, thus enhancing the conductance. The same authors observed similar results for some other amphiphilic ions (16). They state that dimerization seems to be a rather general phenomenon with this type of salt and that this makes it possible to explain numerous hitherto unexplained observations.

The explanation of the phenomenon given by Mukerjee is not, however, universally accepted. It can scarcely be accounted for as due to hydrolysis, since our conductances are all corrected for hydrolysis. Parfitt and Smith (17) find that they can account for the deviation from the Onsager slope by using the Fuoss–Onsager equation (18) i.e. with the incorporation of a term representative of ion size. We, however, find that the Fuoss–Onsager equation is insufficient to account for the deviation here. Again, van Voorst Vader (19) using an e.m.f. method, arrives at the same conclusion. To calculate the distance of closest approach, they use the equation of Falkenhagen and Kelbgk (20), and arrive at an $\mathring{a}$ value of 5.6 Å, comparable with the value of $\mathring{a}$ found by Parfitt and Smith. We do not wish to assume a position in this matter, but it seems to us that our deviations are somewhat too great to be accounted for in this way.

Critical Micelle Concentration

The critical micelle concentration (c.m.c.) is obtained by determining the concentration at which normal behavior of any physical property changes sharply, owing to an association or aggregation of ions: this must not be confused with the simple dimerization dealt with in the previous section. When the specific conductance is plotted against concentration, as in Figures 5, 6, 7, and 8, for sodium octanoate, sodium decanoate, sodium laurate, and sodium myristate, respectively, at both temperatures, an abrupt change of slope is

Can. J. Chem. Downloaded from www.nrcresearchpress.com by 210.87.254.105 on 09/05/12
For personal use only.

Can. J. Chem. Downloaded from www.nrcresearchpress.com by 210.87.254.105 on 09/05/12
For personal use only.

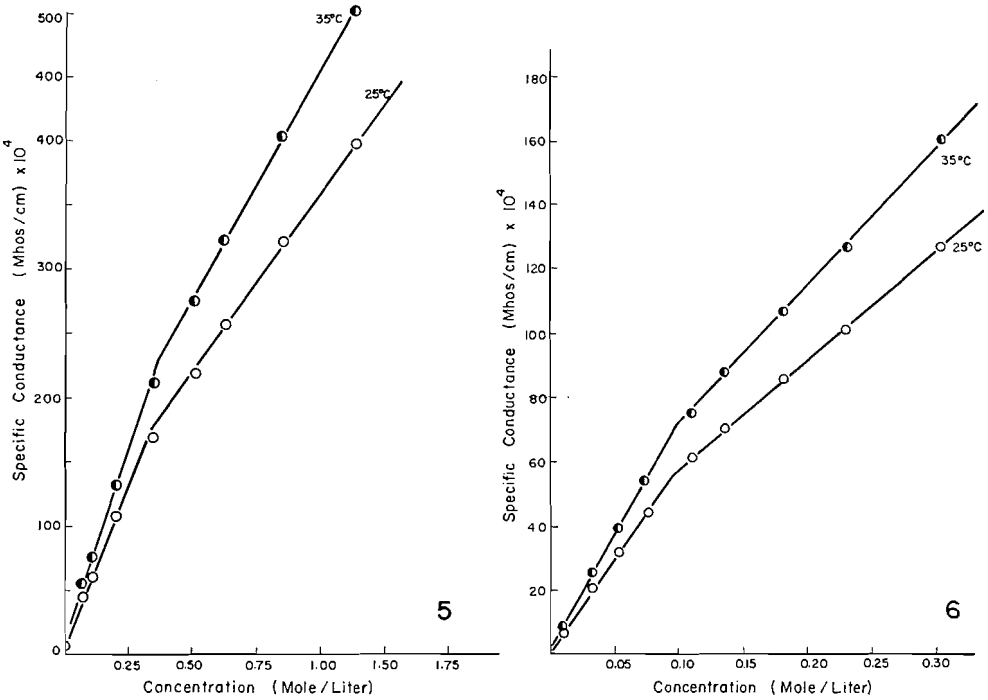

FIG. 5. Specific conductance vs. concentration of sodium octanoate.
FIG. 6. Specific conductance vs. concentration of sodium decanoate.

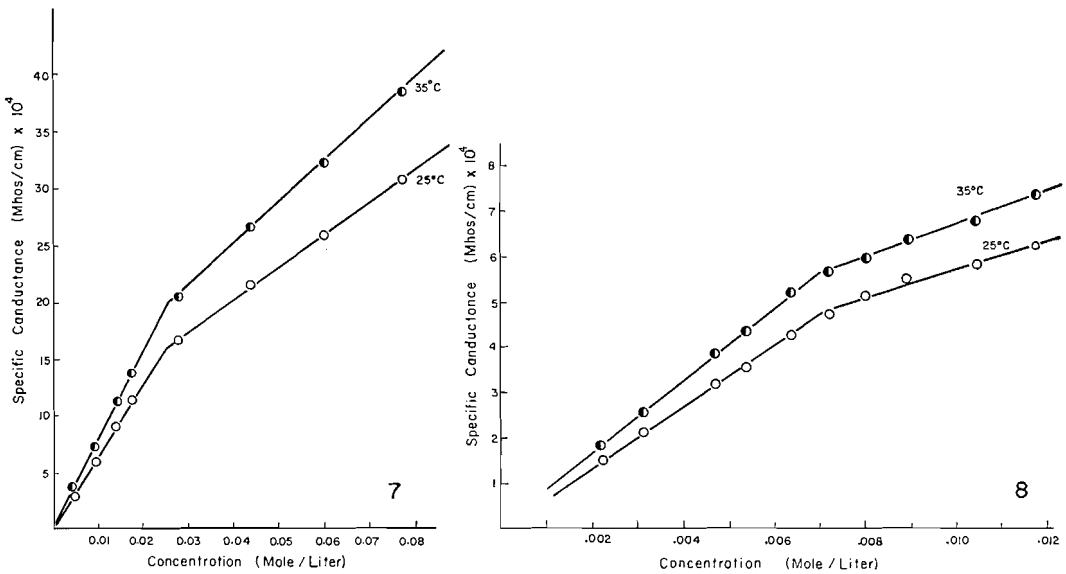

FIG. 7. Specific conductance vs. concentration of sodium laurate.
FIG. 8. Specific conductance vs. concentration of sodium myristate.

observed at the intersection of two curves which are almost straight lines. In a previous publication (1) we reported that sodium octanoate does not form micelles, because we then plotted equivalent conductance against the square root of concentration, a method which is not so sensitive for the detection of the c.m.c. Table III summarizes the critical micelle concentrations, at both temperatures. The value for the critical micelle concentration, at 25°, of sodium laurate agrees closely with that of 0.024 *M*, given by Huff, Brady, and McBain (21).

TABLE III

Comparison of the critical micelle concentrations (m*M*) of sodium salts of fatty acids by different methods at 25, 35, and 50 °C

Sodium salts	Critical concentration at 25 °C by		Critical concentration at 35 °C by conductivity	Critical concentration at 50 °C by surface tension
	Conductivity	Surface tension		
Octanoate	340.0	351.0	360.0	385.0
Decanoate	94.0	95.5	98.0	106.0
Laurate	24.4	23.0	25.0	28.0
Myristate	6.9	6.9	6.95	7.1

Increase of temperature usually raises the c.m.c. In the present case, the effect of temperature is not very great, as shown by Table III. The c.m.c. decreases with increasing chain length, approximately four times from octanoate to decanoate, from decanoate to laurate and so on, both at 25° and at 35°. Similar results were obtained by Harkins (22) and Klevens (23) who found that the c.m.c. increased by a factor of two for the removal of each CH_2 group from the chain.

Evans (24) has proposed an equation for the composition of the micelle in terms of conductance data. If S_1 is the slope of the specific conductivity vs. concentration curve below the c.m.c. and S_2 is the slope above the c.m.c., then according to Evans,

$$1\,000\,S_2 = \frac{(n-m)^2}{n^{4/3}}(1\,000\,S_1 - \Lambda_{Na}) + \frac{n-m}{n}\Lambda_{Na},$$

where n = number of anions in micelle, and m = number of gegenions (cations). An approximate value of n can be calculated, assuming a spherical micelle, from the formula

$$n = \frac{4}{3}\frac{\pi l^3 N d}{10^{24} M},$$

where l = length of hydrocarbon portion attached to the carboxylate group, N = Avogadro number, and d = density.

Using the above equation, from the measured slopes of the specific conductance vs. concentration curves (Figs. 5–8) of all four salts, n and m values have been calculated at both temperatures, and these are summarized in Table IV.

Below the c.m.c. the slope (S_1) increases with increasing chain length and decreasing anion mobility, and above the c.m.c. the gegenion micelle interaction increases, as is seen in the increased value of the ratio of gegenions (m) to single ions (n) with increasing chain length. In fact, the m/n ratio increases linearly with chain length, i.e. the degree of binding of gegenions increases with increase of chain length. The temperature effect upon the ratio m/n is not very great, over the range 25° to 35°.

Can. J. Chem. Downloaded from www.nrcresearchpress.com by 210.87.254.105 on 09/05/12
For personal use only.

TABLE IV

Degree of cation binding in fatty acid salt (sodium) solutions from specific conductance data at 25 and 35 °C

Sodium salt†	Temp. (°C)	1 000 S_1	1 000 S_2	n*	m*	m/n
Octanoate (C_8)	25	50.35	27.94	7	3	0.43
	35	61.74	35.25	7	3	0.43
Decanoate (C_{10})	25	57.88	33.78	14	7	0.50
	35	72.04	42.65	14	7	0.50
Laurate (C_{12})	25	64.72	28.40	23	15	0.65
	35	77.06	36.65	23	15	0.65
Myristate (C_{14})	25	68.03	31.90	35	24	0.69
	35	80.02	36.20	34	24	0.69

*Nearest whole number.
†C_8, C_{10}, etc. refers to number of carbon atoms in the chain.

Viscosity and Fluidity of the Aqueous Solutions of the Salts at 25° and 35°

In the dilute region the changes of viscosity with concentration are not very great, but at higher concentrations an increase of viscosity is observed. The change of slope of the curves, however, is not sufficiently sudden to allow of an exact determination of the c.m.c. Assuming a linear relation to exist both between conductance and temperature and between fluidity and temperature, the temperature coefficients of conductance and of fluidity and the activation energies have been deduced. The similarity in the values of the activation energies of conductance and of fluidity, and the value of practically unity for the ratio of the temperature coefficients, suggest a strong resemblance between the two phenomena (see Table V). Nevertheless, since conductance involves ionic migration through the bulk of the solution and viscosity involves a shearing motion of the whole solution, their mechanisms cannot be identical.

TABLE V

Average values of activation energy of conductance and viscosity (fluidity) and temperature coefficients of conductance and fluidity of sodium salts between 25 and 35 °C

Sodium salt	Activation energy of conductance (kcal/mole)	Activation energy of fluidity (kcal/mole)	Coeffic. of fluidity $\gamma \times 10^2$	Coeffic. of conductance $\beta \times 10^2$	γ/β
Decanoate	4.17	4.38	2.61	2.57	1.02
Laurate	4.29	4.17	2.57	2.64	0.973
Myristate	3.70	3.92	2.39	2.25	1.06

Surface Tensions of Aqueous Solutions of the Salts

If plots are made of surface tension against log concentration, the curves exhibit breaks at the c.m.c. The c.m.c. values for the four salts by the different methods are compared in Table III. Variations of surface tension with concentration follow the same pattern for all four salts. In the dilute region, the addition of salt reduces the surface tension rapidly, sometimes leading to a minimum but in all cases to a pronounced change of slope at the c.m.c. Because of the limited solubility of sodium myristate, the investigation was limited to low concentrations. The minima observed with sodium laurate and sodium myristate are not unusual. Such minima appear to be characteristic of certain colloidal electrolytes (25). In the present case, the minima may be associated with hydrolysis and the formation of mixed monolayers containing undissociated acid and acid anion. Nevertheless, though it may be a coincidence, the concentrations at the minima do correspond with the c.m.c.'s obtained by conductance.

Can. J. Chem. Downloaded from www.nrcresearchpress.com by 210.87.254.105 on 09/05/12
For personal use only.

REFERENCES

1. A. N. CAMPBELL, E. M. KARTZMARK, and G. R. LAKSHMINARAYANAN. Can. J. Chem. **40**, 839 (1962).
2. A. N. CAMPBELL and E. BOCK. Can. J. Chem. **36**, 330 (1958).
3. B. SAXTON and L. S. DARKEN. J. Am. Chem. Soc. **62**, 846 (1940).
4. D. A. MACINNES and T. SHEDLOVSKY. J. Am. Chem. Soc. **54**, 1429 (1932).
5. D. BELCHER. J. Am. Chem. Soc. **60**, 2744 (1938).
6. A. N. CAMPBELL and J. I. FRIESEN. Can. J. Chem. **38**, 1939 (1960).
7. G. C. BENSON and A. R. GORDON. J. Chem. Phys. **13**, 473 (1945).
8. B. D. FLOCKART. J. Colloid Sci. **17**, 305 (1962).
9. J. T. EDWARD. Sci. Proc. Roy. Dublin Soc. **27**, 273 (1956).
10. D. W. KUHN and C. A. KRAUS. J. Am. Chem. Soc. **72**, 3676 (1950).
11. E. J. BLAIR and C. A. KRAUS. J. Am. Chem. Soc. **73**, 1129 (1951).
12. M. J. MCDOWELL and C. A. KRAUS. J. Am. Chem. Soc. **73**, 2173 (1951).
13. P. MUKERJEE, K. J. MYSELS, and C. T. DULIN. J. Phys. Chem. **62**, 1390 (1958).
14. P. MUKERJEE. J. Phys. Chem. **62**, 1397 (1958).
15. P. MUKERJEE and K. J. MYSELS. J. Phys. Chem. **62**, 1400 (1958).
16. P. MUKERJEE. J. Phys. Chem. **62**, 1404 (1958).
17. G. D. PARFITT and A. L. SMITH. J. Phys. Chem. **66**, 942 (1962).
18. R. M. FUOSS and L. ONSAGER. J. Phys. Chem. **61**, 668, (1957); **62**, 1339 (1958).
19. VAN VOORST VADER. Trans. Faraday Soc. **57**, 110 (1961).
20. H. FALKENHAGEN and G. KELBGK. Ann. Physik, **11**, (6), 389 (1952).
21. H. HUFF, J. W. MCBAIN, and A. B. BRADY. J. Phys. Chem. **55**, 311 (1951).
22. W. D. HARKINS. J. Am. Chem. Soc. **69**, 1428 (1947).
23. H. B. KLEVENS. J. Phys. Chem. **52**, 130 (1948).
24. H. C. EVANS. J. Chem. Soc. 579 (1956).
25. H. NEVILLE and C. A. JENSON. J. Phys. Chem. **37**, 1001 (1933).

Can. J. Chem. Downloaded from www.nrcresearchpress.com by 210.87.254.105 on 09/05/12
For personal use only.

Can. J. Chem. Downloaded from www.nrcresearchpress.com by 210.87.254.105 on 09/05/12
For personal use only.

ANALYSIS OF PRODUCTS FROM PERIODATE OXIDATION AND FROM METHYLATION OF A RHAMNAN[1]

G. G. S. DUTTON
Department of Chemistry, University of British Columbia, Vancouver, British Columbia
AND
A. M. UNRAU
Department of Plant Science, University of Manitoba, Winnipeg, Manitoba

Received April 17, 1964

ABSTRACT

A synthetic L-rhamnan containing both rhamnofuranosyl and rhamnopyranosyl units has been used as a model substance in the application of vapor phase chromatography (v.p.c.) to the study of the structure of rhamnose containing polysaccharides. Groups of isomeric methylated sugars obtained from the methylated rhamnan were analyzed by converting them to methylated alditols which had widely different retention times. A Smith periodate degradation of the rhamnan gave 1,2-dihydroxypropane, 1-deoxy-D-erythritol, L-rhamnose, and 5-deoxy-L-arabinose, which were separated by paper chromatography. There were also obtained 1-deoxy-3-*O*-(α-L-rhamnopyranosyl)-D-erythritol and the β-anomer, and 1-deoxy-2-*O*-(L-rhamnopyranosyl)-D-erythritol, separable by v.p.c. as their trimethylsilyl ethers. 1-Deoxy-D-erythritol was synthesized and characterized as the tri-*p*-nitrobenzoate. Of the terminal units in the synthetic rhamnan 35% were furanose and 2,3-di-*O*-methyl-L-rhamnose constituted 75% of the dimethyl fraction indicating that the principal linkage was (1 → 4).

The classical methods for the determination of the structure of polysaccharides have included methylation and periodate oxidation. Separation of the derived methyl ethers has been facilitated by the advent of vapor phase chromatography (v.p.c.), but since the methyl ethers are normally converted to their glycosides prior to separation this introduces an added complication, as most sugars will give two glycosides and may give four (1). The retention times of isomeric glycosides do not always differ greatly, although compounds of varying degrees of methylation are easily separable. The present paper describes a method whereby a group of di-*O*-methylrhamnoses with similar chromatographic behavior may be converted by periodate oxidation and borohydride reduction into a mixture of C_3, C_4, C_5, and C_6 glycitols whose retention times are markedly different and whose separation is thus facilitated. A similar procedure enables the isomeric mono-*O*-methylrhamnoses to be resolved. Each methyl ether gives rise to a characteristic degradation product(s) which enables a mixture of five isomeric ethers to be analyzed rapidly and completely. These separations are described below.

In a similar way the application of the Smith periodate degradation gives isomeric and anomeric glycosides. It has already been shown that in certain cases such mixtures cannot be separated by paper chromatography or paper electrophoresis but may be readily resolved by v.p.c. as their trimethylsilyl ethers (2). These observations are now extended to the separation of anomeric and isomeric rhamnosyl glycosides.

The polysaccharide used in this study was a synthetic rhamnan prepared by the high temperature polymerization of L-rhamnose (3). By analogy with other polysaccharides prepared by this method it was anticipated that the rhamnan would have a highly branched structure and an appreciable proportion of furanosyl units (4). Hydrolysis of the methylated rhamnan would therefore give a mixture of all possible methyl ethers,

[1]*Presented at the 47th Chemical Institute of Canada Meeting, Kingston, Ontario, June 1964.*

furanose and pyranose. Similarly periodate degradation should give several rhamnosyl glycosides. The results obtained have confirmed this general structure of the rhamnan, which is therefore a useful substrate for model studies.

TABLE I

Paper chromatographic separation of L-rhamnose methyl ethers

Fraction	R_f	Color of spot	Weight (mg)	Components
1*a*	0.86	Violet	322	Trimethyl
1*b*	0.84	Yellow		
2*a*	0.72	Violet	655	Dimethyl
2*b*	0.66	Yellow		
2*c*	0.62	Yellow		
2*d*	0.56	Brown		
3*a*	0.37	Yellow	254	Monomethyl
3*b*	0.31	Brown		
3*c*	0.25	Yellow		
4	0.1	Yellow-brown	20	Rhamnose

TABLE II

Identification of di-*O*-methyl-L-rhamnoses

Di-*O*-methyl ether	Reaction	Products
2,5-		1-Hydroxy-2-methoxypropane (I) + 2-*O*-methylglycerol (II)
3,5-		5-Deoxy-2,4-di-*O*-methyl-L-arabinitol (III)
	(*i*) BH_4^- (*ii*) IO_4^- (*iii*) BH_4^-	
2,3-		2,3-Di-*O*-methylerythritol (IV)
2,4-		2,4-Di-*O*-methyl-L-rhamnitol (VI)
3,4-		5-Deoxy-2,3-di-*O*-methyl-L-arabinitol (V)

The fully methylated rhamnan was hydrolyzed and the sugars separated by paper chromatography into groups depending on their degree of methylation, as shown in Table I. The 2,3,4- and 2,3,5-tri-*O*-methyl-L-rhamnoses were readily separated as their lactones by v.p.c. and their relative amounts showed that in the polymer 35% of the terminal units were furanose.

Rechromatography of the dimethyl fraction gave three subfractions 2*a*, 2*b* + 2*c*, and 2*d*. Part of fraction 2*d* was obtained pure and identified as 3,4-di-*O*-methyl-L-rhamnose. Electrophoresis of 2*a* indicated the 2,5- and 3,5-di-*O*-methyl ethers while 2*b* and 2*c* did not migrate and were therefore the 2,3- and 2,4-di-*O*-methyl ethers. None of these could be cleanly separated by paper chromatography and since in the past preparative paper electrophoresis had given poor recoveries, and anyhow would not be applicable to the latter pair, the following analytical scheme was adopted (Table II). Fraction 2*a* was reduced with borohydride, oxidized with periodate, and again reduced. The resulting mixture was subjected to v.p.c. Three components were obtained. The products I, II, and III (Table II) were collected separately and identified by the product obtained on demethylation (for I and II) or by the acetaldehyde formed by periodate oxidation of III after demethylation. Fractions 2*b* and 2*c* were similarly reacted and the fragments separated by v.p.c. to give compounds IV, V, and VI (Table II), the identities of which

Can. J. Chem. Downloaded from www.nrcresearchpress.com by 210.87.254.105 on 09/05/12
For personal use only.

were deduced from the nature of the products obtained on demethylation. It was subsequently shown that if the original fraction 2 was reacted without division into subfractions each of the compounds I–VI was separable by v.p.c. (Fig. 1). It is thus clear that all the di-*O*-methylrhamnoses may be uniquely identified by this method. The fact that 2,3-di-*O*-methyl-L-rhamnose was the major component of this fraction indicates that (1 → 4) linkages predominate although all possible linkages occur in the polymer.

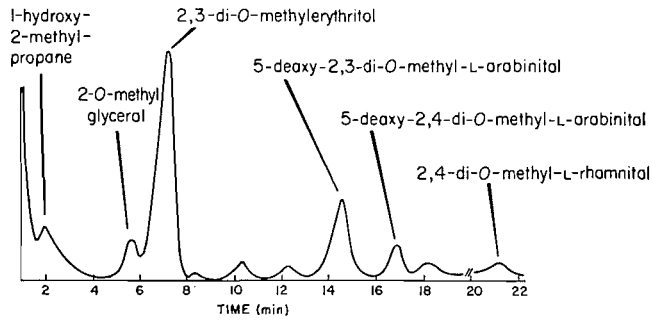

FIG. 1. Vapor phase chromatography of products from di-*O*-methyl-L-rhamnoses.

The mixture of mono-*O*-methylrhamnoses was analyzed by a similar series of reactions except that the free sugars were converted to their methyl glycosides before periodate oxidation. The ether bridge between the two oxidation fragments was cleaved by methanolysis and the products, after hydrolysis, reduced with borohydride. The mixture was then subjected to v.p.c. with the isolation of the products shown in Table III.

TABLE III

Identification of mono-*O*-methyl-L-rhamnoses

Methyl glycoside of mono-*O*-methyl-L-rhamnose		Products	Demethylation product (m.p. of *p*-nitrobenzaote)
2-	(*i*) IO_4^-	2-*O*-Methylglycerol + 1,2-dihydroxypropane	Glycerol (188–192°) + 1,2-dihydroxypropane (125–126°)
3-	(*ii*) MeOH/HCl (*iii*) H^+	3-*O*-Methyl-L-rhamnitol	L-Rhamnitol
4-	(*iv*) BH_4^-	1-Deoxy-3-*O*-methyl-D-erythritol + ethylene glycol	1-Deoxy-D-erythritol (109–110°) + ethylene glycol (148–150°)
5-		1-Deoxy-2-*O*-methyl-D-erythritol + ethylene glycol	

When the rhamnan was subjected to a Smith degradation and the products were analyzed by paper chromatography six distinct fractions were obtained and a seventh which showed considerable trailing. The nature of these fractions, two of which were reducing, is shown in Table IV. The identity of fractions 1, 2, and 4 was readily shown by the preparation of derivatives. Characterization of fraction 3 as a deoxypentose followed from the fact that periodate degradation of its methyl glycoside gave 1,2-ethanediol and 1,2-propanediol. Of greater interest in the present connection were fractions 5 and 6.

Hydrolysis of fraction 5 gave L-rhamnose and 1-deoxy-D-erythritol in equimolecular amounts indicating a glycoside while periodate oxidation and measurement of the formal-

Can. J. Chem. Downloaded from www.nrcresearchpress.com by 210.87.254.105 on 09/05/12
For personal use only.

TABLE IV

Paper chromatographic separation of Smith periodate degradation fragments

Fraction	R_g	Weight (mg)	Identity
1	4.48	230	1,2-Dihydroxypropane
2	3.98	257	1-Deoxy-D-erythritol
3	3.14	20	5-Deoxy-L-arabinose
4	2.16	23	L-Rhamnose
5	1.79	134	Rhamnosyl 1-deoxy-erythritols
6	1.30	58	Dirhamnosyl 1-deoxy-erythritols
7	0.90	25	Oligosaccharides

dehyde suggested that the major part of the 1-deoxy-D-erythritol was linked at C-2 and a minor amount at C-3. The remainder of fraction 5 was accordingly converted to its trimethylsilyl derivative and analyzed by v.p.c. (Fig. 2A). Three components were

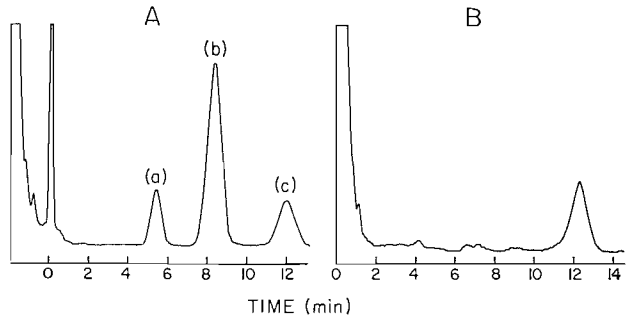

FIG. 2. A. Vapor phase chromatography of trimethylsilyl ethers of (*a*) 1-deoxy-3-*O*-(α-L-rhamnopyranosyl)-D-erythritol, (*b*) the β-anomer, (*c*) 1-deoxy-2-*O*-(β-L-rhamnopyranosyl)-D-erythritol. B. Vapor phase chromatography of trimethylsilyl ethers of L-Rha*p*-(1 → 4)-L-Rha*p*-(1 → 3)-1-deoxy-D-erythritol.

obtained 5*a*, 5*b* (major), and 5*c* and each formed a crystalline *p*-nitrobenzoate. On periodate degradation 5*c* yielded only 1,2-propanediol and hence this component must have been 1-deoxy-2-*O*-(β-L-rhamnopyranosyl)-D-erythritol with the β-linkage inferred from the optical rotation. Both 5*a* and 5*b* gave 1,2-propanediol and 1-deoxy-D-erythritol and on the basis of optical rotation and retention times (5) these components were believed to be 1-deoxy-3-*O*-(α-L-rhamnopyranosyl)-D-erythritol (5*a*) and the corresponding β-anomer (5*b*). The separation of these compounds is further evidence that v.p.c. of trimethyl silyl ethers is capable of separating isomeric and anomeric glycosides. The isolation of these compounds is also evidence that the rhamnan contained 5-*O*-L-rhamnopyranosyl-rhamnose units (5*c*) and 4-*O*-L-rhamnopyranosyl-rhamnose units, both α-linked (5*a*) and β-linked (5*b*).

Investigation of fraction 6 in a similar way showed it to contain L-rhamnose and 1-deoxy-D-erythritol in a 2:1 ratio with not more than 10% of the erythritol residues substituted at C-2. Periodate degradation gave 1,2-propanediol and 1-deoxy-D-erythritol in approximately a 1:2 ratio together with a trace of rhamnose. Conversion to the trimethylsilyl ether and v.p.c. gave only one major component (Fig. 2B) which on desilylation and periodate oxidation gave no formaldehyde. The principal component of this fraction was therefore

L-Rha*p*-(1 → 4)-L-Rha*p*-(1 → 3)-1-deoxy-D-erythritol.

Can. J. Chem. Downloaded from www.nrcresearchpress.com by 210.87.254.105 on 09/05/12
For personal use only.

The preparation of 1-deoxy-D-erythritol needed as a standard in these studies does not appear to have been described and it was accordingly synthesized from methyl α,β-L-rhamnofuranosides.

The results reported have demonstrated that periodate degradation of methylated sugars followed by v.p.c. is a quick and convenient method for the analysis and characterization of groups of isomeric sugars. The selective degradation to fragments of varying molecular weight enhances the differences in retention times and by using the glycitols complications of multiple peaks for the same sugar are avoided. The method is capable of extension to other groups of sugars but is particularly convenient with 6-deoxy compounds and will therefore be of use for studies on seaweed and blood-group polysaccharides. If suitable crystalline derivatives of all the cleavage products were known it would be possible to characterize directly each of the v.p.c. fractions. Lack of such derivatives necessitated the demethylation step. As yet there is no data available on the quantitative aspects of this step and hence this method of analysis may only be used qualitatively. As far as the fragments from a Smith degradation are concerned there is an increasing body of evidence to show that the reaction produces a greater number of fragments than can be separated by existing techniques. The combination of trimethylsilyl ethers and v.p.c. is a welcome step forward but methods must be developed for the separation of higher oligomers if full advantage is to be taken of this method of degradation.

EXPERIMENTAL

General and analytical methods have been described previously (2). Chromatograms were run on Whatman 1 paper using ethyl acetate – acetic acid – water (8:2:2) unless otherwise noted. R_g refers to glucose = 1.0.

Analysis of the Rhamnan

Hydrolysis of the polysaccharide gave an almost quantitative yield of L-rhamnose monohydrate, m.p. 92–93° and $[\alpha]_D$ 8.1° (*c*, 2 in water). Partial hydrolysis of the rhamnan with 0.1 *N* HCl at 50° gave 9% rhamnose (1 h), 12% (2 h), 16% (4 h), and 20% (8 h). Estimation of the formaldehyde produced on periodate oxidation of the reduced rhamnan gave a D.P. of 40 on the assumption that each rhamnitol end group gave 1 mole of formaldehyde. Borohydride reduction of the oxidized polysaccharide followed by hydrolysis gave L-rhamnose, 1,2-propanediol (R_g 4.48, di-*p*-nitrobenzoate, m.p. 124–126°), and 1-deoxy-D-erythritol (R_g 3.98, tri-*p*-nitrobenzoate, m.p. 108–109°) in a 1:7:6 molar ratio.

Methylation of Rhamnan

The rhamnan (1.50 g) was dissolved in *N,N*-dimethylformamide and methylated by Kuhn's procedure. The partially methylated product was reacted with Purdie's reagents for 120 h to give a pale-yellow gum (1.55 g) which showed no hydroxyl absorption in the infrared and had $[\alpha]_D$ −24.6° (*c*, 4.2 in acetone). The methylated polysaccharide was so soluble that no fractionation could be achieved with chloroform – petroleum ether mixtures. The methylated polysaccharide was hydrolyzed with sulfuric acid (6) and the brown, water-insoluble substance which separated was subjected to methanolysis and hydrolysis to yield a further quantity of methylated rhamnoses. The ratio of tri:di:monomethyl:free rhamnose was determined by the phenol – sulfuric acid method and was found to be 23:58:19:2. The mixture was resolved on Whatman 3MM paper using butanone–water azeotrope into the four fractions shown in Table I.

Trimethyl Fraction

This fraction (300 mg) was dissolved in water (20 ml) and oxidized with bromine (3 ml) in the presence of lead carbonate (2 g). After 48 h, excess bromine was removed by aeration, insoluble lead salts were removed by filtration, and the filtrate passed through a column of cation exchange resin. The effluent was evaporated and the sirupy product heated at 75–80° *in vacuo* to achieve lactonization. The product was analyzed by gas chromatography (Table V). The 2,3,4-tri-*O*-methyl-L-rhamnonolactone crystallized in the collection tube, remelted at 41°, and had $[\alpha]_D$ −132° → −78° (*c*, 0.3 in water); lit. (7) m.p. 40–41°, $[\alpha]_D$ −138° → −78° (water). The other component did not crystallize and was reacted with phenylhydrazine. A poor yield of 2,3,5-tri-*O*-methyl-L-rhamnonophenylhydrazide, m.p. 156–159°, was obtained; lit. (8) m.p. 160°.

Can. J. Chem. Downloaded from www.nrcresearchpress.com by 210.87.254.105 on 09/05/12
For personal use only.

TABLE V

Data for vapor phase separations

Mixture	Retention time (min)	Operating conditions
2,3,4-Tri-*O*-methyl-L-rhamnonolactone +	9	*
2,3,5-tri-*O*-methyl-L-rhamnonolactone	7	
1-Hydroxy-2-methoxypropane (I) +	1	
2-*O*-methylglycerol (II) +	4	†
5-deoxy-2,4-di-*O*-methyl-L-arabinitol (III)	15	
2,3-Di-*O*-methyl-erythritol (IV) +	5	
5-deoxy-2,3-di-*O*-methyl-L-arabinitol (V) +	12	‡
2,4-di-*O*-methyl-L-rhamnitol (VI)	18	
1,2-Dihydroxypropane +	2	
ethylene glycol +	4	
2-O-methylglycerol +	5	§
1-deoxy-2- and 3-*O*-methyl-	7	
D-erythritols	8	

Apparatus: Aerograph A90-P2 and F and M 800.
Column: 3 ft by 0.25 in. i.d., 10% versamide on chromosorb W.
Retention times quoted are relative to the solvent peak.
*Column 150°; helium flow 80 ml/min.
†Column 80–190° at 8°/min; helium flow 95 ml/min.
‡Column 80–200° at 8°/min; raised to 230° after 16 min; helium flow 95 ml/min; using these conditions a mixture of I–VI was successfully separated.
§Column 140–240° at 10°/min; helium flow 95 ml/min.

Dimethyl Fraction

Fraction 2a

Rechromatography of fraction 2 gave the fastest moving material (2*a*) substantially pure and electrophoresis (0.1 *M* sodium borate, 2 h at 450 V) showed approximately equal amounts of two components with M_G values 0.05 and 0.39 corresponding with 2,5- and 3,5-di-*O*-methyl-L-rhamnoses. The mixture (90 mg) was dissolved in water (20 ml) and treated with sodium borohydride (150 mg). The glycitols were oxidized with periodate and the yield of formaldehyde (6.0 mg) indicated about 35 mg of 3,5-di-*O*-methyl-L-rhamnitol. After the removal (barium carbonate) of periodate and iodate sodium borohydride was added and 16 h later the solution was acidified with sulfuric acid and boiled. Barium carbonate was added and the filtrate evaporated to a thin sirup which was extracted with acetone. Removal of the solvent left a sirup which was analyzed by gas chromatography (Tables II and V). Three products were collected and each was characterized after demethylation by heating with hydrobromic acid (45%) for 35 min (9). The product from *compound I* was 1,2-dihydroxypropane (di-*p*-nitrobenzoate, melting point and mixed melting point 125–126°) and that from *compound II* was glycerol (tri-*p*-nitrobenzoate, melting point and mixed melting point 189–192°). The product from *compound III* (32 mg) was oxidized with periodate and gave formaldehyde (7.1 mg). Periodate and iodate were removed with barium carbonate and the solution was saturated with sodium bisulfite. The solution was cooled to 5° and the addition compound was collected and decomposed with aqueous alcoholic hydrochloric acid. This solution was then reacted with semicarbazide hydrochloride and sodium acetate (10). The reaction mixture was extracted with chloroform and evaporation of the solvent gave acetaldehyde semicarbazone, melting point and mixed melting point 160–162°.

Fraction 2d

From the second separation on paper of fraction 2*a* described above part of the slowest moving portion was collected separately to give fraction 2*d* and the intermediate material gave fractions 2*b* and 2*c* (which could not be sharply separated) together with the remainder of 2*d*. Paper electrophoresis of these fractions indicated that 2*b* and 2*c* were non-migrating while fraction 2*d* had an M_G value of 0.36. Quantitative estimation showed that fraction 2*d* constituted 7–8% of fraction 2. A portion of fraction 2*d* (18 mg) was reacted with 2,4-dinitrophenylhydrazine to give 3,4-di-*O*-methyl-L-rhamnose 2,4-dinitrophenylhydrazone, m.p. 166–168° (decomp.), $[\alpha]_D$ 75° (*c*, 0.5 in 1,4-dioxane); lit. (11) m.p. 170° (decomp.), $[\alpha]_D$ 75.6° (*c*, 1 in 1,4-dioxane).

Fractions 2b and 2c

This material (550 mg) was dissolved in water (50 ml) and reduced with sodium borohydride (0.9 g). Periodate oxidation gave a small amount of formaldehyde and the product was again reduced. Gas chromatography of the resulting mixture showed three main components (Tables II and V) of which one (IV) was present as the major constituent. The identity of these components is shown in Table II and is based

Can. J. Chem. Downloaded from www.nrcresearchpress.com by 210.87.254.105 on 09/05/12
For personal use only.

on the following evidence. *Compound IV* was demethylated and the product (250 mg) gave erythritol tetra-*p*-nitrobenzoate melting point and mixed melting point 250–252°. *Compound V* was demethylated and the product (45 mg) gave formaldehyde (9.9 mg) on oxidation with periodate. Acetaldehyde was recovered from the oxidation mixture and converted to acetaldehyde semicarbazone melting point and mixed melting point 160–162°. *Compound VI* was demethylated and the product (38 mg) was chromatographically identical with L-rhamnitol. Reaction with acetic anhydride in pyridine gave L-rhamnitol pentaacetate, $[\alpha]_D$ ca. 2° (*c*, 2 in chloroform), but which failed to crystallize.

Monomethyl Fraction

A small amount (13 mg) of fraction 3*a* was obtained pure by rechromatographing fraction 3 on Whatman 1 paper. Reaction with phenylhydrazine gave 5-*O*-methyl-L-rhamnose phenylosazone, m.p. 120–123°; lit. (12) m.p. 123–124°.

The remainder of fraction 3 (195 mg) was refluxed for 6 h with methanolic hydrogen chloride (1%) and the glycosides were oxidized with periodate followed by methanolysis, hydrolysis, and borohydride reduction. A portion of the product was examined by gas chromatography (Table V) which indicated five components. The bulk of the product was demethylated and examined by paper chromatography. The compounds found, their derivatives, and their relation to the monomethylrhamnoses are shown in Table III.

Smith Periodate Degradation

To the rhamnan (2.04 g) was added periodic acid (0.5 *M*, 45 ml) and the solution diluted to 100 ml. The oxidation was carried out in the dark at 5° for 100 h (1.1 mole IO_4^- per rhamnose unit) and the solution, freed from inorganic ions, was extracted with ether. The ether extract yielded acetaldehyde characterized as the semicarbazone m.p. 158–160°. The aqueous solution was reduced with borohydride (1.8 g, 24 h) and after removal of borate, hydrolysis (0.1 *N* HCl, 22°, 8 h), and deionization, chromatography on Whatman 3MM paper gave the products listed in Table IV and fractions 1, 2, and 4 were characterized as shown. Fraction 3 was reducing and was believed to be a methyl pentose, presumably 5-deoxy-L-arabinose, on the following evidence. Refluxing with 1% hydrogen chloride in methanol gave a nonreducing product which was oxidized with periodate followed by borohydride reduction. Hydrolysis, deionization, and chromatographic separation gave a 1:1 molar ratio of 1,2-ethanediol (di-*p*-nitrobenzoate, m.p. 142–143°) and 1,2-propanediol (di-*p*-nitrobenzoate, m.p. 125–126°).

Vapor Phase Chromatography of Fractions 5 and 6

Fraction 5 contained some reducing material, presumably L-rhamnose, which was oxidized by aqueous bromine in the presence of lead carbonate. Deionization gave a nonreducing product (126 mg) from a portion (40 mg) of which there was obtained by hydrolysis a 1:1 molar ratio of L-rhamnose (21 mg, phenylhydrazone, melting point and mixed melting point 157–158°, $[\alpha]_D$ 43° (*c*, 2.5 in water)) and 1-deoxy-D-erythritol (13.7 mg, tri-*p*-nitrobenzoate, melting point and mixed melting point 109–110°, $[\alpha]_D$ 2° (*c*, 2 in pyridine)). Oxidation of the rhamnoside with 0.1 *M* periodic acid at 5° for 24 h gave formaldehyde. Hydrolysis of the borohydride-reduced product gave a 5:3 molar ratio of 1,2-propanediol (di-*p*-nitrobenzoate, m.p. 125–126°) and 1-deoxy-D-erythritol (tri-*p*-nitrobenzoate, m.p. 108–110°).

A portion of the rhamnoside (50 mg) was reacted in pyridine (1 ml) with hexamethyldisilazane (0.1 ml) and trimethylchlorosilane (0.2 ml). The product was examined by vapor phase chromatography on a 4 ft column (0.25 in. i.d.) packed with 20% GESF-96 on 60/80 mesh firebrick with a helium flow rate of 90 ml/min at 180°. Three peaks were obtained (Fig. 2A) and the corresponding substances were separately condensed in glass tubing and desilylated by boiling overnight in 80% ethanol to give components 5*a*, *b*, *c*, in the approximate ratio of 1:4:1. Component 5*a* had $[\alpha]_D$ 15° (*c*, 2 in water) and when a portion (1.7 mg) was oxidized with periodic acid (0.1 *M*, 15 ml) no formaldehyde was detected. After reduction and hydrolysis 1,2-propanediol and 1-deoxy-D-erythritol were found in a 1:1 molar ratio. The rest of component 5*a* (11 mg) was reacted in pyridine with *p*-nitrobenzoyl chloride to give 1-deoxy-3-*O*-(α-L-rhamnopyranosyl)-D-erythritol penta-*p*-nitrobenzoate, m.p. 155–158°, $[\alpha]_D$ 12° (*c*, 2 in pyridine).

Anal. Calcd. for $C_{45}H_{35}N_5O_{22}$: N, 7.04. Found: N, 7.07.

Component 5*b* showed no measurable optical activity and was oxidized as described for 5*a*. The two polyols obtained from 5*a* and 5*b* were pooled and characterized as their *p*-nitrobenzoates. Reaction of a portion of 5*b* (10 mg) with *p*-nitrobenzoyl chloride gave 1-deoxy-3-*O*-(β-L-rhamnopyranosyl)-D-erythritol penta-*p*-nitrobenzoate, m.p. 181–183°.

Anal. Calcd. for $C_{45}H_{35}N_5O_{22}$: N, 7.04. Found: N, 7.05.

Component 5*c* (7 mg) was oxidized with periodic acid (0.1 *M*, 20 ml) and gave formaldehyde (0.83 mg). Only 1,2-propanediol was found on reduction and hydrolysis. Reaction of a portion of 5*c* with *p*-nitrobenzoyl chloride gave 2-*O*-(L-rhamnopyranosyl)-1-deoxy-D-erythritol penta-*p*-nitrobenzoate, m.p. 191–193°.

Anal. Calcd. for $C_{45}H_{35}N_5O_{22}$: N, 7.04. Found: N, 7.15.

Fraction 6 gave rhamnose and 1-deoxy-D-erythritol in a 2:1 molar ratio on hydrolysis. Oxidation with periodic acid (0.1 *M*, 15 ml) of a portion (10 mg) gave some formaldehyde (0.075 mg). Barium carbonate was added and the filtrate reduced with sodium borohydride (30 mg). The hydrolysate of the polyalcohol gave 1,2-propanediol and 1-deoxy-D-erythritol in a 1:2 molar ratio. A trace of L-rhamnose was also detected.

Can. J. Chem. Downloaded from www.nrcresearchpress.com by 210.87.254.105 on 09/05/12
For personal use only.

The remainder of the glycoside (30 mg) was reacted in pyridine (0.5 ml) with hexamethyldisilizane (0.3 ml) and trimethylchlorosilane (0.6 ml) for 1 h at 40°. Using the same conditions as described for fraction 5 only one peak was obtained. A portion (20 mg) of the desilylated product was oxidized with periodic acid (0.1 *M*, 15 ml) and no formaldehyde was detected. On reduction and hydrolysis 1,2-propanediol and 1-deoxy-D-erythritol were obtained in a 1:2 molar ratio.

Fraction 7 was thought to be heterogeneous because of considerable streaking on chromatograms. Hydrolysis of a portion (10 mg) gave L-rhamnose and 1-deoxy-D-erythritol in a molar ratio of about 4:1. Periodate oxidation of a sample (10 mg) gave formaldehyde (0.21 mg) indicating the presence of some C-2 substituted 1-deoxy-D-erythritol units. Mild hydrolysis of the polyalcohol with hydrochloric acid (0.1 *N*) at room temperature for 8 h gave 1,2-propanediol, 1-deoxy-D-erythritol and a nonreducing substance with R_g 1.80 and hence presumed to be similar to fraction 5. Complete hydrolysis of the polyalcohol gave 1,2-propanediol, 1-deoxy-D-erythritol, and L-rhamnose in a molar ratio of 6:4:1.

Synthesis of 1-deoxy-D-erythritol

L-Rhamnose (2.5 g) was converted to the diethyl dithioacetal, m.p. 133–135°, by a published method (13, 14) and this was converted to the methyl α,β-L-rhamnofuranoside mixture (2.3 g) by the method of Green and Pacsu (15). The furanoside mixture was oxidized with periodic acid at 5°. One mole was consumed. Periodate and iodate were precipitated by the addition of barium carbonate and sodium borohydride (1.5 g) was added to the filtrate. The reduction was allowed to proceed for 16 h at room temperature and then the solution was acidified with hydrochloric acid and refluxed for 6 h. Borate was removed by distillation with methanolic hydrogen chloride and inorganic salts were removed by ion exchange. On evaporation an oily residue was obtained which was homogeneous when examined by paper chromatography and had R_g 3.9.

A portion of the product was further purified by vapor phase chromatography and collected as a clear oily liquid having $[\alpha]_D$ 7.4° (*c*, 2 in methanol). A portion (40 mg) was converted to 1-deoxy-D-erythritol tri-*p*-nitrobenzoate which on recrystallization from acetone had m.p. 109–110° and $[\alpha]_D$ 2° (*c*, 2 in pyridine).

Anal. Calcd. for $C_{25}H_{19}N_3O_{12}$: N, 7.60. Found: N, 7.68.

ACKNOWLEDGMENTS

This investigation was supported by grant number GM 07652 from the Division of General Medical Sciences, Public Health Services, U.S.A. We are grateful to Miss J. Hunter for skillful technical assistance and to Dr. P. Mora for providing the rhamnan.

REFERENCES

1. C. T. BISHOP. *In* Methods of biochemical analysis. Vol. X. *Edited by* D. Glick. Interscience, New York. 1962.
2. G. G. S. DUTTON and A. M. UNRAU. Can. J. Chem. **42**, 2048 (1964).
3. P. T. MORA, J. W. WOOD, and V. W. MCFARLAND. J. Am. Chem. Soc. **82**, 3418 (1960).
4. G. G. S. DUTTON and A. M. UNRAU. Can. J. Chem. **40**, 2105 (1962).
5. C. C. SWEELEY, R. BENTLEY, M. MAKITA, and W. W. WELLS. J. Am. Chem. Soc. **85**, 2497 (1963).
6. I. CROON, G. HERRSTRÖM, G. KULL, and B. LINDBERG. Acta Chem. Scand. **14**, 1338 (1960).
7. J. AVERY and E. L. HIRST. J. Chem. Soc. 2466 (1929).
8. F. SMITH. J. Chem. Soc. 1035 (1940).
9. L. HOUGH, J. K. N. JONES, and W. H. WADMAN. J. Chem. Soc. 1702 (1950).
10. R. L. SHRINER, R. C. FUSON, and D. Y. CURTIN. *In* Systematic identification of organic compounds. 4th ed. Wiley, New York. 1958.
11. K. BUTLER, P. F. LLOYD, and M. STACEY. J. Chem. Soc. 1531 (1955).
12. P. A. LEVENE and J. COMPTON. J. Biol. Chem. **114**, 9 (1936).
13. P. A. LEVENE and G. M. MEYER. J. Biol. Chem. **74**, 695 (1927).
14. M. L. WOLFROM. J. Am. Chem. Soc. **52**, 2466 (1930).
15. J. W. GREEN and E. PACSU. J. Am. Chem. Soc. **60**, 2056 (1938).

Can. J. Chem. Downloaded from www.nrcresearchpress.com by 210.87.254.105 on 09/05/12
For personal use only.

Can. J. Chem. Downloaded from www.nrcresearchpress.com by 210.87.254.42 on 09/05/12
For personal use only.

LE SPECTRE INFRAROUGE DE L'OZONIDE D'AMMONIUM ET LA STRUCTURE DE L'ION O_3^-

KAZIMIERA HERMAN ET PAUL A. GIGUÈRE
Département de Chimie, Université Laval, Québec, Québec

Reçu le 28 decembre 1964

RÉSUMÉ

L'oxydation ménagée de l'ammoniac solide par l'ozone gazeux à basse température donne comme intermédiaire l'ozonide d'ammonium selon l'équation:

$$4NH_3 + 3O_3 \rightarrow 2NH_4O_3 + NH_4NO_3.$$

En élevant la température le solide rouge-orangé apparaît vers -130 °C; il atteint sa concentration maximum vers $-115°$, et à $-90°$ il est complètement décomposé. Les spectres infrarouges montrent, outre les bandes caractéristiques des ions NH_4^+ et NO_3^-, deux fortes bandes d'absorption à 800 et 1 140 cm^{-1} et deux autres assez faibles à 1 260 et 2 053 cm^{-1} qui doivent appartenir aux vibrations ν_2, ν_3, ν_1 et $\nu_1 + \nu_2$ de l'ion O_3^-. Ces fréquences sont nettement plus élevées que les fréquences correspondantes de la molécule d'ozone, ce qui indique des liaisons plus fortes dans l'ion, contrairement aux prévisions. Par analogie avec l'ozone on prévoit pour l'ion O_3^- des longueurs de liaisons de 1.22 Å et un angle au sommet d'environ 100°.

ABSTRACT

The slow oxidation of solid ammonia by gaseous ozone at low temperature proceeds through an unstable intermediate, ammonium ozonide, after the equation

$$4NH_3 + 3O_3 \rightarrow 2NH_4O_3 + NH_4NO_3.$$

The red solid appears on warming around -130 °C, reaches maximum concentration at about $-115°$, and is all decomposed by $-90°$. The infrared spectra show, besides the characteristic bands of the NH_4^+ and NO_3^- ions, two strong bands at 800 and 1 140 cm^{-1}, and two faint ones at 1 260 and 2 053 cm^{-1} which must belong to the ν_2, ν_3, ν_1 and $\nu_1 + \nu_2$ modes of the O_3^- ion. These frequencies are appreciably higher than the corresponding ones of the ozone molecule, which indicates a stronger bonding in the ozonide ion contrary to most predictions. By analogy with ozone the bond lengths in the ion are estimated to be 1.22 Å and the interbond angle, about 100°.

INTRODUCTION

L'existence des ozonides de métaux alcalins est maintenant bien établie à la suite des résultats tant de l'analyse chimique (1, 2) que de mesures physiques par les méthodes magnétiques (1, 3, 4) et spectroscopiques (4, 5). A cause de l'intérêt qu'elle présente pour les théories électroniques de la valence la structure de l'ion O_3^- a fait l'objet de plusieurs spéculations. Ainsi Kazarnovskii (1) a représenté cette structure comme un hybride de résonance entre deux formules canoniques avec une liaison à trois électrons et peut-être aussi une troisième avec liaisons simples seulement, ce qui l'a conduit à prédire des longueurs approximatives de liaison $r_{O-O} = 1.38$ Å. En tant que molécule triatomique avec 19 électrons de valence, l'ion O_3^- devrait avoir une structure triangulaire (6)—tout comme la molécule ClO_2 (7)—ce qui a été confirmé par le spectre de résonance de spin électronique (3). Par comparaison avec la série des molécules et ions NO_2^+, NO_2, NO_2^- et NO_2^{2-}, et d'après les données bien connues de la molécule d'ozone, Smith (8) a prévu les valeurs suivantes pour l'ion : $r = 1.34 \pm 0.05$ Å et $\theta = 115 \pm 5°$. Pour sa part Pauling (9) entrevoit des valeurs du même ordre ($r = 1.35$ Å et $\theta = 108°$) en se basant sur les deux structures en résonance,

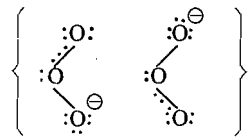

selon la méthode des liaisons de valence, tandis que Green (10) utilise la méthode des orbitales moléculaires et représente ainsi les structures canoniques possibles.

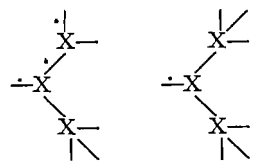

La première, dans laquelle l'ordre de liaison est de $2\frac{1}{2}$, serait la plus importante dans le cas de l'ion ozonide.

Par contre, les données expérimentales sont peu abondantes, sans doute à cause des difficultés de préparation et de l'instabilité chimique des ozonides. Les auteurs russes (1) ont mesuré les premiers le moment magnétique de KO_3 (1.63 magnétons de Bohr, soit très près de la valeur théorique 1.78 pour un électron célibataire), ainsi que la diffraction des rayons X par la méthode des poudres. Ce travail préliminaire a révélé une ressemblance marquée des réseaux cristallins de KO_3 et de KN_3, ce qui semblait indiquer une structure linéaire de l'ion O_3^-. Toutefois une analyse subséquente des figures de diffraction a jeté des doutes sur cette interprétation ; entre autre l'absence des réflexions (121) dans les diagrammes de poudres pouvait selon Zhdanov et Zvonkova (11) être due à une structure triangulaire. Plus récemment encore, alors que le présent travail était en cours, une étude plus poussée de la structure cristalline de KO_3 est parue (12) donnant les coordonnées atomiques suivantes pour l'anion : $r = 1.19$ Å, $\theta = 100°$. Cependant, comme le font remarquer les auteurs, la précision de ces résultats est assez faible à cause de la diffraction excessive par les ions potassium.

Il nous a semblé que la spectroscopie infrarouge était susceptible d'apporter de nouvelles données sur cet intéressant problème. La difficulté, évidemment, résidait dans la préparation d'un échantillon convenable. De nombreuses tentatives pour obtenir un mince film de KO_3 par ozonisation soit de KOH anhydre à 0° (13), soit de KO_2 (14) suivie d'une extraction à l'ammoniac liquide se sont toutes soldées par un échec à cause de la réactivité extrême de ces composés. C'est alors que les récents succès de Solomon et ses collaborateurs (5) dans la préparation de l'ozonide d'ammonium nous ont conduits à étudier ce composé qui offre le grand avantage de pouvoir être synthétisé directement dans la cellule d'absorption à partir des réactifs gazeux à basse pression, et sans manipulation subséquente. Des essais préliminaires ont montré que, malgré son instabilité thermique, il était possible d'obtenir le spectre infrarouge de ce composé en contrôlant rigoureusement la température.

PARTIE EXPÉRIMENTALE

L'ozone a été préparé sur place par dissociation de l'oxygène sous basse pression dans une décharge à micro-ondes. Afin de prévenir toute contamination du premier produit par des oxydes d'azote, nous sommes partis d'oxygène ultra-pur provenant de la décomposition catalytique du peroxyde d'hydrogène (solution à 40% de Becco) soigneusement dégazé sous vide dans le tube A (Fig. 1). Le catalyseur, une fine toile de platine métallique, était suspendu par un fil enroulé sur une tige de verre montée dans l'axe d'un joint rodé B.

Can. J. Chem. Downloaded from www.nrcresearchpress.com by 210.87.254.42 on 09/05/12
For personal use only.

Un petit disque de verre fritté supportant des billes de verre dans l'ampoule C servait à arrêter les gouttelettes de liquide entraînées dans le courant gazeux, tandis que deux pièges à azote liquide D et E débarrassaient l'oxygène de toute trace d'humidité, précaution essentielle pour obtenir un bon rendement en ozone (15).

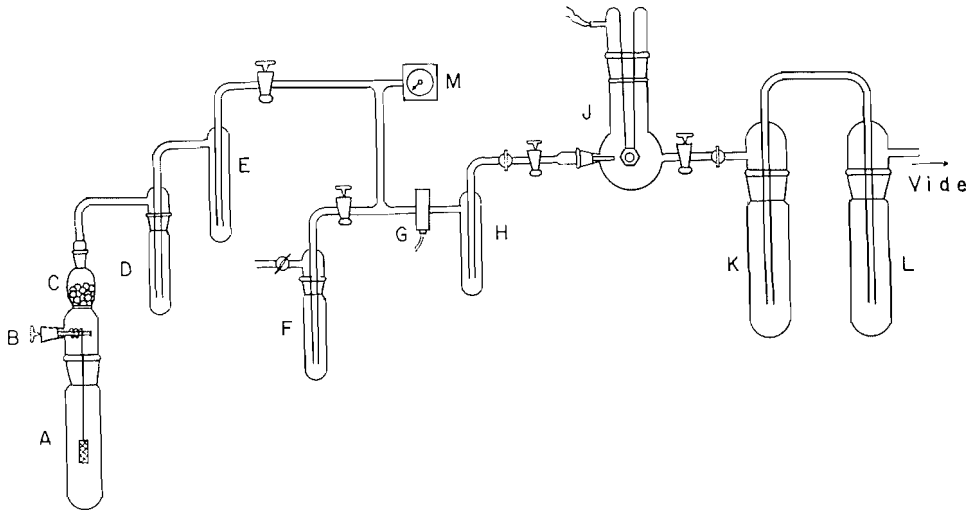

FIG. 1. Schéma de l'appareil utilisé pour préparer l'ozonide d'ammonium.

La pression d'oxygène telle qu'indiquée par le manomètre mécanique M (General Electric, Molecular Vacuum Gage, C-148 388) était amenée à environ 1 mm Hg en ajustant le taux de décomposition du peroxyde d'hydrogène soit en faisant varier la température, soit en manipulant le catalyseur de platine. L'énergie du générateur de micro-ondes ("Raytheon Microtherm"), opérant à 2 400–2 500 Mc, était introduite par le résonateur G placé sur le tube latéral d'un piège à azote liquide H. L'expérience nous a appris qu'il ne se forme pas d'ozone dans le piège quand l'oxygène dissocié est introduit par le tube central, sans doute parce que les atomes se recombinent avant d'atteindre la paroi froide. Cette observation rejoint les conclusions de Schiff (16) et de Ruehrwein et Hashman (17) sur la nécessité d'une température suffisamment basse pour synthétiser l'ozone avec ce genre de décharge électrique. Pour la même raison, il fallait limiter l'énergie (à environ 60 W) afin de prévenir l'échauffement excessif et la désintégration rapide du tube de Pyrex. Une fois allumée (avec une bobine de Tesla) la décharge à micro-ondes était très stable sous une pression voisine de 1 mm Hg. Après quelques minutes l'ozone liquide apparaissait sous forme d'une mince couronne bleue dans le piège au niveau de l'azote liquide. Eventuellement le film liquide glissait jusqu'au fond où il formait une grosse goutte.

L'ammoniac anhydre provenant d'une bouteille (Matheson, 99.99% pur) était liquéfié tel quel dans un piège à carboglace F, d'où il pouvait être distillé au besoin sous basse pression (10^{-2} mm Hg) dans la cellule à absorption J. Celle-ci était en verre, du type courant (18), avec un piège central fermé par un joint verre-métal de Kovar et bloc de cuivre dans lequel était encastré le disque porteur de l'échantillon. Au début ce dernier était en chlorure de sodium comme les fenêtres externes, mais à cause de l'attaque par les réactifs il dut être remplacé par des disques de verres transparents en infrarouge, Eastman Kodak, Irtran-2 (jusqu'à 700 cm^{-1}) ou Irtran-4 (jusqu'à 500 cm^{-1} environ), qui ont l'avantage de résister à la plupart des substances corrosives ainsi qu'aux brusques variations de température. Le seul inconvénient de ces matériaux était leur coloration jaune ; en effet il devenait difficile d'observer la formation ou la disparition de la couleur rouge due à l'ozonide. On pouvait suivre la température de l'échantillon à 1° près au moyen d'un petit thermocouple cuivre–constantan inséré entre le disque porteur et le bloc de cuivre et un potentiomètre de précision (Leeds & Northrup, modèle 8662). La pompe à vide mécanique était protégée par deux pièges à azote liquide K et L montés en série par mesure de précaution contre les explosions (19). Dans le même but toute la verrerie utilisée était soigneusement nettoyée avec de l'acide sulfurique fumant ; les robinets et les rodages étaient lubréfiés avec une graisse de silicone (Dow Corning, High-Vacuum Grease). Nous n'avons jamais observé au cours de ce travail d'explosion ni de décomposition violente des ozonides.

On commençait par déposer un mince film d'ammoniac sur le disque central de la cellule d'absorption en contrôlant la pureté et l'épaisseur par son spectre infrarouge. Après avoir admis l'ozone gazeux, la cellule était détachée du montage, grâce à des joints rodés sphériques, et installée dans le spectromètre à infrarouge (Perkin-Elmer, modèle 12-C). Une fois l'azote liquide évaporé, la température de l'échantillon montait au rythme de 2 °C par minute.

Can. J. Chem. Downloaded from www.nrcresearchpress.com by 210.87.254.42 on 09/05/12
For personal use only.

Can. J. Chem. Downloaded from www.nrcresearchpress.com by 210.87.254.42 on 09/05/12
For personal use only.

RÉSULTATS

Des essais préliminaires ont montré que les premiers signes de coloration jaune du film d'ammoniac coïncidaient avec l'apparition d'une nouvelle bande d'absorption vers 800 cm^{-1} et la déformation, du côté des hautes fréquences, de la bande de NH_3 solide vers 1 055 cm^{-1} (20). En conséquence ces deux régions furent étudiées soigneusement en fonction de la température. Les écarts de température indiqués dans la Fig. 2 viennent de ce que la vitesse de balayage du spectromètre était assez lente par rapport au taux de réchauffement de l'échantillon. En bref, on observe les phénomènes suivants : au début le spectre ne montre que la forte bande de l'ammoniac cristallin à 1 055 cm^{-1}. La pression partielle de l'ozone gazeux est trop basse et le parcours optique trop court (10 cm environ) pour déceler ses bandes d'absorption. Les deux nouvelles bandes qui apparaissent à 800 et 1 140 cm^{-1} vers -150 °C augmentent d'intensité parallèlement avec le degré de coloration rouge-orangé des produits de la réaction. Peu après on voit poindre l'une des bandes de l'ion NO_3^- à 827 cm^{-1}, l'autre vers 1 085 cm^{-1} (21) étant alors masquée

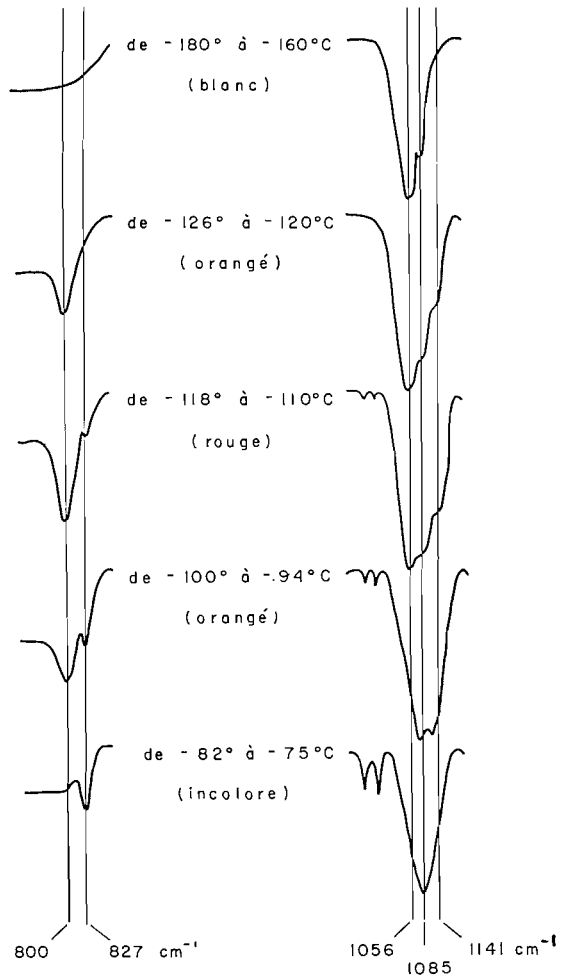

FIG. 2. Evolution des bandes d'absorption en infrarouge vers 9 et 12 μ dans le système $NH_3 + O_3$ entre $-180°$ et -75 °C.

par la forte absorption de NH_3 solide. Au fur et à mesure que celle-ci diminue par suite de la réaction le maximum d'absorption à cet endroit se déplace de 1 055 vers 1 085 cm^{-1}. Concurremment la chaleur de la réaction volatilise une partie de l'ammoniac, d'où le doublet à 932 et 968 cm^{-1}.

Comme il était souhaitable d'observer tout le spectre de vibration (de 3 à 15 μ) du système au moment où la concentration en ozonide d'ammonium a atteint son maximum, nous avons cherché à arrêter la réaction en refroidissant brusquement. Cette opération s'est avérée difficile à cause de l'inertie calorifique de la cellule. En effet si on ajoutait de l'azote liquide dans le piège de la cellule alors que la concentration en ozonide était appréciable, soit vers $-125°$, la réaction continuait et l'ozonide se décomposait presque entièrement avant que l'échantillon ne commence à se refroidir à cause de la mauvaise conductibilité thermique du support (Irtran). Par contre si on refroidissait plus tôt, la réaction s'arrêtait prématurément par suite de la condensation de l'ozone sur la partie supérieure du piège. Pour obvier à cet inconvénient il a fallu entourer ce dernier, de même que le bloc de métal, d'un manchon de Teflon, un bon isolant thermique et, en même temps, parfaitement inerte vis-à-vis de l'ozone et de l'ammoniac. C'est ainsi qu'a pu être obtenu le spectre d'absorption (Fig. 3) du système brusquement refroidi de $-115°$ à $-190°$. En plus des bandes déjà mentionnées on y relève à 1 620 cm^{-1} celle de l'ammoniac

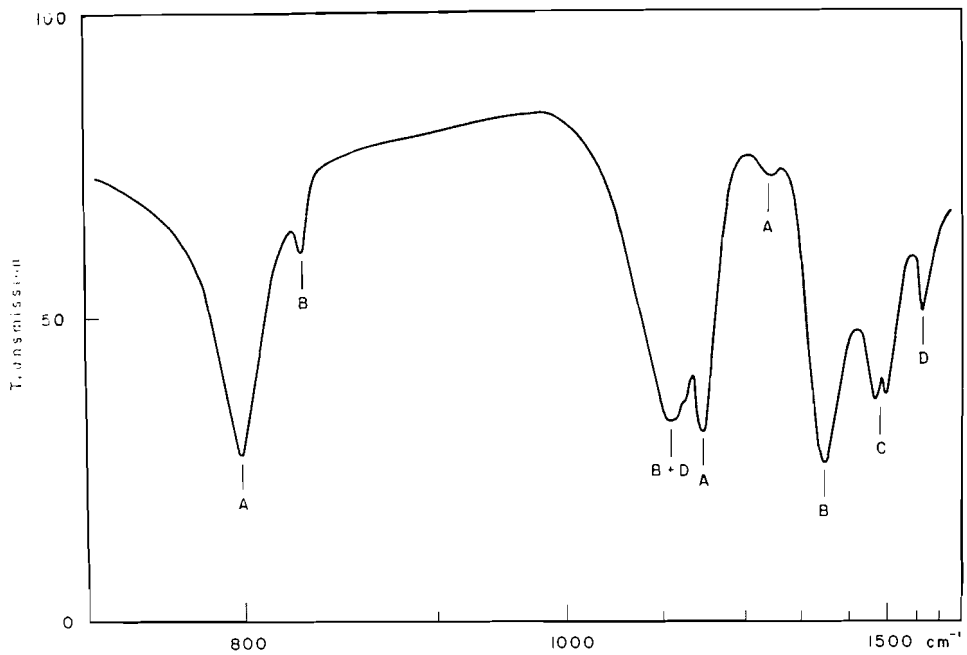

FIG. 3. Spectre infrarouge entre 600 et 1 800 cm^{-1} des produits de la réaction entre l'ozone gazeux et l'ammoniac solide à -115 °C stabilisés à $-190°$: A, O_3^-; B, NO_3^-; C, NH_4^+; D, NH_3.

solide qui n'a pas encore réagi avec l'ozone, ainsi que celles du nitrate d'ammonium à 1 350 et 1 420–1 490 cm^{-1}. Signalons en passant que les maxima d'absorption rapportés ici pour ce composé ne correspondent pas exactement aux données de la littérature (21). Les différences s'expliquent par la nature métastable du produit de la réaction qui ne doit point avoir de structure cristalline régulière; effectivement son apparence est celle d'un verre incoloré.

Can. J. Chem. Downloaded from www.nrcresearchpress.com by 210.87.254.42 on 09/05/12
For personal use only.

Enfin un pic assez faible a été noté à 2 053 cm^{-1} qui ne saurait appartenir aux espèces NH_3 ou NH_4NO_3. Comme son intensité varie de la même façon que pour les nouvelles bandes à 800 et 1 140 cm^{-1}, il doit s'agir d'une harmonique ou d'une combinaison. Des diverses possibilités, soit (*a*) le double de la fréquence 1 140 cm^{-1}, (*b*) une combinaison de celle-ci avec une autre de l'ordre de 930 cm^{-1} ou encore, (*c*) une combinaison de la fréquence 800 cm^{-1} avec une autre d'environ 1 260 cm^{-1}, c'est cette dernière qui s'est avérée correcte. En effet une analyse point par point de la courbe d'absorption dans la région de 8 μ a permis de mettre en évidence un pic très faible à cet endroit. Au contraire la région de 11 μ est toujours apparue libre de toute absorption sélective, même dans des films assez épais. L'intensité relative des nouvelles bandes est indiquée entre parenthèses dans le Tableau I.

TABLEAU I

Comparaison des données spectroscopiques et structurales

		Ozone	Ion ozonide
Fréquences (cm^{-1})	ν_1	1 120 (1)*	1 260 (0.2)
	ν_2	704 (5)*	800 (10)
	ν_3	1 050 (10)*	1 140 (5)
Constantes de force de rappel ($\times 10^{-5}$ dynes cm^{-1})	k_1	5.70†	6.5?
	k_{α/l^2}	1.28†	1.5?
Longueur de liaisons (Å)	r_{O-O}	1.278 ± 0.002	1.22
Angle au sommet	α	116°40′ ± 30′	100°?

*Pour l'ozone solide (23).
†D'après le spectre de micro-ondes (29, 30).

DISCUSSION

L'attribution des nouvelles bandes aux vibrations de l'ion O_3^- ne fait pas de doute. En effet, leur comportement en fonction de la température suit rigoureusement l'évolution de la couleur rouge-orangé caractéristique des ozonides (4, 5). Par ailleurs, les seules autres molécules qui pourraient se former dans ce système et montrer des bandes d'absorption dans la même région sont les oxydes d'azote NO_2, N_2O_3, N_2O_4 et N_2O_5. Mais aucune de ces molécules n'a de fréquences fondamentales correspondant exactement aux présentes (22). De plus leurs propriétés physiques, couleur, point de fusion ou de sublimation, etc. ne coïncident aucunement avec celles de l'ozonide d'ammonium. L'ensemble des observations rapportées plus haut peut s'expliquer parfaitement grâce au schéma suivant:

[1] $$4NH_3 + 3O_3 \rightarrow 2NH_4O_3 + NH_4NO_3$$

[2] $$2NH_4O_3 \rightarrow NH_4NO_3 + 2H_2O + \tfrac{1}{2}O_2$$

Il và sans dire que ces équations ne représentent que la réaction globale. On peut imaginer que le premier acte est la décomposition de l'ozone, suivie de l'attaque de l'ammoniac par l'atome d'oxygène avec formation de diverses espèces transitoires ; NH_3O, NH_2OH, HNO_2, HNO_3, etc. La réaction de décomposition [2] avait déjà été démontrée par voie chimique (5).

Par comparaison avec les fréquences fondamentales de l'ozone (Tableau I) la bande à 800 cm^{-1} doit appartenir au mode de déformation ν_2 ; elle est certainement trop basse pour une vibration de valence O—O. Dans H_2O_2, où la liaison est essentiellement simple, cette vibration se trouve à 880 cm^{-1}. D'ailleurs un examen minutieux du spectre de l'ozonide jusqu'à 600 cm^{-1} n'a révélé aucune autre absorption pouvant provenir d'un mode de déformation de basse fréquence. A noter que le spectre des ozonides dans le visible (4) montre un maximum à 4 500 Å et des pics secondaires décalés du premier,

Can. J. Chem. Downloaded from www.nrcresearchpress.com by 210.87.254.42 on 09/05/12
For personal use only.

d'abord de quelque 800 cm^{-1} puis de valeurs décroissantes jusqu'à environ 700 cm^{-1}. La précision de ces mesures n'est cependant pas très grande vu qu'il s'agit de bandes diffuses.

Les deux autres bandes à 1 140 et 1 260 cm^{-1} ont des fréquences et des intensités appropriées pour les vibrations de valence ν_3 et ν_1 de l'ion O_3^-. Ainsi $\nu_3 < \nu_1$, tout comme pour la molécule d'ozone ; de plus les trois fréquences fondamentales de l'ion sont décalées dans le même sens, et à peu près de la même quantité, par rapport à celles de l'ozone. Tel que mentionné au début ces décalages sont de sens opposé à celui prévu par les théories électroniques de la valence. En effet, des fréquences plus élevées impliquent des liaisons plus courtes. Assurément les fréquences caractéristiques de l'ion O_3^- sont affectées par diverses interactions dans l'ozonide d'ammonium solide : forces de Coulomb, de van der Waals, liaisons hydrogène sans doute assez fortes entre NH_4^+ et O_3^-. La dynamique des oscillations internes des ions polyatomiques en est sûrement modifiée. Par exemple, la bande de combinaison $\nu_1 + \nu_2$ de l'ion O_3^- à 2 053 cm^{-1} n'a pas son équivalent dans le spectre de l'ozone solide (23) où c'est plutôt le mode $\nu_1 + \nu_3$ qui est actif en infrarouge. Mais ce ne sont là que des effets de deuxième ordre, comme on peut s'en rendre compte en comparant les fréquences de l'ion NO_3^- des nitrates d'ammonium avec celles des nitrates alcalins (22). Les déplacements observés ici sont donc bien réels, même si leurs valeurs absolues sont un peu incertaines.

A partir des présents résultats on peut évaluer approximativement la longueur des liaisons dans l'ion O_3^- suivant la règle de Badger (24). Pour plus de précision il vaut mieux utiliser cette relation non pas directement mais par comparaison avec les données de l'ozone,

$$\frac{\nu_a}{\nu_b} = \frac{(r_b - C)}{(r_a - C)},$$

où C est la constante empirique 0.68 Å. On obtient ainsi une valeur moyenne de 1.22 Å pour les liaisons O—O dans l'ion, ce qui s'accorde assez bien avec le résultat 1.19 Å de la diffraction des rayons X dans KO_3 (12). Quant à l'angle au sommet α, il est plus difficile à évaluer car les méthodes usuelles de calcul selon l'approximation des forces de valence (25) conduisent à des valeurs imaginaires pour l'ion O_3^- aussi bien que pour la molécule d'ozone. Par exception l'équation utilisée par Bailey et Cassie pour SO_2 (26) donne exactement la même valeur, 100°, que la diffraction des rayons X. La coïncidence est certainement fortuite vu l'imprécision des deux méthodes. C'est néanmoins une bonne indication que l'angle au sommet est plus petit dans l'ion que dans la molécule O_3, en accord cette fois avec les prévisions théoriques.

Signalons enfin que la simplicité des présents spectres confirme les données cristallographiques aussi bien que les conclusions de la théorie (10) à savoir que l'ion O_3^- n'a pas tendance à se dimériser, contrairement à l'ion isoélectronique NO_2^{2-} (27, 28) et à la molécule NO_2.

REMERCIEMENTS

Ces travaux ont pu être exécutés grâce à l'aide financière du Conseil National de Recherches.

BIBLIOGRAPHIE

1. I. A. KAZARNOVSKII, G. P. NIKOLSKII et T. A. ABLETSOVA. Dokl. Akad. Nauk SSSR, **64**, 69 (1949).
2. T. P. WHALEY et J. KLEINBERG. J. Am. Chem. Soc. **73**, 79 (1951).
3. A. D. MCLACHLAN, M. C. R. SYMONS et M. G. TOWNSEND. J. Chem. Soc. 952 (1959).
4. I. J. SOLOMON, A. J. KACMAREK, J. M. MCDONOUGH et K. HATTORI. J. Am. Chem. Soc. **82**, 5640 (1960).

Can. J. Chem. Downloaded from www.nrcresearchpress.com by 210.87.254.42 on 09/05/12
For personal use only.

5. I. J. SOLOMON, K. HATTORI, A. J. KACMAREK, G. M. PLATZ et M. J. KLEIN. J. Am. Chem. Soc. **84**, 34 (1962).
6. A. D. WALSH. J. Chem. Soc. 2266 (1953).
7. L. E. SUTTON (*Editeur*) Tables of interatomic distances. Chem. Soc. London Spec. Publ. No. 11. 1958.
8. P. SMITH. J. Phys. Chem. **60**, 1471 (1956).
9. L. PAULING. The nature of the chemical bond. 3rd ed. Cornell University Press, Ithaca, N.Y. 1960. p. 354.
10. M. GREEN. J. Chem. Soc. 2819 (1962).
11. G. S. ZHDANOV et Z. V. ZVONKOVA. Zhur. Fiz. Khim. **25**, 100 (1951).
12. L. V. AZAROFF et I. CORVIN. Proc. Natl. Acad. Sci. U.S. **49**, 1 (1963).
13. V. G. KARPENKO et A. S. POTERYAIKO. Khim. Perekisnykh Soedin., Akad. Nauk SSSR, 193 (1963).
14. I. I. VOLNOV et V. V. MATVEEV. Izv. Akad. Nauk SSSR, 1136 (1963).
15. H. P. BROIDA et J. R. PELLAM. J. Chem. Phys. **23**, 409 (1955).
16. H. I. SCHIFF. Ann. N.Y. Acad. Sci. **67**, 518 (1957).
17. R. A. RUEHRWEIN et J. S. HASHMAN. J. Chem. Phys. **30**, 823 (1959).
18. E. L. WAGNER et D. F. HORNIG. J. Chem. Phys. **18**, 296 (1950).
19. P. A. GIGUÈRE et D. CHIN. J. Chem. Phys. **31**, 1685 (1959).
20. P. A. STAATS et H. W. MORGAN. J. Chem. Phys. **31**, 553 (1959).
21. A. THÉORÊT et C. SANDORFY. Can. J. Chem. **42**, 57 (1964).
22. K. NAKAMOTO. Infrared spectra of inorganic and coordination compounds. J. Wiley & Sons, New York. 1963. p. 100.
23. K. B. HARVEY et A. M. BASS. J. Mol. Spectry, **2**, 405 (1958).
24. R. M. BADGER. J. Chem. Phys. **2**, 128 (1934).
25. G. HERZBERG. Infrared and Raman spectra of polyatomic molecules. D. Van Nostrand Co. Inc., New York. 1945.
26. C. R. BAILEY et A. B. D. CASSIE. Proc. Roy. Soc. London, Ser. A, **137**, 622 (1932).
27. R. W. ASMUSSEN. Acta Chem. Scand. **12**, 578 (1958).
28. H. C. CLARK, A. HORSFIELD et M. C. R. SYMONS. J. Chem. Soc. 7 (1961).
29. R. H. HUGHES. J. Chem. Phys. **24**, 131 (1956).
30. L. PIERCE. J. Chem. Phys. **24**, 139 (1956).

Can. J. Chem. Downloaded from www.nrcresearchpress.com by 210.87.254.42 on 09/05/12
For personal use only.

Can. J. Chem. Downloaded from www.nrcresearchpress.com by 210.87.254.105 on 09/05/12
For personal use only.

9,10-DIMETHYL- AND 9,10-DIPHENYL-9,10-DIHYDRO-9,10-ETHANOANTHRACENE BY FRIEDEL–CRAFTS CYCLIALKYLATIONS OF 1,4-DIARYLSUBSTITUTED-1,4-DIOLS

L. R. C. Barclay and Ralph A. Chapman[1]
Department of Chemistry, Mount Allison University, Sackville, New Brunswick
Received November 16, 1964

ABSTRACT

The 1,4-diols, 2,5-diphenylhexane-2,5-diol (I*a*), and 1,1,4,4-tetraphenylbutane-1,4-diol (I*b*) were found to undergo intramolecular cyclodehydrations and dehydration yielding 9,10-disubstituted-9,10-dihydro-9,10-ethanoanthracenes, 2,2,5,5-tetrasubstituted-tetrahydrofurans, and 1,1,4,4-tetrasubstituted-1,3-butadienes when treated with hydrogen fluoride or aluminium chloride. No evidence could be found for intermolecular cyclialkylations of added aromatics such as benzene, anisole, or veratrole. Nuclear magnetic resonance spectra of the products are discussed.

RESULTS AND DISCUSSION

A number of 1,4-diols are readily available from either the action of ketones on acetylenic Grignard reagents or the action of Grignard reagents on appropriate diesters. Bruson (1) reported using two such diols in experiments on the cyclialkylation of various aromatic compounds. The present investigation is concerned with the reactions which take place when the diols 2,5-diphenylhexane-2,5-diol (I*a*) and 1,1,4,4-tetraphenylbutane-1,4-diol (I*b*) are used as alkylating agents in Friedel–Crafts cyclialkylations. In particular it was desirable to determine whether these diols would cyclialkylate an added aromatic or whether they would react intramolecularly. Bruson (1) has reported that the diol (I*b*) cyclialkylated *o*-cresol to yield 5,5,8,8-tetraphenyl-3-methyl-5,6,7,8-tetrahydro-2-naphthol but this structure was based only on a carbon and hydrogen analysis.

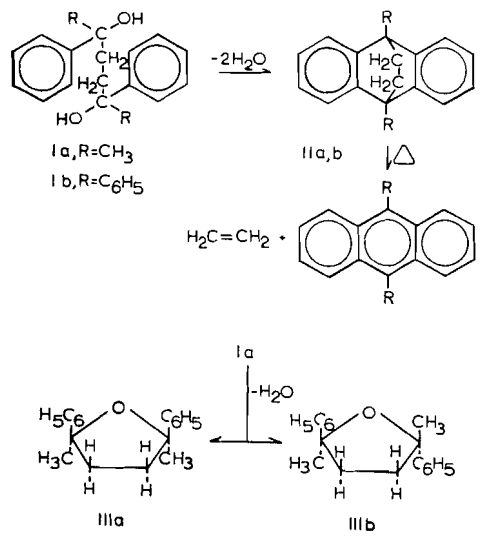

[1]*Recipient of a National Research Council Studentship.*

Can. J. Chem. Downloaded from www.nrcresearchpress.com by 210.87.254.105 on 09/05/12
For personal use only.

The treatment of 2,5-diphenylhexane-2,5-diol (I*a*) with anhydrous hydrogen fluoride in the presence or absence of benzene (Table I, Nos. 1 and 2) yielded a four component mixture. The major component (63%) was found to be the new hydrocarbon, 9,10-dimethyl-9,10-dihydro-9,10-ethanoanthracene (II*a*). The assignment of this structure is based on the following evidence. The ultraviolet spectrum was characteristic of an *o*-disubstituted aromatic with bands at 2 720 Å (ϵ = 1 390), 2 650 Å (ϵ = 1 150) and a slight inflection at 2 580–2 590 Å. The infrared spectrum showed a strong band at 760 cm^{-1} for *o*-disubstitution. The mass spectrum of the compound II*a* showed a parent mass of 234 with a large fragment mass at 206. This fragment mass is attributed to 9,10-dimethylanthracene formed by the loss of the ethano bridge as ethylene from the parent compound. This was further substantiated by the fact that spectral peaks at masses 26, 27, and 28 were in the proper ratio for ethylene and that 9,10-dimethylanthracene was produced when the compound II*a* was heated with selenium at 275°. A similar loss of an ethano bridge has been reported by Campbell and co-workers (2).

The nuclear magnetic resonance (n.m.r.) spectrum of II*a* (see Table II) showed a symmetrical A_2B_2 multiplet centered at 2.73 p.p.m. assigned to the eight aromatic protons of the two ortho-disubstituted rings. It is of interest to note that the methyl protons absorbed on the low field side (8.04) of the methylene protons (8.34). A Stuart-Briegleb model of II*a* showed that the methyls are positioned approximately in the planes of the two aromatic rings. The methyl protons are thus deshielded by the ring current effect and resonate at lower field than normally expected. This effect is similar to that reported by LeGoff (3) for 2,3,6,7-tetraacetoxy-9,10-dimethyl-9,10-dihydro-9,10-ethanoanthracene. The formation of II*a* apparently takes place by a double intramolecular cyclodehydration of the starting diol as shown in the illustration. The remainder of the reaction mixture from hydrogen fluoride treatment of I*a* consisted of a mixture (32%) of *cis*- and *trans*-2,5-dimethyl-2,5-diphenyltetrahydrofuran (III*a*, *b*).

The reaction of the diol (I*a*) with a molar equivalent of aluminium chloride produced a mixture of 59% compound II*a* and 40% of a mixture of the two isomeric furans (III*a*, *b*) mentioned above (Table I, No. 3). On the other hand, reaction of the diol (I*a*) with a catalytic amount of aluminium chloride (Table I, No. 4) produced a mixture of III*a* and *b* (58% and 42%) which were separated by crystallization and repetitive gas–liquid chromatography (g.l.c.) to yield a solid (m.p. 75–76°) and a liquid. Both compounds showed several strong bands in the infrared at 1 000 – 1 100 cm^{-1} characteristic of the furan ethers, as well as strong bands at 705 and 770 cm^{-1} indicating monosubstituted aromatics. On this basis the components were thought to be the isomeric *cis*- and *trans*-2,5-dimethyl-2,5-diphenyltetrahydrofurans. These have been reported previously by Kotlyarevskii and co-workers (4).

The n.m.r. spectra of these compounds (Table II) confirmed their structures to be the *cis*- and *trans*-furan derivatives. The solid isomer showed a singlet at 8.48 p.p.m. assigned to the two methyl groups. The methylene protons absorbed in a well-defined A_2B_2 symmetrical multiplet* centered at 7.83 and the aromatic protons absorbed in a complex multiplet centered near 2.66. The liquid isomer showed a singlet at 8.42 for the methyls, a singlet at 7.77 for the methylenes,* and a complex multiplet centered near 2.75 assigned to the aromatic protons.

The treatment of 1,1,4,4-tetraphenylbutane-1,4-diol (I*b*) with anhydrous hydrogen fluoride in the presence or absence of benzene gave a high yield of the new hydrocarbon,

**This difference in the methylene absorption readily distinguished the two isomers. The determination of the configuration of the isomers by n.m.r. spectroscopy is under investigation and will be reported separately.*

Can. J. Chem. Downloaded from www.nrcresearchpress.com by 210.87.254.105 on 09/05/12
For personal use only.

TABLE I

Cyclodehydration reactions

No.	Reactants (mole)	Catalyst (mole)	Solvent*	Time, h	Products	% yield
1	2,5-Diphenylhexane-2,5-diol (I*a*)(0.010)	HF (0.48)	Benzene	16	Dimethylethanoanthracene (II*a*)	63
					Dimethyldiphenyltetrahydrofurans (III*a,b*)	32
2	I*a* (0.010)	HF (0.48)	CCl_4	16	II*a*	68
					III*a,b*	—
3	I*a* (0.010)	$AlCl_3$ (0.01)	Benzene	23	II*a*	59
					III*a,b*	40
4	I*a* (0.010)	$AlCl_3$ (0.00075)	Benzene	48	III*a,b*	100
5	1,1,4,4-tetraphenylbutane-1,4-diol (I*b*)(0.005)	HF (0.50)	Benzene	24	Diphenylethanoanthracene (II*b*)	100
6	I*b* (0.005)	HF (0.50)	—	24	II*b*	94
7	I*b* (0.01)	$AlCl_3$ (0.01)	Benzene	24	II*b*	14
					1,1,4,4-Tetraphenylbutadiene (IV)	30
8	I*b* (0.005)	$AlCl_3$ (0.00075)	Benzene	19	IV	
					Tetraphenyltetrahydrofuran(?)	
9	I*b* (0.02)+*o*-cresol (0.09)	$AlCl_3$ (0.06)	*n*-Hexane	15	II*b*	70
					IV	—
10	I*b* (0.005)+veratrole (0.022)	$AlCl_3$ (0.015)	Petroleum ether	92	IV	—

*Reactions in hydrogen fluoride were carried out at room temperature; those catalyzed by $AlCl_3$, at reflux temperatures of the solvents. For other details see Experimental.

TABLE II

Nuclear magnetic resonance spectral data

Compound	Chemical shifts		Multiplicity	Relative areas	Assignments
II*a*	8.38*	(4.22)†	Singlet	3.9	2×—CH_2—
	8.04	(3.88)	Singlet	5.7	2×—CH_2
	2.73	(−1.45)	Symmetrical multiplet (A_2B_2)	8.0	Ortho-disubstitution
II*b*		(3.74)†	Singlet	4.0	2×—CH_2—
		(−1.07)	Symmetrical multiplet (A_2B_2)	7.5	Ortho-disubstitution
		(−1.72)	Complex multiplet	10	2×C_6H_5
III (m.p. 75–76°)	8.48		Singlet	6.0	2×—CH_3
	7.83		Symmetrical multiplet (A_2B_2)	4.0	2×—CH_2—
	2.66		Complex multiplet	9.7	2×C_6H_5
III (liquid)	8.42		Singlet	5.9	2×—CH_3
	7.77		Singlet	4.0	2×—CH_2
	2.75		Complex multiplet	10.1	2×C_6H_5
Tetraphenyl-1,3-butadiene IV		(−1.00)†	Singlet	2.1	2×C=C—H
		(−1.35)	Singlet	10.0	2×C_6H_5—
		(−1.54)	Singlet	10.0	2×C_6H_5—
9,10-Diphenylanthracene	2.40		Symmetrical multiplet (A_2B_2)	9‡	9,10-Substituted anthracene
	2.37		Singlet	10‡	2×C_6H_5

*τ values determined in CCl_4.
†Values in parentheses are chemical shifts relative to tetrachloroethane (τ = 5.95) and were recorded in the solvent at 146°.
‡Integrations were approximate due to overlap of bands.

9,10-diphenyl-9,10-dihydro-9,10-ethanoanthracene (II*b*) (Table I, Nos. 5 and 6). The assignment of this structure was based on the following physical and chemical evidence. The ultraviolet spectrum of II*b* gave bands at 2 710 Å (ϵ = 746), 2 642 Å (ϵ = 1 130), and 2 580 – 2 590 Å (ϵ = 1 140). The infrared spectrum showed strong bands at 745 cm^{-1} attributed to *o*-disubstitution and at 707 and 767 cm^{-1} attributed to monosubstitution. The mass spectrum indicated a parent mass at mass 358 with a large fragment mass at 330. This is consistent with the proposed structure. The mass of 330 is due to 9,10-diphenylanthracene produced by the loss of the ethano bridge from the original II*b*. Hydrocarbon II*b* was not soluble in the usual solvents for n.m.r. spectroscopy at room temperature. However, its spectrum was determined at elevated temperatures in tetrachloroethane and this spectrum (see Table II) confirmed the suggested structure.

The singlet at 3.74 (chemical shift from tetrachloroethane) was assigned to the two methylene groups. Under high resolution, the band at −1.07 was resolved into an A_2B_2-type of symmetrical multiplet which could therefore be assigned to the two ortho-disubstituted rings. The two monosubstituted rings absorbed in a complex multiplet in the region near −1.72. Further supporting evidence for this structure was obtained by the thermal decomposition of II*b* yielding 9,10-diphenylanthracene and ethylene which was identified by gas–solid chromatography. The 9,10-diphenylanthracene was identified by its ultraviolet spectrum (see Experimental) and n.m.r. spectrum. The latter showed a symmetrical A_2B_2 multiplet expected of a 9,10-disubstituted anthracene (see Table II). The phenyl protons absorbed as a singlet at 2.37 p.p.m.

The reaction of the diol (I*b*) with a molar equivalent of aluminium chloride (Table I, No. 7) yielded only 14% II*b* with a larger quantity of 1,1,4,4-tetraphenyl-1,3-butadiene (IV). The latter was identified by spectral analyses (see Table II). Reaction of I*b* with a catalytic amount of aluminium chloride yielded what was apparently a mixture of the

Can. J. Chem. Downloaded from www.nrcresearchpress.com by 210.87.254.105 on 09/05/12
For personal use only.

1,3-butadiene (IV) and 2,2,5,5-tetraphenyltetrahydrofuran (No. 8). This mixture was previously reported by Wasserman and Kloetzel (5) as a mixture with a narrow melting range in the vicinity of 160° which was difficult to separate.

The reaction of the diol (I*b*) with *o*-cresol and aluminium chloride (Table I, No. 9) yielded no phenolic reaction product. The products isolated were 70% crude compound II*b* and the 1,3-butadiene (IV). A similar reaction with veratrole (Table I, No. 10) yielded only the 1,3-butadiene (IV). The report by Bruson (1) that *o*-cresol and the diol I*b* yielded 5,5,8,8-tetraphenyl-3-methyl-5,6,7,8-tetrahydro-2-naphthol is open to question. It is most likely that the compound isolated (m.p. 330–332°) was the ethanoanthracene (II*b*) described in this paper.

It is apparent that 1,4-diaryl-1,4-diols such as I*a* and I*b* undergo intramolecular dehydrations exclusively. They fail to alkylate added aromatics under a variety of conditions. With hydrogen fluoride or molar equivalents of aluminium chloride as catalysts, the predominate reaction was a double aromatic intramolecular cyclodehydration. This provided a synthesis of the 9,10-disubstituted-9,10-dihydro-9,10-ethanoanthracenes. Because of the availability of various diols, the convenience of the cyclodehydration, and high yields obtainable, this reaction will be useful in future syntheses of such bridged hydrocarbons.

EXPERIMENTAL

Apparatus and Methods

The ultraviolet spectra were recorded on a Beckman DK-2 Ratio Recording Spectrophotometer. The infrared spectra were recorded on a Perkin–Elmer Model 137 "Infracord" spectrophotometer. Gas–liquid chromatography analyses were carried out on an F & M Model 500 Programmed Temperature Gas Chromatograph equipped with a dual column attachment. Silicone Gum Rubber on Chromosorb P was used as the column material for all high boiling liquids and solids. The mass spectrometer analyses were determined at an independent laboratory. The n.m.r. spectra were recorded on a Varian A-60 spectrometer equipped with a variable temperature probe. Melting points were determined on a Fisher-Johns melting point apparatus equipped with a microscope or a Thomas Hoover "Unimelt" capillary melting point apparatus. Reactions with anhydrous hydrogen fluoride were carried out in a 12 in. stainless steel MD Test Tube Reactor equipped with stainless steel gaskets made by Autoclave Engineers Inc. Samples of pure components for analyses were obtained by gas–liquid chromatography.

Reagents

The 2,5-diphenylhexane-2,5-diol was a gift of the Air Reduction Chemical Co. It was approximately an equal mixture of the two possible diastereoisomers and was used as such. The 1,1,4,4-tetraphenylbutane-1,4-diol (m.p. 203–205°) was prepared by the procedure of Wasserman and Kloetzel (5).

Reaction of 2,5-Diphenylhexane-2,5-diol (Ia) with Hydrogen Fluoride

(a) With Benzene as Solvent

Benzene (15 ml) and 2,5-diphenylhexane-2,5-diol (2.70 g, 0.010 mole) were placed in the reaction tube and it was cooled below 10° in an ice bath. The hydrogen fluoride (9.5 g) was added from a commercial cylinder and the tube was sealed and stirred for 16 h at room temperature. The tube was then cooled to below 10° and opened. The contents were poured onto crushed ice and the organic material extracted with petroleum ether. After the extract was washed free of acid with sodium carbonate and water, it was dried over sodium sulfate. Distillation of the solvent yielded a solid. Gas–liquid chromatography indicated a four component mixture, the respective components being 63, 18, 14, and 4% of the mixture. Chromatography of this product from petroleum ether on alumina and recrystallization of the solid fractions from ethanol yielded a crystalline solid, m.p. 126–128°. The ultraviolet spectrum gave bands at 2 720 Å (ϵ = 1 390), 2 650 Å (ϵ = 1 150), and an inflection at 2 580 – 2 590 Å. The infrared spectrum showed a strong band at 760 cm^{-1}. The mass spectrum of the compound indicated a parent mass of 234, with a large fragment mass at 206. Peaks were also observed at masses 26, 27, and 28 in the proper ratio for ethylene. The n.m.r. spectrum of this compound (II*a*) is outlined in Table II.

Anal. Calcd. for $C_{18}H_{18}$: C, 92.26 H, 7.74. Found: C, 92.08, 92.18; H, 7.72, 7.80.

(b) With Carbon Tetrachloride as Solvent

The reaction was repeated using 10 ml of carbon tetrachloride as solvent in place of benzene. The petroleum ether extract yielded 2.54 g of product which was found to be a similar mixture to that obtained in (*a*). Chromatography on alumina as above yielded a crystalline solid (68%) which was identical with that obtained above.

Can. J. Chem. Downloaded from www.nrcresearchpress.com by 210.87.254.105 on 09/05/12
For personal use only.

Thermal Decomposition of 9,10-Dimethyl-9,10-dihydro-9,10-ethanoanthracene (IIa)

Selenium (0.50 g) and compound II*a* (0.25 g) were ground together and the mixture was heated in a nitrate bath at 275° for 30 h. Crystals which sublimed were periodically returned to the flask. The cooled mixture was shaken with benzene and decolorizing carbon and then filtered. Distillation of the benzene yielded 0.20 g of solid. Chromatography from benzene on alumina and sublimation of the fractions *in vacuo* yielded a yellow crystalline solid. The ultraviolet spectrum of this gave bands at 3 980 Å (log = ϵ 3.91), 3 780 Å (log ϵ = 3.90), 3 580 Å (log ϵ = 3.64), 3 410 Å (log ϵ = 3.29), 3 260 Å (log ϵ = 2.98), 2 610 Å (log ϵ = 5.21), and 2 530 Å (log ϵ = 4.87). This was identified as 9,10-dimethylanthracene by comparison with the spectrum recorded by Jones (6) and with the tabulation of the main absorption bands which were as follows: 3 980 Å (log ϵ = 3.99), 3 780 Å (log ϵ = 4.00), 3 570 Å (log ϵ = 3.77), 3 410 Å (log ϵ = 3.43), 3 260 Å (log ϵ = 3.03), 2 600 Å (log ϵ = 5.24).

Reactions of 2,5-Diphenylhexane-2,5-diol (Ia) with Aluminium Chloride in the Presence of Benzene

(a) With a Molar Equivalent of Catalyst

Benzene (7.8 g, 0.1 mole) and the diol (I*a*) (2.70 g, 0.01 mole) were mixed and 1.33 g (0.01 mole) of aluminium chloride was added over 10 min. The reaction was vigorous with the evolution of a great deal of hydrogen chloride. Water cooling was used to moderate the reaction. After 1 h at room temperature and 22 h refluxing, the mixture was hydrolyzed on crushed ice. Extraction with ether yielded 2.07 g of a semisolid. Gas–liquid chromatography showed that 59% of the semisolid was compound II*a* while 40% of it was a mixture of the two isomeric substituted tetrahydrofurans (III*a* and *b*).

(b) With a Catalytic Amount of Catalyst. Separation of cis and trans-2,5-Dimethyl-2,5-diphenyltetrahydrofuran (IIIa and b)

Benzene (7.8 g, 0.1 mole), the diol (I*a*) (2.70 g, 0.01 mole), and aluminium chloride (0.10 g, 0.00075 mole) were mixed and refluxed for 12½ h and let stand for 36 h at room temperature. The mixture was then hydrolyzed on ice, extracted with benzene, treated as usual to remove acid, and then freed from benzene by distillation. Gas–liquid chromatography of the residue indicated two components representing 58 and 42% of the mixture respectively and with the same retention time as the minor components obtained in the reaction described above. On standing, part of the liquid crystallized. Filtration of the crystals and recrystallization from ethanol yielded a solid, m.p. 75–76°. The major component of the residual liquid was collected as a liquid by repetitive gas–liquid chromatographic fractionation of small samples of the mixture. Both the crystals and the liquid showed several strong bands in the infrared between 1 000 and 1 100 cm^{-1} characteristic of the furan ethers. Bands at 705 and 770 cm^{-1} indicated monosubstituted aromatics. The n.m.r. spectra of the solid and the liquid are outlined in Table II.

Reactions of 1,1,4,4-Tetraphenylbutane-1,4-diol (Ib) with Hydrogen Fluoride

(a) With Benzene as Solvent

Hydrogen fluoride (10 g) was condensed in the cooled tube. The 1,1,4,4-tetraphenylbutane-1,4-diol (1.97 g, 0.005 mole) was added in small quantities and 5 ml of benzene was added dropwise. The tube was sealed and stirred for 24 h at room temperature. The tube was cooled, then opened, and the contents were poured on ice. A solid was observed that apparently would not dissolve in either benzene or chloroform. It was collected by filtration and a total of approximately 1.8 g of crude solid obtained. Sublimation under high vacuum at 220° yielded a solid, m.p. 312° (II*b*) with decomposition. The ultraviolet spectrum gave bands at 2 710 Å (ϵ = 746), 2 642 Å (ϵ = 1 130), and 2 580 – 2 590 Å (ϵ = 1 140). The infrared spectrum showed strong bands at 767 and 707 cm^{-1} attributed to monosubstitution and 745 cm^{-1} attributed to *o*-disubstitution. Mass spectral analysis indicated a parent mass of 358. There was a strong peak for a fragment mass of 330.

Anal. Calcd. for $C_{28}H_{22}$: C, 93.81; H, 6.19. Found: C, 93.91, 94.07; H, 6.08, 6.14.

(b) In the Absence of Solvent

The reaction was repeated using no solvent. After the reaction mixture had been stirred for 24 h, the tube was opened as usual. The contents of the tube was solid. This solid was added to water to remove adhering acid and was collected by filtration to yield 1.68 g (a 94% yield) of solid, m.p. 309–310° with decomposition. The ultraviolet spectrum was identical to the product from (*a*).

Thermal Decomposition of 9,10-Diphenyl-9,10-dihydro-9,10-ethanoanthracene (IIb)

The compound II*b* (0.25 g) was heated at 315° for 20 min in an atmosphere of nitrogen. Samples of the off-gas from the decomposition were analyzed by gas–solid chromatography on a silica gel column. The major component was found to be ethylene by comparison of retention time with that of an authentic sample. The residual solid was sublimed *in vacuo* to yield a crystalline solid, m.p. 252–254° (lit. (7) 9,10-diphenylanthracene, m.p. 250–252°). The ultraviolet spectrum showed bands at 3 920 Å (log ϵ = 4.14), 3 720 Å (log ϵ = 4.15), 3 540 Å (log ϵ = 3.87), 3 370 Å (log ϵ = 3.73), 2 585 Å (log ϵ = 5.27), and 2 260 Å (log ϵ = 4.48). This was essentially identical with the spectrum of 9,10-diphenylanthracene reported by Jones (6).

Anal. Calcd. for $C_{26}H_{18}$: C, 94.51; H, 5.49. Found: C, 94.51, 94.42; H, 5.67, 5.66.

Can. J. Chem. Downloaded from www.nrcresearchpress.com by 210.87.254.105 on 09/05/12
For personal use only.

Reactions of 1,1,4,4-Tetraphenylbutane-1,4-diol (Ib) with Aluminium Chloride in the Presence of Benzene

(a) With a Molar Equivalent of Catalyst

Benzene (7.80 g, 0.1 mole) and the diol (I*b*) (3.94 g, 0.01 mole) were mixed and 1.33 g (0.01 mole) of aluminium chloride was added over 10 min. After 1 h at room temperature and 23 h reflux, the mixture was hydrolyzed on ice and chloroform added. The insoluble solid which formed was collected and after recrystallization from dioxane yielded 0.51 g of II*b*.

From the chloroform-soluble material there was obtained 1.1 g of a solid, m.p. 190–204°. Two recrystallizations from benzene yielded crystals of m.p. 205–207° (hot stage) and 202.5–203.5° (capillary). The infrared spectrum (in Nujol and KBr) showed strong bands near 700 and 770 cm^{-1} attributed to monosubstituted aromatic absorption. There was no hydroxyl absorption. The ultraviolet spectrum had strong broad absorption at 2 480 Å and 3 460 Å consistent with the spectrum of 1,1,4,4-tetraphenylbutadiene (IV) illustrated in the literature (8). The n.m.r. spectrum of IV (see Table II) was also consistent with this structure. The reported melting point for IV was 202.5–203.5° (5).

(b) With a Catalytic Amount of Catalyst

A mixture of benzene (7.8 g, 0.1 mole), the diol (I*b*) (1.82 g, 0.005 mole), and aluminium chloride (0.10 g, 0.00075 mole) were stirred and refluxed for 19 h. The mixture was hydrolyzed on ice and the benzene was allowed to evaporate. The solid which separated was collected by filtration (m.p. 140–165°). Crystallization from ethanol–benzene yielded crystals of m.p. 162–165°. The ultraviolet spectrum of this solid gave broad bands at 3 420 – 3 460 Å and 2 490 – 2 500 Å characteristic of the 1,3-butadiene (IV). The infrared spectrum gave strong bands between 1 000 and 1 100 cm^{-1} indicative of ether absorption. An attempt was made to separate the mixture following the procedure of Wasserman (5) but no pure compounds were obtained.

Reaction of 1,1,4,4-Tetraphenylbutane-1,4-diol (Ib) with Aluminium Chloride

(a) In the Presence of o-Cresol

Following the procedure of Bruson (1), aluminium chloride (8.0 g, 0.06 mole) was suspended in 100 ml of *n*-hexane. The diol (I*b*) (8.0 g, 0.02 mole) and *o*-cresol (10 g, 0.09 mole) were added all at once. After refluxing for 15 h, the mixture was hydrolyzed on 200 ml of 1:4 mixture of hydrochloric acid and water. On treatment with *n*-hexane, there was obtained 5.0 g of insoluble solid which was identified as diphenylethanoanthracene (70%) by its melting point and ultraviolet spectrum. Distillation of the *n*-hexane yielded a mixture of a solid and a liquid. This was found by gas–liquid chromatography to be a mixture of unreacted *o*-cresol and a smaller amount of tetraphenylbutadiene (IV).

(b) In the Presence of Veratrole

A similar reaction was carried out with 3.10 g (0.022 mole) of veratrole, 2.00 g (0.005 mole) of the diol (I*b*), and 2.00 g (0.015 mole) of aluminium chloride. After refluxing for 92 h in 25 ml of low boiling petroleum ether, the mixture was hydrolyzed on ice and extracted with benzene. This product was found to be a mixture of the diene (IV) and veratrole with no compound II*b* or other alkylation product detectable.

ACKNOWLEDGMENTS

The authors thank Dr. A. G. McInnes of the National Research Council, Halifax, Nova Scotia, for recording the n.m.r. spectra of the dimethyl diphenyltetrahydrofurans. Financial assistance from the National Research Council is also gratefully acknowledged. The Varian A-60 n.m.r. spectrometer was purchased with funds from a National Research Council Major Equipment Grant.

REFERENCES

1. H. A. Bruson and J. W. Kroeger. J. Am. Chem. Soc. **62**, 36 (1940).
2. T. W. Campbell, V. E. McCoy, J. C. Kauer, and V. S. Foldi. J. Org. Chem. **26**, 1422 (1961).
3. E. LeGoff. Angew. Chem. **74**, 490 (1962).
4. I. L. Kotlyarevskii, M. S. Schvartsberg, and Z. P. Trotsenko. Zh. Obshch. Khim. **30**, 440 (1960).
5. W. J. Wasserman and M. C. Kloetzel. J. Am. Chem. Soc. **75**, 3036 (1953).
6. R. N. Jones. J. Am. Chem. Soc. **67**, 2127 (1945).
7. L. F. Fieser and H. Heyman. J. Am. Chem. Soc. **64**, 376 (1942).
8. F. Bergman, J. Szmuszkowicz, and E. Dimant. J. Am. Chem. Soc. **71**, 2968 (1949).

Can. J. Chem. Downloaded from www.nrcresearchpress.com by 210.87.254.105 on 09/05/12
For personal use only.

Can. J. Chem. Downloaded from www.nrcresearchpress.com by 210.87.254.105 on 09/05/12
For personal use only.

THEORETICAL STUDIES ON THE ELECTRONIC SPECTRA OF SUBSTITUTED AROMATIC MOLECULES

PART III. SEMIEMPIRICAL SCF CALCULATIONS FOR POLYCYCLIC ALTERNANT HYDROCARBONS

J. E. BLOOR[1] AND N. BREARLEY

British Columbia Research Council, Vancouver, British Columbia

Received November 30, 1964

ABSTRACT

The effect of changing the method of calculating repulsion integrals within the framework of the semiempirical self-consistent field method is investigated with respect to the transition energies of the alternant hydrocarbons benzene, anthracene, phenanthrene, and pyrene. Of the methods investigated, the one originally suggested by Mataga gave the best agreement with experiment. By statistical analysis of the linear relationship between the internuclear distance r_{pq} and the bond order p_{pq}, the regression line

$$r_{pq} = 1.515 - 0.178p_{pq}$$

was obtained.

The success of the Hückel LCAO procedure in correlating observed p-band transition energies with the Hückel energy number

$$K_i^{\mathrm{H}} = \sum_p^{NP} \sum_q^{NP} C_{ip}^{\mathrm{H}} C_{iq}^{\mathrm{H}}$$

(NP = No. of atoms contributing π electrons) for the highest occupied MO was shown to be due to (1) the relative unimportance of configuration interaction for this transition, (2) the invariance of the electron interaction terms calculated by the SCF method for different hydrocarbons, and (3) the identity of the Hückel energy number K_i^{H} with the corresponding term

$$K_i^{\mathrm{SCF}} = \sum_p^{NP} \sum_q^{NP} C_{ip}^{\mathrm{SCF}} C_{iq}^{\mathrm{SCF}}$$

of SCF theory, the latter value being insensitive to the method of choosing repulsion integrals even though the individual AO coefficients C_{ip}^{SCF} were quite sensitive.

INTRODUCTION

Although a number of calculations have been made of the excited states of polycyclic alternant hydrocarbons using the non-iterative antisymmetric molecular orbital configuration interaction (ASMOCI) method suggested by Pariser and Parr (1–3), very few have been done using the self-consistent field method (SCF) suggested by Pople.

To determine whether the use of SCF molecular orbitals (MOs) rather than Huckel MOs in limited configuration interaction (CI) calculations gives better agreement between experiment and theory, we have computed the transition energies and oscillator strengths of a number of hydrocarbons using as MOs for the CI calculations (*a*) the ground state SCF MOs recently made available by Hoyland and Goodman (5) and (*b*) new SCF MOs calculated using the Mataga and Nishimoto (6) method of calculating repulsion integrals. We have then compared the results with similar calculations carried out by others (1–7, 11–13, 20) and with experiment.

[1]*To whom all correspondence concerning this paper should be sent. Present address: The Franklin Institute Research Laboratories, Philadelphia, Pennsylvania 19103, U.S.A.*

Can. J. Chem. Downloaded from www.nrcresearchpress.com by 210.87.254.105 on 09/05/12
For personal use only.

RESULTS

The method of computation has been described in detail in Part II (8) of this series and elsewhere (1, 5). In carrying out CI calculations using SCF MOs and orbital energies, the repulsion integrals were obtained from a curve supplied by Professor L. Goodman constructed as described in (5). The same closed shell MOs were used for both singlets and triplets.

Naphthalene and Anthracene

The spectra of naphthalene and anthracene are fairly well understood, and the polarization of the first two bands of naphthalene has been established experimentally (9). In naphthalene the α band (^1L_b transition) has a 0–0 band at 32 100 cm^{-1}, and the p-band 0–0 band (^1L_a transition) is at 34 700 cm^{-1}. There is an intense band at 44 300 cm^{-1} (^1B_b transition) and a further band in the 50 000 – 60 000 cm^{-1} region.

In anthracene, the ^1L_b transition is not apparent since it is hidden by the intense ^1L_a transition at 26 600 cm^{-1}. The ^1B_b transition is at 39 500 cm^{-1}, and there is a further band around 54 000 cm^{-1} (^1B_a transition). The hidden band in anthracene, whose presence is shown by the behavior of the molecule on substitution of —OH and —NH_2 groups in different positions (10), provides a good means of testing the theory.

A considerable number of SCF CI and ASMO CI calculations have been done on these molecules (3, 4, 6, 11). As can be seen from Table I, there is, for naphthalene, a difference between the results of Gladney (11) and of Pople (4) of 2 200 cm^{-1} in the transition energy for the p band. This is unexpected, since the only difference between these two calculations is that in the former, the repulsion integrals for $r_{pq} > 2.78$ Å are obtained using Pariser and Parr's (2) long-distance formula, whereas in the latter, the inverse distance approximation (4) is used. It is usually assumed (13) that the transition energies are insensitive to repulsion integrals other than those between nearest neighbors. Assuming the absence of numerical error in these two calculations, this implies a very strong sensitivity of the ^1L_a transition energy to the values used for the repulsion integrals between distant atoms. This is a most unexpected conclusion and should be investigated further. In the case of

TABLE I

Experimental and theoretical results for naphthalene and anthracene

Excited state assignment	$E_{exp}(f_{exp})$[a] (cm^{-1})	Calculated $E(f)$ (cm^{-1})				
		Pariser method[b]	Mataga method[a]	Pople method[c]	Gladney method[d]	Present work[e]
Naphthalene						
$^1B_{1u}$ (^1L_b)	32 100 (0.0)	32 400 (0)	34 300 (0)	35 500	35 700	36 600 (0)
$^1B_{2u}$ (^1L_a)	34 700 (0.18)	36 200 (0.26)	36 300 (0.33)	37 500	35 300	39 800 (0.17)
$^1B_{1u}$ (^1B_b)	44 300 (2.0)	47 800 (2.12)	46 700 (2.03)	49 500	50 100	49 100 (1.15)
$^1B_{2u}$ (^1B_a)	58 800	50 800 (0.7)	51 100 (0.46)	50 000	53 100	51 100 (0.72)
$^3B_{3u}$ (^3L_a)	20 900	17 600	20 800	25 000	25 100	23 500
Anthracene						
$^1B_{2u}$ (^1L_a)	26 600 (0.1)	29 600 (0.039)	26 500 (0.26)	30 000	29 000	31 990 (0.26)
$^1B_{1u}$ (^1L_b)	28 200 (0.0)	29 900 (0)	31 400 (0)	33 500	33 500	30 200 (0)
$^1B_{1u}$ (^1B_b)	38 700 (2.20)	44 300 (3.23)	41 100 (2.74)	45 500	45 500	43 080 (2.95)
$^1B_{2u}$ (^1B_a)	48 500 (0.65)	45 900 (0)	53 600 (1.03)	52 000	53 800	46 700 (0.734)
$^3B_{2u}$ (^3L_a)	14 500	13 400	13 800	18 000	18 000	17 500

[a]Ref. 7.
[b]Ref. 3.
[c]Ref. 4.
[d]Ref. 11.
[e]Using SCF MOs of Goodman and Hoyland, ref. 5.

anthracene, the difference between Pople's (4) and Gladney's (11) calculations for the p-band transition energy is 1 000 cm^{-1}, all other transition energies being identical. Calculations using the same parameters as Gladney have recently been reported (12). The results were identical for all transitions.

The present CI calculation using Hoyland and Goodman's SCF MOs predicts the order of the first three bands of naphthalene successfully. Whether or not the observed transition in the 46 000 cm^{-1} region consists of two superimposed transitions, as is predicted by Pople's calculation, is at present uncertain. The apparent splitting of this band on substitution by a group such as the amino group could be explained by the appearance of a new charge transfer band in this region (14). A conclusive assignment requires further experimental work.

The quantitative agreement of our calculations with the experimental results, Table I, is not as good for naphthalene as in the case of the Pople (4) and the Mataga (7) calculations. Both the α and p bands are predicted to appear about 3 000 cm^{-1} higher than is observed, even though more configuration interaction (9 configurations) has been used in our calculation than in the previous work. The first triplet is predicted to have $^3B_{2u}$ symmetry by all the SCF calculations. Experimental studies of phosphorescence (15) report a band at 20 900 cm^{-1}, and if we accept this as being due to emission from a $^3B_{2u}$ excited state then the results of Mataga (7) are in very good agreement with experiment. The present results and those of Pople (4) predict considerably higher values for this state (by 2 600 and 4 000 cm^{-1} respectively), while Pariser's (3) calculation gives a value 3 300 cm^{-1} too low.

The results of the calculation on anthracene are given in Table I. The agreement between experimental results and our calculation is poor. In common with the results of Pople (4) and of Gladney (11), the energies of the α and p bands are considerably everestimated, and the present calculation predicts an inversion of these two bands. However, in contrast to the other calculations noted, ours does predict the right order of separation between these two bands.

Phenanthrene

The results on phenanthrene are given in Table II. The only previous SCF calculation on phenanthrene is that of Gladney (11), in which the repulsion integrals are obtained by the method of Pariser and Parr (1, 2).* The agreement with experiment is rather poor: the p-band transition energy is predicted quite well, but the method also predicts an overlap of the α band by the p band. In fact, the two systems are clearly separated (16) with a separation between the two 0–0 bands of 4 850 cm^{-1}, whereas Gladney predicts a separation of 400 cm^{-1}. Our calculation predicts the right order of separation (5 230 cm^{-1}) although the absolute values of the transition energies are about 2 000 cm^{-1} too high.

One of the β systems is clearly seen in phenanthrene, and the fine structure appears to constitute a single progression with a spacing of approximately 1 220 cm^{-1} (16). Our work and Gladney's predict two bands quite close together in this region (see Table II). However, the predicted oscillator strength of one of these is quite low, and the band could be obscured by another one of higher intensity since the observed spectrum is quite broad even at −100 °C.

The present calculation also shows a fourth band of fairly high intensity at around

We do not recommend this widely used approximation for calculations on transition energies of aromatic compounds because of the low value it gives when used to calculate the ^1L_a transition energy of benzene (5.3 eV compared to an experimental value of 5.9–6.2 eV).

Can. J. Chem. Downloaded from www.nrcresearchpress.com by 210.87.254.105 on 09/05/12
For personal use only.

Can. J. Chem. Downloaded from www.nrcresearchpress.com by 210.87.254.105 on 09/05/12
For personal use only.

TABLE II

Experimental and theoretical results for phenanthrene and pyrene

Excited state assignments	E_{exp}	Calculated $E(f)$ (cm^{-1})					
		Hamm and Ruedenberg[b]	Hummel and Ruedenberg[c]	Gladney[d]	Heilbronner and Murrell[e]	Present calculations: Goodman type[f]	Present calculations: Mataga type[g]
Phenanthrene							
$^1A_1$ (^1L_b)	28 930[a]	27 300 (0.0003)	30 786 (0.017)	35 200	27 500	31 070 (0.005)	31 200 (0)
$^1B_1$ (^1L_a)	34 080[a]	34 300 (0.10)	32 529 (0.392)	34 900	30 300	36 300 (0.358)	34 600 (0.471)
$^1B_1$ (^1B_b)	39 650[a]	45 400 (1.16)	39 992 (0.394)	45 300	34 700	41 774 (0.097)	41 500 (1.434)
$^1A_1$ (^1B_a)		43 000 (2.33)	38 830 (0.087)	46 600	36 700	42 621 (0.522)	41 900 (0.687)
$^3B_1$ (^3L_a)	21 780[a]			26 850		21 190	19 200
Pyrene							
$^1B_{2u}$ (^1L_a)	30 200[h]	30 200 (0.012)	27 409 (0.796)			32 970 (0.752)	30 200 (0.859)
$^1B_{3u}$ (^1L_b)	26 900[h]	26 500 (0.005)	26 818 (0.034)			33 880 (0)	31 000 (0)
$^1B_{3u}$ (^1B_b)	37 900[h]	41 400 (1.53)	39 024 (0.909)			40 440 (0.976)	40 600 (1.068)
$^1B_{2u}$ (^1B_a)	42 500[h]	45 200 (3.44)	45 613 (1.17)			48 020 (1.154)	45 800 (1.327)
$^3B_{2u}$ (^3L_a)	16 800[g]		12 193			18 600	15 100

[a]Singlet 0–0 transitions reported in ref. 16. Triplet ν_{max} reported in ref. 33.
[b]Ref. 31.
[c]Ref. 20, TBM method.
[d]Ref. 11.
[e]Ref. 13.
[f]SCF MOs of Hoyland and Goodman, ref. 5.
[g]Ref. 32.
[h]Ref. 30.

46 000 cm^{-1}, which could correspond to the band which has its first peak observed experimentally at 47 500 cm^{-1} (17).

Two recent experimental studies (18, 19) have been made of the triplet states of phenanthrene. McGlynn (18) reports that the first triplet has its origin at 21 730 cm^{-1} and, on the basis of polarization measurements, that it is ^3B in character. Gladney (11) gives the first ^3B at 26 900 cm^{-1}, i.e., rather high. We predict the transition to be at 21 200 cm^{-1}, in exceptionally good agreement with experiment.

Pyrene

There does not seem to be a previous SCF treatment of this molecule, although calculations have been carried out using non-iterative ASMO CI techniques (20, 21, 22). These calculations are in better agreement with the experimental results of Becker (23) than the present SCF results using Hoyland and Goodman's MOs. In particular, we predict (see Table II) that the ^1L_b band ($^1B_{2u}$ symmetry) is at a slightly higher (300 cm^{-1}) frequency than the ^1L_a band, whereas the experimental data show clearly a separation of the 0–0 bands of 3 500 cm^{-1} in the vapor.

THE MATAGA APPROXIMATION

Although the repulsion integrals and resonance integrals used by Hoyland and Goodman (5) were chosen to fit the ionization potentials and transition energies of benzene and ethylene, the use of their MOs to calculate transition energies for the round-field polycyclic hydrocarbons discussed here, and particularly for the long-field molecules styrene, phenyl acetylene, and diphenyl discussed elsewhere (24), has produced very disappointing results. Comparison of the results using SCF MOs and limited CI with those of Pariser using Hückel MOs (Tables I–II) shows that the use of the former MOs gives poorer results than when the latter, supposedly less accurate, MOs are used.

On the other hand, Mataga *et al.* (7) have found that when they used their approximation for the repulsion integrals for naphthalene and anthracene they found very good agreement between theory and experimental data for both the electronic excited states and the bond lengths (calculated from an empirical bond order – bond length relationship). We have therefore used their method for repulsion integrals in SCF calculations on phenanthrene, which was the one molecule which gave quite good agreement with experiment when Hoyland and Goodman MOs and repulsion integrals were used, and on pyrene, for which the Hoyland and Goodman parameters gave quite poor agreement with experiment. The results are compared with the previous results in Table II. It can be seen that for phenanthrene the results for both calculations are in quite good agreement with experiment, and that the transition energies are not greatly altered by the change in repulsion integrals. The results are much better than when Pariser and Parr's (11) method for repulsion integrals was used. For example, use of the latter predicted the ^1L_b and ^3L_a transitions to be over 5 000 cm^{-1} too high compared with the observed values. For pyrene, the results for the ^1L_a, ^1B_b, ^1B_a are in better agreement with experiment than in the case of our previous calculation. However, for the ^1L_b transition, both our calculation and those carried out by Hummel and Ruedemberg (20), by a non-iterative ASMO CI method, predict it to be overlapped by the more intense ^1L_a transition. Recent experimental results (23) clearly assign the 0–0 transition to be at 26 947 cm^{-1} i.e. below the 0–0 for the ^1L_a transition. However, we have not carried out new variational calculations for each excited state but have constructed them from MOs obtained using the ground state Hamiltonian. It is therefore probably more realistic to compare our calculated

Can. J. Chem. Downloaded from www.nrcresearchpress.com by 210.87.254.105 on 09/05/12
For personal use only.

values with the observed Frank–Condon maxima rather than the 0–0 transition, and this would improve the agreement between calculated and experimental values since the ^1L_b transition is partly overlapped by the ^1L_a transition.

BOND LENGTHS

The bond lengths of the polyacene hydrocarbons under discussion in this paper have been determined by X-ray crystallographic methods to a high order of accuracy and should therefore constitute a good means of testing the widely held supposition (25) that a smooth-curve relationship exists between the calculated bond order (p_{pq}) and observed bond lengths (r_{pq}) provided that there are no abnormal non-bonding interactions and that the atoms forming the bonds do not change their states of hybridization. Statistical analysis does give fairly good linear relationship between p_{pq} and r_{pq}. The calculated regression line is given by eq. [1],

$$r_{pq} = 1.515 - 0.178p_{pq}. \qquad [1]$$

The correlation coefficient is 0.81 and the standard deviation is 0.002. The predicted value for the "ideal single bond" between two single sp^2 hybridized carbon atoms is calculated to be 1.515 Å, in good agreement with Mulliken's (25) estimate of 1.51 ± 0.01 Å and that of Bak and Hansen-Nygaard (27) of 1.517 Å.

For ethylene, eq. [1] predicts a bond length of 1.337 Å, in good agreement with recent experimental determinations (28, 29). For benzene, the predicted bond length is 1.398 Å, again in very good agreement with experiment. It can therefore be stated that the SCF method using the Mataga method of calculating repulsion integrals gives bond orders which can be used satisfactorily in estimations of bond distances in alternant hydrocarbons.

DISCUSSION

The most valuable conclusion to be obtained from this study is that excitation energies are very sensitive to the method of calculating repulsion integrals, and that small differences in values of the two-center integrals can result in changes in transition energy of the order of several thousand cm^{-1}.

We have found that, of the three most commonly used methods of obtaining repulsion integrals, the method suggested by Mataga and Nishimoto gives by far the best agreement with experiment for both the round-field molecules discussed here and the long-field molecules discussed elsewhere (24).

We have also found that the agreement with experiment is not as good when the SCF method is used compared to the non-iterative ASMO CI method.

For alternant hydrocarbons, the main difference between the SCF and the Huckel methods is the appearance of small off-diagonal elements between non-nearest neighbors in the former method as shown by eq. [2] for F_{pq}, the off-diagonal elements of the secular determinant. In eq. [2] β_{pq} is the resonance integral between atoms p and q, γ_{pq} is the repulsion integral between atoms p and q, and p_{pq} is the π-bond order between atoms p and q.

$$F_{pq} = \beta_{pq} - \tfrac{1}{2}p_{pq}\gamma_{pq} \qquad p \neq q \qquad [2]$$

These small off-diagonal elements ($\frac{1}{2}p_{pq}\gamma_{pq}$) for non-nearest neighbors are large when either Pariser's or Hoyland and Goodman's method of choosing γ_{pq} is used, and result in a considerable difference in the atomic orbital coefficients of SCF MOs compared to the

Can. J. Chem. Downloaded from www.nrcresearchpress.com by 210.87.254.105 on 09/05/12
For personal use only.

Hückel MOs used in the ASMOCI method. When the Mataga method is used to calculate the γ_{pq} values, they are found to be smaller in magnitude than in the other methods; consequently the non-nearest neighbor interactions in [2] are smaller and the resulting SCF MOs are much closer to Hückel MOs.

Considerable success has been obtained for the Hückel method in interpreting electronic spectra even though electron repulsion integrals are neglected. For the p bands of alternant hydrocarbons, the success of the simple procedure of equating the p-band transition energy to the difference between the orbital energies in terms of β (25) can be explained by:

(1) the small effect of configuration interaction on the p band making the assumption of a one-configuration wave function for the p band quite accurate;

(2) the correct expression for the transition energy for an excitation of an electron from ψ_i to ψ_k is [3].

$$[3] \qquad E(i \rightarrow k) = E_k - E_i + 2K_{ik} - J_{ik},$$

where for a system of NP atoms, each contributing one π-electron, we have

$$[4] \qquad E_k = \sum_{p}^{NP} \sum_{q}^{NP} C_{kp}C_{kq}F_{pq}$$

$$[5] \qquad = (-I + \tfrac{1}{2}\gamma) + \sum_{p}^{NP} \sum_{q \neq}^{NP} C_{kp}C_{kq}(\beta_{pq} - \tfrac{1}{2}p_{pq}\gamma_{pq})$$

$$[6] \qquad = \alpha + K_k^{SCF}\beta - \tfrac{1}{2} \sum_{p}^{NP} \sum_{q \neq}^{NP} C_{kp}C_{kq}p_{pq}\gamma_{pq}.$$

The symbols in [4] and [5] are quite standard and have been defined elsewhere (8) and in eq. [1]. Equation [6] shows that we can express the SCF orbital energy in a similar way to that of Hückel theory. Thus $(-I + \frac{1}{2}\gamma)$ is equivalent to the Hückel coulomb integral of a carbon atom, β is the standard resonance integral for a C—C bond, and K_i^{SCF} corresponds to the Hückel number K_i^H (25).* The third term of [6] involves electron repulsion terms and has no Hückel counterpart. We have found for the hydrocarbons of Table III the SCF number K_i^{SCF} for the highest occupied MO is very close to the corresponding Hückel number even though the individual SCF AO coefficients are somewhat different from the Hückel ones. This is found to be true for both our SCF calculations for pyrene and phenanthrene, i.e. the number K_i^{SCF} is apparently independent of the choice of repulsion integrals.

We can now write [3] in the form [7].

$$[7] \qquad E_{ik} = (K_k^{SCF} - K_i^{SCF})\beta + \tfrac{1}{2} \sum_{p}^{NP} \sum_{q \neq}^{NP} [(C_{ip}^{SCF}C_{iq}^{SCF} - C_{kp}^{SCF}C_{kq}^{SCF}p_{pq}\gamma_{pq}] + 2K_{ik} - J_{ik}$$

To be able to relate the energy of the p band to a simple difference of K numbers, it is necessary for the last three terms i.e. those involving electron interactions, of [7] to be constant. That this is apparently so, to a first approximation, is shown by the results of column 5 of Table III.

**The Huckel numbers for alternant hydrocarbons are the eigenvalues of the secular determinant when the matrix elements of the determinant are written in units of β, i.e.*

$$E_i^H = \alpha + K_i^H\beta.$$

Can. J. Chem. Downloaded from www.nrcresearchpress.com by 210.87.254.105 on 09/05/12
For personal use only.

Key to Symbols in Boxheads of Table III

E_i = Orbital energy of the highest occupied MO.

E_{ik} = Transition energy of the transition $i \rightarrow k$, where k denotes the lowest unoccupied MO.

$E(p)$ = Calculated transition energy of the p band after CI.

$$\Delta = 2K_{ik} - J_{ik} + \tfrac{1}{2} \sum_{p}^{NP} \sum_{q \neq p}^{NP} (C_{ip}C_{iq} - C_{kp}C_{kq})p_{pq}\gamma_{pq}$$

$$= E_{ik} - 2 \sum_{p}^{NP} \sum_{q}^{NP} C_{ip}C_{iq}\beta_{pq}.$$

TABLE III

Transition energies for p bands of alternant hydrocarbons

Molecule	E_i (eV)	E_{ik} (eV)	$E(p)$ (eV)	Electron interaction contribution Δ (eV)
Naphthalene[a]	−10.53	5.16	4.93	2.25
Anthracene[a]	−9.80	4.16	3.96	2.22
Phenanthrene[a]	−10.10	4.63	4.51	1.74
Pyrene[a]	−9.74	4.28	4.10	2.18
Phenanthrene[b]	−9.36	4.4	4.28	1.60
Pyrene[b]	−8.90	3.85	3.75	1.76

[a]Calculated using Goodman and Hoyland's MOs and repulsion integrals, ref. 5.
[b]Calculated using Mataga's method of calculating repulsion integrals, refs. 6–8.

Thus, for energies calculated using Hoyland and Goodman's (5) repulsion integrals, we can write [8] because of the pairing properties of alternant hydrocarbon MOs which make $K_k^{SCF} = -K_i^{SCF}$ for the highest occupied and lowest unoccupied MO respectively,

$$E_{ik} = 4.73K_i^{SCF} + 2.20. \quad [8]$$

For calculations using Mataga integrals (6), we can write [9],

$$E_{ik} = 4.78K_i^{SCF} + 1.70, \quad [9]$$

where K_i^{SCF} refers to the energy of the highest occupied MO.

If we allow a further lowering of 0.2 eV for the effect of configuration interaction on the p state, we arrive at an electron interaction term of 2.0 when Goodman and Hoyland integrals are used and a value of 1.50 eV when Mataga integrals are used. For the relationship between the observed transition energy and the Hückel number K_i^H several authors have arrived at a number of different regression lines which differ depending on the choice of experimental values for the transition energy and on the number and type of hydrocarbon included. Murrell (34) gives the relationship [10], Koutecky (21) gives [11], Slifkin (26) gives [12], and Streitwieser (25) gives [13].

$$E(p) = 4.44K_i^H + 1.016 \quad [10]$$

$$E(p) = 4.76K_i^H + 1.27 \quad [11]$$

$$E(p) = 5.27K_i^H + 1.13 \quad [12]$$

$$E(p) = 4.92K_i^H + 1.30 \quad [13]$$

From this, it is clear that the electron interaction term calculated using Mataga repulsion integrals is more compatible with that derived statistically than that obtained using Hoyland and Goodman's repulsion integrals. The use of the theoretically derived

Can. J. Chem. Downloaded from www.nrcresearchpress.com by 210.87.254.105 on 09/05/12
For personal use only.

equation [9] to calculate transition energies using K_i^{H} instead of K_i^{SCF} is quite successful, although for some of the larger polyacenes such as pentacene and perylene, the calculated values are somewhat high and it would be preferable to use a constant of 1.3 eV as was used by Koutecky and Streitwieser.* It is, however, clear that the success of simple relationships using Hückel theory is due to (1) the identity between K_i^{H} and K_i^{SCF} and (2) the constancy of the electron interaction terms given in [7]. The magnitude of this electron interaction term as derived from statistical analysis is of the order of 1 eV, and this fact may be used as an extra piece of information in choosing molecular repulsion integrals. It is possible that an alternative method of choosing repulsion integrals can be found which will give a value for the terms in [7] in closer agreement with the statistical regression lines [10–13], but at present, the Mataga method seems to give the best overall results.

ACKNOWLEDGMENTS

We are grateful to the National Research Council of Canada for financial support, and to Professor R. M. Hochstrasser for sponsoring our use of the IBM 1620 computer at the University of British Columbia. We should also like to thank the staffs of the Computing Centres of the University of British Columbia, and of The Franklin Institute for much helpful advice and assistance in the course of this study. The computer programs are available for use at the Franklin Institute Computing Center.

REFERENCES

1. R. G. Parr. Quantum theory of molecular electronic structure. W. A. Benjamin, Inc., New York. 1963.
2. R. Pariser and R. G. Parr. J. Chem. Phys. **24**, 466 (1953); **24**, 767 (1953).
3. R. Pariser. J. Chem. Phys. **24**, 250 (1956).
4. J. A. Pople. Proc. Phys. Soc. London, A, **68**, 81 (1955).
5. J. R. Hoyland and L. Goodman. J. Chem. Phys. **36**, 12 (1962) and private communication.
6. K. Nishimoto and N. Mataga. Z. Physik. Chem. Frankfurt, **12**, 335 (1957); **13**, 140 (1957).
7. N. Mataga, K. Nishimoto, and S. Mataga. Bull. Chem. Soc. Japan, **32**, 395 (1959).
8. J. E. Bloor, P. N. Daykin, and P. Boltwood. Can. J. Chem. **42**, 121 (1964).
9. D. S. McClure. Solid State Phys. **9**, 399 (1959).
10. S. Suzuki and H. Baba. J. Chem. Phys. **38**, 349 (1963).
11. H. M. Gladney. Theoret. Chim. Acta Berlin, **1**, 245 (1963).
12. T. E. Peacock and P. T. Wilkinson. Proc. Phys. Soc. **83**, 525 (1964).
13. E. Heilbronner and J. N. Murrell. Mol. Phys. **6**, 1 (1963).
14. J. E. Bloor and N. Brearley. Unpublished work.
15. D. S. McClure. J. Chem. Phys. **17**, 905 (1949).
16. R. N. Jones and E. Spinner. Spectrochim. Acta, **16**, 1060 (1960).
17. H. B. Klevens and J. R. Platt. Survey of vacuum ultraviolet spectra. Laboratory of Molecular Structure and Spectra, University of Chicago. 1954.
18. T. Azumi and S. P. McGlynn. J. Chem. Phys. **37**, 2143 (1962).
19. M. A. El-Sayed and T. Pavlopoulos. J. Chem. Phys. **39**, 834 (1963).
20. R. L. Hummel and K. Ruedenberg. J. Phys. Chem. **66**, 2334 (1962).
21. J. Koutecky, J. Paldus, and R. Zahradnik. J. Chem. Phys. **36**, 3129 (1962).
22. G. Hoijtink, N. Velthorst, and P. Zandstra. Mol. Phys. **3**, 371 (1960).
23. R. S. Becker, I. S. Singh, and E. A. Jackson. J. Chem. Phys. **38**, 2144 (1963).
24. J. E. Bloor and N. Brearley. To be published.
25. A. Streitwieser. Molecular orbital theory. John Wiley and Sons, Inc. New York. 1961.
26. M. A. Slifkin. Nature, **200**, 877 (1963).
27. B. Bak and L. Nansen-Nygaard. J. Chem. Phys. **33**, 418 (1960).
28. L. S. Bartell and R. A. Bonham. J. Chem. Phys. **27**, 1414 (1957).
29. B. P. Stoicheff. Current Sci. India, **27**, 1 (1958).
30. E. Miller Layton, Jr. J. Mol. Spectry. **5**, 181 (1960).
31. N. S. Ham and K. Ruedenberg. J. Chem. Phys. **29**, 1215 (1958).
32. G. Porter and M. W. Windsor. Proc. Roy. Soc. London, Ser. A, **245**, 238 (1958).
33. D. F. Evans. J. Chem. Soc. 1351 (1957).
34. E. Heilbronner and J. N. Murrell. J. Chem. Soc. 2611 (1962).

It is possible to justify a lower value of the constant in [9] by making an allowance for the red shift in passing from vapor spectra to hydrocarbon solution. This would be of the order of 0.1–0.2 eV.

Can. J. Chem. Downloaded from www.nrcresearchpress.com by 210.87.254.105 on 09/05/12
For personal use only.

Can. J. Chem. Downloaded from www.nrcresearchpress.com by 210.87.254.105 on 09/05/12
For personal use only.

ELECTROPHILIC CATALYSIS IN SOLVOLYTIC REACTIONS

VII. SOLVENT EFFECT

R. ANANTARAMAN AND K. SARAMMA[1]
Chemistry Department, University of Kerala, Trivandrum, India

Received October 13, 1964

ABSTRACT

The rates of mercuric chloride catalyzed solvolysis of some alkyl chlorides in aqueous acetone and ethanol solvents have been compared. It is found that the increase in rate on changing from the acetone to the ethanol solvent is less in the catalyzed than in the normal reaction. On the basis that the electrophilic activity of the catalyst is less in aqueous ethanol than in aqueous acetone an explanation for the anomaly has been suggested. The effect, on the rates of solvolysis, of added chloride ions is in accord with the suggested explanation.

The rates of solvolysis of a number of alkyl chlorides, with and without mercuric chloride, in aqueous acetone and aqueous ethanol, together with the values of the heats and entropies of activation, are given in Tables I and II. The Hughes–Ingold theory requires that the rate of solvolysis of an alkyl chloride should increase on changing from aqueous acetone to aqueous ethanol (1). This can be put on a quantitative basis by using the Winstein equation $\log k/k_0 = m\mathbf{Y}$ (2). The data show that, while this is true of the normal solvolysis of all the alkyl chlorides, regarding the catalyzed reaction, *tert*-butyl and *tert*-amyl chloride behave abnormally, the rates in aqueous ethanol being lower. It can also be seen (Table I) that the ratio $k_{\text{ethanol}}/k_{\text{acetone}}$ for the normal solvolysis (k_{I}) is, in all cases, larger than the corresponding ratio for the catalyzed reaction (k_{II}). Since k_{I} varies over a wide range of values, to obtain a proper idea regarding the extent of abnormality in the rates of the catalyzed reaction of the different alkyl chlorides, a factor k_{III}, defined as $k_{\text{II}}/k_{\text{I}}$, has been calculated and included in the last column of Table I. It is evident that completely normal behavior will correspond to a value of 1 for k_{III}.

Since the k_{III} values of all alkyl chlorides are much less than 1, it was thought likely that the abnormal behavior might be due to a lower electrophilic activity of the catalyst in aqueous ethanol, particularly since Foote has shown that mercuric chloride does not form a complex with chloride ions in dry ethanol (3). This has been confirmed by solubility measurements which show that the $HgCl_2$:Cl^- (combined) ratios in 80% aqueous acetone and 80% aqueous ethanol at 31 °C are, respectively, 1:2.86 and 1:2.21, with a mercuric chloride concentration of 0.4 *M* (4). With a mercuric chloride concentration of 0.2 *M* the ratios have the values 1:4.38 and 1:3.0. It is clear that, since the number of chloride ions combining with a molecule of catalyst is less in aqueous ethanol, the electrophilic activity of the catalyst must be smaller in this solvent.* However, two points, namely the lower rates of catalyzed solvolysis in aqueous ethanol shown by *tert*-butyl and *tert*-amyl chloride and the wide variation in the k_{III} values, require explanation.

In Table II, a factor k_{IV} is introduced, which is the ratio of the rate, in aqueous acetone, due to the catalyst alone and the rate of the normal hydrolysis. If 1-chloropropylbenzene, 1-chloroisobutyl benzene, and (1-chloro-2,2-dimethylpropyl)benzene are excluded from consideration, it can be seen that the order of increasing k_{III} values parallels decreasing

[1]*Government of India Research Scholar.*

**This is an amplification of the argument in ref. 5. However, the effects, on the rate, due to a change in the electrophilic activity can be swamped by new kinetic factors introduced by the catalyst.*

Can. J. Chem. Downloaded from www.nrcresearchpress.com by 210.87.254.105 on 09/05/12
For personal use only.

TABLE I

Kinetics of the solvolysis of alkyl chlorides (alkyl chloride = 0.1 M; $HgCl_2$ = 0.075 M;* T = 20 °C, in all except with p-$ClPhCH_2Cl$ where it is 68.2 °C)

	10^7k_1 (normal)		10^6k_1 (catalyzed)		$k_{EtOH}/k_{acetone}$		
RCl	Acetone	EtOH	Acetone	EtOH	Normal (k_I)	Catalyzed (k_{II})	$k_{III} = k_{II}/k_I$
(*i*) Solvent 80% v/v acetone/ethanol – water							
t-BuCl	10.4	50.9†	58.2	48.8	4.90	0.839	0.17
t-AmCl	14.7	91.6	105.	81.7	6.23	0.778	0.13
CHPhMeCl	4.03†	71.0§,‖	42.9‡	81.3	17.6	1.90	0.11
CHPhEtCl	0.935‡,‖	17.5§,‖	9.58‡,‖	23.0‖	18.7	2.41	0.13
CHPh-*i*-PrCl	0.238‡,‖	2.88§,‖	3.07‡,‖	6.73‖	12.1	2.19	0.18
CHPh-*t*-BuCl	0.0196‡,‖	0.0767§,‖	0.275‡,‖	0.606‖	3.90	2.20	0.56
CH(*p*-MePh)MeCl	178	3 400	3 545	5 237	19.1	1.48	0.077
$PhCH_2Cl$	0.0425‖	0.912‖	0.0240‖	0.212‖	21.46	8.83	0.41
p-$ClPhCH_2Cl$	7.83¶	98.30¶	5.12¶	42.20¶	12.56	8.24	0.65
t-BuCl	306	683	505	396	2.23	0.784	0.35

*For p-$ClPhCH_2Cl$, $HgCl_2$ = 0.3 M.
†Value calculated from ref. 14, 10^7k_1 = 48.7.
‡From ref. 9.
§Value calculated from ref. 27, 10^7k_1; CHPhMeCl = 71.00, CHPhEtCl = 18.10, CHPh-*i*-PrCl = 2.84, CHPh-*t*-BuCl = 0.076.
‖Calculated from higher temperatures.
¶From ref. 7, the temperature was wrongly given as 62.8 °C; it should be 68.2 °C.

Can. J. Chem. Downloaded from www.nrcresearchpress.com by 210.87.254.105 on 09/05/12
For personal use only.

TABLE II

Kinetics of the solvolysis of alkyl chlorides

RCl	$\frac{k_{cat} - k_{normal}}{k_{normal}}(k_{IV})$* (80% aq. acetone)	Normal				Catalyzed			
		$\Delta H_{25}°‡$ (kcal/mole)		$\Delta S_{25}°‡$ (e.u.)		$\Delta H_{25}°‡$ (kcal/mole)		$\Delta S_{25}°‡$ (e.u.)	
		80% aq. acetone	80% aq. EtOH	80% aq. acetone	80% aq. EtOH	80% aq. acetone	80% aq. EtOH	80% aq. acetone	80% aq. EtOH
t-BuCl	57.97	22.0	22.3	−10.8	−6.6	17.9	19.8	−17.1	−11.8
t-AmCl	71.15	—	—	—	—	17.5	19.7	−16.9	−9.9
CHPhMeCl	102.7	21.1	19.8†	−15.5	−15.0	17.6	20.0	−18.5	−8.9
CHPhEtCl	101.5	22.6	20.1†	−13.6	−16.9	17.8	19.1	−20.7	−14.7
CHPh-*i*-PrCl	120.9	22.2	22.3†	−17.5	−12.1	17.9	17.9	−22.9	−21.3
CHPh-*t*-BuCl	148.6	24.9	24.8†	−14.1	− 9.8	19.0	19.6	−24.2	−20.4
CH(*p*-MePh)MeCl	198.2	—	—	—	—	—	—	—	—
$PhCH_2Cl$	4.65	21.4	20.9	−23.8	−23.9	17.5	19.7	−16.9	−9.9
p-$ClPhCH_2Cl$	1.40	—	—	—	—	—	—	—	—

*T = 20 °C in all except *p*-$ClPhCH_2Cl$ where it is 68.2 °C. The k_{IV} value for *p*-$ClPhCH_2Cl$ is not likely to be very different at 20 °C since for $PhCH_2Cl$, which shows similar behavior, the k_{IV} value at 82.3 °C is 2.9.

†Reference 27.

k_{IV} values. This means that the abnormality in the rate of the catalyzed reaction in aqueous ethanol increases with the catalytic efficiency of the hydrolytic process. Provided the catalytic activity remains unchanged,* the sensitivity of the rate of solvolysis to the presence of the catalyst should be quantitatively similar in the two solvents. But any change in the catalytic activity will cause abnormal behavior, its extent varying with the alkyl chloride. Thus a substrate like 1-*p*-tolylethyl chloride, whose rate of hydrolysis is especially sensitive to the presence of the catalyst, will be most affected by such a change. On the other hand, the rates of hydrolysis of benzyl and *p*-chlorobenzyl chloride are little affected by the catalyst and so their rates of catalyzed solvolysis in aqueous ethanol will show the least abnormality, in agreement with observation. It may be noted that the two tertiary alkyl chlorides also fit into this pattern. The fact that the rates of their catalyzed solvolysis in aqueous ethanol is lower than the rate in aqueous acetone is accidental, caused by their abnormally low k_I values.†

The exceptional behavior shown by the other three alkyl chlorides has now to be explained. It has been argued that with the other alkyl chlorides, an inverse relationship exists between the extent of abnormal behavior (as shown by the k_{III} values) and the catalytic efficiency for the hydrolysis (as given by the k_{IV} values). These three alkyl chlorides, however, have k_{IV} values which are much larger than those expected on the basis of their k_{III} values. A possible explanation for this is as follows. The catalytic efficiency must increase with the ease with which the C—Cl bond can be heterolyzed (in other words, must increase with the inherent tendency of the substrate to adopt the S_N1 mechanism), and normally this will be the case. But if the catalyst is able to bring into play additional kinetic factors or to change the factors already present in the normal reaction significantly, the above rule may no longer hold. It has been argued on the basis of experimental evidence that the unduly high catalytic efficiency observed in the reactions of these three alkyl chlorides is due to the catalyst calling into play an additional inductomeric effect of substantial magnitude (9). The conclusion, therefore, is that the abnormally high k_{IV} values shown by these three alkyl chlorides are due to this special cause, which has no particular relevance to the argument presented here, so that its validity is not affected.

A closer inspection of the k_{III} values suggests that the explanation given above is not adequate, by itself, to account for the fact they are so much less than unity, even in favorable cases. Thus, according to the argument presented here, benzyl chloride and *p*-chlorobenzyl chloride should show the least abnormality. Yet the k_{III} values are only 0.42 and 0.65 respectively. In our studies of the kinetics of mercuric chloride catalyzed solvolysis of alkyl chlorides, we have found that the sensitivity of the rate to changes in the polarity of the medium is less in the presence of the catalyst than in its absence. Now, although the rates of solvolytic reactions of alkyl chlorides by both the S_N1 and S_N2 mechanisms are considerably accelerated by a change to a more polar solvent, the magnitude of the effect is greater for the S_N1 reaction (10). We believe that the inclusion of the catalyst molecule in the transition state will confer on it some of the properties of the transition state of an S_N2 reaction, in particular the relatively smaller response of the

**A referee has suggested consideration of the viewpoint that in a more ionizing solvent the effect of the catalyst may be expected to be less. We have not considered this possibility because the evidence available does not support it. Thus the value of the catalytic coefficient for the mercuric chloride catalyzed hydrolysis of benzyl chloride is almost constant over the solvent range 45–80% aqueous acetone (6), which involves a greater variation in the ionizing power than a change of solvent from 80% aqueous acetone to 80% aqueous ethanol. A similar situation obtains for the catalyzed solvolysis of p-chlorobenzyl chloride (7).*

†The low k_I values are presumably due to the fact that the tert-alkyl cations have relatively little stability (8).

Can. J. Chem. Downloaded from www.nrcresearchpress.com by 210.87.254.105 on 09/05/12
For personal use only.

rate of substitution to changes in the polarity of the environment, although we recognize that mercuric chloride is here the catalyst and not the substituting agent (11). This is in agreement with the views of Hammond *et al.* (12) that the transition state of the silver ion catalyzed hydrolysis of alkyl halides has a substantial S_N2 character. Other arguments in support of the above conclusion are as follows. (i) A convenient method of distinguishing solvolytic reactions occurring by the S_N1 and S_N2 mechanisms is by determining their *m* values by using the Winstein equation. The *m* values for the normal and catalyzed reactions of some of the alkyl chlorides are respectively (values taken from Fainberg and Winstein (13)): 1-phenethyl chloride, 1.056 (14), 0.40; *tert*-butyl chloride 1.00 (2), 0.50; *tert*-amyl chloride 1.10, 0.50; 1-chloropropyl benzene 0.62, 0.40; benzyl chloride 0.425 (15), 0.43; *p*-chlorobenzyl chloride 0.56, 0.44. Since a high *m* value signifies that the reaction belongs to the S_N1 category, the conclusion from the data is that the *m* values of the catalyzed reaction are more characteristic of S_N2 reactions. (ii) The magnitude of the ionic-strength effect is much less in the catalyzed than in the normal reaction; thus the ionic-strength effect in the hydrolysis of 1-phenethyl chloride is substantial (16), while it is barely detectable in the catalyzed reaction (17). (iii) The "medium effect" which is so characteristic of S_N1 solvolysis is much less marked in the catalyzed reaction; thus the rate of hydrolysis of *tert*-butyl chloride is rather sensitive to its concentration (18), while this is not the case with the catalyzed reaction (19).

With all alkyl chlorides except 1-chloroisobutyl benzene and (1-chloro-2,2-dimethylpropyl)benzene, the heats of activation for the catalyzed reaction in aqueous acetone are markedly lower than in aqueous ethanol, which contrasts with the normal reaction. It is suggested that this is due to the lower electrophilic activity in the ethanolic solvent. For the other two alkyl chlorides, the heats of activation in the two solvents are almost the same, suggesting that steric resistance to solvation is under observation (20). The trend in the entropy values is more difficult to explain. For the catalyzed reaction, the entropy values are more favorable in aqueous ethanol. This is possibly due to the orientational requirement in the transition state being more easily met in the ethanolic solvent consequent on the greater solvation of the catalyst. For 1-chloroisobutyl benzene and (1-chloro-2,2-dimethylpropyl)benzene, however, steric strain due to crowding in the transition state must be dominant, since the entropy values in the two solvents are relatively rather similar.

Addition of chloride ions reduces the rate of the catalyzed reaction because (i) by decreasing the catalyst concentration through formation of complexes like $HgCl_3^-$, $HgCl_4^=$ and (ii) by inducing a mass-law effect (17). An explanation for the latter observation has been given by Ingold (21) and Bunton (22). Of the alkyl chlorides studied (Table III), the mass-law effect is of importance only in the case of 1-phenethyl chloride (9, 17). So, with this exception, the reduction in rate due to added chloride ions must be due to the inactivation of the catalyst. It can be seen that the magnitude of reduction is approximately equal for the hydrolysis of all alkyl chlorides excepting 1-phenethyl chloride, in agreement with the above conclusion. But, the decrease in rate in aqueous ethanol is consistently smaller than in aqueous acetone. This again must be attributed to the greater solvation of the catalyst in this solvent. Further, while the rate decrease in the hydrolytic reaction appears to be little affected by changes in temperature (thus the rate reductions for five alkyl chlorides are about the same although the temperature varies by over 50 °C), this is not the case in aqueous ethanol where the decrease in rate appears to increase with temperature. It is suggested that this may be due to a negative temperature effect on the interaction between the mercuric chloride and the solvent. If this

Can. J. Chem. Downloaded from www.nrcresearchpress.com by 210.87.254.105 on 09/05/12
For personal use only.

Can. J. Chem. Downloaded from www.nrcresearchpress.com by 210.87.254.105 on 09/05/12
For personal use only.

TABLE III

Effect of added sodium chloride on the rate of the catalyzed reaction ($HgCl_2$ = 0.075 *M*)

RCl	*T* (°C)	Solvent	10^6k_1		% reduction in rate	
			Cl = 0.05 *M*	Cl = 0.10 *M*	Cl = 0.05 *M*	Cl = 0.10 *M*
t-BuCl	20	60% acetone	346	235	31.5	53.5
t-BuCl	20	80% acetone	33.5	11.5	41.5	80.2
t-BuCl	20	60% EtOH	400	338	Nil	14.6
t-BuCl	20	80% EtOH	47.9	42.0	1.9	13.9
t-AmCl	20	60% acetone	508	334	30.5	54.3
t-AmCl	20	80% acetone	53.0	19.6	49.5	81.1
t-AmCl	20	60% EtOH	647	557	2.2	16.5
t-AmCl	20	80% EtOH	75.8	68.0	7.5	16.8
CHPhMeCl	20	80% acetone*	17.6	4.91	59.0	88.4
CHPhMeCl	20	80% EtOH	70.5	55.9	13.3	31.2
CHPhEtCl	45	80% acetone*	54.8	18.8	51.1	83.2
CHPhEtCl	45	80% EtOH	199	165	34.5	45.2
CHPh-*i*-PrCl	54.8	80% acetone*	40.2	14.3	51.2	82.6
CHPh-*i*-PrCl	54.8	80% EtOH	127	103	32.8	45.5
CHPh-*t*-BuCl	80	80% acetone*	35.5	14.6	49.7	79.3
CHPh-*t*-BuCl	80	80% EtOH	108	85.4	41.6	53.8

*Reference 9. Rate in the absence of chloride ions. CHPhEtCl: 80% acetone, 10^6k_1 = 112; 80% EtOH, 10^6k_1 = 304. CHPh-*i*-PrCl: 80% acetone, 10^6k_1 = 82.4; 80% EtOH, 10^6k_1 = 189; CHPh-*t*-BuCl: 80% acetone, 10^6k_1 = 70.5; 80% EtOH, 10^6k_1 = 185.

is the case, the extent of complex formation between mercuric chloride and chloride ions (and hence the rate reduction) should increase with temperature.

EXPERIMENTAL

Materials

1-Phenethyl alcohol, 1-hydroxypropyl benzene, and 1-*p*-tolylethyl alcohol were prepared by the Meerwein-Pondorff reduction of the corresponding ketones. 1-Hydroxyisobutyl benzene and (1-hydroxy-2,2-dimethylpropyl)benzene were prepared by the Grignard reaction with magnesium isopropyl bromide and magnesium *tert*-butyl chloride, respectively. The alcohols were purified through their acid phthalates, prepared in the usual way (23). The alcohols were converted into the chlorides by reaction with thionyl chloride. *tert*-Butyl chloride (24) and *tert*-amyl chloride (25) were prepared by the usual methods.

The physical constants of the alkyl chlorides are given below.

	Boiling point (°C)		n_D^{25}	
Alkyl chlorides	Expt.	Lit.	Expt.	Lit.
CHPhMeCl	78–79/16 mm	81–82/17 mm (26)	1.5250	1.5250 (13)
CHPhEtCl	64/2 mm	61–62/0.5 mm (27)	1.5185	
CHPh-*i*-PrCl	65/1 mm	63–64/0.5 mm (27)	1.5150	
CHPh-*t*-BuCl	87–89/5 mm	89.5–90.5/6.7 mm (20)	1.5149	1.5142 (20)
t-BuCl	50–51/760 mm	50.8/760 mm (28)	1.3818	1.3819 (14)
t-AmCl	86–87/760 mm	86/760 mm (29)	1.4058	1.407 (18°)(29)
CH(*p*-MePh)MeCl	134/80 mm; 101/25 mm		1.5220	

A.R.(B.D.H.) mercuric chloride and sodium chloride were used. The latter was dried at 250 °C.
Acetone was purified and dried by the method of Conant and Kirner (30). Lime-dried ethanol was made absolute by refluxing with sodium and diethyl phthalate.

Kinetic Work

The term $x\%$ aqueous acetone or ethanol signifies solvent made up (at room temperature) with x volumes of dry acetone or ethanol and $(100 - x)$ volumes of distilled water. A large stock of solvent was made up to facilitate comparative measurements.

A conventional thermostat (±0.03°) was used for rate measurements at higher temperatures while for work at below room temperature, a Gallenkamp low temperature thermostat fitted with a Jackson thermoregulator was used (±0.02°).

At the higher temperatures, the sealed-bulb technique was used. The appropriate quantity of alkyl chloride was taken in a 100 ml volumetric flask and accurately weighed quantities of mercuric chloride and (or) sodium chloride were transferred to the flask with the aid of the solvent. After dissolution, the solution was made up to the mark. Aliquots (5 ml) were pipetted into neutral glass ampoules (which conformed to the B.P. test for limits of alkalinity (31)), and the ampoules sealed. They were immersed in the thermostat and vigorously shaken for 2 min. Then one ampoule was taken out, immediately chilled to kill the reaction, washed, and broken, under 150 ml of cold, dry acetone/ethanol. The liberated acid was titrated against carbon dioxide free standard NaOH, lacmoid being used as the indicator. At suitable intervals, the other ampoules were removed and the acid estimated similarly. The "infinity" titer (mean of two concordant values) was taken after an interval equal to 8 half-lives. When mercuric chloride was present, a quantity of concentrated potassium iodide solution (neutralized to lacmoid) just sufficient to destroy the mercuric

TABLE IV

Illustrative kinetic run for the mercuric chloride catalyzed hydrolysis of *tert*-butyl chloride in 60% v/v acetone–water at 20.0 °C (initial concentration *t*-BuCl = 0.0980 *M*; $HgCl_2$ = 0.0750 *M*)

t (s)	NaOH titer (ml)*	10^4k_1	t (s)	NaOH titer (ml)*	10^4k_1
0	0.24	—	480	2.18	4.78
60	0.53	5.18	1 200	3.98	4.19
120	0.81	5.18	1 800	4.98	3.86
180	1.06	5.04	2 400	5.78	3.67
240	1.32	5.06	3 300	6.68	3.54
300	1.56	5.04	4 800	7.70	3.24
360	1.76	4.87	∞	9.70	—
420	1.96	4.78			

*Volume of 0.05050 *N* NaOH solution equivalent to 5.0 ml sample.

Can. J. Chem. Downloaded from www.nrcresearchpress.com by 210.87.254.105 on 09/05/12
For personal use only.

chloride was added before titration. For work at low temperature, the pipetting was done directly from the volumetric flask which served as the reaction vessel.

The first-order rate coefficients were calculated from the formula $k = (1/t) \ln a/(a - x)$ and the values are expressed in reciprocal second. The values given are the mean from two experiments.

One point deserves mention. It was found for the catalyzed reaction (particularly in aqueous acetone) that the first-order rate coefficients were steady only over an initial limited portion of the reaction. This is illustrated in Table IV. The rate coefficients given are the mean of the values which show constancy derived from duplicate runs. The catalyzed hydrolysis of 1-*p*-tolylethyl chloride did not show even this initial constancy in the rate. To obtain the initial rate, therefore, log k was plotted against log $(a - x)$ a good straight line was obtained. The best straight line was obtained by the method of least squares. Duplicate runs gave good agreement.

REFERENCES

1. C. K. INGOLD. Structure and mechanism in organic chemistry. Cornell University Press, Ithaca. 1953. p. 345.
2. E. GRUNWALD and S. WINSTEIN. J. Am. Chem. Soc. **70**, 846 (1948).
3. H. W. FOOTE. Am. Chem. J. **42**, 620 (1905).
4. R. ANANTARAMAN and K. SARAMMA. Indian J. Chem. **2**, 335 (1964).
5. R. ANANTARAMAN and K. SARAMMA. Naturwissenschaften, **50**, 497 (1963).
6. S. KOSHY and R. ANANTARAMAN. J. Am. Chem. Soc. **82**, 1574 (1960).
7. R. ANANTARAMAN and K. SARAMMA. Z. Physik. Chem. Leipzig, **216**, 21 (1961).
8. C. G. SWAIN and B. R. MOSELY. J. Am. Chem. Soc. **77**, 3727 (1955). C. A. BUNTON and B. NAYAK. J. Chem. Soc. 1915 (1959).
9. R. ANANTARAMAN and K. SARAMMA. Tetrahedron. In press.
10. E. D. HUGHES and C. K. INGOLD. J. Chem. Soc. 252 (1935).
11. L. C. BATEMAN, K. A. COOPER, E. D. HUGHES, and C. K. INGOLD. J. Chem. Soc. 925 (1940).
12. G. S. HAMMOND, M. F. HAWTHORNE, J. H. WATERS, and B. M. GRAYBILL. J. Am. Chem. Soc. **82**, 704 (1960).
13. A. H. FAINBERG and S. WINSTEIN. J. Am. Chem. Soc. **78**, 2770 (1956).
14. A. H. FAINBERG and S. WINSTEIN. J. Am. Chem. Soc. **79**, 1597 (1957).
15. S. WINSTEIN, E. GRUNWALD, and H. W. JONES. J. Am. Chem. Soc. **73**, 2700 (1951).
16. E. D. HUGHES, C. K. INGOLD, and A. D. SCOTT. J. Chem. Soc. 1201 (1937).
17. R. ANANTARAMAN. Ph.D. Thesis, University of London. 1950.
18. E. D. HUGHES. J. Chem. Soc. 255 (1935).
19. P. J. CHAKKO. M.Sc. Thesis, Kerala University. 1961.
20. S. WINSTEIN and B. K. MORSE. J. Am. Chem. Soc. **74**, 1133 (1952).
21. C. K. INGOLD. Structure and mechanism in organic chemistry. Cornell University Press, Ithaca. 1953. p. 359.
22. C. A. BUNTON. Nucleophilic substitution at a saturated carbon atom. Elsevier. 1963. p. 154.
23. A. J. H. HOUSSA and J. KENYON. J. Chem. Soc. 2260 (1930).
24. A. I. VOGEL. A textbook of practical organic chemistry. Longmans, Green, London. 1959. p. 276.
25. E. D. HUGHES and B. J. MACNULTY. J. Chem. Soc. 1283 (1937).
26. A. M. WARD. J. Chem. Soc. 445 (1927).
27. G. BADDELEY, J. CHADWICK, and H. T. TAYLOR. J. Chem. Soc. 2405 (1954).
28. J. TIMMERMANS and Y. DELCOURT. J. Chem. Phys. **31**, 98 (1934).
29. C. D. HODGMAN (*Editor*). Handbook of chemistry and physics. Chemical Rubber Publishing Co., Ohio. 1944. p. 665.
30. J. B. CONANT and W. R. KIRNER. J. Am. Chem. Soc. **46**, 246 (1924).
31. British Pharmacopocia. 1953. p. 851.

Can. J. Chem. Downloaded from www.nrcresearchpress.com by 210.87.254.105 on 09/05/12
For personal use only.

Can. J. Chem. Downloaded from www.nrcresearchpress.com by 210.87.254.40 on 09/05/12
For personal use only.

REACTIONS OF IMINO RADICALS WITH HYDROCARBON GASES[1]

J. L. BRASH[2] AND R. A. BACK
Division of Pure Chemistry, National Research Council, Ottawa, Canada

Received February 19, 1965

ABSTRACT

The photolysis of HNCO vapor has been studied in the presence of ethylene, butene, ethane, propane, and neopentane at 51 °C. Both the olefins and paraffins reduced the yield of CO to about one-third of its value in pure HNCO, which is thought to correspond to the CO formed in the primary photolytic step. Yields of N_2 and H_2 were reduced close to zero in the presence of olefins, and it appears that NH radicals were removed by reaction with olefins. No imines, amines, nor other nitrogenous products could be detected, however, and it is suggested that these were lost by polymerization.

Yields of N_2 were also reduced close to zero in the presence of paraffins, and it appears that NH reacted readily with the hydrocarbons. Once again, no amines could be detected. The yield of H_2, a minor product in pure HNCO, was markedly enhanced, and alkyl radical dimers appeared as products. A mechanism is suggested which involves the decomposition of vibrationally excited amines formed by insertion reactions.

INTRODUCTION

In an earlier paper from this laboratory (1), it was observed that the addition of ethylene reduced the yields of CO, N_2, and H_2 in the photolysis of isocyanic acid vapor; this was attributed to the reaction of NH radicals with ethylene. More recently, in the flash photolysis of HNCO, both ethylene and propane were found to have a similar effect (2). The present paper describes a more detailed study of the reactions of NH radicals, produced in the photolysis of HNCO vapor, with olefin and paraffin gases.

EXPERIMENTAL

The photolysis system, procedure, and the analysis of non-condensable gases were all similar to those used previously (1). All experiments were done at 51 °C using unfiltered radiation from an Hanovia S-500 medium-pressure mercury arc. Gas chromatography, using a variety of columns, was used to examine the products condensable at −196 °C.

Isocyanic acid was prepared and purified as before. A sample of DNCO was prepared by pyrolysis of cyanuric acid-d_3 obtained from Merck, Sharp and Dohme of Canada Ltd. Hydrocarbon gases were all Phillips Research Grade, used after simple degassing. Propane-d_8 was obtained from Merck, Sharp and Dohme of Canada Ltd.

RESULTS AND DISCUSSION

Reactions of NH with Olefins

In agreement with Back and Mui (1), it was observed that the addition of ethylene rapidly reduced the yields of N_2 and H_2 to zero, and that of CO to a constant value, about 1/3 of the yield from the photolysis of HNCO alone. It is reasonable to suggest, as before (1), that the residual CO came from the primary photolysis process,

$$\text{HNCO} + h\nu \rightarrow \text{CO} + \text{NH}, \qquad [1]$$

and that at moderate pressures of ethylene, NH radicals were completely removed by reaction with the olefin, so that formation of N_2, H_2, and two-thirds of the CO, all of which arose from secondary reactions of NH radicals in the pure HNCO system, were suppressed.

[1]*Issued as N.R.C. No. 8421.*
[2]*National Research Council Postdoctorate Fellow, 1961–1963. Present address: Stanford Research Institute, Menlo Park, California, U.S.A.*

By analogy with other biradicals, one might expect NH radicals to add to the double bond of ethylene, forming vibrationally excited ethylenimine which could undergo rearrangement or be stabilized by collision.

[2] $$NH + C_2H_4 \longrightarrow [CH_2{-}CH_2]^* \begin{cases} \longrightarrow CH_2{=}CH{-}NH_2 & [a] \\ \longrightarrow CH_3{-}CH{=}NH & [b] \\ \xrightarrow{+M} CH_2{-}CH_2 \ (NH) & [c] \end{cases}$$

Blank experiments showed that both ethylenimine and vinyl amine could have been readily detected by gas chromatography, using a 3 ft column of polyethylene glycol on firebrick at 50 °C. The unsaturated amine postulated in reaction [2*b*] has apparently not been reported, and probably polymerizes spontaneously.

When HNCO was photolyzed in the presence of ethylene at pressures ranging up to 500 torr, neither ethylenimine nor vinyl amine nor any other nitrogen-bearing products could be detected.[3] It may be concluded that any ethylenimine formed in reaction [2] was not stabilized at these pressures. Failure to find vinyl amine or any other rearrangement product could very probably be due to polymerization, either alone or as copolymers with HNCO, to which these unsaturated amines are notoriously prone. Ethylenimine has recently been observed by Jacox and Milligan (3) as a product of the photolysis of hydrazoic acid in the presence of ethylene in an argon matrix at 4 °K, where it presumably arose via reaction [2*c*]. The low temperature and the solid state thus appear to favour stabilization and prevent polymerization.

A few experiments were done with butene-2 in the hope that butenimine, with more vibrational modes, would be more readily stabilized than ethylenimine. At pressures up to 500 torr of butene-2, however, no stabilized product could be detected.

In summary, the effect of olefins on the yields of CO, N_2, and H_2 in the photolysis of HNCO leaves little doubt that NH reacts readily with olefins. The present observations are compatible with a primary addition to form a cyclic imine, followed by rearrangement and polymerization of the resulting unsaturated products, although they by no means prove such a mechanism.

Reactions of NH with Paraffins

Isocyanic acid vapor was photolyzed in the presence of ethane, propane, and neopentane. The three systems showed the same general behavior. The CO yield fell with increasing pressure of hydrocarbon and became constant at about 1/3 of its original value, while the N_2 yield decreased towards zero; these effects are very similar to those observed with olefins. Hydrogen, however, which was a minor product in pure HNCO (probably arising from combination of NH radicals (1, 2)) and was completely absent in the presence of olefin, increased markedly with increasing pressure of paraffin, becoming constant at higher pressures.

Again by analogy with other biradicals, NH might be expected to undergo insertion into the C—H bonds of the paraffins, forming amines. As with the olefins, however, no amines nor other nitrogenous compounds could be detected by gas chromatography. Hydrocarbon pressures approaching 1 atm were used, and 600 torr pressure of CO_2 was added to the propane–HNCO system; no amines could be detected as products of any of

[3]*Hydrogen cyanide, a possible product by analogy with nitrogen-atom reactions, was also not observed, although it could have been detected if present.*

Can. J. Chem. Downloaded from www.nrcresearchpress.com by 210.87.254.40 on 09/05/12
For personal use only.

these experiments. The failure to observe amines indicates either that no insertion reaction occurred, or that the amine formed by insertion decomposed before it could be stabilized by collision.

The only condensable products found from the photolysis of HNCO in the presence of paraffins were *n*-butane and hexane (mostly 2,3-dimethylbutane) from ethane and propane respectively. Decane may have been produced from neopentane but was not analyzed. The dependence of all product yields on hydrocarbon pressure with constant HNCO pressure of 19.6 torr is shown in Fig. 1 and Table I.

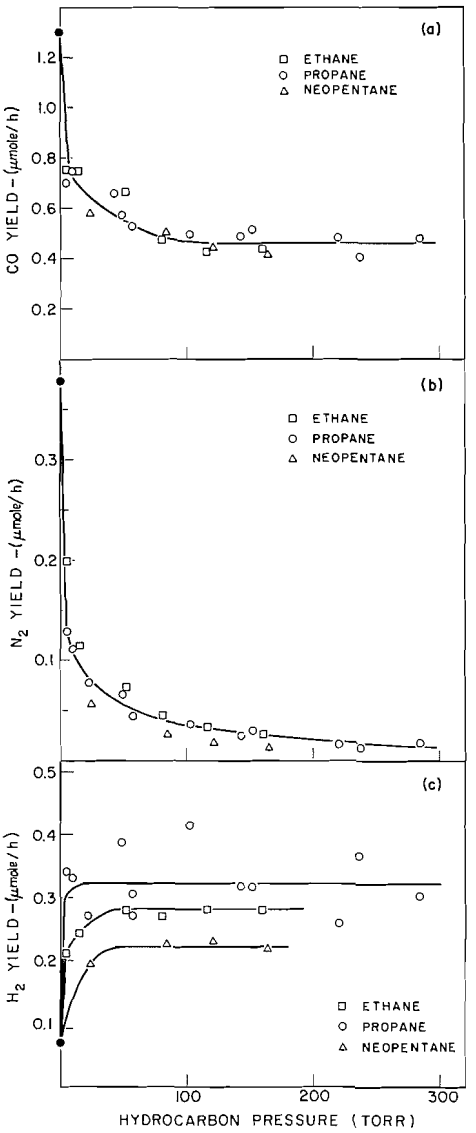

FIG. 1. Production of (*a*) CO, (*b*) N_2, and (*c*) H_2 from the photolysis of HNCO in the presence of paraffin gases.

Can. J. Chem. Downloaded from www.nrcresearchpress.com by 210.87.254.40 on 09/05/12
For personal use only.

TABLE I

Yields of radical dimers from photolysis of HNCO–alkane mixtures (T = 51 °C, HNCO pressure = 19.6 torr)

Ethane pressure (torr)	Yield of butane (μmole/h)	Propane pressure (torr)	Yield of hexane (μmole/h)
5.4	0.072	4.7	0.107
14.7	0.126	10.1	0.087
51.8	0.092	48.7	0.128
80.6	0.113	102.7	0.091
115.9	0.115	151.9	0.068
159.5	0.099	237.0	0.074
	Av. 0.103		Av. 0.093

The reduction in the yields of CO and N_2, products which were attributed (1) to reactions of NH radicals in the photolysis of pure HNCO, suggests that NH was reacting with alkanes, probably by insertion in a C—H bond followed by decomposition of the excited amine,

[4] $$NH + RH \rightarrow [RNH_2]^* \rightarrow R + NH_2,$$

or alternatively by simple abstraction of hydrogen, which from the present data is indistinguishable. The NH_2 radical would have reacted readily to form ammonia,

[5] $$NH_2 + RH \rightarrow NH_3 + R,$$

and combination of the hydrocarbon radicals formed in reactions [4] and [5] would account for the butane and hexane observed as products from ethane and propane. The possibility of abstraction of hydrogen from HNCO is a complicating factor at low pressure of hydrocarbon, which, lacking knowledge of the H—NCO bond energy, is difficult to assess. In fact, the steady reduction in N_2 and CO evident in Fig. 1, (*a*) and (*b*), could represent a shift in the equilibrium,

[6] $$R + HNCO \rightleftharpoons RH + NCO,$$

to the left, thus inhibiting formation of N_2 and CO by the reaction

[7] $$2NCO \rightarrow N_2 + 2CO,$$

rather than a gradual scavenging of NH radicals via reaction [4]. There is an indication from Fig. 1(*b*), however, that this is not so, as it is seen that neopentane, propane, and ethane, in that order, show a decreasing efficiency in reducing the yield of N_2. This order of efficiency is not compatible with the equilibrium, [6], being a controlling factor, since in that case the efficiency should have followed the C—H bond strengths in the hydrocarbons, i.e., propane > ethane and neopentane. It is compatible with a rather indiscriminate reaction [4], as insertion reactions are known to be, depending approximately on the number of C—H bonds in the molecule. Thus tentatively it appears that abstraction of hydrogen from HNCO by alkyl radicals is not important in the present systems.

Reaction [5] requires NH_3 to be a product. As in the photolysis of pure HNCO (1), however, ammonia, while detectable, was very difficult to measure quantitatively in the presence of HNCO.

The production of hydrogen in the HNCO–alkane systems was surprising and is difficult to explain satisfactorily. To investigate its origin, a small pressure of ethylene (about 1 torr) was added to the propane–HNCO and ethane–HNCO systems, at alkane

Can. J. Chem. Downloaded from www.nrcresearchpress.com by 210.87.254.40 on 09/05/12
For personal use only.

pressures of about 150 torr; the hydrogen yield was reduced to about one-quarter and one-sixth of its former value, respectively, in the two systems. The added ethylene should not have been able to compete effectively with the alkanes for NH radicals (ethylene and propane appear to be about equally efficient in suppressing N_2 and CO production from HNCO photolysis), and the marked reduction in H_2 strongly suggests that the hydrogen was produced via hydrogen atoms, which would have been readily removed by reaction with ethylene.

Further evidence concerning the origin of the hydrogen was obtained by studying HNCO–C_3D_8 and DNCO–C_3H_8 mixtures. The isotopic composition of the hydrogen produced is shown in Table II; it is seen that the hydrogen from both mixtures was largely HD. The H_2 in fact can be reasonably attributed to protium impurity in the DNCO and the C_3D_8, and it appears that to a good approximation each molecule of hydrogen contained one atom of hydrogen from isocyanic acid and one from propane.

TABLE II

Isotopic composition of hydrogen from HNCO–C_3D_8 and DNCO–C_3H_8 mixtures

	Propane pressure (torr)	% H_2	% HD	% D_2
HNCO + C_3D_8	33.8	20.6	77.6	1.8
	36.0	19.8	78.1	2.1
	82.3	14.0	83.9	2.1
	146.9	13.0	85.2	1.8
DNCO + C_3H_8	36.0	9.8	88.7	1.5
	144.0	12.0	87.3	1.6

Two mechanisms may be suggested for the formation of hydrogen. In the first, a second primary process is postulated in the photolysis of HNCO:

[8] $$HNCO + h\nu \rightarrow H + NCO.$$

This would be followed in pure HNCO by

[9] $$H + HNCO \rightarrow [NH_2CO]^* \rightarrow NH_2 + CO,$$

(thus accounting for the absence of hydrogen as a major product in pure HNCO) and in the presence of propane by

[10] $$H + C_3H_8 \rightarrow H_2 + C_3H_7.$$

Hydrogen was a major product in the HNCO–alkane systems and, allowing for some scavenging of hydrogen atoms by olefins arising from disproportionation reactions or present as trace impurities, was approximately equal to the residual CO, so that reaction [8] would have had to occur to about the same extent as reaction [1]. The arguments against the occurrence of reaction [8] to such an extent have been discussed previously (1). Most compelling is the persistence of CO production, about one-third of its value in pure HNCO, in the presence of high pressures of both olefins and paraffins. This and the dependence of N_2 and H_2 yields on HNCO pressure, temperature, and light intensity (1, 2, 4) are difficult to reconcile with occurrence of any major primary process other than reaction [1].

An alternative mechanism for hydrogen formation involves the decomposition of the excited amine, formed by insertion, to yield hydrogen atoms; e.g., with propane,

[11] $$NH + C_3H_8 \rightarrow [CH_3\underset{NH_2}{CH}—CH_3]^* \rightarrow CH_3\dot{\underset{NH_2}{C}}—CH_3 + H.$$

Can. J. Chem. Downloaded from www.nrcresearchpress.com by 210.87.254.40 on 09/05/12
For personal use only.

Reaction [11] must then have been followed exclusively by

[12] $$H + HNCO \rightarrow H_2 + NCO,$$

to meet the requirement of one hydrogen atom coming from HNCO and one from propane.

The crux of this mechanism is the energy of the excited amine formed by insertion. For NH in its ground state, reaction [4] cannot be far from thermoneutral, and reaction [11] must be about 15 or 20 kcal endothermic (5, 6), The NH radical is probably formed by photolysis in an excited singlet state, perhaps the lowest $^1\Delta$ state which has been estimated to be about 27 kcal above the ground state, or possibly in one of several higher singlet states (7, 8). The effective light in the present photolysis was of wavelengths from 2 000 to 2 200 Å, corresponding to quantum energies from 130 to 142 kcal/mole. The dissociation energy of the HN—CO bond is uncertain, but by analogy with ketene should be much less than that of a normal N=C double bond, and could be as weak as 80 or 90 kcal. Thus it is probably energetically possible to form NH in an excited singlet state with sufficient energy to make reaction [11] exothermic. For reaction [11] to compete effectively with reaction [4], the amine intermediate would have to be vibrationally excited well beyond the threshold for C—H bond rupture, and the frequency factor for this mode of decomposition would have to be much larger than that for the C—N split (reaction [4]). The failure to stabilize amines in the present experiments lends some support to their being formed in highly excited states.

The mechanism also requires C—H rather than N—H bond rupture in reaction [11]; this is not unreasonable, being favored statistically and probably energetically (9). The apparent absence of C—C bond rupture is somewhat surprising (no CH_4 or C_2H_6 was observed). Another requirement is that reaction [12] would have had to have been at least 100 times faster than reaction [10] in order to predominate at the highest propane/HNCO ratios used in the isotopic experiments.

Of the two suggested mechanisms, the second is perhaps the less unpalatable. A decision between the two and consideration of other mechanisms that might be suggested must await further investigation of some of the suggested reaction steps.

REFERENCES

1. J. Y. P. Mui and R. A. Back. Can. J. Chem. **41**, 826 (1963).
2. R. A. Back. J. Chem. Phys. **40**, 3493 (1964).
3. M. E. Jacox and D. E. Milligan. J. Am. Chem. Soc. **85**, 278 (1963).
4. R. A. Back and R. D. Ketcheson. To be published.
5. T. L. Cottrell. The strengths of chemical bonds. 2nd ed. Butterworths, London. 1958.
6. B. G. Gowenlock, P. Pritchard Jones, and J. R. Majer. Trans. Faraday Soc. **57**, 23 (1961).
7. G. Herzberg. Spectra of diatomic molecules. 2nd ed. Van Nostrand, New York. 1950.
8. G. Pannetier and H. Guenebaut. Acta Chim. Acad. Sci. Hung. **18**, 347 (1959).
9. J. V. Michael and W. A. Noyes. J. Am. Chem. Soc. **85**, 1228 (1963).

Can. J. Chem. Downloaded from www.nrcresearchpress.com by 210.87.254.40 on 09/05/12
For personal use only.

Can. J. Chem. Downloaded from www.nrcresearchpress.com by 210.87.254.42 on 09/05/12
For personal use only.

PERMANGANATE–PERIODATE OXIDATION

VI. THE OXIDATION OF VARIOUS ALIPHATIC COMPOUNDS[1]

E. VON RUDLOFF

National Research Council of Canada, Prairie Regional Laboratory, Saskatoon, Saskatchewan

Received December 4, 1964

ABSTRACT

A study was made of the reaction of the permanganate–periodate reagent with a wide variety of aliphatic alcohols, polyols, aldehydes, acids, oxy-acids, ketones, ethers, and esters. Saturated monols, ketones, and ethers, as well as acetic, pelargonic, pyruvic, lactic, and oxalic acids reacted only very slowly. Glycols, olefinic alcohols, and unsaturated acids were cleaved to give predictable end products. Activated alcohols and ethyl acetoacetate reacted at relatively high rates. Formic, glyoxylic, lactic, and malonic acids as well as 1,3-propanediol and 2,5-hexane dione reacted extensively and diethyl tartrate consumed as much oxidant as did tartaric acid. The oxidation of tetrahydrofurfuryl alcohol gave succinic acid instead of the expected tetrahydro-2-furoic acid. Saturated mono- and di-carboxylic acids, 3-hydroxy propionic acid, γ-valero lactone, and saturated esters were stable towards the reagent.

INTRODUCTION

Since our initial reports on the permanganate–periodate reagent (1–4) this combined oxidant has found extensive use in the lipid field. Gas–liquid chromatographic (g.l.c.) analysis of the acidic oxidation products obtained from unsaturated fatty acids and esters has confirmed the quasi-quantitative oxidation to predictable end products (5–7). This aspect has made the reagent highly successful in routine analysis of lipids (6–10) as well as in locating the position of double bonds in unknown or isomeric unsaturated fatty acids (6, 7, 11–14).

In order to determine whether the reagent may be applied equally well to other fields of organic chemistry, in particular to terpenes, a systematic study of its mode of reaction at pH 7–8 and room temperature with various oxygenated compounds was carried out. The rate of reaction and amount of oxidant consumed by a variety of alcohols, ketones, aldehydes, ethers, esters, and carboxylic acids was determined by back titration of the unconsumed oxidant (1). In a few pertinent instances the reaction products were isolated and characterized.

Previously it was shown (1) that the reagent hydroxylates an olefinic double bond rapidly to give the isomeric 1,2-ketols (preferentially at pH 7–8) and 1,2-diol (preferentially at pH 9–10) and that these are cleaved by the periodate to give aldehydes and carboxylic acids. Since only catalytic amounts of permanganate are used the aldehydes are oxidized smoothly, though more slowly, to the corresponding carboxylic acids. No side reactions were detected. The mechanism of hydroxylation with permanganate was reviewed in 1958 (15) and has since been studied further by Wolfe and Lemieux (16). It was shown that a cyclic hypomanganate ester intermediate is involved which hydrolyzes either to the ketols or diol depending on the pH of the solution. The periodate cleavage step appears to follow the well-known course (17). Since one of the basic properties of the reagent is the reoxidation of permanganate by the excess periodate, care must be taken with highly reactive compounds that may reduce the permanganate beyond the Mn^{V} stage more quickly than reoxidation takes place, thus bringing the permanganate reaction

[1]*Issued as N.R.C. No. 8372.*

to a stop. Slow addition of such a reactant to the reagent or greater dilution usually prevents this extensive reduction of permanganate. The reverse order of addition (18) cannot be recommended.

EXPERIMENTAL

Most of the compounds used were of commercial origin (reagent grade, if available). When required the compounds were purified by fractional distillation. Aldehydes were taken up in ether and washed with small aliquots of aqueous bicarbonate solution. Ethers were treated with aqueous ferrous sulfate solution to remove peroxides. Formaldehyde, *n*-butanal, *cis*-hex-3-en-1-ol, 2-methyl-hept-2-en-6-ol, and all of the acids were used without prior purification.

Gas–liquid chromatography analyses were carried out with an F & M model 500 chromatograph (F & M Scientific Corp.), using a 180 cm × 6 mm O.D. polyethylene glycol (Carbowax 20M, 15% on Gaschrom P, 60–80 mesh) column which was temperature programmed from 55 °C at 4 °C/min. The helium flow rate was 105 ml/min and the retention time of methyl hexanoate was 7.2 min (measured from the time of injection to initial emergence of the peak). Relative retention times (r.r.t) were measured relative to this standard (r.r.t = 1.00). Since methylation of acids with freshly prepared diazomethane was found to give additional peaks and was incomplete with some dicarboxylic acids, some of the free acids were methylated in methanol containing concentrated sulfuric acid (2–3%). The esters were extracted with ether in the usual manner. Esters of high volatility were not recovered quantitatively.

Oxidation Procedure

The compound to be oxidized (0.25 mmole; 0.5 mmole if little or no uptake of oxidant was expected) was dissolved in water (10–30 ml) and transferred quantitatively to a standard volumetric flask (100.0 ml) containing permanganate–periodate stock solution (20.0 ml), potassium carbonate (69 mg; or more if more than 1 equivalent acidic product was expected), and water (20 ml). The stock solution of oxidant consisted of 97.5 mmoles sodium periodate (20.86 g) and 2.5 mmoles potassium permanganate (25.0 ml of a 0.1 *M* standard solution) per liter. The mixture was shaken, made up to 100.0 ml, and maintained at 20 °C (±2 °C). At the desired intervals, aliquots (10.0 ml) were pipetted into Erlenmeyer flasks containing standard 0.1 *N* sodium arsenite solution (5.0 ml) and sodium bicarbonate (1 g). After standing for at least 10 min the excess arsenite was titrated with standard 0.025 *N* iodine solution, using starch indicator for the end point. Duplicate values for blank determinations agreed within ±0.01 equivalents and aqueous blanks remained constant within this value for 3 to 4 days. If the compound studied was only very slightly soluble in water it was weighed into the volumetric flask. The reagent, potassium carbonate, and water were added to give about 90 ml and this mixture was shaken for 1 to 3 h before it was made up to volume and aliquots were withdrawn. Alternatively, 10 to 50% *tert*-butanol was used as solvent. The values obtained in the back titration were converted to equivalents oxidant consumed per mole of reactant and the results obtained are expressed as atoms of oxygen per mole in Tables I to VI.

Ethanol, *n*-propanol, *n*-butanol, isobutanol, *n*-hexanol, and *n*-octanol consumed 0.10 to 0.18 atoms of oxygen per mole in 24 h and 0.40 to 0.50 in 144 h. Methanol, isopropanol, *sec*- and *tert*-butanol consumed 0 to 0.10 and 0.15 to 0.22 equivalents during the same time. Pyruvic, oxalic, and acetic acid gave corresponding values of 0.02 to 0.05 and 0.06 to 0.10 whereas pelargonic acid used up 0.08 and 0.25 atoms of oxygen per mole. Glutaric, *n*-hexanoic, benzoic, and azelaic acid, methyl acetate, ethyl acetate, and γ-valero lactone, as well as methyl stearate and stearodipalmitin (both in 30% *tert*-butanol solution) did not consume more than 0.01 to 0.05 atoms of oxygen per mole in 3 to 6 days. 3-Hydroxy propionic acid consumed 0.15 equivalents in the first hour and was not oxidized further from then on. The initial uptake appears, therefore, to be due to an impurity. Similarly, succinic acid consumed initially 0.08 equivalents without further oxidation in 5 days.

Benzyl alcohol was also oxidized in the presence of 20% *tert*-butanol. The consumption of oxidant was 0.16, 0.43, 0.80, 2.18, 2.54, and 2.84 atoms oxygen per mole after 1, 3, 6, 24, 48, and 72 h respectively.

Preparative Oxidations

1. Benzyl alcohol (108 mg) was shaken vigorously with standard oxidant (40 ml), potassium carbonate (276 mg), and water (160 ml) for 48 h. The excess oxidant was reduced with sodium bisulfite and the weakly alkaline reaction mixture was evaporated *in vacuo* to a small volume. The mixture was acidified and extracted continuously with ether. The ether extract was dried over anhydrous sodium sulfate and evaporated to give crude acid (85 mg), m.p. 118–121 °C. Recrystallization from water raised the m.p. to 121–122° (undepressed in admixture of authentic benzoic acid).

2. n-Butanol (74 mg) was oxidized as above for 2 weeks. The acidic product (52 mg) was worked up as above. The g.l.c. analysis of the derived methyl esters showed only one major peak (99%) corresponding to methyl butyrate (r.r.t. = 0.32) in addition to the solvent peaks (ether, methanol).

3. Tetrahydrofurfuryl alcohol (102 mg) was oxidized for 24 h in the same manner. After reduction of excess oxidant the alkaline solution was extracted with ether to remove neutral compounds (3.8 mg). The acidic

Can. J. Chem. Downloaded from www.nrcresearchpress.com by 210.87.254.42 on 09/05/12
For personal use only.

fraction (35.2 mg) was worked up as above to give a crystalline product, m.p. 188–191.5 °C (undepressed by admixture of authentic succinic acid). The ethereal mother liquor was methylated and the resulting methyl esters were analyzed by g.l.c. Two peaks were recorded with r.r.t. 2.30 (3%; tetrahydrofuroic acid methyl ester r.r.t. = 2.29) and 2.80 (97%; methyl succinate r.r.t. = 2.80). The purity of the starting material was found to be 90% by g.l.c.

4. 2-Methyl-hept-2-en-6-ol (57 mg) (82% pure) was oxidized as above and gave only traces of neutral product (1.5 mg) and an acidic fraction (31.9 mg). When the latter was taken up in ether and washed with alkali virtually all material (30.5 mg) remained in the ether layer. The g.l.c. analysis gave a single peak with the r.r.t. of γ-valero lactone (r.r.t. = 3.05). In a separate oxidation experiment the reduced solution was evaporated to a small volume and the distillate was treated with iodine in 2 *N* sodium hydroxide solution. A yellow percipitate having m.p. 119–121 °C (undepressed by admixture of iodoform) was obtained.

5. n-Hexanal (100 mg, 92% pure) was oxidized as above for 24 h to give an acid fraction (75.0 mg) which was analyzed by g.l.c. after methylation. Two peaks with r.r.t. 0.93 (10%) and r.r.t. 1.00 (90%) were recorded (methyl hexanoate r.r.t. 1.00, methyl pentanoate r.r.t. = 0.60).

6. Glutardialdehyde. A 25% solution of glutardialdehyde (400 mg) was oxidized as above for 18 h. The acid fraction (82 mg) was obtained crystalline, m.p. 91–95° (undepressed by admixture of authentic glutaric acid). The g.l.c. analysis of the derived methyl esters of the mother liquor gave one main peak (98%) with r.r.t. 3.55 (methyl glutarate r.r.t. = 3.55).

Oxidation of Esters

Methyl stearate, m.p. 37.5–38.8 °C (99.20 mg) was dissolved in *tert*-butanol (30 ml) and added to the standard oxidation mixture (see above). After 24 h the excess oxidant was reduced and the reaction mixture was extracted repeatedly with ether. After evaporation of the solvent, the residue was dried *in vacuo* to constant weight (99.25 mg); m.p. 37.2–38.8 °C.

In a similar experiment oxidation of stearodipalmitin m.p. 67.5–68.3 °C (96.10 mg) gave the unreacted starting material, m.p. 67.5–68.3 °C, in almost quantitative amount (94.55 mg).

RESULTS AND DISCUSSION

The rate of oxidation of saturated aliphatic alcohols was found to be very slow (see Experimental). No significant difference in rate was found between lower and higher homologues or between primary, secondary, and tertiary alcohols. Surprisingly, the rate for methanol was one of the lowest. The oxidation of *n*-butanol gave only *n*-butyric acid as acidic reaction product. Since it is generally accepted that alcohols are attacked only slowly by permanganate in neutral media (19), it follows that at pH 7.5–8 the permanganate–periodate reagent behaves like neutral permanganate towards saturated alcohols. This finding permits the selective oxidation of other functional groups in alcohols provided these are not adjacent to the hydroxyl group. Wall and Serota (20) made use of this property in the selective oxidation of steroidal sapogenins with the permanganate–periodate reagent.

Activated alcohols (see Table I) reacted at much higher rates than the saturated aliphatic alcohols. Thus, benzyl alcohol consumed 1 mole of oxidant in less than 6 h and 2 in just over 2 days. Since benzoic acid was isolated in 70% yield the oxidation was essentially that of the primary alcohol group. When benzyl alcohol was oxidized in the presence of 20% *tert*-butanol the rate of oxidation increased and more than 2 moles of oxidant were consumed in 1 day (see Experimental). The oxidation of tetrahydrofurfurol (see Table I) did not proceed in the expected manner since the main product was succinic acid rather than tetrahydro-2-furoic acid. The reaction with cyclic ethers will have to be studied in more detail to clarify the mechanism by which the ring is opened. Allyl alcohol consumed 4 moles of oxidant very rapidly and another 1 in about an hour; oxidation continued more slowly until nearly 6 moles were consumed. This can be rationalized by assuming that allyl alcohol is hydroxylated very rapidly to glycerol, glyceraldehyde, and dihydroxy acetone and that these are cleaved quickly to give formic acid and formaldehyde. Formic acid appears to be oxidized fairly rapidly (see below); the slow oxidation of formaldehyde at pH 7–8 has been described before (1). Hydroxylation and cleavage may proceed so rapidly that oxidation of the activated hydroxyl group in allyl alcohol may take place only to a very small extent.

Can. J. Chem. Downloaded from www.nrcresearchpress.com by 210.87.254.42 on 09/05/12
For personal use only.

TABLE I

Oxidant consumed (atoms oxygen per mole) by some activated or unsaturated alcohols

Reaction time	Allyl alcohol	Benzyl alcohol	Tetrahydro-furfurol	Tetrahydro-pyran-2-methanol	*cis*-Hex-3-en-1-ol	2-Methyl-hept-2-en-6-ol
5 min	4.39	—	—	—	2.32	1.85
10 min	4.45	0.05	—	—	2.40	1.92
20 min	4.58	0.07	—	—	2.65	2.02
30 min	4.71	0.14	0.22	0.05	2.75	2.05
1 h	4.93	0.22	0.30	0.10	3.15	2.20
3 h	5.47	0.85	0.38	0.15	3.35	2.28
6 h	5.61	1.28	0.43	0.18	3.38	2.50
24 h	5.71	1.48	1.09	0.29	3.45	2.85
48 h	—	1.91	1.54	0.33	3.50	2.90
72 h	5.88	2.02	1.99	0.44	3.55	2.94
96 h	5.92	2.08	2.24	0.53	3.60	3.02
144 h	—	—	2.63	0.89	—	—

The oxidation of alcohols with an isolated double bond followed the normal pattern of hydroxylation, cleavage, and subsequent slower oxidation of the oxidizable cleavage products. The overall consumption of 3 moles of oxidant by 2-methyl-hept-2-en-6-ol (see Table I) is in agreement with formation of acetone and 4-hydroxy pentanoic acid. Acetone was characterized by the iodoform reaction and 4-hydroxy pentanoic acid was recovered (as γ-valero lactone) in high yield. It was shown previously (2) that acetone is oxidized only very slowly at pH 7–8 by the reagent. The consumption of almost 4 moles of oxidant by *cis*-hex-3-en-1-ol is in accord with formation of propionic and 3-hydroxy propionic acid. A commercial sample of the latter acid was found to be completely stable towards the reagent (see Experimental).

Simple α-glycols (see Table II) reacted in complete accordance with the concept of periodate cleavage (17, 21, 22) and further oxidation of aldehydic products and formic acid. When the product is formaldehyde, further oxidation is slow (see e.g. ethylene glycol). The rate of oxidation after the initial cleavage of glycerol is somewhat slower than that of formic acid (see Table IV). Similarly, that of 1,2-propanediol is a little slower than the rate of oxidation of acetaldehyde as produced in the oxidation of 2,3-butanediol. This is unexpected since both compounds would also produce formaldehyde, oxidation of which (in addition to either formic acid or acetaldehyde) should lead to a somewhat faster consumption of oxidant. This may be due, at least in part, to a slightly different pH of the respective reaction mixtures. On the other hand, the rate of oxidation of erythritol did approach the expected values closely. The markedly lower rate of cleavage of pinacol is due to steric hindrance (23). Methyl β-L-arabopyranoside consumed slightly more than 3 moles of oxidant rather rapidly without further oxidation. Since cleavage and oxidation of the resulting formic acid require 3 moles of oxidant, the intermediate dialdehyde ether moiety appears to be stable. The formation of cyclic hemialdals (22) in periodate oxidations is well known and it is possible that these are stable towards the permanganate–periodate reagent. Methyl glucoside and free sugars reacted very extensively and their oxidation was not characterized by clearly defined stages.

Water-soluble aldehydes, except formaldehyde, were oxidized smoothly with consumption of 1 mole of oxidant in 6–24 h (see Table III). The oxidation of pelargon aldehyde to pelargonic acid is in agreement with earlier data on the behavior of this aldehyde as part of the oxidation of oleic acid (1). *n*-Octanal also required 3 h shaking to give complete oxidation. *n*-Decanal was too insoluble to give consistent data in the aqueous mixture, but addition of 40% *tert*-butanol resulted in a normal rate of oxidation. The oxidation of *n*-hexanal gave *n*-hexanoic acid in 65% yield. Since no lower homologous acids were

Can. J. Chem. Downloaded from www.nrcresearchpress.com by 210.87.254.42 on 09/05/12
For personal use only.

Can. J. Chem. Downloaded from www.nrcresearchpress.com by 210.87.254.42 on 09/05/12
For personal use only.

TABLE II

Oxidant consumed (atoms oxygen per mole) by some polyols

Reaction time	Ethylene glycol	Glycerol	2,3-Butanediol	1,2-Propanediol	1,3-Propanediol	Erythritol	Pinacol	Methyl arabinoside
10 min	0.98	1.90	1.19	1.07	—	3.38	0.11	2.05
20 min	0.98	1.94	1.36	1.13	—	3.74	—	2.28
30 min	—	1.96	1.50	—	—	3.98	0.22	2.45
1 h	0.98	2.00	1.88	1.34	0.10	4.35	0.37	2.80
2 h	—	2.27	2.40	—	—	—	0.57	3.06
3 h	1.01	—	2.59	1.72	0.10	5.03	0.67	3.18
6 h	1.03	2.69	2.92	1.87	0.25	5.12	0.90	3.26
24 h	1.07	2.83	2.98	1.98	0.41	5.22	1.00	3.24
48 h	1.20	2.94	2.98	1.98	0.50	5.34	1.02	3.21
72 h	1.32	3.01	—	—	0.55	—	1.08	—
144 h	1.50	3.18	3.03	—	0.70	—	1.23	—

TABLE III

Oxidant consumed (atoms oxygen per mole) by some aldehydes

Reaction time (h)	Form-	*n*-Butyl-	*n*-Hexyl-	*n*-Octyl-	*n*-Nonyl-	*n*-Decyl-*	Glutardi-
0.25	0.0	0.45	0.35	—	—	—	—
0.5	0.01	0.60	0.62	—	—	—	0.65
1	0.01	0.81	0.91	—	—	—	1.01
3	0.01	0.88	0.94	0.75	0.48	0.53	1.52
6	0.03	0.96	0.96	0.77	0.62	0.78	1.62
24	0.24	0.98	0.96	0.90	0.91	0.83	1.73
48	—	1.00	0.96	0.94	0.94	0.83	1.76
72	0.58	1.00	—	1.00	—	0.84	—
144	—	1.06	1.10	1.02	1.12	—	1.96

*In 40% *tert*-butanol solution.

found to be present and since some loss of these volatile acids is likely during isolation, the smooth conversion of *n*-aldehydes to the corresponding carboxylic acid is confirmed. The consumption of nearly 2 moles of oxidant by glutardialdehyde and the isolation of glutaric acid from the product indicates that dialdehydes are also oxidized in a predictable manner, except malon dialdehyde which appears to be degraded extensively (see below).

TABLE IV

Oxidant consumed (atoms oxygen per mole) by some carboxylic acids

Reaction time	Formic	Malonic	Glyoxylic	Lactic	Tartaric	Diethyl tartaric	Crotonic
5 min	—	—	—	—	1.28	—	2.98
10 min	—	—	0.69	0.01	1.82	1.09	3.28
20 min	—	—	1.18	—	2.23	1.48	3.45
30 min	0.34	0.04	1.34	0.02	2.71	1.93	3.63
1 h	0.53	0.06	1.69	0.06	3.47	2.74	4.06
3 h	0.78	0.10	1.95	0.12	4.59	3.54	4.44
6 h	0.81	—	1.97	0.27	4.85	4.11	4.55
24 h	0.86	0.23	2.01	0.62	4.89	5.00	4.78
48 h	0.94	0.48	2.00	—	—	—	4.81
72 h	0.97	0.71	2.02	1.08	4.94	—	4.80
144 h	0.98	—	2.04	1.98	—	—	—

Aliphatic acids, benzoic, oxalic, glutaric, azelaic, and pyruvic acid were oxidized only very slowly by the reagent (see Experimental). The fact that oxalic acid did not react to any appreciable extent confirms that manganese is not reduced below the Mn^{V} level, thus preventing the well-known autocatalyzed reaction. Formic acid (see Table IV) consumed 1 mole of oxidant in 1 to 2 days. As found earlier (3), malonic acid is also oxidized slowly (see Table IV), the rate being similar to that of 1,3-propanediol. Hence, it is surprising that 3-hydroxy propionic acid was found to be much more stable. Glyoxylic acid (see Table IV) consumed 2 moles of oxidant fairly rapidly, indicating that this acid was cleaved rather than oxidized to oxalic acid. Pyruvic acid was stable towards the reagent and lactic acid was oxidized only slowly. The latter consumed 2 moles of oxidant in 6 days indicating that cleavage has taken place instead of oxidation of pyruvic acid. Tartaric acid reacted very rapidly and the consumption of almost 5 moles in 24 h suggests again that the intermediate glyoxylic acid must be cleaved, which is in agreement with the above conclusions. This is further supported by the data obtained with diethyl tartrate. Cleavage of this ester would yield 2 moles of ethyl glyoxylate. The consumption of a total of 5 moles of oxidant is in agreement with cleavage of this aldehydo ester

Can. J. Chem. Downloaded from www.nrcresearchpress.com by 210.87.254.42 on 09/05/12
For personal use only.

(possibly after hydrolysis to glyoxylic acid). Hydroxylation and cleavage of crotonic acid would yield acetaldehyde and glyoxylic acid. Further oxidation of these two products would require 3 moles of oxidant if the glyoxylic acid moiety is cleaved. Again, the values of oxidant consumed are in good agreement (see Table IV).

TABLE V

Oxidant consumed (atoms oxygen per mole) by some aliphatic ketones

Reaction time (h)	Methyl ethyl ketone	Methyl isobutyl ketone		Methyl *n*-amyl ketone	2,5-Hexane dione	Ethyl aceto-acetate
		(*a*)*	(*b*)†			
1		—	—	—	—	2.09
3	0.01	0.01	0.01	0	0.01	2.54
6	0.01	0.01	0.04	0.02	0.08	2.94
24	0.03	0.04	0.05	0.09	0.22	3.53
48	0.06	0.05	0.07	0.14	0.40	3.76
120	0.23	0.16	0.20	0.33	0.86	3.90
144	0.30	0.33	0.40	0.55	1.16	3.90

*(*a*) In aqueous solution.
†(*b*) In 20% *tert*-butanol solution.

Ketones were oxidized only very slowly (see Table V). This was anticipated from the very low rate of oxidation of acetone at pH 7–8 (2). The rate of oxidation of methyl isobutyl ketone in the presence of *tert*-butanol was practically the same as in aqueous solution. Noteworthy, again, is the higher rate of oxidation of 2,5-hexanedione, the rate being similar to that of malonic acid and 1,3-propanediol. This would indicate a similar activation of the methylene group in 1,3-diones, although in the ketones it seems more likely that the enol form is the one that reacts. As expected, ethyl acetoacetate reacts rapidly and the consumption of almost 4 moles of oxidant is in agreement with the assumption that the enol form is hydroxylated and cleaved to give acetaldehyde and ethyl glyoxylate as intermediates. The latter two compounds would react further as described above for 2,3-butanediol, crotonic acid, and ethyl tartrate.

As noted previously (3), saturated esters are stable towards the reagent. Methyl and ethyl acetate, as well as methyl stearate and stearodipalmitin, consumed less than 0.05 moles of oxidant in 3 days and the latter two esters were recovered virtually quantitatively (see Experimental). γ-Valero lactone also consumed no oxidant. This confirms that the saturated esters are not hydrolyzed under the ordinary oxidation conditions and this stability accounts in part for the quantitative results obtained in triglyceride analysis (6–9). Some workers have found that in the oxidation of oleic and linoleic acid or their esters a few percent of the next lower homologous monocarboxylic acid (octanoic and pentanoic acid respectively) may be formed in permanganate–periodate oxidation (6, 14, 18). Recent results obtained by Craig and Bhatty (14) indicate that this so-called overoxidation is largely due to the presence of peroxides. However, the very low rate of oxidation of pelargonic acid itself (see Experimental) suggests that a small amount of the next lower homologue may be produced by direct attack on the end products. However, since the reaction time for the oxidation of unsaturated acids and esters is usually less than 24 h, this side reaction cannot amount to more than 3%. In fact, it will normally be smaller since azelaic and hexanoic acids were found to be practically stable towards the reagent. It is also noteworthy that 9,10-epoxy stearic acid was not oxidized by the reagent (1).

Can. J. Chem. Downloaded from www.nrcresearchpress.com by 210.87.254.42 on 09/05/12
For personal use only.

TABLE VI

Oxidant consumed (atoms oxygen per mole) by some aliphatic ethers

Reaction time (h)	Diethyl ether	*n*-Dibutyl ether	Bis-(2-methoxy ethyl)-ether	Bis-(2-ethoxy ethyl)-ether
3	0.03	0.11	0.15	0.13
24	0.41	0.40	0.18	0.42
48	0.49	0.48	0.30	0.64
72	0.70	0.58	0.42	0.78
96	0.80	0.67	0.48	1.00
168	1.30	1.11	0.89	1.17

Finally, a few ethers were investigated (Table VI). These were oxidized at a slow rate and the uptake of oxidant did not cease after 7 days. When *p*-dioxane was used as solvent (2) a slow increase in the blank titration was also noted. This confirms that the ethers are not ideal for use as solvent and *tert*-butanol and possibly also pyridine (4) are to be preferred.

ACKNOWLEDGMENTS

The interesting and stimulating discussions with Drs. R. U. Lemieux and A. S. Perlin are gratefully acknowledged. Thanks are also due to Mr. M. Granat for technical assistance.

REFERENCES

1. R. U. Lemieux and E. von Rudloff. Can. J. Chem. **33**, 1701, 1710 (1955).
2. E. von Rudloff. Can. J. Chem. **33**, 1714 (1955).
3. E. von Rudloff. J. Am. Oil Chemists' Soc. **33**, 126 (1956).
4. E. von Rudloff. Can. J. Chem. **34**, 1413 (1956).
5. B. M. Craig and E. von Rudloff. Unpublished results.
6. A. P. Tulloch and B. M. Craig. Abstract, Oct. Meeting Am. Oil Chemists' Soc. 1960; J. Am. Oil Chemists' Soc. **41**, 322 (1964).
7. T. C. Lo Chang and C. C. Sweeley. J. Lipid Res. **3**, 170 (1962).
8. C. G. Youngs. J. Am. Oil Chemists' Soc. **38**, 62 (1961).
9. M. R. Subbaram and C. G. Youngs. J. Am. Oil Chemists' Soc. **41**, 150, 218 (1964).
10. M. R. Subbaram, M. M. Chakrabarty, C. G. Youngs, and B. M. Craig. J. Am. Oil Chemists' Soc. **41**, 691 (1964).
11. C. R. Smith, T. L. Wilson, T. K. Miwa, H. Zobel, R. L. Lohmar, and J. A. Wolff. J. Org. Chem. **26**, 2903 (1961).
12. C. R. Smith, T. L. Wilson, R. B. Bates, and C. R. Scholfield J. Org. Chem. **27**, 3112 (1962).
13. P. A. J. Gorin, J. F. T. Spencer, and A. P. Tulloch. Can. J. Chem. **39**, 846 (1961).
14. B. M. Craig and M. K. Bhatty. J. Am. Oil Chemists' Soc. **41**, 209, 508 (1964).
15. J. W. Ladbury and C. F. Cullis. Chem. Rev. **58**, 403 (1958).
16. S. Wolfe. Ph.D. Thesis, University of Ottawa, Ottawa. 1957.
17. C. A. Bunton and V. J. Shiner. J. Chem. Soc. 1593 (1950).
18. E. P. Jones and J. A. Stolp. J. Am. Oil Chemists' Soc. **35**, 71 (1958).
19. R. Stewart. *In* Oxidation mechanism. W. A. Benjamin, Inc., New York. 1964. p. 63.
20. M. E. Wall and S. Serota. J. Org. Chem. **24**, 741 (1959).
21. F. R. Duke and V. C. Bulgrin. J. Am. Chem. Soc. **76**, 3803 (1954).
22. R. D. Guthrie. *In* Advances in carbohydrate chemistry. Vol. 16. *Edited by* M. L. Wolfrom. Academic Press, New York. 1961. p. 105.
23. G. J. Buist, C. A. Bunton, and J. H. Miles. J. Chem. Soc. 4567 (1957).

Can. J. Chem. Downloaded from www.nrcresearchpress.com by 210.87.254.42 on 09/05/12
For personal use only.

Can. J. Chem. Downloaded from www.nrcresearchpress.com by 210.87.254.40 on 09/05/12
For personal use only.

A PROTON MAGNETIC RESONANCE STUDY OF N-BIS(2-HALOETHYL)AMINES[1]

GEORGE R. PETTIT, JOSEPH A. SETTEPANI, AND RALPH A. HILL
Department of Chemistry, University of Maine, Orono, Maine

Received September 28, 1964

ABSTRACT

The proton magnetic resonance chemical shifts of N-bis(2-haloethyl)amine hydrohalide salts have been found useful for rapidly assessing organohalide composition. An important illustration of nitogen mustard reactivity was obtained by observing the p.m.r. response of N-bis(2-haloethyl)amine hydrohalide salts (in deuterium oxide) following neutralization. In general, the amines rapidly entered a complex series of intra- and inter-molecular reactions. Among the substances studied N-bis(2-fluoroethyl)amine was by far the most stable and remained essentially unchanged during a 7-day period. By contrast N-bis(2-iodoethyl)amine was completely transformed in less than 6 min. The self-condensation reactions of, for example, N-bis(2-chloroethyl)amine appear to be accompanied by transient formation of N-2-chloroethylaziridine (III*b*). The present investigation indicates that p.m.r. spectroscopy is a valuable technique for evaluating the course of nitrogen mustard self-condensation reactions.

In order to extend both the utility of nitrogen mustards as cancer chemotherapeutic agents and our chemical knowledge of these substances, we have undertaken development of convenient synthetic routes to various symmetrical (with respect to the halogen substituent, e.g., see ref. 2) and unsymmetrical (3) N-bis(2-haloethyl)amines. When it became apparent (2*a*) that even appreciable quantities of incorrectly halogenated impurities accompanying unsymmetrical nitrogen mustards could be difficult to detect, prior to elemental microanalyses, we began to employ proton magnetic resonance (p.m.r.) spectroscopy as a method for rapidly evaluating purity. Prior experience with, and interest in, N-bis(2-chloroethyl)amine (I*b*) self-condensation reactions (4) suggested the potential value of also using p.m.r. measurements to follow and compare the course of such transformations in aqueous solution (at various pH levels) and in other protic and aprotic solvents. The possibility of assessing aziridinium ion (II) formation also appeared attractive. Certain reactions of N-bis(2-chloroethyl)amine are now generally believed to proceed via the corresponding aziridinium salt (5) and additional support for such intermediates[2] in the case of nitrogen mustard reactions would be useful. For example, a meaningful correlation between extent of aziridinium ion formation and antineoplastic activity might then be possible. A summary of initial results obtained in pursuit of these general objectives is presented in the sequel.

Proton magnetic resonance chemical shifts of the four parent N-bis(2-haloethyl)amines (1*a–b* and 1*d–e*), as hydrohalide salts in deuterium oxide solution, allowed each to be readily distinguished from the other members. One unsymmetrically halogenated nitrogen mustard (I*c*) was also studied and as expected the p.m.r. response was again unique. The spectral results summarized in Fig. 1 for the secondary amines and in Fig. 2 for their N-methyl derivatives[3] clearly indicates that proton magnetic resonance spectroscopy provides a very useful means for rapidly distinguishing between the various halogenated

[1]*The present contribution and a previous one (1) may be considered Parts XIV and XIII respectively of our series, Antineoplastic Agents. For Part XII, refer to G. R. Pettit and J. A. Settepani, Chem. Ind. London, 43, 1805 (1964).*

[2]*The structure of 2,2-pentamethylene-1,1-tetramethylene aziridinium perchlorate and related ethylenimonium compounds prepared by Leonard and colleagues (6), however, have been carefully substantiated.*

[3]*Because of insufficient solubility in deuterium oxide (at 20°) a spectrum of N-methyl-N-bis(2-iodoethyl)amine hydrochloride was not included in Fig. 2.*

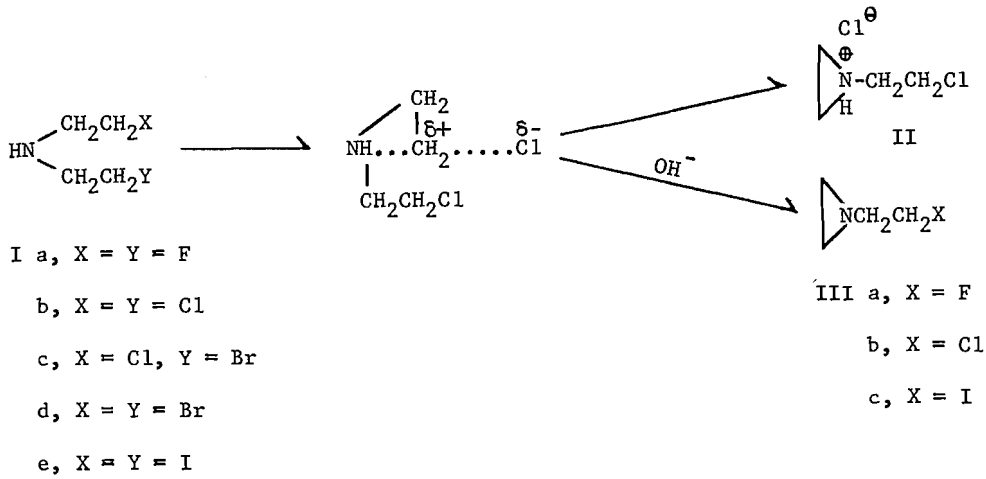

nitrogen mustards. In Fig. 1 the spectrum of N-bis(2-fluoroethyl)amine hydrobromide provides a classical example of fluorine–proton spin–spin coupling (1). The two lowest field triplets centered at 5.56 and 4.8 δ represent methylene protons adjacent to fluorine and the two high field triplets (at 4.15 and 3.68 δ) reflect methylene protons adjacent to nitrogen (1). Coupling constants for the fluorine derivative and N-bis(2-chloroethyl)-amine hydrochloride were essentially equal (J = 5 c.p.s.) but the triplet assignable to methylene protons adjacent to nitrogen in the latter compound was centered at 3.88 δ and the triplet corresponding to methylene protons adjacent to chlorine was centered at 4.28 δ. With N-bis(2-bromoethyl)amine hydrochloride the partially masked triplet arising at 4.05 δ approximates an A_2B_2 case (7). The principal peak exhibited by N-(2-iodoethyl)amine hydrochloride at 3.84 δ resembled that of the bromine analog. As expected N-2-bromoethyl-N-2-chloroethylamine hydrobromide displayed a near composite of the spectra corresponding to chloroamine I*b* and bromoamine I*d* and the principal peak was positioned at 4.05 δ. Except for the $\oplus$N—CH_3 signal (e.g., see ref. 8) at 3.53 δ each of the tertiary amines noted in Fig. 2 displayed a spectrum qualitatively similar to that of the related secondary amine.

Next, each of the secondary amine (I*a–e*) hydrohalide salts was treated with an equivalent amount of sodium deuteroxide in deuterium oxide. Three minutes later p.m.r. scanning was commenced. Since the scanning time was 4 min a total of 7 min elapsed before the complete spectrum was recorded. The mixtures p.m.r. response was then generally ascertained at 15, 30, 60, and 100 to 120 min intervals. Under the experimental conditions employed, fluoroamine I*a* proved quite stable.[4] Three minutes after neutralizing the fluoroamine (I*a*) hydrobromide salt, a p.m.r. spectrum of the solution showed four new, but nicely resolved, triplets centered at 3.05, 3.55, 4.55, and 5.30 δ (J = 5 c.p.s.). Except for a slight shift (0.05 δ) to lower field and emergence of 2 small split peaks at 1.80 and 2.19 δ by the third day, the spectrum remained otherwise unchanged during a 7-day observation period. Meanwhile, the p.m.r. chemical shifts (Table I) of six representative aziridine derivatives were recorded. On the basis of this

[4]*The* ^{19}F *nuclear magnetic resonance of N-bis(2-fluoroethyl)amine has been studied (9) but proton magnetic resonance chemical shifts were not recorded. Our brief mention of fluoroamine Ia, stability as evidenced by p.m.r. studies, in ref. 2b (footnote 3), represents to our knowledge the only prior report of an N-bis(2-haloethyl)amine p.m.r. investigation.* NOTE ADDED IN PROOF. *An excellent p.m.r. study of 2-chloro- and 2-fluoro-ethylamines has now been summarized by P. L. Levins and Z. B. Papanastassiou. J. Am. Chem. Soc. 87, 826 (1965).*

Can. J. Chem. Downloaded from www.nrcresearchpress.com by 210.87.254.40 on 09/05/12
For personal use only.

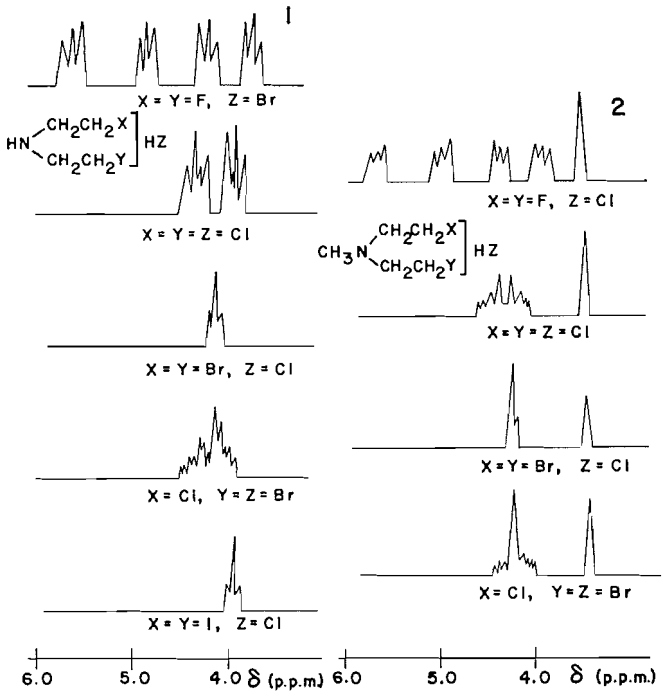

FIG. 1. Proton magnetic resonance spectra of representative N-bis(2-haloethyl)amine hydrohalides in deuterium oxide.

FIG. 2. Proton magnetic resonance spectra of several N-methyl-N-bis(2-haloethyl)amine hydrohalides in deuterium oxide.

study (see also ref. 10) it seemed likely that the aziridinium ion (cf. II) derived from amines such as I*a–e* in deuterium oxide should give rise to a p.m.r. signal at approximately 2.6–3.5 δ and that the parent aziridine (III), in the same solvent, should exhibit a signal at approximately 2.0 δ. Thus, the two small complex signals near 2.0 δ (appearing after 3 days) were tentatively attributed to a small quantity of N-2-fluoroethylaziridine (III*a*).

TABLE I

Nuclear magnetic resonance chemical shifts (δ units) of aziridine ring protons*

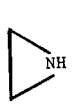	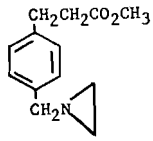		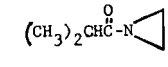	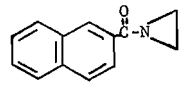	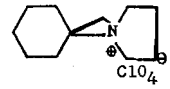
1.52 (broad) 2.0 (sharp)†	1.2 and 1.72‡ (J=2)	2.14	2.17	2.37	3.33†

*Each substance was studied in deuterochloroform solution unless otherwise noted.
†Deuterium oxide as solvent.
‡Middle peak positions of two triplets.

Repeating the neutralization experiment employing N-bis(2-chloroethyl)amine provided the spectral data illustrated in Fig. 3. Within 7 min after neutralization, 2 triplets centered at 3.35 and 4.05 δ (J = 5 c.p.s.) corresponding to essentially pure amine I*b*

Can. J. Chem. Downloaded from www.nrcresearchpress.com by 210.87.254.40 on 09/05/12
For personal use only.

were recorded. By the time 15 min elapsed two small peaks appeared at 1.90 and 2.25 δ and another at approximately 3.0 δ; the original triplets had shifted downfield 0.05 δ. Accordingly, the two peaks at higher field were tentatively assigned to N-2-chloroethylaziridine (III*b*). During the next 15 min period an increase in hydrogen ion concentration was probably responsible for the overall shift to lower field. The three highest field peaks were relocated at 2.45, 2.65, and 3.36 δ and the triplets became centered at 3.75 and 4.25 δ. With passing of 100 min, the p.m.r. spectrum (Fig. 3) qualitatively resembled that of the original hydrochloride derivative (Fig. 1) although the presence of other substances was apparent. Three days later approximately the same p.m.r. response was elicited.

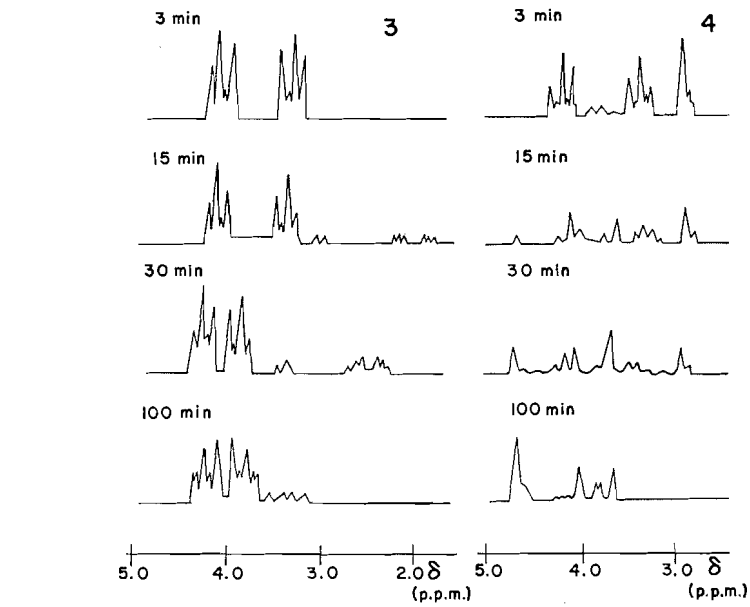

FIG. 3. Proton magnetic resonance spectra of N-bis(2-chloroethyl)amine following neutralization (zero time) of the hydrochloride salt (in deuterium oxide).
FIG. 4. Proton magnetic resonance spectra of N-methyl-N-bis(2-chloroethyl)amine following neutralization (zero time) of the hydrochloride salt (in deuterium oxide).

The two high field partially resolved triplets (centered at 1.85 and 2.20 δ) presented by N-2-bromoethyl-N-2-chloroethylamine hydrobromide 3 min after neutralization were more convincing. The high field signals were assigned to the aziridine ring protons of amine III*b*. Again, the poorly resolved signals in the 3.0 δ region were much less convincing evidence for aziridinium ion ring protons. Fifteen minutes later the spectrum of amine I*c* appeared more complex and the two highest field signals had shifted 0.10 δ to lower field. During the next 15 min a solid began to separate from solution which prohibited further p.m.r. observations.

When the preceding experiment was repeated using N-bis(2-bromoethyl)amine hydrochloride initial reaction of the free base proved quite rapid. The p.m.r. spectrum recorded at time 3 to 7 min displayed two very broad and ill-defined signals centered at 2.5 and 4.0 δ. At a total elapsed time of 16 min a complex multiplet had appeared at 3.39 δ and a partially masked triplet reminiscent of the original hydrobromide salt (of amine I*d*) was positioned at 4.10 δ. Essentially the same p.m.r. spectrum was obtained 2 h later.

Can. J. Chem. Downloaded from www.nrcresearchpress.com by 210.87.254.40 on 09/05/12
For personal use only.

Can. J. Chem. Downloaded from www.nrcresearchpress.com by 210.87.254.40 on 09/05/12
For personal use only.

In keeping with rapid disappearance of amine I*d* a p.m.r. spectrum of N-bis(2-iodoethyl)amine hydrochloride 3 min after neutralization showed, principally, a weak but broad and unresolved signal centered at approximately 3.8 δ. Interestingly, two small barely discernible peaks were positioned at 1.8 and 2.18 δ and suggested the transient presence of aziridine III*c*. The reactions of amine I*e* culminated at time 6 min with separation of a dark semisolid which precluded further spectral study.

Of the tertiary amines, N-methyl-N-bis(2-fluoroethyl)amine and N-methyl-N-bis(2-chloroethyl)amine were selected for initial examination. A p.m.r. spectrum of the fluorine-containing amine, 3 min after neutralizing the corresponding hydrochloride salt in deuterium oxide solution, was consistent with that expected for the pure base; the methyl peak emerged at 2.80 δ and 4 triplets (J = 5 c.p.s.) were centered at 3.02, 3.52, 4.69, and 5.48 δ. Two hours later an identical spectrum was recorded. Four days later approximately 85% of the original amine had been transformed to a new substance displaying p.m.r. signals at 3.95 and 4.59 δ.[5] After a total time of 7 days the reaction was essentially complete. Analogous reaction of the chloro derivative was considerably faster and nearly complete within 2 h (Fig. 4). Similarly, N-methyl-N-bis(2-bromoethyl)amine disappeared during the first 3 min period and 30 min later reaction seemed terminated. Although the early spectra reproduced in Fig. 4 contain a small peak at 2.78 δ which might correspond to aziridinium ring protons, the present evidence is at best only suggestive. In the tertiary amine experiments just described, the concentration of aziridinium ion, if formed at all, must remain low.[6] In general, firm spectral evidence for terminal piperazine formation was lacking and assignments for the end-products (following neutralization) require a definitive chemical study.

The preceding albeit preliminary experimental results indicate that future p.m.r. investigations of N-bis(2-haloethyl)amines under varying conditions of pH and solvent should lead to a clearer understanding of stability, the course of self-condensation reactions, and important intermediates. Thus, it should now be possible to rapidly determine the optimum time requirements and other experimental conditions for production of selected intermediates and terminal products. By this means, isolation and characterization of, for example, the N-2-haloethylaziridines (III)[7] may become practical. Previous attempts (4, 12) at isolation or preparation of aziridine III*b* have met with failure. Experiments related to these problems are now in progress.

EXPERIMENTAL

The proton magnetic resonance data were recorded using a Varian Associates Model A-60 Spectrometer. Each of the N-bis(2-haloethyl)amines was studied in deuterium oxide (10% solute by weight) using a capillary tube filled with tetramethylsilane as external standard (uncorrected for bulk, diamagnetic susceptibility differences). The chemical shifts reported with deuterium oxide as solvent in Table I were obtained in the same manner. When deuterochloroform was employed as solvent (for the measurements recorded in Table I) the solute also amounted to 10% (wt./vol.) and enough tetramethylsilane was added to standardize the instrument. The chemical shifts (at 20 $\pm$ 1°) are reported using the frequency-independent unit δ (p.p.m.) with respect to tetramethylsilane. In each case the scanning time from low to high field was 4 min (120 c.p.s./min).

After collecting the chemical shift data for each N-bis(2-haloethyl)amine hydrohalide salt, exactly 1 equivalent of sodium deuteroxide (by adding the calculated quantity of sodium to deuterium oxide) in deuterium oxide was added and mixing was achieved by twice inverting the n.m.r. sample tube. At this point the opalescent solution had cleared and 3 min after adding base scanning was commenced. The spectrum was recorded again after 15, 30, 60, and 100 to 120 min intervals. Longer periods were employed

[5]*The composition of this substance (possibly a piperazine) will be ascertained as part of a future investigation.*
[6]*The utility of p.m.r. techniques for mechanism studies depends on relatively high concentrations of important intermediates.*
[7]*In vivo transport of N-bis(2-haloethyl)amine has been postulated to involve aziridine IIIb (11).*

in those cases where reaction appeared incomplete. Scanning was terminated whenever a solid product began to separate from solution.

N-Bis(2-haloethyl)amines

The N-bis(2-haloethyl)amines and their N-methyl derivatives were prepared in this laboratory as part of previous (2, 13) or recently completed (3) investigations. Synthesis of the two new nitrogen mustards, N-2-bromoethyl-N-2-chloroethylamine and its N-methyl derivative, will be described in a separate contribution (3).

Aziridines

The specimen of N-chloroaziridine was supplied (cooled to dry ice temperature) by Aerojet-General Corporation, Azusa, California, and its p.m.r. spectrum was recorded within 2 h of delivery. We are indebted to Drs. Goodman (14) and Leonard (6) for providing the second and sixth compounds entered in Table I. The remaining substances (in Table I) were purchased from Aldrich Chemical Company.

ACKNOWLEDGMENTS

This investigation was aided by Grants No. T-79D and T-79E from the American Cancer Society and by National Science Foundation Research Grant GB-249. We are also grateful to the National Institutes of Health for predoctoral fellowship (to J. A. S., 1963–1964) support.

REFERENCES

1. G. R. PETTIT, I. B. DOUGLASS, and R. A. HILL. Can. J. Chem. **42**, 2357 (1964).
2. (*a*) G. R. PETTIT, M. R. CHAMBERLAND, D. S. BLONDA, and M. A. VICKERS. Can. J. Chem. **42**, 1699 (1964). (*b*) G. R. PETTIT and R. L. SMITH. Can. J. Chem. **42**, 572 (1964). (*c*) G. R. PETTIT, D. S. BLONDA, and E. C. HARRINGTON. Can. J. Chem. **41**, 2962 (1963).
3. G. R. PETTIT and M. R. CHAMBERLAND. Can. J. Chem. In preparation.
4. G. R. PETTIT and J. A. SETTEPANI. J. Org. Chem. **27**, 2962 (1962).
5. N. B. CHAPMAN and D. J. TRIGGLE. J. Chem. Soc. 1385 (1963). S. D. ROSS, J. J. BRUNO, and R. C. PETERSEN. J. Am. Chem. Soc. **85**, 3999 (1963). A. YA BERLIN and A. D. CHINAEVA. Zh. Obshch. Khim. **33**, 610 (1963). G. R. PETTIT and J. A. SETTEPANI. J. Med. Pharm. Chem. **5**, 296 (1962). V. M. RAKOVA, A. D. CHINAEVA, and A. YA BERLIN. Zh. Obshch. Khim. **29**, 3962 (1959). A. STREITWIESER, Jr. Chem. Rev. **56**, 571 (1956). M. IZUMI. Pharm. Bull. Tokyo, **3**, 88 (1955).
6. (*a*) N. J. LEONARD, E. P. F. KIEFER, and L. E. BRADY. J. Org. Chem. **28**, 2850 (1964). (*b*) N. J. LEONARD and K. JANN. J. Am. Chem. Soc. **84**, 4806 (1962).
7. K. B. WIBERG and B. J. NIST. Interpretation of NMR spectra. W. A. Benjamin, Inc., New York, N.Y. 1962.
8. H. SUHR. Chem. Ber. **96**, 1720 (1963). E. CAMPAIGNE and N. W. JACOBSEN. J. Org. Chem. **29**, 1703 (1964).
9. N. MULLER, P. C. LAUTERGUR, and G. F. SVATOS. J. Am. Chem. Soc. **79**, 1807 (1957).
10. M. BEROZA and A. B. BOŘKOBEC. J. Med. Chem. **7**, 44 (1964). R. G. KOSTYANOVSKII and B. F. BYSTROV. Izv. Akad. Nauk SSSR Otd. KHIM. NAUK, 1488 (1962). S. J. BROIS. J. Org. Chem. **27**, 3532 (1962). A. T. BOTTINI and J. D. ROBERTS. J. Am. Chem. Soc. **80**, 5203 (1958). R. F. M. WHITE. Physical methods in heterocyclic chemistry. Vol. II. *Edited by* A. R. KATRITZKY. Academic Press, New York. 1963. p. 151.
11. W. C. J. ROSS. Biological alkylating agents. Butterworth, London. 1962. p. 13.
12. F. D. POPP, E. CULLEN, and S. ROTH. Chem. Ind. London, 1017 (1962).
13. A. M. SELIGMAN, O. M. FRIEDMAN, and A. M. RUTENBURG. Cancer Res. **3**, 342 (1950). A. F. CHILDS, L. J. GOLDSWORTHY, G. F. HARDING, F. E. KING, A. W. NINEHAM, W. L. NORRIS, S. G. P. PLANT, B. SELTON, and A. L. L. TOMPSETT. J. Chem. Soc. 2174 (1948).
14. W. A. SKINNER, A. P. MARTINEZ, H. F. GRAM, L. GOODMAN, and B. R. BAKER. J. Org. Chem. **26**, 148 (1961).

Can. J. Chem. Downloaded from www.nrcresearchpress.com by 210.87.254.40 on 09/05/12
For personal use only.

Can. J. Chem. Downloaded from www.nrcresearchpress.com by 210.87.254.5 on 09/05/12
For personal use only.

ANTINEOPLASTIC AGENTS

XV. INTRAMOLECULAR REACTIONS OF N-PHENYL-N′-BIS(2-CHLOROETHYL)UREA[1]

GEORGE R. PETTIT, DAVID S. BLONDA,[2] AND ROGER A. UPHAM
Department of Chemistry, University of Maine, Orono, Maine

Received October 5, 1964

ABSTRACT

Reaction between phenyl isocyanate and N-bis(2-chloroethyl)amine in cold diethyl ether solution yields N-phenyl-N′-bis(2-chloroethyl)urea. The urea was found to rearrange in ethanol solution or upon warming to, respectively, 2-(N-phenylimino)-3-(2′-chloroethyl)-oxazolidine hydrochloride and 1-phenyl-2-oxo-3-(2′-chloroethyl)imidazolidine. Infrared spectral studies, augmented by mass and proton magnetic resonance determinations provided compelling support for the structural formulations. The oxazolidine reaction sequence was also examined employing 4-nitrophenyl isocyanate, 1-naphthyl isocyanate, and N-bis(2-bromoethyl)amine.

Rapid intramolecular rearrangement of N-bis(2-chloroethyl)amides to 2-(2′-chloroethylamino)ethyl esters, in the presence of water, has been well established (for example, see ref. 1). When rearrangement of N-bis(2-chloroethyl)amides to the corresponding ester derivatives was found to be rather general in scope (1*a*), we decided to extend the study to N-substituted-N′-bis(2-chloroethyl)ureas (I). Major impetus for this course resided with the enhanced potential of N-bis(2-chloroethyl)ureas to undergo one of a variety of possible intra- or inter-molecular reactions combined with the possibility of finding a useful antineoplastic agent among substances of this type and (or) their transformation products.

When the present investigation was begun in 1959, one N-phenyl- and one benz(a)anthracene derivative of N-bis(2-chloroethyl)urea had already been described (2, 3). Both urea derivatives were prepared, employing the corresponding isocyanate and N-bis(2-chloroethyl)amine, and purified under mild conditions employing aprotic solvents. No rearrangement reactions of the ureas were reported and the conditions recorded would not have favored transformations of this type. Subsequently, Popp and Swarz (4*a*) reported a series of urea and thiourea[3] derivatives of N-bis(2-chloroethyl)amine which they considered to be the first examples of N-bis(2-chloroethyl)ureas. Here, the crude reaction products were not further purified.[4] Recently, Khedouri, Kim, and Friedman (4*c*) described a series of N-bis(2-chloroethyl)ureas prepared (in benzene solution) from isocyanate derivatives of aspartic acid, glutamic acid, phenylalanine, methionine, and leucine ethyl esters. A reaction employing ethyl L-leucine isocyanate and N-bis(2-chloroethyl)amine was reported to yield (12 and 70% respectively) a crystalline racemate and the optically active urea. The remaining ureas were oils characterized following column chromatography on Florisil. In each case, treating the urea with water, either alone or containing acid or base, provided a hydrochloride salt which was assigned a carbamate structure (e.g. III*b*).

Addition of phenyl isocyanate to a dry ethereal solution of N-bis(2-chloroethyl)amine

[1]*Part XIV. G. R. Pettit, J. A. Settepani, and R. A. Hill. Can. J. Chem. This issue.*
[2]*Present address: E. I. duPont de Nemours and Co., Inc., Wilmington, Delaware.*
[3]*Interestingly, the principal product from reaction between N-bis(2-chloroethyl)amine and phenyl isothiocyanate in diethyl ether solution has been found (in our laboratory) to be N-bis(2-chloroethyl)amine hydrochloride. The same observation has recently been reported by Berlin and Levi (5). A more detailed study of this unexpected reaction is now in progress.*
[4]*Later (4b), a pure specimen of N-(4-fluorophenyl)-N′-bis(2-chloroethyl)urea was reported.*

Can. J. Chem. Downloaded from www.nrcresearchpress.com by 210.87.254.5 on 09/05/12
For personal use only.

was selected for initial study. Conversion to urea I*a* proceeded quite rapidly; the reaction product (I*a*) began to separate from solution within a 3 min period. With several examples described below, the reaction began immediately and was essentially complete within a several minute period. Assignment of an N-phenyl urea structure (I*a*) was considered appropriate on the basis of elemental composition and results of infrared spectral and

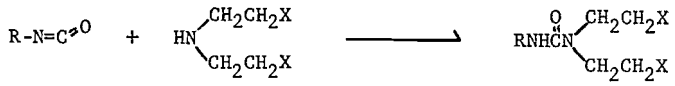

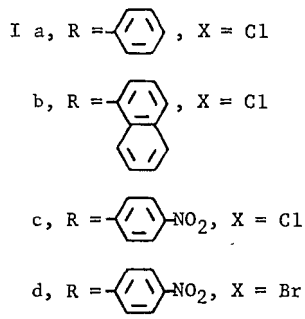

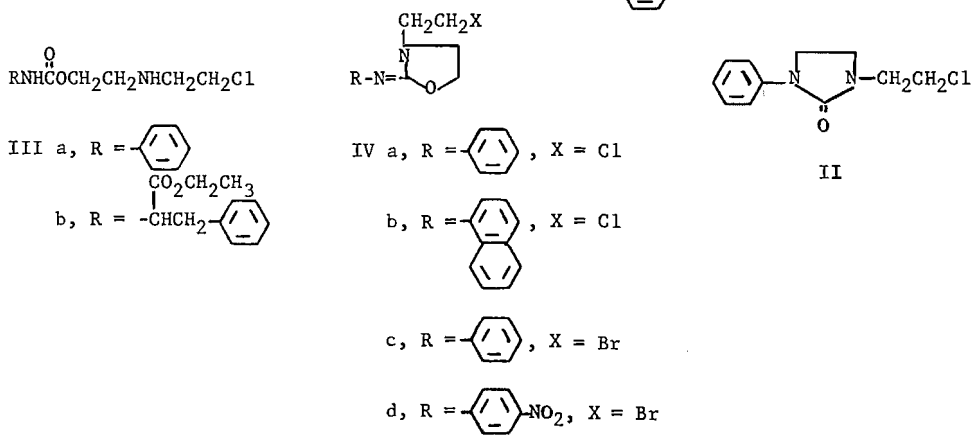

proton magnetic resonance (p.m.r.) determinations. The infrared spectrum of urea I*a* exhibited N—H absorption at 3 100 cm^{-1} and carbonyl absorption at 1 670 and 1 635 cm^{-1}. Proton magnetic resonance signals were observed at 3.58 δ (approximately 8 methylene-type protons) and in the region 6.82–7.15 δ (phenyl protons). During purification of urea I*a*, certain conditions such as heating or contact with protic solvents led to new products. Warming (steam bath) the urea caused intramolecular cyclization to imidazolidone II with concomitant loss of hydrogen chloride. In addition to molecular weight determination (by mass spectrometry) and elemental composition, assignment of the imidazolidine structure[5] was suggested by its infrared spectrum (no N—H absorption and a single carbonyl band at 1 685 cm^{-1}) and p.m.r. response. The p.m.r. spectrum of imidazolidine II exhibited a band at 3.53 δ (partially masked triplet) attributable to the 8 aliphatic-type protons and a complex response in the 6.8–7.4 δ region assignable to the aromatic protons.

[5]*An analogous reaction sequence was reported by Gabriel in 1895 (6). Warming N-phenyl-N'-(2-chloroethyl)-urea in ethanol-containing base yielded a product assigned the corresponding imidazolidone structure.*

Can. J. Chem. Downloaded from www.nrcresearchpress.com by 210.87.254.5 on 09/05/12
For personal use only.

Attention was next focused on transformation of urea I*a* in a polar medium. As the amide → ester rearrangement noted earlier (1) was found to proceed satisfactorily in ethanol solution, intramolecular rearrangement of urea I*a* was allowed to proceed in this solvent. Here, two prominent reaction pathways would appear likely: rearrangement to carbamate[6] III*a* or oxazolidine IV*a*. Reaction of urea I*a* in ethanol, at room temperature, was found to proceed quite readily and yield (quantitative) a hydrochloride salt. An infrared spectrum of the product revealed a strong ammonium band at 2 750 cm^{-1} and a broad carbonyl-type band at 1 660–1 680 cm^{-1}. Absence of absorption in the vicinity of 1 720 cm^{-1} (8) eliminated the carbamate structure (III) from further consideration. In addition, relatively strong absorption bands at 1 030 and 1 230 cm^{-1} suggested a vinyl ether-type[7] linkage. In keeping with these observations and elemental microanalytical data, the salt was assigned 2-(N-phenylimino)-3-(2′-chloroethyl)oxazolidine (IV*a*) hydrochloride.[8] Although a p.m.r. spectrum of the salt observed in deuterium oxide solution did not provide definitive support for the structural formulation, the complex signals observed at 4.4–4.6 and 4.95–5.15 δ appeared to involve 8 methylene protons and be consistent with oxazolidine IV*a*.

The reaction sequence leading to phenyl oxazolidine IV*a* was also utilized to prepare the 1-naphthyl derivative (IV*b*) and two oxazolidines (IV*c* and *d*) derived from N-bis(2-bromoethyl)ureas. As might be expected, N-phenyl-N′-bis(2-bromoethyl)urea proved too reactive to be conveniently isolated and was instead converted to oxazolidine IV*c*. While reaction of 4-nitrophenyl isocyanate with N-bis(2-chloroethyl)amine led to the most stable urea (I*c*) examined, analogous reaction with N-bis(2-bromoethyl)amine again led to a relatively unstable urea which was more conveniently characterized as oxazolidine IV*d*.

EXPERIMENTAL[9]

N-Phenyl-N′-bis(2-chloroethyl)urea(Ia)

A 20 g (0.112 mole) sample of N-bis(2-chloroethyl)amine hydrochloride (ref. 11, footnote 23) was neutralized with cold (ice bath) 10% sodium hydroxide solution. The amine was extracted with diethyl ether (3 × 100 ml) and the combined extract was washed with water and dried successively over magnesium sulfate and calcium sulfate. The ethereal solution was cooled (ice bath) and a solution of phenyl isocyanate (13.4 g, 0.112 mole) in dry diethyl ether (75 ml) was added. After approximately 3 min, the colorless crystalline product began to separate from solution. Cooling was continued for 30 min before collecting the product; yield 21.2 g (73%), m.p. 72–74°. Four recrystallizations from ethyl acetate – benzene provided an analytical sample as needles melting at 76–78° (lit. (3) m.p. 74–75°); p.m.r. response ($CDCl_3$ solution) 3.58 (8 methylene protons) and 6.82–7.15 (5 phenyl protons) δ; ν_{max}^{KBr} 3 100, 1 670, 1 635, 1 595, 1 440, 760–755, and 695 cm^{-1}.

Anal. Calcd. for $C_{11}H_{14}Cl_2N_2O$: C, 50.60; H, 5.41; Cl, 27.15; N, 10.72. Found: C, 50.72; H, 5.11; Cl, 27.16; N, 10.92.

1-Phenyl-2-oxo-3-(2′-chloroethyl)imidazolidine(II)

Method A

A 5.0 g specimen of phenyl urea I*a* was heated (steam bath) for approximately 30 h. The remaining pale-yellow residue weighed 4.3 g. Two recrystallizations from ethanol (95%) – methanol yielded a pure specimen

[6]*In this regard, several N-bis(2-chloroethyl)carbamates have been prepared (7), but possible intramolecular rearrangement reactions involving these substances have apparently not been evaluated.*

[7]*For example, see ref. 8, p. 36.*

[8]*Several reactions pertinent to this assignment have been described (6, 9). The products arising from rearrangement of N-phenyl and N-benzyl-N′-(2-chloroethyl)ureas have been assigned oxazoline structures. See also ref. 10.*

[9]*Melting points were observed employing a Kofler melting point apparatus and are corrected. Dr. R. A. Hill of this laboratory provided the infrared and proton magnetic resonance spectra. The p.m.r. spectra were obtained using a Varian Associates Model A-60 NMR Spectrometer. When deuterium oxide was employed as solvent, a sealed capillary tube containing tetramethylsilane (TMS) was added to the sample tube. Otherwise, enough tetramethylsilane was added to the solution (containing approximately 10% by weight of sample) to standardize the instrument. Scanning was performed from low to high field at a rate of 120 c.p.s. per min and measurements are reported in δ (p.p.m.) units with respect to TMS. Elemental compositions were determined in the microanalytical laboratory of Dr. A. Bernhardt, Max-Planck Institute, Müilheim, Germany. Molecular weight determinations (by mass spectrometry) were provided by Dr. R. Ryhage, Karolinska Institutet, Stockholm, Sweden.*

of colorless leaflets melting at 94–94.5°; p.m.r. response ($CDCl_3$ solution) 3.53 (partially masked triplet corresponding to 8 protons) and 6.8–7.4 (5 phenyl protons) δ; ν_{max}^{KBr} 2 900 (weak), 1 685, 1 594, 1 505, 1 490, 1 285, 1 150, and 755 cm^{-1}.

Anal. Calcd. for $C_{11}H_{13}ClN_2O$(225): C, 58.78; H, 5.83; Cl, 15.79; N, 12.47. Found: C, 58.77; H, 5.65; Cl, 15.75; N, 12.61; molecular weight, 225.

Method B

When the urea (I*a*, 0.3 g) was heated at 140° for 24 h in a sublimation tube (at 0.1 mm), 0.1 g, m.p. 92–93°, of the imidazolidone (II) was collected. Found: C, 58.66; H, 5.75; Cl, 16.02; N, 12.23.

2-(N-Phenylimino)-3-(2'-chloroethyl)oxazolidine(IVa) Hydrochloride

A solution of N-phenyl urea I*a* (1.0 g) was prepared in absolute ethanol (10 ml) at room temperature. Before concentration (*in vacuo*, at room temperature) to a viscous oil, the clear solution was allowed to stand approximately 15 h. The oil crystallized during an overnight drying (*in vacuo*) period. An infrared spectrum of the crude product indicated conversion to the oxazolidine was essentially complete, as absorption attributable to N—H or carbonyl was not observed. Three recrystallizations from ethanol – ethyl ether yielded an analytical sample as colorless needles; m.p. 96–97°; p.m.r. response (D_2O solution) 4.25–4.6, 4.95–5.15, and 7.60 δ; ν_{max}^{KBr} 3 400 (weak), 2 750, 1 670 (broad), 1 590, 1 510, 1 275, 1 230, 1 080, 1 030, 980, 900, and 755 cm^{-1}.

Anal. Calcd. for $C_{11}H_{14}Cl_2N_2O$: C, 50.60; H, 5.41; Cl, 27.15; N, 10.72. Found: C, 50.64; H, 5.40; Cl, 26.99; N, 10.70.

N-(1-Naphthyl)-N'-bis(2-chloroethyl)urea(Ib)

Preparation of urea I*b* (14.8 g, 85% yield, m.p. 123–126°) was accomplished using 1-naphthyl isocyanate (9.5 g) and the amine corresponding to 10 g of N-bis(2-chloroethyl)amine hydrochloride in dry diethyl ether (300 ml) as illustrated for synthesis of phenyl urea I*a*. Recrystallization (three times) from acetone afforded an analytical sample as colorless crystals melting at 124–125°; p.m.r. response ($CDCl_3$ solution) 3.64 and 7.02–7.70 (complex) δ; ν_{max}^{KBr} 3 120, 1 670, 1 630, 1 595, 1 515, 1 500, 790, and 770 cm^{-1}.

Anal. Calcd. for $C_{15}H_{16}Cl_2N_2O$: C, 57.90; H, 5.18; Cl, 22.78; N, 9.00. Found: C, 57.75; H, 5.31; Cl, 22.81; N, 8.97.

Naphthyl urea I*b* did not exhibit any change in its infrared spectrum after storage in a sealed container for approximately 1 year.

2-[N-(1'-Naphthyl)imino]-3-(2'-chloroethyl)oxazolidine(IVb) Hydrochloride

A solution of naphthyl urea I*b* (0.5 g) in absolute ethanol (10 ml) was allowed to stand at room temperature 5 h. Addition of dry diethyl ether (100 ml) precipitated 0.28 g of colorless crystals. An infrared spectrum of the crude product exhibited no absorption in the N—H stretching region. Three recrystallizations from ethyl alcohol – ethyl ether led to needles melting at 147–151°. Further recrystallization (using the same solvent) did not improve the melting point. The p.m.r. spectrum (D_2O) displayed a series of complex responses at 4.38–4.55, 4.86–5.15, and 7.70–8.23 δ. The infrared spectrum (ν_{max}^{KBr}) of oxazolidine IV*b* exhibited principal absorption bands at 2 700 (broad), 1 660 (broad), 1 270, 1 105, and 1 030 cm^{-1}.

Anal. Calcd. for $C_{15}H_{16}Cl_2N_2O$: C, 57.90; H, 5.18; Cl, 22.78; N, 9.00. Found: C, 57.53; H, 5.31; Cl, 22.84; N, 8.86.

N-(4-Nitrophenyl)-N'-bis(2-chloroethyl)urea(Ic)

Employing the amine from 5.45 g of N-bis(2-chloroethyl)amine hydrochloride, and *p*-nitrophenyl isocyanate (5.0 g), preparation of *p*-nitrophenyl urea I*c* was accomplished in 79% yield (7.4 g, m.p. 137–140°). In this case, the colorless urea began to separate from solution within a few seconds after initiation of the reaction. On exposure to the atmosphere, the colorless product became pale yellow. Following three recrystallizations from ethyl acetate – hexane a pure specimen melted at 142–144° (cf. ref. 4*a*); p.m.r. response (CH_3CN solution) 3.65 and a quartet (J = 10 c.p.s.) at 7.38, 7.53, 7.85, and 8.0 (4 phenyl protons) δ; ν_{max}^{KBr} 3 100, 1 642, 1 610, 1 590, 1 545, and 1 500 cm^{-1}.

Anal. Calcd. for $C_{11}H_{13}Cl_2N_3O_3$: C, 43.15; H, 4.28; Cl, 23.17; N, 13.73. Found: C, 43.36; H, 4.22; Cl, 23.16; N, 13.63.

The *p*-nitrophenyl urea (I*c*) remained unchanged (as evidenced by its infrared spectrum) during storage in a sealed container for over 2 years.

2-(N-Phenylimino)-3-(2'-bromoethyl)oxazolidine(IVc) Hydrobromide

A dry ethereal solution of N-bis(2-bromoethyl)amine from 15 g of the corresponding hydrobromide derivative (12) was allowed to react at 0–5° with phenyl isocyanate (5.75 g) as described for preparation of urea I*a*. The solid product (12.5 g, 75%) which separated displayed an infrared spectrum consistent with that expected for *N-phenyl-N'-bis(2-bromoethyl)urea*. However, during a 4-day period at room temperature, the urea rearranged to oxazolidine IV*a* hydrobromide. An infrared spectrum (in potassium bromide) of the product indicated conversion to the oxazolidine was complete. Four recrystallizations of the new product from ethanol (95%) – diethyl ether led to a pure sample of colorless needles; m.p. 118–119° and ν_{max}^{KBr} 2 900 (broad), 1 670 (broad), 1 595, 1 512, 1 280, 1 075, 975, 750, and 690 cm^{-1}. The p.m.r. spectrum (in D_2O) exhibited complex responses at 4.0–4.55 and 5.0–5.17 δ, and a sharp band at 7.62 δ.

Can. J. Chem. Downloaded from www.nrcresearchpress.com by 210.87.254.5 on 09/05/12
For personal use only.

Anal. Calcd. for $C_{11}H_{14}Br_2N_2O$: C, 37.74; H, 4.03; Br, 45.65; N, 8.01. Found: C, 37.94; H, 3.87; Br, 45.92; N, 7.95.

2-[N-(4'-Nitrophenylimino)]-3-(2'-bromoethyl)oxazolidine(IVd) Hydrobromide

Reaction between the amine from N-bis(2-bromoethyl)amine hydrobromide (12.0 g) and *p*-nitrophenyl isocyanate (6.32 g) in diethyl ether (150 ml) was conducted as noted in the case of urea I*a*. The colorless solid which began to separate immediately (from the reaction mixture) was collected after 20 min. On exposure to the atmosphere urea I*d* (12.6 g, 83%), m.p. 121–124°, became pale yellow. The infrared spectrum (in potassium bromide) was in complete accord with a N-(4-nitrophenyl)-N'-bis(2-bromoethyl)urea (I*d*) structure. The urea was found to rearrange readily in polar solvents (such as acetone) and was, therefore, more conveniently characterized as the oxazolidine derivative (IV*d*). A 1.0 g specimen of urea I*d* was dissolved in 25 ml of warm ethanol. Immediately after dissolution the crystalline oxazolidine began to separate. Following a 12 h period at room temperature, the product (0.72 g) was collected. Three recrystallizations from ethanol – ethyl ether yielded an analytical sample of yellow platelets melting over the range 134–144° with sintering from 120°; ν_{max}^{KBr} 2 890 (broad), 1 685, 1 590, 1 520, 1 340, 1 250, and 1 075 cm^{-1}.

Anal. Calcd. for $C_{11}H_{13}Br_2N_3O_3$: C, 33.44; H, 3.32; Br, 40.45; N, 10.63. Found: C, 33.52; H, 3.38; Br, 40.42; N, 10.54.

ACKNOWLEDGMENTS

This investigation was aided by Grants No. T-79D and T-79E from the American Cancer Society. We also wish to acknowledge the assistance of R. C. Bansal, K. Parent, and P. A. Whitehouse with several preliminary experiments.

REFERENCES

1. (*a*) G. R. PETTIT, D. S. BLONDA, and E. C. HARRINGTON. Can. J. Chem. **41**, 2962 (1963). (*b*) F. BERGEL. J. Pure Appl. Chem. **6**, 351 (1963).
2. O. M. FRIEDMAN and A. M. SELIGMAN. J. Am. Chem. Soc. **70**, 3082 (1948).
3. R. PREUSSMANN. Arzneimittel-Forsch. **8**, 9 (1958); Chem. Abstr. **52**, 9439 (1958).
4. (*a*) F. D. POPP and H. SWARZ. J. Org. Chem. **26**, 4764 (1961). (*b*) F. D. POPP and D. W. ALWANI. Can. J. Chem. **42**, 1506 (1964). (*c*) E. KHEDOURI, Y. KIM, and O. M. FRIEDMAN. J. Med. Chem. **7**, 653 (1964).
5. A. Y. BERLIN and I. S. LEVI. Zh. Obshch. Khim. **33**, 846 (1963).
6. S. GABRIEL and R. STELZNER. Chem. Ber. **28**, 2937 (1895).
7. R. RAILEANU and E. CIORANESCU. Acad. Rep. Populare Romine Studii Cercetari Chim. **11**, 433 (1963); Chem. Abstr. **60**, 15938 (1964). M. H. BENN, A. M. CREIGHTON, L. N. OWEN, and G. R. WHITE. J. Chem. Soc. 2365 (1961). T. F. NOGRADY. J. Org. Chem. **26**, 4177 (1961).
8. K. NAKANISHI. Infrared absorption spectroscopy. Holden-Day, Inc., San Francisco. 1962. p. 47.
9. A. F. MCKAY. J. Org. Chem. **16**, 1395 (1951). A. F. MCKAY, M. A. WEINBERGER, J. P. PICARD, W. G. HATTON, M. BEDARD, and H. E. ROONEY. J. Am. Chem. Soc. **76**, 6371 (1954). R. B. MOFFETT. J. Med. Chem. **7**, 319 (1964). F. F. EBETINO. J. Org. Chem. **29**, 2582 (1964). F. L. SCOTT and D. F. FENTON. Tetrahedron Letters, 1681 (1964).
10. M. R. KAMAL and J. E. WICKLATZ. Can. J. Chem. **42**, 1500 (1964).
11. G. R. PETTIT, M. F. BAUMANN, and K. N. RANGAMMAL. J. Med. Pharm. Chem. **5**, 800 (1962).
12. G. R. PETTIT, M. R. CHAMBERLAND, D. S. BLONDA, and M. A. VICKERS. Can. J. Chem. **42**, 1699 (1964).

Can. J. Chem. Downloaded from www.nrcresearchpress.com by 210.87.254.5 on 09/05/12
For personal use only.

Can. J. Chem. Downloaded from www.nrcresearchpress.com by 210.87.254.6 on 09/05/12
For personal use only.

LIGHT SCATTERING OF A CRITICAL BINARY LIQUID MIXTURE: TRIETHYLAMINE–WATER[1]

B. CHU[2] AND W. P. KAO
Chemistry Department, The University of Kansas, Lawrence, Kansas

Received January 22, 1965

ABSTRACT

The coexistence curve and critical opalescence of a binary liquid mixture, triethylamine–water, have been reinvestigated. The measurements showed that the coexistence curve appears to follow a cubic relation to within about 0.003° of the critical solution temperature, and in this range, there is no evidence of a flat region. Furthermore, within the range of the values of s/λ (where $s = 2 \sin(\theta/2)$, λ = wavelength in the medium, and s/λ varied from 1.2×10^{-4} to 7.0×10^{-4} Å^{-1}) and temperatures studied, the light scattering data are in good agreement with the Debye theory (J. Chem. Phys. 31, 680 (1959)). The molecular interaction range of Debye was found to be 5.1 ± 0.3 Å.

The large density fluctuations of any system near its critical point are accompanied by local fluctuations in refractive index. Such a system, being optically inhomogeneous, scatters light very strongly and therefore it looks turbid. This is the so-called "critical opalescence." An equation for light scattering from a critical binary liquid mixture can be formulated as follows (1):

$$[1] \quad I(\theta) = I_d(\theta) + I_c(\theta)$$
$$= I_0 \frac{4\pi^2 V}{\lambda^4 r^2} \frac{1+\cos^2\theta}{2}\left[kT\beta\left(\frac{\rho}{n}\frac{\partial n}{\partial \rho}\right)^2 + \left(\left(\frac{c}{n}\frac{\partial n}{\partial c}\right)^2 \Big/ \left\{\phi_2\left[\frac{\partial}{\partial \phi_2}\left(\frac{P}{kT}\right)\right] + 4\pi^2\phi_2{}^2\left(\frac{H}{kT}\right)\left(\frac{s}{\lambda}\right)^2\right\}\right)\right],$$

where $I(\theta)$ is the intensity of light scattered at an angle θ (between secondary and primary ray) at a large distance r from a scattering volume V, I_d and I_c are scattered intensities due to density and concentration fluctuations, respectively, I_0 is the primary intensity, λ is the wavelength of the light in the medium, k is the Boltzmann constant, T is the absolute temperature, β is the compressibility, ρ is the density, n is the index of refraction, c is the concentration of the second component, P is the osmotic pressure, ϕ_2 is the volume fraction of the second component, and the symbol H represents a factor (2) of the following form.

$$H = \frac{1}{6}\left[\frac{W_{11}}{\omega_1{}^2} l_{11}{}^2 + \frac{W_{22}}{\omega_2{}^2} l_{22}{}^2 - 2\frac{W_{12}}{\omega_1\omega_2} l_{12}{}^2\right],$$

where l_{ij} is the respective range of molecular forces of component 1, component 2, and the mixture. The expressions $W_{ij}/\omega_i\omega_j$ represent the respective cohesive energy densities. Equation [1] is a classical scattering formula corrected for the effect of the energy connected with the existence of local gradients of concentration fluctuations. It is an approximation which breaks down if we extend our measurements over large ranges of s/λ by means of small angle X-ray scattering (3, 4, 5). Furthermore, very long range

[1]*This work was supported by the National Science Foundation (GP 3922).*
[2]*Author to whom requests for reprints should be addressed.*

correlations have not been taken into account. However, it is an adequate representation of experimental facts for critical opalescence of binary liquid mixtures at intermediate temperature distances and in the visible region ($\lambda_0 \cong 365$–600 mμ; $\theta \cong 20$–$145°$). It is also important to note that for a critical binary liquid mixture, the fluctuations are there whether one can observe the opalescence visually or not. The effect may be more pronounced for liquid mixtures with larger refractive index differences in the two components. Therefore, it is somewhat misleading to identify the visibly opalescent region as a separate entity in the one phase region (6). Experimental light scattering data on strongly opalescent critical binary liquid mixtures (7) showed an absence of two kinds of fluctuations as suggested by Hildebrand (8). We chose the system triethylamine–water in order to demonstrate similarities, which may exist in terms of critical opalescence, among systems with upper and lower critical solution points. In fact, triethylamine–water is a relatively troublesome system, partly because it is difficult to make the mixture (water being polar) dust-free and partly because triethylamine seems to attack Pyrex glass.

Reviews of both theory (9, 10) and experiment (7) on critical opalescence have been presented elsewhere. Opalescence of the system, triethylamine–water, near the critical solution temperature has been investigated by Chow (11) and the results on coexistence curves have been summarized (12). Discrepancies in both opalescence (7, 11, 13) and coexistence curve (12, 14) measurements have also prompted us to repeat this system with refined techniques.

EXPERIMENTAL

Materials

Water.—Ion-exchanged water was doubly distilled with an all-Pyrex still fitted with a double vapor bulb (Fisher No. 9-107). Care was taken to exclude CO_2 with a drying tube containing Ascarite.

Triethylamine.—Our triethylamine samples could not be purified by fractional distillation. So, the material was purified by preparative gas chromatography on an Aerograph model A-700 Autoprep vapor fractometer (Wilkens Instrument and Research, Inc.). A 20 ft long × 3/8 in. outside diameter column packed with 30% SE-30 (a General Electric methyl silicone rubber) on 40/60 chromosorb P, operated at 147 °C and 40 p.s.i.g. was used. Flow rates of helium carrier gas were around 200 ml/min. The injection volume was limited to 0.2 ml each time and a short cut in the main peak was collected under helium. Impurities were estimated as being less than 0.01% for the purified triethylamine (purified grade, J. P. Baker Chemical Co.) and less than 0.1% for the purified material purchased from the Matheson, Coleman and Bell Co. The MCB triethylamine had its impurity peak very close to the main peak.

Phase Separation Temperature Measurements

A cleansed 1.3 × 1.3 × 0.1 cm thick flat cell fitted with a 20 cm long and 0.5 cm diameter stem and Teflon stopcock was dried in an oven at 105 °C and stored in a desiccator (or dust-free container) until used. The solutions were prepared from weighed amounts of the purified components. The flat cell was immersed in a large insulated bath fitted with a cooling coil for thermostated circulating cooling fluid and two heaters connected with variable transformers. With vigorous stirring the whole bath could be very slowly heated or cooled from appropriate adjustments of the two heater outputs. This setup was more convenient than a conventional constant temperature bath for phase separation temperature determinations so long as the temperature of the bath could not be changed with the same ease as its controlled precision. With very slow rates of cooling and heating, the phase separation temperature could be determined to 0.001°. In our case, a calibrated Beckman thermometer was used. For concentrations near the critical solution concentration, phase separation temperatures were determined to within 0.002° while for those further away, separation temperatures were determined to within 0.01°. The dead space above the sample in the flat cell was about 4 cc. There should be no appreciable error in composition due to material in the vapor phase.

When measuring the separation temperature of a sample, it was cooled and thoroughly shaken before immersing it in the bath. Then the temperature of the bath was raised (or lowered) slowly and finally at a very slow rate in the vicinity of the phase separation temperature. Two approaches were used: (*a*) slowly heat the homogeneous mixture with shaking until phase separation occurred, and (*b*) slowly cool the separated mixture with shaking until it became homogeneous. Results from (*a*) and (*b*) agreed to within 0.002° for concentrations near the critical solution concentration. Furthermore, phase separation temperatures determined by means of a flat cell agreed, within the limits of error, with those determined in sealed ampuls. It should be noted that the consolute temperature changed with time. At our critical solution concentration, the change amounted to −0.18° over a period of about 105 d for a sample preserved in a

Can. J. Chem. Downloaded from www.nrcresearchpress.com by 210.87.254.6 on 09/05/12
For personal use only.

Pyrex glass cell which was fitted with a Teflon stopcock and then sealed with paraffin wax. Kohler and Rice (14) attributed this lowering of the consolute temperature to possible attacks of ordinary glass by triethylamine and used quartz cells instead. We always tried to complete our measurements in a few days from freshly prepared samples.

Near-Infrared Spectra

The critical solution mixture was prepared from weighed amounts of purified components. The thermostat block was essentially the same as in previous work (15, 16). Measurements were carried out with a Cary model 14 recording spectrophotometer. All measurements were made in cells with 1 cm optical path length. Carbon tetrachloride was filled in the light path of the cell block to ensure uniform temperature control. The absorbancies ($A_s = -\log I/I_0$) were determined relative to a cell that contained CCl_4, which partially compensated for the CCl_4 in the light path of the sample cell block. Background amounting to $A_s = 0.02$ was not corrected. Temperature of the cell block was controlled to $\pm 0.01°$. However, the near-infrared radiation could heat up the sample rapidly, so only the absorption bands of water and triethylamine at room temperature, and the mixture at a large temperature distance ($\Delta T = T_c - T = 11.3°$) in the 0.9–1.3 μ region were recorded. Those for the critical binary liquid mixture at smaller temperature distances ($T_c - T < 1°$) were measured manually point by point. Then, the sample was exposed to the beam only a few seconds at a time for the recorder to register the absorbancy, which was checked until it could be reproduced. The time interval between each measurement was extended to about 25 min to ensure a uniform temperature distance (ΔT) over the whole absorption bands.

Light Scattering Measurements

Detailed descriptions of the light scattering photometer (1, 7, 17), preparation of solutions, phase separation temperature determinations, and attenuation corrections due to critical opalescence are discussed elsewhere (1, 7). The light scattering photometer was further modified as follows: four 10 × 1 mm slits immersed in the thermostated tank were used to define the incident beam, while a receiver nosepiece with dimensions 10 × 1 mm, and 20 mm apart, was used. Each purified component was further treated by filtration through Millipore filters of 50 mμ average pore size directly into the light scattering cell, which was fitted with a Teflon stopcock. The filter was tested to be inert to both components. The temperature of phase separation, T_p, was again determined directly in the light scattering photometer to 0.01° by slowly heating the homogeneous mixture, at a rate of approximately 0.001° per minute, until phase separation occurred. A filtered fluorescein solution was used as a standard for periodic checks of the performance of the photometer.

Refractive indices of the critical liquid mixture at different wavelengths (λ_0 364, 436, and 575 mμ) were calculated from an empirical mixture rule (16) with the aid of known dispersion curves and densities (18). The calculated corresponding wavelengths in the medium are λ = 268, 321, and 428 mμ respectively.

RESULTS AND DISCUSSION

Coexistence Curve

Values of the critical solution temperature for the system, triethylamine–water, varied from 12.4 to 19.9 °C in the literature (12). Since the separation temperature of a mixture is a sensitive indicator of the state of purity of the components, the variations clearly signify a lack of high-precision measurements of coexistence curves on highly purified systems. Our coexistence curve, as shown in Fig. 1, is not comparable to the work of Rice *et al.* on the system perfluoromethylcyclohexane – carbon tetrachloride (19), but approaches the precision of the work on the system aniline–cyclohexane (20). Cox and Herrington (21) have reported that solubility data may be represented as follows:

$$(T_D - T_c) = \left[A' \log \frac{X'}{1-X'} + B' \right]^3$$

and

$$(T_D - T_c) = \left[A'' \log \frac{X''}{1-X''} + B'' \right]^3,$$

in which $'$ and $''$ refer to the two coexisting phases, T_D is the consolute temperature, and T_c is the critical solution temperature corresponding to the minimum consolute temperature. The constants A' and A'' have also been discussed by Rudd and Widom (22). Figure 2 provides another method for determining the critical solution concentration. The result agrees with the value determined from Fig. 1. Our measurements showed that the coexistence curve appears to follow a cubic relation to within about 0.003° of the critical solution temperature, and in this range, there is no evidence of a flat region.

Can. J. Chem. Downloaded from www.nrcresearchpress.com by 210.87.254.6 on 09/05/12
For personal use only.

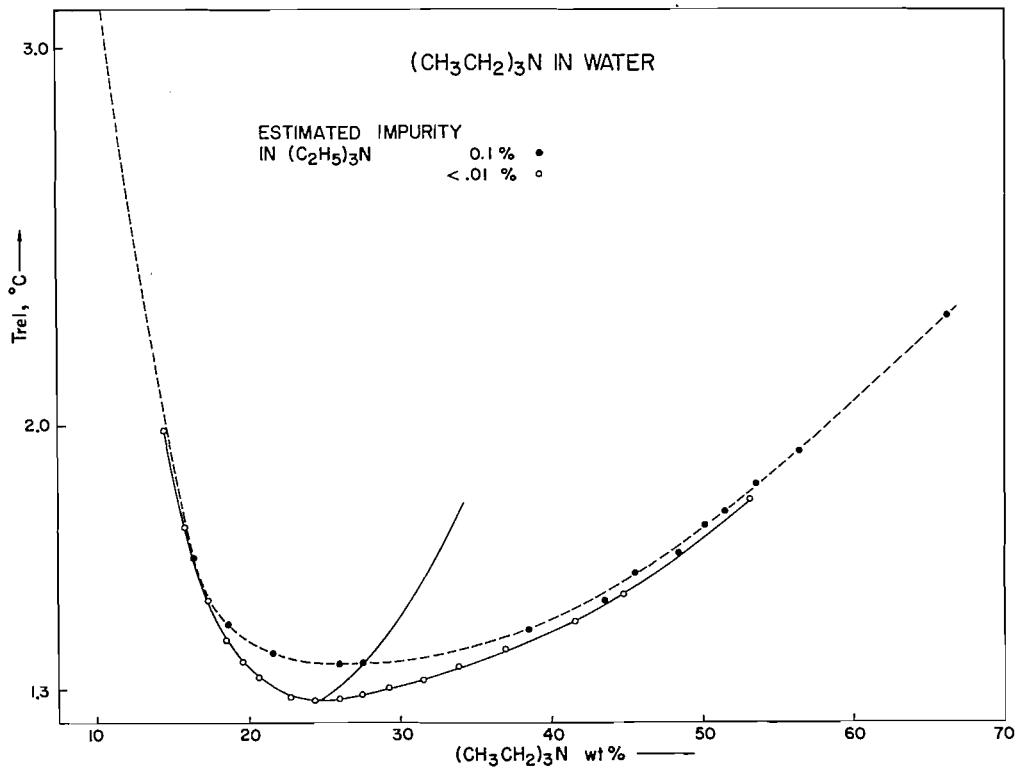

FIG. 1. Plot of phase separation temperature vs. weight concentration. T_p* (minimum phase separation temperature) = T_c = 1.27° (rel. unit) = 18.3$_8$ °C. The curved line segment represents the average concentration of two coexisting phases (<0.01% impurity) at different temperatures.

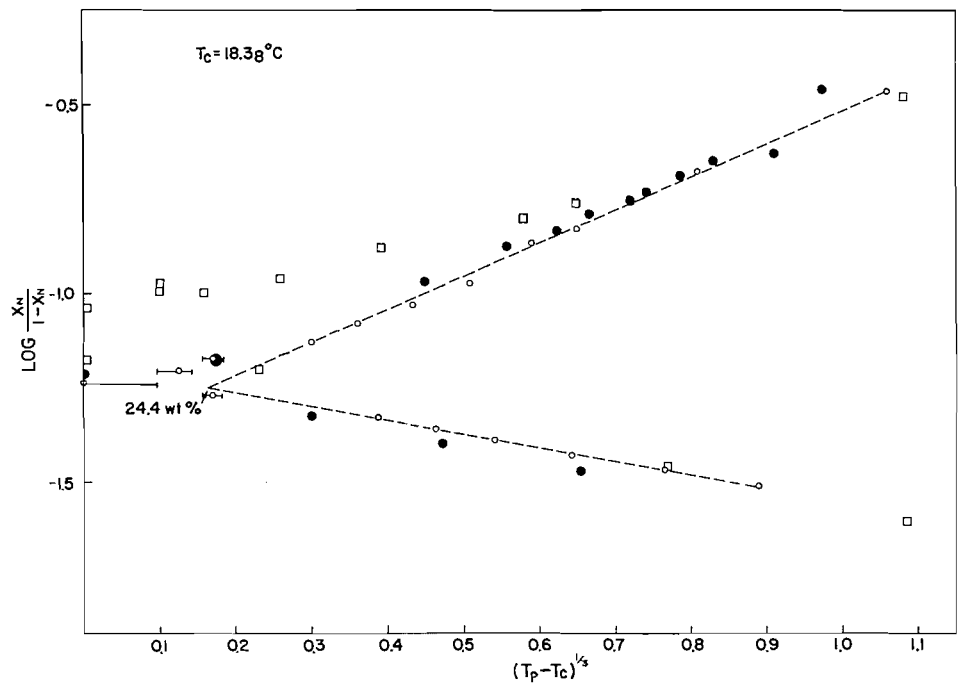

FIG. 2. Plot of log $(X_N/1 - X_N)$ vs. $(T_p - T_c)^{1/3}$, where subscript N denotes triethylamine and X denotes mole fraction: ○ <0.01% impurity; ● 0.1% impurity; □ ref. 14 with T_c = 18.330 °C.

Can. J. Chem. Downloaded from www.nrcresearchpress.com by 210.87.254.6 on 09/05/12
For personal use only.

The data are in qualitative agreement with those of Kohler and Rice (14). In both cases, the cubic equation remains a good representation of the coexistence curve except when $T_p - T_c$ is very small. The discrepancy in the critical solution concentration could possibly be accounted for in terms of impurities in triethylamine. We are, however, unable to prove the possible existence of a small horizontal portion in the coexistence curve. Since the system behaves normally otherwise, we see no compelling reason to hunt for the existence of such a flat top.

Critical Opalescence

The treatment of data according to the Debye theory is described elsewhere (1). Equation (1) may be presented in a simpler form as follows:

$$[2] \qquad \frac{1}{I} = F(T)\left(\frac{T_c}{T}\right)\left[\frac{\Delta T}{T_c} + \frac{8\pi^2}{3} l^2 \frac{\sin^2(\theta/2)}{\lambda^2}\right] = A + B \sin^2(\theta/2).$$

Figure 3 shows a typical set of intensity curves in a plot of reciprocal relative scattered

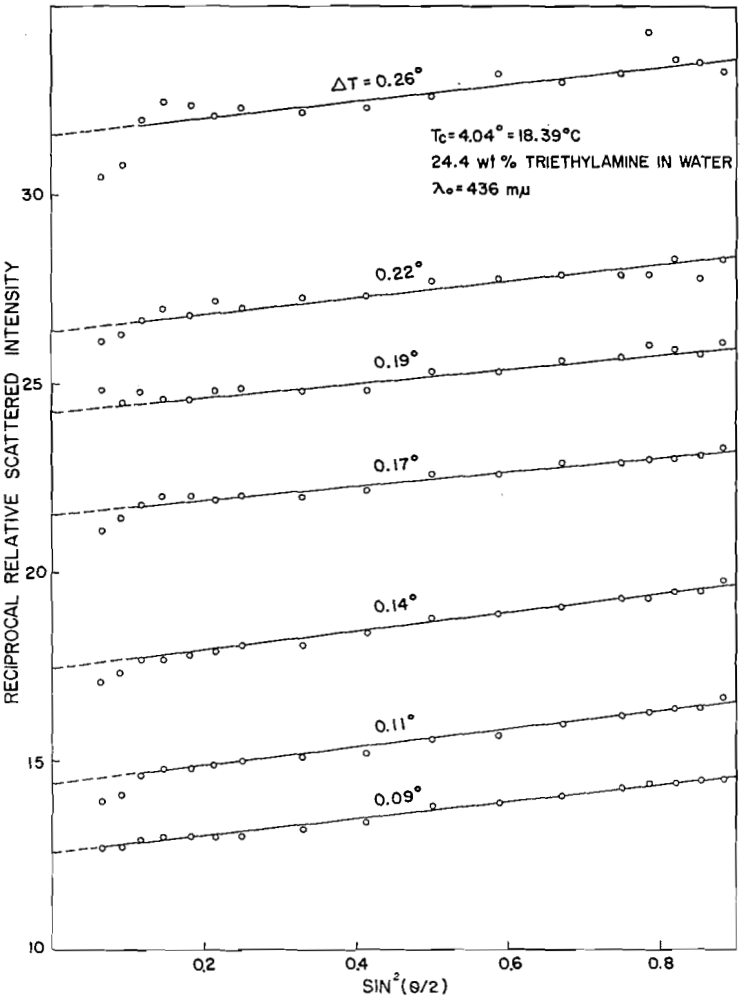

FIG. 3. Plot of reciprocal relative scattered intensity vs. $\sin^2(\theta/2)$.

Can. J. Chem. Downloaded from www.nrcresearchpress.com by 210.87.254.6 on 09/05/12
For personal use only.

intensity vs. $\sin^2(\theta/2)$. Such a plot is sometimes referred to as an OZD plot. Only a faint opalescence could be observed at small fixed temperature distances from the critical solution temperature because of low scattered intensity. For the same reason, the presence of dust was detected at small values of the scattering angle (Fig. 3, curve $\Delta T = 0.26°$). Figure 4 shows a plot of A/B vs. T for the three wavelengths we have investigated.

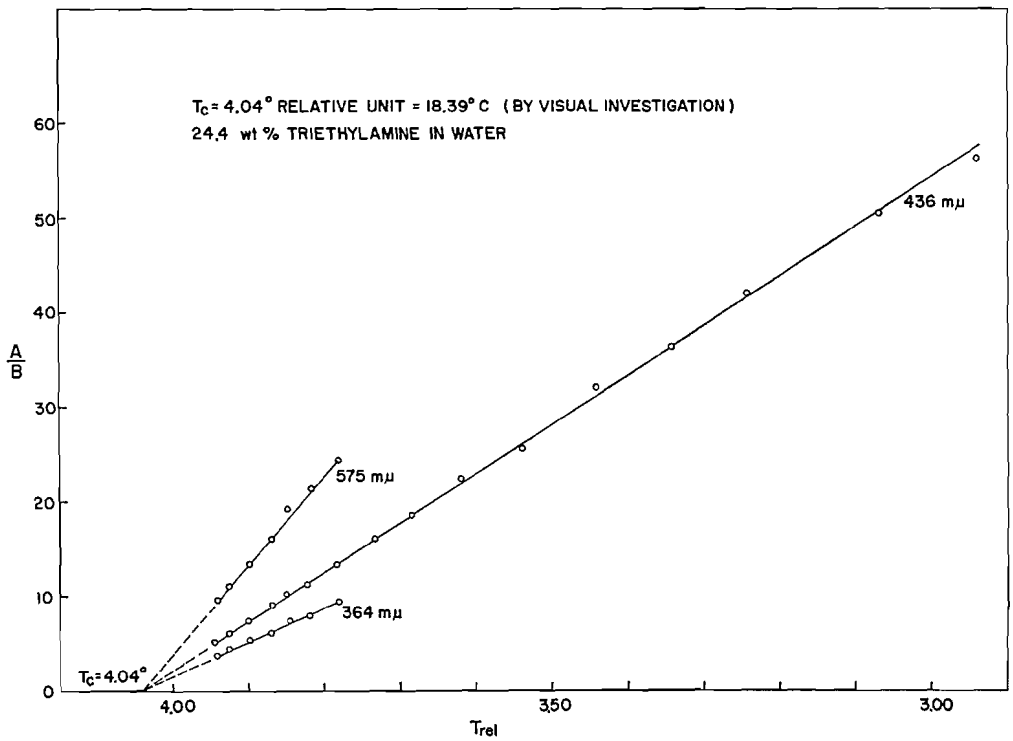

FIG. 4. Plot of A/B vs. temperature.

$$\frac{A}{B} = \left(\frac{3\lambda^2}{8\pi^2 l^2 T_c}\right)(T_c - T),$$

with $T_c = -(\text{intercept/slope})$ of the resulting straight line and $l = 5.1 \pm 0.3$ Å. It should be noted that the molecular interaction range of Debye differs from the short-range correlation length of Fixman (23) by a factor of $(4/15)^{1/2}$ for one component systems. The two lengths do not have exactly the same meaning. According to the (approximate) Debye theory, the interaction range is a property of the averaged intermolecular pair potential and is a constant which should be independent of frequency.

The Critical Region

In the vicinity of the critical point, the equilibrium of the *one* phase system for a binary liquid mixture is near its limit of stability. Appreciable changes in this equilibrium may be induced by outside agencies, such as an applied gravitational field (8) or an electric field (24). In this respect, ultrasonic disturbances may influence the true critical behavior of the system under observation. We question the postulation of two kinds of fluctuations (6, 8): composition variations and fluctuations within such regions; or the system in two phases, yet not distinctly separated phases, but as regions in a type of emulsion when

Can. J. Chem. Downloaded from www.nrcresearchpress.com by 210.87.254.6 on 09/05/12
For personal use only.

strong visible opalescence is observed. The Debye theory (2) is an excellent representation of experimental facts in the intermediate temperature range. As the critical solution temperature is approached, light scattering is increased because of inhomogeneities produced by concentration fluctuations. "Reflection from the composition gradients between the regions of different composition," as stated by Kruus (6), is but another consequence of critical fluctuations. We see no microscopic phase separation in the opalescent one phase region. No abrupt change in intensity was observed as shown in Fig. 5. The behaviors of the strongly opalescent and the weakly opalescent systems are analogous (compare Fig. 5 and ref. 7, Fig. 2). Furthermore, the concentration fluctuation term (eq. [1]) exists even when ΔT is large. It becomes predominant as T approaches T_c. There is no actual separate region in a type of emulsion that one can distinguish optically.

We have also measured the near-infrared spectra of the critical liquid mixture at different fixed temperature distances from the critical solution temperature. Since the

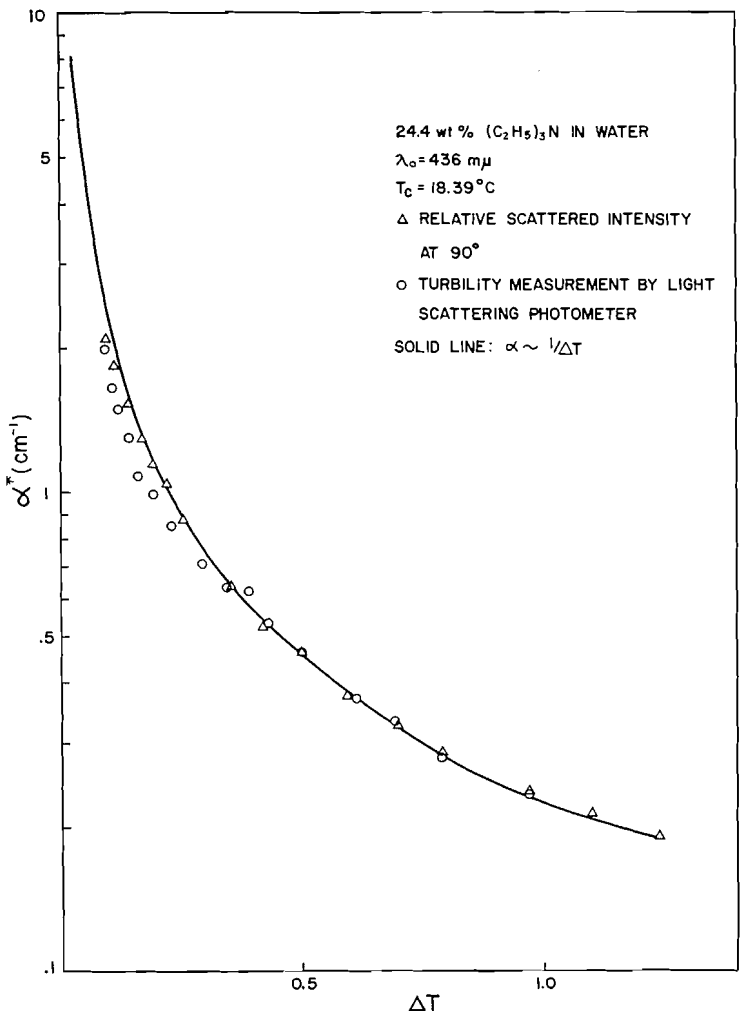

FIG. 5. Plot of extinction coefficient α^* (cm^{-1}) vs. $T_c - T$, where $\alpha^* = 2.303 \log I_0/I$ and I_0 is the transmitted intensity at $T_c - T \sim 5°$.

Can. J. Chem. Downloaded from www.nrcresearchpress.com by 210.87.254.6 on 09/05/12
For personal use only.

system has a minimum critical mixing temperature, resulting from sufficiently large negative deviations from Raoult's law which in many instances can be traced to possible complex formation, the vibrational transition bands in the near-infrared region may reveal changes in the intramolecular structure of the two components. The absorption bands of pure water in the 1.1–1.3 μ region have been measured (25). Within the limits of our experiments, we find a lack of frequency shifts and intensity changes between the homogeneous phase at various temperature distances from T_c and the composite phase, as shown in Fig. 6. Such a lack of change appears to signify that the phase separation behavior is essentially intermolecular in nature. On closer examination, the critical mixture contains only 0.054 mole fraction of triethylamine. So, it is not surprising that the absorption spectra remains approximately unchanged from a homogeneous phase to a heterogeneous phase.

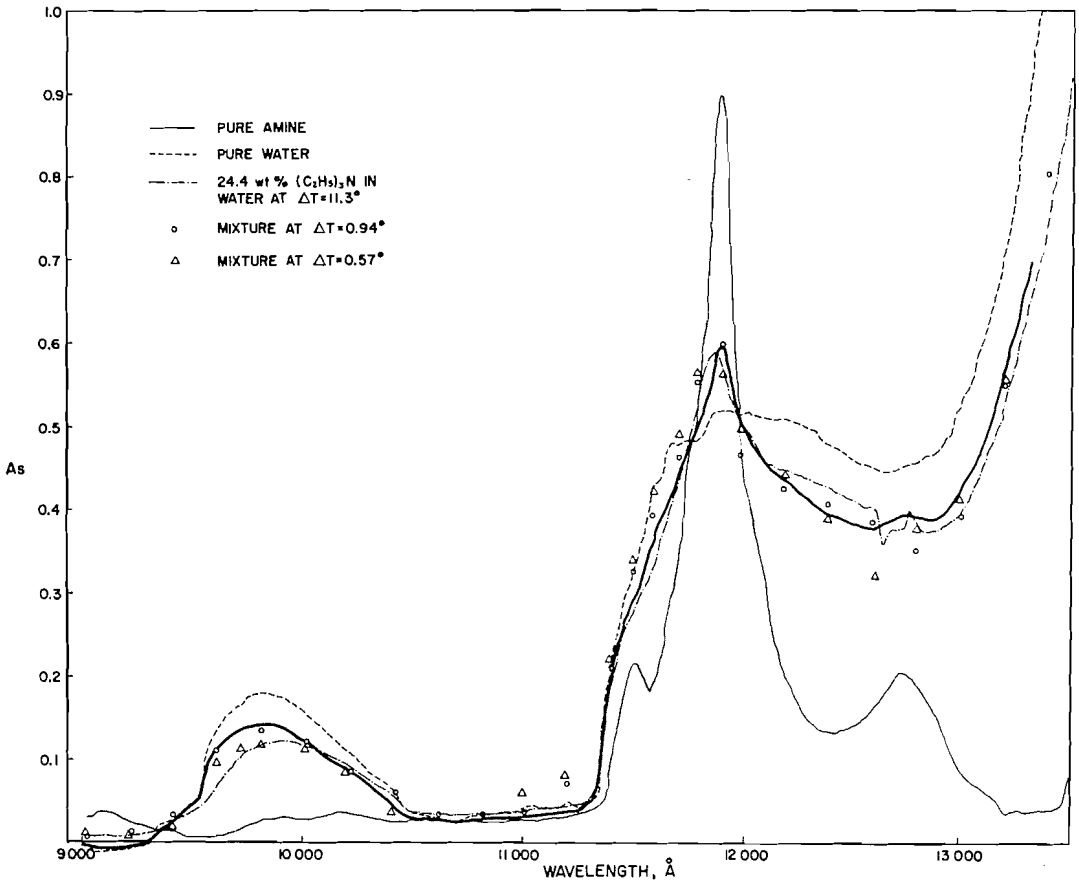

FIG. 6. Absorption bands of water, triethylamine, and the critical binary mixture at different values of $T_c - T$ in the 0.9–1.3 μ region. A_s = log I_0/I. Thick solid line = composite phase;

$$A_s \text{ (composite phase)} = \phi_{H_2O} A_{sH_2O} + \phi_N A_{sN},$$

where ϕ = volume fraction and the subscript N denotes triethylamine.

REFERENCES

1. B. CHU. J. Chem. Phys. **41**, 226 (1964).
2. P. DEBYE. J. Chem. Phys. **31**, 680 (1959).
3. B. CHU. J. Chem. Phys. **42**, 426 (1965).

Can. J. Chem. Downloaded from www.nrcresearchpress.com by 210.87.254.6 on 09/05/12
For personal use only.

4. P. DEBYE, D. CAULFIELD, and J. BASHAW. J. Chem. Phys. **41**, 3051 (1964).
5. B. CHU. Critical opalescence of a binary liquid mixture, *n*-decane-β,β'-dichloroethyl ether. II. Small-angle X-ray scattering. J. Chem. Phys. In press. 1965.
6. P. KRUUS. Can. J. Chem. **42**, 1712 (1964).
7. B. CHU. J. Am. Chem. Soc. **86**, 3557 (1964).
8. J. H. HILDEBRAND, B. J. ALDER, J. W. BEAMS, and H. M. DIXON. J. Am. Chem. Soc. **58**, 577 (1954).
9. M. FIXMAN. Advan. Chem. Phys. **6**, 175 (1964).
10. M. E. FISHER. J. Math. Phys. **5**, 944 (1964).
11. Q. CHOW. Proc. Roy. Soc. London, Ser. A, **224**, 90 (1954).
12. J. TIMMERMANS. The physico-chemical constants of binary systems in concentrated solutions. Vol. IV. Interscience. 1959. p. 77.
13. P. DEBYE, B. CHU, and H. KAUFMANN. J. Chem. Phys. **36**, 3378 (1962).
14. F. KOHLER and O. K. RICE. J. Chem. Phys. **26**, 1614 (1957).
15. P. DEBYE, D. WOERMANN, and B. CHU. J. Chem. Phys. **36**, 851 (1962).
16. B. CHU. J. Phys. Chem. **67**, 1969 (1963).
17. B. CHU. Rev. Sci. Instr. **35**, 1201 (1964).
18. J. TIMMERMANS. Physico-chemical constants of pure organic compounds. Elsevier Publishing Co., New York, N.Y. 1959.
19. D. R. THOMPSON and O. K. RICE. J. Am. Chem. Soc. **86**, 3547 (1964).
20. D. ATACK and O. K. RICE. J. Chem. Phys. **22**, 382 (1954). O. K. RICE. J. Chem. Phys. **23**, 164 (1955).
21. J. D. COX and E. F. G. HERRINGTON. Trans. Faraday Soc. **52**, 926 (1956).
22. DEF. P. RUDD and B. WIDOM. J. Chem. Phys. **33**, 1816 (1960).
23. M. FIXMAN. J. Chem. Phys. **33**, 1357 (1960).
24. P. DEBYE and K. KLEBOTH. An electric field effect on the critical opalescence. J. Chem. Phys. In press.
25 K. BUIJS and G. R. CHOPPIN. J. Chem. Phys. **39**, 2035 (1963).

Can. J. Chem. Downloaded from www.nrcresearchpress.com by 210.87.254.6 on 09/05/12
For personal use only.

Can. J. Chem. Downloaded from www.nrcresearchpress.com by 210.87.254.105 on 09/05/12
For personal use only.

A QUASI-CRYSTALLINE MODEL OF DIFFUSION IN TERNARY LIQUID SYSTEMS[1]

J. E. LANE[2] AND J. S. KIRKALDY[3]
Department of Metallurgy and Metallurgical Engineering, McMaster University, Hamilton, Ontario
Received December 28, 1964

ABSTRACT

A quasi-crystalline model of a dilute ternary liquid system is proposed in which diffusion occurs by an interchange of species on neighboring lattice sites. Nonelectrolyte molecules are assumed to interchange with any type of diffusing species present in the system. In ternary nonelectrolyte systems relatively large cross-effects are associated with the mutual interchange of the two dilute solute species. The symmetry of the L-matrix arises directly through the application of detailed balance (microscopic reversibility) to this unit process.

In electrolyte solutions, the only significant contribution to the ionic fluxes is expected to arise through interchange of ions with uncharged molecules. For diffusion in an aqueous solution of two strong electrolytes with a common ion, large off-diagonal L-coefficients result from the transformation of the lattice-referred diagonal diffusion matrix, written in terms of ionic fluxes and forces, to a form which relates the two independent salt fluxes and forces. Symmetry of the L-matrix in this case arises indirectly through the application of detailed balance to the ion-solvent interchanges. In aqueous electrolyte solutions the dilute solution ternary L-coefficients can be calculated from the independent individual ionic mobilities at infinite dilution, and these are found to be in excellent agreement with the experimental values for the system NaCl–KCl–H_2O. The application of the model to binary electrolyte solutions at infinite dilution correctly yields the Nernst equation.

The model is extended to solutions of two electrolytes with one or both incompletely ionized and to solutions containing a nonelectrolyte and a strong electrolyte. In all applications of the model the derived L-coefficients satisfy the well-known thermodynamic requirements. When appropriate ancillary data is available, the model yields fair to excellent predictions of the diffusion matrix at low concentrations of the solute species. Possible methods of improving the agreement at higher concentrations are discussed.

INTRODUCTION

In a recent paper (1), hereinafter referred to as I, diffusion in multicomponent substitutional alloys was described in terms of two separate microscopic models, an exchange mechanism and a vacancy mechanism. Both models indicate a similar concentration dependence of the L-coefficients in the number-fixed frame of reference, i.e.,

$$[1] \qquad (L_{ii})_N = K_{ii}N_i,$$

and

$$[2] \qquad (L_{ij})_N = -K_{ij}N_iN_j,$$

where the K's are coefficients expected to vary slowly with concentration. In both models the K_{ii} are positive; the K_{ij} are always positive in the exchange model, but may be negative in the vacancy model for some extreme cases. Both models assume microscopic reversibility and hence the derived phenomenological matrix is symmetric (2). The nonzero off-diagonal coefficients arise in a formal manner through the linear dependence of the fluxes imposed by the specification of the frame of reference in which they are measured, and the form of the conjugate thermodynamic forces associated with this particular frame of reference. Nevertheless, there exists a real microscopic coupling of the

[1]*Program on multicomponent diffusion supported by the National Research Council of Canada and the American Iron and Steel Institute.*
[2]*Now at the C.S.I.R.O. Division of Physical Chemistry, Box 4331 G.P.O., Melbourne, Australia.*
[3]*Temporarily at the Département de Physique, Institut de Recherches de la Sidérurgie Française, St. Germain-en-Laye, S. et O., France.*

fluxes in both models. This coupling occurs through the interchange of lattice sites by neighboring atoms in the exchange model, and the Kirkendall shift in the vacancy model.

No sufficiently precise diffusion and thermodynamic data is available to test the applicability of eqs. [1] and [2] to substitutional metallic alloys. Data, suitable for computing the L-coefficients, is available in a few ternary liquid systems. It is worthwhile to consider whether either model, with suitable modification, is suitable for the description of diffusion in such systems. The quasi-crystalline model of a liquid has proved useful in interpreting the equilibrium properties of liquid mixtures (3), and it is now extended to include kinetic properties.

THE DIFFUSION MODEL

Experimental evidence of the Kirkendall shift, coupled with theoretical calculations of activation energies, strongly suggests that diffusion in solids occurs by a vacancy mechanism (4). Similar models of diffusion in liquids have been proposed (5) although there is no experimental evidence of a Kirkendall shift in liquids (6). The analysis of I indicated that the concentration dependence of the L-coefficients was similar for both vacancy and exchange models. For this communication the exchange model has been chosen for liquids because it avoids the problem of the vacancy flux, which is observed in substitutional alloys as a Kirkendall shift.

The model is defined as a quasi-crystalline (close-packed) liquid, each lattice point being occupied by one diffusing unit (atom, ion, or molecule) unless otherwise specified. Diffusion occurs by the direct interchange of neighboring units on the lattice. The frame of reference is arbitrarily chosen as one stationary with respect to the quasi-lattice and parallel to one of the principal crystallographic planes. In this model, this frame of reference is coincident with both the number-fixed frame, defined for a system of n diffusing lattice units as

$$\sum_{i=0}^{n-1} (J_i)_N = 0, \qquad [3]$$

where the solvent is component 0, and the volume-fixed frame, defined by

$$\sum_{i=0}^{n-1} \bar{V}_i (J_i)_V = 0, \qquad [4]$$

where $\bar{V}_i$ is the partial molar volume of the i'th of n components.

The phenomenological description of diffusion in the volume-fixed frame of reference is (see I)

$$(J)_V = (L)_V (X)_V, \qquad [5]$$

where $(J)_V$ is a vector consisting of the $(n-1)$ independent fluxes $(J_i)_V$, $i \neq 0$, $(L)_V$ is a unique, symmetric $(n-1) \times (n-1)$ matrix of phenomenological L-coefficients, and $(X)_V$ is the column vector of the $(n-1)$ independent thermodynamic forces $(X_i)_V$, where

$$(X_i)_V = -\left(\frac{\partial \mu_i}{\partial x} - \frac{\bar{V}_i}{\bar{V}_0}\frac{\partial \mu_0}{\partial x}\right). \qquad [6]$$

The transition state formalism of I is used, but the concentrations, c_i, are in moles l^{-1}, to be consistent with common experimental usage. The flux $J_i^{\leftrightarrows j}$ of molecules of type i, resulting from interchanges with species j on the quasi-lattice, is given in I (eq. [20]) as

$$J_i^{\leftrightarrows j} = -k_{ij} c_i c_j \left(\frac{\partial \mu_i}{\partial x} - \frac{\bar{V}_i}{\bar{V}_0}\frac{\partial \mu_0}{\partial x}\right), \qquad [7]$$

Can. J. Chem. Downloaded from www.nrcresearchpress.com by 210.87.254.105 on 09/05/12
For personal use only.

where $\bar{V}_i/\bar{V}_0$ takes the value of unity for the quasi-crystalline model. The k_{ij} are given by

$$[8] \qquad k_{ij} = (RTN)^{-1}10^{-6}\lambda^2\nu_{ij} \exp[-(\Delta G_{ij}^{\neq})_c/kT]y_iy_j/y_{ij}^{\neq},$$

where RT has its usual meaning, N is the total number of moles per cm^3 of the lattice plane normal to the flux, λ is the lattice spacing in the direction of the flux, ν_{ij} is the frequency of forward transitions through the activated state, $(\Delta G_{ij}^{\neq})_c$ is the standard free energy of formation of the activated complex $ij^{\neq}$ on the molar concentration scale, and the y's are the activity coefficients of the various species, also on the molar scale. A liter has been taken as 10^3 cm^3.

The variables in [8] for an isothermal system are λ, the ν_{ij} and the ratio $y_iy_j/y_{ij}^{\neq}$. The lattice spacing is not strongly concentration dependent, and corrections may be included in the model without any difficulty. There is as yet no simple method of determining the concentration dependence of the ν_{ij} and the $y_{ij}^{\neq}$ so that application of this model is made only to systems dilute enough that the k_{ij} are not significantly different from their values, k_{ij}^0, at infinite dilution.

The total flux of i in an n-component system is therefore,

$$[9] \qquad (J_i)_V = \sum_{j=0}^{n-1} J_i^{i \rightleftarrows j}.$$

Using the method described in I for obtaining the phenomenological coefficients from expressions similar to [7], [8], and [9] gives

$$[10] \qquad (L_{ii})_V = \sum_{j=0(\neq i)}^{n-1} k_{ij}c_ic_j,$$

$$[11] \qquad (L_{ij(i\neq j)})_V = -k_{ij}c_ic_j.$$

Equations [10] and [11] are directly applicable to multicomponent nonelectrolyte solutions.

Values of k_{i0}^0 may be obtained from binary diffusion data. In a binary solution the flux of component i is given by [7] as

$$(J_i)_V = -k_{i0}c_ic_0\left(\frac{\partial\mu_i}{\partial x} - \frac{\bar{V}_i}{\bar{V}_0}\frac{\partial\mu_0}{\partial x}\right),$$

which by means of the Gibbs–Duhem equation,

$$c_0\frac{\partial\mu_0}{\partial x} + c_i\frac{\partial\mu_i}{\partial x} = 0,$$

and the relations,

$$c_0\bar{V}_0 + c_i\bar{V}_i = 10^3,$$

and

$$\frac{\partial\mu_i}{\partial x} = \frac{RT}{c_i}\left(1 + \frac{\partial \ln y_i}{\partial \ln c_i}\right)\frac{\partial c_i}{\partial x},$$

yields

$$[12] \qquad (J_i)_V = -k_{i0}(10^3/\bar{V}_0)RT\left(1 + \frac{\partial \ln y_i}{\partial \ln c_i}\right)\frac{\partial c_i}{\partial x}.$$

Fick's first law gives the flux of the i'th component as

$$[13] \qquad (J_i)_V = -[(D_i)_V/10^3]\frac{\partial c_i}{\partial x},$$

Can. J. Chem. Downloaded from www.nrcresearchpress.com by 210.87.254.105 on 09/05/12
For personal use only.

where $(D_i)_V$ is the diffusion coefficient in the volume-fixed frame of reference, in units of $cm^2\ s^{-1}$.

Comparison of [12] with [13] and taking the limit as $c_i \rightarrow 0$ gives k_{i0}^0 as

$$k_{i0}^0 = (D_i^0)_V/c_0^0 RT10^3. \qquad [14]$$

There is no method of obtaining the $k_{ij(j\neq 0)}^0$, but as these only appear in conjunction with the product c_ic_j which, relative to the product c_ic_0, is small in dilute solutions, an estimate may be obtained from the expression

$$k_{ij(i\neq j)}^0 \approx (k_{i0}^0 + k_{j0}^0)/2. \qquad [15]$$

The application of the model to binary nonelectrolyte solutions gives some information on the validity of the approximation

$$k_{i0} = k_{i0}^0 \qquad [16]$$

The direct comparison of eqs. [12] and [13] gives

$$k_{i0} = (D_i)_V \bar{V}_0/10^6 RT\left(1 + \frac{\partial \ln y_i}{\partial \ln c_i}\right),$$

which combined with [14] yields the ratio

$$k_{i0}/k_{i0}^0 = (D_i)_V \bar{V}_0 c_0^0/(D_i^0)_V\left(1 + \frac{\partial \ln y_i}{\partial \ln c_i}\right)10^3. \qquad [17]$$

If $\bar{V}_0$ does not vary significantly in dilute solutions from its value in the pure solvent, the combination of [16] and [17] gives

$$(D_i)_V = (D_i^0)_V\left(1 + \frac{\partial \ln y_i}{\partial \ln c_i}\right). \qquad [18]$$

Equation [18] is equivalent to the statement that the solute mobility $(M_i)_V$ (velocity of the solute in the volume-fixed frame of reference per unit chemical potential gradient) given by

$$(M_i)_V = (D_i)_V \Big/ \left(1 + \frac{\partial \ln y_i}{\partial \ln c_i}\right)RT$$

is independent of concentration. Precise diffusion measurements in several solutions of nonelectrolytes in water (7, 8, 9) show that in the systems studied the D's given by [18] at finite concentrations are larger than the experimental values, the discrepancy increasing with increase in concentration. The disagreement is of the order of a few percent at concentrations near 1.0 M, and increases rapidly with increase in concentration. Therefore, the ternary model may be most usefully applied to solutions of combined concentration below 1.0 M. The information obtained from these experimental results suggests that $k_{i0} < k_{i0}^0$, and hence the moduli of the L-coefficients given by [16], [10], and [11] are expected to be larger than the experimental values.

By the use of [10], [11], [14], [15], and [16], together with the binary diffusion data of Dunlop (10) and Gosting and Akeley (8), the L-coefficients for the ternary solution of raffinose (component 1) – urea (component 2) in water at molar concentrations of $c_1 = 0.0149$ and $c_2 = 0.5$, have been calculated. Using $D_1^0 = 0.4359 \times 10^{-5}$ and $D_2^0 = 1.381 \times 10^{-5}$, the calculated values of $(L_{11})_V$, $(L_{12})_V$, and $(L_{22})_V$ multiplied by $RT \times 10^8$ were found to be 0.00633, −0.00012, and 0.673 which compare favorably with the values

Can. J. Chem. Downloaded from www.nrcresearchpress.com by 210.87.254.105 on 09/05/12
For personal use only.

of 0.00618, −0.0013, and 0.657 given by Miller (11). Miller's L-coefficients were obtained from the ternary diffusion data of Dunlop (12) and estimates of the thermodynamic derivatives $\partial \ln y_i/\partial \ln c_j$. This system is not a good test of a quasi-crystalline model because of the large molar volume of the raffinose compared with the urea and water. The only significant comparison that can be made between the result given by this model and that given by Miller is for L_{11} and L_{22}. In both cases the predicted value is larger by approximately 2%.

AQUEOUS SOLUTIONS OF TWO STRONG ELECTROLYTES

The following discussion is restricted to electrolytes of the type A_aB_b, and in general will not be applicable to more complex salts such as those of the class $A_aB_bC_c$. For simplicity, the solvent is considered to be un-ionized.

An aqueous solution containing two electrolytes can only be classified as a ternary diffusion system if one ion is common to both salts (11). The three ionic species are designated 1, 2, and 3, component 3 being the common ion. Although there are four diffusing species, the condition of electrical neutrality,

$$[19] \qquad \sum_{i=1}^{3} z_i c_i = 0,$$

where z_i is the ionic charge (including sign) of the i'th species, imposes the restriction,

$$[20] \qquad \sum_{i=1}^{3} z_i J_i = 0,$$

in every frame of reference. The condition [19] together with the definition of the frame of reference,

$$[21] \qquad \sum_{i=0}^{3} \alpha_i J_i = 0,$$

where α_i is the appropriate weighting factor (partial molar volume in the volume-fixed reference frame), allows only two independent fluxes. Similarly, although there are three ionic species, each with its own chemical potential (sometimes distinguished by the use of the term electrochemical potential) the restriction [19] ensures that only certain combinations of the ionic chemical potentials can exist. The Gibbs–Duhem equation provides an additional dependency between the chemical potentials of the salts and the solvent and therefore only two of the four chemical potential gradients are independent.

The order in the distribution of ionic species in aqueous solutions of electrolytes, resulting from the long range electrostatic forces, allows a simplification in the microscopic model previously used for substitutional metallic alloys and nonelectrolyte solutions. The success of the "principle of specific interaction of ions" (13), indicates that ions of like charge are separated enough to render the mutual interaction negligible in determining the thermodynamic properties in dilute solutions. Ions of like charge are therefore unlikely to occupy adjacent sites on the quasi-lattice, and therefore the probability of forming an activated complex consisting of two ions of like charge is small enough to be neglected as a significant contribution to a diffusion flux. There is a higher probability of finding two ions of unlike charge on two adjacent quasi-lattice sites (but due to the diluteness of the solution the probability is very much lower than for ion–solvent pairs) and hence a small proportion of the activated complexes may consist of two ions of opposite charge. However, if the decomposition of this type of complex results

Can. J. Chem. Downloaded from www.nrcresearchpress.com by 210.87.254.105 on 09/05/12
For personal use only.

in an exchange of the original lattice sites, the two ions are now at the center of an ionic atmosphere with similar sign to their own. This configuration of high local energy cannot decay away in the normal manner by thermal interaction with the new neighbors, but only by two alternate processes, (i) by a reversal of the original interchange, or (ii) by a series of interchanges which reverse the sign of the ionic atmosphere.

The first of these mechanisms would seem most probable, with the net result of zero flux. Although the second mechanism is possible, its small probability, together with the small proportion of activated complexes containing two ions of opposite charge, restricts the net flux arising from this mechanism to insignificant values. Therefore, only the fluxes resulting from ion–solvent exchanges are considered, and these are given by [7] and [9] as

$$[22] \qquad (J_{i(i\neq 0)})_V = J_i^{i\rightleftarrows 0} = -k_{i0}c_i c_j\left(\frac{\partial \mu_i}{\partial x} - \frac{\partial \mu_0}{\partial x}\right).$$

Equation [22] is a complete statement of diffusion in electrolytes for this particular model. It only remains to carry out a mathematical transformation to a form composed only of independent, conjugate fluxes and forces, of which there are a number of alternative choices. The following derivation has been influenced by the fact that the experimental phenomenological coefficients for ternary electrolyte solutions have been given in terms of the two independent salt fluxes and the corresponding thermodynamic forces written in terms of the chemical potential gradients of the salts.

The i'th salt, indicated by the subscript is, contains the i'th ion, where i is not the common ion (component 3). The chemical formula of the i'th salt is always written as $i_{z_3}3_{z_i}$, even if z_i and z_3 have a common factor other than unity. The concentration c_{is} is defined as

$$[23] \qquad c_{is} = c_i/|z_3|,$$

where $|\ \ |$ indicates the modulus. The concentration defined in [23] is directly related to the experimental quantities needed to make a ternary solution and is not to be confused with the thermodynamic mean molar concentration $c_{1s}^{\mp}$ defined as

$$[24] \qquad c_{1s}^{\mp} = (|z_i| + |z_3|)\sqrt{(c_i)^{z_3}(c_3)^{z_i}}\ .$$

The concentration of the common ion is given by

$$c_3 = \sum_{j=1}^{2} c_{js}\,|z_j|,$$

and hence [24] becomes

$$[25] \qquad c_{1s}^{\mp} = (|z_i| + |z_3|)\sqrt{(c_{is}|z_3|)^{z_3}\left(\sum_{j=1}^{2} c_{js}|z_j|\right)^{z_i}},$$

which is only equal to c_{is} for a binary uni-univalent salt solution.

The salt flux J_{is} is given by

$$[26] \qquad J_{is} = J_i/|z_3|.$$

The chemical potentials of the salts are given by

$$[27] \qquad \mu_{is} = |z_3|\mu_i + |z_i|\mu_3.$$

Can. J. Chem. Downloaded from www.nrcresearchpress.com by 210.87.254.105 on 09/05/12
For personal use only.

Can. J. Chem. Downloaded from www.nrcresearchpress.com by 210.87.254.105 on 09/05/12
For personal use only.

Each ion is assigned sole occupancy of a quasi-lattice site, so that the ratio of salt to solvent molar volume is

[28] $$\bar{V}_{is}/\bar{V}_0 = |z_3| + |z_i|,$$

and hence the thermodynamic forces are given by [6] and [28] as,

[29] $$X_i = -\left\{\frac{\partial \mu_{is}}{\partial x} - (|z_3| + |z_i|)\frac{\partial \mu_0}{\partial x}\right\},$$

or alternately by means of [27] as

[30] $$X_i = -\left\{|z_3|\left(\frac{\partial \mu_i}{\partial x} - \frac{\partial \mu_0}{\partial x}\right) + |z_i|\left(\frac{\partial \mu_3}{\partial x} - \frac{\partial \mu_0}{\partial x}\right)\right\}.$$

The fluxes of eq. [22] must satisfy the condition [20], hence

[31] $$\sum_{j=1}^{3} -z_j k_{j0} c_j c_0 \left(\frac{\partial \mu_j}{\partial x} - \frac{\partial \mu_0}{\partial x}\right) = 0.$$

As the ionic concentrations and chemical potentials are not all independent, eq. [31] imposes no restrictions on the k_{j0}. The salt fluxes are given by [26], [22], and [31] as

[32] $$(J_{is})_V = -(|z_3|)^{-1}\left\{k_{i0}c_i c_0\left(\frac{\partial \mu_i}{\partial x} - \frac{\partial \mu_0}{\partial x}\right) + \theta_i \sum_{j=1}^{3} k_{j0}c_j c_0\left(\frac{\partial \mu_j}{\partial x} - \frac{\partial \mu_0}{\partial x}\right)\right\},$$

where through [31] we have added a constant θ_i times zero to the right hand side. A value of θ_i is now chosen for which the forces have the form of eqs. [29] or [30] and the fluxes the form of [5]. This yields

$$\theta_i z_3 k_{30} c_3 c_0 = \theta_i \sum_{j=1}^{2} \frac{|z_j|z_j}{|z_3|} k_{j0}c_j c_0 + \frac{|z_i|}{|z_3|} k_{i0}c_i c_0,$$

or

[33] $$\theta_i = |z_i| k_{i0} c_i c_0 \Big/ \left(z_3|z_3|k_{30}c_3 c_0 - \sum_{j=1}^{2} |z_j|z_j k_{j0}c_j c_0\right).$$

Substitution of [33] into [32], with rearrangement of the forces into the form given by eq. [29] results in

[34] $$(J_{is})_V = -k_{i0}c_i c_0 (z_3)^{-2}\left\{1 + |z_i|z_i k_{i0}c_i \Big/ \left(|z_3|z_3 k_{30}c_3 - \sum_{j=1}^{2} |z_j|z_j k_{j0}c_j\right)\right\}$$
$$\times \left\{\frac{\partial \mu_{is}}{\partial x} - (|z_3| + |z_i|)\frac{\partial \mu_0}{\partial x}\right\} - (z_3)^{-2}\left\{k_{10}k_{20}c_1 c_2 c_0 |z_1|z_1 \Big/ \left(|z_3|z_3 k_{30}c_3 - \sum_{j=1}^{2} |z_j|z_j k_{j0}c_j\right)\right\} \times \left\{\frac{\partial \mu_{is(l\neq i)}}{\partial x} - (|z_3| + |z_l|)\frac{\partial \mu_0}{\partial x}\right\}.$$

Noting that z_3 has the opposite sign to z_1 and z_2 and comparing [34] with [5] we find that the L-coefficients for an aqueous solution containing two strong electrolytes with a common ion are given by this model as

[35] $$(L_{il})_V = k_{i0}c_i c_0 (z_3)^{-2}\left\{1 - (z_i)^2 k_{i0}c_i \Big/ \sum_{j=1}^{3} (z_j)^2 k_{j0}c_j\right\}$$

and

[36] $$(L_{12})_V = (L_{21})_V = -k_{10}k_{20}c_1 c_2 c_0 z_1 z_2/(z_3)^2 \sum_{j=1}^{3} (z_j)^2 k_{j0}c_j.$$

If terms involving exchange of ions had been included in eq. [22], and the analysis carried through to eqs. [35] and [36] in an identical manner, then even if

$$k_{ij(j\neq 0)} \approx k_{i0}$$

the dilute solution approximation

$$c_i \ll c_0,$$

would assure that all terms in the k_{ij} could be omitted to give a result identical with [35] and [36]. Indeed, it is expected that the $k_{ij(j\neq 0)}$ are very much smaller than the corresponding k_{i0}, so that their inclusion would be an unnecessary complication.

As the k's must always be positive the L-coefficients of [35] and [36] satisfy all of the thermodynamic requirements (14), i.e.

[37] $$(L_{12})_V = (L_{21})_V;$$

$$(L_{11})_V > 0;\ (L_{22})_V > 0;\ (L_{11})_V(L_{22})_V - (L_{12})_V(L_{21})_V \geqq 0.$$

EVALUATION OF THE k's FOR IONIC SOLUTIONS FROM CONDUCTANCE DATA

The present model, summarized in eq. [22] and without the restriction of electrical neutrality, should describe conductance behavior at infinite dilution where the "time of relaxation effect", normally present in conductance, but not in diffusion, disappears (15). This allows evaluation of the k_{i0} from the corresponding limiting conductance data at infinite dilution. The conductance Ω_i of a solution, due to the presence of the i'th ion is

$$\Omega_i = |z_i| c_i \lambda_i 10^{-3},$$

where λ_i is the equivalent ionic conductance, and hence the flux of ions under an electrical potential gradient $\partial E/\partial x$ is

[38] $$(J_i)_{\text{cell}} = -\frac{|z_i| c_i \lambda_i}{z_i 10^3 F} \frac{\partial E}{\partial x},$$

where the flux is measured with respect to the cell and F is the Faraday. As there is no concentration gradient within the solution the chemical potential gradient of the i'th ion is given by (16),

$$\frac{\partial \mu_i}{\partial x} = z_i F \frac{\partial E}{\partial x}.$$

As the water molecules are assumed to be un-ionized,

$$\frac{\partial \mu_0}{\partial x} = 0.$$

Substitution of the above results into [22] gives

$$(J_i)_V = -k_{10} c_i c_0 z_i F \frac{\partial E}{\partial x},$$

and as the volume-fixed and cell-fixed frames of reference are coincident because the concentration gradient is zero, comparison of this equation with [38] gives

[39] $$k_{i0}^0 = \lambda_i^0 / 10^3 c_0^0 |z_i| F^2$$

at the limit of infinite dilution.

Can. J. Chem. Downloaded from www.nrcresearchpress.com by 210.87.254.105 on 09/05/12
For personal use only.

Can. J. Chem. Downloaded from www.nrcresearchpress.com by 210.87.254.105 on 09/05/12
For personal use only.

BINARY ELECTROLYTE SOLUTIONS

Before proceeding to check the results of the model against the experimental data for ternary solutions, it is instructive to consider the application of the model to binary solutions. For an aqueous solution of a strong electrolyte dissociating into ions 1 and 3, the flux $(J_{1s})_V$ is given by [34] as

$$(J_{1s})_V = -\frac{k_{10}k_{30}c_1c_0c_3}{(z_1)^2k_{10}c_1 + (z_3)^2k_{30}c_3}\left\{\frac{\partial\mu_{1s}}{\partial x} - (|z_3| + |z_1|)\frac{\partial\mu_0}{\partial x}\right\},$$

which by use of eq. [23], the Gibbs–Duhem equation, the relation

$$\mu_{1s} = \mu_{1s}^0 + (|z_1| + |z_3|)RT \ln y_{1s}^{\mp}c_{1s}^{\mp},$$

where μ_{1s}^0 is the standard chemical potential on the molar scale, $y_{1s}^{\mp}$ is the mean molar activity coefficient, and $c_{1s}^{\mp}$ is given by [24] or [25], can be reduced to

$$[40] \quad (J_{1s})_V = -\frac{k_{10}k_{30}(|z_1| + |z_3|)RT}{|z_3|k_{30} + |z_1|k_{10}}\left\{c_0 + (|z_1| + |z_3|)c_{1s}\right\}\left(1 + \frac{\partial \ln y^{\mp}}{\partial \ln c_{1s}}\right)\frac{\partial c_{1s}}{\partial x}.$$

Comparison of [40] with the flux given by Fick's first law (eq. [13]), which is applicable to any type of solution, yields

$$[41] \quad (D_{1s})_V = \frac{k_{10}k_{30}}{z_3k_{30} + z_1k_{10}}(|z_3| + |z_1|)RT\{c_0 + (|z_3| + |z_1|)c_{1s}\}\left(1 + \frac{\partial \ln y_{1s}^{\mp}}{\partial \ln c_{1s}}\right).$$

By substitution for the k's from eq. [39], the limiting value of the diffusion coefficient at infinite dilution is

$$[42] \quad (D_{1s}^0)_V = \frac{(|z_3| + |z_1|)\lambda_1^0\lambda_3^0RT}{|z_3||z_1|(\lambda_1^0 + \lambda_3^0)F^2}.$$

Equation [42] is the Nernst relation which has been experimentally verified for a large number of electrolyte solutions (17).

Combination of [41] and [42] with the approximation [16] gives

$$[43] \quad (D_{1s})_V = (D_{1s}^0)_V\left(1 + \frac{\partial \ln y_{1s}^{\mp}}{\partial \ln c_{1s}}\right)\{c_0 + (|z_3| + |z_1|)c_{1s}\}/c_0^0.$$

In dilute solutions the term $\{c_0 + (|z_3| + |z_1|)c_{1s}\}/c_0^0$, which allows for variations in the quasi-lattice dimensions, is not significantly different from unity. A number of experimental investigations have shown (17, 18) that eq. [43] is a good approximation for solutions of concentration below 10^{-1} M. At higher concentrations the diffusion coefficients given by eq. [43] are invariably higher than the experimental values. Equation [43] is often corrected by dividing the right hand side by the relative viscosity η_{rel} (17, 18), but this arbitrary procedure will be avoided here.

COMPARISON OF THE MODEL FOR AQUEOUS SOLUTIONS CONTAINING TWO STRONG ELECTROLYTES WITH EXPERIMENTAL OBSERVATIONS

L-coefficients have been calculated by means of eqs. [35] and [36] using the approximation [16] in conjunction with [39], for the system NaCl–KCl–H_2O, and these are compared in Table I, section A, with the experimental values of Dunlop and Gosting (20) and Dunlop (19) at a number of concentrations. The experimental L-coefficients were originally given for the solvent-fixed frame of reference, but these have been transformed to the volume-fixed frame by the method of Hooyman *et al.* (21). The quoted value of the

experimental off-diagonal coefficient is the mean of the experimentally determined $(L_{12})_V$ and $(L_{21})_V$. The agreement is good at low concentrations, and as expected the moduli of the calculated values are higher than the experimental values, the disagreement increasing with the concentration.

Miller (11) has determined from experimental ternary diffusion data and estimated thermodynamic data the L-coefficients for the systems LiCl–KCl–H_2O and LiCl–NaCl–H_2O, each at a single concentration, and these are compared in Table I, section B, with those given by equations [35], [36], [16], and [39]. Again the agreement is good.

AQUEOUS SOLUTION OF TWO ELECTROLYTES WITH ONE, OR BOTH, INCOMPLETELY IONIZED

The general mathematical description of this class of ternary system is cumbersome, and therefore a specific example, Na_2SO_4–H_2SO_4–H_2O, is chosen because experimental values of the L-coefficients have been measured (22). Davies *et al.* (23) have shown that the ionic species Na^+, H^+, SO_4^{--}, $NaSO_4^-$, HSO_4^- exist in detectable quantities, and these species are represented by the subscripts 1–5 respectively. The flux J_{1s} of Na_2SO_4 is given by an extension of [26] as

$$J_{1s} = J_1/2 + J_4/2, \qquad [44]$$

i.e. the flux of Na_2SO_4 is one-half of the combined flux of sodium nuclei, and similarly the flux J_{2s} of sulfuric acid is given by,

$$J_{2s} = J_2/2 + J_5/2. \qquad [45]$$

The ions $NaSO_4^-$ and HSO_4^- are each assumed to occupy two adjacent lattice sites, and hence exchange of either type of ion must occur simultaneously with two water molecules. Equation [22] must be modified for these two ionic species, and by the transition state theory of I,

$$(J_{j(j=4,5)})_V = -k_{j0}c_j(c_0)^2\left(\frac{\partial\mu_j}{\partial x} - 2\frac{\partial\mu_0}{\partial x}\right), \qquad [46]$$

with the k_{j0}^0 given by a modified form of [39] as

$$k_{j0(j=4,5)}^{\ 0} = \lambda_i^{\ 0}/10^3(c_0^{\ 0})^2F^2. \qquad [47]$$

Combination of eqs. [44], [46], [22], and [20] yields,

$$(J_{1s})_V = -\frac{1}{2}\left\{k_{10}c_1c_0\left(\frac{\partial\mu_1}{\partial x} - \frac{\partial\mu_0}{\partial x}\right) + k_{40}c_4(c_0)^2\left(\frac{\partial\mu_4}{\partial x} - 2\frac{\partial\mu_0}{\partial x}\right) + \theta_1\sum_{i=1}^{3} z_ik_{i0}c_ic_0\left(\frac{\partial\mu_i}{\partial x} - \frac{\partial\mu_0}{\partial x}\right) + \theta_1\sum_{j=4}^{5} z_jk_{j0}c_j(c_0)^2\left(\frac{\partial\mu_j}{\partial x} - 2\frac{\partial\mu_0}{\partial x}\right)\right\}. \qquad [48]$$

Assuming local equilibrium of the reactions,

$$NaSO_4^- \rightleftharpoons Na^+ + SO_4^{--},\ HSO_4^- \rightleftharpoons H^+ + SO_4^{--},$$

then,

$$\mu_4 = \mu_1 + \mu_3,\ \mu_5 = \mu_2 + \mu_3,$$

and hence

$$\left(\frac{\partial\mu_4}{\partial x} - 2\frac{\partial\mu_0}{\partial x}\right) = \left(\frac{\partial\mu_1}{\partial x} - \frac{\partial\mu_0}{\partial x}\right) + \left(\frac{\partial\mu_3}{\partial x} - \frac{\partial\mu_0}{\partial x}\right),$$

Can. J. Chem. Downloaded from www.nrcresearchpress.com by 210.87.254.105 on 09/05/12
For personal use only.

Can. J. Chem. Downloaded from www.nrcresearchpress.com by 210.87.254.105 on 09/05/12
For personal use only.

TABLE I

Comparison of L-coefficients, for systems containing two strong electrolytes, calculated by means of eqs. [26] and [29] with those obtained from experimental diffusion data in ternary systems

		A*					B†	
		1s = NaCl, 2s = KCl; $\lambda_{Na^+}{}^0 = 50.10$; $\lambda_{K^+}{}^0 = 73.50$; $\lambda_{Cl^-}{}^0 = 76.35$ (ref. 18, p. 463)					1s = LiCl, 2s = KCl; $\lambda_{Li^+}{}^0 = 38.6_8$ (ref. 18, p. 463)	1s = LiCl, 2s = NaCl
c_{1s}		0.2500	0.2500	0.5000	0.5000	1.500	0.25	0.25
c_{2s}		0.2500	0.5000	0.2500	0.5000	1.500	0.20	0.20
c_0		54.69	54.29	54.43	54.02	51.14	54.8	54.8
$(L_{11})_V \times RT \times 10^8$	Expt.	0.260	0.277	0.470	0.510	1.27	0.200	0.189
	Calcd.	0.270	0.289	0.492	0.533	1.51	0.213	0.209
$(L_{12}=L_{21})_V \times RT \times 10^8$	Expt.	−0.077	−0.102	−0.108	−0.163	−0.477	−0.060	−0.041
	Calcd.	−0.088	−0.113	−0.120	−0.173	−0.492	−0.064	−0.047
$(L_{22})_V \times RT \times 10^8$	Expt.	0.345	0.619	0.378	0.691	1.73	0.283	0.206
	Calcd.	0.355	0.629	0.393	0.701	1.99	0.291	0.215

*Experimental L-coefficients obtained by means of experimental thermodynamic data (19, 20).
†Experimental L-coefficients obtained by means of estimated thermodynamic data (11).

Can. J. Chem. Downloaded from www.nrcresearchpress.com by 210.87.254.105 on 09/05/12
For personal use only.

and

$$\left(\frac{\partial \mu_5}{\partial x} - 2\frac{\partial \mu_0}{\partial x}\right) = \left(\frac{\partial \mu_2}{\partial x} - \frac{\partial \mu_0}{\partial x}\right) + \left(\frac{\partial \mu_3}{\partial x} - \frac{\partial \mu_0}{\partial x}\right).$$

Substitution of these relations into [48], and selection of θ_1 such that the thermodynamic forces are in the form given by [29] results in

$$[49]\quad (J_{1s})_V = -\frac{1}{4}c_0\left[k_{10}c_1 + k_{40}c_4c_0 - \left\{(k_{10}c_1 - k_{40}c_4c_0)^2 \Big/ \left(\sum_{i=1}^{3}(z_i)^2k_{i0}c_i + \sum_{j=4}^{5}(z_j)^2k_{j0}c_jc_0\right)\right\}\right] \times \left(\frac{\partial \mu_{1s}}{\partial x} - 3\frac{\partial \mu_0}{\partial x}\right)$$
$$+ \frac{1}{4}c_0\left[(k_{10}c_1 - k_{40}c_4c_0)(k_{20}c_2 - k_{50}c_5c_0) \Big/ \left(\sum_{i=1}^{3}(z_i)^2k_{i0}c_i + \sum_{j=4}^{5}(z_j)^2k_{j0}c_jc_0\right)\right] \times \left(\frac{\partial \mu_{2s}}{\partial x} - 3\frac{\partial \mu_0}{\partial x}\right).$$

Comparison of eq. [49] with eq. [5] gives

$$[50]\quad (L_{11})_V = \frac{1}{4}c_0\left[k_{10}c_1 + k_{40}c_4c_0 - \left\{(k_{10}c_1 - k_{40}c_4c_0)^2 \Big/ \left(\sum_{i=1}^{3}(z_i)^2k_{i0}c_i + \sum_{j=4}^{5}(z_j)^2k_{j0}c_jc_0\right)\right\}\right],$$

$$[51]\quad (L_{12})_V = -\frac{1}{4}c_0\left[(k_{10}c_1 - k_4c_4c_0)(k_{20}c_2 - k_{50}c_5c_0) \Big/ \left(\sum_{i=1}^{3}(z_j)^2k_{i0}c_i + \sum_{j=4}^{5}(z_j)^2k_{j0}c_jc_0\right)\right].$$

The expressions for $(L_{22})_V$ and $(L_{21})_V$ are given by interchanging in [50] and [51] the subscripts 1 and 4 with 2 and 5 respectively. The coefficients given by the above relations satisfy the thermodynamic requirements [37].

TABLE II

Comparison of experimental L-coefficients for the incompletely ionized system Na_2SO_4–H_2SO_4–H_2O with those calculated from eqs. [29], [38], and [41]. Experimental data from Wendt (22)

		1s = Na_2SO_4, 2s = H_2SO_4; ($\lambda_{H^+}{}^0$ = 349.8, $\lambda_{SO_4^{--}}{}^0$ = 80.0$_2$ (ref. 18, p. 463)); $\lambda_{HSO_4^-}{}^0$ = 51.2 (ref. 28)			
c_{1s}		0.5000	1.000	0.5000	1.000
c_{2s}		0.5000	0.5000	1.0000	1.000
c_0		53.47	52.58	52.29	51.24
$(L_{11})_V \times RT \times 10^8$	Expt.	0.231	0.381	0.226	0.371
	Calcd.	0.273	0.496	0.285	0.526
$(L_{12}=L_{21})_V \times RT \times 10^8$	Expt.	−0.072	−0.084	−0.091	−0.146
	Calcd.	−0.153	−0.206	−0.177	−0.272
$(L_{22})_V \times RT \times 10^8$	Expt.	0.515	0.444	0.802	0.725
	Calcd.	0.834	0.956	1.47	1.66

The concentrations of the various ionic species are not available for salt concentrations as high as those used by Wendt (22). By using the crude approximation that the concentration of $NaSO_4^-$ ions is zero, and that the H_2SO_4 dissociates only as far as the first ionization stage, values of the L's have been calculated from eqs. [50] and [51]. These

are compared in Table II with the experimental values given by Wendt (transforming the published solvent-fixed frame data to the volume-fixed frame of reference). As expected, the agreement is poor due to the crude approximations made in the ionic concentrations, and the very high overall concentration of solute.

AQUEOUS SOLUTIONS CONTAINING A NONELECTROLYTE AND A STRONG ELECTROLYTE

In this class of ternary solution, diffusion proceeds by interchange of nonelectrolyte with water molecules, ions with water molecules, and ions with nonelectrolyte molecules. Nonelectrolyte molecules are represented by the subscript 1 and the ionic species by subscripts 2 and 3. The nonelectrolyte fluxes are therefore given by the expression

$$[52]\qquad (J_1)_V = -k_{10}c_1c_0\left(\frac{\partial\mu_1}{\partial x}-\frac{\partial\mu_0}{\partial x}\right)-\sum_{i=2}^{3}k_{i1}c_ic_1\left(\frac{\partial\mu_1}{\partial x}-\frac{\partial\mu_i}{\partial x}\right),$$

$$= -\left(k_{10}c_1c_0+\sum_{i=2}^{3}k_{i1}c_ic_1\right)\left(\frac{\partial\mu_1}{\partial x}-\frac{\partial\mu_0}{\partial x}\right)+\sum_{i=2}^{3}k_{i1}c_ic_1\left(\frac{\partial\mu_i}{\partial x}-\frac{\partial\mu_0}{\partial x}\right).$$

Similarly the ionic fluxes are given by,

$$[53]\qquad (J_{i(i=2,3)})_V = -(k_{i0}c_ic_0+k_{i1}c_ic_1)\left(\frac{\partial\mu_i}{\partial x}-\frac{\partial\mu_0}{\partial x}\right)+k_{i1}c_ic_1\left(\frac{\partial\mu_1}{\partial x}-\frac{\partial\mu_0}{\partial x}\right),$$

the two ionic fluxes again being subject to the condition of electrical neutrality [20].

Combination of [52] and [53], and the use of the condition [20] to bring the electrolyte forces into the form of eq. [29], results in,

$$[54]\qquad (J_1)_V = -\left\{k_{10}c_1c_0+\sum_{i=2}^{3}k_{i1}c_ic_1-\frac{|z_2||z_3|(k_{21}-k_{31})^2c_{2s}(c_1)^2}{\sum_{i=2,3}|z_i|(k_{i0}c_0+k_{i1}c_1)}\right\}$$

$$\times\left(\frac{\partial\mu_1}{\partial x}-\frac{\partial\mu_0}{\partial x}\right)+c_1c_{2s}\left\{\sum_{i(j=2;\,i\neq j)}^{3}|z_i|(k_{i0}c_0+k_{i1}c_1)k_{j1}\Big/\sum_{i=2}^{3}|z_i|(k_{i0}c_0+k_{i1}c_1)\right\}$$

$$\times\left(\frac{\partial\mu_{2s}}{\partial x}-(|z_3|+|z_2|)\frac{\partial\mu_0}{\partial x}\right),$$

$$[55]\qquad (J_{2s})_V = -\left\{c_{2s}\prod_{i=2,3}(k_{i0}c_0+k_{i1}c_1)\Big/\sum_{i=2}^{3}|z_i|(k_{i0}c_0+k_{i1}c_1)\right\}$$

$$\times\left(\frac{\partial\mu_{2s}}{\partial x}-(|z_2|+|z_3|)\frac{\partial\mu_0}{\partial x}\right)$$

$$+c_1c_{2s}\left\{\sum_{i(j=2;\,i\neq j)}^{3}|z_i|(k_{i0}c_0+k_{i1}c_1)k_{j1}\Big/\sum_{i=2}^{3}|z_i|(k_{i0}c_0+k_{i1}c_1)\right\}\times\left(\frac{\partial\mu_1}{\partial x}-\frac{\partial\mu_0}{\partial x}\right).$$

Comparison of [54] and [55] with [5] gives the L-coefficients as,

$$[56]\qquad (L_{11})_V = c_1\left(k_{10}c_0+\sum_{i=2}^{3}k_{i1}c_i\right),$$

where the third term has been omitted because of its relative smallness,

$$[57]\qquad (L_{12}) = (L_{21})_V = -c_1c_{2s}\left\{\sum_{i(j=2;\,i\neq j)}^{3}|z_i|(k_{i0}c_0+k_{i1}c_1)k_{j1}\Big/\sum_{i=2}^{3}|z_i|(k_{i0}c_0+k_{i1}c_1)\right\},$$

Can. J. Chem. Downloaded from www.nrcresearchpress.com by 210.87.254.105 on 09/05/12
For personal use only.

$$[58] \qquad (L_{22})_V = c_{2s} \prod_{i=2,3} (k_{i0}c_0 + k_{i1}c_1) \Big/ \sum_{i=2}^{3} |z_i|(k_{i0}c_0 + k_{i1}c_1),$$

and again the L-coefficients satisfy the requirements [37].

There is no method of obtaining the k_{i1} from binary data, but as the concentration term associated with it is c_1 and not c_0, then any reasonable value assigned to k_{i1} will not seriously influence the calculated L-coefficients for dilute solutions. Accordingly k_{i1} is assigned the same value as k_{i0}.

The approximation [16] was used in conjunction with [14] and [39] to calculate values of the L-coefficients for the system glycine–KCl–H_2O, and these are compared with the experimental values of Woolf *et al.* (24) in Table III, section A. The agreement is good, and as expected, the moduli of the calculated values are greater than the moduli of the experimental values, the discrepancy increasing with concentration.

Table III, section B, contains a similar comparison for the system raffinose–KCl–H_2O. The exchange model is not strictly applicable to this system because of the relatively large partial molar volume of the raffinose. In addition, Miller's L-coefficients (11) have been determined from experimental ternary diffusion data but with estimates of the thermodynamic functions $\partial \ln y_i/\partial \ln c_j$ only. The agreement between the two sets of values is nonetheless good.

DISCUSSION

The simple exchange model provides some insight into the manner in which gross Onsager cross-effects arise in ternary diffusion. In completely nonelectrolyte solutions the off-diagonal coefficients may be directly attributed to interchange of solute molecules. The application of detailed balance (or microscopic reversibility) to the kinetics of this process yields the symmetry property of the diffusion matrix. Direct interchange of solute species (ions) is considered to be negligible in ternary solutions containing two strong electrolytes so diffusion must be attributed to interchange between ions and solvent molecules, each type of exchange being regarded as an independent process. In this case relatively large off-diagonal L-coefficients arise as a result of transforming the lattice referred diagonal diffusion matrix describing the diffusion of the ions to a form which relates the two independent salt fluxes and forces. The fact that one ion must be common to both salts requires a very strong formal "coupling" of the chemical potential gradients of the salts, which ensures that the off-diagonal L-coefficients remain relatively large, even if all of the individual mobilities (or k_{i0}'s in this model) are identical. In an aqueous solution containing a strong electrolyte and a nonelectrolyte, both interchange of ions with nonelectrolyte and the formal requirements of thermodynamics act together to produce a finite off-diagonal coefficient, but by comparison with the case of two strong electrolytes the combined effect is small.

The use of the k's obtained from binary diffusion and conduction data, extrapolated to infinite dilution, places severe restrictions on the use of the model. This approximation, which is equivalent to assuming a constant mobility in the volume-fixed frame of reference, is known to lead to large errors in binary solutions, except at low concentrations. It is therefore not surprising that a similar behavior occurs for ternary solutions. For electrolyte solutions, inclusion of a coupling between interchanges, comparable with the electrophoretic effect (15), would not be sufficient to reduce the error at higher concentrations, and in many cases would increase the discrepancy.

The introduction of a correction based on the relative viscosity of the solution would probably lead to better agreement with real systems. The only models of diffusion in binary

Can. J. Chem. Downloaded from www.nrcresearchpress.com by 210.87.254.105 on 09/05/12
For personal use only.

Can. J. Chem. Downloaded from www.nrcresearchpress.com by 210.87.254.105 on 09/05/12
For personal use only.

TABLE III

Comparison of L-coefficients calculated by means of eqs. [29], [45], and [46] with those obtained from experimental diffusion data in ternary solutions

		A*						B†	
		1 = glycine, 2s = KCl; $D^0 \times 10^5 = 1.059$ (footnote [52] Woolf *et al.* (24))						1 = raffinose, 2s = KCl; $D_1^0 \times 10^5 = 0.4359$ (Dunlop (10))	
c_1		0.2500	0.2500	0.2500	0.5000	0.5000	0.5000	0.015	0.015
c_{2s}		0.1250	0.2500	0.5000	0.1250	0.2500	0.5000	0.1	0.5
c_0		54.55	54.35	53.95	53.94	53.74	53.33	54.9	54.9
$(L_{11})_V \times RT \times 10^8$	Expt.	0.259	0.259	0.258	0.502	0.501	0.498	0.0063	0.0063
	Calcd.	0.263	0.264	0.267	0.517	0.519	0.519	0.0066	0.0069
$(L_{12}=L_{21}) \times RT \times 10^8$	Expt.	0.000	0.000	0.000	0.001	−0.001	−0.002	−0.0003	−0.0019
	Calcd.	−0.001	−0.003	−0.006	−0.003	−0.006	−0.011	−0.0001	−0.0003
$(L_{22})_V \times RT \times 10^8$	Expt.	0.122	0.245	0.486	0.118	0.238	0.467	0.0992	0.495
	Calcd.	0.123	0.246	0.491	0.123	0.244	0.485	0.0989	0.488

*Experimental L-coefficients obtained by means of experimental thermodynamic data (24).
†Experimental L-coefficients obtained by means of estimated thermodynamic data (11).

solutions, which introduce a viscosity factor are those of a quasi-macroscopic nature, based on the application of Stokes' Law. A discussion of this type of model in relation to binary electrolyte diffusion is given by Robinson and Stokes (17). Agreement with experiment is reached only by introducing a parameter in the form of a variable hydration number. Gosting and Akeley (8) and Dunlop and Gosting (7) have shown that the introduction of a viscosity factor does not always lead to agreement, within experimental error, for binary nonelectrolyte solutions. Ellerton *et al.* (25) have used frictional coefficients to describe diffusion in binary aqueous solutions of nonelectrolytes. They show that for the systems studied there is no direct correlation between Stokes' law and the variation of the frictional coefficients with concentration. The exchange model cannot use Stokes' law directly because diffusion is described as a unit rate process, with an overall probability of a flux in a particular direction with a non-zero driving force. Nevertheless, the factors giving rise to a relative viscosity greater than unity must also influence the heat of formation (and hence the activity coefficient), and the frequency of decomposition of the activated complex. It is interesting to note that the system Na_2SO_4–H_2SO_4–H_2O showed the poorest agreement of all the ternary systems considered. The viscosity data of Vinal and Craig (26) for aqueous sulfuric acid solutions, and the more recent discussion of Kaminsky (27) suggests that the SO_4^{--} ions have a very much stronger influence on the relative viscosity of aqueous solutions than any of the ionic species present in the other ternary systems.

It is important to realize that the success of the model in dilute ternary solutions does not prove that diffusion in liquids occurs through a simple exchange mechanism, because the k_{10}'s were obtained from binary diffusion and conductance data, and not from any more fundamental statistical theory. It has been shown in I that both exchange and vacancy models lead to a similar concentration dependence of the L-coefficients in solid solutions. However, the agreement between estimated and experimental L-values in dilute ternary liquid systems lends confidence to the results of the analysis of diffusion in multicomponent alloys given in I, where no experimental data is available to make a direct check of the models.

The exchange model is not restricted to ternary systems. Extension to systems of more than three components is a formal procedure which does not require the introduction of any new principles or assumptions.

ACKNOWLEDGMENT

This research was sponsored by the National Research Council of Canada through a grant to J. S. K.

REFERENCES

1. J. E. LANE and J. S. KIRKALDY. Can. J. Phys. **42**, 1643 (1964).
2. L. ONSAGER. Phys. Rev. **37**, 405; **38**, 2265 (1931).
3. E. A. GUGGENHEIM. Mixtures. Oxford University Press. 1952.
4. A. E. LECLAIRE. Progress in metal physics. Vol. 4. *Edited by* B. Chalmers. Pergamon, London. 1953. p. 265.
5. H. A. WALLS and N. R. UPTHEGROVE. Acta Met. **12**, 461 (1964).
6. R. MILLS. J. Phys. Chem. **67**, 600 (1963).
7. P. J. DUNLOP and L. J. GOSTING. J. Am. Chem. Soc. **75**, 5073 (1953).
8. L. J. GOSTING and D. F. AKELEY. J. Am. Chem. Soc. **74**, 2058 (1952).
9. L. J. GOSTING and M. S. MORRIS. J. Am. Chem. Soc. **71**, 1998 (1949).
10. P. J. DUNLOP. J. Phys. Chem. **60**, 1464 (1956).
11. D. G. MILLER. J. Phys. Chem. **63**, 570 (1959).
12. P. J. DUNLOP. J. Phys. Chem. **61**, 1619 (1957).
13. J. N. BRONSTED. J. Am. Chem. Soc. **44**, 877 (1922).
14. S. R. DEGROOT and P. MAZUR. Non-equilibrium thermodynamics. North-Holland Pub., Amsterdam. 1962. p. 31.

Can. J. Chem. Downloaded from www.nrcresearchpress.com by 210.87.254.105 on 09/05/12
For personal use only.

15. L. ONSAGER and R. M. FUOSS. J. Phys. Chem. **26**, 2689 (1932).
16. E. A. GUGGENHEIM. Thermodynamics. 3rd ed. North-Holland Pub., Amsterdam. 1957. p. 374.
17. H. S. HARNED. Discussions Faraday Soc. **24**, 70 (1957).
18. R. A. ROBINSON and R. H. STOKES. Electrolyte solutions. 2nd ed. Butterworths, London. 1959.
19. P. J. DUNLOP. J. Phys. Chem. **63**, 612 (1959).
20. P. J. DUNLOP and L. J. GOSTING. J. Phys. Chem. **63**, 86 (1959).
21. G. J. HOOYMAN, S. R. DEGROOT, and P. MAZUR. Physica, **21**, 360 (1955).
22. R. P. WENDT. J. Phys. Chem. **66**, 1279 (1962).
23. C. W. DAVIES, H. W. JONES, and C. B. MONK. Trans. Faraday Soc. **48**, 921 (1952).
24. L. A. WOOLF, D. G. MILLER, and L. J. GOSTING. J. Am. Chem. Soc. **84**, 317 (1962).
25. H. D. ELLERTON, G. REINFELDS, D. E. MULCAHY, and P. J. DUNLOP. J. Phys. Chem. **68**, 403 (1964).
26. G. W. VINAL and D. N. CRAIG. J. Res. Natl. Bur. Std. **10**, 781 (1933).
27. M. KAMINSKY. Discussions Faraday Soc. **24**, 171 (1957).
28. M. KERKER. J. Am. Chem. Soc. **79**, 3664 (1957).

Can. J. Chem. Downloaded from www.nrcresearchpress.com by 210.87.254.105 on 09/05/12
For personal use only.

Can. J. Chem. Downloaded from www.nrcresearchpress.com by 210.87.254.40 on 09/05/12
For personal use only.

REACTIONS OF NITRO SUGARS

I. SOME BENZYLIDENE AND ACYL DERIVATIVES OF METHYL 3-DEOXY-3-NITRO-D-HEXOPYRANOSIDES

HANS HELMUT BAER, FRANK KIENZLE, AND THOMAS NEILSON
Department of Chemistry, University of Ottawa, Ottawa, Canada

Received February 10, 1965

ABSTRACT

The 4,6-*O*-benzylidene derivatives VII, VIII, and XVII of methyl 3-deoxy-3-nitro-β-D-mannopyranoside, -β-D-galactopyranoside, and -α-D-glucopyranoside, respectively, were prepared. Acetylation of the β-D-*manno* derivative (VII) led, depending upon the reaction conditions, to its 2-*O*-acetate (IX) and, by way of an unexpected epimerization, to the 2-*O*-acetate (V) of the corresponding β-D-*gluco* isomer. There is evidence that this epimerization proceeds through methyl 4,6-*O*-benzylidene-2,3-dideoxy-3-nitro-β-D-*erythro*-hexopyranos-2-enide (VI). This nitroolefin was obtained by a Schmidt–Rutz reaction from IX (as earlier from V) and was shown to add acetic acid readily giving V. It also added ethanol producing a 2-*O*-ethyl glycoside (XII). Acetylation of the *galacto* derivative (VIII) did not afford an acetate but proceeded with dehydration yielding methyl 4,6-*O*-benzylidene-2,3-dideoxy-3-nitro-β-D-*threo*-hexopyranos-2-enide (X).

A number of further derivatives of methyl 3-deoxy-3-nitro-β-D-glucopyranoside were prepared, viz., the 2-*O*-acetyl (XI), 2-deoxy-6-*O*-tosyl (XIV), and 2,6-dideoxy-6-iodo (XV) derivatives.

A recent article (1) has described the synthesis of 3-amino-2,3-dideoxy-D-*arabino*-hexose via the corresponding methyl 2,3-dideoxy-3-nitro-β-glycoside (XIII). In view of the potential usefulness of nitro sugar intermediates for similar syntheses which may lead to rare amino sugars, a number of additional 3-deoxy-3-nitro-hexose derivatives have been prepared and some of their reactions have been studied.

Nitromethane cyclization of L′-methoxy-D-hydroxymethyldiglycolic aldehyde (periodate-oxidized methyl β-D-hexopyranosides) had afforded (2, 3, 4) crystalline methyl 3-deoxy-3-nitro-β-D-glucopyranoside (I), -D-mannopyranoside (II), and -D-galactopyranoside (III). The 4,6-*O*-benzylidene derivative (IV) of I had been acetylated (1) to methyl 2-*O*-acetyl-4,6-*O*-benzylidene-3-deoxy-3-nitro-β-D-glucopyranoside (V) which was subsequently converted into a nitroolefin, methyl 2,3-dideoxy-3-nitro-β-D-*erythro*-hexopyranos-2-enide (VI) by treatment with sodium bicarbonate in refluxing benzene (Schmidt–Rutz reaction). We have now prepared the 4,6-*O*-benzylidene derivatives VII and VIII from II and III, respectively, and have studied their behavior in similar reaction sequences.

The benzylidene mannoside (VII) furnished its 2-*O*-acetate (IX) on treatment with acetic anhydride in cold pyridine. Acetylation with hot acetic anhydride and anhydrous sodium acetate, however, did not lead to the same acetate but gave, surprisingly, the 2-*O*-acetyl glucoside (V). This glucoside acetate was also obtained when the nitroolefin (VI) was heated with a mixture of acetic anhydride, acetic acid, and sodium acetate. It appears, therefore, that under the more vigorous acetylation conditions the mannoside (VII) undergoes dehydration followed by addition, to intermediate VI, of a molecule of acetic acid in such a way as to favor equatorial orientation of the nitro and acetoxy substituents (i.e., *gluco* configuration).

The 2-*O*-acetyl-mannoside (IX) furnished *isolable* nitroolefin (VI) by Schmidt–Rutz elimination of acetic acid, as did the glucoside (V). It was noted that the reaction rates were of similar magnitude for V and IX; however, this observation should not be stressed

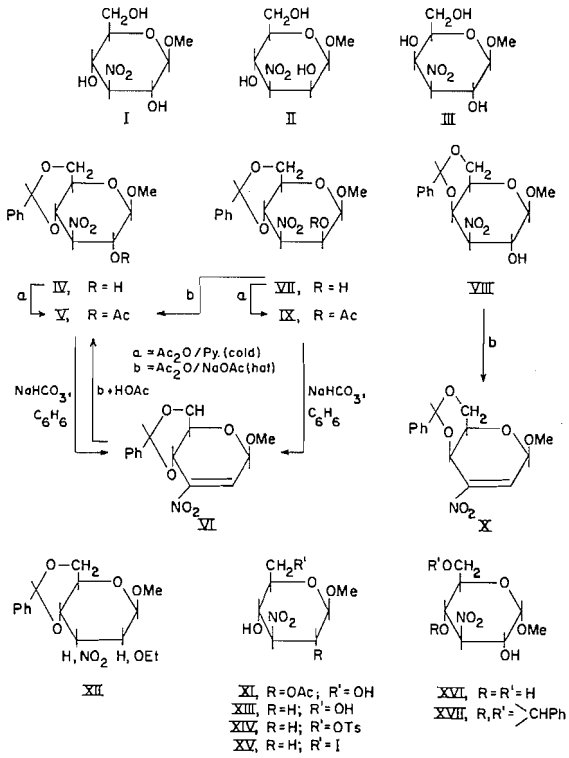

too much since slightly varying conditions may have prevailed in the heterogeneous reaction media.

When acetylation of the benzylidene galactoside (VIII) was attempted with acetic anhydride and pyridine, decomposition occurred; and acetylation with cold acetic anhydride and sodium acetate led to recovery of starting material. When, however, VIII was *heated* for a few minutes in an acetic anhydride – sodium acetate mixture, a new crystalline product was formed in 96% yield. It was not the expected nor any other *O*-acetate, but proved to be the nitroolefin, methyl 4,6-*O*-benzylidene-2,3-dideoxy-3-nitro-β-D-*threo*-hexopyranos-2-enide (X). Further refluxing of (isolated) X in a glacial acetic acid – acetic anhydride mixture for 2.5 h yielded only starting material. A comparison of these results with those in the *manno* and *gluco* series described above shows that the C-4 configuration influences remarkably the stability of the 2,3-olefinic bond.

Further, it was of interest to study the feasibility of preparing nitroolefins by the Schmidt–Rutz reaction in the absence of a benzylidene blocking group at C-4 – C-6. Compound V was therefore debenzylidenated with a cation exchange resin in aqueous methanol, and crystalline methyl 2-*O*-acetyl-3-deoxy-3-nitro-β-D-glucopyranoside (XI) was obtained. Treatment of XI with sodium bicarbonate in refluxing benzene gave only an intractable mixture, possibly owing to intermolecular addition and (or) polymerization reactions of the nitroalkenediol presumably produced. It is of interest in this connection that the benzylidene nitroolefin (VI) readily added ethanol when refluxed in this solvent.[1]

[1]*This was discovered during an attempt to recrystallize VI from hot ethanol. The addition was probably promoted by the presence of a trace of alkali. Alkali-catalyzed additions of alkoxyl to nitroolefins are well known: cf. (5, 6, 7) and earlier literature cited there.*

Can. J. Chem. Downloaded from www.nrcresearchpress.com by 210.87.254.40 on 09/05/12
For personal use only.

The crystalline product obtained had the composition of a methyl 4,6-*O*-benzylidene-3-deoxy-2-*O*-ethyl-3-nitro-β-D-hexopyranoside (XII), but no attempt was made to elucidate its stereochemistry. This type of addition reaction should lend itself to the synthesis also of other 2-*O*-alkylated 3-nitro (and thence amino) sugars and possibly of 2-linked disaccharides.

One of the possible ways to synthesize 3-amino-2,3,6-trideoxy sugars (such as occur in certain antibiotics) was seen in a conversion of a 2,3-dideoxy-3-nitro hexoside into its 6-*O*-*p*-toluenesulfonyl and thence its 6-deoxy-6-iodo derivative, followed by reduction. To explore this route, methyl 2,3-dideoxy-3-nitro-β-D-*arabino*-hexopyranoside (XIII) (1) was monotosylated to XIV. That the tosyloxy group in XIV was indeed a primary one (i.e., located at C-6) was shown by its facile displacement by iodine on refluxing with sodium iodide in acetone. Unfortunately, reduction of the 6-iodo derivative (XV) has as yet been unsuccessful.[2]

All the experiments described above and those done previously (1) relate to the β-D-hexopyranoside series. Their performance was facilitated by the fact that I, II, and III were fairly readily available in pure, crystalline condition. It should be interesting to investigate the course of these reactions in the α-anomeric series as well. However, such undertaking remains unattractive so long as the corresponding α-glycosides, known only as amorphous mixtures of isomers (8, 9), cannot be separated into stereochemically homogeneous compounds. A first step in this direction has now been accomplished by the isolation, through column chromatography, of crystalline methyl 3-deoxy-3-nitro-α-D-glucopyranoside (XVI) and by its conversion into a crystalline 4,6-*O*-benzylidene derivative (XVII). Proof of the identity of XVI was furnished by hydrogenation and acetylation giving the known methyl 3-acetamido-3-deoxy-2,4,6-tri-*O*-acetyl-α-D-glucopyranoside.

EXPERIMENTAL

Unless otherwise indicated, evaporations were carried out *in vacuo* at 35–40° (bath temperature), petroleum ether refers to the fraction boiling at 30–60°, melting points were taken with an aluminium block apparatus and calibrated thermometer, and infrared spectra were measured using the Nujol mull technique and a Parkin-Elmer Infracord instrument.

Methyl 4,6-O-Benzylidene-3-deoxy-3-nitro-β-D-mannopyranoside (VII)

Methyl 3-deoxy-3-nitro-β-D-mannopyranoside (II; 150 mg) (4) was magnetically stirred for 15 h with 2 ml of benzaldehyde and 400 mg of anhydrous zinc chloride. The partly solidified reaction mixture was taken up with 150 ml of water and 50 ml of petroleum ether, and the heterogeneous mixture was vigorously stirred for 30 min. A solid material which separated was filtered off, washed with water and petroleum ether, and dried in a desiccator. The weight was 130 mg (62%). Recrystallization from ethanol containing a few drops of water afforded 70 mg of colorless leaflets melting at 194–196° and showing $[\alpha]_D^{23}$ −107.5° (*c*, 1 in ethanol).

Anal. Calcd. for $C_{14}H_{17}NO_7$ (311.3): C, 54.01; H, 5.51; N, 4.50. Found: C, 54.02; H, 5.62; N, 4.45.

It was not necessary to use pure II for this preparation. Rather, the material that was left in the mother liquor when methyl 3-deoxy-3-nitro-β-D-galactopyranoside (III) was prepared (4) and that consisted largely of II together with remnant III, could be utilized. Scaled-up runs could conveniently be performed. The crude benzylidenated product was then subjected to fractional crystallization from absolute ethanol, in which the *galacto* derivative VIII is less soluble than VII. Thus, in one experiment using about 25 g of a sirup of II and III there was obtained, after several recrystallizations, about 2.5 g of pure VIII from the forefractions and about 9.5 g of pure VII with m.p. 198–199° and $[\alpha]_D^{23}$ −105° (*c*, 1 in dimethylformamide). For characteristic infrared absorption bands see the second paragraph of the next section.

Methyl 4,6-O-Benzylidene-3-deoxy-3-nitro-β-D-galactopyranoside (VIII)

Pure methyl 3-deoxy-3-nitro-β-D-galactopyranoside (4) (III; 200 mg) was benzylidenated as described above for II. After recrystallization of the crude product from absolute ethanol, 140 mg (50%) of VIII

[2]*Hydrogenations using platinum catalyst or Raney nickel were tried. The choice of reducing agents was limited since alkaline conditions had to be avoided because of danger of epimerization in the nitroalcohol part of the molecule.*

Can. J. Chem. Downloaded from www.nrcresearchpress.com by 210.87.254.40 on 09/05/12
For personal use only.

was obtained as colorless, long needles having m.p. 230–231° (decomp.) and $[\alpha]_D^{23}$ +24.8° (*c*, 1 in dimethylformamide). A large run using 7.7 g of crystalline but unpurified III afforded 6.0 g (56%) of pure VIII after recrystallization.

Anal. Calcd. for $C_{14}H_{17}NO_7$ (311.3): C, 54.01; H, 5.51; N, 4.50. Found: C, 54.16; H, 5.50; N, 4.70.

Infrared data:[3] The three stereoisomeric benzylidene derivatives IV, VII, and VIII show sharp hydroxyl bands at 3 450 and nitro bands at 1 560 cm^{-1}. Characteristic differences are seen in the 900–700 cm^{-1} region. IV: 880(w), 857(w), 762–755(s), 730(w), 697(s). VII: 877(s), 850(w), 815(w), 775(ms), 750(s), 725(ms), 697(s). VIII: 872(w), 827(w), 790(w), 755(w), 744(s), 697(s).

*Methyl 2-O-Acetyl-4,6-O-benzylidene-3-deoxy-3-nitro-β-*D*-mannopyranoside (IX)*

Benzylidene mannoside (VII) (200 mg) in pyridine (2 ml) was acetylated at room temperature with acetic anhydride (0.6 ml). The reaction mixture was allowed to stand overnight and was then poured into 50 ml of ice water, and the precipitate which formed was thoroughly washed with water. Recrystallization from aqueous ethanol gave 130 mg (57%) of colorless acetate IX melting at 136–137°.

Anal. Calcd. for $C_{16}H_{19}NO_8$ (353.2): C, 54.40; H, 5.42; N, 3.97. Found: C, 54.52; H, 5.55; N, 3.93.

The infrared spectrum[3] lacked hydroxyl absorption and showed a strong carbonyl peak at 1 740 and a nitro peak at 1 560 cm^{-1}. The spectrum differed from that of V in the 900–700 cm^{-1} region. IX: 917(m), 905(w), 872(m), 760–750–745(m), 722(m), 697(s), 690(w). V: 917(s), 890(m), 875(w), 763(s), 733(w), 703–697(s).

Acetylation of VII with Acetic Anhydride – Sodium Acetate

A sample of VII (300 mg) was refluxed with sodium acetate (1.2 g) in acetic anhydride (5 ml) for 6 min. Decomposition of the reaction mixture with ice water (50 ml) led to the formation of a white solid within 10 min. The solid was collected, washed thoroughly with cold water, and dried in a desiccator. The m.p. of the crude product (290 mg) was 151–154°; it was raised to 191–193° by two recrystallizations from ethyl acetate – petroleum ether. The yield of pure V was 160 mg; its infrared spectrum was identical with that of a sample prepared from IV (1) and differed from that of IX (see preceding section). The m.p. recorded (1) for V is 193–194°.

Acetoxylation of Nitroolefin (VI)

An 80 mg sample of nitroolefin (VI) from previous work (1) was refluxed for 6 min in 1 ml of acetic anhydride containing 240 mg of anhydrous sodium acetate and 40 mg of glacial acetic acid. Decomposition of the reaction mixture with 10 ml of ice water furnished 72 mg of crystals showing an unsharp m.p. of 142–148°. Since recrystallization (ethyl acetate – petroleum ether) failed to give a pure product, the whole material—crystals and evaporated mother liquor of recrystallization—was subjected once more to an identical treatment of acetoxylation, but for 2 min only. Work-up as described then afforded 60 mg of crystals melting at 152–154°. After two recrystallizations from aqueous ethanol the m.p. was 192–193° and the yield was 22 mg. The product was identified as V by its infrared spectrum.

Nitroolefin (VI) from IX

The Schmidt–Rutz elimination of acetic acid from the nitromannoside (IX) was done[4] essentially as described (1) for V. Nitromannoside (IX) (2 g) in dry benzene (50 ml) was refluxed with 10 g of finely ground, dry sodium bicarbonate. Small amounts of the solution were withdrawn from time to time, allowed to evaporate, and inspected by infrared spectroscopy. Progress of the reaction was revealed by diminution of the acetate carbonyl peak at 1 740 cm^{-1} and the nitroalkane peak at 1 560 cm^{-1} with concurrent appearance and increase of a peak at 1 533 cm^{-1} which was due to the olefinic nitro group produced. Progress was slight after 30 min, considerable after 3 and 4.5 h, and very large though incomplete after 27 h. Only VI and no more starting material was detected after 48 h when the reaction mixture was worked up by filtration, evaporation, and recrystallization of the residue from the minimum amount of ethyl acetate – petroleum ether (b.p. 60–80°). There was obtained 1.1 g of VI melting at 140–141° (yield, 70%). The infrared spectrum was identical with that of material prepared (1) from V.

Acetylation of Benzylidene Galactoside (VIII)

(a) Attempted O-Acetylation

Samples of VIII (about 50 mg each) were treated with acetic anhydride in pyridine in the manner described above for VII. The reaction mixtures turned dark brown and black on standing overnight at 0° and 23°, respectively. No crystalline acetate could be isolated, and benzaldehyde was detected during work-up. When acetylation was attempted with sodium acetate and acetic anhydride at 4° (24 h), only starting material was recovered. Under similar conditions but at room temperature a crystalline material was obtained that, according to its infrared spectrum, consisted of starting material and nitroolefin (X) (see under (*b*)).

*(b) Methyl 4,6-O-Benzylidene-2,3-dideoxy-3-nitro-β-*D*-threo-hexopyranos-2-enide (X)*

Pure benzylidene galactoside (VIII) (3 g) was refluxed for 6 min with 12 g of anhydrous sodium acetate

[3]*Frequencies ν_{max} in cm^{-1}. Relative intensities are given in parentheses: s = strong, m = medium, w = weak.*

[4]*We are obliged to Dr. M. C. Cook of this laboratory for performing some confirmatory experiments.*

Can. J. Chem. Downloaded from www.nrcresearchpress.com by 210.87.254.40 on 09/05/12
For personal use only.

in 30 ml of acetic anhydride. The slightly yellowish reaction mixture was allowed to cool under tap water and then poured into 200 ml of ice water. Stirring for 10 min resulted in the separation of a crystalline solid that was collected and washed well with water. The yield was 2.7 g (96%) of desiccator-dried, crude X which melted at 152–155° and was suitable for further experiments. An analytical sample was obtained by recrystallization from ethyl acetate – petroleum ether giving beautiful needles of m.p. 162° and $[\alpha]_D^{23}$ −47.8° (*c*, 1 in dimethylformamide).

Anal. Calcd. for $C_{14}H_{15}NO_6$ (293.3): C, 57.33; H, 5.16; N, 4.78. Found: C, 57.56; H, 5.32; N, 4.99.

When a sample of X was refluxed for 2.5 h in glacial acetic acid containing acetic anhydride, starting material was recovered and no evidence for the formation of an *O*-acetate was obtained.

Characteristic infrared bands[3]: No hydroxyl absorption; olefinic nitro group, 1 525 cm^{-1}. Comparison of X and VI in the 900–700 cm^{-1} region: X, 895(w), 877(w), 855(w), 820(m), 795(m), 752(s), 738(s), 692(s); VI, 890(w), 865(w), 802(m), 751(s), 738(w), 695(s), 675(w).

Methyl 2-O-Acetyl-3-deoxy-3-nitro-β-D-glucopyranoside (XI)

Benzylidene acetate (V) (500 mg) was refluxed for 4 h with 1.5 g of Dowex 50W-X8 (H^+) in 40 ml of methanol and 10 ml of water. The resin was removed and the filtrate was taken to dryness. Crystallization of the colorless residue (370 mg) from ethyl acetate – petroleum ether gave needles or platelets (200 mg, 54%) melting at 190–191°.

Anal. Calcd. for $C_9H_{15}NO_8$ (265.2): C, 40.76; H, 5.70; N, 5.28. Found: C, 40.31; H, 5.80; N, 5.51.

Refluxing of XI in benzene (25 parts) in the presence of solid sodium bicarbonate (5 parts) produced a dark intractable sirup.

Addition of Ethanol to Nitroolefin (VI)

Crude nitroolefin (VI) that had been obtained from 200 mg of benzylidene acetate (V) by a Schmidt–Rutz reaction as previously described (1), was refluxed for 2 h in 25 ml of ethanol. Upon addition of water and cooling there separated 120 mg (63% based on V) of needles with m.p. 122–123° and $[\alpha]_D^{23}$ −88.0° (*c*, 1.16 in ethanol). Analysis and infrared spectrum were in agreement with structure XII of a methyl 4,6-*O*-benzylidene-3-deoxy-2-*O*-ethyl-3-nitro-β-D-hexopyranoside.

Anal. Calcd. for $C_{16}H_{21}NO_7$ (339.3): C, 56.63; H, 6.24; N, 4.13. Found: C, 56.70; H, 6.22; N, 4.31.

Infrared bands (cm^{-1}): no hydroxyl; 1550, 1375 (nitroalkane); 1087, 1075, 990, 970 (ether C—O—C); 763, 700 (benzylidene).

Methyl 2,3-Dideoxy-3-nitro-6-O-p-toluenesulfonyl-β-D-arabino-hexopyranoside (XIV)

To a solution of 840 mg of methyl 2,3-dideoxy-3-nitro-β-D-*arabino*-hexopyranoside (XIII) (1) in 1 ml of pyridine was added a solution of tosyl chloride (810 mg, 1.05 molar equiv) in dichloromethane (25 ml). The mixture was left overnight at room temperature and then extracted thrice with 25 ml of 0.2 *N* hydrochloric acid, washed thrice with 25 ml of water, dried over anhydrous magnesium sulfate and finally evaporated. The colorless residue was crystallized from ethyl acetate – petroleum ether and furnished 955 mg (65%) of XIV as needles with m.p. 115°.

Anal. Calcd. for $C_{14}H_{19}NO_8S$ (361.2): C, 46.51; H, 5.31; N, 3.88; S, 8.87. Found: C, 46.75; H, 5.45; N, 4.01; S, 8.74.

Methyl 6-Iodo-3-nitro-2,3,6-trideoxy-β-D-arabino-hexopyranoside (XV)

Monotosylate (XIV) (380 mg) and sodium iodide (1.6 g) were refluxed in acetone (25 ml) for 24 h. After cooling, sodium tosylate (200 mg, 98%) was filtered off and the filtrate was evaporated. Water (25 ml) was added to the residue, and the mixture was extracted four times with 25 ml of chloroform. The combined chloroform extracts were washed once with a dilute sodium thiosulfate solution in order to remove a small amount of free iodine formed in a side reaction. Washing with water (3 × 25 ml), drying over anhydrous magnesium sulfate, and evaporation of the chloroform gave a crystalline residue which was recrystallized from ethyl acetate – petroleum ether. There was obtained 200 mg of colorless crystals, m.p. 147–148°, and a second crop (150 mg) of crystals of lesser purity. The crops were jointly recrystallized from the same solvents giving 305 mg (91%) of XV melting at 147–148°.

Anal. Calcd. for $C_7H_{12}INO_5$ (317.1): C, 26.51; H, 3.81; I, 40.03; N, 4.42. Found: C, 26.73; H, 3.92; I, 40.28; N, 4.53.

Methyl 3-Deoxy-3-nitro-α-D-glucopyranoside (XVI)

An amorphous mixture of methyl 3-deoxy-3-nitro-α-D-hexopyranosides was prepared, starting from 3.88 g (0.02 mole) of methyl α-D-glucopyranoside, in the fashion described on p. 86 of ref. 9 and relating to the nitromethane condensation in methanolic solution. The product ($[\alpha]_D^{23}$ ca. +100°, in water) was liquefied with a small amount of a chromatographic solvent mixture which consisted of the upper layer formed on mixing 1-butanol – acetic acid – water (4:1:5, v/v), and placed on a column (4.2 × 100 cm) of powdered cellulose. Elution was performed with 1.5 l of the solvent mixture, and 13-ml fractions were collected and checked polarimetrically in a 2-dm tube. Fraction No. 65 was the first to show optical activity (α_D +0.08°); maximum rotation (α_D +2.52°) was observed in fraction No. 77; then followed a gradual decrease with fraction No. 112 showing α_D +0.04° and the subsequent fractions having zero rotation. Paper chromatography using the same solvent system revealed that separation on the column had been rather unsatisfactory,

Can. J. Chem. Downloaded from www.nrcresearchpress.com by 210.87.254.40 on 09/05/12
For personal use only.

as all the fractions gave two or three spots. Some accumulation of product and, probably, removal of impurities was nevertheless achieved resulting in the crystallization of XVI from certain fractions. Fractions 69–73 were combined and evaporated. The residue was taken up in a small amount of tetrahydrofuran, excess ethyl ether was added, and the solution was placed in a refrigerator for crystallization. The same procedure was followed for fractions 77–80. There crystallized in the course of 2 and 4 d 51 and 98 mg of products, melting at 127–133° (decomp.) and 129–133° (decomp.), respectively. Jointly recrystallized from tetrahydrofuran–ether (with an activated charcoal treatment included) the material (59 mg) melted at 136–137° (decomp.). All the other fractions were combined and, together with the mother liquors from fractions 69–73 and 77–80, were worked up in similar fashion. Seeding with the above crystals gave another crop, which upon recrystallization weighed 104 mg and also melted at 136–137° (decomp.).

Pure XVI formed colorless, elongated prisms which were chromatographically uniform; R_f 0.67; $[\alpha]_D^{23}$ +166° (*c*, 1 in water).

Anal. Calcd. for $C_7H_{13}NO_7$ (223.2): C, 37.67; H, 5.87. Found: C, 38.19; H, 5.93.

The anomeric glycosides XVI and I exhibit characteristic differences in their infrared spectra,[3] particularly in the region 950–700 cm^{-1}: XVI, 927(w), 903(m), 860(m), 800(m), 750–700(m, broad, with maximum at 725); I, 935(w), 918(m), 890(m), 790–700(m, broad, with maximum at 740).

To establish the configuration of crystalline XVI it was converted into known methyl 3-acetamido-3-deoxy-2,4,6-tri-*O*-acetyl-α-D-glucopyranoside. An aqueous solution containing 30 mg of XVI and an equivalent amount of (dilute) hydrochloric acid was hydrogenated catalytically over prehydrogenated platinum dioxide. A sirupy but chromatographically uniform amine hydrochloride was obtained; it traveled more slowly than a comparison sample of the corresponding mannoside (8, 9). Acetylation of the amine hydrochloride using 2 ml of acetic anhydride and 500 mg of sodium acetate (5 min at reflux temperature) gave after work-up in the usual manner rectangular prisms (18 mg, from ethanol) with m.p. 180–181° and $[\alpha]_D^{23}$ +108.5° (*c*, 1 in chloroform), in excellent agreement with the literature (9, 10). A mixture melting point with an authentic sample was undepressed and the infrared spectra were identical.

Methyl 4,6-O-Benzylidene-3-deoxy-3-nitro-α-D-glucopyranoside (XVII)

An amorphous mixture of methyl 3-deoxy-3-nitro-α-D-hexopyranosides (0.02 mole) was obtained according to the directions cited in the preceding section. Instead of chromatography the material was subjected to benzylidenation. The material was stirred overnight at room temperature with 4 g of anhydrous zinc chloride in 25 ml of benzaldehyde. To the reaction mixture was then added 150 ml of water and 50 ml of petroleum ether (b.p. 80–100°). When no solid had separated after 30 min of vigorous magnetic stirring, the emulsion was allowed to settle into three layers. The oily middle layer was presumed to contain the desired product. This layer was isolated, washed several times with fresh petroleum ether, then taken up in 10 ml of ethanol, and water was added to incipient turbidity. On standing at 23° for 2 d and at 4° for another day there crystallized 100 mg of XVII melting at 163–164°. Several additional crops totalling 196 mg and having slightly lower melting points were deposited by the mother liquor on prolonged standing. Recrystallization from aqueous ethanol afforded platelets of m.p. 167° and $[\alpha]_D^{23}$ +87.2° (*c*, 1 in ethanol).

Anal. Calcd. for $C_{14}H_{17}NO_7$ (311.3): C, 54.01; H, 5.51. Found: C, 54.03; H, 5.45.

The infrared spectrum shows hydroxyl (3 330 cm^{-1}) and nitro (1 550 cm^{-1}) bands and in the region 900–700 cm^{-1} the following characteristic peaks: 893(w), 865(w), 850(w), 790(m), 757(s), 697(s).

A sample of 50 mg of XVII was hydrogenated at room temperature with a platinum catalyst in 10 ml of *N*/10 hydrochloric acid. The benzylidene group was thereby removed and the nitro group reduced. The resulting amine hydrochloride failed to crystallize but gave on acetylation (as described in the preceding section) crystalline methyl 3-acetamido-3-deoxy-2,4,6-tri-*O*-acetyl-α-D-glucopyranoside, m.p. 179°, which was identified by an undepressed mixture melting point and by its infrared spectrum.

ACKNOWLEDGMENT

This work was supported by the National Institute of Allergy and Infectious Diseases, United States Public Health Service (Grant AI-4697), and by the National Research Council of Canada (Grant A 1350).

REFERENCES

1. H. H. BAER and T. NEILSON. Can. J. Chem. **43**, 840 (1965).
2. H. H. BAER. Chem. Ber. **93**, 2865 (1960).
3. H. H. BAER. J. Am. Chem. Soc. **83**, 1882 (1961).
4. H. H. BAER and F. KIENZLE. Can. J. Chem. **41**, 1606 (1963).
5. H. FEUER and S. MARKOFSKY. J. Org. Chem. **29**, 929 (1964).
6. J. C. SOWDEN, M. L. OFTEDAHL, and A. KIRKLAND. J. Org. Chem. **27**, 1791 (1962).
7. H. O. L. FISCHER and H. H. BAER. Ann. Chem. **619**, 53 (1958).
8. H. H. BAER and H. O. L. FISCHER. J. Am. Chem. Soc. **82**, 3709 (1960).
9. H. H. BAER. J. Am. Chem. Soc. **84**, 83 (1962).
10. H. OGAWA, T. ITO, S. KONDO, and S. INOUE. Bull. Agr. Chem. Soc. Japan, **23**, 289 (1959).

Can. J. Chem. Downloaded from www.nrcresearchpress.com by 210.87.254.40 on 09/05/12
For personal use only.

Can. J. Chem. Downloaded from www.nrcresearchpress.com by 210.87.254.105 on 09/05/12
For personal use only.

STUDIES IN THE BIOCHEMISTRY OF MICROORGANISMS

PART 117.[1] SEPEDONIN, A TROPOLONE METABOLITE OF SEPEDONIUM CHRYSOSPERMUM FRIES[2]

P. V. DIVEKAR[3] AND H. RAISTRICK,

Department of Biochemistry, London School of Hygiene and Tropical Medicine, University of London, London, England,

T. A. DOBSON,[4]

Prairie Regional Laboratory, National Research Council of Canada, Saskatoon, Saskatchewan,

AND

L. C. VINING

Atlantic Regional Laboratory, National Research Council of Canada, Halifax, Nova Scotia

Received December 15, 1964

ABSTRACT

Two yellow substances were isolated from culture filtrates of the fungus *Sepedonium chrysospermum* Fries. One of these, named sepedonin, predominates in growing cultures and is believed to be the direct product of metabolism. The second, an anhydro derivative of sepedonin, was probably formed spontaneously in the culture filtrate, and during the isolation process, by chemical dehydration. Sepedonin, $C_{11}H_{12}O_5$ with one C-methyl group, gave two dimethyl ethers with diazomethane and has the spectral characteristics of a substituted tropolone. Dehydration under mild conditions afforded anhydrosepedonin, from which a monomethyl ether and two dimethyl ethers were prepared. One of the latter was unstable and rearranged slowly to a third dimethyl ether. By fusion with alkali, anhydrosepedonin was converted to a mixture from which two substituted benzoic acids and a product formulated as 6-hydroxy-4-methyltropolone were separated. The bathochromic displacement of the peaks in the ultraviolet spectrum of anhydrosepedonin compared with those in sepedonin indicated an unsaturated group conjugated to the tropolone ring, confirmed by catalytic reduction to a dihydro derivative. By careful oxidation of one of the dimethyl ethers of anhydrosepedonin with permanganate a substance believed to be a tropolone containing ester and carboxyl substituents was obtained, together with a second product formulated as the 3,4-cyclic anhydride. From these results and supporting n.m.r. and spectral evidence anhydrosepedonin is considered to be a 6-hydroxytropolone with a 2′-methylpyran ring fused at the 4,5,4′,5′-positions. Sepedonin differs only by having a 2′-hydroxy-2′-methyldihydropyran ring as the heterocyclic moiety.

Sepedonium chrysospermum (Bull.) Fr., the imperfect stage of *Hypomyces chrysospermus* (Bull.) Tul., has been isolated from soils in Europe and the American continent and is a common parasite of the fleshy fungi. The strain used in the present work was isolated from *Boletus luridus*. Cultures of this hyphomycete developed a yellow color in the broth and the surface mycelium showed patches of orange-yellow color after approximately 10 days undisturbed growth on Raulin-Thom or Czapek-Dox media. The color of the culture fluid later deepened and, in addition, gave an increasingly strong greenish-brown reaction with ferric chloride. Spectrophotometric examination of the solution showed that these changes corresponded with the appearance of a strong absorption peak at 250–275 mμ and weaker absorption in the region between 300 and 360 mμ. The wavelengths at which the maxima appeared varied with the pH of the culture filtrate. The

[1]*Part 116: J. H. Birkinshaw and A. M. L. Dryland, Biochem. J. 93, 478 (1964).*

[2]*Issued as N.R.C. No. 8364.*

[3]*National Research Council of Canada Postdoctorate Fellow, 1957–1959. Some of the work described in this paper forms part of a Ph.D. thesis submitted in October 1956, to the University of London by P. V. Divekar. Present address: Microbiology Department, Defence Research Laboratory, Kanpur, India.*

[4]*National Research Council of Canada Postdoctorate Fellow 1960–1962. Present address: Ayerst, McKenna and Harrison, Montreal, Quebec.*

optical density at 271 mμ of filtrates buffered at pH 7.0 reached a maximum in cultures which had been incubated for approximately 30 days at 25°. At this time more than 90% of the glucose had been exhausted from the medium. Information on the development of cultures grown on Raulin-Thom as well as Czapek-Dox media is summarized in Table I. The main product isolated from metabolism solutions of *S. chrysospermum* was given the trivial name sepedonin.

TABLE I

	Incubation period											
	7 days			14 days			21 days			28 days		
	Batch No.											
	I	II	III	I	II	III	I	II	III	I	II	III
Czapek-Dox medium pH colorimetric	6.2	6.2	6.4	6.8	6.4	6.6	7.2	7.0	6.8	7.2	7.2	6.8
Residual glucose by polarimeter (%)	4.60	4.60	4.03	2.60	2.92	2.50	1.13	1.14	1.06	0.39	0.52	0.50
Raulin-Thom medium pH colorimetric	3.6	3.4	3.6	3.4	3.6	3.6	3.6	3.6	3.6	3.6	3.6	3.6
Residual glucose by polarimeter (%)	4.05	4.33	4.33	2.25	2.42	2.50	1.05	0.97	1.09	0.44	0.82	0.98

Sepedonin obtained by extracting filtrates at pH 3.5 with ethyl acetate and recrystallized from the same solvent retained ethyl acetate tenaciously in the crystals. When freed of solvent the compound gave analyses for a molecular formula of $C_{11}H_{12}O_5$, with one C-methyl but no methoxyl group. Methylation with diazomethane yielded two isomeric dimethyl ethers, the infrared spectra of which still showed hydroxyl absorption. Attempts to methylate the compound under more vigorous conditions, or to prepare other derivatives invariably led to complex mixtures and were accompanied by large bathochromic shifts in the ultraviolet absorption maxima. Similar spectral shifts could be brought about by treating sepedonin with dilute acid or alkali or even by heating a solution in ethanol.

The product obtained after acetic acid treatment was isolated and found to differ from sepedonin by loss of the elements of water. It is identical with the substance which Divekar (1) first isolated directly from culture filtrates of *S. chrysospermum* and named "sepedonin". Spectroscopic examination of the products excreted by stationary cultures of the fungus grown on Czapek-Dox medium has shown that the proportion of anhydro compound present during the early growth phase is less than 15% of the mixture, but increases later as the cultures become alkaline. This is illustrated in Figs. 1 and 2. If the pH of the cultures increases beyond 8.0, as frequently happens after growth has ceased in shaken cultures, anhydrosepedonin is usually the only product which can be isolated. Most of the sepedonin appears in the culture fluid but extraction of the mycelium with organic solvents under mild conditions afforded a very small amount which was difficult to separate in a pure form. Absorption spectra of crude mycelial extracts indicated that the proportion of anhydro form was less than in the corresponding culture filtrates. Because of the susceptibility of sepedonin to dehydration it appears likely that the presence of anhydrosepedonin in cultures is the result of a chemical change. Isolation of the anhydro form directly from culture filtrates may be due to the acidic conditions employed in this procedure, but dehydration would also occur during purification of the product by crystallization from hot ethanol and acetic acid. We now propose to reserve

Can. J. Chem. Downloaded from www.nrcresearchpress.com by 210.87.254.105 on 09/05/12
For personal use only.

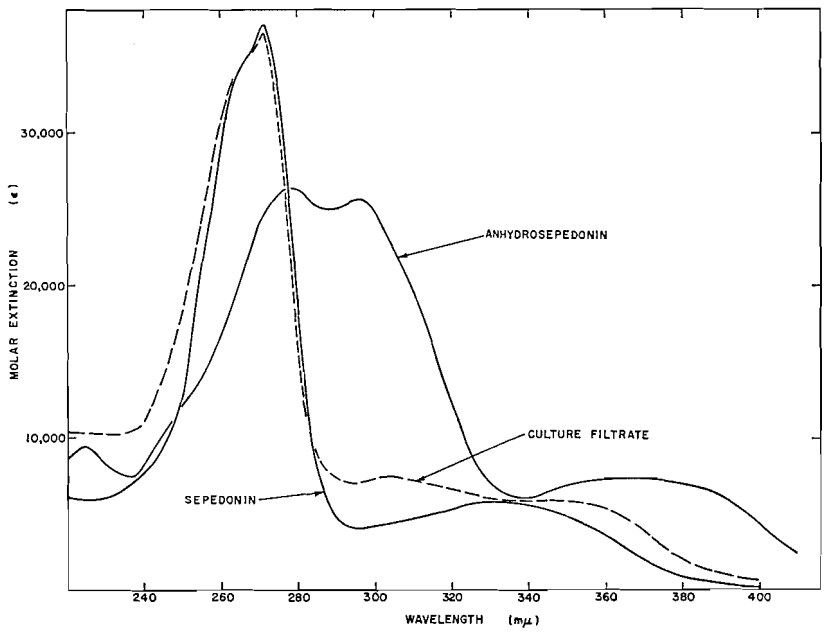

FIG. 1. Absorption spectra of sepedonin and anhydrosepedonin in 0.1 *M* sodium phosphate buffer pH 7.4 compared with that of the filtrate from a 30 day old culture of *S. chrysospermum* grown on Czapek-Dox medium and diluted with the phosphate buffer.

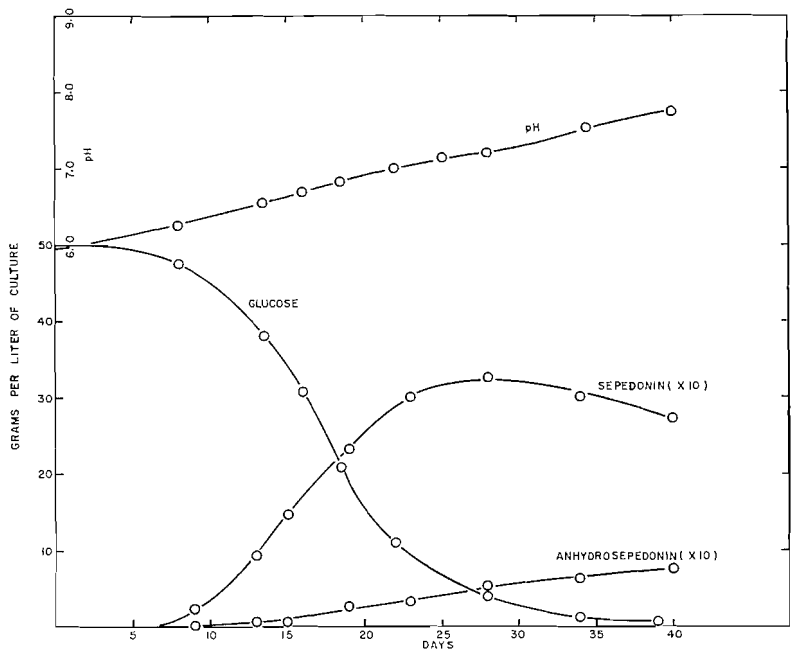

FIG. 2. Changes in glucose, sepedonin, and anhydrosepedonin concentration and pH during growth of *S. chrysospermum* in stationary culture on Czapek-Dox medium.

Can. J. Chem. Downloaded from www.nrcresearchpress.com by 210.87.254.105 on 09/05/12
For personal use only.

use of the name "sepedonin" for the hydrated metabolite of *S. chrysospermum* and to refer in future to the compound first isolated by Divekar (1) as "anhydrosepedonin".

Anhydrosepedonin has the properties of both a weak base and a weak acid. In anhydrous media a monohydrochloride and monoperchlorate could be prepared; both were hydrolyzed rapidly in water. Since anhydrosepedonin lacks nitrogen the basicity must be due to a structural feature involving oxygen or a pseudoaromatic ring. One acidic function could be readily detected by titrating with alkali and, since no decarboxylation occurred when anhydrosepedonin was boiled with either copper chromite catalyst in quinoline or 2 *N* sulfuric acid, this is presumed to be a phenolic group. The conclusion is supported by the absence of absorption maxima in the infrared spectrum which might be assigned to a carboxyl group. Short treatment of anhydrosepedonin with diazomethane yielded a monomethyl derivative which, although no longer soluble in bicarbonate, retained some weakly acidic properties, and the characteristic ferric chloride reaction of the parent compound. Longer exposure to diazomethane gave a mixture of isomeric dimethyl ethers which were no longer acidic and showed no hydroxyl absorption maxima in their infrared spectra. Two of the oxygen functions of anhydrosepedonin are therefore phenolic in character. Attempts to prepare acetyl derivatives of sepedonin or anhydrosepedonin with either basic or acidic catalysts were unsuccessful.

No quinonoid or ketonic groups could be detected in sepedonin or its anhydro derivative by chemical tests. After reduction with zinc and acetic acid, however, anhydrosepedonin gave a copious precipitate with Brady's reagent indicating a masked ketonic function as is the case with the tropolonoid stipitatic acid (2). The infrared absorption spectra of sepedonin and its derivatives show intense maxima in the 1 500 – 1 605 cm^{-1} region with weaker maxima at 1 625 – 1 650 cm^{-1}. These are consistent with the presence of a tropolone nucleus (3–6). Further evidence has been provided by the potentiometric titration of anhydrosepedonin which showed the two acidic functions to have p*K* values similar to those reported for 4-hydroxytropolone (7). By reaction of anhydrosepedonin with fused potassium hydroxide 3-hydroxy-5-methylbenzoic acid (I) and 3,4-dimethyl-5-hydroxybenzoic acid (II) have been isolated (8). Tropolones are known to rearrange to the corresponding benzoic acids under these conditions (2, 9, 10, 11). The alkaline fusion also afforded a third product which could be obtained in better yield under somewhat milder conditions. This was a weak acid analyzing for $C_8H_8O_3$, with one C-methyl substituent, and gave a color reaction with ferric chloride similar to that of sepedonin. The ultraviolet absorption spectrum was tropolonoid rather than benzenoid in character (12) and generally similar to that of sepedonin itself. From the analyses it is assumed that one methyl and one hydroxyl substituent are present on the tropolone ring, and the most plausible structure, in view of the concomitant production of 3-hydroxy-5-methylbenzoic acid during alkaline fusion, would be (III).

If the formation of 3,4-dimethyl-5-hydroxybenzoic acid is also taken into account, anhydrosepedonin may be formulated as a 6-hydroxytropolone with carbon substituents

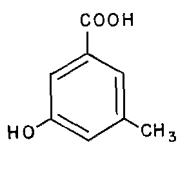

I

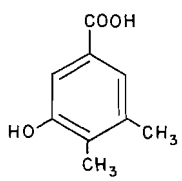

II

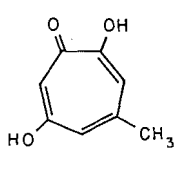

III

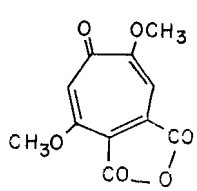

IV

Can. J. Chem. Downloaded from www.nrcresearchpress.com by 210.87.254.105 on 09/05/12
For personal use only.

in the 4 and 5 positions. The ultraviolet absorption spectrum of sepedonin with a strong maximum in 0.01 *N* ethanolic HCl at 258 mμ (ϵ = 51 800) and a weaker peak at 329 mμ (ϵ = 9 310) is comparable with that of 4-hydroxytropolone for which the principal absorption maximum is reported to be just below 250 mμ (13). In the spectrum of anhydrosepedonin measured in acidic ethanol the principal maximum is at about 305 mμ and the longer wavelength maximum at 383 mμ is also bathochromically displaced by comparison with the corresponding maximum of sepedonin. It is apparent that dehydration of sepedonin has introduced additional unsaturation which is conjugated to the tropolone chromophore. A more complete discussion of the absorption spectrum of anhydrosepedonin, for which we are indebted to Dr. G. Aulin-Erdtman, can be found in the experimental section.

The remaining part of the C_4H_6O fragment unaccounted for in anhydrosepedonin must contain one C-methyl group and an inert oxygen atom. Information about this portion of the molecule has come from the oxidation of one of the methyl ethers of anhydrosepedonin with permanganate. From the mixture of products there was isolated an acid, $C_{13}H_{14}O_7$ which retained the two methoxyl and one C-methyl substituents as well as all carbon atoms of the parent compound. The ultraviolet spectrum of this product had reverted to the type of tropolone absorption represented by sepedonin, suggesting that oxidation had resulted in loss of the conjugated double bond of the anhydro compound. Infrared spectral evidence indicated that a carboxyl (ν_{max} 1 720 cm^{-1}) and an ester (ν_{max} 1 738 cm^{-1}) function had been generated. Treatment of the acid with diazomethane afforded a nonacidic ester (ν_{max} 1 725 cm^{-1}).

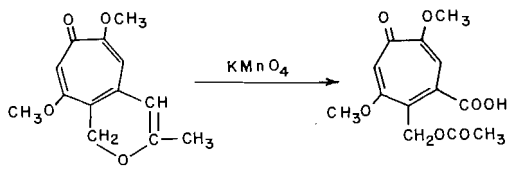

V VI

A second product, obtained in very small yield from the oxidation, analyzed for $C_{11}H_8O_6$ and is considered to be the anhydride (IV) or the isomeric methyl ether. Infrared maxima at 1 850 and 1 775 cm^{-1} attributed to the cyclic anhydride structure are comparable with those at 1 824 and 1 746 cm^{-1} in stipitatonic acid (6), and at 1 830 and 1 770 cm^{-1} in puberulonic acid (3, 4). The reaction with permanganate may be explained as the oxidative fission of a pyran ring fused to the tropolone as in (V), which would represent one of a number of possible isomeric structures of anhydrosepedonin dimethyl ether A. Cleavage of the double bond in (V) would give the acid ester (VI). An analogous reaction has been shown to occur when methyl di-*O*-methylanhydrofulvate (14) is oxidized with permanganate. The presence of a fused pyranotropolone ring system would account for the basicity of anhydrosepedonin, which is greater than expected for a tropolone system alone. It would also explain adequately the formation of formic, acetic, and malonic acids when anhydrosepedonin is oxidized with alkaline hydrogen peroxide. Anhydrosepedonin could be reduced over a suitable catalyst with the uptake of 1 mole of hydrogen. The product, deoxysepedonin, showed ultraviolet absorption maxima similar to those of sepedonin and consistent with the structure (VII) or an isomer.

The mass spectrum of anhydrosepedonin gave peaks above the highest expected molecule–ion peak at 206. This anomalous behavior disappeared upon hydrogenation,

Can. J. Chem. Downloaded from www.nrcresearchpress.com by 210.87.254.105 on 09/05/12
For personal use only.

when the highest molecule–ion peak was at 208, provided the inlet temperature was not above 200°. The nuclear magnetic resonance (n.m.r.) spectrum of anhydrosepedonin measured in a 1:1 mixture of deuterated acetone and deuterated chloroform gave signals at τ values of 2.88 and 3.15 (two tropolone ring hydrogens); 4.15 (vinylmethine), 4.70 (methylene), and 7.89 (methyl). The assignments are consistent with the structure (VIII) or the isomer with reversed substitution at C_4 and C_5. A similar interpretation arrived at independently by Professor H. Erdtman is given in the experimental section. Structure (VIII) is preferred since the formation of 3-hydroxy-5-methylbenzoic acid (I) and 6-hydroxy-4-methyltropolone (III) during alkaline fusion may be then accounted for as the elimination of a hydroxymethyl group β- to the tropolone C_6 ring hydroxyl by means of a reversed aldol reaction. Formation of three isomeric dimethyl ethers by the action of diazomethane on anhydrosepedonin is unexpected. However, one of these, dimethyl ether A, is an unstable product which rearranges slowly to the stable derivative, dimethyl ether A_1. The type of rearrangement involved and the structure of the three products is not yet understood.

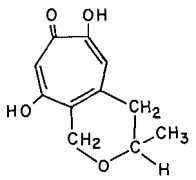

VII

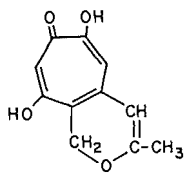

VIII

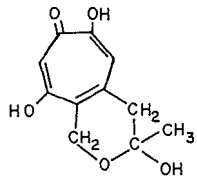

IX

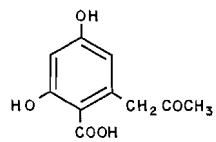

X

The facile dehydration of sepedonin is similar to the conversion of the fungal metabolites fusarubin (15) and fulvic acid (14, 16) to their anhydro derivatives and is presumed to be due to the presence of a similar 2′-hydroxy-2′-methyldihydropyrane ring fused to the aromatic system. Like fusarubin and fulvic acid, sepedonin is optically inactive at the wavelength of sodium light and we propose for it the structure (IX). Assuming that its biosynthesis follows the pathway suggested for other fungal tropolones and now supported by considerable experimental evidence (17), sepedonin should be formed by condensation of acetyl coenzyme A with four units of malonyl coenzyme A. By analogy with the route proposed for stipitatonic and puberulonic acids in which orsellinic acid is an intermediate (18, 19), the phenolic acid (X) which has been isolated by Raistrick (20, 21) from cultures of *Penicillium brevicompactum* may represent an intermediate in the biosynthesis of sepedonin.

EXPERIMENTAL

Culture

The culture of *Sepedonium chrysospermum* Fries used in this work was purchased in July 1939, from the Centraalbureau voor Schimmelcultures, Baarn, Holland, who received it in July 1923 from Boedijn, Hortus Botanicus, Amsterdam, by whom it was isolated from *Boletus luridus*. It was maintained in two separate culture collections under the London School of Hygiene and Tropical Medicine (L.S.H.T.M.) catalogue numbers Ag 39 and B.B. 166. These collections were subcultured at different times and on different media. Nevertheless, comparative experiments have shown no appreciable difference in the yields of anhydrosepedonin obtained from the two cultures.

A transfer of Ag 39 is maintained on Difco malt agar slopes in the Prairie Regional Laboratory culture collection under the catalogue number PRL 1707.

Production, Isolation, and Properties of Sepedonin

Medium

The nutrient used routinely for production of sepedonin was Czapek-Dox solution of the following composition: glucose, 50 g; $NaNO_3$, 2 g; KH_2PO_4, 1 g; KCl, 0.5 g; $MgSO_4 \cdot 7H_2O$, 0.5 g; $FeSO_4 \cdot 7H_2O$,

Can. J. Chem. Downloaded from www.nrcresearchpress.com by 210.87.254.105 on 09/05/12
For personal use only.

Can. J. Chem. Downloaded from www.nrcresearchpress.com by 210.87.254.105 on 09/05/12
For personal use only.

0.01 g; distilled water, 1 l. Portions (350 ml) were dispensed into 1 l Erlenmeyer flasks and autoclaved for 20 min.

Inoculum and Conditions of Culture

A few drops of a spore suspension obtained by shaking an agar slope culture with 10 ml of sterile water proved satisfactory as inoculum only when the nutrient solution was supplemented with biotin at the rate of 5 μg per l. With a large spore inoculum sufficient biotin was introduced to give satisfactory growth without the vitamin supplement. Equally vigorous and more uniform growth was obtained with a vegetative inoculum produced by inoculating a medium consisting of Difco yeast extract (1%) and D-glucose (1%) at pH 7.2–7.4 with a spore suspension of *S. chrysospermum* and incubating at 25° on a rotary shaker at 150 r.p.m. for 3 days. These cultures were macerated in a Waring blendor and 1 ml of the suspension used for each 350 ml of production medium.

The inoculated cultures were left undisturbed in the dark at ambient temperature for 30–35 days.

Estimation of Sepedonin and Anhydrosepedonin in Culture Filtrates

Cultures were grown in triplicate in 1 l Erlenmeyer flasks constructed with a small sidearm below the surface of the 350 ml of nutrient solution. This fitting was closed with a rubber hypodermic cap, through which a sterile hypodermic needle was inserted at intervals and samples (2 ml) withdrawn for analysis of the culture fluid. A portion of the filtered metabolism solution was diluted with 0.1 *M* phosphate buffer pH 7.0, and its ultraviolet absorption spectrum recorded. Fig. 1 shows the spectrum of a 30 day old culture and, for comparison, those of sepedonin and anhydrosepedonin recorded under similar conditions. The quantities of sepedonin and anhydrosepedonin in the culture fluid were calculated by Vierordt's method (22) from the optical densities at 271 and 296 mμ. Glucose remaining in the culture filtrate was estimated with the Somogyi reagent (23). Changes in these values observed during the growth of the fungus are plotted in Fig. 2.

Isolation, Purification, and Properties of Sepedonin

The mycellium was separated by filtration through glass wool. The broth was adjusted with hydrochloric acid to pH 3.5 and allowed to remain overnight at 4°. The clear supernatant was decanted and the remaining turbid portion filtered. The clarified culture fluid was extracted six times with half volumes of ethyl acetate. Partition into ether or chloroform was less favorable, and the use of more polar solvents, such as *n*-butanol or methyl ethyl ketone into which the product was more readily extracted, resulted in decomposition.

The extracts were combined and the solvent removed at 40° *in vacuo*. Sepedonin crystallized from the concentrated solution and was purified by three additional crystallizations from the same solvent as pale-yellow prisms, m.p. 190–205° (decomp.). Found in a sample of this material dried in high vacuum at room temperature: C, 58.58; H, 5.85; OC_2H_5, 3.11. $C_{11}H_{12}O_6 \cdot \frac{1}{6}CH_3COOC_2H_5$ requires C, 58.68; H, 5.63; OC_2H_5, 3.14%. ν_{max} (KBr disk) at 1 730 cm^{-1}. Drying the sample at 80° caused decomposition. However, when the crystals were redissolved in ethanol and immediately evaporated to dryness at 40° *in vacuo*, and this procedure repeated twice, the preparation no longer absorbed energy at 1 730 cm^{-1}. The ultraviolet absorption spectrum was not appreciably changed, and showed $\lambda\lambda_{max}$ 253 mμ (ϵ = 36 800) and 327 mμ (ϵ = 6 400) in ethanol. Principal ν_{max} (KBr disk) at 3 265, 2 920, 2 850, 1 656 (shoulder), 1 600, 1 573, 1 525, 1 462, 1 378, 944, 870, 796, and 705 cm^{-1}. Found: C, 59.11; H, 5.63; OCH_3, nil; CCH_3, 11.83; mol. wt. (osmometer in ethanol) 226; $[\alpha]_D^{26°}$ nil (*c*, 0.2 in ethanol). $C_{11}H_{12}O_6$ requires: C, 58.92; H, 5.40; 1-CCH_3, 12.06%; mol. wt. 224.2.

Sepedonin is insoluble in petroleum ether, carbon tetrachloride, and benzene, poorly soluble in chloroform, ethyl acetate, acetone, or water, and fairly soluble in ethanol, pyridine, or dioxane. It is insoluble in dilute $NaHCO_3$ but dissolves easily in dilute Na_2CO_3 or NaOH solution. It is also soluble in *N* HCl giving a straw-colored solution which rapidly turns bright yellow. The solution in concentrated H_2SO_4 is also yellow. Ferric chloride added to an alcoholic solution gives a deep-green color. Tests with ketonic reagents are negative.

Derivatives of Sepedonin

Methylation of Sepedonin

Sepedonin (123 mg) in a mixture of chloroform (10 ml) and ethanol (10 ml) was treated with a distilled ethereal solution of diazomethane (from 0.5 g of nitrosomethylurea) at 0° for 18 h. The reaction products were adsorbed from chloroform solution on to a column of silicic acid which was developed first with chloroform and then with a gradient of ethyl acetate in chloroform. Two main bands, pale yellow in color, were eluted. The appropriate eluates were evaporated to dryness *in vacuo* at 40° and the residue crystallized from ethyl acetate to give the following. *(a) Sepedonin dimethyl ether A* as pale-yellow silky needles, m.p. 150–158° (decomp.), $\lambda\lambda_{max}$ in ethanol at 252 mμ (ϵ = 23 120) and 322 mμ (ϵ = 5 980), ν_{max} (KBr disk) at 3 270, 1 635 (w), 1 602, 1 592, 1 555, 1 527, 996, 946, 863, and 793 cm^{-1}. Found: C, 61.63; H, 6.50; OCH_3, 24.74. $C_{13}H_{16}O_6$ requires: C, 61.89; H, 6.39; 2-OCH_3, 24.61%. *(b) Sepedonin dimethyl ether B* as pale-cream prisms, m.p. 140–148° (decomp.), $\lambda\lambda_{max}$ in ethanol at 252 mμ (ϵ = 21 700) and 326 mμ (ϵ = 5 600), ν_{max} (KBr disk) 3 290, 1 645 (shoulder), 1 598, 1 555, 1 527, 990, 962, 938, 864, and 789 cm^{-1}. Found: C, 61.71; H, 6.24; OCH_3, 24.87%.

Can. J. Chem. Downloaded from www.nrcresearchpress.com by 210.87.254.105 on 09/05/12
For personal use only.

Anhydrosepedonin (by Direct Isolation from S. chrysospermum)

Two culture media were used for the preparation of anhydrosepedonin. (*a*) Czapek-Dox solution without addition of biotin and (*b*) Raulin-Thom solution: glucose, 75.0 g; tartaric acid, 4.0 g; ammonium tartrate, 4.0 g; $(NH_4)_2HPO_4$, 0.60 g; $(NH_4)_2SO_4$, 0.25 g; K_2CO_3, 0.60 g; $MgCO_3$, 0.40 g; $FeSO_4 \cdot 7H_2O$, 0.07 g; $ZnSO_4 \cdot 7H_2O$, 0.07 g; distilled water, 1.5 l.

These solutions (350 ml/flask) were distributed in 1 l conical flasks which were plugged with cotton wool and sterilized. The contents of the flasks were inoculated with a spore suspension, in sterile water, prepared from mature cultures of *Sepedonium chrysospermum* (strain Ag. 39 or B.B. 166) grown on wort agar, four flasks being inoculated from one slope. The inoculated flasks were incubated at 24° in the dark.

Initially the fungus grew slowly on Czapek-Dox solution, the surface of which was covered after 1 week with a white mycelium which changed to various shades of orange by the middle of the second week. Growth became very luxuriant and brownish orange in color by the end of the fourth week. The culture fluid, initially colorless, was then dark brown.

Growth on Raulin-Thom solution was not quite as heavy as on Czapek-Dox solution but showed a similar range of color. After 4 weeks incubation both mycelium and culture fluid were deep orange in color.

In order to follow the course of metabolism and to determine the optimum time of harvesting the flasks for the preparation of anhydrosepedonin, batches of 25 flasks of each culture medium were inoculated with *Sepedonium chrysospermum.* One flask culture of each medium was harvested after 7, 14, 21, and 28 days incubation. The culture fluid was then separated by filtration from the mycelium and examined. The results obtained in three separate experiments are summarized in Table I. The culture filtrate from each medium gave no color with $FeCl_3$ after 7 days incubation, pale brown after 14 days, brown after 21 days, and deep brown after 28 days, the intensity of the ferric color being a rough measure of the amount of anhydrosepedonin present.

The contents of the remaining 21 flasks of each culture medium after 28 days incubation were filtered and the separated mycelium was washed with water, dried *in vacuo* at 45°, and weighed. The respective weights of mycelium from batches I, II, and III were 78 g, 80 g, and 92 g on Czapek-Dox medium and 58 g, 50 g, and 60 g on Raulin-Thom medium. The respective culture filtrates and washings were evaporated *in vacuo* to about 1/10 volume, acidified with concentrated HCl to pH about 2.0 and exhaustively extracted with ether to separate anhydrosepedonin. The ether extracts were evaporated to dryness and the resulting dark-orange gums weighed. The respective weights of crude anhydrosepedonin from batches I, II, and III were 3.7 g, 3.5 g, and 3.9 g on Czapek-Dox medium and 3.2 g, 3.0 g, and 2.8 g on Raulin-Thom medium.

Hence Czapek-Dox medium was used for the subsequent bulk preparation of anhydrosepedonin and the flasks were harvested after 28 days incubation. The orange-colored ether extract obtained as described above from 100 such flasks was evaporated to dryness. The resulting gum was weighed and triturated with cold acetone, giving an orange solid, m.p. 190–197° (decomp.), which was separated by filtration and purified by crystallization either from absolute ethanol or glacial acetic acid. From four batches, each consisting of 100 flasks of Czapek-Dox medium, there was obtained 16.6, 17.2, 15.3, and 15.8 g of crude ether extract yielding respectively 5.8, 6.2, 4.3, and 4.9 g of pure crystalline *anhydrosepedonin.* From three batches, each consisting of 100 flasks of Raulin-Thom medium, there was obtained 3.9, 3.5, and 3.2 g of pure anhydrosepedonin.

Extraction of the dried and defatted mycelium with a variety of organic solvents failed to yield any crystalline material. However, small amounts of crystalline anhydrosepedonin were obtained from the extraction of Raulin-Thom mycelium with cold dilute aqueous NaOH or Na_2CO_3. The alkaline extracts were acidified and extracted with ether and the residue obtained on removal of the solvent was crystallized from acetone. Yield of anhydrosepedonin, melting point and mixed melting point 203–205°, 50 mg from 25 g of dried mycelium.

Anhydrosepedonin forms glistening yellow needles, m.p. 205° (decomp. and not resetting on cooling). It contains no N, Cl, or S. Found: C, 64.0, 64.2; H, 5.52, 5.29; O, by direct estimation, 31.2; OCH_3, nil; CCH_3, 5.5; active H atoms in pyridine, 0.86%; titration equivalent to phenolphthalein, 204. $C_{11}H_{10}O_4$ requires: C, 64.1; H, 4.89; O, 31.0; 1-CCH_3, 7.3; 2 active H atoms, 0.98%, equivalent titrating as a monobasic acid, 206; $\lambda\lambda_{max}$ in ethanol at 249 mμ (ϵ = 15 750), 286 mμ (ϵ = 29 400), 302 mμ (inflection, ϵ = 18 700), 354 mμ (inflection, ϵ = 8 270), 375 mμ (ϵ = 7 250), and 386 mμ (ϵ = 8 130). Principal ν_{max} (Nujol) at 1 660, 1 607, 1 465, 1 430, 1 370, 1 340, 1 310, 1 230, 1 170, 1 140, 1 105, 885, 835, and 725 cm^{-1}.

Anhydrosepedonin shows no optical activity. It sublimes unchanged in high vacuum at 170°. It is sparingly soluble in water and ether, but appreciably soluble in acetone, ethanol, methanol, ethyl acetate, dioxane chloroform, and benzene. It is insoluble in light petroleum (b.p. 40–60°). It dissolves slowly in aqueous $NaHCO_3$ but readily in aqueous NaOH. It also dissolves readily in concentrated HCl from which it is precipitated unchanged on dilution with water. It gives a strong-brown color in aqueous or ethanol solution with either aqueous or ethanolic $FeCl_3$. It gives no precipitate with Brady's reagent (0.32% 2,4-dinitrophenylhydrazine in aqueous 2*N* HCl). Its yellow ethanolic solution is not decolorized with sodium dithionite, $Na_2S_2O_4$, nor is ammoniacal $AgNO_3$ reduced. It gives a negative color test for primary and secondary alcohols (24).

Anhydrosepedonin (from Sepedonin)

Sepedonin (100 mg) was heated under reflux for 1 h in glacial acetic acid (5 ml). On cooling, bright-yellow needles (47 mg) separated slowly from the solution. After two recrystallizations from ethanol they had m.p.

203–205° (decomp.), unchanged when a specimen was mixed with anhydrosepedonin obtained directly from culture filtrates of *S. chrysospermum*. Found: C, 63.93; H, 5.05; CCH_3, 5.5%; neutralization equivalent by potentiometric titration in 80% ethanol against 0.1 *N* NaOH, 207 ± 3 (p*K* of acid function titrated, 7.15).

Physical Properties of Anhydrosepedonin (by H. Erdtman and G. Aulin-Erdtman)

The sample used for these studies had been obtained through repeated recrystallizations of an old specimen. It may have been slightly impure, as indicated by the fact that it showed lower ultraviolet absorption maxima and a higher minimum at 275 mμ in ethanolic hydrochloric acid than a pure specimen, later obtained from Dr. Vining. The mass spectra of the two specimens, however, were very similar.

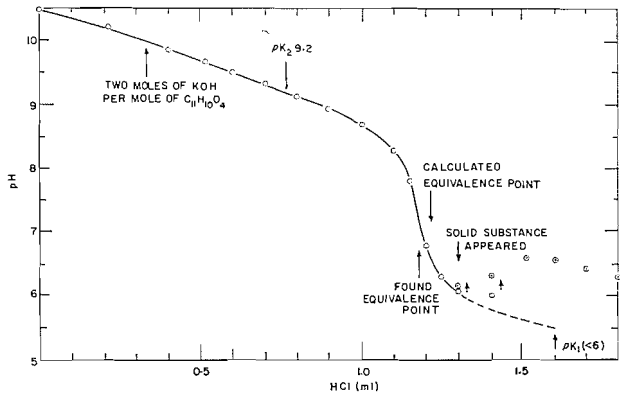

FIG. 3. Potentiometric titration of anhydrosepedonin (see text for details).

Potentiometric titration.—The potentiometric titration in aqueous solution presented difficulties because of the low solubility not only of anhydrosepedonin itself, but also of the presumed monosodium salt. The compound (10.7 mg) was dissolved by keeping it overnight at room temperature in excess (15.0 ml of 0.0084 *M*) aqueous potassium hydroxide solution containing a drop of octanol to wet the crystals, and back-titrated with 0.0613 *M* hydrochloric acid. Since solid precipitated after the first equivalence point had been passed the pK_1 could not be measured. From the titration curve (Fig. 3) an approximate upper limit of 6 is found for the pK_1 and pK_2 can be estimated as 9.2. The two values are in agreement with the dissociation constants of 4-hydroxytropolone for which Yui (7) quoted pK_1 (4-hydroxyl) 5.7 and pK_2 (2-hydroxyl) 9.5.

Ultraviolet absorption.—The absorption curve of anhydrosepedonin, measured in ethanol in the presence of a strong acid to suppress ionization of the acidic functions, showed three principal maxima (Fig. 4). The one at 250–251 mμ (log ε 4.3) may be compared with the nearly twice as high maximum just below 250 mμ reported by Nozoe and Kitahara (13) for 4-hydroxytropolone. The second high maximum, at 305 mμ (log ε 4.5, for the pure preparation 4.6), is probably a property of the entire chromophoric system, for which no close analogies yet seem to exist to enable comparison. β-Isopropenyltropolone shows no strong band in this region (25). The third, long wavelength maximum of anhydrosepedonin occurs at 386 mμ (383 mμ for the pure specimen, log ε 4.0 for both). It is bathochromically displaced and intensified compared with the

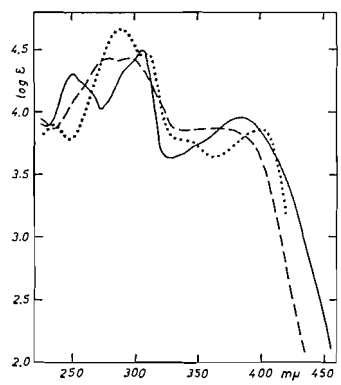

FIG. 4. Ultraviolet absorption curves for anhydrosepedonin: (—) in 0.1 *N* hydrochloric acid in 95% ethanol; (---) in phosphate buffer pH 7.2 (no ethanol added); (...) in 0.1 *N* potassium hydroxide in 95% ethanol.

Can. J. Chem. Downloaded from www.nrcresearchpress.com by 210.87.254.105 on 09/05/12
For personal use only.

long wavelength maxima of tropolones not containing an extended conjugated system. The solution of anhydrosepedonin in 0.1 *M* ethanolic hydrochloric acid showed only very slight spectral changes during the period of measurement but deteriorated when kept for 24 h.

The absorption of anhydrosepedonin in 0.1 *M* ethanolic potassium hydroxide solution should be that of the doubly ionized molecule. This solution was stable for at least 24 h and gave an absorption curve generally similar to that of fully ionized stipitatic acid (12) except for the maximum at 310 mμ (log ε 4.5), which seems to correspond to the 305 mμ peak of the acidic solution. The other maxima were: 236 mμ (log ε 3.9), 289 (4.7), and 401 (3.9).

To measure the absorption of the singly ionized molecule the substance was dissolved in aqueous phosphate buffer of pH 7.2. The solution is calculated to contain only 1% of doubly ionized and not more than 6% of unionized anhydrosepedonin. The difference in absorption between this and the acidic solution, however, is not only due to ionization of the 5-hydroxyl group but also to the change of solvent from ethanol to water. Thus, the hypsochromic shift of the long wavelength absorption on passing from the acidic to the near-neutral solution seems to be caused by the change of solvent. The following maxima were found: 279–280 mμ (log ε 4.4), 295 (4.4), and 350–370 (3.9).

The ultraviolet absorption of the deoxysepedonin, whose mass spectrum is discussed below, is shown in Fig. 5. The 305 mμ peak of anhydrosepedonin has disappeared and the overall absorption is now similar to that of tropolones without extended conjugation, although the absorption does not extend as far into the long wavelength region. The maxima for the acidic solution are: 259–260 mμ (log ε 4.7) and 333 (4.0); for the alkaline solution: 281–282 (4.7), 341 (3.9), and 368 (3.9).

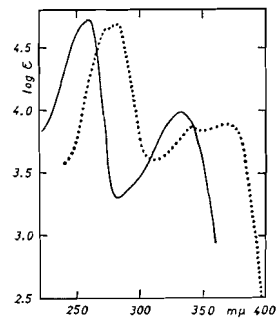

FIG. 5. Ultraviolet absorption curves for hydrogenated anhydrosepedonin (deoxysepedonin): (—) in 0.1 *M* ethanolic hydrogen chloride; (...) in 0.1 *M* ethanolic potassium hydroxide.

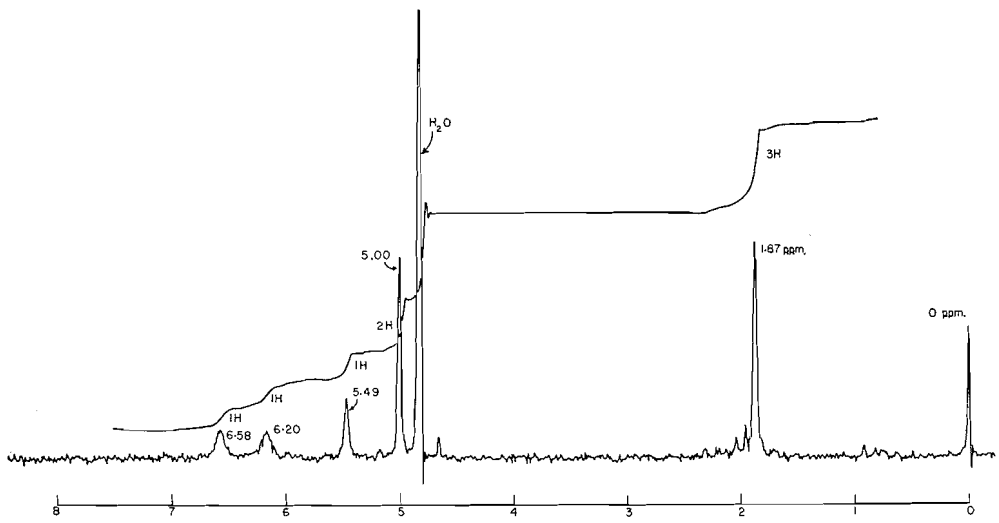

FIG. 6. Nuclear magnetic resonance spectrum of anhydrosepedonin in D_2O containing NaOD at a concentration of approximately 2 *N*. Trimethylsilyl acetic acid was the internal reference.

Can. J. Chem. Downloaded from www.nrcresearchpress.com by 210.87.254.105 on 09/05/12
For personal use only.

Nuclear magnetic resonance spectrum.—The spectrum (Fig. 6) was recorded for a solution in deuterium oxide containing approximately 2 *N* sodium deuteroxide. Trimethylsilyl acetic acid was the internal reference. The two hydrogen atoms of the tropolone ring exhibited resonance at 6.58 and 6.20 p.p.m. The signal at 6.20 p.p.m. is tentatively assigned to the hydrogen atom in position 3. As found for other tropolones examined under similar conditions the peaks were slightly broadened. Signals at 5.49, 5.00, and 1.87 p.p.m. are attributed to the olefinic, methylene, and methyl protons, respectively. An integration of the peaks supports these assignments.

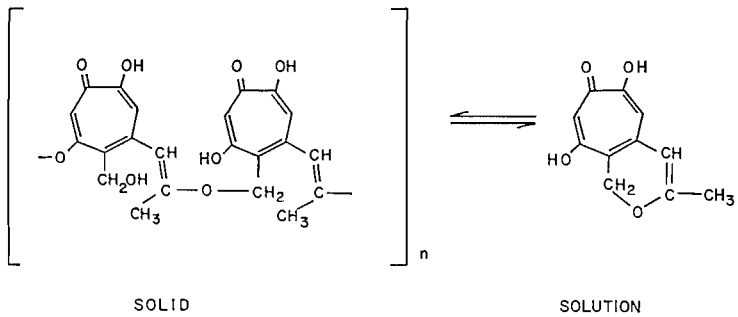

FIG. 7. Suggested oligomerization of anhydrosepedonin in the solid state.

Mass spectrum.—The two preparations of anhydrosepedonin used in these studies invariably gave mass peaks higher than the expected molecule–ion peak at 206 when examined at a range of temperatures. On the assumption that this behavior might be due to the existence of oligomers in the solid state (cf. Fig. 7) one of the samples, of which only a very small amount was available, was hydrogenated over 10% palladium on charcoal catalyst. The product, after purification by repeated sublimation and crystallization, melted in the temperature range 217–224°, with some needles remaining unchanged and sintering with decomposition up to 250°. A mass spectrum on this material at 200° gave the expected molecule–ion peak at 208, and additional peaks at 206, 178, 165, 152, 135, 121, 109, 93, 79, 77, 65, 53, and 43. At a higher temperature (250°) the result was essentially similar, except for the appearance of a lot of small peaks above 208.

Derivatives of Anhydrosepedonin

Hydrochloride.—Concentrated HCl (1 ml) was added to a filtered hot solution of anhydrosepedonin (0.5 g) in glacial acetic acid (35 ml). On cooling, *anhydrosepedonin hydrochloride* (0.35 g) crystallized from the greenish-yellow solution. It was collected and crystallized from acetic acid – concentrated HCl giving yellowish-green prisms (0.30 g) which blackened on heating above 205° but did not melt. Found: C, 54.5; H, 4.66; Cl, 14.7. $C_{11}H_{10}O_4 \cdot HCl$ requires: C, 54.4; H, 4.57; Cl, 14.6%.

The hydrochloride is immediately decomposed by water giving anhydrosepedonin and HCl. It (0.0162 g) was suspended in water for some time and shaken occasionally. The undissolved material was then separated by filtration, and the filtrate and washings were titrated against 0.02 *N* NaOH to phenolphthalein. Found: 3.40 ml 0.02 *N* NaOH = 14.9% Cl in the hydrochloride. The undissolved yellow crystalline material melted at 203–205° unchanged by admixture with anhydrosepedonin.

Perchlorate.—Aqueous $HClO_4$ (60%; 1 ml) was added to a suspension of anhydrosepedonin (0.5 g) in glacial acetic acid (15 ml). The substance dissolved and, on standing, *anhydrosepedonin perchlorate* crystallized out from the orange-colored solution. It was collected and recrystallized from acetic acid – perchloric acid as long yellow needles (0.36 g), m.p. 180–183° (decomp.). Found: C, 41.0; H, 4.22; Cl, 11.5. $C_{11}H_{10}O_4 \cdot HClO_4 \cdot H_2O$ requires: C, 40.7; H, 4.04; Cl, 10.9%. The perchlorate is immediately decomposed by water giving anhydrosepedonin and perchloric acid. Treatment of the perchlorate (0.0180 g) with water and titration as described for the hydrochloride required 2.86 ml of 0.02 *N* NaOH for neutralization to phenolphthalein = 11.3% Cl in the perchlorate. The undissolved residue was collected and dried. It melted at 203–205° unchanged by admixture with anhydrosepedonin.

Methylation Products of Anhydrosepedonin

Monomethyl ether.—An ether solution of diazomethane (from 5 g of nitrosomethylurea) was gradually added to a suspension of anhydrosepedonin (1 g) in methanol (50 ml). After 4 h a clear, greenish-yellow solution was obtained and was then evaporated to 30 ml and held overnight at 0°. The resulting crystals were collected (0.75 g), m.p. 158–160° (decomp.), and recrystallized from ethanol giving *anhydrosepedonin monomethyl ether* as canary-yellow needles (0.50 g), m.p. 163–164° (decomp.), which showed a marked green fluorescence in ultraviolet light. $\lambda\lambda_{max}$ in ethanol at 248.5 mμ (ϵ = 17 400), 285 mμ (ϵ = 28 700), and 383 mμ (ϵ = 5 430). ν_{max} (KBr disk) at 3 190, 3 100 – 2 350 (broad), 1 662, 1 614, 1 590, 1 543, 884, 845, 829, 800, and 770 cm^{-1}. Found: C, 65.15; H, 5.63; OCH_3, 14.2. $C_{12}H_{12}O_4$ requires: C, 65.5; H, 5.49; 1-OCH_3, 14.1%. The ether is insoluble in $NaHCO_3$ but is soluble in Na_2CO_3 and NaOH. Its ethanolic solution gives a brown color with ethanolic $FeCl_3$ which is very similar to that given by anhydrosepedonin itself.

Can. J. Chem. Downloaded from www.nrcresearchpress.com by 210.87.254.105 on 09/05/12
For personal use only.

Dimethyl ether A.—An ether solution of diazomethane (from 10 g of nitrosomethylurea) was added to a suspension of anhydrosepedonin (2 g) in acetone (25 ml) and the mixture was held at room temperature for 24 h. The resulting reddish-brown solution was then evaporated to dryness giving a gum which was dissolved in benzene (50 ml) and passed through a column of alumina (B.D.H. for chromatographic absorption analysis). The column was eluted with ether (3 l) and the eluate was evaporated to dryness. The yellow residue (0.95 g), m.p. 148–151° (decomp.), was crystallized once from benzene and then from toluene giving *anhydrosepedonin dimethyl ether A* as bright-yellow needles, m.p. 153–155° (decomp.). Found: C, 66.1; H, 5.91; OCH_3, 27.0; mol. wt. (Rast), 225. $C_{13}H_{14}O_4$ requires: C, 66.65; H, 6.02; 2-OCH_3, 26.5%; mol. wt. 234. $\lambda\lambda_{max}$ in ethanol 250.5 mμ (ϵ = 15 400), 271 mμ (inflection; ϵ = 18 750), 280.5 mμ (ϵ = 23 600), 370 mμ (ϵ = 16 950). ν_{max} (KBr disk) at 1 650, 1 588, 1 550, 1 504, 902, 841, and 826 cm^{-1}. Dimethyl ether A is readily soluble in water and $CHCl_3$ and moderately soluble in benzene, acetone, ethanol, and methanol. An ethanolic solution gives a clear-orange color with ethanolic $FeCl_3$. An aqueous solution gives a copious precipitate with an aqueous solution of picric acid. Dimethyl ether A is unstable and is converted slowly during storage in the solid state, or in solution, to dimethyl ether A_1.

Ferric chloride complex of dimethyl ether A.—A solution of anhydrous $FeCl_3$ (100 mg) dissolved in concentrated HCl (0.5 ml) was added to a solution of anhydrosepedonin dimethyl ether A (100 mg) in glacial acetic acid (2 ml). The $FeCl_3$ complex separated as orange crystals which were collected, dried, m.p. 150–153°, and recrystallized from glacial acetic acid containing a little concentrated HCl. The complex formed beautiful orange needles (60 mg), m.p. 156–158°, which turned brick red when kept for a few days. Found: OCH_3, 14.4. $C_{13}H_{14}O_4 \cdot HFeCl_4$ requires: 2-OCH_3, 14.3%.

Dimethyl ether B.—The ether-extracted alumina column was further eluted with $CHCl_3$ (200 ml). The eluate was dried *in vacuo* and the gummy residue (0.20 g) was crystallized twice from water giving *anhydrosepedonin dimethyl ether B* as pale-cream-colored needles (80 mg), m.p. 146°. A mixed melting point with dimethyl ether A was 120–125°. Found: C, 66.6; H, 6.2; OCH_3, 26.5. $C_{13}H_{14}O_4$ requires: C, 66.65; H, 6.02; 2-OCH_3, 26.5%. $\lambda\lambda_{max}$ in ethanol: 227 mμ (inflection; ϵ = 7 620), 249 mμ (ϵ = 11 400), 298 mμ (inflection; ϵ = 30 600), 308.5 mμ (ϵ = 38 000), 354 mμ (inflection; ϵ = 10 750), 369 mμ (inflection; ϵ = 9 700), 388 mμ (inflection; ϵ = 6 500). ν_{max} (KBr disk) at 1 648, 1 585, 1 533, 975, 901, and 838 cm^{-1}. Dimethyl ether B is only slightly soluble in water, but its other properties are very similar to those of dimethyl ether A.

Dimethyl ether A_1.—Anhydrosepedonin (2 g) suspended in acetone (25 ml) was treated with a dry ethereal solution of diazomethane prepared from *N*-methyl-*N*-nitroso-*N'*-nitroguanidine (15 g). The reaction mixture, after 16 h at room temperature, was evaporated to dryness, then redissolved in benzene and applied to a column of alumina (Merck, chromatographic grade). The column was developed with a benzene–chloroform (1:1) mixture and fractions collected. Three partially resolved yellow zones were eluted. Thin-layer chromatography (t.l.c.) using silica-gel G (Merck) with chloroform containing 5% glacial acetic acid as solvent was used to follow the separation and appropriate fractions pooled, evaporated, and crystallized to give, in the order of their elution from the column: (*a*) *anhydrosepedonin dimethyl ether A_1*, obtained as clusters of yellow needles (214 mg), m.p. 157–159°, after several recrystallizations from benzene–petroleum ether (b.p. 60–80°); mixed melting point with dimethyl ether A, 140–149°. $\lambda\lambda_{max}$ in ethanol: 226 mμ (ϵ = 12 850), 232 mμ (ϵ = 12 650), 253 mμ (inflection; ϵ = 13 400), 261.5 mμ (ϵ = 17 400), 300 mμ (ϵ = 18 150), 309 mμ (ϵ = 18 700), 340 mμ (ϵ = 7 480), 352 mμ (inflection; ϵ = 7 000), 379 mμ (inflection; ϵ = 4 200). ν_{max} (KBr disk) at 1 658, 1 615 (w), 1 575, 1 553, 1 530, 1 010, 984, 868, 846, and 828 cm^{-1}. Found: C, 66.67; H, 6.27; OCH_3, 26.75; mol. wt. (osmometer with acetone) 242. $C_{13}H_{14}O_4$ requires: C, 66.65; H, 6.02; 2-OCH_3, 26.5%; mol. wt. 234. (*b*) Anhydrosepedonin dimethyl ether A, obtained as glistening bright-yellow needles (80 mg), m.p. 153–155° (decomp.), after recrystallization from toluene or carbon tetrachloride. (*c*) Anhydrosepedonin dimethyl ether B, obtained as pale-cream needles (240 mg), m.p. 146°, by crystallization from toluene and then water.

Methylation with dimethyl sulfate.—Anhydrosepedonin (0.5 g) suspended in dry acetone (30 ml) was heated under reflux for 6 h with anhydrous K_2CO_3 (0.5 g) and dimethylsulfate (0.3 ml). The solution became green after 2 h and then changed slowly to reddish brown. It was filtered and the filtrate evaporated to dryness *in vacuo*. The residue, redissolved in water (25 ml), was extracted continuously with ether. The extract upon evaporation gave a residue (260 mg) from which, in the manner described above, dimethyl ether A (80 mg) and B (3 mg) were obtained.

Methylation with methyl iodide.—Anhydrosepedonin (0.5 g) suspended in dry benzene (50 ml) was heated under reflux for 8 h while seven additions of methyl iodide (1 ml) and silver oxide (200 mg) were made. The reddish-brown reaction mixture was filtered, the filtrate evaporated to dryness and re-extracted into ether. The ethereal solution gave, on evaporation, a residue (280 mg) from which dimethyl ether A (120 mg) and B (6 mg) were obtained in the manner described above.

Dehydration of sepedonin dimethyl ethers A and B.—Sepedonin dimethyl ether A (24 mg) in glacial acetic acid (3 ml) was heated on a steam bath for 1 h. The solvent was removed and the residue, in chloroform, chromatographed on a column of alumina. The yellow band eluted with chloroform was collected and the solvent removed *in vacuo*. Crystallization of the residue gave anhydrosepedonin dimethyl ether A (4 mg).

Sepedonin dimethyl ether B (16 mg) treated similarly gave anhydrosepedonin dimethyl ether B (7 mg).

Deoxysepedonin

Anhydrosepedonin (23 mg) in ethanol (15 ml) was hydrogenated at 29° and atmospheric pressure over

Can. J. Chem. Downloaded from www.nrcresearchpress.com by 210.87.254.105 on 09/05/12
For personal use only.

Adams' catalyst (10 mg). The rate of hydrogen uptake decreased abruptly after the absorption of 1.06 moles per mole. The catalyst was removed and the solution concentrated to a small volume. Buff-colored needles (14 mg) of *deoxysepedonin*, m.p. 234–235°, separated. $\lambda\lambda_{max}$ in ethanol 254.5, and 329 mμ with inflections at 268 and 352 mμ. ν_{max} (KBr disk) at 3 240, 3 100 – 2 550, 1 630 (shoulder), 1 606, 1 568, 1 533, 1 515, 930, 884, 816, and 720 cm^{-1}. Found: C, 63.41; H, 6.07. $C_{11}H_{12}O_4$ requires: C, 63.45; H, 5.81%.

Degradative Studies

Alkaline Degradation of Anhydrosepedonin

Anhydrosepedonin (200 mg) was stirred quickly into a fusion mixture of KOH (7 g) and water (0.5 ml) at 200°. The amber solution was immediately cooled, acidified with concentrated HCl, and extracted five times with ether. The combined ether extracts were washed with 5% $NaHCO_3$ solution, dried over anhydrous Na_2SO_4, and evaporated to dryness. The residue was crystallized from water, sublimed in high vacuum, and finally crystallized from aqueous methanol as colorless plates, m.p. 230–232°. $\lambda\lambda_{max}$ in ethanol: 251.5 mμ (ϵ = 36 500); 267 mμ (inflection; ϵ = 21 400), 331 mμ (ϵ = 7 820), 343 mμ (ϵ = 8 000). ν_{max} (KBr disk) at 3 200–2 600, 1 655 (w), 1 563, 1 478, 1 435, 1 393, 1 370, 1 345, 1 208, 1 045, 920, 870, 852, 778, 723, and 700 cm^{-1}. Found: C, 63.27; H, 5.53; CCH_3, 9.62. $C_8H_8O_3$ requires: C, 63.15; H, 5.30; 1-CCH_3, 9.86%.

The compound is insoluble or sparingly soluble in petroleum ether and benzene, only slightly soluble in water or methanol but more soluble in acetone, chloroform, or dioxane. It is insoluble in dilute $NaHCO_3$ solution but dissolves readily in *N* NaOH. With $FeCl_3$ in ethanolic solution it gives a greenish-brown color.

Oxidation of Anhydrosepedonin with Alkaline Hydrogen Peroxide

Anhydrosepedonin (1 g) was dissolved in *N* sodium hydroxide (40 ml) in a closed reaction vessel through which a slow stream of nitrogen was passed. Hydrogen peroxide (10 ml of 30% aqueous solution) was added and a slow exothermic reaction began. Gases issuing from the vessel were led through traps containing solutions of Brady's reagent and of baryta. After 10 h the reaction mixture had become colorless and was neutralized with *N* hydrochloric acid (40 ml). When carbon dioxide evolution had ceased the yield of barium carbonate in duplicate experiments was equivalent to 1.5 and 1.6 moles of carbon dioxide per mole of anhydrosepedonin used. No precipitation appeared in the trap containing Brady's reagent.

The reaction mixture was distilled *in vacuo* at temperatures not exceeding 50° and the distillate collected. In duplicate experiments the total yields of volatile acids, estimated by titration with 0.1 *N* sodium hydroxide, were 0.97 and 1.00 moles per mole of anhydrosepedonin.

Formic acid was detected by the test with chromotropic acid (26) and isolated as the lead salt. The distillate from one experiment was boiled with lead carbonate (0.75 g) and filtered. The filtrate was concentrated *in vacuo* to 10 ml and diluted with ethanol (50 ml). The product which separated was recrystallized from water as glistening colorless needles (95 mg) which became black on heating above 245°. Found by conversion to lead sulfate: Pb, 67.6, 67.9. Calcd. for $PbC_2H_2O_4$, 69.71%. A similar measurement of the lead content in an authentic sample of lead formate gave 68.4%. The amount of formic acid in the distillate was estimated by allowing it to reduce mercuric chloride. The total volatile acids from an experiment were neutralized and concentrated *in vacuo* to a small volume. Sodium acetate (3 g), mercuric chloride (3 g), and sodium chloride (2.25 g) were added, and the solution filtered, made to 150 ml, and heated on a water bath for 2 h. The yield of mercurous chloride (1.00 g) was equivalent to 0.42 mole formic acid per mole of anhydrosepedonin.

The presence of acetic acid in the volatile acids was established by preparing a *p*-bromophenacyl ester. The neutralized distillate from one experiment was evaporated *in vacuo*. The residue (0.2 g) redissolved in water (2 ml) and made acid with two drops of *N*-hydrochloric acid was heated under reflux with a solution of *p*-bromophenacyl bromide (0.75 g) in ethanol (10 ml). On cooling for several hours at 4° a crystalline product (200 mg), m.p. 70–74°, separated. This, when twice recrystallized from ethanol, had m.p. 85°, undepressed on admixture with an authentic specimen of *p*-bromophenacyl acetate. Found: Br, 31.0. Calcd. for $C_{10}H_9O_3Br$: 31.1%.

The nonvolatile fraction from the oxidation was evaporated to dryness *in vacuo* at 45–50° and the last traces of moisture removed over phosphorus pentoxide. The residue was continuously extracted with dry ether and the ether removed to give from duplicate experiments 0.59 and 0.64 g of ether-soluble material. The product from one such experiment was crystallized from chloroform and twice sublimed in high vacuum at 80° to give colorless plates, m.p. 135°, undepressed by an authentic specimen of malonic acid. Found: C, 34.9; H, 3.8. Calcd. for $C_3H_4O_4$: C, 34.6; H, 3.9%. The substance gave the color changes with acetic anhydride expected of malonic acid and formed fluorescein when heated with resorcinol and sulfuric acid.

Oxidation of Anhydrosepedonin Dimethyl Ether A with Permanganate

To a well-stirred solution of anhydrosepedonin dimethyl ether A (50 mg) in acetone (20 ml) at 0° powdered potassium permanganate (150 mg) was added in small portions over a period of 30 min. The precipitate was removed by filtration, washed with acetone, then extracted with several 2 ml portions of ice-cold water. The combined aqueous extracts were washed twice with chloroform, then acidified and re-extracted with chloroform (5 × 25 ml). The acidic product remaining after evaporation of solvent was washed with a small volume of cold acetone then twice crystallized from water to give feathery white needles (8 mg), m.p. 205–206°. $\lambda\lambda_{max}$ in ethanol at 259 mμ (ϵ = 30 300) and 324 mμ (ϵ = 6 890). ν_{max} (KBr disk) at 3 100 – 2 450,

Can. J. Chem. Downloaded from www.nrcresearchpress.com by 210.87.254.105 on 09/05/12
For personal use only.

1 738, 1 720, 1 600, 1 540, 1 240, 1 028, 997, 891, 875, 788, 742, and 690 cm^{-1}. Found: C, 55.3; H, 5.3; OCH_3, 23.9; CCH_3, 4.6; neutr. equiv., 288. $C_{13}H_{14}O_7$ requires: C, 55.33; H, 5.00; 2-OCH_3, 22.00; 1-CCH_3, 5.33%; mol. wt. 282.

A methyl ester was prepared by treating an ethereal solution of the acid with diazomethane. After sublimation in high vacuum it had m.p. 132°. $\lambda\lambda_{max}$ in ethanol at 251 mμ (ϵ = 29 600), 256 mμ (inflection; ϵ = 20 700) and 323 mμ (ϵ = 7 560). ν_{max} (KBr disk) at 1 738 (shoulder) and 1 725 cm^{-1}. Found: C, 56.4; H, 5.5; OCH_3, 36.4. $C_{14}H_{16}O_7$ requires: C, 56.74; H, 5.44; 3-OCH_3, 31.41%. The ester was insoluble in dilute $NaHCO_3$ but dissolved slowly in dilute NaOH solution.

The acetone soluble fraction of the acidic oxidation products gave, on concentrating and cooling the acetone solution, a crop of orange plates (15 mg). These were recrystallized from acetone to a constant melting point of 221–222° (decomp.). $\lambda\lambda_{max}$ in ethanol at 254 mμ and 353 mμ with an inflection at 414 mμ. ν_{max} (KBr disk) at 1 850, 1 775, 1 632, 1 565, 988, 907, 883, 825, 756, 731, and 700 cm^{-1}. Found: C, 55.8; H, 3.2; OCH_3, 26.5. $C_{11}H_8O_6$ requires: C, 55.9; H, 3.4; 2-OCH_3, 26.3%.

ACKNOWLEDGMENTS

We thank Dr. R. H. Haskins and Mr. L. R. Nesbitt of the Prairie Regional Laboratory for assistance in growing and extracting cultures of *S. chrysospermum*. P. V. Divekar also thanks the Council of Scientific and Industrial Research (India) for the award of an Assam Oil Company Scholarship (1953–1956). The nuclear magnetic resonance spectrum of anhydrosepedonin in deuterated acetone – chloroform was provided by Dr. H. J. Bernstein, Division of Pure Chemistry, National Research Council of Canada, Ottawa.

We are very grateful to Professor Holger Erdtman and Dr. Gunhild Aulin-Erdtman of the Department of Organic Chemistry and the Department of Wood Chemistry, respectively, Royal Institute of Technology, Stockholm, Sweden, for their expert examination of anhydrosepedonin which they assure us is a tropolone.

REFERENCES

1. P. V. Divekar. Ph.D. Thesis, University of London. 1956.
2. J. H. Birkinshaw, A. R. Chambers, and H. Raistrick. Biochem. J. **36**, 242 (1942).
3. G. Aulin-Erdtman and H. Theorell. Acta Chem. Scand. **4**, 1490 (1950).
4. A. W. Johnson, N. Sheppard, and A. R. Todd. J. Chem. Soc. 1139 (1951).
5. W. D. Crow, R. D. Haworth, and P. R. Jeffries. J. Chem. Soc. 3705 (1952).
6. W. Segal. J. Chem. Soc. 2847 (1959).
7. N. Yui. Sci. Rept. Tohoku Univ. First Ser. **40**, 114 (1956).
8. P. V. Divekar and L. C. Vining. Can. J. Chem. **42**, 63 (1964).
9. J. A. Barltrop and J. S. Nicholson. J. Chem. Soc. 116 (1948).
10. H. Erdtman and J. Gripenberg. Acta Chem. Scand. **2**, 625 (1948).
11. R. E. Corbett, A. W. Johnson, and A. R. Todd. J. Chem. Soc. 147 (1950).
12. G. Aulin-Erdtman. Acta Chem. Scand. **5**, 301 (1951).
13. T. Nozoe and Y. Kitahara. Proc. Japan Acad. **30**, 204 (1954).
14. F. M. Dean, R. A. Eade, R. Moubasher, and A. Robertson. J. Chem. Soc. 3497 (1957).
15. H. W. Ruelius and A. Gauhe. Ann. **569**, 38 (1950).
16. A. E. Oxford, H. Raistrick, and P. Simonart. Biochem. J. **29**, 1102 (1935).
17. R. Bentley. Ann. Rev. Biochem. **31**, 589 (1962).
18. T. R. Seshadri. J. Sci. Ind. Res. India, **14B**, 248 (1955).
19. R. Bentley. J. Biol. Chem. **238**, 1895 (1963).
20. H. Raistrick. Proc. Roy. Soc. London Ser. B, **136**, 481 (1949–50).
21. A. E. Oxford and H. Raistrick. Biochem. J. **27**, 634 (1933).
22. A. E. Gillam and E. S. Stern. An introduction to electronic absorption spectroscopy in organic chemistry. Edward Arnold (Publishers) Ltd., London. 1954. p. 186.
23. M. Somogyi. J. Biol. Chem. **160**, 61 (1945).
24. F. Feigl. Spot tests. Vol. II. Organic applications. 4th ed. Elsevier Publishing Company, Amsterdam. 1954. p. 129.
25. T. Nozoe, K. Takase, and M. Ogata. Chem. Ind. London, 1070 (1957).
26. E. Eegriwe. Z. Anal. Chem. **110**, 22 (1937).

Can. J. Chem. Downloaded from www.nrcresearchpress.com by 210.87.254.105 on 09/05/12
For personal use only.

Can. J. Chem. Downloaded from www.nrcresearchpress.com by 210.87.254.5 on 09/05/12
For personal use only.

ON THE USE OF NUCLEAR MAGNETIC RESONANCE FOR THE DETECTION, ESTIMATION, AND CHARACTERIZATION OF N-METHYL GROUPS

J. C. N. MA[1] AND E. W. WARNHOFF[2]
Department of Chemistry, University of Western Ontario, London, Ontario
Received December 18, 1964

ABSTRACT

A useful n.m.r. technique for the detection, estimation, and characterization of N-methyl groups is described. The method depends on the decreased shielding of N_{basic}-methyl protons when the solvent is changed from deuterochloroform to perdeuteroacetic (PDA) (or acetic) acid to trifluoroacetic acid (TFA). The decreased shielding results in a downfield shift of the N-methyl resonance of ca. 0.3–1.3 p.p.m. depending on the type of amine. Most N-methyl groups on neutral nitrogen atoms show little movement. For the majority of aliphatic amines in trifluoroacetic acid the NH exchange rate is slow enough at 38° to permit observation of coupling of H(N) with the N-methyl protons, and thus determination of whether the amine is secondary or tertiary. In some cases information can be obtained about methylene and methine groups attached to basic nitrogen. In acid solution compounds with basic nitrogen attached to, or part of, an aromatic ring show considerable shift of the aromatic proton resonance signals to lower magnetic field. Combination of the n.m.r. technique with the Herzig-Meyer analysis can also reveal the number of methyl groups attached to neutral nitrogen.

INTRODUCTION

The determination of N-alkyl groups in compounds of unknown structure is normally done by the Herzig-Meyer analysis (1) or by means of nuclear magnetic resonance (n.m.r.) spectroscopy (2, 3*a*, 3*b*). To a lesser extent infrared spectroscopy (3*c*), the isolation of a smaller known degradation fragment containing an N-alkyl group, or else Conroy's method (4) have also served. However, all of these methods have limitations.

Occasionally low or negligible values are obtained in the Herzig-Meyer analysis of compounds which do contain N-alkyl groups. Examples are the alkaloids ajaconine (44% of one NCH_3) (5), tazettine (65% of one NCH_3) (6), and α- and β-obscurine (no NCH_3 found in ref. 7*a*, but see ref. 7*b*). On the other hand there are a number of compounds which are known not to have a C_{1-4} N-alkyl group, but which do give rise to a volatile alkyl iodide under the conditions of the Herzig-Meyer reaction. The alkaloids atisine (8), veatchine, garryine (9), aspidospermine (10), aspidosine (4), hetisine, heteratisine (11), undulatine (12), decamine, decodine, decaline, vertaline (13), cassine (14), quebrachamine (15), the alkaloid derivative yohimbol (15), and 3-hydroxypiperidine (14) all have given appreciable N-alkyl values.

The Herzig-Meyer procedure does not distinguish N-methyl from N-ethyl or higher alkyl groups unless the volatile alkyl iodide is isolated as a derivative, usually the trimethylammonium salt. In the past this has led to the assumption that certain compounds possessed an N-methyl group, whereas in fact an N-ethyl group was present. The alkaloids lycoctonine (16), delpheline (17), napelline (18), and ajacine (19) are cases in point. Nor does the analysis reveal whether the N-methyl group is bonded to basic or to neutral nitrogen in those compounds with both types of nitrogen atom present.

The infrared method is complicated by overlapping absorption, while the isolation of a known fragment containing the N-alkyl group may be difficult or tedious. Conroy's

[1]*Present address: National Heart Institute, National Institutes of Health, Bethesda, Maryland, 20014.*
[2]*Fellow of the Alfred P. Sloan Foundation.*

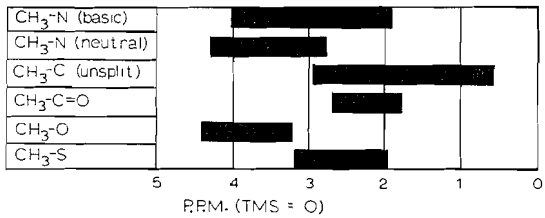

FIG. 1. Ranges of methyl n.m.r. absorption peaks for the compounds in the Varian catalogs 1 and 2, The range given for the CH_3—S group also includes the compounds reported by G. R. Pettit, I. B. Douglass, and R. A. Hill. Can. J. Chem. 42, 2357 (1964), except for methanesulfonyl chloride.

method (4) for proving the presence or absence of N-methyl groups (quaternization with labelled methyl iodide, regeneration of the original free base, and its examination for label incorporation) is restricted to those basic nitrogen-containing compounds which can be reformed from their quaternary metho salts by pyrolysis, reduction, or Hofmann degradation.

Nuclear magnetic resonance spectroscopy is potentially a much better means of detecting the N-methyl function, but it also suffers from a weakness. Several different types of methyl groups give rise to unsplit 3-hydrogen n.m.r. peaks, and their rather broad ranges of absorption overlap considerably as seen from Fig. 1. Moreover, in a complex molecule there is always the possibility of mistaking any sharp peak for a methyl group as happened in the case of aspidospermine (4, 20).

In the present work a simple and useful modification of the n.m.r. method for N-methyl analysis is described. It depends on the pronounced downfield shift of the resonance peak of basic N-methyl groups in solvents of increasing acidity. This effect, due to the decreased shielding of the methyl protons of the positively charged ammonium ion relative to those of the amine, is well known (21). The n.m.r. spectra of a series of 116 compounds containing N-methyl and (or) other methyl groups exhibiting apparent singlet n.m.r. peaks have been recorded in deuterochloroform, perdeuteroacetic acid, and trifluoroacetic acid. These two acidic solvents were chosen for the absence of hydrogen, great difference in acid strength (acetic acid $pK_a^{H_2O}$ 4.76, trifluoroacetic acid $pK_a^{H_2O}$ −0.26), and powerful solvent action on most organic compounds. Perdeuteroacetic acid, while expensive, is not inordinately so, and for most compounds acetic acid is equally satisfactory.[3] Comparison of the peak positions and chemical shift changes for the methyl protons of the compounds studied reveals that the N-methyl groups can be arranged in six and the C-methyl compounds in three categories. There is little variation among the O-methyl groups. These peak positions and chemical shift changes (Δ) are collected in Table I, A–J. Table II summarizes the range of δ values found for the resonance position of each category of methyl group together with the range of differences (Δ) in chemical shift for each two solvents. Chart 1 is a graphical presentation of the ranges for each group in each solvent in the manner of a Colthup chart.

DISCUSSION

For mono-, di-, and tri-methylamine it has been shown that in aqueous acid solution the chemical shift of the methyl protons is a linear function of the concentration of protonated amine (21*a*). Although one might thus expect a linear correlation of the Δ values

[3]*On the Varian A-60 spectrometer the region of the spectrum effectively blocked by the methyl protons in acetic acid is 2.0–2.05 p.p.m. at spectrum amplitude (s.a.) 0.1, 1.95–2.1 p.p.m. at s.a. 1, 1.9–2.2 p.p.m. at s.a. 10, and 1.85–2.25 p.p.m. at s.a. 40 (the appreciable* ^{13}C *satellite peaks at higher s.a. must be taken into account).*

Can. J. Chem. Downloaded from www.nrcresearchpress.com by 210.87.254.5 on 09/05/12
For personal use only.

Can. J. Chem. Downloaded from www.nrcresearchpress.com by 210.87.254.5 on 09/05/12
For personal use only.

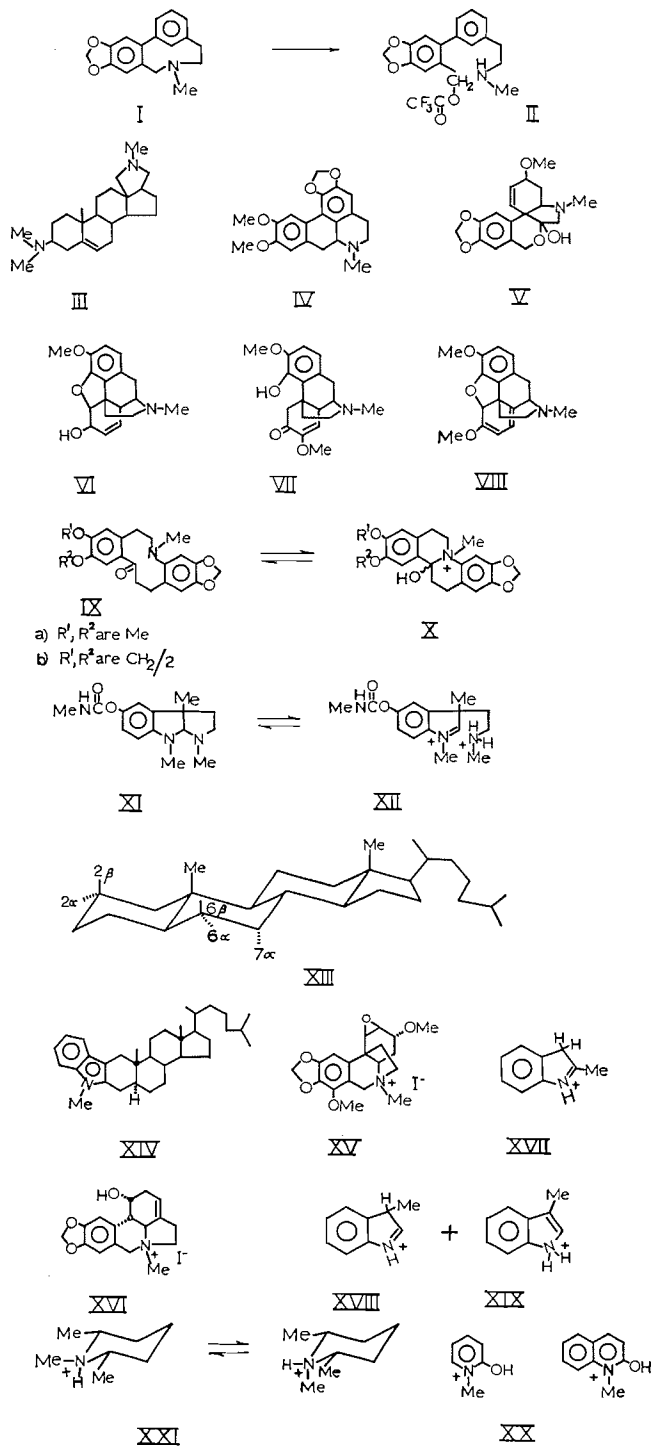

TABLE I

Nuclear magnetic resonance positions and their differences for **N-methyl** groups

No.	Compound	Structure[a]	δ in $CDCl_3$[b]	δ in CD_3COOD[b]	δ in CF_3COOH[b]	$\delta_{CD_3COOD} - \delta_{CDCl_3}$	$\delta_{CF_3COOH} - \delta_{CD_3COOD}$	$\delta_{CF_3COOH} - \delta_{CDCl_3}$
		A. Tertiary aliphatic amines						
1.	Methyldiethylamine	$(CH_3CH_2)_2NMe$	2.19	2.76	2.98 d(5.5)	+0.57	+0.22	+0.79
2.	N,N-Dimethyl-n-butylamine	$CH_3(CH_2)_3NMe_2$	2.18	2.82	2.93 d(5.0)	+0.64	+0.11	+0.75
3.	N,N-Dimethyl-n-dodecylamine	$CH_3(CH_2)_{11}NMe_2$	2.20	2.88	3.04 d(5)	+0.68	+0.16	+0.84
4.	N,N-Dimethyl-n-octadecylamine	$CH_3(CH_2)_{17}NMe_2$	2.20	2.88	3.02 d(5)	+0.68	+0.14	+0.82
5.	Tetramethylmethylenediamine	$Me_2NCH_2NMe_2$	2.22	2.69	2.92 t(5.5)[c]	+0.47	+0.23[c]	+0.70[c]
6.	Tetramethylethylenediamine	$Me_2NCH_2CH_2NMe_2$	2.23	2.81	3.18 d(4)	+0.58	+0.37	+0.95
7.	N,N-Dimethylcyclohexylamine		2.25	2.78	2.91 d(5.5)	+0.53	+0.13	+0.66
8.	N,N-Dimethylbenzylamine		2.22	2.86	3.02 d(5.5)	+0.64	+0.16	+0.80
9.	Gramine		2.29	2.88	3.00 d(5.5)	+0.59	+0.12	+0.71
10.	Belladine		2.26	2.85	3.07 d(5.5)	+0.59	+0.22	+0.81
11.	Caranine anhydromethine	I	2.48	3.14	3.00 t(5.5)[d]	+0.66	-0.14[d]	+0.52[d]
12.	N-Methylpyrrolidine		2.33	2.90	3.03 d(5.5)	+0.57	+0.13	+0.70
13.	N-Methylpiperidine		2.21	2.78	2.93 d(5.5)	+0.57	+0.15	+0.72
14.	cis-1,2,6-Trimethylpiperidine		2.23	2.63[e] 2.92	2.76 d(5.5)[e] 3.03 d(5.5)	+0.40 +0.69	+0.13 +0.11	+0.53 +0.80
15.	N-Methyl-1,2,5,6-tetrahydropyridine		2.33	2.92	3.03 d(5)	+0.59	+0.11	+0.70
16.	Conessine	III	2.18 2.27C_3	2.91 (9H)	3.01(9H) d(5.5)	+0.73 +0.64	+0.10	+0.83 +0.74
17.	Nicotine		2.15	2.85	3.10	+0.70	+0.25	+0.95
18.	N-Methylanabasine		1.97	2.67	2.89 d(5)	+0.70	+0.22	+0.92
19.	Hydrocotarnine		2.44	3.08	3.19 d(5.5)	+0.64	+0.11	+0.75
20.	Dicentrine	IV	2.51	3.10	3.36 d(5)	+0.59	+0.26	+0.85
21.	Arecoline		2.38	3.04	3.18 d(5)	+0.66	+0.14	+0.80
22.	Tropinone		2.48	2.98	3.34 d(5)e 3.14 d(5)a	+0.50	+0.36 +0.16	+0.86 +0.66
23.	Scopoline	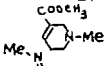	2.56	3.12	3.26 d(5.5)	+0.56	+0.14	+0.70
24.	N-Methylmorpholine		2.27	2.91	3.12 d(5)	+0.64	+0.21	+0.85
25.	N-Methylpiperazine		2.25	2.75	3.22	+0.50	+0.47	+0.97
26.	2-Dimethylaminoethanol	$Me_2NCH_2CH_2OH$	2.26	2.97	3.13 d(5)	+0.71	+0.16	+0.87
27.	1-Dimethylamino-2-propanol	$CH_3CHCH_2NMe_2$ OH	2.26	2.97	3.11 d(5) 3.14 d(5)	+0.71	+0.14 +0.17	+0.85 +0.88
28.	β-N,N-Dimethylaminoethyl acrylate		2.29	2.98	3.16 d(5)	+0.69	+0.18	+0.87
29.	4-Carbamyl-4-(N,N-dimethylamino)-piperidine		Insol.	3.02	3.16	-	+0.14	-

Can. J. Chem. Downloaded from www.nrcresearchpress.com by 210.87.254.5 on 09/05/12
For personal use only.

TABLE I (*Continued*)

Nuclear magnetic resonance positions and their differences for **N-methyl** groups (*Continued*)

No.	Compound	Structure[a]	δ in $CDCl_3$[b]	δ in CD_3COOD[b]	δ in CF_3COOH[b]	$\delta_{CD_3COOD} - \delta_{CDCl_3}$	$\delta_{CF_3COOH} - \delta_{CD_3COOD}$	$\delta_{CF_3COOH} - \delta_{CDCl_3}$
30.	Tazettine	V	2.38	3.08	3.22 d(5)	+0.70	+0.14	+0.84
31.	Codeine	VI	2.42	3.06	3.19 d(5)	+0.64	+0.13	+0.77
32.	Sinomenine	VII	2.43	2.97	3.11 d(4.5)	+0.54	+0.14	+0.68
33.	Thebaine	VIII	2.45	3.05	3.60[f]	+0.60	+0.55	+1.15
34.	Cryptopine	IXa	1.88	3.12[g] 3.20	3.24[g]	+1.24 +1.32	+0.12 +0.04	+1.36
35.	Protopine	IXb	1.91	3.10[g] 3.20	3.25[g]	+1.19 +1.29	+0.15 +0.05	+1.34
36.	Physostigimine (Eserine)	XI	2.53 2.91 Ar	2.90 3.13	3.05[h] 4.35[h]	+0.37 +0.22	+0.15 +1.22	+0.52 +1.44
37.	N,N-Dimethylleucine	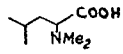	Insol.	2.98	3.13 d(5) 3.18 d(5)	-	+0.15 +0.20	-
38.	N,N-Dimethyliso-leucine	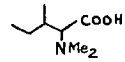	Insol.	2.98	3.18 d(5)	-	+0.20	-
39.	6α-N,N-Dimethylam-inocholestane	6α-Me_2N-XIII	2.19	2.83	2.80 d(5) 3.01 d(5)	+0.64	-0.03 +0.18	+0.61 +0.82
40.	6β-N,N-Dimethylam-inocholestane	6β-Me_2N-XIII	2.24	3.05	3.10 d(5) 3.16 d(5)	+0.81	+0.05 +0.11	+0.86 +0.92
41.	2α-N,N-Dimethylam-inocholestane	2α-Me_2N-XIII	2.27	2.85	2.96 d(5)	+0.58	+0.11	+0.69
42.	2β-N,N-Dimethylam-inocholestane	2β-Me_2N-XIII	2.21	2.88	3.03 d(5)	+0.67	+0.15	+0.82
43.	7α-N,N-Dimethylam-inocholestane	7α-Me_2N-XIII	2.36	3.05	3.12 d(5) 3.16 d(5)	+0.69	+0.07 +0.11	+0.76 +0.80
		B. Secondary aliphatic amines						
44.	N-Methyl-n-butyl-amine	$CH_3(CH_2)_3NHMe$	2.43	2.76	2.96 t(5.5)	+0.33	+0.20	+0.53
45.	N-Methyl-n-octyl-amine	$CH_3(CH_2)_7NHMe$	2.43	2.76	2.96 t(5.5)	+0.33	+0.20	+0.53
46.	N-Methyl-n-octa-decylamine	$CH_3(CH_2)_{17}NHMe$	2.42	2.75	2.94 t(5.5)	+0.33	+0.19	+0.52
47.	N-Methylcyclopen-tylamine		2.39	2.73	2.92 t(5.5)	+0.34	+0.19	+0.53
48.	N-Methyl tetrahydro-furfurylamine		2.44	2.82	3.00 t(5.5)	+0.38	+0.18	+0.56
49.	N-Methylcyclohexyl-amine		2.41	2.67	2.86 t(5.5)	+0.26	+0.19	+0.45
50.	N-Methylbenzyl-amine	$\phi CH_2\overset{H}{N}Me$	2.42	2.76	2.94 t(6.0)	+0.34	+0.18	+0.52
51.	N-Methyl-β-phenyl-ethylamine	$\phi CH_2CH_2\overset{H}{N}Me$	2.35	2.75	2.78 t(5.5)	+0.40	+0.03	+0.43
52.	2-Methylamino-ethanol	$MeHNCH_2CH_2OH$	2.43	2.82	3.03 t(5.5)	+0.39	+0.21	+0.60
53.	Ephedrine	$\phi\underset{OH}{CH}-\underset{CH_3}{CH}NHMe$	2.34	2.88	3.01 t(5.5)	+0.54	+0.13	+0.67
54.	N-Methyl-β-phenyl-alanine methyl ester	$\phi-CH_2\underset{NHMe}{CH}COOCH_3$	2.35	2.83	-	+0.48	-	-

Can. J. Chem. Downloaded from www.nrcresearchpress.com by 210.87.254.5 on 09/05/12
For personal use only.

TABLE I (*Continued*)

Nuclear magnetic resonance positions and their differences for **N-methyl** groups (*Continued*)

No.	Compound	Structure[a]	δ in $CDCl_3$[b]	δ in CD_3COOD[b]	δ in CF_3COOH[b]	$\delta_{CD_3COOD} - \delta_{CDCl_3}$	$\delta_{CF_3COOH} - \delta_{CD_3COOD}$	$\delta_{CF_3COOH} - \delta_{CDCl_3}$
55.	N-Methyl-β-phenyl-alanine	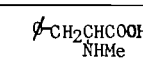	-	2.78	3.02 t(5)	-	+0.24	-
		C. Aromatic and N-heteroaromatic amines						
56.	N-Methylaniline		2.66	2.78	3.17 [3.25 t(4)][i]	+0.12	+0.39	+0.51
57.	N-Methyl-p-toluidine	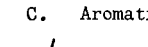	2.79	3.11	3.33 t(5.5)	+0.32	+0.22	+0.54
58.	N-Methyl-α-naphthylamine	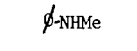	2.68	2.96	3.50	+0.28	+0.54	+0.82
59.	N,N-Dimethylaniline		2.85	3.01	3.46 d(5)	+0.16	+0.45	+0.61
60.	N,N-Dimethyl-p-toluidine	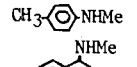	2.88	3.26	3.47 d(5)	+0.38	+0.21	+0.59
61.	N-Methyl-N-benzyl-aniline	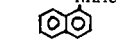	2.86	2.99	3.46[i] d(4.5)	+0.13	+0.47	+0.60
62.	N,N-Dimethyl-α-naphthylamine	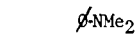	2.86	3.34	3.68 d(5)	+0.48	+0.34	+0.82
63.	α-Methylphenyl-hydrazine	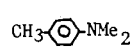	3.06	3.20	3.44	+0.14	+0.24	+0.38
64.	Antipyrine	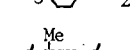	3.02	3.25	3.58	+0.23	+0.33	+0.56
65.	4-Aminoantipyrine	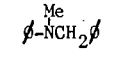	2.82	3.22	3.59	+0.40	+0.37	+0.77
66.	4-(Dimethylamino)-antipyrine	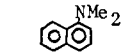	2.78 2.91	3.32 (9H)	3.58(Me_2N) 3.52(MeN)	+0.54 +0.41	+0.26 +0.20	+0.80 +0.61
67.	Pilocarpine	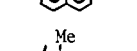	3.57	3.90	3.96	+0.33	+0.06	+0.39
68.	Theobromine	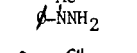	Insol.	3.98	4.30	-	+0.32	-
69.	Caffeine	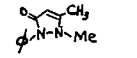	3.99	4.00	4.33	+0.01	+0.33	+0.34
		D. Amides and imides						
70.	N,N-Dimethyl-formamide	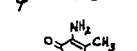	2.85 2.96	2.87 3.01	3.05 3.18	+0.02 +0.05	+0.18 +0.17	+0.20 +0.22
71.	N,N-Dimethyl-acetamide	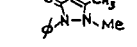	2.90 3.02	2.91 3.04	3.15(6H)	+0.01 +0.02	+0.24 +0.11	+0.25 +0.13
72.	N-Methylurea	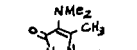	2.77	2.72	3.00	-0.05	+0.28	+0.23
73.	4-N,N-Dimethyl-carboxamido-4-phenyl piperidine	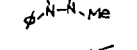	2.71	2.78	2.92	+0.07	+0.14	+0.21
74.	Physostigmine (Eserine)	XI	2.82 d(5.0)	2.82	2.90[h]	0.00	+0.08	+0.08
75.	N-Methyl-2-pyrrolidone	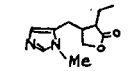	2.82	2.82	3.09	0.00	+0.27	+0.27

Can. J. Chem. Downloaded from www.nrcresearchpress.com by 210.87.254.5 on 09/05/12
For personal use only.

TABLE I (*Continued*)

Nuclear magnetic resonance positions and their differences for **N-methyl** groups (*Continued*)

No.	Compound	Structure[a]	δ in $CDCl_3$[b]	δ in CD_3COOD[b]	δ in CF_3COOH[b]	$\delta_{CD_3COOD} - \delta_{CDCl_3}$	$\delta_{CF_3COOH} - \delta_{CD_3COOD}$	$\delta_{CF_3COOH} - \delta_{CDCl_3}$
76.	N-Methylbenzanilide	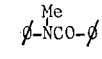	3.48	3.48	3.82	0.00	+0.34	+0.34
77.	N-Methylthiobenzanilide	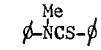	3.89	3.88	4.20	-0.01	+0.32	+0.31
78.	N-Methyl-3-ethyloxindole	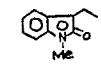	3.11	3.18	3.34	+0.07	+0.16	+0.23
79.	N-Methylphthalimide	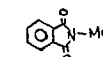	3.16	3.12	3.29	-0.04	+0.17	+0.13
80.	Theobromine	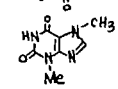	Insol.	3.51	3.77 (N-3)	-	+0.26	-
81.	Theophylline	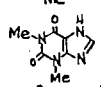	3.49 3.66	3.40 3.58	3.64 (N-1) 3.85 (N-3)	-0.09 -0.08	+0.24 +0.27	+0.15 +0.19
82.	Caffeine	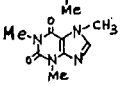	3.38 3.56	3.36 3.53	3.59 (N-1) 3.80 (N-3)	-0.02 -0.03	+0.23 +0.27	+0.21 +0.24
83.	N-Methyl-p-toluene sulfonanilide	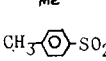	3.16	3.16	3.26	0.00	+0.10	+0.10
		E. Other compounds with neutral nitrogen						
84.	N-Methyl-2-pyridone	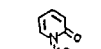	3.53	3.62	4.13	+0.09	+0.51	+0.60
85.	N-Methyl-2-quinolone	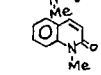	3.68	3.72	4.34	+0.04	+0.62	+0.66
86.	N-Methylpyrrole	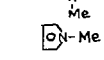	3.50	3.44	dec.	-0.04	-	-
87.	N-Methyl-5-benzyloxyindole	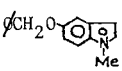	3.66	3.72	4.24	+0.06	+0.52	+0.58
88.	N-Methylindole of cholestan-3-one	XIV	3.57	Insol.	4.08	-	-	+0.51
89.	p-(Dimethylamino)-benzaldehyde	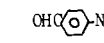	3.04	3.04	3.58	0.00	+0.54	+0.54
90.	4,4'-Bis(dimethylamino)benzophenone		3.02	3.04	3.57	+0.02	+0.53	+0.55
91.	N,N-Dimethyl-p-nitroaniline	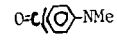	3.09	3.09	3.57	0.00	+0.48	+0.48
		F. Quaternary ammonium compounds						
92.	Tetramethylammonium iodide	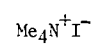	Insol.	3.30	3.35	-	+0.05	-
93.	Phenyl trimethylammonium perchlorate	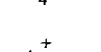	Insol.	3.71	3.72	-	+0.01	-
94.	1,2,6-Trimethylpyridinium iodide	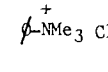	Insol.	4.19	4.24	-	+0.05	-
95.	Undulatine methiodide	XV	Insol.	3.45	3.42[j]	-	-0.03	-
96.	Caranine α- and β-methiodides	XVI	Insol.	Insol.	3.02 3.16	-	-	-

Can. J. Chem. Downloaded from www.nrcresearchpress.com by 210.87.254.5 on 09/05/12
For personal use only.

TABLE I (*Continued*)

Nuclear magnetic resonance positions and their differences for **N-methyl** groups (*Continued*)

No.	Compound	Structure[a]	δ in $CDCl_3$[b]	δ in CD_3COOD[b]	δ in CF_3COOH[b]	$\delta_{CD_3COOD} - \delta_{CDCl_3}$	$\delta_{CF_3COOH} - \delta_{CD_3COOD}$	$\delta_{CF_3COOH} - \delta_{CDCl_3}$
97.	N-Methylquinolinium chloride	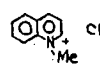	Insol.	4.77	4.79	–	+0.02	–
	G. C-Methyl groups on aromatic rings containing or attached to basic nitrogen							
98.	2-Picoline		2.51	2.62	2.97	+0.11	+0.35	+0.46
99.	3-Picoline		2.27	2.43	2.67	+0.16	+0.24	+0.40
100.	4-Picoline		2.30	2.56	2.78	+0.26	+0.22	+0.48
101.	2,6-Lutidine		2.48	2.72	2.86	+0.24	+0.14	+0.38
102.	2,4,6-Collidine	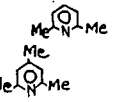	2.20 2.45	2.52 2.69	2.61(4) 2.76(2,6)	+0.32 +0.24	+0.09 +0.07	+0.41 +0.31
103.	2-Methylquinoline		2.60	2.87	3.13	+0.27	+0.26	+0.53
104.	1-Methylisoquinoline		2.82	3.19	3.39	+0.37	+0.20	+0.57
105.	2-Methylpyrazine		2.54	2.60	3.02	+0.06	+0.42	+0.48
106.	3,5-Dimethyl-pyrazole		2.26 (6H)	2.31	2.50	+0.05	+0.19	+0.24
107.	3-Methyl-1-phenyl-5-pyrazolone	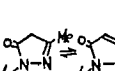 i ii	2.15[k] (i)	2.23	2.50(ii)	+0.08	+0.27	+0.35
108.	Antipyrine	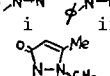	2.21	2.30	2.51	+0.09	+0.21	+0.30
109.	4-Aminoantipyrine	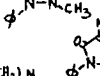	2.12	2.37	2.64	+0.25	+0.27	+0.52
110.	4-(Dimethylamino)-antipyrine	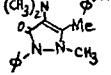	2.16	2.52	2.67	+0.36	+0.15	+0.51
111.	N-Methyl-p-toluidine	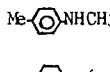	2.24	2.36	2.45	+0.12	+0.09	+0.21
112.	N,N-Dimethyl-p-toluidine		2.25	2.37	2.46	+0.12	+0.09	+0.21
	H. C-Methyl groups on non-basic aromatic rings							
113.	Toluene	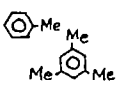	2.32[n]	2.26	2.24	-0.06	-0.02	-0.08
114.	Mesitylene		2.23	2.20	2.20	-0.03	0.00	-0.03
115.	N-Acetyl-p-toluidine	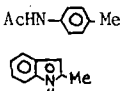	2.30[n]	2.26	2.33	-0.04	+0.07	+0.03
116.	2-Methylindole	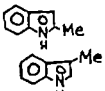	2.32	2.36	3.01[l]	+0.04	+0.65	+0.69
117.	3-Methylindole		2.28[n] d(1)	2.28 d(1)	2.43 and 1.52[m] d(6.5)	0.00	+0.15	+0.15
118.	N-Methyl-p-toluenesulfonanilide	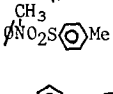	2.40	2.39	2.46	-0.01	+0.07	+0.06
119.	1,2,6-Trimethylpyridinium iodide	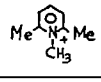	–	2.89	2.92	–	+0.03	–

[a] In the structural formulas Me denotes the methyl group whose absorption is given.

[b] Peak positions are given in p.p.m. from internal tetramethylsilane (= 0). If the peak is not a singlet, the multiplicity is given after the peak position (d = doublet, t = triplet). The apparent coupling constant is given in parentheses.

Can. J. Chem. Downloaded from www.nrcresearchpress.com by 210.87.254.5 on 09/05/12
For personal use only.

TABLE I (*Concluded*)

Nuclear magnetic resonance positions and their differences for **N-methyl** groups (*Concluded*)

No.	Compound	Structure[a]	δ in $CDCl_3$[b]	δ in CD_3COOD[b]	δ in CF_3COOH[b]	$\delta_{CD_3COOD} - \delta_{CDCl_3}$	$\delta_{CF_3COOH} - \delta_{CD_3COOD}$	$\delta_{CF_3COOH} - \delta_{CDCl_3}$
		I. Acetyl groups						
120.	Acetone	MeCOMe	2.14	2.16	2.31	+0.02	+0.15	+0.17
121.	Methyl ethyl ketone	$MeCOCH_2CH_3$	2.13[n]	2.15	2.30	+0.02	+0.15	+0.17
122.	Acetophenone		2.59[n]	2.57	2.73	−0.02	+0.16	+0.14
123.	2-Methyl-1-acetyl cyclohexene		2.21	2.25	2.44	+0.04	+0.19	+0.23
124.	N,N-Dimethyl-acetamide	$MeCON(CH_3)_2$	2.04	2.08	2.31	+0.04	+0.23	+0.27
125.	Acetanilide		2.08	2.17	2.54	+0.09	+0.37	+0.46
126.	N-Acetyl-p-toluidine	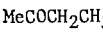	2.12[n]	2.16	2.50	+0.04	+0.34	+0.38
127.	s-Butylacetate		1.99	2.00	2.15	+0.01	+0.15	+0.16
128.	Acetone 2,4-dinitro phenylhydrazone		2.08 2.17	2.08[o] 2.17	2.88 2.94	0.00 0.00	+0.80 +0.77	+0.80 +0.77
		J. Methoxyl groups						
129.	Methyl ester of N-Methylphenyl-alanine	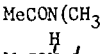	3.64	3.75	-	+0.11	-	-
130.	Arecoline		3.71	3.79	3.92	+0.08	+0.13	+0.21
131.	Tazettine	V	3.44	3.51	3.73	+0.07	+0.22	+0.29
132.	Belladine	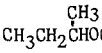	3.75(3H) 3.83(6H)	3.72 3.80	3.93 3.99	−0.03 −0.03	+0.21 +0.19	+0.18 +0.16
133.	Codeine	VI	3.82	3.83	3.98	+0.01	+0.15	+0.16
134.	Sinomenine	VII	3.47 3.79(Ar)	3.49 3.82	3.62 3.91	+0.02 +0.03	+0.13 +0.09	+0.15 +0.12
135.	Thebaine	VIII	3.59 3.84(Ar)	3.65 3.83	(3.99[p] (4.03[p]	+0.06 −0.01	+0.34 +0.20	+0.40 +0.19
136.	Cryptopine	IXa	3.86(6H)	3.86 3.90	3.98(6H)	0.00 +0.04	+0.12 +0.08	+0.12
137.	Hydrocotarnine	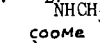	3.96	4.02	4.12	+0.06	+0.10	+0.16
138.	Dicentrine	IV	3.74(6H)	3.81 3.84	4.01 (6H)	+0.07 +0.10	+0.20 +0.17	+0.27
139.	O-Methylcaprolactim		3.55	3.62	4.17	+0.07	+0.55	+0.62

[c]present as dimethylammonium ion; see Discussion.
[d]Present as II; see Discussion.
[e]Present as the equilibrium mixture of axial and equatorial protonated ions XXI. The ratio (32:68 in TFA, 43:57 in PDA) of the two species eliminates the possibility of one of the ions having a *cis*-diaxial-2,6-dimethyl chair conformation; see Discussion.
[f]Has undergone reaction.
[g]Probably present as a mixture of *cis* and *trans* isomers of X, or, less likely, a mixture of the two conformations of *cis* X whose interconversion is slow. In perdeuteroacetic acid one of the two N-methyl peaks might conceivably arise from uncyclized IX; see Discussion.
[h]Present as XII; see Discussion.
[i]Measured on a Varian DP-60 at 27°.
[j]The epoxide ring has undoubtedly been opened.
[k]The infrared spectrum in chloroform has little or no NH absorption.
[l]Present as XVII; see Discussion.
[m]Present as a mixture of XVIII and XIX; see Discussion.
[n]Value taken from the Varian NMR Spectra catalogs.
[o]Solvent was a 2:1 mixture of $CD_3COOD:CDCl_3$.
[p]Assignment uncertain.
Note: The value of 4.17 for compound No. 139 is probably for methyl trifluoroacetate.

Can. J. Chem. Downloaded from www.nrcresearchpress.com by 210.87.254.5 on 09/05/12
For personal use only.

Can. J. Chem. Downloaded from www.nrcresearchpress.com by 210.87.254.5 on 09/05/12
For personal use only.

TABLE II

Ranges of chemical shifts and chemical shift differences in the present study

Type of Methyl	$CDCl_3$ (p.p.m.)	CD_3COOD (p.p.m.)	CF_3COOH (p.p.m.)	$\Delta_{CD_3COOD-CDCl_3}$	$\Delta_{CF_3COOH-CD_3COOD}$	$\Delta_{CF_3COOH-CDCl_3}$
N, aliphatic 3° amines	1.88–2.56	2.63–3.14	2.76–3.26	+0.40 to +0.81	+0.05 to +0.26[a] (or +0.47[b])	+0.53 to +0.92[a] (or +0.97[b])
N, aliphatic 2° amines	2.34–2.44	2.67–2.88	2.78–3.03	+0.26 to +0.54	+0.03 to +0.24	+0.43 to +0.67
N, aromatic and N-heteroaromatic amines	2.66–3.99	2.78–4.00	3.17–4.33	+0.01 to +0.54	+0.06 to +0.54	+0.34 to +0.82
N, amides and imides	2.71–3.89	2.72–3.88	2.90–4.20	−0.09 to +0.07	+0.08 to +0.34	+0.08 to +0.34
N, other neutral nitrogen compounds	3.02–3.68	3.04–3.72	3.57–4.34	−0.04 to +0.09	+0.48 to +0.62	+0.48 to +0.66
N, quaternary ammonium compounds	—	3.30–4.77	3.02–4.79	—	+0.01 to +0.05	—
C, aromatic rings with basic nitrogen	2.12–2.82	2.23–3.19	2.45–3.39	+0.05 to +0.37	+0.07 to +0.42	+0.21 to +0.57
C, nonbasic aromatic nuclei[c]	2.23–2.40	2.20–2.39	2.20–2.46[d]	−0.06 to +0.04	−0.02 to +0.07[d]	−0.08 to +0.06[d]
C, acetyl[e]	1.99–2.59	2.00–2.57	2.15–2.73	−0.02 to +0.09	+0.15 to +0.37	+0.14 to +0.46
O, methoxyl	3.44–3.96	3.49–4.02	3.62–4.17	−0.03 to +0.11	+0.09 to +0.55	+0.12 to +0.62

[a]Excluding compounds with two proximate basic nitrogen atoms, and Nos. 34 and 35.
[b]Including compounds with two proximate basic nitrogen atoms, but excluding Nos. 34 and 35.
[c]Excluding No. 119.
[d]Also excluding Nos. 116 and 117.
[e]Excluding No. 128.

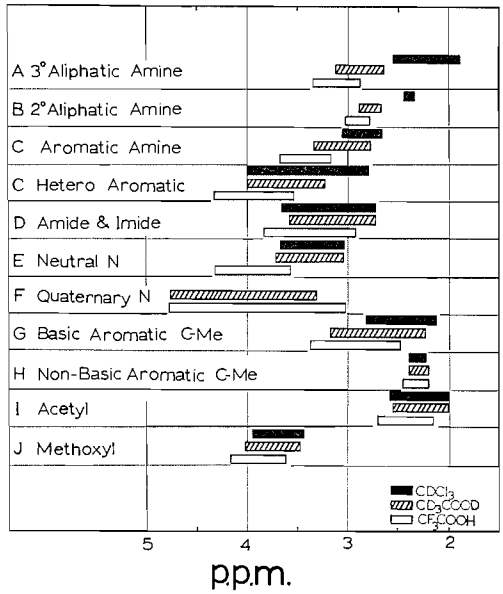

CHART 1. Normal chemical shift ranges for the methyl groups of compounds in the present study (values for compounds that react with a solvent are not included).

with base strength of the amine, perdeuteroacetic or acetic acid is sufficiently strong and is present in sufficient excess that most of the molecules of an aliphatic amine will be present as ammonium ions. Over the range of basicities for which this is true, there should be little variation in the chemical shift increments. Fig. 2, in which are plotted N-methyl chemical shift increments in perdeuteroacetic acid vs. $pK_a^{H_2O}$ values for some of the amines in the present study, bears out this conclusion. Only when the base is as weak as an aromatic amine does the downfield shift decrease considerably. Closer inspection reveals that secondary N-methylamines fall into a group separate from tertiary N-methylamines; a reason for this effect is considered later.

Under the subheadings that follow are discussed generalizations for each of the methyl types. It should be emphasized that these generalizations will be most useful for compounds containing more than one nitrogen atom and (or) unsplit methyl groups, and the following has been written with this point in mind.

Aliphatic Tertiary Amines (Table I, A)

Of the compounds studied, the N-methyl protons of aliphatic tertiary amines show the largest movement in acid toward lower magnetic field ($\sim$ 0.6–0.8 p.p.m. in TFA), and most of this shift ($\sim$ 0.5–0.6 p.p.m.) is already present in perdeuteroacetic acid. There was no difference between tertiary amines with one or two N-methyl groups. Furthermore, the shift is fairly constant regardless of the absorption position in deuterochloroform which varies from 1.97 to 2.56 p.p.m. Not surprisingly, molecules with a second basic nitrogen near the basic methyl-bearing nitrogen atom (Table I, Nos. 6, 17, 18, and 25) give somewhat greater ($\sim$ 0.9–1.0 p.p.m.) downfield increments in the stronger acid. Other electron-attracting atoms or groups in the vicinity of the basic N-methyl function do not have any regular effect on the Δ values provided they are not conjugated (compounds rendered neutral by conjugation are notable exceptions; see Table I, E). In most cases any shielding or deshielding effect of a substituent or group

Can. J. Chem. Downloaded from www.nrcresearchpress.com by 210.87.254.5 on 09/05/12
For personal use only.

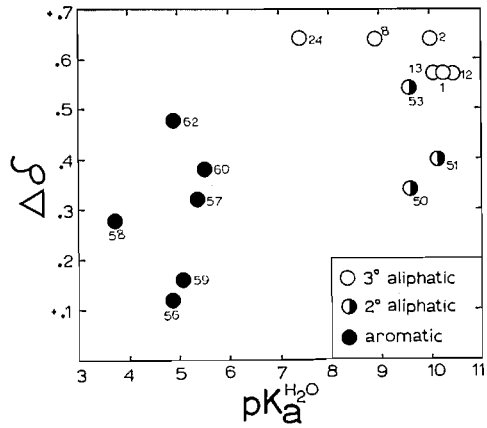

FIG. 2. Variation of N-methyl chemical shift increments ($\Delta_{CD_3COOD-CDCl_3}$) with amine basicity.

would be expected to be present in both unprotonated and protonated amine and therefore to be cancelled. Thebaine (No. 33), cryptopine (No. 34), and protopine (No. 35) are exceptions and these alkaloids are discussed later.

Aliphatic Secondary Amines (Table I, B)

N-Methyl protons in most secondary aliphatic amines are decidedly less deshielded in strong acid (~ 0.45–0.6 p.p.m. in TFA) than N-methyl protons in tertiary amines with about half of this shift occurring in the weaker acid. This can be seen best by comparing values in Table I for secondary and tertiary amines with the same structure: Nos. 2 and 44, 4 and 46, 7 and 49, 8 and 50. The values are sufficiently lower to allow tentative differentiation of secondary and tertiary N-methyl groups, whereas the N-methyl absorption in deuterochloroform alone does not distinguish the two types. A more secure distinction between secondary and tertiary N-methyl groups is possible by noting the coupling between the nitrogen protons and the N-methyl group in trifluoroacetic acid solution (see below).

Although the downfield N-methyl shift in acid will be proportional to the concentration of protonated amine (21), the cause of the discrepancy in shift between secondary and tertiary amines cannot lie in different extents of protonation of the two types, for the aliphatic secondary amines are in general stronger bases than the tertiary amines in hydroxylic solvents. A reasonable explanation is that, since the protonated secondary amine is better solvated (chiefly by hydrogen bonding of the NH protons), the positive charge is more dispersed (23); therefore, the smaller effective positive charge on nitrogen will have a smaller deshielding effect on the N-methyl protons (24).

This effect may be responsible for some of the variations in shift increments within the series of tertiary amines. Of the five dimethylaminocholestanes examined, those (2β, 7α, 6β) with axial dimethylamino groups gave larger $\Delta_{CD_3COOD-CDCl_3}$ shifts (+0.67, +0.69, +0.81 p.p.m., respectively) than those (2α, 6α) with equatorial groups (+0.58, +0.64 p.p.m.). Protonated axial amines are less accessible to solvation than their equatorial epimers as supported by pK_a measurements (22), and therefore the axial ions should have the greater effective positive charge on nitrogen. Furthermore, the axial 6β-dimethylamino derivative, which would be expected to have the most severe steric hindrance to ion solvation (C-10 axial methyl, C-4 and C-8 axial hydrogens), shows the largest shift increment (+0.81 p.p.m.).

Can. J. Chem. Downloaded from www.nrcresearchpress.com by 210.87.254.5 on 09/05/12
For personal use only.

Aromatic and N-Heteroaromatic Amines (Table I, C)

The chemical shift differences for secondary or tertiary aromatic N-methyl groups (~ 0.5–0.8 p.p.m. in TFA) do not differ from each other appreciably and are much the same as those for N-methyl aliphatic amines, except that the shift in perdeuteroacetic acid is somewhat smaller (~ 0.1–0.2 p.p.m.) for most of the aromatic amines. The rather procrustean classification of N-heteroaromatic amines exhibits similar effects in both acids but with wider variations. The fact that the resonance position of aromatic and N-heteroaromatic N-methyl groups in deuterochloroform is at lower field than for aliphatic N-methyl amines permits the former to be distinguished from the latter.

Amides and Imides (Table I, D)

The range of absorption for N-methyl amides and imides in deuterochloroform overlaps most of the values for aromatic amines. However, these compounds give even smaller shift increments (−0.09 to +0.07 p.p.m.) in perdeuteroacetic acid than N-methyl aromatic amines, and, moreover, do not show coupling in trifluoroacetic acid solution as most aromatic N-methyl amines do. Of course, infrared and ultraviolet spectra may also distinguish these functional types.

N-Methyl-2-pyridone (No. 84) and N-methyl-2-quinolone (No. 85) are exceptions and show much larger shifts (0.60 and 0.66 p.p.m.) than normal amides in strong acid. The reason for this behavior is that both types of compound exist largely as hydroxypyridinium derivatives XX at low pH, and the methyl resonance position in trifluoroacetic acid approaches that of N-methylpyridinium salts such as Nos. 94 and 97 in Table I, F. Both of these "amides" show greater similarity to other resonance neutralized nitrogen compounds and have been included in part E of Table I.

Other Compounds with Neutral Nitrogen (Table I, E)

The combination of the low field position (3.02–3.68 p.p.m.) of the N-methyl resonance in deuterochloroform and the negligible change in perdeuteroacetic acid allows this type of N-methyl group to be distinguished from normal aliphatic and aromatic methylamino groups. The greater change (~ 0.5–0.6 p.p.m.) in trifluoroacetic acid differentiates this group from the N-methyl amides and imides. Ultraviolet and infrared spectra will be a useful adjunct in distinguishing these types.

Quaternary Ammonium Salts (Table I, F)

The few examples of this kind were insoluble in deuterochloroform. They are characterized by relatively low field N-methyl absorption in perdeuteroacetic acid (3.30–4.77 p.p.m.) with negligible change (< 0.05 p.p.m.) in trifluoroacetic acid. The latter fact also distinguishes quaternary N-methyl from methoxyl groups which move 0.1–0.3 p.p.m. downfield.

C-Methyl Groups on Aromatic Rings Containing or Attached to Basic Nitrogen (Table I, G)

In deuterochloroform the methyl peaks of this type spread over a range which includes or overlaps categories A–D of N-methyl group. Furthermore, many of them exhibit downfield shifts in perdeuteroacetic and trifluoroacetic acids of the same magnitude as basic aromatic or secondary aliphatic N-methyl groups. For these compounds a negative Herzig-Meyer determination and (or) a positive Kuhn-Roth C-methyl analysis could provide reasonable certainty of the absence of an N-methyl group.

In addition to these aromatic C-methyl compounds, two nonaromatic compounds were found whose methyl groups are unusually sensitive to acid although they are not on basic nitrogen atoms. Acetone 2,4-dinitrophenylhydrazone and O-methyl caprolactim

Can. J. Chem. Downloaded from www.nrcresearchpress.com by 210.87.254.5 on 09/05/12
For personal use only.

(Table I, Nos. 128 and 139) show no shift in deuteroacetic acid, but in trifluoroacetic acid the changes (+0.77, +0.80, and +0.62 p.p.m.) are those expected of tertiary aliphatic amines, the O-methyl caprolactim probably having been solvolyzed to methyl trifluoroacetate.

All of these examples demonstrate that the deshielding effect of a protonated nitrogen atom can be transmitted through several bonds in a conjugated system.

C-Methyl Groups on Nonbasic Aromatic Nuclei (Table I, H)

The narrow range and high field resonance position of these methyl groups in deuterochloroform coupled with their negligible movement in perdeuteroacetic acid and trifluoroacetic acid (unless reaction occurs; see discussion later of Nos. 116 and 117) distinguish them from N-methyl groups and most C-methyl groups on basic N-heterocyclic aromatic nuclei.

Acetyl and Methoxyl Groups (Table I, I and J)

Methoxyl groups and acetyl groups attached to C, N, and O atoms show negligible shifts (−0.03 to +0.11 p.p.m.) on changing from deuterochloroform to perdeuteroacetic acid and only a small (+0.08 to +0.37 p.p.m.) further downfield shift in trifluoroacetic acid. If the acetyl methyl changes are considered in conjunction with the resonance positions in deuterochloroform, the only methyl groups with which they might be confused from n.m.r. data alone are C-methyl groups on nonbasic aromatic compounds. Methoxyl groups are not differentiated from certain N-methyl amides and imides. However, if the n.m.r. data are considered with infrared spectra, Zeisel, Kuhn-Roth and Herzig-Meyer analyses, there need be no ambiguity.

Coupling in Strong Acid

It has been noted previously, e.g. refs. 25 and 26, that hydrogen atoms on the α-carbon atoms of amines are coupled to the NH protons of amine salts of strong acids. In the present study it was found that at 38° in trifluoroacetic acid a proton remains on the nitrogen atom of most aliphatic and aromatic amines long enough to give observable coupling with $J \sim 5$–5.5 c.p.s. (see Table I). The splitting pattern is very useful in the further characterization of basic N-methyl groups. Thus the combination of a methyl n.m.r. peak at higher field than 2.56 p.p.m. in deuterochloroform, a downfield shift of $\sim$ 0.5–0.6 p.p.m. in perdeuteroacetic acid, a $\sim$ 0.6–0.8 p.p.m. shift in trifluoroacetic acid, and splitting of the methyl peak into a doublet (Fig. 3*a*), all taken together provides strong evidence for the N-methyl group of a tertiary aliphatic amine. The two peaks do result from coupling rather then merely from non-equivalent methyl groups or from stereoisomers protonated on opposite sides of the nitrogen atom since some symmetrical molecules with only one N-methyl group have a doublet N-methyl absorption with equal area under each peak. More conclusively, double irradiation of N,N-dimethylbenzylamine in trifluoroacetic in the low field HN^+ region caused the N-methyl doublet (and N-methylene doublet) to collapse to a singlet. In the case of some N,N-dimethylamines with an asymmetric carbon in the α- or β-position, the N-methyl absorption appeared as a pair of doublets in trifluoroacetic acid. These non-equivalent methylamino groups are analogous to the non-equivalent methyls of similarly situated isopropyl groups (27).

Secondary N-methylamines give a symmetrical triplet in trifluoroacetic acid. (Fig. 3*b*) A methyl group which absorbs in the range $\sim$ 2.3–2.4 p.p.m. in deuterochloroform, shifts $\sim$ 0.2–0.3 p.p.m. in perdeuteroacetic acid, shifts $\sim$ 0.4–0.6 p.p.m. in trifluoroacetic acid, and is split into a triplet in the latter solvent is in all probability the N-methyl group of a secondary aliphatic amine.

Can. J. Chem. Downloaded from www.nrcresearchpress.com by 210.87.254.5 on 09/05/12
For personal use only.

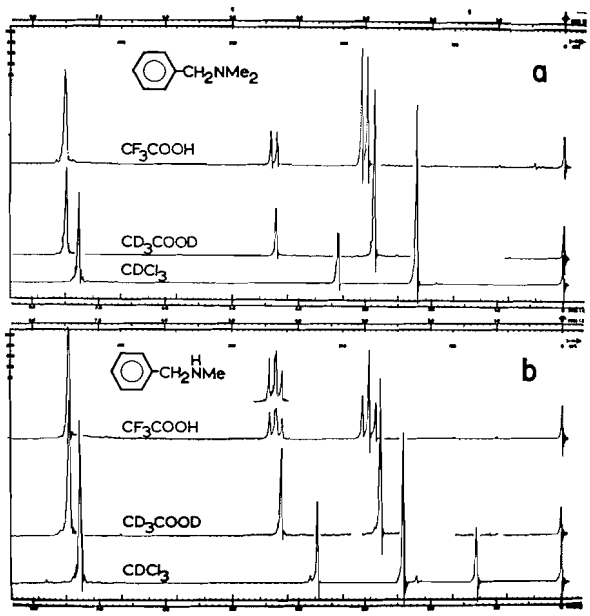

FIG. 3. (*a*) N,N-Dimethylbenzylamine and (*b*) N-methylbenzylamine.

A few aliphatic and aromatic amines gave broadened but unresolved N-methyl peaks in trifluoroacetic acid. Since this situation must be a consequence of too rapid NH exchange rate, the spectra of several of these compounds were recorded at 27° instead of 38° in an attempt to decrease the proton exchange rate. At this temperature the previously broad N-methyl peak of N-methyl-N-benzylaniline (No.61) was resolved into a doublet, and the methyl peak of N-methylaniline (No. 56) was a partially resolved triplet. No resolution of the N-methyl peak of nicotine was observed, but if the temperature were lowered still further, the coupling should become apparent. None of the other types (Table I, D–F) of N-methyl group gave any indication of coupling or peak broadening in trifluoroacetic acid at 38°. Although in trifluoroacetic acid the methyl and methylene peaks of N,N-dimethylbenzylamine (Fig. 3*a*) are symmetrical doublets, in *acetic* acid at 38° there was no resolution or broadening of the singlet peaks from the methyl or methylene groups.

Other Information

In some cases the n.m.r. spectra in weak and strong acid provide more information than just the type of methyl group. The fact that tetramethylmethylene diamine (No. 5) gives a triplet in trifluoroacetic acid is in accord with the molecule being solvolyzed to dimethylamine. Similarly, the appearance of the N-methyl resonance of caranine anhydromethine (No. 11) as a triplet in trifluoroacetic acid shows that the *o,m'*-bridge has been broken with formation of the N-methyl secondary amine II (28). This is corroborated by the appearance of a 2-H singlet at 5.29 p.p.m. due to the methylene group of the benzylic trifluoroacetate.

The anomalously large shift of the N-methyl group of cryptopine and protopine can be attributed to two factors. In deuterochloroform this methyl group is apparently shielded by the long range anisotropic effect of the carbonyl group through space to give an abnormally low δ value, compared to those for other tertiary N-methyl groups, while in acid the compounds exist largely, if not exclusively, as the quaternary ammonium

Can. J. Chem. Downloaded from www.nrcresearchpress.com by 210.87.254.5 on 09/05/12
For personal use only.

salts X (29). The latter point was demonstrated by the identity of the ultraviolet absorption spectrum of cryptopine in ethanol containing either acetic or trifluoroacetic acids with the published spectrum of protopine hydrochloride (29). Thus not only is the shielding effect of the carbonyl group removed, but the methyl absorption is moved toward the lower field region of quaternary N-methyl groups ($\delta > 3$ p.p.m., see Table I, F).

Physostigmine (eserine, No. 36) is another compound having an unusually large Δ value in strong acid because of chemical reaction. The chemical shifts of its aromatic N-methyl group in deuterochloroform and perdeuteroacetic acid are normal values (see Table I, C), but the marked low field δ value in trifluoroacetic acid is that expected of some aromatic quaternary ammonium salts (cf. Table I, F). This is entirely reasonable since in strong acid structures of the physostigmine type are opened to imonium compounds, i.e. XII (30).

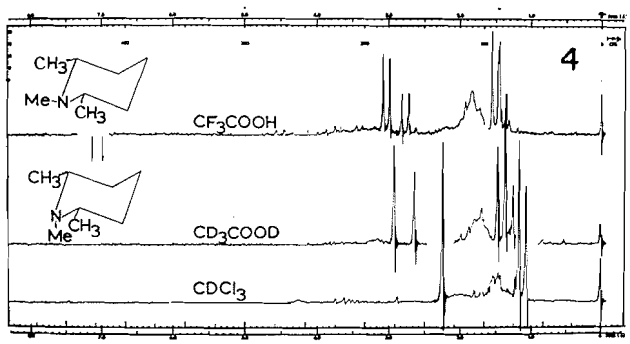

FIG. 4. *cis*-1,2,6-Trimethylpiperidine.

cis-1,2,6-Trimethylpiperidine is an example of a piperidine derivative in which the axial and equatorial N-methyl protonation isomers XXI have long enough life times to permit their observation in perdeuteroacetic and trifluoroacetic acid (Fig. 4). The more intense N-methyl peak (peak ratios 43:57 in PDA) presumably corresponds to the equatorial methyl isomer as found in the case of tropane derivatives (26). The purity of the *cis* amine was assured by reductive methylation of *cis*-2,6-dimethylpiperidine purified through its crystalline hydrochloride.

The large downfield shift (+0.69 p.p.m.) in trifluoroacetic acid reveals that 2-methylindole (No. 116) is protonated at C-3 to form XVII in trifluoroacetic acid, just as in sulfuric acid (31). Confirmation is provided by the peak (2H) at 4.47 p.p.m. arising from the C-3 protons. On the other hand 3-methylindole (No. 117) in trifluoroacetic acid is partly protonated at C-3 (XVIII) (methyl doublet at 1.52 p.p.m., $J \sim 6.5$ c.p.s.) and partly on nitrogen (XIX) (methyl singlet at 2.43 p.p.m.).

Thebaine is known to react with strong acid at room temperature; since its N-methyl resonance in trifluoroacetic acid is not near those of codeine and sinomenine, it has obviously undergone chemical change.

In molecules with more than one basic nitrogen a larger $\delta_{CF_3COOH}-\delta_{CD_3COOD}$ shift ($\sim$ 0.25–0.5 p.p.m.) than usual ($\sim$ 0.1–0.2 p.p.m.) for aliphatic amines may be evidence for close proximity of the basic nitrogen atoms, for in such cases the inductive effect of the second positively charged nitrogen atom will come into play only in strong acid where both nitrogen atoms are appreciably protonated (see Nos. 6, 17, 18, 25).

Can. J. Chem. Downloaded from www.nrcresearchpress.com by 210.87.254.5 on 09/05/12
For personal use only.

Can. J. Chem. Downloaded from www.nrcresearchpress.com by 210.87.254.5 on 09/05/12
For personal use only.

Methylene and Methine Hydrogens

Methylene and methine groups attached to basic nitrogen also show the same downfield shift as methyl groups, but since they usually appear as complex multiplets which overlap other absorption (see Fig. 5) particularly in deuterochloroform, assignment is often difficult. The unambiguous cases among the compounds studied are set forth in Table III. In so far as the limited number of examples permits, the following generalizations can be made.

In perdeuteroacetic acid methylene groups adjacent to tertiary aliphatic nitrogen are shifted almost twice as far downfield ($\sim$ 0.8–0.9 p.p.m.) as methylene groups adjacent to secondary aliphatic nitrogen ($\sim$ 0.4–0.5 p.p.m.). The reason for the difference is presumably the same as that discussed earlier for the difference between secondary and tertiary basic N-methyl groups.

In trifluoroacetic acid and in dilute perdeuteroacetic acid solution, the absorption from methylene protons within an N-heterocyclic ring and adjacent to a tertiary (but not secondary) nitrogen atom is separated into two groups of multiplets (see Fig. 6). One group presumably corresponds to the α,α' protons on the same side of the ring as the NH, while the other group arises from the α,α' protons on the side opposite the NH group. This separation could be useful in deciding whether a basic tertiary nitrogen is part of a ring.

Aromatic Hydrogens

Aromatic rings with basic nitrogen as part of the nucleus or bonded to the nucleus exhibit pronounced shifts of the aromatic protons to lower field in acid solution. The shifts are difficult to specify exactly because of the unsymmetrical nature of most of the bands and the compression of the overall bandwidth which usually takes place in acid (see Fig. 7).[4] For basic N-heterocyclic rings in trifluoroacetic acid the shift is $\sim$ 1 p.p.m. for pyridines and $\sim$ 0.5–1 p.p.m. for the other N-heteroaromatic compounds of Table I, G. For the aromatic amines of Table I, C the downfield shift in trifluoroacetic acid is somewhat less, $\sim$ 0.3–0.5 p.p.m. The aromatic protons of N-methyl-α-pyridone also move downfield more than 1 p.p.m. in trifluoroacetic acid where the molecule is present as the hydroxy pyridinium ion (XX).

EXPERIMENTAL

The compounds used in this work were commercial products, specimens from the authors' file, compounds prepared in this laboratory, or else samples generously donated by other laboratories. In each case the n.m.r. spectrum in deuterochloroform was in agreement with the structure. A few commercial products were contaminated with small amounts of impurities whose effect, if any, was assumed to be negligible.

Eastman 2,6-dimethylpiperidine was converted to the hydrochloride. This salt was recrystallized from methanol to constant m.p. 286–292° (reported (32) for *cis*-2,6-dimethylpiperidine, m.p. 281°). The regenerated pure *cis* amine was methylated by catalytic reduction in the presence of aqueous formaldehyde and 5% palladium-on-carbon catalyst. The perdeuteroacetic acid (99% d_4, Merck, Sharp and Dohme of Canada) and trifluoroacetic acid (Matheson, Coleman and Bell) were used without further purification.

Unless otherwise noted the spectra were recorded on a Varian A-60 spectrometer (measured probe temperature 38°). Concentrations varied between 10% and 20% w/v (g/ml) except for a few compounds whose low solubility or short supply obliged the use of more dilute solutions. Variations in concentration within the range used had little effect on peak positions. Dilution of a 1:3 v/v N-methyl pyrrolidine: chloroform solution to 1:30 v/v moved the N-methyl peak only 1 c.p.s. to lower field. The same control experiment with N-methyl pyrrolidine: trifluoroacetic acid gave an N-methyl downfield shift of only 2 c.p.s.; for N,N-dimethylbenzylamine in acetic acid the downfield shift was 1.5 c.p.s. Peak positions are believed accurate to $\pm$1 c.p.s. For the 19 examples run which were also in the Varian catalogs 1 and 2, the agreement in the

[4] *Although in deuterochloroform the aromatic protons of a compound may give rise to a complex pattern, in trifluoroacetic acid (and to a lesser extent in perdeuteroacetic acid) the chemical shifts of the aromatic hydrogens of some compounds are so closely spaced as to give the appearance of a broadened singlet.*

TABLE III

Nuclear magnetic resonance positions and their differences for **N-methylene** groups

No.[a]	Compound	Structure[b]	δ in $CDCl_3$[c]	δ in CD_3COOD[c]	δ in CF_3-COOH[c]	δ_{CD_3}-COOD− δ_{CDCl_3}	δ_{CF_3}-COOH− δ_{CD_3COOD}	δ_{CF_3}-COOH− δ_{CDCl_3}
			N-Methylene tertiary amines					
1.	Methyldiethylamine	$(CH_3CH_2)_2NMe$	2.40q(7)	3.17q(7)	3.33 m	+0.77	+0.16	+0.93
2.	N,N-Dimethylbutylamine	$CH_3(CH_2)_2CH_2NMe_2$	~2.28 m	~3.06 m	~3.15 m	+0.78	+0.09	+0.87
3.	N,N-Dimethyl-n-dodecylamine	$CH_3(CH_2)_{10}CH_2NMe_2$	~2.25 bm	~3.12 bm	~3.25 bm	+0.87	+0.13	+1.00
4.	N,N-Dimethyl-n-octadecylamine	$CH_3(CH_2)_{16}CH_2NMe_2$	~2.25 bm	~3.10 bm	~3.16 bm	+0.85	+0.06	+0.91
6.	Tetramethylethylenediamine	$Me_2NCH_2CH_2NMe_2$	2.38	3.42	3.88 m	+1.04	+0.46	+1.50
8.	N,N-Dimethylbenzylamine	ϕ-CH_2NMe_2	3.41	4.34	4.37 d(5.5)	+0.93	+0.03	+0.96
9.	Gramine	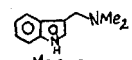	3.63	4.51	4.54 d(5)	+0.88	+0.03	+0.91
10.	Belladine	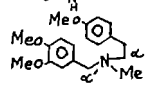	α2.69 m α'3.47	~3.17 bm 4.32	~3.55 bm 4.40 d(5)	+0.48 +0.85	+0.38 +0.08	+0.86 +0.93
12.	N-Methylpyrrolidine		~2.45 m	3.29 m	3.15(2Hm) 3.83(2Hmm)	+0.84	-0.14 +0.54	+0.70 +1.38
13.	N-Methylpiperidine		~2.33 bm	~3.20 bm	~2.94(2Hbm) ~3.60(2Hm)	+0.87	-0.26 +0.40	+0.61 +1.27
15.	N-Methyl-1,2,5,6-tetrahydropyridine		α2.50 m α'2.90 bm	3.35 bm 3.72 bm	-[d]	+0.85 +0.82	-	-
19.	Hydrocotarnine	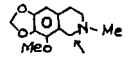	3.43	4.42 m	4.57 m	+0.99	+0.15	+1.14
21.	Arecoline	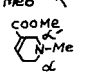	α ~2.42 m α' 3.13 m	~3.44 bm ~4.00 bm	-[d]	+1.02 +0.87	-	-
24.	N-Methylmorpholine		2.39 m	~3.33 bm	3.60 m	+0.94	+0.27	+1.21
25.	N-Methylpiperazine		2.33 m	3.41 bm	3.97 bm	+1.08	+0.56	+1.64
26.	2-Dimethylaminoethanol	$Me_2NCH_2CH_2OH$	2.46 dd (5,5.5)	3.33 m	3.50 m	+0.87	+0.17	+1.04
27.	1-Dimethylamino-2-propanol	$Me_2NCH_2\underset{OH}{C}HCH_3$	2.16 d (6.5)	3.16 d(6.5)	3.36 m	+1.00	+0.20	+1.20
28.	β-N,N-Dimethylaminoethyl acrylate	$CH_2{=}CH\overset{O}{\overset{\|}{C}}OCH_2CH_2NMe_2$	2.60 t (5.5)	3.54 m	3.54 m	+0.94	0.00	+0.94
61.	N-Methyl-N-benzylaniline	ϕ-$CH_2\overset{Me}{N}$-ϕ	4.38	4.48	~4.75 bm	+0.10	+0.27	+0.37
			N-Methylene secondary amines					
12a.	Pyrrolidine		2.85 m	3.27 m	3.46 m	+0.42	+0.19	+0.61
13a.	Piperidine		~2.80 bm	~3.20 bm	~3.34 bm	+0.40	+0.14	+0.54
44.	N-Methyl-n-butylamine	$CH_3(CH_2)_2CH_2\overset{H}{N}Me$	~2.58 bm	~3.05 bm	~3.25 bm	+0.47	+0.20	+0.67

Can. J. Chem. Downloaded from www.nrcresearchpress.com by 210.87.254.5 on 09/05/12
For personal use only.

TABLE III (*Concluded*)

Nuclear magnetic resonance positions and their differences for **N-methylene** and **N-methine** groups

No.[a]	Compound	Structure[b]	δ in $CDCl_3$[c]	δ in CD_3COOD[c]	δ in CF_3COOH[c]	$\delta_{CD_3COOD}-\delta_{CDCl_3}$	$\delta_{CF_3COOH}-\delta_{CD_3COOD}$	$\delta_{CF_3COOH}-\delta_{CDCl_3}$
46.	N-Methyl-n-octadecylamine	$CH_3(CH_2)_{16}CH_2\overset{H}{\underset{}{N}}Me$	~2.57 bm	~3.04 bm	~3.23 bm	+0.47	+0.19	+0.66
48.	N-Methyltetrahydrofurfurylamine	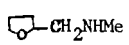	2.62 d(5.5)	~3.20 m	~3.34 bm	+0.58	+0.14	+0.72
50.	N-Methylbenzylamine	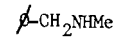	3.71	4.26	4.34 dd (5,6)	+0.55	+0.08	+0.63
51.	N-Methyl-β-phenylethylamine	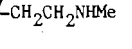	2.74[e]	~3.17 bm	~3.25 bm	+0.43	+0.08	+0.51
52.	2-Methylaminoethanol	$MeHNCH_2CH_2OH$	~2.69 m	~3.25 m	~3.50 bm	+0.56	+0.25	+0.81
73.	4-N,N-Dimethylcarboxamido-4-phenyl piperidine	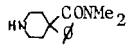	3.05 bm	3.47 bm	3.72 bm	+0.42	+0.25	+0.67
75.	N-Methyl-2-pyrrolidone	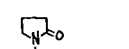	3.39 ~t(6.5)	3.43t (6.5)	3.76t (6.5)	+0.04	+0.33	+0.37
139.	O-Methylcaprolactim	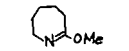	3.36 bm	3.02 bm	3.78 bm	-0.34	+0.76	+0.42
		N-Methine tertiary amines						
7.	N,N-Dimethylcyclohexylamine	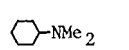	~2.33 bm	~3.12 bm	~3.20 bm	+0.79	+0.08	+0.87
22.	Tropinone	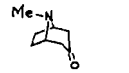	3.43 bm	4.19 bm	4.43 bm	+0.76	+0.24	+1.00
37.	N,N-Dimethylleucine	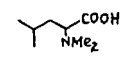	-	3.81 q(5,10)	4.17 m	-	+0.36	-
38.	N,N-Dimethylisoleucine	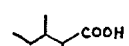	-	3.80 d(4)	4.09 dd (4,8)	-	+0.29	-
		N-Methine secondary amines						
47.	N-Methylcyclopentylamine	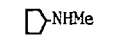	2.98 bm	3.56 bm	3.70 bm	+0.58	+0.14	+0.72
49.	N-Methylcyclohexylamine	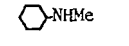	~2.24 bm	3.02 bm	3.14 bm	+0.78	+0.12	+0.90
53.	Ephedrine	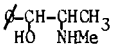	~2.73 bm	~3.54 bm	~3.70 bm	+0.81	+0.16	+0.97
54.	N-Methyl-β-phenylalanine methyl ester	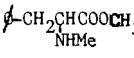	3.44 dd (5.5,7)	4.37 dd (5.5,7)	-	+0.93	-	-
55.	N-Methyl-β-phenylalanine	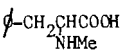	-	4.17 t(5.5)	4.49 bm	-	+0.32	-

[a]The compound numbers are the same as in Table I.
[b]The protons whose absorption is given are indicated by Greek letters or an arrow in ambiguous cases.
[c]Peak positions are given in p.p.m. from internal tetramethylsilane (= 0). If the peak is not a singlet, the multiplicity is given after the peak position (d = doublet, dd = doublet of doublets, t = triplet, q = quartet, m = multiplet with well-defined peaks, bm = broad multiplet with ill-defined or no peaks). The apparent coupling constant is given in parentheses. The symbol ~ means that the band center could not be determined exactly.
[d]Assignment uncertain.
[e]Both methylene groups happen to have the same chemical shift.

Can. J. Chem. Downloaded from www.nrcresearchpress.com by 210.87.254.5 on 09/05/12
For personal use only.

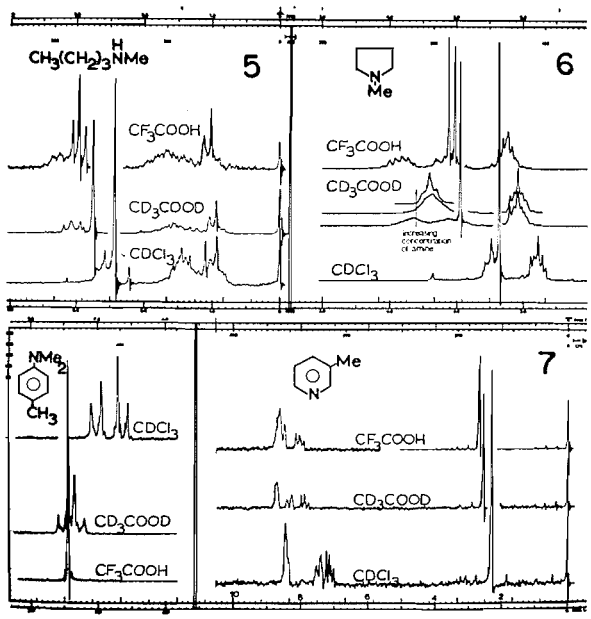

FIG. 5. N-methyl-*n*-butylamine.
FIG. 6. N-Methylpyrrolidine.
FIG. 7. (*a*) N,N-Dimethyl-*p*-toluidine and (*b*) β-picoline.

methyl resonance position in deuterochloroform was within 0.02 p.p.m. for 12 cases, and with one exception (dicentrine −0.06 p.p.m.) all agreed within 0.04 p.p.m. Several spectra were recorded in both acetic acid and perdeuteroacetic acid, and no change in methyl resonance position was observed.

Assignment of peaks in compounds with more than one kind of unsplit methyl signal presented little or no difficulty. The unsplit methyl peaks of such compounds differed in the numbers of similar methyl groups (e.g. Nos. 16, 66, 102) and (or) differed sufficiently in δ to allow clear-cut designation (e.g. Nos. 10, 19, 20, 21, 31, 65, 83), or else differed unambiguously in effect of acid on the methyl peaks (e.g. Nos. 14, 21, 57, 60). Specific assignments to the methyl groups of caffeine, theobromine, and theophylline (Nos. 68, 69, 80, 81, 82) were made by comparing the values of all three bases. The present assignments are the same as those made elsewhere (33) by comparing the spectra of caffeine, ethyl theobromine, and ethyl theophylline. The N-acetyl-*p*-toluidine methyl peaks were assigned by comparison with acetanilide. Thebaine methyl positions were based on comparison with codeine and sinomenine.

ACKNOWLEDGMENTS

Most of the funds for purchase of the Varian A-60 n.m.r. spectrometer were generously provided by the National Research Council. The support of the U.S. National Heart Institute under Grant HE-07394 is gratefully acknowledged. The authors would like to thank Mr. W. D. Chambers for preparation of some of the compounds, and Dr. R. J. Highet and Professor R. C. Cookson for donation of other compounds. Professor J. B. Stothers kindly obtained several spectra on the Varian DP-60 instrument.

REFERENCES

1. (*a*) F. PREGL and J. GRANT. Quantitative organic microanalysis. The Blakiston Co., Philadelphia. 1946. p. 156. (*b*) H. ROTH. *In* Methoden der organischen Chemie (Houben-Weyl). Vol. II. *Edited by* E. Müller. G. Thieme Verlag, Stuttgart. 1953. p. 671.
2. (*a*) J. A. POPLE, W. G. SCHNEIDER, and H. J. BERNSTEIN. High resolution nuclear magnetic resonance. McGraw-Hill Book Co., New York. 1959. p. 280. (*b*) J. B. STOTHERS. *In* Elucidation of structures by physical and chemical methods. Part I. *Edited by* A. Weissberger. Interscience–Wiley, New York. 1963. p. 241.

Can. J. Chem. Downloaded from www.nrcresearchpress.com by 210.87.254.5 on 09/05/12
For personal use only.

3. (*a*) I. R. C. BICK, J. HARLEY-MASON, N. SHEPPARD, and M. J. VERNENGO. J. Chem. Soc. 1896 (1961). (*b*) J. PECHER *et al.* Tetrahedron Letters, No. 8, 270 (1961). (*c*) R. D. HILL and G. D. MEAKINS. J. Chem. Soc. 760 (1958).
4. H. CONROY, P. R. BROOK, M. K. ROUT, and N. SILVERMAN. J. Am. Chem. Soc. **80**, 5178 (1958).
5. J. A. GOODSON. J. Chem. Soc. 245 (1945).
6. E. SPÄTH and L. KAHOVEC. Ber. **67**, 1501 (1934).
7. (*a*) B. P. MOORE and L. MARION. Can. J. Chem. **31**, 952 (1953). (*b*) W. A. AYER, J. A. BEREZOWSKY, and G. G. IVERACH. Tetrahedron, **18**, 567 (1962).
8. A. LAWSON and J. E. C. TOPPS. J. Chem. Soc. 1640 (1937).
9. K. WIESNER, S. K. FIGDOR, M. F. BARTLETT, and D. R. HENDERSON. Can. J. Chem. **30**, 608 (1952).
10. O. O. ORAZI, R. A. CORRAL, J. S. E. HOLKER, and C. DJERASSI. J. Org. Chem. **21**, 979 (1956).
11. W. A. JACOBS and L. C. CRAIG. J. Biol. Chem. **143**, 606 (1942).
12. (*a*) H.-G. BOIT. Chem. Ber. **89**, 1129 (1956). (*b*) E. W. WARNHOFF and W. C. WILDMAN. J. Am. Chem. Soc. **82**, 1472 (1960).
13. J. P. FERRIS. J. Org. Chem. **27**, 2985 (1962).
14. R. J. HIGHET. J. Org. Chem. **29**, 471 (1964).
15. B. WITKOP. J. Am. Chem. Soc. **71**, 2559 (1949).
16. (*a*) H. SCHULZE and E. BIERLING. Arch. Pharm. **251**, 8 (1913). (*b*) W. B. COOK and O. A. BEATH. J. Am. Chem. Soc. **74**, 1412 (1952). (*c*) J. A. GOODSON. J. Chem. Soc. 245 (1945).
17. (*a*) J. A. GOODSON. J. Chem. Soc. 139 (1943). (*b*) J. A. GOODSON. J. Chem. Soc. 665 (1944).
18. L. C. CRAIG and W. A. JACOBS. J. Biol. Chem. **143**, 611 (1942).
19. J. A. GOODSON. J. Chem. Soc. 108 (1944).
20 H. CONROY, P. R. BROOK, M. K. ROUT, and N. SILVERMAN. J. Am. Chem. Soc. **79**, 1763 (1957).
21. (*a*) E. GRUNWALD, A. LOEWENSTEIN, and S. MEIBOOM. J. Chem. Phys. **27**, 641 (1957). (*b*) J. L. SUDMEIER and C. N. REILLEY. Anal. Chem. **36**, 1698 (1964). (*c*) G. FRAENKEL. J. Chem. Phys. **39**, 1614 (1963).
22. C. W. BIRD and R. C. COOKSON. J. Chem. Soc. 2343 (1960).
23. (*a*) A. F. TROTMAN-DICKENSON. J. Chem. Soc. 1293 (1949). (*b*) H. K. HALL. J. Am. Chem. Soc. **79**, 5441 (1957).
24. G. FRAENKEL. Personal communication.
25. E. GRUNWALD, A. LOEWENSTEIN, and S. MEIBOOM. J. Chem. Phys. **27**, 630 (1957).
26. G. L. CLOSS. J. Am. Chem. Soc. **81**, 5456 (1959).
27. G. M. WHITESIDES, D. HOLTZ, and J. D. ROBERTS. J. Am. Chem. Soc. **86**, 2628 (1964).
28. E. W. WARNHOFF and W. C. WILDMAN. J. Am. Chem. Soc. **79**, 2192 (1957).
29. E. H. MOTTUS, H. SCHWARZ, and L. MARION. Can. J. Chem. **31**, 1144 (1953).
30. H. FRITZ and O. FISCHER. Tetrahedron, **20**, 1737 (1964).
31. R. L. HINMAN and E. B. WHIPPLE. J. Am. Chem. Soc. **84**, 2534 (1962).
32. A. MARCUSE and R. WOLFFENSTEIN. Ber. **32**, 2525 (1899).
33. T. G. ALEXANDER and M. MAIENTHAL. J. Pharm. Sci. **53**, 962 (1964).

Can. J. Chem. Downloaded from www.nrcresearchpress.com by 210.87.254.5 on 09/05/12
For personal use only.

Can. J. Chem. Downloaded from www.nrcresearchpress.com by 210.87.254.6 on 09/05/12
For personal use only.

THE SULFUR–CHLORINE STRETCHING BAND IN SULFONYL CHLORIDES

J. F. KING AND DAVID J. H. SMITH

In connection with some questions arising from our general study of the chemistry of sulfenes (1, 2), we wished to have information on the nature of the sulfur–chlorine stretching absorption in sulfonyl chlorides. Studies of the Raman spectra had been reported previously (3–7) and these had concurred in assigning the strong band around 375 cm^{-1} to the sulfur–chlorine stretching mode. But in order to use the corresponding infrared region for the purposes of structural elucidation, we required more information than was already available. To obtain this we have measured the spectra of a number of sulfonyl chlorides, along with a few other sulfonyl halides, using an infrared spectrophotometer equipped with cesium iodide optics. The data are listed in Table I.

Most of the spectra are of methylene chloride solutions using potassium bromide cells, which under the conditions used are limited to frequencies down to about 300 cm^{-1}. The spectra of a number of sulfonyl chlorides in the region above 420 cm^{-1} have been discussed by other investigators (6, 8) and will not be treated here. In the hope of being able to describe the intensities of the bands more precisely than merely as "strong" or "weak", we attempted to measure their extinction coefficients. In many cases this could not be done accurately because, among other things, of the presence of overlapping bands or strong background absorption. As can be seen from Table I, the value of the apparent extinction coefficient in the case of the 375 cm^{-1} band of *p*-toluenesulfonyl chloride apparently varies somewhat with change in concentration; the variation over the range of concentrations commonly used in infrared spectroscopy is, however, not large (if, in fact, real). In the most favorable cases the apparent extinction coefficients are probably accurate to $\pm 10\%$, but with those values indicated as only approximate the error is larger. In some of these cases error is introduced because the sample did not completely dissolve (probably because of partial hydrolysis). The shape of the S—Cl stretching band of *p*-toluenesulfonyl chloride was not changed significantly by running the spectra under conditions of higher resolution, and it seems likely that the uncertainties in the ϵ_{app} values (for bands above 340 cm^{-1} at any rate) deriving from overly large spectral slit widths are of minor significance.

Inspection of Table I reveals that virtually all of the sulfonyl chlorides show a band within the range 380 $\pm$ 10 cm^{-1} which may be assigned to the sulfur–chlorine stretching vibration. It is also evident that the introduction of electron-withdrawing substituents is accompanied by a shift to higher frequencies. Though the S—Cl stretching frequencies of the aromatic sulfonyl chlorides show no precise correlation with the ordinary Hammett substituent parameters, they do give a reasonably good linear plot with Taft's σ_I values (Fig. 1), indicating a direct connection between the stretching frequency and the *inductive* effect of the substituent. With the aliphatic sulfonyl chlorides the same tendency of electron-withdrawing substituents to raise the frequency of the absorption maximum is found, but the correlation with σ^*, for example, is only approximate. The effect of electron-

TABLE I

Infrared spectra of sulfonyl halides in the region 420–300 cm^{-1}

Compound	S—Cl stretching frequency in cm^{-1} (apparent ϵ_{max})	Other bands (apparent ϵ_{max})	Concentration* (*M*) (cell thickness in mm)
(*a*) Aromatic sulfonyl chlorides			
Benzenesulfonyl chloride	373 (11)	318 (5)	2 (0.1)
1-Naphthalenesulfonyl chloride	373 (11)	412 (16), 340 (4)	2 (0.1)
2-Naphthalenesulfonyl chloride	373 (12)	394 (11), 346 (4)	2 (0.1)
o-Toluenesulfonyl chloride	372 (13)	—	2 (0.1)
p-Toluenesulfonyl chloride	375 (24)	334 (7)	2 (0.1)
p-Toluenesulfonyl chloride	375 (28)	334 (?)†	0.2 (1.0)
p-Toluenesulfonyl chloride	375 (33)	334 (?)†	0.04 (5.0)
m-Chlorosulfonylbenzoic acid	378 (13)	318 (8)	0.3 (1.0)
p-Bromobenzenesulfonyl chloride	379 (~21)	418 (~100)	0.1 (1.0)
p-Methoxybenzenesulfonyl chloride	377 (25)	345 (6)	2 (0.1)
p-Hydroxybenzenesulfonyl chloride	377 (12)	354 (11), 343 (13)	2 (0.1)
p-Nitrobenzenesulfonyl chloride	380 (10)	312 (8)	0.2 (1.0)
m-Nitrobenzenesulfonyl chloride	380 (19)	—	0.3 (1.0)
p-Fluorobenzenesulfonyl chloride	382 (25)	348 (5)	0.2 (1.0)
2,4-Dinitrobenzenesulfonyl chloride	390 (5)	340 (18)	0.3 (1.0)
1-Anthraquinonesulfonyl chloride	390 (~24) 381 (shoulder)	418 (~16)	0.1 (1.0)
2-Anthraquinonesulfonyl chloride	379 (49)	404 (82)	0.1 (1.0)
2-Methylanthraquinone-1-sulfonyl chloride (I)	384 (~25)	348 (~21), 336 (~19), 322 (~36)	0.1 (1.0)
(*b*) Aliphatic sulfonyl chlorides			
Methanesulfonyl chloride	377 (13)	—	2 (0.1)
Ethanesulfonyl chloride	372 (12)	410 (25)	2 (0.1)
2-Phenylethanesulfonyl chloride	373 (12)	—	2 (0.1)
1,4-Butanedisulfonyl chloride	376 (33)	416 (36)	0.2 (1.0)
Phenylmethanesulfonyl chloride	373 (15)	338 (8)	0.2 (1.0)
Phenylmethanesulfonyl-*1-d* chloride	369 (13)	337 (9)	0.3 (1.0)
Phenylmethanesulfonyl-*1,1-d*$_2$ chloride	369 (8)	336 (7)	2 (0.1)
p-Nitrophenylmethanesulfonyl chloride	390 (25)	410 (25), 326 (11)	2 (0.1)
p-Nitrophenylmethanesulfonyl-*1-d* chloride	389 (32)	407 (28), 324 (15)	0.2 (1.0)
Trichloromethanesulfonyl chloride	416 (~19)‡ 379 (~12)‡	—	2 (0.1)
Camphor-10-sulfonyl chloride	368 (9) 388 (11)	—	2 (0.1)
Chlorosulfonylacetyl chloride	383 (~3)	345 (~6)	0.3 (1.0)
Chlorosulfonylacetic acid	379 (~13)	348 (~14)	0.2 (1.0)
2-Phenylethenesulfonyl chloride	377 (25)	—	2.0 (0.1)
(*c*) Other sulfonyl halides			
Methanesulfonyl fluoride	—	326 (8)	2 (0.1)
Phenylmethanesulfonyl fluoride	—	—	2 (0.1)
p-Toluenesulfonyl fluoride	—	383 (11), 358 (10)	2 (0.1)
p-Nitrophenylmethanesulfonyl bromide	—	408 (40), 379 (44)	0.2 (1.0)
p-Nitrophenylmethanesulfonyl-*1,1-d*$_2$ bromide§	—	402 (26), 375 (33), 293 (14), 277 (11)	1 (0.1)
Benzenesulfonyl bromide§	—	327 (11), 277 (6)	2 (0.1)
p-Toluenesulfonyl bromide§	—	326 (11), 275 (16)	2 (0.1)
p-Toluenesulfonyl iodide§	—	322 (~11), 274 (~11)	2 (0.1)

*In methylene chloride solution.
†Value uncertain because of strong absorption by solvent.
‡Assignment uncertain, see text.
§Spectrum determined using CsBr cells.

withdrawing substituents leads one to suggest the possibility that the band at 416 cm^{-1} in the spectrum of trichloromethanesulfonyl chloride is the sulfur–chlorine stretching mode and not the band at 379 cm^{-1}, even though the latter falls well within the normal range and might at first glance appear to be the more likely choice.

The position of the S—Cl stretching band does not appear to be particularly sensitive to change in solvent. This is indicated by the following data for the position of this band

Can. J. Chem. Downloaded from www.nrcresearchpress.com by 210.87.254.6 on 09/05/12
For personal use only.

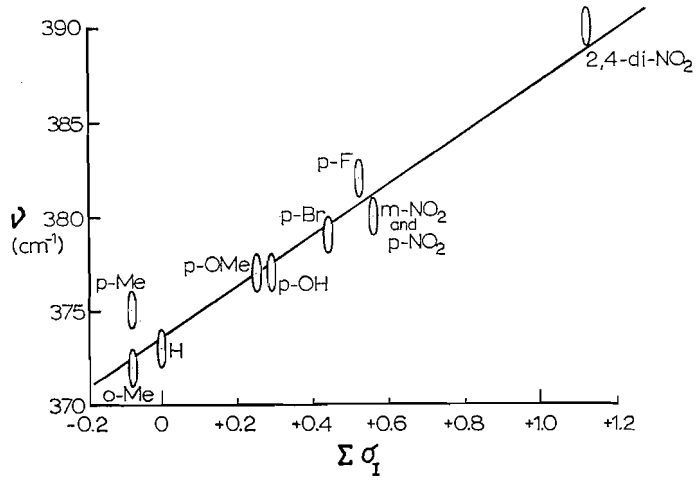

FIG. 1. Plot of the S—Cl stretching frequency for sulfonyl chlorides vs. the Taft inductive substituent parameter, σ_I. The values for σ_I used are those for "normal" solvents obtained from ^{19}F shielding values (9). The straight line was obtained from a least squares fit of the data and corresponds to the equation $\nu = 373.6 + 13.56 \sum\sigma_I$.

in the spectrum of methanesulfonyl chloride in various solvents: acetone, 374 cm^{-1}; benzene, 375 cm^{-1}; nitrobenzene, 375 cm^{-1}; carbon tetrachloride, 376 cm^{-1}; nitromethane, 378 cm^{-1}; methylene chloride, 377 cm^{-1}.

Referring again to Table I it is evident that most of the apparent extinction coefficients fall within the range 20 ± 10, though with a few compounds they lie outside this range. The compounds showing the lowest extinction coefficients, namely chlorosulfonylacetyl chloride and 2,4-dinitrobenzenesulfonyl chloride, both show somewhat broader bands than most of the other materials. Comparison of the integrated absorptions of these bands with those of the more typical cases diminishes the discrepancy in the intensities somewhat, though even by this measure the bands are only about half as intense as the weakest of the other S—Cl stretching absorptions.

Included also in Table I are the spectra of a few sulfonyl fluorides and bromides and one sulfonyl iodide. These compounds, in general, do not absorb in the region assigned to the S—Cl stretching mode, an observation which, of course, supports that assignment. *p*-Toluenesulfonyl fluoride and *p*-nitrophenylmethanesulfonyl bromide, however, do have bands in that region though the origin of these bands is obscure.

Neither the infrared nor the Raman spectra of sulfonyl bromides or iodides seem to have been investigated previously in this region. Though the number of examples is too few to establish any generalizations, it is of interest to note that the three sulfonyl bromides show a band close to 275 cm^{-1}. This is close to the band at 270 cm^{-1} in the spectrum of sulfuryl bromofluoride (SO_2FBr) which has been assigned by Gillespie and Robinson (10) to the sulfur–bromine stretching mode. *p*-Toluenesulfonyl iodide, however, also shows a similar band, and at this juncture any conclusions about the S—Br stretching position in sulfonyl bromides would seem premature.

One of the problems to which it was hoped that these data would be pertinent was concerned with the structure of the product derived by treatment of 2-methylanthraquinone-1-sulfonic acid with inorganic acid chlorides (2, 11). This compound has been assigned the sulfonyl chloride structure (I), but another structure (II) is also readily conceivable and has analogy in the chlorosultone (III) formed by the action of thionyl

Can. J. Chem. Downloaded from www.nrcresearchpress.com by 210.87.254.6 on 09/05/12
For personal use only.

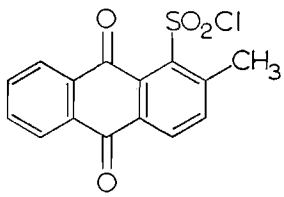

I

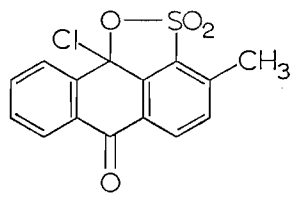

II

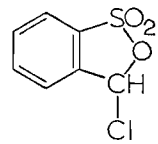

III

chloride on sodium 2-formylbenzenesulfonate. Structure III had been proved by the absence of a carbonyl maximum in the infrared spectrum (12), but an attempt to distinguish between one or two carbonyl groups with the anthraquinone derivative was inconclusive. The compound does, however, show a band at 384 cm^{-1} (see Table I) in excellent agreement with structure I. The compound obtained analogously from anthraquinone-1-sulfonic acid also shows absorption in the same region (see Table I) and is therefore probably anthraquinone-1-sulfonyl chloride, as postulated by previous investigators (13).

EXPERIMENTAL

The spectra were determined using a Beckman IR-7 grating spectrophotometer equipped with cesium iodide optics. Potassium bromide cells were used to obtain the spectra of the sulfonyl chlorides. Control experiments showed that under the conditions used, the spectra obtained with the potassium bromide cells were indistinguishable down to 310 cm^{-1} (and perhaps slightly lower) from those obtained using cesium bromide cells. Cesium bromide cells were used for the spectra of all compounds for which bands below 300 cm^{-1} are listed in Table I. The data in Table I refer to solutions in methylene chloride (Fisher Spectranalyzed, distilled from calcium hydride). The spectrophotometer was calibrated using the water vapor bands in the region from 369 to 401 cm^{-1} as recommended by Blaine, Plyler, and Benedict (14); the frequencies quoted in Table I are believed to be accurate to within ± 1 cm^{-1}. The apparent extinction coefficients were calculated from optical density values obtained directly by double beam operation; control experiments using single beam operation gave essentially identical values.

Most of the compounds were commercial materials; all of these were purified by crystallization or distillation prior to running the spectrum. The following compounds were prepared as described in the accompanying references: 2-phenylethenesulfonyl chloride (15); camphor-10-sulfonyl chloride (16); phenylmethanesulfonyl-*1-d* chloride and phenylmethanesulfonyl-*1,1-d*$_2$ chloride (1); *p*-toluenesulfonyl fluoride (17); phenylmethanesulfonyl fluoride (18); chlorosulfonylacetic acid (19); 1-anthraquinonesulfonyl chloride (20); 2-methyl-1-anthraquinonesulfonyl chloride (2); *p*-nitrophenylmethanesulfonyl chloride (21); 2-phenylethanesulfonyl chloride (22); 1,4-butanedisulfonyl chloride (23). *p*-Hydroxybenzenesulfonyl chloride was prepared by the action of phosphorus pentachloride on sodium *p*-hydroxybenzenesulfonate; m.p. 90–92°. 2-Anthraquinonesulfonyl chloride was prepared by refluxing the corresponding acid with phosphorus pentachloride in chloroform for 1 h; m.p. 210° (vacuum capillary); reported m.p. 193° (24), 197° (25). Benzenesulfonyl bromide and *p*-toluenesulfonyl bromide were prepared by the reaction of bromine with an aqueous solution of the sodium salt of the corresponding sulfinic acid, instead of the sulfinic acid itself as described by Otto and co-workers (26, 27). Benzenesulfonyl iodide was prepared as described by Whitmore and Thurman (28); m.p. 90–92°. Details of the preparation and characterization of *p*-nitrophenylmethanesulfonyl bromide and its deuterated analogue, as well as that of *p*-nitrophenylmethanesulfonyl-*1-d* chloride will be described elsewhere. In a number of instances compounds which had been allowed to stand for some time in the laboratory or which had been obtained from commercial sources were not completely soluble in nonpolar solvents; the residue was found to be water soluble. These observations were taken to indicate that the sample had suffered partial hydrolysis and it was accordingly refluxed for a short time with thionyl chloride prior to recrystallization.

ACKNOWLEDGMENTS

This work was supported by a grant from the Petroleum Research Fund administered by the American Chemical Society. We wish to express our thanks to Dr. T. Durst who prepared some of the compounds, and to Professor D. C. Bradley who kindly lent us the infrared cells used in this study.

Can. J. Chem. Downloaded from www.nrcresearchpress.com by 210.87.254.6 on 09/05/12
For personal use only.

1. J. F. KING and T. DURST. J. Am. Chem. Soc. **86**, 287 (1964).
2. J. F. KING, P. DE MAYO, E. MORKVED, A. B. M. A. SATTAR, and A. STOESSL. Can. J. Chem. **41**, 100 (1963).
3. N. S. HAM and A. N. HAMBLY. Australian J. Chem. **6**, 135 (1953).
4. N. S. HAM and A. N. HAMBLY. Australian J. Chem. **6**, 33 (1953).
5. A. SIMON, H. KRIEGSMANN, and H. DUTZ. Chem. Ber. **89**, 1990 (1956).
6. G. GEISELER and K. O. BINDERNAGEL. Z. Elecktrochem. **63**, 1140 (1959).
7. N. S. HAM, A. N. HAMBLY, and R. H. LABY. Australian J. Chem. **13**, 443 (1960).
8. G. MALEWSKI and H.-J. WEIGMANN. Spectrochim. Acta, **18**, 725 (1962).
9. R. W. TAFT, E. PRICE, I. R. FOX, I. C. LEWIS, K. K. ANDERSEN, and G. T. RITCHIE. J. Am. Chem. Soc. **85**, 709 (1963).
10. R. J. GILLESPIE and E. A. ROBINSON. Can. J. Chem. **39**, 2171 (1961).
11. A. LOCHER and H. E. FIERZ. Helv. Chim. Acta, **10**, 642 (1927). A. LOCHER. Doctoral Thesis, Swiss Federal Institute of Technology, Zurich, Switzerland. 1925.
12. K. A. FREEMAN and C. D. RITCHIE. J. Assoc. Offic. Agr. Chemists, **40**, 1108 (1957).
13. F. ULLMANN and P. KERTESZ. Ber. **52**, 545 (1919).
14. L. R. BLAINE, E. K. PLYLER, and W. S. BENEDICT. J. Res. Natl. Bur. Std. A, **66**, 223 (1962).
15. F. G. BORDWELL, C. M. SUTER, J. M. HOLBERT, and C. S. RONDESTVEDT. J. Am. Chem. Soc. **68**, 139 (1946).
16. S. SMILES and T. P. HILDITCH. J. Chem. Soc. **91**, 519 (1907).
17. W. DAVIES and J. H. DICK. J. Chem. Soc. 2104 (1931).
18. W. DAVIES and J. H. DICK. J. Chem. Soc. 483 (1932).
19. R. L. HINMAN and L. LOCATELL, JR. J. Am. Chem. Soc. **81**, 5655 (1959).
20. H. MEYER and K. SCHLEGL. Monatsh. **34**, 561 (1913).
21. C. ZIEGLER and J. M. SPRAGUE. J. Org. Chem. **16**, 621 (1951).
22. E. B. EVANS, E. E. MABBOTT, and E. E. TURNER. J. Chem. Soc. 1159 (1927).
23. B. HELFERICH and H. GRÜNERT. Ber. **74**, 1531 (1941).
24. D. A. MACHOUL. Ber. **13**, 692 (1880).
25. H. E. FIERZ-DAVID. Helv. Chim. Acta, **10**, 197 (1927).
26. R. OTTO and H. OSTROP. Ann. **141**, 365 (1867).
27. R. OTTO and O. VON GRUBER. Ann. **142**, 92 (1867).
28. F. C. WHITMORE and N. THURMAN. J. Am. Chem. Soc. **45**, 1068 (1923).

RECEIVED JANUARY 14, 1965.
DEPARTMENT OF CHEMISTRY,
UNIVERSITY OF WESTERN ONTARIO,
LONDON, ONTARIO.

Can. J. Chem. Downloaded from www.nrcresearchpress.com by 210.87.254.6 on 09/05/12
For personal use only.

GLUCOPUTRANJIVIN

M. H. BENN AND D. MEAKIN

Long known as a synthetic product (1), isopropyl isothiocyanate was first isolated from natural sources by Puntambekar (2) who obtained it[1] from seeds of the Indian tree *Putranjiva roxburghii* Wall. (Euphorbiaceae). Puntambekar named the (assumed) glucosidic precursor of this mustard oil glucoputranjivan (2).

Although *P. roxburghii* still remains the only well-established example of the occurrence of mustard oils in the family Euphorbiaceae,[2] isopropyl isothiocyanate was subsequently found to be quite widely distributed (5), particularly within the Cruciferae, and in 1959 Kjaer succeeded in isolating glucoputranjivin from seeds of *Lunaria annua* L.[3] and characterized it as the crystalline tetraacetate (6).

[1]*Together with (+)-2-butyl isothiocyanate and a third mustard oil originally identified (2) as phenyl isothiocyanate, but later shown by Kjaer and Friis (3) to be (S)-2-methylbutyl isothiocyanate.*

[2]*The family Euphorbiaceae is normally regarded as taxonomically remote from the order Rhoeadales, which contains the families Cruciferae and Capparidaceae. (Mustard oil glucosides are widely distributed amongst the species of these two families.) However, Hutchinson (4) regards the Euphorbiaceae as a heterogeneous family, probably derived from several stocks, including the Bixales, which he also regards as the ancestral stock from which the Capparidaceae were derived; i.e. the occurrence in the Euphorbiaceae of species containing mustard oil glucosides is not to be entirely unexpected.*

[3]*Synonym, L. biennis Moench.*

1. J. F. KING and T. DURST. J. Am. Chem. Soc. **86**, 287 (1964).
2. J. F. KING, P. DE MAYO, E. MORKVED, A. B. M. A. SATTAR, and A. STOESSL. Can. J. Chem. **41**, 100 (1963).
3. N. S. HAM and A. N. HAMBLY. Australian J. Chem. **6**, 135 (1953).
4. N. S. HAM and A. N. HAMBLY. Australian J. Chem. **6**, 33 (1953).
5. A. SIMON, H. KRIEGSMANN, and H. DUTZ. Chem. Ber. **89**, 1990 (1956).
6. G. GEISELER and K. O. BINDERNAGEL. Z. Elecktrochem. **63**, 1140 (1959).
7. N. S. HAM, A. N. HAMBLY, and R. H. LABY. Australian J. Chem. **13**, 443 (1960).
8. G. MALEWSKI and H.-J. WEIGMANN. Spectrochim. Acta, **18**, 725 (1962).
9. R. W. TAFT, E. PRICE, I. R. FOX, I. C. LEWIS, K. K. ANDERSEN, and G. T. RITCHIE. J. Am. Chem. Soc. **85**, 709 (1963).
10. R. J. GILLESPIE and E. A. ROBINSON. Can. J. Chem. **39**, 2171 (1961).
11. A. LOCHER and H. E. FIERZ. Helv. Chim. Acta, **10**, 642 (1927). A. LOCHER. Doctoral Thesis, Swiss Federal Institute of Technology, Zurich, Switzerland. 1925.
12. K. A. FREEMAN and C. D. RITCHIE. J. Assoc. Offic. Agr. Chemists, **40**, 1108 (1957).
13. F. ULLMANN and P. KERTESZ. Ber. **52**, 545 (1919).
14. L. R. BLAINE, E. K. PLYLER, and W. S. BENEDICT. J. Res. Natl. Bur. Std. A, **66**, 223 (1962).
15. F. G. BORDWELL, C. M. SUTER, J. M. HOLBERT, and C. S. RONDESTVEDT. J. Am. Chem. Soc. **68**, 139 (1946).
16. S. SMILES and T. P. HILDITCH. J. Chem. Soc. **91**, 519 (1907).
17. W. DAVIES and J. H. DICK. J. Chem. Soc. 2104 (1931).
18. W. DAVIES and J. H. DICK. J. Chem. Soc. 483 (1932).
19. R. L. HINMAN and L. LOCATELL, JR. J. Am. Chem. Soc. **81**, 5655 (1959).
20. H. MEYER and K. SCHLEGL. Monatsh. **34**, 561 (1913).
21. C. ZIEGLER and J. M. SPRAGUE. J. Org. Chem. **16**, 621 (1951).
22. E. B. EVANS, E. E. MABBOTT, and E. E. TURNER. J. Chem. Soc. 1159 (1927).
23. B. HELFERICH and H. GRÜNERT. Ber. **74**, 1531 (1941).
24. D. A. MACHOUL. Ber. **13**, 692 (1880).
25. H. E. FIERZ-DAVID. Helv. Chim. Acta, **10**, 197 (1927).
26. R. OTTO and H. OSTROP. Ann. **141**, 365 (1867).
27. R. OTTO and O. VON GRUBER. Ann. **142**, 92 (1867).
28. F. C. WHITMORE and N. THURMAN. J. Am. Chem. Soc. **45**, 1068 (1923).

RECEIVED JANUARY 14, 1965.
DEPARTMENT OF CHEMISTRY,
UNIVERSITY OF WESTERN ONTARIO,
LONDON, ONTARIO.

Can. J. Chem. Downloaded from www.nrcresearchpress.com by 210.87.254.5 on 09/05/12
For personal use only.

GLUCOPUTRANJIVIN

M. H. BENN AND D. MEAKIN

Long known as a synthetic product (1), isopropyl isothiocyanate was first isolated from natural sources by Puntambekar (2) who obtained it[1] from seeds of the Indian tree *Putranjiva roxburghii* Wall. (Euphorbiaceae). Puntambekar named the (assumed) glucosidic precursor of this mustard oil glucoputranjivan (2).

Although *P. roxburghii* still remains the only well-established example of the occurrence of mustard oils in the family Euphorbiaceae,[2] isopropyl isothiocyanate was subsequently found to be quite widely distributed (5), particularly within the Cruciferae, and in 1959 Kjaer succeeded in isolating glucoputranjivin from seeds of *Lunaria annua* L.[3] and characterized it as the crystalline tetraacetate (6).

[1]*Together with (+)-2-butyl isothiocyanate and a third mustard oil originally identified (2) as phenyl isothiocyanate, but later shown by Kjaer and Friis (3) to be (S)-2-methylbutyl isothiocyanate.*

[2]*The family Euphorbiaceae is normally regarded as taxonomically remote from the order Rhoeadales, which contains the families Cruciferae and Capparidaceae. (Mustard oil glucosides are widely distributed amongst the species of these two families.) However, Hutchinson (4) regards the Euphorbiaceae as a heterogeneous family, probably derived from several stocks, including the Bixales, which he also regards as the ancestral stock from which the Capparidaceae were derived; i.e. the occurrence in the Euphorbiaceae of species containing mustard oil glucosides is not to be entirely unexpected.*

[3]*Synonym, L. biennis Moench.*

The now classic studies of Ettlinger and Lundeen (7, 8) established the general structure of the mustard oil glucosides and the mechanism by which they are enzymatically decomposed to mustard oils; thus glucoputranjivin is assigned the structure (V, R = H). We have confirmed this structure by synthesis, using the same approach as that which we developed for the synthesis of glucotropaeolin (9) and subsequently successfully applied to the synthesis of a number of other mustard oil glucosides (10).

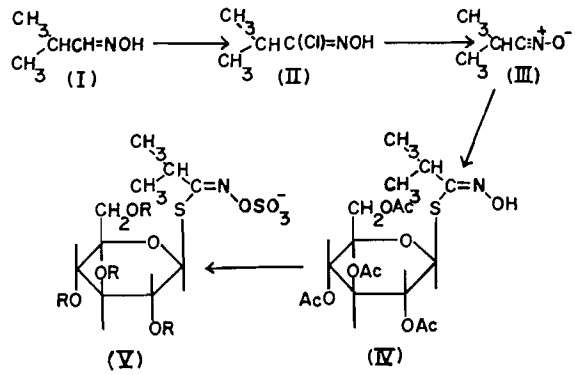

Isobutyraldoxime (I) was chlorinated; the isobutyrohydroxamoyl chloride (II) was converted to the nitrile oxide (III) and condensed, *in situ*, with tetra-*O*-acetyl-β-D-glucopyranosyl mercaptan to give tetraacetylproglucoputranjivin (IV). Sulfonation of this with pyridine – sulfur trioxide, followed by isolation of the product as the potassium salt, gave tetraacetylglucoputranjivin (V, R = $COCH_3$), identical with a sample of natural origin. We deacetylated this material, but although the product, glucoputranjivin (V, R = H) was chromatographically homogeneous it refused to crystallize as either the potassium or tetramethylammonium salt.[4]

Our original and main interest in the mustard oil glucosides was (and remains) in their biogenesis. Inspection of the structures of the glucosides, general structure (VIII), reveals that in many cases the aglycone skeleton is that of commonly encountered α-amino acids,[5] from which the carboxyl groups have been lost. Other aglycones correspond to unknown α-amino acids,[6] implying either that these amino acids remain to be discovered or that alternative biosynthetic pathways exist, which do not necessarily involve α-amino acids.

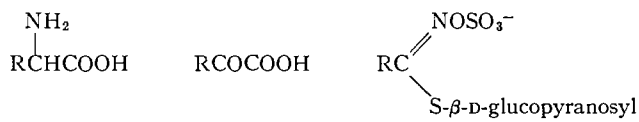

To date, experiments have revealed that some of the mustard oil glucosides are indeed derived from α-amino acids.[7] Glucotropaeolin (VIII, R = $PhCH_2$) is derived from

[4]*The tetramethylammonium salts of the mustard oil glucosides often crystallize better than the potassium salts (7, 8, 10c).*

[5]*For example glucocapparin (VIII,* R = CH_3*) and alanine (VI,* R = CH_3*), glucocochlearin (VIII,* R = $CH_3CH_2CH(CH_3)$*), and isoleucine (VI,* R = $CH_3CH_2CH(CH_3)$*) with the same configuration at the asymmetric center in the side chain (11), and several other examples in addition to those cited in the text (5).*

[6]*For example glucohirsutin (VIII,* R = $CH_3SO(CH_2)_8$*) and a series of sulfides, sulfoxides, and sulfones of closely related structure (5).*

[7]*In addition, gluconasturtiin (VIII,* R = $C_6H_5CH_2CH_2$*) is partly derived from phenylalanine (13). However, the best precursor yet discovered for sinigrin (VIII,* R = CH_2=$CHCH_2$—*) is acetate although there was some conflict in the results reported by the two groups (13, 17).*

Can. J. Chem. Downloaded from www.nrcresearchpress.com by 210.87.254.5 on 09/05/12
For personal use only.

phenylalanine (VI, R = $PhCH_2$) (12, 13, 14), glucobrassicin (VIII, R = β-indolylmethyl) from tryptophan (VI, R = β-indolylmethyl) (15) and sinalbin (VIII, R = p-$HOC_6H_4CH_2$) (16). Interestingly, there appear to be two pathways from α-amino acids, one in which the nitrogen of the α-amino acid is lost (16), biosynthesis proceeding via the keto acid (VIII), and the other in which the nitrogen of the α-amino acid is incorporated directly into the aglycone (14).[8]

In terms of the "α-amino acid hypothesis", glucoputranjivin can be visualized as derived from valine (VI, R = $(CH_3)_2CH$) (5, 19).

T. peregrinum[9] plants fed DL-valine-4-^{14}C were worked up and the mustard oil aglycones isolated as the thiourea derivatives. Paper chromatography revealed that a spot identical with isopropylthiourea contained the bulk of the radioactivity, corresponding to 0.12% incorporation of activity into the mustard oil. This initial result strongly suggests that glucoputranjivin is in fact biosynthesized in *T. peregrinum* from valine.[10]

EXPERIMENTAL

Tetraacetylproglucoputranjivin (IV)

Isobutyrohydroxamoyl chloride, freshly prepared from isobutyraldoxime (2.0 g) (20) and dissolved in ice-cold ether (50 ml), was added to a solution of 2,3,4,6-tetra-*O*-acetyl-β-D-glucopyranosyl mercaptan (1.0 g) in cold, dry ether (100 ml) and was followed by triethylamine (2.8 ml) dissolved in dry ether (10 ml). Triethylamine hydrochloride precipitated and the blue color of the solution was discharged. After 30 min the reaction mixture was washed with ca. 0.6 *N* dilute aqueous sulfuric acid (50 ml); the ether extract was separated, dried, and evaporated to yield a colorless oil which crystallized from concentrated ethereal solution upon addition of petroleum ether. Recrystallization from ether – petroleum ether gave colorless needles of tetraacetylproglucoputranjivin, m.p. 93–95° (0.75 g, 60%). Further recrystallization raised the m.p. to 98–100°. $[\alpha]_D^{25}$ –29° (*c*, 3 in $CHCl_3$). Anal. Calcd. for $C_{18}H_{27}NO_{10}S$; C, 48.10; H, 6.06; N, 3.12. Found: C, 48.31, H, 6.09; N, 3.29.

Tetraacetylglucoputranjivin (V, R = CH_3CO)

Tetracetylproglucoputranjivin (0.37 g) was dissolved in dry pyridine (5 ml), reshly prepared sulfur trioxide – pyridine complex (0.42 g) added and the reaction mixture stirred at room temperature overnight, with exclusion of moisture. The reaction mixture was poured into water (ca. 20 ml) containing potassium bicarbonate (0.75 g). After effervescence ceased the aqueous solution was extracted with ether (2 × 20 ml), the combined ether extracts washed with water (2 × 20 ml), and the combined aqueous extracts freeze dried. The residual solids were extracted with boiling 95% aqueous ethanol (v/v) and filtered hot. On cooling the filtrate deposited fine colorless needles, m.p. 180.5–182° (0.220 g, 47%), $[\alpha]_D^{25}$ –18.3° (*c*, 1.6, H_2O); lit. (6), $[\alpha]_D^{23}$ –15.4° (c, 1.2, H_2O). The infrared spectrum in a KBr disc was superimposable on that of an authentic specimen of natural origin.

Glucoputranjivin (V, R = H).

Tetraacetylglucoputranjivin (0.93 g) was dissolved in anhydrous methanol, previously saturated with ammonia, and kept at room temperature overnight. The solution was evaporated to dryness under reduced pressure to give a gum which refused to crystallize. The gum was taken up in water and passed through a Dowex-50 ion exchange column (in the tetramethylammonium form) and the aqueous eluates freeze dried. Again, the gummy residue of tetramethylammonium glucoputranjivin which was chromatographically homogeneous (21) refused to crystallize.

Biosynthesis of Glucoputranjivin from DL-*Valine-4-*^{14}*C*

The freshly cut stems of the above-ground portion of young *T. peregrinum* plants (27 g) were dipped into an aqueous solution of DL-valine-4-^{14}C(50 μcuries). After 50 h the uptake of radioactivity amounted to 33 μcuries The plants were removed, washed, homogenized in a Waring Blendor, and, after standing at

[8]*We have also performed experiments with doubly labelled phenylalanine-2-*^{14}C,^{15}N *similar to those described by Underhill and Chisholm (14), as well as with phenylpyruvic acid oxime-2-*^{14}C,^{15}N, *and also concluded that the nitrogen of the phenylalanine is retained during incorporation into glucotropaeolin.*

[9]*Synonym T. canariense Hort., the canary bird vine. The seeds of this plant are reported to produce glucocochlearin in addition to glucoputranjivin, but both compounds are only present in small amounts (18).*

[10]*We had insufficient material to carry out the degradation of the thiourea necessary to establish this absolutely. Further, as yet, we have no evidence which permits discrimination between the two possibilities of the nitrogen atom of the valine being lost or retained during incorporation into glucoputranjivin. Since the plant is in the same genus as T. majus in which glucotropaeolin is biosynthesized from phenylalanine with retention of the nitrogen atom, we favor the same process here. However, it is quite possible that in the Cruciferae, e.g. L. biennis, the biosynthesis might proceed by the alternative pathway via the keto acid (VII,* R = $(CH_3)_2CH$*).*

Can. J. Chem. Downloaded from www.nrcresearchpress.com by 210.87.254.5 on 09/05/12
For personal use only.

room temperature for 1 h, steam distilled into ethanolic ammonia. The distillate was kept at room temperature overnight and then freeze dried. The residue (a very small amount of dark-brown solid) was taken up in ethanol and examined by paper chromatography (22). No spot appeared on spraying with Grote's reagent (23) but a radioactive spot could be detected with a Nuclear-Chicago Actigraph II chromatogram scanner in the approximate position expected for isopropylthiourea. The chromatography was repeated with the addition of authentic isopropylthiourea. The chromatogram was examined with the scanner prior to spraying and 95% of the activity was located in the position exactly corresponding to the spot which appeared on spraying. The activity of this spot was further measured by cutting out the area on the paper chromatogram and, after a complete wet combustion (24), counting as carbon dioxide, using a Dynacon 6000 ionization chamber system. The total activity of the isopropylthiourea was calculated to be 0.04 μcuries, an incorporation of 0.12%.

ACKNOWLEDGMENTS

We wish to thank the National Research Council for financial support of this research and Professor Anders Kjaer for an authentic sample of tetraacetylglucoputranjivan. We are also grateful to the Golden West Seed Co. of Calgary for a generous gift of *T. peregrinum* seeds.

1. H. JAHN. Monatsh. **3**, 165 (1882).
2. S. V. PUNTAMBEKAR. Proc. Indian Acad. Sci. Sect. A, **32**, 114 (1950).
3. A. KJAER and P. FRIIS. Acta Chem. Scand. **16**, 936 (1962).
4. J. HUTCHINSON. The families of flowering plants. 2nd ed. Vol. I. Dicotyledons. Clarendon Press, Oxford. 1959.
5. A. KJAER. Fortschr. Chem. Org. Naturstoffe, **18**, 122 (1960).
6. A. KJAER. Acta Chem. Scand. **13**, 851 (1959).
7. M. G. ETTLINGER and A. J. LUNDEEN. J. Am. Chem. Soc. **78**, 4172 (1956).
8. M. G. ETTLINGER and A. J. LUNDEEN. J. Am. Chem. Soc. **79**, 1764 (1957).
9. M. H. BENN. Can. J. Chem. **41**, 2837 (1963).
10. M. H. BENN. (*a*) Can. J. Chem. **42**, 163 (1964); (*b*) J. Chem. Soc. 4072 (1964); (*c*) Can. J. Chem. **43**, 1 (1965).
11. A. KJAER and S. E. HANSEN. Acta Chem. Scand. **11**, 898 (1957).
12. M. H. BENN. Chem. Ind. London, 1907 (1962).
13. E. W. UNDERHILL, M. D. CHISHOLM, and L. R. WETTER. Can. J. Biochem. Physiol. **40**, 1505 (1962).
14. E. W. UNDERHILL and M. D. CHISHOLM. Biochem. Biophys. Res. Commun. **14**, 425 (1964).
15. M. KUTÁČEK, Ž. PROCHÁZKA, and K. VEREŠ. Nature, **194**, 393 (1962).
16. H. KINDL. Monatsh. **95**, 439 (1964).
17. M. MATSUO and M. YAMAZAKI. Chem. Pharm. Bull. Tokyo, **11**, 545 (1963).
18. P. G. DELAVEAU and A. KJAER. Acta Chem. Scand. **17**, 2562 (1963).
19. A. KJAER, J. CONTI, and I. LARSEN. Acta Chem. Scand. **7**, 1276 (1953).
20. M. H. BENN. Can. J. Chem. **42**, 2393 (1964).
21. O.-E. SCHULTZ and R. GMELIN. Z. Naturforsch. **8b**, 151 (1953).
22. A. KJAER and K. RUBINSTEIN. Acta Chem. Scand. **7**, 528 (1953).
23. I. W. GROTE. J. Biol. Chem. **93**, 25 (1931).
24. D. D. VAN SLYKE, J. PLAZIN, and J. WEISIGER. J. Biol. Chem. **191**, 299 (1951).

RECEIVED DECEMBER 28, 1964.
DEPARTMENT OF CHEMISTRY,
UNIVERSITY OF ALBERTA,
CALGARY, ALBERTA.

THE HEAT OF FORMATION OF BORON TRIBROMIDE–ACETONITRILE

J. M. MILLER AND M. ONYSZCHUK

Laubengayer and Sears (1) were the first to suggest that BF_3 is not the strongest electron-pair acceptor in the boron trihalide series. They found that heats of formation of the solid adducts from their gaseous components were 33.8 and 26.5 kcal mole^{-1} for $CH_3CN{\cdot}BCl_3$ and $CH_3CN{\cdot}BF_3$, respectively, in good agreement with their heats of

Can. J. Chem. Downloaded from www.nrcresearchpress.com by 210.87.254.5 on 09/05/12
For personal use only.

room temperature for 1 h, steam distilled into ethanolic ammonia. The distillate was kept at room temperature overnight and then freeze dried. The residue (a very small amount of dark-brown solid) was taken up in ethanol and examined by paper chromatography (22). No spot appeared on spraying with Grote's reagent (23) but a radioactive spot could be detected with a Nuclear-Chicago Actigraph II chromatogram scanner in the approximate position expected for isopropylthiourea. The chromatography was repeated with the addition of authentic isopropylthiourea. The chromatogram was examined with the scanner prior to spraying and 95% of the activity was located in the position exactly corresponding to the spot which appeared on spraying. The activity of this spot was further measured by cutting out the area on the paper chromatogram and, after a complete wet combustion (24), counting as carbon dioxide, using a Dynacon 6000 ionization chamber system. The total activity of the isopropylthiourea was calculated to be 0.04 μcuries, an incorporation of 0.12%.

ACKNOWLEDGMENTS

We wish to thank the National Research Council for financial support of this research and Professor Anders Kjaer for an authentic sample of tetraacetylglucoputranjivan. We are also grateful to the Golden West Seed Co. of Calgary for a generous gift of *T. peregrinum* seeds.

1. H. JAHN. Monatsh. **3**, 165 (1882).
2. S. V. PUNTAMBEKAR. Proc. Indian Acad. Sci. Sect. A, **32**, 114 (1950).
3. A. KJAER and P. FRIIS. Acta Chem. Scand. **16**, 936 (1962).
4. J. HUTCHINSON. The families of flowering plants. 2nd ed. Vol. I. Dicotyledons. Clarendon Press, Oxford. 1959.
5. A. KJAER. Fortschr. Chem. Org. Naturstoffe, **18**, 122 (1960).
6. A. KJAER. Acta Chem. Scand. **13**, 851 (1959).
7. M. G. ETTLINGER and A. J. LUNDEEN. J. Am. Chem. Soc. **78**, 4172 (1956).
8. M. G. ETTLINGER and A. J. LUNDEEN. J. Am. Chem. Soc. **79**, 1764 (1957).
9. M. H. BENN. Can. J. Chem. **41**, 2837 (1963).
10. M. H. BENN. (*a*) Can. J. Chem. **42**, 163 (1964); (*b*) J. Chem. Soc. 4072 (1964); (*c*) Can. J. Chem. **43**, 1 (1965).
11. A. KJAER and S. E. HANSEN. Acta Chem. Scand. **11**, 898 (1957).
12. M. H. BENN. Chem. Ind. London, 1907 (1962).
13. E. W. UNDERHILL, M. D. CHISHOLM, and L. R. WETTER. Can. J. Biochem. Physiol. **40**, 1505 (1962).
14. E. W. UNDERHILL and M. D. CHISHOLM. Biochem. Biophys. Res. Commun. **14**, 425 (1964).
15. M. KUTÁČEK, Ž. PROCHÁZKA, and K. VEREŠ. Nature, **194**, 393 (1962).
16. H. KINDL. Monatsh. **95**, 439 (1964).
17. M. MATSUO and M. YAMAZAKI. Chem. Pharm. Bull. Tokyo, **11**, 545 (1963).
18. P. G. DELAVEAU and A. KJAER. Acta Chem. Scand. **17**, 2562 (1963).
19. A. KJAER, J. CONTI, and I. LARSEN. Acta Chem. Scand. **7**, 1276 (1953).
20. M. H. BENN. Can. J. Chem. **42**, 2393 (1964).
21. O.-E. SCHULTZ and R. GMELIN. Z. Naturforsch. **8b**, 151 (1953).
22. A. KJAER and K. RUBINSTEIN. Acta Chem. Scand. **7**, 528 (1953).
23. I. W. GROTE. J. Biol. Chem. **93**, 25 (1931).
24. D. D. VAN SLYKE, J. PLAZIN, and J. WEISIGER. J. Biol. Chem. **191**, 299 (1951).

RECEIVED DECEMBER 28, 1964.
DEPARTMENT OF CHEMISTRY,
UNIVERSITY OF ALBERTA,
CALGARY, ALBERTA.

THE HEAT OF FORMATION OF BORON TRIBROMIDE–ACETONITRILE

J. M. MILLER AND M. ONYSZCHUK

Laubengayer and Sears (1) were the first to suggest that BF_3 is not the strongest electron-pair acceptor in the boron trihalide series. They found that heats of formation of the solid adducts from their gaseous components were 33.8 and 26.5 kcal mole^{-1} for $CH_3CN{\cdot}BCl_3$ and $CH_3CN{\cdot}BF_3$, respectively, in good agreement with their heats of

Can. J. Chem. Downloaded from www.nrcresearchpress.com by 210.87.254.105 on 09/05/12
For personal use only.

dissociation, 34.4 and 26.5 kcal mole^{-1}, respectively. These results were interpreted as indicating that BCl_3 is a stronger electron-pair acceptor than BF_3, assuming that crystal lattice energies of the adducts are similar. Unfortunately, they did not extend their measurements to $CH_3CN{\cdot}BBr_3$. We have now determined the heat of formation of $CH_3CN{\cdot}BBr_3$ with the object of (*i*) establishing the trend in heats of formation of acetonitrile – boron trihalide adducts, and (*ii*) comparing heats of formation with proton nuclear magnetic resonance (n.m.r.) shifts (2).

The heat of formation of $CH_3CN{\cdot}BBr_3$ was obtained by measuring its heat of hydrolysis using a precision calorimeter (3). The details of these measurements are summarized in

TABLE I

Heat of hydrolysis data for $CH_3CN{\cdot}BBr_3$

Trial	$CH_3CN{\cdot}BBr_3$ (mmole)	Temp. rise $\Delta T - \mu v$	Calibration $\Delta T - \mu v$	Calibration cal μv^{-1}	Heat of hydrolysis (kcal mole^{-1})
1	0.3491	77	48	0.27063	59.6
2	0.5043	108	43	0.29503	63.2
3	0.3176	68	44	0.28781	61.6
				Average	61.5±1.2

Table I. Calculation of the heat of formation of the solid adduct from its gaseous components, following Laubengayer and Sears (1), was based on the reaction

$$CH_3CN(g) + BBr_3(g) \rightarrow CH_3CN{\cdot}BBr_3(s)$$

for which, $-\Delta H = A + B + C + D - E$,

where $-\Delta H$ = heat of formation of the solid adduct from its gaseous constituents; A = heat of hydrolysis of BBr_3 = 83.6 kcal mole^{-1} (4); B = heat of vaporization of BBr_3 = 8.2 kcal mole^{-1} (5); C = heat of vaporization of CH_3CN = 8.0 kcal mole^{-1} (1); D = heat of solution of CH_3CN in H_2O = 1.1 kcal mole^{-1} (1); E = heat of hydrolysis of $CH_3CN{\cdot}BBr_3$ = 61.5 kcal mole^{-1}.

Substitution of these values into the equation gives $-\Delta H = 39.4 \pm 1.2$ kcal mole^{-1}. This value together with those of Laubengayer and Sears (1) for $CH_3CN{\cdot}BF_3$ and $CH_3CN{\cdot}BCl_3$ confirms that heats of formation decrease in the order: $BBr_3 > BCl_3 > BF_3$. Since it seems reasonable to assume that crystal lattice energies will not vary appreciably in this series of closely related adducts, we conclude that the order of acceptor power toward acetonitrile is also $BBr_3 > BCl_3 > BF_3$. Brown and Holmes (6) made the same assumption and drew the same conclusion for pyridine – boron trihalide complexes. Other physical measurements on a variety of donor – boron trihalide complexes have also been interpreted as indicating the above order of boron trihalide acceptor power (ref. 7, and references cited therein).

EXPERIMENTAL

Boron tribromide (Anderson) was purified of bromine by shaking the crude sample with mercury followed by several vacuum distillations at −78°, and its purity was checked by molecular weight (M) and vapor pressure (v.p.) measurements (M: found, 252.0; calcd., 250.6; v.p. at 32.0°: found, 82.8 mm; lit. (5), 84.0 mm). Reagent grade acetonitrile (Fisher) was distilled twice from calcium hydride (b.p.: found, 81.7°; lit. (5), 81.8°).

The complex $CH_3CN{\cdot}BBr_3$ was prepared by reacting BBr_3 with an excess of CH_3CN in a vacuum at 25°, followed by removal of excess CH_3CN by distillation at 233–255°. The resulting white solid complex melted with decomposition at 233–235°. Its heat of hydrolysis was determined with a precision calorimeter (3) designed for measurements of heats of formation of addition compounds.

Can. J. Chem. Downloaded from www.nrcresearchpress.com by 210.87.254.105 on 09/05/12
For personal use only.

ACKNOWLEDGMENTS

We are grateful to the Defence Research Board for support of this work (Grant number 9530-20, Project D46-95-30-20), and to the National Research Council for Scholarships to one of us (J. M. M.).

1. A. W. LAUBENGAYER and D. B. SEARS. J. Am. Chem. Soc. **67**, 164 (1945).
2. J. M. MILLER and M. ONYSZCHUK. To be published.
3. J. M. MILLER. Ph.D. Thesis, McGill University. 1964.
4. Handbook of chemistry and physics. 41st ed. Chemical Rubber Publishing Co., Cleveland, Ohio. 1959.
5. D. R. STULL. Ind. Eng. Chem. **39**, 517 (1947).
6. H. C. BROWN and R. R. HOLMES. J. Am. Chem. Soc. **78**, 2173 (1956).
7. J. M. MILLER and M. ONYSZCHUK. Can. J. Chem. **41**, 2898 (1963).

RECEIVED AUGUST 31, 1964.
INORGANIC CHEMISTRY LABORATORY,
MCGILL UNIVERSITY,
MONTREAL, QUEBEC.

COORDINATION COMPLEXES OF NIOBIUM PENTACHLORIDE WITH TRIPHENYL DERIVATIVES OF GROUP V ELEMENTS

JEAN DESNOYERS AND ROLAND RIVEST

The reactions of niobium pentachloride and triphenyl derivatives of group V elements have been investigated. If a coordination number of VI is assumed for niobium, only the 1:1 complexes would be expected, but it has been found experimentally that two types of coordination compounds are possible. Complexes with the 1:1 and the 2:1 compositions have been obtained.

Preparation of the 1:1 Complexes

Carbon tetrachloride, *n*-hexane, and cyclohexane were used as solvents. A solution of the ligand was added to a solution of niobium pentachloride and a clear solution having a different color for every ligand was obtained. The intensity of the coloration progressively decreased with time and completely vanished in 4 h. During this time a colored precipitate appeared. It was washed several times with the solvent and dried under vacuum for 4 h. It was then analyzed for carbon, hydrogen, niobium, and chloride. Carbon and hydrogen determinations were made by Schwakzkopf Microanalytical Laboratory, 56–19 37th Ave., Woodside, N.Y. Niobium and chloride were determined gravimetrically by the following method. A solid sample of the complex was treated with water and decomposed, and a suspension of the ligand and of niobium pentoxide was obtained. It was heated to boiling, filtered, and washed with water. The filtrate thus obtained was kept for the determination of chloride as silver chloride. The precipitate was then washed with acetone to remove the ligand, calcined, cooled in a desiccator, and weighed as niobium pentoxide. The analytical results and the color of the 1:1 complexes are included in Table I and compared with the theoretical values.

Preparation of the 2:1 Complexes

Using benzene instead of the solvents mentioned above, it has been possible to prepare a series of mixed solutions containing one ligand and niobium pentachloride. The color of these solutions remained almost unchanged after 24 h, but slight precipitation occurred.

Can. J. Chem. Downloaded from www.nrcresearchpress.com by 210.87.254.105 on 09/05/12
For personal use only.

ACKNOWLEDGMENTS

We are grateful to the Defence Research Board for support of this work (Grant number 9530-20, Project D46-95-30-20), and to the National Research Council for Scholarships to one of us (J. M. M.).

1. A. W. LAUBENGAYER and D. B. SEARS. J. Am. Chem. Soc. **67**, 164 (1945).
2. J. M. MILLER and M. ONYSZCHUK. To be published.
3. J. M. MILLER. Ph.D. Thesis, McGill University. 1964.
4. Handbook of chemistry and physics. 41st ed. Chemical Rubber Publishing Co., Cleveland, Ohio. 1959.
5. D. R. STULL. Ind. Eng. Chem. **39**, 517 (1947).
6. H. C. BROWN and R. R. HOLMES. J. Am. Chem. Soc. **78**, 2173 (1956).
7. J. M. MILLER and M. ONYSZCHUK. Can. J. Chem. **41**, 2898 (1963).

RECEIVED AUGUST 31, 1964.
INORGANIC CHEMISTRY LABORATORY,
MCGILL UNIVERSITY,
MONTREAL, QUEBEC.

COORDINATION COMPLEXES OF NIOBIUM PENTACHLORIDE WITH TRIPHENYL DERIVATIVES OF GROUP V ELEMENTS

JEAN DESNOYERS AND ROLAND RIVEST

The reactions of niobium pentachloride and triphenyl derivatives of group V elements have been investigated. If a coordination number of VI is assumed for niobium, only the 1:1 complexes would be expected, but it has been found experimentally that two types of coordination compounds are possible. Complexes with the 1:1 and the 2:1 compositions have been obtained.

Preparation of the 1:1 Complexes

Carbon tetrachloride, *n*-hexane, and cyclohexane were used as solvents. A solution of the ligand was added to a solution of niobium pentachloride and a clear solution having a different color for every ligand was obtained. The intensity of the coloration progressively decreased with time and completely vanished in 4 h. During this time a colored precipitate appeared. It was washed several times with the solvent and dried under vacuum for 4 h. It was then analyzed for carbon, hydrogen, niobium, and chloride. Carbon and hydrogen determinations were made by Schwakzkopf Microanalytical Laboratory, 56–19 37th Ave., Woodside, N.Y. Niobium and chloride were determined gravimetrically by the following method. A solid sample of the complex was treated with water and decomposed, and a suspension of the ligand and of niobium pentoxide was obtained. It was heated to boiling, filtered, and washed with water. The filtrate thus obtained was kept for the determination of chloride as silver chloride. The precipitate was then washed with acetone to remove the ligand, calcined, cooled in a desiccator, and weighed as niobium pentoxide. The analytical results and the color of the 1:1 complexes are included in Table I and compared with the theoretical values.

Preparation of the 2:1 Complexes

Using benzene instead of the solvents mentioned above, it has been possible to prepare a series of mixed solutions containing one ligand and niobium pentachloride. The color of these solutions remained almost unchanged after 24 h, but slight precipitation occurred.

Can. J. Chem. Downloaded from www.nrcresearchpress.com by 210.87.254.42 on 09/05/12
For personal use only.

TABLE I

Analytical results of the 1:1 composition complexes

	% Nb		% Cl		% C		% H		
Ligands	Anal.	Theor.	Anal.	Theor.	Anal.	Theor.	Anal.	Theor.	Colors
Ph_3N	18.12	18.02	34.12	34.38	41.80	41.93	2.81	2.93	Green
Ph_3P	17.66	17.44	22.10	22.02	40.30	40.60	2.76	2.85	Amber
Ph_3As	15.92	16.10	20.32	20.35	37.71	37.50	2.50	2.62	Orange
Ph_3Sb	14.76	14.90	18.76	18.81	34.60	34.68	2.30	2.42	Brown
Ph_3Bi	13.13	13.07	16.61	16.50	30.21	30.42	2.21	2.12	Orange

TABLE II

Analytical results of the 2:1 composition complexes

	% Nb		% Cl		% C		% H		
Ligands	Anal.	Theor.	Anal.	Theor.	Anal.	Theor.	Anal.	Theor.	Colors
Ph_3N	23.26	23.65	44.78	45.12	27.32	27.51	2.01	1.92	Dark green
Ph_3P	23.29	23.14	43.91	44.17	26.79	26.93	1.90	1.88	Brown
Ph_3As	22.60	21.94	42.12	41.88	25.61	25.53	1.89	1.78	Red
Ph_3Sb	20.31	20.79	39.13	39.68	24.30	24.19	1.54	1.69	Blue
Ph_3Bi	18.15	18.94	36.42	36.15	22.11	22.04	1.80	1.54	Red

The precipitates were filtered off and the filtrates used to isolate the complexes by evaporation of the solvent under vacuum. Crystalline precipitates were obtained which were filtered, washed several times with normal hexane, dried under vacuum, and analyzed for carbon, hydrogen, niobium, and chloride as for the 1:1 complexes. The analytical results are listed in Table II and compared with the theoretical values for the 2:1 complexes.

Received January 21, 1965.
Department of Chemistry,
University of Montreal,
Montreal, Quebec.

SYNTHESIS AND REACTIVITY OF SOME ORTHO-SUBSTITUTED DIPHENYL SULFONES

O. Francis Bennett[1]

The influence of the sulfone group on the reactivity of substituents (including hydrogen) at the ortho positions in diaryl sulfones has been noted in several cases. For example, 5-nitro-2-(*p*-nitrophenylsulfonyl)benzaldehyde fails to cyclize to the corresponding thiaxanthone dioxide, whereas 5-nitro-2-(*p*-nitrothiophenoxy)benzaldehyde readily ring closes to the corresponding thiaxanthone. The resistance of the former towards cyclization has been attributed to the oxidation state of sulfur (1). Furthermore, the sulfone group which is normally considered a meta directing substituent in electrophilic substitution reactions, promotes ortho substitution when diphenyl sulfones are metalated by *n*-butyl lithium (2). Resonance and inductive effects of the sulfone group have been invoked to

[1]*Present address: Department of Chemistry, Boston College, Chestnut Hill, Massachusetts 02167.*

Can. J. Chem. Downloaded from www.nrcresearchpress.com by 210.87.254.42 on 09/05/12
For personal use only.

TABLE I

Analytical results of the 1:1 composition complexes

	% Nb		% Cl		% C		% H		
Ligands	Anal.	Theor.	Anal.	Theor.	Anal.	Theor.	Anal.	Theor.	Colors
Ph_3N	18.12	18.02	34.12	34.38	41.80	41.93	2.81	2.93	Green
Ph_3P	17.66	17.44	22.10	22.02	40.30	40.60	2.76	2.85	Amber
Ph_3As	15.92	16.10	20.32	20.35	37.71	37.50	2.50	2.62	Orange
Ph_3Sb	14.76	14.90	18.76	18.81	34.60	34.68	2.30	2.42	Brown
Ph_3Bi	13.13	13.07	16.61	16.50	30.21	30.42	2.21	2.12	Orange

TABLE II

Analytical results of the 2:1 composition complexes

	% Nb		% Cl		% C		% H		
Ligands	Anal.	Theor.	Anal.	Theor.	Anal.	Theor.	Anal.	Theor.	Colors
Ph_3N	23.26	23.65	44.78	45.12	27.32	27.51	2.01	1.92	Dark green
Ph_3P	23.29	23.14	43.91	44.17	26.79	26.93	1.90	1.88	Brown
Ph_3As	22.60	21.94	42.12	41.88	25.61	25.53	1.89	1.78	Red
Ph_3Sb	20.31	20.79	39.13	39.68	24.30	24.19	1.54	1.69	Blue
Ph_3Bi	18.15	18.94	36.42	36.15	22.11	22.04	1.80	1.54	Red

The precipitates were filtered off and the filtrates used to isolate the complexes by evaporation of the solvent under vacuum. Crystalline precipitates were obtained which were filtered, washed several times with normal hexane, dried under vacuum, and analyzed for carbon, hydrogen, niobium, and chloride as for the 1:1 complexes. The analytical results are listed in Table II and compared with the theoretical values for the 2:1 complexes.

Received January 21, 1965.
Department of Chemistry,
University of Montreal,
Montreal, Quebec.

SYNTHESIS AND REACTIVITY OF SOME ORTHO-SUBSTITUTED DIPHENYL SULFONES

O. Francis Bennett[1]

The influence of the sulfone group on the reactivity of substituents (including hydrogen) at the ortho positions in diaryl sulfones has been noted in several cases. For example, 5-nitro-2-(*p*-nitrophenylsulfonyl)benzaldehyde fails to cyclize to the corresponding thiaxanthone dioxide, whereas 5-nitro-2-(*p*-nitrothiophenoxy)benzaldehyde readily ring closes to the corresponding thiaxanthone. The resistance of the former towards cyclization has been attributed to the oxidation state of sulfur (1). Furthermore, the sulfone group which is normally considered a meta directing substituent in electrophilic substitution reactions, promotes ortho substitution when diphenyl sulfones are metalated by *n*-butyl lithium (2). Resonance and inductive effects of the sulfone group have been invoked to

[1]*Present address: Department of Chemistry, Boston College, Chestnut Hill, Massachusetts 02167.*

Can. J. Chem. Downloaded from www.nrcresearchpress.com by 210.87.254.105 on 09/05/12
For personal use only.

explain the observed orientation in this latter example (2*a*). Indeed, these effects adequately explain the reactivity found for a variety of substituted diphenyl sulfones.*

Many years ago, Weedon and Doughty (4) gave brief mention to their observation that 2-carbomethoxyphenyl phenyl sulfone was resistent to alkaline saponification. They offered no explanation for these findings. Since that time, as far as we are aware, no further observations of the effect of the sulfone group on the reactivities of 2-carboalkoxyphenyl phenyl sulfones towards saponification have been reported. Moreover, the susceptibilities of substituted 2-carboxyphenyl phenyl sulfones to esterification have also been neglected.

Recently we had occasion to prepare a number of substituted diphenyl sulfones for use as intermediates. Several of these new compounds clearly demonstrated that for diaryl sulfones, a carboxyl group or carbomethoxy group in the 5-position—which is not affected by neighboring groups—is much more reactive than the corresponding group in the 2-position in esterification and saponification reactions, respectively. Thus, methanolic esterification of the mixture obtained from nitric acid oxidation of 2,5-dimethylphenyl phenyl sulfone (5) afforded 5-carbomethoxy-2-methylphenyl phenyl sulfone, I, and 5-carbomethoxy-2-carboxyphenyl phenyl sulfone, V, in a weight ratio of 1:10, respectively. Compounds I and V were readily converted to their corresponding acids, II and VI, by treatment with dilute base. To demonstrate the difference in reactivity of the 2-carbomethoxy group relative to the 5-carbomethoxy group, 2,5-dicarbomethoxyphenyl phenyl sulfone, III, prepared by reaction of either V or VI with diazomethane, was reacted with 1 equiv of aqueous base. As expected, 2-carbomethoxy-5-carboxyphenyl phenyl sulfone, IV, was the principal product.

Our findings parallel the reactivities found for ortho- and meta-nitrobenzoic acids (6) and their esters (7) as well as the reactivities found for 2-nitroterephthalic acid (8) and its esters (9) in esterification and saponification reactions, respectively. For these latter cases, the refractory nature of the ortho groups has been attributed primarily to steric effects (6–11). It appears likely that similar effects, attributable to the large sulfone group, provide a major contribution to the observed reactivities reported in this paper.

The equations on the next page summarize this work.

EXPERIMENTAL†

2,5-Dimethylphenyl Phenyl Sulfone

This compound (5) was prepared in 92% yield by reaction of benzenesulfonyl chloride with excess *p*-xylene in the presence of aluminium chloride; m.p. 109–110°.

Nitric Acid Oxidation of 2,5-Dimethylphenyl Phenyl Sulfone

Aqueous nitric acid (580 ml, 35%) and 2,5-dimethylphenyl phenyl sulfone, 187.3 g (0.762 mole) were charged into a 2 l stainless steel pressure vessel. An initial pressure of 150 p.s.i.g. of nitrogen was placed on the system which was heated at 190° until no further increase in pressure was evident (3 h). The pressure vessel was cooled, vented to the atmosphere, and the contents allowed to degas overnight. The insoluble materials were collected by suction filtration, washed with cold water, and air dried. Attempts to separate and purify the oxidation products by crystallization from common solvents were not successful.

Separation of Principal Oxidation Products as Methyl Esters

The above oxidation mixture (10.0 g) was treated with 300 ml of methanol containing 10 drops of concentrated sulfuric acid. The stirred reactants were heated to reflux with occasional distillation of methanol until the volume of the reaction mixture was about 75 ml (6 h). Ether (150 ml) was added to the methanolic solution, and the resulting ethereal solution was washed with three 50 ml portions of 10% sodium bicarbonate and two 50 ml portions of water. The combined washings were set aside for subsequent work-up.

**An excellent discussion of both the resonance and the inductive effects of the sulfone group in diphenyl sulfones may be found in ref. 3.*

†*All melting points are corrected. Infrared spectra were obtained on a Perkin-Elmer model 221 spectrophotometer.*

Can. J. Chem. Downloaded from www.nrcresearchpress.com by 210.87.254.105 on 09/05/12
For personal use only.

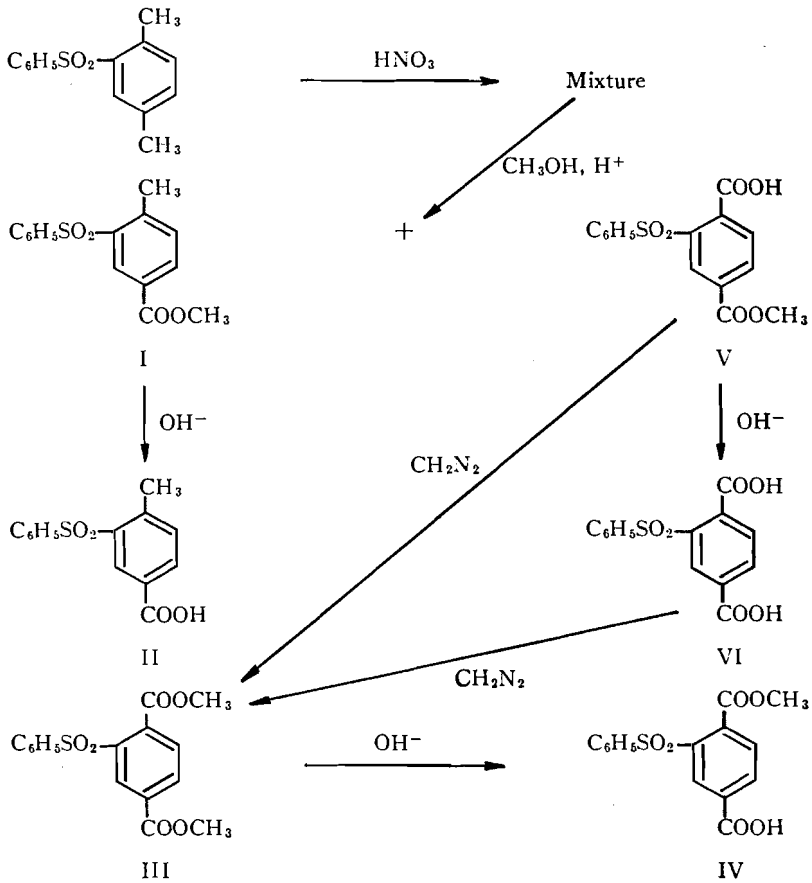

5-Carbomethoxy-2-methylphenyl Phenyl Sulfone (I)

The neutral ethereal solution obtained from the esterification described above was dried over anhydrous magnesium sulfate and filtered, and the ether was removed by evaporation. The oily residue crystallized to a yellow solid (0.85 g) after gentle scratching with a glass rod. Three crystallizations from methanol–water afforded a white solid with m.p. 106–108°.

Anal. Calcd. for $C_{15}H_{14}O_4S$: C, 62.0; H, 4.86; S, 11.0. Found: C, 61.8; H, 4.88; S, 10.71.

Saponification of I in 0.1 *N* sodium hydroxide gave the corresponding acid, 5-carboxy-2-methylphenyl phenyl sulfone, II, m.p. 230.5–231.5°.

Anal. Calcd. for $C_{14}H_{12}O_4S$: C, 61.0; H, 4.38; neut. equiv, 276. Found: C, 60.74; H, 4.53; neut. equiv, 278.

Independent Synthesis of Compounds I and II; 3-Chlorosulfonyl-4-methylbenzoic Acid (VII)

This compound was prepared by modifying the procedure used by Hansch and co-workers (12) to make 3-chlorosulfonyl-4-ethylbenzoic acid.

Chlorosulfonic acid, 200 g (1.71 moles), was added to 66 g (0.426 mole) of *p*-toluoyl chloride at such a rate that the reaction temperature did not exceed 40°. After complete addition of the chlorosulfonic acid, the reactants were heated to 80° for 3 h and then poured cautiously, with stirring, onto cracked ice. The solid was collected by suction filtration and washed thoroughly with cold water. Crystallization of the air-dried product from toluene gave VII as a white solid in 74% yield; m.p. 166–167.6°.

Anal. Calcd. for $C_8H_7O_4SCl$: C, 41.0; H, 3.02; neut. equiv, 78.2. Found: C, 41.07; H, 3.29; neut. equiv, 79.3.

The Friedel–Crafts procedure starting with 100 g (1.28 moles) of benzene, 30 g (0.127 mole) of VII, and 38 g (0.286 mole) of aluminium chloride gave II as silvery plates after crystallization of the crude reaction product from methanol; m.p. 229–231°.

Anal. Calcd. for $C_{14}H_{12}O_4S$: C, 61.0; H, 4.38; neut. equiv, 276. Found; C, 60.68; H, 4.69; neut. equiv, 280.

Methanol esterification of this acid afforded the methyl ester, identical to I in all respects, in 89% yield, m.p. 106.4–108°.

Can. J. Chem. Downloaded from www.nrcresearchpress.com by 210.87.254.105 on 09/05/12
For personal use only.

5-Carbomethoxy-2-carboxyphenyl Phenyl Sulfone (V)

Acidification with 5% sulfuric acid of the combined bicarbonate–water washings from the esterification of the oxidation products afforded 8.5 g of crude V. This product, after crystallization from methanol–water, had m.p. 182.2–183.6°.

Anal. Calcd. for $C_{15}H_{12}O_6S$: C, 56.2; H, 3.78; S, 10.0; neut. equiv, 320. Found: C, 55.93; H, 4.09; S, 9.73; neut. equiv, 323.

Alkaline saponification readily converted V to the known 2,5-dicarboxyphenyl phenyl sulfone, VI (5); m.p. 265–266.5°.

Treatment of both V and VI with ethereal diazomethane gave the known 2,5-dicarbomethoxyphenyl phenyl sulfone, III (5); in each instance, m.p. 110.4–112°. In addition, reaction of both V and VI with thionyl chloride followed by treatment with excess methanol afforded III in each case.

Structure Proof of V

3-Carbomethoxyphenyl Phenyl Sulfone (VIII); Polymorphs of VIII

One gram (0.00313 mole) of V was heated at 180° with 10 ml of quinoline containing a trace of copper powder until gas evolution ceased (½ h). Ether (100 ml) was added to the cooled reaction mixture and the ethereal solution was filtered. The filtrate was washed successively with four 30 ml portions of 3% hydrochloric acid, one 30 ml portion of water, two 50 ml portions of 10% sodium bicarbonate, and one 50 ml portion of water. The neutral ethereal solution was dried over anhydrous magnesium sulfate and filtered, and the ether was evaporated. The dark residual oil crystallized from methanol–water, following treatment with Norite, as a white solid; m.p. 64.5–66.5°. A yield of 50% (0.43 g) was obtained.

Anal. Calcd. for $C_{14}H_{12}O_4S$: C, 61.0; H, 4.38. Found: C, 61.11; H, 4.40.

The following data show that this compound was an unstable polymorphic form (A) of VIII:

When A was heated above its melting point, 64.5–66.5°, solidification occurred at about 68° and the new solid (B) melted at 84–85.2°. Subsequent decarboxylations of V, performed as above, gave only the stable form of VIII, B, m.p. 84–85.2°; the unstable form, A, was not isolated in later preparations.

Anal. Calcd. for $C_{14}H_{12}O_4S$ (B): C, 61.0; H, 4.38. Found: C, 60.88; H, 4.38.

A mixture melting point of forms A and B showed no depression of the melting point of the stable form, B (m.p. of B, 84–85.2°; mixed m.p. 84–85°). The solid phase (Nujol mull) infrared spectrum of A was different from that of B. However, their solution spectra (carbon tetrachloride) were identical in all respects. The unstable form, A, spontaneously converted to the more stable form, B, after standing at room temperature for several months as shown by its m.p. (84–85.2°), and by its solid phase infrared spectrum.

3-Carboxyphenyl Phenyl Sulfone (IX) (2a)

This substance was prepared in almost quantitative yield by saponification of VIII in 0.1 *N* sodium hydroxide, m.p. 184–185.2°.

Infrared and melting point comparisons of IX with a sample of 2-carboxyphenyl phenyl sulfone showed them to be different compounds.

The m.p.'s of VIII and IX were not depressed, in either case, when mixed with authentic samples prepared by the procedures described below. In addition, infrared comparison showed VIII and IX to be identical with the authentic samples.

The Friedel–Crafts procedure starting with 20 g (0.0884 mole) of 3-chlorosulfonyl benzoic acid (13) m.p. 132–133°, 100 g (1.28 moles) of benzene, and 28 g (0.21 mole) of aluminium chloride gave a 43% yield of 3-carboxyphenyl phenyl sulfone; m.p. 184.5–185.5°.

The corresponding methyl ester had a m.p. of 84–85°.

2-Carbomethoxy-5-carboxyphenyl Phenyl Sulfone (IV)

Saponification of 2,5-dicarbomethoxyphenyl phenyl sulfone (2.0 g, 0.0006 mole) in 55 ml of 0.1067 *N* sodium hydroxide afforded this compound in 84% yield; m.p. 200.3–201° from methanol.

Anal. Calcd. for $C_{15}H_{12}O_6S$: C, 56.3; H, 3.78; S, 10.0. Found: C, 56.16; H, 3.84; S, 9.72.

Structure Proof of IV

5-Bromo-2-carbomethoxyphenyl Phenyl Sulfone (X)

2-Carbomethoxy-5-carboxyphenyl phenyl sulfone, IV, 2.7 g (0.0084 mole), was neutralized with 1 equiv of cold 0.3325 *N* sodium hydroxide, and the resulting solution was treated with 10% excess of aqueous silver nitrate solution. The silver salt of IV precipitated at once and was collected by suction filtration, washed with water, and air dried. An 81% yield of the silver salt was obtained.

The procedure of Barnes and Prochaska (14) was followed to convert the silver salt of IV to X.

The silver salt of IV (2.9 g, 0.0068 mole), 50 ml of dried carbon tetrachloride, and 1.085 g (0.0068 mole) of dry bromine were refluxed for 1 h. The warm pale-orange reaction mixture was filtered. Ether (200 ml) was added to the cooled filtrate and the ethereal solution was washed successively with 50 ml of water, two 50 ml portions of 10% sodium bicarbonate, and 50 ml of water. The dried (anhydrous magnesium sulfate) organic solution was evaporated to dryness, and the white solid residue was crystallized from methanol–water. The resultant white needles (55% yield) had m.p. 131.5–133.5°.

Anal. Calcd. for $C_{14}H_{11}O_4SBr$: C, 47.3; H, 3.13. Found: C, 47.3; H, 3.35.

Can. J. Chem. Downloaded from www.nrcresearchpress.com by 210.87.254.105 on 09/05/12
For personal use only.

5-Bromo-2-carboxyphenyl Phenyl Sulfone (XI)

Heating under reflux (5 h) of 0.8 g (0.00225 mole) of X with 60 ml of 0.5 *N* sodium hydroxide containing 40 ml of methanol gave the known (3*a*) XI in 89% yield, m.p. 195–196.3°.

A mixture m.p. of XI and an authentic sample was not depressed; the infrared spectra of both samples were totally superimposable.

ACKNOWLEDGMENTS

The author is indebted to Professors John Roberts and Marvin Carmack for valuable discussions during the course of this work.

The author wishes to thank Professor William E. Truce of Purdue University for the samples of 2-carboxyphenyl phenyl sulfone and 5-bromo-2-carboxyphenyl phenyl sulfone.

1. E. D. Amstutz and C. R. Neumoyer. J. Am. Chem. Soc. **69**, 1925 (1947).
2. (*a*) W. E. Truce and M. F. Amos. J. Am. Chem. Soc. **73**, 3013 (1951).
   (*b*) H. Gilman and D. L. Esmay. J. Am. Chem. Soc. **75**, 278 (1953).
   (*c*) W. E. Truce and O. L. Norman. J. Am. Chem. Soc. **75**, 6023 (1953).
3. C. C. Price and S. Oae. Sulfur bonding. The Ronald Press Co., New York, N.Y. 1962. Chap. 3.
4. W. S. Weedon and H. W. Doughty. Am. Chem. J. **33**, 386 (1905).
5. G. Holt and B. Pagdin. J. Chem. Soc. 2508 (1960).
6. R. J. Hartman and A. M. Borders. J. Am. Chem. Soc. **59**, 2107 (1937).
7. (*a*) D. P. Evans, J. J. Gordon, and H. B. Watson. J. Chem. Soc. 1430 (1937).
   (*b*) K. Kindler. Ann. **450**, 1 (1926).
8. B. H. Chase and D. H. Hey. J. Chem. Soc. 553 (1952).
9. J. B. Cohen and H. S. de Pennington. J. Chem. Soc. **113**, 65 (1918).
10. E. S. Gould. Mechanism and structure in organic chemistry. Henry Holt and Co., New York, N.Y. 1959. p. 324.
11. Reference 10, p. 317 and p. 324.
12. C. Hansch, B. Schmidhalter, F. Reiter, and W. Saltonstall. J. Org. Chem. **21**, 265 (1956).
13. S. Smiles and J. Stewart. J. Chem. Soc. **119**, 1792 (1921).
14. R. A. Barnes and R. J. Prochaska. J. Am. Chem. Soc. **72**, 3188 (1950).

Received February 10, 1965.
E.I. du Pont de Nemours and Company,
Eastern Laboratories, Gibbstown, New Jersey,
and
Department of Chemistry,
Boston College,
Chestnut Hill, Massachusetts.

THE STRUCTURE OF BIS-DIMETHYLAMINOBERYLLIUM

Neil R. Fetter and Frances M. Peters

INTRODUCTION

In connection with other work, bis-dimethylaminoberyllium was prepared from the reaction of dimethylamine with diethylberyllium. Although the method of preparation was slightly different from that described by Coates and Glockling (1), it was noted on several occasions that the melting points of our preparations did not agree with those (1, 2) reported by these authors. Also, nuclear magnetic resonance (n.m.r.) data indicate that $Be(NMe_2)_2$ is not cyclic, but is trimeric as reported by Coates and Glockling (1).

EXPERIMENTAL

We prepared bis-dimethylaminoberyllium by two slightly different methods and with one of them it was possible to obtain $Be(NMe_2)_2$ with the literature (1) melting point.

In the first method, a typical preparation involved adding, under vacuum, a large excess of $HNMe_2$ in four equal portions to 2.5 g (37 mmole) of Et_2Be at 25 °C. After removal of the ethane formed and the excess dimethylamine, the solid product was vacuum sublimed (0.01 mm) at 90 °C onto a cold surface

Can. J. Chem. Downloaded from www.nrcresearchpress.com by 210.87.254.105 on 09/05/12
For personal use only.

5-Bromo-2-carboxyphenyl Phenyl Sulfone (XI)

Heating under reflux (5 h) of 0.8 g (0.00225 mole) of X with 60 ml of 0.5 *N* sodium hydroxide containing 40 ml of methanol gave the known (3*a*) XI in 89% yield, m.p. 195–196.3°.

A mixture m.p. of XI and an authentic sample was not depressed; the infrared spectra of both samples were totally superimposable.

ACKNOWLEDGMENTS

The author is indebted to Professors John Roberts and Marvin Carmack for valuable discussions during the course of this work.

The author wishes to thank Professor William E. Truce of Purdue University for the samples of 2-carboxyphenyl phenyl sulfone and 5-bromo-2-carboxyphenyl phenyl sulfone.

1. E. D. Amstutz and C. R. Neumoyer. J. Am. Chem. Soc. **69**, 1925 (1947).
2. (*a*) W. E. Truce and M. F. Amos. J. Am. Chem. Soc. **73**, 3013 (1951).
   (*b*) H. Gilman and D. L. Esmay. J. Am. Chem. Soc. **75**, 278 (1953).
   (*c*) W. E. Truce and O. L. Norman. J. Am. Chem. Soc. **75**, 6023 (1953).
3. C. C. Price and S. Oae. Sulfur bonding. The Ronald Press Co., New York, N.Y. 1962. Chap. 3.
4. W. S. Weedon and H. W. Doughty. Am. Chem. J. **33**, 386 (1905).
5. G. Holt and B. Pagdin. J. Chem. Soc. 2508 (1960).
6. R. J. Hartman and A. M. Borders. J. Am. Chem. Soc. **59**, 2107 (1937).
7. (*a*) D. P. Evans, J. J. Gordon, and H. B. Watson. J. Chem. Soc. 1430 (1937).
   (*b*) K. Kindler. Ann. **450**, 1 (1926).
8. B. H. Chase and D. H. Hey. J. Chem. Soc. 553 (1952).
9. J. B. Cohen and H. S. de Pennington. J. Chem. Soc. **113**, 65 (1918).
10. E. S. Gould. Mechanism and structure in organic chemistry. Henry Holt and Co., New York, N.Y. 1959. p. 324.
11. Reference 10, p. 317 and p. 324.
12. C. Hansch, B. Schmidhalter, F. Reiter, and W. Saltonstall. J. Org. Chem. **21**, 265 (1956).
13. S. Smiles and J. Stewart. J. Chem. Soc. **119**, 1792 (1921).
14. R. A. Barnes and R. J. Prochaska. J. Am. Chem. Soc. **72**, 3188 (1950).

Received February 10, 1965.
E.I. du Pont de Nemours and Company,
Eastern Laboratories, Gibbstown, New Jersey,
and
Department of Chemistry,
Boston College,
Chestnut Hill, Massachusetts.

THE STRUCTURE OF BIS-DIMETHYLAMINOBERYLLIUM

Neil R. Fetter and Frances M. Peters

INTRODUCTION

In connection with other work, bis-dimethylaminoberyllium was prepared from the reaction of dimethylamine with diethylberyllium. Although the method of preparation was slightly different from that described by Coates and Glockling (1), it was noted on several occasions that the melting points of our preparations did not agree with those (1, 2) reported by these authors. Also, nuclear magnetic resonance (n.m.r.) data indicate that $Be(NMe_2)_2$ is not cyclic, but is trimeric as reported by Coates and Glockling (1).

EXPERIMENTAL

We prepared bis-dimethylaminoberyllium by two slightly different methods and with one of them it was possible to obtain $Be(NMe_2)_2$ with the literature (1) melting point.

In the first method, a typical preparation involved adding, under vacuum, a large excess of $HNMe_2$ in four equal portions to 2.5 g (37 mmole) of Et_2Be at 25 °C. After removal of the ethane formed and the excess dimethylamine, the solid product was vacuum sublimed (0.01 mm) at 90 °C onto a cold surface

Can. J. Chem. Downloaded from www.nrcresearchpress.com by 210.87.254.6 on 09/05/12
For personal use only.

(−15 °C). The sublimate turned yellow slowly at 25 °C and was resublimed under the same conditions. The second sublimate (m.p. 83–130 °C*) also turned yellow slowly at 25 °C.

Anal. Calcd. for $C_4H_{12}N_2Be$: C, 49.44; H, 12.45; N, 28.84; Be, 9.27. Found: C, 49.18; H, 12.31; N, 28.70; Be, 9.54.

In the second method 0.970 g (14.5 mmole) of Et_2Be (prepared by the method of Gilman and Schulze (3)) was dissolved in 15 ml of *n*-heptane and the portions of $HNMe_2$ were condensed on the solution at −78 °C. After each addition, the mixture was allowed to warm to 25 °C and the evolved ethane was removed. A total of 40 mmole of $HNMe_2$ was condensed on the Et_2Be solution. After the solvent was removed at 25 °C via vacuum transfer, the crude product was vacuum sublimed (0.01 mm) at 65 °C yielding approximately 50 mole % of the calculated yield as a white sublimate, I, (m.p. 86–88 °C, lit. (1) 88–90 °C. (2) 94 °C). Anal. Found: C, 49.30; H, 12.58; N, 28.59; Be, 8.97. By continuing the sublimation at 100 °C another 30 mole % of the calculated $Be(NMe_2)_2$ was obtained as a white solid, II, which commenced melting at 85 °C and finally liquefied at 175 °C. Anal. Found: Be, 8.99. The remaining material which did not sublime at 100 °C was a fluffy yellow powder insoluble in benzene. No analysis was made of this material.

The n.m.r. spectra of the N—Me protons were all made at 42 °C on a Varian A-60 spectrometer with the samples 15% by weight in benzene. Molecular weight determinations were made with a Bender-Hobein freezing point apparatus using benzene as the solvent. The differential thermal analyses were made with a du Pont Model 900 DTA apparatus under a nitrogen atmosphere. The samples weighed approximately 5 mg and the heating rate was 20 °C/min. Molecular weight and differential thermal analysis (d.t.a.) data were obtained only from samples of $Be(NMe_2)_2$ prepared by the second method described above.

RESULTS AND DISCUSSION

The differential thermograms obtained from I and II sublimates of the second method explain to some extent the anomalous melting points obtained for many of our preparations of $Be(NMe_2)_2$.

The thermogram of I shows sharp endotherms at 86 and 250 °C, the former being the melting point and the latter either a boiling point or a decomposition temperature as indicated by the deposition of a white substance on the bell-jar cover of the d.t.a. cell. The endotherm at 86 °C was found to be reproducible by stopping the heating cycle at 100 °C and, after cooling, restarting the thermogram at 30 °C on the same sample.

The thermogram of II has four endotherms, sharp ones at 85, 175, and 278 °C and a broad one at 254 °C. The endotherms at 85 and 254 °C indicate the presence of I and the endotherms at 175 and 278 °C indicate the presence of at least one other form of $Be(NMe_2)_2$, if one assumes the endotherms at 254 and 278 °C represent boiling points or decomposition temperatures. A deposit of white material appeared on the bell jar at about 250 °C. Compound II appears, therefore, to be a mixture of at least two components and to obtain one of these in a pure state, the crude product must be vacuum sublimed at a temperature near 65 °C. A thermogram of the crude product also shows the same four endotherms as II, indicating a mixture is obtained during the initial reaction of Et_2Be with $HNMe_2$ between −78 and 25 °C. A thermogram of the nonsublimable yellow powder was featureless to 500 °C. The n.m.r. data are summarized in Table I.

TABLE I

Nuclear magnetic resonance spectra of $Be(NMe_2)_2$

Sample	Resonance peaks (p.p.m., δ benzene = 0)	Peak area ratio
1st Method		
Crude product	4.26, 4.23 (sh)* ; 4.87, 4.77 (sh)	1:2
90 °C sublimate	4.26 ; 4.87, 4.77 (sh)	1:2
2nd Method		
65 °C sublimate I	4.28 ; 4.90	1:2
100 °C sublimate II	4.30, 4.25 ; 4.90, 4.80	1:1:2:2
Crude product	4.28, 4.25 ; 4.87; 4.78	2:1:4:2

*sh = shoulder.

**Melting points are uncorrected.*

Can. J. Chem. Downloaded from www.nrcresearchpress.com by 210.87.254.6 on 09/05/12
For personal use only.

These data show that I from the second method has two NMe proton peaks in a ratio of 1:2 at $\delta = 4.28$ and 4.90 upfield from benzene. All the other spectra contain these two peaks in the same ratio, but other peaks are also present. In the spectra of crude products and in the 90 and 100 °C sublimate from both methods, another pair of peaks is located at approximately $\delta = 4.25$ and 4.78 upfield from benzene and in the ratio of 1:2. These two closely spaced pairs suggest the presence of two forms of $Be(NMe_2)_2$ of similar structure.

If $Be(NMe_2)_2$ were a cyclic trimer as suggested by Coates (1), there should be two types of NMe protons in a ratio of 1:1, that is, there should be 18 methyl protons bonded to terminal NMe_2 groups and 18 protons on the bridging NMe_2 groups. Since the ratio of the two types of NMe protons is 1:2, a trimeric structure of the type

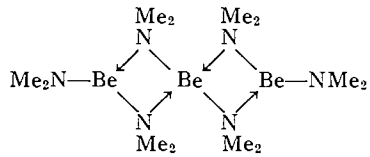

is indicated to achieve a maximum coordination for beryllium. The other form of $Be(NMe_2)_2$ may be another configuration of this trimer; for example, there may exist *cis* and *trans* forms for the terminal NMe_2 groups.

Only I of the second method appears to be a pure compound; hence, the molecular weight of this substance was the only one measured. The values 308 and 311 (calcd. 291.3 for $Be(NMe_2)_2$ trimer) indicate this material is trimeric in freezing benzene; therefore, the form of $Be(NMe_2)_2$ obtained by sublimation at 65 °C is more accurately represented by the structure shown above than by the cyclic form.

ACKNOWLEDGMENTS

The authors wish to acknowledge the assistance of Dr. Charles P. Haber and Dr. Peter J. Slota, Jr. of the U. S. Naval Ordnance Laboratory, Corona, California, and Mr. Donald W. Moore of the U. S. Naval Ordnance Test Station, China Lake, California. We wish to acknowledge the financial support of the Office of Naval Research.

1. G. E. Coates and F. Glockling. J. Chem. Soc. 22 (1954).
2. G. E. Coates and F. Glockling. J. Chem. Soc. 2526 (1954).
3. H. Gilman and F. Schulze. J. Chem. Soc. 2663 (1927).

Received December 18, 1964.
U.S. Naval Ordnance Laboratory,
Corona, California.

THE PHOTOLYSIS OF CARBON DISULFIDE AND CARBON DISULFIDE – OXYGEN MIXTURES

M. de Sorgo, A. J. Yarwood, O. P. Strausz, and H. E. Gunning

The ultraviolet absorption spectrum of carbon disulfide indicates at least two electronic transitions. The absorption at 1 900 Å to 2 100 Å is strong and has been assigned (1) to the transition of $^1B_2 \leftarrow {}^1\Sigma_g^+$. Some of the moderately intense bands in the region 2 800 – 3 600 Å have recently been suggested to be due to the transition from the ground $^1\Sigma_g^+$

Can. J. Chem. Downloaded from www.nrcresearchpress.com by 210.87.254.6 on 09/05/12
For personal use only.

These data show that I from the second method has two NMe proton peaks in a ratio of 1:2 at $\delta = 4.28$ and 4.90 upfield from benzene. All the other spectra contain these two peaks in the same ratio, but other peaks are also present. In the spectra of crude products and in the 90 and 100 °C sublimate from both methods, another pair of peaks is located at approximately $\delta = 4.25$ and 4.78 upfield from benzene and in the ratio of 1:2. These two closely spaced pairs suggest the presence of two forms of $Be(NMe_2)_2$ of similar structure.

If $Be(NMe_2)_2$ were a cyclic trimer as suggested by Coates (1), there should be two types of NMe protons in a ratio of 1:1, that is, there should be 18 methyl protons bonded to terminal NMe_2 groups and 18 protons on the bridging NMe_2 groups. Since the ratio of the two types of NMe protons is 1:2, a trimeric structure of the type

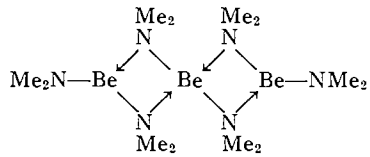

is indicated to achieve a maximum coordination for beryllium. The other form of $Be(NMe_2)_2$ may be another configuration of this trimer; for example, there may exist *cis* and *trans* forms for the terminal NMe_2 groups.

Only I of the second method appears to be a pure compound; hence, the molecular weight of this substance was the only one measured. The values 308 and 311 (calcd. 291.3 for $Be(NMe_2)_2$ trimer) indicate this material is trimeric in freezing benzene; therefore, the form of $Be(NMe_2)_2$ obtained by sublimation at 65 °C is more accurately represented by the structure shown above than by the cyclic form.

ACKNOWLEDGMENTS

The authors wish to acknowledge the assistance of Dr. Charles P. Haber and Dr. Peter J. Slota, Jr. of the U. S. Naval Ordnance Laboratory, Corona, California, and Mr. Donald W. Moore of the U. S. Naval Ordnance Test Station, China Lake, California. We wish to acknowledge the financial support of the Office of Naval Research.

1. G. E. Coates and F. Glockling. J. Chem. Soc. 22 (1954).
2. G. E. Coates and F. Glockling. J. Chem. Soc. 2526 (1954).
3. H. Gilman and F. Schulze. J. Chem. Soc. 2663 (1927).

Received December 18, 1964.
U.S. Naval Ordnance Laboratory,
Corona, California.

THE PHOTOLYSIS OF CARBON DISULFIDE AND CARBON DISULFIDE – OXYGEN MIXTURES

M. de Sorgo, A. J. Yarwood, O. P. Strausz, and H. E. Gunning

The ultraviolet absorption spectrum of carbon disulfide indicates at least two electronic transitions. The absorption at 1 900 Å to 2 100 Å is strong and has been assigned (1) to the transition of $^1B_2 \leftarrow {}^1\Sigma_g^+$. Some of the moderately intense bands in the region 2 800 – 3 600 Å have recently been suggested to be due to the transition from the ground $^1\Sigma_g^+$

Can. J. Chem. Downloaded from www.nrcresearchpress.com by 210.87.254.105 on 09/05/12
For personal use only.

state to the B_2 multiplet component of the $^3A_2$ state (2). Heicklen (3) has observed luminescence from carbon disulfide vapor irradiated with light between 2 800 and 3 600 Å. The vibrational energy of the excited state was not dissipated by collision before emission and the lifetime of the excited state was estimated to be 3.3×10^{-6} s. Predissociation in carbon disulfide vapor has been reported (4) to set in at $\lambda = 2\,068$ Å. In previous flash photolysis studies (5, 6, 7) the possible role of long-lived excited molecules has not been considered and although the presence of atomic sulfur was demonstrated only in the careful work of Callear (5), predissociation was invoked as the sole photolytic act in every case.

The aim of the present study was to examine the mechanism of the luminescence-quenching reaction and to establish whether chemical reaction can occur from the luminescent state.

EXPERIMENTAL

Continuous Photolysis

The vacuum technique, product handling, and analytical procedures were in general similar to those described in other communications (8). The light source was a Hanovia, model 30620, medium-pressure mercury arc, in conjunction with either an interference filter which had a transmission of about 25% at 2 100 ± 150 Å, or a 6 mm thick Vycor 7910 filter, which had a short wavelength cutoff at $\lambda = 2\,290$ Å. The reaction vessel was made of fused quartz.

Flash Photolysis

A 41 μF capacitor, at 9 kV, was discharged through two 55 cm long quartz flash lamps connected in parallel. The two lamps were joined near the ends. The photolysis lamp was filled with 7 Torr N_2 and 80 Torr krypton while the spectroscopic lamp contained 100 Torr krypton. The 3 μF capacitor for the spectroscopic flash was usually charged to 10 kV. The photolysis flash reached its maximum intensity in about 35 μs and the intensity was greater than 50% of the peak value for about 55 μs. The corresponding times for the spectroscopic flash were 10 μs and 40 μs. Transient ultraviolet absorption spectra were recorded on Kodak 103 a-O plates exposed in a Hilger medium quartz spectrograph. Two reaction vessels, both 50 cm long and 4.3 cm in diameter, were used. One was constructed of Vycor 7910 (transmitted wavelength > 2 200 Å), the other of pyrex glass. Both had plane parallel quartz windows.

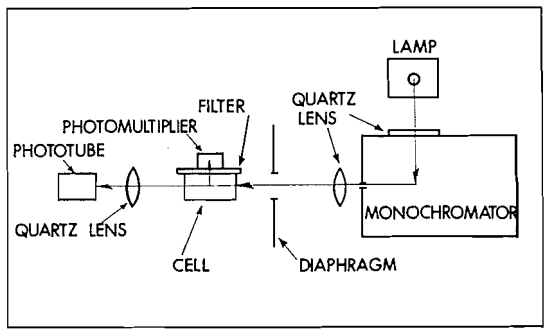

FIG. 1. A schematic illustration of the apparatus for the measurement of luminescence intensities.

Luminescence Intensity Measurements

The apparatus is illustrated schematically in Fig. 1. The lamp was an Osram, type HBO 250, high-pressure mercury arc. The light passed through a Bausch and Lomb 500 mm monochromator with a 1 200 groove/mm grating which was blazed at 5 000 Å. The entrance and exit slits were 1.00 mm wide. The cylindrical quartz cell was 5.0 cm long and 5.3 cm in diameter and was irradiated along its axis. The emerging luminescence was measured perpendicular to the incident beam by an E.M.I. 6256 photomultiplier, operated at 1900 V, from a Jarrell-Ash Recording Electronic System No. 82-110. Only the luminescence in the region 3 350 to 6 500 Å was determined. The short wavelength cutoff was set by an appropriate filter and the long wavelength limit was defined by the response of the photomultiplier. The transmitted radiation was focused by a quartz lens onto a Photovolt 501-M electronic photometer. The incident wavelength was 3 000 Å and the intensity of the luminescent radiation was taken as the difference between the photomultiplier outputs with the cell full and empty.

Can. J. Chem. Downloaded from www.nrcresearchpress.com by 210.87.254.105 on 09/05/12
For personal use only.

Materials

The carbon disulfide used was Baker 'Analyzed' reagent which was purified by low temperature distillation. The carbonyl sulfide (Matheson) was purified by bubbling through caustic soda solution, followed by low temperature distillation. Nitrogen, oxygen, and carbon dioxide were Airco 'Analyzed' reagents and the hydrocarbons were Philips 'Research' grade. The products were fractionated by low temperature distillation and analyzed by gas chromatography and mass spectrometry.

RESULTS AND DISCUSSION

The long wavelength ($\lambda > 2\,300$ Å) continuous photolysis of carbon disulfide vapor (or liquid) yielded only a brown, solid polymeric material. When the photolysis in the vapor phase was carried out in the presence of an excess of hydrogen, ethylene, butene, or propane, the polymer yield decreased but no additional product was observed. However, addition of oxygen (200 Torr to 20 Torr CS_2) resulted in the formation of carbonyl sulfide and sulfur dioxide in a ratio of about 1 to 2, with a simultaneous decrease in the polymer yield. When the effective wavelength region was 1 950 – 2 250 Å, the photolysis of a mixture of 20 Torr CS_2 and 200 Torr C_2H_4 yielded ethylene episulfide. However, no volatile product could be detected from a mixture of 20 Torr CS_2 and 200 Torr propane. Since triplet, ground-state sulfur atoms add readily to ethylene to form episulfide, but do not react with paraffins (8, 9), it follows that the photodissociation of carbon disulfide in this wavelength region leads to S (^3P) atom formation. This conclusion is in agreement with Callear's results (5). By kinetic absorption spectroscopy in the vacuum ultraviolet he demonstrated that the sulfur atoms are formed in the ^3P and not in the ^1D state. From these data it is evident that the photopolymerization and photooxidation of carbon disulfide in the absorption region of $\lambda = 2\,800 - 3\,600$ Å involve long-lived excited CS_2 molecules as the reactive intermediates.

To investigate the mechanism of the reactions, further studies were made in the flash apparatus, and the spectra of transient species recorded photographically. Spectra of both CS and S_2 were obtained when 7 Torr CS_2, with 380 Torr N_2, were flashed in either the pyrex or Vycor 7910 reaction vessel. The 2 600 – 3 000 Å band of S_2 reached its maximum intensity with the photolytic flash (35 μs) and lasted for about 300–500 μs. The prominent band of CS at 2 575.6 Å (0, 0) was visible for several minutes after the photolytic flash and the band at 2 589.6 Å (1, 1) was observed at short delay times. It is quite clear at this point that CS and S_2 must form via an excited CS_2 and atomic sulfur is absent. Further support for the excited molecule mechanism was provided by the results of the following experiments. When 2 Torr of COS with 410 Torr of N_2 were flash photolyzed the transient spectrum of S_2 molecules was detected. However, no S_2 spectrum could be detected when 2 Torr COS with 80 Torr ethylene and 300 Torr N_2 were flash photolyzed. This demonstrated that ethylene is an efficient scavenger for sulfur atoms. When this latter experiment was repeated, but with 20 Torr of added CS_2, the absorption spectrum of S_2 was again detected. (It was shown that flash photolysis of 20 Torr of CS_2 yielded approximately the same amount of S_2 as did 2 Torr of COS.) From the flash photolysis of a mixture of 3 Torr COS, 30 Torr CS_2, 90 Torr butene-2, and 280 Torr N_2, butene-2 episulfide was isolated. However, with 30 Torr CS_2, 90 Torr butene-2, and 280 Torr N_2, no episulfide was formed. The S_2 spectrum was observed in both of the latter two experiments.

The data suggest the following reaction,

$$[1] \qquad CS_2^* + CS_2 \rightarrow 2CS + S_2,$$

and also suggest that the brown polymer observed in the reaction is a mixture of CS and

Can. J. Chem. Downloaded from www.nrcresearchpress.com by 210.87.254.105 on 09/05/12
For personal use only.

sulfur polymers. Taking $D(SC{=}S) \leqslant 90$ kcal/mole, [1] will be energetically possible even at the onset of the absorption (about 3 800 Å).

In the flash photolysis of CS_2 the S_2 spectrum is completely suppressed by oxygen while the CS spectrum is only slightly affected, even at high oxygen pressures (90 Torr O_2, 22 Torr CS_2, and 280 Torr N_2). Sulfur dioxide is the only volatile product and its spectrum only appeared at delay times greater than 1 ms, suggesting its formation via the sulfur superoxide (SOO) intermediate (10). The spectrum of sulfur monoxide, SO, was not detected. In the absence of inert gas, the CS_2–O_2 mixtures exploded, yielding CO_2 and SO_2 in stoichiometric proportions. The experimental results are summarized in Table I.

TABLE I
Results of photolyses

Reactants	Illumination	Products	Conclusions
CS_2	Continuous $\lambda > 2\,300$ Å	Brown polymer	—
CS_2 + hydrocarbon	Continuous $\lambda > 2\,300$ Å	Polymer only product found	No S atom formation
$CS_2 + O_2$	Continuous $\lambda > 2\,300$ Å	COS and SO_2	
$CS_2 + C_2H_4$	Continuous $\lambda = 1\,950 - 2\,250$ Å	$H_2C{-}CH_2$ \S/	S (^3P) atoms produced
$CS_2 + N_2$ + olefin	Flash $\lambda > 2\,200$ Å	CS and S_2 No C—C formed \S/	Products come from CS_2^* and not from predissociation
$CS_2 + O_2$	Flash $\lambda > 2\,200$ Å	$CS + SO_2$ S_2 suppressed No SO observed	$CS_2^* + O_2 \rightarrow CS + SO_2$

A reaction consistent with the experimental observations is

[2] $$CS_2^* + O_2 \rightarrow CS + SOO.$$

The sulfur superoxide then isomerizes to SO_2. The fact that COS is formed in continuous but not in flash photolysis and that the intensity of the CS spectrum decreased only by a factor of less than two upon addition of oxygen could be explained if it is assumed that ground state CS does not react with O_2 but that the electronically excited CS, formed by secondary absorption does.

[3] $$CS + h\nu \rightarrow CS^*,$$
$$CS^* + O_2 \rightarrow COS + O.$$

Step [3] would be possible on both energetic and spin conservation grounds. This mechanism is also supported by the observation that COS is not formed in the continuous photolysis, when the irradiation is carried out in the pyrex vessel (CS does not absorb in the ultraviolet above 2 589.6 Å).

If [1] and [2] are assumed to be the only fluorescence-quenching reactions, the relative rate constant, k_1/k_2, could be determined by the measurement of the luminescence intensities. Figures 2 and 3 show reciprocal Stern–Volmer plots for the intensity of luminescence I_F, vs. the pressure of CS_2 and O_2 respectively. The luminescence intensities were corrected approximately for absorption by dividing the measured intensity by the total percentage of light absorbed. From the ratio of the slopes, $k_1/k_2 \simeq 7.6$.

In the flash photolysis experiments it was observed that a 4.5-fold excess of oxygen was sufficient to suppress S_2 formation below the limit of detectability, when [2] could account only for a decrease of $(7.6 \times 100)/(7.6 + 4.5) \sim 50\%$. Two alternative explanations can be offered. (*a*) S_2 is rapidly removed by oxygen. In this connection it should be

Can. J. Chem. Downloaded from www.nrcresearchpress.com by 210.87.254.105 on 09/05/12
For personal use only.

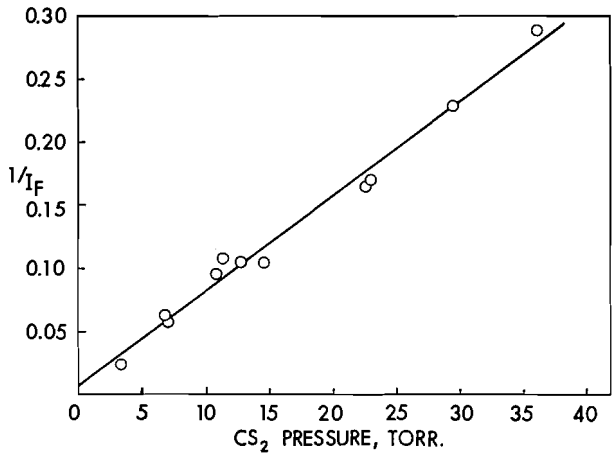

FIG. 2. Reciprocal Stern–Volmer plot for the luminescence intensities vs. carbon disulfide pressure.

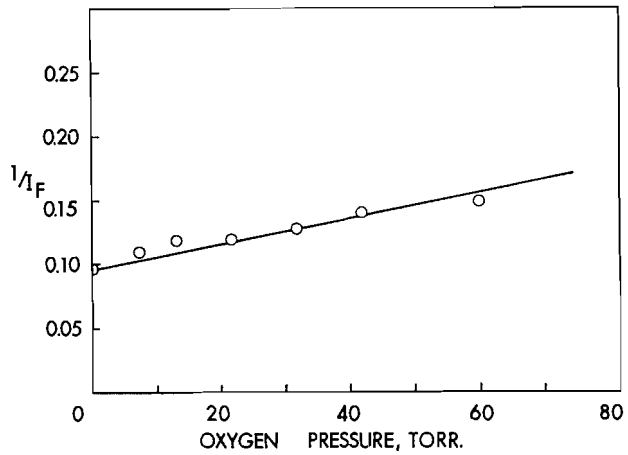

FIG. 3. Reciprocal Stern–Volmer plot for the luminescence intensities vs. added oxygen pressure. (Pressure of CS_2 = 10 Torr.)

mentioned that Wright (6) could not detect any change in the rate of S_2 disappearance upon addition of small amounts of oxygen in the flash photolysis of CS_2. (*b*) There are more than one kind of CS_2* involved. Indeed, the near-ultraviolet absorption system of CS_2 is made up of transitions from the ground state to three or four excited electronic levels (2). Some of these excited species may react with ground state CS_2 as indicated by [1], while others may react according to

$$CS_2^* + CS_2 \rightarrow 2CS_2, \qquad [4]$$

as suggested by Heicklen (3). O_2 on the other hand could react with any of the excited CS_2 molecules present.

CONCLUSION

Electronically excited carbon disulfide molecules, formed by absorption in the region $\lambda > 2\,200$ Å, may react with ground state CS_2 or O_2 molecules. Photodissociation of CS_2 to CS and S (^3P) atoms occurs at wavelength $< 2\,200$ Å.

Can. J. Chem. Downloaded from www.nrcresearchpress.com by 210.87.254.105 on 09/05/12
For personal use only.

ACKNOWLEDGMENTS

The authors wish to express their gratitude to the National Research Council of Canada and to Imperial Oil Limited for financial help. They are also indebted to Mr. H. A. Wiebe for performing one of the experiments.

1. A. D. WALSH. J. Chem. Soc. 2266 (1953).
2. A. E. DOUGLAS and E. R. V. MILTON. J. Chem. Phys. **41**, 357 (1964). J. T. HOUGEN. J. Chem. Phys. **41**, 363 (1964). B. KLEMAN. Can. J. Phys. **41**, 2034 (1963).
3. J. HEICKLEN. J. Am. Chem. Soc. **85**, 3562 (1963).
4. V. KONDRATJEV and A. YAKOVLEVA. J. Phys. Chim. **14**, 853 (1940).
5. A. B. CALLEAR. Proc. Roy. Soc. London Ser. A, **276**, 401 (1963).
6. F. J. WRIGHT. J. Phys. Chem. **64**, 1648 (1960). J. AKRICHE. J. Chim. Phys. **60**, 732 (1963).
7. J. J. MCGARVEY and W. D. MCGRATH. Proc. Roy. Soc. London Ser. A, **278**, 490 (1964).
8. O. P. STRAUSZ and H. E. GUNNING. J. Am. Chem. Soc. **84**, 4080 (1962). A. R. KNIGHT, O. P. STRAUSZ, and H. E. GUNNING. J. Am. Chem. Soc. **85**, 1207, 2349 (1963).
9. H. A. WIEBE, A. R. KNIGHT, O. P. STRAUSZ, and H. E. GUNNING. To be published.
10. A. L. MYERSON, F. R. TAYLOR, and P. L. HANST. J. Chem. Phys. **26**, 1309 (1957).

RECEIVED DECEMBER 9, 1964.
DEPARTMENT OF CHEMISTRY,
UNIVERSITY OF ALBERTA,
EDMONTON, ALBERTA.

ADDENDUM: A SIMPLIFIED PROCEDURE FOR THE ANALYSIS OF COMPLEX NUCLEAR MAGNETIC RESONANCE SPECTRA. I. THE PRINCIPLES OF SUB-SPECTRAL ANALYSIS

P. DIEHL, R. G. JONES, AND H. J. BERNSTEIN

(Ref. Can. J. Chem. 43, 81 (1965))

In Table AII on p. 92 an approximate function diagram has been given for the C_{2v} (planar) group. The detailed function diagram is given below.

C_{2v} (planar)	A_1 species	A_2 species	B_1 species	B_2 species
F_z				
2	—			
1	—	—	—	—
0	— — —	—	—	—
−1	—	—	—	—
−2	—			

None of the results have been altered by this change, which anticipates the situation where more information with regard to sub-spectral breakdown is possible.

On page 87, line 11, ABB′ should read ABC. On line 13, *abb′* should read *abc*.

DIVISION OF PURE CHEMISTRY,
NATIONAL RESEARCH COUNCIL,
OTTAWA, CANADA.

Can. J. Chem. Downloaded from www.nrcresearchpress.com by 210.87.254.105 on 09/05/12
For personal use only.

ACKNOWLEDGMENTS

The authors wish to express their gratitude to the National Research Council of Canada and to Imperial Oil Limited for financial help. They are also indebted to Mr. H. A. Wiebe for performing one of the experiments.

1. A. D. WALSH. J. Chem. Soc. 2266 (1953).
2. A. E. DOUGLAS and E. R. V. MILTON. J. Chem. Phys. **41**, 357 (1964). J. T. HOUGEN. J. Chem. Phys. **41**, 363 (1964). B. KLEMAN. Can. J. Phys. **41**, 2034 (1963).
3. J. HEICKLEN. J. Am. Chem. Soc. **85**, 3562 (1963).
4. V. KONDRATJEV and A. YAKOVLEVA. J. Phys. Chim. **14**, 853 (1940).
5. A. B. CALLEAR. Proc. Roy. Soc. London Ser. A, **276**, 401 (1963).
6. F. J. WRIGHT. J. Phys. Chem. **64**, 1648 (1960). J. AKRICHE. J. Chim. Phys. **60**, 732 (1963).
7. J. J. MCGARVEY and W. D. MCGRATH. Proc. Roy. Soc. London Ser. A, **278**, 490 (1964).
8. O. P. STRAUSZ and H. E. GUNNING. J. Am. Chem. Soc. **84**, 4080 (1962). A. R. KNIGHT, O. P. STRAUSZ, and H. E. GUNNING. J. Am. Chem. Soc. **85**, 1207, 2349 (1963).
9. H. A. WIEBE, A. R. KNIGHT, O. P. STRAUSZ, and H. E. GUNNING. To be published.
10. A. L. MYERSON, F. R. TAYLOR, and P. L. HANST. J. Chem. Phys. **26**, 1309 (1957).

RECEIVED DECEMBER 9, 1964.
DEPARTMENT OF CHEMISTRY,
UNIVERSITY OF ALBERTA,
EDMONTON, ALBERTA.

ADDENDUM: A SIMPLIFIED PROCEDURE FOR THE ANALYSIS OF COMPLEX NUCLEAR MAGNETIC RESONANCE SPECTRA. I. THE PRINCIPLES OF SUB-SPECTRAL ANALYSIS

P. DIEHL, R. G. JONES, AND H. J. BERNSTEIN

(Ref. Can. J. Chem. 43, 81 (1965))

In Table AII on p. 92 an approximate function diagram has been given for the C_{2v} (planar) group. The detailed function diagram is given below.

C_{2v} (planar)	A_1 species	A_2 species	B_1 species	B_2 species
F_z				
2	—			
1	—	—	—	—
0	— — —	—	—	—
−1	—	—	—	—
−2	—			

None of the results have been altered by this change, which anticipates the situation where more information with regard to sub-spectral breakdown is possible.

On page 87, line 11, ABB′ should read ABC. On line 13, *abb′* should read *abc*.

DIVISION OF PURE CHEMISTRY,
NATIONAL RESEARCH COUNCIL,
OTTAWA, CANADA.

Can. J. Chem. Downloaded from www.nrcresearchpress.com by 210.87.254.105 on 09/05/12
For personal use only.

ERRATUM: ULTRASONIC ABSORPTION IN CRITICAL BINARY LIQUID SYSTEMS. II

PEETER KRUUS

(Ref. Can. J. Chem. 42, 1712 (1964))

On page 1716, line 18, the value of l (quoted from ref. 11) is in error. The figure quoted (12.7 Å) is the value of l for the system methanol–cyclohexane. Debye *et al.* estimate the value of l for the system cyclohexane–aniline to be virtually zero.

The author is indebted to Dr. B. Chu for bringing this error to his attention.

DEPARTMENT OF CHEMISTRY,
UNIVERSITY OF TORONTO,
TORONTO, ONTARIO.

Canadian Journal of Chemistry. Volume 43 (1965)

Can. J. Chem. Downloaded from www.nrcresearchpress.com by 210.87.254.105 on 09/05/12
For personal use only.

Can. J. Chem. Downloaded from www.nrcresearchpress.com by 210.87.254.42 on 09/05/12
For personal use only.

Canadian Journal of Chemistry

Issued by THE NATIONAL RESEARCH COUNCIL OF CANADA

VOLUME 43 JULY 1965 NUMBER 7

FULLY FLUORINATED ALKOXIDES

PART I. TRIFLUOROMETHOXIDES OF ALKALI METALS[1]

M. E. REDWOOD AND C. J. WILLIS

Department of Chemistry, University of Western Ontario, London, Ontario

Received January 12, 1965

ABSTRACT

The preparation is described of the trifluoromethoxides of the heavier alkali metals, i.e. $MOCF_3$ where M = K, Rb, or Cs. These are stable, crystalline, ionic solids made by the reversible reaction of carbonyl fluoride with the appropriate metal fluoride. No trifluoromethoxides could be prepared from lithium, sodium, barium, or thallium(I) fluorides. Factors affecting the relative stability of such compounds are discussed.

Trifluoromethanol, CF_3OH, is not known, and is generally assumed to be incapable of existence because of the ease with which compounds having a fluorine atom in a position α to a hydroxyl group would eliminate hydrogen fluoride. Because of this unavailability of the parent alcohol, no metallic trifluoromethoxides have hitherto been reported. We now report the preparation of stable, crystalline trifluoromethoxides of the heavier alkali metals, i.e. $MOCF_3$, where M = K, Rb, or Cs.

A consideration of the possible formation of metallic trifluoromethoxides shows at once that they are likely to be more ionic in nature than the corresponding methoxides. The completely ionic formulation $M^+[OCF_3]^-$ would contain the trifluoromethoxide ion, isoelectronic with the fluoroborate ion, BF_4^-. The charge in the trifluoromethoxide ion rests formally on the oxygen atom, but it would be shared to some extent by the three fluorine atoms because of their greater electronegativity. The distribution of charge over the whole ion achieved in this way should therefore stabilize it, in a manner not possible in the ionic non-fluorinated methoxides of the alkali metals. The stability of a solid ionic trifluoromethoxide would clearly be influenced by the nature of the cation present, since smaller cations, or those with a high ratio of charge to size, would cause greater polarization of the anion and a correspondingly greater tendency towards decomposition to give a fluoride ion and carbonyl fluoride. In other words, the equilibrium:

$$MOCF_3 \rightleftharpoons COF_2 + MF$$

would be displaced to the left by the presence of large cations. An immediate corollary of this suggestion is that by approaching the equilibrium from the direction of formation rather than decomposition one would have available a possible synthetic route to trifluoromethoxides.

[1]*Presented in part at the 48th Annual Conference of the Chemical Institute of Canada, Montreal, May 31–June 2, 1965. For a preliminary communication, see D. C. Bradley, M. E. Redwood, and C. J. Willis. Proc. Chem. Soc. 416 (1964).*

The simple reasoning given above has now been readily confirmed by experiment. We find that visible reaction of carbonyl fluoride with suspensions of potassium, rubidium, or cesium fluorides in acetonitrile proceeds rapidly at 20°. Removal of excess carbonyl fluoride and solvent gives crystalline solids which, when kept *in vacuo*, show no sign of decomposition or evolution of carbonyl fluoride.

The molar ratio in which the carbonyl fluoride reacted with the metal fluoride was initially found to be variable in the ratio 0.5 to 0.95 mole carbonyl fluoride to 1.0 mole metal fluoride. It was therefore assumed that the reaction mixture, contained in a sealed tube, was reaching an equilibrium position, but that this equilibrium was being displaced during the subsequent removal of the volatile reactants, leading to decomposition of some of the trifluoromethoxide. It may readily be seen that the pressure of carbonyl fluoride in the system will affect the position of equilibrium. Since both the metal fluorides and the trifluoromethoxides are only very sparingly soluble in acetonitrile, we may assume their saturated solutions to be completely ionized and write the following equilibria:

$$[1] \qquad MF_{(s)} + \text{solvent} \rightleftharpoons M^{+}_{(sol)} + F^{-}_{(sol)}$$

$$[2] \qquad COF_{2(g)} + \text{solvent} \rightleftharpoons COF_{2(sol)}$$

$$[3] \qquad COF_{2(sol)} + F^{-}_{(sol)} \rightleftharpoons OCF_3^{-}{}_{(sol)}$$

$$[4] \qquad OCF_3^{-}{}_{(sol)} + M^{+}_{(sol)} \rightleftharpoons MOCF_{3(s)} + \text{solvent}$$

giving by summation the overall equilibrium:

$$[5] \qquad MF_{(s)} + COF_{2(g)} \rightleftharpoons MOCF_{3(s)}.$$

The final equilibrium is heterogeneous and the concentrations of solid metal fluoride and trifluoromethoxide are constant. Hence, when both of these solids are simultaneously present, there will be a unique pressure of carbonyl fluoride present at equilibrium at a given temperature. If this equilibrium pressure is exceeded, conversion of metal fluoride to trifluoromethoxide must occur, while at lower pressures of carbonyl fluoride the trifluoromethoxide will decompose to the fluoride. At 20°, however, these reactions only occur in the presence of a solvent, such as acetonitrile. This is demonstrated by the stability of the solid trifluoromethoxides *in vacuo*, by the observation that no reaction occurs between carbonyl fluoride and the metal fluorides in the absence of solvent, and by the fact that carbonyl fluoride is evolved when acetonitrile is added to the pure trifluoromethoxides. The equilibrium pressure of carbonyl fluoride above the solutions of the various trifluoromethoxides will clearly be a measure of their relative stabilities, and measurements of such pressures are now in progress.

In the preparation of the trifluoromethoxides, therefore, it is clear that, by having a sufficiently high pressure of carbonyl fluoride in the equilibrium mixture, the metal fluoride should be quantitatively converted to the trifluoromethoxide. However, when the volatile materials are removed, the carbonyl fluoride (b.p. −83°) must come off before the acetonitrile (b.p. 82°) and some decomposition of the trifluoromethoxide might occur while the solvent is being removed.

To minimize this decomposition, and thus obtain pure samples of the trifluoromethoxides, the reaction mixture was held below −20° while the volatile materials were removed. This had the effect of slowing down the rate of decomposition of the trifluoromethoxides, and also, presumably, of reducing their solubility in acetonitrile, and under these conditions the conversion of the fluorides of rubidium and cesium to their corresponding trifluoromethoxides was essentially quantitative. The molar combining ratio of carbonyl fluoride to metal fluoride was 0.97:1.00 and 0.94:1.00 for cesium and rubidium

Can. J. Chem. Downloaded from www.nrcresearchpress.com by 210.87.254.42 on 09/05/12
For personal use only.

respectively and subsequent analysis of the solid products showed that their composition was that expected for 1:1 adducts. With potassium fluoride, the combining ratio was a little lower (0.82:1.00), indicating that some decomposition had occurred during solvent removal even below −20°. With sodium, lithium, barium, and thallium(I) fluorides there was no evidence of the formation of trifluoromethoxides and virtually complete recovery of unreacted carbonyl fluoride.

In the case of lithium, sodium, and barium it is presumably the greater charge to size ratio of the metal ion which leads to instability of the trifluoromethoxides. For thallium(I), the ionic size alone would lead one to expect that the trifluoromethoxide would be formed, since the ionic radius of Tl^+, given as 1.40 Å (1) or 1.44 Å (2), is between that of K^+ (1.33 Å) and Rb^+ (1.48 Å) (1, 2). However, other factors are clearly involved here, since thallium(I) fluoride differs from the alkali metals in having a distorted sodium chloride structure (3) and a lattice energy of 198 kcal/mole (4) which is higher than that of potassium fluoride (192 kcal/mole) or rubidium fluoride (183 kcal/mole) (5) and this would tend to favor thallium(I) fluoride over the trifluoromethoxide.

The influence of the cationic radius on the relative stabilities of the trifluoromethoxides was also shown in their resistance to thermal decomposition. It was found that breakdown to give carbonyl fluoride and the metal fluoride occurred readily at 80° *in vacuo* and Fig. 1 shows the relative rates of decomposition of the potassium, rubidium, and cesium salts. It is clear that the increasing size of the cation leads to a decreasing rate of decomposition.

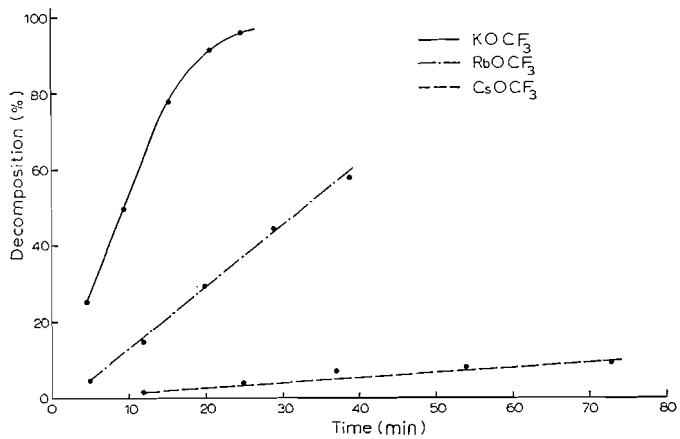

FIG. 1. Decomposition of trifluoromethoxides at 80°.

The results described above have therefore shown that carbonyl fluoride will undergo a reversible reaction with the fluorides of the heavier alkali metals to give solid 1:1 adducts. We suggest that formulation as the metal trifluoromethoxides gives the only structure consistent with the observed properties of the adducts. The only other type of bonding conceivable between carbonyl fluoride and a metallic fluoride would be coordination from the oxygen atom of the carbonyl group to the metal ion, i.e. $[M{\leftarrow}OCF_2]^+F^-$. This may be rejected in the present case for several reasons. The formation of stable complexes by coordination from oxygen to an alkali metal is very rare, and the strongest bonds are formed with the smaller ions. Hence the expected order of stability would be K > Rb > Cs, and the fact that thermal decomposition studies give the reverse order, combined with the fact that no adduct at all could be formed with the even smaller lithium and sodium ions,

Can. J. Chem. Downloaded from www.nrcresearchpress.com by 210.87.254.42 on 09/05/12
For personal use only.

would seem to make oxygen to metal coordination most unlikely. The greater stability of the compounds containing the larger cations is, however, entirely consistent with the trifluoromethoxide formulation, where the smaller cations, having greater polarizing tendencies and yielding fluorides of higher lattice energy, would tend to favor the decomposition of the salts to the fluorides and carbonyl fluoride.

Further support for the trifluoromethoxide structure is obtained from the X-ray powder diffraction patterns of the compounds. The trifluoromethoxide ion is isoelectronic with the fluoroborate ion, and the powder patterns of the corresponding salts are very similar. Detailed indexing has been carried out for the rubidium salt, showing it to be isomorphous with rubidium fluoroborate.

The crystals are orthorhombic, cell dimensions being:

	a	*b*	*c*	Vol.
$RbBF_4$(8)	9.07 Å	5.60 Å	7.23 Å	367 Å^3
$RbOCF_3$	8.86 Å	5.79 Å	7.37 Å	378 Å^3

A density determination on rubidium trifluoromethoxide showed that, like the fluoroborate, it contains four molecules in the unit cell. It is unlikely that such a similarity in unit cells would be fortuitously shown by compounds which did not contain ions of similar shape and size.

The trifluoromethoxides are reactive compounds and are immediately hydrolyzed on contact with water. This presumably occurs by decomposition into fluoride ion and carbonyl fluoride, followed by the known, rapid hydrolysis of carbonyl fluoride.

$$2H_2O + COF_3^- \rightarrow H_2CO_3 + HF + HF_2^-$$

Analysis of solutions resulting from this hydrolysis showed the presence of ionic fluoride ion in conformity with the above stoichiometry. Similar hydrolysis occurred rapidly when samples of the trifluoromethoxides were exposed to moist air, subsequent examination by infrared spectroscopy and X-ray powder pattern showing the presence of bifluoride. It would seem unlikely, therefore, that the unknown trifluoromethanol can be produced by hydrolysis of the trifluoromethoxides, or, indeed, that it is capable of existence.

Since, among the alkali metals, the formation of stable trifluoromethoxides seems to be limited to potassium, rubidium, and cesium (and, by implication, francium), it seems improbable that purely ionic trifluoromethoxides can be formed with any other simple cation, although they are likely to be stable when combined with a large, complex cation.

The non-fluorinated alkali metal alkoxides have been used for some time as valuable intermediates in the preparation of covalent alkoxides of other elements. With the trifluoromethoxides, it is clear that this application will be restricted by the ease with which they decompose to give carbonyl fluoride, but their synthetic uses for preparing covalent trifluoromethoxides are now being investigated.

EXPERIMENTAL

Volatile materials were handled in a conventional vacuum system and separated by fractional condensation. Molecular weights were determined by Regnault's method. Moisture was rigorously excluded throughout, all reaction vessels being flamed out *in vacuo* before use and solid materials being handled in a dry controlled atmosphere enclosure.

Analysis

Fluoride was determined gravimetrically as lead chloride fluoride. Since no interfering ions were present, a preliminary "fluorosilicic acid" distillation was not necessary. Rubidium and cesium were determined gravimetrically as their tetraphenylborates (6).

Can. J. Chem. Downloaded from www.nrcresearchpress.com by 210.87.254.42 on 09/05/12
For personal use only.

Metal Fluorides

The metal fluorides used were commercial samples.* Their purity was checked by analysis and by infrared examination, which showed bifluorides to be absent. They were dried before use by heating to 150° *in vacuo* for 1 h, then finely ground in a dry atmosphere, transferred to the reaction tube, and again heated *in vacuo* before other reactants were added.

Acetonitrile

Redistilled acetonitrile was stored in sealed tubes over phosphorus(V) oxide. When required for use it was transferred directly to the reaction tube, using the vacuum manifold to avoid contact with the atmosphere.

Carbonyl Fluoride

Carbonyl fluoride was prepared in 97% yield by the reaction of carbonyl chloride with sodium fluoride in acetonitrile (7). Carbonyl chloride was a redistilled commercial sample whose purity was checked by infrared examination and molecular weight determination.

In a typical preparation carbonyl chloride (1.47 g, 14.9 mmole) was condensed onto sodium fluoride (8.0 g, 180 mmole) in acetonitrile (15 ml) and the reaction mixture kept at 20° for 24 h in a sealed Pyrex tube (100 ml). Fractionation of the volatile components gave carbonyl fluoride (0.95 g, 14.4 mmole). Infrared examination showed the product to contain traces of silicon tetrafluoride and carbon dioxide but to be free of carbonyl chlorofluoride, COClF. The last compound was formed, however, if a lower ratio of sodium fluoride to carbonyl chloride was employed. The carbonyl fluoride was stored at −196° until required for use, to prevent its reaction with glass to give silicon tetrafluoride.

Reaction of Carbonyl Fluoride with Metal Fluorides

The dried metal fluoride was contained in an evacuated Pyrex tube (100 ml). Acetonitrile (15 ml) was condensed on, followed by carbonyl fluoride. The tube was sealed and allowed to warm up to room temperature with constant shaking, in the absence of which a solid layer of trifluoromethoxide rapidly formed on the surface of the metal fluoride, preventing complete reaction. After keeping at 20° for 48 h with occasional shaking the tube was opened and volatile materials removed below −20°. The unreacted carbonyl fluoride was separated from acetonitrile by fractional condensation and its purity checked by infrared examination. A blank experiment showed that, in the absence of the metal fluoride, the carbonyl fluoride could be quantitatively recovered from the reaction tube, and the amount which had reacted with the metal fluoride was therefore deduced from the weight recovered.

(a) Reaction with Cesium Fluoride

In a typical experiment carbonyl fluoride (4.26 g, 64.5 mmole) was shaken with cesium fluoride (2.50 g, 16.5 mmole). The weight of recovered carbonyl fluoride showed that 1.06 g (16.0 mmole) had reacted, giving a reacting molar ratio, COF_2:CsF, of 0.97:1.00.

Anal. Calcd. for $CsOCF_3$: Cs, 61.0; F, 26.2. Found: Cs, 60.8; F, 26.5.

In an experiment in the absence of acetonitrile, carbonyl fluoride (0.091 g, 1.37 mmole) was condensed onto cesium fluoride (0.60 g, 3.94 mmole) in an evacuated Pyrex tube (20 ml). The mixture was held at −96° for 4 h, then at 20° for 24 h. On opening the tube, unchanged carbonyl fluoride (0.089 g, 1.35 mmole) was recovered, showing that no significant reaction had occurred.

(b) Reaction with Rubidium Fluoride

In a typical experiment carbonyl fluoride (4.99 g, 75.6 mmoles) was shaken with rubidium fluoride (1.25 g, 12.0 mmoles). The weight of recovered carbonyl fluoride showed that 0.74 g (11.2 mmoles) had reacted, giving a reacting molar ratio, COF_2:RbF, of 0.94:1.00.

Anal. Calcd. for $RbOCF_3$: Rb, 50.1; F, 32.6. Found: Rb, 49.9; F, 32.7.

(c) Reaction with Potassium Fluoride

Carbonyl fluoride (5.24 g, 79.5 mmoles) was shaken with potassium fluoride (1.53 g, 26.3 mmoles). The weight of recovered carbonyl fluoride showed that 1.42 g (21.5 mmoles) had reacted, giving a reacting ratio, COF_2:KF, of 0.82:1. This ratio was reproducible.

(d) Reaction with Lithium, Sodium, Barium, and Thallium(I) Fluorides

Reaction with these fluorides was attempted under the same conditions. In all cases virtually complete recovery (96–98%) of the unreacted carbonyl fluoride was obtained.

Thermal Decomposition of Trifluoromethoxides

No evidence was found for the decomposition of the trifluoromethoxides of cesium, rubidium, or potassium at 20°. Samples kept in sealed, evacuated tubes for several weeks showed no gas pressure on opening. Qualitative experiments showed that a gas was evolved when any of the trifluoromethoxides was heated *in vacuo* at 80–100°. The gas was identified in each case by infrared examination and molecular weight measurement as carbonyl fluoride, containing traces of silicon tetrafluoride and carbon dioxide.

For quantitative measurements of the relative rates of decomposition of the potassium, rubidium, and cesium salts a continuously evacuated Pyrex tube was heated to 80°. A sample of the trifluoromethoxide was introduced from a sidearm and evolved gas led through a series of traps cooled to −196° and arranged in such a manner that the gas flow could be diverted from one to the next at regular intervals, the contents of each

**Fluorides of rubidium, cesium, and thallium were supplied by Alfa Inorganics Inc., Beverley, Mass.*

Can. J. Chem. Downloaded from www.nrcresearchpress.com by 210.87.254.42 on 09/05/12
For personal use only.

trap being subsequently weighed. The temperature was finally raised to 120° and heating continued until evolution of carbonyl fluoride ceased, which was considered to represent 100% decomposition of the trifluoromethoxide present. Results are shown in Fig. 1.

X-ray Powder Patterns

These were determined on samples contained in 0.5 mm Pyrex capillaries using an 11 cm camera and Cu K_α radiation with a nickel filter. Data on rubidium trifluoromethoxide are given in Table I, together with the corresponding figures for rubidium fluoroborate as reported by Hoard and Blair (8).

TABLE I

Calculated and observed X-ray data

	$RbBF_4$			$RbOCF_3$		
h,k,l	I_{obs}	d_{obs}	d_{calcd}	I_{obs}	d_{obs}	d_{calcd}
011	m	4.48	4.43	m	4.51	4.55
111	ms	4.02	3.98	m	4.02	4.05
201	f	3.87	3.84	f	3.83	3.80
002	mf	3.68	3.62	m	3.71	3.69
210	s	3.55	3.53	vs	3.53	3.52
102	ms	3.39	3.36	ms	3.41	3.42
				vf	3.28*	
211	s	3.20	3.17	s	3.20	3.18
112	ms	2.90	2.88	s	2.94	2.93
020	m	2.81	2.80	ms	2.84	2.89
301			2.79	ms	2.74	2.74
212	mf	2.53	2.52	mf	2.54	2.54
311	n.o.		2.50	f	2.47	2.48
220	m	2.40	2.38	mf	2.41	2.42
103	m	2.34	2.33	mf	2.37	2.37
302			2.32	s	2.29	2.30
221	ms	2.28	2.26			2.30
113	vs	2.17	2.15	vs	2.19	2.19
312			2.14	s	2.14	2.14
410	ms	2.11	2.10	ms	2.08	2.07
222	f	2.01	1.99	mf	1.99	2.03
321	f	1.99	1.98			1.99
303	m	1.90	1.88	m	1.90	1.89
031	mf	1.82	1.81	m	1.87	1.87
004	f	1.80	1.81	m	1.85	1.84

Abbreviations: vs, very strong; s, strong; m, medium; f, faint; vf, very faint; n.o., not observed.

*Attributed to the (111) reflection of rubidium fluoride (d_{calcd} = 3.26). No other lines attributable to the fluoride were observed.

Density of Rubidium Trifluoromethoxide

The density of the powdered trifluoromethoxide was determined by the displacement method using *n*-hexane. At 24° the density was found to be 2.7 g/cc. The calculated value, based on 4 molecules in an orthorhombic unit cell (a = 8.86, b = 5.79, c = 7.37 Å) is 2.9 g/cc.

ACKNOWLEDGMENTS

The authors thank Dr. D. C. Bradley for valuable discussions and Mrs. C. Rand for assistance in determining and indexing X-ray powder patterns. They also gratefully acknowledge financial support from the National Research Council of Canada.

REFERENCES

1. L. PAULING. The nature of the chemical bond. 3rd ed. Cornell University Press, Ithaca, N.Y. 1960. p. 518.
2. A. F. WELLS. Structural inorganic chemistry. 3rd ed. Oxford University Press. 1962. p. 71.
3. J. A. A. KETELAAR. Z. Krist. **92**, 30 (1935).
4. D. F. C. MORRIS and L. H. AHRENS. J. Inorg. Nucl. Chem. **3**, 263 (1956).
5. M. L. HUGGINS. J. Chem. Phys. **5**, 143 (1937).
6. S. KALLMANN. *In* Treatise on analytical chemistry, Part II. Vol. 1. *Edited by* I. M. Kolthoff and P. J. Elving. Interscience Publishers, New York. 1961. p. 439.
7. F. S. FAWCETT, C. W. TULLOCK, and D. D. COFFMANN. J. Am. Chem. Soc. **84**, 4275 (1962).
8. J. L. HOARD and V. BLAIR. J. Am. Chem. Soc. **57**, 1985 (1935).

Can. J. Chem. Downloaded from www.nrcresearchpress.com by 210.87.254.42 on 09/05/12
For personal use only.

Can. J. Chem. Downloaded from www.nrcresearchpress.com by 210.87.254.40 on 09/05/12
For personal use only.

THE REACTION OF ACTIVE NITROGEN WITH MIXTURES OF ETHYLENE AND NITRIC OXIDE[1]

E. FERSHT[2] AND R. A. BACK
Division of Pure Chemistry, National Research Council, Ottawa, Canada

Received December 3, 1964

ABSTRACT

The reaction of active nitrogen, produced in a condensed discharge at 1 mm pressure, with mixtures of ethylene and nitric oxide has been studied with mixtures ranging in composition from pure ethylene to pure nitric oxide. The sum of HCN + $^{14}N^{15}N$ produced from mixtures of C_2H_4 and ^{15}NO remained constant and equal to the HCN produced from pure C_2H_4 for NO concentrations up to 50 mole %. As more NO was added, this sum rose towards the value of $^{14}N^{15}N$ produced from pure ^{15}NO. These data appear to lend support to the HCN yield from ethylene as the true measure of nitrogen atom concentration. It is suggested that ^{15}NO also undergoes a concerted reaction with excited $^{14}N^{14}N$ molecules, probably in the $A^3\Sigma_u^+$ state, to produce $^{14}N^{15}N$, and that these excited molecules can be quenched by collision with ethylene or methane without consuming nitrogen or forming HCN.

INTRODUCTION

Both ethylene and nitric oxide, when present in sufficient excess, appear to react quantitatively with active nitrogen, and both have been used to measure its activity. The extent of the nitric oxide reaction, however, is consistently higher by about 50% than the maximum yield of hydrogen cyanide from the reaction with ethylene, and despite extensive studies of both systems, this discrepancy remains unexplained (1, 2, 3). It is well established that atomic nitrogen is the major reactive species in active nitrogen (2, 4, 5). There is also little doubt that excited nitrogen molecules are also present in appreciable concentrations in active nitrogen, are responsible for the decomposition of ammonia, and probably initiate the reactions with saturated hydrocarbons (2, 6–9). Suggested explanations of the ethylene–NO discrepancy fall into two general categories. In the first of these it is proposed that the reaction

[1] $$N + NO \rightarrow N_2 + O$$

is the only one of importance in the nitric oxide system, and that the lower yield of hydrogen cyanide from ethylene arises from some inherent inefficiency in the ethylene reaction (10, 11). The nitric oxide reaction has been studied by following the disappearance of nitric oxide (1, 12, 13), the appearance of N_2 (using ^{15}NO) (3), and the formation of oxygen atoms (14), and all the data are compatible with this simple mechanism, which is also apparently supported by recent estimates of atom concentration by electron spin resonance methods (5), and by measurement of the pressure change on combination (15).

In the second category of explanations, it is suggested that in the presence of a sufficient excess of ethylene, the reactions

[2] $$N + C_2H_4 \dashrightarrow HCN + CH_3$$

[3] $$N + CH_3 \dashrightarrow HCN + H_2 \text{ (or } 2H)$$

quantitatively convert nitrogen atoms to hydrogen cyanide, and that the "extra" decomposition of nitric oxide arises from some additional reaction, probably of excited

[1]*Issued as N.R.C. No. 8406. Presented at the Chemical Institute of Canada Annual Conference at Kingston, June 1964.*

[2]*National Research Council of Canada Postdoctorate Fellow, 1961–1963. Present address: Yerkes Research and Development Laboratory, E. I. duPont de Nemours and Co., Buffalo, New York.*

nitrogen molecules, in the nitric oxide system (1, 2). This view is supported by the simplicity of the products of the ethylene reaction, the absence of appreciable amounts of other nitrogenous products, and the fact that a large number of other hydrocarbons and organic compounds give approximately the same maximum yield of hydrogen cyanide (2).

A recent study of the reaction of ^{14}N-active nitrogen with ^{15}NO in this laboratory showed that $^{14}N^{15}N$ was produced in amounts approximately equal to the ^{15}NO destroyed, and that $^{15}N^{15}N$ was completely absent from the products (3). The quantitative production of $^{14}N^{15}N$ in these experiments suggested a means of measuring the extent of the nitric oxide reaction in ethylene–NO mixtures which would avoid the uncertainty, due to possible loss of NO in secondary reactions, inherent in a measurement of NO disappearance. Both $^{14}N^{15}N$ and hydrogen cyanide should be effectively inert to secondary reactions in this system (3, 16), and by simultaneous measurements of both these products from the reaction of active nitrogen with various ethylene–NO mixtures it was hoped that the origin of the ethylene–NO discrepancy might be clarified.

EXPERIMENTAL

Active nitrogen was generated by a condensed discharge in a conventional fast-flow system, previously described (3). Pressure of nitrogen was about 1 mm and the flow rate was 35 μmoles/s. Surfaces were poisoned with phosphoric acid and a trace of water vapor added to the nitrogen stream. The active nitrogen reached the reactant nozzle about 0.15 s after leaving the discharge tube.

The reaction vessel was a fused silica cylinder of 24 mm i.d. and 60 cm long. Nitric oxide and ethylene from separate flowmeters were premixed, and introduced through a nozzle mounted coaxially within the reaction vessel, designed to ensure rapid mixing of the reagent gases with the active nitrogen.

Hydrogen cyanide was trapped at −196 or −210 °C together with other condensable products and unreacted ethylene; it was dissolved in dilute sodium hydroxide solution and titrated with silver nitrate as described previously (3). Suitable blank experiments showed that none of the other products interfered with the titration. In the experiments in which $^{14}N^{15}N$ was measured, solid nitrogen traps (−210 °C) removed nitric oxide and other condensable products or reagents which might have interfered with the mass spectrometric analysis; this was also confirmed by blank experiments. Samples of noncondensable gas were removed from the flow system downstream from the traps by a Toepler pump, and analyzed by a mass spectrometer.* Straightforward corrections were made for $^{14}N^{15}N$ initially present in the isotopically natural active nitrogen, and for about 5% ^{14}NO in the ^{15}N-nitric oxide. Hydrogen, carbon monoxide, oxygen, and methane were minor noncondensable products of the ethylene – nitric oxide reaction with active nitrogen; these were analyzed by gas chromatography, and a small correction applied to the mass spectra for the contributions of carbon monoxide to the mass-28 and mass-29 peaks.

Nitric oxide titrations, based on simple visual observation of the sharp transition from a blue to a yellow–green flame, were performed before each experiment to check the activity of the active nitrogen; these always gave values within the range shown in Fig. 1, in good agreement with the $^{14}N^{15}N$ yield from pure nitric oxide.

All experiments were done at a temperature of 248 ± 2 °C. Linde "Bone dry" (99.98% pure) nitrogen was used throughout without purification. Ethylene and methane were Phillips Research grade, used after the usual degassing and bulb-to-bulb distillation. ^{14}N-Nitric oxide was obtained from Matheson and used after repeated simple distillations to remove traces of N_2O, NO_2, O_2, and N_2 impurities. ^{15}N-Nitric oxide was obtained from Merck, Sharp and Dohme of Canada Ltd., and subjected to similar purification.

RESULTS

Experiments with pure ethylene gave the usual behavior, with the yield of hydrogen cyanide becoming constant at about 3.1 μmoles/s, independent of ethylene flowrate, at ethylene flowrates above about 4 μmoles/s. Experiments with pure ^{15}NO, at flowrates beyond the end point of the flame titration, produced about 4.8 μmoles/s of $^{14}N^{15}N$, corresponding closely to the end point of the flame titration, and about 55% higher than the maximum yield of hydrogen cyanide from pure ethylene. These observations are in good agreement with previous work, and confirm the nitric oxide – ethylene discrepancy (1–3).

*The authors are grateful to Mr. R. Pilon for these analyses.

Can. J. Chem. Downloaded from www.nrcresearchpress.com by 210.87.254.40 on 09/05/12
For personal use only.

Figure 1 shows yields of $^{14}N^{15}N$ and HCN from NO–C_2H_4 mixtures as a function of the mole % of nitric oxide in the reagent mixture. Two sets of experiments were performed. The open squares and circles represent experiments in which the ethylene flowrate was

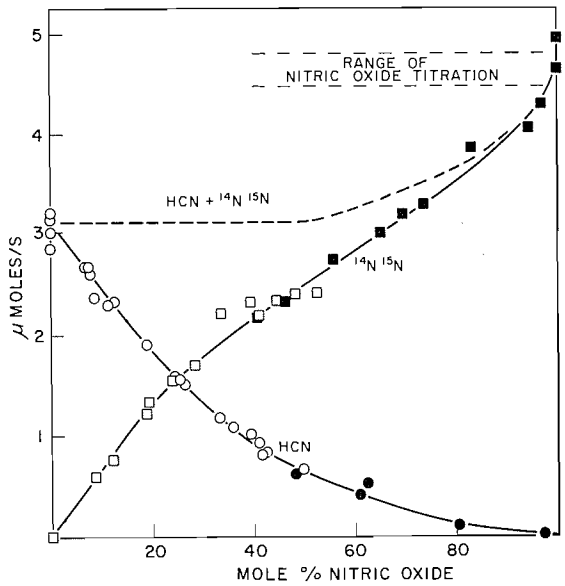

FIG. 1. Yields of HCN and $^{14}N^{15}N$ from the reaction of active nitrogen with NO–C_2H_4 mixtures ranging in composition from pure C_2H_4 to pure NO.

maintained approximately constant at values well up on the HCN "plateau", while increasing increments of nitric oxide were added. The solid squares and circles correspond to experiments in which nitric oxide flowrates were held at values somewhat in excess of the titration end point, while various amounts of ethylene were added. Thus in all the experiments there was always a sufficient excess of one reagent or the other to have ensured complete consumption of nitrogen atoms. The two sets of data overlap somewhat, and appear to lie on the same curves. In some but not all of the overlapping experiments, both reagents were in excess of the flowrates required for complete reaction. In several experiments, considerably more nitric oxide was added than the usual moderate excess; the product yields were indistinguishable from the normal experiments, indicating that nitric oxide was not being seriously depleted by any side reactions, and was always present in excess.

Also shown in Fig. 1 is a curve representing the sum of the yields of HCN and $^{14}N^{15}N$, derived from the smooth curves drawn through the HCN and $^{14}N^{15}N$ data.

Some experiments were also done with mixtures of methane with nitric oxide. Because methane reacts very slowly with active nitrogen (17), only one series of experiments, in which methane was added in increasing amounts to the NO-active nitrogen system with NO present in excess, was possible. Table I shows the effect of added methane on the yield of $^{14}N^{15}N$. There was no detectable hydrogen cyanide produced in these experiments.

DISCUSSION

As increments of ^{15}NO were added to excess ethylene (left hand side of Fig. 1), the HCN decreased from its value with ethylene alone, linearly at first and then more slowly,

Can. J. Chem. Downloaded from www.nrcresearchpress.com by 210.87.254.40 on 09/05/12
For personal use only.

TABLE I

The reaction of active nitrogen with NO–CH_4 mixtures

Mole % NO	$^{14}N^{15}N$ product (μmole/s)
1.00	4.80
0.93	4.61
0.87	4.47
0.82	4.65
0.64	4.36
0.54	4.09

and was replaced by $^{14}N^{15}N$. Because reaction [1] is probably at least 100 times faster than reaction [2] (even at 248 °C) (6, 13, 18), the initial decrease in HCN was limited by complete consumption of NO. As more NO was added, it was not completely consumed, and the relative yields of $^{14}N^{15}N$ and HCN reflected a competition between reactions [1] and [2]. This competition was complicated by reaction [3], which is probably almost as fast as reaction [1], and by the reaction of oxygen atoms, formed in reaction [1], with ethylene (19).

[4] $$O + C_2H_4 \dashrightarrow C_2H_4O^* \dashrightarrow CH_3 + CHO$$

Subsequent reactions probably account for the CH_4, CO, H_2, and C_2H_6 observed as minor products. Methyl radicals formed in reaction [4] also contribute to reaction [3], and it was probably this reaction sequence that kept the HCN yield from falling to zero as rapidly as it should have with a simple competition between reactions [1] and [2]. The abscissa scale in Fig. 1 is simply the mole % of NO initially present in the reagent mixture; it is evident from the complex nature of the competition between reactions [1], [2], and [3] that no simple significance attaches to the shapes of the curves, and that the abscissa scale merely represents a convenient empirical variable.

The most striking feature of Fig. 1 is that within the very considerable experimental error evident from the scatter of the data, the sum of HCN and $^{14}N^{15}N$ remained almost constant, and equal to the HCN yield from pure ethylene, up to about 50 mole % nitric oxide. At this point, HCN had fallen to about 20% of its initial value, and had been replaced almost quantitatively by $^{14}N^{15}N$. Despite the fact that four-fifths of the reaction was thus with nitric oxide, none of the extra reactivity shown by pure nitric oxide was yet in evidence. Only as the nitric oxide was increased beyond 50% did the extra reactivity begin to appear, as the sum of HCN + $^{14}N^{15}N$ rose gradually and then more sharply as 100% nitric oxide was approached.

Conversely, as increments of ethylene were added to the nitric oxide reaction (right hand side of Fig. 1), the yield of $^{14}N^{15}N$ decreased sharply. The decrease was at first only slightly compensated by the production of HCN, so that the sum of HCN + $^{14}N^{15}N$ fell rapidly towards the value of the HCN produced from pure ethylene.

The present observations fit most readily an explanation of the second category discussed earlier, i.e., a two-species explanation, with both ethylene and NO reacting quantitatively with nitrogen atoms, and with NO alone also reacting with a second species. The most likely second species is the metastable $A^3\Sigma_u^+$ state of N_2 (2, 8) and the lack of $^{15}N^{15}N$ in the product requires that this must react with ^{15}NO by a concerted mechanism,

[5] $$^{14}N_2(A^3\Sigma_u^+) + {}^{15}NO \dashrightarrow [{}^{14}N{}^{14}N{}^{15}NO]^* \dashrightarrow {}^{14}N + {}^{14}N{}^{15}N + O$$

Can. J. Chem. Downloaded from www.nrcresearchpress.com by 210.87.254.40 on 09/05/12
For personal use only.

rather than by an energy transfer process (3).* The effect of adding ethylene to the NO reaction would initially be the quenching of $N_2(A^3\,\Sigma_u^+)$ by ethylene, perhaps with some decomposition of the ethylene, but producing no HCN and consuming no nitrogen:

[6] $$N_2(A^3\,\Sigma_u^+) + C_2H_4 \dashrightarrow N_2(\text{ground state}) + C_2H_4 \text{ or other products.}$$

From the rapidity of the decrease in the $^{14}N^{15}N$ yield upon the addition of ethylene, it may be estimated that reaction [6] must have been from 5 to 10 times faster than reaction [5]. The data in Fig. 1 thus would represent two distinct competitions, the first for nitrogen atoms (reactions [1], [2], and [3]), in which the reaction with NO (reaction [1]) was much the faster, and the second a competition for $N_2(A^3\,\Sigma_u^+)$ (reactions [5] and [6]), in which ethylene was the faster reagent.

The effect of methane on the NO reaction (Table I) can also be explained by a similar quenching of $N_2(A^3\,\Sigma_u^+)$ by methane. It was much less efficient than ethylene, as only about half the extra $^{14}N^{15}N$ formed with pure ^{15}NO was eliminated by the addition of 50 mole % methane (cf. ethylene, Fig. 1). Allowing for consumption of NO in reaction [1], the quenching of $N_2(A^3\,\Sigma_u^+)$ by methane would have to be 2 or 3 times slower than reaction [5], and from 10 to 30 times slower than reaction [6]. This is in accord with the relative quenching efficiencies of methane and ethylene for other species (21).

It has been pointed out (2) that reaction [5] is endothermic unless the excited nitrogen molecule possesses at least one quantum of vibrational excitation. The $A^3\,\Sigma_u^+$ molecules can be formed directly by combination of nitrogen atoms or by one of several cascade processes associated with the nitrogen afterglow. In either case vibrational excitation is highly probable, and deactivation, especially below the $v = 1$ level, could be a slow process in pure nitrogen (2). This raises the possibility that ethylene and methane might be acting by deactivating $N_2(A^3\,\Sigma_u^+)$ to its lowest vibrational level rather than by electronic quenching.

The chief objection to the suggested two-species mechanism is the apparent disagreement with the recent physical measurements, mentioned previously, which yielded atom concentrations corresponding closely to the consumption of nitric oxide (5, 15). It is very difficult, however, to explain the present observations in terms of a nitrogen atom flowrate equal to the production of $^{14}N^{15}N$ from pure ^{15}NO, for whatever the data may represent, it is *not* a simple competition for nitrogen atoms. The constancy of the sum of HCN + $^{14}N^{15}N$ for reagent mixtures ranging from pure ethylene to 50% NO, with HCN production ranging from 100 to 20% of its value with pure ethylene, seems almost impossible to explain by a mechanistic inefficiency (such as catalytic combination of atoms (10, 22) for example) in the ethylene reaction. Unless this constant sum is purely fortuitous, it is difficult to avoid the conclusion that it corresponds to the flowrate of nitrogen atoms. A further argument against an explanation in terms of nitrogen atoms alone is the high efficiency of ethylene in reducing the $^{14}N^{15}N$ production from the ^{15}NO reaction, which is markedly at variance with the known (6, 18) relative rates of reactions [1] and [2], which, incidentally, are confirmed by the efficiency with which NO reduced the HCN yield when added to the ethylene reaction. The effect of methane on the production of $^{14}N^{15}N$ from the ^{15}NO reaction is similarly incompatible with its known very slow rate of reaction with nitrogen atoms (17).

**The reaction,* $NO^* + NO \rightarrow N_2 + O_2$, *following excitation of* NO *by energy transfer from* $N_2(A^3\,\Sigma_u^+)$, *suggested by Wright and Winkler (20), would still lead to* $^{15}N^{15}N$ *in the* ^{15}NO *reaction and thus may also be ruled out.*

Can. J. Chem. Downloaded from www.nrcresearchpress.com by 210.87.254.40 on 09/05/12
For personal use only.

Reaction [5] at first sight may seem a rather unlikely process. However, it could be regarded as a radical–radical disproportionation reaction, with transfer of N from the weakly bonded (D_{N-N} = 85 kcal) $N_2(A^3\Sigma_u^+)$ diradical to the monoradical NO, forming N_2O with sufficient vibrational excitation to break the N—O bond; in this light it is perhaps more plausible. Simple energy transfer from $N_2(A^3\Sigma_u^+)$ to NO, with decomposition of NO, is an obvious alternative, but this is not necessarily an efficient process; experimentally it has been shown that it does not occur in the present system (3).

A further difficulty with reaction [5] is the lack of effect of ammonia, added upstream, on the nitric oxide reaction (2), since it has been suggested by several authors (2, 6–8) that ammonia reacts readily with $N_2(A^3\Sigma_u^+)$ molecules. Wright *et al.* (2) reconciled this conflict, but their arguments are not particularly convincing. However, the mechanism of the ammonia reaction is obscure and possesses several very puzzling features, and until it is better understood, any conclusions about the lack of effect of ammonia on the nitric oxide reaction should be treated with considerable reserve.

In summary, it may be concluded that the present results appear to support the HCN production from ethylene as the true measure of the nitrogen atom content of active nitrogen. A second active species that can be destroyed by ethylene or methane without producing HCN is most probably responsible for the extra reactivity shown by nitric oxide. If the second species were $N_2(A^3\Sigma_u^+)$, previous experiments in this laboratory have shown that it must react with NO by a concerted mechanism (reaction [5]), and its concentration in the present system must have been about 27% of the atom concentration. This seems well beyond the margin of error in recent physical measurements of atom concentration, and the disagreement between these and the present conclusions remain unexplained.

REFERENCES

1. G. J. Verbeke and C. A. Winkler. J. Phys. Chem. **64**, 319 (1960).
2. A. N. Wright, R. L. Nelson, and C. A. Winkler. Can. J. Chem. **40**, 1082 (1962).
3. R. A. Back and J. Y. P. Mui. J. Phys. Chem. **66**, 1362 (1962).
4. J. Kaplan, W. J. Schade, C. A. Barth, and A. F. Hildebrandt. Can. J. Chem. **38**, 1688 (1960).
5. A. A. Westenberg and N. de Haas. J. Chem. Phys. **40**, 3087 (1964).
6. A. N. Wright and C. A. Winkler. Can. J. Chem. **40**, 5 (1962); J. Phys. Chem. **67**, 172 (1963).
7. H. B. Dunford. J. Phys. Chem. **67**, 258 (1963).
8. H. B. Dunford, E. R. V. Milton, and D. L. Whalen. Can. J. Chem. **42**, 2504 (1964).
9. W. E. Jones and C. A. Winkler. Can. J. Chem. **42**, 1948 (1964).
10. W. G. Zinman. J. Phys. Chem. **64**, 1344 (1960).
11. M. A. A. Clyne and B. A. Thrush. Proc. Roy. Soc. London, Ser. A, **261**, 259 (1961).
12. G. B. Kistiakowski and G. G. Volpi. J. Chem. Phys. **27**, 1141 (1957).
13. J. T. Herron. J. Chem. Phys. **35**, 1138 (1961).
14. J. E. Morgan, L. Elias, and H. I. Schiff. J. Chem. Phys. **33**, 930 (1960).
15. L. Elias. To be published.
16. H. Brody and C. A. Winkler. Unpublished results. H. Brody. M.Sc. Thesis, McGill University. 1955.
17. P. A. Gartaganis and C. A. Winkler. Can. J. Chem. **34**, 1457 (1956).
18. J. T. Herron. J. Chem. Phys. **33**, 1273 (1960).
19. R. J. Cvetanović. J. Chem. Phys. **23**, 1375 (1955); Can. J. Chem. **33**, 1684 (1955).
20. A. N. Wright and C. A. Winkler. J. Phys. Chem. **66**, 1747 (1962).
21. K. J. Laidler. The chemical kinetics of excited states. Oxford. 1955.
22. W. Forst, H. G. V. Evans, and C. A. Winkler. J. Phys. Chem. **61**, 320 (1957).

Can. J. Chem. Downloaded from www.nrcresearchpress.com by 210.87.254.40 on 09/05/12
For personal use only.

Can. J. Chem. Downloaded from www.nrcresearchpress.com by 210.87.254.40 on 09/05/12
For personal use only.

HALOGEN ATOM REACTIONS

III. LUMINESCENCE FROM THE RECOMBINATION OF BROMINE ATOMS[1]

D. B. GIBBS AND E. A. OGRYZLO

Department of Chemistry, University of British Columbia, Vancouver, British Columbia

Received January 26, 1965

ABSTRACT

The recombination of bromine atoms has been found to result in the emission of an orange–red glow. Analysis of the banded spectrum has resulted in the identification of the transition responsible for the visible emission as $Br_2(^3\Pi_{0u}^+ \rightarrow {}^1\Sigma_{0g}^+)$. The results of a kinetic study of the glow indicate that the emission is second order in [Br] and first order in [Br_2]. Several detailed preassociation mechanisms for the reaction are discussed.

INTRODUCTION

Light emission from electronically excited states formed by the recombination of radicals is potentially an important source of information about the details of the "reactive collision process". For example, an important unanswered question for association reactions is the role of repulsive and weakly bound states. When luminescence from such states can be studied kinetically their role in the total process can be assessed. Because of the interest in reactions which are relevant to the upper atmosphere, chemiluminescence from reactions involving nitrogen and oxygen atoms has received a great deal of attention, but the mode of participation of electronically excited states in the total recombination process is still not clear (1).

Halogen atoms have received much less attention. The continuous "glow-spectrum" obtained by heating the halogens in a quartz container to temperatures in excess of 600 °C has been attributed to the two body recombination of atoms by Kondratjew and Leipunsky (2). A similar "continuous" emission from bromine dissociated in a shock tube has been reported by Palmer (3), for which he also proposed a two body recombination mechanism which can be written

$$Br(^2P_{3/2}) + Br(^2P_{1/2}) \rightleftarrows Br_2(^3\Pi_{0u}^+) \rightarrow Br_2(^1\Sigma_g^+) + h\nu$$

$$Br(^2P_{3/2}) + Br(^2P_{3/2}) \rightleftharpoons \left\{\begin{matrix} Br_2(^1\Pi_{1u}) \\ Br_2(^3\Pi_{1u}) \end{matrix}\right\} \rightarrow Br_2(^1\Sigma_g^+) + h\nu.$$

The discrete "glow-spectrum" of bromine which is obtained when the gas is at low pressures was studied by Uchida (4). The emission was found to originate from between the 4th and 12th vibrational levels of the $^3\Pi_{0u}^+$ state. The system was complicated by the fact that the walls were involved in the production of the excited molecules, and the order of the reaction with respect to bromine atoms could not be directly determined. In view of the many assumptions that Ochida was forced to make, it is doubtful if much significance should be attributed to his conclusion that the emission appears to be 4th order in the atom concentration.

In Part I (5) of this series it was shown that large concentrations of chlorine and bromine atoms could be formed with an electrical discharge in a flow system. A kinetic and spectroscopic study of the light emission accompanying the recombination of chlorine atoms was described in Part II (6). This paper described a similar study for bromine atoms.

[1]*The study was supported by the Air Force Office of Scientific Research Grant No. 158-63 and by the National Research Council of Canada.*

Can. J. Chem. Downloaded from www.nrcresearchpress.com by 210.87.254.40 on 09/05/12
For personal use only.

EXPERIMENTAL

The apparatus used for the kinetic experiments was essentially that described in Part I (5). For the spectroscopic study an optical window was inserted at the end of the reaction tube and the slit of the spectrograph placed against it. Aluminium foil was wrapped around the tube to increase the light gathered by the spectrograph. The reaction tube and gas stream were at room temperature for all experiments.

A 2 450 mc microwave discharge was used to dissociate the bromine. The pyrex walls of the discharge tube and reaction tube were coated with orthophosphoric acid. Bromine was dried with silica gel and purified by trap-to-trap distillation. The atom concentration was measured with a movable nickel wire calorimeter described previously (4). The relative emission intensity along the reaction tube was measured by photographing it with a Konica 35 mm camera with an $f/3.5$, 135 mm focal length lens. Each film was independently calibrated to relate optical density to light intensity by using a number of exposure times. Kodak high speed infrared film was used because the emission was found to peak in the infrared.

The high speed spectrophotometer was constructed from an $f/4.5$ Hilger-Watts model D285 glass prism spectrometer, an R.C.A. 7102 photomultiplier, and a 27.5 c.p.s. a-c. amplifier. For greater resolution an $f/6.3$ Jarell-Ash model 75—000 plane grating spectrograph blazed at 7 500 Å was used with Kodak 1N plates.

RESULTS

Under the usual flow-system operating conditions (p = 1 mm Hg, flow = 25 μmoles/s) a weak orange-red glow can be seen coming from the discharge products for a distance of about 1 m along the gas stream. The spectrum obtained with a low dispersion spectrophotometer is shown in Fig. 1. Comparison with the spectral response of the tube (dotted curve) indicates that the maximum in the emission intensity occurs beyond 10 000 Å under these conditions.

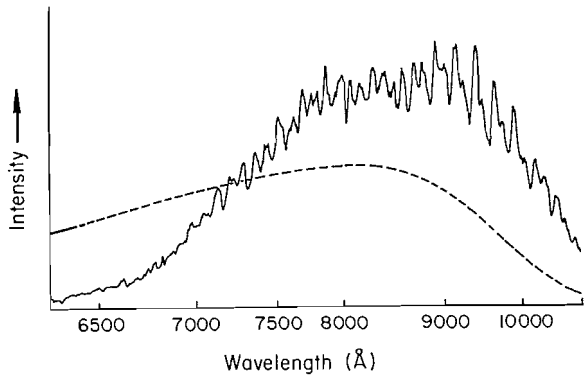

FIG. 1. Spectrum of red glow obtained with an $f/4.5$ low dispersion glass prism spectrometer and an RCA-7102 photomultiplier. Slit = 100 μ. Dotted line gives the spectral response of the photomultiplier.

Figure 2 shows the effect of pressure on the spectral distribution. A wide slit was used to remove the fine structure. It will be observed that there is a decrease in the higher energy emission intensity (relative to that at about 9 000 Å) with increasing pressure.

The spectrum was also taken on a grating spectrograph with a dispersion of 20 Å/mm. Because of the low intensity of the emission the slit width could not be decreased sufficiently to bring out the rotational structure. However, bands belonging to the system $B^3\Pi^+_{0u}$–$X^1\Sigma^+_g$ could easily be picked out. The following series were recorded between 6 200 Å and 8 300 Å:

$B^3\Pi^+_{0u}$	$X^1\Sigma^+_g$
$v' = 0$	$v'' = 5$ to $v'' = 12$
$v' = 1$	$v'' = 5$ to $v'' = 13$
$v' = 2$	$v'' = 6$ to $v'' = 12$
$v' = 3$	$v'' = 9$ to $v'' = 13$

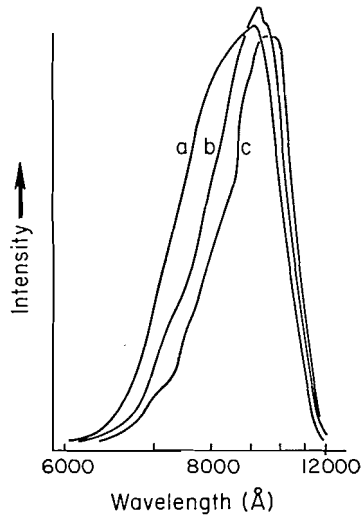

FIG. 2. Spectral distribution of the red glow obtained at three different pressures. (*a*) $P \sim 0.5$ mm Hg, (*b*) $P \sim 2$ mm Hg, (*c*) $P \sim 2.5$ mm Hg. Slit = 700 μ.

No transitions were observed involving v' greater than 3. In addition to these bands others were noted that could not belong to this system. No identification of this new system was possible because of the considerable overlap with the ${}^3\Pi_{0u}^+ - {}'\Sigma_g^+$ system. Though the new system of bands begins further into the red, bands at 7 600 Å, 7 800 Å, and 8 000 Å are quite strong. A complete analysis of this system may be possible if measurements can be extended further into the red.

The dependence of the emission intensity on the atom concentration was determined by assuming a relation of the form

$$I = k[\mathrm{Br}]^n[\mathrm{Br}_2]^m. \qquad [1]$$

At some constant pressure $[Br_2]$ = constant and eq. [1] can be written

$$\log I = n \log [\mathrm{Br}] + \text{constant}. \qquad [2]$$

A plot of log I against log [Br] in a typical experiment is shown in Fig. 3. The slope of the line is equal to 1.9 ± 0.2 which gives the order of the reaction with respect to [Br].

The order with respect to $[Br_2]$ was obtained by observing the change in light emission with the change in pressure at points in the reaction tube where [Br] is the same. Under these circumstances eq. [1] can be written:

$$m = \frac{\log (I'/I'')}{\log ([\mathrm{Br}_2]'/[\mathrm{Br}_2]'')}.$$

A typical change in conditions gave

$$\frac{[\mathrm{Br}_2]'}{[\mathrm{Br}_2]''} = \frac{0.6 \text{ mm Hg}}{1.0 \text{ mm Hg}} = 0.6$$

which resulted in a change in emission intensity (at a point where [Br]′ = [Br]″) given by

$$\frac{I'}{I''} = \frac{2.03}{2.97} = 0.68$$

$$m = 0.8 \pm 0.2.$$

Can. J. Chem. Downloaded from www.nrcresearchpress.com by 210.87.254.40 on 09/05/12
For personal use only.

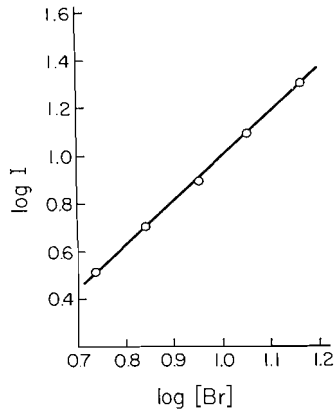

FIG. 3. A typical plot of the log of the emission intensity against the log of the bromine atom concentration (in arbitrary units). Slope ≈ 2 gives the order of the reaction with respect to bromine atoms.

The shift of the peak intensity into the infrared with increasing pressure illustrated in Fig. 2 would have the effect of making the apparent $[Br_2]$ dependence smaller than the actual value (i.e. that obtained if the entire emission were observed). A rigorously quantitative correction cannot be made until the complete spectral distribution is obtained. However, a 20% drop in intensity in the region from 7 000 Å to 9 000 Å seems quite reasonable from Fig. 2. We therefore conclude that the results indicate a first order dependence on $[Br_2]$, and that the following kinetic expression can be written for the light-emitting recombination reaction:

$$I = k[Br]^2[Br_2].$$

DISCUSSION

Some relevant potential energy curves for bromine are shown in Fig. 4. The solid curves have been spectroscopically observed and the dotted portions are drawn according to the suggestions of Rees (7) and Mulliken (8). The most significant fact is that the $^3\Pi_{0u}^+$ state does not correlate with ground state atoms.

It is possible that excited atoms form in the discharge, and direct recombination into $Br_2(^3\Pi_{0u}^+)$ could occur via the reaction:

$$Br(^2P_{1/2}) + Br(^2P_{3/2}) + Br_2 \rightarrow Br_2(^3\Pi_{0u}^+) + Br_2.$$

However, it would seem too fortuitous if the metastable $Br(^2P_{1/2})$ atoms decayed at the same rate as $Br(^2P_{3/2})$ atoms by wall and gas phase recombination to give the second order dependence on [Br] that is observed experimentally. Furthermore, if this were the mode of formation of $Br_2(^3\Pi_{0u}^+)$, emission would be expected from levels above $v' = 3$, since it is observed for chlorine (6) which has a much longer radiative lifetime. From the integrated absorption coefficient it can be established that the radiative lifetime of $^3\Pi_{0u}^+$ is shorter than 10^{-4} s. The possibility that the excited molecules themselves originate in the discharge can therefore be ruled out. It would seem more reasonable to seek an explanation which involves a collision along a potential curve which correlates with ground state atoms. There are at least two curves which might lend themselves to such a process: the $^1\Pi_{1u}$ and the $^3\Pi_{0u}^-$.

Darbyshire (9) has observed that when the rotational constant (B) for the $^3\Pi_{0u}^+$ state is plotted against the vibrational level (v') a change in slope can be seen between $v' = 3$

Can. J. Chem. Downloaded from www.nrcresearchpress.com by 210.87.254.40 on 09/05/12
For personal use only.

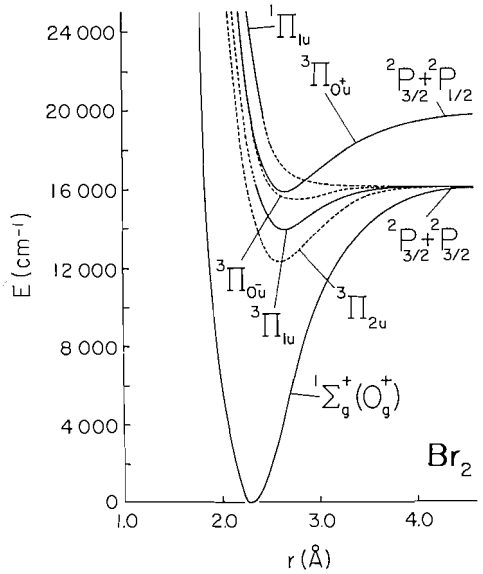

FIG. 4. Potential energy diagram for Br_2. Solid lines give spectroscopically observed states. Dotted lines give extrapolated or estimated states.

and 4. Bayliss and Rees (10) suggested that this perturbation may be due to a crossing of the $^3\Pi_{0u}^+$ curve by the $^1\Pi_{1u}$ curve as shown in Fig. 4. However, there is some evidence (11, 12, 13), that magnetic and collisional predissociation of the $^3\Pi_{0u}^+$ state in the halogens is due to the close proximity of a 0_u^- state. Rees (14) has suggested that this could be the repulsive $^1\Sigma_{0u}^-$ state which would have to intersect the right hand side of the $^3\Pi_{0u}^+$ curve. On the other hand the predissociating state could be the $^3\Pi_{0u}^-$ as suggested by Van Vleck (12) and Zener (13). Mulliken (8) has indicated that this state should lie very close to the $^3\Pi_{0u}^+$ at small internuclear distances as shown in Fig. 4. A consequence of this latter interpretation is that predissociation should occur over a large portion of the $^3\Pi_{0u}^+$ curve. The recent work of Brown and Klemperer (15) seems to indicate just such a situation. Several mechanisms therefore need to be considered.

Mechanism 1

[11] and [12] $$Br(^2P_{3/2}) + Br(^2P_{3/2}) \underset{k_{12}}{\overset{k_{11}}{\rightleftharpoons}} Br_2(^3\Pi_{0u}^- \text{ or } ^1\Pi_{1u})$$

[13] $$Br_2(^3\Pi_{0u}^- \text{ or } ^1\Pi_{1u}) + Br_2 \xrightarrow{k_{13}} Br_2(^3\Pi_{0u}^+) + Br_2$$

[14] $$Br_2(^3\Pi_{0u}^+) \xrightarrow{k_{14}} Br_2 + h\nu$$

[15] $$I = (k_{11}/k_{12})k_{13}[Br]^2[Br_2]$$

This mechanism assumes that a collision between two ground state atoms occurs along the $^3\Pi_{0u}^+$ or the $^1\Pi_{1u}$ curve. The inhomogeneous electric field of a colliding Br_2 molecule is then assumed to induce an intersystem crossing to the $^3\Pi_{0u}^+$ state. The correct kinetic order can be obtained (see eq. [15]) by assuming an equilibrium concentration of $Br_2(^3\Pi_{0u}^-)$ determined by reaction [11] and [12], and a steady state concentration of $Br_2(^3\Pi_{cu}^+)$. The mechanism can then account for all the experimental observations including the fact that emission is observed only from levels below $v' = 4$. The shift of the emission maximum

Can. J. Chem. Downloaded from www.nrcresearchpress.com by 210.87.254.40 on 09/05/12
For personal use only.

to longer wavelength shown in Fig. 2 is consistent with more rapid vibrational relaxation to lower levels of the $^3\Pi_{0u}^+$ state as the pressure is increased. From Fig. 4 it can be seen that such a shift to lower energy emission is consistent with the Franck-Condon principle.

Mechanism 2

Since the $^3\Pi_{0u}^-$ state is probably a weakly bound state, it is possible that direct recombination into that state occurs through a termolecular collision. Transitions to the emitting $^3\Pi_{0u}^+$ state could then conceivably require an additional collision. If the mechanism is written as follows,

[21] and [22] $$Br(^2P_{3/2}) + Br(^2P_{3/2}) + Br_2 \underset{k_{22}}{\overset{k_{21}}{\rightleftharpoons}} Br_2(^3\Pi_{0u}^-) + Br_2$$

[23] and [24] $$Br_2(^3\Pi_{0u}^-) + Br_2 \underset{k_{24}}{\overset{k_{23}}{\rightleftharpoons}} Br_2(^3\Pi_{0u}^+) + Br_2$$

[25] $$Br_2(^3\Pi_{0u}^+) \overset{k_{25}}{\rightarrow} Br_2 + h\nu,$$

the correct kinetic order could still result if the relative rates of the reactions are:

(*a*) [21], [22], and [25] $\gg$ [23] $\gg$ [24]

whence $$I = \frac{k_{21}}{k_{22}} k_{23}[Br_{3/2}]^2[Br_2],$$

(*b*) if reaction [21] is rate controlling

whence $$I = k_{21}[Br_{3/2}][B^2r_2].$$

Mechanism 3

There is increasing evidence that the recombination of halogen atoms occurs through the loosely bound intermediates I_3, Br_3, Cl_3 in the absence of added gases (16, 17). If these species exist in appreciable concentrations in atom-containing systems then the following series of reactions could lead to light emission with the correct kinetic dependence (eq. [35]):

[31] and [32] $$Br(^2P_{3/2}) + Br_2(+ Br_2) \underset{k_{32}}{\overset{k_{31}}{\rightleftharpoons}} Br_3(+ Br_2)$$

[33] $$Br_3 + Br(^2P_{3/2}) \overset{k_{33}}{\rightarrow} Br_2(^3\Pi_{0u}^+) + Br_2$$

[34] $$Br_2(^3\Pi_{0u}^+) \rightarrow Br_2 + h\nu$$

[35] $$I = \frac{k_{31}}{k_{32}} k_{33}[Br]^2[Br_2]$$

The symmetry requirements that prevent the direct formation of $Br_2(^3\Pi_{0u}^+)$ from ground state atoms probably do not apply to metathetical reactions such as [33], in which spin and orbital angular momentum are easily conserved.

Mechanism 3 is attractive because it is applicable to a large number of other preassociation reactions such as Cl—Cl, N—N, N—O, S—O, and S—S where preassociation has also been observed very near the dissociation limit. It is quite likely that a more detailed study of each of these reactions, which includes a determination of the temperature dependence of the emission, will allow a decision between the three mechanisms we have proposed.

Can. J. Chem. Downloaded from www.nrcresearchpress.com by 210.87.254.40 on 09/05/12
For personal use only.

REFERENCES

1. R. A. YOUNG and R. L. SHARPLESS. J. Chem. Phys. **39**, 1071 (1963).
2. V. KONDRATJEW and A. LEIPUNSKY. Z. Physik, **50**, 366 (1928).
3. H. B. PALMER. J. Chem. Phys. **26**, 648 (1957).
4. Y. UCHIDA. Sci. Papers Inst. Phys. Chem. Research Tokyo, **30**, 71 (1936).
5. E. A. OGRYZLO. Can. J. Chem. **39**, 2556 (1961).
6. L. W. BADER and E. A. OGRYZLO. J. Chem. Phys. **41**, 2926 (1964).
7. A. L. G. REES. Proc. Phys. Soc. London, **59**, 1008 (1947).
8. R. S. MULLIKEN. Phys. Rev. **46**, 529 (1934); **57**, 500 (1940).
9. O. DARBYSHIRE. Proc. Roy. Soc. London, Ser. A, **159**, 93 (1937).
10. N. S. BAYLISS and A. L. G. REES. J. Chem. Phys. **7**, 854 (1939).
11. L. A. TURNER. Phys. Rev. **38**, 574 (1931).
12. J. H. VAN VLECK. Phys. Rev. **40**, 544 (1932).
13. C. ZENER. Proc. Roy. Soc. London, **140**, 660 (1933).
14. L. MATHIESON and A. L. G. REES. J. Chem. Phys. **23**, 753 (1956).
15. R. L. BROWN and W. KLEMPERER. J. Chem. Phys. **41**, 3072 (1964).
16. G. PORTER. Discussions Faraday Soc. **33**, 198 (1962).
17. E. A. OGRYZLO. Unpublished results.

Can. J. Chem. Downloaded from www.nrcresearchpress.com by 210.87.254.40 on 09/05/12
For personal use only.

Can. J. Chem. Downloaded from www.nrcresearchpress.com by 210.87.254.6 on 09/05/12
For personal use only.

AN ADIABATIC SOLUTION CALORIMETER USED FOR MEASURING THE MOLAR EXCESS ENTHALPY OF THE SYSTEM CARBON TETRACHLORIDE – BENZENE AT 25 °C[1]

J. E. BENNETT[2] AND G. C. BENSON
Division of Pure Chemistry, National Research Council, Ottawa, Canada

Received February 15, 1965

ABSTRACT

A new adiabatic calorimeter for measuring heats of mixing is described. The design of the mixing cell avoids the presence of a vapor space, and accommodates changes in volume by means of a flexible diaphragm. The apparatus is equipped with automatic adiabatic control and produces a continuous record of the temperature of the mixing cell. An extensive series of measurements was carried out for the system carbon tetrachloride – benzene at 25 °C. The maximum value of the molar excess enthalpy, 113.4 ± 0.5 J mole^{-1}, occurred at a mole fraction of carbon tetrachloride equal to 0.4907. For most of the concentration range, the results are from 1 to 2 J mole^{-1} lower than data reported recently by other investigators.

INTRODUCTION

Criteria governing the choice of a suitable pair of liquids for use in testing a new calorimeter have been discussed by McGlashan (1). He tentatively recommended the pair carbon tetrachloride – benzene for this purpose. However, values reported for the excess enthalpy at 25 °C by various authors (2–7) did not agree well; thus, for example, results for an equimolar mixture were scattered over a range of nearly 10%. Larkin and McGlashan (8) reinvestigated the system using a new calorimeter capable of much higher precision than before. Their results were systematically higher than most previous measurements and were, in fact, 4 J mole^{-1} higher for an equimolar mixture than they had expected on the basis of the earlier data. They suggested that the discrepancies arose from incomplete mixing which occurred to varying degrees in all the previous calorimeters.

More recently Lundberg (9) has also studied the carbon tetrachloride – benzene system and obtained results which are generally lower than those of Larkin and McGlashan for x, the mole fraction of carbon tetrachloride, less than 0.7 and greater for higher x-values. At the equimolar concentration the difference amounts to about 1.7 J mole^{-1} (i.e. 1.5%) and exceeds somewhat the combined estimates of the accuracies of the two calorimeters (about 1.3 J mole^{-1}).

It is clear that further careful studies of the heat of mixing of carbon tetrachloride with benzene are needed before this system can be adopted as a standard for testing calorimeters. The present investigation was undertaken to provide new independent data.

EXPERIMENTAL

The measurements were carried out in a new adiabatic calorimeter. Briefly, this apparatus consists of a stainless steel mixing cell suspended by nylon loops within a thin gold-plated copper shield. The latter is mounted on, but thermally insulated from, a framework inside an evacuated brass can immersed in an oil thermostat.

Since the calorimeter was constructed by modifying an adiabatic solution calorimeter, already described in the literature (10), the outline below is limited mainly to the changes which have been made in the previous equipment. These comprise improved instrumentation, making operation of the calorimeter more automatic, and a new vessel which is more suitable for studying small heat effects associated with the mixing of organic liquids. Reference should be made to the earlier publication (10) for details of those features of the calorimeter which remain unchanged (e.g., the adiabatic shield and can assembly).

[1]*Issued as N.R.C. No. 8434.*
[2]*National Research Council of Canada Postdoctorate Fellow 1961–1963. Present address: Imperial Chemical Industries, Agricultural Division, Billingham, England.*

(i) Automatic Adiabatic Control

The copper shield consists of two cylindrical and two conical sections bolted together, each wound with a manganin wire heater. Four 4-junction copper–constantan thermocouples are used to detect temperature differences between the parts of the shield and between the shield and the mixing cell. The oil thermostat, which is usually maintained at a temperature about 1.5 deg lower than the shield, acts as a heat sink. Heat flow between the shield and the cell is minimized by suitable adjustment of the current through the four shield heaters according to the indications of the four-difference couples. To achieve automatic control, the output of the couple between the shield and the vessel is amplified by a d-c. microvolt amplifier (Leeds and Northrup No. 9835B) and fed to a Speedomax G recorder-controller. Maximum amplification is used and full scale deflection of the recorder corresponds to a temperature difference of 0.3 °C. Deflection of the recorder auxiliary slide wire from zero actuates a Leeds and Northrup Series 60 three-action C.A.T. control unit which provides an output current of from 0 to 5 mA depending on the recorder imbalance and the control-unit settings. The output from the C.A.T. unit regulates the voltage supplied to the shield heaters by a stabilized transistorized d-c. power unit. The power to the four heaters is apportioned by individual rheostats which were adjusted once to equalize the temperatures of the four shield sections and then locked at that setting.

(ii) Cell Temperature Measurement

The temperature of the mixing cell relative to that of a water triple-point cell, external to the calorimeter assembly, is measured by a 12-junction copper–constantan thermocouple. The electromotive force (e.m.f.) of the thermocouple is balanced to the nearest microvolt on a Wenner Potentiometer (Leeds and Northrup No. 7559) and the fractional residue, amplified by a Liston-Becker DC Breaker Amplifier (Model 14) which has been modified to include feedback (11), is displayed on a second Speedomax G recorder. At the amplification normally used, a full scale deflection on the recorder corresponds to 10 μV; an e.m.f. of 0.1 μV (i.e. a temperature difference of 0.0002 °C) is easily measurable.

The coupling between the thermocouple circuit and the shield heaters is fairly high since all the leads to the calorimeter pass through a flexible metal vacuum tube for a distance of about 3 ft (from outside the oil bath to the can inside). To reduce the noise level on the recorder trace of the main thermocouple e.m.f. to an acceptable level it was found necessary to use direct current for the shield heaters.

(iii) The Mixing Cell

The new mixing cell, shown diagrammatically in Fig. 1, is basically similar to a cell used by Brown and Fock (12), but differs in details of the design. It is constructed mainly from stainless steel and consists of two cylindrical parts (A and B) held together by a ring nut (C) which clamps a 0.0005 in. aluminium foil diaphragm (D) between two machined Teflon gaskets (E and F). Part A is closed by a conical end (G) also

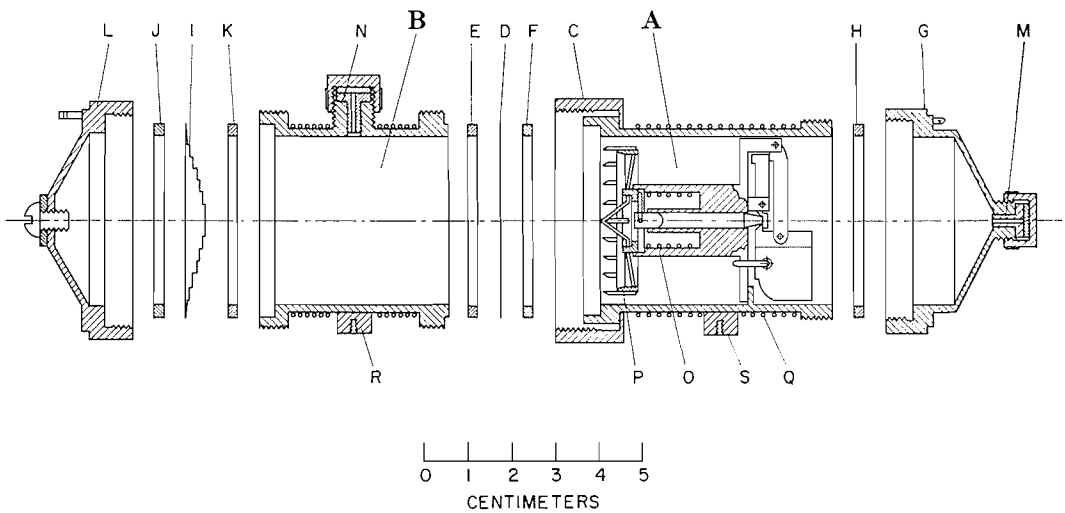

FIG. 1. Exploded sectional diagram of mixing cell.

sealed with a Teflon gasket (H). A flexible corrugated diaphragm (I), pressed from 0.003 in. beryllium–copper alloy and held in place by a pair of gaskets (J and K) and screw-end (L) complete part B. The compartments separated by the aluminium foil are filled through ports (M and N), one in end G and the other in the side of B. The walls of B are dished slightly to facilitate the escape of bubbles through the port. In use, both compartments are filled as completely as possible with the liquids to be mixed and the ports are closed by

Can. J. Chem. Downloaded from www.nrcresearchpress.com by 210.87.254.6 on 09/05/12
For personal use only.

tightly fitting nylon plugs and screw caps. A strong coiled spring device (O), housed in part A, is released by gravity when the cell is rotated vertically through 180° and drives a spiked circular cutting frame (P) through the foil separator. Changes in volume which accompany the mixing are taken up by the diaphragm I; the maximum change which can be accommodated in this way is about 1.3 cm^3. A glass-fiber-insulated manganin wire heater (Q) is wound in the outside of the cell and thermocouple junctions can be screwed on to copper lugs (R and S) soldered to parts A and B. Various mixing ratios are obtained by employing several parts B of different size.

(iv) Some Operational Details

The calorimeter, with cell loaded, is left overnight in the oil thermostat (at 25 °C) to reach thermal equilibrium. About an hour before the measurements are to be started, the oil bath temperature is reduced by 1.5 deg and the C.A.T. control system is switched on to maintain the shields and the cell at the original bath temperature. When the oil bath has settled at its new control setting and the cell temperature is steady (as evidenced by the recorder trace of the main thermocouple e.m.f.), the liquids are mixed by rotating the calorimeter through 180°. Ten seconds after initiating an endothermic mixing process (as in the case of the carbon tetrachloride – benzene system) the current through a dummy resistor, similar to the cell heater, is diverted through the heater, and an amount of electrical energy very nearly balancing the expected heat of mixing is dissipated in the heater. The 10 s delay in switching the current was found to improve the C.A.T. control characteristics greatly during the mixing period. The heater voltage can range from 2 to 12 V and is chosen so that current is passed through the cell heater for about 5 min. During this period, readings of the voltage difference across the terminals of the heater and across those of a standard resistor in series with the heater are taken on a White Double Potentiometer. The calorimeter is rotated backwards and forwards 25 times during the mixing period which lasts about 20 min; after this time the cell temperature is again steady and is followed for a further 10 min. The effect of tipping is then determined by tipping the calorimeter assembly 100 times and measuring the increase in the thermocouple e.m.f. between the steady fore- and after-periods. This is usually repeated once or twice and an average is adopted. In order to allow for inexact compensation of the heat of mixing, the calorimeter is calibrated by carrying out two or three further heating periods. The heat dissipated in each of these is about 8 J; agreement between two calibrations is better than 1.5%. The heat effect associated with breaking the aluminium foil was determined in a series of separate experiments. It is exothermic and amounts to 0.18 J.

During the calibration periods and the determination of the heat of tipping, the control system keeps the temperature difference between the cell and its surroundings quite small and heat exchange is negligible. The mixing process, however, usually involves an initial rapid change in temperature and, in a measurement of a large heat of mixing, the difference between the cell and shield may be as large as 0.1 °C for a brief period. In these cases a correction is applied for the heat exchange; this is based on estimates of the net area under the recorder trace from the controller and of the cooling constant for the calorimetric system.

The heat of mixing was usually determined at a temperature differing from 25 °C by less than 0.05 °C. All results were corrected to 25.00 °C using the temperature coefficient given in ref. 8. The largest correction required was 0.25 J $mole^{-1}$ (for a temperature difference of 0.2 °C).

In a typical experiment involving about 1.317 moles of material at a mole fraction of carbon tetrachloride equal to 0.4052, the observed heat of mixing was 143.9 J. About 150.6 J were dissipated in the cell heater, of which 6.7 J gave a net rise in the cell temperature equivalent to 7.6 μV (about 0.016 °C). The energy gained by the cell as a result of exchange with the shield during the mixing period was estimated to be about 0.5 J. The temperature increases due to two lots of 100 tips were 0.54 and 0.48 μV respectively. Two determinations of the heat capacity of the system were 0.4% apart and gave a calibration factor of the order of 0.88 J μV^{-1}.

Mixtures with a final mole fraction of carbon tetrachloride from 0.3 to 0.7 were obtained directly from the pure liquids. Others outside this concentration range were made with one side of the cell filled with a mixture for which the heat of mixing was already established. The compositions were determined from weighings of the cell and components during the loading process. Weighings were made to 1 mg and all weights were corrected to *vacuo*. The total amount of material used for a measurement varied from 1.1 to 1.5 moles. At the equimolar concentration there were about 110 g of carbon tetrachloride and 54 g of benzene in the cell.

(v) Consideration of Errors

The equipment used for the electrical energy measurement is the same as that described by Benson and Benson (13). The accuracy of determination is limited primarily by the accuracy of measuring the time interval. In the present work, a 5 min period can be measured to about 0.05 s (i.e. 0.02%).

A reasonable estimate of the error in determining changes in the e.m.f. of the main thermocouple is 0.15 μV. This corresponds, for the amounts of material used, to an error of 0.1 J $mole^{-1}$. The largest energy exchange, which occurred between cell and shield during the mixing, lead to a correction of only 0.6 J $mole^{-1}$. It is believed that this correction could be estimated to better than 30%.

We feel quite certain that mixing was complete in the experiments reported in this paper. After rupture of the foil, there were pieces of the breaking mechanism loose in the cell, which acted as stirrers when the cell was rotated. The heat of tipping, measured immediately after the mixing period, was small (about 0.5 J for 100 tips) and exothermic. Repeat determinations of the heat of tipping always agreed to better than 20%.

Can. J. Chem. Downloaded from www.nrcresearchpress.com by 210.87.254.6 on 09/05/12
For personal use only.

Although the presence of a vapor space in the cell cannot be detected readily, every precaution was taken, both in the design and loading procedure, to ensure the absence of such a space. However errors arising from a vapor space (1) would be small in the present instance, due to the large quantities of material in the cell and the similarity of the vapor pressures of benzene and carbon tetrachloride as well as to the ability of the diaphragm to accommodate the increase in volume on mixing.

(vi) Materials

The carbon tetrachloride used for most of the measurements was Analytical Reagent (Mallinkrodt Chemical Works) which had been fractionally distilled 3 times; potassium hydroxide pellets were added prior to the third distillation. The density and refractive index of the final product were $d^{25} = 1.5842_5$ g cm^{-3} and $\mu_D^{25} = 1.4575$.

Reagent Grade benzene (Nichols Chemical Company) was treated with concentrated sulfuric acid, washed until neutral, and fractionally distilled 3 times after refluxing with sodium wire. The values of the density and refractive index were $d^{25} = 0.8734_5$ g cm^{-3} and $\mu_D^{25} = 1.4979$.

In addition to the above materials, some measurements were also made using Chromatoquality Reagent carbon tetrachloride (Matheson, Coleman and Bell) and Research Reagent benzene (Phillips Petroleum Company). No significant difference was detected in the results obtained with these materials.

RESULTS AND DISCUSSION

The experimental results for the mixing of carbon tetrachloride and benzene at 25 °C are summarized in Table I. This gives h^e, the molar excess enthalpy in J mole^{-1}, for various values of x, the mole fraction of carbon tetrachloride. In the previous investigations by Larkin and McGlashan (8) and by Lundberg (9), data for $h^e/x(1 - x)$ were fitted with polynomials in $(1 - 2x)$. A least square treatment of our results leads to the form

$$[1] \qquad h^e = x(1 - x)[453.5 + 15.7(1 - 2x) + 29.8(1 - 2x)^2].$$

Deviations, δ, between the experimental values and those calculated from eq. [1] are included in Table I. The root mean square value of δ is 0.5_2 J mole^{-1}, which is somewhat larger than might be expected from the above consideration of errors (i.e. about 0.3 J mole^{-1}). The values of δ show a tendency to vary systematically with x and it appears that eq. [1] gives a slightly broader and flatter curve than observed experimentally. Adding terms with higher powers of $(1 - 2x)$ did not improve the fit significantly. Alternative forms in which the mole fraction was replaced by the volume fraction, or in which $x(1 - x)/h^e$ was fitted by a polynomial in $(1 - 2x)$, were also tried, but neither of these led to a better representation of the data.

TABLE I

Experimental results for the molar excess enthalpy of carbon tetrachloride – benzene solutions at 25.00 °C

x*	h^e (J mole^{-1})	δ† (J mole^{-1})	x*	h^e (J mole^{-1})	δ† (J mole^{-1})
0.0716	32.6	0.1	0.4880	114.0	0.6
0.1417	58.3	−0.1	0.5099	113.6	0.4
0.1934	74.1	0.1	0.5136	113.7	0.5
0.2618	90.1	−0.3	0.5572	111.1	−0.5
0.3545	104.6	−0.8	0.5579	111.8	0.3
0.3553	104.7	−0.8	0.6051	107.0	−0.9
0.4052	109.8	−0.4	0.6080	107.1	−0.5
0.4486	113.5	0.9	0.6598	100.6	−0.8
0.4490	113.5	0.8	0.7241	90.5	0.1
0.4499	113.2	0.5	0.7793	78.2	0.1
0.4504	112.8	0.1	0.8415	60.9	0.0
0.4532	113.5	0.7	0.9338	28.7	0.1

*x = mole fraction of carbon tetrachloride.
†$\delta = h^e$(obs.) − h^e(calcd. from eq. [1]).

Can. J. Chem. Downloaded from www.nrcresearchpress.com by 210.87.254.6 on 09/05/12
For personal use only.

Can. J. Chem. Downloaded from www.nrcresearchpress.com by 210.87.254.6 on 09/05/12
For personal use only.

Equation [1] was adopted as a basis for comparing our results with those of other workers. The points plotted in Fig. 2 show the deviations of the experimental data from the values calculated with eq. [1]. Lundberg's results (9) are available only as an equation and the deviations of his data are represented as a dashed curve. In general, our results are much higher than the older data in the literature and in this sense confirm more recent findings (8, 9). According to eq. [1] the maximum value of h^e, 113.4 ± 0.5 J mole^{-1}, occurs at $x = 0.4907$. The standard deviations between eq. [1] and the forms given by Larkin and McGlashan (8) and by Lundberg (9) are 1.6 and 0.8 J mole^{-1} respectively. For comparison the standard deviation between these two other sets of data is 1.3 J mole^{-1}. It appears that our results agree fairly well with those of Lundberg over the lower half of the concentration scale. For larger x-values Lundberg's data are systematically higher; the maximum deviation (1.5 J mole^{-1}) occurs near $x = 0.85$. Over the central concentration range $0.25 < x < 0.75$ our results are about 2 J mole^{-1} lower than those in ref. 8. The latter difference is much larger than the combined experimental errors of the two investigations. Leakage around the gaskets of the central diaphragm in our cell would, of course, lead to premixing and the subsequent observation of smaller heat effects. In tests where a soluble dye was placed in the liquid on one side of the diaphragm, no evidence of leakage was detected over periods of several days.

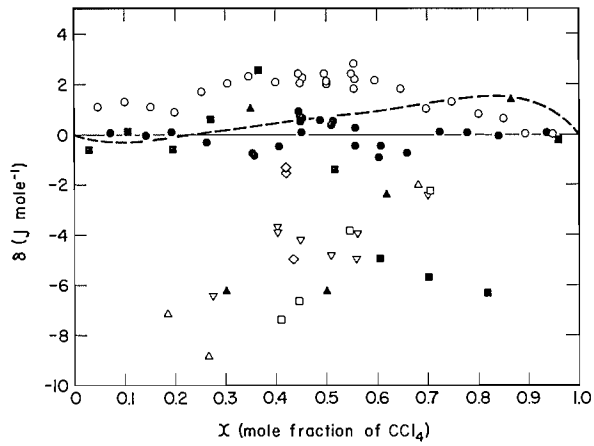

FIG. 2. Plot of the deviation $\delta = h^e$(obs.) − h^e(calcd. from eq. [1]) against the mole fraction of carbon tetrachloride. All data for 25 °C. ● This research; ▲ Hirobe (2); ■ Schulze (3); ▽ Cheesman and Whitaker (4) corrected to 25° as in ref. 8; △ Brown, Mathieson, and Thynne (5); ◇ Brown and Fock (6); □ Goates, Sullivan, and Ott (7); ○ Larkin and McGlashan (8); - - Lundberg (9).

It has been pointed out that in some instances the heat of mixing of liquids may be affected by the presence of dissolved gases (1). In our work the components were loaded into the cell with pipettes and syringes; exposure to water vapor was avoided but in most cases, the liquids must have been saturated with air. However, in several experiments, an effort was made to decrease the dissolved gas content by "boiling" the components under reduced pressure just prior to the filling, and then transferring them to the cell as quickly as possible and with a minimum of turbulence. No significant difference was observed in results obtained with these partially degassed solvents.

Larkin and McGlashan noted that a few measurements made with a sample of certified high purity benzene gave higher results than those obtained with material of their own

purification. Lundberg suggested that the presence of trace impurities might account for the difference between his results and those of Larkin and McGlashan. In our work, some initial measurements were made with materials of about 99% purity; these gave heats of mixing 5 to 6 J $mole^{-1}$ lower than those reported in Table I. If, indeed, the discrepancies between the various investigations of the carbon tetrachloride – benzene system must be attributed to trace impurities which are not readily removed by normal purification procedures, the suitability of this system as a calorimetric standard seems questionable.

NOTE ADDED IN PROOF: Since this paper was written we have learned of another investigation of the carbon tetrachloride – benzene system by Van Ness and co-workers at Rensselaer Polytechnic Institute. The precision of the results appears to be very good and the values are in closer agreement with Lundberg's curve than the values reported above. We are indebted to Professor H. C. Van Ness for sending us a copy of his data.

ACKNOWLEDGMENTS

The help of Mr. G. O. Grummett in constructing the mixing cell and of Mr. B. Weston in designing the d-c. power supply for the shield heaters is gratefully acknowledged. We also wish to thank Mr. P. J. D'Arcy for invaluable technical assistance during the calorimetric measurements.

REFERENCES

1. M. L. MCGLASHAN. *In* Experimental thermochemistry. Vol. II. *Edited by* H. A. Skinner. Interscience Publishers, New York. 1962.
2. H. HIROBE. J. Fac. Sci. Univ. Tokyo, **1**, 155 (1926).
3. W. SCHULZE. Z. Physik. Chem. Leipzig, **197**, 105 (1951).
4. G. H. CHEESMAN and A. M. B. WHITAKER. Proc. Roy. Soc. London, Ser. A, **212**, 406 (1952).
5. C. P. BROWN, A. R. MATHIESON, and J. C. J. THYNNE. J. Chem. Soc. London, 4141 (1955).
6. I. BROWN and W. FOCK. Australian J. Chem. **8**, 361 (1955).
7. J. R. GOATES, R. J. SULLIVAN, and J. B. OTT. J. Phys. Chem. **63**, 589 (1959).
8. J. A. LARKIN and M. L. MCGLASHAN. J. Chem. Soc. London, 3425 (1961).
9. G. W. LUNDBERG. J. Chem. Eng. Data, **9**, 193 (1964).
10. G. C. BENSON, E. D. GODDARD, and C. A. J. HOEVE. Rev. Sci. Instr. **27**, 725 (1956).
11. R. W. ATTREE, R. L. CUSHING, J. A. LADD, and J. J. PIERONI. Rev. Sci. Instr. **29**, 491 (1958).
12. I. BROWN and W. FOCK. Australian J. Chem. **14**, 385 (1961).
13. G. C. BENSON and G. W. BENSON. Rev. Sci. Instr. **26**, 477 (1955).

Can. J. Chem. Downloaded from www.nrcresearchpress.com by 210.87.254.6 on 09/05/12
For personal use only.

Can. J. Chem. Downloaded from www.nrcresearchpress.com by 210.87.254.5 on 09/05/12
For personal use only.

SYNTHESIS OF β-D-MANNOSE 1,2-ORTHOACETATES[1]

M. MAZUREK AND A. S. PERLIN
National Research Council of Canada, Prairie Regional Laboratory, Saskatoon, Saskatchewan

Received February 4, 1965

ABSTRACT

Synthesis of 3,4,6-tri-*O*-acetyl-β-D-mannopyranose 1,2-orthoacetates (I) from 2,3,4,6-tetra-*O*-acetyl-α-D-mannopyranosyl bromide (II) and various alcohols in the presence of pyridine and substituted pyridines is described. 2,6-Lutidine is a particularly effective acid acceptor in these condensations, and the use of chloroform as a diluent is advantageous. The lutidine-buffered system has afforded a good yield of orthoacetate (I) with several alcohols that barely react with II in the presence of silver ion; this difference is attributed to the dominance of side reactions under the latter conditions. The N-bases also promote a more highly stereoselective orthoester synthesis than does the silver-catalyzed reaction, leading to formation of the OR-*exo*-diastereoisomer almost exclusively.

An earlier paper (1) reports that the two possible diastereoisomers of 3,4,6-tri-*O*-acetyl-D-mannopyranose 1,2-(methyl orthoacetate) (I) are formed when 2,3,4,6-tetra-*O*-acetyl α-D-mannopyranosyl bromide (II) is treated with methanol in the presence of silver carbonate (2, 3, 4). The isomers co-crystallize and are not readily separable, but both were found to be present in the mixture by nuclear magnetic resonance (n.m.r.) spectroscopy. The spectral data also suggested that the OR group of the isomer giving a C-methyl signal at 1.75 p.p.m. is oriented *exo* to the fused ring system (IA), and is *endo* in the isomer that gives a C-methyl signal at 1.51 p.p.m. (IB). By preparing the benzyl analogue of I, it was possible to separate and characterize two diastereoisomeric orthoacetates as distinct crystalline entities; each of these gave only one of the orthoacetyl resonance signals shown by the mixture of IA and IB (1).

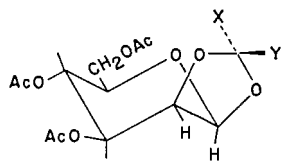

I

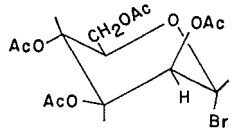

II

A (X = CH_3; Y = OCH_3)

B (X = OCH_3; Y = CH_3)

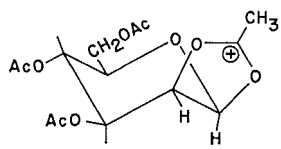

III

In continuing these studies, the synthesis of analogues of I containing yet other OR groups was undertaken. Since most orthoesters described in the literature (5) have been derived from primary aliphatic alcohols, it was of particular interest to test the condensation of less reactive types of hydroxylic compounds with II in the presence of silver

[1]*Presented in part at the 148th Meeting of the American Chemical Society, Chicago, Ill., August 30–September 4, 1964. Issued as N.R.C. No. 8419.*

Can. J. Chem. Downloaded from www.nrcresearchpress.com by 210.87.254.5 on 09/05/12
For personal use only.

carbonate. However, attempts to utilize several secondary alcohols and halogenated benzyl alcohols afforded little or no orthoester. Rather, side reactions (6) resulting from decomposition of the bromide (II) occurred at the expense of the condensation step. Since tetra-*O*-acetyl-α-D-mannosyl bromide is relatively stable in pyridine (6), and since the latter and various derivatives of it have occasionally been used for orthoester syntheses (5), pyridine and substituted pyridines were tested for the present purposes as acid acceptors in place of silver ion. This change in the reaction medium proved to be highly advantageous. 2,6-Lutidine was found to be especially effective, and permitted the synthesis of several new crystalline orthoester derivatives in very good yield. Among alcohols used in preparing these latter derivatives (Table I), none of which had given more than a trace of orthoester in the presence of silver carbonate, were 1,3-*O*-benzylidene-glyceritol, diphenylmethanol, *o*- and *p*-bromobenzyl alcohol, and *p*-iodobenzyl alcohol.[2]

The course of these condensations was conveniently examined by n.m.r. spectroscopy, since the intensity of the C-methyl signal provided a ready assay of orthoester yield. A striking property of the lutidine (or pyridine) buffered system was the fact that only one C-methyl signal, that at about 1.8 p.p.m., was prominent in the spectra of the reaction mixtures, whereas the signal at about 1.5 p.p.m., characteristic of IB, was usually almost completely absent. Hence each of the crystalline D-mannose 1,2-orthoacetates isolated in the current study (Table I) is essentially a single diastereomer, and is assumed to be an analogue of IA, i.e., the OR-*exo*-isomer.

Orthoester formation was more rapid and a better yield was obtained in the presence of a diluent such as chloroform, than when lutidine itself was used as the solvent. This deleterious effect of a high concentration of the N-base was particularly marked for the reaction of the mannosyl bromide with *p*-iodobenzyl alcohol: in lutidine alone the yield of orthoester was about 15%, whereas using chloroform and 2.5 molar equivalents of lutidine the yield of crystalline product was 67%. Reaction mixtures in which only 1 mole of lutidine was present per mole of mannosyl bromide, appeared to be insufficiently buffered, but 2 to 3 molar equivalents of the base was adequate to insure an optimum yield. The importance of buffering capacity was shown further by the fact that substituted pyridines having relatively low pK_a values were less effective than lutidine (pK_a, 6.7). Thus, with 3- or 4-hydroxypyridine (pK_a, 4.9 and 3.3, respectively), methanol and II gave 50–75% of the yield of I obtained in the presence of lutidine, whereas with 2-hydroxy- or 2-bromo-pyridine (pK_a 0.8 and 0.9, respectively), no orthoester was detected.

The overwhelming predominance of the diastereomer corresponding to IA in these reaction mixtures was at first attributed solely to a much more favored approach of the "hindered" alcohols towards the acetoxonium-ion intermediate (III) from a direction *exo* to the fused ring system (7). In fact, it was this expectation that partly prompted the use of these alcohols. However, in the presence of lutidine, methanol itself was found to yield IA almost entirely (the ratio of IA to IB was about 12:1), showing that the N-base induces a specific orientation effect unrelated to the reactivity of the hydroxylic component.[3] Lemieux and Morgan (8) have suggested that a transient pyridinium complex of an ion analogous to III is formed during the reaction of tetra-*O*-acetyl-α-D-glucopyranosyl bromide (or -β-D-glucopyranosyl chloride) with pyridine. They provided support for this

[2]*Not unexpectedly, o-bromobenzyl alcohol was the least reactive of this group, and required an elevated temperature whereas the other alcohols reacted smoothly at room temperature.*

[3]*A control experiment, in which a mixture of IA and IB was introduced at the outset of the condensation between the mannosyl bromide (II) and methanol, showed that IB remained unaltered during the succeeding reaction. Hence its virtual absence from the normal lutidine-buffered mixture is due not to its relative instability but to kinetic factors.*

Can. J. Chem. Downloaded from www.nrcresearchpress.com by 210.87.254.5 on 09/05/12
For personal use only.

TABLE I

Properties of some 1,2-orthoacetates of D-mannose 3,4,6-triacetate

Hydroxylic component (ROH)	m.p. (°C)	$[\alpha]_D$*	Anal. (%) Calcd. C	Calcd. H	Found C	Found H	Resonance signals† (δ, p.p.m.) H_1	$C—CH_3$	OR protons
1,3-*O*-Benzylidene-glyceritol (m.p. 83–84 °C)	176–176.5	−8.4°	56.5	5.9	56.7	5.6	—	1.80	—
Diphenylmethanol	150–151	+10.4°	63.0	5.9	62.9	6.2	5.40	1.80	—
Benzyl alcohol (1)	146–147	−1.0°	—	—	—	—	5.62	1.85	4.66‡
p-Bromobenzyl alcohol	182–182.5	+1.5°	48.8 (Br, 15.5)	4.9	48.8 (Br, 15.8)	4.9	5.55	1.80	4.50‡
p-Iodobenzyl alcohol	178–179	+0.9°	44.7 (I, 22.5)	4.5	44.7 (I, 22.7)	4.6	5.50	1.80	4.50‡
o-Bromobenzyl alcohol	119–121	+3.9°	48.8	4.9	48.8	5.1	5.38	1.75	4.55‡
1,2,3,4-Tetra-*O*-acetyl β-D-glucose	172–173	+18.3°	49.6	5.6	49.7	5.6	—	1.75	—
Glyceritol (diorthoester)	164–165	−8.6°	49.5	5.9	49.3	6.0	5.50	1.75	—
Methanol	111–113	−23.5°	49.7	6.1	49.7	6.1	5.52	1.75	3.29
Methanol (L-rhamnose derivative)	84–86	+34.7°	51.3	6.6	51.4	6.7	5.65	1.70	3.25
Methanol (D-lyxose derivative)	90–93	−107.3°	49.7	6.3	49.9	6.4	5.62	1.75	3.27

*In chloroform.
†The n.m.r. spectra were measured with a Varian A60 high resolution spectrometer using chloroform as solvent and tetramethylsilane as the internal reference.
‡Methylene protons.

Can. J. Chem. Downloaded from www.nrcresearchpress.com by 210.87.254.5 on 09/05/12
For personal use only.

proposal by showing that the addition of methanol to the reaction mixture resulted in the formation of methyl orthoacetate comprised chiefly of one diastereomer, believed to be the OR-*exo*-isomer. The current finding shows that pyridine and its analogues produce the same type of effect in the D-mannose series. However, this would not necessarily be anticipated because acetobromo-D-mannose, unlike the D-glucosyl halides, appears to be quite stable when dissolved in these bases (6). Consequently there is little reason to assume that a D-mannose pyridinium complex (analogous to the D-glucose complex) is an intermediate in the formation of diastereomer IA, although this would be required according to the mechanism of Lemieux and Morgan (8). In fact, these latter workers have now found that *sym*-collidine, which reacts far more slowly than does pyridine with D-glucosyl halides, is also more satisfactory for synthesis of D-glucose 1,2-orthoesters (9).

Although isomer IA and analogues of it may be obtained easily by the procedure described here, a stereospecific route to isomer IB and its analogues has not yet been found. Reaction conditions much more favorable to synthesis of IB were those in which II was treated with methanol and silver carbonate at relatively low temperatures.[4] Thus, at −10 °C the product contained twice as much of IB as of IA. This temperature effect was not consistent, however, for with benzyl alcohol as the hydroxylic component the direction was reversed and the relative proportion of the diastereomer corresponding to IA was even higher than at ambient temperature (i.e., 5:1 vs. 2:1). Such changes in composition with temperature suggest that the silver-catalyzed reaction may not proceed *entirely* through an intermediate such as III. With pyridine or lutidine the results are more consistent with a single, ionic, pathway: the ratio of IA to IB was the same at −10 °C as at room temperature and the rate of orthoacetate formation, as measured by changes in optical rotation or in intensity of the developing C-methyl signal, was that expected of a first-order process.

During the course of this study several other orthoesters have been synthesized with the lutidine-buffered system. Among these is a disaccharide derivative having m.p. 173 °C and $[\alpha]_D$ +18° (Table I), which was obtained from the reaction (18 h at 50 °C) of II with 1,2,3,4-tetra-*O*-acetyl-β-D-glucopyranose. This corresponds to one of two disaccharide orthoesters that have been isolated (10) from the silver-catalyzed condensation of the same compounds, an experiment that we were unable to duplicate successfully. Another derivative is one prepared for its potential use in synthesis of 2-substituted monoglycerides or 2-*O*-glycosyl-glyceritols. This is a diorthoester (Table I), undoubtedly the 1,3-diglyceride, and was obtained by treating glyceritol with two equivalents of II in dioxane–lutidine. Fischer, Bergmann, and Rabe (11) prepared 3,4-di-*O*-acetyl-β-L-rhamnopyranose (1,2-methyl orthoacetate) using quinoline as the acid acceptor and, not unexpectedly, the pure diastereomer prepared in the current study had the same physical constants as reported by them. Quinoline has been used also in a synthesis of the corresponding D-lyxose derivative (12) although its yield was only 6% whereas, now, with lutidine as base and chloroform as diluent the yield was 49%. Both of these methyl orthoacetates are analogues of IA since all three compounds give C-methyl signals at δ 1.70–1.75 p.p.m. and *O*-methyl signals at 3.25–3.29 p.p.m. However, H_1—H_2 coupling in the mannose and rhamnose derivatives ($J_{1,2}$ = 2.8 c.p.s.) is considerably smaller than in the lyxose derivative ($J_{1,2}$ = 4.7 c.p.s.). The latter value is, in fact, in the range ($J_{1,2}$ = 4.5–5.0 c.p.s.) characteristic of 1,2-orthoacetates of D-glucose (1, 9), D-galactose, and D-xylose. The apparent H_1—H_2 dihedral angles (13) represented by these two different

[4] *Variations with temperature in the relative yields of orthoester, methyl α- and β-D-mannosides, and D-mannose tetraacetate formed in this reaction have already been examined by Frush and Isbell (4).*

coupling values suggest that the chair conformation of mannopyranose (or rhamnopyranose) is distorted less by fusion of the orthoester ring than occurs with the other four sugars.

The preparation of *p*-bromobenzyl and *p*-iodobenzyl alcohol, used as hydroxylic components in this study, deserves some comment. Gilman and Melstrom (14) reported that the *p*-bromo alcohol is obtained in lower yield from *p*-bromobenzyl chloride than from *p*-bromobenzyl bromide. In addition, it has now been found that the chloride leads to a product contaminated with 15% of *p*-chlorobenzyl alcohol. This mixture was inadvertantly used initially in preparing the *p*-bromobenzyl orthoester described above. Although the orthoester also was crystalline, it too was a mixture of *p*-chloro- and *p*-bromo-derivatives, in which the ratio of the two halogens was the same as in the starting material. *p*-Iodobenzyl alcohol was prepared by lithium aluminium hydride reduction of readily available *p*-iodobenzoic acid. Fang *et al.* (15) obtained the alcohol in 25% yield from admixture with far larger amounts of benzyl alcohol. Gas–liquid chromatographic analysis of the reaction mixture showed that reduction of the carboxyl group proceeds far more rapidly than does replacement of the iodine atom. Hence, use of a relatively short reduction period affords the iodo-alcohol almost exclusively.

EXPERIMENTAL

3,4,6-Tri-O-acetyl-β-D-mannopyranose 1,2-(p-Iodobenzyl Orthoacetate)

The procedure for synthesis of this orthoester is typical of most syntheses reported herein.

A solution of *p*-iodobenzyl alcohol (250 mg) and 2,6-lutidine (0.14 ml) in chloroform (1 ml) was added to crystalline 2,3,4,6-tetra-O-acetyl-α-D-mannopyranosyl bromide (200 mg), and the reaction mixture was stored at room temperature for 24 h. Additional chloroform (15 ml) was added, the solution was washed successively with ice-cold sodium bicarbonate solution and ice water, then dried with sodium sulfate, and concentrated to dryness *in vacuo* at 55 °C. The solid residue was taken up in acetone (1.5 ml) and crystallization was promoted by addition of 1.0 ml each of ether and hexane; yield, 160 mg (69%). After recrystallization from the same solvent mixture the product had m.p. 178.5–179.0 °C; $[\alpha]_D$ 0.9° (*c*, 5.4, chloroform).

In most instances the course of the reactions was followed by n.m.r. spectroscopy, and if some unreacted acetobromo-α-D-mannose was still present (as shown by persistence of its signal for H_1) the reaction period was extended or the temperature was increased. With 1,3-*O*-benzylidene-glyceritol (m.p. 83–84 °C) for example, reaction was incomplete after 1 day but appeared to be at an end in 4 days, when the yield of crystalline product recovered was 68%. In another instance, there was little apparent reaction between II and *o*-bromobenzyl alcohol in 24 h at room temperature, but orthoester formed readily when the reaction mixture was heated under reflux. After a reflux period of 4.5 h, a 58% yield of the orthoacetate was isolated. Based on the intensity of C-methyl signals given by crude reaction products, estimated yields of orthoacetate were frequently close to 90%.

Reaction of 2,3,4,6-Tetra-O-acetyl-α-D-mannopyranosyl Bromide with Glyceritol

Glyceritol (0.44 g) was dissolved in dioxane (17 ml) containing lutidine (2.8 ml) and anhydrous calcium sulfate (6.0 g). The glycosyl bromide (4.1 g; 2.1 equivalents) was added and the reaction mixture was stored at room temperature for 5 days. Most of the dioxane was evaporated off, chloroform was added, and the chloroform solution was washed successively with ice-cold sodium bicarbonate and ice water, dried, and concentrated; yield of syrup, 2.8 g. Crystallization took place from solution in acetone–ether (yield, 0.74 g) and, after recrystallization, the solid had m.p. 164–165 °C; $[\alpha]_D$ −8.6° (*c*, 4.2, chloroform).

The mother liquor contained other orthoester material, part of which behaved chromatographically like a monosubstituted glyceryl derivative.

Reaction of 2,3,4,6-Tetra-O-acetyl-α-D-mannopyranosyl Bromide with Methanol in the Presence of 2,6-Lutidine

The glycosyl bromide (206 mg) was added to a solution (1.0 ml) of methanol and 2,6-lutidine containing 0.14 ml of the base. The reaction mixture was examined by polarimetry and also by n.m.r. spectroscopy; measurements were made over a period of 45 min of the rate of rotatory change (at 28 °C) and of the increase in intensity of the (major) C-methyl signal (probe temperature of about 35 °C). Typical of the first-order rate constant values (min^{-1}) calculated from these data are the following:

Time (min)	By n.m.r. spectroscopy	By polarimetry
10	0.0248	0.0226
15	0.0260	0.0235
20	0.0267	0.0237
40	0.0240	0.0273

Can. J. Chem. Downloaded from www.nrcresearchpress.com by 210.87.254.5 on 09/05/12
For personal use only.

At 40 min reaction time the yield of orthoacetate IA estimated from the intensity of its C-methyl signal was 62%.

With *sym*-collidine as base the polarimetrically estimated first-order rate constant was (average of 12 values) 0.0243 min^{-1}; with pyridine, the corresponding average value was 0.0297 min^{-1}.

p-Bromobenzyl Alcohol

Prepared from *p*-bromobenzyl bromide according to the procedure of Gilman and Melstrom (14), *p*-bromobenzyl alcohol had m.p. 77–78 °C and was analytically pure. When the starting material for its synthesis was *p*-bromobenzyl chloride (14), the alcohol obtained had the same melting point, but an incorrect elemental composition, and gave a positive test for chloride. Gas–liquid chromatographic analysis of the product showed the presence of *p*-bromobenzyl alcohol (83%) and a minor component (17%) having a shorter emergence time.

p-Iodobenzyl Alcohol

This was prepared by reduction of *p*-iodobenzoic acid with lithium aluminium hydride in ether (15). When the reduction was carried out for 1 h (15) the product was found by gas–liquid chromatographic analysis to consist of benzyl alcohol (55%) and *p*-iodobenzyl alcohol (45%). However, when the reduction period was 10 min, analysis of the product showed the presence of only 8% benzyl alcohol. The yield of *p*-iodobenzyl alcohol was 74%; after recrystallization from chloroform the melting point was 74 °C.

ACKNOWLEDGMENTS

The authors express their thanks to Dr. W. Klöker who carried out several experiments preliminary to this study, and to Dr. B. M. Craig for assistance in gas–liquid chromatographic analyses.

REFERENCES

1. A. S. Perlin. Can. J. Chem. **41**, 399 (1963).
2. J. K. Dale. J. Am. Chem. Soc. **46**, 1046 (1924).
3. H. G. Bott, W. N. Haworth, and E. L. Hirst. J. Chem. Soc. 1395 (1930).
4. H. L. Frush and H. S. Isbell. J. Res. Natl. Bur. Std. **27**, 413 (1941).
5. E. Pacsu. Advan. Carbohydrate Chem. **1**, 77 (1945).
6. H. R. Goldschmid and A. S. Perlin. Can. J. Chem. **39**, 2025 (1961).
7. R. U. Lemieux and J. D. T. Cipera. Can. J. Chem. **34**, 906 (1956).
8. R. U. Lemieux and A. R. Morgan. J. Am. Chem. Soc. **85**, 1889 (1963).
9. R. U. Lemieux and A. R. Morgan. Private communication.
10. E. A. Talley, D. D. Reynolds, and W. L. Evans. J. Am. Chem. Soc. **65**, 575 (1943).
11. E. Fischer, M. Bergmann, and A. Rabe. Ber. **53**, 2362 (1920).
12. P. A. Levene and M. L. Wolfrom. J. Biol. Chem. **78**, 525 (1928).
13. M. Karplus. J. Chem. Phys. **30**, 11 (1959).
14. H. Gilman and D. S. Melstrom. J. Am. Chem. Soc. **70**, 4177 (1948).
15. F. T. Fang, J. K. Kochi, and G. S. Hammond. J. Am. Chem. Soc. **80**, 563 (1958).

Can. J. Chem. Downloaded from www.nrcresearchpress.com by 210.87.254.5 on 09/05/12
For personal use only.

Can. J. Chem. Downloaded from www.nrcresearchpress.com by 210.87.254.42 on 09/05/12
For personal use only.

THE SYSTEM: BISMUTH–CADMIUM–MERCURY

A. N. Campbell and E. M. Kartzmark
Chemistry Department, University of Manitoba, Winnipeg, Manitoba
Received January 15, 1965

ABSTRACT

The liquidus surface of this ternary alloy has been determined, together with the nature of the solid phase separating from various melts. The densities and molar volumes of the binary system: Cd—Hg have been determined and it is shown that there is marked contraction when the α and β phases form from the components. X-ray powder photographs of various Cd—Hg alloys at room temperature have been made and the limits of homogeneity determined.

The binary systems from which the ternary system Bi—Cd—Hg is derived, have all been investigated previously. The system Bi—Cd is of the simple eutectic type, the eutectic lying at 144 ° and 40% Cd by weight: there appears not to be any appreciable solid solubility (1). The system Bi—Hg is also of the simple eutectic type, the eutectic lying close to the freezing point of pure mercury and containing only a trace of bismuth (2).

The system Cd—Hg is of much greater theoretical and practical interest, since the universally used cadmium standard cell makes use of a cadmium–mercury alloy of defined concentration. According to Bijl (3), Puschin (2), and Mehl and Barrett (4), this system exhibits two peritectic points, one at 190° and 50% by weight of the components, and one at −34° with a corresponding liquidus content of something less than 1% of cadmium. Corresponding to these two peritectics there are three series of solid solutions α and γ showing the cadmium and mercury lattices respectively, and β, the intermediate phase, which is said to be face-centered tetragonal. The solid solubility curves rest principally on the dilatometric work of Bijl (3). Because of the slowness with which equilibrium is established, they are highly indefinite. The careful work of Mehl and Barrett gives the limits of β and γ at the lower peritectic (−34 °) with more accuracy.

EXPERIMENTAL

The liquidus curves of the binary systems Bi—Hg and Cd—Hg, as well as certain points on the liquidus surface of the ternary system Bi—Cd—Hg, were determined, using a copper–constantan thermocouple and a Brown recorder. The system Bi—Cd is too well known to merit further attention.

All alloys were prepared by direct weighing. The mercury used was Johnson, Matthey and Mallory "technical grade", redistilled. The cadmium was "Fisher Certified Reagent", stated to contain 99.9% Cd, with traces of Cu, Pb, Fe, and Zn. The bismuth was "Fisher Certified Reagent", with traces of As, Cu, Fe, Pb, and Sb.

The weighed components were sealed in Pyrex glass containers, with inserts for the thermocouple junction. For the purposes of thermal analysis after complete fusion and shaking, the alloys were allowed to cool in the resistance furnace in which they had been prepared, after the heating current had been turned off.

The densities and molar volumes of alloys containing only cadmium and mercury were determined. The X-ray patterns of the Cd—Hg alloys were taken, using a copper anticathode and nickel filter. For this purpose, the alloys were allowed to cool over a period of 6 h in the furnace in which they were prepared. That they were in a stable state seems to be indicated by the fact that some 40 X-ray pictures of different alloys were beautifully clear and exactly reproducible. In so far as comparison is possible, our data agree with those of Mehl (5). The lattice structures of the α, β, and γ alloys had already been worked out by Mehl (5) and by Mehl and Barrett (4), but some doubt still existed as to the solid solubility curves. Our powder pictures, which reveal many more lines than those given by Mehl, indicate that the system Cd—Hg is homogeneous, at room temperature, from pure Cd up to 39 ± 3% Hg (Cd lattice), is heterogeneous from 39 ± 3% up to 45 ± 3% Hg, and after that is homogeneous (intermediate β lattice) presumably up to 92.5% Hg (Mehl and Barrett's figures). The data of our X-ray powder pictures have been accepted by A.S.T.M.

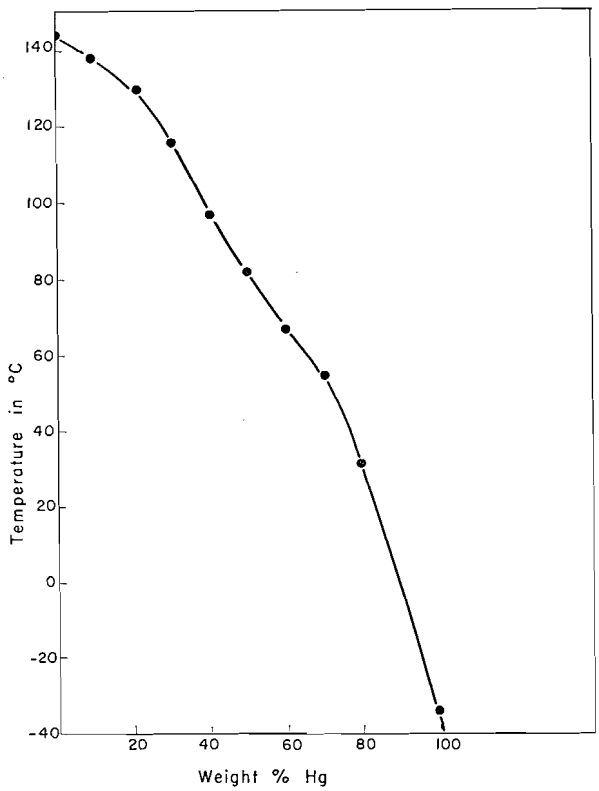

FIG. 1. Temperatures of primary crystallization vs. concentration.

The eutectic trough running across the triangular diagram from the binary eutectic of the Bi—Cd system to the low temperature (−34 °C) peritectic in the Cd—Hg system (or for that matter the eutectic of the Bi—Hg system) was determined by making up the binary eutectic of the Bi—Cd system adding increasing quantities of mercury, and submitting these pseudo-binary systems to thermal analysis. We assume that the eutectic trough is a straight line running across the diagram to the freezing point of mercury. This assumption seems to be justified by the absence of points of inflection on the cooling curve, prior to the main halt when the trough is reached.

Mixtures of the ternary system, on both sides of the eutectic trough, were made up and submitted to thermal analysis. Two halts on the cooling curves were obtained, one that of primary crystallization and the other when the eutectic trough was attained. From these data, the crystallization path and the nature of the primary crystallization were readily deduced (Fig. 1).

RESULTS

TABLE I

Densities and molar volumes of Cd—Hg alloys

Wt. % Hg	Atomic % Hg	Density at 25 °C (g/cc)	Molar volume (cc)
0.00	0.00	8.6454	13.00
10.00	5.82	9.0456	13.01
20.00	12.44	9.4762	13.02
30.00	19.36	9.9064	13.07
40.00	27.20	10.3490	13.18
51.65	37.45	10.8987	13.34
61.18	46.90	11.4114	13.47
70.55	57.31	12.0346	13.54
80.17	69.38	12.7397	13.63
100.00	100.00	13.546	14.81

Can. J. Chem. Downloaded from www.nrcresearchpress.com by 210.87.254.42 on 09/05/12
For personal use only.

TABLE II

Temperatures of primary crystallization and compositions along the pseudo-binary eutectic trough

Binary eutectic: Bi—Cd + Hg	Temperature (°C)
Pure eutectic (60% Bi : 40% Cd)	143
9.5% Hg	138
21.44% Hg	125
30.59% Hg	116
40.36% Hg	97
49.92% Hg	82
59.81% Hg	67
69.63% Hg	55
79.94% Hg	32
Pure Hg	−39

TABLE III

Thermal analysis of ternary mixtures

	Composition in wt. %				
Mixture No.	Bi	Cd	Hg	t_1 (°C)	t_2 (°C)
I	19.67	58.56	21.77	203	120
II	39.93	39.78	20.29	140	130
III	59.43	20.00	20.58	180	115
IV	11.07	78.49	10.43	270	130
V	40.24	20.18	39.60	114	94
VI	19.72	20.09	60.19	88	82

DISCUSSION

The results of our thermal analysis of the system Bi—Hg are not reproduced since they are in excellent agreement with those of Puschin (2). If the solution of mercury in bismuth can by considered ideal, and in very dilute solution perhaps it can, the well-known equation

$$\Delta H/R \cdot (1/T_0 - 1/T) = \ln X_A$$

is applicable. In this formula ΔH is taken to be the molar heat of fusion of the solvent (bismuth). If, however, the solution is not infinitely dilute, the heat effect becomes the sum of the heats of fusion and the heats of mixing of molten bismuth with liquid mercury, neglecting differences in the specific heats of the component metals and the fluid amalgams. Applying this equation to our data, we obtain Table IV.

TABLE IV

Calculated heat effects

Wt. % Bi	ΔH (kcal/mole)
5	5.812
10	4.136
20	3.877
30	3.255
40	2.990
50	2.783
90.2	2.283
100.0	2.132*

*Calculated from experimental heat of fusion.

Can. J. Chem. Downloaded from www.nrcresearchpress.com by 210.87.254.42 on 09/05/12
For personal use only.

As the composition approaches that of pure bismuth, the calculated ΔH approaches the (experimental) heat of fusion of bismuth as, of course, it must. It would be unsafe to assume that the large discrepancies at lower concentrations of bismuth represent heats of mixing of molten bismuth with mercury: they more probably represent nonideality of the melt. Nevertheless, it appears that solutions containing up to 10% mercury behave in a fairly ideal manner.

Our thermal analysis figures for the system Cd—Hg confirm those of Bijl (3), who did the classical work on this system. It must be confessed, however, that our results would not reveal the existence of a peritectic at 190° and, indeed, if Bijl's own results are plotted, they could easily be interpreted as representing a smooth curve. There is no doubt of the existence of this peritectic but it does not appear very evidently as the result of thermal analysis. As the peritectic cannot be detected by thermal analysis, in the binary system, Cd—Hg, it is hopeless to attempt to determine the position of the peritectic trough by thermal analysis in the ternary system. For diagrammatic purposes we have joined the binary peritectic by a dotted line to the Bi apex, terminating it at its intersection with the eutectic trough: this intersection occurs at a composition of 21% Hg, 47.5% Bi, 31.5% Cd and corresponds to a temperature on the eutectic trough of 120° (Fig. 2).

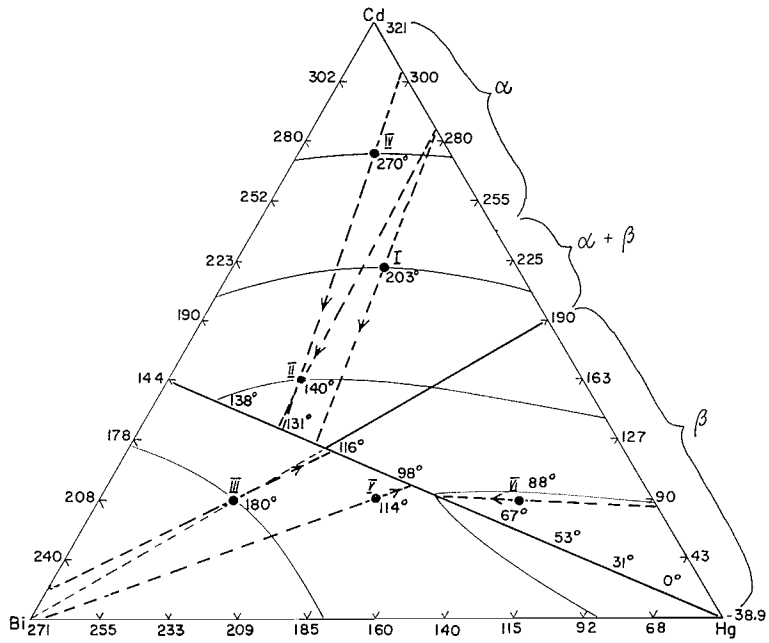

FIG. 2. Isothermal lines and crystallization paths.

When the molar volumes of cadmium–mercury alloys (Table III) are plotted against mole %, a three-branch curve, lying well below the straight line of ideal behavior, is obtained. The discontinuities correspond roughly to the limits of α and β solid solubility, as given by Mehl and Barrett (4). Since the molar volumes are always less, sometimes considerably less, than the sum of the volumes of the components, it is obvious that α and β solid solutions form with lattice contraction or, more exactly, that the cadmium lattice does not expand very greatly with the entrance of mercury atoms. The β lattice

Can. J. Chem. Downloaded from www.nrcresearchpress.com by 210.87.254.42 on 09/05/12
For personal use only.

is face-centered tetragonal and, therefore, different from those of cadmium or mercury. For this modification also the total volume is much less than the sum of those of the components. In fact, at the mercury limit of the β range, the molar volume differs by about 0.7 cc from the ideal (straight line) molar volume of 14.25 cc, a contraction of 5%. We did not push our measurements beyond 70 mole % mercury, i.e. we dealt only with alloys that are completely solid at room temperature.

The temperature arrests on cooling of ternary mixtures have been plotted on the triangular diagram of Fig. 2. These points have been joined by smooth curves to the corresponding temperatures on the sides of the diagram, thus generating isothermal lines, which give indications of the curvature of the liquidus surface. The compositions have been joined by straight lines to those compositions on the eutectic trough, corresponding to the observed eutectic inflections on the cooling curves. When these straight lines are produced backwards to the corresponding binary system, the nature of the primary phase separating becomes apparent, in other words these lines represent crystallization paths. This procedure is only justified on the assumption that the phase separating contains no bismuth. Tammann and Rocha (6) have shown that the solubility of Bi in Cd is less than 0.05% at the eutectic temperature. These primary phases are read off as follows.

Mixture No. (Table II)	Primary phase separating
I	α containing 18% Hg
II	α containing 12% Hg
III	bismuth
IV	α containing 7% Hg
V	bismuth
VI	β containing 81.5% Hg

REFERENCES

1. K. Honda and T. Ishigaki. Sci. Rept. Tohoku Univ. **14**, 221 (1925).
2. N. A. Puschin. Z. Anorg. Allgem. Chem. **36**, 201 (1903).
3. H. C. Bijl. Z. Physik. Chem. **41**, 641 (1902).
4. R. F. Mehl and C. S. Barrett. Trans. Am. Inst. Mining Met. Engrs. Inst. Metals Div. 578 (1930).
5. R. F. Mehl. J. Am. Chem. Soc. **50**, 381 (1928).
6. G. Tammann and H. J. Rocha. Z. Metallk. **25**, 133 (1933).

Can. J. Chem. Downloaded from www.nrcresearchpress.com by 210.87.254.42 on 09/05/12
For personal use only.

Can. J. Chem. Downloaded from www.nrcresearchpress.com by 210.87.254.42 on 09/05/12
For personal use only.

PRESSURE-INDEPENDENT FLOW SYSTEM PYROLYSIS OF DIMETHYL CADMIUM

M. KRECH AND S. J. PRICE
Department of Chemistry, University of Windsor, Windsor, Ontario
Received January 26, 1965

ABSTRACT

The pyrolysis of $CdMe_2$ has been investigated in a benzene carried flow system using temperatures from 743 °K to 800 °K and pressures from 1.63 cm to 16.2 cm. High pressure limiting rate constants were obtained above approximately 8 cm pressures. The high pressure activation energy, E_0, of 48.8 ± 1 kcal/mole is identified with D(MeCd—Me) within the limits $D < E_0 < D + RT$.

INTRODUCTION

Three previous investigations of the pyrolysis of $CdMe_2$ have been reported (1, 2, 3). In the first investigation a marked surface reaction was noted but no attempt was made to isolate the homogeneous components of the reaction (1). The second study was carried out in a toluene carrier flow system by one of the present authors (2). This gave log $k = 11.9 - (45\,800/2.3RT)$ at 18 mm pressure. Under the experimental conditions used k was still a function of pressure. No appreciable surface effects were noted. The third investigation was carried out in a static system in the absence of any inhibitors (3). Rate constants were calculated on the basis of the undecomposed alkyl. A marked surface effect was again noted. To obtain the homogeneous rate, reactions were carried out at a number of surface to volume ratios and extrapolated to zero. The reaction was studied at only one temperature and a selected value of log $A = 13.08$ was used to calculate an experimental activation energy of 43.5 ± 1.4 kcal/mole.

EXPERIMENTAL

Materials

(*a*) Dimethyl cadmium was prepared from $CdCl_2$ by a procedure identical to that previously used to make dimethyl mercury (4). The fraction with b.p. 105 °C at 754 mm was collected and stored under its own vapor pressure at −78 °C.

(*b*) Spectro grade benzene was prepared for use by refluxing over sodium for 24 h and then degassing twice by bulb-to-bulb distillation. The benzene used in each experiment was freshly degassed by bulb-to-bulb distillation immediately before use.

Apparatus and Procedure

The apparatus and procedure used were similar to those previously employed in the study of dimethyl mercury (4). Contact of dimethyl cadmium vapor with mercury was minimized by replacing the mercury manometer of the alkyl injection system used in the dimethyl mercury work with a spoon gauge. The temperature control trap was kept at −100 °C so that any propane formed would be collected with the other gaseous products. Analysis of gaseous products was carried out by gas chromatography using a 1 m silica gel column at 80 °C and a flow rate of 20 cc/min. Analysis of the liquid products from the dry ice – acetone trap was carried out using a 1 m diisodecyl phthalate on diatomaceous earth column at 120 °C with a helium flow rate of 15 cc/min.

RESULTS AND DISCUSSION

The results are shown in Table I. They may be represented by a mechanism similar to that proposed for the decomposition of $Cd(CH_3)_2$ in a toluene carrier system (2):

[1] $$Cd(CH_3)_2 \rightarrow CdCH_3 + CH_3$$

[2] $$CdCH_3 \rightarrow Cd + CH_3$$

Can. J. Chem. Downloaded from www.nrcresearchpress.com by 210.87.254.42 on 09/05/12
For personal use only.

TABLE I

Temp. (°K)	Contact time (s)	Total press. (cm)	Length of run (min)		$Cd(Me)_2$* (10^{-4} mole)	CH_4 (10^{-4} mole)	C_2H_6 (10^{-4} mole)	C_2H_4 (10^{-6} mole)	C_3H_8 (10^{-6} mole)	Toluene (10^{-5} mole)	k (s^{-1})
			Total	Alkyl							
798	1.07	11.12	8	5	9.27	6.14	3.14	8.1	3.2	4.45	1.050
797.5	1.04	10.60	8	5	9.68	5.82	3.18	6.4	8.7	7.56	1.020
799	1.23	8.80	8	5	18.20	8.40	7.85	20.9	14.4	10.22	0.971
799	1.15	8.80	8	5	7.51	4.72	2.77	6.1	6.1	5.50	1.050
799	1.21	8.48	8	5	7.36	4.08	3.56	12.8	36.0	3.60	1.180
799	1.23	7.48	8	5	11.22	6.24	4.83	11.7	13.1	8.12	1.110
799	1.13	6.28	8	5	4.63	3.09	1.89	1.0	1.0	3.99	1.140
797	1.41	4.60	25	15	10.80	6.53	4.64	9.4	8.6	6.27	0.959
800	2.20	2.61	60	50	16.99	7.38	7.63	15.4	15.4	12.61	0.563
799	2.02	2.12	80	60	16.29	7.89	6.70	16.3	16.3	7.15	0.569
800.5	2.41	1.63	60	50	16.43	6.60	8.56	19.6	26.7	8.32	0.600
775	1.10	16.18	8	5	12.36	4.47	2.05	8.4	1.9	5.33	0.396
775	1.10	14.90	8	5	10.53	3.86	1.83	6.2	1.7	4.94	0.406
777	1.11	12.10	8	5	16.50	4.83	3.32	6.3	8.8	4.08	0.394
777	1.11	11.86	10	7	13.27	4.59	2.47	6.7	5.0	5.59	0.415
776	1.12	10.42	8	5	12.36	3.57	2.46	6.0	5.5	5.11	0.387
778	1.12	9.70	8	5	14.80	4.18	3.25	6.0	9.1	3.55	0.407
777	1.14	8.44	8	5	12.00	3.80	2.74	5.8	5.8	3.46	0.432
779	1.28	6.00	20	15	14.40	5.27	3.63	5.9	5.9	5.03	0.457
777	1.34	5.60	18	13	18.80	4.69	4.15	9.4	11.3	4.34	0.330
777	1.29	4.70	20	15	10.39	3.03	2.20	3.8	1.3	4.26	0.339
777	1.59	3.22	25	20	9.55	2.51	2.27	4.2	4.3	3.56	0.287
777	2.03	2.58	45	35	11.59	3.27	2.95	7.7	9.0	3.35	0.254
777	2.72	1.88	60	50	12.00	3.56	3.36	6.4	7.8	2.90	0.207

Can. J. Chem. Downloaded from www.nrcresearchpress.com by 210.87.254.42 on 09/05/12
For personal use only.

TABLE I (*Concluded*)

Temp. (°K)	Contact time (s)	Total press. (cm)	Length of run (min)		$Cd(Me)_2$* (10^{-4} mole)	CH_4 (10^{-4} mole)	C_2H_6 (10^{-4} mole)	C_2H_4 (10^{-6} mole)	C_3H_8 (10^{-6} mole)	Toluene (10^{-5} mole)	k (s^{-1})
			Total	Alkyl							
758	1.16	16.20	8	5	11.51	1.79	1.56	1.9	0.7	4.28	0.203
759	1.08	13.80	8	5	10.24	2.74	1.13	4.2	2.9	2.20	0.247
760.5	1.06	13.76	8	5	12.01	2.68	1.16	3.9	2.3	2.22	0.209
760	1.11	12.74	8	5	14.75	2.65	1.52	3.4	4.4	4.40	0.195
760	1.10	11.70	8	5	11.92	2.67	1.49	3.0	2.7	2.31	0.227
761	1.14	10.36	10	7	14.68	3.48	1.98	5.3	3.8	2.93	0.253
761	1.16	8.80	8	5	11.79	2.54	1.68	3.9	2.8	1.63	0.234
762	1.26	8.12	15	12	10.81	3.09	1.54	3.7	3.3	2.50	0.257
762.5	1.42	5.86	20	15	14.26	3.16	2.18	3.9	4.8	2.84	0.212
761	1.32	5.64	20	15	16.85	3.10	2.25	5.0	5.5	2.03	0.190
761	1.43	5.60	20	15	13.90	2.74	1.86	4.3	3.1	4.21	0.185
762	1.68	3.50	60	50	34.13	5.18	4.84	6.2	8.7	7.57	0.152
761	1.98	2.66	40	30	5.97	1.86	0.80	3.7	2.5	1.31	0.154
763	2.29	2.24	60	50	19.45	3.78	3.90	6.6	8.6	5.34	0.160
761	2.06	2.09	80	70	11.80	2.34	1.49	2.7	1.4	3.45	0.121
743	1.27	13.46	8	5	18.33	2.14	1.19	3.3	4.5	3.12	0.102
744	1.13	10.50	8	5	17.28	1.99	1.14	1.9	1.9	1.83	0.108
744	1.17	10.32	8	5	20.22	2.38	1.45	4.7	2.2	2.16	0.114
744	1.15	10.26	8	5	12.92	1.79	1.08	2.4	2.0	1.75	0.132
744	1.18	10.04	8	5	9.69	1.39	0.64	1.8	1.1	1.67	0.107
744	1.18	8.40	8	5	12.56	1.46	0.71	2.2	1.2	1.56	0.090
744	1.38	5.76	13	10	9.69	1.49	0.79	1.5	1.8	0.66	0.105
745	1.33	5.36	20	15	14.68	1.69	0.95	1.8	2.4	1.96	0.090
745	2.31	2.27	40	30	16.57	1.58	1.32	3.8	4.6	2.11	0.057
744	2.06	2.16	60	50	14.40	2.04	1.18	4.0	2.8	1.73	0.075

*Amount used in a given run.

[3] $CH_3 + C_6H_6 \rightarrow CH_4 + C_6H_5$

[4] $2CH_3 \rightarrow C_2H_6$

[5] $2C_6H_5 \rightarrow C_{12}H_{10}$

[6] $CH_3 + C_6H_5 \rightarrow C_6H_5CH_3$

[7] $CH_3 + C_2H_6 \rightarrow C_2H_5 + CH_4$

[8] $C_2H_5 \rightarrow C_2H_4 + H$

[9] $H + C_6H_6 \rightarrow C_6H_5 + H_2$

[10] $C_2H_6 + CH_3 \rightarrow C_3H_8$

where reaction [2] is much faster than reaction [1]. In the present investigation the extent of reaction [6] has been quantitatively determined and analyses for ethylene and propane have been made in each run. Rate constants have therefore been calculated from the usual first-order rate equation assuming fraction decomposed =

$$\frac{\frac{1}{2}(\text{moles } CH_4 + \text{moles toluene}) + \text{moles } C_2H_6 + \text{moles } C_2H_4 + \frac{3}{2}\text{ moles } C_3H_8}{\text{moles } Cd(CH_3)_2} .$$

A blank correction of 3×10^{-5} mole of methyl radicals was subtracted to allow for decomposition that occurred in the alkyl injection system.

The rate constant was studied as a function of pressure at four temperatures. From plots of log k vs. log P, it is apparent that at all temperatures used k_1 is independent of pressure above approximately 8 cm. Figure 1 shows the Arrhenius plots for the high pressure limit and for 18 mm. The lines may be represented respectively by:

$$\log k\ (s^{-1}) = 13.4 - (48\,800/2.3RT)$$

and

$$\log k\ (s^{-1}) = 12.3 - (45\,800/2.3RT).$$

The results at 18 mm are in good agreement with the previous flow system study of dimethyl cadmium if due allowance is made for the different energy transfer efficiencies of benzene and toluene.

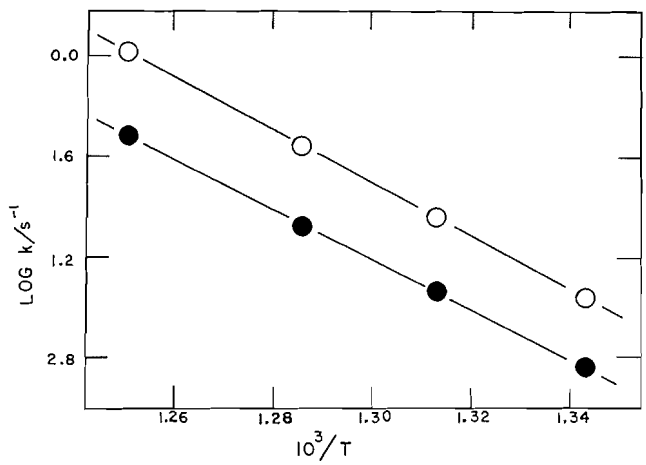

FIG. 1. Arrhenius plots for the decomposition of dimethyl cadmium at the high pressure limit (○), and at 18 mm pressure (●).

Can. J. Chem. Downloaded from www.nrcresearchpress.com by 210.87.254.42 on 09/05/12
For personal use only.

The high pressure activation energy may be related to D(MeCd—Me). The best value for the sum of the two metal–carbon bond dissociation energies is 65.6 kcal/mole (5). Hence:

$$D(\text{MeCd—Me}) = 48.8 \text{ kcal/mole}$$

$$D(\text{Me—Cd}) = 16.8 \text{ kcal/mole.}$$

If the present high pressure frequency factor is used to recalculate D(MeCd—Me) from the results of Laurie and Long (3) a value of 44.3 kcal/mole is obtained. This value would seem to be too low, indicating complexities in the static system work which have not been taken into account.

ACKNOWLEDGMENT

This work has been supported by a grant from the National Research Council of Canada.

REFERENCES

1. C. A. Heller and H. A. Taylor. J. Phys. Chem. **57**, 226 (1953).
2. S. J. Price and A. F. Trotman-Dickenson. Trans. Faraday Soc. **53**, 939 (1957).
3. C. M. Laurie and L. H. Long. Trans. Faraday Soc. **53**, 1431 (1957).
4. M. Krech and S. J. Price. Can. J. Chem. **41**, 224 (1963).
5. L. H. Long. Pure Appl. Chem. **2**, 61 (1961).

Can. J. Chem. Downloaded from www.nrcresearchpress.com by 210.87.254.42 on 09/05/12
For personal use only.

Can. J. Chem. Downloaded from www.nrcresearchpress.com by 210.87.254.42 on 09/05/12
For personal use only.

THE PHOTOLYSIS OF CYCLOPENTANONE AND CYCLOBUTANONE[1]

R. F. KLEMM, D. N. MORRISON, P. GILDERSON, AND A. T. BLADES
Research Council of Alberta, Edmonton, Alberta

Received February 1, 1965

ABSTRACT

The vapor phase photolysis of cyclopentanone, cyclopentanone-d_8, and cyclobutanone have been investigated at 3 130 Å and 2 537 Å under a variety of conditions. In cyclopentanone photolysis a pressure- and wavelength-dependent "falloff" has been observed in the product ratio cyclobutane:ethylene, while a similarly dependent effect in the ratio cyclopropane:propylene exists in cyclobutanone photolysis. In the light of this data a reappraisal has been made of existing concepts regarding the photodecomposition of these ketones.

INTRODUCTION

The photochemistry of cyclic ketones has been summarized by Srinivasan (1). Thus, it has been affirmed that the photolysis of cyclopentanone vapor at temperatures up to 125° at 3 130 Å, and at shorter wavelengths up to 300°, involves a stoichiometry given by the following reactions,

$$\overbrace{CH_2CH_2CH_2CH_2CO} \xrightarrow{h\nu} 2C_2H_4 + CO$$
$$\rightarrow \text{cyclo-}C_4H_8 + CO$$
$$\rightarrow H_2C{=}CHCH_2CH_2CHO,$$

wherein the importance of 4-pentenal relative to total products increases with pressure at any given temperature. In addition, cyclopentanone exhibits fluorescence in all three phases with a maximum at 4 100 Å; however, the phosphorescence observed in condensed phases does not appear in the vapor (2).

The photolysis of cyclobutanone has not been as thoroughly studied as that of cyclopentanone; but in a similar way, the products of cyclobutanone photolysis are presumed to arise by

$$\overbrace{CH_2CH_2CH_2CO} \xrightarrow{h\nu} C_2H_4 + CH_2CO$$
$$\rightarrow \text{cyclo-}C_3H_6 + CO$$
$$\rightarrow C_3H_6 + CO.$$

Unfortunately, however, CO was found in excess of (cyclo-C_3H_6 + C_3H_6), while the equivalence of C_2H_4 and CH_2CO is difficult to establish analytically.

The important observation from the present standpoint is that the ratio cyclobutane: ethylene in cyclopentanone photolysis at 3 130 Å and 2 537 Å appears to have a constant value independent of temperature in the pressure range investigated (10–300 mm Hg). In contrast, the cyclopropane:propylene ratio in cyclobutanone ratio in cyclobutanone photolysis is wavelength sensitive and preliminary suggestions of a pressure dependence have also been reported (1). This implies a common energetic precursor for these products which may be distinct from the precursor of the other products, ethylene and ketene. Such a possibility and the seemingly dissimilar behavior in cyclopentanone prompted a reexamination of both systems with particular reference to temperature, pressure, and wavelength effects to further clarify the situation. The study of these systems also bears

[1]*Contribution No. 291 from the Research Council of Alberta, Edmonton, Alberta, Canada.*

relevantly upon the thermal reactions of cyclic molecules. Furthermore it seemed of some importance to repeat the experiments of Flowers and Frey (3), in which the ability of ethylene to react with polymethylene diradicals was described.

MATERIALS

Cyclopentanone (Eastman Kodak White Label) was distilled on a 1 m pyrex helices-packed column with a vapor takeoff. Gas chromatographic analysis using a polyethylene glycol 400 column in conjunction with a hot wire detector indicated the absence of impurities. When not in use the cyclopentanone thus prepared was stored in the dark and under vacuum at −80°. Cyclopentanone-d_8 was supplied by Merck, Sharp, and Dohme, Montreal, and was used without further purification. The cyclobutanone, an Aldrich Chemical Co. product, was treated in the same way as the cyclopentanone. Crude 4-pentenal was obtained from the thermal isomerization of allyl vinyl ether (4). It was purified by preparative scale gas chromatography on a polyethylene glycol 400 column. Toluene was prepyrolyzed, dried, distilled on an efficient column with vapor takeoff, and stored under vacuum in sealed ampoules. Ethylene (Phillips Research Grade) was distilled from −160° to −196° prior to use to ensure its purity with respect to C_5 and C_6 hydrocarbons.

APPARATUS AND PROCEDURE

The customary static vacuum system employing metal Hoke valves sufficed for experiments at 3 130 Å, while experiments at 2 537 Å were similarly conducted but in a mercury-free system. Cylindrical quartz cells of 172 cc and 535 cc were used and enclosed in lagged aluminium furnaces. The 3 130 Å radiation from a Hanovia-type SH medium pressure lamp entered the cell after passing through a 2 mm pyrex filter followed by a 2 mm Corning 0–54 filter. A low pressure mercury resonance lamp provided 2 537 Å, the 1 849 Å component being removed by a Corning 7–54 filter. The ketones were admitted to the cell either from small gas-metering volumes or weighed ampoules, or measured directly by a calibrated Pirani gauge. Exposure times ranged from a few minutes to 4 h.

After irradiation the procedure with cyclopentanone was to remove most of the substrate at −64° while distilling the more volatile products into a small U trap filled with activated silica gel at −196°. The latter trap heated to 150° formed the sample inlet to a 10 ft polypropylene glycol column which was followed by either a Gow-Mac hot wire detector or an Aerograph model 600 hydrogen-flame detector. The above chromatographic column provided an adequate separation of C_2H_4 from cyclobutane in particular and by a suitable choice of column temperature all hydrocarbons through C_6's. An essentially similar procedure was used for cyclobutanone; in this case, however, the propylene and cyclopropane were better resolved by a 20 ft squalane column. Where CO analyses were warranted, a 2 ft charcoal column at 0° was found adequate.

RESULTS AND DISCUSSION

A. Cyclopentanone

Results

It was again confirmed that over the temperature range 28-225° and the pressure interval 0.09–30 mm cyclopentanone the only hydrocarbon products appearing at low extent of reaction are C_2H_4 and cyclo-C_4H_8. The relationship $\Phi(CO) = \frac{1}{2}\Phi(C_2H_4) + \Phi(\text{cyclo-}C_4H_8)$ was also verified.

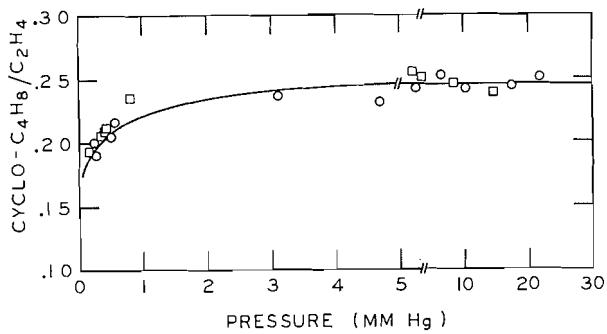

FIG. 1. Ratio of product yields, cyclo-C_4H_8:C_2H_4 vs. cyclopentanone pressure. □ Cyclopentanone, ○ cyclopentanone-d_8; at 3 130 Å and 100°.

Can. J. Chem. Downloaded from www.nrcresearchpress.com by 210.87.254.42 on 09/05/12
For personal use only.

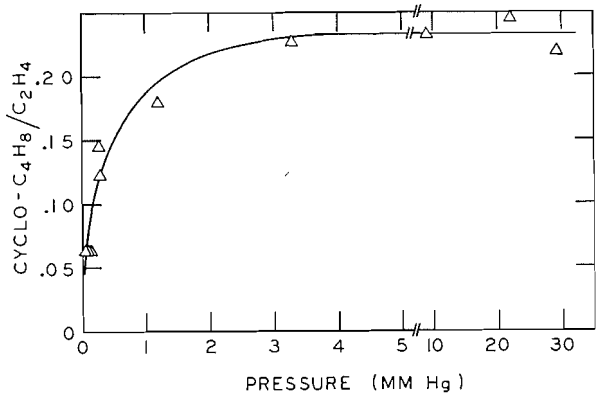

FIG. 2. Ratio of product yields, cyclo-C_4H_8:C_2H_4 vs. cyclopentanone pressure; at 2 537 Å and 100°.

The variation in R with cyclopentanone pressure at 3 130 Å presented in Fig. 1 shows R to definitely decrease at substrate pressures below 4 mm Hg for both the normal and deuterated compound, while Fig. 2 presents the more dramatic effect observed at 2 537 Å. The results with normal cyclopentanone represent overlapping data from two photolysis cells of similar geometry but differing by a factor of 3 in volume. It was further demonstrated that, over the entire pressure range studied, R was not a function of light intensity. The data in Table I also indicate that no apparent change in R with irradiation time or percent decomposition occurs over the same pressure interval. This is to be contrasted with the observations of Butler, *et al.* (5) which indicated an asymptotic decrease in R taking place from 0.075–0.75% reaction, albeit in the interval 6–10 mm cyclopentanone, where, perhaps, only the last of the three sets of data in Table I would then be a relevant comparison.

TABLE I

Effect of irradiation time on [cyclo-C_4H_8]/[C_2H_4] at 3 130 Å, 102°

Cyclopentanone pressure, mm	Duration of photolysis, min	R([cyclo-C_4H_8]/[C_2H_4])	% decomp. based on CO
0.188	30	0.19_6	0.55
0.194	18	0.19_6	0.34
0.494	30	0.20_8	0.8
0.432	90	0.21_2	2.6
13.7	10	0.24_6	0.070
19.7	180	0.23_8	0.62

Furthermore, in contrast to the work of Flowers and Frey (3), no C_6 olefins or cyclohexane were detected upon photolysis of 5–6 mm cyclopentanone in the presence of up to 850 mm C_2H_4. In fact, experiments indicate addition of C_2H_4 has little or no effect on R at this pressure other than reducing the actual amounts of C_2H_4 and cyclo-C_4H_8 formed. This conclusion rests upon the measurement of CO and cyclo-C_4H_8 in the presence of added C_2H_4 and assuming the relation [CO] = $\frac{1}{2}$[C_2H_4] + [cyclo-C_4H_8] still holds.

It seemed entirely possible that subsequent to energy absorption, cyclopentanone isomerized rapidly to either an electronically or a vibrationally excited state of 4-pentenal from which the observed hydrocarbons then arose. Consequently it was deemed relevant to look at both the photolysis and pyrolysis of 4-pentenal. Photolysis of well-characterized

Can. J. Chem. Downloaded from www.nrcresearchpress.com by 210.87.254.42 on 09/05/12
For personal use only.

samples of 4-pentenal at 3 130 Å and 100° over the range 1.0–30 mm 4-pentenal afforded butene-1 as the major (90%) hydrocarbon product along with smaller amounts ($\sim 2\%$) of C_2H_4, C_3H_6, butene-2, and pentene-1; formaldehyde and acetaldehyde were also evident. These products suggest concomitant molecular and free radical reaction modes. Pyrolysis of 4-pentenal by the toluene carrier technique at 575° and 0.1–0.2 s contact time yielded propylene and C_2H_4 as major hydrocarbon products plus smaller amounts of butene-1 and butene-2. No cyclo-C_4H_8 was evident in either photolysis or pyrolysis of 4-pentenal.

Discussion

A mechanism for the photolysis of cyclopentanone must allow for the following salient features: (*a*) variation of the 4-pentenal:CO ratio with pressure, wavelength, and temperature (6); (*b*) invariance of cyclo-C_4H_8:C_2H_4 ("*R*") with pressure and wavelength at high pressures (6); and (*c*) the wavelength-dependent decrease in *R* at low pressure. Srinivasan (6) originally suggested the vibrational energy possessed by the electronically excited cyclopentanone at the instant of its decomposition determines its mode of photolysis. His mechanism may be schematically represented as

$$\overline{CH_2CH_2CH_2CH_2CO} \xrightarrow{h\nu} (C_4H_8CO)^* \xrightarrow{k'M} \text{4-pentenal}$$
$$(C_4H_8CO)^* \xrightarrow{k_1} 2C_2H_4 + CO \qquad (C_4H_8CO)^* \xrightarrow{k_2} \square + CO$$

and is adequate to explain (*a*) and (*b*) above. To the extent that such a scheme appears to be insufficient to cope with (*c*), further definition is needed to allow for an added source of ethylene at low pressure, most likely at the expense of cyclobutane. A modification which essentially retains the concept of three independent reaction paths is the following.

$$\overline{CH_2CH_2CH_2CH_2C{=}O} \xrightarrow{h\nu} (C_4H_8CO)^* \xrightarrow{k'M} \text{4-pentenal}$$
$$(C_4H_8CO)^* \xrightarrow{k_1} C_2H_4 + C_2H_4CO \xrightarrow{k_4} C_2H_4 + CO$$
$$(C_4H_8CO)^* \xrightarrow{k_2} \square^* + CO \xrightarrow{k_3} 2C_2H_4 \qquad \square^* \xrightarrow{kM} \square$$

The species $C_4H_8CO^*$ initially presents a rather narrow spectrum of energies defined by the absorbed radiation and the thermal energy distribution of cyclopentanone. This designation may in fact include several discrete species representing various photophysical processes such as intersystem crossing and internal conversion. That the structure of $C_4H_8CO^*$ is in part like 4-pentenal might conceivably be inferred from its collisional conversion to 4-pentenal. However, the failure of 4-pentenal, on pyrolysis or photolysis, to give any trace of cyclo-C_4H_8 must be invoked against such a possibility. A diradical structure for $C_4H_8CO^*$ ties in well with its proposed unimolecular reactions; but this should not be construed as definite evidence for such a configuration. The decomposition of $C_4H_8CO^*$ into C_2H_4 and C_2H_4CO (which subsequently affords C_2H_4 and CO) is necessary to formally distinguish this route to C_2H_4, and hence k_1, from the additional source of C_2H_4 represented by the sequence involving k_2 and k_3. The reaction path utilizing k_1 has an obvious analogy to the formation of C_2H_4 and ketene in cyclobutanone photolysis. Further justification for considering such a similarity will be made in the discussion arising out of the cyclobutanone data.

Because of the energy partitioning with CO during its formation, cyclo-$C_4H_8^*$ carries a wider range of energies than its parent, $C_4H_8CO^*$. As with $C_4H_8CO^*$, no direct evidence has been obtained on its precise configuration; but one real possibility would be for

Can. J. Chem. Downloaded from www.nrcresearchpress.com by 210.87.254.42 on 09/05/12
For personal use only.

$C_4H_8CO^*$ to yield cyclo-C_4H_8 and CO directly, as Srinivasan (1) supposes. The formation of cyclo-C_4H_8 and CO from cyclopentanone requires around 26 kcal/mole. When this figure is combined with the 91 kcal/mole representing 3 130 Å radiation, one finds that 65 kcal/mole plus the thermal energy of $C_4H_8CO^*$ are to be partitioned between cyclo-C_4H_8 and CO. Because of its many more vibrational degrees of freedom it is likely that cyclo-C_4H_8 will carry away the majority of this energy. A similar energy calculation suggests even more convincingly the participation of vibrationally excited cyclo-C_4H_8 at 2 537 Å. Thus it is proposed that this species contains enough energy at both 3 130 Å and 2 537 Å to yield two molecules of C_2H_4 (a process for which an activation energy of 61 kcal/mole has been reported (7)) if it is not collisionally deactivated first.

Having thus delimited the various reactive species and their possible fates, comparison between mechanistic predictions and experimental observations opens further areas for discussion. A mathematical analysis of the mechanism with the usual steady-state assumptions gives for R, the ratio cyclo-C_4H_8:C_2H_4

$$R = \frac{k_2 k M}{2k_1 k M + 2k_3(k_2 + k_1)}.$$

At high pressure R approaches $k_2/2k_1$ independent of substrate pressure. Figures 1 and 2 indicate this high pressure limit is independent of wavelength and deuterium substitution, while Srinivasan's (6) data indicate R does not vary with temperature either. It seems possible to suggest two explanations for such behavior: either the Rice, Ramsperger, Kassel (RRK) expressions, $k = A(1 - (E_a/E))^{s-1}$, for k_1 and k_2 are congruent over the range of energies involved or C_4H_8 is already so highly excited as a result of 3 130 Å absorption that the decompositional modes represented by k_1 and k_2 are insensitive to the further gross change in energy when irradiating with 2 537 Å. A choice of explanations is not possible unless one makes the rather dubious assumption that the collisional deactivation efficiency k' does not change with wavelength. This allows one to turn to other information to resolve the point. Thus, the mechanism proposed above demands [4-pentenal]/[CO] = $k'M/(k_1 + k_2)$, a linear relationship which has been observed by Srinivasan (6) at 125° and 3 130 Å. The limited data provided by Srinivasan indicates a lower slope for [4-pentenal]/[CO] at 2 537 Å, and hence $(k_1 + k_2)$ appears to change with energy. Therefore the constancy of R would result from the former assumption, namely that of coincident RRK expressions for k_1 and k_2, at least over the energy interval 3 130 – 2 537 Å.

In the high pressure region the refined mechanism concurs additionally with the results obtained from the photolysis of cyclopentanone-2,2,5,5-d_4 where only ethylene-1,1-d_2 was found (1). Since these experiments were done above 11 mm cyclopentanone and in the region where only k_1 determines the source of C_2H_4, the more statistical distribution of deuterated ethylene which would indicate the participation of "hot" cyclobutane is not expected.

As the pressure tends to zero, R becomes a function of M, the substrate pressure:

$$R(M \to 0) \simeq \frac{k_2 k M}{2k_3(k_2 + k_1)}$$

in accord with the behavior observed. However, a strictly linear dependence of R on M in the limit is to be qualified by a concurrent decrease in k_3 with decreasing pressure. This occurs because the lower the pressure the greater is the relative contribution to the formation of ethylene from molecules of cyclo-$C_4H_8^*$ with smaller reaction probabilities,

Can. J. Chem. Downloaded from www.nrcresearchpress.com by 210.87.254.42 on 09/05/12
For personal use only.

i.e. smaller values of k_3, so that an increasingly more positive slope is expected in the R vs. pressure plots as one approaches zero pressure. In this low pressure region the lower value of R at 2 537 Å compared to that at 3 130 Å for a given substrate pressure reflects the higher energy content of cyclo-C_4H_8* and the consequently larger value of k_3. No doubt a lower efficiency for collisional deactivation contributes to the lower values of the ratio R at 2 537 Å, also.[2]

Since the expression above for the ratio R involves k_3, the rate constant which describes the unimolecular decomposition of activated cyclo-C_4H_8, it is in this low pressure range that photolysis of cyclopentanone-2,2,5,5-d_4 might serve to support our proposal for participation of vibrationally excited cyclo-C_4H_8.

B. Cyclobutanone

Results

As in earlier literature (1) the products observed were C_2H_4, CH_2CO, C_3H_6, cyclo-C_3H_6, and CO. At 3 130 Å and 100° $[CO]/([C_3H_6] + [\text{cyclo-}C_3H_6]) = 1.1 \pm 0.1$ over the range 10–200 mm cyclobutanone, contrary to previous data indicating CO to be formed much in excess of C_3's (8). However, equivalence of CO with total C_3's is to be expected if their formation is concurrent and CH_2CO photolysis negligible. At 100 °C and over the pressure range 10–200 mm cyclobutanone the ratio C_2H_4:CO was 1.7 ± 0.1 at both 3 130 Å and 2 537 Å. A slight ($\sim$ 1 kcal/mole) temperature coefficient was noted in the latter ratio at 3 130 Å. Other than this, at a given substrate pressure, no temperature variation in the product distribution was detectable. As with cyclopentanone, irradiation of 2–5 mm cyclobutanone in a large excess of C_2H_4 failed to yield the pentenes previously attributed to the interaction of trimethylene and C_2H_4 (3). The pressure dependence of R at 3 130 Å is depicted in Fig. 3 and in Fig. 4 for data obtained at 2 537 Å, all experiments performed at 100°. Thirty-fold variation in lamp intensity again did not alter the data.

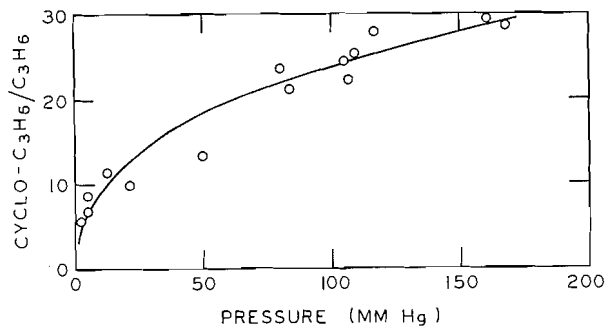

FIG. 3. Ratio of product yields cyclo-C_3H_6:C_3H_6 vs. cyclobutanone pressure; at 3 130 Å and 100°.

Discussion

Although the data obtained in cyclobutanone photolysis parallel, in general, that from cyclopentanone, the products of cyclobutanone photolysis show a number of differences: (*a*) a very minor isomerization product analogous to 4-pentenal (1); (*b*) two distinct sets of decomposition products; and (*c*) potential rearrangement rather than decomposition of the cyclic hydrocarbon if sufficient energy is available. Lack of the rearrangement product, 3-butenal, is to be expected for reasons based on the geometry of the nearly

[2]*A referee has kindly pointed out that if a single collision does not render cyclo-C_4H_8* incapable of decomposition, then the effect of a series of collisions would be to lower the average energy of cyclo-C_4H_8*, and thus lower the average k_3 with increasing pressure.*

Can. J. Chem. Downloaded from www.nrcresearchpress.com by 210.87.254.42 on 09/05/12
For personal use only.

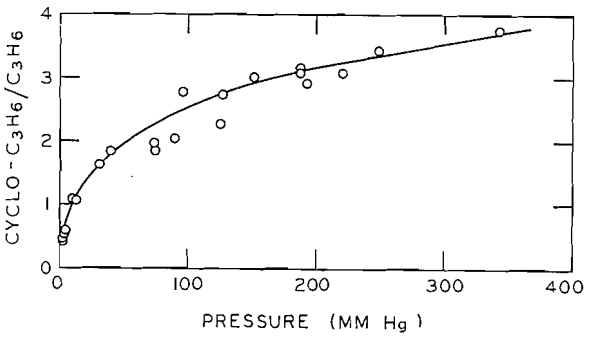

FIG. 4. Ratio of product yields, cyclo-C_3H_6:C_3H_6 vs. cyclobutanone pressure; at 2 537 Å and 100°.

planar cyclobutanone ring, provided such an isomerization is viewed as a concerted four-center process (1). In addition, compared to cyclopentanone, cyclobutanone contains half the number of β-hydrogens that are directly involved in aldehyde formation. On energetic grounds less 3-butenal would be expected simply because a comparable energy must be distributed among fewer degrees of freedom and a greater tendency exists for a 3-butenal precursor to decompose. The formation of C_2H_4 and CH_2CO may be considered a parallel to that reaction of cyclopentanone affording initially C_2H_4 and C_2H_4CO. The pressure effect shown in Figs. 3 and 4 implies that allowance must be made both for the unimolecular rearrangement of an excited cyclopropane and its deactivation or stabilization by collision.

Pursuant to this line of reasoning the following mechanism is proposed in analogy with that developed for the cyclopentanone photolysis:

$$CH_2CH_2CH_2C{=}O \xrightarrow{h\nu} (C_3H_6CO)^* \dashrightarrow H_2C{=}CH{-}CH_2CHO$$

$$(C_3H_6CO)^* \xrightarrow{k_1} C_2H_4 + CH_2O$$

$$(C_3H_6CO)^* \xrightarrow{k_2} \text{cyclo-}C_3H_6^* + CO$$

$$\text{cyclo-}C_3H_6^* \xrightarrow{k_3} C_3H_6$$

$$\text{cyclo-}C_3H_6^* \xrightarrow{kM} \text{cyclo-}C_3H_6.$$

Here $(C_3H_6CO)^*$ is considered to initially have that rather narrow energy spectrum characteristic of the absorbed radiation. The same loose definition of $(C_3H_6CO)^*$ applies here as was developed in the case of $(C_4H_8CO)^*$. The dotted arrow to 3-butenal indicates the absence, or extremely small importance, of this reaction path while preserving the analogy to cyclopentanone. According to this reaction sequence it is obvious that the ratio C_2H_4:CO is given by k_1/k_2. Experimentally a value 1.7 ± 0.1 has been found to be independent of wavelength and pressure. This is compared with the similar value from cyclopentanone of $k_1/k_2 = 2$, which is the high pressure limit of $[C_2H_4]/2[\text{cyclo-}C_4H_8]$ and is likewise wavelength independent. Such coincidence in value and behavior, though possibly fortuitous, adds a measure of reinforcement to such a unified mechanism for both ketones.

Simultaneous with its elimination of CO, $C_3H_6CO^*$ is allowed to form a cyclo-C_3H_6 structure, for which process, beginning with cyclobutanone, about 16 kcal/mole are required. At 3 130 Å cyclo-C_3H_6 and CO must partition $91 - 16 \simeq 75$ kcal/mole, which,

Can. J. Chem. Downloaded from www.nrcresearchpress.com by 210.87.254.42 on 09/05/12
For personal use only.

if it is accepted that cyclo-C_3H_6 retains the major portion, is sufficient energy to isomerize the cyclo-C_3H_6 to propylene. The extent of this conversion is dependent upon the rate of collisional deactivation and the exact energy content of cyclo-C_3H_6*. Hence, although a steady-state treatment of the mechanism predicts

$$\frac{[\text{cyclo-}C_3H_6]}{[C_3H_6]} = \frac{kM}{k_3}$$

in fact k_3 is a function of the energy allowed cyclo-C_3H_6*, which at 2 537 Å is on the average up to 21 kcal greater than at 3 130 Å; this accords with the smaller slope depicted in Fig. 4 compared with that in Fig. 3. In the low pressure region of Figs. 3 and 4 curvature of R vs. pressure plots is expected in the direction observed because of the wide variation in the excess energy of cyclo-C_3H_6*, the exact curvature determined by the energy of excitation distribution curve and the variation of k_3 with energy.

Although the success of the present slight modifications of the original proposals of Srinivasan (1) in correlating the photochemical behavior of cyclopentanone and cyclobutanone is certainly appealing, the type and accuracy of the data accumulated to date do not prompt the more precise definition of mechanism desired. Certainly the experimental evidence definitely establishes a pressure falloff in the ratios cyclo-C_4H_8:C_2H_4 and cyclo-C_3H_6:C_3H_6. Such behavior means the interdependent formation of cyclic hydrocarbon and its decomposition or rearrangement product will require appropriate consideration in the further elucidation of the photolysis of these cyclic ketones.

REFERENCES

1. R. SRINIVASAN. *In* Recent advances in photochemistry. Vol. I. *Edited by* W. A. Noyes, Jr., G. S. Hammond, and J. N. Pitts. Interscience. 1963. pp. 83–114.
2. S. R. LA PAGLIA and B. C. ROQUITTE. J. Phys. Chem. **66**, 1739 (1962); Can. J. Chem. **41**, 287 (1963).
3. M. C. FLOWERS and H. M. FREY. J. Chem. Soc. 2758 (1960).
4. C. D. HURD and M. A. POLLACK. J. Am. Chem. Soc. **60**, 1905 (1938).
5. J. N. BUTLER, A. T. DRAKE, J. C. MITCHELL, and P. SINGH. Can. J. Chem. **41**, 2704 (1963).
6. R. SRINIVASAN. J. Am. Chem. Soc. **83**, 4344 (1961).
7. C. T. GENAUX and W. D. WALTERS. J. Am. Chem. Soc. **73**, 4497 (1951); **75**, 6196 (1953).
8. F. E. BLACET and A. MILLER. J. Am. Chem. Soc. **79**, 4327 (1957).

Can. J. Chem. Downloaded from www.nrcresearchpress.com by 210.87.254.42 on 09/05/12
For personal use only.

Can. J. Chem. Downloaded from www.nrcresearchpress.com by 210.87.254.40 on 09/05/12
For personal use only.

THE RELATIVE SIGNS OF THE PROTON COUPLING CONSTANTS IN DIKETENE AND VINYL FORMATE

F. HRUSKA,[1] H. M. HUTTON, AND T. SCHAEFER[2]
Department of Chemistry, University of Manitoba, Winnipeg, Manitoba

Received February 2, 1965

ABSTRACT

The relative signs of the proton coupling constants in diketene and vinyl formate have been determined by the field-sweep selective decoupling method. In both compounds, the couplings between protons separated by an even number of bonds are of the same sign, but of opposite sign to the couplings between protons separated by an odd number of bonds. The coupling mechanisms, especially in vinyl formate, are discussed briefly.

INTRODUCTION

In proton magnetic resonance, coupling between protons separated by more than three bonds is called "long-range coupling" and is observed in many molecules. A recent review by Sternhell collects a considerable body of data on this topic (1). One of the uses of these data will be in the establishment of configurations and conformations of organic molecules (1). Less is known about the relative signs of the coupling constants, which can be determined sometimes by the analysis of strongly coupled spectra (2). However, the method of double irradiation is more powerful in this respect (3–8).

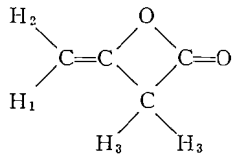

I

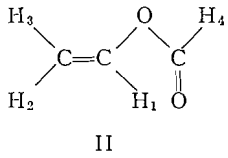

II

In this paper we describe the determination of the relative signs of the coupling constants in diketene and vinyl formate (I and II) by Freeman's selective double irradiation method (4, 5). Although the magnitudes of the coupling constants are known for both diketene (9) and vinyl formate (measured in this laboratory (12)), the spectra at 40 or 60 Mc/s are not strongly coupled and the relative signs had not been determined. The long-range couplings in diketene, $H_{1,2}$—C=C—C—H_3, are known as allylic couplings (1), while the long-range couplings in vinyl formate are an example of coupling across a hetero atom, oxygen.

EXPERIMENTAL

1. Materials

Diketene was obtained from the Aldrich Chemical Company and vinyl formate from the Borden Chemical Company. Both chemicals were used without further purification. Diketene was studied as a 6 mole % solution in benzene with tetramethylsilane (TMS) as an internal reference. At this concentration the proton spectrum was approximately an AKX_2 system (11). Vinyl formate was studied with 2 mole % TMS as internal reference and the spectrum was nearly an AKRX system (11).

2. Single Resonance Measurements

The spectra of the two solutions were recorded on a Varian DP60 spectrometer at room temperature and calibrated by the side-band technique. The spectra were analyzed as ABX_2 (diketene) and ABRX (vinyl formate) systems using an average of at least 10 spectra.

[1]*Holder of a N.R.C. Studentship, 1964–1965.*
[2]*Holder of an N.R.C. Senior Research Fellowship, 1964–1965.*

3. Double Resonance Experiments

The double resonance experiments involved a Varian integrator V3521A and Hewlett-Packard 200CD audio oscillator to which a set of reduction gears was attached, allowing changes in frequency settings of 0.1 c/s at about 2 kc/s. The frequency of the 2kc/s side band of the integrator varied slightly from day to day and was remeasured before each set of experiments. The required frequency settings for the selective double irradiation experiments by field-sweep methods were obtained from the measured line positons in the single resonance spectra and are reliable to ±0.2 c/s. All calculated decoupling frequencies for various relative sign possibilities were examined for complete decoupling.

RESULTS

The chemical shifts with respect to internal TMS and the coupling constants are given in Table I. The numbering is as in I and II above. Figures 1 and 2 show the single resonance spectra obtained for these two compounds. For the convenience of tabulating the decoupling data below, the proton peaks for vinyl formate are numbered in Fig. 2, starting from high field.

TABLE I

Coupling constants and chemical shifts in diketene and vinyl formate in c/s at 60 Mc/s

Coupling constants*		Chemical shifts†	
Diketene	Vinyl formate	Diketene	Vinyl formate
$J_{12} = -3.87\ (3.92)$‡	$J_{12} = 6.4\ (6.3)$§	$H_1 = -271.5$	$H_1 = -439.8$
$J_{13} = -1.94\ (1.82)$	$J_{13} = 13.9\ (13.8)$	$H_2 = -236.8$	$H_2 = -279.5$
$J_{23} = -1.36\ (1.34)$	$J_{23} = -1.7\ (-1.7)$	$H_3 = -182.0$	$H_3 = -297.3$
	$J_{14} = -0.7\ (0.6)$		$H_4 = -484.1$
	$J_{24} = 1.6\ (1.7)$		
	$J_{34} = 0.8\ (0.8)$		

*The relative signs were determined by the double resonance experiments and are assumed to be negative for protons separated by an even number of bonds.
†Chemical shifts relative to internal TMS for a 6 mole % solution of diketene in benzene and for neat vinyl formate.
‡Reference 9.
§Reference 10.

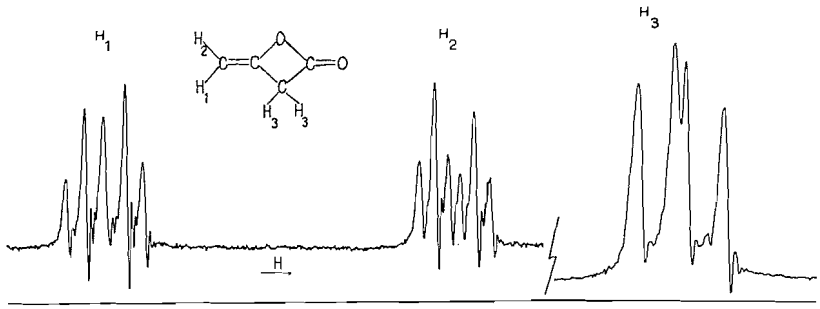

FIG. 1. Proton magnetic resonance spectrum of a 6 mole % solution of diketene in benzene at 60 Mc/s; the H_3 spectrum was obtained at a different sweep rate and gain than the H_1 and H_2 spectra.

1. Diketene

Two sets of experiments were necessary to find the relative signs of the three couplings. In the first, the peaks of proton H_3 (in the first order limit) were irradiated collapsing the multiplet due to the coupling J_{13}, while the H_1 peaks were observed with the low power modulation frequency. Figure 3*a* shows the collapse of the high-field triplet in the H_1 spectrum for a decoupling frequency of 90.7 c/s. In the second experiment, the peaks of H_3 were again irradiated collapsing the multiplet due to the J_{23} coupling, while the H_2 peaks were observed. Although other possible experiments were also performed as a check, the results of the two experiments are sufficient and are given in Table II.

Can. J. Chem. Downloaded from www.nrcresearchpress.com by 210.87.254.40 on 09/05/12
For personal use only.

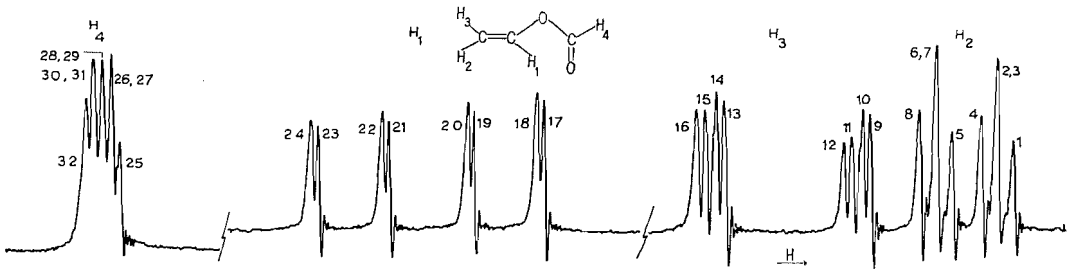

FIG. 2. Proton magnetic resonance spectrum of neat vinyl formate at 60 Mc/s. The lines are numbered from high field to indicate the transitions for each proton in an AKRX system. Each proton group was not obtained at the same sweep rate and gain.

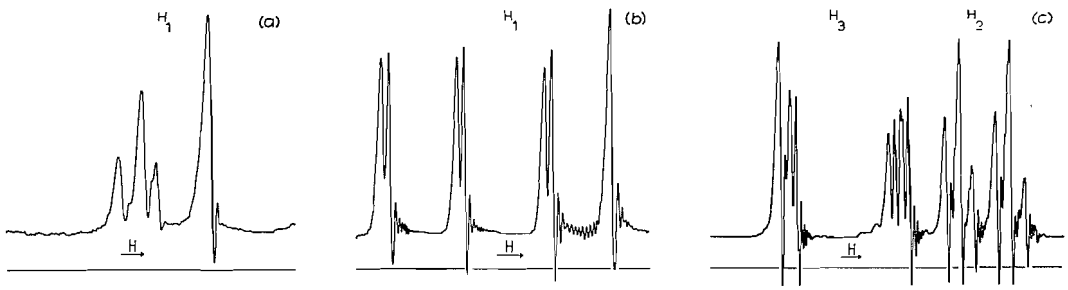

FIG. 3. Examples of decoupled spectra. (*a*) The H_1 spectrum of diketene while irradiating H_3 with a decoupling frequency of 90.7 c/s. (*b*) The collapse of lines 17, 18 of the H_1 spectrum of vinyl formate while irradiating H_4 with a decoupling frequency of 53.0 c/s. (*c*) The collapse of lines 15, 16 of the H_3 spectrum of vinyl formate while irradiating H_4 with a decoupling frequency of 177.7 c/s. The fields were swept from low to high field.

TABLE II

Calculated and experimental frequencies for the decoupling of diketene

	Decoupling frequencies (c/s)			
	J_{12}/J_{23}		J_{12}/J_{13}	
Relative signs	(*a*)* Collapse of low-field H_1 triplet	(*b*) Collapse of high-field H_1 triplet	(*c*) Collapse of low-field H_2 triplet	(*d*) Collapse of high-field H_2 triplet
+	88.2	90.8	53.8	55.9
−	86.8	92.2	51.9	57.8
Experimental value	88.1±0.2	90.7±0.2	53.7±0.2	55.8±0.2

*Values calculated from calibrated line positions, accurate to about ±0.2 c/s.

2. Vinyl Formate

At least three experiments were necessary (although others were performed). Each of the three yielded the relative signs of two sets of coupling constants. In the first experiment, the H_4 peaks were irradiated to collapse the multiplet due to J_{14} while observing the H_1 peaks. A typical result for this experiment is shown in Fig. 3*b*. In the second experiment, the H_1 peaks were observed while a J_{12} multiplet was collapsed by irradiation in the H_2 spectrum. For the third experiment, the H_3 peaks were observed while a J_{34} multiplet was collapsed by irradiation of the H_4 spectrum. Figure 3*c* shows a typical result for this last experiment. The results of these experiments are given in Table III.

Can. J. Chem. Downloaded from www.nrcresearchpress.com by 210.87.254.40 on 09/05/12
For personal use only.

TABLE III

Calculated and experimental frequencies for the decoupling of vinyl formate

Relative signs J_{12} J_{13} / J_{24} J_{34}	Decoupling frequencies* (c/s)			
	Collapse of† H_1 lines 17, 18	Collapse of H_1 lines 19, 20	Collapse of H_1 lines 21, 22	Collapse of H_1 lines 23, 24
+ +	53.3	48.5	40.0	35.4
+ −	54.0	49.2	39.2	34.7
− +	54.9	46.9	41.6	33.8
− −	55.6	47.6	40.9	33.0
Experimental value	53.0±0.2	48.1±0.2	40.0±0.2	35.0±0.2

Relative signs J_{14} J_{13} / J_{24} J_{23}	Decoupling frequencies* (c/s)			
	Collapse of H_1 lines 17, 19	Collapse of H_1 lines 18, 20	Collapse of H_1 lines 21, 23	Collapse of H_1 lines 22, 24
+ +	154.7	153.7	167.0	165.9
+ −	153.0	152.0	168.6	167.6
− +	153.0	155.4	165.3	167.6
− −	151.3	153.7	167.0	169.3
Experimental value	151.6±0.1	153.9±0.1	167.0±0.1	169.5±0.1

Relative signs J_{13} J_{23} / J_{14} J_{24}	Decoupling frequencies* (c/s)			
	Collapse of H_3 lines 9, 10	Collapse of H_3 lines 11, 12	Collapse of H_3 lines 13, 14	Collapse of H_3 lines 15, 16
+ +	193.4	193.3	180.4	180.2
+ −	195.1	191.7	182.0	178.6
− +	194.1	194.0	179.6	179.5
− −	195.7	192.4	181.3	177.9
Experimental value	195.5±0.1	192.3±0.1	181.0±0.1	177.7±0.1

*Calculated decoupling frequencies accurate to about ±0.2 c/s.
†Line numbers are those indicated in Fig. 2.

DISCUSSION

1. *Diketene*

The sign of the geminal coupling is of the same sign as the long-range allylic couplings. Allylic couplings are transmitted mainly through the π-electron system and are expected theoretically (10) and found experimentally to be negative and to lie in the range 0–3 c/s (1). Presumably, therefore, the geminal coupling in diketene is negative. This sign agrees with that found for geminal couplings in vinyl esters (13). The magnitude of these is about 1.5–1.7 c/s (see vinyl formate) and it would appear that ring strain in diketene causes a considerable increase in the magnitude of this coupling. This may be due to hybridization changes in the carbon atom on ring formation, but at present there is no published theory which accounts for this increase in magnitude.

The magnitude of the allylic coupling J_{23} (transoid) is generally found to be smaller in magnitude than J_{13} (cisoid). Our numbering system in I above therefore agrees with these findings (1). It also seems likely (1) that the magnitude of the allylic couplings should depend on the angle θ made by the C—H_3 bond and the plane of the double bond. This possibility depends on the amount of σ–π overlap and would be at a maximum for $\theta = \pi/2$ and a minimum for $\theta = 0$. An intermediate angle would be expected for diketene, leading to the observed finite values of the allylic couplings.

Can. J. Chem. Downloaded from www.nrcresearchpress.com by 210.87.254.40 on 09/05/12
For personal use only.

2. Vinyl Formate

The two and three bond couplings have been adequately discussed for vinyl compounds elsewhere (14, 15). The vicinal proton couplings, J_{12} and J_{13}, are almost certainly positive (14, 16). In that case the signs of the couplings between protons separated by an odd number of bonds are positive and those for an even number of bonds are negative, as predicted by the Dirac vector model (17).

(a) Five Bond Couplings

Freeman and Bhacca (18) and others (1, 14) have suggested that the resonance structure III contributes, which makes vinyl formate analogous to a conjugated system. Furthermore, Rao and Curl (20) predict from microwave data that the most stable conformation

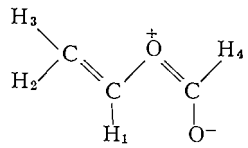

III

is approximately as in III, with the carbonyl oxygen near H_1. The structure III connects H_2 and H_4 by a "straighter" zig-zag path than H_3 and H_4, which appears to be particularly favorable for a five bond coupling in a number of molecules (14, 18, 19). Indeed J_{24} is about twice as large as J_{34}.

The formal structure for vinyl formate is analogous to H—C=C—C—C—H (with one carbon replaced by oxygen). For the former, a σ–π interaction is calculated to give +2.0 c/s for the proton coupling (12). This mechanism, however, predicts the same magnitude for J_{24} and J_{34}. It may be that $J_{34} = 0.8$ c/s is caused by the σ–π mechanism, while $J_{24} = 1.6$ c/s has an additional contribution from a mechanism, favored by the "straight" zig-zag path. In this connection it is interesting to note that in other molecules we know of in which this "straight" five bond coupling (analogous to J_{24}) is present, the coupling analogous to J_{34} is usually too small to measure (1, 14, 18, 19). The latter molecules are all aromatic for which valence bond theory predicts a very small (<0.2 c/s) contribution by the σ–π mechanism (21). In aromatic molecules, of course, there is no localized π bond.

On the other hand, there is a five bond coupling of about 0.5 c/s (sign unknown) in the alkyl formates (22). It is true that for ethyl formate, for instance, one could write a "straight" zig-zag structure, as in IV, and interpret this as evidence in favor of a σ mechanism in vinyl formate in addition to the σ–π mechanism. In IV there is no formal

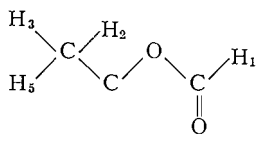

IV

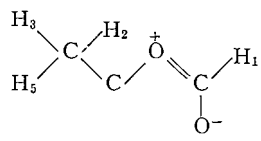

V

double bond but, of course, the resonance structure V may well contribute. There is also the question of the rotation about the C—C bond, since the measured coupling is an average of J_{15}, J_{13}, and J_{12} and not the "straight" J_{15} coupling alone. (A somewhat similar objection can be levelled against structure III for vinyl formate.)

Can. J. Chem. Downloaded from www.nrcresearchpress.com by 210.87.254.40 on 09/05/12
For personal use only.

(b) Four Bond Coupling

J_{14} is formally an example of allylic coupling if III is considered (one double and three single bonds). J_{14} has the right sign for such a coupling but the C—H_4 bond in III makes an angle of $\theta = 0$ with the plane of the $^{+}$O=C bond. This minimizes the σ–π overlap and entails a small J_{14}.

$J_{14} = 0.8$ c/s is of the same magnitude as found for the analogous coupling in the alkyl formate, which range from 0.80–0.96 c/s (sign unknown (22)). If steric effects are important, as implied in the above discussion for both four and five bond couplings, then a change in conformer populations by solvent or temperature effects may lead to changes in magnitude of the long range couplings. Such experiments are being carried out on vinyl formate.

ACKNOWLEDGMENTS

We are grateful to Dr. K. McLauchlan for discussions on diketene. His unpublished sign determinations for this molecule are in agreement with ours. We are grateful to the National Research Council for financial support.

REFERENCES

1. S. STERNHELL. Rev. Pure Appl. Chem. **14**, 15 (1964).
2. J. A. POPLE and T. SCHAEFER. Mol. Phys. **3**, 547 (1961).
3. R. FREEMAN. Mol. Phys. **3**, 435 (1960).
4. J. P. MAHER and D. F. EVANS. Proc. Chem. Soc. 208 (1961).
5. R. FREEMAN and D. H. WHIFFEN. Mol. Phys. 4, 321 (1961).
6. W. A. ANDERSON and R. FREEMAN. J. Chem. Phys. **37**, 85 (1962); **37**, 2053 (1962); **39**, 806 (1963).
7. J. D. BALDESCHWIELER and E. W. RANDALL. Chem. Rev. **63**, 81 (1963).
8. D. W. TURNER. J. Chem. Soc. 847 (1962).
9. D. W. MOORE. J. Chem. Phys. **34**, 1470 (1961).
10. T. SCHAEFER. J. Chem. Phys. **36**, 2235 (1962).
11. J. A. POPLE, W. G. SCHNEIDER, and H. J. BERNSTEIN. High resolution nuclear magnetic resonance. McGraw-Hill Book Co., New York. 1959. Chap. 6.
12. M. KARPLUS. J. Chem. Phys. **33**, 1842 (1960).
13. W. BRÜGEL, TH. ANKEL, and F. KRÜCKEBERG. Z. Elektrochem. **62**, 1121 (1960).
14. C. N. BANWELL and N. SHEPPARD. Discussions Faraday Soc. **34**, 115 (1962).
15. M. KARPLUS. J. Am. Chem. Soc. **85**, 2870 (1963).
16. A. D. BUCKINGHAM and K. A. MCLAUCHLAN. Proc. Chem. Soc. 144 (1963).
17. H. M. MCCONNELL. J. Chem. Phys. **23**, 2454 (1955).
18. R. FREEMAN. Private communication.
19. G. J. KARABATSOS and F. M. VANE. J. Am. Chem. Soc. **85**, 3886 (1963).
20. V. M. RAO and R. F. CURL, JR. J. Chem. Phys. **40**, 3688 (1964).
21. H. M. MCCONNELL. J. Chem. Phys. **30**, 126 (1959).
22. D. G. KOWALEWSKI and V. J. KOWALEWSKI. Mol. Phys. **8**, 93 (1964).

Can. J. Chem. Downloaded from www.nrcresearchpress.com by 210.87.254.40 on 09/05/12
For personal use only.

Can. J. Chem. Downloaded from www.nrcresearchpress.com by 210.87.254.105 on 09/05/12
For personal use only.

ELECTRON SPIN RESONANCE SPECTRA OF $S_2O_2^-$ IN IRRADIATED THIOSULFATE SINGLE CRYSTALS[1]

J. R. MORTON
Division of Applied Chemistry, National Research Council, Ottawa, Canada

Received February 8, 1965

ABSTRACT

Single crystals of $Na_2S_2O_3.5H_2O$ were irradiated and examined, at room temperature, with an e.s.r. spectrometer. Two radicals are present: the species present in highest concentration is $S_2O_2^-$; the other species has not yet been identified.

INTRODUCTION

It has been suggested (1), as a result of electron spin resonance (e.s.r.) experiments on microcrystalline samples, that the radical SO_2^- is trapped in thiosulfates irradiated at room temperature. In view of recent studies of this radical in dithionite systems (2–5) and the possibility of comparison with the isoelectronic species ClO_2 (6) and SeO_2^- (7), the spectra of oriented SO_2^- radicals would be of considerable interest.

It has been shown (8) that two types of radical are trapped in irradiated thiosulfate crystals. In the present work it is demonstrated that one species is $S_2O_2^-$, and also that the other radical is unlikely to be SO_2^-.

EXPERIMENTAL

Crystals of $Na_2S_2O_3.5H_2O$ tend to effloresce, and to prevent this they were coated with a film of Saran (vinylidene chloride) by dipping them into a 25% acetone solution and allowing the solvent to evaporate. The crystals were irradiated at room temperature with X rays from a Philips tube type 25623-62; they were 5 cm from the copper target and radiation times of approximately 2 h were given. The electron spin resonance spectra were examined at room temperature with a Varian V-4502 spectrometer, and a V-4012A 12 in. magnet. The magnetic field was controlled by a VFR-2100 Fieldial Hall-effect regulator and monitored with an F-8A n.m.r. fluxmeter. The frequency of the latter was measured with a C.M.C. type 707B frequency counter, which was also used to measure the frequency of an H.P. type 540B transfer oscillator from which harmonics are generated in the X band microwave region.

Crystals of $Na_2S_2O_3.5H_2O$ are monoclinic (9) having the unit-cell parameters $a = 5.94$, $b = 21.57$, $c = 7.53$ Å, $\beta = 103°58'$, $Z = 4$, in the space group $P2_1/c$. The crystals were prismatic and elongated along the a-axis, developing the faces {011} and, less strongly, {001}, {010}. The irradiated crystals were mounted on a two-circle Teflon goniometer (10) so that the a-axis was horizontal and the crystals could be rotated in the magnetic field about the a-axis or about any axis perpendicular to the a-axis. The axis-system chosen was crystallographic abc^* axis-system, to which all direction cosines therefore refer.

RESULTS

The freshly irradiated crystals of $Na_2S_2O_3.5H_2O$ were brown in color and the e.s.r. spectrum indicated the presence of two radicals, designated A and B. Radical A had an average g-value (one-third diagonal sum) of 2.0054, whereas that of radical B was 2.0143. Initially the concentration ratio A:B exceeded 20:1, but after a few days at room temperature the concentration ratio became 1:1 or less, because of the more rapid decay of the signal from radical A. During this time the brown coloration also faded. It will be shown that radical A is $S_2O_2^-$; radical B has not yet been identified, but, if an isotropic g-value of 2.005 is a prerequisite for SO_2^- (2–5), B is not SO_2^- either.

Figure 1 shows the spectrum of a freshly irradiated crystal of $Na_2S_2O_3.5H_2O$ for the orientation H_0 parallel to c^*. The hyperfine interaction of two non-equivalent ^{33}S nuclei

[1]*Issued as N.R.C. No. 8429.*

(spin 3/2, abundance 0.74%) in radical A is revealed, although for this orientation only the outer component of one quartet is visible. The tensors for the two ^{33}S hyperfine interactions in radical A were determined, using second-order theory (11) for the larger interaction. The g-tensors of radicals A and B (normal isotopic species) were also assembled. The tensors are listed in Table I together with the principal values and their direction cosines.

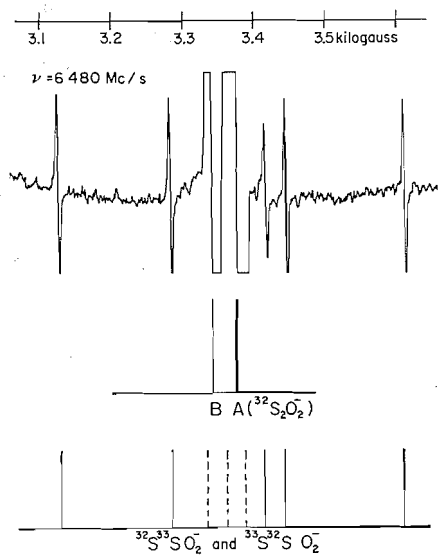

FIG. 1. First derivative electron spin resonance spectrum of a crystal of $Na_2S_2O_3.5H_2O$ irradiated at 300 °K; H_0 parallel to c^*.

TABLE I

^{33}S hyperfine tensors (Mc/s) and g-tensors of radicals trapped in irradiated $Na_2S_2O_3.5H_2O$ crystals

Radical	Tensor			Principal values	Principal directions in abc^* axis-system		
$^{32}S_2O_2^-$ (g)	2.0048	0	−0.0013	2.0083±0.0002	(0.262,	±0.613,	−0.746)
	0	2.0055	∓0.0024	2.0050	(0.857,	∓0.503,	−0.112)
	−0.0013	∓0.0024	2.0060	2.0030	(0.443,	±0.610,	0.657)
$^{32}S^{33}SO_2^-$ (^{33}S hfs)	406	0	0	513±10	(0.000,	±0.831,	0.557)
	0	480	±49	407	(0.000,	∓0.557,	0.831)
	0	±49	440	406	(1.000,	0.000,	0.000)
$^{33}S^{32}SO_2^-$ (^{33}S hfs)	45	0	−18	114±5	(0.191,	∓0.665,	−0.722)
	0	80	±31	59±10	(0.598,	±0.662,	−0.452)
	−18	±31	80	32±10	(0.779,	∓0.345,	0.524)
B	2.0042	0	−0.0041	2.0287	(0.164,	∓0.129,	−0.978)
	0	2.0108	±0.0023	2.0106	(0.074,	±0.990,	−0.118)
	−0.0041	±0.0023	2.0278	2.0035	(0.984,	∓0.053,	0.172)

DISCUSSION

A comparison of the principal values of the larger ^{33}S hyperfine tensor and the g-tensor of radical A with the same parameters (12) for $^{33}SO_3^-$ suggests that the two radicals are very similar and that A is $S_2O_2^-$. In radical A the major hyperfine tensor has principal

Can. J. Chem. Downloaded from www.nrcresearchpress.com by 210.87.254.105 on 09/05/12
For personal use only.

values 513, 407, and 406 Mc/s, whereas in $^{33}SO_3^-$ values of 428, 316, and 314 Mc/s were reported. In radical A the isotropic g-value is 2.0054, and the tensor possesses some anisotropy; the g-factor of SO_3^- was isotropic and equal to 2.0036 ± 0.0007.

The orbital scheme proposed (12) for the ground state of SO_3^-, a pyramidal radical with C_{3v} symmetry, was

$$\ldots . (3a_1)^2(3e)^4(4e)^4(1a_2)^2(4a_1)^1(5a_1)^0(5e)^0, {}^2A_1.$$

Contributions to the singly occupied $4a_1$ orbital were estimated (12) to be 0.13 from sulfur 3s and 0.49 from sulfur $3p_z$. Lowering the symmetry to C_{1h} by the substitution of a second sulfur atom for an oxygen atom, the ground state becomes $^2A'$, and approximate contributions[2] to the singly occupied orbital are 0.16 and 0.45 from central sulfur 3s and $3p_\sigma$ respectively.

The lower symmetry also removes the requirement that the central-atom hyperfine tensor and the g-tensor be coaxial and have cylindrical symmetry. It will be seen from the data in Table I that these two tensors are not diagonal in a common axis-system, and the g-tensor is not cylindrically symmetrical. One requirement of C_{1h} symmetry is that one of the principal g-values be perpendicular to the unique direction of the central ^{33}S hyperfine tensor. The principal value 2.0083 fulfills this requirement, being $\cos^{-1}$ 0.094, or 84.6° from the direction corresponding to the 513 Mc/s hyperfine interaction. The same symmetry requirement is fulfilled by the principal value 59 Mc/s of the small ^{33}S hyperfine tensor, being $\cos^{-1}$ 0.298 or 72.7° from the direction corresponding to the 513 Mc/s hyperfine interaction. The correlation in this case is less exact, owing to experimental difficulties in determining the smaller principal values and directions of the hyperfine tensor in $^{33}S^{32}SO_2^-$.

Within the experimental error, therefore, it appears that the direction normal to the symmetry plane of the radical (z) is to be associated with the largest principal g-value (2.0083) and the intermediate principal value (59 Mc/s) of the (terminal) ^{33}S hyperfine interaction, the angle between these directions being $\cos^{-1}$ 0.900 or 25.9°.

The deviation from cylindrical symmetry in the principal values (assumed positive) of the smaller ^{33}S hyperfine tensor is real, although not of great significance in view of the experimental errors involved in the determination of the smaller principal values of this tensor. It may be diagnostic of configuration interaction giving rise to positive spin-density in the terminal sulfur $3p_\pi$ orbital, and negative spin-densities in the oxygen $2p_\pi$ orbitals, the mechanism (13) for which would involve admixture into the $^2A'$ ground state of configurations involving unpaired spins in a'' orbitals. An objection to this mechanism is the large excitation energy between the $1a_2$ orbital and the $5e$ orbital, which, under C_{1h}, would correspond to the required $(a'')^2 \rightarrow (a'')^0$ promotion. An alternative possibility not quite so energetically unfavorable involves negative spin-density in a terminal sulfur $3p_\sigma$ orbital due to $(a') \rightarrow (a')$ promotion. In any event, the contributions to the singly occupied a' orbital from the terminal sulfur atom are: 3s, 0.02; and $3p_\sigma$, at least 0.23.

In SO_3^- (12) it was deduced that each oxygen $2p_z$ orbital contributed 0.13 to the singly occupied $4a_1$ orbital, and in $S_2O_2^-$ it appears that the contribution from the terminal sulfur atom has increased at the expense of that from the oxygen atoms. This can be attributed (14) to the lower electronegativity of the substituted sulfur atom.

It has been demonstrated that the largest g-shift observed in $S_2O_2^-$ corresponds to the

[2]*In calculating spin-densities for* ^{33}S *the following parameters were used (12):*

$$(8\pi g\beta\gamma/3h)\psi_{3s}^2(0) = 2\,715 \text{ Mc/s},$$
$$(2g\beta\gamma/5h)\langle r^{-3}\rangle_{3p} = 78 \text{ Mc/s}.$$

Can. J. Chem. Downloaded from www.nrcresearchpress.com by 210.87.254.105 on 09/05/12
For personal use only.

direction (z) normal to the symmetry plane ($\Delta g_{zz} = +0.006$). Under C_{1h}, R_z (rotation about an axis perpendicular to the symmetry plane) belongs to the representation A', and so the non-zero Δg_{zz} must arise from spin–orbit interaction between the ground $^2A'$ state and an excited A' state. The first excited $^2A'$ state in $S_2O_2^-$ probably corresponds to the configuration . . . $[(a'')^2 + (a')](a'')^2(a')^2$; where the square brackets enclose orbitals deriving from the $4e$ orbital in SO_3^-. Spin–orbit interaction between this state and the ground state would account for a positive Δg_{zz}.

The signal from radical B was too weak to allow detection of ^{33}S hyperfine structure. An identification based on the principal g-values alone is somewhat conjectural, but one possibility is that B is polyatomic sulfur biradicals. In molten sulfur (15) such radicals have an isotropic g-value of 2.024, and the spectrum of sulfur dissolved in certain amines and cooled to 77 °K (16) was indicative of principal g-values 2.055, 2.035, 2.003. Radicals can also be detected in sublimed sulfur (17) where the principal values are 2.039, 2.025, 2.000. The correlation of these data with those of radical B is not compelling, but the possibility that B is elemental sulfur in some form must be borne in mind, since colloidal sulfur is formed when irradiated thiosulfates are dissolved in water (18).

Another possibility is that B is $S_2O_3^-$. Tetrahedral radicals such as SO_4^- and PO_4^{2-} have been detected (19), and the principal g-values for SO_4^- in persulfate are 2.033, 2.008, 2.004 (average 2.0149). Such radicals are expected to possess a . . . t_1^5 ground configuration (20) under T_d symmetry. The anisotropy of the g-tensor is thought to be due to crystal-field or Jahn-Teller distortion, resulting in an effective $^2A_2$ ground state under C_{2v} symmetry. If B is $S_2O_3^-$, a similar mechanism must be operative, lowering the symmetry from C_{3v} to C_{1h}. In a monoclinic unit cell there are no three-fold axes and the environment could distort the radical.

ACKNOWLEDGMENT

The author thanks Dr. L. D. Calvert for determining the unit-cell directions of the crystals, and Dr. D. H. Whiffen for a stimulating discussion.

REFERENCES

1. R. L. Eager and D. S. Mahadevappa. Can. J. Chem. **41**, 2106 (1963).
2. W. G. Hodgson, A. Neaves, and C. A. Parker. Nature, **178**, 489 (1956).
3. R. G. Rinker, T. P. Gordon, D. M. Mason, and W. H. Corcoran. J. Phys. Chem. **63**, 302 (1959).
4. P. W. Atkins, A. Horsfield, and M. C. R. Symons. J. Chem. Soc. 5220 (1964).
5. R. G. Rinker, T. P. Gordon, and W. H. Corcoran. Inorg. Chem. **3**, 1467 (1964).
6. T. Cole. Proc. Natl. Acad. Sci. U.S. **46**, 506 (1960).
7. R. J. Cook, J. R. Rowlands, and D. H. Whiffen. Mol. Phys. **8**, 195 (1964).
8. R. Servant and J. Rocher. J. Phys. Radium, **24**, 285 (1963).
9. P. G. Taylor and C. A. Beevers. Acta Cryst. **5**, 341 (1952).
10. G. Roberts and W. Derbyshire. J. Sci. Instr. **38**, 511 (1961).
11. W. C. Lin and C. A. McDowell. Mol. Phys. **7**, 223 (1964).
12. G. W. Chantry, A. Horsfield, J. R. Morton, J. R. Rowlands, and D. H. Whiffen. Mol. Phys. **5**, 233 (1962).
13. D. W. Ovenall and D. H. Whiffen. Mol. Phys. **4**, 135 (1961).
14. J. R. Morton. Chem. Revs. **64**, 453 (1964).
15. D. M. Gardner and G. K. Fraenkel. J. Am. Chem. Soc. **78**, 3279 (1956).
16. W. G. Hodgson, S. A. Buckler, and G. Peters. J. Am. Chem. Soc. **85**, 543 (1963).
17. H. E. Radford and F. O. Rice. J. Chem. Phys. **33**, 774 (1960).
18. R. L. Eager and D. S. Mahadevappa. Can. J. Chem. **43**, 614 (1965).
19. P. W. Atkins, J. A. Brivati, A. Horsfield, M. C. R. Symons, and P. A. Trevalion. Sixth Intern. Symp. Free Radicals, Cambridge, England. 1963.
20. M. Wolfsberg and L. Helmholz. J. Chem. Phys. **20**, 837 (1952).

Can. J. Chem. Downloaded from www.nrcresearchpress.com by 210.87.254.105 on 09/05/12
For personal use only.

Can. J. Chem. Downloaded from www.nrcresearchpress.com by 210.87.254.40 on 09/05/12
For personal use only.

THE CHROMIC ACID OXIDATION OF 2-PROPANOL IN TRIFLUOROACETIC ACID

DONALD G. LEE AND DANIEL T. JOHNSON
Camrose Lutheran College, Camrose, Alberta

Received January 14, 1965

ABSTRACT

The mechanism of the chromic acid oxidation of 2-propanol in trifluoroacetic acid solutions has been studied. The general features of this reaction strongly resemble those observed in aqueous solutions of other strong acids. A "normal" primary kinetic isotope effect is observed, similar thermodynamic parameters are obtained, and the rate behaves in similar way towards changes in acidity.

An extensive study of the effect of added salts on this reaction has substantiated that the identity of added anions has a profound effect on the rate of reaction and that any complete reaction mechanism must take this into consideration.

It has been established that chromic acid is a very effective reagent for the oxidation of alcohols and that under similar conditions of acidity and temperature the rate of oxidation is much faster in acetic acid solutions than in aqueous solutions (1). The kinetics and mechanism of this reaction have been investigated quite thoroughly and it appears that the enhanced rate in acetic acid solutions is due in part to incorporation of an acetate ligand into the chromic acid ester, which acts as an intermediate in this reaction (1, 2). It seemed probable to us that the details of the mechanism of this reaction could be further exposed by undertaking a kinetic study of the chromic acid oxidation of 2-propanol in trifluoroacetic acid solutions. The following paper reports the results of this investigation.

EXPERIMENTAL

Kinetic Methods

All kinetic measurements were made spectrophotometrically using a Unicam model SP 500 spectrophotometer with a thermostated cell compartment. Solutions were made up by adding a weighed amount of anhydrous trifluoroacetic acid (Halocarbon Products) to a dilute aqueous solution of $K_2Cr_2O_7$ (Fisher Reagent). This solution was then brought to 25.0 ± 0.2° in a thermostated bath and an excess of 2-propanol was added volumetrically either from a pipet or a microsyringe fitted with a Chaney adaptor. The optical density of these solutions at 3 500 Å was then determined at intervals and a plot of log $[Cr^{VI}]$ against time was prepared. A typical rate plot is presented in Fig. 1.

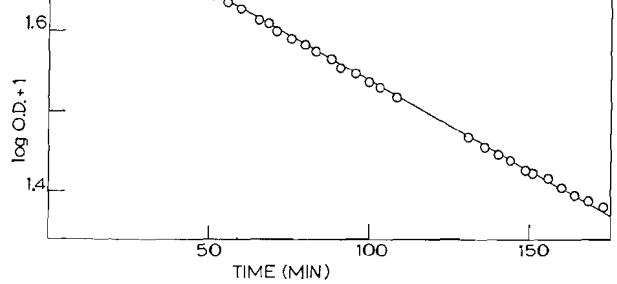

FIG. 1. Typical pseudo first order rate plot for the chromic acid oxidation of 2-propanol in aqueous trifluoroacetic acid solutions.

Can. J. Chem. Downloaded from www.nrcresearchpress.com by 210.87.254.40 on 09/05/12
For personal use only.

pK_a Measurements

Previous work (3) has shown that the protonation of $HCrO_4^-$ does not involve simple addition of a proton to give H_2CrO_4, but that the change is accompanied by incorporation of the conjugate base of the proton-supplying acid.

$$HCrO_4^- + H^+ + HA \rightleftharpoons HCrO_3A + H_2O.$$

To determine the apparent "pK_a" for this equilibrium it is necessary to obtain a measure of the ratio of the concentration of $HCrO_4^-$ to the concentration of $HCrO_3A$ over a wide range of acidities (4).

It was found possible to obtain such a ratio by measuring the extinction coefficients at 3 500 Å of aqueous trifluoroacetic acid solutions containing Cr^{VI}. Then the ratio

$$\frac{C_{HCrO_3A}}{C_{HCrO_4^-}} = \frac{\epsilon_{HCrO_4^-} - \epsilon}{\epsilon - \epsilon_{HCrO_3A}},$$

where $\epsilon_{HCrO_4^-}$ is the extinction coefficient for $HCrO_4^-$, ϵ_{HCrO_3A} is the extinction coefficient for $HCrO_3A$, and ϵ is the extinction coefficient for solutions containing both species. The plot of ϵ against H_0 (Fig. 2) shows that at 3 500 Å a typical sigmoidal curve is obtained. The H_0 scale reported by Randles and Tedder was used (5).

Materials

Chromic acid stock solutions were prepared by dissolving weighed amounts of $K_2Cr_2O_7$ in definite volumes of distilled water. Isopropyl alcohol was refluxed over calcium oxide for 2 h and then distilled. A middle fraction boiling at 81.5–82.0° was collected and used for the kinetic experiments. The 2-propanol-2-*d* was prepared in the manner described by Leo and Westheimer (6) and was purified by use of vapor phase chromatography. Salt solutions were prepared from commercially available reagent grade salts.

Trifluoroacetic acid was distilled through an all-glass apparatus and a middle fraction boiling at 71.0–72.0° was collected and used. Attempts were made to distil trifluoroacetic acid from both $K_2Cr_2O_7$ and $KMnO_4$. When it was distilled from $K_2Cr_2O_7$ through a 14 in. all-glass Vigreux column, the distillate was observed to have a pale-yellow color that rapidly disappeared when treated with easily oxidizable substances such as alcohols or aldehydes. Such observations suggested that Cr^{VI} was forming a volatile trifluoroacetic acid complex which was being carried over into the distillate. Titration with standardized sodium thiosulfate indicated that the concentration of Cr^{VI}, though somewhat larger in the initial stages of the distillation, was about 1×10^{-5} *M* in later fractions.

When trifluoroacetic acid was distilled from $KMnO_4$ a bright green distillate was obtained. The ultraviolet–visible spectrum of the distillate was similar to that reported by Symons *et al.* (4) for $HMnO_4$. When water was added to this anhydrous trifluoroacetic acid solution the familiar purple color of permanganate was obtained. From the amount of permanganate obtained it was possible to calculate that the $HMnO_4$ concentration in the sample of CF_3COOH was 1.4×10^{-3} *M*.

From these results we have concluded that Cr^{VI} and Mn^{VII} form volatile complexes with trifluoroacetic acid. However, it is possible that H_2CrO_4 and $HMnO_4$ are themselves volatile, but so strongly solvated in water that they cannot be distilled from aqueous solutions.

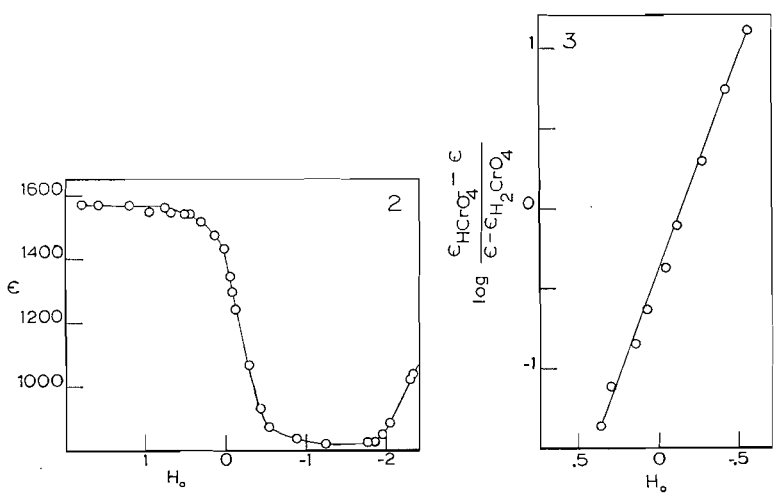

FIG. 2. The extinction coefficient of Cr^{VI} at 3 500 Å in trifluoroacetic acid solutions of varying acidity.
FIG. 3. Ionization plot for chromic acid dissolved in trifluoroacetic acid (slope = 2.7).

Can. J. Chem. Downloaded from www.nrcresearchpress.com by 210.87.254.40 on 09/05/12
For personal use only.

RESULTS

pK_a Measurements

It has been found in previous work that a plot of the function $H_- + \log (a_{H_2O}/a_{HA})$ against $\log (C_{HCrO_3A}/C_{HCrO_4^-})$ should give a straight line of unit slope for the protonation of $HCrO_4^-$ in aqueous solutions of mineral acid HA (3). This function was used rather than the conventional H_- function because evidence had shown eq. [1] to be the correct protonation equilibrium.

$$[1] \qquad HCrO_4^- + H^+ + HA \rightleftharpoons HCrO_3A + H_2O.$$

It was also found, however, that good straight lines, though not of unit slope, could be obtained by plotting $\log (C_{HCrO_3A}/C_{HCrO_4^-})$ against H_0. Figure 3 indicates that the apparent pK_a for this equilibrium is at -0.14 on the H_0 scale. The large deviation from unit slope emphasizes that H_0 is not the best function to use in this case. However, since literature values for neither H_-, a_{H_2O}, nor a_{HA} were available for trifluoroacetic acid solutions, the latter method was used. Presumably use of the function $H_- + \log (a_{H_2O}/a_{HA})$ would give a plot with a slope closer to unity.

Reaction Rates

The rates of oxidation of 2-propanol by Cr^{VI} at 25° were determined for aqueous solutions of trifluoroacetic acid varying from 0.36 to 96.2% CF_3COOH. The logarithms of the second-order rate constants which were obtained are plotted against H_0 in Fig. 4. This plot is strongly reminiscent of the one obtained for the same reaction in aqueous solutions of other strong acids (3). In these acids the linear region at lower acidities ($+1$ to -0.3 H_0 units) was ascribed to oxidation by $HCrO_4^-$, and the other linear region at higher acidities (-0.3 to -1.9 H_0 units) was attributed to oxidation by $HCrO_3A$, where A is the conjugate base of the mineral acid used as a proton supplier.

When this reaction was previously studied in aqueous solutions of HNO_3, $HClO_4$, H_2SO_4, HCl, and H_3PO_4 it was found that in each case the slope of the plot of log k_2 against H_0 changed at an acidity near the apparent pK_a of H_2CrO_4 in that medium. In the present case the intersection of the two slopes occurred at an H_0 of -0.30 while the apparent pK_a was -0.14. This evidence suggests that in accordance with previous results the active oxidant at acidities below the apparent pK_a is $HCrO_4^-$ while at higher acidities the active species is $HOCrO_2$—$OCOCF_3$.

The rate of oxidation of 2-propanol in concentrated sulfuric acid solutions has been observed to become nearly independent of acid concentrations in solutions containing 58–100% H_2SO_4 (7, 8). In fact the slope tends to have a slight negative value. This has also been observed in the present medium where the rate is observed to remain almost constant between -1.9 and -3.2 H_0 units.

Thermodynamic Parameters

The variation of the reaction rate with temperature can be utilized to obtain the heat and entropy of activation, $\Delta H^{\neq}$ and $\Delta S^{\neq}$ respectively. Transition state theory predicts that if log k_2/T(°K) is plotted against $1/T$(°K) (over a limited temperature range) the slope of the straight line and the intercept would give respectively $\Delta H^{\neq}$ and $\Delta S^{\neq}$ (9). The second-order rate constants for the reaction under consideration were determined at five different temperatures. The rate constants obtained are presented in Table I and a plot of log k_2/T(°K) against $1\,000/T$(°K) is presented in Fig. 5. Table II compares the thermodynamic parameters for the oxidation of 2-propanol in aqueous trifluoroacetic acid with the parameters obtained under other conditions. Since the reaction under consideration

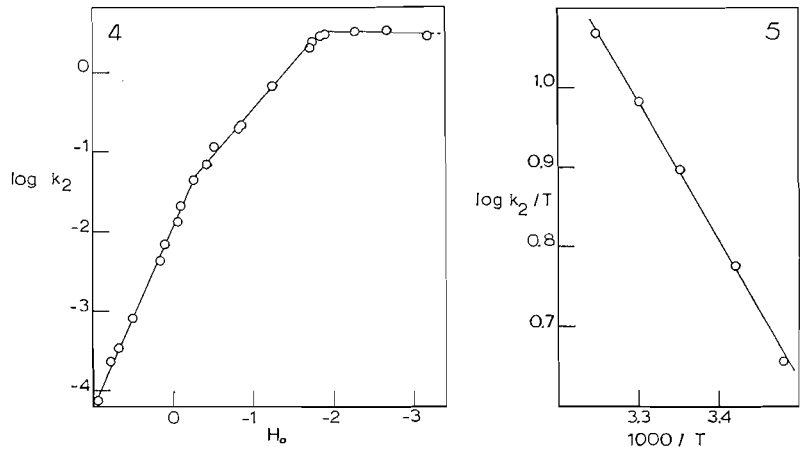

FIG. 4. Variation of rate with acidity for the chromic acid oxidation of 2-propanol in trifluoroacetic acid solutions.
FIG. 5. Plot for evaluating thermodynamic parameters.

is not a simple one (the rate-determining step follows a preliminary equilibrium) it is difficult to interpret the significance of heats and entropies which have been derived from kinetic data. However, the fact that the parameters determined in trifluoroacetic acid solutions are not greatly different from those obtained in other media would seem to substantiate accompanying evidence which indicates that use of this solvent does not produce any basic changes in the reaction mechanism.

TABLE I

Effect of temperature on the rate of oxidation of 2-propanol ($Cr^{VI} = 5.13 \times 10^{-4}$ *M*, alcohol $= 2.18 \times 10^{-2}$ *M*, $CF_3COOH = 8.6$ *M*)

Temperature (°C)	k_2 (l moles^{-1} s^{-1})
15.0	0.131
15.0	0.130
20.0	0.175
20.0	0.176
25.0	0.236
25.0	0.234
30.0	0.286
30.0	0.294
34.3	0.360
34.3	0.364

TABLE II

Thermodynamic parameters for the oxidation of 2-propanol by Cr^{VI} under various conditions

Conditions	Reference	$\Delta H^{\ddagger}$ (kcal/mole)	$\Delta S^{\ddagger}$ (cal/mole deg)
5.29% H_2SO_4	(8)	10.38	−35.7
6.8% H_2SO_4	(7)	12.4	−27.5
70% AcOH	(10)	12.86	−34.57
8.6 *M* CF_3COOH	Present work	8.02	−34.5

Can. J. Chem. Downloaded from www.nrcresearchpress.com by 210.87.254.40 on 09/05/12
For personal use only.

Salt Effects

It has previously been suggested that in the region of acidity beyond the pK_a of H_2CrO_4 in a particular mineral acid, HA, the intermediate of the oxidation reaction is an ester of the type $R_2HC—O—CrO_2A$, which is formed from a molecule of alcohol and one of $HOCrO_2A$ (3). At acid concentrations below the pK_a, the active oxidant was thought to be $HCrO_3^-$. It should be possible to test these ideas by examining the effect on the reaction rate when a salt MA′ is added to the solution. If the effect of the added salt on the acidity of the solution is subtracted, then this theory would predict that above the pK_a the nature of the salt effect observed would be dependent to a large extent on the nature of A′, since there would probably be an exchange between A and A′ in the Cr^{VI} species. Below the pK_a, however, where the anion does not become intimately attached to the chromium species, the added salt would cause only medium effects and all salts would be expected to cause somewhat similar changes in rate.

In the present investigation the effect of chloride ion, nitrate ion, and perchlorate ion was studied at 0.298 *M* CF_3COOH ($H_0 = 0.60$) and at 7.35 *M* CF_3COOH ($H_0 = -0.61$). These acidities are on either side of −0.14, the observed pK_a for H_2CrO_4 in this medium. The results are summarized in Table III and are presented graphically in Figs. 6 and 7.

The values for k_{cor} were obtained by use of the formula

$$\log k_{cor} = \log k_{obs} + m\Delta H_0,$$

where k_{obs} is the observed second-order rate constant, ΔH_0 is the change in acidity caused

TABLE III

The effect of added salts on the rate of oxidation of 2-propanol by Cr^{VI} in 0.298 and 7.35 *M* CF_3COOH

$[CF_3COOH]$ (*M*)	Salt	Molarity	H_0	k_{obs}	log k_{obs}	log k_{cor}
0.298	NaCl	0	0.60	7.82×10^{-4}	−3.107	−3.107
		0.311	0.52	4.94×10^{-4}	−3.306	−3.486
		0.779	0.40	3.59×10^{-4}	−3.445	−3.895
		1.94	0.16	2.82×10^{-4}	−3.550	−4.540
		2.72	−0.05	3.33×10^{-4}	−3.476	−4.936
	$NaNO_3$	0.171	0.52	8.37×10^{-4}	−3.077	−3.257
		0.857	0.18	10.4×10^{-4}	−2.983	−3.926
		2.14	−0.23	16.6×10^{-4}	−2.780	−4.645
		2.98	−0.54	23.2×10^{-4}	−2.634	−5.194
	$NaClO_4$	0.312	0.52	7.50×10^{-4}	−3.125	−3.300
		0.780	0.40	9.43×10^{-4}	−3.025	−3.475
		1.95	0.16	17.7×10^{-4}	−2.752	−3.742
		2.73	−0.05	31.3×10^{-4}	−2.504	−3.967
7.35	NaCl	0	−0.61	0.175	−0.757	−0.757
		0.00516	−0.65	0.108	−0.967	−1.007
		0.0103	−0.65	0.0884	−1.053	−1.093
		0.0155	−0.65	0.0764	−1.117	−1.157
		0.0206	−0.65	0.0704	−1.152	−1.192
		0.0516	−0.65	0.0406	−1.391	−1.431
		0.103	−0.66	0.0243	−1.614	−1.664
		0.206	−0.68	0.0146	−1.836	−1.906
		0.516	−0.72	0.00753	−2.123	−2.233
	$NaNO_3$	0.326	−0.79	0.170	−0.770	−0.950
		0.652	−0.96	0.183	−0.737	−1.087
		0.978	−1.14	0.185	−0.733	−1.263
		1.30	−1.29	0.192	−0.717	−1.397
	$NaClO_4$	0.637	−0.81	0.163	−0.777	−0.997
		1.27	−1.02	0.167	−0.788	−1.198
		1.91	−1.19	0.194	−0.712	−1.292

Can. J. Chem. Downloaded from www.nrcresearchpress.com by 210.87.254.40 on 09/05/12
For personal use only.

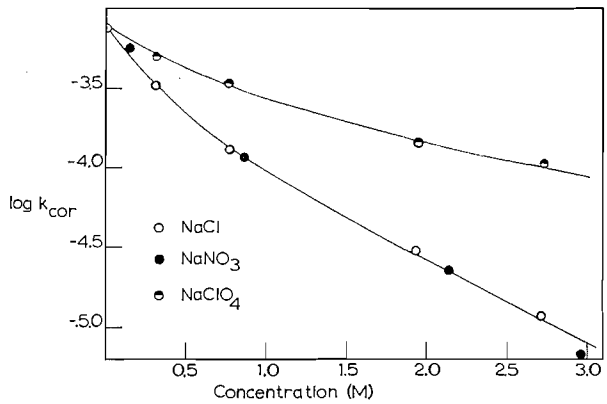

FIG. 6. Effect of added salts on the rate of oxidation of 2-propanol by Cr^{VI} in 0.298 *M* trifluoroacetic acid.

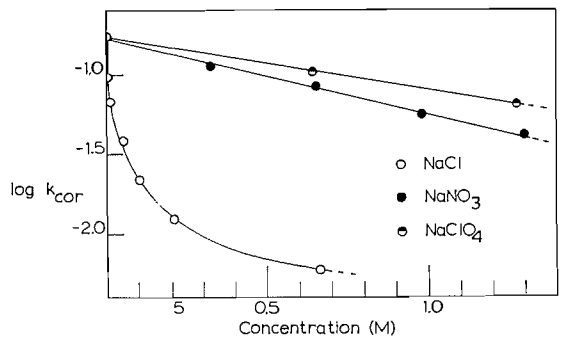

FIG. 7. Effect of added salts on the rate of oxidation of 2-propanol by Cr^{VI} in 7.35 *M* trifluoroacetic acid.

by the addition of salt, and m is the slope of the plot of log k_2 vs. H_0 taken from Fig. 4. In every case acidities were determined by use of the indicators *p*-nitroaniline, *o*-nitroaniline, and 4-chloro-2-nitroaniline. Use of the formula subtracts any increment in rate that is due to an enhanced acidity caused by the addition of salt to the solution, but it does not correct for other salt effects such as the change in ionic strength of the medium.

At low acid concentrations the results indicate that, aside from their effect on acidity, NaCl, $NaNO_3$, and $NaClO_4$ all have approximately the same effect on the rate of oxidation. In fact NaCl and $NaNO_3$ seem to be identical in their ability to depress the rate of reaction while $NaClO_4$ is slightly less effective. However, at higher acidities the salts show independent effects with small concentrations of chloride ion slowing down the reaction greatly, while nitrate and perchlorate ion also slow down the rate but to a much lesser extent. This is in accord with the work of Cohen and Westheimer (1) and of Lee and Stewart (3) who showed that formation of the species $HOCrO_2Cl$ leads to a much slower rate of reaction than does formation of the corresponding Cr^{VI} species with either acetate, nitrate, or perchlorate replacing chloride.

The dramatic decrease caused by even small concentrations of chloride ion indicates that equilibrium [2],

[2] $$HOCrO_2—OCOCF_3 + Cl^- \rightleftharpoons HOCrO_2Cl^- + CF_3COO^-,$$

Can. J. Chem. Downloaded from www.nrcresearchpress.com by 210.87.254.40 on 09/05/12
For personal use only.

must lie far to the right. An attempt was made to follow this exchange spectrophotometrically in the ultraviolet–visible region of the spectrum where chromium absorbs strongly. While the most interesting part of the spectrum, below 3 000 Å, was blanked out by trifluoroacetic acid absorption it was possible to make a partial study at about 3 500 Å. The pertinent data are reported in Table IV. From the data it can be seen that as the chloride ion concentration increases the extinction coefficient steadily increases until it almost equals that observed for HCl solutions of the same acidity.

TABLE IV
Spectral data

Acid concentration	Chloride conc. (M)	ϵ	λ_{max} (Å)
7.35 M CF_3COOH	0	859	3 500
	0.0130	981	3 570
	0.0206	1 090	3 570
	0.0516	1 132	3 570
	0.103	1 190	3 580
	0.206	1 208	3 580
	0.516	1 218	3 600
2.02 M HCl	0	1 240	3 580
	0.50	1 240	3 580

In the case of nitrate and perchlorate ions the fact that significant rate changes did not occur until the concentration of these ions was quite great would seem to indicate that the equilibrium constants for nitrate or perchlorate ion exchange must be smaller than for chloride ion, i.e. chloride ion more readily forms a covalent bond with chromium.

Isotope Effects

Westheimer and coworkers have shown that a primary kinetic isotope effect of approximately 7:1 is observed for the oxidation of 2-propanol-2-*d* in either aqueous or acetic acid solutions (1, 11, 12). In the present investigation the primary kinetic isotope effect was determined at 25° for two different concentrations of trifluoroacetic acid. The results presented in Table V indicate that in this case also the rate-determining step is cleavage of the α-C—H bond.

TABLE V
Primary kinetic isotope effects on the rate of oxidation in trifluoroacetic acid solutions at 25°

Alcohol	$[CF_3COOH]$ (M)	k_2 (l moles^{-1} s^{-1})	k_H/k_D
2-Propanol	0.298	7.88×10^{-4}	
	0.298	7.76×10^{-4}	
	7.35	0.178	
	7.35	0.169	
	7.35	0.178	
2-Propanol-2-*d*	0.298	1.09×10^{-4}	
	0.298	1.10×10^{-4}	7.0
	7.35	2.43×10^{-2}	
	7.35	2.56×10^{-2}	
	7.35	2.71×10^{-2}	6.8

Can. J. Chem. Downloaded from www.nrcresearchpress.com by 210.87.254.40 on 09/05/12
For personal use only.

Can. J. Chem. Downloaded from www.nrcresearchpress.com by 210.87.254.40 on 09/05/12
For personal use only.

DISCUSSION

The results of this investigation indicate that the general features of the chromic acid oxidation of 2-propanol in trifluoroacetic acid solution strongly resemble those observed in aqueous solutions of most other strong acids. A "normal" primary kinetic isotope effect is observed, similar thermodynamic parameters are obtained, and the rate behaves in a similar way towards changes in acidity.

The change of slope in Fig. 4 indicates, in analogy with other strong acids, that trifluoroacetic acid becomes incorporated into the Cr^{VI} species only after protonation of the monoanion, i.e., equilibrium [3] would seem to be to the right but equilibrium [4] to the left.

[3] $$H_2O + {}^-OCrO_2—OCOCF_3 \rightleftharpoons {}^-OCrO_2OH + CF_3CO_2H,$$

[4] $$H_2O + HOCrO_2—OCOCF_3 \rightleftharpoons H_2CrO_4 + CF_3COOH.$$

Results from the effect of added salts also indicate that it is possible for an exchange of conjugate base groups to take place, and that such an exchange can have a profound effect on the reaction rate.

[5] $$HOCrO_2—OCOCF_3 + Cl^- \rightleftharpoons HOCrO_2Cl + CF_3CO_2^-.$$

Current theories suggest that chromic acid oxidations involve formation of an intermediate ester which subsequently decomposes to products (13, 14). It is not clear from our results whether the presence of the conjugate base is felt more strongly in ester formation or ester decomposition, i.e., the A group could have an effect either on equilibrium [6] or on the rate-determining step [7].

[6] $$HOCrO_2A + (CH_3)_2CHOH \rightleftharpoons (CH_3)_2CH—O—CrO_2A + H_2O$$

[7] $$(CH_3)_2CH—O—CrO_2A \rightarrow (CH_3)_2C{=}O + Cr^{IV}.$$

The evidence which is available would seem to indicate that the decomposition step [7] involves intermolecular transfer of 2 electrons from the alcohol part of the ester to the chromium part, with the exact mode of transfer depending on the relative amount of overlap between the bonding orbitals in the transition state (15). Regardless of the mode of transfer an electron-attracting group attached to chromium would increase the rate of decomposition. The salt effect results presented in this paper have substantiated this idea. The second-order rate constant for oxidation of 2-propanol in HCl solutions with an H_0 of -0.61 is 1.0×10^{-3} l moles^{-1} s^{-1} (3), while the second-order rate constant for the oxidation of 2-propanol in trifluoroacetic acid solutions of the same acidity is 0.175 l moles^{-1} s^{-1}. Addition of NaCl to this trifluoroacetic acid solution steadily decreases the rate until at a salt concentration of 0.516 M the rate constant is only 7.52×10^{-3} (corrections being made for acidity changes). At the same time as the rate is being decreased spectral changes indicate the formation of a new Cr^{VI} species which has an extinction coefficient at 3 600 Å, closer to that observed for $HOCrO_2Cl$. From this it appears that chlorine is able to form a stronger covalent bond with chromium than is the trifluoroacetate group and is consequently displacing this group.

Addition of nitrate or perchlorate ions also effects a decrease in the rate of reaction after corrections are made for acidity changes. The second-order rate constant for oxidation of 2-propanol in either HNO_3 or $HClO_4$ solutions with an H_0 of -0.61 is 2.82×10^{-2} l moles^{-1} s^{-1} (3) while the second-order rate constant for the same reaction in trifluoroacetic acid solutions of the same acidity is 0.175 l moles^{-1} s^{-1}. However, addition of $NaNO_3$ steadily decreases the rate (corrected for changes in acidity) until at a concentration of

1.30 M $NaNO_3$ the rate constant is only 4.01×10^{-2} l moles^{-1} s^{-1}. Similarly addition of $NaClO_4$ decreases the rate constant until at a concentration of 1.91 M $NaClO_4$ the corrected rate constant is only 5.1×10^{-2} l moles^{-1} s^{-1}.

These results substantiate the fact that the identity of the conjugate base has a profound effect on the rate. Any complete mechanism of this reaction must take this fact into consideration.

ACKNOWLEDGMENT

The financial support of the National Research Council is gratefully acknowledged, as is a gift of trifluoroacetic acid from Halocarbon Products, Hackensack, New Jersey, U.S.A.

REFERENCES

1. M. COHEN and F. H. WESTHEIMER. J. Am. Chem. Soc. **74**, 4387 (1952).
2. M. C. R. SYMONS. J. Chem. Soc. 4331 (1963).
3. D. G. LEE and R. STEWART. J. Chem. Soc. **86**, 3051 (1964).
4. N. BAILEY, A. CARRINGTON, K. A. LOTT, and M. C. R. SYMONS. J. Chem. Soc. 290 (1960).
5. J. E. R. RANDLES and J. M. TEDDER. J. Chem. Soc. 1218 (1955).
6. A. LEO and F. WESTHEIMER. J. Am. Chem. Soc. **45**, 419 (1949).
7. J. ROCEK and J. KRUPICKA. Collection Czech. Chem. Commun. **23**, 2068 (1958).
8. R. STEWART and D. G. LEE. Unpublished results.
9. K. J. LAIDLER. Chemical kinetics. McGraw-Hill Book Co., Inc., Toronto. 1950. p. 75.
10. N. VENKATASUBRAMENIAN. Proc. Indian Acad. Sci. **50**, 156 (1959).
11. F. WESTHEIMER and N. NICOLAIDES. J. Am. Chem. Soc. **71**, 25 (1949).
12. A. LEO and F. WESTHEIMER. J. Am. Chem. Soc. **74**, 4383 (1952).
13. R. STEWART. Oxidation mechanisms: applications to organic chemistry. W. A. Benjamin, Inc., New York. 1963. Chap. 4.
14. R. ROCEK, F. H. WESTHEIMER, A. ESCHENMOSER, L. MOLDOVANYI, and J. SCHREIBER. Helv. Chim. Acta, **45**, 2554 (1962).
15. R. STEWART and D. G. LEE. Can. J. Chem. **42**, 439 (1964).

Can. J. Chem. Downloaded from www.nrcresearchpress.com by 210.87.254.40 on 09/05/12
For personal use only.

Can. J. Chem. Downloaded from www.nrcresearchpress.com by 210.87.254.105 on 09/05/12
For personal use only.

THE PYROLYSIS OF TRIMETHYLTHALLIUM

M. G. JACKO[1] AND S. J. W. PRICE
Department of Chemistry, University of Windsor, Windsor, Ontario
Received February 1, 1965

ABSTRACT

The pyrolysis of trimethylthallium has been studied in a toluene carrier flow system from 458 to 591 °K using total pressures from 5.6 to 33.0 mm. The progress of the reaction was followed by measuring the amount of methane, ethane, ethylene, and ethylbenzene formed and, in 21 runs, by direct thallium analysis. All preparative and kinetic work was carried out in total darkness where possible. A shielded 10 W lamp was used when some illumination was necessary.

The decomposition is approximately 80% heterogeneous in an unconditioned vessel and 14–27% heterogeneous in a vessel pretreated with hot 50% HF for 10 min. The reaction proceeds by the simple consecutive release of three methyl radicals. The rate constant depends only slightly on the total pressure in the system so that the activation energy of the homogeneous process, 27.4 kcal/mole, may be equated to $D[(CH_3)_2Tl—CH_3]$.

INTRODUCTION

No previous studies of the thermal decomposition of trimethylthallium have been reported. The pyrolysis of trimethylgallium and trimethylindium has been studied (1, 2). In each case two of the three metal–carbon bond dissociation energies were determined from the kinetic data. The reactions showed a marked surface dependence which could be substantially reduced by carrying out a number of runs to condition the reaction vessels. Somewhat similar behavior was expected in the pyrolysis of trimethylthallium.

EXPERIMENTAL

Materials

(*a*) Trimethylthallium was prepared by adding dropwise an ether solution of methyllithium to a suspension of dry powdered thallous iodide in anhydrous ether containing methyl iodide (3, 4). The methyllithium was prepared by adding methyl iodide dropwise to a suspension of finely cut lithium metal in ether (5). The thallous iodide suspension was stirred at room temperature under a dry nitrogen atmosphere. As each drop of methyllithium hit the suspension, a black dot (finely divided, highly reactive thallium) formed momentarily and then disappeared. As the addition of methyllithium progressed, the suspension became darker. After standing for 36 h the mixture cleared. The overall reaction is given by:

$$2CH_3Li + CH_3I + TlI \rightarrow Tl(CH_3)_3 + 2LiI.$$

The reaction mixture was heated in a water bath at 75 °C to distill the ether. The crude metallic alkyl was distilled into a degassing system where the remaining ether was removed by repeated bulb-to-bulb distillations with the cold trap at 0 °C. The final product had a melting point of 38.5 °C (literature value 37.5–39 °C). Trimethylthallium was handled and stored in the dark as it is sensitive to light. Vapour pressures were measured from −25 °C (1.0 mm) to 60 °C (17.5 mm).

(*b*) Toluene from sulfonic acid (Eastman Organic, X325) was dried by refluxing over sodium under vacuum and then degassed by bulb-to-bulb distillation.

Apparatus and Procedure

The toluene carrier system used was identical with that used for the study of trimethylindium (2). The volume of the reaction zone was 171 cc in the unpacked vessel and 141 cc in the packed vessel. The apparatus was operated in total darkness except for two shielded 10 W lamps which were used to take manometer readings.

In 11 runs the contents of the reaction zone were analyzed for thallium by dissolving the deposit in the reaction zone in concentrated hydrochloric acid (12 *N*). The resulting thallium trichloride solution was evaporated to 1–2 cc, diluted to 50 ml with distilled water, buffered with hexamethylenetetramine, and titrated with 0.02 *M* EDTA using xylenol orange as indicator (6). In four of these runs the contents of the

[1]*Recipient of a National Research Council of Canada Studentship. Present address: Research Division, Imperial Oil Ltd., Sarnia, Ontario.*

acetone – dry ice trap were similarly analyzed. The total moles of thallium found was always better than 99% of the moles of trimethylthallium used. Subsequently an additional 10 runs were carried out in which thallium analyses were made only on the contents of the trap.

Chromatographic analysis of the gaseous products was carried out on a 2 m silica-gel column at 80 °C with a helium flow rate of approximately 20 cc/min. The contents of the acetone – dry ice trap were analyzed using a Perkin-Elmer model 800 gas chromatograph equipped with a 150 ft Golay column, 0.02 in. i.d. coated with poly(propylene glycol).

RESULTS AND DISCUSSION

The complete experimental results are given in Tables I–V. They may be discussed in terms of the following mechanism:

[1] $$Tl(CH_3)_3 \rightarrow Tl(CH_3)_2 + CH_3,$$

[2] $$Tl(CH_3)_2 \rightarrow Tl(CH_3) + CH_3,$$

[3] $$Tl(CH_3) \rightarrow Tl + CH_3,$$

[a] $$CH_3 + C_6H_5—CH_3 \rightarrow C_6H_5—CH_2 + CH_4,$$

[r] $$2CH_3 \rightarrow CH_3—CH_3,$$

[4] $$2C_6H_5—CH_2 \rightarrow (C_6H_5—CH_2)_2.$$

The abstraction reaction [a] was a composite reaction proceeding mainly as written but with a small percentage of abstraction from the ring. The ethylene and the hydrogen observed in very small amounts (usually less than 0.05%) result from the reactions:

[5] $$CH_3 + C_2H_6 \rightarrow C_2H_5 + CH_4,$$

[6] $$C_2H_5 \rightarrow C_2H_4 + H,$$

[7] $$H + C_6H_5—CH_3 \rightarrow C_6H_5—CH_2 + H_2.$$

In runs with low toluene-to-alkyl ratios, propane, ethylbenzene, and xylenes observed in small amounts result from the reactions:

[8] $$CH_3 + C_2H_5 \rightarrow C_2H_5—CH_3,$$

[9] $$CH_3 + C_6H_5—CH_2 \rightarrow C_6H_5—CH_2—CH_3,$$

[10] $$CH_3 + CH_3—C_6H_4 \rightarrow CH_3—C_6H_4—CH_3.$$

The Arrhenius plot of $k_a/k_r^{1/2}$ shown in Fig. 1 shows no characteristic break at 33% or 67% theoretical yield of methyl radicals indicating that at all temperatures reactions [2] and [3] follow rapidly after reaction [1]. Thus the rate constants were calculated assuming that three methyl radicals were released for each trimethylthallium molecule undergoing decomposition.

Although the continuity of the Arrhenius curve of $k_a/k_r^{1/2}$ was indicative of the process outlined (2), independent tests have been made to verify the mechanism.

(*a*) In 14 runs (see Table V), the contents of the acetone – dry ice trap located at the outlet of the furnace were analyzed for thallium. Over the entire temperature range, the thallium found in this trap was equal to the quantity of undecomposed trimethylthallium expected if each alkyl molecule that decomposed liberated three methyl radicals.

(*b*) In 11 runs, the contents of the reaction vessel were analyzed for thallium. In all cases the quantity of thallium deposited in the reaction zone was in agreement with the postulated release of three methyl radicals. To insure that the deposit was actually thallium, 0.082 g of the deposit was scraped from the reaction zone while in an inert atmosphere and analyzed for thallium; 19.0 ml of 0.02 *M* EDTA were required giving a thallium analysis of 99.8%. No evidence was found for the formation of polymer of the type $(TlCH_3)_n$, as found in the pyrolysis of trimethylgallium or trimethylindium.

Can. J. Chem. Downloaded from www.nrcresearchpress.com by 210.87.254.105 on 09/05/12
For personal use only.

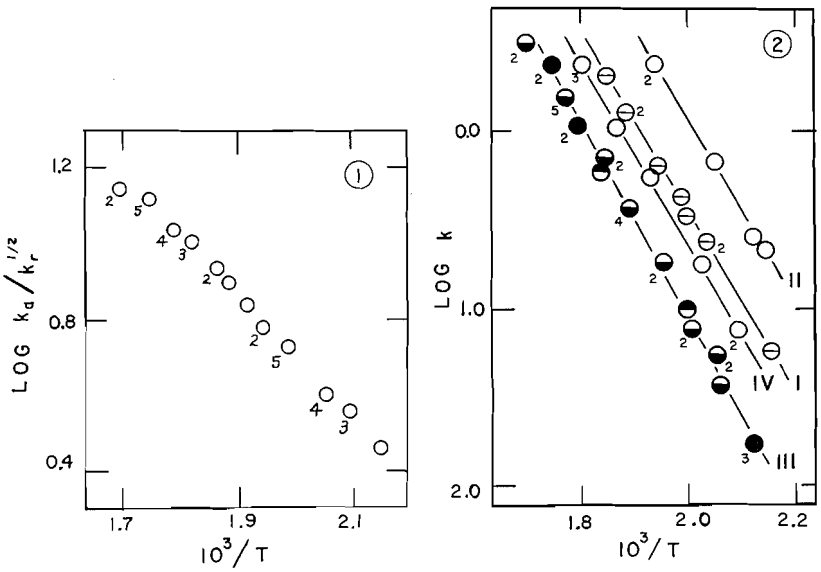

FIG. 1. Arrhenius plot for the reaction of methyl radicals with toluene when trimethylthallium is used as the source of methyl radicals. The experimental points cover 1–95% decomposition of the alkyl. Subscripts indicate the number of points averaged to obtain the given point.

FIG. 2. Arrhenius plots for the decomposition of trimethylthallium: ⊖, runs in unpacked unconditioned vessel (curve I); ○, runs in packed unconditioned vessel (curve II); ◒, runs in unpacked conditioned vessel (curve III) (◓, based on metal analysis); ○, runs in packed conditioned vessel (curve IV). Subscripts denote the number of runs averaged to obtain the given point.

Starting with a clean vessel (I), the rate constants did not decrease over several runs to a fixed minimum value as in the case of trimethylgallium or trimethylindium but remained at a constant value. These runs would have deposited enough thallium to change the surface, but no effect due to coating the surface with thallium was observed. In another series of runs, small amounts of air introduced into the reaction zone between runs produced no observable effect on the rate constants. The experimental data under these conditions (unconditioned and unpacked vessel) are given in Table I and constitute curve I in Fig. 2.

TABLE I

The pyrolysis of trimethylthallium (in an unpacked unconditioned vessel)

Temp. (°K)	t_c (s)	P† (mm)	Millimoles of					k (s^{-1})
			Toluene*	$TlMe_3$*	CH_4	C_2H_6	ϕ—C_2H_5	
543	0.969	13.0	134	0.630	0.060	0.765	0.040	2.05
531	0.983	13.0	241	1.148	0.075	1.192	0.034	1.30
528	1.015	13.0	199	1.069	0.070	1.121	0.044	1.29
513	1.058	13.0	196	0.910	0.040	0.647	0.031	0.651
504	1.100	13.0	151	0.645	0.022	0.350	0.000	0.424
501	1.074	13.0	103	0.758	0.017	0.336	0.010	0.340
499	1.118	13.0	191	1.642	0.036	0.579	0.017	0.255
491	1.111	13.0	333	1.132	0.029	0.374	0.000	0.234
481	1.170	13.0	79.6	1.242	0.009	0.189	0.014	0.095
475	1.125	13.0	167	0.872	0.010	0.110	0.000	0.082
464	1.103	13.0	280	1.614	0.012	0.135	0.000	0.054

*Quantities used in a given run.
†Total pressure.

Can. J. Chem. Downloaded from www.nrcresearchpress.com by 210.87.254.105 on 09/05/12
For personal use only.

TABLE II

The pyrolysis of trimethylthallium (in a packed unconditioned vessel)

Temp. (°K)	t_c (s)	P† (mm)	Millimoles of Toluene*	$TlMe_3$*	CH_4	C_2H_6	ϕ—C_2H_5	k (s^{-1})
522	0.732	13.0	251	1.000	0.067	1.220	0.029	2.50
512	0.769	13.0	207	0.748	0.040	0.912	0.024	2.31
486	0.781	13.0	277	0.644	0.033	0.527	0.006	0.674
471	0.809	13.0	118	0.847	0.012	0.229	0.013	0.259
466	0.847	13.0	220	1.218	0.018	0.290	0.002	0.212

*Quantities used in a given run.
†Total pressure.

The percentage of heterogeneous reaction was estimated by carrying out a series of runs in a packed vessel (II) with a surface-to-volume ratio 12 times that of the unpacked vessel I, and the results are given in Table II and constitute curve II of Fig. 2. The rate constants obtained using vessel II were a factor 3.7 greater than those obtained in vessel I. The overall reaction in vessel I was therefore apparently about 25% heterogeneous.

In an attempt to reduce the amount of surface reaction, the unpacked vessel was treated with hot 50% hydrofluoric acid for 10 min and then baked out under vacuum at 350 °C. The experimental results are given in Table III and constitute curve III of Fig. 2. The rate constants in vessel III could never be reduced below this curve even by longer treatments with hot 50% hydrofluoric acid. Therefore, vessels treated as described above are termed conditioned vessels.

TABLE III

The pyrolysis of trimethylthallium (in an unpacked conditioned vessel)

Temp. (°K)	t_c (s)	P† (mm)	Millimoles of Toluene*	$TlMe_3$*	CH_4	C_2H_6	ϕ—C_2H_5	k (s^{-1})
591	0.870	13.0	226	0.710	0.100	0.925	0.073	3.48
589	0.860	13.0	139	0.390	0.054	0.478	0.058	2.82
571	0.935	13.0	144	0.676	0.058	0.872	0.032	2.69
571	0.963	13.0	213	0.878	0.105	1.018	0.100	1.99
568	0.995	13.0	181	0.732	0.100	0.734	0.072	1.36
567	0.890	13.0	203	0.790	0.099	0.799	0.075	1.52
567	1.030	13.0	127	0.687	0.054	0.727	0.044	1.35
560	0.914	13.0	179	0.780	0.053	0.633	0.040	0.950
559	0.860	13.0	311	1.348	0.105	1.580	0.070	2.01
558	1.250	13.0	122	0.500	0.057	0.599	0.044	1.57
556	0.937	13.0	152	0.465	0.053	0.402	0.045	1.09
543	1.022	13.0	146	0.883	0.042	0.551	0.029	0.565
542	0.890	13.0	101	0.369	0.029	0.206	0.011	0.718
541	0.953	13.0	208	0.672	0.047	0.428	0.034	0.655
528	1.440	5.6	138.5	0.744	0.027	0.457	0.020	0.391
528	0.985	13.2	183.5	0.569	0.034	0.236	0.010	0.385
530	1.050	28.0	182.5	0.905	0.043	0.478	0.030	0.451
529	1.047	33.0	265	1.128	0.058	0.567	0.040	0.430
512	1.085	13.0	234	0.838	0.031	0.228	0.000	0.197
509	1.038	13.0	117	0.666	0.0147	0.165	0.000	0.179
501	0.996	13.0	214	0.748	0.0176	0.0728	0.000	0.0694
500	1.000	13.0	149	0.358	0.0851	0.0700	0.000	0.0990
487	1.077	13.0	183	0.590	0.0174	0.0244	0.000	0.0364
486	1.105	13.0	160	0.544	0.0059	0.0451	0.000	0.0541
473	1.145	13.0	126	0.533	0.0044	0.0146	0.000	0.0181
470	1.111	13.0	212	0.918	0.0275	0.0007	0.000	0.0186

*Quantities used in a given run.
†Total pressure.

Can. J. Chem. Downloaded from www.nrcresearchpress.com by 210.87.254.105 on 09/05/12
For personal use only.

With a conditioned vessel, successive runs producing an increasing deposit of thallium metal on the surface raised the rate constant to the level of the unconditioned vessels. Consequently, conditioning with hot 50% hydrofluoric acid was required between runs to obtain reproducible results in the conditioned vessel. However, if the amount of trimethylthallium used in a run was varied from 0.5 to 2.0 millimoles, no variation in the rate constant was observed signifying that the maximum amount of alkyl used in one run did not deposit enough thallium to significantly increase the rate. Therefore the rate constants observed in the individual runs were a true indication of the decomposition in the conditioned vessel.

To estimate the percentage of heterogeneous reaction in vessel III, a packed pyrex vessel (IV) with a surface-to-volume ratio 9 times that of vessel III was treated with hot 50% hydrofluoric acid for 10 min. This gave a rate constant high by a factor of 13. Further conditioning with the hot acid reduced the rate constants to approximately a factor of 4 times those obtained in vessel III. These results are tabulated in Table IV and constitute curve IV in Fig. 2. These results indicated that the reaction in vessel III was approximately 13% heterogeneous at the highest temperatures used and approximately 27% at the lowest.

TABLE IV

The pyrolysis of trimethylthallium (in a packed conditioned vessel)

Temp. (°K)	t_c (s)	P† (mm)	Millimoles of					k (s^{-1})
			Toluene*	$TlMe_3$*	CH_4	C_2H_6	ϕ—C_2H_5	
495‡	1.340	13.0	159	0.393	0.043	0.476	0.001	1.38
501§	0.893	13.0	126	0.540	0.024	0.270	0.001	0.515
479‖	0.970	13.0	118	0.630	0.0566	0.0306	0.000	0.0765
560	0.807	13.0	203	1.050	0.107	1.272	0.061	2.47
550	0.872	13.0	191	0.900	0.084	1.060	0.048	2.06
539	1.008	13.0	78.8	0.500	0.037	0.473	0.006	1.05
518	1.094	13.0	121	0.805	0.068	0.523	0.000	0.556
490	1.100	13.0	170	0.531	0.044	0.142	0.000	0.178
484	0.947	13.0	135	0.580	0.042	0.036	0.000	0.073

*Quantities used in a given run.
†Total pressure.
‡Run 95 (vessel only partially conditioned).
§Run 96 (vessel almost completely conditioned).
‖Run 97 (first run in fully conditioned vessel).

Comparison of curves I and III indicated that the reaction in vessel I was about 79% heterogeneous. This large percentage heterogeneous reaction is consistent with the greater than 45% heterogeneous reaction that would be indicated by comparison of curve I with the initial runs in the partially conditioned packed vessel (vessel IV before it was fully conditioned). The low estimate of percent heterogeneous reaction in vessel I obtained by comparison of runs in vessels I and II was probably due to the fact that vessel II had been washed with hydrofluoric acid before being stored at the conclusion of previous work.

The pressure dependence of $k_a/k_r^{1/2}$ is shown in Fig. 3. The falloff with increasing pressure is similar to that previously observed in similar studies with trimethylgallium, trimethylindium, and other metallic alkyls (1, 2, 7, 8, 9).

The rate constant k depended on the total pressure in the system, although the pressure dependence was very slight (Fig. 4). This slight pressure dependence was very similar to that observed for the thermal decomposition of trimethylgallium or trimethylindium.

Can. J. Chem. Downloaded from www.nrcresearchpress.com by 210.87.254.105 on 09/05/12
For personal use only.

TABLE V

Runs with thallium analyses

Temp. (°K)	Percentage gas (%)	Decomposition metal (%)	Trap analysis (%)	k_g (s^{-1})	k_m (s^{-1})
591‡	95.2	98.5		3.48	4.84
571‡	90.5	91.6		2.60	2.65
571‡	85.3	88.9		1.99	2.28
568‡	74.0	71.6		1.36	1.27
567‡	74.2		25.3	1.52	
560‡	58.2	60.5	38.7	0.955	1.020
558‡	86.7	87.6		1.57	1.80
543*	86.3		11.0	2.05	
543‡	43.9	45.0		0.565	0.585
542‡	47.4	45.0	54.2	0.718	0.671
513*	50.0		47.3	0.651	
501‡	6.8	8.0		0.069	0.084
500‡	9.5	9.3	89.8	0.099	0.097
494‡	8.6		91.8	0.087	
491*	22.9		77.1	0.234	
486‡	5.9		93.2	0.054	
481*	10.5		89.4	0.095	
475*	8.8		89.5	0.082	
473‡	1.3	1.8	97.9	0.012	0.016
470‡	2.0		95.0	0.019	
466†	16.4		82.2	0.212	

*Runs in the unpacked unconditioned vessel.
†Runs in the packed unconditioned vessel.
‡Runs in the unpacked conditioned vessel.

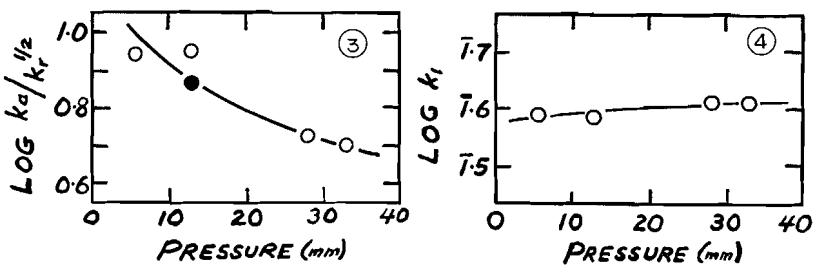

FIG. 3. Variation of $k_a/k_r^{1/2}$ with pressure at 528 °K: ○, individual runs; ●, point taken from Fig. 1.
FIG. 4. Variation of rate constant with pressure for trimethylthallium at 528 °K.

The overall reaction in the unpacked conditioned vessel may be represented by the equation:

$$\log_{10} k\ (s^{-1}) = 10.3 - (26\,000/2.303RT).$$

However, at low temperatures the heterogeneous component was 27% while at higher temperatures the heterogeneous component was only 13%. The homogeneous reaction in the unpacked conditioned vessel may therefore be represented by:

$$\log_{10} k\ (s^{-1}) = 10.8 - (27\,400/2.303RT).$$

No studies on the mean bond energy of trimethylthallium have been reported. From the known total metal–methyl bond strengths of the neighboring elements, a value of 65 ± 5 kcal/mole may be estimated.

The experimental evidence indicates that $D(Me_2Tl—Me) = 27.4$ kcal/mole, so that D_2 plus D_3 is therefore approximately equal to 38 ± 5 kcal/mole.

Can. J. Chem. Downloaded from www.nrcresearchpress.com by 210.87.254.105 on 09/05/12
For personal use only.

ACKNOWLEDGMENTS

This work has been supported by a grant from the National Research Council of Canada.

REFERENCES

1. M. G. JACKO and S. J. W. PRICE. Can. J. Chem. **41**, 1560 (1963).
2. M. G. JACKO and S. J. W. PRICE. Can. J. Chem. **42**, 1198 (1964).
3. H. GILMAN and R. G. JONES. J. Am. Chem. Soc. **68**, 517 (1946).
4. H. GILMAN and R. G. JONES. J. Am. Chem. Soc. **72**, 1760 (1950).
5. H. GILMAN, E. A. ZOELLNER, and W. M. SELBY. J. Am. Chem. Soc. **56**, 1252 (1933).
6. J. KINNUNEN and B. WINNESTRAND. Chemist-Analyst, **46**, 92 (1957).
7. S. J. W. PRICE and A. F. TROTMAN-DICKENSON. Trans. Faraday Soc. **53**, 1208 (1957).
8. S. J. W. PRICE and A. F. TROTMAN-DICKENSON. Trans. Faraday Soc. **53**, 939 (1957).
9. S. J. W. PRICE and A. F. TROTMAN-DICKENSON. Trans. Faraday Soc. **54**, 1630 (1958).

Can. J. Chem. Downloaded from www.nrcresearchpress.com by 210.87.254.105 on 09/05/12
For personal use only.

Can. J. Chem. Downloaded from www.nrcresearchpress.com by 210.87.254.5 on 09/05/12
For personal use only.

THE FLOW OF GASES THROUGH MICROPOROUS CARBON[1]

R. F. BARTHOLEMEW[2] AND E. A. FLOOD
Division of Pure Chemistry, National Research Council, Ottawa, Canada

Received December 14, 1964

ABSTRACT

Steady state flow rates are reported for He, Ar, N_2, Kr, methane, propane, and *n*-butane flowing through a microporous carbon rod at room temperature.

I. INTRODUCTION

Flow rates of He, Ar, N_2, Kr, methane, propane, and *n*-butane through a small circular cylinder of microporous 'saran' carbon at 25 °C have been measured. The corresponding adsorption isotherms have also been measured. The experimental results are reported below. The observed flow rates of propane and butane are compared with those calculated by means of a theoretical equation deduced previously. The theoretical equation is based on a laminar viscous flow of liquid-like films and correlates flow rates with pore dimensions and adsorption isotherms (1).

II. EXPERIMENTAL

Materials

The microporous carbon used for the permeability and adsorption measurements was a polyvinylidene or 'saran' carbon activated by heating in vacuum to about 1 100 °C for about 1 h. The sample No. 139 Plug 2A had the following properties: 99.9% carbon, surface area (B.E.T., N_2) 1 073 m^2/g, helium density 1.87 (not corrected for the adsorption), weight 56.4 mg, mean length 4.01 mm, mean diameter 4.53 mm, apparent density $\rho' = 0.872$, void volume per gram $v = 0.6112$, porosity 0.5334.

Helium.—A high grade helium for use in a helium cryostat. Minimum purity 99.99%. Supplied by Air Reduction Sales.

Argon.—Minimum purity, 99.99%. Supplied by Union Carbide, Linde Gas Division.

Nitrogen.—Super dry. Minimum purity 99.7%. Impurity mainly O_2.

Krypton.—Spectroscopically pure. Supplied by Dominion Oxygen Co.

Methane.—Phillips Research Grade. 99.58%. Lot No. 985. Probable impurities N_2, ethane, O_2, and propane.

Propane.—Phillips Research Grade, 99.99%, Lot No. 847. Main impurity, ethane.

n-Butane.—Phillips Research Grade, 99.91%, Lot No. 885. Main impurities isobutane and butenes.

Apparatus

The flow apparatus was similar to that described previously, but was provided with improved automatic input and output measuring devices. In all flow rates reported, where the output pressure was greater than zero, the input and output mass flow rates showed no trends and were the same within a few percent. An important experimental feature is the mercury seal sample or 'plug' holder which allows the carbon 'plug' to expand or contract without causing appreciable changes in leaks through the mercury–carbon interface. For samples of reasonably high permeabilities a pressure of about 40 cm of Hg is necessary to reduce the annulus leak to negligible values.

Adsorption isotherms were determined volumetrically using a microvariant of the standard volumetric equipment. In the case of the more strongly adsorbed gases, propane and butane, the volumetrically determined isotherms were checked by the McBain balance technique. The helium density of the small carbon plug was determined in the device shown in Fig. 1, the operation of which is obvious. All flow and adsorption isotherm measurements were carried out at 25.0 °C ± 0.1. All pressures quoted are in cm Hg (25 °C).

Results

Adsorption isotherm data appear in Figs. 2 to 4.

In Table I the observed flow rates in K units corresponding to various mean pressures, $\bar{p}$, are shown. K units are cc per minute measured at the input gas pressure, p_1, multiplied by this pressure, and divided by the difference between the input and output pressures, i.e., divided by $p_1 - p_2$. The mean pressure, $\bar{p}$, is $(p_1 + p_2)/2$. Molecular weight and gas viscosities in micropoise are given in Table II.

[1]*Issued as N.R.C. No. 8451.*
[2]*National Research Council Postdoctorate Fellow.*

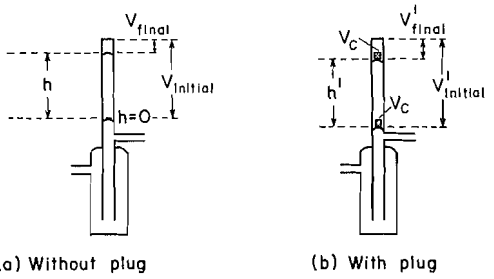

FIG. 1.

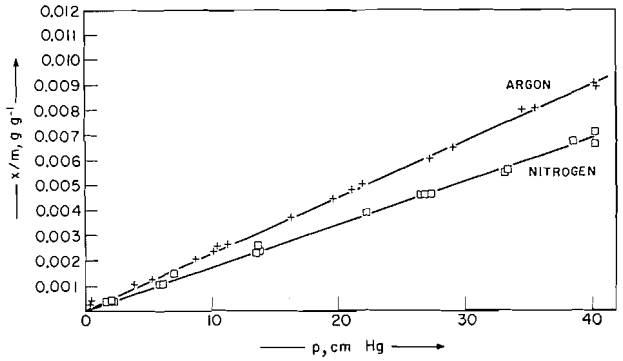

FIG. 2.

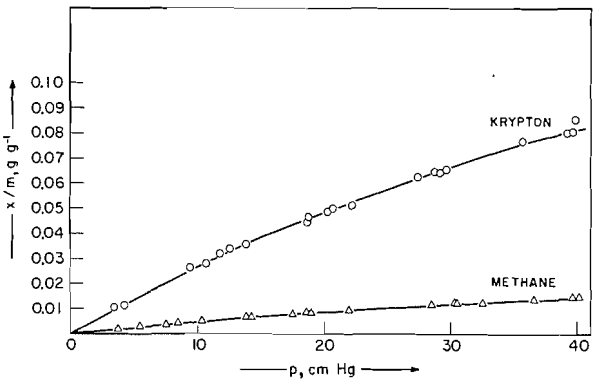

FIG. 3.

III. DISCUSSION

It has been shown by a number of investigators that flow rates of gases through microporous bodies are materially influenced by surface forces (2–5). There are two, more or less, distinct mechanisms in vogue for describing 'surface' flow rates, namely diffusion mechanisms and hydrodynamic mechanisms, the former being the more popular. Assuming that the adsorbate consists of thin liquid-like films as in Polanyi adsorption and that the dimensions of rate-controlling pores are large enough for laminar flow of these films, the following equation has been deduced (1),

[1] $$K = A\sqrt{T/M} + B\bar{p}/\eta_g + (CT^2/M^2\eta_l) \times \overline{|X^2/p|},$$

Can. J. Chem. Downloaded from www.nrcresearchpress.com by 210.87.254.5 on 09/05/12
For personal use only.

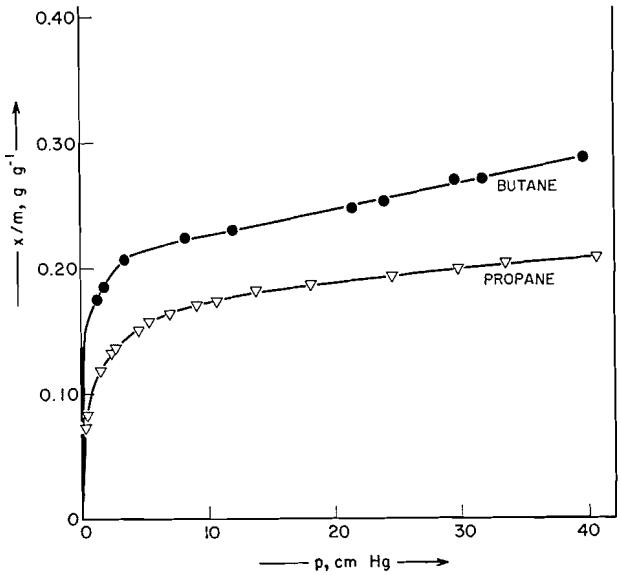

FIG. 4.

TABLE I

Gas	$\bar{p}$	K	Gas	$\bar{p}$	K
He ($\Delta p = 5.180$)	41.025	0.02395	CH_4 ($\Delta p = 5.170$)	41.310	0.1046
	32.940	0.02318		32.410	0.0990
	24.685	0.02181		24.568	0.0970
	19.260	0.02230*		16.923	0.0929
	16.760	0.02124		9.583	0.0896
	7.555	0.01928		4.373	0.0863
	2.593	0.01878		2.593	0.08473
				35.330	0.10014
N_2 ($\Delta p = 5.180$)	42.643	0.04570			
	34.493	0.04386	C_3H_8 ($\Delta p = 5.170$)	41.865	0.06606
	25.900	0.04158		33.723	0.07125
	17.288	0.03964		24.228	0.08287
	8.625	0.03768		15.688	0.1036
	5.163	0.03586		7.818	0.1529
	2.595	0.03506		2.595	0.2768
Ar ($\Delta p = 5.170$)	40.815	0.03658	n-C_4H_{10} ($\Delta p = 5.185$)	41.378	0.03506
	33.073	0.03525		32.265	0.03636
	24.725	0.03371		24.878	0.03922
	15.488	0.03295		16.828	0.04749
	7.802	0.02947		8.710	0.07202
	2.595	0.02882		5.447	0.1001
	13.968	0.03152		2.600	0.2203
	5.428	0.02892			
Kr ($\Delta p = 5.225$)	45.700	0.05625			
	34.780	0.05492			
	25.325	0.05318			
	16.401	0.05235			
	9.688	0.05065			
	6.183	0.05024			
	2.640	0.04838			

*Measured after runs using N_2, Ar, Kr, CH_4, and C_3H_8.

where A, B, and C are constants largely descriptive of the pore structure; T is the absolute temperature, M the molecular weight, $\bar{p}$ the mean gas pressure, η_g the gas viscosity,

Can. J. Chem. Downloaded from www.nrcresearchpress.com by 210.87.254.5 on 09/05/12
For personal use only.

η_1 the liquid viscosity and $\overline{|X^2/p|}$ is given by

$$\overline{|X^2/p|} \times (p_1 - p_2) = \int_{p_1}^{p_2} X^2/p \cdot dp,$$

where X is the weight adsorbed per gram of adsorbent. A and B are determined from helium flow data and C chosen so as to fit the data at one point. Equation [1] has been shown to describe the flow of water vapor through a sample of active carbon reasonably well over a considerable range of pressure and temperature (6).

TABLE II

Gas	Molecular weight	η
He	4.003	196.0
N_2	28.016	177.4
Ar	39.944	225.4
Kr	83.80	251.7
CH_4	16.042	111.2
C_3H_8	44.097	81.3
		950*
n-C_4H_{10}	58.124	74.9
		1 600*

*Liquid viscosities, 25 °C.

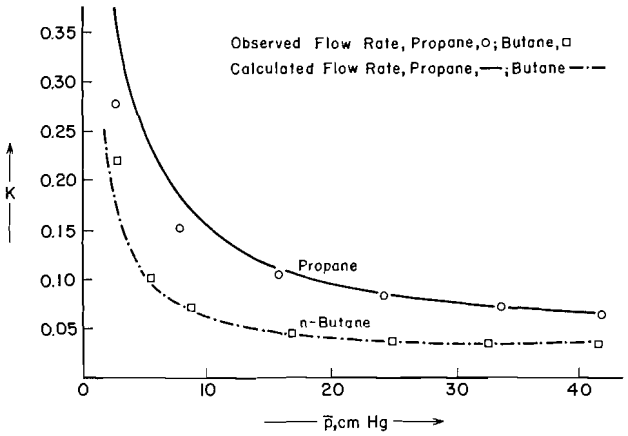

FIG. 5.

In Fig. 5 observed values of flow rates of propane and n-butane are compared with those calculated from eq. [1]. The value of $CT^2/\eta_1 M^2$ for propane is taken as 45.0 while that for n-butane is 8.63.

Since C is supposed descriptive of the pore structure only, in the absence of any molecular sieve action and other complications, the ratios of these two values should be 45/15.36 instead of 45/8.63. We believe that surface forces should increase viscosities of liquid-like films. If the differential heat of adsorption of butane (in the higher relative pressure ranges) is greater than that of propane by about 1 kcal more than the difference in their heats of evaporation, this viscosity ratio η(butane adsorbed)/η(propane adsorbed) would be about 1.78 times the ratio of their normal liquid viscosities. Hence the ratio 45/8.63 in place of 45/15.26 would be obtained.

Can. J. Chem. Downloaded from www.nrcresearchpress.com by 210.87.254.5 on 09/05/12
For personal use only.

For various pore models the mean pore radii of rate-controlling pores can be estimated from eq. [1]. If these pores are more or less circular or square in cross section the pores appear to have diameters of the order of 15 to 20 Å for reasonably plausible pore models. If the pores are slit-like spaces between carbon platelets they appear to be about 10 to 15 Å apart.

The observed flow rates of Ar, N_2, Kr, and methane can be described quite well by equations where the third term on the right hand side of eq. [1] is replaced by (*a*) terms descriptive of a hydrodynamic flow with slip of gaseous adsorbate, (*b*) a term descriptive of a two-dimensional molecular random walk surface flow mechanism, i.e. a term descriptive of surface diffusion. It is difficult to distinguish between gaseous hydrodynamic flow with slip, Knudsen flow, and random walk surface diffusion mechanisms, especially in these microporous bodies, since in the lower concentration regions these mechanisms are all related more or less directly to $(RT/M)^{1/2}$ and to mean step lengths, and they all contribute to a greater or lesser extent to the net flow phenomena.

In the case of the gases Ar and N_2 we consider that the equation in which the third term of eq. [1] represents a random walk surface diffusion mechanism describes the net flow most faithfully. From our data the mean step lengths (resolved in the direction of flow) for Ar and N_2 appear to be surface controlled and of the order of 5 to 8 Å, increasing slightly with surface coverage. Thus in the cases of Ar and N_2 if we write

$$J = -\frac{1}{2}\bar{v}_x\bar{x}\frac{\mathrm{d}N}{\mathrm{d}x} = -D\frac{\mathrm{d}N}{\mathrm{d}x}$$

where J is the number of molecules passing unit length per second on the surface, $\bar{v}_x$ is the mean speed resolved in the direction of flow, the x direction, $\bar{x}$ is the mean step length resolved in the x direction and N the number of molecules per unit area, D is of the order $10^{-4}(1 + (4.59 \times 10^{-3}p_{cm}))$. If we follow Barrer (2) and write $J' = -D'\frac{dC}{dx}$ where J' refers to the number of molecules per second passing unit area of the input surface of the whole plug and C is the total number of molecules both in the gas space and on the surface that is contained in unit volume of sample, the value of D' is about the same as D.

REFERENCES

1. E. A. Flood, R. H. Tomlinson, and A. E. Leger. Can. J. Chem. **30**, 389 (1952).
2. R. Ash, R. M. Barrer, and C. G. Cope. Proc. Roy. Soc. London, Ser. A, **271**, 1 (1963).
3. P. C. Carman. Flow of gases through porous media. Butterworths, London. 1956.
4. J. R. Dacey. *In* Solid surfaces and the solid-gas interface. Advances in Chemistry Series, American Chemical Society. 1961.
5. E. R. Gilliland, R. F. Baddour, and J. L. Russell. Am. Inst. Chem. Eng. J. **4**, 90 (1958).
6. M. E. Huber, E. A. Flood, and R. D. Heyding. Can. J. Chem. **34**, 1284 (1956).

Can. J. Chem. Downloaded from www.nrcresearchpress.com by 210.87.254.5 on 09/05/12
For personal use only.

Can. J. Chem. Downloaded from www.nrcresearchpress.com by 210.87.254.105 on 09/05/12
For personal use only.

THE REACTIONS OF 2-METHYL ETHYLENIMINE AND AZACYCLOBUTANE WITH ATOMIC HYDROGEN

J. W. S. JAMIESON, G. R. BROWN, AND W. K. HANCOCK
Department of Chemistry, St. John's College, University of Manitoba, Winnipeg, Manitoba
Received December 23, 1964

ABSTRACT

The reactions of hydrogen atoms with 2-methyl ethylenimine and azacyclobutane have been investigated at various temperatures. Between 100 and 300 °C both reactions have been found to be rapid and complete, so that the maximum disappearance of either cyclic imine under these conditions may be regarded as a satisfactory measure of atomic hydrogen flow rates. At 300 °C ethane has been found to be a major product, and it has been inferred from this and other results at this temperature that the other major product of both reactions is cyanogen, which could not be isolated since it appears to form compounds with both cyclic imines.

INTRODUCTION

The reactions of 2-methyl ethylenimine and azacyclobutane with atomic hydrogen have been studied with the hope that either or both of these cyclic imines would be capable of giving even more accurate estimates of the flow rates of atomic hydrogen in a Wood-Bonhöffer apparatus than it has previously been possible to make on the basis of the maximum extent of the reactions of ethyl chloride (1), formamide (1), or ethylenimine (2) with hydrogen atoms.

EXPERIMENTAL

A 50 g sample of 2-methyl ethylenimine (b.p. 64.0–65.5 °C) was kindly donated by Chemirad Corporation, East Brunswick, N.J., U.S.A., and azacyclobutane (1,3-propylenimine, trimethylenimine) of research grade was purchased from the Borden Company, Chemical Division, Monomer–Polymer Laboratories, Philadelphia, Pa., U.S.A. These reactants were further purified by bulb-to-bulb distillation under vacuum, the first and last fractions being discarded.

Cyanogen was prepared either by heating mercuric cyanide alone (3) or in the presence of $HgCl_2$ (4) (which did not prove to be a very satisfactory method) or by dropping saturated KCN solution into a solution of $CuSO_4$ (5).

The apparatus was a conventional fast flow system which has recently been described (1, 6). Gaseous products of the reactions have been identified by comparing temperatures for separation from a Le Roy still and retention times in gas chromatography for known gases, gases produced in the reactions studied, and mixtures of known gases and reaction products. Experimental procedures, including volumetric analysis of cyanide and analysis of ethane and ethylene by gas chromatography were as previously described (1, 6). Unreacted imine was determined by titration with standard acid to the methyl red end point. A column (7) of triacetin on Chromosorb P at 70 °C was used whenever possible to separate HCN and cyanogen by gas chromatography.

In all experiments the flow rate of molecular hydrogen was 8.82×10^{-5} mole/s, which gave a pressure in the reaction system of 1.10 mm. The atomic hydrogen flow rate was estimated at several temperatures from the reactions of ethyl chloride (1), formamide (1), and ethylenimine (2) with hydrogen atoms. At 300 °C the best estimate thus obtained is 2.1×10^{-6} mole/s, which is applicable to most of the experiments reported.

RESULTS AND DISCUSSION

The data of Table I and Fig. 1 show that 2-methyl ethylenimine reacted rapidly and completely with hydrogen atoms at 300 °C. At high imine flow rates the amount of imine reacted per second was found to be equal to the estimated hydrogen atom flow rate. The reaction was slower at 96 °C but the same maximum extent of reaction was observed at high imine flow rates, while at 36 °C (in the unheated reaction vessel) the reaction was slow and incomplete.

Can. J. Chem. Downloaded from www.nrcresearchpress.com by 210.87.254.105 on 09/05/12
For personal use only.

TABLE I

Data for the 2-methyl ethylenimine reaction*

T, °C	Imine		Cyanide produced	Ethane produced
	Flowed	Reacted		
36±3	0.80	0.20	0.11	
	2.12	0.31	0.20	
	4.70	0.74	0.30	
	7.32	1.05	0.46	
96±2	2.20	0.92	0.55	
	4.91	1.83	0.51	
	7.90	2.03	0.49	
	8.79	2.07	0.54	
	9.45	2.08	0.51	
	10.62	2.01	0.52	
	11.50	2.13	0.49	
300±4	0.80	0.50	0.50	
	1.50	1.00	0.83	
	1.73			0.82
	1.92	1.22	1.00	
	2.10			0.91
	3.00	1.65	1.09	
	4.70	2.02	1.06	
	4.82			1.55
	6.10	2.06	1.03	
	7.35			1.87
	7.50	2.02	1.11	
	8.50	2.10	1.02	
	10.00			2.02
	10.65	2.06	1.04	
	11.60			2.08

*All flow rates are in μmole/s.

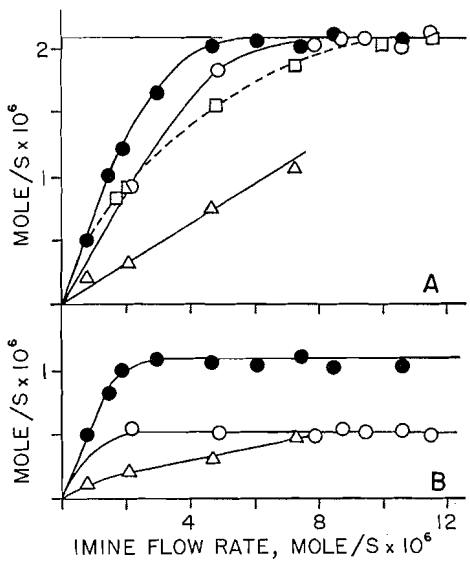

FIG. 1. The reaction of 2-methyl ethylenimine with atomic hydrogen. A. Imine reacted at 36 °C (△), 96 °C (○), and 300 °C (●); ethane produced at 300 °C (□). NOTE. The light horizontal line denotes the flow rate of hydrogen atoms. B. Cyanide produced at 36 °C (△), 96 °C (○), and 300 °C (●).

In the experiments at 300 °C the maximum amount of ethane produced was equal not only to the maximum amount of imine reacted but also to the flow rate of hydrogen atoms. The maximum amount of cyanide produced at the high temperature was about half the maximum amount of imine reacted.

A number of experiments at higher hydrogen atom flow rates (about 4 and 5 μmoles/s) and at various temperatures have given similar results, some of which have previously been reported (6).

As in the reaction of ethylenimine (2) the most probable primary reaction is abstraction of the imine hydrogen.

[1] 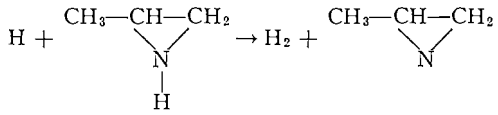

It is unlikely that ethane is formed by decomposition of the imino radical thus formed, except possibly at very low imine flow rates where some HCN may be produced by reaction of the excess hydrogen atoms with imino radicals. Trace amounts of HCN were detected by gas chromatography in some experiments at very low imine flow rates, although consideration of a material balance for carbon and nitrogen at the high temperature and high imine flow rates seems to imply that the product which gives the cyanide titration is cyanogen, which during the analysis hydrolyzes to the cyanate ion and the cyanide ion. Titration of the latter ion would then give a measure of the amount of cyanogen produced in the reaction of the imine with atomic hydrogen. Thus ethane and cyanogen are probably formed mainly by combination of two of the imino radicals produced in reaction [1] so that, in agreement with the experimental results at 300 °C, one molecule of ethane and half a molecule of cyanogen are produced for each molecule of 2-methyl ethylenimine reacted with atomic hydrogen.

Cyanogen has not been positively identified among the products, except in trace amounts, either by separation from a Le Roy still at −125 °C or by gas chromatography. In an attempt to understand how cyanogen could give the cyanide titration but could not be determined by other means some cyanogen was prepared and studied. The freshly prepared cyanogen was further purified in a Le Roy still, from which it was distilled at −125 °C. The pure material was then measured in a gas burette, after which it was analyzed by gas chromatography. After passage through a suitable column (7) the cyanogen gave a distinct peak which was easily separated from HCN when it was added. The pure cyanogen was also found to give the cyanide titration with silver nitrate.

When some of either imine was added to cyanogen in the Le Roy still no gas was evolved at −125 °C. Similarly when either imine was introduced into a gas burette containing cyanogen there was an immediate and substantial drop in pressure. When some of the mixture of either imine with cyanogen was taken into the gas chromatograph no cyanogen was detected. On the other hand, when either mixture was distilled into a removable cold trap it was found to give the cyanide titration.

It appears, therefore, that there is conclusive evidence that cyanogen forms compounds in the gas phase with both 2-methyl ethylenimine and azacyclobutane. Evidently both compounds decompose either in aqueous solution or in the presence of silver nitrate solution. In view of these experiments it is hardly surprising that cyanogen could not be isolated from the mixtures of unreacted imines and other products of the reactions of atomic hydrogen with the cyclic imines.

Can. J. Chem. Downloaded from www.nrcresearchpress.com by 210.87.254.105 on 09/05/12
For personal use only.

The results for the reaction of azacyclobutane with atomic hydrogen are shown in Table II and in Fig. 2. This reaction was found to be even more rapid than the 2-methyl ethylenimine reaction. Destruction of azacyclobutane and formation of products were almost independent of temperature from 41 to 300 °C. Again, at high imine flow rates and at both temperatures, all the available hydrogen atoms were consumed by the imine. In all experiments the maximum amount of cyanide determined by titration with silver nitrate was about half the maximum amount of imine reacted.

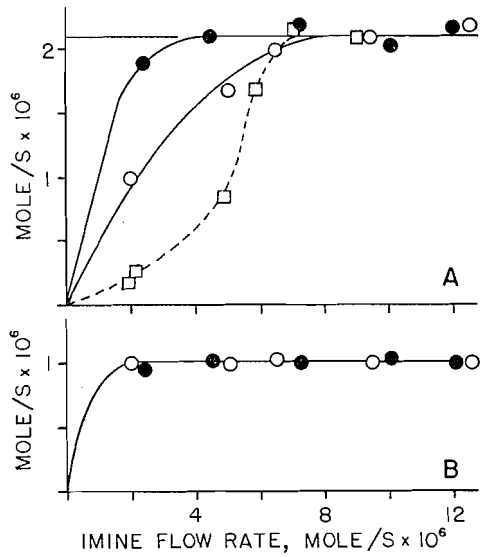

FIG. 2. The reaction of azacyclobutane with atomic hydrogen. A. Imine reacted at 41 °C (○) and 300 °C (●); ethane plus ethylene produced at 300 °C (□). NOTE. The light horizontal line denotes the flow rate of hydrogen atoms. B. Cyanide produced at 41 °C (○) and 300 °C (●).

TABLE II

Data for the azacyclobutane reaction*

	Imine			
T, °C	Flowed	Reacted	Cyanide produced	$C_2H_6 + C_2H_4$ produced
41±2	2.00	1.00	1.00	
	5.03	1.69	0.99	
	6.58	2.00	1.03	
	9.49	2.10	1.00	
	12.60	2.19	1.00	
300±3	1.91			0.18
	2.20			0.26
	2.41	1.90	0.95	
	4.57	2.12	1.01	
	4.93			0.84
	5.95			1.68
	7.15			2.17
	7.33	2.20	1.00	
	9.07			2.09
	10.10	2.04	1.03	
	12.10	2.17	1.00	

*All flow rates are in μmole/s.

Can. J. Chem. Downloaded from www.nrcresearchpress.com by 210.87.254.105 on 09/05/12
For personal use only.

Analysis by gas chromatography showed that both ethane and ethylene were among the products of the azacyclobutane reaction at 300 °C. Since separation of the peaks for these gases was incomplete the results are reported as ethane plus ethylene, although it is estimated that there was about twice as much ethane as ethylene. The total amount of these two products was equal to the extent of the azacyclobutane reaction at 300 °C and high flow rates.

Again, as previously reported (6), similar results were obtained in several experiments at higher hydrogen atom flow rates and at various temperatures.

By analogy with the reactions of atomic hydrogen with ethylenimine (2) and 2-methyl ethylenimine it seems likely that hydrogen atoms first attack azacyclobutane to abstract the imine hydrogen.

[2] 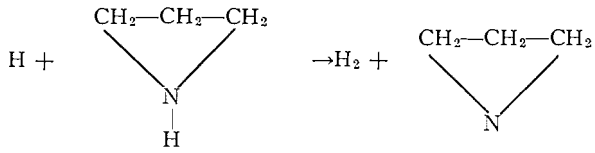

Except at very low imine flow rates the main subsequent reactions would seem to involve combination of two imino radicals to give cyanogen and either ethane predominately or ethylene and hydrogen, although it has not been possible, for the reason already given, to confirm the presence of cyanogen among the products.

The formation of small quantities of HCN at very low imine flow rates might again be due to reaction of the imino radicals with any excess hydrogen atoms.

As anticipated, both 2-methyl ethylenimine and azacyclobutane reacted rapidly and completely with atomic hydrogen, particularly at temperatures above 100 °C, so that both reactants at high flow rate seem to be very suitable for the estimation of atomic hydrogen flow rates. Their use for this purpose in a study of the kinetics of the reaction of atomic hydrogen with methane has already been reported (6).

ACKNOWLEDGMENT

The authors are grateful to the National Research Council for financial assistance.

REFERENCES

1. J. W. S. JAMIESON. Can. J. Chem. **41**, 1568 (1963).
2. J. W. S. JAMIESON and C. A. WINKLER. J. Phys. Chem. **60**, 1542 (1956).
3. W. L. JOLLY. Synthetic inorganic chemistry. Prentice-Hall, Englewood Cliffs, N.J. 1960.
4. J. R. PARTINGTON. A text-book of inorganic chemistry. 6th ed. Macmillan, London. 1950.
5. F. A. COTTON and G. WILKINSON. Advanced inorganic chemistry. Interscience, Wiley, New York. 1962.
6. J. W. S. JAMIESON and G. R. BROWN. Can. J. Chem. **42**, 1638 (1964).
7. R. E. ISBELL. Anal. Chem. **35**, 255 (1963).

Can. J. Chem. Downloaded from www.nrcresearchpress.com by 210.87.254.105 on 09/05/12
For personal use only.

Can. J. Chem. Downloaded from www.nrcresearchpress.com by 210.87.254.6 on 09/05/12
For personal use only.

THE DISSOLUTION OF COPPER IN AMMONIACAL POTASSIUM BROMATE SOLUTIONS[1]

M. KULKARNI AND D. R. WILES
Department of Chemistry, Carleton University, Ottawa, Canada

Received January 15, 1965

ABSTRACT

The dissolution of copper in ammonia solutions was found earlier to be bimolecular in ammonia, involving a fast equilibrium adsorption of one molecule, followed by attack by a second molecule of ammonia (or an ammonium ion). The present work, differing in that potassium bromate is used as oxidizing agent rather than oxygen under pressure, shows that the dissolution process is essentially similar in many respects. The most striking difference is that the oxidation step can now be seen and proves to be quite complex. In particular two quite different oxidation mechanisms appear to operate: one is a simple adsorption of $KBrO_3$ and the other is a higher order reaction interpreted as involving a multiple adsorption on the reaction site, for which ammonia and ammonium also compete.

INTRODUCTION

The dissolution of metallic copper in aqueous ammonia solutions has been shown in earlier work (1) to involve two steps in addition to the oxidation stage. The first of these appears to be a fast equilibrium adsorption of ammonia on an oxidized site in the metal surface. The second, the rate-determining step, is an attack on the same site by either an ammonia molecule or an ammonium ion. These steps are illustrated by eqs. [1] and [2].

$$[1] \qquad Cu_o + NH_3 \overset{K}{\rightleftharpoons} Cu_oNH_3$$

$$[2a] \qquad Cu_oNH_3 + NH_3 \overset{k_1}{\rightarrow} Cu(NH_3)_2^{++}$$

$$[2b] \qquad Cu_oNH_3 + NH_4^+ \overset{k_2}{\rightarrow} Cu(NH_3)_2^{++} + H^+$$

The symbol Cu_o is used to denote a copper atom at an oxidized site in the metal surface, although the nature of this site is at present not known. Direct observation of this adsorption has recently been made by Nagi (2) using carbon-14-labelled methylamine.

The same mechanism was found to hold for the simple aliphatic amines as well as for ammonia. The reaction rate was well expressed by eq. [3], which can easily be derived from the mechanism given.

$$[3] \qquad \text{Rate} = \frac{d[Cu^{++}]}{dt} = \frac{K[NH_3]S}{1 + K[NH_3]} (k_1[NH_3] + k_2[NH_4^+])$$

The supposition that the sites for reactions [1] and [2] are the same was confirmed by the observation (3) that the same reaction is monomolecular in ethylenediamine. It is interesting to note that in 1,4-butanediamine the dissolution is bimolecular, while in 1,3-propanediamine both a bimolecular and a monomolecular reaction can be observed (3).

These studies allowed no investigation of the role of the oxidizing agent (O_2 under 8 atm pressure) because of transport problems in the solution. In the present study, oxidation was effected by the use of $KBrO_3$. This reagent was chosen as a convenient one for use in basic solutions: one which is stable toward decomposition and gives no reaction with Cu^{++}.

[1]*Paper presented to the 46th Annual Conference of the Chemical Institute of Canada, Toronto, June 6, 1963.*

Can. J. Chem. Downloaded from www.nrcresearchpress.com by 210.87.254.6 on 09/05/12
For personal use only.

EXPERIMENTAL METHODS

The copper used was 99.9% pure, supplied by J. T. Baker Chemical Company. The metal was vacuum melted and cast into ingots and then stressed and annealed to effect grain refinement.* The resultant sample was a polycrystalline material whose average grain size was a few tenths of a millimeter. No determination was made of crystal orientation, which is assumed to be essentially random. After being machined to size (14.0 mm diameter) the metal samples were mounted in Bakelite to expose a constant surface area. The samples were polished by hand down to number 0 emery paper before each use. No etching treatment was used, since it was shown earlier (1) that etching makes no difference in the rate. Failure to etch the samples may lead to a variation in the true zero time, but this time was not of concern in determining the rate.

All other reagents were the best grade available. Ammonia stock solutions were kept in stoppered containers and checked frequently to detect possible changes in concentration.

The dissolution studies were done in a vessel essentially similar to the one used before, except that the use of atmospheric pressure made possible the use of a Pyrex container and Lucite internal parts. A diagram showing the essential features is given in Fig. 1.

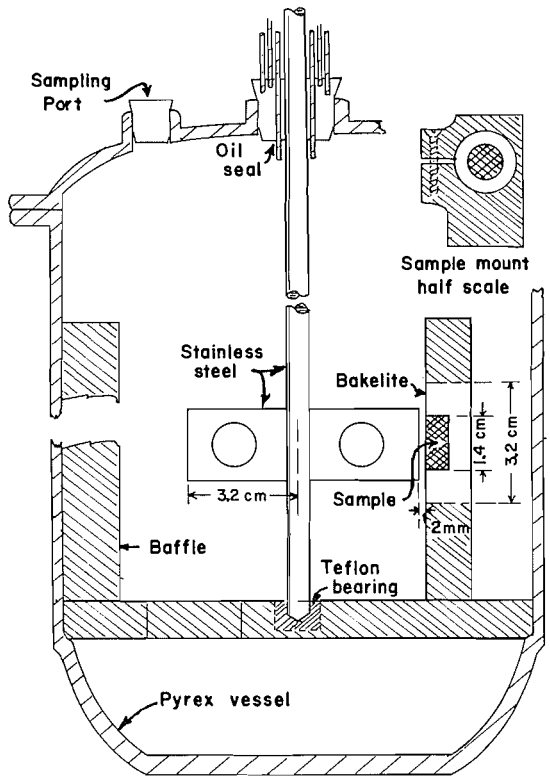

FIG. 1. Diagram of dissolution apparatus.

In any heterogeneous system, it is important to make sure that the observed rate is not merely the rate of transport of the reactants to the reaction interface (4, 5). While in the case of very slow reactions mild agitation is adequate (6, 7) in the case of more rapid dissolution the rate of stirring of the solution is occasionally of greatest importance (8, 9). We have employed two criteria to convince ourselves that transport of the reactants was not a limiting factor in the experiments described here: (i) The reaction rate was found to be essentially independent of stirring rate† between 750 r.p.m. and 1 100 r.p.m. so a stirring rate of 900 r.p.m. was used. (ii) The system was tested for transport control also by the method suggested by Bircumshaw and Riddiford (5). The dissolution was done using 0.02 M I_2 in KI solution as oxidant. A dissolution rate of ~ 250

*We are grateful to Mr. H. Weld for assistance in preparing the copper samples.

†*This is one of the criteria of King (4). Another criterion is that the activation energy not be too low, e.g.* $\Delta H^{\ddagger} > 5$ *kcal/mole. This seems to be a somewhat uncertain test, however, since some of the activation energies observed in chemically controlled dissolution reactions are disturbingly close to the suggested limit (13).*

mg Cu^{++} cm^{-2} h^{-1} was found, corresponding to a diffusion layer ~ 0.003 mm thick. Using available (10) mobility data for NH_3 and assuming the mobilities of NH_4^+ and BrO_3^- to be not greatly different, it was computed that transport control would be no problem unless the dissolution rate exceeded 500 mg Cu^{++} cm^{-2} h^{-1}. The rates observed were seldom in excess of 150 mg Cu^{++} cm^{-2} h^{-1}, and transport of reactants to the surface is concluded to play no limiting part in determining the kinetics of the reaction.

Each experiment involved stirring 3.0 l of solution of the chosen concentrations of $KBrO_3$, NH_3, and NH_4ClO_4, adjusted in advance to the proper temperature, in contact with the copper samples. The solution was sampled by withdrawing 10 ml aliquots at regular intervals. These samples were analyzed for copper by the carbamate method (11). The temperature was controlled by the use of a thermistor controller.* Temperatures were adjusted to ± 0.1 °C and controlled to about ± 0.05 of the adjusted value.

Rates were determined from the slope of the plot of $[Cu^{++}]$ vs. time. Correction was not made for the amount of solution removed in samplings and a systematic error of about 0.5% is thus introduced. In the light of other uncertainties, however, this is not of a magnitude to warrant concern. These rate plots were invariably linear, which fact was taken to indicate that (*a*) there is no reaction between BrO_3^- and NH_3 or NH_4^+ which might affect the dissolution rate, and that (*b*) the cupric ion has no effect on the reaction. Thus, autocatalytic mechanisms such as that of Lu and Graydon (12), involving some cupric species as oxidant, are not relevant here.

RESULTS AND DISCUSSION

The dissolution rates are shown, as a function of $[NH_3]$ for various values of $[NH_4^+]$, in Figs. 2 and 3.

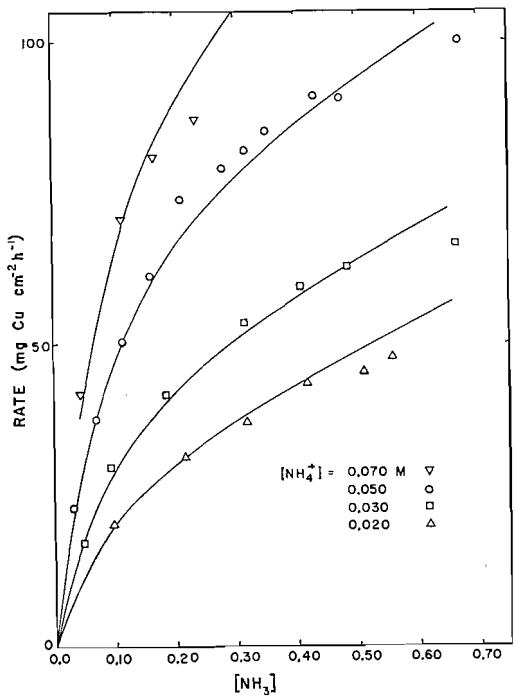

FIG. 2. Rates of dissolution as a function of $[NH_3]$. $[KBrO_3] = 0.033$ *M*, temperature 25 °C, $[NH_4^+]$ as shown on figure. Solid lines calculated using eq. [3].

The most striking feature of the rate plots is a sudden remarkable decrease in the rate which occurs as higher ammonia concentrations are reached. The "turnover point", which clearly marks the change from one reaction mechanism to another, is also a function of the ammonium ion concentration and, as is seen in Fig. 4, of the bromate concentration.

**Model 71, Yellow Springs Instrument Co., Yellow Springs, Colorado.*

Can. J. Chem. Downloaded from www.nrcresearchpress.com by 210.87.254.6 on 09/05/12
For personal use only.

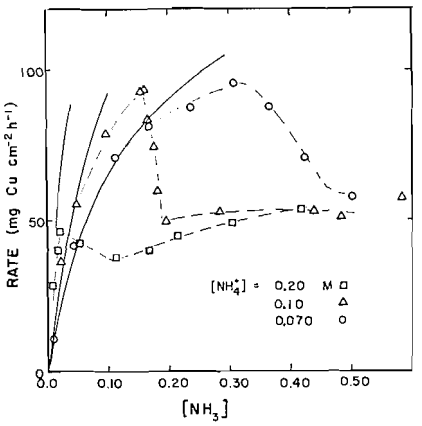

FIG. 3. Rates of dissolution as a function of $[NH_3]$. $[KBrO_3] = 0.033\ M$, temperature 25 °C, $[NH_4^+]$ as shown on figure. Solid lines calculated using eq. [3].

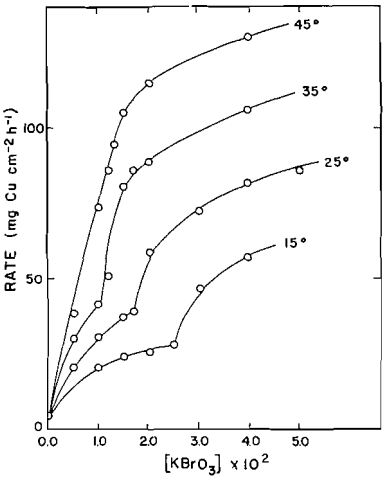

FIG. 4. Rates of dissolution as a function of $[KBrO_3]$. $[NH_3] = 0.35\ M$, $[NH_4^+] = 0.050\ M$.

We will find it convenient to refer to the "high-bromate region" and the "low-bromate region." These are quite distinct in Fig. 4.

In the high-bromate region, the dependence of the rate on the ammonia and ammonium concentrations is the same as that observed earlier using O_2 as oxidant. At constant acidity eq. [3] becomes:

$$\text{rate} = \frac{K[NH_3]^2 S}{1 + K[NH_3]} (k_1 + k_2\alpha) \qquad [4]$$

where $\alpha = [NH_4^+]/[NH_3]$. The results at constant acidity are shown in Figs. 5 and 6, for various values of α.

It is evident that the data are not precise enough to permit unequivocal computation of the constants of eqs. [3] and [4]. However, a self-consistent set is given in Table I.

It is these values which have been used in computing the solid curves drawn in Figs. 2, 3, 5, and 6. Comparison of the values for the constants determined in this work with the

Can. J. Chem. Downloaded from www.nrcresearchpress.com by 210.87.254.6 on 09/05/12
For personal use only.

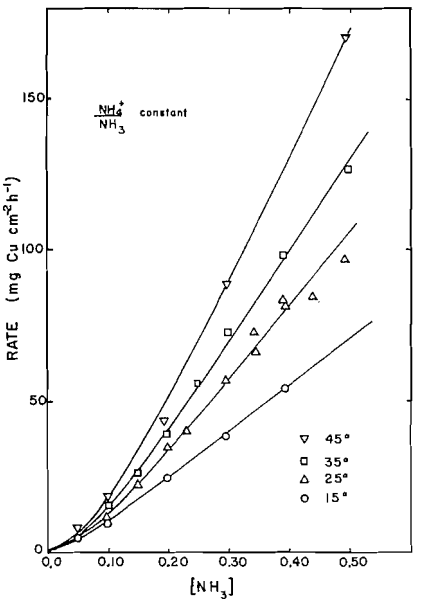

FIG. 5. Rates of dissolution at constant acidity. $[NH_4^+]/[NH_3] = 0.10$, $[KBrO_3] = 0.033$ *M*. Solid curves calculated using eq. [4].

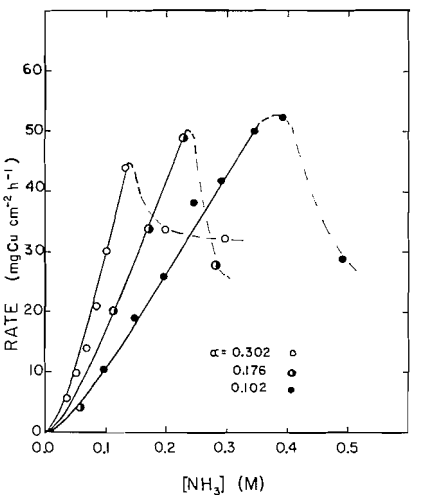

FIG. 6. Rates of dissolution at constant acidity. $[NH_4^+]/[NH_3]$ ($= \alpha$) given on graph, $[KBrO_3] = 0.011$ *M*, temperature 25 °C. Solid curves calculated using eq. [4].

values obtained by Sircar (1) shows that the adsorption and reaction mechanisms are fairly similar, although there is a quantitative dependence on both the nature and concentration range of the oxidant.

The concentration of ammonia seems to have a much smaller effect on the rate in the low-bromate region, although the nature of this effect is not clear at present. The ammonium ion appears to have a rather more pronounced effect but too few data have been obtained to make a detailed analysis possible.

Can. J. Chem. Downloaded from www.nrcresearchpress.com by 210.87.254.6 on 09/05/12
For personal use only.

TABLE I
Constants for eqs. [3] and [4]

$KBrO_3$ (M)	Temperatures (°C)	K	k_1	k_2
0.012	25	16.5	(~10)	1.6×10^3
0.033	15	22	45	0.95×10^3
0.033	25	10.0	45	1.8×10^3
0.033	35	8.0	15	3.1×10^3
0.033	45	7.0	(~25)	4.0×10^3
Activation energies (kcal/mole)		~6	—	10.7
O_2 at 8.2 atm (ref. 1)	25	4.7	80	2.5×10^3

The effect of changing bromate ion concentration (Fig. 4) suggests that the low-bromate region involves simple Langmuir adsorption of a single bromate ion, leading to the production of oxidized sites, which may then react with ammonia. Reasonable fit of the data is obtained at 25 °C by using a value $K = 140$ for the adsorption equilibrium constant. It must be emphasized that only few data are available, and a definite conclusion is not possible.

The turnover point varies in a rather complicated manner with the concentrations of bromate, ammonia, and ammonium. A sudden break in curves of this type has been observed in other cases. For example, in the dissolution of zinc in oxygenated ammoniacal solutions (14) the rate decreases suddenly as the oxygen pressure is increased. This was shown to result from the formation of a protective layer of zinc oxide.

This interpretation seems unsatisfactory in the present case, however, on the following grounds: (i) A pH-potential diagram (15) was drawn up for the copper–ammonia system, and it clearly showed that the formation of any kind of oxide layer is most unlikely under the conditions used. (ii) Zogović showed (16) that CuO, under similar experimental conditions, dissolves very slowly indeed. The present experiments show an increase in rate under conditions where formation of any sort of layer would lead to a decrease in rate.

An attractive possibility is that of a competitive adsorption at a surface site, S.

[5] $$S(NH_3)_x(NH_4^+)_y + zBrO_3^- \rightleftharpoons S(BrO_3^-)_z + xNH_3 + yNH_4^+$$

It is hoped that continuation of our carbon-14 experiments (2) may shed further light on this question. The final steps in the reaction of the oxidized site produced by this competition are the same as was found earlier for sites produced by molecular oxygen (1).

An attempt was made to apply Moelwyn-Hughes' molecular statistics (17) to the final step (i.e. eq. [2*a*] or [2*b*]). In this approach, one calculates the total number, $N^{\ddagger}$, of molecules of a given species striking the surface with energy greater than the activation energy for the reaction using the formula,

[6] $$N^{\ddagger} = n_s \sqrt{\frac{RT}{2\pi M}}\ e^{-\Delta H^{\ddagger}/RT}.$$

In cases which Moelwyn-Hughes feels the agreement is satisfactory, this number $N^{\ddagger}$ is larger than the experimental reaction rate by a factor of perhaps 40. Using this technique to look at the ammonium reaction (eq. [2*b*]) for which both the rate and the activation energy are fairly reliable, one finds the observed rate to be some 30 times the maximum theoretical rate. Considering the uncertainties involved, this may be regarded as satisfactory agreement.

Can. J. Chem. Downloaded from www.nrcresearchpress.com by 210.87.254.6 on 09/05/12
For personal use only.

ACKNOWLEDGMENT

The financial support of the National Research Council is gratefully acknowledged.

REFERENCES

1. S. C. SIRCAR and D. R. WILES. J. Electrochem. Soc. **107**, 164 (1960).
2. F. I. NAGI and D. R. WILES. To be published.
3. S. C. SIRCAR and D. R. WILES. J. Electrochem. Soc. **107**, 366 (1960).
4. C. V. KING. *In* Surface chemistry of metals and semiconductors. *Edited by* H. C. Gatos. Wiley, New York. 1959.
5. A. C. RIDDIFORD and L. L. BIRCUMSHAW. J. Chem. Soc. 698 (1952).
6. G. R. HILL. J. Electrochem. Soc. **100**, 345 (1953).
7. J. R. WEEKS and G. R. HILL. J. Electrochem. Soc. **103**, 203 (1956).
8. G. C. BOND, B. M. HILL, and R. TENNYSON. J. Chem. Soc. 33 (1959).
9. G. C. BOND and G. WEBB. J. Chem. Soc. 2122 (1962).
10. B. E. CONWAY. Electrochemical data. Elsevier. 1952.
11. E. B. SANDELL. Colorimetric determination of traces of metals. Interscience, New York. 1950.
12. B. C-Y. LU and W. F. GRAYDON. J. Am. Chem. Soc. **77**, 6136 (1955).
13. J. HALPERN. J. Electrochem. Soc. **100**, 421 (1953).
14. L. R. DILWORTH. M.A.Sc. Thesis, University of British Columbia. 1960.
15. M. POURBAIX. Thermodynamics of dilute aqueous solutions. Edward Arnold and Co., London. 1949.
16. D. R. WILES and B. ZOGOVIĆ. Unpublished work, Carleton University. 1960.
17. E. A. MOELWYN-HUGHES. Kinetics of reactions in solution. Clarendon Press, Oxford. 1950.

Can. J. Chem. Downloaded from www.nrcresearchpress.com by 210.87.254.6 on 09/05/12
For personal use only.

THE REACTION OF UNSATURATED CARBOHYDRATES WITH CARBON MONOXIDE AND HYDROGEN

IV. STRUCTURE AND STEREOCHEMISTRY OF ANHYDRODEOXYHEPTITOLS FROM 3,4,6-TRI-*O*-ACETYL-D-GALACTAL

ALEX ROSENTHAL AND DEREK ABSON
Department of Chemistry, University of British Columbia, Vancouver, British Columbia
Received February 24, 1964

ABSTRACT

3,4,6-Tri-*O*-acetyl-D-galactal reacted with carbon monoxide and hydrogen in the presence of dicobalt octacarbonyl to yield 2,6-anhydro-3-deoxy-D-*galacto*-heptitol (I) and 2,6-anhydro-3-deoxy-D-*talo*-heptitol (II). The stereochemistry of (I) and (II) has been established by correlation with 2,6-anhydro-3-deoxy-D-*gluco*-heptitol (VI) of known configuration. Evidence that both (I) and (II) are formed by the addition of a hydroxmethyl group to C-1 of the glycal is also furnished by the proton n.m.r. spectra of the normal and deuterated anhydrodeoxyheptitols.

Part I of this series (1) described the action of carbon monoxide and hydrogen on 3,4,6-tri-*O*-acetyl-D-galactal, and presented evidence for the formation of an anhydrodeoxyheptitol of unknown stereochemistry. It has since been found that 3,4,6-tri-*O*-acetyl-D-galactal reacts under oxo conditions in a manner entirely analogous to other glycals investigated (2, 3) to yield as the major products a pair of isomeric anhydrodeoxyheptitols (I) and (II), formed by the addition of a hydroxymethyl group to C-1 of the unsaturated carbohydrate. The stereochemistry of (I) and (II) has been elucidated by an analysis of their proton n.m.r. spectra and by correlation with 2,6-anhydro-3-deoxy-D-*gluco*-heptitol (VI), whose structure has been proved by crystallographic X-ray analysis (4).

3,4,6-Tri-*O*-acetyl-D-galactal (5) was reacted in a high-pressure apparatus with carbon monoxide and hydrogen in the presence of dicobalt octacarbonyl, under conditions similar to those described previously (1). The reaction product was separated from the catalyst by chromatography on a Florisil column, and deacetylated with methanolic sodium methoxide. The two major reaction products (I) and (II), after separation by preparative paper chromatography, were obtained in approximately equal amounts.

DISCUSSION

Both (I) and (II) consumed 1 molar equivalent of periodate (0.95 and 0.98 respectively) as measured by the spectrophotometric method of Dixon and Lipkin (6). Fraction (II) reacted with acetone in the presence of sulfuric acid to form a monoisopropylidene derivative (VII), which on treatment with *p*-toluenesulfonyl chloride in pyridine gave a compound (VIII) containing two tosyloxy groups. The latter compound on heating with sodium iodide in acetone solution liberated 2 equivalents of sodium *p*-toluenesulfonate. Thus it is highly likely that (II) contains two primary hydroxyl groups and two adjacent *cis* secondary hydroxyl groups. Compound (I) was characterized as the tetra-*O*-(*p*-nitrobenzoyl) derivative.

Evidence that both (I) and (II) have unbranched carbon skeletons was furnished by their proton nuclear magnetic resonance (n.m.r.) spectra, measured in D_2O solution (Fig. 1*a* and *c*). These both show a group of signals at lower field (3.3–4.3 p.p.m.) with total area corresponding to 8 hydrogens, and a further group at higher field (1.3–2.3 p.p.m.), area = 2 hydrogens. The higher field signals can clearly be assigned to hydrogens attached

Can. J. Chem. Downloaded from www.nrcresearchpress.com by 210.87.254.42 on 09/05/12
For personal use only.

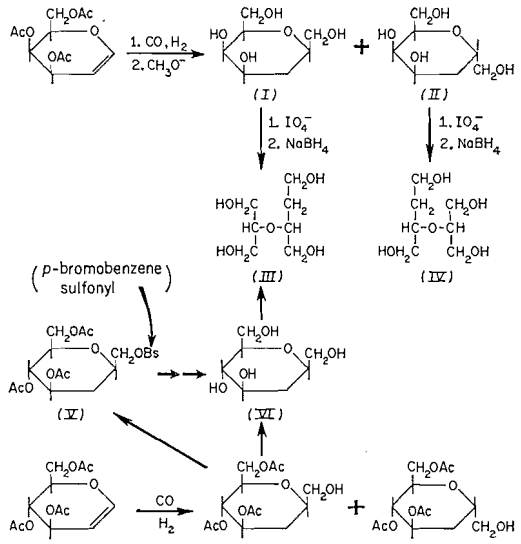

to C-3 of the anhydrodeoxyheptitols, this being the only carbon atom which is not directly linked to oxygen, and the fact that two such hydrogens are present in both (I) and (II) must mean that the two compounds differ only in the configuration of the hydroxymethyl group about C-2. This tentative assignment was then rigorously established by classical chemical methods in the following way. Oxidative cleavage of (I) and (II) with periodic acid followed by sodium borohydride reduction of the resulting dialdehydes gave a pair of enantiomeric tetrol ethers (III) and (IV). Each had only one asymmetric center, and the enantiomers had similar infrared spectra, and equal and opposite specific rotations. Treatment of (III) and (IV) with *p*-nitrobenzoyl chloride in pyridine afforded the enantiomeric tetra-*O*-(*p*-nitrobenzoyl) derivatives, which had identical infrared spectra and melting points and differed only in the sign of rotation.

The configuration of C-2 of both epimeric 2,6-anhydro-3-deoxyheptitols was readily established by application of proton n.m.r. spectroscopy, as previously described (2), to the 3-deoxy-3-deuterioanhydroheptitols (IX) and (X) which were produced when 3,4,6-tri-*O*-acetyl-D-galactal was reacted with carbon monoxide and deuterium. Thus, as shown in Fig. 1*b*, the narrow quartet structure (width about 17 c.p.s.) of the signal of intensity 1 at around $\delta = 1.7$ requires the C-3 proton to be in an equatorial orientation and coupled with the C-2 and C-4 axial hydrogens. On the other hand, as depicted in Fig. 1*d*, the corresponding wider multiplet of signals (width about 35 c.p.s.) of intensity 1 at the field ($\delta = 1.9$) suggests the C-3 proton of compound (X) to be in an axial orientation and coupled with the C-4 axial and C-2 equatorial hydrogens. Therefore, compounds (IX) and (X) are 2,6-anhydro-3-deoxy-D-*galacto*-heptitol-1,1,3-$^2H_3$ and 2,6-anhydro-3-deoxy-D-*talo*-heptitol-1,1,3-$^2H_3$, respectively.

Unequivocal confirmation of the C-2 configuration of the anhydrodeoxyheptitols (I) and (II) was provided by correlating (I) and (II) with 2,6-anhydro-3-deoxy-D-*gluco*-heptitol (VI). The latter compound had been produced by application of the oxo reaction to 3,4,6-tri-*O*-acetyl-D-glucal (4). The absolute configuration of the 1-*O*-(*p*-bromobenzenesulfonyl) derivative (V) had been previously proved by X-ray analysis (4), and (V) has been converted by standard procedures into (VI). The latter compound on periodate oxidation followed by sodium borohydride reduction of the dialdehyde gave a tetrol ether

Can. J. Chem. Downloaded from www.nrcresearchpress.com by 210.87.254.42 on 09/05/12
For personal use only.

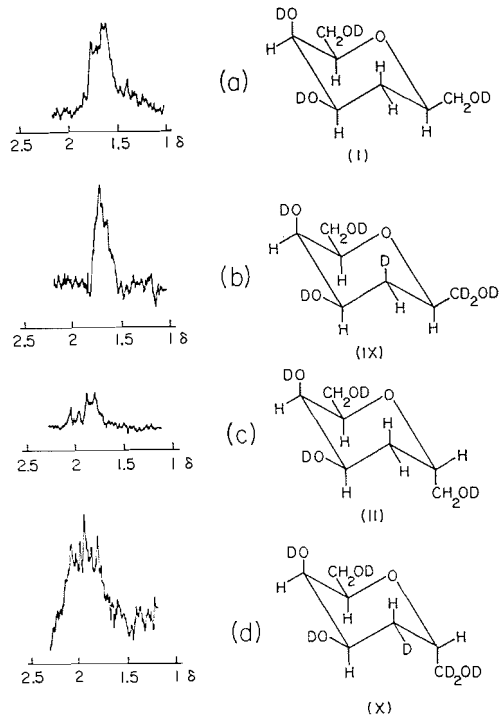

FIG. 1. Proton n.m.r. spectra in D_2O solution at 60 mc with chemical shifts given in p.p.m. from tetramethylsilane as zero; (*a*) 2,6-anhydro-3-deoxy-D-*galacto*-heptitol (I); (*b*) 2,6-anhydro-3-deoxy-D-*galacto*-heptitol-1,1,3-$^2H_3$ (*cis*) (IX); (*c*) 2,6-anhydro-3-deoxy-D-*talo*-heptitol (II); (*d*) 2,6-anhydro-3-deoxy-D-*talo*-heptitol-1,1,3-$^2H_3$ (*cis*) (X). (Only signals of protons attached to C-3 are shown.)

having an infrared spectrum and specific rotation similar to the dextrorotatory tetrol ether (III) derived from the anhydrodeoxyhexitol (1), and formed a tetra-*O*-(*p*-nitrobenzoyl) derivative identical with that obtained from (III) on the basis of melting point, mixed melting point, infrared spectrum, and specific rotation. Therefore (I), having the same configuration at C-2 as 2,6-anhydro-3-deoxy-D-*gluco*-heptitol, is 2,6-anhydro-3-deoxy-D-*galacto*-heptitol, and (II), the C-2 isomer of (I), is 2,6-anhydro-3-deoxy-D-*talo*-heptitol.

EXPERIMENTAL

General Considerations

Conditions for chromatographic separations and measurement of n.m.r. and infrared spectra have been described previously (2).

Preparation of *p*-nitrobenzoyl derivatives was carried out by a procedure similar to that of Gorin (7).

Microanalyses were by Mrs. Aldridge of this department and by Dr. A. Bernhardt, Mülheim (Ruhr), West Germany.

*Reaction of 3,4,6-Tri-O-acetyl-*D*-galactal with Carbon Monoxide and Hydrogen to Yield 2,6-Anhydro-3-deoxy-*D*-galacto-heptitol (I) and 2,6-Anhydro-3-deoxy-*D*-talo-heptitol (II)*

A solution of 3,4,6-tri-*O*-acetyl-D-galactal (15 g) and dicobalt octacarbonyl (3.5 g) in dry purified benzene (50 ml) was shaken with carbon monoxide (1 300 p.s.i.) and hydrogen (1 900 p.s.i.) in a high-pressure autoclave at a temperature of 130–135° for approximately 2 h. The resulting solution was transferred to a column (14 × 8 cm diameter) of Florisil and the catalyst was eluted with 30–60° petroleum ether. Elution with benzene–ethanol (9:1, v/v) and evaporation of solvent then gave 13.5 g of syrupy product. Deacetylation with 0.1 *N* sodium methoxide in methanol at room temperature for 18 h and removal of solvent gave a water-soluble product which, after deionization with Amberlite IR 120 (H^+) resin and freeze drying, afforded a partially crystalline mixture of (I) and (II) in approximately equal amounts, together with traces of sugars. Fractionation of the mixture of anhydrodeoxyheptitols was carried out by preparative paper chromatography. From an amount of 0.43 g of crude mixture, 0.16 g (37%) of fraction I and 0.14 g (33%) of fraction II were isolated.

Can. J. Chem. Downloaded from www.nrcresearchpress.com by 210.87.254.42 on 09/05/12
For personal use only.

Characterization of Fractions (I) and (II)

*Fraction (I) (2,6-anhydro-3-deoxy-*D*-galacto-heptitol)* was crystallized from methanol – isopropyl ether; m.p. 158–159°; $[\alpha]_D^{27}$ +24° (*c*, 0.8 in water);* R_F = 0.24.

Anal. Calcd. for $C_7H_{14}O_5$: C, 47.18; H, 7.92. Found: C, 47.50; H, 8.07.

*2,6-Anhydro-3-deoxy-1,4,5,7-tetra-O-(p-nitrobenzoyl)-*D*-galacto-heptitol*

Fraction (I) (35 mg) was treated with *p*-nitrobenzoyl chloride in pyridine to yield a tetra-*O*-(*p*-nitrobenzoyl) derivative (95 mg, 72%), which was recrystallized from ethyl acetate – petroleum ether (30–60°); m.p. 210–211°; $[\alpha]_D^{23}$ −12° (*c*, 2.0 in chloroform).

Anal. Calcd. for $C_{35}H_{26}O_{17}N_4$: C, 54.28; H, 3.38; N, 7.23. Found: C, 54.61; H, 3.50; N, 7.47.

*Fraction (II) (2,6-anhydro-3-deoxy-*D*-talo-heptitol)* was crystallized from methanol – isopropyl ether; m.p. 168°; $[\alpha]_D^{27}$ +68° (*c*, 1.1 in water); R_F = 0.21.

Anal. Calcd. for $C_7H_{14}O_5$: C, 47.18; H, 7.92. Found: C, 46.94; H, 8.22.

*2,6-Anhydro-3-deoxy-4,5-O-isopropylidene-*D*-talo-heptitol (VII)*

Fraction (II) (55 mg) in dry, purified acetone (2 ml) containing 4% H_2SO_4 was stirred at room temperature for 20 h. Neutralization with sodium hydroxide solution, filtration, and evaporation of solvent gave an oil, which was extracted with boiling carbon tetrachloride to yield the mono-*O*-isopropylidene derivative (23 mg). Further treatment of the carbon tetrachloride insoluble residue with acidified acetone gave an additional amount (21 mg) of product (66% overall yield). The combined extracts were recrystallized from carbon tetrachloride; m.p. 104–105°; $[\alpha]_D^{21}$ +12° (*c*, 1.6 in chloroform).

Anal. Calcd. for $C_{10}H_{18}O_5$: C, 55.03; H, 8.31. Found: C, 54.82; H, 7.97.

*2,6-Anhydro-3-deoxy-4,5-O-isopropylidene-1,7-di-O-tosyl-*D*-talo-heptitol (VIII)*

To a solution of (VII) (33 mg) in dry pyridine (1.0 ml) was added *p*-toluenesulfonyl chloride (66 mg). After standing for 18 h at room temperature the solution was stirred with water (0.1 ml). More water was added until the solution became turbid, and on standing, crystals (50 mg, 63%) of the di-*O*-tosyl derivative formed. The product was recrystallized from methanol; m.p. 135°; $[\alpha]_D^{23}$ −42° (*c*, 1.7 in chloroform).

Anal. Calcd. for $C_{24}H_{30}O_9S_2$: C, 54.78; H, 5.74. Found: C, 55.08; H, 6.01.

When a solution of the di-*O*-tosyl derivative (VIII) (8.4 mg) and sodium iodide (25 mg) in acetone (0.4 ml) was heated in a sealed tube at 118° for 26 h sodium *p*-toluenesulfonate (6.4 mg) was precipitated in an amount equivalent to the replacement of two tosyloxy groups by iodine. When the reaction was carried out at 100° for 30 min the amount of sodium *p*-toluenesulfonate isolated was approximately equivalent to the replacement of only one tosyloxy group.

Structure and Stereochemistry of Fractions (I) and (II)

*2-Deoxy-3-O-(1,3-dihydroxy-2-propyl)-*L*-glycero-tetritol (III) from 2,6-Anhydro-3-deoxy-*D*-gluco-heptitol (VI)*

Oxidation of (VI) with 0.1 *M* periodic acid followed by reduction of the resulting dialdehyde with sodium borohydride in water, according to the procedure described previously (2), gave the tetrol ether (III), $[\alpha]_D^{22}$ +26° (*c*, 2.9 in water), which formed a tetra-*O*-(*p*-nitrobenzoyl) derivative; m.p. 151–152°; $[\alpha]_D^{21}$ +22° (*c*, 1.2 in chloroform).

Periodate oxidation and sodium borohydride reduction of (I) under similar conditions gave the tetrol ether (III); $[\alpha]_D^{25}$ +21° (*c*, 3.7 in water). This formed a tetra-*O*-(*p*-nitrobenzoyl) derivative which was recrystallized from ethyl acetate; m.p. 150–151°, undepressed on admixture with the corresponding derivative of the tetrol ether derived from (VI); $[\alpha]_D^{24}$ +23° (*c*, 0.9 in chloroform).

Anal. Calcd. for $C_{35}H_{28}O_{17}N_4$: C, 54.13; H, 3.63; N, 7.21. Found: C, 54.46; H, 3.55; N, 7.29.

In a similar manner (II) gave the tetrol ether (IV) (2-deoxy-3-*O*-(1,3-dihydroxy-2-propyl)-D-*glycero*-tetritol), $[\alpha]_D^{25}$ −23° (*c*, 3.2 in water), which formed a tetra-*O*-(*p*-nitrobenzoyl) derivative; m.p. 150–151°; $[\alpha]_D^{24}$ −23° (*c*, 1.1 in chloroform).

Anal. Calcd. for $C_{35}H_{28}O_{17}N_4$: C, 54.13; H, 3.63. Found: C, 54.55; H, 3.71.

The infrared spectra of the tetra-*O*-(*p*-nitrobenzoyl) derivatives of the tetrol ethers (III) and (IV) were identical.

*Reaction of 3,4,6-Tri-O-acetyl-*D*-galactal with Carbon Monoxide and Deuterium to Yield 2,6-Anhydro-3-deoxy-*D*-galacto-heptitol-1,1,3-$^2H_3$ (cis) (IX) and 2,6-Anhydro-3-deoxy-*D*-talo-heptitol-1,1,3-$^2H_3$ (cis) (X)*

3,4,6-Tri-*O*-acetyl-D-galactal was reacted with carbon monoxide and deuterium at 130°, under similar conditions to those used in the preparation of the normal anhydrodeoxyheptitols, to yield the above-mentioned deuterated heptitols (IX) and (X). The configuration of C-2 of both heptitols was determined by proton n.m.r. analysis (see Discussion).

ACKNOWLEDGMENTS

The authors gratefully acknowledge the financial assistance of the National Cancer Institute of Canada, the National Research Council, and the University of British

**It is now thought that the compound previously reported as having* $[\alpha]_D$ *+38° (1) was not pure.*

Can. J. Chem. Downloaded from www.nrcresearchpress.com by 210.87.254.42 on 09/05/12
For personal use only.

Columbia Research Grant. One of us (D. A.) gratefully acknowledges the Standard Oil Fellowship and the University of British Columbia Research Fellowship.

The sample of the tetra-*O*-(*p*-nitrobenzoyl) derivative of the tetrol ether derived from (VI) was prepared by Mr. H. J. Koch.

REFERENCES

1. A. ROSENTHAL and D. READ. Can. J. Chem. **35**, 788 (1957). A. Rosenthal and D. Read. Methods in carbohydrate chemistry. Vol. II. *Edited by* R. L. Whistler and M. L. Wolfrom. Academic Press, New York, N.Y. 1963. p. 457.
2. A. ROSENTHAL and D. ABSON. Can. J. Chem. **42**, 1811 (1964).
3. A. ROSENTHAL and H. J. KOCH. Can. J. Chem. **42**, 2025 (1964).
4. A. CAMERMAN, J. TROTTER, A. ROSENTHAL, and H. J. KOCH. Can. J. Chem. **42**, 2630 (1964).
5. B. HELFERICH, E. N. MULCAHY, and H. ZIEGLER. Ber. **87**, 233 (1954).
6. J. S. DIXON and D. LIPKIN. Anal. Chem. **26**, 1092 (1954).
7. P. A. J. GORIN. Can. J. Chem. **38**, 641 (1960).

Can. J. Chem. Downloaded from www.nrcresearchpress.com by 210.87.254.42 on 09/05/12
For personal use only.

Can. J. Chem. Downloaded from www.nrcresearchpress.com by 210.87.254.42 on 09/05/12
For personal use only.

LA RÉACTION DU PENTACHLORURE DE PHOSPHORE SUR LES ACYLOXY-3β-Δ⁴-CETO-6 STÉROIDES

I. SÉRIE DU PREGNANE[1]

YVON LEFEBVRE ET ROGER GAUDRY
Ayerst Research Laboratories, Montréal, Québec

Reçu le 20 janvier 1965

RÉSUMÉ

Le pentachlorure de phosphore réagit sélectivement avec la fonction carbonyle en position 6 des acyloxy-3β pregnène-4 diones-6,20, diversement substituées en 17 et 21, dans le tétrachlorure de carbone, pour donner les acyloxy-3β chloro-6 pregnadiène-4,6 ones-20 correspondantes. L'activité biologique de ces produits est rapportée.

L'influence du système Δ⁶-chloro-6 sur l'activité orale des progestérones I substituées en positions 17 et 21 est maintenant bien connue: la chloro-6 méthyl-17 pregnadiène-4,6 dione-3,20 I*a* (1, 2), la chloro-6 fluoro-21 méthyl-17 pregnadiène-4,6 dione-3,20 I*b* (1, 2), l'acétoxy-17 chloro-6 pregnadiène-4,6 dione-3,20 I*c* (3) et la chloro-6 éthyl-17 pregnadiène-4,6 dione-3,20 I*d* (2, 4) sont parmi les agents progestationnels les plus actifs actuellement connus.

Dans les cadres d'un vaste programme de recherches sur l'activité biologique en rapport avec la structure, nous avons préparé une série d'acyloxy-3β chloro-6 pregnadiène-4,6 ones-20 II, substituées en positions 17 et 21, afin de les comparer avec les cétones correspondantes I et d'étudier l'effet sur l'activité biologique de la réduction du carbonyle 3.[2,3]

Les substances de structure générale II (R′ = acyloxyles) s'obtiennent facilement par l'action du pentachlorure de phosphore, à température ambiante, dans le tétrachlorure de carbone, sur les acyloxy-3β pregnène-4 diones-6,20 III (R′ = acyloxyles). Il en résulte le remplacement du carbonyle en position 6 par un groupement Δ⁶-chloro-6.[4,5] La structure des produits formés est confirmée à l'aide des données micro-analytiques, des spectres ultraviolets et par leur transformation chimique en dicétones correspondantes I. Bien que les deux groupes carbonyles, présents dans les produits de départ III, soient susceptibles de réagir avec le pentachlorure de phosphore pour donner des substances dichlorées, les micro-analyses montrent qu'un seul atome de chlore a été introduit au cours de la chloruration. De plus, les spectres ultraviolets sont caractéristiques du système diénique 4,6, montrant un maximum d'absorption de forte intensité à 243 mμ, et deux épaulements, également de forte intensité, à 237 et 250 mμ. Par contre, les produits de départ n'ont qu'un maximum de faible intensité à 236 mμ (Tableau I). Il est par conséquent, évident d'après ces résultats que seule la cétone en position 6 a été remplacée par un groupe Δ⁶-chloro-6 et que le carbonyle en position 20 n'est pas appréciablement

[1]*Travail présenté au 31ème Congrès annuel de l'Association Canadienne-Française pour l'Avancement des Sciences, Québec, novembre 1963.*

[2]*Dans les cadres du même programme, d'autres hydroxy-3β pregnènes-4, hydroxy-3β pregnadiènes-4,6 et leurs esters ont été préparés dans nos laboratoires. Les méthodes de synthèse et les activités biologiques ont déjà été rapportées (5).*

[3]*Récemment, G. R. Allen Jr. et M. J. Weiss (6) ont obtenu la chloro-6 éthyl-17 hydroxy-3β pregnadiène-4,6 one-20 par réduction sélective du carbonyle en 3 de la dione correspondante Id.*

[4]*Une série de chloro-3 diènes-3,5 stéroides, préparée dans nos laboratoires a déjà été décrite (7).*

[5]*Bien que la réaction du pentachlorure de phosphore sur les cétones cycliques soit bien connue (8), seulement quelques céto-stéroides ont été transformés (9–12).*

TABLEAU I

Spectres ultraviolets des acyloxy-3β pregnène-4 diones-6,20 et des acyloxy-3β chloro-6 pregnadiène-4,6 ones-20

Substituants			Produits de départ III		Produits chlorés	
R	X	R′	λ_{max}(mμ)	ϵ	λ_{max}(mμ)	ϵ
CH_3-	H	CH_3CO-	236	7 400	243	24 600
CH_3-	F	CH_3CO-	236	7 700	243	24 700
CH_3COO-	H	CH_3CO-	236	7 600	243	26 200
CH_3COO-	H	$CH_3(CH_2)_4CO$-	236	8 000	243	25 500
CH_3COO-	H	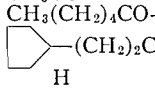 $-(CH_2)_2CO$-	236	8 220	243	26 200
CH_3COO-	H	H	241	6 800	243	24 000

effecté par le réactif. De plus les produits II (R′ = CH_3CO-) sont facilement transformés an dicétones I par hydrolyse alcaline, suivie d'une oxydation des alcools ainsi formés.

Nous avons remarqué la même sélectivité dans la réaction de l'acétoxy-3β pregnène-4 one-20 avec le pentachlorure de phosphore. Bien qu'il nous ait été impossible de purifier complètement l'acétoxy-3β chloro-6 pregnadiène-4,6 one-20 formée, sa structure ne fait aucun doute, la bande caractéristique de la fonction cétonique en 20 se voyant très clairement dans le spectre infrarouge.[6]

Le pentachlorure de phosphore réagit aussi sur les diones III dans d'autres solvants tels le benzène et l'acétate d'éthyle. Cependant les rendements en produits chlorés II sont nettement inférieurs à ceux obtenus dans le tétrachlorure de carbone. La chloruration ne se produit pas en milieu basique (pyridine, dioxane, tétrahydrofurane, *N*,*N*-diméthyl formamide), les produits de départ étant habituellement retrouvés inchangés.[7] De plus, nous n'avons pu obtenir de produits chlorés II à l'aide d'autres réactifs (chlorure de thionyle, oxychlorure de phosphore, trichlorure de phosphore et chlorure d'oxalyle (7)), les produits de départ demeurant souvent inchangés.

Quant aux acyloxy-3β pregnène-4 diones-6,20 de départ, elles sont préparées à partir des pregnénolones appropriées IV. Ces dernières sont transformées par deux voies distinctes en acétoxy-3β hydroxy-5α pregnanediones VII. D'une part les acétates de pregnénolones de départ IV (R′ = CH_3CO-) sont époxydés par l'acide peracétique et le mélange des époxydes V est traité par l'acide periodique dans l'acétone (14) ou par l'acide perchlorique dans l'acétone (15) pour donner les diols VI, qui sont ensuite oxydés par l'acide chromique en hydroxy-diones VII. D'autre part les pregnénolones IV (R′ = H) (ou leurs esters) sont transformées selon la méthode de Fieser (14) en dérivés trihydroxylés VIII, qui par oxydation sélective de l'alcool en 6 par la *N*-bromo succinimide (14), suivie d'une acétylation donnent les acétoxy-3β hydroxy-5α pregnanediones-6,20 VII. Ces dernières sont facilement déshydratées par le chlorure de thionyle dans la pyridine en acétoxy-3β pregnène-4 diones-6,20 III (R′ = CH_3CO-). Les esters III*d* et III*e* s'obtiennent par estérification de l'alcool correspondant III*f*, préparé par hydrolyse alcaline de l'acétate III*c*.

[6]*Bien que les spectres infrarouges des produits II confirment la disparition du système Δ^4-céto-6 (1 690 et 1 637 cm^{-1}), présent dans les produits de départ, ils ne sont d'aucune utilité pour déceler la présence de la fonction cétonique en 20. En effet, dans la plupart des cas la bande caractéristique coïncide avec la bande de l'acyloxyle en 3. Le cas de l'acétoxy-3β chloro-6 méthyl-17 pregnadiène-4,6 one-20 IIa est encore plus probant, la bande de la méthyl-17 cétone-20 se trouvant à 1 690 cm^{-1}.*

[7]*Ce fait est en accord avec le mécanisme général de réaction du pentachlorure de phosphore sur les cétones (13). Cependant il est intéressant de mentionner que l'addition de dioxane après le début de la chloruration dans le benzène ne nuit pas à la réaction. Bien au contraire, les rendements en produits chlorés sont sensiblement améliorés (voir Partie Expérimentale).*

Can. J. Chem. Downloaded from www.nrcresearchpress.com by 210.87.254.42 on 09/05/12
For personal use only.

Can. J. Chem. Downloaded from www.nrcresearchpress.com by 210.87.254.42 on 09/05/12
For personal use only.

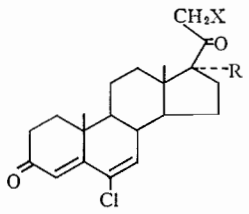

I

Ia: R = CH_3-; X = H
Ib: R = CH_3-; X = F
Ic: R = CH_3COO-; X = H
Id: R = CH_3CH_2-; X = H

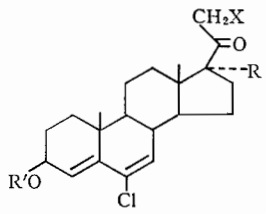

II

IIa: R = CH_3-; X = H; R′ = CH_3CO-
IIb: R = CH_3-; X = F; R′ = CH_3CO-
IIc: R = CH_3COO-; X = H; R′ = CH_3CO-
IId: R = CH_3COO-; X = H; R′ = $CH_3(CH_2)_4CO$-
IIe: R = CH_3COO-; X = H; R′ = 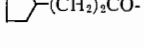
IIf: R = CH_3-; X = H; R′ = H
IIg: R = CH_3COO-; X = H; R′ = H

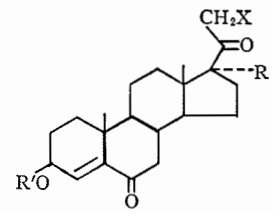

III

IIIa: R = CH_3-; X = H; R′ = CH_3CO-
IIIb: R = CH_3-; X = F; R′ = CH_3CO-
IIIc: R = CH_3COO-; X = H; R′ = CH_3CO-
IIId: R = CH_3COO-; X = H; R′ = $CH_3(CH_2)_4CO$-
IIIe: R = CH_3COO-; X = H; R′ = 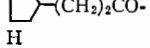
IIIf: R = CH_3COO-; X = H; R′ = H

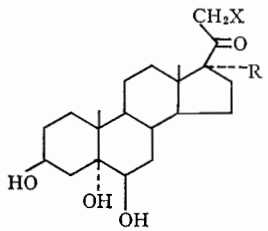

VIII

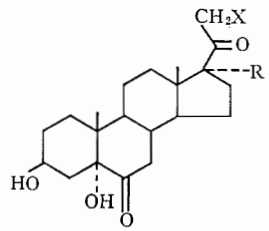

IX

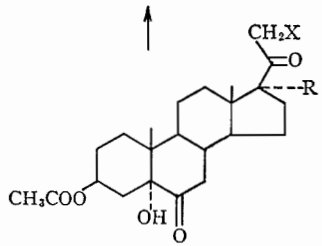

VII

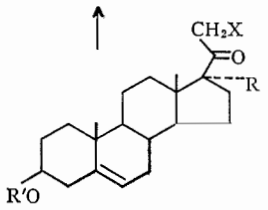

IV

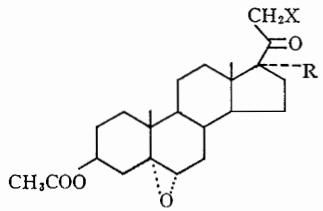

V

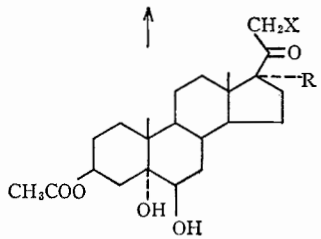

VI

Va: R = CH_3-; X = H
Vb: R = CH_3-; X = F
Vc: R = CH_3COO-; X = H

Dans le test de Clauberg–McPhail (16) les acétoxy-3β chloro-6 diènes II (R′ = CH_3CO-) montrent une activité progestationnelle très puissante. Ils ont une activité comparable à celle des dicétones I. Dans le cas de la chloro-6 diacétoxy-3β,17 pregnadiène-4,6 one-20 II*c*, l'activité orale est près de trois fois celle de la dicétone correspondante I*c* (Tableau II) (17).

TABLEAU II

Activités biologiques comparées des produits II et I dans le test de Clauberg–McPhail

Substituants			Produits II		Dicétones I	
R	X	R′	S.C.	Oral	S.C.	Oral
CH_3-	H	CH_3CO-	2	10	10	20
CH_3-	F	CH_3CO-	—	10	5	10
CH_3COO-	H	CH_3CO-	50	100	50	35–50
CH_3-	H	H	1	5	10	20
	Progestérone		1	—		
	Noréthindrone		—	1		

PARTIE EXPÉRIMENTALE[8]

*Acétoxy-3β hydroxy-5α méthyl-17 pregnanedione-6,20 VII*a

Première méthode

On agite à température ambiante pendant 4 h une solution de 31.5 g de méthyl-17 pregnénolone brute IV*a* (R′ = H) dans 155 ml d'acide formique 88%. On ajoute un volume égal d'eau et on filtre le solide qui résulte. Après lavage à l'eau et séchage, on recrystallise dans un mélange de chlorure de méthylène–hexane et on obtient 16.7 g de formiate de méthyl-17 pregnénolone IV*a* (R′ = HCO-) p.f. 187–190°. On agite pendant 2 h à température ambiante une solution de 19.2 g de ce formiate, 19.2 ml d'une solution 30% de H_2O_2 et 192 ml d'acide formique. La solution est jetée dans l'eau et la glace. Le solide formé est filtré et après lavage à l'eau est dissout dans 200 ml de méthanol. Après l'addition de 60 ml de potasse alcoolique 10%, on porte cette solution à reflux pendant 10 min. L'addition d'eau donne 15 g de triol VIII*a* p.f. 293–296°. Une solution de 15 g de ce triol dans 1 120 ml de méthanol et 720 ml d'éther est mélangée avec une solution de 20 g de *N*-bromo succinimide dans 440 ml d'eau. Après 2 h à 5°, on évapore l'éther sous pression réduite. On ajoute de l'eau et on obtient 14.1 g de diol IX*a*, qui sans autre purification sont acétylés pendant la nuit avec 140 ml d'anhydride acétique et 140 ml de pyridine. On obtient 17.25 g d'acétate brut VII*a*, purifié par plusieurs cristallisations dans un mélange de chlorure de méthylène–hexane p.f. 234–236°, $[\alpha]_D = -79°$.

Anal. Calc. pour $C_{24}H_{36}O_5$: C, 71.25; H, 8.97. Trouvé: C, 71.31; H, 9.12.

Deuxième méthode

On ajoute, en maintenant la température entre −2 et 2°, une solution de 8 g d'acétate de méthyl-17 pregnénolone IV*a* (R′ = CH_3CO-) (1, 18) dans 60 ml de chloroforme à un mélange de 700 mg d'acétate de sodium anhydre et 8 ml d'acide peracétique. Après 2 h entre 0 et 5°, la solution chloroformique est lavée successivement à l'eau, au bicarbonate de sodium et à l'eau jusqu'à neutralité. Après séchage et évaporation 8.1 g d'époxydes V*a* sont obtenus. Ce mélange d'époxydes est dissout dans 212 ml d'acétone et après l'addition de 4 ml d'acide perchlorique 70% et 28 ml d'eau, on laisse reposer à température de la pièce pendant 3 h. Le mélange réactionnel est dilué avec de l'eau et le précipité est recristallisé dans l'acétone pour donner 6 g de diol VI*a* p.f. 217–218°.

Ces 6 g de diol sont dissouts dans 70 ml de *N*,*N*-diméthyl formamide. A cette solution, on ajoute un mélange de 12 ml d'acide chromique 8 *N* (19) et 30 ml de diméthyl formamide. Après 15 min à température ambiante, l'excès d'oxydant est détruit par une solution de bisulfite de sodium. Par l'addition d'eau, on récolte 5.1 g d'un produit p.f. 234–241°, identique par comparaison des spectres infrarouges, à l'acétoxy-3β hydroxy-5α méthyl-17 pregnanedione-6,20 obtenue par la première méthode.

*Acétoxy-3β méthyl-17 pregnène-4 dione-6,20 III*a

Une solution de 5.1 ml de chlorure de thionyle dans 10 ml de pyridine est ajoutée à une solution de 5.1 g d'hydroxy-dione VII*a* dans 51 ml de pyridine, refroidie à 0°. La température est maintenue à 0° pendant

[8]*Les points de fusion ont été déterminés en tube capillaire et ne sont pas corrigés. Les rotations ont été déterminées en solution chloroformique, sauf mention spéciale, à une concentration d'environ 1% et à 23 °C. Les spectres ultraviolets ont été pris en solution dans l'éthanol 95% sur un appareil Perkin–Elmer, modèle 350, et les spectres infrarouges sur un appareil Perkin–Elmer, modèle 21, en solution chloroformique à 10%.*

Can. J. Chem. Downloaded from www.nrcresearchpress.com by 210.87.254.42 on 09/05/12
For personal use only.

l'addition. Après 1 h à 0°, le mélange réactionnel est jeté dans l'eau et la glace. Le précipité est filtré et lavé jusqu'à neutralité. Par recristallisation dans un mélange de chlorure de méthylène–hexane, on obtient 3 g d'acétoxy-3β méthyl-17 pregnène-4 dione-6,20 p.f. 205–207°. L'échantillon analytique fond à 206–208°, $[\alpha]_D = -69.2°$.

Anal. Calc. pour $C_{24}H_{34}O_4$: C, 74.57; H, 8.78. Trouvé: C, 74.42; H, 8.69.

Acétoxy-3β chloro-6 méthyl-17 pregnadiène-4,6 one-20 IIa et chloro-6 hydroxy-3β méthyl-17 pregnadiène-4,6 one-20 IIf

Chloruration dans le benzène

On agite pendant 30 min à température ambiante une solution de 2.37 g de III*a*, 2.37 g de PCl_5 dans 110 ml de benzène. On jète le mélange réactionnel dans l'eau et la glace. La phase organique est lavée jusqu'à neutralité, séchée et évaporée. Le résidu est cristallisé dans le méthanol et on obtient 193 mg p.f. 119–126°. Par chromatographie des eaux-mères sur le florisil on obtient une quantité additionnelle p.f. 120–130°. La cristallisation des fractions combinées donne 224 mg d'acétoxy-3β chloro-6 méthyl-17 pregnadiène-4,6 one-20 p.f. 137–139°. Un échantillon analytique fond à 139–141°, $[\alpha]_D = -67.6°$.

Anal. Calc. pour $C_{24}H_{33}O_3Cl$: C, 71.18; H, 8.21; Cl, 8.75. Trouvé: C, 70.94; H, 8.28; Cl, 8.78, 8.67.

Chloruration dans le benzène–dioxane

On agite une solution de 1 g de III*a*, 1 g de PCl_5 dans 50 ml de benzène. Après 1 min, on ajoute 0.5 ml de dioxane et on continue l'agitation pendant 30 min. Le produit de la réaction est isolé comme précédemment. Par purification chromatographique et par cristallisation dans le méthanol, on obtient 301 mg de produit chloré II*a* p.f. 136–141°. Selon les préparations le point de fusion varie entre 136 et 145°. Par contre, l'indice de rotation se situe entre −66 et −69.5°.

Chloruration dans le CCl_4

On dissout à chaud 5 g de III*a* dans 250 ml de CCl_4. Après refroidissement à la température ambiante, on ajoute 5 g de PCl_5 et on agite le mélange pendant 45 min. On arrête la réaction par l'addition de 10 ml de pyridine. Le mélange est jeté dans une solution glacée de bicarbonate de sodium; la phase organique est séparée, lavée, séchée et évaporée. Deux recristallisations dans le méthanol donne 1.25 g d'acétoxy-3β chloro-6 méthyl-17 pregnadiène-4,6 one-20 p.f. 148–150°. L'échantillon analytique fond à 149–151°, $[\alpha]_D = -64.8°$.

Anal. Calc. pour $C_{24}H_{33}O_3Cl$: C, 71.18; H, 8.21; Cl, 8.75. Trouvé: C, 71.27; H, 8.39; Cl, 8.66, 8.69.

Une quantité additionnelle de 924 mg p.f. 146–149° est obtenue par chromatographie des eaux-mères.

Hydrolyse de IIa

On chauffe à reflux pendant 30 min sous atmosphère d'azote un mélange de 530 mg de II*a*, 137 mg de bicarbonate de potassium, 21.5 ml de méthanol et 2.5 ml d'eau. L'addition d'eau donne 415 mg de chloro-6 hydroxy-3β méthyl-17 pregnadiène-4,6 one-20 II*f* dont le point de décomposition varie entre 182 et 193° (chlorure de méthylène–hexane). Un échantillon analytique montre un point de décomposition de 182–184°. $[\alpha]_D = -45.5°$.

Anal. Calc. pour $C_{22}H_{31}O_2Cl$: C, 72.79; H, 8.61; Cl, 9.78. Trouvé: C, 72.83; H, 8.66; Cl, 9.88, 9.98.

L'acétylation de 95 mg de cet alcool, selon la méthode usuelle, avec 1 ml d'anhydride acétique et 1 ml de pyridine donne après recristallisation dans le méthanol 60 mg de II*a* p.f. 148–150°.

Chloro-6 méthyl-17 pregnadiène-4,6 dione-3,20 Ia

A une solution, agitée et maintenue à 0°, de 500 mg d'alcool II*f* dans 60 ml d'acétone on ajoute 1 ml d'acide chromique 8 *N*. Le mélange est immédiatement jeté dans l'eau et la glace et est extrait à l'éther. La solution éthérée est lavée à l'eau, séchée et évaporée. Par chromatographie du résidu sur l'alumine et par cristallisation dans l'hexane on obtient 180 mg de chloro-6 méthyl-17 pregnadiène-4,6 dione-3,20 I*a* p.f. 122–124° (point de fusion rapporté 125–126° (1)).

Acétoxy-3β fluoro-21 hydroxy-5α méthyl-17 pregnanedione-6,20 VIIb

On agite pendant 3 h à température ambiante un mélange de 16.2 g d'acétoxy-3β fluoro-21 méthyl-17 pregnène-5 one-20 IV*b* (R′ = CH_3CO-) (1), 160 ml d'acide formique et 16.2 ml d'une solution 30% de H_2O_2. Après ce temps, on dilue la solution avec de l'eau et on récolte un solide qui est lavé à l'eau et séché. Ce solide est dissout dans 240 ml de méthanol et après l'addition de 80 ml de potasse 10% on porte à reflux pendant 1 h. Par l'addition d'eau on obtient 13.6 g de triol VIII*b* p.f. 288–291°.

Sans autre purification, ce triol est dissout dans 1 000 ml de méthanol et 680 ml d'éther. Après l'addition de 17 g de *N*-bromo succinimide dissouts dans 300 ml d'eau, on laisse le mélange à 5° pendant 2 h. Le brome qui s'est formé est détruit par l'addition de 325 ml de thiosulfate de sodium 0.1 *N*. On évapore l'éther sous pression réduite en chauffant entre 40 et 50°. La solution résiduelle est mélangée avec de l'eau et on obtient 11.25 g de diol IX*b*, qui sont acétylés selon la méthode habituelle avec 110 ml d'anhydride acétique et 110 ml de pyridine. L'acétate brut est cristallisé dans un mélange de chlorure de methylène–hexane puis dans un mélange de chlorure de méthylène–ether pour donner 8.95 g d'acétoxy-3β fluoro-21 hydroxy-5α pregnanedione-6,20 p.f. 263–266°, $[\alpha]_D = -83.9°$.

Anal. Calc. pour $C_{24}H_{35}O_5F$: C, 68.22; H, 8.35; F, 4.50. Trouvé: C, 68.18; H, 8.11; F, 4.53, 4.40.

Can. J. Chem. Downloaded from www.nrcresearchpress.com by 210.87.254.42 on 09/05/12
For personal use only.

Can. J. Chem. Downloaded from www.nrcresearchpress.com by 210.87.254.42 on 09/05/12
For personal use only.

Acétoxy-3β fluoro-21 méthyl-17 pregnène-4 dione-6,20 IIIb

La déshydratation de 8.66 g de VII*b* par le chlorure de thionyle (9 ml) dans la pyridine (104 ml), selon la méthode utilisée plus haut pour le composé VII*a*, conduit à 6.96 g de produit brut, purifié par chromatographie sur le florisil. Les fractions éluées avec des mélanges benzène–ether sont combinées et cristallisées dans un mélange de chlorure de méthylène–hexane. On obtient 3.95 g d'acétoxy-3β fluoro-21 méthyl-17 pregnène-4 dione-6,20 p.f. 196–197.5°, $[\alpha]_D = -76.6°$.

Anal. Calc. pour $C_{24}H_{33}O_4F$: C, 71.26; H, 8.22; F, 4.70. Trouvé: C, 70.91; H, 7.76; F, 4.70, 4.78.

Acétoxy-3β chloro-6 fluoro-21 méthyl-17 pregnadiène-4,6 one-20 IIb

On agite à température de la pièce une solution de 4.15 g de III*b*, 4.15 g de PCl_5 dans 200 ml de benzène. Après 1 min on ajoute une solution de 1.6 ml de dioxane dans 20 ml de benzène et la réaction est continuée pendant 30 min. On ajoute 2.8 ml de pyridine et le produit de la réaction est isolé comme on a fait plus haut pour II*a*. Le résidu est cristallisé dans le méthanol et on obtient 891 mg d'acétoxy-3β chloro-6 fluoro-21 méthyl-17 pregnadiène-4,6 one-20 II*b* p.f. 170–173°. L'échantillon analytique fond à 172–173°, $[\alpha]_D = -73.5°$.

Anal. Calc. pour $C_{24}H_{32}O_3FCl$: C, 68.14; H, 7.63; F, 4.49; Cl, 8.39. Trouvé: C, 67.90; H, 7.71; F, 4.44; Cl, 8.18, 8.17.

Diacétoxy-3β,17 dihydroxy-5α,6β pregnanone-20 VIc

On ajoute une solution de 30 g de diacétoxy-3β,17 pregnène-5 one-20 IV*c* (R′ = CH_3CO-) dans 218 ml de chloroforme à un mélange de 2.67 g d'acétate de sodium et 30 ml d'acide peracétique. La température est maintenue entre −2 et 2° pendant l'addition puis entre 0 et 5° pendant 2 h. La solution chloroformique est lavée à l'eau, au bicarbonate et à l'eau jusqu'à neutralité. Après l'évaporation du solvant, on obtient 30 g d'époxydes V*c*.

On dissout ces 30 g dans 300 ml d'acétone et après addition d'une solution de 18 g d'acide periodique dans 90 ml d'eau, on porte à reflux pendant 30 min. L'addition d'eau donne 27.6 g de diacétoxy-3β,17 dihydroxy-5α,6β pregnanone-20 p.f. 301–303°. Par recristallisation dans le méthanol aqueux, on obtient l'échantillon analytique p.f. 304–306°, $[\alpha]_D = -44.5°$.

Anal. Calc. pour $C_{25}H_{38}O_7$: C, 66.64; H, 8.51. Trouvé: C, 66.85; H, 8.48.

On peut aussi obtenir ce diol à partir du mélange d'époxydes de la façon suivante. On laisse à température ambiante pendant 3 h une solution de 45 g d'époxydes, 1 020 ml d'acétone et une solution de 23 ml d'acide perchlorique et 161 ml d'eau. Pendant la réaction des cristaux de diol se forment. On ajoute un volume égal d'eau. On filtre le solide et après séchage, on obtient 45.8 g of diol VI*c* p.f. 303–305°.

Diacétoxy-3β,17 hydroxy-5α pregnanedione-6,20 VIIc

On ajoute à une solution de 2 g de diol VI*c* dans 40 ml de diméthyl formamide, une solution de 4 ml d'acide chromique 8 *N* dans 11 ml de diméthyl formamide. Après 15 min l'excès d'oxydant est détruit par l'addition de 7 ml d'une solution de bisulfite de sodium 10%. Le mélange est jeté dans l'eau et on récolte 1.78 g de diacétoxy-3β,17 hydroxy-5α pregnanedione-6,20 pf. 270–273°. Par recristallisation dans un mélange de chlorure de méthylène–hexane, on obtient l'échantillon analytique p.f. 273–275°, $[\alpha]_D = -75.2°$.

Anal. Calc. pour $C_{25}H_{36}O_7$: C, 66.94; H, 8.09. Trouvé: C, 66.68; H, 8.36.

Diacétoxy-3β,17 pregnène-4 dione-6,20 IIIc

La déshydration de 25 g de VII*c*, selon la méthode usuelle par le chlorure de thionyle dans la pyridine, donne 18.1 g de diacétoxy-3β,17 pregnène-4 dione-6,20, de pureté suffisante pour la chloruration par le pentachlorure de phosphore. On obtient un échantillon analytique, après chromatographie sur le florisil, en recristallisant dans un mélange de chlorure de méthylène–hexane les fractions éluées par des mélanges benzène–éther p.f. 200–202°, $[\alpha]_D = -70.6°$.

Anal. Calc. pour $C_{25}H_{34}O_6$: C, 69.74; H, 7.96. Trouvé: C, 69.95; H, 8.02.

Acétoxy-17 hydroxy-3β pregnène-4 dione-6,20 IIIf

On porte à reflux pendant 30 min sous atmosphère d'azote un mélange de 430 mg de III*c*, 110 mg de bicarbonate de potassium, 15 ml de méthanol et 1.5 ml d'eau. On dilue la solution avec de l'eau et on extrait par l'acétate d'éthyle. La solution organique est lavée, séchée et évaporée, laissant un résidu (387 mg) qui cristallise dans l'éther. Par recristallisation dans un mélange de chlorure de méthylène–éther on obtient un échantillon analytique d'acétoxy-17 hydroxy-3β pregnène-4 dione-6,20 III*f* p.f. 214–222°, $[\alpha]_D = 33.3°$.

Anal. Calc. pour $C_{23}H_{32}O_5$: C, 71.11; H, 8.30. Trouvé: C, 71.39; H, 8.16.

Acétoxy-17 hexanoyloxy-3β pregnène-4 dione-6,20 IIId

On laisse à température ambiante pendant 32 h une solution de 9.4 g de III*f*, 9.4 ml d'anhydride hexanoique et 94 ml de pyridine. L'hexanoate est isolé de la façon habituelle. On obtient un solide jaune purifié par chromatographie sur l'alumine. Les fractions éluées par un mélange benzène–hexane 3:1 et par le benzène pur sont combinées et cristallisées dans l'hexane pour donner 5.07 g d'acétoxy-17 hexanoyloxy-3β pregnène-4 dione-6,20 p.f. 158–159°, $[\alpha]_D = -70.2°$.

Anal. Calc. pour $C_{29}H_{42}O_6$: C, 71.58; H, 8.70. Trouvé: C, 71.45; H, 8.82.

Une quantité additionnelle de 1.13 g p.f. 155–158° s'obtient des eaux-mères.

Acétoxy-17 (cyclopentyl)-3′ propionyloxy-3β pregnène-4 dione-6,20 IIIe

On laisse à température ambiante pendant la nuit une solution de 9 g d'alcool III*f*, 9 ml de chlorure de cyclopentyl-3′ propionyle et 90 ml de pyridine. L'ester est isolé de la façon usuelle. Après chromatographie sur l'alumine, on obtient 5.78 g d'acétoxy-17 (cyclopentyl)-3′ propionyloxy-3β pregnène-4 dione-6,20 (méthanol) p.f. 163–166°, $[\alpha]_D = -60.2°$.

Anal. Calc. pour $C_{31}H_{44}O_6$: C, 72.63; H, 8.65. Trouvé: C, 72.70; H, 8.48.

Une quantité additionnelle (779 mg) p.f. 163–167° s'obtient des eaux-mères.

Chloro-6 diacétoxy-3β,17 pregnadiène-4,6 one-20 IIc

Chloruration dans le benzène-dioxane

On agite une solution de 3 g de diacétoxy-3β,17 pregnène-4 dione-6,20 III*c* et 3 g de PCl_5 dans 150 ml de benzène. Après 1 min, on ajoute une solution de 1.2 ml de dioxane dans 15 ml de benzène. Après 30 min, on ajoute 2.2 ml de pyridine. Le produit de la réaction est isolé comme à l'habitude. La cristallisation du résidu donne 1.06 g de II*c* p.f. 206–207° (décomp.). Selon les préparations le point de décomposition varie entre 202 et 215°. Un échantillon analytique fond à 202–204° (décomp.), $[\alpha]_D = -89.5°$.

Anal. Calc. pour $C_{25}H_{33}O_5Cl$: C, 66.87; H, 7.41; Cl, 7.91. Trouvé: C, 66.79; H, 8.07; Cl, 8.07, 8.06.

Chloruration dans le CCl_4

On agite pendant 30 min à température ambiante un mélange de 5 g de III*c* et 5 g de PCl_5 dans 250 ml de CCl_4. Après l'addition de 10 ml de pyridine, on isole le produit de la réaction. Par recristallisation dans le méthanol, on récolte 1.62 g de chloro-6 diacétoxy-3β, 17 pregnadiène-4,6 one-20 p.f. 203–204° (décomp.).

Acétoxy-17 chloro-6 hydroxy-3β pregnadiène-4,6 one-20 IIg

On chauffe à reflux sous azote une solution de 10 g de II*c*, 2.6 g de bicarbonate de potassium, 200 ml de tétrahydrofurane, 300 ml de méthanol et 50 ml d'eau. L'addition d'eau donne 9 g d'un solide, purifié par chromatographie sur l'alumine. On obtient par cristallisation 5.12 g d'alcool II*g* p.f. 218–221° (décomp.). Il n'a pas été possible d'obtenir un échantillon analytiquement pur. Cependant, 100 mg de cet alcool, acétylé selon la méthode habituelle, donnent après cristallisation dans le méthanol 82 mg de II*c* p.f. 213–214 (décomp.), $[\alpha]_D = -93.5°$.

Acétoxy-17 chloro-6 pregnadiène-4,6 dione-3,20 Ic

On ajoute à une solution de 1 g de l'acool II*g* dans 100 ml d'acétone, 1 ml d'acide chromique 8 *N*. Après 2 ou 3 min d'agitation, l'excès d'oxydant est détruit par l'addition d'alcool isopropylique. Le mélange est dilué avec de l'eau et est extrait par l'éther. La solution éthérée est lavée, séchée et évaporée. Le résidu est cristallisé dans le méthanol pour donner 634 mg d'acétoxy-17 chloro-6 pregnadiène-4,6 dione-3,20 p.f. 208–210°, $[\alpha]_D = -3.9°$.

Le spectre infrarouge est identique à celui d'un échantillon authentique de I*c*.

Acétoxy-17 chloro-6 hexanoyloxy-3β pregnadiène-4,6 one-20 IId

La chloruration de 5.05 g de III*d*, effectuée comme plus haut dans CCl_4, donne, après chromatographie du produit brut sur l'alumine et par cristallisation dans le méthanol du produit purifié, 3.1 g d'acétoxy-17 chloro-6 hexanoyloxy-3β pregnadiène-4,6 one-20 p.f. 94.5–98°. L'échantillon analytique fond à 95.5–98.5°, $[\alpha]_D = -80.7°$.

Anal. Calc. pour $C_{29}H_{41}O_5Cl$: C, 68.97; H, 8.32; Cl, 7.03. Trouvé: C, 68.95; H, 8.18; Cl, 7.00, 6.93.

Acétoxy-17 chloro-6 (cyclopentyl)-3′ propionyloxy-3β pregnadiène-4,6 one-20, IIe

La chloruration de 6.1 g de III*e* est faite comme plus haut. Le produit brut est purifié par chromatographie et par cristallisation dans le méthanol. On obtient 2.16 g d'acétoxy-17 chloro-6 (cyclopentyl)-3′ propionyloxy-3β pregnadiène-4,6 one-20 p.f. 106–111°. L'échantillon analytique fond à 109–112°, $[\alpha]_D = -79.3°$.

Anal. Calc. pour $C_{31}H_{43}O_5Cl$: C, 70.10; H, 8.16; Cl, 6.68. Trouvé: C, 69.85; H, 8.21; Cl, 6.69, 6.57.

REMERCIEMENTS

Nous tenons à remercier tout particulièrement Monsieur le professeur H. Favre de l'Université de Montréal dont les conseils nous ont été très utiles et Monsieur P. Abonyi dont l'aide technique nous a été très précieuse. Nous voulons également remercier le docteur G. Papineau-Couture et Madame J. Jachner pour les spectres infrarouges, Monsieur M. Boulerice pour les spectres ultraviolets et Monsieurs W. Turnbull et ses collaborateurs pour les microanalyses. Nous remercions finalement les docteurs C. Revesz et C. Chappel pour les données biologiques.

Can. J. Chem. Downloaded from www.nrcresearchpress.com by 210.87.254.42 on 09/05/12
For personal use only.

BIBLIOGRAPHIE

1. R. DEGHENGHI, Y. LEFEBVRE, P. MITCHELL, P. F. MORAND et R. GAUDRY. Tetrahedron, **19**, 289 (1963).
2. R. DEGHENGHI, C. REVESZ et R. GAUDRY. J. Med. Pharm. Chem. **6**, 301 (1963).
3. H. J. RINGOLD, E. BATRES, A. BOWERS, J. E. EDWARDS et J. ZDERIC. J. Am. Chem. Soc. **81**, 3485 (1959).
4. M. J. WEISS, R. E. SCHAUB, J. F. POLETTO, G. R. ALLEN, JR. et C. J. COSCIA. Chem. Ind. London, 118 (1963). M. J. WEISS, R. E. SCHAUB, J. F. POLETTO, G. R. ALLEN, JR. et C. C. PIDACKS. Steroids, **1**, 608 (1963).
5. D. J. MARSHALL, P. F. MORAND, C. REVESZ et R. GAUDRY. J. Med. Pharm. Chem. **7**, 355 (1964).
6. G. R. ALLEN, JR. et M. J. WEISS. J. Med. Pharm. Chem. **7**, 684 (1964).
7. R. DEGHENGHI et R. GAUDRY. Can. J. Chem. **40**, 818 (1962).
8. M. MOUSSERON et R. JACQUIER. Bull. Soc. Chim. France, 648 (1950).
9. U. WESTPHAL, Y. L. WANG et H. HELLMANN. Chem. Ber. **72**, 1233 (1939).
10. L. MAMLOK et J. JACQUES. Bull. Soc. Chim. France, 484 (1960).
11. A. BOWERS, J. EDWARDS et J. C. ORR. U.S. Patent No. 3,055,916 (25 Sept., 1952).
12. A. BOWERS et P. G. HOLTON. U.S. Patent No. 3,127,426 (31 Mars, 1964).
13. M. S. NEWMAN et L. L. WOOD, JR. J. Am. Chem. Soc. **81**, 4000 (1959). M. S. NEWMAN, G. FRAENKEL et W. M. KIRN. J. Org. Chem. **28**, 1851 (1963).
14. L. F. FIESER et S. RAJAGOPALAN. J. Am. Chem. Soc. **71**, 3938 (1949).
15. F. SONDHEIMER, O. MANCERA et G. ROSENKRANZ. J. Am. Chem. Soc. **76**, 5020 (1954).
16. M. K. MCPHAIL. J. Physiol. London, **83**, 145 (1934).
17. C. REVESZ. Travaux non encore publiés.
18. PL. A. PLATTNER, H. HEUSSER et P.TH. HERZIG. Helv. Chim. Acta, **32**, 270 (1949).
19. K. BOWDEN, I. M. HEILBRON, E. R. H. JONES et B. C. L. WEEDON. J. Chem. Soc. 39 (1946).

Can. J. Chem. Downloaded from www.nrcresearchpress.com by 210.87.254.42 on 09/05/12
For personal use only.

Can. J. Chem. Downloaded from www.nrcresearchpress.com by 210.87.254.40 on 09/05/12
For personal use only.

THE ALCOHOLYSIS OF TRIALKYLALKOXYSILANES

PART I. A KINETIC STUDY OF THE METHANOLYSIS OF METHYL 2,3,4,6-TETRA-*O*-TRIMETHYLSILYL-α-D-GLUCOPYRANOSIDE TO FORM METHYL 2,3,4-TRI-*O*-TRIMETHYLSILYL-α-D-GLUCOPYRANOSIDE[1]

A. G. McINNES

Atlantic Regional Laboratory, National Research Council and Dalhousie University, Halifax, Nova Scotia

Received January 29, 1965

ABSTRACT

The selective methanolysis of the trimethylsilyl group on the primary 6-position of methyl 2,3,4,6-tetra-*O*-trimethylsilyl-α-D-glucopyranoside (I) to form methyl 2,3,4-tri-*O*-trimethylsilyl-α-D-glucopyranoside (II) is catalyzed by acid or base. In the latter case the reaction follows second-order kinetics in I and methoxide ion, and the rate of reaction is independent of the nature of the cation of the metal methoxide used to catalyze the reaction. Successive replacement of the methyl hydrogens in the methoxide ion by methyl groups is accompanied by a corresponding decrease in the rate of reaction. The rate constant for removal of trimethylsilyl groups at the secondary 2-, 3-, and 4-positions of I and II is smaller by a factor of 25 than for removal of the corresponding group at the primary 6-position, and the energies of activation for the two processes are 10.8 and 9.1 kcal mole^{-1}.

When an alcohol undergoes an interchange reaction with an organosilicon alkoxide as shown in [*a*], equilibrium between the reactants and products is established slowly unless catalyzed by acid or base (1*a*).

[*a*] $$R_3SiOR' + R''OH \rightleftharpoons R_3SiOR'' + R'OH.$$

In a recent publication (2) Eaborn and co-workers demonstrated that the rate of methoxy–methoxy exchange between methanol and optically active methoxymethyl-α-naphthylphenylsilane, containing tritium in the methoxyl group, was one-half the rate of racemization regardless of whether an acidic or basic catalyst was used. Their data established that methoxide ion or methanol, depending on the nature of the catalyst, reacts with inversion of configuration at the asymmetric silicon atom. The work of Sommer and his co-workers on the stereochemistry of reactions at asymmetric silicon (3, 4, 5), on the other hand, established that organosilicon alkoxides react with solid potassium hydroxide in nonpolar solvents with retention of configuration (4). It seems probable, therefore, that if reaction [*a*] was carried out in nonpolar solvents using solid metal alkoxide and an organosilicon alkoxide, containing an asymmetric silicon atom, the reaction would also proceed with retention of configuration.

However, apart from the interesting studies described above, reaction [*a*] has been used principally to prepare organosilicon phenoxides and higher alkoxides from the corresponding methoxide or ethoxide (—OR′) derivatives (1*b*). The syntheses of the former compounds have been achieved by making the equilibrium in [*a*] favor the production of the desired product, R_3SiOR'', by removing R′OH by distillation, or by using a large excess of R″OH to shift the position of the equilibrium to the right. It should be noted that all previous investigations of this nature have been concerned only with the production of an organosilicon compound. No previous attempt has been made to carry

[1]*Presented at the 47th Annual Conference, The Chemical Institute of Canada, Kingston, Ontario, June 1–3, 1964.*
Issued as N.R.C. No. 8431.

out a detailed kinetic study of reaction [*a*], and to determine if the nature of R, R′, and R″ influences the reaction. Consequently, work was initiated in this laboratory to study this problem, and initially to make a kinetic study of the rates of methanolysis of the trimethylsilyl ethers of a variety of compounds containing different types of alcoholic hydroxyl groups. It soon became apparent that considerable differences do exist in the rates of methanolysis of different types of hydroxyl groups (primary, secondary, etc.), and that these differences in rate could be utilized for synthetic purposes in the chemistry of polyhydroxy compounds. The present communication reports a kinetic study of the methanolysis of methyl 2,3,4,6-tetra-*O*-trimethylsilyl-α-D-glucopyranoside (I) using basic and acidic catalysts. In reaction [*b*] the trimethylsilyl group on the 6-position of the glucose moiety is removed preferentially with the concomitant formation of methyl 2,3,4-tri-*O*-trimethylsilyl-α-D-glucopyranoside (II) in high yield.

[*b*]

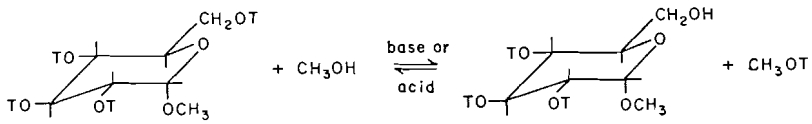

I II

[T = $-Si(CH_3)_3$]

A description of the preparation, structure, and chemistry of II is reported in Part II of this series (6). The synthetic implications of the latter encouraged us to anticipate the results of our more general study of the alcoholysis reaction, which will be the subject of future communications.

EXPERIMENTAL

Materials

The methanol was dried by distillation from magnesium methoxide. Diphenylmethane, 4-methylquinaldine, and compounds I and II each had a purity greater than 99.5% when analyzed by gas–liquid partition chromatography (g.l.p.c.).

The preparation of I and II from methyl α-D-glucopyranoside is described elsewhere (6).

Standard Alcoholysis Reaction Conditions

An aliquot (80 μl) of a methanolic solution containing metal methoxide (0.02 millimole) was injected, by means of a calibrated micro syringe, into a methanolic solution (10 ml) of compound I (0.25 millimole) which also contained 4-methylquinaldine or diphenylmethane (0.32 millimole) as an internal standard. Both solutions were allowed to come to constant temperature in an oil bath before mixing, and care was taken to exclude moisture from the reaction solutions. The progress of the methanolysis reaction was followed by withdrawing aliquots (90 μl) of the reaction solution periodically and stopping the reaction by injecting it into a 0.9% methanolic solution (100 μl) of potassium hydrogen phthalate. An aliquot (2.5 μl) of the resulting solution was analyzed by g.l.p.c. Details of the experimental conditions and rate constants are given in Table I.

The g.l.p.c. apparatus used for the analyses was an F & M gas chromatograph, model 609, equipped with a flame ionization detector, which gave a linear response for all compounds under our reaction conditions.

RESULTS AND DISCUSSION

A typical g.l.p.c. separation of I, 4-methylquinaldine, and II is shown in Fig. 1. Compounds I and II had retention volumes relative to 4-methylquinaldine of 0.37 and 1.49, and relative to diphenylmethane of 0.53 and 2.07.

The effect of temperature on the rate of methanolysis of I is shown in Fig. 2, and the rates of alcoholysis of this compound in ethanol, isopropanol, and *tert*-butanol, using the appropriate alkoxide ion as catalyst, are depicted in Fig. 3.

Can. J. Chem. Downloaded from www.nrcresearchpress.com by 210.87.254.40 on 09/05/12
For personal use only.

Under our standard reaction conditions the disappearance of I in [*b*] follows pseudo first-order kinetics (k_1) in I (see Fig. 2). Furthermore, the magnitude of k_1 is directly proportional to the methoxide ion concentration (Table I; experiments C, D, and E). Consequently, the overall methanolysis reaction must be of second order and involve

TABLE I

Rate constants for the methanolysis of the trimethylsilyl group(s) at the primary 6-position of compound I and at the secondary positions of compound II*

Expt.	Cpd.	Temp. (°C)	Catalyst	Catalyst concentration (m*M*)	k_1 ($s^{-1} \times 10^3$)	k_2 (l $mole^{-1}$ s^{-1})	k_2'† (l $mole^{-1}$ s^{-1})
A	I	26.4	LiOMe	1.97	2.10	1.07	1.02
B	I	26.4	NaOMe	1.97	2.06	1.05	1.01
C	I	26.4	KOMe	1.98	2.08	1.06	1.02
D‡	I	26.4	—	—	0.02	—	—
E	I	26.4	KOMe	0.99	1.01	1.02	—
F	I	1.4	NaOMe	1.98	0.51	0.257	—
G	II	27.0	KOMe	1.98	0.0852	0.043	—
H	II	0	KOMe	1.98	0.0142	0.0071	—
J	I	27.0	CH_3COOH	9.57	0.7	—	—

*The solvent in each case was methanol. 4-Methylquinaldine was used as the internal standard for all experiments except J, in which diphenylmethane was used. The values for the rate constants are the mean values obtained from several experiments, and the individual rate constants could be reproduced to within ±2% of the mean values.
†Rate constant for formation of II from I.
‡There was no difference in the value of k_1 in the presence or absence of 4-methylquinaldine although it is a weak base.

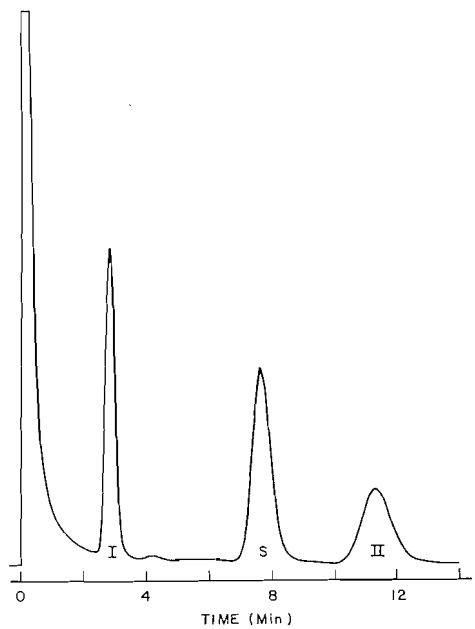

FIG. 1. The g.l.p.c. separation of methyl 2,3,4,6-tetra-*O*-trimethylsilyl-α-D-glucopyranoside (I), 4-methylquinaldine (S), and methyl 2,3,4-tri-*O*-trimethylsilyl-α-D-glucopyranoside (II) on a 5 ft column (20% w/w Carbowax 20M on Chromosorb W). Nitrogen flow rate was 84 ml/min and column temperature was 203°.

the nucleophilic attack of methoxide ion on the organosilicon compound. The rate of methanolysis of I, therefore, should be dependent only on the concentrations of methoxide ion and I. However, the observed rate of reaction will depend on the rate at which I is reformed by reaction of the anion of II with trimethylmethoxysilane, and on the rate at

Can. J. Chem. Downloaded from www.nrcresearchpress.com by 210.87.254.40 on 09/05/12
For personal use only.

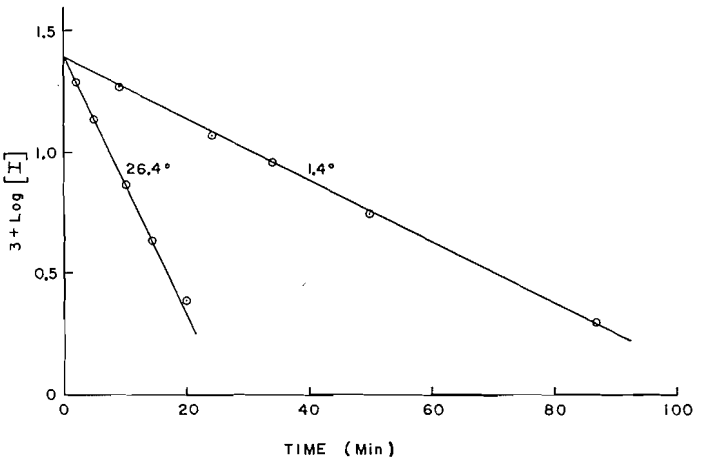

FIG. 2. The plot of the logarithm of the methyl 2,3,4,6-tetra-*O*-trimethylsilyl-α-D-glucopyranoside (I) concentration against time for the standard methanolysis reaction at 26.4° and 1.4°.

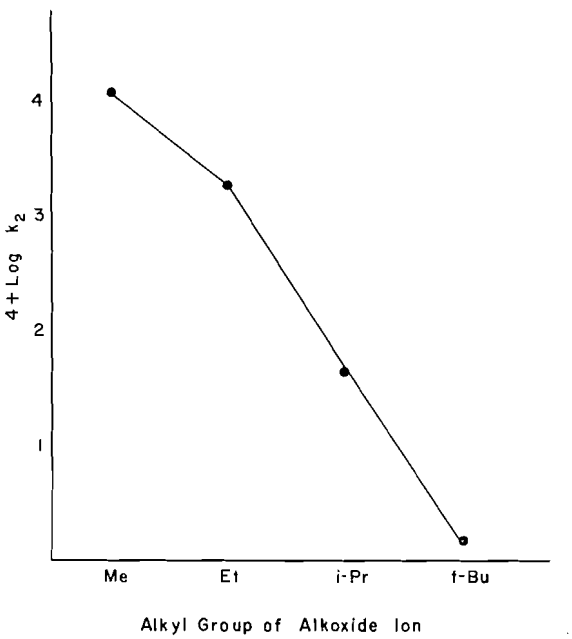

FIG. 3. The effect of structural differences in the alkyl group of the alkoxide ion on the second-order rate constant (k_2) for the alcoholysis of methyl 2,3,4,6-tetra-*O*-trimethylsilyl-α-D-glucopyranoside (I) in methanol, ethanol, isopropanol and *tert*-butanol at 30°.

which II itself reacts with methoxide ion. The latter makes only a slight contribution to the overall rate of reaction (Table I; experiments C and G). Furthermore, the linear plots in Fig. 2 require that the methoxide concentration remain constant throughout the reaction. The high methanol concentration and relative acidity of the hydroxyl proton in methanol, as compared to the corresponding proton in II, ensure that the concentration of the anion of II remains so low that the rate of reformation of I from II is negligible. Therefore, the observed second-order rate constants (k_2) for the methanolysis of I, using

Can. J. Chem. Downloaded from www.nrcresearchpress.com by 210.87.254.40 on 09/05/12
For personal use only.

basic catalysis, reported in Table I differ only in a minor degree from the true rate constant for the conversion of I to II. It is not surprising, therefore, that the second-order rate constant for the formation of II from I (Table I; k_2') is essentially the same as for the methanolysis of I (Table I; k_2).

The nature of the metal methoxide cation, as expected, does not affect the rate of reaction (Table I; experiments A, B, and C), and the complete removal of the trimethylsilyl groups from II using base or acid catalysis yields methyl α-D-glucopyranoside. Since no change in configuration has occurred at the asymmetric centers of the latter compound during methanolysis, the reaction mechanism must involve cleavage of the Si—O bonds and not the C—O bonds. This result is in agreement with published results on the acidic or basic hydrolysis of organosilicon alkoxides containing an asymmetric carbon atom attached to the ether oxygen atom (3, 4, 5, 7).

The rate constant for removal of the trimethylsilyl groups at the *primary* 6-position of the glucose moiety of I was greater by a factor of approximately 25 than for removal of the corresponding groups at the *secondary* 2-, 3-, and 4-positions (Table I; experiments C and G). It was possible, therefore, to prepare and isolate crystalline II in high yield (6). The selectivity of this reaction appears to be quite general and has been used, for example, to prepare the derivatives corresponding to II of other methyl glycosides. Our more general studies on the methanolysis of trimethylalkoxysilanes also indicate that an even greater difference exits in the rates of methanolysis of appropriate derivatives of secondary and tertiary alcohols.

The effect of temperature on the rate of methanolysis of the trimethylsilyl group at the *primary* 6-position of the glucose moiety of I is shown in Fig. 2. This reaction was found to have an energy of activation of 9.1 kcal mole^{-1}, and an Arrhenius frequency factor of 4×10^6 l mole^{-1} s^{-1} (Table I; experiments B and F). From the transition-state theory (8) the following constants were calculated, $\Delta F^{\ddagger} = 17.5$ kcal mole^{-1}, $\Delta H^{\ddagger} = 8.5$ kcal mole^{-1}, and $\Delta S^{\ddagger} = -30$ entropy units. The large negative entropy and low frequency factor are characteristic of reactions associated with electrorestriction of solvent molecules by a highly polar activated complex (9, 10). In a similar manner the corresponding activation energy for the removal of the trimethylsilyl groups at the *secondary* 2-, 3-, and 4-positions in the glucose residue was calculated to be 10.8 kcal mole^{-1} (Table I; experiments G and H). It must be realized that there are three secondary positions in compound II and that the kinetic study measured only the rate of disappearance of II. Since the removal of any of the trimethylsilyl groups in this compound would contribute to the overall rate of reaction, and since no evidence has been found for the specific reaction at one of the secondary positions, it is probable that the value for the activation energy given above represents the average value for the secondary position in the molecule. The activation energies given above differ in magnitude by 1.7 kcal mole^{-1} and, therefore, the difference in reactivity at the primary and secondary positions in II is mainly due to a change in the enthalpy rather than the entropy of activation for the reaction.

It was also considered desirable to determine whether structural differences in the alkyl substituent of the alkoxide ion influenced the rate of alcoholysis. Figure 3 clearly illustrates that the successive substitution of the methyl hydrogens by methyl groups is accompanied by a corresponding decrease in the rate of alcoholysis of I. The relative rate constants using methoxide, ethoxide, isopropoxide, and *tert*-butoxide ion as catalysts decreased in the ratio 10^4:1.7×10^3:40:1. Compound II was not formed in the reactions using isopropoxide or *tert*-butoxide ion. Since the reaction using the latter was extremely slow, it is possible that II underwent further equilibration with the formation of lower substituted derivatives of methyl α-D-glucopyranoside. The decrease in rate of reaction

Can. J. Chem. Downloaded from www.nrcresearchpress.com by 210.87.254.40 on 09/05/12
For personal use only.

on going from methoxide to *tert*-butoxide ion is undoubtedly due to an increase in steric interaction in the transition state as the number of methyl substituents is increased on the carbon bearing the basic oxygen atom. In this respect the methanolysis reaction resembles the reaction of different alkoxide ions with tri-*o*-tolylsilyl chloride (11) in which *tert*-butoxide ion in *tert*-butanol could not convert the chloride into the corresponding alkoxide.

Reaction [*b*] can be catalyzed by an organic acid instead of an alkoxide ion (Table I; experiment J). In the present experiments acetic acid was used and proved to be a less efficient catalyst than methoxide ion since the acid concentration had to be 12 times the methoxide concentration to obtain the same value for k_1 (Table I; experiments A, B, C, and J). Mineral acids such as HCl and H_2SO_4, on the other hand, were at least 4 times more efficient as catalysts for the reaction than methoxide ion. The reaction kinetics using these catalysts appeared to be more complex, and the yields of II very much poorer than when using our standard reaction conditions. Since we did not obtain consistent, reproducible rate data using these catalysts we have not included the results in this report. Nevertheless, it would appear that the methanolysis reaction is less selective if protons are used in place of alkoxide ion to catalyze the reaction. Acetic acid exists in the dissociated as well as undissociated form in methanolic solution, and it is probable that all of these species can act as catalysts for the methanolysis reaction. The yields of II using acetic acid as the catalyst are comparable with those obtained by using methoxide ion. Compound II can therefore be prepared from I under basic, acidic, or neutral conditions (Table I; experiments C, D, and J), although the rate of formation in the last case would be comparatively slow. It is interesting to note that Akerman found that the hydrolysis of trialkylphenoxysilanes proceeded much more rapidly in basic than in acidic solution (12), an observation opposite to that which we observe in the methanolysis reaction.

Although our present results do not enable us to draw conclusions about the exact nature of the mechanism of the alcoholysis reaction, it seems likely that it proceeds either by an S_N2 mechanism or by a mechanism involving a pentacovalent-silicon intermediate in which the silicon orbitals are dsp^3 hybridized. The presence of such an intermediate has been suggested by Swain, Esteve, and Jones (13) as a result of kinetic studies on the hydrolysis of triphenylsilyl fluoride and tri-*p*-tolysilyl fluoride in aqueous acetone. Eaborn has pointed out, however, that their kinetic data *do not* in fact distinguish between the two mechanisms (1*c*).

ACKNOWLEDGMENTS

The author would like to acknowledge the excellent technical assistance of Mr. D. R. Johnson and Mrs. H. J. Levy.

REFERENCES

1. C. EABORN. Organosilicon compounds. Butterworths Scientific Publications, London. 1960. (*a*) p. 295, (*b*) p. 297, (*c*) p. 111.
2. R. BAKER, R. W. BOTT, C. EABORN, and D. W. JONES. J. Organometal. Chem. **1**, 37 (1963).
3. L. H. SOMMER, C. L. FRYE, G. A. PARKER, and K. W. MICHAEL. J. Am. Chem. Soc. **86**, 3271 (1964).
4. L. H. SOMMER, C. L. FRYE, and G. A. PARKER. J. Am. Chem. Soc. **86**, 3276 (1964).
5. L. H. SOMMER, G. A. PARKER, and C. L. FRYE. J. Am. Chem. Soc. **86**, 3280 (1964).
6. D. T. HURST and A. G. McINNES. Can. J. Chem. In press. 1965.
7. R. H. KRIEBLE and C. A. BURKHARD. J. Am. Chem. Soc. **69**, 2689 (1947).
8. S. GLASSTONE, K. J. LAIDLER, and H. EYRING. The theory of rate processes. McGraw-Hill Book Co., Inc., New York. 1941. p. 195.
9. K. J. LAIDLER and P. A. LANDSKROENER. Trans. Faraday Soc. **52**, 200 (1956).
10. C. T. BURRIS and K. J. LAIDLER. Trans. Faraday Soc. **51**, 1497 (1955).
11. H. GILMAN and G. N. R. SMART. J. Org. Chem. **19**, 441 (1954).
12. E. AKERMAN. Acta Chem. Scand. **10**, 298 (1956); **11**, 373 (1957).
13. C. G. SWAIN, R. M. ESTEVE, and R. H. JONES. J. Am. Chem. Soc. **71**, 965 (1965).

Can. J. Chem. Downloaded from www.nrcresearchpress.com by 210.87.254.40 on 09/05/12
For personal use only.

Can. J. Chem. Downloaded from www.nrcresearchpress.com by 210.87.254.6 on 09/05/12
For personal use only.

THE ALCOHOLYSIS OF TRIALKYLALKOXYSILANES

PART II. THE PREPARATION AND CHEMISTRY OF METHYL 2,3,4-TRI-*O*-TRIMETHYLSILYL-α-D-GLUCOPYRANOSIDE[1]

D. T HURST[2] AND A. G. MCINNES

Atlantic Regional Laboratory, National Research Council of Canada, Halifax, Nova Scotia

Received January 29, 1965

ABSTRACT

The trimethylsilyl group on the 6-position of methyl 2,3,4,6-tetra-*O*-trimethylsilyl-α-D-glucopyranoside is preferentially removed by methanolysis, using basic or acidic catalysts, giving methyl 2,3,4-tri-*O*-trimethylsilyl-α-D-glucopyranoside in high yield (>80%). Reaction of the latter with acetic anhydride, benzoyl chloride, or phenyl isocyanate produces the corresponding 6-substituted derivatives in quantitative yield. The trimethylsilyl residues from the latter compounds are hydrolyzed by 50% aqueous methanol with the concomitant formation of 6-*O*-acetyl, 6-*O*-benzoyl, or 6-carbanilate derivatives of methyl α-D-glucopyranoside in excellent yield. Chemical and proton magnetic resonance (p.m.r.) studies established the structure of methyl 2,3,4-tri-*O*-trimethylsilyl-α-D-glucopyranoside, and of subsequent derivatives prepared from this compound. Infrared and p.m.r. evidence is offered to support conclusions regarding the conformation of the groups or atoms attached to C_6 and C_5 of the glucoside residue in some of these compounds.

INTRODUCTION

Although general methods used for the preparation of trialkylalkoxysilanes (trialkylsilyl ethers), or trialkylaryloxysilanes, have been described by Eaborn in his excellent book (1*a*), it is only the trimethylsilyl residue which has been used extensively to protect hydroxyl (2) and amino groups (1*b*). These derivatives are easily prepared, are resistant to oxidation, and have more volatility and thermal stability than the parent compound (3). Moreover, they are readily hydrolyzed under neutral conditions by hot aqueous ethanol or methanol, and the hydrolysis is catalyzed by acids or bases (1*c*). Derivatives of this type, therefore, have been used for the separation and purification of compounds containing hydroxyl groups by fractional distillation (2), and in the gas–liquid partition chromatography (g.l.p.c.) of sugars (4). The physical properties of trimethylsilyl ethers are also utilized in mass spectrometry to prevent the elimination of water from alcohols on volatilization (5).

Recently the primary hydroxyl groups in sucrose have been selectively substituted with tricyclohexylsilyl groups (6). This work, however, also established that tricyclohexylsilyl and triphenylsilyl groups are only hydrolyzed by hot solutions of a strong acid or base. Consequently, one of the advantages in using trimethylsilyl residues as blocking groups, namely their ease of hydrolysis, is lost when a tricylcohexylsilyl residue is used. Nevertheless, a literature survey reveals no other case in which advantage was taken of the relative rates of substitution of different types of hydroxyl groups by trialkylsilyl residues. Moreover, it was not realized until the present work (7) that trialkylsilyl derivatives of primary, secondary, or tertiary alcohols might have different rates of alcoholysis (or hydrolysis) and that this property could be used for synthetic purposes.

The present communication describes a method for the preparation of methyl 2,3,4-tri-*O*-trimethylsilyl-α-D-glucopyranoside in high yield by the preferential methanolysis of the

[1]*Presented at the 47th Annual Conference, The Chemical Institute of Canada, Kingston, Ontario, June 1–3, 1964.*

Issued as N.R.C. No. 8432.

[2]*National Research Council Postdoctorate Fellow 1963–1964. Present address: Department of Chemistry, Kingston College of Technology, Kingston-upon-Thames, Surrey, England.*

trimethylsilyl residue on the primary 6-position of the corresponding fully substituted trimethylsilyl derivative of methyl α-D-glucopyranoside. Further work has shown that this reaction can probably be applied to any polyhydroxyl compound since the trimethylsilyl groups of primary, secondary, and tertiary hydroxyl groups have significantly different rates of methanolysis under acidic, basic, and neutral conditions, and this work will be the subject of future publications. It would also be of interest to establish whether the corresponding derivatives of phenolic and carboxylic hydroxyl groups in different chemical environments also differ in their rates of methanolysis.

EXPERIMENTAL

Methyl 2,3,4,6-Tetra-O-trimethylsilyl-α-D-glucopyranoside (I) from Methyl α-D-Glucopyranoside

The procedure for the preparation and purification of I has been described previously by Hedgley and Overend (3). Methyl α-D-glucopyranoside (0.31 mole) was reacted with trimethylchlorosilane (1.8 moles) in pyridine (500 ml) at 0° to yield I (0.29 mole), b.p. 115–120° at 0.25 mm, $[\alpha]_D^{22}$ +86.7° (*c*, 0.67 in chloroform), η_D^{22} 1.4410. Reported physical constants for this compound (3) are b.p. 109–110° at 0.1 mm, η_D^{25} 1.4415, $[\alpha]_D^{20}$ +92.5° (*c*, 0.692 in chloroform).

Methyl 2,3,4-Tri-O-trimethylsilyl-α-D-glucopyranoside (II) from I

The methanolysis of I (0.105 mole) in anhydrous methanol (200 ml) at 0° using a solution of potassium carbonate (0.8 millimole in 25 ml methanol) as catalyst, with the concomitant formation of II, was followed by analyzing aliquots of the reaction mixture by g.l.p.c. (7). After 45 min the relative intensities of the peaks corresponding to I and II on the g.l.p.c. tracing indicated that the reaction was complete, so the catalyst was destroyed by the addition of an equivalent amount of acetic acid to the reaction solution. Distilled water was then added to the latter, with vigorous shaking, until the solution remained cloudy. This turbidity was carefully removed by the addition of a few drops of methanol, and the resulting solution was placed in a refrigerator at 5°. When crystallization of II (0.088 mole) was complete, the product was recrystallized from cold aqueous methanol to yield II (0.081 mole) as a white crystalline compound, m.p. 98.5–99.5°, $[\alpha]_D^{24}$ +91.48° (*c*, 5.0 in chloroform).

Anal. Calcd. for $C_{16}H_{38}O_6Si_3$: C, 46.83; H, 9.27. Found: C, 46.88; H, 9.53.

A similar yield of II was obtained when acetic acid was used instead of a base as catalyst for the methanolysis reaction. However, for a comparable reaction rate the concentration of acetic acid has to be approximately 15 times that of a basic catalyst (7).

Methyl 6-O-Acetyl-2,3,4-tri-O-trimethylsilyl-α-D-glucopyranoside (III) from II

A solution of II (10 millimoles) and acetic anhydride (11 millimoles) in anhydrous pyridine (20 ml) was heated on a steam bath for 1 h and was then taken to dryness under reduced pressure. The residue was distilled under reduced pressure to obtain III (9.3 millimoles) as a colorless oil, b.p. 145–147° at 0.34 mm, $[\alpha]_D^{23}$ +90.26° (*c*, 1.047 in chloroform), and η_D^{21} 1.4502.

Anal. Calcd. for $C_{18}H_{40}O_7Si_3$: C, 47.79; H, 8.85. Found: C, 47.51; H, 9.08.

Methyl 6-O-Acetyl-α-D-glucopyranoside (IV) from III

Distilled water was added to a solution of III (5 millimoles) in methanol (40 ml) until cloudy, and then the solution was refluxed for 4 h. Subsequently, the solution was taken to dryness under reduced pressure and the oily residue was dissolved in distilled water and filtered. The clear filtrate was taken to dryness and dried over phosphorus pentoxide *in vacuo* to yield IV (4.55 millimoles) as an oil $[\alpha]_D^{21}$ +150.1° (*c*, 1.12 in acetone).

Anal. Calcd. for $C_9H_{16}O_7$: C, 45.75; H, 6.83. Found: C, 46.10; H, 6.97.

Methyl 6-O-Acetyl-α-D-glucopyranoside 2,3,4-Tricarbanilate (V) from IV

A solution containing IV (5 millimoles) and phenyl isocyanate (17.25 millimoles) in anhydrous pyridine (10 ml) was heated on a steam bath for 1 h, and then the excess phenyl isocyanate was destroyed by the addition of ethanol (1 ml). The reaction solution was subsequently taken to dryness under reduced pressure, and the residue was crystallized several times from ethanol. Compound V (4.3 millimoles) was obtained as needles, m.p. 244–246° and $[\alpha]_D^{24}$ +73.4° (*c*, 0.105 in acetone).

Anal. Calcd. for $C_{30}H_{31}O_{10}N_3$: C, 60.70; H, 5.26; N, 7.08. Found: C, 60.73; H, 5.44; N, 7.05.

Reported physical constants for V (8) are m.p. 235–237° and $[\alpha]_D^{25}$ +71° (*c*, 0.1 in acetone). A satisfactory melting point for V could not be obtained on a hot stage micro melting point apparatus (the compound appeared to sublime) so the melting point was determined by the capillary method.

Methyl 6-O-Benzoyl-2,3,4-tri-O-trimethylsilyl-α-D-glucopyranoside (VI) from II

Compound II (10 millimoles) was reacted, overnight, with benzoyl chloride (11 millimoles) in pyridine (30 ml) at 0°, and the reaction mixture was worked up in the usual manner. However, when the chloroform solution of the reaction product was washed with acid, to remove traces of pyridine, care was taken to ensure

Can. J. Chem. Downloaded from www.nrcresearchpress.com by 210.87.254.6 on 09/05/12
For personal use only.

that the aqueous phase did not become strongly acidic. The latter condition could lead to the hydrolysis of the trimethylsilyl groups. Distillation of the residue obtained from the chloroform solution under reduced pressure yielded VI (8.8 millimoles), b.p. 208–212° at 0.47 mm, $[\alpha]_D^{23}$ +80.12° (*c*, 0.92 in chloroform) and η_D^{22} 1.4780.

Anal. Calcd. for $C_{16}H_{38}O_6Si_3$: C, 53.70; H, 8.30. Found: C, 53.52; H, 8.30.

Methyl 6-O-Benzoyl-α-D-glucopyranoside (VII) from VI

The trimethylsilyl groups of VI (5 millimoles) were hydrolyzed in aqueous methanol by the procedure described above for the preparation of IV. Removal of the solvent under reduced pressure left a solid residue. Crystallization of the latter from ethyl acetate yielded VII (4.1 millimoles) as prisms, m.p. 132–133° (reported m.p. 174–175° (9)), $[\alpha]_D^{24}$ +104° (*c*, 1.45 in chloroform).

Anal. Calcd. for $C_{14}H_{18}O_7$: C, 56.37; H, 6.08. Found: C, 56.33; H, 6.13.

Methyl α-D-Glucopyranoside 6-Carbanilate (IX) from II

Compound II (10 millimoles) was reacted with phenyl isocyanate (11 millimoles) in pyridine (10 ml) by the same procedure described for the preparation of V above. The residue (VIII) from the reaction mixture was immediately hydrolyzed in aqueous methanol (35 ml) to remove the trimethylsilyl groups, using 1 drop of glacial acetic acid as a catalyst (see procedure described for the preparation of IV and VII above). Removal of the solvent under reduced pressure left a solid residue which crystallized from water to yield IX (8.5 millimoles) as long needles, m.p. 141–143°, $[\alpha]_D^{23}$ +126.2° (*c*, 0.93 in pyridine).

Anal. Calcd. for $C_{14}H_{19}O_7N$: C, 53.67; H, 6.11; N, 4.47. Found: C, 53.62; H, 6.16; N, 4.43.

Precipitation of IX from ethyl acetate gave an amorphous white powder, m.p. 131–132.5°. Reported physical constants for IX (10) are m.p. 131–133° (from ethyl acetate), $[\alpha]_D^{25}$ +115° (*c*, 1.0 in pyridine).

Methyl 2,3,4-Tri-O-acetyl-α-D-glucopyranoside 6-Carbanilate (X) from IX

Acetylation of IX (3.2 millimoles) with acetic anhydride (3.92 millimoles) in pyridine (20 ml) in the usual manner gave a product which crystallized from methanol to yield X (3.01 millimoles) as prisms, m.p. 146–147°, $[\alpha]_D^{24}$ +1.43° (*c*, 1.1 in chloroform).

Anal. Calcd. for $C_{20}H_{25}O_{10}N$: C, 54.66; H, 5.73; N, 3.19. Found: C, 54.57; H, 5.72; N, 3.20.

Reported physical constants for X(10) are m.p. 147–148° (from methanol), $[\alpha]_D^{24}$ +145° (*c*, 1 in chloroform).

Methyl 2,3,4-Tri-O-methyl-α-D-glucopyranoside 6-(N-Methyl)-carbanilate (XI) from IX

Compound IX (5 millimoles) was methylated (11) in anhydrous *N,N*-dimethylformamide (DMF) (20 ml) using methyl iodide (0.11 mole) and freshly prepared silver oxide (40 millimoles). The reaction was assisted by vigorous agitation of the reaction solution on a mechanical shaker for 30 h. At the end of the reaction period the solution was filtered and the clear filtrate was diluted with chloroform (250 ml) to precipitate silver iodide. The latter was removed by filtration and the chloroform/DMF solution was taken to dryness *in vacuo* on a rotary evaporator. Drying under reduced pressure over phosphorous pentoxide left an oily residue (1.29 g). The residue was further purified by distillation under reduced pressure, followed by chromatography on neutral Wöelm alumina using chloroform as the eluant. Removal of the chloroform under reduced pressure yielded XI (3.14 millimoles) as a colorless oil, $[\alpha]_D^{22}$ +89.8° (*c*, 1.314 in acetone), η_D^{21} 1.5006.

Anal. Calcd. for $C_{18}H_{27}O_7N$: C, 58.52; H, 7.37; N, 3.79. Found: C, 58.58; H, 7.63; N, 3.81.

Periodate Oxidation of IX

Compound IX (0.348 millimole) was oxidized with sodium metaperiodate (1.44 millimoles) in acetate buffer solution (100 ml; pH 4) as described by Guthrie (12). The periodate consumed by IX was determined periodically on aliquots of the reaction solution by the Fleury–Lange method (13). Aliquots of the solution (5 ml) were pipetted into a solution of saturated sodium bicarbonate (10 ml) and 0.01 *N* sodium arsenite (20 ml) and left standing in the dark for 15 min. Subsequently, a 20% solution of potassium iodide was added and the excess arsenite was titrated against 0.1 N iodine solution, using a 1% starch solution (1 ml) as indicator. The results are given in Fig. 2.

All p.m.r. spectra were taken on a Varian A60 spectrometer fitted with a variable temperature probe, and using tetramethylsilane (TMS) as an internal standard. The infrared spectra were recorded on a Perkin-Elmer model 521 spectrometer.

RESULTS AND DISCUSSION

The reaction scheme for the preparation and chemistry of II is depicted in Fig. 1.

The experimental procedures which were used to make a kinetic study of the controlled methanolysis of I to produce II have already been described in this issue (7). Essentially the same reaction conditions were used for the production of II on a preparative scale (see Experimental), apart from changes in the relative concentrations of reagents, and g.l.p.c. was again used to follow the course of the reaction. However, no g.l.p.c. internal standard (7) was present in the reaction solution since the course of the reaction could be estimated in a qualitative manner by observing the relative intensities of I and II on the g.l.p.c. tracing.

Can. J. Chem. Downloaded from www.nrcresearchpress.com by 210.87.254.6 on 09/05/12
For personal use only.

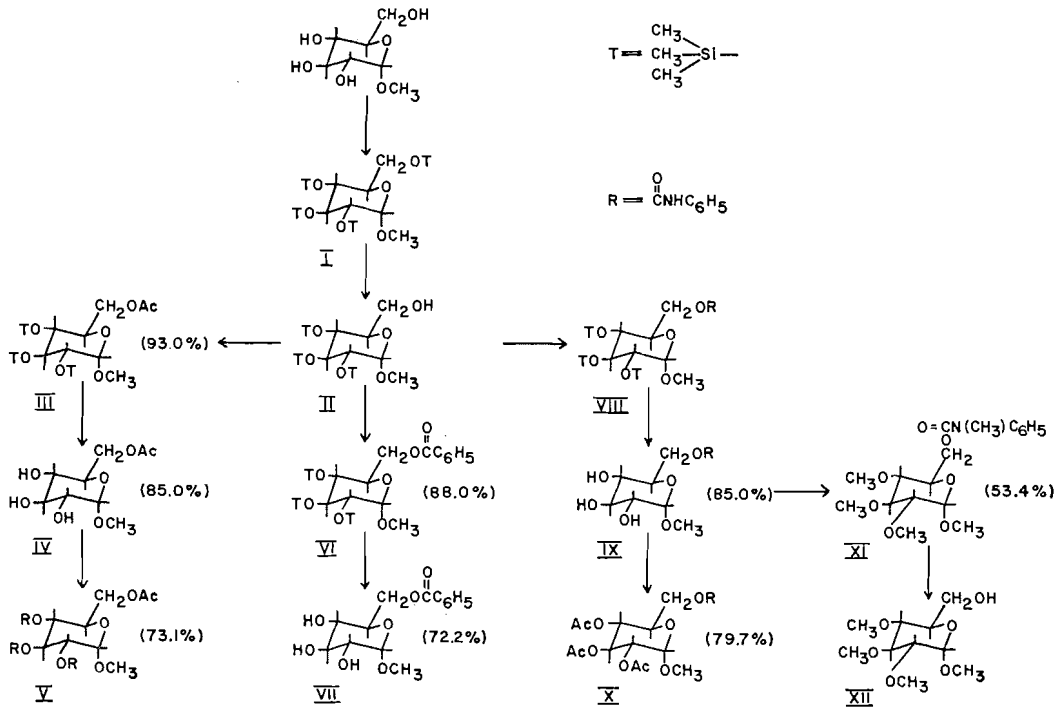

FIG. 1. The preparation and chemistry of methyl 2,3,4-tri-*O*-trimethylsilyl-α-D-glucopyranoside (II).

When the reaction was complete, II crystallized from the methanolic reaction solution on addition of water. This simple experimental procedure enabled II to be isolated in greater than 70% yield based on methyl α-D-glucopyranoside, or over 80% yield based on I. Moreover, studies in this laboratory have shown that the reaction of trimethylchlorosilane with polyhydroxy compounds in pyridine is virtually instantaneous at room temperature. Consequently, a supply of II for synthetic purposes can be obtained quickly provided it is prepared from crude (undistilled) I. The latter may be obtained sufficiently pure for this purpose by removing the pyridine under reduced pressure and dissolving I in petroleum ether, in which pyridinium hydrochloride is insoluble.

Compound II reacted with phenyl isocyanate in pyridine to form the corresponding monocarbanilate derivative VIII, which was subsequently hydrolyzed in aqueous methanol to give compound IX. The position of the carbanilate residue in IX could be determined by periodate oxidation studies. If the substituent was at carbon-6 of the glucose moiety of this compound it would consume 2 moles of periodate due to the presence of three secondary hydroxyl groups on contiguous carbon atoms, whereas the corresponding 2- and 4-derivatives, with only two secondary hydroxyl groups on adjacent carbon atoms, would require only 1 mole of the reagent. The remaining derivative with the substituent on the 3-position, and containing no secondary hydroxyl groups on adjacent carbon atoms, would not be oxidized by periodate. From Fig. 2 it can be seen that compound IX consumed 2 moles of periodate and consequently must have the substituent at carbon-6. This result requires that compounds VIII and II have the structures shown in Fig. 1, since the carbanilate residue of IX occupies the same position as the original hydroxyl group in II.

It was not possible to deduce the structure of IX by comparing its physical constants with those reported in the literature (10). Although the melting point of the latter agreed

Can. J. Chem. Downloaded from www.nrcresearchpress.com by 210.87.254.6 on 09/05/12
For personal use only.

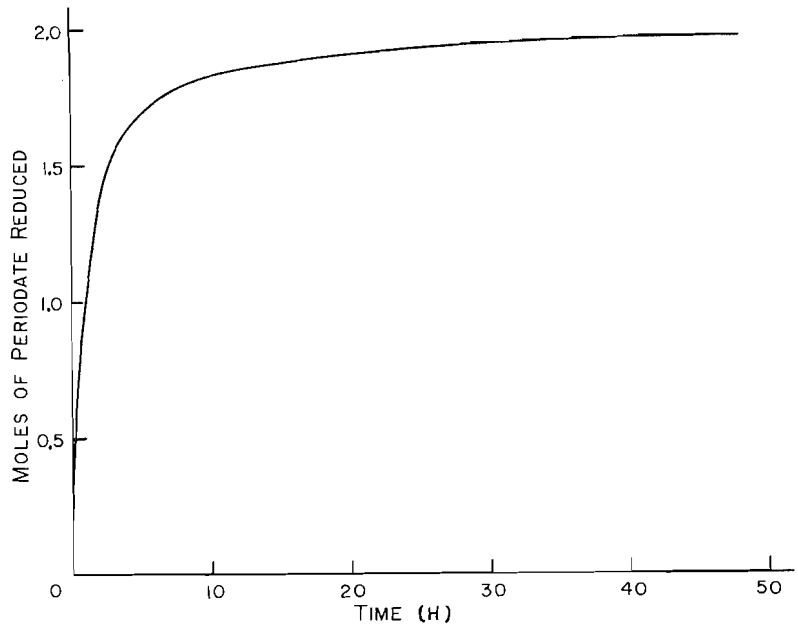

FIG. 2. A plot of the number of moles of periodate consumed by methyl α-D-glucopyranoside 6-carbanilate (IX) against time.

with the literature value it was obtained as an amorphous powder from ethyl acetate and not crystalline as reported by Hearon *et al.* Compound IX, however, could be obtained as long crystalline needles from water. Moreover, the specific rotation of our compound was 11° higher than the reported value. However, the physical constants for X, prepared by the reaction of IX with acetic anhydride in pyridine, were in excellent agreement with those reported (10). Since Hearon and co-workers prepared IX by the deacetylation of X with boiling methanolic hydrogen chloride, it seems probable that any differences in the two sets of physical constants for IX may be due to the presence of some of the corresponding β-isomer in their product which must be present after this treatment. It is of interest that Hearon *et al.* obtained IX in 15% yield using a standard five step synthesis (i.e. tritylation, acetylation, carbanilation, etc.) whereas by the present method this compound can be obtained in >60% yield based on the methyl glucoside, and without the possibility of side reactions occurring. Compound XI was prepared from IX by the Kuhn procedure (11), and the former was converted to XII when treated with ethanolic barium hydroxide. The latter (XII) was identified (14) and isolated by g.l.p.c., and the physical constants of this compound agreed with those reported in the literature for methyl 2,3,4-tri-*O*-methyl-α-D-glucopyranoside (15). Consequently, the carbanilate residues of IX and XI, and the hydroxyl group of II, must have been attached to carbon-6 of the glucose moieties of these compounds. Moreover, the differences in the infrared spectra of IX and XI were consistent with those expected for *N*-methylation as well as *O*-methylation of IX by the Kuhn procedure. *N*-Alkylation of carbanilate groups under similar experimental conditions has been reported previously by Bouveng (16). This behavior is also observed in urethans and is in contrast to that exhibited by thiourethans which apparently can undergo *S*-alkylation (17), to produce dialkyl esters of ortho-thiocarbonic anil, RN=C(OR′)(SR″), or *N*-alkylation (18) depending on the basic catalyst.

Can. J. Chem. Downloaded from www.nrcresearchpress.com by 210.87.254.6 on 09/05/12
For personal use only.

The structure of XI was also confirmed by p.m.r. studies (see Fig. 3). At low field the five aromatic protons of the phenyl group appear as a broad singlet at 2.79, and the equatorial anomeric hydrogen occurs at 5.38 with the spacing of 3.3 c.p.s. (19) characteristic of protons in the *cis* orientation at carbon-1 and -2. The geminal hydrogens on carbon-6, which are not magnetically equivalent because of the presence of the asymmetric center at carbon-5, constitute the AB part of the ABX system shown in Fig. 4, R = —CH_3; R′ = —$OCN(CH_3)C_6H_5$, and are consequently present as two characteristic overlapping quartets centered at 5.83. Analysis of the AB multiplet gave values of 17.9 c.p.s. for the

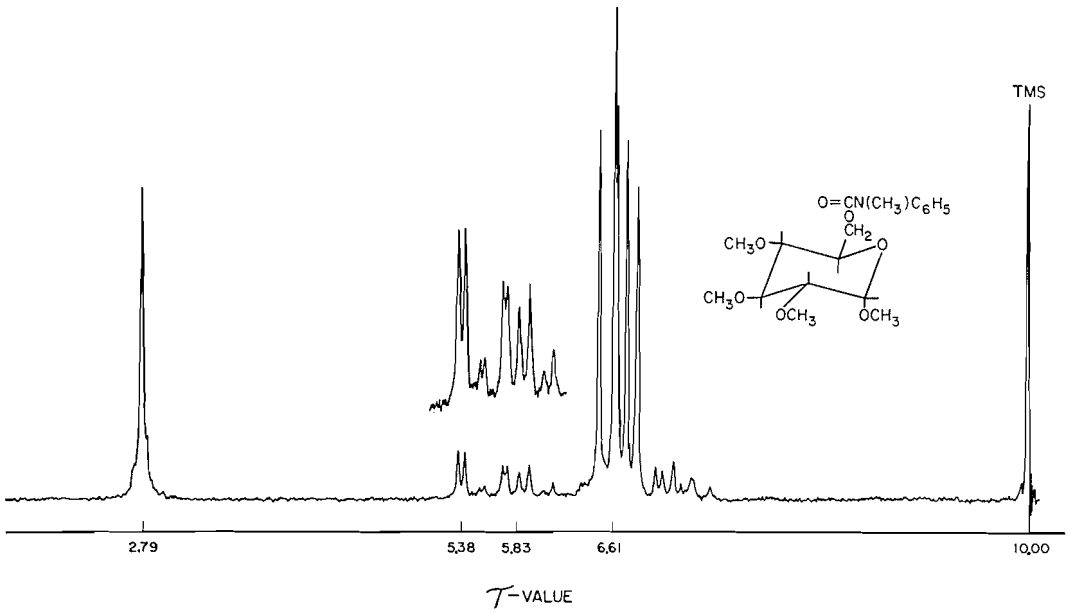

FIG. 3. The p.m.r. spectra of methyl 2,3,4-tri-*O*-methyl-α-D-glucopyranoside 6-(*N*-methyl)-carbanilate (XI) in CCl_4 using TMS as an internal standard.

chemical shift δ_{AB}, −11.7 c.p.s. for J_{AB}, 5.4 c.p.s. for J_{AX}, and 2.0 c.p.s. for J_{BX}. Although no information can be obtained about the absolute or relative signs of these coupling constants from the p.m.r. signals for the two geminal protons, it is known that geminal coupling constants (i.e. J_{AB}) are negative (20, 21), and of opposite sign to vicinal coupling constants (i.e. J_{AX} and J_{BX}) in substituted alkanes. Consequently, the above coupling constants were arbitrarily given appropriate signs. Calculation of the theoretical line positions and intensities for the AB multiplet, using the values for the chemical shift and coupling constants given above, gave results in excellent agreement with those obtained experimentally. Furthermore, the protons of the *N*-methyl and four methoxyl groups of XI appear as singlets at 6.5, 6.61, 6.63, 6.74, and 6.83. The remaining protons of the pyranose ring are partly hidden under the latter peaks or appear on the high-field side of the singlet at 6.83.

If compound XI exists solely in conformation 1*a* (R′ = —$OCN(CH_3)C_6H_5$; R = —CH_3) (see Fig. 4) in carbon tetrachloride solution the protons H_A and H_X, which are in a *trans* relationship to one another, would be expected to have a value of from 8 to 12 c.p.s. for J_{AX} (22, 23). The low experimental value of 5.4 c.p.s. for this coupling constant therefore suggests that there is free rotation about the C_5—C_6 bond resulting in a rapid interconversion of the three possible conformations (see Fig. 4; 1*a*, 1*b*, and 1*c*) with a concomitant

Can. J. Chem. Downloaded from www.nrcresearchpress.com by 210.87.254.6 on 09/05/12
For personal use only.

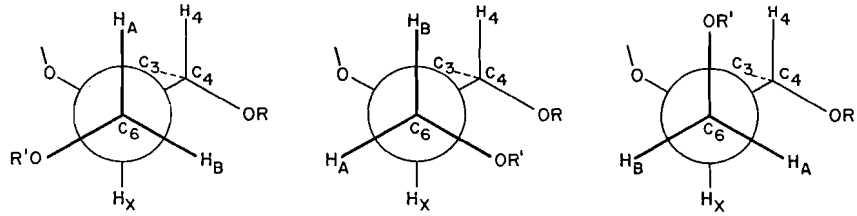

1a 1b 1c

FIG. 4. The three possible conformations of the groups or atoms attached to the fifth and sixth carbon atoms in the glucose moiety of compounds XI and II.

decrease in the value of J_{AX} (22). However, the coupling constants J_{AX} and J_{BX} remained unchanged when the spectrum of XI was recorded over a temperature range of 60° to −60°, and when a solvent of high dielectric constant such as acetone-d_6 was used as a solvent instead of carbon tetrachloride. Since changes in coupling constants resulting from a changing equilibrium between conformations of different dipole moments on varying the polarity of the solvent have already been found by Sheppard (24), and since similar changes can occur by varying the temperature of the solution (25), the results only seem to be compatible with the presence of a single conformer. Consideration of the *gauche* interactions of the substituents on carbon-5 and carbon-6, together with the 1,3-interactions between the substituents on the latter and on carbon-4, leaves little doubt that 1*a* is the most stable and 1*b* the least stable conformation (see Fig. 4). Indeed the differences in non-bonded interactions in the three conformations make it unlikely that they would be equally populated in solution under all of the experimental conditions described above. Consequently, compound XI probably exists almost entirely in conformation 1*a*. The low value obtained for J_{AX} may be due to the fact that the 1,3-interactions in 1*a* would tend to repel H_A and H_4 thereby reducing the dihedral angle subtended by the C_6—H_A and C_5—O bonds. This would result in a reduction in the angle subtended by the C_5—H_X and C_6—H_A bonds, which would result in a decrease in the value of J_{AX} (23). It should also be remembered that the electronegativity of the R′ group (see Fig. 4) could also have a profound effect on the value of J_{AX} (23).

The infrared spectrum of a 5×10^{-3} *M* solution of II in carbon tetrachloride gave a single absorption band in the O—H stretching region in the infrared at 3 609 cm^{-1}. Since free primary hydroxyl groups under similar experimental conditions give absorption bands with little variation at 3 636 – 3 641 cm^{-1} (26, 27) it would appear that the primary hydroxyl group of II is involved in a *weak* intramolecular hydrogen bond corresponding to a shift to lower frequency of approximately 30 cm^{-1}. The only conformations in which the primary hydroxyl group could form a hydrogen bond are 1*a* and 1*b*, see Fig. 4; R′ = —H; R = —$Si(CH_3)_3$, and the single absorption band at 3 609 cm^{-1} implies that there is only one conformer present, or that the hydrogen bonds formed in the two conformations are of equal energy. It is unlikely, however, that II exists in conformation 1*b* since the short O—O distance (≈2.4 Å) (28) and the high electron density at the oxygen atom attached to carbon-4, due to the ionic character of the Si—O bond (1*d*), would require the presence of a much stronger hydrogen bond. Indeed, the experimental results can be explained if II exists in the same conformation as XI, namely 1*a*. In this case if the angle between the C_6—O and C_5—O bonds was increased because of the 1,3-interactions discussed above, the O—O distance in this conformation could easily be about 3 Å, and this

Can. J. Chem. Downloaded from www.nrcresearchpress.com by 210.87.254.6 on 09/05/12
For personal use only.

large distance would of course result in a weak hydrogen bond (28) between the hydroxyl group and the oxygen atom in the pyranose ring. It is possible, however, that 3 609 cm^{-1} is the normal O—H stretching frequency for the free primary hydroxyl group in compounds such as II, although there is no evidence in the literature to support such a contention.

In conclusion compounds III and VI were prepared by the reaction of II with acetic anhydride or benzoyl chloride in pyridine, and hydrolysis of these compounds with boiling aqueous methanol gave IV, and VII, in excellent yield. The former has not been synthesized previously, and the physical constants of the latter reported in the literature (7) are in error (see Experimental). Inspection of the p.m.r. spectra of III and VI in $CDCl_3$ reveals that the signals for the two geminal protons on carbon-6 are present as two overlapping quartets centered at τ values of 5.74 and 5.50. Calculation as in the case of compound XI gave values for III of 18.5 c.p.s. for δ_{AB}, −12.2 c.p.s. for J_{AB}, 4.7 c.p.s. for J_{AX}, and 1.5 c.p.s. for J_{BX} and corresponding values for VI of 20.0 c.p.s. for δ_{AB}, −12.4 c.p.s. for J_{AB}, 5.4 c.p.s. for J_{AX}, and 1.6 c.p.s. for J_{BX}. Although V was prepared by the reaction of IV with phenyl isocyanate in pyridine, it was not possible to confirm the identity of the latter by preparing this derivative because the melting point and $[\alpha]_D$ reported for this compound (8) were lower than the values obtained in this laboratory (see Experimental). Proton magnetic resonance temperature studies on III and IV also indicate that the atoms and groups attached to carbon-5 and -6 have the same conformation as described above for XI and II.

ACKNOWLEDGMENTS

We should like to acknowledge the excellent technical assistance of Mrs. M. G. Flack and the help of our colleague Mr. D. G. Smith in recording the p.m.r. spectra.

REFERENCES

1. C. EABORN. Organosilicon compounds. Butterworths Scientific Publications, London. 1960. (*a*) p. 288, (*b*) p. 339, (*c*) p. 301, (*d*) p. 89.
2. J. F. W. MCOMIE. Advances in organic chemistry. Vol. III. Interscience Publishers Inc., New York. 1963. pp. 218, 231.
3. E. J. HEDGLEY and W. G. OVEREND. Chem. Ind. London, 378 (1960).
4. C. C. SWEELEY, R. BENTLEY, M. MAKITA, and W. W. WELLS. J. Am. Chem. Soc. **85**, 2497 (1963).
5. A. G. SHARKEY, Jr., R. A. FRIENDEL, and S. H. LANGER. Anal. Chem. **29**, 770 (1957).
6. S. A. BARKER, J. S. BRIMACOMBE, M. R. HARDEN, and J. A. JARVIS. J. Chem. Soc. 3403 (1963).
7. A. G. MCINNES. Can. J. Chem. In press. 1965.
8. W. M. HEARON. J. Am. Chem. Soc. **70**, 297 (1948).
9. TH. LIESER and E. LECKZYCK. Ann. **519**, 271 (1935).
10. W. M. HEARON, G. D. HIATT, and C. R. FORDYCE. J. Am. Chem. Soc. **66**, 995 (1944).
11. R. KUHN, H. TRISCHMANN, and I. LÖW. Angew. Chem. **67**, 32 (1955).
12. R. D. GUTHRIE. Methods in carbohydrate chemistry. Vol. I. Academic Press, New York. 1962. p. 436.
13. R. F. FLEURY and J. LANGE. J. Pharm. Chim. **17**, 107, 196 (1933).
14. C. T. BISHOP and F. P. COOPER. Can. J. Chem. **38**, 388 (1960).
15. A. ROBERTSON and R. B. WATERS. J. Chem. Soc. 1709 (1931).
16. H. O. BOUVENG. Acta Chem. Scand. **15**, 87 (1961).
17. C. LIEBERMAN. Ann. **207**, 121 (1881).
18. B. R. BAKER, K. HEWSON, L. GOODMAN, and A. BENITEZ. J. Am. Chem. Soc. **80**, 6577 (1958).
19. R. U. LEMIEUX, R. K. KULLNIG, H. J. BERNSTEIN, and W. G. SCHNEIDER. J. Am. Chem. Soc. **80**, 6098 (1958).
20. A. D. BUCKINGHAM and K. A. MCLAUCHLAN. Proc. Chem. Soc. 144 (1963).
21. F. A. L. ANET. J. Am. Chem. Soc. **84**, 3767 (1962).
22. F. A. L. ANET. J. Am. Chem. Soc. **84**, 747 (1962).
23. M. KARPLUS. J. Am. Chem. Soc. **85**, 2870 (1963).
24. N. SHEPPARD and J. J. TURNER. Proc. Roy. Soc. London, Ser. A, **252**, 506 (1959).
25. L. M. JACKMAN. Applications of nuclear magnetic resonance spectroscopy in organic chemistry. Pergamon Press, Oxford. 1959. p. 102.
26. R. N. JONES and C. SANDORFY. Techniques of organic chemistry. Vol. IX. *Edited by* Weissberger. Interscience Publishers Inc., New York. 1956. pp. 417–432.
27. A. R. H. COLE, G. T. A. MILLER, D. W. THORNTON, and R. L. S. WILLIX. J. Chem. Soc. 1220 (1959).
28. G. C. PIMENTEL and A. L. MCCLELLAN. The hydrogen bond. W. H. Freeman and Co., San Francisco. 1960. p. 88.

Can. J. Chem. Downloaded from www.nrcresearchpress.com by 210.87.254.6 on 09/05/12
For personal use only.

Can. J. Chem. Downloaded from www.nrcresearchpress.com by 210.87.254.5 on 09/05/12
For personal use only.

THE STRUCTURE OF RETAMINE AND THE PARTIAL SYNTHESIS OF THE (−)-ENANTIOMORPH[1]

KJU HI SHIN,[2] L. FONZES,[2] AND LÉO MARION
Division of Pure Chemistry, National Research Council, Ottawa, Canada

Received March 3, 1965

ABSTRACT

Previous work by many authors has led to the assumption that retamine might be (+)-12-hydroxysparteine. A partial synthesis of the enantiomorph of this compound has been effected by dehydration of (+)-13-hydroxylupanine and hydroboration of the product. The dehydration product consisted of two components that were separated by thin-layer chromatography and identified by the characteristics of their nuclear magnetic resonance (n.m.r.) spectra as $\Delta^{12,13}$- and $\Delta^{13,14}$-dehydrolupanine. Hydroboration of the $\Delta^{12,13}$-isomer gave rise to (−)-12-hydroxysparteine having, in thin-layer chromatography, the same R_f value as natural retamine and the same optical rotation numerically, although of opposite sign. The synthetic base had the same infrared and n.m.r. spectra as the alkaloid and the two had superimposable Debye–Scherrer patterns. Evidence is given showing the hydroxyl to be equatorial.

The lupin alkaloid retamine, $C_{15}H_{26}ON_2$, m.p. 168°, $[\alpha]_D$ +46.2°, was first isolated by Battandier and Malosse (1). It was suggested by White (2) that it was probably a hydroxysparteine, and by Ribas, Sanchez, and Primo (3) that it was likely 6-hydroxysparteine (I). Later Ribas and Fraga (4) recognized that the properties of retamine could not be accommodated by a 6-hydroxy structure and, since the base could not be oxidized to a ketone, they suggested that it was either a 7- or a 9-hydroxy-(+)-sparteine. More recently, in the light of new evidence, Ribas and his co-workers (5) abandoned the 7- or 9-hydroxy structure in favor of 8-hydroxy-(+)-sparteine, notwithstanding the fact that retamine did not produce a ketone on oxidation. Finally, Bohlmann and his co-workers (6, 7) synthesized both epimers of each 7-hydroxy and 9-hydroxy-(+)-sparteine as well as the two epimers of 8-hydroxy-(+)-sparteine and established that none of these was identical with retamine.

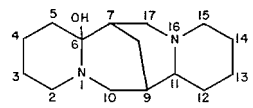

I

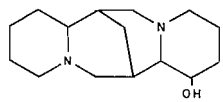

II

From the results of Ribas *et al.* (5) the hydroxyl in retamine can be present only in ring A or ring D. Since, however, anhydroretamine obtained by the dehydration of the base at high temperature gives rise on catalytic hydrogenation to a mixture of sparteine and α-isosparteine, it must be concluded that the hydroxyl is located in ring D. Furthermore, retamine is not a carbinolamine and, therefore, the hydroxyl cannot occupy positions 11 or 15. Also both epimers of 13-hydroxysparteine are known (8) and neither is identical with the alkaloid. Consequently, Bohlmann *et al.* (7) have suggested that retamine was either 12-hydroxysparteine II or 14-hydroxysparteine. It was assumed that the dehydration of 12-hydroxysparteine would give rise to $\Delta^{11,12}$-dehydrosparteine, and since this product on catalytic hydrogenation should form α-isosparteine exclusively (9, 10) whereas the dehydration product of retamine, depending on the temperature at which it was

[1]*Issued as N.R.C. No. 8459.*
[2]*National Research Council of Canada Postdoctorate Fellow.*

formed (5), produced on hydrogenation either sparteine or a mixture of sparteine and α-isosparteine, Bohlmann (8) considered 14-hydroxysparteine as the more likely structure for retamine.

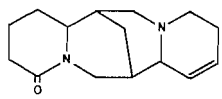

III

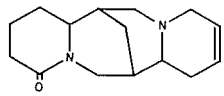

IV

From a consideration of the optical activity, the possibility that retamine could be a hydroxy-α-isosparteine can be discarded. The molecular rotation of retamine is +115 and, on the assumption that it is a hydroxysparteine, the calculated molecular rotation of its hydroxy epimer, isoretamine, should be −35° in agreement with the found value (5). Were retamine a hydroxy-α-isosparteine, the molecular rotation of its hydroxy epimer should be +145.

In an attempt to establish the structure of retamine we have sought to synthesize its (−)-enantiomorph from naturally occurring (+)-13-hydroxylupanine. The dehydration of this hydroxy base would be expected to give a mixture of $\Delta^{12,13}$-dehydrolupanine III and the $\Delta^{13,14}$-isomer. In fact when 13-hydroxylupanine was dehydrated by heating at 170° with phosphoric anhydride the product showed two main spots in thin-layer chromatography.

Hydroboration of the mixed dehydrolupanines produced a mixture, one of the components of which, after purification by chromatography and sublimation, corresponded to the (−)-enantiomorph of retamine. It melted at 166–167° and depressed the melting point of the alkaloid when the two were mixed, but its infrared and n.m.r. spectra were identical, respectively, with those of retamine. It can be concluded from this result that retamine must be either 12-hydroxy- or 14-hydroxysparteine. It had been ascertained in a preliminary experiment that diborane reduced the lactamic carbonyl and converted (+)-lupanine to (−)-sparteine. Brown and Heim (11) have since shown that amides generally are reduced by diborane.

In $\Delta^{12,13}$-dehydrolupanine III the system $\rangle CH \cdot CH{=}CH \cdot CH_2-$ is present while in $\Delta^{13,14}$-dehydrolupanine IV there is the sequence $-CH_2 \cdot CH{=}CH \cdot CH_2-$. The n.m.r. spectrum of the mixture of the two dehydrolupanines isolated from the product of the dehydration of 13-hydroxylupanine contains in the ethylenic region a symmetrical quartet centered at δ 5.07 which should be assigned to the protons of the symmetrically substituted ethylenic system of $\Delta^{13,14}$-dehydrolupanine, and an unsymmetrical signal at σ 5.64, 5.48 assignable to $\Delta^{12,13}$-dehydrolupanine. The mixture of dehydrolupanines was separated into its two components by preparative scale chromatography. The component with R_f 0.49 which, in the n.m.r., showed an unsymmetrical signal (δ 5.72, 5.53, 5.32), but no symmetrical quartet, was taken to be $\Delta^{12,13}$-dehydrolupanine III while the component with R_f 0.55 containing a symmetrical quartet in its n.m.r. spectrum was considered to be $\Delta^{13,14}$-dehydrolupanine IV.[3] Hydroxylation of $\Delta^{12,13}$-dehydrolupanine by treatment with diborane yielded a product showing in thin-layer chromatography three main spots (R_f 0.64, 0.47, and 0.33), of which the intermediate one corresponded to retamine, plus four other weak spots.

[3]*Such an assignment is not always reliable, particularly when dealing with a single compound. With a mixture of two compounds, however, representing both systems and giving the coupling patterns expected of each, the assignment becomes much more reliable, especially since after separation one component gives only the unsymmetrical pattern and the other component produces exclusively the symmetrical pattern.*

Can. J. Chem. Downloaded from www.nrcresearchpress.com by 210.87.254.5 on 09/05/12
For personal use only.

Can. J. Chem. Downloaded from www.nrcresearchpress.com by 210.87.254.5 on 09/05/12
For personal use only.

The components of the reaction mixture were separated by preparative scale thin-layer chromatography with developing solvent No. 3. The band corresponding to retamine was eluted and the product after distillation *in vacuo* crystallized spontaneously. The crystals, washed with acetone and dried, melted at 166–167°. In admixture with the synthetic retamine enantiomorph described above, the melting point was unaltered, but in admixture with naturally occurring (+)-retamine (m.p. 168°)[4] it melted at 146–147.5°. The synthetic base had $[\alpha]_D^{24}$ −47.3°, which is in good agreement numerically, but of opposite sign, with the optical rotation of authentic retamine. The infrared and n.m.r. spectra and the X-ray powder pattern of synthetic (−)-12-hydroxysparteine III were identical, respectively, with those of authentic retamine, and the mobilities of the two in thin-layer chromatography were the same. It can be concluded that retamine is (+)-12-hydroxysparteine.

The direction of elimination in the dehydration of retamine is temperature dependent. If the temperature of the reaction is kept below 170° the dehydro derivative formed gives rise to sparteine on hydrogenation. When the dehydration is carried out at 200° the product gives rise to α-isosparteine on hydrogenation so that in this case the double bond must be in the $\Delta^{11,12}$ position. It is most unlikely that a 14-hydroxysparteine could give rise to $\Delta^{11,12}$-dehydrosparteine and therefore on chemical grounds can be rejected.

Since an axial hydroxyl would be expected to give $\Delta^{11,12}$-dehydrosparteine readily on dehydration, the experimental results of Ribas (5) showing that this isomer is formed only under drastic conditions and is still accompanied by the $\Delta^{12,13}$-isomer militate in favor of an equatorial hydroxyl in retamine. Such a configuration of 12-hydroxy-(+)-sparteine would favor acid-catalyzed elimination of trans-diequatorial hydroxyl and hydrogen and formation of $\Delta^{12,13}$-dehydrosparteine, whereas an axial hydroxyl would not favor the formation of this compound.

Furthermore, hydroboration proceeds preferentially from the less hindered side of cyclic or bicyclic olefins (12). An examination of a Dreiding model shows that a C-12 equatorial hydroxyl is less hindered than an axial hydroxyl, so that in accordance with the foregoing generalization the former would be favored.

In the light of the established structure of retamine the peculiarities of the dehydration of the alkaloid are readily explained. Dehydration at the lower temperature gives rise to $\Delta^{12,13}$-dehydrosparteine, which on hydrogenation produces sparteine. On the other hand at ca. 200° the predominant product is $\Delta^{11,12}$-dehydrosparteine accompanied by some of the $\Delta^{12,13}$-isomer, because of the partial rearrangement of the latter. Catalytic hydrogenation of the mixture would give rise to both α-isosparteine and sparteine.

NOTE ADDED IN PROOF: After this manuscript had been accepted for publication a paper on the structure and synthesis of retamine (F. Bohlmann, H. Overwien, and D. Schumann, Chem. Ber. 98, 659, 1965) received in Ottawa April 23 appeared in print. The constitution assigned to retamine in that paper is the same as that we have assigned, although the configuration is different. The interpretation of our evidence led us to the conclusion that the hydroxyl in retamine is equatorial.

EXPERIMENTAL

The distillations were carried out in glass bulbs blown in a tube and the temperatures cited were those of the air bath surrounding the end bulb. The n.m.r. spectra were obtained on an A-60 Varian spectrometer, in deutero-chloroform solution with tetramethylsilane as an internal indicator. For thin-layer chromatography, silica gel G was used with one of the following developing solvents: cyclohexane–chloroform–diethylamine

[4]*Very kindly sent by Professor I. Ribas, whom we thank cordially.*

7:2:1 (solvent No. 1); methanol–diethylamine 9:1 (solvent No. 2); heptane–methylethylketone–diethylamine 7.5:2:0.5 (solvent No. 3). The spots were brought out by spraying with modified Dragendorf's reagent.

Dehydration of (+)-13-Hydroxylupanine

Finely powdered (+)-13-hydroxylupanine (3.0 g) mixed with phosphorus pentoxide (17.0 g) was heated during 6 h in a metal bath at 170–175°. After cooling, cracked ice was added gradually, the reaction mixture was made strongly basic with potassium hydroxide and extracted with methylene chloride. The extract was dried over sodium sulfate and the solvent evaporated *in vacuo*. There was left a slightly colored residual oil (2.3 g). A small sample showed in thin-layer chromatography two quite close spots corresponding to the anhydrolupanines (R_f 0.49, solvent No. 1), one spot corresponding to the starting material (R_f 0.12) and three other spots that were very faint.

The residual oil was dissolved in benzene and chromatographed on neutral grade I alumina (70 g). The column was eluted and the eluate collected in 100 ml fractions. The results of the elution are given in the following table. Combined fractions 1–11 gave 1.360 g of the mixture of anhydrolupanines. This mixture

Fractions	Eluant	Residue, mg	Product
1–5	Benzene	105	Anhydrolupanines
6	Benzene–chloroform 9:1	15	,,
7	Benzene–chloroform 8:2	50	,,
8	Benzene–chloroform 7:3	75	,,
9	Benzene–chloroform 5:5	300	,,
10	Benzene–chloroform 4:6	400	,,
11	Benzene–chloroform 3:7	415	,,
12	Benzene–chloroform 2:8	50	,, and starting product
13–15	Chloroform	110	Starting product
16–18	Methanol	440	Starting product

contained in its n.m.r. spectrum in the ethylenic region a symmetrical quartet centered at δ 5.07 attributable to the protons of the symmetrically substituted ethylenic system of $\Delta^{13,14}$-anhydrolupanine and an unsymmetrical signal at δ 5.64, 5.48 assignable to $\Delta^{12,13}$-anhydrolupanine.

Synthesis of Retamine

A solution of diborane was first prepared by the addition of freshly distilled boron fluoride ethyl ether (5 ml) to a solution of sodium borohydride (5.9 g) in tetrahydrofurane (100 ml) kept magnetically stirred and cooled in an ice bath. The addition was carried out in the course of 20 min in a stream of nitrogen. The reaction mixture was then kept at room temperature for 16 h.

To the mixture of anhydrolupanines (900 mg) obtained by dehydration of (+)-13-hydroxylupanine dissolved in tetrahydrofurane (50 ml) and cooled in ice while magnetically stirred, the above solution of diborane was added in the course of 10 min in a stream of nitrogen. After 30 min the ice bath was removed and the stirring continued under an atmosphere of nitrogen for $2\frac{1}{2}$ h at room temperature. The reaction mixture was again cooled in an ice bath, made alkaline by the gradual addition of 20% aqueous sodium hydroxide, followed by the dropwise addition of 30% hydrogen peroxide (5 ml). The mixture was heated on the steam bath for 15 min, cooled, and decanted. The aqueous layer was extracted with benzene, the benzene extract combined with the tetrahydrofurane layer, dried over sodium sulfate, and evaporated to dryness under reduced pressure. The residue consisted of a slightly colored oil (900 mg) which, in thin-layer chromatography, showed two main spots (R_f 0.64 and 0.47, solvent No. 3), the second of which (R_f 0.47) was identical with that of retamine. There is also a spot (R_f 0.33) corresponding to an important quantity of unchanged starting material, and four other much weaker spots (R_f 0.54, 0.24, 0.18, 0.12).

Separation of Retamine

The above product (900 mg) obtained from the hydroboration reaction was distributed onto 10 plates (20 × 20 cm) covered with silica gel G of 0.5 mm thickness and the chromatograms were developed with solvent No. 3. The spots were brought out on strips of the chromatograms with Dragendorf's reagent and the parts corresponding to the retamine spot were scraped off, and eluted with methanol containing 5% of diethylamine. The substance obtained from this elution (200 mg) was again chromatographed on two plates (20 × 20 cm) exactly as before. It yielded on elution a crystalline residue (100 mg) that was further purified by two sublimations at 115° under 10^{-3} mm, wt. 60 mg. The substance then melted at 166–167° and in admixture with authentic (+)-retamine[4] melted at 144–148°, $[\alpha]_D^{24}$ −47.3° (c = 0.97 in 95% EtOH). Its infrared and n.m.r. spectra and X-ray powder pattern were identical, respectively, with those of (+)-retamine.

Can. J. Chem. Downloaded from www.nrcresearchpress.com by 210.87.254.5 on 09/05/12
For personal use only.

Separation of $\Delta^{12,13}$- and $\Delta^{13,14}$-Anhydrolupanine

The mixture of $\Delta^{12,13}$- and $\Delta^{13,14}$-anhydrolupanine (300 mg) was applied on five plates (20 × 20 cm) covered with silica gel and the chromatograms developed with solvent No. 1. Two fractions were obtained: fraction A ($\Delta^{13,14}$-anhydrolupanine), R_f 0.55, had a higher mobility than fraction B ($\Delta^{12,13}$-anhydrolupanine, R_f 0.49). Both fractions were located after spraying a strip on each plate with modified Dragendorf's reagent. Fraction B was scraped off and eluted with methylene chloride containing about 5% of diethyl amine. The eluate, evaporated *in vacuo*, left a residual, slightly yellow oil containing fraction B still contaminated with a very small quantity of fraction A. The separation by preparative scale thin-layer chromatography was repeated. It yielded pure $\Delta^{12,13}$-anhydrolupanine (fraction B), which produced a single spot in thin-layer chromatography. The product was distilled at 140° under 0.01 mm, wt. 102 mg. Its n.m.r. spectrum contained signals at δ 5.72, 5.53, 5.32.

Fraction A was also scraped off the plates, eluted with methylene chloride containing 5% of diethylamine. It was purified again by preparative scale thin-layer chromatography. The product thus obtained ($\Delta^{13,14}$-anhydrolupanine) showed a single spot in thin-layer chromatography and its n.m.r. spectrum contained a symmetrical quartet centered at δ 5.07.

Conversion of $\Delta^{12,13}$-Anhydrolupanine to (−)-Retamine

To a solution of $\Delta^{12,13}$-anhydrolupanine (102 mg) in tetrahydrofurane cooled in an ice-water bath and stirred under a nitrogen atmosphere, a diborane solution prepared as above (6 ml) was added in the course of 10 min. The reaction was completed exactly as described above, and the product isolated by the same procedure. It was purified by preparative scale chromatography, followed by distillation at 130° under 0.01 mm it crystallized spontaneously, m.p. 155–164°. The undistilled residue was dissolved in methylene chloride, chromatographed on grade III alumina, and eluted with chloroform. Evaporation of the eluate left a residue which was crystallized from acetone, m.p. 164–167°. Both crystalline fractions (m.p. 155–164° and 164–167°) were combined and distilled at 135° under 0.01 mm. The distillate crystallized spontaneously and was washed with a little acetone, m.p. 166–167°. The melting point was not depressed by admixture with the synthetic sample described above, but in admixture with authentic retamine, m.p. 146–147.5°. The synthetic product had the same mobility in thin-layer chromatography as authentic retamine; its infrared and n.m.r. spectra and X-ray powder pattern were identical, respectively, with those of the alkaloid.

Action of Diborane on (−)-Lupanine

(−)-Lupanine (380 mg) was dissolved in tetrahydrofurane (30 ml) and treated with diborane exactly as described above. The product, worked up as described for retamine and distilled at 150° under 0.01 mm, was an oil that formed a crystalline perchlorate. After recrystallization from methanol, the salt melted at 173° either alone or in admixture with an authentic sample of (+)-sparteine perchlorate.

ACKNOWLEDGMENTS

We express our gratitude to Mr. R. Lauzon for measuring the infrared spectra and Mr. M. Lesage for the n.m.r. spectra. We acknowledge also our indebtedness to Dr. M. Przybylska, who produced the X-ray powder patterns, and to Professor I. Ribas, who gave us a generous sample of retamine.

REFERENCES

1. J. Battandier and T. Malosse. Compt. Rend. **125**, 360, 450 (1897).
2. E. P. White. New Zealand J. Sci. Technol. B, **27**, 474 (1946).
3. I. Ribas, A. Sanchez, and E. Primo. Anales Fis. y Quim. Madrid, Ser. B, **42**, 516 (1946).
4. I. Ribas and F. Fraga. Anales Fis. y Quim. Madrid, Ser. B, **45**, 1426 (1949).
5. F. Fraga, J. M. Gavilan, A. Duran, E. Seoane, and I. Ribas. Tetrahedron, **11**, 78 (1960).
6. F. Bohlmann, E. Winterfeldt, D. Schumann, and U. Zarnack. Angew. Chem. **73**, 771 (1961).
7. F. Bohlmann, E. Winterfeldt, U. Zarnack, and P. Wandrey. Chem. Ber. **95**, 2365 (1962).
8. F. Bohlmann, E. Winterfeldt, and H. Brackel. Chem. Ber. **91**, 2194 (1958).
9. K. Winterfeld and C. Rauch. Arch. Pharm. **272**, 273 (1934).
10. L. Marion and N. J. Leonard. Can. J. Chem. **29**, 355 (1951).
11. H. C. Brown and P. Heim. J. Am. Chem. Soc. **86**, 3566 (1964).
12. H. C. Brown. Hydroboration. W. A. Benjamin, Inc., New York. 1962. p. 126.

Can. J. Chem. Downloaded from www.nrcresearchpress.com by 210.87.254.5 on 09/05/12
For personal use only.

Can. J. Chem. Downloaded from www.nrcresearchpress.com by 210.87.254.42 on 09/05/12
For personal use only.

BIOSYNTHESIS OF BERBERINE AND BERBERASTINE

INCORPORATION OF CATECHOLAMINES[1]

IVO MONKOVIĆ AND IAN D. SPENSER

Department of Chemistry and Research Unit in Biochemistry, Biophysics and Molecular Biology, McMaster University, Hamilton, Ontario

Received February 15, 1965

ABSTRACT

Dopamine serves as a precursor of berberastine, berberine, hydrastine, and canadine in *Hydrastis canadensis* L. Noradrenaline serves as a precursor of berberastine but is not incorporated into the other three bases. It is shown that the incorporation of labelled dopamine into berberine and of labelled noradrenaline into berberastine takes place without randomization of radioactivity.

Two C_6—C_2 units, derived from tyrosine, are incorporated into the alkaloids which are biogenetically related to norlaudanosoline. The carbon skeleton of some of these bases (e.g., papaverine (3) and morphine (4)) is accounted for in its entirety by two such units. To complete the skeleton of other bases belonging to this group (e.g., hydrastine (5, 6), narcotine (7), berberine (6, 8), and chelidonine (9)) an additional one-carbon unit is required, which is derived from the S-methyl group of methionine (10).

We have presented evidence that the two C_6—C_2 units differ from one another. The first experimental indications came from our finding that even though tyrosine gave rise to both of the C_6—C_2 units which are incorporated into hydrastine the efficiency of incorporation of the two units was unequal (5), and from the results of Rapoport, Levy, and Stermitz on the nonrandom incorporation of carbon dioxide into morphine (11). We obtained direct evidence for the inequality of the two C_6—C_2 units in the biosynthesis of hydrastine with the demonstration that 3,4-dihydroxyphenylethylamine (dopamine) supplied only one of these units (12). Analogous results have now been reported by Leete and Murrill and by Battersby and Francis in studies of the biosynthesis of chelidonine (13) and of morphine (13, 14).

It appears that the conversion of tyrosine into dopa (15) and thence into two dissimilar intermediates, presumably dopamine and 3,4-dihydroxyphenylpyruvic acid, represents a common early stage of the routes leading to the different structural variants among the alkaloids related to norlaudanosoline (XII). In extension of the evidence for the generality of this biosynthetic pathway we now report that dopamine supplies only one of the two C_6—C_2 units which are incorporated into berberine.

Six small plants of *Hydrastis canadensis* L. were allowed to grow for 6 days with their roots immersed in aerated nutrient solution containing 1-^{14}C-dopamine hydrobromide (expt. 1). Berberine and hydrastine were extracted from roots and rhizomes by standard methods (6), and were found to be radioactive. Radiochemical yields in this experiment were of the same magnitude as those obtained in an earlier experiment with the same precursor (ref. 6, expt. 10), even though the duration of the feeding, the modes of administration of tracer, and the number and size of the plants and therefore also the chemical yield of alkaloids were different. In Table I the chemical and radiochemical yields obtained in these two experiments are compared.

[1]*Parts of this work have been reported in preliminary communications (1, 2).*

TABLE I

Chemical and radiochemical yields

	Expt. 10 (6)	Expt. 1
Tracer		
1-^{14}C-Dopamine hydrobromide		
Weight (mg)	13.0	16.1
Specific activity (counts min^{-1} $mmole^{-1} \times 10^{-9}$)	0.61±0.006	0.73±0.01
Total activity (counts $min^{-1} \times 10^{-7}$)	2.16±0.02*	5.04±0.07
Mode of administration	Wick	Root
Duration (days)	10	6
No. of plants	6	6
Products		
Roots and rhizomes		
Dry weight (g)	36	9
Berberine hydrochloride dihydrate		
Yield (mg)	825	280
Specific activity (counts min^{-1} $mmole^{-1} \times 10^{-4}$)	4.50±0.08	6.67±0.05
Specific radiochemical yield† $\times 10^4$	73.5	91.3
% incorporation‡	0.42	0.91
Hydrastine		
Yield (mg)	555	140
Specific activity (counts min^{-1} $mmole^{-1} \times 10^{-4}$)	0.87±0.02	0.48±0.01
Specific radiochemical yield† $\times 10^4$	14.2	6.57
% incorporation‡	0.058	0.0035

*Cf. ref. 6.

†Specific radiochemical yield $= \frac{\text{specific activity of product}}{\text{specific activity of precursor}} \times 100.$

‡% Incorporation $= \frac{\text{total activity of product}}{\text{total activity of precursor}} \times 100.$

Limits are standard deviation of the mean.

TABLE II

Degradation of berberine derived from 1-^{14}C-dopamine

Compound	Specific activity (counts min^{-1} $mmole^{-1}$ $\times 10^{-3}$)	Relative specific activity (%) (berberine = 100)
Berberine hydrochloride (IV)*	1.81±0.09	100±5
Benzyldihydroberberine	1.95±0.09	108±8
Des-*N*-methylstyryltetrahydroberberine	1.71±0.11	95±8
Hydrastinine (V)	1.72±0.07	95±6
6-Vinylpiperonylic acid (VI)	1.77±0.06	98±6
6-Bromo-α-hydroxyhomopiperonyl bromide (VII)	1.75±0.06	97±6
6-Bromopiperonylic acid (VIII)	0.01±0.06	0.3±3.3

*Diluted with carrier.

The labelled berberine from expt. 1 was diluted with carrier, crystallized to constant activity, and degraded by the method previously reported (6) (Fig. 1). The specific activities of some of the intermediates of the degradation sequence are summarized in Table II. No loss of activity occurred in the eight-step conversion of berberine (IV) into 6-bromo-α-hydroxyhomopiperonyl bromide (VII). Oxidation of this compound, which removed a single carbon atom, led to 6-bromopiperonylic acid (VIII), which was essentially inactive. All activity of the original berberine was therefore confined to C-6 of the berberine nucleus, showing that dopamine is specifically incorporated into berberine and that only one dopamine unit enters the molecule. This result is in complete agreement with those on the incorporation of dopamine into hydrastine, chelidonine, and morphine.

Can. J. Chem. Downloaded from www.nrcresearchpress.com by 210.87.254.42 on 09/05/12
For personal use only.

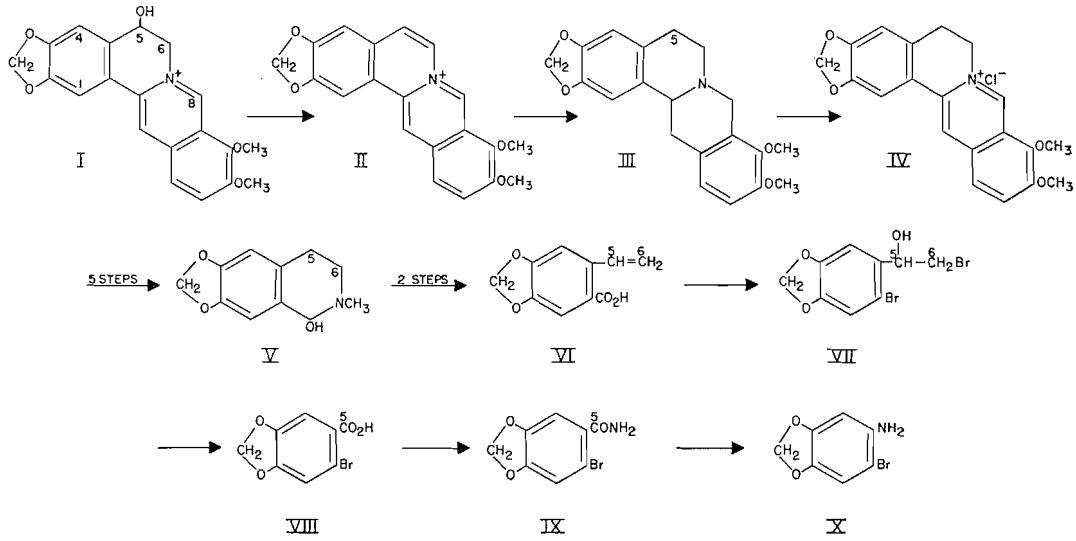

FIG. 1. Steps in the degradation of berberastine and berberine.

An outstanding experimental gap in the present understanding of the biosynthesis of the alkaloids of *H. canadensis* concerns the metabolic interrelationship of berberine (IV), hydrastine (XI), and canadine (III), which until recently were the only alkaloids known to occur in this plant. It had long been postulated that berberine is derived by partial aromatization of canadine (16), which in turn is formed from the benzylisoquinoline system of norlaudanosoline (XII) by intervention of a one-carbon unit (16). Recent evidence is consistent with this hypothesis (10, 15, 17). The third alkaloid, hydrastine, may arise from berberine (18, 19), or else directly from norlaudanosoline (XII) by a route which excludes canadine and berberine (16, cf. ref. 10). The specific incorporation of norlaudanosoline into narcotine (7) lends substance to these possibilities. Alternatively, hydrastine may originate from dopamine (6, 12) and a second tyrosine-derived C_6—C_2 unit (5, 6) by a pathway which excludes norlaudanosoline. The observation that labelled reticuline, an *O,O,N*-trimethylnorlaudanosoline, was not incorporated into hydrastine in an experiment with *H. canadensis* which yielded specifically labelled berberine (15) would appear to leave this possibility open.

One of the structural features of hydrastine, absent in berberine, is the benzylic oxygen function at C-7′. A rational biogenetic scheme for the introduction of this oxygen function in the course of the elaboration of berberine into hydrastine has been put forward (19). It was conceivable, however, that this benzylic hydroxyl group is introduced into a C_6—C_2 unit prior to formation of the benzylisoquinoline skeleton.

To test this possibility, noradrenaline (XIII), a C_6—C_2 compound which is derivable

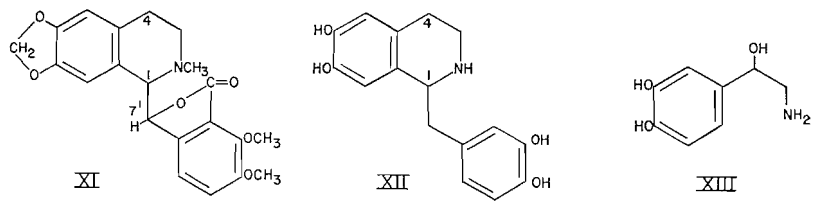

Can. J. Chem. Downloaded from www.nrcresearchpress.com by 210.87.254.42 on 09/05/12
For personal use only.

Can. J. Chem. Downloaded from www.nrcresearchpress.com by 210.87.254.42 on 09/05/12
For personal use only.

from tyrosine (20) and contains the required structural features, was administered to *H. canadensis* by infusion into the stem in an exploratory experiment (expt. 2). Extraction of roots and rhizomes by standard methods gave crude hydrastine (339 mg) and berberine hydrochloride (564 mg), both of which, surprisingly, appeared to be highly radioactive. Recrystallization of berberine hydrochloride from water left the specific activity of the compound virtually unchanged. Paper chromatography of this sample with ethanol as the solvent appeared to give a single spot (R_f 0.18). When a portion of the berberine sample was subjected to the usual degradation procedure, however, inconsistent results were obtained. Conversion of 500 mg of the berberine, through four stages, into des-*N*-methylstyryltetrahydroberberine, led to a loss of more than half of the specific activity even though not a single carbon atom of the original alkaloid had been removed at this stage. It became clear that a re-examination of the radio-purity of the original berberine was indicated.

The remaining quantity of the berberine sample was repeatedly chromatographed on an alumina column, and a virtually inactive sample of berberine was eventually obtained. All activity was contained in a yellow fraction weighing no more than 300 μg, which closely followed, but was discrete from, the berberine fraction. The crude hydrastine lost most of its activity after repeated crystallization from ethanol.

Even though the experiment had failed in its original purpose, the use of noradrenaline as a tracer had serendipitously led to the detection of hitherto unrecognized alkaloid constituents of *H. canadensis* by a novel type of activation analysis.

At this time we became aware of the elegant work of Nijland (21) on the isolation and structure[2] of a new alkaloid, berberastine (I), from *Hydrastis* extract. We suspected that our berberine contaminant might be identical with berberastine, since the R_f value of our compound in Nijland's solvent system matched that of berberastine.[3] The berberine contaminant was isolated on a larger scale from a commercial *Hydrastis* extract by an improved method. The entire protoberberine components of the extract were precipitated in the form of their acetone adducts and the dried mixture, which also contained co-precipitated hydrastine and small quantities of other tertiary bases, was chromatographed on an alumina column, using chloroform and chloroform–methanol mixtures of increasing polarity as eluents. Chloroform eluted the acetone adduct of berberine as well as the tertiary bases. Some free berberine appeared in the effluent with chloroform containing up to 4% methanol. Chloroform of higher methanol content brought out the yellow material which was recognized as the berberine contaminant. The berberine contaminant was rechromatographed in the same manner and converted into the sparingly soluble iodide, whose infrared spectrum was identical with Nijland's published spectrum of berberastine iodide.

In this manner 120 mg berberastine iodide was isolated from 1 lb of extract.

Amongst the tertiary bases obtained from the commercial *Hydrastis* extract in trace quantity was a compound which was identical in paper-chromatographic behavior with the reduction product (21) of berberastine. This compound is presumably one of the stereoisomers of 5-hydroxycanadine. Three other unknown components of the system

[2]*Of the two possible structures for berberastine deduced by Nijland, 5-hydroxyberberine (I) was favored over the alternative 6-hydroxyberberine (21). In fact her evidence eliminates the latter. Reduction of 5-hydroxyberberine would yield 5-hydroxycanadine. The hydroxy group of 6-hydroxyberberine, a carbinolamine derivative, would not be expected to survive reduction. Reduction of berberastine with zinc/platinum (21), and also with borohydride, gave a product which retained the hydroxy group. The structure of berberastine as 5-hydroxyberberine is thus established by Nijland's work.*

[3]*We are indebted to Dr. M. M. Nijland for sending us a paper chromatogram of berberastine. In her letter she predicted independently that noradrenaline might serve as a precursor of berberastine.*

Can. J. Chem. Downloaded from www.nrcresearchpress.com by 210.87.254.42 on 09/05/12
For personal use only.

were detected chromatographically in quantities too small for isolation and characterization. These fractions are under investigation.

Having gained some qualitative insight into the nature of the labelled products derived from the feeding experiment with radioactive noradrenaline, it became desirable to ascertain whether noradrenaline served as a specific precursor of berberastine, and to gather quantitative data on its incorporation into the other alkaloids. Since our earlier samples of berberine had presumably contained minute amounts of radio-berberastine as impurity, it was of importance also to obtain information on the relative efficiencies of incorporation into the alkaloids of at least one of the labelled precursors, tyrosine or dopamine, whose specific incorporation into these contaminated samples of berberine had been established by chemical degradation (6, 8).

In separate feeding experiments 1-^{14}C-dopamine (expt. 3) and DL-2-^{14}C-noradrenaline (expt. 4) were administered to *Hydrastis* plants by infusion into the stem over a period of 6 days. The alkaloids were extracted, and berberine, hydrastine, canadine, and berberastine were isolated by column chromatography on alumina, as described in the experimental section. Each alkaloid sample was purified by column chromatography and crystallized to constant activity. Chemical and radiochemical yields obtained in these experiments are summarized in Table III. Every one of the four alkaloids derived from the dopamine experiment was labelled. The noradrenaline experiment gave radioactive berberastine of high specific activity. Berberine, canadine, and hydrastine obtained from this experiment contained little radioactivity.

The incorporation figures in Table III make it abundantly clear why consistent results had been obtained in the degradation experiments with dopamine-derived berberine which was contaminated with berberastine (expt. 1), whereas contamination became immediately apparent on degradation of the contaminated noradrenaline-derived berberine (expt. 2). In the latter instance a contaminant of less than 1% by weight contained 97% of the total activity. In the former case a contaminant of less than 1% by weight contained less than 1% of the total activity.

Even though it is now recognized that the samples of berberine obtained from feeding experiments with tyrosine, dopamine, methionine, and formate, which were used in earlier degradation experiments (6, 8, 10), probably contained berberastine as a contaminant, it is not likely that the earlier results are invalidated. The tracers used in all these experiments almost certainly serve as precursors not only of berberine but also of berberastine, as is now shown to be the case for dopamine. It is probable that the relationship with respect to yield and activity between berberine and the contaminating berberastine in these earlier experiments was similar to the relationship between berberine and berberastine found in expt. 3. In the degradation experiments on these earlier berberine samples the limits of standard deviation in the radioactivity assays were higher than 1%. Within these limits all activity of the degraded samples was accounted for. Clearly, the error due to contamination was also within these limits, and does not therefore affect the results or the conclusions based on them.

Since recrystallization removed the contaminating activity from the hydrastine sample obtained in the exploratory noradrenaline experiment, the earlier results with hydrastine (5, 6, 10, 12) stand.

The noradrenaline-derived berberastine (expt. 4) was diluted with carrier and degraded. Acid-catalyzed dehydration gave 5,6-dehydroberberine (II) (21, 22) which was not isolated but was directly reduced to canadine by means of sodium borohydride (cf. refs. 21, 22). The (±)-canadine (III) so obtained was further diluted with carrier and oxidized to

TABLE III

Chemical and radiochemical yields

	Expt. 3	Expt. 4
Tracer	1-^{14}C-Dopamine hydrobromide	DL-2-^{14}C-Noradrenaline bitartrate
Weight (mg)	3.90	3.94
Specific activity (counts min^{-1} $mmole^{-1} \times 10^{-9}$)	2.18±0.03	4.43±0.06
Total activity (counts $min^{-1} \times 10^{-7}$)	3.65±0.05	4.88±0.07
Mode of administration	Wick	Wick
Duration	6	6
No. of plants	6	6
Products		
Roots and rhizomes		
Dry weight (g)	30	22
Berberastine iodide		
Yield (mg)	3	6
Specific activity (counts min^{-1} $mmole^{-1} \times 10^{-4}$)	14.2±0.34	396±6.7
Specific radiochemical yield $\times 10^4$	65.2	894
% incorporation	0.0024	0.10
Canadine		
Yield (mg)	21	24
Specific activity (counts min^{-1} $mmole^{-1} \times 10^{-4}$)	12.4±0.14	0.22±0.003
Specific radiochemical yield $\times 10^4$	56.7	0.49
% incorporation	0.021	0.00032
Berberine hydrochloride dihydrate		
Yield (mg)	945	895
Specific activity (counts min^{-1} $mmole^{-1} \times 10^{-4}$)	4.62±0.03	0.073±0.005
Specific radiochemical yield $\times 10^4$	21.2	0.16
% incorporation	0.29	0.0033
Hydrastine		
Yield (mg)	594	600
Specific activity (counts min^{-1} $mmole^{-1} \times 10^{-4}$)	0.31±0.02	0.028±0.002
Specific radiochemical yield $\times 10^4$	1.42	0.062
% incorporation	0.013	0.00088

TABLE IV

Degradation of berberastine derived from 2-^{14}C-noradrenaline

Compound	Specific activity (counts min^{-1} $mmole^{-1}$ $\times 10^{-4}$)	Relative specific activity (%) (berberastine = 100)
Berberastine (I)*	57.74±1.22	100±2
(±)-Canadine (III)	57.69±0.64	100±2
(±)-Canadine (III) (diluted)†	1.52±0.021	100±1
Berberine hydrochloride (IV)	1.54±0.027	101±2
Benzyltetrahydroberberine	1.54±0.022	101±2
Des-*N*-methylstyryltetrahydroberberine	1.49±0.018	98±2
Hydrastinine (V)	1.47±0.020	97±2
6-Vinylpiperonylic acid (VI)	1.50±0.028	99±2
6-Bromo-α-hydroxyhomopiperonyl bromide (VII)	1.50±0.029	99±2
6-Bromopiperonylic acid (VIII)	1.49±0.021	98±2
2-Bromo-4,5-methylenedioxyaniline (X)	0.003±0.001	0.3±0.2

*Diluted with carrier.

†The (±)-canadine (26 mg), specific activity 57.69 (±0.64) × 10^4 counts min^{-1} $mmole^{-1}$, obtained by sodium borohydride reduction of the radio-berberastine, was diluted with inactive (±)-canadine (960 mg), to yield, after recrystallization, (±)-canadine (964 mg, 98%) specific activity 1.52 (±0.021) × 10^4 counts min^{-1} $mmole^{-1}$. The relative specific activity of further intermediates of the degradation sequence, given in the table, relates to this diluted (±)-canadine.

Can. J. Chem. Downloaded from www.nrcresearchpress.com by 210.87.254.42 on 09/05/12
For personal use only.

Can. J. Chem. Downloaded from www.nrcresearchpress.com by 210.87.254.42 on 09/05/12
For personal use only.

berberine (IV) (23). This berberine was dissected in 10 steps, by the method previously reported (6), to yield 6-bromopiperonylic acid (VIII) of a specific activity identical with that of the original alkaloid. In the final step of the degradation sequence the acid was converted to the corresponding amide (IX) which, in a Hofmann rearrangement, yielded inactive 2-bromo-4,5-methylenedioxyaniline (X). The specific activities of the intermediates of the degradation sequence are tabulated in Table IV. It is evident that all activity of the original berberastine was located at C-5, indicating that noradrenaline is incorporated without randomization of activity, and that only one noradrenaline unit enters the berberastine molecule.

Because of the low yield, systematic degradation of the dopamine-derived berberastine was not feasible.

A number of conclusions regarding the interrelationship of the alkaloids can be drawn on the basis of the present experiments.

Since the specific activity of berberastine obtained in the dopamine experiment was found to be substantially higher than that of the berberine isolated from the same experiment, and since the noradrenaline experiment yielded highly active berberastine and virtually inactive berberine and canadine, neither berberine nor canadine can be precursors of berberastine.

Also excluded as a stage between noradrenaline and berberastine is norlaudanosoline (XII), whose *N*- and *O,O,N*-methyl derivatives, laudanosoline (17) and reticuline (15), have been shown to serve as specific precursors of berberine. The present evidence suggests that the benzylic hydroxyl group is generated at an early stage of biosynthesis, prior to formation of the benzylisoquinoline system. If noradrenaline is an obligatory stage of the pathway to berberastine, intermediacy of a 4-hydroxynorlaudanosoline must be postulated, which is directly derived from noradrenaline and a second C_6—C_2 unit, presumably 3,4-dihydroxyphenylpyruvic acid.

It remains to demonstrate unequivocally that the bases, whose presence in *H. canadensis* in trace amounts has now been detected for the first time by virtue of the selective incorporation of labelled noradrenaline into their skeleton, are indeed the hydroxyanalogs of hydrastine and canadine, and to show that berberastine is the first representative of a larger group of compounds, which are related to 4-hydroxynorlaudanosoline.

It will be of even greater significance to apply 'noradrenaline activation analysis' to other plants which contain alkaloids related to norlaudanosoline, e.g., the opium poppy, in order to establish whether hitherto undiscovered bases of the 4-hydroxynorlaudanosoline series, e.g., 15-hydroxymorphine, accompany the known alkaloid components. This work is in progress.

EXPERIMENTAL

Isolation of Berberastine from Commercial Plant Extract

The extract (Soft solid extract, Goldenseal root, Pennick Canada Ltd., 9–11% alkaloid content) (100 g) was dissolved in warm aqueous acetone (33%, 600 ml) and the solution was made basic by addition of 10% sodium hydroxide (100 ml). After 12 h a crystalline precipitate was obtained which consisted[4] mainly of 8-acetonylanhydrodihydroberberine (berberineacetone) and contained all the berberastine present in the original extract, either as the acetone adduct or as a co-precipitate, together with hydrastine and small amounts of other weak bases. The precipitate was washed with water and dried in air to yield crude material (20 g) which melted over a wide range (148–156°).

The dried precipitate from several duplicate experiments (80 g) was dissolved in chloroform[5] and applied to a column (3.2 cm diameter × 38 cm length) of alumina[6] (300 g) in chloroform. The column was eluted in

[4]*At every stage of the separation, product analysis was carried out by ascending paper chromatography, using Nijland's solvent, 2% aqueous potassium dihydrogen phosphate solution (21). Unless otherwise stated, R_f values in the present paper refer to this solvent.*

[5]*Commercial chloroform, containing ethanol (0.75%), was used in all experiments.*

[6]*Unless otherwise stated neutral alumina, grade I, was used in all experiments.*

succession with chloroform (1 000 ml), chloroform containing 4% methanol (1 500 ml), chloroform containing 5.5% methanol (1 500 ml), and finally with a mixture of chloroform and methanol (2:3) (500 ml). The rate of elution for the first two solvents was approximately 50 ml per hour. The elution rate with the final two solvents was increased to 150 ml per hour.

The chloroform fraction contained berberineacetone, hydrastine, and minor quantities of other tertiary bases. Free berberine was eluted with chloroform / 4% methanol, and most of the berberastine appeared in the eluent from chloroform / 5.5% methanol. The last traces of berberastine were removed from the column by the chloroform/methanol (2:3) mixture. Small quantities of phenolic bases closely preceded or followed but did not overlap with the berberastine band. The conditions which are responsible for the variation of the elution pattern of the phenolic materials have not yet been investigated.

To achieve further purification, the berberastine fraction was rechromatographed on a second alumina column (1 × 13 cm, 13 g), using the same sequence of solvents.

The berberastine so obtained was dissolved in a minimum quantity of hot methanol, and 5% aqueous ammonium iodide (20 ml) was then added. Berberastine iodide (120 mg) separated and was recrystallized from hot water containing a small amount of charcoal. The iodide does not melt, but darkens from 220°. (Found: C, 50.4; H, 4.0; I, 26.3; N, 2.7. Calcd. for $C_{20}H_{18}INO_5$: C, 50.1; H, 3.8; I, 26.5; N, 2.9%.)

The infrared spectrum of the product was identical with that reported by Nijland (21). On paper chromatography with 2% aqueous potassium dihydrogen phosphate as the solvent the material gave a single, yellow, fluorescent, elongated spot, R_f 0.20.

Isolation of the Alkaloids from Roots and Rhizomes

Hydrastine and Canadine

Dried and finely powdered roots and rhizomes (22 g) of *H. canadensis* were extracted with ether and then with ethanol, as described earlier (6).

The ether extract was evaporated and the residue dissolved in ethanol. Hydrastine, R_f 0.72, crystallized, and after two recrystallizations from ethanol, melted at 131–132°. Yield 600 mg. The combined ethanolic mother liquids were evaporated to dryness, the residue (200 mg) was dissolved in benzene (15 ml) and the solution was applied to a column (1.8 × 20 cm) prepared from 60 g alumina of 12% water content, slurried in benzene. The column was eluted in succession with benzene (100 ml), benzene containing 10% chloroform (60 ml), benzene/chloroform 1:1 (60 ml), chloroform (60 ml), chloroform containing 1% methanol (60 ml), and finally with chloroform containing 2% methanol (60 ml). (−)-Canadine (20–25 mg), R_f 0.26, melting at 132–133°, emerged with the benzene. The benzene/chloroform solutions eluted a mixture of canadine and hydrastine, contaminated by small amounts of other bases, including traces of two substances, R_f 0.30 to 0.45, which may have been isomers of hydroxycanadine, since this R_f value is identical with that of one of the reduction products of berberastine (21). Hydrastine (90–105 mg) emerged with the chloroform. The chloroform–methanol mixtures removed traces of berberine and berberastine from the column.

Berberine and Berberastine

The alcohol extract of the root material was evaporated to dryness, the residue was dissolved in 33% aqueous acetone (30 ml), and the solution was filtered through glass wool and basified with 10% aqueous sodium hydroxide (5 ml). The precipitate (805 mg), melting range 150–158°, which had separated after 12 h, was dried in air, dissolved in chloroform, and chromatographed on a column (1 × 13 cm) containing alumina (13.5 g), slurried in chloroform. Elution with chloroform (30 ml) at a rate of 10 ml per hour removed berberineacetone (650 mg). Chloroform containing 4% methanol (30 ml) then eluted most of the berberine (180 mg). By increasing the polarity of the solvent (chloroform containing 6% methanol, 30 ml) as well as the elution rate berberastine was removed. It was purified by chromatography on a second alumina column, (3 g, 0.7 × 6 cm) using the same solvent sequence, and was converted into berberastine iodide (4–6 mg) (*vide supra*).

The berberine fractions were combined and crystallized from aqueous hydrochloric acid, yielding berberine hydrochloride (960 mg).

This method for the isolation of the four alkaloids was used in the work-up of tracer experiments 3 and 4.

Conversion of Berberastine Iodide into Tetrahydroberberine ((±)-Canadine) (cf. Ref. 21)

Berberastine iodide (6 mg) was refluxed for 12 min in 2 *N* hydrochloric acid (6 ml). The solution was cooled and neutralized with 0.880 ammonia. The mixture was warmed, and methanol (7 ml) was added to redissolve the dehydroberberine which separated. Sodium borohydride (20 mg) was added in one portion to the warm solution. A vigorous reaction ensued and the solution became colorless, indicating that reduction was complete. To decompose the reduction complex the reaction mixture was acidified with 5 *N* hydrochloric acid, and was then made basic with 5 *N* ammonia. The product was extracted into ether (4 × 15 ml) and the combined ether extracts were evaporated. The residue was dissolved in *N* hydrochloric acid (1 ml), the solution was filtered and the product (3.6 mg, 81%) was precipitated by addition of 0.880 ammonia. Two crystallizations from aqueous acetone gave (±)-canadine melting at 170–172°. Reported melting point 167° (24), 174° (25).

Conversion of Berberine Hydrochloride into Tetrahydroberberine ((±)-Canadine) (cf. Refs. 26, 27)

Berberine hydrochloride (200 mg) was dissolved in methanol containing 20% water (5 ml). The solution

Can. J. Chem. Downloaded from www.nrcresearchpress.com by 210.87.254.42 on 09/05/12
For personal use only.

was warmed to 50° and sodium borohydride (100 mg) was added in one portion, with stirring. After the vigorous reaction had ceased the mixture was refluxed for 5 min, cooled, acidified with 5 *N* hydrochloric acid, and warmed to redissolve the precipitate which had separated. Addition of 5 *N* ammonia gave (±)-canadine (145 mg, 88%), which after two recrystallizations from aqueous acetone melted at 170–172°. The sodium borohydride reduction of berberine has been reported (27) to yield dihydroberberine. In fact both berberine and dihydroberberine yield (±)-canadine on sodium borohydride reduction (26).

Conversion of (±)-Canadine into Berberine Hydrochloride (cf. Ref. 23)

(±)-Canadine (960 mg) was dissolved in glacial acetic acid (9 ml). Mercuric acetate (3.82 g) was dissolved in water (40 ml) to which a few drops of acetic acid had been added. The solutions were combined and the mixture was kept 3 days at room temperature. The precipitate of mercurous acetate was filtered off, the filtrate was refluxed for 30 min, cooled, and a second crop of mercurous acetate was removed. Hydrogen sulfide was passed through the filtrate, the sulfide precipitate was filtered off, and the solution was acidified with concentrated hydrochloric acid (5 ml). On cooling berberine hydrochloride (1.12 g, 97%) was obtained.

Conversion of 6-Bromopiperonylic Acid (VIII) into 6-Bromopiperonylamide (IX)

6-Bromopiperonylic acid (6) (49 mg) and thionyl chloride (0.5 ml) were heated under reflux until the acid had dissolved. Excess thionyl chloride was removed under reduced pressure and the residue was dissolved in anhydrous ether (3 ml). Anhydrous ammonia was bubbled through the ether solution for several minutes and the solvent was then evaporated. Ammonia (5 *N*, 0.5 ml) was added to the solid residue to dissolve ammonium chloride and any unchanged acid. *6-Bromopiperonylamide* (45 mg, 92%) was obtained, which after recrystallization from water melted at 170–171°. Reported melting point 163–164.5° (28). (Found: C, 39.6; H, 2.5; N, 5.6. $C_8H_6BrNO_3$ requires C, 39.4, H, 2.5, N, 5.7%.)

Conversion of 6-Bromopiperonylamide (IX) into 2-Bromo-4,5-methylenedioxyaniline (X)

Bromine (0.12 ml) was added to an ice-cold solution of sodium hydroxide (0.5 g) in water (4 ml) and the mixture was cooled and shaken until the bromine had dissolved. A portion (0.4 ml) of this hypobromite solution was added to 6-bromopiperonylamide (49 mg) and the reaction mixture was swirled in an ice bath until the amide had dissolved (15 min). The solution was heated for 30 min and was evaporated to dryness under reduced pressure. Distillation of the residue at 80° and 3×10^{-2} mm yielded *2-bromo-4,5-methylenedioxyaniline* (25 mg, 58%), melting at 83–84°. Reported melting point 80° (29). (Found: C, 39.2; H, 3.0; N, 6.3. $C_7H_6BrNO_2$ requires: C, 38.9; H, 2.8; N, 6.5%.)

A portion of the base was converted to the *picrate*, melting at 160–161°. (Found: C, 35.3; H, 2.3; N, 12.4. $C_{13}H_9BrN_4O_9$ requires C, 35.1; H, 2.0; N, 12.6%.)

Administration of ^{14}C-Labelled Compounds to Hydrastis Canadensis L. and Extraction of Labelled Alkaloids

1-^{14}C-Dopamine hydrobromide (expts. 1 and 3) and DL-2-^{14}C-noradrenaline (expts. 2 and 4) were administered to mature plants of *H. canadensis* L. either hydroponically (expt. 1) or by infusion into the stem (expts. 2, 3, and 4) by reported methods (6). Alkaloids were extracted from roots and rhizomes. In expt. 1, hydrastine and berberine were isolated by conventional methods (6). Experiment 2 demonstrated the limitations of these methods. Isolation of berberine, hydrastine, canadine, and berberastine from expts. 3 and 4 was carried out by the method described in an earlier section of this paper. Chemical and radiochemical yields from expts. 1, 3, and 4 are shown in Tables I and III.

Degradation of Radioactive Alkaloids

Labelled berberine derived from plants fed with 1-^{14}C-dopamine (expt. 1) and labelled berberastine from plants exposed to 2-^{14}C-noradrenaline (expt. 4) were degraded. The method for the degradation of berberine into 6-bromopiperonylic acid has been fully reported (6). Degradation of berberastine involved conversion of the compound into canadine and then into berberine, by the methods described above. The berberine so obtained was degraded to 6-bromopiperonylic acid as before. The final steps, conversion to the corresponding amide and Hofmann rearrangement to the aniline derivative, were carried out by the method used in the pilot experiments with inactive material. A minimum of 800 mg berberine hydrochloride was required to carry a degradation sequence to completion. To obtain sufficient material the active alkaloid samples were diluted with carrier. The specific activity of the intermediates in the two degradation sequences are tabulated in Tables II and IV. Limits shown are standard deviation of the mean.

The degradation products were crystallized to constant activity. Their radioactivity was assayed on samples of finite thickness on aluminium planchettes, using a Nuclear Chicago Corp. gas flow counter (Model 1052) in a low-background sample changer (C115). Counts were recorded on a printing timer (C111B) in association with a scaler (181B).

The usual corrections for background and self-absorption were applied. For plating a 1% solution of collodion in dimethylformamide was used as the solvent.

ACKNOWLEDGMENTS

We are grateful to Mr. R. E. Halward, Propagator of the Royal Botanical Gardens, Hamilton, for maintaining a colony of *H. canadensis* L. for our work.

Can. J. Chem. Downloaded from www.nrcresearchpress.com by 210.87.254.42 on 09/05/12
For personal use only.

This investigation was supported by Research Grant GM-10034 from the National Institute of General Medical Sciences, United States Public Health Service, and by a grant from the National Research Council of Canada.

REFERENCES

1. I. MONKOVIČ and I. D. SPENSER. Proc. Chem. Soc. 223 (1964).
2. I. MONKOVIČ and I. D. SPENSER. J. Am. Chem. Soc. **87**, 1137 (1965).
3. A. R. BATTERSBY and B. J. T. HARPER. Proc. Chem. Soc. 152 (1959); J. Chem. Soc. 3526 (1962).
4. A. R. BATTERSBY and B. J. T. HARPER. Chem. Ind. London, 364 (1958). E. LEETE. Chem. Ind. London, 977 (1958); J. Am. Chem. Soc. **81**, 3948 (1959). A. R. BATTERSBY, R. BINKS, and D. J. LECOUNT. Proc. Chem. Soc. 287 (1960). A. R. BATTERSBY, R. BINKS, and B. J. T. HARPER. J. Chem. Soc. 3534 (1962).
5. J. R. GEAR and I. D. SPENSER. Nature, **191**, 1393 (1961).
6. J. R. GEAR and I. D. SPENSER. Can. J. Chem. **41**, 783 (1963).
7. A. R. BATTERSBY and D. J. MCCALDIN. Proc. Chem. Soc. 365 (1962).
8. I. D. SPENSER and J. R. GEAR. Proc. Chem. Soc. 228 (1962).
9. E. LEETE. J. Am. Chem. Soc. **85**, 473 (1963).
10. R. N. GUPTA and I. D. SPENSER. Biochem. Biophys. Res. Commun. **13**, 115 (1963); Can. J. Chem. **43**, 133 (1965).
11. H. RAPOPORT, N. LEVY, and F. R. STERMITZ. J. Am. Chem. Soc. **83**, 4298 (1961).
12. I. D. SPENSER and J. R. GEAR. J. Am. Chem. Soc. **84**, 1059 (1962).
13. E. LEETE and J. B. MURRILL. Tetrahedron Letters, 147 (1964).
14. A. R. BATTERSBY and R. J. FRANCIS. J. Chem. Soc. 4078 (1964).
15. D. H. R. BARTON, R. H. HESSE, and G. W. KIRBY. Proc. Chem. Soc. 267 (1963).
16. R. ROBINSON. J. Chem. Soc. **111**, 876 (1917).
17. A. R. BATTERSBY, R. J. FRANCIS, M. HIRST, and J. STAUNTON. Proc. Chem. Soc. 268 (1963).
18. W. H. PERKIN, JR. and R. ROBINSON. J. Chem. Soc. **97**, 305 (1910).
19. E. LEETE. *In* Elucidation of structures by physical and chemical methods. *Edited by* K. W. Bentley. Interscience Publishers, New York. 1963. p. 440; *in* Biogenesis of natural compounds. *Edited by* P. Bernfeld. Pergamon Press, New York. 1963. p. 766.
20. S. UDENFRIEND and J. B. WYNGAARDEN. Biochim. Biophys. Acta, **20**, 48 (1956). McC. GOODALL and N. KIRSHNER. J. Biol. Chem. **226**, 213 (1957).
21. M. M. NIJLAND. Pharm. Weekblad, **96**, 640 (1961); **98**, 301 (1963).
22. C. K. BRADSHER and N. L. DUTTA. J. Am. Chem. Soc. **82**, 1145 (1960).
23. J. GADAMER. Arch. Pharm. **253**, 274 (1915).
24. J. W. MCDAVID, W. H. PERKIN, JR., and R. ROBINSON. J. Chem. Soc. **101**, 1218 (1912).
25. W. H. PERKIN, JR. J. Chem. Soc. **113**, 722 (1918).
26. R. MIRZA. J. Chem. Soc. 4400 (1957).
27. S. BOSE. J. Indian Chem. Soc. **32**, 450 (1955).
28. Y. YAMAGUCHI. Nippon Kagaku Zasshi, **77**, 591 (1956).
29. G. K. HUGHES, N. K. MATHESON, A. T. NORMAN, and E. RITCHIE. Australian J. Sci. Research, Ser. A, **5**, 206 (1952).

Can. J. Chem. Downloaded from www.nrcresearchpress.com by 210.87.254.42 on 09/05/12
For personal use only.

Can. J. Chem. Downloaded from www.nrcresearchpress.com by 210.87.254.42 on 09/05/12
For personal use only.

SYNTHESIS IN AQUEOUS SOLUTIONS OF BINARY COMPOUNDS OF THE TRANSITION METALS WITH GROUP VA AND VIA ELEMENTS

G. E. Cranton and R. D. Heyding
Department of Chemistry, Queen's University, Kingston, Ontario
Received February 19, 1965

ABSTRACT

Some of the compounds in the systems Cu/Se, Cu/As, Cu/Sb, Ni/Se, Ni/As, Ni/Sb, and Ni/Bi have been synthesized by precipitation from aqueous solutions, following procedures similar to those described by Kulifay. The precipitates were finely divided and of relatively low purity. No new compounds were observed. None of the compounds in the Fe/As and Co/As systems were obtained, nor were any intermediate phases formed in the systems Fe/Bi, Co/Bi, and Cu/Bi.

INTRODUCTION

Transition metal pnictides and chalicides[1] are usually prepared by direct combination of the elements at temperatures above 500 °C. This method presupposes that the rate of transition in the solid to low temperature polymorphs or compounds will be appreciable in the temperature range in which these phases are stable. In the event that a transformation is slow, the stable low temperature phase may not be observed. Such polymorphs and compounds might be obtained by syntheses requiring lower temperatures.

Aqueous methods involving temperatures below 100 °C have been known for some time. These fall into four classifications: (i) reaction of a gaseous hydride (H_3Z or H_2Y) with a metal ion in solution (1–3); (ii) heterogeneous reaction of an element with ions in solution (4–14); (iii) chemical reduction of ions or complex ions of both components in solution (15–19); and (iv) electrochemical methods (20). Of the third group, the methods described by Kulifay appear to be the most promising, inasmuch as a large number of binary pnictides, chalicides, and intermetallic compounds have been prepared in this way (18, 19). Accordingly, syntheses of compounds in several binary systems were attempted using methods similar to those of Kulifay, with particular reference to new or known low temperature phases.

EXPERIMENTAL

General Procedure

Solutions of the appropriate elements as ions or complex ions were added to a solution containing a reducing agent (eg. hydrazine, hypophosphorous acid), and boiled for specified periods. Ratios of metal to metalloid ions did not necessarily correspond to those of known compounds. Quantities were used to yield approximately 0.02 mole of product. The initial and final pH of the solutions were determined, but in general no attempt was made to control the pH during the reaction. Modifications to this general procedure are given in the detailed procedures below.

The products were recovered in tared sintered glass crucibles, washed, rinsed in methanol, and dried at 70–80 °C. Chemical analyses were made by standard analytical procedures (21). Powder diffraction patterns were obtained in 11.46 cm Debye–Scherrer cameras using Ni-filtered Cu radiation ($\lambda_{K\alpha_1}$ = 1.5405 Å).

To assist in the identification of phases, 'standard' diffraction patterns were available, or were obtained for compounds prepared by mixing high purity elements in the appropriate ratios, heating, and annealing in sealed evacuated Vycor tubes in the usual manner.

The experimental conditions and product identifications are summarized in Table I.

[1]*The terms pnictide and chalicide have been proposed by Professor A. E. van Arkel for compounds of the group VA and VIA elements. Professor van Arkel has also proposed that just as 'X' is often used to denote halide atoms and ions, 'Y' and 'Z', respectively, might be used for chalicide and pnictide atoms and ions.*

TABLE I

Products formed by metal and metalloid ions in reducing media

Reducing agent	Initial metal/metalloid ratio	Total product metal/metalloid ratio	Products identified by X-ray diffraction
Copper/selenium system			
Basic hydrazine (pH 11–8)	1.00	1.01	CuSe
	1.19–1.80	0.90–1.49	CuSe + Se or Cu_2O
	1.90–2.35	1.90–2.44	$Cu_{2-x}Se$ + Cu_3Se_2 or Cu_2O
Neutral hydrazine (pH 8–5)	1.00–1.50	1.02–1.50	CuSe + Se or $Cu_{2-x}Se$
	1.80	1.86–1.89	$Cu_{2-x}Se$
	2.00	2.05	$Cu_{2-x}Se$
Ammonium sulfite (sealed tube)	1.00	1.02–1.09	CuSe + $Cu_{2-x}Se$
	1.80	1.73	$Cu_{2-x}Se$ + Cu_3Se_2
		1.83	$Cu_{2-x}Se$
Basic hydrazine on $CuSeO_3.2H_2O$	1.00	0.94–1.07	CuSe or CuSe + Se
Sulfite on $CuSeO_3.2H_2O$	1.00	1.30	CuSe + $Cu_{2-x}Se$
Nickel/selenium system			
Basic hydrazine (pH 8 or 9)	1.00	0.90–0.96	NiSe
	0.75	0.76	$NiSe_{1.30}$
	0.50	0.48–0.49	$NiSe_2$ + Se
Copper/arsenic system			
Hypophosphorous acid plus hydrazine	0.50–2.50	—	βCu_3As + Cu_2O or As_2O_3
	3.00	2.85–3.02	βCu_3As + Cu_2O
	6.00	—	βCu_3As + Cu
Hypophosphorous acid	0.50–2.50	—	βCu_3As + As_2O_3
	3.00	2.84	βCu_3As + traces Cu_2O
	6.00–9.00	—	βCu_3As + Cu, traces Cu_2O
Copper/Antimony System			
Hypophosphorous acid	1.00	—	Cu_2Sb + Sb
	2.00	2.00	Cu_2Sb
	2.75	—	Cu_2Sb
Nickel/antimony system			
Alkaline hydrazine	1.00	1.15	NiSb
	0.50–3.00	—	NiSb
Nickel/bismuth system			
Alkaline hydrazine	0.33	0.32–0.36	$NiBi_3$ + Bi
	1.00	—	$NiBi_3$ + Ni
Nickel/arsenic system			
Hypophosphorous acid plus hydrazine	1.00	0.92	NiAs
Alkaline hydrazine	0.50 (1.5 h)	—	$Ni_{2.61}As$ + $Ni_{11}As_8$
	1.00 (0.5 h)	2.03	$Ni_{11}As_8$ + $Ni_{2.61}As$
	(1.5 h)	—	$Ni_{11}As_8$
	(2.5 h)	1.42	$Ni_{11}As_8$
	1.38 (0.5 h)	2.10	$Ni_{11}As_8$ + $Ni_{2.61}As$
	(1.5 h)	2.06	Ni_5As_2
	(2.5 h)	—	$Ni_{11}As_8$
	2.00 (1.5 h)	—	Ni + Ni_5As_2
	(40 h)	—	$Ni_{11}As_8$ + Ni_5As_2
	2.50 (1.5 h)	2.30	$Ni_{2.39}As$
	(2.5 h)	—	$Ni_{2.61}As$
	3.00 (1.5 h)	—	$Ni_{2.61}As$

The Copper–Selenium System

(a) Reduction with Hydrazine

Solutions of copper(II) oxide in 10 ml of 6 *N* HCl and selenium in a minimum amount of 8 *N* HNO_3 were mixed and added slowly to a boiling aqueous solution consisting of 6 g of hydrazine dihydrochloride, 150 ml of distilled water, and sufficient concentrated ammonium hydroxide to give an initial pH of either 11 (basic conditions) or 8.5 (neutral conditions). The solutions were boiled for 1.5 h. The final pH of the basic solutions was 8, and of the 'neutral' solutions, 5.

In the initial stages of the reaction, the selenite ion was reduced to red selenium which transformed rapidly to the stable hexagonal (black) modification. During the reaction the red form again appeared, and was slowly replaced by a fine precipitate of the copper selenides. Relatively pure CuSe and $Cu_{2-x}Se$ were obtained for initial stoichiometric Cu/Se ratios from basic and neutral solutions, respectively. At other concentration ratios mixtures of products were obtained, with Se and Cu_2O appearing as impurities. (See Table I.) Cu_3Se_2

Can. J. Chem. Downloaded from www.nrcresearchpress.com by 210.87.254.42 on 09/05/12
For personal use only.

Can. J. Chem. Downloaded from www.nrcresearchpress.com by 210.87.254.42 on 09/05/12
For personal use only.

was observed, but only in small amounts in precipitates of $Cu_{2-x}Se$. Analysis of $Cu_{2-x}Se$ samples indicated the composition $Cu_{1.85}Se$.

(b) Reduction by Sulfite in Sealed Tubes

Copper(II) chloride dihydrate and selenious acid (ca. 0.005 mole of each) were dissolved in water and mixed with a solution containing 3 g of ammonium sulfite to give a total volume of 20 to 40 ml in a heavy walled glass tube. The tube was sealed, leaving a void volume of 10 ml, and heated at 85–95 °C for 2 to 6 h. The final pH was 5. When the solutions were mixed, dark precipitates were formed which are believed to have contained red selenium. $Cu_{2-x}Se$ was the only relatively pure product obtained by this method.

(c) Reduction of Copper Selenite

Copper selenite was prepared by mixing solutions of copper(II) chloride dihydrate and sodium selenite. The solid selenite was then added to the reducing solution of either ammoniacal hydrazine or of ammonium sulfite. The solid dissolved in the former solution, and the subsequent reactions were identical to the reductions with hydrazine described above. The selenite did not dissolve in the sulfite solution, but was gradually replaced by a mixture of CuSe and $Cu_{2-x}Se$.

The Nickel–Selenium System

Solutions of nickel acetate tetrahydrate in 10 ml of water and selenium dissolved in ca. 12 ml of 8 *N* HNO_3 were mixed and added to a boiling solution of 7 g of hydrazine dihydrochloride, 45 ml of ammonium hydroxide, 2 g of tartaric acid, and 130 ml of water. Aliquots of ammonium hydroxide were added at intervals to maintain the pH between 8 and 9. The total boiling time was 2.5 h. The reactions followed the same general path observed during the reduction of copper and selenium ions with hydrazine. The compounds NiSe, $NiSe_{1.30}$, and $NiSe_2$ were observed, although Se was always present with the diselenide. There was some indication in the powder diffraction patterns that a number of compositions were formed in the $NiSe_{1+x}$ phase, with $0 \leqslant x \leqslant 0.30$. Analyses indicated that impurities in most of the precipitates were of the order of 5%.

The Copper–Arsenic System

(a) Reduction with Hypophosphorous Acid and Hydrazine

Copper(II) oxide was dissolved in 10 ml of 6 *N* HCl and added to a boiling solution of 18 ml of 50% H_3PO_2, 50 ml of water, and 30 ml of concentrated HCl. A solution containing arsenite ion, prepared by dissolving arsenious oxide in 25 ml dilute NH_4OH and acidifying with HCl, was immediately added to this mixture, and the solution returned to the boiling point. A solution containing 10 g of hydrazine dihydrochloride in 50 ml of water and 100 ml of ammonium hydroxide was added slowly, raising the pH to 11. After the solution was boiled for 1.5 h, the pH had decreased to 5. A brown precipitate (probably amorphous arsenic) formed immediately on addition of the reactants to the hypophosphorous solution. Addition of the ammoniacal hydrazine solution finally produced dark precipitates containing βCu_3As and Cu_2O, Cu, or As_2O_3.

(b) Reduction with Hypophosphorous Acid

The copper(II) and arsenite solutions, as prepared above, were added to 25 ml of 50% H_3PO_2 in 100 ml of water, and the mixture boiled for 1.5 h. The pH of the solution remained at 4 throughout the reaction. On addition to the hypophosphorous solution, the blue color due to the aquo-cupric ion disappeared, indicating reduction to copper(I). Again βCu_3As was recovered, contaminated with Cu_2O or Cu.

The Nickel–Arsenic System

(a) Reduction with Hypophosphorous Acid and Hydrazine

The procedure used in the copper–arsenic system was repeated, substituting solutions of nickel chloride for those of cupric chloride. The NiAs phase was the only arsenide formed, and that with purity less than 90%.

(b) Reduction by Hydrazine

Nickel acetate tetrahydrate was dissolved in 15 ml of water containing 2 g of tartaric acid, and arsenious oxide in 25 ml of dilute ammonium hydroxide. The nickel(II) solution was added to a boiling solution of 8 ml of hydrazine hydrate, 10 g of potassium hydroxide, 2 g of tartaric acid, and 100 ml of water. Upon reduction of nickel to the metal, the arsenite solution was added rapidly. The solution was strongly alkaline throughout the reaction. The effects of nickel/arsenic concentration ratios and boiling times were determined (Table I).

On addition of nickel ion to the alkaline hydrazine solution a blue nickel–hydrazine complex was formed, which was gradually reduced to spongy nickel metal. The reaction of this precipitate with the arsenite ions was vigorous, and yielded $Ni_{2.61}As$, $Ni_{2.50}As$, $Ni_{2.39}As$, and $Ni_{11}As_8$, depending on initial concentration and reaction times. The precipitates became progressively richer in arsenic with increasing reaction time, but neither NiAs nor higher arsenides were observed.

The Copper–Antimony System

Potassium antimonyl tartrate hemihydrate was dissolved in 40 ml of water, and copper(II) oxide in 10 ml of 6 *N* HCl. The cupric and then the arsenite solutions were added to a boiling reducing solution of 125 ml of 17% H_3PO_2, and the mixture boiled for 1.5 h. As in the copper–arsenic experiments, the Cu(II) was apparently reduced immediately to Cu(I). After a short induction period, a white precipitate formed which

darkened with boiling to produce precipitates containing Cu_2Sb, in some instances contaminated with antimony.

The Nickel–Antimony System

Solutions of nickel acetate tetrahydrate in 15 ml of water and potassium antimonyl tartrate hemihydrate in 40 ml of water were added to the hydrazine / potassium hydroxide reducing solution described in the nickel–arsenic syntheses. Boiling time was 1.5 h. The reactions were similar to those observed in the nickel–arsenic system. NiSb was the only antimonide recovered.

The Nickel–Bismuth System

Solutions of bismuth(III) oxide in 30 ml of 8 *N* HCl and of nickel acetate tetrahydrate in 15 ml of water, both containing 2 g of tartaric acid, were added to a reducing solution of hydrazine in potassium hydroxide, as used in the nickel–arsenic syntheses. Again the reactions were similar to those observed in the nickel–arsenic systems. $NiBi_3$ was the only bismuthide recovered.

The Cobalt- and Iron–Arsenic Systems, and the Cobalt–, Iron–, and Copper–Bismuth Systems

Attempts were made to prepare cobalt and iron arsenides, and cobalt, iron, and copper bismuthides using the various techniques and reagents described above. None of these attempts was successful. For systems containing iron, various hydrolysis products were obtained. In the cobalt–arsenic and cobalt–bismuth preparations, elemental arsenic (largely amorphous) and bismuth were precipitated, together with essentially all of the cobalt in such a finely divided form that no diffraction pattern registered through a nickel screen. In the copper–bismuth system the elements were precipitated, but the reduction was incomplete.

DISCUSSION

The compounds obtained are given in Table II with all of the compounds believed to exist in these binary systems at low temperatures. Several iron and cobalt diarsenides are known to exist, but none were obtained. No bismuthides of iron, cobalt, or copper have been reported, and none were formed in our experiments. The phases which were formed were found to depend on the reducing agent, pH, and reaction time, as well as initial concentrations of the reactants.

TABLE II

Comparison of observed phases and compounds known to exist

System	Compounds
Cu/Se	($Cu_{2-x}Se$, Cu_3Se_2*, CuSe),† $CuSe_2$
Ni/Se	Ni_3Se_2, (NiSe, $NiSe_{1+x}$, $NiSe_2$)
Cu/As	ϵCu_3As, αCu_3As, (βCu_3As), $Cu_{5-x}As_2$, Cu_2As
Ni/As	($Ni_{5-x}As_2$), β',γ, Ni/As, ($Ni_{11}As_8$, NiAs), α,$\beta NiAs_2$
Cu/Sb	$\epsilon Cu_{4.5}Sb$, (Cu_2Sb)
Ni/Sb	$Ni_{15}Sb$, Ni_3Sb, Ni_7Sb_3, (NiSb), $NiSb_{2+x}$
Ni/Bi	NiBi, ($NiBi_3$)

*Cu_3Se_2 obtained only in small amounts in presence of $Cu_{2-x}Se$.
†Phases obtained in this study are in parenthesis.

TABLE III

Unit cell dimensions of compounds prepared in aqueous solutions

Compound	System	*a* (Å)	*b* (Å)	*c* (Å)
$Cu_{2-x}Se$*	Cubic	5.735±8		
$Cu_{2-x}Se$†	Cubic	5.755±7		
$Cu_{2.8}As$	Trigonal	7.11±1		7.28±1
Cu_2Sb	Tetragonal	4.00±1		6.09±1
$NiBi_3$	Orthorhombic	8.88±1	4.115±4	11.48±1
$NiBi_3$‡	Orthorhombic	8.84±1	4.117±7	11.42±3

*Reduction with ammoniacal hydrazine.
†Reduction with ammonium sulfite. Pattern with two very weak unindexed lines at d = 3.68 and 2.25 Å.
‡Specimen prepared by heating mixture of elements in conventional manner; annealed and air quenched from 230 °C. Bi also present.

Can. J. Chem. Downloaded from www.nrcresearchpress.com by 210.87.254.42 on 09/05/12
For personal use only.

Can. J. Chem. Downloaded from www.nrcresearchpress.com by 210.87.254.42 on 09/05/12
For personal use only.

Although comments on the mechanisms involved in these reactions are largely speculative, it was obvious in nearly all instances that reduction of the metal and metalloid did not occur simultaneously. In those reactions involving nickel and hydrazine in potassium hydroxide, the metal was precipitated, and reaction apparently occurred between the metal and complex metalloid ions in solution. In the reduction of nickel and arsenite ions, for example, nickel-rich phases were first produced which became progressively richer in arsenic with increasing reaction time. These observations are reminiscent of the reaction of nickel powder with solutions of arsenic trichloride in hydrochloric acid, for which the arsenic content of the product depended on the reaction time (22). In the majority of systems involving copper, on the other hand, the metalloid was precipitated first, although the subsequent reactions may have occurred homogeneously between redissolved metalloid ions and copper ions or complex ions. In separate experiments it was observed that relatively pure $Cu_{2-x}Se$ was formed when solid CuSe and aqueous copper(II) ions were added to ammoniacal hydrazine at 100 °C; similarly some CuSe was formed when $Cu_{2-x}Se$ was treated with selenite ion under the same reducing conditions.

Known compounds which were not observed are not necessarily unstable at 100 °C. The conditions required for their appearance in appreciable quantities may not have been employed. However, compounds which did appear must be stable at 100 °C. Hence Cu_3Se_2, believed to be unstable at some temperature below 170 °C (23), is still stable at 100 °C. Similarly, these syntheses confirm the contention that the trigonal β modification of Cu_3As is stable at relatively low temperatures (24).

The products, as one might expect, were all finely divided. In many instances the diffraction patterns were so diffuse that accurate determinations of lattice dimensions were impossible. For those compounds whose patterns could be indexed at high Bragg angles, the calculated lattice dimensions agree well with those reported in the literature (Table III).

Two anomalies observed in the diffraction studies should be mentioned. The diffraction pattern of precipitated $NiBi_3$ was indexed assuming the orthorhombic unit cell given by Zhdanov (25). However, $NiBi_3$ prepared from the elements in the conventional manner at 720 °C, annealed at 230 °C, and air quenched, had the somewhat smaller unit cell recorded in Table III. Since the pattern of this specimen also contained reflections due to bismuth, the implication is that $NiBi_3$ may have a small range of variable composition on the nickel-rich side. Secondly, the diffraction patterns of a precipitated $Cu_{2-x}Se$ phase and of $Cu_{1.80}Se$ prepared in the conventional way, annealed at 230 °C, and air quenched, showed two very weak reflections at relatively low orders, which may be indicative of ordering in this compound.

In no instances, even when only one component was evident in the diffraction pattern, could the precipitated phases be regarded as pure in the semiconductor sense. Quite aside from the adsorbed impurities to be expected in any finely divided precipitate, analyses and microscopic examinations indicated the presence of phases not revealed by X-ray diffraction. Moreover, reproducibility of the syntheses was less than satisfactory. It is our opinion that the synthesis of semiconductor grade compounds by these methods, as suggested by Benzing *et al.* (17), would be most difficult, if not impossible.

ACKNOWLEDGMENTS

We gratefully acknowledge the award of Operating Grants from the National Research Council of Canada, and the award to G. E. C. of Ontario Fellowships for Graduate Study.

REFERENCES

1. A. BRUKL. Z. Anorg. Allgem. Chem. **131**, 236 (1923).
2. L. MOSER and K. ATYNSKI. Monatsh. **54**, 235 (1925).
3. S. ROTHSCHILD. Brit. Patent No. 819,090 (1959).
4. F. GARELLI. Rec. Trav. Chim. **42**, 818 (1923).
5. L. M. CLARK. J. Chem. Soc. 2888 (1928).
6. H. PÉLABON. Bull. Soc. Chim. France, **51**, 377 (1932).
7. G. SCHOTT. Wiss. Z. Univ. Leipzig, Math.-Naturw. Reihe, No. 2 (1951–52), No. 4, 39; Chem. Abstr. **47**, 10390.
8. R. NITSCHE. Angew. Chem. **69**, 333 (1957).
9. G. ARRIVAUT. Compt. Rend. **190**, 1506 (1930).
10. G. ARRIVAUT. Compt. Rend. **192**, 1238 (1931).
11. A. MUZZUCCHELLI and A. VERCILLO. Atti Accad. Nazl. Lincei, [VI] **1**, 233 (1925).
12. R. WEIL and R. HOCART. Compt. Rend. **233**, 559 (1951).
13. R. WEIL and R. HOCART. Compt. Rend. **233**, 880 (1951).
14. R. WEIL, R. HOCART, and J. C. MONIER. Bull. Soc. Franc. Mineral Crist. **77**, 1084 (1954).
15. W. GEILMANN and FR. W. WRIGGE. Z. Anorg. Allgem. Chem. **197**, 375 (1931).
16. W. GEILMANN and FR. W. WRIGGE. Z. Anorg. Allgem. Chem. **210**, 373 (1933).
17. W. C. BENZING, J. B. CONN, J. V. MAGEE, and E. J. SHEEHAN. J. Am. Chem. Soc. **80**, 2657 (1958).
18. S. M. KULIFAY. J. Am. Chem. Soc. **83**, 4916 (1961).
19. S. M. KULIFAY. J. Inorg. Nucl. Chem. **25**, 75 (1963).
20. A. J. PANSON. Inorg. Chem. **3**, 940 (1964).
21. A. I. VOGEL. A textbook of quantitative inorganic analysis. 3rd ed. Longmans. 1961.
22. R. D. HEYDING and L. D. CALVERT. Can. J. Chem. **35**, 1205 (1957).
23. P. RAHLFS. Z. Physik. Chem. Leipzig, B, **31**, 157 (1936).
24. R. D. HEYDING and G. J. G. DESPAULT. Can. J. Chem. **38**, 2477 (1960).
25. G. S. ZHDANOV. Tr. Inst. Kristallogr. Akad. Nauk SSSR, **10**, 99 (1954).

Can. J. Chem. Downloaded from www.nrcresearchpress.com by 210.87.254.42 on 09/05/12
For personal use only.

Can. J. Chem. Downloaded from www.nrcresearchpress.com by 210.87.254.6 on 09/05/12
For personal use only.

TERPENOIDS

X. PRE-SENEGENIN, A QUITE NORMAL TRITERPENOID

J. J. DUGAN AND P. DE MAYO
Department of Chemistry, University of Western Ontario, London, Ontario
Received February 22, 1965

ABSTRACT

Pre-senegenin has been obtained by a combination of oxidative and hydrolytic cleavage of the saponin, and has been shown to be a member of the normal and unrearranged oleanolic acid series: 2β,27-dihydroxy-23-carboxyoleanolic acid (XXII). On treatment with ethanolic hydrochloric acid it is converted quantitatively to a mixture of polygalic acid (XXI) and senegenin.

Previous work (1) has shown that senegenin is a triterpenoid of empirical formula $C_{30}H_{45}O_6Cl$ with a 2β,3β-glycol system and a 4α-carboxyl group. A second carboxyl group is also present. It has now been found to be a member of the β-amyrin-oleanolic acid series in which a carbon atom at C_{14} has migrated to C_{12} with concomitant movement of the double bond to the C_{13}—C_{14} position, and that it has the structure (XX).*

In our earlier study of the triterpenoid senegenin, we showed that, surprisingly, it contained chlorine and that it had the empirical formula $C_{30}H_{45}O_6Cl$. Four of the oxygen atoms were found to be present as shown in the part-structure (I), and the remaining two, in agreement with the conclusions of previous workers (3, 4), formed part of a carboxyl function.

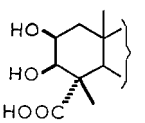

(I)

By heating senegenin with quinoline a substance, de(hydrochloro)senegenin, was obtained which showed the ultraviolet absorption spectrum of a conjugated diene. This compound could also be obtained, under defined conditions, as the product of the alkali treatment of senegenin, the "extra", and third, equivalent of alkali required in the titration of senegenin being consumed by the liberated hydrochloric acid.

The ultraviolet absorption spectrum of de(hydrochloro)senegenin (λ_{max} 243, 249, 256 mμ) was clearly indicative of a heteroannular diene and the nuclear magnetic resonance (n.m.r.) spectrum, which showed a multiplet (one proton) at τ 4.65 and a broad singlet (ca. three protons) at τ 8.19 suggested that a methyl group and a proton were substituents on this diene. However, none of the methyl groups of senegenin, of which there were clearly five, provided the methyl group of the diene, and indeed the mere presence of but five methyl groups in senegenin derivatives suggested that the biogenetically to be expected sixth bore the chlorine atom. This could give rise, eventually, to the vinylic methyl group.

The n.m.r. spectrum of senegenin esters was obscured by the signals from the methoxyl groups in the region where —CH_2Cl signals were to be expected. The spectrum of senegenin itself, determined in pyridine, showed a multiplet in the expected region of about two

**Part of this material formed a preliminary communication (2).*

protons. The fact that a complex pattern was observed further suggested that there was at least one proton attached to the terminus of the chloromethyl group. Since senegenin derivatives showed no vinyl proton signal in their n.m.r. spectra, these observations suggested, though subject to other interpretations in detail, that the changes observed in the conversion of senegenin to de(hydrochloro)senegenin could be represented as (II) → (III). An obvious point requiring clarification was the nature of the prototropic shift apparently occurring under basic conditions. This will be returned to later.

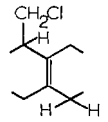

(II)

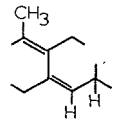

(III)

These experiments at least indicated the proximity of the chlorine to the one double bond present in senegenin. It was also necessary to relate these functions, spatially, to the remaining carboxyl group.

For these experiments dechlorosenegenin (1), obtained from senegenin monoacetate by reduction with lithium and liquid ammonia, was used.

Oxidation of dechlorosenegenin diacetate with hydrogen peroxide in acetic acid gave, after esterification with diazomethane, an oily lactonic ester. This showed absorption in the infrared compatible with the presence of a hydroxyl group (3 500 cm^{-1}) and of a γ-lactone (1 767 cm^{-1}). The tertiary alcohol in this compound (no methine proton on carbon bearing an oxygen) could be dehydrated with thionyl chloride in pyridine to give an anhydro lactone (VI) which appeared to contain a vinylic proton.

Merely on heating in methanol, this unsaturated lactone was isomerized into a new lactone (VII), likewise a γ-lactone (ν_{max} 1 773 cm^{-1}). This isomeric lactone, however, had no vinylic proton, but had, instead, a doublet (one proton) at τ 5.19 suggestive of the presence of a proton on carbon bearing an oxygen.

The mildness of the isomerism conditions (the isomerism was also achieved by hydrolysis of the anhydro lactone with base followed by reacetylation) seemed only compatible with an allylic rearrangement. This required that both ends of the allylic system be γ to the carboxyl group. The sequence of reactions could then be represented as in (IV) → (VII).

The ready isomerism of VI to VII, presumably through an allylic cation, suggested that if this cation could be induced to lose a proton the familiar chromophore of III would

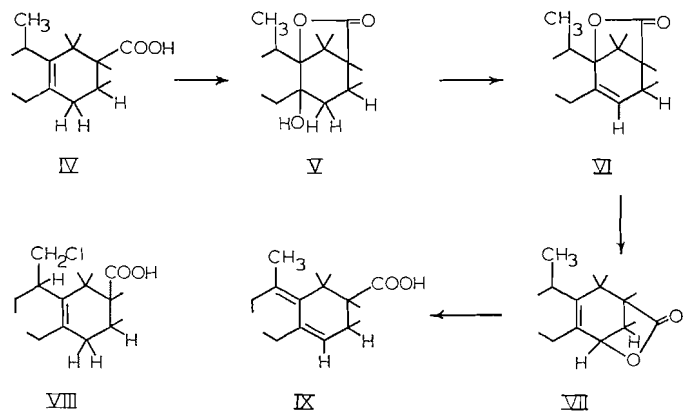

Can. J. Chem. Downloaded from www.nrcresearchpress.com by 210.87.254.6 on 09/05/12
For personal use only.

be obtained. When the unacetylated ester of (VII) was allowed to stand in 5% methanolic hydrochloric acid at room temperature the diene was indeed rapidly formed and the monocarboxylic acid (IX) could be obtained in quantitative yield. This, when converted to the ester with diazomethane, gave the dimethyl ester of de(hydrochloro)senegenin.

The spatial relationship of the three functional groups in senegenin under discussion appeared to be as represented in (VIII). It was in addition, because of the difficulty of hydrolysis of the corresponding ester, probable that the carboxyl was attached to quaternary carbon. However, the mode of fusion of the remaining ring systems onto the ring in (VIII) remained to be ascertained.

One method by which information could be obtained appeared to be, in principle, by partial aromatization. Should the carboxyl be the only blocking group, then its removal should engender ready aromatization. The route selected was that used by Barton in the study of tomentosolic acid (6) and for this purpose it was desirable to have an unsaturated derivative of senegenin in which the ring A carboxyl was esterified and the other was not. Partial hydrolysis of a diester could not serve since the ring A carboxyl was the more readily hydrolyzed, but such a compound was available, by a devious route, in IX, which after acetylation gave de(hydrochloro)senegenin diacetate monomethyl ester. Conversion of this to the acid chloride, followed by pyrolysis, with loss of carbon monoxide and hydrogen chloride, gave the desired aromatic product represented now in terms of the completed structure as (X). Some difficulty was experienced in the purification of X until it was found that brief treatment with ozone after partial separation removed some olefinic contaminant.

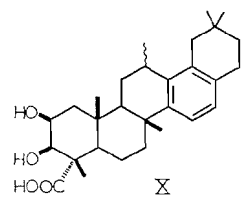

X

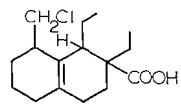

XI

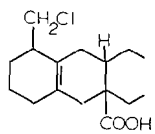

XIIa

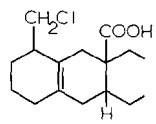

XIIb

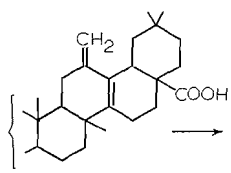

XIII

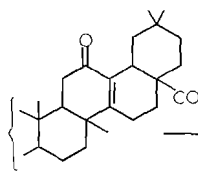

XIV

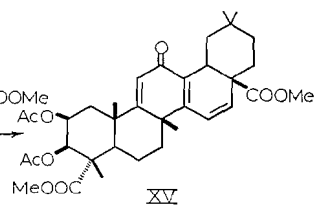

XV

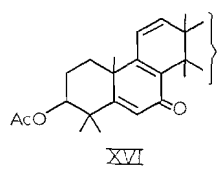

XVI

Can. J. Chem. Downloaded from www.nrcresearchpress.com by 210.87.254.6 on 09/05/12
For personal use only.

The nature of X rests on the following evidence, other than its mode of genesis. It has the ultraviolet absorption of an alkylated benzene (λ_{max} 269 mμ). Two, and only two, aromatic protons are present in the n.m.r. spectrum as a near singlet at τ 3.05 (indicating their nearly identical environment). All four remaining positions of the benzenoid ring must be occupied by carbon (there is no aromatic methyl group) and represent the points of fusion of the adjacent rings. Part-structure (VIII) can therefore be expanded to (XI) or (XII*a*, *b*). Of these (XII*a*) may be excluded since (IX), aside from the mechanistic requirements of its genesis, does not have the properties of a β,γ-unsaturated acid.

Although there were suggestions that (XI), and therefore (X), was correct (the vinylic proton in (IX) was not a clean doublet, for instance) this sequence of reactions did not provide unequivocal evidence which allowed a decision between (XI) and (XII*b*) to be made.

Whilst the conversion of (II) to (III) under the influence of quinoline at high temperatures could be envisaged (the quinoline hydrochloride could supply a proton for a prototropic shift) the same change under the action of dilute sodium hydroxide would be impressive. The action of base was re-investigated and, indeed, in alkaline solution a new heteroannular diene could be observed. This was partly, or wholly, destroyed by casual acidification but by careful adjustment of pH to near 6 with phosphate buffer and extraction followed by esterification, an isode(hydrochloro)senegenin dimethyl ester could be obtained. Rearrangement into the de(hydrochloro) series was easily effected at room temperature with hydrochloric acid in dioxane.

Isode(hydrochloro)senegenin (XIII) showed the presence of the expected exocyclic methylene group by exhibiting bands at τ 5.13, 5.40. Ozonolysis gave, in agreement, an α,β-unsaturated ketone (λ_{max} 253 mμ) (XIV). Reduction of this gave an allylic alcohol which was readily dehydrated to a heteroannular diene absorbing at shorter wavelength than in the de(hydrochloro) series. Acetylation of the unsaturated ketone gave the expected keto-diacetate which was characterized as the allylic alcohol.

This conjugated ketone was a suitable substance for the introduction of further unsaturation in a classical procedure for structural elucidation. Bromination of the keto-diacetate resulted in the uptake of two atoms of bromine. Direct dehydrobromination of the crude dibromo compound with lithium chloride in dimethyl formamide then gave a trienone (XV).

The ultraviolet absorption spectrum of XV was characteristic of a cross-conjugated carbonyl system which, to a first approximation, shows the absorption of the separate chromophores. In the present case, excellent analogy was available in the lanosterol derivative (XVI) (5) which showed λ_{max} 258, 326 mμ (ϵ 8 500 and 8 500) as against λ_{max} 260, 320 mμ (ϵ 8 200, 7 200) for (XV) (see also (14)). The n.m.r. spectrum of (XV) showed all the signals to be expected of such a molecule. In particular, five singlets for the methyl groups were observable (Fig. 1) as were appropriate signals for three vinyl protons, two of which were strongly coupled. One of the latter shows weak long-range coupling probably with the methine proton at C_{18}.

The existence of the chromophore also requires that a blocking group, represented in (XV) by the C_8 methyl group, be present to prevent the formation, by tautomerism, of a phenol.

The summation of the part-formula (1) and the requirements for senegenin itself implied by (XV) leads, most plausibly, to the structure (XVII) for senegenin, where the weaker lines are those for which no direct evidence has been adduced. It should be noted that, in fact, only six carbon atoms have not been specifically located, and that of these three are

Can. J. Chem. Downloaded from www.nrcresearchpress.com by 210.87.254.6 on 09/05/12
For personal use only.

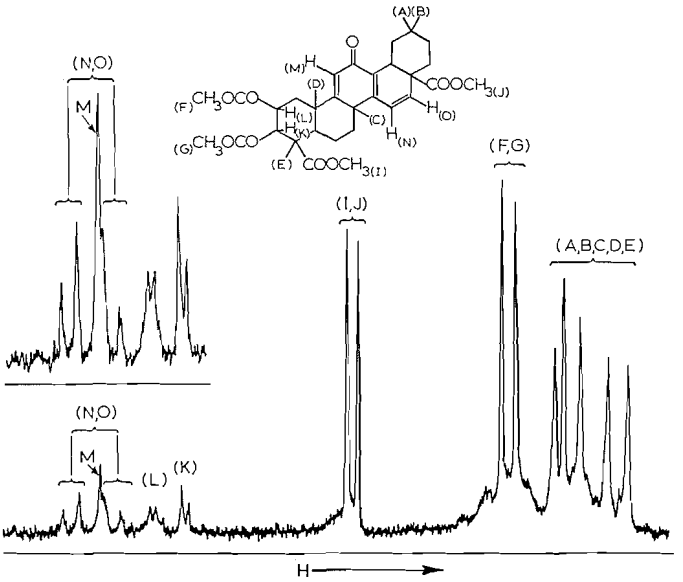

FIG. 1. Nuclear magnetic resonance spectrum of trienone (XV), with expanded inset of the vinyl region.

methyl groups attached to quaternary carbon. The formulation (XVII), that of a simply modified oleanane derivative, acquired added verisimilitude with knowledge that polygalacic acid, (XVIII) another oleanane derivative, has recently been isolated and characterized from a related species of polygala, *Polygala paenea* L., by Polonsky and her collaborators (7).

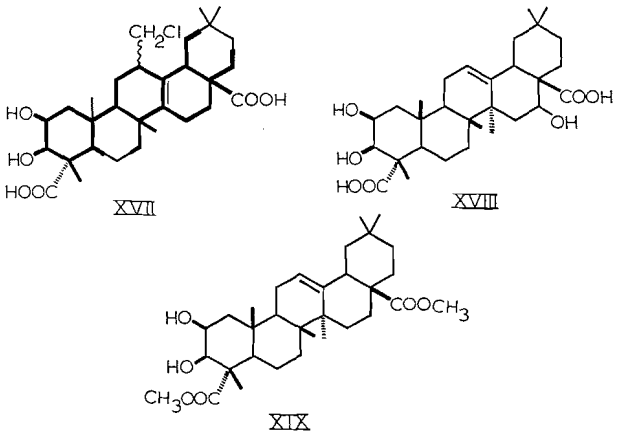

In the hope of obtaining direct evidence for the original ring system in senegenin, and in particular the location of the double bond in it, the mass spectrum of dechlorosenegenin dimethyl ester was obtained. For comparison that of dimethyl medicagenate (XIX) was also recorded.

Dimethyl medicagenate showed peaks at *m/e* values to be expected for an oleanolic acid derivative. These peaks, following the interpretation of Budzikiewicz, Wilson, and Djerassi (8), and irrespective of the accuracy of the interpretation of the sources of certain

Can. J. Chem. Downloaded from www.nrcresearchpress.com by 210.87.254.6 on 09/05/12
For personal use only.

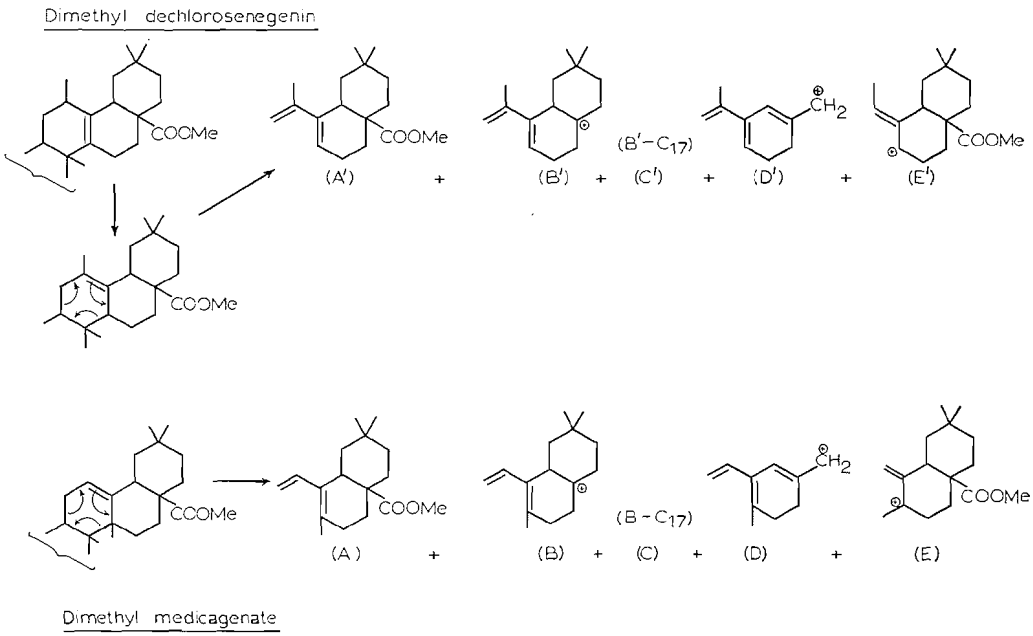

SCHEME 1. Breakdown scheme for dimethyl dechlorosenegenin and dimethyl medicagenate.

of these peaks, are to be attributed to the fragments illustrated in Scheme 1 (A–E). In this sense the pattern fully confirms the suggested importance of the retro-Diels–Alder reaction in this series, with the retention of the charge in the D/E system.

The spectrum of dechlorosenegenin dimethyl ester up to $m/e \sim 300$ is shown in Fig. 2. Comparison with the spectrum of dimethyl medicagenate shows a striking similarity in the ratios and, with one exception, an identity of position of the more important peaks. The only important difference is the presence, in dechlorosenegenin dimethyl ester, of an additional peak at 241.

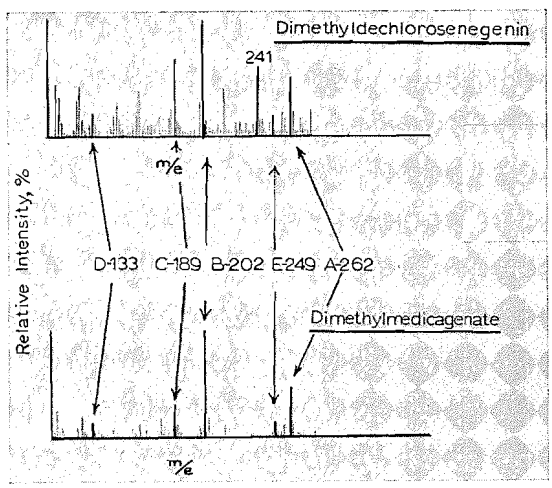

FIG. 2. Mass spectra of dimethyl dechlorosenegenin and dimethyl medicagenate.

Can. J. Chem. Downloaded from www.nrcresearchpress.com by 210.87.254.6 on 09/05/12
For personal use only.

This impressive identity would suggest (8) that senegenin belonged to the Δ^{12}-unsaturated oleanene or ursene series, a conclusion which would be, in view of the facts already presented, totally unacceptable. This seeming contradiction, however, serves to complete the structure of senegenin.

If it be assumed that after impact the ion produced may transfer the hydrogen atom at C_{12}, either in one or two stages, to C_{14} then (without charge indication) a series of fragments (A′–E′) may be written differing from, but isomeric with, the series (A–E) from dimethyl medicagenate, which will produce a series of peaks of identical *m/e* with those of that series.* If it be assumed, as appears reasonable, that the retro-Diels–Alder is energetically the most desirable mode of fragmentation other modes may be sufficiently slow to permit hydrogen transfer and breakdown by this route.

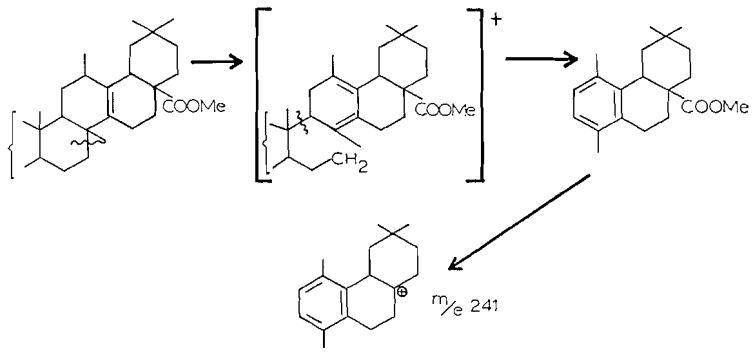

SCHEME 2. Possible origin of the peak at *m/e* 241 in the mass spectrum of dimethyl dechlorosenegenin.

The remaining feature requiring explanation is the peak at *m/e* 241 in the spectrum of dechlorosenegenin dimethyl ester. Since this has no equivalent in dimethyl medicagenate it could arise from fragmentation in the unrearranged molecule. Such a scheme is represented in Scheme 2. If this interpretation be correct the peak at *m/e* 241 should be independent of substitution in ring A. The spectrum of dechlorosenegenin diacetate was accordingly obtained and the same series of peaks, including that at *m/e* 241 was observed.†

These observations suffice, therefore, to permit the attribution of the structure (XX) to senegenin. No evidence has been provided for the stereochemistry of the methyl group at C_8, but it seems probable that it is β as in all known members of the oleanene series.

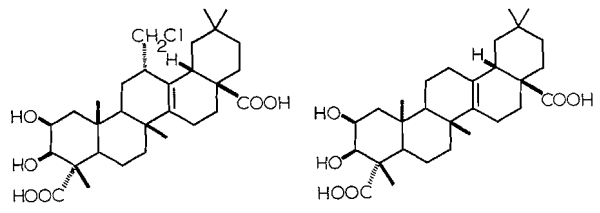

XX XXI

The stereochemistry of the chloromethyl group will have been determined by the mechanism of transfer of what was evidently the C_{14} methyl in a precursor to C_{12}. On the assumption, for the moment, that the migration is intramolecular, then the chloromethyl

Thermal rearrangement prior to ionization is also conceivable.
†*Mass spectra by Dr. R. Ryhage, Karolinska Institutet, Stockholm, Sweden.*

Can. J. Chem. Downloaded from www.nrcresearchpress.com by 210.87.254.6 on 09/05/12
For personal use only.

group surely lies on the same face of the molecule as did the original methyl group (or equivalent); that is, α. The configuration at C_{18} follows from the relationship to polygalic acid (see below).

At this point it was possible to direct attention to the structure of pre-senegenin the presumed precursor of senegenin. The structure of polygalic acid (XXI), the substance (as the monoethyl ester) accompanying senegenin when prepared by the normal isolation procedure, has been determined by conversion into the unsaturated ketone (XIV) (9). From other evidence Professor Pelletier and his colleagues have arrived at the same conclusion (10).* It seemed most probable that the carbon atom transferred in the formation of senegenin from pre-senegenin was lost in the concomitant formation of polygalic acid by a reverse Prins reaction or some equivalent on a different oxygen level.

The saponin from *polygala senega*, as already demonstrated, contains no halide (1), but attempts to hydrolyze the saponin under milder acid conditions in an attempt to isolate pre-senegenin were, in our hands, unavailing. It seemed possible, as an alternative approach, that preliminary cleavage with periodic acid might produce carbonyl functions in a suitable position for activated release of the ethereal linkage retaining the sapogenin. The cleavage might then be induced by the action of base through some process such as β-elimination. Even if not suitably placed, then, by ketol equilibration, the carbonyl function might reach such a position.

Whilst the details of the reaction are unknown the overall result was that desired. The saponin, after cleavage with sodium metaperiodate (the excess oxidant being destroyed reductively) was heated with 5% potash under nitrogen. From this medium, after adjustment to pH $\sim$ 3, the sapogenin could be extracted and was obtained crystalline as the dimethyl ester. It had the empirical formula $C_{32}H_{50}O_7$ and on acetylation gave a triacetate. By another chromatographic procedure, pre-senegenin was itself obtained crystalline. The material was accompanied by *p*-coumaric acid identified by comparison with an authentic specimen.†

When pre-senegenin was heated with ethanolic hydrochloric acid it was converted in high yield into a mixture of senegenin and polygalic acid which was separated, after methylation, and the individual components identified spectroscopically and, in the case of dimethyl polygalate, also by mixed melting point. The new sapogenin was, therefore, the sought-for precursor.

Pre-senegenin differed in composition from polygalic acid by the elements of formaldehyde. If the concept of a reverse Prins were correct, formaldehyde itself should be eliminated during the conversion of pre-senegenin into polygalic acid. By conducting the acid treatment in the presence of 2,4-dinitrophenylhydrazine the 2,4-dinitrophenylhydrazone of formaldehyde could, in fact, be isolated. The yield of polygalic acid remained unaffected by the presence of the reagent as it was when the acid treatment was conducted in the presence of a large excess of formaldehyde. The structure of pre-senegenin could then be represented by (XXII) or (XXIII), the former being a normal derivative of the oleanene series whilst (XXIII) would be that of a member of taraxerene series. In either case, the geometry of ring C, it was considered, should be such as to facilitate a Cope rearrangement through a six-center transition state including C_{12}, C_{13}, C_{14}, and the primary hydroxyl group (as in (XXIV)) with the eventual transfer of the hydroxyl proton to C_{12} and the

Professor Pelletier has used the term 'senegenic acid' for polygalic acid. Aside from observing the slight confusion possibly engendered between, for instance, dimethyl senegenin and dimethyl senegenate, we have no particular preference. The term 'polygalic acid' coined by Shamma and Irwin (18) was used in our earlier publication and we use it here for simplicity.

†*We thank Dr. A. Stoessl (Department of Agriculture) for a specimen of this substance.*

Can. J. Chem. Downloaded from www.nrcresearchpress.com by 210.87.254.6 on 09/05/12
For personal use only.

liberation of formaldehyde. Under these conditions untoward migration of the double bond prior to the reverse Prins could be discounted, a possibility which could not be excluded in the more vigorous acid treatment.

At 220° the dimethyl ester of pre-senegenin smoothly underwent the desired rearrangement and entrainment of the volatile material into aqueous dimedone gave a 73% yield of the dimedone derivative of formaldehyde. The other product was identified as dimethyl polygalate. Since, in this transformation, no possibility of inversion at C_{18} is presented this must be the same in polygalic acid as in pre-senegenin.

The identity of pre-senegenin as either (XXII) or (XXIII) was thus confirmed. In agreement there was a single vinyl proton in the n.m.r. spectrum of the pre-senegenin esters. The rearrangement just discussed offered a simple means of distinguishing between these formulations. Equilibration of pre-senegenin dimethyl ester with deuterium oxide in dioxane converted the hydroxyl proton in (XXIV) to a deuteron. Removal of the solvents and pyrolysis in a sealed tube under high vacuum gave after crystallization dimethyl polygalate, as previously, in which deuterium (1.4% excess) had been incorporated. Since the incorporation of one deuterium atom (at C_{12} or C_{15}) should have resulted in about 2% excess deuterium, inefficient exchange or insufficiently vigorous exclusion of water may be responsible for its incompleteness.

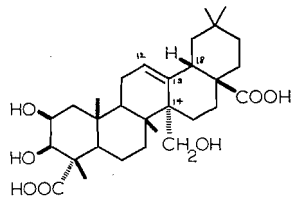

XXII

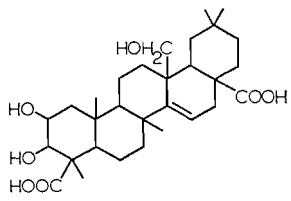

XXIII

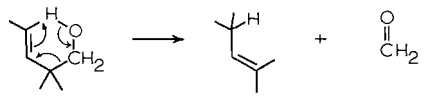

XXIV

To distinguish between structures (XXII) and (XXIII) for pre-senegenin it was necessary only to ascertain the position of the introduced deuteron. Oxidation of the deuteriopolygalate ester diacetate to the unsaturated ketone (XIV) gave material containing no excess deuterium. The deuteron was therefore required to be at C_{12} unless during the oxidation, by equilibration with the solvent, a deuteron had been removed from C_{15}. This was intrinsically unlikely since this would require enolization, and such an enol would be expected to be trapped by the oxidant to give the transoid cross-conjugated ene-dione. However, the possibility was rendered even more remote by performing an equivalent oxidation of dimethyl polygalate in chromium trioxide – acetic acid-*d*. No deuterium was incorporated into the unsaturated ketone obtained. The structure of pre-senegenin is thus (XXII); bathetically, that of a normal oleanene triterpenoid.

Three points remain for discussion. Under the original isolation procedure (4) senegenin was obtained largely as the free dicarboxylic acid whilst polygalic acid was obtained in a partly esterified condition. Since normal oleanane derivatives would not be expected to be

Can. J. Chem. Downloaded from www.nrcresearchpress.com by 210.87.254.6 on 09/05/12
For personal use only.

esterified significantly under Fischer-Speier conditions, some explanation is required. The simplest is that the change in geometry implied by the introduction of a C_{13-14} ethylenic linkage may reduce hindrance to a point where partial esterification may take place under, what are for this type of procedure, forcing conditions. In agreement, use of milder conditions for the transformation of pre-senegenin gave senegenin and polygalic acid which were only $\sim 10\%$ esterified.

Treatment of polygalic acid diacetate and senegenin monoacetate with refluxing methanolic hydrochloric acid (2.4 *N*) for 6 h resulted in $\sim 100\%$ and 24% esterification respectively, as estimated by n.m.r. measurements of the methoxyl signal. Under the same conditions oleanolic acid was 7% esterified. The difference in rate between senegenin and polygalic acid may be attributed to interaction of the bulky chloromethyl group with ring E resulting in slight torsional movement of the 17-carboxyl towards ring C and somewhat increased difficulty of steric access.

Secondly, since the configuration at C_{18} in pre-senegenin is presumably β as in other oleanene derivatives this configuration must obtain in polygalic acid (because of relationship through the Cope rearrangement) and in senegenin (because of its relationship to polygalic acid through the unsaturated ketone (XIV)).

The last point, the mechanism of the evidently intramolecular conversion of pre-senegenin to senegenin is discussible in terms of cyclobutonium ions, but such discussion will be deferred until present investigations in this area are completed. It should be noted that the solvolysis of the system present in pre-senegenin has been studied (for instance refs. 11, 12) and has in fact been used for the synthesis of the triterpenoid phyllanthol (13). However, these studies were performed under essentially irreversible conditions.

The isolation of substances apparently closely related to senegenin (15–17) from *Polygala* species suggests that these, too, contain substances of the type of pre-senegenin.

NOTE ADDED IN PROOF: Professor Pelletier has very recently reported* the formation of a cyclosenegenin by the action of alkali on senegenin: a reaction with ample analogy. With hydrochloric acid senegenin (but not polygalic acid) is formed. The title of the communication requires that cyclosenegenin be present in *Polygala senega*, and the text suggests that it may be the precursor. We have also noted the formation of cyclosenegenin, but an n.m.r. study of the saponin failed to show any signals near τ 10.0 of an intensity sufficient to render possible the presence of a combined cyclosenegenin.

EXPERIMENTAL

Unless otherwise stated the following are implied: light petroleum refers to the fraction of b.p. 60–80°, rotations and infrared spectra are in chloroform solution, ultraviolet spectra are in 95% ethanol solution, and melting points were determined in evacuated capillaries. Thin-layer chromatography was done using Camag silica gel DF-5 with fluorescent indicator. The n.m.r. spectra were determined in deuteriochloroform using 1% tetramethylsilane as internal standard using a Varian D.P. 60 spectrometer (peak positions being determined using an audio oscillator calibrated with a Hewlett Packard 522-B frequency counter) or a Varian A-60. Band positions are in tau (τ) units.

Senegenin

The Anhydro Lactone Methyl Ester Diacetate (VI)

Dechlorosenegenin diacetate (290 mg) was heated in acetic acid (10 ml) containing hydrogen peroxide (4.5 ml, 30%) at 85° for 1.5 h. Dilution with water and extraction into ether followed by methylation (diazomethane) gave, after thin-layer chromatography (t.l.c.) (eluant: ether : isopropyl ether, 3:7) and extraction of the appropriate band, the hydroxy lactone (V) as an oil (250 mg), $[\alpha]_D$ +38° (*c*, 2.05), ν_{max} 3 500, 1 767, 1 742 cm^{-1}, n.m.r. bands at 9.09, 9.05, 8.85, 8.63, 8.07 (3H, singlet), 7.96 (3H, singlet), 6.32 (3H, singlet), 4.64 (2H, multiplet), which was used directly for dehydration.

The hydroxy lactone (115 mg) was dissolved in dry pyridine (8 ml), thionyl chloride (0.5 ml, purified)

* *Y. Shimizu and S. W. Pelletier. J. Am. Chem. Soc. 87, 2065 (1965).*

Can. J. Chem. Downloaded from www.nrcresearchpress.com by 210.87.254.6 on 09/05/12
For personal use only.

added dropwise with stirring, and the solution allowed to stand at room temperature for 1 h. Pouring into sodium acetate (75 ml, 10%) with stirring, extraction into ether, and washing with dilute hydrochloric acid to remove pyridine followed by careful evaporation in the cold gave crystalline anhydro lactone. Crystallization from methanol (in the cold) gave pure material, m.p. 187–192° (decomposition, rapid heating), m.p. 180–185° (decomposition, slow heating), $(\alpha)_D$ +50° (*c*, 1.94), ν_{max} 1 742 cm^{-1} (broad band), λ_{max} 200 (ϵ 5 000), n.m.r. bands at 8.98, 8.77, 8.57, 8.04 (3H, singlet), 7.94 (3H, singlet), 6.34 (3H, singlet), and near 4.7 (3H, complex multiplet).

Anal. Calcd. for $C_{35}H_{50}O_8$: C, 70.20; H, 8.42. Found: C, 69.77; H, 8.31.

Isoanhydro Lactone Ester Diacetate (VII)

Anhydro lactone ester diacetate (60 mg) was refluxed for 35 min in methanol (25 ml). Evaporation of the solvent and crystallization from methanol, after separation by t.l.c. (eluant: ether:benzene, 1:1), gave the isoanhydro lactone ester diacetate (30 mg), m.p. 223–225°, $[\alpha]_D$ +10° (*c*, 1.20), ν_{max} 1 745 cm^{-1} (broad band), ν_{max} 1 773, 1 745 cm^{-1} (dioxane), n.m.r. bands at 9.05, 8.93, 8.88, 8.76, 8.61, 8.05 (3H, singlet), 7.96 (3H, singlet), 6.35 (3H, singlet), 5.19 (1H, doublet $J \sim 5$ c.p.s.), 4.62 (2H, multiplet).

Anal. Calcd. for $C_{35}H_{50}O_8$: C, 70.20; H, 8.42. Found: C, 69.98; H, 8.34.

Isoanhydro Lactone Ester

Anhydro lactone ester diacetate (115 mg) was refluxed for 10 min in methanolic potassium hydroxide (15 ml, 5%) under nitrogen. Dilution with water and extraction into ether followed by crystallization from acetone gave the isoanhydro lactone ester (90 mg), m.p. 215–219°, $[\alpha]_D$ −4° (*c*, 1.32), ν_{max} 3 500, 1 760, 1 721 cm^{-1}, n.m.r. bands at 9.02, 8.91, 8.85, 8.81, 8.75, 8.65, 6.28 (3H, singlet), 5.90 (2H, multiplet), 5.17 (1H, doublet $J \sim 5$ c.p.s.).

Anal. Calcd. for $C_{31}H_{46}O_6$: C, 72.34; H, 9.01. Found: C, 71.70; H, 8.63.

Isoanhydro lactone ester (50 mg) was acetylated (pyridine – acetic anhydride, 3:1) by heating for 2.5 h at 90° under nitrogen. Isolation of the product and crystallization from methanol gave a diacetate, m.p. 223–225°, $[\alpha]_D$ +10° (*c*, 1.20) showing no melting point depression on admixture with a sample prepared by refluxing the unrearranged lactone in methanol and having an n.m.r. spectrum identical with that sample

Monomethyl(A) De(hydrochloro)senegenin (IX)

Isoanhydro lactone ester (30 mg) was allowed to stand at room temperature for 15 min in methanol – hydrochloric acid (5%). Isolation of the product and crystallization from acetone gave a quantitative yield of monomethyl (A) de(hydrochloro)senegenin. Recrystallization from acetone gave material which softens at 200°, resolidifies, and melts at 299–301°, $[\alpha]_D$ +71° (*c*, 1.05), λ_{max} 242, 249, 258 mμ (ϵ 14 000, 16 100, 10 100), n.m.r. bands at 9.21, 9.06, 8.95, 8.75, 8.63, 8.23, 6.31 (3H each, all singlets), 5.96 (2H, multiplet), 4.66 (1H, multiplet).

Anal. Calcd. for $C_{31}H_{46}O_6$: C, 72.34; H, 9.01. Found: C, 71.74; H, 8.82.

Methylation with diazomethane and crystallization from acetone gave de(hydrochloro)senegenin dimethyl ester, m.p. 234–235°, $[\alpha]_D$ +82° (*c*, 1.12), showing no melting point depression on admixture with an authentic sample and having an n.m.r. spectrum identical with that of the authentic material.

Monomethyl (A) de(hydrochloro)senegenin (140 mg) was acetylated (pyridine – acetic anhydride, 3:1) by heating 2.5 h at 95° under nitrogen. Isolation of the product and crystallization from acetone – light petroleum gave a diacetate, m.p. 175–180°, $[\alpha]_D$ +60° (*c*, 1.43), ν_{max} 1 739, 1 695 cm^{-1}, λ_{max} 242, 249, 256 mμ (ϵ 15 000, 16 900, 11 700), n.m.r. bands at 9.22, 9.08, 8.97, 8.80, 8.58, 8.25, 8.05, 7.95, 6.35 (3H each, all singlets), 4.56 (3H, multiplet).

Anal. Calcd. for $C_{35}H_{50}O_8$: C, 70.20; H, 8.42. Found: C, 69.60; H, 8.11.

Acid Chloride (IX, COCl Instead of COOH) Formation and Pyrolysis

Monomethyl (A) de(hydrochloro)senegenin diacetate (57 mg) was refluxed in a dry atmosphere for 45 min in carbon tetrachloride (10 ml, dried) containing thionyl chloride (1 ml). Evaporation to dryness gave an oily acid chloride, ν_{max} 1 745, 1 792 cm^{-1}, which on contact with wet solvents was hydrolyzed to the corresponding acid. The freshly made acid chloride (350 mg total) was heated in five equal portions under nitrogen at 265° for 30 min. Separation by t.l.c. (eluant: ether:benzene, 3:7) gave a major portion (130 mg) (R_f near 0.5) which was treated in ethyl acetate solution with a stream of ozone for 5 min at −70°. Nitrogen was then blown through (15 min) to remove excess ozone. Reseparation by t.l.c. and crystallization from methanol gave the pure benzene derivative (X) (53 mg), m.p. 302–303°, ν_{max} 1 739 cm^{-1}, $[\alpha]_D$ +50° (*c*, 0.91), λ_{max} 269 (ϵ 535), n.m.r. bands at 9.06, 9.00, 8.89, 8.85, 8.58, 8.02, 7.91, 6.35 (3H each, all singlets), 4.6 (2H, multiplet), 3.05 (2H, broad singlet).

Anal. Calcd. for $C_{34}H_{48}O_6$: C, 73.88; H, 8.75. Found: C, 73.49; H, 8.96.

Isode(hydrochloro)senegenin Dimethyl Ester

Senegenin monoacetate (495 mg) was refluxed for 18 h under nitrogen in aqueous alcoholic (1:3) sodium hydroxide (85 ml, 5%). Dilution with water and neutralization with saturated KH_2PO_4 solution to pH ~ 6 and extraction into ether gave material which, after methylation (diazomethane) and crystallization from methanol, gave isode(hydrochloro)senegenin dimethyl ester (XIII) (250 mg), m.p. 228–230°, $[\alpha]_D$ +23° (*c*, 1.17), λ_{max} 249 mμ (ϵ 13 100), ν_{max} 3 500, 1 715, 1 616, 1 592 cm^{-1}, n.m.r. bands at 9.13, 8.98, 8.83, 8.70, 6.48 (3H, singlet), 6.36 (3H, singlet), 6.0 (2H, multiplet), 5.40 (1H, singlet), 5.13 (1H, singlet).

Anal. Calcd. for $C_{32}H_{48}O_6$: C, 72.69; H, 9.15. Found: C, 72.75; H, 9.43.

Can. J. Chem. Downloaded from www.nrcresearchpress.com by 210.87.254.6 on 09/05/12
For personal use only.

Rearrangement of Isode(hydrochloro)senegenin Dimethyl Ester

The ester (50 mg) was allowed to stand for 15 min at room temperature in dioxane (5 ml) containing hydrochloric acid (0.5 ml, concentrated). Isolation of the product and crystallization from methanol gave de(hydrochloro)senegenin dimethyl ester, melting point and mixed melting point 221–223°, λ_{max} 243, 249, 258 mμ (ϵ 12 700, 14 700, 10 300). The n.m.r. spectrum was identical with that of an authentic sample.

The α,β-Unsaturated Ketone (XIV)

Isode(hydrochloro)senegenin dimethyl ester (99 mg) was dissolved in methanol (5 ml), the solution cooled to −70°, and ozone bubbled in for 2 min. Nitrogen was blown through the solution for 15 min and acetic acid (0.5 ml) and potassium iodide (0.5 ml, 50% aqueous) was added. The solution was then allowed to warm up to room temperature and after 30 min it was poured into dilute sodium thiosulfate (5%) and extracted into ether. Separation by t.l.c. (eluant: ether:benzene, 3:7) and crystallization from methanol gave the α,β-unsaturated ketone (32 mg), m.p. 228–230°, $[\alpha]_D$ +41° (*c*, 1.38), λ_{max} 253 mμ (ϵ 9 400), ν_{max} 3 500, 1 721, 1 653, 1 613 cm^{-1}.

Anal. Calcd. for $C_{31}H_{46}O_7$: C, 70.16; H, 8.74. Found: C, 70.81; H, 8.50.

The ketone (90 mg) was acetylated (pyridine – acetic anhydride, 3:1) by heating for 3 h at 95° under nitrogen. Extraction into ether and crystallization from methanol gave a diacetate (85 mg), m.p. 245–247°, $[\alpha]_D$ +46° (*c*, 1.88), λ_{max} 253 mμ (ϵ 9 400), ν_{max} 1 745, 1 661, 1 613 cm^{-1}, n.m.r. bands at 8.97, 8.78, 8.62, 8.06, 7.94, 6.44, 6.33 (3H each, all singlets), 4.6 (2H, multiplet).

Anal. Calcd. for $C_{35}H_{50}O_9$: C, 68.38; H, 8.20. Found: C, 68.15; H, 7.89.

Reduction of the α,β-Unsaturated Ketone

The unsaturated ketone dimethyl ester diacetate (72 mg), in three equal portions, was allowed to stand at room temperature for 20 min in methanol (5 ml) containing sodium borohydride (120 mg). The product was poured into dilute acetic acid, neutralized with sodium carbonate (5%), and extracted into ether. Crystallization from methanol gave an alcohol, m.p. 223–224°, $[\alpha]_D$ +33° (*c*, 1.17), λ_{max} 205 mμ (ϵ 7 000), ν_{max} 3 450, 1 733 cm^{-1}. The compound had n.m.r. bands at 9.06 (~ 9H, singlet), 8.86 (3H, singlet), 8.66 (3H, singlet), 8.10 (3H, singlet), 7.97 (3H, singlet), 6.36 (6H, singlet), 5.84 (1H, multiplet), 4.58 (2H, multiplet).

Anal. Calcd. for $C_{35}H_{52}O_9$: C, 68.15; H, 8.50. Found: C, 68.56; H, 8.61.

Norde(hydrochloro)senegenin Dimethyl Ester

The unsaturated ketone dimethyl ester (19 mg) was allowed to stand at room temperature for 15 min in methanol (4 ml) and sodium borohydride (89 mg). The product was isolated as above and dehydrated by warming on a steam bath for 15 min in methanolic hydrochloric acid (10 ml, 5%). Isolation and crystallization from methanol gave the diene (15 mg), m.p. 200–210°, $[\alpha]_D$ +58° (*c*, 1.40), λ_{max} 238, 246, 254 mμ (ϵ 11 800, 13 800, 9 750), n.m.r. bands at 9.17, 9.10, 9.02, 8.77, 8.65, 6.46, 6.31 (3H each, all singlets), 5.99 (2H, multiplet), 5.60 (2H, multiplet).

Anal. Calcd. for $C_{31}H_{46}O_6$: C, 72.34; H, 9.01. Found: C, 71.91; H, 9.00.

Bromination of the Unsaturated Ketone

The unsaturated ketone dimethyl ester diacetate (16.0 mg) was dissolved in 10 ml of a bromine solution (232 mg Br_2 / ml of acetic acid containing 0.05% HBr). Aliquots (1 ml) were withdrawn and dropped into a solution containing potassium iodide (1 ml, 5%), water (5 ml), thiodene indicator (1 ml, 5% aqueous) and titrated with standard *N*/100 sodium thiosulfate. After 90 min the uptake was 1.99 atoms of bromine which increased to 2.05 atoms after a further 90 min.

Preparation of the Trienone (XV)

The unsaturated ketone dimethyl ester diacetate (175 mg) was brominated by allowing it to stand for 2.25 h at room temperature in a mixture of acetic acid (10 ml) and a bromine solution (4 ml, acetic acid containing 46 mg Br_2 / ml and 0.05% HBr). Pouring into sodium thiosulfate solution (25 ml, 10%) and neutralization with bicarbonate (5%), followed by extraction into ether and evaporation in the cold gave the crude dibromo compound (212 mg).

The material so obtained was heated at 105–110° under nitrogen for 5.25 h in dimethyl formamide (12 ml) containing lithium chloride (180 mg). Dilution with water, extraction into ether, and separation by t.l.c. (eluant: ether:benzene, 1:3) followed by crystallization from methanol gave the trienone (88 mg), m.p. 312–314°, $[\alpha]_D$ +136° (*c*, 1.44), λ_{max} 260, 320 mμ (ϵ 8 200, 7 200), ν_{max} 1 742, 1 650, 1 623, 1 570 cm^{-1}. The n.m.r. spectrum showed bands at 9.16, 8.97, 8.68, 8.52, 8.43, 8.05, 7.91, 6.47, 6.36 (3H each, all singlets), 4.73 (1H, doublet $J \sim 4.5$ c.p.s.), 5.40 (1H, complex multiplet), 3.88 (1H, singlet), 3.77 (2H, AB pattern, $J_{AB} = 10$ c.p.s., $\delta_B - \delta_A = 20.7$ c.p.s.).

Anal. Calcd. for $C_{35}H_{46}O_9$: C, 68.83; H, 7.59. Found: C, 69.11; H, 7.55.

Pre-senegenin

Cleavage of the Saponin and Isolation of the Sapogenin

The saponin (30 g) was dissolved in water (1 l) and sodium metaperiodate (41 g) was added over a period of ½ h while the solution was being stirred and cooled in an ice bath. The solution was allowed to stand in the dark at room temperature for 24 h. Then while the solution was stirred, potassium iodide was added (20 g) and then sodium arsenite until the iodine color disappeared. The mixture was neutralized with solid potassium hydroxide, and then an additional 50 g were added. The solution was heated at 100° under

Can. J. Chem. Downloaded from www.nrcresearchpress.com by 210.87.254.6 on 09/05/12
For personal use only.

nitrogen with stirring for 1 h, cooled, and carefully acidified with hydrochloric acid to pH ~ 3. Extraction with ether gave 4.5 g of crude sapogenin. Methylation (diazomethane) and chromatography on silica gel (100 g, BDH) gave a crystalline sapogenin ester (1.5 g). Several recrystallizations from ethyl acetate gave the sapogenin dimethyl ester, m.p. 214–215°, $[\alpha]_D$ +78° (*c*, 2.22), ν_{max} 3 500, 1 718 cm^{-1}, n.m.r. bands at 9.37, 9.12, 9.07, 8.82, 8.68, 6.38, 6.32 (3H each, all singlets), 5.98 (2H, multiplet), 4.16 (1H, multiplet).

Anal. Calcd. for $C_{32}H_{50}O_7$: C, 70.30; H, 9.22. Found: C, 70.42; H, 9.28.

Acetylation of Pre-senegenin Dimethyl Ester

The ester was acetylated (pyridine – acetic anhydride, 3:1) by heating at 95° for 3 h under nitrogen. Evaporation and extraction into ether gave a triacetate which, on crystallization from methanol, had m.p. 219–220°, $[\alpha]_D$ +110° (*c*, 2.32), ν_{max} 1 727, 1 739 cm^{-1}, n.m.r. bands at 9.30, 9.13, 9.07, 8.80, 8.60, 8.07, 7.98, 7.96, 6.26, 6.23 (~ 3H each, all singlets), 5.90 (2H, broad singlet), 4.56 (3H, complex multiplet).

Anal. Calcd. for $C_{38}H_{50}O_{10}$: C, 67.83; H, 8.39. Found: C, 67.85; H, 8.45.

Isolation of Pre-senegenin

The crude sapogenin (1.4 g) was separated by t.l.c. (eluant: acetic acid : chloroform, 1:4) to give 450 mg of sapogenin. Crystallization from aqueous alcohol (care being taken not to heat the solvent excessively) gave pure pre-senegenin, m.p. 310–311°, $[\alpha]_D$ +91° (*c*, 1.16, MeOH).

Anal. Calcd. for $C_{30}H_{46}O_7 \cdot 0.5H_2O$: C, 68.28; H, 8.98. Found: C, 67.95; H, 8.82.

Identification of p-Methoxy Cinnamic Acid

Chromatography of the methylated crude sapogenin mixture on silica gel (BDH) yielded, besides the terpenoid ester, *p*-methoxy methyl cinnamate as identified by melting point, mixed melting point, and infrared spectrum. Separation of the crude sapogenin gave, besides the sapogenin, *p*-methoxy cinnamic acid as identified by melting point and mixed melting point.

Conversion of Pre-senegenin to Senegenin and Polygalic Acid

The sapogenin (167 mg) was refluxed for 1.25 h in a mixture of ethanol (10 ml), water (3 ml), and hydrochloric acid (1.35 ml, concentrated). Dilution with water and extraction into ether followed by re-extraction into aqueous sodium bicarbonate (5%) gave neutral (17 mg) and bicarbonate-soluble material (140 mg). Methylation of the latter with diazomethane and separation on t.l.c. (eluant: ether:benzene, 3:1) gave senegenin dimethyl ester (61 mg), $[\alpha]_D$ +14° (*c*, 1.12) and dimethyl polygalate (50 mg), m.p. 211–212°, $[\alpha]_D$ +23° (*c*, 1.11). The dimethyl senegenin was identified by comparison of the n.m.r. spectrum, infrared spectrum, and R_F (t.l.c.) with an authentic specimen. The dimethyl polygalate was identified by melting point and mixed melting point determination with an authentic specimen prepared from polygalic acid by esterification with diazomethane. Crystallized from methanol this had m.p. 211–212°, $[\alpha]_D$ +22° (*c*, 1.00).

Anal. Calcd. for $C_{31}H_{48}O_6$: C, 72.06; H, 9.36. Found: C, 71.62; H, 8.93.

No other product could be detected by t.l.c.

Treatment of Pre-senegenin Dimethyl Ester with HCHO:HCl

(*a*) The ester (4 mg) was refluxed 1.25 h in a mixture of ethanol (1.5 ml), water (0.5 ml), and hydrochloric acid (0.2 ml, concentrated). The product was diluted with water and extracted into ether.

(*b*) The ester (4 mg) was refluxed 1.25 h in a mixture of ethanol (1.5 ml), water (0.18 ml), formaldehyde (0.32 ml, 3.7% aqueous solution), and hydrochloric acid (0.2 ml, concentrated). The product was isolated as above.

Running a series of spots of various concentrations, from the above experiments, using t.l.c. (eluant: ether:benzene, 3:1) indicated no detectable difference in the ratio of senegenin ester to polygalic acid ester in the two experiments (the plates were sprayed with 50% H_2SO_4 and charred).

Pyrolysis of Pre-senegenin Dimethyl Ester

The ester (75 mg) was heated at 220° for 30 min under a stream of nitrogen that bubbled into an aqueous dimedone solution (40 ml, 0.45%). A precipitate formed immediately. The solution was allowed to stand for 2 h and the precipitate collected. The product (29 mg, 73% yield) was identified as the dimedone derivative of formaldehyde by melting point and mixed melting point comparison with an authentic sample; t.l.c. (eluant: ether:benzene, 3:1) showed only one pyrolysis product which, on crystallization from methanol, was identified as dimethyl polygalate (57 mg) by melting point, mixed melting point, and rotation.

Acid Treatment of Pre-senegenin Dimethyl Ester in the Presence of 2,4-Dinitrophenylhydrazine

Pre-senegenin dimethyl ester (86 mg) and 2,4-dinitrophenylhydrazine (89 mg) were refluxed for 2.5 h in a mixture of methanol (13 ml), water (4 ml), and hydrochloric acid (2 ml, concentrated). Isolation of the products and separation by t.l.c. (eluant: chloroform) gave formaldehyde 2,4-dinitrophenylhydrazone (4.7 mg) identified by melting point and mixed melting point comparison with an authentic sample.

*Deuterium Experiments**

Pre-senegenin dimethyl ester (215 mg) was dissolved in dried dioxane (1 ml), D_2O (10 drops, 99.65%) added, and the mixture evaporated to dryness. This process was repeated three times, the tube sealed under high vacuum and heated at 220° for 20 min. The product was separated by t.l.c. (eluant: ether:benzene, 3:1) and crystallized from methanol to give dimethyl polygalic acid-d_1 (106 mg).

**Deuterium analyses by Josef Nemeth, 303 Washington St., Urbana, Illinois.*

Can. J. Chem. Downloaded from www.nrcresearchpress.com by 210.87.254.6 on 09/05/12
For personal use only.

Anal. Calcd. for $C_{31}H_{47}O_6D$: 2.08% excess deuterium. Found: 1.40% excess deuterium.

Dimethyl polygalate-d_1 (80 mg) was acetylated (pyridine – acetic anhydride) to give the diacetate. The product was dissolved in acetic acid (1 ml), chromic acid (5 ml, 0.4 *N* in acetic acid) added, and the solution allowed to stand for 1 h at room temperature. The product was poured into a bisulfite solution and extracted into chloroform. Separation by thin-layer chromatography and crystallization gave the α,β-unsaturated ketone (XIV) (10 mg), m.p. 245–247°.

Found: 0.00% excess deuterium.

Dimethyl polygalate diacetate (87 mg) was allowed to stand 1 h at room temperature in 5 ml of 0.5 *N* chromic acid in acetic acid-d_1. The solution was poured into D_2O (30 ml), bisulfite added, and the solution extracted into chloroform. Purification in the usual way gave the α,β-unsaturated ketone (XIV) (16 mg).

Found: $< 0.04\%$ excess deuterium.

Esterification Experiments

Polygalic acid diacetate (113 mg) was refluxed for 6 h in a mixture of methanol (20 ml) and hydrochloric acid (5 ml, concentrated). This was poured into water and extracted into ether. The n.m.r. was taken in pyridine indicating $\sim 100\%$ methylation.

Senegenin monoacetate (87 mg) was treated under exactly the same conditions as above and the n.m.r. spectrum of the crude product was taken in pyridine showing $\sim 24\%$ methylation.

Oleanonic acid (91 mg) was treated as above and the n.m.r. spectrum of the crude product, taken in deuteriochloroform, indicated $\sim 7\%$ methylation.

ACKNOWLEDGMENTS

The authors wish to thank the National Research Council of Canada for financial support and for a scholarship to one of us (J. J. D.).

REFERENCES

1. J. J. DUGAN, P. DE MAYO, and A. N. STARRATT. Can. J. Chem. **42**, 491 (1964).
2. J. J. DUGAN, P. DE MAYO, and A. N. STARRATT. Proc. Chem. Soc. 264 (1964).
3. M. SHAMMA and L. P. RIEFF. Chem. Ind. London, 1272 (1960).
4. W. A. JACOBS and O. ISLER. J. Biol. Chem. **119**, 155 (1937).
5. D. H. R. BARTON and B. R. THOMAS. J. Chem. Soc. 1842 (1953).
6. D. H. R. BARTON, H. T. CHEUNG, P. J. L. DANIELS, K. G. LEWIS, and J. F. MCGHIE. J. Chem. Soc. 5163 (1962).
7. J. RONDEST and J. POLONSKY. Bull. Soc. Chim. France, 1253 (1963).
8. H. BUDZIKIEWICZ, J. M. WILSON, and C. DJERASSI. J. Am. Chem. Soc. **85**, 3688 (1963).
9. J. J. DUGAN, P. DE MAYO, and A. N. STARRATT. Tetrahedron Lettors, **37**, 2567 (1964).
10. S. W. PELLETIER, N. ADITYACHAUDHURY, M. TOMASZ, J. J. REYNOLDS, and R. MECHOULAM. Tetrahedron Letters, **41**, 3065 (1964).
11. J. W. ROWE, A. MELERA, D. ARIGONI, O. JEGER, and L. RUCZICKA. Helv. Chim. Acta, **40**, 1 (1957).
12. W. G. DAUBEN and J. B. ROGAN. J. Am. Chem. Soc. **79**, 5002 (1957).
13. A. ZURCHER, O. JEGER, and L. RUCZICKA. Helv. Chim. Acta, **37**, 2145 (1954).
14. A. I. SCOTT. The ultraviolet spectra of natural products. Pergamon Press. 1964. p. 59.
15. T. Q. CHOU, J. H. CHU, and P. F. MEI. J. Am. Pharm. Assoc. Sci. Ed. **36**, 241 (1947).
16. R. TSCHESCHE and A. K. SEN GUPTA. Chem. Ber. **93**, 1903 (1960).
17. M. FUJITA and H. ITOKAWA. Chem. Pharm. Bull. Tokyo, **9**, 1006 (1961).
18. W. E. IRWIN. Ph.D. Thesis, The Pennsylvania State University. 1962.

Can. J. Chem. Downloaded from www.nrcresearchpress.com by 210.87.254.6 on 09/05/12
For personal use only.

Can. J. Chem. Downloaded from www.nrcresearchpress.com by 210.87.254.6 on 09/05/12
For personal use only.

INFRARED EMISSION SPECTRA OF FATTY ACIDS ON STEEL SURFACES[1]

M. J. D. Low and H. Inoue
School of Chemistry, Rutgers, The State University, New Brunswick, New Jersey
Received March 5, 1965

ABSTRACT

Infrared emission spectra of oleic, linoleic, linolenic, and stearic acids, and of methyl linolenate, on the surfaces of steel plates were measured at 100, 150 and 200° from 5 to 10 microns. Reactions occur to produce complex iron soaps.

The study of molecular species chemisorbed on infrared-transmitting solids has advanced markedly since the application of infrared absorption techniques to surface problems (1). However, relatively little work has been done with surfaces of bulk materials that are opaque to infrared radiation. Although reflection techniques have been developed (2, 3), these are delicate and tedious. Little attention has been paid to the alternate technique of infrared emission spectroscopy.

Some exploratory emission experiments were made by Eischens and Pliskin (1), but with little success. More recent experiments (4), however, indicated that emission methods could be used in special cases for the examination of the surface of opaque bulk solids. Infrared emission spectra of fatty acids on steel surfaces have now been obtained.

EXPERIMENTAL

A Perkin–Elmer Model 521 spectrometer fitted with a high sensitivity thermocouple* was used. Samples were placed between NaCl or CaF_2 plates for absorption spectra. Soft steel plates 1 mm thick were used as emitters for emission spectra, in conjunction with a heating device described elsewhere (4). All emission spectra shown are differential spectra obtained with slits fixed at 290 microns. The calculated spectral slit width at 1 600 cm^{-1} was 3 cm^{-1}. Units of emission and absorption ordinates are arbitrary. The fatty acids and methyl ester were of 99+% purity, obtained from The Hormel Institute.

The emitter plates were polished with grade 000 sandpaper, dipped in dilute nitric acid polished with alumina, and were washed and dried prior to use. A pair of plates was brought to constant temperature, and a thin layer of fatty acid was then quickly spread on one plate with a filter paper or glass-wool brush. Excess acid was wiped off, so that the plate surface appeared to be dry. Emission spectra were then recorded.

EXPERIMENTS, RESULTS, AND DISCUSSION

A pronounced feature of an infrared spectrum of oleic acid is a carbonyl stretching mode at about 1 700 cm^{-1} that is characteristic of C=O associated with the acid hydroxyl group. Ionization of the carboxyl group brings about bands at higher frequencies, spectra of ionic oleates showing bands near 1 555 cm^{-1} as well as in the region 1 470 – 1 400 cm^{-1}, corresponding to antisymmetrical and symmetrical vibrations of the ionized carboxyl group, respectively. Attention is therefore focused on the region from 1 800 cm^{-1} to about 1 300 cm^{-1}, on the assumption that a surface reaction would involve the formation of a carboxylate species. That region is shown in the figures presented.

Figure 1 shows examples of emission spectra of oleic acid coated steel, as well as an absorption spectrum of oleic acid. Greater detail is shown by the spectra of Fig. 2. These and similar results showed that stable spectra were obtained with the emitter plates at

[1]*Report of work done, in part, under contract with the U.S. Department of Agriculture and authorized by the Research and Marketing Act. The contract was supervised by the Northern Utilization Research and Development Division of the Agricultural Research Service.*
**C. M. Reeder Co., 173 Victor Ave., Detroit, Michigan.*

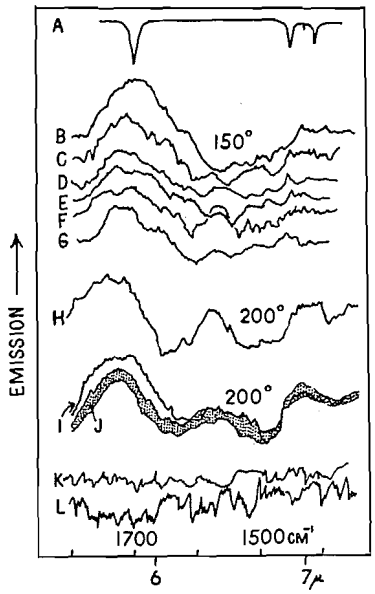

FIG. 1. Emission spectra of oleic acid on steel. All emission spectra were measured at 1× ordinate scale expansion. A. Schematic absorption spectrum of oleic acid. B–G. Emission at 150°. The time in min elapsed after oleic acid addition were: B, none; C, 17; D, 28; E, 38; F, 49; G, 60. H. Emission at 200° after a coated plate had been kept at 150° for 1 h. I. Emission at 200° immediately after acid addition. J. The dotted region represents 6 consecutive scans lasting 41 min, made after spectrum I. K. 150° background. L. 200° background.

100°. At 150° and 200°, however, some evaporation of oleic acid from the emitter plates occurred initially and, also, some changes occurred in the spectra with the passage of time. Slight decreases in intensity of all bands occurred at 200°, but even after 5 h the spectra could be readily observed. The emitter plates initially were and remained bright during the experiment, so that the oxide coating was minimal. Satisfactory emission spectra could not be obtained with plates deliberately oxidized to a great extent.

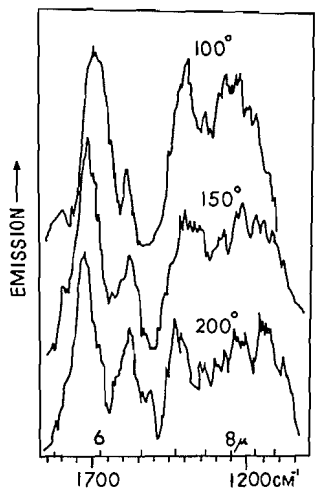

FIG. 2. Emission spectra of oleic acid on steel. Each spectrum was measured immediately after oleic acid addition, at 5× ordinate scale expansion.

Can. J. Chem. Downloaded from www.nrcresearchpress.com by 210.87.254.6 on 09/05/12
For personal use only.

The results of similar experiments at 100, 150, and 200° with linoleic and linolenic acids were like those obtained with oleic acid and need not be discussed separately. The position of emission bands observed at 100° with stearic acid were like those of oleic acid, but satisfactory spectra could not be obtained at higher temperatures because band intensities declined rapidly.

Similar experiments were made with methyl linolenate. Emission and absorption spectra are shown in Fig. 3. Emission band intensities declined rapidly even at 100°, so that structure could not be observed in the spectrum after about 20 min. This suggests that relatively rapid evaporation occurred. Also, the stearic acid and ester spectra were comparatively "noisy". This could be caused by cooling of the emitter surface through evaporation.

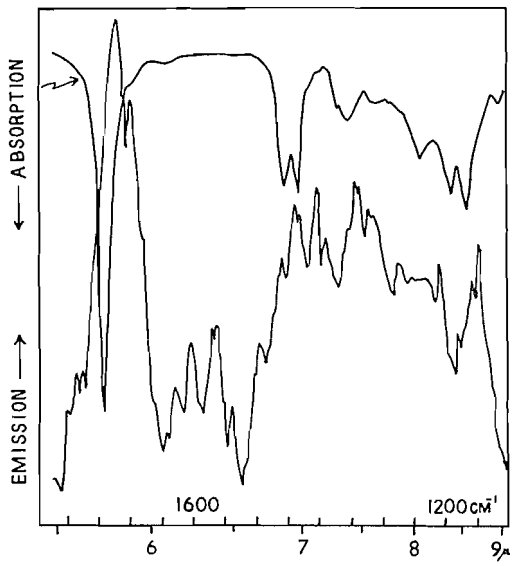

FIG. 3. Spectra of methyl linolenate. The emission spectrum was obtained at 100° immediately after ester addition, at 5× ordinate scale expansion.

The greater retention on the surface of oleic, linoleic, and linolenic acids than of methyl oleate would imply that the reaction at double bonds alone to form carbon-to-surface bonds was not significant. The relatively rapid removal of stearic acid, however, suggests that both carboxyl groups and double bonds could be involved, possibly through the formation of a surface species similar in structure to the complex zinc oleate described by Jacobsen and Gardner (5), involving a coordination of the 9,10 double bond to a Zn atom and a bond to that same atom from one of the oxygen atoms of the carboxyl group of the same acid radical. An alternative is the degeneration of the unsaturated acids to form polymers on the surface.

The 100° spectra of Figs. 1 and 2 showed strong bands near 1 700 cm^{-1}, indicating the presence of oleic acid. At 150°, however, that band gradually shifted to 1 720 cm^{-1}. If acid was placed on an emitter plate at 200°, however, a band appeared immediately at 1 720 cm^{-1}. Also, bands appeared in the region 1 120 – 1 140 cm^{-1} at 200°, as shown in Fig. 2. As this shift might be caused by the formation of degradation products, absorption spectra were obtained of oleic acid after heating in air in Erlenmeyer flasks. Heating at 140° for

Can. J. Chem. Downloaded from www.nrcresearchpress.com by 210.87.254.6 on 09/05/12
For personal use only.

24 h caused a shoulder near 1 720 cm^{-1} to appear on the original 1 703 cm^{-1} band, and a weak band was detected at 1 170 cm^{-1}. After 48 h at 140° the shoulder had grown into a distinct band at 1 730 cm^{-1} and the 1 173 cm^{-1} band had increased. After 168 h at 140°, broad bands were found at 1 740 and 1 720 cm^{-1}, and a general loss of structure occurred in the 1 500 – 900 cm^{-1} region. Heating at 200° for 4 h had no effect, however. The spectrum obtained after heating for 48 h at 200° was similar to the 140°, 48 h spectrum. The results indicate a slow degeneration of oleic acid in air, and suggest that the 1 700 to 1 720 cm^{-1} shift is caused by the formation of a surface polymer.

It is interesting to note, however, that this shift was observed only with Fe and Co, but not with Al (4), Cu, Zn, Cd, Ag, Au, or Sn (6). There is also similarity between the 200° acid emission spectra and that of the methyl ester, which shows a strong carbonyl band at 1 720 cm^{-1} and a characteristic band at 1 170 cm^{-1} that is ascribed to the linear C—O vibration (7). The 1 700 – 1 720 cm^{-1} shift may thus be brought about through the formation of ester linkages.

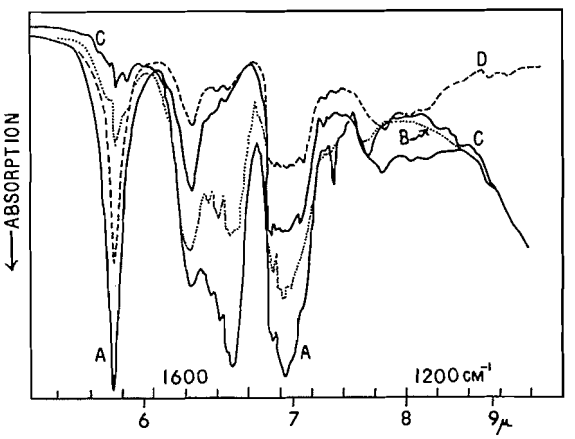

FIG. 4. Absorption spectra of iron oleates. Aqueous solution of sodium oleate (I) and $Fe(NO_3)_3$ (II) or $Fe(NH_4)_2(SO_4)_2$ (III) were mixed, and the precipitate extracted with isooctane. The mole ratios were: A, I/II = 1; B, I/II = 1/3; C, I/III = 1; D, I/II = 1/3.

The emission spectra also show structure in the 1 650 – 1 500 cm^{-1} region that is absent in the oleic acid absorption spectrum, suggesting that reactions involving the carboxylate group had occurred. Bands and shoulders were found near 1 570 and 1 580 cm^{-1} and near 1 550 cm^{-1}. The centers of broad bands from about 1 600 to 1 500 cm^{-1} centering near 1 570 cm^{-1} were occasionally shifted to near 1 550 cm^{-1}. To obtain further information, as iron oleate spectra do not seem to have been reported, some precipitates were prepared from sodium oleates and iron salts. The absorption spectra are given in Fig. 4. The sharp bands near 1 710 cm^{-1} point to the presence of free oleic acid. The relative intensities of bands near 1 590, 1 550, and 1 530 cm^{-1} changed with the proportion of reactants, suggesting the existence of at least two iron oleate structures. As the aqueous oleate ion has a band near 1 555 cm^{-1}, the 1 550 cm^{-1} band could be ascribed to sodium oleate impurity as well as to the free oleate ion of an iron salt. The structures of the iron oleates are not known. Complex iron acetates (8) are known, however. Also, binuclear acetate complexes $Cr(ac)_4 \cdot 2H_2O$ and $Cu(ac)_4 \cdot 2H_2O$ (9) and the analogous copper oleates and stearates (10), with structure I, were reported to give bands at 1 575, 1 605, 1 588, and 1 585 cm^{-1}, respectively, assigned to the asymmetric OCO vibration. It seems possible that the 1 590

Can. J. Chem. Downloaded from www.nrcresearchpress.com by 210.87.254.6 on 09/05/12
For personal use only.

cm^{-1} band of the precipitates and the emission bands near 1 570 cm^{-1} may be caused by the same vibration of species such as I or II.

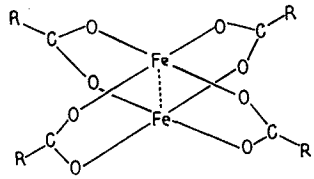

I

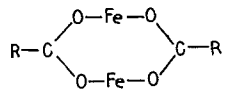

II

The emission spectra are, unfortunately, not well enough resolved for adequate characterization of the carboxylate species present on the surface. The presence of shoulders and bands over a relatively wide spectral region and the shifting of the bands suggest, however, that species other than unassociated carboxylate ions are formed involving in part, the abstraction of iron atoms from the surface. The shifting of bands to lower wave numbers on heating suggests that some change occurs in the complexes, possibly a dissociation to $RCOO^-$.

ACKNOWLEDGMENTS

Support from the U.S. Department of Agriculture is gratefully acknowledged, as is a National Science Foundation Instrument Grant GP 1434.

REFERENCES

1. R. P. Eischens and W. A. Pliskin. Advan. Catalysis, **9**, 1 (1958).
2. H. L. Pickering and H. C. Eckstrom. J. Phys. Chem. **63**, 512 (1959).
3. S. A. Francis and A. H. Ellison. J. Opt. Soc. Am. **49**, 131 (1959); J. Chem. Eng. Data, **6**, 83 (1961).
4. M. J. D. Low and H. Inoue. Anal. Chem. **36**, 2397 (1964).
5. A. E. Jacobsen and W. H. Gardner. Ind. Eng. Chem. **33**, 1254 (1941).
6. M. J. D. Low. Unpublished results.
7. L. J. Bellamy. The infrared spectra of complex molecules. John Wiley & Sons, Inc., New York. 1960. pp. 178 ff.
8. W. D. Treadwell and W. Fish. Helv. Chim. Acta, **13**, 1209, 1219 (1930); **18**, 200 (1935).
9. K. Nakamoto, Y. Morimoto, and A. E. Martell. J. Am. Chem. Soc. **83**, 4528 (1961).
10. I. Satake and R. Matuura. Kolloid-Z. **176**, 31 (1961).

Can. J. Chem. Downloaded from www.nrcresearchpress.com by 210.87.254.6 on 09/05/12
For personal use only.

Can. J. Chem. Downloaded from www.nrcresearchpress.com by 210.87.254.42 on 09/05/12
For personal use only.

CHEMISTRY OF THE COMPLEXES OF URANYL AND PLUTONYL IONS WITH ORGANIC LIGANDS

P. V. BALAKRISHNAN, S. K. PATIL, H. D. SHARMA, AND H. V. VENKATASETTY
Radiochemistry and Isotope Division, Atomic Energy Establishment, Trombay, Bombay

Received August 24, 1964

ABSTRACT

A series of complexes of uranyl and plutonyl ions with different organic ligands have been prepared and investigated by infrared spectra and magnetic susceptibility measurements. The uranyl complexes were found to be weakly diamagnetic and the plutonyl complex was found to be paramagnetic. Two ligand series are defined on the basis of the infrared asymmetric stretching frequency of the uranyl and plutonyl groups.

The chemistry of the oxometal ions is of interest because of the existence of a strong multiple metal–oxygen covalent bond persisting in various chemical environments. This can be employed as an internal molecular probe to understand more about the nature of metal–ligand bonds in the complexes of these ions (1). Many coordination compounds of uranyl ion have been prepared and their properties studied, but the problems of the coordination number of the uranium atom and the nature of binding are as yet not well understood (2–6). From the available experimental data it would seem that there is a definite preference for a coordination number of eight for the uranium atom, the axial oxygens being considered as ligands, and that all the other ligands are directly bonded to the uranium atom in a plane perpendicular to the axial U—O bonds. In the case of plutonyl ion there have been very little data in the literature both on the magnetic susceptibility and on the infrared spectra of the solid complexes (1, 2).

This paper describes the preparation of the complexes of uranyl nitrate with dimethyl sulfoxide (DMSO), pyridine (py), 2,2′-dipyridyl (dipy), 2,2′-dipyridyl-N,N′-dioxide (dipy·O_2), and *o*-phenanthroline (phen), and of the complexes of plutonyl chloride with dipy, dipy·O_2, and phen as well as the investigation of their properties by infrared spectra and magnetic susceptibility measurements.

EXPERIMENTAL

$UO_2(NO_3)_2 \cdot 2DMSO$

Uranyl nitrate hexahydrate (4.0 g) in ethanol was added to pure dimethyl sulfoxide (10 ml). On standing a yellow compound precipitated. This was filtered, washed with ethanol, and dried *in vacuo*. This compound was insoluble in benzene and carbon tetrachloride, but soluble in acetone, methanol, acetonitrile, and water. Found: U, 43.13; C, 9.04; H, 2.25. Calcd. for $UO_2(NO_3)_2 \cdot 2DMSO$: U, 43.27; C, 8.7; H, 2.2.

$UO_2(NO_3)_2 \cdot H_2O \cdot py$

Uranyl nitrate hexahydrate (4.0 g) in *n*-butyl acetate was mixed with reagent grade pyridine (2.0 g). The greenish-yellow precipitate obtained was filtered, recrystallized from ethanol, and dried *in vacuo*. It was insoluble in benzene and carbon tetrachloride, slightly soluble in acetone and acetonitrile, but more soluble in methanol and water. Found: U, 47.9; C, 11.8; H, 1.3. Calcd. for $UO_2(NO_3)_2 \cdot H_2O \cdot py$: U, 48.2; C, 12.2; H, 1.4. Thermogravimetric analysis confirmed this formula.

$UO_2(NO_3)_2 \cdot dipy$

Uranyl nitrate hexahydrate (4.0 g) in ethanol was mixed with 2,2′-dipyridyl (3.0 g) in ethanol. The resulting yellow precipitate was removed by filtration, washed with ethanol, and dried *in vacuo*. It was insoluble in benzene, carbon tetrachloride, acetone, and water, but slightly soluble in methanol and acetonitrile. Found: U, 42.5; N, 10.4; C, 22.3; H, 1.4. Calcd. for $UO_2(NO_3)_2 \cdot dipy$: U, 43.27; N, 10.21; C, 21.8; H, 1.45. Thermogravimetric analysis confirmed this formula.

$UO_2(NO_3)_2(dipy{\cdot}O_2)$

2,2′-Dipyridyl-N,N′-dioxide was prepared from 2,2′-dipyridyl as described elsewhere (7). Uranyl nitrate hexahydrate (2.0 g) in ethanol was mixed with dipy·O_2 (10.0 g) in boiling ethanol. The resulting light-yellow precipitate was filtered, washed with ethanol, and dried *in vacuo*. It was insoluble in benzene, carbon tetrachloride, and acetone, slightly soluble in methanol and acetonitrile, but more soluble in water. Found: U, 41.08; N, 9.2; C, 20.9; H, 1.34. Calcd. for $UO_2(NO_3)_2$(dipy·O_2): U, 40.88; N, 9.6; C, 20.6; H, 1.37.

$UO_2(NO_3)_2{\cdot}phen$

Uranyl nitrate hexahydrate (4.0 g) in ethanol was mixed with *o*-phenanthroline (4.0 g) in ethanol. The resulting pale-yellow precipitate was filtered, washed with ethanol, and dried *in vacuo*. It was insoluble in benzene, carbon tetrachloride, acetone, and water but slightly soluble in methanol and acetonitrile. Found: U, 40.1; N, 9.73; C, 26.9; H, 1.5. Calcd. for $UO_2(NO_3)_2$·phen: U, 41.45; N, 9.81; C, 25.1; H, 1.4. Thermogravimetric analysis confirmed this formula.

Plutonium purified by ion exchange method was oxidized by ozone to plutonium(VI) in 1 *M* HCl (8) and used for the preparation of the complexes.

$PuO_2Cl_2(dipy{\cdot}HCl)_2$

About 5 ml of a solution containing about 30 mg of plutonium as plutonium(VI) in 1 *M* HCl was mixed with about 150 mg of 2,2′-dipyridyl in acetone. The resulting clear solution was treated with excess of dioxane until a yellow, oily layer separated. This layer was separated, treated with more dioxane and alcohol, and dried. A yellowish-brown solid was thus obtained. Found: Pu, 32.3; Cl, 19.08. Calcd. for PuO_2Cl_2(dipy·HCl)$_2$: Pu, 32.8; Cl, 19.5.

$PuO_2Cl_2(phen{\cdot}HCl)_2$

About 5 ml of a solution containing about 30 mg of plutonium as plutonium(VI) in 1 *M* HCl was mixed with about 150 mg of phenanthroline. On treating the resulting clear solution with dioxane a yellowish-brown solid separated. It was thoroughly washed with ethanol and dried. Found: Pu, 29.73; Cl, 16.44; Calcd. for PuO_2Cl_2(phen·HCl)$_2$: Pu, 30.8; Cl, 18.3.

$PuO_2Cl_2(dipy{\cdot}O_2{\cdot}HCl)_2$

About 5 ml of a solution containing about 30 mg of plutonium as plutonium(VI) in 1 *M* HCl was mixed with about 150 mg of 2,2′-dipyridyl-N,N′-dioxide. The resulting clear solution gave on standing a reddish-brown precipitate. It was thoroughly washed with dioxane and ethanol and dried. Found: Pu, 27.8; Cl, 16.5; Calcd. for PuO_2Cl_2(dipy·O_2·HCl)$_2$: Pu, 30.2; Cl, 17.9. Thermogravimetric analysis of the compound confirmed the above formula.

The infrared spectra of these complexes were obtained in Nujol mull in the region 4 000 – 625 cm^{-1}, using a Perkin–Elmer Model 237 Spectrophotometer. The wave numbers in the region 2 000 – 625 cm^{-1} are accurate to ± 3 cm^{-1}. The magnetic susceptibility measurements were made in the solid phase by the Gouy method using water and nickel chloride solution as standards. The susceptibility values are accurate to $\pm 2\%$. The thermogravimetric measurements were made in a silica spring thermobalance with a sensitivity of 2.5 mm/mg. The rate of heating was maintained at 5 °C/min. About 10 mg of the sample was taken for each thermogravimetric study.

RESULTS AND DISCUSSION

Recent X-ray diffraction work (9) and the infrared (10, 11) and Raman spectral studies (12) on uranyl and plutonyl ions (11) show that these ions are linear and the strong absorption band in the region between 900–950 cm^{-1} was assigned to the asymmetric stretching mode of the metal–oxygen bonds. Not much work has been reported on the infrared spectra of the actinide complexes. Barr and Harton (13), who studied the infrared spectrum of the pyridine complex of uranyl nitrate, made some qualitative observations regarding the C=C and C=N stretching modes of the pyridine ring. Jones (14) studied the infrared spectra of the sodium acetate complexes of U(VI), Np(VI), Pu(VI), and Am(VI) and calculated the approximate values of the force constants for the metal–oxygen bonds from their symmetric and asymmetric stretching frequencies. Gatehouse, Livingston, and Nyholm (15) studied the infrared spectra of uranyl nitrate hydrates and alkalimetal uranyl nitrates in order to differentiate a coordinatively bound nitrate group from a nitrate ion.

The infrared spectra of the complexes of the uranyl and plutonyl ions with pyridine, 2,2′-dipyridyl, and *o*-phenanthroline have several absorption peaks characteristic of the

Can. J. Chem. Downloaded from www.nrcresearchpress.com by 210.87.254.42 on 09/05/12
For personal use only.

Can. J. Chem. Downloaded from www.nrcresearchpress.com by 210.87.254.42 on 09/05/12
For personal use only.

TABLE I

The assignments of the main infrared bands in cm^{-1}

Assignment	$UO_2(NO_3)_2 \cdot 2DMSO$	$UO_2(NO_3)_2 \cdot H_2O \cdot py$	$UO_2(NO_3)_2 \cdot dipy \cdot O_2$	$UO_2(NO_3)_2 \cdot dipy$	$UO_2(NO_3)_2 \cdot phen$
U—O asymmetric stretching	922 (S)	926 (S)	929 (S)	943 (S)	937 (S)
N—O asymmetric stretching	1 510 (S)	1 525 (S)	1 510 (S)	1 515 (S)	1 525 (S)
N—O symmetric stretching	1 282 (S)	1 270 (S)	1 280 (S)	1 280 (S)	1 280 (S)
S—O stretching	985 (S)	—	—	—	—
O—H bending	—	1 648 (W)	—	—	—
O—H stretching	—	3 530 (S) 3 230 (S) 3 160 (S) 3 105 (S) 3 070 (S)	—	—	—
N—O stretching*	—	—	1 222 (S) 1 205 (M)	—	—

Abbreviations: S = strong; M = medium; W = weak.
*N—O stretching mode of the ligand in the complex.

C═C, C═N, and C—H groups of the ligands. These absorption bands are shifted appreciably from those of free ligands. In addition the complex $UO_2(NO_3)_2.H_2O.py$ has a peak around 1 648 cm^{-1}, characteristic of the bending vibration of the water molecule, and a pair of bands in the region 3 000 – 3 530 cm^{-1}, characteristic of the stretching modes of the bonded water molecule (16) (Table I). The asymmetric stretching mode (ν_3) of U—O bond of the uranyl group in these complexes appears at 926 cm^{-1} in $UO_2(NO_3)_2.H_2O.py$, at 937 cm^{-1} in $UO_2(NO_3)_2.phen$, and at 943 cm^{-1} in $UO_2(NO_3)_2.dipy$ (Fig. 1). McGlynn, Smith, and Nealy (17), who made similar studies on the pyridine and *o*-phenanthroline complexes of uranyl nitrate, found ν_3 at 926 cm^{-1} for the pyridine complex and ν_3 at 945 cm^{-1} for the *o*-phenanthroline complex. Similarly the infrared studies on the *o*-phenanthroline and dipyridyl complexes of the plutonyl ion show that the asymmetric stretching mode (ν_3) of the Pu—O bond of the plutonyl group appears at 912 cm^{-1} in the plutonyl phenanthroline complex and at 918 cm^{-1} in the plutonyl dipyridyl complex (Fig. 2).

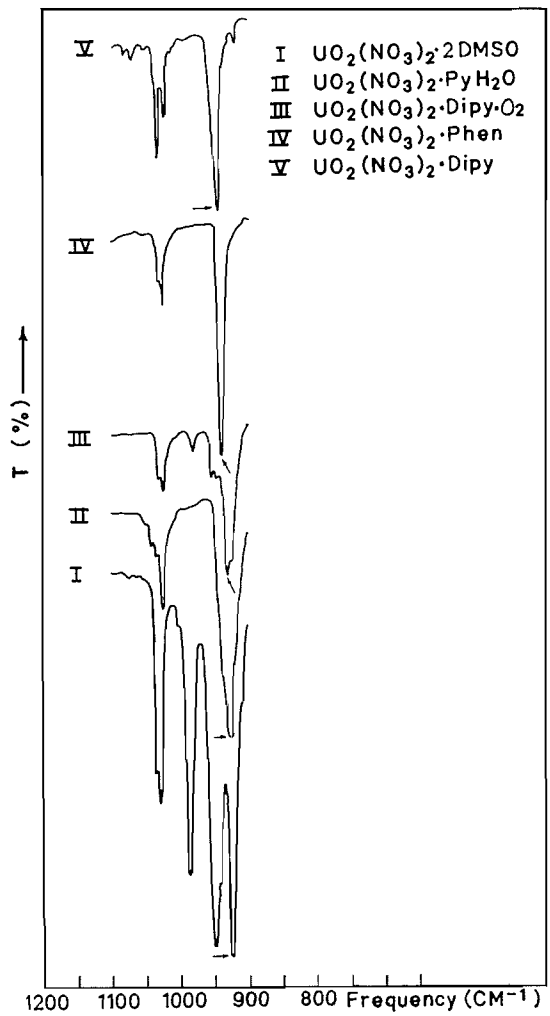

FIG. 1

Can. J. Chem. Downloaded from www.nrcresearchpress.com by 210.87.254.42 on 09/05/12
For personal use only.

In the complex $UO_2(NO_3)_2(dipy{\cdot}O_2)$, the ligand dipy-$O_2$, which forms a seven-membered chelate ring with the metal, very likely is present in a staggered conformation (7). In the spectrum of the complex, of the two ν(N—O) stretching vibrations, one appears as a sharp band at 1 222 cm^{-1} and the other appears as a medium band at 1 205 cm^{-1} (Table I). This lowering of the N—O stretching frequencies from the free ligand values of 1 262 cm^{-1} and 1 255 cm^{-1} (7) is attributed to oxygen–metal coordination. The sharp band at 929 cm^{-1} (Fig. 1) is assigned to the asymmetric (ν_3) stretching mode of the U—O bond of the uranyl group. Similarly for the plutonyl dipyridyl-N,N′-dioxide complex, the sharp band at 908 cm^{-1} (Fig. 2) is assigned to the asymmetric (ν_3) stretching mode of the Pu—O bond of the plutonyl group.

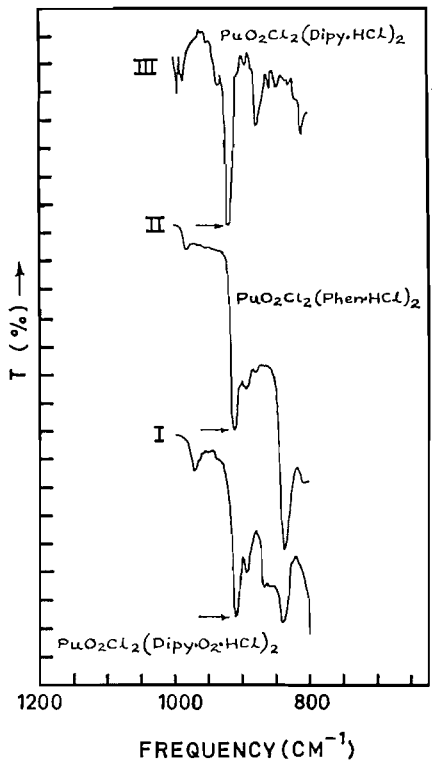

FIG. 2

The infrared spectrum of $UO_2(NO_3)_2.2DMSO$ is particularly informative because the S—O stretching frequency should indicate whether the ligand DMSO is coordinated through the oxygen or through the sulfur atom (18). Recent infrared studies on DMSO complexes of Th(IV), U(IV), and Pu(IV) show that for these metals coordination takes place through the oxygen of the ligand (19). The infrared spectrum of the complex $UO_2(NO_3)_2.2DMSO$ shows that the S—O stretching frequency is shifted to 985 cm^{-1}, from the free ligand value of 1 055 cm^{-1} (18). The strong absorption band at 922 cm^{-1} can be assigned to the asymmetric stretching mode (ν_3) of the U—O bond of the uranyl group (Fig. 1).

The infrared absorption bands assigned to the nitrate groups in the complexes indicate that these are coordinated to the metal (15, 20–23). The presence of bidentate nitrate

Can. J. Chem. Downloaded from www.nrcresearchpress.com by 210.87.254.42 on 09/05/12
For personal use only.

groups and of eight-coordinated hexavalent uranium has been observed for crystalline rubidium uranyl nitrate (24), and an analogous structure has recently been established by X-ray diffraction studies (25) for the crystalline uranyl nitrate triethyl phosphate complex. By analogy with these structures it is, therefore, reasonable to propose an eight-coordination structure for the hexavalent uranium in our complexes, assuming the nitrate group to act as bidentate ligand.

In the case of plutonyl diamine hydrochloride complexes, it is very likely that each diamine is in the form of a monohydrochloride (26, 27, 28) and can act only as a monodentate ligand and therefore plutonium(VI) in these complexes can have six-coordination structure (29).

The uranium and plutonium of uranyl and plutonyl ions contain a large number of vacant orbitals (5f, 6d) available for coordination. A ligand which forms strong bonding with the metal can effectively hinder the shift of electrons from the oxygen to the metal, thus leading to a decrease in the strength of the multiple metal–oxygen covalent bond. The characteristic absorption frequency of the asymmetric vibration of the U—O bond of the uranyl ion and of the Pu—O bond of the plutonyl ion are shifted to lower values in all the complexes, from the free ion values of $965 \pm 1\ cm^{-1}$ and $962 \pm 1\ cm^{-1}$ respectively (11). Using the magnitude of this shift as a criterion of the relative complexing ability of the ligand, ligand series can be deduced (30) (Table I). The order of complexing ability of the ligands with the uranyl ion seem to be DMSO > py > dipy·O_2 > phen > dipy, and with the plutonyl ion the order is dipy·O_2 > phen > dipy. This order may also be taken qualitatively as a measure of the order of stability of these complexes.

The high stability of the uranyl dimethyl sulfoxide complex may be attributed to the ability of the oxygen atom of the ligand to form multiple bonds with atoms or groups which can readily accept π-bonding electrons available in the compact 2p level. The stability of the uranyl pyridine complex may also be attributed to the aromatic character of the nitrogen atom. The higher stability of the dipy·O_2 complex compared with that of *o*-phenanthroline and dipyridyl complexes may be attributed to the strength of the coordinative bond formed between an oxygen donor and the metal atom. In the case of phenanthroline and 2,2′-dipyridyl complexes, the highly conjugated phenanthroline is expected to form a stronger complex than that of dipyridyl.

Thermogravimetric experiments on $UO_2(NO_3)_2.H_2O$.py show that at 125 °C the water molecule is lost, giving rise to the anhydrous complex. At 195 °C the pyridine molecule is also lost and at about 550 °C the decomposition is complete, giving rise to U_3O_8. In the case of $UO_2(NO_3)_2$.dipy, at 310 °C the dipyridyl molecule is lost and further decomposition to U_3O_8 takes place at about 500 °C. The complex PuO_2Cl_2(dipy·O_2·HCl)$_2$ loses the two molecules of HCl at 170 °C and further decomposition to PuO_2 takes place at about 350 °C.

The magnetic susceptibility measurements show that the uranyl complexes are, as expected, weakly diamagnetic with X_m values ranging from -27×10^{-6} c.g.s. units to -103×10^{-6} c.g.s. units. The observed susceptibilities are $UO_2(NO_3)_2$.2DMSO, -69×10^{-6} c.g.s. units; $UO_2(NO_3)_2.H_2O$·py, -27×10^{-6} c.g.s. units; $UO_2(NO_3)_2$(dipy·O_2), -51×10^{-6} c.g.s. units; $UO_2(NO_3)_2$.phen, -103×10^{-6} c.g.s. units; and $UO_2(NO_3)_2$.dipy, -40×10^{-6} c.g.s. units. The plutonyl dipyridyl complex is paramagnetic. The magnetic susceptibility measurements were made over a limited temperature range. The X_m values are $2\,747 \times 10^{-6}$ c.g.s. units at 300 °K, $2\,649 \times 10^{-6}$ c.g.s. units at 311 °K, and $2\,483 \times 10^{-6}$ c.g.s. units at 328 °K. The effective magnetic moment is 2.6 BM. This value is much lower than that expected for $5f^2\ ^3H_4$ configuration with $\mu = 3.58$ BM. by

Can. J. Chem. Downloaded from www.nrcresearchpress.com by 210.87.254.42 on 09/05/12
For personal use only.

Russell-Saunders coupling scheme. Similar deviations have been observed for Pu(IV) and Pu(III) compounds (19, 31, 32) and are attributed to the spin–orbit interaction for 5f electrons. The greater spatial extension of the 5f wave functions results in large splitting of the 5f electrons by the crystalline field and the mixing of the ground multiplet $^3H_4$ levels of the free ion with the upper level (33, 34) and possibly to orbital angular momentum (L) reduction by covalent bonding (35).

ACKNOWLEDGMENT

The authors thank Professor Glenn H. Brown, Kent State University, Ohio, U.S.A. for reading this manuscript and offering valuable suggestions.

REFERENCES

1. J. SELBIN. J. Chem. Ed. **41**, 86 (1964).
2. A. E. COMYNS. Chem. Rev. **60**, 115 (1960).
3. E. GLUECKAUF and H. A. C. MCKAY. Nature, **165**, 574 (1950).
4. R. E. CONNICK and Z. Z. HUGUS, JR. J. Am. Chem. Soc. **74**, 6012 (1952).
5. A. E. COMYNS, B. H. GATEHOUSE, and E. WAIT. J. Chem. Soc. 4655 (1958).
6. L. SACCONI and Y. GIANNONI. J. Chem. Soc. 2368, 2751 (1954).
7. P. G. SIMPSON, A. VINCIGUERRA, and J. V. QUAGLIANO. Inorg. Chem. **2**, 282, 286 (1963).
8. J. J. KATZ and G. T. SEABORG. Chemistry of the actinide elements. John Wiley and Sons, New York. 1951.
9. W. H. ZACHARIASEN. Acta Cryst. **8**, 847 (1954).
10. L. H. JONES. Spectrochim. Acta, **10**, 395 (1958); **11**, 409 (1959).
11. L. H. JONES and R. A. PENNEMAN. J. Chem. Phys. **21**, 542 (1953).
12. J. SUTTON. Nature, **160**, 235 (1952).
13. J. T. BARR and C. A. HARTON. J. Am. Chem. Soc. 74, 4430 (1952).
14. L. H. JONES. J. Chem. Phys. **23**, 2105 (1955).
15. B. M. GATEHOUSE, S. E. LIVINGSTON, and R. S. NYHOLM. J. Chem. Soc. 4222 (1957).
16. L. J. BELLAMY. Infrared spectra of complex molecules. John Wiley and Sons, New York. 1956.
17. S. P. MCGLYNN, J. K. SMITH, and W. C. NEALY. J. Chem. Phys. **35**, 105 (1961).
18. F. A. COTTON, R. FRANCIS, and W. D. HORROCKS, JR. J. Phys. Chem. **64**, 1536 (1960).
19. H. D. SHARMA *et al.* To be published.
20. F. A. MILLER and C. H. WILKINS. Anal. Chem. **24**, 1253 (1952).
21. J. C. D. BRAND and T. M. CAWTHON. J. Am. Chem. Soc. **77**, 319 (1955).
22. F. A. COTTON and J. G. BERGMAN. J. Am. Chem. Soc. **86**, 2941 (1964).
23. A. ZALKIN, J. D. FORRESTER, and D. H. TEMPLETON. J. Chem. Phys. **39**, 2881 (1963).
24. G. H. DIEKE and A. B. F. DUNCAN. Spectroscopic properties of uranium compounds. McGraw-Hill Books, Inc., New York. 1949.
25. J. E. FLENING and H. LYNTON. Chem. Ind. London, 1409 (1959).
26. E. A. HEALY and R. K. MURMANN. J. Am. Chem. Soc. **79**, 5827 (1957).
27. MIROSTAW SZAFRAN. Spectrochim. Acta, **19**, 2132 (1963).
28. F. H. WESTHEIMER and O. T. BENFEY. J. Am. Chem. Soc. **78**, 5309 (1956).
29. B. G. HARVEY, H. G. HEAL, A. G. MADDOCK, and (MISS) E. L. ROWLEY. J. Chem. Soc. 1011 (1947).
30. J. SELBIN, L. H. HOLMES, JR., and S. P. MCGLYNN. J. Inorg. Nucl. Chem. **25**, 1359 (1963).
31. N. ELLIOTT and W. B. LEWIS. AECD-2910. LADC-806 (August 12, 1950).
32. D. B. MCWHAN. UCRL-9695. Thesis. May 1961.
33. D. M. GRUEN and C. A. HUTCHISON, JR. J. Chem. Phys. **22**, 396 (1954).
34. R. A. SATTEN, D. YOUNG, and D. M. GRUEN. J. Chem. Phys. **33**, 1140 (1960).
35. K. H. W. STEVENS. Proc. Roy. Soc. London, Ser. A, **219**, 542 (1953).

Can. J. Chem. Downloaded from www.nrcresearchpress.com by 210.87.254.42 on 09/05/12
For personal use only.

Can. J. Chem. Downloaded from www.nrcresearchpress.com by 210.87.254.105 on 09/05/12
For personal use only.

SUBSTITUTIONAL AND CONFIGURATIONAL EFFECTS ON CHEMICAL SHIFT IN PYRANOID CARBOHYDRATE DERIVATIVES[1]

R. U. LEMIEUX AND J. D. STEVENS[2]
Department of Chemistry, University of Alberta, Edmonton, Alberta
Received January 25, 1965

ABSTRACT

The effects of long-range and virtual long-range coupling on the observed spectra of acetylated hexopyranoses and pentopyranoses are examined. Use is made of both spin decoupling and specific deuteration for the assignment of signals. It is seen that specific solvent effects on chemical shift can be superior to increasing the applied magnetic field for the resolution of the signals of closely related protons. The alteration of virtual long-range coupling effects in these ways can be useful in the diagnosis of spectra. Empirical rules are derived for estimating the long-range shielding effects which occur on changing configurations. It is seen that the inversion of a center can lead to deshielding of axial protons and to shielding of equatorial protons at other centers relative to the chemical shifts observed in reference compounds wherein all the acetoxy groups are in equatorial orientation. The effects in several cases result in equatorial protons giving their signal to higher field than chemically similar but axial protons. The conformational properties of pentopyranose tetraacetates as estimated from chemical shifts and coupling constants are seen to be in good agreement with expectations based on non-bonding interaction free energies. As expected, 2-deoxy-β-D-ribopyranose triacetate has the 1C-conformation when dissolved in chloroform.

INTRODUCTION

In 1958, Lemieux *et al.* (1) reported a study of the nuclear magnetic resonance (n.m.r.) spectra of a number of six-membered ring compounds. It was concluded that the proton of an equatorially oriented hydrogen comes into resonance at lower field than that of a chemically similar but axially oriented hydrogen. Also, the coupling constant between hydrogens on adjacent carbon atoms was observed to be two to three times greater when their projected bond angle is about 180° (anti-periplanar (2)) than when the angle is about 60° (*gauche* or syn-clinal (2)). These observations, which have since been used extensively (3–6) in structural and stereochemical studies, came primarily from a study of the acetylated aldopyranoses in which the hydrogen on C-1 (known as the anomeric carbon) is strongly deshielded, appearing as a doublet at low field, well removed from the signals produced by other hydrogens in the molecules. Although the spacing for this doublet was taken as the coupling constant, $J_{H\text{-}1,H\text{-}2}$, the spectra obtainable at that time were of poor quality by present standards and many of the signals were poorly resolved. As will be seen later on, due to virtual long-range coupling (7) the spacings were, in general, only approximately the coupling constant.

Since the time of this early study, advances in instrumentation have allowed us to examine in more detail the spectra of carbohydrate derivatives. Chemical shifts reported in this paper will be in parts per million (p.p.m.) from the internal standard, tetramethylsilane, and unless otherwise specified, spectra were recorded at 60 Mc.p.s. with a Varian A60 spectrometer.

A detailed assignment of the signals in the spectrum (Fig. 1A) of β-D-glucopyranose pentaacetate (I) in chloroform solution serves as an illustration of the chemical shifts observed for protons in this type of compound. The doublet of intensity one at lowest field

[1]*Presented at the 45th National Meeting of the Chemical Institute of Canada, Edmonton, Alberta, May 28–30 1962.*
[2]*Corn Industries Research Foundation Postdoctorate Fellow 1960–1962.*

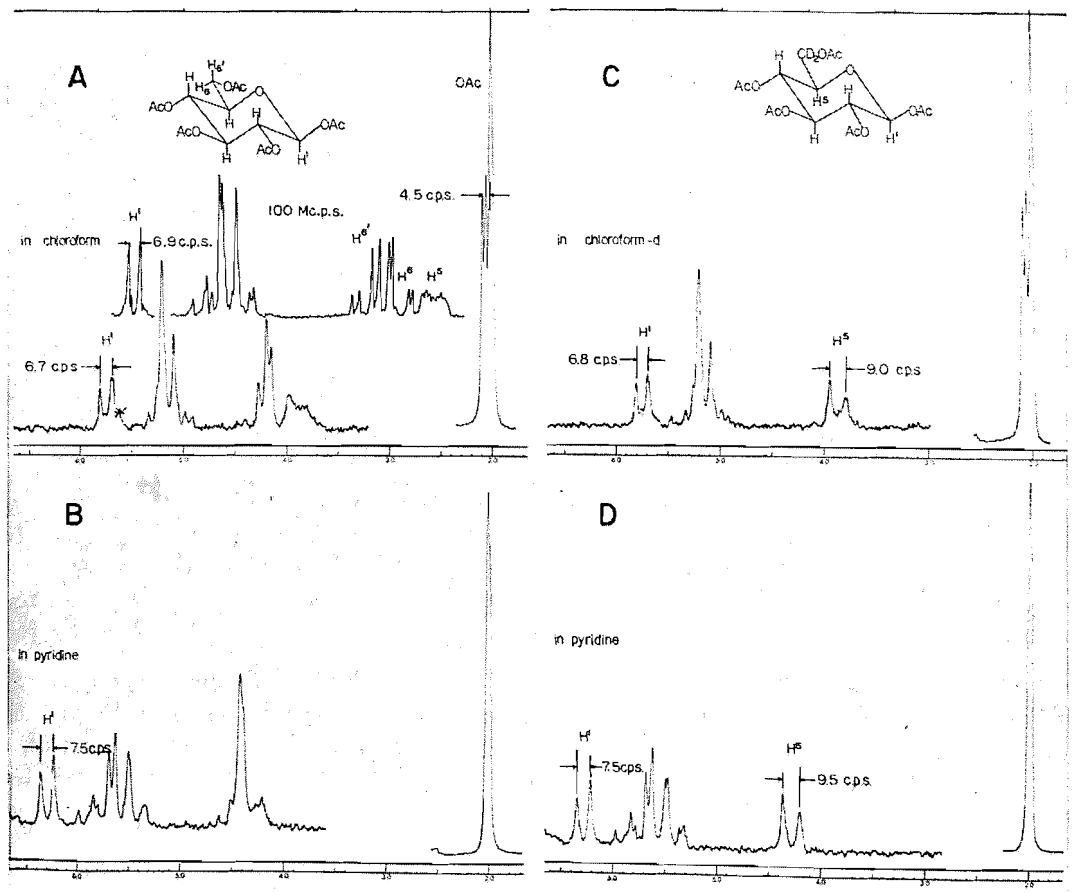

FIG. 1. Effects of solvent and deuteration on the n.m.r. spectrum of β-D-glucopyranose pentaacetate (I). A. I in chloroform. B. I in pyridine. C. 6,6′-Dideuterio-I in deuterated chloroform. D. 6,6′-Dideuterio-I in pyridine.

was assigned to the anomeric hydrogen and this assignment was verified by showing that the signal was absent in the spectrum of the C-1 deuterated derivative (1). The multiplets of total intensity three in the region 3.5–4.5 p.p.m. were assigned to the C-5 and C-6 hydrogens (1). 6,6′-Dideuterio-β-D-glucopyranose pentaacetate was now prepared from D-glucurone (8) and, as seen in Fig. 1C, the signal in this region was in fact reduced to a one-proton doublet arising from the H-5 proton. The spacings observed are in the range expected for the anti-periplanar arrangement of H-4 and H-5. The n.m.r. spectrum of I in deuterated chloroform at 100 Mc.p.s. is also shown in Fig. 1A. It is seen that the signals for the H-5, H-6, and H-6′ protons are now well shifted chemically. However, the group of signals arising from H-2, H-3, and H-4 in the region 4.8–5.5 p.p.m. remained virtually unchanged. That some increased shift between H-2 and H-3 took place is indicated by the change in the spacing of the signal for H-1 from 6.7 c.p.s. at 60 Mc.p.s. to 6.9 c.p.s. at 100 Mc.p.s. Furthermore, it is seen that the spacing for the H-1 signal increased to 7.5 c.p.s. when the spectrum (Fig. 1B) was measured at 60 Mc.p.s. using pyridine as solvent and, therefore, this solvent must have increased the chemical shift between H-2 and H-3.

Although the change in the solvent from chloroform to pyridine shifted H-3 from H-2,

Can. J. Chem. Downloaded from www.nrcresearchpress.com by 210.87.254.105 on 09/05/12
For personal use only.

the change caused a decrease in the chemical shifts between H-5, H-6, and H-6′. It is seen therefore that specific solvent effects on chemical shift (c.p.s.) complement those obtained by changing the applied magnetic field. The signals for H-6′ and H-6 in the 100 Mc.p.s. spectrum (Fig. 1A) appear as an octet to lower field than the signal for H-5 at 3.87 p.p.m. Treating these three protons as an isolated ABX system, the following n.m.r. parameters were obtained, $\delta_A - \delta_B = 0.18$ p.p.m., $J_{AB} = 12.4$ c.p.s., $\delta_A - \delta_X = 0.4$ p.p.m., $J_{AX} = 4.7$ c.p.s., $J_{BX} = 1.9$ c.p.s. with $\delta_A = 4.27$ p.p.m. If one assumes staggered conformations for the substituents on C-5 and C-6 and that the conformation wherein the 4- and 6-acetoxy are opposed has negligible population, the A-proton can be assigned to the proton at C-6 which is anti-periplanar with H-5 in one of the conformations wherein the 6-acetoxy group is *gauche* (syn-clinal) to the ring-oxygen, namely H-6′. As can be seen in Fig. 4A, the signals for H-6′ and H-6 of β-D-mannopyranose pentaacetate show, as would be expected, a very similar pattern. The H-6 and H-6′ protons are well resolved in the 100 Mc.p.s. spectrum for α-D-gulopyranose pentaacetate (Fig. 2D). The coupling constants calculated for these protons (5.3 and 7.6 c.p.s.) are of magnitudes which require a low population for the conformation wherein the 4- and 6-acetoxy groups are in opposition and H-5 is *gauche* to both H-6 and H-6′.

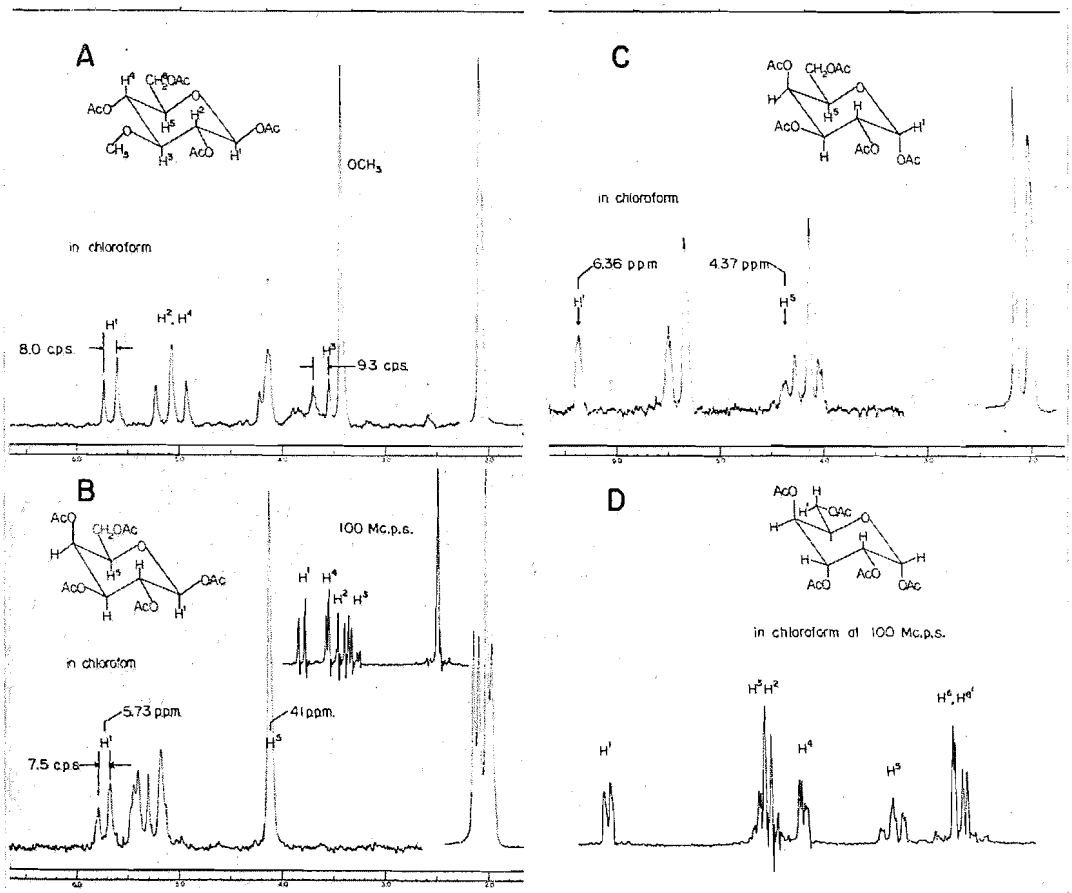

FIG. 2. Substitutional and configurational effects on n.m.r. spectra. A. 3-*O*-Methyl-β-D-glucopyranose tetraacetate. B. β-D-Galactopyranose pentaacetate. C. α-D-Galactopyranose pentaacetate. D. α-D-Gulopyranose pentaacetate.

Can. J. Chem. Downloaded from www.nrcresearchpress.com by 210.87.254.105 on 09/05/12
For personal use only.

Can. J. Chem. Downloaded from www.nrcresearchpress.com by 210.87.254.105 on 09/05/12
For personal use only.

Virtual long-range coupling (7) refers to second-order effects on the signal of X in a system of protons, ABCX (9), wherein J_{AB} is large as compared to δ_{AB} and B is not appreciably coupled to X. Under these circumstances, B has a long-range effect on the spin states of X although it may not be directly coupled to X. Anet (10) has described this effect in connection with the structure of signals of *C*-methyl groups. The occurrence of this phenomenon is well displayed in the spectra of the 6,6′-dideuterio derivative of I. It is seen that both the signals for H-1 and H-5 are not well defined in the spectrum (Fig. 1C) obtained using chloroform as solvent. On the other hand, these signals are better defined sharper doublets in the spectrum (Fig. 1D) using pyridine as solvent. That virtual long-range coupling effects were probably still present in the latter spectrum is suggested by the larger spacing of 8.0 c.p.s. observed for the signal of H-1 in the spectrum of 3-*O*-methyl-β-D-glucopyranose tetraacetate in the same solvent (see Fig. 2A). The signal for H-3 ($\delta_{H\text{-}3}$ = 3.87 p.p.m.) is now well shifted from those for H-2 and H-4 ($\delta_{H\text{-}2} \simeq \delta_{H\text{-}4} \simeq$ 5.42 p.p.m.). The signals for H-2 and H-4 remained virtually superimposed in the spectrum which was obtained using pyridine as solvent. This may be related to their both being in axial orientation on the same side of the ring. This type of phenomenon, like that observed (11) for specific deshielding by chloride ions, may prove of value in stereochemical studies. For example, it could be speculated that, in the spectrum for I in pyridine (Fig. 1A), it is the signal for H-3 that is shifted downfield from the signals for H-2 and H-4 which are on the same side of the pyranose ring.

As seen in Fig. 2B, the signal for the anomeric proton of β-D-galactopyranose pentaacetate appears at 60 Mc.p.s. as a quartet with the smaller spacing amounting to 1.0 c.p.s. Superficially, this spacing could be considered to arise from long-range coupling. However, when the spectrum was measured at 100 Mc.p.s., the signal for the anomeric proton appeared as a sharp doublet with a spacing of 8.4 c.p.s. with the two branches of much more nearly the same intensity. Obviously, therefore, the anomeric proton is not long-range coupled but, instead, the quartet structure of the signal observed at 60 Mc.p.s. must have arisen from virtual long-range coupling. This observation renders it clear that caution must be exercised in assigning long-range coupling to spectra subject to the phenomenon of virtual long-range coupling. The occurrence of virtual long-range coupling in this compound was not surprising in view of the fact that H-2 and H-3 were estimated to be chemically shifted by only about 0.2 p.p.m. and coupled to an extent of 10.2 c.p.s. In the case of α-D-gulopyranose pentaacetate (Fig. 2D), H-1 appeared definitely long-range coupled (about 1.3 c.p.s.) to H-3. This observation is not surprising in view of the equatorial orientations for both these hydrogens (12). Similarly, the equatorial H-5 of α-D-ribopyranose tetraacetate was found to be long-range coupled (about 0.7 c.p.s.) to the equatorial H-3 (see Fig. 5B). Irradiation of H-1 of α-D-gulopyranose pentaacetate caused the complex multiplet due to H-4 to collapse to a quartet. This coupling, about 0.7 c.p.s., over five bonds appears less commonly observed than the coupling over four bonds. It is noteworthy that spin-decoupling experiments at 100 Mc.p.s. (see Fig. 3B) showed the axial H-3 of 6,6′-dideuterio-α-D-glucopyranose pentaacetate to be weakly long-range coupled to both the equatorial H-1 and the axial H-5.

In contrast to the case of β-D-glucopyranose pentaacetate (I), the signal produced by H-1 in α-D-glucopyranose pentaacetate (II) did not change in spacing, 3.3 c.p.s., or sharpness on changing the solvent from chloroform to pyridine (compare Figs. 3A and 3C). This is not surprising since there was virtually no change in the structure of the band of signals arising from H-2, H-3, and H-4. That the signal for H-3 in these spectra is centered at about 5.5 p.p.m. (chloroform) and 5.89 p.p.m. (pyridine) and about 0.4 p.p.m. to lower

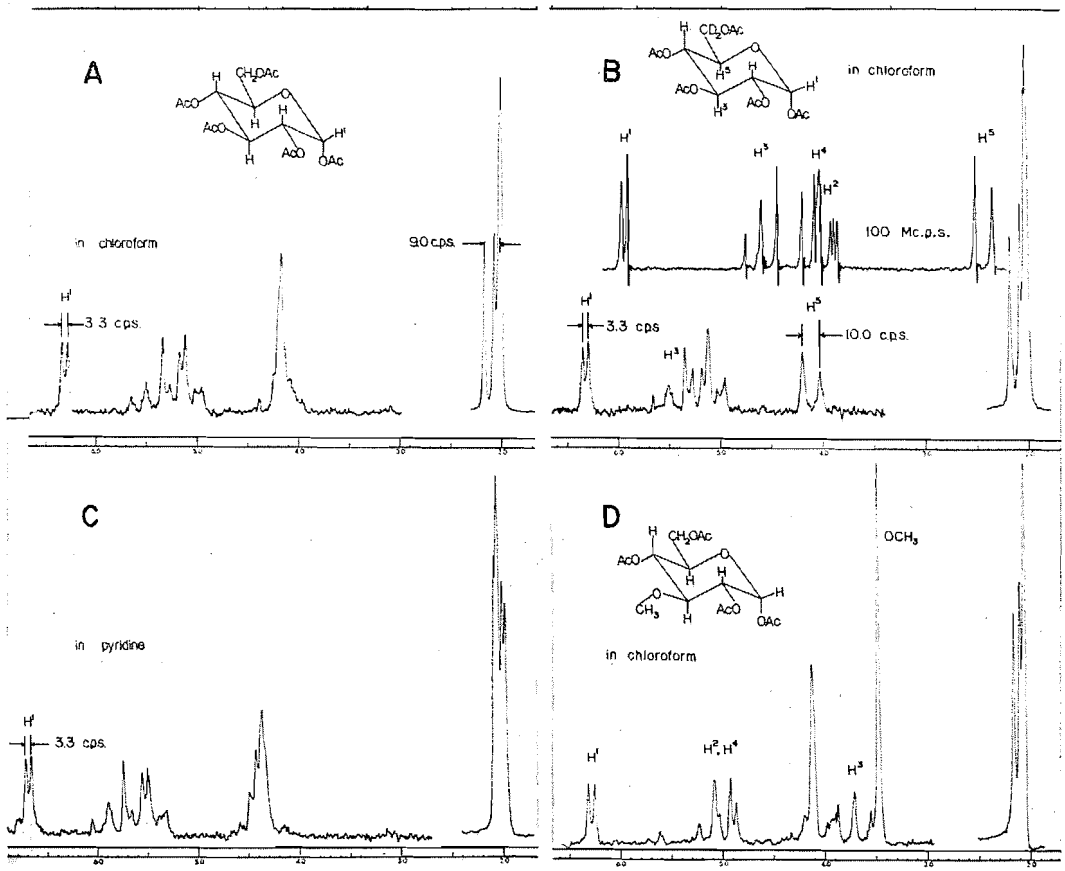

FIG. 3. Substitutional and solvent effects on the n.m.r. spectrum of α-D-glucopyranose pentaacetate (II). A. II in chloroform. B. 6,6′-Dideuterio-II in chloroform. C. II in pyridine. D. 3-*O*-Methyl-α-D-glucopyranose tetraacetate.

field than the signals for H-2 and H-4 in both spectra was deduced from the effect of the change in configuration on the chemical shift for H-5. This is best considered on the basis of the spectra obtained for the 6,6′-dideuterio derivatives of I and II. It is seen that the signal for H-5 is at 3.88 p.p.m. for the β-anomer (Fig. 1C) and at 4.12 p.p.m. (Fig. 3B) for the α-form. This deshielding effect by an axial oxygen on opposing axial hydrogens was consistently observed in all the pyranose compounds examined. It is on this basis that the above-mentioned assignment of the signal for H-3 could be made. In accordance with this assignment, irradiation of the H-5 signal in the 100 Mc.p.s. spectrum of 6,6′-dideuterio-α-D-glucopyranose pentaacetate in chloroform caused the collapse of a triplet signal at 5.13 p.p.m., with a spacing of 10.0 c.p.s. which must arise from H-4. Therefore, the now well-defined quartet at 5.5 p.p.m. with spacings of 9.4 and 10.0 c.p.s. must indeed arise from H-3. In the spectrum, H-2 appeared as a quartet centered at about 5.08 p.p.m. with spacings of 4.0 and 10.0 c.p.s. The signal for H-3 of 3-*O*-methyl-α-D-glucopyranose tetraacetate (III) was 0.22 p.p.m. to lower field than the signal for the corresponding hydrogen in the β-anomer (compare Figs. 2A and 3D). The signal for H-5 in III was obscured by the signals for the two hydrogens at the 6-position but evidently to substantially lower field than the corresponding signal in the spectrum, under the same conditions, for the β-anomer.

Can. J. Chem. Downloaded from www.nrcresearchpress.com by 210.87.254.105 on 09/05/12
For personal use only.

This deshielding effect by axial oxygen in opposing axial hydrogens has proven very useful in this laboratory for the assignment of configurations to anomeric pairs of compounds and is particularly useful when the signals for the anomeric protons are obscured or when the coupling constants for the anomeric protons do not allow an unequivocal conclusion. An example of the latter situation is provided by the anomeric pair of the D-mannopyranose pentaacetates (see Figs. 4A and 4B). For both these compounds, H-1 and H-2 are in *gauche* relationship and an assignment of the anomeric configurations based on the spacings of the signals for the anomeric proton would not be feasible. An assignment could be made on the basis of their relative chemical shifts by assigning the equatorial orientation (α-configuration) to the anomer with the signal for H-1 at lower field (1). However, as will be seen later on, this generalization that equatorial protons produce their signals at lower field than chemically similar but axial protons can have exceptions depending on the overall shielding effects operating in the molecule. Therefore, it is useful to note that the configurational assignment is supported by the relative positions of the signals for H-5 in this pair of anomers. As expected, the axial 1-acetoxy group of the α-anomer has a deshielding effect on H-5.

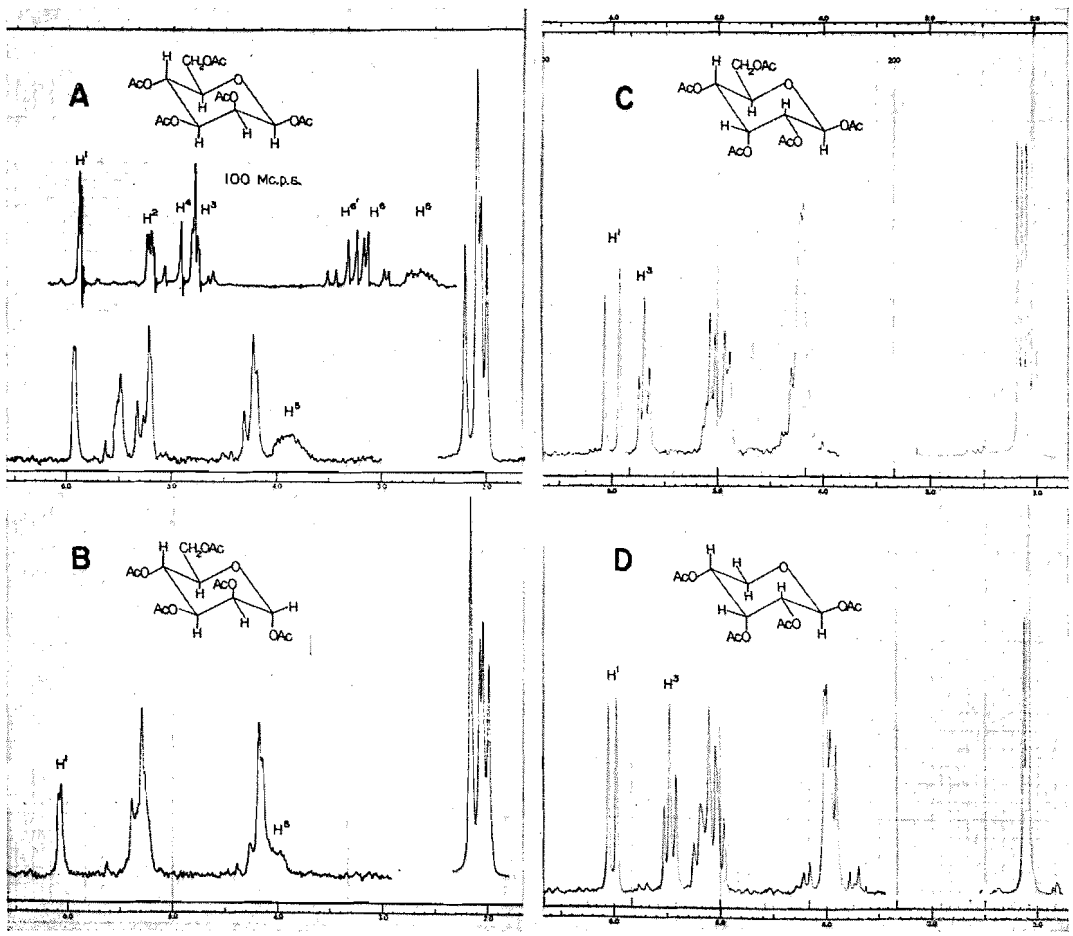

FIG. 4. Nuclear magnetic resonance spectra of sugar acetates in chloroform solution. A. β-D-Mannopyranose pentaacetate. B. α-D-Mannopyranose pentaacetate. C. β-D-Allopyranose pentaacetate. D. β-D-Ribopyranose tetraacetate.

Can. J. Chem. Downloaded from www.nrcresearchpress.com by 210.87.254.105 on 09/05/12
For personal use only.

Can. J. Chem. Downloaded from www.nrcresearchpress.com by 210.87.254.105 on 09/05/12
For personal use only.

The chemical shift of an equatorial proton in acetylated pyranose structures is strongly influenced by the orientation of the acetoxy groups at the neighboring centers. The chemical shifts for the anomeric protons of α-D-glucopyranose pentaacetate (II) and α-D-mannopyranose pentaacetate are 6.33 and 6.07 p.p.m., respectively. Thus, inversion of the 2-position from the equatorial to the axial orientation for the acetoxy group shielded the equatorial 1-proton by 0.26 p.p.m. It is seen in Fig. 4A that one of the protons at the 2-, 3-, or 4-position of β-D-mannopyranose pentaacetate produced its signal at substantially lower field (about 0.25 p.p.m.) than the other two protons. Spin decoupling at 100 Mc.p.s. showed the low field signal to arise from H-2. It is seen that this signal moved to higher field on changing the configuration at the 1-position to form the α-anomer. Thus, again we see a greater shielding effect on an equatorial proton by a neighboring axial acetoxy group than by an equatorial acetoxy group.

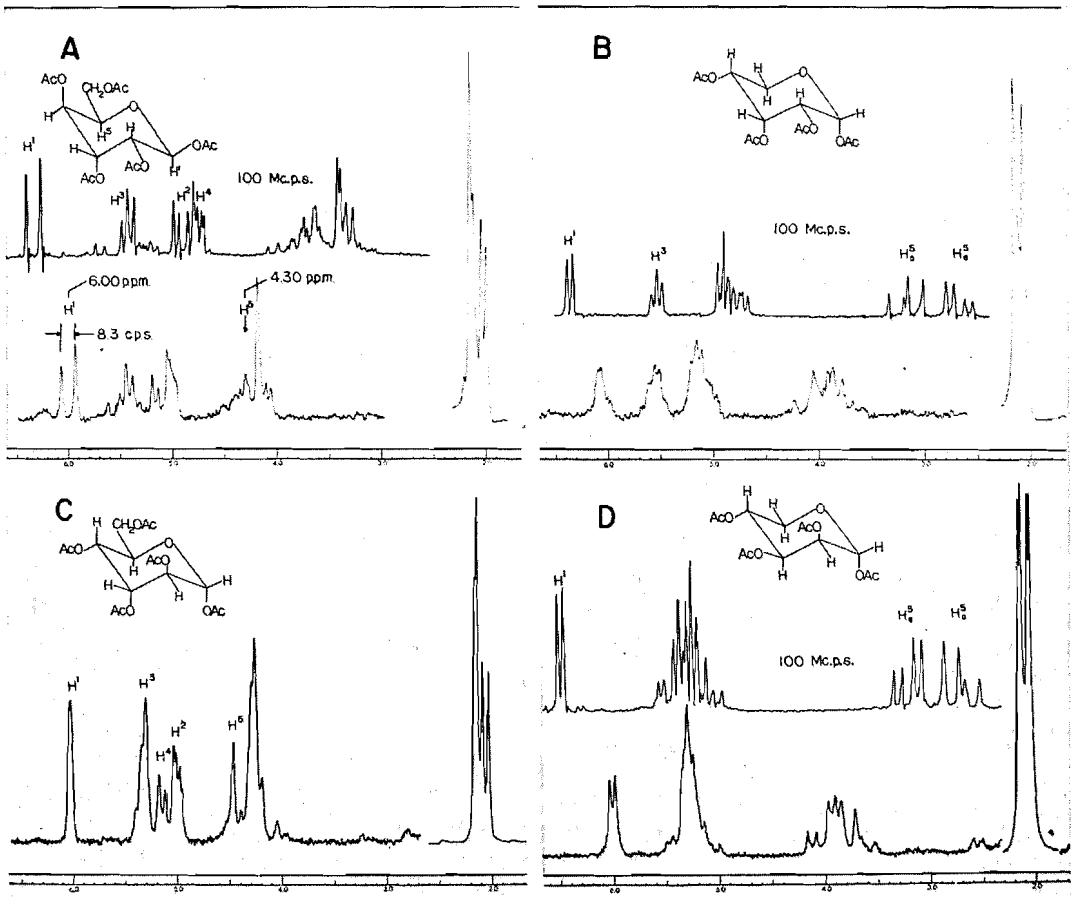

FIG. 5. Nuclear magnetic resonance spectra of sugar acetates in chloroform solution. A. β-D-Gulopyranose pentaacetate. B. α-D-Ribopyranose tetraacetate. C. α-D-Altropyranose pentaacetate. D. α-D-Lyxopyranose tetraacetate.

The spectra for the pentaacetates of β-D-allopyranose, β-D-gulopyranose, and α-D-altropyranose are presented in Figs. 4C, 5A, and 5C, respectively. The sharp triplet at 5.69 p.p.m. in the spectrum of the allose derivative is readily assigned on the basis of the spacings, 2.8 c.p.s., to the equatorial H-3. When the configuration was changed at the

Can. J. Chem. Downloaded from www.nrcresearchpress.com by 210.87.254.105 on 09/05/12
For personal use only.

4-position to produce the gulose derivative, as expected, the signal for the 3-proton shifted upfield by at least 0.25 p.p.m. When the configuration of the allose derivative was changed at both the 1- and 2-positions to form the α-altrose derivative, the position of H-3 was shifted from 5.69 p.p.m. to 5.34 p.p.m. The position of H-3 in the spectrum for the altrose derivative was established by detailed examination at 100 Mc.p.s. The position of the equatorial H-2 was found to be at 5.00 p.p.m. Thus, the axial acetoxy groups at both the neighboring positions have strongly shielded this equatorial proton, to such an extent that it produces its signal to substantially higher field than the chemically similar but axial proton at the 4-position. This exception to the rule for the chemical shifts of chemically similar axial and equatorial protons arises mainly because of the superposition in this molecule of deshielding of the axial H-4 by the axial 2- and 3-acetoxy groups and the shielding of the equatorial H-2 by the axial acetoxy groups at the 1- and 3-positions. That an equatorial acetoxy has a greater shielding effect on a neighboring axial proton than has a neighboring axial acetoxy group is apparent from a comparison of the chemical shifts for the anomeric protons of β-D-glucopyranose pentaacetate, 5.75 p.p.m., and β-D-mannopyranose pentaacetate, 5.93 p.p.m. Also, the signal for H-5 in β-D-glucopyranose pentaacetate is 0.25 p.p.m. to higher field than the signal for the corresponding proton in β-D-galactopyranose. The n.m.r. spectra of both the anomeric pairs of the tetraacetates of methyl D-glucopyranuronate and methyl D-galactopyranuronate were measured in chloroform solution. The signals for the H-5 protons in these compounds appeared as doublets with spacings of 9.5 c.p.s. for the *gluco*-configuration and 1.5 c.p.s. for the *galacto*-configuration. The signals for H-5 were 4.20 and 4.58 p.p.m. for the *β-gluco* and *β-galacto* compounds, respectively, and 4.41 and 4.78 p.p.m. for the α-anomers, respectively. The positions of the signals for the H-5 protons of the α-anomers to lower field (0.2 p.p.m.) than the corresponding signals for the β-forms is attributed to the deshielding effect of the axial 1-acetoxy groups in the α-compounds. It is seen that changing the configuration at the 4-position in each case caused a deshielding of the H-5 proton. Therefore, it is apparent that a change in the configuration of an asymmetric center in these compounds which brings an acetoxy group from the equatorial to the axial orientation produces a deshielding effect on a neighboring axial proton but a shielding effect on a neighboring equatorial proton. On this basis, the chemical shifts observed for the ring protons in α-D-altropyranose pentaacetate are understandable with the compound in the chair conformation with the acetoxy groups at the 1-, 2-, and 3-positions in axial orientation. This conformation is also supported by the coupling of H-4. The spacings of the signal observed in the 100 Mc.p.s. spectrum were 9.2 and 3.3 c.p.s. Therefore, H-4 must define a dihedral angle of about 180° with H-5.

The following approximate empirical rules account well for the observed effects of changes in configuration on chemical shift using the chemical shifts of the ring protons of β-D-glucopyranose pentaacetate as the reference signals.

(1) If the proton under consideration has remained axial; (*a*) add 0.20 p.p.m. for an axial acetoxy group at a neighboring position, (*b*) add 0.25 p.p.m. for an opposition of the proton by an axial acetoxy group.

(2) If the proton under consideration has achieved the equatorial orientation; (*a*) add 0.60 p.p.m. because of the change from the environment of an axial hydrogen to that of an equatorial hydrogen (1, 13), (*b*) subtract 0.20 p.p.m. for an axial acetoxy group at a neighboring position, (*c*) subtract 0.20 p.p.m. for an axial acetoxy group at the next to neighboring position. This latter rule was derived primarily from a consideration of the spectra for pentopyranose tetraacetates. Thus, it is seen that, whereas axial acetoxy

groups have deshielding effects on axial protons (relative to the effects of equatorial acetoxy groups), shielding effects are observed when the ring-proton is in equatorial orientation.

TABLE I

Configurational effects on chemical shift observed in the n.m.r. spectra of hexopyranose pentaacetates dissolved in chloroform

	Chemical shift, p.p.m.			
	H-1		H-5	
Compound	Found	Calcd.*	Found	Calcd.*
β-D-*gluco*	5.76	5.75	3.9	3.9
β-D-*manno*	5.93	5.95	3.9	3.9
β-D-*allo*	6.00	6.00	4.2	4.15
β-D-*galacto*	5.74	5.75	4.1	4.1
β-D-*gulo*	6.00	6.00	4.3	4.35
α-D-*gluco*	6.34	6.35	4.1	4.15
α-D-*manno*	6.09	6.15	4.1	4.15
α-D-*galacto*	6.36	6.35	4.4	4.35
α-D-*altro*	6.02	5.95	4.5	4.4
α-D-*gulo*	6.25	6.15	4.6	4.6

*Calculated using the empirical rules described in the text and β-D-glucopyranose pentaacetate as the reference compound.

Table I shows the agreement obtained between the chemical shifts observed for the H-1 and H-5 protons of a number of hexopyranose pentaacetates and those estimated using this procedure. It is seen that the agreement is quite good and the procedure therefore well summarizes the main conclusions reached in this study of configurational effects on chemical shift. The agreement was not nearly as good for the protons at the 2-, 3-, and 4-positions. The worst discrepancy was with the 2- and 4-protons of β-D-allopyranose pentaacetate. The above-mentioned rules would predict a chemical shift of about 5.4 p.p.m. for these protons when in fact the chemical shift was about 5.0 p.p.m. The position of the 3-proton was at 5.68 p.p.m. in better agreement with the calculated value of 5.8 p.p.m. In the case of β-D-mannopyranose pentaacetate, the above rules would require the signal for the axial H-4 to be about 0.05 p.p.m. to lower field than that for the axial H-3. Spin-decoupling experiments at 100 Mc.p.s. in fact showed this to be the case, $\delta_{H-3} = 5.21$, $\delta_{H-4} = 5.30$ p.p.m. Similarly, for β-D-galactopyranose pentaacetate, the axial H-2 was found at lower field than the axial H-3, $\delta_{H-2} = 5.34$, $\delta_{H-3} = 5.16$ p.p.m. This substantiates the conclusion that in general the deshielding of an axial hydrogen by an opposing axial acetoxy group is somewhat greater than that by a neighboring axial acetoxy group.

The readily derived n.m.r. parameters for six acetylated pentoses and 2-deoxy-β-D-ribopyranose triacetate are presented in Table II. Judging from the coupling constants between a number of the vicinal protons, it is obvious that some of the compounds when dissolved in chloroform are either in conformations other than the chair forms or have appreciable populations for both the chair conformations. There can be little doubt that none of these structures have boat conformations. Certainly, the polysubstituted six-membered pyranose rings of sugar structures cannot be expected to have exactly chair conformations. Some deviation from the precisely staggered arrangement for neighboring groups must be expected. Nevertheless, it is considered that the chair conformation provides a useful approximation of the conformations possessed by acetylated sugar structures. The following discussion of the conformations of the pentopyranose tetraacetates support this contention.

Can. J. Chem. Downloaded from www.nrcresearchpress.com by 210.87.254.105 on 09/05/12
For personal use only.

Can. J. Chem. Downloaded from www.nrcresearchpress.com by 210.87.254.105 on 09/05/12
For personal use only.

TABLE II

Nuclear magnetic resonance parameters for acetylated pentopyranoses dissolved in chloroform

	Chemical shift, p.p.m.						Coupling constants, c.p.s.					
	H-1		H-5		H-5′*							
Configuration	Found	Calcd.	Found	Calcd.	Found	Calcd.	H-1,H-2†	H-2,H-3†	H-3,H-4†	H-4,H-5‡	H-4,H-5′*‡	H-5,H-5′*‡
1. C1-conformation												
β-D-*xylo*	5.75	5.75	3.6	—	4.20	—	6.6	—	—	8.5	4.3	12.0
α-D-*xylo*	6.27	6.35	3.77	3.85	4.00	4.0	3.3	9.5	9.5	11.0	5.6	11.3
α-D-*lyxo*	6.02	6.15	3.75	3.85	4.04	4.0	3.2	—	—	8.4	4.4	11.4
β-D-*ribo*	6.03	6.00	3.90	3.85	4.02	4.0	4.7	3.4	3.4	6.2	2.8	12.6
α-D-*ribo*	6.08	6.15	4.03	4.1	3.75	3.8	3.3	3.3	3.3	8.85	4.55	11.5
β-L-*arabino*	6.35	6.35	4.08	4.05	3.83	3.8	<1.0	—	—	<1†	1.66†	13.1
2. 1C-conformation												
2-Deoxy-β-D-*ribo*	6.27	6.35	3.87	3.8	4.03	4.05	5.5§	—	—	2.3	1.6	13.0

*H-5′ is the hydrogen at the 5-position in equatorial orientation when the compound has the C1-conformation.
†Observed spacing only.
‡Calculated as part of an isolated ABX system (9).
§The outside spacing of a triplet.

Can. J. Chem. Downloaded from www.nrcresearchpress.com by 210.87.254.105 on 09/05/12
For personal use only.

Application of the non-bonded interaction free energies derived by Lemieux and Chü (14) for the anomerization equilibria of hexose pentaacetates suggests that, except for the compounds possessing the β-D-*ribo* and β-L-*arabino* configurations, at least 90% of the pentose tetraacetates listed in Table II should exist in chloroform solution in the C1-conformation (15). On this basis, it would be expected that the configurational effects on chemical shift mentioned above in connection with the spectra of the hexose pentaacetates could be used to predict the changes in chemical shift which would result from changes in the configuration of the reference compound, β-D-xylopyranose tetraacetate. The results of the calculations for the H-1, H-5, and H-5′ protons are given in Table II. It is seen that in general the calculated chemical shifts are in good agreement with the observed chemical shifts. With the exception of the β-L-*arabino* and 2-deoxy-β-D-*ribo* compounds, the assignment of the signals arising from H-5 and H-5′ are readily made on the basis of their coupling constants with H-4. It is clear, however, from the coupling constants obtained for β-D-ribopyranose tetraacetate (the spectrum is reproduced in Fig. 4D) that this compound must exist to an appreciable extent in the 1C-conformation. In fact, an estimate of the position of the chair–chair equilibrium based on the non-bonded interaction energies (14) suggests that this compound should exist to about equal extents in the C1- and 1C-conformations. On this basis and using $J_{H\text{-}1,H\text{-}2} = 7.0$, $J_{H\text{-}4,H\text{-}5} = 12.0$, and $J_{H\text{-}4,H\text{-}5'} = 5.2$ c.p.s. for the C1-conformation and $J_{H\text{-}1,H\text{-}2} = 2.8$, $J_{H\text{-}4,H\text{-}5} = 2.3$, and $J_{H\text{-}4,H\text{-}5'} = 1.6$ c.p.s. for the 1C-conformation, the expected coupling constants are 4.7, 7.2, and 3.4 c.p.s., respectively, in fairly good agreement with the observed values. The above expected coupling constants are estimated from the data for the xylose tetraacetates and the 2-deoxy-β-D-ribose triacetate given in Table II. No greater precision is expected from this treatment other than to show that the two chair conformations are in fact abundant for this compound. That the compound exists in chair conformations seems evident from the values for $J_{H\text{-}2,H\text{-}3}$ and $J_{H\text{-}3,H\text{-}4}$. The predicted chemical shifts for H-1, H-5, and H-5′ for the compound in the 1C-conformation are 6.15, 3.8, and 4.05, respectively, and therefore virtually the same as those anticipated on the basis of the C1-conformation. The agreement found between the observed and calculated chemical shifts for this compound given in Table II is therefore not surprising. On the basis of the conformational properties of β-D-ribopyranose tetraacetate and of β-L-arabinopyranose tetraacetate [about 80% C1-conformation (14)], 2-deoxy-β-D-ribopyranose triacetate must be expected to exist in solution virtually completely in the 1C-conformation. In fact, the chemical shifts and coupling constants observed for this compound can only be rationalized using the 1C-conformation.

The data given in Table II require that, in the case of α-D-ribopyranose tetraacetate, the signal for the equatorial hydrogen at the 5-position is at higher field than that for the similar but axial geminal hydrogen. It seems probable that the same situation exists for the β-L-*arabino* and 2-deoxy-β-D-*ribo* compounds. The assignments given for these compounds in Table II are made on this basis. As was seen above in the spectrum of α-D-altropyranose pentaacetate, long-range shielding effects arising from substituents at other positions can more than compensate for the shift normally found between similar hydrogens differing in orientation. A similar situation was encountered in the spectra for the anomeric D-gulopyranose pentaacetates. In each case the signal for the axial H-2 was at lower field than that for the equatorial H-4 as shown by spin-decoupling experiments at 100 Mc.p.s. Nickon and co-workers (16) have observed a similar phenomenon for the α-protons of steroidal α-haloketones. Thus, it is abundantly clear that the assignment of configurations based on the simple generalization that equatorial hydrogens produce

signals at lower field than chemically similar but axial protons is a hazardous procedure when applied to complex structures. On the other hand, it is apparent that with the development of sufficient insight on the nature of long-range effects on chemical shift, the chemical shift data will prove as valuable as coupling constants for the determination of points of configuration. Hall (17) has recently reviewed and commented on the effects of changes in the configuration at the 2-position of sugar structures on the chemical shifts of the anomeric protons.

A consideration of the signals for the protons of the acetoxy groups in the spectra of the sugar acetates presented in Figs. 1–5 shows that, as previously noted (1), axial acetoxy groups tend in general to produce their signal to lower field than equatorial acetoxy groups. It is clearly evident, however, that there is no definite regularity to the chemical shift involved and, indeed, exceptions to the rule are seen in several instances. Also, the spectra in Fig. 1 show the effect to be strongly solvent dependent. Therefore, although useful as guides toward the determination of configurations, these chemical shifts are unreliable as evidence for configurational assignments. Any doubts thus cast on the assignment of the signals for the acetyl groups in 1-trideuterio-*O*-acetyl-β-L-arabinose triacetate (14) seem dispelled by the chemical shift data given in Table II.

EXPERIMENTAL

Except for β-D-gulopyranose pentaacetate and 3-*O*-methyl-α-D-glucopyranose tetraacetate, the compounds used in this investigation were prepared by well-established procedures (1). The preparation of the 6,6′-dideuterio-D-glucose is reported elsewhere (8).

β-D-Gulopyranose pentaacetate was prepared as a sirup, $[\alpha]_D$ +2.4° (*c*, 5 in chloroform), by reaction of sirupy tetra-*O*-acetyl-D-gulopyranosyl bromide with silver acetate in acetic acid.

Sirupy 3-*O*-methyl-α-D-glucopyranose tetraacetate was prepared by anomerization of the crystalline β-form (18) by the standard procedure using sulfuric acid in acetic anhydride and was purified by chromatography on silicic acid using chloroform as eluant.

The 100 Mc.p.s. spectra were measured on a Varian HR-100 spectrometer and the spin-decoupling experiments were performed as previously described (13, 19).

ACKNOWLEDGMENTS

The 60 Mc.p.s. spectra were measured by Mr. R. Swindlehurst and Mrs. G. Conway and those at 100 Mc.p.s. by Mr. G. Bigam of this department.

REFERENCES

1. R. U. Lemieux, R. K. Kullnig, H. J. Bernstein, and W. G. Schneider. J. Am. Chem. Soc. **80**, 6098 (1958).
2. W. Klyne and V. Prelog. Experientia, **16**, 521 (1960).
3. J. B. Stothers. Technique of organic chemistry. A Weisberger (*Editor*). Vol. 11, Part 1. *Edited by* K. Bentley. Interscience Publishers, Inc., New York. 1963. p. 175.
4. L. D. Hall. Advan. Carbohydrate Chem. **19**, 51 (1964).
5. H. Conroy. Advances in organic chemistry. Methods and results. Vol. II. R. A. Raphael, E. C. Taylor, and H. Wynberg (*Editors*). Interscience Publishers, Inc., New York. 1960. p. 265.
6. O. Jardetzky and C. D. Jardetzky. Methods of biochemical analysis. Vol. IX. D. Glick (*Editor*). John Wiley and Sons, Inc., New York. 1962. p. 235.
7. J. I. Musher and E. J. Corey. Tetrahedron, **18**, 791 (1961).
8. R. U. Lemieux and J. D. Stevens. Unpublished results.
9. H. J. Bernstein, J. A. Pople, and W. G. Schneider. Can. J. Chem. **35**, 65 (1957).
10. F. A. L. Anet. Can. J. Chem. **39**, 2262 (1961).
11. R. U. Lemieux, Jun-ichi Hayami, and J. Martin. Unpublished results.
12. S. Sternhell. Rev. Pure Appl. Chem. **14**, 15 (1964).
13. R. U. Lemieux and J. W. Lown. Can. J. Chem. **42**, 893 (1964).
14. R. U. Lemieux. Molecular rearrangements. Part 2. Paul de Mayo (*Editor*). Interscience Publishers. 1963. pp. 735–743.
15. R. E. Reeves. Advan. Carbohydrate Chem. **6**, 107 (1951).
16. A. Nickon, M. A. Castle, R. Harada, C. E. Berkoff, and R. O. Williams. J. Am. Chem. Soc. **85**, 2185 (1963).
17. L. D. Hall. Tetrahedron Letters, No. 23, 1457 (1964).
18. B. Helferich and O. Lang. J. Prakt. Chem. **132**, 321 (1932); Chem. Abstr. **26**, 1903 (1932).
19. L. F. Johnson. Varian Associates Technical Bulletin No. 87-100-082. May 1962.

Can. J. Chem. Downloaded from www.nrcresearchpress.com by 210.87.254.105 on 09/05/12
For personal use only.

TRIDENTATE COMPLEXES OF PERIODATE AND SOME FURANOSE DERIVATIVES[1]

A. S. PERLIN AND E. VON RUDLOFF
National Research Council of Canada, Prairie Regional Laboratory, Saskatoon, Saskatchewan
Received March 4, 1965

ABSTRACT

1,2-*O*-Isopropylidene-α-D-glucofuranose (I) is highly resistant to glycol scission by periodate in alkaline solution. This atypical effect is caused by preferential formation of a stable periodate complex. Proton magnetic resonance spectroscopy shows that the 3-, 5-, and 6-protons of I (and the 3- and 5-protons of I-6,6′-d_2) become strongly deshielded during this process, which, together with accompanying changes in proton–proton coupling, establishes that the complex (II) has a 3,5,6-tridentate structure. Variations in the stability of II with pH suggest that it can exist either as a monoanion or dianion. A complex analogous to II is formed by ethyl α-D-thioglucofuranoside, whereas methyl β-D-galactofuranoside forms a complex that probably has the 2,5,6-structure. The characteristics of these tridentate complexing reactions support the general concept that a five-membered cyclic complex is a transient intermediate of α-glycol oxidation by periodate.

Can. J. Chem. Downloaded from www.nrcresearchpress.com by 210.87.254.40 on 09/05/12
For personal use only.

During recent studies (1) on the oxidation of various *vic*-diols with a weakly alkaline solution of periodate containing a small proportion of permanganate (2), it was found that the 5,6-diol group of 1,2-*O*-isopropylidene-α-D-glucofuranose (I) is cleaved far more slowly than it is by periodate in acid solution (Table I, Nos. 1 and 2). Although the rate of glycol scission by periodate may be retarded as the pH is raised (3, 4), the lessened reactivity of I appeared far too marked to be attributed to such a cause.[2] Another effect of pH has been encountered (5) with some sugars possessing a *cis*,*cis*-1,2,3-triol grouping on a six-membered ring. Several moles of periodate are consumed rapidly by these sugars at pH 4.5, but only 1 mole is taken up quickly at pH 7. This periodate is not actually *reduced*, but is complexed so strongly with the polyol that it is not backtitrated by arsenite. Although the isopropylidene derivative (I) did not show an *apparent* uptake of this kind, the likelihood has been examined that its slow oxidation rate in the presence of alkali is due to the competitive formation of a stable periodate complex.

The type of complex discovered by Barker and Shaw (5) requires proper orientation of three hydroxyl groups and hence probably has a tridentate structure. It appeared feasible that the 3-, 5-, and 6-hydroxyl groups of I might also satisfy steric requirements of a tridentate complex in which iodine is the central atom, as illustrated in II (the periodate moiety is only partially represented here for simplicity). Thus, for example, triorthoesters of I are known (6, 7). In such an event, the fact that the 5,6-diol group is not oxidized at higher pH, whereas numerous structurally related *vic*-diols are, could be attributed to the presence in I of a suitably positioned 3-hydroxyl group. Therefore, it is pertinent that 3-*O*-ethyl-1,2-*O*-isopropylidene-α-D-glucofuranose (III) behaves normally, rapidly consuming 1 mole of periodate under alkaline conditions (Table I, No. 8).

A clear demonstration that a tridentate complex such as II is formed between the isopropylidene derivative (I) and periodate at a pH of 8.5 is afforded by n.m.r. spectroscopy. The spectrum of I in deuterium oxide containing potassium carbonate (Fig. 1A) is altered drastically when sodium metaperiodate is added (Fig. 1B). That these changes are not due to oxidation is readily apparent from the different sort of spectrum obtained when

[1]*Issued as N.R.C. No. 8474.*
[2]*The presence of permanganate was not a factor in the reaction (Table I, No. 2).*

TABLE I

Periodate uptake (moles/mole)

No.	Compound	pH	Titration method*	Reaction time (min) 1	5	10	30
1	1,2-*O*-Isopropylidene-α-D-glucofuranose (I)	4.6	*a*	0.84	0.92	0.94	—
2		7.5†,‡	*b*	0.01	0.04	0.11	0.20
3		8.5§	*a*	0.01	0.05	0.08	0.12
4		8.5§	*b*	0.64	0.67	0.67	—
5		9.8‖	*b*	0.60	0.63	0.64	—
6		9.0¶	*a*	0.07	0.14	0.24	0.44
7		9.0¶	*b*	0.66	0.75	0.75	—
8	3-*O*-Ethyl-1,2-*O*-isopropylidene-α-D-glucofuranose (III)	7.5‡	*b*	—	0.73	0.78	0.95
9	Ethyl α-D-thioglucofuranoside (IX)	7.5‡	*b*	0.80	1.00	1.15	1.56
10		8.5§	*a*	0.05	0.15	0.20	—
11		8.5§	*b*	0.08	0.20	0.27	0.32
12	Methyl α-D-mannofuranoside (X)	7.5‖	*b*	—	1.80	2.22	2.94
13		8.4§	*a*	0.85	0.93	0.96	—
14		8.4§	*b*	0.90	0.98	0.95	—
15	Methyl β-D-galactofuranoside (XI)	7.5‡	*b*	1.00	1.35	1.50	2.20
16		7.5**	*a*	0.27	0.47	0.52	0.62
17		8.4§	*b*	—	0.03	0.05	0.12

*Titration methods: (*a*) thiosulphate (18); (*b*) arsenite (19) (15 min, cold).
†With added permanganate (2) or without the permanganate.
‡1 equivalent K_2CO_3; 4 equivalents $NaIO_4$.
§2 equivalents K_2CO_3; 1 equivalent $NaIO_4$.
‖4 equivalents K_2CO_3; 1 equivalent $NaIO_4$.
¶2 moles Na_2HPO_4; 1 equivalent $NaIO_4$.
**1 equivalent K_2CO_3; 1 equivalent $NaIO_4$.

TABLE II

Reaction of complex II* with arsenite (19). Apparent periodate uptake (mole/mole)

	Reaction time (min) 15	30	60	120
At 25°	0.67†	0.35	0.18	0.12
At 95°	0.10†	—	—	—

*Formed by 5 min reaction at pH 8.5 as in experiment No. 4, Table I.
†The uptake according to the thiosulphate method was 0.05 mole/mole (No. 3, Table I).

I is oxidized at pH 4.5 (see ref. 8), or when the 3-*O*-ethyl derivative (III) is oxidized at pH 8.5.[3] To preclude appreciable oxidation of I at pH 8.5, the interaction must be not only extremely rapid but also essentially quantitative; its quantitative nature can be assessed independently, in fact, since the various resonance signals in Fig. 1B are integer values. A particularly noticeable difference between Figs. 1A and 1B is the marked displacement towards lower field in the latter spectrum of signals for the 3-, 5-, and 6-protons such as occurs when hydroxyl groups in α-position are acylated (9) or are involved in borate complexing (10). Although these signals are well differentiated and hence readily identified with the corresponding protons in II, a clear confirmation of these assignments was obtained by using 1,2-*O*-isopropylidene-D-glucofuranose-6,6′-d_2.[4] The complex now

[3]*Compound I was oxidized slowly under these conditions, however, this reaction being easily detectable by the appearance of a sharp singlet due to the protons of liberated formaldehyde (C_6) at 12 c.p.s. downfield from the* DOH *signal. The intensity of this signal increased progressively over a period of 24 h, at which time 1 mole of periodate per mole of I had been reduced and the spectrum had become closely similar to that obtained in the oxidation at pH 4.5 (8).*

[4]*This di-deuterio- derivative was kindly provided by Dr. W. Mackie.*

Can. J. Chem. Downloaded from www.nrcresearchpress.com by 210.87.254.40 on 09/05/12
For personal use only.

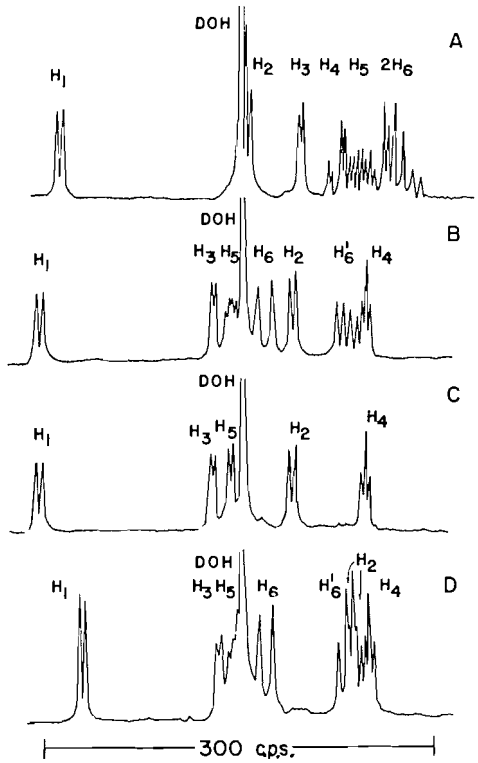

FIG. 1. Nuclear magnetic resonance spectra (100 Mc/s) in deuterium oxide – potassium carbonate solution (pH 8.5) of (A) 1,2-*O*-isopropylidene-α-D-glucofuranose, (B) 1,2-*O*-isopropylidene-α-D-glucofuranose *plus* 1 molar equivalent of sodium periodate, (C) 1,2-*O*-isopropylidene-α-D-glucofuranose-6,6′-d_2 *plus* 1 molar equivalent of sodium periodate, (D) ethyl α-D-thioglucofuranoside *plus* 1 molar equivalent of sodium periodate. In A, B, and C the two signals for the protons of the two C-methyl groups are omitted, and in D signals for the ethyl protons are omitted; the chemical shift of these protons is virtually unaffected by complexing.

afforded a spectrum (Fig. 1C) in which the signals that had been ascribed to H_6 and H_6' (Fig. 1B) are absent. Also, the quartet ascribed to H_5 in Fig. 1B is reduced to a doublet, as is to be expected when detectable coupling with H_6' has been eliminated. Hence the spectral data show that compound I forms a complex with the periodate ion at high pH and also, by directly implicating the 3-, 5-, and 6-hydroxyl groups, clearly demonstrate that this complex has a tridentate structure.

In contrast to the strong deshielding of the 3-, 5-, and 6-protons, H_2 and H_4 experience a notable increase in shielding as I is converted into II. Noteworthy also is the fact that the signal for one of the 6-protons (6′ in II) is not displaced nearly so far towards lower field as is that of the other. This intermediate result could conceivably be due to an interplay of two opposing effects: i.e., the proton may be subjected not only to the intense deshielding introduced when complexing occurs at the α-position, but also to the moderate shielding influence such as evident for H_2 and H_4.

Proton–proton coupling values in Fig. 1 agree well with measurements of carbon–hydrogen bond dihedral angles in molecular models of I and II. In making these comparisons the model of I was oriented so that C_2 was below and C_3 above a plane defined by the C_1, ring O, and C_4 atoms. Such a conformation has been depicted by Abraham *et al.* (11) for various derivatives of I, and should apply equally well for I itself since the ring

Can. J. Chem. Downloaded from www.nrcresearchpress.com by 210.87.254.40 on 09/05/12
For personal use only.

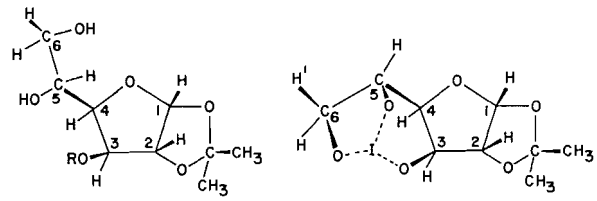

I (R = H)
III (R = C_2H_5)

II

proton coupling values in spectrum 1A are very close to those reported in ref. 11. According to the models the reaction I → II need involve little change in H_1—H_2 coupling and H_3—H_4 coupling, and a comparison of the pertinent signals in Figs. 1, A, B, and C shows that these values do, in fact, remain constant. Hence, the conformation of the fused 1,3-dioxalane and furanose rings in II is probably the same as in I. The fact that complexing occurs does not in itself serve to define this conformation, because a model of II can be constructed readily when the rings are puckered in the opposite sense (i.e., with C_3 down and C_2 up). However, the 3-, 4-, and 5 protons of the complex must be staggered in a nearly symmetrical fashion since H_3 and H_5 are coupled equally with H_4 (Fig. 1, B or C). Such an arrangement is found in the conformation depicted, with C_3 above the plane of the furanose ring, but is not possible in the alternative conformation.

The major change to be expected when the complex is formed is a realignment of the 5- and 6-carbinol groups from an orientation in which they likely are directed away from the furanose ring in I (perhaps as in formula I) to an arrangement (as in II) in which they have been rotated upon the C_4—C_5 bond in an arc of about 120° towards the ring. The spectral data are in good agreement on this point with what would be predicted by the Karplus relationship (12, 13). Thus, the change in $J_{4,5}$ (evident most clearly in the H_4 signals of Fig. 1, A and B and the H_5 signal of Fig. 1C) corresponds to a decrease in the C_4H–C_5H dihedral angle from a value of perhaps 180° in I to a value of 40–50° in II. Similarly, the data are consistent regarding the orientation of the 5- and 6-protons in the complex. According to the model of II, H_5 subtends an angle of 90° with H_6 and 30° with H_6' and the corresponding dihedral angles estimated from the observed values of J (i.e., 0 and 5 c.p.s.) are 90° and 35° (12, 13).

The tridentate type of structure (II) may be regarded as one of a variety of cyclic periodate complexes that can arise as a result of changes in the degree of dissociation and hydration of periodate at different hydrogen ion concentrations (14). According to Bunton and colleagues (4, 15) the monocyclic type formed as a transient intermediate in glycol-scission reactions (3, 16, 17) is a singly charged anionic species (IV, V) in weakly acid or neutral media, but exists largely as a dianion (VI) at pH 9. These workers contend also that the entity that actually decomposes to products must be the *dehydrated* form, i.e. IV. Therefore, they regard dianion VI as highly stable because it cannot likewise suffer dehydration (thus accounting for the relatively slow rate of periodate oxidations at high pH (4, 15)). Tridentate complexes corresponding to V and VI are represented by VII and VIII. All four species are considered to be in equilibrium if the third hydroxyl group of the polyol can readily be accommodated within the octahedral structure of the periodate anion. We do not know if these tridentate complexes can decompose to yield products, but if they can, their rates of decomposition are exceedingly slow. It is possible that the tridentate type of structure cannot undergo an internal rearrangement with the ease that

Can. J. Chem. Downloaded from www.nrcresearchpress.com by 210.87.254.40 on 09/05/12
For personal use only.

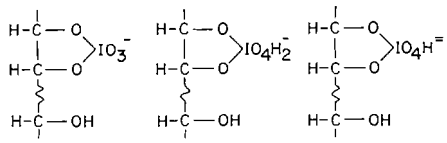

IV V VI

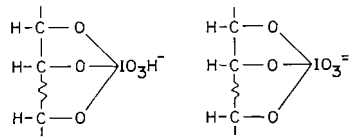

VII VIII

characterizes the decomposition of IV to a dialdehyde (15, 16), and hence is inherently more stable than a monocyclic complex. However, an extension of Bunton's views on the mechanism of periodate oxidation would suggest that neither VII nor VIII fulfills the requirements of a decomposing entity, since neither can be converted into a dehydrated form.

There is no indication that tridentate complexing takes place at pH 4.5. Glycol-cleavage rates are usually optimal in this region (3, 4) and, therefore, if IV, V, and VII are in equilibrium with each other the irreversible process IV $\rightarrow$ products should rapidly displace the system at the expense of tridentate complexing. As the pH is raised and the rate of the oxidation reaction is thereby retarded (3, 4) the formation of tridentate complexes should be progressively favored. It appears possible also that the stability of anion VII is increased at a higher pH because the complexing reaction competes effectively with oxidation in the region of pH 7 (5) to 7.5, where glycol scission can still be relatively vigorous (4). In more strongly alkaline media, a high yield of dianion VIII would be ensured by the now sluggish behavior of the competing oxidation process.

Some evidence has been obtained that, in fact, two different tridentate complexes of 1,2-*O*-isopropylidene-α-D-glucose (I) are formed as the pH is raised. As noted above, a very slow reaction takes place between I and periodate at pH 7.5, as measured titrimetrically by the arsenite method (Table I, No. 2). However, at a pH of 8.5 an immediate uptake of about 0.65 moles of periodate per mole of I was detected by the same titration method (Nos. 4 and 5). Such a result was clearly at variance with the spectral data (Fig. 1B) and, in addition, iodimetric analysis of the reaction mixture showed that no reduction of periodate had actually taken place (No. 3).[5] Hence, this spurious uptake indicated that part of the complex formed at pH 8.5 is relatively stable in the presence of added arsenite (see ref. 5). This was confirmed readily by treating the reaction mixture with the arsenite for more than the usual 15 min reduction period or at an elevated temperature (Table II), which showed that under relatively vigorous conditions the complex is broken down with release of the periodate. Since the complex that is formed at pH 7.5 did not exhibit such stability towards the arsenite reagent it must represent a second species of II. Accordingly, this latter complex probably corresponds to VII and the more stable complex, to the dianion VIII.

The arrangement of the 3,5,6-triol grouping in ethyl α-D-thioglucofuranoside (IX) or methyl α-D-mannofuranoside (X) appears to be closely similar to that in I, although the

[5]*Similar results were obtained at pH 9.0 with the use of disodium hydrogen phosphate as the base (Table I, compare No. 6 with No. 7).*

Can. J. Chem. Downloaded from www.nrcresearchpress.com by 210.87.254.40 on 09/05/12
For personal use only.

3-hydroxyl group of these compounds is itself part of a second *vic*-diol located on the five-membered ring. A *cis*-diol as in X usually is extremely reactive towards glycol-cleaving agents, whereas a *trans*-diol as in IX is relatively sluggish. At pH 7.5, in contrast to the behavior of I, both of these glycosides were rapidly oxidized (Table I, Nos. 9 and 12). When the pH was raised to 8.5, the thioglucoside now reacted much more slowly (Table I, Nos. 10 and 11) and n.m.r. spectroscopy (Fig. 1D) showed that complex formation occurs

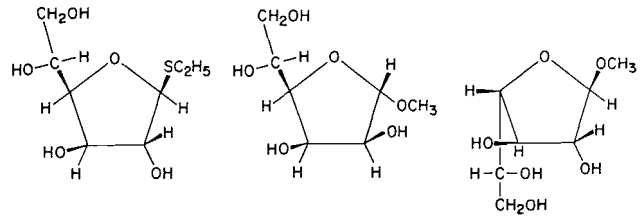

IX X XI

under these conditions. Moreover, the structure of this complex must be closely similar to that of tridentate II, because signals for the 3-, 4-, 5-, and 6 protons in Fig. 1D are almost exact counterparts of the corresponding signals in Fig. 1B. With the manno-furanoside (X), however, oxidation of the 2,3-diol group took precedence over tridentate complex formation (Table I, Nos. 13 and 14; no formaldehyde was liberated when 1 mole of periodate was reduced). Although the complexing reaction as it applies to I and IX must be exceedingly rapid, it is not clear whether X is oxidized because scission of its 2,3-diol group is far too rapid a reaction, or because it cannot complex readily despite its presumed structural similarity to I and IX.

Molecular models suggested that a galactofuranoside also might form a stable tridentate complex with periodate, but one involving the 2-, rather than 3-hydroxyl group together with the 5,6-diol. In agreement with this possibility, it was found that methyl β-D-galactofuranoside (XI) does not readily reduce periodate at pH 8.4 (Table I, No. 17). Further, its n.m.r. spectrum was markedly altered on addition of the reagent, with several proton signals being shifted strongly towards lower field, but a detailed analysis of this spectrum has not yet been completed. However, the galactofuranoside was rapidly oxidized at pH 7.5 (Table I, Nos. 15 and 16) so that, like the thioglucofuranoside, it requires more strongly alkaline conditions for stable tridentate complexing. Presumably the complex of both these compounds attains sufficient stability only in the dianionic form (VIII).

From the current and earlier (5) data it is seen that the stability of periodate tridentate complexes varies over a wide range. D-Ribose forms a complex at the relatively low pH value of 7 (5) and this complex, probably a monoanion (VII), is stable in the presence of arsenite. The complex formed between periodate and 1,2-*O*-isopropylidene-α-D-glucose at pH 7.5 is likely also of type VII, but is far more easily decomposed by arsenite, whereas the dianionic species (VIII) formed at pH 8.5 is not readily decomposed. Tridentates of the thioglucofuranoside and galactofuranoside are detected only under the more strongly alkaline conditions that favor the dianionic form, but neither of these complexes is stable towards arsenite. These variations reinforce an earlier suggestion (5) that the tridentate-complexing reaction might provide a useful basis for comparing conformation and (or) inductive effects among series of related polyols.

Can. J. Chem. Downloaded from www.nrcresearchpress.com by 210.87.254.40 on 09/05/12
For personal use only.

EXPERIMENTAL

Proton magnetic resonance (n.m.r.) spectra were recorded with a Varian HA-100 high resolution spectrometer.

Reaction of Periodate with Furanose Derivatives

(a) Nuclear Magnetic Resonance Experiments

In a typical experiment 1,2-*O*-isopropylidine-D-glucofuranose (20 mg) was dissolved in deuterium oxide (0.6 ml), anhydrous potassium carbonate (20 mg) was added, and the n.m.r. spectrum was recorded (Fig. 1A). Sodium metaperiodate (20 mg, 1 molar equivalent) was then added to the solution, after which the n.m.r. spectrum was again measured (Fig. 1B).

(b) Titration Measurements

The polyol (0.025 mmole) and base (0.0 to 0.10 mmole) were dissolved in water (1.0 ml) and to this was added 1.0 ml of 0.025 molar sodium metaperiodate (0.025 mmole) solution. After the desired time of reaction the reaction mixture was added to either (*a*) a solution (5.0 ml) of potassium iodide (5%) in 0.2 molar potassium dihydrogen (4 parts) and disodium hydrogen (6 parts) phosphate buffer (pH 7.0) (18) or, (*b*) a mixture of 0.1 *N* sodium arsenite solution (2.0 ml) containing potassium iodide (0.01%) and sodium bicarbonate (0.5 g) (19). In the former method (thiosulphate method, Table I), the liberated iodine was titrated with 0.025 *N* thiosulphate solution, and in the latter (arsenite method, Table I) the excess arsenite was titrated (after 15 min, unless otherwise indicated) with 0.025 *N* iodine solution. Starch indicator (2%) was used in both titrations for the end point.

Under the conditions of permanganate–periodate oxidation (2) the concentration of periodate was 0.1 mmole per ml and that of potassium carbonate 0.0125 mmole.

ACKNOWLEDGMENTS

The authors thank M. Mazurek for recording the n.m.r. spectra and M. Granat for technical assistance.

REFERENCES

1. E. VON RUDLOFF. Can. J. Chem. In press.
2. R. U. LEMIEUX and E. VON RUDLOFF. Can. J. Chem. **33**, 1701 (1955).
3. C. C. PRICE and M. KNELL. J. Am. Chem. Soc. **64**, 552 (1942).
4. G. J. BUIST and C. A. BUNTON. J. Chem. Soc. 1406 (1954).
5. G. R. BARKER and D. F. SHAW. J. Chem. Soc. 584 (1959).
6. K. FREUDENBERG and W. JACOB. Chem. Ber. **80**, 325 (1947).
7. B. S. SHASHA, W. M. DOANE, C. R. RUSSELL, and C. E. RIST. Nature, **204**, 186 (1964).
8. A. S. PERLIN. Can. J. Chem. **42**, 1365 (1964).
9. L. M. JACKMAN. Applications of nuclear magnetic resonance spectroscopy in organic chemistry. Pergamon Press. 1959. p. 55.
10. M. MAZUREK and A. S. PERLIN. Can. J. Chem. **41**, 2403 (1963).
11. R. J. ABRAHAM, L. D. HALL, L. HOUGH, and K. A. MCLAUCHLIN. J. Chem. Soc. 3699 (1962).
12. M. KARPLUS. J. Chem. Phys. **33**, 316 (1960).
13. F. A. L. ANET. Can. J. Chem. **39**, 789 (1961).
14. C. E. CROUTHAMEL, A. M. HAYES, and D. S. MARTIN. J. Am. Chem. Soc. **73**, 82 (1951).
15. G. J. BUIST, C. A. BUNTON, and J. H. MILES. J. Chem. Soc. 743 (1959).
16. R. CRIEGEE. Sitzber. Ges. Befoerder Ges. Naturw. Marburg, **69**, 25 (1934).
17. L. J. HEIDT, E. K. GLADDING, and C. B. PURVES. Paper Trade J. **121**, No. 9, 35 (1945).
18. G. NEUMÜLLER and E. VASSEUR. Arkiv. Kemi, Mineral. Geol. **5**, 235 (1935).
19. P. F. FLEURY and J. LANGE. J. Pharm. Chim. **17**, 107, 196 (1933).

Can. J. Chem. Downloaded from www.nrcresearchpress.com by 210.87.254.40 on 09/05/12
For personal use only.

Can. J. Chem. Downloaded from www.nrcresearchpress.com by 210.87.254.6 on 09/05/12
For personal use only.

ACETONATION OF ALDOSE DIETHYL THIOACETALS[1]

P. A. J. GORIN
National Research Council of Canada, Prairie Regional Laboratory, Saskatoon, Saskatchewan
Received February 2, 1965

ABSTRACT

Acetonation of hexose diethyl thioacetals using copper sulphate catalyst gave rise to 5,6-*O*-substituted products. The exception was D-galactose diethyl thioacetal, which underwent some 4,5-*O*-substitution. D-Threose and 2,3-di-*O*-methyl-D-galactose diethyl thioacetals also underwent predominant α-terminal substitution although some β-terminal substitution took place, particularly with the latter thioacetal. Acetone – sulphuric acid caused preferential α-T acetonation of D-threose and 2,3-di-*O*-methyl-D-galactose diethyl thioacetals. The product from D-threose diethyl thioacetal contained 90% of the 2,3-*O*-isopropylidene and 10% of the 3,4-*O*-isopropylidene derivatives.

D-Glucurono-δ-lactone diethyl thioacetal in acetone – sulphuric acid acetonated mainly on the 2,4- positions although a smaller proportion of 4,5-*O*-isopropylidene derivative was present.

The synthesis of sugars with septanose rings has been recorded in the literature on only a few occasions (1, 2, 3). The starting compound used by Micheel and co-workers for preparation of a series of septanosyl derivatives was 2,3,4,5-tetra-*O*-acetyl-D-galactose hydrate. However, in view of the ready migration of acetyl groups, compounds of this type have only a limited application. Attempts have now been made to synthesize compounds with the 6-hydroxyl free, but with the 4- and 5-hydroxyls blocked as in the 4,5-*O*-isopropylidene hexoses derived from 4,5-*O*-isopropylidene hexose thioacetals.

The *O*-isopropylidene aldose thioacetals, first synthesized by E. and J. Pacsu and coworkers (4–7), required reinvestigation since structures were assigned on the basis of methylation experiments in which the products were improperly characterized. The compound obtained on treatment of mannose diethyl thioacetal with copper sulphate acetone was assigned a 2,3-*O*-isopropylidene structure (4), which now appears unlikely since it would contain a *cis*-disubstituted 2,2-dimethyl-1,3-dioxolane ring. 2,3-*O*-Substitution was also claimed for the copper sulphate catalyzed acetonation product of galactose dibenzyl thioacetal (5) and for the condensation product from methyl ethyl ketone and glucose dibenzyl thioacetal (6). The former derivative was unambiguously characterized later as a mixture of 4,5- (7) and 5,6-*O*-isopropylidene galactose dibenzyl thioacetal (8). Mono-*O*-isopropylidene glucose dibenzyl thioacetal was obtained by action of sulphuric acid (9) and copper sulphate (10) in acetone on glucose dibenzyl thioacetal. In the latter experiment, Schinle also isolated 2,3,5,6-di-*O*-isopropylidene glucose dibenzyl thioacetal. Formation of 2-*O*-methyl glucose dibenzyl thioacetal by partial methylation of the mono-*O*-isopropylidene derivative followed by partial hydrolysis led the author to assign a 5,6-*O*-isopropylidene structure.

In the present work the mono-*O*-isopropylidene diethyl thioacetals of mannose, glucose, altrose, and galactose were prepared by the action of copper sulphate in acetone on the corresponding hexose diethyl thioacetal. Optimum conditions for synthesis were found by examination of the products, at intervals, by silica gel thin-layer chromatography. *O*-Isopropylidene derivatives were isolated by crystallization except in the glucose series, which required silicic acid chromatography before crystallization was possible. Demercaptalation of the *O*-isopropylidene hexose diethyl thioacetals with mercuric chloride in

[1]*Issued as N.R.C. No. 8478.*

aqueous acetone, in the presence of cadmium carbonate, yielded the free *O*-isopropylidene hexoses. The parent *O*-isopropylidene hexose diethyl thioacetals were identified by oxidation with sodium periodate at neutral pH, followed by sodium borohydride reduction and acid hydrolysis. Formation of glycerol from the glucose, mannose, and altrose derivatives indicated 5,6-*O*-isopropylidene substitution. The galactose derivative gave rise mainly to threitol, showing 4,5- or 4,6-substitution. Of these two possibilities, the 4,5-assignment was shown to be correct by converting the thioacetal via a series of steps into methyl tri-*O*-methyl $\alpha\beta$-D-galactoside. Gas chromatographic analysis (g.l.c.) showed that the trimethyl derivative had the 2,3,6- rather than the 2,3,5-structure (see the acetonation of 2,3-di-*O* methyl galactose diethyl thioacetal described in the experimental section). Some 2,3,4-tri-*O*-methyl derivative (11%) was also detected showing that 5,6-*O*-isopropylidene-D-galactose diethyl thioacetal had been present as an impurity in the isolated crystals.

Since acetonation of the above diethyl thioacetals was complicated by the formation of di-*O*-isopropylidene derivatives, the diethyl thioacetals of 2,3-di-*O*-methyl-D-galactose and D-threose were used as substrates. Unlike D-galactose diethyl thioacetal, the 2,3-di-*O*-methyl substituted derivative gave rise, after 18 h, to 5,6-*O*-isopropylidene (63%) and 4,6-*O*-isopropylidene derivatives (37%) with the copper sulphate catalyst. These structures and percentages were deduced from a methylation experiment described in the experimental section.

The acetonation of D-threose diethyl thioacetal was followed more readily since the three possible products were separable by g.l.c. as their acetates. Acetonation was complete after 8 h and the main product was the 3,4-isomer with smaller proportions of the 2,3- and 2,4-isomer[2] (Fig. 1). It was apparent that, although the 2,4-*O*-isopropylidene derivative was formed initially, most of it was transformed at later stages of the reaction. However,

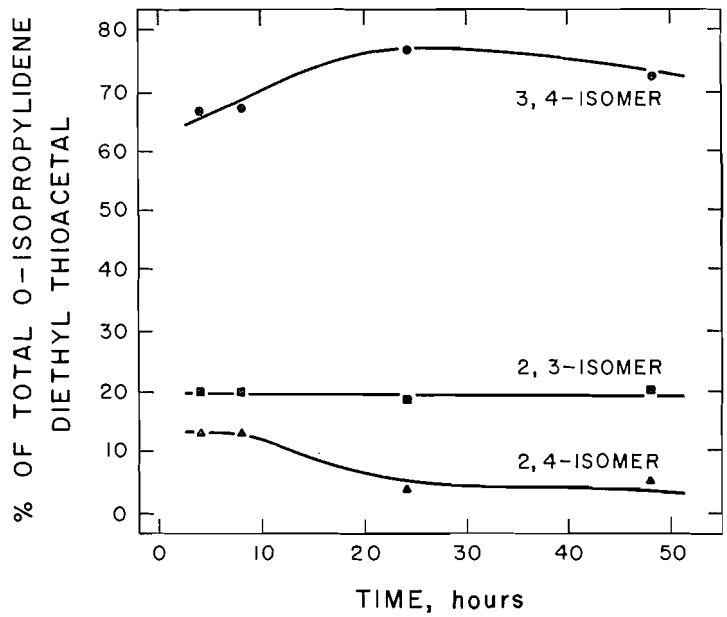

FIG. 1. Gas–liquid chromatography signal response variation with time of acetates derived from *O*-isopropylidene-D-threose diethyl thioacetals which were formed by the action of copper sulphate–acetone.

[2]*For characterization data see the experimental section.*

Can. J. Chem. Downloaded from www.nrcresearchpress.com by 210.87.254.6 on 09/05/12
For personal use only.

hydrolysis of the initially formed products was slow so that kinetic control of the copper sulphate catalyzed acetonation was virtually effected. Barker *et al.* (11) noted that ketones prefer to substitute primary rather than secondary hydroxyls. Rapid equilibration does not occur and since the intermediate in formation of an *O*-isopropylidene derivative should be a hemiketal, it follows that preferential substitution should take place at the more active primary hydroxyl. Since condensation depends on the reactivity of the participating groups and their relative proximity, it is not surprising that the β-terminal ring should be formed in addition to the α-terminal ring, although examples of this are rare in the ketal series (12).

In contrast, the more rapid reactions of sugar thioacetals with acetone – sulphuric acid are thermodynamically controlled and give rise to different proportions of products than the above copper sulphate catalyzed reactions. 2,3-Di-*O*-methyl-D-galactose diethyl thioacetal was converted mainly to its 4,5-*O*-isopropylidene derivative, as shown by a methylation experiment. The products from D-threose diethyl thioacetal were shown to

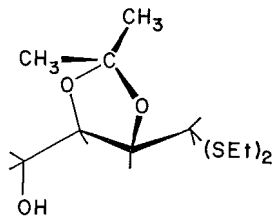

I

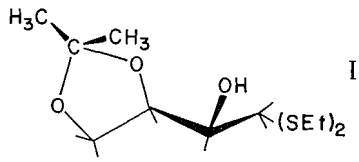

II

consist of the 2,3-*O*-isopropylidene- (90%; I) and 3,4-*O*-isopropylidene- (10%; II) derivatives by g.l.c. of their acetates. The preferential formation of an αT-ring over a corresponding terminal α-ring has been briefly rationalized by Mills (13). Known instances are the pyridinium chloride catalyzed conversion of 1,2;4,5-di-*O*-isopropylidene DL-galactitol to its 2,3;4,5-isomer (14) and the acetonation of D-galactose dibenzyl thioacetal to give the 2,3;4,5-*O*-isopropylidene rather than the 2,3;5,6-*O*-isopropylidene derivative (15).

An attempt to prepare 4,5-*O*-isopropylidene D-glucose starting from the acetonation product of D-glucurono-δ-lactone diethyl thioacetal did not succeed because of low yields. Using the acetone – sulphuric acid reagent a crystalline mono-*O*-isopropylidene derivative was obtained. The product gave a nuclear magnetic resonance (n.m.r.) spectrum which appeared to be a superimposition of two sets of signals. Reduction with sodium borohydride yielded a waxy material which was substituted mainly in the 2,4-position since demercaptalation followed by borohydride reduction gave 2,4-*O*-isopropylidene-D-sorbitol. The mother liquors contained a small proportion of 4,5-*O*-isopropylidene-D-sorbitol since periodate oxidation followed by sodium borohydride reduction and hydrolysis yielded erythritol in addition to xylitol. A crystalline sample of mono-*O*-isopropylidene D-mannurono-δ-lactone diethyl thioacetal was prepared in a similar way and also appeared to be a mixture, as indicated by its n.m.r. spectrum. The quantities of material isolated precluded a definite characterization. However, the two most likely structures are the 2,4- and

Can. J. Chem. Downloaded from www.nrcresearchpress.com by 210.87.254.6 on 09/05/12
For personal use only.

4,5-*O*-isopropylidene derivatives since the 2,5-substituted derivative would contain a 7-membered ketal ring.

EXPERIMENTAL

Acetonation of Hexose Diethyl Thioacetals

(1) Mannose Series

The acetone derivative was prepared in a somewhat better yield than that described by Pacsu and Kary (4). D-Mannose diethyl thioacetal (11 g) was shaken for 3 h in acetone (200 ml) containing anhydrous copper sulphate (50 g). Filtration and evaporation gave material which was recrystallized from ether–*n*-hexane to give the mono-*O*-isopropylidene derivative (9.4 g). This was chromatographically pure on thin-layer silica gel plates using chloroform as solvent and 50% sulphuric acid as spray reagent.

A portion (5.5 g) was treated according to the method of Micheel and Suckfull (1) and stirred vigorously in 90% aqueous acetone (100 ml) containing cadmium carbonate (35 g) at 0 °C. Mercuric chloride (7.3 g; 1.6 moles) in acetone (30 ml) was added and the mixture was stirred at room temperature for 18 h. After heating at 50 °C for 30 min the solids were filtered off and the filtrate evaporated to a syrup in the presence of cadmium carbonate. Chromatography on cellulose (eluant, benzene–ethanol–water 500:50:1 v/v) yielded 5,6-*O*-isopropylidene-D-mannose (2.3 g), which was recrystallized twice from ethyl acetate to yield material with m.p. 76–78 °C and $[\alpha]_D$ +27° (*c*, 1.0, H_2O).

Anal. Calcd. for $C_9H_{16}O_6$: C, 49.08; H, 7.32. Found: C, 48.7; H, 7.4.

The *O*-isopropylidene mannose (100 mg) was treated with sodium borohydride (40 mg) in water (5 ml). After 1 h the pH was adjusted to 7 and the solution evaporated to a crust. The residue was dissolved in methanol, which was then evaporated. After this process was repeated three times the product was chromatographed on cellulose using benzene–ethanol–water (500:50:1 v/v) as eluant. 5,6-*O*-Isopropylidene-D-mannitol, thus isolated, was twice recrystallized from ethyl acetate and had m.p. 164–166 °C (Vargha (16) reported m.p. 167 °C for this material).

Anal. Calcd. for $C_9H_{18}O_6$: C, 48.64; H, 8.16. Found: C, 48.3; H, 8.1.

(2) Glucose Series

D-Glucose diethyl thioacetal was shown by thin-layer silica gel chromatography to acetonate rapidly and accordingly 6.0 g was shaken for 3 h in acetone (100 ml) containing anhydrous copper sulphate (25 g). The solution was then filtered, evaporated, and chromatographed on a column of silicic acid using chloroform as solvent. Initially two fractions were eluted, firstly, a di-*O*-isopropylidene-D-glucose diethyl thioacetal (0.39 g) with $[\alpha]_D$ −9° (*c*, 1.6, MeOH).

Anal. Calcd. for $C_{16}H_{30}O_5S_2$: C, 52.45; H, 8.25. Found: C, 52.1; H, 8.5.

Secondly, the major di-*O*-isopropylidene-D-glucose diethyl thioacetal (1.34 g) with $[\alpha]_D$ −44° (*c*, 1.9, MeOH), was eluted. Found: C, 52.3; H, 8.7. The above structures were probably substituted 3,4,5,6- and 2,3,5,6-respectively by analogy with the compounds obtained by Curtis and Jones in the dimethyl thioacetal series (17).

The mono-*O*-isopropylidene glucose derivative was eluted later and this was crystallized from ether–*n*-hexane. The product (3.2 g) had m.p. 68–69 °C and $[\alpha]_D$ −11° (*c*, 1.2, MeOH).

Anal. Calcd. for $C_{13}H_{26}O_5S_2$: C, 47.84; H, 8.03. Found: C, 47.8; H, 8.2.

Demercaptalation of 0.78 g by the previously described procedure provided 5,6-*O*-isopropylidene-D-glucose (0.32 g). Recrystallization from ethyl acetate gave material with m.p. 111–113 °C and $[\alpha]_D$ +17° (*c*, 0.7, H_2O).

Anal. Calcd. for $C_9H_{16}O_6$: C, 49.08; H, 7.32. Found: C, 48.9; H, 7.6.

(3) Altrose Series

D-Altrose diethyl thioacetal (18) (1.0 g) was shaken in acetone (20 ml) containing copper sulphate (5 g) for 3 h. Filtration and evaporation gave material which was recrystallized twice from ether–*n*-hexane to give a derivative with m.p. 70–71 °C and $[\alpha]_D$ +8° (*c*, 1.2, MeOH). Yield, 0.56 g.

Anal. Calcd. for $C_{13}H_{26}O_5S_2$: C, 47.84; H, 8.03. Found: C, 47.5; H, 8.1.

(4) Galactose Series

D-Galactose diethyl thioacetal (19.5 g) was treated overnight in acetone (250 ml) containing copper sulphate (25 g). The product gave two zones on silica gel thin-layer chromatography using chloroform as solvent. Filtration and evaporation gave material which appeared to be a crystalline mixture, and fractional crystallization three times from ether gave a product (6.1 g) with m.p. 82–83 °C and $[\alpha]_D$ +19° (*c*, 3.1, MeOH).

Anal. Calcd. for $C_{13}H_{26}O_5S_2$: C, 47.84; H, 8.03. Found: C, 47.8; H, 8.3.

The slower moving component on thin-layer plates was considerably concentrated by the recrystallization processes.

Characterization of Mono-O-isopropylidene Hexose Diethyl Thioacetals

(1) Mannose, Glucose, and Altrose Derivatives

These were oxidized overnight with 10 equivalents of 0.1 *M* sodium periodate in the presence of sodium bicarbonate buffer. Salts were removed with mixed Amberlite IR120 and Dowex 1 (bicarbonate form) and

Can. J. Chem. Downloaded from www.nrcresearchpress.com by 210.87.254.6 on 09/05/12
For personal use only.

the filtrate treated with excess sodium borohydride. After 2 h the reducing agent was removed. Hydrolysis of the products in 5% aqueous acetic acid at 100° gave glycerol as shown by paper chromatograms (solvent: butanol–ethanol–water 40:11:19 v/v; spray: ammoniacal silver nitrate) thus indicating a 5,6-*O*-isopropylidene structure in the starting materials.

(2) Galactose Derivative

A treatment similar to that described above gave threitol and a trace of glycerol. The *O*-isopropylidene group was therefore either in the 4,5- or 4,6-position.

The *O*-isopropylidene derivative was methylated by the Haworth procedure (19) at room temperature using dimethyl sulphate and aqueous sodium hydroxide containing 5% of acetone. Excess reagent was destroyed by being heated for 3 h on a steam bath and the product was isolated by extraction with benzene. The methylated derivative was demercaptalated (1) and converted to a methylated methyl galactosidic mixture by being heated under reflux in 3% methanolic hydrogen chloride for 4 h. The product was examined by g.l.c. using 2% neopentyl glycol succinate (20) on HMDS Chromosorb W (80–100 mesh) in a 5 ft × 1/4 in. o.d. copper tube at 143 °C with helium (30 p.s.i.) as carrier gas. The g.l.c. unit was of conventional design using thermal conductivity detectors.

The following galactosides were detected, their proportion being expressed as the percentage of the total signals; the other figures in parentheses are the emergence times: methyl 2,3,6-tri-*O*-methyl-D-galactosides (89%; three signals at 1.1, 1.5, and 1.6 min), methyl 2,3,4-tri-*O*-methyl-D-galactosides (11%; one signal at 2.8 min). Identification was made by comparison of retention times and signal patterns with those of authentic glycosides.

Acetonation of D-Glucurono-δ-lactone Diethyl Thioacetal

D-Glucurono-δ-lactone diethyl thioacetal prepared by the method of Zinner and Dässler (21) was shown to be acetonated readily by 0.1% sulphuric acid in acetone. Zinc chloride and copper sulphate in acetone at room temperature gave only partial acetonation after 18 h as shown by chromatography on thin-layer silica gel plates using chloroform as solvent.

D-Glucurono-δ-lactone diethyl thioacetal (12.5 g) was treated overnight in acetone (300 ml) containing 0.1% sulphuric acid. The acid was removed with barium carbonate and the solution filtered and evaporated. Two crystallizations from ether gave the mono-*O*-isopropylidene derivative (6.7 g) with m.p. 108–111 °C and $[\alpha]_D$ +78° (*c*, 0.9, MeOH).

Anal. Calcd. for $C_{13}H_{22}O_5S_2$: C, 48.44; H, 6.88. Found: C, 48.8; H, 7.4. Examination of the product in chloroform by nuclear magnetic resonance (n.m.r.) spectroscopy showed two sets of four methylene proton signals superimposed. Absorption at 1 780 cm^{-1} in the infrared corresponded to a δ-lactone.

The mono-*O*-isopropylidene-D-glucurono-δ-lactone diethyl thioacetal (1.2 g) in dioxane (50 ml) was treated with sodium borohydride (0.3 g) in water (5 ml). After 18 h the reaction mixture was added to excess water and the solution adjusted to pH 7. Chloroform extraction removed the product, which was crystallized from ether–*n*-hexane to give a waxy product (0.73 g) with an indefinite melting point. The carbon and hydrogen analyses corresponded to those of mono-*O*-isopropylidene-D-glucose diethyl thioacetal.

Anal. Calcd. for $C_{13}H_{26}O_5S_2$: C, 47.84; H, 8.03. Found: C, 47.9; H, 8.1.

A sample of the thioacetal was demercaptalated and reduced with sodium borohydride. The product after two recrystallizations from acetone had m.p. 158–160 °C and $[\alpha]_D$ +11° (*c*, 0.9, MeOH).

Anal. Calcd. for $C_9H_{18}O_6$: C, 48.64; H, 8.16. Found: C, 48.4; H, 8.3. The mono-*O*-isopropylidene D-sorbitol after 1 h consumed 0.94 moles of sodium periodate without formation of acid.

The mother liquors (containing 30% by weight of the reduction product) were evaporated and oxidized with sodium periodate at neutral pH and the product reduced with sodium borohydride and then hydrolyzed. A small proportion of erythritol in addition to xylitol pointed to the presence of 4,5-*O*-isopropylidene-D-sorbitol.

Preparation of O-Isopropylidene-D-mannurono-δ-lactone Diethyl Thioacetal

Synthesis of the mannurono-δ-lactone derivative was carried out in a manner analogous to that used in the glucurono-δ-lactone series. After silicic acid column chromatography (chloroform 3 : hexane 2 as eluant) *O*-isopropylidene-D-mannurono-δ-lactone was obtained in very low yield. After two crystallizations from ether–*n*-hexane the product had m.p. 78–85 °C, $[\alpha]_D$ +53° (*c*, 1.1, EtOH) and an infrared absorption band at 1 785 cm^{-1} corresponded to a δ-lactone.

Anal. Calcd. for $C_{13}H_{22}O_5S_2$: C, 48.44; H, 6.88. Found: C, 48.2; H, 6.8. In the n.m.r. spectrum the methylene proton signals appeared to consist of two distinct overlapping quadruplets.

Acetonation of D-Threose Diethyl Thioacetal

D-Threose, prepared from D-galactose (5.0 g) (22), was shaken with ethanethiol (3 ml) and concentrated hydrochloric acid (3 ml) for 30 min. The reaction mixture was neutralized by addition to a stirred suspension of lead carbonate (15 g) in methanol (100 ml). Filtration and evaporation yielded a syrup which crystallized and two recrystallizations from ether gave D-threose diethyl thioacetal (1.65 g) with m.p. 69–70 °C and $[\alpha]_D$ −13° (*c*, 2.0, EtOH).

Anal. Calcd. for $C_8H_{18}O_3S_2$: C, 42.47; H, 8.02. Found: C, 42.7; H, 8.1.

Can. J. Chem. Downloaded from www.nrcresearchpress.com by 210.87.254.6 on 09/05/12
For personal use only.

(1) Acetonation using Copper Sulphate

D-Threose diethyl thioacetal (1.0 g) in acetone (20 ml) was shaken with copper sulphate (5.0 g). At intervals samples were abstracted, filtered, and evaporated to residues which were acetylated with acetic anhydride in pyridine. Examination of the products by g.l.c. using a column of neopentyl glycol succinate on HMDS Chromosorb W (80–100 mesh) (see analysis of methyl tri-*O*-methyl galactosides described earlier) at 160 °C showed that tri-*O*-acetyl D-threose diethyl thioacetal had disappeared after 8 h.

The three possible acetylated *O*-isopropylidene threose diethyl thioacetal isomers had the following retention times: 3,4-*O*-isopropylidene derivative, 2.1 min; 2,4-isomer, 2.4 min;[3] 2,3-isomer, 3.2 min. The variation of the relative signals produced by these isomers with time are recorded in Table I.

TABLE I

The copper sulphate catalyzed acetonation of D-threose diethyl thioacetal

Isomer of *O*-acetyl-*O*-isopropylidene D-threose diethyl thioacetal	Time (h)					
	4	8	24	48	72	144
	% total signal response					
3,4-*O*-Isopropylidene-	66	67	77	73	65	67
2,4-*O*-Isopropylidene-	13	13	4	6	5	0
2,3-*O*-Isopropylidene-	20	20	19	21	30	33

A portion of the *O*-isopropylidene D-threose diethyl thioacetals formed after 24 h was isolated. The mixture was chromatographed on silicic acid using chloroform–hexane (1:1 v/v) as eluant. The product was syrupy and consisted of the 3,4-isomer and had $[\alpha]_D$ −18° (*c*, 1.8, $CHCl_3$).

Anal. Calcd. for $C_{11}H_{22}O_3S_2$: C, 49.61; H, 8.33. Found: C, 49.1; H, 8.3.

A small sample of the crude acetonated mixture was demercaptalated and the product reduced with sodium borohydride to *O*-isopropylidene-D-threitol. This was oxidized with excess sodium periodate and the resulting mixture reduced with sodium borohydride and the *O*-isopropylidene groups removed by hydrolysis. The product consisted mainly of glycerol arising from 3,4-*O*-isopropylidene-D-threitol diethyl thioacetal and a small amount of threitol from the other isomers.

(2) Acetonation using Zinc Chloride

The products arising from the action of zinc chloride (45 mg) in acetone (10 ml) on D-threose diethyl thioacetal were similar to those in the copper sulphate experiment. After 2 h and 8 h the relative signal responses produced by the 3,4-, 2,4-, and 2,3-isomers were 64%, 16%, 20%, and 74%, 11%, and 15%, respectively, on g.l.c. of the acetylated mixtures.

(3) Acetonation using 1% Sulphuric Acid

D-Threose diethyl thioacetal (1.0 g) was treated for 3 h with acetone (150 ml) containing sulphuric acid (0.5 ml). The mixture was added to aqueous sodium bicarbonate which was then extracted with chloroform. The extract was evaporated to a syrup which, after purification by silicic acid chromatography, had $[\alpha]_D$ +47° (*c*, 1.8, $CHCl_3$).

Anal. Calcd. for $C_{11}H_{22}O_3S_2$: C, 49.6; H, 8.33. Found: C, 49.6; H, 8.4.

The product was shown to be 2,3-*O*-isopropylidene-D-threose diethyl thioacetal by methylation with dimethyl sulphate and aqueous sodium hydroxide containing 5% acetone. The product was demercaptalated and reduced with sodium borohydride. Removal of the isopropylidene group with 5% aqueous acetic acid at 100 °C gave mono-*O*-methyl-D-threitol, which was separated from a little unmethylated threitol by cellulose chromatography (eluant: benzene–ethanol–water 200:50:1 v/v). It had $[\alpha]_D$ −6.5° (*c*, 1.5, EtOH) and on a paper chromatogram in *n*-butanol–ethanol–water (40:11:19 v/v) ran at 1.2 times the rate of glycerol. Oxidation with sodium periodate resulted in the uptake of 1.6 moles of oxidant with formation of 0.7 moles of acid. These data are consistent with slightly impure 4-*O*-methyl-D-threitol and distinguishes it from 3-*O*-methyl-D-threitol.

The above structure was confirmed by conversion to 4-*O*-methyl-D-threitol tris-*p*-nitrobenzoate, which, on three recrystallizations from ethyl acetate *n*-hexane, had melting point and mixed melting point 80–83 °C and $[\alpha]_D$ −32° (*c*, 1.0, $CHCl_3$). The product gave an X-ray diffraction pattern identical with that of authentic material.

Authentic 4-*O*-methyl-D-threitol was prepared by oxidation of 6-*O*-methyl-D-galactose with 2 moles of lead tetraacetate followed by reduction of the product with sodium borohydride. The product had $[\alpha]_D$ −9° (*c*, 1.7, EtOH) and gave a crystalline tris-*p*-nitrobenzoate with m.p. 79–83 °C and $[\alpha]_D$ −34° (*c*, 1.0, $CHCl_3$).

Anal. Calcd. for $C_{26}H_{21}O_{13}N_3$: C, 53.52; H, 3.63. Found: C, 53.6; H, 3.8.

On g.l.c. examination, 4-*O*-acetyl-2,3-*O*-isopropylidene-D-threose diethyl thioacetal gave 1.42 times the

[3]*The 2,4-isomer was identified by process of elimination after chemical characterization of the 2,3- and 3,4-isomers.*

Can. J. Chem. Downloaded from www.nrcresearchpress.com by 210.87.254.6 on 09/05/12
For personal use only.

response obtained with the corresponding 2-*O*-acetyl-3,4-*O*-isopropylidene derivative. The products formed after treatment of D-threose diethyl thioacetal with acetone containing 1% sulphuric acid for 1 h and 24 h were analyzed after acetylation with pyridine – acetic anhydride. Using the above correction factor 10% of the 3,4-*O*-isopropylidene and 90% of the 2,3-*O*-isopropylidene derivatives were shown to be present in each acetonation product.

Acetonation of 2,3-Di-O-methyl-D-galactose Diethyl Thioacetal

2,3-Di-*O*-methyl-D-galactose (5.0 g) was mercaptalated by the method described previously. The product (1.4 g) was twice crystallized from ether–*n*-hexane and had m.p. 53–54 °C and $[\alpha]_D$ −25° (*c*, 1.1, EtOH).

Anal. Calcd. for $C_{12}H_{26}O_5S_2$: S, 20.40. Found: S, 20.6.

(1) Acetonation using 1% Sulphuric Acid

2,3-Di-*O*-methyl-D-galactose diethyl thioacetal was acetonated for 1 h by the method described for D-threose diethyl thioacetal. The product contained almost exclusively one compound as shown by silica gel thin-layer chromatography and had $[\alpha]_D$ +7° (*c*, 1.0, EtOH).

Anal. Calcd. for $C_{15}H_{30}O_5S_2$: C, 50.83; H, 8.53. Found: C, 51.1; H, 8.4.

Methylation and conversion to a methyl tri-*O*-methyl galactosidic mixture was carried out by the method described for 4,5-*O*-isopropylidene-D-galactose diethyl thioacetal. The products corresponded to methyl 2,3,6-tri-*O*-methyl-D-galactosides, thus indicating a 4,5-*O*-isopropylidene-2,3-di-*O*-methyl-D-galactose structure. A trace of the 2,3,4-tri-*O*-methyl isomers was present.

(2) Acetonation using Copper Sulphate

2,3-Di-*O*-methyl-D-galactose diethyl thioacetal (0.25 g) was treated with copper sulphate (1.25 g) in acetone (10 ml). After 18 h the reaction mixture was added to aqueous sodium bicarbonate, which was extracted with chloroform. The extract was evaporated to a syrup.

Anal. Calcd. for $C_{15}H_{30}O_5S_2$: C, 50.83; H, 8.53. Found: C, 50.6; H, 8.3.

The product was examined on silica gel thin-layer plates using chloroform as solvent. Two spots moving at a greater rate than 4,5-*O*-isopropylidene 2,3-di-*O*-methyl-D-galactose diethyl thioacetal were detected. These were, by process of elimination, the 5,6- and 4,6-*O*-isopropylidene derivatives.

Methylation of the *O*-isopropylidene mixture was carried out and was followed by conversion to a methyl tri-*O*-methyl galactosidic mixture. Examination by g.l.c. showed that methyl 2,3,4-tri-*O*-methyl galactosides (63%) were the main products arising from the 5,6-*O*-isopropylidene derivative. The minor component (37%) consisted of methyl 2,3,5-tri-*O*-methyl galactosides with emergence times of 1.3 min and 1.7 min. The signal pattern differed from that of the methyl 2,3,6-tri-*O*-methyl galactosides, which had emergence times of 1.1, 1.5, and 1.6 min.

ACKNOWLEDGMENTS

The author would like to thank Mr. M. Mazurek for carrying out microanalytical determinations and Mr. W. C. Haid for obtaining n.m.r. spectra.

REFERENCES

1. F. MICHEEL and F. SUCKFULL. Ann. **502**, 85 (1933).
2. F. MICHEEL and F. SUCKFULL. Ann. **507**, 138 (1933).
3. F. MICHEEL and W. SPRUCK. Chem. Ber. **67B**, 1665 (1934).
4. E. PACSU and C. KARY. Chem. Ber. **62**, 2811 (1929).
5. J. PACSU and A. LOB. Chem. Ber. **62**, 3104 (1929).
6. E. PACSU. Chem. Ber. **58**, 1455 (1925).
7. E. PACSU, S. M. TRISTER, and J. W. GREEN. J. Am. Chem. Soc. **61**, 2444 (1939).
8. E. PACSU and S. M. TRISTER. J. Am. Chem. Soc. **62**, 2301 (1940).
9. E. PACSU. Chem. Ber. **57**, 849 (1924).
10. R. SCHINLE. Chem. Ber. **65**, 315 (1932).
11. S. A. BARKER, E. J. BOURNE, and D. H. WHIFFEN. J. Chem. Soc. 3865 (1952).
12. F. VALENTIN and D. TOMKULJAK. Chem. Zvesti, **3**, 146 (1949).
13. J. A. MILLS. Advan. Carbohydrate Chem. **10**, 27 (1955).
14. R. M. HANN, W. D. MCCLAY, and C. S. HUDSON. J. Am. Chem. Soc. **61**, 2432 (1939).
15. J. MUNRO and E. G. PERCIVAL. J. Chem. Soc. 640 (1936).
16. L. VON VARGHA. Chem. Ber. **66**, 1394 (1933).
17. E. J. C. CURTIS and J. K. N. JONES. Can. J. Chem. **38**, 890 (1960).
18. E. ZISSIS and N. K. RICHTMYER. J. Am. Chem. Soc. **74**, 4373 (1952).
19. W. N. HAWORTH. J. Chem. Soc. 8 (1915).
20. Y. C. LEE and C. E. BALLOU. J. Biol. Chem. **239**, 1316 (1964).
21. H. ZINNER and C. G. DÄSSLER. Chem. Ber. **93**, 1597 (1960).
22. A. S. PERLIN and C. BRICE. Can. J. Chem. **34**, 541 (1956).

Can. J. Chem. Downloaded from www.nrcresearchpress.com by 210.87.254.6 on 09/05/12
For personal use only.

Can. J. Chem. Downloaded from www.nrcresearchpress.com by 210.87.254.105 on 09/05/12
For personal use only.

THE CHEMISTRY OF D-APIOSE

PART II. THE CONFIGURATION OF D-APIOSE IN APIIN

R. K. HULYALKAR,[1] J. K. N. JONES, AND M. B. PERRY[1]

Department of Organic Chemistry, Queen's University, Kingston, Ontario

Received March 10, 1965

ABSTRACT

The tri-*O*-methyl-D-apiose derivative obtained from the hydrolysis products of methylated apiin was found to be identical with 2,3,4-tri-*O*-methyl-D-apio-D-furanose prepared synthetically. Periodate oxidation studies support the suggested *cis* relationship of the hydroxyl groups at C_2 and C_3 of the apiose moiety in apiin, and consideration of optical rotation data suggest that a β-type linkage unites the D-apiosyl unit to C_2 of the D-glucopyranose residue in apiin.

INTRODUCTION

Apiose (I) is an unusual branched-chain pentose first found in parsley, in which it occurs as the flavanoid glycoside apiin (1), and reported to occur in other plant species (2–5*a*).

On conversion of the open-chain structural formulation of D-apiose (I) to its furanose ring forms, carbon atom 3 becomes asymmetric, giving rise to four possible isomers (II–V).

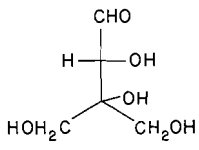

I

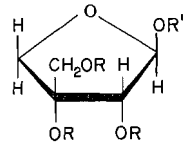

II, R = R' = H

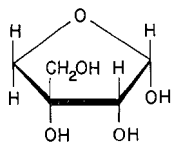

III

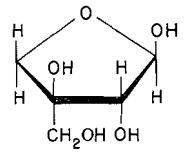

IV

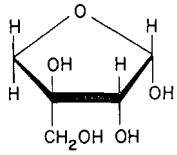

V

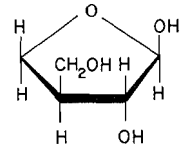

VI

It may be noted that cordycepose (VI) (5*b*) can also exist in four possible forms. Although previous workers (6, 7) had shown that apiin contains a β-glycosidically linked 2-*O*-(D-apiofuranosyl)-D-glucopyranose disaccharide moiety at C_7 of the flavone residue, the absolute configuration of the D-apiofuranose residue at C_3 was not determined. The present paper describes work directed towards establishing the configuration of the D-apiofuranose residue in apiin.

[1]*Present address: Division of Biosciences, National Research Council, Ottawa, Canada.*

Can. J. Chem. Downloaded from www.nrcresearchpress.com by 210.87.254.105 on 09/05/12
For personal use only.

DISCUSSION

Apiin was isolated from parsley (8, 9) and characterized as its crystalline octa-*O*-acetate (9). The pure apiin was fully methylated, thus fixing the configuration at C_3 of the D-apiofuranose residue, and hydrolysis of the product with an aqueous acetic acid – hydrochloric acid mixture (10) resulted in the precipitation of 5,4′-di-*O*-methyl-apigenin, leaving a solution from which 3,4,6-tri-*O*-methyl-D-glucose, characterized as its phenylosazone derivative, and 2,3,4-tri-*O*-methyl-D-apiofuranose were isolated in approximately equal molar amounts.

2,3,4-Tri-*O*-methyl-D-apio-D-furanose (II, R = Me; R′ = H) of known configuration at C_3 was synthesized. Methylation of 2,3-*O*-isopropylidene-D-apio-D-furanose (5*a*) with methyl iodide and silver oxide yielded methyl 2,3-*O*-isopropylidene-4-*O*-methyl-$\alpha+\beta$-D-apio-D-furanoside, which on treatment with methanolic hydrogen chloride, gave methyl 4-*O*-methyl-$\alpha+\beta$-D-apio-D-furanoside. Methylation of methyl 4-*O*-methyl-$\alpha+\beta$-D-apio-D-furanoside with methyl iodide and silver oxide gave methyl 2,3,4-tri-*O*-methyl-$\alpha+\beta$-D-apio-D-furanoside, which on hydrolysis with dilute sulphuric acid, yielded 2,3,4-tri-*O*-methyl-D-apio-D-furanose.

The synthetic 2,3,4-tri-*O*-methyl-D-apio-D-furanose and the tri-*O*-methyl-D-apiose isolated from methylated apiin had identical infrared spectra, and paper, thin-layer, and gas–liquid partition chromatography did not distinguish between the two products (see Tables I and II). Gas–liquid partition chromatograms of the synthetic methyl $\alpha+\beta$-glycosides from 2,3,4-tri-*O*-methyl-D-apio-D-furanose and from the tri-*O*-methyl-D-apiose isolated from apiin each showed two peaks and were indistinguishable. Gas chromatographic examination of the product obtained by direct methylation of D-apiose showed four peaks of which the faster two had the same retention times as the methyl glycosides from 2,3,4-tri-*O*-methyl-D-apio-D-furanose. The slower two peaks are probably due to the methyl α- and β-glycosides of the remaining two of the four possible isomers of D-apiofuranose. Attempts to prepare crystalline derivatives of 2,3,4-tri-*O*-methyl-D-apio-D-furanose were unsuccessful.

TABLE I

Comparison of 2,3,4-tri-*O*-methyl-D-apiose from parsley with the synthetic 2,3,4-tri-*O*-methyl-D-apio-D-furanose

	Tri-*O*-methyl-D-apiose	
	Natural	Synthetic
Paper chromatography		
1. R_G values in solvent *a*	0.96	0.96
2. R_G values in solvent *b*	0.91	0.91
3. R_G values in solvent *c*	0.95	0.95
Thin-layer chromatography		
R_G values in solvent *b*	0.91 1.06 (methyl glycosides)	0.91 1.06 (methyl glycosides)
Gas–liquid partition chromatography (see Table II)		
T_g values on column *a* at 150°	2.34	2.34

NOTE: R_G values are quoted relative to the rate of movement of 2,3,4,6-tetra-*O*-methyl-D-glucose (= 1.00). T_g values are quoted relative to the retention time of methyl 2,3,4,6-tetra-*O*-methyl-α-D-glucoside (= 1.00).

Periodate oxidation (11, 12, 13) of apiin [VII, X = 7-*O*-(D-glucopyranosyl)-apigenin] was found to proceed with a rapid consumption of 2.3 moles of periodate and release of 0.7 mole of formaldehyde (30 min oxidation) followed by a slow reaction leading to a total

TABLE II

Gas–liquid partition chromatography of 2,3,4-tri-*O*-methyl-D-apiose (natural and synthetic) and their derivatives (columns at 150°)

Compound	Natural T_g values	Synthetic T_g values
Column *a*		
1. 2,3,4-Tri-*O*-methyl-D-apio-D-furanose	2.34	2.34
2. Methyl 2,3,4-tri-*O*-methyl-$\alpha+\beta$-D-apio-D-furanoside	0.343	0.343
	0.483	0.483
3. Fully methylated methyl D-apiosides	0.343	
	0.483	
	0.582	
	0.905	
Column *b*		
4. Trimethylsilyl 2,3,4-tri-*O*-methyl-$\alpha+\beta$-D-apioside	0.316 (major)	0.316 (major)
	0.355 (minor)	0.355 (minor)
5. 2,3,4-Tri-*O*-methyl-1,4′-di-*O*-trimethylsilyl-D-apiitol	0.206	0.206

NOTE: T_g values are quoted relative to the retention time of methyl 2,3,4,6-tetra-*O*-methyl-α-D-glucoside (= 1.00).

consumption of 2.93 moles of periodate and release of 0.88 mole of formaldehyde (40 hours) per mole apiin. Periodate oxidation of 1 mole of apiin with 1 mole of metaperiodate released 0.35 mole of formaldehyde, and the reduced periodate-oxidized product on hydrolysis gave a 90% recovery of glucose; paper chromatographic examination of the hydrolyzed reduced products showed the presence of glycerol, tetritol, and sorbitol. Oxidation of apiin with 2 moles of periodate resulted in the release of 0.85 mole of formaldehyde.

TABLE III

Periodate oxidation of apiin

Time, h	Uptake of periodate, moles/mole	Formaldehyde production, moles/mole
0.50	2.22	0.70
1.00	2.34	0.75
14.00	2.78	0.88
22.00	2.88	0.88
44.00	2.93	0.88

The above periodate oxidation studies support the conclusion that the secondary and tertiary hydroxyl groups at C_2 and C_3, respectively, of the apiose moiety in apiin are *cis*-related having the D-*erythro* configuration. It can be expected that, if the hydroxyl groups at C_2 and C_3 in the apiofuranose moiety were *cis*-related, their cleavage by periodate would be much faster than that of the trans C_3 and C_4 glycol system in the glucopyranose moiety. The release of formaldehyde on selective oxidation of apiin with 1 and with 2 moles of periodate suggests that the initial attack by the first mole of periodate results in about 65% splitting of the C_2–C_3 glycol system of apiose and about 35% at the C_3–C_4 bond, this latter step proceeding with the release of formaldehyde. The release of 0.85 mole of formaldehyde on oxidation of apiin by 2 moles periodate shows that the intermediates produced by the initial attack on the apiose residue are more easily oxidized than is the hexose molecule since the glucose residue is almost unaffected under these conditions.

Apiin has a molecular rotation $[M]_D$* of −754° and 7-*O*-(D-glucopyranosyl)-apigenin, which is the aglycon of apiose in apiin, has a molecular rotation $[M]_D$ of −349°. The

*$[M]_D = ([\alpha]_D \times m.wt.)/100$. *These values are approximate.*

Can. J. Chem. Downloaded from www.nrcresearchpress.com by 210.87.254.105 on 09/05/12
For personal use only.

molecular rotation $[M]_D$ of apiin minus the molecular rotation $[M]_D$ of 7-*O*-(D-glucopyranosyl)-apigenin is $-405°$, which is the molecular rotation $[M]_D$ of the corresponding methyl glycoside of D-apiose (14, 15, 16). It is highly improbable that the alpha form of methyl D-apio-D-furanoside would have such a high negative value as the sugar is in the D-series and the di-*O*-isopropylidene derivative, the formation of which involves an α-glycosidic hydroxyl group, has a positive rotation (5*a*). Also it may be noted that methyl α-D-erythrofuranoside (VIII) and β-D-erythrofuranoside (IX) have approximate $[M]_D$ values of $+199°$ and and $-217°$, respectively (calculated from the results of Ballou (17)).

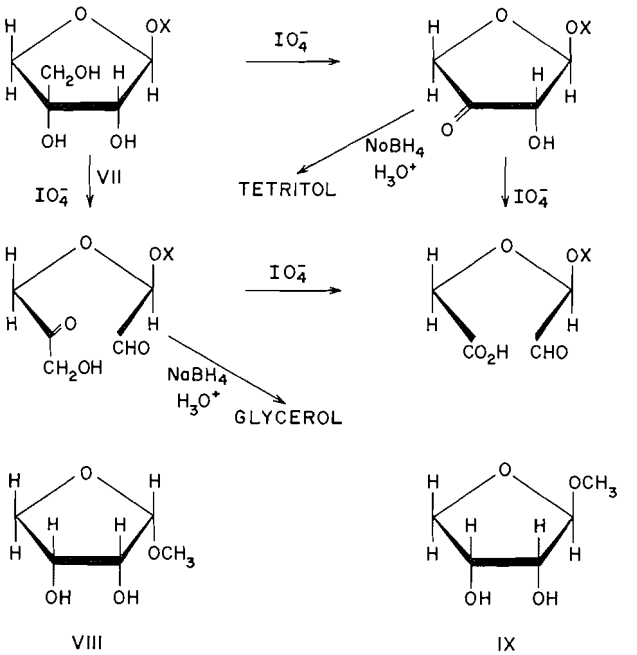

Further evidence is given by the optical rotations of the 4-*O*-methyl- and 2,3,4-tri-*O*-methyl-D-apio-D-furanoses, which are very close to zero. It would appear therefore that methyl α-D-apio-D-furanoside should not have a negative optical rotation and hence the contribution from the anomeric linkage of the D-apiose residue corresponds to that of the β-glycoside. The evidence suggests that the D-apio-D-furanose residue in apiin is joined to C_2 of the D-glucopyranose residue by a β-glycosidic linkage. There is a structural resemblance between the glycosides of D-cordycepose (VI), D-apiose (I), and L-streptose (X, R″ = H) which may have biological significance.

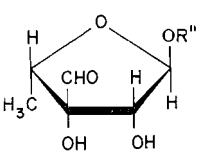

X

EXPERIMENTAL

Paper chromatography was performed by the descending method on Whatman No. 1 filter paper using the following solvent systems: (*a*) butan-1-ol–pyridine–benzene–water (10:6:2:6 v/v); (*b*) butan-1-ol–ethanol–water (10:3:3 v/v); (*c*) butan-1-ol–ethanol–benzene–water (10:3:5:3 v/v); (*d*) ethyl acetate – acetic acid – formic acid – water (18:3:1:4 v/v). Thin-layer chromatoplates were prepared using silica gel G in water

Can. J. Chem. Downloaded from www.nrcresearchpress.com by 210.87.254.105 on 09/05/12
For personal use only.

suspension (1:2 w/v) and were dried at 110° for 10 h before use. Sugars were detected with the spray reagents 2% *p*-anisidine hydrochloride in butan-1-ol (18) and 1% silver nitrate in acetone followed by 2% sodium hydroxide in ethanol (19).

Gas–liquid partition chromatography was carried out using a Pye Argon chromatograph fitted with an ionization detector (^{90}Sr-80 μc) and employing straight glass columns (120 × 0.5 cm, I.D.) packed with either (*a*) 10% Carbowax 6000 on 80–100 mesh Chromosorb W or (*b*) 10% neopentylglycol sebacate polyester on 80–100 mesh Chromosorb W. Samples (5–10 γ) were placed on the top of the columns and development was made with dry argon at a flow rate of 100 ml per min.

Melting points were determined on a Kofler hot stage and are uncorrected. Optical rotations were measured at 22 ± 2°. Solutions were concentrated under reduced pressure below 50°.

Isolation of Apiin from Parsley

Washed fresh parsley stems and leaves (510 g) were blended with acetone (5 l) and the mixture was heated under reflux for 18 hours and filtered. The filtrate was concentrated to about 150 ml, and the resulting insoluble gelatinous material was collected and repeatedly extracted with petrol (b.p. 40–60°). The residue (15 g) was then washed with water (2 × 100 ml) and collected by filtration. The aqueous filtrate, which showed the presence of glucose, arabinose, and xylose, was discarded, and the dried insoluble residue of crude apiin (5.1 g), having m.p. 195–210°, was purified via its lead salt (9) to yield pure apiin, which, after recrystallization from ethanol, gave crystals having m.p. 228–230° and $[\alpha]_D$ −130° (*c*, 0.12 methanol).

The prepared apiin (0.5 g) was dissolved in acetic anhydride (6 ml) and pyridine (2 ml), and the solution was refluxed for 3 hours and then poured onto crushed ice. The insoluble product (0.8 g) was collected and recrystallized from a chloroform–methanol mixture to give crystalline apiin octa-*O*-acetate having $[\alpha]_D$ −53° (*c*, 1.0 chloroform) and m.p. 253–254° (lit. value m.p. 249–251° (9)).

Methylation of Apiin (20, 21)

Barium oxide (10 g) was added portionwise over 5 h to a stirred solution of apiin (5 g) in dimethyl sulphoxide (35 ml) and methyl iodide (30 ml), and after 48 hours the reaction mixture was filtered, the residue washed with chloroform, and the combined filtrate and washings were treated with more chloroform until no more inorganic material precipitated. On removal of the inorganic material the brown-colored solution was washed with 15% sodium thiosulphate solution (100 ml) and water (2 × 60 ml), and the dried (Na_2SO_4) solution was concentrated to a syrup (5.7 g). The syrup (5.7 g) was further methylated three times using methyl iodide (30 ml) and silver oxide (15 g) (22) to yield a final product (4.75 g) which showed no hydroxyl absorption at 3 500 cm^{-1} and had $[\alpha]_D$ −91° (*c*, 2.3 chloroform).

Anal. $C_{34}H_{42}O_{15}$ requires OMe, 35.5%. Found OMe, 35.1%.

Fission of Methylated Apiin

Methylated apiin (4.6 g) was heated for 8 hours on a boiling water bath with a mixture of acetic acid (50 ml) and 5% aqueous hydrochloric acid (100 ml), and after cooling, the insoluble 5,4′-di-*O*-methyl apigenin (1.4 g) (m.p. 293–295° (8)) was removed by filtration. The filtrate was neutralized by passing it through Duolite A4 (OH^-) ion-exchange resin, and the solution was concentrated to a syrup which was extracted with water (15 ml). Paper chromatographic examination of the aqueous extract using solvent system *c* showed the presence of 3,4,6-tri-*O*-methyl-D-glucose (R_G 0.82) and 2,3,4-tri-*O*-methyl-D-apiose (R_G 0.95).

Separation of 2,3,4-Tri-O-methyl-D-apiose and 3,4,6-Tri-O-methyl-D-glucose

The aqueous extracts (15 ml) of the sugars obtained from the fission of the methylated apiin were extracted with chloroform (4 × 10 ml). Concentration of the dried (anhydrous $MgSO_4$) chloroform extracts gave 2,3,4-tri-*O*-methyl-D-apiose (820 mg) having $[\alpha]_D$ −1.7° (*c*, 2.3 methanol), while concentration of the aqueous solution gave 3,4,6-tri-*O*-methyl-D-glucose (950 mg), which had $[\alpha]_D$ +70° (*c*, 1.5 water) (literature value $[\alpha]_D$ +71° (water) (23, 24)) and gave a crystalline phenylosazone derivative with m.p. 80–81° (literature value m.p. 80° (23)).

Synthesis of 2,3,4-Tri-O-methyl-D-apio-D-furanose

(A) Methyl 2,3-O-Isopropylidene-4-O-methyl-α+β-D-apio-D-furanoside

2,3-*O*-Isopropylidene-D-apio-D-furanose (1.4 g) (5*a*) in methyl iodide (75 ml) was heated under reflux while silver oxide (15 g) was added portionwise over 8 hours, and after a further 24 hours the reaction mixture was filtered, the residue was washed with chloroform, and the combined filtrate and washings were concentrated to a syrup. Thin-layer chromatographic examination of the syrup using solvent system *d* showed a major component (about 90% visual ratio) having R_f 0.68 and a minor component having R_f 0.88. Distillation of the syrup gave a fraction (1.1 g) collected at 90–95°/0.35 mm which had η_D^{23} 1.43915 and $[\alpha]_D$ −66° (*c*, 3.6 methanol).

Anal. $C_{10}H_{18}O_5$ requires: C, 55.1%; H, 8.2%; OMe 28.4. Found: C, 55.1%; H, 8.1%; OMe, 27.9.

(B) Methyl 4-O-Methyl-α+β-D-apio-D-furanoside

Methyl 2,3-*O*-isopropylidene-4-*O*-methyl-D-apio-D-furanoside (1.1 g) was heated on a boiling water bath for 3 hours with dry 2% methanolic hydrogen chloride, and, after neutralization of the cooled reaction mixture

Can. J. Chem. Downloaded from www.nrcresearchpress.com by 210.87.254.105 on 09/05/12
For personal use only.

with Duolite A4 (OH^-) ion-exchange resin (previously washed with methanol), the solution was concentrated to yield syrupy methyl 4-*O*-methyl-$\alpha+\beta$-D-apio-D-furanoside (0.8 g) having $[\alpha]_D$ 0° (*c*, 1.9 methanol).

Anal. $C_7H_{14}O_5$ requires: OMe, 34.8%. Found: OMe, 35.2.

(C) 4-O-Methyl-D-apio-D-furanose

Methyl 4-*O*-methyl-$\alpha+\beta$-D-apio-D-furanoside (0.8 g) was heated for 2 h at 100° with *N* sulphuric acid (10 ml) and after neutralization (Duolite A4(OH^-)) the solution was concentrated to a syrup (0.75 g) which had $[\alpha]_D$ 0° (*c*, 2.3 methanol). Paper chromatographic examination of the product using solvent system *d* showed a single spot having R_G 0.16.

Anal. $C_6H_{12}O_5$ requires: OMe, 18.9. Found: OMe, 18.5.

(D) Methyl 2,3,4-Tri-O-methyl-$\alpha+\beta$-D-apio-D-furanoside

4-*O*-Methyl-D-apio-D-furanose (0.74 g) was refluxed for 8 h with 2% methanolic hydrogen chloride (15 ml) and, after neutralization (Duolite A4(OH^-)) filtration and concentration of the filtrate, the residual syrupy furanoside was methylated in the usual way using three successive treatments with methyl iodide (25 ml) and silver oxide (10 g) to yield a final product (510 mg) which had $[\alpha]_D$ +2° (*c*, 2.2 methanol) and gave a single spot on thin-layer chromatograms.

Anal. $C_9H_{18}O_5$ requires: OMe, 60.2%. Found: OMe, 58.8%.

(E) 2,3,4-Tri-O-methyl-D-apio-D-furanose

Methyl 2,3,4-tri-*O*-methyl-$\alpha+\beta$-D-apio-D-furanoside (500 mg) was hydrolyzed with *N* sulphuric acid (15 ml) for 2 h at 100° and, after neutralization (Duolite A4(OH^-)) and concentration, the product was obtained as a syrup (450 mg) having $[\alpha]_D$ −7° (*c*, 2 methanol) and R_G 0.91 (solvent *b*).

Anal. $C_8H_{16}O_5$ requires: OMe, 48.4%. Found: OMe, 47.3%.

Periodate Oxidation of Apiin

(A) Oxidation of Apiin with Excess Periodate

Apiin (28.8 mg) dissolved in 50% aqueous ethanol (49 ml) was oxidized in the dark at room temperature by the addition of 0.3 *M* sodium metaperiodate (1 ml). At intervals, samples were withdrawn for the determination of periodate uptake (25) and release of formaldehyde (26). The results are recorded in Table III.

(B) Oxidation of Apiin with 1 Mole of Periodate

Sodium metaperiodate (32.1 mg in water (3 ml)) was added to a solution of apiin (87 mg) in 50% aqueous ethanol (72 ml) and the mixture was kept at 5° for 16 h at which time 0.35 mole of formaldehyde had been released per mole apiin. The solution was deionized by passing it through Amberlite IR-120 (H^+) and Duolite A4 (OH^-) ion-exchange resins, the eluate and washings were combined, and the oxidized apiin was reduced by addition of sodium borohydride (30 mg). After 30 min, the reduced product was hydrolyzed with *N* sulphuric acid for 3 h at 100°, and, after neutralization (Duolite A4 (OH^-)), the solution was divided into three parts. The first part, examined directly by paper chromatography, showed only the presence of glucose, and the second part, after the addition of xylose as an internal standard, showed by quantitative evaluation that 90% of the glucose present in the apiin had been recovered. The third part was reduced by $NaBH_4$ (20 mg) and subsequent paper chromatographic analysis of the product showed the presence of glycerol, tetritol, and sorbitol.

(C) Oxidation of Apiin with 2 Moles of Periodate

Oxidation of apiin as described in (B) above using twice the amount of periodate showed after 16 hours oxidation at 5° that 0.85 mole of formaldehyde was released per mole of apiin.

REFERENCES

1. C. S. HUDSON. Advan. Carbohydrate Chem. 4, 57 (1949).
2. D. J. BELL, N. E. HARDWOCK, F. A. ISHERWOOD, and R. S. CAHN. J. Chem. Soc. 2702 (1954).
3. J. S. D. BACON. Biochem. J. **89**, 103P. (1963).
4. R. B. DUFF and A. H. KNIGHT. Biochem. J. **88**, 33P. (1963).
5. (*a*) D. T. WILLIAMS and J. K. N. JONES. Can. J. Chem. **42**, 69 (1964).
   (*b*) H. R. BENTLEY, K. G. CUNNINGHAM, and F. S. SPRING. J. Chem. Soc. 2301 (1951).
6. N. NARSIMHACHARI and T. R. SESHADRI. Proc. Indian Acad. Sci. Sect. A, **30**, 151 (1949).
7. R. HEMMING and W. D. OLLIS. Chem. Ind. London, 85 (1953).
8. A. G. PERKIN. J. Chem. Soc. **71**, 805 (1897).
9. S. R. GUPTA and T. R. SESHADRI. Proc. Indian Acad. Sci. Sect. A, **35**, 242 (1952).
10. W. BAKER, R. HEMMING, and W. D. OLLIS. J. Chem. Soc. 691 (1951).
11. L. MALAPRADE. Bull. Soc. Chim. France, **43**, 683 (1928).
12. P. F. J. FLEURY. Pharm. Chim. **17**, 409 (1933).
13. E. L. JACKSON. *In* R. Adams. Organic reactions. Vol. II. John Wiley and Sons, Inc., New York, N.Y. 1944. p. 347.
14. W. KLYNE. Biochem. J. **47**, XLI (1950).
15. J. STANĚK. Chem. Ind. London, 488 (1956).
16. T. REICHSTEIN *et al.* Almost all papers entitled Glycosides and aglycons. *In* Helv. Chim. Acta (1950–1960).
17. C. E. BALLOU. J. Am. Chem. Soc. **82**, 2587 (1960).
18. L. HOUGH, J. K. N. JONES, and W. H. WADMAN. J. Chem. Soc. 1702 (1950).

Can. J. Chem. Downloaded from www.nrcresearchpress.com by 210.87.254.105 on 09/05/12
For personal use only.

19. W. E. TREVELYAN, D. P. PROCTOR, and J. S. HARRISON. Nature, **166**, 444 (1950).
20. H. C. SHRIVASTAVA, S. N. HARSHE, and P. P. SINGH. Ind. J. Chem. **1**, 304 (1963).
21. H. C. SHRIVASTAVA, S. N. HARSHE, and P. P. SINGH. Tetrahedron Letters, No. 27, 1869 (1963).
22. T. PURDIE and J. C. IRVINE. J. Chem. Soc. **83**, 1021 (1903).
23. E. W. PUTMAN, A. L. POTTER, R. HODGSON, and W. Z. HASSID. J. Am. Chem. Soc. **72**, 5024 (1950).
24. W. N. HAWORTH, E. L. HIRST, and L. PANIZZON. J. Chem. Soc. 154 (1934).
25. G. NEUMULLER and E. VASSEUR. Arkiv Kemi, **5**, 235 (1953).
26. J. F. O'DEA and R. A. GIBBONS. Biochem. J. **55**, 580 (1953).

Can. J. Chem. Downloaded from www.nrcresearchpress.com by 210.87.254.105 on 09/05/12
For personal use only.

Can. J. Chem. Downloaded from www.nrcresearchpress.com by 210.87.254.40 on 09/05/12
For personal use only.

SURFACE EFFECTS IN THE UNINHIBITED AND THE INHIBITED PYROLYSES OF ISOMERIC HEXANES

PARTS I–III. *n*-HEXANE, 2-METHYL PENTANE, 3-METHYL PENTANE

J. CHRYSOCHOOS[1] AND W. A. BRYCE[2]

Department of Chemistry, University of British Columbia, Vancouver, British Columbia

Received December 9, 1964

ABSTRACT

The rates of pyrolysis of *n*-hexane, 2-methyl pentane, and 3-methyl pentane decrease with increasing S/V ratio in the pressure range of 15 to 90 mm at temperatures around 520 °C. The partial pressure of nitric oxide required for maximum inhibition which appears to be independent of the hydrocarbon pressure and is approximately constant for all isomers, namely 12–14 mm, for hydrocarbon ranging from 50 to 100 mm, increases slightly with increasing S/V ratio. Nitric oxide affects the product distribution markedly. The simultaneous increase in the yield of C_2H_4 and decrease in the yield of C_2H_6 with increasing NO pressure can be attributed to the set of competitive reactions

$$C_2H_5 + NO \rightarrow C_2H_4 + HNO$$

$$C_2H_5 + RH \rightarrow C_2H_6 + R.$$

Similarly, the slight decrease in the yield of C_3H_8 with increasing NO pressure can be accounted for by the competition

$$i\text{-}C_3H_7 + NO \rightarrow C_3H_6 + HNO$$

$$i\text{-}C_3H_7 + RH \rightarrow C_3H_8 + R.$$

Increased S/V ratios favor the formation of C_2H_6 in both the uninhibited and the inhibited pyrolyses, but has no effect on the yields of such products as C_3H_6, 1-C_4H_8, and i-C_4H_8. The analytical balance becomes less complete at higher NO pressures for the inhibited decomposition, which can be attributed to the formation of some nitrogen-containing compounds undetectable by the analytical methods used. Mechanisms are proposed accounting qualitatively for the products of the uninhibited and the inhibited pyrolyses.

INTRODUCTION

Although there has been a large number of investigations of the inhibition of the thermal decomposition of organic compounds, comparatively little work has appeared on higher hydrocarbons. Peard *et al.* (1) investigated the inhibited pyrolyses of 2-methyl pentane and 3-methyl pentane, but they focused their study on the apparent chain lengths and the kinetic parameters. The same authors have investigated the variation of the activation energy with the hydrocarbon pressure for the thermal decomposition of the above-mentioned compounds (2).

The role of nitric oxide in various decomposition reactions has not yet been completely clarified. However, a number of theories have been proposed to interpret the effects. In the early theories of Hobbs and Hinshelwood (3, 4) on the thermal decomposition of ethane and propane, nitric oxide was assumed to capture the chain-propagating radical, which inevitably causes reduction in rate. More recently, the inhibitor has been associated with both initiation and termination processes (5–8). This idea has been applied to various hydrocarbons, leading to rate expressions in good agreement with experiment.

The inhibitor is also assumed to capture β or μ radicals and to be regenerated from the bound states (βI) and (μI) (9). An attempt has been made to explain the inhibition

[1]*Present address: Department of Chemistry, Harvard University, Cambridge, Mass. 02138.*

[2]*The premature death of Professor Bryce has deprived kineticists of an able scientist and his colleagues of a trusted friend.*

phenomenon on the occurrence of degenerate chain branching of some intermediate oximes formed in the system of NO and hydrocarbon (10). The rate expressions derived on this basis also agree well with experimental results for the isomeric pentanes (11). In all of these examples inhibition was considered to be a fully homogeneous reaction. Voevodsky (12) assumed that inhibition is heterogeneous. Covering of the active centers at the wall of the vessel by the inhibitor was suggested as the cause of the rate reduction. Such surface effects have been found in the case of isopentane (13). A thorough investigation of the isomeric hexanes with respect to the effect of S/V ratio and presence of inhibitor on both reaction rates and product distributions has been carried out. The details of the decomposition of *n*-hexane, 2-methyl pentane, and 3-methyl pentane are described here.

EXPERIMENTAL

The *n*-hexane, 2-methyl pentane, and 3-methyl pentane used were Research grade (99.9, 99.7, and 99.83% respectively) obtained from the Phillips Petroleum Corp., Bartlesville, Okla. They were subjected to repeated trap-to-trap distillation at −196 and −78°. No impurities could be detected by conventional gas chromatographic methods. The nitric oxide (99%), supplied by the Matheson Co., East Rutherford N.J., was further purified by repeated trap-to-trap distillation. The absence of NO_2 in the purified NO was confirmed by infrared spectroscopy.

The pyrolyses were done in a conventional static system. For all of the inhibited and some of the uninhibited pyrolyses, a 300 ml quartz reaction vessel, held in an insulated brass block furnace, was used in which the temperature could be controlled to within 1 deg at 500 °C. Packing of the vessel was done with fire-polished quartz tubes. When necessary, hydrocarbons and NO were premixed before admitting them to the reaction vessel.

Manometric rates were obtained throughout the study, after establishing a 1:1, 0.98:1 and 0.95:1 correspondence between the initial rates so obtained and those found from the rate of disappearance of *n*-hexane, 2-methyl pentane, and 3-methyl pentane respectively by direct analysis. This correspondence was established in the uninhibited pyrolyses and it was assumed to apply to the inhibited pyrolyses too.

For some of the uninhibited pyrolyses, two 160 ml quartz reaction vessels, one packed with fire-polished quartz and the other unpacked, were placed in a well-insulated, double furnace. The increase in pressure due to decomposition was recorded for each vessel under otherwise identical conditions with a sensitive pressure transducer (9 mm recorder response per mm of mercury pressure).

Complete analytical mass balances were obtained by conventional gas chromatographic techniques supplemented by infrared analysis.

PART I. *n*-HEXANE

Results

A typical set of data for the uninhibited decomposition of *n*-hexane at 500 °C is given in Table I.

TABLE I

Analytical results (mole %) for the decomposition of *n*-hexane (T = 500 °C, $\Delta P/P_i$ = 0.20)

	P_i (mm)			
Product	112	100	70	50
n-Hexane	72.50	74.00	77.00	78.00
CH_4	4.20	4.00	3.80	3.70
C_2H_6	2.50	2.60	1.90	2.00
C_2H_4	5.40	5.20	4.80	4.25
C_3H_6	9.60	8.50	7.80	7.00
1-C_4H_8	5.00	4.20	3.80	3.70
H_2	0.50	0.50	0.50	0.50
C_3H_8	Trace	Trace	Trace	Trace
Total	99.7	99.0	99.6	99.1

The effect of an 11-fold increase in S/V ratio on the reaction initial rates was examined over a wide range of initial pressures of *n*-hexane at various temperatures with the

Can. J. Chem. Downloaded from www.nrcresearchpress.com by 210.87.254.40 on 09/05/12
For personal use only.

pressure transducer. One such pressure time curve is shown in Fig. 1. The solid line is drawn by the pen of the recorder and the discontinuities correspond to alternate connection of the transducer to the packed and unpacked vessels. In all cases, the reaction rate was lower in the packed than in the unpacked vessel. The percentage reduction in rate brought about by packing is given in Fig. 2 as a function of the initial pressure of *n*-hexane.

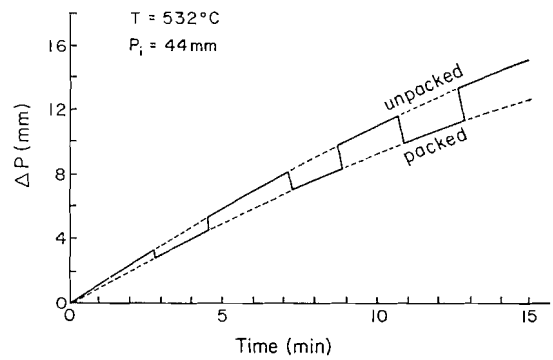

FIG. 1. Pressure–time curves for packed and unpacked vessels recorded through a pressure transducer

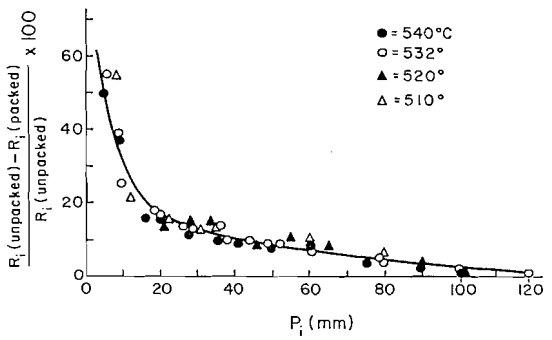

FIG. 2. Percentage reduction in rate due to packing for various initial pressures of *n*-hexane.

The data on the effect of this same increase in surface area on the product distribution are given in Table II. The ratios CH_4/C_2H_6 and C_2H_4/C_2H_6 decrease markedly when the vessel is packed.

TABLE II

Variation of product ratios with pressure in packed (P) and unpacked (U) vessels

	CH_4/C_2H_6		C_2H_4/C_2H_6		C_3H_6/1-C_4H_8		$(C_2H_6 + C_2H_4)/C_3H_6$	
P_i (mm)	U	P	U	P	U	P	U	P
40	2.20	1.60	3.50	2.80	—	—	—	—
50	2.00	1.50	3.20	2.70	1.85	1.80	1.62	1.50
60	1.75	—	2.50	—	1.79	—	1.50	1.56
70	1.40	1.30	2.02	1.90	1.76	1.85	1.45	1.40
80	1.37	1.27	2.36	2.10	—	—	1.50	1.52
90	1.40	0.91	2.30	2.00	1.76	1.74	1.75	1.62
100	1.40	1.00	1.85	1.56	1.85	1.78	1.76	1.76

Can. J. Chem. Downloaded from www.nrcresearchpress.com by 210.87.254.40 on 09/05/12
For personal use only.

The activation energies and frequency factors were calculated from the Arrhenius equation using rate constants obtained at the temperatures 490, 510, and 520 °C which are given in Table III. The kinetic parameters are pressure dependent yet approach constant values at high pressures. The average from 3 different determinations are given in Table IV. The rate constants can be related to the A factors and activation energies by the expressions

$$k = A(P_i) \exp -(E_{act}(P_i)/RT).$$

This in fact means that the whole mechanism depends on the initial pressure.

TABLE III

Rate constants for the decomposition of n-hexane $\times 10^2$ min^{-1}

	T (°K)		
P (mm)	763	783	793
0–40	0.45	1.30	2.25
40–60	0.49	1.40	2.25
60–70	0.48	1.40	2.20
70–80	0.48	1.42	2.20
80–90	0.47	1.42	2.18
90	0.47	1.42	2.18
100	0.46	1.39	2.15
110	0.46	1.35	2.10
120	0.46	1.35	2.10

TABLE IV

Variation of activation energies and frequency factors with initial pressure of n-hexane

P_i (mm)	E_{act} (kcal)	A (s^{-1}) $\times 10^{12}$
0–40	64.0±1.0	170.
40–60	60.0±2.0	11.
60–80	59.5±2.5	8.2
90	59.4±4.0	5.3
100	59.0±4.0	3.5
120	58.5±3.5	3.3

The overall reaction order, which was measured from the slope of the plot, log (initial rate) vs. log (P_i), was found to be unity, in fact 1.09, at the temperatures 500, 510, and 520 °C over a hydrocarbon pressure range of 10 to 120 mm (Fig. 3).

Nitric oxide reduces the reaction rate quite significantly even when present only in trace quantities. The pressure time curves were sigmoid in the presence of NO, and initial rates were obtained. The NO pressure required for maximum reduction in initial rate is 12–14 mm for the pressure range of 50 to 100 mm of n-hexane at 520 °C (Fig. 4*a*). An increase in S/V ratio from 1 cm^{-1} to 5 and 10 cm^{-1} shifts the NO pressure required for maximum inhibition from 12–14 mm to 16 and 18 mm respectively (Fig. 4*b*). Nitric oxide also changes the product distribution. The yields of C_2H_4 and CH_4 increase with increasing NO pressure while that of C_2H_6 decreases. The distribution of the products C_3H_6 and 1-C_4H_8 are independent of NO (Fig. 5).

The relationship between the yield of the products and time in the fully inhibited decompositions was found to be very nearly linear for conversions up to 40% (Fig. 6). This indicates that the inhibited reaction is not affected by the products of the reaction.

Can. J. Chem. Downloaded from www.nrcresearchpress.com by 210.87.254.40 on 09/05/12
For personal use only.

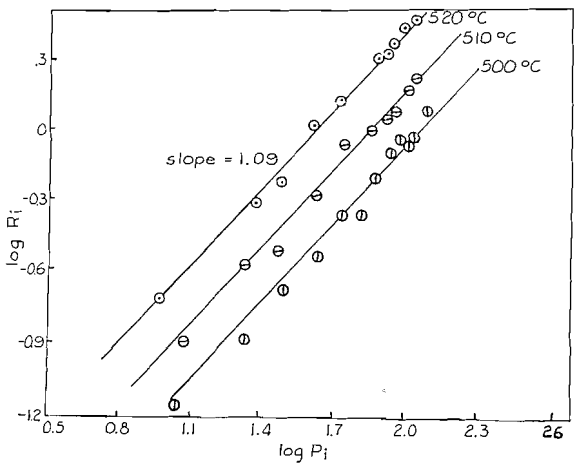

FIG. 3. Plots of the logarithm of the rate against the logarithm of the pressure for the uninhibited decomposition of *n*-hexane.

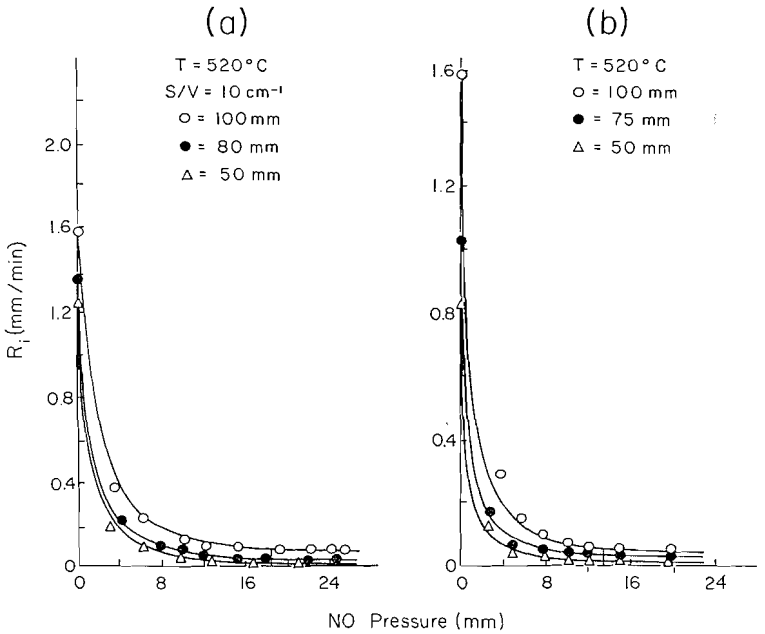

FIG. 4. Dependence of the initial rate on NO pressure in (*a*) the unpacked and (*b*) the packed vessels.

This relationship is not linear in the uninhibited decompositions at such high conversions. Thus the fully inhibited decomposition may obey a purely homogeneous mechanism.

An increase in the surface area does not affect the yields of C_3H_6 and 1-C_4H_8 as illustrated in Fig. 7. The ratio C_2H_4/C_2H_6, however, increases with increasing NO pressure and for all NO pressures decreases with increasing S/V ratio (Fig. 8).

Because of the remarkable effect of the surface on the initial rates of the decomposition, it was felt necessary to obtain some information as far as the relative adsorption of *n*-hexane and NO on quartz is concerned. Binary mixtures of *n*-hexane and NO of known

Can. J. Chem. Downloaded from www.nrcresearchpress.com by 210.87.254.40 on 09/05/12
For personal use only.

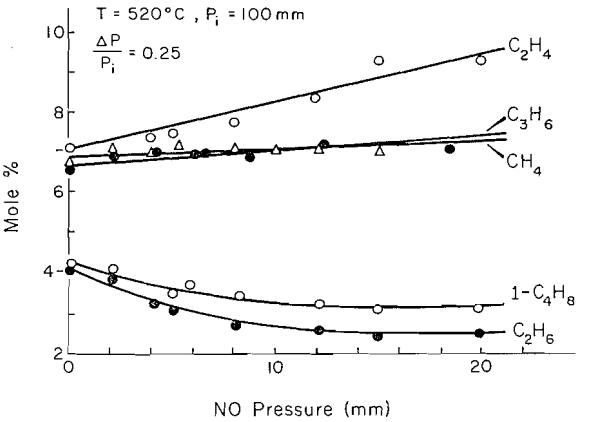

FIG. 5. Variation of the product distribution with NO pressure.

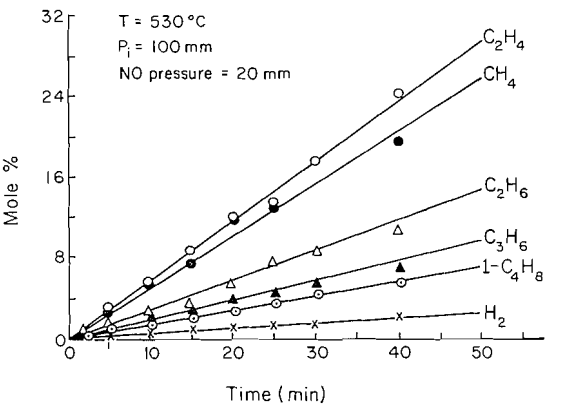

FIG. 6. Variation of the product distribution with time for the fully inhibited decomposition.

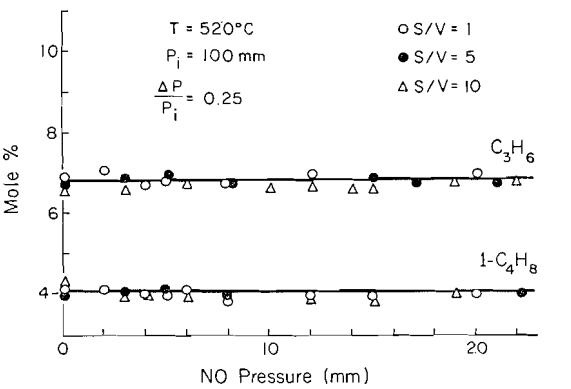

FIG. 7. Variation of the C_3H_6 yield with NO pressure and with S/V ratio.

Can. J. Chem. Downloaded from www.nrcresearchpress.com by 210.87.254.40 on 09/05/12
For personal use only.

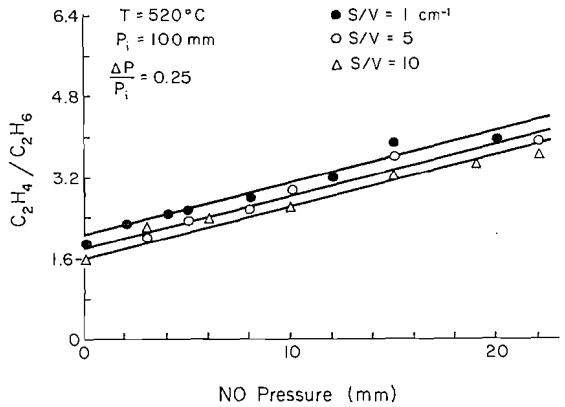

FIG. 8. Variation of the C_2H_4/C_2H_6 ratio with NO pressure and with S/V ratio.

composition were passed through a thermally insulated glass tube packed with quartz wool to give an $S/V \simeq 60\ cm^{-1}$, and then analyzed by gas chromatography. Any differences in the relative adsorption of the components of the mixture on the quartz wool would change the composition of the mixture in the gas phase. However, this experiment was primitive and the results have only qualitative significance. Although it was desirable to establish the same conditions with those in the thermal decomposition of *n*-hexane, yet it was impossible because at about 400 °C decomposition was occurring rapidly, in spite of the high pressure of NO present and the short contact time (2 min). Some of the results are given in Table V. It is seen that the ratio is higher at low initial pressures of the mixture and tends to its initial value at high pressures. Therefore, at lower initial pressures, the amount of NO in the gas phase is smaller relative to the amount of *n*-hexane. In other words NO is adsorbed more than *n*-hexane on quartz wool. At higher pressures this effect fades completely.

TABLE V

Variation of *n*-hexane/NO ratio with initial pressure of the mixture after adsorption on quartz wool $(n\text{-hexane/NO})_{init} = 2.50$, $T = 350$ °C, contact time = 2 min)

Initial pressure of the mixture (mm)	$(n\text{-Hexane/NO})_{final}$
18	2.85
27	2.66
36	2.70
51	2.70
68	2.70
93	2.50

Discussion

The following reactions are sufficient to account for the products of the uninhibited decomposition. Additional reactions which could be written only add to the complexity.

Initiation reactions:

[1*a*] $$n\text{-}C_6H_{14} \rightarrow CH_3 + n\text{-}C_5H_{11}$$

[1*b*] $$n\text{-}C_6H_{14} \rightarrow C_2H_5 + n\text{-}C_4H_9$$

[1*c*] $$n\text{-}C_6H_{14} \rightarrow 2(n\text{-}C_3H_7).$$

Can. J. Chem. Downloaded from www.nrcresearchpress.com by 210.87.254.40 on 09/05/12
For personal use only.

Propagation reactions:

[2*a*] $$CH_3 + n\text{-}C_6H_{14} \rightarrow CH_4 + n\text{-}C_6H_{13}$$

[2*b*] $$CH_3 + n\text{-}C_6H_{14} \rightarrow CH_4 + CH_3CH_2CH_2CH_2CHCH_3$$

[2*c*] $$CH_3 + n\text{-}C_6H_{14} \rightarrow CH_4 + CH_3CH_2CH_2CHCH_2CH_3$$

[3*a–c*] $$C_2H_5 + n\text{-}C_6H_{14} \rightarrow C_2H_6 + n\text{-hexyl radicals.}$$

Radical decompositions:

[4*a–c*] $$n\text{-hexyl radicals} \rightarrow C_2H_5 + 1\text{-}C_4H_8$$

[5*a–c*] $$n\text{-hexyl radicals} \rightarrow n\text{-}C_3H_7 + C_3H_6$$

[6] $$n\text{-}C_5H_{11} \rightarrow CH_3 + 1\text{-}C_4H_8$$

[7] $$n\text{-}C_5H_{11} \rightarrow C_2H_5 + C_3H_6$$

[8] $$n\text{-}C_4H_9 \rightarrow CH_3 + C_3H_6$$

[9] $$n\text{-}C_4H_9 \rightarrow C_2H_5 + C_2H_4$$

[10] $$n\text{-}C_3H_7 \rightarrow CH_3 + C_2H_4$$

[11] $$n\text{-}C_3H_7 \rightarrow H + C_3H_6$$

[12] $$C_2H_5 \rightarrow H + C_2H_4.$$

Termination reaction:

[13] $$2CH_3 \xrightarrow{\beta\beta M} C_2H_6.$$

The comparatively small amount of hydrogen can be accounted for by such reactions as

$$H + RH \rightarrow H_2 + R$$

which may participate to a slight extent. Hydrogen atoms are formed through reactions [11] and [12]. However, reaction [10] predominates in the competing set of reaction [10] and [11], because of a difference in activation energy of about 17 kcal (14). Thus a very small fraction of n-C_3H_7 produces H atoms. The overall order of decomposition is unity and according to the terminology of Goldfinger *et al.* (15) for first order initiations there are only two choices of termination leading to an overall order of unity: $\beta\beta$M and $\beta\mu$. The $\beta\mu$ termination is canceled because of the lack of C_4H_{10} and the only trace of C_3H_8. For second order initiation the only two choices leading to unity order, namely $\mu\mu$ and $\beta\mu$M are canceled again because of the lack of C_4H_{10} in the system.

Propylene appears in greater amounts than 1-butene, and therefore reactions [5*a–c*] must play a more important role than the competing reactions [4*a–c*].

The lower yield of C_2H_6 compared with that of CH_4 can be attributed to the difference in activation energies for the sets of the reactions [2*a–c*] and [3*a–c*]. Methyl radicals are produced mainly through reactions [5*a–c*] and [10] which are the main propagating processes and C_2H_5 are formed through reaction [4*a–c*] which play less important roles as it is revealed from the ratio $C_3H_6/1\text{-}C_4H_8$. This is the main reason for the higher yield of CH_4 over C_2H_6.

The initiation processes can take place both homogeneously and heterogeneously. A molecule chemisorbed on the walls of the reaction vessel can decompose more easily than a molecule in the gas phase because of the weakening of the various bonds due to chemisorption. In addition, termination can take place in both phases. That is, chemisorbed radicals on the walls react with other radicals more readily than if both radicals are in the gas phase. An active center on the walls can play the role of a third body, M, as well as a

Can. J. Chem. Downloaded from www.nrcresearchpress.com by 210.87.254.40 on 09/05/12
For personal use only.

molecule in the gas phase. Therefore, the surface has a twofold effect on the decomposition; acceleration because of the effect on the initiation and reduction because of the effect on the termination. The net effect can be expressed as

$$\text{net effect} = \text{effect on initiation} - \text{effect on termination.}$$

Nitric oxide is adsorbed more than *n*-hexane on quartz wool. Therefore in a competition between NO and *n*-hexane molecules for active centers, the NO molecules will expel the *n*-hexane ones. This will result in suppression of the heterogeneous initiation to a very significant extent. It is not known how much the energy of dissociation of *n*-hexane is reduced because of the chemisorption on the wall. The heat of adsorption of *n*-hexane on ferrous and ferric oxide has been found to be about 15 kcal (16). If the same value is assumed for quartz it is to be expected that the chemisorbed molecules may require 10–15 kcal less than the energy in the gas phase to dissociate. In other words the heterogeneous initiation may be more than 100 times faster than the homogeneous initiation at 500 °C.

From this point of view it is understood that NO, even in very small amounts, can reduce the rate very sharply by simply suppressing the heterogeneous initiation. However, such a heterogeneous effect of NO can be assigned only in the initial stage of the reaction. Once the initiation will take place, propagation will continue in the gas phase. In this case the effect of NO, if any, will be associated with the gas phase. The strong induction period in the initial rate of the inhibited decomposition can be attributed to this effect of NO. At maximum inhibition, an equilibrium between adsorbed and desorbed NO molecules may be established. Therefore the effect of NO on the heterogeneous initiation will cease and the rate will be independent of NO. Certainly, initiatory effects of NO will appear whose significance will increase with increasing NO pressure.

Surface-to-volume ratio has no effect on the yield of C_3H_6 or 1-C_4H_8, therefore, the propagation reactions involved in their formation must occur homogeneously. The effect of NO in causing an increase in the yield of C_2H_4 can be accounted for by the reaction

[14] $$C_2H_5 + NO \rightarrow C_2H_4 + HNO.$$

Reaction [14] would compete with reactions [3*a*–*c*] and consequently any increase in the yield of C_2H_4 would be associated with a decrease in the yield of C_2H_6.

The role of HNO in the system is not known. However, its existence has been established by flash photolysis and its lifetime was found to be about 0.1 s under these conditions (17). Some controversies exist as far as D(H—NO) is concerned. The value of 48.6 kcal was obtained from spectroscopy measurements (18, 19) while a minimum of 56 kcal was assigned from infrared chemiluminescence studies (20). In either case, reaction [14] is exothermic by at least 11 kcal (based on $D(C_2H_4\text{—H}) = 38$ kcal (21)). The HNO molecule can further participate in termination processes which regenerate nitric oxide. In addition, NO, a free readical itself, can recombine with free radicals leading to a variety of nitrogen-containing products. However, such products were not detected in the present study by the analytical method used. Slight consumption of NO was found for NO pressures above 5 mm.

It is interesting to note that the rate expressions derived by Norrish and Pratt (10) applied to the present study, gives curves approximately of the same shape as the experimental ones. However, some more or less severe assumptions have to be made because many rate constants are unknown for the *n*-hexane system.

Can. J. Chem. Downloaded from www.nrcresearchpress.com by 210.87.254.40 on 09/05/12
For personal use only.

PART II. 2-METHYL PENTANE

Results

Two typical sets of analytical results for the uninhibited and the inhibited decomposition of 2-methyl pentane at 520 °C are given in Tables VI and VII.

TABLE VI

Analytical results (mole %) for the decomposition of 2-methyl pentane (T = 520 °C, $\Delta P/P_i$ = 0.20)

	P_i (mm)		
Product	154	102	80
2-Methyl pentane	65.00	69.00	72.00
CH_4	5.60	4.70	4.00
C_2H_6	5.20	4.20	3.20
C_2H_4	3.20	2.80	2.20
C_3H_8	1.90	1.60	0.90
C_3H_6	7.20	6.80	7.20
i-C_4H_8	6.00	5.60	5.60
H_2	5.40	4.50	4.00
Total	99.5	99.7	99.6

TABLE VII

Analytical results (mole %) with various NO pressures for the decomposition of 2-methyl pentane (T = 500 °C, $\Delta P/P_i$ = 0.25, P_i = 100 mm)

	NO pressure (mm)			
Product	0	5	12	15
2-Methyl pentane	64.60	64.00	61.00	59.00
CH_4	5.50	6.50	8.60	8.80
C_2H_6	6.80	5.30	4.50	4.40
C_2H_4	3.20	4.70	5.60	6.80
C_3H_8	2.10	1.20	1.00	1.00
C_3H_6	7.50	7.50	7.50	8.00
i-C_4H_8	5.40	5.30	6.20	6.40
H_2	4.70	5.20	4.70	4.60
Total	99.8	99.7	99.1	99.0

The effect of an 11-fold increase in the S/V ratio on the decomposition rate is less marked than that observed with *n*-hexane. The percentage reduction in rate due to packing is illustrated in Fig. 9. At about 110 mm of 2-methyl pentane the effect of S/V ratio disappears. No marked effect of the surface on the product distribution was observed in the uninhibited decomposition.

Overall activation energies and frequency factors were calculated from the Arrhenius equation, using rate constants obtained at three temperatures, 500, 510, and 520 °C. The rate constants are given in Table VIII. The kinetic parameters are pressure dependent and decrease at high hydrocarbon pressures as shown in Table IX. The overall order was found to be 1.3 for hydrocarbon pressures less than 40 mm and tends to unity for pressures above 40 mm (Fig. 10).

Can. J. Chem. Downloaded from www.nrcresearchpress.com by 210.87.254.40 on 09/05/12
For personal use only.

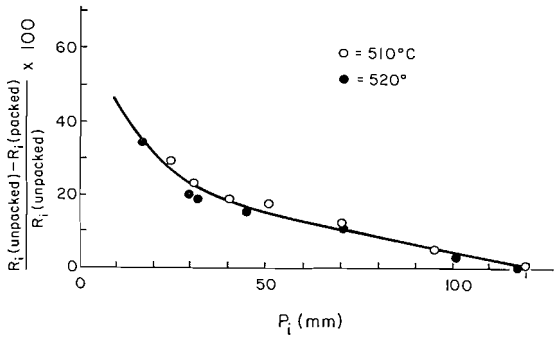

FIG. 9. Percentage reduction in rate due to the packing for various pressures of 2-methyl pentane.

TABLE VIII

Rate constants for the decomposition of 2-methyl pentane $\times 10^2$ min^{-1}

	T (°K)		
P (mm)	773	783	793
0–20	0.80	1.33	2.20
30	0.80	1.33	2.40
40–60	0.90	1.45	2.30
60–80	0.85	1.40	2.20
80–90	0.83	1.40	2.20
90–100	0.83	1.40	2.18
120	0.80	1.30	2.00

TABLE IX

Variation of activation energies and frequency factors with initial pressure of 2-methyl pentane

P_i (mm)	E_{act} (kcal)	A (s^{-1}) $\times 10^{11}$
0–30	62.0±1.0	470
30–60	60.0±2.0	550
60–90	58.0±3.0	120
90–100	58.5±4.0	55
120	56.0±2.0	8.4

Over a large pressure range and at constant extent of decomposition (20%), the yields of CH_4, C_2H_6, C_3H_8, and H_2 increase with increasing hydrocarbon pressure. The yields of the rest of the products increase slightly with increasing hydrocarbon pressure approaching more or less constant values at higher hydrocarbon pressures (Fig. 11).

Nitric oxide, even in small amounts, reduces the rate of decomposition significantly (Fig. 12*b*). However, the reduction in rate is less sharp in the decomposition of 2-methyl pentane than in the decomposition of *n*-hexane. The nitric oxide pressure required for maximum inhibition is about 14 mm for hydrocarbon pressures in the range of 50 to 100 mm. It also shifts to higher pressures for higher S/V ratios (Fig. 12*a*). Nitric oxide also affects the product distribution. The yields of CH_4 and C_2H_4 increase while those of C_2H_6 and C_3H_8 decrease with increasing NO pressure. The yields of products such as C_3H_6 and *i*-C_4H_8 are independent of the NO pressure as shown in Fig. 13.

Can. J. Chem. Downloaded from www.nrcresearchpress.com by 210.87.254.40 on 09/05/12
For personal use only.

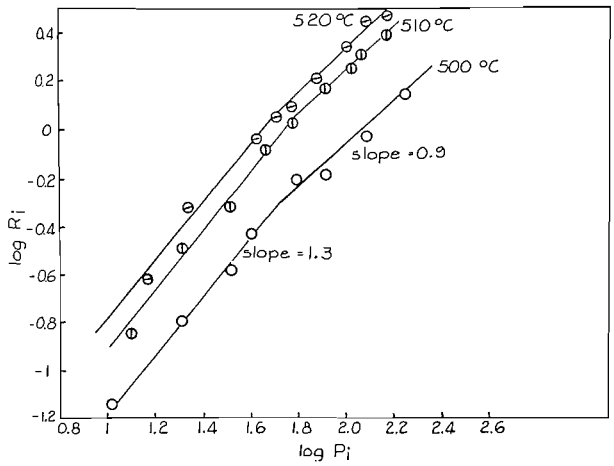

FIG. 10. Plots of the logarithm of the rate against the logarithm of the pressure for the uninhibited decomposition of 2-methyl pentane.

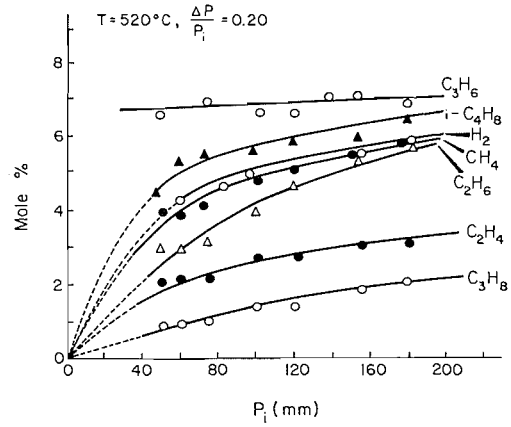

FIG. 11. Variation of the product distribution with initial pressure of 2-methyl pentane.

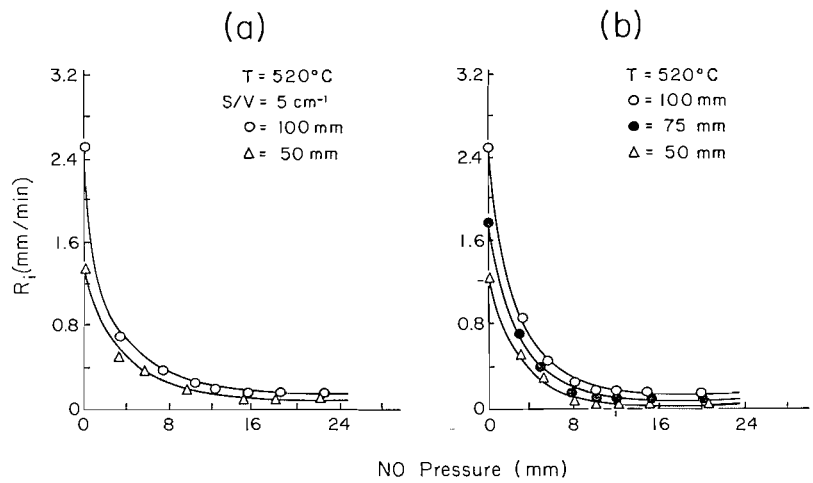

FIG. 12. Dependence of the initial rate on NO pressure in (*a*) the packed and (*b*) the unpacked vessels.

Can. J. Chem. Downloaded from www.nrcresearchpress.com by 210.87.254.40 on 09/05/12
For personal use only.

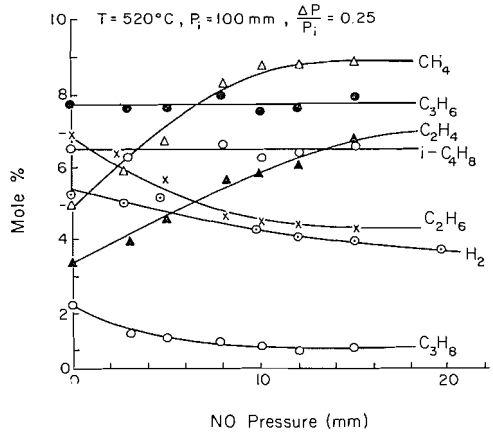

FIG. 13. Variation of the product distribution with NO pressure.

The variation of the product distribution with time is almost linear for extents of decomposition up to 40% in the fully inhibited reaction (Fig. 14). This indicates that no self-inhibition by the products occurs, at least in the fully inhibited decomposition. Self-inhibition is obvious in the case of the uninhibited decompositions under the same conditions.

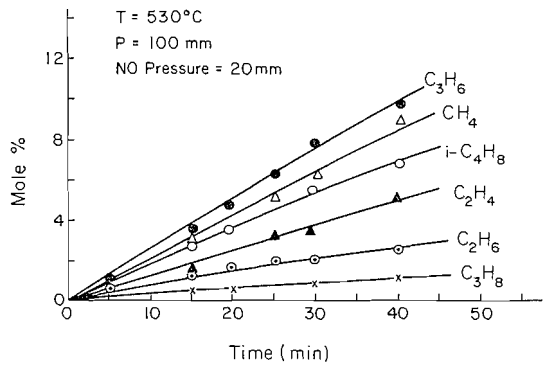

FIG. 14. Variation of the product distribution with time for the fully inhibited decomposition.

No definite effect was found on the formation of C_2H_6, C_2H_4, or C_3H_8 by the surface. The ratio C_2H_4/C_2H_6 which increases steadily with increasing NO pressure, is not significantly affected by variation in S/V ratio (Fig. 15). However, the data are scattered enough to mask any small variation in the ratio.

Results on the adsorption of 2-methyl pentane relative to NO are given in Table X. Nitric oxide is still adsorbed more than 2-methyl pentane on quartz.

Discussion

The products of the uninhibited pyrolysis at pressures of 2-methyl pentane in the range of 40 to 200 mm can be accounted for by the following reactions.

Initiation reactions:

[15*a*] $(CH_3)_2CHCH_2CH_2CH_3 \rightarrow CH_3 + (CH_3)_2CHCH_2CH_2$

[15*b*] $(CH_3)_2CHCH_2CH_2CH_3 \rightarrow CH_3 + CH_3CHCH_2CH_2CH_3$

Can. J. Chem. Downloaded from www.nrcresearchpress.com by 210.87.254.40 on 09/05/12
For personal use only.

[15c] $(CH_3)_2CHCH_2CH_2CH_3 \rightarrow C_2H_5 + (CH_3)_2CHCH_2$

[15d] $(CH_3)_2CHCH_2CH_2CH_3 \rightarrow i\text{-}C_3H_7 + n\text{-}C_3H_7.$

Propagation reactions:

[16a] $CH_3 + (CH_3)_2CHCH_2CH_2CH_3 \rightarrow CH_4 + (CH_3)_2CHCH_2CH_2CH_2$

[16b] $CH_3 + (CH_3)_2CHCH_2CH_2CH_3 \rightarrow CH_4 + (CH_3)_2CHCH_2CHCH_3$

[16c] $CH_3 + (CH_3)_2CHCH_2CH_2CH_3 \rightarrow CH_4 + (CH_3)_2CHCHCH_2CH_3$

[16d] $CH_3 + (CH_3)_2CHCH_2CH_2CH_3 \rightarrow CH_4 + (CH_3)_2CCH_2CH_2CH_3$

[16e] $CH_3 + (CH_3)_2CHCH_2CH_2CH_3 \rightarrow CH_4 + CH_3\underset{\displaystyle CH_2}{\underset{|}{C}}HCH_2CH_2CH_3.$

[17a–e] $C_2H_5 + (CH_3)_2CHCH_2CH_2CH_3 \rightarrow C_2H_6 +$ 2-methyl pentyl radicals

[18a–e] $i\text{-}C_3H_7 + (CH_3)_2CHCH_2CH_2CH_3 \rightarrow C_3H_8 +$ 2-methyl pentyl radicals

[19a–e] $H + (CH_3)_2CHCH_2CH_2CH_3 \rightarrow H_2 +$ 2-methyl pentyl radicals.

Radical decompositions:

[20a–e] 2-methyl pentyl radicals $\rightarrow C_2H_5 + i\text{-}C_4H_8$

[21a–e] 2-methyl pentyl radicals $\rightarrow i\text{-}C_3H_7 + C_3H_6$

[22] $(CH_3)_2CHCH_2CH_2 \rightarrow C_2H_5 + C_3H_6$

[23] $CH_3CHCH_2CH_2CH_3 \rightarrow C_2H_5 + C_3H_6$

[24] $(CH_3)_2CHCH_2 \rightarrow CH_3 + C_3H_6$

[25] $(CH_3)_2CHCH_2 \rightarrow H + i\text{-}C_4H_8$

[26] $n\text{-}C_3H_7 \rightarrow CH_3 + C_2H_4$

[27] $n\text{-}C_3H_7 \rightarrow H + C_3H_6$

[28] $i\text{-}C_3H_7 \rightarrow CH_3 + C_2H_4$

[29] $i\text{-}C_3H_7 \rightarrow H + C_2H_4$

[30] $C_2H_5 \rightarrow H + C_2H_4.$

Termination reaction:

[31] $2CH_3 \xrightarrow{\beta\beta M} C_2H_6.$

For first order initiation a $\beta\beta$M termination type leads to unity order (15) while for second order initiation a $\beta\mu$M termination leads to the same order. However, the $\beta\mu$M termination is canceled because no C_4H_{10} was detected among the products. For pressures lower than 40 mm the order tends to 3/2, in fact is 1.3, therefore two termination types will participate, $\beta\beta$ and $\beta\beta$M for first and second order initiation respectively. The $\beta\beta$ is canceled because β radicals are CH_3 and H whose recombination involves a third body. Therefore the above-outlined mechanism may be valid for pressures higher than 40 mm, involving a first order initiation.

Hydrogen is formed in quite significant amounts compared with those found in the decomposition of *n*-hexane. This can be attributed to the decomposition of the isopropyl radical, one of the major radicals in the mechanism. Isopropyl radical can undergo isomerization, direct decomposition, or chain propagation.

[28] $CH_3CHCH_3 \rightarrow (CH_3CH_2CH_2) \rightarrow CH_3 + C_2H_4$

[29] $CH_3CHCH_3 \rightarrow H + C_3H_6$

[18] $CH_3CHCH_3 + RH \rightarrow C_3H_8 + R$

Can. J. Chem. Downloaded from www.nrcresearchpress.com by 210.87.254.40 on 09/05/12
For personal use only.

At temperatures around 500 °C, Jackson and McNesby (22) found that reaction [29] is faster by a factor of at least 14 than reaction [28]. Therefore reaction [29] predominates. The small amount of C_3H_8 formed indicates that reaction [18] participates to a minor extent. The dependence of the yields of CH_4, C_2H_6, C_3H_8, and H_2 on the hydrocarbon pressure can be accounted for by reactions [16] to [19] which are favored as the hydrocarbon pressure is increased. The complexity of the mechanism, however, makes any relation between the yields of products and the hydrocarbon pressure impossible.

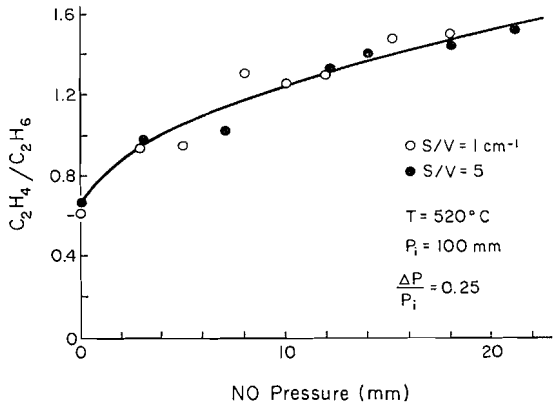

FIG. 15. Variation of the C_2H_4/C_2H_6 ratio with NO pressure.

TABLE X

Variation of 2-methyl pentane / NO ratio with initial pressure of the mixture after adsorption on quartz wool (2-methyl pentane / NO)$_{init}$ = 1.82, T = 310 °C, contact time = 2 min)

Initial pressure of the mixture (mm)	(2-Methyl pentane / NO)$_{final}$
11	2.00
31	1.94
44	1.88
61	1.86
66	1.86
96	1.80

The net effect of the surface is less marked in the decomposition of 2-methyl pentane than in the decomposition of *n*-hexane. From the mechanism of decomposition of *n*-hexane and 2-methyl pentane, it can be inferred that termination processes involve similar radicals and therefore it is rather unlikely that the effect of the surface on termination reactions would be much different in the two cases. Consequently, the less marked effect of the surface on the decomposition of 2-methyl pentane can be associated with the initiation rather than the termination processes. From Tables V and X we can infer that NO expels *n*-hexane from adsorption sites easier than 2-methyl pentane. Nitric oxide reduces the rate of decomposition of 2-methyl pentane also by suppressing the herogeneous initiation as in the case of *n*-hexane. For this reason the reduction in rate is also very sharp.

As the amount of NO increases, the inhibitor starts functioning in both phases. This is revealed by the effect of NO on the products of decomposition. The product distribution is markedly affected by NO. The simultaneous increase in the yield of C_2H_4 and decrease in that of C_2H_6 with increasing NO pressure can arise from the competing reactions discussed earlier in this paper.

Can. J. Chem. Downloaded from www.nrcresearchpress.com by 210.87.254.40 on 09/05/12
For personal use only.

[14] $$C_2H_5 + NO \rightarrow C_2H_4 + HNO$$

[3] $$C_2H_5 + RH \rightarrow C_2H_6 + R$$

The decrease in the yield of C_3H_8 with increasing NO pressure is attributed to similar competing reactions.

[32] $$i\text{-}C_3H_7 + NO \rightarrow C_3H_6 + HNO$$

[33] $$i\text{-}C_3H_7 + RH \rightarrow C_3H_8 + R$$

The effect of NO on the yield of CH_4 is particularly dramatic; it almost doubles from the uninhibited to the fully inhibited reaction, yet in the case of *n*-hexane there is almost no effect of NO on the yield of methane.

Although the reaction

[34] $$R + NO \rightarrow HNO + \text{olefins}$$

becomes more exothermic as the size of R increases, the instability of the larger R radicals rules out almost completely reactions of the type [34] in comparison to their unimolecular decomposition.

The fully inhibited decomposition appears to be of the same nature as that of *n*-hexane. The linearity in the relationship of the yields of the products to time indicates that the fully inhibited decomposition is not self-inhibited by any of its products either in the gas phase or adsorbed on the walls. This may indicate that the fully inhibited decomposition involves only homogeneous initiation while the heterogeneous one is completely suppressed by NO.

The analytical balance becomes less complete as the NO pressure is increased. This observation fits with the addition reaction of NO with radicals.

[35] $$R + NO \rightarrow RNO$$

These nitroso compounds can isomerize and decompose further into nitrogen-containing products which, however, were not observed here because of the analytical method used. Similar products have been observed by mass spectrometry in a system containing NO and methyl radicals (23). For low pressures of NO, at which NO was recovered completely, it is assumed that reaction [35] and subsequent isomerization are not important.

PART III. 3-METHYL PENTANE

Results

Two typical sets of analytical results are given in Tables XI and XII.

TABLE XI

Analytical results (mole %) for the uninhibited decomposition of 3-methyl pentane (T = 510 °C, $\Delta P/P_i$ = 0.20)

	P_i (mm)		
Products	100	50	40
3-Methyl pentane	69.50	75.50	76.50
CH_4	7.20	4.90	4.70
C_2H_6	4.20	3.20	2.80
C_2H_4	3.80	3.00	3.00
C_3H_6	3.00	2.60	2.60
$i\text{-}C_4H_8$ + 1-C_4H_8	1.50	1.50	1.20
trans-Butene-2	2.50	2.80	2.00
cis-Butene-2	2.20	2.00	1.90
2-Methyl butene-1	3.80	2.50	3.40
H_2	1.90	1.50	1.60
Total	99.6	99.5	99.7

Can. J. Chem. Downloaded from www.nrcresearchpress.com by 210.87.254.40 on 09/05/12
For personal use only.

TABLE XII

Analytical results (mole %) for various NO pressures in the inhibited pyrolysis of 3-methyl pentane (T = 520 °C, $\Delta P/P_i$ = 0.25, P_i = 100 mm)

Products	NO pressure (mm)		
	0	8	18
3-Methyl pentane	64.00	61.00	57.00
CH_4	9.80	13.00	14.00
C_2H_6	6.20	5.40	4.80
C_2H_4	5.60	6.00	7.10
C_3H_6	3.20	3.30	3.30
i-C_4H_8 + 1-C_4H_8	1.50	1.30	1.60
trans-Butene-2	3.00	2.40	2.70
cis-Butene-2	2.60	2.40	2.50
2-Methyl butene-1	2.00	2.90	2.90
H_2	1.90	1.70	1.80
Total	99.8	99.4	97.7

The effect of an 11-fold increase in S/V ratio upon the decomposition of 3-methyl pentane is the same as on the decomposition of 2-methyl pentane (Fig. 16). The percentage reduction in rate vanishes at about 100 mm of hydrocarbon. The overall reaction order obtained at 490, 500, 510, and 520 °C is a little higher than unity, namely 1.2 (Fig. 17). Rate constants obtained at the above-mentioned temperatures are given in Table XIII. The kinetic parameters are pressure dependent and tend to more or less constant values at higher pressures. Average of 6 values are given in Table XIV.

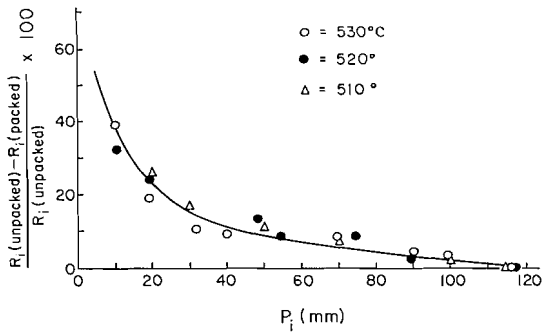

FIG. 16. Percentage reduction in rate due to packing for various initial pressures of 3-methyl pentane.

Nitric oxide inhibits the thermal decomposition of 3-methyl pentane to a similar degree as it does the decomposition of 2-methyl pentane. The NO pressure required for maximum inhibition is 12–14 mm for the hydrocarbon pressure range of 50 to 100 mm (Fig. 18*b*). This NO pressure increases slightly with increasing S/V ratio (Fig. 18*a*). Nitric oxide affects the product distribution in the thermal decomposition of 3-methyl pentane fo some extent. The yields of CH_4 and C_2H_4 increase slowly with increasing NO pressure. This result is consistent with previous investigations on isopentane (13). Finally the yield of 2-methyl butene-1 reaches a maximum with increasing NO pressure and then decreases (Fig. 19).

The variation of the product distribution of the fully inhibited decomposition is almost linear with time, with the exception of 2-methyl butene-1 which reaches a maximum and then decreases (Fig. 20), which may be attributed to further pyrolysis of this product when it is accumulated in significant amounts.

Can. J. Chem. Downloaded from www.nrcresearchpress.com by 210.87.254.40 on 09/05/12
For personal use only.

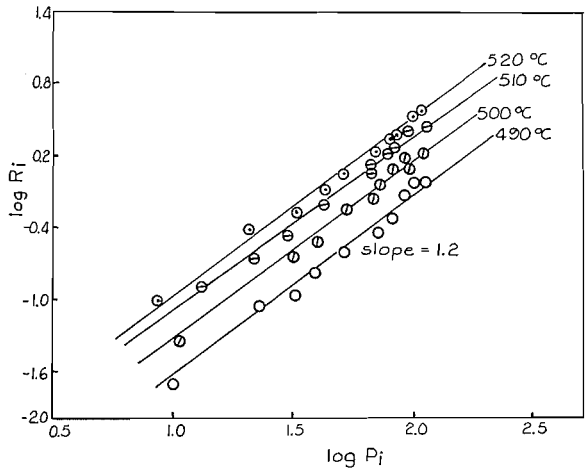

FIG. 17. Plots of the logarithm of the rate against the logarithm of the pressure for the uninhibited decomposition of 3-methyl pentane.

TABLE XIII

Rate constants for the decomposition of 3-methyl pentane $\times 10^2$ min^{-1}

	T (°K)			
P (mm)	763	777	783	793
0–30	0.38	0.63	1.10	1.87
30–50	0.60	1.00	1.60	2.55
50–60	0.60	1.05	1.60	2.70
60–70	0.72	1.10	1.70	2.70
70–80	0.66	1.10	1.70	2.60
80–90	0.66	1.10	1.60	2.60
100	0.65	1.05	1.60	2.50
120	0.63	1.00	1.55	2.40

TABLE XIV

Variation of activation energies and frequency factors with initial pressure of 3-methyl pentane

P_i (mm)	E_{act} (kcal)	A (s^{-1}) $\times 10^{12}$
0–30	65.0±2	95
40	59.0±2	4
50	59.0±7	4.4
60–80	55.5±3.5	0.66
90	54.5±5	0.80
100	54.0±4	0.66
120	54.0±4	0.25

High S/V ratios favor the formation of C_2H_6 in the inhibited reaction. The C_2H_4/C_2H_6 ratio increases with increasing NO pressure and for a given NO pressure it decreases with increasing S/V ratio (Fig. 21). However, this effect is not marked. The other decomposition products are independent of the S/V rtaio. This S/V ratio independence is shown for one of the products, C_3H_6 (Fig. 22).

Nitric oxide is adsorbed on quartz wool to a similar degree as 3-methyl pentane (Table XV). Therefore both compounds will compete for adsorption sites with equal probability.

Can. J. Chem. Downloaded from www.nrcresearchpress.com by 210.87.254.40 on 09/05/12
For personal use only.

Can. J. Chem. Downloaded from www.nrcresearchpress.com by 210.87.254.40 on 09/05/12
For personal use only.

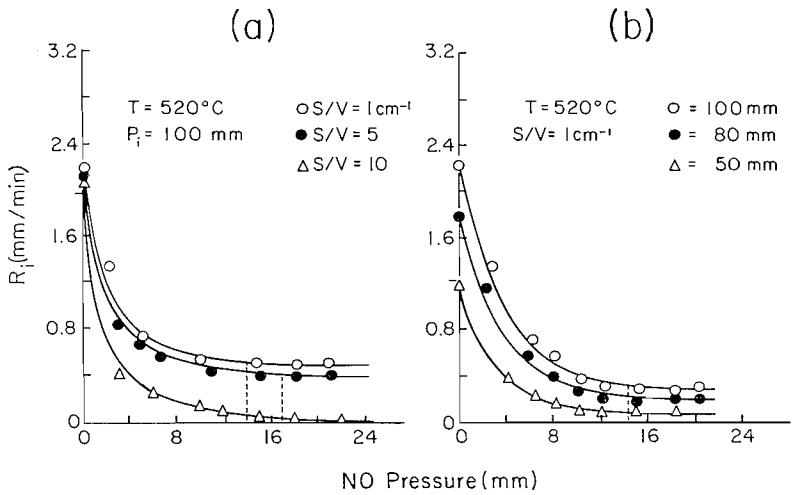

FIG. 18. Dependence of the initial rate on NO in (*a*) the packed and (*b*) the unpacked vessels.

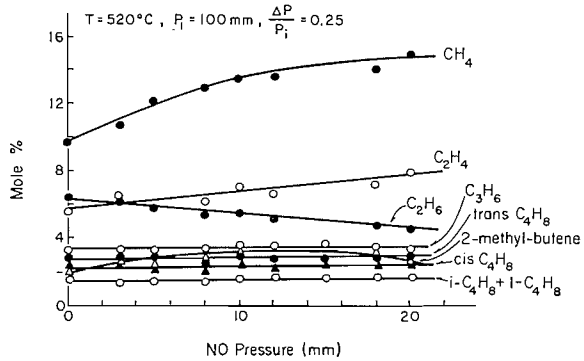

FIG. 19. Variation of the product distribution with NO pressure.

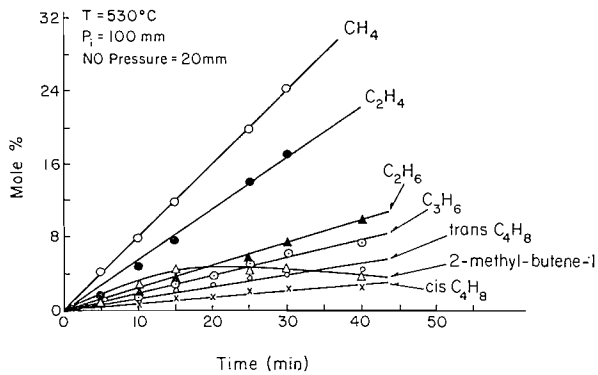

FIG. 20. Variation of the product distribution with time for the fully inhibited decomposition of 3-methyl pentane.

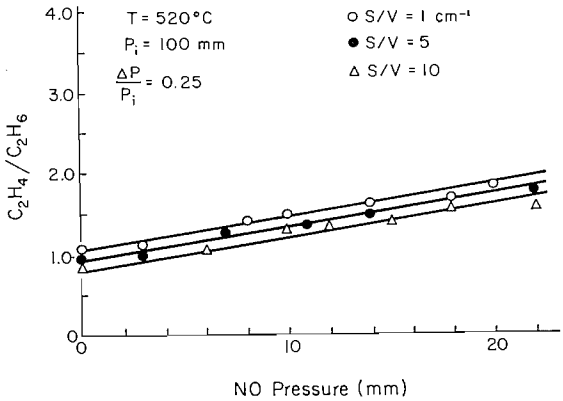

FIG. 21. Variation of the C_2H_4/C_2H_6 ratio with NO pressure and S/V ratio for 3-methyl pentane.

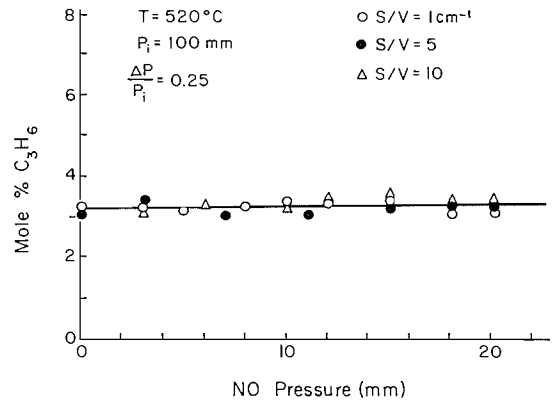

FIG. 22. Variation of the C_3H_6 yield with NO pressure and S/V ratio.

TABLE XV

Variation of (3-methyl pentane / NO) ratio with initial pressure of the mixture after adsorption on quartz wool $(3\text{-methyl pentane / NO})_{init} = 2.12$, $T = 310$ °C, contact time = 2 min)

Initial pressure of the mixture (mm)	$(3\text{-Methyl pentane / NO})_{final}$
22	2.10
30	2.14
47	2.22
64	2.04
97	2.16

Discussion

The products of the uninhibited pyrolysis of 3-methyl pentane can be accounted for at lower pressures by the following mechanism.

Initiation reactions:

[36*a*] $CH_3CH_2CH(CH_3)CH_2CH_3 \rightarrow CH_3 + CH_3CH_2CH(CH_3)CH_2$

[36*b*] $CH_3CH_2CH(CH_3)CH_2CH_3 \rightarrow C_2H_5 + CH_3CH_2CHCH_3$

36*c*] $CH_3CH_2CH(CH_3)CH_2CH_3 \rightarrow CH_3 + CH_3CH_2CHCH_2CH_3.$

Can. J. Chem. Downloaded from www.nrcresearchpress.com by 210.87.254.40 on 09/05/12
For personal use only.

Propagation reactions:

[37*a–d*] $CH_3 + CH_3CH_2CH(CH_3)CH_2CH_3 \rightarrow CH_4 +$ 3-methyl pentyl radicals

[38*a–d*] $C_2H_5 + CH_3CH_2CH(CH_3)CH_2CH_3 \rightarrow C_2H_6 +$ 3-methyl pentyl radicals

[39*a–d*] $H + CH_3CH_2CH(CH_3)CH_2CH_3 \rightarrow H_2 +$ 3-methyl pentyl radicals.

Radical decompositions:

[40*a–d*] 3-methyl pentyl radicals $\rightarrow C_2H_5 + CH_3CH{=}CHCH_3$

[41*a–d*] 3-methyl pentyl radicals $\rightarrow C_2H_5 + CH_2{=}CHCH_2CH_3$

[42*a–d*] 3-methyl pentyl radicals $\rightarrow CH_3 + CH_2{=}C(CH_3)CH_2CH_3$

[43] $CH_3CH_2CH(CH_3)CH_2 \rightarrow CH_3 + CH_2{=}C(CH_3)_2$

[44] $CH_3CH_2CH(CH_3)CH_2 \rightarrow C_2H_5 + C_3H_6$

[45] $CH_3CH_2CHCH_2CH_3 \rightarrow CH_3 + CH_3CH{=}CHCH_3$

[46] $CH_3CH_2CHCH_2CH_3 \rightarrow C_2H_5 + C_3H_6$

[47] $CH_3CH_2CHCH_3 \rightarrow CH_3 + C_3H_6$

[48] $CH_3CH_2CHCH_3 \rightarrow C_2H_5 + C_2H_4$

[49] $CH_3CH_2CHCH_3 \rightarrow H + CH_3CH{=}CHCH_3$

[50] $C_2H_5 \rightarrow H + C_2H_4$.

Termination reaction:

[51] $2CH_3 \xrightarrow{\beta\beta M} C_2H_6$.

For first order initiation, $\beta\mu$ and $\beta\beta$M termination types lead to unity overall order (15), while for second order initiation $\mu\mu$ and $\beta\mu$M termination types lead to the same order. However $\beta\mu$, $\beta\mu$M, and $\mu\mu$ terminations are canceled because of the lack of C_4H_{10} and C_3H_8 among the products. Therefore only one choice remains, namely a $\beta\beta$M termination type leading to unity overall order. The experimental overall order was found to be slightly higher than unity. Therefore, it is not clear whether or not another mechanism will also participate leading to 3/2 order. In such a case, only one termination type can occur, $\beta\beta$M, for second order initiation. Thus we face two choices: (i) The overall order can be considered unity, so that one mechanism can account for the decomposition involving a first order initiation and a $\beta\beta$M termination. (ii) Another mechanism also participates to a smaller extent involving a second order initiation and a $\beta\beta$M termination type. The overall order in such a case will be between unity and 3/2.

The observation that the NO pressure required for maximum inhibition is approximately the same for hydrocarbon pressures of 50 to 100 mm and that it has the same magnitude to that required for maximum inhibition in the decomposition of *n*-hexane and 2-methyl pentane, indicates that NO inhibition is associated with the particular experimental conditions more than with the nature of the hydrocarbon. It must be pointed out that any small difference could be well masked, since this NO pressure is not defined accurately. However, it is rather obvious that the NO pressure required for maximum inhibition is not a fixed percentage of the hydrocarbon pressure.

Nitric oxide and 3-methyl pentane are adsorbed on quartz wool to similar extents. Therefore, NO can expel 3-methyl pentane molecules from the active sites and it can be expelled with equal probabilities. Under these circumstances, one would expect that heterogeneous initiation still exist to some extent, even in the fully inhibited decomposition. Since heterogeneous initiation is suppressed less in the decomposition of 3-methyl pentane than in the decomposition of *n*-hexane and 2-methyl pentane by NO, it is expected that

Can. J. Chem. Downloaded from www.nrcresearchpress.com by 210.87.254.40 on 09/05/12
For personal use only.

the reduction in rate due to the inhibitor will be less steep in this isomer, which is the case. On the other hand, since heterogeneous initiation participates even to a small extent, in the fully inhibited decomposition, it is expected that the initial rate of the fully inhibited decomposition of 3-methyl pentane will be larger than the corresponding initial rates of the fully inhibited decomposition of *n*-hexane and 2-methyl pentane. This has been observed too.

Nitric oxide also functions homogeneously, as can be revealed from its effect on the decomposition products.

The effect of NO on CH_4, C_2H_6, and C_2H_4 has been discussed earlier in this paper. The special behavior of 2-methyl butene-1 can be attributed to further reaction of it with NO when the latter is in significant amount. Thus

[52] $$CH_2{=}C(CH_3)CH_2CH_3 + NO \rightarrow CH_2{=}C(CH_3)CHCH_3 + HNO.$$

The C—H bond located in a β-position to the double bond is very weak, namely $D(C—H) \simeq 76$ kcal/mole. This value is assigned on the basis of the following (24, 25)

$$D(CH_2{=}CHCH_2—H) = 77 \text{ kcal/mole}$$

and

$$D(CH_2{=}C(CH_3)CH_2—H) = 76 \text{ kcal/mole}$$

and the fact that the dissociation energies in primary, secondary, and tertiary C—H bonds in molecules with infinity long side chains differ by a small quantity B (26).

$$D(C—H)_{pr} = D(C—H)_{sec} + B = D(C—H)_{tert} + 2B$$

Thus the endothermicity of reaction [52] can be estimated as follows

$$\Delta H = D(C—H) - D(H—NO) \leq 76 - 48.6 = 27 \text{ kcal/mole.}$$

Higher radicals could be attacked by NO as easily as C_2H_5, leading to olefins and HNO. However, this does not happen here because of the instability of the higher radicals for which the unimolecular decomposition must predominate.

The analytical balance becomes less complete with increasing NO pressure. It may be attributed to the possibility that reactions like

$$R + NO \rightarrow RNO \rightarrow \text{oxime} \rightarrow \text{nitrogen containing products}$$

gain significance with increasing NO pressure. In the special case of CH_3 radical we obtain

[53] $$CH_3 + NO \rightarrow CH_3NO$$

For reaction [53] it was found (27) that

$$E_A = 5.7 \text{ kcal/mole for } P \simeq 1$$

or

$$E_A = 0 \text{ kcal/mole for } P = 1.5 \times 10^{-4}.$$

Nitrosomethane is unstable and it decomposes to products such as HCN, H_2O, NH_3, CO, N_2, CO_2, CH_3CN, etc. (23).

The energy of dissociation of CH_3NO is not accurately known but it is supposed to be (28)

$$D(CH_3—NO) \simeq 30 \text{ kcal/mole.}$$

This indicates that dissociation of CH_3NO to CH_3 and NO will compete with any further isomerization of CH_3NO, but the latter cannot predominate because an activation energy of 40 kcal/mole has been found for the reaction (29)

$$CH_3NO \rightarrow CH_2{=}NOH.$$

Can. J. Chem. Downloaded from www.nrcresearchpress.com by 210.87.254.40 on 09/05/12
For personal use only.

Direct evidence for the isomerization of primary and secondary nitroso compounds has been found from the infrared spectrum of these compounds (30).

ACKNOWLEDGMENTS

We are grateful to the National Research Council and to the Petroleum Research Fund of the American Chemical Society for financial support. We are also greatly indebted to Dr. G. B. Porter for many valuable discussions.

REFERENCES

1. M. G. PEARD, F. J. STUBBS, and C. N. HINSHELWOOD Proc. Roy. Soc. London, Ser. A, **214**, 339 (1952).
2. M. G. PEARD, F. J. STUBBS, and C. N. HINSHELWOOD. Proc. Roy. Soc. London, Ser. A, **214**, 471 (1952).
3. J. E. HOBBS and C. N. HINSHELWOOD. Proc. Roy. Soc. London, Ser. A, **167**, 439 (1938).
4. J. E. HOBBS and C. N. HINSHELWOOD. Proc. Roy. Soc. London, Ser. A, **167**, 447 (1938).
5. B. W. WOJCIECHOWSKI and K. J. LAIDLER. Can. J. Chem. **38**, 1027 (1960).
6. K. J. LAIDLER, N. H. SAGERT, and B. W. WOJCIECHOWSKI. Proc. Roy. Soc. London, Ser. A, **270**, 254 (1962).
7. N. H. SAGERT and K. J. LAIDLER. Can. J. Chem. **41**, 838 (1963).
8. N. H. SAGERT and K. J. LAIDLER. Can. J. Chem. **41**, 848 (1963).
9. T. REE, K. YANG, and H. ERYING. Trans. Faraday Soc. **58**, 2375 (1962).
10. R. G. W. NORRISH and G. L. PRATT. Nature, **197**, 143 (1963).
11. D. R. BLACKMORE and C. N. HINSHELWOOD. Proc. Roy. Soc. London, Ser. A, **268**, 36 (1962).
12. V. V. VOEVODSKY. Trans. Faraday Soc. **55**, 65 (1959).
13. W. A. BRYCE and J. CHRYSOCHOOS. Trans. Faraday Soc. **59**, 1842 (1963).
14. E. W. R. STEACIE. Atomic and free radical reactions. Vol. II. Reinhold Publ. Corp. 1954.
15. P. GOLDFINGER, M. LETORT, and M. NICLAUSE. Contributions à l'étude de la structure moléculaire. Victor Henri Commemorative Volume. Desoer, Liege. 1948. p. 283.
16. YOUNG FANG and YU YAA. J. Phys. Chem. **67**, 2055 (1962).
17. F. W. DALBY. Can. J. Phys. **36**, 1336 (1958).
18. M. A. CLYNE and B. A. THRUSH. Trans. Faraday Soc. **57**, 1305 (1961).
19. M. A. CLYNE and B. A. THRUSH. Discussions Faraday Soc. **33**, 139 (1962).
20. J. K. CASHION and J. C. POLANYI. J. Chem. Phys. **30**, 317 (1959).
21. N. N. SEMENOV. Some problems in chemical kinetics and reactivity. Vol. I. Princeton University Press. 1958. p. 66.
22. W. M. JACKSON and J. R. MCNESBY. J. Chem. Phys. **36**, 2272 (1962).
23. W. A. BRYCE and K. U. INGOLD. J. Chem. Phys. **23**, 1968 (1955).
24. M. SZWARC. Chem. Rev. **47**, 75 (1950).
25. N. N. SEMENOV. Some problems in chemical kinetics and reactivity. Vol. I. Princeton University Press. 1958. p. 19.
26. V. V. VOEVODSKY. Dokl. Akad. Nauk SSSR, **79**, 455 (1951).
27. E. W. R. STEACIE. Atomic and free radical reactions. Vol. I. Reinhold Publishing Corp. 1954. p. 127.
28. B. G. GOWENLOCK. Discussions Faraday Soc. **37**, 287 (1962).
29. L. BATT and B. G. GOWENLOCK. Trans. Faraday Soc. **56**, 682 (1960).
30. W. LÜTTKE. Z. Elektrochem. **61**, 302 (1957).

Can. J. Chem. Downloaded from www.nrcresearchpress.com by 210.87.254.40 on 09/05/12
For personal use only.

Can. J. Chem. Downloaded from www.nrcresearchpress.com by 210.87.254.6 on 09/05/12
For personal use only.

NOTES

THE PREPARATION OF ANHYDROUS ZIRCONIUM DICHLORIDE

B. SWAROOP AND S. N. FLENGAS

INTRODUCTION

The existence of zirconium dichloride was first noticed by de Boer and Fast (1) while zirconium tetrachloride was heated with zirconium metal in the presence of aluminium chloride. Later, Larsen and Leddy (2) and Turnbull and Watts (3) confirmed the formation of zirconium dichloride while studying the disproportionation of zirconium trichloride. However, the production of high purity, anhydrous zirconium dichloride was not achieved by these investigators. In the present investigation, zirconium dichloride of a purity between 95 and 99% was produced by the direct reaction between zirconium trichloride powder and zirconium metal.

EXPERIMENTAL AND RESULTS

The anhydrous zirconium trichloride was prepared by a two-step reduction of zirconium tetrachloride with zirconium metal as described in the previous investigation (4). The reduction stages are indicated by the following equations:

$$[i] \qquad Zr(s) + ZrCl_4(\text{vap. 1 atm}) = 2ZrCl_2(s) \qquad \text{at 700 °C}$$

$$[ii] \qquad 2ZrCl_2(s) + 2ZrCl_4(\text{vap. 1 atm}) = 4ZrCl_3(s) \qquad \text{at 400 °C.}$$

Hence the overall reaction is:

$$[iii] \qquad 3ZrCl_4(\text{vap. 1 atm}) + Zr(s) = 4ZrCl_3(s).$$

The direct preparation of zirconium dichloride by the reduction of zirconium tetrachloride vapor with zirconium metal, as shown in eq. [*i*], was not adopted as the procedure because of difficulty in preventing the formation of $ZrCl_3$ during the cooling cycle of the reaction cell. Zirconium dichloride was prepared by reducing zirconium trichloride with zirconium metal according to the reaction,

$$[iv] \qquad Zr(s) + 2ZrCl_3(s) = 3ZrCl_2(s) \qquad \text{at 675 °C.}$$

In order to complete the reduction of zirconium trichloride, zirconium metal in excess of the stoichiometric amount was used. The possible contamination of the product, due to the disproportionation of zirconium dichloride, as shown in reaction [*i*], was prevented by reducing the free volume of the reaction site to a minimum.

The reaction apparatus consisted of a 4 in. long quartz tube of 1 in. in diameter, closed at one end. To prevent the reaction between quartz and the charge, the tube was lined with platinum foil 0.010 in. thick. The platinum lining could be used only twice, as there was some evidence of alloy formation with zirconium.

Finely divided reactor grade zirconium metal, containing less than 70 p.p.m. hafnium and a total of other metallic impurities of 400 p.p.m, was obtained by filling the metal in a dry box containing oxygen-free argon gas. Particle sizes between −80 and +100

mesh were separated by screening and used for the experiments. About 2 g of zirconium trichloride was mixed with about 1 g of the zirconium metal powder (50% excess), and the mixture was placed in the reaction tube. The tube was then sealed under vacuum, and gradually heated to 675 °C in a vertical furnace. The reaction was allowed to continue at 675 °C for a period of 30 to 35 h, and then the tube was quenched to room temperature. The tube was opened in a dry box containing purified argon. The product was screened through a −200 mesh and a −325 mesh sieve to separate the unreacted metal, and the finely divided zirconium dichloride powder was stored in sealed containers. The −325 mesh product was analyzed as follows: (*a*) The total chlorine content was determined by a modified Volhard's method (5). To this purpose, concentrated sulfuric acid was added to the material contained in a conical flask. The flask was connected to a distillation column through ground glass joints. The chlorine of zirconium dichloride was then boiled off as hydrogen chloride, and was collected and precipitated in a standardized solution of silver nitrate. The distillation was carried out in a stream of purified argon. (*b*) The total zirconium content was determined by precipitating zirconium as zirconium phosphate following the standard method. (*c*) The reducing power of the materials in solution was determined with an $N/10$ ceric ammonium sulfate solution. (*d*) X-ray powder diffraction patterns were obtained using a 57.3 mm camera with Cu K_α radiation. The lines were indexed by the film measuring device, and the intensities were estimated visually.

The X-ray information is shown in Table II, and the results of analyses of selected batches of zirconium dichloride are given in Table I.

TABLE I

Analysis of zirconium dichloride

Batch No.	Zirconium analysis			Chlorine analysis			Atomic ratio Zr:Cl	Redox titration		
	Wt. of sample	Zr (wt. %)		Wt. of sample	Cl_2 (wt. %)			Wt. of sample	$ZrCl_2$ content	Wt. % $ZrCl_2$
		Theor.	Expt.		Theor.	Expt.				
1	0.0946	56.2	52.6	0.1010	43.7	43.5	1:2.12	0.1349	0.1332	98.7
2	0.1469	56.2	56.1	0.1513	43.7	43.3	1:1.99	0.0910	0.084	92.3
3	0.0754	56.2	61.0	0.0572	43.7	45.1	1:1.92	0.1649	0.1650	100.0
4	0.1244	56.2	58.2	0.1244	43.7	42.7	1:1.92	0.0943	0.0936	99.2

The X-ray diffraction data indicate clearly new lines that do not belong to zirconium metal, zirconium trichloride (6), or zirconium tetrachloride. Furthermore, there is no evidence that the product contains any detectable amounts of metallic platinum or platinum dichloride.

The results of the chemical analyses indicate that zirconium dichloride of a purity between 95 and 99% was produced by this method. Zirconium dichloride is a black powder which was found to be more stable in air than the trichloride. Material contaminated with zirconium metal in the form of a chemical powder appears to be much more reactive and becomes pyrophoric. Zirconium dichloride does not dissolve in water readily. The solutions after long standing produce a greyish precipitate. There is no evidence of rapid hydrogen evolution as observed with zirconium trichloride.

The overall reaction recovery after screening the product lies between 50 and 56%. This recovery is certainly dependent upon reaction temperature (675°), the reaction time (30 to 35 h), and the particle size of the reactants.

Can. J. Chem. Downloaded from www.nrcresearchpress.com by 210.87.254.6 on 09/05/12
For personal use only.

TABLE II
X-ray data for zirconium dichloride

No.	$2\theta \pm 0.05$	d (A°)	I (obs.)
1	17.50	5.067	W
2	24.15	3.686	M
3	28.20	3.164	VS
4	31.45	2.844	S
5	34.10	2.630	MS
6	35.40	2.535	W
7	38.60	2.332	VW
8	40.90	2.206	M
9	43.40	2.015	VW
10	45.15	2.008	M
11	49.10	1.855	M
12	50.20	1.817	M
13	52.30	1.750	VW
14	53.90	1.701	W
15	55.35	1.660	M
16	56.90	1.618	W
17	57.90	1.593	VW
18	59.60	1.551	MW
19	61.10	1.516	VW
20	62.65	1.482	W
21	64.00	1.455	VW
22	65.40	1.427	MW
23	67.40	1.389	VW
24	68.60	1.368	VW
25	70.75	1.331	MW
26	72.10	1.310	VW
27	74.50	1.274	MW
28	76.00	1.252	W
29	78.40	1.220	W

Abbreviations: W, weak; M, medium; S, strong.

ACKNOWLEDGMENTS

The authors are indebted to the Defence Research Board of Canada for a grant in support of this work.

1. J. H. DE BOER and J. D. FAST. Z. Anorg. Allgem. Chem. **187**, 177 (1930).
2. E. N. LARSEN and J. J. LEDDY. J. Am. Chem. Soc. **78**, 5983 (1956).
3. A. G. TURNBULL and J. A. WATTS. Australian J. Chem. **16**, 947 (1963).
4. B. SWAROOP and S. N. FLENGAS. Can. J. Chem. **42**, 1495 (1964).
5. J. R. CALDWELL and H. V. MOYER. Ind. Eng. Chem. **7**, 1, 38 (1935).
6. B. SWAROOP and S. N. FLENGAS. Can. J. Phys. **42**, 1886 (1964).

RECEIVED NOVEMBER 16, 1964.
DEPARTMENT OF METALLURGY AND MATERIALS SCIENCE,
UNIVERSITY OF TORONTO,
TORONTO, ONTARIO.

REACTIONS OF PHENYL-SUBSTITUTED HETEROCYCLIC COMPOUNDS. VI. NITRATION OF 5-PHENYLISOXAZOLE

BRIAN M. LYNCH AND LIZZIE SHIU

References cited in a recent review (1) of isoxazole chemistry indicate the possibility of some confusion between the nitro compounds derived from 5-phenylisoxazole (I) and

Can. J. Chem. Downloaded from www.nrcresearchpress.com by 210.87.254.6 on 09/05/12
For personal use only.

TABLE II
X-ray data for zirconium dichloride

No.	$2\theta \pm 0.05$	d (A°)	I (obs.)
1	17.50	5.067	W
2	24.15	3.686	M
3	28.20	3.164	VS
4	31.45	2.844	S
5	34.10	2.630	MS
6	35.40	2.535	W
7	38.60	2.332	VW
8	40.90	2.206	M
9	43.40	2.015	VW
10	45.15	2.008	M
11	49.10	1.855	M
12	50.20	1.817	M
13	52.30	1.750	VW
14	53.90	1.701	W
15	55.35	1.660	M
16	56.90	1.618	W
17	57.90	1.593	VW
18	59.60	1.551	MW
19	61.10	1.516	VW
20	62.65	1.482	W
21	64.00	1.455	VW
22	65.40	1.427	MW
23	67.40	1.389	VW
24	68.60	1.368	VW
25	70.75	1.331	MW
26	72.10	1.310	VW
27	74.50	1.274	MW
28	76.00	1.252	W
29	78.40	1.220	W

Abbreviations: W, weak; M, medium; S, strong.

ACKNOWLEDGMENTS

The authors are indebted to the Defence Research Board of Canada for a grant in support of this work.

1. J. H. DE BOER and J. D. FAST. Z. Anorg. Allgem. Chem. **187**, 177 (1930).
2. E. N. LARSEN and J. J. LEDDY. J. Am. Chem. Soc. **78**, 5983 (1956).
3. A. G. TURNBULL and J. A. WATTS. Australian J. Chem. **16**, 947 (1963).
4. B. SWAROOP and S. N. FLENGAS. Can. J. Chem. **42**, 1495 (1964).
5. J. R. CALDWELL and H. V. MOYER. Ind. Eng. Chem. **7**, 1, 38 (1935).
6. B. SWAROOP and S. N. FLENGAS. Can. J. Phys. **42**, 1886 (1964).

RECEIVED NOVEMBER 16, 1964.
DEPARTMENT OF METALLURGY AND MATERIALS SCIENCE,
UNIVERSITY OF TORONTO,
TORONTO, ONTARIO.

REACTIONS OF PHENYL-SUBSTITUTED HETEROCYCLIC COMPOUNDS. VI. NITRATION OF 5-PHENYLISOXAZOLE

BRIAN M. LYNCH AND LIZZIE SHIU

References cited in a recent review (1) of isoxazole chemistry indicate the possibility of some confusion between the nitro compounds derived from 5-phenylisoxazole (I) and

Can. J. Chem. Downloaded from www.nrcresearchpress.com by 210.87.254.105 on 09/05/12
For personal use only.

its 3-isomer (II). Thus, Kochetkov and Khomutova (2) report that treatment of 5-phenylisoxazole by mixed nitrating acids at 20° yields two products, having m.p. 171–172° and 115.5–116.5°: these are assigned as 5-*p*-nitrophenylisoxazole (III) and 4-nitro-5-phenylisoxazole (IV). However, Musante (3) reports that 3-phenylisoxazole is nitrated to 3-*p*-nitrophenylisoxazole (V), m.p. 174–176°, while Wieland (4) obtained 4-nitro-3-phenylisoxazole (VI), m.p. 116°, from the action of nitrous fumes on cinnamaldehyde.

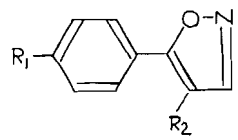

I, $R_1 = R_2 = H$
III, $R_1 = NO_2, R_2 = H$
IV, $R_1 = H, R_2 = NO_2$
VII, $R_1 = R_2 = NO_2$

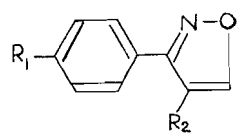

II, $R_1 = R_2 = H$
V, $R_1 = NO_2, R_2 = H$
VI, $R_1 = H, R_2 = NO_2$

In addition to the closely coincident melting points, doubt arises since the structures proposed by the Russian and Italian workers are based in part upon oxidative degradations to *p*-nitrobenzoic or benzoic acid, which would not distinguish between III and V, or between IV and VI. Wieland's assignment of structure VI, which is based on alkaline degradation to benzonitrile, is firmly based.

Since 5- and 3-phenylisoxazoles have quite similar physical properties (5), and syntheses from hydroxymethyleneacetophenone and hydroxylamine (6) yield mixtures of the two isomers, an obvious possibility is that the lower-melting product obtained by Kochetkov and Khomutova is VI, reflecting the presence of some 3-phenylisoxazole in their starting material. This possibility was checked by nitration of a sample of 5-phenylisoxazole prepared by a route claimed to yield only the 5-isomer (7). Our sample was homogeneous on two different gas–liquid chromatographic columns, and its retention times differed from those for a sample of 3-phenylisoxazole, prepared from benzoylvinyl benzoate and hydroxylamine (8). Our 5-phenylisoxazole was further authenticated by conversion into benzoylacetonitrile by methanolic sodium methoxide (9). Experiments using identical conditions with 3-phenylisoxazole showed that 3-phenylisoxazole was largely unaffected by sodium methoxide, although ca. 5% conversion into benzonitrile (identified by comparison of relative retention times on two different chromatographic columns, and also by its infrared absorption) occurred. Neither 3-phenylisoxazole nor benzonitrile could be detected in the reaction mixtures when our sample of 5-phenylisoxazole was treated with methanolic sodium methoxide.

Using this sample, several repetitions of Kochetkov and Khomutova's experiments, and also nitrations using acetyl nitrate (which favors substitution in the *heterocyclic ring* of arylazoles over attack at the aryl groups (10, 11)) yielded *one* mononitro compound, m.p. 176–178°, accompanied in some experiments by a dinitro compound, m.p. 115–117°. The dinitro compound was obtained readily from the mononitro compound using mixed nitrating acids at 80°.

In view of the authentication of our 5-phenylisoxazole sample, the mononitro compound is certainly 5-*p*-nitrophenylisoxazole. Unequivocal proof is furnished by its conversion into *p*-nitrobenzoylacetonitrile by brief refluxing with methanolic sodium methoxide, and is confirmed by its proton magnetic resonance (p.m.r.) spectrum. A solution in dimethyl sulfoxide at 60° shows the following proton signals: four protons in an A_2B_2 aromatic system centered at δ 8.25 (resolved (see (12)) into an A component, δ 8.37, and a B component, δ 8.13, with J_{AB} 9.1 c/s), and two 1-proton doublets (J, 2 c/s) at δ 8.73 (the 3-proton) and δ 7.25 (the 4-proton).

Can. J. Chem. Downloaded from www.nrcresearchpress.com by 210.87.254.105 on 09/05/12
For personal use only.

Can. J. Chem. Downloaded from www.nrcresearchpress.com by 210.87.254.105 on 09/05/12
For personal use only.

Treatment of the dinitro compound with methanolic sodium methoxide yields a high-melting solid showing both carbonyl (1 681 cm^{-1}) and nitrile (2 220 cm^{-1}) infrared absorption bands, but this information is not sufficient for a decision between a 5-(dinitrophenyl) isoxazole and 4-nitro-5-*p*-nitrophenylisoxazole (VII). The proton magnetic resonance spectrum establishes VII as the correct structure: a solution of the dinitro compound in dimethyl sulfoxide shows a 1-proton signal at δ 11.37, and a 4-proton A_2B_2 pattern from the 5-*p*-nitrophenyl group, now centered at δ 7.97 (A component, δ 8.25, B component, δ 7.69, J_{AB} 8.7 c/s). The increased shielding of all the protons of the 5-*p*-nitrophenyl group in VII as compared with III, and the increased internal chemical shift between the A and B protons, may be rationalized readily in terms of mutual twisting of the two rings resulting from the presence of the 4-nitro group, with consequent reduction of inter-ring paramagnetic effects (11, 13). The signal at δ 11.37 is assigned tentatively to the 3-proton, deshielded both by the adjacent ring nitrogen and the nitro group. Although similarly substituted compounds have highly deshielded protons (for example, the 5-proton signal from 4-nitro-1-*p*-nitrophenylpyrazole in dimethyl sulfoxide appears at δ 9.78 (11), and the 2-proton signal from 3-nitroquinoline in acetone appears at δ 9.56 (14)), the 3-proton does appear surprisingly acidic.* It is possible that the highly deshielded proton signal might reflect ring opening of VII in the dimethyl sulfoxide solvent to yield the tautomers VIII and IX: the enolic proton in VIII, or the methine proton in IX, would be expected to be highly deshielded. However, the infrared spectrum of the fission product from the dinitro compound shows little indication that the enol form is significant, while the *p*-nitrobenzoyl fragment of IX would not be expected to generate the observed A_2B_2 pattern (the chemical shifts expected for the A and B protons in *p*-nitroacetophenone (a reasonable model for IX) using parameters suggested by Corio and Dailey (15) would be δ 8.49 and 8.20). In any event, whether ring fission occurs or not, the key finding is an A_2B_2 pattern characteristic of a paradisubstituted compound, which eliminates the possibility of a 5-(dinitrophenyl)isoxazole structure.

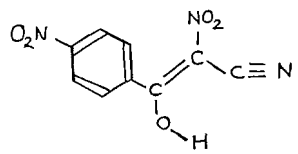

VIII

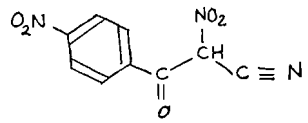

IX

Although the melting range of the dinitro compound VII falls near that quoted by Kochetkov and Khomutova for their lower-melting nitration product, the two materials are not identical, since the Russian workers quote elementary analyses consistent with a mononitro compound, in addition to oxidative degradation to benzoic acid.

We conclude that 4-nitro-5-phenylisoxazole has yet to be prepared, and also suggest that reexamination of the nitration of 3-phenylisoxazole is in order, in view of the close agreement in melting range for our authenticated 5-*p*-nitrophenylisoxazole and Musante's claimed 3-*p*-nitrophenylisoxazole.

EXPERIMENTAL†

5-Phenylisoxazole, b.p. 246°, was prepared from the anil of benzoylacetaldehyde (anilinomethyleneacetophenone) and hydroxylamine, using Panizzi and Monti's method (7). The sample showed only a single peak on gas–liquid chromatography using either Silicone SE-52 or Cyanosilicone XF-1150 partitioning phases supported on Chromosorb P (Aerograph A-90P3 instrument, helium carrier gas, column temperatures 200°

**We are indebted to a referee for bringing this point to our attention.*

†*Analytical services, measurements of melting points, and infrared and p.m.r. spectra were as described in ref. 11.*

and 170°). Its retention time at 170° with the Cyanosilicone column (30% partitioning phase, 10 ft. × 3/8 in., flow rate 60 ml/min) was 8.0 min, while a sample of 3-phenylisoxazole, b.p. 245°, prepared by Panizzi and Sbrillo-Siena's method (8), gave a major peak (95%) with retention time 7.2 min, and a minor peak (5%) at 8.0 min. The minor peak disappeared from the sample after brief refluxing (10 min) with 0.5 *N* methanolic sodium methoxide, and a new minor peak appeared with retention time 2.0 min (area 5% of the 7.2 min component). This minor peak was identified as benzonitrile by comparison of retention times and by direct trapping and measurement of its infrared absorption spectrum. Corresponding treatment of the 5-phenylisoxazole sample with sodium methoxide, followed by acidification and collection of the resulting precipitate, yielded benzoylacetonitrile (40%), m.p. 76° (lit. (9) 81°), ν_{max} 2 247 cm^{-1} (nitrile) and 1 681 cm^{-1} (carbonyl). Neither 3-phenylisoxazole nor benzonitrile could be detected by gas–liquid chromatographic analysis of the mother liquor from the sodium methoxide treatment.

Nitrations

5-Phenylisoxazole was nitrated by mixed nitric acid (*d* 1.42) and sulfuric acid (*d* 1.84), or by nitric acid – acetic anhydride, or by mixed nitric acid (*d* 1.50) and sulfuric acid (*d* 1.84) at 15–20°, using reaction periods ranging from 0.25–1 h (these are the general conditions used in previous work on nitrations of phenyl-substituted heterocyclic compounds (10, 11, 16), and include those used by Kochetkov and Khomutova (2)). The products were collected after pouring the reaction mixtures into ice water, and were purified by careful fractional crystallization or by adsorption chromatography on alumina. 5-*p*-Nitrophenylisoxazole, m.p. 176–178° (p.m.r. spectrum, see above; nitro group infrared absorption at 1 515 and 1 333 cm^{-1}) was obtained in yields of ca. 50% starting from 1 g of 5-phenylisoxazole. The infrared spectra of all crystalline fractions were examined routinely, but there was no evidence for the presence of another mononitro compound in any of the reaction mixtures. In one experiment using mixed nitrating acids and a reaction period of 1 h, a small quantity (ca. 5% yield based on 1 g of 5-phenylisoxazole) of 4-nitro-5-*p*-nitrophenylisoxazole, m.p. 115–117°, was obtained from the fraction most readily soluble in ethanol. This material was identical with a sample prepared by nitration of 5-*p*-nitrophenylisoxazole with mixed nitrating acids for 1 h at 80°, which after crystallization from ethanol had m.p. 115–117° (p.m.r. spectrum, see above; nitro group infrared absorption at 1 504, 1 339, and 1 310 cm^{-1}; anal. calcd. for $C_9H_5N_3O_5$: C, 45.96; H, 2.14; N, 17.87%; found: C, 45.84; H, 2.38; N, 18.10%).

Fission of Nitrophenylisoxazoles by Methoxide

5-*p*-Nitrophenylisoxazole yielded *p*-nitrobenzoylacetonitrile, m.p. 133° (lit. (17) 135°) (infrared absorption: 2 273 (nitrile), 1 690 (carbonyl), 1 515, 1 351 (nitro group) cm^{-1}), when refluxed (10 min) in 0.5 *N* methanolic sodium methoxide, followed by acidification and isolation by ether extraction. Similar treatment of 4-nitro-5-*p*-nitrophenylisoxazole yielded a product, m.p. over 300°, with strong infrared absorption at 1 681, 2 220 (carbonyl, nitrile), 1 511, 1 342, and 1 310 (nitro groups) cm^{-1}.

ACKNOWLEDGMENTS

We thank the National Research Council for support of our work through Operating Grant No. A-964, and Mr. D. G. Smith (Atlantic Regional Laboratory, National Research Council, Halifax) for the measurements of proton magnetic resonance spectra.

1. N. K. KOCHETKOV and S. D. SOKOLOV. *In* Advances in heterocyclic chemistry. Vol. 2. *Edited by* A. R. Katritzky. Academic Press, New York. 1963. p. 365.
2. N. K. KOCHETKOV and E. D. KHOMUTOVA. Zh. Obshch. Khim. **28**, 359 (1958).
3. C. MUSANTE. Farm. sci. e tec. Pavia, **6**, 32 (1951).
4. H. WIELAND. Ann. **328**, 160, 195, 245, 263 (1903).
5. L. CLAISEN. Ber. **42**, 65 (1909).
6. K. v. AUWERS and H. WUNDERLING. Ber. **67**, 638 (1934).
7. L. PANIZZI and E. MONTI. Gazz. Chim. Ital. **77**, 556 (1947).
8. L. PANIZZI and M. SBRILLO-SIENA. Gazz. Chim. Ital. **73**, 335 (1943).
9. K. BOWDEN and E. R. H. JONES. J. Chem. Soc. 953 (1946).
10. M. A. KHAN, B. M. LYNCH, and Y. HUNG. Can. J. Chem. **41**, 1540 (1963).
11. B. M. LYNCH and Y. HUNG. Can. J. Chem. **42**, 1605 (1964).
12. R. E. RICHARDS and T. P. SCHAEFER. Trans. Faraday Soc. **54**, 1280 (1958).
13. L. M. JACKMAN. Applications of nuclear magnetic resonance spectroscopy in organic chemistry. Pergamon Press, London. 1959. p. 126.
14. P. J. BLACK and M. L. HEFFERNAN. Australian J. Chem. **17**, 558 (1964).
15. P. L. CORIO and B. P. DAILEY. J. Am. Chem. Soc. **78**, 3043 (1956).
16. B. M. LYNCH and T. CHAN. Can. J. Chem. **41**, 274 (1963).
17. S. CUSMANDO. Gazz. Chim. Ital. **78**, 764 (1948).

RECEIVED FEBRUARY 8, 1965.
DEPARTMENT OF CHEMISTRY,
ST. FRANCIS XAVIER UNIVERSITY,
ANTIGONISH, NOVA SCOTIA.

Can. J. Chem. Downloaded from www.nrcresearchpress.com by 210.87.254.105 on 09/05/12
For personal use only.

A SYNTHESIS OF 2,2,4-TRIMETHYL-4-HYDROXYTETRAHYDROFURAN, A PRODUCT OF THE PHOTOLYSIS OF 4-METHYL-4-METHOXY-2-PENTANONE

M. A. GIANTURCO AND P. FRIEDEL

It has recently been reported (1) that the photolysis of 4-methyl-4-methoxy-2-pentanone yields methanol, acetone, mesityl oxide, and a "hydroxyfuran." The elemental analysis and the spectral properties suggested that this latter substance should have structure I, which could be derived from the methoxyketone via a seven-membered ring intermediate (1). However, this important product of the photolytic reaction was not compared with a synthetic sample.

We wish to report that compound I can be conveniently obtained by reacting methyl β-methylcrotonate with the oxanion of methyl glycolate in dimethyl sulfoxide, decarboxylating the resultant β-ketoester (2,2-dimethyl-3-carbomethoxytetrahydrofuran-4-one, II) and treating the 2,2-dimethyltetrahydrofuran-4-one so obtained (III) with methylmagnesium iodide. The syntheses of the intermediates II and III were patterned after those of other tetrahydrofuranone derivatives which have been recently prepared in this laboratory (2).

When the synthesis of the intermediate III was attempted by treatment of 4-methylpent-2-yn-1,4-diol (IV) with mercuric oxide and sulfuric acid, a mixture resulted, whose main constituent was identical with a sample of III prepared from II. Two other substances, isolated from the reaction mixture by vapor phase chromatography (v.p.c.) and not submitted to elemental analysis, had infrared spectra which are compatible with the structures of two anticipated by-products of the reaction, i.e., 4-methylpent-4-en-2-yn-1-ol and 4-methylpent-4-en-3-on-1-ol. It was found, however, that the use of the less acidic catalyst described by Colonge *et al.* (3) (mercuric sulfate with no excess of sulfuric acid) suppresses the formation of these by-products and permits another convenient synthesis of III.

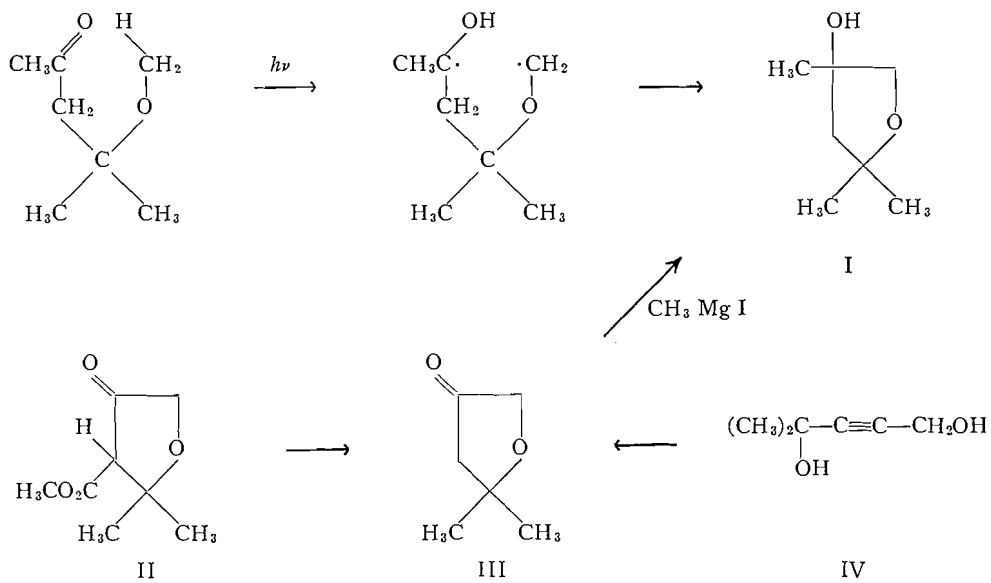

Can. J. Chem. Downloaded from www.nrcresearchpress.com by 210.87.254.5 on 09/05/12
For personal use only.

The identity of synthetic I with the "hydroxyfuran" obtained by photolysis of 4-methyl-4-methoxy-2-pentanone was proved by a comparison of the spectral properties of the two substances (infrared, nuclear magnetic resonance (n.m.r.), and mass spectra), effected through the courtesy of Dr. Petersen of the Aerospace Corporation, El Segundo, California (1).

The potentialities of the now easily available (2) tetrahydrofuran-3-ones as intermediates in the synthesis of 2,3-dihydrofurans (via tosylhydrazones), furans, and γ-lactones are currently being investigated.

EXPERIMENTAL

The infrared spectra were determined on CCl_4 solutions. The n.m.r. spectra were measured in CCl_4 at 60 Mc, with tetramethylsilane as internal standard; chemical shifts are in p.p.m. The mass spectra were determined on a CEC 21-103C instrument. The v.p.c. retention times (R_T) are expressed in minutes and refer to the following conditions: 2m × 0.25 in. silicone rubber column, 15% on acid-washed Chromosorb W (60–80 mesh), 75°, 70 ml He/min.

2,2-Dimethyl-3-carbomethoxytetradrofuran-4-one (II)

This compound was prepared in 40% yield from methyl glycolate and methyl β-methylcrotonate by a procedure completely analogous to that previously employed for the synthesis of other tetrahydrofuranone derivatives (2). Boiling point 41–42° at 0.1 mm; n_D^{23} 1.4497; infrared bands at 5.58, 5.69, 5.92, and 6.07 μ indicate the coexistence of keto and enol forms.

Anal. Calcd. for $C_8H_{12}O_4$: C, 55.81; H, 7.02. Found: C, 55.87; H, 7.25.

Methyl 3-methoxyisovalerate, the only important by-product of the reaction, was isolated by v.p.c. of the forerun of distillation, and was identified by comparison of its infrared spectrum and retention time with those of an authentic sample (4).

2,2-Dimethyltetrahydrofuran-4-one (III)

The decarboxylative hydrolysis of II was effected by 1 h refluxing in 10% H_2SO_4. The usual work-up (ether extraction, drying over Na_2SO_4, removal of the solvent, and distillation) gave III in 73% yield. Boiling point 64° at 50 mm; R_T 5.6; n_D^{25} 1.4259; $\lambda_{CO}^{CCl_4}$ 5.63 μ; $\lambda_{C-O-C}^{CCl_4}$ 9.36 μ; n.m.r.: singlets at δ = 3.88, 2.23, and 1.35, in ratios of 1:1:3.

Anal. Calcd. for $C_6H_{10}O_2$: C, 63.13, H, 8.83. Found: C, 62.98; H, 8.93.

Semicarbazone, m.p. 187–188°.

Anal. Calcd. for $C_7H_{13}N_3O_2$: N, 24.55. Found: N, 24.36.

Treatment of 4-methylpent-2-yn-1,4-diol (IV) as described for the synthesis of 2,2,5,5-tetramethyltetrahydrofuran-3-one from 2,5-dimethylhex-3-yn-2,5-diol (5) resulted in a mixture, which was separated into its components by v.p.c. The main constituent (R_T 5.6) was identical (R_T, infrared) with a sample of III prepared from II. The principal infrared bands of two by-products (see text) occur at the following wavelengths: Compound A (R_T 7.6): 2.75 and 2.90 μ, free and bonded O—H stretching; 3.22 μ, asymmetric stretching olefinic CH_2; 5.54 μ, overtone of δ_{C-H} out-of-plane; 6.15 μ, C=C stretching; 9.80 and 9.90 μ, C—O stretching; 11.10 μ, δ_{C-H} out-of-plane. Compound B (R_T 13.1): 2.85 μ, O—H stretching (intramolecular bond); 5.85, 6.08, and 9.65 μ, C=O, C=C, and C—O stretching; 10.95 μ, δ_{C-H} out of plane; λ_{max}^{EtOH} 231 mμ. However, when a less acidic reaction medium was employed (see text and ref. 3), the formation of compounds A and B was suppressed, and III was obtained in 30% yield.

2,2,4-Trimethyl-4-hydroxytetrahydrofuran (I)

Refluxing for 2 h an ether solution of compound III and methylmagnesium iodide (10% excess) gave, after the usual work-up and distillation, an 87% yield of I. Boiling point 63–64° at 12 mm; n_D^{25} 1.4259; n.m.r.: doublet, 2 protons, centered at δ = 3.60; singlet, 1 proton, δ = 3.27; doublet, 2 protons, centered at δ = 1.80; singlet, 6 protons, δ = 1.30; singlet, 3 protons, δ = 1.20. The mass spectrum showed an extremely weak molecular ion peak (m/e = 130); the principal peaks were at the following m/e values: 43 (100%), 85 (69%), 57 (31%), 115 (30%), and 41 (27%).

Anal. Calcd. for $C_7H_{14}O_2$: C, 64.58; H, 10.84. Found: C, 64.68; H, 10.83.

1. D. J. Coyle, R. V. Petersen, and J. Heicklen. J. Am. Chem. Soc. **86**, 3850 (1964).
2. M. A. Gianturco, P. Friedel, and A. S. Giammarino. Tetrahedron, **20**, 1763 (1964).
3. J. Colonge, R. Falconet, and R. Gaumant. Bull. Soc. Chim. France, 211 (1958).
4. R. B. Wagner. J. Am. Chem. Soc. **71**, 3217 (1949).
5. M. S. Newman (*Editor*). Organic syntheses. Vol. 40. John Wiley and Sons, New York. 1960. p. 88.

Received February 1, 1965.
Fundamental Research Department of the Coca-Cola Co.,
Linden, New Jersey.

Can. J. Chem. Downloaded from www.nrcresearchpress.com by 210.87.254.5 on 09/05/12
For personal use only.

THE EFFECT OF PHENOLS ON THE POLYMERIZATION OF VINYL ACETATE

R. A. BIRD AND K. E. RUSSELL

In studies of the effect of phenols on the free radical polymerization of styrene (1, 2) and methyl methacrylate (3), it was shown that polymer radicals attack phenols by hydrogen abstraction at the OH group. The rates of hydrogen abstraction by polystyryl radicals vary widely with the phenol; the transfer constants for simple phenols at 60 °C are in the range 0.001 to 0.008 while that for pyrogallol is 1.04. Phenols are much less reactive towards polymethyl methacrylate radicals, the transfer constant for pyrogallol being only 0.0026 at 45 °C.

The effect of phenols on the polymerization of vinyl acetate was investigated because polyvinyl acetate radicals have a much higher reactivity in transfer reactions (4) and the transfer constants for simple phenols are more easily measured. The results for such phenols provide information concerning the extent to which polar factors influence the rates of hydrogen abstraction by polymer radicals. Both deuterated and undeuterated phenols were used in the study in order to test the validity of Bagdasar'ian and Sinitsina's conclusion (5) that hydrogen atoms of phenolic OH groups do not participate directly in reactions with polyvinyl acetate radicals. A large isotope effect shows that polyvinyl acetate radicals attack almost exclusively at the OH group but a smaller effect indicates that there is a simultaneous addition to the ring to give a stabilized cyclohexadienyl radical.

EXPERIMENTAL

Vinyl acetate was fractionally distilled and prepolymerized at 70 °C under nitrogen using azobisisobutyronitrile as initiator. After approximately 10% had polymerized, the monomer was again distilled and the middle fraction retained. It was dried over calcium chloride, degassed, and distilled three times on the high vacuum line. The phenols were purified by distillation or recrystallization. Azobisisobutyronitrile was recrystallized from ether and stored at 0 °C.

The procedure was similar to that used with methyl methacrylate (3). Initiator concentrations were close to 0.004 M and phenol concentrations were usually in the range 0.002–0.02 M. In experiments with deuterated phenols, 0.05 g heavy water was added to the reaction mixture and it was shown that heavy water did not affect the rate of polymerization or molecular weight in the absence of phenol. After about 3% conversion of monomer to polymer, the reaction tubes were cooled to 0 °C on removal from the bath at 45 °C, and the contents diluted with acetone. The solution was added dropwise with vigorous stirring to 500 ml petroleum ether and allowed to stand for 5 h before filtration. The polymer was dried *in vacuo* at 60 °C, weighed, and stored in dry stoppered tubes to prevent absorption of moisture.

Intrinsic viscosities of the polyvinyl acetate samples were determined at 25 °C using acetone as solvent. Average degrees of polymerization $\bar{P}_n$ were calculated using the relationship quoted by Fuhrman and Mesrobian (6)

$$\bar{P}_n = 2.57[\eta_l]^{1.40}$$

where η_l is the limiting viscosity number.

RESULTS AND DISCUSSION

Phenols act as fairly strong retarders in the polymerization of vinyl acetate, the rate of polymerization at 45 °C being reduced to two thirds of its normal value by the addition of phenol at a concentration of 0.009 M or 2,3,4,6-tetramethylphenol at a concentration of 0.0002 M. With the exceptions of 3-acetyl- and 3-cyano-phenols, the deuterated phenols are much weaker retarders than the corresponding phenols so that the main transfer reaction occurs by attack of the polyvinyl acetate radical on the OH group.

The transfer constant C is the ratio k_{tr}/k_p where k_{tr} is the rate constant of reaction [1] and k_p is the rate constant for the propagation process. When the polymerization of

Can. J. Chem. Downloaded from www.nrcresearchpress.com by 210.87.254.5 on 09/05/12
For personal use only.

[1] 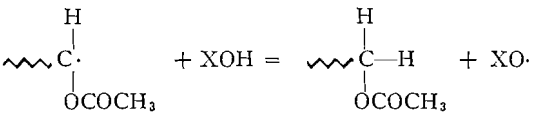

vinyl acetate is retarded by phenols, the proportion of XO· radicals lost in cross-termination reactions with polyvinyl acetate radicals or by mutual termination is not known. Three estimates of the transfer constant for each phenol have been made from the molecular weight data, using equations derived assuming various fates for the XO· radicals (1), and the mean values are given as C_1 in Table I. The required transfer constant to monomer at 45 °C was determined experimentally to be 2.0×10^{-4}; a value of 20.5 mole l^{-1} s was used for $2k_t/k_p^2$ (7, 8), $2k_t$ being the rate constant for the mutual termination of polyvinyl acetate radicals, a process which occurs almost entirely by disproportionation (9). Transfer constants may also be derived from the rates of polymerization provided that it is assumed that none of the XO· radicals formed by reaction [1] reinitiate polymerization. Three estimates of the transfer constant have been made using equations derived by Jenkins (10) and the mean values are given as C_2 in Table I. The uncertainty in C_1 and C_2 arises largely from the lack of knowledge concerning the termination reactions, individual estimates differing by as much as 35% from the mean.

TABLE I

Transfer constants for phenols and deuterated phenols at 45 °C

	Phenols		Deuterated phenols		
	C_1	C_2	C_1	C_2	Ratios (r)
Phenol	0.019	0.024	0.002	0.005	6.1
3-Chlorophenol	0.027	0.014	0.007	0.007	2.9
3-Methylphenol	0.046	0.029	0.012	0.005	4.4
3-Acetylphenol	0.160	0.121	0.137	0.121	1.1
3-Cyanophenol	0.069	0.095	0.067	0.094	1.0
4-Chlorophenol	0.046	0.034	0.010	0.006	5.0
4-Methylphenol	0.071	0.071	0.015	0.011	5.5
2,3,4,6-Tetramethylphenol	0.94	1.32	0.075	0.085	14.1

The ratios r of the means of C_1 and C_2 for each phenol and its deuterated counterpart are given in Table I. The fairly large values of r for phenol, the chlorophenols, the cresols, and 2,3,4,6-tetramethylphenol confirm that the main rate-determining step in the transfer process is the hydrogen abstraction reaction [1]. The greatest isotope effect is observed for 2,3,4,6-tetramethylphenol and the lower value of r for phenol suggests that addition to the nucleus, which is now less sterically hindered, may compete with hydrogen transfer. A referee points out that preferential activation of the nucleus towards the addition of a polyvinyl acetate radical appears to occur when the phenol contains a meta substituent. For the electron-withdrawing substituents the ratio r decreases through chlorine ($r = 2.9$) and acetyl ($r = 1.1$) to a minimum ($r = 1.0$) with cyano in 3-cyanophenol, corresponding to the increasing importance of addition to the nucleus relative to attack at the OH group.

Analysis of the results by the method of Allen, Merrett, and Scanlan (11) shows that the efficiency of reinitiation of polymerization by XO· radicals formed in the transfer process is generally low. This conclusion is supported by the fair agreement between values of C_1 and C_2, since C_2 has been calculated on the assumption that no reinitiation occurs. In contrast, the efficiency of reinitiation of the polymerization of methyl methacrylate by XS· radicals derived from aromatic thiols is greater than 90% (3).

Can. J. Chem. Downloaded from www.nrcresearchpress.com by 210.87.254.5 on 09/05/12
For personal use only.

Of the meta-substituted phenols investigated, only 3-chloro- and 3-methyl-phenol are attacked primarily at the OH group. Their transfer constants are not greatly different from that of phenol and it is probable that inductive effects are not of great importance in this hydrogen-abstraction reaction. 4-Methyl- and 4-chloro-phenol have higher transfer constants than the corresponding meta-substituted phenols, presumably due to weak contributions to the transition state of polar structures in which an electron has been donated by the phenol to the radical (12). Inductive and resonance effects from these single substituents are small but the total effect of the four methyl groups in 2,3,4,6-tetramethylphenol is large enough to increase its transfer constant to 1.

The ratios of transfer constants for 2,3,4,6-tetramethylphenol towards polymethyl methacrylate (3), polystyryl (1), and polyvinyl acetate radicals are approximately 0.02:1:18 while those for the hydrocarbon toluene are 4:1:170. The difference in relative reactivities of polystyryl and polymethyl methacrylate radicals towards phenols and toluene is interpreted (3) in terms of contributions to the transition state of polar structures in which an electron has been donated by the radical to the phenol. Such contributions are significant in reactions between polystyryl radicals and phenols but are not important in polymethyl methacrylate reactions because of the electron-withdrawing character of the ester group (13). On this interpretation, polar structures with the polyvinyl acetate radical as donor and 2,3,4,6-tetramethylphenol as acceptor contribute to the transition state of this hydrogen-abstraction reaction but are less important than those involved in the corresponding reaction with polystyryl radicals.

ACKNOWLEDGMENTS

The authors are grateful to the National Research Council for a grant. The vinyl acetate was a gift from Du Pont of Canada.

1. M. P. Godsay, G. A. Harpell, and K. E. Russell. J. Polymer Sci. **57**, 641 (1962).
2. R. A. Bird, G. A. Harpell, and K. E. Russell. Can. J. Chem. **40**, 601 (1962).
3. S. C. Barton, R. A. Bird, and K. E. Russell. Can. J. Chem. **41**, 2737 (1963).
4. S. R. Palit and S. K. Das. Proc. Roy. Soc. London, Ser. A, **226**, 82 (1954).
5. Kh. S. Bagdasar'ian and Z. A. Sinitsina. J. Polymer Sci. **52**, 31 (1961).
6. N. Fuhrman and R. B. Mesrobian. J. Am. Chem. Soc. **76**, 3281 (1954).
7. M. S. Matheson, E. E. Auer, E. B. Bevilacqua, and E. J. Hart. J. Am. Chem. Soc. **71**, 2610 (1949).
8. C. Walling. Free radicals in solution. John Wiley and Sons, New York. 1957. p. 95.
9. B. L. Funt and W. Pasika. Can. J. Chem. **38**, 1865 (1960).
10. A. D. Jenkins. Trans. Faraday Soc. **54**, 1885 (1958).
11. P. W. Allen, F. M. Merrett, and J. Scanlan. Trans. Faraday Soc. **51**, 95 (1955).
12. J. A. Howard and K. U. Ingold. Can. J. Chem. **41**, 1744 (1963).
13. C. Walling. Free radicals in solution. John Wiley and Sons, New York. 1957. p. 157.

Received February 8, 1965.
Department of Chemistry,
Queen's University,
Kingston, Ontario.

PREPARATION OF 4,4″-BIS(DIPHENYLAMINES) BY THE CHAPMAN REARRANGEMENT

Robert Barclay, Jr.

Very few applications of 4,4″-bis(diphenylamines) to the synthesis of condensation polymers have been reported. Exploratory studies in this area required the development of a convenient laboratory preparation of the diamines, preferably from the corresponding

Can. J. Chem. Downloaded from www.nrcresearchpress.com by 210.87.254.5 on 09/05/12
For personal use only.

Of the meta-substituted phenols investigated, only 3-chloro- and 3-methyl-phenol are attacked primarily at the OH group. Their transfer constants are not greatly different from that of phenol and it is probable that inductive effects are not of great importance in this hydrogen-abstraction reaction. 4-Methyl- and 4-chloro-phenol have higher transfer constants than the corresponding meta-substituted phenols, presumably due to weak contributions to the transition state of polar structures in which an electron has been donated by the phenol to the radical (12). Inductive and resonance effects from these single substituents are small but the total effect of the four methyl groups in 2,3,4,6-tetramethylphenol is large enough to increase its transfer constant to 1.

The ratios of transfer constants for 2,3,4,6-tetramethylphenol towards polymethyl methacrylate (3), polystyryl (1), and polyvinyl acetate radicals are approximately 0.02:1:18 while those for the hydrocarbon toluene are 4:1:170. The difference in relative reactivities of polystyryl and polymethyl methacrylate radicals towards phenols and toluene is interpreted (3) in terms of contributions to the transition state of polar structures in which an electron has been donated by the radical to the phenol. Such contributions are significant in reactions between polystyryl radicals and phenols but are not important in polymethyl methacrylate reactions because of the electron-withdrawing character of the ester group (13). On this interpretation, polar structures with the polyvinyl acetate radical as donor and 2,3,4,6-tetramethylphenol as acceptor contribute to the transition state of this hydrogen-abstraction reaction but are less important than those involved in the corresponding reaction with polystyryl radicals.

ACKNOWLEDGMENTS

The authors are grateful to the National Research Council for a grant. The vinyl acetate was a gift from Du Pont of Canada.

1. M. P. Godsay, G. A. Harpell, and K. E. Russell. J. Polymer Sci. **57**, 641 (1962).
2. R. A. Bird, G. A. Harpell, and K. E. Russell. Can. J. Chem. **40**, 601 (1962).
3. S. C. Barton, R. A. Bird, and K. E. Russell. Can. J. Chem. **41**, 2737 (1963).
4. S. R. Palit and S. K. Das. Proc. Roy. Soc. London, Ser. A, **226**, 82 (1954).
5. Kh. S. Bagdasar'ian and Z. A. Sinitsina. J. Polymer Sci. **52**, 31 (1961).
6. N. Fuhrman and R. B. Mesrobian. J. Am. Chem. Soc. **76**, 3281 (1954).
7. M. S. Matheson, E. E. Auer, E. B. Bevilacqua, and E. J. Hart. J. Am. Chem. Soc. **71**, 2610 (1949).
8. C. Walling. Free radicals in solution. John Wiley and Sons, New York. 1957. p. 95.
9. B. L. Funt and W. Pasika. Can. J. Chem. **38**, 1865 (1960).
10. A. D. Jenkins. Trans. Faraday Soc. **54**, 1885 (1958).
11. P. W. Allen, F. M. Merrett, and J. Scanlan. Trans. Faraday Soc. **51**, 95 (1955).
12. J. A. Howard and K. U. Ingold. Can. J. Chem. **41**, 1744 (1963).
13. C. Walling. Free radicals in solution. John Wiley and Sons, New York. 1957. p. 157.

Received February 8, 1965.
Department of Chemistry,
Queen's University,
Kingston, Ontario.

PREPARATION OF 4,4″-BIS(DIPHENYLAMINES) BY THE CHAPMAN REARRANGEMENT

Robert Barclay, Jr.

Very few applications of 4,4″-bis(diphenylamines) to the synthesis of condensation polymers have been reported. Exploratory studies in this area required the development of a convenient laboratory preparation of the diamines, preferably from the corresponding

Can. J. Chem. Downloaded from www.nrcresearchpress.com by 210.87.254.105 on 09/05/12
For personal use only.

diphenols. The method of choice, involving the Chapman rearrangement (1) in its key step, is a standard synthesis of diarylamines, but has apparently not previously been applied to diphenols.

Imido esters (Table I) are prepared from the phenol and the imidoyl chloride in the presence of an acid-acceptor. While anhydrous conditions are commonly employed (2), it was found at least equally convenient to carry out this reaction under conditions suitable for the preparation of polyphenyl esters by interfacial polycondensation (3). In suitable reaction media, both N-arylimidoyl chlorides (4) and acyl halides (5) undergo solvolysis by mechanisms involving a rate-determining ionization step, the rates being increased by the addition of amines; therefore, the similarity in their reactions with aqueous aryloxide ions was not unexpected. The yields were good, but not quantitative; small amounts of benzanilide and of unchanged diphenol were often recovered. Although the pure imido esters are solids with fairly high melting points, it was often difficult to obtain them in a crystalline form. It was, nevertheless, expedient to purify the imido esters, since pure benzamides could not be isolated from the products of rearrangement of crude intermediates.

Rearrangement was effected by heating the molten imido esters in a nitrogen atmosphere at temperatures in the range 220–280° (Table II). In most cases the reaction could be followed by observation of changes in the infrared spectra, especially in the C—O and C—N stretching region. The imido esters exhibited strong bands in the ranges 1206–1225 and 1266–1271 cm^{-1}, while the amides absorbed at 1326–1339 and 1289–1294 cm^{-1}. As reported by Chapman (6) and others (7), reaction is facilitated by electron-attracting substituents in the aryl groups derived from the original phenol. With the benzimidates I and II, for example, rearrangement was complete within 1 h at 240° and 3 h at 220°, respectively.

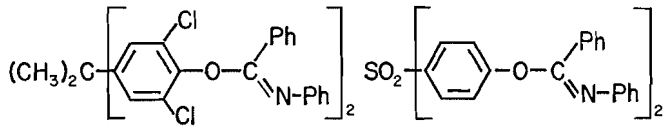

I II

The dibenzoyl derivatives were hydrolyzed to the free 4,4″-bis(diphenylamines) (Table III) by treatment with potassium hydroxide in hot aqueous ethanol. Conversion in this step appeared to be essentially quantitative. A sample of 4,4″-methylenebis(diphenylamine) prepared in this way was identical with the diamine obtained (8) by the condensation of diphenylamine with formaldehyde.

The methods described above were extended to the preparation of the polymeric substances IV and V. Since the reduced viscosities of IV and V were 0.15 and 0.12, respectively, it is probable that little change in molecular weight accompanied the rearrangement.

EXPERIMENTAL

Melting points are uncorrected. Infrared spectra (except those of the polymers) were determined on glasses obtained by cooling the molten substance or as Nujol mulls; a Beckman IR5 spectrophotometer was used. Tabulated yields refer to once-recrystallized material. Microanalyses were performed by Galbraith Laboratories, Inc., Knoxville, Tennessee. Reduced viscosities were measured in methylene chloride at 25° (0.2 g of polymer/100 ml of solution).

Diphenol N-phenylbenzimidates.—In a 250-ml, three-necked Morton-type flask with stirrer, dropping funnel, and thermometer were placed 0.04 mole of the diphenol, 0.0816 mole of sodium hydroxide, 3.3 g of

Can. J. Chem. Downloaded from www.nrcresearchpress.com by 210.87.254.105 on 09/05/12
For personal use only.

Can. J. Chem. Downloaded from www.nrcresearchpress.com by 210.87.254.105 on 09/05/12
For personal use only.

TABLE I

Diphenol N-phenylbenzimidates

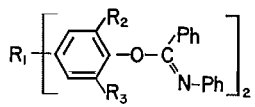

						C, %		H, %		N, %	
R_1	R_2	R_3	Yield, %	M.p., °C	Formula	Calcd.	Found	Calcd.	Found	Calcd.	Found
$C(CH_3)_2$	H	H	74	138–139*	$C_{41}H_{34}N_2O_2$	83.93	83.82	5.84	5.77	4.77	4.61, 4.53
$C(CH_3)_2$	Cl	Cl	74	170.5–174*	$C_{41}H_{30}Cl_4N_2O_2$	67.97	68.05	4.17	4.21	3.87	—
SO_2	H	H	80	141.5–144†	$C_{38}H_{28}N_2O_4S$	74.98	74.63	4.64	4.77	4.60	—
CH_2	H	H	60	124–127‡	$C_{39}H_{30}N_2O_2$	83.85	83.76	5.41	5.32	5.01	4.97

*Recrystallized from benzene–ethanol.
†Recrystallized from acetone–ethanol.
‡Recrystallized from toluene–heptane.

Can. J. Chem. Downloaded from www.nrcresearchpress.com by 210.87.254.105 on 09/05/12
For personal use only.

TABLE II

Dibenzoyl derivatives of 4,4″-bis(diphenylamines)

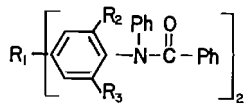

R_1	R_2	R_3	Reaction Time, h	Reaction Temp., °C	Yield, %	M.p., °C	Formula	C, % Calcd.	C, % Found	H, % Calcd.	H, % Found	N, % Calcd.	N, % Found
$C(CH_3)_2$	H	H	20	260–280	92	170–171*	$C_{41}H_{34}N_2O_2$	83.93	83.66	5.84	5.97	4.77	4.81, 4.74
$C(CH_3)_2$	Cl	Cl	2.7	234–241	83	207–209*,†	$C_{41}H_{30}Cl_4N_2O_2$	67.97	67.76	4.17	4.10	3.87	—
SO_2	H	H	4	218–222	97‡	208–210§	$C_{38}H_{28}N_2O_4S$	74.98	76.44, 76.52	4.64	4.78, 4.83	4.60	—
CH_2	H	H	19	265–275	69	197–198.5‖	$C_{39}H_{30}N_2O_2$	83.85	84.02	5.41	5.59	5.01	4.95
2,2″-$CH_2[C_6H_4$—N(Ph)—C(Ph)=O]$_2$			21.5	260–270	26¶	201.5–206¶	$C_{39}H_{30}N_2O_2$	—	—	—	—	—	—

*Recrystallized from ethanol.
†Melt cloudy to about 234°.
‡Yield of crude product, m.p. 205.5–208.5°.
§Recrystallized from benzene; evidently not pure.
‖Recrystallized from toluene.
¶Prepared from an impure, resinous imido ester; recrystallized from toluene–ethanol, but not obtained pure.

Can. J. Chem. Downloaded from www.nrcresearchpress.com by 210.87.254.105 on 09/05/12
For personal use only.

TABLE III

4,4″-Bis(diphenylamines)

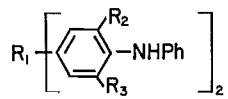

						C, %		H, %		N, %	
R_1	R_2	R_3	Yield, %	M.p., °C	Formula	Calcd.	Found	Calcd.	Found	Calcd.	Found
$C(CH_3)_2$	H	H	85	98.5–99.5*,†	$C_{27}H_{26}N_2$	—	—	—	—	7.40	7.74 7.40
$C(CH_3)_2$	Cl	Cl	74	172–173.5*	$C_{27}H_{22}Cl_4N_2$‡	62.81	62.86	4.30	4.29	5.43	5.38
SO_2	H	H	85	221–223§	$C_{24}H_{20}N_2O_2S$‖	71.97	72.14	5.03	5.24	7.00	7.01
CH_2	H	H	80	121–122*,¶	$C_{25}H_{22}N_2$	—	—	—	—	—	—
2,2″-$CH_2(C_6H_4NHPh)_2$			62	121–122*, **	$C_{25}H_{22}N_2$	85.68	84.79 84.54	6.33	6.10 5.99	7.99	7.75

*Recrystallized from ethanol.
†D. Craig (11) reported m.p. 99–100°.
‡Anal. Calcd.: Cl, 27.47. Found: Cl, 27.28.
§Recrystallized from acetone–ethanol.
‖Anal. Calcd.: S, 8.01. Found: S, 8.27.
¶D. Craig (8) reported m.p. 122–123° (higher melting form).
**This compound was evidently not pure. Mixture melting point with the 4,4″-isomer exhibited strong depression.

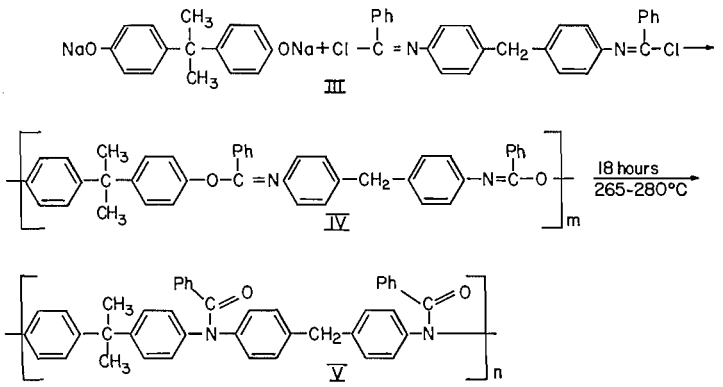

sodium chloride, 30 ml of water, and 40 ml of methylene chloride. A solution of 0.08 mole of N-phenylbenzimidoyl chloride (9) in 70 ml of methylene chloride was added with rapid stirring over 2–3 hours at 23–27°. The solution was diluted with 200 ml of water, the layers were separated, and the aqueous phase was extracted with three 100-ml portions of methylene chloride. The combined organic solution was washed with three 100-ml portions of water and dried over anhydrous magnesium sulfate. The methylene chloride was removed by distillation, leaving the crude imido ester as a residue product.

Rearrangement.—The purified imido ester was heated by means of an oil bath in a large test tube with side arm. Dry nitrogen gas was bubbled through the melt. When the reaction was complete, the cooled glassy reaction product was recrystallized from a suitable solvent.

Hydrolysis.—The preparation of 4,4″-isopropylidenebis(diphenylamine) is typical. A mixture of 32.9 g (0.0561 mole) of 4,4″-isopropylidenebis(diphenylbenzamide), 16.5 g (0.25 mole) of potassium hydroxide pellets, 135 ml of ethanol, and 15 ml of water was heated under reflux for 22 hours. The cooled reaction mass was diluted with 500 ml of water and extracted with a total of 500 ml of methylene chloride in three portions. The combined extract was washed with three 150-ml portions of water and dried over magnesium sulfate. Removal of methylene chloride by distillation left as a residue 19.84 g (94%) of crude diamine. Recrystallization from 180 ml of ethanol gave 18.10 g (85%) of 4,4″-isopropylidenebis(diphenylamine), m.p. 98–100°.

4,4″-Methylenebis(diphenylamine).—This compound was prepared via the Chapman rearrangement. However, preparation by the condensation of diphenylamine with formaldehyde (8) is more convenient.

A mixture of 2 249 g (13.29 moles) of diphenylamine, 136 g (1.68 moles) of 37% formaldehyde solution, 9 ml of concentrated hydrochloric acid, and 2.2 l of ethanol was heated under reflux (80–81°) for 1 h. The solution was cooled and divided into six portions, each of which was added to a mixture of 3 g of sodium hydroxide, 1.65 l of water, and 1.0 kg of crushed ice in a Waring Blendor. The precipitated solids were collected by filtration, washed thoroughly with water, and dried in a vacuum oven at 40°. The unchanged diphenylamine (1 700 g) was recovered by distillation to a final pot temperature of 230° (0.2 mm), and a crude product fraction was obtained by heating to a pot temperature of 358° (0.75 mm). The diamine was purified by redistillation, 294.8 g being collected, b.p. 259–286° (0.25–0.55 mm). Recrystallization from 5.75 l of ethanol gave 207.8 g (36.6%, based on diphenylamine not recovered) of 4,4″-methylenebis(diphenylamine), m.p. 121–123°.

Imidoyl chloride III.—Reaction of 4,4′-methylenedianiline with benzoyl chloride and pyridine in chloroform gave the dibenzoyl derivative, m.p. 250–251.7° (250° (10)). A mixture of 20.4 g (0.0502 mole) of the latter and 22 ml (0.30 mole) of thionyl chloride was heated under reflux for 3.5 h by means of an oil bath kept at 110–113°. Unchanged thionyl chloride was removed by distillation under reduced pressure (bath temperature 125°), giving 22.1 g (99%) of the yellow imidoyl chloride III. After two recrystallizations from toluene–heptane there remained 16.3 g (73%) of nearly pure III, m.p. 140–143°.

Anal. Calcd. for $C_{27}H_{20}Cl_2N_2$: Cl, 16.0. Found: Cl, 15.7, 15.8.

Poly-(imido ester) IV.—The polymer was prepared from 10.27 g (0.0450 mole) of bisphenol A, 19.95 g (0.0450 mole) of III and 3.72 g (0.091 mole) of sodium hydroxide essentially as described above for the N-phenylbenzimidates. Addition of III required 3 hours, the temperature being maintained at 14–16°. The polymer was precipitated by addition of the water-washed methylene chloride solution to 1.6 l of ethanol in a Waring Blendor and dried overnight in a vacuum oven at 60°. The yield of polymer, reduced viscosity 0.15, was 22.3 g (83%).

The infrared spectrum, measured as a potassium bromide pellet, included typical imido ester bands at 1 208 and 1 267 cm^{-1}.

Polyamide V.—The polymer IV was heated in a nitrogen atmosphere for 18 h at 265–270°. The resulting polymer, reduced viscosity 0.12, exhibited infrared absorption bands at 1 294 and 1 330 cm^{-1}, typical of N,N-diarylbenzamides.

Can. J. Chem. Downloaded from www.nrcresearchpress.com by 210.87.254.105 on 09/05/12
For personal use only.

ACKNOWLEDGMENT

The technical assistance of Mr. Arno Lehmann and Mr. Arthur E. Dieffenbach is gratefully acknowledged.

1. F. MÖLLER. *In* Methoden der organischen Chemie. Houben-Weyl. Vol. XI/1. 4th ed. *Edited by* E Müller. Georg Thieme Verlag, Stuttgart. 1957. pp. 910–913.
2. A. P. T. EASSON. J. Chem. Soc. 1029 (1961).
3. W. M. EARECKSON III. J. Polymer Sci. **40**, 399 (1959).
4. I. UGI, F. BECK, and U. FETZER. Chem. Ber. **95**, 126 (1962).
5. R. F. HUDSON and G. E. MOSS. J. Chem. Soc. 5157 (1962).
6. A. W. CHAPMAN. J. Chem. Soc. 1743 (1927).
7. K. B. WIBERG and B. I. ROWLAND. J. Am. Chem. Soc. **77**, 2205 (1955).
8. D. CRAIG. J. Am. Chem. Soc. **55**, 3723 (1933).
9. J. v. BRAUN and W. PINKERNELLE. Ber. **67B**, 1218 (1934).
10. J. v. BRAUN and O. KRUBER. Ber. **45**, 2977 (1912).
11. D. CRAIG. J. Am. Chem. Soc. **60**, 1458 (1938).

RECEIVED FEBRUARY 5, 1965.
UNION CARBIDE CORPORATION, PLASTICS DIVISION,
RESEARCH AND DEVELOPMENT DEPARTMENT,
BOUND BROOK, NEW JERSEY.

THE IONIZATION OF SOME TYPICAL WEAK BASES IN CONCENTRATED PERCHLORIC ACID

KEITH YATES AND HENRY WAI

In connection with a study of the acidity of 0–80% perchloric acid, we have investigated the behavior of nine typical weak organic bases in this medium. These include representatives of the amine, carbonyl, and ether type of base. All these classes have been extensively investigated in sulfuric acid (1) but little is known of their stability, spectral changes, and basicity constants in perchloric acid. We find that the amines and carbonyl compounds are quite stable even at the highest acid concentrations used and although there is some evidence of slow decomposition of phenol and anisole in these solutions, even these compounds are quite stable within the usual time required to measure ultraviolet spectra. This is in contrast to their behavior in sulfuric acid where rapid and irreversible sulfonation of phenols and anisoles occurs at the acidities required to measure their pK values.

TABLE I

Ultraviolet absorption in perchloric acid at 25 °C

Compound	λ_B* (mμ)	ϵ_B*	λ_{BH^+}† (mμ)	ϵ_{BH^+}†
2-Chloro-4,6-dinitroaniline	350	13 000	350	390
N,*N*-Dimethyl-2,4,6-trinitroaniline	385	13 600	385	110
Benzoic acid	230	10 300	258	14 100
Benzamide	225	8 900	240	11 900
Benzaldehyde	250	11 400	295	19 200
Acetophenone	250	12 000	295	20 200

*Measured in acid solutions about 2 H_0 units greater than pK.
†Measured in acid solutions about 2 H_0 units less than pK.

Can. J. Chem. Downloaded from www.nrcresearchpress.com by 210.87.254.105 on 09/05/12
For personal use only.

ACKNOWLEDGMENT

The technical assistance of Mr. Arno Lehmann and Mr. Arthur E. Dieffenbach is gratefully acknowledged.

1. F. MÖLLER. *In* Methoden der organischen Chemie. Houben-Weyl. Vol. XI/1. 4th ed. *Edited by* E Müller. Georg Thieme Verlag, Stuttgart. 1957. pp. 910–913.
2. A. P. T. EASSON. J. Chem. Soc. 1029 (1961).
3. W. M. EARECKSON III. J. Polymer Sci. **40**, 399 (1959).
4. I. UGI, F. BECK, and U. FETZER. Chem. Ber. **95**, 126 (1962).
5. R. F. HUDSON and G. E. MOSS. J. Chem. Soc. 5157 (1962).
6. A. W. CHAPMAN. J. Chem. Soc. 1743 (1927).
7. K. B. WIBERG and B. I. ROWLAND. J. Am. Chem. Soc. **77**, 2205 (1955).
8. D. CRAIG. J. Am. Chem. Soc. **55**, 3723 (1933).
9. J. v. BRAUN and W. PINKERNELLE. Ber. **67B**, 1218 (1934).
10. J. v. BRAUN and O. KRUBER. Ber. **45**, 2977 (1912).
11. D. CRAIG. J. Am. Chem. Soc. **60**, 1458 (1938).

RECEIVED FEBRUARY 5, 1965.
UNION CARBIDE CORPORATION, PLASTICS DIVISION,
RESEARCH AND DEVELOPMENT DEPARTMENT,
BOUND BROOK, NEW JERSEY.

THE IONIZATION OF SOME TYPICAL WEAK BASES IN CONCENTRATED PERCHLORIC ACID

KEITH YATES AND HENRY WAI

In connection with a study of the acidity of 0–80% perchloric acid, we have investigated the behavior of nine typical weak organic bases in this medium. These include representatives of the amine, carbonyl, and ether type of base. All these classes have been extensively investigated in sulfuric acid (1) but little is known of their stability, spectral changes, and basicity constants in perchloric acid. We find that the amines and carbonyl compounds are quite stable even at the highest acid concentrations used and although there is some evidence of slow decomposition of phenol and anisole in these solutions, even these compounds are quite stable within the usual time required to measure ultraviolet spectra. This is in contrast to their behavior in sulfuric acid where rapid and irreversible sulfonation of phenols and anisoles occurs at the acidities required to measure their pK values.

TABLE I

Ultraviolet absorption in perchloric acid at 25 °C

Compound	λ_B* (mμ)	ϵ_B*	λ_{BH^+}† (mμ)	ϵ_{BH^+}†
2-Chloro-4,6-dinitroaniline	350	13 000	350	390
N,*N*-Dimethyl-2,4,6-trinitroaniline	385	13 600	385	110
Benzoic acid	230	10 300	258	14 100
Benzamide	225	8 900	240	11 900
Benzaldehyde	250	11 400	295	19 200
Acetophenone	250	12 000	295	20 200

*Measured in acid solutions about 2 H_0 units greater than pK.
†Measured in acid solutions about 2 H_0 units less than pK.

Can. J. Chem. Downloaded from www.nrcresearchpress.com by 210.87.254.105 on 09/05/12
For personal use only.

Can. J. Chem. Downloaded from www.nrcresearchpress.com by 210.87.254.105 on 09/05/12
For personal use only.

The ultraviolet spectra of most of the bases studied change in the expected way with increasing acid concentration. The absorption characteristics of the bases and their conjugate acids are listed in Table I. Plots of extinction coefficient against acidity (H_0) give the usual smooth sigmoid plots for the amines and carbonyl compounds, allowing pK values to be determined for these bases using standard methods (2). The upper and lower arms of these sigmoid curves should be flat in the absence of complicating medium effects which are not associated with protonation, and in fact are generally less sloping than those obtained for the same bases in sulfuric acid. This indicates that medium effects on spectra are less serious in perchloric acid. However, the spectra of anisole, phenol, and *p*-nitroanisole do not change with acidity in any simple way. The main absorption peaks in the 260 mμ region decrease continuously in intensity over a wide range of acid until by about 70% $HClO_4$ they are about half as intense as in dilute acid. It is unlikely that this change can be associated with protonation since it takes place over a range of 8–9 H_0 units and does not give any inflection point. At higher acidities new absorption bands appear as shoulders in the 285 mμ region and plots of ϵ at these wavelengths against H_0 give the beginnings of typical sigmoid ionization curves, suggesting that protonation does not occur with these bases until H_0 is less than -9.

TABLE II

Comparison of pK values* and indicator slopes of typical weak bases in perchloric and sulfuric acids at 25 °C

Base	Perchloric acid		Sulfuric acid†		Ref.	ΔpK
	pK	Slope	pK	Slope		
Benzamide	−2.03	0.77	−2.1	0.66	6	0.07
	−2.10				7	
N,*N*-Dimethyl-2,4,6-trinitroaniline	−4.54	1.22	−4.98	1.30	8	0.44
2-Chloro-4,6-dinitroaniline	−6.83	0.99	−6.68	0.98		−0.15
Acetophenone	−7.00	0.56	−6.45	0.73	9	−0.55
			−6.36		10	
Benzaldehyde	−7.90	0.72	−7.39	0.82		−0.53
			−7.47		11	
Benzoic acid	−8.85	0.83‡	−7.62	0.84‡		−1.23
			−7.66		12	
Phenol	<-9	—	−7.06	—	3	—
Anisole	<-9	—	−6.82	—	3	—
4-Nitroanisole	−10.01	0.92	—	—		—

*These were obtained by plotting log $(\epsilon_B - \epsilon)/(\epsilon - \epsilon_{BH^+})$ versus H_0. The wavelength chosen was that which gave the smoothest sigmoid titration curve on a nonlogarithmic plot. All H_0 values were taken from ref. 5.
†Values in sulfuric acid redetermined in the present work except where noted.
‡The method of Stewart and Granger (2*b*) gives somewhat higher slopes.

The pK values of the bases have been obtained, where possible, from conventional plots of log $[BH^+]/[B]$ against H_0. These resulted in good linear plots and the slopes and pK values are listed in Table II. According to the defining equation for H_0 these slopes should be equal to unity if the bases exhibit similar activity coefficient behavior to the Hammett indicators (1). This is important since if the indicator slope deviates from unity this means the base is following some other acidity function and the pK value obtained is not referred back to the same standard state as the H_0 scale, and is not a true pK value. It is clear from the indicator slopes in Table II that only 2-chloro-4,6-dinitroaniline obeys the H_0 function in its ionization. Thus the "pK" values of the other bases are not valid thermodynamic equilibrium constants. For this reason it is interesting to compare these "pK" values with those reported in sulfuric acid. (These should be the same if the pK values are

valid equilibrium constants.) It can be seen that except for 2-chloro-4,6-dinitroaniline and benzamide the agreement is not good, especially for the weaker bases. This again illustrates that caution must be used in interpreting numerical values of pK based on the H_0 function (1), unless the base in question has been shown to follow this acidity function. This is particularly true for the very weak bases which are measurably ionized only in the more concentrated acid region. Although the relative order of base strengths in Table II is the same in perchloric acid as in sulfuric acid, the absolute values of pK can only be taken as approximate estimates of basicity. Particularly striking is the discrepancy between the pK values for benzoic acid. Although the indicator slope has practically the same value in either acid, the two equilibrium constants differ by a factor of 17. We have checked our measurements of this pK carefully and have also redetermined its value in sulfuric acid and the observed difference in pK is well outside the experimental error. Arnett has already pointed out that benzoic acid is probably unusual in its activity coefficient behavior (1) and the present finding confirms this. It was not possible to obtain even approximate pK values for anisole and phenol for the reasons described above. However, our results, which have been obtained over a wider range of acid concentrations than is possible in sulfuric acid, indicate that these bases are considerably weaker than previous estimates (3). It was, however, possible to estimate a "pK" for *p*-nitroanisole by the method of Arnett and Wu (3) since this compound gave more pronounced spectral changes than anisole or phenol. This gave a value of -10.0 which is in good agreement with the value -10.26 reported for *p*-nitrophenol (4, 5) which should be very similar in base strength to the corresponding anisole.

EXPERIMENTAL

Compounds used were commercially available samples and purified by fractional distillation or repeated recrystallization. Spectra were recorded at 25 ± 0.1 °C on a Bausch and Lomb 505 Recording Spectrophotometer. Indicator solutions and acids were prepared essentially as described previously (13).

ACKNOWLEDGMENTS

This study was supported in part by a grant from the Defense Research Board of Canada. We are also grateful to the National Research Council for financial support. We are grateful to Mr. Brian Scott for redetermining the pK of benzoic acid.

1. E. M. ARNETT. *In* Progress in physical organic chemistry. Vol. I. *Edited by* S. G. Cohen, A. Streitwieser, Jr., and R. W. Taft. Interscience, New York. 1963. p. 223.
2. (*a*) J. T. EDWARD and I. C. WANG. Can. J. Chem. **40**, 966 (1962).
(*b*) R. STEWART and M. R. GRANGER. Can. J. Chem. **39**, 2508 (1961).
3. E. M. ARNETT and C-Y. WU. J. Am. Chem. Soc. **82**, 5660 (1960).
4. V. GOLD and D. P. N. SATCHELL. J. Chem. Soc. 3609 (1955).
5. M. J. JORGENSON and D. R. HARTTER. J. Am. Chem. Soc. **85**, 878 (1963).
6. A. R. KATRITZKY, A. J. WARING, and K. YATES. Tetrahedron, **19**, 465 (1963).
7. R. B. MOODIE, P. D. WALE, and T. J. WAITE. J. Chem. Soc. 4273 (1963).
8. E. M. ARNETT and G. W. MACH. J. Am. Chem. Soc. **86**, 2671 (1964).
9. L. A. FLEXSER, L. P. HAMMETT, and A. DINGWALL. J. Am. Chem. Soc. **57**, 2103 (1935).
10. R. STEWART and K. YATES. J. Am. Chem. Soc. **80**, 6355 (1958).
11. K. YATES and R. STEWART. Can. J. Chem. **37**, 664 (1959).
12. R. STEWART and K. YATES. J. Am. Chem. Soc. **82**, 4059 (1960).
13. K. YATES and H. WAI. J. Am. Chem. Soc. **86**, 5408 (1964).

RECEIVED MARCH 12, 1965.
DEPARTMENT OF CHEMISTRY,
UNIVERSITY OF TORONTO,
TORONTO, ONTARIO.

Can. J. Chem. Downloaded from www.nrcresearchpress.com by 210.87.254.105 on 09/05/12
For personal use only.

ERRATUM: NEW NITROCHALCONES. VII

T. SZELL, A. M. EASTHAM, AND GY. SIPOS

(Ref. Can. J. Chem. 42, 2417 (1964).

On page 2418, Table I, the melting point for chalcone No. 37 should read 197–198.

On page 2419, Table I, Chalcone No. 69 should read 3′-NO_2-4′-OH-4-CHO-.

On page 2422, Experimental, the quantity for NaOH should read 9.6 g. All melting points are uncorrected.

INSTITUTE OF APPLIED CHEMISTRY,
UNIVERSITY OF SZEGED,
SZEGED, HUNGARY.

Canadian Journal of Chemistry. Volume 43 (1965)

Can. J. Chem. Downloaded from www.nrcresearchpress.com by 210.87.254.6 on 09/05/12
For personal use only.

Can. J. Chem. Downloaded from www.nrcresearchpress.com by 210.87.254.6 on 09/05/12
For personal use only.

Canadian Journal of Chemistry

Issued by THE NATIONAL RESEARCH COUNCIL OF CANADA

VOLUME 43 AUGUST 1965 NUMBER 8

HINDERED INTERNAL ROTATION IN BORON HALIDE COMPLEXES OF N,N-DIMETHYLFORMAMIDE

E. S. GORE,[1] D. J. BLEARS,[2] AND S. S. DANYLUK[2]

Department of Chemistry, University of Toronto, Toronto, Ontario

Received March 2, 1965

ABSTRACT

The barriers to internal rotation about the CN partial double bond in N,N-dimethylformamide (DMF) and its complex with BF_3 have been determined in tetrachloroethane (TCE) by nuclear magnetic resonance measurements. The activation energy for rotation E_a, increased from 6.2 ± 0.3 kcal mole^{-1} for DMF to 14.5 ± 1.1 kcal mole^{-1} for DMF·BF_3. Values of $\Delta H^{\neq}$ and $\Delta S^{\neq}$ were also derived. Low field shifts of the methyl resonances and an increase in the relative shifts between the two methyl groups were observed on complex formation. The formyl coupling constant to the methyl groups was larger for the complex than for pure DMF. In addition, for DMF—BCl_3 evidence for the presence of two types of complex was found. The present results are compatible with BF_3 and BCl_3 complexing to the amide oxygen atom. The energy changes for internal rotation and J variation are attributed to changes in the π character of the CN bond due to stabilization of the charged resonance from $(CH_3)_2N{=}C{<}^{H}_{O}$ upon complex formation.

During the past few years the site of protonation of amides and the structure of the resulting proton adduct has been the subject of considerable controversy (1, 2, 3). Recent nuclear magnetic resonance (n.m.r.) studies confirm that protonation occurs at the oxygen atom and leads to stabilization of a planar structure of the form,

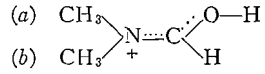

I

The amides also form relatively stable 1:1 molecular complexes with boron halides. Although the structure of such complexes has not been studied as extensively as the protonated species the infrared and n.m.r. studies of Gerrard and co-workers (4) indicate that the lone pair of the oxygen is involved in bonding to the boron halide. The planar configuration of I is presumably retained in the boron halide complex II,

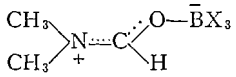

II

[1]*Now at University of Illinois, Urbana, Illinois.*
[2]*Now at Argonne National Laboratory, Argonne, Illinois.*

Protonation and complex formation at the oxygen atom would stabilize resonance forms favoring a higher π-bond character in the C—N bond and it would be expected that the energy barrier for rotation about the C—N bond would increase over that for the free amide. This has been confirmed by Fraenkel and Franconi (5) who observed an increase in the rotational barrier from 9.6 kcal mole^{-1} for pure N,N-dimethylformamide (DMF) to 12.7 kcal mole^{-1} for the protonated DMF. In this work we have studied the effects of complex formation between boron halides and DMF on the parameters E_a, $\Delta H^{\ddagger}$, and $\Delta S^{\ddagger}$ for internal rotation about the C—N bond.

Low field chemical shifts together with increases in the relative chemical shifts between the two methyl peaks are observed on complex formation. The formyl coupling constants to the methyl peaks also increase on complexing, reflecting changes in the electronic configuration at the CN bond.

EXPERIMENTAL

The N,N-dimethylformamide was Fisher Certified Reagent, dried by passing through a 50 cm column of Linde Molecular Seive 5A. The solvent, 1,1,2,2-tetrachloroethane (TCE), was washed with concentrated sulfuric acid and then with dilute sodium hydroxide solution and finally purified by distillation. The boron trifluoride and trichloride were Matheson C.P. gases and were further purified on a vacuum-transfer system.

Samples were made up by adding equimolar amounts of boron halide and DMF under vacuum to degassed TCE. The final concentration of the complex was approximately 4 mole %.

All spectra were recorded on a Varian A-60 spectrometer equipped with a variable temperature accessory. Three or four spectra were recorded at each temperature. The temperatures were accurate to ± 1 °C, chemical shifts to ± 0.10 c/s, and coupling constants to ± 0.05 c/s.

CALCULATIONS

The activation energies for rotation were calculated by the procedure of Gutowsky and Holm (6) in which the rotation about the CN bond can be regarded as a rate process which intramolecularly interchanges the two methyl groups between two environments. Solution of the Gutowsky and Holm equations yields τ from the experimental values of methyl group separations at a given temperature. Numerical calculations for τ were carried out on an IBM 7090 computer. The activation energy for the barrier to internal rotation was then computed by fitting a least squares curve to an Arrhenius equation. The computer programme also gave standard deviations in E_a and ν_0.

The free energy and entropy of activation were calculated from the Eyring equation.

RESULTS

The partial double bond character of the CN bond (4, 5) and the planar configuration of DMF (4) give rise to two separate methyl resonances of equal intensity, each split into doublets by spin–spin coupling to the formyl proton (5).

The 60 Mc/s spectrum of the methyl protons of DMF in solution in TCE at 25 °C consists of two doublets chemically shifted from each other by $\Delta_{AB} = 5.6$ c/s. The doublet at lower field has a splitting $J = 0.50$ c/s, while the higher field doublet has a splitting $J = 0.80$ c/s. This compares with the values of $J = 0.28$ c/s and $J = 0.56$ c/s obtained by Woodbrey and Rogers (7) for pure DMF. By analogy with ethylenic systems (8) the coupling of the methyl group *trans* to the formyl proton is larger than the formyl coupling to the *cis* methyl group and hence the higher field doublet is assigned to the *trans* methyl group. The relative shift of the methyl resonances would also be expected in view of the high electron density at the carboxyl oxygen atom and the high anisotropy of the carbonyl bond (9). This produces a greater shielding effect at the methyl group *cis* to the oxygen atom and results in its resonance to higher field.

Can. J. Chem. Downloaded from www.nrcresearchpress.com by 210.87.254.6 on 09/05/12
For personal use only.

The midpoint of the two methyl peaks of $DMF \cdot BF_3$ measured at 25 °C in TCE appears at 23.5 c/s to lower field from DMF. The peak separation is 7.1 c/s while the high and low field peak splittings are $J = 1.10$ c/s and $J = 0.70$ c/s respectively.

For $DMF \cdot BCl_3$ at 25 °C there are two sets of methyl doublets (Fig. 1). One set shifted by 26.5 c/s to lower field from DMF has a methyl group separation of 10.6 c/s and splitting of $J = 0.90$ c/s and $J = 1.30$ c/s for the low and high field peaks respectively. The other set is shifted by 21.3 c/s to lower field from DMF and has a methyl group separation of 8.4 c/s and splittings of $J = 0.90$ c/s and $J = 1.20$ c/s for the low and high field peaks respectively.

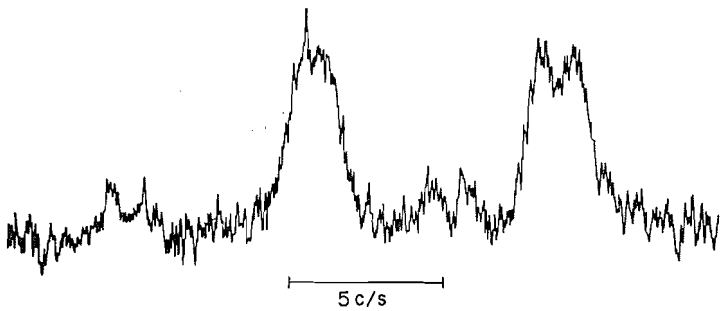

FIG. 1. Nuclear magnetic resonance spectrum of a 4 mole % solution of $DMF \cdot BCl_3$ in TCE at 25 °C.

The signals for the DMF and $DMF \cdot BF_3$ methyl groups broadened and moved closer together with increasing temperature and eventually coalesced at $T_c = 115$ °C and $T_c = 135$ °C respectively. This data is shown in Table I. Spectra were recorded under "slow passage" conditions and radio-frequency saturation avoided since the analysis is only valid provided that these conditions are maintained.

TABLE I

Collapse of the methyl group doublets in 4 mole % solutions of DMF and $DMF \cdot BF_3$ in TCE

DMF		$DMF \cdot BF_3$	
T (°C)	Δ_{AB} (c/s)	T (°C)	Δ_{AB} (c/s)
90	4.27	104	6.30
92	4.27	108	6.42
94	4.16	110	5.87
96	4.15	112	5.96
98	4.05	115	5.54
100	3.83	116	5.60
102	3.42	118	4.95
104	3.09	119	4.65
106	2.49	120	4.55
140	1.3*	122	3.75

*Line width at half height after coalescence.

Similar observations were noted for $DMF \cdot BCl_3$ complexes but in this case accurate data were not obtainable because of the overlap of the two sets of signals. An approximate coalescence temperature of 145 °C was indicated for the 1:1 complex.

The formyl coupling to the methyl groups of DMF and $DMF \cdot BX_3$ complexes in TCE is not observed at temperatures below ~ -15 °C due to a combination of freezing out of rotational isomers and signal broadening arising from viscosity effects.

Can. J. Chem. Downloaded from www.nrcresearchpress.com by 210.87.254.6 on 09/05/12
For personal use only.

A summary of the parameters E_a, $\Delta H^{\ddagger}$, and $\Delta S^{\ddagger}$ calculated for DMF and DMF·BF_3 is given in Table II.

TABLE II

Energy parameters for internal rotation (4 mole % in TCE solutions)

	E_a (kcal mole^{-1})	ν_0 (s^{-1})	$\Delta H^{\ddagger}$ (kcal mole^{-1})	$\Delta S^{\ddagger}$ (e.u.)*	T_c
DMF	6.2±0.3	$4.02\pm0.02\times10^{4}$	6.5±1.0	−54±1.0	115
DMF·BF_3	14.5±1.1	$1.33\pm0.02\times10^{9}$	11.8±0.4	−55±1.0	135

*e.u. = entropy units.

DISCUSSION

1. *Factors Affecting Line Shape*

A variety of factors can affect the line shapes of n.m.r. spectra with the most important being intermolecular phenomena such as chemical exchange and solvent perturbations and intramolecular effects such as internal rotation.

Intermolecular exchange of the amide can occur between the free and complexed forms in solution and may result in line-shape changes with temperature. However, the stability of the BX_3 complexes (4, 15) and the good linearity obtained for plots of $(1/2\tau)$ vs. temperature indicate that changes in the equilibrium constant for complex formation are unimportant. Intermolecular solvent effects on line shapes were minimized by working with low concentrations of the complex in an inert solvent TCE. The variation of the line shapes with temperature is therefore compatible with the variation of the rate constant for the rotation of the methyl groups about the CN bond. The rate constants were evaluated from the separation between the two methyl peaks near the coalescence temperature. Although other methods of evaluation of $1/\tau$ are available (10) they are not as reliable in this region where the separation shows good sensitivity to temperature change.

2. *Coupling Constant Changes*

The long-range formyl proton–methyl group coupling constants observed for DMF in TCE in the present work are somewhat larger than the values reported earlier (7) for the neat compound. It is likely that these small differences result from solvent perturbations of the rotational and (or) H-bonding equilibrium.

The formation of DMF·BX_3 complexes significantly increases the long-range coupling between the formyl proton and the methyl group protons. A similar increase has been noted on protonation of DMF (5). In both cases the addition stabilizes the resonance form having a greater double bond (π bond) character of the CN bond and leads to an increase of the long-range coupling constant (11, 12). A similar mechanism has been evoked to explain the increase in the long-range couplings in aqueous solutions of N-methylformamide and DMF (17, 18).

The J increase for DMF·BCl_3 is slightly greater than for DMF·BF_3 as would be expected on the basis of the weaker acceptor properties of BF_3 (13). The value of J_{trans} in the 1:2 complex of DMF·BCl_3 is slightly greater than in the 1:1 complex. This would occur provided the stabilization of (II) caused by 1:1 complex formation is enhanced on 1:2 complexing. The additional increased s character of the CN bond would give rise to the larger J_{trans} value.

3. *Changes in the Rotational Barrier*

Boron trichloride is a stronger electron acceptor than BF_3 (13) and hence in the

Can. J. Chem. Downloaded from www.nrcresearchpress.com by 210.87.254.6 on 09/05/12
For personal use only.

amide–BX_3 complexes the former will stabilize from (II) more than will BF_3. The higher coalescence temperature, $T_c \gtrsim 145$ °C for the BCl_3 complex as compared with $T_c = 135$ °C for $DMF \cdot BF_3$ is in agreement with this. The enhanced stabilization and resulting increased CN double bond character is reflected in the magnitude of the activation energies for the barriers hindering internal rotation. For DMF, $E_a = 6.2 \pm 0.3$ kcal mole^{-1} and for $DMF \cdot BF_3$, $E_a = 14.5 \pm 1.1$ kcal mole^{-1}. The DMF result is compatible with previous values of $E_a = 7.3 \pm 3$ kcal mole^{-1} (ref. 6) and $E_a = 9.6 \pm 1.5$ kcal mole^{-1} (ref. 5) for pure DMF, but differs markedly from the value reported by Rogers and Woodbrey (7) of 18.3 kcal mole^{-1}. The value of E_a was found to increase on protonation to 12.7 ± 1.5 kcal mole^{-1}, in agreement with the present result for $DMF \cdot BF_3$.

The variation in the values obtained by different authors for the activation energy hindering rotation about the CN bond in DMF is probably due to solvent and concentration effects and to the presence of acidic impurities, all of which can combine to stabilize the ionic form (II) and result in an increased value of E_a.

A large increase of approximately five orders of magnitude occurs in the value of the frequency factor ν_0 on going from DMF to $DMF \cdot BF_3$. Large variations in ν_0 are also noted for similar systems, i.e. DMF, investigated under different solvent conditions by different authors (5, 6, 7). Such changes appear to be typical of these systems and are not readily interpreted at the present time. However, it seems likely that the variation of ν_0 reflects subtle influences of the solvent on the frequency of rotation about the CN bond.

The large, approximately equivalent negative values of $\Delta S^{\ddagger}$ for DMF and $DMF \cdot BF_3$ are somewhat surprising and are suggestive of a rigidly defined transition state intermediate.

4. Changes in the Chemical Shifts

Significant differences are noted between the relative shifts for the methyl groups of DMF in TCE and the values reported previously (5, 6, 7). As in the case of coupling constants these differences arise because of the influence of the solvent on the methyl shieldings. Similar solvent effects on the shifts and rotational energy barriers have been noted recently for N,N-dimethylnitrosamine (16).

Complex formation results in the low field shifts for the methyl protons in DMF in agreement with recent observations for a number of ether–BX_3 (13) and amine–BX_3 (14) addition compounds. The deshielding effect can be attributed to a flow of electron density from the donor molecule to the acceptor and would be expected to fall off with increasing number of intervening bonds. A comparison of the data for the ether and amide complexes, Table III, indicates that the deshielding effect drops off by a factor of 2 to 3 in going from the α to the β position.

Although the shift changes observed for protons on different donors upon complex formation are subject to a variety of complicating influences, the magnitudes of the shift changes for methyl protons in stable 1:1 $DMF \cdot BX_3$ complexes, ~ 0.400 p.p.m., are consistent with coordinate bond formation at the oxygen atom.

The appearance of two sets of methyl peaks in the $DMF \cdot BCl_3$ complex indicates the presence of two types of complex. The more abundant complex, -21.3 c/s downfield from DMF is due to a 1:1 adduct involving complexing at the DMF carboxyl oxygen atom. The second pair of methyl peaks at -26.5 c/s, is of much lower intensity and is probably due to a 1:2 adduct. The site of complexing in this case cannot be established unequivocally although the deshielding effect, -0.443 p.p.m., would favor the O site.

Can. J. Chem. Downloaded from www.nrcresearchpress.com by 210.87.254.6 on 09/05/12
For personal use only.

TABLE III

Chemical shifts of protons in $D \cdot BX_3$ addition compounds

Addition compound	$\delta_{D \cdot BX_3} - \delta_D$ (p.p.m.)	Group
$(CH_3)_2O \cdot BF_3$ (13)	−1.04	CH_3
$(CH_3CH_2)_2O \cdot BF_3$ (13)	−0.333	CH_3
	−0.851	CH_2
$(CH_3CH_2)_2O \cdot BCl_3$ (13)	−0.378	CH_3
	−1.24	CH_2
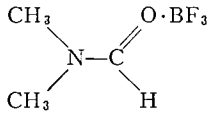	−0.392	CH_3
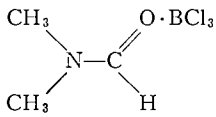	−0.356	CH_3
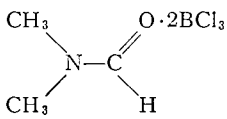	−0.443	CH_3
$Me_2S \cdot BF_3$ (14)	−0.250	CH_3

ACKNOWLEDGMENTS

The financial assistance of the National Research Council and the National Cancer Institute is gratefully acknowledged. The authors also wish to thank the Ontario Research Foundation for use of their A-60 Spectrometer.

REFERENCES

1. R. A. Y. Jones and A. R. Katritzky. Chem. Ind. London, 722 (1961).
2. G. Fraenkel and C. Niemann. Proc. Natl. Acad. Sci. U.S. 44, 688 (1958).
3. R. J. Gillespie and T. Birchall. Can. J. Chem. **41**, 148 (1963).
4. W. Gerrard, M. F. Lappert, H. Pyszova, and J. W. Wallis. J. Chem. Soc. 2144 (1960).
5. G. Fraenkel and C. Franconi. J. Am. Chem. Soc. **82**, 4478 (1960).
6. H. S. Gutowsky and C. H. Holm. J. Chem. Phys. **25**, 1228 (1956).
7. M. T. Rogers and J. C. Woodbrey. J. Phys. Chem. **66**, 540 (1962).
8. R. R. Fraser and D. E. McGreer. Can. J. Chem. **39**, 505 (1961).
9. P. T. Narasimhan and M. T. Rogers. J. Phys. Chem. **63**, 1388 (1959).
10. J. Lee. Symposium on high resolution n.m.r. spectroscopy, Boulder, Colorado. 1962.
11. M. Karplus and D. M. Anderson. J. Chem. Phys. **30**, 6 (1959).
12. H. McConnell. J. Chem. Phys. **30**, 126 (1959).
13. E. S. Gore and S. S. Danyluk. J. Phys. Chem. In press.
14. T. D. Coyle and F. G. A. Stone. J. Am. Chem. Soc. **83**, 4138 (1961).
15. N. N. Greenwood and R. L. Martin. Quart. Rev. London, **8**, 1 (1954).
16. D. J. Blears. J. Chem. Soc. In press, and unpublished results.
17. E. W. Randall and J. D. Baldeschwieler. J. Mol. Spectry. **8**, 365 (1962).
18. A. J. R. Bourn and E. W. Randall. Mol. Phys. **8**, 567 (1964).

Can. J. Chem. Downloaded from www.nrcresearchpress.com by 210.87.254.6 on 09/05/12
For personal use only.

Can. J. Chem. Downloaded from www.nrcresearchpress.com by 210.87.254.40 on 09/05/12
For personal use only.

ELECTRON SPIN RESONANCE DETERMINATION OF THE RADIOLYTIC YIELDS OF TRAPPED ELECTRONS AND OTHER SPECIES IN AN ORGANIC GLASS[1]

D. R. SMITH AND J. J. PIERONI

Research Chemistry Branch, Atomic Energy of Canada Limited, Chalk River Nuclear Laboratory, Chalk River, Ontario

Received April 7, 1965

ABSTRACT

The radiolytic yields, at liquid nitrogen temperature, of trapped electrons and radicals or radical-ions in 2-methyltetrahydrofuran and the yields of these species plus the biphenyl anion in solutions containing biphenyl have been determined by e.s.r. These measurements were also carried out after photolysis of the trapped electrons. The combined results are interpreted in terms of the identity of the intermediates and the reactions which they undergo. "Dual e.s.r. cavity" techniques have enabled greater accuracy and precision than is normally obtained when concentrations of paramagnetic species are determined by e.s.r.

INTRODUCTION

The work of Hamill *et al.* (1, 2) has provided convincing evidence of the role of electrons and ions in the radiation chemistry of certain organic compounds at low temperature. From optical absorption measurements, they found that electrons become trapped in the matrix during the radiolysis of 2-methyltetrahydrofuran (MTHF) at 77 °K. They also found that a solute such as biphenyl ($C_{12}H_{10}$) could compete with the solvent for electrons by forming $C_{12}H_{10}^-$. By assuming that the optical extinction coefficient of the chemically generated anion equals that of the radiolytically generated anion they determined that during radiolysis the maximum value of G(solute anion) was 2.6 to 3.0,* depending on the solute. From this they assumed that in the absence of solute, G(trapped electron) was approximately 3.0. They estimated a minimum oscillator strength $f \sim 0.8$ for trapped electrons in MTHF (3). f is expected to be close to unity and has been found to equal 0.8 to 0.9 for F centers in alkali halides (4).

In view of the importance of these results, it was decided to repeat the experiment and make observations using electron spin resonance spectroscopy (e.s.r.). Electron spin resonance measurements detect paramagnetic species and these can often be identified with greater certainty from their e.s.r. spectra than from their optical absorption spectra. In particular, and as is the case in MTHF, many free radicals which are easily detected by e.s.r. have only a weak optical absorption. A concentration measurement can be made by e.s.r. whose accuracy does not depend on any factor analogous to the extinction coefficient in optical absorption measurements. Hence this work provides a check of the results obtained by Hamill *et al.*, independent of the assumptions made by them.

In a previous paper (5) we described results which supported Hamill and co-workers' conclusion that trapped electrons are formed by radiolysis of MTHF. From microwave saturation studies, and measurements of rates of thermal disappearance, it was concluded that the "trapped electron" in MTHF is a distinct entity distinguishable from a free radical. It was also concluded that it is trapped, along with radicals or radical-ions, in clusters or regions containing higher local concentrations than the bulk of the matrix.

[1]*AECL No. 2304.*

**G equals the number of molecules of a species formed per 100 eV energy deposited in the sample.*

The results suggested that the electron is trapped by the solvent at an average distance of about 40 Å from the parent positive ion.

The e.s.r. spectrum of another species was also detected (6, 7). Salmon (7) ascribes a weak ultraviolet absorption to this species. We choose to identify this species as the ion-radical I while Dainton *et al.* (8) suggest it is the free radical II and that the H^+ migrates to a neighboring solvent molecule to form III. Since the arguments presented earlier are not conclusive (5) this species will be referred to as I or II. Where no distinction need be made we will refer to species I or II as species A. Species IV, the primary ion, is defined here for convenience.

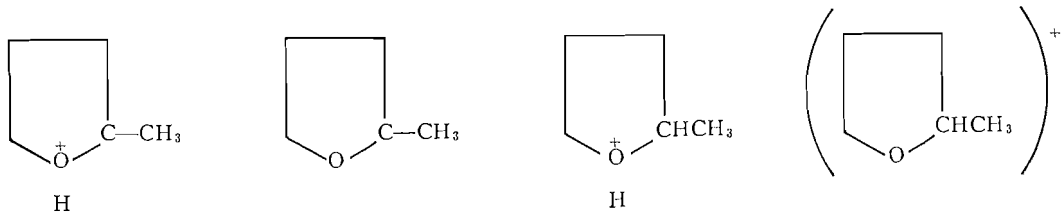

I II III IV

This paper reports the results of concentration measurements by e.s.r. of paramagnetic species formed and trapped during radiolysis of MTHF and solutions of MTHF containing various amounts of $C_{12}H_{10}$. These measurements have been carried out both before and after photolysis of the irradiated sample.

EXPERIMENTAL

Techniques of preparation of pure MTHF samples, ^{60}Co gamma irradiation, dosimetry, and measurement of e.s.r. spectra have been described (5, 6). A linear reproducible magnetic field scan was provided by a Varian fieldial. These experiments were all carried out at liquid nitrogen temperature. Solutions of $C_{12}H_{10}$ in MTHF were irradiated to a dose of 9.4×10^{18} eV ml^{-1}.

To prepare solutions of $C_{12}H_{10}$ of known concentration, the required amount of $C_{12}H_{10}$ was weighed into a volumetrically calibrated tube to which a spectrosil e.s.r. tube was attached. The apparatus was then evacuated while cooling the $C_{12}H_{10}$ with liquid nitrogen to avoid sublimation. A measured volume of purified degassed MTHF was then distilled under vacuum into the tube and the $C_{12}H_{10}$ dissolved. The resulting solution was subjected to several degassing cycles to ensure the absence of dissolved air. The entire apparatus was then detached from the vacuum line by sealing off at a constriction. The solution of $C_{12}H_{10}$ in MTHF was poured into the e.s.r. tube and this was in turn detached from the apparatus by sealing off under vacuum.

The chemically formed anion $C_{12}H_{10}^-$ was prepared by the method of Paul, Lipkin, and Weissman (9).

Both unknown and reference sample were present in a Varian TE_{104} "dual" cavity at the same time and both were observed at liquid nitrogen temperature. Each was in a Spectrosil tube of the same dimensions, filled and positioned so that the sample filled the vertical dimension of the cavity. The spectra were obtained consecutively without retuning the spectrometer. The reference sample spectrum was obtained both before and after that of the unknown, to check for fluctuations in spectrometer sensitivity. The reference was the stable free radical in nuclear reactor irradiated terphenyl coolant which had been stored at room temperature for 3 years. To avoid errors due to microwave saturation both samples were measured at a cavity input power of 8 μW. Identical modulation amplitudes were used for both reference and unknown sample spectra and amplifier gain switches were calibrated in terms of absorption spectrum intensity. This procedure of comparing samples in a dual cavity under identical conditions of cavity Q, cavity input power, temperature, sample dimension, etc., has considerable advantage over the more common practice of using a single cavity. The latter necessitates substitution of samples, retuning the spectrometer, etc. Unless the two samples being compared by the single cavity technique have identical dielectric properties, the spectrometer sensitivity may vary greatly between the two measurements and errors as great as $\pm 50\%$ are usually involved. In pure MTHF we estimate our precision to be $\pm 5\%$. In the series of solutions containing $C_{12}H_{10}$, the precision is poorer, $\pm 15\%$, because the graphical double integrals of spectra having different shapes are being compared. The accuracy depends on the graphical integration and on our calibration of the reference, described earlier (5). Briefly, the concentration of free radicals in the reference sample was determined by comparison

Can. J. Chem. Downloaded from www.nrcresearchpress.com by 210.87.254.40 on 09/05/12
For personal use only.

with a solution of 2,2-diphenyl-1-picryl-hydrazl (DPPH) in CCl_4. The concentration of DPPH was determined by its optical absorption using the known optical extinction coefficient. The accuracy of the extinction coefficient is based on a measured weight of purified DPPH and on the accuracy of dilution of this material. Hence our major source of error in calibrating the reference, probably ±10%, arises from the graphical double integration of the spectra.

After irradiation, the concentrations of paramagnetic species in a sample were determined. The sample was then photolyzed by illuminating it with light of wavelength longer than about 6 000 Å. The concentrations of paramagnetic species remaining after photolysis were then determined. The total concentration of paramagnetic species was determined by comparison of the double integral (obtained graphically) of the first derivative e.s.r. spectrum with that of the free radical reference spectrum (5). In most of these measurements an absorption due to trapped electrons, $C_{12}H_{10}^-$, or both was superimposed on the central line of the septet absorption due to species A. In these cases the concentration of A was calculated from the intensity of the third and fifth absorption peaks and the measured double integral for a given intensity of these peaks. The concentration of trapped electrons, in pure MTHF, and of trapped electrons plus $C_{12}H_{10}^-$, in solutions of $C_{12}H_{10}$, was equated to the difference between the total concentration and that of A.

RESULTS

1. *Pure MTHF*

The e.s.r. spectra and the identification of the species causing them have been discussed (5). A singlet absorption due to trapped electrons is superimposed on the center line of a septet absorption due to species A and the sample is colored blue. Photolysis eliminates the blue color and the e.s.r. absorption due to trapped electrons while the e.s.r. absorption due to species A remains, although diminished in intensity. Figure 1A shows the yields of trapped electrons and of species A before and after photolysis as a function of irradiation dose up to 7.09×10^{19} eV ml^{-1}. Figure 1B is an expansion of Fig. 1A in the low dose region. Note that each graph in Fig. 1A is slightly curved and that about one-third of species A disappears when the trapped electrons are totally eliminated by photolysis. This was also observed by the e.s.r. difference spectrum method (6). Below about 5×10^{18} eV ml^{-1}, the yields are linear with dose. From the initial slopes in Fig. 1B $G(e^-_{trapped}) = 2.6$, $G(A) = 3.0$ before photolysis, and $G(A) = 2.0$ after photolysis.

We previously observed that on warming an unphotolyzed sample to 92–95 °K, the trapped electrons disappeared along with about one-third of species A (5).

2. *Solutions of $C_{12}H_{10}$ in MTHF*

Solutions containing 0.01, 0.03, 0.066, 0.098, 0.20, and 0.39 mole % $C_{12}H_{10}$ have been studied. The results are illustrated by the e.s.r. spectra in Fig. 2 and the data in Table I.

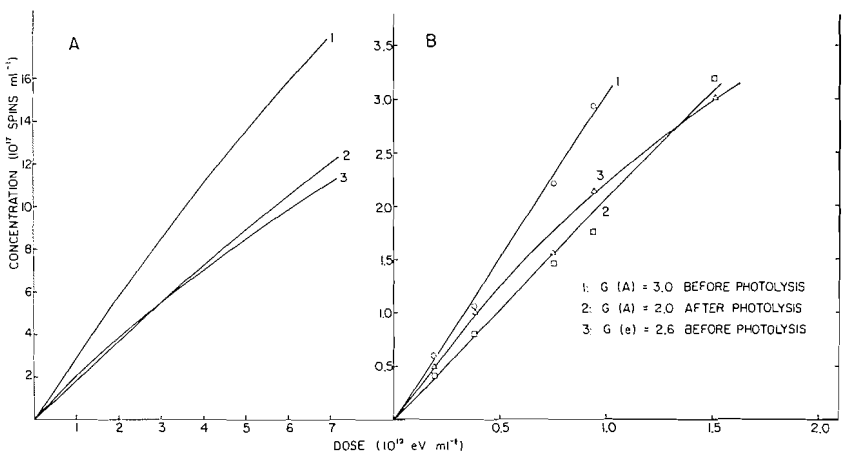

FIG. 1. Yields of trapped electrons and species A (before and after photolysis) as a function of radiation dose. Fig. 1B is an expansion of the low dose portion of Fig. 1A.

Can. J. Chem. Downloaded from www.nrcresearchpress.com by 210.87.254.40 on 09/05/12
For personal use only.

In Fig. 2 only the central absorption plus part of the third and fifth lines of the spectrum due to A is shown. The relative intensity of the spectra in the figure should be ignored, since different gain settings were used to obtain some of them.

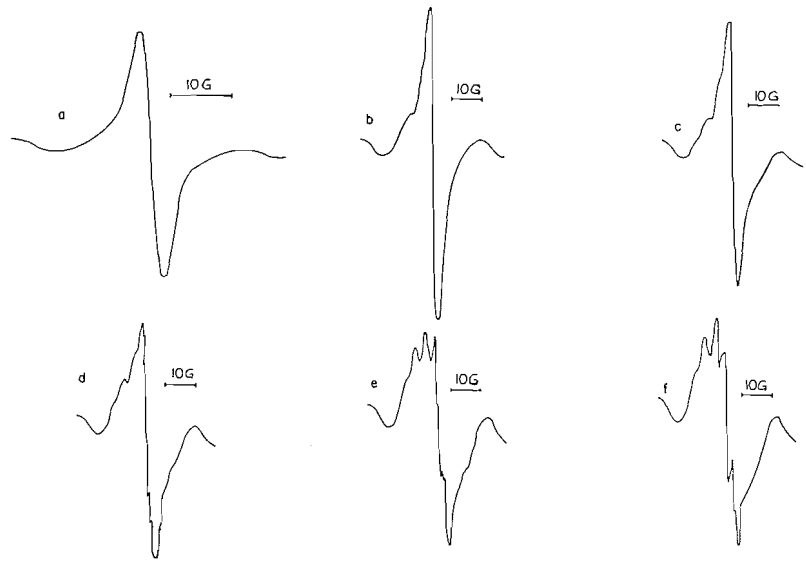

FIG. 2. Central portions of the first derivative e.s.r. spectra obtained by radiolysis of solutions of $C_{12}H_{10}$ in MTHF. Mole % $C_{12}H_{10}$ concentrations are (*a*) 0.01, (*b*) 0.031, (*c*) 0.066, (*d*) 0.098, (*e*) 0.20, (*f*) 0.39.

TABLE I

Radiolytic yields of species trapped in solutions of $C_{12}H_{10}$ in MTHF

Mole % $C_{12}H_{10}$	G(A)*	$G(e^- + C_{12}H_{10}^-)$*	G(A)†	$G(C_{12}H_{10}^-)$†
0.01	3.33	2.40	2.66	1.20
0.031	3.32	2.22	3.08	2.44
0.066	3.45	2.29	3.77	2.53
0.098	3.37	2.60	3.38	2.90
0.20	3.11	2.72	3.37	2.66
0.39	3.53	2.43	3.53	3.00
Average‡ G	3.4	2.5	3.4	2.7

*Before photolysis.
†After photolysis.
‡The averages do not include the data for the 0.01% solution.

Radiolysis generates the septet e.s.r. absorption of A. Superimposed on the center line of the septet is the sum of the absorptions due to trapped electrons and a species formed from $C_{12}H_{10}$ (concluded to be $C_{12}H_{10}^-$, see Discussion). The ratio of $C_{12}H_{10}$ species absorption to trapped electron absorption increases (the sum remaining constant) with $C_{12}H_{10}$ concentration up to 0.1 mole %. At 0.2 and 0.39 mole % only the absorption due to the $C_{12}H_{10}$ species superimposed on the central line of the spectrum of species A was observed, the absorption intensity being the same in both cases. The color of the sample changes from blue to green-blue as the absorption due to the $C_{12}H_{10}$ species increases and that due to trapped electrons decreases.

Photolysis of the samples containing up to 0.098 mole % $C_{12}H_{10}$ changed the e.s.r.

Can. J. Chem. Downloaded from www.nrcresearchpress.com by 210.87.254.40 on 09/05/12
For personal use only.

spectrum to that obtained in irradiated samples containing 0.20 or 0.39 mole %. Photolysis did not affect the e.s.r. spectrum of the $C_{12}H_{10}$ species nor, in the presence of 0.03 mole % $C_{12}H_{10}$ or greater, was the intensity of the e.s.r. septet due to A diminished. However, photolysis did reduce the intensity of the septet in the 0.01 mole % $C_{12}H_{10}$ solution. It was qualitatively observed that much less photolysis time was required to convert the trapped electron absorption to that of the $C_{12}H_{10}$ species, compared to that required to eliminate the trapped electron absorption in pure MTHF.

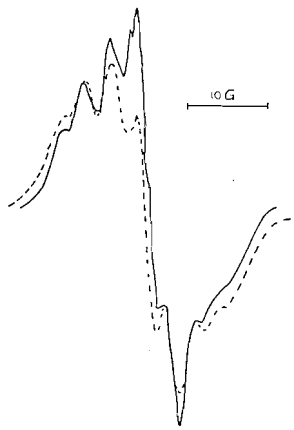

FIG. 3. (—) First derivative e.s.r. spectrum of the $C_{12}H_{10}$ species formed during radiolysis of 0.2 mole % solution of $C_{12}H_{10}$ in MTHF. (- -) First derivative e.s.r. spectrum at 77 °K of $C_{12}H_{10}^-$ formed in MTHF by reaction with Na.

The solid curve in Fig. 3 is the first derivative e.s.r. spectrum of the $C_{12}H_{10}$ species in a 0.2 mole % $C_{12}H_{10}$ solution, obtained by the e.s.r. difference spectrum technique (6). It is the difference between the absorption of the $C_{12}H_{10}$ solution, irradiated to 9.4×10^{18} eV ml^{-1} and that due to a pure MTHF sample irradiated to 14.1×10^{18} eV ml^{-1} and photolyzed. The higher dose for the pure MTHF sample was required to match the intensity of the spectrum due to A in both samples because one-third of A also disappears during photolysis. The dashed curve is the spectrum of the chemically generated $C_{12}H_{10}^-$ for comparison. The average hyperfine splitting in Fig. 3 is 3.1 G.

DISCUSSION AND CONCLUSIONS

1. *Pure MTHF*

A tentative reaction scheme to account for the results is outlined below. A possible physical mechanism for reaction [2] has been discussed (5).

[1]* $$\text{MTHF} \xrightarrow{\sim\sim} \text{IV} + e^-_{\text{untrapped}}$$

[2] $$e^-_{\text{untrapped}} \rightarrow e^-_{\text{trapped}}$$

[3*a*] $$\text{IV} \rightarrow \text{I}$$

or

[3*b*] $$\text{IV} + \text{MTHF} \rightarrow \text{II} + \text{III}$$

[4] $$e^-_{\text{trapped}} + \text{visible light or heat} \rightarrow e^-_{\text{untrapped}}$$

[5*a*] $$e^-_{\text{untrapped}} + \text{I} \rightarrow \text{II} + \text{H}\cdot$$

or

[5*b*] $$e^-_{\text{untrapped}} + \text{III} \rightarrow \text{MTHF} + \text{H}\cdot$$

**The symbol* —∿∿→ *means "produces during irradiation with γ-rays from* ^{60}Co".

Can. J. Chem. Downloaded from www.nrcresearchpress.com by 210.87.254.40 on 09/05/12
For personal use only.

[6] $$H\cdot + II \rightarrow MTHF$$

[7] $$H\cdot + H\cdot \rightarrow H_2$$

Either reaction sequence ([3*a*] + [5*a*] + [6]) or ([3*b*] + [5*b*] + [6]) accounts for the disappearance of all the trapped electrons and a fraction of A as a result of photolysis or warming. Our arguments favoring reactions ([3*a*] + [5*a*]) over ([3*b*] + [5*b*]) were presented earlier (5). Salmon did not observe any disappearance of A by e.s.r. (7), possibly because of the errors involved in making concentration measurements with a "single" TE_{102} e.s.r. cavity. The slight optical absorption in the ultraviolet which Dainton *et al.* attributed to species II did not decrease when the trapped electrons were eliminated by photolysis (8).

$G(e^-_{trapped}) = 2.6$ is 13% less than the value deduced by Hamill and co-workers from their value of $G(C_{12}H_{10}^-) = 3.0$. If $G = 2.6$ is more nearly correct, the oscillator strength must be close to $f = 0.9$. The value $G(A) = 3.0$ suggests that a small amount of recombination competes with trapping via reactions [8] and [9] and causes the ratio $G(e^-_{trapped})/G(A)$ to be less than unity.

[8] $$e^-_{untrapped} + IV \rightarrow (MTHF)\dagger$$

[9] $$(MTHF)\dagger \rightarrow II + H\cdot$$

The thermal reaction observed at liquid nitrogen temperature (5) accounts for the curvature in Fig. 1.

2. Solutions of $C_{12}H_{10}$ in MTHF

In Fig. 3 the hyperfine splittings in the e.s.r. spectra of the radiolytically generated $C_{12}H_{10}$ species and of the chemically generated $C_{12}H_{10}^-$ ion are the same. Trace absorption by trapped electrons in the irradiated sample would account for the small difference in central peak intensity. The average value of $G(e^-_{trapped} + C_{12}H_{10}$ species) before photolysis and the average value of G(biphenyl species) after photolysis are equal within experimental error to the value of $G(e^-_{trapped}$ electrons) = 2.6 obtained in pure MTHF.

The spectra in Fig. 2 show qualitatively that the ratio of the concentration of the $C_{12}H_{10}$ species to that of trapped electrons increases in solutions containing up to 0.1 mole % $C_{12}H_{10}$. At the same time the sum of their concentrations is constant (Table I) and equals the yield of trapped electrons obtained when $C_{12}H_{10}$ is absent. Above 0.2 mole % $C_{12}H_{10}$ virtually all the electrons are captured to form the $C_{12}H_{10}$ species. Thus each $C_{12}H_{10}$ species formed results in the observation of one less trapped electron. It is concluded that the $C_{12}H_{10}$ species is $C_{12}H_{10}^-$ formed in competition with electron trapping by the solvent. The average maximum $G(C_{12}H_{10}^-)$ observed by e.s.r. is slightly lower than the value of 3.0 obtained in the optical work (2). These e.s.r. results qualitatively agree with those obtained by optical measurements (ref. 2, Fig. 2) and support the assumption of Hamill *et al.* (2) that $G(e^-_{trapped})$ in the absence of $C_{12}H_{10}$ can be equated to the maximum $G(C_{12}H_{10}^-)$ obtained in the more concentrated $C_{12}H_{10}$ solutions. However, the e.s.r. results do suggest that the value of $G(e^-_{trapped}) = G(C_{12}H_{10}^-)_{max} = 3.0$ deduced from optical measurements may be 10 or 15% high.

The yield of species A in all but the 0.01% solution was unchanged during photolysis in contrast to the behavior in pure MTHF where photolysis of the trapped electrons reduced the concentration of A by one-third via reactions ([5*a*] + [6]) or ([5*b*] + [6]). This may be due to prevention of reactions ([5*a*] + [6]) or ([5*b*] + [6]) by the $C_{12}H_{10}$ competition reaction [10].

[10] $$C_{12}H_{10} + e^-_{untrapped} \rightarrow C_{12}H_{10}^-$$

Can. J. Chem. Downloaded from www.nrcresearchpress.com by 210.87.254.40 on 09/05/12
For personal use only.

G(A) appears to be about 10% higher than in pure MTHF but this may not be significant.

Comparison of the above results with those in Fig. 2 of ref. 2 shows one difference. Our work indicates total capture of $e^-_{untrapped}$ by $C_{12}H_{10}$ during photolysis in samples containing as little as 0.031 mole % $C_{12}H_{10}$. However, optical measurements indicate considerable loss of electrons during photolysis in solutions containing as much as 0.13 mole % $C_{12}H_{10}$ (2). The only apparent difference in experimental conditions is that the optical measurements were made at a dose nearly 10 times lower than that used in our work. The explanation apparently involves an effect of dose on the competition between reaction [10] and reaction [5*a*] or [5*b*]. This is supported by our observation that at a dose of 9.4×10^{18} eV ml^{-1} photolysis of a 0.01 mole % solution does not result in quantitative capture of $e^-_{untrapped}$ by $C_{12}H_{10}$ while at the same time 20% of species A disappears.

REFERENCES

1. P. S. Rao, J. R. Nash, J. P. Guarino, M. R. Ronayne, and W. H. Hamill. J. Am. Chem. Soc. **84**, 500 (1962).
2. M. R. Ronayne, J. P. Guarino, and W. H. Hamill. J. Am. Chem. Soc. **84**, 4230 (1962).
3. J. P. Guarino and W. H. Hamill. J. Am. Chem. Soc. **86**, 777 (1964).
4. R. H. Silsbee. Phys. Rev. **103**, 1675 (1956).
5. D. R. Smith and J. J. Pieroni. Can. J. Chem. **43**, 876 (1965).
6. D. R. Smith and J. J. Pieroni. Can. J. Chem. **42**, 2209 (1964).
7. A. Salmon. Discussions Faraday Soc. **36**, 286 (1963).
8. F. S. Dainton, J. P. Keene, T. J. Kemp, G. A. Salmon, and J. Teply. Proc. Chem. Soc. 265 (1964).
9. D. E. Paul, D. Lipkin, and S. I. Weissman. J. Am. Chem. Soc. **78**, 116 (1956).

Can. J. Chem. Downloaded from www.nrcresearchpress.com by 210.87.254.40 on 09/05/12
For personal use only.

Can. J. Chem. Downloaded from www.nrcresearchpress.com by 210.87.254.40 on 09/05/12
For personal use only.

POSSIBLE CALORIMETRIC METHOD FOR MEASUREMENT OF THE LIGAND FIELD SPLITTING ENERGIES FOR THE HEXAAQUO CATIONS OF SOME TRANSITION ELEMENTS

J. W. S. JAMIESON, G. R. BROWN, D. W. GRUENER, R. V. PEILUCK, AND R. A. LAMONTAGNE

Department of Chemistry, St. John's College, University of Manitoba, Winnipeg, Manitoba

Received November 26, 1964

ABSTRACT

High energy modifications of the lower hydrates of the divalent sulfates of manganese, iron, cobalt, and nickel have been prepared by vacuum dehydration. The heats of solution of these materials have been measured and compared with the heats of solution of the normal crystalline lower hydrates. The maximum heats of transition appear to be proportional to the ligand field splitting energies for the corresponding hexaaquo divalent cations, although theoretical justification for this correlation is not yet obvious.

INTRODUCTION

In 1930, Slonim (1) showed that certain salts can be dehydrated at low pressure to give intermediates which were thought to be amorphous. Quantitative measurements of the heat evolved when such samples change spontaneously to normal crystalline lower hydrates have been made by Volmer and Seydel (2), Khomyakov (3), and, more recently, by Frost and his co-workers (4, 5). The heat of solution method was used in all of these investigations since there is usually a substantial heat of transition. Many values may be found in the literature (6, 7, 8) for the heats of solution of anhydrous salts and their crystalline hydrates but there are few available data for the high energy forms which are obtainable from these by dehydration *in vacuo*.

The present investigation was undertaken not only to extend the data for vacuum dehydration products but also to test an approximate method, which will be proposed, for predicting the occurrence of such high energy dehydration products and estimating upper limits of the magnitude of their heats of solution, and heats of transition to normal crystalline form, from the known heats of solution of the various salts and their crystalline hydrates.

The results reported here deal with the products of dehydration of $MnSO_4.5H_2O$, $FeSO_4.7H_2O$, $CoSO_4.7H_2O$, and $NiSO_4.6H_2O$.

EXPERIMENTAL

All of the inorganic salts were J. T. Baker Analyzed reagents, except for $MnSO_4.5H_2O$ of analytical reagent grade, which was supplied by May and Baker, Ltd. Quantitative analysis of these salts has given close agreement with the analyses reported by the manufacturers. Samples of each of the salts were lightly ground in a mortar and dehydrated in various ways to obtain mixtures of the lower crystalline hydrates for measurement of heats of solution. Crystalline samples containing between 4 and 7 moles of water per mole of sulfate were usually prepared by dehydration over sulfuric acid in a desiccator for 48 h or less. Other crystalline samples containing less water were obtained by heating the higher hydrates in an oven or an Abderhalden drying apparatus, usually at 100 °C or higher. Since the iron(II) sulfate was readily oxidized, this salt was dehydrated in an atmosphere of nitrogen.

Vacuum dehydration to various water contents was carried out in a vacuum desiccator, a vacuum oven, or an Abderhalden drying apparatus, connected to a good vacuum line. The system was evacuated at ambient temperature (usually about 25 °C) and at pressures from about 30 microns to below 1 micron for sufficient time to give a product of approximately the composition desired. In some experiments barium oxide was used as desiccant. The water content of each dehydrated sample was calculated from the loss in weight.

All samples were lightly ground in a mortar before measurement of their heats of solution.

Integral heats of solution were measured in a rather crude calorimeter (9) consisting of a silvered Dewar flask equipped with a mechanical stirrer and a Beckmann thermometer. Samples which usually weighed between 0.2 and 0.5 g were dissolved in 1 000 ml of distilled water at 29.0 °C.

The heat capacity of the calorimetric system was determined from the change in temperature caused by application of a known quantity of electrical energy for a measured time to a heater made of B. and S. 28 chromel wire. Rectified power was supplied by an Eico low ripple battery eliminator (manufactured by Electronic Instrument Co. Inc., L. I. City 1, N.Y.). Throughout the heating period the current and voltage remained steady at, for example, 0.801 ± 0.002 A and 5.99 ± 0.02 V. Time was measured with a stopwatch to about 600 ± 0.1 s.

Determination of the temperature change due to either energy input or solution of a sample, which is probably the limiting factor, appears to be accurate to about ±0.002 deg, since a Beckmann thermometer can be read to the nearest 0.001 deg, and the corrections for thermal radiation, calculated from the cooling curves before and after energy input or salt addition, are probably not subject to comparable errors. For each experiment the heat capacity was calculated by dividing the energy input in calories by the temperature change caused by the energy input. An average value of 1.24×10^3 cal/deg for the heat capacity of the calorimeter, based on many individual determinations, has been used in all calculations of heats of solution.

Since measured temperature differences are probably accurate to about ±0.002 deg, it appears that individual heats of solution are known to $1.24 \times 10^3 \times 0.002$ cal or about ±2.5 cal. Independent calibrations of the calorimeter to this accuracy or better have been made with several substances, including $Na_2SO_4.10H_2O$ and oxalic acid, which have well-known heats of solution.

RESULTS

The results are given in Tables I to IV and also in Figs. 1 to 4, where it may be seen that it has been established empirically that certain linear relations are obtained by plotting the heats of solution in calories per gram of solute against the percentages of water in the samples. For convenience the various sets of results will also be expressed in the form of straight line equations, calculated by the method of least squares. The vertical lines in Figs. 1 to 4 are at the monohydrate compositions.

TABLE I

Heats of solution for various hydrates of iron(II) sulfate

% water in sample	Heat of solution (cal/g)	Nature of sample or method of dehydration
13.20	40.9	Dehydrated at 100 °C
29.69	12.1	Dehydrated at 100 °C
32.54	6.1	Dehydrated over H_2SO_4
40.81	−8.8	Dehydrated over H_2SO_4
45.36	−16.1	Crystalline heptahydrate
12.11	144.7	Vacuum dehydration
18.32	115.9	Vacuum dehydration
22.60	92.1	Vacuum dehydration
32.28	46.5	Vacuum dehydration
38.69	17.8	Vacuum dehydration
41.11	1.2	Vacuum dehydration
45.36	−16.1	Crystalline heptahydrate

Iron(II) Sulfate

The heats of solution for samples of $FeSO_4.7H_2O$ which were dehydrated by various methods are given in Table I and in Fig. 1. The line AB joins de Forcrand's values (10) for the crystalline monohydrate (10.60% water) and the anhydride. The present line BC for the higher crystalline hydrates gives close agreement with values reported by de Forcrand (10) for the monohydrate, the tetrahydrate (32.18% water), and the heptahydrate (45.36% water) and has the equation

$$y = -1.78x + 64.5.$$

Can. J. Chem. Downloaded from www.nrcresearchpress.com by 210.87.254.40 on 09/05/12
For personal use only.

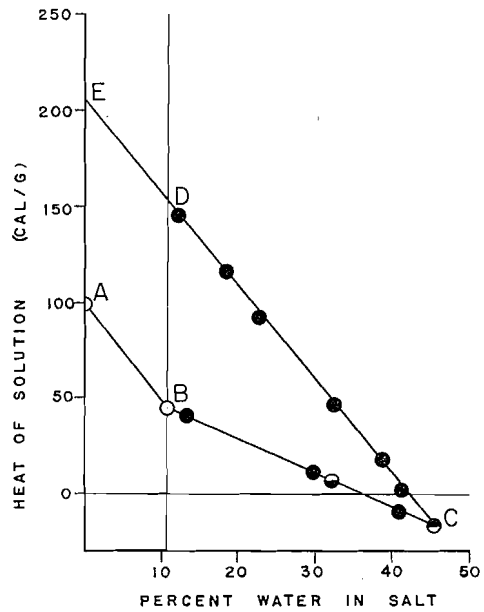

FIG. 1. Heats of solution for various hydrates of iron(II) sulfate: (○) earlier data, (●) present results.

Vacuum dehydration of $FeSO_4.7H_2O$ gave heat of solution results on the line CE with the equation

$$y = -4.86x + 203.6.$$

This line seems to be virtually parallel to the line AB for crystalline samples between the monohydrate and the anhydrous salt.

The heat of transition at any composition is just the difference in cal/g between the points on the two lines CD and BC at any desired percentage of water. Evidence that the vacuum dehydration products of $FeSO_4.7H_2O$ do revert to normal crystalline form has been reported (4). It is apparent that the maximum heat of transition DB to normal crystalline form of the high energy intermediates produced by vacuum dehydration of the heptahydrate is about 106.5 cal/g, which could be expressed as 18.1 kcal/mole of monohydrate or about 30 kcal/mole of $FeSO_4.7H_2O$. This maximum heat of transition is very much larger than the values (4, 5) which have been reported for other divalent metal sulfates.

Cobalt(II) Sulfate

Samples obtained by dehydration of $CoSO_4.7H_2O$ gave the results shown in Table II and in Fig. 2. The heat of solution of the heptahydrate (44.86% water) is in reasonable agreement with Thomsen's earlier value (6, 8). Again the lines AB and BC refer to crystalline samples. The equation of the line BC is

$$y = -2.80x + 114.7$$

while that of the line FH for samples dehydrated *in vacuo* is

$$y = -5.52x + 200.0.$$

Can. J. Chem. Downloaded from www.nrcresearchpress.com by 210.87.254.40 on 09/05/12
For personal use only.

TABLE II

Heats of solution for various hydrates of cobalt(II) sulfate

% water in sample	Heat of solution (cal/g)	Nature of sample or method of dehydration
10.98	85.5	Dehydrated at 100 °C
12.51	78.9	Dehydrated at 100 °C
23.48	46.4	Dehydrated at 100 °C
28.33	36.9	Dehydrated at 100 °C
30.92	30.3	Dehydrated over H_2SO_4
31.96	23.8	Dehydrated over H_2SO_4
44.86	−10.8	Crystalline heptahydrate
3.80	179.5	Vacuum dehydration
8.80	150.4	Vacuum dehydration
14.25	124.0	Vacuum dehydration
17.86	99.5	Vacuum dehydration
23.76	67.5	Vacuum dehydration
31.74	(25.9)	Calculated for crystalline tetrahydrate from line BC
25.41	98.7	Vacuum dehydration with BaO
26.43	88.0	Vacuum dehydration with BaO
40.93	8.8	Vacuum dehydration with BaO
44.86	−10.8	Crystalline heptahydrate

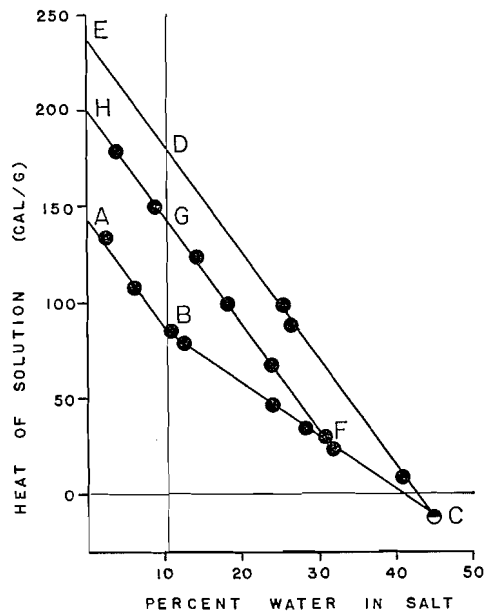

FIG. 2. Heats of solution for various hydrates of cobalt(II) sulfate: (○) earlier data, (●) present results.

Vacuum dehydration has been found to give results on this line unless barium oxide was present as desiccant, when the line CE was obtained. Again it appears that the lines AB, FH, and CE are all essentially parallel, so that the maximum heat of transition DB may be estimated as about 93.7 cal/g, which is 16.8 kcal/mole of monohydrate or about 26 kcal/mole of $CoSO_4.7H_2O$.

Can. J. Chem. Downloaded from www.nrcresearchpress.com by 210.87.254.40 on 09/05/12
For personal use only.

TABLE III

Heats of solution for various hydrates of nickel(II) sulfate

% water in sample	Heat of solution (cal/g)	Nature of sample or method of dehydration
29.07	28.8	Dehydrated at 100 °C
30.39	25.8	Dehydrated at 100 °C
33.16	17.7	Dehydrated at 100 °C
36.89	6.4	Dehydrated at 100 °C
38.25	0.0	Dehydrated at 100 °C
41.13	−6.0	Crystalline hexahydrate
10.85	128.9	Dehydrated at 100 °C
14.36	110.5	Dehydrated at 100 °C
14.89	109.4	Dehydrated at 100 °C
15.70	105.4	Dehydrated at 100 °C
17.81	93.8	Dehydrated at 100 °C
6.73	182.0	Vacuum dehydration
12.44	149.1	Vacuum dehydration
14.67	138.8	Vacuum dehydration
23.17	88.9	Vacuum dehydration
27.94	65.2	Vacuum dehydration
29.31	57.6	Vacuum dehydration
34.68	27.2	Vacuum dehydration
41.13	−6.0	Crystalline hexahydrate

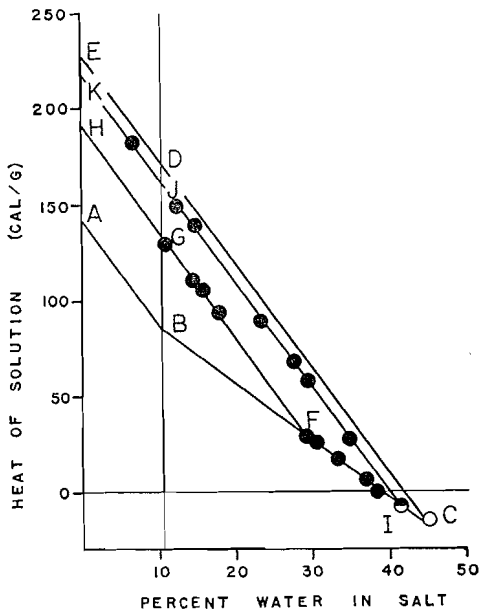

FIG. 3. Heats of solution for various hydrates of nickel(II) sulfate: (○) earlier data, (●) present results.

Nickel(II) Sulfate

The results obtained for samples of $NiSO_4.6H_2O$ dehydrated by various methods are given in Table III and in Fig. 3. Again there is reasonable agreement with previous values for the hexahydrate (11) and the heptahydrate (6, 8). The line BC for crystalline lower hydrates,

$$y = -3.00x + 116.2,$$

Can. J. Chem. Downloaded from www.nrcresearchpress.com by 210.87.254.40 on 09/05/12
For personal use only.

has been calculated for samples containing more than 29% water, since it has not been possible to prepare samples which give heats of solution on this line between B and F. Attempts to make crystalline hydrates with less than 29% water have given either insoluble samples or samples with heats of solution which fell on the line FG, which has the equation

$$y = -5.55x + 191.1.$$

In a previous rather cursory study (12) of this salt it was found that samples dehydrated either at 100 °C or *in vacuo* gave heats of solution in the vicinity of the point G. The vacuum dehydration products showed the complete absence of X-ray diffraction patterns. Vacuum dehydration in this laboratory, by a technique which is not obviously different from that previously used, except that ambient temperature was used instead of 40 °C, gave samples having heats of solution on the line IK, with the equation

$$y = -5.48x + 218.0.$$

Parallel lines AB and CE have been drawn through the points for the monohydrate (10.43% water) and the heptahydrate (44.90% water). Thus the maximum heat of transition DB to normal crystalline form of the high energy intermediates produced by vacuum dehydration of the heptahydrate has been estimated as 85.7 cal/g, which is 14.8 kcal/mole of monohydrate or about 24 kcal/mole of $NiSO_4.7H_2O$.

TABLE IV

Heats of solution for various hydrates of manganese(II) sulfate

% water in sample	Heat of solution (cal/g)	Nature of sample or method of dehydration
10.66	56.5	Crystalline monohydrate
37.37	17.2	Crystalline pentahydrate
8.53	114.7	Dehydrated at 100 °C
11.02	104.4	Dehydrated at 100 °C
13.07	95.6	Dehydrated at 100 °C
9.32	123.1	Vacuum dehydration
10.12	120.7	Vacuum dehydration
11.06	116.1	Vacuum dehydration
12.25	111.2	Vacuum dehydration
16.05	98.7	Vacuum dehydration
37.37	17.2	Crystalline pentahydrate

Manganese(II) Sulfate

The heats of solution for samples of $MnSO_4.5H_2O$ which were dehydrated by various methods are given in Table IV and in Fig. 4. The line BI has been calculated from the heats of solution of commercial samples of the monohydrate (10.66% water) and the pentahydrate (37.37% water) as

$$y = -1.47x + 72.2.$$

This line for the crystalline hydrates has been extrapolated to the heptahydrate composition at C (45.51% water).

When samples of the pentahydrate were heated at 100 °C in an attempt to prepare lower crystalline hydrates it was found that this salt had a marked tendency to form lower hydrates of high energy instead. The resulting samples gave heats of solution on the line FH, which has the equation

$$y = -3.76x + 145.9.$$

Can. J. Chem. Downloaded from www.nrcresearchpress.com by 210.87.254.40 on 09/05/12
For personal use only.

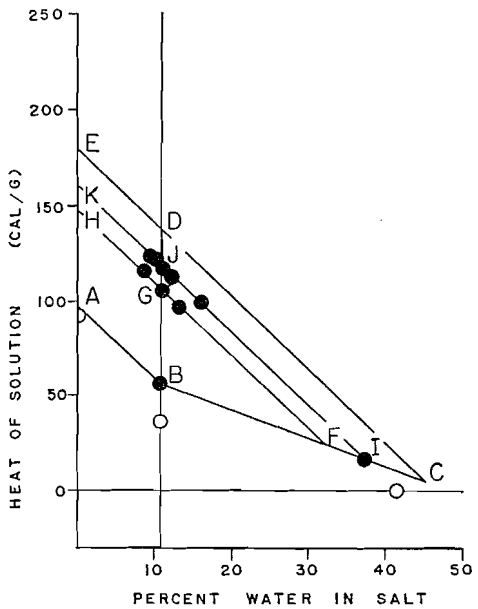

FIG. 4. Heats of solution for various hydrates of manganese(II) sulfate: (○) earlier data, (●) present results.

Similarly, vacuum dehydration of the pentahydrate gave results which fell along the line IK, with the equation

$$y = -3.77x + 158.3.$$

The lines AB and CE have been drawn parallel to FH and IK to facilitate comparison of the results for the hydrate system of manganese(II) sulfate with the results for the other three salts. Thus it is estimated that the maximum heat of transition DB for vacuum dehydration products of the heptahydrate would be about 80.2 cal/g, which could be expressed as 13.6 kcal/mole of monohydrate or about 22 kcal/mole of $MnSO_4.7H_2O$.

DISCUSSION

The maximum heats of transition DB to normal crystalline form of the high energy intermediates produced by vacuum dehydration of the heptahydrates have been directly measured for the sulfates of iron and cobalt, and obtained by extrapolation of the heat of solution data for lower hydrates of manganese sulfate and nickel sulfate. These values have been plotted in Fig. 5, from which it may be seen that the measured or calculated maximum heats of transition appear to be directly proportional to the original ligand field splitting energies of Jørgensen, quoted by Orgel (13), for the hexaaquo divalent cations of the same transition elements. The latter values are usually expressed in either cm^{-1} or kK (1 kilokayser (kK) = 1 000 cm^{-1}).

The data of Table V show that the maximum heats of transition, expressed as kcal/mole of each heptahydrate, are virtually identical with the ligand field splitting energies. It appears, however, that further study will be needed to definitely establish whether or not the correlation is valid and, if possible, to provide theoretical justification for it.

On the basis of the present results and the few other data available (2–5) it seems likely that high energy vacuum dehydration products can be obtained for any salt for which

Can. J. Chem. Downloaded from www.nrcresearchpress.com by 210.87.254.40 on 09/05/12
For personal use only.

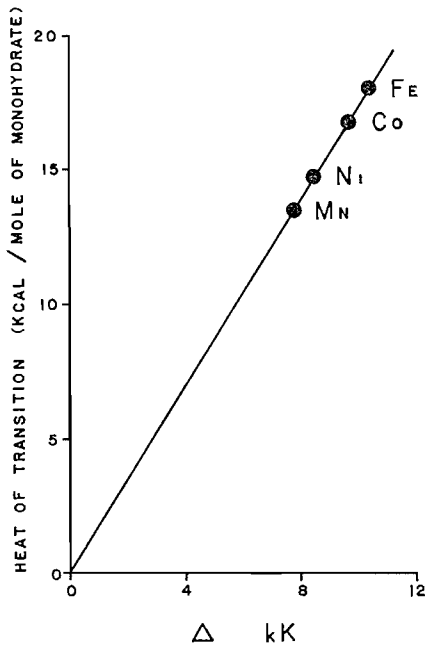

FIG. 5. Direct proportionality between maximum heats of transition and the corresponding ligand field splitting energies.

TABLE V

Ligand field deltas and maximum heats of transition

	Ligand field splitting energy		Maximum heat of transition	
Metal	kK	kcal/mole	kcal/mole	kK
Mn	7.8	22	22	7.8
Fe	10.4	30	30	10.4
Co	9.3	27	26	9.2
Ni	8.5	24	24	8.5

the heat of solution of the normal anhydride is higher than would be expected from an extrapolation of the values for the higher crystalline hydrates. For all the salts which have been found to form such high energy intermediates there has been a break in the heat of solution line for the crystalline hydrates as the anhydride has been approached. This break has usually appeared at the monohydrate composition.

When the heats of solution in cal/g are plotted against the percentages of water in various samples it may be seen that the maximum heats of transition DB for each high energy monohydrate and EA for the corresponding high energy anhydride are approximately equal. Hence, for any such simple salt for which the heats of solution of the anhydride and several crystalline hydrates are known, a line CE may be drawn (or calculated) through the point C for the heptahydrate and parallel to the line AB between the normal anhydride and the crystalline monohydrate. Points on the upper line CE may then be assumed to represent, at least approximately, the maximum possible heats of solution for vacuum dehydration products of the heptahydrate. Lower heats of solution,

Can. J. Chem. Downloaded from www.nrcresearchpress.com by 210.87.254.40 on 09/05/12
For personal use only.

and heats of transition to normal crystalline form may, however, be obtained if the method of dehydration allows the formation of one of the lower crystalline hydrates before high energy intermediates are formed.

The formation, in the presence of barium oxide as desiccant, of high energy vacuum dehydration products of $CoSO_4.7H_2O$ having heats of solution of the line CE, which seems to be the theoretical maximum high energy line, is not yet fully understood. It has, however, been established in similar experiments that vacuum dehydration of the manganese, iron, and nickel salts in the presence of barium oxide does not yield forms having higher energy, presumably because ordinary vacuum dehydration gives samples with heats of solution on the maximum possible high energy lines for the starting materials, i.e., the line IJK for $MnSO_4.5H_2O$, the line CD for $FeSO_4.7H_2O$, and the line IJK for $NiSO_4.6H_2O$.

ACKNOWLEDGMENTS

Financial assistance from the National Research Council is gratefully acknowledged. The authors are also grateful to Messrs. W. G. Baldwin, K. E. Stones, and W. K. Hancock, as well as to Miss B. A. Pattern, for their assistance at various stages of the experimental investigation.

REFERENCES

1. C. Slonim. Z. Elektrochem. **36**, 439 (1930).
2. M. Volmer and G. Seydel. Z. Physik. Chem. Leipzig, **A179**, 153 (1937).
3. K. G. Khomyakov. J. Phys. Chem. (USSR) **11**, 805 (1938).
4. G. B. Frost, K. A. Moon, and E. H. Tompkins. Can. J. Chem. **29**, 604 (1951).
5. J. W. S. Jamieson and G. B. Frost. Can. J. Chem. **34**, 583 (1956).
6. J. Thomsen. Thermochemische Untersuchungen. Barth, Leipzig. pp. 1882–1886.
7. J. Thomsen. Thermochemistry. Longmans, Green & Co., Ltd., London. 1908.
8. F. R. Bichowsky and F. D. Rossini. The thermochemistry of the chemical substances. Reinhold, New York. 1936.
9. D. P. Shoemaker and C. W. Garland. Experiments in physical chemistry. McGraw-Hill, New York. 1962.
10. R. de Forcrand. Compt. Rend. **158**, 20 (1914).
11. J. W. Mellor. A comprehensive treatise on inorganic and theoretical chemistry. Vol. XV. Longmans, Green & Co., Inc., New York. 1936.
12. J. W. S. Jamieson. M.Sc. Thesis, Queen's University, Kingston, Ontario. 1953.
13. L. E. Orgel. An introduction to transition-metal chemistry: ligand field theory. Methuen, London. 1960. p. 46.

Can. J. Chem. Downloaded from www.nrcresearchpress.com by 210.87.254.40 on 09/05/12
For personal use only.

THE DETERMINATION OF THE SATURATION VAPOR PRESSURE OF SOLID HYDROXYLAMINE USING A PISTON PRESSURE GAUGE[1]

R. A. BACK AND J. BETTS[2]
Division of Pure Chemistry, National Research Council, Ottawa, Canada
Received March 12, 1965

ABSTRACT

The saturation vapor pressure of solid hydroxylamine has been determined at temperatures from −12 to 7 °C and found to fit the equation

$$\log_{10} P \text{ (Torr)} = 11.7102 - 3352.6/T \text{ (°K)}.$$

From this have been calculated several thermochemical quantities, including a heat of sublimation of 15.34 kcal/mole, and a dissociation energy of 61.3 kcal/mole for the NH_2—OH bond. Vapor density measurements showed that hydroxylamine vapor consisted of single molecules of NH_2OH at 0.27 Torr and 25 °C.

A novel pressure gauge used in the measurements is described. Pressures were determined with an accuracy of ±0.001 Torr by measuring the force acting on a piston, moving freely in a glass cylinder, suspended on the arm of a torsion balance.

INTRODUCTION

In connection with a study of the photolysis of hydroxylamine vapor (1), an accurate knowledge of the saturation vapor pressure was required. Values for the liquid between temperatures of 39 and 110 °C are quoted in a review by Stull (2); the source of these data is not clear. They appear to be based on an extrapolation from reported boiling points of 57° at 22 Torr (3) and 70° at 60 Torr (4), and because the liquid is notably unstable at these temperatures, the data are of dubious merit. To minimize thermal decomposition both of the vapor (in which decomposition increases sharply with rising pressure (1, 5)) and of the condensed phase, our present measurements and photolysis experiments have been made with the solid well below its melting point (32 °C) and with correspondingly low vapor pressures.

The pressures involved (0.08 to 0.5 Torr) fall in a somewhat awkward region for accurate measurement of the absolute pressure of a condensable vapor. A simple gauge of novel design was devised in which the pressure of the vapor acting on a glass piston moving freely in a close-fitting glass cylinder was measured by a torsion balance. In theory such a gauge promises high sensitivity, since 1 Torr pressure with a piston of 1 cm^2 area gives a force of about 1.4 g, a quantity easily measured to one part in a thousand by a very ordinary torsion balance. In practice its performance was close to these expectations.

EXPERIMENTAL

The glass cylinder and piston used in the pressure gauge were from a 5 cc, "Super Ward" hypodermic syringe made by Becton, Dickinson and Co., taken from stock. The piston, about 12 mm in diameter, was cut to a length of about 20 mm and weighed about 3 g; its weight was approximately balanced by a counterpoise. The torsion balance was a Precision Torque Balance obtained from Vereenigde Draadfabrieken, Nijmegen, Holland, with a tungsten torsion wire, a rated capacity of 3.5 g, and a sensitivity of ±1 mg. The balance was returned to a null position by rotation of one end of the torsion wire, with 300° rotation corresponding to about 1 g. The balance was modified to permit evacuation of the chamber enclosing the balance arm, the torsion wire, and the cylinder above the piston, with the torsion wire controls operating through rubber "O" rings. Continuous pumping maintained a pressure of about 0.001 Torr which was added to all pressure readings.

[1]*Issued as N.R.C. No. 8492.*
[2]*National Research Council Postdoctorate Fellow, 1962–1964. Present address: Department of Chemistry, Carleton University, Ottawa, Canada.*

To measure the pressure of a gas or vapor, it was admitted to the cylinder below the piston, and the torsion wire was rotated to balance the force on the piston, restoring the balance to its null position. A tendency of the piston to stick slightly in the cylinder was countered by gently thumping the bench supporting the pressure gauge. The null point could be set with an accuracy corresponding to ±0.001 Torr.

The gauge was calibrated with nitrogen against a sloping (about 1 in 10) one-armed manometer filled with Octoil-S (2-ethyl hexyl sebacate) with a measured density of 0.9108 g/cc at 24.5 °C. This calibration is shown in Fig. 1, and gave a value of 0.5716 Torr for full-scale rotation of the torsion head. This value was in fair agreement with one calculated from the specified sensitivity of the balance, the area of the piston, and the length of the cross arm; the latter is a less accurate value.

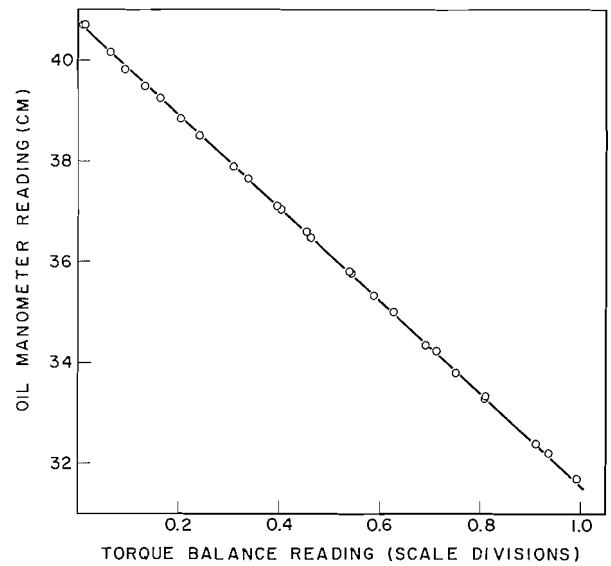

FIG. 1. Calibration of piston pressure gauge against an oil manometer.

The hydroxylamine, prepared by the method of Hurd and Brownstein (6), had a melting point close to the accepted value of 32.05 °C. It was stored in the vacuum line at −78 °C and purified as required by repeated sublimation in vacuo from 0 °C to −60 °C until the saturation vapor pressure reached a constant minimum value.

The saturated vapor pressure was measured by holding the solid at constant temperature and allowing the vapor to fill a volume of about 0.2 l. Pressure readings taken over a period of about 10 min showed a steady increase due to thermal decomposition (about 0.025 Torr/h at 0 °C); these were extrapolated to zero time to obtain the vapor pressure. The molecular weight of hydroxylamine vapor was determined by allowing it to fill a volume of 5.44 l at about 0.27 Torr pressure and room temperature, and then condensing it at −196 °C into a thin-walled Pyrex phial. The phial was sealed off, weighed, and weighed again after opening and standing over concentrated sulfuric acid in a desiccator for several days. In this way, hydroxylamine, or ammonia and water formed by its decomposition, were removed, while any mercury that had condensed out with the hydroxylamine was retained (mercury was present in the vacuum line). Buoyancy corrections were applied for the air displaced by the phial.

RESULTS AND DISCUSSION

The saturation vapor pressure data are plotted in Fig. 2. A least-squares treatment gave the equation

$$\log_{10} P \text{ (Torr)} = 11.7102 - 3352.6/T \text{ (°K)}.$$

From this equation were calculated the vapor pressures and standard molar enthalpies, free energies, and entropies of sublimation, at 0 °C and at the melting point, shown in Table I. These data are not in good agreement with those quoted by Stull (2) for liquid hydroxylamine, which gave a heat of vaporization of 17 kcal/mole and an extrapolated saturation vapor pressure of 2.6 Torr at 32.05 °C. The latter data are of uncertain origin and subject to error caused by thermal decomposition of the liquid, as discussed earlier.

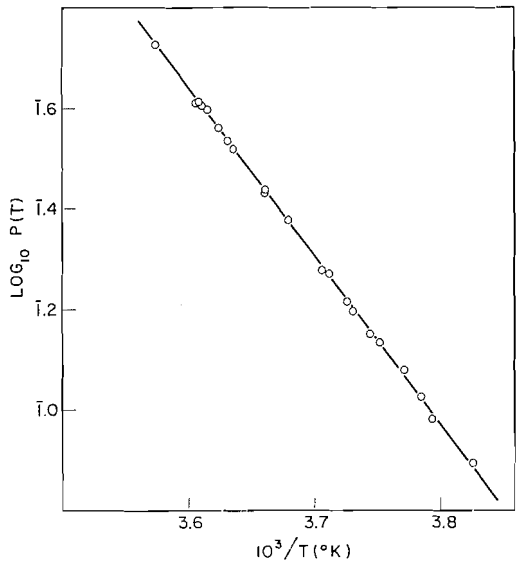

FIG. 2. Saturation vapor pressure of hydroxylamine.

TABLE I

Thermochemical data for the sublimation of hydroxylamine vapor

T (°C)	Saturated vapor pressure (Torr)	ΔH (kcal/mole)	ΔF (kcal/mole)	ΔS (cal/deg mole)
0	0.273	15.34	4.30	40.4
32.05 (m.p.)	5.31	15.34	3.01	40.4

From our extrapolated value for the vapor pressure at the melting point, combined with Bruhl's reported boiling point of 57° at a pressure of 22 Torr (3), vapor pressure data for the liquid can be computed which should be more reliable than those quoted by Stull. Estimates of the heat of vaporization (11.4 kcal/mole) and thence of the heat of fusion, and the hypothetical boiling point of the liquid at atmospheric pressure, can also be made; in Table II, these and other physical constants of hydroxylamine are compared with those of hydrazine (7) and hydrogen peroxide (8). With the notable exceptions of the high melting point and the related high heat of fusion, the properties of hydroxylamine lie, not unexpectedly, between those of the other two. The volatility of hydroxylamine as reflected in the vapor pressure, the boiling point, and the heat of sublimation, is considerably closer to that of hydrogen peroxide than to that of hydrazine.

TABLE II

Physical constants of hydrazine, hydroxylamine, and hydrogen peroxide

	N_2H_4	NH_2OH	H_2O_2
Melting point (°C)	2	32.05	−0.43
Boiling point at 760 Torr (°C)	113.5	~142 (extrapolated)	150.2
Vapor pressure at 0 °C (Torr)	2.69	0.273	0.26
Vapor pressure at melting point (Torr)	3.2	5.31	0.26
Heat of sublimation at 0 °C (kcal/mole)	14.6	15.34	15.6
Heat of fusion (kcal/mole)	3.025	3.94	2.987

The molecular weight determinations confirmed that hydroxylamine vapor at room temperature and 0.27 Torr pressure consisted largely of single molecules of NH_2OH. Experimental values, determined from the ideal gas equation, were 32.9, 34.6, and 33.9 for three samples (theoretical value = 33.03). These data also provide a rough confirmation of the purity of the hydroxylamine.

Taking the standard heats of formation of solid hydroxylamine (9) and the hydroxyl (10) and amino (11) radicals to be -25.5, $+10.1$, and $+41$ kcal/mole respectively, we can calculate a heat of formation of gaseous NH_2OH of -10.2 and thence a bond dissociation energy of 61.3 kcal/mole for the NH_2—OH bond. Cottrell (10) has calculated a value of 48 by a very similar process, using an estimated heat of sublimation. The reason for the large discrepancy is not clear; one possibility is that Cottrell took the wrong sign for the heat of solution of solid hydroxylamine (9), -3.8 kcal, and slightly overestimated the heat of sublimation. Our value of 61.3 kcal for the NH_2—OH bond may be compared with 51 for HO—OH and 60 for NH_2—NH_2 (10); it is apparent that the extreme thermal instability of hydroxylamine is not a matter of bond energy, but probably depends on a higher susceptibility to surface reaction than hydrazine or hydrogen peroxide.

Finally, the piston pressure gauge deserves some comment. This instrument showed excellent sensitivity and reproducibility (Fig. 2) which could probably be improved further. It measures absolute pressure directly, and glass is the only material in contact with the gas being measured. The cost of the gauge was about one-tenth that of commercially available diaphragm or quartz spiral gauges with about the same sensitivity. Its chief limitations are the tendency of the piston to stick in the cylinder, and leakage of gas past the piston. The latter, measured with air at a pressure of 1 Torr, was about 4 μmole/h and probably varies linearly with pressure. This was of no consequence in the present experiments, but could be inconvenient in a static system of small volume. The sticking of the piston was minimized by keeping the system free of grease and dust. Both the leakage and the sticking might be improved by more precise fitting of the piston to the cylinder. No attempt was made to do so; the piston and cylinder were simply taken from a stock hypodermic syringe without special care or selection. The piston was also heavier than it needed to be, which overloaded the torsion balance somewhat and reduced its sensitivity; this could be remedied by a specially made piston. All things considered, the gauge shows considerable promise as a convenient absolute pressure gauge for an awkward region of pressure.

Several piston pressure gauges have been described previously (12, 13, 14), with that of Ernsberger and Pitman (12) most closely resembling ours. They employed a mica-disc piston suspended on a quartz spiral whose deflection was proportional to the pressure difference across the piston. The working range of the gauge was lower than ours (0.5 to 20 microns) and leakage was probably greater. Hutton's gauge (13) operated at higher pressures than ours (0.1 to 12.5 Torr), while that of Douslin and McCullough (14) was oil-lubricated and measured pressures from 0.01 to 40 Torr. Both these latter gauges operated on a tilting deadweight piston principle, with Hutton (13) using a rotating cylinder to avoid sticking of the air-lubricated piston. The gauge of Ernsberger and Pitman could have probably been modified for our present purposes, although leakage might well have been a serious problem at the higher pressures. A compromise probably must be struck between leakage and sticking, and a quartz spiral suspension might be more affected by a sticking piston than was the torsion balance used in the present instrument.

REFERENCES

1. J. BETTS and R. A. BACK. To be published.
2. D. R. STULL. Ind. Eng. Chem. **39**, 517 (1947).
3. J. W. BRÜHL. Ber. **26**, 2508 (1893).
4. M. C. A. LOBRY DE BRUYN. Rec. Trav. Chim. **10**, 100 (1891).
5. R. N. SMITH and P. A. LEIGHTON. J. Am. Chem. Soc. **66**, 172 (1944).
6. C. DE W. HURD and H. J. BROWNSTEIN. J. Am. Chem. Soc. **47**, 67 (1925).
7. C. C. CLARK. Hydrazine. Mathieson, Baltimore. 1953.
8. W. C. SCHUMB, C. N. SATTERFIELD, and R. L. WENTWORTH. Hydrogen peroxide. Reinhold, New York. 1955.
9. F. R. BICHOWSKY and F. D. ROSSINI. The thermochemistry of chemical substances. Reinhold, New York. 1936.
10. T. L. COTTRELL. The strengths of chemical bonds. 2nd ed. Butterworths, London. 1958.
11. M. SZWARC. Chem. Rev. **47**, 75 (1950).
12. F. M. ERNSBERGER and H. W. PITMAN. Rev. Sci. Instr. **26**, 584 (1955).
13. V. O. HUTTON. J. Res. Natl. Bur. Std. C, **63**, 47 (1959).
14. D. R. DOUSLIN and J. P. MCCULLOUGH. U.S. Bureau of Mines Report No. 6149. 1963.

Can. J. Chem. Downloaded from www.nrcresearchpress.com by 210.87.254.42 on 09/05/12
For personal use only.

THE MECHANISM OF THE ANOMERIZATION OF THE TETRA-*O*-ACETYL-D-GLUCOPYRANOSYL CHLORIDES

R. U. LEMIEUX AND JUN-ICHI HAYAMI[1]
Department of Chemistry, University of Alberta, Edmonton, Alberta
Received January 25, 1965

ABSTRACT

The anomerization of the tetra-*O*-acetyl-D-glucopyranosyl chlorides in acetonitrile is first order in chloride ion. Experiments with ^{36}Cl-labelled chloride ion showed the reaction to involve nucleophilic attack (S_N2) by chloride ion at the anomeric center. The reaction is accompanied by a faster dissociation of the β-anomer (I) to the 1,2-acetoxonium ion. Although the rate of anomerization was slightly accelerated by addition of benzene, the ionic reaction was strongly suppressed. Bromide ion was less effective than chloride ion in catalyzing the reaction and iodide ion was least effective. Reaction of tetra-*O*-acetyl-α-D-glucopyranosyl bromide with tetraethylammonium chloride in acetonitrile rapidly gave I in high yield. The anomeric effect for chlorine appears to be about 2 kcal/mole.

INTRODUCTION

The acetylated glycosyl halides have played a central role in the chemical synthesis of a wide variety of glycosides. Although the reaction properties of these important compounds have received considerable attention (1), there has not been reported, to date, a study of the anomerization of these compounds. Such studies gained immediate importance through the observation by Lemieux and Morgan (2) that the presence of bromide ion can strongly influence the course of the reaction of tetra-*O*-acetyl-α-D-glucopyranosyl bromide by catalyzing its anomerization to the β-form.

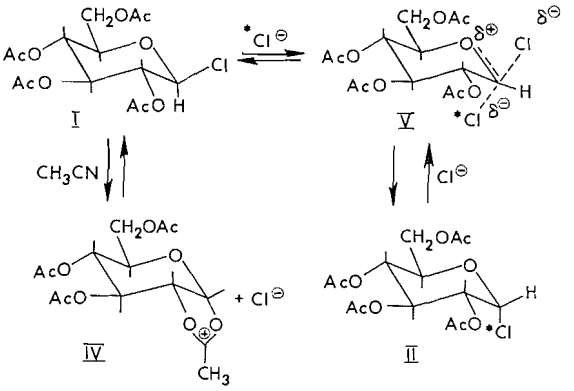

Lemieux and Brice (3) observed the anomerization of tetra-*O*-acetyl-β-D-glucopyranosyl chloride (I) to the α-anomer in the course of the reaction of β-D-glucopyranose pentaacetate with titanium tetrachloride. Recently, Korytnyk and Mills (4) anomerized I using aluminum chloride in refluxing chloroform. The reaction properties of I early indicated that the compound possesses the 1,2-*trans*-configuration and this conclusion was later fully substantiated by the nuclear magnetic resonance (n.m.r.) spectra for I and its anomer (5, 6). Furthermore, the n.m.r. spectra required the chlorine in I to be in

[1]*Postdoctorate Fellow, 1963–1964.*

equatorial orientation and to be axially disposed in the more stable α-anomer. This apparent anomaly has been termed the "anomeric effect" and is attributed to presence of strong intramolecular dipole–dipole interactions (7, 8).

Although the β-chloride (I) has often been reported to give rise to mutarotation in chloroform solution, Korytnyk and Mills (4) traced this phenomenon to hydrolysis and showed that the compound is highly stable under strictly anhydrous conditions. Tetra-*O*-acetyl-β-D-glucopyranosyl bromide was recently prepared (9) and shown to have reaction properties closely analogous to those of the β-chloride (I).

This communication is primarily concerned with the results of a detailed study of the halide-ion catalyzed anomerization of the tetra-*O*-acetyl-D-glucopyranosyl chlorides in acetonitrile. It is shown that these and closely related reactions proceed by way of a mechanism which corresponds kinetically to bimolecular nucleophilic substitution reactions.

DISCUSSION OF RESULTS

Although tetra-*O*-acetyl-β-D-glucopyranosyl chloride (I) remained virtually unchanged over several hours when dissolved in pure dry acetonitrile at room temperature, addition of chloride ion in the form of tetraethylammonium chloride produced a rapid reaction as evidenced by the change in the rotation of the solution. The course of the reaction could be followed polarimetrically and, as expected, after the optical rotation had reached a constant value the product consisted of the equilibrium mixture of I and its α-anomer (II). The equilibrium constant at 30°, starting with a 0.2 *M* solution of I in acetonitrile and 0.2 *M* in tetraethylammonium chloride, was 20.6 as determined by isotopic dilution analysis for the β-anomer (I) and 13.1 as determined by a similar analysis for the α-anomer (II). On this basis, at equilibrium, the solution contained 4.6 to 7.0% of the β-anomer I. The specific rotations of I and II under the reaction conditions were $-8.0°$ and $+162°$, respectively. On the basis of these rotations and the results of the isotopic dilution analyses of the equilibrium mixture, equilibrium specific rotations in the range 150–154° are expected. In fact, in all the equilibration studies conducted at 30°, equilibrium specific rotations in the range 141–148° were obtained. As will be seen later on, evidence was obtained that all the reactions involved some hydrolysis because of our inability to completely exclude water. Therefore, it was to be expected that the observed equilibrium rotations would be somewhat lower than those calculated from the results of the isotopic dilution analyses.

The isotopic dilution analyses require 93–95% of the α-anomer (II) in the equilibrium mixture. To calculate velocity constants from the polarimetric data, an equilibrium constant of 16 (94% of II) for the reaction I $\rightleftarrows$ II was assumed. The *A*-value [$-\Delta G$ (10)] for chlorine appears to be in the order of 0.5 kcal/mole (10, 11). On this basis, the anomeric effect for chlorine would be about 2 kcal/mole. This value may be high since the *A*-value for chlorine is probably greater for the 1-position of a pyranose ring than for a cyclohexane ring. Nevertheless, it is evident that the anomeric effect is considerably greater for chlorine than that [about 1.5 kcal/mole (8)] for the acetoxy group. This result is in accord with expectation based on the relative magnitudes of the dipole moments (12) for the C—O (1.5 D) and C—Cl (2.2 D) bonds and the theory advanced by Lemieux and Chü (7, 8) for the origin of the anomeric effect (13).

Table I reports some results of a kinetic study of the anomerizations of I and II, and the data provide an indication of the quality of the results which were obtained. It is seen that, under the conditions studied, the polarimetric data provided good first-order

Can. J. Chem. Downloaded from www.nrcresearchpress.com by 210.87.254.42 on 09/05/12
For personal use only.

TABLE I

Polarimetric rates for the anomerization of tetra-*O*-acetyl-β-D-glucopyranosyl chloride (I)*

Expt. No.	Time, min	Observed rotation, degrees	$k_\alpha + k_\beta \times 10^3$, min^{-1}
1	22	0.590	3.82
	52	1.080	3.73
	72	1.380	3.81
	132	2.170	3.74
	172	2.605	3.75
	192	2.799	3.74
	452	4.392	3.83
	∞	5.30	3.77†
2	12	0.904	4.15
	32	1.324	4.26
	52	2.059	4.19
	92	3.383	4.17
	132	4.517	4.18
	232	6.639	4.19
	462	9.202	4.24
	∞	10.77	4.20†
3	3	0.038	(−17)
	5	0.132	(−2.4)
	9	0.317	(2.8)
	15	0.481	3.93
	20	0.575	3.96
	30	0.756	3.97
	40	0.930	3.98
	∞	5.20	3.96†

*The reactions were conducted at 30° in dry acetonitrile 0.2 *M* in both I and tetraethylammonium chloride.
The specific rotations at equilibrium (t_∞) were 144.5°, 146.8°, and 141.5° for experiments 1, 2, and 3, respectively. The initial observed rotations obtained by extrapolation of the linear part of a log plot were −0.350, −0.008 and +0.195° for experiments 1, 2, and 3, respectively.
†Average values.

kinetics after the reaction had been allowed to proceed for at least 10 min. However, the rotations at zero time obtained by extrapolation of the linear part of the log plots varied considerably and, as seen from experiment 3, velocity constants calculated from the data obtained in the first few minutes of the reaction are meaningless. We attribute this initial behavior to the presence of traces of water present in the system which are involved in a fast reaction. As will be seen later on, the anomerization reaction under these conditions is accompanied by a faster dissociation of the β-chloride (I) to the 1,2-acetoxonium ion (IV). The situation is closely similar to that observed by Lemieux and Brice (3) for the anomerization of β-D-glucopyranose pentaacetate in acid media, a phenomenon which has received detailed study (14, 15). Lemieux and Cipera (16) have shown that the acetoxonium ion is an extremely effective scavenger for water. It was recently shown that the first isolable product of this reaction is 1,3,4,6-tetra-*O*-acetyl-α-D-glucopyranose (17), a strongly dextrorotatory compound, $[\alpha]_D$ +141.1° (*c*, 3 in chloroform). In fact, when the β-chloride was added to the presumably dry acetonitrile, there was observed a slight increase in the rotation of the mixture, from −0.21 (initial) to +0.10° over a period of about 12 min. The rate of the increase then diminished greatly. This initial side reaction could not be excluded by the means at our disposal and, unfortunately, precluded the achievement of highly precise measurements of certain features of the reaction. Nevertheless, as will be seen later on, the important features of the reaction were not obscured. We estimate the amounts of water required for the interference noted to be in the order of 0.02% of the reaction mixture.

Can. J. Chem. Downloaded from www.nrcresearchpress.com by 210.87.254.42 on 09/05/12
For personal use only.

TABLE II

Polarimetric rates for the anomerization of tetra-*O*-acetyl-β-D-glucopyranosyl chloride 0.2 *M* in acetonitrile at 30° and 40°

Temp., °C	Concentration of added tetraethylammonium salt		Velocity constant, $(k_\alpha + k_\beta) \times 10^3$, min^{-1}
	Chloride	Perchlorate	
30	0.2	0	3.9
	0.2	0.1	3.9
	0.2	0.2	3.9
	0.4	0	7.8
	0.6	0	10.6
40	0.2	0	12.4

Table II presents data related to the effect of the chloride ion concentration on the rate of the anomerization. It is seen that the rate was essentially doubled by doubling the concentration of the chloride ion. That this effect was not related to the increase in salt concentration is evident from the experimentally insignificant effects on rate observed on the addition of tetraethylammonium perchlorate. It is clearly evident, therefore, that the reaction is first order both in chloride ion and the acetochloroglucose (I or II). As indicated in Table II, the rate of the reaction was increased by a factor of 3.2 on raising the temperature from 30° to 40°. It was not possible at this time to obtain reliable data at other temperatures. The polarimetric rates for anomerization conducted under the conditions reported in Table I provide the sum of the velocity constants, $k_\alpha + k_\beta$, to be about 4.0×10^{-3} min^{-1}. On the basis of an equilibrium constant of $16 = k_\beta/k_\alpha$, the values for the individual velocity constants are $k_\alpha = 0.23 \times 10^{-3}$ and $k_\beta = 3.77 \times 10^{-3}$ min^{-1}.

The results of a study of the incorporation of ^{36}Cl-labelled chloride ion into both the β-chloride (I) and the α-chloride (II) are presented in Table III. In view of the inevitable small loss of the β-chloride to the traces of water, it was decided to determine its change in concentration in the course of the reaction by isotopic dilution analysis. The amounts present after 15, 30, and 90 min reaction times are given in Table III. This rate of disappearance of I requires a velocity constant of 3.6×10^{-3} min^{-1} for the reaction, in good agreement with the polarimetric rate. On the basis of these data, it is calculated that 94.2% of the β-chloride (I) survived hydrolysis. From this amount of I as the initial amount in the reaction mixture the percentages of I present after the various reaction times were calculated, and the results of these calculations are presented in Table III.

The procedure used to follow the incorporation of radioactivity from the chloride ion into the acetochloroglucoses was as follows. In view of the problem of excluding water from the system, the experiments were conducted batchwise in sealed tubes. After each of the reaction times noted in Table III, a solution was diluted with benzene and extracted four times with water under carefully standardized conditions. The fourth aqueous extract was devoid of appreciable radioactivity. The total activity in the combined aqueous extracts was then determined and the specific activity of the chloride ion calculated. The total activity in the benzene solution was also determined. The sum of the radioactivities found in the aqueous and benzene layers agreed with the amount expected from the radioactivity of the chloride ion introduced into the reaction mixture.

The experiments listed in Table III were conducted to only about 50% conversion of I since it was necessary to isolate pure I from the reaction mixture. This could only be accomplished with these relatively high concentrations of I in the reaction product. To

Can. J. Chem. Downloaded from www.nrcresearchpress.com by 210.87.254.42 on 09/05/12
For personal use only.

Can. J. Chem. Downloaded from www.nrcresearchpress.com by 210.87.254.42 on 09/05/12
For personal use only.

TABLE III

Rate of the exchange of tetra-*O*-acetyl-β-D-glucopyranosyl chloride (I) with tetraethylammonium chloride-^{36}Cl (III) in acetonitrile at 30°*

Reaction time, min	Unreacted I, %			Spec. activity of I × 10^{-5}, c.p.m./mmole	Total act. of I × 10^{-5}, c.p.m./mmole	Total act. org. layer × 10^{-5}, c.p.m.	Spec. act. of II × 10^{-5}, c.p.m./mmole	Spec. act. of Cl^- × 10^{-5}, c.p.m./mmole
	Found†	Calcd.‡	In org. layer§					
0	—	94.2	—	—	—	—	—	—
5	—	92.5	88.5	0.31	0.22	0.475	19.8	17.7
15	89.8	89.3	85.5	1.68	1.15	1.80	17.5	16.2
30	84.4	84.6	81.0	3.05	1.98	3.02	14.3	15.0
45	—	80.2	76.7	4.75	2.92	4.41	14.0	12.9
90	68.4	68.4	65.5	—	—	—	—	—
180	—	49.7	47.5	8.96	3.40	7.14	11.1	9.3

*The initial concentrations were 0.2 *M* in I and 0.2 *M* in III with a specific activity of 19.46 × 10^5 c.p.m./mmole and total activity of 15.57 × 10^5 c.p.m.
†By isotopic dilution analysis.
‡Calculated from the isotopic dilution analyses.
§Corrected for hydrolysis during the isolation.

Can. J. Chem. Downloaded from www.nrcresearchpress.com by 210.87.254.42 on 09/05/12
For personal use only.

insure that the radioactivity found in I did not in part arise from the α-anomer (II) as a contaminant, after I had been recrystallized twice, a 10% amount of radioinactive II was added as hold-back carrier. After two recrystallizations, pure I was obtained and its specific activity was determined. The specific activities of I after various reaction times are given in Table III.

To obtain the total activity present in I after the various reaction times listed in Table III, it was necessary to be sure that the acetochloroglucoses underwent negligible hydrolysis in the course of the isolation procedure. In fact, it was found that the α-anomer (II) could be quantitatively recovered from solutions in acetonitrile. However, in repeated experiments only 95.7% of the expected radioactivity was found in the benzene layer when the β-chloride was used. Since this result was highly reproducible and had to arise from hydrolysis of I in the course of the isolation, the amounts of I in the benzene layers were taken as 95.7% of the amounts calculated to be present. From these amounts and the specific activities determined for the samples of I which were isolated, the activities expected to arise from I in each of the benzene layers were calculated. The results of these calculations are presented in Table III. The differences between these activities and the total activities found in the benzene layers were than taken as arising from the α-chloride (II). The number of millimoles of II present in each of the benzene layers was calculated from the expected extents of anomerization. On this basis, the specific activities of the samples of II present in each of the benzene layers were calculated and the results are listed in Table III. The specific activities of the chloride ions present in each of the aqueous layers could be calculated from the total activities found in the aqueous layers and the expected number of millimoles responsible for this activity. The number of millimoles was taken in each case as the initial 0.8 millimoles plus 5.8% of 0.8 mmoles due to hydrolysis of the β-chloride (I) during the first 10–15 min of the reaction. The specific activities for the chloride ion after the various reaction times are listed in Table III.

A consideration of the last two columns in Table III shows a good correspondence between the specific activity of the chloride ion and that calculated for the α-anomer (II) after each of the reaction times. Over the period of the reaction studied, only a very small amount of the α-anomer would have undergone reversion to the β-form. Consequently, unless there existed an intramolecular mechanism for the anomerization of I to II, as known to occur for methyl tetra-*O*-acetyl-β-D-glucopyranoside (18), the specific activity of the α-anomer (II) formed from I should be virtually the same as that of the ambient chloride ion. In fact, this is seen to be the case and the results exclude an intramolecular mechanism. Therefore, it is apparent that, as expected from the kinetic data, the mechanism of the anomerization involves nucleophilic attack by chloride at the anomeric center with subsequent inversion of the anomeric center. This conclusion was substantiated by a study of the relative rates of exchange and anomerization of the α-chloride (II).

The α-chloride (II) was reacted with ^{36}Cl-labelled tetraethylammonium chloride under the conditions shown in Table IV. After the various reaction times, benzene was added and the salt was removed by washing with water. The radioactivity in the benzene solution was then determined. This radioactivity was incorporated into both the β-(I) and α-(II) chlorides and is a measure of the extent to which the α-chloride (II) had reacted with chloride ion in the specified reaction time. The rate of the incorporation of radioactivity should be the same as the rate of the α to β anomerization if the process involves a nucleophilic attack by chloride ion with inversion of the anomeric center.

TABLE IV

Rate of the exchange of tetra-*O*-acetyl-α-D-glucopyranosyl chloride (II) with tetraethylammonium chloride-^{36}Cl (III) in acetonitrile at 30°*

Reaction time, min	Total activity incorporated $\times 10^{-5}$, c.p.m.	Velocity constant for the incorporation $\times 10^{4}$, min^{-1}	Spec. activity of II $\times 10^{-5}$, c.p.m./mmole
0	0	—	—
240	0.382	2.17	0.255
360	0.511	1.95	0.432
600	0.789	1.84	0.787
1200	1.552	1.93	1.661
∞	(7.50)	—	—
		Av. 2.0	

*The initial concentrations were 0.2 *M* in II and 0.2 *M* in III with a specific activity of 18.8×10^5 c.p.m./mmole and total activity of 15.0×10^5 c.p.m.

It is seen that, in fact, the velocity constant for the incorporation, average value = 2.0×10^{-4} min^{-1}, is in close agreement with the polarimetric value for $k_\alpha = 2.3 \pm 0.4 \times 10^{-4}$ min^{-1}. Table IV also contains the specific activities found for the α-chloride (II) after the various reaction times. It can be shown by obvious approximate methods of analysis that these specific activities correspond reasonably closely to those expected on the basis that the radioactive II arises from first-formed radioactive I. An exact mathematical treatment was not attempted. Nevertheless, it is clearly apparent that the α-chloride did not undergo direct exchange with the chloride ion. This was not the case for the β-anomer (I).

The specific activities found for the β-chloride (I) in the course of the exchange reaction reported in Table III are too high for the radioactivity to have been incorporated by way of the α-anomer. Therefore, the β-chloride, unlike the α-anomer, underwent exchange of the chlorine by way of mechanism other than anomerization. This exchange is readily accounted for on the basis of dissociation of I to the 1,2-acetoxonium ion (IV) followed by the return reaction of IV with chloride ion to reform I. It is seen from Table V that

TABLE V

Velocity constants, k_β, for the exchange of tetra-*O*-acetyl-β-D-glucosyl chloride (I) with tetraethylammonium chloride-^{36}Cl (III) at 30°

Reaction time, min	$k_\beta \times 10^3$, min^{-1}						
	Expt. 1* exchange	Expt. 1* anomerization	Expt. 2† exchange	Expt. 3‡ exchange	Expt. 3‡ anomerization	Expt. 4§ exchange	Expt. 4§ anomerization
15	12.7	3.77‖	17.6	14.9	3.87‖	0.86	4.31‖
30	12.3		17.5	17.7		1.78	
45	15.2						

*Acetonitrile 0.2 *M* in both I and III.
†Acetonitrile 0.2 *M* in I, 0.1 *M* in III, and 0.1 *M* in tetraethylammonium perchlorate.
‡Acetonitrile 0.2 *M* in each of I, III, and tetraethylammonium perchlorate.
§Acetonitrile containing 40 mole % of benzene and 0.2 *M* in both I and III.
‖Average value determined polarimetrically using 16 for the equilibrium constant.

the rate of the incorporation of radioactivity from the chloride ions by the β-chloride under the conditions reported in Table III is about 4 times greater than its anomerization. That the exchange resulted from dissociation of I is clear from the data reported in Table V. It is seen from experiment 3 that neither the rates of exchange nor of anomerization were affected appreciably by the addition of tetraethylammonium perchlorate. The

Can. J. Chem. Downloaded from www.nrcresearchpress.com by 210.87.254.42 on 09/05/12
For personal use only.

slight increase in rate of exchange may be a reflection of the increased ionic strength of the solution. On the other hand, the addition of benzene to reduce the dielectric constant of the medium, as seen from the results of experiment 4, reduced the rate of exchange by a factor of about 10. This is clearly in accord with the premise that the direct exchange of the β-chloride (I) involves dissociation of I and recombination of ions with overall retention of configuration. For the reasons stated above, the mechanism in all likelihood involves dissociation to the 1,2-acetoxonium ion. Of course, a 1,2-orthoacetyl chloride may have existence as a transient intermediate and would have observable properties similar to the 1,2-acetoxonium ion. However, the results of experiment 2 (Table V) show that the process is not catalyzed by chloride ion since reduction of the chloride ion concentration to one-half of that in experiment 1, while keeping the salt concentration constant, had no experimentally significant effect on the rate of exchange.

A comparison of the polarimetric rates of anomerization using both acetonitrile and mixtures of acetonitrile and benzene as solvent indicated, as seen from the experimental result reported in Table V, that the addition of benzene accelerated the reaction to a small extent. This result is consistent with the notion that the anomerization involves nucleophilic attack by chloride ion in the rate-controlling step. It would be predicted on this basis that bromide ion would be less effective than chloride ion in catalyzing the reaction and that iodide ion would be the least effective halide ion. This would follow from the established order of nucleophilicity for these ions as quaternary ammonium salts in non-hydroxylic solvents (19). The data in Table VI show this to be the case.

TABLE VI

Effect of the type of halide ion on the rate of anomerization of tetra-*O*-acetyl-β-D-glucopyranosyl chloride (I)*

Salt	Velocity constant $\times 10^4$, min^{-1} (average value)	Relative rate
Tetraethylammonium chloride	40	15
Tetra-*n*-butylammonium bromide	14	5
Tetra-*n*-butylammonium iodide	2.6	1

*The reactions were carried out at 30° using a 0.2 *M* solution of I in acetonitrile 0.2 *M* in the halide salt.

Chloride ion catalyzed the reaction 3 times more effectively than bromide ion and the latter ion was 5 times more effective than iodide ion. In all cases, the product was the equilibrium mixture of the α(II)- and β(I)-chlorides. Undoubtedly, the anomerizations catalyzed by bromide and iodide ion proceeded by way of unstable tetra-*O*-acetyl-D-glucopyranosyl bromides and iodides, respectively, and these intermediates were formed by way of both the acetoxonium ion and the bimolecular substitution processes.

The results of this investigation provide evidence that, as previously noted for reactions with thiophenoxide ion (20), replacements at the anomeric center of sugar structures can proceed by way of bimolecular nucleophilic displacement processes accelerated by the participation of the ring-oxygen in delocalization of the positive charge at the reacting center of the transition state. It is not possible to be sure of the nature of the bonding between the reacting center and the entering and leaving groups in the transition state (V). The bonding may be akin to that between ions in intimate ion-pairs (21) and thus represent an intimate ion-triplet. Lemieux and Chü (7, 22) have reported evidence that the anomerization of the acetylated aldoglycopyranoses in acetic acid – acetic anhydride mixtures catalyzed by mineral acid proceed by way of the glycosyloxocarbonium ion

Can. J. Chem. Downloaded from www.nrcresearchpress.com by 210.87.254.42 on 09/05/12
For personal use only.

bonded (complexed) to two molecules of solvent one on each side of the reacting center. Thus, in this case, the transition state involves intimate ion–molecule complexing. Lemieux and Fraser-Reid (23) obtained evidence that the halogenomethoxylation of acetylated glycals proceeds by way of transition states wherein methanol is complexed with the anomeric center in the transition state. Therefore, it is becoming apparent that reactions at the anomeric center of glycosidic structures have a strong tendency to be bimolecular in nature although a main driving force for the reaction is participation of the ring-oxygen in delocalization of the charge at the reacting center. Thus, the high degree of inversion normally observed in reactions of acylated 1,2-*cis*-glycosyl halides is perhaps best viewed as arising not from shielding by the departing group (20) but instead from bonding (electrostatic solvation*) of the nucleophile with the reacting center in the transition state. Doering and Zeiss (24) have suggested that the greater the ability of a carbonium ion to disperse its positive charge internally the less likely is covalent bonding at the rear of the reacting center in the transition state. On this basis, the dissociation of a glycosyl halide should not be highly dependent on a stabilization of the transition state by covalent bond formation with the entering group. Instead, simple electrostatic solvation can be expected, especially for a structure approaching the glycosyloxocarbonium ion. Thus, the role of the chloride ion in the anomerization reaction can be considered to provide stabilization of the developing ion-pair by leading to an ion-triplet. To rationalize the S_N2 kinetics which were observed, the stabilization needs only to be sufficiently great (about 5 kcal/mole) to render the ion-triplet clearly a more favorable route of reaction than that provided by the ion-pair. These conclusions are of possible pertinence to a understanding of the high degree of stereospecificity observed in carbohydrase-catalyzed reactions. Also, it can be envisaged that the catalysis provided by these enzymes is to an important measure the result of specific electrostatic solvation of the transition state.

The results of a kinetic study of the halide ion catalyzed anomerization of the 3,4,6-tri-*O*-acetyl-β-D-glucopyranosyl chloride are reported in Table VII. It is seen that, except

TABLE VII

Polarimetric rates for the anomerization of 0.05 *M* 3,4,6-tri-*O*-acetyl-β-D-glucopyranosyl chloride in acetonitrile 0.1 *M* in *sym*-collidine at 25° catalyzed by halide ion

	Concentration of salt, *M*	Velocity constant, $(k_\alpha + k_\beta) \times 10^2$, min^{-1}	Relative rate
Tetraethylammonium chloride	0.005	8.7	1
	0.01	16.0	1.85
	0.015	24.7	2.84
Tetra-*n*-butylammonium bromide	0.05	7.5	1
	0.10	15.4	2.1

for the much higher rates, the reaction has the same characteristics as that described above for tetra-*O*-acetyl-β-D-glucopyranosyl chloride. It is seen that, for the triacetate, the bromide ion was about 10 times less effective as catalyst in contrast to the factor of 3 noted above with reference to Table VI. It seems likely that the factor of 10 represents a better measure of the difference in the abilities of the chloride and bromide ions to electrostatically solvate the transition state under these conditions since, presumably, the

*For a recent review of the literature, see ref. 24.

Can. J. Chem. Downloaded from www.nrcresearchpress.com by 210.87.254.42 on 09/05/12
For personal use only.

Can. J. Chem. Downloaded from www.nrcresearchpress.com by 210.87.254.42 on 09/05/12
For personal use only.

reaction of the triacetate was not complicated by the solvolytic reaction involving participation of the 2-substituent. Lemieux, Hayami, and Martin (6) have shown that the highly specific electrostatic deshielding (n.m.r.) of the 1, 3, and 5 protons of acetylated β-glucopyranosyl compounds by halide ions in acetonitrile most likely arises from electrostatic solvation of these hydrogens. The stabilities of the complexes increased ($Cl^- > Br^- > I^-$) with decreasing atomic radius for the halide ion present as a quaternary ammonium salt. Lemieux and Huber (25) have shown that both the α- and β-forms of 3,4,6-tri-*O*-acetyl-D-glucosyl chloride undergo replacement of the chlorine by acetate with virtually complete inversion when dissolved in acetic acid. The observation that the rate of reaction remained unchanged on the addition of potassium acetate does not preclude the possibility that the developing carbonium ion was appreciably solvated by acetic acid in the transition state. It is evident from the high stability of the biacetate ion as present in quaternary ammonium biacetates that acetic acid strongly solvates acetate ion and, as a consequence, acetate ion may not be profitably available for stabilization of the transition state by contributing to a weak ionic bond since this bond may be weaker than the bonds involved in the electrostatic solvation of the acetate ion by the acetic acid. This situation would resemble the great loss in the nucleophilicity of chloride ion on going to hydroxylic solvents (19). Similar conditions may apply to methoxide ion in methanol and be mainly responsible for the absence of an effect on the rate of the methanolysis of tetra-*O*-methyl-α-D-glucopyranosyl chloride (20). It may be noted that the mechanistic notions advanced in 1955 for the difference in the rates of acetolysis of the anomeric 3,4,6-tri-*O*-acetyl-D-glucosyl chlorides (25) must now be disregarded. The discovery of the anomeric effect (8) provides an adequate basis for explaining the 100-fold difference in reactivity based on the difference in stabilities of the ground states.

Preliminary experiments showed that reaction of tetraethylammonium acetate, as the equimolar complex with acetic acid, with the β-chloride (I) in acetonitrile led to appreciable (about 50%) replacement of the chlorine by the acetoxy group with inversion of the anomeric center. The initial reaction to yield α-D-glucopyranose pentaacetate was rapid but the reaction seemed to slow down after about 50% completion. This indication that, under appropriate conditions, I can undergo nucleophilic attack much faster than its dissociation with participation of the 2-acetoxy group suggests that it may indeed prove possible to prepare derivatives of α-D-glucose from *O*-acetylated β-D-glucopyranosyl halides, and this possibility will receive further attention. It was found in the course of this study that treatment of tetra-*O*-acetyl-α-D-glucopyranosyl bromide with tetraethylammonium chloride resulted in a rapid replacement of the bromine by chlorine with inversion of the anomeric center. The β-chloride (I) could be obtained in high yield and the reaction proved useful to prepare ^{36}Cl-labelled I.

EXPERIMENTAL

Solvents and Reagents

Unless otherwise stated, the materials used in this study were prepared by standard methods (26) and had the following physical constants: tetra-*O*-acetyl-β-D-glucopyranosyl chloride (I), m.p. 101–102°, $[\alpha]_D$ −7.2° (*c*, 4 in chloroform), −8.0° (*c*, 3.7 in acetonitrile); tetra-*O*-acetyl-α-D-glucopyranosyl chloride (II), m.p. 75–76°, $[\alpha]_D$ +166° (*c*, 2 in chloroform), +162 (*c*, 3.6 in acetonitrile); 3,4,6-tri-*O*-acetyl-β-D-glucopyranosyl chloride, m.p. 155–156°, $[\alpha]_D$ +28.9 (*c*, 1 in chloroform).

The acetonitrile was purified and dried by first distilling at least five times from phosphorus pentoxide and then distillation from anhydrous potassium carbonate. The benzene was dried by distillation and stored over sodium wire.

Tetra-*n*-butylammonium iodide and tetraethylammonium chloride were commercial reagents dried at 80° over phosphorous pentoxide. Tetra-*n*-butylammonium bromide was prepared by heating under reflux equimolar amounts of *n*-butyl bromide and tri-*n*-butylamine in an equal volume of acetonitrile for 36 h.

Evaporation left a crystalline product which was washed with acetonitrile recrystallized from ethyl acetate and dried *in vacuo* over phosphorous pentoxide.

^{36}Cl-labelled tetraethylammonium chloride was prepared by adding tetraethylammonium biacetate to a 0.3644 *N* aqueous solution of H^{36}Cl obtained from Atomic Energy of Canada and which had 4 microcuries of radioactivity per milliliter. The resulting solution was freeze dried and the residue was dried *in vacuo* at 80°. The substance was recrystallized from dry chloroform by the addition of petroleum ether. The crystals were dried *in vacuo* over phosphorus pentoxide.

Tetra-*O*-acetyl-β-D-glucopyranosyl chloride-^{36}Cl was prepared by reacting 1 mmole of tetra-*O*-acetyl-α-D-glucopyranosyl bromide with an equivalent amount of tetraethylammonium chloride-^{36}Cl (18.3×10^5 c.p.m./mmole) in 2 ml of dry acetonitrile. After 90 min at 30°, the reaction mixture was diluted with 20 ml of benzene containing 2 mmole of tetra-*O*-acetyl-β-D-glucopyranosyl chloride to serve as carrier. The resulting solution was washed four times with 5 ml volumes of water. The radioactivity of the aqueous washings indicated that 83% of the initial radioactivity remained in the benzene solution. This solution was dried by filtration through paper wetted with benzene and evaporated to a residue which was recrystallized three times from dry ether and dry petroleum ether (Skellysolve B). The yield was 800 mg (2.18 mmole) with a specific activity of 5.05 c.p.m./mmole.

Tetracetyl-α-D-glucopyranosyl chloride-^{36}Cl was prepared in the same manner as described above for the β-anomer except that the reaction mixture was kept at 30° for 60 min and then at 100° for 90 min in order to complete the anomerization of the first-formed β-chloride. The radioactive yield was near quantitative.

Methods

The polarimetric rates were determined using a Rudolph recording polarimeter operating at 589 mμ (27). In a typical experiment, 146.7 mg (0.4 mmole) of tetra-*O*-acetyl-β-D-glucopyranosyl chloride and 66.3 mg (0.4 mmole) of tetraethylammonium chloride were dissolved at zero time in acetonitrile and the solution was rapidly diluted to 2 ml and transferred to a prewarmed 0.5 dm jacketed polarimeter tube maintained at 30° by the circulation of thermostatted water. All transfers were made as quickly as possible to prevent the solvent or solutions from coming into contact with the atmosphere. The change in rotation with reaction time was provided by the chart record.

The rates of exchange were determined batchwise using sealed, double-stem tubes maintained at 30° in a water bath. In a typical experiment, 2 ml volumes of freshly prepared 0.4 *M* solutions of tetra-*O*-acetyl-β-D-glucopyranosyl chloride and of tetraethylammonium chloride-^{36}Cl were added separately one to each stem of the tube. After it had been sealed, the tube was brought to thermal equilibrium by keeping it immersed in the thermostatted bath for 30 min. The tube was then shaken to thoroughly mix the contents and the time of mixing was taken as zero time. After a given reaction time, the tube was opened and the content was immediately diluted with 20 ml of benzene. The mixture was then extracted four times with 5 ml volumes of water. The water extracts were combined in a 25 ml volumetric flask and diluted to 25ml. The resulting benzene solution was also transferred to a flask for dilution to 25 ml. The radioactivities of the solutions were determined by counting the solutions resulting on adding 1 ml samples to 15 ml volumes of an organic phosphor solution which contained 120 g of naphthalene, 7 g of PPO, and 0.05 g of POPOP per liter of dioxane. A Nuclear Chicago 700 liquid scintillation counter was used; the standard error in counting was less than 1% and the two solutions had radioactivities which totalled within 99% of that expected from the amount of radioactivity used in the experiment.

The benzene solution was evaporated to dryness and the tetra-*O*-acetyl-D-glucopyranosyl chloride-^{36}Cl was induced to crystallize from dry ether by the addition of petroleum ether. The crystalline compound (either crude I or II, depending on the experiment) was recrystallized to high purity (melting point determination) and its weight was determined. A 10% amount of the non-radioactive anomer was added to serve as hold-back carrier. The mixture was then recrystallized until the radioactive product appeared pure. Two recrystallizations normally sufficed. The compound, 18.3 mg (1 mmole), was dissolved in 1 ml of benzene for counting using 15 ml of the above mentioned organic phosphor solution.

To determine the rates of reaction by isotopic dilution analysis, reactions were conducted in the same manner as described above for the determination of rates of exchange except that non-radioactive starting materials were used. At the end of a given reaction time, the tube was opened and 100 mg of a radioactive sample of the component to be determined was added. The work-up procedure was then performed and the radioactivity of the compound isolated from the benzene layer was determined.

ACKNOWLEDGMENTS

This research was supported by a grant (N.R.C. T-172) to R. U. L. by the National Research Council of Canada.

REFERENCES

1. L. J. Haynes and F. H. Newth. Advan. Carbohydrate Chem. **10**, 207 (1955).
2. R. U. Lemieux and A. R. Morgan. J. Am. Chem. Soc. **85**, 1889 (1963).
3. R. U. Lemieux and C. Brice. Can. J. Chem. **30**, 295 (1952).

Can. J. Chem. Downloaded from www.nrcresearchpress.com by 210.87.254.42 on 09/05/12
For personal use only.

4. W. KORYTNYK and J. A. MILLS. J. Chem. Soc. 636 (1959).
5. R. U. LEMIEUX, R. K. KULLNIG, H. J. BERNSTEIN, and W. G. SCHNEIDER. J. Am. Chem. Soc. **80**, 6098 (1958).
6. R. U. LEMIEUX, JUN-ICHI HAYAMI, and J. MARTIN. In preparation.
7. R. U. LEMIEUX and N. J. CHÜ. Abstr. of Papers, Am. Chem. Soc. **133**, 31N (1958).
8. R. U. LEMIEUX. Molecular rearrangements. Part 2. P. de Mayo (*Editor*). Interscience Publishers, New York. 1964. p. 735.
9. F. WEYGAND, H. ZIEMANN, and H. J. BESTMANN. Chem. Ber. **91**, 2534 (1958).
10. E. L. ELIEL, N. L. ALLINGER, S. J. ANGYAL, and G. A. MORRISON. Conformational analysis. Interscience Publishers, New York. 1965. p. 44.
11. R. U. LEMIEUX and J. W. LOWN. Can. J. Chem. **42**, 893 (1964).
12. J. W. SMITH. Electric dipole moments. Butterworths Scientific Publications, London. 1955. p. 92.
13. J. T. EDWARD, P. F. MORAND, and I. PUSKAS. Can. J. Chem. **39**, 2069 (1961).
14. R. U. LEMIEUX, C. BRICE, and G. HUBER. Can. J. Chem. **33**, 134 (1955).
15. W. A. BONNER. J. Am. Chem. Soc. **83**, 962 (1961).
16. R. U. LEMIEUX and J. D. T. CIPERA. Can. J. Chem. **34**, 906 (1956).
17. A. R. MORGAN. Ph.D. thesis, Department of Chemistry, University of Alberta, Edmonton. 1964.
18. R. U. LEMIEUX and W. P. SHYLUK. Can. J. Chem. **33**, 120 (1955).
19. S. WINSTEIN, L. G. SAVEDOFF, S. SMITH, I. D. R. STEVENS, and J. S. GALL. Tetrahedron Letters, No. 9, 24 (1960).
20. A. J. RHIND-TUTT and C. A. VERNON. J. Chem. Soc. 4637 (1960).
21. S. WINSTEIN, P. E. KLINEDINST, JR., and G. C. ROBINSON. J. Am. Chem. Soc. **83**, 885 (1961).
22. N. J. CHÜ. Ph.D. thesis, Department of Chemistry, University of Ottawa. 1959.
23. R. U. LEMIEUX and B. FRASER-REID. In preparation.
24. A. STREITWEISER, JR. Solvolytic displacement reactions. McGraw-Hill Book Co., Inc., New York. 1962.
25. R. U. LEMIEUX and G. HUBER. Can. J. Chem. **33**, 128 (1955).
26. R. L. WHISTLER and M. L. WOLFROM (*Editors*). Methods in carbohydrate chemistry. Vol. II. Academic Press Inc., New York. 1963.
27. R. U. LEMIEUX and D. R. LINEBACK. Can. J. Chem. **43**, 94 (1965).

Can. J. Chem. Downloaded from www.nrcresearchpress.com by 210.87.254.42 on 09/05/12
For personal use only.

Can. J. Chem. Downloaded from www.nrcresearchpress.com by 210.87.254.40 on 09/05/12
For personal use only.

SYNTHÈSES DE PEPTIDES CONTENANT DES THIOACIDES

CASIMIR BERSE ET GILLES DUPUIS
Département de Chimie, Université de Montréal, Montréal, Québec
Reçu le 19 février 1965

RÉSUMÉ

L'introduction de la cystéine dans une chaîne peptidique présente toujours certaines difficultés. D'autre part, la présence des atomes de soufre dans un grand nombre de substances naturelles possédant certaines actions physiologiques permet de supposer que le remplacement de la cystéine par un autre résidu peut affecter l'activité caractéristique des peptides. Les thioacides semblent présenter une alternative intéressante pour la cystéine comme molécules remplaçantes. La présente publication décrit des condensations de *S*-benzyl thioacides (mercapto-2 acétique, (±)-mercapto-2 propionique, (±)-mercapto-2 succinique et mercapto-3 propionique) avec des esters éthyliques d'acides α-aminés (glycine, (±)-phénylalanine et L-phénylalanine) par la méthode du *N,N'*-dicyclohexylcarbodiimide.

Un très grand nombre de substances naturelles, essentielles aux différents organismes vivants, contiennent au moins une molécule de cystéine; par exemple, oxytocine, insuline, vasapressine, glutathion . . . etc. Le groupement sulfhydryle de ces substances peut être oxydé soit pour former un pont —S—S— comme dans le cas de l'oxytocine ou un dimère $(—S—R)_2$ comme le glutathion, par exemple.

Des études récentes (1) ont montré que certaines propriétés physiologiques de ces substances sont reliées à la présence de soufre dans leur structure. Du Vigneaud et ses collaborateurs ont montré que si la cystéine en position 1 de la séquence de l'oxytocine était remplacée par l'acide mercapto-3 propionique, l'hormone non naturelle ainsi obtenue (désamino-oxytocine) possède des propriétés physiologiques supérieures à celles de l'hormone naturelle (2, 3).

Dans ce présent travail, nous étudions les condensations de quatre thioacides différents avec les esters éthyliques de la glycine et de la phénylalanine. Les thioacides utilisés (mercapto-2 acétique, mercapto-3 propionique, (±)-mercapto-2 propionique et (±)-mercapto-2 succinique) possèdent une activité physiologique (4–10). Nous croyons que lorsque l'un de ces acides est incorporé dans une chaîne peptidique autre que celle de l'oxytocine le peptide obtenu pourrait jouer un rôle pharmacodynamique.

La méthode de condensation par formation d'anhydride mixte a été essayée sans succès. Le produit obtenu forme une huile que nous n'avons pu cristalliser. Cependant, la méthode de condensation par le *N,N'*-dicyclohexylcarbodiimide s'est avérée efficace dans la plupart des cas, sauf pour les condensations avec le glycinate d'éthyle. La fonction sulfhydryle des thioacides est bloquée par le groupement benzyle, et la fonction acide de l'acide aminé par formation de l'ester éthylique suivant la méthode de Fischer. La condensation est ensuite effectuée suivant le schéma indiqué (DDC = *N,N'*-dicyclohexylcarbodiimide, DCU = *N,N'*-dicyclohexylurée).

Comme nous le mentionnons précédemment, les essais de condensation du glycinate d'éthyle avec les *S*-benzyl thioacides ne donnent pas les peptides attendus (sauf dans le cas de l'acide *S*-benzyl (±)-mercapto-2 succinique).

La réaction qui a lieu est probablement la condensation du *N,N'*-dicyclohexylcarbodiimide avec le *S*-benzyl thioacide. Khorana rapporte une étude sur ce sujet (11).

Pour vérifier cette hypothèse, nous avons fait réagir équimoléculairement le DCC et l'acide *S*-benzyl mercapto-2 acétique dans le chloroforme. Le point de fusion du produit

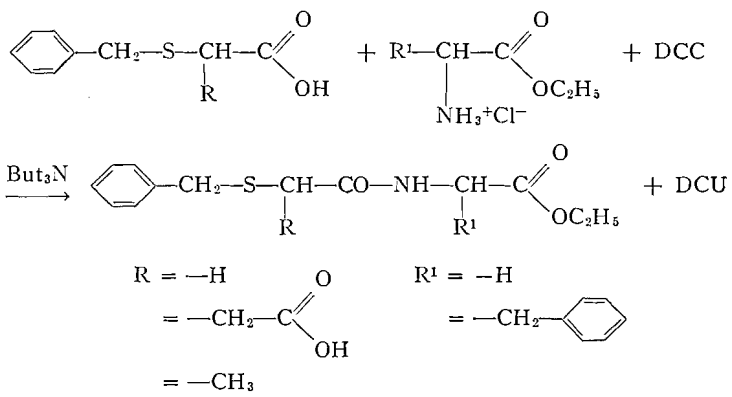

obtenu (*S*-benzyl *N*-mercapto-2 acétyl *N,N'*-dicyclohexylurée) est le même que celui obtenu par essai de condensation de l'acide *S*-benzyl mercapto-2 acétique avec le glycinate d'éthyle en présence de DCC. L'analyse quantitative du pourcentage de carbone et d'hydrogène montre de plus l'identité des deux produits.

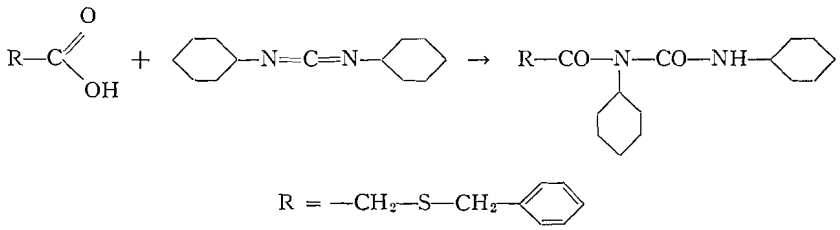

PARTIE EXPÉRIMENTALE

Les points de fusion ont été déterminés dans des tubes capillaires, sauf indications contraires, et ne sont pas corrigés. Les indices de rotations ont été déterminés sur un appareil de Rudolph and Sons, modèle 80. Les analyses sont de C. Daesslé, Montréal, et de J. Maciak, Indianapolis.

Préparation générale des dérivés S-benzyle des thioacides

A une solution aqueuse de thioacide, dans le volume de 4 *N* NaOH calculé, refroidie à 0° sous agitation, une quantité équimoléculaire de α-chlorotoluène, dans quatre fois son volume de dioxanne est ajoutée en cinq portions approximativement égales sur une période de 30 min. Le mélange est ensuite agité 30 min à la température de la pièce. La solution aqueuse lavée à l'éther, acidifiée par 6 *N* HCl jusqu'au pH 3, concentrée in vacuo à 40°, est ensuite laissée au repos pour cristallisation. Les détails sur la recristallisation et les propriétés physiques des *S*-benzyl thioacides sont résumés dans le Tableau I.

S-Benzyl mercapto-2 acétate d'éthyle (V)

Une solution d'acide *S*-benzyl mercapto-2 acétique (6.0 g; 0.033 mole) dans de l'éthanol absolu (100 ml) saturé 0.5 h par un courant de chlorure d'hydrogène anhydre est portée à reflux pendant 2 h. La solution filtrée est ensuite évaporée in vacuo à 40°. Le *S*-benzyl mercapto-2 acétate d'éthyle est purifié par distillation sous vide; p.é. 265° à 760 mm, $n_D^{20} = 1.5352$.

Anal. Calc. pour $C_{11}H_{14}O_2S$ (210.28): C, 62.80; H, 6.67. Trouvé: C, 63.03; H, 7.17.

S-Benzyl N-mercapto-2 acétyl N,N'-dicyclohexylurée (VI)

(*a*) Une solution de glycinate d'éthyle (2.1 g; 0.015 mole) libéré de son chlorhydrate par la tributylamine (7 ml) dans le chlorure de méthylène (150 ml) est ajoutée à 0°, sous agitation, à une solution d'acide *S*-benzyl mercapto-2 acétique (2.7 g; 0.015 mole) dans le chlorure de méthylène (50 ml). La condensation est réalisée en présence de *N,N'*-dicyclohexylcarbodiimide (3.1 g; 0.015 mole) dans le chlorure de méthylène (50 ml). Le mélange est agité 0.5 h à 0° et 24 h à la température de la pièce. On sépare le précipité de DCU par filtration, puis la solution est lavée par *N* HCl (3 × 25 ml), H_2O (3 × 25 ml), 10% $NaHCO_3$ (3 × 25 ml), H_2O (3 × 25 ml), séchée sur Na_2SO_4 anhydre et évaporée à sec *in vacuo*. Le résidu cristallise d'éthanol–eau; rendement: 1.2 g (20%), p.f. 119°. Contrairement au peptide attendu (*S*-benzyl mercapto-2 acétylglycinate d'éthyle), l'analyse montre que l'on obtient le *S*-benzyl *N*-mercapto-2 acétyl *N,N'*-dicyclohexylurée.

Anal. Calc. pour $C_{22}H_{32}N_2O_2S$ (388.56): C, 68.00; H, 8.30. Trouvé: C, 68.36; H, 8.30.

Can. J. Chem. Downloaded from www.nrcresearchpress.com by 210.87.254.40 on 09/05/12
For personal use only.

Can. J. Chem. Downloaded from www.nrcresearchpress.com by 210.87.254.40 on 09/05/12
For personal use only.

TABLEAU I

Dérivés *S*-benzyle des thioacides

Composés	Rendement (%)	p.f. (°C)	Lit.	Purification et cristall.	Calculé (%)		Trouvé (%)	
					C	H	C	H
Mercapto-2 acétique (I)	88	60.5–63.5	(12)	Distillation				
Mercapto-2 succinique (II)	100	185–187	(13)	Eau	55.20	4.61	54.79	4.87
Mercapto-2 propionique (III)	94	79–80		Isopropanol	61.20	6.10	60.79	5.95
Mercapto-3 propionique (IV)	48	80–82	(14)	Eau	61.20	6.10	60.49	6.06

Can. J. Chem. Downloaded from www.nrcresearchpress.com by 210.87.254.40 on 09/05/12
For personal use only.

TABLEAU II

Peptides contenant des thioacides

Composés	Rendement (%)	p.f. (°C)	Cristallisation	Calculé (%) C	Calculé (%) H	Trouvé (%) C	Trouvé (%) H
S-Benzyl *N*-mercapto-2 acétyl *N,N'*-dicyclohexylurée (VI) (*a*)	20	119	Éthanol–eau	68.00	8.30	68.36	8.30
(*b*)	66	119–120*	Éthanol–eau	68.00	8.30	68.94	9.08
S-Benzyl(±)-mercapto-2 succinyl-diglycinate d'éthyle (VII)	15	121–124	Acétate d'éthyle – éther de pétrole	55.59	6.39	55.99	6.51
S-Benzyl mercapto-2 acétyl (±)-phénylalanate d'éthyle (VIII)	93	100–101	Isopropanol	67.20	6.48	67.61	6.65
S-Benzyl (±)-mercapto-2 propionyl (±)-phénylalanate d'éthyle (IX)	70	108*	Éthanol–eau	67.84	6.78	67.88	7.31
S-Benzyl mercapto-3 propionyl (±)-phénylalanate d'éthyle (X)	36	56–57	Isopropanol	67.89	6.78	67.93	6.98
S-Benzyl (±)-mercapto-2 succinyl (±)-diphénylalanate d'éthyle (XI)	40	148–149	Acétate d'éthyle – éther de pétrole	67.09	6.43	67.27	6.91
S-Benzyl (±)-mercapto-2 propionyl L-phénylalanate d'éthyle (XII)†	20	76*	Isopropanol–eau	67.89	6.78	67.82	6.90
S-Benzyl (±)-mercapto-2 succinyl L-diphénylalanate d'éthyle (XIII)‡	23	159–160	Acétate d'éthyle – éther de pétrole	67.09	6.43	66.92	6.15
S-Benzyl mercapto-2 acétyl (±)-phénylalanine (XIV)	85	138–140	Éthanol–eau	65.62	5.81	65.12	6.04
S-Benzyl (±)-mercapto-2 propionyl (±)-phénylalanine (XV)	77	114	Éthanol–eau	66.47	6.15	66.45	6.22
S-Benzyl (±)-mercapto-2 succinyl (±)-diphénylalanine (XVI)	75	202	Isopropanol	64.90	5.64	65.04	5.24
S-Benzyl mercapto-2 acétyl (±)-phényl-alanyl (±)-phénylalanate d'éthyle (XVII)	36	124–125	Éthanol	69.02	6.39	68.81	6.46
				N, 5.55		N, 5.26	

*p.f. déterminés sur bloc maquenne.
†$[\alpha]_D^{26} = +68.6$ ($c = 1.0$, isopropanol).
‡$[\alpha]_D^{27} = -9.18$ ($c = 0.29$, acétate d'éthyle).

(*b*) Des quantités équimoléculaires d'acide *S*-benzyl mercapto-2 acétique (1.8 g; 0.01 mole) et de DCC (2.1 g; 0.01 mole) sont dissoutes dans le chloroforme et agitées 1 h à la température de la pièce. Après filtration du précipité de DCU (800 mg), la solution est lavée de façon habituelle, séchée et évaporée à sec *in vacuo*. Le résidu cristallise de l'éthanol–eau; rendement: 2.5 g (66%), p.f. 119–120° (bloc maquenne).

Anal. Calc. pour $C_{22}H_{32}N_2O_2S$ (388.56): C, 68.00; H, 8.30. Trouvé: C, 68.94; H, 9.08.

Le point de fusion mixte des produits obtenus en (*a*) et (*b*) est de 117° (bloc maquenne).

S-Benzyl (±)-mercapto-2 succinyl-diglycinate d'éthyle (VII)

Une solution de glycinate d'éthyle (21.0 g; 0.150 mole) libéré de son chlorhydrate par la triéthylamine (30.4 ml) dans le DMF (200 ml) est, après filtration du chlorhydrate de triéthylamine, ajoutée à 0°, sous agitation, à une solution d'acide *S*-benzyl (±)-mercapto-2 succinyl (18.0 g; 0.075 mole) dans le DMF (100 ml). La condensation est réalisée en présence de DCC (31.2 g; 0.150 mole) dans le chloroforme (100 ml). Le mélange est agité pendant 0.5 h à 0° et 2 jours à la température de la pièce. On sépare le précipité de DCU par filtration et on concentre le filtrat *in vacuo* à 50°. Le résidu est repris dans l'acétate d'éthyle; la solution obtenue est lavée de façon habituelle, séchée et évaporée à sec *in vacuo*. Le produit cristallise de l'acétate d'éthyle – éther de pétrole (60–110°); rendement: 6.0 g (15%), p.f. 121–124°.

Anal. Calc. pour $C_{19}H_{26}N_2O_6S$ (410.49): C, 55.59; H, 6.39. Trouvé: C, 55.99; H, 6.51.

S-Benzyl mercapto-2 acétyl (±)-phénylalanate d'éthyle (VIII)

Une solution de phénylalanate d'éthyle (6.9 g; 0.03 mole) libéré de son chlorohydrate par la tributylamine (7 ml) dans le chloroforme (75 ml) est ajoutée à 0°, sous agitation, à une solution d'acide *S*-benzyl mercapto-2 acétique (5.5 g; 0.03 mole) dans le chloroforme (75 ml). La condensation est réalisée en présence de DCC (6.2 g; 0.03 mole) dans le chloroforme (50 ml). Le mélange est agité pendant 0.5 h à 0° et 12 h à la température de la pièce. On sépare le DCU par filtration puis la solution est lavée de façon habituelle, séchée et évaporée à sec. Le produit cristallise de l'isopropanol; rendement: 10 g (93%), p.f. 100–101°.

Anal. Calc. pour $C_{20}H_{23}NO_3S$ (357.46): C, 67.20; H, 6.48. Trouvé: C, 67.61; H, 6.65.

S-Benzyl (±)-mercapto-2 propionyl (±)-phénylalanate d'éthyle (IX)

Ce composé est préparé de la même façon que VIII en condensant l'acide *S*-benzyl (±)-mercapto-2 propionique (9.8 g; 0.05 mole) avec le chlorhydrate de (±)-phénylalanate d'éthyle (11.5 g; 0.05 mole) en présence de DCC (10.2 g; 0.05 mole) et de tributylamine (11.6 ml) dans le chloroforme (quantité totale: 200 ml). Le produit cristallise d'éthanol–eau; rendement: 13 g (70%), p.f. 108° (bloc maquenne).

Anal. Calc. pour $C_{21}H_{25}NO_3S$ (371.49): C, 67.89; H, 6.78. Trouvé: C, 67.88; H, 7.31.

S-Benzyl mercapto-3 propionyl (±)-phénylalanate d'éthyle (X)

Ce composé est préparé de la même façon que VIII en condensant l'acide *S*-benzyl mercapto-3 propionique (5.9 g; 0.03 mole) avec le chlorhydrate de (±)-phénylalanate d'éthyle (6.9 g; 0.03 mole) en présence de DCC (6.2 g; 0.03 mole) et de tributylamine (7 ml) dans le chloroforme (quantité totale: 200 ml). Le produit cristallise de l'isopropanol; rendement: 4 g (36%), p.f. 56–57°.

Anal. Calc. pour $C_{21}H_{25}NO_3S$ (371.49): C, 67.89; H, 6.78. Trouvé: C, 67.93; H, 6.98.

S-Benzyl (±)-mercapto-2 succinyl (±)-diphénylalanate d'éthyle (XI)

Ce composé est préparé de la même façon que VIII en condensant l'acide *S*-benzyl (±)-mercapto-2 succinique (3.6 g; 0.015 mole) dans le DMF (25 ml) avec le chlorhydrate de (±)-phénylalanate d'éthyle (6.9 g; 0.03 mole) dans le chlorure de méthylène (40 ml) en présence de DCC (6.2 g; 0.03 mole) et de tributylamine (7 ml). Après filtration du précipité de DCU et évaporation *in vacuo* du filtrat, le résidu est repris dans l'acétate d'éthyle lavé, séché et évaporé. Le produit cristallise d'acétate d'éthyle – éther de pétrole (60–110°); rendement: 3.6 g (40%), p.f. 148–149°.

Anal. Calc. pour $C_{23}H_{38}N_2O_6S$ (590.70): C, 67.09; H, 6.43. Trouvé: C, 67.27; H, 6.91.

S-Benzyl (±)-mercapto-2 propionyl L-*phénylalanate d'éthyle (XII)*

Ce composé est préparé de la même façon que VIII en condensant l'acide *S*-benzyl (±)-mercapto-2 propionique (9.8 g; 0.05 mole) avec le chlorhydrate de L-phénylalanate d'éthyle (11.5 g; 0.05 mole) en présence de DCC (10.2 g; 0.05 mole) et de tributylamine (11.6 ml) dans le chlorure de méthylène (quantité totale: 200 ml). Le produit cristallise de l'isopropanol–eau; rendement: 3.7 g (20%), p.f. 76° (bloc maquenne), $[\alpha]_D^{26} = +68.6°$ ($c = 1.0$, isopropanol).

Anal. Calc. pour $C_{21}H_{25}NO_3S$ (371.49): C, 67.89; H, 6.78. Trouvé: C, 67.82; H, 6.90.

S-Benzyl (±)-mercapto-2 succinyl L-*diphénylalanate d'éthyle (XIII)*

Ce composé est préparé de la même façon que XI en condensant l'acide *S*-benzyl (±)-mercapto-2 succinique (3.6 g; 0.015 mole) avec le chlorhydrate de L-phénylalanate d'éthyle (6.9 g; 0.030 mole) en présence de DCC (6.2 g; 0.030 mole) et de tributylamine (7 ml) dans les mêmes solvants. Le produit est purifié après plusieurs cristallisations de l'acétate d'éthyle – éther de pétrole (60–110°); rendement: 2.0 (23%), p.f. 159–160°, $[\alpha]_D^{27} = -9.18°$ ($c = 0.29$, acétate d'éthyle).

Anal. Calc. pour $C_{33}H_{38}N_2O_6S$ (590.70): C, 67.09; H, 6.43. Trouvé: C, 66.92; H, 6.15.

Can. J. Chem. Downloaded from www.nrcresearchpress.com by 210.87.254.40 on 09/05/12
For personal use only.

S-Benzyl mercapto-2 acétyl (±)-phénylalanine (XIV)

A une solution de *S*-benzyl mercapto-2 acétyl (±)-phénylalanate d'éthyle (10 g; 0.028 mole) dans l'éthanol absolu (200 ml) on ajoute *N* NaOH (30 ml). Le mélange est agité 2 h à la température de la pièce, acidifié par 6 *N* HCl jusqu'à virage du tournesol et concentré *in vacuo* à 40°. Le précipité cristallise de l'éthanol–eau; rendement: 7.8 g (85%), p.f. 139–140°.

Anal. Calc. pour $C_{18}H_{19}NO_3S$ (329.41): C, 65.62; H, 5.81. Trouvé: C, 65.12; H, 6.04.

S-Benzyl (±)-mercapto-2 propionyl (±)-phénylalanine (XV)

A une solution de *S*-benzyl (±)-mercapto-2 propionyl (±)-phénylalanate d'éthyle (1.5 g; 0.004 mole) dans le dioxanne (100 ml) on ajoute *N* NaOH (6 ml). Le mélange est agité 20 h à la température de la pièce. Le précipité est filtré, dissout dans l'eau et acidifié par *N* HCl jusqu'au pH 3. Le précipité cristallise d'éthanol–eau; rendement: 1.1 g (77%), p.f. 114°.

Anal. Calc. pour $C_{19}H_{21}NO_3S$ (343.43): C, 66.47; H, 6.15. Trouvé: C, 66.45; H, 6.22.

S-Benzyl (±)-mercapto-2 succinyl (±)-diphénylalanine (XVI)

Ce composé est préparé de la même façon que XV par saponification de *S*-benzyl (±)-mercapto-2 succinyl (±)-phénylalanate d'éthyle (1.2 g; 0.002 mole) par *N* NaOH (5.4 ml) dans le dioxanne (100 ml). Le produit cristallise de l'isopropanol–eau; rendement: 0.80 g (75%), p.f. 202°.

Anal. Calc. pour $C_{29}H_{30}N_2O_6S$ (536.61): C, 64.90; H, 5.64. Trouve: C, 65.04; H, 5.24.

S-Benzyl mercapto-2 acétyl (±)-phénylalanyl (±)-phénylalanate d'éthyle (XVII)

Ce composé est préparé de la même façon que VIII en condensant le *S*-benzyl mercapto-2 acétyl (±)-phénylalanine (3.3 g; 0.01 mole) avec le chlorhydrate de (±)-phénylalanate d'éthyle (2.3 g; 0.01 mole) en présence de DCC (2.0 g; 0.01 mole) et de tributylamine (2.3 ml) dans le chlorure de méthylène (quantité totale: 125 ml). Le produit cristallisé d'éthanol; rendement: 1.8 g (36%), p.f. 124–125°.

Anal. Calc. pour $C_{29}H_{32}N_2O_4S$ (504.63): C, 69.02; H, 6.39; N, 5.55. Trouvé: C, 68.81; H, 6.46; N, 5.26.

REMERCIEMENTS

Les auteurs remercient le Conseil National de Recherches pour l'aide financière apportée sous forme d'octroi de recherches et de bourse d'étude (G. D.).

BIBLIOGRAPHIE

1. Howard Rasmussen, Irving L. Schwartz, Richard Young et Julien Marc-Aurèle. J. Gen. Physiol. **46**, 1171 (1963).
2. Derek B. Hope, V. V. S. Murti et Vincent du Vigneaud. J. Biol. Chem. **237**, 1563 (1962).
3. Derek B. Hope et Vincent du Vigneaud. J. Biol. Chem. **237**, 3146 (1962).
4. J. Sos *et al.* Schweiz. Med. Wochschr. **86**, 1077 (1956). CA **52**, 2281*i*.
5. Bunkichi Yokoya. Osaka Daigaku Igaku Zasshi, **10**, 1 (1958). CA **52**, 7504*h*.
6. Seiichiio Yamasaki. Fukuoka Acta Med. **45**, 234 (1954).
7. H. Thiers et J. Pellerat. J. Med. Lyon, **30**, 699 (1949).
8. E. Friedberger. Berl. Klin. Wochschr. **45**, 1714 (1909).
9. M. Klein, J. H. Brewer, J. E. Perez et B. Day. J. Immunol. **59**, 135 (1948).
10. M. Klein, B. J. Brewer et R. Joiner. Arch. Biochem. **7**, 415 (1945).
11. H. G. Khorana. J. Chem. Soc. 2081 (1952).
12. E. Larsson. Chem. Ber. B, **63**, 1347 (1930).
13. Bror Holmberg. Arkiv. Kemi, Mineral. Geol. **24A**, 10 (1946).
14. Bror Holmberg. Arkiv. Kemi, Mineral. Geol. **14A**, 13 (1940).

Can. J. Chem. Downloaded from www.nrcresearchpress.com by 210.87.254.40 on 09/05/12
For personal use only.

Can. J. Chem. Downloaded from www.nrcresearchpress.com by 210.87.254.105 on 09/05/12
For personal use only.

THE ALKALOIDS OF PAPAVERACEOUS PLANTS

LIII. ESCHSCHOLTZIA CALIFORNICA CHAM.

RICHARD H. F. MANSKE AND KJU HI SHIN
Research Laboratory, Dominion Rubber Co. Ltd., Guelph, Ontario

Received November 13, 1964

ABSTRACT

Several lots of *Eschscholtzia californica* have been investigated and the following alkaloids have been identified, in addition to a new alkaloid which has been named eschscholtzine: protopine, allocryptopine, cryptopine, chelerythrine, and lauroscholtzine, which is a new name for *N*-methyllaurotetanine. Some plant lots did not yield cryptopine and not sufficient chelerythrine for positive identification.

The presence of alkaloids, and particularly of protopine and of allocryptopine, in *Eschscholtzia californica* Cham. has long been known (1, 2). Other alkaloids have been suspected and (or) reported and the author has recorded the presence of a new alkaloid, eschscholtzine (3).

More plant material has become available and a more complete examination is now reported. A small quantity of plant material (4 kg) grown locally yielded protopine, allocryptopine, cryptopine, chelerythrine, eschscholtzine, and a small amount of a phenolic base melting at 254° but not further characterized. The main lot (270 kg) did not yield this phenolic base nor cryptopine, and chelerythrine was found in only trace amounts and then evidently contaminated with sanguinarine. Eschscholtzine has now been obtained crystalline and is $C_{19}H_{17}O_4N$. The phenolic fraction yielded *N*-methyllaurotetanine for which the trivial name lauroscholtzine is now proposed.

EXPERIMENTAL

The smaller lot of material (4 kg) consisted largely of plants grown from seed of the wild plant. The large lot (270 kg) was grown from seed kindly supplied by Bodgers Seeds Limited, El Monte, California, and consisted of a mixture of cultivated varieties. The plants were grown on a plot of the Ontario Agricultural College, Guelph, Ontario, and special thanks are due to Dr. R. J. Hilton who made the necessary arrangements.

The dried and gound plant material was extracted with methanol and the extract was largely freed of solvent. The residue was then acidified with dilute hydrochloric acid (Congo test paper) and the remaining solvent was expelled in a current of steam. While still hot paraffin was added to the mixture. After settling and cooling the lower aqueous layer was withdrawn, reheated with paraffin, and after cooling once more was filtered with the aid of Filtercel. The water insoluble portions were washed with a fresh portion of acidified water and this extract was added to a subsequent methanol extract. By this countercurrent procedure it was possible to extract all of the alkaloid and do it with about 1 l of final solution per 2 kg of plant material.

The total alkaloid mixture was recovered from the aqueous solution by chloroform extraction after making alkaline with ammonia. Much non-alkaloid material was obtained in the chloroform extract and this was largely eliminated by extracting the residue from the extract with dilute hydrochloric acid. The water soluble fraction thus obtained was extracted with chloroform (4) and yielded the following fractions:

BC, bases whose hydrochlorides are extracted from aqueous solution with chloroform—eschscholtzine; some allocryptopine;

BCE and BEC, phenolic bases—lauroscholtzine;

BS, bases whose hydrochlorides are not extracted from aqueous solution with chloroform—protopine; cryptopine; most of the allocryptopine; chelerythrine; and

BSE and EES, phenolic bases—lauroscholtzine.

Eschscholtzine

The chloroform extract from the hydrochloric acid solution of the total alkaloids was evaporated to a syrupy consistency. After several days a few crystal nuclei made their appearance and the addition of a mixture of chloroform and carbon tetrachloride to incipient turbidity hastened crystallization. Filtration

and washing with the mixed solvent yielded the eschscholtzine hydrochloride in pale-yellow crystals which were recrystallized by adding chloroform to a concentrated methanol solution. Colorless well shaped needles were then obtained which effervesce slightly at 225° and melt to a colorless liquid at 246°. By reworking mother liquors there was obtained a total of 140 g of the hydrochloride from 270 kg of plant material. Analytical figures indicated a variable amount of solvent of crystallization.

Crystallization of the free base occurred only after many trials over a number of years. When nuclei were ultimately obtained, eschscholtzine crystallized with great facility from an ethereal solution which had been dried with potassium hydroxide. It will also crystallize from methanol in which, however, it is moderately soluble. The colorless stout prisms melt sharply at 128°* (λ_{max}^{EtOH} 295 mμ, log ε 4.04).

Anal. Calcd. for $C_{19}H_{17}O_4N$: C, 70.57; H, 5.30; N, 4.33. Found: C, 70.59, 70.43; H, 5.53, 5.63; N, 3.95.

The alkaloid is optically active showing $[\alpha]_D^{20}$ −202 (*c*, 1.00 in methanol).

Eschscholtzine acid oxalate crystallizes slowly from methanol and then melts with previous effervescence and sintering at 140°. A variable amount of solvent results in analytical figures of questionable value.

Protopine and Allocryptopine

The bases in the hydrochloric acid solution which had been extracted with chloroform were precipitated by adding an excess of potassium hydroxide, filtering, and washing with water until the filtrate was colorless. (The phenolic bases in the filtrate were regenerated by the addition of excess ammonium chloride and extraction with chloroform. The mixture of non-phenolic bases was redissolved in the minimum amount of dilute hydrochloric acid and the filtered solution was evaporated slightly. On cooling a copious crop of protopine hydrochloride was obtained. By reworking mother liquors it was possible to obtain a total of 58 g of protopine from the large lot of plant material. Its identity was established by melting point, mixed melting point (210°), and other characteristics.

The bases in the mother liquor from the above were regenerated by adding ammonia and extracting with chloroform. The residue from the chloroform extract crystallized readily in contact with methanol and one recrystallization from chloroform–methanol yielded pure allocryptopine melting at 160° either alone or in admixture with an authentic specimen. By reworking mother liquors there was obtained a total of 61 g of this alkaloid, but no other base, and specifically no cryptopine, could be isolated in pure form.

However, the plant material grown earlier from what was purported to be the wild species yielded cryptopine as its sparingly soluble oxalate (from methanol) and the regenerated base melted at 221° either alone or in admixture with an authentic specimen. From another lot of plant material there was obtained an oxalate which crystallized in contact with acetone. The base regenerated from this and recrystallized from chloroform–methanol melted sharply at 207°, either alone or in admixture with chelerythrine. The ψ-cyanide prepared from this melted at 257 °C.

The mother liquors from the eschscholtzine hydrochloride yielded some allocryptopine and a trace of protopine.

Lauroscholtzine

The phenolic bases from both the BC and BS fractions were worked up in parallel experiments. They were redissolved in cold aqueous sodium hydroxide, filtered to remove a turbidity, acidified with dilute acid, filtered once more, basified with ammonia, and extracted with chloroform. Further purification was effected by dissolving the residues from the chloroform extracts in aqueous oxalic acid, filtering from some amorphous residue, and repeatedly extracting the acid solutions with ether. The solutions were then diluted with water, basified with ammonia, and extracted with large volumes of ether. The residues from the ether extracts consisted of pale amber colored resins which could not be crystallized in contact with a number of solvents.

It was possible however to isolate about half of the bases in the form of glaucine perchlorate (m.p. 232–243°) from small portions which had been treated with diazomethane. It was then observed that either fraction of the phenolic bases yielded a sparingly soluble *l*-tartrate when treated with the theoretical amount of *l*-tartaric acid in absolute ethanol. Crystallization was virtually immediate. The tartrate was conveniently recrystallized by dissolving it in a small volume of hot water, evaporating to incipient crystallization, and adding hot absolute ethanol. As thus prepared the salt melted at 238–239° with some darkening. It was virtually insoluble in cold methanol or ethanol. About one half of the total phenolic fraction of alkaloids was obtainable in the form of this salt, and the yield was ca. 8 g. Though the regenerated base did not crystallize in contact with ether or with methanol it readily yielded a hydrobromide which when recrystallized once from methanol and dried at 110° melted at 237–238° and this melting point was not depressed when the salt was admixed with an authentic specimen of *N*-methyllaurotetanine hydrobromide which melted at 235–236° and which was kindly supplied by Dr. A. Rüegger of Sandoz Ltd., Basle, Switzerland (5).

The *O*-ethyl ether prepared by the action of diazoethane yielded an *l*-tartrate melting at 206° and a methiodide melting at 213°. Hofmann degradation yielded a methine whose methiodide melted at 285° and this in turn yielded 1-vinyl-7-ethoxy-3,4,6-trimethoxyphenanthrene melting at 141°. Except for the last these melting points are not always the same as reported (4) but they are of the right order. There is no doubt that lauroscholtzine is identical with the base previously described as *N*-methyllaurotetanine and the ultraviolet spectrum confirmed this identity. The maxima and their intensities were the same as those recorded by Rüegger (5).

**All melting points are corrected.*

Can. J. Chem. Downloaded from www.nrcresearchpress.com by 210.87.254.105 on 09/05/12
For personal use only.

Before it had been discovered that lauroscholtzine formed such a characteristic *l*-tartrate, attempts had been made to separate the phenolic bases by chromatography through alumina, but without success. However, the *O*-acetyl derivative, though not obtained crystalline, was obtained in ca. 50% yield as the ether eluate from a column of neutral alumina. It had R_f 0.6 in the system cyclohexane–chloroform–diethylanine (4:10:1) on thin-layer chromatography (silica gel G) and showed a phenolic acetate band at 1 760 cm^{-1} in the infrared spectrum. A hydroxyl band was absent.

Anal. Calcd. for $C_{22}H_{25}O_5N$: C, 68.91; H, 6.57; N, 3.65. Found: C, 68.77; H, 6.20; N, 3.79.

The n.m.r. spectrum of this acetyl derivative showed three methoxyl proton signals at 6.12, 6.15, and 6.31 τ, the last being undoubtedly due to the sterically hindered methoxyl at position 1 (5). Protons of the acetyl and *N*-methyl groups occurred at 6.21 and 7.50 τ respectively.

Hydrogenolysis of the acetyl derivative with lithium aluminium hydride in tetrahydrofurane regenerated lauroscholtzine characterized as its hydrobromide.

REFERENCES

1. R. FISCHER. Arch. Pharm. **239**, 421 (1901).
2. R. FISCHER and M. E. TWEEDEN. Pharm. Arch. **5**, 117 (1902).
3. R. H. F. MANSKE. The alkaloids. Academic Press, New York. 1954. p. 82.
4. R. H. F. MANSKE. Can. J. Research, **8**, 210 (1933).
5. A. RÜEGGER. Helv. Chim. Acta, **42**, 754 (1959).

Can. J. Chem. Downloaded from www.nrcresearchpress.com by 210.87.254.105 on 09/05/12
For personal use only.

Can. J. Chem. Downloaded from www.nrcresearchpress.com by 210.87.254.105 on 09/05/12
For personal use only.

THE ALKALOIDS OF PAPAVERACEOUS PLANTS

LIV. THE STRUCTURE OF ESCHSCHOLTZINE

RICHARD H. F. MANSKE AND KJU HI SHIN
Research Laboratories, Dominion Rubber Co., Ltd., Guelph, Ontario
AND
A. R. BATTERSBY AND D. F. SHAW
Robert Robinson Laboratories, University of Liverpool, Liverpool, England
Received January 22, 1965

ABSTRACT

Eschscholtzine, a new alkaloid from *Eschscholtzia californica*, has been shown to be the bismethylenedioxy analogue of *N*-methylpavine (argemonine). The mass spectrometric fragmentation of alkaloids of the pavine type is discussed.

Two of us have reported the isolation of a new alkaloid, eschscholtzine, from *Eschscholtzia californica* Cham. (1) and a mass spectrum* of it showed the molecular formula to be $C_{19}H_{17}O_4N$. In the meantime, a fuller mass spectrometric study of eschscholtzine at Liverpool allowed the correct structure to be derived which had independently been determined by nuclear magnetic resonance (n.m.r.) and chemical degradation at Guelph. The mass spectrum of eschscholtzine shows a very small parent peak at *m/e* 323 when the hot inlet system was used; however, by direct inlet of the sample, the parent peak increased to about one-third the size of the base peak. In both spectra (hot inlet or direct inlet) only one intense fragment peak appeared at *m/e* 188. This behavior is similar to that of the 1-benzylisoquinoline alkaloids (2) but on this basis the only reasonable structure for the fragment ion is (I) which corresponds to *m/e* 190 and is thus unacceptable. However, the spectra of pavine (IV, R = H) and *N*-methylpavine (IV, R = Me) parallel that of eschscholtzine in showing a single intense fragment ion at *m/e* 190 and one at *m/e* 204. These ions are formulated as II (R = H) and II (R = Me) and their formation can be rationalized as shown below. The nature of the ion from eschscholtzine can now be understood as the aromatic ion (III) and its formation strongly indicated the methylenedioxy analogue (V) of *N*-methylpavine (IV, R = Me) (argemonine) as the structure of eschscholtzine.

The striking similarity of the n.m.r. spectra of argemonine (IV, R = Me) (3, 4) and eschscholtzine (V) supported this indication. Both n.m.r. spectra exhibit impressive symmetry and they are largely superimposable except for the slight shifts described in Table I. The aromatic and *N*-methyl protons call for no special comment but the protons of the two methylenedioxy groups appear as a quartet of lines of almost equal intensity: 4.17, 4.21, 4.22, and 4.26 τ. The two methylenedioxy groups are thus almost equivalent but the two protons of the O—CH_2—O system are not identical as a result of their being in different environments with respect to the aromatic rings. The eschscholtzine molecule is non-planar and may resemble a partly opened hinge. A similar non-equivalence of the methylenedioxy protons has been encountered in the aporphine alkaloids, dicentrine and bulbocapnine methyl ether (5).

**Kindly determined for us by Professor D. B. MacLean of McMaster University, Hamilton, Ontario.*

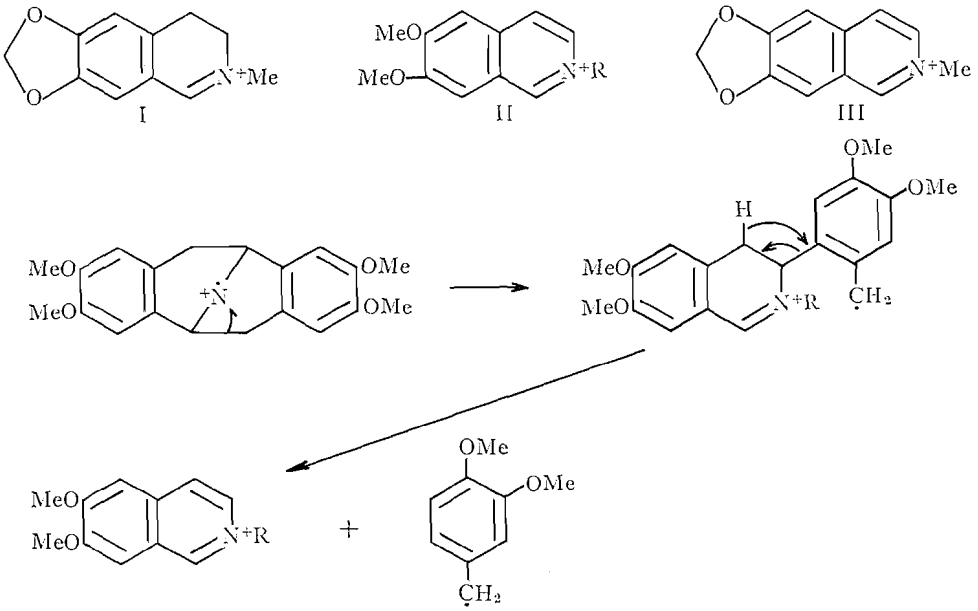

The ultraviolet spectra of argemonine and eschscholtzine are given in Table II. The bathochromic shift from 287 mμ to 295 mμ (with increase of intensity) resulting from the replacement of four methoxyl groups in the former by two methylenedioxy groups in the latter is as expected and these changes are evident in the degradation products as well.

The final proof of the structure of eschscholtzine came from chemical degradation by a route parallel to that used for *N*-methylpavine (6) to afford 2,3,8,9-tetramethoxydibenzo[*a*,*e*]cyclooctadiene (XI). The course of the degradation is outlined in the chart.

The n.m.r. spectrum of the first Hofmann degradation product (VI) exhibited a doublet centered at 3.39 τ (2H) (J = 1.5 c.p.s.) in accordance with a *cis*-stilbene structure, since *cis*- and *trans*-silbene give signals at 3.45 τ and 2.9 τ respectively (7). The n.m.r. spectrum also showed a singlet (6H) at 7.87 τ for NMe_2 and a multiplet (3H) at ca. 6.1–7.8 τ corresponding to the protons at C_{11} and C_{12}, and the aromatic protons (4H) gave signals at 3.58 τ and 3.43 τ. Finally the methylenedioxy protons appeared as singlets at 4.30 τ and 4.23 τ (2H for each) showing that now the methylenedioxy protons are equivalent. Again similar phenomena have been reported for the aporphine methines (5).

Quantitative catalytic hydrogenation of the methine (VI) yielded the dihydro derivative (VII) in which an n.m.r. multiplet (7H) corresponding to C_5, C_6, C_{11}, and C_{12} appeared between ca. 6.7 and 7.5 τ. The four protons of the two methylenedioxy groups became equivalent and appeared as a singlet at 4.33 τ. The second Hofmann degradation product (VIII) derived from the dihydromethine (VII) had a new signal as a singlet (2H) at 3.43 τ indicating once more a *cis*-stilbene. A singlet (4H) at 6.96 τ can be assigned to the protons on C_{11} and C_{12}. Reduction of the cyclooctatriene (VIII) yielded the 2,3,8,9-bismethylenedioxydibenzo[*a*,*e*]cyclooctadiene (IX) which because of symmetry gave a simple n.m.r. spectrum; singlets appeared at 7.07 τ (8H at C_5, C_6, C_{11}, and C_{12}), at 4.2 τ (4H of the methylenedioxy group), and at 3.45 τ (4H of aromatic nuclei).

Can. J. Chem. Downloaded from www.nrcresearchpress.com by 210.87.254.105 on 09/05/12
For personal use only.

Can. J. Chem. Downloaded from www.nrcresearchpress.com by 210.87.254.105 on 09/05/12
For personal use only.

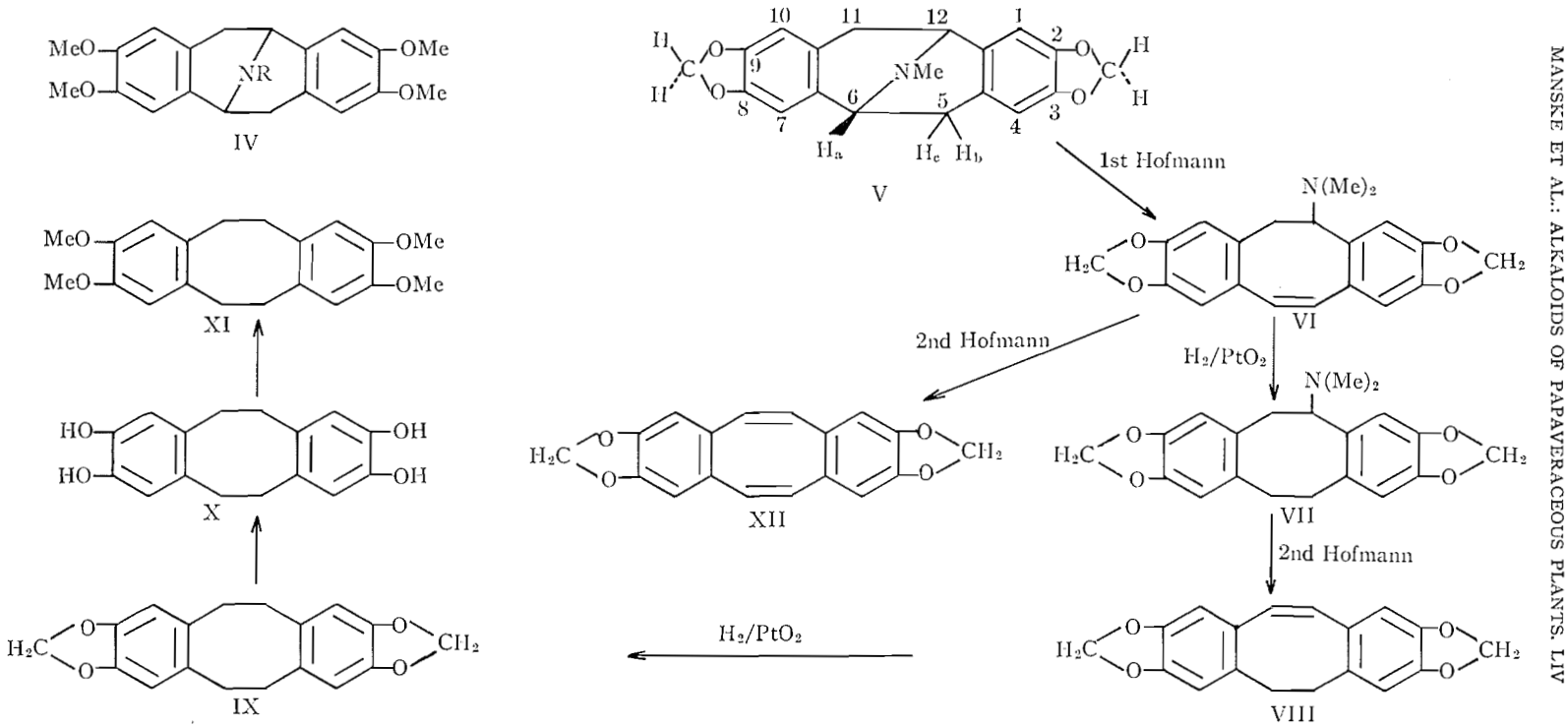

Can. J. Chem. Downloaded from www.nrcresearchpress.com by 210.87.254.105 on 09/05/12
For personal use only.

TABLE I

Nuclear magnetic resonance spectra

Argemonine (3, 4)					Eschscholtzine				
Proton	τ	J(c.p.s.)	Splitting	No. of protons	Proton	τ	J(c.p.s.)	Splitting	No. of protons
H_a	5.92	$J_{a-b}=6.0$ $J_{a-c}=0$	Doublet	2	H_a	6.07	$J_{a-b}=6.0$ $J_{a-c}=0$	Doublet	2
H_b	6.47 6.58	J_{b-a} J_{b-c}	A pair of doublets	2	H_b	6.51 6.78		Two pair of doublets	2
H_c	7.38	$J_{c-b}=17$ $J_{a-c}=0$	Doublet	2	H_c	7.52	$J_{c-b}=17$ $J_{a-c}=0$	Doublet	2
Aromatic H	3.24 3.41		Singlet Singlet	2 2	Aromatic H	3.42 3.60		Singlet Singlet	2
N—Me	7.43		Singlet	3	$\rangle$N—CH_3	7.51		Singlet	3
O—Me	6.08 6.16		Singlet Singlet	6 6	—O —O$\rangle CH_2$	4.19 4.23		A pair of doublets	4

Can. J. Chem. Downloaded from www.nrcresearchpress.com by 210.87.254.105 on 09/05/12
For personal use only.

TABLE II

Ultraviolet spectra (95% ethanol)

Eschscholtzine series			*N*-Methylpavine series		
	λ_{max}^{EtOH}	ϵ (log ϵ)		λ_{max}^{EtOH}	ϵ (log ϵ)
Eschscholtzine (V)	295	11 000 (4.04)	*N*-Methylpavine	287	10 000 (4.00)
Eschscholtzinemethine (VI)	298.4	11 100 (4.04)	*N*-Methylpavinemethine	290.5	9 450 3.98)
Eschscholtzinemethine hydrochloride	297.5	11 100 (4.05)	*N*-Methylpavinemethine hydrochloride	290.5	9 540 (3.98)
Dihydroeschscholtzinemethine hydrochloride	238.5* 294	8 260 (3.92) 8 500 (3.93)	Dihydro-*N*-methylpavinemethine hydrochloride	225* 286	16 600 (4.22) 6 050 (3.78)
Bismethylenedioxydibenzo[*a*,*e*]-cyclooctatriene	303.7†	12 500 (4.10)	Tetramethoxydibenzo[*a*,*e*]-cyclooctatriene	296 345*	11 040 (4.04) 2 420 (3.38)
The dibenzocyclooctadiene (XI)	225* 286	15 960 (4.20) 6 920 (3.85)	Dibenzocyclooctadiene	225* 285.5	15 960 (4.20) 7 020 (3.85)

*Inflection.
†Solvent: MeOH.

Can. J. Chem. Downloaded from www.nrcresearchpress.com by 210.87.254.105 on 09/05/12
For personal use only.

The above compound (IX) was a new substance but it was possible to convert it into the known tetramethoxy derivative (XI) by converting it first into the tetrahydroxy compound (X). Reaction of the ether (IX) with phosphorus pentachloride, hydrolysis of the presumed tetrachloro intermediate, and methylation of the tetrahydroxy compound (X) with dimethyl sulfate or with methyl iodide in the presence of anhydrous potassium carbonate yielded the tetramethoxy compound (XI). Direct comparison of this compound (m.p. 200–203°) with that reported by Battersby and Binks (6) (m.p. 200–203°) proved that the two are identical. The n.m.r. spectrum was in agreement with the structure of the final product; three singlets appeared at 7.07 τ (8H of C_5, C_6, C_{11}, and C_{12}), at 6.25 τ (12H of four methoxyls), and at 3.5 τ (4H of aromatic nuclei).

In contrast to the *N*-methylpavine series (6), further Hofmann degradation of the methine (VI) yielded 2,3,8,9-bismethylenedioxydibenzo[*a*,*e*]cyclooctatetraene (XII), $C_{18}H_{12}O_4$. The structure was confirmed by the n.m.r. spectrum which exhibited three singlets at 4.18 τ (4H of the methylenedioxy groups), at 3.53 τ (4 aromatic protons), and at 3.47 τ (4 olefinic protons). The infrared spectrum of this product showed no hydroxyl band and the ultraviolet absorption (λ_{max}^{MeOH} 3.062 mμ; log ϵ = 3.97) is in keeping with the cyclooctatetraene formulation.

EXPERIMENTAL

All analytical samples were dried at room temperature *in vacuo* over phosphorus pentoxide. Thin layer chromatography was carried out using Silica Gel G, and the developing solvent was cyclohexane:chloroform:diethylamine (7:2:1). All melting points were determined with a Leitz hot-stage microscope and are uncorrected. Infrared absorption spectra were taken on a Perkin–Elmer, model 13713 spectrophotometer; ultraviolet absorption spectra were recorded using a Bausch & Lomb, spectronic 505. The n.m.r. spectra were determined in deuterochloroform with tetramethylsilane internal standard using a Varian A-60 spectrometer.

Eschscholtzine Methiodide

A solution of Eschscholtzine in methanol was treated with excess methyl iodide. Ether was added to complete the separation of the methiodide (quantitative yield) which when washed with ether and recrystallized from methanol melted at 286–287° with decomposition.

Anal. Calcd. for $C_{19}H_{17}O_4N.MeI$: C, 51.63; H, 4.33; N, 3.01; I, 27.27. Found: C, 51.78; H, 4.27; N, 2.96; I, 27.18.

Eschscholtzinemethine Hydrochloride

A solution of eschscholtzine methiodide (0.62 g) in aqueous methanol (30 ml of 50%) was reacted with silver oxide (from 1.5 g silver nitrate). The filtrate from this mixture was evaporated *in vacuo* at 40° to ca. 12 ml and heated under reflux for 5 h with 12 g potassium hydroxide. The resulting oily methine was separated by ether extraction and when dried and freed of solvent weighed 0.42 g (89%). The *hydrochloride* was obtained in colorless needles melting at 215–220° from methanol–ether. R_f: 0.51 (cf. eschscholtzine, R_f: 0.47); thin layer chromatography (t.l.c.) gives a single spot with strong fluorescence under ultraviolet lamp.

Anal. Calcd. for $C_{20}H_{19}O_4N.HCl.H_2O$: C, 61.30; H, 5.66; N, 3.58; Cl, 9.05. Found C, 61.15; H, 5.51; N, 3.19; Cl, 9.37.

Dihydroeschscholtzinemethine Hydrochloride

The catalytic hydrogenation (PtO_2 catalyst) of the methine hydrochloride in methanol proceeded to completion in 40 min. The *hydrochloride* isolated from the filtered solution crystallized readily from a small volume of methanol and the purified product melting at 275–284° (decomp.) was obtained in 80% yield. It was only very sparingly soluble in water; R_f: 0.71.

Anal. Calcd. for $C_{20}H_{21}O_4N.HCl$: C, 63.91; H, 5.90; N, 3.73; Cl, 9.43. Found: C, 63.96; H, 5.94; N, 3.35; Cl, 9.47. Nuclear magnetic resonance spectrum of free base; a multiplet (7H) at 6.7–7.5 (protons at C_5, C_6, C_{11}, and C_{12}); a singlet (4H) at 4.33 ($2CH_2O_2$=); a singlet (6H) at 7.82 (—NMe_2); and aromatic protons (4H) at ca. 3.70.

Dihydroeschscholtzinemethine Methiodide

The free base (the dihydromethine) was prepared by shaking the above hydrochloride with aqueous sodium hydroxide and ether. The dried ether solution was treated with an excess of methyl iodide and the precipitated methiodide thus formed in 60% yield melted at 180–181° with decomposition. The infrared spectrum showed a hydroxyl band at 3 500 cm^{-1} due to water of crystallization.

Anal. Calcd. for $C_{20}H_{21}O_4N.MeI.H_2O$: C, 50.51; H, 5.25; N, 2.81; I, 25.41. Found: C, 50.52; H, 5.22; N, 2.71; I, 25.73.

Dihydroeschscholtzinebismethine (VIII)

A suspension of the above methiodide (3.48 g) and fresh silver oxide (from 10 g silver nitrate) in aqueous methanol (30 ml MeOH; 10 ml H_2O) was shaken for 1 h and the clear filtrate from this was concentrated to ca. 25 ml. Potassium hydroxide (30 g) was then added and the mixture heated under reflux for 5 h and exhaustively extracted with ether. The ether extract was washed with water, with dilute hydrochloric acid, and again with water. The crystalline residue from the dried ether solution was only sparingly soluble in methanol or acetone but readily so in benzene and ethyl acetate. It was recrystallized from *n*-propanol and then melted at 146–152° (1.2 g; 59%).

Anal. Calcd. for $C_{18}H_{14}O_4$: C, 73.46; H, 4.80. Found: C, 73.45; H, 5.01. Nuclear magnetic resonance spectrum: a singlet (2H) at 3.43 (olefinic protons); a singlet (4H) at 6.96 (protons at C_{11} and C_{12}); a singlet (4H) at 4.19 ($2CH_2O_2$=); and a singlet (4H) at 3.48 (aromatic protons).

2,3,8,9-Bismethylenedioxydibenzo[a,e]cyclooctadiene (IX)

The above dihydromethine was easily hydrogenated in ethyl acetate in the presence of Adam's catalyst and crystallized from the same solvent. The colorless crystals melted at 215–218° (76% yield) and were virtually insoluble in ethanol or chloroform.

Anal. Calcd. for $C_{18}H_{16}O_4$: C, 72.96; H, 5.44. Found: C, 73.14; H, 5.45.

2,3,8,9-Tetrahydroxydibenzo[a,e]cyclooctadiene (X)

A mixture of 100 mg of the foregoing substance and 300 mg phosphorus pentachloride in 25 ml benzene was heated under reflux for 90 min. The cooled solution was treated with ice and then evaporated *in vacuo*. The precipitated solid which was virtually insoluble in organic solvents was washed with water and without further treatment converted into the following.

2,3,8,9-Tetramethoxydibenzo[a,e]cyclooctadiene (XI)

(*a*) A suspension of 80 mg of the tetrahydroxy compound in 3 ml of 2 *N* sodium hydroxide and 0.5 ml methanol was treated with dimethyl sulfate (total amount, 1.7 g) in three portions. The pH was maintained at ca. 10 by the further addition of sodium hydroxide solution and the whole was stirred and maintained under nitrogen for 3 h. The mixture was then extracted with three portions of ether and the dried extract concentrated to ca. 100 ml which solution was passed through a column of alkaline alumina. Evaporation of the eluate to a small volume yielded a crop of colorless plates which when recrystallized from ethanol melted at 201–203° (lit. 201–203°).

(*b*) A mixture of the tetrahydroxy compound (50 mg), methyl iodide (1.0 g), and anhydrous potassium carbonate (0.9 g) in acetone (30 ml) was gently heated under reflux with stirring for 21 h. The acetone was evaporated, water was added to the residue, and the mixture extracted with ether. Removal of the ether from the extract yielded colorless plates (58 mg) which melted at 201–203° either alone or in admixture with the prepraration described under (*a*). Furthermore, this compound in admixture with that prepared from pavine (6) also melted at 201–203°.

Eschscholtzinemethine Methiodide

The methine was regenerated from its hydrochloride by treatment with ammonium hydroxide and ether extraction. The dried and clarified solution was treated with excess methyl iodide. The methiodide obtained in 60% yield melted at 158–161° with gas evolution. The infrared spectrum showed a band at 3 500 cm^{-1}.

Anal. Calcd. for $C_{20}H_{19}O_4N.MeI.\frac{1}{2}H_2O$: C, 51.65; H, 4.75; N, 2.87; I, 25.99. Found: C, 51.57; H, 4.96; N, 2.62; I, 25.84.

2,3,8,9-Bismethylenedioxydibenzo[a,e]cyclooctatetraene (XII)

A suspension of 0.46 g of the above methiodide in 36 ml water was shaken for 1 h with an excess of silver oxide. The filtrate from this mixture was heated under reflux after the addition of 40 g potassium hydroxide. The resulting precipitate was filtered from the cooled solution and washed with water. It was dissolved in a large volume (250 ml) of ether and the solution extracted with dilute hydrochloric acid, washed with water, dried, and evaporated. The residue (0.19 g) which was only sparingly soluble in methanol was recrystallized once from ethyl acetate – pentane and twice from benzene. It then melted at 230–233°.

Anal. Calcd. for $C_{18}H_{12}O_4$: C, 73.96; H, 4.14. Found: C, 74.26; H, 4.14.

REFERENCES

1. R. H. F. MANSKE and K. H. SHIN. Can. J. Chem. This issue.
2. H. BUDZIKIEWCZ, C. DJERASSI, and D. H. WILLIAMS. Structure elucidation of natural products by mass spectrometry. Holden-Day. 1964. p. 173.
3. M. J. MARTELL, JR., T. O. SOINE, and L. B. KIER. J. Am. Chem. Soc. **85**, 1022 (1963).
4. F. R. STERMITZ, S.-Y. LWO, and G. KALLOS. J. Am. Chem. Soc. **85**, 1551 (1963).
5. S. GOODWIN, J. N. SHOOLERY, and L. H. JOHNSON. Proc. Chem. Soc. 306 (1958).
6. A. R. BATTERSBY and R. BINKS. J. Chem. Soc. 2888 (1955).
7. N. S. BHACCA, L. H. JOHNSON, and J. N. SHOOLERY. NMR Spectra Catalog, Varian Associates. 1962. Spectra No. 305.

Can. J. Chem. Downloaded from www.nrcresearchpress.com by 210.87.254.105 on 09/05/12
For personal use only.

Can. J. Chem. Downloaded from www.nrcresearchpress.com by 210.87.254.6 on 09/05/12
For personal use only.

THE SYNTHESIS OF β-D-GLUCOPYRANOSYL 2-DEOXY-α-D-*ARABINO*-HEXOPYRANOSIDE[1]

R. U. LEMIEUX AND A. R. MORGAN[2]
Department of Chemistry, University of Alberta, Edmonton, Alberta
Received January 25, 1965

ABSTRACT

D-Glucal triacetate reacted with iodonium and bromonium di-*sym*-collidine perchlorate complexes in the presence of 2,3,4,6-tetra-*O*-acetyl-β-D-glucopyranose to yield, after deacetylation, crystalline β-D-glucopyranosyl 2-deoxy-2-halogeno-α-D-mannopyranosides. The halogen was hydrogenolyzed catalytically to yield β-D-glucopyranosyl 2-deoxy-α-D-*arabino*-hexopyranoside (2-deoxy-neotrehalose) isolated as the crystalline heptaacetate. A correction of the literature is made regarding the preparation of "2,3,4,6-tetra-*O*-acetyl-α-D-glucopyranose".

INTRODUCTION

Lemieux and Levine (1)* proved that the reaction of D-glucal triacetate with iodine and silver benzoate in dry benzene (2) formed an approximately equimolar mixture of the products of *trans*-addition to the double bond, namely, 1-*O*-benzoyl-2-deoxy-2-iodo-β-D-glucopyranose triacetate and the stereoisomer with the α-D-*manno*-configuration. In a later paper (3), they extended this type of reaction to the preparation of glycosides by reacting D-glucal triacetate in benzene with equimolar amounts of an alcohol, iodine, silver perchlorate, and *sym*-collidine.

In view of the limited solubility of silver perchlorate in inert, non-polar solvents, it seemed probable that the conditions for the glycoside synthesis would be improved by the use of preformed positive halogen complexes with *sym*-collidine. For example, Carlsohn (4) prepared salts containing cationic iodine complexes with *sym*-collidine such as the hydroxide corresponding to the formula $[I(sym\text{-collidine})_{3.5}]OH$. In a later paper (5), he described the preparation of bromonium dipyridine perchlorate and referred to iodonium di-2,6-lutidine nitrate. The analogous complex with *sym*-collidine was given the formula $[I(sym\text{-collidine})_{3.5}]NO_3$. We accordingly prepared a number of complexes of "halonium perchlorates" with pyridine and substituted pyridines.

The general methods used may be summarized as follows:

$$AgNO_3 + NaClO_4 + 2B \rightarrow [Ag(B)_2]ClO_4\downarrow + NaNO_3,$$

$$[Ag(B)_2]ClO_4 + X_2 \rightarrow [X(B)_2]ClO_4 + AgX\downarrow,$$

where B is the pyridine base and X_2 is the halogen.

The first stage was carried out in aqueous solution and quantitative yields of the complexed silver perchlorate were obtained. As expected from the highly reactive state of positive halogens, the second stage, in which the halonium complex was produced, was more difficult to carry out. The stabilities and solubilities of the complexes varied widely. Colorless crystalline preparations of the bromonium and iodonium complexes with

[1]*Presented by R. U. Lemieux at the International Symposium on Carbohydrate Chemistry sponsored by the Chemical Society and the University of Birmingham (Chem. Ind. 1703 (1962)).*

[2]*Submitted by A. R. M. in a thesis in partial fulfillment of the requirements for the degree of Doctor of Philosophy, University of Alberta, 1964.*

**The rotations reported in ref. 1 for methyl 2-deoxy-2-iodo-β-D-glucopyranoside and its triacetate are erroneous. The specific rotations at room temperature are* $[\alpha]_D$ *+31° (c, 0.9 in methanol) and* $[\alpha]_D$ *+61° (c, 2 in chloroform) (10), respectively. In a private communication, P. W. Kent reported* $[\alpha]_D^{25}$ *+25.4 (c, 0.92 in methanol) for the former compound.*

pyridine, 2-methylpyridine, and *sym*-collidine were readily obtained. The analyses always corresponded closely to 2 molecules of the base per positive halogen, even in the case of *sym*-collidine complexes, compounds for which Carlsohn (4, 5) usually obtained 3.5 molecules. Uschakow and Tchistow prepared various halonium complexes and later they isolated chloronium dipyridine nitrate (6). When we attempted to prepare chloronium di-*sym*-collidine perchlorate, all that was obtained was a mixture of *sym*-collidinium perchlorate and chlorinated *sym*-collidine.

As expected (3), reaction of D-glucal triacetate with equimolar amounts of methanol and either iodonium or bromonium di-*sym*-collidine complexes dissolved in chloroform gave virtually quantitative yields of acetylated methyl 2-deoxy-2-halogenoglycosides. When these halonium complexes were reacted with D-glucal triacetate in absence of the alcohol, only a very slow disappearance of the olefin took place leading to intractable materials. On the other hand, the halonium complexes with either pyridine or 2-methylpyridine rapidly gave rise to the *N*-(tri-*O*-acetyl-2-deoxy-2-halogenoglycosyl) pyridinium or 2-methylpyridinium perchlorates (7). Thus, the steric hindrance to *N*-glycoside formation provided by the methyl groups at the 2- and 6-positions of *sym*-collidine is required for a successful *O*-glycoside synthesis using these pyridine bases as buffers.

In view of the high yields obtained in the preparation of 2-deoxy-2-halogenoglycosides of simple alcohols, it was believed of interest to attempt the synthesis of non-reducing disaccharides and, for this purpose, 2,3,4,6-tetra-*O*-acetyl-β-D-glucose (8) was used as the "alcohol". The 2-deoxy-2-halogenodisaccharide heptaacetates (mainly II and III) were not obtained crystalline but deacetylation with triethylamine in aqueous methanol (9) yielded crystalline samples of both β-D-glucopyranosyl 2-deoxy-2-iodo-α-D-mannopyranoside (IV) and the corresponding bromide (V). The structures of these compounds were determined as follows.

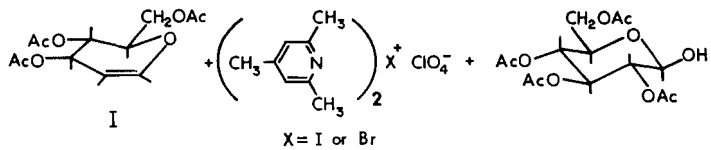

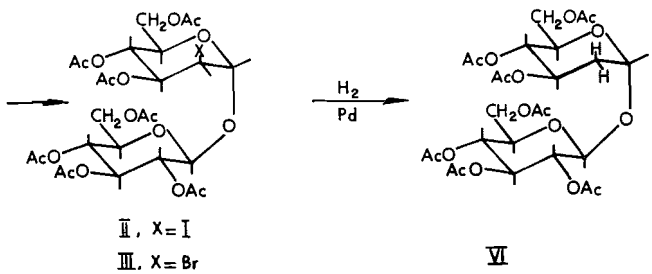

Compound IV was hydrogenolyzed with palladium on charcoal as the catalyst, and acetylation of the product yielded the crystalline heptaacetate (VI). The deacetylated product was rapidly hydrolyzed by dilute hydrochloric acid (typical of 2-deoxyglycosides), to give D-glucose and 2-deoxy-D-*arabino*-hexose as shown by paper chromatography. A compound identical to VI was obtained on hydrogenolysis followed by acetylation of the

Can. J. Chem. Downloaded from www.nrcresearchpress.com by 210.87.254.6 on 09/05/12
For personal use only.

Can. J. Chem. Downloaded from www.nrcresearchpress.com by 210.87.254.6 on 09/05/12
For personal use only.

bromo-compound V. Therefore, compounds IV and V have identical anomeric configurations. The n.m.r. spectrum of IV in deuterium oxide had signals of intensity one at τ 4.35 (spacing, <1 c.p.s.) and τ about 5.25 (obscured by another signal) which can be assigned to anomeric protons. The n.m.r. spectrum of V in deuterium oxide containing a little pyridine had signals of intensity one at τ 4.7 and τ 5.52 with spacings of <1 c.p.s. and 8 c.p.s., respectively. The low field signals in these spectra show very small coupling of the anomeric proton with the H-2 proton. This is characteristic of compounds with the *α-manno-* or *β-manno-* configurations (10). Since the 2-deoxy-disaccharide (VI) formed on hydrogenolysis of both IV and V was found to have the deoxyglucose residue in the α-configuration, both compounds IV and V must have the residue containing the halogen atom in the α-D-*manno-* configuration. This conclusion is in accord with expectations based on the experience of Lemieux and Levine as to the preferred stereochemical route in these halogenoalkoxylation reactions. The configuration of the deoxyglycoside obtained on deacetylation of VI was clearly evident from its n.m.r. spectrum in deuterium oxide. The signals for the anomeric protons appeared as two "doublets" at τ 4.6 and τ 5.3. The latter signal had a spacing of 7.0 c.p.s. and can be assigned to the β-D-glucopyranosyl portion of the compound. The low field signal was actually an ill-defined "doublet" resembling closely the signal for the anomeric proton of 2-deoxy-α-D-*arabino*-hexopyranosides (3). Well-resolved quartets are obtained for the β-D-isomers (3). Also, the structures of the signals for the protons at the 2-position were very similar to those observed for 2-deoxy-α-D-*arabino*-hexopyranosides (3). The molar rotations of compounds IV, V, and VI are approximately those which would be expected from rotations of closely related compounds. However, it is of interest to note that, according to Brewster's rules of atomic and conformational asymmetry (11), the bromo compound V should be more dextrorotatory than the iodo analog IV. In fact, V ($[M]_D$ +140°) was more dextrorotatory than IV ($[M]_D$ +123°). However, caution must be exercised in extending Brewster's rules to screw patterns involving atoms of high rotational rank. For example, according to Brewster's rules, methyl β-D-glucopyranoside ($[M]_D$ −66°) and methyl 2-deoxy-2-iodo-β-D-glucopyranoside ($[M]_D$ +94°) (1) should have the same rotation.

In preliminary experiments, when Celite chromatography (12) was used to isolate the deacetylated 2-deoxy-2-halogenodisaccharides, no crystalline material with the 2-deoxy-2-iodo-β-D-*gluco*-configuration could be obtained. Paper chromatograms also showed no evidence for the formation of stereoisomers other than the 2-deoxy-2-iodo-α-D-*manno* isomer. On the other hand, both the 2-deoxy-2-iodo- and 2-bromo-2-deoxy-disaccharides IV and V crystallized extremely slowly and incompletely from the crude syrup, possibly suggesting an impurity. Only trace amounts of glucose could be detected chromatographically as an impurity of the crude syrup. It is therefore likely that these compounds were formed in substantially higher yields than those (30–40%) calculated on the basis of the amounts of crystalline products obtained.

In attempting to extend the reaction to the formation of the α,α-linked disaccharide, it was necessary to prepare 2,3,4,6-tetra-*O*-acetyl-α-D-glucose.

Schlubach and Wolf (13) reacted 2,3,4,6-tetra-*O*-acetyl-β-D-glucopyranosyl chloride with silver carbonate in either ether or acetone containing a little water to obtain a product melting at 107–108°, $[\alpha]_D$ +138.9°, (*c*, 0.9 in chloroform). The compound was assigned the structure of 2,3,4,6-tetra-*O*-acetyl-α-D-glucose.

Georg (14) treated tetra-*O*-acetyl-α-D-glucopyranosyl bromide with silver nitrate in ether containing a little water. He isolated material of m.p. 99–100°, $[\alpha]_D$ +135° (*c*, 4 in chloroform), and claimed its structure to be 2,3,4,6-tetra-*O*-acetyl-α-D-glucose. The

Can. J. Chem. Downloaded from www.nrcresearchpress.com by 210.87.254.6 on 09/05/12
For personal use only.

mechanism for its formation was postulated as Walden inversion at the anomeric center of the glucosyl bromide with replacement of bromide by the nitrate, followed by a second Walden inversion as water attacks the β-nitrate. Georg could not raise the melting point of his product to that of Schlubach and Wolf's material in spite of repeated recrystallization from ether – petroleum ether. Georg obtained a sample of Schlubach's material and on recrystallization from ether – petroleum ether the melting point fell to 98–99°, but when he recrystallized the compound from ether alone, the melting point rose immediately to 112–113°. He then obtained the same result with his own sample. Georg therefore concluded that dimorphic forms had been obtained.

Lemieux and Brice (15) reacted tetra-*O*-acetyl-β-D-glucopyranosyl chloride with silver acetate in 90% aqueous acetic acid and isolated crystals of m.p. 96–98°, $[\alpha]_D$ +138° (*c*, 0.44 in chloroform). The mutarotation displayed by an aqueous solution of the compound and the good agreement with Georg's values for the physical constants led them to assume they had prepared the 2,3,4,6-tetra-*O*-acetyl-α-D-glucose.

We repeated Lemieux and Brice's directions to obtain a product of m.p. 110–111°, $[\alpha]_D$ +149° (*c*, 1 in chloroform), and the n.m.r. spectrum shown in Fig. 1. The same spectrum was obtained for a product, melting in the range 90–95° obtained in second preparation. It was possible to raise the melting point to 110–111° by recrystallization from ether – Skellysolve B and seeding with the crystals of m.p. 110–111°.

The n.m.r. spectrum (Fig. 1) requires (16) the compound to be 1,3,4,6-tetra-*O*-acetyl-α-D-glucopyranose. The spacing of 3.75 c.p.s. in the signal for the anomeric proton at τ 3.77 is characteristic of protons in *gauche* orientation (17). Therefore, the anomeric configuration is α-D. The chemical shift of the proton requires the presence of an acetoxy group at the 1-position; for example, α-D-glucopyranose pentaacetate gives a signal for the anomeric proton at τ 3.63, spacing 3.3 c.p.s. The presence of a signal for an acetyl group at τ 7.82 is indicative of an axial acetoxy group. The doublet at τ 6.77 and with a spacing of 7.5 c.p.s. is assigned to the hydroxyl proton since the signal was not present in the spectrum after the chloroform solution had been shaken with deuterium oxide. The coupling of the hydroxyl proton with the 2-proton was not always observed. The signal for the 2-proton was in the region τ 5.7–6.3 and superimposed by the signals from the protons at the 5- and 6-positions.

Lemieux and Huber (18) prepared 1,3,4,6-tetra-*O*-acetyl-α-D-glucose, $[\alpha]_D$ +145° (in chloroform), m.p. 97–98°, by reacting 3,4,6-tri-*O*-acetyl-β-D-glucopyranosyl chloride with silver acetate in acetic acid. Matsuda (19) has substituted mercuric acetate for the silver acetate. His material melted at 98–100°, $[\alpha]_D$ +143° (*c*, 3 in chloroform). Recently, Helferich and Zirner (20) prepared 1,3,4,6-tetra-*O*-acetyl-α-D-glucose m.p. 98–100°, $[\alpha]_D$ +141.1° (*c*, 3.2 in chloroform), by a new route. Although Helferich and Zirner reported their compound to depress the melting point of Georg's material, it seems probable that the compounds were identical.

The formation of 1,3,4,6-tetra-*O*-acetyl-α-D-glucose from 2,3,4,6-tetra-*O*-acetyl-β-D-glucosyl chloride is most readily understood in terms of participation of the 2-acetoxy group in the solvolysis of the chloride to yield in the presence of water a transient ortho-acid, which can then rearrange to either the 1,3,4,6- or 2,3,4,6-tetra-*O*-acetyl-α-D-glucose. Our results indicate that, in the glucose series at any rate, the major first product is the 1,3,4,6-tetraacetate. That 1,3,4,6-tetra-*O*-acetyl-α-D-glucose in aqueous solution is thermodynamically less stable than the 2,3,4,6-isomer was established as follows. Although the 1,3,4,6-tetraacetate did not mutarotate in dry pyridine, the specific rotation of an aqueous solution changed from 147.5° to 71° in 12 h. That the product consisted essentially of

Can. J. Chem. Downloaded from www.nrcresearchpress.com by 210.87.254.6 on 09/05/12
For personal use only.

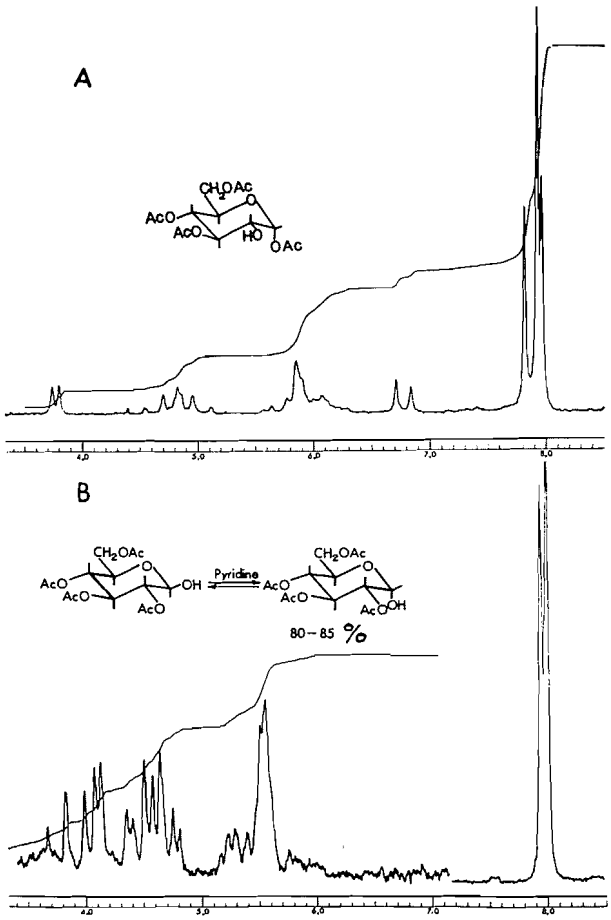

FIG. 1. A. The n.m.r. spectrum of 1,3,4,6-tetra-*O*-acetyl-α-D-glucopyranose in chloroform solution. B. The n.m.r. spectrum of the equilibrium mixture of the anomeric 2,3,4,6-tetra-*O*-acetyl-D-glucoses in pyridine solution.

2,3,4,6-tetra-*O*-acetyl-α- and -β-D-glucose in about equal amounts was evident from the n.m.r. spectrum in chloroform. The signal for the anomeric proton at τ 3.77 disappeared, and no trace of the signal at τ 7.82 characteristic of the 1-*O*-acetyl group of the 1,3,4,6-tetraacetate was present. The equilibrium mixture obtained when 2,3,4,6-tetra-*O*-acetyl-β-D-glucose was dissolved in water had the same spectrum and rotation. That the mutarotation was due to acetyl group migration followed by $\alpha \rightleftarrows \beta$ interconversion was evident since the intensity of the signals for acetyl groups required the product to be a mixture of tetraacetates.

A solution of 2,3,4,6-tetra-*O*-acetyl-β-D-glucose in pyridine displayed mutarotation. The n.m.r. spectrum (see Fig. 1) of the product in pyridine solution after equilibrium was achieved, showed a triplet with spacings of 9.5 c.p.s. at τ 3.92, and a doublet with a spacing of 3.0 c.p.s. at τ 4.16. In view of its spacing and chemical shift, the doublet is assigned to the anomeric proton of the α-anomer. This configuration is supported by the position of the triplet which is assigned to the 3-proton and which is 0.7 τ-values to lower field than the signals for the protons at the 2- and 4-positions. This decreased shielding of

the 3-proton is expected for the α-anomer wherein the 1-hydroxyl group is in axial orientation (21). The intensities of these signals relative to the total of the intensities of the other signals in the spectrum indicated that the equilibrium mixture contained about 80% of the α-anomer. The greater abundance of this isomer in the equilibrium mixture obtained from pyridine as compared to water was expected (22). Benzoylation of the product gave an 80–85% yield of 2,3,4,6-tetra-*O*-acetyl-1-*O*-benzoyl-α-D-glucose. The isomerization of the 1,3,4,6-tetraacetate of α-D-glucose in aqueous solution was independently established by Helferich and Zirner (20) during the course of this investigation.

When the syrup containing about 80% of 2,3,4,6-tetraacetyl-α-D-glucose was used as the "alcohol" in an attempt to form an α,α-linked isomer of compound IV, only IV was obtained and the yield was about the same as when pure 2,3,4,6-tetra-*O*-acetyl-β-D-glucose was used. Presumably, therefore, mutarotation took place more rapidly than did the reaction of the α-anomer, and the α-anomer reacted only very slowly as compared to the β-anomer in the iodoalkoxylation reaction.

With regard to the formation of 1,3,4,6-tetra-*O*-acetyl-α-D-glucose, it is of interest to note that Perlin (23) found the acid hydrolysis of the diastereoisomeric β-D-mannose 1,2-(benzyl orthoacetates) yielded 2-*O*-acetyl-D-mannose. Evidently, the configuration is important in determining whether the acetyl group materializes at the 1- or the 2-poisiton. Ness and Fletcher (24) showed that 1,3,5-tri-*O*-benzoyl-α-D-ribose is formed both on hydrolysis of tri-*O*-benzoyl-D-ribofuranosyl bromide and on hydrogenolysis of 3,4-di-*O*-benzoyl-α-D-ribose 1,2-(benzoyl orthobenzoate). The 1-*O*-benzoyl group was found to migrate to the 2-position in alkaline solution. The isolation by Antia (25) of 1,3,4-tri-*O*-acetyl-α-D-xylose as a product of the reaction of tri-*O*-acetyl-α-D-xylopyranosyl bromide in aqueous acetone and in the presence of silver carbonate is noteworthy.

EXPERIMENTAL

The melting points were taken on a heating stage and are uncorrected. The rotations were measured at room temperature, 23–25°.

The nuclear magnetic resonance (n.m.r.) spectra were determined, unless otherwise stated, in deuterium oxide with a Varian A60 spectrometer and the chemical shifts are reported in *tau* (τ) values with tetramethylsilane (TMS) as external standard.

Deacetylated material was chromatographed on Whatman No. 1 paper and developed with the lighter phase of 1-butanol, ethanol, and water mixture (5:1:4) (26). Silver nitrate (27), periodate–permanganate (28), *p*-anisidine hydrochloride (29), and aniline hydrogen phthalate (30) sprays were used. The R_G numbers refer to the R_f values relative to that of glucose.

Chloroform, when used in preparative procedures, was purified by passing down a column of activated alumina. A column 1.9 cm × 28 cm gave 400 ml chloroform with no trace of hydroxyl absorption in the infrared.

It is important to realize that perchlorates are potentially powerful explosives. Although none of the preparations described below caused trouble, the compounds detonated on strong heating. Due precautions must be taken (31).

Silver Di-sym-collidine Perchlorate

sym-Collidine, 20 ml, was added with vigorous stirring to a solution of silver nitrate, 9 g, and sodium perchlorate, 11 g, in 100 ml of water to give a white curdy precipitate. After washing repeatedly with water, the product was washed with ethanol and ether and finally dried under vacuum over phosphorus pentoxide. The yield was 24 g (100%).

Iodonium Di-sym-collidine Perchlorate

It is important in the preparation of halonium complexes to make sure the conditions are anhydrous. Otherwise, the halogen tends to be reliberated. Powdered iodine, 20.2 g (79.5 mmoles), was added to a suspension of the silver di-*sym*-collidine perchlorate, 35.7 g (79.5 mmoles), in about 200 ml of chloroform and 5 ml of *sym*-collidine. After shaking for 15 min, the yellow precipitate of silver iodide was removed by filtration through a bed of Celite, and the iodonium complex crystallized directly from the filtrate on standing in the cold. The mother liquors gave further fine white crystals on the addition of ether. The combined crystals were dried under high vacuum and analyzed for positive iodine by titration of the iodine liberated in

Can. J. Chem. Downloaded from www.nrcresearchpress.com by 210.87.254.6 on 09/05/12
For personal use only.

the reaction with potassium iodide in aqueous acid. The yield of iodine was 97.5% of theoretical based on the formula $(C_8H_{11}N)_2ICIO_4$.

Bromonium Di-sym-collidine Perchlorate

Silver di-*sym*-collidine perchlorate, 13.47 g (30 mmoles), was suspended in 150 ml pure chloroform and 1 ml *sym*-collidine, and 1.65 ml bromine (30 mmoles) was added. Silver bromide was rapidly precipitated and was collected by filtration on Celite. The clear faint-yellow filtrate gave a fine, white crystalline precipitate on the addition of ether. A 70% yield was obtained of a product which, on analysis contained 93% of the positive bromine expected $(C_8H_{11}N)_2BrClO_4$. The n.m.r. spectrum in methylene chloride was that expected for complexed *sym*-collidine. The intensities of the signals at τ 2.72, 7.15, and 7.57 were 2:6:3, respectively. *sym*-Collidine in methylene chloride gave signals of corresponding relative intensities at higher field τ 3.22, 7.59, and 7.77, respectively. The melting point was ill-defined but a clear liquid was obtained at 230°.

Methyl 3,4,6-tri-O-Acetyl-2-deoxy-2-iodo-α-D-mannopyranoside and the Corresponding β-Glucoside

Anhydrous methanol, 0.12 ml (2.8 mmoles), and 1.3 g of the iodonium complex (titration gave 86% of the theoretical iodine) were added to D-glucal triacetate, 0.755 g (2.78 mmoles), dissolved in 15 ml of pure chloroform. A homogeneous faint-yellow solution was obtained from which, almost immediately, *sym*-collidinium perchlorate separated. The mixture was filtered after a 20 min reaction time, and the filtrate was washed first with water, then with 2 *N* sulfuric acid, and finally with water. After drying by filtration through chloroform-wetted paper, the solution was evaporated at high vacuum to a syrup, 1.115 g (93% yield of methyl tri-*O*-acetyl-2-deoxy-2-iodoglycosides). The n.m.r. spectrum was almost identical to that obtained by Lemieux and Levine (3) except that integration of the methoxyl peaks indicated 82% of the *α-manno* and 18% of the *β-gluco*-configurations.

β-D-Glucopyranosyl 2-Deoxy-2-iodo-α-D-mannopyranoside (IV)

The iodonium complex, 12.17 g (23.7 mmoles of positive iodine as determined by titration) was added to D-glucal triacetate, 6.45 g (23.7 mmoles), and 8.25 g (23.7 mmoles) of 2,3,4,6-tetra-*O*-acetyl-β-D-glucopyranose dissolved in 50 ml of pure chloroform. As the iodonium salt dissolved on stirring the mixture, *sym*-collidinium perchlorate was precipitated. After 20 min, a sample of the solution was added to aqueous potassium iodide solution containing soluble starch. A strong blue color developed. After 6 h, the brownish solution was filtered to remove the *sym*-collidinium perchlorate and the filtrate was washed with 0.1 *M* sodium thiosulfate, 60 ml, to give a light-brown chloroform layer. Iodine was liberated on standing. On passing the chloroform layer down a silicic acid column (1.8 cm × 19.5 cm), a band with the violet color of iodine moved down the column followed by a brown band from which a syrup was isolated. The syrup was deacetylated by allowing a solution, in 20 ml of methanol containing 2 ml of triethylamine and water added to turbidity, to stand overnight at room temperature. A paper chromatogram of the deacetylated syrup showed a spot with R_G = 1.19 and a trace of glucose (aniline hydrogen phthalate as spray reagent). The compound, 2.84 g, crystallized from water on seeding with crystals obtained in an earlier experiment from a chromatographic purification on a Celite column using 1-butanol–water (12). A further 0.5 g was obtained by crystallization of the residual syrup from methanol. The total yield was 33%. Recrystallization from ethanol–water gave material which decomposed around 100°, $[\alpha]_D$ +26.3° (*c*, 2 in water).

Anal. Calcd. for $C_{12}H_{21}O_{10}I.1.5H_2O$: C, 30.08; H, 5.05; I, 26.48. Found: C, 30.19; H, 5.00; I, 27.94.

Further elution of the silicic acid column gave 0.6 g of syrup which, on deacetylation, gave spots corresponding to glucose and glucal on paper chromatograms.

2,3,4,6-Tetra-O-acetyl-β-D-glucopyranosyl 2-Deoxy-3,4,6-tri-O-acetyl-α-D-arabino-hexopyranoside (VI)

The above described compound (IV), 0.163 g (0.36 mmoles), dissolved in 2.5 ml water and 0.3 ml triethylamine, was hydrogenolyzed with a 10% palladium-on-charcoal catalyst. After stirring for 2 h under hydrogen at slightly above atmospheric pressure, the theoretical quantity of hydrogen was taken up. The catalyst was removed by filtration using Celite. Silver carbonate, 10 mmoles, was added to the filtrate to precipitate the iodide ion. Filtration followed by passage of hydrogen sulfide to remove traces of silver salts and evaporation of the clarified solution left 0.135 g of brown residue which was acetylated in 5 ml pyridine and 5 ml acetic anhydride. After standing overnight, the solvents were evaporated to leave 0.207 g of a semicrystalline syrup. Two recrystallizations from ethanol gave fine crystals, m.p. 163.5° and $[\alpha]_D$ +66.5° (*c*, 0.8 in chloroform).

Anal. Calcd. for $C_{26}H_{36}O_{17}$: C, 50.25; H, 5.80. Found: C, 50.25; H, 5.79.

The compound was deacetylated with sodium methoxide in methanol to give a fine, white amorphous powder, R_G = 0.43. The n.m.r. spectrum in deuterium oxide had signals of intensity one (relative to the intensity of a broad band in the τ 5.6–6.9 region and taken as arising from 11 protons) at τ 4.60, 5.28, about 7.6, and about 8.2. The structures of the signals at τ 4.60, 7.6, and 8.2 were very similar to those with similar chemical shifts in the spectrum of methyl 2-deoxy-α-D-*arabino*-hexopyranoside (3). The signal at τ 5.28 was a doublet with a spacing of 7.0 c.p.s. as expected for the anomeric proton of the β-D-glucosyl portion of VII. A 0.05 g sample of the deacetylated product was dissolved in 5 ml of 0.2 *N* hydrochloric acid. The observed rotation of 0.65° (1 dm tube) after 0.5 h fell to 0.55° after 1 day. The reaction was also followed chromatographically and after 1 d essentially all the starting material, R_G = 0.43, had hydrolyzed to glucose and 2-deoxy-D-*arabino*-hexose as seen by direct comparison with authentic samples on a paper chromatogram.

Can. J. Chem. Downloaded from www.nrcresearchpress.com by 210.87.254.6 on 09/05/12
For personal use only.

Can. J. Chem. Downloaded from www.nrcresearchpress.com by 210.87.254.6 on 09/05/12
For personal use only.

Methyl 3,4,6-Tri-O-acetyl-2-bromo-2-deoxy-α-D-mannopyranoside and the Corresponding β-D-Glucoside

The bromonium complex, 0.965 g (2.12 mmoles of positive bromine as determined by titration), was added to D-glucal triacetate, 0.576 g (2.12 mmoles), and 0.2 ml methanol (4.9 mmoles) in 5 ml chloroform. The reaction was exothermic and a rapid precipitation of *sym*-collidinium perchlorate was obtained. After stirring for 10 min, the solution was washed with dilute hydrochloric acid containing potassium iodide. Iodine was liberated, but 6 ml of 0.1 *M* thiosulfate solution rendered both phases colorless. The chloroform layer was then washed with sodium bicarbonate, filtered, and evaporated overnight in a high vacuum. The residue, 0.818 g (quantitative yield) of a light-yellow syrup, had an n.m.r. spectrum which showed the presence of three methyl glycosides. From the chemical shifts of the methoxy-group signals, the compounds were identified as the methyl tri-*O*-acetyl-2-bromo-2-deoxy-D-glycopyranosides with the *β-gluco-* (25%), *α-manno-* (about 65%), *α-gluco-* (about 10%) (32) configurations.

β-D-Glucopyranosyl 2-Bromo-2-deoxy-α-D-mannopyranoside (V)

The bromonium di-*sym*-collidine perchlorate, 13.5 g (27.3 mmoles of bromonium ion by titration), was added to D-glucal triacetate, 7.17 g (26.4 mmoles), and 2,3,4,6-tetra-*O*-acetyl-*β*-D-glucopyranose, 9.17 g (26.4 mmoles), in chloroform. There resulted an exothermic reaction with precipitation of *sym*-collidinium perchlorate. After 5 min, a sample did not liberate iodine when shaken with potassium iodide solution. The reaction mixture was cooled to 0° and about 6 g (27 mmoles) of *sym*-collidinium perchlorate was obtained on filtration. The chloroform filtrate was washed with dilute acid and then sodium bicarbonate.

Evaporation left a syrup which was dissolved in 40 ml of methanol containing 6.5 ml of triethylamine, and water was added to turbidity. The solution turned green and, on standing overnight, became purple. The deacetylated syrup very slowly deposited crystals from methanol, 3.5 g after a month (33% yield). Recrystallization from methanol–water mixture gave material which carbonized around 180°, $[\alpha]_D$ +39.4° (*c*, 1 in water).

Anal. Calcd. for $C_{12}H_{21}O_{10}Br$: C, 35.56; H, 5.32. Found: C, 35.46; H, 5.32.

Since the R_G value was 0.95, the compound was difficult to distinguish from glucose in the chromatogram of the crude deacetylated syrup.

The compound was hydrogenolyzed for 2 d under the same conditions as described above for compound IV using palladium-on-charcoal catalyst. The syrup obtained from the reaction was acetylated and worked up exactly as described for the preparation of the deoxy-glycoside VI. The melting point, 163°, was not depressed on admixture with VI.

1,3,4,6-Tetra-O-acetyl-α-D-glucose

2,3,4,6-Tetra-*O*-acetyl-*β*-D-glucopyranosyl chloride, 36.6 g (100 mmoles), was dissolved in about 100 ml of glacial acetic acid, and 5 ml water (110 mmoles) and 20 g silver acetate (120 mmoles) were added. The mixture was shaken vigorously for 2 min and then frozen in a dry ice and acetone mixture. The volatile components were removed *in vacuo*. The residue was finally warmed to 80° *in vacuo* to remove the last traces of acetic acid. The residue was extracted five times with ether and the silver salts were removed on Celite. To the ether filtrate was added Skellysolve B just to the point of turbidity. The crystalline precipitate, 13.7 g (40% yield), m.p. 90–95° had the n.m.r. spectrum expected for the 1,3,4,6-tetraacetate. Recrystallization from ether – Skellysolve B gave material of m.p. 110–111°, $[\alpha]_D$ +149° (*c*, 1 in chloroform). The n.m.r. spectrum (Fig. 1) is described in the above discussion.

1,3,4,6-Tetra-*O*-acetyl-*α*-D-glucopyranose did not mutarotate in dry pyridine but did in water to a final rotation of $[\alpha]_D$ +71° (*c*, 1.8 in water). 2,3,4,6-Tetra-*O*-acetyl-*β*-D-glucopyranose mutarotated in water to an equilibrium point of $[\alpha]_D$ +71° (*c*, 1.5 in water). The n.m.r. spectra of the equilibrium products dissolved in chloroform were identical and it was apparent that the *α*- and *β*-anomers were present in about equal amounts.

When the product from the equilibration in water was dissolved in pyridine further mutarotation occurred and the n.m.r. spectrum in pyridine indicated that about 80% of the mixture was 2,3,4,6-tetra-*O*-acetyl-*α*-D-glucopyranose. This was confirmed by benzoylation in the usual manner using benzoyl chloride in pyridine. The n.m.r. spectrum of the crude syrupy product, $[\alpha]_D$ +93.5° in chloroform, contained a doublet at τ 3.35, spacing 3.5 c.p.s. This signal is readily assigned to the anomeric proton of 1-*O*-benzoyl-*α*-D-glucopyranose tetraacetate, which must comprise about 80% of the product as determined from the relative intensities of the signals in the n.m.r. spectrum. The syrup readily provided a 75% yield of crystalline product from a solution in ethanol and water, $[\alpha]_D$ +74.3° in chloroform, m.p. 65–70°, and the n.m.r. spectrum indicated now only 75% of the 1-*O*-benzoyl-*α*-D-glucopyranose tetraacetate. However, a further crop of crystals was obtained from the mother liquors which, after repeated recrystallizations, melted at 67–68°, $[\alpha]_D$ +132° (*c*, 0.3 in chloroform). The n.m.r. spectrum was that expected for pure 2,3,4,6-tetra-O-acetyl-1-*O*-benzoyl-*α*-D-glucopyranose and half a molecule of ethanol of solvation. The literature values (33) for 2,3,4,6-tetra-*O*-acetyl-1-*O*-benzoyl-*α*- and -*β*-D-glucopyranoses are, respectively, m.p. 60–63°, $[\alpha]_D^{15}$ +113.5° (*c*, 3 in chloroform) and m.p. 143° $[\alpha]_D^{20}$ −28.1° (*c*, 3 in chloroform). Treatment of the benzoate with hydrogen bromide in acetic acid gave a crystalline product identical to tetra-*O*-acetyl-*α*-D-glucopyranosyl bromide.

Reaction of Syrupy 2,3,4,6-Tetra-O-acetyl-α-D-glucopyranose with Iodonium Di-sym-collidine Perchlorate and D-Glucal Triacetate

The reaction of the mixture of the α- and β-anomers of 2,3,4,6-tetra-*O*-acetyl-D-glucose, obtained by equilibration in pyridine, was performed under the same conditions as described above starting with the pure 2,3,4,6-tetra-*O*-acetyl-β-D-glucose.

On deacetylation, a 39% yield of virtually pure 2-deoxy-2-iodo-α-D-glucopyranosyl β-D-glucopyranoside was obtained as evidenced by the n.m.r. spectrum and optical rotation, and its catalytic reduction and acetylation to VI.

ACKNOWLEDGMENTS

The research was supported by grants (N.R.C.-T 172) to R. U. Lemieux and three North Atlantic Treaty Organization Studentships to A. R. M. (1961–1964). The n.m.r. spectra were determined by Mrs. Gail Conway.

REFERENCES

1. R. U. LEMIEUX and S. LEVINE. Can. J. Chem. **40**, 1926 (1962).
2. J. STANĚK and V. SCHWARZ. Collection Czech. Chem. Commun. **20**, 42 (1955).
3. R. U. LEMIEUX and S. LEVINE. Can. J. Chem. **42**, 1473 (1964).
4. H. CARLSOHN. Angew. Chem. **46**, 747 (1933).
5. H. CARLSOHN. Ber. **68**, 2209 (1935).
6. M. J. OUCHAKOW and W. O. TSCHITOW. Bull. Soc. Chim. France, Ser. 5, **3**, 2142 (1935).
7. R. U. LEMIEUX and A. R. MORGAN. Can. J. Chem. In press. 1965.
8. P. Z. ALLEN. Methods in carbohydrate chemistry. Vol. I. R. L. Whistler and M. L. Wolfrom (*Editors*). Academic Press, New York. 1962. p. 372.
9. W. J. WHELAN. Private communication.
10. R. U. LEMIEUX and B. FRASER-REID. Can. J. Chem. **42**, 532 (1964).
11. J. H. BREWSTER. J. Am. Chem. Soc. **81**, 5475, 5483 (1959).
12. R. U. LEMIEUX, C. T. BISHOP, and G. E. PELLETIER. Can. J. Chem. **34**, 1365 (1956).
13. H. H. SCHLUBACH and I. WOLF. Ber. **62**, 1507 (1929).
14. A. GEORG. Helv. Chim. Acta, **15**, 924 (1932).
15. R. U. LEMIEUX and C. BRICE. Can. J. Chem. **33**, 109 (1955).
16. R. U. LEMIEUX, R. K. KULLNIG, H. J. BERNSTEIN, and W. G. SCHNEIDER. J. Am. Chem. Soc. **80**, 6098 (1958).
17. M. KARPLUS. J. Chem. Phys. **30**, 11 (1959).
18. R. U. LEMIEUX and G. HUBER. Can. J. Chem. **31**, 1040 (1953).
19. K. MATSUDA. Nature, **180**, 985 (1957).
20. B. HELFERICH and J. ZIRNER. Chem. Ber. **95**, 2604 (1962).
21. R. U. LEMIEUX and J. W. LOWN. Can. J. Chem. **42**, 893 (1964).
22. R. U. LEMIEUX. Advan. Carbohydrate Chem. **9**, 1 (1954).
23. A. S. PERLIN. Can. J. Chem. **41**, 399 (1963).
24. R. K. NESS and H. G. FLETCHER, JR. J. Am. Chem. Soc. **78**, 4710 (1956).
25. N. J. ANTIA. J. Am. Chem. Soc. **80**, 6138 (1958).
26. E. L. HIRST and J. K. N. JONES. Discussions Faraday Soc. **7**, 271 (1949).
27. W. E. TREVELYAN, D. P. PROCTOR, and J. S. HARRISON. Nature, **166**, 444 (1950).
28. R. U. LEMIEUX and H. F. BAUER. Anal. Chem. **26**, 920 (1954).
29. L. HOUGH, J. K. N. JONES, and W. H. WADMAN. J. Chem. Soc. 1702 (1950).
30. S. M. PARTRIDGE. Nature, **164**, 443 (1949).
31. J. C. SCHUMACHER (*Editor*). Perchlorates, their properties, manufacture and uses. Reinhold Publishing Corp., N.Y. 1960. p. 187.
32. R. U. LEMIEUX and B. FRASER-REID. Can. J. Chem. **43**, 1460 (1965).
33. E. FISCHER and M. BERGMANN. Ber. **52**, 829 (1919).

Can. J. Chem. Downloaded from www.nrcresearchpress.com by 210.87.254.40 on 09/05/12
For personal use only.

Can. J. Chem. Downloaded from www.nrcresearchpress.com by 210.87.254.40 on 09/05/12
For personal use only.

THE PREPARATION AND CONFIGURATIONS OF TRI-*O*-ACETYL-α-D-GLUCOPYRANOSE 1,2-(ORTHOESTERS)[1]

R. U. LEMIEUX AND A. R. MORGAN[2]
Department of Chemistry, University of Alberta, Edmonton, Alberta
Received January 25, 1965

ABSTRACT

Reaction of tri-*O*-acetyl-2-*O*-acyl (acetyl, benzoyl, pivalyl, and methoxycarbonyl)-α-D-glucopyranosyl halides with a variety of alcohols in *sym*-collidine containing a tetraalkylammonium halide gave the 1,2-orthoesters in near quantitative yields. In each case one of the two diastereoisomeric orthoesters was obtained in high yield and was shown by application of n.m.r. spectroscopy to be that isomer which has the alkoxy group on the dioxolan ring *trans* to the pyranose ring (*exo*-configuration). Participation of a methoxycarbonyloxy group allowed the preparation of a 1,2-(dimethyl orthocarbonate). 1,2-(Phenyl orthoacetates) were prepared.

INTRODUCTION

Helferich and co-workers (1, 2) observed that reaction of tetra-*O*-acetyl-α-D-glucopyranosyl bromide (I) with alcohols in the presence of *sym*-collidine (2,4,6-trimethylpyridine) gave tri-*O*-acetyl-α-D-glucopyranose 1,2-(alkyl orthoacetates). Our study of the

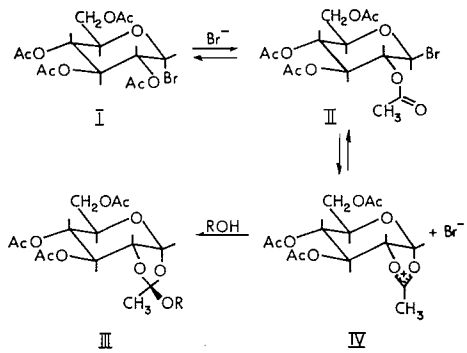

reaction of I with pyridine (3, 4) led to the conclusion that the orthoesters must form from the β-anomer of I which arises in the reaction mixture as a result of the liberation of bromide ion. A recent study of the equilibration of the tetra-*O*-acetyl-D-glucopyranosyl chlorides has in fact shown that the anomerization reaction is strongly catalyzed by halide ions (5). It has long been established that the reaction of tetra-*O*-acetyl-β-D-glucopyranosyl chloride with alcohols, preferably in the presence of pyridine, yields the alkyl 1,2-orthoacetates (6, 7). Tetra-*O*-acetyl-β-D-glucopyranosyl bromide (II) has recently been prepared and this highly labile compound was shown to give the 1,2-orthoacetate when reacted with methanol (8). Particularly in view of the promise that the 1,2-orthoesters of sugars will play an important role in the chemical synthesis of α-glycopyranosides (9), it seemed important to examine their preparation from the readily available *O*-acylated glycopyranosyl halides which possess a 1,2-*cis*-configuration. 1,2-Orthoesters are readily prepared from those sugars which provide the 1,2-*trans*-acylated glycopyranosyl

[1]*Presented by R. U. Lemieux at 148th Meeting of the American Chemical Society, Chicago, Illinois, August 30 – September 4, 1964.*

[2]*This research was part of a thesis submitted by A. R. M. in partial fulfillment of the requirements for the degree of Doctor of Philosophy, 1964.*

halide as the more stable anomer (10). This communication is concerned with the preparation of a variety of 1,2-orthoesters and a 1,2-orthocarbonate from derivatives of D-glucopyranose in near quantitative yield. It is apparent that the method should be generally applicable to the preparation of 1,2-orthoesters from *O*-acylated 1,2-*cis*-glycopyranosyl halides.

The preparation of orthoesters requires that the reaction medium be strongly buffered against acid. Although pyridine can be used for this purpose, its use requires the reaction to yield orthoesters to be substantially more rapid than the formation of the pyridinium glycosides (3). Since this need not generally be the case, it seemed desirable to employ a more hindered base. Since tetra-*O*-acetyl-α-D-glucopyranosyl bromide (I) did not react with *sym*-collidine after 5 d at room temperature, *sym*-collidine was chosen as a suitable base. Of course, other 2,6-disubstituted pyridines should also be useful in this regard. In fact, Mazurek and Perlin (11) have found 2,6-dimethylpyridine to be a solvent of choice in the preparation of 1,2-orthoacetates from tetra-*O*-acetyl-α-D-mannopyranosyl bromide.

Since the formation of a 1,2-orthoester from a 1,2-*cis*-glycopyranosyl halide is dependent on the epimerization of the latter compound to the 1,2-*trans*-anomer, it was evident that the anomerization reaction should be promoted by the addition of halide ion. Quaternary ammonium halide salts were used for this purpose in view of their solubilities in non-polar solvents such as *sym*-collidine and their effectiveness in promoting anomerization (5).

Reaction of I with a wide variety of alcohols using *sym*-collidine as solvent and tetra-*n*-butylammonium bromide as catalyst has provided near quantitative yields of the 1,2-orthoacetate (III). The preparations wherein R = ethyl, isopropyl, *t*-butyl, and phenyl are presented in the experimental section in order to illustrate the generality of the method. In all cases one of the diastereoisomers was formed in large excess (over 85%) except for the reaction with phenol (about 70%). Lemieux and Cipera (7) have suggested that this high degree of partial asymmetric synthesis probably arose because of a more facile approach by the alcohol to the side of the 1,2-acetoxonium ion intermediate (IV) which is *trans* to the glucopyranose ring to yield the *exo*-orthoester (the isomer with the alkoxy group in the *exo*-orientation at the 2-position of the dioxolane ring). Evidence that this is in fact the case was obtained by a comparison of the n.m.r. spectra of the 1,2-(methyl orthoacetate), 1,2-(methyl orthopivalate), and 1,2-(dimethyl orthocarbonate) derivatives of 3,4,6-tri-*O*-acetyl-α-D-glucopyranose. The orthopivalate was originally prepared in the anticipation that the bulk of the *t*-butyl group would prevent the formation of the *exo*-isomer. However, that this was probably not the case was apparent from the chemical shifts of the methoxy-group protons in the above mentioned compounds, the chemical shifts of the pyranose-ring protons in a series of 1,2-(alkyl orthoacetates), and the difference in the conformations of the pyranose rings of the orthoacetates and the orthopivalate as indicated by their n.m.r. spectra. As is seen in Table I, the major isomers in the reaction products obtained in preparing the orthoacetate and the orthopivalate both had the methoxy group signal at τ 6.71. This undoubtedly means that these isomers have the same configuration. The chemical shifts of the methoxy groups in the orthocarbonate agree well with those which would be anticipated from the chemical shifts of the methoxy groups of the diastereoisomeric orthoacetates. This is to be expected since the change in the configuration of the orthoacetates places the methoxy group in one of the environments of the methoxy groups in the orthocarbonate. The chemical shift data reported in Table II show that the change in the alkyl group from methyl to ethyl, to isopropyl, to *t*-butyl, and to phenyl had an appreciable effect on the chemical shifts of the pyranose-ring protons only at the anomeric center (H-1). Therefore, it is evident that

Can. J. Chem. Downloaded from www.nrcresearchpress.com by 210.87.254.40 on 09/05/12
For personal use only.

TABLE I

N.m.r. parameters and yields of derivatives of 3,4,6-tri-*O*-acetyl-α-D-glucopyranose

Derivative	% yield	Chemical shifts of methoxy groups, τ
1,2-(Methyl orthoacetate)		
exo-Isomer	89	6.71
endo-Isomer	11	6.55
1,2-(Methyl orthopivalate)		
exo-Isomer	92	6.71
endo-Isomer	8	6.53
1,2-(Dimethyl orthocarbonate)		
exo-Methoxy	—	6.67
endo-Methoxy	—	6.55

TABLE II

Chemical shifts (τ) and approximate coupling constants (c.p.s.) for tri-*O*-acetyl-α-D-glucopyranose 1,2-(alkyl orthoesters) in chloroform*

		H-1		H-3			H-4	
Alkyl group	Orthoester	τ	$J_{1,2}$	τ	$J_{2,3}$	$J_{3,4}$	τ	$J_{4,5}$
Methyl	Acetate	4.26	5.0	4.81	2.8	2.8	5.09	9.0
Ethyl	Acetate	4.28	5.0	4.81	2.8	2.8	5.09	9.0
Isopropyl	Acetate	4.30	5.0	4.81	2.8	2.8	5.09	9.0
t-Butyl	Acetate	4.35	5.0	4.82	2.6	2.6	5.09	9.0
Phenyl	Acetate	4.32	5.0	4.80	2.8	2.8	5.09	9.0
Methyl	Pivalate	4.17	5.0	4.70	4.0	6.5	5.07	7.0

*The diastereoisomer formed in the greater amount.

these groups are in *cis*-relationship to H-1 and that the compounds have the alkoxy and phenoxy groups in the *exo*-orientation. It is seen in Table II that a change in the bulk of the alkoxy group of the 1,2-orthoacetates had no appreciable effect on the coupling constants for the pyranose-ring protons. It can therefore be concluded that these substitutional changes have no effect on the conformation of the ring. It is evident in view of the magnitudes of the coupling constants that these compounds have the pyranose ring distorted so that H-3 defines a dihedral angle of about 120° with both H-2 and H-4, and H-4 and H-5 define an angle of about 180°. A precise space-filling model of this conformation shows that H-5 is axially oriented and very close to the *endo*-*C*-methyl group of the *exo*-isomer. Replacement of the *C*-methyl group of the methyl 1,2-(orthoacetate) by a *t*-butyl group results in extensive interaction between the *t*-butyl group and H-5, which can only be relieved by a decrease of the dihedral angle defined by H-4 and H-5 and an increase of that defined by H-3 and H-4. Thus, it may have been predicted that $J_{3,4}$ should be greater and $J_{4,5}$ smaller for the orthopivalate than for the orthoacetate when both have the *exo*-configuration. It is seen that this was in fact the case, namely, $J_{3,4}$ increased from 2.8 to 6.5 c.p.s. and $J_{4,5}$ decreased from 9.0 to 7.0 c.p.s. Therefore, the more rapidly formed isomer in each case must have the *exo*-configuration. That the above changes in the n.m.r. parameters were not due to a change in the conformation of the dioxolane ring is clear from the constancy of $J_{1,2} = 5$ c.p.s. There is no basis to expect that an *exo*-*t*-butyl group could influence the conformation of the pyranose ring.

Can. J. Chem. Downloaded from www.nrcresearchpress.com by 210.87.254.40 on 09/05/12
For personal use only.

Can. J. Chem. Downloaded from www.nrcresearchpress.com by 210.87.254.40 on 09/05/12
For personal use only.

The 1,2-(methyl orthopivalate) and a 1,2-(isopropyl orthobenzoate) were prepared as syrups by reaction of the tri-*O*-acetyl-2-*O*-pivalyl-α-D-glucopyranosyl bromide and tri-*O*-acetyl-2-*O*-benzoyl-α-D-glucopyranosyl bromide with the appropriate alcohol in *sym*-collidine containing tetra-*n*-butylammonium bromide. Reaction of tri-*O*-acetyl-2-*O*-methoxycarbonyl-α-D-glucopyranosyl chloride with methanol in *sym*-collidine containing tetraethylammonium chloride gave the 1,2-(dimethyl carbonate). However, the syrupy product was considerably less pure than that obtained on reaction of tri-*O*-acetyl-2-*O*-methoxycarbonyl-β-D-glucopyranosyl chloride with methanol and silver di-(*sym*-collidine) perchlorate (12) using methylene chloride as solvent. Both the preparation of this β-chloride and of the orthocarbonate show that, as expected, the methoxycarbonyloxy group can participate effectively in replacements at a neighboring position. Although the methoxycarbonyloxy group is probably less nucleophilic than the acetoxy group, the delocalization of the positive charge in the resulting oxocarbonium ion is greater than in the acetoxonium ion.

EXPERIMENTAL

Tri-O-acetyl-α-D-glucopyranose 1,2-(Ethyl Orthoacetate)

Tetra-*O*-acetyl-α-D-glucopyranosyl bromide, 4.1 g (10 mmoles), was dissolved in 10 ml of *sym*-collidine and 0.6 ml of dry ethanol (10 mmoles). Tetra-*n*-butyl-ammonium bromide, 1 g (3.1 mmoles), was added, and when the mixture was heated to 50° with shaking, a homogeneous solution was obtained. Crystals of *sym*-collidinium hydrobromide soon began to separate. After 12 h at 50°, the almost solid reaction mixture was dissolved in the minimum chloroform and washed with just sufficient hydrochloric acid to neutralize the collidine, then with aqueous sodium bicarbonate, and finally water. After drying the chloroform layer by filtration through chloroform-wetted filter paper, evaporation at reduced pressure left a semicrystalline mass. The n.m.r. spectrum of this product indicated that the two diastereoisomers of the 1,2-orthoacetate had formed in theoretical yield, 3.8 g (10 mmoles). Recrystallization from hot ethanol with a drop of *sym*-collidine and water added just to turbidity resulted in a heavy crystalline precipitate. The crystals were collected by filtration, washed with water, and dried *in vacuo*. The yield of the *exo*-isomer was 85%, m.p. 95–96°; reported 97–97.5° (7), after two recrystallizations from ethanol. When a 10 *M* excess of ethanol over the tetra-*O*-acetyl-α-D-glucopyranosyl bromide was used, the product still contained only 14% of the *endo*-isomer.

Tri-O-acetyl-α-D-glucopyranose 1,2-(Isopropyl Orthoacetate)

The standard conditions above but with isopropanol in place of ethanol were used to obtain a theoretical yield of the *endo*- and *exo*-diastereoisomers. Crystallization from ethanol with a trace of *sym*-collidine, and water added to turbidity, gave an 85% yield of the *exo*-isomer, m.p. 116–117°. On repeated recrystallization, the m.p. was raised to 120–121°, $[\alpha]_D$ +30° (*c*, 2.4 in chloroform).

Anal. Calcd. for $C_{17}H_{26}O_{10}$(390.4): C, 51.8; H, 6.67. Found: 384; C, 51.54; H, 6.82.

Tri-O-acetyl-α-D-glucopyranose 1,2-(t-Butyl Orthoacetate)

Again the above conditions were employed but with *t*-butanol, except that the acid washing was omitted because of the very high sensitivity of the orthoacetate. The *sym*-collidine was finally removed *in vacuo* with warming at 80° to give a crystalline mass in theoretical yield. The pure *exo*-isomer was obtained on dissolving the crude crystals in hot ethyl acetate and adding Skellysolve B to turbidity. A 75% yield of the orthoester, m.p. 152.5–154.5°, $[\alpha]_D$ +34.5° (*c*, 1.6 in chloroform), was obtained.

Anal. Calcd. for $C_{18}H_{28}O_{10}$ (404.4): C, 53.46; H, 6.98. Found: 394; C, 53.1; H, 6.71.

Tri-O-acetyl-α-D-glucopyranose 1,2-(Phenyl Orthoacetate)

The standard conditions above with phenol as the alcohol were used to obtain a syrup which could not be induced to crystallize. The n.m.r. spectrum required the formation of the diastereoisomeric orthoacetates as the only products with 68% of the *exo*- and 32% of the *endo*-isomers as judged from the relative intensities of the signals for the orthoacetyl group at τ 8.22 and τ 8.42, respectively. The compounds are exceedingly sensitive to hydrolysis.

Tri-O-acetyl-α-D-glucopyranose 1,2-(Isopropyl Orthobenzoate)

1,3,4,6-Tetra-O-acetyl-α-D-glucopyranose (12) was benzoylated in pyridine solution using benzoyl chloride under the usual conditions. The syrupy product resisted crystallization and was treated with 30% hydrogen bromide in acetic acid to produce tri-*O*-acetyl-2-*O*-benzoyl-α-D-glucopyranosyl bromide. This product also failed to crystallize. Nevertheless, its n.m.r. spectrum was precisely that expected for this compound in that the presence of three *O*-acetyl groups and one benzoyl group was evident. The signal for the anomeric proton

Can. J. Chem. Downloaded from www.nrcresearchpress.com by 210.87.254.40 on 09/05/12
For personal use only.

was a doublet at τ 3.23, spacing 3.8 c.p.s.; H-3 and H-4 gave triplet signals at τ 4.21 and 4.72, respectively, with spacings of 9.5 c.p.s. The signal for H-2 was a quartet centered at τ 4.90. The signals for the protons at the 5- and 6-positions were in the usual positions with the signal for H-5 to somewhat lower field, about τ 5.6. The syrup, 2.3 g, was dissolved in 4 ml of *sym*-collidine and 0.25 g of tetra-*n*-butylammonium bromide, and 0.47 ml of isopropanol were added. When the mixture was warmed to obtain a homogeneous solution, a fine precipitate appeared, and after 20 h at 42°, the solution had set solid with crystals. The chloroform solution of the reaction mixture was washed with excess 2 *N* sulfuric acid, followed by aqueous sodium bicarbonate. The n.m.r. spectrum of the syrup obtained on evaporation of the chloroform layer had doublets each of spacing 5 c.p.s. at τ 4.13 and 4.24 with relative intensities of about 2:1. This evidence that both the diastereoisomeric orthobenzoates had formed was supported by the complex structures of the signals for the acetyl groups (five signals) and the methyl groups of the isopropyl group. The pattern of signals for the protons on the pyranose ring was very similar to that observed for the tri-*O*-acetyl-α-D-glucopyranose 1,2-(alkyl orthoesters). Crystalline material was not obtained. It was apparent that these orthoesters were substantially more susceptible to hydrolysis than the corresponding orthoacetates.

Tri-O-acetyl-α-D-glucopyranose 1,2-(Methyl Orthopivalate)

1,3,4,6-Tetra-*O*-acetyl-α-D-glucopyranose (12), 3 g (8.62 mmoles), in 9 ml of pyridine was treated with pivalyl chloride, 3.08 g (25.6 mmoles). After 3 h, the product was isolated in the normal way, and crystals were obtained from the syrup on evaporation at high vacuum. Two recrystallizations from methanol–water yielded crystal plates, m.p. 109.5–110°, $[\alpha]_D$ +93.2° (*c*, 1.2 in chloroform). The n.m.r. spectrum was in complete agreement with the assigned structure.

Anal. Calcd. for $C_{19}H_{29}O_{11}$: C, 52.77; H, 6.52. Found: C, 52.63; H, 6.20.

The above crystals, 1.486 g (3.44 mmoles), were dissolved in 5 ml of 30% hydrogen bromide in acetic acid, 1 ml of acetic acid, and 1 ml of acetic anhydride. After 9 h, the product was isolated in the normal fashion. The syrup obtained could not be crystallized, but had the n.m.r. spectrum required for tri-*O*-acetyl-2-*O*-pivalyl-α-D-glucopyranosyl bromide. The yield was quantitative.

The above syrup, 0.55 g (1.21 mmoles), was dissolved in 2 ml of *sym*-collidine and 1 ml of methanol (24.7 mmoles), and 0.2 g of tetra-*n*-butylammonium bromide were added. The reaction time required was significantly longer than that for the formation of the methyl orthoacetate. After 1 d at 60°, the reaction mixture was shaken with carbon tetrachloride and the *sym*-collidinium bromide was removed by filtration. The carbon tetrachloride filtrate was washed with water and then evaporated to a syrup, 0.3 g (61% yield). The n.m.r. spectrum of the compound is described in Tables I and II and is discussed in detail in the introduction to this paper.

Tri-O-acetyl-α-D-glucopyranose 1,2-(Dimethyl Orthocarbonate)

3,4,6-Tri-*O*-acetyl-β-D-glucopyranosyl chloride (13), 20 g (61.5 mmoles), was dissolved in 20 ml of *sym*-collidine and 100 ml of methyl chloroformate. On warming the solution, gases were evolved. Carbon dioxide and methyl chloride are presumably formed by nucleophilic attack of the chloride ion produced in the reaction on the methyl chloroformate. This reaction amounts to a decomposition of the methyl chloroformate which must therefore be added in a large excess. The reaction was carried out until almost all the methyl chloroformate had disappeared, around 4 h. The products were extracted with carbon tetrachloride, and the insoluble salts were removed by filtration. The carbon tetrachloride solution was washed with dilute sulfuric acid and aqueous sodium bicarbonate, and finally evaporated to a syrup. The n.m.r. spectrum of the product was in all respects precisely that expected for tri-*O*-acetyl-2-*O*-methoxycarbonyl-α-D-glucopyranosyl chloride. The yield was 90%.

The above syrup, 21 g (55 mmoles), was dissolved in 100 ml of acetic acid and 10 ml of acetic anhydride. Silver acetate, 15 g (89.8 mmoles), was added and the mixture was refluxed for 2 h. The silver salts were removed by filtration on Celite and the filtrate was evaporated down to a semi-crystalline mass *in vacuo*. The ethanolic solution of the crystals was decolorized with Darco G 60 and water was added to the clear solution. Shiny needle-like crystals, m.p. 129.5–130°, $[\alpha]_D$ +13.4° (*c*, 1.12 in chloroform) were obtained. The n.m.r. spectrum was that expected for tetra-*O*-acetyl-2-*O*-methoxycarbonyl-β-D-glucopyranose.

Anal. Calcd. for $C_{16}H_{22}O_{12}$: C, 47.29; H, 5.46. Found: C, 46.98; H, 5.20.

The above crystals, 0.5 g (1.23 mmoles), reacted with aluminium chloride, 0.164 g (1.23 mmoles), in 6 ml of methylene chloride over half an hour with stirring. Dry benzene, 15 ml, was added to the reaction mixture, which was passed through a bed of 1/2 g of dry silicic acid. The benzene – methylene chloride solution was washed with ice-cold water and evaporated to a crystalline mass, 0.31 g (66% yield). Recrystallization from benzene–Skellysolve B yielded material, m.p. 55–80°, $[\alpha]_D$ +5.45° (*c*, 3 in chloroform). Recrystallization did not alter the properties, but crystallization from benzene alone, followed by grinding the crystals to a fine powder before drying *in vacuo* for 1 d, raised the m.p. to 103.5–104°. The n.m.r. spectrum in deuterated chloroform indicated the presence of about one-third mole of benzene per mole of tri-*O*-acetyl-2-*O*-methoxycarbonyl-β-D-glucopyranosyl chloride.

Anal. Calcd. for $C_{14}H_{19}O_{10}Cl$. 1/3 C_6H_6: C, 47.18; H, 5.20. Found: C, 47.44; H, 5.30.

The above β-chloride, 0.765 g (2 mmoles), silver di-*sym*-collidine perchlorate (12), 0.9 g (2 mmoles), and methanol, 0.5 ml (12.13 mmoles), were allowed to react in 3 ml of methylene chloride with stirring overnight. After the removal of insoluble salts on Celite, the filtrate was washed with aqueous sodium bicarbonate and

water and finally evaporated to a syrup. The n.m.r. spectrum required that virtually pure tri-*O*-acetyl-α-D-glucopyranose 1,2-(dimethyl orthocarbonate) was the product of the reaction. The same compound was formed but in a less pure condition by reacting the syrupy tri-*O*-acetyl-2-*O*-methoxycarbonyl-α-D-glucopyranosyl chloride with methanol in *sym*-collidine containing tetraethylammonium chloride. The spacing of the signal for the anomeric proton at τ 4.32 was 5.2 c.p.s. The signal for H-3 was a quartet centered at τ 4.69 with spacings of about 4 and 6 c.p.s. which must correspond closely to $J_{2,3}$ and $J_{3,4}$, respectively. The quartet signal for H-4 was centered at τ 5.11 and showed a spacing of 9 c.p.s. which must correspond to $J_{4,5}$. Thus the *endo*-methoxy group distorts the pyranose ring from the conformation in the *exo*-1,2-(alkyl orthoacetates) toward that in the *exo*-1,2-(methyl orthopivalate).

ACKNOWLEDGMENTS

The research was supported by grants (N.R.C.-T 172) to R. U. L. and three North Atlantic Treaty Organization Studentships to A. R. M. (1961–1964). The n.m.r. spectra were determined at 60 Mc.p.s. by Mrs. Gail Conway.

REFERENCES

1. B. HELFERICH, A. DOPPSTADT, and G. A. GOTTSCHLICH. Naturwissenschaften, **40**, 441 (1953).
2. B. HELFERICH and K. WEIS. Chem. Ber. **89**, 314 (1956).
3. R. U. LEMIEUX and A. R. MORGAN. Can. J. Chem. In press. 1965.
4. R. U. LEMIEUX and A. R. MORGAN. J. Am. Chem. Soc. **85**, 1889 (1963).
5. R. U. LEMIEUX and JUN-ICHI HAYAMI. Can. J. Chem. In press. 1965.
6. R. U. LEMIEUX and C. BRICE. Can. J. Chem. **33**, 109 (1955).
7. R. U. LEMIEUX and J. D. T. CIPERA. Can. J. Chem. **34**, 906 (1956).
8. F. WEYGAND, H. ZIEMANN, and H. J. BESTMANN. Chem. Ber. **91**, 2534 (1958).
9. R. U. LEMIEUX and A. R. MORGAN. Can. J. Chem. In press. 1965.
10. E. PACSU. Advan. Carbohydrate Chem. **1**, 77 (1945).
11. M. MAZUREK and A. S. PERLIN. Private communication.
12. R. U. LEMIEUX and A. R. MORGAN. International Symposium on the Chemistry of Natural Products, Kyoto, Japan. May 12–18, 1964. Abstracts of Papers, p. 151.
13. P. BRIGL. Z. Physiol. Chem. **122**, 245 (1922).

Can. J. Chem. Downloaded from www.nrcresearchpress.com by 210.87.254.40 on 09/05/12
For personal use only.

Can. J. Chem. Downloaded from www.nrcresearchpress.com by 210.87.254.42 on 09/05/12
For personal use only.

THE ABNORMAL CONFORMATIONS OF PYRIDINIUM α-GLYCOPYRANOSIDES

R. U. LEMIEUX AND A. R. MORGAN[1]
Department of Chemistry, University of Alberta, Edmonton, Alberta
Received January 25, 1965

ABSTRACT

The nuclear magnetic resonance spectra for *N*-(tetra-*O*-acetyl-α-D-glucopyranosyl)-pyridinium and 4-methylpyridinium bromides and *N*-(tri-*O*-acetyl-2-deoxy-2-iodo-α-*D*-mannopyranosyl)-pyridinium perchlorate (V) require these compounds to exist in the 1C-conformation wherein the pyridinium group is in equatorial orientation. The highly strained condition of V was evidenced by its high reactivity as compared to the β-D-*gluco* diastereoisomer (IV). It is suggested that the instability of the C1-conformation is partly attributable to the reverse of the anomeric effect, and the probable importance of this phenomenon is discussed. The optical rotatory dispersion properties of these and a number of other pyridinium glycosides are presented.

INTRODUCTION

In 1910, Fischer and Raske (1) reported the preparation of *N*-(tetra-*O*-acetyl-β-D-glucopyranosyl)-pyridinium bromide (I). Recently, Lemieux and Morgan (2) reported the preparation of the α-anomer as a syrup. Application of these synthetic methods has now yielded both the anomers for the 4-methylpyridine analogs in pure crystalline condition. The unique conformational properties of these compounds stimulated a study of related compounds, and the results obtained are the subject of this communication.

The 100 Mc.p.s. spectrum (Fig. 1) of the crystalline *O*-acetylated 4-methylpyridinium α-glucoside (III), for reasons of the expected change in the coupling constant for protons on neighboring carbons with change in the dihedral angle defined by the protons (3, 4), appeared to require that the compound has the pyranose ring strongly distorted from the C1-conformation. It is seen that the signals for the five ring protons are all well separated and, consequently, the spectrum is subject to first-order analysis. On this basis, the coupling constants $J_{1,2} = 2.8$, $J_{2,3} = 3.1$, $J_{3,4} = 3.2$, and $J_{4,5} = 5.7$ c.p.s. are indicated. In view of these coupling constants, the compound appears to have a conformation which is close to the 1C-conformation wherein the acetoxy groups at the 2-, 3-, and 4-positions are in axial orientation. In fact, the signals for three of the acetoxy groups are in the region *normally* found for axial acetoxy groups (3). Such a strong distortion of the pyranose ring from the C1-conformation, wherein the substituents at the 2 to 5 positions would be in the equatorial orientation, must arise from powerful non-bonding interactions arising from the 4-methylpyridinium group when in axial orientation at the anomeric center. Since the *A* value for the benzene ring is believed to be in the order of only 2–3 kcal/mole (5), the distortion noted in III could not have been expected on steric grounds. However, the N—C bond length in quaternary ammonium compounds is substantially shorter, 1.48 Å (maximum), than the C—C bond in a compound such as toluene, 1.52 ± 0.01 Å (6). It is to be noted, however, that the establishment of a positively charged atom in axial orientation at the anomeric center must be expected to meet a strongly destabilizing effect (relative to when the group is in equatorial orientation) arising from the electrostatic interaction between the C-1 to N and C-5 to O bonds, when the N and C-5 atoms are in

[1]*Submitted in part by A. R. M. in partial fulfillment of the requirements for the degree of Doctor of Philosophy, University of Alberta, 1964.*

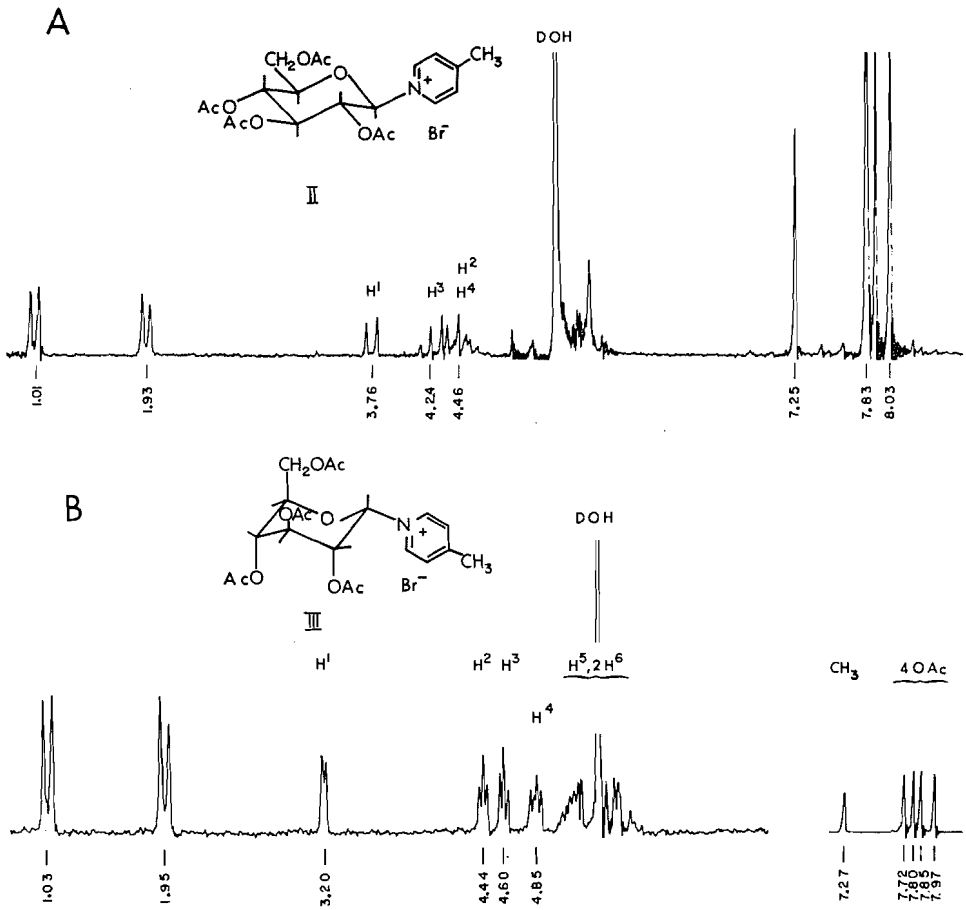

FIG. 1. N.m.r. spectra measured at 100 Mc.p.s. with deuterium oxide as solvent. A, *N*-(Tetra-*O*-acetyl-β-D-glucopyranosyl)-4-methylpyridinium bromide (II). B, *N*-(Tetra-*O*-acetyl-α-D-glucopyranosyl)-4-methylpyridinium bromide (III).

gauche relationship. This interaction amounts to the *reverse* of the anomeric effect (7, 8). Since, for example, the anomeric effect for the tetra-*O*-acetyl-D-glucopyranosyl chlorides amounts to about 3 kcal/mole in favor of the α-anomer wherein the chlorine is in axial orientation (9), it can be anticipated that the *reverse* anomeric effect may well amount to an even stronger destabilizing interaction for the 4-methylpyridinium α-glucoside (III) in the C1-conformation than that arising from the space requirements of the 4-methylpyridinium group. Thus, the fact that the n.m.r. spectrum of III requires the compound to exist in a conformation approaching the 1C-conformation in order to have the aglycone in equatorial orientation may arise from both steric and dipolar interactions, both of which destabilize the α-anomer. The n.m.r. spectrum of the syrupy preparation of the pyridinium α-glucoside (2) was virtually identical with that of III.

The above-mentioned evidence that a quaternized nitrogen at the anomeric position of a lactol ring structure is strongly demanding for an equatorial orientation could be of great importance for a number of reasons. First of all, the phenomenon would have an important bearing on the conformation and conformational rigidity of such important

Can. J. Chem. Downloaded from www.nrcresearchpress.com by 210.87.254.42 on 09/05/12
For personal use only.

biological compounds as the pyridine nucleosides. Secondly, it is evident that the protonation of an axial aglycon at the atom bonded to the anomeric center will cause strong destabilization of the conformation of the sugar ring relative to that wherein the aglycon is in equatorial orientation. Thus, it can be speculated that for α-glucosides, the preferred point of protonation in the course of acid-catalyzed hydrolysis would be at the ring-oxygen atom. On the other hand, for β-glucosides, the reverse anomeric effect would tend to lead to protonation at the oxygen of the aglycon since, in this case, protonation of the ring-oxygen would have to disturb the orientation of the aglycon from the sterically and electronically most favorable position wherein the first carbon of the aglycon is *gauche* to the ring-oxygen as depicted in structure VII (10).

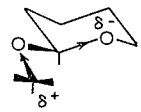

VII

Thirdly, an attack by a molecule at the anomeric center which leads to development of positive charge on the entering group must be expected to be much more favorable when the entering group leads to the equatorial product. For example, it would be expected on the basis of the reverse anomeric effect that the transition state VIII would be considerably more favorable than that represented by IX.

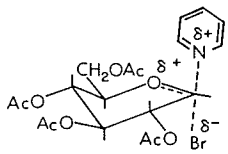

VIII

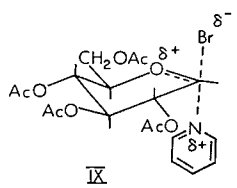

IX

In view of the above mentioned probable importance of the *reverse anomeric effect*, it was desirable to further examine the phenomenon. First of all, it was necessary to gain better evidence that compound III actually possesses the unusual conformation indicated by its n.m.r. spectrum. Although it seemed very unlikely, there was the possibility that the Karplus relationship for coupling constants broke down completely for this kind of structure. To test this possibility, it was of interest to determine the n.m.r. spectrum of a compound such as *N*-(tetra-*O*-acetyl-α-D-mannopyranosyl)-pyridinium bromide. Should, for the reasons outlined above, this compound exist in the 1C-conformation, then H-1 and H-2 would define a dihedral angle of about 180° and, under these circumstances, the protons should be coupled to an extent of about 9 c.p.s. However, reaction of tetra-*O*-acetyl-α-D-mannopyranosyl bromide with pyridine, with or without the addition of tetra-*n*-butylammonium bromide,* gave only the pyridinium β-mannoside. It was possible, however, to obtain pyridinium glycosides with the *α-manno* configuration by reacting D-glucal triacetate with halonium dipyridine perchlorates (11). One of these compounds, *N*-(tri-*O*-acetyl-2-deoxy-2-iodo-α-D-mannopyranosyl)-pyridinium perchlorate (V) was obtained in a pure crystalline condition. The n.m.r. spectrum of this compound is shown in Fig. 2. It is seen that, indeed, the spectrum corresponds closely with that expected for

**These experiments were conducted by Mr. M. Ponpipom.*

Can. J. Chem. Downloaded from www.nrcresearchpress.com by 210.87.254.42 on 09/05/12
For personal use only.

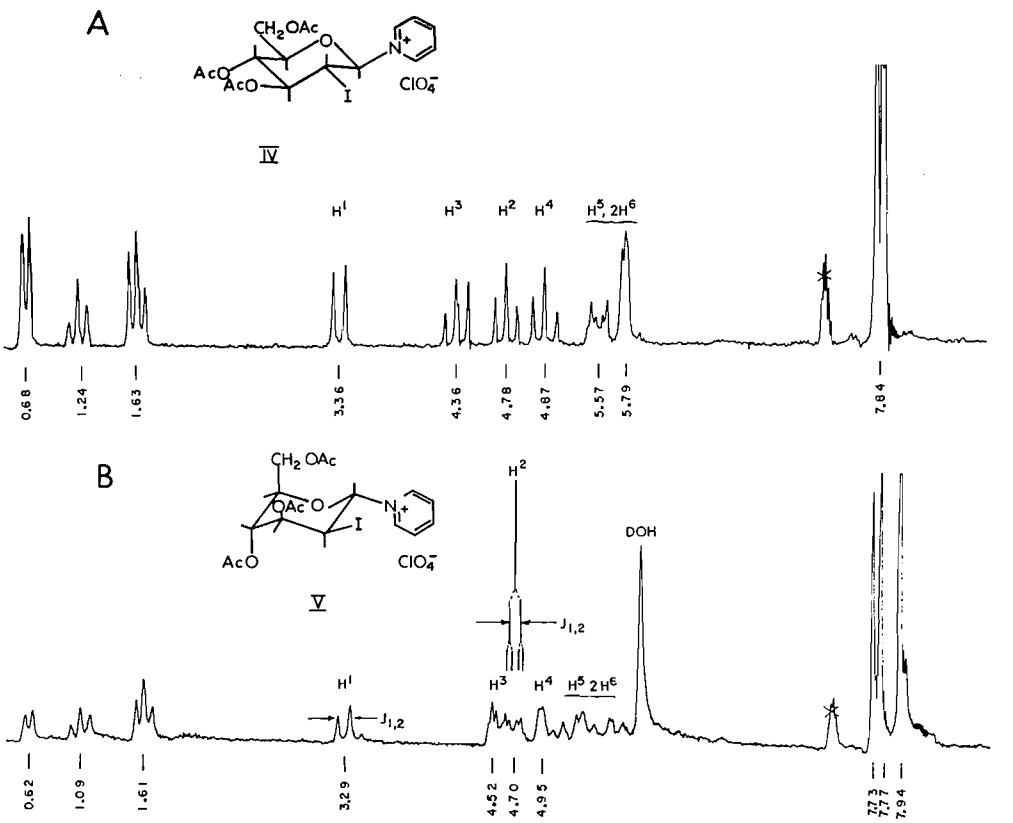

FIG. 2. N.m.r. spectra at 100 Mc.p.s. A, *N*-(Tri-*O*-acetyl-2-deoxy-2-iodo-β-D-glucopyranosyl)-pyridinium perchlorate (IV) dissolved in deuterated dimethylsulfoxide. B, *N*-(Tri-*O*-acetyl-2-deoxy-2-iodo-α-D-manno-pyranosyl)-pyridinium perchlorate (V) dissolved in deuterated dimethylsulfoxide containing a drop of deuterium oxide.

the compound in the 1C-conformation. Since there was a chemical shift of only τ 0.18 for H-2 and H-3, the structure of the doublet signal for the anomeric proton at τ 3.29 was undoubtedly affected by virtual long-range coupling (12). Nevertheless, the spacing of 9.0 c.p.s. clearly indicates that both these protons are in axial orientation. The signal for H-4 appeared at τ 4.95 as a rough singlet with a half-band width of 7 c.p.s. Therefore, the coupling of H-4 with both H-3 and H-5 must be in the range, about 3 c.p.s., expected for hydrogens in *gauche* relationship. Furthermore, the presence of signals for two acetyl groups at τ 7.73 and τ 7.77 lends support to the presence of two axial acetoxy groups as required by the 1C-conformation. The two acetyl groups gave their signals at 10–15 c.p.s. to lower field than did the other acetyl group in a variety of solvents, namely, dimethylsulfoxide, methylene chloride, acetone, pyridine, and methanol. Also, the β-D-*gluco* isomer (IV) of the above compound was prepared and the signal for the anomeric proton was found to be in almost the same position, τ = 3.36, as observed for that of the α-D-manno compound, τ = 3.29, in dimethylsulfoxide as the solvent. Also, as seen in Fig. 2, the n.m.r. spectrum of the β-D-*gluco* isomer (IV) corresponds well with that expected for the compound in the all equatorial C1-conformation. That is, the coupling constants agree well in magnitude to those normally observed in derivatives of β-D-glucopyranose (13). Therefore,

Can. J. Chem. Downloaded from www.nrcresearchpress.com by 210.87.254.42 on 09/05/12
For personal use only.

there can be no doubt that the Karplus relationship applies well enough to these compounds to allow the conclusion that definitely compounds III and V exist in conformations closely approaching the 1C-conformation. The coupling constants are not compatible with boat conformations.

In view of their highly strained conformations, compounds III and V would be expected to display somewhat abnormal properties. This was in fact the case. Compound IV was readily deacetylated in methanol using triethylamine as catalyst. On the other hand, the *α-manno* isomer (V) decomposed too readily to allow deacetylation. Although IV showed no reaction with aqueous potassium iodide solution, V rapidly decomposed to iodine and D-glucal triacetate. Furthermore, V readily isomerized to IV when dissolved in pyridine at room temperature.

Reaction of D-glucal triacetate with bromonium dipyridine perchlorate readily gave crystalline *N*-(tri-*O*-acetyl-2-bromo-2-deoxy-*β*-D-glucopyranosyl)-pyridinium perchlorate (VI). The *α-manno* isomer in the residual syrup could not be induced to cyrstallize. However, it was evident from the n.m.r. spectrum that the compound had formed and possessed the 1C-conformation of the 2-iodo analog (V). On standing in pyridine solution, the *α-manno* compound isomerized to VI.

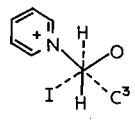

X

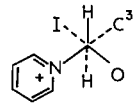

XI

The optical rotatory dispersion curves for the *O*-acetylated pyridinium glycosides IV and V support the conformations assigned above on the basis of the n.m.r. spectral data. Following Brewster's rules (14) for predicting rotation on the basis of conformational asymmetry, it would be expected that the screw pattern described by the conformational unit X for compound IV in the C1 conformation would make an important contribution to rotation. Since the pyridinium group absorbs in the 260 mμ region and is present in this unit, the exhaltation of the rotation with decreasing wavelength toward the region of absorption should render the contributions to rotation by other portions of the molecule negligible as compared to contribution by the conformational unit X. On this basis, therefore, compound IV can be expected to display a Cotton effect characteristic of the conformational unit X. From Fig. 3, it is seen that IV in water provided a plain positive curve. The strong absorption prevented a measurement of the full Cotton effect. For the above mentioned reasons, the *α-manno* isomer (V) in the 1C conformation, wherein the conformational unit XI is the mirror image of that in X, would be expected to display a plain negative o.r.d. curve. Indeed, as seen in Fig. 3, this was the case. Of course, this o.r.d. data provides only circumstantial evidence for the 1C conformation of V since it is not possible to predict the rotational properties of V in the C1 conformation. The *N*-(tri-*O*-acetyl-2-bromo-2-deoxy-*β*-D-glucopyranosyl)-pyridinium perchlorate (VI) also gave a plain positive curve. The o.r.d. curves for the *α*- and *β*-anomers of the *N*-D-glucopyranosides derived from pyridine and 4-methylpyridine were very similar to those previously reported (15) for the corresponding glucosides derived from nicotinamide. For the free glucosides, both the anomers gave plain positive curves.

The addition of iodonium dipyridine perchlorate to D-glucal triacetate in chloroform gave an immediate precipitation of *N*-(tri-*O*-acetyl-2-deoxy-2-iodo-*β*-D-glucopyranosyl)-pyridinium perchlorate in 70% yield. Since the isomerization of the *α-manno* isomer did

Can. J. Chem. Downloaded from www.nrcresearchpress.com by 210.87.254.42 on 09/05/12
For personal use only.

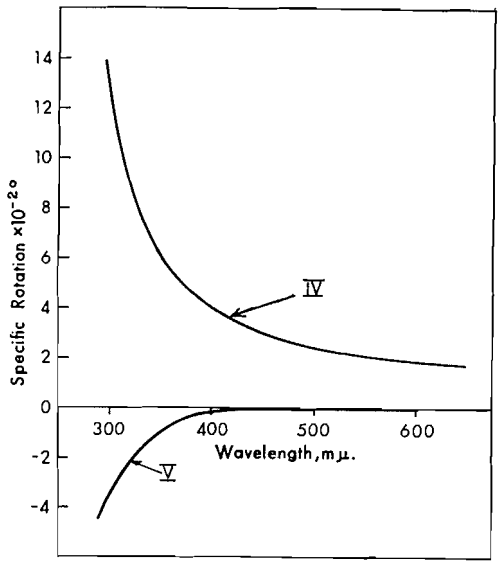

FIG. 3. The optical rotatory dispersion curves for *N*-(tri-*O*-acetyl-2-deoxy-2-iodo-D-glycopyranosyl)-pyridinium perchlorates with the *β-gluco* (IV) and *α-manno* (V) configurations.

not take place in chloroform solution, the reaction gave the product with the *β*-D-*gluco* configuration in preference to that with the *α*-D-*manno* configuration. This route of reaction is opposite to that observed in the reaction of D-glucal triacetate with alcohols in the presence of iodonium di-*sym*-collidine perchlorate (16, 17). These results support the contention (16) that the rate-controlling step in these reactions is not the formation of a 1,2-cyclic iodonium complex. Therefore, the transition state must be related to the nucleophilic attack. The reverse anomeric effect can be expected to influence the relative stabilities of these transition states. Since the reverse anomeric effect must be strong in an axial attack by pyridine and since the change in the yield of the *α-manno* product was only from about 70% for alcohols to about 30% for pyridine, it seems probable that the oxygen of the alcohol is positively charged in the transition states leading to the *O*-glycosides (18).

Although iodonium di-(2,4,6-trimethylpyridine) perchlorate did not form an isolable product when reacted with D-glucal triacetate (11), iodonium di-(2-methylpyridine) perchlorate readily formed the expected *N*-(tri-*O*-acetyl-2-deoxy-2-iodo-*β*-D-glucopyranosyl)-2-methylpyridinium perchlorate. The bromine analog was also prepared.

Reduction of IV with sodium dithionite gave a very unstable 1,4-dihydro derivative.

EXPERIMENTAL

The physical and chemical methods of analysis were described previously (15).

N-(Tetra-O-acetyl-β-D-glucopyranosyl)-pyridinium Bromide (I)

The compound, m.p. 170°, $[\alpha]_D$ −5.9° (*c*, 10 in water) was prepared following the directions of Fischer and Raske (1). The n.m.r. spectrum and o.r.d. curve of solutions in deuterium oxide were very similar to those published for the 3-carboxamido derivative (15). The signal for the anomeric proton was at τ 3.63, spacing 8.0 c.p.s.

Compound I, 3.2 g, was set aside in 320 ml of 3% hydrobromic acid for 15 h at 40° (19). Evaporation left a syrup which was crystallized from ethanol. After two recrystallizations from ethanol and water mixtures, the compound, *N*-(*β*-D-glucopyranosyl)-pyridinium bromide, melted at 176–177°, $[\alpha]_D$ +45.5° (*c*, 1.2 in water). The signal for the anomeric proton in the n.m.r. spectrum using deuterium oxide as solvent was at τ 4.10, spacing 8 c.p.s.

Anal. Calcd. for $C_{11}H_{16}NO_5Br$: C, 41.01; H, 5.01; N, 4.35. Found: C, 40.98; H, 4.87; N, 4.27.

Can. J. Chem. Downloaded from www.nrcresearchpress.com by 210.87.254.42 on 09/05/12
For personal use only.

N-(Tetra-O-acetyl-β-D-glucopyranosyl)-4-methylpyridinium Bromide (II) and the α-Anomer (III)

Tetra-*O*-acetyl-α-D-glucopyranosyl bromide, 3.78 g, was dissolved in 5 ml of 4-methylpyridine, and after 2 d the solution became filled with crystals. Ethyl acetate was added and the crystals were removed by filtration. Recrystallization from 95% ethanol – ethyl acetate gave crystals, m.p. 202–203°. The n.m.r. spectrum showed that 0.5 of a molecule of each of ethanol, ethyl acetate and water per molecule of II was present in the crystals. After drying at high vacuum the crystals melted at 207–208.5°, $[\alpha]_D$ −10.2° (*c*, 1 in water). The n.m.r. spectrum of II is shown in Fig. 1. The o.r.d. curve was similar to that found for compound I and showed a plain negative curve. The specific rotations at 300, 350, 400, 450, and 500 mμ were −128, −61, −35, −22, and −17°, respectively.

Anal. Calcd. for $C_{20}H_{26}NO_9Br.0.5H_2O$: C, 46.80; H, 5.30; N, 2.73. Found: C, 46.95; H, 5.30; N, 2.62.

On standing, the filtrate from the isolation of II deposited crystals which were recrystallized from 95% ethanol – ethyl acetate. The material, m.p. 175°, $[\alpha]_D$ +43° (*c*, 1 in water), provided the n.m.r. spectrum reproduced in Fig. 1, and assigned to *N*-(tetra-*O*-acetyl-α-D-glucopyranosyl)-4-methylpyridinium bromide (III). The assignments of signals shown in Fig. 1 are based on spin-decoupling experiments and are unequivocal. The o.r.d. gave a plain positive curve with specific rotations of 138, 121, 90, 66, and 51° at 300, 350, 400, 450, and 500 mμ, respectively.

Anal. Calcd. for $C_{20}H_{26}NO_9Br.H_2O$: C, 45.98; H, 5.40. Found: C, 46.20; H, 5.14.

N-(β-D-Glucopyranosyl)-4-methylpyridinium Bromide

Compound II, 0.65 g, was kept at 40° for 12 h in 65 ml of 3% hydrobromic acid. Evaporation left a syrup which crystallized from ethanol – ethyl acetate, m.p. 162–162.5°, $[\alpha]_D$ +38.3° (*c*, 1.2 in methanol). The n.m.r spectrum was in complete agreement with the assigned structure. A plain positive o.r.d. curve was obtained with specific rotations of 127, 92, 70, and 55° at 350, 400, 450, and 500 mμ, respectively, in methanol.

N-(α-D-Glucopyranosyl)-4-methylpyridinium Bromide

Deacetylation of III under the conditions described above for the β-anomer gave a syrup which could not be induced to crystallize. The n.m.r. spectrum required the assigned structure. The o.r.d. was a plain positive curve with specific rotations of 267, 175, 125, 94, 73, and 59° at 300, 350, 400, 450, 500, and 550 mμ, respectively.

Iodonium Di-(2-methylpyridine) Perchlorate

2-Methylpyridine, 10 ml, and sodium perchlorate, 12.2 g, in 125 ml of water were added with stirring to 5.7 g of silver nitrate dissolved in 25 ml of water. The precipitate, 13.1 g, was washed with water and dried under high vacuum over phosphorus pentoxide. The silver di-(4-methylpyridine) perchlorate thus produced, 39 g, was dissolved in the minimum amount of dry dimethylformamide, and 25.4 g of iodine and 5 ml of 2-methylpyridine were added. After being briefly stirred, the precipitated silver iodide was removed by filtration. Crystals of the iodonium salt soon began to form in the filtrate. Ether was added to provide a 21.2 g yield. The content of positive iodine as determined by iodometric titration was quantitative on the basis of the formula $(C_6H_7N)_2IClO_4$.

Iodonium Dipyridine Perchlorate

Silver dipyridine perchlorate was prepared as described above and 46.5 g was dissolved in the minimum amount of pyridine. Finely powdered iodine, 27.8 g, was added with stirring and silver iodide precipitated at once. The precipitate was removed by filtration and, on the addition of chloroform, a white crystalline product was deposited in the filtrate. The positive iodine content was 97.5% of the theoretical for $(C_5H_5N)_2IClO_4$.

Bromonium Complexes

Procedures very similar to those described above for the preparation of the iodonium complexes were used to prepare bromonium dipyridine perchlorate, $(C_5H_5N)_2BrClO_4$, and bromonium di-(2-methylpyridine) perchlorate, $(C_6H_7N)_2BrClO_4$. In each case the content of positive bromine was that expected from the formula given.

N-(Tri-O-acetyl-2-deoxy-2-iodo-β-D-glucopyranosyl)-pyridinium Perchlorate (IV) and the Corresponding α-D-manno-Stereoisomer (V)

D-Glucal triacetate, 22.2 g (81.7 mmoles), and the iodonium dipyridine perchlorate, 31.4 g (81.7 mmoles), reacted rapidly in 200 ml of chloroform. As the latter dissolved a fine precipitate of the pyridinium glucoside (IV) appeared. The reaction mixture was shaken for 1 h and the product was isolated by filtration. Fine, needle-like crystals of the pyridinium mannoside (V) were obtained from the filtrate on standing at 0°.

Compound IV, 33 g (70% yield), was recrystallized from methanol to constant physical properties, m.p. 163–164°, $[\alpha]_D$ +109.8° (*c*, 1.1 in methanol), $[\alpha]_D$ +133° (*c*, 0.4 in acetone). The n.m.r. spectrum is shown in Fig. 2 and the o.r.d. curve in Fig. 3.

Anal. Calcd. for $C_{17}H_{21}NO_{11}ClI$: C, 35.34; H, 3.66; N, 2.43; I, 22.0. Found: C, 35.55; H, 3.56; N, 2.59; I, 21.1.

The pyridinium glucoside (IV), 4.0 g, was dissolved in 100 ml of methanol and 1 ml of triethylamine. After 1 d, the solvents were evaporated and the crystalline residue was recrystallized from water. A 72% yield,

Can. J. Chem. Downloaded from www.nrcresearchpress.com by 210.87.254.42 on 09/05/12
For personal use only.

2.25 g, was obtained. Further recrystallization from methanol with a little water gave an analytical sample, m.p. 155–157° (decomposition of the liquid phase to a black tar), $[\alpha]_D$ +132.5° (*c*, 1 in water). The n.m.r. spectrum agreed throughout with the assigned structure. The compound dissolved in water gave a plain positive o.r.d. curve with specific rotations of 1 610, 595, 301, 239, 214, and 194° at 300, 350, 400, 450, 500, and 550 mμ, respectively.

Anal. Calcd. for $C_{11}H_{15}NO_8ClI$: C, 29.25; H, 3.35; N, 3.10. Found: C, 29.01; H, 3.23; N, 3.02.

A 5.08 g sample of IV was dissolved on warming in 100 ml of water and 40 ml of methanol. Addition of anhydrous sodium bicarbonate, 5.02 g, and sodium dithionite, 5.5 g, in 40 ml of water immediately produced a yellow coloration. The solution then became turbid and a gummy precipitate was deposited. After 1 h, the gum was washed with water. It dissolved on gently warming in ethanol and, on cooling, crystals were obtained, m.p. 68.5–69.5°. The n.m.r. spectrum in chloroform initially gave a spectrum similar to that for the compound obtained on the dithionite reduction of *N*-(tetra-*O*-acetyl-β-D-glucopyranosyl)-pyridinium bromide (I). However, the solution soon liberated iodine and the signal at about τ 7.0 disappeared in 10 min.

Recrystallization of the crude mannoside (V), m.p. 97–102°, 14 g (30% yield), from chloroform was accomplished with difficulty as there was a tendency to obtain an oil, but seeding gave crystals, m.p. 103–104°, $[\alpha]_D$ −22.6° (*c*, 1 in methanol), $[\alpha]_D$ −15.5° (*c*, 2 in acetone). The n.m.r. spectrum is given in Fig. 2 and the o.r.d. curve in Fig. 3. The iodine content, 19%, agreed well with the theoretical amount for V, 22%. The assignments of the signals shown in Fig. 2 are based on spin-decoupling experiments and are unequivocal.

When pure pyridinium mannoside (V) was dissolved in pyridine, crystals were obtained after 1 week in about 80% yield. The melting point, mixed melting point and the n.m.r. spectrum of the product were identical with those of IV. Treatment of V with aqueous potassium iodide gave a rapid liberation of iodine. The iodine was destroyed by the addition of sodium thiosulfate. Extraction with chloroform gave D-glucal triacetate, m.p. 53–54° in 94% yield. The pyridinium glucoside (IV) did not liberate iodine under similar conditions even after 1 d. Iodine was liberated when the solution was heated to the boiling point. Compound V decomposed to dark-brown products when an attempt was made to deacetylate the compound under the conditions which proved useful to deacetylate the diastereoisomer IV.

N-(Tri-O-acetyl-2-bromo-2-deoxy-β-D-glucopyranosyl)-pyridinium Perchlorate (VI)

Bromonium dipyridine perchlorate, 19.5 g, reacted rapidly with D-glucal triacetate, 15.7 g (58 mmoles), dissolved in pure chloroform to yield a fine crystalline precipitate. Recrystallization from ethanol, with a little methanol to facilitate solution, gave a product of m.p. 117–119°, $[\alpha]_D$ +78.8° (*c*, 1.2 in methanol). Cooling of the mother liquors resulted in a further crop of crystals which, when crystallized from methanol, melted at 152.5–155°. After drying *in vacuo* both lots of crystals had the same n.m.r. spectrum. Those with melting point 117–119°, on dissolving in methanol and seeding with the crystals melting at 152.5–155°, yielded crystals with the latter melting point. The n.m.r. spectrum was in agreement with the assigned structure and the specific rotation in water was 690, 377, 253, 140, 68, and 45° at 300, 350, 400, 450, 500, and 550 mμ, respectively.

Anal. Calcd. for $C_{17}H_{21}NO_{11}ClBr$: C, 38.47; H, 3.17; N, 2.64. Found: C, 38.24; H, 3.99; N, 2.81.

On adding ether to the filtrate, a syrup separated which could not be induced to crystallize. The n.m.r. spectrum of the syrup in methylene chloride was very similar to that shown in Fig. 2 for *N*-(tri-*O*-acetyl-2-deoxy-2-iodo-α-D-mannopyranosyl)-pyridinium perchlorate (IV). When the syrup was dissolved in pyridine, crystals of VI were deposited after the solution had been kept at room temperature for several days.

N-(3,4,6-Tri-*O*-acetyl-2-bromo-2-deoxy-β-D-glucopyranosyl)-pyridinium bromide, m.p. 130–133°, $[\alpha]_D$ +79.2° (*c*, 1.2 in methanol), was prepared by dissolving the syrupy mixture of tri-*O*-acetyl-2-bromo-2-deoxy-D-glucopyranosyl bromides (20) in pyridine.

The n.m.r. spectrum was very similar to that of the perchlorate VI.

Anal. Calcd. for $C_{17}H_{21}NO_7Br_2.H_2O$: C, 38.58; H, 4.38; N, 2.63. Found: C, 38.50; H, 4.30; N, 2.52.

N-(Tri-O-acetyl-2-bromo-2-deoxy-β-D-glucopyranosyl)-2-methylpyridinium Perchlorate

The compound, m.p. 223–224° (decomp.), $[\alpha]_D$ +100° (*c*, 0.5 in methanol), was prepared in a manner similar to that described above for the preparation of VI. The n.m.r. spectrum agreed with the assigned structure.

Anal. Calcd. for $C_{18}H_{23}NO_{11}ClBr$: C, 39.69; H, 4.26; N, 2.57. Found: C, 39.69; H, 4.36; N, 2.68.

N-(Tri-O-acetyl-2-iodo-2-deoxy-β-D-glucopyranosyl)-2-methylpyridinium Perchlorate

Reaction of D-glucal triacetate with iodonium di-(2-methylpyridine) perchlorate in chloroform solution gave a syrup which was extracted with hot water. On cooling, the extract deposited crystals, m.p. 186–187°. The n.m.r. spectrum was very similar, except for the signals from the 2-methylpyridine residue, to that for compound IV and left no doubt as to its identity.

ACKNOWLEDGMENTS

The research was supported by grants (N.R.C.-T 172) to R. U. L. and three North Atlantic Treaty Organization Studentships to A. R. M. (1961–1964). The n.m.r. spectra at 60 Mc.p.s. were determined by Mrs. Gail Conway and those at 100 Mc.p.s. by G. Bigam of this department.

Can. J. Chem. Downloaded from www.nrcresearchpress.com by 210.87.254.42 on 09/05/12
For personal use only.

REFERENCES

1. E. FISCHER and K. RASKE. Ber. **43**, 1750 (1910).
2. R. U. LEMIEUX and A. R. MORGAN. J. Am. Chem. Soc. **85**, 1889 (1963).
3. R. U. LEMIEUX, R. K. KULLNIG, H. J. BERNSTEIN, and W. G. SCHNEIDER. J. Am. Chem. Soc. **80**, 6098 (1958).
4. M. KARPLUS. J. Chem. Phys. **30**, 11 (1959).
5. E. L. ELIEL. J. Chem. Educ. **37**, 126 (1960).
6. L. E. SUTTON (*Editor*). Tables of interatomic distances and configuration in molecules and ions. Chem. Soc. London Spec. Publ. No. 11. 1958. pp. 513, 516.
7. R. U. LEMIEUX and N. J. CHU. Abstracts of Papers, Am. Chem. Soc. **133**, 31N (1958).
8. J. T. EDWARD and I. PUSKAS. Can. J. Chem. **40**, 711 (1962).
9. R. U. LEMIEUX and J. HAYAMI. Can. J. Chem. In press. 1965.
10. R. U. LEMIEUX and N. J. CHU. Abstract of Papers, Am. Chem. Soc. **135**, 5E (1959).
11. R. U. LEMIEUX and A. R. MORGAN. Can. J. Chem. In press. 1965.
12. J. I. MUSHER and E. J. COREY. Tetrahedron, **18**, 791 (1962).
13. R. U. LEMIEUX and J. D. STEVENS. Can. J. Chem. In press. 1965.
14. J. H. BREWSTER. J. Am. Chem. Soc. **81**, 5475, 5483 (1959).
15. R. U. LEMIEUX and J. W. LOWN. Can. J. Chem. **41**, 889 (1963).
16. R. U. LEMIEUX and S. LEVINE. Can. J. Chem. **42**, 1473 (1964).
17. R. U. LEMIEUX and A. R. MORGAN. Can. J. Chem. In press. 1965.
18. R. U. LEMIEUX and B. FRASER-REID. Can. J. Chem. **43**, 1458 (1965).
19. M. VISCONTINI and F. HURZELER-JUCKER. Helv. Chim. Acta, **39**, 1620 (1956).
20. R. U. LEMIEUX and B. FRASER-REID. Can. J. Chem. **42**, 532 (1964).

Can. J. Chem. Downloaded from www.nrcresearchpress.com by 210.87.254.42 on 09/05/12
For personal use only.

Can. J. Chem. Downloaded from www.nrcresearchpress.com by 210.87.254.40 on 09/05/12
For personal use only.

MECHANISMS FOR THE REACTIONS OF THE ANOMERIC TETRA-*O*-ACETYL-D-GLUCOPYRANOSYL BROMIDES WITH PYRIDINE AND 2-PYRIDONE

R. U. LEMIEUX AND A. R MORGAN[1]
Department of Chemistry, University of Alberta, Edmonton, Alberta

Received January 25, 1965

ABSTRACT

Reaction of tetra-*O*-acetyl-α-D-glucopyranosyl bromide (I) with pyridine at high dilution gives a high yield of *N*-(tetra-*O*-acetyl-β-D-glucopyranosyl)-pyridinium bromide (II). The addition of tetra-*n*-butylammonium bromide diverts the reaction to the formation of the highly strained α-anomer (III) of II. It is contended that III arises from the β-anomer (IV) of I by way of a rearrangement of an intermediate formed between pyridine and the 1,2-acetoxonium ion (VIII) which readily arises by dissociation of IV. The formation of 2-pyridyl tetra-*O*-acetyl-α-D-glucopyranoside in >60% yield in the reactions of I with either 2-ethoxypyridine or 2-pyridone in the presence of tetra-*n*-butylammonium bromide is taken as supporting evidence for this novel type of rearrangement.

INTRODUCTION

Fischer and Raske (1) prepared *N*-(2,3,4,6-tetra-*O*-acetyl-β-D-glucopyranosyl)-pyridinium bromide (II), through the reaction of tetra-*O*-acetyl-α-D-glucopyranosyl bromide (I) with pyridine in the presence of phenol. On repeating the preparation, II was obtained in 47% yield and its anomeric configuration was confirmed by the n.m.r. spectrum (2). Since the role of the phenol in the reaction mixture was not evident, it was decided to examine the course of the reaction in its absence. When a 34.4% solution of I in pyridine was allowed to react to constant rotation, a syrupy, water-soluble product was obtained. The n.m.r. spectrum in deuterium oxide showed doublet signals at τ 3.60 (spacing 8 c.p.s.) and τ 3.12 (spacing 3 c.p.s.). These signals were found to arise from the anomeric protons of II and its α-anomer (III), respectively (2, 3). The relative intensities of the signals indicated that the two compounds were present in the ratio 11:9 in favour of the α-anomer.

The change in optical rotation during the reaction of I with pyridine was followed polarimetrically. When the initial concentration was low, 1.95% (w/v), the rate of change corresponded closely to a first-order process and virtually only the β-anomer (II) was formed. The yield was greater than 90% as judged from the n.m.r. spectrum of the product in pyridine. When the initial concentration of I was 34.4%, an induction period in the polarimetric change was noted and, therefore, it was apparent that the product of the initial reaction became involved in a faster process. The induction period was also present when the initial concentration of I was about 16%, and the anomers were formed in about equal amounts. The same course of reaction was obtained when half of the pyridine was replaced by acetonitrile, although the more polar solvent gave rise to a somewhat increased rate of reaction. When the reaction of I (16% initial concentration) was carried out in pyridine containing 1 mole of tetra-*n*-butylammonium bromide per mole of I, the rate of the reaction was greater and the induction period was not present. Virtually only the α-pyridinium glucoside (III) was formed as judged from the n.m.r. spectrum of the product. When tetra-*n*-butylammonium perchlorate was used instead of the bromide, the induction period reappeared and the product comprised a 3:2 mixture of the α- and β-forms, respectively. These results are summarized in Table I.

[1]*Presented in part in a thesis by A. R. M. in partial fulfillment of the requirements for the degree of Doctor of Philosophy, University of Alberta, 1964.*

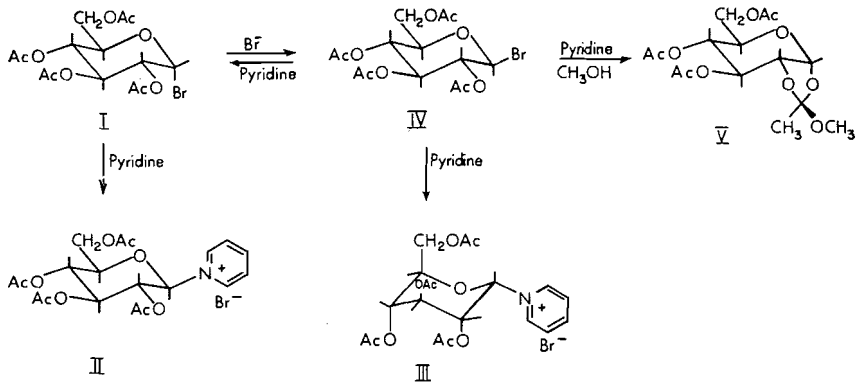

TABLE I

Effect of concentration and the addition of bromide ion on the rate and stereochemical route of the reaction of tetra-*O*-acetyl-α-D-glucopyranosyl bromide (I) with pyridine

Experiment	Concentration of I, % w/v	Final specific rotation, deg	Time for completion of reaction, h	Yields of *N*-glucosides, %	
				α-Anomer	β-Anomer
1	1.95	7.2	30	—	>90
2	34.4	13.4	9	55	45
3	16.3	10.3	12	50	50
4	15.8*	18.4	5	>90	—
5	15.9†	9.65	—	60	40

*The solution contained 13.5% tetra-*n*-butylammonium bromide.
†The solution contained 13.2% tetra-*n*-butylammonium perchlorate.

The most reasonable interpretation of these results was that initially I underwent nucleophilic attack by pyridine with inversion of the anomeric center to produce the β-pyridinium bromide (II). The bromide ion, thus liberated, then participated in a faster process involving a nucleophilic attack on I to form its anomer, tetra-*O*-acetyl-β-D-glucopyranosyl bromide (IV), and the latter compound was the precursor of the α-pyridinium glucoside (III). To test this hypothesis, tetra-*O*-acetyl-β-D-glucopyranosyl chloride was reacted with pyridine at room temperature. Five days were required for the rotation of the solution to reach a constant value. To the syrupy product obtained, water was added, and the mixture was extracted with chloroform. The chloroform extract gave a syrup (40% yield), the n.m.r. spectrum of which showed it to be virtually pure tetra-*O*-acetyl-α-D-glucopyranosyl chloride. Evaporation of the aqueous phase gave a syrup which was assigned the structure of *N*-(tetra-*O*-acetyl-α-D-glucopyranosyl)-pyridinium chloride in view of the very close similarity of its n.m.r. spectrum to that of compound III. No evidence was present in the spectrum for the formation of the β-anomer. When the reaction of the β-chloride with pyridine was repeated under the same conditions, except that tetraethylammonium chloride was added, a time of about 2 d was required for the rotation to reach a constant value and the only product found in appreciable amount was that of anomerization, the α-chloride. That the bromide ion can catalyze the anomerization of the tetra-*O*-acetyl-D-glucopyranosyl bromides was supported by a recent study of the anomerization of the anomeric chloride (4). It was found that, in acetonitrile, the rate of anomerization was first-order in tetraethylammonium chloride. The more rapid exchange of the chlorine of the β-anomer with ^{36}Cl-labelled chloride ion was interpreted as resulting from

Can. J. Chem. Downloaded from www.nrcresearchpress.com by 210.87.254.40 on 09/05/12
For personal use only.

dissociation of the β-chloride to 1,2-acetoxonium ion (4). The β-bromide (IV) has recently been isolated (5), and its reaction properties correspond closely to those previously established for tetra-*O*-acetyl-β-D-glucopyranosyl chloride (6).

Since the reaction of this β-chloride in pyridine containing an alcohol leads to the formation of tri-*O*-acetyl-α-D-glucopyranose 1,2-(alkyl orthoacetate) (6, 7), the observations related to the formation of the α-pyridinium glucoside (III) led to the prediction that the addition of I to pyridine containing methanol would result in the formation of the 1,2-(methyl orthoacetate) (V). In fact, the reaction of I in pyridine containing 3 moles of methanol per mole of I, under conditions which in the absence of methanol provided the α- and β-pyridinium glucosides in the ratio 3:2, respectively, gave a mixture of the methyl orthoacetate (V) and the β-pyridinium glucoside (II). That is, the presence of the methanol blocked the route to the formation of the α-pyridinium glucoside (III), precisely the result expected should the latter compound arise from the β-bromide (IV). The n.m.r. spectrum of the crude 1,2-orthoacetate (V) showed the presence of the two possible diastereoisomers arising from a change in the configuration of the new asymmetric center in the dioxalane ring (8). It thus became apparent why Fischer and Raske (1) found it useful to add phenol to the reaction mixture to form the β-pyridinium glucoside (II). That is, the phenol prevented the formation of the α-anomer. In fact, the n.m.r. spectrum of the reaction product showed the presence of only II and the phenyl orthoesters (9).

The formation of the β-pyridinium glucoside (II) undoubtedly involves nucleophilic attack by pyridine at the anomeric center of I. Bimolecular reactions of this type at the anomeric center of glycosyl halides are known to occur (10, 11). The mechanism for the formation of the α-pyridinium glucoside (III) is more difficult to anticipate. An obvious possibility is attack by pyridine at the anomeric center of the β-bromide (IV). However, this course of reaction seems unattractive for a number of reasons. First of all, it is to be noted that compound III is highly strained (2) and must be thermodynamically considerably less stable than the β-anomer (II). Consequently, the mechanism must account for the ability of bromide ion to divert the reaction to the formation of a less stable product. That is, the formation of III is kinetically controlled. It is well established that I is more stable than the β-anomer (IV) and is the anomer with the bromine in axial orientation (n.m.r. spectrum). Judging from the yields of I obtained from reactions mixtures where it must have been at equilibrium with IV (12), the equilibrium constant for the anomerization must be at least 9. The equilibrium constant for the $\beta \rightleftarrows \alpha$ anomerization of the acetochloroglucoses is about 16 (4). Assuming that, in the presence of tetra-*n*-butylammonium bromide, compounds I and IV were at equilibrium throughout the course of reaction, then the concentration of I was at least nine times that of IV. Control experiments showed that the presence of the β-*N*-glucoside (II) in mixtures of II with its α-anomer (III) could easily be detected when II formed 10% of the mixture. Therefore, the yield of III in the experiment using tetra-*n*-butylammonium bromide as catalyst must have been greater than 90%. It is seen therefore that the reaction of IV with pyridine would have to be at least 80 times faster than the reaction of the α-anomer (I) with pyridine.

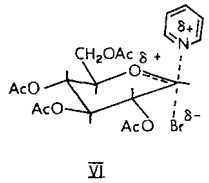

VI

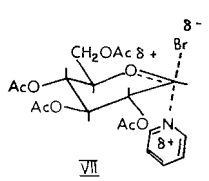

VII

Can. J. Chem. Downloaded from www.nrcresearchpress.com by 210.87.254.40 on 09/05/12
For personal use only.

Can. J. Chem. Downloaded from www.nrcresearchpress.com by 210.87.254.40 on 09/05/12
For personal use only.

Assuming that the reactions proceed by nucleophilic attack at the anomeric centers of I and IV, the transition states depicted in VI and VII, respectively, would be anticipated and the transition state VII would have to be at least 1 kcal/mole more stable than VI. In fact, VII must be expected to be less stable than VI especially if those factors related to the anomeric effect are important in the transition states (2). Evidence in support of this contention was obtained by reaction of tri-*O*-acetyl-2-chloro-2-deoxy-α-D-glucopyranosyl bromide (13) with pyridine in the presence of tetra-*n*-butylammonium bromide. The main product of the reaction had the n.m.r. spectrum expected for 2-chloro-D-glucal triacetate. This product of dehydrobromination (11) was formed in about 78% yield. *N*-(Tri-*O*-acetyl-2-chloro-2-deoxy-β-D-glucopyranosyl)-pyridinium bromide crystallized directly from the reaction mixture in 17% yield. Therefore, if the reaction mixture contained the equilibrium amounts of the α- and β-glucosyl bromides, the reaction of the α-bromide with pyridine was substantially faster than that of the β-anomer. Although it was not possible to obtain direct evidence for the rates of anomerization of the 2-chloroglucosyl bromides under these reaction conditions, the α-bromide reacts rapidly with tetraethylammonium chloride in acetonitrile to yield tri-*O*-acetyl-2-chloro-2-deoxy-β-D-glucopyranosyl chloride and this reaction is substantially faster than the analogous reaction of I under comparable conditions (13). Thus, there is no reason to doubt that the bromide ion led to equilibration of the 2-chloroglucosyl bromides as was observed in the reactions of I with pyridine in the presence of bromide ion. On this basis, the results obtained in the reaction of tri-*O*-acetyl-2-chloro-2-deoxy-α-D-glucopyranosyl bromide with pyridine in the presence of a high concentration (0.51 *M*) of tetra-*n*-butylammonium bromide support the contention that nucleophilic attack by pyridine at the anomeric center of the β-bromide (IV) leads to a less favorable transition state (VII) than that (VI) involving attack of the α-anomer (I).

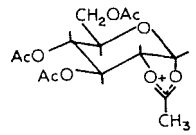

VIII

It seems more likely that the ready formation of III from IV relative to the formation of II from I is related to the ability of IV to readily dissociate to the 1,2-acetoxonium ion (VIII). This is consistent with the observation that the cation VIII is formed more rapidly than the α-glucoside (III) and can be a precursor of III. The experimental results require the reaction of the acetoxonium ion (VIII) with pyridine to form the β-glucoside (II) to be much slower than the process which leads to the formation of the α-anomer (III).

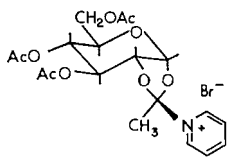

IX

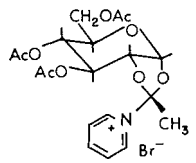

X

In pyridine, the 1,2-cyclic carbonium ion must lead rapidly to the complexes IX and X. In view of the ease of the acid-catalyzed hydrolysis or alcoholysis of orthoesters, these complexes must be expected to be highly labile and of only transient existence. For

example, tri-*O*-acetyl-α-D-glucopyranose 1,2-(phenyl orthoacetate) was found to be solvolyzed in *sym*-collidine saturated with water (9). Therefore, IX and X can be expected to readily revert to the acetoxonium ion.

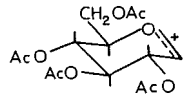

XI

Formation of III from the acetoxonium ion (VIII) would have to involve rearrangement of the acetoxonium ion *toward* the glucosyloxocarbonium ion (XI) in the first stage of the reaction. It is reasonable to expect that this would be a facile process since it is first-order process and merely involves a reallocation of the positive charge. In contrast, the formation of the transition state VII requires charge separation in a second-order process conducted in a weakly polar solvent. It could be speculated that the ion XI is closer to the 1C- than the C1-conformation and provides α-pyridinium glucoside (III) for this reason. However it is well established that the 1,2-acetoxonium ion is formed in the anomerization of both penta-*O*-acetyl-β-D-glucopyranose (14) and tetra-*O*-acetyl-β-D-glucopyranosyl chloride (4) and that the ion does not offer a facile route to the formation of the α-anomers. For this reason, it seems best to assume that the α-glucoside (III) is formed by a rearrangement of a pyridine – acetoxonium ion complex. That is, an intimate ion–molecule pair could be involved as an intermediate in a 1,3-shift of the pyridine via the *endo*-complex X. Thus, an energetically economical route for the formation of the highly-strained α-glucoside (III) would be provided.

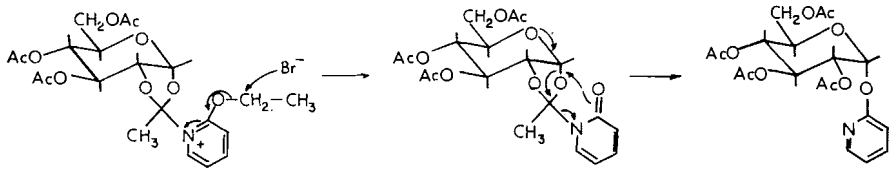

XII XIII XIV

In view of the unexpected conformational properties of III, it was desired to examine the conformation of *N*-(tetra-*O*-acetyl-α-D-glucopyranosyl) 2-pyridone. Therefore, I was reacted with 2-ethoxypyridine in an excess of tetra-*n*-butylammonium bromide; n.m.r. examination of the product showed the presence of a complex mixture containing about 60% of an acetylated *O*-glucoside. The compound was readily isolated by chromatography on silicic acid and found to be 2-pyridyl tetra-*O*-acetyl-α-D-glucopyranoside, m.p. 84–84.5°, $[\alpha]_D$ +147° (*c*, 0.5 in chloroform). The anomeric proton gave a doublet signal at τ 3.22 with a spacing of 3.5 c.p.s. The four aromatic protons gave signals with chemical shifts and structures very similar to those in the spectrum of 2-ethoxypyridine. The signal for H-3 was a triplet (spacing 9.5 c.p.s.) at τ 4.24, about 0.5 p.p.m. to lower field than the signals for H-2 and H-4. It was therefore evident that the compound was the α-anomer in the C1-conformation. The tetra-*O*-acetyl-α- and -β-*N*-glucosides of 2-pyridone were also formed but did not separate on the silicic acid column. The n.m.r. spectrum of the mixture isolated from the chromatogram indicated that β-anomer was formed to about three times the extent of the α-form. Spin-decoupling experiments at 100 Mc.p.s. showed the anomeric protons of the α- and β-forms to give doublet signals at τ 3.44 and τ 3.60, respectively.

Can. J. Chem. Downloaded from www.nrcresearchpress.com by 210.87.254.40 on 09/05/12
For personal use only.

The spacings were 2.5 and 9.0 c.p.s., respectively. It was not possible to draw conclusions as to the structures of the signals for other ring-protons of the α-anomer. The spectra were devoid of signals for the ethyl group which, as expected (15), was lost in the course of the reaction. In these reactions, the ethyl group must be lost after the nitrogen has been quaternized. The quaternization which was involved in producing the α-*O*-glucoside must have taken place at a position other than the anomeric center. It seems probable *in view of the high yield of the O-glucoside*, that the 2-ethoxypyridine attacked the 1,2-acetoxonium ion to yield the intermediate (XII). This would activate the nucleophilic attack by bromide ion to remove the ethyl group and yield the *N*-orthoacetyl pyridone derivative (XIII). Such a compound can be expected to be highly labile and its rearrangement to the *O*-glucoside (XIV) following a route similar to that described above for the formation of the α-pyridinium glucoside (III) appears plausible. Reaction of I with 2-pyridone in *sym*-collidine containing tetra-*n*-butylammonium bromide gave a 70% yield of the *O*-α-glucoside (XIV) but none of the *N*-glycosides. The formation of an α-glucoside under these conditions is abnormal and presumably arose by way of the intermediate XIII. The small amount of the *N*-α-glucoside which was formed in the reaction of I with 2-ethoxypyridine in the presence of bromide ion was likely the result of nucleophilic attack by the 2-ethoxypyridine at the anomeric center of the β-bromide (IV).

EXPERIMENTAL

The experimental methods were similar to those previously described (9, 11, 16).

Reactions of Pyridine with Tetra-O-acetyl-α-D-glucopyranosyl Bromide (I)

Solutions of I in pyridine, with or without the addition of salt, were made up in the concentrations reported in Table I. The solutions were kept at room temperature and their optical rotations were determined from time to time. The initial specific rotations, 194.5°, were those expected for I. The reaction times reported in Table I correspond to the time required for the rotational change to become near asymptotic. The rotational changes observed in experiments 2, 3 and 5 showed points of inflection indicating increases in the rates of optical change in the first periods of the reactions.

After the solutions had achieved constant rotations, the pyridine was rapidly removed *in vacuo* and a sample of the residue was dissolved in deuterium oxide for analysis by n.m.r. spectroscopy. The relative amounts of the α- and β-anomers of *N*-(tetra-*O*-acetyl-D-glucopyranosyl)-pyridinium bromide were estimated from the relative intensities of the signals for the anomeric protons at τ 2.8–3.1 and 3.4–3.6, respectively, depending on the salt concentration. When the α-anomer (III) was dissolved in pyridine, the n.m.r. spectrum showed a signal for one of the acetoxy to lower field, τ 7.47, than the signals for the other acetyl groups centered at τ 7.86. Under the same conditions, the acetyl groups of the β-anomer all gave their signals above τ 7.9. The relative amounts of the anomers in mixtures could therefore be estimated by integrating over the acetyl group signals. This method of analysis confirmed in each case the results obtained by comparing the intensities of the signals from the anomeric protons.

Reactions of Tetra-O-acetyl-β-D-glucopyranosyl Chloride

(*a*) The compound, 0.25 g, was dissolved in 5 ml of dry pyridine. After 2.5 min, the observed rotation was −1.09° and the rotation steadily rose to a constant value of 4.50° after 125 h. Most of the pyridine was evaporated *in vacuo* and the product was distributed between 20 ml of water and 20 ml of chloroform. The solutions were taken to dryness. The chloroform layer gave 0.10 g of tetra-*O*-acetyl-α-D-glucopyranosyl chloride (40% yield) identified by its n.m.r. spectrum. The residue from the aqueous layer was dissolved in deuterium oxide for examination by n.m.r. spectroscopy. The spectrum was that expected for *N*-(tetra-*O*-acetyl-α-D-glucopyranosyl)-pyridinium chloride. It was therefore concluded that the yield of this compound was about 60%. No indication of the β-anomer was present in the n.m.r. spectrum.

(*b*) The compound, 0.25 g, was taken up in 5 ml of dry pyridine saturated with tetraethylammonium chloride. After 15 min the observed rotation was −0.5° and the rotation rose to +6.52° in 45 h. The pyridine was evaporated *in vacuo* and the product was worked up as described above. The chloroform layer contained 0.19 g of virtually pure tetra-*O*-acetyl-α-D-glucopyranosyl chloride (n.m.r. spectrum). The aqueous layer gave a crystalline solid which had the n.m.r. spectrum of tetraethylammonium chloride. The spectrum indicated that a mere trace of *N*-(tetra-*O*-acetyl-α-D-glucopyranosyl)-pyridinium chloride had formed.

Tri-O-acetyl-α-D-glucopyranose 1,2-(Methyl Orthoacetate)

Tetra-*O*-acetyl-α-D-glucopyranosyl bromide (I), 3.03 g, was dissolved in 10 ml of pyridine containing 0.89 ml of methanol and the solution was kept at room temperature. The observed rotation after 5 min was

Can. J. Chem. Downloaded from www.nrcresearchpress.com by 210.87.254.40 on 09/05/12
For personal use only.

47° and fell to a constant value of 2.81° after 19 h. An induction period was noted in the rotational change. The solvent was removed *in vacuo* and the residue was partitioned between water and chloroform. The chloroform layer gave a sirupy product, the n.m.r. spectrum of which showed it to be tri-*O*-acetyl-α-D-glucopyranose 1,2-(methyl orthoacetate) (9). Evaporation of the aqueous layer left a residue which was dissolved in deuterium oxide for n.m.r. spectroscopy. Except for pyridinium hydrobromide, the substance was virtually pure *N*-(tetra-*O*-acetyl-β-D-glucopyranosyl)-pyridinium bromide (2).

Reaction of Tri-O-acetyl-2-chloro-2-deoxy-α-D-glucopyranosyl Bromide

The compound, m.p. 97–98°, $[\alpha]_D$ +250° (*c*, 3 in chloroform) (13), 0.94 g, and 0.83 g of tetra-*n*-butylammonium bromide were taken up in pyridine to give 5 ml of solution. The solution was kept at room temperature. After 40 min, the observed rotation had fallen to 11.3° at which time the solution became turbid due to deposition of a crystalline solid. After 16 h, the crystals were collected and washed with pyridine. The n.m.r. spectrum of this product required it to be *N*-(tri-*O*-acetyl-2-chloro-2-deoxy-β-D-glucopyranosyl)-pyridinium bromide contaminated by tetra-*n*-butylammonium bromide. It was estimated that the β-*N*-glucoside was formed in 17% yield based on the starting material. Recrystallization of the compound from ethanol – ethyl acetate gave material, m.p. 129.5–131.5°, $[\alpha]_D$ +67° (*c*, 0.5 in water). The n.m.r. spectrum in deuterium oxide showed the signal for the anomeric proton at τ 3.55 with a spacing of 9.2 c.p.s. The signals for H-3 and H-4 were broadly (about 9 c.p.s.) spaced triplets centered at τ 4.24 and 4.60, probably respectively. The presence of ethanol in the crystals was indicated.

The filtrate was evaporated to dryness *in vacuo* and the residue was partitioned between water and chloroform. The aqueous layer was evaporated to dryness and taken up in deuterium oxide for analysis by n.m.r. The material was mainly a mixture of tetra-*n*-butylammonium bromide and pyridinium hydrobromide. The spectrum was devoid of signals for the above mentioned β-*N*-glucoside. However, weak signals at τ 2.75 and 4.5 can be taken as evidence that some of the *N*-(tri-*O*-acetyl-2-chloro-2-deoxy-α-D-glucopyranosyl)-pyridinium bromide had formed.

The chloroform layer was taken to dryness to leave 1.19 g of syrup. The n.m.r. spectrum in chloroform showed this product to be an equimolar mixture of tetra-*n*-butylammonium bromide and 2-chloro-D-glucal triacetate. On this basis the yield of the latter compound was estimated to be 78%. The identity of the 2-chloro-D-glucal triacetate was evident from its n.m.r. spectrum which had a one-proton singlet at τ 3.22 and was otherwise virtually identical to that of 2-acetoxy-D-glucal triacetate (17).

2-Pyridyl Tetra-O-acetyl-α-D-glucopyranoside and N-(Tetra-O-acetyl-D-glucopyranosyl)-2-pyridone

(*a*) Tetra-*O*-acetyl-α-D-glucopyranosyl bromide, 5.91 g, and tetra-*n*-butylammonium bromide, 3.96 g, were dissolved in 2-ethoxypyridine, 10 ml, and the homogeneous solution obtained at 75° was allowed to react for 1 d. The volatile components were then removed *in vacuo* and the residue was dissolved in chloroform. The chloroform solution was washed three times with 2 *N* hydrochloric acid and finally with aqueous sodium bicarbonate solution. The n.m.r. spectrum of the syrup obtained from the chloroform layer showed the mixture to consist essentially of 2-pyridyl tetra-*O*-acetyl-α-D-glucopyranoside (60%) and *N*-(tetra-*O*-acetyl-D-glucopyranosyl)-2-pyridone (<40%). This was determined in the following manner. The *p*-anisidin spray reagent (18) revealed only two spots when a sample of the syrup was chromatographed on a thin layer of silicic acid. A 0.42 g sample was therefore chromatographed on a column of silicic acid, 25 g (100 mesh), with reagent chloroform as the eluant. The bands which could be observed to separate on the column were collected. The first band corresponded to ~10% yield of 2-acetoxy-D-glucal triacetate as determined by the direct comparison of n.m.r. spectra (17).

The second band showed absorptions in the ultraviolet, λ_{max} 266 mμ (ε 3 670) and 208 mμ [2-ethoxypyridine, λ_{max} 270 mμ (ε 4 500) and 214 mμ]. The n.m.r. spectrum was that expected for 2-pyridyl tetra-*O*-acetyl-α-D-glucopyranoside and this was confirmed by crystallization of the syrup. Recrystallization from ethanol–water to constant physical properties resulted in material of m.p. 84–84.5°, $[\alpha]_D$ +148° (*c*, 0.5 in chloroform).

Anal. Calcd. for $C_{19}H_{23}NO_{10}$: C, 53.64; H, 5.45; N, 3.29. Found: C, 53.70; H, 5.77; N, 3.20.

The n.m.r. spectrum contained a doublet at τ 3.22, spacing 3.5 c.p.s., and signals in the τ 1.7 to 3.2 region closely resembling those in the spectrum of 2-ethoxypyridine. The remainder of the spectrum was that expected for a tetra-*O*-acetyl-α-D-glucopyranoside.

The material in the third band absorbed in the ultraviolet, λ_{max} 300 mμ (ε 4 720) and 226 mμ (2-pyridone, λ_{max} 300 mμ (ε 6 120) and 224 mμ). The n.m.r. spectrum at 100 Mc.p.s. showed the material to be a mixture, and it was established by integration of the signals and by spin-decoupling experiments that the compounds were both *N*-(tetra-*O*-acetyl-D-glucopyranosyl) 2-pyridones. The signal for the anomeric proton of the α-anomer was a doublet at τ 3.44, spacing 2.5 c.p.s., and that for the β-form was a doublet at τ 3.60, spacing 9 c.p.s. The ratio of the α- to β-forms was estimated to be about 1:3. Pure compounds were not obtained.

(*b*) Tetra-*O*-acetyl-α-D-glucopyranosyl bromide, 0.21 g, 0.19 g of 2-pyridone, and 0.16 g of tetra-*n*-butylammonium bromide were dissolved in 0.4 ml of *sym*-collidine. The solution was kept at 75° for 18 h. Chloroform was added and the solution was washed three times with dilute hydrochloric acid and then with aqueous bicarbonate. Solvent removal gave a syrup. Integration of the n.m.r. spectrum required the material to be about 70% 2-pyridyl tetra-*O*-acetyl-α-D-glucopyranoside. There was no evidence that *N*-glycosides had formed.

Can. J. Chem. Downloaded from www.nrcresearchpress.com by 210.87.254.40 on 09/05/12
For personal use only.

ACKNOWLEDGMENTS

The research was supported by grants (N.R.C.-T 172) to R. U. Lemieux and three North Atlantic Treaty Organization Studentships to A. R. M. (1961–1964). The n.m.r. spectra were determined by Mrs. G. Conway (60 Mc.p.s.) and G. Bigam (100 Mc.p.s.) of this department.

REFERENCES

1. E. Fischer and K. Raske. Chem. Ber. **43**, 1750 (1910).
2. R. U. Lemieux and A. R. Morgan. Can. J. Chem. In press. 1965.
3. R. U. Lemieux and A. R. Morgan. J. Am. Chem. Soc. **85**, 1889 (1963).
4. R. U. Lemieux and Jun-ichi Hayami. Can. J. Chem. In press. 1965.
5. F. Weygand, H. Ziemann, and H. J. Bestmann. Chem. Ber. **91**, 2534 (1958).
6. R. U. Lemieux and C. Brice. Can. J. Chem. **33**, 109 (1955).
7. R. U. Lemieux and J. D. T. Cipera. Can. J. Chem. **34**, 906 (1956).
8. A. S. Perlin. Can. J. Chem. **41**, 399 (1963).
9. R. U. Lemieux and A. R. Morgan. Can. J. Chem. In press. 1965.
10. A. J. Rhind-Tutt and C. A. Vernon. J. Chem. Soc. 4637 (1960).
11. R. U. Lemieux and D. R. Lineback. Can. J. Chem. **43**, 94 (1965).
12. R. U. Lemieux. *In* Methods in carbohydrate chemistry. Vol. II. R. L. Whistler and M. L. Wolfrom (*Editors*). Academic Press Inc., New York. 1963. p. 221.
13. R. U. Lemieux and R. J. Bose. Unpublished results.
14. R. U. Lemieux, C. Brice, and G. Huber. Can. J. Chem. **33**, 134 (1955).
15. J. J. Fox and I. Wempen. Advan. Carbohydrate Chem. **14**, 328 (1959).
16. R. U. Lemieux and J. W. Lown. Can. J. Chem. **41**, 889 (1963).
17. R. U. Lemieux, D. R. Lineback, M. L. Wolfrom, F. B. Moody, E. G. Wallace, and F. Komitsky, Jr. J. Org. Chem. In press.
18. L. Hough, J. K. N. Jones, and W. H. Wadman. J. Chem. Soc. 1702 (1950).

Can. J. Chem. Downloaded from www.nrcresearchpress.com by 210.87.254.40 on 09/05/12
For personal use only.

Can. J. Chem. Downloaded from www.nrcresearchpress.com by 210.87.254.6 on 09/05/12
For personal use only.

ÉTUDE DES EFFETS ÉLECTROSTATIQUES SUR LE MÉCANISME D'ACTION CATALYTIQUE DE LA PHOSPHATASE ALCALINE INTESTINALE DE VEAU

MICHEL LAZDUNSKI,[1] JACQUES BROUILLARD ET LUDOVIC OUELLET
Département de Chimie, Université Laval, Québec, Québec

Reçu le 5 mars 1965

ABSTRACT

The influence of dioxane and ethanol on the rate of hydrolysis of *p*-nitrophenyl phosphate in the presence of an intestinal alcaline phosphatase can be interpreted as a dielectric constant effect, at high substrate concentration. The dielectric constant effect is a function of the pH of the medium and is maximum around pH 9.4 at 25 °C and pH 9.0 at 15 °C. An interpretation suggesting that the change in diameter of the enzyme molecule becoming an activated complex is minimum at a pH of maximum activity is proposed. The same model can take into account the influence of the ionic strength on the same reaction.

INTRODUCTION

L'étude de l'influence du pH sur l'activité de la phosphatase alcaline intestinale (1) et l'analyse cinétique de différents mécanismes d'inhibition (2) ont permis de proposer une description et un mode de fonctionnement du centre actif de l'enzyme. Pour mieux connaître l'importance des contributions électrostatiques associées au mécanisme d'action catalytique de l'enzyme nous avons étudié l'influence cinétique des effets de solvant et de force ionique.

PARTIE EXPÉRIMENTALE

A. Réactifs

Le sel disodique utilisé comme substrat provient de Mann Research Laboratories Inc. Sa richesse en phosphate de *p*-nitrophényle est de 99.7%; il a été utilisé sans purification ultérieure. Les solutions à différentes concentrations de substrat ont été obtenues par dilution du sel dans l'eau distillée. L'enzyme utilisée est la phosphatase alcaline intestinale purifiée préparée selon une méthode décrite précédemment (3). Les tampons THAM (0.01 *M*) – HCl ont été utilisés au-dessus de pH 9 et éthanolamine (0.01 *M*) – HCl pour les valeurs de pH supérieures à 9. Les pH ont été mesurés avec un pH-mètre Radiometer TTT 1-B utilisant une électrode de verre Radiometer type B.

B. Mode opératoire

(1) Détermination de la vitesse initiale d'hydrolyse, v

L'hydrolyse du phosphate de *p*-nitrophényle est suivie par mesure colorimétrique du *p*-nitrophénol libéré lors de la réaction:

$$NO_2C_6H_4OPO_3^{=} + H_2O \rightarrow NO_2C_6H_4O^- + PO_4H^{=} + H^+.$$

Des essais préliminaires ont montré que la réaction d'hydrolyse s'arrêtait par passage en milieu très alcalin.

Le déroulement des opérations est le suivant: 14 ml d'une solution de phosphate de *p*-nitrophényle, de concentration adéquate, sont ajoutés à 15 ml de solution tampon. Ce mélange est porté dans un bain à thermostat (à 15.3 °C ou 25.7 °C ± 0.1 °C) et y est laissé pendant 30 min. Ce laps de temps écoulé, la réaction est démarrée par injection d'un millilitre d'une solution de l'enzyme également à température voulue. La réaction est suivie pendant 5–10 min suivant le cas. Des prélèvement de 5 ml sont faits chaque minute et versés dans 0.3 ml d'une solution de soude 4 *N*. La réaction s'arrête. Le *p*-nitrophénol est, dans ces conditions de basicité, sous forme ionisée et les lectures sont faites au spectrophotomètre Beckman DU à la longueur d'onde de 407 mμ correspondant au maximum de densité optique.

(2) Détermination de la vitesse maximum d'hydrolyse en présence de dioxanne

Le coefficient d'extinction du *p*-nitrophénol à 407 mμ n'est pas sensiblement affecté par la présence de dioxanne.

[1]*Adresse actuelle: Institut de Chimie Biologique, Faculté des Sciences, Marseille (Bouches-du-Rhône), France.*

Chaque essai utilise 30 ml de mélange composé comme suit: 11 ml de tampon, 1 ml d'enzyme de concentration adéquate, 1 ml de phosphate de *p*-nitrophényle de concentration suffisante pour que la vitesse initiale déterminée puisse être considérée comme une vitesse maximum, le nombre de millilitres de dioxanne nécessaire à l'obtention de la concentration de dioxanne désirée dans le milieu, et la quantité d'eau distillée nécessaire pour compléter le volume à 30 ml.

Il n'existe dans la littérature aucune mention d'un tampon standard permettant de définir de façon satisfaisante l'échelle de pH dans les mélanges eau–dioxanne. Marshall et Grunwald (4) ont montré que l'électrode de verre et l'électrode à hydrogène répondent de la même manière à des variations de l'activité des ions hydrogène dans des solutions contenant jusqu'à 82% de dioxanne en poids. Inagami et Sturtevant (5) ont constaté que les appareils de mesure de pH habituels, utilisant une électrode de verre Beckman, fonctionnent parfaitement et de façon reproductible dans des solutions contenant jusqu'à 88% de dioxanne. Les pH des tampons utilisés dans cette étude ont été déterminés par la méthode déjà utilisée par Sturtevant (5) qui consiste à étalonner le pH-mètre à pH 7 avec le tampon Beckman standard, et à l'utiliser ensuite directement dans les mélanges eau–dioxanne. Les valeurs des pH apparents, lues de cette manière, sont assez peu éloignées des valeurs de pH lues en milieux purement aqueux. Le pH d'un tampon éthanolamine–HCl de force ionique 0.1 passe de la valeur 9.05 aux valeurs 8.9 et 8.65, lorsque la concentration de dioxanne dans le milieu passe de 0% à 20% puis 50% en volume. Le pH des tampons THAM–HCl est moins affecté. Un tampon THAM–HCl de force ionique 0.1 ayant un pH de 8.15 dans l'eau prend successivement des pH de 8.11 à 8.07 dans des solutions à 20% puis 50% de dioxanne en volume.

(3) Étude de l'influence de la force ionique du milieu réactionnel sur la vitesse initiale d'hydrolyse

Les vitesses de réaction ont été évaluées par titrage de l'acide phosphorique libéré par hydrolyse du phosphate de *p*-nitrophényle.

L'appareillage manufacturé par Radiometer (Copenhague) est composé d'un pH-mètre TTT 1-b muni d'une électrode à calomel et d'une électrode de verre type B, d'un enregistreur type SBr2b et d'une seringue microburette type SBU1a.

Le déroulement des opérations est le suivant: le mélange réactionnel est composé de 19 ml d'une solution contenant les quantités adéquates de phosphate de *p*-nitrophényle et de chlorure de potassium ou de bromure de tétraéthylammonium utilisés comme modificateurs de force ionique. Lorsque ce mélange a atteint la température constante de 15.3 °C, il est porté par le système pH-stat, à la valeur de pH choisie. La réaction d'hydrolyse est alors amorcée par addition de 1 ml d'une solution de phosphatase alcaline également à température de 15.3 °C. Le titrigraphe enregistre, en fonction du temps, les quantités de soude nécessaires au maintien du pH. Les pentes initiales des courbes obtenues sont utilisées à l'évaluation des vitesses initiales de réaction. La quantité de soude ajoutée au cours de la réaction représente en moyenne 1 à 2% du volume réactionnel total. La manipulation est faite en atmosphère d'air débarrassée de gaz carbonique.

PARTIE THÉORIQUE

A. Effet de solvant

Les théories de cinétique chimique s'accordent à reconnaître que la vitesse d'une réaction est déterminée par une variation de l'énergie libre $\Delta G^{\neq}$ qui se manifeste lors du passage des réactifs de l'état initial à l'état activé.

L'expression générale décrivant la constante de vitesse est:

$$[1] \qquad k = \frac{RT}{Nh} \exp\left[-\frac{\Delta G_{\text{n.e.s.}}^{\neq}}{RT}\right] \times \exp\left[\frac{\Delta G_{\text{e.s.}}^{\neq}}{RT}\right]$$

où $\Delta G_{\text{n.e.s.}}^{\neq}$ et $\Delta G_{\text{e.s.}}^{\neq}$ représentent respectivement les contributions non électrostatiques et électrostatiques à l'énergie libre d'activation, h est la constante de Planck, R, la constante des gaz et N, le nombre d'Avogadro.

Barnard et Laidler (6) ont appliqué ces concepts aux interactions entre le centre actif de l'enzyme et le substrat. Nous avons tenté de considérer toute la molécule d'enzyme comme un ion dont la charge varie avec pH du milieu.

(1) Formation du complexe enzyme–substrat

La réaction de formation du complexe enzyme–substrat est représentée schématiquement dans la Fig. 1A. La protéine est figurée par une grosse sphère de rayon R_B et de charge nette $Z_B e$ située en son centre. Le substrat est figuré par une petite sphère de rayon R_A et de charge $Z_A e$. Le complexe activé, formé par association des deux espèces ioniques,

Can. J. Chem. Downloaded from www.nrcresearchpress.com by 210.87.254.6 on 09/05/12
For personal use only.

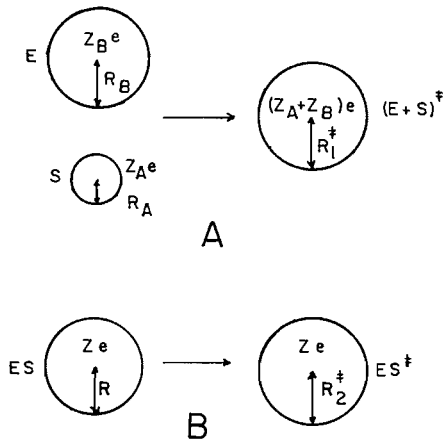

FIG. 1A. Mécanisme de formation du complexe enzyme–substrat.
FIG. 1B. Mécanisme de décomposition du complexe enzyme–substrat.

a la forme d'une sphère unique de rayon $R_1^{\ddagger}$ ayant pour charge $(Z_A + Z_B)e$. La variation d'énergie libre, $\Delta G_{e.s.}^{\ddagger}$, dérivée de l'équation de Born, est donnée par:

$$[2] \qquad \Delta G_{e.s.}^{\ddagger} = \frac{e^2}{2D}\left[\frac{(Z_A + Z_B)^2}{R_1^{\ddagger}} - \frac{Z_A^2}{R_A} - \frac{Z_B^2}{R_B}\right]$$

où e représente la charge de l'électron et D, la constante diélectrique; d'où

$$[3] \qquad \ln k_1 = \ln k_1^0 - \frac{Ne^2}{2DRT}\left[\frac{(Z_A + Z_B)^2}{R_1^{\ddagger}} - \frac{Z_A^2}{R_A} - \frac{Z_B^2}{R_B}\right]$$

k_1^0 est la constante de vitesse de formation du complexe enzyme–substrat en solution infiniment diluée.

(2) Décomposition du complexe enzyme–substrat

Le mécanisme hypothétique de cette décomposition est représenté dans la Fig. 1B. Le complexe enzyme–substrat est présenté sous la forme d'un ion sphérique de rayon R et de charge $Ze = (Z_A + Z_B)e$ qui, en passant à l'état activé, à charge constante, change de rayon $(R \rightarrow R_2^{\ddagger})$ sans changer de forme; $R_2^{\ddagger}$ peut être inférieur, égal ou supérieur à R

$$[4] \qquad \Delta G_{e.s.}^{\ddagger} = \frac{e^2}{2D} Z^2\left[\frac{1}{R_2^{\ddagger}} - \frac{1}{R}\right]$$

$$[5] \qquad \ln k_2 = \ln k_2^0 - \frac{Ne^2Z^2}{2DRT}\left[\frac{1}{R_2^{\ddagger}} - \frac{1}{R}\right]$$

k_2^0 est la constante de vitesse de décomposition du complexe enzyme–substrat en solution infiniment diluée.

Comme la suite le montrera, ces équations permettent une interprétation satisfaisante des résultats expérimentaux.

B. Effet de la force ionique

L'équation de Brönsted–Bjerrum permet d'évaluer la constante de vitesse d'une réaction dont le mécanisme serait du type:

$$A + B \rightarrow X^{\ddagger} \rightarrow \text{produits.}$$

Can. J. Chem. Downloaded from www.nrcresearchpress.com by 210.87.254.6 on 09/05/12
For personal use only.

Can. J. Chem. Downloaded from www.nrcresearchpress.com by 210.87.254.6 on 09/05/12
For personal use only.

[6] $$k = k_0 \frac{\gamma_A \gamma_B}{\gamma_X}$$

γ_A, γ_B, γ_X sont les coefficients d'activité des espèces A, B et du complexe activé X; k_0 est la constante de vitesse en solution infiniment diluée. L'expression familière du coefficient d'activité est donnée par l'équation de Debye et Hückel:

[7] $$\ln \gamma_i = -\frac{Ne^2 Z_i^2}{2DRT} \frac{\kappa}{1 + \kappa a_i}$$

a_i est le rayon d'exclusion de l'espèce i qui possède une charge Z_i. Le paramètre κ représente l'inverse de la dimension de l'atmosphère ionique.

À 15 °C, l'éq. [7] peut s'écrire:

[8] $$\log \gamma_i = -0.500^* \frac{\sqrt{\mu}}{1 + a_i B \sqrt{\mu}} Z_i^2$$

où $B = 0.33 \times 10^8$ et μ est la force ionique.

Dans le cas le plus commun où A et B sont de petits ions, la quantité $a_i B\sqrt{\mu}$ peut être négligée en comparaison de 1, dans le terme $1 + a_i B\sqrt{\mu}$. L'équation [6] peut alors être écrite:

[9] $$\log k = \log k_0 + Z_A Z_B \sqrt{\mu}$$

Cette équation classique est utilisée à tort en cinétique enzymatique; la protéine a, en général, un rayon d'exclusion tel qu'il est impossible de négliger la quantité $a_i B\sqrt{\mu}$ dans le terme $1 + a_i B\sqrt{\mu}$; pour des valeurs arbitraires $a_i = 20$ Å et $\sqrt{\mu} = 0.1$, $a_i B\sqrt{\mu} = 0.66$.

(1) Formation du complexe enzyme–substrat

Cette réaction de formation, représentée schématiquement dans la Fig. 1A, fait appel à un mécanisme bimoléculaire. Les équations [6] et [8] permettent d'obtenir l'éq. [10] qui rend compte de l'influence de la force ionique sur la constance de vitesse k_1:

[10] $$\log \frac{k_1}{k_1^0} = -0.500\sqrt{\mu}\left[\frac{Z_A^2}{1 + a_A B\sqrt{\mu}} + \frac{Z_B^2}{1 + a_B B\sqrt{\mu}} - \frac{(Z_A + Z_B)^2}{1 + a_1^{\ddagger} B\sqrt{\mu}}\right]$$

a_A, a_B et $a_1^{\ddagger}$ représentent les rayons d'exclusion du substrat, de l'enzyme et du complexe activé. Les autres paramètres ont été définis dans la section précédente.

(2) Décomposition du complexe enzyme–substrat

Si la décomposition du complexe enzyme–substrat se fait selon le modèle unimoléculaire représenté dans la Fig. 1B, la vitesse de décomposition est donnée par l'équation:

[11] $$k_2 = k_2^0 \frac{\gamma}{\gamma^{\ddagger}}$$

γ et $\gamma^{\ddagger}$ sont les coefficient d'activité du complexe ES et du complexe activé ES‡. L'équation [12] rend compte de l'influence de la force ionique sur la constante de vitesse k_2.

[12] $$\log \frac{k_2}{k_2^0} = -0.500 Z^2 \sqrt{\mu}\left[\frac{1}{1 + aB\sqrt{\mu}} - \frac{1}{1 + a_2^{\ddagger} B\sqrt{\mu}}\right]$$

a et $a_2^{\ddagger}$ représentent les rayons d'exclusion du complexe ES et du complexe activé ES‡; $Z = Z_A + Z_B$.

Les équations qui ont été décrites permettent d'interpréter les résultats obtenus avec la papaine (8), la myosine (7) et l'uréase (9).

**Ce terme est égal à 0.509 à 25 °C.*

Can. J. Chem. Downloaded from www.nrcresearchpress.com by 210.87.254.6 on 09/05/12
For personal use only.

RÉSULTATS

A. Influence de la constante diélectrique sur la vitesse maximum de la réaction d'hydrolyse

Avant de traiter l'effet produit par le dioxanne sur la cinétique de la réaction enzymatique comme un effet purement électrostatique, il convient de s'assurer que les concentrations de dioxanne utilisées n'ont pas d'action spécifique tendant à supprimer l'activité phosphatasique. A 20 ml de mélange eau–dioxanne de concentration adéquate sont ajoutés 5 ml d'une solution d'enzyme à concentration de 2 / 1 000 (en poids). Le mélange est laissé à 25.7 °C pendant 30 min. Ce laps de temps écoulé, on se sert d'un millilitre de cette solution d'enzyme pour provoquer la réaction d'hydrolyse du phosphate de *p*-nitrophényle. Cette expérience a été faite à pH 9.3 en milieu d'incubation de concentration en dioxanne allant de 0 à 50%. La vitesse initiale déterminée est indépendante de la concentration en dioxanne du milieu d'incubation. Nous avons observé le même phénomène en utilisant comme solvant mixte le mélange éthanol–eau.

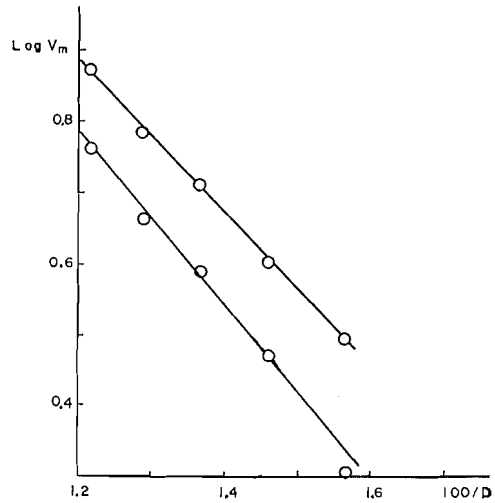

FIG. 2. Représentations de log $\bar{V}_m$ en fonction de $1/D$. Courbe supérieure: pH 7.45. Courbe inférieure: ph 10.42. Température: 15.3 °C.

La Fig. 2 représente un certain nombre de données caractéristiques obtenues à différents pH en adoptant la représentation classique qui consiste à évaluer log $\bar{V}_m$ en fonction de $1/D$. Aux deux températures, 15.3 °C et 25.7 °C, et à tous les pH étudiés, cette représentation est linéaire. Les valeurs de D utilisées sont celles d'Akerlof et Short (10).

Les valeurs des pentes d log $\bar{V}_m$/ d$(1/D)$ calculées avec les valeurs d'Akerlof ont été représentées en fonction du pH, aux températures de 15.3 et 25.7 °C dans la Fig. 3. Nous avons obtenu des résultats semblables avec les mélanges éthanol–eau à 25.7 °C (Fig. 4). Dans les deux cas, l'effet de constante diélectrique passe par un maximum pour la même valeur de pH. Des résultats semblables ont été rapportés pour la chymotrypsine par Castañeda-Agullo et Castillo (11).

B. Influence de la force ionique sur la vitesse maximum et la constante de Michaelis de la réaction d'hydrolyse

La Fig. 5 représente les résultats obtenus en portant le logarithme de la vitesse relative d'hydrolyse, v, en fonction de la racine carrée de la force ionique. L'expérience

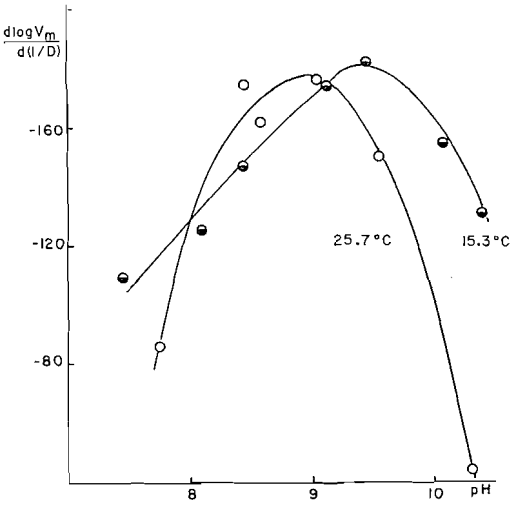

FIG. 3. Influence du pH sur la quantité $\frac{d \log \bar{V}_m}{d(1/D)}$ en présence de dioxanne.

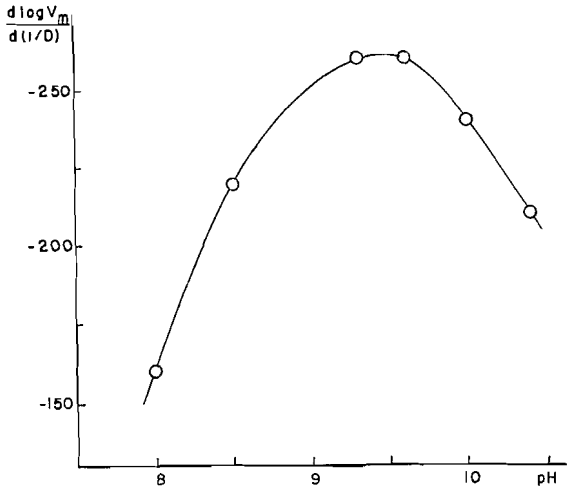

FIG. 4. Influence du pH sur la quantité $\frac{d \log V_m}{d(1/D)}$ en présence d'éthanol à 25.7 °C.

a été faite à pH 7.5, à une température de 15.3 °C et pour plusieurs concentrations de substrat. Le modificateur de force ionique utilisé est le chlorure de potassium.

La même expérience a été réalisée dans les mêmes conditions de pH et de température en utilisant le bromure de tétraéthylammonium comme modificateur de force ionique. L'accord satisfaisant entre les résultats obtenus avec les deux substances permet d'assurer que l'effet observé est bien essentiellement un effet de force ionique.

Les données représentées dans la Fig. 5 permettent d'obtenir des courbes de Lineweaver-Burk à force ionique constante. Elles permettent à leur tour l'évaluation des grandeurs $\bar{K}_m$, $\bar{V}_m$ et $\bar{K}\bar{V}_m$ en fonction de la racine carrée de la force ionique. Les résultats ainsi obtenus ont été représentés dans les Figs. 6, 7 et 8.

Can. J. Chem. Downloaded from www.nrcresearchpress.com by 210.87.254.6 on 09/05/12
For personal use only.

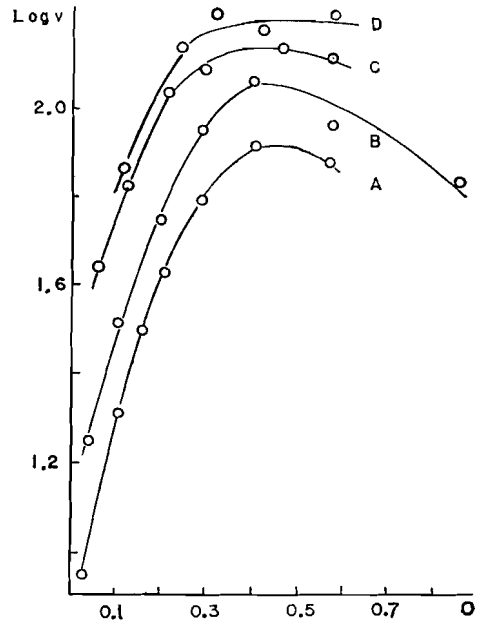

FIG. 5. Influence de μ sur le logarithme de la vitesse d'hydrolyse, en unités arbitraires, à pH 7.5 et température 15.3 °C. (A) [S] = 2.5×10^{-4} M; (B) [S] = 5×10^{-4} M; (C) [S] = 1.5×10^{-3} M; (D) [S] = 6×10^{-3} M.

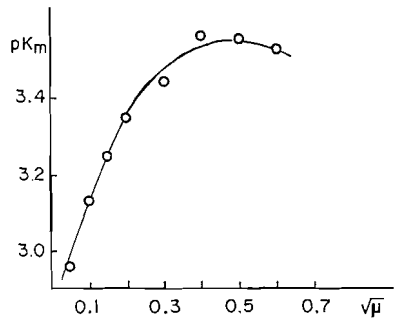

FIG. 6. Influence de $\sqrt{\mu}$ sur $p\bar{K}_m$ à 15.3 °C.

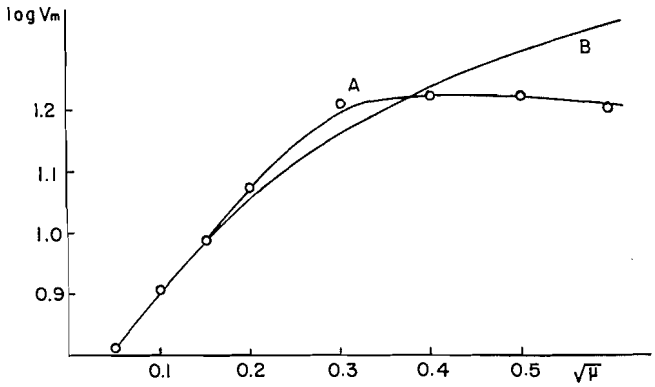

FIG. 7. Influence de $\sqrt{\mu}$ sur log $\bar{V}_m$ exprimé en unités arbitraires. Les points sont expérimentaux. (A) Tracé expérimental; (B) tracé théorique: $a_2^{\mp} = 20$ Å, $a = 22.3$ Å.

Can. J. Chem. Downloaded from www.nrcresearchpress.com by 210.87.254.6 on 09/05/12
For personal use only.

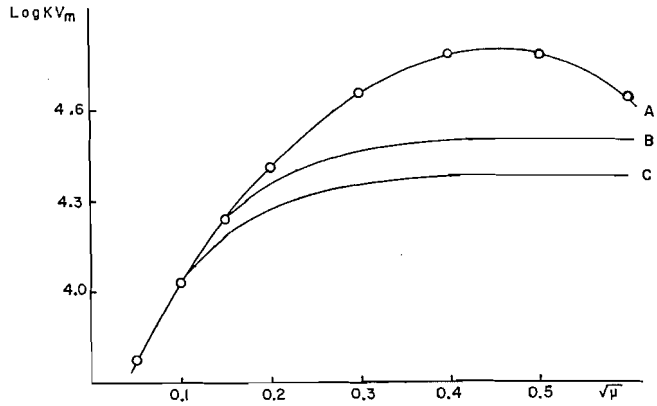

FIG. 8. Influence de $\sqrt{\mu}$ sur la quantité log $\bar{K}\bar{V}_m$ en unités arbitraires. Les points sont expérimentaux. (A) Tracé expérimental; (B) tracé théorique: $a_1^{\mp} = 20$ Å, $a_B = 19$ Å, $a_A = 4$ Å; (C) tracé théorique: $a_1^{\mp} = 20$ Å, $a_B = 18$ Å, $a_A = 4$ Å.

Influence du pH sur l'effet de force ionique

La même expérience a été faite à pH 9.55 et à 15.3 °C. L'effet de force ionique observé à ce pH est faible tant sur $\bar{V}_m$ que sur $\bar{K}_m$. La Fig. 9 traduit l'influence de $\sqrt{\mu}$ sur log $\bar{V}_m$. Les résultats ont été obtenus en présence de chlorure de potassium et de bromure de tétraéthylammonium.

DISCUSSION

A. Effet de solvant

(1) Influence des facteurs de nature non électrostatique

Si l'on a l'intention d'interpréter les données expérimentales obtenues en analysant l'effet de solvant, il convient de ne pas oublier les facteurs de nature non électrostatique dont la contribution pourrait expliquer les phénomènes observés. Les plus importants de ces facteurs sont les suivants:

(*a*) Une diminution de la concentration en eau peut provoquer une décroissance des vitesses si l'étape déterminante fait intervenir la participation de molécules d'eau (ce qui peut bien être le cas dans une réaction d'hydrolyse).

(*b*) Une inhibition possible par le composant non aqueux du solvant mixte.

(*c*) Une dénaturation de l'enzyme causée par l'addition du solvant organique.

L'influence du facteur (*a*) observée par Inagami et Sturtevant (5) par l'étude de la catalyse due à la trypsine en milieu eau–dioxanne ne se manifeste qu'à des concentrations de dioxanne supérieures à 80%. Les expériences réalisées dans cette étude, avec la phosphatase alcaline, n'ont pas fait intervenir de concentrations en dioxanne supérieures à 30%. Dans un tel milieu, la concentration en eau est encore de 39 *M* et certainement très suffisante pour que l'on puisse négliger l'influence de ce premier facteur dans l'interprétation des résultats. L'expérience exposée plus haut a montré que l'incubation de l'enzyme en présence de fortes quantités de dioxanne n'apporte aucune modification de la vitesse d'hydrolyse. Elle ôte beaucoup de son importance au facteur (*c*). L'influence du facteur (*b*) est certainement négligeable puisque les effets observés sont les mêmes avec deux molécules aussi différentes que l'éthanol et le dioxanne.

Enfin, et surtout, le fait qu'à tous les pH et températures étudiés, l'influence de $1/D$ sur log $\bar{V}_m$ se représente par une droite, comme le laissent prévoir les théories qui traitent uniquement des effets électrostatiques, enlève beaucoup d'importance aux facteurs secondaires.

Can. J. Chem. Downloaded from www.nrcresearchpress.com by 210.87.254.6 on 09/05/12
For personal use only.

(2) Essai de détermination du mécanisme intime de la réaction de décomposition du complexe enzyme–substrat

Si la réaction se déroule selon le modèle monomoléculaire décrit dans la Fig. 1B, la pente théorique a pour expression:

$$[13] \qquad A' = -\frac{NZ^2e^2}{2.3 \times 2RT}\left[\frac{1}{R_2^{\neq}} - \frac{1}{R}\right].$$

La représentation la plus intéressante (Fig. 12) consiste à figurer la valeur $A = A'T$ en fonction de la charge Z du complexe enzyme–substrat évaluée à partir des courbes de titrage (Figs. 10 et 11). Ce changement de variable fait disparaître l'effet de température qui apparaissait dans la Fig. 3. Comme le prévoit l'éq. [13], l'extrapolation du côté des charges faibles indique que $A = 0$ lorsque $Z = 0$.

La pente des courbes log $\bar{V}_m$ en fonction de $1/D$ est négative quel que soit le pH d'étude; la quantité

$$\left[\frac{1}{R_2^{\neq}} - \frac{1}{R}\right]$$

doit donc être positive. Le rayon équivalent de la molécule de complexe enzyme–substrat

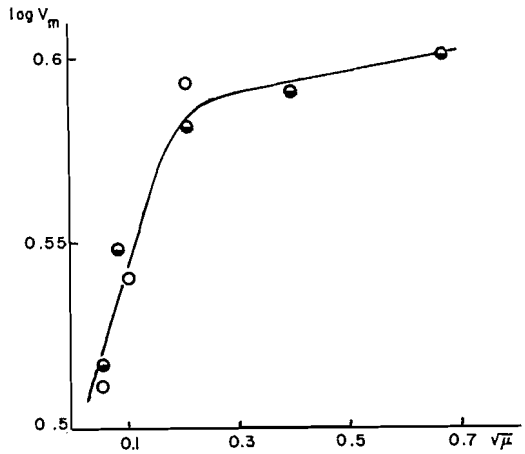

FIG. 9. Influence de $\sqrt{\mu}$ sur log $\bar{V}_m$ exprimé en unités arbitraires; pH 9.55; température 15.3 °C. ◒ KCl; ○ $(C_2H_5)_4NBr$.

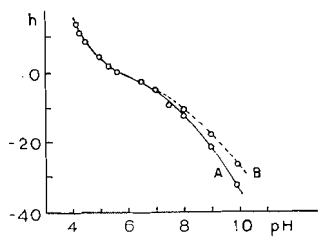

FIG. 10. Influence de la température sur la charge de l'enzyme de poids moléculaire 80 000. (A) Température 24.8 °C; (B) température 15.3 °C.

Can. J. Chem. Downloaded from www.nrcresearchpress.com by 210.87.254.6 on 09/05/12
For personal use only.

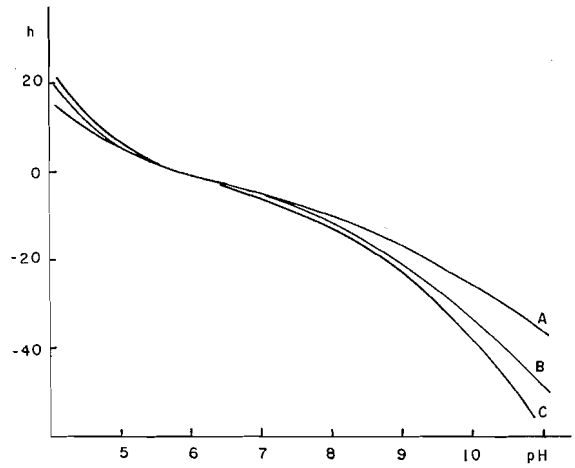

FIG. 11. Influence de la force ionique sur la charge de l'enzyme de poids moléculaire 80 000 à 24.8 °C. (A) $\mu = 0.02$; (B) $\mu = 0.1$; (C) $\mu = 0.5$.

est plus grand à l'état initial qu'à l'état activé. De toute évidence, la figure n'est pas décrite par une équation du type $y = ax^2$ (éq. [13]). La quantité

$$\frac{1}{R_2^{\neq}} - \frac{1}{R}$$

varie donc en fonction du pH. La fonction

$$\sqrt{\frac{1}{R_2^{\neq}} - \frac{1}{R}} = \sqrt{-\frac{2.3 \times 2RA}{Z^2e^2N}}$$

a été calculée pour chaque valeur de Z à partir des données expérimentales qui apparaissent dans la Fig. 12. Cette fonction ainsi obtenue est représentée par la Fig. 13, de façon

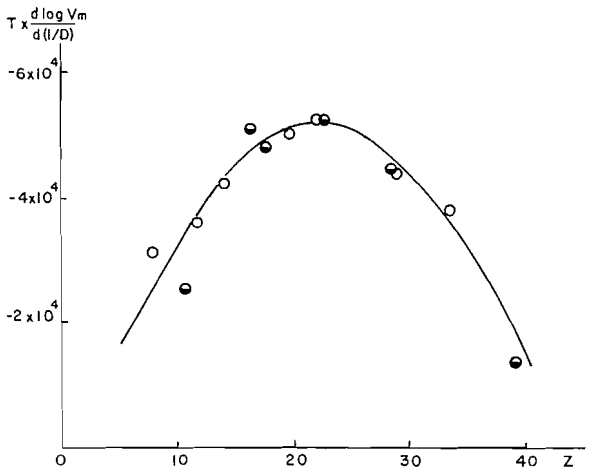

FIG. 12. Influence de la charge Z du complexe enzyme–substrat sur la quantité $T \times \frac{\mathrm{d} \log V_m}{\mathrm{d}(1/D)}$. ◒ 25.7 °C; ○ 15.3 °C.

Can. J. Chem. Downloaded from www.nrcresearchpress.com by 210.87.254.6 on 09/05/12
For personal use only.

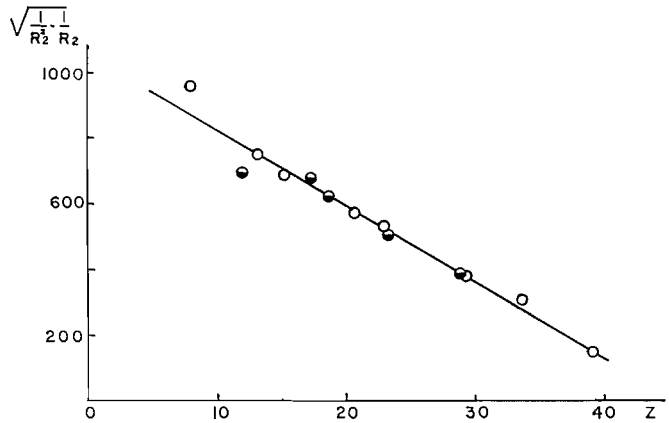

FIG. 13. Influence de la charge Z du complexe enzyme–substrat sur la quantité $\sqrt{\frac{1}{R_2^{\ddagger}} - \frac{1}{R}}$. ○ 25.7 °C; ◒ 15.3 °C.

linéaire. L'activation se fait sans changement de dimensions lorsque la charge du complexe enzyme–substrat devient $Z = -45$. Selon la température d'étude, les pH correspondants à cette charge sont compris entre 10.5 et 11. Il est intéressant de remarquer que la différence entre R et $R_2^{\ddagger}$ est minimum dans une région de pH correspondant à une vitesse maximum de décomposition du complexe enzyme–substrat (1).

Cette constatation est à rapprocher des conclusions de Bruice et Pandit (12) à l'issue d'une étude sur la catalyse intramoléculaire de l'hydrolyse des monoesters de diacides. Ces auteurs ont montré qu'une décomposition à catalyse intramoléculaire non enzymatique est d'autant plus rapide que la conformation de l'état fondamental de la molécule est plus voisine de celle de son état activé.

B. Effet de force ionique

(1) Formation du complexe enzyme–substrat

Les difficultés de mesure directe de la constante de vitesse k_1 rendent difficile, sinon impossible, l'étude systématique de l'influence de la force ionique sur la vitesse de formation du complexe enzyme–substrat. Néanmoins, si $\bar{K} = 1/\bar{K}_m$ ne représente pas, comme Michaelis l'admettait implicitement, la constante d'équilibre k_1/k_{-1} de la réaction

$$E + S \underset{k_{-1}}{\overset{k_1}{\rightleftharpoons}} ES$$

mais plutôt le rapport k_1/k_2, il est évident que la quantité $\bar{K}\bar{V}_m$ est égale à $k_1[E]_0$.

Toutes les études les plus sûres, faites avec la catalase (13, 14), les trypsines (15), la peroxydase (16, 17), la carboxypeptidase (18, 19) et la myosine (20) ont montré que k_2 était très supérieure à k_{-1}, de sorte que $\bar{K} = k_1/k_2$. Nous admettrons que ceci est également vrai pour la phosphatase alcaline et interprèterons la courbe expérimentale (A) de la Fig. 8, donnant log $\bar{K}\bar{V}_m$ en fonction de $\sqrt{\mu}$, comme s'il s'agissait de la courbe log (k_1 relative) en fonction de $\sqrt{\mu}$. La courbe (A) a l'allure d'une droite aux très faibles forces ioniques entre $\sqrt{\mu} = 0.05$ et 0.2. Lorsque la force ionique augmente, ensuite, son influence sur log $\bar{K}\bar{V}_m$ devient de moins en moins considérable, passe par un maximum entre $\sqrt{\mu} = 0.4$ et 0.5 et diminue sensiblement dès que $\sqrt{\mu} = 0.6$.

Can. J. Chem. Downloaded from www.nrcresearchpress.com by 210.87.254.6 on 09/05/12
For personal use only.

L'équation [10] permet de calculer les courbes théoriques log k_1/k_1^0 en fonction de $\sqrt{\mu}$.

La courbe (B) de la Fig. 8 a été calculée avec les valeurs suivantes: $a_1^{\neq} = 20$ Å, $a_B = 19$ Å et $a_A = 4$ Å; la courbe (C) avec les valeurs: $a_1^{\neq} = 20$ Å, $a_B = 18$ Å et $a_A = 4$ Å.

L'allure des courbes théoriques est très semblable à celle de la courbe expérimentale (A). Les valeurs choisies pour les rayons d'exclusion ne permettent pas d'obtenir de maximum entre $\sqrt{\mu} = 0.4$ et 0.5. On ne saurait trop attracher d'importance à cette différence; l'équation de Debye–Hückel ne s'applique plus parfaitement à des forces ioniques aussi élevées. L'expérience montre que les réactions entre petits ions ne suivent la loi décrite par l'éq. [9] que pour des valeurs de $\sqrt{\mu}$ généralement inférieures à 0.3 (21). Les courbes théoriques (B) et (C), par ailleurs, ont le mérite d'avoir entre $\sqrt{\mu} = 0.05$ et 0.2, des pentes moyennes qui sont en accord satisfaisant avec la pente 4.2 obtenue expérimentalement.

(2) Décomposition du complexe enzyme–substrat

Puisque le phosphate d'enzyme, E—$PO_3^=$, semble être l'intermédiaire le plus stable formé au cours de la catalyse phosphatasique (22–24), la courbe (A) de la Fig. 5 (log $\bar{V}_m$ en fonction de $\sqrt{\mu}$) représente en fait l'influence de la force ionique sur la vitesse k_2 de décomposition du complexe E—$PO_3^=$. Cette décomposition, qui est certainement à catalyse intramoléculaire, procède par un mécanisme unimoléculaire du type représenté dans la Fig. 1B. La courbe expérimentale (A) a l'allure d'une droite aux très faibles forces ioniques, entre $\sqrt{\mu} = 0.05$ et 0.2. Lorsque la racine carrée de la force ionique continue à augmenter, ensuite, son influence sur log $\bar{V}_m$ devient moins considérable et atteint un palier dès que $\sqrt{\mu} = 0.3$.

L'éq. [12] permet de calculer les courbes théoriques log k_2/k_2^0, c'est-à-dire log $\bar{V}_m$ en unités arbitraires, en fonction de $\sqrt{\mu}$. Pour calculer théoriquement une droite de pente positive semblable à celle obtenue expérimentalement à faibles forces ioniques, il faut nécessairement choisir des valeurs de $a_2^{\neq}$, rayon d'exclusion du complexe activé $ES^{\neq}$, inférieures à a, rayon d'exclusion du complexe enzyme–substrat ES. La courbe (B) de la Fig. 6 a été calculée en remplaçant dans l'éq. [12] les valeurs de $a_2^{\neq}$ et de a par: $a_2^{\neq} = 20$ Å et $a = 22.3$ Å.

La pente de la courbe (B) entre $\sqrt{\mu} = 0.05$ et 0.2 est en bon accord avec la pente 1.6 obtenue expérimentalement. En outre, l'allure des courbes théoriques est semblable à celle de la courbe expérimentale (A).

À pH 9.55, l'influence de $\sqrt{\mu}$ sur log $\bar{V}_m$ est beaucoup plus faible qu'à pH 7.5. Les seuls résultats qui seront interprétés sont ceux situés au-dessous de $\sqrt{\mu} = 0.4$. La pente expérimentale moyenne entre $\sqrt{\mu} = 0.05$ et 0.2 est de 0.45. En remplaçant dans l'éq. [12] les valeurs de a et $a_2^{\neq}$ par: $a = 20$ Å et $a_2^{\neq} = 19.87$ Å pour la courbe (A) et $a = 22.3$ Å et $a_2^{\neq} = 22.17$ Å pour la courbe (B), et en utilisant la charge de la phosphatase à pH 9.55 pour une force ionique de 0.02 à 15.3 °C, les pentes ainsi calculées sont respectivement 0.39 et 0.43. Elles sont en bon accord avec la valeur expérimentale.

Les interprétations données aux effets de force ionique et celles données aux effets de solvant montrent que la molécule entière de phosphatase alcaline joue, par sa charge, un rôle important dans la catalyse. Les deux études sont en bon accord; le rayon R du complexe enzyme–substrat est toujours supérieur au rayon $R_2^{\neq}$ du complexe activé correspondant; de même le rayon d'exclusion, a, du complexe enzyme–substrat est toujours supérieur au rayon d'exclusion $a_2^{\neq}$ du complexe activé correspondant. La différence $(a - a_2^{\neq})$ comme la différence $(R - R_2^{\neq})$ est d'autant plus faible que la charge de la protéine est plus élevée. Elle passe de 2.3 Å à pH 7.5 à 0.13 Å à pH 9.55. Les valeurs a_A du rayon d'exclusion du substrat utilisées dans les calculs sont nécessairement du bon

Can. J. Chem. Downloaded from www.nrcresearchpress.com by 210.87.254.6 on 09/05/12
For personal use only.

ordre de grandeur puisqu'elles ont été choisies en conséquence. Elles déterminent l'évaluation des rayons d'exclusion de l'enzyme, du complexe enzyme–substrat et des complexes activés. Ces rayons sont d'environ 20 Å; cette dimension est à peu près satisfaisante vu les simplifications faites en considérant la molécule comme sphérique et en négligeant la répartition des charges. En solution de chlorure de potassium, la valeur de $(a - R)$ pour une molécule de protéine est environ de 2.5 Å (25). À pH 7.5, le rayon d'exclusion du complexe enzyme–substrat qui permet de mieux décrire les données expérimentales est $a = 22.3$ Å. Si l'on choisit $R = 20$ Å pour que $a - R = 2.3$ Å, le rayon $R_2^{\neq}$ du complexe activé correspondant, déterminé à partir de la Fig. 13, est de 17.4 Å. Au rayon d'exclusion $a = 22.3$ Å correspond un rayon d'exclusion $a_2^{\neq} = 20$ Å (Fig. 7). La différence $(a_2^{\neq} - R_2^{\neq}) = 2.6$ Å est, elle aussi, en bon accord avec la valeur prévue (25).

CONCLUSION

Les résultats présentés peuvent s'accorder avec les schémas proposés et les équations établies dans la partie théorique. Si l'on admet ces hypothèses, les développements mathématiques décrits permettent d'interpréter les effets de force ionique et de constante diélectrique en cinétique enzymatique. Mais surtout ces résultats mettent l'accent sur un deuxième aspect de la catalyse enzymatique, sur le rôle des résidus ionisables situés en dehors du centre actif. Par la charge qu'ils confèrent à la protéine, ces résidus ont une action électrostatique directe sur les constantes de vitesses des différentes étapes de la catalyse. Cette influence électrostatique serait, en partie, le fruit d'un effet de la charge sur la configuration relative du complexe enzyme-substrat en de son état activé. La différence de rayon entre le complexe activé et son état fondamental est fonction du pH du milieu réactionnel.

Depuis deux ans, un certain nombre de preuves directes s'accumulent qui montrent que la conformation des enzymes est profondément affectée par la fixation du substrat. Tels sont les résultats de Parker et Lumry (26), obtenus par étude du système chymotrypsine – *p*-nitrophényl – triméthylacétate par dispersion rotatoire, qui sont d'ailleurs confirmés par les travaux de Hess (27). Les conformations de l'α-chymotrypsine et les acyl-chymotrypsines dépendent du pH de façon différente. Les différences de conformation entre enzyme et complexe enzyme–substrat sont minimum aux environs de pH 7.5. Avec la chymotrypsine comme avec la phosphatase alcaline, la différence entre l'état fondamental et l'état activé du complexe enzyme–substrat est minimum à un pH voisin du domaine d'activité maximum des enzymes.

REMERCIEMENTS

Ces travaux ont été subventionnés par le Conseil National de Recherches. L'un de nous (M. L.) a été boursier des Canadian Industries Limited.

BIBLIOGRAPHIE

1. M. Lazdunski et L. Ouellet. Can. J. Chem. **39**, 1928 (1961).
2. M. Lazdunski et L. Ouellet. Can. J. Biochem. Physiol. **40**, 1620 (1962).
3. M. Lazdunski et L. Ouellet. Can. J. Biochem. Physiol. **39**, 1933 (1961).
4. H. P. Marshall et E. Grunwald. J. Chem. Phys. **21**, 2143 (1953).
5. T. Inagami et J. M. Sturtevant. Biochim. Biophys. Acta, **38**, 64 (1960).
6. M. L. Barnard et K. J. Laidler. J. Am. Chem. Soc. **74**, 6099 (1952).
7. K. Linderstrøm-Lang. Compt. Rend. Trav. Lab. Carlsberg, **15**, No. 7 (1923–25).
8. A. Stockell et E. L. Smith. J. Biol. Chem. **227**, 1 (1957).
9. G. B. Kistiakowsky et W. H. T. Shaw. J. Am. Chem. Soc. **75**, 2751 (1953).
10. G. Akerlof et O. A. Short. J. Am. Chem. Soc. **58**, 1243 (1936).
11. M. Castañeda-Agullo et L. del Castillo. J. Gen. Physiol. **44**, 19 (1960).
12. T. C. Bruice et U. K. Pandit. Proc. Natl. Acad. Sci. U.S. **46**, 402 (1960).

Can. J. Chem. Downloaded from www.nrcresearchpress.com by 210.87.254.6 on 09/05/12
For personal use only.

13. B. CHANCE, D. S. GREENSTEIN et J. F. W. ROUGHTON. Arch. Biochem. Biophys. **37**, 301 (1952).
14. B. CHANCE, D. S. GREENSTEIN, J. HIGGINS et C. C. YANG. Arch. Biochem. Biophys. **37**, 322 (1952).
15. M. LAZDUNSKI. Bull. Soc. Chim. Biol. Sous presses.
16. B. CHANCE. J. Biol. Chem. **151**, 533 (1942).
17. B. CHANCE. Science, **109**, 204 (1949).
18. R. LUMRY, E. L. SMITH et R. R. GLANTZ. J. Am. Chem. Soc. **73**, 4330 (1951).
19. R. LUMRY et E. L. SMITH. Discussions Faraday Soc. **20**, 105 (1955).
20. L. B. NANNINGA et W. F. H. M. MOMMAERTS. Proc. Natl. Acad. Sci. U.S. **46**, 1166 (1960).
21. E. W. DAVIE et H. NEURATH. J. Biol. Chem. **212**, 515 (1955).
22. D. E. KOSHLAND. Arch. Biochem. Biophys. **39**, 229q (1952).
23. R. K. MORTON. Biochem. J. **70**, 139 (1958).
24. L. ENGSTRÖM. Biochim. Biophys. Acta, **54**, 179 (1961).
25. G. SCATCHARD, A. C. BATCHELDER et A. BROWN. J. Am. Chem. Soc. **68**, 2320 (1946).
26. R. LUMRY et H. PARKER. Federation Proc. **21**, 246 (1962).
27. B. LABOUESSE, B. H. HAVSTEEN et G. P. HESS. Proc. Natl. Acad. Sci. U.S. **48**, 2137 (1962).

Can. J. Chem. Downloaded from www.nrcresearchpress.com by 210.87.254.6 on 09/05/12
For personal use only.

Can. J. Chem. Downloaded from www.nrcresearchpress.com by 210.87.254.6 on 09/05/12
For personal use only.

THE THERMAL DECOMPOSITION OF METHYL HYDROPEROXIDE

ALEXANDER D. KIRK
Department of Chemistry, University of Victoria, Victoria, British Columbia
Received March 1, 1965

ABSTRACT

The thermal decomposition of methyl hydroperoxide has been studied in solution and in the gas phase. The decomposition was found to be partly heterogeneous in solution in dimethyl phthalate and no reliable rate constants were obtained. Use of the toluene carrier method for the gas phase work enabled measurement of the rate constant for the homogeneous decomposition. The first order rate constants obtained range from 0.19 s^{-1} at 292 °C to 1.5 s^{-1} at 378 °C, leading to log A, 11 ± 2, and activation energy, 32 ± 5 kcal/mole. These results are compared with the expected values of log A, 13–14, and activation energy, 42 kcal/mole. The significance of these findings is discussed.

Although the mechanism of its production has not been unambiguously established, and indeed may not be unique, methyl hydroperoxide has now been recognized as a significant product in the low temperature (1), radiolytic (2), and mercury photosensitized oxidation (3) of methane, the photooxidation of azomethane (4, 5), acetone (6), and methyl iodide (7), and the oxidation of methyl radicals (8). Although frequently not found in the products, it seems likely to be formed in any system involving methyl radicals and oxygen below about 400 °C. The possibility that methyl hydroperoxide acts as a chain-branching agent in the low temperature oxidation of methane has been in dispute and appears to be still uncertain (9). This uncertainty exists largely because the rate of homogeneous decomposition of the hydroperoxide is not known.

Early work (10) showed that decomposition of methyl hydroperoxide in a stream of nitrogen led to a complex mixture of products, almost certainly arising from simultaneous homogeneous and heterogeneous reaction. Recently, Fisher and Tipper (9) have studied the decomposition of the pure vapor in a static system and found the half-life of the peroxide to be up to 30 s at 395 °C depending on the condition of the reaction vessel surface. The lack of more complete data may be due to the difficulty of obtaining the hydroperoxide pure and its fairly ready heterogeneous decomposition. In this work, it was found that pure methyl hydroperoxide could be obtained safely by fractionation at reduced pressure and could be reliably estimated by iodine liberation and thiosulfate titration. The latter contrasts with other literature reports (11, 9). Details are given in the Experimental section.

This research was undertaken to obtain evidence for the homogeneous decomposition of methyl hydroperoxide into radicals

[1] $$(M +) CH_3OOH \rightarrow CH_3O\cdot + OH\cdot (+ M)$$

and to measure the rate constants and Arhennius parameters both in solution and in the gas phase. For the gas phase work, the toluene carrier method was adopted despite the criticisms which may be levelled against it (12). The facile heterogeneous decomposition of methyl hydroperoxide with low activation energy necessitates working at high temperature and short reaction times if the homogeneous reaction is to be favored. In addition, the relative effectiveness of toluene as a radical scavenger reduces secondary reactions and gives a measure of radical concentration by dibenzyl production.

Can. J. Chem. Downloaded from www.nrcresearchpress.com by 210.87.254.6 on 09/05/12
For personal use only.

EXPERIMENTAL

Materials

Methyl hydroperoxide was best prepared as described by Eggersglüss (13) with the slight modification that the product was removed directly from the reaction mixture by continuous ether extraction. The extract, after removal of the ether, was fractionated at reduced pressure in a Fenske helix column. Yields were only of the order of 5%, but, in the best case, the middle fraction of 1.5 g, with b.p.$_{184mm}$ 45.5–46.5° C, $n_D^{21} = 1.3654$, had a purity of 99% by iodimetric titration.

The dangers associated with low alkyl peroxides are well known, but the two explosions that occurred in this work are both notable in their spontaneity. In the first, dimethyl sulfate had been added over 4 h to alkaline H_2O_2, stirring through a mercury seal. The system vented through a small tube into a well-ventilated fume hood. The flask exploded violently when the temperature of the reaction mixture was only 19 °C. In retrospect, it seems certain that the explosion was caused by dimethyl peroxide and that the gas was not ignited. It has been observed previously that violent agitation may cause dimethyl peroxide vapor to detonate (14). In the second explosion, three containers containing methyl hydroperoxide samples, of purity 99%, 80%, and 50%, were allowed to warm to room temperature in a Dewar flask after being stored in liquid nitrogen for some weeks. The samples exploded completely spontaneously after about a 1 h interval. Since samples of methyl hydroperoxide of 80–90% purity were treated similarly for every run without mishap, it seems very probable that the 50% sample contained some dimethyl peroxide which initiated the explosion.

Unpurified Eastman Kodak dimethyl phthalate was used as solvent in the solution work.

Eastman Kodak sulfur-free toluene was used without purification as it gave no dibenzyl when pyrolyzed at 400 °C.

Analysis

Methyl hydroperoxide was estimated by a modification of the iodimetric method of Wagner, Smith, and Peters (15). The hydroperoxide was dissolved in 50 ml isopropanol; 1 ml glacial acetic acid and 1 g of sodium iodide was added and dissolved while warming gently. When the sodium iodide was in solution, the mixture was heated and maintained just at the boiling point for 10 min. Water (50 ml) was then added and the cooled solution titrated with 0.05 *M* sodium thiosulfate. No problem was experienced with air oxidation, and toluene, dimethyl phthalate, and formaldehyde did not interfere. Erratic results were obtained when the solutions were rapidly heated before the sodium iodide was completely in solution, but the temperature and the time of heating were not critical. No loss of iodine occurred when a standard solution of iodine in isopropanol was maintained at 82 °C in an open Erlenmeyer flask for 30 min.

In a few runs, the dibenzyl was analyzed for impurity by gas chromatography on a 3 ft silicone column at 200 °C.

Gases volatile at −196 °C were analyzed for oxygen, methane, and carbon monoxide using a 4 ft molecular sieve column at 60 °C. In one run, a 4 ft alumina column was used to analyze the gases volatile at −130 °C.

Apparatus and Procedure

(a) Decomposition in Solution

A degassed solution of methyl hydroperoxide was used to fill six calibrated 10 ml ampoules which were then sealed off under vacuum leaving just sufficient vapor space to fill them on heating to the reaction temperature. They were then heated in an oil bath thermostatted to 1 °C, removed at intervals, quenched in ice water, and analyzed iodimetrically. The first was taken as time zero and all times measured from its removal. Experiments with an ampoule having a thermocouple sealed into its center showed that the ampoules came up to bath temperature in 3 min and quenched in 30 s.

(b) Decomposition in the Gas Phase

A conventional flow system was used for the work (16); the cylindrical reaction vessel was 28 mm in outside diameter and 134 ml in volume and was heated by an aluminium block furnace. The rates of flow of toluene and methyl hydroperoxide and the overall contact time were controlled by capillaries. The pressure was measured with a Bourdon gauge and the reaction vessel temperature with a thermocouple. Degassed samples of methyl hydroperoxide and toluene were stored in containers removable for weighing.

The duration of a run was generally 10–20 min and toluene alone was passed through the apparatus for 2 min at the beginning and the end to stabilize the flow and sweep out the products. The concentration of methyl hydroperoxide was calculated from the loss in weight of the container and the exact percentage purity (about 90%) and, except for one run, was always about 0.5 mole % or less. After reaction, the products and reactants were collected in two removable traps, a small double U trap at −5 to −10 °C to collect dibenzyl and a large trap to collect all other products except permanent gases. The latter were collected in a Teopler pump and analyzed by gas chromatography. The undecomposed hydroperoxide was estimated by iodimetric titration.

RESULTS

(a) Decomposition in Solution

A conventional paraffin solvent could not be used due to the limited solubility of the polar methyl hydroperoxide. Initial runs with glycerin showed that methyl hydroperoxide

reacted with the solvent and that glycerin interfered with the iodimetric estimation of the hydroperoxide. Dimethyl phthalate was found to be a suitable solvent.

Figure 1 shows a plot of methyl hydroperoxide concentration versus time for typical data obtained for the decomposition in dimethyl phthalate. Packing experiments showed the scatter evident in the data to be due to heterogeneous decomposition. A degassed solution of methyl hydroperoxide was placed in six ampoules, three unpacked (surface/volume ≈ 4 cm^{-1}), two packed with glass tubing (surface/volume ≈ 13 cm^{-1}), and one packed with glass wool (surface/volume unknown), and heated at 155 °C for 30 min. Titration of the hydroperoxide remaining gave thiosulfate titers (corrected to 10 ml of solution) of 12.9, 12.4, and 12.0 ml for the unpacked vessels, 1.93 and 1.31 ml for the glass tube packed vessels, and 0.17 ml for the glass wool packed vessel.

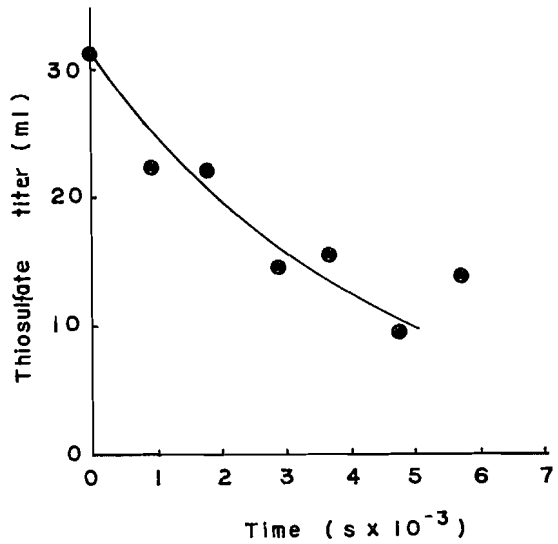

FIG. 1. Plot of undecomposed methyl hydroperoxide versus time. Solid line calculated for a first order reaction. Solvent dimethyl phthalate. Volume of solutions 10 ml. Temp. 153 °C. $[S_2O_3^{2-}] = 0.055$ *M*.

The first order rate constants obtained in unpacked vessels ranged from 3×10^{-5} s^{-1} at 112 °C to 2×10^{-4} s^{-1} at 153 °C, but, in view of the irreproducibility and the fact that heterogeneous reaction was clearly contributing to the rate, these values are of little significance. In agreement is the observation that the rate constants are much larger than would be expected by extrapolation of the gas phase data for the homogeneous reaction.

(b) Decomposition in Gas Phase

The main results are shown in Table I. Analyses were carried out primarily for dibenzyl and undecomposed hydroperoxide, but methane, carbon monoxide, oxygen, and ethane were minor products (together about 6% of the total decomposition). Analysis of the liquid products for methanol, formaldehyde, and water would have precluded titration of the unchanged hydroperoxide. Analysis of the dibenzyl showed no impurities (limit of detection $< 1\%$). The identity of the dibenzyl was confirmed by comparison of the infrared spectrum with that of an authentic sample. Test runs with toluene alone and toluene with small amounts of oxygen gave no dibenzyl.

Table I shows that the percentage decomposition rose from 15 to 75% over the temperature range 290 °C to 380 °C while the ratio mole dibenzyl / mole hydroperoxide

Can. J. Chem. Downloaded from www.nrcresearchpress.com by 210.87.254.6 on 09/05/12
For personal use only.

TABLE I

Experimental data and rate constants for the gas phase decomposition of methyl hydroperoxide

Temp. (°K)	Press. (mm)	$\frac{P_{MeO_2H}}{P_{toluene}} \times 100$	Contact time (s)	% decomposition MeO_2H	ϕ	k_{tot} (s^{-1})	k_1 (s^{-1})
565	25.3	0.53	0.93	16	0.03	0.19	0.005
574	23.5	0.42	0.88	27	0.07	0.66	0.044
582	24.0	0.41	0.87	20	0.22	0.26	0.057
584	20.7	0.41	0.87	30	0.24	0.44	0.11
591	23.3	0.55	0.77	40	0.12	0.66	0.079
597	42.0	0.21	0.89	44	0.38	0.64	0.244
598	25.5	0.45	0.86	24	0.37	0.32	0.12
613	22.2	0.37	0.77	51	0.38	0.95	0.36
614	23.7	4.0	0.85	58	0.27	1.05	0.28
627	38.0	0.41	1.36	45	0.82	0.58	0.47
633	49.0	0.12	0.89	57	0.76	0.94	0.71
649	23.5	0.47	0.83	75	0.86	1.65	1.41
651	22.3	0.41	0.84	71	0.76	1.47	1.12

ϕ = mole dibenzyl / mole MeO_2H decomposed.

decomposed (ϕ) rose from 0.05 to 0.80 over the same range. This suggests competition between a heterogeneous decomposition of low activation energy and a homogeneous decomposition of higher activation energy. The ready heterogeneous decomposition of methyl hydroperoxide is well known and packing experiments were regarded as superfluous. The production of dibenzyl is unambiguous evidence for the decomposition of methyl hydroperoxide into radicals.

The total first order rate constants were calculated from the contact time and the initial and final concentrations of methyl hydroperoxide. If the mechanism presented in the discussion is assumed, the total first order rate constant may be divided into a heterogeneous and a homogeneous rate constant by

$$k_1 = k_{tot}\,\phi$$

$$k_{het} = k_{tot} - k_1.$$

DISCUSSION

Since the gas phase decomposition of methyl hydroperoxide in the presence of toluene gave dibenzyl in yields up to 85%, reactions [1]–[4] must occur.

[1] $(M +)\ CH_3OOH \rightarrow CH_3O\cdot + OH\cdot\ (+ M)$

[2] $CH_3O\cdot + C_6H_5CH_3 \rightarrow CH_3OH + C_6H_5CH_2\cdot$

[3] $OH\cdot + C_6H_5CH_3 \rightarrow H_2O + C_6H_5CH_2\cdot$

[4] $2C_6H_5CH_2\cdot \rightarrow C_6H_5CH_2CH_2C_6H_5$

The other possible reactions of methyl hydroperoxide and methoxyl, hydroxyl, and benzyl radicals must also be considered.

[5] $C_6H_5CH_2\cdot + OH\cdot \rightarrow C_6H_5CH_2OH$

[6] $C_6H_5CH_2\cdot + CH_3O\cdot \rightarrow C_6H_5CH_2OCH_3$

[7] $(M +)\ CH_3O\cdot + OH\cdot \rightarrow CH_2O + H_2O$ (or CH_3OOH) $(+ M)$

[8] $CH_3O\cdot + CH_3O\cdot \rightarrow CH_3OH + CH_2O$ (or CH_3OOCH_3)

[9] $M + OH\cdot + OH\cdot \rightarrow H_2O_2 + M$

[10] $CH_3OOH + CH_3O\cdot \rightarrow CH_3OH + CH_3OO\cdot$

Can. J. Chem. Downloaded from www.nrcresearchpress.com by 210.87.254.6 on 09/05/12
For personal use only.

[11] $$CH_3OOH + OH\cdot \rightarrow H_2O + CH_3OO\cdot$$

[12] $$CH_3OOH \xrightarrow{\text{walls}} CH_3OH,\ CH_2O,\ O_2,\ H_2O,\ \text{etc.}$$

Alternate ring abstraction reactions from toluene are suggested by the recent work of Cher (17).

[13] $$CH_3O\cdot + C_6H_5CH_3 \rightarrow CH_3OH + \cdot C_6H_4CH_3$$

[14] $$OH\cdot + C_6H_5CH_3 \rightarrow H_2O + \cdot C_6H_4CH_3$$

Several pieces of evidence suggest that the recombination reactions involving methoxyl and hydroxyl radicals are unimportant. First, no benzyl alcohol or benzyl methyl ether was found in the dibenzyl, direct evidence against reactions [5] and [6]. Secondly, the higher temperature runs consistently gave dibenzyl in 80% yield which, remembering the likelihood of heterogeneous decomposition, indicates quantitative conversion of methoxyl and hydroxyl into dibenzyl. Since the reactions of methoxyl and hydroxyl radicals are all of zero or low activation energy, this situation probably carries over to the low temperature runs. Finally, reaction [8] will be faster than [7] or [9] since the hydroxyl radical almost certainly reacts more rapidly with toluene than methoxyl. It is interesting then to compare the relative rate of reaction of methoxyl with toluene [2] and with methoxyl [8]. Assuming $E_8 = 0$, $A_8 = 10^{11}$ l mole^{-1} s^{-1}, $k_1 = 0.3$ s^{-1} (this work), $A_2 = 10^{11}\ P_2$ l mole^{-1} s^{-1}, and $E_2 = 5.0$ kcal/mole (the value for hydrogen abstraction by methoxyl from methyl acetate (18)), then at 610 °K, if P_2 is 10^{-2}, reaction [8] accounts for only 0.1% of the methoxyls, if P_2 is 10^{-3} it accounts for 10%. Thus it seems likely that no serious error is incurred by the neglect of reactions [5], [6], [7], [8], and [9].

The experimental evidence does not entirely preclude the possibility of some chain reaction, [10] and [11], particularly at the lower temperatures. Benson has indeed suggested (19) that previous work (20) on alkyl hydroperoxides has led to high rate constants due to chain decomposition. It must be noted, however, that in this study the molar concentration of hydroperoxide was always less than or equal to 0.5% of the toluene. Since $D(CH_3OO—H) \simeq 87$ kcal/mole (19) and $D(C_6H_5CH_2—H) \simeq 83$ kcal/mole (21), one would expect a slightly lower activation energy for hydrogen abstraction from toluene. Thus, unless the steric factor for abstraction from hydroperoxide is markedly greater than from toluene, chain reaction does not occur.

Reactions [13] and [14] are unimportant since no dimethyl diphenyl or phenyl tolyl methane was found, indicating, as Cher has suggested (17), that the tolyl radical rapidly reverts to the benzyl radical when excess toluene is present. Even if this were not so, the results of this study would not be affected.

If the main reactions in the system are [1], [2], [3], [4], and [12], and if [1] and [12] are assumed to be first order, then the first order rate constants for reaction [1] may be calculated as described in the previous section. These rate constants are shown in Table I together with the total first order constants. The latter show the greater scatter confirming that the method of calculation is in fact correcting for an irreproducible heterogeneous contribution to the decomposition.

Figure 2 is the Arhennius plot of the homogeneous rate constants for reaction [1], and leads to

$$k_1 = 10^{11\pm2} \exp \frac{-(32 \pm 5) \times 10^3}{RT}$$

The 95% error limits were obtained by least squares treatment excluding the single point at the low temperature extreme.

Can. J. Chem. Downloaded from www.nrcresearchpress.com by 210.87.254.6 on 09/05/12
For personal use only.

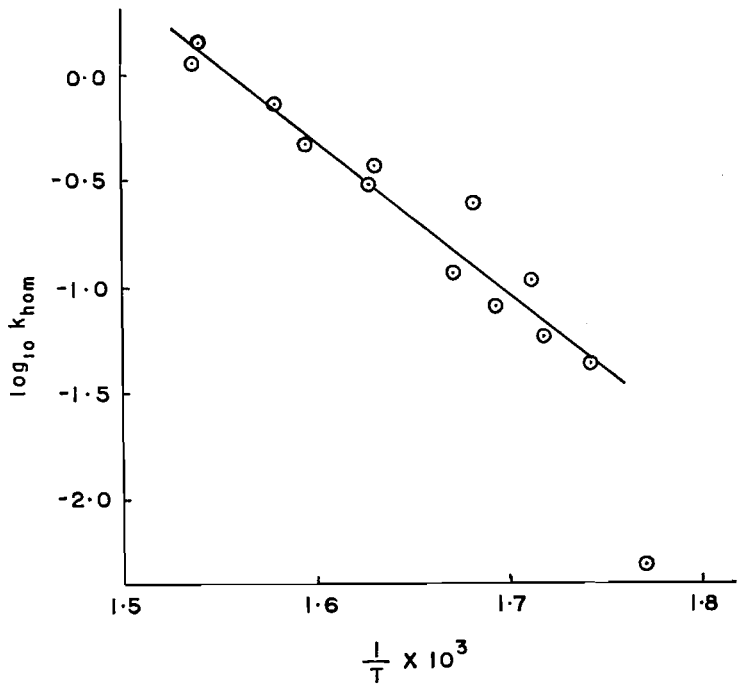

FIG. 2. Arhennius plot for the homogeneous gas phase decomposition of methyl hydroperoxide. $k_{hom} \equiv k_1$.

If the recombination of methoxyl and hydroxyl radical is assumed to have zero activation energy, then E_1 may be equated with $D(CH_3O—OH)$. The value obtained of 32 kcal/mole is much lower than would be expected on the basis of thermochemical calculations. Using group energy values (22), the heat of formation of methyl hydroperoxide is calculated to be −32.1 kcal/mole. Together with $\Delta H_f(OH) = 8$ kcal/mole (19) and $\Delta H_f(CH_3O) = 2.0$ kcal/mole (rather than −0.5 kcal/mole (23) since it is more consistent with the data on dimethyl peroxide), then $D(CH_3O—OH) = 42$ kcal/mole.

The combination of low activation energy and low A factor suggests that the rate constants are of the correct order of magnitude but are sufficiently in error to lead to these large errors in E and log A. Benson (24) has emphasized the high precision required to measure Arhennius parameters.

If this is so, it is likely that the fault lies with the data obtained at the lower end of the temperature range as there the heterogeneous reaction predominates and the mechanistic uncertainties are most important. It is significant in this regard that the high temperature rate constants are of the magnitude to be expected for a reaction of activation energy 42 kcal/mole and a "normal" A factor. Thus, using the rate constant obtained at 649 °K and assuming $E = 42$ kcal/mole, we find log $A = 14.2$. Thus the disagreement lies not in the magnitude of the rate constants but in their interrelationship.

The rate constants are lower by a factor of about three than the values previously obtained for ethyl and isopropyl hydroperoxides (20). At these temperatures, this is equivalent to an activation energy difference of 0.9 kcal/mole.

Fisher and Tipper have recently reported the half-life of methyl hydroperoxide as up to 30 s at 395 °C (9). The present work suggests a value of 0.2 s. One is tempted to favor the longer lifetime for obvious reasons. However, the following considerations support our

Can. J. Chem. Downloaded from www.nrcresearchpress.com by 210.87.254.6 on 09/05/12
For personal use only.

value. 1. The longer half-life corresponds to a minimum activation energy for reaction [1] of 45–48 kcal/mole for the normal range of A factors while our value corresponds to 38–41 kcal/mole, in better agreement with the thermochemical data. 2. Our value was obtained in circumstances where 80% of the hydroperoxide decomposed led to dibenzyl, leaving little doubt about the mechanism of that proportion of the decomposition. Any errors in the assumptions regarding the remaining 20% do not affect the homogeneous rate constants significantly.

One may conclude that, in the temperature range 300–400 °C, methyl hydroperoxide will cause branching in oxidation systems if formed, but that its lifetime is too short for it to be involved in degenerate chain branching.

Because of the relative simplicity of the methyl hydroperoxide molecule, it is quite likely that, at the pressures used in this work, the rate constants are pressure dependent. Unfortunately, the experimental technique was unsuitable for any study of the pressure dependence of the rate constant. As the runs reported were all at approximately the same pressure of toluene, the present results would not be affected.

ACKNOWLEDGMENTS

The author wishes to thank W. Hyslop for assistance with the solution work, W. R. Newman for much of the gas phase work, and the National Research Council and the University of Victoria for research grants. The author would also like to thank one of the referees for drawing attention to the work of Barnard and Honeyman (25) who obtained an estimate of the lifetime of methyl hydroperoxide at 284 °C as 1–4 min, consistent with the present results.

REFERENCES

1. I. P. Fisher and C. F. H. Tipper. Trans. Faraday Soc. **59**, 1163 (1963).
2. G. R. A. Johnson and G. A. Salmon. J. Phys. Chem. **65**, 177 (1961).
3. J. A. Gray. J. Chem. Soc. 3150 (1952).
4. N. R. Subbaratnam and J. G. Calvert. J. Am. Chem. Soc. **84**, 1113 (1962).
5. M. Shanin and K. O. Kutschke. J. Phys. Chem. **65**, 189 (1961).
6. H. S. Johnston and J. Heicklen. J. Am. Chem. Soc. **86**, 4249 (1964).
7. J. Heicklen and H. S. Johnston. J. Am. Chem. Soc. **84**, 4030 (1962).
8. L. I. Avramenko and L. N. Postnikov. Izv. Akad. Nauk SSSR, **11**, 1921 (1960).
9. I. P. Fisher and C. F. H. Tipper. Trans. Faraday Soc. **59**, 1174 (1963).
10. S. Medvedev and A. Podyapolskaya. Acta Physicochim. U.R.S.S. **2**, 487 (1935).
11. A. Rieche and F. Hitz. Chem. Ber. **62B**, 2458, 74 (1929).
12. E. W. R. Steacie. Atomic and free radical reactions. Reinhold. 1954. p. 94.
13. W. Eggersglüss. Organic peroxides. Monograph, N.R.C. 1-793. 1959. p. 68. Angew. Chem. **61** (1951).
14. A. Reiche and W. Brumshagen. Chem. Ber. **61B**, 951 (1928).
15. C. O. Wagner, R. H. Smith, and E. D. Peters. Anal. Chem. **19**, 976 (1947).
16. M. Szwarc, B. N. Ghosh, and A. H. Sehon. J. Chem. Phys. **18**, 1142 (1950).
17. M. Cher. J. Phys. Chem. **68**, 1316 (1964).
18. M. J. Wignen. J. Chem. Phys. **27**, 710 (1957).
19. S. W. Benson. J. Chem. Phys. **40**, 1007 (1964).
20. A. D. Kirk and J. H. Knox. Trans. Faraday Soc. **56**, 1296 (1960).
21. A. H. Sehon and M. Szwarc. Ann. Rev. Phys. Chem. **8**, 439 (1957).
22. S. W. Benson and J. H. Buss. J. Chem. Phys. **29**, 546 (1958).
23. P. Gray and A. Williams. Chem. Rev. **59**, 239 (1959).
24. S. W. Benson. The foundations of chemical kinetics. McGraw-Hill. 1960.
25. J. A. Barnard and T. W. Honeyman. Proc. Roy. Soc. London, Ser. A, **279**, 248 (1964).

Can. J. Chem. Downloaded from www.nrcresearchpress.com by 210.87.254.6 on 09/05/12
For personal use only.

KINETICS OF VAPOR-PHASE HYDROCARBON–OZONE REACTIONS

J. J. BUFALINI AND A. P. ALTSHULLER

Laboratory of Engineering and Physical Sciences, Division of Air Pollution, and Robert A. Taft Sanitary Engineering Center, Public Health Service, U.S. Department of Health, Education, and Welfare, Cincinnati, Ohio

Received August 10, 1964

ABSTRACT

The reactions of nine olefinic and aromatic hydrocarbons with ozone in the vapor phase have been investigated in static and dynamic systems. Some of the rate constants for the olefin–ozone reactions are in good agreement with previously published data, whereas others are larger than values previously reported. Rate constants for *trans*-2-butene–, isobutene–, and ethylene–ozone reactions were measured between 30 and 100 °C. The activation energies for the reaction of ozone with *trans*-2-butene, isobutene, and ethylene are 0.2 ± 0.3, 2.8 ± 0.4, and 4.2 ± 0.4 kcal/mole. In general, the reactions of hydrocarbons with ozone are non-stoichiometric. However, these reactions do appear to be second order. The rates of reaction between alkylbenzenes and ozone are too low to be of importance in air pollution studies.

INTRODUCTION

The ozonization of hydrocarbons in the liquid phase has been the subject of considerable investigation (1). The vapor-phase counterpart has received less attention. Since Haagen-Smit (2) observed that eye irritation and plant damage resulted from ozone–hydrocarbon reactions, considerable effort has been directed toward a better understanding of the role of ozone–hydrocarbon reactions in air pollution. In the ensuing investigations numerous disagreements have arisen concerning the stoichiometries and magnitudes of the rate constants for many of the ozone–olefin reactions.

Hydrocarbons that are present in the atmosphere are generally thought to react with atomic oxygen, ozone, and free radicals. Since accurate rate constants are necessary for determining the relative importance of each of these reactants in polluted air, the present study was undertaken.

EXPERIMENTAL

Reactions were carried out in dynamic and in static systems. For the dynamic system the volume of the reaction vessel depended upon the particular hydrocarbon under consideration. (Reaction vessels of 0.5, 1, 2, 6, and 12 l capacity were employed.) For the static system a 12 l round-bottom flask and a Teflon (FEP) bag were used. Except for a few butt-to-butt glass connections jointed by Teflon tubing, an all-glass system with ball and socket connectors was employed. Fluorocarbon grease was used sparingly as a lubricant for the stirrer employed with the 12 l flask. Most dynamic experiments were conducted at 30 ± 0.1 °C. Several of the reactions also were studied at temperatures between 30 and 100 °C. The static runs were conducted at room temperatures ($T = 25 \pm 2$ °C).

Prepurified air was metered at a rate of 400 cc/min through the ozone generator. The ozone-producing lamps were of the small mercury vapor type operating on 4 W (G.E. 0Z4S11). The ballasts for the lamps were connected to a constant-voltage transformer to ensure steady ozone output. Because the 1 849 Å line is extremely dependent upon voltage, it was imperative that a steady line voltage be maintained. The ozone produced in this manner was stored in a double-walled 100 l FEP (fluorinated ethylene propylene copolymer) plastic container and was either used in test runs or vented into the air (3).

The hydrocarbons were introduced by means of syringes into a previously evacuated 34 l stainless steel tank equipped with a silicon rubber septum. The 34 l tank was then pressurized with tank air to approximately 200 p.s.i. (gauge pressure) and placed in an oven (~ 75 °C) overnight. This operation was necessary to ensure proper mixing under the high pressure.

For dynamic reactions known mixtures of hydrocarbon and ozone were metered through a venturi and into the reaction flask. The total inlet volume was checked against the total outlet volume. Enough time was allowed for the dynamic chamber to reach steady-state conditions. The calculated value for charging was in excellent agreement with the experimental value.

For static reactions the 12 l flask was evacuated with a mechanical vacuum pump. The specified amount of hydrocarbon was introduced through a silicon rubber septum by means of a syringe. A known volume of ozone was then introduced from the FEP bag.

Can. J. Chem. Downloaded from www.nrcresearchpress.com by 210.87.254.40 on 09/05/12
For personal use only.

The ozone concentration was measured by the usual procedure involving the oxidation of iodide to triiodide in neutral solution. In some instances the Mast ozone meter was employed. The meter value was multiplied by a factor of 1.48 to equal the colorimetric value. Hydrocarbons were measured by a gas–liquid chromatograph (g.l.c.) equipped with a flame-ionization detector. Selection of the column material depended upon the hydrocarbon to be reacted. A column packed with medium-activity silica gel was used for the lighter olefins; a column packed with bis-2(2 methoxyethyl)adipate (BMEA) on C-22 firebrick was used for the higher olefins but was later replaced by a column packed with 10% silicon fluid (SF96) on C-22 firebrick. Aromatic hydrocarbons were separated on a column packed with 5 to 10% Carbowax 1540 on C-22 firebrick. The gas flow rates for the gas chromatograph were H_2, 22 cc/min; air, 300 cc/min; and He, 31 cc/min.

Most of the hydrocarbons were obtained from Phillips Petroleum Company. 1,3,5-Trimethylbenzene was obtained from Aldrich Chemical Company; styrene from Matheson-Coleman Company; *tert*-butyl hydroperoxide from K and K Laboratories; peracetic acid from the FMC Corporation; *n*-butyl hydroperoxide was prepared by the method of Williams and Mosher (4); and the tank air for ozone generation was obtained from the Matheson Company.

METHOD OF CALCULATION

The dynamic reaction flask was treated as a continuous stirred flow reactor. With such a reactor, materials leave at a constant concentration at steady state.
At steady state

$$F(x_0 - x) = kVxy \quad [1]$$

where F is the flow rate, x_0 is the hydrocarbon concentration entering the reactor, x is the hydrocarbon concentration leaving the reactor, y is the ozone concentration leaving the reactor, V is the reactor volume, and k is the rate constant.

In the static method, the integrated second-order rate equation was employed.

$$k = \frac{2.303 \log (C_0/C)}{\int_0^t [O_3]\, dt} \quad [2]$$

RESULTS

The values for the absolute rate constants for various hydrocarbons are shown in Table I for the dynamic system and Tables II and III for the static system.

The rate constant for mesitylene was calculated on the basis of its detectability with the gas chromatograph, i.e., it was based on the fact that if 5% of the mesitylene had reacted, the gas chromatographic analysis would detect this difference.

TABLE I

Absolute rates of reaction of various hydrocarbons with ozone at 30 °C

Compound	Rate constant (l mole^{-1} s^{-1} × 10^{-3})	Activation energy (kcal/mole^{-1})	Literature k (l mole^{-1} s^{-1} × 10^{-3})
Ethylene	1.6±0.2	4.2±0.4	1.6*, 0.8†
Styrene	18		
1,3,5-Trimethylbenzene	<0.06		
trans-2-Butene	260±40	0.2±0.3	100‡, 17§
cis-2-Butene	200		30‡, 13§
1-Hexene	6.8±0.1		6.9‡, 4.6§, 6.1*, 6.1†, 5.5‖
1-Butene	6.2		3.9§
2-Methylpropene	14±2	2.8±0.4	3.6§, 3.7†, 8.8‡
2-Methyl-2-Butene	450		12§

*Cadle and Schadt, ref. 13.
†Hanst *et al.*, ref. 7.
‡Schuck *et al.*, ref. 17.
§Vrbaski and Cvetanovic, ref. 18.
‖Saltzman and Gilbert, ref. 19.

Can. J. Chem. Downloaded from www.nrcresearchpress.com by 210.87.254.40 on 09/05/12
For personal use only.

TABLE II

Experimental data for the reactions of ozone with various olefins

Time (min)	Log $\frac{C_1}{C_2}$	$\int_{t_1}^{t_2}[O_3]\,dt$ (p.p.m. min)	k (l mole^{-1} s^{-1} $\times$ 10^{-3})
Ethylene			
0–20	0.105	49.2	2.0
20–40	0.0635	35.4	1.8
40–60	0.0465	23.4	1.9
60–80	0.036	16.0	2.1
80–120	0.059	26.3	2.1
			Average =2.0
1-Butene			
0–20	0.166	18.4	8.5
20–40	0.124	13.6	8.5
40–60	0.097	10.9	8.3
60–100	0.147	16.7	8.2
100–150	0.143	15.2	8.8
			Average = 8.5
trans-2-Butene			
0–2	0.171	0.820	200
2–4	0.142	0.740	180
4–6	0.148	0.708	200
6–12	0.455	1.98	220
			Average = 200
1-Hexene			
0–30	0.690	22.1	7.5
30–60	0.129	16.6	7.3
60–90	0.095	11.2	7.3
90–120	0.074	8.97	7.7
			Average = 7.5

TABLE III

Experimental data for the reaction of 0.40 p.p.m. of *trans*-2-butene with 0.34 p.p.m. of ozone in the presence of 1.6 p.p.m. of hexene-1 at 27 °C

Time (min)	Log $\frac{C_1}{C_2}$	$\int_{t_1}^{t_2}[O_3]\,dt$ (p.p.m. min)	k (l mole^{-1} s^{-1} $\times$ 10^{-5})
0–2	0.1265	0.605	2.0
2–6	0.217	0.890	2.3
6–12	0.187	0.930	1.9
12–16	0.105	0.504	2.0

The olefin-to-ozone consumption ratios increased with increasing olefin concentration. These ratios did level off, however, when the initial olefin concentration was in excess of the initial ozone concentration. The consumption ratios at higher olefin concentrations were 1.5 for *trans*-2-butene, 1.6 for ethylene, 1.8 for 1-hexene, 2.0 for 1-butene, 1.5 for isobutene, and 2.0 for 2-methyl-2-butene. Styrene showed 1:1 stoichiometry within experimental error. There is also some evidence that the consumption ratio decreased with increasing flow rate. The consumption ratios for equal *trans*-2-butene concentrations were 1.47 for a flow rate of 655 cc/min, 1.27 for 790 cc/min, and 1.11 for 900 cc/min. Some of the data obtained on the static runs for the olefin–ozone reactions are shown in Figs. 1, 2, and 3. The dashed line in Fig. 1 is the calculated ozone concentrations assuming 1:1 stoichiometry. It is noted that the calculated ozone concentration goes to zero at 60 min reaction time when 1:1 stoichiometry is assumed.

In Figs. 2 and 3 are shown the reactions of 1-butene, *trans*-2-butene, and 1-hexene with ozone. The data show that more ozone was consumed in the 1-hexene–ozone reaction;

Can. J. Chem. Downloaded from www.nrcresearchpress.com by 210.87.254.40 on 09/05/12
For personal use only.

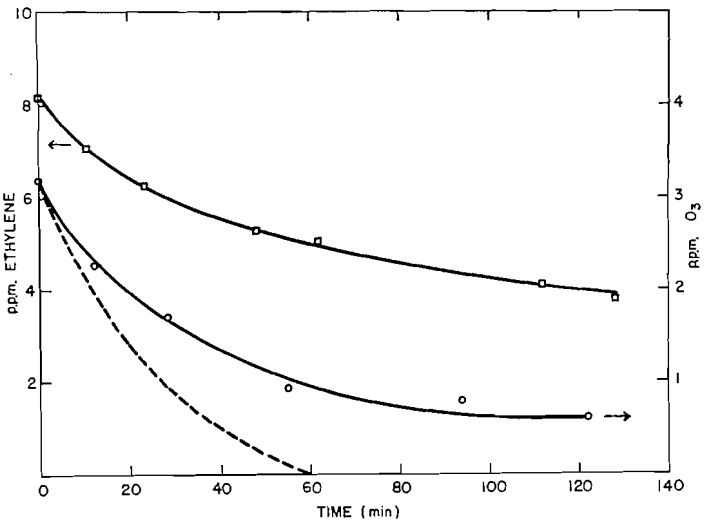

FIG. 1. Concentration vs. time curves for ozone–ethylene reaction.

however, part of the decrease in ozone concentration can be attributed to surface and thermal decomposition. It was found that 1 p.p.m. of ozone dissociated 13.6% for a period of 2 h in the Teflon bag.

Since we were primarily interested in rate constants for the ozone–olefin reactions, a thorough product analysis for reaction products was not performed. The products listed are those that were easily observed by ordinary g.l.c. analysis or by wet analysis in the case of ethylene. The reader is referred to three excellent papers (5, 6, 7) for a more complete product analysis.

The major product formed from the *trans*-2-butene–ozone reaction is acetaldehyde. Approximately 1 mole of this product is formed for every mole of olefin consumed. One

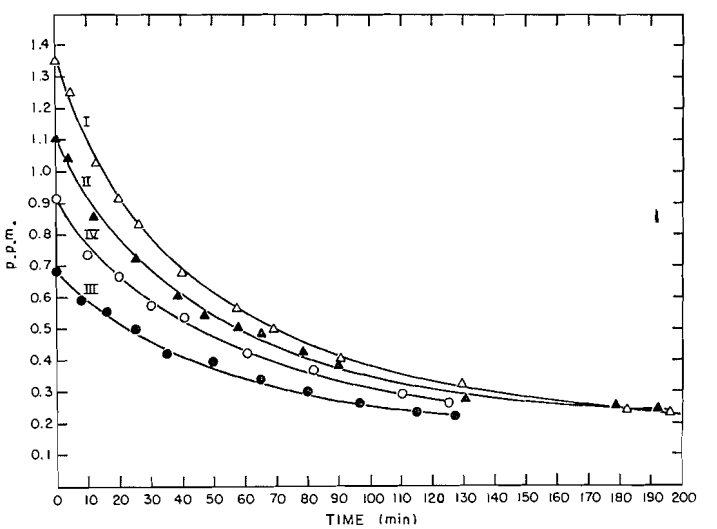

FIG. 2. Concentration vs. time curves for ozone–olefin reactions. The curves are: I and II for 1-butene and ozone, respectively; III and IV for 1-hexene and ozone, respectively.

Can. J. Chem. Downloaded from www.nrcresearchpress.com by 210.87.254.40 on 09/05/12
For personal use only.

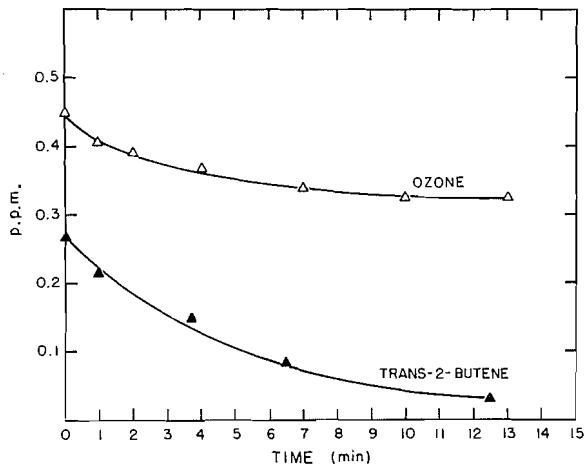

FIG. 3. Concentration vs. time curves for *trans*-2-butene–ozone reaction.

mole of acetone is formed for every 2 moles of isobutene reacted. About 0.7 mole of formaldehyde was observed for every mole of ethylene reacted. Approximately 0.2 mole of acetone was formed for every mole of 2-methyl-2-butene reacted. Because the amount of acetaldehyde formed from the 2-methyl-2-butene–ozone reaction fluctuated, a definite ratio was difficult to establish. It was noticed, however, that the reaction formed more acetaldehyde than acetone. The 1-butene–ozone reaction showed ethane to be a minor product. A quantitative study was not made on this product. The 1-hexene–ozone reaction showed pentanal as a major product and butane as a minor product. Again no quantitative studies were made.

DISCUSSION

The olefin-to-ozone consumption ratio suggests that an intermediate is formed that reacts further with the olefin. The Criegee mechanism (8) that is usually accepted for gas-phase ozone–olefin reactions is compatible with this observation. The mechanism can be written as follows.

[3] $$RHC{=}CHR + O_3 \rightarrow \text{initial product}$$

[4] $$\text{initial product} \rightarrow RH\overset{+}{C}{-}O{-}\bar{O} + RCHO$$

[5] $$RH\overset{+}{C}{-}O{-}\bar{O} + \text{olefin} \rightarrow \text{product(s)}$$

[6] $$RH\overset{+}{C}{-}O{-}\bar{O} \rightarrow RH + CO_2$$

[7] $$RH\overset{+}{C}{-}O{-}\bar{O} + O_2 \rightarrow RCHO + O_3$$

[8] $$RH\overset{+}{C}{-}O{-}\bar{O} \rightarrow ROH + CO$$

Reactions [5] and [7] can explain the high olefin-to-ozone consumption ratio that was observed. If reactions [3] and [4] are treated as one and if steady-state conditions are assumed for the zwitterion, the rate of disappearance of the olefin becomes

[9] $$-\frac{d[ol]}{dt} = k_3[ol][O_3] + \frac{k_5k_3[ol]^2[O_3]}{k_5[ol] + k_7[O_2] + k_6 + k_8}.$$

A recent study by Wei and Cvetanovic (6) in which ozone–olefin reactions were studied both in the presence and absence of molecular oxygen, seems to corroborate reaction [7].

Can. J. Chem. Downloaded from www.nrcresearchpress.com by 210.87.254.40 on 09/05/12
For personal use only.

They found that there was an increase in aldehyde and (or) ketone concentration(s) when molecular oxygen is present. Also, they observed that in the presence of molecular oxygen the olefin–ozone consumption ratio varied between 1.4 and 2 for different olefins. The reactions were stoichiometric in the absence of molecular oxgyen, however. This observation strongly suggests that reaction [5] is unimportant. Therefore, eq. [9] was reduced to the simple second-order rate eq. [2].* The rate constants obtained from this equation by use of the data from Fig. 1, 2, and 3 are shown in the last column of Table II.

It is conceivable that other olefin-consuming reactions could occur. If a free radical were formed as an intermediate between olefin and ozone a rapid direct attack of the olefin could occur. If such a free radical were formed, a pronounced effect would be noticed when a rapid-reacting olefin is mixed with a large excess of a slower reacting olefin. Table III shows the data when *trans*-2-butene is reacted with ozone in the presence of hexene-1. Column 4 of Table III shows good agreement with the corresponding rate constant of the *trans*-2-butene–ozone reaction shown in Table III.

The presence of ethane and butane in the ozone–1-butene and ozone–1-hexene reactions can be explained by reaction [6]. The aldehyde and ketone formation can be explained by reaction [4]. We were unable with this study to determine whether the initial product resulting from reaction [3] is a four- or five-membered ring. The more acceptable form of the initial ozonide in liquid phase reactions is the five-membered ring (9).

It has been shown that the reactivity of mesitylene approaches that of many 1-alkenes in photooxidation-type reactions (10, 11, 12). Since the rate of reaction of mesitylene with ozone is very slow in the concentration range of interest, the overall rates of hydrocarbon consumption in photooxidations cannot be attributed to the reaction with ozone. The atomic oxygen – mesitylene reaction has been measured in this laboratory and found to be slow. The computed rate of reaction of atomic oxygen with mesitylene accounts for only a small fraction of the overall rate of mesitylene consumption. If the rapid photooxidation of mesitylene in the presence of oxides of nitrogen is to be explained, it must be done by introducing reacting species other than atomic oxygen and ozone. The hypothesis most compatible with these observations is that free-radical attack on the hydrocarbon is more important in the photooxidation of olefins. It would appear that electrophilic or radical species must be formed that may be capable of much more vigorous reaction with aromatic hydrocarbons than are ether ozone or atomic oxygen.

The pre-exponential factors for the three compounds studied at various temperatures are 3.6×10^8 cc mole^{-1} s^{-1} for *trans*-2-butene, 1.4×10^9 cc mole^{-1} s^{-1} for isobutene, and 1.7×10^9 cc mole^{-1} s^{-1} for ethylene.

Cadle and Schadt (13) studied ethylene–ozone and 1-hexene–ozone reactions at various temperatures. Their data showed no statistically significant change in the rate constants with increasing temperatures for both ethylene and 1-hexene. The pre-exponential factors calculated from their rate constants are 1.6×10^5 cc mole^{-1} s^{-1} and 6.1×10^6 cc mole^{-1} s^{-1} for ethylene and 1-hexene, respectively. These results are open to doubt. The largest contribution to the activation entropy comes from a loss in translational degrees of freedom. This loss in translational degrees of freedom increases with increasing masses of the reacting species. One should therefore expect that the 1-hexene–ozone reaction would have a smaller pre-exponential factor (14).

It has been suggested (15) that the nonstoichiometric behavior of olefin–ozone reactions may be due in part to oxidizing products interfering with the titration of ozone by neutral

**Other reactions can be written for the decomposition of the zwitterion (see ref. 15, pp. 175–178). However, since the rate constants for these reactions will also appear in the denominator in the last term of eq. [9], they will not contribute to the equation and have not been included.*

Can. J. Chem. Downloaded from www.nrcresearchpress.com by 210.87.254.40 on 09/05/12
For personal use only.

KI. To test this possibility, *tert*-butyl hydroperoxide, *n*-butyl hydroperoxide, and peracetic acid were tested with neutral KI solutions. The hydroperoxides liberated iodine very slowly while the peracid liberated iodine quickly. Since no slow-reacting product was observed with any of the ozone–olefin reactions, it was concluded that either hydroperoxides were absent or their reactions with olefins are so rapid that only small steady-state concentrations are present. To eliminate the latter possibility, *tert*-butyl and *n*-butyl hydroperoxides were added to isobutene in two separate experiments. No reaction was observed over a period of 12 h. It was therefore concluded that hydroperoxides are not formed from ozone–olefin reactions. It is not possible to distinguish between ozone and peracids with the neutral KI. It is possible, however, to determine whether peracids are present by appropriate kinetic experiments. Peracetic acid and 1-hexene were introduced into a Teflon (FEP) bag, and no reaction was observed over a period of several hours. Since the rate constants appearing in Table II show no trend with increasing time, it must be concluded that no peracids are formed. It is assumed that if peracids were formed, they would have to react with olefins at the same rate as ozone in order to maintain any constancy in the rate constants. Since peracids do not react quickly with olefins, if formed, they would remain in the reaction chamber. Their buildup would be appreciable over a period of time. Since this oxidant buildup would show a decrease in the rate constants by use of eq. [2] and no such decrease was observed, it must be concluded that no significant concentrations of peracids were formed.

The other possible oxidant product usually associated with ozone–olefin type reactions is an ozonide. Scott and co-workers (16) found no ozonides from the ozone–olefin reactions in the gas phase. The same group of workers in a later publication (7) did detect ozonides as minor products. A yield of 8% ozonide was observed by these workers when 20 p.p.m. each of 1-pentene and ozone were reacted. With 11 p.p.m. each of ozone and 1-hexene, 13% ozonide was detected. Little or no ozonide was observed with the lower olefins (C_2–C_4).

We did not test ozonides with neutral KI so it is entirely possible that a reaction could occur with this reagent. The rate constants given in Tables I, II, and III are dependent upon ozonides not reacting with neutral KI. Since no trend could be detected in the static studies (Column 4, Tables II and III) we feel that ozonide interference is small.

ACKNOWLEDGMENT

The authors wish to thank Dr. R. J. Cvetanovic for his valuable comments and discussions.

REFERENCES

1. P. S. Bailey. Chem. Rev. **58**, 925 (1958).
2. A. J. Haagen-Smit, E. F. Darley, N. Zeitlin, H. Hall, and W. Noble. Plant Physiol. **27**, 18 (1952).
3. A. P. Altshuller, A. F. Wartburg, I. R. Cohen, and S. F. Sleva. Intern. J. Air Water Pollution, **6**, 75 (1962).
4. H. R. Williams and H. S. Mosher. J. Am. Chem. Soc. **76**, 2984 (1954).
5. T. Vrbaski and R. J. Cvetanovic. Can. J. Chem. **38**, 1063 (1960).
6. Y. K. Wei and R. J. Cvetanovic. Can. J. Chem. **41**, 913 (1963).
7. P. L. Hanst, E. R. Stephens, W. E. Scott, and R. C. Doerr. Atmospheric ozone–olefin reactions. The Franklin Institute, Philadelphia, Pa. 1958.
8. R. Griegee, G. Blust, and H. Zinke. Chem. Ber. **87**, 766 (1954).
9. P. S. Bailey, S. B. Manthia, and C. J. Abshire. J. Am. Chem. Soc. **82**, 6136 (1960).
10. J. J. Bufalini and A. P. Altshuller. Intern. J. Air Water Pollution, **7**, 769 (1963).
11. S. L. Kopczynski. Intern. J. Air and Water Pollution **8**, 107 (1964).
12. E. R. Stephens and W. E. Scott. Relative reactivities of various hydrocarbons in polluted atmospheres. *Presented at* the Research Conference on Motor Vehicle Exhaust Emissions and their Effects. University of Southern California. Dec. 5, 1961.
13. R. D. Cadle and C. Schadt. J. Am. Chem. Soc. **74**, 6002 (1952); J. Chem. Phys. **21**, 163 (1953).
14. S. W. Benson. The foundations of chemical kinetics. McGraw-Hill Book Co., New York. 1960. p. 287.

Can. J. Chem. Downloaded from www.nrcresearchpress.com by 210.87.254.40 on 09/05/12
For personal use only.

15. P. A. LEIGHTON. Photochemistry of air pollution. Academic Press, New York, N.Y. 1961. p. 159.
16. W. E. SCOTT, E. R. STEPHENS, P. L. HANST, and R. C. DOERR. Proc. Am. Petrol. Inst. Sect. III, **37**, 171 (1957).
17. E. A. SCHUCK, G. J. DOYLE, and N. Endow. Air pollution foundation, Rept. No. 31, San Marino, California. 1960.
18. T. VRBASKI and R. J. CVETANOVIC. Can. J. Chem. **38**, 1053 (1960).
19. B. E. SALTZMAN and N. GILBERT. Ind. Eng. Chem. **51**, 1415 (1959).

Can. J. Chem. Downloaded from www.nrcresearchpress.com by 210.87.254.40 on 09/05/12
For personal use only.

SYNTHESIS OF 1-ARYL SUBSTITUTED 9*H*-PYRIDO[3,4-*b*]INDOLES

W. A. SKINNER AND R. M. PARKHURST
Department of Pharmaceutical Chemistry, Stanford Research Institute, Menlo Park, California
Received March 12, 1965

ABSTRACT

A series of 1-aryl substituted 9*H*-pyrido[3,4-*b*]indoles (1,2,3,4-tetrahydro-β-carbolines) were synthesized by cyclization of tryptamine with a number of substituted benzaldehydes in the presence of hydrochloric acid. Four modifications of reaction conditions were found necessary in order to obtain the desired products containing a variety of substituents on the 1-aryl group. Nuclear magnetic resonance spectra of the products enabled definitive assignment of structure.

Can. J. Chem. Downloaded from www.nrcresearchpress.com by 210.87.254.42 on 09/05/12
For personal use only.

A number of naturally occurring β-carboline derivatives having marked physiological effects are known. Among these are harmine, harmaline, and tetrahydroharmine. A review of the synthetic methods and biological activities of these compounds was recently published (1). The psychotomimetic activity of harmine appears to be less than that of the crude extract *B. caapi* (2) leading to the suggestion that harmaline and 1,2,3,4-tetrahydroharmine may also have this type of activity (3). Yohimbine, which caused anxiety in humans (4), also contains the 1,2,3,4-tetrahydroharmine moiety.

Only a few references to the synthesis of 1-aryl-9*H*-pyrido[3,4-*b*]indoles (1-aryl-1,2,3,4-tetrahydro-β-carbolines) appear in the literature. However, quite a number of 1-alkyl-1,2,3,4-tetrahydro-β-carbolines have been reported as well as some 1-benzyl derivatives. Recently, Taborsky and McIsaac (5) reported the synthesis of some 9*H*-pyrido[3,4-*b*]indoles. None of these derivatives were 1-aryl substituted, however. Some exhibited a significant effect on the conditioned behavioral response rates of rats. A series of 6-acetyl-1,2,3,4-tetrahydro-β-carbolines were synthesized by von Strandtmann, Puchalski, and Shavel (6). The only 1-aryl derivative of this group was the phenyl-substituted compound. Protiva, Vejdělek, and Rajsner (7) reported the synthesis of 1-(3′-methoxyphenyl)-1,2,3,4-tetrahydro-β-carboline; 1-(4′-methoxyphenyl)-1,2,3,4-tetrahydro-β-carboline and 1-(4′-dimethylaminophenyl)-1,2,3,4-tetrahydro-β-carboline from the corresponding Schiff bases.

We wish to report the synthesis of a series of substituted 1-aryl-1,2,3,4-tetrahydro-β-carbolines (Table I) utilizing modifications of the Pictet and Spengler reaction (8). It was necessary to use four different reaction conditions for cyclization of tryptamine to the desired compounds.

Attempts to prepare the tetrahydro-β-carbolines from syringaldehyde and tryptamine by methods I, III, and IV failed. During isolation, the lighter colored product darkened rapidly upon contact with air indicating that rapid air oxidation was occurring, probably involving the 4′-hydroxyl group. It is interesting that the *m*-hydroxyphenyl derivative, which cannot form a quinoidal structure, and the 3′-methoxy-4′-hydroxy-5′-nitro derivative, in which the hydroxyl group is hydrogen bonded to the adjacent nitro group, were obtained without difficulty. The 2′-hydroxyphenyl derivative was also obtained. Hydrogen bonding of the hydroxyl group with the 2-nitrogen of the β-carboline moiety is probably responsible for its stability.

Nuclear magnetic resonance spectra of this series of 1-aryl-1,2,3,4-tetrahydro-β-carbolines using an A-60 instrument and TMS as an internal reference were extremely

Can. J. Chem. Downloaded from www.nrcresearchpress.com by 210.87.254.42 on 09/05/12
For personal use only.

TABLE I

1-Aryl-1,2,3,4-tetrahydro-β-carbolines

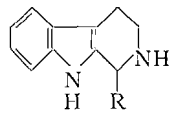

R	Formula	melting point °C	Yield, %	Analyses*			Prep. method
				% C	% H	% N	
Phenyl	$C_{17}H_{17}ClN_2$	267–270†	38	71.6 (71.7)	5.81 (6.02)	10.3 (9.85)	IV
m-Tolyl	$C_{18}H_{19}ClN_2$	248–251‡	40	72.4 (72.6)	6.36 (6.44)	—	IV
p-Tolyl	$C_{18}H_{19}ClN_2$	283–286	53	72.0 (72.3)	6.44 (6.40)	9.46 (9.38)	I
o-Hydroxyphenyl	$C_{17}H_{17}ClN_2O$	235–237	50	68.3 (68.1)	5.55 (5.72)	9.42 (9.32)	III
m-Hydroxyphenyl	$C_{17}H_{17}ClN_2O$	282–284	42	68.2 (68.1)	5.88 (5.72)	—	III
p-Methoxyphenyl	$C_{18}H_{19}ClN_2O$	283–285§	56	68.7 (68.7)	6.20 (6.08)	8.92 (8.90)	III
3,4-Dimethoxyphenyl	$C_{19}H_{21}ClN_2O_2$	295–297	75	66.3 (66.3)	6.39 (6.11)	8.22 (8.13)	IV
3,4-Methylenedioxyphenyl	$C_{18}H_{17}ClN_2O_2$	270–273	64	65.8 (66.0)	5.37 (5.21)	8.40 (8.54)	III
3,4,5-Trimethoxyphenyl	$C_{20}H_{23}ClN_2O_3$	270–273	16	64.1 (64.0)	6.04 (6.20)	7.44 (7.50)	III
4-Hydroxy-3-methoxynitrophenyl	$C_{18}H_{18}ClN_3O_4$	260(decomp.)	59	57.0 (57.5)	4.96 (4.83)	11.0 (11.2)	III
p-Nitrophenyl	$C_{17}H_{16}ClN_3O_2$	240–250 (decomp.)	91	62.1 (62.0)	4.96 (4.89)	12.6 (12.8)	III
4-Chloro-3-nitrophenyl	$C_{17}H_{15}Cl_2N_3O_2$	270(decomp.)	72	56.4 (56.1)	3.84 (4.15)	11.7 (11.6)	III
o-Chlorophenyl	$C_{17}H_{16}Cl_2N_2$	283	56	63.9 (64.0)	5.18 (5.06)	9.04 (8.77)	I
p-Chlorophenyl	$C_{17}H_{16}Cl_2N_2$	280–281	65	63.8 (64.0)	5.25 (5.06)	8.80 (8.77)	III
m-Fluorophenyl	$C_{17}H_{16}ClFN_2$	269–273	73	67.4 (67.3)	5.46 (5.35)	9.48 (9.30)	I
p-Fluorophenyl	$C_{17}H_{16}ClFN_2$	267–270	66	67.0 (67.3)	5.33 (5.35)	9.51 (9.30)	I
p-Bromophenyl	$C_{17}H_{16}BrClN_2$	290	14	56.0 (56.2)	4.60 (4.43)	7.56 (7.70)	III
4-Pyridyl	$C_{16}H_{15}N_3$	252‖	36	77.4 (77.1)	5.68 (6.06)	—	III
p-Dimethylamino	$C_{19}H_{21}N_3$	173–174‖¶	24	78.4 (78.3)	7.19 (7.27)	—	II

*Calculated values are given in parentheses for comparison.
†Literature m.p., 157–159° (free base) ref. 9.
‡The ortho derivative has been reported, ref. 10.
§Literature m.p., 273–274°, ref. 7.
‖Isolated as the free base.
¶Literature m.p., 168–169°, ref. 7.

valuable in assigning the tetrahydro-β-carboline structures to them. The absence of a band due to H—C=N at low field and the presence of a singlet 1H band at 5.00–5.20 τ assigned to the 1-position hydrogen indicated that the intermediate Schiff's base had closed to the tetrahydro-β-carboline structure. The 3,4-methylene triplets near 7 τ and the singlet NH at 8.10–8.56 τ strengthened this evidence for a saturated β-carboline ring. Addition of D_2O to the samples in the n.m.r. tubes resulted in a loss of the bands at 8.10–8.56 τ and 1.10–1.80 τ for the 9H pyrido and indole NH respectively.

EXPERIMENTAL

Method I. 1-(4'-Methylphenyl)-1,2,3,4-tetrahydro-β-carboline Hydrochloride

A mixture of 2 g (0.01 mole) of tryptamine hydrochloride, 1.2 g (0.01 mole) of 4-tolylaldehyde, and 25 ml of absolute ethanol was refluxed under nitrogen for 5 h. After this time, 0.1 ml of concentrated hydrochloric acid was added and refluxing was continued overnight. Upon cooling, a white precipitate was deposited, 1.57 g (53%), m.p. 283–286°, after recrystallization from ethanol–water; $\lambda_{max(\mu)}^{Nujol}$ 3.14 (indole NH); 6.20 (aryl); 12.2 (1,4-disubstituted benzene); 13.6 (1,2-disubstituted benzene).

The n.m.r. spectrum of the free base in $CDCl_3$ showed: NH (singlet, 1.80 τ); 8 φH (multiplet, 2.50–3.25 τ); CH (singlet, 5.20 τ); CH_2 (triplet, 7.05 τ); CH_2 (triplet, 7.30 τ); CH_3 (singlet, 7.75 τ); NH (singlet, 8.56 τ).

Method II. 1-(4'-Dimethylaminophenyl)-1,2,3,4-tetrahydro-β-carboline

A mixture of 1 g (0.005 mole) of tryptamine hydrochloride and 0.8 g (0.005 mole) of *p*-dimethylaminobenzaldehyde in 50 ml of ethanol containing a drop of concentrated hydrochloric acid was allowed to stand at room temperature for a week. The mixture was poured into excess aqueous ammonia to precipitate the product as the free base. Crystallization of the crude product from benzene – petroleum ether (b.p. 30–60°) afforded 350 mg (24%) of yellow colored platelets, m.p. 173–174°; $\lambda_{max(\mu)}^{Nujol}$ 3.15, 3.25 (indole NH and β-carboline NH); 6.18 (aryl); 6.55 (aryl); 12.2, 12.5 (1,4-disubstituted benzene); 13.3, 13.4, 13.6 (1,2-disubstituted benzene).

The n.m.r. spectrum of the free base in $CDCl_3$ showed: NH (singlet, 1.10 τ); 8 φH (multiplet, 2.50–3.25 τ); CH (singlet, 5.00 τ); CH_2 (triplet, 6.80 τ); $2CH_3$ (singlet, 7.10 τ); CH_2 (triplet, 7.20 τ); NH (singlet, 8.25 τ).

Method III. 1-(4'-Methoxyphenyl)-1,2,3,4-tetrahydro-β-carboline Hydrochloride

A solution of 2 g (0.01 mole) of tryptamine hydrochloride and 1.36 g (0.01 mole) of *p*-methoxy-benzaldehyde in 25 ml of ethanol containing 1 drop of concentrated hydrochloric acid and enough water to dissolve the tryptamine hydrochloride (5 drops) was refluxed overnight under nitrogen. Upon cooling, the product separated as colorless needles and was recrystallized from ethanol–water, 1.75 g (56)%, m.p. 283–285°; $\lambda_{max(\ )}^{Nujol}$ 3.05 (indole NH); 3.60–3.95 (NH^+); 6.12, 6.55 (aryl); 7.95 (C—O); 9.63 (C—O—C); 12.0 (1,4-disubstituted benzene); 13.5 (1,2-disubstituted benzene).

The n.m.r. spectrum of the free base in $CDCl_3$ showed: NH (singlet, 1.5 τ), 8 φH (multiplet, 2.40–3.30 τ); CH (5.10 τ); CH_3O (6.33 τ); CH_2—CH_2 (6.8–7.4 τ); NH (8.40 τ).

Method IV. 1-(3',4'-Dimethoxyphenyl)-1,2,3,4-tetrahydro-β-carboline

A mixture of 2 g (0.01 mole) of tryptamine hydrochloride, 1.66 g (0.01 mole) of veratraldehyde, 25 ml of ethanol, 0.5 ml of water, 1 drop of concentrated hydrochloric acid, and 10 ml of benzene was refluxed and the water was removed by azeotropic distillation. Upon cooling the product, 2.6 g (75%) of colorless needles precipitated. Recrystallization from ethanol–water afforded an analytical sample, m.p. 295–297°; $\lambda_{max(\mu)}^{Nujol}$ 3.00 (indole NH); 6.30, 6.66 (aryl); 8.80 (C—O—C); 12.5 (1,2,4-trisubstituted benzene); 13.5 (1,2-disubstituted benzene).

The n.m.r. spectrum of the free base showed: NH (singlet, 1.35 τ); 7 φH (multiplet, 2.20–3.20 τ); CH (singlet, 5.05 τ); OCH_3 (singlet, 6.25 τ); OCH_3 (singlet, 6.40 τ); CH_2 (multiplet, 6.90 τ); CH_2 (multiplet, 7.20 τ); NH (singlet, 8.10 τ).

REFERENCES

1. D. F. Downing. Quart. Rev. London, **16**, No. 2, 133 (1962).
2. H. H. Pennes and P. H. Hoch. Am. J. Psychiatry, **113**, 887 (1957).
3. F. A. Hochstein and A. M. Paradies. J. Am. Chem. Soc. **79**, 5735 (1957).
4. G. Holmberg and S. Gershon. Psychopharmacologia, **2**, 93 (1961).
5. R. G. Taborsky and W. M. McIsaac. J. Med. Chem. **7**, 135 (1964).
6. M. von Strandtmann, C. Puchalski, and J. Shavel. J. Med. Chem. **7**, 141 (1964).
7. M. Protiva, Z. J. Vejdělek, and M. Rajsner. Collection Czech. Chem. Commun. **28**, 629 (1963).
8. A. Pictet and T. Spengler. Ber. **44**, 2030 (1911).
9. M. Protiva, J. O. Jílek, E. Hachová, L. Novák, Zdenk, J. Vejdělek, and E. Adlerova. Chem. Listy, **51**, 1915 (1957).
10. S. Wawzonek and G. E. Nelson. J. Org. Chem. **27**, 1377 (1962).

Can. J. Chem. Downloaded from www.nrcresearchpress.com by 210.87.254.42 on 09/05/12
For personal use only.

Can. J. Chem. Downloaded from www.nrcresearchpress.com by 210.87.254.105 on 09/05/12
For personal use only.

α-DEUTERIUM KINETIC ISOTOPE EFFECTS IN SOLVOLYSES OF *endo*-NORBORNYL *p*-BROMOBENZENESULFONATE

C. C. LEE AND EDWARD W. C. WONG[1]

Department of Chemistry, University of Saskatchewan, Saskatoon, Saskatchewan

Received February 12, 1965

ABSTRACT

endo-Norbornyl-2-*d* *p*-bromobenzenesulfonate was synthesized and the isotope effects, as measured by k_H/k_D, were determined over a range of temperatures for solvolyses in 30% water – 70% dioxane, acetic acid, and formic acid. Values of k_H/k_D are of the order of 1.20. The data appear to indicate slightly higher isotope effects as the solvents are changed from aqueous dioxane to acetic acid to formic acid, as well as somewhat higher isotope effects at lower temperatures. Possible mechanistic implications of these results are presented. Relative titrimetric acetolysis rates, k_{exo}/k_{endo}, at different temperatures, and enthalpies and entropies of activation for these acetolyses are evaluated and discussed.

INTRODUCTION

The difference in kinetic behaviors of the *endo*- and *exo*-isomers and the stereospecific nature of the products of solvolyses (1, 2), the great propensity for rearrangement (3), and the relatively recent controversy on the "equilibrating classical" or "nonclassical" structure of the norbornyl cation (4, 5) have led to intensive studies on the norbornyl (bicyclo[2.2.1]heptyl) system. Recently, the n.m.r. spectra of the norbornyl cation at various temperatures have been reported by Schleyer and co-workers (6, 7), who also adequately gave a list of the pertinent literature. Since solvolyses involving carbonium ion intermediates are known to give rise to secondary α-deuterium kinetic isotope effects (8), preliminary studies have been made (9) in an attempt to measure the kinetic isotope effects in the acetolyses of *endo*- and *exo*-norbornyl-2-*d* *p*-bromobenzenesulfonates. Because of internal returns (2, 10), which would lead to scrambling of the deuterium atom during acetolysis of the *exo*-isomer, it is difficult to interpret the overall kinetic results from solvolyses of *exo*-norbornyl-2-*d* *p*-bromobenzenesulfonate. The present paper reports more extensive measurements of α-deuterium kinetic isotope effects on the *endo*-system, the solvolyses of which are not complicated by internal returns.

RESULTS AND DISCUSSION

Reduction of norcamphor with lithium aluminium deuteride gave chiefly *endo*-norborneol-2-*d* which was converted to the *p*-bromobenzenesulfonate. The small amount (about 10%) of *exo*-isomer present was removed by selective solvolysis in aqueous acetone (3), pure *endo*-norbornyl-2-*d* *p*-bromobenzenesulfonate (I-*d*) being recovered. The n.m.r. spectrum of I-*d* showed that the absorption corresponding to the C-2 proton essentially disappeared (11) and deuterium analysis* indicated that it contained 0.94 D atoms per molecule.

The kinetics of solvolysis of *endo*-norbornyl *p*-bromobenzenesulfonate (I) and I-*d* at a number of temperatures were followed titrimetrically in 30% water – 70% dioxane (by volume), in glacial acetic acid (reagent grade, minimum 99.8% CH_3COOH), and in reagent grade 98–100% formic acid. The resulting first-order specific rate constants, together with the corresponding 95% confidence limits (standard deviation × 1.96), and the kinetic isotope effects as measured by k_H/k_D, are summarized in Table I.

[1]*Holder of a National Research Council of Canada Studentship, 1963–1964.*

By Josef Nemeth, Urbana, Illinois.

Can. J. Chem. Downloaded from www.nrcresearchpress.com by 210.87.254.105 on 09/05/12
For personal use only.

TABLE I

Isotope effects in solvolyses of *endo*-norbornyl and *endo*-norbornyl-2-*d* *p*-bromobenzenesulfonates

Hydrolysis in aqueous dioxane				Acetolysis				Formolysis			
Temp. (°C)	10^5k_H (s^{-1})	10^5k_D (s^{-1})	k_H/k_D	Temp. (°C)	10^5k_H (s^{-1})	10^5k_D (s^{-1})	k_H/k_D	Temp. (°C)	10^5k_H (s^{-1})	10^5k_D (s^{-1})	k_H/k_D
50.20	2.02±0.03	1.68±0.02	1.20	20.00	0.0152*	0.0125*	1.22	25.00	7.28±0.02	5.85±0.04	1.24
55.18	3.62±0.05	3.04±0.05	1.19	50.07	0.955±0.008	0.794±0.005	1.20	25.00	7.09±0.11	5.83±0.04	1.22
60.65	6.62±0.11	5.55±0.06	1.19	50.07	0.956±0.007	0.794±0.005	1.20	30.20	13.4±0.1	10.9±0.1	1.23
65.12	11.0±0.2	9.22±0.15	1.19	55.18	1.76±0.02	1.47±0.01	1.20	30.20	13.4±0.1	11.2±0.1	1.20
70.00	18.2±0.4	15.3±0.2	1.19	60.65	3.33±0.02	2.84±0.02	1.17	35.20	25.9±0.1	21.6±0.2	1.20
				65.14	5.81±0.05	4.92±0.05	1.18	35.20	26.2±0.4	21.8±0.1	1.20
				70.00	10.1±0.3	8.40±0.06	1.20				

*Extrapolated values.

Can. J. Chem. Downloaded from www.nrcresearchpress.com by 210.87.254.105 on 09/05/12
For personal use only.

While interpretations of secondary deuterium isotope effects are still of some controversy, a recent critical review has been presented by Halevi (12). Among the current hypotheses is one by Streitwieser (8, 13) who suggests that the α-deuterium kinetic isotope effect is largely due to "the decrease in a bending force constant from a starting tetrahedral C—H bending vibration to the generally lower out-of-plane bending motion in the transition state leading to the carbonium ion" (8). For a reaction involving an isolated carbonium ion, the α-deuterium kinetic isotope effect was estimated to be about 1.4 (13). The generally smaller observed effect of about 15% rate retardation per α-deuterium atom for reactions such as acetolysis is postulated as attributable to the nearby leaving group in the transition state, which impedes the out-of-plane bending motion of the C—H bond (8, 13), and possibly also to the electron-releasing inductive effect of deuterium (12, 14). For a direct displacement reaction, the α-deuterium kinetic isotope effect virtually vanishes or becomes inverse. This again may be attributed to a combination of the inductive effect of deuterium and the further stiffening of the out-of-plane C—H bending motion by the presence of the entering group at the rear (8, 13).

The data in Table I indicate that solvolyses of I and I-*d* gave an isotope effect of about 1.20 which may be regarded as normal for an S_N1 or limiting solvolysis. For the different solvents employed, the differences in k_H/k_D were very small, although the results appear to suggest a tendency towards a higher isotope effect as the solvents are changed from aqueous dioxane to acetic acid to formic acid. A similar trend for k_H/k_D has been noted in solvolyses of 2-(Δ^3-cyclopentenyl)ethyl *p*-nitrobenzenesulfonate and its 1,1-dideuterio-analog when the solvent was changed from aqueous dioxane to acetic acid (15). If this trend is real, it could be regarded as support of Streitwieser's interpretation of the α-deuterium kinetic isotope effect that, in a solvent such as formic acid, the leaving group would have receded farther from the developing carbonium ion in the transition state and would impede the out-of-plane C—H bending motion to a lesser extent, thus resulting in a higher k_H/k_D, nearer to the calculated value of 1.4 per α-deuterium atom.

The influence of varying temperature on the isotope effects recorded in Table I is very slight. The data, however, do appear to indicate somewhat higher isotope effects for lower temperatures. Leffek, Robertson, and Sugamori (16) have treated temperature effects by plotting log (k_H/k_D) against reciprocals of absolute temperature, and from the slope and intercept, $\Delta\Delta H^{\ddagger}$ (i.e. $\Delta H_D^{\ddagger} - \Delta H_H^{\ddagger}$) and $\Delta\Delta S^{\ddagger}$ (i.e. $\Delta S_D^{\ddagger} - \Delta S_H^{\ddagger}$) were evaluated. Although the precision of the present data likely may not be as high as that attained by Robertson's group, if the present results are calculated with the inclusion of one extra figure and the temperature effects are treated by the method of Leffek and co-workers, the values of $\Delta\Delta H^{\ddagger}$ and $\Delta\Delta S^{\ddagger}$ obtained appear to suggest that the rate retardation by α-deuterium substitution may be regarded as largely due to differences in enthalpy of activation (9, 15). This observation would be consistent with the assumption that differences in zero point energies contribute mainly to α-deuterium kinetic isotope effects (13).

Aside from the isotope effect considerations, it is of interest to compare the kinetic data for acetolysis of *endo*-isomer I (k_H, acetolysis, Table I) with the rates obtained previously (9) from acetolysis of *exo*-norbornyl *p*-bormobenzenesulfonate (II). The specific rate constants for the acetolysis of II at various temperatures are given in Table II. The activation parameters for these acetolyses, summarized in Table III, indicate that differences in rate may be largely attributable to a difference in enthalpy of activation. Professor H. C. Brown (17) has informed us that his group has also noted that the entropies of activation for the acetolyses of *endo*- and *exo*-isomers I and II do not differ very significantly, and that this would not be in agreement with expectation if anchimeric assistance

TABLE II

Specific rate constants from acetolysis of *exo*-norbornyl *p*-bromobenzenesulfonate

Temp. (°C)	$10^5 k_H$ (s^{-1})
20.00	4.94±0.05
20.00	5.00±0.02
24.85	9.52±0.05
30.02	18.6±0.1
35.00	34.1±0.1
50.00	195*

*Extrapolated value.

TABLE III

Activation parameters calculated for acetolysis of *endo*-norbornyl *p*-bromobenzenesulfonate (I) at 50 °C and of *exo*-norbornyl *p*-bromobenzenesulfonate (II) at 20 °C

	ΔH^* (kcal/mole)	ΔS^* (cal/deg mole)
endo-I	25.3±0.4	−3.5±1.2
exo-II	22.3±0.1	−2.0±0.3

were associated with a higher entropy of activation (18) and if anchimeric assistance were taking place in the acetolysis of *exo*- but not *endo*-norbornyl *p*-bromobenzenesulfonate. However, Professor Winstein (19) has pointed out that entropies of activation as a criterion of anchimeric assistance have been used only *empirically* in 2-arylethyl systems (18) and that this application does not necessarily have to include the norbornyl system.

Professor Brown (17) also drew attention to the fact that relative rates calculated from k_H for acetolyses of I and II (Tables I and II) appear to be less than the well-known value of k_{exo}/k_{endo} of 350 at 25 °C reported by Winstein and co-workers (20). The latter value was based on rate constants at 25 °C calculated from experimental results obtained at two other temperatures. When the kinetic data from the present studies were extrapolated to 20 °C for the acetolysis of the *endo*-isomer I and to 50 °C for the *exo*-isomer II, the relative rate obtained for k_{exo}/k_{endo} was 330 at 20 °C but was only about 200 at 50 °C. The lower value at the higher temperature is, of course, attributable to the differences in activation parameters for the acetolyses of I and II (Table III), the predominance of a greater enthalpy of activation for the *endo*-isomer I being responsible for a proportionally greater rise in its rate constant as the temperature is increased. When this temperature effect and small differences in experimental conditions (the chief of which may be the fact that acetolyses in the present work were carried out in commercially obtained glacial acetic acid while Winstein and coworkers used anhydrous acetic acid containing about 0.2% acetic anhydride prepared from glacial acetic acid, potassium acetate, and acetic anhydride (21)) are taken into consideration, it is not surprising that absolute values of rate constants may be somewhat different. It is believed that the present results constitute a self-consistent set of data and that the relative rate of 330 for k_{exo}/k_{endo} calculated for 20 °C is in substantial agreement with the reported relative titrimetric acetolysis rates of Winstein and co-workers.

Can. J. Chem. Downloaded from www.nrcresearchpress.com by 210.87.254.105 on 09/05/12
For personal use only.

EXPERIMENTAL

endo-Norbornyl-2-d p-Bromobenzenesulfonate (I-d)

Reduction of 27.0 g (0.25 mole) of norcomphor by 3.0 g (0.071 mole) of lithium aluminium deuteride in anhydrous ether in the usual manner gave 26.5 g (96%) of norborneol-2-*d*, m.p. 148–149 °C. The alcohol was converted to the *p*-bromobenzenesulfonate which was selectively solvolyzed in 25% water – 75% acetone at 45 °C for 15 min (3). Titration of the *p*-bromobenzenesulfonic acid liberated indicated the presence of 10% *exo*-isomer. Pure *endo*-norbornyl-2-*d* *p*-bromobenzenesulphonate, m.p. 62–63 °C, was recovered in 83% yield after the selective solvolysis.

Kinetic Measurements

All reaction kinetics were followed titrimetrically. The procedures used for hydrolysis in 30% water – 70% dioxane and for acetolysis were as described earlier in analogous studies with 2-(Δ^3-cyclopentenyl)ethyl and related systems (15). For formolysis, titrations were carried out according to the method of Winstein and Heck (18). The initial concentration of I or I-*d* in all experiments was 0.0500 *M*. At each reaction temperature, corresponding protio- and deuterio-analogs were solvolysed simultaneously to minimize possible variations between experiments. The specific rate constants and the activation parameters were calculated from the slopes of least squares plots of the appropriate data (15), with the aid of a digital computer.*

ACKNOWLEDGMENT

The financial support given by the National Research Council of Canada is gratefully acknowledged.

REFERENCES

1. S. WINSTEIN and D. S. TRIFAN. J. Am. Chem. Soc. **74**, 1147 (1952).
2. S. WINSTEIN and D. S. TRIFAN. J. Am. Chem. Soc. **74**, 1154 (1952).
3. J. D. ROBERTS, C. C. LEE, and W. H. SAUNDERS, JR. J. Am. Chem. Soc. **76**, 4501 (1954).
4. H. C. BROWN. *In* The transition state. Chem. Soc. London Spec. Publ. No. 16. 1962. pp. 140–158; 175–178.
5. S. WINSTEIN. J. Am. Chem. Soc. **87**, 381 (1965).
6. P. VON R. SCHLEYER, W. E. WATTS, R. C. FORT, JR., M. B. COMISAROW, and G. A. OLAH. J. Am. Chem. Soc. **86**, 5679 (1964).
7. M. SAUNDERS, P. VON R. SCHLEYER, and G. A. OLAH. J. Am. Chem. Soc. **86**, 5680 (1964).
8. A. STREITWIESER, JR. Solvolytic displacement reactions. McGraw-Hill Book Co., New York. 1962. pp. 172–175.
9. C. C. LEE and E. W. C. WONG. J. Am. Chem. Soc. **86**, 2752 (1964).
10. S. WINSTEIN and K. C. SCHREIBER. J. Am. Chem. Soc. **74**, 2165 (1952).
11. E. W. C. WONG and C. C. LEE. Can. J. Chem. **42**, 1245 (1964).
12. E. A. HALEVI. *In* Progress in physical organic chemistry. Vol. 1. *Edited by* S. G. Cohen, A. Streitwieser, Jr., and R. W. Taft. Interscience Publishers, New York. 1963. pp. 101–221.
13. A. STREITWIESER, JR., R. H. JAGOW, C. R. FAHEY, and S. SUZUKI. J. Am. Chem. Soc. **80**, 2326 (1958).
14. A. STREITWIESER, JR. and H. S. KLEIN. J. Am. Chem. Soc. **85**, 2759 (1963).
15. C. C. LEE and E. W. C. WONG. Tetrahedron, **21**, 539 (1965).
16. K. T. LEFFEK, R. E. ROBERTSON, and S. E. SUGAMORI. Can. J. Chem. **39**, 1989 (1961).
17. H. C. BROWN. Private communications.
18. S. WINSTEIN and R. HECK. J. Am. Chem. Soc. **78**, 4801 (1956).
19. S. WINSTEIN. Discussion at the Symposium on Reactive Intermediates in Organic Chemistry, The Chemical Institute of Canada, held at Laval University, Quebec, August 27–29, 1964.
20. S. WINSTEIN, B. K. MORSE, E. GRUNWALD, H. W. JONES, J. CORSE, D. TRIFAN, and H. MARSHALL. J. Am. Chem. Soc. **74**, 1127 (1952).
21. S. WINSTEIN, E. GRUNWALD, and L. L. INGRAHAM. J. Am. Chem. Soc. **70**, 821 (1948).

**All computer programming were kindly worked out by Professor N. Sklov of the Mathematics Department.*

Can. J. Chem. Downloaded from www.nrcresearchpress.com by 210.87.254.105 on 09/05/12
For personal use only.

FORMATION OF *O*-β-D-GLUCOPYRANOSYL- AND *O*-β-D-GALACTOPYRANOSYL-MYO-INOSITOLS BY GLYCOSYL TRANSFER[1]

P. A. J. GORIN, K. HORITSU,[2] AND J. F. T. SPENCER
National Research Council of Canada, Prairie Regional Laboratory, Saskatoon, Saskatchewan

Received February 2, 1965

ABSTRACT

Enzyme extracts or growing cells of *Sporobolomyces singularis* catalyzed glycosyl transfer from cellobiose or lactose to polyhydroxylic acceptors. The substituted hydroxyl, in each instance, had hydroxylic neighbors which appeared to have a role in the reaction. To show whether the pyranoid ring oxygen of glycosyl acceptors has an effect on the reaction, the substitution positions on pyranoid and myo-inositol acceptors are compared. Glucosyl transfer to the 1- and 5-positions of (1R)-myo-inositol[3] and galactosyl transfer to the 5-position occurs. The configuration of hydroxyl groups adjacent to the position substituted is the same in these products as in the corresponding pyranoid derivatives. The pyranoid ring oxygen, therefore, has little effect on the glycosyl transfer reactions.

Formation of disaccharides by transfer of β-galactopyranosyl residues from lactose to carbohydrate acceptors using growing cultures and enzyme extracts of *Sporobolomyces singularis* has been observed. When cellobiose was used in place of lactose, analogous β-glucopyranosyl transfer took place. The substituted position in the polyhydroxylic acceptor generally had a vicinal hydroxyl and it was postulated that one or more of these participated in the reaction by interaction in the transitory enzyme–substrate complex (2). In most cases the glycosyl transfer was stereospecific so that virtually only one product was formed. In acceptors containing four consecutive hydroxyl groups such as D-galactose, D-fucose, and L-arabinose the 3-positions were substituted (D-arabinose and L-fucose were poor acceptors). The 3-positions of D-glucose (using enzyme extract), 6-deoxy-D-glucose, and D-xylose were also substituted.

The reaction involved in glycosyl transfer is complex and groups in the acceptor other than neighboring hydroxyls could be involved in the enzyme–substrate complex. To establish the role of the pyranoid oxygen, if any, in the reaction, myo-inositol was tested as an acceptor. If the oxygen atom had no effect the myo-inositol molecule should be substituted in the 1- and (or) 5-positions which are similar, in respect to the configuration of the neighbouring hydroxyl groups, to the 3-positions of D-galactose and D-glucose (and configurationally similar pyranose sugars) respectively.

The products of transfer from lactose to myo-inositol in growing cultures of *Sporobolomyces singularis* were therefore examined. A mixture of galactosyl and galactobiosyl inositols was formed and the galactosyl inositol portion was isolated by chromatography. The total fraction was methylated and then hydrolyzed, and the derived penta-*O*-methyl myo-inositols were examined by gas phase chromatography (g.l.c.) (3). 1,2,3,4,6-Penta-*O*-methyl myo-inositol (74%; V) derived from 5-*O*-β-D-galactopyranosyl myo-inositol (I) was the main product and was kindly identified by Prof. C. E. Ballou.[4] Other fragments corresponded to the (1S)-1,2,4,5,6-isomer (IV) and (or) its enantiomer (3%) and other isomers (23%). 5-*O*-β-D-Galactopyranosyl myo-inositol was isolated in 23% yield (based

[1]*Issued as N.R.C. No. 8468.*
[2]*National Research Council of Canada Postdoctorate Fellow, 1963–1964.*
[3]*The prefixes 1S and 1R are according to the nomenclature used by Angyal and Gilham (1).*
[4]*By g.l.c. 1,2,3,4,6-penta-O-methyl myo-inositol was identified as a partial methylation product of 1,3,4,6-tetra-O-methyl myo-inositol since the other product, the 1,3,4,5,6-isomer, could be prepared from 1,4,5,6-tetra-O-methyl myo-inositol (3).*

Can. J. Chem. Downloaded from www.nrcresearchpress.com by 210.87.254.42 on 09/05/12
For personal use only.

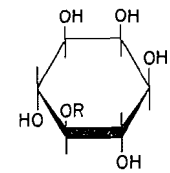

(I) R = D- Galp
(II) R = D- Gp

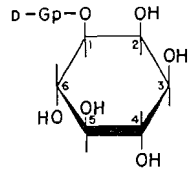

III

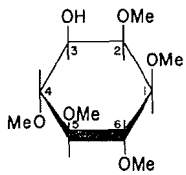

IV

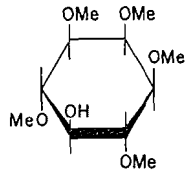

V

on lactose) by crystallization of the galactosyl inositol fraction. A methylation experiment similar to that described above provided methylated fragments corresponding to methyl 2,3,4,6-tetra-*O*-methyl $\alpha\beta$-galactoside and penta-*O*-methyl myo-inositols (g.l.c.). The cyclitol portion consisted of the 1,2,3,4,6-isomer (91%) and the (1S)-1,2,4,5,6-isomer and (or) its enantiomer (9%).

Transfer of β-D-galactopyranosyl residues to myo-inositol in the presence of enzyme extract from *Sporobolomyces singularis* cells was also followed. In contrast with growing cultures the glucose liberated from lactose was not utilized. This hexose competed with myo-inositol and reduced the yields of galactosyl and galactobiosyl inositols. Analyses by g.l.c. of penta-*O*-methyl myo-inositols formed on methylation of the original reaction mixture followed by hydrolysis were obtained. Examination at intervals up to 24 h showed that only the 1,2,3,4,6-isomer was formed, and that 5-linked myo-inositol residues were present.

Transfer of β-glucopyranosyl units from cellobiose to myo-inositol was also studied in growing cultures of *Sporobolomyces singularis* and using enzyme extracts from cells. The two main β-D-glucopyranosyl myo-inositols formed in growing cultures were isolated chromatographically and crystallized. The major component was 1-*O*-β-D-glucopyranosyl-(1R)-myo-inositol, which accounted for 38% of the glucosyl inositol fraction. Methylation gave a crystalline nona-*O*-methyl derivative. It was hydrolyzed in aqueous acid and the product was treated with methanolic hydrogen chloride. The resulting mixture was examined by g.l.c. and contained materials corresponding to methyl 2,3,4,6-tetra-*O*-methyl $\alpha\beta$-glucoside and a penta-*O*-methyl myo-inositol, identified after crystallization as the 1S-1,2,4,5,6-isomer[5] (IV) (4). Because of the presence of the minor glucosyl transfer product, 5-*O*-β-D-glucopyranosyl myo-inositol (II), the mixture of penta-*O*-methyl myo-inositols obtained on hydrolysis of the permethylated product, prior to its crystallization, contained 16% of the 1,2,3,4,6-isomer (V). This glucosyl inositol crystallized as a monohydrate in 18% yield based on the total glucosyl inositol fraction and was also characterized by methylation followed by hydrolysis. The fragments corresponded on g.l.c. to methyl 2,3,4,6-tetra-*O*-methyl $\alpha\beta$-glucoside and 1,2,3,4,6-penta-*O*-methyl myo-inositol, the latter being isolated and crystallized after silicic acid chromatography.

[5]*Its specific rotation of −18° was less than that of −3.5° reported for the product derived from galactinol (4). However, repetition of the galactinol experiment showed the former value to be correct.*

Can. J. Chem. Downloaded from www.nrcresearchpress.com by 210.87.254.42 on 09/05/12
For personal use only.

A small portion of the mixture of β-glucopyranosyl myo-inositols formed on glucosyl transfer was methylated. Hydrolysis of the permethylated product followed by methanolysis provided methyl 2,3,4,6-tetra-*O*-methyl αβ-glucoside and penta-*O*-methyl myo-inositols. The cyclitol mixture was examined by g.l.c. and shown to consist of the 1,2,3,4,6-isomer (30%) and the (1S)-1,2,4,5,6-isomer and (or) its enantiomer (56%). In view of the good yield of 1-*O*-β-D-glucopyranosyl-(1R)-myo-inositol, (1S)-1,2,4,5,6-penta-*O*-methyl myo-inositol should be the predominant isomer in the mixture.

The configurations of the glucosidic linkages in II and III were confirmed as β since they were readily hydrolyzed by emulsin, a β-glucosidase. The configuration of galactosyl inositol (I) was shown to be β also by using Hudson's rules of isorotation (5). The $[M]_D$ of 5-*O*-β-D-galactopyranosyl myo-inositol should equal

$[M]_D$ of II − ($[M]_D$ of methyl-β-D-glucopyranoside − $[M]_D$ of methyl β-D-galactopyranoside),

and using known $[M]_D$ values this expression comes to −560°. This value corresponds to a specific rotation of −2° which is in agreement with the found value of 0°.

β-Glucosyl transfer proceeded more rapidly than the β-galactosyl transfer in a system containing cellobiose, myo-inositol and cell enzyme extract, scission of cellobiose being virtually complete after 30 min whereas complete scission of lactose took 6 h. The reaction was complex giving glucose in addition to glucosyl inositols. Several penta-*O*-methyl myo-inositols were formed on methylation of the reaction mixture followed by hydrolysis in aqueous acid. The ratios of these derivatives compared with tetra-*O*-methyl-D-glucose and their variations with reaction time are given in Fig. 1. These results show that 5-*O*-β-D-glucopyranosyl myo-inositol is formed most rapidly but later undergoes hydrolytic exchange to give, most likely, 1-*O*-β-D-glucopyranosyl (1R)-myo-inositol, which would be represented by (1S)-1,2,4,5,6-penta-*O*-methyl myo-inositol. Although the presence of the latter material is not proven it appears likely that it is formed predominantly, at least in early stages, by analogy with the reaction with growing cultures described earlier.

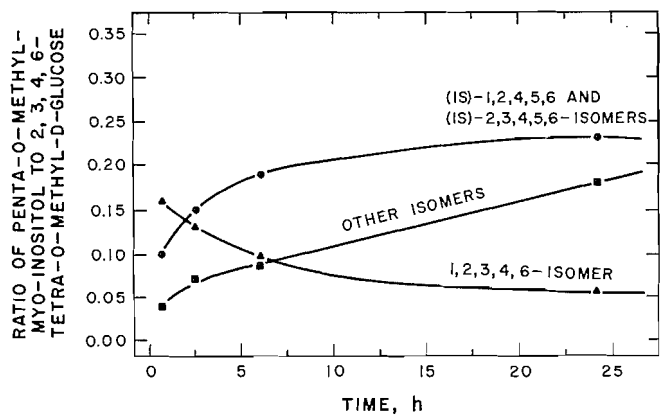

FIG. 1.

Transfer of β-galactosyl units to myo-inositol takes place preferentially at the 5-position which is configurationally analogous to the 3-positions of D-glucose, 6-deoxy-D-glucose, and D-xylose which have been shown to be prone to substitution (2). In contrast with the acceptors examined previously the products of galactosyl transfer differ from those of glucosyl transfer which are (1R)-1- and 5-substituted myo-inositol derivatives. The

Can. J. Chem. Downloaded from www.nrcresearchpress.com by 210.87.254.42 on 09/05/12
For personal use only.

(1R)-1-position is analogous to the 3-position of L-arabinose, which is similarly substituted in the glucosyl transfer reaction (2). These results show that the pyranoid oxygen has little effect on the transfer reactions, and in all likelihood does not have a role in forming the intermediate enzyme–substrate complex.

EXPERIMENTAL

Preparation of β-Glycopyranosyl myo-Inositols

1. 5-O-β-D-Galactopyranosyl myo-Inositol (I)

Culture conditions used are described in a previous publication (2). The products obtained by growth of *Sporobolomyces singularis* on medium (50 ml) containing 5% lactose and 2.5% myo-inositol were examined on paper chromatograms (solvent: acetone–water (4:1 v/v), dip method: silver nitrate – sodium hydroxide (6)). In addition to myo-inositol, spots with R_I 0.88 and 0.68 (R_I refers to the mobility of the compound on a paper chromatogram compared with myo-inositol) were detected. The new products were isolated by cellulose chromatography using acetone–water (5:1 v/v) as eluant. The material with R_I 0.88 was isolated (yield 0.76 g) and was crystallized twice from aqueous methanol. The galactosyl inositol (I) (0.57 g) had m.p. 248–252° and $[\alpha]_D^{25}$ 0° (*c*, 1.0, H_2O).

Anal. Calcd. for $C_{12}H_{22}O_{11}$: C, 42.1; H, 6.5. Found: C, 42.3; H, 6.5.

Hydrolysis with 1 *N* sulfuric acid at 100° gave galactose and myo-inositol as shown by paper chromatogtography.

The fraction having R_I 0.68 was isolated (yield 0.49 g) and was probably a galactobiosyl inositol since acid hydrolysis gave a higher proportion of galactose to inositol than the above galactosyl inositol(paper chromatograms).

A complete identification of the fraction with R_I 0.68 was not carried out.

2. 5-O- and 1-O-β-D-Glucopyranosyl-(1R)-myo-inositol (II and III Respectively)

The products from 50 ml of 5% cellobiose and 2.5% myo-inositol were examined and shown to consist of materials with R_I's 0.87 and 0.95. They were isolated by cellulose chromatography using acetone–water (6:1 v/v) as eluant. The material with R_I 0.95 (0.44 g) was crystallized from aqueous methanol to give a hydrated glucosyl inositol (II) (0.13 g; 5% yield) with m.p. 158–162° and $[\alpha]_D^{25}$ −20° (*c*, 1.0, H_2O).

Anal. Calcd. for $C_{12}H_{22}O_{11}.H_2O$: C, 40.0; H, 6.7. Found: C, 40.2; H, 6.7.

The fraction with R_I 0.87 (0.35 g) which was crystallized from aqueous methanol was also a glucosyl inositol (III; 0.27 g; 11% yield) and had m.p. 256–260° and $[\alpha]_D^{25}$ −17.5°. Anal. Calcd. for $C_{12}H_{22}O_{11}$: C, 42.1; H, 6.5. Found: C, 41.8; H, 6.5.

Compound II (10 mg) was dissolved in water (0.2 ml) and almond emulsin (2.5 mg) was added. Examination of the solution, at intervals, on a paper chromatogram (solvent: *n*-butanol–ethanol–water 40:11:19 v/v; spray: ammoniacal silver nitrate) showed that hydrolysis was almost complete after 30 min. Compound III was similarly hydrolyzed using identical proportions.

Method of Characterization of β-Glycopyranosyl myo-Inositols

These were methylated at room temperature by the sodium hydroxide – dimethyl sulfate procedure of Haworth (7). After destruction of dimethyl sulfate by heating at 100° the solutions were neutralized and extracted continuously for 3 d with chloroform. The extracts were further methylated with treatment for 4 d with silver oxide in refluxing methyl iodide (8). Hydrolysis for 24 h in 1 *N* hydrochloric acid at 100° converted the fully methylated products to a mixture of 2,3,4,6-tetra-*O*-methyl-D-hexose and penta-*O*-methyl myo-inositols. Full methylation was attained under the above conditions as shown by examination of the products on silica gel thin layer plates (solvent: chloroform–methanol 50:1 v/v; spray: 50% aqueous sulfuric acid at 130°). Tetra-*O*-methyl hexoses and penta-*O*-methyl myo-inositols ran at virtually the same rates, and complete methylation was shown by absence of slower moving spots. Treatment of the fragments with refluxing 5% methanolic hydrogen chloride for 3 h converted the hexose derivative to its αβ-methyl glycoside, thus rendering the mixture more readily separable by g.l.c. and silicic acid chromatography.

Gas phase chromatography was carried out using 2% neopentyl glycol succinate (3) on HMDS Chromosorb W (80–100 mesh) in a 5 ft × 1/4 in. o.d. copper tube at 143° and 160° with helium as carrier gas injected at 30 p.s.i. The g.l.c. unit was of conventional design using thermal conductivity detectors.

Identification of 1,2,3,4,6-penta-*O*-methyl myo-inositol (V) was kindly carried out by Prof. C. E. Ballou (see footnote 4 in the theoretical section). This compound had a different retention time from other penta-*O*-methyl myo-inositols (3).

Characterization of Total O-β-D-Galactopyranosyl myo-Inositols Formed on Glycosyl Transfer

Methylated fragments were obtained from a sample of the total galactosyl inositol fraction which was formed on glycosyl transfer from lactose to myo-inositol in growing culture. These were shown by g.l.c. to consist of methyl 2,3,4,6-tetra-*O*-methyl αβ-D-galactoside and a mixture of methylated inositols consisting of 1,2,3,4,6-penta-*O*-methyl myo-inositol (V; 74%), the (1S)-1,2,4,5,6-isomer (IV) and (or) its enantiomer (3%) and other isomers (23%).

Can. J. Chem. Downloaded from www.nrcresearchpress.com by 210.87.254.42 on 09/05/12
For personal use only.

Characterization of 5-O-β-D-Galactopyranosyl myo-Inositol (I)

Fractional crystallization of the *O*-β-D-galactopyranosyl myo-inositol mixture from aqueous methanol yielded compound I. A methylation experiment gave rise to methyl 2,3,4,6-tetra-*O*-methyl αβ-D-galactoside and 1,2,3,4,6-penta-*O*-methyl myo-inositol (91%), the (1S)-1,2,4,5,6-isomer and (or) its enantiomer (5%) and other isomers (4%). Three recrystallizations of the galactosyl inositol from aqueous methanol resulted in the formation of a less pure sample. The penta-*O*-methyl myo-inositols obtained consisted of 83% of the 1,2,3,4,6-isomer and 17% of the (1S)-1,2,4,5,6-isomer and (or) its enantiomer.

Characterization of Total O-β-D-Glucopyranosyl myo-Inositols Formed on Glycosyl Transfer

The mixture of glucosyl inositols was isolated by chromatography from the culture medium as described earlier in the experimental section. Methylation followed by hydrolysis and methanolysis yielded as the only products methyl 2,3,4,6-tetra-*O*-methyl αβ-D-glucoside and a mixture of penta-*O*-methyl myo-inositols consisting of the (1S)-1,2,4,5,6-isomer and (or) its enantiomer (56%), 1,2,3,4,6-isomer (30%), and other isomers (14%). The major methylated fraction, the (1S)-1,2,4,5,6-isomer was derived from 1-*O*-β-D-glucopyranosyl-(1R)-myo-inositol (III; R_I 0.87). This material was isolated crystalline in 38% yield from the total glucosyl inositol fraction.

Characterization of 5-O-β-D-Glucopyranosyl myo-Inositol (II; R_I 0.95)

Methylation (as before) of II (0.18 g) gave 0.16 g of fully methylated glucosyl inositol. This was hydrolyzed in aqueous acid and the product was treated with methanolic hydrogen chloride. The g.l.c. analysis showed that it contained as the only products methyl 2,3,4,6-tetra-*O*-methyl αβ-D-glucoside and 1,2,3,4,6-penta-*O*-methyl myo-inositol. The mixture was fractionated on silicic acid. Chloroform eluted the glycosides (70 mg) and chloroform–acetone (4:1 v/v) eluted the inositol derivative (57 mg). Two recrystallizations of the latter from *n*-hexane gave material (29 mg) with m.p. 85–86° and $[\alpha]_D^{25}$ 0° (*c*, 1.0, H_2O).

Anal. Calcd. for $C_6H_7O.(OCH_3)_5$: OCH_3, 62.0. Found: OCH_3 61.75.

Characterization of 1-O-β-D-Glucopyranosyl-(1R)-myo-Inositol (III; R_I 0.87)

Methylation of III (0.31 g) yielded 0.18 g of fully methylated glucosyl inositol, a small portion of which was hydrolyzed and the product treated with methanolic hydrogen chloride. The penta-*O*-methyl myo-inositols consisted of 84% of the (1S)-1,2,4,5,6-isomer and 16% of the 1,2,3,4,6-isomer. Crystallization from *n*-hexane yielded the nona-*O*-methyl ether (0.12 g) of the major glucosyl inositol with m.p. 95–98° and $[\alpha]_D^{25}$ −10° (*c*, 1.0, EtOH). Anal. Calcd. for $C_{21}H_{40}O_{11}$: C, 53.8; H, 8.6. Found: C, 54.1; H, 8.45.

Hydrolysis of the nona-*O*-methyl derivative (91 mg) followed by treatment with methanolic hydrogen chloride gave a mixture of methyl 2,3,4,6-tetra-*O*-methyl αβ-glucoside and a penta-*O*-methyl myo-inositol as shown by g.l.c. The latter was crystallized from *n*-hexane (yield 31 mg) and a further crystallization gave material with m.p. 111–114° and $[\alpha]_D$ −18° (*c*, 1.0, H_2O). Anal. Calcd. for $C_{11}H_{22}O_6$: C, 52.8; H, 8.9. Found: C, 53.2; H, 8.9.

The material gave an X-ray diffraction diagram identical with that of (1S)-1,2,4,5,6-penta-*O*-methyl myo-inositol (4). The material prepared in this laboratory in a similar manner from galactinol had $[\alpha]_D$ −19° (*c*, 0.8, H_2O).

Formation of Glycosyl Inositols Using Enzyme Extract from Sporobolomyces Singularis

To a mixture of lactose (2.5 g) and myo-inositol an extract (14 ml) from wet *Sporobolomyces singularis* cells (2) isolated from 250 ml of medium was added. The reaction mixture was examined at intervals up to 24 h on a paper chromatogram with acetone–water (4:1 v/v) as solvent. After 30 min only a small amount of galactosyl inositol had been formed, but after 6 h most of the lactose originally present had been utilized in forming galactose, glucose, galactosyl inositols (R_I 0.88), and galactobiosyl inositols (R_I 0.68). The reaction was also followed by methylation of portions of the mixture. The products, on hydrolysis with aqueous acid and examination by g.l.c., provided 1,2,3,4,6-penta-*O*-methyl myo-inositol as the only cyclitol derived from galactosyl and galactobiosyl inositols.

Greater complexity was observed in the reaction of cellobiose and myo-inositol. Paper chromatography showed that most of the cellobiose had been hydrolyzed after 30 min and that glucose and two glucosyl inositols with R_I 0.87 and 0.95 were formed. The relative amounts of penta-*O*-methyl myo-inositols formed on methylation followed by hydrolysis are shown in Fig. 1. The amount of penta-*O*-methyl myo-inositols is expressed as a ratio by comparison with the 2,3,4,6-tetra-*O*-methyl glucose formed simultaneously from glucose.

ACKNOWLEDGMENTS

The authors would like to thank Dr. H. G. Fletcher, Jr. for a sample of galactinol, and Prof. C. E. Ballou for authentic (1S)-1,2,4,5,6-penta-*O*-methyl myo-inositol. Thanks are also due to Mr. M. Mazurek for carrying out microanalytical determinations and Mr. N. R. Gardner for technical assistance.

Can. J. Chem. Downloaded from www.nrcresearchpress.com by 210.87.254.42 on 09/05/12
For personal use only.

REFERENCES

1. S. J. ANGYAL and P. T. GILHAM. J. Chem. Soc. 3691 (1957).
2. P. A. J. GORIN, J. F. T. SPENCER, and H. J. PHAFF. Can. J. Chem. **42**, 2307 (1964).
3. C. E. BALLOU and Y. C. LEE. Biochemistry, **3**, 682 (1964).
4. E. A. KABAT, D. L. MACDONALD, C. E. BALLOU, and H. O. L. FISCHER. J. Am. Chem. Soc. **75**, 4507 (1953).
5. C. S. HUDSON. Bur. Std. Sci. Papers, **21**, 241 (1926).
6. W. E. TREVELYAN, D. P. PROCTER, and J. S. HARRISON. Nature, **166**, 444 (1950).
7. W. N. HAWORTH. J. Chem. Soc. 8 (1915).
8. T. PURDIE and J. C. IRVINE. J. Chem. Soc. 1021 (1903).

Can. J. Chem. Downloaded from www.nrcresearchpress.com by 210.87.254.42 on 09/05/12
For personal use only.

Can. J. Chem. Downloaded from www.nrcresearchpress.com by 210.87.254.105 on 09/05/12
For personal use only.

REACTIVITIES IN PHOTOSENSITIZED OLEFIN OXIDATIONS

KARL R. KOPECKY AND HANS J. REICH
University of Alberta, Edmonton, Alberta

Received January 15, 1965

ABSTRACT

The rate of the methylene blue photosensitized oxidation of olefins increases in the order: 1-nonene < 4-methylcyclohexene < cyclohexene < 2,3-dimethyl-1-butene < 2-hexene < cyclopentene < 1-methylcyclohexene < 2,3-dimethylcyclohexene < 1-methylcyclopentene <1,2-dimethylcyclohexene < 2,3-dimethyl-2-butene. The last compound is oxidized 5 500 times as fast as cyclohexene. Comparison of this reactivity sequence with those obtained in other reactions confirms that the reactive intermediate in the photosensitized oxidations is electrophilic. The relative rates (k_A/k_B) of photo-oxidation of 1-methylcyclopentene (A) and of 1-methylcyclohexene (B) are 10 and do not vary significantly with five different sensitizers. Thus the same reactive intermediate, presumably singlet oxygen, is formed using each of the five sensitizers.

INTRODUCTION

The dye-photosensitized oxidation of olefins to allylic hydroperoxides has been studied extensively by Schenck and his co-workers (1). A shift of the double bond was reported always to take place. The reaction is stereospecific in cyclic systems (2) and has recently been used to advantage in several synthetic studies (3–5).

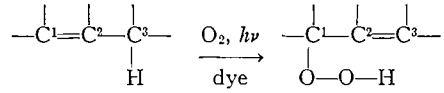

Two mechanisms for this transformation are currently popular.

Schenck, adapting a mechanism suggested by Schönberg (6) has proposed the following mechanism for the photosensitized oxidation of mono-olefins (1).

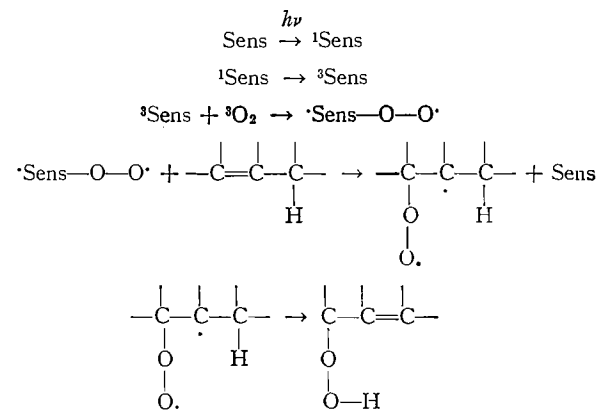

In this mechanism a sensitizer molecule (Sens) is excited by radiation (light absorbed only by the dye molecule is sufficient for reaction) to an excited singlet state which undergoes internal conversion to give the triplet (7). This reacts with oxygen to give a "diradical" adduct ('Sens—O—O'). The adduct reacts with an olefinic double bond, regenerating the sensitizer and forming a "diradical" adduct of oxygen and olefin. Hydrogen transfer then yields the allylic hydroperoxide.

Kautsky (8), and, more recently, Sharp (9) and Foote (10, 11) have suggested that the metastable $^1\Delta_g$ state of the oxygen molecule is the reactive intermediate involved in photosensitized oxidations.

$$^3\text{Sens} + {}^3\text{O}_2 \rightarrow \text{Sens} + {}^1\text{O}_2$$
$$^1\text{O}_2 + \text{olefin} \rightarrow \text{hydroperoxide}$$

Energy transfer from triplet sensitizer to triplet oxygen yields the ground state sensitizer and singlet oxygen, because of conservation of electron spin angular momentum during energy transfer (12, 13). Singlet oxygen then reacts with the olefin to produce the hydroperoxide.

In support of the second mechanism Foote (10) has shown that products identical to those formed in dye photosensitized photo-oxidations are produced when sodium hypochlorite is added to solutions containing hydrogen peroxide and an oxidizable substrate. Singlet oxygen has been observed spectroscopically when sodium hypochlorite was added to hydrogen peroxide (14–17). In addition, singlet oxygen generated by electrodeless discharge oxidizes anthracenes to the corresponding endoperoxides (18).

The rate of disappearance of the reactive intermediate in the sensitized oxidation of α-terpinene to ascaridole is independent of sensitizer used (19*a*). It has been suggested that a common intermediate is thus involved when different sensitizers are used (11). However, the activation energy for this reaction is only ca. 0.5 kcal/mole (19*a*), and the only conclusion one may safely make regarding any intermediates in these reactions is that they are all very reactive.

Schenck (19*b*) and Sharp (9) have measured the rate of sensitized oxidation of several olefins and found that increasing substitution of the double bond greatly increased reactivity. We report here similar reactivity studies but find that the response of the reactive intermediate to variation in olefin structure is much greater than that reported by Sharp but similar to that found by Schenck. We also compare the relative rates of photo-oxidation of olefins with the relative rates of their reactions with a number of free radicals and electrophiles. In addition, it is shown that the relative rates of photo-oxidation of two mono-olefins, a reaction which must proceed with activation energy (19*a*), does not vary with several sensitizers.

RESULTS AND DISCUSSION

Schenck's adduct would be expected to show radical reactivity while singlet oxygen

$$(:\ddot{O}{=}\ddot{O}: \leftrightarrow :\ddot{O}{-}\overset{\oplus}{\ddot{O}}:\overset{\ominus}{})$$

(9) may be electrophilic. A number of studies have been made in which the relative reactivities of a number of olefins toward a variety of reagents have been measured. A comparison of the relative reactivities of olefins of different structural types toward photosensitized oxidation and towards the other reagents can thus be made.

We have measured the relative rates of the photo-oxidation, sensitized by methylene blue, of a number of olefins. These were measured by oxidizing olefins in pairs, thus allowing them to compete for the reactive intermediate, and measuring the amounts of olefin remaining at various intervals by g.l.c. analysis. The relative rates are summarized in Table I along with the relative rates of the reactions of a variety of olefins with peracetic acid (20), phthaloyl peroxide (21), bromine (22), methyl radical (23), trifluoromethyl radical (24), and trichloromethyl radical (25, 26). The photo-oxidation reaction is seen to be extremely sensitive to structure. Indeed, the reactive intermediate involved is the most discriminating reagent of those listed in Table I. There is a close similarity in the

Can. J. Chem. Downloaded from www.nrcresearchpress.com by 210.87.254.105 on 09/05/12
For personal use only.

Can. J. Chem. Downloaded from www.nrcresearchpress.com by 210.87.254.105 on 09/05/12
For personal use only.

TABLE I

Relative reactivity of olefins towards various reagents

Olefin	Photo-oxidation	Peracetic acid[a]	Phthaloyl peroxide[b]	Bromine[c]	Methyl radical[d]	Trifluoromethyl radical[e]	Trichloromethyl radical[f]
Ethylene				1	1	1	
Alkylethylene	0.1[g]	0.032[i]	0.021[e]	2.03[i]	0.65[l]	1.4	4.2[n]
2-Methylpropene	1.7[h]	0.71		5.5	1.1	3.8	
cis-2-Butene		0.71[j]			0.1	1.3	
trans-2-Butene					0.2	1.3	
2-Hexene	9	0.76					
4-Methylcyclohexene	0.67						
Cyclohexene	1	1	1				1
Cyclopentene	16	1.51					3.3
1-Methylcyclohexene	45						
2-Methyl-2-butene		9.61	9.3	10.4			3.8
1-Methylcyclopentene	390	17.2	31.3				
1,2-Dimethylcyclohexene	29 00						
2,3-Dimethyl-2-butene	55 00	3 000[k]	100	14		1.2[m]	

[a]Reference 20.
[b]Reference 21.
[c]Reference 22.
[d]Reference 23.
[e]Reference 24.
[f]References 25, 26.
[g]1-Nonene.
[h]2,3-Dimethyl-1-butene.
[i]Propylene.
[j]Isomer not indicated.
[k]Estimated by Greene (27) from data collected by Swern (20).
[l]1-Decene.
[m]Calculated from data of ref. 28.
[n]1-Octene.

variation of rate with structure between the photosensitized oxidation of olefins and their reaction with peracetic acid, bromine, and phthaloyl peroxide. No such similarity exists at all between the rate of the photosensitized oxidation of olefins and the rate of addition of any of the radical reagents listed in Table I to olefins. Even the electrophilic trifluoromethyl radical (24) does not respond to structural changes in the manner that the reactive intermediate in the photosensitized oxidation reaction does. This intermediate thus has strong electrophilic character and does not exhibit any radical properties. It is quite unlikely that the intermediate has the structural features of the diradical described by Schenck (29). The reactivity is best explained by the suggestion (9–11) that singlet oxygen is the reactive intermediate.

Product formation is best described by the suggestion of Sharp (9) that an intermediate perepoxide is formed which rearranges with a concurrent proton shift to yield the allylic hydroperoxide (Chart I). However, our data do not provide evidence against a concerted cycloaddition as proposed by Nickon (30).

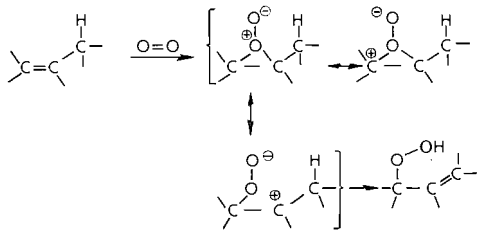

CHART I.

Sharp reports that the relative rates of tetraphenylporphine sensitized photo-oxidation of 1-hexene, 2-methyl-2-butene, and 2,3-dimethyl-2-butene are 1, 94, and 100, respectively. We find a much greater difference in reactivity with comparably substituted olefins, as does Schenck (19*b*). The relative rates of photo-oxidation of 1-nonene, 1-methylcyclohexene, 1-methylcyclopentene, and 2,3-dimethyl-2-butene are, from Table I, 1, 450, 3 900, and 55 000, respectively. The reason for this discrepancy is not clear. It is probably not due to a difference in sensitizer. The relative rates of photo-oxidation of 1-methylcyclohexene and 1-methylcyclopentene with a variety of sensitizers are listed in Table II and do not vary with sensitizer. It may be that Sharp's relative rates were measured indirectly. If so, the relative errors may have accumulated to yield the data reported.[1]

TABLE II

Effect of sensitizer on relative reactivities

Sensitizer	k_A/k_B*
Methylene blue	8.6±0.9
Eosin Y	10.8±1.4
Rose bengal	11.5±1.9
Erythrosin B	8.8±1.6
Hematoporphyrin	9.4±1.8

*A = 1-methylcyclopentene, B = 1-methylcyclohexene.

The oxidation reactions reported in this paper must have an activation energy significantly different from zero. The data of Table II therefore provide the first evidence that a common reactive intermediate is formed in oxidations involving different sensitizers.

[1]*A referee has pointed out that reactivity depends upon concentration, and that the descrepancies may be due to this factor.*

Can. J. Chem. Downloaded from www.nrcresearchpress.com by 210.87.254.105 on 09/05/12
For personal use only.

The activation energies of the rose bengal sensitized photo-oxidation of dicyclohexylidene and β-pinene are reported to be 1.3 and 4.5 kcal, respectively (19*a*). Dicyclohexylidene is thus about 700 times as reactive as β-pinene at 25°. This is in good agreement with the reactivity difference to be expected on the basis of the data in Table I.

EXPERIMENTAL

Preparation of Olefins

Cyclohexene (Eastman Kodak White Label), 2-hexene (Phillips 66 Pure Grade) and 4-methylcyclohexene (Eastman Kodak White Label) were distilled from lithium aluminium hydride. Pyrolysis of 1-nonylacetate yielded 1-nonene. The remaining olefins were obtained from the phosphoric acid catalyzed dehydration of the appropriate alcohols. The physical properties of those olefins obtained in the pure state were (boiling points in this study were obtained at 700 mm unless otherwise indicated and are uncorrected; the boiling points cited in the literature references are all for 760 mm unless otherwise indicated): cyclohexene b.p. 79–80°, n_D^{25} 1.4441 (reported (31) b.p. 82.9°, n_D^{25} 1.4438); cyclopentene b.p. 43°, n_D^{25} 1.4199 (reported b.p. 44° (32), n_D^{25} 1.4194 (33)); 1-methylcyclopentene b.p. 72–74°, n_D^{25} 1.4293 (reported (34) b.p. 75.8°, n_D^{20} 1.4330); 1-methylcyclohexene b.p. 106–107°, n_D^{25} 1.4478 (reported (31) b.p. 110°, n_D^{25} 1.4478); 4-methylcyclohexene b.p. 98–99°, n_D^{25} 1.4392 (reported (31) b.p. 102.7°, n_D^{25} 1.4389); 2-hexene b.p. 65–66°, n_D^{25} 1.3941 (reported for *cis*-2-hexene (35) b.p. 68.8°, n_D^{25} 1.3948; for *trans*-2-hexene (35) b.p. 67.8°, n_D^{25} 1.3907); 2,3-dimethyl-2-butene b.p. 70–71°, n_D^{25} 1.4098 (reported (35) b.p. 73°, n_D^{25} 1.4094); 1-nonene b.p. 61–62° at 48 mm, n_D^{25} 1.4136 (reported b.p. 33.5° at 11 mm (36), n_D^{25} 1.4133 (37)). These olefins were shown to be more than 97% pure by g.l.c. analysis.

Dehydration of 1,2-dimethylcylohexanol produced a mixture, shown by g.l.c. analysis to consist of 58% 1,2-dimethylcyclohexene, 37% 2,3-dimethylcyclohexene, and 5% of an unidentified compound. This mixture was used as such in the rate studies. The small amount of 2,3-dimethyl-1-butene, which was formed along with 2,3-dimethyl-2-butene upon dehydration of 2,3-dimethyl-2-butanol and which was used in the rate studies, was shown by g.l.c. analysis to contain 16% ether and 9% 2,3-dimethyl-2-butene as the only detectable impurities. The results obtained from these impure compounds fit well into the general pattern and are considered accurate enough for the present purpose.

Determination of Relative Reactivities of Olefins

Pairs of olefins were chosen for the competition reactions on the basis of suitable reactivity. Approximately equimolar amounts of the two olefins (0.5 to 2.0 ml), 1.0 ml of an internal standard (benzene, toluene, or ethylbenzene) and 30 mg of methylene blue were dissolved in 200 ml of redistilled methanol. The resulting solution was poured into an immersion photochemical reactor (38) just filling the annular space. A slow stream of oxygen was passed through the solution which was kept at 15 °C while it was being irradiated. The light source was a 200 W Hanovia mercury vapor lamp, type S, No. 654A. A filter sleeve, Hanovia No. 516-27-116 was used to cut off all radiation below 3 600 °A. Samples were withdrawn from the solution initially and at intervals, after mixing, during the irradiation until one component had decreased to about 10% of its original concentration. The samples were analyzed by g.l.c. using the internal standard method of Keulemans (39). A Wilkins Aerograph 202 gas chromatographic instrument was used with a 5 ft column packed with Apiezon M on 60–80 Chromosorb W which gave good separation between methanol and all the olefins. From the relative amounts of olefins remaining, the relative rate constants were calculated by the method of Ingold and Shaw (40). The results are summarized in Table III. The relative rates given represent the average of several determinations and the average errors are indicated. Control experiments showed that no olefin was consumed in the absence of light or in the absence of dye when the lamp was on for the time required for 90% oxidation of the more reactive component except in the case where 1-nonene was a

TABLE III

Relative rates of photosensitized oxidation of olefins

Expt. No.	Olefin A	Olefin B	k_B/k_A
1	1-Nonene	Cyclohexene	10*
2	4-Methylcyclohexene	Cyclohexene	1.5±0.2
3	Cyclohexene	2-Hexene	8.5±0.2
4	2-Hexene	Cyclopentene	1.8±0.4
5	Cyclopentene	2,3-Dimethylcyclohexene	3.0±0.1
6	1-Methylcyclohexene	2,3-Dimethylcyclohexene	1.07±0.03
7	1-Methylcyclohexene	1-Methylcyclopentene	8.6±0.9
8	1-Methylcyclopentene	1,2-Dimethylcyclohexene	7.5±0.7
9	1,2-Dimethylcyclohexene	2,3-Dimethyl-2-butene	1.9±0.2
10	Cyclohexene	2,3-Dimethyl-1-butene	1.7±0.4

*Estimated value. Oxidation of 1-nonene proceeded so slowly that evaporation losses became significant.

Can. J. Chem. Downloaded from www.nrcresearchpress.com by 210.87.254.105 on 09/05/12
For personal use only.

competitor. In another control experiment a solution containing 0.4 g of 2,3-dimethyl-3-hydro-peroxy-1-butene (41) and 1.0 g of 2,3-dimethyl-2-butene were photolyzed in the above apparatus. After 15 min 5% of the olefin had been consumed. Thirty mg methylene blue was added and the photolysis was continued. After 15 min 90% of the olefin had been consumed. The relative reactivities reported in Table II were determined in the manner described above using solutions made up from 2.0 ml ethylbenzene, 1.0 ml each of 1-methylcyclopentene and 1-methylcyclohexene, 30 mg of sensitizer, and 200 ml of distilled methanol.

ACKNOWLEDGMENT

This research was supported in part by a grant from the National Research Council.

REFERENCES

1. G. O. SCHENCK. Angew. Chem. **69**, 579 (1957).
2. A. NICKON and J. F. BAGLI. J. Am. Chem. Soc. **83**, 1498 (1961).
3. R. A. BELL and R. E. IRELAND. Tetrahedron Letters, No. 4, 269 (1963).
4. S. MASAMUNE. J. Am. Chem. Soc. **86**, 290 (1964).
5. A. NICKON and W. L. MENDELSON. J. Am. Chem. Soc. **85**, 1894 (1963).
6. A. SCHÖNBERG. Ann. **518**, 299 (1935).
7. G. N. LEWIS and M. KASHA. J. Am. Chem. Soc. **66**, 2100 (1944).
8. H. KAUTSKY and H. DE BRUIJN. Naturwiss. **19**, 1943 (1931).
9. D. B. SHARP. Abstracts, 138th National Meeting of the American Chemical Society, New York, N.Y. September, 1960. p. 79 P.
10. C. S. FOOTE and S. WEXLER. J. Am. Chem. Soc. **86**, 3879 (1964).
11. C. S. FOOTE and S. WEXLER. J. Am. Chem. Soc. **86**, 3880 (1964).
12. G. PORTER and M. R. WRIGHT. J. Chem. Phys. **55**, 705 (1958).
13. G. PORTER and M. R. WRIGHT. Discussions Faraday Soc. **27**, 18 (1959).
14. E. J. BOWEN and R. A. LLOYD. Proc. Chem. Soc. 305 (1963).
15. R. J. BROWNE and E. A. OGRYZLO. Proc. Chem. Soc. 117 (1964).
16. A. U. KHAN and M. KASHA. J. Chim. Phys. **39**, 2105 (1963).
17. S. J. ARNOLD, E. A. OGRYZLO, and H. WITZKE. J. Chem. Phys. **40**, 1769 (1964).
18. E. J. COREY and W. C. TAYLOR. J. Am. Chem. Soc. **86**, 3881 (1964).
19. (*a*) G. O. SCHENCK and E. KOCH. Z. Electrochem. **64**, 170 (1960). (*b*) G. O. SCHENCK, H. MERTENS, W. MÜLLER, E. KOCH, and O. P. SCHMIEMENZ. Angew. Chem. **68**, 303 (1956).
20. D. SWERN. J. Am. Chem. Soc. **69**, 1692 (1947).
21. F. D. GREENE and W. W. REES. J. Am. Chem. Soc. **80**, 3432 (1958).
22. S. V. ANANTAKRISHNANA and R. VENKATARAMAN. Chem. Rev. **33**, 27 (1943).
23. R. P. BUCKLEY and M. SZWARC. Proc. Roy. Soc. London, Ser. A, **240**, 396 (1957).
24. A. P. STEFANIC, L. H. HERK, and M. SZWARC. J. Am. Chem. Soc. **83**, 4732 (1961).
25. P. S. SKELL and A. Y. GARNER. J. Am. Chem. Soc. **78**, 5430 (1956).
26. C. WALLING. Free radicals in solution. John Wiley and Sons, Inc., New York, N.Y. 1957. p. 254.
27. F. W. GREENE and W. ADAM. J. Org. Chem. **29**, 136 (1964).
28. H. KOMAZAWA, A. P. STEFANIC, and M. SZWARC. J. Am. Chem. Soc. **85**, 2043 (1963).
29. G. O. SCHENCK, O.-A. NEUMULLER, and R. KOCH. Strahlentherapie, **114**, 321 (1961).
30. A. NICKON and J. F. BAGLI. J. Am. Chem. Soc. **83**, 1498 (1961).
31. F. D. ROSSINI *et al.* Selected values of chemical thermodynamic properties. U.S. Government Printing Office, Washington, D.C. 1955. p. 65.
32. A. I. VOGEL. J. Chem. Soc. 1323 (1938).
33. Reference 31, p. 64.
34. C. E. BOORD, A. L. HENNE, K. W. GREENLEE, W. L. PERILSTEIN, and J. M. DERFER. Ind. Eng. Chem. **41**, 609 (1949).
35. Reference 31, p. 55.
36. A. W. SCHMIDT, V. SCHOELLER, and K. EBERLEIN. Ber. **74**, 1314 (1941).
37. Reference 31, p. 52.
38. K. R. KOPECKY, G. S. HAMMOND, and P. A. LEERMAKERS. J. Am. Chem. Soc. **84**, 1015 (1962).
39. A. I. M. KEULEMANS. Gas chromatography. Reinhold Publishing Corp., New York, N.Y. 1957. p. 32.
40. C. K. INGOLD and F. R. SHAW. J. Chem. Soc. 2918 (1927).
41. G. O. SCHENCK and K. H. SCHULTE-ETTE. Ann. **618**, 185 (1958).

Can. J. Chem. Downloaded from www.nrcresearchpress.com by 210.87.254.105 on 09/05/12
For personal use only.

Can. J. Chem. Downloaded from www.nrcresearchpress.com by 210.87.254.42 on 09/05/12
For personal use only.

RAMAN SPECTRUM OF CRYSTALLINE AND LIQUID SO_2

A. Anderson and R. Savoie
Frick Chemical Laboratory, Princeton University, Princeton, New Jersey
Received February 8, 1965

ABSTRACT

The Raman spectrum of crystalline sulfur dioxide has been recorded at several temperatures between 9 and 185 °K. The main features are in accord with those predicted from the factor group analysis for the known structure of the crystal. Additional peaks were also observed, some arising from isotopic species and lattice fundamentals. As an aid to the assignment of several other bands, the spectrum of the liquid has also been recorded to distinguish the specifically crystalline features. Possible causes of these extra peaks, such as combinations with lattice modes, crystalline defects, and impurities, are briefly discussed.

INTRODUCTION

The infrared spectrum of solid SO_2 at liquid air temperature was first reported by Wiener and Nixon (1), and a somewhat more detailed investigation was independently published by Giguère and Falk (2). In both cases, extra peaks occurring close to the main bands were assigned as combination or difference bands involving lattice modes with frequencies of 10 to 25 cm^{-1}. The far infrared spectrum (20 to 400 cm^{-1}) recently measured (3) has shown, however, that these optically active lattice modes have much higher frequencies (67 to 160 cm^{-1}). In an attempt to clarify the situation, Raman spectra of the crystal at 9, 77, and 185 °K, and of the liquid at 225 °K have been recorded.

EXPERIMENTAL

The cryostats and techniques used to grow crystals for investigation at liquid helium and nitrogen temperatures in a Cary 81 Raman spectrophotometer have been described elsewhere (4). The spectrophotometer was calibrated with mercury vapor lines from the lamp, and the frequencies given below are estimated to be correct to ± 2 cm^{-1}. Anhydrous SO_2, from the Matheson Co., was used without further purification. This was stated to be 99.98% pure, and a mass spectrometric check showed only small traces of N_2 and CO_2.

It was remarkably easy to grow transparent crystals, 3 in. long and $\frac{1}{2}$ in. in diameter, around the cold finger of the Raman cryostat in about 30 min. Little cracking of these samples occurred on cooling to the temperatures of the refrigerants, and the resultant low Rayleigh scattering made it possible to scan as close as 30 cm^{-1} to the exciting line. Spectra were recorded with the crystal either immersed in liquid nitrogen or cooled by a flow of cold helium gas escaping from the main refrigerant chamber. In the latter case, the temperature measured by a calibrated carbon resistor embedded in the crystal was about 7 °K, rising to 9 °K when the tail section of the cryostat was placed inside the Toronto arc lamp.

The crystal at 185 °K and the liquid at 225 °K were obtained by condensing the gas in a simple cell inside a glass Dewar vessel, using a flow of cold nitrogen gas as coolant. The solid formed in this way was polycrystalline and highly scattering. Besides the observation of the frequency shifts with temperature, another purpose of this experiment was to see if there was any dependence of the spectrum on the crystalline quality. The Raman spectrum of the liquid has been measured previously (5), but in the present work, special emphasis was placed on the possible presence of the weaker bands observed in the solid.

RESULTS

A typical spectrum of the crystal, recorded at 9 °K, is shown in Fig. 1. There are four regions of interest, corresponding to the lattice vibrations (translational T, and librational R), bending mode (υ_2), symmetric stretch (υ_1), and asymmetric stretch (υ_3). Apart from shifts in frequency (more marked for the lattice modes) and the broadening of the lines, no significant changes are seen at 77 °K and 185 °K. The spectrum of the liquid at 225 °K is shown in Fig. 2. The observed frequencies of the three main peaks are in good agreement with those obtained by Gerding and Nijveld (5). Frequencies at maximum intensity

for both phases, together with the infrared data and possible assignments are listed in Table I. The spectral slit widths for the different regions scanned are shown in Figs. 1 and 2.

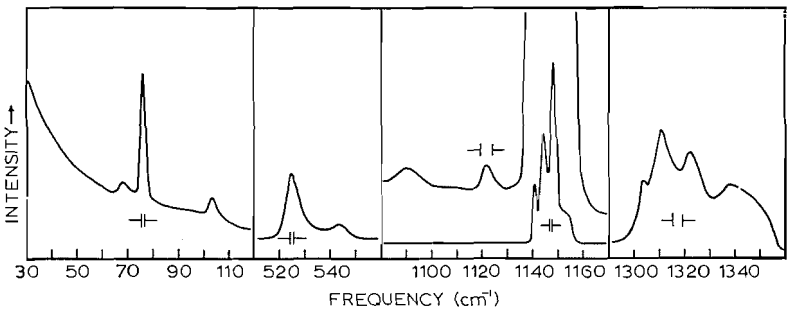

FIG. 1. Raman spectrum of crystalline SO_2 at 9 °K.

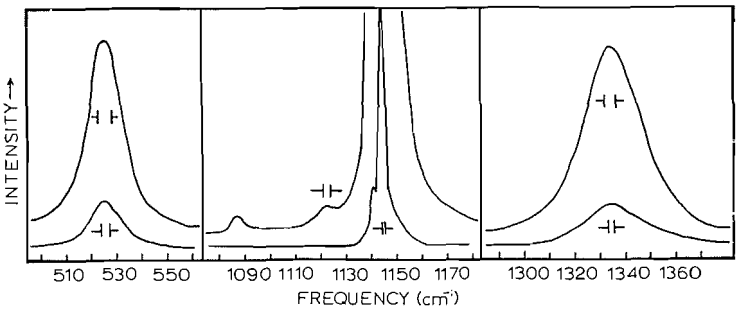

FIG. 2. Raman spectrum of liquid SO_2 at 225 °K.

DISCUSSION

Intramolecular Fundamentals

An X-ray diffraction study of a single crystal of sulfur dioxide (6) has shown the unit cell to be orthorhombic with space group C_{2v}^{17} (Aba), thus confirming earlier results obtained from powder diagrams (7). There are four molecules per unit cell (two per primitive cell) on sites of symmetry C_2. From this result, by usual group theoretical procedures (8, 9), it is easy to deduce the number of infrared and Raman components of the intramolecular and lattice modes, as shown in the correlation diagram, Fig. 3. It is seen that all of the observed infrared fundamental bands should have their Raman counterparts at the same frequencies. Comparison of the two spectra with the predictions from the factor group analysis shows only partial agreement. However, as will be shown, the extra features observed can be explained by effects other than the breakdown of the selection rules.

The doublet expected for ν_1 in Raman is nicely resolved at 1 144 and 1 148 cm^{-1} (the Raman frequencies referred to in the text are those at 77 °K for better comparison with the corresponding infrared values at 93 °K). The first component has exactly the same frequency as the singlet observed in the infrared (2). On the basis of this coincidence, the band at 1 144 cm^{-1} would belong to the A_1 species, although it is somewhat surprising that the one at 1 148 cm^{-1} is more intense, since completely symmetric modes are usually stronger in the Raman effect. In the other infrared study (1), the ν_1 peak is at 1 147 cm^{-1}, and this would support the alternative assignment $\nu_1(A_1)$ = 1 148 cm^{-1}. However, in

Can. J. Chem. Downloaded from www.nrcresearchpress.com by 210.87.254.42 on 09/05/12
For personal use only.

TABLE I

Molecular spectra of sulfur dioxide (frequencies at maximum intensity (in cm^{-1}))

Raman*				Infrared†	
Liquid	Crystal			Crystal	
225 °K	185 °K	77 °K	9 °K	93 °K	Assignment
—	56	67	69	67‡	$R_z(A_2)$ or R_y or T
—	64	74	76	79‡	$R_z(A_1)$
—	86	100	104	101‡	T
—	—	—	—	141/160‡	$R_x(B_1$ and $B_2)$
—	—	—	—	517	ν_2,$^{34}SO_2$
524	523	524	525	521/528	$\nu_2(A_1)$
—	537	542	543	535	$\nu_2(A_2)$
1 044	—	—	—	—	$2\nu_2$
1 088	1 089	1 090	1 091	—	Impurity
1 121	1 122	1 122	1 122	1 121	ν_1, $S^{16}O^{18}O$
1 141	1 140	1 141	1 141	1 140	ν_1, $^{34}SO_2$
1 145	1 144	1 144	1 144	1 144	$\nu_1(A_1)$
~1 150	1 148	1 148	1 148	—	$\nu_1(A_2)$
—	1 152	1 153	1 153	—	Disorder?
—	1 308	1 304	1 304	1 303	ν_3,$^{34}SO_2$
—	1 315	1 312	1 311	1 310	}
—	1 325	1 324	1 323	1 322	} $\nu_1 + R_x$
1 334	1 341	1 341	1 339	1 334	} $\nu_3(B_1$ and $B_2)$
—	1 351	1 351	1 349	—	Disorder?

*Present results.
†Reference 2.
‡Reference 3; 77 °K.

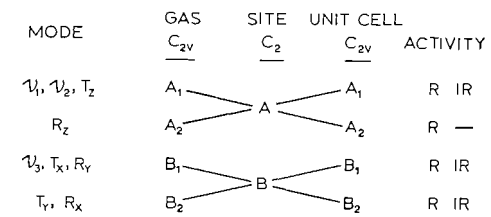

FIG. 3. Correlation between the gas and crystal symmetries for SO_2.

general our frequencies are in better agreement with those of Giguère and Falk. One of the components of the expected doublet for ν_2 is observed at 524 cm^{-1} (521 cm^{-1} in the infrared). The weaker band at 542 cm^{-1} is assigned to the second component of the bending mode (A_2), although a splitting of 18 cm^{-1} seems abnormally large in this case. No further splitting was observed in this region, even at the lowest temperature.

The ν_3 region is more complicated. The predictions for infrared and Raman are identical (two active components) and the two spectra are indeed very similar, but four or five maxima are observed in the broad band in this region. Comparison with the infrared spectrum would suggest that the bands at 1 312 and 1 324 cm^{-1} are the fundamental components, the lower frequency band (at 1 304 cm^{-1}) arising from an isotopic species. This, however, leaves the medium intensity band at 1 341 cm^{-1} (presumably the counterpart of the weaker band observed at 1 334 cm^{-1} in the infrared) unexplained. It is believed that this region is complicated by Fermi resonance between ν_3 and the combination ($\nu_1 + R_x$) with subsequent frequency shifts and intensity redistribution.

The weak peaks at 1 141 and 1 304 cm^{-1} on the low frequency side of ν_1 and ν_3 have almost the same frequency at the corresponding bands observed in the infrared and have

Can. J. Chem. Downloaded from www.nrcresearchpress.com by 210.87.254.42 on 09/05/12
For personal use only.

been assigned by Giguère and Falk to the isotopic molecule $^{34}SO_2$ (natural abundance: 4.2%). However, the very weak band at 1 122 cm^{-1} cannot be a difference between ν_1 and a lattice mode, as was previously assigned, since it appears in the spectrum of the liquid. Furthermore its frequency and intensity in the Raman spectrum makes it a reasonable choice for the isotopic species $S^{16}O^{18}O$ (natural abundance: 0.4%).

Lattice Modes

Only three lattice modes were observed instead of the nine predicted, although careful scans to within 30 cm^{-1} of the exciting line were made. The peak at 74 cm^{-1} is the strongest in the entire spectrum and is probably characteristic of an A_1 representation. One component of the R_z libration falls in this class. The other two bands are very close in frequency to two of the five observed in the far infrared (3). In that spectrum, bands at 141 and 160 cm^{-1} were assigned to the R_x librational doublet, since the principal moment of inertia about the x axis (in the molecular plane, perpendicular to the C_2 or z axis) is much less than the other two. The same doublet should appear in the Raman, but was not observed, possibly because this region is complicated by two spurious peaks characteristic of the spectrometer. These peaks are always present, but their intensity is dependent upon the sample quality, so that exact compensation is difficult. On the basis of the relative moments of inertia, the band at 67 cm^{-1} could be assigned to the R_y librational mode, but it may also be either the second component of R_z or a translational mode. The band at 100 cm^{-1} has been tentatively assigned as translational by Anderson and Walmsley (3) by comparison with the spectrum of crystalline CO_2 (10). In any case, an exact separation of translational and librational modes may not be meaningful here, because of possible mixing between like symmetric species.

In both infrared investigations (1, 2) peaks or shoulders on the high frequency side of the fundamentals were assigned to combinations with lattice modes in the frequency range 10 to 25 cm^{-1}, and in one paper (1) a calculation was made to support this. Although these bands are also observed in Raman, there is no direct evidence from the lattice regions of either the Raman or the far infrared spectrum to support the existence of lattice fundamentals at such low frequencies. However, the evidence is not complete, since even in the far infrared only five of the total of nine bands were observed. In an attempt to resolve this difficulty, the specific heat of the crystal has been calculated according to the Einstein model, using the frequencies observed spectroscopically, as suggested by Ichijima (11). This method will be described in some detail since the original paper is not readily available in English.

A crystal containing N molecules has $6N$ fundamental intermolecular vibrations, the frequency distribution of these being obviously very complicated. Ichijima has shown that although the frequencies of the lattice modes should have a continuous distribution, they have a tendency to concentrate around the optically active modes. His treatment leads to the conclusion that fairly good values can be obtained for the specific heat and entropy of molecular crystals by calculating the contributions of the six degrees of freedom (three translational, three rotational in character) of each molecule, as well as those of the internal modes. The calculation is done using spectroscopically observed frequencies and the Einstein function for a harmonic oscillator in the usual way. Furthermore, the contribution arising from the thermal expansion of the lattice is taken into account in the treatment by using a correction factor based on the temperature dependence of the lattice modes.

Can. J. Chem. Downloaded from www.nrcresearchpress.com by 210.87.254.42 on 09/05/12
For personal use only.

The specific heat at a given temperature T is given by:

$$C_p = C_v(\mathrm{i}) + \sum_{n=1}^{6} C_v(\mathrm{l})_n \left(\frac{\upsilon_n^0}{\upsilon_n}\right)$$

where $C_v(\mathrm{i})$ is the contribution from the internal modes of vibration, and $C_v(\mathrm{l})$ that of the lattice modes. υ_n^0 is the frequency (obtained by extrapolation) at 0 °K of a lattice vibration corresponding to one of the six degrees of freedom, whilst υ_n is the frequency of the same mode at a temperature T. The frequency of a lattice mode can usually be expressed as a linear function of the temperature:

$$\upsilon_n = \upsilon_n^0 - a_n T$$

where T is the temperature in °K, and a_n the temperature coefficient of the frequency.

In the case of crystalline SO_2, the coupling between the vibrations of the two molecules in a unit cell can give rise to two components for a particular mode. For example, R_x is observed as a doublet (141, 160 cm^{-1}) in the far infrared spectrum. Thus, an average value of 150 cm^{-1} was chosen for the degree of freedom corresponding to the libration around the x axis. The band at 100 cm^{-1} was chosen as corresponding to another degree of freedom; whether it is a rotational or translational mode is of no consequence in the calculation. As for the two bands observed at 67 and 74 cm^{-1}, they may be the two components of the R_z libration and an average value of 70 cm^{-1} was chosen for this degree of freedom.

The frequencies of the three bands observed in the lattice region of the Raman spectrum (Table I) have almost the same temperature dependence: the ratio of their frequency at 9 and 185 °K is close to 1.21 in all three cases. It was assumed that the R_x libration, which is seen only in the infrared, and the unseen lattice vibrations follow this trend. Thus three of the six degrees of freedom required for the calculation of the heat capacity have been obtained from spectroscopically observed lattice vibrations. The frequencies were expressed as a function of the temperature.

$$R_x = 163 - 0.1591T \ (cm^{-1})$$

$$T? = 105 - 0.1027T$$

$$R_z = 73 - 0.0703T$$

The contributions of these to the specific heat were then calculated for various temperatures between 20 and 180 °K and added to those of the internal modes (of which only the bending mode at 524 cm^{-1} contributes appreciably). The contributions from the three other degrees of freedom, taken as having the same frequency, were next calculated for various frequencies between 20 and 80 cm^{-1}, and the results added to the first to give the total specific heat. It was found that a value of 70 cm^{-1} (at 0 °K), with the same temperature dependence as the observed modes, yields a curve which agrees very well with the experimental one (12) between 20 and 150 °K (Fig. 4). The small deviation at higher temperatures could possibly be caused by the anharmonicity of the lattice modes. It should also be noted that replacing several or all of the Einstein distributions by Debye functions would increase the contribution to the specific heat at low temperature, thus yielding even worse agreement with experiment in the 25 cm^{-1} case. Because of the approximations involved, particularly the treatment of acoustic modes, one should be

Can. J. Chem. Downloaded from www.nrcresearchpress.com by 210.87.254.42 on 09/05/12
For personal use only.

wary of concluding too much from these calculations alone, especially since in SO_2 the intermolecular interactions are quite strong and may invalidate some of Ichijima's premises. The good agreement for the 70 cm^{-1} case could be fortuitous, and it is felt that the method gives only a crude representation of the true lattice spectrum. Nevertheless, so great is the descrepancy for the assumption of three (or even two) 25 cm^{-1} vibrations (and as it is most unlikely that only one lattice mode is at 25 cm^{-1} and all the others above 60 cm^{-1}) that it is felt that the thermal data supports the conclusion from the Raman studies that the structure on the intramolecular fundamentals is not caused by combinations with lattice modes, and the explanations given in Table I are preferred.

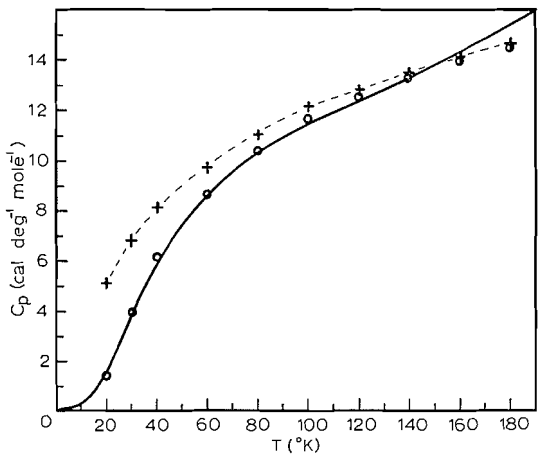

FIG. 4. Heat capacity curve of SO_2: experimental (solid curve, ref. 12), and calculated with three of the six degrees of freedom having experimentally determined frequencies, and the other three equal frequencies of 25 cm^{-1} (+) and 70 cm^{-1} (○).

Other Bands

Several weak bands, none of which was observed in the infrared spectrum, remain to be discussed. The peak at 1 044 cm^{-1}, which was only detected in the spectrum of the liquid, is readily assigned to $2\upsilon_2$, the only overtone observed in this work. Like the first overtone of υ_1 (2), the anharmonicity is quite small. The peak at 1 090 cm^{-1} is believed to arise from an impurity since its intensity is many hundred times weaker than υ_1 and it is impossible to find an overtone or combination that can fit this frequency. Weak bands at 1 153 and 1 351 cm^{-1}, on the high frequency side of υ_1 and υ_3 respectively, are more difficult to explain. Since both frequencies are close to those of the gaseous molecule, it is possible that they are caused by imperfect crystallization of the samples or by lattice defects. The same explanation could hold for the shoulder observed on the high frequency side of υ_2 in the infrared spectrum. If a finite fraction of the domains of the crystal have alternative or disordered structures, a relaxation of the selection rules and a broadening of the band is to be expected (13), and the inactive A_2 component may become active under these circumstances. In the case of crystalline CO_2, an unexpected shoulder was also observed on the high frequency side of υ_2 (14). It was shown by Osberg and Hornig to be a reflection peak since its intensity was strongly dependent upon the film thickness. It was ascertained by Giguère and Falk that no similar effect occurred in the case of crystalline SO_2, and therefore the hypothesis of partial disorder as an explanation for the complicated structure of υ_2 in the infrared is preferred.

Can. J. Chem. Downloaded from www.nrcresearchpress.com by 210.87.254.42 on 09/05/12
For personal use only.

The Spectrum of the Liquid

In the Raman spectrum of liquid SO_2, the ν_2 and ν_3 bands are broad and structureless. The symmetric stretch, ν_1, is, however, remarkably sharp (half width less than 3 cm^{-1}) showing that this vibration is much less perturbed by intermolecular interactions. The corresponding band from the isotopic species $^{34}SO_2$ is readily resolved, although it is separated from the main peak by only 4 cm^{-1}. Another striking feature is the presence of a shoulder on the high frequency side of ν_1. Careful surveys have shown that this becomes more pronounced as the temperature is lowered. The band appears to be somewhat broader than ν_1 itself, and is comparable in intensity (at −70 °C) to the isotopic band at 1 141 cm^{-1}. It is therefore too strong to arise from an impurity, nor can it be accounted for as a combination or overtone, or as another isotopic species. Its temperature dependence eliminates rotational structure as a possible explanation.

The shoulder must therefore arise from the particular structure of the liquid. If one regards a liquid as an ever rearranging framework of molecular aggregates, regions would exist where the molecules are closely packed and have frequencies close to those of the crystal. Also, some molecules would be on sites adjacent to holes and defects, and these would have frequencies intermediate between those of the crystal and gas. This picture, however attractive, is inadequate here since one would expect more holes and defects at higher temperatures, so that the high frequency shoulder, contrary to experiment, should become more intense with increasing temperature. A liquid can also be regarded as made of a large number of regions, some highly ordered, with a crystal-like structure, and some more or less disordered, with a glass-like type of structure. Molecules in the latter type of environment would have an average frequency of 1 145 cm^{-1} in SO_2. Those with a crystal-like type of environment on the other hand would have a frequency distribution more or less similar to that of the crystal. The shoulder could then be explained as the band corresponding to the 1 148 cm^{-1} peak in the crystal, the weaker component (at 1 144 cm^{-1}) being obscured by the main liquid peak. Ordering of molecules in the liquid would then explain the growth in intensity of the shoulder as the temperature is lowered. The weak point in this argument is that different explanations are needed for what appear to be similar features in both liquid and solid.

SUMMARY

The general features of the Raman spectrum of crystalline sulfur dioxide show good agreement with infrared studies and have been assigned using a factor group analysis based on the known structure of the crystal. However, neither direct spectroscopic observation nor comparison with thermal data supports the assignment of very low frequency lattice modes previously postulated.

ACKNOWLEDGMENTS

We are indebted to the Office of Naval Research for its financial support and to Prof. D. F. Hornig for several helpful discussions. We are also grateful to Mr. S. Chubachi for translating the paper by Ichijima, and to Dr. J. A. Morrison for his constructive criticism of the original manuscript.

REFERENCES

1. R. N. Wiener and E. R. Nixon. J. Chem. Phys. **25**, 175 (1956).
2. P. A. Giguère and M. Falk. Can. J. Chem. **34**, 1833 (1956).
3. A. Anderson and S. H. Walmsley. Mol. Phys. To be published.
4. R. Savoie and A. Anderson. J. Opt. Soc. Am. **55**, 133 (1965).
5. H. Gerding and W. J. Nijveld. Nature, **137**, 1070 (1936).

Can. J. Chem. Downloaded from www.nrcresearchpress.com by 210.87.254.42 on 09/05/12
For personal use only.

6. B. POST, R. S. SCHWARTZ, and I. FANKUCHEN. Acta Cryst. **5**, 372 (1952).
7. T. SUGAWARA and E. KANDA. Sci. Rept. Res. Inst., Tohoku Univ. Ser. A, **2**, 216 (1950).
8. D. F. HORNIG. J. Chem. Phys. **16**, 1063 (1948).
9. H. WINSTON and R. S. HALFORD. J. Chem. Phys. **17**, 607 (1949).
10. A. ANDERSON and S. H. WALMSLEY. Mol. Phys. **7**, 583 (1964).
11. I. ICHIJIMA. J. Chem. Soc. Japan, **71**, 551 (1950).
12. W. F. GIAUQUE and C. C. STEPHENSON. J. Am. Chem. Soc. **60**, 1389 (1938).
13. D. F. HORNIG. J. Chem. Phys. **17**, 1346 (1949).
14. W. E. OSBERG and D. F. HORNIG. J. Chem. Phys. **20**, 1345 (1952).

Can. J. Chem. Downloaded from www.nrcresearchpress.com by 210.87.254.42 on 09/05/12
For personal use only.

Can. J. Chem. Downloaded from www.nrcresearchpress.com by 210.87.254.5 on 09/05/12
For personal use only.

THE ROLE OF Hg 6^3P_0 ATOMS IN MERCURY PHOTOSENSITIZATION

III. REACTIONS WITH Hg 6^1S_0 ATOMS

J. E. McAlduff and D. J. Le Roy
Department of Chemistry, University of Toronto, Toronto, Ontario

Received February 9, 1965

ABSTRACT

Metastable Hg 6^3P_0 atoms were produced in a flow system by reaction of Hg 6^3P_1 atoms with nitrogen. Concentrations of the metastable atoms were studied as a function of Hg 6^1S_0 and N_2 concentration by absorption spectrometry. Rate constants have been obtained for the deactivation of Hg 6^3P_0 to the ground state and for its activation to the 6^3P_1 state by collisions with nitrogen, as well as for its reaction with Hg 6^1S_0 atoms to form a relatively long-lived diatomic species, presumably in the $A(^3O_u^-)$ state. The last process involves stabilization by collision with nitrogen.

In a previous paper (1) we described the results of an investigation of the steady-state concentration of $Hg(6^3P_0)$ as a function of nitrogen pressure in mixtures of mercury vapor and nitrogen irradiated with 2 537 Å mercury resonance radiation. Definite evidence was found for, among other reactions, a first-order disappearance of $Hg(6^3P_0)$. A measure of the steady-state concentration was obtained by observing both the absorption of 4 047 Å ($7^3S_1 - 6^3P_0$) and the emission of the forbidden line 2 656 Å ($6^3P_0 - 6^1S_0$). At nitrogen pressures up to about 10 mm the emission and absorption measurements correlated reasonably well and the first-order decay was attributed to the reaction,[1]

[6] $$Hg^0 = Hg + h\nu^0.$$

From the value obtained for k_6 the radiative lifetime of Hg^0 was calculated to be 4.2×10^{-4} s, considerably shorter than the value of 5 s calculated by Garstang (2).

Callear and Norrish (3), in flash photolysis experiments, also observed a first-order decay of Hg^0. Although radiative decay had been unequivocally established under our conditions (1), they argued that their observed first-order process could not be reaction [6] because if it were, the forbidden line would have been observed with an intensity comparable with that found for the emission of 2 537 Å fluorescence when argon–mercury mixtures were flashed. They assumed that in the presence of argon most of the Hg* atoms would disappear by reaction [2],

[2] $$Hg^* = Hg + h\nu^*,$$

whereas in the presence of nitrogen most of them would disappear by [4],

[4] $$Hg^* + N_2 = Hg^0 + N_2.$$

Although they used a constant mercury pressure (1.2×10^{-3} mm) they assumed that the observed first-order rate constant (5.4×10^3 s^{-1}) was actually the product of a second-order rate constant and the mercury concentration. The second-order constant calculated in this way was 8.2×10^{13} cm^3 mole^{-1} s^{-1}.

More recently, Callear and Williams (4), again using the flash photolysis technique, have varied the mercury vapor pressure from 3.8×10^{-4} to 23.8×10^{-4} mm and the nitrogen pressure from 500 to 1 000 mm and obtained evidence for their hypothesis. They found the second-order rate constant for the deactivation of Hg^0 by Hg to be

[1]*We are numbering the various reactions by the scheme used previously (1), and using* Hg, Hg^0, *and* Hg* *to represent* 6^1S_0, 6^3P_0, *and* 6^3P_1, *respectively.*

3.4×10^{13} cm^3 mole^{-1} s^{-1}; they also found evidence for a similar deactivation by N_2 with a rate constant of 8.7×10^7 cm^3 mole^{-1} s^{-1}.

Our previous measurements (1) were made at a constant mercury pressure of 7.7×10^{-4} mm. In the light of the more recent work it would seem reasonable to assume that Kimbell and Le Roy had observed the pseudo-first-order reaction [10] in addition to [6],

[10′] $$Hg^0 + Hg = ?$$

and that reaction [11] may have been involved in addition to, or instead of [7],

[11′] $$Hg^0 + Hg + N_2 = ?$$

[7] $$Hg^0 + N_2 = Hg + N_2.$$

We are now able to report the results of a detailed study of the steady-state concentration of Hg^0 over a wide range of mercury pressures up to 12×10^{-4} mm and over a range of nitrogen pressures up to 8 mm. Under these conditions pressure broadening effects should be small and corrections for imprisonment of resonance radiation can be made with some confidence.

EXPERIMENTAL

Little modification was required in the apparatus and procedures used previously (1). For increased stability and precision a Curtis-Wright Dynamic Capacitor electrometer was used in the double-beam photoelectric bridge circuit. The cell was of all-quartz construction and consisted of an outer tube 28 cm long and 5.5 cm o.d. and an inner tube 20 cm long and 3.1 cm i.d.; polished quartz windows were sealed to each end of the outer tube. An aqueous nickel sulfate solution was circulated through the annular space between the two tubes. This served to remove essentially all of the 4 047 Å radiation arising from the primary lamps and to keep the reaction cell at a constant temperature of 25 °C. The elimination of the 4 047 Å radiation was necessitated not simply to avoid the possibility of it appearing as scattered light, but to avoid depletion of Hg^0 by the process

$$6^3P_0 \xrightarrow{4\,047} 7^3S_1,$$

which has been observed previously in this laboratory. Because of the very low intensity of the 4 047 Å analysis beam no appreciable error arises from this cause.

The 4 047 Å analysis beam was derived from a microwave discharge through natural mercury (5). A special shutter was designed to cut off all light from the primary lamps while making the 100% transmission reading. The analysis beam passed down the axis of the cell. It had a diameter of 6 mm, defined by apertures at each end.

Close fitting metal cylinders covered each end of the reaction cell, leaving a central portion 18 cm long exposed to the light from the primary lamps. Thus the path length L of the analysis beam was effectively approximately 18 cm. The path length x, for the absorption of 2 537 Å from the primary lamps, was set at 1.5 cm, the internal radius of the cell.

The rate of formation of Hg* by reaction [1],

[1] $$Hg + h\nu^* = Hg^*,$$

can be defined as I_a^*, and if the absorption of 2 537 Å radiation can be fitted to a Beer's Law expression (see below) then

[i] $$I_a^* = 2.303K^*I_0^*[Hg]10^{-K^*[Hg]x},$$

where K^* is the decadic extinction coefficient, I_0^* is the intensity of the incident resonance radiation, and x is the path length (1.5 cm). The quantity K^* is an *effective* extinction coefficient, dependent on the nature of the emission line from the primary lamps as well as on the conditions in the reaction cell.

The value of K^* for the present experiments was measured by placing one of the primary lamps in the position usually occupied by the 4 047 Å lamp; the intensity of 2 537 Å transmitted was then determined for a series of mercury concentrations at various nitrogen pressures. For these particular measurements a Westinghouse WL-775 photocell was used. Tests using a monochromator to isolate 2 537 Å radiation from the primary lamp showed that this photocell was not sensitive to other radiation from the primary lamp.

The path length provided by the reaction cell for the absorption of 2 537 Å in these particular experiments was 28 cm. For any given nitrogen pressure up to 8 mm the logarithm of the transmitted intensity was linear in [Hg] over the range 0.6×10^{-4} mm to 1.8×10^{-4} mm and independent of nitrogen pressure. The

Can. J. Chem. Downloaded from www.nrcresearchpress.com by 210.87.254.5 on 09/05/12
For personal use only.

value of K^* calculated was 80 mm^{-1} cm^{-1} or 2.5×10^{-15} cm^2 $atom^{-1}$. At higher mercury pressures the points lay above the Beer's Law line. At higher nitrogen pressures K^* gradually increased, reaching a value of 230 mm^{-1} cm^{-1} at a nitrogen pressure of 80 mm (7.2×10^{-15} cm^2 $atom^{-1}$). For a somewhat similar lamp Pinder and Le Roy (6) found K^* equal to 6.5×10^{-15} cm^2 $atom^{-1}$ in the presence of 300 mm of propane. A constant value of $K^* = 80$ mm^{-1} cm^{-1} was assumed throughout the present work since the maximum pressure of nitrogen did not exceed 8 mm and the value of $[Hg]x$ did not exceed the value $1.8 \times 10^{-4} \times 28$.

RESULTS AND DISCUSSION

The results were interpreted in terms of the following reactions:

[1] $$Hg + h\nu^* = Hg^*$$

[2] $$Hg^* = Hg + h\nu^*$$

[4] $$Hg^* + N_2 = Hg^0 + N_2$$

[5] $$Hg^0 = Hg \text{ (on the wall)}$$

[6] $$Hg^0 = Hg + h\nu^0$$

[7] $$Hg^0 + N_2 = Hg + N_2$$

[8] $$Hg^0 + N_2 = Hg^* + N_2$$

[10′] $$Hg^0 + Hg = ?$$

[11′] $$Hg^0 + Hg + N_2 = ?$$

The rate of [1] is equal to I_a^*, which is given by eq. [i]. Nitrogen is assumed to deactivate Hg* mainly to the Hg^0 state, and so reaction [3] of the previous scheme (1) (quenching to the ground state) is not included. The rate of [5] is assumed to be diffusion-controlled and equal to $k_5 [Hg^0]/[N_2]$. Reaction [9] of the previous scheme (1) (collision-induced emission of the forbidden line ν^0) has not been included because it is kinetically indistinguishable from [7] in the present experiments. The possible products of [10′] and [11′] will be discussed below.

It was necessary to take into consideration the imprisonment of resonance radiation, which has the effect of decreasing k_2 with increasing Hg concentration. It might be noted that this correction was not required in the work of Callear and Williams (4) because the nitrogen pressures used by them were orders of magnitude larger than those used in the present work so that the rate of [2] was negligible compared to that of [4].

If τ is the true lifetime of Hg* with respect to radiation (1.08×10^{-7} s (7)), then in the range of mercury pressures used here we may write

[ii] $$k_2 = (1 - q[Hg])/\tau.$$

By assuming steady state concentrations for [Hg*] and $[Hg^0]$ one readily obtains an expression for $1/[Hg^0]$. However, the latter is not directly observable, and it is more convenient to use, instead, a quantity which is directly proportional to it, namely $K^0[Hg^0]L$, where L is the path length of the analysis beam in the region of the cell containing Hg^0 atoms (18 cm) and K^0 is the decadic extinction coefficient for the absorption of 4 047 Å by Hg^0 atoms. The latter quantity is assumed to be constant throughout the experiments, and hence

[iii] $$K^0[Hg^0]L = -\log_{10} (I_T/I_0)_0,$$

in which the right hand side is an observable, namely the negative of the logarithm of the fraction of analysis beam absorbed.

Can. J. Chem. Downloaded from www.nrcresearchpress.com by 210.87.254.5 on 09/05/12
For personal use only.

Can. J. Chem. Downloaded from www.nrcresearchpress.com by 210.87.254.5 on 09/05/12
For personal use only.

TABLE I

Fraction of analysis beam transmitted and values of Ψ for various pressures of mercury at nitrogen pressures below 0.5 mm

[Hg] = 4.94×10^{-4} mm			[Hg] = 6.15×10^{-4} mm			[Hg] = 10.65×10^{-4} mm			[Hg] = 9.75×10^{-4} mm			[Hg] = 7.90×10^{-4} mm		
$[N_2]$, mm	$(I_T/I_0)_0$	Ψ, mm $\times 10^4$	$[N_2]$, mm	$(I_T/I_0)_0$	Ψ, mm $\times 10^4$	$[N_2]$, mm	$(I_T/I_0)_0$	Ψ, mm $\times 10^4$	$[N_2]$, mm	$(I_T/I_0)_0$	Ψ, mm $\times 10^4$	$[N_2]$, mm	$(I_T/I_0)_0$	Ψ, mm $\times 10^4$
0.118	0.938	154.3	0.080	0.958	278.8	0.086	0.929	247.6	0.082	0.934	249.3	0.075	0.944	252.6
0.166	0.894	89.1	0.146	0.892	104.3	0.141	0.858	119.2	0.095	0.907	175.6	0.086	0.929	199.4
0.230	0.829	53.1	0.184	0.851	74.3	0.186	0.798	81.2	0.166	0.796	75.4	0.121	0.896	133.0
0.314	0.743	33.4	0.241	0.787	50.1	0.241	0.702	51.7	0.227	0.680	44.5	0.175	0.811	70.0
0.330	0.746	33.9	0.305	0.722	36.8	0.323	0.615	37.6	0.273	0.648	39.6	0.221	0.755	52.2
0.394	0.672	25.0	0.498	0.528	18.8	0.396	0.549	30.5	0.344	0.580	31.6	0.271	0.706	42.0
						0.446	0.511	27.2	0.409	0.516	25.9	0.389	0.572	26.2
						0.464	0.485	25.8				0.469	0.507	21.6

TABLE II

Fraction of analysis beam transmitted and values of Ψ for various pressures of mercury at nitrogen pressures above 0.5 mm

$[N_2]$ = 0.68 mm			$[N_2]$ = 1.30 mm			$[N_2]$ = 3.18 mm			$[N_2]$ = 5.40 mm			$[N_2]$ = 7.95 mm		
[Hg], mm $\times 10^4$	$(I_T/I_0)_0$	Ψ, mm $\times 10^4$	[Hg], mm $\times 10^4$	$(I_T/I_0)_0$	Ψ, mm $\times 10^4$	[Hg], mm $\times 10^4$	$(I_T/I_0)_0$	Ψ, mm $\times 10^4$	[Hg], mm $\times 10^4$	$(I_T/I_0)_0$	Ψ, mm $\times 10^4$	[Hg], mm $\times 10^4$	$(I_T/I_0)_0$	Ψ, mm $\times 10^4$
2.34	0.693	13.80	2.47	0.521	8.14	3.21	0.437	8.17	2.46	0.454	6.70	2.88	0.413	7.13
3.47	0.605	14.46	3.76	0.499	11.22	4.31	0.424	10.28	4.00	0.411	9.27	4.29	0.381	9.10
4.80	0.559	16.65	4.95	0.453	12.58	6.29	0.395	13.10	5.80	0.367	11.36	5.62	0.348	10.52
5.46	0.561	18.70	6.21	0.433	14.40	6.77	0.376	13.24	7.58	0.349	13.48	7.48	0.339	12.94
7.37	0.499	19.95	8.21	0.421	17.42	7.41	0.380	14.35	8.66	0.366	15.60	9.47	0.307	14.25
8.70	0.497	22.54	10.05	0.403	19.32	7.62	0.358	13.85	10.52	0.341	16.86	11.13	0.326	16.82
10.62	0.465	23.84	11.10	0.397	20.38	8.36	0.371	15.40	12.63	0.328	18.46			
						8.43	0.377	15.79						
						10.86	0.357	18.00						
						11.87	0.365	19.57						

Further simplification of the steady state expression yields the relation,

$$[\text{iv}] \qquad \Psi = \frac{1}{\tau\alpha}\{k_5/[N_2]^2 + (k_6 + \tau k_4 k_5)/[N_2] + (\tau k_4 k_6 + k_7 + k_8) + \tau k_4 k_7[N_2] + [Hg](k_{10'}/[N_2] + (k_{11'} + \tau k_4 k_{10'}) + \tau k_4 k_{11'}[N_2] - qk_5/[N_2]^2 - qk_6/[N_2] - q(k_7 + k_8)) - [Hg]^2(qk_{10'}/[N_2] + qk_{11'})\},$$

in which Ψ is an experimental quantity,

$$\Psi = \frac{[Hg]}{K^0[Hg^0]L}\, 10^{-K^*[Hg]z};$$

α is not a directly observable quantity but its value can be obtained as described below; it is defined by the relation $\alpha = 2.303K^*K^0I_0^*Lk_4$.

To evaluate q and α a series of measurements was made at various constant Hg pressures at nitrogen pressures below 0.5 mm, where only the smallest powers of $[N_2]$ in [iv] are effective. These data are given in Table I. In Fig. 1 the corresponding values of $\Psi[N_2]^2$ are plotted against $[N_2]$. It follows from [iv] that the intercepts should be equal to $k_5(1 - q[Hg])/\tau\alpha$, and hence linear in [Hg]. The intercepts are plotted against [Hg] in Fig. 2, and while the precision is not high the predicted form is indicated. A least squares treatment gave $k_5/\tau\alpha = 2.0 \pm 0.3 \times 10^{-4}$ mm^3, and since $\tau = 1.08 \times 10^{-7}$ s and $k_5 = 206$ mm s^{-1} at room temperature (1), it follows that $\alpha = 9.5 \pm 1.5 \times 10^{12}$ mm^{-2} s^{-2}.

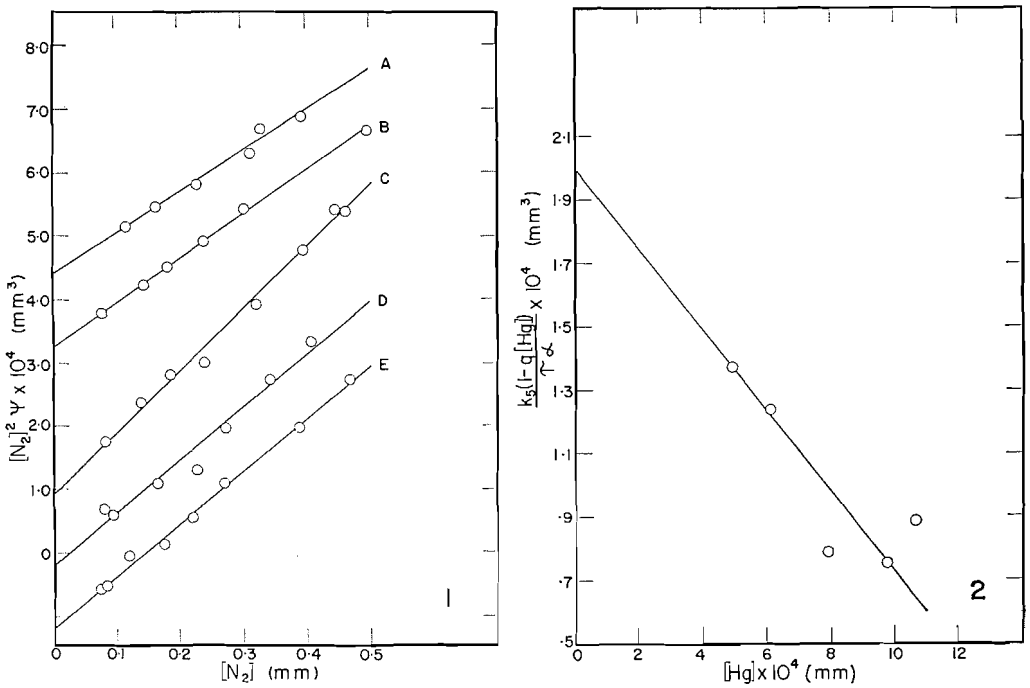

FIG. 1. $[N_2]^2\Psi$ vs. $[N_2]$ for various values of [Hg]. A, [Hg] = 4.94×10^{-4} mm, ordinates increased by 3.0; B, [Hg] = 6.15×10^{-4} mm, ordinates increased by 2.0; C, [Hg] = 10.65×10^{-4} mm; D, [Hg] = 9.75×10^{-4} mm, ordinates decreased by 1.0; E, [Hg] = 7.90×10^{-4} mm, ordinates decreased by 2.0.

FIG. 2. Intercepts of Fig. 1 plotted as function of [Hg].

Can. J. Chem. Downloaded from www.nrcresearchpress.com by 210.87.254.5 on 09/05/12
For personal use only.

The value of q derived from the ratio of the slope to the intercept of Fig. 2 is 640 ± 100 mm^{-1}. This would correspond to a doubling of the effective lifetime of Hg* at a mercury pressure of 8×10^{-4} mm, about one third of the imprisonment effect observed by Webb and Messenger (8). The magnitude of the effect will, of course, depend on the dimensions of the reaction cell as well as on the nature of the 2 537 Å source.

Equation [iv] predicts that the slopes of Fig. 1 should have a parabolic dependence on [Hg]. However, the precision with which $(I_T/I_0)_0$ could be measured at these low nitrogen pressures (*v.* Table I) placed a limitation on the range of Hg pressures that could be used, so that these measurements were not designed to test this aspect of the mechanism or to evaluate the constants involved. Values of the other constants in [iv] were evaluated from a series of experiments at higher nitrogen pressures. The experimental data are given in Table II.

In Fig. 3 the experimental quantity Ψ is plotted against [Hg] for a series of nitrogen pressures above 0.5 mm. From [iv] it is evident that these curves should be of the form

$$\Psi = a + b[\mathrm{Hg}] + c[\mathrm{Hg}]^2, \qquad [v]$$

where

$$a = \frac{1}{\tau\alpha}\{k_5/[\mathrm{N_2}]^2 + (k_6 + \tau k_4 k_5)/[\mathrm{N_2}] + (\tau k_4 k_6 + k_7 + k_8) + \tau k_4 k_7[\mathrm{N_2}]\}, \qquad [vi]$$

$$b = \frac{1}{\tau\alpha}\{-qk_5/[\mathrm{N_2}]^2 + (k_{10'} - qk_6)/[\mathrm{N_2}] + (k_{11'} + \tau k_4 k_{10'} - qk_7 - qk_8) + \tau k_4 k_{11'}[\mathrm{N_2}]\}, \qquad [vii]$$

$$c = \frac{1}{\tau\alpha}\{-qk_{10'}/[\mathrm{N_2}] - qk_{11'}\}. \qquad [viii]$$

It is evident from Fig. 3 that the terms in $[Hg]^2$ in [v] are not important in the range of Hg pressures used. It was not considered desirable to use higher Hg pressures because of the deviations from the Beer's law expression that would occur, as mentioned earlier.

As the nitrogen pressure is increased, the contribution of the term $k_5/[N_2]^2$ in eq. [vi] becomes relatively unimportant and it is convenient to use the value of $k_5/\tau\alpha$ found previously and plot $a[N_2] - (k_5/\tau\alpha)/[N_2]$ against $[N_2]$ in order to evaluate the other constants in the expression for a. This has been done in Fig. 4. No deviation from linearity is indicated, showing that the term $\tau k_4 k_7[N_2]$ in [vi] is negligible at the nitrogen pressures used. It was not desirable to use higher nitrogen pressures because of the possibility of pressure-broadening effects.

From the intercept of Fig. 4, $k_6/\tau\alpha + k_4 k_5/\alpha$ was found to be $1.3_5 \pm 0.6_1 \times 10^{-4}$. Using the value of k_4 given by Matland (9) (2.1×10^5 mm^{-1} s^{-1}) and the values of τ, α, and k_5 used previously, k_6 was calculated to be 133 ± 80 s^{-1}. The major part of the probable error in k_6 arises in the intercept of Fig. 4. It should be pointed out that the value obtained was not derived from observations on the forbidden line. However, the positive intercept of Fig. 4 does indicate the occurrence of a first-order process leading to the removal of Hg^0 atoms which can probably be identified with the emission of the forbidden line, since this has been observed (1). The radiative lifetime of Hg^0 obtained from the present results ($1/k_6 = 7.5 \times 10^{-3}$ s) is about 18 times larger than the value calculated by Kimbell and Le Roy (1). Their value would, of course, be in error because of the occurrence of [10′], which would be pseudo-first order under their conditions and hence indistinguishable from

Can. J. Chem. Downloaded from www.nrcresearchpress.com by 210.87.254.5 on 09/05/12
For personal use only.

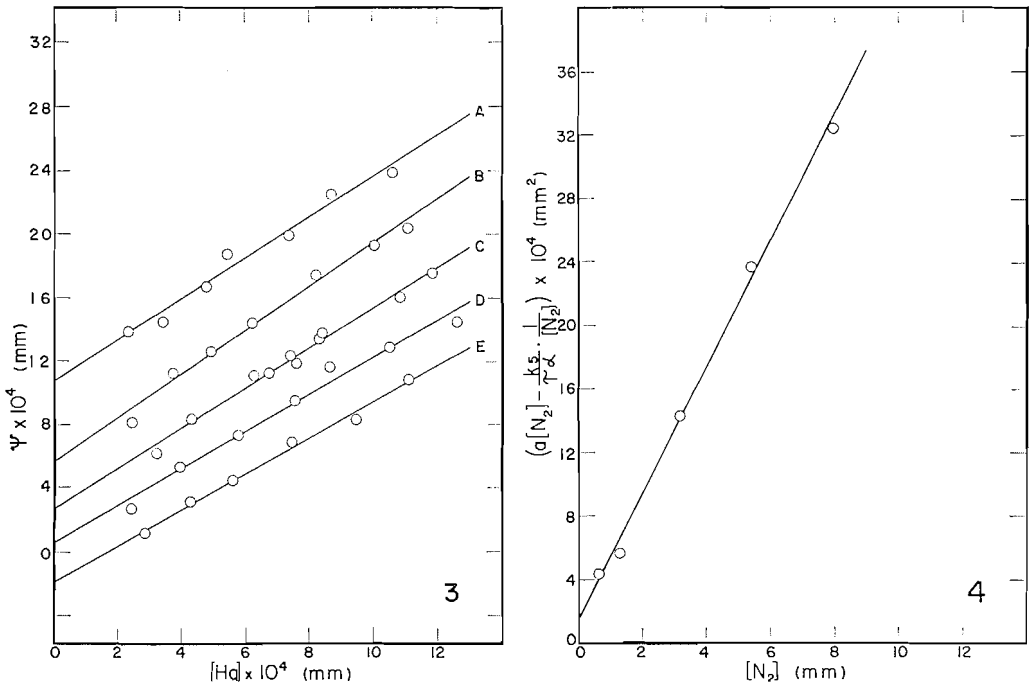

FIG. 3. Ψ as a function of [Hg] for various values of [N_2]. A, [N_2] = 0.68 mm; B, [N_2] = 1.30 mm; C, 3.18 mm, ordinates decreased by 2.0; D, [N_2] = 5.40 mm, ordinates decreased by 4.0; E, [N_2] = 7.95 mm, ordinates decreased by 6.0.

FIG. 4. Evaluation of $(k_6 + \tau k_4 k_5)$ and $(\tau k_4 k_6 + k_7 + k_8)$ from the intercepts of Fig. 3 (*v.* eq. [vi]).

[6]. The present value would seem to be not out of line with the criterion used by Callear and Williams (4) in criticizing our previous value.

The slope of Fig. 4 can be identified with the quantity $(1/\tau\alpha)$ $(\tau k_4 k_6 + k_7 + k_8)$, the least squares value of which was found to be $4.0 \pm 0.1_3 \times 10^{-4}$ mm. With the values of τ, α, k_4, and k_6 given above we obtain the value $(k_7 + k_8) = 7.6 \times 10^9$ cm^3 mole^{-1} s^{-1} with a probable error of $\pm 1.5 \times 10^9$. Since the term $\tau k_4 k_6$ is less than 1% of the value found for $k_7 + k_8$, any error in k_6 will have a negligible effect.

As mentioned previously, Callear and Williams obtained a value of 8.7×10^7 cm^3 mole^{-1} s^{-1} for the rate constant for the second-order removal of Hg^0 by N_2, almost 100 times smaller than our value of $k_7 + k_8$. The explanation would seem to lie in the difference between the experimental methods used. Whereas in our experiments we observe the steady state concentration of Hg^0, Callear and Williams observed the rate of decay of Hg^0 concentration after the removal of the primary radiation. At the high pressures of nitrogen used by them (ca. 780 mm), Hg* atoms formed in [8] would immediately re-form Hg^0 atoms by [4] so that the occurrence of [8] could not be detected from measurements of the rate of decay. Their value of 8.7×10^7 can therefore be attributed solely to reaction [7]. Using this value for k_7 we obtain $k_8 = 7.5 \times 10^9$ cm^3 mole^{-1} s^{-1}.

Reaction [8] is the reverse of reaction [4], and hence k_8/k_4 should be equal to

$$\frac{g^*}{g^0} e^{-(E^*-E^0)/RT}.$$

Using our value for k_8 and Matland's value (9) for k_4, $k_8/k_4 = 1.9 \times 10^{-3}$ at 300 °K;

Can. J. Chem. Downloaded from www.nrcresearchpress.com by 210.87.254.5 on 09/05/12
For personal use only.

the theoretical value calculated from the electronic degeneracies and the energy difference for the two energy levels of mercury involved is 0.7×10^{-3} at 300 °K. The agreement is remarkably good.

The values of $k_{10'}$ and $k_{11'}$ were obtained from the slopes of Fig. 3 as expressed in eq. [vii]. As in treating the intercepts, it was convenient to plot the quantity $b[N_2]$ plus the relatively small correction term $(qk_5/\tau\alpha)/[N_2]$ against $[N_2]$. This has been done in Fig. 5. The linearity of the curve shows that the last term in [vii] is negligible at the pressures of nitrogen used. The intercept of Fig. 5, $(k_{10'} - qk_6)/\tau\alpha$, is equal to 0.47 ± 0.10 mm. The term $qk_6/\tau\alpha$ contributes only 14% to this value so the value of $k_{10'}$ ($1.05 \pm 0.5 \times 10^{13}$ cm^3 mole^{-1} s^{-1}) is not greatly affected by uncertainties in k_6. The probable error in $k_{10'}$ arises largely from that of the intercept itself and from that of α.

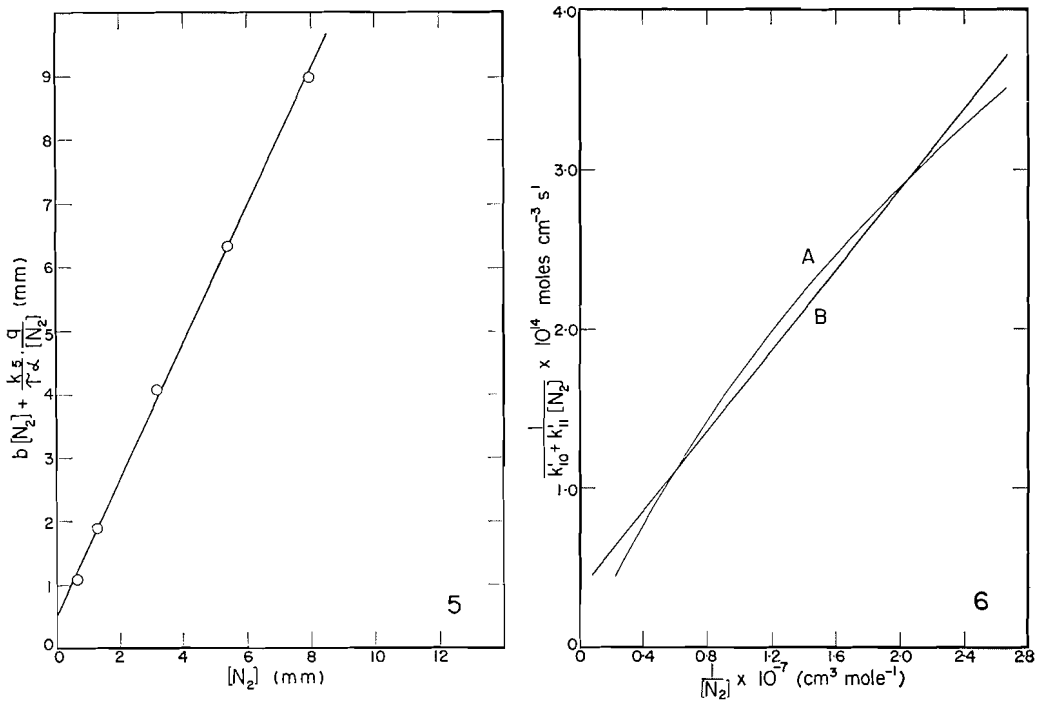

FIG. 5. Evaluation of $(k_{10'} - qk_6)$ and $(k_{11'} + \tau k_4 k_6 - qk_7 - qk_8)$ from the slopes of Fig. 3. (*v.* eq. [vii]).
FIG. 6. A, Experimental curve of $(k_{10'} + k_{11'}[N_2])^{-1}$ vs. $1/[N_2]$; B, Least squares linear approximation to curve A for the range $[N_2] = 0.7$ to 8.0 mm.

From the slope of Fig. 5 we obtain the value $(k_{11'} + \tau k_4 k_{10'} - qk_7 - qk_8)/\tau\alpha = 1.08 \pm 0.02$. The term $k_4 k_{10'}/\alpha$ contributes less than 2% and the term $qk_8/\tau\alpha$ about 25%; the term $qk_7/\tau\alpha$ contributes a negligible amount. The value of $k_{11'}$ obtained is $4.8 \pm 1.0 \times 10^{20}$ cm^6 mole^{-2} s^{-1}; the probable error is largely determined by that of α.

Our value of $k_{10'}$ is about one third of that given by Callear and Williams (4) for the bimolecular removal of Hg° by collision with Hg atoms. However, they found no evidence for the trimolecular reaction [11']. A possible explanation lies in a re-interpretation of both their mechanism and ours. Instead of reactions [10'] and [11'] we will postulate the following:

[10] $$Hg^0 + Hg = Hg_2\dagger^*,$$

Can. J. Chem. Downloaded from www.nrcresearchpress.com by 210.87.254.5 on 09/05/12
For personal use only.

[12] $$Hg_2\dagger^* = Hg^0 + Hg,$$

[13] $$Hg_2\dagger^* + N_2 = Hg_2^* + N_2.$$

The rate of disappearance of Hg^0 by these reactions will be given by $k_{10}k_{13}[Hg^0][Hg][N_2]/(k_{12} + k_{13}[N_2])$. Callear and Williams' measurements were made at high pressures of nitrogen (780 mm, except one at 500 mm and one at 1 000 mm), and under these conditions the term $k_{13}[N_2]$ could be considerably greater than k_{12}. The rate of disappearance of Hg^0 by these reactions would then be equal to $k_{10}[Hg^0][Hg]$, or second order, as found by them. However, our present measurements were made at pressures of nitrogen two or three orders of magnitude smaller than theirs, so it is not surprising that we found evidence for a third-, as well as a second-order process while they did not.

If reactions [10], [12], and [13] are substituted for [10′] and [11′] in the mechanism given previously, eq. [vi] remains the same and the values of α, q, k_6, and k_8 are unchanged. However, eq. [vii] takes a more complex form. Rather than using this it will be assumed that the expression given above is correct (reactions [10], [12], [13]) and that the expression $k_{10'}[Hg^0][Hg] + k_{11'}[Hg^0][Hg][N_2]$ is an approximation to it in the experimental pressure range 0.7 to 8.0 mm of nitrogen. Thus,

[ix] $$\frac{1}{k_{10'} + k_{11'}[N_2]} \approx \frac{1}{k_{10}} + \frac{k_{12}}{k_{10}k_{13}[N_2]}.$$

Using the values of $k_{10'}$ and $k_{11'}$ obtained previously, the left hand side of [ix] was fitted by the method of least squares to a linear function of $1/[N_2]$. The deviation from linearity is not large in the range 0.7 to 8.0 mm, as can be seen from Fig. 6. The least squares calculation gave $k_{10} = 2.7_0 \times 10^{14}$ cm^3 mole^{-1} s^{-1} and $k_{12}/k_{13} = 3.4 \times 10^{-7}$ mole cm^{-3}. The value obtained for k_{10} is about eight times larger than the high-pressure value obtained by Callear and Williams. In view of the considerable difference in experimental conditions, particularly with regard to the nature and possibly spacial dependence of the light absorption by Hg in the experiments of Callear and Williams, we do not consider that their results are in disagreement with the mechanism proposed here.

The value of k_{10} derived from the present experiments corresponds to a collision cross section of 6×10^{-15} cm^2. This is some orders of magnitude larger than collision cross sections for the quenching of Hg^0 by other gases (4), where deactivation to the ground electronic state is indicated. It is for this reason that we have postulated the formation of $Hg_2\dagger^*$, a highly vibrationally excited state of the $A(^3O_u^-)$ electronic state of Hg_2, the products of dissociation of which are Hg^0 and Hg (10).

If we assume a conventional collision cross section for reaction [13] our value of k_{12}/k_{13} predicts a natural lifetime for $Hg_2\dagger^*$ of the order of 3×10^{-7} s. On the other hand, the stabilized Hg_2^* molecule is believed to have a rather long lifetime (11) since the visible fluorescence coming from it persists for some distance downstream in a flowing stream of gas. Berberet and Clark (12) have studied this fluorescence and have concluded that the species responsible is formed by a process such as [11′]. Kimbell and Le Roy (13) have reached a similar conclusion. Further work is now being done in this laboratory in an attempt to establish a correlation between the intensity of the band fluorescence and the mechanism proposed in the present paper.

ACKNOWLEDGMENTS

The authors are pleased to acknowledge the financial assistance of the National Research Council. They would like to thank Dr. Callear for giving them his results (4) before publication.

Can. J. Chem. Downloaded from www.nrcresearchpress.com by 210.87.254.5 on 09/05/12
For personal use only.

REFERENCES

1. G. H. KIMBELL and D. J. LE ROY. Can. J. Chem. **38**, 1714 (1960).
2. R. H. GARSTANG. J. Opt. Soc. Am. **52**, 845 (1962).
3. A. B. CALLEAR and R. G. W. NORRISH. Proc. Roy. Soc. London, Ser. A, **266**, 299 (1962).
4. A. B. CALLEAR and G. J. WILLIAMS. Trans. Faraday Soc. **60**, 2158 (1964).
5. G. H. KIMBELL and D. J. LE ROY. Can. J. Chem. **40**, 1229 (1962).
6. J. A. PINDER and D. J. LE ROY. Can. J. Chem. **35**, 588 (1957).
7. P. H. GARRETT. Phys. Rev. **40**, 779 (1932).
8. H. W. WEBB and H. A. MESSENGER. Phys. Rev. **33**, 319 (1929).
9. C. G. MATLAND. Phys. Rev. **92**, 637 (1953).
10. P. PRINGSHEIM. Fluorescence and phosphorescence. Interscience Publishers, Inc., New York. 1949.
11. LORD RAYLEIGH. Proc. Roy. Soc. London, Ser. A, **125**, 1 (1929).
12. J. A. BERBERET and K. C. CLARK. Phys. Rev. **100**, 506 (1955).
13. G. H. KIMBELL and D. J. LE ROY. Unpublished.

Can. J. Chem. Downloaded from www.nrcresearchpress.com by 210.87.254.5 on 09/05/12
For personal use only.

Can. J. Chem. Downloaded from www.nrcresearchpress.com by 210.87.254.105 on 09/05/12
For personal use only.

INFRARED SPECTRA AND STRUCTURE OF POLYALDEHYDES

VI. POLYFLUORAL[1]

W. K. BUSFIELD[2] AND E. WHALLEY
Division of Applied Chemistry, National Research Council, Ottawa, Canada

Received March 18, 1965

ABSTRACT

The infrared spectrum of oriented polyfluoral is reported. The number and polarization of the bands suggest that the chain is helicoidal.

I. INTRODUCTION

It was reported first by Shechter and Conrad (1) that fluoral polymerizes to a waxy solid on standing, and Husted and Ahlbrecht (2) studied the free-radical and cationic polymerization. More recently Cairns, Clyne, and Graham (3) have described a copolymer of formaldehyde and fluoral, but no other work appears to have been reported on these polymers. In this paper, earlier work (4, 5) on the infrared spectra of polyaldehydes is extended to polyfluoral.

II. METHODS AND RESULTS

Polymer Preparation

Fluoral (b.p. −20 °C) was prepared by dehydrating fluoral methyl hemiacetal, obtained from Columbia Organic Chemical Company Inc., with concentrated sulfuric acid, and was purified by several vacuum distillations from —78 to −196 °C. Its infrared spectrum was identical with that recorded in the literature (1). The fluoral was stable indefinitely at low temperature. Even at room temperature in an air-free ampoule, solid polymer did not separate for at least 3 weeks.

Fluoral was polymerized in six ways using typical free-radical, cationic, and anionic catalysts. Details of the methods are given in Table I and some of the properties of the

TABLE I

Preparation of the polyfluoral samples

Polymer	Catalyst	Solvent	Temp. (°C)	Time	Approx. yield
RB	0.1 mole % Bz_2O_2 with respect to monomer	None	22	18 hours	90%
RS	None	None	22	3 weeks	30%
AN	0.5 mole % BuLi with respect to monomer	None	−78°	<1 second	100%
AH	0.5 mole % BuLi with respect to monomer	*n*-Hexane [monomer] = 10% by volume	−78°	<1 second	100%
CM	1 mole % H_2SO_4 with respect to monomer	Methylene chloride [monomer] = 7% by volume	22	7 days	50%
CT	0.5 mole % H_2SO_4 with respect to monomer	Toluene [monomer] = 5% by volume	22	2 weeks	10%

[1]*N.R.C. No. 8489.*
[2]*National Research Council Postdoctorate Fellow, 1960–1962.*

resulting polymers are summarized below. The rate of formation, the crystallinity of the polymer, and its physical properties depended on the catalyst and the solvent. None of the polymers melted on heating, but all depolymerized to monomeric fluoral at various temperatures which are summarized below.

Polymer	Appearance	Solvent action	Crystallinity	Decomposition temp.
RB	Deformable, stiff solid, low elongation	Unaffected by alcohol, ether, or chloroform	Moderate	Negligible decomposition below 300 °C
RS	Similar to RB	Similar to RB	Similar to RB	Similar to RB
AN	Deformable solid, softer and higher elongation than RB	No action by chloroform or alcohol; swells and slowly depolymerizes in acetone; small fraction dissolves in ether	Low	Negligible decomposition below 300 °C
AH	Soft and foamy solid, low elongation	No action by chloroform; swells and slowly depolymerizes in alcohol or acetone	Moderate	Negligible decomposition below 300 °C
CM	Brittle solid, easily ground, transformed into solid similar to RB on standing for several days	Depolymerizes in alcohol	High	Begins to depolymerize at ~150 °C
CT	Similar to RB	Similar to RB	Similar to RB	Similar to RB

X-ray Measurements

X-ray diffraction photographs were taken with a Debye-Scherrer 114.7 mm camera using nickel-filtered copper radiation. The patterns ranged from two diffuse halos in sample AN to a number of sharp rings in sample CM. The relative positions of the lines were the same for each sample. The approximate intensities of the lines in the sharpest spectrum (sample CM), and the corresponding interplanar spacings are listed in Table II. There appear to be at least two phases; the spacings marked with an asterisk in Table II appear to be characteristic of one phase. The strongest line of the second phase is at 4.3 Å. The other lines are characteristic of both phases. It seems likely that the variations in the patterns are due to variations in morphology or in stacking faults.

Spectroscopic Measurements

Samples of polyfluoral were rolled in a set of jeweller's rollers to form films suitable for infrared investigation. Samples thinner than about 0.001 in. were unable to support themselves, and were prepared by rolling in a silver chloride sandwich. Sample CM, which was a brittle solid, was examined in a potassium bromide disc.

The spectra were recorded on a Perkin-Elmer model 21 in the range 4 000 to 650 cm^{-1} with a rock salt prism, a Beckman IR7 in the range 4 000 to 250 cm^{-1} with gratings and

Can. J. Chem. Downloaded from www.nrcresearchpress.com by 210.87.254.105 on 09/05/12
For personal use only.

TABLE II

Interplanar spacings and approximate intensity of the X-ray diffraction lines of polyfluoral CM

Interplanar spacing (Å)	Intensity	Interplanar spacing (Å)	Intensity
7.9*	s	3.16	s
7.4	vw	2.67	vw
6.8*	m	2.43	m–w
4.8*	m–w	2.30	m
4.2	vs	2.16	w
3.98*	s	2.09	vw
3.77	m	1.93	w
3.45	s		

*These lines are characteristic of one phase. The remaining lines are characteristic of both phases (see text).

fore prisms, and a Perkin-Elmer model 301 in the range 550 to 160 cm^{-1} with gratings and filters. A silver chloride polarizer was placed in the sample beam of the spectrophotometer so that the plane of polarization of the light was at $\pm 45°$ to the instrument vertical to reduce polarization effects of mirrors, prisms, and gratings within the instrument. Oriented specimens of polyfluoral were mounted so that the plane of polarization of the incident light was either parallel or perpendicular to the direction of rolling. In the interpretation, the chains are assumed to be oriented in this direction. The frequency range investigated for each sample was: RB and AN, 4 000 to 450 cm^{-1}; AH, 4 000 to 160 cm^{-1}; CM and CT, 4 000 to 600 cm^{-1}. Various thicknesses were used as required. The thinnest rolled samples were well oriented, and the polarization of the strong bands in the range 1 450 to 500 cm^{-1} was easily determined. Oriented samples of about 0.001 in. thickness were not produced, and the polarization of most of the weaker bands was not determined.

The spectra of all samples studied were identical, except for an absorption band at 1 403 cm^{-1} whose relative intensity varied from sample to sample. A composite spectrum is shown in Fig. 1, and the wave numbers, the relative intensities, and the polarization of the strong bands are listed in Table III.

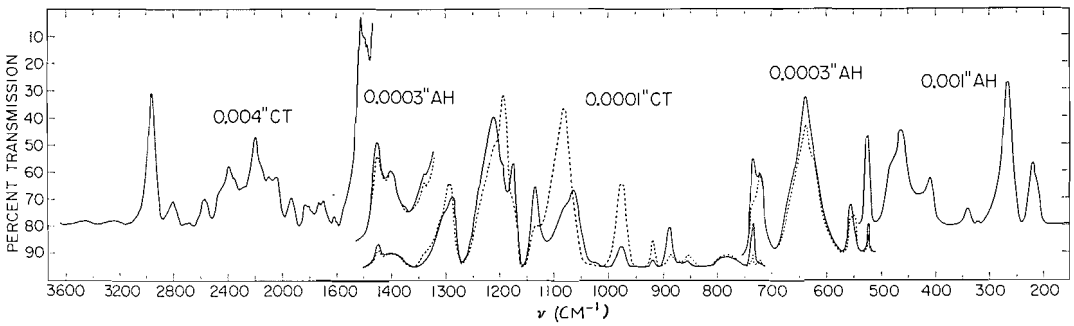

FIG. 1. Infrared spectrum of polyfluoral in the range 4 000 to 160 cm^{-1} showing the polarization of bands in the range 1 500 to 500 cm^{-1}. Full line: electric vector perpendicular to the direction of rolling. Broken line: electric vector parallel to the direction of rolling. There is a change of scale at 1 450 cm^{-1}.

A 0.0003 in. thick specimen of polyfluoral AH was well oriented, as shown by the spectrum in Fig. 1. Nevertheless, the transmission of the 2 963 cm^{-1} band was unaffected by rotation of the polarizer. It is likely, therefore, that the band is a superposition of a π (parallel to chain) band and a σ (perpendicular to chain) band, which could not be resolved in the unpolarized spectrum.

Can. J. Chem. Downloaded from www.nrcresearchpress.com by 210.87.254.105 on 09/05/12
For personal use only.

TABLE III

Infrared spectrum of polyfluoral

Wave number (cm^{-1})	Relative intensity	Polarization	Tentative approximate description of motion
3 460	vvw,b		Sample CT only; end group OH stretching
3 250	vvw,b		"
2 963	m	$\sigma+\pi$?	CH stretching
2 803	vw		Overtone or combination
2 690	vvw		"
2 579	vw		"
~ 2 450	vvw,sh		"
2 390	w		"
2 345	vvw		"
2 295	vvw		"
2 198	mw		"
~ 2 150	vvw,sh		"
2 100	vvw		"
2 050	vw		"
1 935	vw		"
1 830	vw		"
1 803	vvw		"
1 780	vvw		"
1 732	vw		"
1 700	vw		"
1 617	vw		"
1 600	vvw		"
1 525	vvw,sh		"
1 500	vvw,sh		"
1 455	vvw,sh		"
1 422	s	σ	CH bending
1 403	Variable	?	Not observed in spectrum of sample CM, non-crystalline CH_2 bending?
1 376	vw,sh	σ?	734 + 637; CH bending?
1 334	w	π	CF stretching; CH_2 bending
1 293	vs	π	CF stretching
1 288	vs	σ	"
1 212	vvs	σ	"
1 193	vvs	π	"
1 175	vs	σ	"
1 134	vs	σ	Mainly CO stretching
1 082	vvs	π	"
1 065	vs	σ	"
1 025	vw	σ?	CH bending or combination?
976	vs	π	CO stretching
919	s	σ	Mainly CC stretching
888	vs	σ	"
854	vw	π	CH bending?
734	m	σ	CF_3 deformation
722	w	π	"
637	s	σ	CF_3 deformation and (or) CO bending
624	vvw,sh	π	CF_3 deformation
553	m	σ	"
548	w	π	"
522	m–w	σ	"
476?	sh		CF_3 rocking, skeletal bending
462	m		"
423?			CH_2 rocking, CF_2 torsion, skeletal bending
409	w		"
338	vw		"
320?			"
266	m		"
219	w		"
213	sh		"

Abbreviations: v, very weak; w ,weak; m, medium; s, strong; b, broad; sh, shoulder; σ, perpendicular to chain, π, parallel to chain.

Can. J. Chem. Downloaded from www.nrcresearchpress.com by 210.87.254.105 on 09/05/12
For personal use only.

The band at 1 403 cm^{-1} was absent from the most crystalline specimen CM, and increased in intensity relative to the 1 422 cm^{-1} band with decreasing crystallinity as measured by the sharpness of the X-ray diffraction patterns. Its intensity is almost certainly caused by a breakdown in selection rules due to the presence of disorder.

III. DISCUSSION

The chemical structure of polyfluoral is doubtless $(CHCF_3 \cdot O)_n$. The main evidence for this is that when it is heated it depolymerizes to fluoral, and that the infrared spectrum, which is discussed in detail below, can be well interpreted on the basis of this structure. The spectrum of a thick sample of CT had weak absorption at 3 460 and 3 250 cm^{-1}. This indicates that there are OH end groups, as expected for a polymer prepared by sulfuric acid catalysis.

In contrast to the X-ray diffraction photographs, the infrared spectra of the various samples were very similar, except for the 1 403 cm^{-1} band. In particular, the breadths of the bands in the spectra of the most and the least crystalline sample are nearly the same. This indicates that the order within the chains is essentially preserved in the non-crystalline specimens, although the presence of the 1 403 cm^{-1} band shows that it is not perfectly preserved. This probably means that the polyfluoral chains, like polychloral chains (*4b*), are fairly stiff at room temperature, and indicates why it is difficult to find a good solvent for polychloral and polyfluoral. Part of sample AN was soluble in ether, and was probably of low molecular weight. The infrared spectrum of the ether-soluble fraction was similar to that of the other samples except that the bands were much broader, particularly in the region 1 350 to 800 cm^{-1}, and there were small differences in other bands. This indicates that in sample AN the order within the chain is considerably less than in the other samples, as would be expected if the chains are short.

We now consider in detail the spectrum of the polymer. The crystal structure is not known; in particular it is not known how many chains pass through the unit cell. We must, therefore, assume that the interaction between the chains can be neglected and that the spectrum can be interpreted on the basis of a single chain. The fact that the infrared spectra of samples of widely different crystallinity are almost identical suggests that interaction between the chains does not affect the spectrum very much. The general arguments are similar to those used previously for polychloral and are given here only briefly; more detail can be obtained from ref. *4b*.

The physical structure of the chain of polyfluoral is not known, but some information can be obtained from the infrared spectrum. Only those fundamentals can be optically active in which all repeating units move in phase. If there is one monomer unit $(CHCF_3 \cdot O)$ in the repeat unit, then the number of potentially infrared-active fundamentals is 17, excluding the rotation about the chain axis. They can be divided approximately into one CH stretching, two CH bending, six skeletal (CF, CO, CC) stretching, and eight skeletal bending vibrations.

The CH stretching bands are expected to be near 2 900 cm^{-1}. There is one band at 2 963 cm^{-1} which is assigned to a CH stretching fundamental; the polarization measurements (Section II) indicate that this may in fact be a superposition of two bands.

Two CH bending frequencies are expected if there is one monomer unit in the repeat, one approximately in the local symmetry plane, and one perpendicular to it. One is expected in the region 1 450 – 1 300 cm^{-1} and the other below 1 200 cm^{-1}. Only one band, the σ-polarized band at 1 422 cm^{-1} can be identified as a CH bending band with any assurance. In polychloral (*5b*), by contrast, there were two CH bending bands in this region, one π-polarized and one σ-polarized.

Can. J. Chem. Downloaded from www.nrcresearchpress.com by 210.87.254.105 on 09/05/12
For personal use only.

CF_3 stretching vibrations are expected in the region 1 350 to 1 050 cm^{-1} (6). The CO and CC stretching bands are expected to be between 1 250 and 750 cm^{-1}, and no doubt the CF, CO, and CC stretching motions are well mixed. There are 15 bands in this region, of which 4, at 1 376, 1 334, 1 025, and 854 cm^{-1} are weak and of uncertain origin. There are therefore 11 skeletal stretching bands compared with the 6 expected for a one-monomer repeating unit.

Below 750 cm^{-1}, bands due to the bending vibrations are expected. These are the CF_3 symmetrical and asymmetrical deformations; the CF_3 rocking, wagging, and twisting vibrations; the CF_3 torsional vibration; and the COC and OCO bending vibrations. Sixteen bands were observed in this region, most of them being probably fundamentals, compared with the eight expected for a one-monomer repeating unit.

The fact that there are more skeletal stretching and bending fundamentals than are expected for one monomer unit in the repeat unit strongly suggests that there is more than one monomer unit in the repeat. The alternative explanation, that many of the bands arise because of interaction between the chains, is unlikely. A planar zig-zag carbon–oxygen backbone with isotactic (same side) placement of the CF_3 groups can therefore be eliminated.

A planar zig-zag carbon–oxygen backbone with syndiotactic (alternate) placement of the side groups, and a helicoidal carbon–oxygen backbone with isotactic placement of the side groups, and p (where $p \geqslant 3$) monomer units in m turns of the coil in the repeat unit, are the simplest structures that are consistent with the observed number of bands. The polarization of the bands allows one to obtain more information.

The symmetry of the isotactic plane zig-zag is such that few π-polarized bands are expected in the spectrum. In particular, only three should occur in the range 1 400–850 cm^{-1} due to CF_3 and skeletal stretching and CH bending vibrations. Seven, of which five were very strong, were observed in this frequency range, and consequently the spectrum is inconsistent with a planar zig-zag syndiotactic structure.

The helicoidal structure, on the other hand, predicts equal numbers of σ-polarized and π-polarized bands. In the range 1 450 – 800 cm^{-1}, eight σ- and eight π-bands are expected for this structure. Seven σ- and seven π-bands, which are almost certainly fundamentals, and two other weak bands of doubtful polarization which may be combinations, were observed, in good agreement with the prediction. Below 750 cm^{-1} there are approximately equal numbers of σ- and π-polarized bands, and, while detailed interpretation is not possible, the numbers are consistent with the helicoidal isotactic structure. The lack of polarization of the 2 963 cm^{-1} CH stretching band, which is probably due to its being a superposition of a σ- and a π-band, is also consistent with a helicoidal chain.

A tentative assignment of the bands, based on the assignments of smaller molecules, is given in Table III.

ACKNOWLEDGMENT

We are indebted to Dr. L. D. Calvert for the X-ray diffraction.

REFERENCES

1. H. SCHECTER and F. CONRAD. J. Am. Chem. Soc. **72**, 3371 (1950).
2. D. R. HUSTED and A. H. AHLBRECHT. Brit. Patent No. 719,877 (1954).
3. T. L. CAIRNS, E. T. CLYNE, and P. J. GRAHAM. U.S. Patent No. 2,828,287 (1958).
4. A. NOVAK and E. WHALLEY. Trans. Faraday Soc. (*a*) **55**, 1484 (1959); (*b*) **55**, 1490 (1959).
5. A. NOVAK and E. WHALLEY. Can. J. Chem. (*a*) **37**, 1710 (1959); (*b*) **37**, 1718 (1959); (*c*) **37**, 1722 (1959).

Can. J. Chem. Downloaded from www.nrcresearchpress.com by 210.87.254.105 on 09/05/12
For personal use only.

6. R. E. DODD, H. L. ROBERTS, and L. A. WOODWARD. J. Chem. Soc. 2783 (1957). W. F. EDGELL and C. E. MAY. J. Chem. Phys. **22**, 1808 (1954). J. R. NIELSEN *et al.* Papers I to XI. *See* J. Chem. Phys. **30**, 1375 (1959). W. F. EDGELL, T. R. RIETHOFF, and C. WARD. J. Mol. Spectry. **11**, 92 (1963). J. MASON and J. DUNDERDALE. J. Chem. Soc. 754, 759 (1956). D. F. EGGERS, H. E. WRIGHT, and D. W. ROBINSON. J. Chem. Phys. **35**, 1045 (1961). O. RISGIN and R. C. TAYLOR. Spectrochim. Acta, **15**, 1036 (1959). P. R. MCGEE, F. F. CLEVELAND, A. G. MEISTER, and C. E. DECKER. J. Chem. Phys. **21**, 242 (1953). C. V. BERNEY, L. R. COUSINS, and F. A. MILLER. Spectrochim. Acta, **19**, 2019 (1963). J. R. NIELSEN and C. Y. LIANG. J. Chem. Phys. **21**, 1060 (1953). R. THEIMER and J. R. NIELSEN. J. Chem. Phys. **27**, 887 (1957). A. NOVAK and E. WHALLEY. Spectrochim. Acta, **16**, 521 (1960). J. R. NIELSEN, C. M. RICHARDS, and H. L. MCMURRAY. J. Chem. Phys. **16**, 67 (1948). J. R. NIELSEN and C. W. GULLIKSON. J. Chem. Phys. **21**, 1416 (1953).

Can. J. Chem. Downloaded from www.nrcresearchpress.com by 210.87.254.105 on 09/05/12
For personal use only.

Can. J. Chem. Downloaded from www.nrcresearchpress.com by 210.87.254.105 on 09/05/12
For personal use only.

THE ACID HYDROLYSIS OF GLYCOSIDES

II. EFFECT OF SUBSTITUENTS AT C-5

T. E. TIMELL, W. ENTERMAN, F. SPENCER, AND E. J. SOLTES
Department of Forest Chemistry, State University College of Forestry, Syracuse, New York
Department of Chemistry, McGill University, Montreal, Que.
and
The Pulp and Paper Research Institute of Canada, Montreal, Que.

Received March 5, 1965

ABSTRACT

First-order rate coefficients at three temperatures, and energies and entropies of activation, have been determined for the acid-catalyzed hydrolysis of methyl glucopyranosides containing various substituents at C-5 and for glycopyranosiduronic acids with different aglycones. Substitution at C-5 increased the stability towards acids of methyl α- and β-D-glucopyranosides, but there was no correlation between either the polarity or the size of the substituent and the rates of hydrolysis. The operation of either an inductive or a conformational effect alone was accordingly deemed unlikely.

Methyl α- and β-D-glucopyranosiduronic acids and methyl α-D-galactopyranosiduronic acid were only slightly more stable towards acids than the glycoside analogs, while benzyl β-D-glucopyranosiduronic acid was three times more stable. The presence of a methyl ester group at the carboxyl function increased the stability of the glycuronide bond. Isopropyl, *n*-butyl, isobutyl, and neopentyl β-D-glucopyranosiduronic acids were hydrolyzed approximately twice and cyclohexyl β-D-glucopyranosiduronic acid five times as fast as the corresponding glucosides. This appears to be the first time that glycuronides have been found to be hydrolyzed by dilute acid at a higher rate than their glycoside analogs.

The energies and, especially, the entropies of activation were, throughout, lower for the glycuronides than for the glycosides. The difference in entropy suggests that the two classes of compounds are hydrolyzed by different mechanisms.

INTRODUCTION

The mechanism of the acid hydrolysis of glycosides containing a carboxylic acid group at C-5 (glycopyranosiduronic acids, glycuronides) has attracted considerable attention in recent years, partly, no doubt, because polysaccharides with uronic acid residues are common in nature.

The glycuronide linkages have, so far, always been found to be hydrolyzed by moderately concentrated acids at a lower rate than the corresponding glycosidic bonds. Several investigators have attributed this to an inductive effect of the electron-attracting carboxyl group (1–8). Two alternatives are possible in the case of a glycopyranosiduronic acid. Either the polar effect is transmitted via one oxygen and two carbon atoms, which does not appear very likely, or, as has recently been suggested (8), the electrons at the ring oxygen are pulled by the carboxyl groups towards C-5, thus decreasing the ability of the ring oxygen to release electrons to the exocyclic oxygen. It is interesting in this connection to note that xylothiapyranosides are hydrolyzed faster than their oxygen analogs, apparently because of the ability of the less electronegative sulfur to furnish electrons to the glycosidic oxygen (9).

Alternative explanations for the stability of the glycuronide linkage have also been offered. Easty (10) noted that both the energy and the entropy of activation were lower for the acid hydrolysis of methyl α-D-glucopyranosiduronic acid as compared to methyl

α-D-glucopyranoside.[1] This was not considered compatible with the operation of an inductive effect, and Easty concluded that the mechanisms by which the two compounds hydrolyzed probably differed in some unknown manner. McKee and Dickey (11) have recently suggested that the entire uronic acid residue but not the carboxyl group, as such, stabilizes the xylosidic bond in *O*-(4-*O*-methyl-α-D-glucopyranosyluronic acid)-(1 → 2)-*O*-β-D-xylopyranosyl-(1 → 4)-D-xylose. A conformational rather than a polar effect was accordingly assumed to operate.

In a previous paper in this series, the general conditions for the acid-catalyzed hydrolysis of glycosides were discussed, as well as the influence of the nature of the aglycone (12). The present investigation is concerned with the influence on the rate parameters of substituents at C-5, and especially with the acid hydrolysis of glycopyranosiduronic acids. A brief account of some preliminary results has been given elsewhere (13).

RESULTS AND DISCUSSION

Hydrolyses were carried out with 0.05 *M* glycoside solutions in 0.5 *M* aqueous sulfuric acid. The extent of hydrolysis was determined polarimetrically. Kinetic parameters and deviations from the mean were calculated as described previously (12). All compounds studied were chromatographically pure, and all except five were crystalline.

TABLE I

Rate coefficients and kinetic parameters for the hydrolysis of methyl α-D-glucopyranosides with different substituents at C-5 (0.05 *M*) in 0.5 *M* sulfuric acid

Compound	$k \times 10^{-6}$ s^{-1}			*E*, kcal mole^{-1}	$\Delta S^{\ddagger}$ at 60 °C, cal deg^{-1} mole^{-1}
	60 °C	70 °C	80 °C		
Methyl α-D-xyloside	3.06	13.9	57.9	33.4	+14.9
Methyl 6-deoxy-α-D-glucoside	3.22	14.4	61.8	34.6	+18.6
Methyl α-D-glucoside	0.637	2.85	12.6	35.1	+16.9
Methyl α-D-glucuronide	0.572	1.93	7.41	30.2	+2.0
Methyl 6-deoxy-6-chloro-α-D-glucoside	0.092	0.441	1.92	35.7	+14.9
Methyl 6-deoxy-6-iodo-α-D-glucoside	0.099	0.445	1.82	34.2	+10.5
Methyl 6-amino-6-deoxy-α-D-glucoside	0.065	0.284	1.04	33.0	+6.1
Methyl 6-*O*-methyl-α-D-glucoside	0.449	1.90	8.52	34.2	+13.5

Kinetic data for a series of eight methyl α-D-glycopyranosides carrying different substituents at C-5 are presented in Table I. The greater stability of the glucoside as compared to the xyloside is well known (14). The stability towards acids of the 6-iodo- and the 6-amino glucosides has also been noted previously (15, 16). In view of the postulated inductive effect of the carboxyl group, it is of interest to compare the electron affinity of the C-5 substituents with their rate coefficients. Such a comparison is seen in Table II, where the rate constant at 60° and Taft's (17) polar substituent constant σ^* are used as parameters.

There is obviously little or no correlation between the polarity of the C-5 substituents and the rate coefficients, an inverse correlation being expected if the inductive effect alone were operating. The carboxymethyl and the chloromethyl groups, for example, have the

[1]*In Part I of this series (Table III), the rate coefficient reported by D. B. Easty in ref. 10 was erroneously stated to be 6.79 × 10^{-6} s^{-1}, when it was assumed that the original value was given in min^{-1} and 10-logarithms, while actually min^{-1} and natural logarithms had been used. The correct value, 2.95 × 10^{-6} s^{-1} is in excellent agreement with the corresponding value found in these studies, namely 2.85 × 10^{-6} s^{-1}. The authors are thankful to Dr. Alexander Meller, Australian Paper Manufacturers Limited, Melbourne, Australia, for drawing his attention to this error.*

Can. J. Chem. Downloaded from www.nrcresearchpress.com by 210.87.254.105 on 09/05/12
For personal use only.

TABLE II

Rate coefficients at 60 °C and polar substituent constants (σ^*) for some C-5-substituted methyl α-D-glucopyranosides

Substituent	$k \times 10^{-6}$ s^{-1}	σ^*
—CH_2CO_2H	0.572	+1.05
—CH_2Cl	0.092	+1.05
—CH_2I	0.099	+0.85
—CH_2OH	0.637	+0.56
—CH_2OCH_3	0.449	+0.52

same σ^* -values, yet the glucuronide was hydrolyzed more than six times faster than the 6-deoxy-6-chloro compound. The glucoside and the 6-*O*-methylglucoside were both hydrolyzed at approximately the same rate as the glucuronide, yet the σ^* -value for the hydroxymethyl and methoxymethyl groups is only about half of that of the carboxymethyl substituent. It is obvious that in these cases an inductive effect is not the only factor involved. The stability of the 6-deoxy-6-amino compound could be at least partly due to the electrostatic shielding effect of the positive ammonium ion present in acid solution.

TABLE III

Rate coefficients and kinetic parameters for the hydrolysis of methyl β-D-glucopyranosides with different substituents at C-5 (0.05 *M*) in 0.5 *M* sulfuric acid

Compound	$k \times 10^{-6}$ s^{-1}			E	$\Delta S\ddagger$
	60 °C	70 °C	80 °C		
Methyl β-D-xyloside	6.56	28.6	121	33.9	+17.9
Methyl β-D-glucoside	1.38	6.25	24.1	32.5	+10.6
Methyl β-D-glucuronide	1.16	4.14	14.4	29.3	+0.8
Methyl 6-*O*-methyl-β-D-glucoside	0.840	3.88	16.1	34.9	+16.8
Methyl 6-*O*-ethyl-β-D-glucoside	1.01	4.22	18.2	34.4	+15.8
Methyl 6-*O*-isopropyl-β-D-glucoside	1.11	5.08	20.6	34.8	+17.1

Corresponding data obtained for a series of six methyl β-D-glucopyranosides are given in Table III. Again, the difference in rate of hydrolysis between the glucuronide and the glucoside is quite small. All three 6-*O*-alkyl glucosides were hydrolyzed more slowly than the glucuronide.

There can be little doubt that some of the present results can be more rationally explained in terms of conformational rather than of polar effects. As first pointed out by Edward (14), the carbonium–oxonium ion present as an intermediate in the hydrolysis will tend to assume a half-chair conformation, a transformation which will be hindered by any substituent at C-5 relative to C-4. Rates of hydrolysis should thus decrease with increasing size of a C-5 substituent. This would explain the well-known increase in stability towards acids in the series pentosides, hexosides, and heptosides. It is evident, however, from the data in Tables I and III that this conformational effect cannot be adduced to explain all of the present results. The C-5 substituents are not of the same size in the 6-deoxy-6-chloro and 6-deoxy-6-iodo compounds, yet their rates of hydrolysis are almost the same. The methyl 6-deoxy-α-D-glucoside is hydrolyzed as rapidly as the methyl α-D-xyloside, which is also unexpected. The increase in rate of hydrolysis is less than the increase in size of the C-5 substituents in the series 6-*O*-methyl, 6-*O*-ethyl, and 6-*O*-isopropyl β-D-glucosides.

Can. J. Chem. Downloaded from www.nrcresearchpress.com by 210.87.254.105 on 09/05/12
For personal use only.

With a view of obtaining more information on this point, a number of methyl α- and β-D-glycopyranosiduronic acids were synthesized, and their kinetic parameters were compared with those previously obtained for their glycopyranoside analogs. Similar data were also established for a series of seven β-D-glucopyranosiduronic acids containing different aglycones. The results are presented in Tables IV and V.

TABLE IV

Rate coefficients and kinetic parameters for the hydrolysis of methyl glycopyranosiduronic acids and the corresponding glycopyranosides (0.05 *M*) in 0.5 *M* sulfuric acid

Compound	$k \times 10^{-6}$ s^{-1}			E	$\Delta S‡$
	60 °C	70 °C	80 °C		
Methyl α-D-galactoside	3.04	13.6	56.4	34.0	+16.7
Methyl α-D-galacturonide	3.01	13.3	43.0	31.1	+8.0
Methyl α-D-galacturonide*	2.87	10.7	38.6	30.3	+5.3
Methyl β-D-galactoside	5.87	23.3	94.4	32.0	+12.0
Methyl β-D-galacturonide	0.852	3.50	12.8	32.2	+8.8
Methyl α-D-mannoside	1.45	6.56	28.9	34.7	+17.3
Methyl α-D-mannuronide	3.72	9.10	28.4	31.0	+8.1

*Using the methyl ester as starting material.

TABLE V

Rate coefficients and kinetic parameters for the hydrolysis of six β-D-glucopyranosiduronic acids and the corresponding β-D-glucopyranosides (0.05 *M*) in 0.5 *M* sulfuric acid

Compound	$k \times 10^{-6}$ s^{-1}			E	$\Delta S‡$
	60 °C	70 °C	80 °C		
Isopropyl β-D-glucoside	2.65	11.3	44.5	33.2	+14.0
Isopropyl β-D-glucuronide	4.87	17.7	52.6	28.3	+0.5
n-Butyl β-D-glucoside	1.62	6.98	27.9	33.6	+14.3
n-Butyl β-D-glucuronide	4.20	14.4	49.2	29.3	+3.3
Isobutyl β-D-glucoside	1.90	8.21	34.4	33.8	+15.2
Isobutyl β-D-glucuronide	3.74	14.9	51.4	29.5	+3.7
Neopentyl β-D-glucoside	2.41	10.6	39.9	36.2	+22.9
Neopentyl β-D-glucuronide	4.65	16.9	57.2	30.0	+5.6
Cyclohexyl β-D-glucoside	3.25	13.9	56.4	33.5	+15.3
Cyclohexyl β-D-glucuronide	18.5	63.7	217	28.7	+4.5
Benzyl β-D-glucoside	1.56	6.75	28.3	33.6	+14.2
Benzyl β-D-glucuronide	0.587	2.29	8.44	30.9	+4.1

The methyl α-D-glucuronide and methyl α-D-galacturonide were hydrolyzed at a rate which was only slightly lower than that of the corresponding neutral glycosides, which is in agreement with the previous observations of Morell and Link (18), Nakano and Rånby (7), and Easty (10). The same applies to the methyl β-D-glucuronide, while the methyl β-D-galacturonide was hydrolyzed approximately seven times more slowly than the galactoside. The methyl α-D-mannuronide was hydrolyzed 2.5 times faster than the mannoside.

In the series of β-D-glucuronides, the benzyl β-D-glucuronide was approximately three times more stable than the corresponding glucoside. The isopropyl *n*-butyl, isobutyl, and neopentyl compounds were all hydrolyzed about twice as fast as their glucoside analogs, while the cyclohexyl β-D-glucuronide reacted five times more rapidly than the β-D-glucoside. The fact that certain glucuronides are less stable towards dilute acids than their neutral analogs does not seem to have been observed previously. Nakano and Rånby (7) noted that methyl α- and β-D-glucopyranosiduronic acids were both hydrolyzed more

Can. J. Chem. Downloaded from www.nrcresearchpress.com by 210.87.254.105 on 09/05/12
For personal use only.

rapidly in 81% phosphoric acid than the corresponding glucopyranosides. The activation energies were unusually low, however, and it was also found that the acid solutions quickly became colored, indicating the occurrence of secondary reactions.

During the acid hydrolysis of methyl esters of glycuronides the ester groups are rapidly eliminated. When the hydrolysis of methyl (methyl α-D-galactosid) uronate was followed with the aid of thin-layer chromatography, the results showed that ester linkage was hydrolyzed at a much higher rate than the galacturonide bond. The rate coefficients increased gradually during the initial stage of the reaction, indicating that the methyl ester group stabilized the galacturonide. After this period, the rate coefficients became constant and were those of methyl α-D-galacturonide, as can be seen from Table IV. Similar results were obtained with methyl (methyl β-D-galactosid) uronate and methyl (methyl β-D-glucosid) uronate. This is in agreement with the data of Dyer, Glaudemans, Koch, and Marchessault (6), who have shown that ethyl tetrahydro-6-methoxypyran-2-carboxylate is hydrolyzed in 0.001 *N* hydrochloric acid at 30 °C 7.4 times faster than is tetrahydro 6-methoxypyran-2-carboxylic acid. In this case, the extremely labile nature of the 6-methoxy group made it possible to establish quantitatively the effect of the ester group. The electron affinity of an ester group is greater than that of a carbylate ion, and the above investigators attributed the stabilization exerted by the ethyl ester group to an inductive effect. It seems more likely, however, that also in this case conformational factors are involved.

Inspection of the data in Tables I and III shows that nearly all values for the activation energy of the neutral glycosides fall within the range of 33 to 35 kcal $mole^{-1}$. The entropy of activation of the neutral glycosides ranges from +10 to +18 cal deg^{-1} $mole^{-1}$, indicating that the reaction is unimolecular (19). With the single exception of the β-D-galacturonide, all glycuronides and the methyl 6-amino-6-deoxy-α-D-glucoside have energies of activation which are 3 to 5 kcal $mole^{-1}$ lower than those of their neutral analogs, and the entropies of activation are in the range of +0.5 to +8 cal deg^{-1} $mole^{-1}$.

It is clear that the lower rate coefficients of the methyl and benzyl glucuronides and of the methyl galacturonides are entirely due to their lower entropies of activation. Differences in entropies of activation for the acid hydrolysis of esters, acetals, and lactones have previously been found to be associated with differences in reaction mechanisms (20). Whether the present glycosides and glycuronides differ in this respect cannot be decided on the basis of the evidence now available.

The energies of activation of the larger alkyl and the cyclohexyl β-D-glycuronides are 1 to 2 kcal $mole^{-1}$ lower than those of the methyl glycuronides. It is possible that this decrease in activation energy is sufficient to overcome the influence of the low entropy values, thus causing an increase rather than a decrease in rate of hydrolysis. It is interesting to note that these aglycones are all groups with a low electron affinity, while the benzyl group is electron-attracting. Semke, Thompson, and Williams (8) have recently reported that the phenyl, *p*-cresyl, and *p*-chlorophenyl β-D-glucopyranosiduronic acids, all compounds with an electron attracting aglycone, are hydrolyzed 16, 19, and 13 times more slowly, respectively, at 95 °C than the corresponding glycosides. In this case both glucuronides and glucosides had entropies of activation of +10 cal deg^{-1} $mole^{-1}$, and the authors concluded that both classes of compounds were hydrolyzed by the same mechanism.

CONCLUSIONS

The present data indicate that the effect of a carboxyl substituent at C-5 in a glycopyranosiduronic acid, whether deactivating or activating, is probably due to neither polar nor

Can. J. Chem. Downloaded from www.nrcresearchpress.com by 210.87.254.105 on 09/05/12
For personal use only.

conformational factors alone. Instead, both effects might be operative, each contributing to a different extent under different conditions. A reaction mechanism other than that by which most neutral glycosides are hydrolyzed might, however, also be involved. In view of their conspicuously low entropies of activation it is, for example, possible that glycopyranosiduronic acids might be at least partially hydrolyzed by a bimolecular reaction mechanism, which would then involve the participation of a mole of water (19, 20).

A more definite rationalization of the present experimental evidence does not appear feasible at the moment. More data for glycopyranosiduronic acids containing aglycones with different steric and polar characteristics would be particularly desirable. Investigations with such compounds are now in progress.

EXPERIMENTAL

Most experimental conditions were the same as in the previous study in this series (12). One-third of the polarimetric measurements were carried out at 436 mμ with a Perkin–Elmer model 141 photoelectric polarimeter.

Thin-layer chromatography was carried out with Silica Gel H and pyridine – ethyl acetate – acetic acid – water (5:5:1:3). One set of chromatograms was sprayed with 72% sulfuric acid and the other with *o*-aminobiphenyl. After hydrolysis for 6 h at 60 °C, methyl (methyl α-D-galactosid) uronate had been completely replaced by methyl α-D-galacturonide. Galacturonic acid was observed after 24 h and onward. Data for the hydrolysis of methyl (methyl α-D-galactosid) uronate at 60 °C are found in Table VI.

TABLE VI

Kinetic data for the hydrolysis of methyl (methyl α-D-galactosid) uronate (0.05 *M*) in 0.5 *M* sulfuric acid at 60 °C

Time, h	0	12	24	30	54	78	96		
α_{405}, degrees	+3.515	3.365	3.145	3.025	2.625	2.340	2.145		
$k \times 10^4$ min^{-1}	—	0.402	0.523	0.571	0.643	0.652	0.669		
Time, h	108	120	126	144	150	168	179	180	∞
α_{405}, degrees	2.075	1.980	1.910	1.815	1.775	1.168	1.660	1.620	1.330
$k \times 10^4$ min^{-1}	0.645	0.649	0.672	0.658	0.664	0.669	0.663	0.677	—

Mean value: 0.656×10^{-4} min^{-1}, 2.52×10^{-6} s^{-1} (excluding the first three values)
Mean deviation: 2.3%

MATERIALS

Methyl 6-Deoxy-β-D-glucopyranoside

Methyl α-D-glucopyranoside was treated with *p*-toluenesulfonyl chloride in pyridine (16, 21), giving methyl 6-*O*-*p*-toluenesulfonyl-α-D-glucopyranoside, m.p. 122–124 °C and $[\alpha]_D$ +95° (*c*, 1.0 in water) (22). The compound was reduced with lithium aluminium hydride in tetrahydrofuran (23, 24) to give methyl 6-deoxy-α-D-glucopyranoside (methyl α-D-quinovoside) with m.p. 96-98° and $[\alpha]_D$ +145° (*c*, 1.0 in water) (25).

Methyl 6-Amino-6-deoxy-α-D-glucopyranoside

This compound was prepared from methyl 6-*O*-*p*-toluenesulfonyl-α-D-glucopyranoside by treatment with methanolic ammonia at 120° (22). The hydrochloride of methyl 6-amino-6-deoxy-α-D-glucopyranoside melted with decomposition at 180–190° and had $[\alpha]_D$ +136° (*c*, 1.0 in water) (16).

Methyl 6-Chloro-6-deoxy-α-D-glucopyranoside

This compound was prepared by a combination of the methods reported by Helferich and his co-workers (26, 27). Methyl 2,3,4-tri-*O*-acetyl-6-*O*-trityl-α-D-glucopyranoside on treatment with phosphorus pentachloride and subsequent removal of the trityl group with hydrogen bromide in acetic acid gave methyl 2,3,4-tri-*O*-acetyl-6-chloro-6-deoxy-α-D-glucopyranoside. Saponification with aqueous barium hydroxide yielded methyl 6-chloro-6-deoxy-α-D-glucopyranoside with m.p. 108–110° and $[\alpha]_D$ +141° (*c*, 1.0 in water) (25, 26).

Methyl 6-Deoxy-6-iodo-α-D-glucopyranoside

The method of Compton (21) was followed. Methyl 6-*O*-*p*-toluenesulfonyl-α-D-glucopyranoside on acetylation in pyridine gave methyl 2,3,4-tri-*O*-acetyl-6-*O*-*p*-toluenesulfonyl-α-D-glucopyranoside in a yield of 41%, m.p. 169–170° and $[\alpha]_D$ +7.4° (*c*, 3.7 in chloroform). Treatment with sodium iodide in boiling cyclopentanone gave methyl 2,3,4-tri-*O*-acetyl-6-deoxy-6-iodo-α-D-glucopyranoside in a yield of 70%, m.p. 148.5–149.5° and

Can. J. Chem. Downloaded from www.nrcresearchpress.com by 210.87.254.105 on 09/05/12
For personal use only.

$[\alpha]_D$ +111° (*c*, 1.3 in chloroform) (15, 27). The compound was treated with alcoholic hydrochloric acid and crystallized from ethanol – ethyl acetate to give methyl 6-deoxy-6-iodo-α-D-glucopyranoside in a yield of 50%, m.p. 136–137° and $[\alpha]$ +102° (*c*, 1.0 in water).

Methyl 6-O-Methyl-α-D-glucopyranoside

This compound was prepared essentially as described by Helferich and co-workers (25, 28), namely by methylation, according to the method of Kuhn, Trischmann, and Löw (29), of methyl 2,3,4-tri-*O*-benzoyl-α-D-glucopyranoside. The crystalline compound had m.p. 146–149° and $[\alpha]_D$ +143.5° (*c*, 1.0 in water).

Anal. Calcd. for $C_8H_{14}O_6$: OCH_3, 29.8. Found: OCH_3, 29.1.

Methyl 6-O-Methyl-β-D-glucopyranoside

1,2; 3,5-Di-*O*-methylene-D-glucofuranose (14 g, m.p. 57–58°, $[\alpha]_D$ +51° in water) (30) was methylated with methyl iodide (100 ml) and silver oxide for 24 h at room temperature. After addition of chloroform, filtration through Celite, treatment with Darco G-60 charcoal, and concentration, a sirup (13 g) was obtained which could not be induced to crystallize; $[\alpha]_D$ +52° (*c*, 1.4 in water).

Anal. Calcd. for $C_9H_{14}O_6$: OCH_3, 14.2. Found: OCH_3, 14.3.

The 6-*O*-methyl bismethylene glucose was refluxed with *N* sulfuric acid (400 ml) for 5 h. After neutralization with barium carbonate and treatment with Amberlite IR-120 exchange resin, an aqueous solution of the reaction mixture was extracted with chloroform. The water layer was concentrated to a sirup. Crystallization from ethanol gave 6-*O*-methyl-D-glucose (5.5 g), m.p. 141–143.5° and $[\alpha]$ +55° (*c*, 1.0 in water) (31, 32).

6-*O*-Methyl-D-glucose (4.0 g) was acetylated in the usual way with hot acetic anhydride in the presence of anhydrous sodium acetate. Yield of crude, crystalline product: 8.1 g. After recrystallization from absolute ethanol the 1,2,3,4-tetra-*O*-acetyl-6-*O*-methyl-β-D-glucose (5.1 g) had m.p. 92–94° and $[\alpha]_D$ +20° (*c*, 1.0 in chloroform) (32, 33). The compound (5.0 g) was treated with glacial acetic acid (30 ml), saturated at 0° with hydrogen bromide to give the sirupy α-acetobromo compound (6.4 g) which was not characterized.

The 6-*O*-methyl acetobromoglucose (6.0 g) was dissolved in anhydrous methanol (50 ml) and shaken overnight with silver oxide (6.0 g) in the presence of some Drierite and iodine. After filtration through Celite, treatment with charcoal, and concentration, the reaction product was recrystallized from ethyl ether – petroleum ether to give 4.3 g of methyl 2,3,4-tri-*O*-acetyl-6-*O*-methyl-β-D-glucopyranoside, m.p. 103–105° and $[\alpha]_D$ −14.8° (*c*, 1.0 in chloroform) (32, 33). The compound (4.2 g) was deacetylated with anhydrous methanol (150 ml) containing sodium methoxide (1 g). After 2 h at room temperature, sodium ions were eliminated with Amberlite IR-120, and the solution was decolorized with charcoal and concentrated to dryness, yielding 2.9 g of a crude product which was crystallized from ethyl acetate. The methyl 6-*O*-methyl-β-D-glucopyranoside (1.5 g) had m.p. 133–135° and $[\alpha]_D$ −27.8° (*c*, 1.0 in water).

Anal. Calcd. for $C_8H_{16}O_6$: OCH_3; 29.9. Found: OCH_3, 30.5.

Methyl 6-O-Ethyl-β-D-glucopyranoside

Bismethylene glucose (14 g) was treated with ethyl iodide and silver oxide in the presence of dimethyl formamide (29). The sirupy product obtained (9.0 g) gave an infrared diagram with no hydroxyl band. Hydrolysis with *N* sulfuric acid yielded, after crystallization from absolute ethanol, 6-*O*-ethyl-D-glucopyranose (7.9 g), m.p. 163–167° and $[\alpha]_D$ −51.6° (*c*, 1.3 in water). The product (7.5 g) was acetylated with hot acetic anhydride in the presence of anhydrous sodium acetate, giving 1,2,3,4-tetra-*O*-acetyl-6-*O*-ethyl-β-D-glucose (12 g) as a sirup. After deacetylation of a portion of the sirup (8 g) with methanol – sodium methoxide, contaminating glucose was removed by fermentation with baker's yeast. The 6-*O*-ethyl-D-glucopyranose, after crystallization from ethanol (5.0 g) had m.p. 166–168° and $[\alpha]_D$ −53° (*c*, 1.3 in water) (34). Another portion of the crude product (4 g) was converted to the acetobromo compound, which was condensed with methanol in the usual way, giving methyl 2,3,4-tri-*O*-acetyl-6-*O*-ethyl-β-D-glucoside (2.7 g), m.p. 102–102.5° and $[\alpha]_D$ +1.2° (*c*, 1.3 in chloroform). Deacetylation of 1.5 g of this material gave methyl 6-*O*-ethyl-β-D-glucopyranoside (0.8 g) with m.p. 125.5–127.5° and $[\alpha]$ −25.5° (*c*, 1.5 in water).

Methyl 6-O-Isopropyl-β-D-glucopyranoside

Bismethylene glucose (20 g) was dissolved in dimethyl formamide and treated with silver oxide and isopropyl iodide in the usual way, giving the 6-*O*-isopropyl compound (9 g). Hydrolysis with *N* sulfuric acid, removal of glucose with yeast, and crystallization from ethanol gave 6-*O*-isopropyl-D-glucose (4.9 g) m.p. 128–130° and $[\alpha]_D$ +49° (*c*, 1.1 in water) (34). The 1,2,3,4-tetra-*O*-acetyl-6-*O*-isopropyl-β-D-glucose, after recrystallization from ethanol had m.p. 120–121° and $[\alpha]_D$ +16.6° (*c*, 1.0 in chloroform).

Condensation of the acetobromo derivative (3.0 g) with methanol yielded a sirup (2.7 g) which crystallized from ethyl ether – petroleum ether (1.8 g). The methyl 2,3,4-tri-*O*-acetyl-6-*O*-isopropyl-β-D-glucoside had m.p. 57–59° and $[\alpha]_D$ +12.2° (*c*, 1.5 in chloroform). This compound (1.7 g) was deacetylated in the usual way. After crystallization from ethyl acetate – petroleum ether, methyl 6-*O*-isopropyl-β-D-glucopyranoside (1.0 g) had m.p. 83.5–84° and $[\alpha]_D$ −24.1° (*c*, 1.0 in water).

Methyl α-D-Glucopyranosiduronic Acid

Methyl 2,3,4-tri-*O*-benzoyl-α-D-glucopyranoside (15 g) was oxidized with potassium permanganate (16 g) in a solution consisting of 150 ml each of acetone, glacial acetic acid, and water (35). After 3 days at room temperature, the solution was treated with potassium sulfite and extracted with chloroform to yield

Can. J. Chem. Downloaded from www.nrcresearchpress.com by 210.87.254.105 on 09/05/12
For personal use only.

11.3 g of a crude product. Benzoyl groups were eliminated by treatment with methanol and sodium methylate, and the methyl benzoate formed was removed by extraction with chloroform. The crude uronic acid was purified by adsorption on a column containing Dowex 1-X4 (acetate form) exchange resin. Neither the free acid nor the potassium salt of methyl α-D-glucopyranosiduronic acid could be induced to crystallize. The chromatographically pure product had $[\alpha]_D$ +129° (*c*, 1.0 in water).

Anal. Calcd. for $C_7H_{12}O_7$: OCH_3, 14.9. Found: OCH_3, 14.6.

Methyl β-D-Glucopyranosiduronic Acid

Methyl 1,2,3,4-tetra-*O*-acetyl-α-D-glucuronate and the corresponding β-anomer were prepared as described by Bollenback and co-workers (36). The α-compound had m.p. 111–112° and $[\alpha]_D$ +98° (*c*, 1.0 in chloroform). The β-anomer had m.p. 177–178° and $[\alpha]_D$ +8.6° (*c*, 1.0 in chloroform) (37, 38). Methyl 2,3,4-tri-*O*-acetyl-1-bromo-1-deoxy-α-D-glucuronate was obtained in a yield of 82% with m.p. 104–105.5° and $[\alpha]_D$ +198° (*c*, 1.0 in chloroform) (36, 38).

The acetobromo sugar (18 g) was dissolved in methanol (300 ml), and the solution was shaken in the dark with silver carbonate (20 g) in the presence of Drierite (10 g) and some iodine. After 40 h at room temperature, the solids were removed by filtration, and the methanol solution was decolorized with charcoal and evaporated to dryness. After recrystallization from ethanol, the methyl (methyl 2,3,4-tri-*O*-acetyl-β-D-glucopyranosid) uronate (10.5 g) had m.p. 153–155° and $[\alpha]_D$ −30° (*c*, 1.0 in chloroform) (39). A portion of the product (6.2 g) was treated with barium hydroxide (14 g) in water (100 ml) at 60° for 3 h. The reaction mixture was neutralized with carbon dioxide, filtered through Celite, treated with charcoal and Amberlite IR-120, and evaporated to dryness. The methyl β-D-glucopyranosiduronic acid was crystallized from acetone containing some methanol to give 3.1 g, m.p. 68–70° and $[\alpha]_D$ −55.3° (*c*, 1.0 in water).

Anal. Calcd. for $C_7H_{12}O_7$: OCH_3, 14.9. Found: OCH_3, 14.9.

Methyl (Methyl β-D-Glucopyranosid) Uronate

This compound was obtained by treating methyl (methyl 2,3,4-tri-*O*-acetyl-β-D-glucopyranosid) uronate with methanol – sodium methylate, followed by re-esterification with diazomethane. It had $[\alpha]_D$ −45° (*c*, 1.0 in water).

Anal. Calcd. for $C_8H_{14}O_7$: OCH_3, 27.9. Found: OCH_3, 26.0.

Methyl α-D-Galactopyranosiduronic Acid

This compound was prepared from D-galacturonic acid in a yield of 50%, essentially as described by Jones and Stacey (40). After two recrystallizations from ethanol, the methyl α-D-galactopyranosiduronic acid sintered at 88–90° and melted at 107–108°. It had $[\alpha]$ +128° (*c*, 1.4 in water) (41).

Methyl (Methyl α-D-Galactopyranosid) Uronate

D-Galacturonic acid (30 g) was boiled under reflux for 15 h with 0.7 *N* methanolic hydrogen chloride (300 ml) in the presence of Drierite (20 g). After neutralization with silver carbonate, treatment with charcoal, and filtration through Celite, evaporation of the solution gave a pale yellow sirup which was dissolved in a minimum amount of boiling methanol. The crystals deposited on cooling to room temperature were recrystallized from hot methanol, giving methyl (methyl α-D-galactopyranosid) uronate (4.0 g) with m.p. and mixed m.p. 147–148 °C and $[\alpha]_D$ +128° (*c*, 2.0 in water) (42–44).

Anal. Calcd. for $C_8H_{14}O_7 \cdot H_2O$: OCH_3, 25.9. Found: OCH_3, 25.9.

Methyl β-D-Galactopyranosiduronic Acid

Methyl (methyl 2,3,4-tri-*O*-acetyl-β-D-galactopyranosid) uronate, prepared from methanol and the acetobromo derivative of D-galacturonic acid, was saponified with barium hydroxide. The resulting methyl β-D-galactopyranosiduronic acid, after crystallization from acetone–chloroform, had m.p. 161–163° and $[\alpha]_D$ −40.2° (*c*, 1.1 in water) (42, 45).

Methyl (Methyl β-D-Galactopyranosid) Uronate

The above compound was obtained on deacetylation of the triacetate derivative with methanol – sodium methylate. It had $[\alpha]_D$ −27.5° (*c*, 1.0 in water).

Methyl α-D-Mannopyranosiduronic Acid

Methyl 2,3,4-tri-*O*-acetyl-α-D-mannopyranosiduronic acid (46) was oxidized with potassium permanganate as described for the corresponding glucoside derivative (35). The methyl α-D-mannopyranosiduronic acid had m.p. 114–115° and $[\alpha]_D$ +57° (*c*, 1.4 in water) (42, 47). The potassium salt had $[\alpha]_D$ +52° (*c*, 1.0 in water) (42).

Anal. Calcd. for $C_7H_{11}O_7K$: K, 15.8. Found: K, 14.9.

Both the mannuronide and the derived mannuronic acid gave only one sharp peak on ion exchange resin chromatography (48).

Cyclohexyl β-D-Glucopyranosiduronic Acid

Methyl 2,3,4-tri-*O*-acetyl-1-bromo-1-deoxy-α-D-glucuronate (12.1 g) (36) was added to a suspension of silver carbonate (10 g), Drierite (20 g), and a little iodine in cyclohexanol (150 ml). The mixture was shaken in the dark at room temperature for 24 h. The crystalline product was recovered in the usual way. After

Can. J. Chem. Downloaded from www.nrcresearchpress.com by 210.87.254.105 on 09/05/12
For personal use only.

recrystallization from 75 ml of absolute ethanol, the long needles of methyl (cyclohexyl 2,3,4-tri-*O*-acetyl-β-D-glucopyranosid) uronate (10.6 g, 83%) had m.p. 140–141.5° and $[\alpha]_D$ −31.7° (*c*, 1.5 in chloroform) (49). Use of mercuric cyanide instead of silver carbonate, as suggested by Helferich and Berger (49), gave the same crystalline compound in a yield of 70%.

The above compound (10.3 g) was treated with barium hydroxide (20 g) in water (200 ml) at 60° for 3 h. The reaction product was recovered in the usual way and crystallized from ethanol to give cyclohexyl β-D-glucopyranosiduronic acid (4.0 g) with m.p. 168–170° and $[\alpha]$ −59° (*c*, 1.0 in water) (51).

Neopentyl β-D-Glucopyranosiduronic Acid[2]

Methyl 2,3,4-tri-*O*-acetyl-1-bromo-1-deoxy-α-D-glucuronate (12.0 g) was condensed with neopentyl alcohol (20 g) in benzene (125 ml) in the presence of silver carbonate (10 g), Drierite (20 g), and some iodine. After it was shaken at room temperature for 24 h, the solution was recovered by filtration through Celite. Filtrate and washings (benzene) were evaporated to dryness, leaving a crystalline residue which was recrystallized from ethanol. The methyl (neopentyl 2,3,4-tri-*O*-acetyl-β-D-glucopyranosid) uronate (11.0 g) had m.p. 153–154° and $[\alpha]_D$ −51.3° (*c*, 3.0 in chloroform). A portion of the product (10.0 g) was treated with barium hydroxide (22 g) in the usual way, giving neopentyl β-D-glucopyranosiduronic acid (5.1 g); m.p. 149–151° and $[\alpha]_D$ −51.3° (*c*, 3.0 in chloroform).

Isopropyl β-D-Glucopyranosiduronic Acid[2]

The methyl (isopropyl 2,3,4-tri-*O*-acetyl-β-D-glucopyranosid) uronate, obtained as described above in a yield of 71%, had m.p. 143.5–145.5° and $[\alpha]$ −33.4° (*c*, 1.5 in chloroform). The isopropyl β-D-glucopyranosiduronic acid had $[\alpha]$ −45° (*c*, 1.0 in water). It could not be induced to crystallize.

n-Butyl β-D-Glucopyranosiduronic Acid[2]

The methyl (*n*-butyl 2,3,4-tri-*O*-acetyl-β-D-glucopyranosid) uronate was obtained in a yield of 68% and had m.p. 92–93° and $[\alpha]_D$ −26.1° (*c*, 1.3 in chloroform). The sirupy *n*-butyl β-D-glucopyranosiduronic acid had $[\alpha]_D$ −44° (*c*, 1.0 in water).

Isobutyl β-D-Glucopyranosiduronic Acid[2]

The methyl (isobutyl 2,3,4-tri-*O*-acetyl-β-D-glucopyranosid) uronate, obtained in a yield of 38%, had m.p. 138.5–139.5° and $[\alpha]_D$ −24.3° (*c*, 1.3 in chloroform). The isobutyl β-D-glucopyranosiduronic acid, which could not be induced to crystallize, had $[\alpha]_D$ −51.8° (*c*, 1.4 in water).

ACKNOWLEDGMENTS

The authors express their gratitude to Mr. N. Roy for the gift of methyl (methyl α-D-galactopyranosid) uronate and to Mr. B. W. Simson for technical assistance. This investigation was supported by a United States Public Health Service Research Grant (AM 07193 MCHA) from the National Institute of Arthritis and Metabolic Diseases, Public Health Service.

REFERENCES

1. J. K. Hamilton and N. S. Thompson. J. Am. Chem. Soc. **79**, 6464 (1957).
2. R. L. Whistler and G. N. Richards. J. Am. Chem. Soc. **80**, 4888 (1958).
3. R. H. Marchessault and B. G. Rånby. Svensk Papperstid. **62**, 230 (1959).
4. B. G. Rånby and R. H. Marchessault. J. Polymer Sci. **36**, 561 (1959).
5. B. G. Rånby. J. Polymer Sci. **53**, 131 (1961).
6. E. Dyer, C. P. J. Glaudemans, M. J. Koch, and R. H. Marchessault. J. Chem. Soc. 3361 (1962).
7. J. Nakano and B. G. Rånby. Svensk Papperstid. **65**, 29 (1962).
8. L. K. Semke, N. S. Thompson, and D. G. Williams. J. Org. Chem. **29**, 1041 (1964).
9. R. L. Whistler and T. Van Es. J. Org. Chem. **28**, 2303 (1963).
10. D. B. Easty. J. Org. Chem. **27**, 2102 (1962).
11. S. C. McKee and E. E. Dickey. J. Org. Chem. **28**, 1561 (1963).
12. T. E. Timell. Can. J. Chem. **42**, 1456 (1964).
13. T. E. Timell. Chem. Ind. London, 503 (1964).
14. J. T. Edward. Chem. Ind. London, 1102 (1955).
15. M. Zief and R. C. Hockett. J. Am. Chem. Soc. **67**, 1967 (1945).
16. F. Cramer, H. Otterbach, and H. Springmann. Ber. **92**, 384 (1959).
17. R. W. Taft. *In* Steric effects in organic chemistry. *Edited by* M. S. Newman. John Wiley and Sons, Inc., New York, New York. 1956. pp. 556–675.
18. S. Morell and K. P. Link. J. Biol. Chem. **104**, 183 (1934).
19. W. G. Overend, C. W. Rees, and J. S. Sequeira. J. Chem. Soc. 3429 (1962).
20. F. A. Long, J. G. Pritchard, and F. E. Stafford. J. Am. Chem. Soc. **79**, 2362 (1957).
21. J. Compton. J. Am. Chem. Soc. **60**, 395 (1938).

[2]*These compounds are new.*

Can. J. Chem. Downloaded from www.nrcresearchpress.com by 210.87.254.105 on 09/05/12
For personal use only.

22. B. HELFERICH and E. HIMMEN. Ber. **61**, 1831 (1928); **62**, 2136 (1929).
23. P. KARRER and A. BOETTCHER. Helv. Chim. Acta, **36**, 570 (1953).
24. W. W. ZORBACH and C. O. TIO. J. Org. Chem. **26**, 3543 (1961).
25. B. HELFERICH, W. KLEIN, and W. SCHÄFER. Ber. **59**, 79 (1926). Ann. **447**, 19 (1926).
26. B. HELFERICH and H. BREDERECK. Ber. **60**, 1995 (1927).
27. J. W. H. OLDHAM. J. Chem. Soc. **127**, 2844 (1925).
28. B. HELFERICH and J. BECKER. Ann. **440**, 1 (1924).
29. R. KUHN, H. TRISCHMANN, and I. LÖW. Angew. Chem. **67**, 32 (1955).
30. L. HOUGH, J. K. N. JONES, and M. S. MAGSON. J. Chem. Soc. 1525 (1952).
31. H. OHLE and L. VARGHA. Ber. **62**, 2425 (1929).
32. P. A. LEVENE and A. L. RAYMOND. J. Biol. Chem. **97**, 751 (1932).
33. B. HELFERICH and E. GÜNTHER. Ber. **64**, 1276 (1931).
34. H. OHLE and K. TESSMAR. Ber. **71**, 1843 (1938).
35. M. STACEY. J. Chem. Soc. 1539 (1939).
36. G. N. BOLLENBACK, J. W. LONG, D. G. BENJAMIN, and J. A. LINDQUIST. J. Am. Chem. Soc. **77**, 3310 (1955).
37. W. F. GOEBEL and F. H. BABERS. J. Biol. Chem. **106**, 63 (1934).
38. W. D. S. BOWERING and T. E. TIMELL. J. Am. Chem. Soc. **82**, 2827 (1960).
39. W. F. GOEBEL and F. H. BABERS. J. Biol. Chem. **111**, 347 (1935).
40. J. K. N. JONES and M. STACEY. J. Chem. Soc. 1340 (1947).
41. S. MORELL and K. P. LINK. J. Biol. Chem. **100**, 385 (1933).
42. C. A. MARSH. J. Chem. Soc. 1578 (1952).
43. J. E. CADOTTE, F. SMITH, and D. SPRIESTERSBACH. J. Am. Chem. Soc. **74**, 1501 (1952).
44. H. W. H. SCHMIDT and H. NEUKOM. Helv. Chim. Acta, **47**, 865 (1964).
45. S. MORELL, L. BAUR, and K. P. LINK. J. Biol. Chem. **110**, 719 (1935).
46. R. A. EDINGTON, E. L. HIRST, and E. E. PERCIVAL. J. Chem. Soc. 2281 (1955).
47. R. G. AULT, W. N. HAWORTH, and E. L. HIRST. J. Chem. Soc. 517 (1935).
48. O. SAMUELSON and L. WICTORIN. Svensk Papperstid. **67**, 555 (1964).
49. B. HELFERICH and A. BERGER. Ber. **90**, 2492 (1957).

Can. J. Chem. Downloaded from www.nrcresearchpress.com by 210.87.254.105 on 09/05/12
For personal use only.

Can. J. Chem. Downloaded from www.nrcresearchpress.com by 210.87.254.5 on 09/05/12
For personal use only.

1,4-DIMETHYLBICYCLO[2.2.1]HEPTANE DERIVATIVES

PETER YATES AND THOMAS R. LYNCH[1]
Lash Miller Chemical Laboratories, University of Toronto, Toronto, Ontario
Received April 15, 1965

ABSTRACT

The product from the action of methylmagnesium iodide on bicyclo[2.2.1]heptane-2,5-dione gave 2-exo-5-endo-diacetoxy-1,4-dimethylbicyclo[2.2.1]heptane on treatment with sulfuric acid in acetic acid. This has been converted to 1,4-dimethylbicyclo[2.2.1]heptane-2-exo-5-endo-diol, to 1,4-dimethylbicyclo[2.2.1]heptane-2,5-dione, and to 1,4-dimethylbicyclo[2.2.1]heptane-2-endo-5-endo-diol. The stereochemical assignments have been made on the basis of the interpretation of the nuclear magnetic resonance spectra of these compounds. The exo–endo diacetoxy compound is shown to be the expected product from a double Wagner–Meerwein rearrangement.

In the course of other work, we required 1,4-dimethylbicyclo[2.2.1]heptane derivatives with functional groups in both of the two-carbon bridges. The only bicyclo[2.2.1]heptane derivatives with methyl groups at both bridgeheads which had been prepared previously were compounds I–III, obtained from compounds of natural origin (1, 2, 3). Since none of these was suitable for our purpose we investigated other routes to 1,4-dimethylbicyclo-[2.2.1]heptane derivatives. We report now the preparation of such compounds from bicyclo[2.2.1]heptane-2,5-dione (IV). After the completion of this work (4) the preparation of 1,4-dimethylbicyclo[2.2.1]heptane-2,5-dione (V) by a different route was reported (5).

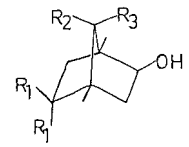

I, $R_1=R_3=H, R_2=CH_3$
II, $R_1=H, R_2=R_3=CH_3$
III, $R_1=CH_3, R_2=R_3=H$

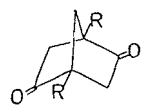

IV, R=H
V, $R=CH_3$

The diketone IV was prepared from bicyclo[2.2.1]heptadiene by the method of Meinwald, Crandall, and Gassman (6). Treatment of IV with a large excess of methylmagnesium iodide gave a viscous, colorless liquid which decomposed on attempted distillation or chromatography. This product is considered to consist largely of the 2-exo-5-exo-dimethyl-2,5-diol VI[2] (the presence of a small amount of a carbonyl compound was indicated by a very weak band in the infrared spectrum of the product at 5.7 μ). Its gross structure is assigned on the basis of its mode of formation and its reactions (*vide infra*). Its n.m.r. spectrum shows a single methyl signal, consistent with its consisting largely of a single diastereomer with both methyl groups either exo or endo. The preponderance of the stereoisomer VI would be expected on mechanistic grounds. Thus Sauers (7) has found that the product obtained by the action of methylmagnesium iodide on norcamphor is the exo-methyl compound VII, "substantially free" of the corresponding endo-methyl compound. It would be anticipated that the steric factors which favor attack by the Grignard

[1]*Sir Joseph Flavelle Fellow, 1961–62; Union Carbide Research Fellow, 1962–63.*
[2]*All products are racemic, and no absolute configuration is implied by this and other formulae.*

reagent on the less hindered exo side of norcamphor would favor similar attack on each of the carbonyl groups of IV (8); electrostatic effects would also be expected to favor *exo* attack in the case of the introduction of the second methyl group via the intermediate VIII. It may further be noted that the positions of the methyl proton signals in the n.m.r. spectra of VI (δ 1.28) and VII (δ 1.24) are very similar.

Treatment of the diol VI with 75% sulfuric acid in acetic acid at 70–80° for 2 h gave a colorless liquid, $C_{13}H_{20}O_4$. This product is assigned the structure IX on the basis of the

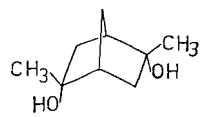

VI

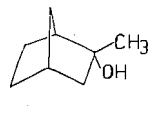

VII

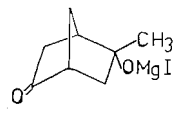

VIII

following evidence. Its infrared spectrum includes bands at 5.74 and 8.1 μ, characteristic of the acetate group and shows no bands attributable to a hydroxyl group. Its n.m.r. spectrum shows signals due to two methyl groups in slightly different magnetic environments at δ 0.95 and 1.09 (cf. X, δ 1.07). The methyl groups of the acetoxyl groups give a

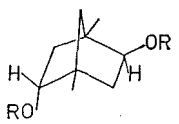

IX, R=COCH3

XI, R=H

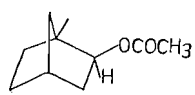

X

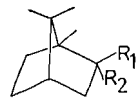

XII, R1=OH, R2=H

XIII, R1=H, R2=OH

single signal at δ 1.97 (cf. X, δ 1.95). Multiplets due to the hydrogen atoms at C.2 and C.5 partially overlap to give a complex pattern in the region δ 4.5–4.8 (cf. X, multiplet centered at δ 4.5 due to the C.2 hydrogen atom).

Removal of the acetyl groups with methanolic sodium methoxide gave the exo–endo diol XI, m.p. 98.5–99.5°. The n.m.r. spectrum again shows two methyl group signals at slightly different positions (δ 1.05 and 1.09). The hydroxyl protons give rise to a singlet at δ 1.70; this assignment is confirmed by the shift of this signal to δ 2.05 in the spectrum of a sample dissolved in deuteriochloroform containing a small amount of ethanol. The multiplets due to the hydrogen atoms at C.2 and C.5 again overlap, but they are sufficiently distinct in this case to permit approximate resolution of the overlapping signals into two multiplets, centered at δ 3.58 and 3.83, which are assigned to the C.2 and C.5 protons, respectively (cf. the corresponding proton signals in isoborneol (XII) (multiplet centered at δ 3.52) and borneol (XIII) (multiplet centered at δ 3.91) (cf. ref. 9).

Oxidation of the diol XI with chromium trioxide in acetone gave the diketone V, m.p. 127.5–128°. This was shown to have two carbonyl groups by the preparation of a bis-2,4-dinitrophenylhydrazone. That these are not in a β relationship is evident from the stability of the diketone under basic conditions. The situation of both carbonyl groups in five-membered rings was confirmed by the infrared spectrum of V, which shows a single carbonyl-stretching band at 5.70 μ (cf. IV, 5.68 μ). This spectrum also has a band at 7.10 μ, characteristic of a deformation vibration of a CH_2 group adjacent to a C=O group, and a band at 7.22 μ characteristic of a symmetrical deformation of a CH_3 group not adjacent to a C=O group (as anticipated, the infrared spectrum of IV shows the former band, but not the latter). The ultraviolet maximum of the diketone V (287.5 mμ (ϵ 47))

Can. J. Chem. Downloaded from www.nrcresearchpress.com by 210.87.254.5 on 09/05/12
For personal use only.

is similar in position and intensity to that of IV (291 mμ (ε 44)) (6). Its n.m.r. spectrum shows apparent singlets at δ 1.22, 1.79, and 2.09, whose positions and relative intensities are in accord with their assignment to the protons of the two CH_3 groups, the C.7 methylene group, and the C.3 and C.6 methylene groups, respectively. Under very high resolution fine splittings of the 2.09 signal and broadening of the 1.79 signal can be observed; these effects are attributable to the non-equivalence of the exo and endo protons on the C.2 and C.5 methylene groups, and long-range coupling of the C.7 methylene protons with the endo C.3 and C.6 protons (9, 10).

Reduction of the diketone V with lithium aluminium hydride gave a syrupy crude product from which a crystalline diol, m.p. 124.5–125°, was isolated in low yield. This was shown to be a stereoisomer of the exo–endo diol XI by its re-oxidation to the diketone V. Although reduction by lithium aluminium hydride of bicyclo[2.2.1]heptan-2-ones without substituents at C.7 normally occurs by attack from the less hindered exo side (*vide supra*) to give the endo alcohol, it has been observed that reduction of the diketone IV with lithium aluminium tri-*t*-butoxy hydride gives, in addition to the corresponding endo–endo diol as the major product, detectable amounts of the exo–endo diol (6). The fact that the tri-*t*-butoxy hydride, which should be particularly susceptible to steric effects, does not react stereospecifically suggests that lithium aluminium hydride might give significant amounts of products derived by endo attack in related cases. Thus caution must be exercised in the assignment of stereochemistry to the product isolated on reduction of V, particularly since it is obtained in low yield. Nevertheless, the n.m.r. spectrum of the crude product, which was obtained in high yield, showed it to consist largely of the isomer, m.p. 124.5–125°, together with less than 20% of another product whose n.m.r. signals correspond to those of the exo–endo diol. Now, it may be counted highly unlikely that endo attack would predominate at both carbonyl groups of V to such a degree that the exo–exo diol (XIV) would be formed to the virtual exclusion of the endo–endo diol (XV). It is therefore concluded that exo attack largely preponderates and that the reduction product is the endo–endo diol XV. This view is corroborated by the following interpreta-

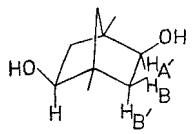

XIV

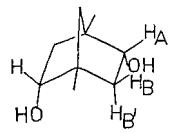

XV

tion of the n.m.r. spectrum of the reduction product. A sharp singlet of relative intensity six at δ 1.01 is assigned to the two equivalent bridgehead methyl groups. A broadened singlet at δ 1.25 of relative intensity two is assigned to the equivalent C.7 methylene protons coupled weakly to the C.3 and C.6 endo protons (cf. refs. 9, 10). A signal at δ 2.55 (in 2.5 mole % solution in $CDCl_3$) of relative intensity two can be attributed to the hydroxyl protons since its position is concentration dependent. The remaining signals consist of an unsymmetrical doublet (97 and 104 c.p.s.)[3] and triplet (226, 233, and 240 c.p.s.)[3] of relative intensities four and two, respectively. These can be interpreted in terms of two identical systems of the ABB′ type (11) with the low-field triplet assigned to the C.2 and C.5 protons (A) coupled respectively with the C.3 and C.6 pairs of protons (BB′). This interpretation requires that $|J_{BB'}|$ be large, as is expected, and that $\delta_B \simeq \delta_{B'}$. Restricted first-order analysis (11) gives the following approximate values: $\delta_A = 3.89$,

[3]*Down-field shifts from Me_4Si (int.) in $CDCl_3$ at 60 Mc.*

Can. J. Chem. Downloaded from www.nrcresearchpress.com by 210.87.254.5 on 09/05/12
For personal use only.

$\delta_B = \delta_{B'} = 1.68$, $|J_{AB} + J_{AB'}| = 14$ c.p.s. Now, Musher's studies of the spectra of a series of bicyclo[2.2.1]heptan-2-ols (9) indicate that for XIV and XV the AB coupling constants should have the following approximate absolute magnitudes: $J_{A'B} = 3$, $J_{A'B'} = 6.5$, $J_{AB} = 9.5$, $J_{AB'} = 3.5$ c.p.s. Thus, the observed value for the sum of the coupling constants confirms that the reduction product is the endo–endo diol XV, for the expected sum in the case of the exo–exo diol, XIV, would be $|J_{A'B'} + J_{A'B}| \simeq 9.5$ c.p.s. Indeed, Musher (9) has observed a triplet signal for the endo >CHOH proton of the exo alcohol, isoborneol (XII) with $|J_{A'B'} + J_{A'B}| = 9.3$ c.p.s. These comparisons are approximate only because of (i) approximations inherent in the restricted first-order analysis, (ii) band broadening or splitting due to further, long-range spin couplings,[4] (iii) changes in the coupling constants of the bicyclo[2.2.1]heptan-2-ols engendered by the introduction of a second hydroxyl group at C.5. However, any inaccuracies arising from these factors are expected to be relatively small and unlikely to jeopardize the structural assignment.

We turn finally to the consideration of the reaction pathway for the formation of the exo–endo diacetate IX by the acid-catalyzed rearrangement of the diol VI. It has been found (8, 12) that similar rearrangement of the corresponding monohydric tertiary endo alcohol VII, or its exo epimer, gives the exo acetate X. It may readily be seen that two successive rearrangements of this type would necessarily lead to a product with the exo–endo stereochemistry, as observed:[5]

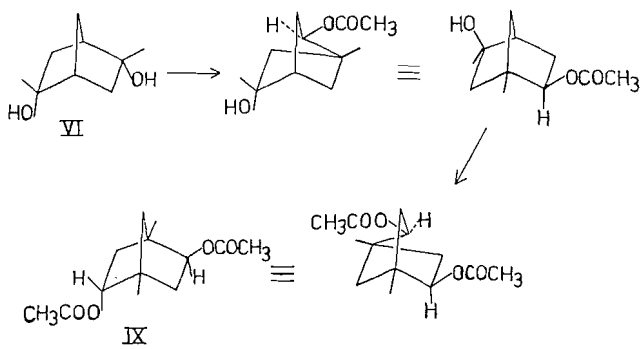

EXPERIMENTAL

Melting points were determined on a Fisher-Johns hot stage and are uncorrected. Solutions in organic solvents were dried with anhydrous sodium sulfate and evaporated on a rotary evaporator, unless otherwise stated.

2-exo-5-exo-Dimethylbicyclo[2.2.1]heptane-2,5-diol (VI)

Bicyclo[2.2.1]heptan-2,5-dione (6) (15.4 g, 0.124 mole) in anhydrous ether (50 ml) was added with mechanical stirring to a Grignard solution made from methyl iodide (88.7 g, 0.629 mole) and magnesium (15.1 g, 0.62 g atom) in anhydrous ether (500 ml). After it had been left to stand for 7 days, with intermittent stirring, the solution was poured into ice-water (310 ml) containing ammonium chloride (40 g). The aqueous solution was extracted four times with ether, and then subjected to continuous extraction for 2 days. Combination of the ethereal extracts, followed by drying and removal of the solvent gave a viscous yellow liquid (15. 8 g, 82%). This was dissolved in ether, washed with aqueous 10% sodium sulfite, dried, and freed of solvent to give a colorless, viscous liquid (15.0 g, 78%); λ_{max} (CCl_4):2.79, 5.72 (v.w.), 7.30, 8.95 μ; δ (CCl_4):1.28 (singlet), 1.95, 2.95 p.p.m.

Attempts to purify this compound by distillation and chromatography were unsuccessful.

[4]*Strong long-range spin coupling involving the C.7 protons of norbornane derivatives of the type reported recently (13) cannot be operative here since the signal due to these protons is unsplit.*

[5]*It may be noted that this result is independent of the stereochemistry assigned to VI.*

Can. J. Chem. Downloaded from www.nrcresearchpress.com by 210.87.254.5 on 09/05/12
For personal use only.

2-exo-5-endo-Diacetoxy-1,4-dimethylbicyclo[2.2.1]heptane (IX)

Compound VI (10.0 g, 64 mmoles) was dissolved in glacial acetic acid (80 ml), and sulfuric acid (75%; 3 ml) was added. The solution was heated at 70–80° for 2 h on the steam bath and when cool, poured into ice-water (150 ml). A solution of sodium hydroxide (43 g) in water (150 ml) was added with rapid stirring to the reaction solution immersed in an ice bath, and neutralization was completed with solid sodium bicarbonate. The aqueous solution was thoroughly extracted with ether and the combined ethereal extracts were washed with saturated brine and dried. Removal of the solvent was effected by distillation through a column of glass helices, and the residue was distilled through a spinning band column to give IX as a colorless liquid (12.15 g, 50%), b.p. 74–75° (0.2 mm), $n_D^{25.6}$ 1.4560; λ_{max} (CCl_4):5.74, 8.1 μ; δ (CCl_4):0.95, 1.09, 1.97, 4.64 (multiplet) p.p.m.

Anal. Calcd. for $C_{13}H_{20}O_4$: C, 64.98; H, 8.39. Found: C, 64.97; H, 8.39.

1,4-Dimethylbicyclo[2.2.1]heptane-2-exo-5-endo-diol (XI)

To a solution of IX (9.8 g, 41 mmoles) in anhydrous methanol (50 ml) was added sodium (200 mg) and the resulting solution was slowly distilled to dryness through a column of glass helices. The last traces of solvent were removed on the rotary evaporator and ether (200 ml) was added. The ethereal solution was washed with water (2 × 10 ml) and dried, and the solvent was distilled as above to give the crude diol as a gum (5.88 g). Crystallization from ether/hexane gave crystalline material (5.0 g, 86%) in crops with melting point ranging from 85–95° to 93–95°. Six further crystallizations gave an analytical sample, m.p. 98.5–99.5°; λ_{max} (CCl_4):2.78, 9.0, 9.72, 11.06 μ; δ ($CDCl_3$):1.05, 1.09, 1.70, 3.58 (multiplet), 3.83 (multiplet) p.p.m.

Anal. Calcd. for $C_9H_{16}O_2$: C, 69.19; H, 10.32. Found: C, 69.24; H, 10.34.

1,4-Dimethylbicyclo[2.2.1]heptane-2,5-dione (V) from XI

A solution of the diol XI (m.p. 93–97°; 200 mg, 1.2 mmoles) in acetone (20 ml) was cooled in an ice bath. A solution of chromium trioxide (760 mg) in sulfuric acid (96%; 0.63 ml) and water (2.2 ml) was added dropwise with rapid stirring until a yellow-brown color persisted. The solution was stirred for a further 3 h, and ether was added and the solution was dried over anhydrous sodium carbonate. Removal of the solvent, followed by one sublimation and crystallization from ether–hexane gave the diketone as long needles (120 mg, 60%), m.p. 127.5–128°; λ_{max} (CCl_4):5.70, 7.10, 7.22, 8.85, 9.35 μ; λ_{max} (MeOH):287.5 mμ (ϵ 47); δ (CCl_4):1.22, 1.79, 2.09 p.p.m.

Anal. Calcd. for $C_9H_{12}O_2$: C, 71.02; H, 7.95. Found: C, 70.94; H, 7.99.

The diketone was recovered unchanged when treated for 24 h with aqueous ethanolic potassium hydroxide.

A *bis-2,4-dinitrophenylhydrazone*, m.p. 280–282°, was prepared in dioxane/aqueous hydrochloric acid, and recrystallized three times from dioxane/ethanol.

Anal. Calcd. for $C_{21}H_{20}N_8O_8$: C, 49.21; H, 3.91; N, 21.87. Found: C, 48.88; H, 4.11; N, 22.09.

1,4-Dimethylbicyclo[2.2.1]heptane-2-endo-5-endo-diol (XV)

A solution of the dione V (110 mg, 0.72 mmole) in anhydrous ether (10 ml) was added dropwise to a solution of lithium aluminium hydride (50 mg) in ether (5 ml) and the solution was stirred overnight under a flow of nitrogen. Water (1 ml) was added and the mixture was vigorously shaken, dried, and filtered. Removal of the solvent gave the crude diol (108 mg) from which pure material (22 mg, 20%), m.p. 124.5–125°, was obtained after two crystallizations from ether/hexane; λ_{max} (CH_2Cl_2):2.80, 7.18, 8.20, 11.50 μ; δ ($CDCl_3$):1.01, 1.25, 1.68 (doublet, 'J' = 7 c.p.s.), 2.55, 3.89 (triplet, 'J' = 7 c.p.s.) p.p.m.

Anal. Calcd. for $C_9H_{16}O_2$: C, 69.19; H, 10.32. Found: C, 68.98; H, 10.31.

1,4-Dimethylbicyclo[2.2.1]heptane-2,5-dione (V) from XV

To a solution of the diol XV (7.5 mg) in acetone (2 ml) were added, with rapid stirring, two drops of a solution of chromium trioxide (260 mg) in water (2.2 ml) and sulfuric acid (96%; 0.63 ml). After 5 min, ether was added and the solution was dried over sodium carbonate. Removal of the solvent gave a white solid (4.5 mg), m.p. 120–122°, which, on crystallization from ether/hexane, gave material (2 mg), m.p. 127–128°, whose infrared spectrum was identical with that of V prepared from XI. A mixed melting point with a sample of V prepared from XI showed no depression.

ACKNOWLEDGMENT

The support of the National Research Council is gratefully acknowledged.

REFERENCES

1. N. J. Toivonen. Suomen Kemistilehti, **88**, 44 (1935).
2. S. Nametkin and L. Brussoff. Ann. **459**, 144 (1927); J. Prakt. Chem. [ii] **135**, 155 (1932).
3. G. A. Nyman and A. M. Kuvaja. Ann. **538**, 68 (1939).
4. T. R. Lynch. M.A. Thesis, University of Toronto. 1963.
5. A. N. Elizarova. Zh. Obshch. Khim. **34**, 3205 (1964).
6. J. Meinwald, J. K. Crandall, and P. G. Gassman. Tetrahedron, **18**, 815 (1962).
7. R. Sauers. J. Am. Chem. Soc. **81**, 4874 (1959).

Can. J. Chem. Downloaded from www.nrcresearchpress.com by 210.87.254.5 on 09/05/12
For personal use only.

8. J. A. BERSON, J. S. WALIA, A. REMANICK, S. SUZUKI, P. REYNOLDS-WARNHOFF, and D. WILLNER. J. Am. Chem. Soc. **83**, 3986 (1961).
9. J. I. MUSHER. Mol. Phys. **6**, 93 (1963).
10. S. STERNHELL. Rev. Pure Appl. Chem. **14**, 15 (1964).
11. R. E. RICHARDS and T. SCHAEFER. Mol. Phys. **1**, 331 (1958). R. J. ABRAHAM and H. J. BERNSTEIN. Can. J. Chem. **39**, 216 (1961). J. I. MUSHER and E. J. COREY. Tetrahedron, **18**, 791 (1962).
12. S. BECKMANN, R. SCHABER, and R. BAMBERGER. Chem. Ber. **87**, 997 (1954). N. J. TOIVONEN, E. SILTANEN, and K. OJALA. Ann. Acad. Sci. Fennicae, Ser. **A II**, No. 64 (1955).
13. J. MEINWALD, Y. C. MEINWALD, and T. N. BAKER III. J. Am. Chem. Soc. **86**, 4074 (1964).

Can. J. Chem. Downloaded from www.nrcresearchpress.com by 210.87.254.5 on 09/05/12
For personal use only.

Can. J. Chem. Downloaded from www.nrcresearchpress.com by 210.87.254.105 on 09/05/12
For personal use only.

NUMERICAL SOLUTIONS OF SMOLUCHOWSKI'S EQUATIONS FOR THE COAGULATION OF UNCHARGED AEROSOLS

J. M. BEECKMANS

Department of Physiological Hygiene, School of Hygiene, University of Toronto, Toronto, Ontario

Received March 3, 1965

ABSTRACT

Smoluchowski's equations for the coagulation of uncharged aerosol particles were programmed for solution by electronic computer. Terms representing differential sedimentation, turbulence, and mean aggregate density in solid aerosols were included. The effect of heterogeneity in the particle-size distribution of the aerosols on their rate of coagulation was illustrated by means of a slip-corrected coagulation factor F_c, which assumes a value of unity in all non-turbulent homogeneous aerosols. Curves of F_c vs. σ_g, the geometrical standard deviation, were calculated for aerosols of various mean particle-size. The effects due to turbulence, and to differential sedimentation, were illustrated in a similar manner. It was also found that the process of coagulation gives rise to a degree of dispersion which is independent of the original dispersion parameter, and depends only slightly on the mean particle-size of the aerosol over a wide range of particle-sizes. In the particle-size range in which differential sedimentation is inappreciable, the relatively constant value of the dispersion parameter implies that heterogeneous aerosols must obey the simplified integrated form of Smoluchowski's equation, which is applicable to homogeneous aerosols. The coagulation constant exceeds that predicted by the simple theory by about 10% for liquid aerosols of 0.1 μ or less.

INTRODUCTION

The theory of coagulation on uncharged and monodispersed colloid particles developed by Smoluchowski (1) is applicable to aerosols when the appropriate correction is made for slip. It has been reasonably well substantiated by experiment when the effects due to wall losses, turbulence, and differential sedimentation are taken into account (2, 3). Essentially, the theory consists of a basic differential equation concerning the rate of coagulation between two different species of particles (i.e., of differing particle-sizes), which must then be integrated over all pairs of species present in the aerosol. The solution consists of a family of particle-size distribution curves, each corresponding to a certain time following the start of coagulation. If the assumption is made that the aerosol is intially homogeneous, and remains homogeneous during the course of coagulation, then a simple analytical solution to the problem is obtained. If this assumption is not made, then numerical solutions must be sought. The success of the simplified treatment, particularly with homogeneous liquid aerosols (2), is taken as evidence that the basic differential equation is essentially correct. Observed deviations from this simple theory are ascribed to three causes, viz., electrical charges, the non-spherical nature of solid aerosol particles, particularly where there exists a tendency to form chain-like agglomerates, and heterogeneity in the particle-size distribution. In this paper the latter factor will be investigated by means of numerical solutions of the basic differential equation, which are compared with the analytical solutions applicable to homogeneous aerosols. In addition, terms representing turbulence and differential sedimentation, which cannot be taken into account in the simple treatment, have been included.

METHOD OF CALCULATION

A. Basic Equations

The derivation of Smoluchowski's equations will not be given here, since this subject has been given adequate treatment in numerous books and papers. (See, e.g., Whytlaw-Gray and Patterson (4) and Green and Lane (5) for expositions in English.) The differential

equation for collisions between particles of species i and particles of species j, including turbulence and differential sedimentation terms, is as follows:

$$[1] \quad -\left(\frac{dn_i}{dt}\right)_j = -\left(\frac{dn_j}{dt}\right)_i = \{K_D\left(\frac{C_i}{d_i} + \frac{C_j}{d_j}\right)(d_i + d_j) + K_c(d_i^2 C_i - d_j^2 C_j)(d_i + d_j)^2 + K_T(d_i + d_j)^3\} n_i n_j \quad (d_i \geqslant d_j).$$

n_i is the concentration of particle species i, C_i the Cunningham slip correction factor for particle species i (see eq. [5]), and d_i is the diameter of particle species i.

The values of the constants are as follows:

$$[2] \quad K_D = \frac{kT}{3\mu} \quad \text{(diffusional collision constant)},$$

μ being the viscosity of the medium.

At 25 °C in air, $K_D = 7.38 \times 10^{-11}$ cm^3 s^{-1}.

$$[3] \quad K_c = \frac{2\pi\rho g}{9\mu} \quad \text{(differential sedimentation collision constant)}.$$

At 25 °C in air, for unit density particles, $K_c = 3.7 \times 10^6$ s^{-1} cm^{-1}.

$$[4] \quad K_T = \frac{4}{3}\left(\frac{\overline{du}}{dz}\right) \quad \text{(turbulence collision constant)}.$$

$\frac{\overline{du}}{dz}$ is the mean rate of shear due to turbulence. The Cunningham slip correction factor was calculated by the equation

$$[5] \quad C_i = 1 + (10^{-4}(0.1664 + 0.053 \exp(-8.325 \times 10^4 d_i))/d_i).$$

This particular form of Cunningham's equation is due to Davies (6).

B. Numerical Integration

Goldman (7) published the complete integro-differential equation based on eq. [1], without the differential sedimentation and turbulence terms. A similar equation was published by Zebel (8), who presented a solution derived on an electronic computer. He did not, however, systematically investigate the effects of heterogeneity, or of any other factor.

In the calculations, 80 particle-sizes were represented in the computer. The particle-size of the smallest particle class, and its density, served as input parameters. The masses of all other particle species were integral multiples of that of the first particle species. The range of masses between the smallest and the largest was 1.58×10^8. Intermediate particle masses were spaced at approximately equal logarithmic intervals. Their diameters were calculated by an equation proposed by Beeckmans (9) for aerosol agglomerates.

$$[6] \quad d_i = d_1(m_i/m_1)^\psi$$

The value of 0.333 for ψ gives the correct diameter for coalescing liquid droplets. Solid particle agglomerates generally have a value between 0.33 and 0.55, if chain formation is not too pronounced.

The procedure followed, after reading in the initial boundary conditions, and the initial particle-size distribution, was to compute values of dn_i/dt for all i by direct summation.

$$[7] \quad \frac{dn_i}{dt} = \sum_{j=1}^{i}\left(\frac{dn_i}{dt}\right)_j$$

Can. J. Chem. Downloaded from www.nrcresearchpress.com by 210.87.254.105 on 09/05/12
For personal use only.

(The values for $(dn_i/dt)_i$ were multiplied by one-half to correct for duplication implied in the above counting scheme.)

Each collision between species i and species j produced an increase in the concentration of particles of species k, the value of k being determined by the equations

$$\begin{cases} m_k \leqslant m_i + m_j \\ m_{k+1} > m_i + m_j. \end{cases} \quad [8]$$

During the summation [7], the computer made additions to the values of the appropriate (dn_k/dt)'s corresponding to each combination of i and j.

$$\left(\frac{dn_k}{dt}\right)_{i,j} = -\left(\frac{dn_i}{dt}\right)_j (1 - Q_{i,j}) \quad [9]$$

$$\left(\frac{dn_{k+1}}{dt}\right)_{i,j} = -Q_{i,j}\left(\frac{dn_i}{dt}\right)_j \quad [10]$$

$$Q_{i,j} = \frac{m_i + m_j - m_k}{m_{k+1} - m_k} \quad [11]$$

The factor $Q_{i,j}$ partitions the particles produced by collisions between particles i and j in such a way as to conserve mass on averaging over many collisions. If $m_k = m_i + m_j$, then $Q_{i,j} = 0$.

All terms of the type of eqs. [9], [10], and [7] were summed to give the total net rate of particle diminution in the aerosol.

$$\frac{dn}{dt} = \sum_{i=1}^{80} \frac{dn_i}{dt} \quad [12]$$

The fractional decrease in total particle number per cycle was held constant, equal to a parameter β.

Thus

$$\frac{dn}{dt}\frac{t_c}{n} = \beta, \quad [13]$$

where

$$n = \sum_{i=1}^{80} n_i$$

and t_c is the cycle time, or the time required to reduce the particle concentration by a fraction β. Equation [13] allows its value to be calculated for a given β. The particle-size distribution was then adjusted as follows in each class.

$$n_i \rightarrow n_i + \left(\frac{dn_i}{dt}\right)t_c \quad [14]$$

Finally, the values of n_i in classes 71–80 were set equal to zero at each cycle. This was necessary to avoid collisions of the type which would produce new particles outside the size range under consideration. The computer reported on the percent of the total mass originally present in the system and removed in this manner. A number of parameters derivable from the altered particle-size distribution were calculated at certain selected cycles. They included the arithmetic and geometrical mean diameters, and the geometrical standard deviation. The following parameters were also calculated:

(i) Coagulation constant. (Calculated with n at its mid-cycle value.)

Can. J. Chem. Downloaded from www.nrcresearchpress.com by 210.87.254.105 on 09/05/12
For personal use only.

[15] $$K = \left(\frac{dn}{dt}\right) \Big/ n^2(1 - \beta/2)^2$$

(ii) Coagulation factor.

[16] $$F = K/4K_D$$

(iii) Slip-corrected coagulation factor.

[17] $$F_c = \frac{F}{C_g} = \frac{K}{4K_D C_g}$$

C_g is the Cunningham slip correction factor for a particle with diameter equal to d_g, the geometrical mean diameter, and was calculated by means of eq. [5]. It may be noted that F_c equals unity for a homogeneous aerosol in which turbulence and differential sedimentation contribute to a negligible degree to the total rate of coagulation. Thus, in aerosols of relatively small particle-size, F_c is essentially a measure of the effects of heterogeneity on the coagulation constant.

RESULTS

Figure 1 shows the effect of heterogeneity, expressed as σ_g, the geometrical mean diameter, on the corrected coagulation factor F_c, for various values of d_g. K_T equalled zero for all curves. The parameter β equalled 0.001, and only one cycle was completed for each value of σ_g, and d_g, since temporal effects were not under consideration. Figure 2 shows the same data plotted as F vs. σ_g, and Fig. 3 shows F_c vs. σ_g in the presence of turbulence ($K_T = 500\ s^{-1}$ in Fig. 3, and $\psi = 0.333$ for all figures).

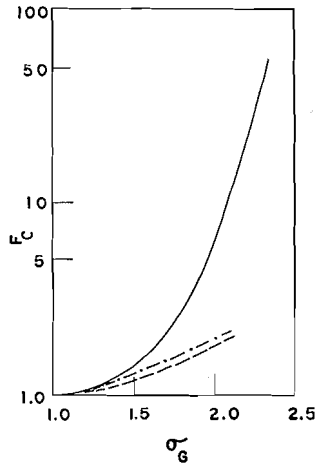

FIG. 1. Corrected coagulation factor F_c vs. σ_g; (—) $d_g = 1\ \mu$, (- -) $d_g = 0.1\ \mu$, (···) $d_g = 0.01\ \mu$.

In runs involving the effect of time on the particle-size distribution, it was first necessary to select a value for β, the fractional particle concentration decrease per cycle. Ideally this number should be as close to zero as possible. On the other hand, since the smaller, the value of β, the greater the amount of time required to compute the course of a given degree of coagulation, practical considerations made it desirable to use the largest value of β giving substantially correct results. In order to test the effect of variations in β, the course of coagulation was computed with three successive values of β and the same starting

Can. J. Chem. Downloaded from www.nrcresearchpress.com by 210.87.254.105 on 09/05/12
For personal use only.

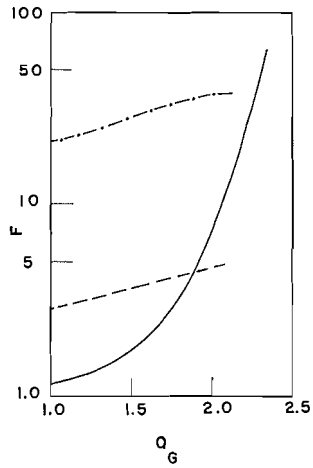

FIG. 2. Coagulation factor F vs. σ_g; (—) $d_g = 1\,\mu$, (- -) $d_g = 0.1\,\mu$, (···) $d_g = 0.01\,\mu$.

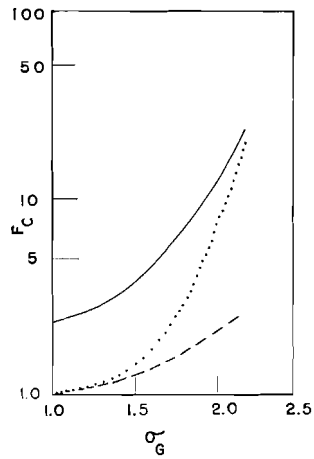

FIG. 3. Corrected coagulation factor F_c vs. σ_g for a turbulent aerosol ($K_T = 500\ s^{-1}$); (—) $d_g = 1\,\mu$, (- -) $d_g = 0.1\,\mu$, (··) $d_g = 1\,\mu$ and $K_T = 0$. (Same curve as in Fig. 1.)

conditions. The results are given in Table I, and indicate that values of β in the range 0–0.1 give substantially similar results. Consequently, a value of 0.05 was used in all subsequent runs involving time.

TABLE I*

Effect of the parameter β on the calculated course of coagulation†

β	t (s)	d_g (μ)	$N \times 10^{-10}$
0.025	0.4283	0.09218	0.1769
0.05	0.4283	0.09314	0.1731
0.10	0.4283	0.09505	0.1666

*Figures obtained by interpolation between cycles where necessary.
†Initial conditions: $d_g = 0.02\,\mu$, $N = 0.2321 \times 10^{12}$.

Can. J. Chem. Downloaded from www.nrcresearchpress.com by 210.87.254.105 on 09/05/12
For personal use only.

A preliminary inspection of the particle-size curves of coagulating aerosols showed that they were approximately logarithmically normal in shape, and, for this reason, the geometric-mean parameters have been preferred for characterization purposes in this paper. It was also found that within relatively wide ranges of mean particle-sizes the geometrical standard deviation of the coagulating aerosol tended to assume a constant value. This is illustrated in Fig. 4, which shows the effect of time on σ_g in three aerosols, each with an initial geometrical mean diameter of 0.1 μ and with geometrical standard deviations of 1.0, 1.3, and 1.5, respectively. It is seen that all three aerosols eventually attain a value of approximately 1.35 for σ_g. The equilibrium values of σ_g for liquid non-turbulent, liquid turbulent, and solid non-turbulent aerosols of three particle-sizes are given in Table II.

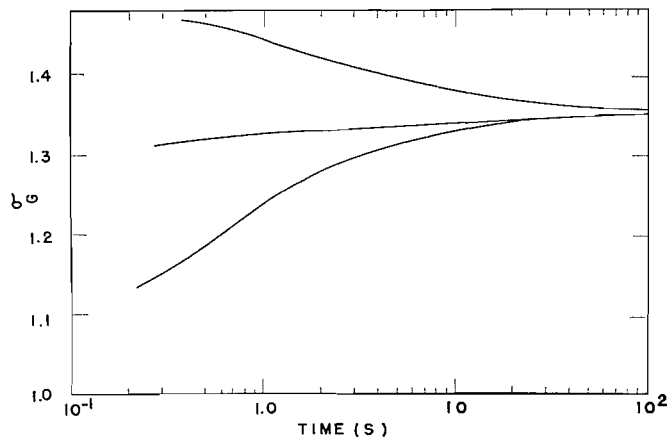

FIG. 4. Asymptotic approach of σ_g to a constant value. Initial values 1.5, 1.3, and 1.0.

TABLE II

Equilibrium σ_g values

	Geometrical mean diameter (μ)		
	0.01	0.1	1.0
Liquid	1.35	1.35	1.70
Liquid turbulent*	1.35	1.36	1.87
Solid†	1.44	1.51	1.67

*$K_T = 500\ s^{-1}$.
†$\psi = 0.5$.

DISCUSSION OF RESULTS

For a homogeneous aerosol, the simplified treatment predicts

$$K = \frac{4kTC_g}{3\mu} = 4K_D C_g. \qquad [18]$$

Since C_g increases with decreasing particle-size, K must also increase with decreasing particle-size, as must F, to which it is proportional. This is borne out in Fig. 2, where F is greater than unity, even in homogeneous aerosols. On the other hand, F_c equals unity for all particle-sizes in non-turbulent aerosols, since $F_c = F/C_g$ (Fig. 1). Values of F_c

Can. J. Chem. Downloaded from www.nrcresearchpress.com by 210.87.254.105 on 09/05/12
For personal use only.

exceeding unity in non-turbulent heterogeneous aerosols arise because the term proportional to K_D in eq. [1] is at a minimum for $d_i = d_j$, irrespective of the values of C_i and C_j, so that the sum of all such terms in a heterogeneous aerosol always exceeds the corresponding sum in the homogeneous case. In addition to this factor, if the mean particle-size of the aerosol is sufficiently large so that differential sedimentation effects come into play, this will also increase the value of F_c. These points are illustrated in Fig. 1. The curves for $d_g = 0.1\ \mu$ and $d_g = 0.01\ \mu$ are very similar because at this particle-size the effects of differential sedimentation are negligible. A curve for $d_g = 1\ \mu$, and $K_c = 0$, and not shown in the figure, was also found to be very similar. On the other hand, the curve for $d_g = 1\ \mu$, with K_c having its proper value, diverges sharply, due to differential sedimentation effects.

Figure 3 shows that even strong turbulence has little influence on F_c for aerosols of 0.1 μ or less. On the other hand, aerosols of a particle-size of 1 μ or more, whether homogeneous or not, coagulate much more rapidly under turbulent conditions.

The relative constancy in σ_g attained in coagulating aerosols presumably derives from the fact that the natural tendency towards widening the distribution which arises through chance collisions of particles is countered by the greater collision rate between particles of differing sizes relative to the collision rate between particles of similar size. This would tend to make the aerosol more homogeneous, since particles differing greatly from the mean size would collide more rapidly than most. It may also be noted that the success of the simplified treatment in predicting the course of coagulation follows as a consequence of the temporal constancy in σ_g. By reference to Fig. 1, it is seen that the value of F_c for an aerosol 0.1 μ or 0.01 μ in mean particle-size, having a value of 1.35 for σ_g, is approximately 1.1. This implies that the rate of coagulation of a heterogeneous, aged aerosol in this particle-size range is approximately 10% greater than the rate predicted by the simplified theory for a homogeneous aerosol of the same mean particle-size. Since this factor is constant, the form of the relation between time and the particle concentration is the same in both cases. Unfortunately, accurate measurements of the particle-size distribution of coagulated aerosols do not appear to have been made, so that the calculated pseudo-equilibrium values of σ_g cannot be directly confirmed.

ACKNOWLEDGMENT

This work was made possible by Public Health Research Grant No. 605-7-229, from the Department of National Health and Welfare, Ottawa, and by facilities made available by the Institute of Computer Science, University of Toronto.

REFERENCES

1. M. VON SMOLUCHOWSKI. Z. Physik. Chem. Leipzig, **92**, 129 (1917).
2. S. DEVIR. J. Colloid Sci. **18**, 744 (1963).
3. G. O. LANGSTROTH and T. GILLESPIE. Can. J. Res. B, **25**, 455 (1947).
4. R. WHYTLAW-GRAY and H. S. PATTERSON. Smoke. Arnold. 1932.
5. H. L. GREEN and W. R. LANE. Particulate clouds, dusts, smokes and mists. Spon. 1957.
6. C. N. DAVIES. Proc. Phys. Soc. **57**, 259 (1945).
7. D. E. GOLDMAN. Handbook on aerosols. U.S. Atomic Energy Commission. 1950.
8. G. ZEBEL. Kolloid-Z. **156**, 102 (1958).
9. J. M. BEECKMANS. Ann. Occupational Hyg. **7**, 299 (1964).

Can. J. Chem. Downloaded from www.nrcresearchpress.com by 210.87.254.105 on 09/05/12
For personal use only.

Can. J. Chem. Downloaded from www.nrcresearchpress.com by 210.87.254.40 on 09/05/12
For personal use only.

THE THERMODYNAMIC PROPERTIES AND PHASE DIAGRAM OF THE GOLD–CADMIUM SYSTEM BY THE ISOPIESTIC METHOD[1]

L. J. BARTHA[2] AND W. A. ALEXANDER
Division of Applied Chemistry, National Research Council, Ottawa, Canada

Received September 2, 1964

ABSTRACT

Activities of cadmium in gold alloys with up to 50 atom % Cd have been determined by an isopiestic method. The partial molar free energy, entropy, and heat of solution in the alpha and beta phases are calculated between 500 and 600 °C. The phase boundaries have been observed between 16 and 60 atom % above 400 °C. The boundaries of the two-phase regions $\alpha_2 + \beta$ and $\beta + \delta'$ are found at somewhat different concentrations than before, but the two-phase region $\alpha + \alpha_2$ was not observed.

INTRODUCTION

Measurements of the vapor pressure of the volatile element in alloys having only one volatile component may be used to calculate the thermodynamic properties of these alloys using well-known relations. These properties furnish a detailed picture of the alloy's energic quantities. The method is restricted by the requirement that only one component be significantly volatile, but several procedures have been developed for this purpose (8, 16, 17). Advantages are that the vapor pressure is very sensitive to changes in temperature or composition and that a clear interpretation of the results is possible.

A limited amount of information has been published on the thermochemical data for the gold–cadmium system. The first investigation of this system was by Ölander (1) using electromotive force measurements of a suitable cell. He calculated the heat effects at only a few phase transitions. Schneider and Schmid (2) made calculations from vapor pressure measurements over four liquid alloys above 45 atom % cadmium. These data are summarized and discussed by Kubaschewski and Catterall (3). Calorimetric measurements of heats of formation have been made for a number of alloys at 450 °C by Kleppa (10). Vapor pressure measurements of this system by Herasymenko are referred to in the literature (9) and are available as a report of limited circulation. In this report indications of ordering at a number of compositions are stressed for both the gold–cadmium and the silver–cadmium systems. However, Kleppa's results for gold–cadmium (10) and Filby and Pratt's work on silver–cadmium (11) did not show any such ordering, so its presence in the gold–cadmium system is questionable.

There is also disagreement in the literature on the gold–cadmium phase diagram, especially on the low cadmium side. Ölander's electromotive force measurements (1) indicate an alpha phase up to about 34 atom % Cd, and a two-phase region from 34 to 42% at temperatures of 500–600 °C. Below 420 °C an alpha prime phase was shown between about 18 and 28% Cd. Owen *et al.* (4, 5) found four alpha phases and suggested that the beta phase begins at 50% Cd. Hansen's more recent summary (6) does not show an alpha three phase. This phase was not found in a reinvestigation of the whole system by Rivlin *et al.* (7). On the above information then the phases present at 500–600 °C up to 55 atom % Cd should be: alpha, alpha two and beta, and two two-phase regions between them.

[1]*Issued as N.R.C. No. 8535.*
[2]*National Research Council Postdoctorate Fellow, 1962–1964. Present address: Kossuth Lajos Tudományegyetem, Fizikai-kémiai Intézete, Debrecen 10, Hungary.*

From both these points of view then a further investigation of this system by the vapor pressure method appeared desirable.

APPARATUS, MATERIALS, AND EXPERIMENTAL PROCEDURE

The apparatus was essentially the same as that used by Herasymenko (8) with some minor modifications as described in ref. 12. In the present work the silica tube was horizontally disposed so that the liquid cadmium distilled to the temperature minimum, which determines its pressure in the system. The equilibrium concentration of cadmium in its gold alloys is determined by this cadmium pressure and by the temperature of the alloy. The gold absorbs cadmium until the cadmium vapor pressure of the alloy is the same as that of the pure cadmium at the temperature minimum. The data for each experiment or vapor pressure are plotted as alloy temperature versus alloy composition. Isobaric curves of alloy temperature versus composition obtained in this manner will show horizontal sections in the two-phase regions of the phase diagram.

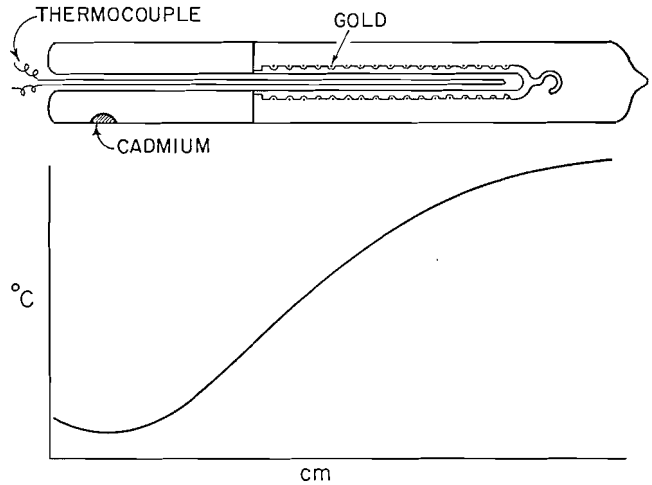

FIG. 1. Quartz vessel and temperature distribution.

The silica vessel used is shown in Fig. 1 with a schematic temperature gradient. The furnace heated by three separate windings was large enough to contain two reaction vessels with different cadmium pressures. The temperature was controlled by electronic instruments actuated by platinum resistance elements placed close to the heating windings. The desired temperature gradient was achieved by placing variable resistances in parallel with portions of the heating elements. The temperatures were measured daily by a platinum–rhodium thermocouple calibrated before and after each experiment.

Gold wire was drawn from doubly electrolyzed gold crystals cast into a bar. The cadmium was used as filings from a high purity bar with any iron particles removed by a strong magnet. Analyses of these materials showed:

Gold.—Impurities close to those in commerical samples of spectroscopically pure material. Au $\geqslant$ 99.999%.

Cadmium.—Lead, copper, and silver— one to two tenths p.p.m. Other elements not detected and therefore less than this level. Cd $\geqslant$ 99.9999%.

The vessels were charged with accurately weighed gold wires 0.254 mm diameter and 4.2 cm long and about twice the calculated amount of cadmium. Degassing was effected by evacuating to about 2×10^{-4} mm Hg while the portion of the vessel containing the gold wires was heated to about 500 °C and the remainder gently warmed. Then the vessel was sealed off under vacuum. The tubes were charged in the furnace near the required temperature and final temperature adjustments made during the next 2 or 3 days. At temperatures of this work annealing times of 3 weeks or more were employed to ensure attainment of equilibrium, although calculations from the available diffusion data (14) would indicate that a considerably shorter time should be sufficient. The vessels were air cooled to about 600 °C and then quenched in oil. Oil quenching much above 600 °C produced a light deposit, probably of carbon or tar, inside the quartz tube. The composition was determined by reweighing the wires or by chemical analysis in the few cases where the ends were fused after alloying.

The cadmium vapor pressure equation used is that of Maier (15):

$$\log p = 12.2870 - 5819.4T^{-1} - 1.2572 \log T.$$

Can. J. Chem. Downloaded from www.nrcresearchpress.com by 210.87.254.40 on 09/05/12
For personal use only.

This is the equation quoted in recent summaries of vapor pressure data and is the result of a critical survey and recalculation of earlier data (cf. ref. 11).

Besides the errors in the original determination of the vapor pressure of cadmium, the following errors apply. The error in weight of the gold wires was $\pm 2\ \mu g$ in a total weight of about 50 mg. The potential of the thermocouple was read to the nearest $\frac{1}{2}\ \mu V$, or 0.05 deg. The distribution of the sample wires in the grooves along the carrier tube was determined to about ± 0.02 mm by a travelling microscope. The location of the thermocouple was measured by a steel meter rule to ± 0.25 mm, which at the maximum temperature gradient was equivalent to about ± 0.3 deg. The day-to-day error or variation in temperature of the furnace was about ± 1 deg at the maximum temperatures and about ± 0.5 deg at the minimum temperatures. This amounts to about $\pm 1.5\%$ error in the cadmium vapor pressure. The radial temperature gradient in the furnace tube was examined. It is believed that this is insignificant under experimental conditions.

EXPERIMENTAL RESULTS AND DISCUSSION

The internal consistency and the reproducibility of the data indicate that final equilibrium was attained. The consistency of the data is shown by the smooth curve obtained when the logarithm of the vapor pressure is plotted against temperature for a given alloy composition, each point being determined from a separate experiment. As should follow from the Clausius–Clapeyron equation, the curve obtained by plotting the logarithm of the vapor pressure of an alloy versus temperature is approximately a straight line. The slope and slight curvature of these curves plotted for a few representative alloy compositions were very close to those of the curve for pure cadmium. The vapor pressures found by Schneider and Schmid (2) for liquid alloys are considerably lower than we observed for the solid alloys. The reproducibility is indicated by the isobars of Fig. 3.

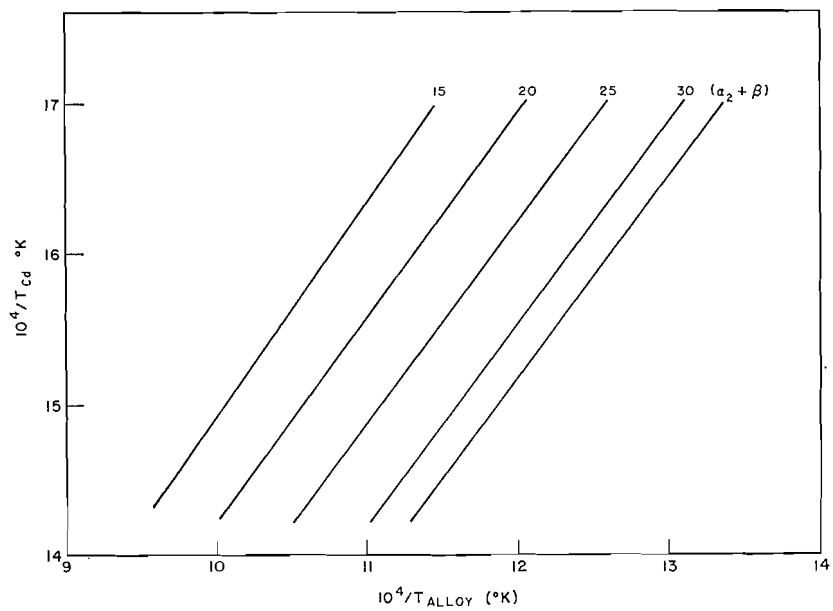

FIG. 2. Relationship between the reciprocal temperatures of the gold-cadmium alloys and of pure cadmium.

Further, two curves obtained at cadmium vapor pressures of 1.74 and 1.75 mm, only one of which is shown, lay close together and parallel over their whole course, indicating a high sensitivity for this method. The self-consistency of the data may also be checked by the method used by Birchenall and Cheng (13) with the following equation derived

Can. J. Chem. Downloaded from www.nrcresearchpress.com by 210.87.254.40 on 09/05/12
For personal use only.

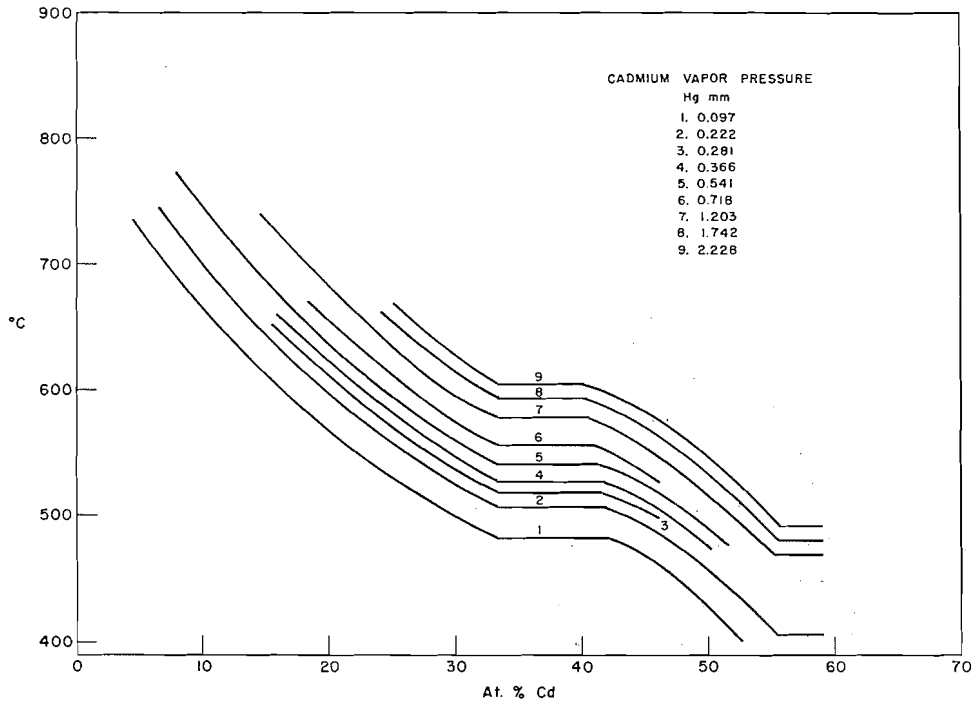

FIG. 3. Experimental isobars for the gold–cadmium alloys.

from the Clausius–Clapeyron relation, which will hold at equilibrium:

$$\frac{1}{T_0} = \frac{\Delta H_1}{\Delta H_0}\frac{1}{T_1} + (C_0 - C_1)\frac{R}{\Delta H_0},$$

where T_0 and T_1 are the absolute temperatures of the pure cadmium and of the alloy at equilibrium at a common pressure, ΔH_0 and ΔH_1 the respective heats of vaporization, C_0 and C_1 the integration constants, and R is the gas constant. The values $1/T_0$ and $1/T_1$ will be proportional if the heats of vaporization are independent of temperature or if their temperature coefficients are the same. In Fig. 2 a few of these curves are shown for some concentrations between 15 and 42 atom % cadmium. These are straight lines within experimental error.

The experimentally determined isobars obtained by plotting temperature against atomic percent showed two sections parallel to the concentration axis corresponding to the two-phase regions $\alpha_2 + \beta$ and $\beta + \delta'$, but no indication of the two-phase region $\alpha + \alpha_2$. Herasymenko (9) also found no indication of this region. The experimental results are shown in Fig. 3 where some isobars lying close together are omitted. X-ray examination of suitable samples showed that the hexagonal alpha two phase was present in these alloys. It is possible that the two-phase region $\alpha + \alpha_2$ is much narrower than shown on current diagrams in which case it would not be evident on the isobars. The phase boundaries from 0 to 60 atom % cadmium based on our results and on those of other investigators are shown in Fig. 4.

From the isobars of composition and temperature (Fig. 3) the activities of cadmium at each integral alloy composition were calculated over the temperature range using the

Can. J. Chem. Downloaded from www.nrcresearchpress.com by 210.87.254.40 on 09/05/12
For personal use only.

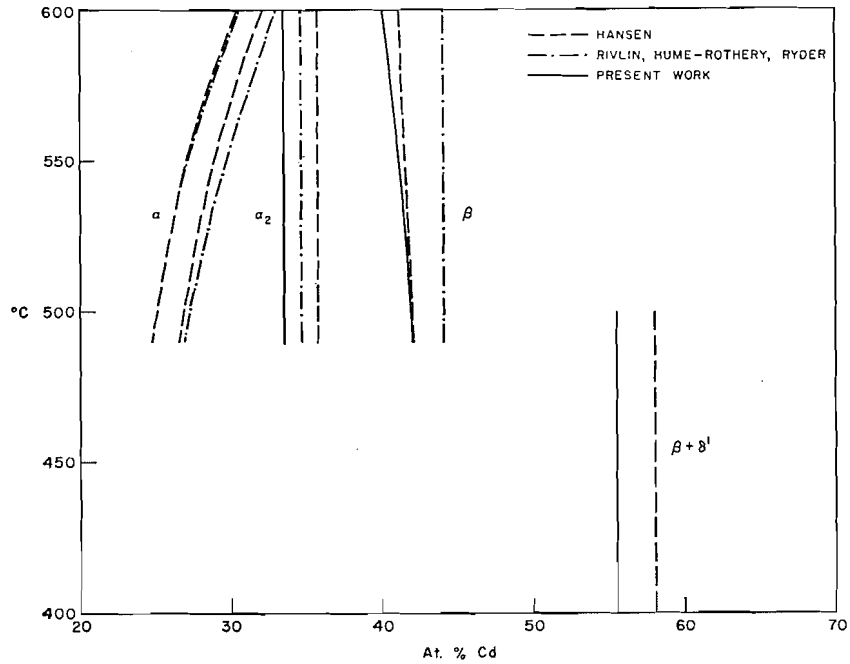

FIG. 4. Phase boundaries of the gold–cadmium system in the alpha–beta region between 490 and 600 °C and the beta – beta plus delta prime boundary between 400 and 500 °C.

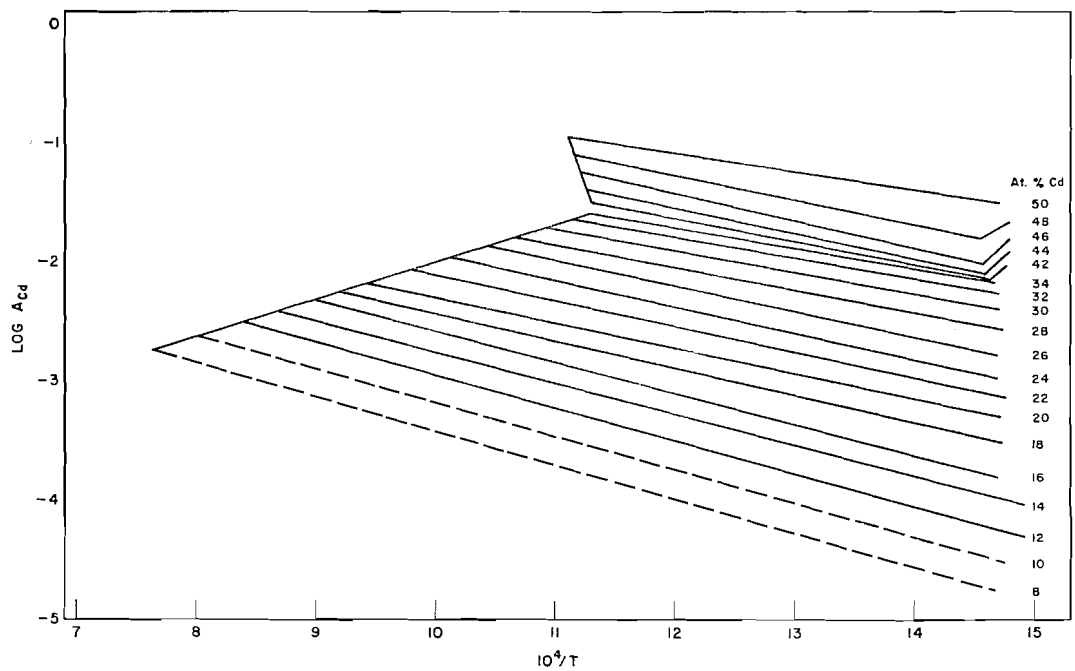

FIG. 5. Calculated curves of the activity of cadmium versus temperature for integral cadmium contents.

Can. J. Chem. Downloaded from www.nrcresearchpress.com by 210.87.254.40 on 09/05/12
For personal use only.

equation given above for the relation of cadmium vapor pressure to temperature. To eliminate errors of estimation, the results were tabulated and the equation of the best straight line through the points for each percent cadmium was determined by a least squares machine computation. The results are shown in Fig. 5. From a larger scale plot of these lines the values for log a were read off at 500, 550, and 600 °C, and the partial molar free energy $\Delta\bar{G}$ was calculated from the equation

$$\Delta\bar{G} = RT \ln a.$$

The free energy of the reference state G_0 is taken as the value for pure liquid cadmium at the temperatures of the experiments. From the same values of log a the partial molar heat of formation and partial molar entropy were calculated using the following relations:

$$\Delta\bar{H} = -RT^2 \, \mathrm{d} \ln a / \mathrm{d}T,$$

$$\Delta\bar{S} = -R(T \, \mathrm{d} \ln a / \mathrm{d}T + \ln a).$$

It is important to note that small experimental errors in the activity values are greatly magnified in the values of $\Delta\bar{H}$ and $\Delta\bar{S}$. The above-mentioned least squares calculation to obtain the best curve of log a vs. temperature was undertaken to minimize this error. Calculations have been made by standard methods (18) of the error in $\Delta\bar{G}$, $\Delta\bar{H}$, and $\Delta\bar{S}$ caused by the various experimental errors mentioned above. The errors in the calculated quantities when the relatively large day-to-day furnace temperature variation is included as an error are considerably greater than the observed scatter of the experimental points. Since these variations are probably cyclic in nature with a period which is relatively short compared with the diffusion time of cadmium through the gold wire, it is apparently safe to neglect them. The errors in the calculated quantities shown in Table I were estimated on this basis and are close to the scatter of the experimental points. The maximum values of the various experimental errors were used in this calculation, while the minima would give about one-half these errors. The data of Table I are plotted in Fig. 6. The gaps in the curves are due to the two-phase region from 34 to 42 atom % cadmium. An inflection in the $\Delta\bar{S}$ curve which is still present at 28–30 atom % cadmium might be caused by an ordering of the atoms related to the alpha two phase formation mentioned above. As would be anticipated, the $\Delta\bar{S}$ curve also shows a sharp minimum at about 47 atom % cadmium which is undoubtedly due to the superlattice formation in the Cd–Au beta phase (19). Our values of $\Delta\bar{S}$ agree reasonably with those of Herasymenko and of Ölander (9) for this phase. Otherwise, all the curves show a smooth variation with composition, in some contradiction to the results of Herasymenko (9) for the partial heat of formation and for the partial entropy. The integral heats of formation appeared to involve a large extrapolation to low cadmium contents and therefore have not been estimated.

Activity isotherms of these alloys are shown in Fig. 7 for 500 and 600 °C compared with the ideal isotherm. Our results depart strongly from the ideal in the direction of lower activities. However, the curves show a pronounced swing towards the ideal curve at 45–50 atom % cadmium.

Comparison with the vapor pressures found by Herasymenko (9) shows our data to be consistently higher by some 25–35%. Our partial free energy values are about 10% lower than those of Herasymenko. The $\Delta\bar{H}$ values found by Herasymenko and those calculated from Ölander's data (9) are both approximately 0 to 15% lower than those found here. Using the method suggested by Lumsden (21), we have estimated the partial heats of formation from 0–50 atom % Cd from the integral calormetric data of Kleppa (10). These

Can. J. Chem. Downloaded from www.nrcresearchpress.com by 210.87.254.40 on 09/05/12
For personal use only.

TABLE I

Thermodynamic data for the system Au–Cd at 550 °C

At. % Cd	$-\Delta\bar{G}$, cal/g-atom (±0.3%)	$-\Delta\bar{H}$, cal/g-atom (smoothed) (±3.7%)	$\Delta\bar{S}$, cal/deg (±5%)
8	15 304	15 880	0.750
9	15 042	15 220	0.28
10	14 208	14 800	0.10
11	13 881	14 380	−0.08
12	13 129	13 970	−0.22
13	12 704	13 570	−0.34
14	12 295	13 120	−0.52
15	12 001	12 700	−0.52
16	11 658	12 320	−0.58
17	11 314	11 960	−0.62
18	10 938	11 640	−0.73
19	10 611	11 310	−0.77
20	10 268	11 040	−0.85
21	9 924	10 750	−0.93
22	9 581	10 460	−1.03
23	9 254	10 210	−1.13
24	8 943	9 930	−1.21
25	8 616	9 670	−1.31
26	8 306	9 410	−1.43
27	7 979	9 160	−1.51
28	7 701	8 920	−1.57
29	7 439	8 680	−1.61
30	7 259	8 440	−1.57
31	7 030	8 220	−1.59
32	6 802	8 020	−1.63
33	6 654	7 840	−1.55
34	6 537	7 660	−1.41
42	6 475	10 760	−4.77
43	6 197	10 790	−5.38
44	5 984	10 760	−5.74
45	5 755	10 700	−6.00
46	5 526	10 540	−6.20
47	5 232	10 220	−6.20
48	4 970	9 660	−5.58
49	4 594	8 800	−4.75
50	4 284	6 460	−2.64

estimated values show a considerably smaller decrease with increasing cadmium content than our results. They are all less than our data, but at the point of nearest approach (32 atom % Cd) Kleppa's value is only about 1.2 kcal lower. Our $\Delta\bar{S}$ values for the alpha phase are generally somewhat lower than those of both Ölander and Herasymenko (9). These differences are nearly all greater than the experimental errors estimated in Table I.

ADDENDUM: Since the above work was completed and prepared for publication, a paper by Filby and Pratt (20) has appeared in which the vapor pressures of solid Au–Cd alloys from 8.4–25.1 atom % Cd only are measured by the dew-point method at temperatures largely coinciding with those reported here. Seven liquid alloys from 11.1–31.8 atom % Cd were also measured at higher temperatures. The ΔH values of Filby and Pratt show a much greater scatter and a different variation with increasing Cd content than those reported here, but they are approximately equal at about 15 atom % Cd. The $\Delta\bar{S}$ values also show a large scatter in contrast to our data, and are notably more positive. However, Filby and Pratt do not definitely suggest that these variations are associated with ordering.

Can. J. Chem. Downloaded from www.nrcresearchpress.com by 210.87.254.40 on 09/05/12
For personal use only.

Can. J. Chem. Downloaded from www.nrcresearchpress.com by 210.87.254.40 on 09/05/12
For personal use only.

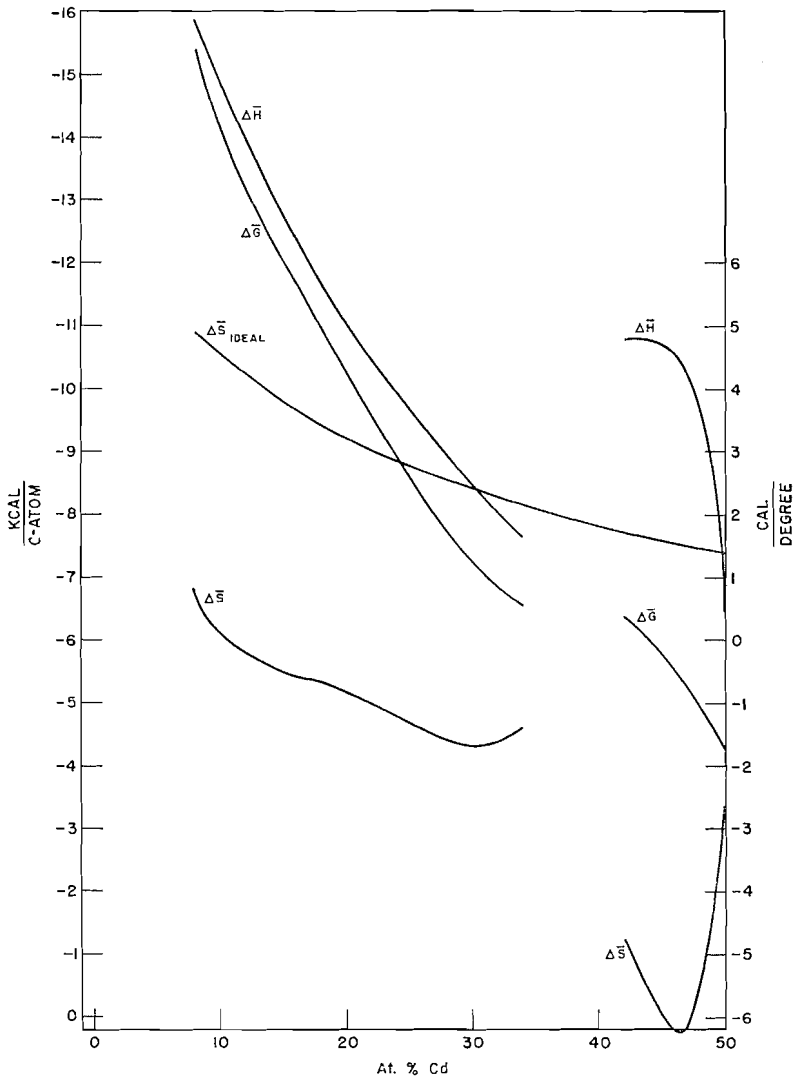

FIG. 6. The partial molar free energy, entropy, and heat of solution of cadmium at 550 °C.

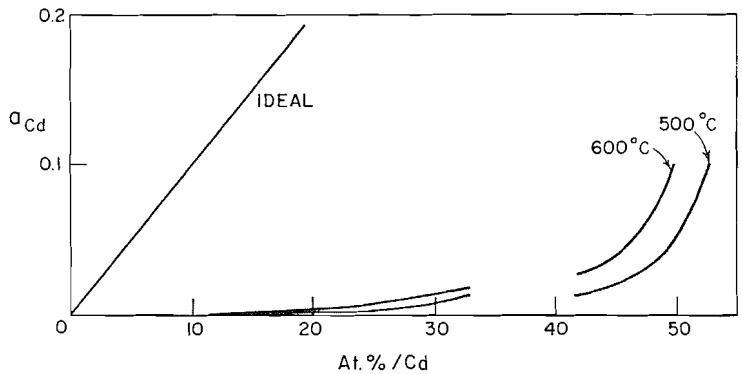

FIG. 7. The activities of cadmium at 500 and 600 °C.

ACKNOWLEDGMENTS

We are indebted to Mr. E. C. Goodhue and Mr. A. Desaulniers for the chemical analyses and to Dr. L. D. Calvert for identification of the alpha two phase by X-ray diffraction.

REFERENCES

1. A. Ölander. J. Am. Chem. Soc. **54**, 3819 (1932).
2. A. Schneider and H. Schmid. Z. Elektrochem. **48**, 627 (1942).
3. O. Kubaschewski and J. A. Catterall. Thermochemical data of alloys. Pergamon Press, Inc., New York. 1956. p. 75.
4. E. A. Owen and E. A. O'Donnell Roberts. J. Inst. Metals, **66**, 389 (1940).
5. E. A. Owen and W. H. Rees. J. Inst. Metals, **67**, 141 (1941).
6. M. Hansen and K. Anderko. Constitution of binary alloys. McGraw-Hill Book Co., Inc., New York. 1958. p. 190.
7. V. G. Rivlin, W. Hume-Rothery, and B. Ryder. Acta Met. **10**, 1143 (1962).
8. P. Herasymenko. Acta Met. **4**, 1 (1956).
9. P. Herasymenko. Phys. Rev. **99**, 614 (1955); Nucl. Sci. Abstr. **9**, 569 (#4454) (1955).
10. O. J. Kleppa. J. Phys. Chem. **60**, 858 (1956).
11. J. D. Filby and J. N. Pratt. Acta Met. **11**, 427 (1963).
12. H. W. Rayson and W. A. Alexander. Acta Met. **8**, 833 (1960).
13. C. E. Birchenall and C. H. Cheng. J. Metals, **1**, 428 (1949).
14. Devendra Gupta, Doctoral Dissertation, University of Illinois, Urbana, Ill. (1961).
15. C. G. Maier. J. Am. Chem. Soc. **48**, 356 (1926).
16. R. Hargreaves. J. Inst. Metals, **64**, 115 (1939).
17. B. Predel. Z. Metallk. **49**, 226 (1958).
18. J. B. Scarborough. Numerical mathematical analysis. The Johns Hopkins Press, Baltimore. 1958. pp. 4–20.
19. W. Class and D. S. Lieberman. J. Australian Inst. Metals, **6**, 11 (1961).
20. J. D. Filby and J. N. Pratt. Trans. Faraday Soc. **60**, 1934 (1964).
21. J. Lumsden. Thermodynamics of alloys. The Institute of Metals, 4 Grosvenor Gardens, London. 1952. p. 158.

Can. J. Chem. Downloaded from www.nrcresearchpress.com by 210.87.254.40 on 09/05/12
For personal use only.

THE H_A ACIDITY FUNCTION AND THE MECHANISM OF AMIDE HYDROLYSIS IN HYDROCHLORIC ACID

KEITH YATES AND J. C. RIORDAN
Department of Chemistry, University of Toronto, Toronto, Ontario
Received March 16, 1965

ABSTRACT

Values of the H_A acidity function have been determined for 0–35% hydrochloric acid using a set of amide indicators. The indicator pK values agree with those previously obtained in sulfuric acid. The H_A scale decreases less steeply than H_0 in the high concentration region, but the difference between the two functions is less marked than in sulfuric acid. The reasons for this are discussed. The values of H_A have been combined with available rate and water activity data to obtain information about the mechanism of amide hydrolysis. Eleven sets of rate data, consisting of 64 rate constants obtained under a variety of experimental conditions, give similar hydration parameters for this reaction. The temperature dependence of hydration parameters is discussed.

INTRODUCTION

An acidity function based on the ionization of amide indicators has recently been determined (1) for aqueous sulfuric acids. This amide-based acidity scale is significantly different numerically from other well-known Hammett type acidity functions, and has been shown (2) to be generally applicable to equilibria of the type

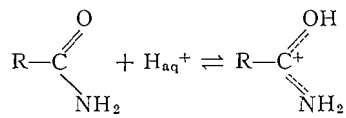

It is defined in an analogous way to other acidity functions,

$$H_A = -\log a_{H^+} f_A / f_{AH^+} = pK_{AH^+} - \log [AH^+]/[A],$$

where A and AH^+ refer specifically to amides and their conjugate acids. An attempt was made (2) to use the H_A scale to explain the dependence of amide hydrolysis rates on the acidity and water activity of the reaction medium in terms of the hydration requirements of the transition state. We have now extended these investigations of the ionization behavior of amides to aqueous hydrochloric acids because in addition to providing useful acidity function data in another medium, there is available a greater amount of appropriate kinetic data in this acid. This has been used to develop rate–acidity relationships for a wider range of amide hydrolysis reactions and provide more general information about the reaction mechanism.

EXPERIMENTAL

Reagents

The indicators used were 2-nitroaniline, 2-pyrrolecarboxamide, and 4-methoxy-, 3,4,5-trimethoxy-, 3-nitro,3,5-dinitro-4-methyl-, and 2,3,6-trichloro-benzamides. These were obtained and purified as described previously (1). Hydrochloric acid solutions from 0–35% by weight were prepared by diluting Fisher reagent grade concentrated acid (36.5% min.) and concentrations determined by titrating weighed samples with standard base.

Indicator Measurements

Solutions of indicators were prepared and their indicator ratios ($[AH^+]/[A] = I$) were determined spectrophotometrically as described previously (2) using a Unicam SP500 instrument thermostatted at 25 ± 0.1 °C. The spectral data were treated essentially as described previously (2) to obtain a set of indicator pK values and from these and the log I values a final set of H_A values was calculated. As before,

only log I values in the range -1.0 to $+1.0$ were used in calculating pK and acidity function values. It was necessary to use the method of Arnett and Wu (3) to obtain ϵ_{AH^+}, the conjugate acid extinction coefficient, and hence pK, for the last indicator, 2,3,6-trichlorobenzamide.*

Treatment of Kinetic Data

Data for the rates of hydrolysis of amides were taken directly from the literature in most cases. We are also grateful to Professor J. T. Edward for supplying us with some unpublished data. Water activity data at 25 °C was taken from Randall and Young (4). Data were used only if the rates had been measured in at least three different acid concentrations, and only if there was a significant change in the measured water activity over the acid range studied. All data were subjected to the standard least mean squares treatment to obtain slopes and correlation coefficients. In cases where a reaction rate had been followed in five or more different acid concentrations, the standard deviation of the slope (5) was also calculated.

RESULTS AND DISCUSSION

Indicator pK Values

The pK values of the six amide indicators were determined spectrophotometrically using changes in ultraviolet absorption on protonation, essentially as described previously (1). These were based on the reference indicator, 2-nitroaniline, whose pK is well established (6). The validity of the standard stepwise method of measuring pK values of very weak bases (6, 7) is shown by the parallelism of the indicator curves in Fig. 1. This indicates that the Hammett activity coefficient postulate (7) is being obeyed for each pair of indicators whose ionization ranges overlap, including 2-nitroaniline and the strongest amide base used, 2-pyrrolecarboxamide. As a check, the pK of the former was determined in the present study and a value of -0.31 was obtained, in excellent agreement with previously reported values in several different mineral acids (6). The pK values and absorption maxima are listed in Table I, along with the corresponding pK values obtained in sulfuric acid solutions. If these pK's are to be considered as valid thermodynamic dissociation constants† the value for each base should be independent of the acid used to establish it. That this is nearly the case can be seen by the agreement between the two sets of values. In view of the fact that the usual estimate of the uncertainty in any pK value measured in concentrated acids is about 0.05 to 0.1 pK unit, depending on the acid range used, the agreement is good.

The H_A Scale in Hydrochloric Acid

Using the above pK values and measured ionization ratios, values of the H_A function were obtained for 20 different hydrochloric acid concentrations in the range 0–35% by weight acid. Because of good ionization range overlap between the various indicators, the H_A value in any one acid solution is an average of values based on measurements involving several different indicators. Thus no part of the scale is based too heavily on any particular indicator. All the H_A values fall on a smooth curve when plotted against acid concentration. Values of H_A are listed in Table II at small concentration intervals, with the corresponding H_0 values of these solutions for comparison. It can be seen that up to about 15% acid there is essentially no difference between the two scales, but after this the H_A scale becomes significantly less negative than H_0 with increasing acid concentration, the difference amounting to 0.55 log units at the highest concentration studied. This means

*We are grateful to Miss Caroline Haynes for running duplicate spectrophotometric measurements on most of the compounds studied.

†*It has been pointed out by a referee that criteria such as indicator slope values, parallelism of successive indicator curves, and equality of pK values obtained in different acids are necessary but not in themselves* sufficient *conditions for the pK values to be accepted as thermodynamic dissociation constants. The question of the validity of pK values obtained by the standard stepwise method has been discussed in detail previously by ourselves (2) and other workers (7, 16). Since the data needed to answer this question are not experimentally accessible at present, we are forced to assume that in the absence of evidence to the contrary, amides do not show anomalous activity coefficient behavior in regions where their ionization ratios are too small to measure.*

TABLE I

Absorption maxima and pK values of indicators at 25 °C

Indicator	pK_{AH^+}*	n†	pK‡ (H_2SO_4)	Base λ_{max} (mμ)	Base (Log ϵ_{max})	Conjugate acid λ_{max}§ (mμ)	Conjugate acid (Log ϵ_{max})
2-Pyrrolecarboxamide	−1.23±0.02	7	−1.23	263	(2.81)	289	(4.28)
4-Methoxybenzamide	−1.46±0.02	9	−1.44	253	(3.23)	283	(4.17)
3,4,5-Trimethoxybenzamide	−1.86±0.02	8	−1.82	256	(3.48)	283	(3.92)
3-Nitrobenzamide	−2.25±0.03	6	−2.42	215	(4.06)	230	(4.24)
3,5-Dinitro-4-methyl-benzamide	−2.77±0.04	7	−2.69	217	(4.09)	235	(4.20)
2,3,6-Trichlorobenzamide	−3.10±0.05	9	−3.30	230	Shoulder	258	(3.63)‖

*Average value ± mean deviation.
†Number of experimental points used to calculate each pK value.
‡Previously determined in sulfuric acid (ref. 1).
§Wavelength used to determine indicator ratio from $I = (\epsilon_A - \epsilon)/(\epsilon - \epsilon_{AH^+})$.
‖Obtained by the method of Arnett and Wu (ref. 3).

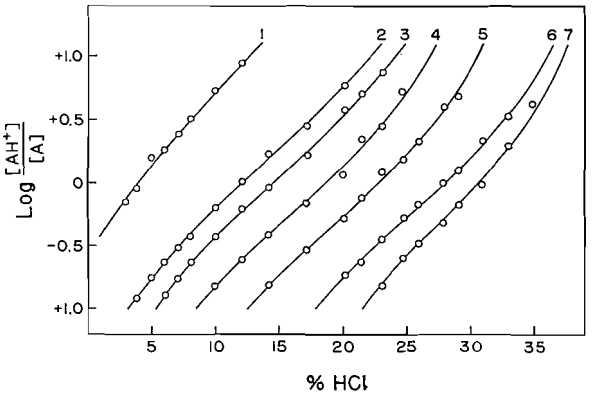

FIG. 1. Ionization curves for amide indicators in hydrochloric acids (for indicator numbers see Table II).

that HCl can be up to three or four times less effective at transferring a proton to an amide than it is towards a corresponding aniline type base. This is qualitatively the same type of difference between the two acidity functions as found for sulfuric acid (1, 8), but is much less pronounced in hydrochloric acid. For example in 66.5% sulfuric acid, which has roughly the same H_A acidity as 35% hydrochloric acid, $(H_0 - H_A)$ has a value of −1.77 log units. The H_A scale in hydrochloric acid is also linear in acid concentration over a wide range, as found for sulfuric acid, $dH_A/d\%HCl$ being nearly constant at −0.1 from 8–35% HCl.

The possible reasons for the difference in the ability of an aqueous mineral acid to protonate primary amides and primary amines have been discussed previously (1) in terms of the hydration requirements of the various indicator species. It is again concluded that the changes in hydration requirements on protonating amides are greater than the corresponding changes on protonating anilines. Whether or not this is primarily due to differences in the hydration numbers of the conjugate acids is not known, but recent measurements of the activity coefficients of *neutral* amides in this laboratory (9) suggest strongly that contributions of the f_A and f_B terms to the overall behavior of H_A and H_0 respectively are significantly different and therefore cannot be ignored. It is clear that

TABLE II

Values of H_A in hydrochloric acid at 25 °C

% HCl	$-H_A$	Mean deviation	Indicators used†	$-H_0$‡	$(H_0 - H_A)$
3	0.13	±0.02	1–3	0.13	0.0
4	0.31	±0.02	1–3	0.29	0.02
5	0.47	±0.02	1–3	0.43	0.04
6	0.59	±0.01	1–3	0.57	0.02
7	0.71	±0.02	1–3	0.69	0.02
8	0.82	±0.005	1–4	0.81	0.01
10	1.03	±0.01	1–4	1.01	0.02
12	1.23	±0.01	1–4	1.23	0.0
14	1.43	±0.01	2–5	1.44	−0.01
16	1.63	±0.02	2–5	1.64	−0.01
18	1.82	±0.03	2–5	1.87	−0.05
20	2.01	±0.02	2–6	2.11	−0.10
22	2.21	±0.02	3–6	2.35	−0.14
24	2.42	±0.04	3–7	2.60	−0.18
26	2.61	±0.02	4–7	2.87	−0.26
28	2.81	±0.03	5–7	3.12	−0.31
30	3.02	±0.03	6,7	3.39	−0.37
32	3.22	±0.005	6,7	3.67	−0.45
34	3.44	±0.05	6,7	3.95	−0.51
35	3.56§	—	—	4.11	−0.55

*Mean deviation between H_A values obtained using different indicators.
†Individual H_A values determined from the following indicators: 1, 2-nitroaniline; 2, 2-pyrrolecarboxamide; 3, 4-methoxybenzamide; 4, 3,4,5-trimethoxybenzamide; 5, 3-nitrobenzamide; 6, 3,5-dinitro-4-methylbenzamide; 7, 2,3,6-trichlorobenzamide.
‡Taken from ref. 6.
§Obtained by a short extrapolation.

differences in the behavior of the two types of base are not as marked in hydrochloric acid as they are in sulfuric acid. The only explanation we are able to offer is that the competition for "free" water is less severe in the former acid, resulting in smaller variations in individual activity coefficients. This may be because the indicator species are able to compete more effectively with chloride ion for available water than they are with bisulfate ion. This explanation receives some support from the fact that over a wide range, a_{H_2O} decreases less steeply with acid concentration in hydrochloric acid than it does in sulfuric acid (4). Wyatt has also concluded that chloride ion is considerably less hydrated than bisulfate (10). When one considers the water activity dependence of acidity functions it is a striking fact that H_0 in sulfuric, perchloric, hydrochloric, and nitric acids is a unique function of a_{H_2O} for these acids. This was first pointed out by Wyatt (10) and has recently been confirmed for the first two acids over a very wide concentration range to a remarkable degree of precision (11). However, plots of H_A versus a_{H_2O} for sulfuric and hydrochloric acids result in two separate curves. Although these curves are similar in appearance they diverge by up to 1.7 H_A units. We have also checked the water activity dependence of the H_R function using published data for sulfuric, perchloric, and nitric acids (12, 13) and find again that similar but clearly separate curves result for each acid. It is therefore apparent that although acidity functions in general are strongly dependent on a_{H_2O} of the medium, the unique character of the H_0–a_{H_2O} relationship for different acids must at least be partly fortuitous.

Dependence of Amide Hydrolysis Rates on Acidity and Water Activity

The following relationships between the rate constant and the acidity and water activity of the reaction medium have been derived previously (2) for amide hydrolysis in concentrated acid solutions. For the hydrolysis of weakly basic amides, which are present in

the reaction medium essentially as unprotonated amide, the relationship is

$$\log k_{obs} + H_A = r \log a_{H_2O} + \text{constant.} \quad [1]$$

For more basic amides, which are present as a mixture of the amide and its conjugate acid, the corresponding relationship is

$$\log k_{obs} - \log (h_A/K_{AH^+} + h_A) = r \log a_{H_2O} + \text{constant.} \quad [2]$$

In these equations k_{obs} is the observed pseudo first order rate constant, K_{AH^+} is the dissociation constant of protonated amide, and r is a hydration parameter which gives a direct measure of the number of water molecules needed to convert a protonated substrate molecule to transition state in the general hydrolysis scheme.

$$A(H_2O)_s + H(H_2O)_n^+ \overset{\text{fast}}{\rightleftharpoons} AH(H_2O)_p^+ + (s + n - p)H_2O$$

$$AH(H_2O)_p^+ + rH_2O \overset{\text{slow}}{\rightarrow} A^+(H_2O)_t \rightarrow \text{products.}$$

If the assumptions involved in the derivation of eqs. [1] and [2] are justified, plots of either ($\log k_{obs} + H_A$) or $\log k_{obs} - \log (h_A/K_{SH^+} + h_A)$ against $\log a_{H_2O}$ should be linear. We have tested this by using 64 reported rate constants obtained by measuring the rates of hydrolysis of six different amides in solutions ranging from 0.6 to 10.1 M hydrochloric acid. Good linear plots resulted in every case. The least squares slopes and correlation coefficients of the 11 linear relationships obtained are listed in Table III. The reactions

TABLE III

Water activity dependence of hydrolysis rates in hydrochloric acid

Reaction	Temp. (°C)	n*	r	σ_r†	c‡	Reference
Simple amides:§ $\log k_{obs} - \log (h_A/K_{SH^+} + h_A) = r \log a_{H_2O} + \text{constant}$						
Acetamide	50	8	3.10	0.19	0.996	17
	61.0	7	2.66	0.27	0.990	18
Propionamide	40.5	5	2.60	0.20	0.991	19
	59.6	5	2.40	0.20	0.990	19
Benzamide	25.0	9	3.14	0.30	0.966‖	20
	59.6	3	3.17	—	0.983	19
	78.6	3	3.04	—	0.984	19
Heterocyclic amides: $\log k_{obs} + H_A = r \log a_{H_2O} + \text{constant}$						
Picolinamide	85	7	3.43	0.18	0.996	21
Nicotinamide	76.0	7	3.60	0.14	0.993	22
Isonicotinamide	68	7	3.59	0.20	0.993	21

*Number of experimental rate constants obtained in different acid concentrations up to 10 M HCl.
†Standard deviation of slope r.
‡Least squares correlation coefficient.
§K_{SH^+} values of amides taken from ref. 2.
‖With one widely deviating point in dilute solution omitted, the data give a much better linear plot with $r = 2.75$, $\sigma_r = 0.22$, and $c = 0.991$.

fall into two series. For simple amides like acetamide, propionamide, and benzamide, which are measurably protonated in the acids used for kinetic measurements, eq. [2] was used. For heterocyclic amides like picolinamide, eq. [1] for weakly basic substrates was used. Although the latter are in fact completely protonated in most of the acids used, it is presumably the ring nitrogen which is protonated first. However, the hydrolysis reaction requires preliminary protonation of the amide group as well.

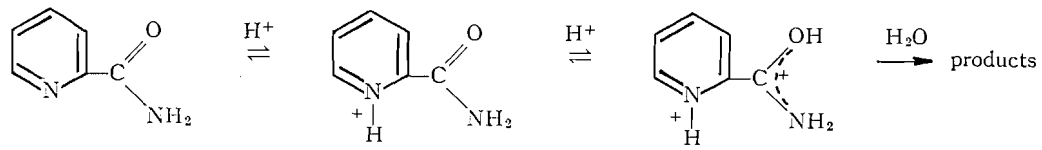

Since it is unlikely that the second protonation equilibrium is established to any measurable extent even in moderately concentrated acids, these amides can be treated as weakly basic substrates. Hence eq. [1] is more appropriate, and in fact does give very good linear plots. It can be seen from Table III that the r-values are all similar in magnitude, particularly for the simple amides which have an average r-value of 2.91 ± 0.27. This would be expected if r is a useful indicator of mechanism since all these compounds presumably react in a very similar way. The above value compares very well with r-values of 2.6 and 2.7 obtained for the hydrolyses of benzamide and p-nitrobenzamide in sulfuric acid (2), and again suggests that in the rate-determining step one water molecule attacks the conjugate acid as a nucleophile and two more water molecules on the average assist by hydrogen bonding. The transition state for acid-catalyzed hydrolysis can thus be represented by the following structure:

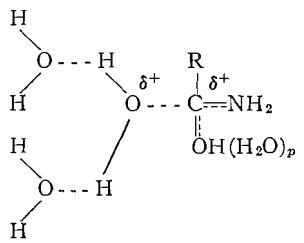

The higher r-values obtained for the heterocyclic amides may reflect a somewhat different mechanism, but it seems more probable that this small difference is due to the fact that H_A is based on the ionization of uncharged amides whereas strictly speaking some acidity function of the $H+$ type should be used for the pyridine derivatives. In any event the range of hydration parameters for all 11 cases studied is fairly narrow (r = 3.1 ± mean deviation 0.3).

The theoretical relationships represented by eqs. [1] and [2] are formally equivalent to the empirical w-parameter treatment of Bunnett (14). However, the present treatment is a modification of the Bunnett approach in which the acidity of the reaction medium is based on a function strictly appropriate to the type of substrate whose reaction mechanism is being considered. This is preferable to the use of only one acidity function, namely H_0, for reactions of all types of basic substrates as is the case with the w-parameter treatment, particularly since it is now clear that many organic bases do not follow H_0 even approximately (1, 15, 16). It is noteworthy that the w-values for the reactions listed in Table III range from 1.18 to 4.94.

Effect of Temperature on Hydration Parameters

Ideally, in any treatment of rate dependence on acidity and water activity, it would be desirable to have all the data measured at the same temperature. However, such data are not always available in practice, since acidity functions and water activities are usually measured at 25 °C whereas rate constants are obtained at whatever temperature affords a conveniently measurable rate. For example, of the 158 sets of rate data in

moderately concentrated acids listed by Bunnett (14), only 78 had been studied at or near 25 °C and the rest at temperatures ranging from 0 to 131 °C. However, it can easily be shown that it is not a serious disadvantage if the kinetic data can not be obtained at 25 °C. If we let t_1 correspond to 25 °C and t_2 to some other temperature, then in the ideal case we have, for weakly basic substrates,

$$\log k_{t_1} + (H_A)_{t_1} = r \log (a_{H_2O})_{t_1} + C.$$

This can be combined with the Arrhenius relationship

$$\log k_{t_1} = \log k_{t_2} + E_a/2.3R(1/T_2 - 1/T_1)$$

to yield

$$\log k_{t_2} + (H_A)_{t_1} = r \log (a_{H_2O})_{t_1} + C^1$$

providing E_a is temperature independent over the range t_1–t_2. In the case of more strongly basic substrates the equation

$$\log k_{t_2} - \log [(h_A)_{t_1}/K_{AH^+} + (h_A)_{t_1}] = r \log (a_{H_2O})_{t_1} + C^1$$

can be arrived at in a similar way, providing K_{AH^+} for the substrate in question does not change appreciably over the range t_1–t_2. Thus, correlating kinetic data at one temperature with acidities and water activities obtained at a different temperature should just mean that each curve is shifted vertically by a constant amount $E_a/2.3R(1/T_2 - 1/T_1)$ and that the slope r is unaffected by the temperature at which the rates were measured. The data in Table III and the earlier observations of Bunnett appear to bear this out, since variations of hydration parameters with temperature appear to be small and random. However, it would be interesting to test this experimentally in a more systematic way, and we are at present investigating this.

Finally, in view of the fact that all available amide hydrolysis data, obtained under a wide variety of reaction conditions, yield good linear relationships when treated as described above, with approximately the same r-value in all cases, it is concluded that this treatment provides a useful criterion of reaction mechanism and can be extended to yield detailed information about transition states in other acid-catalyzed reactions.

ACKNOWLEDGMENTS

We wish to express gratitude to the National Research Council of Canada for continued financial support and for the award of an Overseas Postdoctorate Fellowship to one of us (J. C. R.).

REFERENCES

1. K. YATES, J. B. STEVENS, and A. R. KATRITZKY. Can. J. Chem. **42**, 1957 (1964).
2. K. YATES and J. B. STEVENS. Can. J. Chem. **43**, 529 (1965).
3. E. M. ARNETT and C-Y. WU. J. Am. Chem. Soc. **82**, 5660 (1960).
4. M. RANDALL and L. E. YOUNG. J. Am. Chem. Soc. **50**, 989 (1928).
5. W. J. YOUDEN. Statistical methods for chemists. Wiley, New York. 1951. Chap. 5.
6. M. A. PAUL and F. A. LONG. Chem. Rev. **57**, 1 (1957).
7. E. M. ARNETT. *In* Progress in physical organic chemistry. Vol. 1. *Edited by* S. G. Cohen, A. Streitwieser, Jr., and R. W. Taft. Interscience, New York. 1963. pp. 233 ff.
8. M. J. JORGENSON and D. R. HARTTER. J. Am. Chem. Soc. **85**, 878 (1963).
9. K. YATES and L. M. SWEETING. Unpublished results.
10. P. A. H. WYATT. Discussions Faraday Soc. **24**, 162 (1957).
11. K. YATES and H. WAI. J. Am. Chem. Soc. **86**, 5408 (1964).
12. J. N. PEARCE and A. F. NELSON. J. Am. Chem. Soc. **55**, 3075 (1933). R. A. ROBINSON and O. J. BAKER. Trans. Proc. Roy. Soc. New Zealand, **76**, 256 (1946). A. POTIER. Ann. Fac. Sci. Univ. Toulouse Sci. Math. Sci. Phys. **20**, 1 (1956).
13. N. C. DENO, J. J. JARUSZELSKI, and A. SCHRIESHEIM. J. Am. Chem. Soc. **77**, 3044 (1955). N. C. DENO, H. E. BERKHEIMER, W. L. EVANS, and H. J. PETERSON. J. Am. Chem. Soc. **81**, 2344 (1959).

14. J. F. BUNNETT. J. Am. Chem. Soc. **83**, 4956 (1961).
15. E. M. ARNETT and G. W. MACH. J. Am. Chem. Soc. **86**, 2671 (1964).
16. R. L. HINMAN and J. LANG. J. Am. Chem. Soc. **86**, 3796 (1964).
17. D. ROSENTHAL and I. T. TAYLOR. J. Am. Chem. Soc. **79**, 2684 (1957).
18. J. T. EDWARD, H. P. HUTCHINSON, and S. C. R. MEACOCK. J. Chem. Soc. 2520 (1955).
19. R. S. RABINOVITCH and C. A. WINKLER. Can. J. Res. B, **20**, 73 (1942).
20. J. T. EDWARD and S. C. R. MAECOCK. J. Chem. Soc. 2000 (1957).
21. H. H. G. JELLINEK and J. R. URWIN. J. Phys. Chem. **57**, 900 (1953).
22. H. H. G. JELLINEK and A. GORDON. J. Phys. Colloid Chem. **53**, 996 (1949).

Can. J. Chem. Downloaded from www.nrcresearchpress.com by 210.87.254.105 on 09/05/12
For personal use only.

THE OXIDATION OF DITERPENOID ALKALOIDS[1]

O. ACHMATOWICZ, JR.,[2] Y. TSUDA,[2] AND LÉO MARION
Division of Pure Chemistry, National Research Council, Ottawa, Canada
Received March 12, 1965

ABSTRACT

The highly oxygenated diterpenoid alkaloids possessing the same C—N ring structure fall into two groups: group A containing the aconitine-like bases in which the C-6 methoxyl is α-oriented, and group B containing the lycoctonine-like bases in which the C-6 methoxyl is β-oriented. The alkaloids of both groups are oxidized rapidly at room temperature by neutral potassium permanganate. The oxidation dealkylates the amino group in the bases of group A giving rise to secondary bases while it converts the bases of group B to the corresponding lactams. The different course of the oxidation from one group to the other is due to the different orientation of the C-6 methoxyl, and can be used to determine the stereochemistry at C-6.

The highly oxygenated diterpenoid alkaloids can be classified into two groups: group A containing the aconitine-like alkaloids I and group B or the lycoctonine-like bases II. The latter contain a ditertiary vicinal glycol and the former do not. More particularly in I the C-6 methoxyl is α whereas in II it is β.

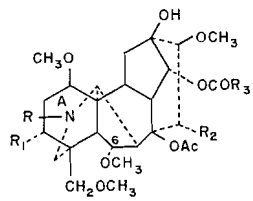

I

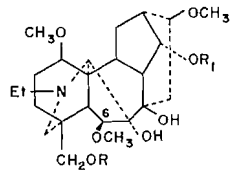

II

There has been no method reported of determining the orientation of this group except X-ray crystallography. We now wish to report a method of ascertaining the stereochemistry at C-6 through an oxidation of the bases.

Oxidation of these alkaloids involving the attack of the reagent on the nitrogen is complicated and gives variable results depending on reaction conditions and the structure of the alkaloids. Of the various oxidizing agents tried, potassium permanganate proved the most promising. In the presence of acid, however, the oxidation gave rise to mixtures. The oxidation of aconitine with potassium permanganate in acetone containing acetic acid produced several neutral compounds and from the mixture oxonitine was isolated in 20% yield. Although oxonitine is N-formyl-N-deethylaconitine (1) it was not possible to find N-deethylaconitine among the reaction products. Under identical conditions mesaconitine I (R = Me, $R_1 = R_2 = OH$, $R_3 = C_6H_5$) is oxidized to oxonitine, and delphinine to α-oxodelphinine, which is N-formyl-N-demethyldelphinine I (R = CHO, $R_1 = R_2 = H$, $R_3 = C_6H_5$) and β-oxodelphinine claimed to be delphinine lactam (2).

In contrast, lycoctonine II (R = H; $R_1 = CH_3$) is oxidized under the same acidic

[1]*Issued as N.R.C. No. 8516.*
[2]*National Research Council of Canada Postdoctorate Fellow.*

conditions to a mixture of the lactam oxolycoctonine, deoxymethylene oxolycoctonine, and lycoctonamic acid (3). Similarly delpheline and acetylbrowniine are oxidized to oxodelpheline (4) and acetyloxobrowniine (5) respectively. In neither group of alkaloids was the formation of a secondary base observed.

In the absence of acid, however, the course of the oxidation with potassium permanganate was quite different and straightforward. In the course of the work that led to the determination of the structure of chasmanine, $C_{25}H_{41}O_6N$, III (R = Et), it was found that the alkaloid could be smoothly dealkylated when treated at room temperature for

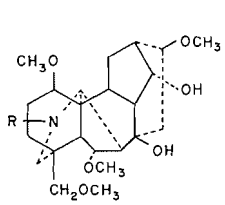

III

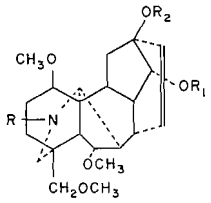

IV

5 min with potassium permanganate in acetone–water solution (6). The product no longer showed the signal characteristic of the ethyl group in the n.m.r. spectrum and hence the product is III (R = H). That dealkylation was the only change brought about by the oxidation was shown by reconversion of the product (N-deethylchasmanine) to chasmanine with the aid of ethyl iodide and to the lower homologue, N-methyl-N-deethylchasmanine $C_{24}H_{39}O_6N$, III (R = CH_3) by treatment with methyl iodide.

In connection with an attempted correlation of chasmanine with bikhaconine (6) a derivative of the latter, diacetyldemethoxyisopyrobikhaconine IV (R = Et, $R_1 = R_2 = Ac$) (7), was found to undergo ready dealkylation in good yield when oxidized for 5 min with potassium permanganate in aqueous acetone at room temperature. A single product was obtained, m.p. 200–204°, which was the deethyl derivative IV (R = H, $R_1 = R_2 = Ac$). It still showed signals from the olefinic protons in the n.m.r. spectrum but no longer showed the N-Et signal. On acetylation, the product gave the neutral N-acetyl derivative IV (R = $R_1 = R_2 = Ac$), which, when treated with lithium aluminium hydride, produced demethoxyisopyrobikhaconine IV (R = Et, $R_1 = R_2 = H$). Direct ethylation of the oxidation product gave back the starting material IV (R = Et, $R_1 = R_2 = Ac$). The triacetyl derivative IV (R = $R_1 = R_2 = Ac$), when hydrogenated catalytically and subsequently saponified with methanolic sodium hydroxide, was converted to N-acetyl-N-deethyldihydrodemethoxyisopyrobikhaconine $C_{24}H_{35}O_6N$, showing an N-acetylcarbonyl band at 1 600 cm^{-1} in the infrared. Hence oxidation under the conditions described does not affect any part of the molecule besides removing the N-alkyl group. This interesting result prompted us to examine systematically the diterpenoid alkaloids of group A and group B.

First we studied the effect of the reaction on the alkaloids of group A, related structurally to aconitine and, like chasmanine, bearing an α-methoxyl group at C-6. With these ester alkaloids the reaction was slower and was allowed to proceed for a somewhat longer time. In spite of this the oxidation was not complete and for all except bikhaconitine an appreciable quantity of unchanged starting material was recovered. The predominant product was the N-dealkyl ester alkaloid accompanied by a small quantity of the neutral

Can. J. Chem. Downloaded from www.nrcresearchpress.com by 210.87.254.105 on 09/05/12
For personal use only.

Can. J. Chem. Downloaded from www.nrcresearchpress.com by 210.87.254.105 on 09/05/12
For personal use only.

TABLE I

Oxidation of ester alkaloids

Alkaloid	mg	Time, min	N-dealkyl base mg	N-dealkyl base %	Recovered starting base mg	Recovered starting base %	Net yield	Neutral compound mg	Neutral compound %	Structural formula of alkaloid
Aconitine	664	10	135	20	450	68	63	78	10	R = Et; $R_1 = R_2 = OH$; $R_3 = C_6H_5$
Aconitine	1950	20	578	30	522	27	40	600	31	
Deoxyaconitine	161	10	75	47	77	48	90	—	—	I, R = Et; $R_1 = H$; $R_2 = OH$; $R_3 = C_6H_5$
Deoxyindaconitine	248	10	92	37	111	45	67	17	7	I, R = Et; $R_1 = R_2 = H$; $R_3 = C_6H_5$
Pseudaconitine	464	10	246	53	136	30	75	32	7	I, R = Et; $R_1 = OH$; $R_2 = H$; $R_3 = C_6H_3(OCH_3)_2$
Indaconitine	430	10	177	41	207	48	80	21	5	I, R = Et; $R_1 = OH$; $R_2 = H$; $R_3 = C_6H_5$
Bikhaconitine	183	10	65	35	101	55	80	2	1	I, R = Et; $R_1 = R_2 = H$; $R_3 = C_6H_3(OCH_3)_2$
Bikhaconitine	540	50	479	89	12	2	91	32	6	
Delphinine	679	10	171	25	351	52	52	24	4	I, R = Me; $R_1 = R_2 = H$; $R_3 = C_6H_5$
Anhydropseudaconitine	568	10	134	24	224	40	40	—	—	

Can. J. Chem. Downloaded from www.nrcresearchpress.com by 210.87.254.105 on 09/05/12
For personal use only.

N-dealkyl oxobase (Table I). All the N-dealkyl ester bases prepared except N-demethyldelphinine (identical with N-deethyldeoxyindaconitine, I, R = R_1 = R_2 = H; R_3 = C_6H_5)[3] were amorphous. The lowest yield of N-dealkyl ester base obtained was 40% and the highest was 91%, calculated after subtraction of the recovered unchanged starting material.

The neutral product in each case was the N-deethyl-oxobase. Those obtained in the oxidation of the various ester alkaloids are listed in Table IV (see experimental). The N-deethyl-ester alkaloids obtained in each case as the main product were all smoothly methylated to the corresponding N-methyl derivatives. Thus the N-deethyl derivatives of aconitine (I, R = H; R_1 = R_2 = OH; R_3 = C_6H_5), deoxyaconitine (I, R = R_1 = H; R_2 = OH; R_3 = C_6H_5), and deoxyindaconitine (I, R = R_1 = R_2 = H; R_3 = C_6H_5) yielded respectively mesaconitine, hypaconitine, and delphinine, while the N-deethyl derivatives of pseudaconitine, indaconitine, and bikhaconitine yielded lower homologues which have not yet been reported as occurring in nature (see Table III). The N-methyl bases having properties very similar to those of the corresponding N-ethyl alkaloids are not separable from the latter in thin-layer chromatography, and to obtain them pure it is essential to purify the secondary base before methylation.

The C-3 hydroxyl in ring A seems to have no effect on the course of the oxidation nor on the yield of deethyl base produced. The presence of a double bond in ring A, however, probably because of the half-chair conformation assumed by the ring, complicated the reaction. Oxidation of anhydropseudaconitine, for instance, gave only 64% yield of combined N-deethyl compound and unreacted starting base, while no oxoderivative was present.

TABLE II

Oxidation of alkamines

Alkamine	Wt., mg	Time, min	N-dealkyl base		Recovered starting base		Net yield, %	Neutral product
			mg	%	mg	%		
Chasmanine	245	5	215	94	—	—	94	
Bikhaconine	312	5	208	69	80	25	90	Trace
Pseudaconine	150	5	95	65	45	30	95	Trace
Diacetyl-demethoxy-isopyrobikhaconine	396	5	320	90	Trace	Trace	90	—
Monoacetyl-demethoxy-isopyrobikhaconine	113	5	101	95	—	—	95	Trace

Naturally occurring alkamines of group A and those obtained by saponification of the corresponding ester alkaloids underwent oxidation to the dealkyl base under the same conditions not only more rapidly but more completely in better yield and without the accompanying formation of the oxoderivative (Table II). Owing to their higher solubility in water, however, the products were more difficult to isolate. The dealkyl alkamines also were methylated smoothly to the corresponding N-methyl compounds. In most cases the product was acetylated. Thus bikhaconine gave triacetyldelphonine, and pseudaconine was converted into the new N-methyl-N-deethyl-pseudaconine tetraacetate ($C_{32}H_{47}O_{12}N$).

The bases of group B, which contain a β-C-6 methoxyl were rapidly oxidized by potassium permanganate in aqueous acetone, but with quite different results. With the

[3]*N-Deethyldeoxyindaconitine crystallized readily from ether, although when prepared previously by a different method it could not be induced to crystallize (8).*

three bases of this group that were oxidized, the main product was the oxoderivative. Lycoctonine (II, R = H; $R_1 = CH_3$) produced oxolycoctonine exclusively. Browniine (II, R = CH_3; R_1 = H) gave mostly oxobrowniine accompanied by 7.5% of deethylbrowniine. Delcosine produced mainly anhydrohydroxydelcosine, a carbinolamine ether, accompanied by 15% of deethyldelcosine. As described already (9) delcosine carries a hydroxyl at C-1 of ring A oriented on the same side of ring A as the nitrogen ring, and readily forms a carbinolamine ether by condensation of this hydroxyl with the carbinolamine hydroxyl initially produced in the oxidation. Hence in the oxidation now described, the formation of anhydrohydroxydelcosine is equivalent to the formation of a lactam, but the reaction is stopped half way by the formation of the stable ether.

The characteristic difference between the alkaloids of group A and those of group B is that the C-6 methoxyl is α in the former and β in the latter. Without exception it has been found that the oxidation product of the group A alkaloids is predominantly the N-dealkyl derivative with the oxoderivative as a minor product, whereas the oxidation product of the group B alkaloids is predominantly the oxoderivative with the dealkyl base as a minor product.

The results obtained show that the ease of oxidation of a highly oxygenated diterpenoid alkaloid possessing the C—N-skeleton I or II to either a dealkyl derivative or to the oxo-base can be taken as an indication of the orientation of the C-6 methoxyl, which must be α in the first case and β when the product is mostly the lactam.

An examination of models shows that when the C-6 methoxyl is α it sterically hinders the vulnerable C-16 methylene group and prevents or restricts its oxidation to a lactamic carbonyl, thus favoring the attack on the imino-ethyl group. In contrast the β-oriented C-6 methoxyl in the alkaloids of group B does not interfere with the C-16 methylene, which is normally oxidized to a lactam carbonyl.

A possible mechanism of the oxidation reaction involves an initial complexing of MnO_4^- with the free pair of electrons on the nitrogen. The presence or absence of steric hindrance then determines the observed specificity of the reaction.

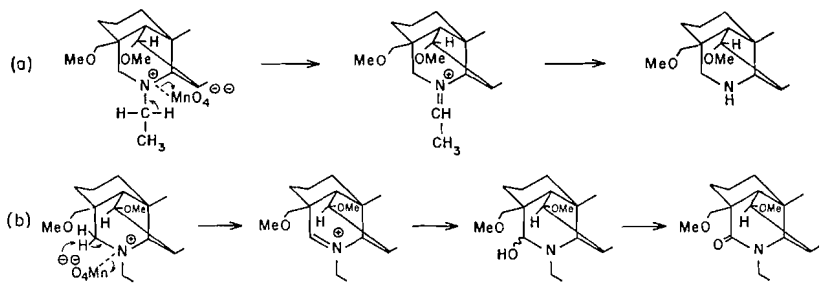

The ring methylene being more reactive is the favored point of attack, but if it is sterically hindered by the α-oriented C-6 methoxyl, as in the alkaloids of group A, the attack is on the ethyl group as in scheme *a* with the resulting elimination of that group. If there is no steric hindrance as in the group B alkaloids in which the C-6 methoxyl is β-oriented, the attack occurs as in scheme *b* and results in the production of the lactam. In the latter case there is a *trans* proton elimination with formation of an anhydronium intermediate which, in the basic medium, is rapidly oxidized, probably via the carbinolamine, to the lactam.

Can. J. Chem. Downloaded from www.nrcresearchpress.com by 210.87.254.105 on 09/05/12
For personal use only.

Can. J. Chem. Downloaded from www.nrcresearchpress.com by 210.87.254.105 on 09/05/12
For personal use only.

EXPERIMENTAL

Unless otherwise stated Analar acetone was used as a solvent in the oxidations, grade IV Woelm neutral alumina for column chromatography, and Merck's silica gel G as adsorbent and cyclohexane–chloroform–diethylamine as developing solvent for thin-layer chromatography. Infrared spectra were measured in nujol mulls for crystalline substances and in chloroform solution for amorphous compounds. The n.m.r. spectra were all measured on an A-60 instrument in $CDCl_3$ solution with tetramethylsilane as an internal standard. All melting points have been taken on a Kofler hot stage and are uncorrected.

Oxidation of Group A Alkaloids (General Procedure)

Oxidation of Bikhaconitine

Bikhaconitine (I, R = Et; $R_1 = R_2 = H$; $R_3 = C_6H_3(OCH_3)_2$) (183 mg) was dissolved in 80% acetone–water (50 ml) and potassium permanganate (160 mg) in 50% acetone–water (70 ml) was added all at once. The mixture was stirred for 10 min at room temperature and the excess permanganate reduced with sulfurous acid. The acetone was evaporated under reduced pressure and the residual aqueous solution after addition of sodium carbonate was extracted with chloroform. The dried chloroform extract on evaporation left a residue (192 mg) that was dissolved in 1% sulfuric acid (10 ml) and extracted with benzene to remove neutral substances. The aqueous solution was made basic with sodium carbonate and extracted with chloroform. Evaporation of the dried chloroform extract left a foam (180 mg) that was dissolved in benzene and chromatographed on alumina. The chromatogram was eluted first with benzene and then with 50% chloroform benzene. The benzene eluate gave unchanged bikhaconitine (101 mg) while the chloroform–benzene eluate yielded N-deethylbikhaconitine (65 mg), both homogeneous in thin-layer chromatography. The n.m.r. spectrum of the product no longer contained the triplet characteristic of the N-ethyl group. For analyses of N-methyl derivatives, see Table III.

The benzene extract containing the neutral fraction left, on evaporation, a residue that crystallized on contact with ethanol, m.p. 220–222°, wt. 2 mg. This product proved to be N-deethyloxobikhaconitine (cf. Table IV). This lactam becomes the main product of oxidation when the time of reaction is prolonged to 50 min.

Oxidation of Aconitine

Aconitine (1.950 g) in acetone (200 ml) was oxidized at room temperature with potassium permanganate (2.0 g) dissolved in 50% acetone–water (400 ml) for 20 min. The product was treated with 1% sulfuric acid and separated as above into a neutral and a basic fraction. The neutral fraction yielded N-deethyloxoaconitine (600 mg, see below) and the basic fraction gave N-deethylaconitine (578 mg) and unchanged aconitine (522 mg), which were separated by chromatography on alumina.

Oxidation of Anhydropseudaconitine

Anhydropseudaconitine (7) (568 mg) was oxidized with potassium permanganate (616 mg) in 50% acetone–water. The product (598 mg) in thin-layer chromatography showed the presence of two main compounds and five minor ones. The two main compounds were unchanged starting material and N-deethylanhydropseudaconitine. The product was chromatographed in benzene solution on alumina. Elution with benzene gave the unchanged starting material (174 mg) and elution with 20% chloroform–benzene gave a mixture (109 mg) of starting material and the N-deethyl base in which the latter predominated. Further elution with the same solvent yielded pure N-deethyl base (26 mg) as a gum. Final elution with chloroform gave material (80 mg) which included the N-deethyl base and the other minor products of low mobility. In the n.m.r. spectrum N-deethylanhydropseudaconitine produced signals at δ 6.20–5.80 (ethylenic protons), δ 3.91, 3.89 (veratroyl methoxyls), δ 3.54, 3.33, 3.30, 3.17 (four methoxyls), δ 1.33 (O-acetyl), but showed no imino ethyl signals.

N-Deethyl Bases

N-Deethylaconitine (I, R = H; $R_1 = R_2 = OH$; $R_3 = C_6H_5$), N-deethyldeoxyaconitine (I, R = R_1 = H; R_2 = OH; $R_3 = C_6H_5$), N-deethylindaconitine (I, R = R_2 = H; R_1 = OH; $R_3 = C_6H_5$), N-deethylanhydropseudaconitine, N-deethylpseudaconitine (I, R = R_2 = H; R_1 = OH; $R_3 = C_6H_3(OCH_3)_2$) and N-deethylbikhaconitine (I, R = $R_1 = R_2$ = H; $R_3 = C_6H_3(OCH_3)_2$) were amorphous. They all lacked the N-ethyl signal in the n.m.r. spectrum. N-Demethyldelphinine, identical with N-deethyldeoxyindaconitine (I, R = $R_1 = R_2$ = H; $R_3 = C_6H_5$) crystallized from ether as fine colorless needles, m.p. 162–164°. The compound obtained from two different sources also lacked the iminoethyl signal in the n.m.r. spectrum. Gilman and Marion (8), who had previously obtained this substance, reported it to be amorphous.

Methylation of N-Deethyl Bases

The N-deethyl base was refluxed in 50% methanol–ether with excess methyl iodide and powdered potassium carbonate for 1 h. In each case the product was purified by chromatography on alumina. Every one of the N-methyl-N-deethyl bases prepared showed an imino-methyl signal at δ 2.30 in the n.m.r. spectrum. They are listed in Table III together with their analytical figures.

N-Dealkyloxo Bases

The neutral fraction of the product of oxidation of the ester alkaloids mentioned above was in each case the N-dealkyloxo-derivative. It was purified by chromatography over alumina. The crystal forms, melting points, and analytical figures are given in Table IV.

Oxidation of Group A Alkamines

Oxidation of Chasmanine

Chasmanine (245 mg) was dissolved in 80% acetone–water (60 ml) and a solution of potassium permanganate (242 mg) in 50% acetone–water (200 ml) was added. The resulting solution was stirred at room temperature for 5 min and the product worked up as usual. It gave N-deethylchasmanine (215 mg), crystallizing as colorless prisms from chloroform–hexane, m.p. 230–231°.

Anal. Calcd. for $C_{23}H_{37}O_6N$: C, 65.22; H, 8.81. Found: C, 64.71; H, 8.67.

On treatment with ethyl iodide by the method described above, the product gave back chasmanine, while treatment with methyl iodide by the same method yielded N-methyl-N-deethylchasmanine, which separated from *n*-hexane as colorless prisms, m.p. 90–92°. In the n.m.r. spectrum: δ 2.29 ($N\text{-}CH_3$) (6).

Anal. Calcd. for $C_{24}H_{39}O_6N$: C, 65.87; H, 8.98; N, 3.20. Found: C, 65.64; H, 9.10; N, 3.19.

Oxidation of Diacetyldemethoxyisopyrobikhaconine

To a stirred solution of the compound (7) (396 mg) in acetone (72 ml) and water (8 ml), potassium permanganate (214 mg) dissolved in acetone (40 ml) was added all at once. After 5 min stirring at room temperature, the excess permanganate was decomposed by the addition of sulfurous acid ($Na_2SO_3 + H_2SO_4$) and the acetone evaporated under reduced pressure below 40°. Extraction of the acid liquor with chloroform removed 5 mg of neutral material which was not further investigated. The solution was made basic with sodium carbonate and extracted with chloroform. Evaporation of the dried extract yielded a colorless gum (440 mg) showing in thin-layer chromatography one strong spot (N-deethyl compound) and two weak spots, one of which corresponded to the starting material.

Crystallization of the product from ether gave N-deethyldiacetyldemethoxyisopyrobikhaconine as fine colorless needles (320 mg) m.p. 200–204°. In the n.m.r. spectrum signals at δ 6.20–5.45 (olefinic protons), δ 3.30, 3.29, 3.21 (three OMe), δ 2.05, 2.01 (two acetyl groups).

Anal. Calcd. for $C_{26}H_{35}O_7N\cdot H_2O$: C, 63.52, H, 7.59. Found: C, 63.83, H, 7.62.

Some of the N-deethyl compound (200 mg) in pyridine (5 ml) and acetic anhydride (2.5 ml) was heated on the steam bath for 4 h. The product of the reaction, a triacetate (200 mg) was a gum that could not be induced to crystallize. In the n.m.r. spectrum signals at δ 6.20–5.40 (olefinic protons), δ 3.29 (6H), 3.19 (3 OMe), δ 2.11, 2.09, 2.03 (three acetyl groups).

Reduction of the triacetate (50 mg) with lithium aluminium hydride in tetrahydrofurane (5 ml) overnight gave a product that was dissolved in benzene and chromatographed on alumina. The chloroform eluate yielded demethoxyisopyrobikhaconine, which crystallized from ether-*n*-hexane as colorless fine needles, m.p. 147–150°, identical with an authentic sample (8).

Some of the triacetate (300 mg) dissolved in ethanol (20 ml) was hydrogenated over platinum oxide (200 mg). The product, worked up as usual, was a colorless gum. It was saponified by refluxing with 3% sodium hydroxide in methanol, the methanol was evaporated, water added, and the solution extracted with chloroform. Evaporation of the extract left N-acetyl-N-deethyldihydrodemethoxyisopyrobikhaconine as a colorless gum (290 mg) which crystallized from methanol–ether as colorless prisms (256 mg), m.p. 242–245°.

Anal. Calcd. for $C_{24}H_{35}O_6N\cdot 0.5H_2O$: C, 65.01; H, 8.13. Found: C, 65.36; H, 8.42.

Oxidation of Bikhaconine

Bikhaconine (312 mg) oxidized with potassium permanganate by the procedure already described gave N-deethylbikhaconine (120 mg) and unchanged starting material (80 mg) separated by chromatography, together with a small quantity of neutral material.

A quantity of N-deethylbikhaconine (90 mg) was methylated with methyl iodide and acetylated. There was obtained a triacetate that crystallized from methanol as colorless prisms (64 mg) m.p. 182–184°.

Anal. Calcd. for $C_{30}H_{45}O_{10}N$: C, 62.16; H, 7.83. Found: C, 61.66, H, 7.41.

The triacetate was identical with triacetyldelphonine, m.p. 182–184°, prepared by hydrolysis and acetylation of delphinine.

Oxidation of Pseudaconine

Pseudaconine (150 mg) was oxidized as above for 5 min and the excess permanganate was reduced with sulfurous acid. After evaporation of the acetone under reduced pressure and extraction with chloroform to remove any neutral product, the solution was made basic with sodium carbonate and extracted for 3 days with chloroform in a liquid–liquid extractor. Evaporation of the extract left N-deethylpseudaconine (140 mg) as a gum. The gummy residue was treated with methyl iodide as described above and the product acetylated. This gave rise to the tetraacetate of N-methyl-N-deethylpseudaconine obtained as colorless prisms from ethanol, m.p. 235°.

Anal. Calcd. for $C_{32}H_{47}O_{12}N$: C, 60.19; H, 7.36. Found: C, 59.61; H, 7.08.

Can. J. Chem. Downloaded from www.nrcresearchpress.com by 210.87.254.105 on 09/05/12
For personal use only.

Can. J. Chem. Downloaded from www.nrcresearchpress.com by 210.87.254.105 on 09/05/12
For personal use only.

TABLE III

N-Methyl-N-deethyl alkaloids

N-Methyl-N-deethyl derivative of:	Crystal form**	m.p.	Formula	Analysis				Identical with:
				Calcd.		Found		
				% C	% H	% C	% H	
Bikhaconitine*	Needles (*a*)	187–190°	$C_{35}H_{49}O_{11}N$*	63.64	7.43	63.75	7.78	
Bikhaconitine $HClO_4$	Needles (*b*)	200–204°	$B.HClO_4 \cdot H_2O$	53.99	6.69	54.24	6.69	
Aconitine†	Prisms (*c*)	196–198°	$C_{33}H_{45}O_{11}N$†	62.74	7.12	62.50	7.16	Mesaconitine
Deoxyaconitine‡	Prisms (*c*)	184–186°	$C_{33}H_{45}O_{10}N$‡	64.37	7.37	64.57	7.29	Hypaconitine
Indaconitine§	Prisms (*d*)	204–205°	$C_{33}H_{47}O_{10}N$§	64.16	7.67	64.05	7.58	
Pseudaconitine‖	Prisms (*b*)	208–211°	$C_{35}H_{49}O_{12}N.H_2O$	60.61	7.36	60.83	7.41	
Deoxyindaconitine¶	Prisms (*a*)	187–189°	$C_{33}H_{49}O_9N$¶	66.09	7.56	66.30	7.66	Delphinine

*I, R = CH_3; $R_1 = R_2 = H$; $R_3 = C_6H_3(OCH_3)_2$.
†I, R = CH_3; $R_1 = R_2 = OH$; $R_3 = C_6H_6$.
‡I, R = CH_3; $R_1 = H$; $R_2 = OH$; $R_3 = C_6H_5$.
§I, R = CH_3; $R_1 = OH$; $R_2 = H$; $R_3 = C_6H_5$.
‖I, R = CH_3; $R_1 = OH$; $R_2 = H$; $R_3 = C_6H_3(OCH_3)_2$.
¶I, R = CH_3; $R_1 = R_2 = H$; $R_3 = C_6H_3(OCH_3)_2$.
**Crystallized from (*a*) ether, (*b*) ethanol, (*c*) methanol, (*d*) benzene.

TABLE IV

N-Dealkyloxo alkaloids

Compound	Crystal form*	m.p.	Formula	Analysis			
				Calcd.		Found	
				% C	% H	% C	% H
N-Deethyloxoaconitine	Prisms (*a*)	266–267°	$C_{32}H_{41}O_{12}N$	60.28	6.83	60.84	6.54
N-Deethyloxobikhaconitine	Prisms (*b*)	222–223°	$C_{34}H_{45}O_{12}N$				
N-Demethyloxodelphinine N-Deethyloxodeoxyindaconitine	Needles (*c*)	211–212°	$C_{32}H_{41}O_{10}N$	64.09	6.89	64.43	7.42
N-Deethyloxoindaconitine	Prisms (*b*)	273–280°	$C_{32}H_{41}O_{11}N$	62.44	6.83	62.23	7.34
N-Deethyloxopseudaconitine	Needles (*b*)	256–262°	$C_{34}H_{45}O_{11}N$				

*Crystallized from (*a*) chloroform–acetone, (*b*) ethanol, (*c*) acetone.

Oxidation of Group B Alkaloids

Oxidation of Lycoctonine

Lycoctonine (380 mg) was oxidized with potassium permanganate (380 mg) for 4 min under the conditions described above. It yielded a single product (386 mg) which crystallized on standing, m.p. 93–95°, and proved identical in every respect with an authentic sample of oxolycoctonine (3).

Oxidation of Browniine

Browniine (213 mg) liberated from its perchlorate was oxidized with potassium permanganate (220 mg) for 3 min under the conditions already described. The excess permanganate was decomposed with sulfurous acid. After evaporation of the acetone under reduced pressure, the aqueous solution was extracted with chloroform to remove the neutral fraction (170 mg). The aqueous solution was made basic with sodium carbonate and extracted with chloroform. This second chloroform extract yielded the basic fraction (43 mg). The neutral fraction crystallized immediately and after recrystallization from ether was obtained as colorless needles, m.p. 170–171°, identical by melting point, mixture melting point, and infrared spectra with an authentic sample of oxobrowniine (5).

The basic fraction still contained oxobrowniine. On chromatography in benzene solution on alumina and elution with benzene and then chloroform–benzene (1:1), it yielded a further crop of oxobrowniine (27 mg) and amorphous N-deethylbrowniine (16 mg).

N-Deethylbrowniine (76 mg) was methylated with methyl iodide by the method already described and the resulting amorphous N-methyl-N-deethylbrowniine (28 mg) was characterized as its perchlorate, colorless needles from methanol – ethyl acetate, m.p. 215°.

Anal. Calcd. for $C_{24}H_{39}O_7N \cdot HClO_4$: C, 51.99; H, 7.40. Found: C, 51.89; H, 7.28.

Oxidation of Delcosine

Delcosine (212 mg) was oxidized with potassium permanganate (150 mg) for 7 min under the conditions described and the product worked up as usual. By means of chromatography the product was separated into anhydrohydroxydelcosine (165 mg), m.p. 186–188°, unchanged delcosine (15 mg), and N-deethyldelcosine (30 mg), m.p. 240–241° (decomp.). The identity of these compounds was confirmed by direct comparison with authentic specimens (9).

ACKNOWLEDGMENT

The authors acknowledge their indebtedness to Mr. H. Seguin for the microanalyses, Mr. M. Lesage for the n.m.r. spectra, and Mr. R. Lauzon for the infrared spectra.

REFERENCES

1. W. A. Jacobs and S. W. Pelletier. Chem. Ind. 591 (1960).
2. S. W. Pelletier and W. A. Jacobs. J. Org. Chem. **21**, 1514 (1956).
3. O. E. Edwards and L. Marion. Can. J. Chem. **30**, 627 (1952).
4. R. C. Cookson and M. E. Trevett. J. Chem. Soc. 3121, 3864 (1956).
5. M. H. Benn, M. A. M. Cameron, and O. E. Edwards. Can. J. Chem. **41**, 477 (1963).
6. O. Achmatowicz, Jr., Y. Tsuda, L. Marion, T. Okamoto, M. Natsume, H.-H. Chang, and K. Kajima. Can. J. Chem. **43**, 825 (1965).
7. Y. Tsuda and L. Marion. Can. J. Chem. **41**, 3055 (1963).
8. R. E. Gilman and L. Marion. Can. J. Chem. **42**, 2700 (1964).
9. V. Skaric and L. Marion. J. Am. Chem. Soc. **80**, 4434 (1958).

Can. J. Chem. Downloaded from www.nrcresearchpress.com by 210.87.254.105 on 09/05/12
For personal use only.

Can. J. Chem. Downloaded from www.nrcresearchpress.com by 210.87.254.5 on 09/05/12
For personal use only.

CARBOHYDRATES CONTAINING NITROGEN IN A FIVE-MEMBERED RING AND AN ATTEMPTED SYNTHESIS OF A CARBOHYDRATE WITH NITROGEN IN A SEVEN-MEMBERED RING[1]

W. A. SZAREK[2] AND J. K. N. JONES
Department of Chemistry, Queen's University, Kingston, Ontario

Received March 18, 1965

ABSTRACT

Lead tetraacetate oxidation of 6-acetamido-6-deoxy-D-galactose (IX) yielded a syrup which was converted to a compound formulated as 4-acetamido-4-deoxy-1,2-*O*-isopropylidene-D-threofuranose (XII). The same syrup was obtained by alkaline degradation of the product of oxidation of 5-acetamido-5-deoxy-D-xylose diethyl dithioacetal (XVII) with peroxypropionic acid. Treatment of compound XII with *p*-toluenesulfonyl chloride yielded crystalline 4-acetamido-4-deoxy-1,2-*O*-isopropylidene-3-*O*-*p*-tolylsufonyl-D-threofuranose (XIII).

Demercaptalation of 6-acetamido-2,3,4,5-tetra-*O*-acetyl-6-deoxy-D-galactose diethyl dithioacetal (XX) with mercuric chloride and cadmium carbonate in aqueous acetone did not yield a nitrogen-containing septanose ring but an acyclic derivative.

CARBOHYDRATES CONTAINING NITROGEN IN A FIVE-MEMBERED RING

In a previous paper (1) from this laboratory the synthesis of methyl 4-acetamido-4-deoxy-L-erythrofuranoside (I), the first example of a sugar with nitrogen in a five-membered ring, was described. Very shortly after this announcement, Hanessian and Haskell (2) reported that they had obtained syrupy 4-acetamido-4-deoxy-L-erythrofuranose by the alkaline degradation of 5-acetamido-5-deoxy-L-arabinose diethylsulfonal. In the same paper Hanessian and Haskell reported the preparation of a novel sugar derivative, 4-amino-4-deoxy-D-erythronolactam (II). In the present publication we describe the synthesis by two different routes of derivatives of 4-acetamido-4-deoxy-D-threofuranose (XI).

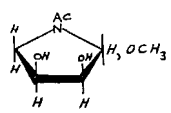

I

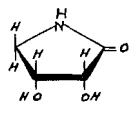

II

1,2;3,4-Di-*O*-isopropylidene-α-D-galactopyranose (IV) (3) was prepared from D-galactose (III) and treated with *p*-toluenesulfonyl chloride in pyridine to give 1,2;3,4-di-*O*-isopropylidene-6-*O*-*p*-tolylsulfonyl-α-D-galactopyranose (V) (4). Compound V reacted with sodium azide in *N*,*N*-dimethylformamide to afford a homogeneous pale yellow oil, the infrared spectrum of which showed the highly characteristic azide group absorption at 2 100 cm^{-1} but no aromatic ring and sulfonate group absorptions. The new substance is therefore 6-azido-6-deoxy-1,2;3,4-di-*O*-isopropylidene-α-D-galactopyranose (VI). This derivative could be reduced to 6-amino-6-deoxy-1,2;3,4-di-*O*-isopropylidene-α-D-galactopyranose (VII) (5) by merely stirring it with an excess of Raney nickel, a procedure described by Wolfrom *et al.* (6). Treatment of compound VII with acetic anhydride in pyridine afforded a glass which gave a negative ninhydrin reaction. The glassy product

[1]*Presented in part at the International Symposium on Carbohydrate Chemistry, Münster, July 13–17, 1964.*
[2]*Present address: Ohio State University, Columbus, Ohio.*

showed amide I and amide II bands in the infrared, and thus is 6-acetamido-6-deoxy-1,2;3,4-di-*O*-isopropylidene-α-D-galactopyranose (VIII). Hydrolysis of VIII with Amberlite IR-120 (H form) resin yielded glassy 6-acetamido-6-deoxy-D-galactose (IX), which was characterized by its conversion to crystalline 6-acetamido-6-deoxy-D-galactitol (X) on sodium borohydride reduction.

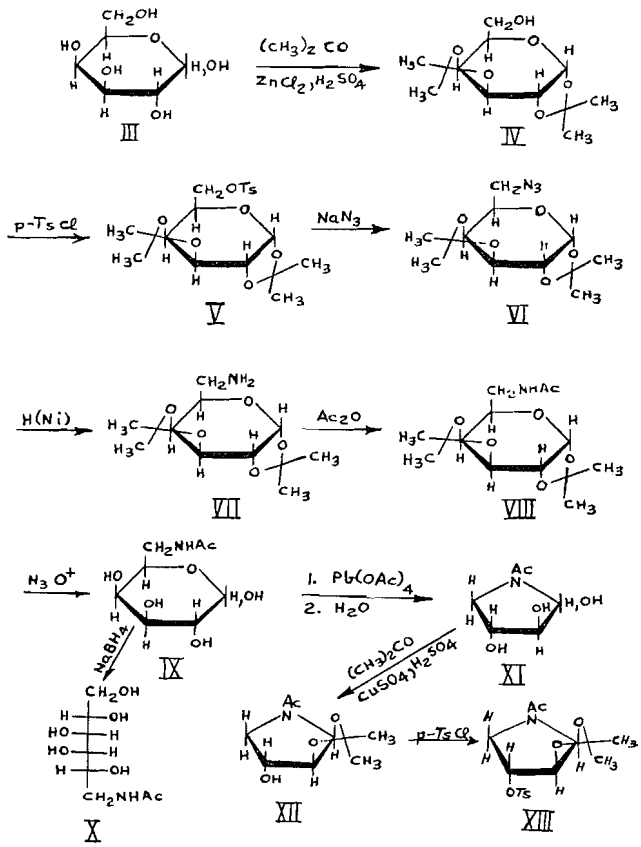

It has been known for some time that aldohexoses, when treated with lead tetraacetate, rapidly consume 2 moles of oxidant, after which the reaction becomes very slow (7, 8). Thus, Perlin and Brice (8) were able to degrade D-glucose selectively to di-*O*-formyl-D-erythrose by oxidation with 2 moles of lead tetraacetate. The ester groups were easily hydrolyzed, giving D-erythrose in an overall yield of at least 80% of theory. D-Galactose showed similar behavior, but the product formed was D-threose esterified with 1.8 formate groups per molecule (9). Significantly, substitution of the C-6 hydroxyl group in D-glucose did not alter the rate of uptake of lead tetraacetate (10). This result implies that the primary carbinol group is not involved in the oxidation of D-glucose itself.

The results cited above suggested that oxidation of 6-acetamido-6-deoxy-D-galactose (IX) with 2 moles of lead tetraacetate would yield a 4-acetamido-4-deoxy-D-threose derivative in which there existed the possibility of formation of a nitrogen-containing furanose ring. Oxidation of compound IX with 2 moles of lead tetraacetate followed by hydrolysis of the ester groups by heating of the product in water afforded a syrup which was reducing towards Fehling's solution and whose infrared spectrum showed absorption

Can. J. Chem. Downloaded from www.nrcresearchpress.com by 210.87.254.5 on 09/05/12
For personal use only.

attributable to *OH* and a very broad amide I band, but no significant amide II band. The infrared data suggested that the new substance exists primarily in the furanose form (XI). The results of periodate oxidation in unbuffered aqueous solution were consistent also with the proposed structure. The n.m.r. spectrum in deuterium oxide (Fig. 1) could

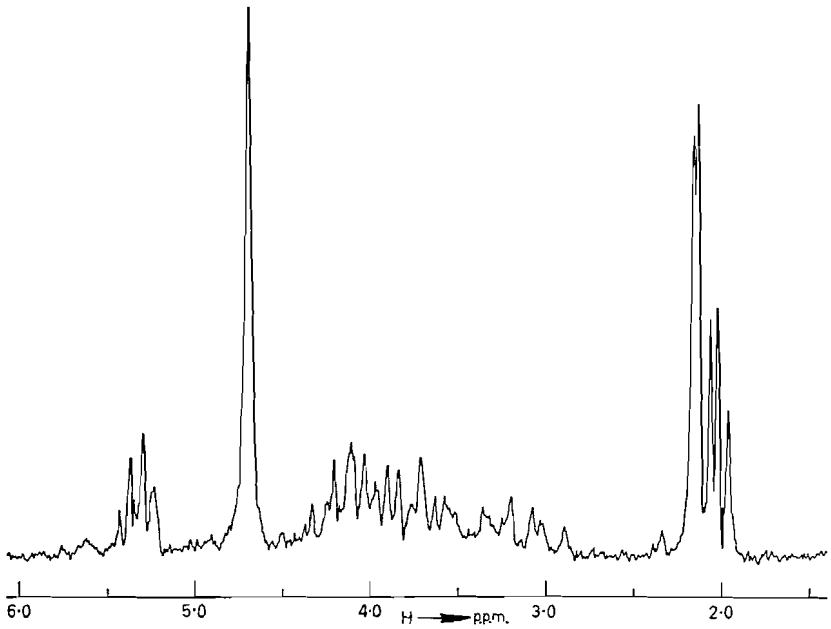

FIG. 1. Nuclear magnetic resonance spectrum of "4-acetamido-4-deoxy-D-threofuranose" at room temperature.

not be satisfactorily interpreted, however, on the basis of this formulation. In the region 1.96–2.15 p.p.m., characteristic of the protons of an *N*-acetyl group (11), there are five peaks. The portion of the spectrum from 5.24 p.p.m. to 5.43 p.p.m., which can be attributed to anomeric protons (12), is also unusually complex. An attractive suggestion is that the new substance is a mixture of α- and β-anomers, and that each anomer displays restricted rotation about the *CO—N* bond. Such hindered internal rotation has been demonstrated in methyl 4-acetamido-4-deoxy-L-erythrofuranoside and in two nitrogen-containing pyranose sugars (13). In addition there may be present a small amount of the acyclic form of the compound.

The new substance appeared on both paper and thin-layer chromatograms as two spots which moved very close to one another. A separation of the two components by preparative paper chromatography was attempted. The zones were located and extracted with methanol. Examination of the two extracts on paper chromatograms still showed in each case, however, the presence of the two original components. This observation indicated that a transformation of one component into the other occurred during the extraction or chromatography process.

Treatment of the oxidation product with dry acetone in the presence of anhydrous copper (II) sulfate and concentrated sulfuric acid afforded a pale yellow syrup. In contrast to the starting material, the product migrated as a homogeneous spot on a thin-layer chromatogram. The infrared spectrum of this material showed a doublet of approximately equal intensity attributable to a $C(CH_3)_2$ grouping, absorption attributable to *OH*,

Can. J. Chem. Downloaded from www.nrcresearchpress.com by 210.87.254.5 on 09/05/12
For personal use only.

and an amide I band but no amide II band. This evidence is consistent with structure XII for the new compound, which is named 4-acetamido-4-deoxy-1,2-*O*-isopropylidene-D-threofuranose. The n.m.r. spectrum in deuterium oxide at room temperature (Fig. 3) shows two peaks at 1.36 and 1.41 p.p.m. which may be assigned to the protons of an isopropylidene group, and two peaks at 2.08 and 2.16 p.p.m. in the region characteristic of the protons of *N*-acetyl groups. Since there is no possibility of anomers in 4-acetamido-4-deoxy-1,2-*O*-isopropylidene-D-threofuranose, the two signals in the *N*-acetyl region may

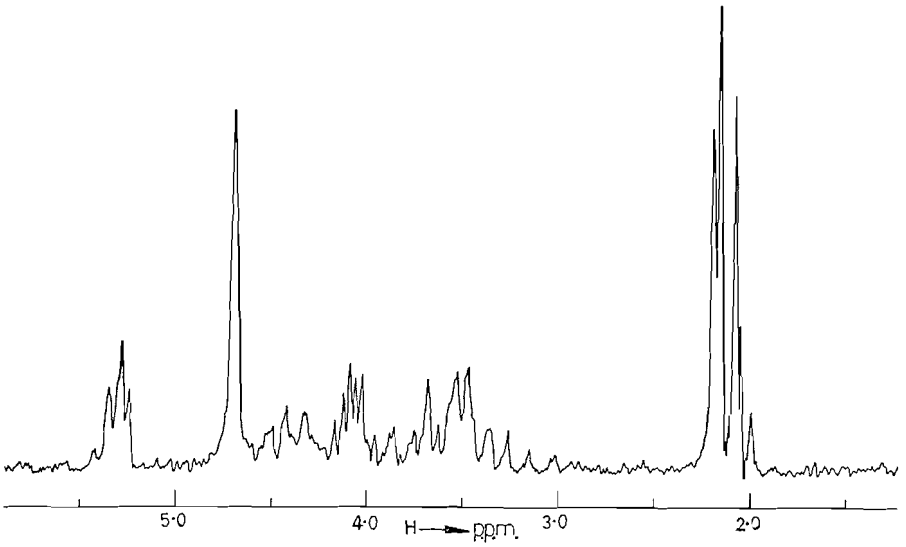

FIG. 2. Nuclear magnetic resonance spectrum of "4-acetamido-4-deoxy-L-erythrofuranose" at room temperature.

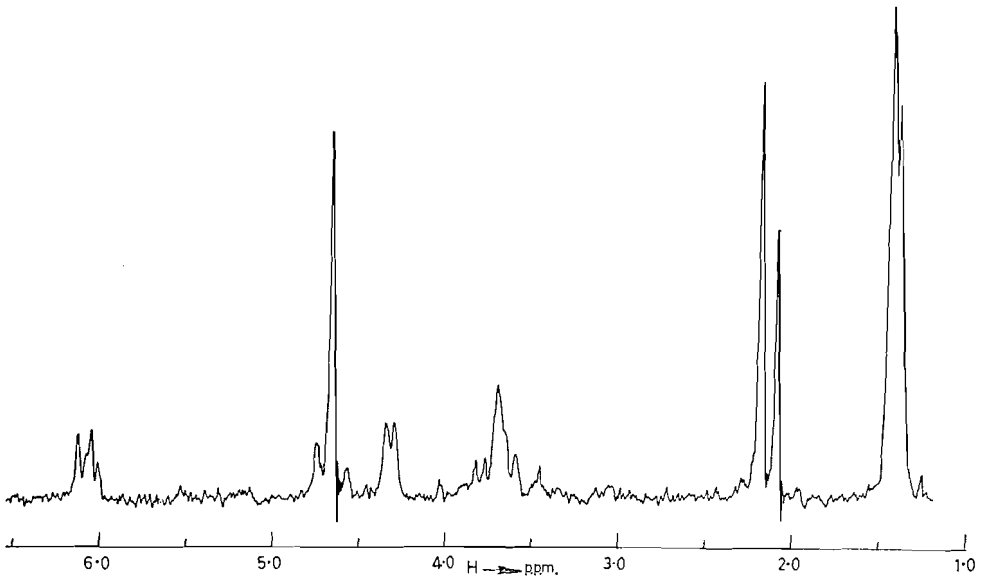

FIG. 3. Nuclear magnetic resonance spectrum of 4-acetamido-4-deoxy-1,2-*O*-isopropylidene-D-threofuranose (LXXXVI) at room temperature.

Can. J. Chem. Downloaded from www.nrcresearchpress.com by 210.87.254.5 on 09/05/12
For personal use only.

Can. J. Chem. Downloaded from www.nrcresearchpress.com by 210.87.254.5 on 09/05/12
For personal use only.

arise from restricted rotation about the *CO*—*N* bond. At 80°, however, there was no measurable merging of the two signals. Treatment of compound XII with *p*-toluenesulfonyl chloride in pyridine yielded crystalline 4-acetamido-4-deoxy-1,2-*O*-isopropylidene-3-*O*-*p*-tolylsulfonyl-D-threofuranose (XIII). The five-membered ring structure of XIII was indicated by the absence of the amide II band in its infrared spectrum. The n.m.r. spectrum of 4-acetamido-4-deoxy-1,2-*O*-isopropylidene-3-*O*-*p*-tolylsulfonyl-D-threofuranose in deuterochloroform at room temperature is presented in Fig. 4. The group of peaks centered at 7.60 p.p.m. with an intensity corresponding to four protons may be assigned to tosyl ring protons. The peak at 2.47 p.p.m., corresponding to three protons, is assigned to the tosyl methyl group. The n.m.r. spectrum shows also two peaks at 1.35 and 1.39 p.p.m. attributable to the protons of an isopropylidene group. Evidence in favor of restricted rotation about the *CO*—*N* bond was obtained by the appearance of two peaks at 2.00 and 2.17 p.p.m. which may be assigned to the protons of the *N*-acetyl group, and two doublets at 5.90 and 6.20 p.p.m. in the general region characteristic of anomeric protons.

In the present work the preparation of the syrupy product obtained by lead tetraacetate oxidation of 6-acetamido-6-deoxy-D-galactose was accomplished also by a different approach. 1,2-*O*-Isopropylidene-5-*O*-*p*-tolylsulfonyl-D-xylose (XIV) was prepared from D-xylose by the method of Levene and Raymond (14). Treatment with sodium azide in *N*,*N*-dimethylformamide gave crystalline 5-azido-5-deoxy-1,2-*O*-isopropylidene-D-xylose (XV). This compound was readily reduced with Raney nickel at room temperature to give a crystalline product which, when treated with aqueous acetic anhydride, gave 5-acetamido-5-deoxy-1,2-*O*-isopropylidene-D-xylose (XVI) (15). The furanose ring of XVI could be opened by treatment with ethanethiol and hydrochloric acid to give crystalline 5-acetamido-5-deoxy-D-xylose diethyl dithioacetal (XVII). Oxidation of compound XVII with peroxypropionic acid afforded a glass, probably 5-acetamido-5-deoxy-D-xylose diethylsulfonal. Treatment of this material with aqueous ammonia afforded crystalline bis (ethylsulfonyl) methane and a syrup. The infrared and proton magnetic resonance spectra and chromatographic properties of this material were the same as those of the syrup obtained from the lead tetraacetate oxidation.

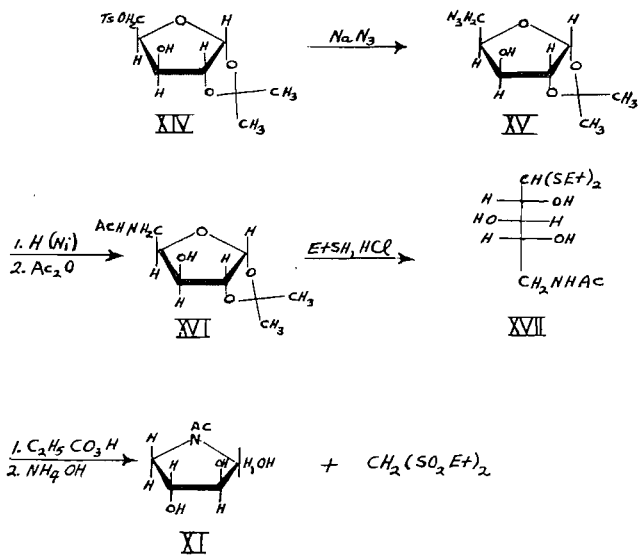

Can. J. Chem. Downloaded from www.nrcresearchpress.com by 210.87.254.5 on 09/05/12
For personal use only.

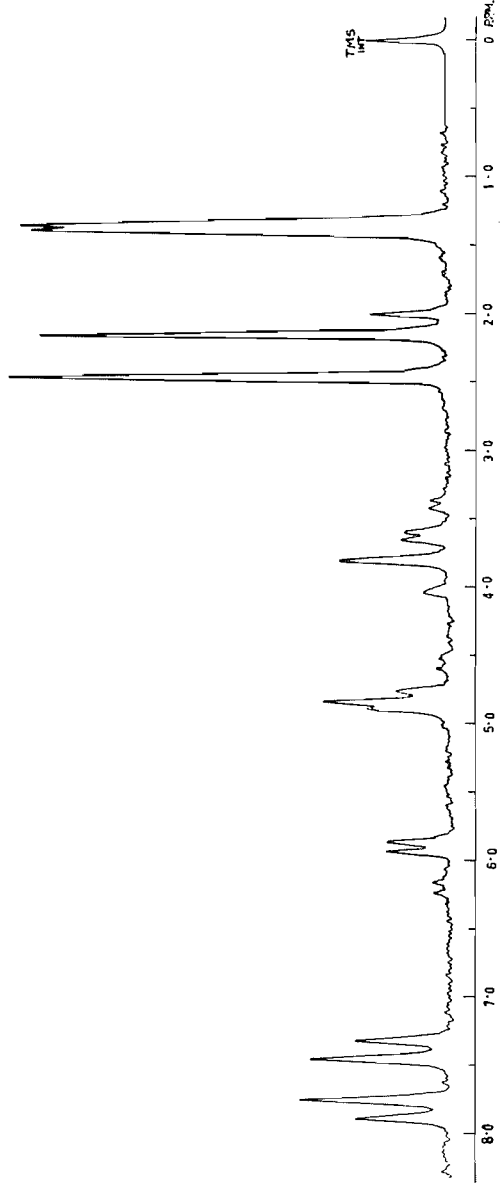

FIG. 4. Nuclear magnetic resonance spectrum of 4-acetamido-4-deoxy-1,2-*O*-isopropylidene-D-threofuranose 3-*p*-tolylsulfonate.

It is of interest to note that hydrolysis with Amberlite IR-120 (H form) resin of methyl 4-acetamido-4-deoxy-L-erythrofuranoside (I) (1) afforded a reducing syrup which exhibited behavior entirely analogous to that shown by the product derived from the two degradation procedures described above. The infrared spectrum of the syrup showed absorption attributable to *OH* and a broad amide I band, but no significant absorption in the region characteristic of an amide II band. On the basis of the infrared data and the structure of the precursor I, a reasonable formulation of the new syrup would be that shown by XVIII.

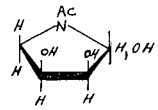

XVIII

The results of periodate oxidation in unbuffered aqueous solution could be accommodated also by this structure. The n.m.r. spectrum in deuterium oxide (Fig. 2), however, is very complex but resembles closely the spectrum shown in Fig. 1. Two spots were detected again by both paper and thin-layer chromatography, and an attempted separation of the components by preparative paper chromatography indicated that they are interconvertible.

ATTEMPTED SYNTHESIS OF A CARBOHYDRATE CONTAINING NITROGEN IN A SEVEN-MEMBERED RING

The synthesis of derivatives of seven-membered ring sugars or septanoses has been achieved by Micheel *et al.* (16–18). By a series of reactions α- and β-1,2,3,4,5-penta-*O*-acetyl-D-galactoseptanose were prepared. The septanose structure was confirmed by conversion of the pentaacetate to a methyl tetra-*O*-methyl-D-galactoseptanoside which, upon oxidation with nitric acid, gave tetra-*O*-methylmucic acid (17). In the present work the synthesis of a sugar derivative with nitrogen as the hetero atom in a seven-membered ring was attempted by a method analogous to that described by Micheel and Suckfüll (16).

Treatment of 6-acetamido-6-deoxy-1,2;3,4-di-*O*-isopropylidene-α-D-galactopyranose (VIII) (*vide supra*) with ethanethiol and hydrochloric acid gave crystalline 6-acetamido-6-deoxy-D-galactose diethyl dithioacetal (XIX). Acetylation of XIX with acetic anhydride in pyridine then afforded crystalline 6-acetamido-2,3,4,5-tetra-*O*-acetyl-6-deoxy-D-galactose diethyl dithioacetal (XX). Demercaptalation of compound XX with mercuric chloride and cadmium carbonate in aqueous acetone, by the method employed by Wolfrom (19) to prepare the monoethyl alcoholate of 2,3,4,5,6-penta-*O*-acetyl-*aldehydo*-galactose, gave a crystalline product XXI which, on heating, reduced Fehling's solution. The infrared spectrum of this material showed strong absorption attributable to *OH*, absorption owing to *O*-acetyl groups, an amide I band, and an amide II band. Thus compound XXI is presumably the aldehydrol of 6-acetamido-2,3,4,5-tetra-*O*-acetyl-6-deoxy-*aldehydo*-D-galactose. Accordingly, compound XXI was allowed to stand in dry pyridine for 24 h and then treated with acetic anhydride. The presence of an amide II band in the infrared spectrum of the product indicated, however, that the desired cyclization to form a nitrogen-containing septanose ring had not occurred.

EXPERIMENTAL

Melting points were determined on a Fisher-Johns melting point apparatus. Optical rotations were measured with a Hilger standard polarimeter. Infrared spectra were measured with a Perkin–Elmer model 21 spectrophotometer. The n.m.r. spectra were determined at 60 Mc/s with a Varian A-60 n.m.r. spectrometer

Can. J. Chem. Downloaded from www.nrcresearchpress.com by 210.87.254.5 on 09/05/12
For personal use only.

using approximately 10% by weight solutions; chemical shifts were determined as p.p.m. downfield from tetramethylsilane as an external standard for the deuterium oxide solutions and as an internal standard for the deutero chloroform solutions. Paper chromatography was carried out by the descending method at room temperature on Whatman No. 1 filter paper for qualitative purposes or on Whatman 3 MM filter paper for preparative purposes in the following solvent systems (v/v): (A) butan-1-ol:ethanol:water, 3:1:1; (B) ethyl acetate:acetic acid:formic acid:water, 18:3:1:4. Sugars were detected on paper chromatograms by the following spray reagents: (i) alkaline silver nitrate (20); (ii) *p*-anisidine hydrochloride (21); (iii) sodium metaperiodate – potassium permanganate (22). Rates of movement of the sugars on paper chromatograms are given relative to that of rhamnose (R_{rh}). Thin-layer chromatography was carried out on Silica Gel G supplied by Research Specialties Company, Richmond, California. The developed plates were dried in air, sprayed with concentrated sulfuric acid, and then heated in an oven at about 150°. Raney nickel catalyst in water was supplied by Aldrich Chemical Co., Inc., Milwaukee, Wisconsin.

1,2;3,4-Di-O-isopropylidene-6-O-p-tolylsulfonyl-α-D-galactopyranose (V)

1,2;3,4-Di-*O*-isopropylidene-α-D-galactopyranose (IV) was prepared from D-galactose (36 g) according to Tipson (3). The crude product (33 g) was dissolved in dry pyridine (65 ml) and *p*-toluenesulfonyl chloride (36.8 g, 1.5 moles) was added at room temperature. After 3 h the mixture was poured into 400 ml of ice-water and the precipitated product (44.1 g, 84%) was isolated in the usual way. After two recrystallizations from methanol the compound had m.p. 101.5–102.5° and $[\alpha]_D^{25} = -62°$ (*c*, 4.33 in chloroform containing 0.75% ethanol). Foster *et al.* (4) report m.p. 89–91° and $[\alpha]_D = -63.4°$ (chloroform); Freudenberg and Raschig (23) report m.p. 102–103°.

6-Azido-6-deoxy-1,2;3,4-di-O-isopropylidene-α-D-galactopyranose (VI)

To a solution of 1,2;3,4-di-*O*-isopropylidene-6-*O*-*p*-tolylsulfonyl-α-D-galactopyranose (V) (27.0 g) in *N*,*N*-dimethylformamide (230 ml) was added water (12 ml), sodium azide (6.38 g, 1.5 moles), and urea (0.8 g). The mixture was heated for 19 h at 120° under a stream of nitrogen. The cooled solution was poured into 600 ml of ice water and extracted several times with chloroform. The combined extracts were washed with aqueous sodium hydrogen carbonate, then with water, dried over anhydrous magnesium sulfate, and concentrated under reduced pressure to leave a pale yellow oil (15.6 g, 84%), $[\alpha]_D^{21} = -92.1°$ (*c*, 1.48 in chloroform containing 0.75% ethanol). Thin-layer chromatography in methanol:benzene, 1:9 (v/v), showed only one component. The infrared spectrum of this material in chloroform showed azide absorption at 2 100 cm^{-1}, but no aromatic ring and sulfonate group absorptions, and no hydroxyl group absorption.

6-Amino-6-deoxy-1,2;3,4-di-O-isopropylidene-α-D-galactopyranose (VII)

A solution of 6-azido-6-deoxy-1,2;3,4-di-*O*-isopropylidene-α-D-galactopyranose (VI) (14.4 g) in methanol (300 ml) was treated with Raney nickel (80 g) for 44 h, filtered, and concentrated to give a pale yellow syrup (13.7 g). The infrared spectrum of this material in chloroform showed *N*—*H* deformation vibration at 1 587 cm^{-1} and *N*—*H* stretching vibration in the 3 300 cm^{-1} region, but no absorption attributable to an azide grouping. The product was distilled to yield a mobile colorless syrup which had $[\alpha]_D^{23} = -44.0°$ (*c*, 1.31 in methanol). Veksler *et al.* (5) report $[\alpha]_D^{21} = -40.1°$ (in methanol) for syrupy 6-amino-6-deoxy-1,2;3,4-di-*O*-isopropylidene-α-D-galactopyranose.

6-Acetamido-6-deoxy-1,2;3,4-di-O-isopropylidene-α-D-galactopyranose (VIII)

To a solution of 6-amino-6-deoxy-1,2;3,4-di-*O*-isopropylidene-α-D-galactopyranose (VII) (12.2 g) in reagent pyridine (45 ml) was added acetic anhydride (17 ml) portionwise with ice-cooling. After 20 h at room temperature the solution was poured into 400 ml of ice water, and the mixture was extracted several times with chloroform. The combined chloroform extracts were washed with water, then shaken with an aqueous solution of cadmium chloride (to remove pyridine). The pyridine – cadmium chloride complex was filtered, the chloroform solution washed with water, dried over anhydrous magnesium sulfate, and concentrated under reduced pressure to leave an almost colorless glass (15.5 g). This material gave a negative ninhydrin reaction and had $[\alpha]_D^{23} = -8.3°$ (*c*, 1.81 in chloroform containing 0.75% ethanol). The infrared spectrum in chloroform showed *N*—*H* stretching vibration absorption at 3 440 cm^{-1}, an amide I band at 1 663 cm^{-1}, an amide II band at 1 520 cm^{-1}, and a doublet at 1 387 cm^{-1} and 1 376 cm^{-1} attributable to *C*—*H* deformation vibrations of a $C(CH_3)_2$ grouping.

6-Acetamido-6-deoxy-D-galactose (IX)

A suspension of 6-acetamido-6-deoxy-1,2;3,4-di-*O*-isopropylidene-α-D-galactopyranose (VIII) (1.5 g) in water (225 ml) was stirred with 7.5 g of Amberlite IR-120 (H form) resin at 60° for 3½ h. The resin was then removed by filtration, and the filtrate was shaken briefly with a small amount of Duolite A-4 (OH form) resin to remove any trace of acid. The resin was removed, and the clear colorless solution was concentrated under reduced pressure to leave a colorless glass (1.2 g). This material was reducing towards Fehling's solution, and had $[\alpha]_D^{22} = +81°$ (constant, during 24 h) (*c*, 1.24 in water). Thin-layer chromatography in 2-propanol:benzene, 1:2 (v/v), showed only one component; paper chromatography also showed only one component with R_{rh} 0.50 (solvent A, sprays i and ii).

Can. J. Chem. Downloaded from www.nrcresearchpress.com by 210.87.254.5 on 09/05/12
For personal use only.

*6-Acetamido-6-deoxy-*D*-galactitol (X)*

To a cold solution of 6-acetamido-6-deoxy-D-galactose (IX) (0.26 g) in water (10 ml) 0.26 g of sodium borohydride was added, with shaking. The solution was allowed to stand in a refrigerator for 3 h and then 30 min at room temperature. Excess sodium borohydride was destroyed by the addition of acetone, and the solution was then passed through Amberlite IR-120 (H form) exchange resin. The eluate and washings were concentrated to dryness under reduced pressure. Boric acid was removed by repeated distillation with methanol. A white crystalline material was obtained which was recrystallized from methanol to give crystals (0.12 g) which had $[\alpha]_D^{21} = +20.4°$ (*c*, 1.38 in water), R_{rh} 0.6 (solvent A, spray i), and m.p. 183–183.5°. The infrared spectrum in Nujol mull showed strong absorption at 3 280 cm^{-1} attributable to *OH* and *NH*, an amide I band at 1 645 cm^{-1}, and an amide II band at 1 557 cm^{-1}.

Anal. Calcd. for $C_8H_{17}O_6N$: C, 43.04; H, 7.68; N, 6.28. Found: C, 42.78; H, 7.58; N, 6.48.

*Lead Tetraacetate Oxidation of 6-Acetamido-6-deoxy-*D*-galactose (IX)*

To a rapidly stirred solution of 6-acetamido-6-deoxy-D-galactose (0.53 g, 0.00238 mole) in 2 ml of water and 50 ml of acetic acid was added lead tetraacetate (2.2 g, 0.00497 mole), prepared according to the procedure of Vogel (24), over a period of 3 to 4 min. After 18 min oxalic acid dihydrate (ca. 0.7 g), dissolved in glacial acetic acid, was added, and the suspension was stirred for an additional 30 min; a negative potassium iodide – starch test was then obtained. The precipitate was filtered off and washed with acetic acid, and the filtrate was concentrated under reduced pressure at 35° to a volume of a few milliliters. Ethyl acetate was added and the precipitate which formed was triturated with several portions of ethyl acetate. The extracts were combined, filtered, and concentrated to a syrup which was further purified by extraction with ethyl acetate. The product was a pale yellow syrup (0.40 g).

The yellow syrup was taken up in water (25 ml) and heated on a stream bath for 3 h. The solution was then concentrated under reduced pressure to yield a light brown syrup (0.26 g) which was examined on paper chromatograms. Sprays i and ii showed the presence of 6-acetamido-6-deoxy-D-galactose at R_{rh} 0.5 and two closely moving components at R_{rh} 1.05 and 1.32 (solvent A). The two components having R_{rh} 1.05 and 1.32 were separated as one fraction from the 6-acetamido-6-deoxy-D-galactose by preparative paper chromatography in solvent A. The syrupy fraction was purified by dissolving it in water and washing the solution with chloroform. Concentration of the aqueous phase under reduced pressure gave an almost colorless syrup (ca. 0.14 g) which reduced Fehling's solution in a few minutes on heating, and had $[\alpha]_D^{24} = -15.5°$ (*c*, 1.68 in methanol). In solvent B the syrup was revealed as two spots at R_{rh} 1.06 and 1.13 (sprays i and ii). Two spots were detected also by thin-layer chromatography in 2-propanol:benzene, 1:2 (v/v). The infrared spectrum of this material (smear between "IRTRAN-2" plates) showed strong absorption at 3 380 cm^{-1} attributable to *OH*, and a very broad band at 1 627 cm^{-1} attributable to *N*-Ac.

A separation of the two components was attempted by preparative paper chromatography using solvent A. The zones were located (spray i), cut, and extracted with methanol. Examination of the two extracts on paper chromatograms still showed in each case the presence of the two original components.

*4-Acetamido-4-deoxy-1,2-O-isopropylidene-*D*-threofuranose (XII)*

To a portion (0.096 g) of the lead tetraacetate oxidation product were added dry acetone (20 ml), anhydrous copper sulfate (2 g), and concentrated sulfuric acid (1 drop). The mixture was shaken mechanically for 24 h and filtered, and the filtrate was then poured into a rapidly stirred saturated aqueous solution (ca. 24 ml) of sodium hydrogen carbonate. Most of the acetone was removed by evaporation under reduced pressure and the solution was then continuously extracted with chloroform overnight. The chloroform extract was dried over anhydrous magnesium sulfate and concentrated under reduced pressure to leave a pale yellow syrup (0.058 g). This material was distilled under vacuum to yield a syrup which had $[\alpha]_D^{25} = +162°$ (*c*, 1.64 in methanol). Thin-layer chromatography in methanol:benzene, 1:9 (v/v), showed only one component. The infrared spectrum of this material in chloroform showed absorption at 3 420 cm^{-1} attributable to *OH*, a doublet of approximately equal intensity at 1 382 and 1 391 cm^{-1} caused by an isopropylidene grouping, and an amide I band at 1 645 cm^{-1} but no amide II band.

Anal. Calcd. for $C_9H_{15}O_4N \cdot \frac{1}{2}H_2O$: C, 51.5; H, 7.62; N, 6.68. Found: C, 51.9; H, 7.28; N, 6.15.

*4-Acetamido-4-deoxy-1,2-O-isopropylidene-3-O-p-tolylsulfonyl-*D*-threofuranose (XIII)*

Syrupy 4-acetamido-4-deoxy-1,2-*O*-isopropylidene-D-threofuranose (0.51 g) was dissolved in dry pyridine (10 ml) and *p*-toluenesulfonyl chloride (0.57 g, 1.2 moles) was added at room temperature. After 24 h the solution was poured into ice water; a crystalline material separated after a few min. The product (0.61 g) was recrystallized from ether to give crystals which had m.p. 129–129.5° and $[\alpha]_D = +84°$ (*c*, 1.73 in chloroform containing 0.75% ethanol). The infrared spectrum in (KBr) showed absorption at 1 600 cm^{-1} attributable to an aromatic ring, and an amide I band at 1 653 cm^{-1}, but no absorption attributable to *OH*, nor an amide II band.

Anal. Calcd. for $C_{16}H_{21}O_6NS$: C, 54.07; H, 5.96; N, 3.94. Found: C, 53.86; H, 5.76; N, 4.05.

*1,2-O-Isopropylidene-5-O-p-tolylsulfonyl-*D*-xylose (XIV)*

This compound was prepared from D-xylose (33 g) by the method of Levene and Raymond (14). The

Can. J. Chem. Downloaded from www.nrcresearchpress.com by 210.87.254.5 on 09/05/12
For personal use only.

crystalline product (44 g, 58)% was recrystallized from ethyl acetate and it then melted at 133–134° and had $[\alpha]_D = -12.4°$ (*c*, 2.9 in chloroform containing 0.75% ethanol). Levene and Raymond report m.p. 133–134° and $[\alpha]_D^{20} = -13.0°$ (*c*, 2.0 in chloroform).

*5-Azido-5-deoxy-1,2-O-isopropylidene-*D*-xylose (XV)*

To a solution of 1,2-*O*-isopropylidene-5-*O*-*p*-tolylsulfonyl-D-xylose (14.0 g) in *N*,*N*-dimethylformamide (125 ml) was added water (6.5 ml), sodium azide (3.4 g), and urea (0.25 g). The mixture was heated overnight at 110° under a stream of nitrogen. The cooled solution was poured into 150 ml of ice water and extracted with chloroform. The combined extracts were washed with aqueous sodium hydrogen carbonate, then with water, dried over anhydrous magnesium sulfate, and concentrated under reduced pressure to leave a yellow syrup (9.2 g) which appeared as one spot on a thin-layer chromatogram run in methanol:benzene, 1:9 (v/v). This syrup was crystallized from chloroform:*n*-hexane, ca. 1:15 (v/v), as long needles. A further recrystallization gave material of m.p. 58.5–60° and $[\alpha]_D^{21} = 44°$ (*c*, 1.55 in methanol). The infrared spectrum in chloroform showed absorption at 3 480 cm^{-1} attributable to *OH*, a doublet of approximately equal intensity at 1 382 and 1 391 cm^{-1} caused by an isopropylidene grouping, and strong absorption at 2 115 cm^{-1} caused by an azide group, but no aromatic absorptions.

Anal. Calcd. for $C_8H_{13}O_4N_3$: C, 44.64; H, 6.09; N, 19.53. Found: C, 44.66; H, 6.07; N, 19.62.

*5-Acetamido-5-deoxy-1,2-O-isopropylidene-*D*-xylose (XVI)*

To a solution of 5-azido-5-deoxy-1,2-*O*-isopropylidene-D-xylose (2.0 g) in methanol (60 ml) was added Raney nickel (35 g). The mixture was shaken mechanically overnight, fresh catalyst (10 g) was added, and, after it was shaken for an additional 4 h, the solution was filtered and concentrated under reduced pressure to give a crystalline product (1.1 g). This material could be readily recrystallized from ether. A sharp melting point was not obtained, however, but rather the crystals started to soften at 104° and finally melted at 107.5–109°. The substance is hygroscopic, and satisfactory analytical results were not obtained. The infrared spectrum in chloroform showed absorption at 3 350 cm^{-1} attributable to *OH* and *NH* and absorption at 1 382 and 1 392 cm^{-1} caused by an isopropylidene grouping, but was devoid of azide absorption.

A portion (0.95 g) of the crystalline compound obtained above was dissolved in water (7.7 ml) and treated with acetic anhydride (1.1 ml). The solution was allowed to stand for 20 min with occasional shaking, then was concentrated under reduced pressure to leave a light brown syrup (0.98 g) which crystallized on standing. Recrystallization from chloroform–hexane–ether gave rectangular plates with the same melting point and infrared spectrum as those of the previously reported (15) 5-acetamido-5-deoxy-1,2-*O*-isopropylidene-D-xylose.

*5-Acetamido-5-deoxy-*D*-xylose Diethyl Dithioacetal (XVII)*

5-Acetamido-5-deoxy-1,2-*O*-isopropylidene-D-xylose (0.4 g) was suspended in ice-cold concentrated hydrochloric acid (2.8 ml). Cold ethanethiol (2.8 ml) was then added, and the mixture was stirred in an ice-water bath for 7 h and finally left to stand in a refrigerator overnight. The mixture was then diluted with cold methanol and neutralized with lead carbonate and filtered, and the filtrate concentrated under reduced pressure to leave a clear colorless syrup which crystallized immediately (0.4 g, 78%). This material was recrystallized from methanol–ether to give white glistening crystals which had m.p. 106–107°, $[\alpha]_D^{23} = 0°$ (*c*, 2.50 in methanol), and R_{rh} 2.3 (solvent A, spray iii and iodine vapor). The infrared spectrum in chloroform showed absorption at 3 460 cm^{-1} attributable to *OH* and *NH*, an amide I band at 1 662 cm^{-1} and an amide II band at 1 525 cm^{-1}.

Anal. Calcd. for $C_{11}H_{23}O_4NS_2$: C, 44.4; H, 7.80; N, 4.71. Found: C 44.33; H, 7.85; N, 4.73.

Sulfone Degradation

To a solution of 5-acetamido-5-deoxy-D-xylose diethyl dithioacetal (0.30 g) in dioxane (5 ml) was added, dropwise with shaking, peroxypropionic acid (25) (15% excess over the required 4 molar equivalents) over a period of 10 min. The solution was allowed to stand for 10 min and then cooled in ice for 1 h. The clear solution was then concentrated under reduced pressure to a syrup which was repeatedly dissolved in methanol and reconcentrated until only traces of peroxypropionic acid remained. The syrup was dried over potassium hydroxide in a desiccator to yield a colorless glass (0.38 g), the infrared spectrum (chloroform) of which showed amide bands at 1 653 and 1 545 cm^{-1}. Spray iii showed the presence of only one component at R_{rh} 2.02 (solvent A).

The preceding product (0.33 g) was dissolved in dilute aqueous ammonia (5 ml, pH 8–9). After 5 min the pH fell to 5 and was restored with more ammonia solution. Paper chromatography indicated that degradation was nearly complete in 5 h. The solution was allowed to stand at room temperature overnight. A small amount of a fine precipitate appeared which was removed by filtration. The pH of the filtrate was adjusted to 3–4 with dilute acetic acid, and the solution was then passed through Amberlite IR-120 (H form) and Duolite A-4 (OH form) ion exchange resins. The eluate was extracted three times with chloroform, and the combined extract was dried over anhydrous magnesium sulfate and concentrated under reduced pressure to yield a white solid (0.087 g). After recrystallization from water this material melted at 101–102°, and showed no depression on the melting point on admixture with an authentic sample of bis-(ethylsulfonyl)-methane. The aqueous phase was concentrated under reduced pressure to leave a syrup (0.10 g) whose infrared and

Can. J. Chem. Downloaded from www.nrcresearchpress.com by 210.87.254.5 on 09/05/12
For personal use only.

n.m.r. spectra and chromatographic properties were the same as those of the product from the lead tetraacetate oxidation.

Hydrolysis of Methyl 4-Acetamido-4-deoxy-L-erythrofuranoside (I)

An aqueous solution (25 ml) of methyl 4-acetamido-4-deoxy-L-erythrofuranoside (I) (0.094 g), purified through the di-*O*-acetyl derivative (1), was stirred with 1 g of Amberlite IR-120 (H form) resin at 60° for 1 h. The resin was then removed by filtration, and the filtrate was shaken briefly with a small amount of Duolite A-4 (OH) form) resin to remove any trace of acid. The resin was removed, and the solution was concentrated under reduced pressure to leave an almost colorless syrup (0.075 g) which was examined on paper chromatograms. Sprays i, ii, and iii showed the presence of components at R_{rh} 1.00 and 1.18 (solvent A). In solvent B an elongated spot at R_{rh} 1.12 (possibly two spots) was detected. Two spots were detected also by thin-layer chromatography in 2-propanol:benzene, 1:2 (v/v). The syrup was reducing towards Fehling's solution and had $[\alpha]_D^{24} = -6.6°$ (*c*, 1.54 in methanol). The infrared spectrum of this material (smear between "IRTRAN-2" plates) showed strong absorption at 3 360 cm^{-1} (*OH*) and a very broad band at 1 617 cm^{-1} (*N*-Ac). Attempts were made to separate the two components by preparative paper chromatography using solvents A and B. The zones were located (spray i), cut, and extracted with methanol. Examination of the extracts on paper chromatograms still showed in every case the presence of the two original components.

Periodate Oxidations

The compound under examination (10–15 mg) was dissolved in water containing 0.3 *M* sodium metaperiodate solution (1 ml). The total volume was made up to 25 ml with additional water. A blank experiment was carried out at the same time. The oxidation was carried out in the dark and at room temperature. Formic acid yield and periodate uptake were determined in the usual fashion (26). The results are summarized in Table I.

TABLE I

Periodate oxidations

	(*a*) "4-Acetamido-4-deoxy-D-threofuranose"					
Time (h)	0.35	1.35	4.92	9.94	25.1	76.1
Periodate (moles/mole)	1.08	1.24	1.39	1.75	1.74	1.77
Formic acid (moles/mole)		0.79	0.93	1.13	1.51	2.04
	(*b*) "4-Acetamido-4-deoxy-L-erythrofuranose"					
Time (h)	0.35	1.28	5.85	10.8	25.6	74.7
Periodate (moles/mole)	1.42	1.60	1.77	1.70	1.75	1.84
Formic acid (moles/mole)	0.72	0.97	1.10	1.25	1.29	1.35

6-Acetamido-6-deoxy-D-galactose Diethyl Dithioacetal (XIX)

A solution of 6-acetamido-6-deoxy-1,2;3,4-di-*O*-isopropylidene-α-D-galactopyranose (VIII) (7.7 g) in concentrated hydrochloric acid (45 ml) at 0 °C was stirred with ethanethiol (45 ml) for 12 h at 0 °C. The mixture was then diluted with cold methanol and neutralized with an excess of lead carbonate. The solution was filtered and concentrated under reduced pressure to a volume of about 100 ml, whereupon a white crystalline material separated from solution (5.0 g). This solid was recrystallized from methanol–ether to give crystals which had m.p. 182.5–184°, $[\alpha]_D = +16.6°$ (*c*, 1.00 in methanol), and R_{rh} 2.18 (solvent A, spray iii, and iodine vapor). The infrared spectrum (Nujol mull) showed strong absorption at 3 270 cm^{-1} attributable to *OH* and *NH*, and amide I band at 1 645 cm^{-1} and an amide II band at 1 564 cm^{-1}.

Anal. Calcd. for $C_{12}H_{25}O_5NS_2$: C, 44.0; H, 7.64; N, 4.28. Found: C, 44.2; H, 7.82; N, 4.68.

6-Acetamido-2,3,4,5-tetra-O-acetyl-6-deoxy-D-galactose Diethyl Dithioacetal (XX)

A solution of 6-acetamido-6-deoxy-D-galactose diethyl dithioacetal (4.7 g) in dry pyridine (100 ml) was cooled in an ice-water bath and treated with acetic anhydride (28 ml). The clear colorless solution was left to stand in a refrigerator for 22 h, then at room temperature for 1 h and poured into ice water (800 ml), and the mixture extracted several times with chloroform. The combined extracts were washed with water, then shaken with an aqueous solution of cadmium chloride. The pyridine – cadmium chloride complex was filtered, and the chloroform solution was washed with water, dried over anhydrous magnesium sulfate, and concentrated under reduced pressure to leave a white crystalline material (6.9 g, 97%). Two recrystallizations from methanol–water gave crystals which melted at 131°, and had $[\alpha]_D = 84°$ (*c*, 1.73 in chloroform containing 0.75% ethanol). The infrared spectrum in chloroform showed *NH* stretching vibration at 3 430 cm^{-1}, absorption at 1 743 cm^{-1} caused by *O*-acetyl groups, an amide I band at 1 675 cm^{-1}, and an amide II band at 1 520 cm^{-1}.

Anal. Calcd. for $C_{20}H_{33}O_9NS_2$: C, 48.48; H, 6.71. Found: C, 48.36; H, 6.53.

Demercaptalation of 6-Acetamido-2,3,4,5-tetra-O-acetyl-6-deoxy-D-galactose Diethyl Dithioacetal

6-Acetamido-2,3,4,5-tetra-*O*-acetyl-6-deoxy-D-galactose diethyl dithioacetal (1 g) was dissolved in acetone (14 ml). Water (6 ml) and an excess (2 g) of cadmium carbonate were added, and under rapid stirring a

Can. J. Chem. Downloaded from www.nrcresearchpress.com by 210.87.254.5 on 09/05/12
For personal use only.

solution of mercuric chloride (1.96 g, 3.6 moles) in acetone (8 ml) was gradually added. Stirring was maintained at room temperature for 24 h with occasional additions of cadmium carbonate. The solution was then filtered, an excess of fresh cadmium carbonate being placed in the suction flask, and the precipitate was washed with acetone. The filtrate and washings were then concentrated under reduced pressure (water bath temperature 35°) and in the presence of excess cadmium carbonate. The residue was extracted several times with warm chloroform; the combined extracts were then cooled and filtered. The chloroform filtrate was washed with water, with aqueous solution of potassium iodide and again with water. The chloroform solution was dried over anhydrous magnesium sulfate and concentrated under reduced pressure to leave a thick syrup (0.35 g). Thin-layer chromatography of this material in 2-propanol:benzene, 1:2 (v/v), showed an elongated spot (possibly two spots) which moved at a slower rate than the starting material. The syrupy product crystallized on contact with ether. The ether was evaporated and the crude product was dissolved in acetone:ether, 2:1 (v/v); hexane was then added to opalescence. The crystals (XXI) which separated (0.10 g) reduced Fehling's solution on heating and migrated as a single spot with slight tailing on a thin-layer chromatogram. The mother liquors had trace quantities of two faster moving components. The crystals did not melt sharply, but rather started to soften at 90° and finally melted at 116°. The infrared spectrum (Nujol mull) showed strong absorption at 3 400 cm^{-1} attributable to *OH*, absorption at 1 753 cm^{-1} caused by *O*-acetyl groups, an amide I band at 1 663 cm^{-1}, and an amide II band at 1 553 cm^{-1}.

Attempted Cyclization of XXI

The preceding product XXI (0.072 g) was allowed to stand in dry pyridine (5 ml) for 24 h at room temperature. In a few hours the solution assumed a yellow color and finally darkened to orange. The solution was then cooled in an ice bath and treated with acetic anhydride (0.75 ml). After 1 h at 0° and at room temperature overnight, the solution was poured into ice water, and the product extracted with chloroform. The extract was washed with water, then shaken with an aqueous solution of cadmium chloride. The pyridine – cadmium chloride complex was filtered off, the chloroform filtrate washed with water, dried over anhydrous magnesium sulfate, and concentrated under reduced pressure to leave a slight brown syrup (0.026 g). This material was distilled under vacuum to yield a yellow syrup. Thin-layer chromatography in 2-propanol:benzene, 1:2 (v/v), showed the presence of only one component which migrated faster than XXI. The infrared spectrum in chloroform showed weak absorption at 3 525 cm^{-1} attributable to *NH* stretching vibrations, strong absorption at 1 757 cm^{-1} caused by *O*-acetyl groups, an amide I band at 1 685 cm^{-1}, and an amide II band at 1 528 cm^{-1}.

ACKNOWLEDGMENTS

The authors thank the National Research Council for a grant (N.R.C. T-19) which made this work possible, and for a scholarship (to W. A. S.). They also wish to thank Miss Anne P. Fletcher for excellent technical assistance during the summers of 1963 and 1964.

REFERENCES

1. W. A. Szarek and J. K. N. Jones. Can. J. Chem. **42**, 20 (1964).
1. S. Hanessian and T. H. Haskell. J. Heterocyclic Chem. **1**, 57 (1964).
3. R. S. Tipson. *In* Methods in carbohydrate chemistry. Vol. II. *Edited* by R. L. Whistler and M. L. Wolfrom. Academic Press, N.Y. 1963. p. 247.
4. A. B. Foster, W. G. Overend, M. Stacey, and L. F. Wiggins. J. Chem. Soc. 2542 (1959).
5. V. I. Veksler, L. N. Kovalenko, and A. V. Markovich. Zh. Obshch. Khim. **34**, 704 (1964).
6. M. L. Wolfrom, J. Bernsmann, and D. Horton. J. Org. Chem. **27**, 4505 (1962).
7. R. C. Hockett and M. Zief. J. Am. Chem. Soc. **72**, 2130 (1950).
8. A. S. Perlin and C. Brice. Can. J. Chem. **33**, 1216 (1955).
9. A. S. Perlin and C. Brice. Can. J. Chem. **34**, 541 (1956).
10. A. J. Charlson and A. S. Perlin. Can. J. Chem. **34**, 1200 (1956).
11. L. M. Jackman. Applications of nuclear magnetic resonance spectroscopy in organic chemistry. Pergamon Press, London. 1959. p. 56.
12. L. D. Hall. Tetrahedron Letters, 1457 (1964).
13. W. A. Szarek, S. Wolfe, and J. K. N. Jones. Tetrahedron Letters, 2743 (1964).
14. P. A. Levene and A. L. Raymond. J. Biol. Chem. **102**, 317 (1933).
15. J. K. N. Jones and W. A. Szarek. Can. J. Chem. **41**, 636 (1963).
16. F. Micheel and F. Sückfull. Ann. **502**, 85 (1933).
17. F. Micheel and F. Sückfull. Ann. **507**, 138 (1933).
18. F. Micheel and W. Spruck. Chem. Ber. **67**, 1665 (1934).
19. M. L. Wolfrom. J. Am. Chem. Soc. **52**, 2464 (1930).
20. W. E. Trevelyan, D. P. Proctor, and J. S. Harrison. Nature, **166**, 444 (1950).
21. L. Hough, J. K. N. Jones, and W. H. Wadman. J. Chem. Soc. 1702 (1950).
22. R. U. Lemieux and H. F. Bauer. Anal. Chem. **26**, 920 (1954).
23. K. Freudenberg and K. Raschig. Chem. Ber. **60**, 1633 (1927).
24. A. I. Vogel. Practical organic chemistry. Longmans, Green and Co., Inc., New York. 1951. p. 194.
25. R. Barker and D. L. MacDonald. J. Am. Chem. Soc. **82**, 2297 (1960).
26. G. Neumüller and E. Vasseur. Arkiv. Kemi, **5**, 235 (1953).

Can. J. Chem. Downloaded from www.nrcresearchpress.com by 210.87.254.5 on 09/05/12
For personal use only.

Can. J. Chem. Downloaded from www.nrcresearchpress.com by 210.87.254.5 on 09/05/12
For personal use only.

SUR LE SPECTRE INFRAROUGE DE SO_2 À HAUTE TEMPÉRATURE

PAUL A. GIGUÈRE ET RODRIGUE SAVOIE
Département de Chimie, Université Laval, Québec, Québec
Reçu le 8 mars 1965

ABSTRACT

The infrared spectra of SO_2 have been recorded both in absorption and emission over the range 400 to 3 000 cm^{-1} at atmospheric pressure and at temperatures up to 700 °C. Two weak bands were found at 1 075 and 1 290 cm^{-1} which represent a downward shift of some 75–80 cm^{-1} from the fundamental stretching vibrations of the SO_2 molecule. They cannot fit the hypothetical isomer SOO, suggested sometime to account for the perturbations in the ultraviolet spectrum at high temperature. Other possibilities, such as "hot" bands involving a low-lying, electronically excited state of SO_2 are discussed. A third, very weak band at about 680 cm^{-1}, detected in emission only, must be due to the formation of traces of disulfur monoxide S_2O.

RÉSUMÉ

On a mesuré en absorption et en émission le spectre infrarouge de SO_2 entre 400 et 3 000 cm^{-1} à pression atmosphérique et à des températures allant jusqu'à 700 °C. Deux faibles bandes sont apparues à 1 075 et 1 290 cm^{-1}, soit à quelque 75–80 cm^{-1} de moins que les vibrations de valence de SO_2. Elles ne sauraient provenir d'un isomère hypothétique SOO, invoqué parfois comme cause des perturbations dans le spectre ultraviolet à haute température. On discute la possibilité d'un état électronique excité, mais relativement bas, de la molécule SO_2. Une troisième bande, très faible, à 680 cm^{-1}, décelée en émission seulement révèle la formation de traces d'hémioxyde S_2O.

INTRODUCTION

On sait depuis longtemps déjà (1) que le spectre ultraviolet de SO_2 subit des transformations importantes à des températures au-dessus de 450 °C. Ces dernières années diverses études de spectroscopie cinétique ont confirmé et précisé la nature de ces transformations. Ainsi Norrish et Zeelenberg (2) ont remarqué que dans la photolyse éclair de SO_2, le spectre d'absorption dans le proche ultraviolet s'effaçait temporairement pour réapparaître graduellement sur une période de plusieurs millisecondes. Un phénomène semblable a été noté par Myerson et ses collaborateurs (3) dans les explosions de mélanges de CS_2 et O_2. L'apparition du spectre électronique de SO_2 était d'abord masquée par une absorption continue à partir de 2 100 Å apparemment causée par quelque intermédiaire. Après avoir écarté la possibilité d'un état excité de SO_2, à cause de la vie moyenne relativement trop longue (10^{-2} s) de cet intermédiaire, ces auteurs en ont conclu à l'existence d'un isomère de formule probable SOO. Par ailleurs Norrish et Oldershaw (4) ont montré que l'absorption continue résultant de la photolyse éclair est un phénomène thermique et non photochimique. Sans se prononcer sur la nature de l'intermédiaire ils admettent la possibilité d'une forme isomère de la molécule. Enfin plus récemment McGarvey et McGrath (5) ont poussé l'examen spectroscopique des réactions de combustion de H_2S et CS_2 jusque dans l'ultraviolet lointain; ils sont observé un nouveau spectre transitoire dont la structure fine pourrait d'après eux s'interpréter selon le spectre de vibration de l'isomère hypothétique SOO.

Etant donné que ces phénomènes sont d'origine thermique et qu'ils apparaissent déjà à des températures de l'ordre de 500 °C, ils nous a semblé utile de les étudier en système statique par spectroscopie infrarouge. En effet, l'isomère mentionné plus haut devrait avoir un spectre de vibration passablement différent de celui de SO_2 normal. Ce travail

préliminaire (6) a également montré que l'émission produite par SO_2 au-dessous de 500° est suffisamment intense pour être enregistrée avec un spectromètre infrarouge conventionnel.

MÉTHODE EXPÉRIMENTALE

Du point de vue expérimental la principale difficulté résidait dans la construction d'une cellule d'absorption appropriée. En effet, cette cellule devait permettre de chauffer l'échantillon de gaz de façon aussi uniforme que possible, et jusqu'à des températures de l'ordre de 700 °C. De plus, elle devait être relativement étanche et inerte vis-à-vis de SO_2, assez longue pour réaliser une absorption mesurable, même aux plus hautes températures, et enfin transmettre l'infrarouge jusqu'à 20 μ. Ces objectifs ont put être assez bien satisfaits, sauf pour ce qui est de l'étanchéité. Le corps de la cellule se composait d'un tube de Pyrex (Fig. 1) de quelque 13 cm de long et 25 mm de diamètre, portant deux tubulures latérales, l'une de diamètre moyen (3 mm) pour l'entrée du gaz, l'autre, capillaire, pour la sortie. Les fenêtres étaient des disques de NaCl ou KBr, selon la région étudiée. Faute de trouver un matériau de garniture à la fois souple et réfractaire pour étancher le joint, les fenêtres ainsi que les extrémités du tube d'absorption ont été polies pour donner des surfaces de contact aussi planes que possible. Les fenêtres elles-mêmes étaient protégées par des manchons de verre pouvant glisser à frottement doux sur le tube central et son prolongement. Le tout était maintenu ensemble sous faible pression par quatre minces tiges d'acier munies de ressort à un bout.

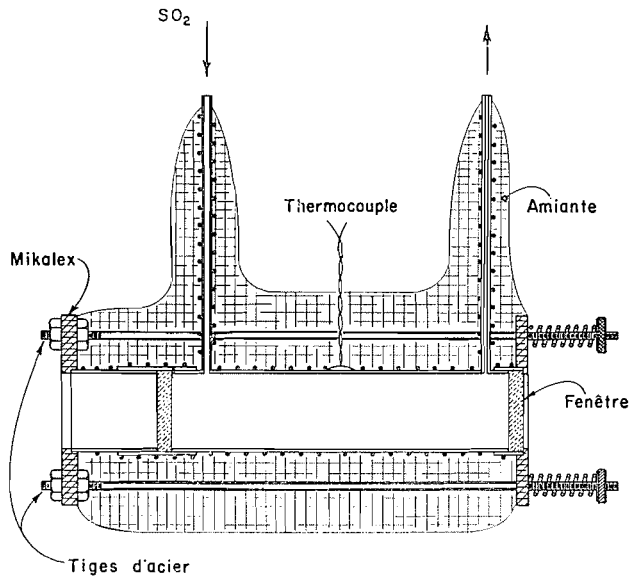

FIG. 1. Cellule d'absorption infrarouge pour les gaz à haute température.

La cellule était chauffée électriquement par un enroulement de fil de résistance (Chromel "A") de 25 Ω (environ 4.5 m) recouvert de plusieurs tours de ruban d'amiante tressé. Ce dernier avait au préalable été flambé pour éliminer le liant qui brûle à haute température et dégage des vapeurs qui auraient pu nuire à l'enregistrement des spectres. Pour atteindre un maximum de 700 °C il fallait un courant de près de 2 A sous 75 V; le chauffage devait se faire très graduellement (jusqu'à 1.5 h) pour éviter l'éclatement des fenêtres de sel. Pour cette même raison, et aussi pour empêcher les courants de convection trop violents à l'intérieur de la cellule, la température des fenêtres était maintenue assez près de celle de la cellule même. A cette fin le manchon de chauffage avait été prolongé de quelque 3 cm à une extrémité, tandis que l'autre fenêtre était montée tout près de la source (Globar) du spectromètre.

La température était mesurée à l'aide d'un petit thermocouple fer–constantan fixé sur la paroi externe du tube d'absorption, et un potentiomètre de précision (Leeds and Northrup, modèle 8662). Le thermocouple avait été calibré au point d'ébullition de l'eau ainsi qu'au point de fusion de l'étain (232 °C) et du zinc (419.5 °C). On avait également vérifié que la température à l'intérieur de la cellule était uniforme partout à 10 deg près, de sorte que la limite d'erreur sur les valeurs données ici ne dépasse pas 3%.

Le bioxyde de soufre (Mathieson 99.7% min.) passait directement de la bouteille à la cellule sans purification préalable. Le courant gazeux sortant de la cellule circulait à travers un flacon laveur contenant de

Can. J. Chem. Downloaded from www.nrcresearchpress.com by 210.87.254.5 on 09/05/12
For personal use only.

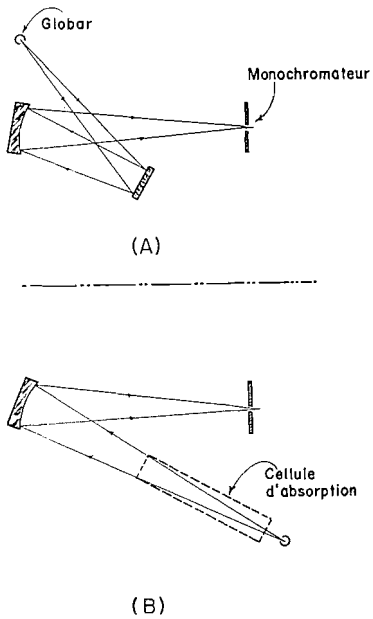

FIG. 2. Schéma du montage optique original (A) et modifié (B) du spectromètre infrarouge.

'lacide sulfurique concentré et se condensait ensuite dans un piège à carboglace. Le débit du gaz était ajusté à peu près à une bulle par seconde à travers un tube de 3 mm de diamètre intérieur. Des traces de SO_2 parvenaient toujours à s'échapper de la cellule autour des fenêtres, ce qui a necessité une ventilation très active au-dessus de l'appareil. Le spectromètre (Perkin–Elmer, modèle 12-C, avec prismes de NaCl ou de CsBr) a dû être légèrement modifié (Fig. 2) pour accommoder la cellule.

RÉSULTATS

Quelques spécimens des spectres obtenus sont reproduits dans la Fig. 3 à côté du spectre d'absorption de SO_2 à température ordinaire pour fin de comparaison. Ce dernier est tiré du travail de Pierson, Fletcher et Gantz (7). On sait que les fréquences fondamentales de la molécule sont $\nu_1 = 1\,151.38$, $\nu_2 = 517.69$ et $\nu_3 = 1\,361.76$ cm^{-1} (8). A haute température, la densité du gaz étant naturellement moindre, l'absorption infrarouge s'en trouvait diminuée d'autant. De plus l'émission sélective par le gaz contribuait à réduire davantage l'intensité apparente des bandes d'absorption. En effet, il était malheureusement impossible de séparer ces deux phénomènes avec notre système optique vu la position, juste en avant du thermocouple, de l'interrupteur de faisceau. De façon générale on vois que les bandes sont élargies par l'agitation thermique; ainsi on ne peut plus discerner let branches P et R des deux bandes de valence même lorsque l'absorption ne dépasse pas 50%. Quant à la bande de déformation, son intensité est considérablement réduite et son contour mal défini, bien que le maximum (vers 520 cm^{-1}) ne soit pas déplacé de façon notable. Phénomène tout à fait inattendu, deux nouvelles bandes apparaissent à ces températures: l'une assez faible, mais très nette à 1 075 cm^{-1}, l'autre qui se confond avec la bande ν_3 de SO_2, et dont le maximum doit correspondre assez bien au minimum à 1 290 cm^{-1} dans le spectre à température ordinaire.

En émission les bandes de valence S—O ont *grosso modo* la même allure qu'en absorption, sauf que la bande additionnelle à 1 290 cm^{-1} se détache bien de la fondamentale ν_3, et la bande de déformation est beaucoup plus intense. Ses branches P et R sont maintenant

Can. J. Chem. Downloaded from www.nrcresearchpress.com by 210.87.254.5 on 09/05/12
For personal use only.

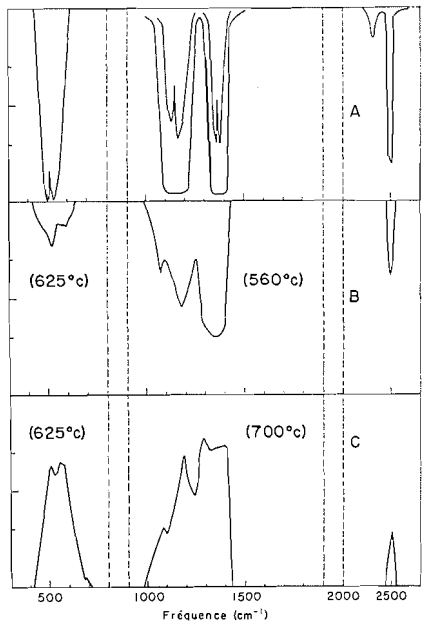

FIG. 3. Spectres infrarouges de SO_2. A. Absorption à température ordinaire (7). B. Absorption à température élevée. C. Emission.

bien visibles, et leur séparation au maximum, 505–560 cm^{-1}, est nettement plus large qu'en absorption à température ordinaire à cause, entre autre, du déplacement de population vers les niveaux de rotation supérieurs. Enfin, du côté des hautes fréquences le contour semble indiquer un pic additionnel à 620–640 cm^{-1} (tout comme en absorption quoique moins nettement) en plus d'un faible épaulement vers 680 cm^{-1} au pied de la bande principale. A propos des intensités relatives des bandes rapportées ici il convient de noter que, outre le fait que dans nos expériences l'absorption et l'émission par l'échantillon s'annulaient en partie, d'où l'impossibilité de mesures quantitatives de l'intensité en fonction de la température, l'énergie admise par la fente dans le monochromateur était contrôlée, en émission comme en absorption, par un servomécanisme basé sur le rayonnement du corps noir.

Une dernière observation faite au cours de ce travail a trait aux fenêtres de sel de la cellule d'absorption qui finissaient par se couvrir d'une fine poudre blanchâtre sous l'action de SO_2 à chaud. Le spectre d'absorption de cette poudre pris une fois les fenêtres refroidies a montré deux bandes de faible intensité à 1 110 et 640 cm^{-1} et deux autres encore beaucoup plus faibles à 1 045 et 965 cm^{-1} attribuables à des sulfites et des bisulfates (9). Comme ces bandes ne se formaient que très lentement, il était assez facile d'écarter cette cause d'erreur en repolissant les fenêtres périodiquement.

DISCUSSION

Plusieurs possibilités sont à considérer pour rendre compte des nouvelles bandes. D'abord la formation à haute température de quelque composé à partir des impuretés contenues dans le gaz SO_2 semble fort peu probable étant donné la faible concentration (moins de 0.3%) et la nature de celles-ci (O_2, N_2 et SO_3). De même on peut écarter toute réaction avec les gaz atmosphériques vu que SO_2 était sous une légère surpression dans la cellule.

Can. J. Chem. Downloaded from www.nrcresearchpress.com by 210.87.254.5 on 09/05/12
For personal use only.

Autres oxydes de soufre

Des divers oxydes de soufre connus, et dont certains sont sans doute présents, du moins en traces, dans notre système, aucun n'a un spectre de vibration correspondant aux nouvelles bandes. Ainsi l'hémioxyde S_2O, dont la formation a déjà été rapportée dans la photolyse éclair de SO_2 (4), et se trouve confirmée ici par la faible bande d'émission vers 680 cm^{-1}, possède deux autres vibrations fondamentales à 1 165 cm^{-1} (10), donc submergée par la forte bande de SO_2, et à 387 cm^{-1} (11) au-delà de la région couverte ici. Le monoxyde SO, qui lui aussi est produit dans la photolyse éclair de SO_2 (2, 4), n'a évidemment qu'une seule vibration fondamentale dont la fréquence est de 1 138 cm^{-1} d'après l'analyse de Norrish et Oldershaw (4). Quant au trioxyde SO_3, ses bandes infrarouges se confondent assez bien avec celles de SO_2 (13). Deux de ses fréquences fondamentales à 1 271 et 1 068 cm^{-1} appartiennent à des modes symétriques, et donc ne sont actives qu'en Raman (14), bien que la dernière ait été signalée dans le spectre infrarouge du liquide (15) sans doute à cause des interactions moléculaires.

L'isomère hypothétique SOO

Qualitativement la grande stabilité thermique (16) de SO_2 milite contre l'hypothèse d'un isomère quelconque. La formule SOO proposée par Myerson pour cet isomère apparaît également assez improbable du point de vue des théories de la valence. En effet, la liaison O—O devrait être passablement plus faible que les liaisons S—O dans SO_2. Des trois formules canoniques que l'on peut imaginer, seule la première contribuerait de façon

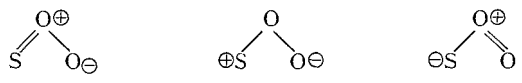

I II III

appréciable à la structure de cet isomère, car la seconde ne donne pas un octet à l'atome de soufre, tandis que la troisième conduit à une séparation de charges formelles sur le soufre et l'oxygène médian à l'encontre de leur électronégativité respective (2.5 et 3.5 selon l'échelle de Pauling). D'ailleurs on ne connaît à peu près pas d'exemple de molécule triatomique ABC dont l'atome médian soit notablement plus électronégatif que l'un des deux autres. Enfin l'existence d'orbitales d sur l'atome de soufre, qui participent effectivement aux liaisons π dans la molécule SO_2 (17), favorise sa position au milieu de la molécule.

Malgré que l'isomère hypothétique SOO soit peu favorisé des points de vue thermodynamique et structure électronique, on peut quand même spéculer sur la nature de son spectre moléculaire. La vibration de valence S—O devrait se situer dans la même région que celles de SO_2. Par contre la liaison O—O étant essentiellement simple, sa fréquence de vibration devrait être de l'ordre de 900 cm^{-1} (v.g. 880 cm^{-1} dans H_2O_2). Or cette région était parfaitement libre dans nos spectres; pas la moindre absorption n'y a été décelée en aucun cas.

État excité de SO_2

La possibilité d'un état excité de SO_2 a déjà été considérée (3, 5) pour expliquer les modifications dans le spectre ultraviolet au cours de la photolyse éclair; c'est-à-dire l'apparition d'un continuum à partir de 3 000 Å et un nouveau système de bandes entre 1 840 et 1 740 Å (5). Cette hypothèse a dû être écartée à cause de la vie moyenne beaucoup trop longue de cette espèce (représentée par la formule $[SO_2]$) soit quelques millisecondes. Mais il se peut que cette valeur soit fictive et ne dépende que du taux de refroidissement du gaz après la photolyse. Il est également possible que la même espèce moléculaire $[SO_2]$ soit à l'origine, et des spectres supposés transitoires en ultraviolet, et des nouvelles

Can. J. Chem. Downloaded from www.nrcresearchpress.com by 210.87.254.5 on 09/05/12
For personal use only.

bandes de vibrations rapportées ici; d'autant plus que les deux phénomènes apparaissent vers la même température. Cependant la nature de l'excitation de [SO_2] soulève de sérieuses difficultés. En effet, elle ne saurait être d'origine vibrationnelle vu le décalage considérable des fréquences observé ici. Le spectre de vibration de SO_2 ne révèle qu'une anharmonicité assez faible (8), de l'ordre de quelques cm^{-1}, comme on peut s'y attendre.

D'autre part l'existence d'un niveau électronique excité qui serait suffisamment bas pour être peuplé de façon appréciable déjà vers 750–800 °K semble assez problématique au premier abord. La transition correspondante devrait apparaître dans le proche infrarouge, à moins qu'elle ne soit interdite. Dans son analyse de la structure électronique de SO_2, Walsh (18) a conclu à l'existence d'une première transition

$$.. (a_2'')^2 (b_2')^2 (a_1') (b_1'') \, {}^1B_1 \leftarrow ..... (a_2'')^2 (b_2')^2 (a_1')^2 \, {}^1A_1 ..$$

Or cette transition est permise et elle devrait donner en ultraviolet un système de bandes perpendiculaires. En outre elle conduirait à une légère augmentation, et de l'angle au sommet, et de la longueur des liaisons S—O. Il est vrai que les décalages rapportés ici sont bien dans ce sens; ils correspondent à un allongement de quelque 0.03 Å de ces liaisons d'après la règle de Badger.

CONCLUSIONS

Les résultats de ce travail préliminaire sont intéressants, mais forcément incomplets. En particulier ils ne permettent pas d'identifier l'espèce moléculaire responsable des nouvelles bandes infrarouges, et peut-être aussi, des anomalies dans les spectres électroniques de SO_2 à haute température. Il apparaît cependant que l'hypothèse d'un isomère de formule SOO doive être écartée. Nous nous proposons de poursuivre cette étude avec un appareil différent de façon a pouvoir distinguer entre l'absorption et l'émission. Il serait également souhaitable de reprendre les mesures de Wieland (1) sur les spectres ultraviolets à température élevée en système statique. Notons enfin qu'une situation analogue semble exister dans le cas du composé SeO_2. Ainsi la fluorescence jaune-verdâtre qui apparaît en chauffant au-dessus de 300 °C (19) a peut-être la même origine que les nouvelles bandes décelées récemment à la même température en infrarouge (20).

BIBLIOGRAPHIE

1. K. Wieland. Trans. Faraday Soc. **30**, 260 (1934).
2. R. G. W. Norrish et A. P. Zeelenberg. Proc. Roy. Soc. London, Ser. A, **240**, 293 (1957).
3. A. L. Myerson, F. R. Taylor et P. L. Hanst. J. Chem. Phys. **26**, 1309 (1957).
4. R. G. W. Norrish et G. A. Oldershaw. Proc. Roy. Soc. London, Ser. A, **249**, 498 (1958).
5. J. J. McGarvey et W. D. McGrath. Proc. Roy. Soc. London, Ser. A, **278**, 490 (1964).
6. R. Savoie. Thèse de B.Sc., Université Laval, Québec, Qué. 1960.
7. R. H. Pierson, A. N. Fletcher et E. St. C. Gantz. Anal. Chem. **28**, 1237 (1956).
8. R. D. Shelton, A. H. Nielsen et W. H. Fletcher. J. Phys. Chem. **21**, 2178 (1953).
9. K. Nakamoto. Infrared spectra of inorganic and coordination compounds. John Wiley & Sons, New York. 1962.
10. A. V. Jones. J. Chem. Phys. **18**, 1263 (1950).
11. D. J. Meschi et R. J. Myers. J. Mol. Spectry. **3**, 405 (1959).
12. E. V. Martin. Phys. Rev. **41**, 167 (1932).
13. R. W. Lovejoy, J. H. Colwell, D. F. Eggers, Jr. et G. D. Halsey, Jr. J. Chem. Phys. **36**, 612 (1962).
14. H. Gerding et W. J. Nijveld. Rec. Trav. Chim. **59**, 1206 (1940).
15. H. Gerding et J. Lecomte. Physica, **6**, 737 (1939).
16. G. St. Pierre et J. Chipman. J. Am. Chem. Soc. **76**, 4787 (1954).
17. W. Moffitt. Proc. Roy. Soc. London, Ser. A, **200**, 409 (1950).
18. A. D. Walsh. J. Chem. Soc. 2266 (1953).
19. D. M. Yost et J. B. Hatcher. J. Am. Chem. Soc. **54**, 151 (1932).
20. K. Sathianandan, T. C. Ehlert et J. L. Margrave. Résultats inédits.

Can. J. Chem. Downloaded from www.nrcresearchpress.com by 210.87.254.5 on 09/05/12
For personal use only.

Can. J. Chem. Downloaded from www.nrcresearchpress.com by 210.87.254.40 on 09/05/12
For personal use only.

THE MAGNETIC ANISOTROPY OF THE CARBONYL BOND

D. L. Hooper and R. Kaiser

Departments of Chemistry and Physics, University of New Brunswick, Fredericton, New Brunswick

Received September 21, 1964

ABSTRACT

The magnetic susceptibility components of the carbonyl bond have been determined from chemical shift differences in the n.m.r. spectra of amides. Correction of the experimental chemical shift differences for the effect of internal electric fields is found to overestimate the shielding of groups close to the carbonyl bond and it is shown that the sets of susceptibility components determined without this correction give a satisfactory correlation of structure and chemical shifts in amides, α,β-unsaturated ketones, and exo-methylene cycloketones.

Four sets of susceptibility components are derived from formamide or acetamide spectra and depending on whether the effect of the carbonyl bond is assumed to be shielding or deshielding. These sets are, in units of 10^{-6} cm^3 mole^{-1}:

	$\chi_{xx}^{C=O}$	$\chi_{yy}^{C=O}$	$\chi_{zz}^{C=O}$
From acetamide spectra			
Shielding assumed	18	−14	−19
Deshielding assumed	−38	0.6	23
From formamide spectra			
Shielding assumed	0.5	−9	−7
Deshielding assumed	−12	−0.7	−3

Spectra of 1-ethylpyrrolidinone-2 are interpreted as showing that the effect of the carbonyl bond is to shield distant protons in the plane of the carbonyl group and its substituents.

INTRODUCTION

A knowledge of the anisotropy of the magnetic susceptibility of the carbonyl bond is of importance in the interpretation of the nuclear magnetic resonance (n.m.r.) spectra of large molecules (1). If the bond lengths and bond angles of a molecule are known, the contribution of each magnetically anisotropic bond to the chemical shift of protons in the molecule may be calculated (2). Conversely, Narasimhan and Rogers (3) determined the magnetic susceptibility components of the carbonyl bond from measured chemical shift differences in the n.m.r. spectra of amides.

When the susceptibility components determined by Narasimhan and Rogers are used to calculate chemical shift differences in some of the substituted acetamides discussed below, the results differ considerably from experimental values. A similar discrepancy between calculated and observed chemical shifts has been reported for the exo-methylene protons of α-methylene cycloketones (4, 5). We wish to report the results of an investigation which had as its aim the determination of susceptibility components suitable for the calculation of chemical shift differences in a variety of molecules containing carbonyl bonds.

THEORY

The effect of the magnetic anisotropy of the carbonyl bond on the screening constants $\sigma(A)$ and $\sigma(B)$ of protons H_A and H_B of a substituted acetamide (Fig. 1) is given by the theory of Narasimhan and Rogers in the form

$$[1]\qquad 3L_0(\sigma(A) - \sigma(B)) = f_1(\varphi_A,\varphi_B)\chi_{xx}^{C=O} + f_2(\varphi_A,\varphi_B)\chi_{yy}^{C=O} + f_3(\varphi_A,\varphi_B)\chi_{zz}^{C=O} + f_4(\varphi_A,\varphi_B)\Delta\chi^{C-C}.$$

x, y, and z are the axes of a right-handed coordinate system with its origin at the point in the carbonyl bond at which a magnetic dipole is assumed to be induced. The system is

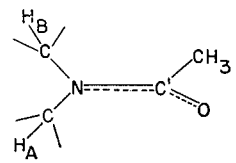

FIG. 1. Symmetrically disubstituted acetamide.

chosen such that the susceptibility tensor is diagonal, with z axis directed along the bond toward the oxygen atom, the y axis in the NC'O plane and directed away from the C'—CH_3 bond, and the x axis perpendicular to the NC'O plane. φ_A and φ_B are the rotation angles of the N-alkyl bonds with respect to the plane of the N-acetyl group. For a given choice of the origin of the coordinate system, the functions f_1, f_2, f_3, and f_4 are easily calculated from the known molecular geometry (6).

One of the four equations necessary to solve for the four unknowns $\chi_{xx}^{C=O}$, $\chi_{yy}^{C=O}$, $\chi_{zz}^{C=O}$, and $\Delta\chi^{C-C}$ was obtained from a recent quantum mechanical calculation (7) of the value of $\chi_{av}^{C=O}$, the mean bond susceptibility. For a carbonyl bond with bond order between 1 and 2, a reasonable value is $\chi_{av}^{C=O} = -5.0 \times 10^{-6}$ cm^3 mole^{-1} which leads to the equation

$$[2] \qquad \chi_{av}^{C=O} = \tfrac{1}{3}(\chi_{xx}^{C=O} + \chi_{yy}^{C=O} + \chi_{zz}^{C=O}) = -5.0 \times 10^{-6} \text{ cm}^3 \text{ mole}^{-1}.$$

Further simplification is obtained if the number of unknowns is reduced to three by treating $\Delta\chi^{C-C}$ (or $\Delta\chi^{C-H}$ for formamides) as a parameter with one of the many reported values (8–13). The remaining two equations must be obtained from experimental chemical shift differences between protons with known φ_A and φ_B values, i.e. from the spectra of molecules of known configuration. Such spectra normally show a pair of signals that may be assigned to hydrogen atoms A and B, but a decision on which signal arises from H_A and which from H_B is frequently ambiguous. Only the absolute value of the chemical shift difference can then be determined and thus the question of the sign of $(\sigma(A) - \sigma(B))$ arises. This is equivalent to the question of whether the effect of the carbonyl bond is shielding or deshielding. In Part A of the Results both possibilities are considered, while Part B discusses an experiment designed to permit a choice to be made.

EXPERIMENTAL

The n.m.r. spectra were obtained on a Varian V-4302 spectrometer operating at 56.4 Mc/s and equipped with a Varian temperature control assembly. The temperature at the sample was monitored by a copper–constantan thermocouple.

Five factors known to affect the chemical shifts of amide protons were initially taken into account in the planning and evaluation of the n.m.r. measurements: (i) interaction between amide molecules in solution (14), (ii) amide–solvent interactions (14), (iii) the averaging of chemical shifts caused by rotation of the central C'—N partial double bond (15), (iv) the possibility of structural differences between acetamides and formamides which is suggested by the differences in barriers to internal rotation (16), (v) the effect of internal electric fields arising from the polar structure of amides.

The first three factors were minimized by the extrapolation of chemical shift differences to the freezing point at infinite dilution in CCl_4. Factor iv was taken into account by considering separately the data for acetamides and formamides, and the electric field shift was estimated by means of the relation

$$[3] \qquad \sigma_E = 2 \times 10^{-12} E_z$$

derived by Buckingham (17) where σ_E is in p.p.m. and E_z is the component of the field at the H atom parallel to the C—H or N—H bond in electrostatic units.

Can. J. Chem. Downloaded from www.nrcresearchpress.com by 210.87.254.40 on 09/05/12
For personal use only.

Can. J. Chem. Downloaded from www.nrcresearchpress.com by 210.87.254.40 on 09/05/12
For personal use only.

RESULTS

Part A. Determination of the Susceptibility Components

The components of the carbonyl bond susceptibility in acetamides were determined from the chemical shift difference between the N—CH_3 groups in N,N-dimethylacetamide and that between the two sets of CH_2 protons α to the acetyl group in N-acetylpyrrolidine. Similarly, the carbonyl bond susceptibility components in formamides were determined from the corresponding chemical shift differences in N,N-dimethylformamide and N-formylpyrrolidine. The experimental chemical shift differences between the two N-substituents of these compounds are given in the second column of Table I. The values result from extrapolation of a series of measurements to low temperature and infinite dilution in CCl_4. The third column gives the electric field shift difference estimated by means of eq. [3]. E_z was assumed to be the sum of contributions originating from an electric dipole of moment 2.3 D located 1.20 Å from C′ on the axis of the C′=O bond, and from a point charge of −0.1 e located on the oxygen atom (18). Columns 4 and 5 give the difference between the experimental values in column 2 and the calculated electric field contribution in column 3, and this differential shift is assumed to be caused by the bond magnetic anisotropy. The anisotropy shift difference derived in this manner is seen to depend on whether the experimental values are taken as positive or negative, i.e. whether the signal of the A substituent is at higher or lower field respectively than that of the B substituent. The following computations were carried out for both choices.

TABLE I

Experimental chemical shift differences of amides in CCl_4 solution and electric field correction. All values are in p.p.m.

Compound		Experimental shift difference	$\sigma_E(A) - \sigma_E(B)$	Anisotropy shift difference: A at higher field	Anisotropy shift difference: B at higher field
1. N,N-Dimethylacetamide*	(CH_3)	±0.150	−0.024	+0.174	−0.126
2. N-Acetylpyrrolidine*	(CH_2)	±0.090	−0.088	+0.178	−0.002
3. N,N-Dimethylformamide*	(CH_3)	±0.155	−0.024	+0.179	−0.131
4. N-Formylpyrrolidine*	(CH_2)	±0.165	−0.088	+0.253	−0.077
5. N-Acetylnortropine	(CH)	±0.510	−0.152	+0.662	−0.358
6. Formamide†	(NH)	±0.214	−0.195	+0.409	−0.019
7. 1-Ethylpyrrolidinone-2	(CH_2)	+0.108	−0.002	+0.110	

*Extrapolated to low temperature and infinite dilution.
†B. Sunners, L. H. Piette, and W. G. Schneider. Can. J. Chem. 38, 681 (1960).

TABLE II

Values of the orientation functions for substituted amides in units 10^{22} cm^{-3}

Compound		f_1	f_2	f_3	f_4
N,N-Dimethylacetamide	(CH_3)	1.72	−6.82	4.96	−7.09
N-Acetylpyrrolidine	(CH_2)	1.64	−8.08	6.33	−9.29
N,N-Dimethylformamide	(CH_3)	1.72	−6.82	4.96	−6.70
N-Formylpyrrolidine	(CH_2)	1.64	−8.08	6.33	−8.90
N-Acetylnortropine	(CH)	5.22	−15.78	10.54	−12.51
Formamide	(NH)	2.99	−7.82	4.84	−16.77

Table II shows the values of the orientation functions used in eq. [1]. The magnetic dipole was assumed to be induced on the C′=O bond at a point 1.20 Å from the carbon atom. This location was chosen because it is believed that the strong electronegativity of

oxygen places the electronic center of charge very near the oxygen nucleus. Free rotation of the methyl group was assumed for the N,N-dimethylamides, while for the pyrrolidine derivatives the values $\varphi_A = \varphi_B = 60°$ were substituted. Equation [1] was combined with eq. [2] for compounds 1 and 2 and separately for compounds 3 and 4 to solve for the three susceptibility components of acetamides and formamides separately, with $\Delta\chi$ as a parameter. Selected values of $\Delta\chi$ (8–13) were then substituted to obtain the results listed in columns 2, 3, and 4 of Tables III and IV.

TABLE III

Susceptibility components in units 10^{-6} cm^3/mole for acetamides and calculated anisotropy shift difference in p.p.m. for N-acetylnortropine for several values of $\Delta\chi^{C-C}$. Electric field correction applied

	$\Delta\chi^{C-C}$	$\chi_{xx}^{C=O}$	$\chi_{yy}^{C=O}$	$\chi_{zz}^{C=O}$	$\delta(A) - \delta(B)$	
A at higher field						
	1.21	+2.0	−10	−6.7	+0.48	
	4.0	−0.4	−11	−3.3	+0.50	
	10.0	−5.4	−14	+4.0	+0.56	∩
B at higher field						
	1.21	−44	+6.9	+22	−0.68	
	4.0	−46	+5.8	+25	−0.65	
	10.0	−51	+3.6	+32	−0.59	∩

TABLE IV

Susceptibility components in units 10^{-6} cm^3/mole for formamides and calculated anisotropy shift difference in p.p.m. for formamide for several values of $\Delta\chi^{C-H}$. Electric field correction applied

	$\Delta\chi^{C-H}$	$\chi_{xx}^{C=O}$	$\chi_{yy}^{C=O}$	$\chi_{zz}^{C=O}$	$\delta(A) - \delta(B)$	
A at higher field						
	−0.74	−13	−5.0	+3.2	+0.15	∩
	0	−14	−5.3	+4.1	+0.11	
	+0.48	−14	−5.4	+4.7	+0.08	
B at higher field						
	−0.74	−25	+3.0	+7.1	−0.29	∩
	0	−26	+2.8	+8.0	−0.33	
	+0.48	−26	+2.6	+8.6	−0.36	

In order to select an optimum set of values from those given in Tables III and IV, the anisotropy difference was calculated by means of eq. [1] for N-acetylnortropine (Fig. 2) and for formamide. Hydrogen atoms A and B in N-acetylnortropine have rotation angles $\varphi_A = \varphi_B = 0$ and the corresponding values of the orientation functions are included in Table II. When these calculated values in column 5 of Tables III and IV are compared with the corresponding anisotropy shift differences in Table I, it is seen that only a very poor agreement results. The optimum values are those marked ∩ in the last column.

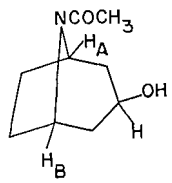

FIG. 2. N-Acetylnortropine.

Can. J. Chem. Downloaded from www.nrcresearchpress.com by 210.87.254.40 on 09/05/12
For personal use only.

It appears that the principal source of error is an overestimation of the electric field effect, especially at small values of φ_A and φ_B when the protons are close to the charges. The determination of the electric field shift by means of eq. [3] is apparently not very accurate at small distances although the field strengths are still small enough to make the quadratic term in Buckingham's equation (17) negligibly small in comparison with the linear term.

Better agreement between calculated and observed shift differences for N-acetylnortropine and formamide is obtained when the electric field effect is disregarded entirely, as was done by Narasimhan and Rogers (3). The entire experimental shift difference in column 1 of Table I is then assumed to be caused by the bond magnetic anisotropy. The resulting susceptibility components are listed in Tables V and VI, and the optimum values are marked ∪. It will be shown in the Discussion that these values are successful in the interpretation of the spectra of a variety of molecules.

TABLE V

Susceptibility components in units 10^{-6} cm³/mole for acetamides and calculated anisotropy shift difference in p.p.m. for N-acetylnortropine for several values of $\Delta\chi^{C-C}$. Electric field correction neglected

	$\Delta\chi^{C-C}$	$\chi_{xx}^{C=O}$	$\chi_{yy}^{C=O}$	$\chi_{zz}^{C=O}$	$\delta(A) - \delta(B)$	
A at higher field						
	1.21	+18	−14	−19	0.59	∪
	4.0	+15	−15	−15	0.62	
	10.0	+10	−17	−7.9	0.68	
B at higher field						
	1.21	−31	+3.8	+12	−0.60	
	4.0	−33	+2.8	+16	−0.57	
	10.0	−38	+0.6	+23	−0.52	∪

TABLE VI

Susceptibility components in units 10^{-6} cm³/mole for formamides and calculated anisotropy shift difference in p.p.m. for formamide for several values of $\Delta\chi^{C-H}$. Electric field correction neglected

	$\Delta\chi^{C-H}$	$\chi_{xx}^{C=O}$	$\chi_{yy}^{C=O}$	$\chi_{zz}^{C=O}$	$\delta(A) - \delta(B)$	
A at higher field						
	−0.74	+1.2	−8.6	−7.6	0.31	
	0	+0.5	−8.8	−6.7	0.21	∪
	+0.48	0.0	−9.0	−6.0	0.18	
B at higher field						
	−0.74	−11	−0.5	−3.5	−0.19	
	0	−12	−0.7	−2.7	−0.23	∪
	+0.48	−12	−0.9	−1.9	−0.26	

Part B. Determination of the Sign of the Experimental Shift Difference

In Part A, both choices $\sigma(B) > \sigma(A)$ and $\sigma(A) > \sigma(B)$ were used in calculating susceptibility components. There is evidence for each choice. The argument of Narasimhan and Rogers (3) leads to the acceptance of only those sets which were calculated with the assumption that B is at higher field. It has been shown (19) that the largest contribution to the diamagnetic susceptibility of urea is directed perpendicular to the carbonyl bond, i.e. in the x direction. Pople (20) has postulated paramagnetic circulations in the plane of a carbonyl bond and its substituents. These ought to give a positive contribution to $\chi_{yy}^{C=O}$ and $\chi_{zz}^{C=O}$, while the results observed for urea indicate that $\chi_{xx}^{C=O}$ should be

Can. J. Chem. Downloaded from www.nrcresearchpress.com by 210.87.254.40 on 09/05/12
For personal use only.

negative. Only the sets of components derived with the assumption that B is more shielded than A satisfy these requirements.

On the other hand, the opposite choice is favored by consideration of the magnitude of the long range spin couplings through the C—N partial double bond. The analogous long range coupling H—C=C—C—H has been analyzed (21) as the sum of a positive contribution $J(\sigma)$ through the σ-bond frame and a negative contribution $J(\pi)$ through the π electrons of the C=C double bond. The first part is different for the *cis* and *trans* configurations with $J(\sigma)_{trans} > J(\sigma)_{cis}$, while for the second part $J(\pi)_{trans} = J(\pi)_{cis}$. The magnitude of the total coupling constants $|J_{cis}|$ and $|J_{trans}|$ thus depends on the magnitude of $J(\pi)$, and if $|J(\pi)| < \frac{1}{2}(J(\sigma)_{cis} + J(\sigma)_{trans})$ then $|J_{trans}| > |J_{cis}|$. The magnitude of $J(\pi)$ may be expected to depend on the double bond character of the central bond, and this dependence may be the cause of the observed variation of the total coupling constants of amides in solvents of high dielectric constant (22). It appears permissible to assume that the double bond character of the central bond in amides is sufficiently small to warrant the conclusion that $|J_{trans}| > |J_{cis}|$. This conclusion is confirmed by recent work on unsymmetrically disubstituted amides (23) in which the spectral assignments based on the assumption $|J_{trans}| > |J_{cis}|$ were corroborated by the differential solvent shift in benzene (24). In all cases that allow observation of the long range coupling it is the signal at higher field that shows the stronger coupling. If $|J_{trans}| > |J_{cis}|$ this signal must be assigned to the group *cis* to the carbonyl group, i.e. the A substituent must be more shielded than the B substituent.

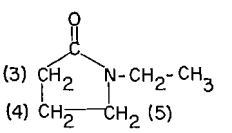

FIG. 3. 1-Ethylpyrrolidinone-2.

We have attempted to reach a decision between the two alternatives by means of the following experiment. In 1-ethylpyrrolidinone-2 (Fig. 3) the —CH_2— protons of the ethyl group and those on C_5 may be compared to the —CH_2— protons of ethyl groups *cis* and *trans* to the carbonyl bond of an acetamide. In the acetamide the two —CH_2— groups can be distinguished only by making an assumption about the relative magnitude of *cis* and *trans* coupling across the C—N partial double bond. However, in 1-ethylpyrrolidinone-2 they can be distinguished by the coupling patterns of their signals, a quadruplet being expected for —CH_2— protons of an ethyl group and a triplet for those on C_5. The relative positions of the centers of these multiplet signals enables us to decide which CH_2 group is more shielded.

The low field multiplets in the spectra of dilute solutions of 1-ethylpyrrolidinone-2 in CCl_4 and benzene are shown in Figs. 4*a* and 4*b* respectively. Figure 4*a* shows the expected seven peaks, but it is impossible to decide which four peaks are those of the quadruplet and which belong to the triplet. Figure 4*b* shows the strong separation of the quadruplet and triplet structures produced by benzene dilution of the compound. Since all four peaks of the quadruplet must be shifted identically by the change of solvent, as must the three peaks of the triplet, the peaks in the spectrum of the CCl_4 solution were assigned by the measurement of spectral positions of individual peaks in each spectrum. The peaks are labelled in order of increasing field strength in the spectrum of the benzene solution.

Can. J. Chem. Downloaded from www.nrcresearchpress.com by 210.87.254.40 on 09/05/12
For personal use only.

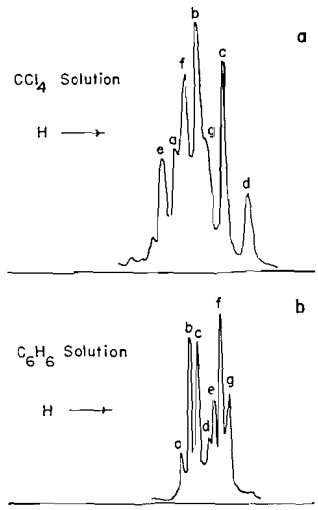

FIG. 4. (*a*) Low field peaks in the n.m.r. spectrum of 1-ethylpyrrolidinone-2 in CCl_4. (*b*) Low field peaks in the n.m.r. spectrum of 1-ethylpyrrolidinone-2 in C_6H_6.

Table VII summarizes the assignment of the peaks of the CCl_4 solution and shows agreement with the rule developed by Hatton and Richards (24) in that the group farthest from the carbonyl group (—C^5H_2—) experiences additional shielding in benzene solution.

TABLE VII

Room temperature spectral positions of low field 1-ethylpyrrolidinone-2 peaks with respect to benzene as internal standard

Peak	$-\delta$ (c.p.s.) CCl_4 soln.	$-\delta$ (c.p.s.) C_6H_6 soln.	$\delta_{CCl_4} - \delta_{C_6H_6}$ (c.p.s.)
a	220.3	218.3	−2.0
b	227.1	225.3	−1.8
c	234.2	232.3	−1.9
d	241.4	239.3	−2.1
e	218.1	247.9	29.8
f	224.8	254.9	30.1
g	231.1	261.9	30.8

A double resonance experiment in which the quadruplet was collapsed by irradiation of the high field methyl triplet confirmed that the peaks *a*, *b*, *c*, *d* are the signal of the —CH_2— protons of the ethyl group.

Table VII shows that in CCl_4 solution the signal of the A substituent (center of the quadruplet) is located at higher field than the signal of the B substituent (center of the triplet) by 6.08 c.p.s. = 0.108 p.p.m., confirming the assumption made for the long range spin coupling.

DISCUSSION

The results presented in Tables III–VI must be criticized because of the failure to achieve consistency when the shift caused by the electric field is taken into account. The discrepancy between calculated and observed shift differences is greatest for protons close to the carbonyl bond. This suggests that at distances of 1 to 2 Å the approximation

Can. J. Chem. Downloaded from www.nrcresearchpress.com by 210.87.254.40 on 09/05/12
For personal use only.

of a continuous electronic distribution by localized charges and dipoles is inadequate. Indeed, values from 0 (25) to 0.4 e (6) have been suggested for the charge on the oxygen atom in amides, and the decomposition of the electric field into a polar and dipolar part is somewhat ambiguous. The same criticism, of course, applies also to the description of the magnetic effect of the carbonyl bond in terms of an induced magnetic dipole. A calculation for the C—C bond (26) indicates the complexity of the actual physical situation.

The reaction field caused by polarization of the solvent surrounding the amide molecule has been neglected in the calculation of the electric field shift, and the values given in Table I must therefore be too large. A detailed consideration of this effect is probably of little significance in view of the use of a single model for a variety of molecules of different shapes and sizes.

It does appear, however, that the susceptibility components derived by neglecting the effect of the electric field are useful for correlating chemical shift differences with the structure of molecules containing a carbonyl bond. For example, the optimum results given in Table V have been used to explain the dependence of the chemical shift difference for the exo-methylene protons of α-methylenecycloketones on ring size (5). It was shown that the *s-trans* conformation is preferred unless the *s-cis* conformation is required by small ring size. Similar results are obtained for the open chain α,β-unsaturated ketones $CH_3CO—C{=}CRR'$. The calculated and observed shift differences $|\delta(R) - \delta(R')|$ in p.p.m. are for

		Calculated		
		s-cis	*s-trans*	Observed
methyl vinyl ketone	(R, R′) = H	0.63	0.15	0.13
mesityl oxide	(R, R′) = CH_3	0.55	0.33	0.27

To give another application, the spectra of a series of disubstituted acetamides may be considered. The observed shift differences may be rationalized by distinguishing two groups of compounds:

Group I with N—CH_2R substituents show

$$|\delta(H_A) - \delta(H_B)| \simeq 0 \text{ and } |\delta(R_A) - \delta(R_B)| \simeq 0.09 \text{ p.p.m.;}$$

Group II with N—CHRR′ substituents show

$$|\delta(H_A) - \delta(H_B)| \simeq 0.58 \text{ p.p.m. and } |\delta(R_A) - \delta(R_B)| \simeq 0.$$

The shift differences calculated with the optimum susceptibility components of Table V agree with these observations if it is assumed that the two groups of compounds exist mainly in the following conformations:

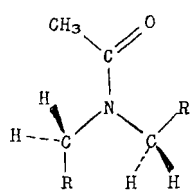

Group I

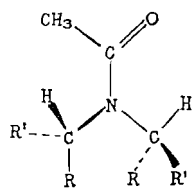

Group II

We have not been able to prove the existence of distinct rotational isomers, but a similar proposal (27) for the closely related nitrosamines lends some support to this hypothesis.

The magnitude of the calculated shift difference is in these cases nearly independent

Can. J. Chem. Downloaded from www.nrcresearchpress.com by 210.87.254.40 on 09/05/12
For personal use only.

of whether the susceptibility components derived for A at higher field or those for B at higher field are used. The results reported in Part B, however, indicate that the assumption that A is at higher field is the better choice. Although this conclusion is in agreement with deductions made from long range spin coupling patterns and also with results for the isoelectronic nitroso group (28), it does contradict Narasimhan and Rogers' argument based on the sign of the individual susceptibility components. It is also contrary to the empirical rule that in complex molecules protons are deshielded by the influence of neighboring carbonyl bonds (1).

The susceptibility components derived for formamides differ considerably from those derived for acetamides. It appears possible that some fundamental difference in the electronic structure between formamides and acetamides is reflected in both the susceptibilities of the carbonyl bond and in the barriers for internal rotation (16).

ACKNOWLEDGMENTS

We wish to gratefully acknowledge the assistance of the National Research Council of Canada in the form of a grant in aid of research and the award of a studentship to one of us (D. L. H.).

REFERENCES

1. L. M. JACKMAN. Applications of nuclear magnetic resonance spectroscopy in organic chemistry. Pergamon Press, New York. 1959.
2. H. M. MCCONNELL. J. Chem. Phys. **27**, 226 (1957).
3. P. T. NARASIMHAN and M. T. ROGERS. J. Phys. Chem. **63**, 1388 (1959).
4. G. KLOSE. Mol. Phys. **6**, 585 (1963).
5. R. KAISER and D. L. HOOPER. Mol. Phys. **8**, 403 (1964).
6. L. PAULING. The nature of the chemical bond. 3rd ed. Cornell University Press, Ithaca. 1960.
7. A. PACAULT, J. HOARAU, and A. MARCHAND. Aspects récents du diamagnetism. *In* Advances in chemical physics. Vol. III. *Edited by* I. Prigogine. Interscience Publishers, New York. 1961. p. 171.
8. J. TILLIEU and J. GUY. J. Chem. Phys. **24**, 1117 (1956).
9. J. A. POPLE. Discussions Faraday Soc. **34**, 7 (1962).
10. R. F. ZÜRCHER. J. Chem. Phys. **37**, 2421 (1962).
11. A. A. BOTHNER-BY and C. NAAR-COLIN. Ann. N.Y. Acad. Sci. **70**, 833 (1958).
12. P. T. NARASIMHAN and M. T. ROGERS. J. Chem. Phys. **31**, 1302 (1959).
13. J. I. MUSHER. J. Chem. Phys. **35**, 1159 (1961).
14. J. V. HATTON and R. E. RICHARDS. Mol. Phys. **3**, 253 (1960).
15. J. A. POPLE, W. G. SCHNEIDER, and H. J. BERNSTEIN. High resolution nuclear magnetic resonance. McGraw-Hill, New York. 1959.
16. M. T. ROGERS and J. C. WOODBREY. J. Phys. Chem. **66**, 540 (1962).
17. A. D. BUCKINGHAM. Can. J. Chem. **38**, 300 (1960).
18. W. D. KUMLER and C. W. PORTER. J. Am. Chem. Soc. **56**, 2549 (1934).
19. K. LONSDALE. Proc. Roy. Soc. London, Ser. A, **177**, 272 (1944).
20. J. A. POPLE. Proc. Roy. Soc. London, Ser. A, **239**, 550 (1957).
21. M. Y. DEWOLF and J. D. BALDESCHWIELER. J. Mol. Spectry. **13**, 344 (1964).
22. E. W. RANDALL and J. D. BALDESCHWIELER. J. Mol. Spectry. **8**, 365 (1962).
23. L. A. LAPLANCHE and M. T. ROGERS. J. Am. Chem. Soc. **85**, 3728 (1963).
24. J. V. HATTON and R. E. RICHARDS. Mol. Phys. **5**, 139 (1962).
25. W. W. BATES and M. E. HOBBS. J. Am. Chem. Soc. **73**, 2151 (1951).
26. J. R. DIDRY and J. GUY. Compt. Rend. **256**, 3042 (1963).
27. G. J. KARABATSOS and R. A. TALLER. J. Am. Chem. Soc. **86**, 4373 (1964).
28. H. W. BROWN and D. P. HOLLIS. J. Mol. Spectry. **13**, 305 (1964).

Can. J. Chem. Downloaded from www.nrcresearchpress.com by 210.87.254.40 on 09/05/12
For personal use only.

Can. J. Chem. Downloaded from www.nrcresearchpress.com by 210.87.254.105 on 09/05/12
For personal use only.

REACTIONS OF SUGAR CHLOROSULFATES

PART V. THE SYNTHESIS OF CHLORODEOXY SUGARS[1]

H. J. JENNINGS[2] AND J. K. N. JONES
Department of Chemistry, Queen's University, Kingston, Ontario

Received February 1, 1965

ABSTRACT

The reaction of sulfuryl chloride with reducing sugars and their methyl glycopyranosides was shown to produce fully substituted pyranose derivatives containing both chlorodeoxy and chlorosulfate ester groups. It was demonstrated that the chlorodeoxy groups were formed by nucleophilic displacement (S_N2) by chloride ion of specific reactive chlorosulfate groups in fully chlorosulfated intermediates. The degree of chloro-substitution was shown to be determined by both steric and electronic effects in the individual pyranose derivatives.

INTRODUCTION

The first direct nucleophilic substitution (S_N2) at a secondary carbon atom in a pyranose ring was achieved by Helferich (1) through the use of sulfuryl chloride. Proof of the expected change of sterochemistry at C_4 of methyl α-D-glucopyranoside when it reacts with sulfuryl chloride to give methyl 4,6-dichloro-4,6-dideoxy α-D-galactopyranoside 2,3-cyclic sulfate was given later (2). When a reduced pyridine – sulfuryl chloride ratio was employed, both D-glucose (3) and methyl α-D-glucopyranoside (4) also gave 4,6-dichloro-4,6-dideoxy-D-galactopyranoside derivatives but with positions C_2 and C_3 substituted by chlorosulfate ester groups. Most of the work recorded to date on the reaction of sulfuryl chloride with pyranose sugars (1–7) has been concerned with those in the xylo- or arabino-configuration and has indicated that position C_4 is the only secondary hydroxyl group to be converted readily to a chlorodeoxy group, with inversion of configuration. This inversion of configuration probably occurs via intermediate chlorosulfate ester groups (1–7). Positions C_2 and C_3 were found to be comparatively unreactive to chloro-substitution. This result is analogous to the substitution of the tosyl esters of methyl glucopyranosides with chloride ion (8), although the conclusion of the authors that the C_4 secondary tosyl ester group is more prone to nucleophilic substitution than the primary exocyclic C_6 tosyl ester in monosubstitution is probably incorrect. The isolation of chloro-sulfate esters under conditions which suppressed the formation of the cyclic sulfate ester derivatives (3) prompted a further study of the individual reactivities of all the chloro-sulfate esters of pyranose sugars in regard to competitive nucleophilic substitution. Besides the obvious objective of the synthesis of chlorodeoxy sugars, it was hoped to relate the high degree of selectivity found in the substitution of chlorosulfate esters in the pyranose ring structures to steric effects in each individual molecule.

DISCUSSION

Structural Determinations

In a previous communication (4) it was reported that methyl α-D-glucopyranoside when treated with sulfuryl chloride gave, at room temperature, methyl 4,6-dichloro-4,6-dideoxy-α-D-galactopyranoside 2,3-dichlorosulfate (III). When the above reaction was repeated, except that the product was isolated from the reaction mixture at low temperature (−70°), a crystalline tetrachlorosulfate ester derivative (I) was obtained. It was

[1]*Part IV in this series was a paper by H. J. Jennings and J. K. N. Jones. Can. J. Chem. 41, 1151 (1963).*
[2]*Present address: Department of Chemistry, The University of Bristol, Bristol, England.*

shown to be a derivative of methyl α-D-glucopyranoside because, on treatment with 1 mole of pyridine hydrochloride, it gave crystalline methyl 6-chloro-6-deoxy-α-D-glucopyranoside 2,3,4-trichlorosulfate (II). Compound II had been obtained previously from the product when the reaction of methyl α-D-glucopyranoside with sulfuryl chloride was carried out at 0°. The structure of II was ascertained by removal of the chlorosulfate ester groups (4) to give crystalline methyl 6-chloro-6-deoxy-α-D-glucopyranoside (9). Periodate oxidation of this monochloro-hexoside led to an uptake of periodate (1.99 mole) and the production of acid (1.07 mole). These figures are those expected from the oxidation of a 6-chloro-substituted derivative.

Methyl β-D-glucopyranoside, when treated with sulfuryl chloride, using the conditions which previously gave III, yielded a crystalline product which was shown to be methyl 6-chloro-6-deoxy-β-D-glucopyranoside 2,3,4-trichlorosulfate (IV), since dechlorosulfation gave crystalline methyl 6-chloro-6-deoxy-β-D-glucopyranoside (10). Periodate oxidation of this monochloro-hexoside gave results consistent only with those expected from a 6-chloro-substituted pyranose derivative. When IV was heated with pyridine hydrochloride in chloroform solution, there resulted further chloro-substitution, and the major product was shown to be V. The syrupy reaction product was dechlorosulfated and gave a non-reducing crystalline mixture from which a pure component could not be isolated. The major component of this mixture was methyl 4,6-dichloro-4,6-dideoxy-β-D-galactopyranoside (3) since its acid hydrolysis gave three reducing components (paper chromatography), the major and fastest running of which was characterized as crystalline 4,6-dichloro-4,6-dideoxy-D-galactose (2).

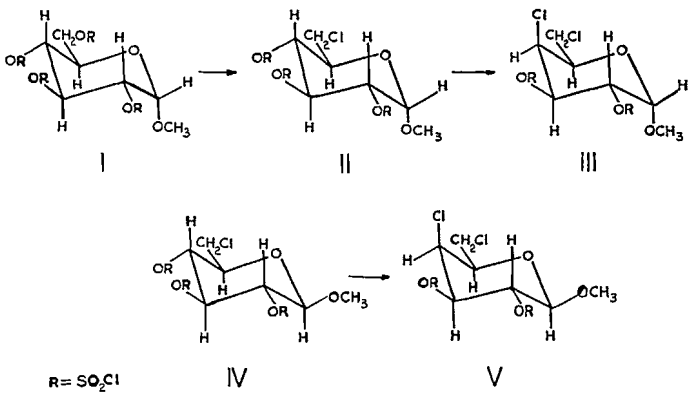

D-Mannose, when treated with sulfuryl chloride, gave a crystalline product (VI) which was shown to be 6-chloro-6-deoxy-α-D-mannosyl chloride 2,3,4-trichlorosulfate on the following evidence. The compound (VI) was considered to be the α-anomer by the similarity of its specific rotation to that of α-tetra-*O*-acetyl-D-mannopyranosyl chloride (11). Methanolysis and subsequent dechlorosulfation of VI gave a non-reducing syrupy mixture, the major component of which was shown to be methyl 6-chloro-6-deoxy-α-D-mannopyranoside. Hydrolysis of the syrupy mixture gave another syrup, which was shown to be a mixture containing three reducing components (paper chromatography), one of which (major component) was characterized as 6-chloro-6-deoxy-D-mannose in the following manner. The syrupy mixture of reducing compounds gave a crystalline 3,5-dichlorophenylhydrazone in good yield, from which a chromatographically pure monochloro-hexose was regenerated (12). The pure monochloro-hexose did not crystallize, but

Can. J. Chem. Downloaded from www.nrcresearchpress.com by 210.87.254.105 on 09/05/12
For personal use only.

gave a crystalline phenylhydrazone, which, on further heating with phenylhydrazine, gave a crystalline phenylosazone identical with the phenylosazone of authentic 6-chloro-6-deoxy-D-glucose (3). Dechlorosulfation of the crystalline derivative (VII) obtained from the reaction of sulfuryl chloride with methyl α-D-mannopyranoside gave a syrupy non-reducing mixture which had the same specific rotation as the mixture of glycosides obtained previously by the methanolysis and dechlorosulfation of VI. The syrupy mixture obtained from VII was converted to crystalline methyl 3,6-anhydro-α-D-mannopyranoside (13) by base, while hydrolysis of the mixture gave 6-chloro-6-deoxy-D-mannose as the major product (characterized as its crystalline phenylhydrazone).

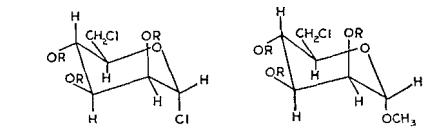

Methyl α-D-galactopyranoside, when treated with sulfuryl chloride, gave methyl 4,6-dichloro-4,6-dideoxy-α-D-glucopyranoside 2,3-dichlorosulfate (VIII), the structure of which was proved by dechlorosulfation of VIII to give crystalline methyl 4,6-dichloro-4,6-dideoxy-α-D-glucopyranoside (IX) (2). Hydrolysis of IX, which required vigorous conditions, gave crystalline 4,6-dichloro-4,6-dideoxy-D-glucose (X). D-Galactose, when treated with sulfuryl chloride, gave a syrupy product which was shown to contain 3,4,6-trichloro-3,4,6-trideoxy-D-allopyranosyl chloride 2-chlorosulfate (XI). Methanolysis and subsequent dechlorosulfation of XI gave a crystalline derivative (XII) which was shown to have the structure methyl 3,4,6-trichloro-3,4,6-trideoxy-α-D-allopyranoside on the basis of the following evidence. Elemental analysis of XII and of its crystalline tosyl ester and methyl ether derivatives proved it to be a trichloro-substituted compound. Hydrolysis of XII gave a crystalline trichlorohexose (XIII), which was also obtained directly from the syrupy mixture containing XI, by treatment of an aqueous acetone solution of the syrupy mixture with sodium iodide. The trichlorohexose (XIII) gave a crystalline *p*-nitrophenylhydrazone also containing three chlorine atoms. The same crystalline trichlorohexose was also formed in the hydrolysis of XV, which was obtained by dechlorosulfation of the reaction product (XIV) of methyl β-D-galactopyranoside with sulfuryl chloride. This implied that XV was the β-anomer of XII. That chloro-groups were present on C_6 and C_4 of XII, the one at C_4 having been introduced with inversion of configuration, was ascertained by the fact that further reaction of 4,6-dichloro-D-glucose (X) with sulfuryl chloride gave a syrupy product, which, on methanolysis and subsequent dechlorosulfation, gave XV as the major product of a mixture of methyl glycosides (thin-layer chromatography). Hydrolysis of the mixture of methyl glycosides also gave crystalline XIII as the major component of the hydrolysate. Evidence that XII was a 3,4,6-trichloro-trideoxy-D-allose derivative was obtained, although some preliminary experiments had suggested that the third chloro-group was in fact situated at C_2 of XIII. These later experiments included (*a*) the inability to reform the methyl glycoside of XIII using methanolic hydrogen chloride; (*b*) the failure to obtain a phenylosazone or a 1;2-*O*-isopropylidene derivative of XIII; (*c*) the failure to form a trichlorotrideoxy hexitol by reduction under acidic conditions of XIII; (*d*) the unusually slow uptake of periodate by XIII (14); and (*e*) a negative tetrazolium red test (15) on XIII. A probable explanation for some of these anomalous reactions can be attributed to an axial chloro-group on C_3 of XIII which is in close proximity to C_1, and could hinder reactions at this site. That the third chloro-group was,

Can. J. Chem. Downloaded from www.nrcresearchpress.com by 210.87.254.105 on 09/05/12
For personal use only.

in fact, at C_3 of XII was established by paper electrophoresis of XIII in borate buffer, where XIII had a comparable electrophoretic mobility to 3,4,6-tri-*O*-methyl-D-glucose, whereas 2,4,6-tri-*O*-methyl-D-glucose is known not to move under these conditions (16). Evidence for chloro-substitution having occurred with inversion of configuration on C_3 of XII (allo-configuration) is the fact that elimination of chloride ion did not take place under basic conditions and this is consistent with the chloro-group at C_3 of XII being cis to the hydroxyl group at C_2 (2). Also the trichlorohexose (XIII) obtained from XII was immediately converted to a crystalline non-reducing derivative (XVI) by 1 mole of sodium hydroxide. The elemental analysis of XVI was consistent with the structure 1,6-anhydro-3,4-dichloro-3,4-dideoxy-β-D-allopyranose, and as the formation of the 1,6-anhydro derivative (XVI) requires the trichlorohexose (XIII) to change to the Cl conformation, it is likely that the axial chloro-group on C_3 of XIII facilitated this change.

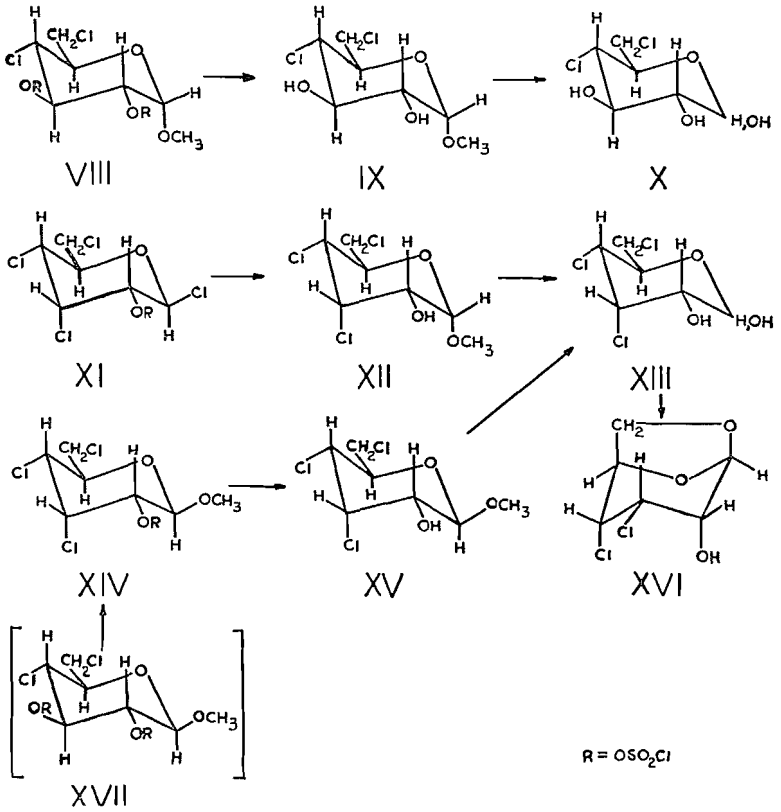

Although the structure of XII has been fairly well established, a further experiment was performed to avoid the complication of three-chloro-groups being attached to the product. A configurational analogue of X methyl 4,6-*O*-benzylidene-β-D-glucopyranoside (17) was treated with sulfuryl chloride on the assumption that chloro-substitution with inversion of configuration would take place at C_3 of the 4,6-*O*-benzylidene derivative. The product of the reaction was a syrup, which on dechlorosulfation gave a mixture of two components, the minor component of which was characterized as the crystalline starting compound. The major component was characterized as syrupy methyl 3-chloro-3-deoxy-4,6-*O*-benzylidene-β-D-allopyranoside (XVIII) on the following evidence. Mild hydrolysis of

Can. J. Chem. Downloaded from www.nrcresearchpress.com by 210.87.254.105 on 09/05/12
For personal use only.

XVIII gave a syrupy derivative (XIX) which had lost the benzylidene group and was shown to be pure by gas–liquid chromatographic analysis of its triacetate derivative. The triacetate derivative of XIX did not crystallize but analyzed as a monochloro-triacetate methyl glycoside. That the chloro-group of XIX was on C_3 was indicated by the fact that XIX remained resistant to periodate oxidation and also that hydrolysis of XIX gave a syrupy monochlorohexose (XX), the electrophoretic mobility of which in borate buffer was comparable to that of 3-*O*-methyl-D-glucose and not to that of 2-*O*-methyl-D-glucose (16). Finally, XIX was assigned the allo-configuration as treatment of XIX with base gave no elimination of chloride ion; it is known that 3-chloro-3-deoxy-α-D-glucopyranoside as its 4,6-*O*-benzylidene derivative eliminates chloride ion under basic conditions (18). It might be supposed, however, that XIX might eliminate chloride ion under more drastic conditions to give methyl 3,6-anhydro-β-D-glucopyranoside. To check this possibility, XIX was heated in sodium hydroxide solution but was recovered unchanged. The triacetate derivative of the product had the same retention time as the triacetate derivative of XIX (gas–liquid partition chromatography). Also, hydrolysis of the recovered product gave a compound which had the same electrophoretic mobility as XX in borate buffer and a different mobility from that of 3,6-anhydro-D-glucose (13) in molybdate buffer.

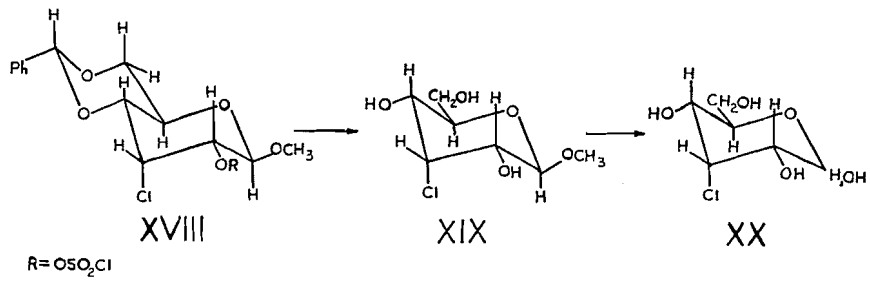

Mechanism of the Substitution Reaction

In all the cases studied so far (2–4) and in the evidence submitted in this publication, the chlorodeoxy products formed from secondary pyranose ring hydroxyl groups have been shown to be formed with inversion of configuration. Thus the reaction seems to fall into the category of a bimolecular nucleophilic substitution reaction (S_N2) on stereochemical grounds. That the chlorosulfate ester group is the precursor of the chlorodeoxy groups is well established. Low temperature isolations of the products of the reaction of methyl α-D-glucopyranoside with sulfuryl chloride in the presence of pyridine gave the tetrachlorosulfate (I) and the 6-chloro-trichlorosulfate (II) intermediates (isolated at −70° and 0° respectively), whereas the usual reaction conditions (3) gave the 4,6-dichloro-dichlorosulfate derivative (III). It is probable therefore that at higher temperatures the reactive chlorosulfate groups on C_6 and C_4 of I are replaced by chloride ion (pyridine hydrochloride), which is itself formed in the esterification of the hydroxyl groups. Both the intermediates (I and II) were converted smoothly to the 4,6-dichloroderivative (III) by excess pyridine hydrochloride in chloroform solution and also the tetrachlorosulfate derivative (I) was converted to the 6-chloro derivative (II) by 1 mole of pyridine hydrochloride using similar conditions. The latter experiment eliminates the possibility of the regeneration of pyridine hydrochloride in the substitution reaction (catalytic effect) and also the thermal decomposition of the chlorosulfate ester group under the conditions used.

Can. J. Chem. Downloaded from www.nrcresearchpress.com by 210.87.254.105 on 09/05/12
For personal use only.

Can. J. Chem. Downloaded from www.nrcresearchpress.com by 210.87.254.105 on 09/05/12
For personal use only.

It is interesting to note that treatment of the chlorosulfate ester derivatives with iodide ion (sodium iodide) in 6% aqueous methanol solution did not give the corresponding iododeoxy compounds. For example, the 6-chloro-trichlorosulfate derivative (II) gave only methyl 6-chloro-6-deoxy-α-D-glucopyranoside (9) on treatment with sodium iodide. This removal of chlorosulfate ester groups to give the corresponding hydroxyl groups with retention of configuration was found to be of wide application and constitutes an efficient and fast method of dechlorosulfation. Only one exception to this general reaction pattern has been recorded (4) where vicinal chlorosulfate ester groups in the open-chain hexitol series gave a cyclic-sulfate ester derivative when treated with sodium iodide.

Steric Effects

In all the experiments carried out on the reaction of sulfuryl chloride with hexopyranoses and hexopyranosides, chloro-substitution on the primary C_6 position (via the intermediate 6-chlorosulfate ester) was facile. That the C_6 chlorosulfate ester was also the most reactive one was demonstrated by the fact that methyl α-D-glucopyranoside tetrachlorosulfate (I) gave only the 6-chloro-substituted derivative (II) when treated with 1 mole of pyridine hydrochloride. These results were expected on the basis of previous work (19) and a probable explanation is that the approach of the chloride ion to the exocyclic C_6 position is not sterically hindered by other large groups in the pyranose ring.

Only the derivatives in the D-manno-configuration failed to give chloro-substitution at position C_4 under the normal conditions of the reaction (3). This result could be interpreted as due to 1;3-diaxial interaction between the approaching chloride ion at C_4 and the large axial chloro-sulfate group at C_2 in VI and VII. This is supported by the fact that II, which differed from VII only in the configuration of the C_2 chlorosulfate group, gave good yields of the methyl 4,6-dichloro-D-galactoside derivative (III) under similar experimental conditions. Further evidence of these 1;3-diaxial interactions was found in the D-galacto-series. Both D-galactose and methyl β-D-galactopyranoside gave 3,4,6-trichloro-D-allose derivatives (XI and XIV respectively) whereas methyl α-D-galactopyranoside under similar reaction conditions gave only a 4,6-dichloro-D-glucose derivative (VIII), which was shown to be resistant to further chloro-substitution even when heated at 50° with pyridine hydrochloride in chloroform solution. Crystalline VIII was recovered from the reaction mixture and examination (g.l.p.c.) of the dechlorosulfated residual syrupy product indicated a preponderance of the 4,6-trichloro-derivative (IX) and only a very minor quantity of the 3,4,6-trichloro-derivative (XII). This evidence indicated an effect that was due to the anomeric substituent of VIII, which could be interpreted as 1;3-diaxial interaction to the approach of the chloride ion to C_3 by the axial methyl-glycosidic group of VIII. This effect is not present in XIV (methyl β-glycoside) and there is some evidence that is not present in XI since it is probable that XI is the β-chloro anomer ($[\alpha_D] = -30°$). In any event, even if XI were the α-chloro anomer, it is likely that anomerization could occur under the reaction conditions used. Another example of the 1;3-diaxial interaction effect, concerning the methyl glycosidic group, is found in the reaction of sulphuryl chloride with the 4,6-*O*-benzylidene derivatives of methyl α- and β-D-glucopyranosides. The α-anomer has been shown to give a 2,3-dichlorosulfate derivative (4), whereas under similar reaction conditions the β-anomer gave mainly a 3-chloro-substituted D-alloside derivative (XVIII).

Although nucleophilic substitution by chloride ion at position C_3 is controlled by the configuration of the anomeric substituent, other factors have to be considered. Both methyl α- and β-D-glucopyranoside gave only 4,6-dichloro-substituted derivatives (III

and V respectively), whereas it might have been expected that the methyl β-glycoside would have given a 3,4,6-trichloro-D-gulose derivative. The fact that no substitution by chloride ion occurred on C_3 of V indicated a deactivating effect by the axial chloro-group at C_4 of V. This deactivating effect by an axial substituent at C_4 was also observed in the reaction of sulfuryl chloride with D-glucose and 4,6-*O*-ethylidene-D-galactose: the former gave a 4,6-dichloro-D-galactose derivative (3) and the latter only a 2,3-dichloro-sulfate derivative. In contrast, compounds which had a configuration identical with that of V except for an equatorial substituent at C_4 (methyl 4,6-*O*-benzylidene-β-D-glucopyranoside and 4,6-dichloro-4,6-dideoxy-D-glucose (X)) gave facile chloro-substitution at C_3. In view of this evidence it is also probable that XVII was the unidentified intermediate in the formation of XIV.

The deactivation of an equatorial chlorosulfate ester group by a vicinal axial substituent cannot be explained by steric affects because of the approach of the chloride ion at C_3 of V, as an examination of a model of V indicates that there are no large groups in proximity to this approach. However, a possible explanation can be found by consideration of the transition state in the substitution reaction. Reaction of V with Cl^- would involve the formation of a transition state possessing considerable skew interactions due to the near-eclipsed conformation of the large substituents on C_3 and C_4. This is illustrated in XXI

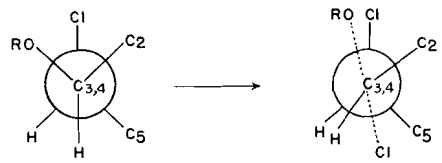

XXI XXII

and XXII, representing the end-on views (20) of the C_3—C_4 bond of V and of the transition state respectively. This could raise the energy requirements of the transition state (XXII) considerably. When the chloro-group on C_4 is equatorial as in X and in the intermediate XVII, similar skew interactions would be avoided, giving a transition state (XXIV) of lower energy than XXII. This is indicated by the end-on representations of the C_3—C_4 bond of XVI in the ground state (XXIII) and in the transition state (XXIV). Similar skew interactions have been postulated to explain the large differences in the rates of nucleophilic substitution of highly substituted erythro- and threo-bromobenzenesulfonate derivatives (21).

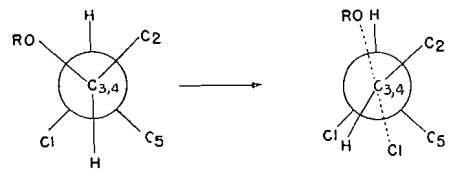

XXIII XXIV

$R = SO_2Cl$

All of the derivatives discussed so far have, as a common feature, the relative inertness of the C_2 chlorosulfate ester group to nucleophilic substitution by chloride ion. This observation cannot be justified on the basis of steric interactions as it might be expected that the chlorosulfate ester groups on C_2 and C_4 of IV would be equally active as they are

Can. J. Chem. Downloaded from www.nrcresearchpress.com by 210.87.254.105 on 09/05/12
For personal use only.

Can. J. Chem. Downloaded from www.nrcresearchpress.com by 210.87.254.105 on 09/05/12
For personal use only.

both in a similar conformational environment. However, compound IV gave mainly a 4,6-dichloro-D-galactoside derivative (V), when heated with pyridine hydrochloride in chloroform solution. This might be explained by the fact that the ester groups on C_2 and C_4 of IV are in different electronic environments. Thus position C_2 of IV is in the proximity of two β-oxygen atoms (ring oxygen and anomeric group) whereas C_4 is only in the proximity of one (ring oxygen). This explanation has some credence as it is known that β-methoxyl substituents do retard considerably the rate of nucleophilic substitution (22). However, it is possible that C_2 chloro-substitution may have occurred in D-mannose as discussed below. The 6-chloro-substituted derivative (VI), obtained from the reaction of D-mannose with sulfuryl chloride, gave a tetrachloro-substituted derivative on further heating with pyridine hydrochloride in chloroform solution, whereas VII was resistant to further chloro-substitution. It could be argued that to obtain further substitution of VI the deactivating influence of the axial C_2 chlorosulfate ester group would have to be removed. This could be achieved by chloro-substitution at C_2 of VI to produce an equatorial chlorodeoxy group at this position. This would then allow the normally reactive C_4 ester group VI to be substituted and thus one might postulate a 1,2,4,6-tetrachloro-D-galacto-configuration for the product. Further structural studies on this tetrachloro-substituted product are being carried out.

EXPERIMENTAL

Optical rotations were measured at 21 ± 3°. Melting points were determined on a Kofler hot stage and were uncorrected. All solutions were concentrated under reduced pressure below 50°. Aqueous solutions were deionized by passage through Amberlite I.R. 120 (H form) and Duolite A.4 (OH form) ion exchange resins. Paper chromatography was carried out by the descending method on Whatman No. 1 filter paper using the following solvent systems (v/v): (*a*) butan-1-ol, ethanol, water (3:1:1), (*b*) ethyl acetate, acetic acid, formic acid, water (18:3:1:4). The rates of movement of the sugars are quoted relative to that of D-xylose (R_x). Paper electrophoresis was performed using Whatman 3 MM filter paper impregnated with buffer solutions: (i) 0.05 *M* borate solution (23) and (ii) 2% aqueous solution of sodium molybdate (24). The rates of movement of sugars in (i) are given relative to that of D-glucose (M_g) and in (ii) relative to that of sorbitol (M_s). Sugars were detected on paper chromatograms and electrophoretograms by *p*-anisidine hydrochloride (25) and (or) alkaline silver nitrate (26) spray reagents. Thin-layer chromatographic analysis (t.l.c.) was carried out on prepared silica gel G plates.

Analytical gas–liquid chromatographic analysis (a.g.l.c.) was carried out using a Pye Argon gas chromatograph with the following column packings: (A) 1:1:2 intimate mixture of 20% w/w butanediol–succinate polyester on 60–80 mesh Chromosorb W, 20% w/w Apiezon M grease on 60–80 mesh silver-coated Chromosorb W, 0.3% w/w Apiezon M grease on 60 plus mesh silver-coated glass beads, at 175° with a flow rate of 145 ml per min; (B) 10.7% of LAC-4R-886 on 100–120 mesh Chromosorb W at 207° with a flow rate of 160 ml per min.

Anhydrous pyridine hydrochloride was made by passing dry gaseous hydrogen chloride into a petrol solution of anhydrous pyridine. The precipitated pyridine hydrochloride was collected by filtration, quickly washed with petrol, and stored in a desiccator over phosphoric oxide.

Periodate oxidations were carried out in the dark at 25°, using a small sample (20 mg) of the compounds in distilled water (25 ml) containing 0.3 *M* sodium metaperiodate (1 ml). Aliquots (1 ml) were removed at intervals and the consumption of periodate (27) and the production of acid (28) were measured.

Methyl α-D-Glucopyranoside 2,3,4,6-Tetrachlorosulfate (I)

Methyl α-D-glucopyranoside (10 g) was treated with sulfuryl chloride (26 ml) and pyridine (40 ml) in chloroform solution as described in a previous communication (3), except that the reaction mixture, while still at the temperature of the acetone – solid carbon dioxide bath (ca. −70°), was quickly poured into a vigorously stirred solution of ice-cold 10% sulfuric acid (1 000 ml). The product (8.7 g, 29%) was recrystallized from chloroform–petrol (b.p. 50–60°) and gave colorless needles (7 g, 23%) of m.p. 118° and $[\alpha]_D$ +92° (*c*, 0.8 in chloroform).

Anal. Found: C, 14.6; H, 1.7; Cl, 24.6; S, 22.5. Calcd. for $C_7H_{10}Cl_4O_{14}S_4$: C, 14.6; H, 1.7; Cl, 24.2; S, 21.8.

Methyl 6-Chloro-6-deoxy-α-D-glucopyranoside 2,3,4-Trichlorosulfate (II)

The above reaction was repeated using methyl α-D-glucopyranoside (10 g), except that the reaction mixture was allowed to warm up slowly to 0° and then was poured, at this temperature, into a vigorously stirred

solution of ice-cold 10% sulfuric acid (1 000 ml). The crystalline chloroform-soluble product was recrystallized twice from chloroform–petrol (b.p. 35–60°) and gave large colorless prisms (15.5 g, 59%) of m.p. 90–91° and $[\alpha]_D$ +115° (*c*, 0.9 in chloroform).

Anal. Found: C, 16.3; H, 1.9; Cl, 28.2; S, 19.0. Calcd. for $C_7H_{10}Cl_4O_{11}S_3$: C, 16.5; H, 2.0; Cl, 27.9; S, 18.9.

Methyl 6-Chloro-6-deoxy-α-D-glucopyranoside

The compound II (5 g) was dissolved in methanol and dechlorosulfated as described previously (4). The product (2.5 g, 60%) was recrystallized from benzene–methanol to give colorless plates (1.5 g, 36%) of m.p. 110–111° and $[\alpha]_D$ +187° (*c*, 1.25 in water). The physical constants are consistent with those reported for methyl 6-chloro-6-deoxy-α-D-glucopyranoside (9).

Periodate Oxidation of Methyl 6-Chloro-6-deoxy-α-D-glucopyranoside

The moles of periodate consumed and the moles of formic acid produced were respectively as follows: 0.57, 0.26 (1 h); 1.60, 0.71 (7 h); 1.91, 1.05 (21 h); 1.99, 1.07 (46 h).

Methyl 6-Chloro-6-deoxy-α-D-glucopyranoside 2,3,4-Trichlorosulfate (II)

Methyl α-D-glucopyranoside 2,3,4,6-tetrachlorosulfate (8 g) was dissolved in chloroform (70 ml) and anhydrous pyridine hydrochloride (1.6 g, 1 mole) was added, and the solution was heated at 40–50° for 2 h. The chloroform solution was then washed with sodium bicarbonate solution and distilled water and dried over anhydrous sodium sulfate. Concentration of the chloroform solution gave a syrup which crystallized. Recrystallization from chloroform–petrol (b.p. 40–60°) gave large colorless plates (4.5 g, 65%) of m.p. 90–91°, undepressed on admixture with previously prepared methyl 6-chloro-6-deoxy-α-D-glucopyranoside 2,3,4-trichlorosulfate.

Methyl 4,6-Dichloro-4,6-dideoxy-α-D-galactopyranoside (III)

Compound I (1.1 g) was dissolved in chloroform (20 ml) and after the addition of anhydrous pyridine hydrochloride (1 g, 4.4 mole) the solution was heated at 40–50° for 8 h. The product isolated as described above was dechlorosulfated (4) and the resulting solid was recrystallized from chloroform–petrol (b.p. 40–60°) to give needles (0.42 g, 84%) of m.p. 158°, undepressed on admixture with authentic methyl 4,6-dichloro-4,6-dideoxy-α-D-galactopyranoside (2).

Methyl 6-Chloro-6-deoxy-β-D-glucopyranoside 2,3,4-Trichlorosulfate (IV)

Methyl β-D-glucopyranoside (4.5 g), prepared from acetobromglucose (29), was treated with sulfuryl chloride (12 ml) and pyridine (18 ml) in chloroform solution (3). Removal of the solvent gave a product (6 g, 54%) which was recrystallized from chloroform–petrol (b.p. 40–60°) to give colorless needles (1.1 g, 10%)* of m.p. 134–135° and $[\alpha]_D$ +1.7° (*c*, 1.2 in chloroform).

Anal. Found: C, 16.7; H, 2.0; Cl, 27.5; S, 18.9. Calcd. for $C_7H_{10}Cl_4O_{11}S_3$: C, 16.5; H, 2.0; Cl, 27.9; S, 18.9.

Methyl 6-Chloro-6-deoxy-β-D-glucopyranoside

The crystals of IV (0.5 g) were dechlorosulfated as described previously (4) and the product (0.2 g, 95%) was recrystallized from benzene–methanol to give large colorless crystals of m.p. 157–159° and $[\alpha]_D$ −50° (*c*, 1.0 in water) (10).

Periodate Oxidation of Methyl 6-Chloro-6-deoxy-β-D-glucopyranoside

The moles of periodate consumed and the moles of formic acid produced per mole of sugar were respectively as follows: 0.60, 0.28 (1 h); 1.65, 0.75 (7 h); 1.90, 0.98 (21 h); 1.98, 1.00 (46 h).

Methyl 4,6-Dichloro-4,6-dideoxy-β-D-galactopyranoside (V)

The crystals of methyl 6-chloro-6-deoxy-β-D-glucopyranoside 2,3,4-trichlorosulfate (4 g) were dissolved in chloroform and anhydrous pyridine hydrochloride (4 g) was added to the solution. The chloroform solution was heated at 50° for 14 h and the syrupy product (3 g) isolated in the usual way had $[\alpha]_D$ −5.5° (*c*, 0.9 in chloroform). Dechlorosulfation (4), followed by continuous extraction with chloroform, gave a crystalline residue of m.p. 142°. Recrystallization from chloroform–petrol (b.p. 35–60°) gave colorless needles (1.2 g, 75%) of m.p. 144–146° and $[\alpha]_D$ −16° (*c*, 1.2 in water). Successive recrystallizations from ether did not raise the melting point to that of authentic methyl 4,6-dichloro-4,6-dideoxy-β-D-galactoside (m.p. 154°) (3).

4,6-Dichloro-4,6-dideoxy-D-galactose

A solution of the above impure preparation of V (0.4 g) was refluxed in *N* sulfuric acid (50 ml) for 16 h. The acidic solution was neutralized ($BaCO_3$) and filtered. Concentration of the aqueous solution gave colorless, syrupy crystals (0.3 g), paper chromatographic analysis in solvent *a* indicated the presence of three reducing components at R_x 1.4 (slight), R_x 2.2 (slight), and R_x 2.9 (intense). The component at R_x 2.9 was found to be chromatographically indistinguishable from 4,6-dichloro-4,6-dideoxy-D-galactose (5). Recrystallization of the syrupy crystals from methanol–water gave colorless crystals (0.1 g, 27%) of m.p. 184–186°, undepressed in admixture with authentic 4,6-dichloro-4,6-dideoxy-D-galactose (5).

**A repetition of this experiment, by Mr. A. Cottrell, showed (t.l.c.) that the non-crystalline material was mainly the 4,6-dichloro-4,6-dideoxy-β-D-galactopyranoside derivative.*

Can. J. Chem. Downloaded from www.nrcresearchpress.com by 210.87.254.105 on 09/05/12
For personal use only.

6-Chloro-6-deoxy-α-D-mannosyl Chloride 2,3,4-Trichlorosulfate (VI)

D-Mannose (25 g) was treated with sulfuryl chloride (63 ml) and pyridine (100 ml) in chloroform solution (3), and the reaction mixture was allowed to stand at room temperature for 7 h before isolation of the product as described above. Concentration of the chloroform extracts and recrystallization of the residue (31 g,) 44% from chloroform–petrol (b.p. 40–60°) gave large colorless crystals (15 g, 21%) of m.p. 156° and $[\alpha]_D$ +52° (*c*, 1.2 in chloroform).

Anal. Found: C, 14.3; H, 1.2; Cl, 34.5; S, 18.5. Calcd. for $C_6H_7Cl_5O_{10}S_3$: C, 14.1; H, 1.3; Cl, 34.6; S, 18.6.

Methyl 6-Chloro-6-deoxy-α-D-mannopyranoside

A solution of VI (10 g) in anhydrous methanol (100 ml) was refluxed for 8 h. The resulting glycoside(s) were dechlorosulfated (4) and the product, a colorless syrup (4.0 g, 96%) had $[\alpha]_D$ +60° (*c*, 1.0 in water). Paper chromatograms developed in solvent *a* and sprayed with periodic acid – *p*-anisidine hydrochloride (30) indicated that the syrup contained three components at R_x 2.1 (trace), R_x 2.5 (slight), and R_x 3.0 (intense). All of the components were non-reducing (negative test with *p*-anisidine hydrochloride).

6-Chloro-6-deoxy-D-mannose

The above syrup (3.0 g) was dissolved in *N* sulfuric acid and the solution was boiled for 7 h. The solution was neutralized with barium carbonate and filtered. Concentration of the aqueous solution gave a syrup (2.5 g). Paper chromatographic analysis in solvent *a* indicated three reducing components at R_x 0.7 (trace), R_x 1.6 (slight), and R_x 2.1 (intense). The syrup (0.8 g) gave a crystalline 3,5-dichloro phenylhydrazone which was recrystallized from chloroform–ethyl acetate to give yellow plates (0.9 g, 62%) of m.p. 149° (decomp.).

Anal. Found: C, 39.9; H, 4.1; Cl, 29.6; N, 8.0. Calcd. for $C_{12}H_{15}Cl_3N_2O_4$: C, 40.2; H, 4.2; Cl, 29.8; N, 7.8.

The 3,5-dichlorophenylhydrazone (0.8 g) was converted to the reducing sugar by the procedure of Sowden and Fischer (12). Concentration of the water-soluble fraction gave a colorless syrup (0.35 g, 79%) $[\alpha]_D$ +18° (*c*, 1.0 in water) which was shown to be chromatographically pure in solvents *a* and *b*. The syrup with phenylhydrazine in the cold gave a crystalline phenylhydrazone, m.p. 141–142° (decomp.).

Anal. Found: C, 50.1; H, 6.1; Cl, 12.3; N, 9.7. Calcd. for $C_{12}H_{17}ClN_2O_4$: C, 49.9; H, 5.9; Cl, 12.3; N, 9.7.

The phenylhydrazone, on further heating with phenylhydrazine acetate, gave a crystalline phenylosazone. Two recrystallizations from ethanol–water gave yellow needles of m.p. 165–168° (decomp.), undepressed on admixture with 6-chloro-6-deoxy-D-glucose phenylosazone (3). The infrared spectra of the two phenylosazones were also identical (0.8% in potassium bromide).

Further Chloro-substitution of 6-Chloro-6-deoxy-α-D-mannosyl Chloride 2,3,4-Trichlorosulfate (VII)

The crystals of the 6-chloro-6-deoxy-D-mannosyl chloride derivative (8 g) were dissolved in chloroform (150 ml) and anhydrous pyridine hydrochloride (6 g) was added to the solution. The chloroform solution was heated at 50° for 20 h the product isolated in the usual way, was recrystallized from chloroform–petrol (b.p. 40–60°) yielding large prisms (1.5 g, 27%) of m.p. 147° (decomp.) and $[\alpha]_D$ +65° (*c*, 1.2 in chloroform).

Anal. Found: C, 20.5; H, 2.1; Cl, 50.5; S, 9.4. Calcd. for a tetrachloro-monochlorosulfate derivative $C_6H_7Cl_5O_4S$: C, 20.4; H, 2.0; Cl, 50.0; S, 9.1.

Methyl Trichloro-trideoxy-α-D-hexoside

A solution of VII (2.5 g) in anhydrous methanol (200 ml) was boiled under reflux. The resultant glycoside was dechlorosulfated (4) and the product was crystallized from chloroform–petrol (b.p. 40–60°) to give colorless needles (0.4 g, 33%) of m.p. 122–123° and $[\alpha]_D$ +81° (*c*, 0.9 in chloroform), and +122° (*c*, 0.9 in methanol).

Anal. Found: C, 33.5; H, 4.1; Cl, 43.1. Calcd. for $C_7H_{11}Cl_3O_3$: C, 33.6;H, 4.4; Cl, 42.6.

Hydrolysis of the Methyl Trichloro-trideoxy-α-D-hexoside

The above glycoside was unaffected by boiling *N* sulfuric acid during 16 h. Hydrolysis in 25% sulfuric acid for 5 h yielded a complex mixture of reducing components as was indicated by thin-layer chromatographic analysis. All attempts to obtain a crystalline derivative of the hydrolysis product have so far failed.

Methyl 6-Chloro-6-deoxy-α-D-mannopyranoside 2,3,4-Trichlorosulfate (VII)

Methyl α-D-mannopyranoside (20 g) was treated with sulfuryl chloride (52 ml) and pyridine (80 ml) in chloroform solution (3). The chloroform extracts were concentrated to give a syrup which rapidly crystallized. Recrystallization from chloroform–petrol (b.p. 40–60°) (×2) gave large colorless prisms (15 g, 29%) of m.p. 134° and $[\alpha]_D$ +19° (*c*, 1.2 in chloroform).

Anal. Found: C, 16.7; H, 2.0; Cl, 27.8; S, 18.9. Calcd. for $C_7H_{10}Cl_4O_{11}S_3$: C, 16.5; H, 2.0; Cl, 27.9; S, 18.9.

Methyl 6-Chloro-6-deoxy-α-D-mannopyranoside

Compound VII (10 g) was dechlorosulfated and the syrupy product (4 g, 100%) which was isolated in the usual way had $[\alpha]_D$ +59° (*c*, 1.1 in water). Paper chromatograms developed in solvent *a* and sprayed with periodic acid – *p*-anisidine hydrochloride (30) indicated that the syrup contained two components at R_x 2.5 (slight) and R_x 3.0 (intense). Hydrolysis of the syrup (*N* sulfuric acid, 7 h at 100°) gave a reducing syrupy product, which yielded a crystalline phenylhydrazone derivative of m.p. 140° (decomp.), undepressed on admixture with an authentic sample.

Can. J. Chem. Downloaded from www.nrcresearchpress.com by 210.87.254.105 on 09/05/12
For personal use only.

Methyl 3,6-Anhydro-α-D-mannopyranoside

The syrupy methyl 6-chloro-6-deoxy-D-mannoside (0.5 g) (above) was dissolved in *N* sodium hydroxide (5 ml), and the solution was allowed to stand at room temperature for 10 h. The solution was deionized and concentrated to a syrup (0.4 g, 100%) which crystallized when seeded with authentic methyl 3,6-anhydro-α-D-mannopyranoside. Recrystallization from benzene gave colorless crystals (0.15 g, 36%) of m.p. 129°, undepressed on admixture with the authentic compound (13).

Attempt to Obtain Further Chloro-substitution of Methyl 6-Chloro-6-deoxy-α-D-mannopyranoside 2,3,4-Trichlorosulfate (VII)

The crystals of the methyl glycoside (6 g) (VII) were dissolved in chloroform (40 ml) and anhydrous pyridine hydrochloride (4 g) was added to the solution. After the solution had been heated at 50° for 12 h the product was recrystallized from chloroform–petrol (b.p. 40–60°) to yield colorless prisms (4.5 g, 75%) of m.p. 134°, undepressed on admixture with the starting material.

Methyl 4,6-Dichloro-4,6-dideoxy-α-D-glucopyranoside 2,3-Dichlorosulfate (VIII)

Methyl α-D-galactopyranoside (31) (10 g) was treated with sulfuryl chloride (26 ml) and pyridine (40 ml) in chloroform solution (3). The reaction mixture was allowed to stand at room temperature for 12 h before the chloroform-soluble product was isolated. It was recrystallized from chloroform–petrol (b.p. 40–60°) to give large colorless prisms (6 g, 27%) of m.p. 122–124° and $[\alpha]_D$ +68° (*c*, 2.66 in chloroform).

Anal. Found: C, 19.6; H, 2.2; Cl, 32.9; S, 14.6. Calcd. for $C_7H_{10}Cl_4O_8S_2$: C, 19.6; H, 2.3; Cl, 33.2; S, 15.0.

Methyl 4,6-Dichloro-4,6-dideoxy-α-D-glucopyranoside

Compound VIII (6 g) was dechlorosulfated (4) and the product isolated in the usual way. It (3 g, 93%) was recrystallized from chloroform–petrol (b.p. 40–60°) and had m.p. 119–121°, undepressed on admixture with authentic methyl 4,6-dichloro-4,6-dideoxy-α-D-glucopyranoside (2).

4,6-Dichloro-4,6-dideoxy-α-D-glucose

The crystalline methyl glycoside was unaffected by hot *N* sulfuric acid. Therefore, more drastic conditions were tried.

The glycoside (3 g) was dissolved in 3 *N* sulfuric acid and the solution was refluxed for 24 h. The solution was neutralized ($BaCO_3$) and filtered and the filtrate was concentrated to a solid. Recrystallization from chloroform gave colorless needles of m.p. 136–137° and $[\alpha]_D$ +49° (10 minutes) → +25° (24 h, equilibrium) (*c*, 1.1 in water). The crystals reduced Fehlings' solution and gave a positive tetrazolium red test (15).

Anal. Found: C, 33.0; H, 4.6; Cl, 32.9. Calcd. for $C_6H_{10}Cl_2O_4$: C, 33.2; H, 4.6; Cl, 32.8.

The crystals formed a crystalline phenylosazone which, when recrystallized from ethanol–water, had m.p. 129–131° (decomp.).

Anal. Found: C, 54.4; H, 4.8; Cl, 18.0; N, 14.4. Calcd. for $C_{18}H_{20}Cl_2N_4O_2$: C, 54.6; H, 5.1; Cl, 18.0; N, 14.2.

Attempt to Obtain Further Chloro-substitution of Methyl 4,6-Dichloro-4,6-dideoxy-α-D-glucopyranoside 2,3-Dichlorosulfate

The crystals of the 2,3-dichlorosulfate (4.5 g) were dissolved in chloroform (25 ml) and anhydrous pyridine hydrochloride (4 g) was added to the chloroform solution. The solution was heated at 50° for 18 h, and the products were then isolated in the usual way. Recrystallization from methanol–water gave large crystals (1.5 g, 33%) of m.p. 124°, undepressed on admixture with the starting compound. The mother liquors were concentrated to a syrup (2.5 g) which was dechlorosulfated (4). The dechlorosulfated products were examined by gas–liquid chromatographic analysis using a column (A) and the results are shown in Table I.

TABLE I

Gas–liquid chromatographic analysis of the dechlorosulfated products from VIII

Compound or mixture	Components	Retention time relative to compound 1	Estimated % of individual compounds in mixture
(1) Methyl 4,6-dichloro 4,6-dideoxy-α-D-glucopyranoside	1	1.000	—
(2) Methyl 3,4,6-trichloro 3,4,6-trideoxy-α-D-allopyranoside	1	0.545	—
(3) Syrup from experiment above	1	0.246	3–4
	2	0.324	3–4
	3	0.545	1
	4	1.000	90

3,4,6-Trichloro-3,4,6-trideoxy-D-allosyl Chloride 2-Monochlorosulfate (XI)

D-Galactose (10 g) was treated with sulfuryl chloride (26 ml) and pyridine (40 ml) in chloroform solution (3). Concentration of the chloroform extracts gave a syrup (9.5 g) which had $[\alpha]_D$ −7° (*c*, 5.0 in chloroform).

Can. J. Chem. Downloaded from www.nrcresearchpress.com by 210.87.254.105 on 09/05/12
For personal use only.

Can. J. Chem. Downloaded from www.nrcresearchpress.com by 210.87.254.105 on 09/05/12
For personal use only.

Paper chromatograms developed in solvent *a* and sprayed with aniline-pyridine reagent (3) indicated that the syrup was a mixture of two components.

*Methyl 3,4,6-Trichloro-3,4,6-trideoxy-β-*D*-allopyranoside (XII)*

The above syrup (XI) (9 g) was dissolved in anhydrous methanol and the solution was refluxed to form the methyl glycoside(s). The methyl glycoside(s) was dechlorosulfated (4) and the product was crystallized from water to give colorless needles (1.5 g, 11%) of m.p. 116° and $[\alpha]_D$ +159° (*c*, 1.8 in methanol).

Anal. Found: C, 33.6; H, 4.4; Cl, 42.3. Calcd. for $C_7H_{11}Cl_3O_3$: C, 33.6; H, 4.4; Cl, 42.6.

The overall yield of this product could be increased to 36% by first dissolving the original syrup, obtained from the reaction of sulfuryl chloride with D-galactose, in chloroform, and heating the resultant solution with anhydrous pyridine hydrochloride at 50° for 16 h, followed by the methanolysis and dechlorosulfation of the product. Methylation of the methyl trichlorotrideoxy glycoside by the method of Purdie (32) gave a crystalline monomethyl derivative which, when recrystallized from *n*-hexane, gave colorless needles of m.p. 68–69° and $[\alpha]_D$ +116° (*c*, 1.12 in methanol).

Anal. Found: C, 36.7; H, 4.8; Cl, 39.7. Calcd. for $C_8H_{13}Cl_3O_3$: C, 36.5; H, 4.9; Cl, 40.0.

The methyl trichloro-trideoxy glycoside also gave a crystalline monotosylate which, when recrystallized from ethanol, had m.p. 120–121°.

Anal. Found: C, 41.9; H, 4.2; Cl, 26.6; S, 8.1. Calcd. for $C_{14}H_{17}Cl_3O_5S$: C, 41.6; H, 4.2; Cl, 26.4, S, 7.9.

*Attempted Reaction of Methyl 3,4,6-Trichloro-3,4,6-trideoxy-α-*D*-allopyranoside (XII) with Sodium Hydroxide*

The crystals of the methyl glycoside (0.05 g) were dissolved in methanol (5 ml) and 0.1 *N* sodium hydroxide (5 ml) was added to the solution. The reaction mixture was left at room temperature for 8 h, and then was deionized. The solution was concentrated to a solid which was recrystallized from water. It had m.p. 116°, which was undepressed on admixture with the starting compound.

*3,4,6-Trichloro-3,4,6-trideoxy-*D*-allose (XIII)*

The original syrup obtained from the reaction of sulfuryl chloride with D-galactose (10 g) was dissolved in acetone (200 ml) and barium carbonate (30 g) was added and the heterogeneous mixture was stirred. Sodium iodide solution (5 g in 20 ml water) was added drop by drop until the formation of iodine had ceased. The solution was filtered and the filtrate was concentrated. The residue was dissolved in water and the aqueous solution was continuously extracted with chloroform for 10 h. Concentration of the chloroform solution and recrystallization from chloroform gave colorless crystals (1.9 g, 29%) of m.p. 170–171°. The crystals reduced Fehling's solution and gave a negative tetrazolium red test (15). The same crystalline compound was also obtained by the hydrolysis of methyl 3,4,6-trichloro-3,4,6-trideoxy-α-D-alloside with *N* sulfuric acid under reflux for 10 h.

The crystals failed to give a phenylosazone or a *p*-nitrophenylosazone but gave a crystalline *p*-nitrophenylhydrazone, which, when recrystallized from methanol–water, had m.p. 105° (decomp.) and $[\alpha]_D$ −58° (*c*, 0.75 in methanol).

Anal. Found: Cl, 28.5; N, 11.4. Calcd. for $C_{12}H_{13}Cl_3N_3O_4$: Cl, 28.8; N, 11.3.

Paper electrophoresis of the crystalline trichlorohexose in buffer solution i gave the results shown in Table II.

TABLE II

Paper electrophoresis of 3,4,6-trichloro-3,4,6-trideoxy-D-allose (XIII)

Compound	Electrophoretic mobility, mg × 10^2
3,4,6-Trichloro-3,4,6-trideoxy-D-allose	23
3,4,6-Tri-*O*-methyl-D-glucose	29
2,4,6-Tri-*O*-methyl-D-glucose	0

The crystalline trichlorohexose failed (*a*) to form an 1,2,-*O*-isopropylidene derivative, (*b*) to re-form the methyl glycoside by refluxing the sugar in a 2% (w/w) anhydrous solution of hydrochloric acid in methanol, and (*c*) to be reduced to the trichloro-trideoxy-hexitol (33). In each case the crystalline starting material was obtained.

*1,6-Anhydro-3,4-dichloro-3,4-dideoxy-*D*-allose (XVI)*

The crystals of the trichlorohexose (0.5 g) were dissolved in water and treated with 0.1 *N* sodium hydroxide (21 ml, 1 mole). The alkali reacted rapidly and the neutral solution was then continuously extracted with chloroform. The chloroform extracts were concentrated to a solid which, on recrystallization from benzene–petrol (b.p. 60–80°), gave colorless crystals (0.3 g, 77%) of m.p. 94° and $[\alpha]_D$ −96° (*c*, 1.1 in methanol). The crystals did not reduce Fehling's solution and did not appear as reducing spots when paper chromatograms developed in solvent *a* were sprayed with *p*-anisidine hydrochloride, or with the alkaline silver nitrate spray.

Anal. Found: C, 36.3; H, 4.0; Cl, 35.4. Calcd. for $C_6H_8Cl_2O_3$: C, 36.2; H, 4.0; Cl, 35.7.

Methyl 3,4,6-Trichloro-3,4,6-trideoxy-β-D-allopyranoside 2-Monochlorosulfate (XIV)

Methyl β-D-galactopyranoside (5 g) was treated with sulfuryl chloride (13 ml) and pyridine (20 ml) in chloroform solution (3). The reaction mixture was allowed to stand at room temperature for 12 h. The chloroform extracts on concentration gave a dark-colored syrup which was decolorized (5 g, 56%).

Methyl 3,4,6-Trichloro-3,4,6-trideoxy-β-D-allopyranoside (XV)

The above syrup (XIV) (5 g) was dechlorosulfated (4) and the syrupy product (2.5 g, 71%) of $[\alpha]_D$ −12.8° (*c*, 1.18 in methanol) was isolated in the usual way.

Anal. Found: C, 34.4; H, 4.3; Cl, 41.7. Calcd. for $C_7H_{11}Cl_3O_3$: C, 33.6; H, 4.4; Cl, 42.6.

The syrup appeared homogeneous by thin-layer chromatographic analysis, also hydrolysis of the syrupy glycoside in 2 *N* sulfuric acid gave a crystalline trichlorohexose of m.p. 170°, undepressed on admixture with the previously isolated 3,4,6-trichloro-3,4,6-trideoxy-D-allose.

Formation of 3,4,6-Trichloro-3,4,6-trideoxy-D-allose from 4,6-Dichloro-4,6-dideoxy-D-glucose

Crystalline 4,6-dichloro-4,6-dideoxy-D-glucose (0.15 g) was treated with sulfuryl chloride (0.4 ml) and pyridine (0.6 ml) in chloroform solution (3). The chloroform soluble product was redissolved in chloroform and heated at 50° for 8 hours with anhydrous pyridine hydrochloride (0.2 g). The syrupy product (0.2 g), isolated from the reaction mixture in the usual way, on methanolysis and dechlorosulfation (4) gave a syrup (0.1 g) which was shown by thin-layer chromatography to be chromatographically indistinguishable from methyl 3,4,6-trichloro-3,4,6-trideoxy-β-D-allopyranoside. Hydrolysis of the syrupy glycoside in *N* sulfuric acid gave a crystalline trichlorohexose of m.p. 171°–172°, undepressed on admixture with 3,4,6-trichloro-3,4,6-trideoxy-D-allose.

Reaction of Sulfuryl Chloride with 4,6-O-Ethylidene-D-galactopyranose

4,6-*O*-Ethylidene-D-galactose (10 g) (34) was treated with sulfuryl chloride (21 ml) and pyridine (40 ml) in chloroform solution (3). Concentration of the chloroform extracts gave a solid which was recrystallized from chloroform–petrol (b.p. 40–60°) to give large colorless prisms (6 g, 30%) of m.p. 133–135° and $[\alpha]_D$ +207° (*c*, 1.12 in chloroform).

Anal. Found: C, 22.7; H, 2.5; Cl, 25.4; S, 15.1. Calcd. for $C_8H_{11}Cl_3O_9S_2$: C, 22.8; H, 2.6; Cl, 25.3; S, 15.2.

A small quantity of the crystals were dechlorosulfated (4), and paper chromatographic analysis of the resultant methanol solution in solvents *a* and *b* indicated two reducing components which were chromatographically indistinguishable from D-galactose and 4,6-*O*-ethylidene-D-galactose (34).

Methyl 4,6-O-Benzylidene-3-chloro-3-deoxy-β-D-allopyranoside (XVIII)

Methyl 4,6-*O*-benzylidene-β-D-glucopyranoside (4 g) (17) was treated with sulfuryl chloride (10.4 ml) and pyridine (16 ml) in chloroform solution (3). The chloroform extracts were concentrated to a syrup (6 g) (XVIII). The substance was dechlorosulfated (4) in the presence of barium carbonate to prevent the removal of the benzylidene group. The resulting syrupy product (4 g) was extracted with a solution of benzene–petrol (b.p. 40–60°) (1:2) leaving a crystalline residue (0.2 g). Recrystallization of the residue from acetone gave needles of m.p. 199°, undepressed on admixture with authentic methyl 4,6-*O*-benzylidene-β-D-glucoside (7). The benzene–petrol extract was concentrated to a syrup (2.8 g) which had $[\alpha]_D$ −30° (*c*, 1.05 in methanol) and was shown to be homogeneous by thin-layer chromatographic analysis (XVIII, R = H).

Methyl 3-Chloro-3-deoxy-β-D-allopyranoside (XIX)

The above syrup (XVIII) (2.8 g) was dissolved in methanol (15 ml) and 0.1 *N* sulfuric acid (15 ml) was added to the solution. The solution was heated at 50° for 2 h, neutralized ($BaCO_3$) and filtered, and the filtrate was extracted with ether to remove the liberated benzaldehyde. The aqueous solution was deionized and concentrated to a syrup (1.5 g, 75%) of $[\alpha]_D$ −49° (*c*, 1.0 in water) which was shown to be homogeneous by thin-layer chromatographic analysis. Periodate oxidation of the syrup resulted in no consumption of periodate up to a reaction time of 60 h.

The syrup gave a syrupy triacetate derivative which had $[\alpha]_D$ −21° (*c*, 1.15 in methanol).

Anal. Found: C, 46.1; H, 6.0; Cl, 10.4. Calcd. for $C_{13}H_{19}ClO_8$; C, 46.1; H, 5.6; Cl, 10.5.

Gas liquid chromatographic analysis of the triacetate using column (B) gave one sharp peak which had a retention time of 12.3 min.

3-Chloro-3-decxy-D-allose (XX)

The syrupy monochloro methyl glycoside (XIX) (0.3 g) was refluxed in 2 *N* sulfuric acid for 16 h. The solution was neutralized and concentrated to a syrup (0.25 g, 89%), which had $[\alpha]_D$ +5.4° (*c*, 0.92 in water). Attempts to form phenylosazone, *p*-nitrophenylosazone, and *p*-nitrophenylhydrazone derivatives were unsuccessful. Paper chromatographic analysis of the syrup in solvent *a* indicated one reducing component at R_x 1.5. The syrup also gave a negative tetrazolium red test (15). Paper electrophoresis of the syrup in buffer solutions i and ii gave the following results shown in Tables III and IV respectively.

Effect of Sodium Hydroxide on Methyl 3-Chloro-3-deoxy-β-D-allopyranoside

The syrupy monochloro methyl glycoside (0.25 g) was dissolved in *N* sodium hydroxide (5 ml) and the solution was allowed to stand for 16 h at room temperature. It was deionized, and concentrated to a syrup (0.2 g) which had $[\alpha]_D$ +28° (*c*, 1.0 in methanol). It was hydrolyzed by the same method used in the previous

Can. J. Chem. Downloaded from www.nrcresearchpress.com by 210.87.254.105 on 09/05/12
For personal use only.

TABLE III

Paper electrophoresis of 3-chloro-3-deoxy-D-allose in buffer solution i

Compound	Electrophoretic mobility, mg × 10^2
Hydrolysis product (above)	84.5
2-*O*-Methyl-D-glucose	23
3-*O*-Methyl-D-glucose	80
3,6-Anhydro-D-glucose	82

TABLE IV

Paper electrophoresis of 3-chloro-3-deoxy-D-allose in buffer solution ii

Compound	Electrophoretic mobility, mg × 10^2
Hydrolysis product (above)	0
3,6-Anhydro-D-glucose	29

experiment and gave another syrup. Paper chromatography in solvent *a* and paper electrophoresis in buffer solutions i and ii of the syrup, all indicated one component indistinguishable from 3-chloro-3-deoxy-D-allose.

The reaction with *N* sodium hydroxide solution was repeated and the solution was heated at 50–60° for 10 h and then allowed to stand at room temperature for a further 16 h. The solution was deionized, and concentrated to a syrup (0.22 g) which had $[\alpha]_D$ −27° (*c*, 0.93 in methanol). The syrup gave an acetate derivative which did not crystallize and had $[\alpha]_D$ −22° (*c*, 1.32 in methanol). Gas–liquid chromatographic analysis of the derived acetate gave one sharp peak with a retention time (12.3 minutes) identical with that of methyl 3-chloro-3-deoxy-β-D-allopyranoside triacetate, when carried out using similar conditions.

ACKNOWLEDGMENTS

The authors thank the National Research Council (N.R.C. T-19) for a grant. They also thank Dr. E. Buncel for helpful discussions and Dr. H. G. Jones for carrying out the gas–liquid chromatographic analysis and for a gift of 3,4,6-tri-*O*-methyl-D-glucose.

REFERENCES

1. B. HELFERICH. Ber. **54**, 1082 (1921).
2. J. K. N. JONES, M. B. PERRY, and J. C. TURNER. Can. J. Chem. **38**, 1122 (1960).
3. H. J. JENNINGS and J. K. N. JONES. Can. J. Chem. **40**, 1408 (1962).
4. H. J. JENNINGS and J. K. N. JONES. Can. J. Chem. **41**, 1151 (1963).
5. P. D. BRAGG, J. K. N. JONES, and J. C. TURNER. Can. J. Chem. **37**, 1412 (1959).
6. B. HELFERICH, A. LOWA, W. NIPPE, and H. RIEDEL. Ber. **56**, 1083 (1923).
7. B. HELFERICH, G. SPROEK, and E. BESLER. Ber. **58**, 886 (1925).
8. K. HESS and H. STENZEL. Ber. **68**, 981 (1935).
9. B. HELFERICH, W. KLEIN, and W. SCHÄFER. Ber. **59**, 79 (1926).
10. B. HELFERICH and A. SCHNEIDMÜLLER. Ber. **60**, 2002 (1927).
11. E. PACSU. Ber. **61**, 1508 (1928).
12. J. C. SOWDEN and H. O. L. FISCHER. J. Am. Chem. Soc. **69**, 1963 (1947).
13. R. B. DUFF and E. G. V. PERCIVAL. J. Chem. Soc. 830 (1941).
14. H. J. JENNINGS. Ph.D. Thesis, Queen's University, Kingston, Ontario. 1964.
15. K. WALLENFELS, E. BERNT, and C. LINBURG. Angew. Chem. **65**, 581 (1953).
16. J. L. FRAHN and J. A. MILLS. Australian J. Chem. **12**, 65 (1959).
17. K. FREUDENBURG, H. TOEPFFER, and C. C. ANDERSON. Ber. **61**, 1758 (1928).
18. F. H. NEWTH, W. G. OVEREND, and L. F. WIGGINS. J. Chem. Soc. 10 (1947).
19. J. W. H. OLDHAM and J. K. RUTHERFORD. J. Am. Chem. Soc. **54**, 366 (1932).
20. M. S. NEWMAN. J. Chem. Educ. **32**, 344 (1955).
21. D. J. CRAM and F. A. ABD. ELHAFEZ. J. Am. Chem. Soc. **74**, 5851 (1952).
22. F. B. TUTWILER and R. L. MCKEE. J. Am. Chem. Soc. **76**, 6342 (1954).
23. J. L. FRAHN and J. A. MILLS. Chem. Ind. London, 578 (1956).
24. E. J. BOURNE, D. H. HUTSON, and H. WIEGEL. J. Chem. Soc. 4252 (1960).
25. L. HOUGH, J. K. N. JONES, and W. H. WADMAN. J. Chem. Soc. 1702 (1950).
26. W. E. TREVELYAN, D. D. PROCTOR, and J. S. HARRISON. Nature, **166**, 444 (1950).
27. G. NEUMÜLLER and E. VASSEUR. Arkiv. Kemi, **5**, 235 (1953).
28. D. M. W. ANDERSON, C. T. GREENWOOD, and E. L. HIRST. J. Chem. Soc. 225 (1955).

Can. J. Chem. Downloaded from www.nrcresearchpress.com by 210.87.254.105 on 09/05/12
For personal use only.

29. M. BÁRCZAI-MARTOS and F. KOROSY. Nature, **165**, 369 (1950).
30. J. A. CIFONELLI and F. SMITH. Anal. Chem. **26**, 1132 (1954).
31. J. K. DALE and C. S. HUDSON. J. Am. Chem. Soc. **52**, 2534 (1930).
32. T. PURDIE. J. Chem. Soc. **83**, 1021 (1903).
33. H. C. BROWN. J. Org. Chem. **22**, 1136 (1957).
34. D. H. BALL and J. K. N. JONES. J. Chem. Soc. 905 (1958).

Can. J. Chem. Downloaded from www.nrcresearchpress.com by 210.87.254.105 on 09/05/12
For personal use only.

THE NATURE OF ASSOCIATION BETWEEN MOLECULES OF N-METHYLPYRROLE

HUGH J. ANDERSON
Department of Chemistry, Memorial University of Newfoundland, St. John's, Newfoundland
Received April 2, 1965

ABSTRACT

The dilution of N-methylpyrrole by an inert solvent causes a change in the values of the proton chemical shifts which has been interpreted to support a "closed cyclic dimer" type of association between molecules. Equilibrium constants have been computed for the monomer–dimer system at two temperatures. The proton chemical shifts have been determined for the pure liquid at a series of temperatures covering a wide range. The effects of dilution in several different solvents have also been investigated.

Can. J. Chem. Downloaded from www.nrcresearchpress.com by 210.87.254.40 on 09/05/12
For personal use only.

There has been some dispute over the nature of the association which takes place between pyrrole molecules in the pure liquid as related to the interpretation of infrared spectra (1, 2). However, the investigations of dipole moments by Lumbroso (3) and of nuclear magnetic resonance spectra by Happe (4) lend much support to their view that the association involves two molecules in the form of a "closed cyclic dimer" where the N-H of each molecule is hydrogen bonded by the π-electron cloud of the other molecule. Since these hydrogen bonds are non-linear, the force of attraction involved is far less than that of the usual hydrogen bond, probably of the order of 20–30% of the energy according to dipole moment calculations. Values for the self-association constant, as determined by the two methods, using a series of concentrations approaching infinite dilution in cyclohexane, were found to be in reasonable agreement when converted to the same units (5), and temperature differences were considered.

A dipole moment study of N-methylpyrrole (3(*a*)) indicated that this compound was also associated to some extent in an apparently similar spatial arrangement. This equilibrium system was found to have roughly similar self-association constants in both cyclohexane and carbon tetrachloride solutions to those found for the pyrrole equilibrium by the same method.

While assembling data on the n.m.r. chemical shifts of pyrrole derivatives in carbon tetrachloride we observed a variation with dilution of all of the proton signals of N-methylpyrrole. The changes of δ involved were of a magnitude similar to those observed during the dilution of pyrrole itself. To provide a comparison with the dipole moment results a series of measurements was carried out on N-methylpyrrole at increasing dilution in cyclohexane at the normal probe temperature (38 °C).

Table I shows the change in chemical shifts observed for the protons of N-methylpyrrole as this compound was diluted with cyclohexane. A similar series of measurements on solutions at 0 °C are shown in Table II. The assumption was made that the only associated form present was the dimer and that, with dilution, its concentration would decrease until at infinite dilution only monomeric N-methylpyrrole would be present. Thus the chemical shifts at infinite dilution would be those of the pure monomeric form, while in more concentrated solutions increasing amounts of the dimer would be present.

Following the arguments of Happe and of Lumbroso it was decided to assume the simplest possible situation where the only association was a dimeric one. Although other polymeric forms might well be present in liquid N-methylpyrrole, calculations involving

TABLE I

Chemical shifts of protons of N-methylpyrrole in cyclohexane at 38 °C*

Molarity	N-CH_3, c.p.s.	α-, c.p.s.	β-, c.p.s.
10.03	187.8	381.2	365.6
8.01	190.5	381.5	365.0
5.02	195.4	382.1	363.7
4.01	197.2	382.3	363.1
2.51	201.0	382.7	362.1
2.00	202.9	383.2	362.1
1.26	206.2	384.3	362.2
1.00	207.3	384.5	362.0
0.50	210.2	385.4	362.1
0.20	212.2	386.0	362.1
0.10	213.0	386.0	362.0
0.05	213.1	386.0	362.0
0.01	213.1	386	362

*TMS as internal standard taken as 0.00 c.p.s.

TABLE II

Chemical shifts of protons of N-methylpyrrole in cyclohexane at 0 °C

Molarity	N-CH_3, c.p.s.	α-, c.p.s.	β-, c.p.s.
10.00	185.0	377.8	366.0
8.01	186.8	379.3	364.3
5.00	191.1	379.8	363.0
4.00	193.7	380.2	362.5
2.50	198.0	381.5	362.0
2.00	199.7	381.9	361.9
1.25	204.5	384.0	362.5
1.00	205.0	383.5	362.0
0.40	208.8	384.1	361.4
0.20	211.1	384.3	360.9
0.10	212.3	386.8	362.8
0.05	Frozen	Frozen	Frozen

them would be too complex. It was found (Tables I and II) that the plots of concentration vs. the signal position of the N-methyl group were smooth curves with no abrupt change of curvature. The values of K were computed through extrapolation to infinite dilution and thus it seemed probable that at these low concentrations the only important associated species would be the dimer.

Using the series of shifts observed for the N-methyl group protons at the various dilutions as listed in Tables I and II, as well as the assumptions mentioned above, it was possible to compute, for each temperature, an infinite dilution equilibrium constant for the dissociation: dimer $\leftrightharpoons$ monomer. It was also possible to obtain the chemical shift of the N-methyl protons of both pure monomer and pure dimer.* The values at 0° are somewhat less reliable than those at 38° since the solution froze when at a concentration of 0.05 M. Nevertheless the computed chemical shifts for pure monomer and dimer at the two temperatures are in quite close agreement. These were found to be 213.5 c.p.s. for the monomer, and 153.4 c.p.s. for the dimer at 38 °C; and 213.1 c.p.s., monomer, and 150.1 c.p.s., dimer, at 0 °C. The values of K_{diss} were 15.7 $\pm$ 1.7 mole/liter at 38 °C and 10.6 $\pm$ 1.9 mole/liter at 0 °C. These values differ from the value obtained by Lumbroso

*These computations were carried out by Dr. S. Ehrenson and by Professor R. L. Taft, Jr., using a program developed to determine these values in a series of fluorinated aromatics.

Can. J. Chem. Downloaded from www.nrcresearchpress.com by 210.87.254.40 on 09/05/12
For personal use only.

at 25 °C in cyclohexane (inverted to give a K_{diss} of 18.2 moles/liter). However, they are of similar magnitude. From the values for K_{diss} at the two temperatures it was calculated that for this equilibrium $\Delta S_0 = 11.2 \pm 4.4$ e.u. and $\Delta H_0 = 4 \pm 3$ kcal/mole. These values are consistent with the weak association expected in the "closed cyclic dimer" structure.

Qualitatively, the change in the n.m.r. spectrum observed on dilution of N-methylpyrrole with cyclohexane (or with carbon tetrachloride) is similar to that for pyrrole and may be explained in the same way. It is evident that, with dilution, some of the N-methyl protons are being removed from the environment of the dimer where they are strongly shielded. This is consistent with the N-methyl group lying in the π-cloud of another molecule while in the associated form, and the breaking up of this dimer with dilution (4, 6, 7). The smaller downfield shift of the α-protons and the even smaller upfield shift of the β-protons in cyclohexane solution may be deduced from an examination of the location of these protons in scale models where two molecules form an associated pair with the aromatic rings antiparallel and face-to-face (see the figure). Here the α-protons are inside but close to the edge of the shielding zone above, or below, the aromatic ring of the other molecule. The β-protons lie just outside this zone and are thus partially deshielded. This arrangement would produce the observed changes with dilution of the signal positions.

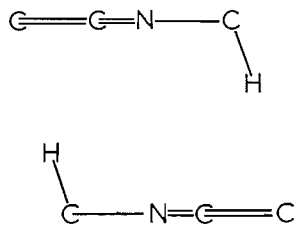

As Lumbroso has pointed out the arrangement of N-methylpyrrole molecules must be in an antiparallel face-to-face rather than an "open" or perpendicular arrangement since the dipole moment of the neat liquid is less than that of the vapor. The assemblages may be dimeric or multimeric in the neat liquid but at low concentrations the dimer is probably the most important associated species.

Hatton and Richards (6) observed a similar downfield movement of the methyl group signal in 4-picoline when it was diluted with carbon tetrachloride. The actual change was about 5.1 c.p.s., but this was from pure liquid to 0.10 mole fraction rather than to infinite dilution. These authors suggested the same sort of antiparallel face-to-face arrangement of molecules in the pure liquid to explain the change observed on dilution. It is most interesting to note that the doublet signal of the protons ortho to the methyl group (i.e. 3- and 5-) moved, on the average, 0.9 c.p.s. to higher field and the doublet of the protons meta to the methyl (i.e. 2- and 6-) moved, on the average, 4.5 c.p.s. to higher field on dilution with carbon tetrachloride. These positions approximate our α- and β-positions in their location with respect to the methyl group. However, it would appear that in 4-picoline the shape of the 6-membered ring and the arrangement of the molecules in space is such as to place the 3- and 5- protons just outside the shielding zone, and the 2- and 6-protons in the deshielding zone of the other molecule of the pair.

A series of measurements, shown in Table III, has been carried out on pure liquid N-methylpyrrole at temperatures from $-70°$ (supercooled) to $+100$ °C. These samples contained tetramethylsilane (TMS) as an internal reference. At higher temperatures it was necessary to use larger amounts of TMS; however, the dilution involved was relatively

Can. J. Chem. Downloaded from www.nrcresearchpress.com by 210.87.254.40 on 09/05/12
For personal use only.

very small. A plot of temperature vs. the chemical shift of the N-methyl protons was a straight line throughout this range of temperatures. It is possible that if several multimeric species were present there would be breaks in this curve. As the temperature increased, the values for chemical shift of the N-CH_3, α-, and β-protons all changed in the same fashion as they did when the pure liquid was diluted with cyclohexane at a given temperature. That is, N-CH_3 and α- moved to lower field while β- shifted only very slightly and to higher field. It is felt that this represents a change in the equilibrium in favor of a higher concentration of monomer at higher temperature. This should not have been caused by the expansion of the liquid since an internal standard was used. It must have been caused by the effect of the thermal energy on the weak binding forces between the molecules in the dimeric form. The values for the K_{diss} given above are indicative of the instability of dimer formed. Hatton and Schneider (7) reported a similar change of shift in methyl group protons arising from the effect of temperature on the toluene–acetonitrile complex.

TABLE III

The effect of temperature on the chemical shifts for pure N-methylpyrrole

Temp.	N-CH_3, c.p.s.	α-, c.p.s.	β-, c.p.s.
−70°	175.8	376.7	369.0
−50°	178.2	377.5	367.7
−30°	180.2	378.0	366.9
−10°	182.5	378.6	366.1
+10°	184.1	379.2	365.4
+30°	186.7	380.2	365.7
+38°	188.0	381.4	366.0
+40°	187.9	381.0	365.5
+60°	189.7	381.9	365.6
+80°	191.6	382.4	365.4
+100°	193.4	383.7	366.0

Values for the chemical shifts of all the protons in solutions of N-methylpyrrole at concentrations approaching infinite dilution were found for other solvents and are listed in Table IV. The changes taking place on dilution with carbon tetrachloride, though in the same direction, were larger than those for dilution in cyclohexane. This may well be caused by the different reaction fields of these solvents, carbon tetrachloride shifting all the signals to lower field than cyclohexane did. However, the β-proton signal is moved, instead, to higher field and to a greater extent than in cyclohexane. This cannot be explained by our simple picture. It should be noted, however, that there is also a difference in the values for K_{diss} calculated by dipole moment measurements for both N-methylpyrrole and pyrrole in these two solvents (3 (*a*)).

TABLE IV

The effect of solvent on signal positions of N-methylpyrrole*

Solvent	N-CH_3, c.p.s.	α-, c.p.s.	β-, c.p.s.
Reference cyclohexane	213.1	386.0	362.0
CCl_4	−8.0	−2.4	+3.0
Mesitylene	+28.0	+7.0	−6.5
Nitrobenzene	−3.3	−16.0	−10.6
N-Methylpyrrole (pure liquid)	+25.1	+4.6	−4.0

*A + value means a shift to higher field.

Can. J. Chem. Downloaded from www.nrcresearchpress.com by 210.87.254.40 on 09/05/12
For personal use only.

Dilution in mesitylene caused all signals to be moved in the opposite direction to those observed in cyclohexane, but only to a small extent. This would be expected if the N-methylpyrrole molecule had been transferred from the environment of the dimer suggested above into a different and slightly greater induced field belonging to the other aromatic molecule, mesitylene.

This picture of associating N-methylpyrrole molecules corresponds to that suggested by Lumbroso. The chemical shifts obtained by Happe for pyrrole in cyclohexane over the range from 0.9675 to 0.0000 mole fraction change by N-H = -0.455, α-H = -0.215 and β-H = $+0.088$ p.p.m. These values are quite close to the observed changes for the corresponding protons in N-methylpyrrole in cyclohexane, over about the same concentration range. For these reasons it is felt that all our observations on N-methylpyrrole fit well with the picture of self-association for both pyrrole and N-methylpyrrole molecules in the pure liquid and in concentrated solutions suggested by Happe and by Lumbroso. That is, the "closed cyclic dimer" type of structure, involving in N-methylpyrrole some sort of dipole–dipole or charge transfer attraction, is an important associated form, and probably the most important one at lower concentrations.

Finally, dilution with nitrobenzene shifted all the proton signals of N-methylpyrrole to lower field in amounts that are in the order of their presumed polarizability: $\alpha- > \beta- > CH_3-$, as shown in Table IV. Thus, while mesitylene appears to associate with N-methylpyrrole by forming a complex similar to that formed by N-methylpyrrole with itself, the same does not seem to be true for nitrobenzene. The latter solvent apparently is acting in a selective manner on individual protons, possibly through the nitro group (8). Schneider (9) has observed a similar shift to low field of the protons of benzene in a nitrobzenene solution. He reported the change in shift from cyclohexane to be 12.9 c.p.s., the same order as observed here for the difference in chemical shift at infinite dilution of the aromatic protons of N-methylpyrrole in these two solvents.

EXPERIMENTAL

The nuclear magnetic resonance spectra were determined at 60 Mc/s using a Varian A-60 spectrometer with tetramethylsilane as internal reference. The variable Temperature Probe was calibrated against ethylene glycol above, and methanol below, ambient.

ACKNOWLEDGMENT

The author is deeply indebted to Professors J. M. W. Scott and E. Bullock for many stimulating discussions. He also thanks Dr. S. Ehrenson and Professor R. L. Taft, Jr., for the computations, and the National Research Council for continued financial support.

REFERENCES

1. M. L. Josien and N. Fuson. J. Chem. Phys. **22**, 1169 (1954).
2. P. Tuomikoski. J. Chem. Phys. **22**, 2096 (1954).
3. (*a*) M. Gomel and H. Lumbroso. Bull. Soc. Chim. France, 2200 (1954). (*b*) H. Lumbroso. J. Chim. Phys. 132 (1954).
4. J. A. Happe. J. Phys. Chem. **65**, 72 (1961).
5. H. J. Wimette and R. H. Linnell. J. Chem. Phys. **36**, 1401 (1962).
6. J. V. Hatton and R. E. Richards. Mol. Phys. **5**, 153 (1962).
7. J. V. Hatton and W. G. Schneider. Can. J. Chem. **40**, 1285 (1962).
8. L. W. Reeves and W. G. Schneider. Can. J. Chem. **35**, 251 (1957).
9. W. G. Schneider. J. Phys. Chem. **66**, 2653 (1962).

Can. J. Chem. Downloaded from www.nrcresearchpress.com by 210.87.254.40 on 09/05/12
For personal use only.

Can. J. Chem. Downloaded from www.nrcresearchpress.com by 210.87.254.105 on 09/05/12
For personal use only.

CONCERNING THE ORTHO SHIFT IN PROTON AND FLUORINE MAGNETIC RESONANCE OF SOME CONJUGATED HYDROCARBONS

F. HRUSKA,[1] H. M. HUTTON, AND T. SCHAEFER[2]
Department of Chemistry, University of Manitoba, Winnipeg, Manitoba
Received February 25, 1965

ABSTRACT

A linear correlation with Q is found for the shifts of protons or fluorines placed ortho or *cis* to the substituent in monosubstituted benzenes, ethylenes, propenes, monofluorobenzenes, and perfluorobenzenes. The substituent X corresponds to H, F, Cl, Br, I, and Q equals P/Ir^3 where P is the polarizability of the C—X bond, r is the C—X bond length, and I is the first ionization potential of atom X. The correlation is useful for predicting some as yet unknown shifts in the above compounds. The significance of this correlation is discussed in an inconclusive manner.

INTRODUCTION

The observed proton shifts in the ortho position correlate well with the para proton shifts and reactivity parameters in monosubstituted benzenes (1). The exceptions are iodo-, bromo-, and chloro-benzenes. As pointed out by Wu and Dailey (2), factors other than pi electron densities are important in determining the observed shieldings in this position. It has been suggested (1) that these anomalies are caused by the magnetic anisotropy $\Delta\chi$ of the halogens, but it appears that a consistent assignment of $\Delta\chi$ cannot be made (3). This is perhaps not surprising since a shift of about 1 p.p.m. would be expected from $\Delta\chi$ effects of this sort, while the anomalous ortho fluorine shifts in the substituted fluorobenzenes are about 20 times as large as the analogous proton shifts (4, 5, 6).

There has been the suggestion (7) that the origin of the ortho shift lies in an increased paramagnetic term in Ramsey's equation (8), arising from smaller values of the electron excitation energies associated with a fluorine atom at a position ortho to a substituent. This explanation agrees with the increasing magnitude of the ortho effect as the substituent increases in size or when it is a transition metal with low-lying excited states of suitable symmetry. The appropriate ΔE values are, however, not known.

Others (6, 9, 10) have suggested that the ortho effect has its origin in the presence of time-dependent electric fields arising from the substituent. These electric fields are taken to be those which give rise to the van der Waal's forces between non-bonded atoms. Raynes *et al.* (11) calculate the intermolecular time average fields as $E^2 = 3PIr^{-6}$ where P is the polarizability of the molecule, I is the first ionization potential, and r is the intermolecular distance. This equation represents the long-range contribution to the shielding but in molecular collisions shorter range effects may be appreciable. Although there appears to be no real justification for it, Boden *et al.* have applied this equation in an attempt to explain the ortho effect for C_6F_5X (X = halogen) compounds with some success (6). In this intramolecular situation one may well question the use of this long-range equation, and it is interesting to note that it failed badly when applied to X = H.

As there appears to be no adequate theoretical model at present, it may be worthwhile to have an empirical correlation of the ortho shifts with some properties of the substituent. Such a correlation should be capable of predicting presently unknown shifts and

[1]*Holder of a N.R.C. Studentship, 1964–65.*
[2]*N.R.C. Senior Research Fellow, 1964–65.*

should be easy to use. The halogens (and hydrogen) are the substituents for which considerable shift data are available. We report here that we find a linear correlation of the low-field ortho shift with the quantity $Q = P/Ir^3$. P is the polarizability of the C—X bond (X = H, F, Cl, Br, I), r is the C—X bond length, and I is the first ionization potential of X.

The shift has been correlated with Q for (1) ortho protons in monosubstituted benzenes, (2) *cis* protons in the vinyl halides, (3) protons *cis* to the substituent in 1- or 2-halopropenes, (4) ortho fluorines in ortho-substituted monofluorobenzenes, (5) ortho fluorines in monosubstituted perfluorobenzenes.

Correlation of Shifts with $Q = P/Ir^3$

In Table I the bond and atom parameters for X = H, F, Cl, Br, I are given. The ionization potentials for the free atoms are given since no data are available on bond

TABLE I

Parameters for the C—H and C—halogen bonds

X	r_{C-X} (A°)[a]	P_{C-X} ($\times 10^{24}$ cm^3)[b]	I_X ($\times 10^{12}$ ergs)[c]	$Q = P/Ir^3$ ($\times 10^{-14}$ ergs^{-1})
H	1.09	0.645	21.8	2.28
F	1.30	0.633	27.8	1.04
Cl	1.70	2.604	20.8	2.55
Br	1.85	3.754	18.8	3.16
I	2.05	5.752	16.7	3.98

[a]Tables of interatomic distances and configuration in molecules and ions. *Editor* L. E. Sutton. The Chemical Society, London. 1958.
[b]C. P. Smyth. Dielectric constant and molecular structure. The Chemical Catalogue Company, New York. 1931.
[c]American Institute of Physics Handbook. *Editor* D. E. Gray. Second edition. McGraw-Hill Book Company, New York. 1963.

TABLE II

Chemical shifts of protons and fluorines in ortho or *cis* position to the substituent X in some conjugated molecules. The resonant nucleus is set in italic type in the formulae

X	*o*-C_6H_5X[a]	*cis*-CH_2=CHX[b]	*cis*-CH_2=CXCH$_3$[e]	*cis*-CHX=CHCH$_3$[e]	*o*-C_6H_4FX[i]	*o*-C_6F_5X[j]
H	0	−318.0[c]	−293.0[f]	−344.0[f]	0	−23.4
F	18.5	−281.5[d]	−264.0[k]	−317.9[g]	25.9	0
Cl	−1.2	−324.0[d]	−301.5[h]	−349.2[h]	2.7	−21.7
Br	−13.4	−345.0[d]	−316.7[h]	−365.2[h]	−5.5	−29.7
I	−24.0	−371.3[d]	—	—	−19.3	−43.1

[a]In c/s at 60 Mc/s in cyclohexane solution. Reference 1.
[b]In c/s at 60 Mc/s from tetramethylsilane in tetramethylsilane.
[c]Reference 13.
[d]Reference 17.
[e]In c/s at 60 Mc/s relative to internal tetramethylsilane.
[f]In carbon tetrachloride solution. Reference 14.
[g]Pure compound. Reference 15.
[h]In cyclohexane or tetramethylsilane solution. Reference 16.
[i]In p.p.m. Reference 4.
[j]In p.p.m. Reference 6.
[k]In CCl_3F solution. Reference 18.

excitation energies (see the discussion below). In Table II, experimental data are given for the types of compounds indicated above. The data were selected from the literature with the criterion that, if possible, the shift measurements were made in a common inert solvent for each set and that an internal reference was used. In this way, solvent effects (12) and bulk susceptibility corrections (12) were either small or nonexistent.

Can. J. Chem. Downloaded from www.nrcresearchpress.com by 210.87.254.105 on 09/05/12
For personal use only.

1. Proton Shifts

In Fig. 1*a* the ortho proton shifts in C_6H_5X are plotted versus Q. The largest deviations from the linear relationships are about 1.5 c/s in a range of over 40 c/s. In Fig. 1*b* the

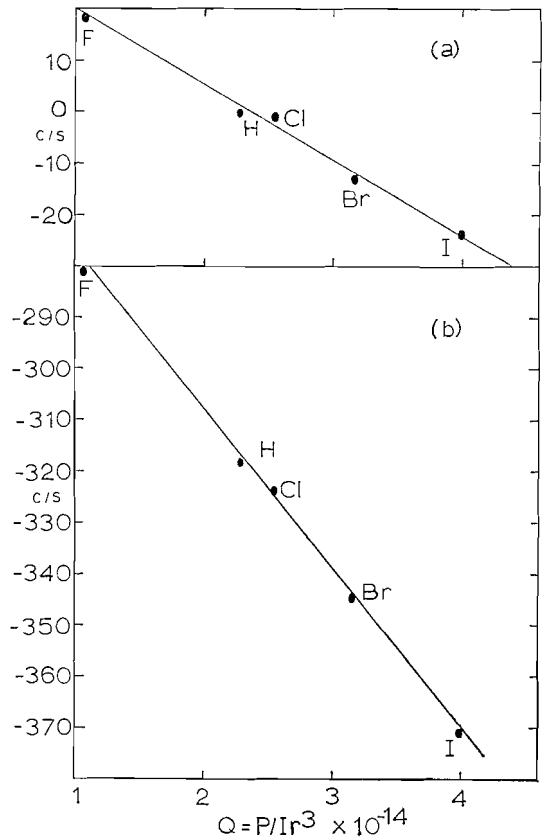

FIG. 1. In (*a*) the ortho proton shifts in c/s at 60 Mc/s in monosubstituted benzenes are plotted versus P/Ir^3. In (*b*) the shifts of the protons *cis* to the substituent are similarly plotted for monosubstituted ethylenes. Data are taken from Tables I and II.

cis proton shift in ethylene and the vinyl halides is similarly plotted. The largest deviation is about 2 c/s in a range of 90 c/s.

In Fig. 2 the shift of the protons *cis* to the substituent in the 1- and 2-halopropenes is plotted against Q. The shift for propene itself (14) was measured in carbon tetrachloride but the other values are for the neat compound (15) or cyclohexane or tetramethylsilane solutions (16). Again, the maximum deviation is about 1 c/s in the 1-halopropenes. The predicted shifts for 2-iodopropene is −337.5 c/s from internal tetramethylsilane. Similarly, the predicted shift for 1-iodopropene is −384 c/s. (The 1-iodo compound does not appear to have been made and we are presently engaged in its synthesis.)

2. The Fluorine Shifts

In Fig. 3*b* the ortho fluorine shifts in C_6F_5X are plotted versus Q. The linear correlation is considered satisfactory, although the deviation for X = H is 3.7 p.p.m. in a range of 43 p.p.m. (Boden *et al.* found a deviation as large as 23 p.p.m. for their calculation (6)).

Can. J. Chem. Downloaded from www.nrcresearchpress.com by 210.87.254.105 on 09/05/12
For personal use only.

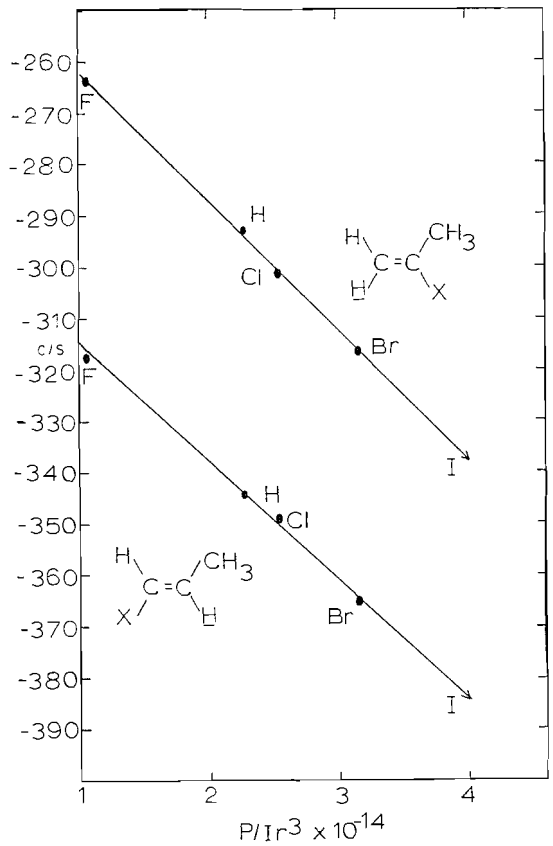

FIG. 2. The shifts, in c/s relative to internal tetramethylsilane, of the protons *cis* to the substituent in 1- and 2-substituted propenes are plotted versus P/Ir^3. The arrowheads indicate the predicted values for the iodo compounds. Data are taken from Tables I and II.

Part of the deviation of 3.7 p.p.m. may be a result of the CCl_4 solvent. Intermolecular van der Waals shifts in halogenated solvents are particularly large (12) and since hydrogen is such a small substituent it may allow a closer approach of the solvent molecules to the ortho fluorine atoms. The deviation is in fact to low field in Fig. 3*b*.

In Fig. 3*a* the ortho fluorine shifts in ortho-substituted monofluorobenzenes are plotted versus Q. The deviation for X = H from the very good straight line of X = halogen is 6.3 p.p.m., again to low field. The measurements were made on the pure compounds and not in an inert solvent (4).

DISCUSSION

1. Range of Observed Shifts

The range of proton shifts in the monosubstituted benzenes is 0.7 p.p.m. while for the *cis* proton in vinyl halides it is 1.5 p.p.m. For the *cis* proton in the 2-substituted propenes it is 1.2 p.p.m. and it is 1.1 p.p.m. for the *cis* proton in the 1-substituted propenes (using the predicted values for the 1- and 2-iodopropenes). The range of fluorine shifts is 45 p.p.m. for the mono- and 43 p.p.m. for the per-fluorobenzenes.

It is therefore fairly certain that the cause of the ortho effect is not $\Delta\chi$ of the substituents. On the other hand, it is impossible to decide whether the paramagnetic term

Can. J. Chem. Downloaded from www.nrcresearchpress.com by 210.87.254.105 on 09/05/12
For personal use only.

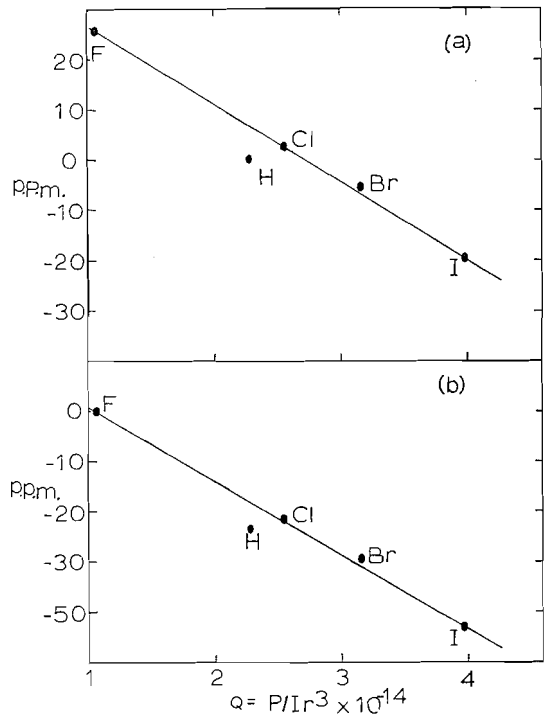

FIG. 3. In (*a*) the shifts in p.p.m. of the ortho fluorines in ortho-substituted fluorobenzenes, *o*-C_6H_4FX, are plotted versus P/Ir^3. In (*b*) the ortho fluorine shifts of monosubstituted perfluorobenzenes are similarly plotted. Data are taken from Tables I and II.

in Ramsey's equation or the intramolecular van der Waals effect is the origin of these low field shifts (but see below).

2. Correlation of Other Shifts with $Q = P/Ir^3$

The shift of the proton *trans* to the substituent in the vinyl halides and the ethylene itself gives a very good linear correlation with Q (it has not been plotted here). Furthermore, the range of shifts is 2.2 p.p.m. and is therefore larger than the 1.5 p.p.m. for the *cis* proton. This fact argues against an intramolecular van der Waals effect as the origin of the ortho shifts. The gem proton shifts do not correlate with Q.

The protons *trans* to the substituent in the 1- and 2-substituted propenes also correlate linearly with Q and we have used this correlation to predict the unknown shifts in 1- and 2-iodopropenes. The gem proton shifts do not correlate with Q.

Other shifts which do not correlate with Q are the meta and para proton shifts in the monosubstituted benzenes, monofluoro- and perfluoro-benzenes.

3. Significance of the Correlation with $Q = P/Ir^3$

If one treats the correlation function P/Ir^3 seriously, then it predicts that a perfectly hard C—X bond ($P = 0$, $I = \infty$) is to be taken as the reference and that low-field shifts will be observed for any real C—X bond in the molecules under consideration. This is reasonable in that a perturbation usually causes a low-field shift in nuclear magnetic resonance. Normally, in these compounds, the reference point is taken as the C—H bond, and the shifts in Figs. 1 to 3 are then all to high field for the C—F bond. This is

Can. J. Chem. Downloaded from www.nrcresearchpress.com by 210.87.254.105 on 09/05/12
For personal use only.

usually interpreted as due to conjugative electron release from the fluorine substituent. We consider that since the linear correlation holds for the halogens *and* for hydrogen, it is something more than a coincidence.

One rationalization of Q is as follows. The paramagnetic contribution (second term in Ramsey's equation) should be roughly inversely proportional to a mean excitation energy ΔE. Since ΔE is not known, we are forced to use the first ionization potential, I, of the substituent X. The quantity P/r^3 (dimensionless) is then a factor which corrects for the use of I.

On this view, the ortho shifts are closely related to the paramagnetic contribution and then the linear correlation with Q of, for instance, the *trans* protons in the vinyl halides is not entirely unreasonable.

ACKNOWLEDGMENTS

We thank the National Research Council, Ottawa, for financial aid. T. S. thanks the members of the Basic Physics Division, National Physical Laboratory, Teddington, for their hospitality. Part of this paper was written there.

REFERENCES

1. H. SPIESECKE and W. G. SCHNEIDER. J. Chem. Phys. **35**, 731 (1961).
2. T. K. WU and B. P. DAILEY. J. Chem. Phys. **41**, 2796 (1964).
3. J. S. MARTIN and B. P. DAILEY. J. Chem. Phys. **39**, 1722 (1963).
4. H. S. GUTOWSKY, D. W. MCCALL, B. R. MCGARVEY, and L. H. MEYER. J. Am. Chem. Soc. **74**, 4809 (1952).
5. A. J. R. BOURNS, D. G. GILES, and E. W. RANDALL. Proc. Chem. Soc. 200 (1963).
6. N. BODEN, J. W. EMSLEY, J. FEENEY, and L. H. SUTCLIFFE. Mol. Phys. **8**, 133 (1964).
7. E. PITCHER, A. D. BUCKINGHAM, and F. G. A. STONE. J. Chem. Phys. **36**, 124 (1962).
8. N. F. RAMSEY. Phys. Rev. **78**, 609 (1951).
9. T. SCHAEFER, W. F. REYNOLDS, and T. YONEMOTO. Can. J. Chem. **41**, 2969 (1963).
10. V. M. S. GILL and W. A. GIBBONS. Mol. Phys. **8**, 199 (1964).
11. W. T. RAYNES, A. D. BUCKINGHAM, and H. J. BERNSTEIN. J. Chem. Phys. **36**, 3481 (1962).
12. A. D. BUCKINGHAM, T. SCHAEFER, and W. G. SCHNEIDER. J. Chem. Phys. **32**, 1227 (1960).
13. J. H. GOLDSTEIN and G. S. REDDY. J. Chem. Phys. **36**, 2644 (1962).
14. A. A. BOTHNER-BY and C. NAAR-COLIN. J. Am. Chem. Soc. **83**, 231 (1961).
15. R. A. BEAUDET and J. D. BALDESCHWIELER. J. Mol. Spectry. **9**, 30 (1962).
16. G. S. REDDY and J. H. GOLDSTEIN. J. Am. Chem. Soc. **83**, 2045 (1961).
17. R. E. MAYO and J. H. GOLDSTEIN. J. Mol. Spectry. **14**, 173 (1964).
18. M. Y. DE WOLF and J. D. BALDESCHWIELER. J. Mol. Spectry. **13**, 344 (1964).

Can. J. Chem. Downloaded from www.nrcresearchpress.com by 210.87.254.105 on 09/05/12
For personal use only.

Can. J. Chem. Downloaded from www.nrcresearchpress.com by 210.87.254.6 on 09/05/12
For personal use only.

CYCLOHEXANE COMPOUNDS

V. THE REACTION OF 1-METHOXYCYCLOHEXENE-2 WITH AQUEOUS N-BROMOSUCCINIMIDE. THE 1-METHOXY-2-BROMO-3-HYDROXYCYCLOHEXANES[1]

R. A. B. BANNARD, A. A. CASSELMAN, AND L. R. HAWKINS
Defence Chemical Biological and Radiation Laboratories, Defence Research Board, Ottawa, Canada
Received April 6, 1965

ABSTRACT

Interaction of 1-methoxycyclohexene-2 and aqueous N-bromosuccinimide gave a mixture of stereoisomeric bromohydrins, which, on treatment with aqueous sodium hydroxide, furnished 1β-methoxy-2α,3α-epoxycyclohexane (I) and 1α-methoxy-2α,3α-epoxycyclohexane (II) in the ratio 3:1. The mixture from the N-haloimide-olefin reaction was separated by preparative vapor phase chromatography into three isomeric bromohydrins, 1α-methoxy-2α-hydroxy-3β-bromocyclohexane (IV), 1α-methoxy-2α-bromo-3β-hydroxycyclohexane (V), and 1α-methoxy-2β-bromo-3α-hydroxycyclohexane (VI) in the relative proportions 1:10:4. The 3-bromo isomer IV was identified by comparison with an authentic specimen prepared by the action of hydrobromic acid on the oxide II. Compounds V and VI were shown to have the indicated structures by deetherification to the corresponding bromodiols VII and VIII in high yield, followed by debromination of the latter to *trans*- and *cis*-1,3-cyclohexanediol respectively. The product distribution is considered in relation to the intervention of electronic and steric factors in a possible mechanism suggested for the reaction between aqueous N-bromosuccinimide and 1-methoxycyclohexene-2.

Several years ago (1) we reported that the action of hydrobromic acid on the stereoisomeric 1-methoxy-2,3-epoxycyclohexanes I and II led to the formation of 1α-methoxy-2β-hydroxy-3α-bromocyclohexane (III) and 1α-methoxy-2α-hydroxy-3β-bromocyclohexane (IV) respectively. The structures of these substances were established by a variety of chemical means (1) because we wished to determine their relationship to the mixture of bromohydrins resulting from the action of aqueous N-bromosuccinimide upon 1-methoxycyclohexene-2. The latter bromohydrin mixture furnishes the oxides I and II in the ratio of 3:1 on treatment with aqueous sodium hydroxide and since 1,2-halohydrin to oxide conversions involve a *trans* ring closure (3, 4), it is apparent that the trans oxide I could have arisen from either or both of 1α-methoxy-2β-hydroxy-3α-bromocyclohexane (III) and 1α-methoxy-2α-bromo-3β-hydroxycyclohexane (V). Likewise the *cis*-oxide II would be formed if the mixture contained either 1α-methoxy-2α-hydroxy-3β-bromocyclohexane (IV) or 1α-methoxy-2β-bromo-3α-hydroxycyclohexane (VI) or both. The present communication describes the manner in which the composition of the bromohydrin mixture from the olefin-N-haloimide reaction was determined and provides an unequivocal proof of structure for 1α-methoxy-2α-bromo-3β-hydroxycyclohexane (V) and 1α-methoxy-2β-bromo-3α-hydroxycyclohexane (VI).

Attempts to separate the components of the bromohydrin mixture by fractional distillation *in vacuo* and by column chromatography on alumina were unsuccessful. We therefore explored chemical separations based upon the formation of crystalline derivatives. In this connection, the possible utility of acetate, *p*-toluenesulfonate, 2,4-dinitrobenzenesulfenate, dichloroacetate, 3-nitrophthalate, phenylurethane, and naphthylurethane derivatives was examined, but only by means of the latter was a partial separation of the isomers achieved. The crude solid resulting from the prolonged action of 1-naphthylisocyanate on the bromohydrin mixture was fractionally crystallized furnishing two methoxycyclohexene bromohydrin 1-naphthylurethanes, m.p. 151° and 196–197.5°, in 64.1% and

[1]*Issued as DCBRL Report No. 457.*

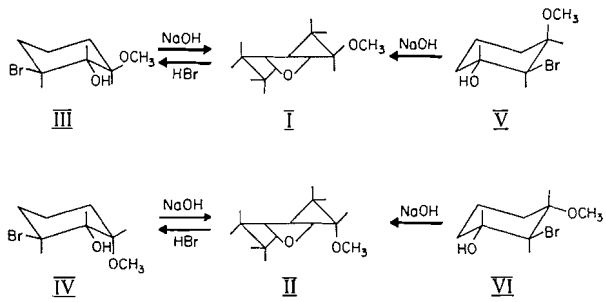

10.5% yield respectively. These compounds were shown to be completely different from the 1-naphthylurethanes of the 3-bromo compounds III and IV (1) (Table II) by mixture melting points and comparison of infrared spectra. Preparative paper chromatography of the mixture on Whatman seed test paper using hexane saturated with 90% methanol also gave a partial separation into two fractions, R_F 0.14 and 0.35. The slower-moving band (66.6%) consisted of the two 2-bromo compounds V and VI as shown by conversion to the 1-naphthylurethanes mentioned above. The faster-moving band accounted for 8.5% of the mixture and was identified as 1α-methoxy-2α-hydroxy-3β-bromocyclohexane (IV) by its infrared spectrum and its conversion to the 1-naphthylurethane of m.p. 122–124° (Table II).

These experiments demonstrated the presence of the bromohydrins IV, V, and VI in the mixture and indicated the great predominance of the 2-bromo compounds. From the ratio of the oxides I and II obtained from the bromohydrin mixture by the action of alkali (1), it was also concluded that the 1-naphthylurethanes of m.p. 151° and 196–197.5° are derived from V and VI respectively. However, these partial separations did not eliminate the possibility that III is also present as a minor component and, moreover, did not provide us with the bromohydrins V and VI which we wished to obtain for comparison of their physical properties and chemical reactivity with those of the 3-bromo isomers III and IV. Although it was considered probable that a satisfactory separation of the components of the mixture might be achieved using another solvent system for paper chromatography or thin-layer chromatography (and this actually proved to be the case later (5)) such separations on a preparative scale are frequently unduly tedious (6, 7) in comparison to those obtainable with a variety of preparative vapor phase chromatographic (v.p.c.) equipment which is now commercially available.

Preparative vapor phase chromatography at 150° on the Wilkens Autoprep Model A-700 gas chromatograph, using a column packed with 30% XF-1150 on Chromosorb P as described in the experimental section, gave the fractions shown in Table I. Fraction 1 consisted of two very minor components with retention times of 12 and 30 min. These substances differed from the four bromohydrins in question as shown by their infrared spectra, which contained a prominent carbonyl band at 1 700 cm^{-1}, which was not, of course, present in those of the bromohydrins. Fraction 2 was identified as 1α-methoxy-2α-hydroxy-3β-bromocyclohexane (IV) by its infrared spectrum. Fractions 3 and 4 were the pure 1-methoxy-2-bromo-3-hydroxycyclohexanes. From the relative amounts of fractions 3 and 4 it was deduced that the former, which is a crystalline solid, m.p. 55.5–57.0°, is 1α-methoxy-2β-bromo-3α-hydroxycyclohexane (VI)* and that the latter, which is a liquid

*We are indebted to Prof. R. Y. Moir, Mr. T. McMullen, and Mr. E. J. Langstaff for first isolating this compound during a partial v.p.c. separation of V and VI obtained using 20% butane-1,4-diolsuccinate as the substrate on a column packed with Chromosorb W.

Can. J. Chem. Downloaded from www.nrcresearchpress.com by 210.87.254.6 on 09/05/12
For personal use only.

TABLE I

Vapor phase chromatographic separation of the 1-methoxycyclohexene-2 bromohydrins

Fraction No.	Retention time (min)	Weight* (mg)	% of total recovery
1	0–36	64.5	1.04
2	41	414	6.73
3	69	1 570	25.6
4	91	4 100	66.7

*Total recovery 6 150 mg (84.0%), weight of mixture processed 7.33 g.

n_D^{25} 1.5145, is 1α-methoxy-2α-bromo-3β-hydroxycyclohexane (V). These deductions were confirmed by unambiguous chemical methods as indicated later.

The two new bromohydrins V and VI were characterized by preparation of their 1-naphthylurethanes and acetyl derivatives, the physical constants of which are recorded in Table II together with the corresponding data for the 3-bromo compounds. It is noteworthy that the structural assignments which were tentatively made on the basis of the proportions of the 1-naphthylurethanes isolated from the bromohydrin mixture were completely confirmed when these derivatives were prepared from the pure bromohydrins.

That 1α-methoxy-2β-hydroxy-3α-bromocyclohexane (III) can be formed to the extent of only 0.5% or less was established in two ways after it was discovered that the chromatographic column used in the work just described would *not* separate III from V.* Thin-layer chromatography of the bromohydrins III, IV, V, and VI on silica gel G in hexane: N,N-dimethylformamide: 90% methanol, (100:25:100) gave the R_F values 0.27, 0.40, 0.21, and 0.36 respectively, and it was demonstrated that as little as 0.5% of III could be detected in the presence of the other three by this means (5). Likewise, vapor phase chromatography at 150° in the same apparatus used previously, but employing a 5 ft column packed with 10% Versamid-900 on 45/60 mesh acid-washed and silanized Chromosorb P gave a clean separation of a synthetic mixture of the four isomers with retention times of 23, 14.5, 28, and 17 min respectively (5). Similar treatment of the bromohydrin mixture from the N-bromosuccinimide–olefin reaction failed to reveal the presence of the 3-bromo isomer III. It is therefore concluded that the bromohydrin mixture consists of compounds IV, V, and VI in the relative amounts 1:10:4, together with minor amounts of two other unidentified compounds which are not bromohydrins.

It was previously shown (1) that the most straightforward chemical method for establishing the structures of the alkoxycyclohexene bromohydrins is by deetherification and debromination to the cyclohexanediols, the structures of which, together with the predictable behavior of *trans*-1,2-bromohydrins (3, 4) provide an unambiguous configurational proof. Accordingly, the deetherification of compound VI with 68% aqueous hydrobromic acid at 65–68° gave the bromodiol VIII, m.p. 136.5–138° in 98% yield. The latter substance was converted to *cis*-1,3-cyclohexanediol (X), m.p. 85.0–86.5° (8) in 87% yield by debromination with Raney nickel and hydrogen in the presence of Amberlite IR-4B (OH) resin (9, 1). Since the bromine atom must have been *trans* to the hydroxyl group in the original bromohydrin to give the *cis*-oxide II on treatment with alkali, it follows that the structure of the bromodiol is 2β-bromo-1α,3α-cyclohexanediol (VIII) and that of the

**Difficulties encountered in the separation of the chloro analogues of III and V during their preparative v.p.c. separation were brought to our attention by Prof. R. Y. Moir and E. J. Langstaff. It was then found that the XF-1150 substrate would not separate a prepared mixture of III and V.*

Can. J. Chem. Downloaded from www.nrcresearchpress.com by 210.87.254.6 on 09/05/12
For personal use only.

Can. J. Chem. Downloaded from www.nrcresearchpress.com by 210.87.254.6 on 09/05/12
For personal use only.

TABLE II

Physical properties of the 1-methoxy-2(3)-bromo-3(2)-hydroxycyclohexanes and their derivatives

	Cyclohexane		Derivative (m.p. or b.p. °C)			
			1-Naphthylurethane	Acetate	Diol	Diol diacetate
III	1α-Methoxy-2β-hydroxy-3α-bromo-	68.5–69	185–186	56–56.5	98–99	65–66.5
IV	1α-Methoxy-2α-hydroxy-3β-bromo-	62–63/0.01 n_D^{25} 1.5080	122–124	63–65/0.01 n_D^{25} 1.4828	70.5–71	85–86/0.1 n_D^{25} 1.4810
VI	1α-Methoxy-2β-bromo-3α-hydroxy-	55.5–57	196–197.5	44–45	136.5–138	80.2–81.2
V	1α-Methoxy-2α-bromo-3β-hydroxy-	61–61.5/0.04 n_D^{25} 1.5145	151	69–70/0.03 n_D^{25} 1.4861	104–105	82–83/0.05 n_D^{25} 1.4817

bromohydrin is 1α-methoxy-2β-bromo-3α-hydroxycyclohexane (VI). Similarly, deetherification of the liquid bromohydrin (V), n_D^{25} 1.4145, gave the bromodiol VII, m.p. 104–105°, in 91% yield. Debromination of VII furnished *trans*-1,3-cyclohexanediol (IX), m.p. 118.5–119.5° (8), in 93% yield. Since the liquid bromohydrin leading to IX yields the *trans*-oxide I it must have the structure 1α-methoxy-2α-bromo-3β-hydroxycyclohexane (V) and the corresponding bromodiol must be 2α-bromo-1α,3β-cyclohexanediol (VII). That the two bromodiols in question are not 1,2-diols was shown by the fact that they are not oxidized by sodium metaperiodate as are their isomers derived from the bromohydrins

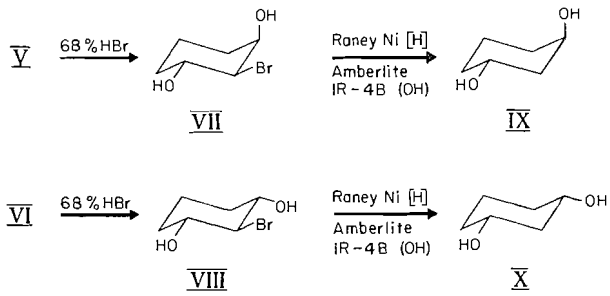

III and IV (1). The bromodiols VII and VIII were further characterized by preparation of their diacetyl derivatives, some physical constants of which are shown in Table II, together with those of the corresponding 3-bromo compounds.

The structural assignments which were made on chemical grounds as described above were fully confirmed by first-order analysis (10, 11, 12) of the multiplet patterns of the C_2 methine protons in the nuclear magnetic resonance spectra of the bromohydrin acetates and bromodiol diacetates. These spectra will be discussed in a forthcoming paper.

The composition of the bromohydrin mixture is of considerable interest from the standpoint of the mechanism of the reaction which leads to its formation. The synthetic utility of N-bromoimides in aqueous, alcoholic, or acetic acid media for adding the elements of hypobromous acid, alkyl hypobromite, or acetyl hypobromite across double bonds has been recognized for many years (13–20). No detailed studies appear to have been conducted on the mechanism of additions to double bonds via the use of N-bromoimides in polar solvents (or on the addition reactions which often accompany allylic brominations of olefins by N-bromosuccinimide in non-polar solvents). However, it has been generally assumed that such reactions proceed by a polar mechanism (14, 15, 18, 19, 21, 23, 24) involving attack by a brominium ion or another electrophilic species containing bromine to yield a cyclic bromonium ion (14, 18, 23, 24), a pi-complex (14, 25), or a carbonium ion (14, 25), which reacts subsequently with a nucleophile to form the final product. Some evidence in favor of this mechanism is derived from the *trans* stereochemistry of the resultant addition products. It has also been stated (21, 22) that when N-bromosuccinimide reacts in water or alcohols, it is converted by hydrolysis or alcoholysis to hypobromous acid or alkyl hypobromite and this viewpoint is strengthened by Traynham and Pascual's observation (25) that the substitution of aqueous N-bromosuccinimide for aqueous hypobromous acid in reactions with methylene cycloalkanes causes no change in product distribution. If the function of aqueous N-bromosuccinimide is indeed to generate hypobromous acid, there is good reason to believe that the mechanism just referred to is valid, since the extensive work of de la Mare and co-workers (26–29) on the addition of aqueous hypohalous acids to olefins has produced convincing evidence in favor of an electrophilic

Can. J. Chem. Downloaded from www.nrcresearchpress.com by 210.87.254.6 on 09/05/12
For personal use only.

mechanism. These workers, however, favor, as an intermediate, a carbonium ion which is shielded against configurational equilibration by participation of the neighboring halogen atom during the subsequent attack by the nucleophile, as depicted in formula XI.

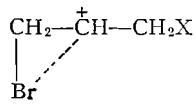

XI

If the viewpoint is accepted that the first stage in the reaction under consideration involves the electrophilic addition of a brominium ion or its equivalent to 1-methoxycyclohexene-2, then it could be considered that a pi-complex is first formed then transformed to the bromonium ion or shielded carbonium ion which represent slight variations of the reactive intermediate undergoing subsequent nucleophilic attack. For convenience in the subsequent discussion we shall designate the cyclic bromonium ion as the postulated intermediate. We shall then examine the products obtained from the reaction in relation to those predicted on opening the bromonium ring in a manner analogous to the nucleophilic scission of epoxides.

1-Methoxycyclohexene-2 should exist in two conformations XII and XIII, the first of which is the more stable (30). The inversion free energy change for the methoxyl group has been estimated as 0.74 kcal/mole (31) from which it follows that the percentage population of XII should be at least 75% (32). The use of Courtaulds molecular models indicated that the formation of the *trans* bromonium ions XVI and XVII and the *cis* bromonium ion XIV would not be appreciably hindered by steric interactions during the approach of the brominium ion to XII and XIII. However, the formation of the *cis* bromonium ion XV from XIII is severely hindered by the quasi-axially oriented oxygen atom of the methoxyl group. From these considerations it may be assumed that XVI and XIV will be formed in almost equal amounts and that XVII will be formed in considerably greater quantity than XV. Also, the sum of XIV and XVI should be appreciably larger than the sum of XVII and XV.*

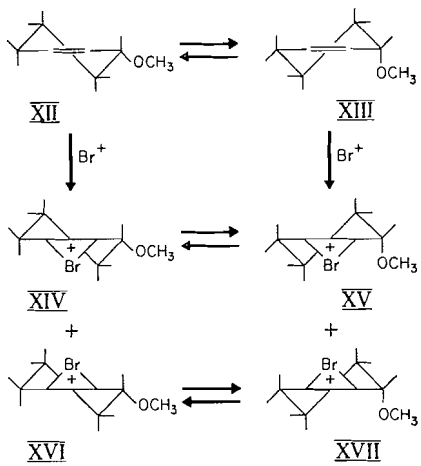

**In this analysis the possibility that approach of the brominium ion cis to the methoxyl group in XII or XIII might be electronically assisted to a degree sufficient to overcome the less favorable steric ease of approach from that side was considered but rejected on the grounds that such electronic assistance did not intervene during the addition of hypobromous acid to 5α-cholest-1-en-3β-ol (18).*

Can. J. Chem. Downloaded from www.nrcresearchpress.com by 210.87.254.6 on 09/05/12
For personal use only.

Can. J. Chem. Downloaded from www.nrcresearchpress.com by 210.87.254.6 on 09/05/12
For personal use only.

It was mentioned previously (1) that no completely satisfactory picture of the role of polar and steric effects in determining the point of attack by nucleophiles on 1,2-epoxides has emerged. Moir and coworkers (10, 33) have pointed out that ring opening at C_3 in the 1-alkoxy-2,3-epoxycyclohexanes is to be expected if it is recognized that bond-breaking is more important than bond-making in the transition state of S_N2 epoxide scissions (34–37) and that the electron-withdrawing effect of the alkoxyl group predominates over steric factors. This interpretation predicts major attack at C_3, but not exclusive (1, 2, 10) opening at that point, since some of the experiments which led to its evolution (35–37) gave mixtures containing large amounts of isomeric products. The system was thought to be so mobile (due to the low conformation-holding energy barrier provided by the methoxyl group (33)) that it could readily accommodate itself to the polar demands of the bonds being made and broken without violating the steric requirements for diaxial opening of the ring to yield a chair form (38–39). In our view, steric factors such as the ease of approach of the nucleophile and the energy needed to bring the molecule into a reacting conformation suitable for diaxial opening to the chair form should be more carefully considered, both in the reaction of the alicyclic oxides under consideration, and in the scission of their bromonium ion analogs XIV–XVII. If it is assumed that polar and steric factors are both important, with the former slightly predominant, it seems reasonable to expect that major products will be formed when these effects operate in unison and that minor products will result when they are opposed.

In the reaction of XIV according to these principles, attack at C_3 is favored by both the polar effect of the methoxyl group and the unhindered approach of the nucleophile to yield a chair on diaxial opening, while attack at C_2 is unfavorable on both electronic and steric grounds. Consequently, XIV reacts rapidly to produce the 2-bromo compound V in major amount. In the reaction of the other major conformer XVI, opening at C_3 is favored electronically but is opposed by the steric condition that a less stable boat form would result. On the other hand, the unhindered approach of the nucleophile at C_2 would give a chair form, but is opposed by the unfavorable polar effect of the methoxyl group. The result is a decreased rate of reaction for XVI. Since XVI is in equilibrium with its conformer XVII and the latter can react more rapidly to yield VI as indicated below, the latter substance is produced at a rate faster than attack at C_2 yields the 3-bromo isomer IV. Consequently, IV is only a minor product of the reaction. In conformer XVII, diaxial opening at C_3 to yield a chair form is facilitated by the inductive effect of the methoxyl group and although the approach of the nucleophile to C_3 is impeded by 1,3-interaction with the axial methoxyl group, the hindrance is not as severe as that caused by approach to C_2. Consequently, rapid reaction at C_3 ensues, yielding the 2-bromo isomer VI. The latter compound is obtained in major amount since it is also formed from XVI via XVII as mentioned earlier. In the least abundant bromonium ion XV, opening at C_3 is favored by polar but opposed by steric factors, and for attack at C_2 the interplay of these effects is reversed. The rate of reaction of XV is thereby decreased and since its conformer XIV can react by a more favorable pathway to produce the 2-bromo isomer V, only a negligible amount of the 3-bromo compound III resulting from attack of XV at C_2 would be expected.

According to these predictions it would be anticipated that the relative amounts of the isomeric bromohydrins would be in the order V $\approx$ VI $>$ IV $>$ III. The proportions found experimentally were 10:4:1:0 and thus agree qualitatively with the above interpretation except that the presence of III could not be established by the methods employed. Also, Moir and co-workers (33) in studying the reaction between 1-methoxycyclohexene-2 and

aqueous N-chlorosuccinimide obtained a similar distribution of the corresponding chloro-isomers and demonstrated the absence of the 3-chloro analogue of III. These results provide some support for the mechanistic interpretation just presented, but it is difficult to reconcile the exclusive formation of 3-substituted products from scission of the oxides I and II under acidic and alkaline conditions (1, 2, 10) with the results presented above if the analogy in the behavior of epoxides and cyclic bromonium ions used herein is valid. It was mentioned earlier (1), however, that the methods of analysis which established 3-substituted derivatives as exclusive products in the oxide openings just referred to may not have been sufficiently sensitive to reveal the presence of minor amounts of the 2-substituted derivatives. Now that the more sensitive methods afforded by vapor phase chromatography can be brought to bear on the problem, reinvestigation of the ammonlysis and hydrobromic acid scission of these oxides is warranted to establish whether the 2-substituted products predicted by the above interpretation are actually formed.

EXPERIMENTAL*,†

1-Methoxycyclohexene-2 Bromohydrin

The mixture of positionally and stereoisomeric bromohydrins was prepared by the action of aqueous N-bromosuccinimide on 1-methoxycyclohexene-2 as described by Bannard and Hawkins (2).

Partial Separation of the 1-Methoxycyclohexene-2 Bromohydrins via 1-Naphthylurethane Formation

A portion of the bromohydrin mixture (1.00 g, 4.79 $\times$ 10^{-3} mole) and 1-naphthylisocyanate (1.0 g) were mixed and kept at 65–68° for 2 days in an apparatus protected from entry of moisture, after which a further portion of 1-naphthylisocyanate was added and the heating was repeated. The resultant crude solid product was collected and washed with heptane. A portion of this material proved to be soluble in hot carbon tetrachloride, and after separation, was recrystallized from ether–heptane, yielding 1.16 g (64.1%) of *dl*-1α-methoxy-2α-bromo-3β-hydroxycyclohexane 1-naphthylurethane, as colorless needles, m.p. 151°.

Anal. Calcd. for $C_{18}H_{20}NO_3Br$: C, 57.15; H, 5.33; N, 3.70; Br, 21.13. Found: C, 57.38; H, 5.35; N, 3.91; Br, 21.02.

The carbon tetrachloride insoluble material was recrystallized from acetone–heptane, yielding 0.19 g (10.5%) of *dl*-1α-methoxy-2β-bromo-3α-hydroxycyclohexane 1-naphthylurethane as colorless needles, m.p. 196–197.5°.

Anal. Calcd. for $C_{18}H_{20}NO_3Br$: C, 57.15; H, 5.33; N, 3.70; Br, 21.13. Found: C, 57.41; H, 5.54; N, 3.82; Br, 20.86.

In admixture the compounds had m.p. 143–182° and the infrared spectra (KBr pellet) were quite different.

Partial Separation of the 1-Methoxycyclohexene-2 Bromohydrins via Chromatography on Seed Test Paper

The bromohydrin mixture (1.5 g in 1 ml 95% ethanol) was applied as a streak to a sheet (18 in. $\times$ 22 in.) of Whatman seed-test paper which had been washed chromatographically with the following solvents in the order named: 0.01 *N* hydrochloric acid (3 days), water (2 days), 95% ethanol (2 days). The chromatogram was developed by the descending technique in a "Chromatocab" for 10 h using hexane saturated with 90% methanol. After air-drying the chromatogram was sprayed with 95% ethanol until damp and pressed against a sheet of Whatman No. 1 paper to produce a print. The print was sprayed with 2 *N* potassium hydroxide followed by 0.05 *N* silver nitrate and placed under ultraviolet light for 3.5 min. The bromohydrins were revealed as two dark brown bands against a light brown background at R_F values of 0.14 and 0.35. The bands were cut from the chromatogram and eluted with 95% ethanol. Corresponding eluates from four such chromatograms were combined, evaporated to dryness *in vacuo*, and distilled *in vacuo* in a Späth tube. The colorless oil obtained from the material of R_F 0.14 weighed 4.00 g (66.6%); b.p. 55–60° (air-bath temperature) /0.005 mm; n_D^{25} 1.5137. This material was shown to be a mixture of *dl*-1α-methoxy-2α-bromo-3β-hydroxycyclohexane (V) and *dl*-1α-methoxy-2β-bromo-3α-hydroxycyclohexane (VI) by separation and identification of the 1-naphthylurethanes of m.p. 151° and 196–197.5° as described above. The colorless oil obtained from the material of R_F 0.35 weighed 0.51 g (8.5%), b.p. 50–55° (air-bath temperature)/0.005 mm, n_D^{25} 1.5080; and was identified as *dl*-1α-methoxy-2α-hydroxy-3β-bromocyclohexane (IV) (1) via its infrared spectrum and conversion to the corresponding 1-naphthylurethane, m.p. 122–124°.

Separation of the 1-Methoxycyclohexene-2 Bromohydrins by Vapor Phase Chromatography

The bromohydrin mixture was separated into three major components by vapor phase chromatography on the Wilkens Autoprep Model A-700 gas chromatograph, using a 5 ft 3/8 in. diameter, aluminium column packed with 30% XF-1150 (cyanosilicone) on acid-washed and dimethyldichlorosilane-treated 45/60 mesh

**All melting-points are uncorrected.*

†Microanalyses by J. Helie of these laboratories.

Can. J. Chem. Downloaded from www.nrcresearchpress.com by 210.87.254.6 on 09/05/12
For personal use only.

Chromosorb P. Optimum conditions for the separation were column and collector temperature 150°, injector temperature 168°, detector temperature 175°, helium flow rate 300 ml/min, filament current 200 mA. Serial injections of the neat bromohydrin mixture 150 μl (221 mg) were made every 2 h and the fractions recovered from processing 7.33 g of the mixture in this manner gave the results shown in Table I. Fraction 2, which was a liquid, n_D^{25} 1.5080, was identified as *dl*-1α-methoxy-2α-hydroxy-3β-bromocyclohexane (IV) by comparison of its infrared spectrum with that of an authentic specimen (1). Fraction 3 was redistilled in a Späth tube at 0.04 mm pressure at an air bath temperature of 30°, yielding a colorless oil, which crystallized on standing. Recrystallization from *n*-pentane furnished colorless prisms, m.p. 55.5–57.0°, which were shown to have the structure *dl*-1α-methoxy-2β-bromo-3α-hydroxycyclohexane (VI) (see below).

Anal. Calcd. for $C_7H_{13}O_2Br$: C, 40.22; H, 6.27; Br, 38.22. Found: C, 40.34; H, 6.44; Br, 38.06.

Fraction 4 was redistilled in a micro Bantamware still yielding a colorless liquid, b.p. 61–61.5°/0.04 mm n_D^{25} 1.5145, which was identified as *dl*-1α-methoxy-2α-bromo-3β-hydroxycyclohexane (V) (see below).

Anal. Calcd. for $C_7H_{13}O_2Br$: C, 40.22; H, 6.27; Br, 38.22. Found: C, 40.24; H, 6.26; Br, 38.12.

The infrared spectra of the two 1-methoxy-2-bromo-3-hydroxycyclohexanes taken in carbon tetrachloride solution were quite different from one another and from those of the isomeric 1-methoxy-2-hydroxy-3-bromocyclohexanes.

Derivatives of dl-1α-Methoxy-2β-bromo-3α-hydroxycyclohexane (VI)

The acetyl derivative was obtained in 90.5% yield, m.p. 44–45° as colorless prisms after recrystallization from anhydrous ether.

Anal. Calcd. for $C_9H_{15}O_3Br$: C, 43.04; H, 6.02; Br, 31.82. Found: C, 42.85; H, 5.84; Br, 32.02.

The 1-naphthylurethane was obtained in 96.0% yield, m.p. 196–197.5°, as colorless needles after recrystallization from acetone. This substance was identical in all respects with the 1-naphthylurethane, which was isolated in the smaller amount from the bromohydrin mixture.

Derivatives of dl-1α-Methoxy-2α-bromo-3β-hydroxycyclohexane (V)

The acetyl derivative, b.p. 69–70°/0.03 mm, n_D^{25} 1.4861, was obtained in 96.2% yield as a colorless viscous oil.

Anal. Calcd. for $C_9H_{15}O_3Br$: C, 43.04; H, 6.02; Br, 31.82. Found: C, 43.20; H, 6.01; Br, 31.67.

The 1-naphthylurethane was obtained in 91.6% yield as colorless needles, m.p. 151°, after recrystallization from anhydrous ether. This substance was identical in all respects with the 1-naphthylurethane, which was isolated in the larger amount from the bromohydrin mixture.

Deetherification of dl-1α-Methoxy-2β-bromo-3α-hydroxycyclohexane (VI) to dl-2β-Bromo-1α,3α-cyclohexanediol (VIII)

dl-1α-Methoxy-2β-bromo-3α-hydroxycyclohexane (2.09 g, 0.01 mole) was heated for 1½ h in a sealed tube at 65–70° with 68% hydrobromic acid (2.0 ml, 2.14×10^{-2} mole). The pale yellow solution was transferred quantitatively to a 500 ml round-bottomed flask in ca. 40 ml of water, the excess acid was neutralized by the addition of solid sodium bicarbonate (3.0 g), and the solution was evaporated to dryness *in vacuo*. The colorless residue was ground in a mortar, transferred to a Soxhlet extractor, and extracted for 16 h with anhydrous ether, and the extract was evaporated to dryness. Crystallization of the product from anhydrous ether furnished 1.91 g (97.4%) of *dl*-2β-bromo-1α,3α-cyclohexanediol (VIII) as colorless needles, m.p. 136.5–138°.

Anal. Calcd. for $C_6H_{11}O_2Br$: C, 36.94; H, 5.68; Br, 40.97. Found: C, 37.17; H, 5.55; Br, 40.73.

dl-2β-Bromo-1α,3α-diacetoxycyclohexane

This substance was obtained in 94.5% yield as colorless needles, m.p. 80.2–81.2°, after recrystallization from ether–heptane.

Anal. Calcd. for $C_{10}H_{15}O_4Br$: C, 43.03; H, 5.42; Br, 28.63. Found: C, 43.29; H, 5.44; Br, 28.70.

Debromination of dl-2β-Bromo-1α,3α-cyclohexanediol (VIII) to cis-1,3-Cyclohexanediol (X)

dl-2β-Bromo-1α,3α-cyclohexanediol (390 mg, 2.0×10^{-3} mole) was dissolved in ethanol (50 ml), Raney nickel W-7 (40) catalyst (10 g), and Amberlite IR-4B (OH) resin (3 ml) were added and the mixture was shaken at 50 p.s.i. hydrogen pressure for 18 h at room temperature. The catalyst was separated from the solution by centrifugation and decantation and was washed thrice with 50-ml portions of ethanol. The combined solutions were filtered, taken to dryness *in vacuo*, dissolved in ethanol (5 ml), and transferred to a 25 ml flask. The ethanol was removed *in vacuo* and the residue was heated at 60°–90° at 0.001 mm pressure in a stirred oil bath. The colorless sublimate which collected during this process was recrystallized from anhydrous ether yielding 203 mg (87.4%) of colorless platelets, m.p. 85.0–85.6°, alone, and 84.8–85.5° in admixture with an authentic specimen of *dl-cis*-1,3-cyclohexanediol of mp. 84.5–85.5°. The infrared spectra (KBr pellet) of the specimens were also identical.

Deetherification of dl-1α-Methoxy-2α-bromo-3β-hydroxycyclohexane (V) to dl-2α-Bromo-1α,3β-cyclohexanediol (VII)

The procedure was identical with that described above for the stereoisomeric bromohydrin. Recrystallization of the product from anhydrous ether gave 1.63 g of *dl*-2α-bromo-1α,3β-cyclohexanediol (VII) as colorless

Can. J. Chem. Downloaded from www.nrcresearchpress.com by 210.87.254.6 on 09/05/12
For personal use only.

rosettes, m.p. 104–105°. The yield was 90.6% based on the bromohydrin used; 0.16 g of unreacted starting material was recovered and identified by its infrared spectrum.

Anal. Calcd. for $C_6H_{11}O_2Br$: C, 36.94; H, 5.68; Br, 40.97. Found: C, 36.85; H, 5.70; Br, 40.92.

dl-2α-Bromo-1α,3β-diacetoxycyclohexane

This compound was obtained in 96.8% yield as a colorless mobile oil, b.p. 82–83°/0.05 mm, n_D^{25} 1.4817.

Anal. Calcd. for $C_{10}H_{15}O_4Br$: C, 43.03; H, 5.42; Br, 28.63. Found: C, 43.00; H, 5.58; Br, 28.79.

Debromination of dl-2α-Bromo-1α,3β-cyclohexanediol (VII) to trans-1,3-Cyclohexanediol (IX)

The procedure was identical with that described above for the stereoisomeric bromodiol. Recrystallization of the sublimate from anhydrous ether furnished 215 mg (92.6%) of colorless rosettes, m.p. 118.5–119.5°, which was undepressed on admixture with an authentic sample of *dl-trans*-1,3-cyclohexanediol of m.p. 118–119.5°. The infrared spectra (KBr pellet) of the specimens were also identical.

ACKNOWLEDGMENTS

We are indebted to Mr. J. H. Parkkari and Mr. J. Legari for assistance with the preparative v.p.c. separation of the bromohydrins; to Prof. R. Y. Moir and Mr. E. J. Langstaff for helpful discussions and access to their results on the analogous chlorohydrins prior to publication; and to Dr. G. Rigby for providing us with authentic samples of *cis*- and *trans*-1,3-cyclohexanediol.

REFERENCES

1. R. A. B. Bannard and L. R. Hawkins. Can. J. Chem. **39**, 1530 (1961).
2. R. A. B. Bannard and L. R. Hawkins. Can. J. Chem. **36**, 1241 (1958).
3. P. D. Bartlett. J. Am. Chem. Soc. **57**, 224 (1935).
4. D. H. R. Barton, D. A. Lewis, and J. F. McGhie. J. Chem. Soc. 2907 (1957).
5. A. A. Casselman and R. A. B. Bannard. Unpublished results.
6. A. A. Casselman, R. Greenhalgh, H. H. Brownell, and R. A. B. Bannard. Can. J. Chem. **38**, 1277 (1960).
7. R. A. B. Bannard and A. A. Casselman. Can. J. Chem. **39**, 1879 (1961).
8. W. Rigby. J. Chem. Soc. 1856 (1949).
9. G. E. McCasland and E. C. Horswill. J. Am. Chem. Soc. **75**, 4020 (1953).
10. R. U. Lemieux, R. K. Kullnig, and R. Y. Moir. J. Am. Chem. Soc. **80**, 2237 (1958).
11. R. U. Lemieux, R. K. Kullnig, H. J. Bernstein, and W. G. Schneider. J. Am. Chem. Soc. **80**, 6098 (1958).
12. F. A. L. Anet, R. A. B. Bannard, and L. D. Hall. Can. J. Chem. **41**, 2331 (1963).
13. E. Schmidt, W. Knilling, and A. Ascherl. Ber. **59**, 1279 (1926).
14. S. Winstein and H. J. Lucas. J. Am. Chem. Soc. **61**, 1576 (1939).
15. R. A. Raphael. J. Chem. Soc. 544 (1949).
16. C. O. Guss and R. Rosenthal. J. Am. Chem. Soc. **77**, 2549 (1955).
17. L. R. Hawkins and R. A. B. Bannard. Can. J. Chem. **36**, 220 (1958).
18. H. B. Henbest and R. A. L. Wilson. J. Chem. Soc. 4136 (1959).
19. A. Ivochev. Compt. Rend. Acad. Bulgare. Sci. **12**, 235 (1959); Chem. Abstr. **54**, 22351*a* (1960).
20. A. Jovtscheff. Chem. Ber. **93**, 2048 (1960).
21. S. D. Ross, M. Finkelstein, and R. C. Petersen. J. Am. Chem. Soc. **80**, 4327 (1958).
22. L. F. Fieser and M. Fieser. Advanced organic chemistry. Reinhold Publishing Corp., New York. 1961. p.523.
23. D. J. Cram and G. S. Hammond. Organic chemistry. McGraw-Hill Book Co., New York. 1959. p. 542.
24. E. A. Braude and E. S. Waight. J. Chem. Soc. 116 (1952).
25. J. G. Traynham and O. S. Pascual. J. Am. Chem. Soc. **79**, 234 (1957).
26. P. B. D. de la Mare and J. G. Pritchard. J. Chem. Soc. 3910 (1954).
27. P. B. D. de la Mare and J. G. Pritchard. J. Chem. Soc. 3990 (1954).
28. P. B. D. de la Mare and A. Salma. J. Chem. Soc. 3337 (1956).
29. P. B. D. de la Mare, P. G. Naylor, and D. H. L. Williams. J. Chem. Soc. 443 (1962).
30. D. H. R. Barton, R. C. Cookson, W. Klyne, and C. W. Shoppee. Chem. Ind. London, 21 (1954).
31. D. S. Noyce and L. J. Dolby. J. Org. Chem. **26**, 3619 (1961).
32. E. L. Eliel. Stereochemistry of carbon compounds. McGraw-Hill Book Co., New York. 1962. p. 207.
33. R. Y. Moir, E. J. Langstaff, E. Hamanaka, and G. Neville. To be published.
34. R. E. Parker and N. S. Isaacs. Chem. Rev. **59**, 737 (1959).
35. A. Feldstein and C. A. Vander Werf. J. Am. Chem. Soc. **76**, 1626 (1954).
36. R. M. Laird and R. E. Parker. J. Am. Chem. Soc. **83**, 4277 (1961).
37. H. Kwart and A. L. Goodman. J. Am. Chem. Soc. **82**, 1947 (1960).
38. S. J. Angyal. Chem. Ind. London, 1230 (1954).
39. A. Fürst and Pl. A. Plattner. Abstracts of Papers. 12th International Congress of Pure and Applied Chemistry, New York. 1951. p. 405.
40. H. Adkins and H. R. Billica. J. Am. Chem. Soc. **70**, 695 (1948).

Can. J. Chem. Downloaded from www.nrcresearchpress.com by 210.87.254.6 on 09/05/12
For personal use only.

Can. J. Chem. Downloaded from www.nrcresearchpress.com by 210.87.254.105 on 09/05/12
For personal use only.

STUDIES IN THE CYCLIZATION OF THE PRODUCTS OF STOBBE CONDENSATION WITH PROPIOPHENONE

A. M. El-Abbady and S. H. Doss

Department of Chemistry, University College for Girls, Ain Shams University and National Research Centre, Cairo, U.A.R.

Received August 7, 1964

ABSTRACT

The isomeric mixture of the half-esters resulting from the Stobbe condensation of propiophenone with diethyl succinate is cyclized with stannic chloride as well as with sodium acetate in acetic anhydride. Cyclization of the ethyl half-ester chlorides with stannic chloride gives the keto-ester "4-carbethoxy-2-methyl-3-phenylcyclopent-2-enone." This on acid hydrolysis and decarboxylation yields 2-methyl-3-phenylcyclopent-2-enone, from which 2-methyl-3-phenylcyclopentanone is prepared by catalytic reduction. The keto-ester on Clemmensen reduction gives the corresponding unsaturated ester from which 3-methyl-2-phenylcyclopentane-1-carboxylic acid is obtained by catalytic hydrogenation and hydrolysis. 2-Methyl-3-phenylcyclopentanone and 3-methyl-2-phenylcyclopentane-1-carboxylic acid are of interest as intermediates for analogues of steroid hormones. From the latter 3-methyl-2-phenylcyclopentyl hydroxymethyl ketone and its acetate are prepared.

Cyclization of the isomeric mixture of the ethyl half-esters with sodium acetate in acetic anhydride gives methyl 4-acetoxy-1-ethyl-2-naphthoate which is converted into 1-ethyl-4-methoxy-2-naphthoic acid.

In previous studies propiophenone was shown to condense with diethyl succinate in the presence of sodium ethoxide (1) or potassium *tert*-butoxide (2) giving a quantitative yield of an oily isomeric mixture of the half-esters (I*a*, main product, and I*b* *cis* and *trans*; R = C_2H_5). Stobbe (1) was able to separate and identify the three isomeric dibasic acids (I*a*, 80% and I*b* *cis* and *trans*, 9%; R = H). In the present investigation the cyclization of this isomeric mixture of half-esters was carried out aiming to synthesise a cyclopentenone by the use of anhydrous stannic chloride as well as a mixture of fused sodium acetate in acetic anhydride as cyclizing agents. The Stobbe condensation products from alicyclic (3) and aliphatic ketones (4) give normally cyclopentenones on cyclization, but as far as we are aware, no alkyl aryl ketone products have been cyclized in this way.

Stannic Chloride Method

The mixture of the ethyl half-esters was converted into its acid chlorides (II*a* and *b*) by the action of thionyl chloride in the presence of one molecular proportion of pyridine (5). Cyclization of the crude half-ester chlorides was achieved with anhydrous stannic chloride (4). The mixture of products thus obtained was completely neutral to carbonate but partially soluble in cold dilute sodium hydroxide solution. The alkaline solution was acidified and the solid product obtained was acidic to carbonate and melted over a wide range. This mixture when boiled with aqueous caustic soda gave a single substance which was identified as γ-ethyl-γ-phenylisoitaconic acid (I*b* *trans* Ph—CH_2COOH, R = H) (1). This result showed that the alkali-soluble fraction was exclusively the anhydride mixture (III) which was hydrolyzed by the cold alkali to the corresponding known dibasic acid mixture (I*b* *cis* and *trans*, R = H) and then converted by the boiling alkali to I*b* *trans* Ph—CH_2COOH, (R = H). This same isomerization and a similar one were previously reported (1, 6). Now the possibility of the formation of the phenolic ester (XI) can be excluded. The neutral fraction was an oil, which showed bands in the infrared region at 1 750 (m), 1 720 (s), 1 690 (s); 1 610 (m); 765 (s), and 700 (s) cm^{-1}, characteristic of the stretching frequencies of the carbonyl groups of esters, ketones, and conjugated esters and

Can. J. Chem. Downloaded from www.nrcresearchpress.com by 210.87.254.105 on 09/05/12
For personal use only.

ketones; the stretching frequencies of olefinic linkages; and the bending frequencies (out of plane) of aromatic 5H atoms adjacent respectively (7, 12). It gave a single semicarbazone and one 2,4-dinitrophenylhydrazone. Theoretically, such a product may be an unsaturated γ-keto-ester which can have any one of the structures IV, XII, or XIII. Acid hydrolysis and decarboxylation of the product was effected by refluxing with a mixture of glacial acetic acid, constant-boiling hydrobromic acid, and water (8) to yield the previously reported unsaturated ketone (V), as a crystalline solid, m.p. 53–55° (cf. ref. 9*a*, *b*, *c*, *d*, m.p. 50–51°, 47–48°, 49–50°, 51–52° respectively). This ketone gave a semicarbazone, m.p. 251–253° (cf. ref. 9*b*, m.p. 238°), and a 2,4-dinitrophenylhydrazone, m.p. 232–233° (cf. refs. 9*a*, *c*, *d*, m.p. 232–233°, 232–232.5°, 218–220° respectively). Since there are some variations in the published melting points of this ketone and its derivatives, it was thought necessary to confirm its structure through oxidation with concentrated sulfuric acid and mercuric sulfate (10). Benzoic acid was found to be the only insoluble product from this experiment. This indicated that the cyclization took place on the olefinic linkage and not on the aromatic ring, giving 4-carbethoxy-2-methyl-3-phenylcyclopent-2-enone (IV) from the half-ester chloride (II*a*, R = C_2H_5). This agrees with the findings of Dahn (11) in a similar cyclization. The infrared spectrum of the unsaturated ketone showed the expected stretching frequencies at 1 700 and 1 620 cm^{-1} (cf. ref. 9*c*, *e*) and aromatic γ-CH at 765 and 700 cm^{-1}, characteristic of 5H adjacent (12) which further confirmed structure V. Both the unsaturated keto-ester and ketone showed absorption maxima in the ultraviolet spectra at 270, 243, 236 mμ (log ε 4.06, 4.02, 4.00), and 275 mμ (log ε 4.23) respectively (for the unsaturated ketone, cf. ref. 9*c* and *d*, λ_{max} 279.5, 242 mμ (log ε 4.013, 3.18) and 278 mμ (log ε 4.28) respectively; for similar compounds, cf. ref. 13, λ_{max} 276 mμ (log ε 4.20)).

The unsaturated ketone (V) was then hydrogenated at a platinum oxide catalyst, absorbing 1 mole of hydrogen and giving the known 2-methyl-3-phenylcyclopentanone VI (9*a*, *b*), as a colorless oil. Its infrared spectrum showed the expected stretching frequencies at 1 745 cm^{-1} and bending frequencies (out of plane) at 765 and 700 cm^{-1} (7, 12). It gave a semicarbazone, m.p. 220–221° (cf. ref. 9*b*, m.p. 209–210°) and a 2,4-dinitrophenylhydrazone, m.p. 199–200° (cf. ref. 9*a*, m.p. 203–204°).

Clemmensen reduction of the keto-ester (IV) yielded a mixture of neutral (main product) and acid fractions. The neutral fraction consisted mainly of the unsaturated ester (VII; R = C_2H_5), which on alkaline hydrolysis gave the corresponding acid (VII; R = H). This was characterized as *p*-toluidide. The acid fraction was found to be the unsaturated acid (VII; R = H), as it gave the same *p*-toluidide derivative. The structure of the unsaturated ester and its acid was inferred from their ultraviolet spectra ($\lambda_{max}^{ethanol}$ 248.5 mμ; log ε 3.57 and 243 mμ; log ε 3.58, respectively) which showed a styryl structure (14).

The unsaturated ester (VII; R = C_2H_5) was then hydrogenated with Adam's catalyst. It absorbed 1 mole of hydrogen to yield the ester (VIII; R = C_2H_5), whence alkaline hydrolysis gave the corresponding acid (VIII; R = H). 2-Methyl-3-phenylcyclopentanone (VI) and 3-methyl-2-phenylcyclopentane-1-carboxylic acid (VIII; R = H) are of interest, as they could serve as intermediates in the preparation of analogues of steroid hormones. 3-Methyl-2-phenyl-cyclopentane-1-carboxylic acid on treatment with thionyl cloride (15) yielded the corresponding acid chloride, which with diazomethane (16) gave the corresponding diazomethyl ketone. This when treated with glacial acetic acid or with 2 *N* sulfuric acid gave 3-methyl-2-phenylcyclopentyl acetoxymethyl ketone (IX, R = $COCH_3$) or 3-methyl-2-phenylcyclopentyl hydroxymethyl ketone (IX, R = H) respectively. Both compounds (IX, R = H and R = $COCH_3$) reduced ammoniacal silver

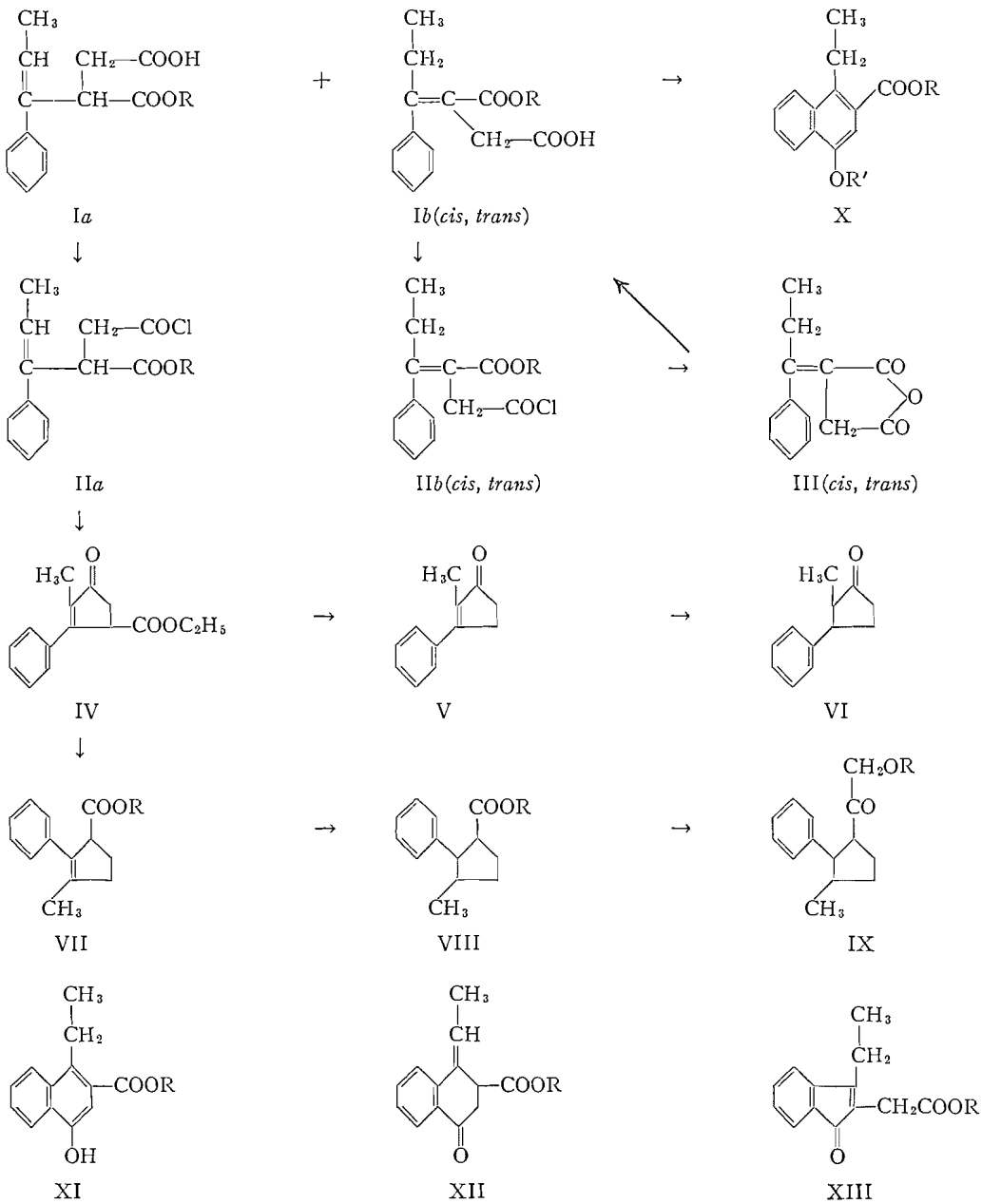

nitrate solution, and their infrared spectra showed the expected stretching frequencies at 3 600 (—OH), 1 720 (>C=O) and 1 730 (—$COCH_2OCO$—) cm^{-1} respectively. They also showed the aromatic γ-CH at 765 and 700 cm^{-1}.

Sodium Acetate Acetic Anhydride Method

Cyclization of the crude mixture of the half-esters using fused sodium acetate in acetic anhydride (17) gave a mixture of acid and neutral fractions. The acid fraction, probably

Can. J. Chem. Downloaded from www.nrcresearchpress.com by 210.87.254.105 on 09/05/12
For personal use only.

unreacted half-ester, was a viscous brownish oil, which on hydrolysis with baryta solution gave the known dibasic acid (I*a*, R = H) (1). The neutral fraction was a viscous oil and found to be ethyl 4-acetoxy-1-ethyl-2-naphthoate (X, R = C_2H_5, R′ = CH_3CO) formed from the half-ester I*b cis* (Ph—CH_2COOH). Trials to isolate any trace of the half-ester I*b trans* (Ph—CH_2COOH) were unsuccessful, indicating that it is present in a very small amount. The fact that the *cis* isomer in the *cis–trans* mixture of the alkylidene succinic half-ester (I*b*) is predominant can be explained by consideration of the two conformations which are favorable for the formation of the two intermediate paraconic esters. These two conformers are represented by XIV and XV. It is clear that the conformer XIV, which leads to the *cis* isomer, is more stable because of the eclipse of the bulky phenyl group with the small hydrogen atom (18).

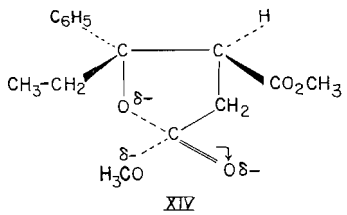

XIV

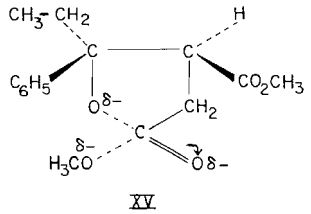

XV

The crude acetoxy ester (X, R = C_2H_5, R′ = CH_3CO) on alkaline hydrolysis afforded 1-ethyl-4-hydroxy-2-naphthoic acid (X, R = R′ = H) in a higher yield than expected. Although Stobbe (1) stated that the ratio of I*a* to I*b* is 9:1, yet the above cyclization yield evokes the possibility of partial conversion of I*a* to I*b* under the conditions of the experiment. The hydroxynaphthoic acid was then treated with dimethyl sulfate and potassium carbonate in acetone to give the methoxy methyl ester (X, R = R′ = CH_3), which on alkaline hydrolysis yielded the methoxynaphthoic acid (X, R = H, R′ = CH_3) as a colorless crystalline solid.

EXPERIMENTAL*

4-Carbethoxy-2-methyl-3-phenylcyclopent-2-enone (IV)

The crude ethyl half-ester (14 g) obtained from the Stobbe condensation of propiophenone with diethyl succinate (2), in dry benzene (140 ml) was treated with pyridine (7 ml) and then redistilled thionyl chloride (6 ml) at 0° for half an hour. The benzene solution of the acid chlorides (II*a* and II*b*) was decanted from the solid cake, which was then pulverized and washed by decantation with benzene. The acid chlorides solution and washings were treated with stannic chloride (10 ml) for 15 h at 0°; the benzene solution was then poured on ice and concentrated hydrochloric acid (40 ml) and shaken. The benzene layer was separated and the aqueous layer washed with ether. The combined ether–benzene extract was washed with saturated sodium bicarbonate solution. Acidification of the bicarbonate washings gave no products. The organic layer was then extracted with cold 10% sodium hydroxide solution. Acidification of the sodium hydroxide washings with cold dilute hydrochloric acid gave a colorless solid, m.p. 158–175° (2.2 g). This mixture was completely soluble in $NaHCO_3$ solution and when refluxed in 10% sodium hydroxide solution (30 ml) for 1.5 h it gave after acidification γ-ethyl-γ-phenylisoitaconic acid (*Ib trans* Ph—CH_2COOH, R = H), m.p. 184–185° (from water) (cf. ref. 1).

Anal. Calcd. for $C_{13}H_{14}O_4$: C, 66.65; H, 6.02. Found: C, 66.36; H, 5.85.

The organic layer after drying (Na_2SO_4), evaporation of the solvents, and distillation gave 4-carbethoxy-2-methyl-3-phenyl-cyclopent-2-enone, IV, (6.8 g, 52% crude yield), b.p. 120–122° at 0.3 mm. Infrared spectrum (liquid): 1 700, 1 690, 1 610, 765, 700 cm^{-1}. Ultraviolet spectrum: $\lambda_{max}^{ethanol}$ 270, 243, 236 mμ (log ε, 4.06, 4.02, 4.00).

Anal. Calcd. for $C_{15}H_{16}O_3$: C, 73.75; H, 6.60. Found: C, 73.23; H, 6.69.

It gave a semicarbazone, m.p. 195–196° (from benzene). Ultraviolet spectrum $\lambda_{max}^{ethanol}$ 290 mμ (log ε 4.39).

Anal. Calcd. for $C_{16}H_{19}O_3N_3$: C, 63.77; H, 6.36; N, 13.95. Found: C, 63.56; H, 6.58; N, 13.83.

**All melting points and boiling points are uncorrected. Infrared spectra were recorded on a Perkin-Elmer Infracord 137B spectrophotometer. The ultraviolet absorption spectra were determined with a Perkin-Elmer Spectracord 4000A.*

Can. J. Chem. Downloaded from www.nrcresearchpress.com by 210.87.254.105 on 09/05/12
For personal use only.

Its 2,4-dinitrophenylhydrazone melted at 192–193° (from ethanol). Ultraviolet spectrum: $\lambda_{max}^{CHCl_3}$ 389 mμ (log ε 4.46).

Anal. Calcd. for $C_{21}H_{26}O_6N_4$: C, 59.43; H, 4.75; N, 13.20. Found: C, 59.30; H, 4.87; N, 13.24.

2-Methyl-3-phenylcyclopent-2-enone (V) (9)

The keto-ester IV (12 g distilled) was refluxed with glacial acetic acid (120 ml), constant-boiling hydrobromic acid (80 ml) and water (40 ml) for 1 h, during which carbon dioxide was evolved. The acidic mixture was cooled and poured carefully on crystalline sodium carbonate (320 g) in sufficient water to form a slurry. The ketone was extracted with ether and dried over Na_2SO_4, and the solvent was evaporated to give a brown oily residue (8.4 g). This after distillation, b.p. 101–103° at 0.35 mm, solidified on standing giving 2-methyl-3-phenylcyclopent-2-enone (V) as colorless needles, m.p. 53–55° (from petroleum ether, b.p. 40–60°). Infrared spectrum (Nujol mull): 1 700, 1 620, 765, 700 cm^{-1}. Ultraviolet spectrum: $\lambda_{max}^{ethanol}$ 275 mμ (log ε 4.23).

Anal. Calcd. for $C_{12}H_{12}O$: C, 83.69; H, 7.02. Found: C, 83.86; H, 7.04.

It gave a semicarbazone, m.p. 251–253° (from ethanol).

Anal. Calcd. for $C_{13}H_{15}ON_3$: N, 18.33. Found: N, 17.74.

Its 2,4-dinitrophenylhydrazone melted at 232–233° (from acetic acid).

Anal. Calcd. for $C_{18}H_{16}O_4N_4$: C, 61.36; H, 4.58; N, 15.90. Found: C, 61.11; H, 4.81; N, 15.51.

The unsaturated ketone (1 g) was treated with mercuric sulfate (0.6 g) and concentrated sulfuric acid (8 ml) at 250° for 10 min, then at 300–310° for 50 min using a metal bath and an air condenser. A colorless solid sublimed and was collected from the air condenser, m.p. 119–121°. This on admixing with an authentic specimen of benzoic acid, m.p. 122° (B.D.H.), gave no depression.

2-Methyl-3-phenylcyclopentanone (VI) (9a, b)

A solution of 2-methyl-3-phenylcyclopent-2-enone (2.5 g) in glacial acetic acid (30 ml) was shaken with hydrogen in presence of Adams platinum oxide (0.2 g) until the absorption of hydrogen was ceased. After filtration, the acetic acid was neutralized with sodium carbonate solution. The product was extracted with ether and dried over Na_2SO_4, and the solvent was evaporated to give an oily residue. This on distillation yielded 2-methyl-3-phenyl-cyclopentanone as a colorless liquid (2.3 g), b.p. 81–82° at 0.25 mm. Infrared spectrum (liquid): 1 745, 765, 700 cm^{-1}.

Anal. Calcd. for $C_{12}H_{14}O$: C, 82.72; H, 8.10. Found: C, 82.24; H, 8.54.

It gave a semicarbazone, m.p. 220–221° (from methanol).

Anal. Calcd. for $C_{13}H_{17}ON_3$: C, 67.50; H; 7.41; N, 18.17. Found: C, 67.56; H, 7.37; N, 18.15.

Its 2,4-dinitrophenylhydrazone melted at 199–200° (from acetic acid).

Anal. Calcd. for $C_{18}H_{18}O_4N_4$: C, 61.01; H, 5.12; N, 15.81. Found: C, 60.93; H, 5.38; N, 15.92.

Clemmensen Reduction of the Keto-ester (IV)

To amalgamated zinc wool (80 g) in water (70 ml) and concentrated hydrochloric acid (160 ml) was added the ethyl keto-ester (IV) (20 g) in toluene (150 ml). The whole was refluxed for 30 h; every 6 h, 30 ml of hydrochloric acid was added. After cooling, the toluene layer was separated from the aqueous layer, the latter was extracted with ether, and then the ether–toluene mixture was extracted with sodium bicarbonate solution. The organic layer, after washing with water and drying (Na_2SO_4), afforded a pale-yellow oil (13.4 g), which on distillation gave ethyl 3-methyl-2-phenylcyclopent-2-ene-1-carboxylate (VII; R = C_2H_5), b.p. 97–101° at 0.2 mm. Ultraviolet spectrum: $\lambda_{max}^{ethanol}$ 248.5 mμ (log ε 3.57).

Anal. Calcd. for $C_{15}H_{18}O_2$: C, 78.23; H, 7.88. Found: C, 78.44; H, 7.84.

The bicarbonate solution after washing with ether and acidification afforded a viscous oil (6.2 g) which on distillation yielded 3-methyl-2-phenylcyclopent-2-ene-1-carboxylic acid (VII; R = H), b.p. 130–135° at 0.45 mm. Ultraviolet spectrum: $\lambda_{max}^{ethanol}$ 243 mμ (log ε 3.58).

Anal. Calcd. for $C_{13}H_{14}O_2$: C, 77.20; H, 6.98. Found: C, 76.67; H, 6.48.

It gave a *p*-toluidide, m.p. 131–133° (from methanol).

Anal. Calcd. for $C_{20}H_{21}ON$: C, 82.41; H, 7.26; N, 4.81. Found: C, 82.70; H, 7.25; N, 4.47.

Alkaline hydrolysis of the unsaturated ester (VII; R = C_2H_5) (1.2 g) for 2 h yielded an unsaturated acid (1 g), which gave the same *p*-toluidide as that obtained directly from the Clemmensen reduction, m.p. and mixed m.p. 130–133°.

Ethyl 3-Methyl-2-phenylcyclopentane-1-carboxylate (VIII; R = C_2H_5)

A solution of the unsaturated ethyl ester (VII; R = C_2H_5) (3.6 g) in glacial acetic acid (40 ml) was shaken with hydrogen in presence of Adams platinum oxide (0.3 g). The hydrogenation was ceased when 1 mole of hydrogen absorbed. After filtration and removal of acetic acid under reduced pressure, the residual oil was distilled at 92–96° at 0.2 mm, to give ethyl 3-methyl-2-phenylcyclopentane-1-carboxylate (VIII; R = C_2H_5) as colorless liquid (3.3 g);

Anal. Calcd. for $C_{15}H_{20}O_2$: C, 77.55; H, 8.68. Found: C, 77.76; H, 8.38.

The ester failed to decolorize bromine in carbon tetrachloride.

3-Methyl-2-phenylcyclopentane-1-carboxylic acid (VIII, R = H)

A mixture of the ester (VIII; R = C_2H_5; 5.3 g) and 10% sodium hydroxide solution (70 ml) was refluxed for 3 h; after cooling it was ether-extracted. The ice-cold alkaline solution was acidified with hydrochloric

Can. J. Chem. Downloaded from www.nrcresearchpress.com by 210.87.254.105 on 09/05/12
For personal use only.

acid and was then ether-extracted. The ethereal solution was dried over sodium sulfate and the solvent was removed. The residue (4 g) gave the acid (VIII; R = H) as a colorless viscous oil, b.p. 132–135° at 0.7 mm.

Anal. Calcd. for $C_{13}H_{16}O_2$: C, 76.44; H, 7.90. Found: C, 76.13; H, 7.63.

3-Methyl-2-phenylcyclopentyl Acetoxymethyl Ketone (IX, R = CH_3CO)

3-Methyl-2-phenylcyclopentane-1-carboxylic acid (VIII; R = H; 2.2 g) in dry benzene (20 ml) was allowed to stand 3 d at room temperature with redistilled thionyl chloride (20 ml). Excess thionyl chloride and benzene were removed *in vacuo*, and the final traces of thionyl chloride were removed by addition and subsequent removal of two 10 ml portions of dry benzene. The dry residue was then dissolved in dry ether (30 ml) and added to an ethereal solution of diazomethane (350 ml) (from 20 g of *N*-nitrosomethyl urea) at 0°; after standing for 30 min at 0° and then overnight at room temperature, removal of ether and excess diazomethane *in vacuo* left the corresponding diazoketone as a residual oil (3.5 g). This was dissolved in glacial acetic acid (50 ml); and gradually heated on a water bath. After 45 min (nitrogen evolution complete), the contents of the flask were diluted with water and ether-extracted. After the ether solution was washed with 5% sodium carbonate and then water, it was dried (Na_2SO_4) and evaporated to give a pale-yellow oil (2.5 g). This on distillation gave 3-methyl-2-phenylcyclopentyl acetoxymethyl ketone, b.p. 130–135° at 0.4 mm, which darkens on keeping. This oil reduced ammoniacal silver nitrate. Infrared spectrum (liquid): 1 730, 765, 700 cm^{-1}.

Anal. Calcd. for $C_{16}H_{20}O_3$: C, 73.82; H, 7.74. Found: C, 73.35; H, 7.42.

3-Methyl-2-phenylcyclopentyl Hydroxymethyl Ketone (IX, R = H)

The diazoketone from 1.7 g 3-methyl-2-phenylcyclopentane-1-carboxylic acid, as in the previous experiment, was dissolved in 40 ml pure dioxane, and 20 ml 2 *N* sulfuric acid was added. The evolution of nitrogen started when the mixture was warmed on a water bath and ceased after 45 min. The mixture was then diluted with water and thoroughly extracted with ether. The ethereal solution was washed with small amounts of 5% sodium bicarbonate solution, then with sodium chloride solution. After drying, the ether was removed *in vacuo* and the residual oil (1.8 g) distilled at 112–115° at 0.2 mm. This oil reduced ammoniacal silver nitrate solution.

Anal. Calcd. for $C_{14}H_{18}O_2$: C, 77.03; H, 8.31. Found: C, 77.21; H, 8.42.

1-Ethyl-4-hydroxy-2-naphthoic Acid (X, R = R′ = H)

The crude ethyl half-ester (10 g) and anhydrous sodium acetate (5 g) in acetic anhydride (80 ml) were refluxed for 5 h and then worked up by removing the acetic anyhdride under reduced pressure, adding water, and extracting the precipitate with ether. The ethereal solution was washed with sodium bicarbonate solution, washed with water, and dried (Na_2SO_4). Evaporation left crude methyl 4-acetoxy-1-ethyl-2-naphthoate (X; R = CH_3, R′ = CH_3CO) as a brown viscous oil (5 g), which on hydrolysis with 10% sodium hydroxide solution (100 ml; 2 h refluxing), gave after acidification pale brownish needles (2.5 g). This on crystallization from aqueous ethanol yielded 1-ethyl-4-hydroxy-2-naphthoic acid (X; R = R′ = H), m.p. 189–191°.

Anal. Calcd. for $C_{13}H_{12}O_3$: C, 72.21; H, 5.59. Found: C, 72.34; H, 5.83.

This phenolic acid gave a violet color with alcoholic ferric chloride solution. Acidification of the carbonate washing gave a viscous brown oil (3.6 g), which on treatment with hot saturated barium hydroxide solution (100 ml; 2 h refluxing), gave after acidification γ-ethylidene-γ-phenyl methylsuccinic acid (I*a*; R = H) (1) as colorless crystals (2.4 g), m.p. 136–138° (from water). Its mixed melting point with an authentic specimen, m.p. 137–138°, which had been prepared by alkaline hydrolysis ($Ba(OH)_2$) of the crude half-ester followed by fractional crystallization, gave no depression.

Methyl 1-Ethyl-4-methoxy-2-naphthoate (X; R = R′ = CH_3)

The phenolic acid (X, R = R′ = H; 6 g), dimethyl sulfate (18 g), and anhydrous potassium carbonate (24 g) in acetone (180 ml) were refluxed for 12 h, affording a solid (5.8 g). This after crystallization from methanol gave methyl 1-ethyl-4-methoxy-2-naphthoate (X; R = R′ = CH_3) as colorless plates, m.p. 92–93°.

Anal. Calcd. for $C_{15}H_{16}O_3$: C, 73.75; H, 6.60. Found: C, 73.79; H, 6.57.

1-Ethyl-4-methoxy-2-naphthoic Acid (X; R = H, R′ = CH_3)

Hydrolysis of the ester (X; R = R′ = CH_3; 0.9 g) using 10% sodium hydroxide solution (20 ml) for 1.5 h refluxing, gave a solid (0.7 g). This on crystallization from methanol afforded 1-ethyl-4-methoxy-2-naphthoic acid as colorless crystals, m.p. 199–200°.

Anal. Calcd. for $C_{14}H_{14}O_3$: C, 73.02; H, 6.13. Found: C, 73.15; H, 6.26.

ACKNOWLEDGMENT

The authors thank Dr. F. G. Baddar, Professor of Organic Chemistry, Faculty of Science, Ain Shams University, for spectral determinations.

Can. J. Chem. Downloaded from www.nrcresearchpress.com by 210.87.254.105 on 09/05/12
For personal use only.

REFERENCES

1. H. STOBBE and K. NIEDENZU. Ann. **321**, 94 (1902).
2. W. S. JOHNSON, W. PETERSEN, and W. P. SCHNEIDER. J. Am. Chem. Soc. **69**, 74 (1947).
3. W. S. JOHNSON *et al.* J. Am. Chem. Soc. **67**, 1360 (1945); **67**, 1366 (1945); **72**, 505 (1950). W. E. BACHMANN and R. E. HOLMER. J. Am. Chem. Soc. **73**, 3660 (1951); A. M. EL-ABBADY, J. Am. Chem. Soc. **79**, 1757 (1957).
4. M. ELLIOTT. J. Chem. Soc. 2231 (1956).
5. J. W. COOK and C. A. LAWRENCE. J. Chem. Soc. 1637 (1935).
6. E. H. RODD. Chemistry of carbon compounds. Vol. III, Part B. Elsevier Publishing Co., New York. 1956. p. 1022.
7. L. J. BELLAMY. The infrared spectra of complex molecules. Methuen & Co. Ltd., London. 1958. pp. 34, 64, 132, 178.
8. W. S. JOHNSON, A. GOLDMAN, and W. P. SCHNEIDER. J. Am. Chem. Soc. **67**, 1357 (1945).
9. (*a*) A. KOLNER and R. ROBINSON. J. Chem. Soc. 566 (1941).
   (*b*) A. WEIDLICK and G. H. DANIELS. Ber. **72**, 1590 (1939).
   (*c*) H. O. HOUSE and R. L. WASSON. J. Org. Chem. **22**, 1157 (1957).
   (*d*) R. JACQUIER, M. MOUSSERON, and S. BOYER. Bull. Soc. Chem. France, 1653 (1956).
   (*e*) P. YATES and L. L. WILLIAMS. J. Am. Chem. Soc. **80**, 5896 (1958).
10. A. SCHOMBERG, W. I. AWAD, and G. A. MOUSA. J. Am. Chem. Soc. **77**, 385 (1955).
11. H. DAHN. Helv. Chim. Acta, **34**, 1087 (1951).
12. J. C. P. SCHWARZ. Physical methods in organic chemistry. Oliver and Boyd, London. 1964. p. 52.
13. H. S. FRENCH. J. Am. Chem. Soc. **74**, 514 (1952).
14. A. E. GILAM and E. S. STERN. An introduction to electronic absorption spectroscopy in organic chemistry. Edward Arnold (Publishers) Ltd., London. 1960. p. 126.
15. W. S. KNOWLES, J. A. KUCK, and R. C. ELDERFIELD. J. Org. Chem. **7**, 374 (1942).
16. M. STEIGER and T. REICHSTEIN. Helv. Chim. Acta, **20**, 1164 (1937).
17. W. BORCHE, S. KETTNER, M. GILLIES, H. KUHN, and R. MANTEUFELL. Ann. **526**, 1 (1936).
18. W. I. AWAD, F. G. BADDAR, and M. I. B. SELIM. J. Chem. Soc. 1854 (1962).

Can. J. Chem. Downloaded from www.nrcresearchpress.com by 210.87.254.105 on 09/05/12
For personal use only.

Can. J. Chem. Downloaded from www.nrcresearchpress.com by 210.87.254.105 on 09/05/12
For personal use only.

NOTES

SYNTHESIS OF THE ISOMERIC METHYL *vic*-BROMOFLUOROPROPANOATES

F. H. DEAN[1] AND F. L. M. PATTISON

The two isomeric methyl *vic*-bromofluoropropanoates I and II were required for a detailed n.m.r. study involving heteronuclear spin decoupling (1). Our recent work on the "BrF" addition to aliphatic alkenes (2) provided a route to these esters.

Initially we examined "BrF" addition to methyl acrylate.[2] This addition proceeded in low yield using *N*-bromoacetamide and anhydrous hydrogen fluoride in ether–pyridine at −20°. In addition to the expected methyl 2-bromo-3-fluoropropanoate (I), small quantities of the unexpected methyl 3-bromo-2-fluoropropanoate (II) and a methyl bromoethoxypropanoate (III) were formed; formation of ethers in this addition reaction has been discussed earlier (2). The yield of the required product was later raised to 45% by using 1,3-dibromo-5,5-dimethylhydantoin (in place of *N*-bromoacetamide) in ether – carbon tetrachloride or in chloroform at −30°. The structure of the main product I was proved by elemental analysis, n.m.r. spectroscopy (1), high-resolution infrared spectroscopy, and dehydrohalogenation to methyl α-bromoacrylate. The methyl bromoethoxypropanoate was tentatively assigned the structure III on the basis of dehydrohalogenation experiments; moreover, the isomer, methyl 2-bromo-3-ethoxypropanoate, has been reported to be unstable (5).

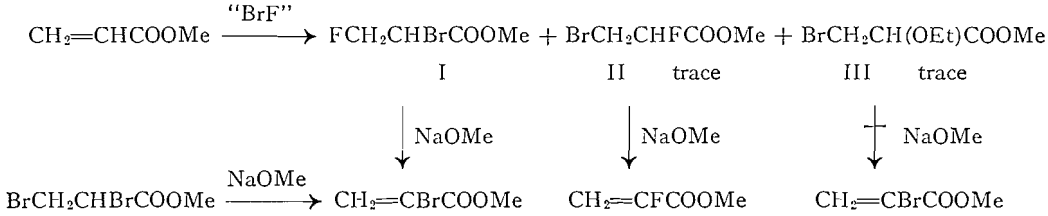

The addition of "BrF" to methyl methacrylate proceeded in good yield to give methyl 3-bromo-2-fluoro-2-methylpropanoate as the single product. The n.m.r. spectrum provided unequivocal proof of structure, as described in the Experimental section.

To obtain methyl 3-bromo-2-fluoropropanoate (II) in reasonable yield, it was necessary to select a precursor which did not have the electronic features of the α-alkenoic acids. Allyl acetate was first examined, and was found to give in low yield a mixture of the required 3-bromo-2-fluoropropyl acetate (IV) and the corresponding hydrolyzed product (V); the similarity in boiling points of these two materials caused difficulty in separation. The ester IV on acid hydrolysis gave the alcohol V. The presence of 3-bromo-2-fluoro-1-propanol was undesirable in the next step in the synthesis, so allyl trichloroacetate was chosen as an alternative precursor; trichloroacetates have been reported to undergo acid-catalyzed hydrolysis 115 times more slowly than acetates (6). Moreover, the large difference in boiling point between the resultant saturated trichloroacetate and the hydrolyzed product would simplify the isolation of the pure products even if some hydrolysis did

[1]*Present address: Department of Chemistry, University of Delaware, Newark, Delaware.*
[2]*While the work was in progress, Bose et al. reported the same reaction (3, 4).*

occur. The "BrF" addition gave a good (69%) yield of pure adduct (VI), which was found to be unstable at room temperature; it was therefore stabilized with 0.05% of pyridine and stored in a refrigerator. Its relationship to the ester from allyl acetate was proved by hydrogenolysis in ethanol; during the hydrogenation, some ethanolysis occurred, thus giving a mixture of the same two products (IV and V) which were isolated from the allyl acetate reaction. The ester VI was converted to the required methyl 3-bromo-2-fluoropropanoate by treatment with nitric acid (7) followed by esterification. Analysis by β-elimination gave methyl α-fluoroacrylate, thus proving the course of the reaction sequence. A very small amount of methyl α-bromoacrylate was isolated, indicating that some anti-Markovnikov addition had also occurred.

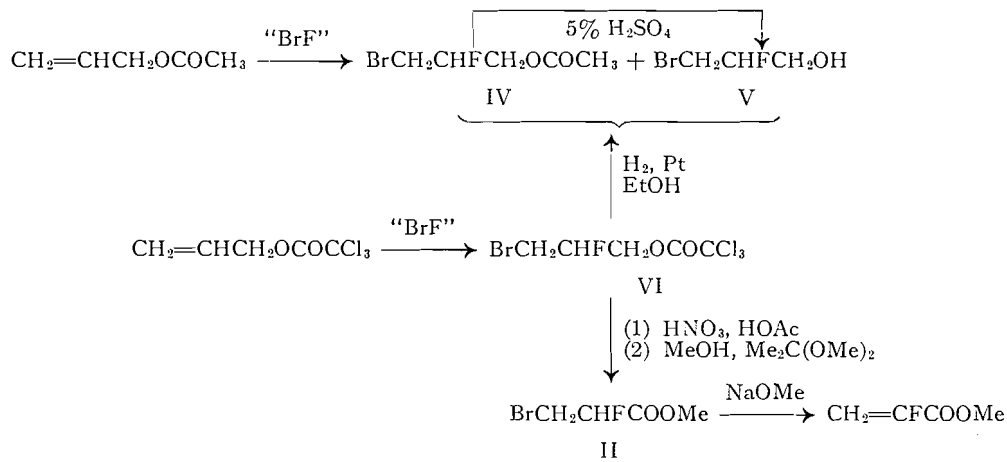

EXPERIMENTAL

The n.m.r. spectra were obtained with Varian A-60 and DP-60 spectrometers. Fractionations were carried out on a 23-plate platinum-plated spinning-band column. Infrared spectra were obtained with Beckman IR-7 and IR-5 infrared spectrophotometers.

Methyl 2-Bromo-3-fluoropropanoate (I)

Methyl acrylate (30 g, 0.35 mole) was added dropwise over 30 min to a stirred mixture of 1,3-dibromo-5,5-dimethylhydantoin (50 g, 0.175 mole), hydrogen fluoride (50 g, 2.5 moles), and chloroform (200 ml) at −40°. After being stirred at −30° for 4 h, the mixture was worked up in the usual way (2) to give the required ester (29.0 g, 45%), b.p. 49.5° at 10.5 mm, n_D^{25} 1.4408, d_4^{20} 1.646; (lit. (8, 9) gives b.p. 80–81.5° at 46 mm, 92–94° at 80 mm; n_D^{24} 1.4432, n_D^{30} 1.4389). The infrared spectrum (4.3% in CCl_4) showed bands at 1 760 (C=O) and at 1 013 and 1 044 (C—F) cm^{-1}. Dehydrohalogenation (see below) gave methyl α-bromoacrylate and a trace of methyl α-fluoroacrylate.

Anal. Calcd. for $C_4H_6BrFO_2$: C, 25.97; H, 3.27; Br, 43.20. Found: C, 25.85; H, 3.31; Br, 43.37.

When the reaction was carried out using *N*-bromoacetamide and anhydrous hydrogen fluoride in ether–pyridine, a higher boiling fraction was ultimately obtained (6%), b.p. 70° at 3.7 mm, n_D^{25} 1.4510, d_4^{20} 1.383. Dehydrohalogenation gave no methyl α-bromoacrylate. The infrared spectrum (CCl_4) showed bands at 1 753 (s; C=O) and 1 110 (v.s.; ether C—O) cm^{-1}.

Anal. Calcd. for $C_6H_{11}BrO_3$: C, 34.14; H, 5.25; Br, 37.86. Found: C, 34.15; H, 5.32; Br, 38.10. Structure III is therefore reasonable for this product.

Dehydrohalogenation of I and II

Absolute ether (0.3–0.5 ml) was added to dry sodium methoxide (50–100 mg) and hydroquinone (5 mg) in a 5-ml pear-shaped flask. One or two drops of the test compound were added, the flask was stoppered and the mixture was swirled. A small sample of the ether solution was then withdrawn using a microliter syringe and injected into the gas chromatograph. The retention times of the products were compared with authentic samples of methyl α-bromoacrylate and methyl α-fluoroacrylate, using both polar (DEGS) and non-polar (Apiezon-L) columns. A temperature of 90–125° was used for the fluoroacrylate and of 125–155° for the bromoacrylate.

Can. J. Chem. Downloaded from www.nrcresearchpress.com by 210.87.254.105 on 09/05/12
For personal use only.

Methyl 3-Bromo-2-fluoro-2-methylpropanoate

A solution of methyl methacrylate (70 g, 0.70 mole) in chloroform (100 ml) was added over 10 min to a stirred solution of 1,3-dibromo-5,5-dimethylhydantoin (100 g, 0.35 mole) and hydrogen fluoride (50 g, 2.5 moles) in chloroform (400 ml) at −50°. The resulting slurry was then stirred at −20° for 4 h. Work-up in the usual way (2) gave unchanged methyl methacrylate (17 g) followed by methyl 3-bromo-2-fluoro-2-methylpropanoate (82.5 g, 78% yield, 59% conversion), b.p. 80.5° at 14 mm, n_D^{25} 1.4423. Gas chromatography indicated a single product.[3] The n.m.r. spectrum was measured in $CDCl_3$ solution, positions being relative to tetramethylsilane. The CH_2Br absorption appeared as the AB portion of an ABX pattern between 200 and 250 c.p.s., and the 2-methyl group as a doublet centered at 1.68 p.p.m. (J_{HF} 21 c.p.s.). The ester CH_3 appeared as a singlet centered at 3.83 p.p.m. The structure of the product is therefore unambiguous.

Anal. Calcd. for $C_5H_8BrFO_2$: C, 30.17; H, 4.05; Br, 40.15. Found: C, 30.37; H, 3.93; Br, 40.14.

3-Bromo-2-fluoropropyl Acetate (IV) and 3-Bromo-2-fluoro-1-propanol (V)

Allyl acetate (50 g, 0.5 mole) and *N*-bromoacetamide (69.7 g, 0.505 mole) were added in the usual way (2) to a solution of hydrogen fluoride (95 g, 4.75 moles) in ether (200 ml). The reaction mixture was stirred at −80° for 75 min, and the products (40.0 g) were isolated in the usual way. From this was isolated crude V (see below) and, in very low yield, pure IV, b.p. 85° at 12 mm, n_D^{25} 1.4521, d_4^{20} 1.515. The infrared spectrum (CCl_4) showed a C=O band at 1 752 cm^{-1}.

Anal. Calcd. for $C_5H_8BrFO_2$: C, 30.17; H, 4.05; Br, 40.15. Found: C, 30.34; H, 4.09; Br, 40.30.

The alcohol V was obtained pure by hydrolyzing a portion of the mixture of IV and V. Using this pure product as a standard, we then proved the presence of V in the original mixture by vapor phase chromatographic analysis on two different columns (polar DEGS and non-polar Apiezon-L) and by infrared spectroscopy. The mixture (11 g) was heated under reflux with 4% sulfuric acid in 60% aqueous dioxane (52 ml), until homogeneous (ca. 30 min). Isolation by ether extraction, washing, drying, and fractionation[4] gave V (4.4 g), b.p. 73–75° at 12 mm, n_D^{25} 1.4683, d_4^{20} 1.770. The infrared spectrum (CCl_4) showed bands at 3 613 (free OH) and 3 408 (hydrogen-bonded OH) cm^{-1}.

Anal. Calcd. for C_3H_6BrFO: C, 22.95; H, 3.85; Br. 50.90. Found: C, 22.93; H, 3.79; Br, 50.79.

3-Bromo-2-fluoropropyl Trichloroacetate (VI)

Anhydrous hydrogen fluoride (120 g, 6.0 moles) was diluted (*caution*!) with a solution of pyridine (17 g) in ether (140 ml). Allyl trichloroacetate (47.3 g, 0.232 mole) and *N*-bromoacetamide (36.0 g, 0.261 mole) were then added at −80° over 10 min. The mixture was stirred at −80° for 1 h and then was gradually warmed to 0° with stirring. Neutralization, isolation, and purification in the usual way[4] gave VI (48.33 g, 69%), b.p. 60° at 0.025 mm, n_D^{25} 1.4895, d_4^{20} 1.760. The infrared spectrum showed a C=O band at 1 776 cm^{-1}.

Anal. Calcd. for $C_5H_5BrCl_3FO_2$: C, 19.86; H, 1.67. Found: C, 20.08; H, 1.73. Treatment of VI with hydrogen (atmospheric pressure) and platinum catalyst in ethanol for 8 h at room temperature gave a mixture of IV and V (by hydrogenolysis of the α-chlorine atoms and considerable ethanolysis of the ester).

Methyl 3-Bromo-2-fluoropropanoate (II)

3-Bromo-2-fluoropropyl trichloroacetate (16.1 g, 0.053 mole) was dissolved in a mixture of glacial acetic acid (35 ml) and nitric acid (35 ml). The solution was warmed at 50° for 32 h and then was allowed to stand at room temperature for 44 h. The nitric and acetic acids were removed by distillation at 11 mm pressure. The residual crude acid was esterified by adding methanol (7.92 g, 0.25 mole), 2,2-dimethoxypropane (20.8 g, 0.20 mole), and *p*-toluenesulfonic acid (10 mg) and allowing the mixture to stand at room temperature for 19 h. The excess methanol and 2,2-dimethoxypropane were distilled off at atmospheric pressure. The residual dark liquid was dissolved in ether, washed with 5% $NaHCO_3$, and dried (Na_2SO_4). Removal of the ether and fractional distillation of the residue gave II (4.15 g, 42%), b.p. 65° at 3.5 mm, n_D^{25} 1.4468, d_4^{20} 1.642. The infrared spectrum (4% in CCl_4) showed bands at 1 747, 1 764 and 1 775 (C=O), and at 1 020 and 1 090 (C—F) cm^{-1}. Dehydrohalogenation gave methyl α-fluoroacrylate and a trace of methyl α-bromoacrylate.

Anal. Calcd. for $C_4H_6BrFO_2$: C, 25.97; H, 3.27; Br, 43.20. Found: C, 26.16; H, 3.41; Br, 42.99.

ACKNOWLEDGMENTS

We wish to express our indebtedness to Canadian Industries Limited, Montreal for the award of a Fellowship (F. H. D.); to the National Research Council for financial support; to Dr. J. B. Stothers of this department for help with the nuclear magnetic resonance spectra; to Dr. D. A. V. Peters of this department for help with some of the preparations; and to Dr. J. J. Baron, Jr., Central Research Laboratory, General Aniline and Film Corporation, Easton, Pa., for a gift of methyl α-fluoroacrylate.

[3]*This ester contains no α-hydrogen atom and is therefore stable to gas chromatographic analysis; α,β-dihaloesters bearing an α-hydrogen atom decompose when this type of analysis is attempted, so are best studied by dehydrohalogenation (see above).*

[4]*Dry, powdered* $CaCO_3$ *should be added to the fractionation flask to prevent autocatalytic decomposition.*

Can. J. Chem. Downloaded from www.nrcresearchpress.com by 210.87.254.105 on 09/05/12
For personal use only.

1. J. B. STOTHERS, J. D. TALMAN, and R. R. FRASER. Can. J. Chem. **42**, 1530 (1964).
2. F. L. M. PATTISON, D. A. V. PETERS, and F. H. DEAN. Can. J. Chem. **43**, 1689 (1965).
3. A. K. BOSE, K. G. DAS, and T. M. JACOB. Chem. Ind. London, 452 (1963).
4. A. K. BOSE, K. G. DAS, and P. T. FUNKE. J. Org. Chem. **29**, 1202 (1964).
5. W. HUBER, R. O. CLINTON, J. S. BUCK, E. J. LAWSON, and P. BEAL. J. Am. Chem. Soc. **67**, 1148 (1945).
6. R. W. TAFT, JR. J. Am. Chem. Soc. **74**, 2729 (1952).
7. F. L. M. PATTISON, R. L. BUCHANAN, and F. H. DEAN. Can. J. Chem. **43**, 1700 (1965).
8. V. TOLMAN and K. VEREŠ. Collection Czech. Chem. Commun. **28**, 421 (1963).
9. A. L. HENNE and C. J. FOX. J. Am. Chem. Soc. **76**, 479 (1954).

RECEIVED MARCH 4, 1965.
DEPARTMENT OF CHEMISTRY,
UNIVERSITY OF WESTERN ONTARIO,
LONDON, ONTARIO.

Can. J. Chem. Downloaded from www.nrcresearchpress.com by 210.87.254.105 on 09/05/12
For personal use only.

THE N.M.R. SPECTRUM OF 2,3,5-TRIMETHYL-2,3,5-TRICYANOHEXANE. UNUSUAL TEMPERATURE DEPENDENCE OF MAGNETIC NONEQUIVALENCE*

P. SMITH AND J. J. MCLESKEY III†

The n.m.r. spectra of short- and long-chain polymers have drawn considerable recent attention (1–4). The compound 2,3,5-trimethyl-2,3,5-tricyanohexane, I, may be regarded as a simple example of a short-chain polymer. Moreover, I is interesting in its own right,

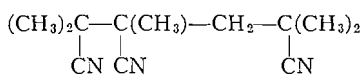

I

since it has an asymmetric carbon atom, the effect of which might show up in its n.m.r. spectrum (5–9). The n.m.r. spectrum of I was first reported for a benzene solution at about 25 °C as part of another study (10). All five methyl groups of I were magnetically nonequivalent, but the protons of the methylene group appeared magnetically equivalent.

Presented here are results of a comprehensive solvent and temperature dependence study of the n.m.r. spectrum of I. In 9 of the 18 solvents employed the methylene group protons of I appeared magnetically nonequivalent at 36 °C. A representative selection of 11 solvents was employed for the temperature dependence investigation. An interesting feature of the results obtained is that for those solvents displaying methylene group nonequivalence which were subjected to a temperature dependence study, this nonequivalence increased with increase in temperature in every case except one. A possible interpretation for this unusual temperature dependence is given.

EXPERIMENTAL

Compound I was prepared and purified as before (11) (m.p. 81 ± 2 °C uncorr.). The 18 solvents employed were reagent grade or better and showed no significant impurities in the n.m.r. region of interest. Spectra were obtained on a Varian A-60 spectrometer equipped with a V-6057 variable temperature accessory, tetramethylsilane (TMS) being used as internal standard. Unsealed sample tubes were employed. Concentrations were 0.2 *M* and, unless otherwise indicated, the probe temperature was 36 ± 1 °C. A minimum of two spectra were run for each solution for each temperature. In the case of the temperature dependence studies, measurements were taken about every 15 °C depending on the observed spectral changes for the following 11 representative solvents listed together with the corresponding temperature range in °C: acrylonitrile (−40 to +74); benzonitrile (−9 to +176); carbon tetrachloride (−9 to +74); chloroacetonitrile (−40 to +114); chlorobenzene (−40 to +123); chloroform (−40 to +63); *o*-dichlorobenzene

**This investigation was supported by United States Public Health Grant GM 07653, Division of General Medical Sciences.*
†*National Defense Education Act Predoctoral Fellow, 1961–1964.*

1. J. B. STOTHERS, J. D. TALMAN, and R. R. FRASER. Can. J. Chem. **42**, 1530 (1964).
2. F. L. M. PATTISON, D. A. V. PETERS, and F. H. DEAN. Can. J. Chem. **43**, 1689 (1965).
3. A. K. BOSE, K. G. DAS, and T. M. JACOB. Chem. Ind. London, 452 (1963).
4. A. K. BOSE, K. G. DAS, and P. T. FUNKE. J. Org. Chem. **29**, 1202 (1964).
5. W. HUBER, R. O. CLINTON, J. S. BUCK, E. J. LAWSON, and P. BEAL. J. Am. Chem. Soc. **67**, 1148 (1945).
6. R. W. TAFT, JR. J. Am. Chem. Soc. **74**, 2729 (1952).
7. F. L. M. PATTISON, R. L. BUCHANAN, and F. H. DEAN. Can. J. Chem. **43**, 1700 (1965).
8. V. TOLMAN and K. VEREŠ. Collection Czech. Chem. Commun. **28**, 421 (1963).
9. A. L. HENNE and C. J. FOX. J. Am. Chem. Soc. **76**, 479 (1954).

RECEIVED MARCH 4, 1965.
DEPARTMENT OF CHEMISTRY,
UNIVERSITY OF WESTERN ONTARIO,
LONDON, ONTARIO.

Can. J. Chem. Downloaded from www.nrcresearchpress.com by 210.87.254.40 on 09/05/12
For personal use only.

THE N.M.R. SPECTRUM OF 2,3,5-TRIMETHYL-2,3,5-TRICYANOHEXANE. UNUSUAL TEMPERATURE DEPENDENCE OF MAGNETIC NONEQUIVALENCE*

P. SMITH AND J. J. MCLESKEY III†

The n.m.r. spectra of short- and long-chain polymers have drawn considerable recent attention (1–4). The compound 2,3,5-trimethyl-2,3,5-tricyanohexane, I, may be regarded as a simple example of a short-chain polymer. Moreover, I is interesting in its own right,

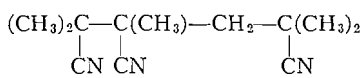

I

since it has an asymmetric carbon atom, the effect of which might show up in its n.m.r. spectrum (5–9). The n.m.r. spectrum of I was first reported for a benzene solution at about 25 °C as part of another study (10). All five methyl groups of I were magnetically nonequivalent, but the protons of the methylene group appeared magnetically equivalent.

Presented here are results of a comprehensive solvent and temperature dependence study of the n.m.r. spectrum of I. In 9 of the 18 solvents employed the methylene group protons of I appeared magnetically nonequivalent at 36 °C. A representative selection of 11 solvents was employed for the temperature dependence investigation. An interesting feature of the results obtained is that for those solvents displaying methylene group nonequivalence which were subjected to a temperature dependence study, this nonequivalence increased with increase in temperature in every case except one. A possible interpretation for this unusual temperature dependence is given.

EXPERIMENTAL

Compound I was prepared and purified as before (11) (m.p. 81 ± 2 °C uncorr.). The 18 solvents employed were reagent grade or better and showed no significant impurities in the n.m.r. region of interest. Spectra were obtained on a Varian A-60 spectrometer equipped with a V-6057 variable temperature accessory, tetramethylsilane (TMS) being used as internal standard. Unsealed sample tubes were employed. Concentrations were 0.2 *M* and, unless otherwise indicated, the probe temperature was 36 ± 1 °C. A minimum of two spectra were run for each solution for each temperature. In the case of the temperature dependence studies, measurements were taken about every 15 °C depending on the observed spectral changes for the following 11 representative solvents listed together with the corresponding temperature range in °C: acrylonitrile (−40 to +74); benzonitrile (−9 to +176); carbon tetrachloride (−9 to +74); chloroacetonitrile (−40 to +114); chlorobenzene (−40 to +123); chloroform (−40 to +63); *o*-dichlorobenzene

**This investigation was supported by United States Public Health Grant GM 07653, Division of General Medical Sciences.*
†*National Defense Education Act Predoctoral Fellow, 1961–1964.*

(−9 to +162); formamide (+33 to +163); methanol (−40 to +62); pyridine (−40 to +106); toluene (−40 to +106). The solvents examined only at 36 °C were acetonitrile, benzaldehyde, benzene, benzotrichloride, dioxane, hexachloroacetone, and *p*-toluonitrile.

RESULTS

At 36 °C the results were as follows. All five methyl groups appeared nonequivalent only in benzene, benzotrichloride, chlorobenzene, toluene, and pyridine. In the remaining solvents, as many as three of the methyl groups appeared equivalent.* The methylene group protons appeared nonequivalent only in acetonitrile, acrylonitrile, benzaldehyde, benzonitrile, chloroacetonitrile, formamide, methanol, pyridine, and *p*-toluonitrile. When an AB quartet† was observed for the methylene group protons the low-field half of the quartet was noticeably broadened, except in the case of formamide.

The temperature dependence of the spectrum of I for the six solvents representative of those in which the methylene group protons appeared nonequivalent at 36 °C, i.e., acrylonitrile, benzonitrile, chloroacetonitrile, formamide, methanol, and pyridine, was as follows: in every case the nonequivalence of the methylene group protons of I increased with increase in temperature over the temperature interval investigated. For the five solvents representative of those in which the methylene group protons appeared equivalent at 36 °C the investigation of the temperature dependence of I gave the following results: in both chloroform and carbon tetrachloride I showed apparently magnetically equivalent methylene group protons over the entire temperature range; however, for the spectrum of I in chlorobenzene and *o*-dichlorobenzene as the temperature was increased above about 100 and 45 °C, respectively, and in toluene as the temperature was decreased below about −10 °C the methylene group protons became increasingly magnetically nonequivalent. A selection of the temperature dependence data is summarized in Table I.

DISCUSSION

The results mentioned above provide a further example of magnetic nonequivalence in a molecule containing an asymmetric carbon atom (5–9, 13, 14). Their most interesting feature is the *increase* in $\delta_{1,2}$ with *increasing* temperature illustrated in Table I and fully tabulated elsewhere (12). This increase occurs for each solvent showing nonequivalent methylene group protons in the temperature range investigated, with one exception. For solutions of I in toluene, $\delta_{1,2}$ fell with rising temperature. In the case of formamide there is only a slight increase in methylene nonequivalence with increase in temperature, which, when considered with the apparent absence of long-range broadening of one of the methylene proton resonances, might be construed as supporting relatively free rotation. However, as may be inferred from the discussion below, this may be an oversimplification. It seems that an increase in $\delta_{1,2}$ with increase in temperature for nonequivalent methylene group protons has not been previously described for any compound. As far as we are aware, in every case so far reported the temperature dependence of $\delta_{1,2}$ for nonequivalent methylene group protons (5, 9, 13, 14) has been a slow reduction in $\delta_{1,2}$ with increasing temperature.

An explanation of this novel temperature dependence of $\delta_{1,2}$ in terms of conformational effects in an asymmetric system would postulate that as the temperature is lowered, for a majority of solvents, the conformation in which the methylene group protons are most

**The methyl resonances are incidental to the present report and are discussed elsewhere (12). These resonances could not be definitely assigned on the basis of available model compounds, e.g., tetramethylsuccinonitrile (10) and 2,4-dicyanopentane (1).*

†The AB nature of the methylene resonance was confirmed by a 100 Mc spectrum of I in benzonitrile kindly provided by Dr. S. G. Levine, North Carolina State University, Raleigh, N.C.

Can. J. Chem. Downloaded from www.nrcresearchpress.com by 210.87.254.40 on 09/05/12
For personal use only.

TABLE I*

Temperature dependence of methylene group chemical shifts

Solvent	Temp., °C†	ν_1	ν_2	$\delta_{1,2}$‡	$J_{1,2}$
Acrylonitrile	−40	117.9	123.6	5.7	14.5
	+20	115.9	123.7	7.8	14.5
	+74	144.5	123.5	9.0	14.5
Chlorobenzene	−40	98.9	98.9	—	—
	+33	101.6	101.6	—	—
	+106	102.8	108.2	5.4	14.5
	+123	103.1	109.1	6.0	14.5
Chloroform	−40	121.9	121.9	—	—
	0	119.7	119.7	—	—
	+63	118.0	118.0	—	—
o-Dichlorobenzene	−9	109.0	109.0	—	—
	+43	107.4	112.8	5.4	14.4
	+162	108.5	117.8	9.3	14.4
Formamide	+33	116.4	127.4	11.0	14.5
	+163	114.7	126.3	11.6	14.5
Pyridine	−40	133.7	139.7	6.0	14.5
	+33	123.1	130.8	7.7	14.5
	+106	118.0	126.9	8.9	14.5
Toluene	−40	78.7	89.1	10.4	14.4
	−9	84.1	90.1	6.0	14.4
	+43	91.9	91.9	—	—
	+106	98.0	98.0	—	—

*Protons 1 and 2 refer to the methylene group protons and ν_1 and ν_2, respectively, are their calculated chemical shifts. The quantity $J_{1,2}$ is the measured coupling constant and $\delta_{1,2}$ is the difference in the 1,2-proton chemical shifts. The data are all in c.p.s., downfield from TMS. Coupling constants and chemical shifts are expressed to the nearest 0.1 c.p.s. Each coupling constant value is the arithmetical mean of all data taken; single measurements for each constant varied from the reported value by as much as a few tenths of a cycle per second.

The methyl resonances each had a width at half height of about 1.0 c.p.s. compared against a corresponding value of about 0.6 c.p.s. for internal TMS.

†Temperature, ±2 °C.

‡When an apparent singlet appeared for protons 1 and 2, this is indicated by no entry for $\delta_{1,2}$. For these cases, the full width of this peak at half height was about 0.9 c.p.s., compared with about 0.6 c.p.s. for internal TMS. This suggests that $\delta_{1,2}$ may be as large as about 4 c.p.s.

equivalent is preferred. But as several contributions to the observed nonequivalence are thought to be important in systems of this kind (7), a final explanation of these results is impossible at present. Nevertheless, the observed temperature dependence of $\delta_{1,2}$ is sufficiently unusual to merit special attention and may serve to warn against too simple explanations of the temperature dependence of the magnetic nonequivalence of methylene group protons.

1. H. G. Clark. Makromol. Chem. **63**, 69 (1963).
2. D. Doskocilova. J. Polymer Sci. **B2**, 421 (1964).
3. F. A. Bovey and G. V. D. Tiers. Fortschr. Hochpolymer.-Forsch. **3**, 139 (1963).
4. D. J. Worsfold and S. Bywater. Can. J. Chem. **42**, 2884 (1964).
5. J. C. Randall, J. J. McLeskey III, P. Smith, and M. E. Hobbs. J. Am. Chem. Soc. **86**, 3229 (1964).
6. H. S. Gutowsky. J. Chem. Phys. **37**, 2196 (1962).
7. E. I. Snyder. J. Am. Chem. Soc. **85**, 2624 (1963).
8. G. M. Whitesides, D. Holtz, and J. D. Roberts. J. Am. Chem. Soc. **86**, 2628 (1964).
9. H. M. Hutton and T. Schaefer. Can. J. Chem. **41**, 1857 (1963).
10. P. Smith, N. Muller, and W. C. Tosch. J. Polymer Sci. **57**, 823 (1962).
11. A. F. Bickel and W. A. Waters. Rec. Trav. Chim. **69**, 1490 (1950).
12. J. J. McLeskey III. Ph.D. Dissertation, Duke University, Durham, North Carolina. 1965.
13. D. Doskocilova and B. Schneider. Collection Czech. Chem. Commun. **29**, 2290 (1964).
14. C. D. Jung and A. A. Bothner-By. J. Am. Chem. Soc. **86**, 4025 (1964).

Received March 22, 1965.
Department of Chemistry,
Duke University,
Durham, North Carolina,
U.S.A.

Can. J. Chem. Downloaded from www.nrcresearchpress.com by 210.87.254.40 on 09/05/12
For personal use only.

LIGNIN MODEL COMPOUNDS. III. DETECTION OF 1-HYDROXY-1-(4-HYDROXY-3-METHOXYPHENYL)-2-PROPANONE IN THE ACIDOLYSIS PRODUCTS OF LIGNIN

J. A. F. Gardner and Harold MacLean

INTRODUCTION

In previous papers of this series (1, 2) and in the results of Adler (3) and Lundgren (4), strong experimental support was provided for Hibbert's proposal that the ethanolysis ketones are derived from lignin via the ketols 1-hydroxy-3-(4-hydroxy-3-methoxyphenyl)-2-propanone (ω-hydroxy-guaiacylacetone) (I) and 1-hydroxy-1-(4-hydroxy-3-methoxyphenyl)-2-propanone (α-hydroxyguaiacylacetone) (II) by a series of rearrangements. If this explanation is accepted, then, in the absence of etherification conditions during an acidic hydrolysis of lignin, both of these ketols as well as ketol III, 2-hydroxy-1-(4-hydroxy-3-methoxyphenyl)-1-propanone (α-hydroxypropioguaiacone), should be formed and, if conditions are not severe, be detectable in the reaction mixture. Ketols I and III have previously been shown to be present in the acidolysis products of Bjorkman lignin (3), but ketol II has not been detected heretofore.

An examination of lignin acidolysis products for the presence of II was made possible by the preparation of reference samples reported in the previous paper (2). Since II has been found to be unstable in basic solution, being quantitatively converted thereby to the ketol III, care was taken in working up the acidolysis products to avoid any contact with even mildly basic solutions.

Extractive-free, native lignin-free western hemlock (*Tsuga heterophylla* (Raf.) Sarg.) sapwood sawdust meal was treated with dioxane–water containing hydrochloric acid according to Pepper *et al.* (5). The pH of the filtered dioxane–water media was adjusted to 6.5 with sodium carbonate solution and evaporated under reduced pressure to a heavy oil. The higher molecular weight lignin fraction was precipitated by diluting the oil with acetone and adding it dropwise to a large volume of vigorously stirred water. The lignin low molecular fraction was reclaimed from the aqueous layer by extraction with chloroform. The resulting oil was separated by partitioning between ether and bisulfite solution, as outlined in the preparation of the synthetic ketol II (2).

Comparison with authentic samples using descending paper chromatography in three different solvent systems (Table I) showed the bisulfite soluble oil to be mainly ketol I together with a small amount of ketol II. Final proof of identity of these products was obtained by thick-paper chromatography separations and infrared spectral comparisons with authentic samples.

The isomeric ketol III was identified in the ether-soluble fraction by a similar procedure. The remaining possible isomeric ketol, 3-hydroxy-1-(4-hydroxy-3-methoxyphenyl)-1-propanone (ω-hydroxypropioguaiacone) could not be detected in the acidolysis products.

Goldschmid's study (6) of the mild aqueous hydrolysis of western hemlock lignin suggested the presence of ketol II by its detection color with diazotized sulfanilic acid

Can. J. Chem. Downloaded from www.nrcresearchpress.com by 210.87.254.42 on 09/05/12
For personal use only.

Can. J. Chem. Downloaded from www.nrcresearchpress.com by 210.87.254.42 on 09/05/12
For personal use only.

TABLE I

R_f values and detection colors of lignin acidolysis monomers

Compound	R_f value*			Detection colors				
	Developing solvent			Ultraviolet		D.S.A.† color	D.S.A. ultraviolet	
	BEAW‡	THF‡	Lindstedt‡	Short§	Long§		Short§	Long§
1-Hydroxy-3-(4-hydroxy-3-methoxyphenyl)-2-propanone (ketol I)	0.72	0.08	0.06	Dark purple	Purple	Pinkish brown	Dark purple	Dark red
1-Hydroxy-1-(4-hydroxy-3-methoxyphenyl)-2-propanone (ketol II)	0.76	0.19	0.16	Purple	Faint purple	Orange with pink edge. Pink in low concentration	Dark red	Dark red
2-Hydroxy-1-(4-hydroxy-3-methoxyphenyl)-1-propanone (ketol III)	0.51	0.35	0.24	Bright blue fl.	Purple fl.	Weak tan	Light purple fl.	Bright blue fl.
3-Hydroxy-1-(4-hydroxy-3-methoxyphenyl)-1-propanone	0.47	0.08	0.03	Purple fl.	Bright blue fl.	Tan	Bright purple fl.	Bright purple fl.

*R_f values are variable depending on the amount of saturation of paper and chromatographic tank atmosphere.
†Sulfanilic acid (9 g) concentrated HCl (90 ml) diluted to 1 liter with water, 2 vol.: sodium nitrite (5%), 1 vol. Let stand in refrigerator 15 min and add potassium carbonate (20%), 2 vol. Spray while freshly prepared.
‡BEAW = Butanol–ethanol–ammonia–water (40:10:1:49 v/v). THF = Tetrahydrofuran – petroleum ether 65/110 – water (3:7:5 v/v). Lindstedt = Benzene – petroleum ether 80/100 – methanol – water (50:50:1:50 v/v organic phase).
§Short ultraviolet, 253.7 mμ; long ultraviolet, 366 mμ.

(DSA) in paper chromatography. This suggestion has now been shown to be correct. However, he was unable to confirm the presence of ketol I.

EXPERIMENTAL

Air-dried western hemlock sapwood was reduced in a Wiley mill to approximately 40–80 mesh and made extractive-free, native-lignin free by soxhlet treatment with alcohol–benzene (1:2) for 48 h, water for 120 h, and absolute ethanol for 48 h, the wood meal being air-dried between each treatment.

Hemlock wood meal (150 g) in dioxane–water (9:1 v/v) (1 200 ml) containing concentrated HCl (19.95 ml) was refluxed with stirring for 2 h under a nitrogen atmosphere. After filtering of the wood meal residue, the reddish dioxane–water solution was partially neutralized to pH 6.5 with sodium carbonate (10%) and evaporated under reduced pressure to a dark brown oil. The oil was thinned with acetone (20 ml) and sprayed in a fine stream into vigorously stirred water (4 liters). The lignin may also be precipitated by using hexane as solvent, giving a smaller yield of a much lighter colored oil. The flocculent lignin precipitate was filtered and the water extracted with chloroform (6 × 50 ml), the emulsion residues being broken by centrifuging. The chloroform extracts were combined, dried over sodium sulfate, and evaporated to a brownish oil (1.23 g).

The oil was taken up in ether (25 ml), separated from additional lignin precipitate by decanting, and treated as outlined in the preparation of synthetic ketol II (2) using half quantities of solvent. This procedure yielded bisulfite-soluble (48 mg) and bisulfite-insoluble (210 mg) fractions.

Paper chromatography of the bisulfite-soluble oil in tetrahydrofuran – petroleum ether (65–110 °C) – water (3:7:5 v/v) (THF), butanol – ethanol – ammonia – water (40:10:1:49 v/v) (BEAW), and the organic phase of benzene – petroleum ether (80–100 °C) – methanol – water (50:50:1:50 v/v) (Lindstedt) (7) together with synthetic samples showed the two main components to be ketol I and ketol II.

Detection was by ultraviolet light and by DSA. R_f values in the respective solvent systems and detection colors are shown in Table I. The remaining oil from the bisulfite solubles (45 mg) was diluted with acetone and streaked on 9 in. wide Whatman No. 17 paper. After the chromatograms were developed in THF solvent, the compounds were detected with ultraviolet light, cut out, and eluted from the paper with additional THF solvent, yielding ketol I in partially crystalline form (25 mg) and ketol II as an oil (3 mg). Infrared spectra were found to be identical with authentic samples using KBr pellets for ketol I and oil smears for ketol II.

Similar thick-paper chromatography on a portion of the bisulfite-insoluble ether residue (80 mg) yielded crystalline ketol III (10 mg) identical with an authentic sample by infrared spectral comparison. Paper chromatographic comparison of all fractions with an authentic sample of the remaining isomeric ketol 3-hydroxy-1-(4-hydroxy-3-methoxyphenyl)-1-propanone (ω-hydroxypropioguaiacone) indicated that this compound was not among the acidolysis products of western hemlock sapwood.

1. J. A. F. Gardner. Can. J. Chem. **32**, 532 (1954).
2. J. A. F. Gardner, D. W. Henderson, and H. MacLean. Can. J. Chem. **40**, 1672 (1962).
3. E. Adler. Paperi Puu, **43**, 11, 634 (1961).
4. R. Lundgren. Paperi Puu, **43**, 11, 670 (1961).
5. J. M. Pepper, P. E. T. Baylis, and E. Adler. Can. J. Chem. **37**, 1241 (1959).
6. O. Goldschmid. Tappi, **38**, 728 (1955).
7. G. Lindstedt. Acta Chem. Scand. **4**, 448 (1950).

Received March 30, 1965.
Forest Products Research Branch,
Department of Forestry,
Ottawa, Canada.

THE IDENTITY OF OXYJAVANICIN WITH FUSARUBIN[1]

G. P. Arsenault

The antibiotic pigments javanicin and oxyjavanicin were isolated from *Fusarium javanicum* by Arnstein, Cook, and Lacey (1, 2). The structure of javanicin was recently established by synthesis (3) but the structure of oxyjavanicin remains unknown. Ruelius and Gauhe isolated fusarubin from *Fusarium solani*, and suggested that fusarubin and oxyjavanicin were identical (4). However, they were unable to make a direct comparison of the two compounds because of the lack of authentic oxyjavanicin.

[1]*Issued as N.R.C. No. 8470.*

Can. J. Chem. Downloaded from www.nrcresearchpress.com by 210.87.254.42 on 09/05/12
For personal use only.

(DSA) in paper chromatography. This suggestion has now been shown to be correct. However, he was unable to confirm the presence of ketol I.

EXPERIMENTAL

Air-dried western hemlock sapwood was reduced in a Wiley mill to approximately 40–80 mesh and made extractive-free, native-lignin free by soxhlet treatment with alcohol–benzene (1:2) for 48 h, water for 120 h, and absolute ethanol for 48 h, the wood meal being air-dried between each treatment.

Hemlock wood meal (150 g) in dioxane–water (9:1 v/v) (1 200 ml) containing concentrated HCl (19.95 ml) was refluxed with stirring for 2 h under a nitrogen atmosphere. After filtering of the wood meal residue, the reddish dioxane–water solution was partially neutralized to pH 6.5 with sodium carbonate (10%) and evaporated under reduced pressure to a dark brown oil. The oil was thinned with acetone (20 ml) and sprayed in a fine stream into vigorously stirred water (4 liters). The lignin may also be precipitated by using hexane as solvent, giving a smaller yield of a much lighter colored oil. The flocculent lignin precipitate was filtered and the water extracted with chloroform (6 × 50 ml), the emulsion residues being broken by centrifuging. The chloroform extracts were combined, dried over sodium sulfate, and evaporated to a brownish oil (1.23 g).

The oil was taken up in ether (25 ml), separated from additional lignin precipitate by decanting, and treated as outlined in the preparation of synthetic ketol II (2) using half quantities of solvent. This procedure yielded bisulfite-soluble (48 mg) and bisulfite-insoluble (210 mg) fractions.

Paper chromatography of the bisulfite-soluble oil in tetrahydrofuran – petroleum ether (65–110 °C) – water (3:7:5 v/v) (THF), butanol – ethanol – ammonia – water (40:10:1:49 v/v) (BEAW), and the organic phase of benzene – petroleum ether (80–100 °C) – methanol – water (50:50:1:50 v/v) (Lindstedt) (7) together with synthetic samples showed the two main components to be ketol I and ketol II.

Detection was by ultraviolet light and by DSA. R_f values in the respective solvent systems and detection colors are shown in Table I. The remaining oil from the bisulfite solubles (45 mg) was diluted with acetone and streaked on 9 in. wide Whatman No. 17 paper. After the chromatograms were developed in THF solvent, the compounds were detected with ultraviolet light, cut out, and eluted from the paper with additional THF solvent, yielding ketol I in partially crystalline form (25 mg) and ketol II as an oil (3 mg). Infrared spectra were found to be identical with authentic samples using KBr pellets for ketol I and oil smears for ketol II.

Similar thick-paper chromatography on a portion of the bisulfite-insoluble ether residue (80 mg) yielded crystalline ketol III (10 mg) identical with an authentic sample by infrared spectral comparison. Paper chromatographic comparison of all fractions with an authentic sample of the remaining isomeric ketol 3-hydroxy-1-(4-hydroxy-3-methoxyphenyl)-1-propanone (ω-hydroxypropioguaiacone) indicated that this compound was not among the acidolysis products of western hemlock sapwood.

1. J. A. F. Gardner. Can. J. Chem. **32**, 532 (1954).
2. J. A. F. Gardner, D. W. Henderson, and H. MacLean. Can. J. Chem. **40**, 1672 (1962).
3. E. Adler. Paperi Puu, **43**, 11, 634 (1961).
4. R. Lundgren. Paperi Puu, **43**, 11, 670 (1961).
5. J. M. Pepper, P. E. T. Baylis, and E. Adler. Can. J. Chem. **37**, 1241 (1959).
6. O. Goldschmid. Tappi, **38**, 728 (1955).
7. G. Lindstedt. Acta Chem. Scand. **4**, 448 (1950).

Received March 30, 1965.
Forest Products Research Branch,
Department of Forestry,
Ottawa, Canada.

THE IDENTITY OF OXYJAVANICIN WITH FUSARUBIN[1]

G. P. Arsenault

The antibiotic pigments javanicin and oxyjavanicin were isolated from *Fusarium javanicum* by Arnstein, Cook, and Lacey (1, 2). The structure of javanicin was recently established by synthesis (3) but the structure of oxyjavanicin remains unknown. Ruelius and Gauhe isolated fusarubin from *Fusarium solani*, and suggested that fusarubin and oxyjavanicin were identical (4). However, they were unable to make a direct comparison of the two compounds because of the lack of authentic oxyjavanicin.

[1]*Issued as N.R.C. No. 8470.*

Can. J. Chem. Downloaded from www.nrcresearchpress.com by 210.87.254.5 on 09/05/12
For personal use only.

In studies on the chemical nature of pigments from fusaria, we obtained, from the Commonwealth Mycological Institute, a culture of the strain of *F. javanicum* used by Cook and co-workers, and isolated javanicin and oxyjavanicin. Oxyjavanicin was shown to be identical with fusarubin. We suggest that the name fusarubin be retained rather than oxyjavanicin since the structure of the compound was fully elucidated (5) under the name fusarubin.

EXPERIMENTAL

F. javanicum Koorders, IMI 29,817, was grown as described by Arnstein and Cook (2). The pigment mixture was isolated from the culture filtrate as described in method *a* of these workers, in yields of 14 mg per liter. The pigment mixture (301 mg) was separated into two components by ascending thin-layer chromatography on 3 × 2 mm thick plates (200 mm × 200 mm) of silica gel G using three passes of 2% methanol in chloroform as developer. The material in each zone was eluted separately with acetone, and recrystallized from chloroform-*n*-hexane. The upper and lower zones afforded 161 mg of javanicin and 25 mg of fusarubin, respectively. Identification of the two compounds was made by direct comparison (by thin-layer chromatography, infrared spectrum, ultraviolet–visible spectrum, melting point, and mixed melting point) with authentic samples.

ACKNOWLEDGMENTS

The author is indebted to Dr. D. Brewer for the culturing of *F. javanicum*, and to Professor F. F. Nord and Dr. H. W. Ruelius for samples of javanicin and fusarubin, respectively.

1. H. R. V. Arnstein, A. H. Cook, and M. S. Lacey. Nature, **157**, 333 (1946).
2. H. R. V. Arnstein and A. H. Cook. J. Chem. Soc. 1021 (1947).
3. E. Hardegger, E. Widmer, K. Steiner, and A. Pfiffner. Helv. Chim. Acta, **47**, 2031 (1964).
4. H. W. Ruelius and A. Gauhe. Ann. Chem. **569**, 38 (1950).
5. E. Hardegger, K. Steiner, E. Widmer, and A. Pfiffner. Helv. Chim. Acta, **47**, 2027 (1964).

Received March 22, 1965.
Atlantic Regional Laboratory,
National Research Council,
Halifax, Nova Scotia.

Can. J. Chem. Downloaded from www.nrcresearchpress.com by 210.87.254.5 on 09/05/12
For personal use only.

THE EFFECT OF ALPHA AND ALPHA′ DEUTERIUM UPON THE P.M.R. OF 2-BUTANONE

O. S. Tee and J. Warkentin

In our work on the relative rates of hydrogen–deuterium exchange at the reactive sites in ketones (1), as followed by n.m.r. spectroscopy, we have observed the effect of α- and α'-deuterium substitution upon the proton resonance of 2-butanone, I. The spectrum of I, in CCl_4 against internal TMS, shows the β-methyl triplet centred at $\tau = 9.00$, the α'-methyl singlet at $\tau = 7.93$, and the α-methylene quartet at $\tau = 7.60$. The coupling constant $J_{H_\alpha H_\beta}$ for the protons of the ethyl group is 7.35 c/s (cf. ref. 2).

If I is exchanged with D_2O in the presence of base,* the α-CH_2 and α'-CH_3 signals decay according to first-order rate laws. As the α-CH_2 is successively deuterated, the β-methyl triplet collapses until at full deuteration it is a close quintet with a splitting $J_{D_\alpha H_\beta} = 1.1$–$1.2$ c/s (Fig. 1), centered about 0.84 c/s upfield from the original β-methyl triplet. It arises

*$OD^\ominus$, $AcO^\ominus$, *and* p-$NO_2PhO^\ominus$ *were employed.*

In studies on the chemical nature of pigments from fusaria, we obtained, from the Commonwealth Mycological Institute, a culture of the strain of *F. javanicum* used by Cook and co-workers, and isolated javanicin and oxyjavanicin. Oxyjavanicin was shown to be identical with fusarubin. We suggest that the name fusarubin be retained rather than oxyjavanicin since the structure of the compound was fully elucidated (5) under the name fusarubin.

EXPERIMENTAL

F. javanicum Koorders, IMI 29,817, was grown as described by Arnstein and Cook (2). The pigment mixture was isolated from the culture filtrate as described in method *a* of these workers, in yields of 14 mg per liter. The pigment mixture (301 mg) was separated into two components by ascending thin-layer chromatography on 3 × 2 mm thick plates (200 mm × 200 mm) of silica gel G using three passes of 2% methanol in chloroform as developer. The material in each zone was eluted separately with acetone, and recrystallized from chloroform-*n*-hexane. The upper and lower zones afforded 161 mg of javanicin and 25 mg of fusarubin, respectively. Identification of the two compounds was made by direct comparison (by thin-layer chromatography, infrared spectrum, ultraviolet–visible spectrum, melting point, and mixed melting point) with authentic samples.

ACKNOWLEDGMENTS

The author is indebted to Dr. D. Brewer for the culturing of *F. javanicum*, and to Professor F. F. Nord and Dr. H. W. Ruelius for samples of javanicin and fusarubin, respectively.

1. H. R. V. Arnstein, A. H. Cook, and M. S. Lacey. Nature, **157**, 333 (1946).
2. H. R. V. Arnstein and A. H. Cook. J. Chem. Soc. 1021 (1947).
3. E. Hardegger, E. Widmer, K. Steiner, and A. Pfiffner. Helv. Chim. Acta, **47**, 2031 (1964).
4. H. W. Ruelius and A. Gauhe. Ann. Chem. **569**, 38 (1950).
5. E. Hardegger, K. Steiner, E. Widmer, and A. Pfiffner. Helv. Chim. Acta, **47**, 2027 (1964).

Received March 22, 1965.
Atlantic Regional Laboratory,
National Research Council,
Halifax, Nova Scotia.

Can. J. Chem. Downloaded from www.nrcresearchpress.com by 210.87.254.105 on 09/05/12
For personal use only.

THE EFFECT OF ALPHA AND ALPHA′ DEUTERIUM UPON THE P.M.R. OF 2-BUTANONE

O. S. Tee and J. Warkentin

In our work on the relative rates of hydrogen–deuterium exchange at the reactive sites in ketones (1), as followed by n.m.r. spectroscopy, we have observed the effect of α- and α'-deuterium substitution upon the proton resonance of 2-butanone, I. The spectrum of I, in CCl_4 against internal TMS, shows the β-methyl triplet centred at $\tau = 9.00$, the α'-methyl singlet at $\tau = 7.93$, and the α-methylene quartet at $\tau = 7.60$. The coupling constant $J_{H_\alpha H_\beta}$ for the protons of the ethyl group is 7.35 c/s (cf. ref. 2).

If I is exchanged with D_2O in the presence of base,* the α-CH_2 and α'-CH_3 signals decay according to first-order rate laws. As the α-CH_2 is successively deuterated, the β-methyl triplet collapses until at full deuteration it is a close quintet with a splitting $J_{D_\alpha H_\beta} = 1.1$–$1.2$ c/s (Fig. 1), centered about 0.84 c/s upfield from the original β-methyl triplet. It arises

*$OD^\ominus$, $AcO^\ominus$, *and* p-$NO_2PhO^\ominus$ *were employed.*

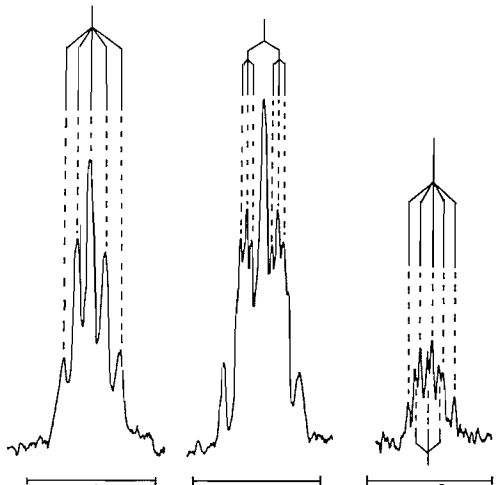

FIG. 1. FIG. 2. FIG. 3.

from the splitting of the β-methyl protons by the two deuterons ($I = 1$) of the CD_2 group, each of which can have $m_s = 1, 0, -1$.

At partial deuteration (ca. 50%), two spectra superimposed can be seen for the β-methyl protons (Fig. 2), viz., the original triplet from molecules still possessing $—CH_2CH_3$, and a pair of triplets arising from β-methyl protons adjacent to a CHD group, their signal first being split into a doublet by the proton ($I = \frac{1}{2}$) and then into triplets by the deuteron ($I = 1$). The splitting $J_{H_\alpha H_\beta}$ due to the proton of the CHD group is 7.25 c/s and the shift associated with the isotopic substitution is about 0.42 c/s upfield. The splitting $J_{D_\alpha H_\beta}$ of the triplets (Fig. 2) is 1.0–1.1 c/s.

As the α'-methyl group is exchanged its signal passes from a singlet (CH_3), through a triplet (CH_2D), to a quintet (CHD_2), which then disappears (CD_3). At approximately 50% exchange the α'-methyl spectrum shows the triplet of CH_2D and the quintet of CHD_2, superimposed (Fig. 3). For both these triplet and quintet spectra $J_{H_\alpha D_\alpha}$ is 2.3–2.4 c/s, and the shift associated with exchange of each proton is about 1.0 c/s upfield.

The results, summarized in Table I, agree with those of Gutowsky for acetone-d_5 (3), and those of Tiers (4, 5), and others (6, 7) on other types of systems. While we have found no previous reference to $J_{D_\alpha H_\beta}$ through saturated bonds, Tiers *et al.* have observed $J_{T_\alpha H_\beta}$ in tritiated ethylbenzene (10).

TABLE I

Group	Shifts relative to signal in undeuterated substrate (p.p.m.)	Shifts relative to signal in undeuterated substrate (c/s)	Coupling constants $J_{H_\alpha H_\beta}$ (c/s)	Coupling constants $J_{D_\alpha H_\beta}$ (c/s)	Coupling constants $J_{H_\alpha D_\alpha}$ (c/s)
CH_2CH_3	0	0	7.35±0.05	—	—
$CHDCH_3$	−.007	−0.42±0.05	7.25±0.05	1.0–1.1	(2.3–2.4)*
CD_2CH_3	−.014	−0.84±0.05	—	1.1–1.2	—
CH_3	0	0	—	—	—
CDH_2	−.017	−1.0±0.05	—	—	2.3–2.4
CD_2H	−.034	−2.0±0.05	—	—	2.3–2.4

*$J_{H_\alpha D_\alpha}$ for the —CHD— group is difficult to measure as the methylene region is complex. However, it is probably 2.3 to 2.4 c/s (cf. α'-CDH_2, CD_2H, and ref. 3).

Can. J. Chem. Downloaded from www.nrcresearchpress.com by 210.87.254.105 on 09/05/12
For personal use only.

The shifts upfield associated with the deuterium substitution are consistent with the accepted view (4, 5, 8, 9) that C—D bonds are more electron-releasing than C—H bonds.

All spectra were recorded on a Varian A-60 spectrometer with the probe temperature at ca. 35 °C.

1. J. WARKENTIN and L. K. M. LAM. Can. J. Chem. **42**, 1676 (1964).
2. L. M. JACKMAN. Applications of n.m.r. spectroscopy to organic chemistry. Pergamon Press, London. 1959. p. 87.
3. H. S. GUTOWSKY. J. Chem. Phys. **31**, 1683 (1959).
4. G. V. D. TIERS. J. Am. Chem. Soc. **79**, 5585 (1957).
5. G. V. D. TIERS. J. Chem. Phys. **29**, 963 (1958).
6. E. I. SNYDER. J. Phys. Chem. **67**, 2873 (1963).
7. C. G. MACDONALD, J. S. SHANNON, and S. STERNHELL. Australian J. Chem. **17**, 38 (1964).
8. E. A. HALEVI. Tetrahedron, **1**, 174 (1957).
9. E. A. HALEVI. Secondary isotope effects. *In* Progress in physical organic chemistry. *Edited by* V. Gold. Vol. 1. Interscience Publishers Inc., New York. 1963, and references therein.
10. G. V. D. TIERS, C. A. BROWN, R. A. JACKSON, and T. N. LAHR. J. Am. Chem. Soc. **86**, 2526 (1964).

RECEIVED MARCH 5, 1965.
DEPARTMENT OF CHEMISTRY,
MCMASTER UNIVERSITY,
HAMILTON, ONTARIO.

Can. J. Chem. Downloaded from www.nrcresearchpress.com by 210.87.254.105 on 09/05/12
For personal use only.

ORTHO-CHLOROBENZALMALONAMIDE AND RELATED COMPOUNDS

RAYMOND P. MARIELLA AND TERRY CONWAY[1]

Recent synthetic techniques (1–11), showing great promise in ring closure reactions, use aryne type intermediates. It was hoped to prepare, for the first time, unsaturated or aromatic type heterocycles directly in one step, via an amide-aryne type intermediate (i.e.):

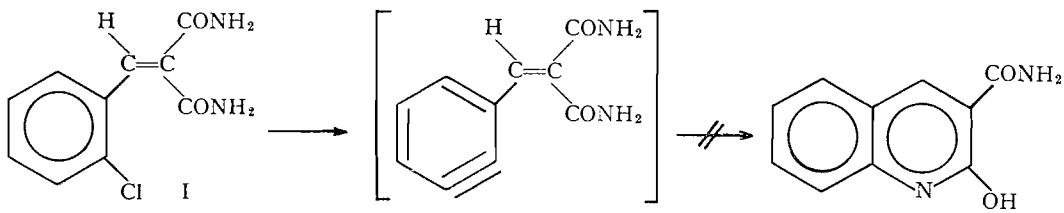

Since one of the carboxamides was locked in the cisoid position, it was hoped that favorable conditions for the desired reaction would prevail. However, repeated experiments on I using potassium in liquid ammonia were unsuccessful in that the original compound was always isolated. Since I had never been synthesized before, subsequent reactions were performed to confirm its expected chemical behavior.

2-Chlorobenzalmalonamide (I) was synthesized from 2-chlorobenzaldehyde and malonamide. Initial attempts to prepare I using the reagents indicated under basic conditions were not practical. The reaction did proceed successfully under acidic conditions, and it was later found that I did undergo a reverse Knoevenagel reaction under basic conditions. Preliminary attempts to prepare I from II via the acid chloride were not successful, and attempts to hydrolyze III to I by means of concentrated sulfuric acid were also unsuccessful. However, in this latter reaction, 2-chlorobenzalcyanoacetamide (IV) was isolated,

[1]*Taken in part from the M.S. thesis of Terry Conway (February 1965).*

The shifts upfield associated with the deuterium substitution are consistent with the accepted view (4, 5, 8, 9) that C—D bonds are more electron-releasing than C—H bonds.

All spectra were recorded on a Varian A-60 spectrometer with the probe temperature at ca. 35 °C.

1. J. WARKENTIN and L. K. M. LAM. Can. J. Chem. **42**, 1676 (1964).
2. L. M. JACKMAN. Applications of n.m.r. spectroscopy to organic chemistry. Pergamon Press, London. 1959. p. 87.
3. H. S. GUTOWSKY. J. Chem. Phys. **31**, 1683 (1959).
4. G. V. D. TIERS. J. Am. Chem. Soc. **79**, 5585 (1957).
5. G. V. D. TIERS. J. Chem. Phys. **29**, 963 (1958).
6. E. I. SNYDER. J. Phys. Chem. **67**, 2873 (1963).
7. C. G. MACDONALD, J. S. SHANNON, and S. STERNHELL. Australian J. Chem. **17**, 38 (1964).
8. E. A. HALEVI. Tetrahedron, **1**, 174 (1957).
9. E. A. HALEVI. Secondary isotope effects. *In* Progress in physical organic chemistry. *Edited by* V. Gold. Vol. 1. Interscience Publishers Inc., New York. 1963, and references therein.
10. G. V. D. TIERS, C. A. BROWN, R. A. JACKSON, and T. N. LAHR. J. Am. Chem. Soc. **86**, 2526 (1964).

RECEIVED MARCH 5, 1965.
DEPARTMENT OF CHEMISTRY,
MCMASTER UNIVERSITY,
HAMILTON, ONTARIO.

ORTHO-CHLOROBENZALMALONAMIDE AND RELATED COMPOUNDS

RAYMOND P. MARIELLA AND TERRY CONWAY[1]

Recent synthetic techniques (1–11), showing great promise in ring closure reactions, use aryne type intermediates. It was hoped to prepare, for the first time, unsaturated or aromatic type heterocycles directly in one step, via an amide-aryne type intermediate (i.e.):

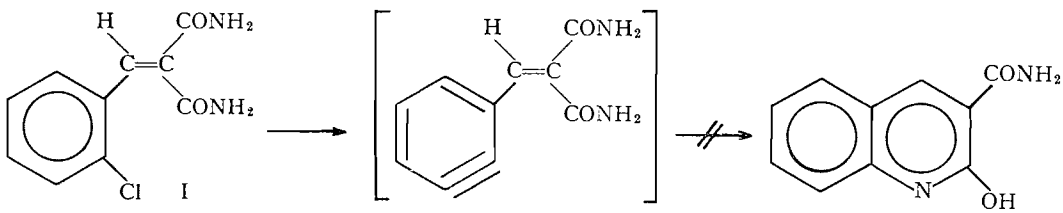

Since one of the carboxamides was locked in the cisoid position, it was hoped that favorable conditions for the desired reaction would prevail. However, repeated experiments on I using potassium in liquid ammonia were unsuccessful in that the original compound was always isolated. Since I had never been synthesized before, subsequent reactions were performed to confirm its expected chemical behavior.

2-Chlorobenzalmalonamide (I) was synthesized from 2-chlorobenzaldehyde and malonamide. Initial attempts to prepare I using the reagents indicated under basic conditions were not practical. The reaction did proceed successfully under acidic conditions, and it was later found that I did undergo a reverse Knoevenagel reaction under basic conditions. Preliminary attempts to prepare I from II via the acid chloride were not successful, and attempts to hydrolyze III to I by means of concentrated sulfuric acid were also unsuccessful. However, in this latter reaction, 2-chlorobenzalcyanoacetamide (IV) was isolated,

[1]*Taken in part from the M.S. thesis of Terry Conway (February 1965).*

Can. J. Chem. Downloaded from www.nrcresearchpress.com by 210.87.254.42 on 09/05/12
For personal use only.

which was identical to the product prepared from cyanoacetamide and 2-chlorobenzaldehyde.

The reduction of I to V was readily accomplished using a platinum catalyst. It is interesting that treatment of VI with zinc metal and zinc chloride in 95% ethanol also gave V. The bromination of I was very slow and was accomplished under heterogeneous conditions in CCl_4 after 20 h. The dibromide (VI) was of variable stability: stable in cold and refluxing 95% ethanol, and unstable in cold absolute methanol. The dibromide (VI) was unstable in refluxing toluene as evidenced by the formation of benzyl bromide (no nuclear bromination was observed). In this regard, VI seems to be a selective solid brominating reagent.

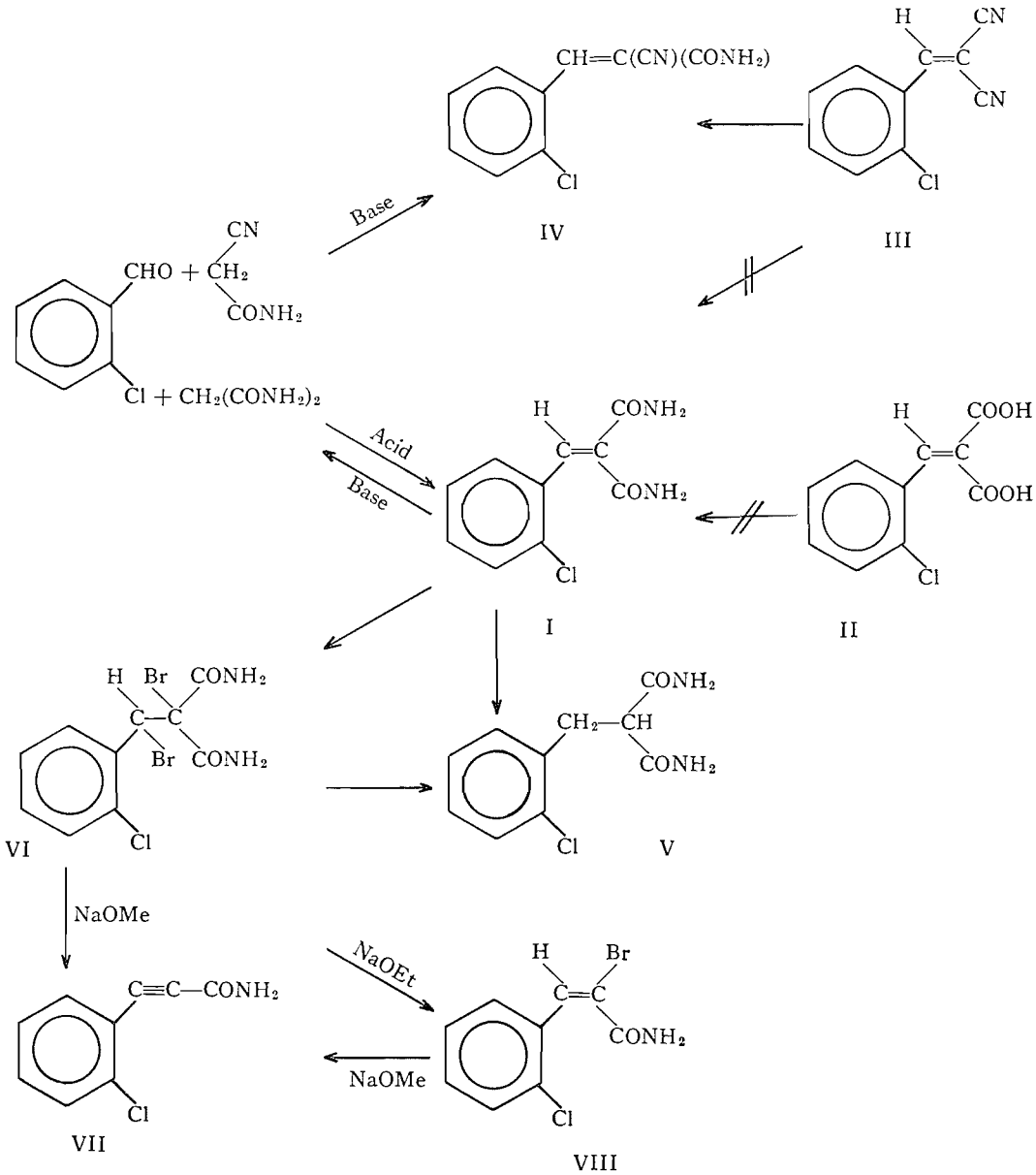

Can. J. Chem. Downloaded from www.nrcresearchpress.com by 210.87.254.42 on 09/05/12
For personal use only.

The treatment of VI with sodium methoxide converted VI to VII directly in one step in fairly good yield. The treatment of VI with sodium *ethoxide*, however, gave IX exclusively. To show that the effect was indeed a selective one, the subsequent treatment of IX with sodium *methoxide* also gave VII, which was identical in all respects to the product prepared from VI.

EXPERIMENTAL

All melting points were determined on a Fisher-Johns melting point apparatus and are corrected. Analyses were performed by Micro-Tech Laboratories, Skokie, Illinois. The following chemicals were commercially available and were purchased from the Fisher Scientific Co.: malonamide, malonic acid, malononitrile, cyanoacetamide, and 2-chlorobenzaldehyde. The ultraviolet spectra were determined on a Beckman Spectrophotometer, model DU; infrared spectra were determined on a Perkin–Elmer spectrophotometer, model 21, and the nuclear magnetic resonance (n.m.r.) spectra were determined on a Varian instrument, model A60.

2-Chlorobenzalmalonamide (I)

Malonamide (10 g, 0.1 mole) and 20 ml of glacial acetic acid were refluxed until the malonamide dissolved. 2-Chlorobenzaldehyde (10.7 ml, 0.1 mole) was added, refluxing was continued for 1 h, and the reaction mixture was steam distilled to remove any unreacted aldehyde. The reaction mixture was then cooled and allowed to stand 2 h, and the white solid which formed was filtered off and washed with ether (8.5 g, 37% yield). Repeated crystallizations from 95% ethanol gave fine white crystals, m.p. 196.5–198°.

Anal. Calcd. for $C_{10}H_9ClN_2O_2$: C, 53.46; H, 4.04; N, 12.47. Found: C, 53.52; H, 4.50; N, 12. 34.

The ultraviolet (methanol) showed an absorption maximum (broad band) at 269 mμ, log ϵ = 4.0720. The infrared (KBr disc) showed characteristic strong absorption at 5.9, 6.0, and 6.15 μ indicating an α,β-unsaturated amide. The N—H amide bands at 2.9, 3.0, and 3.1 μ were strong. The n.m.r. (CD_3OD solvent, $(CH_3)_4Si$ standard) showed a sharp singlet at 7.9 p.p.m. for the vinylic proton, the characteristic multiplet for the aromatic protons at 7.1–7.8 p.p.m., and a broad peak at 4.2–5.0 p.p.m. for the amide protons.

2-Chlorobenzalmalonic Acid (II)

2-Chlorobenzaldehyde and malonic acid were allowed to react according to the method of Stuart (12) and the product was obtained in a 63% yield with a melting point identical to that previously reported, m.p. 192°.

2-Chlorobenzalmalononitrile (III)

2-Chlorobenzaldehyde and malononitrile were allowed to react according to the method of Corson (13) and the product was obtained in an 80% yield, m.p. 98 °C (lit. m.p. 95–96 °C (13)).

2-Chlorobenzalcyanoacetamide (IV)

From III

2-Chlorobenzalmalononitrile (III) (35 g, 0.14 mole) was added to 50 ml concentrated sulfuric acid. The mixture was heated with stirring at 100° for 5 min. The warm, dark-orange-colored reaction mixture was then slowly added to 150 ml of ice water. The white precipitate which formed was filtered off and washed with water, giving 20 g of fine white needles (66%). Recrystallization from 95% ethanol gave material, m.p. 171°.

From 2-Chlorobenzaldehyde and Cyanoacetamide

Cyanoacetamide (4.2 g, 0.05 mole), 2-chlorobenzaldehyde (7.0 g, 0.05 mole), 0.3 ml of 2 *M* NaOH, and 150 ml of 95% ethanol were refluxed for 3 h and then allowed to cool. The white precipitate which formed was filtered off and washed well with water (8.1 g, 80%). Recrystallization from 95% ethanol gave a white solid, m.p. 169.5–171°. The mixed melting point with the product formed from III was not depressed, and the infrared spectra of the two products were identical.

Anal. Calcd. for $C_{10}H_7ClN_2O$: C, 58.28; H, 3.52; N, 13.13. Found: C, 58.13; H, 3.42; N, 13.56.

The infrared spectra (KBr) consisted of strong bands at 5.9 and 6.15 μ indicating an unsaturated amide, and strong bands at 2.9 and 3.15 μ indicating N—H vibrations. Also, a very characteristic peak at 4.5 μ showed the presence of the nitrile group.

2-(2-Chlorobenzyl)-malonamide (V)

From I

Into a Parr bomb containing 0.2 g of prehydrogenated platinum oxide and 29 ml of 95% ethanol was added 2.0 g (0.009 mole) of I dissolved in a mixture of 125 ml of 95% ethanol and 1.5 ml of glacial acetic acid. The hydrogenation was completed in 15 min. The reaction mixture was then heated to reflux and the platinum catalyst was filtered from the hot solution. After the filtrate had cooled, the white solid which had separated was filtered off and washed with ether (1.2 g, 51%). Final purification was achieved by sublimation *in vacuo*, m.p. 246.5–247.5°.

Can. J. Chem. Downloaded from www.nrcresearchpress.com by 210.87.254.42 on 09/05/12
For personal use only.

From VI

To a 250 ml three-necked round-bottom flask, equipped with an addition funnel, a mechanical stirrer, and a condenser protected by a drying tube, was added 2.18 g (0.03 mole) of zinc dust, a pinch of zinc chloride, and 25 ml of 95% ethanol. This was heated to reflux with stirring and then 8.57 g (0.02 mole) of 2-chlorobenzalmalonamide dibromide (VI) dissolved in 150 ml of 95% ethanol was slowly added. Refluxing was stopped after 7 h, and the reaction mixture was filtered while hot to remove the zinc dust. The filtrate was then cooled and the precipitate which formed was filtered off and washed with cold 95% ethanol and then ether (1.6 g, 72%) (white shiny flakes from ethanol), m.p. 247–248.5°. The material was identical with the product obtained above from I, the mixed melting point was non-depressed, and the infrared spectra were identical.

Anal. Calcd. for $C_{10}H_{11}ClN_2O_2$: C, 53.00; H, 4.86; N, 12.35. Found: C, 52.84; H, 4.77; N, 12.32.

The ultraviolet spectra indicated no absorption (in methanol) between 230 mμ and 340 mμ. The infrared showed very strong carbonyl amide absorption at 5.95 μ and strong N—H amide bands at 2.9, 2.95, and 3.1 μ. The n.m.r. spectra in trifluoroacetic acid showed a broad multiplet for the amide and aromatic protons from 7.2–8.1 p.p.m., a triplet at 4.15 p.p.m. for the CH group, and a doublet at 3.7 p.p.m. for the methylene group adjacent to the aromatic ring.

2-Chlorobenzalmalonamide Dibromide (VI)

Into a 200 ml three-necked round-bottom flask, equipped with an addition funnel, a mechanical stirrer, and a condenser, were added 50 ml of carbon tetrachloride (which had been dried over calcium chloride) and 5.0 g (0.025 mole) of I. The suspension was brought to reflux and bromine (4.16 g, 0.025 mole) dissolved in 50 ml of carbon tetrachloride was slowly added as the suspension was stirred. The refluxing was continued for approximately 20 h. After the refluxing had been stopped and the mixture cooled, the precipitate was filtered off and washed with carbon tetrachloride and ether. The yield was 7.6 g of shiny, white plates (75%), m.p. 149–150° (decomp.), after several recrystallizations from 95% ethanol. (Decomposition begins at 120°.)

Anal. Calcd. for $C_{10}H_9Br_2ClN_2O_2$: C, 30.84; H, 2.33. Found: C, 31.36, H, 2.26.

The product seemed to be much more stable in 95% ethanol than in absolute methanol. The infrared showed strong amide absorption at 5.95 μ, and medium N—H amide bands at 2.9, 2.95, and 3.15 μ.

2-Chlorophenylpropargylic Acid Amide (VII)

From VI

Into a 50 ml round-bottom flask containing 25 ml of absolute methanol (prepared by the Grignard method) was added 0.5 g of sodium metal. VI (5 g, 0.0125 mole) was added; the mixture was refluxed for 45 min and then cooled and diluted to twice its volume with cold water. The light-yellow precipitate that formed was filtered off and washed with water. The yield was 1.55 g (69%) of light-yellow crystals, m.p. 120.5–121.5° from water.

Anal. Calcd. for C_9H_6ClNO: C, 60.18; H, 3.37; N, 7.80. Found: C, 60.35; H, 3.35; N, 8.28.

The ultraviolet indicated an absorption maximum (broad band) at 250 mμ (log ϵ = 4.158). The infrared showed an amide band at 6.0 μ (strong), triple bond absorption at 4.4 μ (strong), and N=H bands at 2.95, 3.1, and 3.2 (medium). The n.m.r. ($CDCl_3$ solvent against Me_4Si as standard) showed a multiplet for the aromatic protons from 7.0–7.7 p.p.m. and a broad peak for the amide protons from 5.6–6.6 p.p.m. The signal area ratio of the two peaks was 2:1 as expected.

From IX

IX (1.6 g, 0.006 mole) was added to a solution of 0.4 g of sodium in 20 ml of absolute methanol. The reaction mixture was refluxed for 30 min and then diluted to twice its volume with cold water. The precipitate which formed was filtered off and washed with water (0.6 g, 58% of a light-yellow solid), m.p. 120°. This material did not depress the melting point of a sample of VII prepared for VI and the infrared spectra of both samples were identical. When VII was hydrolyzed with 6 *N* NaOH and then acidified, the known 2-chlorophenylpropargylic acid m.p. 131° was obtained (lit. m.p. 132–133° (14)), and our sample did not depress the melting point of an authentic sample.

α-Bromo-β-(2-chlorophenyl)-acrylamide (IX)

VI (20 g, 0.053 mole) was added to a solution of sodium ethoxide (2 g of sodium in 100 ml of absolute ethanol). The mixture was refluxed with stirring for 1 h. The reaction mixture was then cooled, and filtered. The filtrate was evaporated almost to dryness *in vacuo*. The yellow precipitate which formed was heated with 10 ml of water. The solution was allowed to cool, and the precipitate was filtered off and finally washed with ether (4.6 g white needles m.p. 110°, sublimes).

Anal. Calcd. for $C_9H_7ClBrNO$: C, 41.50; H, 2.71; N, 5.38. Found: C, 41.52; H, 2.65; N, 5.45.

The ultraviolet showed a maximum of 264 mμ (broad band) log ϵ = 4.114. The infrared showed strong absorption characteristics of unsaturated amides at 5.9 μ and 6.1 μ. N—H bands (medium) were present at 2.9, 3.0, and 3.15 μ. (KBr disc). The n.m.r. (CD_3OD solvent and Me_4Si standard) showed a multiplet for the aromatic protons from 7.2–8.0 p.p.m., a sharp singlet at 8.25 p.p.m. for the vinylic proton, and a broad peak from 4.4–5.0 p.p.m. for the amide protons.

Can. J. Chem. Downloaded from www.nrcresearchpress.com by 210.87.254.42 on 09/05/12
For personal use only.

1. R. HUISGEN and H. KÖNIG. Angew. Chem. **69**, 268 (1957).
2. R. HUISGEN and H. KÖNIG. Chem. Ber. **92**, 203 (1959).
3. R. HUISGEN *et al.* Chem. Ber. **92**, 424 (1959).
4. H. HÖNIG and R. HUISGEN. Chem. Ber. **92**, 429 (1959).
5. B. F. HRUTFIORD and J. F. BUNNETT. J. Am. Chem. Soc. **80**, 2021 (1958).
6. B. F. HRUTFIORD and J. F. BUNNETT. J. Am. Chem. Soc. **80**, 4745 (1958).
7. C. R. HAUSER and G. F. MORRIS. J. Org. Chem. **26**, 4740 (1961).
8. J. F. BUNNETT and B. F. HRUTFIORD. J. Am. Chem. Soc. **83**, 1691 (1961).
9. J. F. BUNNETT and J. A. SKORCZ. J. Org. Chem. **27**, 3836 (1962).
10. E. CAMPAIGNE, G. BULBENKO, W. KREIGHBAUM, and D. MAULDING. J. Org. Chem. **27**, 4428 (1962).
11. J. F. BUNNETT *et al.* J. Org. Chem. **28**, 1 (1963).
12. C. M. STUART. J. Chem. Soc. 141 (1888).
13. B. CORSON and R. W. STOUGHTON. J. Am. Chem. Soc. **50**, 2825 (1928).
14. F. G. BODDAR, L. S. EL-ASSAL, and N. A. DOSS. J. Chem. Soc. 461 (1955).

RECEIVED APRIL 12, 1965.
DEPARTMENT OF CHEMISTRY,
LOYOLA UNIVERSITY,
CHICAGO, ILLINOIS.

Can. J. Chem. Downloaded from www.nrcresearchpress.com by 210.87.254.42 on 09/05/12
For personal use only.

THE PHOTOLYSIS OF MALEIC HYDRAZIDE: EVIDENCE FOR AN INTERMOLECULAR HYDROGEN TRANSFER

A. STOESSL

A previous communication (1) has shown that photolysis of aqueous maleic hydrazide (MH) (I) under nitrogen leads to a complex mixture from which succinic acid was isolated in 26% yield. The structure of MH and the nature of the identified product suggested that a pathway of the photolysis might be analogous to that of six-membered carbocyclic dienes (2). For MH, it would be expressed as in eq. [1]. The intermediate (II) could decompose in a number of ways (for instance, [*a*], [*b*], or [*c*]) in which diimide could, but need not, be involved. The products would be succinic acid (via the ketene) and nitrogen, together with either hydrogen or the products of a hydrogen transfer to one or several acceptors.

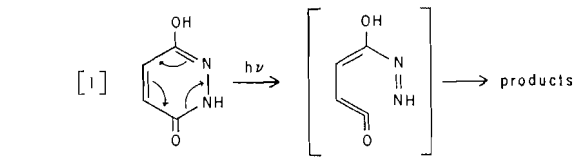

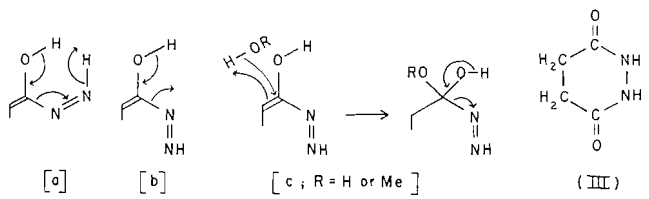

The results of some further experiments reported in this communication went only a little way towards providing positive support for these concepts. No further work is planned but the studies uncovered an intermolecular hydrogen transfer which may be of some interest in itself.

1. R. HUISGEN and H. KÖNIG. Angew. Chem. **69**, 268 (1957).
2. R. HUISGEN and H. KÖNIG. Chem. Ber. **92**, 203 (1959).
3. R. HUISGEN *et al.* Chem. Ber. **92**, 424 (1959).
4. H. HÖNIG and R. HUISGEN. Chem. Ber. **92**, 429 (1959).
5. B. F. HRUTFIORD and J. F. BUNNETT. J. Am. Chem. Soc. **80**, 2021 (1958).
6. B. F. HRUTFIORD and J. F. BUNNETT. J. Am. Chem. Soc. **80**, 4745 (1958).
7. C. R. HAUSER and G. F. MORRIS. J. Org. Chem. **26**, 4740 (1961).
8. J. F. BUNNETT and B. F. HRUTFIORD. J. Am. Chem. Soc. **83**, 1691 (1961).
9. J. F. BUNNETT and J. A. SKORCZ. J. Org. Chem. **27**, 3836 (1962).
10. E. CAMPAIGNE, G. BULBENKO, W. KREIGHBAUM, and D. MAULDING. J. Org. Chem. **27**, 4428 (1962).
11. J. F. BUNNETT *et al.* J. Org. Chem. **28**, 1 (1963).
12. C. M. STUART. J. Chem. Soc. 141 (1888).
13. B. CORSON and R. W. STOUGHTON. J. Am. Chem. Soc. **50**, 2825 (1928).
14. F. G. BODDAR, L. S. EL-ASSAL, and N. A. DOSS. J. Chem. Soc. 461 (1955).

RECEIVED APRIL 12, 1965.
DEPARTMENT OF CHEMISTRY,
LOYOLA UNIVERSITY,
CHICAGO, ILLINOIS.

Can. J. Chem. Downloaded from www.nrcresearchpress.com by 210.87.254.40 on 09/05/12
For personal use only.

THE PHOTOLYSIS OF MALEIC HYDRAZIDE: EVIDENCE FOR AN INTERMOLECULAR HYDROGEN TRANSFER

A. STOESSL

A previous communication (1) has shown that photolysis of aqueous maleic hydrazide (MH) (I) under nitrogen leads to a complex mixture from which succinic acid was isolated in 26% yield. The structure of MH and the nature of the identified product suggested that a pathway of the photolysis might be analogous to that of six-membered carbocyclic dienes (2). For MH, it would be expressed as in eq. [1]. The intermediate (II) could decompose in a number of ways (for instance, [*a*], [*b*], or [*c*]) in which diimide could, but need not, be involved. The products would be succinic acid (via the ketene) and nitrogen, together with either hydrogen or the products of a hydrogen transfer to one or several acceptors.

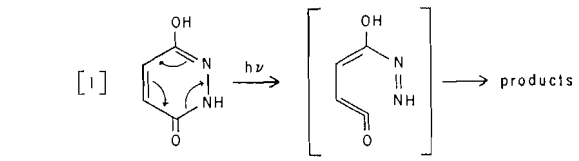

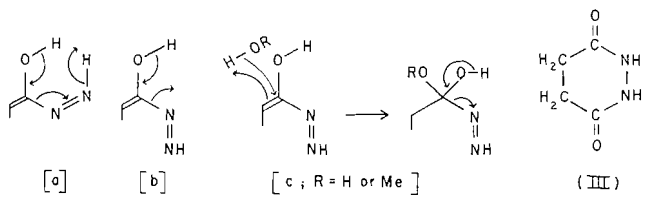

The results of some further experiments reported in this communication went only a little way towards providing positive support for these concepts. No further work is planned but the studies uncovered an intermolecular hydrogen transfer which may be of some interest in itself.

Irradiation of aqueous MH in a sealed, evacuated vessel showed that hydrogen was liberated only in traces or, in some runs, not at all. Nitrogen (40%) and carbon dioxide (1.5%) were products of the photolysis from which succinic acid was again isolated in 25% yield. Pathway [*a*] was therefore eliminated from further consideration but the possibility of a hydrogen transfer remained. It occurred to us that MH itself might act as an acceptor in such a step. The expected product, cyclic succinhydrazide (III), was then shown to have the chromatographic properties of one of the components of the irradiation product. This was isolated and found to be identical with the authentic compound in every respect. The yield was estimated as about 3% of photolyzed MH or 13% of the succinic acid formed. Treatment of MH in a dark reaction, with diimide prepared *in situ* from a large excess of azodicarboxylate, did not lead to any reduction. Diimide in a more highly activated state, or an active precursor, would thus be required.

Proof of the intermediacy of ketenes was attempted by the irradiation of MH in dry methanol (2). This produced some of the expected dimethylsuccinate together with cyclic succinhydrazide and nitrogen. No dicarboxylic acids nor the dimethyl esters of fumaric and maleic acids could be detected. The yield of dimethylsuccinate was very low (0.45%) but this was due in part to the high and, in our hands, unavoidable losses during the working-up (more than 67% of the ester was lost in an appropriate control experiment). Further, photolysis in methanol was much more rapid than in water and the product was even more complex. This indicated that competing reactions, which must account for at least some of the photolysis in water, might have been relatively more important in the alcohol. But this is a surmise and the experimental facts give, at the most, only tentative support to scheme [1].

EXPERIMENTAL

General Methods

The reaction vessel was an unsilvered double-walled Dewar flask of Pyrex glass, the annular space A (capacity, ca. 700 ml) of which was provided with an entry B and an outlet C fitted with a break-off seal D. With the solution in A, the flask was evacuated and sealed at B. A Hanovia lamp CH-3 (85W) was placed in the central well of the flask which was cooled by an airstream to 40–44° during the irradiation. The apparatus was then sealed to a Topler pump at C and the gaseous products transferred to the burette via the break-off seal D. Aliquots of the gas were analyzed quantitatively by chromatography on Perkin–Elmer columns I (synthetic zeolite) and J (silica gel, type 15) with helium as carrier and O_2, N_2, H_2, CO_2, and CO as standards.

Fractionation of the aqueous product was followed by paper chromatography in *n*-BuOH–H_2O–HOAc (4:5:1). Melting points were taken on the Kofler stage.

Irradiations in Water

MH (12 millimoles) in water (600 ml) was irradiated for 144 hours; 0.94 millimole had been photolyzed (absorbance at λ_{max} 302 mμ). The gaseous product consisted of N_2 (0.38 millimole) and CO_2 (0.014 millimole). Hydrogen was not detected (traces, 1–2 μl, were found in other runs).

The vacuum distillate from a major portion (91.8%) of the aqueous product was neutral and did not give a precipitate with 2,4-dinitrophenylhydrazine. The distillation residue was extracted with water (several small portions), most of the unchanged MH (m.p. and mixed m.p., 1.12 g) remaining undissolved. The extracts were filtered through a strongly acidic cation exchange resin (Dowex 50W-X8 (4 ml)) with precautions against entry of atmospheric NH_3. Filtrate and washings were distributed by the single withdrawal procedure (3) in *n*-BuOH–H_2O–HOAc (4:5:1; 100 × 25 ml lower, 365 × 25 ml upper phase).

Fractions $\rho = 70$ to $\rho = 169$ (for the terminology, see ref. 3, p. 12) in water, were continuously extracted with ether. Filtration of the extract through silica gel gave crude succinic acid (26 mg). The pure compound (m.p., mixed m.p., infrared spectrum; 20 mg) was obtained on sublimation.

Fractions $\rho = 240$ to $r = 85$ (at least five components) were chromatographed on thin layers of silica gel (*n*-BuOH–H_2O) and the zones containing the desired compound (ultraviolet) extracted with very dilute acetic acid. Re-extraction of the product into ethanol and sublimation furnished cyclic succinhydrazide, m.p. and mixed m.p. 208°, with resetting and decomposition at 275–285°. The infrared (KBr disc) and ultraviolet spectra were identical with those of the authentic compound (4) (λ_{max} 241 mμ, E 7 250).

In another run (0.81 millimole MH photolyzed; 0.19 millimole crude succinic acid isolated), the yield

Can. J. Chem. Downloaded from www.nrcresearchpress.com by 210.87.254.40 on 09/05/12
For personal use only.

of cyclic succinhydrazide was estimated as 0.025 millimole by semiquantitative paper chromatography (5).

The basic portion of the photolysis product was eluted from the ion exchanger with $N/1$ HCl, to give a small amount of salts. Paper chromatography in three systems showed the presence of ammonia and hydrazine as the main components. The amount of the latter was estimated as 0.0084 millimole by a colorimetric procedure (6) with which the other components did not interfere.

Irradiations in Methanol

MH (5 millimoles) in dry MeOH (250 ml) was irradiated for 96 hours (4 millimoles photolyzed). The solution was evaporated *in vacuo* without warming, the temperature falling to below 0 °C. The residue was extracted with ether and the extracts washed, dried, filtered, evaporated as above, and refiltered in ether into a microtube, most of the solvent being removed in a current of N_2. Quantitative vapor phase chromatography (Perkin–Elmer Carbowax 30%, 6 ft × 0.25 in. at 185°, 70 ml He/min; with the dimethyl esters of succinic, maleic, and fumaric acids as standards) showed the presence of only dimethylsuccinate (2.6 mg). Similar evaporation and ether extraction of dimethylsuccinate (58 mg) in MeOH (250 ml) gave a residue of only 19 mg.

The product from another experiment (12 millimole MH, 600 ml MeOH, 67 hours' irradiation, 2.85 millimoles photolyzed) was shown to contain cyclic succinhydrazide (4.85 mg; 1.5%) by semiquantitative paper chromatography (5). Ammoniacal silver nitrate reagent revealed the presence of at least 10 other distinct spots superimposed on heavy streaking. No succinic, maleic, or fumaric acid was detected (limit < 1 mg).

Attempted Diimide Reduction

MH (0.2 millimole) in water (10 ml) containing acetic acid (1 ml 6 N) was stirred with potassium azodicarboxylate (7) (2 millimoles added in five equal portions). No reduction occurred (ultraviolet and paper chromatography). The same result was obtained with MeOH–HOAc as solvent. Maleic acid in water as above gave succinic acid in 15% yield.

ACKNOWLEDGMENTS

Thanks are due to Drs. D. M. Miller and E. Y. Spencer for discussions and encouragement, to Mr. T. Dumas for the gas analyses, and to Mr. G. Rock for skilled experimental assistance.

1. A. Stoessl. Chem. Ind. 580 (1964).
2. P. de Mayo and S. T. Reid. Quart. Rev. London, **15**, 402 (1961).
3. E. Hecker. Verteilungsverfahren im Laboratorium. Verlag Chemie, Weinheim. 1955. p. 64.
4. H. Feuer, G. B. Bachman, and E. H. White. J. Am. Chem. Soc. **73**, 4716 (1951).
5. W. A. Andreae. Can. J. Biochem. Physiol. **36**, 71 (1958).
6. Snell and Snell. Colorimetric methods of analysis. Vol. IIA. Van Nostrand Co. Inc., New York. 1959. p. 707.
7. E. E. van Tamelen, R. S. Dewey, and R. J. Timmons. J. Am. Chem. Soc. **83**, 3725 (1961).

Received March 19, 1965.
Research Institute,
Canada Department of Agriculture,
University Sub P.O.,
London, Ontario.

THE CHLORINATION OF MONOFLUOROACETONE WITH SULFURYL CHLORIDE

D. P. Wyman,[1] B. L. Shapiro,[2] and P. R. Kaufman[3]

In previous papers (1, 2) the chlorination of a variety of active methyl, methylene, and methine compounds with sulfuryl chloride under mild reaction conditions was described. The reactions were apparently ionic and similar in some respects to acid-catalyzed halogenations with molecular halogens but different in others. One important difference

[1]*Present address: Marbon Chemical, Washington, West Virginia.*
[2]*Present address: Department of Chemistry, Illinois Institute of Technology, Chicago, Illinois.*
[3]*Present address: The Lubrizol Corporation, Cleveland 17, Ohio.*

Can. J. Chem. Downloaded from www.nrcresearchpress.com by 210.87.254.40 on 09/05/12
For personal use only.

of cyclic succinhydrazide was estimated as 0.025 millimole by semiquantitative paper chromatography (5).

The basic portion of the photolysis product was eluted from the ion exchanger with $N/1$ HCl, to give a small amount of salts. Paper chromatography in three systems showed the presence of ammonia and hydrazine as the main components. The amount of the latter was estimated as 0.0084 millimole by a colorimetric procedure (6) with which the other components did not interfere.

Irradiations in Methanol

MH (5 millimoles) in dry MeOH (250 ml) was irradiated for 96 hours (4 millimoles photolyzed). The solution was evaporated *in vacuo* without warming, the temperature falling to below 0 °C. The residue was extracted with ether and the extracts washed, dried, filtered, evaporated as above, and refiltered in ether into a microtube, most of the solvent being removed in a current of N_2. Quantitative vapor phase chromatography (Perkin–Elmer Carbowax 30%, 6 ft × 0.25 in. at 185°, 70 ml He/min; with the dimethyl esters of succinic, maleic, and fumaric acids as standards) showed the presence of only dimethylsuccinate (2.6 mg). Similar evaporation and ether extraction of dimethylsuccinate (58 mg) in MeOH (250 ml) gave a residue of only 19 mg.

The product from another experiment (12 millimole MH, 600 ml MeOH, 67 hours' irradiation, 2.85 millimoles photolyzed) was shown to contain cyclic succinhydrazide (4.85 mg; 1.5%) by semiquantitative paper chromatography (5). Ammoniacal silver nitrate reagent revealed the presence of at least 10 other distinct spots superimposed on heavy streaking. No succinic, maleic, or fumaric acid was detected (limit < 1 mg).

Attempted Diimide Reduction

MH (0.2 millimole) in water (10 ml) containing acetic acid (1 ml 6 N) was stirred with potassium azodicarboxylate (7) (2 millimoles added in five equal portions). No reduction occurred (ultraviolet and paper chromatography). The same result was obtained with MeOH–HOAc as solvent. Maleic acid in water as above gave succinic acid in 15% yield.

ACKNOWLEDGMENTS

Thanks are due to Drs. D. M. Miller and E. Y. Spencer for discussions and encouragement, to Mr. T. Dumas for the gas analyses, and to Mr. G. Rock for skilled experimental assistance.

1. A. Stoessl. Chem. Ind. 580 (1964).
2. P. de Mayo and S. T. Reid. Quart. Rev. London, **15**, 402 (1961).
3. E. Hecker. Verteilungsverfahren im Laboratorium. Verlag Chemie, Weinheim. 1955. p. 64.
4. H. Feuer, G. B. Bachman, and E. H. White. J. Am. Chem. Soc. **73**, 4716 (1951).
5. W. A. Andreae. Can. J. Biochem. Physiol. **36**, 71 (1958).
6. Snell and Snell. Colorimetric methods of analysis. Vol. IIA. Van Nostrand Co. Inc., New York. 1959. p. 707.
7. E. E. van Tamelen, R. S. Dewey, and R. J. Timmons. J. Am. Chem. Soc. **83**, 3725 (1961).

Received March 19, 1965.
Research Institute,
Canada Department of Agriculture,
University Sub P.O.,
London, Ontario.

THE CHLORINATION OF MONOFLUOROACETONE WITH SULFURYL CHLORIDE

D. P. Wyman,[1] B. L. Shapiro,[2] and P. R. Kaufman[3]

In previous papers (1, 2) the chlorination of a variety of active methyl, methylene, and methine compounds with sulfuryl chloride under mild reaction conditions was described. The reactions were apparently ionic and similar in some respects to acid-catalyzed halogenations with molecular halogens but different in others. One important difference

[1]*Present address: Marbon Chemical, Washington, West Virginia.*
[2]*Present address: Department of Chemistry, Illinois Institute of Technology, Chicago, Illinois.*
[3]*Present address: The Lubrizol Corporation, Cleveland 17, Ohio.*

Can. J. Chem. Downloaded from www.nrcresearchpress.com by 210.87.254.40 on 09/05/12
For personal use only.

in the case of ketones was the marked preference, in many cases, for *gem* dichlorination with sulfuryl chloride, a reaction which does not occur readily in halogenation with molecular halogens (3). Thus, the major product from the chlorination of acetone with sulfuryl chloride (4) was 1,1-dichloroacetone rather than monochloroacetone. On this basis it was expected *a priori* that the predominant product from the chlorination of monofluoroacetone (I) probably would be 1-fluoro-1-chloroacetone which was desired for other studies.

Contrary to expectations it was found that only very little reaction occurred on the CH_2F group of I and, instead, substitution occurred mainly on the CH_3 group to yield (depending upon conditions) either 1-fluoro-3-chloroacetone (II) or 1-fluoro-3,3-dichloroacetone (III). It was also evident that I was generally less reactive than acetone or monochloroacetone. Thus, whereas 1,1-dichloroacetone was formed very rapidly (and exothermically) during the chlorination of acetone, a similar chlorination of I was much slower and even after several hours (see Experimental) sulfuryl chloride could be recovered and mainly II was formed. On the other hand, after long reaction times (Table I) the major product from a 1:1 (molar) reaction of I with sulfuryl chloride was III. This shows that the CH_2Cl group of II is somewhat more active than the CH_3 group of I but not to the extent that the CH_2Cl group of chloroacetone is more reactive than a CH_3 group of acetone. The fact that relatively short reaction times can lead to a monochlorinated major product is explainable on the basis that under these conditions I is in excess (relative to both the starting material and the monochlorination product) and even acetone can be made to yield mainly monochloroacetone when it is reacted in excess with sulfuryl chloride (1, 4).

TABLE I

Chlorination results

Reactants	[Ketone]:[SO_2Cl_2]*	Products (% based on SO_2Cl_2)†
Monofluoroacetone	1:1	1-Fluoro-3,3-dichloroacetone(60.1) + 1-fluoro-3-chloroacetone(31.3) + 1-fluoro-1-chloroacetone(4.5) + 1-fluoro-1,3,3-trichloroacetone(3.3)
Monofluoroacetone‡	4:1	1-Fluoro-3-chloroacetone‖
Monofluoroacetone + monochloroacetone	1:1:1	1,1-Dichloroacetone(62.5) + 1-fluoro-3,3-dichloroacetone (7.8) + 1-fluoro-3-chloroacetone(9.5)
Monofluoroacetone‡ + monochloroacetone	5:5:1	1,1-Dichloroacetone¶
Monofluoroacetone + acetone	1:1:1	1,1-Dichloroacetone(52) + monochloroacetone(30) + 1-fluoro-3-chloroacetone(15)
Monofluoroacetone§ + acetone	5:5:1	Monochloroacetone(65) + 1,1-dichloroacetone(15) + 1-fluoro-3-chloroacetone(5)

*In each case the last number given is the relative molar ratio of sulfuryl chloride with respect to the relative molar ratio of the ketones.
†Unless otherwise specified, reaction times of 24 h and reaction temperatures of ~25–30° were used.
‡A reaction time of ~1/2 h was used.
§A reaction time of ~2 h was used.
‖Only 50% of SO_2Cl_2 had reacted and this was essentially the only product.
¶About 80% of sulfuryl chloride had reacted and this was essentially the sole product.

In direct competitions (Table I) both acetone and monochloroacetone reacted much more rapidly with sulfuryl chloride than I. This conclusively establishes that I is generally less active towards sulfuryl chloride than acetone or monochloroacetone.

It is reasonably well established that the acid-catalyzed halogenations of active methylene compounds with molecular halogens proceed through enolic intermediates and that in most (5–8), but not all (9, 10), cases enolization is rate-determining. The same sort of scheme has been suggested for chlorinations with sulfuryl chloride (1, 2)

Can. J. Chem. Downloaded from www.nrcresearchpress.com by 210.87.254.40 on 09/05/12
For personal use only.

with the exception that chloronium abstraction by the enol often appears to be a slow (rate-determining) step (2) along with enolization.

It has been suggested that the fact that the reactions of fluoro-olefins which lead to saturated derivatives are more exothermic than those of the corresponding fluorine-free olefins (11, 12) might be a result of a decrease in stability of olefins to which are bonded one or more fluorine atoms (13). Obviously, such a tenet fits into the enol mechanism and could explain why the CH_2F group of I is so difficult to substitute, i.e., formation of

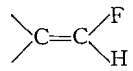

is energetically unfavorable. Another factor might also be contributing; if, in the sulfuryl chloride reaction, the base which extracts the carbon-bonded proton in the enol formation step is a halide (8, 14, 15) ion, the approach to a proton in the CH_2F group might be repelled by a direct field effect of the very electronegative fluorine atom.

The decrease in activity of the methyl group in I is not entirely unexpected. Thus, the chlorination of the methyl group in 1,1-dichloroacetone is very slow (16) even in the presence of an excess of sulfuryl chloride. A partial explanation is that the electron-withdrawing substituents polarize the enol intermediates in the "wrong direction", i.e., the electron flow involved in rehybridization during the formation of the carbon–chlorine band is unfavorable.

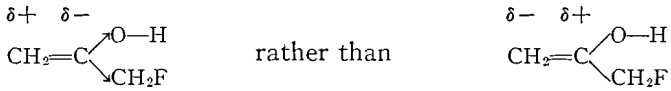

Thus with sulfuryl chloride, this may be a slow step.

Finally, initial attempts to extend these studies to bromo- and iodoacetone were made and the reactions were found to be very complex. In the case of bromoacetone n.m.r. evidence showed that (1) bromide was considerably displaced by chloride and that (2) much more methyl than methylene substitution occurred, as expected. With iodoacetone, a great deal of molecular iodine was rapidly liberated and a complex mixture of products resulted. These compounds have not been studied further to date.

EXPERIMENTAL

General

Nuclear magnetic resonance, n.m.r., spectra were obtained of the neat liquids using TMS as an internal reference. A Varian A-60 spectrometer (r.f. 60 Mc/s; sample temperature 37 ± 2 °C) was used for these measurements. Gas chromatographic determinations were performed with a column composed of 10% Apiezon-L on 80–90 mesh Anakrom-ABS. Elemental analyses were performed by the Galbraith Laboratories, Inc., Knoxville, Tennessee. Monofluoroacetone was purchased from Mr. David Starr, Department of Chemistry, University of South Carolina, Columbia, South Carolina.

Preparation of 1-Fluoro-1-chloro- and 1-Fluoro-3-chloroacetone

A 500 ml round-bottom flask equipped with a magnetic stirrer, dropping funnel, thermometer, and condenser (protected from atmospheric moisture with a calcium chloride drying tube) was charged with 96 g (1.2 moles) of monofluoroacetone. Sulfuryl chloride (135 g, 1 mole) was added dropwise over a period of 40 min. The temperature of the reaction mixture did not rise above 30 °C during this period. After addition was complete the reaction mixture was stirred 4 h at room temperature after which it was distilled through a large heated and insulated vigreux column (~20 plates) as follows:

Fraction	*B.p. (°C)*	*Pressure (mm Hg)*	*Product (g yield)*
1	15–25	75	SO_2Cl_2(~15) + CH_3—CO—CH_2F(?)
2	26–26.5	78	CH_2F—CO—CH_3(5.3) + CHFCl—CO—CH_3(7.6)
3	82	76	CH_2F—CO—CH_2Cl(30.4) + CH_2F—CO—$CHCl_2$(8.4)
4	82	76	CH_2F—CO—CH_2Cl(23.0) + CH_2F—CO—$CHCl_2$(4.1)
5	69	61	CH_2F—CO—CH_2Cl(13.2) + CH_2F—CO—$CHCl_2$(2.9)

Can. J. Chem. Downloaded from www.nrcresearchpress.com by 210.87.254.40 on 09/05/12
For personal use only.

Can. J. Chem. Downloaded from www.nrcresearchpress.com by 210.87.254.40 on 09/05/12
For personal use only.

TABLE II

Nuclear magnetic resonance data*

CH_3—CO—$CH_2'F$		$ClCH_2$—CO—$CH_2'F$		CH_3—CO—$CH'ClF$		Cl_2CH—CO—$CH_2'F$	
$\bar{\nu}$† = 471.3	$\bar{\nu}$ = 304.9	$\bar{\nu}$ = 343.0	$\bar{\nu}$ = 300.0	$\bar{\nu}$ = 472	$\bar{\nu}$ = 229.9	$\bar{\nu}$ = 226	$\bar{\nu}$ = 279
τ‡ = 7.81	τ = 5.05	τ = 5.72	τ = 5.0	τ = 7.87	τ = 3.84	τ = 3.78	τ = 4.66
$\lvert J_{HF}\rvert$§ = 4	$\lvert J_{H'F}\rvert$ = 47	$\lvert J_{HF}\rvert$ = 2.5	$\lvert J_{H'F}\rvert$ = 47	$\lvert J_{HF}\rvert$ = 3.5	$\lvert J_{H'F}\rvert$ = 51	$\lvert J_{HF}\rvert$ = 1.8	$\lvert J_{H'F}\rvert$ = 46.7

*The n.m.r. spectra will be discussed in more detail in future publications by B. L. Shapiro and co-workers.
Most of the τ values reported in this table are for neat liquids rather than dilute solutions and, therefore, are only approximate since the chemical shifts and coupling constants (see footnotes* and ‡) of halogenated ketones are quite solvent dependent.
†$\bar{\nu}$ = frequency in c.p.s. The values are probably accurate to ±0.5 c.p.s.
‡The tau scale as defined by G. V. D. Tiers in ref. 17 with τ_{TMS} = 10.0 p.p.m. (= 600 c.p.s.).
§The units of the coupling constants, $|J|$, are c.p.s. and the absolute magnitudes are probably accurate to ±0.3 c.p.s.

The yield of each product listed above was computed from the total weight of the fraction and the percentage, by weight, of each component as determined by gas chromatography. The structures of the products were assigned on the basis of their n.m.r. spectra (Table II). Fraction 4 above, which was mostly 1-fluoro-3-chloroacetone, was subjected to elemental analysis.

Anal. Calcd. for C_3H_4ClFO: C, 32.76; H, 3.62. Found: C, 32.41; H, 3.19.

It is of interest that a significant quantity of sulfuryl chloride was recovered unchanged in this experiment (~5 h reaction time) and that the major product under these conditions was 1-fluoro-3-chloroacetone rather than 1-fluoro-3,3-dichloroacetone which is obtained as a major product under similar conditions when longer (15–24 h) reaction times are used and essentially complete conversion of the sulfuryl chloride occurs (Table I). Complete separations were difficult to obtain via column fractionation under the conditions employed.

Stepwise Chlorination of Monofluoroacetone

To verify the results obtained above, monofluoroacetone was chlorinated by incremental additions of sulfuryl chloride and the products obtained were followed by quantitative n.m.r. This was done by converting the numbers of protons of specific peaks (e.g. Table II) into relative mole ratios. Typically, to 65 mmoles of monofluoroacetone were added 16.3 mmoles of sulfuryl chloride all at once at room temperature. The temperature rose to ~29 °C. After 0.5 h, 12% of the monofluoroacetone had been converted to 1-fluoro-3-chloroacetone (~50% yield based on sulfuryl chloride). An additional 16.3 mmoles of sulfuryl chloride was then added and after 2 h the reaction mixture contained 35% 1-fluoro-3-chloroacetone (70% yield based on sulfuryl chloride) and traces of 1-fluoro-3,3-dichloroacetone. Addition of a further 16.3 mmole portion of sulfuryl chloride resulted, after 2.5 h, in a mixture containing 60% 1-fluoro-3-chloroacetone (80% yield based on sulfuryl chloride), 5% 1-fluoro-3,3-dichloroacetone (10% based on sulfuryl chloride) and 1% of 1-fluoro-1-chloroacetone. About 34% of the original monofluoroacetone was present at this point. A final 16.3 mmole portion of sulfuryl chloride was added and the reaction mixture was stirred at room temperature for 17 h. The reaction mixture now contained 35% 1-fluoro-3,3-dichloroacetone (70% based on sulfuryl chloride), 25% 1-fluoro-3-chloroacetone, and ~1% 1-fluoro-1-chloroacetone. From these results it is apparent that the CH_2Cl group of 1-fluoro-3-chloroacetone is slightly more reactive than the CH_3 group of monofluoroacetone.

Competitive Chlorinations

Equimolar mixtures of acetone with monofluoroacetone and monofluoroacetone with monochloroacetone, as well as monofluoroacetone, alone were treated with sulfuryl chloride as shown in Table I. The reactions were allowed to proceed for ~24 h at room temperature and, in each case, >95% of the sulfuryl chloride reacted. Analyses were done mainly by means of gas chromatography, although estimates were sometimes made by n.m.r.

ACKNOWLEDGMENTS

We are indebted to Mr. Carl Lindemann for the gas chromatographs and to Mr. William Freeman for assistance with some of the experiments.

1. D. P. Wyman and P. R. Kaufman. J. Org. Chem. **29**, 1956 (1964).
2. D. P. Wyman, P. R. Kaufman, and W. R. Freeman. J. Org. Chem. **29**, 2706 (1964).
3. E. S. Gould. Mechanism and structure in organic chemistry. Henry Holt and Co., N.Y. 1959. p. 383.
4. E. R. Buchman and H. Sargent. J. Am. Chem. Soc. **67**, 401 (1945).
5. P. D. Bartlett and C. H. Stauffer. J. Am. Chem. Soc. **57**, 2580 (1935).
6. L. A. Hammett and L. Zucker. J. Am. Chem. Soc. **61**, 2791 (1939).
7. R. C. Arora, V. M. Bhale, and S. L. Bafna. Vikram, J. Vikram Univ. **4**, 127 (1960); Chem. Abstr. **57**, 5335 (1962).
8. R. F. W. Cieciuch and F. W. Westheimer. J. Am. Chem. Soc. **85**, 2591 (1963).
9. R. P. Bell and N. Spiro. J. Chem. Soc. 424 (1953).
10. R. P. Bell and K. Yates. J. Chem. Soc. 2285 (1962).
11. C. R. Patrick. Advances in fluorine chemistry. Vol. 2. Butterworths, Washington, D.C. 1961. Chap. 1.
12. C. R. Patrick. Tetrahedron, **4**, 26 (1958).
13. J. Hine. J. Am. Chem. Soc. **85**, 3239 (1963).
14. S. Winstein, L. G. Savedoff, S. Smith, I. D. R. Stevens, and J. S. Gall. Tetrahedron Letters, No. 9, 124 (1960).
15. D. N. Kevill and N. H. Cromwell. J. Am. Chem. Soc. **83**, 3812 (1961).
16. D. P. Wyman and W. R. Freeman. Unpublished results.
17. G. V. D. Tiers. J. Phys. Chem. **62**, 1150 (1958).

Received March 9, 1965.
Mellon Institute,
Pittsburgh 13, Pennsylvania.

Can. J. Chem. Downloaded from www.nrcresearchpress.com by 210.87.254.40 on 09/05/12
For personal use only.

THE SYNTHESIS OF POTENTIALLY PHYSIOLOGICALLY ACTIVE β-PHENYLETHYLAMINES. PART III. SOME β-ALKOXY-β-(3,4-DIHYDROXYPHENYL)ETHYLAMINES[1,2]

R. A. HEACOCK,[3] O. HUTZINGER,[4] AND B. D. SCOTT

Can. J. Chem. Downloaded from www.nrcresearchpress.com by 210.87.254.5 on 09/05/12
For personal use only.

Adrenaline methyl ether (i.e. β-(3,4-dihydroxyphenyl)-β-methoxyethylmethylamine) has recently been reported to produce considerable stimulation of the central nervous system; however, it was much less active than adrenaline peripherally (1, 2). In view of these interesting pharmacological results a number of compounds analogous to adrenaline methyl ether have been prepared.

The methyl and ethyl ethers of both adrenaline and noradrenaline can be obtained by boiling solutions of the catecholamine hydrochlorides in the appropriate alcohols (3, 4, 5, 6). The highly reactive 3,4-dihydroxybenzyl chloride derivative, obtained by treatment of adrenaline with thionyl chloride, is readily converted to the corresponding alkoxy compound by being heated under reflux with an aliphatic alcohol (7, 8); adrenaline methyl, ethyl, and isopropyl ethers have recently been prepared by this procedure (8). This note reports the application of this general procedure to the preparation of the methyl and ethyl ethers of (i) noradrenaline, (ii) 3,4-dihydroxynorephedrine, and (iii) *N*-isopropylnoradrenaline.

Attempts to recrystallize noradrenaline methyl ether hydrochloride from acetone–ethanol mixtures gave an azomethine derivative (i.e. *N*-isopropylidenenoradrenaline methyl ether hydrochloride), from which *N*-isopropylnoradrenaline methyl ether hydrochloride could be obtained by catalytic hydrogenation.

EXPERIMENTAL

Preparation of β-Alkoxy-β-(3,4-dihydroxyphenyl)ethylamines

General Procedure

The catecholamine (2.5 g; free base) was added to thionyl chloride (25 ml) in a dry nitrogen atmosphere and the product maintained under nitrogen at 50°[5] for 30 min.[6] Undissolved solids were removed by filtration of the reaction mixture and dry benzene (15 ml) added to the clear filtrate. The resulting solution was allowed to stand at 5° for several hours and the β-chloro-β-(3,4-dihydroxyphenyl)ethylamine derivative separated out as a colorless crystalline solid. The crude β-chloro derivative, which was obtained by filtration, was washed with a little dry benzene and immediately transferred to a flask containing methanol or ethanol (30 ml). The resulting solution was boiled under reflux for 20 min in a nitrogen atmosphere. The crude semisolid β-alkoxy derivative was obtained by removal of the solvent *in vacuo* and purified by recrystallization from an ethanol – ethyl acetate mixture.

N-isopropylidenenoradrenaline Methyl Ether Hydrochloride

Attempts to recrystallize noradrenaline methyl ether hydrochloride from an ethanol–acetone mixture gave colorless prisms of *N*-isopropylidenenoradrenaline methyl ether hydrochloride, m.p. 188° (with decomposition), which depressed the melting point of the starting material, ν_{max}^{Nujol} 1 680 cm^{-1} ($\rangle C{=}\overset{+}{N}\langle$, cf. ref. 9).

Anal. Calcd. for $C_{12}H_{18}NO_3Cl$: C, 55.49; H, 6.98; N, 5.39; Cl, 13.65. Found: C, 55.61; H, 7.12; N, 5.31; Cl, 13.66.

[1]*This investigation was supported by grants from the Department of National Health and Welfare (Ottawa) and the Saskatchewan Department of Public Health.*

[2]*Part II. Can. J. Chem. 40, 133 (1962).*

[3]*Present address of R.A.H., to whom all correspondence should be addressed: Atlantic Regional Laboratory, National Research Council, 1411 Oxford Street, Halifax, Nova Scotia.*

[4]*Present address of O.H.: Department of Plant Pathology, The University of California, Davis, California, U.S.A.*

[5]*25° for N-isopropylnoradrenaline.*

[6]*10 minutes for 3,4-dihydroxynorephedrine.*

Can. J. Chem. Downloaded from www.nrcresearchpress.com by 210.87.254.5 on 09/05/12
For personal use only.

TABLE I

β-Alkoxy-β-(3,4-dihydroxyphenyl)ethylamine hydrochlorides

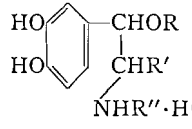

Compd.	R	R′	R″	Yield, %	M.p., °C*	Formula	Found, % C	H	N	Cl	Calculated, % C	H	N	Cl
I	CH_3	H	H	65	178†	$C_9H_{14}NO_3Cl$	49.13	6.51	6.30	16.24	49.21	6.42	6.38	16.14
II	C_2H_5	H	H	30	178‡	$C_{10}H_{16}NO_3Cl$	51.14	7.04	6.04	15.32	51.38	6.90	5.99	15.17
III	CH_3	CH_3	H	63	197	$C_{10}H_{16}NO_3Cl$	51.41	6.93	6.01	15.24	51.38	6.90	5.99	15.17
IV	C_2H_5	CH_3	H	74	190	$C_{11}H_{18}NO_3Cl$	53.22	7.29	5.61	14.11	53.34	7.32	5.66	14.32
V	CH_3	H	i-C_3H_7	88	188	$C_{12}H_{20}NO_3Cl$	55.15	7.80	5.36	13.55	55.08	7.70	5.35	13.55
VI	C_2H_5	H	i-C_3H_7	46	166–167	$C_{13}H_{22}NO_3Cl$	56.49	8.14	4.97	12.58	56.65	8.05	5.08	12.87

*The melting points of these compounds are markedly affected by the rate of heating; they were measured in a capillary tube in an apparatus preheated to about 20° below the melting point of the compound in question. All the products described in Table I, except β-ethoxy-β-(3,4-dihydroxyphenyl)-*N*-isopropylethylamine hydrochloride, melt with decomposition.

†Melting point reported in the literature: 170–171° (5).

‡Melting point reported in the literature: 171–172° (6).

A solution of *N*-isopropylidenenoradrenaline methyl ether hydrochloride (0.2 g) in methanol (50 ml) containing 10% palladium-charcoal (0.1 g) was shaken in an atmosphere of hydrogen for 18 h (room temperature and atmospheric pressure). After this time the catalyst was removed by filtration and the crude product, obtained on concentration of the clear filtrate, was recrystallized from ethanol – ethyl acetate and afforded colorless prisms of *N*-isopropylnoradrenaline methyl ether hydrochloride, m.p. 186° (with decomposition), identical with an authentic specimen (i.e. identical infrared spectra and no depression of melting point).

1. J. A. PAGE and A. HOFFER. Diseases Nervous System, **25**, 558 (1964).
2. A. HOFFER. Mind, **2**, 166 (1964).
3. C. FUNK and L. FREEDMAN. J. Am. Chem. Soc. **45**, 1792 (1923).
4. H. ÖPPINGER and H. VETTER. Med. Chem. **4**, 343 (1942). Chem. Abstr. **38**, 5927 (1944).
5. B. F. TULLAR. J. Am. Chem. Soc. **70**, 2067 (1948).
6. I. SERLIN and M. GOLDENBERG. Biochem. J. **54**, 483 (1953).
7. F. F. BLICKE and W. K. JOHNSON. J. Am. Pharm. Assoc. Sci. Ed. **45**, 437 (1956).
8. J. HUKKI and N. SEPPÄLÄINEN. Acta Chem. Scand. **12**, 1231 (1958).
9. B. WITKOP. J. Am. Chem. Soc. **78**, 2873 (1956).

RECEIVED MARCH 30, 1965.
THE PSYCHIATRIC RESEARCH UNIT,
UNIVERSITY HOSPITAL,
SASKATOON, SASKATCHEWAN.

THE ELECTRON SPIN RESONANCE SPECTRUM OF $\overset{+}{N}(CH_3)_3$ IN γ-IRRADIATED BETAINE[1]

R. DREWS, D. CADENA, JR., AND J. ROWLANDS

INTRODUCTION

Electron spin resonance studies of irradiated single crystals of both inorganic and organic compounds have been shown in many studies (1) to lead to detailed knowledge of both the identity and electronic structure of the radicals formed. The present study of the effects of γ irradiation on a single crystal of betaine $[(CH_3)_3\overset{+}{N}CH_2CO_2H]OH^-$ was motivated by the thought that a detailed study of it might help in the further understanding of the radiation chemistry of choline chloride $[(CH_3)_3\overset{+}{N}CH_2CH_2OH]Cl^-$ (2). Unlike choline chloride, however, in which no trace of the species $\overset{+}{N}(CH_3)_3$ was reported, in betaine at room temperature it was the only species observed. Further studies at liquid nitrogen temperature are required to elucidate the radiation chemistry of the system. The radical $\overset{+}{N}(CH_3)_3$ has already been reported in an irradiated single crystal of tetramethyl ammonium chloride (3). In this lattice the radical was shown to be executing restricted rotation at room temperature. In the betaine lattice the radical is seen to exhibit a nitrogen hyperfine tensor whose principal values more closely approximate the cylindrical symmetry to be expected from a planar radical. A comparison of the anisotropic interaction with that found in similar radicals $N(SO_3^-)_2$ (4) and $H_2\overset{+}{N}SO_3^-$ (5) indicates, however, that the restricted rotation of the radical is not completely quenched.

EXPERIMENTAL

Betaine crystals were grown from saturated aqueous solution. The crystals were hexagonal plates. Crystal axes were found by examination of the crystal under a polarizing microscope. The crystal was shown to be

[1]*Initial phases of this work were performed by R. Drews and J. Rowlands while at General Dynamics Astronautics, San Diego.*

Can. J. Chem. Downloaded from www.nrcresearchpress.com by 210.87.254.5 on 09/05/12
For personal use only.

A solution of *N*-isopropylidenenoradrenaline methyl ether hydrochloride (0.2 g) in methanol (50 ml) containing 10% palladium-charcoal (0.1 g) was shaken in an atmosphere of hydrogen for 18 h (room temperature and atmospheric pressure). After this time the catalyst was removed by filtration and the crude product, obtained on concentration of the clear filtrate, was recrystallized from ethanol – ethyl acetate and afforded colorless prisms of *N*-isopropylnoradrenaline methyl ether hydrochloride, m.p. 186° (with decomposition), identical with an authentic specimen (i.e. identical infrared spectra and no depression of melting point).

1. J. A. Page and A. Hoffer. Diseases Nervous System, **25**, 558 (1964).
2. A. Hoffer. Mind, **2**, 166 (1964).
3. C. Funk and L. Freedman. J. Am. Chem. Soc. **45**, 1792 (1923).
4. H. Öppinger and H. Vetter. Med. Chem. **4**, 343 (1942). Chem. Abstr. **38**, 5927 (1944).
5. B. F. Tullar. J. Am. Chem. Soc. **70**, 2067 (1948).
6. I. Serlin and M. Goldenberg. Biochem. J. **54**, 483 (1953).
7. F. F. Blicke and W. K. Johnson. J. Am. Pharm. Assoc. Sci. Ed. **45**, 437 (1956).
8. J. Hukki and N. Seppäläinen. Acta Chem. Scand. **12**, 1231 (1958).
9. B. Witkop. J. Am. Chem. Soc. **78**, 2873 (1956).

Received March 30, 1965.
The Psychiatric Research Unit,
University Hospital,
Saskatoon, Saskatchewan.

THE ELECTRON SPIN RESONANCE SPECTRUM OF $\overset{+}{N}(CH_3)_3$ IN γ-IRRADIATED BETAINE[1]

R. Drews, D. Cadena, Jr., and J. Rowlands

INTRODUCTION

Electron spin resonance studies of irradiated single crystals of both inorganic and organic compounds have been shown in many studies (1) to lead to detailed knowledge of both the identity and electronic structure of the radicals formed. The present study of the effects of γ irradiation on a single crystal of betaine $[(CH_3)_3\overset{+}{N}CH_2CO_2H]OH^-$ was motivated by the thought that a detailed study of it might help in the further understanding of the radiation chemistry of choline chloride $[(CH_3)_3\overset{+}{N}CH_2CH_2OH]Cl^-$ (2). Unlike choline chloride, however, in which no trace of the species $\overset{+}{N}(CH_3)_3$ was reported, in betaine at room temperature it was the only species observed. Further studies at liquid nitrogen temperature are required to elucidate the radiation chemistry of the system. The radical $\overset{+}{N}(CH_3)_3$ has already been reported in an irradiated single crystal of tetramethyl ammonium chloride (3). In this lattice the radical was shown to be executing restricted rotation at room temperature. In the betaine lattice the radical is seen to exhibit a nitrogen hyperfine tensor whose principal values more closely approximate the cylindrical symmetry to be expected from a planar radical. A comparison of the anisotropic interaction with that found in similar radicals $N(SO_3^-)_2$ (4) and $H_2\overset{+}{N}SO_3^-$ (5) indicates, however, that the restricted rotation of the radical is not completely quenched.

EXPERIMENTAL

Betaine crystals were grown from saturated aqueous solution. The crystals were hexagonal plates. Crystal axes were found by examination of the crystal under a polarizing microscope. The crystal was shown to be

[1]*Initial phases of this work were performed by R. Drews and J. Rowlands while at General Dynamics Astronautics, San Diego.*

Can. J. Chem. Downloaded from www.nrcresearchpress.com by 210.87.254.6 on 09/05/12
For personal use only.

orthorhombic. The extinction directions were parallel and perpendicular to the long diagonal and perpendicular to the surface of the plate. A sketch of the crystal is reproduced in Fig. 1 which also defines the axis system chosen. The crystal was irradiated at room temperature using a ^{60}Co source. An estimated 5 Mrads of irradiation was delivered to the crystal. The crystal was rotated about each of its three orthogonal axes in turn, and spectra were measured at 10° intervals. Measurements were made at room temperature using a Varian V4500 spectrometer using 100 kc/s modulation. The spectra were calibrated by comparison with a solution of Fremy's salt, $(SO_3)_2NO^{2-}$.

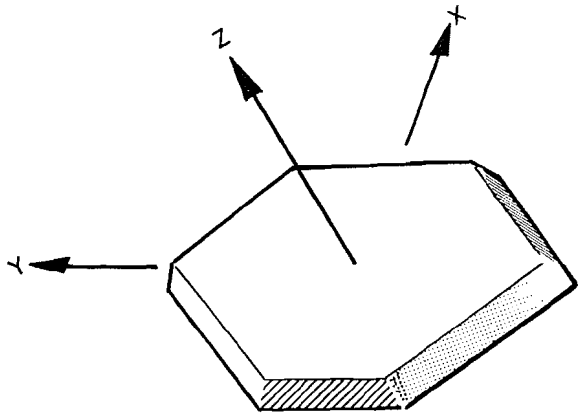

FIG. 1. Sketch of crystal defining crystal axes.

DISCUSSION

The spectra taken along the three crystal axes were consistent with three groups of lines each containing 10 lines of relative intensity 1:9:36:84:126:126:84:36:9:1 required by a radical showing hyperfine interaction to 9 equivalent hydrogens and a nitrogen nucleus. Spectra taken at points between crystal axes were complicated because of the anisotropic nature of the nitrogen coupling, the crystallographic site splitting leading to much overlapping of lines from the two sites. The analysis of these positions was made by assuming the methyl couplings to be isotropic and concentrating on the total spread of the patterns for the two inequivalent sites. The spectrum obtained with the x-axis parallel to the applied field is presented in Fig. 2. Table I gives the direction cosines of principal values of the nitrogen tensor with respect to the crystal axes. The principal values of the nitrogen tensor are all taken to be positive in sign in order to be consistent with values quoted for related species (3, 4, 5), in particular the measured isotropic coupling of the nitrogen nucleus in the radical $\overset{+}{N}H_3$ (6).

TABLE I

Principal values and directions of nitrogen tensor (mc/s with respect to crystal axes)

Nucleus	Tensor (mc/s)²			Principal values (mc/s)	Principal directions
^{14}N	94.0	21.0	41.0	+109	(0.887−0.375−0.267)
	21.0	9.0	5.8	+16	(0.194−0.830−0.523)
	41.0	5.8	28.0	+33	(0.417−0.412−0.809)

In Table II we present the principal values of the nitrogen and methyl couplings. Also included are values obtained for related radicals. From examination of the table it may be seen that the nitrogen principal values in the betaine lattice approximate more closely to

Can. J. Chem. Downloaded from www.nrcresearchpress.com by 210.87.254.6 on 09/05/12
For personal use only.

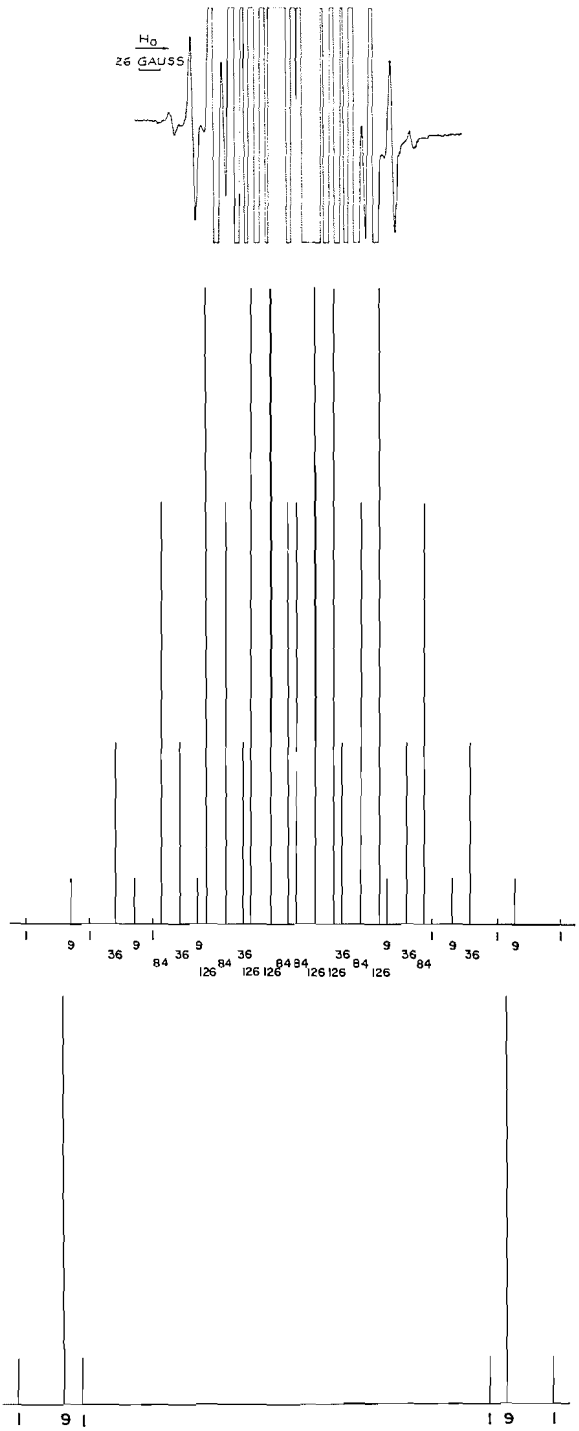

FIG. 2. First derivative spectrum taken with H parallel to the X-axis.

Can. J. Chem. Downloaded from www.nrcresearchpress.com by 210.87.254.6 on 09/05/12
For personal use only.

the expected cylindrical symmetry than they do in the corresponding values for the radical in tetramethyl ammonium chloride (3). In fact they are almost identical to the principal values of the nitrogen tensor for the radical $H_2\overset{+}{N}SO_3^-$ in irradiated sulfamic acid. That this radical was exercising restricted rotation was shown by a study of the change in nitrogen coupling with temperature (5). Because of this restricted rotation we are unable to derive a 2p spin population for the unpaired electron (cf. ref. 4). The isotropic nitrogen coupling compares favorably with the value found for $(CH_3)_3\overset{+}{N}$ in tetramethyl ammonium chloride and the radicals $H_2\overset{+}{N}SO_3^-$ (5) and $\overset{+}{N}H_3$ (6). The methyl coupling is, as to be expected, identical within experimental error with that reported for the same radical by Tench (3).

TABLE II

Principal values of nitrogen and methyl couplings in $\overset{+}{N}(CH_3)_3$ and related radicals

Principal value	$(CH_3)_3\overset{+}{N}$	$(CH_3)_3\overset{+}{N}$*	$H_2\overset{+}{N}SO_3^-$†	$N(SO_3^-)_2$‡	$H_3\overset{+}{N}$§
A^1	109	37	103	106	
A_2	16	57	17	0	
A_3	33	57	33	6	
a_N	53	55	51	37	55
a_H	73	75			

*Reference 3.
†Reference 5.
‡Reference 4.
§Reference 6.

1. J. R. MORTON. Chem. Rev. **64**, 453 (1964).
2. R. O. LINDBLOM. *In* Free radicals in biological systems. *Edited by* M. S. Blois. Academic Press, New York. 1961
3. A. J. TENCH. J. Chem. Phys. **38**, 593 (1963).
4. J. R. MORTON, A. J. HORSFIELD, J. R. ROWLANDS, and D. H. WHIFFEN. Mol. Phys. **5**, 241 (1962).
5. J. R. ROWLANDS and D. H. WHIFFEN. Nature, **193**, 61 (1962).
6. T. COLE. J. Chem. Phys. **35**, 1169 (1961).

RECEIVED JANUARY 4, 1965.
XEROX RESEARCH LABS,
ROCHESTER, NEW YORK,
AND
SOUTHWEST RESEARCH INSTITUTE,
SAN ANTONIO, TEXAS.

AN ELECTRON SPIN RESONANCE STUDY OF ULTRAVIOLET PHOTOLYZED SOLID CARBONYL SULFIDE

D. A. STILES, R. KEWLEY,[1] O. P. STRAUSZ, AND H. E. GUNNING

The gas phase photolysis of carbonyl sulfide has been shown to be a clean source of atomic sulfur (1). No work, however, has been reported on its condensed phase photolysis. A brief electron spin resonance (e.s.r.) study of the solid phase irradiation of COS, both in its pure form and in a variety of matrices at liquid nitrogen temperature, has been undertaken in this laboratory as part of a general program for the study of the reactions

[1]*Present address: Department of Chemistry, Queen's University, Kingston, Ontario.*

Can. J. Chem. Downloaded from www.nrcresearchpress.com by 210.87.254.6 on 09/05/12
For personal use only.

the expected cylindrical symmetry than they do in the corresponding values for the radical in tetramethyl ammonium chloride (3). In fact they are almost identical to the principal values of the nitrogen tensor for the radical $H_2\overset{+}{N}SO_3^-$ in irradiated sulfamic acid. That this radical was exercising restricted rotation was shown by a study of the change in nitrogen coupling with temperature (5). Because of this restricted rotation we are unable to derive a 2p spin population for the unpaired electron (cf. ref. 4). The isotropic nitrogen coupling compares favorably with the value found for $(CH_3)_3\overset{+}{N}$ in tetramethyl ammonium chloride and the radicals $H_2\overset{+}{N}SO_3^-$ (5) and $\overset{+}{N}H_3$ (6). The methyl coupling is, as to be expected, identical within experimental error with that reported for the same radical by Tench (3).

TABLE II

Principal values of nitrogen and methyl couplings in $\overset{+}{N}(CH_3)_3$ and related radicals

Principal value	$(CH_3)_3\overset{+}{N}$	$(CH_3)_3\overset{+}{N}$*	$H_2\overset{+}{N}SO_3^-$†	$N(SO_3^-)_2$‡	$H_3\overset{+}{N}$§
A^1	109	37	103	106	
A_2	16	57	17	0	
A_3	33	57	33	6	
a_N	53	55	51	37	55
a_H	73	75			

*Reference 3.
†Reference 5.
‡Reference 4.
§Reference 6.

1. J. R. MORTON. Chem. Rev. **64**, 453 (1964).
2. R. O. LINDBLOM. *In* Free radicals in biological systems. *Edited by* M. S. Blois. Academic Press, New York. 1961
3. A. J. TENCH. J. Chem. Phys. **38**, 593 (1963).
4. J. R. MORTON, A. J. HORSFIELD, J. R. ROWLANDS, and D. H. WHIFFEN. Mol. Phys. **5**, 241 (1962).
5. J. R. ROWLANDS and D. H. WHIFFEN. Nature, **193**, 61 (1962).
6. T. COLE. J. Chem. Phys. **35**, 1169 (1961).

RECEIVED JANUARY 4, 1965.
XEROX RESEARCH LABS,
ROCHESTER, NEW YORK,
AND
SOUTHWEST RESEARCH INSTITUTE,
SAN ANTONIO, TEXAS.

AN ELECTRON SPIN RESONANCE STUDY OF ULTRAVIOLET PHOTOLYZED SOLID CARBONYL SULFIDE

D. A. STILES, R. KEWLEY,[1] O. P. STRAUSZ, AND H. E. GUNNING

The gas phase photolysis of carbonyl sulfide has been shown to be a clean source of atomic sulfur (1). No work, however, has been reported on its condensed phase photolysis. A brief electron spin resonance (e.s.r.) study of the solid phase irradiation of COS, both in its pure form and in a variety of matrices at liquid nitrogen temperature, has been undertaken in this laboratory as part of a general program for the study of the reactions

[1]*Present address: Department of Chemistry, Queen's University, Kingston, Ontario.*

Can. J. Chem. Downloaded from www.nrcresearchpress.com by 210.87.254.105 on 09/05/12
For personal use only.

of sulfur atoms. The study included the behavior of the radical concentration (as measured by the signal intensity) upon warming the sample *in situ* (internal warm-up), and by externally warming the samples and repeating the spectra at the lower temperature (external warm-up). The radical species was identified as a polyatomic sulfur chain and a maximum value of its mean chain length was calculated.

RESULTS

The spectrum observed from an irradiated sample of pure COS is shown in Fig. 1. It is characterized by three lines having g-values of 2.042 ± 0.003, 2.028 ± 0.003, and 2.002 ± 0.003. The total spread of the spectrum as measured between the two outer peaks was 65 ± 0.5 G and the central line had a width of 9.2 ± 0.5 G. The intensity of the signal grew steadily with irradiation time until it levelled off after approximately 6 h. The sample turned from colorless to pink when removed from the ultraviolet source for several seconds but this color could be bleached by further irradiation. The radical species were very stable since the intensity did not diminish if the sample was stored for several days at 77 °K.

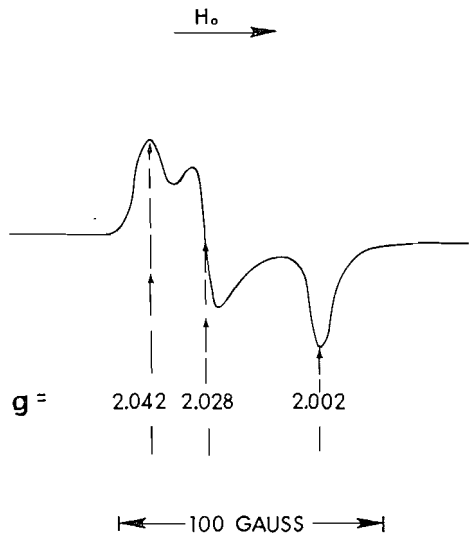

FIG. 1. Electron spin resonance spectrum of ultraviolet photolyzed COS.

Samples containing 1.0 and 0.1 mole % COS in xenon were also irradiated, and gave an identical e.s.r. spectrum to that obtained from pure COS. The intensity increased linearly with time over a period of 12 h, and the same pink aftercolor was observed, although of much weaker intensity. As the sample was warmed the signal intensity began to diminish at −160 °C and continued to do so as the temperature was raised. Because of the low melting points of the substances involved it was not possible to anneal these matrices much above −140 °C, but the e.s.r. spectra recorded after annealing at these temperatures showed the same characteristics as those obtained immediately following irradiation. The samples retained their pink color during warm-up. When each sample was opened to the atmosphere a yellow powder was observed at the bottom of the sample tube.

Further experiments were performed in a cyclodecane matrix (m.p. 10.5 °C) which

Can. J. Chem. Downloaded from www.nrcresearchpress.com by 210.87.254.105 on 09/05/12
For personal use only.

permitted annealing of the samples at higher temperatures. A 0.1 mole % sample of COS in cyclodecane was irradiated at 77 °K and a spectrum was obtained similar to that using a xenon matrix. The intensity of the signal increased linearly with time over a 24 h period but no pink coloration was observed. Although the g-values of the three lines were unchanged, considerable sharpening was evident and the width of the central line decreased to 6.8 ± 0.5 G (see Fig. 2).

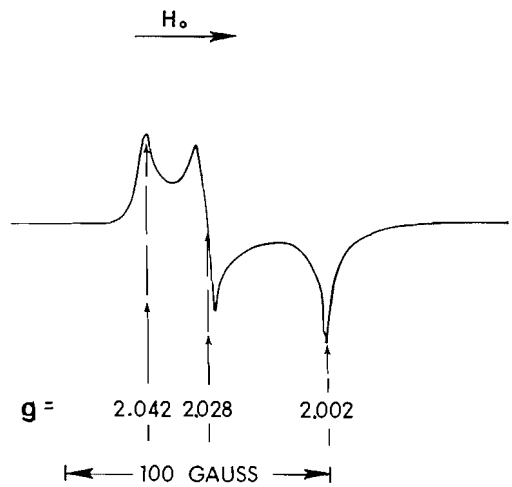

FIG. 2. Electron spin resonance spectrum of ultraviolet photolyzed COS using cyclodecane matrix.

Samples annealed either internally or externally showed similar spectral behavior. The intensity of the signal decreased without change in its basic shape over a warm-up range from −196 °C to −90 °C. The rate of signal decay was most noticeable above −160 °C. This made the recording of spectra of internally warmed samples difficult and it was impossible to make accurate measurements of radical intensity at temperatures above −196 °C. No signal was ever observed after annealing at temperatures higher than −90 °C, nor for values of H_0 corresponding to g-values other than those cited. When the above samples were warmed to room temperature a faint white turbidity was observed.

The numbers of free spins in the different matrices were obtained from the integrated e.s.r. signals by comparison with those from standards of known concentrations.

DISCUSSION

Carbonyl sulfide photolyzes to give carbon monoxide and sulfur atoms (1). The former is diamagnetic and gives no e.s.r. signal while the latter exists in a triplet state and is thus paramagnetic.* It is expected, therefore, that the observed spectrum is due to either sulfur atoms or polyatomic sulfur molecules formed from sulfur atom recombination.

If we assume that the unpaired electrons of a triplet sulfur atom are contained in degenerate 3p orbitals, the Landé g-factor for such a species is calculated at 1.5. The signal observed at $g = 2$ cannot, therefore, be due to free sulfur atoms. A long chain sulfur radical, however, would be expected to have an e.s.r. spectrum centered on a g-value approximately 1% higher than the free spin value (2, 3). The fact that the same characteristic asymmetric spectrum observed for sulfur radicals in the liquid (3) and solid states

**The condensed phase photolysis of* COS *gives* (^3P) *ground state sulfur atoms, while the gas phase photolysis leads to* S(^1D) *atoms.*

Can. J. Chem. Downloaded from www.nrcresearchpress.com by 210.87.254.105 on 09/05/12
For personal use only.

(4, 5) has been obtained suggests that the paramagnetic species are polyatomic sulfur chains. The solids formed on sample warm-up support this view.

Annealing characteristics are interesting because they indicate whether chemical or physical changes occur to the spin system as its temperature is raised. For instance, a change in the spectrum of a sample as it was annealed externally would indicate that there was a chemical change taking place in the system. However, if an external warm-up caused no change in the spectrum but an internal warm-up did, it would mean that a physical effect such as the averaging of g-value or hyperfine anisotropy by rotation of the species was taking place. Since the only effect of warming COS samples either inside or outside the cavity was to diminish the intensity of the signal, it is concluded that only one radical species was present and that this decayed at about −90 °C. The failure to observe any sharpening of the spectrum on internal warm-up may be attributed to the fact that the rate of radical decay by bimolecular collisions was rapid compared to the averaging of g-value anisotropy.

Because of the necessity of conserving spin, a sulfur atom chain formed from atoms in a ^3P state must be a biradical and if the chain is sufficiently long there will be no interactions between the unpaired electrons on the terminal sulfur atoms. From a theoretical standpoint the spectrum is consistent with that expected from a polyatomic sulfur biradical. Kneubühl (6) has developed a theory of line shapes for a system in which a single unpaired electron is associated with either axially symmetric or non-axially symmetric molecules. In cases where there is no hyperfine interaction, as would be the case for a polyatomic sulfur chain (^{32}S, $I = 0$), three lines are predicted for non-axially symmetric molecules. This would pertain to a rigid polyatomic sulfur biradical chain since the dihedral sulfur angle in such a chian is 102° (7). On the other hand, if the radical were able to rotate sufficiently rapidly, the anisotropies of the g-factor would be averaged to the isotropic value. It is interesting to note that averaging the three g-values obtained from the spectrum of photolyzed COS gives the same g-factor, within experimental error, as was obtained from the spectrum of liquid sulfur (2).

These results are in broad agreement with those of Buttet and Châtelain (8) although the annealing experiments did not indicate the growth of a second and third radical species at the expense of the first, as were their findings. The fact that lines from different matrices were of different widths, which remained constant during warm-up, suggests that the difference in observations is due to a change in matrix material. Sulfur, a solid at room temperature, would be expected to form a fairly rigid matrix which would allow radicals to recombine in stages. On the other hand, in the photolysis of COS, it is difficult to use a matrix which is solid at room temperature since it must be able to dissolve the substrate. For this reason these matrices do not show the same characteristics of rigidity as sulfur at −90 °C, and allow total annihilation of sulfur biradicals at this temperature.

Although evidence points to the formation of a single radical species, it does not account for the fairly broad central line observed by Radford and Rice (4) and Châtelain and Buttet (5), under certain conditions at 77 °K. It appears that these investigators obtained two radical species and that the broader spectrum was the superposition of a broadened signal from a fairly labile radical, on the asymmetric triplet of the more stable species, which is observed in the photolysis of COS.

From the stoichiometry of the photolytic reaction

$$COS + h\nu \longrightarrow CO + S$$

and from the assumption that the species responsible for the e.s.r. signals are the polysulfur biradicals $\cdot S(S)_nS\cdot$ (2, 3) a maximum value for the mean chain length can be

Can. J. Chem. Downloaded from www.nrcresearchpress.com by 210.87.254.105 on 09/05/12
For personal use only.

calculated from the relation

$$(2 \times \text{moles of CO})/(\text{number of free spins}) = \text{mean chain length.}$$

The values found for samples of 100% COS, 0.1 mole % COS in Xe, and 0.1 mole % COS in cyclodecane are given in Table I.

TABLE I

Specimen	Spin intensity in spins/cm of sample measured by: Standard 1	Standard 2	Carbon monoxide content, μmoles	Chain length in terms of sulfur atoms
1. 100% COS	8.5×10^{14}	8.0×10^{14}	2.52	2.5×10^{3}
2. 0.1% COS in Xe	8.5×10^{14}	8.0×10^{14}	1.29	1.3×10^{3}
3. 0.1% COS in cyclodecane	19×10^{14}	17×10^{14}	1.14	0.5×10^{3}

Length of sample is assumed to be 1.5 cm for samples 1 and 2, and was measured as 1.5 for sample 3.

Table I shows a decrease in biradical chain length as the matrix is changed from pure COS to saturated hydrocarbon. Although these figures are not completely consistent they suggest that the radical species is a polymer of length about 1 000 units. The accuracy of the intensity measurements was checked and one of the most serious sources of error was found to occur in measuring the length of a sample in a given tube. It was estimated that this error could be as large as 50% in the cases of COS and COS–xenon samples. An upper limit was taken in these cases, so the average chain length could be as high as 4×10^3.

For the cyclodecane sample the measurement of sample length could be made much more accurately; the main source of error in this calculation was in measuring graphical first moments. Since these were checked against two standards for a number of spectral displays, this measurement of spin intensity is considered to have an error of ±10%.

It is possible to explain the variation in the values of chain length obtained if it is assumed that neither the COS nor the xenon matrices were sufficiently rigid to trap completely the products of photolysis. Although these matrices may be more rigid than that of cyclodecane once photolysis is complete, it is likely that the heat of reaction during irradiation will melt them sufficiently to allow some recombination of radicals. This loss of free spins would cause an apparent increase in the mean chain length. This hypothesis is supported by the formation of the pink color when such samples are removed from the ultraviolet source for a few seconds. The color brings to mind the experiment of Radford and Rice (4) in which sulfur was γ-irradiated without the formation of free radicals.

It is concluded that the stable paramagnetic species formed in the photolysis of COS is a biradical sulfur chain whose average length is no more than several hundred atoms. It is likely that either S atoms or S_2 biradicals are the species responsible for propagation, since it is improbable that entities of higher molecular weight could permeate the matrix.

If the steady-state concentration of these species were high enough, the intensity of the e.s.r. signal would be expected to increase after irradiation had ceased. As no such increase was found, the steady-state concentration of the propagating species was probably too low to permit their detection.

EXPERIMENTAL

Preparation of Samples

Samples were prepared by vacuum distillation of the various constituents into a quartz sample tube attached by a graded seal to a pyrex break seal for product analysis. Each was irradiated at 77 °K in a

Can. J. Chem. Downloaded from www.nrcresearchpress.com by 210.87.254.105 on 09/05/12
For personal use only.

quartz Dewar with either a Hanovia medium pressure mercury lamp emitting discontinuously between 2 200 Å and 2 600 Å or an Osram cadmium lamp (λ = 2 288 Å) 3 to 5 cms from the specimen. After irradiation the samples were transferred manually to the spectrometer.

Spectrometer Details

Spectra were recorded as the first derivative of the resonance absorption using a Varian EPR spectrometer, type 4502, fitted with the V-4532 dual cavity and operating at a nominal frequency of 9.5 Gc/s. Normally samples under investigation were kept at 77 °K in the cavity by an insert Dewar filled with liquid nitrogen. For external annealing a Varian type V-4547 variable temperature accessory was set up outside the magnet gap, and specimens were allowed to equilibrate at the desired temperature for about 5 min. When internal annealing was used, the Dewar portion of the variable temperature accessory was placed inside the cavity and the same procedure adopted as for external annealing.

The *g*-values were measured by reference to the parabenzosemiquinone spectrum, which has a central line of $g = 2.0057$ and a spacing of 2.33 G between adjacent hyperfine components (9).

Calibration of Standard

The usual method employs the use of a dual cavity where the standard is placed in one position modulated at 400 c/s, while the unknown is placed in a second position and modulated at 100 kc/s. After the spectra from both samples are recorded under certain gain conditions, the positions of the sample and standard are reversed and the spectra rerecorded using the same modulation amplitudes as before, but the amplifier gains adjusted so that good graphical presentation is still obtained. Comparison of the integrated areas under the absorption curves then determines the number of free spins in the unknown.

A solution of 1,1-diphenyl 2-picryl hydrazyl (DPPH) in benzene was prepared, and the quantity of DPPH dissolved calculated from spectro-photometric data (10). A quantity of solid DPPH was then mixed intimately with powdered potassium chloride and a portion introduced into a sample tube (standard 1). These two samples were used to determine the number of free spins in 'standard 1' using the above procedure.

Although this method was satisfactory in this instance there was sufficient cross talk between the two channels to make the calibration of photolyzed COS samples very difficult to assess quantitatively. Thus an alternative procedure was adopted whereby the sample and standard were run in the same channel consecutively. Intensity measurements on Varian sample 904450-01 (standard 2) containing 3×10^{15} spins per centimeter of length, against standard solutions of DPPH in benzene, showed that this method was at least as accurate as the one discussed previously. By this means 'standard 1' was found to contain 1.8×10^{14} spins per centimeter of length.

Materials

The xenon used was assayed reagent grade, from Airco, and was used without further purification.

The carbonyl sulfide was Matheson reagent grade, which was washed four times with saturated sodium hydroxide, and dried over Drierite. It was then vacuum distilled using *n*-pentane and methanol slushes.

The cyclodecane was a special sample supplied by Columbian Carbon. It was purified by three washings with equal volumes of 1/1 H_2SO_4/HNO_3 and water, and then with concentrated H_2SO_4 until the acid layer remained colorless. After passage through a 20 ft SE30 silicone–rubber gas chromatographic column, it was washed once more with concentrated sulfuric acid, and distilled in a greaseless system at 10 Torr.

ACKNOWLEDGMENTS

The authors are indebted to the National Research Council and to Imperial Oil Limited for financial assistance.

1. O. P. Strausz and H. E. Gunning. J. Am. Chem. Soc. **84**, 4080 (1962). A. R. Knight, O. P. Strausz, and H. E. Gunning. J. Am. Chem. Soc. **85**, 1207, 2349 (1963).
2. D. M. Gardner and G. K. Fraenkel. J. Am. Chem. Soc. **78**, 3279 (1956).
3. W. G. Hodgson, S. A. Buckler, and G. Peters. J. Am. Chem. Soc. **85**, 543 (1963).
4. H. E. Radford and F. O. Rice. J. Chem. Phys. **33**, 774 (1960).
5. A. Châtelain and J. Buttet. Helv. Phys. Acta, **37**, 78 (1964).
6. F. K. Kneubühl. J. Chem. Phys. **33**, 1074 (1960).
7. L. Pauling. Proc. Natl. Acad. Sci. U.S. **35**, 495 (1949).
8. J. Buttet and A. Châtelain. Colloque Ampère, Bordeaux. 1963. p. 16. Compt. Rend.
9. B. Venkataraman and G. K. Fraenkel. J. Am. Chem. Soc. **77**, 2707 (1955).
10. J. A. Lyons and W. F. Watson. J. Polymer Sci. **87**, 141 (1955).

Received March 11, 1965.
Department of Chemistry,
University of Alberta,
Edmonton, Alberta.

Can. J. Chem. Downloaded from www.nrcresearchpress.com by 210.87.254.105 on 09/05/12
For personal use only.

THERMODYNAMIC EXCESS FUNCTIONS IN THE SYSTEMS ACETIC ACID – WATER AND ACETIC ACID – CHLOROFORM

J. M. T. M. GIESKES[1]

Campbell and Gieskes (1) recently studied the heats of mixing of the system acetic acid – chloroform – water, and its contiguous binary systems. It was suggested by Scott (2) that these data be combined with the earlier results of Campbell, Kartzmark, and Gieskes (3) on the isothermal vapor–liquid equilibria of this system. In the earlier paper it was shown that the vapor–liquid equilibrium data are in good agreement with the Gibbs–Duhem conditions when a dimerization equilibrium with a single equilibrium constant is taken into account. In the later study of the heats of mixing and the volumes of mixing, the functions $H^E(x)$ and $V^E(x)$ were based on an ideal solution of acetic acid monomers as the most convenient reference state, even though it was recognized that dimerization occurs in both the liquid and vapor phases.

In order to relate the excess free energy of mixing as calculated from the liquid–vapor equilibria to the heats of mixing, it is, of course, necessary to adopt the same reference state. In this case the excess free energy of mixing is defined by the following formulae:

$$\mu_{H_2O}{}^E = RT \ln \frac{P_{H_2O}}{x_{H_2O} P_{H_2O}{}^0}$$

$$\mu_{CHCl_3}{}^E = RT \ln \frac{P_{CHCl_3}}{x_{CHCl_3} P_{CHCl_3}{}^0}$$

$$\mu_{HAc}{}^E = RT \ln \frac{P_1}{x_{HAc} P_1{}^0}$$

and

$$G^E = x_{H_2O}\mu_{H_2O}{}^E + x_{CHCl_3}\mu_{CHCl_3}{}^E + x_{HAc}\mu_{HAc}{}^E$$

where $p_1{}^0$ is the partial pressure of acetic acid monomers above pure acetic acid liquid, and the mole fractions are the formal mole fractions based upon monomeric acetic acid. Corrections for deviations of the vapor from "ideal" behavior will never be more than a few calories, because the second virial coefficients will only be of the order 1 000 cm^3 $mole^{-1}$ at these low pressures. Consequently G^E can be estimated to a very good approximation from the above formulae by postulating that the true species, i.e. water, chloroform, dimeric acetic acid, and monomeric acetic acid behave as an ideal gas mixture.

The System Acetic Acid – Water at 25 °C

From the data of Campbell *et al.* (3) the values of the G^E function were calculated, and plotted. From the smoothed curve through these values a Redlich–Kister (4) equation was calculated having the form

$$G^E = x_1x_2[768 + 472(x_1 - x_2) - 158(x_1 - x_2)^2 - 1060(x_1 - x_2)^3]$$

where x_1 = mole fraction acetic acid and x_2 = mole fraction water.

Campbell and Gieskes (1) reported the heat of mixing at 25 °C to be represented by the equation

$$H^E = x_1x_2[296 + 166(x_1 - x_2) + 19(x_1 - x_2)^2 + 321(x_1 - x_2)^3].$$

[1]*Holder of a C.I.L. Fellowship 1964–1965. Present address: Woods Hole Oceanographic Institution, Woods Hole, Massachusetts, U.S.A.*

Can. J. Chem. Downloaded from www.nrcresearchpress.com by 210.87.254.5 on 09/05/12
For personal use only.

The excess entropy of mixing can then be calculated from the relation

$$TS^E = H^E - G^E$$

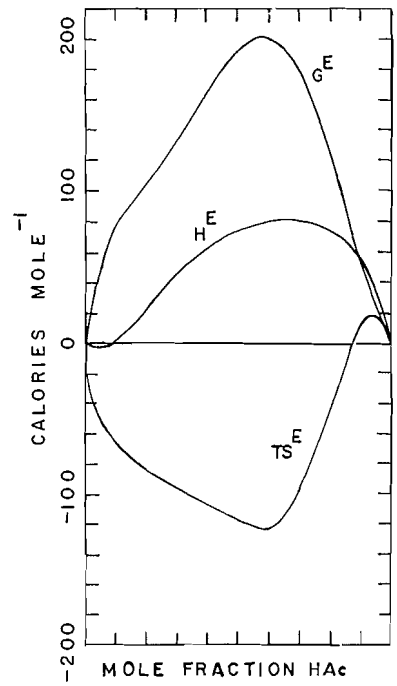

FIG. 1. Thermodynamic excess functions in the system acetic acid – water at 25 °C.

In Fig. 1 the curves for these functions are plotted. It can be seen that the shape of all three thermodynamic functions is very irregular. In view of the complicated interactions (5, 6) which may occur in this system this is not surprising. Of interest is the behavior of the excess entropy of mixing. At high concentrations of acetic acid a positive value occurs. This may well be due to the break up of acetic acid ring dimers as suggested by Cucurezeanu (5) and by Fénéant-Eymard (6). Campbell *et al.* (3) measured the excess volume of mixing for this system, and found it to be negative and quite symmetrical. The Redlich–Kister (4) formula was found to be

$$V^E = x_1x_2[4.58 - 1.25(x_1 - x_2)^2]$$

where V^E is in ml mole^{-1}.

The System Acetic Acid – Chloroform at 25 °C

The excess free energy of mixing was calculated, and the smoothed values fitted the equation

$$G^E = x_1x_2[568 - 291(x_1 - x_2) + 301(x_1 - x_2)^2 + 380(x_1 - x_2)^3]$$

where x_1 = mole fraction acetic acid and x_2 = mole fraction chloroform. Campbell and Gieskes (1) determined the heats of mixing as

$$H^E = x_1x_2[-574 - 71(x_1 - x_2) + 78(x_1 - x_2)^2]$$

and therefore also the excess entropy of mixing can be calculated.

Can. J. Chem. Downloaded from www.nrcresearchpress.com by 210.87.254.5 on 09/05/12
For personal use only.

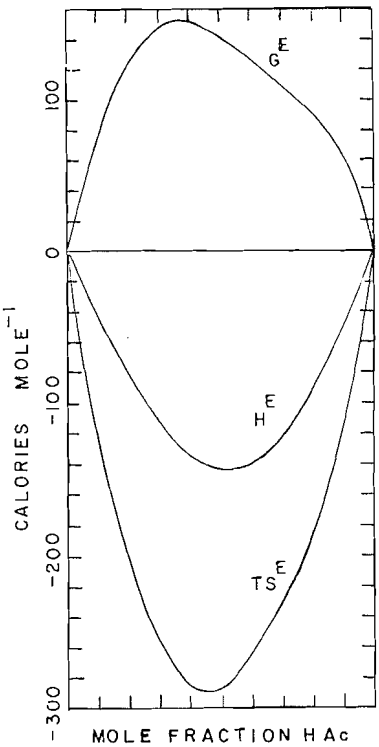

FIG. 2. Thermodynamic excess functions in the system acetic acid – chloroform at 25 °C.

In Fig. 2 the excess functions of mixing are represented. The curves have a fairly regular shape. The excess volume of mixing was determined by Campbell *et al.* (3), and was found to be positive over the entire region of concentration. A Redlich–Kister (4) expression was calculated for this function.

$$V^E = x_1x_2[2.200 + 0.521(x_1 - x_2) - 0.18(x_1 - x_2)^2]$$

where V^E is in ml mole^{-1}.

Haase (7) remarks that in general V^E and S^E have the same sign. This, however, is clearly not the case in the system acetic acid – chloroform. Scott *et al.* (8) found a similar phenomenon in the system $C_7F_{15}H$–acetone. The positive value of V^E and the negative value of S^E seems to the author yet another indication that in this system the antiparallel dipole association of acetic acid ring dimers with chloroform molecules is predominant. This problem was discussed extensively by Campbell and Gieskes (1, 9).

1. A. N. CAMPBELL and J. M. T. M. GIESKES. Can. J. Chem. **43**, 1004 (1965).
2. R. L. SCOTT. Private communication.
3. A. N. CAMPBELL, E. M. KARTZMARK, and J. M. T. M. GIESKES. Can. J. Chem. **41**, 407 (1963).
4. O. REDLICH and A. T. KISTER. Ind. Eng. Chem. **40**, 345 (1948).
5. I. CUCUREZEANU. Acad. Rep. Populare Romine Studii Cercetari Fiz. **9**, 269 (1958).
6. S. FÉNÉANT-EYMARD. Mem. Serv. Chim. Etat Paris, **37**, 297 (1952).
7. R. HAASE. Thermodynamik der Mischphasen. Springer, Berlin. 1956. p. 447.
8. D. L. ANDERSON, R. A. SMITH, D. B. MEYERS, S. A. ALLEY, A. G. WILLIAMSON, and R. L. SCOTT. J. Phys. Chem. **66**, 621 (1962).
9. A. N. CAMPBELL and J. M. T. M. GIESKES. Can. J. Chem. **42**, 1379 (1964).

RECEIVED MARCH 22, 1965.
DEPARTMENT OF CHEMISTRY,
UNIVERSITY OF MANITOBA,
WINNIPEG, MANITOBA.

Can. J. Chem. Downloaded from www.nrcresearchpress.com by 210.87.254.5 on 09/05/12
For personal use only.

ERRATUM: CARBON-13 ISOTOPE EFFECTS IN SYSTEMS CONTAINING CARBON DIOXIDE, BICARBONATE, CARBONATE, AND METAL IONS

H. G. THODE, M. SHIMA, C. E. REES, AND K. V. KRISHNAMURTY

(Ref. Can. J. Chem. 43, 582 (1965))

On page 590, Table V, the K value quoted in the last six rows of Table V is not the equilibrium constant but a comparison of gas phase ^{13}C:^{12}C ratios, i.e.

$$\frac{(^{13}C/^{12}C) \text{ gas phase, } Na^+ \text{ present}}{(^{13}C/^{12}C) \text{ gas phase, } Na^+ + \text{ other ions}}.$$

MCMASTER UNIVERSITY,
HAMILTON, ONTARIO.

Canadian Journal of Chemistry. Volume 43 (1965)

Can. J. Chem. Downloaded from www.nrcresearchpress.com by 210.87.254.5 on 09/05/12
For personal use only.

2453-3549

Canadian Journal of Chemistry

Issued by THE NATIONAL RESEARCH COUNCIL OF CANADA

VOLUME 43 SEPTEMBER 1965 NUMBER 9

EFFECT OF PRESSURE AND TEMPERATURE ON THE RATE OF THE ACID-CATALYZED HYDRATION OF ETHYLENE[1]

B. T. BALIGA AND E. WHALLEY

Division of Applied Chemistry, National Research Council, Ottawa, Canada

Received April 9, 1965

ABSTRACT

The rate of hydration of ethylene in dilute aqueous perchloric acid has been measured in the range 170–190 °C at 100 bars and 100 to 3 000 bars at 180 °C. The energy, entropy, and volume of activation are 33.3 ± ~1 kcal mole^{-1}, −5.7 ± ~2.5 cal deg^{-1} mole^{-1}, and −15.5 ± ~1.5 cm^3 mole^{-1} respectively. The volume of activation shows that at least one molecule of water is strongly bound in the transition state.

The acid-catalyzed hydration of olefins has been much studied in recent years, particularly of relatively highly substituted olefins (see ref. 1 for references). Little has been reported on the hydration of the parent compound ethylene, probably largely because its hydration rate is fast enough for convenient study in dilute aqueous acids only at temperatures above 150 °C. This is well above the boiling point of aqueous acids, and consequently the measurements can be done only under pressure.

The hydration of ethylene is a reaction of considerable importance both theoretically, as the simplest olefin hydration, and technically, as a manufacturing method for both ethanol and (by the reverse reaction) ethylene. The hydration of propylene and isobutylene has recently been studied in this laboratory (1), and the same techniques have now been applied to ethylene. The volume of activation for propylene and isobutylene proved of considerable value in the determination of the mechanism, and consequently the effect of pressure as well as temperature has been studied.

EXPERIMENTAL

Materials

Ethylene was Phillips Petroleum Co. research grade, *n*-heptane was Anachemia Chemicals Ltd. pure grade, and other chemicals were reagent grade.

Analysis of Ethanol

The hydration of ethylene was followed by estimating the alcohol produced. The method of analysis was reported earlier (1).

Kinetic Measurements

The thermostat bath was an aluminum block 14 in. long and 10 in. in diameter, with a hole of 4 in. in diameter and 12 in. long bored centrally to hold the reaction vessel. The outer surface of the block was covered with layers of asbestos paper and wound evenly with two coils of resistance wire, one to serve as the main heater, and one to serve as the intermittent heater. The block was insulated on all sides by transite or vermiculite. The temperature of the block was measured by a platinum resistance thermometer inserted in a hole in the block. It was controlled by a second platinum resistance thermometer connected to a Mueller

[1]*N.R.C. No. 8476.*

Can. J. Chem. Downloaded from www.nrcresearchpress.com by 210.87.254.40 on 09/05/12
For personal use only.

bridge whose galvanometer operated a photo-relay and switched the intermittent heater, which usually delivered 15 to 20 W. The temperature of the block was controlled to ±0.02 deg.

The catalyst used for the hydration was perchloric acid. The reaction solution was made by bubbling ethylene through the acid solution at 0 °C until it was nearly saturated. To reduce the loss of ethylene while assembling the vessel and placing it in the thermostat, the same procedure as used for propylene (1) was followed. To compensate for the fall in temperature when the pressure vessel was put into the thermostat block, the block was previously heated to temperatures higher than was desired. Under these conditions, about 60 min was sufficient to reach temperature equilibrium, and the first sample was taken at least 90 min after immersing the vessel. About seven samples were taken during each run and three samples were taken for the infinity reading, which was taken after at least 10 half-lives.

The pressure techniques were the same as those used previously (2, 3). A small cylindrical stainless-steel pressure vessel of about 6 cm^3 capacity was interposed between the valve F and the head (see Fig. 1 of ref. 3). This was to ensure that the oil added to the vessel when a sample was taken was at the same temperature as the vessel.

It was verified by the following experiment that the hydration of ethylene was essentially unidirectional and that no significant amount of olefin was present at equilibrium. An acid solution (0.7 M in perchloric acid) of ethanol of concentration such as to give an optical density about three times that of the infinity reading ($\sim$ 0.26) of the kinetic runs was kept at 180.00 °C and 100 bars for 24 h, which was more than the time taken to complete a run in the hydration experiment. There was no change in concentration of the alcohol within the reproducibility (± ~0.3%) of the measurements. At higher pressures and at this temperature the amount of olefin present would be expected to be even smaller because alcohols dehydrate with an increase of volume.

RESULTS

The hydration of ethylene was first-order in ethylene, and the first-order rate constants k_1 were obtained in the usual way (1). The accuracy of the rate constants was about 3%. The second-order rate constants k_a were obtained by dividing the first-order constants by the concentration of hydrogen-ion at the temperature and pressure of the experiment, assuming the solution compressed as water (4, 5). The results are given in Table I. The runs at 180.00 °C and 100 bars in 0.3145 and 0.6250 M perchloric acid prove that the reaction is first-order in perchloric acid. The effect of temperature on the reaction was also measured in the range 170–190 °C and at a constant pressure of 100 bars.

TABLE I

Rate constants for the acid-catalyzed hydration of ethylene in water

Temp., °C	p/bar	c_{HClO_4}/M^*	$10^6\ k_a$/l mole^{-1} s^{-1}
170.00	100	0.6279	52.4
180.00	100	0.3145	120
		0.6250	119
	400	0.6365	134
	1 000	0.6596	162
	2 000	0.3484	209
	3 000	0.3638	233
190.00	100	0.3071	265

*c_{HClO_4} is the concentration of perchloric acid at the temperature and pressure of the experiment.

The volume of activation $\Delta V^{\neq}$ at zero pressure was obtained graphically by plotting mean volumes of activation $\Delta V_{mean}^{\neq}$ calculated between any two pressures p_1 and p_2 from the formula

$$\ln \frac{k_a(p_2)}{k_a(p_1)} = \frac{-\Delta V_{mean}^{\neq}(p_2 - p_1)}{RT}$$

against $(p_1 + p_2)/2$, where $k_a(p_1)$ and $k_a(p_2)$ are the rate constants at pressures p_1 and p_2, and extrapolating to zero pressure. A graph of this plot for the acid-catalyzed hydration of ethylene is shown in Fig. 1. The advantages of using this method to evaluate $\Delta V^{\neq}$

423612

Can. J. Chem. Downloaded from www.nrcresearchpress.com by 210.87.254.40 on 09/05/12
For personal use only.

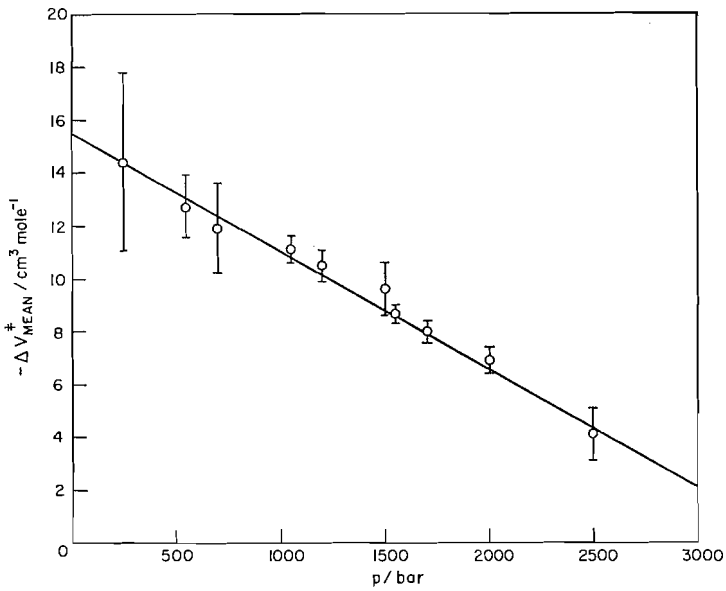

FIG. 1. Effect of pressure on volume of activation for the acid-catalyzed hydration of ethylene in water at 180 °C.

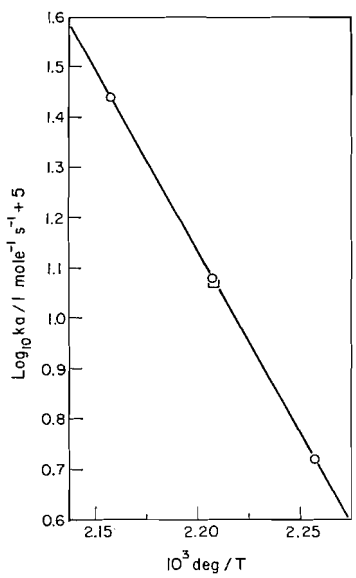

FIG. 2. Effect of temperature on the rate of the acid-catalyzed hydration of ethylene in water at 100 bars.

have been discussed elsewhere (6). The volume of activation $\Delta V^{\ddagger}$ for the acid-catalyzed hydration of ethylene is $-15.5 \pm \sim 1.5$ cm^3 mole^{-1} at 180.00 °C.

The effect of temperature on the reaction is shown by an Arrhenius plot in Fig. 2. The parameters of the Arrhenius equation obtained from this plot are,

$$E_A = 33.3 \pm \sim 1.0 \text{ kcal mole}^{-1},$$

$$\log_{10} A/\text{l mole}^{-1}\text{ s}^{-1} = 12.2,$$

Can. J. Chem. Downloaded from www.nrcresearchpress.com by 210.87.254.40 on 09/05/12
For personal use only.

and the entropy of activation $\Delta S^{\ddagger} = R \ln (A/1 \text{ mole}^{-1})\ (h/ekT)$ is $-5.7 \pm \sim 2.5$ cal deg^{-1} mole^{-1}. The difference between these values and those for zero pressure or 1 bar will be quite inappreciable.

DISCUSSION

The various activation parameters for the acid-catalyzed hydration of ethylene, propylene, and isobutylene are summarized in Table II.

TABLE II

Activation parameters for the acid-catalyzed hydration of olefins in water

Olefin	Ethylene	Propylene (1)	Isobutylene
p/b	100	100	1
Temperature range for $\Delta H_p^{\ddagger}$ and $\Delta S_p^{\ddagger}$, °C	170–190	90–110	25–50
$\Delta H_p^{\ddagger}$/kcal mole^{-1}	32.4±∼1.0	26.4±∼1.0	21.1±∼0.2 (7)
$\Delta S_p^{\ddagger}$/cal deg^{-1} mole^{-1}	−5.7±∼2.5	−5.4±∼2.5	−7.7±∼0.7 (7)
Temperature for $\Delta V^{\ddagger}$, °C	180	100	35
$\Delta V^{\ddagger}$/cm^3 mole^{-1}	−15.5±∼1.5	−9.6±∼1.0	−11.5±∼1.0 (1)

The volume of activation for the acid-catalyzed hydration of ethylene is $-15.5 \pm \sim 1.5$ cm^3 mole^{-1} at 180 °C. Clearly, a loss of volume of this magnitude, which is almost the volume of a water molecule, indicates that the transition state for the hydration of ethylene contains at least one firmly bound molecule of water, and so can be represented as $[\text{ethylene}.H^+.H_2O]^{\ddagger}$. As in the case of propylene and isobutylene, this rules out a mechanism in which a π-protonated ethylene isomerizes unimolecularly to a carbonium ion. The entropy of activation for the hydration of ethylene is $-5.7 \pm \sim 2.5$ cal deg^{-1} mole^{-1}. This is similar to the entropies of activation for the hydration of propylene and isobutylene (see Table II) and confirms the conclusion derived from the volume of activation. It is not in our opinion possible as yet to specify the structure of the transition state in more detail; there are several possibilities which have been discussed in ref. 1 in relation to the hydration of propylene and isobutylene.

The enthalpies of activation show a constant decrease of about 5 kcal mole^{-1} in the series ethylene, propylene, and isobutylene. This is no doubt due largely to the fact that the carbonium ion becomes more stable in the series ethyl, isopropyl, *t*-butyl, and so the olefin can more easily accept the partial positive charge in the transition state.

The volumes of activation for the hydration of propylene and isobutylene are nearly the same, but that of ethylene is nearly 50% more negative. This difference is likely caused at least partly by the higher temperature used for ethylene. The interaction of ethylene with the solvent is small and so its thermal vibrations have relatively large amplitude. They are therefore probably relatively anharmonic, and so cause a large thermal expansivity. The partial expansivity of ethylene is, therefore, probably greater than that of water, of H_3O^+, and of the transition state. This tends to make the volume of activation more negative at higher temperatures.

REFERENCES

1. B. T. BALIGA and E. WHALLEY. Can. J. Chem. **42**, 1019 (1964).
2. A. R. OSBORN and E. WHALLEY. Can. J. Chem. **39**, 1094 (1961).
3. J. KOSKIKALLIO and E. WHALLEY. Trans. Faraday Soc. **55**, 809 (1959).
4. W. T. HOLSER and G. C. KENNEDY. Am. J. Sci. **256**, 744 (1958).
5. G. C. KENNEDY. Am. J. Sci. **248**, 540 (1950).
6. E. WHALLEY. Advances in physical organic chemistry. Vol. II. Academic Press, London. 1964. p. 93.
7. E. L. PURLEE, R. W. TAFT, and C. A. DEFAZIO. J. Am. Chem. Soc. **77**, 837 (1955).

Can. J. Chem. Downloaded from www.nrcresearchpress.com by 210.87.254.40 on 09/05/12
For personal use only.

Can. J. Chem. Downloaded from www.nrcresearchpress.com by 210.87.254.5 on 09/05/12
For personal use only.

SURFACE EFFECTS IN THE UNINHIBITED AND THE INHIBITED PYROLYSES OF ISOMERIC HEXANES

PART V. 2,2-DIMETHYL BUTANE (NEOHEXANE)

J. CHRYSOCHOOS[1] AND W. A. BRYCE[2]
Department of Chemistry, University of British Columbia, Vancouver, British Columbia
Received March 24, 1965

ABSTRACT

The rate of pyrolysis of neohexane decreases slightly with increasing S/V ratio in the pressure range of 15–100 mm at 510–530 °C. The yields of CH_4, C_2H_6, and C_3H_6 increase with increasing hydrocarbon pressure while the yields of i-C_4H_8 and H_2, which increase with increasing hydrocarbon pressure, tend to level off at higher pressures. The rest of the products are pressure independent. The nitric oxide required for maximum inhibition is 12–14 mm for hydrocarbon pressures in the range of 50–120 mm and shifts to slightly higher values for higher S/V ratios. Nitric oxide affects the product distribution slightly. The yields of CH_4 and C_2H_4 increase while the yields of C_2H_6 and 2-methyl butene-2 decrease with increasing NO pressure. Surface-to-volume (S/V) ratio has no effect on the product distribution in the inhibited pyrolysis of neohexane, indicating the role of the inhibitor to be limited to the gas phase for this isomer. The analytical balance does become less complete with increasing NO pressure because of such reactions as

$$R + NO \rightarrow RNO \rightarrow \text{isomerization} \rightarrow \text{further decomposition.}$$

INTRODUCTION

In spite of the great deal of work on the inhibition in the thermal decomposition of gaseous organic compounds the nature of the phenomenon is not yet fully understood. Nitric oxide does reduce the rate of decomposition of many organic compounds to a limiting rate which, although small, is definitely not zero. In earlier attempts to solve this problem, it was contended that the fully inhibited reaction follows a molecular mechanism, with the chain reactions suppressed completely by NO through capture of the chain-propagating radical (1–3). However, some experimental results seem to be imcompatible with the postulate of a molecular mechanism. Hydrogen–deuterium exchange was found to take place in both the uninhibited and the fully inhibited decomposition, indicating that chains exist in both cases (4–6). Recently many attempts have been made to deal with the problem quantitatively. In one of them the inhibitor has been associated with both initiation and termination processes (7–9). A summary of the recent approaches to the phenomenon of inhibition have been given earlier (10–12).

As a part of the comparative study of the decomposition of the isomeric hexanes an investigation has been made of the effect of variation in S/V ratio on both reaction rates and product distribution. Surface effects have been found in the thermal decomposition of isopentane (13).

EXPERIMENTAL

The neohexane used was research grade (99.90%) obtained from the Phillips Petroleum Co., Bartlesville, Okla. The nitric oxide, supplied by the Matheson Co., East Rutherford, N.J., was 99% pure. The methods of purification of the materials and the apparatus used have been described earlier (10, 11).

[1]*Present address: Chemistry Department, Harvard University, 12 Oxford Street, Cambridge, Mass. 02138.*
[2]*The premature death of Professor Bryce has deprived kineticists of an able scientist and his colleagues of a trusted friend.*

Can. J. Chem. Downloaded from www.nrcresearchpress.com by 210.87.254.5 on 09/05/12
For personal use only.

RESULTS

Initial rates were obtained manometrically throughout the whole investigation, after establishing a 0.95 to 1 correspondence between the initial rates so obtained and those found from the rate of disappearance of neohexane by direct analysis. The initial rates were obtained by taking the slopes of the pressure–time curves at $t = 0$. Fairly complete analytical mass balances were obtained by conventional gas chromatographic techniques supplemented by infrared analyses. However, the mass balance becomes less complete with increasing NO pressure in the inhibited decomposition. Two typical sets of results for the uninhibited and the inhibited decomposition are given in Tables I and II.

TABLE I

Analytical results (mole %) for the decomposition of neohexane (T = 510 °C, $\Delta P/P_i$ = 0.20)

	P_i (mm)		
Product	180	143	120
CH_4	7.2	6.2	6.5
C_2H_6	3.3	2.3	2.5
C_2H_4	3.5	3.0	4.1
C_3H_6	1.1	0.8	0.2
i-C_4H_8	7.9	8.0	8.0
2-Methyl butene-2	3.7	3.2	3.2
H_2	5.0	5.0	4.5
Neohexane	67.0	71.0	70.0
Total	98.7	99.5	99.0

TABLE II

Analytical results (mole %) for various NO pressures in the inhibited decomposition of neohexane (T = 510 °C, $\Delta P/P_i$ = 0.30, P_i = 100 mm)

	NO (mm)			
Product	0	3	10	12
CH_4	10.6	10.6	11.8	12.5
C_2H_6	3.2	3.0	2.6	2.4
C_2H_4	6.5	6.5	6.8	7.5
C_3H_6	0.6	0.6	0.8	0.8
i-C_4H_8	8.0	8.1	8.7	9.0
2-Methyl butene-2	3.5	3.5	3.2	3.0
H_2	4.4	4.4	4.0	3.9
Neohexane	63.0	63.0	60.0	59.0
Total	99.8	99.7	97.9	98.1

The effect of an 11-fold increase in S/V ratio on the rates was investigated for a hydrocarbon pressure range of 15 to 120 mm. The decomposition rates are lower for the packed vessel at lower pressures and become identical for pressures around 110 mm (Fig. 1). However, the reduction in rate due to the packing is less marked than that of the less branched isomeric hexanes (10).

Most of the decomposition products are pressure dependent. Ethane displays a significant increase with increasing neohexane pressure while CH_4 and C_3H_6 are pressure dependent to a less extent. The yields of i-C_4H_8 and H_2 increase with increasing neohexane pressure and tend to level off at higher pressures (Fig. 2).

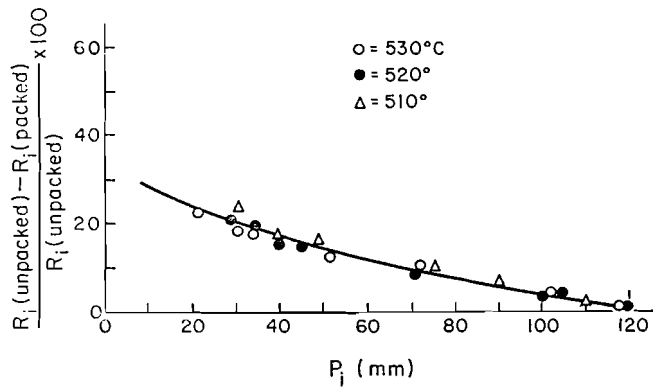

FIG. 1. Percentage reduction in rate due to packing for various initial pressures of neohexane.

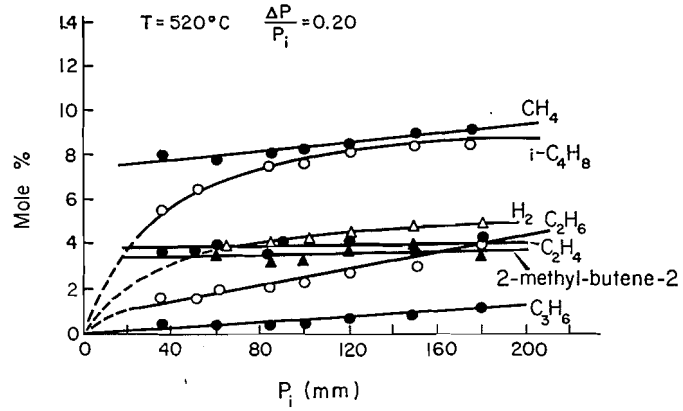

FIG. 2. Variation of product distribution with initial pressure of neohexane.

Nitric oxide reduces the rate of decomposition by about 55%. The reduction in rate is more gradual in comparison to the less branched isomeric hexanes (10). The NO pressure required for maximum inhibition is the same, namely 12–14 mm, for hydrocarbon pressures ranging from 50 to 120 mm (Fig. 3*a*). An increase in S/V ratio from 1 to 5 and 10 cm^{-1} shifts the NO pressure required for maximum inhibition to slightly higher values and reduces the limiting rate (Fig. 3*b*). Nitric oxide does not have a large effect on the product distribution. Methane and C_2H_4 increase slightly while C_2H_6 and 2-methyl butene-2 decrease slightly with increasing NO pressure. The other products appear to be independent of the NO pressure, but there is enough scatter in the results to mask any small changes (Fig. 4). The yield of H_2 is not plotted in Fig. 4 because such a curve would be between the curves for 2-methyl butene-2 and C_2H_6 causing inevitable overlap between them.

An increase in S/V ratio from 1 to 5 and 10 cm^{-1} has no effect on the product distribution. The surface independence of some of the products is illustrated below. The effect of S/V ratio on the C_2H_4/C_2H_6 ratio is shown in Fig. 5. The ratio increases steadily with increasing NO pressure but no effect of S/V ratio on the C_2H_4/C_2H_6 ratio is observed. The independence of the yield of C_3H_6 on both the NO pressure and the S/V ratio is shown in Fig. 6.

Can. J. Chem. Downloaded from www.nrcresearchpress.com by 210.87.254.5 on 09/05/12
For personal use only.

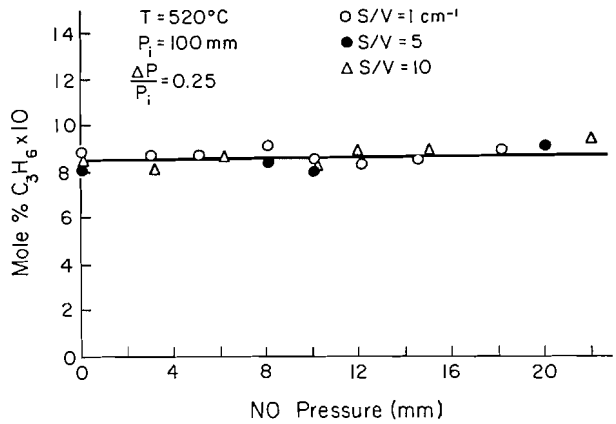

FIG. 3. (*a*) Dependence of the initial rate on NO pressure in the inhibited pyrolysis of neohexane. (*b*) Dependence of the initial rate on NO pressure at various S/V ratios in the inhibited pyrolysis of neohexane.

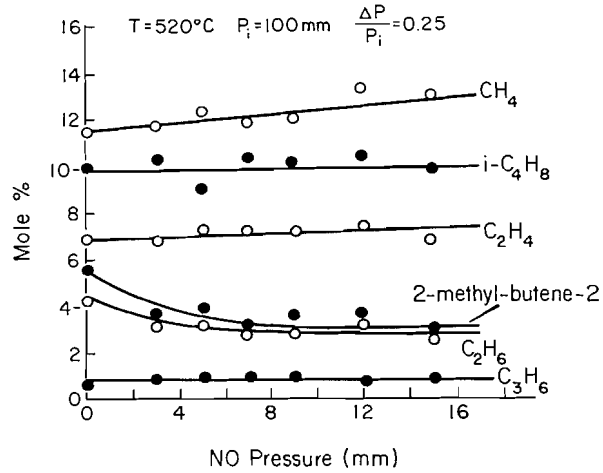

FIG. 4. Variation of product distribution with NO pressure in the inhibited pyrolysis of neohexane.

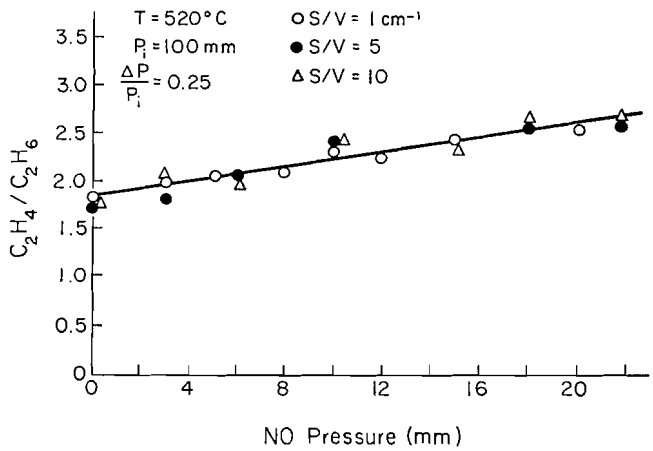

FIG. 5. Variation of the C_2H_4/C_2H_6 ratio with NO pressure and S/V ratios in the inhibited pyrolysis of neohexane.

Can. J. Chem. Downloaded from www.nrcresearchpress.com by 210.87.254.5 on 09/05/12
For personal use only.

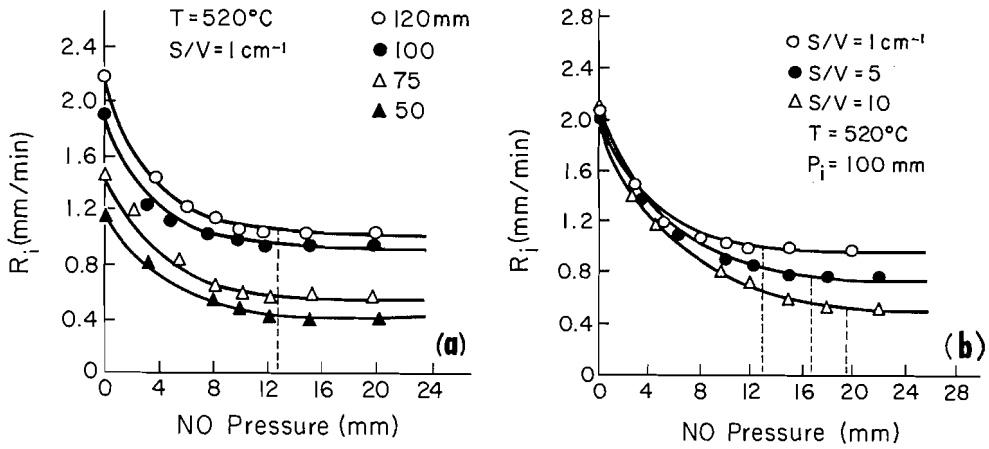

FIG. 6. Variation of the C_3H_6 yield with NO pressure and S/V ratios in the inhibited pyrolysis of neohexane.

TABLE III

Variation of the neohexane/NO ratio with initial pressure of the mixture after adsorption on quartz wool ($(\text{neohexane/NO})_{init} = 3.34$, $T = 310$ °C, contact time = 2 min)

Initial pressure of the mixture (mm)	$(\text{Neohexane/NO})_{final}$
17	2.77
39	3.15
55	3.00
70	3.00
100	3.30

Nitric oxide appears to be less adsorbed on the quartz wool than neohexane. Some results from the relative adsorption of NO and neohexane on quartz wool are given in Table III. Mixtures of neohexane and NO were prepared and after complete mixing their composition was measured by gas chromatography. Change in the composition of the mixture, after adsorption, is observed at low pressures of the mixture. At higher pressure of the mixture no appreciable change is observed in its composition. Certainly results at 310 °C are not necessarily comparable with results at 510 °C. However, it was impossible to obtain results at 510 °C because at temperatures about 400 °C the hydrocarbon was found to decompose rapidly in spite of the small contact time and the amount of NO present. It seems that the large surface of the quartz wool has a significant catalytic effect on the thermal decomposition of neohexane.

DISCUSSION

The products of the uninhibited decomposition can be accounted for by the following mechanism. Addition of more reactions which can be written simply adds to the complexity.

Initiation reactions:

[1*a*] $$(CH_3)_3CCH_2CH_3 \rightarrow CH_3 + (CH_3)_3CCH_2$$

Can. J. Chem. Downloaded from www.nrcresearchpress.com by 210.87.254.5 on 09/05/12
For personal use only.

[1*b*] $\rightarrow CH_3 + (CH_3)_2CCH_2CH_3$

[1*c*] $\rightarrow C_2H_5 + (CH_3)_3C.$

Propagation reactions:

[2*a*] $CH_3 + (CH_3)_3CCH_2CH_3 \rightarrow CH_4 + (CH_3)_3CCH_2CH_2$

[2*b*] $\rightarrow CH_4 + (CH_3)_2C(CH_2)CH_2CH_3$

[2*c*] $\rightarrow CH_4 + (CH_3)_3CCHCH_3$

[3*a–c*] $C_2H_5 + (CH_3)_3CCH_2CH_3 \rightarrow C_2H_6 +$ neohexyl radicals

[4*a–c*] $H + (CH_3)_3CCH_2CH_3 \rightarrow H_2 +$ neohexyl radicals

[5*a–c*] neohexyl radicals $\rightarrow CH_3 + (CH_3)_2C{=}CHCH_3$

[6*a–c*] $\rightarrow C_2H_5 + (CH_3)_2C{=}CH_2$

[7*a–c*] $\rightarrow (CH_3)_3C + C_2H_4$

[8] $(CH_3)_3CCH_2 \rightarrow CH_3 + (CH_3)_2C{=}CH_2$

[9] $(CH_3)_2CCH_2CH_3 \rightarrow CH_3 + (CH_3)_2C{=}CH_2$

[10] $\rightarrow C_2H_6 + C_3H_6$

[11] $(CH_3)_3C \rightarrow H + (CH_3)_2C{=}CH_2.$

Recombination reaction:

[12] $CH_3 + CH_3 \rightarrow C_2H_6.$

Propylene appears in very small amount. Therefore reaction [10] participates to a slight extent. Since reaction [10] is directly related to the initiation the yield of C_3H_6 compared to the yields of CH_4, C_2H_6, and H_2 which are formed through the propagation processes, indicates that the chain is not very large. The yield of H_2 is significant. Its main source is assumed to be the $(CH_3)_3C$ radical. Part of this radical is formed through reaction [1*c*] and part through reactions [7*a–c*].

Methane is the major product. This may indicate that reaction [5*a*] was a major mode of decomposition of neohexyl radical. However, the yield of 2-methyl butene-2 is smaller than the yield of CH_4. This might indicate that 2-methyl butene-2 undergoes further decomposition when accumulated in significant amounts.

The initiation processes can take place in both phases (10). The net reduction in rate due to packing is less marked than that for the less branched isomeric hexanes (10). From the relative adsorption of NO and the isomeric hexanes on quartz wool it appears that neohexane is adsorbed more than the less branched isomers. Therefore, a more pronounced effect of the surface on the initiation is expected. The termination involves similar processes in both neohexane and the less branched isomeric hexanes. Therefore, the net reduction in rate should be less marked in neohexane because of the expression

$$\text{net reduction} = \text{effect on initiation} - \text{effect on termination.}$$

Surface-to-volume ratio has no effect on the propagation processes (10, 11).

Nitric oxide reduces the rate up to 55%. However, this reduction is more gradual than it was in the less isomeric hexanes (10). Nitric oxide cannot expell neohexane molecules from the active sites of the wall efficiently and therefore it is expected that NO will suppress the heterogeneous initiation slightly. Even in the fully inhibited decomposition the heterogeneous initiation will participate. This is supported from the observation that the limiting rate is fairly significant in magnitude. Since the heterogeneous function of the inhibitor is more limited in this isomer it is expected that the inhibition phenomenon can be attributed more to homogeneous than heterogeneous processes in this particular case.

Can. J. Chem. Downloaded from www.nrcresearchpress.com by 210.87.254.5 on 09/05/12
For personal use only.

The effect of NO in the gas phase can be revealed through its effect on the product distribution. Simultaneous increase in the yield of C_2H_4 and decrease in the yield of C_2H_6 with increasing NO pressure may be attributed to the competitive set of reactions

[13] $$C_2H_5 + NO \rightarrow C_2H_4 + HNO$$

[3*a*–*c*] $$C_2H_5 + RH \rightarrow C_2H_6 + R$$

which has been discussed earlier (10). The HNO, whose existence has been verified by flash photolysis (14), may participate in such reactions as

[15] $$CH_3 + HNO \rightarrow CH_4 + NO$$

accounting for the slight increase in the yield of CH_4 with increasing NO pressure. Reaction [15] is highly exothermic by about 52 kcal, based on the values

$$D(CH_3—H) = 101 \text{ kcal/mole (15)}$$

and

$$D(H—NO) = 48.6 \text{ kcal/mole (16, 17).}$$

The yield of 2-methyl butene-2 decreases with increasing NO pressure. This decrease can be accounted for as follows: (i) Nitric oxide can abstract hydrogen from the CH_3 groups of $(CH_3)_2C{=}CCH_3$ relatively easier than from neohexane because the double bond weakens the C—H bonds located in β-position to the double bond. Certainly such H-abstraction reactions will be favored as the amounts of NO and 2-methyl butene-2 increase. (ii) 2-methyl butene-2 is formed from the decomposition of neohexyl radicals. Reactions [2*c*], [3*c*], and [4*c*] are related to the yield of 2-methyl butene-2. A possible recombination between NO and neohexyl radicals could form a relatively stable nitroso compound, namely $(CH_3)_3CCH(NO)CH_3$. Whether this compound remains or decomposes further to nitrogen-containing products, it causes a reduction in the yield of 2-methyl butene-2. Similar recombination might take place between NO and $(CH_3)_3C$. Since the latter radical is assumed to be the source of H atoms, a reduction in the yield of H_2 would be expected with increasing NO pressure. Such a reduction has been discussed earlier for all the isomeric hexanes (18).

The possible formation of stable nitroso compounds or of nitrogen-containing products can account for two main observations in the inhibited decomposition of neohexane. First, nitric oxide was recovered for initial NO pressures up to 5 mm, but for NO pressures higher than 5 mm some consumption was observed, increasing with increasing NO pressure. This indicates that NO can be used up through such reactions as

$$R + NO \rightarrow RNO \rightarrow \text{oxime} \rightarrow \text{further decomposition}$$

which, however, gain importance as the NO pressure increases. Nitroso compounds were not detected, perhaps because of the analytical method used. However, in a system containing CH_3 and NO, decomposition products like HCN, H_2O, NH_3, CO, N_2, CO_2, and CH_3CN were found by mass spectrometry (19). Secondly, the analytical mass balance does become less complete as the NO pressure increases, indicating that such nitrogen-containing products may exist but were not detected.

In addition to the above observations another observation can support the argument outlined above. From Table II it is seen that for constant extent of decomposition ($\Delta P/P_i$) the consumption of neohexane increases with increasing NO pressure. If stable nitroso compounds are formed through such reactions as

$$(CH_3)_3C + NO \rightarrow (CH_3)_3CNO$$

Can. J. Chem. Downloaded from www.nrcresearchpress.com by 210.87.254.5 on 09/05/12
For personal use only.

the pressure of NO will be reduced and at the same time the decomposition of $(CH_3)_3C$ will be suppressed. Therefore one compound would be formed, $(CH_3)_3CNO$, instead of three fragments namely NO, H, and $(CH_3)_2C{=}CH_2$. Under these circumstances to attain the same extent of decomposition in terms of $\Delta P/P_i$ more neohexane must be used up.

ACKNOWLEDGMENTS

We are grateful to the National Research Council and to the Petroleum Research Fund of the American Chemical Society for financial support. We are also greatly indebted to Dr. G. B. Porter for many valuable discussions.

REFERENCES

1. E. W. STEACIE. Atomic and free radical reactions. Reinhold Publishing Corp., New York. 1954.
2. F. J. STUBBS and C. N. HINSHELWOOD. Discussions Faraday Soc. **10**, 129 (1951).
3. D. R. BLACKMORE and C. N. HINSHELWOOD. Proc. Roy. Soc. London, Ser. A, **268**, 21 (1962).
4. V. V. VOEVODSKY and V. A. POLTORAK. Dokl. Akad. Nauk SSSR, **91**, 585 (1953).
5. F. O. RICE and R. E. VARNERIN. J. Am. Chem. Soc. **76**, 324 (1954).
6. R. E. VARNERIN and J. S. DOOLING. J. Am. Chem. Soc. **78**, 2042 (1956).
7. B. W. WOJCIECHOWSKI and K. J. LAIDLER. Can. J. Chem. **38**, 1027 (1960).
8. K. J. LAIDLER, N. H. SAGERT, and B. W. WOJCIECHOWSKI. Proc. Roy. Soc. London, Ser. A, **270**, 254 (1962).
9. N. H. SAGERT and K. J. LAIDLER. Can. J. Chem. **41**, 848 (1963).
10. J. CHRYSOCHOOS and W. A. BRYCE. Can. J. Chem. **43**, 2092 (1965).
11. J. CHRYSOCHOOS and W. A. BRYCE. Part IV. J. Phys. Chem. In press.
12. J. CHRYSOCHOOS and W. A. BRYCE. Part VI. Trans. Faraday Soc. Submitted.
13. W. A. BRYCE and J. CHRYSOCHOOS. Trans. Faraday Soc. **59**, 1842 (1963).
14. F. W. DALBY. Can. J. Phys. **36**, 1336 (1958).
15. N. N. SEMENOV. Some problems in chemical kinetics and reactivity. Princeton University Press, Princeton, N.J. 1958.
16. M. A. A. CLYNE and B. A. THRUSH. Trans. Faraday Soc. **57**, 1305 (1961).
17. M. A. A. CLYNE and B. A. THRUSH. Discussions Faraday Soc. **33**, 139 (1962).
18. J. CHRYSOCHOOS. Chim. Chronica Athens, Greece. In press.
19. W. A. BRYCE and K. U. INGOLD. J. Chem. Phys. **23**, 1968 (1955).

Can. J. Chem. Downloaded from www.nrcresearchpress.com by 210.87.254.5 on 09/05/12
For personal use only.

Can. J. Chem. Downloaded from www.nrcresearchpress.com by 210.87.254.105 on 09/05/12
For personal use only.

STUDIES IN THE WAGNER–MEERWEIN REARRANGEMENT

PART V. RATES OF FORMOLYSIS OF SOME 9-ALKYL-9-FLUORENYLMETHYL TOSYLATES[1]

F. A. L. ANET
University of California at Los Angeles, Los Angeles, California

AND

P. M. G. BAVIN
Smith Kline and French Laboratories, Ltd., Welwyn Garden City, England

Received March 18, 1965

ABSTRACT

For a series of 9-alkyl-9-fluorenylmethyl *p*-toluenesulfonates, the rates of decomposition in formic acid increase with the size of the alkyl group. Changes in the rate constants are associated with changes in $\Delta S^{\ddagger}$.

When this work was initiated the effect of increasing alkyl substitution at the β-position of neopentyl systems on the rates of rearrangement had not been investigated. The esters (I, X = *p*-toluenesulfonate) appeared well-suited for such a study because the products of solvolysis are known to be completely rearranged and were probably formed by an ionization mechanism, for example, the chlorides (I, X = Cl) and the *p*-toluenesulfonates (I, X = *p*-$CH_3C_6H_4SO_3$) decompose at their melting points and in hot formic acid (1, 2, 3). This method has been found useful for the preparation of a wide range of 9-substituted phenanthrenes (1, 2, 3, 4, 5, 6, and references therein).

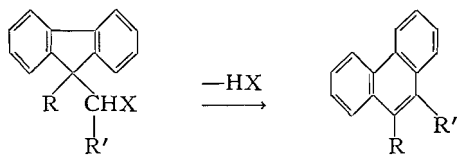

I II

The *p*-toluenesulfonates (I, X = *p*-$CH_3C_6H_4SO_3$) decomposed smoothly in 98% formic acid between 30° and 60°. Sodium formate (20 g/l) served as a buffer and had only a small effect on the rates. The rates of appearance of the 9-alkylphenanthrenes (II) were measured spectrophotometrically using the longest wavelength peak of the ultraviolet spectrum (at approximately 345 mμ (7)). This peak is free from end absorption of the fluorene spectrum and gave accurately first-order rate constants reproducible to ±0.2–0.5% having an estimated (8) accuracy of ±0.9–1.6%. Data derived from the third peak (at approximately 330 mμ) were less reliable but provided a useful check. Runs could be followed to greater than 90% completion but rate constants were generally derived from the first two half lives. The yields of 9-alkylphenanthrenes were 98–101% estimated spectrophotometrically and greater than 90% by isolation. As the rates of appearance of the 9-alkylphenanthrenes were accurately first order, they were equated with the rates of decomposition of the *p*-toluenesulfonates. Our results, evaluated by the method of

[1]*Work carried out at The University of Ottawa during the tenure of a National Research Council Postdoctorate Fellowship (1954–56).*

least squares (8), are summarized in Tables I and II. (For the application of spectrophotometric methods to the measurement of rate constants see refs. 9, 10).)

TABLE I

Rate constants for the decomposition of 9-alkyl-9-fluorenylmethyl *p*-toluenesulfonates in 98% formic acid containing 20 g/l sodium formate (min^{-1} multiplied by 10^4)

I	38.4°		60.2°
R = CH_3, R′ = H	6.49		86.9
R = C_2H_5, R′ = H	9.68	42.5°	160.7 (60.3°)
		18.6	
R = $(CH_3)_2CH$, R′ = H	22.6_5		317
R = $(CH_3)_3C$, R′ = H	31.6_2*	46.0°	481
		88.2	
R = $C_6H_5CH_2$, R′ = H	6.41		95.9
R = CH_3, R′ = CH_3	425		Not measurable

*33.5 in absence of sodium formate.

TABLE II

Heats and enthalpies of activation for the rates of decomposition of 9-alkyl-9-fluorenylmethyl *p*-toluenesulfonates (I, R′ = H)

I	$\Delta H^{\ddagger}$, °C	$\Delta S^{\ddagger}$, e.u.
R = CH_3	24.6	+0.5
R = C_2H_5	25.3	+3.5
R = $(CH_3)_2CH$	25.0	+7.1
R = $(CH_3)_3C$	25.7	+13.1
R = $C_6H_5CH_2$	25.6	+6.2

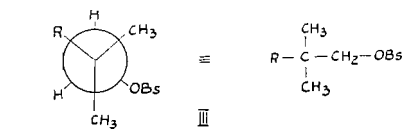

III

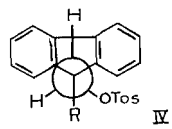

IV

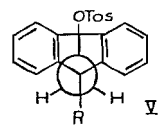

V

The rate constants increase with increasing size of the substituent R, as reported (11) for β-substituted neopentyl *p*-bromobenzenesulfonates (III) (see Table III). Of the rotameric forms (12) of I when R_1 = H, shown in IV and V, only IV is likely to be involved in aryl migration leading to ring expansion (11; 13, p. 270 et seq.). Consequently the effect of increasing the size of R can be interpreted as increasing the tendency of the leaving group to ionize and thereby relieve the interaction between R and the toluenesulfonate group (cf. 14, 15 for data confirming this trend). The increase in rate constants is associated with changes in $\Delta S^{\ddagger}$ rather than ΔH (Table II) but unfortunately the data for the *p*-bromobenzene sulfonates (III) (11) show no such consistency.*

Several pieces of information suggest that the *p*-toluenesulfonates (I, X = *p*-$CH_3C_6H_4SO_2$) decompose by a S_N1 process. Thus the secondary *p*-toluenesulfonate

**The accuracy of the rate constants (±1–4%) for the p-bromobenzenesulfonates makes the enthalpies $\Delta S^{\ddagger}$ unreliable (11).*

Can. J. Chem. Downloaded from www.nrcresearchpress.com by 210.87.254.105 on 09/05/12
For personal use only.

TABLE III

Comparison of rates of decomposition of *p*-toluenesulfonates (I, R′ = H, X = *p*-$CH_3C_6H_4SO_2$) and *p*-bromobenzenesulfonates (III) (comparisons are in column only and not between series)

R	I at 60.2°	III at 59.7°
CH_3	1.0	1.0
C_2H_5	1.84 (60.3°)	2.4
$(CH_3)_2CH$	3.65	4.1
$(CH_3)_3C$	5.54	34.0

(I, R = R′ = CH_3) decomposes 70 times as fast as the primary ester (I, R = CH_3, R′ = H) (cf. ethyl and isopropyl bromides in 'moist' formic acid which show (16) relative rates of 1 to 26). The effect of increasing the size of R in I parallels that found for a series of complex tertiary chlorides known to decompose by a S_N1 process (for a summary, see ref. 17, p. 664). Conclusions concerning the degree of participation accompanying the decomposition of I are not warranted.

Preliminary experiments showed that the formolysis of 2,2-diphenylpropyl *p*-toluene sulfonate (18) gave a mixture of *cis* and *trans*-α-methylstilbene, the *cis* isomer isomerizing at a lower rate to the *trans* isomer (cf. ref. 19). These experiments will not now be completed.

EXPERIMENTAL

Spectroscopic measurements were made with a Beckmann DK-2 spectrophotometer, using matched quartz cells. Formic acid (98%, Fischer Scientific Co.) containing anhydrous sodium formate (20 g/l) was used as solvent. The *p*-toluenesulfonates have been described elsewhere (1, 18).

Sample concentrations were arranged at the start of each run to provide absorption readings in the range 10–80%. Kinetic data were derived from the first two half-lives. Bath temperatures were kept at ±0.05°. (For quantitative data on the spectra of 9-alkylphenanthrenes see ref. 7.) The general precautions to be observed in determining rate constants spectrophotometrically are described elsewhere (9, pp. 176–181). Data were processed by the method of least squares (8), the constants in Table I being the mean of two independent runs. The reproducibility of the method and the effect of added sodium formate were examined by a large number of runs with the *t*-butyl compound (I, R = $(CH_3)_3C$, R′ = H, X = *p*-$CH_3C_6H_4SO_3$).

REFERENCES

1. F. A. L. Anet and P. M. G. Bavin. Can. J. Chem. **34**, 991 (1956).
2. P. M. G. Bavin. Can. J. Chem. **37**, 2023 (1959).
3. P. M. G. Bavin. Can. J. Chem. **38**, 1099 (1960).
4. E. J. Greenhow, D. McNeil, and E. N. White. J. Chem. Soc. 986 (1952).
5. M. Matyen, S. Glazer-Tarasiejska, and R. H. Martin. Bull. Soc. Chim. Belges, **69**, 551 (1960).
6. P. M. G. Bavin. Can. J. Chem. **42**, 1409 (1964).
7. F. A. L. Anet and P. M. G. Bavin. Can. J. Chem. **41**, 2160 (1963).
8. H. Margenau and G. M. Murphy. The mathematics of physics and chemistry. D. Van Nostrand Company, Inc., Princeton, N.J. 1956.
9. R. P. Linstead, J. A. Elvidge, and M. Whalley. A course in modern techniques of organic chemistry. Butterworths Scientific Publications, London. 1955.
10. H. N. Koning and K. G. Van Senden. Rec. Trav. Chim. **81**, 49, 1024 (1962).
11. F. N. McElrath, R. M. Fritz, G. Brown, C. Y. LeGall, and R. B. Duke. J. Org. Chem. **25**, 2195 (1960).
12. M. S. Newman. J. Chem. Educ. **32**, 344 (1955).
13. M. S. Newman (*Editor*). Steric effects in organic chemistry. John Wiley & Sons, Inc., New York. 1956.
14. R. Spitzer and K. S. Pitzer. J. Am. Chem. Soc. **70**, 1261 (1948).
15. H. C. Brown and W. H. Bonner. J. Am. Chem. Soc. **75**, 14 (1953).
16. L. C. Bateman and E. D. Hughes. J. Chem. Soc. 945 (1940).
17. A. Streitweiser. Chem. Rev. **56**, 664 (1956).
18. F. A. L. Anet and P. M. G. Bavin. Can. J. Chem. **35**, 1084 (1957).
19. E. Ellingboe and R. C. Fuson. J. Am. Chem. Soc. **55**, 2960 (1933).

Can. J. Chem. Downloaded from www.nrcresearchpress.com by 210.87.254.105 on 09/05/12
For personal use only.

Can. J. Chem. Downloaded from www.nrcresearchpress.com by 210.87.254.6 on 09/05/12
For personal use only.

CHEMICAL STRUCTURE AND ADSORPTION OF ORGANIC MOLECULES AT THE POLARIZED MERCURY–ELECTROLYTE INTERFACE

R. G. BARRADAS AND P. G. HAMILTON[1]
Department of Chemistry, University of Toronto, Toronto, Ontario
Received March 9, 1965

ABSTRACT

Previous studies on electrochemical adsorption at mercury of a series of heterocyclic and aromatic nitrogen bases and their respective conjugate ions by electrocapillary measurements are extended to simple saturated heterocyclic compounds containing oxygen and to aliphatic alcohols with different degrees of unsaturation. Adsorption isotherms for various electrode potentials are derived, and standard electrochemical free energies of adsorption are calculated as before, to relate the influence of molecular and electronic structure of the adsorbates on the properties of the electrical double layer. Oxygen as the heteroatom in cyclic compounds and in the hydroxyl group of the alcohols plays a distinct role in the characteristics of metal–adsorbate and adsorbate–solvent interactions through its higher electronegativity as compared with nitrogen. Considerations of the different geometric areas of adsorbed molecules due to isomerism of the saturated heterocyclic compounds, and the varying unsaturation of the alcohols lead to more realistic interpretation of orientation effects, surface coverages, and degrees of adsorbability. Improvement in pressure control in the electrocapillarometer assembly gives better precision in surface tension measurements. Some preliminary results on the adsorption of furfurylamines and related analogues which constitute a newly available class of corrosion inhibitors are briefly discussed.

INTRODUCTION

A comprehensive review of recent work on adsorption of organic substances at solid and liquid electrodes has been published (1). The adsorption of organic compounds as electroinactive additives, or as electroactive reactants, intermediates, or products, plays an important part in the kinetics of electrode reactions, corrosion inhibition, suppression or creation of anomalous polarographic effects, chronopotentiometry, fuel cells, and other electrochemical processes. The advantages of using the mercury electrode for systematic studies of electrochemical adsorption have been discussed (2). The electrocapillary method for investigating adsorption is preferred to differential capacity measurements of greater sensitivity, because the former gives more complete information on the properties of the electrical double layer (3). Electrocapillary measurements of surface excess (Γ_A) are based on unambiguous thermodynamic foundations (4), but the determination of Γ_A from capacitance data is dependent on non-thermodynamic assumptions (5). Despite this fundamental difference the two lines of experimental approach are generally regarded as complementary to one another.

Our principal objectives in the present work on electrochemical adsorption are (i) to examine further the π-orbital interactions on mercury by considering the influence of the triple bond (hitherto uninvestigated) in propargyl alcohol by comparison with the double bond in allyl alcohol and the absence of unsaturation in *n*-propanol; (ii) to study the role of oxygen in the aliphatic alcohols and also as the heteroatom(s) in morpholine and 1,4-dioxane in comparison with pyridine and piperidine, in order to evaluate the contribution of its higher electronegativity and greater availability of lone pair electrons; and (iii) to determine the influence of isomerism in the saturated cyclic compounds (boat and chair conformations). The resolution of these aims will facilitate a clearer interpretation of adsorbate–solvent interactions, surface coverages (Θ), and orientation effects at the

[1]*Holder of Province of Ontario Government Fellowships for 1963–1965.*

polarized mercury–electrolyte interface. The above-mentioned factors are also helpful in the clarification of adsorption behavior of a new class of corrosion inhibitors, namely furfurylamine, its saturated analogue, and their respective derivatives. Some preliminary results of the electrocapillary measurements of these inhibitors will be reported here, but a detailed discussion will be presented elsewhere in conjunction with complementary data from capacitance measurements using a square wave pulse technique (6). Finally, it is hoped that these studies of simple oxygenated compounds may be of some value in elucidating the more complex adsorption behavior of high molecular weight surfactant materials such as the Tritons, polyoxyethylene dodecyl and lauryl ethers, etc. These surfactants form micelles at low bulk phase concentrations, and have practical applications as wetting agents and detergents at the solid/liquid and oil/water interfaces respectively. They are also widely used as maxima suppressors and inhibitory agents in polarographic analysis, but their adsorption mechanism, kinetics, and structure at the mercury electrode are not well understood (7).

EXPERIMENTAL

Apparatus and Method

The method and experimental details employed for obtaining electrocapillary curves are essentially the same as those previously described in detail (2, 8). Since the potentials of the mercury electrode are measured with respect to the calomel electrode immersed in the same electrolyte solution in order to avoid liquid junction potentials, an all-glass cell, having two compartments only, was used for convenience. A third compartment is necessary when potentials of the mercury electrode are also measured with respect to the hydrogen electrode. The capillary was observed by a binocular microscope (Bushnell W × 15 or a Bausch and Lomb SVB-12). The latter model is a stereomicroscope, and is preferred because of the improved viewing of the capillary in "3-dimensions". A significant change in the electrocapillarometer assembly was the use of copper bellows in the nitrogen line. Compression and expansion of the bellows permitted extremely sensitive pressure control which improved the precision and accuracy of surface tension (γ) determinations. The reproducibility of pressure measurements on the anodic side of the potential of zero charge (pzc) for the KCl base electrolyte was ± 0.01 mm. At the pzc variations were less than ± 0.01 mm, but at potentials very cathodic to the pzc (ca. $-1\,200$ mV) the precision of pressure readings was about ± 0.05 mm. The same approximate order of precision in the determination of γ's was experienced for KCl base electrolyte solutions containing organic additives.

Materials Used

Doubly distilled mercury was further purified according to the procedure outlined by Ives and Janz (9). Potassium chloride base electrolyte solution in "equilibrium water" was used as previously described (2). The following substances were investigated in aqueous solutions of 1.0 *N* KCl at 25 ± 1 °C: piperidine, pyridine, morpholine, dioxane, *n*-propanol, allyl alcohol, and propargyl alcohol. The initial organic materials were of the highest purity available commercially and were freshly distilled under nitrogen to avoid atmospheric oxidation prior to use in the electrocapillarometer. The additives are electroinactive within the range of potentials examined of the mercury electrode.

RESULTS

Two sets of electrocapillary curves are shown in Figs. 1 and 2 for pyridine, piperidine, morpholine, and dioxane, and for the three aliphatic alcohols respectively. Electrocapillary curves for piperidine and pyridine have been reported before (2) but they were redetermined here in view of the improved precision due to refinement in the pressure-controlling device. The new results in general compare favorably with the ones reported before, but the new data are used in this paper not only because of the greater precision in γ values, but also because measurements have been made at shorter intervals of 20 mV each over a range of 100 mV in the vicinity of the pzc. This provides more accurate location of the coordinates in the respective shifts of the pzc's (ΔE_{pzc} and $\Delta\gamma_{pzc}$). At other potentials, measurements of γ were taken at 100 mV intervals. As before, all potential measurements were accurate to within 1 mV. At least three pressure readings were taken for each potential step within the range of 0 to $-1\,200$ mV, and in between each reading a

Can. J. Chem. Downloaded from www.nrcresearchpress.com by 210.87.254.6 on 09/05/12
For personal use only.

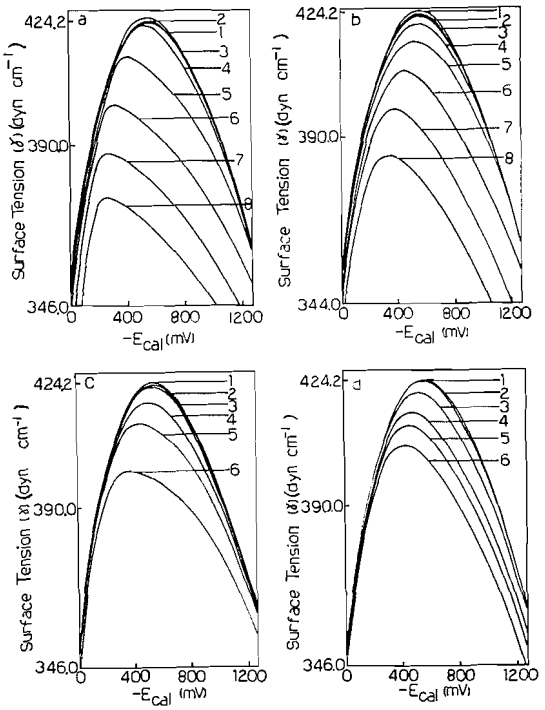

FIG. 1. Electrocapillary curves. (*a*) Piperidine in 1.0 *N* KCl: (1) 1.0 *N* KCl, (2) 1.0×10^{-3} *M*, (3) 3.0×10^{-3} *M*, (4) 1.0×10^{-2} *M*, (5) 3.0×10^{-2} *M*, (6) 1.0×10^{-1} *M*, (7) 3.0×10^{-1} *M*, (8) 1.0 *M*. (*b*) Pyridine in 1.0 *N* KCl: (1) 1.0 *N* KCl, (2) 1.0×10^{-3} *M*, (3) 3.0×10^{-3} *M*, (4) 1.0×10^{-2} *M*, (5) 3.0×10^{-2} *M*, (6) 1.0×10^{-1} *M*, (7) 3.0×10^{-1} *M*, (8) 1.0 *M*. (*c*) Dioxane in 1.0 *N* KCl: (1) 1.0 *N* KCl, (2) 1.0×10^{-3} *M*, (3) 1.0×10^{-2} *M*, (4) 3.0×10^{-2} *M*, (5) 1.0×10^{-1} *M*, (6) 1.0 *M*. (*d*) Morpholine in 1.0 *N* KCl: (1) 1.0 *N* KCl, (2) 1.0×10^{-2} *M*, (3) 1.0×10^{-1} *M*, (4) 3.0×10^{-1} *M*, (5) 5.0×10^{-1} *M*, (6) 1.0 *M*.

small amount of mercury was expelled from the capillary in order to provide a fresh surface before the subsequent measurement was made.

Surface Excess, Adsorption Isotherms, and Adsorption Coefficients

The amount of organic substance adsorbed at mercury is expressed in terms of the surface excess Γ_A of the organic species as defined in previous papers (2, 10, 11), and obtained from the Gibbs adsorption equation (2, 12) as

$$[1] \qquad -(\partial\gamma/\partial\mu_A)_{E,\mu_{KCl}} = \Gamma_A.$$

Determinations of γ at various activities of the organic substance then give

$$[2] \qquad -(\partial\gamma/RT\partial \ln a_A)_{E,\mu_{KCl}} = \Gamma_A.$$

In neutral KCl solutions, the activities of the organic materials were assumed to be equal to their concentrations. Systematic errors in Γ_A are approximately 10% (2, 8). Figures 3 and 4 give adsorption isotherms for the substances examined, i.e. they show surface coverage in terms of Γ_A as a function of solution concentration of adsorbate c_A at constant potentials. Table I shows Γ_m for calculated planar, perpendicular, and stereoisomeric requirements for a monolayer compared with the highest Γ_m observed experimentally ($\pm 5\%$).

Can. J. Chem. Downloaded from www.nrcresearchpress.com by 210.87.254.6 on 09/05/12
For personal use only.

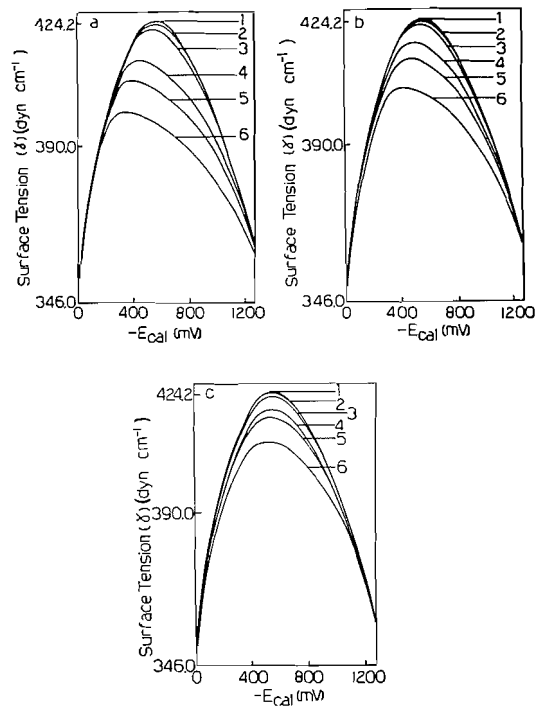

FIG. 2. Electrocapillary curves. (*a*) *n*-Propanol in 1.0 *N* KCl: (1) 1.0 *N* KCl, (2) 3.0×10^{-2} *M*, (3) 1.0×10^{-1} *M*, (4) 3.0×10^{-1} *M*, (5) 5.0×10^{-1} *M*, (6) 1.0 *M*. (*b*) Allyl alcohol in 1.0 *N* KCl: (1) 1.0 *N* KCl, (2) 3.0×10^{-2} *M*, (3) 1.0×10^{-1} *M*, (4) 3.0×10^{-1} *M*, (5) 5.0×10^{-1} *M*, (6) 1.0 *M*. (*c*) Propargyl alcohol in 1.0 *N* KCl: (1) 1.0 *N* KCl, (2) 3.0×10^{-2} *M*, (3) 1.0×10^{-1} *M*, (4) 3.0×10^{-1} *M*, (5) 5.0×10^{-1} *M*, (6) 1.0 *M*.

The adsorption coefficient k (cm^3 mole^{-1}) and the net free energy of adsorption $\Delta\overline{G_A^0}$, i.e. the difference between the standard electrochemical free energies of adsorption of an adsorbate and water, has been given by Blomgren *et al.* (13) as

$$[3] \qquad \frac{\Gamma_A}{\Gamma_m - \Gamma_A} = kc_A = \frac{c_A \exp\left(-\Delta\overline{G_A^0}/RT\right)}{0.0555}$$

where c_A is expressed in mole cm^{-3}. This relation is based on the assumption in Langmuir's isotherm that the total number of sites on the electrode available for water and for the organic adsorbate are the same. This model becomes increasingly inapplicable as the size of the organic molecules increases. Our adsorbates are much smaller than those examined by Blomgren *et al.* (13), and we should expect a smaller degree of error in our estimates of k. The values of k, which represent the adsorbability as a function of structure at the pzc, are given in Table II for various Θ's, where Γ_m's are taken as the highest experimentally observed values.

Standard Electrochemical Free Energy of Adsorption as a Function of Potential for Constant Coverage and as a Function of Surface Coverage at Constant Potentials

In a previous paper (2) an equation for the Langmuir isotherm has been presented in

Can. J. Chem. Downloaded from www.nrcresearchpress.com by 210.87.254.6 on 09/05/12
For personal use only.

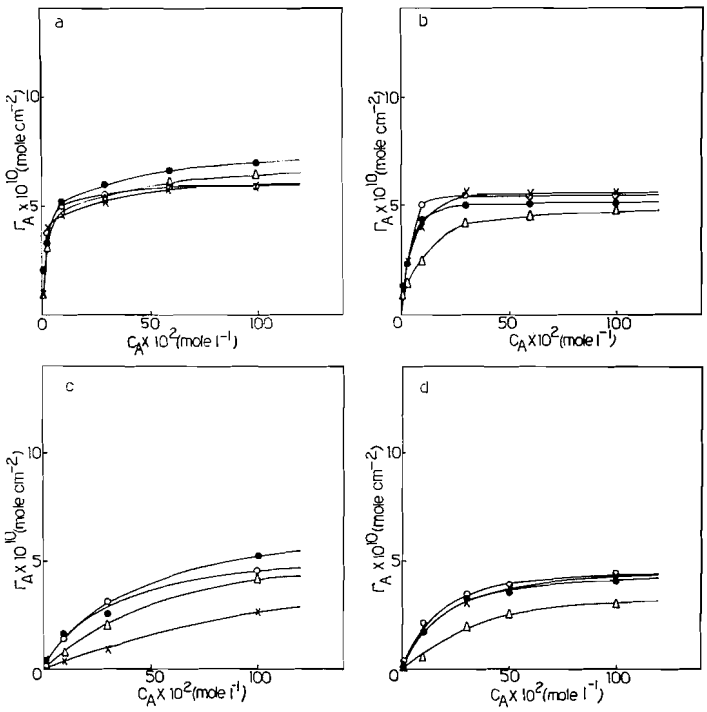

FIG. 3. Adsorption isotherms. (*a*) Piperidine, (*b*) pyridine, (*c*) dioxane, (*d*) morpholine. (△) 400 mV, (●) 600 mV, (○) 800 mV, (×) 1 000 mV (similar legends representing electrode potentials for all four compounds).

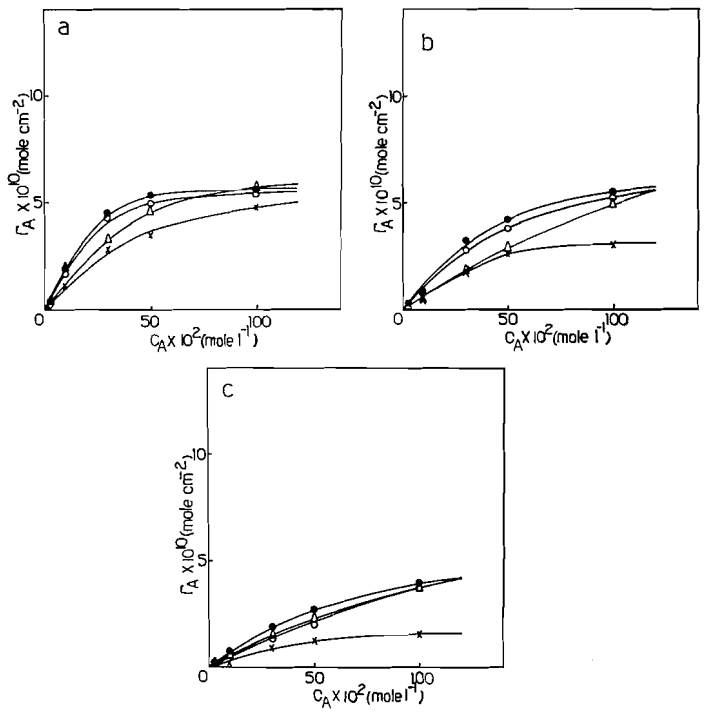

FIG. 4. Adsorption isotherms. (*a*) *n*-Propanol, (*b*) allyl alcohol, (*c*) propargyl alcohol. (△) 400 mV, (●) 600 mV, (○) 800 mV, (×) 1 000 mV (similar legends representing electrode potentials for all three compounds).

Can. J. Chem. Downloaded from www.nrcresearchpress.com by 210.87.254.6 on 09/05/12
For personal use only.

Can. J. Chem. Downloaded from www.nrcresearchpress.com by 210.87.254.6 on 09/05/12
For personal use only.

TABLE I

Orientation of adsorbed molecules

Substance	Area/molecule (Å²)				$\Gamma_m \times 10^{10}$ (mole cm^{-2}) (calcd.)				$\Gamma_m \times 10^{10}$ (mole cm^{-2}) (experimental)
	Planar	Perpendicular	Boat	Chair	Planar	Perpendicular	Boat	Chair	
Piperidine	—	—	33	35	—	—	5.03	4.74	7.02±0.35
Pyridine	40	21	—	—	4.15	7.90	—	—	5.6±0.28
Dioxane	—	—	30	33	—	—	5.53	5.03	5.33±0.27
Morpholine	—	—	33	34	—	—	5.03	4.88	4.38±0.22
n-Propanol	33	21	—	—	5.03	7.90	—	—	6.08±0.30
Allyl alcohol	32	21	—	—	5.19	7.90	—	—	5.68±0.28
Propargyl alcohol	32	21	—	—	5.19	7.90	—	—	5.68±0.28

TABLE II

Adsorbabilities of organic substances on mercury at the pzc in terms of k (cm^3 $mole^{-1}$) for different surface coverages

Substance	k for $\Theta = 0.10$	k for $\Theta = 0.25$	k for $\Theta = 0.50$
Piperidine	3.7×10^4	3.3×10^4	5.0×10^4
Pyridine	2.8×10^4	2.2×10^4	1.6×10^4
Morpholine	0.27×10^4	0.32×10^4	0.39×10^4
Dioxane	0.35×10^4	0.34×10^4	0.37×10^4
n-Propanol	0.39×10^4	0.39×10^4	0.47×10^4
Allyl alcohol	0.24×10^4	0.27×10^4	0.36×10^4
Propargyl alcohol	0.20×10^4	0.23×10^4	0.31×10^4

$\Theta = \Gamma_A/(\Gamma_m)_{experimental}$.

terms of the standard electrochemical free energy of adsorption $\Delta\overline{G_A}^0$, analogously to that reported elsewhere for the adsorption of organic ions (5) in the following form:

$$[4] \qquad \ln\left[\frac{55.5}{c_A}\cdot\frac{\Theta}{1-\Theta}\right] = -\Delta\overline{G_A}^0/RT$$

and surface interactions are accounted for by writing [4] as

$$[5] \qquad \ln\left[\frac{55.5}{c_A}\cdot\frac{\Theta}{1-\Theta}\right] = -\frac{\Delta\overline{G_A}^0}{RT} - \frac{P\Theta^{3/2} - Q\Theta^3}{RT}$$

where P and Q are constants depending on the dipole moment, the area occupied by the adsorbed molecules, and on some other characteristics of the particles adsorbed as well as on the dielectric constant of the surface layer. The term $\Theta^{3/2}$ takes account of the electrostatic repulsion between parallel-oriented dipoles, and the term with Θ^3 represents the van der Waals attraction. Hence eq. [5] permits us to evaluate the deviation from eq. [4] as an apparent change of $\Delta\overline{G_A}^0$ with $\Theta^{3/2}$. Figure 5 shows a plot of $\Delta\overline{G_A}^0$ as a function of potential for constant surface coverage of $\Theta = 0.5$ (in terms of experimental Γ_m values) for all the substances examined. Figure 6 shows some typical plots of $\Delta\overline{G_A}^0$ as a function of $\Theta^{3/2}$ at constant potentials.

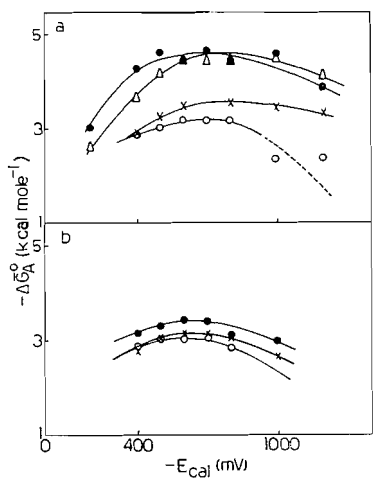

FIG. 5. Values of $\Delta\overline{G_A}^0$ as a function of electrode potential at $\Theta = 0.5$. (*a*) (●) Piperidine, (△) pyridine, (×) morpholine, (○) dioxane. (*b*) (●) n-Propanol, (×) allyl alcohol, (○) propargyl alcohol.

Can. J. Chem. Downloaded from www.nrcresearchpress.com by 210.87.254.6 on 09/05/12
For personal use only.

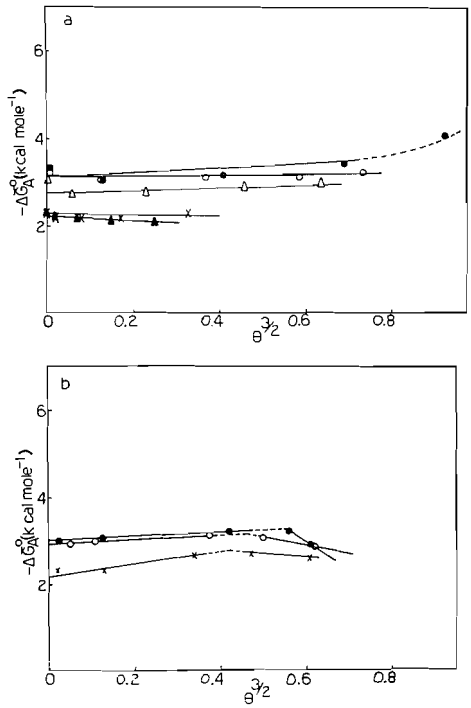

FIG. 6. Plots of $\Delta\overline{G_A^0}$ against $\theta^{3/2}$ at various electrode potentials. (*a*) dioxane, (*b*) *n*-propanol. (▲) 200 mV, (△) 400 mV, (●) 600 mV, (○) 800 mV, (×) 1 000 mV (similar legends represent electrode potentials for both compounds but the lower anodic potentials were not plotted for *b*).

Surface Charge

The surface charge on the metal q_M is obtained from the Gibbs–Lippman equation as

$$-q_M = (\partial\gamma/\partial E)_{\mu_{KCl},\mu_A}. \quad [6]$$

It may be noted that $-q_M = q_S$, where q_S is the net electric charge on the solution side of the double layer. Values of q_M for most of the substances investigated at various electrode potentials and concentrations are shown in Figs. 7 and 8.

DISCUSSION

(a) Morphology of the Electrocapillary Curves

Figures 1 and 2 show the systematic effect of concentration and electrode potentials on the depression of γ. The electrocapillary curves for the heterocyclic compounds indicate that at higher concentrations of additive the order of γ depression is as follows: piperidine > pyridine > dioxane > morpholine. The maximum of these curves is progressively shifted towards positive potentials when concentration of additives is increased. The shifts of the maximum seem to parallel the order of γ depression. On the positive branch with respect to the pzc all the curves diverge without noticeable break except for piperidine at the highest concentrations. Also on the anodic side γ for pyridine is somewhat lower than that of piperidine which indicates some effect due to unsaturation in comparison with its saturated analogue.

On the cathodic side the curves for sufficiently large amounts of additives are at a sharp angle to the base electrolyte curve, and again the most pronounced effect is observed

Can. J. Chem. Downloaded from www.nrcresearchpress.com by 210.87.254.6 on 09/05/12
For personal use only.

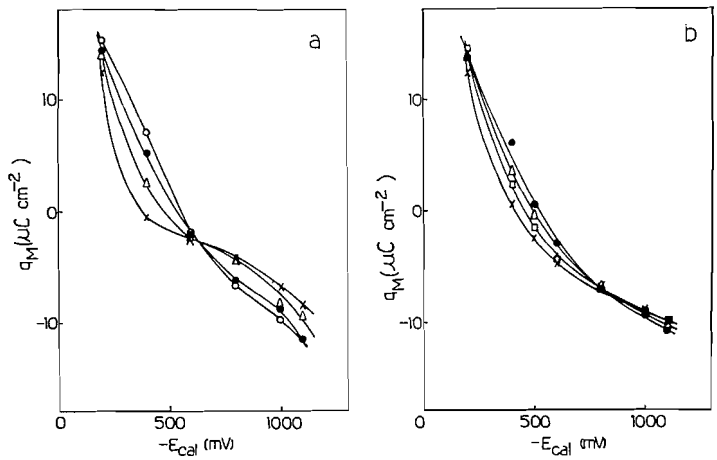

FIG. 7. Charges upon the metal surface as a function of additive concentration in 1.0 N KCl solution and electrode potential. (*a*) Dioxane. (○) 1.0×10^{-2} M, (●) 1.0×10^{-1} M, (△) 3.0×10^{-1} M, (×) 1.0 M. (*b*) Morpholine. (●) 1.0×10^{-1} M, (△) 3.0×10^{-1} M, (□) 5.0×10^{-1} M, (×) 1.0 M.

with piperidine. In general, the electrocapillary curves for the alcohols are less asymmetrical than the cyclic compounds and the order of $\Delta\gamma$ is as follows: n-propanol > allyl alcohol > propargyl alcohol. No break is observed for all three alcohols on both extremes of anodic and cathodic potentials. The least shift of maximum and the attainment of greater symmetry parallels the increasing degree of unsaturation of the three alcohols. $\Delta\gamma$ appears to be the greatest on the anodic branch for propargyl alcohol and relatively smaller for allyl alcohol and n-propanol respectively.

From inspection of Fig. 1, the introduction of oxygen in the cyclic compounds seems to give smaller $\Delta\gamma$ values for morpholine and dioxane in spite of the increased electronegativity of the oxygen atom(s). The unexpected result of dioxane showing greater $\Delta\gamma$ and ΔE_{pzc} than morpholine for correspondingly equal concentrations of additive appears to contradict the trend of increasing electronic density within the ring due to the presence of oxygen. The larger $\Delta\gamma$ for dioxane may perhaps be partly accounted for by the greater field–dipole interaction energy if the molecule can be assumed to adsorb in a boat conformation on mercury (cf. sections *c* and *g* below). Simple considerations of bond moments for C—O and C—N indicate that their respective contributions to the vectorial component of the net dipole moment perpendicular to the mercury surface for both compounds adsorbed in a boat conformation will lead to greater field–dipole interaction energy for dioxane than for morpholine. The shifts in E_{pzc} are not so easily explained as will be seen in section *g*.

(b) Adsorption Isotherms

The adsorption isotherms show in general that the highest values of surface coverage are attained at potentials close to the pzc. Saturation coverage corresponding to a monolayer does not seem to have been reached for all the substances examined (cf. Table I). In general lower values of surface excess were obtained for high negative and positive fields with respect to the pzc.

(c) Maximum Surface Coverage as a Function of Structure

Table I shows the highest Γ_m observed experimentally, and compares with perpendicular, planar, and conformational isomeric space requirements for a monolayer. The molecular

Can. J. Chem. Downloaded from www.nrcresearchpress.com by 210.87.254.6 on 09/05/12
For personal use only.

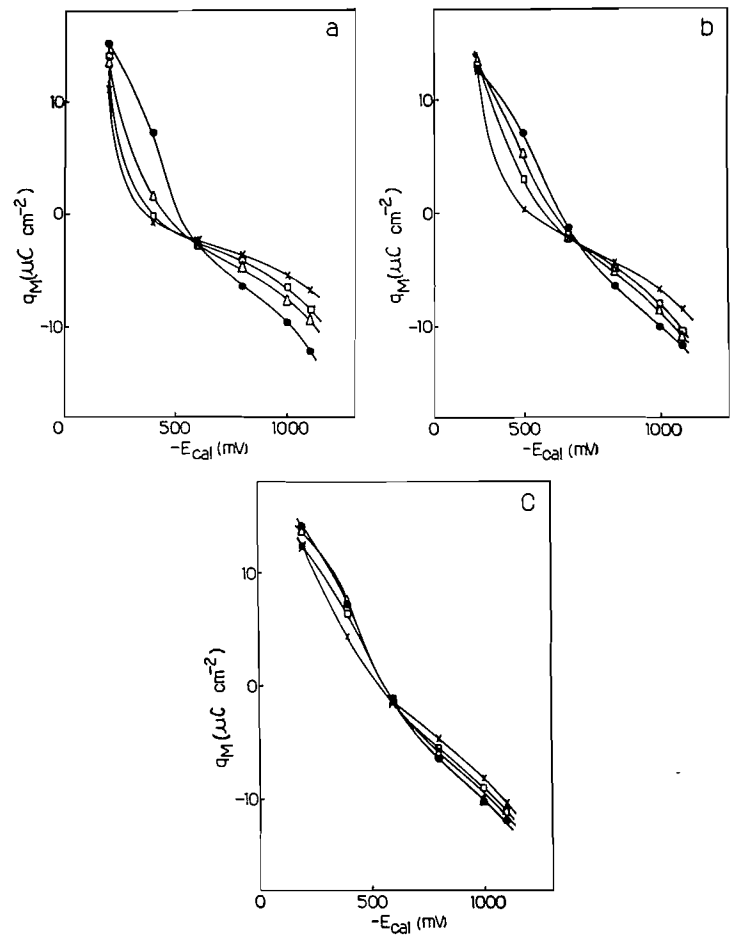

FIG. 8. Charges upon the metal surface as a function of additive concentration in 1.0 N KCl solution and electrode potential. (*a*) *n*-Propanol, (*b*) allyl alcohol, (*c*) propargyl alcohol. (●) 1.0×10^{-1} M, (△) 3.0×10^{-1} M, (□) 5.0×10^{-1} M, (×) 1.0 M (similar legends representing concentrations for all three compounds).

areas have been derived from Leybold space-filling models. The models of the molecules were arranged in the appropriate adsorption positions using a flat surface to represent the metal surface. Photographs of each molecule were taken with a 35 mm camera from a vertical position directly centered over the model. The total area covered by each molecule was calculated by projecting the colored photographic slides outlined on graph paper. Proper allowance in area was made for the molecules to rotate on the surface instead of assuming that they fitted in a close-packed condensed film structure (15). In the cases of morpholine and piperidine the orientation of the N—H bond was taken as perpendicular to the plane of the four central carbon atoms of the ring. If the N—H bond was rotated to a position parallel to the plane of the four central carbon atoms our areas would have to be increased by about 10% for both the chair and boat conformations respectively. Some of our calculated areas are in reasonable agreement with those reported elsewhere (5, 13, 21) but are different from the values given by Hackerman and his co-workers (16, 17, 18). In one paper (16) pyrrolidine and piperidine were given as 45.4 Å^2 and 58.1 Å^2

Can. J. Chem. Downloaded from www.nrcresearchpress.com by 210.87.254.6 on 09/05/12
For personal use only.

respectively from measurements obtained from the maximum radii using atomic models. We have no cause to dispute this choice of area determination except to point out that in a subsequent paper (17) pyrrolidine was retained as 45.5 Å^2 and piperidine was reported as 1.21 × 45.4 Å^2 = 54.9 Å^2. Apart from this inconsistency, it is obvious that an incorrect planar model for piperidine was assumed. In a more recent paper (18) 4-ethylpiperidine was reported as 33 Å^2 in the chair form derived by a method of measurement comparable to ours. In Table I we report 35 Å^2 for piperidine in the chair conformation from a model with the hydrogen atom attached to nitrogen in an axial position. For the hydrogen atom in an equatorial position the value of 38 Å^2 would be obtained. In view of the rapid dynamic situation which may occur between the boat and chair conformations and also between the respective axial and equatorial positions of the hydrogen atom, it is likely that a more realistic value of the molecular area for piperidine (similarly for the other saturated heterocyclic compounds) would be an average one intermediate between 35 and 38 Å^2. Hence, 4-ethylpiperidine may show correspondingly higher areas in view of the size of the ethyl substituent group on the 4-carbon position. For the adsorption of 4-ethylpiperidine on steel powder from cyclohexane solution (18) θ was reported as 0.84 ± 0.28. It was concluded from this finding, in conjunction with a reported "heat of differential adsorption" of 13 kcal per mole, that the molecules are adsorbed in the chair configuration and bonded to the steel surface at nitrogen. In view of the uncertainties in the experimental value of θ and also in the calculated geometrical area of 4-ethylpiperidine it would be difficult to arrive unequivocally at the conclusion regarding the preferred orientation of the adsorbed molecule on steel. The conclusion is not substantiated by any information regarding the dependence of adsorption on potential of the metal in solution.

Our experimental values of Γ_m are generally consistent with the models reported in Table I. The only anomaly is observed with piperidine which could be easily explained if the molecule assumed a perpendicular orientation but this is rather unlikely (cf. section *g*). One may conclude that for piperidine, surface coverage in excess of $\theta = 1$ occurs at the mercury–electrolyte interface, and such behavior could be qualitatively explained in terms of its high basicity ($pK_a = 11.2$), as compared to pyridine $pK_a = 5.2$ and morpholine $pK_a = 8.7$ (14). If piperidine adsorbs on the metal at the nitrogen end of the molecule through lone pair electron interaction, then the effect of withdrawal of the lone pair electrons from nitrogen would tend to affect the attached hydrogen atom by giving this proton an increased "degree of acidity". Such an effect will increase the possibility of intermolecular hydrogen bonding with the lone pair electrons on another piperidine mloecule and thereby drawing the second molecule closer to the interface. The same argument may be applied to morpholine if it adsorbed with the nitrogen atom on the metal but in view of its lower pK_a value there is a corresponding decrease in the "degree of acidity" of the hydrogen atom and a lesser tendency for morpholine to show intermolecular hydrogen bonding. Qualitative support for this argument may be cited from the high resolution n.m.r. spectra of *p*-chloroaniline (19) and 2-methyl piperidine (20). The chemical shifts for the proton on the nitrogen atom are 1.34 and 3.60 p.p.m. for *p*-chloroaniline and 2-methyl piperidine respectively. The latter compound is more basic than the aromatic substance and corresponding withdrawal of the lone pair electrons towards the aromatic ring is greater than that for the saturated heterocyclic compound. This is indicated by the respective effect on the nuclear magnetic resonance (n.m.r.) spectra and it is known that the chemical shift of a proton increases qualitatively with its relative "acidity".

Can. J. Chem. Downloaded from www.nrcresearchpress.com by 210.87.254.6 on 09/05/12
For personal use only.

Can. J. Chem. Downloaded from www.nrcresearchpress.com by 210.87.254.6 on 09/05/12
For personal use only.

(d) Standard Electrochemical Free Energies

Figure 5 shows that $\Delta\overline{G_A}^0$ has a maximum at slightly negative potentials with respect to the pzc at $\Theta = 0.5$ for all the compounds studied. This behavior is consistent with the trend observed by Blomgren *et al.* (13) for aliphatic neutral compounds. For the alcohols the curves are relatively similar to one another but the lowest $\Delta\overline{G_A}^0$ values are observed for the least saturated compounds. For the heterocyclic compounds the introduction of oxygen into the ring system seems to lower $-\Delta\overline{G_A}^0$ values close to those shown by the alcohols. For constant surface coverage of $\Theta = 0.5$ the variation of $\Delta\overline{G_A}^0$ is less symmetrical over the potential range plotted for the heterocyclic compounds than for the alcohols. The $\Delta\overline{G_A}^0$ values for the alcohols at low anodic potentials have not been plotted because at these high positive fields surface coverages were below 0.5. The values of $\Delta\overline{G_A}^0$ at constant Θ can be regarded as a measure of the inherent strength of the net adsorption forces acting on the organic molecules (13) and this is reflected by comparison of the respective k values computed from eq. [3] and shown in Table II (see section *e*).

Figure 6 shows the linear variation of $\Delta\overline{G_A}^0$ with $\Theta^{3/2}$ calculated according to eq. [5] for dioxane and *n*-propanol. The surface coverage was computed from theoretical values of Γ_m for the boat conformation of dioxane and the planar configuration of *n*-propanol. However, it is to be noted that similar qualitative behavior was observed if experimental values of Γ_m were used for calculating Θ's. The choice of experimental Γ_m values results in systematic displacements of the curves but their *forms* do not change. Pyridine and *n*-propanol show significant breaks in the plots at different potentials, which are comparable to previously reported behavior observed for π-deficient (14) aromatic and heterocyclic bases (2). This has been attributed to sudden orientation effects due to lateral interactions of the adsorbed molecules. There are no sharp inflections in the $\Delta\overline{G_A}^0$ vs. $\Theta^{3/2}$ plots for dioxane, which indicate that any orientation of the adsorbed molecules between upright or inverse positions of either the boat or chair conformations is not detectable in terms of surface coverage because the molecular areas of the four possible configurations are approximately equal to one another. Further support regarding the indecisiveness concerning planar to perpendicular orientation of the adsorbed molecules may also be seen from the zero slopes for most of the plots shown in Fig. 6*a*. The zero slopes mean that there is no net repulsion lateral to the surface so that orientations may possibly be "random" for dioxane. The same general dependence of $\Delta\overline{G_A}^0$ on $\Theta^{3/2}$ was observed for piperidine and morpholine, and can be explained by similar reasons offered for dioxane. There were also no inflections in the plots for allyl and propargyl alcohols since these molecules would probably prefer to adsorb in a planar position on the metal due to π-orbital interaction (2). At high coverages, van der Waals attractive forces dominate between the molecules and this behavior is demonstrated by the typical plot at -600 mV for dioxane where the curve tends to turn upwards at $\Theta = 0.8$. The $\Delta\overline{G_A}^0$ vs. $\Theta^{3/2}$ behavior for all the substances examined confirm the trend of orientation effects presented in Table I.

(e) Degree of Adsorbability

For adsorption on mercury Blomgren *et al.* (13) defined adsorbability at the pzc in terms of the adsorption coefficient k for $\Theta = 0.25$, and Laitinen and Mosier (22) used the adsorption index β for $\Theta = 0.5$ at potentials varying from about -0.6 to -0.8 V saturated calomel electrode (s.c.e.). Both terms have been derived from considerations of

the Langmuir isotherm but it is difficult to make extensive comparisons of the two parameters because of the different adsorbates and base electrolytes used by the respective authors. For the adsorption of β-naphthol in an aqueous phthalate buffer 0.1 M (pH 4.4) with 0.1 M KCl, β was given as 13.0 l mmole^{-1} or 1.3×10^7 cm^3 mole^{-1} for $\Theta = 0.5$ (22). For the adsorption of α-naphthol in 0.1 N aqueous HCl, Blomgren *et al.* (13) reported $k = 5.0 \times 10^7$ cm^3 mole^{-1} for $\Theta = 0.25$, which is possibly based on a theoretical value of Γ_m assuming planar adsorption of the molecule on mercury. From their Γ_A vs. c_A isotherm at -400 mV (with respect to the hydrogen electrode) (13) we calculated $k = 2.0 \times 10^7$ cm^3 mole^{-1} for $\Theta = 0.25$ by using the experimental value of Γ_m. In a similar manner k was estimated as 2.8×10^7 cm^3 mole^{-1} for $\Theta = 0.5$.

The adsorption behavior of quinoline and isoquinoline was found to be quantitatively similar on solid or liquid electrodes (23). Furthermore, it is noted that despite the difference in base electrolytes used, and that β and k values were calculated from capacitance and electrocapillary data respectively, there appears to be some reasonable order of agreement between k and β for the two isomeric naphthols examined. We list in Table II the adsorbability of our organic substances investigated in terms of k at the pzc for different values of Θ. Laitinen and Mosier concluded that higher β values indicate increasing surface activity and decreasing polarity. For some compounds there is also a qualitative parallelism between β and the basicity of the molecule (22). Table II shows a regular trend in the degree of adsorbability which is related to the chemical and physical properties of the respective substances, e.g. piperidine has the highest β and basicity of the compounds investigated. For pyridine Laitinen and Mosier reported $\beta = 0.013$ ($\Theta = 0.5$ at -0.8 V (s.c.e.)) and our value of $k = 1.6 \times 10^4$ cm^3 mole^{-1} is equivalent to $\beta = 0.016$ ($\Theta = 0.5$ at 0.56 V normal calomel electrode (n.c.e.)). The close agreement for the only compound that we have examined in common with Laitinen and Mosier is remarkably coincidental. However, if we calculated $\Theta = 0.5$ on the basis of a theoretical Γ_m corresponding to a planar configuration of the adsorbed molecule, $\beta = 0.032$.

(f) Surface Charge as a Function of Coverage and Electrode Potential

Values of q_M at various concentrations and electrode potentials for dioxane and morpholine are shown in Fig. 7 and for the alcohols in Fig. 8. These plots for piperidine and pyridine are essentially similar to those previously reported (2) and are omitted in this paper for that reason. Morpholine and dioxane are different from those of piperidine and pyridine in that the curves of the oxygen-containing compounds do not show independence of potential at negative potentials with respect to the pzc. Morpholine, pyridine, and piperidine display q_M values which decrease numerically with increasing concentration (cf. ref. 2).

For ease of discussion one can divide the q_M vs. E curves into three sets: (i) pyridine and piperidine (2); (ii) morpholine; (iii) dioxane and the alcohols. The isolation of morpholine is based on the fact that at negative potentials with respect to the pzc, the curves are intermediate in form between sets i and iii. The distinction between i and ii as compared with iii is clearly due to the absence of nitrogen in the latter set of compounds. Dioxane and the alcohols show a common crossing point at about -600 mV for all concentrations, and the numerical value of q_M changes in a reverse order with increasing concentration on the anodic and cathodic sides of the pzc respectively. The general shape of set iii resembles those reported by Blomgren *et al.* (13) for aliphatic substances such as *n*-butanol, *n*-valeric acid, and *n*-valeronitrile, which show a common point of intersection at about -250 mV with respect to the hydrogen electrode. It appears that the nitrogen

Can. J. Chem. Downloaded from www.nrcresearchpress.com by 210.87.254.6 on 09/05/12
For personal use only.

atom in the nitrilo functional group does not exert such a profound influence on the adsorptive properties of the aliphatic molecule as it does for the cyclic compounds.

It may not be very conventional to equate the structural effects on adsorption of an aliphatic alcohol with that of a cyclic ether, but it is difficult to ignore the resemblance of the q_M vs. E curves for n-propanol and dioxane, which share the common absence of unsaturation. The divergence of q_M values for the alcohols at various comparable concentrations on the anodic and cathodic sides of the pzc, antiparallels the respective degree of unsaturation in the three compounds. The presence of nitrogen and oxygen in the cyclic compounds, and the degree of unsaturation in the aliphatic alcohols seem to contribute distinctive effects on the changes of shape in the q_M vs. E curves, which are again related in a systematic way to the respective adsorbabilities of the different substances.

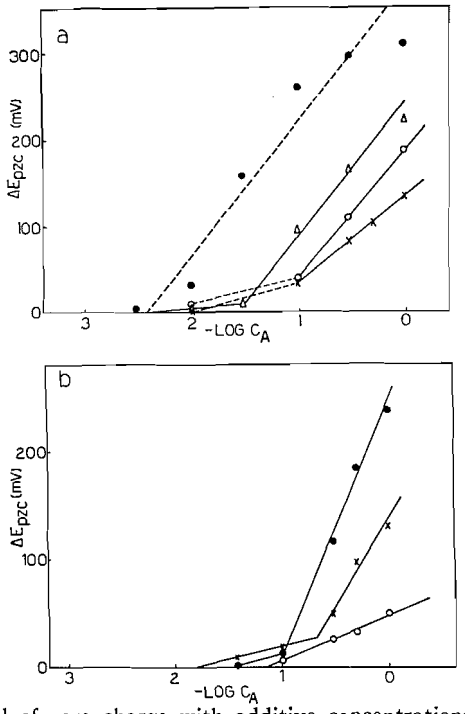

FIG. 9. Shifts of the potential of zero charge with additive concentrations in 1.0 N KCl solution. (*a*) (●) Piperidine, (△) pyridine, (×) morpholine, (○) dioxane. (*b*) (●) n-Propanol, (×) Allyl alcohol, (○) propargyl alcohol.

(g) Variation of ΔE_{pzc} *with log* c_A *and with* $(\Gamma_A)_{pzc}$

Figures 9 and 10 show that $d(\Delta E_{pzc})/d \log c_A$ and $d(\Delta E_{pzc})/d(\Gamma_A)_{pzc}$ change abruptly with increasing c_A and $(\Gamma_A)_{pzc}$ for some of the compounds. Similar behavior was previously shown for several heterocyclic and aromatic amines, and was interpreted as sudden orientations (cf. section *d*) of the adsorbed molecules at critical $(\Gamma_A)_{pzc}$ and c_A values. The sharpest changes of slope at low $(\Gamma_A)_{pzc}$ and c_A values were observed for π-deficient compounds, and conversely, π-excessive compounds showed less pronounced changes of slope at higher $(\Gamma_A)_{pzc}$ and c_A. The relative contributions of π-orbital interaction on mercury for the two classes of cyclic amines were associated with the orientation effects (2).

Can. J. Chem. Downloaded from www.nrcresearchpress.com by 210.87.254.6 on 09/05/12
For personal use only.

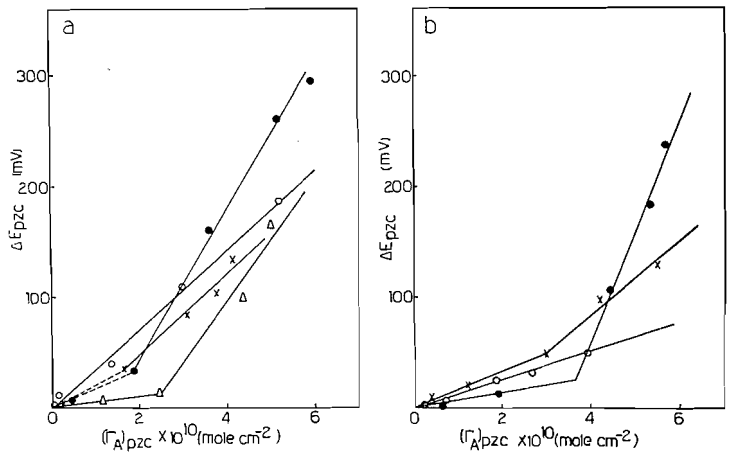

FIG. 10. Shifts of the potential of zero charge against surface excess at the pzc in 1.0 *N* KCl. (*a*) (●) Piperidine, (△) pyridine, (×) morpholine, (○) dioxane. (*b*) (●) *n*-Propanol, (×) allyl alcohol, (○) propargyl alcohol.

In Fig. 9 the repeated results for pyridine and piperidine (both classified as π-deficient (14)) can still be correlated in terms of the respective presence and absence of a partly conjugated π-orbital system. Figures 9*b* and 10*b* present further confirmation of the previously suggested hypothesis of π-orbital effect in relation to orientation (2). At low surface coverage *n*-propanol may adsorb in a planar configuration on the metal but would probably orient to a vertical position with the hydrocarbon end of the molecule attached to mercury at a critical $(\Gamma_A)_{pzc}$ value. This is more consistent with the information in Table I and agrees with the adsorption behavior described for *n*-butanol (13, 21).

Allyl and propargyl alcohols have increasing degrees of unsaturation and these molecules would show greater tendency to adsorb in a planar position on mercury through π-orbital interaction. As surface coverage increases allyl alcohol may orient to a perpendicular position with the hydrophilic end of the molecule pointing towards the solution. The sudden changes in slope for allyl alcohol occur at much higher $(\Gamma_A)_{pzc}$ and c_A values than for *n*-propanol. Propargyl alcohol shows no orientation effects at the respective c_A and $(\Gamma_A)_{pzc}$ values investigated.

The comparative behavior of piperidine, dioxane, and morpholine cannot be explained in terms of π-orbital effects. Moreover, any explanation of sudden orientation from "planar" to "perpendicular" positions on mercury would be erroneous since these compounds exhibit isomeric boat and chair conformations. The areas of the two conformations shown in Table I are approximately identical in magnitude. Furthermore, there is some ambiguity in the choice of models with the hydrogen atom in an axial position when attached to nitrogen in piperidine and morpholine (see Discussion section *c*). There is also an error of about 10% in the computation of Γ_A. Under these circumstances it is not possible to discern any sudden or even gradual orientation of these adsorbed molecules from Fig. 10*a*. The data for piperidine in Fig. 9*a* are so widely scattered that it is difficult to ascertain whether there has been any change in slope at all. It is impossible to draw any valid conclusions from the changes in slope represented by the broken and solid lines shown in Figs. 9*a* and 10*a*.

Cyclohexane has been reported by Selwood (24) to adsorb on nickel in the boat conformation. By analogy it may be possible that the saturated heterocyclic compounds

Can. J. Chem. Downloaded from www.nrcresearchpress.com by 210.87.254.6 on 09/05/12
For personal use only.

Can. J. Chem. Downloaded from www.nrcresearchpress.com by 210.87.254.6 on 09/05/12
For personal use only.

could preferentially adsorb in a similar position on mercury. Some support for this suggestion may be obtained by considering their dipole moments. In the gas phase, dioxane $\mu = 0$, but in solution at room temperature a zero moment has also been quoted (26) although a categorical denial of the boat form has not been made. In benzene $\mu = 0.45$ (25) and the apparent dipole moments μ_S are 3.19, 2.21, and 3.56 in nitrobenzene, *t*-butyl chloride, and acetonitrile respectively (27). The latter values suggest that there must be a reasonable predominance of the boat form in certain nonpolar solvents. Adsorption in the chair form for piperidine and morpholine through lone pair electrons of the nitrogen atom interacting on the metal cannot be ruled out but the same situation for either of the symmetrical oxygens in dioxane appears less feasible. Moreover, the greater $\Delta\gamma$, k values at $\Theta = 0.1$ and 0.25, and (Γ_m) experimental observed for dioxane in comparison with morpholine would favor the preferred adsorption of the dioxane molecule in the boat form.

Although Figs. 9 and 10 do not offer any unequivocal experimental evidence for "planar to perpendicular" orientation of the adsorbed molecules of dioxane, morpholine, and piperidine (cf. Discussion section *d*), it is possible that these adsorbates may orient through any of the four upright or inverse positions of the two conformations. If such orientations occur, we suggest that the preferred form will likely be the boat conformation,* and with the heteroatoms pointing outwards to the solution side of the interface. The latter suggestion is in conformity with reported postulates for molecules which do not exhibit conformational isomerism (2, 13, 21, 28). A better test of orientational effects from one isomeric form to another would be to determine the adsorption of substituted derivatives of the saturated heterocyclic compounds, e.g. with a large aliphatic or aromatic group on the 4-carbon position in piperidine. Such a derivative would have less molecular symmetry, and different Γ_m values should result for various preferred orientational positions on the surface. It would also be interesting to examine the effects of *cis–trans* isomerism on adsorption in a way analogous to that described above.

Figures 9 and 10 indicate that an Esin and Markov effect (29) exists for the adsorption of neutral molecules. This effect has been examined for inorganic ions from a general thermodynamic standpoint (30) and will be reported in detail elsewhere (31) for organic ions and for a wide variety of organic molecules including the ones investigated in this paper.

(h) Five-Membered Heterocyclic Compounds

Difficulties were reported in the adsorption studies on solid electrodes for five-membered heterocyclic compounds such as pyrrole (32). The problem is largely resolved by the availability of a new class of corrosion inhibitors (Miles Chemical Co., Elkhart, Indiana), comprising of furfurylamine, tetrahydrafurfurylamine, and their respective derivatives. These compounds contain oxygen as the cyclic heteroatom and are very π-excessive in properties (14). The amino group on the side chain confers high basicity and complete miscibility with water. The adsorptions of these compounds as neutral molecules and ions have been investigated by electrocapillary and capacitance methods, and comparison with their analogous alcohols, e.g. furfuryl alcohol, is presently being carried out.

Furfuryl alcohol is completely miscible with water but the solution decomposes on standing. This has been attributed to gradual change by "resinification" through intermolecular dehydration, which is catalyzed by heat and increasing acidity (33), but the

**The adsorbed molecules are under the influence of the electrode field which may stabilize the conformation with the higher dipole moment (31). This is comparable to a previously published postulate that displacement of the isomeric equilibrium toward the boat form occurs under the influence of coulombic field (35).*

decomposition may be retarded by traces of cyclic or aromatic amines (34). The varying inhibitory action of cyclic amines, e.g. piperidine, furfurylamine, etc., on the decomposition of furfuryl alcohol is currently being examined on a quantitative basis. There appears to be some relation with the varying mitigating effects on corrosion of metals for these organic bases. The electrocapillary curves for the unsaturated furfurylamines in KCl solutions resemble those of allyl and propargyl alcohols. In HCl, the electrocapillary curves are much more symmetrical on both sides of the pzc. The furfurylamines appear to satisfy the most favorable structural requirements for general purpose corrosion inhibition in acidic media since they are adsorbed on the cathodic side of the pzc by virtue of the positive charge on the protonated amino group, and on the anodic side by π-bonding with the metal. Further theoretical and experimental analysis of the Esin and Markov effect (31), and the comparison of electrocapillary and capacitance results (6) for these compounds will be presented in detail later. The descriptions of structural and other effects due to oxygen and nitrogen reported in this paper for the aliphatic alcohols and the six-membered heterocyclic compounds are undoubtedly of value in the interpretation of the adsorptive and (or) corrosion inhibitory properties of these five-membered heterocyclic bases and their analogous alcohols.

ACKNOWLEDGMENTS

We are indebted to the National Research Council and to the University of Toronto for financial support of this work. The pressure-regulation device described in the Experimental section is due to the kind suggestion of Professor B. E. Conway of Ottawa University. The assistance of Mr. F. M. Kimmerle in the determination of the projected molecular areas is gratefully acknowledged. Finally we wish to thank Professor A. G. Brook for helpful discussions on some aspects of organic chemistry of the saturated heterocyclic compounds.

REFERENCES

1. A. N. FRUMKIN and B. B. DAMASKIN. *In* Modern aspects of electrochemistry. Vol. III. *Edited by* J. O'M. Bockris and B. E. Conway. Butterworths, London. 1964. p. 149.
2. B. E. CONWAY and R. G. BARRADAS. Electrochim. Acta, **5**, 319 (1961).
3. B. B. DAMASKIN. Russ. Chem. Rev. English Transl. **30**, 78 (1961).
4. D. C. GRAHAME. Chem. Rev. **41**, 441 (1947).
5. E. BLOMGREN and J. O'M. Bockris. J. Phys. Chem. **63**, 1475 (1959).
6. R. G. BARRADAS, P. G. HAMILTON, and E. VALERIOTE. (*a*) Abstracts, Corrosion Inhibitor Symposium, Electrochemical Society Meeting, Buffalo, New York. 1965; (*b*) J. Electrochem. Soc. In preparation.
7. R. G. BARRADAS and F. M. KIMMERLE. J. Electroanal. Chem. In press.
8. R. G. BARRADAS and B. E. CONWAY. Electrochim. Acta, **5**, 349 (1961).
9. D. J. G. IVES and G. J. JANZ (*Editors*). Reference electrodes. Academic Press, New York. 1961. pp. 133–135.
10. J. A. V. BUTLER. Proc. Roy. Soc. London, Ser. A, **122**, 399 (1929).
11. E. A. GUGGENHEIM. Trans. Faraday Soc. **36**, 397 (1940).
12. B. E. CONWAY, R. G. BARRADAS, and T. ZADWIDZKY. J. Phys. Chem. **63**, 1475 (1959).
13. E. BLOMGREN, J. O'M. BOCKRIS, and C. JESCH. J. Phys. Chem. **65**, 2000 (1961).
14. A. ALBERT. Heterocyclic chemistry. Athlone Press, London. 1959.
15. J. C. HANSON and F. E. STAFFORD. J. Chem. Educ. **42**, 88 (1965).
16. H. F. FINLEY and N. HACKERMAN. J. Electrochem. Soc. **107**, 259 (1960).
17. N. HACKERMAN. Corrosion **18**, 332 (1962).
18. R. R. ANNAND, R. M. HURD, and N. HACKERMAN. J. Electrochem. Soc. **112**, 138 (1965).
19. High Resolution NMR Spectra Catalog No. 1. Varian Associates Inc. 1962. Spectrum Number 123.
20. High Resolution NMR Spectra Catalog No. 2. Varian Associates Inc. 1963. Spectrum Number 477.
21. J. O'M. BOCKRIS, M. A. DEVANATHAN, and K. MÜLLER. Proc. Roy. Soc. London, Ser. A, **274**, 55 (1963).
22. H. A. LAITINEN and B. MOSIER. J. Am. Chem. Soc. **80**, 2363 (1958).
23. R. G. BARRADAS. Ph.D. Thesis, University of Ottawa, Ottawa, Can. 1960.
24. P. W. SELWOOD. J. Am. Chem. Soc. **79**, 4637 (1957).
25. B. E. CONWAY. Electrochemical data. Elsevier Press, New York. 1952.
26. S. WALKER. *In* Physical methods in heterocyclic chemistry. Vol. I. *Edited by* A. R. Katritzky. Academic Press, New York. 1963. p. 198.

Can. J. Chem. Downloaded from www.nrcresearchpress.com by 210.87.254.6 on 09/05/12
For personal use only.

27. J. W. SMITH. Electric dipole moments. Butterworths, London. 1955.
28. L. GIERST, D. BERMANE, and P. CORBUSIER. Ric. Sci. Rend. **4**, 3 (1959).
29. O. A. ESIN and B. F. MARKOV. Acta Physicochim. SSSR, **10**, 353 (1939).
30. R. PARSONS. Proc. 2nd Int. Congress of Surface Activity; Electrical Phenomena and Solid/Liquid Interfaces. *Edited by* J. H. Schulman. Butterworths, London. 1957. p. 38.
31. R. G. BARRADAS, P. G. HAMILTON, and B. E. CONWAY. J. Phys. Chem. To be published.
32. R. G. BARRADAS and B. E. CONWAY. J. Electroanal. Chem. **6**, 314 (1963).
33. A. P. DUNLOP and F. N. PETERS. The furans. Reinhold Publishing Corporation, New York. 1953.
34. A. P. DUNLOP and F. N. PETERS. Ind. Eng. Chem. **34**, 814 (1942).
35. J. B. HYNE. J. Am. Chem. Soc. **85**, 304 (1963).

Can. J. Chem. Downloaded from www.nrcresearchpress.com by 210.87.254.6 on 09/05/12
For personal use only.

Can. J. Chem. Downloaded from www.nrcresearchpress.com by 210.87.254.105 on 09/05/12
For personal use only.

THE PYROLYSIS OF OXIMES OF SOME GAMMA CYANO- AND GAMMA NITRO-KETONES

C. F. H. ALLEN
Rochester Institute of Technology, Rochester, New York
Received January 19, 1965

ABSTRACT

Oximes of gamma cyano- and gamma nitro-ketones are decomposed by heat as well as by acids. From the very complex mixtures resulting there have been isolated arylated pyrroles, arylated 2-aminopyridines, and the corresponding pyridones, as well as several minor products. This behavior constitutes a new synthesis of these heterocyclic compounds. In a Beckmann rearrangement γ-benzoyl-α,β-diphenylbutyronitrile gave an anilide, the structure of which was confirmed by an independent synthesis. By physical methods both structures of gamma ketonic amides are confirmed.

The thermal reversal of the Michael addition reaction has recently been shown to proceed in two ways, termed *normal* and *abnormal* (1, 2, 3). To prevent the normal reaction, the use of the cyano-oxime (II), prepared from the parent cyanoketone (I) and hydroxylamine acetate, was selected. Because the reagent can attack both carbonyl and cyano groups, it was important, at the outset, to know the structure of the oxime (II) with certainty. This was demonstrated by an examination of the cyano-anilide formed after its Beckmann rearrangement. The oxime gave an acetate (III) when treated with acetic anhydride or acetyl chloride, from which the parent could be regenerated, but with thionyl chloride it was rearranged to the cyano-anilide (IV). The latter was synthesized independently from the known acid (V)(4) for structure confirmation. Since oxime rearrangement is known to involve groups in the *trans* positions (5), the configuration of II must be the one shown. Concentrated sulfuric acid likewise brought about rearrangement to the anilide, but a by-product was the amide-anilide (VI), formed by addition of water to the cyano group; the nitrile (IV) could be re-formed by treatment of the amide with thionyl chloride (Chart I). The amide-anilide (VI) is isomeric with the amide-oxime (VII), which was isolated in small amount from the residues of the recrystallization of the oxime (II).

In view of the recently established value of the mass spectrometer for predicting the course of degradation reactions (1, 2, 3), most of the new substances described in this paper were so examined, and the presence of possible products noted without resort, at each examination, to isolation by classical procedures. The compounds were given an opportunity to decompose in the all-glass heated inlet (230°) of the mass spectrometer. The resulting mass spectra, therefore, represent the decomposition mixtures. Under these conditions the spectra of the cyano-oxime (II) and its acetate (III) gave several spectral peaks which were considered as probably parent molecule-ions of decomposition products. Of these the large ones at 322 and 295 can be accounted for by assuming a loss of water for the first, and of water plus hydrogen cyanide for the second. The products, formed in approximately equal amounts and actually isolated by classical methods, were the new aminopyridine (IX) and the known (6) pyrrole (X); a secondary product was the already known (7) corresponding pyridone (XI) resulting from hydrolysis of the latter. The structure of the aminopyridine (IX) was clearly demonstrated by its independent conversion to the known pyridone (XI) by the action of nitrous acid, and to the known

CHART I

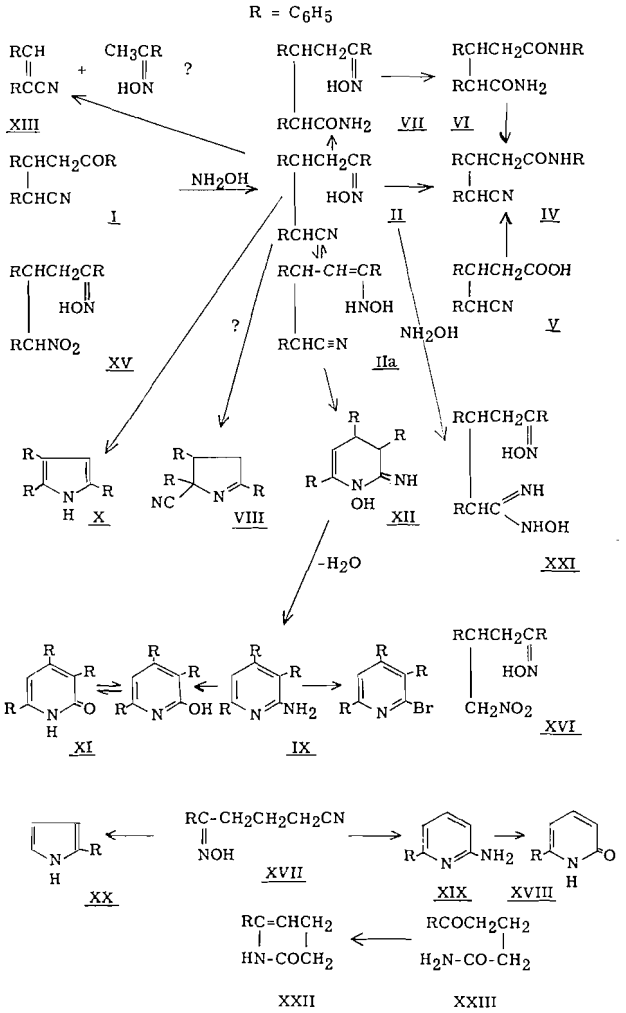

2-bromo-3,4,6-triphenylpyridine (7) following the procedure used by Case (8) in an analogous instance. The oxime (II) can cyclize in two ways; one is by a direct loss of water to give a pyrroline (mol. wt. 322) (VIII). The other follows a path analogous to that for a modification of the Hantzsch pyridine synthesis from monoximes of 1,5-diketones, as was discovered by Wislicenus (9). In line with this, the aminopyridine is slowly formed by treatment of the parent cyanoketone (I) with hydroxylamine hydrochloride. The reaction path involves the hydrogen atom on the oxime nitrogen in the tautomeric form (II*a*); this adds to the cyano group (XII), with concomitant transannular loss of water, to give the aminopyridine (mol. wt. 322)(IX).

Comparisons of the several mass spectra of the decomposition products of the oxime (II) and those of reference samples of the pyrrole (X) and the aminopyridine (IX) confirmed their presence. In each examination of the oxime (II) there was an excess of peak at *m/e* 322 which varied slightly from one examination to another. It was also noted that a peak at *m/e* 218, not present in mass spectra of the aminopyridine (IX), the pyrrole (X), or 2,4-diphenylpyrrole, appeared to vary slightly in size, correlating with

Can. J. Chem. Downloaded from www.nrcresearchpress.com by 210.87.254.105 on 09/05/12
For personal use only.

the amount of excess peak at *m/e* 322. A pyrroline (VIII), if present in the decomposition mixture, would be expected to give a parent peak at *m/e* 322. Although no reference sample of known composition (VIII) was available for comparison, one might expect ring cleavage at the two bonds which are beta to the ring nitrogen, which would be analogous to the fragmentation of pyrrolidines (22). This would leave an ion of *m/e* 218. An alternate process which might also contribute to the *m/e* 218 peak would involve a rearrangement with the loss of a phenyl group and HCN (22).

One of the small ion peaks occurs at *m/e* 205, the molecular weight of α-phenylcinnamonitrile (XIII). This identification not only was supported by comparison with the mass spectrum of an authentic specimen, but also was confirmed in the vapor phase chromatographic estimation of the amount as 2–3% of the thermal products. Its presence suggests that there has been a little abnormal dissociation (1) of the oxime (I), considered as a Michael adduct. The other expected product would be acetophenoneoxime; the latter could not be identified, however.

The cyano-anilide (IV) gave a relatively weak mass spectrum, showing the presence of α-phenylcinnamonitrile (confirmed by reference spectrum). Other components were not completely resolved because of overlapping contributions to peaks in common. It is possible that the peak at 135 may represent some acetanilide (N-methylbenzamide and phenylacetamide were excluded by comparison with reference spectra). The mass spectrum of the products from the cyano-semicarbazone (XIV) showed the presence of small amounts of the same products obtained from the cyano-oxime (I), but there was no evidence for acetophenone semicarbazone.

The formation of the triphenylpyrrole is not limited to the cyano-oxime (II), but is also found with the analogous nitro-oxime (XV). In this instance oxides of nitrogen and water are eliminated. Benzonitrile was present and estimated by gas chromatography in the oily product resulting from a chemical degradation at the bench. The decompositions of both these oximes constitute a new synthesis of triarylpyrroles (10). However, the yields from either oxime are not high enough to make the reaction competitive with that starting with desylacetophenone (6).

In an analogous manner the oxime (XVI) of γ-nitro-β-phenylbutyrophenone decomposed in the heated inlet, yielding 2,4-diphenylpyrrole as the only recognizable product (confirmed by reference mass spectrum), but difficulties in the preparation of the oxime render this approach impractical.

In the case of γ-benzoylbutyronitrile oxime (XVII) there was a mass peak at 188, the molecular weight of the undecomposed parent compound, which decreased with time. There were also peaks at masses 171, 170, and 143, the molecular weights of 2-oxo-6-phenylpyridone (XVIII) (11), 2-amino-6-phenylpyridine (XIX), and 2-phenylpyrrole (XX). These increased with time as would be expected. Identification of the pyrrole was supported by comparison with the complete mass spectrum of an authentic specimen (12). In the laboratory, when this oxime is heated in bulk, it decomposed violently. The only recognizable products were water and the known 2-oxo-6-phenyltetrahydropyridine (XXII) (11).

The hydroximidate (XXI) is a minor product, isolated from the residues in the preparation of the oxime (II). In the heated inlet of the mass spectrometer the hydroximidate gave a very complex spectrum. Peaks were present at *m/e* 322, 321 (characteristic of 2-amino-3,4,6-triphenylpyridine), and at 296 (the molecular weight of 2,3,5-triphenylfuran), but there was none at *m/e* 218. These were confirmed by the identity of their complete mass spectral patterns with those of authentic specimens. The peak at 296 does not occur in the mass spectrum of the pure oxime (II).

Can. J. Chem. Downloaded from www.nrcresearchpress.com by 210.87.254.105 on 09/05/12
For personal use only.

Can. J. Chem. Downloaded from www.nrcresearchpress.com by 210.87.254.105 on 09/05/12
For personal use only.

EXPERIMENTAL

Preparation of the Oximes

Since the delta ketonic nitriles have two groups that can react with hydroxylamine (13) a mixture of products was to be expected; fortunately, with the adduct I, the major portion of the desired oxime (II) was in the first crystalline portion to separate. The best yield was obtained by 1 h heating, under reflux, of a mixture of 20 g of either diastereomeric nitrile (I) with the hydroxylamine acetate solution resulting from the interaction of 12 g of hydroxylamine hydrochloride in 160 ml of dry methanol, and 33 g of fused potassium acetate in 120 ml of the same solvent, with filtration of the salt; the nitrile slowly went into solution. When the solution had been allowed to stand overnight, most of the oxime separated as clear, hard prisms, containing methanol of crystallization (II*a*). If ethyl alcohol was used, no product separated until the volume was reduced one-half. The oxime was recrystallized first from hot benzene, and then from propyl alcohol. The properties of all new compounds are collected in Table I.

TABLE I

Properties of new substances

No.	Substance	M.p., °C	Empirical formula	Analyses					
				Calcd.			Found		
				C	H	N	C	H	N
II	Cyano-oxime (triphenyl)	137	$C_{23}H_{20}N_2O$	81.2	5.9	8.2	81.6	5.6	8.0
II*a*	II plus CH_3OH	136*	$C_{24}H_{24}N_2O_2$	77.4	6.5	7.5	77.5	6.6	7.6
III	Acetate of II	155	$C_{25}H_{22}N_2O_2$	78.5	5.8	7.3	78.3	6.0	7.4
IV	Cyano-anilide	152	$C_{23}H_{20}N_2O$	81.2	5.9	8.2	81.3	5.6	8.4
VI	Amide-anilide	227–8†	$C_{23}H_{22}N_2O_2$	76.8	6.1	7.9	76.8	6.2	7.9
VII	Amide-oxime	226–7†	$C_{23}H_{22}N_2O_2$	76.8	6.1	7.9	76.9	6.1	7.6
IX	The aminopyridine	156–7	$C_{23}H_{18}N_2$	85.7	5.6	8.7	85.8	5.2	8.7
XI	The pyridone	300–1	$C_{23}H_{17}NO$	85.4	5.2	4.3	85.2	5.4	4.3
XIV	Semicarbazone	214 dec.	$C_{24}H_{22}N_4O$	75.4	5.8	14.7	75.3	5.8	14.5
XV	Nitro-oxime (triphenyl)	175	$C_{22}H_{20}N_2O_3$	73.3	5.6	7.8	73.6	5.8	7.6
XVI	Nitro-oxime (biphenyl)	110–11	$C_{16}H_{16}N_2O_3$	67.6	5.6	9.9	67.9	5.8	9.7
XVII	Cyano-oxime (monophenyl)	100–1	$C_{11}H_{12}N_2O$	70.2	6.4	14.9	70.4	6.7	14.9
XXI	The hydroximidate	167–8	$C_{23}H_{23}N_3O_2$	74.0	6.2	11.2	74.0	6.4	11.0

*On block, shrinks at about 85°.
†Mixture shrinks at 210°, melts 219–220°.

The residual solution was treated in two ways: by pouring it into water to precipitate the organic components and get rid of the potassium salts, followed by systematic recrystallization; or (*b*) by direct, tedious fractional crystallization using various solvents. The products identified were a little more of the cyano-oxime (II); 8–10% of unreacted adduct (I) if the reaction time was less than 2 h; the amide-oxime (VII) (5–6%) arising from water, formed in the reaction, and adding to the cyano group; and the hydroximidate (XXI) resulting from the addition of hydroxylamine (13) (13–14%). Doubling the period of heating dropped the yield of oxime to 67–70% and increased those of the amide-oxime and hydroximidates.

The Hydroximidate (XXI)

When a benzene solution of the uncrystallizable, gummy residue was shaken with aqueous copper acetate, very little copper derivative separated. Upon analysis this was found to contain the expected amount of metal for formula XXI, but to have had *one* =NH replaced by =O.

The cyano-oxime (II) dissolves slowly in methanolic sodium methoxide on shaking; it does not give a copper derivative when shaken with aqueous copper acetate. The acetate (III) was obtained by dissolving 1 g of the oxime in 5 ml of hot chloroform, and adding 20 drops of acetyl chloride; when the evolution of hydrogen chloride subsided, an equal volume of acetyl chloride was added and the whole left over night to crystallize. The residual oil, which had a very bright blue fluorescence when illuminated by a source of ultraviolet light,[1] was taken up in methanol, from which 0.4 g of the acetate (II) crystallized. The same acetate was less conveniently obtained by the use of acetic anhydride. If the acetate was boiled for a few minutes with sodium hydroxide in a mixture of water and alcohol, the oxime was quantitatively regenerated.

The oxime (XV) was formed in 95–96% yield by the same general procedure, using the adduct from phenylnitromethane and chalcone (14). As above, both diastereomers gave the same oxime. The preparation of the oxime (XVI) from the nitromethane adduct (15) was erratic, a green oil being formed from which

[1]"*Spectroline*," *Spectronics Corp., Westbury, N.Y. Model SL 3660.*

the oxime separated only after some days. The yields were 0–68%. During manipulative trials a small amount of a blue dye was obtained; this was probably identical with the Knott-Rogers dye (16, 17)—black needles with a bronze reflex, m.p. (on block) 238°.

γ-Butyrophenoneoxime (XVII) was prepared from γ-benzoylbutyronitrile (18) essentially by the procedure employed with II, using methanol. After 80 min, 3 ml of water was added and most of the solvent evaporated. The cooled solution was then inoculated with a little of the previously prepared oxime and left to crystallize overnight (a very slow process); the product separated as very large (up to 5 mm diameter), hard prisms (yield, 27–36%).

The semicarbazone (XIV) corresponding to the oxime (II) was obtained in the usual way, the ethanolic solution being heated under reflux for 80 min. The yield was almost quantitative. Propyl alcohol is preferred for crystallization; acetic acid is unsuitable. The derivative is insoluble in water and in methylene chloride. Both nitriles (I) gave the same semicarbazone.

Rearrangement of Oxime II

To a solution of 1 g of the oxime in 5 ml of hot methylene chloride was slowly added 40 drops of thionyl chloride; gas evolution was rapid. After the oily residual solid was recrystallized from methanol several times, the pure cyanoanilide (IV) was obtained. Its synthesis was accomplished by first converting 1 g of the acid (V) to its chloride by thionyl chloride in hot benzene, evaporating the solution nearly to dryness, and adding more benzene and 1.1 ml of aniline. The white solid formed was worked up by appropriate manipulation, and yielded the same cyano-anilide (mixture melting point, identical infrared and mass spectra).

γ-Carbamoyl-β,γ-diphenylbutyranilide (VI) was obtained when 1 g of the oxime and 10 ml of concentrated sulfuric acid was stirred for 1 h and left overnight at room temperature. The clear solution was poured over ice, and the solid was collected and recrystallized to constant melting point. This amide was dehydrated to the nitrile (IV) by warming its methylene chloride solution with thionyl chloride, removing the excess of reagent by methanol, and recrystallizing the amide from this solvent. There was no depression of melting point on a mixture with an authentic sample of the nitrile.

γ-Benzoylbutyramide

The current availability of γ-benzoylbutyronitrile (18) made mild hydrolysis the preferred route to this amide. The nitrile (6.3 g) was added, in portions, to 20 ml of concentrated sulfuric acid at room temperature. After 3 h the reddish solution was poured into 150 ml of warm water, and the precipitate collected on a filter. It was well-mixed with dilute ammonia to remove γ-benzoylbutyric acid (1.2 g), washed once with water, and, while still wet, dissolved, in 25 ml of 95% ethyl alcohol. Most of the product crystallized on cooling, and a second crop was obtained on concentration. The combined yield was 85–6%. It was used for cyclodehydration to XXII by acetyl chloride (11).

Distillation of the Oximes

The oxime (II) is very sensitive to acidic reagents, to irradiation by ultraviolet light (GE purple X), and to heat, giving uncrystallizable, sticky gums that have a brilliant blue fluorescence when illuminated;[1] this is attributed to the presence of the 2-amino-3,4,6-triphenylpyridine (IX). Numerous small-scale distillations, using 2–5 g of the oxime, were made in miniature apparatus, in vain hope of finding the optimum conditions. Condensing drops of water were visible up to 200°; at this point the pressure was lowered to 1 mm, and the heating was continued as long as any distillate could be observed. The initially thick yellow oil became red and viscous, and a white solid collected in the neck and side of the distilling flask. By gas chromatography it was found that the pyrrole (X) amounted to 19–22%, and the aminopyridine (IX) to 16–20%, with 2–3% of α-phenylcinnamonitrile, b.p., 178–9 at 1 mm. The pyridone was isolated in yields of 12–14%. Larger runs (20–23 g) were than made, using a vacuum throughout (1–0.4 mm) (1.5 h required). Fractions were collected as follows: (A) up to 275–290°, 0.9–1.1 g; (B) 306–315°, 9.5–10.1 g; (C) 365–375°, 2.1–3.5 g; residue. Fraction B set to a thick yellow wax, while C was a red tar. Both were heated under reflux with boiling acetone or ethyl acetate, until a filterable suspension of the pyridone (XI) was formed. Similarly the condensate in the neck and sidearm of the distilling flask was removed. Owing to the large amount of non-crystallizable sticky pitch, yields were not sharply defined. The pyrrole and aminopyridine were separated from each other and from contaminating pyridone by tedious fractional crystallization. The pyridone appeared to have a high vapor pressure for it co-distilled and was found in all fractions collected above 290°, and in the residue; it even persisted through several recrystallization. Metal catalysts (silver solder, stainless steel) had no marked effect, but in the presence of copper only the pyrrole could be isolated; in this instance the aminopyridine appeared to have been hydrolyzed to the pyridone. Added potassium acetate, however, diminished the yield of pyrrole to 6%.

The thermal decomposition were also carried out in various solvents (cumene, dimethylformamide, 1-chloronaphthalene), of which only the latter gave a useful result. After the obvious reaction was over, the solvent was steam distilled, and the residual organic material was treated by appropriate solvents. Column chromatography was not extensively investigated, since preliminary results were not encouraging. A small quantity of the pyrrole was isolated in one sample.

Can. J. Chem. Downloaded from www.nrcresearchpress.com by 210.87.254.105 on 09/05/12
For personal use only.

Under similar conditions, the product from decomposition of the nitro-oxime (XV) showed 15–19% of triphenylpyrrole and 0.5–1.5% of benzonitrile by gas chromatography. The 2,3,5-triphenylpyrrole (X) was identified by comparison with an authentic specimen (6), using the melting and mixture melting points of it and its trinitrobenzene complex (19), violet fluorescence, and infrared and mass spectra. It boils at 254–6° at 1 mm.

2-Amino-3,4,6-triphenylpyridine (IX) crystallized from an acetone extract of cut B, and was recrystallized from propyl alcohol. It was also formed, in a 6.5% yield, by the heating of the adduct I and hydroxylamine hydrochloride under reflux for 24 h (Wislicenus' procedure (see ref. 6)). The infrared spectrum (KBr pressing) of the amine is very similar to that of the simpler 2-aminopyridine in the 2–7 micron region. A series of sharp bands are found near 2.9, 3.05, and 3.15 μ, along with a strong sharp band at 6.13 μ.

2-Bromo-3,4,6-triphenylpyridine from the Amino Compound

To a suspension of 0.6 g of the latter in 6 ml of 48% hydrobromic acid was added a solution of 0.2 ml of bromine in 2 ml of hydrobromic acid. After the mixture was cooled to 3°, 2 g of sodium nitrite in 3 ml of water was added. The red tar formed was taken up in ether, and separated from a little of the pyridone; after removal of the ether, the residual tar was taken up in alcohol from which more pyridone separated. After 3 days, most of the bromopyridine had crystallized in rosettes. The yield was 0.3 g (50%) and of pyridone, 0.1 g (16%). Attempts to synthesize the amine from the bromo compound and sodium amide in boiling butyl ethyl ether were unsuccessful.

The pyridone (XI) was easily separated from the various oils and gums by virtue of its relative insolubility in acetone or ethyl acetate. It was also formed by the action of nitrous acid on the aminopyridine. Once dissolved in a solvent it separates slowly, holding traces of the solvent tenaciously; this may result in an apparent low melting point (7). When mixed with the aminopyridine the melting point of the latter is not depressed, but a clear melt is not obtained until 215–230°. Thus, a 2:1 mixture of IX and XI melts at 272–273°. Although acetic acid can be used, dimethylformamide is the preferred solvent; dimethyl sulfoxide is unsatisfactory. The infrared spectrum (KBr pressing) of the pyridone is very similar to that of the simpler compound, 2-pyridone, and includes a broad absorption band in the 6.15–6.4 μ region. The pyridone has a blue fluorescence.

When the oxime (XVII) of γ-benzoylbutyronitrile was heated, there was an extremely rapid decomposition at 190°, with evolution of much steam, but very little hydrogen cyanide. The latter (collected as silver cyanide) corresponded to a 0.2% yield of 2-phenylpyrrole. The residual black pitch was either distilled at a low pressure or extracted with cold benzene (90–95% is left as residue), and the extract examined by thin-layer and column chromatography. Only the 2-oxo-6-phenyltetrahydropyridone (XXII) (yield, 5–10%) was isolated from all fractions of distillate.

Nuclear Magnetic Resonance

The 2-oxo-6-phenyltetrahydropyridine and γ-benzoylbutyramide were examined by n.m.r., and the findings were consistent with the structure written for the first. There was one imino hydrogen (δ = 8.05) (exchangeable by deuterium), one ethylenic hydrogen (δ = 5.48), four methylenic (δ = 2.53, 2.57), and five aromatic hydrogens (δ = 7.43).

Structures of Gamma Ketonic Amides

There has always been some question whether γ-benzoylbutyramides have the open-chain form or are cyclic, as a result of intramolecular addition (11, 20). In the infrared spectrum of the solid (potassium bromide pressing) the two carbonyl groups show up strongly, indicating the open-chain arrangement, but when the amides are dissolved in dimethyl sulfoxide and examined by n.m.r., the cyclic form is favored, since two different kinds of exchangeable hydrogen appear. The presence of the cyclic form of delta ketonic amides in solution was postulated many years ago (21), and has been independently demonstrated by a simple dehydration of such amides by acetyl chloride in the absence of water or hydrogen chloride (11, 20).

Gas Chromatography

The samples were chromatographed on a 6 × 1 200 mm glass column, containing 25% by weight of Dow Corning 200 silicon fluid on acid and base-washed Celite 545. The detector was a Gow-Mac thermal conductivity cell, Model No. 9285, operated at 260°. The column was operated at 250° and the F. H. heater at 280°. The flow rate was 100 ml of helium per minute, the column being thermostatted with boiling *n*-butyl benzoate. The retention times, as related to octadecane, were α-phenylcinnamonitrile, 1.67; for 2,4,5-triphenylpyrrole, 15.5; and for 2-amino-3,4,5-triphenylpyridine, 20.6.

ACKNOWLEDGMENTS

I am greatly indebted to former associates in the Research Laboratories of the Eastman Kodak Company: Mr. John Stenberg for the preparation of γ-benzoylbutyronitrile; Mr. G. P. Happ for the mass spectrometry; Miss Thelma Davis for the infrared spectra; Dr. T. H. Regan for the n.m.r. spectra; Dr. O. E. Schupp for the vapor phase chromatography;

Can. J. Chem. Downloaded from www.nrcresearchpress.com by 210.87.254.105 on 09/05/12
For personal use only.

and Mr. D. Ketchum and staff of the microanalytical department for the microanalyses. Dr. Robert Gilman of this laboratory carried out the thin-layer chromatography and Mr. E. Vasiliauskas prepared the phenylnitromethane and its adduct with chalcone.

REFERENCES

1. C. F. H. ALLEN and G. P. HAPP. Can. J. Chem. **42**, 641 (1964).
2. C. F. H. ALLEN and G. P. HAPP. Can. J. Chem. **42**, 650 (1964).
3. C. F. H. ALLEN and G. P. HAPP. Can. J. Chem. **42**, 655 (1964).
4. S. AVERY and G. R. MCDOLE. J. Am. Chem. Soc. **30**, 596 (1908).
5. J. MEISENHEIMER. Ber. **54**, 3206 (1921).
6. F. ANGELICO and E. CALVELLO. Gazz. **30**, II 268 (1900); Zentr. **72**, II 778 (1901).
7. E. P. KOHLER and C. F. H. ALLEN. J. Am. Chem. Soc. **46**, 1522 (1924).
8. F. H. CASE. J. Am. Chem. Soc. **68**, 2575 (1946).
9. J. WISLICENUS and F. H. NEWMANN. Ann. **302**, 236 (1898).
10. C. F. H. ALLEN. Can. J. Chem. **42**, 696 (1964).
11. C. F. H. ALLEN and W. L. BALL. J. Am. Chem. Soc. **59**, 686 (1937).
12. C. F. H. ALLEN, M. R. GILBERT, and D. M. YOUNG. J. Org. Chem. **2**, 227 (1937).
13. R. L. SHRINER, R. C. FUSON, and D. Y. CURTIN. The systematic identification of organic compounds. 5th ed. John Wiley and Sons, Inc., New York. 1964. p. 137.
14. E. P. KOHLER. J. Am. Chem. Soc. **46**, 1733 (1924).
15. E. P. KOHLER. J. Am. Chem. Soc. **38**, 892 (1916).
16. M. A. T. ROGERS. J. Chem. Soc. 590 (1943).
17. E. B. KNOTT. J. Chem. Soc. 1196 (1947).
18. M. I. LUR'E, I. S. TRUBNIKOV, N. P. SHUSHERINE, and R. I. LEVINA. J. Gen. Chem. USSR Engl. Transl. **28**, 1410 (1958).
19. J. J. SUDBOROUGH. J. Chem. Soc. **109**, 1347 (1916).
20. C. F. H. ALLEN. J. Am. Chem. Soc. **47**, 1733 (1925).
21. C. BARAT. J. Indian Chem. Soc. **7**, 321 (1930).
22. H. BUDZIKIEWICZ, C. DJERASSI, and D. H. WILLIAMS. Interpretation of mass spectra of organic compounds. Holden-Day, Inc., San Francisco, Calif. 1964. pp. 98, 99, 111–114.

Can. J. Chem. Downloaded from www.nrcresearchpress.com by 210.87.254.105 on 09/05/12
For personal use only.

Can. J. Chem. Downloaded from www.nrcresearchpress.com by 210.87.254.42 on 09/05/12
For personal use only.

INDEPENDENT YIELDS OF ^{124}Sb AND ^{126}Sb IN THERMAL NEUTRON INDUCED FISSION AND THEIR IMPLICATION ON THE EMPIRICAL Z_p FUNCTION

P. O. STROM,[1] G. R. GRANT,[2] AND A. C. PAPPAS
Department of Chemistry, University of Oslo, Oslo, Norway
Received March 22, 1965

ABSTRACT

The independent fission yields in thermal neutron induced fission of ^{235}U have been measured to be $(9.5 \pm 1.4) \cdot 10^{-6}\%$ and $(1.04 \pm 0.17) \cdot 10^{-3}\%$ for ^{124g}Sb and ^{126g}Sb, respectively. The total independent yields for all isomers of these nuclides are estimated to be $(1.2 \pm 0.2) \cdot 10^{-5}\%$ for ^{124}Sb and $(3.7 \pm 0.6) \cdot 10^{-3}\%$ for ^{126}Sb using a Huizenga–Vandenbosch approach for estimating population of isomeric states.

These data do not seem to support a 50 proton shell effect on the Z_p function, using the "unique" charge distribution curve of Wahl. A revised Wahl plot based on recent information on neutron emission from individual fission fragments is given and discussed in view of shell effects in fission. It is shown that the effect of the Z_p function of the 50 proton shell is very small.

INTRODUCTION

A study of the division of nuclear charge in fission requires determinations of independent yields of individual fission products preferably along single mass chains. Because of inherent difficulties in such measurements (genetic relationships between species concerned and short half-lives) our knowledge of the isobaric charge distributions in fission is quite scanty. However, in thermal neutron induced fission of ^{235}U Wahl *et al.* (1) have shown that in the limited number of cases (six) where more than one independent yield is known for a given mass chain the data indicate that the Gaussian relation

$$[1] \qquad P(Z) = (c\pi)^{-1/2} \exp\left[-(Z - Z_p)^2/c\right]$$

adequately represents isobaric charge distributions. In this equation $P(Z)$ is the fractional chain yield of the fission product Z and Z_p is the most probable primary charge in the chain under consideration.

While these authors have determined a best value 0.94 ± 0.15 for the constant c which allows a reasonable fit to the experimental data from the six mass chains studied (A = 91, 139–143), there may be no unique charge distribution function applicable to all mass chains as suggested by a number of authors (1–5).

A determination of the most probable primary charge for other mass chains is therefore subject to the uncertainties present in the postulates regarding the distribution itself. Despite this indeterminancy the results of measurements of independent and cumulative yields indicate (1) that the charge distribution along any given mass chain can reasonably well be represented by the Gaussian relation in eq. [1] or by a curve approximately Gaussian in character (2, 4).

On the assumption that the charge distribution curve given in eq. [1] is unique and applicable to all mass chains in thermal and low energy fission, Wahl *et al.* (1) were able

[1]*On leave 1963–1964 from the United States Naval Radiological Defense Laboratory, San Francisco, California, U.S.A.*

[2]*Postdoctorate Fellow 1961–1963 under the fellowship program of the Royal Norwegian Council for Scientific and Industrial Research. Present address: Whiteshell Nuclear Research Establishment, Atomic Energy of Canada, Ltd., Pinawa, Manitoba, Canada.*

to fix the most probable primary charge for any mass chain in which an independent yield or cumulative yield early in the chain was available.

To obtain the prompt masses (A') involved corrections for neutron emission from the primary fragments were necessary. These were estimated from experimental data on neutron emission as a function of prompt mass as corrected and correlated by Terrell (6). After a number of unsuccessful attempts to correlate their Z_p values with various charge distribution postulates (2, 4, 7) Wahl *et al.* (1) drew a smooth continuous Z_p function through the "experimental" values in their plot of the distribution of charge given by $[Z_p - A'(Z_f/A_f)]$ versus mass number A' before neutron emission, the fissioning nucleus being characterized by (Z_f, A_f). (Cf. Fig. 3.)

One important feature in their plot is the lack of data in the region $108 < A' < 128$. Thus it is very uncertain how the Z_p function behaves in this region. It seems, however, that the function may enter the region with a sharp rise near the 50 proton shell as indicated by the high independent yield of ^{128}I (8). Such a tendency was previously suggested also by Wahl (5) on the basis of low independent yields of ^{96}Nb and ^{98}Tc. On the other hand the function $[Z_p - A'(Z_f/A_f)]$ may presumably equal zero at the point of symmetry, i.e. $A' = 118$ for ^{235}U(th,f).

The kinetic energy distribution resulting from thermal neutron induced fission has been carefully reinvestigated by Milton and Fraser (9). Two possible ways of explaining the observed dip near symmetric fission in the kinetic energy distribution were discussed by these authors. One of these is based on the assumption that the total excitation energy is nearly constant for all fission fragments and then attribute the decrease in kinetic energy to a decrease in energy release caused by unfavorable splitting of the charge of the fissioning nucleus. Following this idea the kinetic energy measurements would give Z_p values which at no time should fall below the 50 proton shell for the heavy fragment, thus eventually leading to a 50 proton shell effect on Z_p much stronger than anticipated by Wahl *et al.* (1). In view of such ideas and the uncertainty of the "experimental" Z_p function in this region it was desirable to measure independent yields in the mass region 108 to 128. This is rather difficult, however, because of extremely low yields and highly complicated genetic relationships for the nuclides concerned. But, one possibility suggested itself in 1962 when Dropesky and Orth (10) found that ^{126}Sb is "quasi-shielded" by its tin parent, the $\sim 10^5$ y ^{126}Sn.

In a preliminary run using natural uranium and designed to give a measure of the independent yield of the 12.5 d ^{126g}Sb, the 60 d ^{124g}Sb was also observed. Since ^{124}Sb is a shielded nuclide ^{124g}Sb must have been produced either independently in fission or from neutron capture in ^{123}Sb from antimony impurity in the target. The experiments in the present paper were therefore designed to eliminate or to correct, as much as possible, for the contribution to ^{124g}Sb from sources other than fission.

EXPERIMENTAL

Irradiations

Natural uranium (sample no. 1), uranium enriched to 19.9% ^{235}U (sample no. 2), both in the form of UO_3 (respectively 800 mg and 25 mg), uranium enriched to 93.3% ^{235}U[3] (samples nos. 3 and 4) in the form of U_3O_8[4] ($\sim$ 10 mg), together with blank samples (quartz ampoules) were irradiated with thermal neutrons[5] in order to minimize possible adverse effects from fast neutrons on the measurements. The flux (constant within $\pm$10%) was approximately $2 \cdot 10^{12}$ thermal neutrons/cm^2 s and the cadmium ratio was

[3]*The amount of other uranium isotopes in this target was: 1.1% ^{234}U, 0.2% ^{236}U, and 5.4% ^{238}U.*

[4]*The samples enriched in ^{235}U were highly purified and obtained from the U.S. National Bureau of Standards, Washington, D.C.*

[5]*The irradiations were performed in the thermal column of the DR-2 reactor of the Danish Atomic Energy Commission, Risø.*

Can. J. Chem. Downloaded from www.nrcresearchpress.com by 210.87.254.42 on 09/05/12
For personal use only.

close to 50. The blank samples were irradiated under the same conditions and subjected to the same chemical treatment as the samples themselves. During the irradiations, which lasted from 1 to 2 weeks, the reactor was operated intermittently. This was taken into consideration as described later. After the irradiation the ampoules were allowed to "cool" for about 1 month prior to radiochemical separations.

Radiochemical Separations

The irradiated target was dissolved in 2 ml of conc. HCl and 1 drop of H_2O_2. The solution was heated to boiling. The quartz ampoule was removed and washed with 7 ml H_2O. A known amount of antimony carrier was added and Sb^{+3} oxidized to Sb^{+5} using several drops of Br_2. After excess Br_2 was expelled by boiling, Sb^{+5} was reduced to Sb^{+3} with $N_2H_4 \cdot HCl$. Saturated oxalic acid (1.5 ml) was added, followed by 1 drop of aerosol solution and 2 ml of 5% thioacetamide to precipitate Sb_2S_3. Heating (water bath) promoted coagulation of the precipitate which was then centrifuged and washed twice with dilute HCl. Two different procedures were then followed:

A. In samples 1 and 2 the Sb_2S_3 was dissolved in 1 ml of conc. H_2SO_4, adding a few drops of HNO_3, and excess HNO_3 removed by fuming. Antimony was further purified as stibine using a procedure similar to that given by Greendale and Love (11).

B. In samples 3 and 4 the Sb_2S_3 was dissolved by boiling with 4 ml of conc. HCl. Antimony was then further purified following essentially the method given by Barnes (12) based on specific sulfide precipitations, alternated with purification steps.

In both procedures antimony was finally converted to metal by reduction with a freshly prepared solution of $CrCl_2$. It was filtered onto a pretreated, weighed filter paper, washed with water and absolute methanol, then dried for $\frac{1}{2}$ h at 100 °C, cooled, and weighed to determine the chemical yield. The samples were then mounted in a standard way. The chemical yield was checked after the decay of the samples through the use of the spectrophotometric determination with rhodamine B given by Greenhalgh and Riley (13).

The 12.80 d ^{140}Ba with a fission yield of 6.35% (14) served as fission monitor. Barium was isolated by following essentially the method described by Minkhinen (15) and mounted as chromate. The chemical yield was determined by weighing.

Counting

The final samples were counted using a methane flow β-proportional counter similar to that described by Forsén and Rydberg (16). An Oltronix power supply (type LS 28) was used for the detector high voltage and a Baird-Atomic preamplifier (model 255) fed a Philips electronic counter (model PW 4032). The samples were also studied using an Intertechnique 400 channel γ-pulse height analyzer with a $2\frac{1}{2}$ in. × 3 in. Harshaw thallium-activated sodium iodide crystal.

Nuclides Present

The antimony isotopes (with their decay products) which were present in the samples counted were:

1. ^{127}Sb, which is unshielded and is formed in relatively high yield. It had, however, decayed substantially during the approximate 1 month "cooling" time prior to the isolation of antimony.

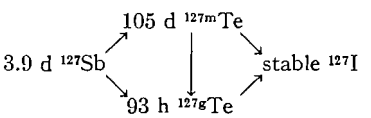

2. ^{126}Sb, which at formation consists of two "quasi-shielded" isomers of which only the 12.5 d ^{126g}Sb was present in the counted samples. The decay scheme reported by Dropesky and Orth (10, 17) is given in Fig. 1.

$$12.5 \text{ d } {}^{126g}\text{Sb} \rightarrow \text{stable } {}^{126}\text{Te}$$

3. ^{125}Sb, which is not shielded. Therefore the majority of the mass 125 chain yield was present.

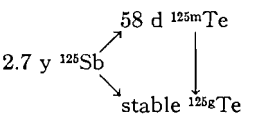

4. ^{124}Sb, which is shielded and formed as three isomers of which only the 60 d ^{124g}Sb was present in the counted samples. The decay scheme reported by Vanhorenbeeck (18) is given in Fig. 2.

$$60 \text{ d } {}^{124g}\text{Sb} \rightarrow \text{stable } {}^{124}\text{Te}$$

The β-counting was done through a 55.3 mg/cm^2 aluminium absorber (total absorption thickness $\sim$ 60 mg/cm^2 including source cover, air, and counter window). This reduced appreciably the weak β-rays from ^{125}Sb, ^{127m}Te, and ^{127g}Te, and absorbed completely the conversion electrons from ^{125m}Te and ^{127m}Te. The hard β-branches from ^{124g}Sb and ^{126g}Sb were relatively unaffected by the absorber.

Can. J. Chem. Downloaded from www.nrcresearchpress.com by 210.87.254.42 on 09/05/12
For personal use only.

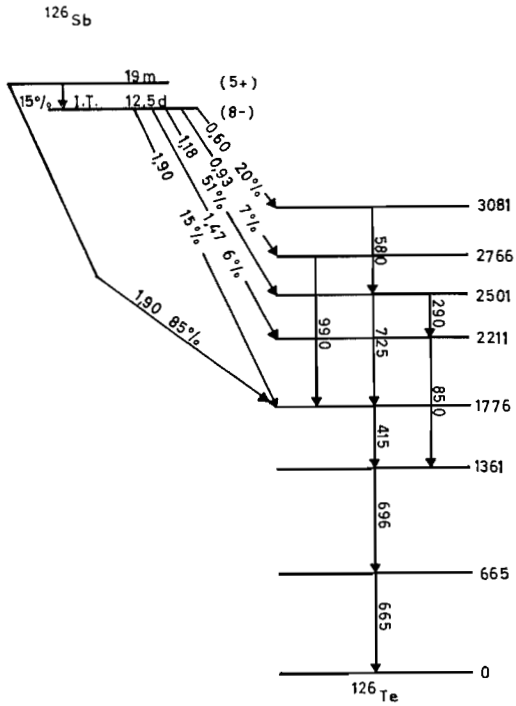

FIG. 1. Decay scheme of ^{126}Sb from ref. 17.

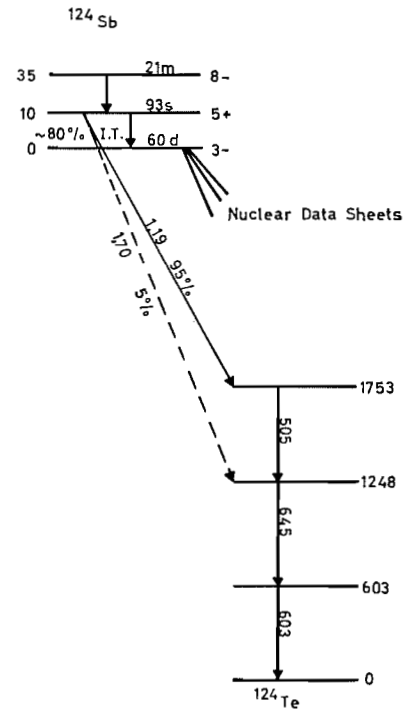

FIG. 2. Decay scheme of ^{124}Sb from ref. 18.

Can. J. Chem. Downloaded from www.nrcresearchpress.com by 210.87.254.42 on 09/05/12
For personal use only.

Gamma spectra taken 50 days after the end of irradiation showed peaks at 0.175, 0.427, and 0.595 MeV almost entirely due to 2.7 y ^{125}Sb. Peaks at 1.15, 1.42, 1.85, and 2.15 MeV were attributed to ^{126g}Sb, as these decayed with a half-life of about 12 days. Herrmann (19) has reported sum peaks at 1.12 and 1.41 MeV for this nuclide and it seems likely that the peaks at 1.85 and 2.15 MeV also are sum peaks; however, this was not explicitly checked. Gamma spectra taken 150 days after the end of irradiation showed besides lines due to 2.7 y ^{125}Sb peaks at 1.37, 1.69, 2.08, and 2.3 MeV in accordance with the γ-spectrum of a pure sample of 60 d ^{124g}Sb.

No contamination could be detected either in the γ-spectra or in the β-decay curves. The half-lives observed are (12.1 $\pm$ 0.3) d for ^{126g}Sb and (3.9 $\pm$ 0.2) d for ^{127}Sb. These are in accordance with the values (12.5 $\pm$ 0.2) d and (3.87 $\pm$ 0.07) d reported by Dropesky and Orth (10).

Determination of Counting Efficiencies

^{124g}Sb.—This nuclide was produced by thermal neutron irradiation of about 15 mg of "specpure" $SbCl_3$. Two months "cooling" time removed the short-lived isomers of ^{122}Sb (3.5 min, 2.8 d), ^{124}Sb (21 min, 93 s), and ^{38}Cl (1 s, 37.3 min). The remaining activity was almost entirely due to ^{124g}Sb as that of ^{36}Cl ($3 \cdot 10^5$ y) could be considered as negligible. From a 250 ml stock solution of ^{124g}Sb, samples for low geometry β-counting were prepared by adding aliquots (25 λ) to known amounts of Sb^{+3} and subsequent quantitative antimony metal precipitation as previously described. These samples were counted in the proportional counter both with and without the 55.3 mg/cm^2 aluminium absorber. In addition aliquots (25 λ) were pipetted onto gold-coated VYNS films, dried, and counted in a $4\pi\beta$ counter and the counting efficiencies obtained. The determinate error was found to be about $\pm 1\%$. Indeterminate errors, however, associated with nonuniform sample thickness in particular, were such that an error of about $\pm 10\%$ is considered more realistic.

The counting efficiency was also determined for the γ-pulse height analyzer using the 1.69 MeV γ-peak with background subtracted. This efficiency was found by comparing the counts under the peak with the number of disintegrations, over the same time period, in the sample when this was counted in the $4\pi\beta$ counter. The estimated error (largely indeterminate due to the background subtraction) is about $\pm 10\%$.

^{126g}Sb.—The counting efficiency for this nuclide was calculated from the relation

$$[2] \qquad \epsilon = \sum_i (f_B)_i (f_M)_i (f_{SA})_i (f_{AB})_i (f_\beta)_i G$$

where G is the geometry used. The correction factors for backscattering f_B, mylar absorption f_M, self-scattering and self-absorption f_{SA}, for absorber, air, and window f_{AB}, were taken from Pappas (3), Rudstam (20), and Buset (21). The fractions of total β-emission f_β were taken from Dropesky and Orth (17) and the summation carried out over all β-branches i. The error estimated in this efficiency is $\pm 10\%$.

^{140}Ba.—Since ^{140}La grows in the ^{140}Ba samples, the counting efficiency of ^{140}La was first measured in a matrix of $BaCO_3$ in a way similar to that described for ^{124g}Sb using a stock solution made up of thermal neutron irradiated "specpure" La_2O_3. With standard parent–daughter equations the counting efficiency for ^{140}Ba could be calculated from the activity of the ^{140}Ba samples measured at different times after separation from lanthanum. The error in the efficiency so obtained is estimated to be $\pm 10\%$. The counting efficiency of ^{140}Ba was also calculated using eq. [2] and data from ref. 3 in good agreement with the results from the more direct determination.

RESULTS

The number of atoms N, of a fission product with essentially no ("quasi-shielded") or entirely no (shielded) growth from parent activities or of one with short-lived precursors, present at the end of an intermittent irradiation is given by

$$[3] \qquad N = \sum_{j=1}^{n} \frac{y\phi N_{235}\sigma}{\lambda} [1 - \exp(-\lambda T_j)] \exp(-\lambda t_j)$$

where y = independent or cumulative yield, ϕ = thermal neutron flux, N_{235} = number of atoms of ^{235}U in the target, σ = thermal neutron fission cross section of ^{235}U, λ = decay constant, T_j = duration of the jth irradiation, and t_j = elapsed time from the end of the jth irradiation to the end of all irradiations.

The summation is carried out over all irradiation periods, n.

The Number of Fissions in the Samples

The decay of the 12.8 d ^{140}Ba – 40 h ^{140}La couple was followed for about 80 days. The number of atoms N_{Ba} of ^{140}Ba present at the end of the irradiation was found from the

Can. J. Chem. Downloaded from www.nrcresearchpress.com by 210.87.254.42 on 09/05/12
For personal use only.

observed activity through use of standard parent–daughter equations and the efficiencies determined for ^{140}Ba and ^{140}La. The total number of fissions F

$$[4] \qquad F = \phi N_{235}\sigma \sum_{j=1}^{n} T_j$$

in the sample is obtained by equating N_{Ba} to N in eq. [3] when this refers to ^{140}Ba. One finds

$$[5] \qquad F = N_{Ba}/C$$

where C is a constant characteristic for each irradiation, given by

$$[5a] \qquad C = \sum_{j=1}^{n} y_{Ba}[1 - \exp(-\lambda_{Ba}T_j)] \exp(-\lambda_{Ba}t_j) \Big/ \lambda_{Ba} \sum_{j=1}^{n} T_j.$$

The determinate error in the number of fissions is $\pm 10\%$.

Independent Yield of ^{124g}Sb

Because of the relatively low β-activity of ^{124g}Sb caused by the use of the absorber, the 60 d half-life could not easily be resolved in the long-lived tail of the β-decay curve. The number of atoms of ^{124g}Sb present at the end of irradiation was therefore determined by γ-ray spectroscopy. This was done by measuring the 1.69 MeV γ-ray associated with its decay, using the efficiency determined above and correcting for chemical yield. The atoms present at the end of irradiation are given in Table I for samples 3 and 4, i.e. those from targets with 93.3% ^{235}U in the uranium.

TABLE I

Contribution to ^{124g}Sb from different sources

	Sample	
	3*	4
Atoms at end of irradiation	$8.00 \cdot 10^7$	$3.55 \cdot 10^8$
Atoms due to Sb in target	$<1.6 \cdot 10^5$	$<7.0 \cdot 10^5$
Atoms due to Sb in ampoule	$1.7 \cdot 10^6$	$8.3 \cdot 10^6$
Atoms due to fission in ^{235}U	$7.81 \cdot 10^7$	$3.46 \cdot 10^8$

*Only about 20% of the target was used for this study.

The values given in Table I represent the atoms actually present in the samples, but might not all be due to fission of ^{235}U as the following processes could have influenced the results.

^{124g}Sb$(n,\gamma)^{125}$Sb. According to Murin *et al.* (22) the capture cross section for thermal neutrons in ^{124g}Sb is about 2 000 barns, while Regier (23) reports 16 barns. The conditions of the present experiments were, however, such that the influence of such a high cross section as suggested in ref. 22 would be quite negligible.

^{123}Sb$(n,\gamma)^{124g}$Sb. This reaction will take place in a possible antimony impurity in the target and might therefore significantly influence the results. Sufficiently sensitive equipment was not available to measure the low concentrations of antimony which would cause difficulties. Therefore targets with increasing enrichment in ^{235}U were used as it was expected that the enrichment procedure would remove antimony. This is borne out by the decreasing "apparent" fission yield of ^{124g}Sb with increasing enrichment of ^{235}U in the target as seen from Table II. The maximum amount of antimony impurity in uranium purified in a tributyl phosphate – hexane extraction system is less than 0.01

Can. J. Chem. Downloaded from www.nrcresearchpress.com by 210.87.254.42 on 09/05/12
For personal use only.

p.p.m. based on uranium according to Nelson and Lang (24). If one makes the very conservative assumption that this limit represents the amount of impurity in the highly purified targets with 93.3% ^{235}U one should be on the safe side. The resulting corrections are given in Table I and amount to only about 0.2%.

^{124}Te(n,p)^{124}Sb and ^{127}I(n,α)^{124}Sb. The average cross sections for these reactions in a fission neutron spectrum have been estimated by Roy and Hawton (25) to be 70 μbarns and 2.6 μbarns, respectively. In the present irradiations, however, where the cadmium ratio was about 50 in the region of exposure the average cross sections should be much smaller. On the basis, however, of the above cross sections the concentrations of tellurium and iodine impurities required to obtain an amount of ^{124g}Sb comparable with that from an antimony impurity of the order discussed above, would be of the order of 10^3 to 10^4 p.p.m. These are orders of magnitude higher than those reported as prominent impurities in uranium purification. Thus, charged particle reactions are considered to be without influence on the results.

Other sources. The quartz ampoules used as target containers were handled as little as possible prior to irradiation. To remove volatile material, they were heated at 500 °C for 3/4 h just before addition of the target material and heat sealing. Blank samples were also irradiated and the number of atoms of ^{124g}Sb produced in the ampoules measured. A correction of about 2% was necessary in the number of atoms of ^{124g}Sb from the highly enriched targets (Table I). Thus all foreseeable corrections amount to only 2 to 3% in the results from the highly enriched targets. Using the corrected values for the number of atoms present at the end of irradiation (Table I) the fission yields obtained are given in Table II for samples 3 and 4.

The results for samples 1 and 2, natural uranium and 19.8% enriched in ^{235}U, are, as seen, seriously influenced by contamination. Only samples 3 and 4 are therefore used in the average value. The error is estimated to be ±15%. The yield given $(9.5 \pm 1.4)\cdot 10^{-6}$% is "apparent" independent yield as it includes parts of the yields of the higher isomeric states (cf. Fig. 2).

TABLE II

Apparent independent fission yields of ^{124g}Sb and ^{126g}Sb

Sample	^{235}U (%)	^{124g}Sb (%)	^{126g}Sb (%)
1	0.72	$1.35\cdot 10^{-4}$	$0.91\cdot 10^{-3}$
2	19.9	$0.55\cdot 10^{-4}$	$0.88\cdot 10^{-3}$
3	93.3	$9.3\cdot 10^{-6}$	$1.11\cdot 10^{-3}$
4	93.3	$9.6\cdot 10^{-6}$	$1.23\cdot 10^{-3}$
Average*		$(9.5\pm 1.4)\cdot 10^{-6}$	$(1.04\pm 0.18)\cdot 10^{-3}$

*For ^{124}Sb see text.

Independent Yield of ^{126g}Sb

The activity of ^{126g}Sb at the end of irradiation was obtained by analytical extrapolation of the β-decay curve observed through the aluminium absorber after subtraction of the long-lived background due to 2.7 y ^{125}Sb and 60 d ^{124g}Sb. The amount of the latter was estimated from the 1.69 MeV γ-peak using the appropriate conversion factor for counting efficiency determined above.

The only non-fission reaction which would influence the number of atoms of ^{126g}Sb present at the end of the irradiation would be:

^{126}Te(n,p)^{126}Sb in tellurium impurity in the target. The average cross section for this

Can. J. Chem. Downloaded from www.nrcresearchpress.com by 210.87.254.42 on 09/05/12
For personal use only.

reaction in a fission neutron spectrum is estimated by Roy and Hawton (25) to be 20 μbarns. Thus the same arguments as used in connection with ^{124g}Sb are applicable and result in a negligible influence of charged particle reactions.

The calculated fission yield is given in Table II. The error is estimated to be ±18%. This yield $(1.04 \pm 0.18) \cdot 10^{-3}\%$ is given also as "apparent" yield for the same reasons as stated in connection with ^{124g}Sb (cf. Fig. 1).

The independent yield of ^{126g}Sb has, during the course of the present investigation, also been measured by Lange and Herrmann (26) who found $(0.90 \pm 0.25) \cdot 10^{-3}\%$. Thus the results from the two groups are in excellent agreement.

DISCUSSION

Estimate of Total Independent Yields of ^{124}Sb and ^{126}Sb (All States)

Both ^{124}Sb and ^{126}Sb have isomeric states with branched decay (Figs. 1 and 2). Therefore, to obtain the total independent fission yields of these nuclides from the measured "apparent" yields knowledge of the manner in which the different isomeric states are populated is required. The ground state of ^{124}Sb has a spin 3 (measured) and negative parity (27). On the basis of careful decay scheme studies Vanhorenbeeck (18) assigns spin and parity 8− to the upper (21 min) state and 5+ to the intermediate (93 s) state. These assignments are supported by the second rule given by Brennan and Bernstein (28) for spin coupling in odd–odd nuclei. For ^{126}Sb Dropesky and Orth (17) assign 8− for the ground (12.5 d) state and 5+ for the upper (19 min) state, based on careful decay scheme studies. The Brennan–Bernstein rule (28), however, is not decisive in this case and predicts 3 or 8 for the ground state, but these should form a closely spaced doublet as in ^{124}Sb. According to Dropesky and Orth (17) the 3− state probably exists as an excited level above the 19 min isomer.

The statistical model of Huizenga and Vandenbosch (29, 30) has been used to estimate the population of states in the isomers concerned as follows:

On the basis of correlation studies of fission fragments and prompt γ-rays from thermal neutron induced fission in ^{235}U, Hoffman (31) concludes that the observations indicate an average angular momentum in fission fragments (after neutron emission) of 6 to 8 units. The initial angular momentum distribution required to account for observed isomer ratios in fission has been calculated by Warhanek and Vandenbosch (32) using the Huizenga–Vandenbosch model (29, 30). Basing their calculations on the measured ratio of the ^{134}Cs isomers and assuming that the primary fragments have an angular distribution of the following form

$$[6] \qquad N(J) = (2J + 1) \exp\left[- \frac{J(J + 1)}{2b^2} \right]$$

they obtain a value of about 7.4 for the root mean square angular momentum

$$\sqrt{(\overline{J^2})} = b\sqrt{2}.$$

In connection with the present problem it should be kept in mind that the number of neutrons emitted from the prompt fragments leading to ^{124}Sb, ^{126}Sb, and ^{134}Cs is about the same (6, 9) and that the results of Warhanek and Vandenbosch (32) show very little difference if 1 or 2 neutrons are assumed to be emitted. Furthermore, the nuclides considered are all of the same nuclear type (odd–odd) and the spins involved very similar. Those of ^{134}Cs are measured as 4 and 8 for the ground and excited state, respectively (27).

Hoffman (31) has, however, also shown that one should expect the angular momentum

Can. J. Chem. Downloaded from www.nrcresearchpress.com by 210.87.254.42 on 09/05/12
For personal use only.

of prompt fragments to increase with their kinetic energy. The latter is somewhat higher in the 134 mass region than in the region of interest for the present work. Therefore it is probably reasonable to assume that the prompt fragments leading to ^{124}Sb and to ^{126}Sb have an angular distribution characterized by $\sqrt{(\overline{J^2})} = 6.5$. One neutron with energy 1 MeV is assumed to be emitted from these fragments.

The probability of a state with angular momentum J_c to emit a neutron with orbital angular momentum l and energy E leading to a final state J_t is expressed by (30):

$$[7] \qquad P(J_t) \propto \rho(J_t) \sum_{S=|Jt-\frac{1}{2}|}^{J_t+\frac{1}{2}} \sum_{l=|Jc-S|}^{J_c+S} T_l(E).$$

The barrier transmission coefficient $T_l(E)$ for a 1 MeV neutron with angular momentum l is taken from the curves by Feld *et al.* (33). $\rho(J_t)$ is the density of levels with spin J_t, given by

$$[8] \qquad \rho(J_t) = \rho(0)(2J_t + 1) \exp\left[-(J_t + \tfrac{1}{2})^2/2\sigma^2\right]$$

where $\rho(0)$ is the density of levels with zero spin. The parameter σ characterizes the distribution function and the value of $\sigma = 3$ was chosen as this is known to give a reasonable fit to experimental data (30).

In accordance with Warhanek and Vandenbosch (32) it is expected that the fragments decay either to high or low spin states predominantly by dipole radiations and that the number of γ-rays emitted will be between 2 and 3. Therefore, in the present calculations two dipole radiations followed by a third γ-ray are assumed to take place, the latter having the lowest multipolarity necessary to reach the final state concerned. The relative probability for a nucleus with spin J to decay by dipole radiation to states with spin $J - 1$, J, and $J + 1$ is given by the level density factor in eq. [8].

The computer programme given by Hafner, Huizenga, and Vandenbosch (34) for calculating isomer yield ratios was used. The distribution to be expected after emission of one neutron and two γ-rays is given in Table III. The third and final γ-emission is then assumed to populate the states in the final isomers as follows:

TABLE III

Distribution of states after emission of one 1 MeV neutron and two dipole radiations from an initial distribution characterized by $\sqrt{(\overline{J^2})} = 6.5$

	Final spin						
	0–2	3	4	5	6	7	8–13
Probability of state being populated	0.05	0.11	0.25	0.32	0.12	0.08	0.07

A state in Table III *exactly* half-way between two final states is assumed to populate both to the same amount. All other states in Table III are assumed to populate the closest final state. The populations thus obtained are given in Table IV.

If one takes into consideration the branched decays of the isomeric states (Figs. 1 and 2) the amount of ^{124}Sb counted as the long-lived isomer ^{124g}Sb is 0.82. For ^{126}Sb one finds that 0.28 is counted as ^{126g}Sb.

The total independent yields thus obtained are given in Table V. In the values given the uncertainty in branching and population of states is indeterminate for both species.

Can. J. Chem. Downloaded from www.nrcresearchpress.com by 210.87.254.42 on 09/05/12
For personal use only.

TABLE IV

Population of isomeric states in ^{124}Sb and ^{126}Sb
(g = ground state, m = metastable state)

State	^{124}Sb	^{126}Sb
3−	0.28 g	
5+	0.57 m_1	0.85 m
8−	0.15 m_2	0.15 g

TABLE V

Total independent fission yields of ^{124}Sb and ^{126}Sb

	Nuclide	
	^{124}Sb	^{126}Sb
Independent yield (%)	$(1.16\pm0.17)\cdot10^{-5}$	$(3.72\pm0.61)\cdot10^{-3}$
Chain yield (%)	$1.7\cdot10^{-2}$	0.10
Fractional independent yield	$(6.8\pm1.0)\cdot10^{-4}$	$(3.7\pm0.6)\cdot10^{-2}$

The Z_p Function

The cumulative yields for mass chains 124 and 126 are respectively $1.7\cdot10^{-2}$% and 0.10% (14). With these values the fractional independent fission yields of ^{124}Sb and ^{126}Sb (all isomers) are obtained and given in Table V. Assuming that the empirical charge distribution curve given by eq. [1] also is valid in this mass region one obtains:

$$Z_p = 48.49 \pm 0.20 \text{ for } A = 124$$

$$Z_p = 49.39 \pm 0.14 \text{ for } A = 126.$$

The limits reflect either the uncertainty in the constant c in eq. [1] or the errors assigned to the independent yields, whatever has the largest effect. The prompt masses A' corresponding to final masses A are obtained by use of the "smoothed" equations given by Wahl *et al.* (1) for the neutron emission from a fission fragment as a function of final mass. This has the following form for the heavy fragments:

[9] $$\nu_h = 0.531\nu + 0.062(A_h - 143).$$

Using $\nu = 2.50$ as the total number of neutrons emitted in thermal neutron fission of ^{235}U, one obtains

$$A_{124}' = 124.2 \text{ and } A_{126}' = 126.3.$$

Recently Troutner, Wahl, and Ferguson (35) have been able to measure the fractional independent yield of the 3.9 d ^{127}Sb and report a value $(5.7 \pm 1.0)\cdot10^{-2}$. The most probable primary charge is therefore $Z_p = 49.5 \pm 0.1$ for $A' = 127.3$.

In Fig. 3 these new data are plotted in the Wahl type of plot. All previously known data (1) are included, but limits given only to the new values. The solid curve represents the empirical Z_p function as given by Wahl *et al.* (1).

The information available in 1962 on the most probable primary charge evaluated from independent and cumulative fission yields indicated that the empirical Z_p function might follow the $Z = 50$ line and thus be strongly influenced by the closed shell of 50 protons (1). A greater preference in fission for isotopes of Sn ($Z = 50$) rather than for low Z elements could be one of two possible explanations to the observed minimum in the total kinetic energy distribution of fission fragments in near symmetric fission (9).

Can. J. Chem. Downloaded from www.nrcresearchpress.com by 210.87.254.42 on 09/05/12
For personal use only.

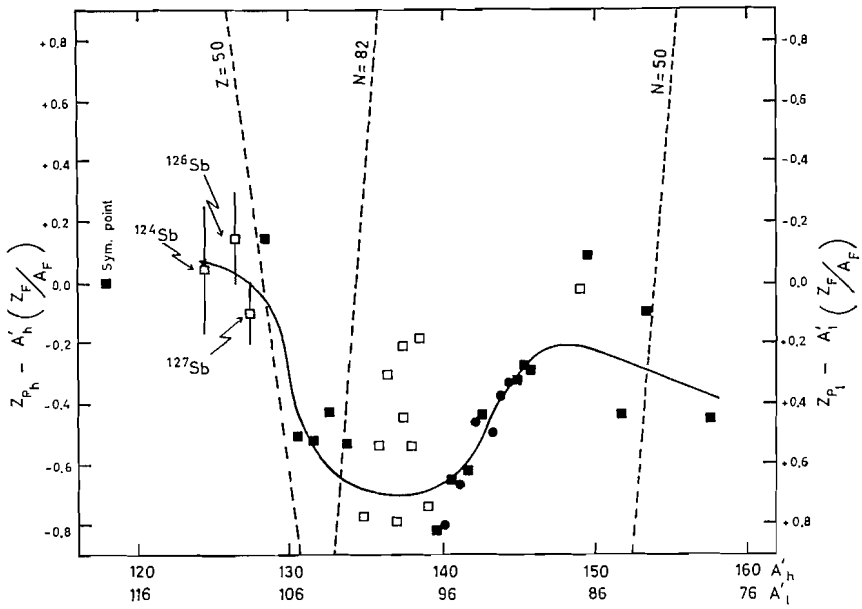

FIG. 3. Wahl plot including data for ^{124}Sb, ^{126}Sb (this work), and ^{127}Sb (35): ● = based on two or more fractional yield values; ■ = based on fractional yield of one fission product not close to a shell edge; □ = based on fractional yield of one fission product within ±1 charge or neutron number of a major closed shell or its complement.

Preference for a 50 proton shell effect might also be drawn from other experimental evidence, as discussed in the paper by Wahl *et al.* (1).

The aim of this investigation was to obtain additional information on this question by "measuring" Z_p values in the region of interest. According to the data plotted in Fig. 3, however, it seems unlikely that the 50 proton shell has as large an effect on the Z_p function as earlier suggested. The Z_p function seems to cross the $Z = 50$ line at a rather high mass number ($A' \sim 128$).

Before proceeding further in the discussion, however, attention should be drawn to an important point in the presentation of the data where our knowledge today is much more detailed than in 1962. This concerns the average number of neutrons emitted from individual fission fragments. As these enter strongly in the $[Z_p - A'(Z_t/A_t)]$ function the results in Fig. 3 might be considerably changed in a more detailed study.

On the basis of the data presented by Terrell (36) and his suggestion that neutron emission is primarily a function of fragment mass and not of mass ratio, Milton and Fraser (9) gave a neutron emission curve applicable to all fissioning nuclei. These authors have quite recently (37) also given further evidence for the general applicability of this curve. The curve is replotted in Fig. 4 for neutron emission as a function of residual mass A. In the same figure are also drawn the functions (linear) used by Wahl *et al.* (1). The latter was based on the overall trend of the neutron emission data, but as can be seen there are in reality large local deviations. The largest deviation is found in the mass region 112 to 130, i.e. just in the region where proton shell effects are discussed. It should, however, be pointed out that the original Milton–Fraser curve was interpolated in this region, but that recent measurements by Apalin *et al.* (38) have proved this proper and heavily supports the curve as drawn in Fig. 4.

Can. J. Chem. Downloaded from www.nrcresearchpress.com by 210.87.254.42 on 09/05/12
For personal use only.

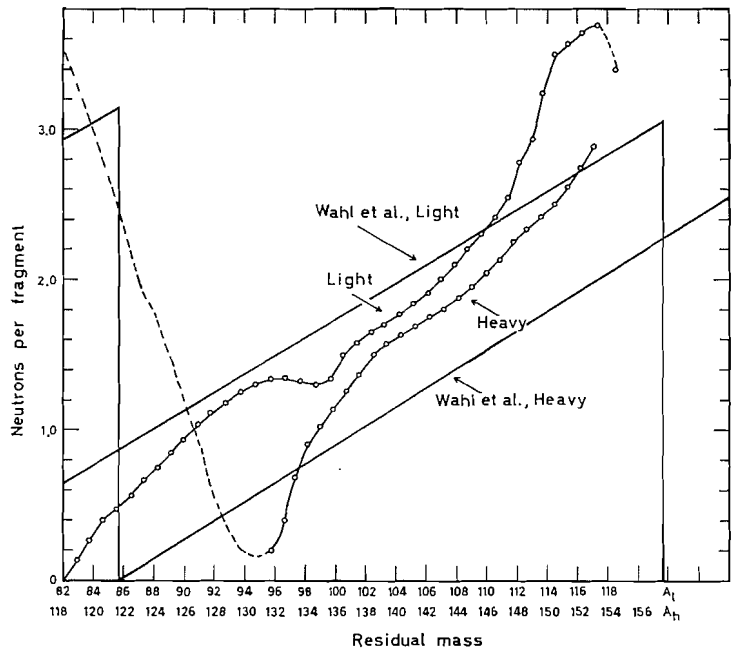

FIG. 4. Neutron emission as function of residual mass, adapted from ref. 9.

The empirical Z_p values from ref. 1 together with the additional values are replotted in Fig. 5, where the solid line A represents the Z_p function from ref. 1 (cf. Fig. 3). The general trend does not seem to have changed at high mass ratios (to the right of the $N = 82$ line). But the new curve rises from its minimum around mass ratio 1.4 more sharply than the old one as if it is "feeling" the approach of the $Z = 50$ shell. This does, however, not last long. At mass ratio 1.3 the curve turns and breaks through the 50 shell (around mass ratio 1.2) whereafter it seems to be heading towards the point of symmetry. Thus it should be concluded that there seems to be a rather limited effect of the 50 proton shell on the Z_p curve.

Therefore the dip in the kinetic energy distribution near symmetric fission should not be explained by a 50 proton shell effect, but should be sought in the large amount of energy going into excitation energy in near symmetric fission fragments, resulting in the emission of a large number of neutrons from these fragments as also observed by Apalin *et al.* (38). This explanation was also given as an alternative by Milton and Fraser (9); however, while this paper was being written (1964), they chose the latter alternative and abandoned the 50 proton shell effect (39).

The conclusions, arrived at in the present study, are supported by the recent determination of the fractional independent yield of ^{121}Sn measured by Wahl and Nethaway (40), 0.07 ± 0.10 or ≤ 0.17. These authors conclude that the value of Z_p is definitely less than 50, thus no proton shell effect seems present at such low masses as $A = 121$.

The discoverers of the double closed shell nuclide $^{132}_{50}Sn_{82}$, Pappas and Wiles (41) and others, expected this nuclide to be especially favored in the fission act due to its special structure. The Z_p value 51.26 reported by Wahl *et al.* (1) for mass number 132 does not seem to support this view. The independent yield, however, used in ref. 1 for estimating Z_p is that for ^{132}Te as reported by Pappas (3), obtained as the difference between measured

Can. J. Chem. Downloaded from www.nrcresearchpress.com by 210.87.254.42 on 09/05/12
For personal use only.

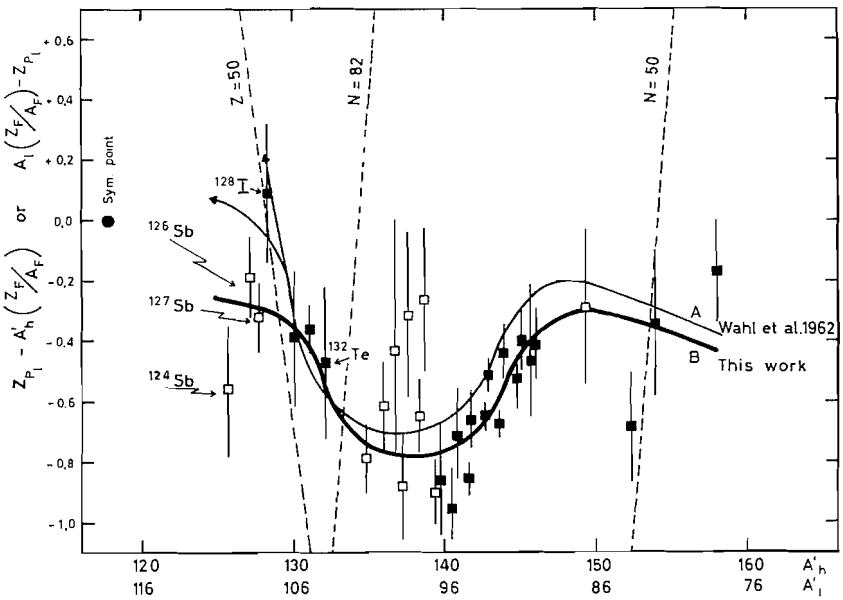

FIG. 5. Revised Wahl plot of empirical Z_p values: ■ = based on fractional yields of fission products not close to a shell edge; □ = based on fractional yield of one fission product within ±1 charge or neutron number of a major closed shell or its complement.

cumulative yields of ^{132}Te and ^{132}Sb. While it was possible in ref. 3 to measure the former to a high degree of accuracy, the latter could only be measured very crudely to ≈ 3%. Improved measurements of the cumulative yield of ^{132}Sb (i.e. cumulative yield of ^{132}Sn and independent yield of ^{132}Sb) are now made available through measurements by Greendale *et al.* (42) who report 3.4 ± 0.4%. With this value together with the chain yield for 132 the corrected fractional independent yield for ^{132}Te is 0.23 ± 0.09. On this basis a value of Z_p = 51.0 ± 0.3 is obtained for mass number 132 (prompt mass 132.2) in agreement with the curve drawn in Fig. 5.

In recent studies Greendale *et al.* (42) have been able to measure the cumulative yield of ^{132}Sn and the independent yields of ^{132}Sb and ^{132}Te. These three values are not inconsistent with the "unique" charge distribution curve of Wahl, but substantially narrower than the empirical curve (2) previously often used in charge distribution studies. As no perturbations are disclosed in the 132 mass chain no effect of double closed shell is indicated.

This leads to the point in Fig. 5 representing ^{128}I, the only nuclide with a strong indication of a 50 proton shell effect. The fact, however, that ^{128}I possesses high independent yield in thermal fission of ^{233}U, ^{235}U, and ^{239}Pu (8) supports an exceptional behavior of this nuclide; a behavior which needs further investigation, as the probability of variations in the width of the charge distribution curve might be especially high in the vicinity of the 50 proton – 82 neutron shell. Conceivably the charge distribution curve may even lack symmetry in this region. In this connection it should be realized that it is just those nuclides that have a nuclear composition within one proton or neutron number removed from a major nuclear closed shell or its complement (indicated by open squares in Fig. 5) that show the greatest scatter in the Wahl type of presentation. This is very likely more than just coincidence.

Can. J. Chem. Downloaded from www.nrcresearchpress.com by 210.87.254.42 on 09/05/12
For personal use only.

Can. J. Chem. Downloaded from www.nrcresearchpress.com by 210.87.254.42 on 09/05/12
For personal use only.

ACKNOWLEDGMENTS

The authors are indebted to Dr. G. Herrmann of the Johannes Gutenberg Universität, Drs. D. L. Love and A. E. Greendale of the U.S. Naval Radiological Defense Laboratory, Dr. J. C. D. Milton of the Atomic Energy of Canada Ltd., and Dr. C. J. Orth of the Los Alamos Scientific Laboratory for making available some of their unpublished results. They are also pleased to express their thanks to Drs. A. Kjelberg and L. Westgaard, both of the University of Oslo, for many helpful discussions and their interest in this work, to Dr. K. Madshus of the Norsk Hydro's Institute for Cancer Research for many valuable measurements with their low level γ-counter, and to Dr. E. Hagebø of CERN for discussions concerned with computation of isomer yield ratios.

This work has been financially supported by the Nansen Foundation in Norway to which the authors express their sincere thanks. One of the authors (G. R. G.) thanks the Royal Norwegian Council for Scientific and Industrial Research for financial support in the form of a Postdoctorate Fellowship during 1961–1963, and P. O. S. is indebted to the United States Navy for financial support and to Drs. E. Cooper, E. Tompkins, L. Gevantman, N. Ballou, and E. Roth, Captain, USN, all of the United States Naval Radiological Defense Laboratory for their support and leave granted in 1963–1964.

REFERENCES

1. A. C. Wahl, R. L. Ferguson, D. R. Nethaway, D. E. Troutner, and K. Wolfsberg. Phys. Rev. **126**, 1112 (1962).
2. L. E. Glendenin, C. D. Coryell, and R. R. Edwards. *In* Radiochemical studies: the fission products. National Nuclear Energy Series, **9**, Div. IV. *Edited by* C. D. Coryell and N. Sugarman. McGraw-Hill Book Co., Inc., New York. 1951. Paper 52.
3. A. C. Pappas. U.S.A. Rept. MIT-LNS-63 (AECU-2806); Inaugural Dissertation, University of Oslo, Oslo, Norway. 1953.
4. A. C. Pappas. Proc. Intern. Conf. Peaceful Uses At. Energy, Geneva, 1955. Vol. 7. United Nations, Geneva. 1956. p. 19.
5. A. C. Wahl. J. Inorg. Nucl. Chem. **6**, 263 (1958).
6. J. Terrell. Bull. Am. Phys. Soc. **6**, 16T (1961).
7. C. D. Coryell, M. Kaplan, and R. D. Fink. Can. J. Chem. **39**, 646 (1961).
8. T. J. Kennett and H. G. Thode. Phys. Rev. **103**, 323 (1956).
9. J. C. D. Milton and J. S. Fraser. Can. J. Phys. **40**, 1626 (1962).
10. B. J. Dropesky and C. J. Orth. J. Inorg. Nucl. Chem. **24**, 1301 (1962).
11. A. E. Greendale and D. L. Love. Anal. Chem. **35**, 632 (1963).
12. J. W. Barnes. *In* Collected radiochemical procedures. *Edited by* J. Kleinberg. U.S.A. Rept. LA-1721. 2nd ed. 1958.
13. R. Greenhalgh and J. P. Riley. Anal. Chim. Acta, **27**, 305 (1962).
14. S. Katcoff. Nucleonics, **18**, (11), 201 (1960).
15. C. O. Minkhinen. *In* Collected radiochemical procedures. *Edited by* J. Kleinberg. U.S.A. Rept. LA-1721. 2nd ed. 1958.
16. S. Forsèn and J. Rydberg. Nucl. Instr. Methods, **7**, 204 (1960).
17. B. J. Dropesky and C. J. Orth. Bull. Am. Phys. Soc. **8**, 377 (1963); personal communication from C. J. Orth. 1964.
18. J. Vanhorenbeeck. Nucl. Phys. **37**, 90 (1962).
19. G. Herrmann. Personal communication. 1962.
20. G. Rudstam. Inaugural Dissertation, University of Uppsala, Sweden. 1956.
21. A. Buset. Personal communication. 1963.
22. A. N. Murin, V. D. Nefedov, D. K. Popov, and V. L. Baranovskij. Kernenergie **1**, 302 (1958).
23. R. B. Regier. U.S.A. Rept. IDO 16633. 1960. p. 21.
24. S. D. Nelson and G. P. Lang. U.S.A. Rept. MCW-1453. 1960.
25. J. C. Roy and J. J. Hawton. Can. Rept. CRC-1003/AECL-1181. 1960.
26. G. Lange and G. Herrmann. Personal communication from G. Herrmann. 1964.
27. Nuclear Data Sheets. National Academy of Sciences – National Research Council, Washington, D.C.
28. M. M. Brennan and A. M. Bernstein. Phys. Rev. **120**, 927 (1960).
29. J. R. Huizenga and R. Vandenbosch. Phys. Rev. **120**, 1305 (1960).
30. R. Vandenbosch and J. R. Huizenga. Phys. Rev. **120**, 1313 (1960).
31. M. M. Hoffman. Phys. Rev. **133**, B714 (1964).
32. H. Warhanek and R. Vandenbosch. J. Inorg. Nucl. Chem. **26**, 669 (1964).
33. B. T. Feld, H. Feshbach, M. L. Goldberger, H. Goldstein, and V. F. Weisskopf. U.S.A. Rept. NYO-636. 1951. J. M. Blatt and V. F. Weisskopf. Theoretical nuclear physics. John Wiley and Sons, Inc., New York. 1952.

34. W. L. HAFNER, Jr., J. R. HUIZENGA, and R. VANDENBOSCH. U.S.A. Rept. ANL-6662. 1962.
35. D. E. TROUTNER, A. C. WAHL, and R. L. FERGUSON. Phys. Rev. **134**, B1027 (1964).
36. J. TERRELL. Phys. Rev. **127**, 880 (1962).
37. J. C. D. MILTON and J. S. FRASER. Bull. Am. Phys. Soc. **8**, RA11 (1963); personal communication by J. C. D. Milton. 1964.
38. V. F. APALIN, Y. N. GRITSYUK, I. Y. KUTIKOV, V. I. LEBEDEV, and L. A. MIKAELYAN. Nucl. Phys. **38**, 193 (1962); Soviet Phys. JETP English Transl. **16**, 235, 1451 (1963).
39. J. S. FRASER and J. C. D. MILTON. III. U.N. Intern. Conf. Peaceful Uses At. Energy, Geneva. Sept. 1964. Can. Rept. AECL-2013. 1964.
40. A. C. WAHL and D. R. NETHAWAY. Phys. Rev. **131**, 830 (1963).
41. A. C. PAPPAS and D. R. WILES. J. Inorg. Nucl. Chem. **2**, 69 (1956).
42. D. L. LOVE, A. E. GREENDALE, and P. O. STROM. Personal communication by P. O. Strom. 1964.

Can. J. Chem. Downloaded from www.nrcresearchpress.com by 210.87.254.42 on 09/05/12
For personal use only.

Can. J. Chem. Downloaded from www.nrcresearchpress.com by 210.87.254.105 on 09/05/12
For personal use only.

SYNTHESIS OF 4-*O*-β-D-GALACTOPYRANOSYL-D-GALACTOSE

E. J. C. CURTIS AND J. K. N. JONES
Department of Chemistry, Queen's University, Kingston, Ontario
Received May 3, 1965

ABSTRACT

The disaccharide named in the title, 6-*O*-β-D-galactopyranosyl-D-galactose, and the 2(?)-substituted isomer have been synthesized in low yield by the condensation of acetobromo-D-galactose and di-*O*-isopropylidene-aldehydo-D-galactose dimethyl acetal.

INTRODUCTION

The two disaccharides 4-*O*-β-D-galactopyranosyl-D-galactose (I) and 6-*O*-β-D-galactopyranosyl-D-galactose (II) have been isolated from the partial hydrolysis products of

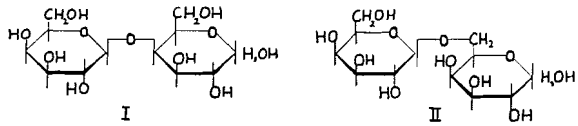

polysaccharides (1, 2). The disaccharide (II) had earlier been synthesized by the condensation of acetobromo-D-galactose with 1,2;3,4-di-*O*-isopropylidene-D-galactose followed by acidic hydrolysis of the isopropylidene residues (3). We now report the synthesis of both II and I. Previous work (4) had shown that acetobromo sugars will readily form glycosides with acyclic sugar derivatives which possess a free hydroxyl group. In the present study aldehydo-D-galactose diethyl dithioacetal (5) was condensed with acetone to yield a mixture containing the 2,3;4,5-(III*a*, R = SEt) and 2,3;5,6-di-*O*-isopropylidene (III*b*, R = SEt) derivatives (cf. the formation of α- and β-di-*O*-isopropylidene-dulcitols

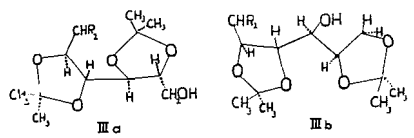

(6)). These thioacetals were readily converted (7) to the mixture of dimethyl acetals (III*a*, III*b*) (R = OMe) which was purified by distillation. Condensation of the dimethyl acetals with acetobromo-D-galactose gave the disaccharide derivatives. After removal of acetyl and isopropylidene residues the mixture of sugars was fractionated first on a charcoal column (8) and then on cellulose (9).

The 1,6-linked disaccharide, the major product, was eluted last in a pure form. It was indistinguishable from an authentic specimen and gave a phenylosazone which was identical with a specimen prepared from the authentic sugar. The fastest-moving fraction on chromatograms was a disaccharide which was provisionally identified as the 1,2-linked isomer since it gave a negative tetrazolium red test (10). The 1,4-linked disaccharide was eluted after this material.

The 1,2(?)-linked isomer was a syrup; it did not give a crystalline phenylosazone; it consumed rapidly 3 moles of periodate and gave rapidly 1.5 moles of formic acid. The sugar underwent overoxidation, the extrapolated values for consumption of periodate and molar yields of formic acid being 4.2 and 3.1 per mole of sugar respectively (Table

I). The disaccharide after reduction with sodium borohydride was oxidized with sodium metaperiodate and then consumed 4.9 moles of periodate and produced 2.8 moles of formic acid per mole of sugar, with no overoxidation (Table II). The values expected from the oxidation of 1 → 2 linked disaccharide are 5 moles and 3 moles respectively.

The 4-*O*-β-D-galactopyranosyl-D-galactose fraction was crystalline and was indistinguishable from an authentic specimen. On oxidation with sodium metaperiodate it yielded 1.7 moles of formic acid and consumed 3.9 moles of metaperiodate per mole. The values expected from a 1 → 4 linked disaccharide are 2 moles and 4 moles respectively (Table III). The yield of formic acid is probably low because of the formation of formyl esters.

EXPERIMENTAL

Paper chromatography was carried out at room temperature on Whatman No. 1 filter paper using the descending method. The following solvent systems were used.

(A) Ethyl acetate:acetic acid:water (9:2:2 v/v)

(B) Butan-1-ol:ethanol:water (3:1:1 v/v)

Sugars were located on chromatograms by spraying either with *p*-anisidine hydrochloride (1% w/v) in butan-1-ol or with silver nitrate in acetone followed by sodium hydroxide in ethanol.

Solutions were concentrated at 40°, under reduced pressure using a water pump. Optical rotations were measured at room temperature either in water or in a specified solvent. All melting points are uncorrected.

*Di-O-isopropylidene-*D*-galactose Diethyl Dithioacetal*

D-Galactose diethyl dithioacetal (71 g) was added to a cold solution of dry acetone (1 l) which contained dry hydrogen chloride (36 g). The mixture was shaken until solution was complete (20 h). After an additional 16 h the solution was neutralized ($PbCO_3$) and filtered, and the filtrate was evaporated to a syrup (92 g).

*Di-O-isopropylidene-*D*-galactose Dimethyl Acetal*

A portion (37 g) of the above dithioacetal derivative plus cadmium carbonate (70 g) was added to dry methanol (250 ml). The resulting mixture was stirred vigorously while a solution of mercuric chloride (80 g) in dry methanol (250 ml) was added portionwise during 22 h. The mixture was then heated under reflux for 6 h. The hot solution was filtered and the solids were washed with hot methanol. The filtrate and washings were concentrated to a small volume and the residue was diluted with chloroform (400 ml). The chloroform solution was extracted with water until it was free of chloride and was then dried over calcium chloride. The solution was passed down a column of activated alumina to remove color and the effluent was evaporated to a syrup. The product was distilled and a fraction (12 g) of b.p. 134–138° at 0.4 mm was collected.

Anal. Calcd. for $C_{14}H_{26}O_7$; C, 54.9; H, 8.5; OMe, 20.2. Found: 54.7; H, 8.5; OMe, 19.8.

*Condensation of Di-O-isopropylidene-*D*-galactose Dimethyl Acetal with Acetobromo-*D*-galactose*

The dimethyl acetal (5.8 g, 0.019 mole) was dissolved in dry, alcohol-free chloroform (40 ml), and silver carbonate (27 g) and Drierite (23 g) were added and the mixture was shaken in the dark at room temperature.

After 3.5 h a solution of acetobromo-D-galactose (11.5 g; 0.028 mole) in dry alcohol-free chloroform (50 ml) plus a few crystals of iodine were added and shaking was then continued. After 23 h a further quantity of acetobromo-D-galactose (7 g, 0.017 mole) in dry chloroform (20 ml) plus Drierite (3.5 g) were added. After 5 days the test for ionizable bromine was negative. The mixture was filtered through a pad of Celite which was washed with chloroform. The filtrate and washings were concentrated and the residual syrup (23 g) was dissolved in dry methanol and the product de-*O*-acetylated by the addition of a catalytic quantity of sodium methoxide in methanol. The solution was evaporated, and the residue was hydrolyzed with warm sulfuric acid (0.1 *N*) until isopropylidene residues had been removed from the sugars. The solution was neutralized ($BaCO_3$) and filtered, and the filtrate was evaporated to a syrup (19 g). Chromatography showed the presence of galactose (mainly) and four components of R_{gal} 3.0, 0.21, 0.32, and 0.64 (solvent A), the last two being present in small amounts only. The fast-moving material presumably still contained isopropylidene or acetate residues.

The syrup was fractionated on a column of charcoal (4.5 × 15 cm). Elution with water removed the bulk of the monosaccharide material, and elution with 5% ethanol:water mixture removed the slower-moving compounds. These were fractionated on a cellulose column (45 × 4.5 cm) using *n*-propanol:ethanol:water (7:1:1 v/v) as solvent.

Can. J. Chem. Downloaded from www.nrcresearchpress.com by 210.87.254.105 on 09/05/12
For personal use only.

In this fashion pure *6-O-β-D-galactopyranosyl-D-galactose* (1.09 g) with R_{gal} 0.21 (solvent A) and 0.20 (solvent B) was obtained. Acid hydrolysis (*N* sulfuric acid at 80° for 15 h) of a portion of the sugar gave galactose only. The disaccharide was crystallized from methanol containing a small percentage of butan-1-ol. The product which contained methanol of crystallization melted at 120–121° and had $[\alpha]_D$ +24° (5 min) → +29° (constant value) (*c* 2.37 in H_2O). The sugar gave a phenylosazone m.p. 207° (decomp.) indistinguishable, by infrared analysis, from an authentic specimen.

A fraction (0.8 g) which had preceded 6-*O*-β-D-galactopyranosyl-D-galactose was a mixture. It was refractionated on Whatman 3MM paper to yield *2(?)-O-β-D-galactopyranosyl-D-galactose*, a syrup (0.13 g) which had $[\alpha]_D$ +35° (*c*, 0.285 in water) and R_{gal} 0.64 (solvent A) and 0.48 (solvent B). Hydrolysis of a portion of this disaccharide with acid gave galactose only. The alkaline triphenyltetrazolium red test (10) was negative under conditions which gave a positive test with D-galactose and 6-*O*-β-D-galactopyranosyl-D-galactose.

Periodate Oxidation of the Syrup

A portion (10.2 mg) of the syrup was oxidized with 0.3 *M* sodium metaperiodate (2 ml) in a total volume of 10 ml. Uptake of metaperiodate and production of formic acid were measured in the usual way.

TABLE I

Periodate oxidation of 2(?)-*O*-β-D-galactopyranosyl-D-galactose

Time	Periodate uptake (moles/mole of sugar)	Formic acid (moles/mole of sugar)
10 min	0.97	0.39
30 min	1.73	0.65
1 h 20 min	2.59	0.99
2 h 30 min	3.19	1.21
4 h 40 min	3.63	1.64
18 h 35 min	4.98	3.06
20 h 50 min	5.27	3.25

Periodate Oxidation of 2(?)-O-β-D-galactopyranosyl-D-galactitol

The sugar (24 mg) was dissolved in water (5 ml) and reduced with sodium borohydride (30 mg) added in two portions over 3 h. The excess of sodium borohydride was destroyed (acetic acid), the solution was deionized (Amberlite IR120 resin) and concentrated, and the boric acid was removed from the residue as methyl borate. The residue (21 mg) did not give a color with the *p*-anisidine hydrochloride spray. A portion of the product (8.5 mg) was oxidized as described above.

TABLE II

Periodate oxidation of 2(?)-*O*-β-D-galactopyranosyl-D-galactitol

Time	Periodate uptake (moles/mole of sugar)	Formic acid (moles/mole of sugar)
10 min	3.44	1.82
30 min	3.85	1.96
1 h 0 min	4.40	2.21
2 h 0 min	4.70	2.43
4 h 0 min	4.94	2.61
6 h 0 min		2.71
19 h 0 min	5.05	2.77
22 h 10 min		2.77
24 h 30 min	5.06	2.79

A second fraction (0.29 g) isolated from the 3MM paper was identified as *4-O-β-D-galactopyranosyl-D-galactose*. It crystallized on nucleation with an authentic specimen and was recrystallized from methanol. It had m.p. 200–202°, not depressed with an authentic specimen (m.p. 204°) and had $[\alpha]_D$ +63° → +69° constant value (*c*, 0.32 in water). Its rates of movement on chromatograms were indistinguishable from authentic specimens, R_{gal} 0.32 (solvent A) and 0.21 (solvent B).

Can. J. Chem. Downloaded from www.nrcresearchpress.com by 210.87.254.105 on 09/05/12
For personal use only.

TABLE III

Periodate oxidation of 4-*O*-β-D-galactopyranosyl D-galactose

Time	Periodate uptake (moles/mole of sugar)	Formic acid (moles/mole of sugar)
12 min	2.37	0.30
30 min		0.45
46 min	2.51	
1 h 5 min	2.78	0.73
2 h 30 min	3.02	1.00
5 h 2 min	3.41	1.20
18 h 50 min	3.94	1.70
21 h 5 min	3.97	1.75
46 h 0 min	4.11	1.83

ACKNOWLEDGMENTS

The authors thank the National Research Council for financial assistance (N.R.C. T-19).

REFERENCES

1. J. K. GILLHAM, A. S. PERLIN, and T. E. TIMELL. Can. J. Chem. **36**, 1741 (1958).
2. S. HAQ and G. A. ADAMS. Can. J. Chem. **39**, 1563 (1961).
3. K. FREUDENBERG, A. WOLF, E. KNOPF, and S. H. ZAHUR. Chem. Ber. **61**, 1743 (1928).
4. E. J. C. CURTIS and J. K. N. JONES. Can. J. Chem. **37**, 358 (1959).
5. M. L. WOLFROM. J. Am. Chem. Soc. **54**, 2464 (1930).
6. R. M. HANN, W. D. MACLAY, and C. S. HUDSON. J. Am. Chem. Soc. **61**, 2432 (1939).
7. M. L. WOLFROM, L. T. TANGHE, R. W. GEORGE, and S. W. WAISBROT. J. Am. Chem. Soc. **60**, 132 (1938).
8. R. L. WHISTLER and D. F. DURSO. J. Am. Chem. Soc. **72**, 677 (1950).
9. L. HOUGH, J. K. N. JONES, and W. H. WADMAN. J. Chem. Soc. 1702 (1950).
10. D. J. BELL and R. DEDONDER. J. Chem. Soc. 2866 (1954).

Can. J. Chem. Downloaded from www.nrcresearchpress.com by 210.87.254.105 on 09/05/12
For personal use only.

Can. J. Chem. Downloaded from www.nrcresearchpress.com by 210.87.254.42 on 09/05/12
For personal use only.

SYNTHESIS OF 2,2-DISUBSTITUTED-5-CYANOCYCLOPENTANONES[1]

STUART S. KULP,[2] VELMER B. FISH, AND NELSON R. EASTON[3]
Wm. H. Chandler Chemistry Laboratory, Lehigh University, Bethlehem, Pennsylvania
Received April 21, 1965

ABSTRACT

The synthesis of a series of 2,2-disubstituted-5-cyanocyclopentanones by hydrolysis of the precursor 3,3-disubstituted-2-amino-1-cyanocyclopentenes (2,2-disubstituted-5-cyanocyclopentanoneimines) is described. The new compounds possess the following substituents: dimethyl, diethyl, phenyl hydrogen, and ethyl phenyl.

The difficulty in hydrolyzing 2,2-diphenyl-5-cyanocyclopentanoneimine to 2,2-diphenyl-5-cyanocyclopentanone (1) led us to the preparation of other compounds of this series and a study of the hydrolyses of these materials. The synthetic approach is outlined in Scheme 1. The new compounds reported here involve the preparation of IV A–D.

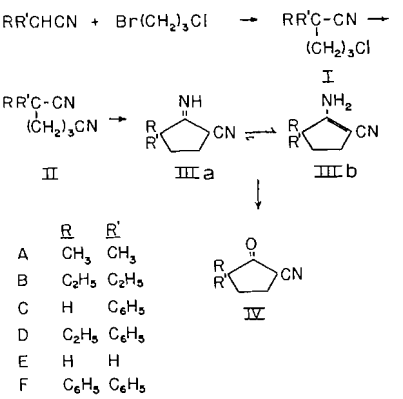

SCHEME 1.

The intermediate chloro compounds (I) were obtained by alkylation of the appropriately substituted acetonitrile with 1-bromo-3-chloropropane at −70°. When the dihalide was added at 0°, both halogens were replaced and dicondensation to a substituted pimelonitrile occurred. This is in contrast to the alkylation of diphenylacetonitrile which gave IF in quantitative yield at 0° (1). The dicondensation product from dimethylacetonitrile was 2,2,6,6-tetramethylpimelonitrile which was characterized and hydrolyzed to its corresponding diamide and diacid.

The dinitriles (II) were prepared by treating the chloro nitriles (I) with potassium cyanide. The dinitriles were characterized by hydrolyzing IIA to the amide acid, IIB to its amide acid and diacid, and IIC to its diamide.

Cyclization of the dinitriles (II) was best accomplished with sodium hydride in dioxane. The alicyclics obtained (III A–D) are best represented as enamines (III*b*) rather than iminonitriles (III*a*) as previously found for IIIE (2). These compounds are listed in Table I.

[1]*From the Ph.D. dissertation of S. S. K., Lehigh University, 1957.*
[2]*To whom inquiries should be addressed. Present address: Moravian College, Bethlehem, Pennsylvania.*
[3]*Present address: Eli Lilly and Company, Indianapolis, Indiana.*

TABLE I

Substituted 2-amino-1-cyanocyclopentenes (III*b*)

Compd.	Yield (%)	Melting point (°C)	Formula	% carbon		% hydrogen		% nitrogen	
				Calcd.	Found	Calcd.	Found	Calcd.	Found
IIIA	90	110–111*	$C_8H_{12}N_2$	70.54	70.75	8.88	8.76	20.60	20.80
IIIB	70	104–106†	$C_{10}H_{16}N_2$	73.10	73.30	9.83	9.92	17.07	17.12
IIIC	98	109–110.5‡	$C_{12}H_{12}N_2$	78.22	78.40	6.57	6.50	15.23	15.15
IIID	85	120–121.5*	$C_{14}H_{16}N_2$	79.20	79.30	7.60	7.81	13.20	12.97

*Recrystallized from methanol.
†Recrystallized from ether.
‡Recrystallized from ethyl acetate.

TABLE II

Substituted 2-cyanocyclopentanones (IV)

Compd.	Boiling point (mm)	Yield (%)	Formula	% carbon		% hydrogen		% nitrogen	
				Calcd.	Found	Calcd.	Found	Calcd.	Found
IVA	114–117 (2)	70	$C_8H_{11}NO$*	70.04	69.75	8.08	7.97	10.21	10.00
IVB	160–163 (20)	66	$C_{10}H_{15}NO$	72.69	72.42	9.15	9.15	8.47	8.41
IVC	174–175 (2)	90	$C_{12}H_{11}NO$†	77.81	77.90	5.99	6.02	7.56	7.70
IVD	144–145 (0.15)	82	$C_{14}H_{15}NO$	78.84	78.61	7.09	7.28	6.56	6.58

*The 2,4-dinitrophenylhydrazone melted at 149°. Anal. Calcd. for $C_{14}H_{18}N_5O_4$: C, 52.99; H, 4.77; N, 22.07. Found: C, 53.08; H, 4.90; N, 21.95.
†The 2,4-dinitrophenylhydrazone melted at 204°. Anal. Calcd. for $C_{18}H_{18}N_5O_4$: C, 59.17; H, 4.14; N, 19.17. Found: C, 59.35; H, 4.20; N,19.25.

Hydrolyses of the enamines (III) proceeded readily to the α-cyanocyclopentanones (IV A–D) which is in marked contrast to the findings with the diphenyl analog (IVF) (1). The keto nitriles IV A–D are listed in Table II. Only the dimethyl (IVA) and the monophenyl (IVC) ketones formed 2,4-dinitrophenylhydrazones under the usual conditions.

Additional evidence for the anomalous behaviour of the *gem*-diphenyl enamine (IIIF), previously ascribed to steric hindrance, was sought. The infrared and ultraviolet spectra of compounds III A–F are listed in Table III and show no significant deviation from those reported for the parent compound (IIIE) (2). Likewise, the infrared spectra of IV A–F

TABLE III

Infrared and ultraviolet spectra of substituted 2-amino-1-cyanocyclopentenes (III*b*)

Compd.	Infrared (μ)					Ultraviolet (mμ)	
	NH	NH	CN	NH	C=C	Max.	a_M
IIIA	2.88	2.98	4.58	6.10	6.26	263	12 500
IIIB	2.85	2.93	4.57	6.09	6.25	263	13 700
IIIC	2.87	2.94	4.57	6.09	6.25	263	14 080
IIID	2.86	2.94	4.57	6.08	6.24	264	13 050
IIIE	2.85*	2.93*	4.56*	6.07*	6.22*	265	13 200*
IIIF†	2.87	2.94	4.56	6.07	6.25	269	13 650

*See ref. 2 for reported values of 2.85, 2.92, 4.57, 6.08, 6.23 μ and 263 mμ (13 000).
†Preparation reported in ref. 1.

are similar and are listed in Table IV. The β-keto nitriles (IV) have absorption maxima around 235 mμ in acid or neutral ethanolic solutions except IVD and IVF. The latter compounds exhibit no absorption maxima in the ultraviolet other than carbonyl absorption at ca. 297 mμ in acid or neutral medium. Most of the keto nitriles have absorption at

Can. J. Chem. Downloaded from www.nrcresearchpress.com by 210.87.254.42 on 09/05/12
For personal use only.

TABLE IV

Infrared and ultraviolet spectra of substituted α-cyanocyclopentanones (IV)

	Infrared (μ)			Ultraviolet (mμ)			
				Acid and neutral		Basic	
Compd.	OH	CN	C=O	Max.	a_M	Max.	a_M
IVA	2.86	4.45	5.79	235	1 630	264	10 500
IVB	2.87	4.45	5.70	235	2 640	264	11 100
IVC	2.85	4.45	5.66	238	5 940	264	13 000
IVD	2.87	4.45	5.70	297*	144	270	11 400
IVE	2.89	4.47†	5.75†	235	2 400	262	16 840
IVF‡	2.87	4.44	5.68	296*	246	278	13 750

*No absorption peak in the 235 mμ region.
†See ref. 2 for values of 4.44 and 5.70 μ.
‡Preparation reported in ref. 4.

about 264 mμ in basic ethanolic solution; however, IVD and IVF have peaks at 270 and 278 mμ under these conditions. Thus, the bathochromic shift of about 29 mμ in changing from neutral to basic solution is comparable to shifts of 36 and 31 mμ as noted for other β-keto nitriles (3).

The enolization of the β-keto nitriles will be reported later.

EXPERIMENTAL

All melting points were determined in an oil bath and are uncorrected. Ultraviolet spectra were determined with a Warren Spectracord in 95% alcohol. Infrared spectra were determined on a Perkin–Elmer model 21 instrument in $CHCl_3$ solution.

5-Chloro-2,2-dimethylpentanenitrile (IA)

An ether solution of 1 mole of the lithium salt of dimethylacetonitrile was prepared from lithium diethylamide as described previously (5). After cooling to −70°, 1 mole of 1-bromo-3-chloropropane was added dropwise over 1 h at a rate to maintain the reaction temperature below −60°. The mixture warmed to room temperature overnight as the acetone – dry ice bath evaporated. After refluxing for 1 h, cooling, and decomposition in the usual manner, the solvent was removed. The remaining liquid was heated to 70° at 20 mm and the crude residue, 136 g (93%), was satisfactory for further synthesis. The following analogs were prepared: IB-diethyl, 70%, b.p. 123° at 10 mm; IC-phenyl, 81%; ID-ethyl-phenyl, 68%, 145–147° at 2 mm.

Addition of the 1-bromo-3-chloropropane to the reaction mixture at 0° gave a quantitative amount of dicondensation product, 2,2,6,6-tetramethylpimelonitrile, m.p. 118–119° from methanol.

Anal. Calcd. for $C_{11}H_{18}N_2$: C, 74.11; H, 10.18. Found: C, 74.20; H, 10.02.

2,2,6,6-Tetramethylpimelamide

Hydrolysis of the pimelonitrile with 80% sulfuric acid on a steam bath for 3 h gave a white solid, m.p. 193–194°.

Anal. Calcd. for $C_{11}H_{22}O_2N_2$: N, 13.05. Found: N, 12.97.

2,2,6,6-Tetramethylpimelic Acid

The above pimelamide gave the diacid by the butyl nitrite procedure (6). The m.p. was 168–169.5° from methanol.

Anal. Calcd. for $C_{11}H_{20}O_4$: C, 61.15; H, 9.32. Found: C, 61.25; H, 9.10.

Attempts to prepare this diacid by basic hydrolysis of either the precursor dinitrile or diamide were unsatisfactory

2,2-Dimethyladiponitrile (IIA)

A mixture of 55 g (1.41 mole) of sodium cyanide in 125 ml of dimethylformamide and 1 ml of water was stirred under reflux. To this was added 125 g (0.86 mole) of crude 5-chloro-2,2-dimethylpentanenitrile over 0.4 h. After refluxing for 2 h the mixture was cooled slightly and 25 ml of water was added. The mixture was refluxed 0.5 h, cooled, poured into a large volume of water, and allowed to stand overnight. The layers were separated, the aqueous layer was extracted with ether, and the combined organic layers were washed with ice-cold 50% sulfuric acid. The ether layer was dried over magnesium sulfate and filtered, and the solvent was distilled and gave a clear distillate, b.p. 145–151° at 14 mm with only a slight forerun and about 8 g of

Can. J. Chem. Downloaded from www.nrcresearchpress.com by 210.87.254.42 on 09/05/12
For personal use only.

residue. The product weighed 93 g (80%). The following analogs were prepared: IIB-diethyl, b.p. 144–146° at 5 mm, 76%; IIC-phenyl, b.p. 170° at 0.5 mm, 60%; IID-ethyl-phenyl, b.p. 180–200° at 3 mm, 52%, after standing several days this oil solidified, m.p. 45.5–47°.

5-Carbamoyl-5,5-dimethylpentanoic Acid

Hydrolysis of IIA with 80% sulfuric acid on a steam bath for 3 h gave a white solid, m.p. 159–161°. Recrystallization from ethyl acetate with a little methanol gave m.p. 160.5–161°.

Anal. Calcd. for $C_8H_{15}O_3N$: N, 8.10. Found: N, 8.19.

5-Carbamoyl-5,5-diethylpentanoic Acid

A mixture of 300 g of IIB and 1 500 ml of 80% sulfuric acid was heated at 110° for 16 h. Sufficient water was cautiously added to decrease the sulfuric acid concentration to about 50%. This mixture was heated at 110° for 24 h, poured on crushed ice, and allowed to stand for 3 days. The solid was collected and dissolved in sodium hydroxide; acidification gave a dark brown solid. Recrystallization from methanol with charcoal did not improve the quality of the product. The solid was distilled, b.p. 190–200° at 0.1 mm. This distillate after two recrystallizations from methanol melted at 152–153.5°.

Anal. Calcd. for $C_{10}H_{19}O_3N$: N, 6.97. Found: N, 6.97.

2,2-Diethyladipic Acid

Obtained from the above amide-acid by the butyl nitrite procedure (6). The crude product, m.p. 99–102°, after three recrystallizations from methanol–water had constant m.p. 102.5–103.5° (reported (7) 90–92°).

Anal. Calcd. for $C_{10}H_{18}O_4$: C, 59.40; H, 8.96. Found: C, 59.40; 59.50; H, 8.83, 8.95.

The infrared spectrum ($CHCl_3$ solution) was in agreement with this structure.

2-Phenyladipamide

A small sample of IIC was treated with 30% hydrogen peroxide and sodium hydroxide (8) and melted at 171–171.5°.

Anal. Calcd. for $C_{12}H_{16}O_2N_2$: C, 65.43; H, 7.32; N, 12.72. Found: C, 65.50; H, 7.63; N, 12.72.

3,3-Dimethyl-2-amino-1-cyanocyclopentene (IIIA)

A suspension of 12 g (0.55 mole) of active sodium hydride (added as 50% dispersion in oil) and 250 ml of dry dioxane was vigorously stirred under reflux in a large 3-neck flask equipped as usual. To this was added 66 g (0.48 mole) of 2,2-dimethyladiponitrile very carefully over 1.5 h. The mixture was refluxed an additional 3 h and then cooled in ice. Water was added cautiously, acetic acid was added to acidify, and the mixture was allowed to stand in ice overnight. The crude brown solid, 60 g (90%), had m.p. 106–108°. Recrystallization raised the melting point to the value reported in Table I. Compounds III B–D were similarly prepared.

5-Cyano-2,2-diethylcyclopentanone (IVB)

A mixture of 30 g (0.18 mole) of IIIB, 15 ml of concentrated HCl (0.18 mole), 85 ml of 8 *N* sulfuric acid, and 100 ml of toluene was heated under reflux for 1 h. The toluene layer was separated, washed with water, and extracted with 10% sodium hydroxide. The aqueous basic solution was cooled and acidified, and the acid solution was extracted with ether. The ether solution was dried (magnesium sulfate), filtered, concentrated, and distilled to give the product reported in Table II. Compounds IVA, IVC, and IVD were similarly prepared.

REFERENCES

1. S. S. KULP, V. B. FISH, and N. R. EASTON. J. Med. Chem. **6**, 516 (1963).
2. C. F. HAMMER and R. A. HINES. J. Am. Chem. Soc. **77**, 3649 (1955).
3. P. B. RUSSELL and J. MENTHA. J. Am. Chem. Soc. **77**, 4245 (1955). S. BALDWIN. J. Org. Chem. **26**, 3280 (1961).
4. S. S. KULP and S. A. IOBST. J. Med. Chem. **7**, 813 (1964).
5. R. F. BROWN and N. M. VAN GULICK. J. Am. Chem. Soc. **77**, 1083 (1955).
6. N. SPERBER, D. PAPA, and E. SCHWENK. J. Am. Chem. Soc. **70**, 3091 (1948).
7. H. MEERWEIN. Ann. **396**, 229 (1913).
8. C. NOLLER. Org. Syn. **2**, 586 (1943).

Can. J. Chem. Downloaded from www.nrcresearchpress.com by 210.87.254.42 on 09/05/12
For personal use only.

Can. J. Chem. Downloaded from www.nrcresearchpress.com by 210.87.254.5 on 09/05/12
For personal use only.

MASS SPECTRA OF SOME FUROQUINOLINE ALKALOIDS

D. M. CLUGSTON AND D. B. MACLEAN
Department of Chemistry, McMaster University, Hamilton, Ontario
Received May 7, 1965

ABSTRACT

The mass spectra of six furoquinoline alkaloids have been recorded and mechanisms have been proposed for their fragmentation upon electron impact. Strong metastable peaks, present in all spectra, have aided in the interpretation of the fragmentation of these alkaloids. The three alkaloids with a methoxyl group in the 8-position of the quinoline ring may be differentiated from the other three by the presence of relatively intense peaks at M-1 and M-29.

In this investigation we wish to report upon the fragmentation of some furoquinoline alkaloids upon electron impact. The alkaloids which we have examined include dictamnine I and several of its derivatives containing methoxy and methylenedioxy substituents in the benzenoid ring. They are represented in the general formula shown below.

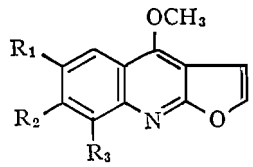

I. Dictamnine	$R_1 = R_2 = R_3 = H$
II. Maculine	$R_1 = R_2 = —OCH_2O—$, $R_3 = H$
III. Kokusaginine	$R_1 = R_2 = OMe$, $R_3 = H$
IV. Skimmianine	$R_2 = R_3 = —OCH_3$, $R_1 = H$
V. Maculosidine	$R_1 = R_3 = —OCH_3$, $R_2 = H$
VI. Flindersiamine	$R_1 = R_2 = —OCH_2O—$, $R_3 = OCH_3$

The spectra of furan and some of its derivatives have been studied (1, 2) but very little has been reported on the spectra of quinoline and its derivatives (3). No studies to our knowledge have been reported on the furoquinoline system itself. Oxygenated benzene systems have, however, been investigated in detail (2, 4, 5) and since all of these alkaloids with the exception of dictamnine carry oxygenated substituents in the benzene ring one might expect to observe fragmentation processes akin to those of the oxygenated benzenes.

The spectra of the six alkaloids are shown in Fig. 1. All show an intense molecular ion peak as one would expect of this aromatic system. In each case they also exhibit a peak at M-15 owing to the loss of a methyl group characteristic of the presence of methoxyl substituents. Of structural interest is the fact that the three alkaloids with an 8-methoxyl substituent show strong peaks at M-1 and M-29. This behavior is also characteristic of 8-methoxy quinolines which we have measured in this laboratory. It seems very likely, therefore, that an 8-methoxyl substituent will give this characteristic pattern in all furoquinoline alkaloids.

In attempting to rationalize the fragmentation of these alkaloids we have first examined the spectrum of dictamnine, the simplest member of the group, and have then examined the spectra of the other alkaloids to ascertain if they undergo similar fragmentation processes.

Can. J. Chem. Downloaded from www.nrcresearchpress.com by 210.87.254.5 on 09/05/12
For personal use only.

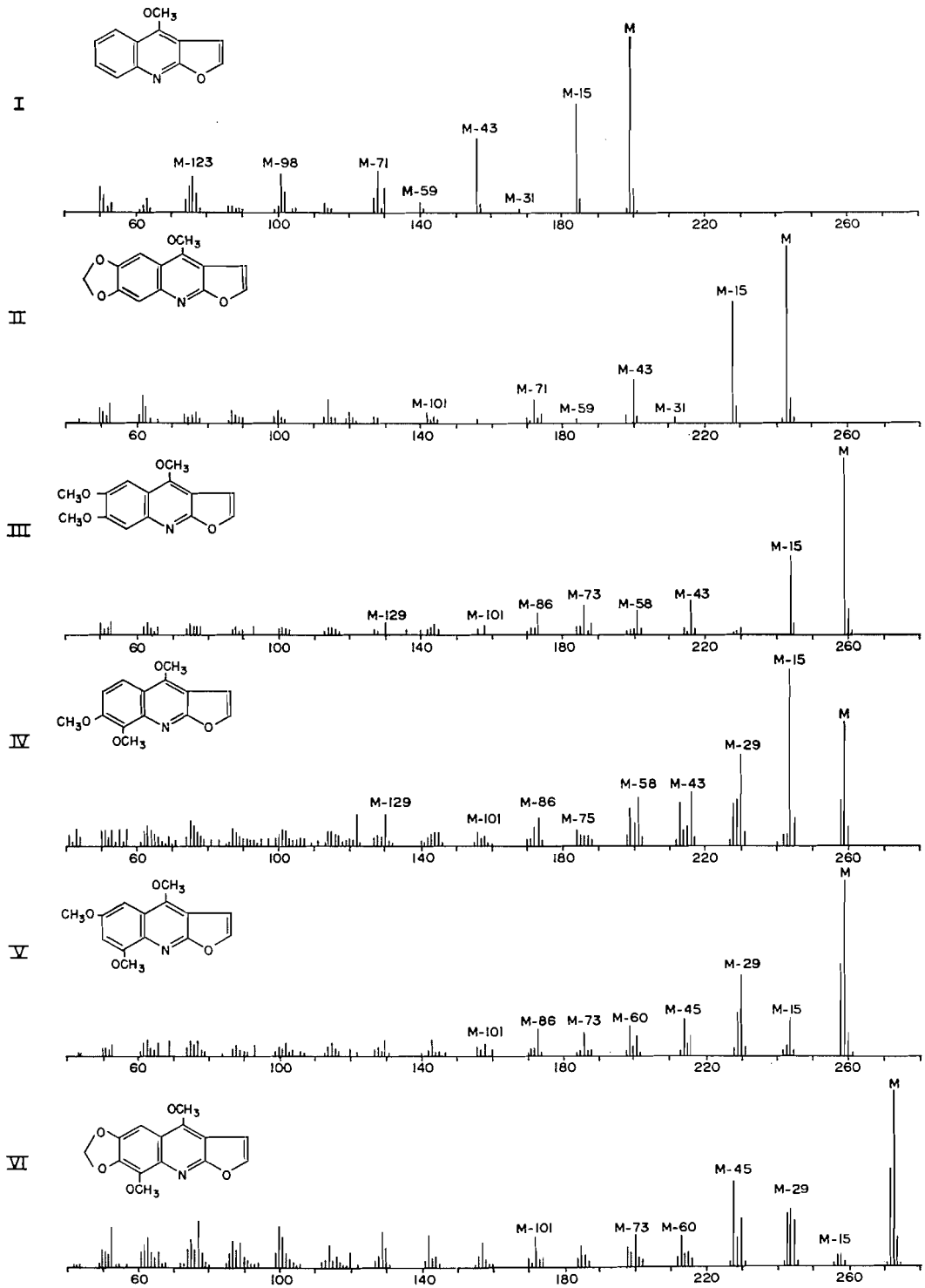

FIG. 1. Mass spectra of I, dictamnine, mol. wt. = 199; II, maculine, mol. wt. = 243; III, kokusaginine, mol. wt. = 259; IV, skimmianine, mol. wt. = 259; V, maculosidine, mol. wt. = 259; and VI, flindersiamine, mol. wt. = 273.

In Scheme 1 a mechanism is advanced to account for the major peaks present in the spectrum of dictamnine. The molecular ion loses a methyl radical leading to the peak at M-15 which then eliminates carbon monoxide leading to the species M-43. This is followed

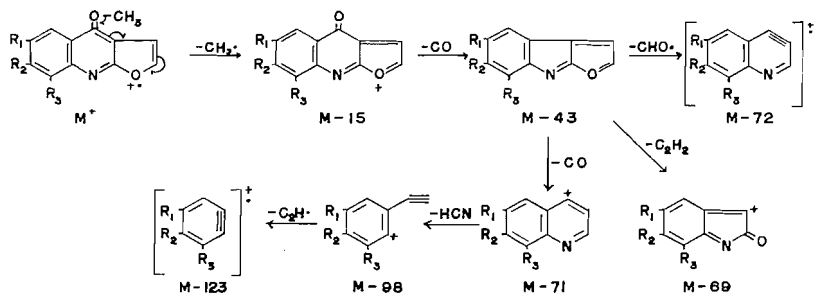

SCHEME 1.

by a further loss of carbon monoxide yielding the ion at M-71, depicted as a ring-expanded quinoline ion in Scheme 1. We have proposed that initial loss of carbon monoxide involves C_4 of the quinoline ring and that the second CO fragment has its origin in the furan system. It is possible that the order may be the inverse of that above or that no differentiation exists. The problem could be resolved only by synthesis and examination of the fragmentation of suitably labelled compounds. The ion M-43 may also lose a formyl radical ·CH=O leading to the peak at M-72. Loss of CHO is the characteristic behavior of furan (1); however, such a fragmentation seems to be of secondary importance to the loss of CO from benzofuran (2) as well as from the furoquinoline system. We have depicted the M-72 species as a ring-expanded "benzyne" ion-radical. Alternately M-72 may form by loss of H from M-71. Another pathway from the M-43 ion leads to an ion at M-69 which we have attributed to loss of an acetylene molecule. The peak at M-98 is considered to arise from M-71 by loss of HCN and this ion may fragment further to the benzyne ion-radical at M-123.

We have examined the spectra of II–VI inclusive to ascertain if they exhibit analogous behavior. Only in the case of maculine II do we find this scheme in its entirety. For III, IV, V, and VI, however, peaks are observed at M-15, M-43, M-71 and M-72.

The spectra of all of these alkaloids are characterized by strong metastable peaks. In Table I the calculated and observed positions of metastable peaks are recorded corresponding to the transitions outlined in Scheme 1 for the six alkaloids. The presence of these metastable peaks lends support, therefore, to the proposals advanced in Scheme 1.

In the spectrum of dictamnine, peaks of relatively low intensity appear at M-31, M-59, and M-86. These peaks are also present in the other alkaloids (an exception being the

TABLE I

Metastable peaks for transitions of Scheme 1

	M → M-15		M-15 → M-43		M-43 → M-71		M-71 → M-98	
	Calcd.	Obsd.	Calcd.	Obsd.	Calcd.	Obsd.	Calcd.	Obsd.
I	170.1	170.2	132.3	132.5	105.0	105.3	79.7	80.0
II	213.9	214.0	175.4	176.0	147.9	148.1	122.2	122.5
III	229.9	230.0	191.2	191.5	163.6	164.0	—	—
IV	229.9	230.0	191.2	191.5	—	—	—	—
V	229.9	230.0	191.2	191.5	—	—	—	—
VI	243.8	244.5	—	—	—	—	—	—

Can. J. Chem. Downloaded from www.nrcresearchpress.com by 210.87.254.5 on 09/05/12
For personal use only.

absence of an M-86 peak in maculine). In dictamnine and maculine loss of the 4-methoxyl must account for the formation of the M-31 peak although in the other four alkaloids the loss of another methoxyl is possible. The peak at M-59 may formally be derived from M-31 by loss of CO and that at M-86 by further loss of HCN. Although no attempt is made to formulate a mechanism for these fragmentations, it should be noted that metastable peaks are observed in the spectra of III, IV, and V at 201.0, m^* calcd. M → M-31 = 200.7 and in VI at 214.8, m^* calcd. = 214.5. The transition M-31 → M-59 is supported by metastable peaks in the spectra of IV and V, m^* calcd. 175.4, m^* obsd. 175.9.

Scheme 1 accounts for the major peaks present in the dictamnine spectrum and for most of those in maculine. In the latter, however, there are peaks at M-73, M-99, and M-101. We consider that the M-73 peak may arise by loss of formaldehyde from the methylenedioxy function and the M-101 peak by subsequent elimination of CO from M-73 as depicted below or by loss of CO from the furan system as in Scheme 1. The M-43 ion is depicted as a resonance hybrid of that shown in Scheme 1 for sake of convenience

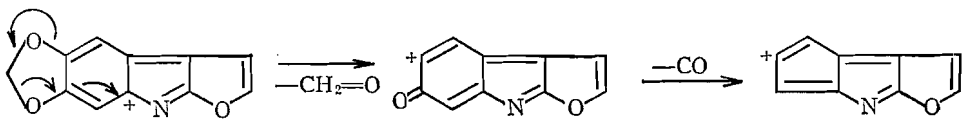

M-43 M-73 M-101

in depicting the mechanism. The M-99 peak in maculine might result from a similar loss of a formaldehyde molecule from the ion M-69 of Scheme 1.

Alkaloids III, IV, and V each contain two methoxyl groups in the benzenoid ring. They exhibit peaks at M-73 and M-101 and at M-58, M-86, and M-129. In Scheme 2 a fragmentation mechanism is advanced to account for the formation of these peaks in III.

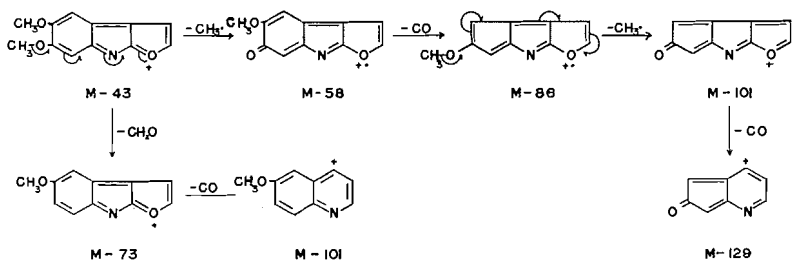

SCHEME 2.

The same mechanism with but slight variation may also be applied to IV and V. In this mechanism the ion of M-43 is considered to lose formaldehyde from one of the two methoxyl groups of the benzenoid ring yielding the M-73 species. Loss of CO from the furan ring leads to an ion of M-101, depicted as a ring-expanded quinoline ion in Scheme 2. The M-43 species may also lose a methyl radical forming the ion-radical of M-58 which by successive loss of CO, CH_3, and CO leads to the ions observed at M-86, M-101, and M-129. Two processes are depicted for the formation of the M-101 ion. A high resolution spectrum would allow one to determine if one or both are operative. In the case of flindersiamine VI the M-43 → M-73 → M-101 sequence is possible through loss of the C_8 methoxyl. Similarly the sequence M-43 → M-58 → M-86 may apply but further fragmentation of flindersiamine via this route is not possible on structural grounds. The transitions M-43 → M-58 are supported by metastable peaks in the spectra of III, IV,

Can. J. Chem. Downloaded from www.nrcresearchpress.com by 210.87.254.5 on 09/05/12
For personal use only.

and V where m^* calcd. = 187.0 and the peaks are observed at 187.5, 187.1, and 187.2, respectively. Similarly the transition M-43 → M-73 is supported by the presence of metastable peaks in the spectra of III and V where m^* calcd. = 160.2 and the peaks are observed at 160.2 and 160.5, respectively.

Other schemes may be written which lead to ions of the same composition as those depicted in Scheme 2. Thus the molecular ion might lose a CH_3 radical from one of the methoxyls on the benzenoid ring and this in turn fragment further by loss of CO to an ion of M-43. The M-43 ion formed in this process would then fragment through loss of the same species and in the same order as that depicted in Scheme 2.

In Scheme 3 a mechanism is postulated to account for the formation of the M-1 and

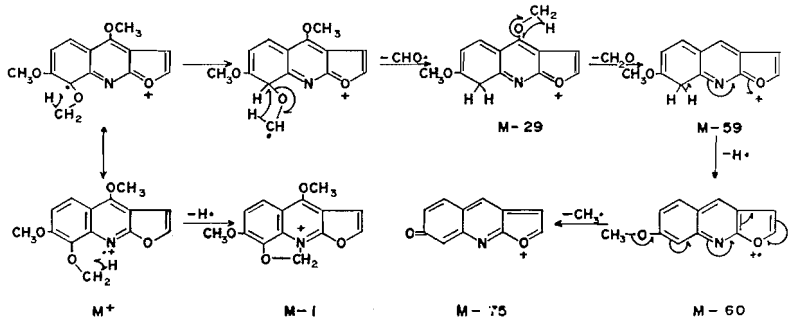

SCHEME 3.

M-29 peaks present in IV, V, and VI. These peaks as noted before differentiate those alkaloids carrying an 8-methoxy substituent from those which lack this structural feature. The formation of the ion M-1 is considered to arise by loss of H from the 8-OMe group and stabilization of the charge by the electron pair on nitrogen, either as shown by formation of a formal C—N bond or alternately by stabilization through space. In each case this transition is supported by a metastable peak at 257.0 in IV and V and at 271.1 in VI.

To account for the loss of 29 mass units (m.u.) in the spectra of IV, V, and VI, an insignificant process in I, II, and III, one must invoke a process involving the 8-OMe group. Loss of 29 m.u. from 1,3-dimethoxy benzene has been reported (4) and a similar fragmentation is shown in Scheme 3 for the generation of the M-29 ion. The loss of 29 m.u. in a concerted fashion is supported by the presence of metastable peaks in the spectra of IV and V, m^* calcd. M → M-29 = 204.2, m^* obsd. = 204.5 in each case. The peak appearing at M-60 in IV, V, and VI may form from M-29 through loss of OCH_3 radical in a single step or in a stepwise fashion by loss of $CH_2{=}O$ and a H radical. Barnes and Occolowitz (4) state that CH_3O is always lost in two steps. However, we have observed one-step loss of CH_3O as discussed previously. In Scheme 3 we have depicted the M-60 radical-ion arising from the M-29 ion by loss of formaldehyde from the C-4 methoxyl followed by loss of H from C_8. In IV and V a peak at M-75 may form by loss of methyl radical from the ion of M-60 but this is not possible in the case of flindersiamine, VI.

Flindersiamine and to a lesser degree skimmianine and maculosidine exhibit peaks at M-28. In the case of flindersiamine the formation of this ion in a concerted elimination is supported by a metastable peak at 220.1 (calcd. 219.9). It is difficult to see how the presence of an 8-methoxyl substituent favors loss of CO involving the furan oxygen. An attractive alternative involves migration of methyl from the 8-OMe group to nitrogen followed by elimination of CO from position 8. Another, but less attractive route, is the loss of HCN from M-1.

Can. J. Chem. Downloaded from www.nrcresearchpress.com by 210.87.254.5 on 09/05/12
For personal use only.

In the spectra of IV, V, and VI peaks are observed at M-30 and M-45. The M-30 peak may arise by loss of formaldehyde from the molecular ion or alternately by loss of CH_3 from the M-15 species. In the case of IV a metastable peak is present corresponding to the transition M-15 → M-30 (m^* calcd. 214.9) m^* obsd. = 215.1 but no metastable peak corresponding to this transition is present in the spectra of V and VI. It is likely that both processes are operative and the loss of 15 m.u. from M-30 would appear more likely through the sequence M → M-30 → M-45 than the alternate M-15 → M-30 → M-45. In fact the latter is impossible in the case of VI. It is worthwhile to point out that the M-30 ion derived from VI by loss of formaldehyde from C_8 is identical with the molecular ion of II and thus all the peaks observed in the maculine spectrum should be present in VI as in fact they are. Flindersiamine is the only alkaloid of the group which shows a relatively intense peak at M-16. Its formation through the transition M-1 → M-16 is supported by the presence of a metastable peak at 243.0 (m^* calcd. 272 → 257 = 242.8). It is likely that the small M-16 peak observed in the spectra of IV and V may also be attributed to fragmentation via a similar route.

EXPERIMENTAL

The spectra were recorded on a Hitachi Perkin-Elmer RMU-6A mass spectrometer fitted with an all-glass inlet system maintained at 200 °C at an ionizing potential of 80 eV and an ionizing current of 50 μA.

All spectra are plotted in terms of relative abundance with the most intense peak (base peak) being taken as 100%. Only those peaks with an intensity equal to or greater than 2% of the base peak are recorded.

ACKNOWLEDGMENTS

We wish to thank Dr. E. Ritchie, Department of Organic Chemistry, The University of Sydney, Sydney, N.S.W., Australia, for samples of the alkaloids used in this investigation. This work was supported by a grant from the National Research Council of Canada.

REFERENCES

1. J. Collin. Bull. Soc. Chim. Belges, **69**, 449 (1960).
2. C. S. Barnes and J. L. Occolowitz. Australian J. Chem. **17**, 975 (1964).
3. H. Budzikiewicz, C. Djerassi, and D. H. Williams. Interpretation of mass spectra of organic compounds. Holden-Day Inc., San Francisco. 1964. p. 257.
4. C. S. Barnes and J. L. Occolowitz. Australian J. Chem. **16**, 219 (1963).
5. Z. Pelah, J. M. Wilson, M. Ohashi, H. Budzikiewicz, and C. Djerassi. Tetrahedron, **19**, 2233 (1963).

Can. J. Chem. Downloaded from www.nrcresearchpress.com by 210.87.254.5 on 09/05/12
For personal use only.

Can. J. Chem. Downloaded from www.nrcresearchpress.com by 210.87.254.40 on 09/05/12
For personal use only.

EFFECT OF WATER VAPOR ON THE FORMATION OF $CaSO_4 \cdot \frac{1}{2}H_2O$ MODIFICATIONS

R. A. KUNTZE

Cementitious Materials Section, Department of Materials Chemistry, Ontario Research Foundation, Toronto, Ontario

Received April 9, 1965

ABSTRACT

The two recognized forms of calcium sulfate hemihydrate can be identified by the position of a relatively small exothermic peak in their differential thermograms. Hemihydrates prepared at various water vapor pressures up to 760 mm Hg were found to produce this exothermic peak in a position which is characteristic for the β-form. These results indicate that α-hemihydrate cannot be made at atmospheric pressure, as was previously suggested on the basis of heat solution measurements. The typical differential thermogram of α-hemihydrate is only obtained with material made by dehydration in solution or by autoclaving. The effect of ambient water vapor pressure on the position of the three peaks that occur in the differential thermogram of $CaSO_4.2H_2O$ has also been studied. It was found that the incipient temperature of the second endothermic peak, corresponding to the transition of hemihydrate to soluble anhydrite, is displaced independent of the rate of heating from 145 °C to 187 °C with increasing water vapor pressures up to 760 mm Hg. This indicates that, for each temperature, a threshold water vapor pressure exists, above which soluble anhydrite cannot be formed.

Calcium sulfate hemihydrate can be prepared from dihydrate ($CaSO_4.2H_2O$) by three types of dehydration methods, i.e., calcination at atmospheric pressures, digesting in salt solutions, and autoclaving in lump form followed by grinding. The hemihydrates obtained differ in a variety of properties, such as density (1), gauging water requirement (2), heat of solution (3, 4), differential thermal analysis (d.t.a.) exotherms (5, 6), and possibly X-ray diffraction pattern (7). There is general agreement that these differences, which reflect the degree of crystal lattice perfection and surface characteristics, indicate the existence of at least two hemihydrate modifications. This has led to the development of the α- and β-hemihydrate theory (4, 8). Based on limited heat of solution data, the theory states that α-hemihydrate is not only produced by solution processes or autoclaving but also at atmospheric pressure, if the atmosphere is saturated with water vapor. In the absence of water vapor the resulting hemihydrate is of the β-form and at intermediate water vapor pressures the heats of solution indicate mixtures of the two modifications. For example, approximately 75% α-hemihydrate and 25% β-hemihydrate are obtained by dehydration in an atmosphere "nearly saturated with water vapor" (4).

A number of objections have been raised against the part of the theory which deals with dehydrations at atmospheric pressures (9, 10). Hence, a study has been made of the effect of the ambient water vapor pressure present during dehydration on the formation of hemihydrate modifications. For this purpose, differential thermal analysis has been used under controlled atmospheric conditions, such as dry nitrogen, steam, and a number of intermediate partial water vapor pressures. This method has the advantage that it permits the preparation of the hemihydrate and its subsequent identification in one uninterrupted experimental procedure. With the same experiment, it is also possible to study the effect of the ambient water vapor pressure on all dehydration processes occurring within the same temperature range.

EXPERIMENTAL

The differential thermal analysis instrument and the sample holder geometry have been described in detail in an earlier publication (6).

A heating rate of 6 deg min^{-1} was used below 200 °C, since this rate was found to give the best combination of peak definition and resolution. Above 200 °C, a heating rate of 12 deg min^{-1} was necessary to obtain a satisfactory definition of the smaller exothermic peak. The differences between the temperatures of the block and the sample did not exceed 1.5 deg over the entire range of temperatures up to 500 °C. The incipient and peak temperatures reported are those of the block at the time when these points occurred in the thermogram.

The water vapor pressure surrounding the sample was controlled within ±4 mm Hg by passing through the furnace a stream of nitrogen containing known amounts of water vapor. Experiments were carried out at various partial water vapor pressures, in dry nitrogen, and in a steam atmosphere.

The differential thermograms were obtained with −325 mesh samples of a relatively pure form of natural gypsum from San Marcus, Mexico, analyzed to be 99.5% $CaSO_4.2H_2O$. All samples were diluted to 20% with ignited alumina, which was also used as reference material. The results were verified in a number of cases with synthetic gypsum and natural gypsums of different origin.

The gauging water requirement of hemihydrates, obtained at different water vapor pressures, was determined according to ASTM C-472 (11). In order to produce the larger quantities necessary for this determination, each dehydration experiment was repeated with the sample holder being replaced by a ceramic boat, not containing differential thermocouples. In these experiments, heating was discontinued at 200 °C. Additional differential thermal analyses were carried out with these materials to identify the hemihydrate modification, and to establish the absence of residual dihydrate and soluble anhydrite (12).

RESULTS

For the purpose of the present series of experiments, the differential thermograms were considered to consist of two stages (as shown schematically in Fig. 1). During the first stage, hemihydrate is prepared by dehydration of the dihydrate (gypsum) under controlled conditions of partial water vapor pressure. This stage is characterized by one relatively large endothermic peak and is always completed at 150 °C. During the second stage, the hemihydrate formed is further dehydrated to soluble anhydrite, producing an endothermic peak below 200 °C, and this anhydrite is subsequently converted to insoluble anhydrite, as indicated by a smaller exothermic peak. The exact position of the exothermic peak within the differential thermogram can be used for the identification of the hemihydrate form obtained during the first stage.

In Fig. 2, the results are shown in form of actual differential thermograms, obtained

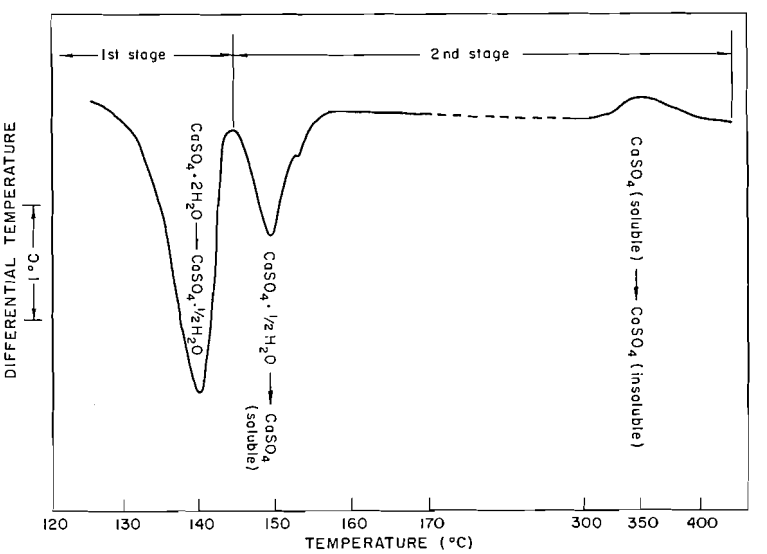

FIG. 1. Formation of $CaSO_4.\frac{1}{2}H_2O$ (1st stage) and subsequent identification (2nd stage) during differential thermal analysis.

Can. J. Chem. Downloaded from www.nrcresearchpress.com by 210.87.254.40 on 09/05/12
For personal use only.

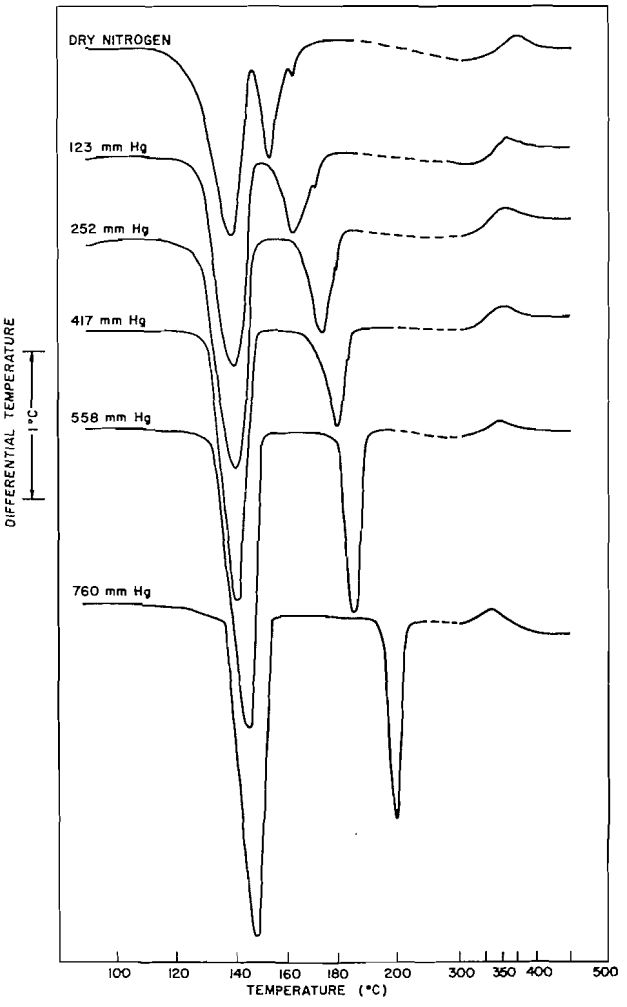

FIG. 2. Differential thermograms of $CaSO_4.2H_2O$ at increasing water vapor pressures.

with increasing ambient water vapor pressures from 0 to 760 mm Hg. The first endothermic peaks, corresponding to the dehydration process

$$CaSO_4.2H_2O_{(s)} = CaSO_4.\tfrac{1}{2}H_2O_{(s)} + 1\tfrac{1}{2}H_2O_{(v)}$$

are affected only to the extent that their incipient temperature increases from 110 °C to 120 °C, while the temperature of the peak does not change. The height of the peaks increases somewhat, indicating a small increase in the rate of dehydration at higher vapor pressures. The first stage of the experimental procedure is completed when these endothermic peaks have appeared, since the hemihydrate present has been prepared under the desired conditions. The second endothermic peaks, representing the continued dehydration

$$CaSO_4.\tfrac{1}{2}H_2O_{(s)} = CaSO_4(\text{soluble})_{(s)} + \tfrac{1}{2}H_2O_{(v)}$$

are effected by the increasing water vapor pressure to a much greater extent than the first endothermic peak. As shown in Fig. 2, the second endothermic peaks become sharper with higher partial water vapor pressures, indicating that hemihydrate is dehydrated at

Can. J. Chem. Downloaded from www.nrcresearchpress.com by 210.87.254.40 on 09/05/12
For personal use only.

faster rates. In Fig. 3, the incipient temperatures of these peaks, which are displaced from 145 °C in dry nitrogen to 187 °C at 760 mm Hg, are plotted against ambient water vapor pressure. These data agree with published calculations for isothermal dehydrations (4, 13), also shown in Fig. 3, except in one case, for which contradicting data are reported (14).

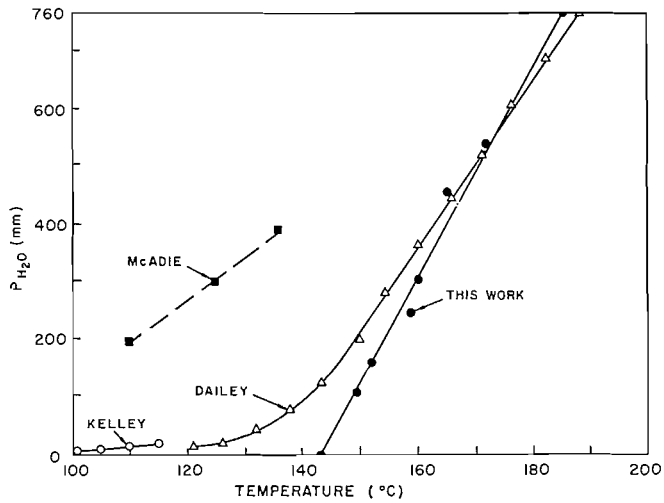

FIG. 3. The incipient temperature of $CaSO_4$ (sol.) formation depending upon water vapor pressure.

The displacement of the incipient temperature of the second endothermic peak, and the shapes of these peaks, suggest that for each temperature a threshold water vapor pressure exists, above which soluble anhydrite cannot be formed. This threshold effect can be demonstrated by producing differential thermograms at different rates of heating. Although the shapes of the second endothermic peaks vary slightly with the rate of heating, because of small differences in the rates of decomposition of hemihydrate, the incipient temperature of these peaks does not change due to the threshold effect of the water vapor pressure.

The third or exothermic peaks are important for the identification of the hemihydrate form produced during the first stage of the experimental procedure (5, 6). In the case of β-hemihydrates, the exothermic peaks occur at approximately 350 °C, whereas with α-hemihydrate, these peaks are observed below 250 °C, immediately following the second endotherms (Fig. 4). All exothermic peaks, obtained in this series of experiments, indicated the presence of the β-modification exclusively, independent of the ambient water vapor pressure present during the dehydration of the dihydrate.

The exclusive production of β-hemihydrate was verified by isothermal dehydration of larger quantities of dihydrate under controlled conditions of water vapor pressure. Subsequent differential thermal analyses at various rates of heating identified the hemihydrate produced in all cases as the β-form. The gauging water requirement of these hemihydrates was above 75 ml per 100 g and decreased to 55 ml per 100 g on exposure to 90% relative humidity at room temperature. The magnitude of the gauging water requirement, and the lack of stability on exposure to 90% relative humidity, is indicative of β-hemihydrate also. The water requirement of α-hemihydrate is approximately 35 ml per 100 g and does not change on exposure to 90% relative humidity.

Can. J. Chem. Downloaded from www.nrcresearchpress.com by 210.87.254.40 on 09/05/12
For personal use only.

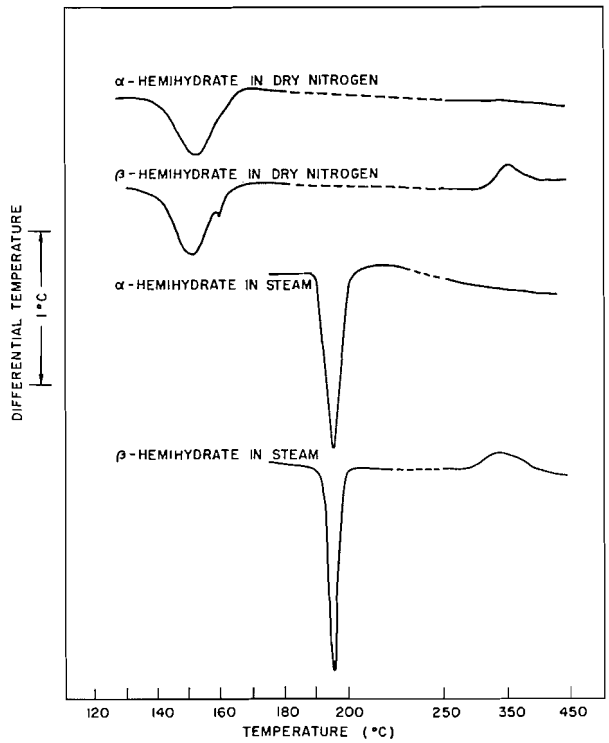

FIG. 4. Differential thermograms of $CaSO_4.\frac{1}{2}H_2O$ modifications.

DISCUSSION

The different physical properties of hemihydrates have been discussed extensively in a number of publications (1–8). In general, it is agreed that the method of dehydration is the most important single factor determining the hemihydrate properties. For example, it is recognized that dehydration in solution or by autoclaving produces the hemihydrate by recrystallization, and the resulting crystals are well developed, dense, and extinguish polarized light uniformly. Hemihydrate, or commercial plaster, made by these processes, has a low gauging water requirement, defined as ml water per 100 g hemihydrate to form a slurry with an arbitrarily established yield point. In contrast, atmospheric dehydration methods do not permit recrystallization and produce poorly defined crystals, or crystalline grains, which are porous and do not uniformly extinguish polarized light. Hemihydrate, or commercial plaster, made by this method, has a high gauging water requirement. The two types of hemihydrate can be prepared reproducibly by the appropriate dehydration methods, and it appears that they are defined adequately by the terms α- and β-hemihydrate, respectively.

It is important to realize that the properties of hemihydrates depend not only on the method of dehydration, but also on a number of other factors, such as particle size distribution and shape, impurities, etc. Therefore, it is obvious that the properties of α- and β-hemihydrates cannot be identical in all cases; instead, they must be expected to cover a range depending on the origin and the past history of the sample. Although these facts are established, an attempt has been made in the case of atmospheric dehydration processes to explain the range of properties obtained by the existence of mixtures of α- and β-hemihydrate. This theory is supported by a single set of heat of solution data (3)

Can. J. Chem. Downloaded from www.nrcresearchpress.com by 210.87.254.40 on 09/05/12
For personal use only.

which indicate that hemihydrate obtained at atmospheric pressures is identical to autoclaved hemihydrate or hemihydrate precipitated from acid or salt solutions. Mixtures of the two hemihydrate forms are obtained, therefore, whenever the water vapor pressure falls below 760 mm Hg.

Other experimental observations contradict this theory. For example, the increase in water vapor pressure during dehydration at atmospheric pressures increases the gauging water requirement. Since α-hemihydrate is characterized by a low water requirement, and since artificial mixtures of the two forms show the expected intermediate water requirements (Table I), it is difficult to accept that this modification is formed under conditions of high water vapor pressure. There is also no evidence to show that any other property of the hemihydrate, such as density, appearance under polarized light, rates of hydration or solution, etc., approaches that of α-hemihydrate when the water vapor pressure is increased. Of particular interest is the observation that the water requirements, and some other properties of hemihydrate prepared at atmospheric pressures, change noticeably on exposure to relative humidities above 50%. An increase in the ambient water vapor pressure increases the magnitude of the changes, although α-hemihydrate, prepared by solution processes, etc., does not change in water requirement on exposure.

Differential thermal analysis is the only known alternative method to heats of solution measurement for the identification of hemihydrate modifications. The results of the present work show clearly that α-hemihydrate is not obtained at atmospheric pressures. All differential thermograms of hemihydrates, prepared at atmospheric pressures, have the characteristic shape of β-hemihydrate shown in Fig. 4. The ambient water vapor pressure during dehydration has no effect on the position or the height of the third, i.e., exothermic peak in the differential thermograms. Since artificial mixtures of α- and β-hemihydrate are easily identified by differential thermal analysis (12), it can be concluded that an ambient water vapor pressure between 0 and 760 mm Hg does not produce mixtures of α- and β-hemihydrate.

In the light of the evidence presented in various publications (1–8) and in this paper, it appears that the α- and β-hemihydrate theory must be limited to the following statements.

1. α-Hemihydrate is prepared by dehydration methods, which permit recrystallization, i.e., by solution processes or autoclaving. This hemihydrate form can be identified by its differential thermogram in conjunction with its other properties, such as high density, uniform appearance under polarized light, and low water requirement, which is not affected by exposure to relative humidities above 50%.

2. β-Hemihydrate is prepared by atmospheric dehydrations independent of the ambient water vapor pressure. This hemihydrate form is characterized by its differential thermogram, as well as its low density, heterogeneous appearance under polarized light, and water requirement, which is always considerably higher than that of the α-form, and decreases on exposure to relative humidities above 50%.

Any conclusions based on heat of solution measurements should be treated with caution until additional supporting evidence has been reported.

ACKNOWLEDGMENTS

This work was carried out with a research grant to the Ontario Research Foundation, received from the Department of Economics & Development, Province of Ontario. The author also wishes to thank Mr. D. Renton and Mr. D. Kupke for the preparation of some of the differential thermograms.

Can. J. Chem. Downloaded from www.nrcresearchpress.com by 210.87.254.40 on 09/05/12
For personal use only.

Can. J. Chem. Downloaded from www.nrcresearchpress.com by 210.87.254.40 on 09/05/12
For personal use only.

TABLE I

Comparison of methods for the identification of hemihydrate forms

Method of dehydration	Heat of solution (kcal/mole)	Form identified by heat of solution	Position of exothermic peak (°C)	Form identified by peak position	Gauging water requirement (ml / 100 g)		Form identified by water requirement
					Not aged	Aged*	
In $CaCl_2$ solution	1.56	α	<250	α	32	30	α
In autoclave	1.56	α	<250	α	35	34	α
In steam at atmospheric pressure	1.56	α	350	β	98	64	β
In vacuum at 100 °C	1.11	β	350	β	79	61	β
In commercial kettle	1.45	75% α / 25% β	350	β	87	62	β
In dry nitrogen	1.11	100% β	350	β	80	61	β
In 123 mm Hg water	1.18	16% α / 84% β	350	β	>80	61	β
In 252 mm Hg water	1.27	33% α / 67% β	350	β	>80	62	β
In 417 mm Hg water	1.37	58% α / 42% β	350	β	>80	62	β
In 558 mm Hg water	1.46	78% α / 22% β	350	β	>80	61	β
In 760 mm Hg water							
25% autoclaved†, 75% in dry nitrogen	1.22	25% α / 75% β	<250 and 350	25% α / 75% β	70	56	25% α / 75% β
50% autoclaved†, 50% in dry nitrogen	1.34	50% α / 50% β	<250 and 350	50% α / 50% β	59	49	50% α / 50% β
75% autoclaved†, 25% in dry nitrogen	1.45	75% α / 25% β	<250 and 350	75% α / 25% β	48	42	75% α / 25% β

*Exposed to 90% relative humidity, 70 °F for 14 days.
†Artificial mixtures.

REFERENCES

1. E. EIPELTAUER. Zement-Kalk-Gips, **11**, 264 (1958).
2. C. M. LAMBE and J. S. OFUTT. Am. Ceram. Soc. Bull. **33**, 272 (1954).
3. J. C. SOUTHARD. Ind. Eng. Chem. **32**, 442 (1940).
4. K. K. KELLEY, J. C. SOUTHARD, and C. T. ANDERSON. U.S. Bur. Mines, Tech. Paper No. 625. 1941.
5. D. A. POWELL. Nature, **182**, 792 (1958).
6. W. E. P. FLECK, M. H. JONES, R. A. KUNTZE, and H. G. MCADIE. Can. J. Chem. **38**, 936 (1960).
7. R. J. MORRIS. Nature, **198**, 1298 (1963).
8. W. C. RIDDELL. Rock Products, **53**, 68 (1950).
9. E. EIPELTAUER. Zement-Kalk-Gips, **9**, 501 (1956).
10. R. A. KUNTZE. Mater. Res. Std. **2**, 640 (1962).
11. R. A. KUNTZE. ASTM Bull. May 1960.
12. R. A. KUNTZE. Mater. Res. Std. **2**, 232 (1961).
13. M. C. DAILEY. Can. Patent 564,225, 1958.
14. H. G. MCADIE. Can. J. Chem. **42**, 792 (1964).

Can. J. Chem. Downloaded from www.nrcresearchpress.com by 210.87.254.40 on 09/05/12
For personal use only.

Can. J. Chem. Downloaded from www.nrcresearchpress.com by 210.87.254.40 on 09/05/12
For personal use only.

^{35}Cl AND ^{37}Cl MAGNETIC RESONANCE OF SIMPLE CHLORINE COMPOUNDS[1]

YASUKAZU SAITO[2]
Division of Pure Chemistry, National Research Council, Ottawa, Canada

Received April 27, 1965

ABSTRACT

The nuclear magnetic resonances of ^{35}Cl and ^{37}Cl in a number of simple chlorine compounds were measured. Since both the paramagnetic contribution for chemical shift and the quadrupole coupling constant of the atom are determined by the same radial distribution of the electron, a linear relationship between the chemical shifts and the quadrupole coupling constants may be expected for compounds for which the electronic excitation energies are comparable. This was demonstrated for the series of chloro-substituted methanes. By graphical extrapolation the absolute chemical shift of the reference compound, NaCl aqueous solution, was obtained. The chemical shift of Cl^- aq. ion can be interpreted as the sum of the diamagnetic shift of Cl^- spherical ion and a paramagnetic shift resulting from its hydration. The experimental and theoretical values of the paramagnetic chemical shift of the Cl_2 molecule were -2.06×10^{-3} and -2.17×10^{-3}, respectively. Paramagnetic chemical shifts and line widths of resonance spectra of simple chlorine compounds are discussed, as well as the feasibility of high-resolution chlorine resonances for structural applications.

I. INTRODUCTION

While fluorine resonances have been extensively studied, both experimentally and theoretically, the resonances of other halogen nuclei have remained virtually unexplored. It was the purpose of this work to investigate to what extent chlorine resonances of simple covalently bonded compounds could be measured and what information could be derived therefrom.

All of the halogen nuclei, other than ^{19}F, possess large electric quadrupole moments and accordingly, in most molecular environments, they will have short nuclear relaxation times and greatly broadened resonance lines. The most favorable systems are the simple halide ions (e.g. Cl^-) in aqueous solution, which, because of the more symmetrical electronic environment, have relatively narrow lines (1). In covalently bonded compounds, and since halogens are monovalent, the nucleus is in a highly asymmetric field to which it is strongly coupled. In such cases the resonance lines are often broadened beyond detection. The ^{35}Cl resonance in CCl_4 and in $CHCl_3$ have been previously measured by Diehl (2).

In Table I, nuclear properties of chlorine are shown.

TABLE I

Nuclear properties of chlorine

Isotope	Natural abundance (%)	Magnetic moment μ (in multiples of the nuclear magneton $(eh/4\pi Mc)$)	Spin I (in multiples of $h/2\pi$)	Electric quadrupole moment Q (in multiples of $e \times 10^{-24}$ cm^2)
^{35}Cl	75.4	0.82089	3/2	-7.97×10^{-2}
^{37}Cl	24.6	0.68329	3/2	-6.21×10^{-2}

II. EXPERIMENTAL

The chlorine resonances were measured using a Varian V4210A broad-line spectrometer incorporating a lock-in amplifier with audio phase-sensitive detection at a magnetic field of 14.1 kG (5.89 Mc/s for ^{35}Cl and

[1]*Issued as N.R.C. No. 8545.*
[2]*National Research Council Postdoctorate Fellow, 1963–1964. Present address: Department of Chemistry, Northwestern University, Evanston, Illinois, U.S.A.*

4.90 Mc/s for ^{37}Cl). To avoid modulation broadening the modulation amplitude was progressively reduced until the width of the resonance being observed showed no further narrowing. The radio-frequency power and sweep rate were also optimized. Chemical shifts and line widths were measured for the derivative of the dispersion mode and of the absorption mode, respectively, by keeping H_0 fixed and sweeping the frequency using a Hewlett Packard frequency counter.

All experiments were done at room temperature. Cylindrical sample tubes with about 13 mm inside diameter were employed except for liquid chlorine which was sealed off after distillation in a spherical sample tube with capillary inlet. All compounds were available as commercial products and were measured as the neat liquid except for ionic compounds. Aqueous solutions of NaCl were prepared in various concentrations: 6.14 *M* (saturated solution), 5.00 *M*, 1.00 *M*, 0.50 *M*, and 0.10 *M*. The compounds $NaClO_4$ and $NaClO_3$ were measured as the saturated aqueous solution.

III. RESULTS AND DISCUSSION

Chemical shifts of the chlorine resonance of simple chlorine compounds may be written (3)

[i] $$\delta = \delta_d + K\langle r^{-3}\rangle_{av}\Delta E^{-1}.$$

The first term is the diamagnetic contribution of the chlorine atom and the second term the paramagnetic contribution, in which $\langle r^{-3}\rangle_{av}$ is the average of $1/r^3$ over the radial part of the wave function for the electron, where r is measured with respect to the nucleus, ΔE is an average value of all the electronic excitation energies, and K is a constant. The quadrupole coupling constant e^2qQ is proportional to the same average radial distribution of the electron $\langle r^{-3}\rangle_{av}$ as

[ii] $$e^2qQ = e^2Q\left(\frac{l+1}{2l-1}\right)\left(\frac{2l}{2l+3}\right)\langle r^{-3}\rangle_{av}R',$$

where l is the orbital angular momentum of the electron ($l = 1$ for p electron) and R' is a relativistic correction factor (4). Then eq. [i] may be written

[iii] $$\delta = \delta_d + K'(\Delta E^{-1})(e^2qQ).$$

The chemical shifts of chloro-substituted methanes, CH_3Cl, CH_2Cl_2, $CHCl_3$, and CCl_4, have been measured in p.p.t. (parts per thousand) relative to Cl^- as an aqueous solution of NaCl ($\delta = (H - H_{Cl^-})/H_{Cl^-} \times 10^3$, cf. Table II) and are plotted against the quadrupole coupling constants of these compounds in Fig. 1. This gives an approximately linear relationship, which suggests that the electronic excitation energies of these compounds are almost the same. This is confirmed from the electronic absorption spectra measured by Lacher *et al.* (5) from which ΔE of CCl_4, $CHCl_3$, and CH_2Cl_2 can be estimated as 5.25 eV, 5.42 eV, and 5.77 eV, respectively.

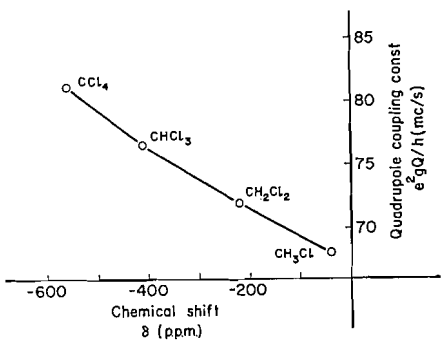

FIG. 1. ^{35}Cl chemical shifts vs. ^{35}Cl quadrupole coupling constants of chloro-substituted methanes. Chemical shifts are relative to chlorine aqueous ion.

Can. J. Chem. Downloaded from www.nrcresearchpress.com by 210.87.254.40 on 09/05/12
For personal use only.

Can. J. Chem. Downloaded from www.nrcresearchpress.com by 210.87.254.40 on 09/05/12
For personal use only.

The concentration dependence of the chemical shift of Cl^- as an aqueous solution of NaCl was studied from 6.14 M of the saturated solution to 0.10 M and no variation was detected. Therefore, the observed shift cannot be interpreted as the result of ion–ion interaction as in the case of CsBr (6), but rather as the sum of the diamagnetic shift of Cl^- spherical ion and the paramagnetic shift caused by its hydration. Dickinson calculated the diamagnetic shift of Cl^- ion as 1.15 p.p.t., using Hartree-type self-consistent functions for S-state Cl^- ion (7). When we extrapolate the quadrupole coupling constants to zero by using the linear relationship in Fig. 1, we obtain a chemical shift of −2.90 p.p.t., from which the paramagnetic chemical shift of Cl^- caused by hydration can be derived as −1.75 p.p.t. (The reference substance of chemical shifts in Fig. 1 is chlorine aqueous ion.) This value appears reasonable. By comparison the calculated paramagnetic shift of the F_2 molecule is 20×10^{-4} (8), and its observed shift relative to F^- aqueous ion, −548.2 p.p.m. (9), so by difference the paramagnetic chemical shift of hydrated fluorine ion is −1.45 p.p.t. The kind of derivation used for the Cl^- ion is impossible for fluorine aqueous ion, since the fluorine nucleus has no quadrupole moment.

The chemical shift of liquid chlorine has been measured as −0.31 p.p.t. relative to chlorine aqueous ion. Therefore, the true paramagnetic component of the chemical shift of Cl_2 must be −2.06 p.p.t. Applying the theoretical treatment of paramagnetic shifts by Saika and Slichter (8) to the Cl_2 molecule instead of the F_2 molecule yields

$$\text{[iv]} \qquad \delta_p = -\frac{2}{3}\frac{e^2\hbar^2}{m^2c^2}\langle r^{-3}\rangle_{av}\,\Delta E^{-1}.$$

Using 3.67 eV (3380A) for ΔE (10) and 8.24 a_0^{-3} for $\langle r^{-3}\rangle_{av}$ (11), we obtain $\delta_p = -2.17$ p.p.t. from eq. [iv], in good agreement with the observed value.

Chemical shifts of ^{35}Cl resonances and absorption line widths of both ^{35}Cl and ^{37}Cl in several chlorine compounds are listed in Table II. The values of the paramagnetic chemical shifts of these compounds, obtained by adding −1.75 p.p.t. to the observed chemical shifts, are shown in the fourth column. The quadrupole coupling constants as well as viscosity and molecular volume data are also shown in this table.

As shown in Table II, ClO_4^- aqueous ion and ClO_3^- aqueous ion give the largest paramagnetic shift, which may be due to the double bond character in the Cl—O bond. Among carbon-bound chlorine compounds, the paramagnetic shifts are well understood in terms of the electronegativity of the group to which chlorine is bonded. Thus, the more ionic character, the less paramagnetic contribution.

The line widths of ^{35}Cl resonance in Table II could be related to their corresponding quadrupole coupling constants by the equation (12),

$$\text{[v]} \qquad \Delta H = \frac{1}{T_1} = \frac{3}{8}\left(\frac{e^2qQ}{\hbar}\right)^2\left(\frac{4\pi\eta a^3}{3kT}\right),$$

where ΔH is the absorption line width, T_1 the spin lattice relaxation time, η the viscosity of the liquid, and a the effective molecular radius. Accordingly the ratio R, defined by

$$\text{[vi]} \qquad R = (\Delta H)/\left(\frac{e^2qQ}{h}\right)^2(\eta)(a^3),$$

should be a constant. As shown in the eighth column of Table II, this is approximately confirmed. The line widths of chlorine resonances are thus to be understood from the viewpoint of quadrupole interaction.

Can. J. Chem. Downloaded from www.nrcresearchpress.com by 210.87.254.40 on 09/05/12
For personal use only.

TABLE II

Results of magnetic resonance and some properties of simple chlorine compounds

Compound	Chemical shift observed δ (p.p.t.)	Line width observed ΔH (G)		Paramagnetic chemical shift* δ_p (p.p.t.)	Quadrupole coupling constant† e^2qQ/h (mc/s)	Viscosity η_{20} (cP)	Molecular volume a^3 (cm^3)	Ratio‡ R
	^{35}Cl	^{35}Cl	^{37}Cl	^{35}Cl	^{35}Cl			
Cl^- aq. ion	0	<0.1	<0.1	−1.75	—	—	—	—
ClO_4^- aq. ion	−1.00	<0.1	<0.1	−2.75	—	—	—	—
ClO_3^- aq. ion	−1.05	18.7	11.3	−2.80	59.6	—	—	—
Cl_2	−0.31	11.8	7.3	−2.06	109.0	—	—	—
CCl_4	−0.56	22.5	12.5	−2.31	81.2	0.97	95.8	2.2
$CHCl_3$	−0.41	17.6	10.7	−2.16	76.2	0.58	79.5	1.2
CH_2Cl_2	−0.22	10.4	6.7	−1.97	72.0	0.43	63.5	1.1
CH_3Cl	−0.04	4.4	2.9	−1.79	68.0	0.18	52.5	0.8
CH_3COCl	−0.20	6.6	4.1	−1.95	57.4	0.38	71.0	0.9
C_6H_5Cl	—	33.5	—	—	69.2	0.80	109	1.0

*Paramagnetic chemical shift was calculated by adding the chemical shift observed relative to chlorine aqueous ion to the paramagnetic chemical shift of chlorine aqueous ion.
†Data of quadrupole coupling constants were taken from ref. 4. The value of CH_3COCl was estimated by extrapolation on the series of CCl_3COCl, $CHCl_2COCl$, and $CH_2ClCOCl$.
‡See eq. [vi]. C_6H_5Cl was taken as basis.

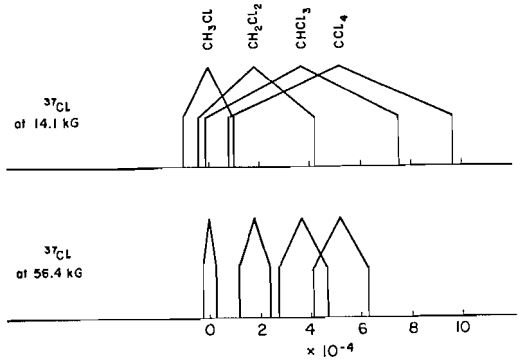

FIG. 2. ^{37}Cl chemical shifts and line widths of chloro-substituted methanes at different magnetic field. Top diagram shows measured resonances at 14.1 kG. Bottom diagram indicates resolution expected at 56.4 kG.

As shown in Table I the ^{37}Cl nucleus has a smaller natural abundance and magnetic moment than ^{35}Cl, which causes weaker signal strengths than the former. But its smaller quadrupole moment favors the resolution of resonance spectra. ^{37}Cl resonance of 1-chloro-2-dichloroethane $CH_2ClCHCl_2$ and chloroacetyl chloride $CH_2ClCOCl$ in which the two non-equivalent Cl's were distinguished by pure quadrupole resonance experiments (13) have been tried, but unfortunately the spectra of these compounds were not resolved at 14.1 kG. However, as illustrated in Fig. 2 where line widths are shown schematically, resolution would be possible if the strength of magnetic field is increased, e.g. four times. The required magnetic field inhomogeneity is of the order to 1×10^{-4}, owing to the large intrinsic line widths. Therefore, chlorine resonances by use of superconducting magnets should be quite favorable for structural applications in chlorine chemistry.

ACKNOWLEDGMENT

The author wishes to express his gratitude to Dr. W. G. Schneider for helpful discussions and encouragement. He is also indebted to Dr. A. D. Buckingham for valuable suggestions and Mr. J. Nicholson and Mr. Y. Lupien for technical help.

REFERENCES

1. Y. MASUDA and T. KANDA. J. Phys. Soc. Japan **9**, 82 (1954). T. KANDA. J. Phys. Soc. Japan, **10**, 85 (1955). J. B. WERTZ. J. Chem. Phys. **24**, 484 (1956).
2. P. DIEHL. Helv. Phys. Acta, **29**, 219 (1956).
3. J. A. POPLE, W. G. SCHNEIDER, and H. J. BERNSTEIN. High-resolution nuclear magnetic resonance. McGraw-Hill Book Co., Inc., New York. 1959. p. 170.
4. T. P. DAS and E. L. HAHN. Nuclear quadrupole resonance spectroscopy. *In* Solid state physics. Suppl. 1. Academic Press, Inc., New York. 1958. p. 120.
5. J. P. LACHER, L. E. HUMMEL, E. F. BOHMFALK, and J. D. PARK. J. Am. Chem. Soc. **72**, 5486 (1950).
6. R. E. RICHARDS and B. A. YORKE. Mol. Phys. **6**, 289 (1963).
7. W. C. DICKINSON. Phys. Rev. **80**, 563 (1950).
8. A. SAIKA and C. P. SLICHTER. J. Chem. Phys. **22**, 26 (1954).
9. H. S. GUTOWSKY and C. J. HOFFMAN. Phys. Rev. **80**, 110 (1950).
10. A. EUCKEN and K. H. HELLWEGE (*Editors*). Landolt-Bornstein Zahlenwerte und Funktionen aus Physik, Chemie, Astronomie, Geophysik, und Tecknik. 6 Aufl. Band I. Springer-Verlag, Berlin. 1951. Teil 3.
11. R. STERNHEIMER. Phys. Rev. **84**, 244 (1951).
12. J. A. POPLE, W. G. SCHNEIDER, and H. J. BERNSTEIN. High-resolution nuclear magnetic resonance. McGraw-Hill Book Co., Inc., New York. 1959. p. 214.
13. P. J. BRAY. J. Chem. Phys. **23**, 704 (1955).

Can. J. Chem. Downloaded from www.nrcresearchpress.com by 210.87.254.40 on 09/05/12
For personal use only.

Can. J. Chem. Downloaded from www.nrcresearchpress.com by 210.87.254.42 on 09/05/12
For personal use only.

THE CHEMISTRY OF THE AMINOCHROMES. PART VIII

THE PREPARATION AND PROPERTIES OF 4- AND 7-METHYLADRENOCHROME[1]

R. A. HEACOCK[2] AND O. HUTZINGER[3]

The Psychiatric Research Unit, University Hospital, Saskatoon, Saskatchewan

Received April 15, 1965

ABSTRACT

Two new catecholamines, 2- and 5-methyladrenaline, have been prepared from 3-methylcatechol and they gave 4- and 7-methyladrenochrome, respectively, on oxidation. 7-Iodo-4-methyladrenochrome was obtained on oxidation of 2-methyladrenaline with potassium iodate; however, an iodoaminochrome could not be obtained in a similar manner from 5-methyladrenaline. The expected 5,6-dihydroxyindole derivatives were obtained on reduction of these aminochromes.

It has been known for many years that the oxidation of adrenaline with potassium iodate leads to the formation of deep-violet products (1, 2). The compound responsible for the violet color was first isolated in 1937 by Richter and Blaschko who described it as 3-hydroxy-2-iodo-1-methylindoline-5,6-quinone (i.e. 2-iodoadrenochrome) (3). However, it has recently been shown that iodination actually occurs in the 7-position of the adrenochrome nucleus and it was further demonstrated that iodination (and bromination) invariably occurs in the 7-position and not the 2-position in the aminochrome molecule (4).

As part of a research program into the chemistry of the aminochromes, that is being carried out in these laboratories, it was decided to prepare 2- and 5-methyladrenaline (I and II respectively) and to investigate the effects of the methyl substitution of the aromatic ring on the oxidation of these hitherto unknown catecholamines with several different oxidizing agents.

It was possible to prepare I and II by procedures similar to that originally described by Stolz for the preparation of adrenaline (5). ω-Chloro-3,4-dihydroxy-2-methylacetophenone (III) was prepared from 3-methylcatechol (IV) by a Friedel–Crafts condensation with chloracetyl chloride in the presence of aluminium chloride in carbon disulfide solution. Methylation of the phenolic hydroxy groups of III gave ω-chloro-3,4-dimethoxy-2-methylacetophenone (V), a compound that had previously been described in the literature (6), proving that the chloroacetyl residue had entered the aromatic ring of IV in the position ortho to the methyl group. The n.m.r. spectrum of III in hexadeuteroacetone showed two well separated doublets centered at δ 7.38 and δ 6.92 with a coupling constant of ca. 8.5 c.p.s., indicating the presence of two ortho aromatic hydrogens in the molecule and confirming the position of the chloroacetyl residue. ω-Methylamino-3,4-dihydroxy-2-methylacetophenone (VI) was prepared by treating III with methanolic methylamine at room temperature (cf. ref. 7). Treatment of III with sodium iodide in acetone gave 3,4-dihydroxy-ω-iodo-2-methylacetophenone (cf. ref. 6). Preliminary experiments indicated that there was no advantage in using the ω-iodo derivative to prepare VI. 2-Methyladrenaline (I) was obtained in good yield by catalytic hydrogenation of VI. The hydrochloride of I was hygroscopic, but the acid oxalate salt of I was not and was readily purified by recrystallization from aqueous ethanol.

[1]*This investigation was supported by grants from the Department of National Health and Welfare, Ottawa, and the Saskatchewan Department of Public Health.*

Part VII. J. Chem. Soc. In press. 1965.

[2]*Present address: The Atlantic Regional Laboratory, The National Research Council, 1411 Oxford St., Halifax, Nova Scotia.*

[3]*Present address: The Department of Plant Pathology, The University of California, Davis, California, U.S.A.*

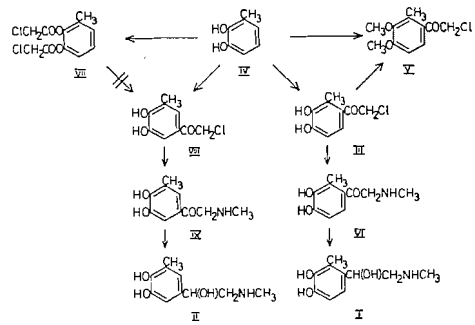

SCHEME 1.

The condensation of 3-methylcatechol (IV) with chloroacetyl chloride in boiling benzene, in the presence of phosphorus oxychloride (i.e. using conditions similar to those originally employed for synthesis of compounds of this type (cf. ref. 5, 8, 9), gave a chloroacetyl derivative of 3-methylcatechol, isomeric with, but different to, ω-chloro-3,4-dihydroxy-2-methylacetophenone (III), obtained by the conventional Friedel–Crafts procedure. This new ω-chloroacetophenone derivative was probably formed by a Fries rearrangement (cf. ref. 10) of an initially formed chloroacetyl ester of IV. In general this type of reaction can be carried out by either isolating a suitable ester of the catechol and subsequently rearranging it with either phosphorus oxychloride (9) or aluminium chloride (11), or by carrying out the entire procedure, without the isolation of the intermediate ester, in the presence of phosphorus oxychloride (9). In the present investigation, the latter procedure was employed. All attempts to bring about a direct Fries-type rearrangement of preformed 2,3-di(chloroacetoxy)toluene (VII) were unsuccessful. The n.m.r. spectrum of the second chloroacetophenone derivative in hexadeuteroacetone showed only a single peak (δ 7.5), corresponding to two hydrogens, in the aromatic proton region, effectively ruling out one of the two alternative structures, i.e., ω-chloro-2,3-dihydroxy-4-methylacetophenone, since the n.m.r. spectrum of this latter compound should indicate the presence of two ortho aromatic protons. Therefore, the only possible structure for this chloroactophenone derivative is ω-chloro-3,4-dihydroxy-5-methylacetophenone (VIII). 3,4-Dihydroxy-ω-methylamino-5-methylacetophenone (IX) was prepared by treatment of VIII with methanolic methylamine, and 5-methyladrenaline (II) was obtained by catalytic reduction of the aminoketone (IX). The hydrochloride, sulfate, and oxalate of 5-methyladrenaline (II) were prepared but were too hygroscopic to purify completely; however, it was possible to prepare a pure nonhygroscopic picrate of II.

4-Methyladrenochrome (X) was obtained as a deep-red crystalline solid on oxidation of 2-methyladrenaline (I) with silver oxide in dry methanol (cf. ref. 12); aqueous solutions of X were readily obtained by oxidizing the base (I) with potassium ferricyanide, buffered with sodium bicarbonate (cf. ref. 13). A crystalline monosemicarbazone of X could be prepared by standard procedures. 7-Iodo-4-methyladrenochrome (XI) was readily obtained as a violet-brown crystalline solid, when an aqueous solution of I was oxidized with potassium iodate.

5,6-Dihydroxy-1,4-dimethylindole (XII) was obtained on reduction of 4-methyladrenochrome (X) with ascorbic acid, and reduction of 7-iodo-4-methyladrenochrome (XI) with sodium borohydride gave 5,6-dihydroxy-7-iodo-1,4-dimethylindole (XIII); all attempts to reduce 7-iodo-4-methyladrenochrome (X I) with ascorbic acid, however, were

Can. J. Chem. Downloaded from www.nrcresearchpress.com by 210.87.254.42 on 09/05/12
For personal use only.

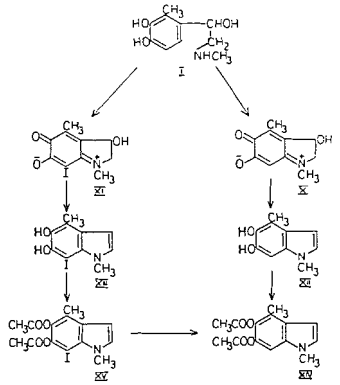

SCHEME 2.

unsuccessful. 5,6-Diacetoxy-1,4-dimethylindole (XIV) and 5,6-diacetoxy-7-iodo-1,4-dimethylindole (XV) were obtained on acetylation of XII and XIII respectively. Deiodination of XV with zinc and acetic acid gave XIV.

The red color of aqueous solutions of 4-methyladrenochrome (X) was discharged by alkali, with the formation of pale-yellow solutions, exhibiting the typical intense yellow green fluorescence associated with 5,6-dihydroxyindoxyls (see ref. 14 for references), indicating that the expected rearrangement of X to 4-methyladrenolutin had occurred. Treatment of an aminochrome with an acetic anhydride – pyridine mixture usually leads to the formation of a 3,5,6-triacetoxyindole derivative (cf. refs. 13, 15). However, solutions of 7-iodo-4-methyladrenochrome (XI) in acetic anhydride – pyridine mixtures did not lose their violet color, even after they had stood for several weeks at room temperature or had been heated at 80° for 2 h, suggesting that no reaction had occurred in this case.

7-Methyladrenochrome (XVI) was obtained as a dark violet, almost black, crystalline solid by the oxidation of 5-methyladrenaline (II) with potassium ferricyanide, in aqueous solution; it could also be prepared, in relatively poor yield, by the oxidation of II by silver oxide in methanol. The properties of the aminochrome (XVI) are unusual in several respects. The low water-solubility of XVI is unusual for non-halogenated aminochromes; aqueous solutions of XVI are violet, and not red in color, showing visible absorption maxima at 534 mμ in water and at 530 mμ in methanol, i.e. at longer wavelengths than are usual for unhalogenated aminochromes (cf. refs. 14, 15, 16). This shift of the visible absorption maxima towards longer wavelengths appears to be associated with 7-substitution. All known 7-halogenoaminochromes absorb in the 530 mμ region (cf. ref. 14). Two other 7-methyl substituted aminochromes have been described; solutions of 7-methyldopachrome and 4,7-dimethylnorepinochrome were prepared by Cromartie and Harley-Mason, and were reported to be deep violet in color (17). It was not possible to prepare an iodo derivative of XVI by the oxidation of II with potassium iodate under a wide variety of conditions; the iodine-free aminochrome (XVI) was invariably obtained. It would appear, therefore, that when the 7-position of the aminochrome nucleus is blocked the iodine atom will not enter any of the alternative free positions in the molecule.

The violet color of aqueous solutions of XVI was also discharged by alkali; yellow fluorescent solutions, presumably containing the corresponding 5,6-dihydroxyindoxyl, were obtained. 5,6-Dihydroxy-1,7-dimethyindole (XVIII: R = H), was obtained on the reduction of 7-methyladrenochrome (XVI) by ascorbic acid; this 5,6-dihydroxyindole

Can. J. Chem. Downloaded from www.nrcresearchpress.com by 210.87.254.42 on 09/05/12
For personal use only.

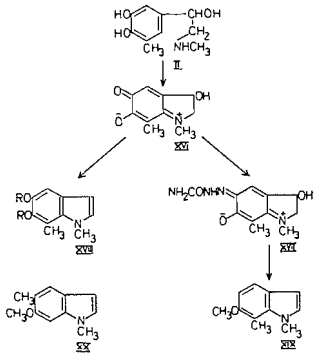

SCHEME 3.

derivative oxidizes readily in air, and was converted to its more stable diacetyl derivative (XVIII: R = CH_3CO).

The n.m.r. spectra of the three 5,6-diacetoxyindole derivatives (in deuterochloroform solution) described above (i.e. XIV, XV, and XVIII: R = CH_3CO) are fully compatible with the structures assigned to them on other grounds. The n.m.r. spectrum of 5,6-diacetoxy-1,4-dimethylindole (XIV) exhibited a singlet peak at δ 6.95, corresponding to the aromatic hydrogen in the 7-position; the hydrogens in the 2- and 3-positions of the indole nucleus in XIV gave rise to two doublets centered at δ 6.96 and δ 6.43 respectively, with a coupling constant of ca. 3 c.p.s. In the case of 5,6-diacetoxy-1,7-dimethylindole (XVIII: R = $COCH_3$), the 4-hydrogen was observed as a singlet at δ 7.19; the 2- and 3-hydrogens gave rise to two doublets centered at δ 6.89 and δ 6.35 respectively with a coupling constant of ca. 3 c.p.s. As would have been expected the n.m.r. spectrum of 5,6-diacetoxy-7-iodo-1,4-dimethylindole (XV) only showed two doublets, due to the 2- and 3-hydrogens, centered at δ 6.96 and δ 6.38 respectively, with a coupling constant of ca. 3 c.p.s. The positions (δ values) of the signals (and the coupling constants) due to the various hydrogen atoms in these substituted indole nuclei are quite compatible with what would have been expected from a consideration of the literature on the n.m.r. spectra of indoles (cf. refs. 4, 18, 19, 20).

5-Methyladrenaline (II) has two positions ortho to the ethanolamine side chain at which intramolecular cyclization might occur during aminochrome formation. However, theoretical considerations and consideration of all reported aminochrome cyclizations suggest that cyclization would occur at the 6-position (after the initial oxidation of the catocholamine to an uncyclized *o*-quinone derivative). If the cyclization occurred in the above manner a normal aminochrome (i.e. 7-methyladrenochrome (XVI)) would result. However, if cyclization had taken place at the 2-position in II, an abnormal aminochrome with the *o*-quinone function in the 6,7-position of the indole ring system would have resulted. To show that abnormal cyclization had not occurred, the monosemicarbazone (XVII) obtained from this aminochrome was treated with hot aqueous alkali, a procedure known to remove the semicarbazide residue from adrenochrome monosemicarbazones (21). The n.m.r. spectrum of the degradation product demonstrated that it was derived from 7-methyladrenochrome (XVI), since the degradation product was clearly 6-methoxy-1,7-dimethylindole (XIX). If abnormal cyclization had occurred during the aminochrome formation from II, the final product would have been 6-methoxy-1,5-dimethylindole (XX). The n.m.r. spectra of the degradation product (i.e. 6-methoxy-1,7-dimethylindole

Can. J. Chem. Downloaded from www.nrcresearchpress.com by 210.87.254.42 on 09/05/12
For personal use only.

(XIX)) in carbon tetrachloride and deuterochloroform both clearly show the presence of two aromatic hydrogens in an ortho relationship to each other. These aromatic hydrogen peaks are observed as doublets with a coupling constant of ca. 8.5 c.p.s. In the alternative structure (i.e. XX) the two hydrogens would be in a para relationship to each other and would not be expected to show a coupling constant of this magnitude. The δ values obtained are given in Table I.

TABLE I

Nuclear magnetic resonance spectral data for 6-methoxy-1,7-dimethylindole*

	Values of δ			
Solvent	4-H	5-H	2-H	3-H
CCl_4	7.16	6.62	6.62	6.16
$CDCl_3$	7.35	6.79	6.81	6.33

*All peaks are doublets; the δ values are calculated from the observed doublets.
The coupling constants observed for the 4- and 5-hydrogens are ~8.5 c.p.s. and those for the 2- and 3-hydrogens are ~3.2 c.p.s.

EXPERIMENTAL

Unless otherwise stated the infrared spectra were recorded on a Beckman IR-8 recording spectrophotometer; the ultraviolet and visible absorption spectra were recorded on a Unicam SP.800 recording spectrophotometer and the nuclear magnetic resonance spectra were recorded on either a Varian A-60 or HA-100 instrument. Only the more important peaks in the infrared and nuclear magnetic resonance spectra of certain compounds, which are relevant to the discussion, are reported.

The light petroleum used throughout this investigation was B.D.H. AnalaR grade (b.p. 80–100°). Peroxide-free ether was invariably used to minimize loses of readily oxidizable indole derivatives.

ω-Chloro-3,4-dihydroxy-2-methylacetophenone (III)

Powdered anhydrous aluminium chloride (50 g) was added cautiously, with stirring, to a solution of 3-methylcatechol[4] (25 g) and chloroacetyl chloride (20 g) in carbon disulfide[5] (300 ml), at 10°, with the rigorous exclusion of moisture. The resulting suspension was boiled, under reflux, until the evolution of hydrogen chloride had virtually ceased (ca. 45 min). Ice water (1 000 ml) and concentrated hydrochloric acid (50 ml) were added cautiously to the reaction mixture after it had been allowed to cool to room temperature. The crude product which separated out as an "off-white" solid was removed by filtration, washed with water, and on recrystallisation from water gave ω-chloro-3,4-dihydroxy-2-methylacetophenone (24 g) in colorless needles, m.p. 178°, ν_{max}^{Nujol} 3 480; 3 340; 1 665 cm^{-1}. The n.m.r. spectrum of III in acetone-d_6 showed signals at δ 7.38 (doublet) and δ 6.92 (doublet); J = 8.5 c.p.s.

Anal. Calcd. for $C_9H_9ClO_3$: C, 53.96; H, 4.55; Cl, 17.22. Found: C, 54.16; H, 4.51; Cl, 18.08.

ω-Chloro-3,4-dimethoxy-2-methylacetophenone (V)

A solution of ω-chloro-3,4-dihydroxyacetophenone (1 g) and dimethyl sulfate (1.25 g) in acetone (30 ml) containing anhydrous potassium carbonate (1.4 g) was stirred and boiled under reflux for 8 h. After this time the suspension was poured into water (150 ml), and the aqueous reaction mixture was cooled to 5°. The crude crystalline product was removed by filtration, washed with water, and recrystallized from benzene – light petroleum. It gave ω-chloro-3,4-dimethoxy-2-methylacetophenone in colorless prisms (0.8 g), m.p. 101°, undepressed on admixture with an authentic sample, prepared by the method of Hornbaker and Burger (6). These two samples of this compound also had identical infrared spectra.

3,4-Dihydroxy-ω-iodo-2-methylacetophenone

A solution containing ω-chloro-3,4-dihydroxy-2-methylacetophenone (2 g) and sodium iodide (1.7 g) in acetone (250 ml) was stirred, at room temperature, for 30 min. After this time the solution was filtered, and the filtrate was evaporated to dryness. 3,4-Dihydroxy-ω-iodo-2-methylacetophenone (1.8 g) was obtained in pale-yellow needles, m.p. 171–172°, on recrystallization of the residue from aqueous ethanol.

Anal. Calcd. for $C_9H_9IO_3$: C, 37.01; H, 3.11. Found: C, 37.17; H, 3.11.

[4]*Obtained from the Aldrich Chemical Co.*

[5]*Two other solvents: 1,2-dichloroethane and nitromethane, were tried in place of the carbon disulfide, to reduce the danger of fire, since the carbon disulfide system is very inflammable, but these alternate solvents gave unsatisfactory results.*

Can. J. Chem. Downloaded from www.nrcresearchpress.com by 210.87.254.42 on 09/05/12
For personal use only.

3,4-Dihydroxy-2-methyl-ω-methylaminoacetophenone (VI)

ω-Chloro-3,4-dihydroxy-2-methylacetophenone (4 g) was added in portions to a stirred, cooled mixture of methanol (5 ml) and a solution of methylamine (Matheson Co.) in methanol (15 ml, saturated at 5°); stirring was continued until solution was complete (ca. 5 min). The resulting brown solution was allowed to stand at 5° for 2 h, during which time tan-colored prisms of 3,4-dihydroxy-2-methyl-ω-methylaminoacetophenone (2.3 g), m.p. 218–222° (with decomposition) separated out, ν_{max}^{Nujol} 3 200 – 2 600; 1 630 cm^{-1}. It was not possible to purify this product by recrystallization since it does not dissolve in most of the common solvents.

Anal. Calcd. for $C_{10}H_{13}NO_3$: C, 61.52; H, 6.71; N, 7.18. Found: C, 60.81; H, 6.72; N, 7.17.

The hydrochloride of 3,4-dihydroxy-2-methyl-ω-methylaminoacetophenone was prepared by stirring a suspension of the base in ethanol with excess concentrated hydrochloric acid; the base dissolved and colorless needles of 3,4-dihydroxy-2-methyl-ω-methylaminoacetophenone hydrochloride, m.p. 256° (with decomposition), separated out after the solution had been stirred at room temperature for a short time (ca. 5–15 min).

Anal. Calcd. for $C_{10}H_{14}ClNO_3$: C, 51.84; H, 6.12; N, 6.08; Cl, 15.30. Found: C, 51.90; H, 5.95; N, 5.76; Cl, 15.20.

Treatment of a solution of ω-chloro-3,4-dihydroxy-2-methylacetophenone (0.5 g) in ether (50 ml) with methanolic methylamine (3 ml) for a few minutes at room temperature gave pale-yellow needles (0.3 g), m.p. 155°. This product, which is readily soluble in water and ethanol, is probably a phenolic methylamine salt of ω-chloro-3,4-dihydroxy-2-methylacetophenone[6] (cf. refs. 5, 22).

Anal. Calcd. for $C_{10}H_{14}ClNO_3$: C, 51.84; H, 6.12; Found: C, 52.04; H, 6.24.

2-Methyladrenaline (I) Hydrogen Oxalate (i.e. 2-Methyl-α-methylaminomethylprotocatechuyl Alcohol Hydrogen Oxalate)

A suspension of 3,4-dihydroxy-2-methyl-ω-methylaminoacetophenone (5 g), oxalic acid dihydrate (3. 25 g), and 5% palladium–charcoal (3 g) in water (300 ml) at 40° was shaken in an atmosphere of hydrogen at atmospheric pressure for 30 h. After this time the reaction mixture was filtered, and the aqueous filtrate concentrated *in vacuo* (nitrogen "leak") to ca. 15 ml; colorless prisms of 2-methyladrenaline hydrogen oxalate (4.2 g) separated out after the concentrate had stood at room temperature overnight. A small sample of the product, purified for microanalysis by recrystallization from water, had m.p. 181° (with decomposition).

Anal. Calcd. for $C_{12}H_{17}NO_7$: C, 50.17; H, 5.97; N, 4.88. Found: C, 50.12; H, 6.11; N, 4.74.

2-Methyladrenaline (I) (Free Base)

A solution of 3,4-dihydroxy-2-methyl-ω-methylaminoacetophenone hydrochloride (3 g) in water (220 ml), containing 5% palladium–charcoal (1 g), was shaken in an atmosphere of hydrogen at atmospheric pressure for 8 h. The catalyst was removed by filtration and the clear filtrate was concentrated *in vacuo* (nitrogen "leak") below 40° to ca. 15 ml. Solid potassium carbonate (2 g) was added to the stirred solution; the crude base (2.6 g), which separated out after the reaction mixture had been allowed to stand at 5° for 1 h, was removed by filtration and was sufficiently pure for the next step in the synthesis of 4-methyladrenochrome. A sample of 2-methyladrenaline, purified for microanalysis by recrystallization from a large volume of methanol, was obtained in colorless prisms (m.p. 190–192° (with decomposition)).

Anal. Calcd. for $C_{10}H_{15}NO_3$: C, 60.89; H, 7.67; N, 7.10. Found: C, 60.85; H, 7.82; N, 6.82.

4-Methyladrenochrome (X) (cf. the Preparation of Adrenochrome by the Method of Heacock et al. (12))

2-Methyladrenaline (1 g) was suspended in absolute methanol (30 ml), and 98% formic acid was added dropwise, with stirring, until a clear solution was obtained. Freshly prepared silver oxide was added in portions to the vigorously stirred solution. After being stirred, at room temperature for 3 min, the reaction mixture was filtered through a Dowex-1 (Cl^-) resin bed (cf. ref. 12). 4-Methyladrenochrome (0.11 g) was obtained in dark-red needles (totally decomposed without melting by 132°)[7] from the deep-red filtrate after it had been allowed to stand at −20° for 4 h. A second crop (0.06 g) of crystalline 4-methyladrenochrome was obtained by adding anhydrous ether (15 ml) to the remaining filtrate and keeping the solution at −20° overnight, $\lambda_{max}^{H_2O}$ 222, 312, 490 mμ; $\lambda_{max}^{CH_3OH}$ 221, 308, 484 mμ.

Anal. Calcd. for $C_{10}H_{11}NO_3$: C, 62.16; H, 5.74; N, 7.25. Found: C, 62.12; H, 5.82; N, 7.01.

4-Methyladrenochrome Monosemicarbazone

A solution of 2-methyladrenaline hydrochloride, prepared by suspending 2-methyladrenaline (0.2 g) in water (1.5 ml) and cautiously adding 2 *N* hydrochloric acid, with shaking, until all the solid had dissolved, was oxidized with a solution of potassium ferricyanide (1.15 g) and sodium bicarbonate (0.4 g) in water (3 ml). A deep-red solution of 4-methyladrenochrome formed rapidly and considerable frothing occurred (due to the evolution of carbon dioxide). After this solution had been allowed to stand at room temperature for 5 min, a solution containing semicarbazide hydrochloride (0.2 g) and sodium acetate (0.2 g) in water (1.5 ml) was added; the reaction mixture, after being stirred at room temperature for 10 min and standing at 5° for 5 h,

[6]*ω-Chloro-3,4-dihydroxy-2-methylacetophenone could be extracted with ether from aqueous solutions of the yellow product which had been made alkaline with sodium hydroxide.*

[7]*The decomposition points of all the aminochromes and aminochrome semicarbazones described in this paper were measured on a Leitz hot-stage instrument.*

Can. J. Chem. Downloaded from www.nrcresearchpress.com by 210.87.254.42 on 09/05/12
For personal use only.

deposited dark reddish-orange crystals of the crude semicarbazone. 4-Methyladrenochrome monosemicarbazone (0.125 g) was obtained in deep-orange needles (totally decomposed without melting by 248°) on recrystallization of the crude product from a pyridine–water (1.1) mixture.

Anal. Calcd. for $C_{11}H_{14}N_4O_3$: C, 52.79; H, 5.64; N, 22.39. Found: C, 52.95; H, 5.72; N, 22.44.

7-Iodo-4-methyladrenochrome (XI)

Potassium iodate (1.7 g) was added, at room temperature with stirring, to an aqueous solution of 2-methyladrenaline hydrochloride (prepared by cautiously adding 2 *N* hydrochloric acid to a suspension of 2-methyladrenaline (1 g) in water (350 ml) until a clear solution was obtained). The reaction mixture was stirred for 3 h at 5°; during this time deep-violet needles of 7-iodo-4-methyladrenochrome (1.1 g) separated out (totally decomposed without melting by ca. 110°), $\lambda_{max}^{H_2O}$ 234, 314, 534 mμ; $\lambda_{max}^{CH_3OH}$ 234, 309, 530 mμ.

Anal. Calcd. for $C_{10}H_{10}INO_3$: C, 37.64; H, 3.16; I, 39.78; N, 4.38. Found: C, 37.74; H, 3.15; I, 39.85; N, 4.45.

5,6-Dihydroxy-1,4-dimethylindole (XII)

Ascorbic acid was added in portions to a vigorously stirred two-phase system, consisting of an aqueous solution of 4-methyladrenochrome (prepared as described above by the oxidation of 2-methyladrenaline (0.3 g) with potassium ferricyanide) and ether (20 ml), until the red color of the aqueous phase had disappeared. The ether layer was separated and the aqueous phase was extracted with a further quantity of ether. Dry benzene (10 ml) was added to the combined, dried (Na_2SO_4) ether solutions, and the resulting solution was concentrated to ca. 5 ml *in vacuo* (nitrogen "leak"); colorless prisms of 5,6-dihydroxy-1,4-dimethylindole (0.11 g), m.p. 140–141°, were obtained by the addition of a small quantity of *n*-heptane to the warm concentrated benzene solution.

Anal. Calcd. for $C_{10}H_{11}NO_2$: C, 67.78; H, 6.26; N, 7.91. Found: C, 67.56; H, 6.25; N, 7.87.

5,6-Diacetoxy-1,4-dimethylindole (XIV)

A mixture of dry pyridine (2 ml) and acetic anhydride (2 ml) was added to a dried ethereal solution of 5,6-dihydroxy-1,4-dimethylindole (prepared by the method described above). The light-brown solution, obtained after removal of the ether *in vacuo*, was allowed to stand overnight at room temperature and then poured into an ice–water mixture. The crude diacetate, that separated out, afforded colorless needles of 5,6-diacetoxy-1,4-dimethylindole (0.22 g), m.p. 135–136°, on recrystallization from benzene – light petroleum.

Anal. Calcd. for $C_{14}H_{15}NO_4$: C, 64.37; H, 5.79; N, 5.36. Found: C, 64.47; H, 5.82; N, 5.52.

5,6-Dihydroxy-7-iodo-1,4-dimethylindole (XIII)

Sodium borohydride was added cautiously to a vigorously stirred two-phase system, consisting of a suspension of 7-iodo-4-methyladrenochrome (0.5 g) in water (20 ml) and ether (20 ml), until the violet color of the aminochrome had been totally discharged. The ether layer was separated and the aqueous phase was extracted with a further quantity of ether. Dry benzene (10 ml) was added to the combined, dried (Na_2SO_4) ether extracts and the resulting solution was concentrated to ca. 5 ml *in vacuo* (nitrogen "leak"); colorless prisms of 5,6-dihydroxy-7-iodo-1,4-dimethylindole (0.19 g) were obtained by the addition of a small quantity of *n*-heptane to the warm concentrated benzene solution. This substance did not melt, but turned black somewhere between 140 and 180°, depending on the rate of heating.

Anal. Calcd. for $C_{10}H_{10}INO_2$: C, 39.62; H, 3.33; N, 4.62; I, 41.87. Found: C, 39.65; H, 3.24; N, 4.55; I, 42.04.

5,6-Diacetoxy-7-iodo-1,4-dimethylindole (XV)

A mixture of dry pyridine (2 ml) and acetic anhydride (2 ml) was added to a dried ethereal solution of 5,6-dihydroxy-7-iodo-1,4-dimethylindole, and the reaction mixture was worked up as described above. Colorless prisms of 5,6-diacetoxy-7-iodo-1,4-dimethylindole (0.22 g), m.p. 192–193°, were obtained on recrystallization of the crude product from benzene – light petroleum. The n.m.r. spectrum of this substance in deuterochloroform showed two doublets centered at δ 6.96 and δ 6.38 (J = 3.2).

Anal. Calcd. for $C_{14}H_{14}INO_4$: C, 43.43; H, 3.65; I, 32.79; N, 3.62. Found: C, 43.26; H, 3.72; I, 32.37; N, 3.57.

Deiodination of 5,6-Diacetoxy-7-iodo-1,4-dimethylindole (XV)

Zinc powder (0.8 g) was added in portions to a solution of 5,6-diacetoxy-7-iodo-1,4-dimethylindole in glacial acetic acid (5 ml). The suspension was boiled under reflux, with stirring, for 5 min and filtered, and the residual zinc was washed with a small quantity of hot glacial acetic acid. Crushed ice was added to the combined filtrate and washings and the resulting aqueous product was extracted several times with ether. The combined ether extracts were washed with aqueous sodium bicarbonate until free of acetic acid and finally with water. Dry benzene (5 ml) was added to the dried (Na_2SO_4) ether solution and the volume of the solution was reduced to ca. 3 ml. 5,6-Diacetoxy-1,4-dimethylindole (32 mg), identical in all respects with the sample prepared by the method described above, was obtained on the addition of a small quantity of light petroleum to the concentrated benzene solution.

Can. J. Chem. Downloaded from www.nrcresearchpress.com by 210.87.254.42 on 09/05/12
For personal use only.

2,3-Di(chloroacetoxy)toluene (VII)

A mixture of 3-methylcatechol (2 g) and chloroacetyl chloride (6 g) was heated in an oil bath at 120–130°, under anhydrous conditions, until hydrogen chloride evolution had ceased (i.e. ca. 90 min). The reaction mixture was poured into water (100 ml) and the product was stirred, at room temperature, for 30 min. The solid which precipitated after the aqueous product had been stored at 5° overnight gave colorless needles of 2,3-di(chloroacetoxy)toluene (3.8 g), m.p. 64°, on repeated recrystallization from aqueous ethanol, ν_{max}^{Nujol} 1 745, 1 770 cm^{-1}.

Anal. Calcd. for $C_{11}H_{10}Cl_2O_4$: C, 47.68; H, 3.63; Cl, 25.59. Found: C, 47.64; H, 3.81; Cl, 25.51.

ω-Chloro-3,4-dihydroxy-5-methylacetophenone (VIII)

A mixture of 3-methylcatechol (54 g), chloroacetic acid (47.3 g), pure phosphorus oxychloride[8] (28 g), and dry benzene was boiled, under reflux, in a nitrogen atmosphere, for 3½ h. Carbon tetrachloride (150 ml) was added and the reaction mixture allowed to stand overnight at 5°. The crude ω-chloro-3,4-dihydroxy-5-methylacetophenone (24 g), m.p. 178°, which separated as a pale-pink solid, was sufficiently pure for use in the next stage of the synthesis and was used directly, after washing with water and carbon tetrachloride. A sample was purified for analysis by recrystallization from water and had m.p. 180°, ν_{max}^{Nujol} 3 490, 3 290, 1 670 cm^{-1}. The n.m.r. spectrum of this substance in acetone-d_6 showed a single singlet peak (δ 7.5) in the aromatic hydrogen region.

Anal. Calcd. for $C_9H_9ClO_3$: C, 53.96; H, 4.55; Cl, 17.72. Found: C, 53.87; H, 4.29; Cl, 17.85.

3,4-Dihydroxy-ω-iodo-5-methylacetophenone

3,4-Dihydroxy-ω-iodo-5-methylacetophenone (pale-yellow needles, m.p. 177°) was prepared from the corresponding chloro compound by a procedure identical to that described above for the preparation of the analogous 2-methylacetophenone derivative.

Anal. Calcd. for $C_9H_9IO_3$: C, 37.01; H, 3.11. Found: C, 37.25; H, 3.38.

3,4-Dihydroxy-5-methyl-ω-methylaminoacetophenene (IX)

A mixture of methanol (5 ml) and a solution of methylamine in methanol (15 ml, saturated at 5°) was added at 0° to solid 3,4-dihydroxy-5-methyl-ω-chloroacetophenone (5 g), and the resulting suspension was shaken in a tightly stoppered flask for 6 min. Excess methylamine and the solvent was then removed *in vacuo*, below 90°; the brownish solid residue was triturated with ethanol (30 ml) and afforded tan prisms of 3,4-dihydroxy-5-methyl-ω-methylaminoacetophenone (2.1 g), m.p. 203–205°. The product, after filtration and washing with ethanol, was sufficiently pure for the next stage in the synthesis. A sample of IX was purified for analysis by recrystallization from a large volume of methanol and was obtained in light tan-colored prisms (m.p. 205–206° (with decomposition)).

Anal. Calcd. for $C_{10}H_{13}NO_3$: C, 61.52; H, 6.71; N, 7.18. Found: C, 61.23; H, 6.87; N, 7.09.

3,4-Dihydroxy-5-methyl-ω-methylaminoacetophenone hydrochloride (colorless needles; m.p. 235°, with decomposition) was prepared from the base in an analogous manner to that described above for the preparation of the 2-methyl derivative.

Anal. Calcd. for $C_{10}H_{14}ClNO_3$: C, 51.84; H, 6.12; N, 6.08; Cl, 15.30. Found: C, 51.86; H, 5.87; N, 5.94; Cl, 15.56.

Treatment of ω-chloro-3,4-dihydroxy-5-methylacetophenone with methanolic methylamine in ether, in a manner similar to that described above for the analogous 3-methyl compound, gave pale-yellow needles (m.p. 80°). The microanalytical values for carbon and hydrogen are not incompatible with this substance being a methylamine salt of ω-chloro-3,4-dihydroxy-5-methyl acetophenone (cf. refs. 5, 22).

Anal. Calcd. for $C_{10}H_{14}ClNO_3$: C, 51.84; H, 6.12. Found: C, 52.19, H, 6.30.

5-Methyladrenaline (i.e. 5-Methyl-α-methylaminomethylprotocatechuyl Alcohol (II))

A solution of 3,4-dihydroxy-5-methyl-ω-methylaminoacetophenone hydrochloride (2.4 g) in water (200 ml), containing 5% palladium–charcoal (1 g), was shaken in an atmosphere of hydrogen at atmospheric pressure for 5 h. After this time the catalyst was removed by filtration and the clear filtrate was concentrated *in vacuo* (nitrogen "leak"), below 40°, to ca. 12 ml; solid potassium carbonate (1.5 g) was added, with stirring, and the crude base separated out, after the solution had been allowed to stand at 5° for 1 h. The product obtained in this manner was pure enough for oxidation directly to the corresponding aminochrome. A sample of 5-methyladrenaline was purified for microanalysis by recrystallization from a large volume of methanol and was obtained as colorless prisms, m.p. 195–197° (with decomposition).

Anal. Calcd. for $C_{10}H_{15}NO_3$: C, 60.89; H, 7.67; N, 7.10. Found: C, 60.89; H, 7.84; N, 6.93.

5-Methyladrenaline picrate was prepared by adding a solution of picric acid (0.1 g) in dry benzene (8 ml) to a stirred suspension of the base (0.1 g) in ethanol (1 ml). The solid dissolved and dark-yellow needles of the

[8]*Commercial phosphorus oxychloride was purified by the procedure described by Ott (9), i.e. by washing a solution of the impure product in chloroform with ice water; removing the solvent in vacuo and fractional distillation of the product. The fraction boiling in the range 103–105° was collected and used directly. The direct use of the commercial product, which contains phosphorus pentachloride and phosphorus trichloride, leads to extensive tar formation and low yields of product.*

Can. J. Chem. Downloaded from www.nrcresearchpress.com by 210.87.254.42 on 09/05/12
For personal use only.

crude picrate were obtained after the solution had stood at 5° for 3 h. 5-Methyladrenaline picrate (0.12 g) m.p. 183°, was obtained in yellow needles on recrystallization of the crude product from a benzene–alcohol (9:1) mixture.

Anal. Calcd. for $C_{16}H_{18}N_4O_{10}$: C, 45.07; H, 4.26; N, 13.14. Found: C, 45.07; H, 4.32; N, 13.08.

7-Methyladrenochrome (XVI)

5-Methyladrenaline (0.6 g) was suspended in water (5 ml) and 2 *N* hydrochloric acid was added cautiously, with stirring, until a clear solution was obtained. A solution containing potassium ferricyanide (3.5 g) and sodium bicarbonate (1.2 g) in water (10 ml) was added, with stirring; the solution became deep violet in color and vigorous effervescence occurred. 7-Methyladrenochrome (0.18 g) (totally decomposed without melting by 105°) was obtained in deep violet (almost black) needles after the reaction mixture had been allowed to stand at 5° for 1 h, $\lambda_{max}^{H_2O}$ 232, 305, 534 mμ;

Anal. Calcd. for $C_{10}H_{11}NO_3$: C, 62.16; H, 5.74; N, 7.25. Found: C, 62.60; H, 5.72; N, 6.92.

Attempted Preparation of an Iodo-7-methyladrenochrome

An aqueous solution of 5-methyladrenaline hydrochloride (prepared from 0.3 g of the base) was treated with potassium iodate (0.5 g), at pH 7.2 (the pH of the solution was adjusted to 7.2 by the cautious addition of solid sodium carbonate), in an identical manner to that described above for the preparation of 7-iodo-4-methyladrenochrome. A deep-violet solution, having ultraviolet and visible spectral characteristics identical to those of 7-methyladrenochrome was obtained. The spectrum of the solution was not affected by prolonged reaction time (i.e. ca. 2 h), or by the addition of a further quantity of potassium iodate (0.5 g).

7-Methyladrenochrome monosemicarbazone (0.21 g) (totally decomposed without melting by 245°) was obtained, when a solution of semicarbazide hydrochloride (0.2 g) and sodium acetate (0.2 g) in water (3 ml) was added to a solution of 5-methyladrenaline hydrochloride that had been oxidized with potassium iodate. The sample of 7-methyladrenochrome monosemicarbazone, obtained in this manner, was identical to the product prepared by the method described below.

7-Methyladrenochrome Monosemicarbazone (XVII)

A solution of 7-methyladrenochrome, prepared by the oxidation of an aqueous solution of 5-methyladrenaline hydrochloride (from 1 g of base) with potassium ferricyanide, was treated with a solution of semicarbazide hydrochloride and sodium acetate in the manner described above for the analogous 4-methyl derivative. 7-Methyladrenochrome monosemicarbazone (0.95 g) (totally decomposed without melting by 245°) was obtained in wine-red needles on recrystallization of the crude product from a pyridine–water (1:1) mixture.

Anal. Calcd. for $C_{11}H_{14}N_4O_3$: C, 52.79; H, 5.64; N, 22.39. Found: C, 52.62; H, 5.61; N, 22.22.

5,6-Dihydroxy-1,7-dimethylindole (XVIII: R = H)

Ascorbic acid was added in portions, with stirring, to a two-phase system consisting of ether and an aqueous solution of 7-methyladrenochrome, prepared by the potassium ferricyanide oxidation of 5-methyladrenaline (0.6 g) by the method described above, until the deep-violet color of the solution had disappeared. The ether layer was removed and the aqueous phase was extracted with a further quantity of ether. Dry benzene (10 ml) was added to the combined, dried (Na_2SO_4) ethereal extracts, and the resulting solution concentrated to ca. 5 ml. Colorless prisms of 5,6-dihydroxy-1,7-dimethylindole (0.18 g) were obtained on addition of a small quantity of *n*-heptane to the warm benzene solution. The product could be further purified (m.p. 155°) by high vacuum sublimation at 160° (bath temperature) at 0.2 mm.

Anal. Calcd. for $C_{10}H_{11}NO_2$: C, 67.78; H,6.26; N, 7.91. Found: C, 67.64; H, 6.32; N, 7.87.

5,6-Diacetoxy-1,7-dimethylindole (XVIII: R = $COCH_3$)

A mixture of dry pyridine (3 ml) and acetic anhydride (3 ml) was added to a dry ethereal solution of 5,6-dihydroxy-1,7-dimethylindole, prepared by the method described above. The ether was removed *in vacuo*, and the concentrated reaction mixture was poured into an ice–water mixture, after it had been allowed to stand overnight at room temperature. Recrystallization of the crude product from benzene – light petroleum gave 5,6-diacetoxy-1,7-dimethylindole (0.35 g) in small colorless prisms, m.p. 137–138°.

Anal. Calcd. for $C_{14}H_{15}NO_4$: C, 64.37; H, 5.79; N, 5.36. Found: C, 64.01; H, 5.68; N, 5.21.

6-Methoxy-1,7-dimethylindole (XIX): Prepared by the Alkaline Degradation of 7-Methyladrenochrome Monosemicarbazone and Subsequent O-Methylation (cf. ref. 21)

Solid potassium hydroxide (2 g) was added, with stirring, in a nitrogen atmosphere, to a suspension of 7-methyladrenochrome monosemicarbazone (0.5 g) in water (20 ml) at 90°, the resulting deep red-brown solution was boiled (in an atmosphere of nitrogen) until effervescence had ceased (ca. 2–5 min). The temperature of the solution was then reduced to ca. 50° by the addition of crushed ice; dimethyl sulfate (2.5 ml) was added dropwise and the reaction mixture was cautiously heated to 80°, and maintained at this temperature for 5 minutes. The resulting solution was cooled to room temperature and extracted several times with ether. The combined extracts were washed with *N* potassium hydroxide solution, dried (Na_2SO_4), and evaporated to dryness. The crude product was purified by recrystallization from light petroleum and

Can. J. Chem. Downloaded from www.nrcresearchpress.com by 210.87.254.42 on 09/05/12
For personal use only.

gave 6-methoxy-1,7-dimethylindole in colorless prisms (0.19 g); m.p. 93°: $\lambda_{max}^{C_2H_5OH}$ 224, 275, 292 (sh), 304 (sh) mμ. The significant n.m.r. peaks are given in Table I.

Anal. Calcd. for $C_{11}H_{13}NO$: C, 75.40; H, 7.48; N, 7.99. Found: C, 75.55; H, 7.31; N, 7.98.

ACKNOWLEDGMENTS

The authors wish to express their thanks to Dr. K. McCallum of the University of Saskatchewan for the use of the Varian A-60 nuclear magnetic resonance spectrometer. The authors are also grateful to Dr. R. G. Micetich of R. & L. Molecular Research Ltd., Edmonton, Alberta, and to Dr. R. Greenhalgh and his colleagues in the Defence Chemical, Biological and Radiation Laboratories, Ottawa, Ontario, for assistance in obtaining some of the n.m.r. spectra and to the latter group for some useful comments on the interpretation of the spectra.

REFERENCES

1. S. Frankel and R. Allers. Biochem. Z. **18**, 40 (1909).
2. L. Kraus. Biochem. Z. **22**, 131 (1909).
3. D. Richter and H. Blaschko. J. Chem. Soc. 601 (1937).
4. R. A. Heacock, O. Hutzinger, B. D. Scott. J. W. Daly, and B. Witkop. J. Am. Chem. Soc. **85**, 1825 (1963).
5. F. Stolz. Ber. **37**, 4149 (1904).
6. E. Hornbaker and A. Burger. J. Am. Chem. Soc. **77**, 5314 (1955).
7. F. Külz and C. Horning. Ger. Patent No. 682,394 (September 28th, 1939); Chem. Abstr. **36**, 3011 (1942).
8. S. K. Dzerzgovsky. J. Russ. Chem. Soc. **25**, 154 (1893); J. Chem. Soc. **66**, Abstr. I, 73 (1894).
9. E. Ott. Ber. **59**, 1068 (1926).
10. A. H. Blatt. Chem. Rev. **27**, 413 (1940); Org. Reactions, **1**, 343 (1942).
11. K. W. Rosenmund and H. Lohfert. Ber. **61**, 2601 (1928).
12. R. A. Heacock, C. Nerenberg, and A. N. Payza. Can. J. Chem. **36**, 853 (1958).
13. J. D. Bu'Lock and J. Harley-Mason. J. Chem. Soc. 712 (1951).
14. R. A. Heacock. Chem. Rev. **59**, 181 (1959).
15. R. A. Heacock and B. D. Scott. Can. J. Chem. **38**, 516 (1960).
16. R. A. Heacock and G. L. Mattok. Can. J. Chem. **41**, 139 (1963).
17. R. I. T. Cromartie and J. Harley-Mason. J. Chem. Soc. 3525 (1953).
18. L. A. Cohen, J. W. Daly, H. Kny, and B. Witkop. J. Am. Chem. Soc. **82**, 2184 (1960).
19. T. J. Mabry, H. Wyler, G. Sassu, M. Mercier, I. Parikh, and A. S. Dreiding. Helv. Chim. Acta, **45**, 640 (1962).
20. R. V. Jardine and R. K. Brown. Can. J. Chem. **41**, 2067 (1963).
21. R. A. Heacock and O. Hutzinger. J. Chem. Soc. In press. 1965.
22. H. D. Dakin. Proc. Roy. Soc. London, Ser. B, **76**, 491 (1905).

Can. J. Chem. Downloaded from www.nrcresearchpress.com by 210.87.254.42 on 09/05/12
For personal use only.

Can. J. Chem. Downloaded from www.nrcresearchpress.com by 210.87.254.6 on 09/05/12
For personal use only.

STEREOSPECIFIC SYNTHESIS OF A DIBENZO[*a*,*g*]QUINOLIZINE ANALOG OF 18-HYDROXYALLOYOHIMBANE

B. BELLEAU AND D. DVORNIK[1]
Department of Chemistry, University of Ottawa, Ottawa, Ontario
Received April 7, 1965

ABSTRACT

Starting from 4-cyclohexene-*cis*-1,2-dicarboxylic acid, the stereospecific synthesis of the dibenzo[*a*,*g*]quinolizine analog IV of epialloyohimbane is described. The synthetic method of approach is outlined in Chart 1. As the trimethoxybenzoic acid ester, the base IV proved to be devoid of significant pharmacological properties.

The alkaloid reserpine (I, R = 3,4,5-trimethoxybenzoyl) and several 18-ester analogs possess unique physiological properties, the most striking being their ability to interfere with the storage mechanism of the catecholamine hormones and serotonin (1). Other

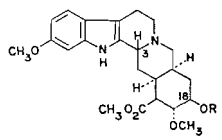

I

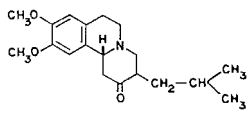

II

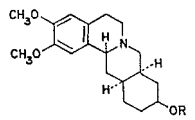

III

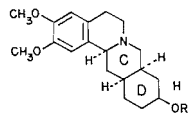

IV

types of analogs such as the 18-ethers (I, R = alkyl) share this property (1) but differ in one important respect: whereas the action of reserpine is protracted, that of the ether derivatives is of shorter duration (1). It seems therefore that an acyl function at position 18 may be essential for prolonged in vivo activity. Quantitatively, reserpine produces effects that are characteristic of irreversible inhibitors such as the alkylating adrenergic blocking agents of the Dibenamine class of drugs (2). It is conceivable that reserpine may be a prototype of selective acylating agents, a hypothesis which readily accounts for the irreversibility characteristics of its action.

Some time ago, it was discovered that a simple benzoquinolizidine derivative (II) known under the name of Tetrabenazine displays reserpine-like activity (3). However, in contrast to reserpine, it is a short-acting compound, a feature which is in accord with the non-acylating properties of the molecule. Evidence is thought to have been produced that Tetrabenazine interacts with the same physiological receptors that serve to bind reserpine (4). This was surprising to us in view of the remote structural analogy between these two drugs. It is apparent that should the same receptors mediate the physiological effects of both reserpine and Tetrabenazine, the formal transformation of the latter to an acylating agent ought to markedly intensify its reserpine-like properties. To this end,

[1]*National Research Council of Canada Postdoctorate Fellow, 1958–1959.*

a close structural analogy to reserpine should be maintained, and accordingly, we elected to synthesize a trimethoxybenzoyl ester of the 3,4-dimethoxyphenyl analog of 18-hydroxy-epialloyohimbane (III). It is the purpose of this communication to report on a stereo-specific approach which led to the synthesis of the isomeric alloyohimbane analog IV (R = 3,4,5-trimethoxybenzoyl). The synthesis of the desired epiallo isomer III was eventually accomplished as described in an accompanying communication (5).

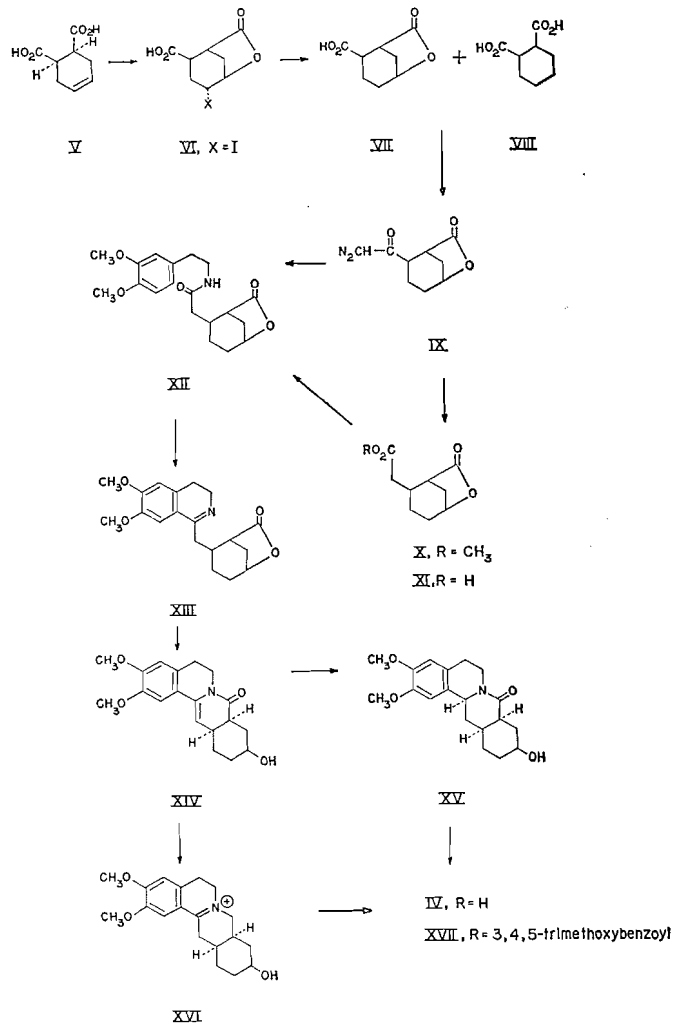

CHART 1.

Our synthetic approach (Chart 1) was based on the readily available starting material *cis*-Δ^4-tetrahydrophthalic acid (V) which provided for the desired *cis* fusion of rings C and D in the end product III. Iodolactonization of V proceeded normally (6) to give iodolactone acid (VI). The lactone VI has recently been described by others (7). Absorption in the infrared at 1 750 cm^{-1} confirmed the exclusive formation of a γ-lactone ring in which the potential 18-hydroxyl function of III assumes the proper configuration.

Can. J. Chem. Downloaded from www.nrcresearchpress.com by 210.87.254.6 on 09/05/12
For personal use only.

Can. J. Chem. Downloaded from www.nrcresearchpress.com by 210.87.254.6 on 09/05/12
For personal use only.

Catalytic hydrogenolysis of the iodolactone acid afforded the lactone acid VII accompanied in various proportions by *cis*-hexahydrophthalic acid (VIII). On a preparative scale, the separation of the hydrogenolysis mixture presented some difficulty. The formation of *cis*-hexahydrophthalic acid was unexpected; it seems probable on the basis of related experiments (5) that the lactone acid VII is the immediate precursor of the diacid VIII. It has been noted before that γ-lactones with an axial ring oxygen can be susceptible to hydrogenolysis (8). However, this process is slower than reductive dehalogenation. Homologation of the lactone acid VII by way of the intermediate diazoketone IX followed by Wolff rearrangement in the presence of homoveratrylamine offered directly the lactone homoamide XII in good yield. The Wolff rearrangement is known to proceed with retention of configuration (9). Alternatively, the rearrangement was carried out in methanol whereupon the methyl ester X was formed; saponification gave the homoacid lactone XI from which the same oily amide XII could be readily prepared. Bishler–Napieralsky ring closure of the amide led to the dihydroisoquinoline lactone XIII in high yield. It was initially characterized as the picrate but the hydrochloride was later obtained in pure form (5). Cyclization of XIII to the tetracyclic ene-lactone XIV was accomplished in moderate yield by boiling in xylene for several hours. The infrared spectrum of the lactam XIV was in agreement with expectations (see Experimental). Conversion of the ene-lactam XIV to the corresponding reduced base IV involved either catalytic hydrogenation of the double bond to give the reduced lactam XV followed by lithium aluminium hydride reduction to IV or hydride treatment to give the intermediate XVI followed by reduction to IV. Thus, reduction of the iminium ion XVI with lithium aluminium hydride, sodium borohydride, zinc and hydrochloric acid, or with sodium in liquid ammonia – *t*-butanol uniformly produced the same tetracyclic base in a homogeneous state. Surprisingly, zinc – acetic acid reduction, a method which is successful in the yohimbane series (10), led only to unchanged starting material. The reasons for this are not clear. The tetracyclic base IV was readily oxidized to the imine XVI by mercuric acetate (10).

Since it has been shown that the sodium – liquid ammonia – *t*-butanol system leads to the thermodynamically more stable isomer in the analogous yohimbane series (11), it follows that the tetracyclic base obtained by us in this manner must possess the configuration IV in which both the phenyl and 18-hydroxyl substituents are equatorial. In agreement with this conclusion, the tetracyclic base IV gave rise to Bohlmann bands (12) in the region 2 800 – 2 700 cm^{-1} of the infrared spectrum; the stable conformation of IV which places the phenyl and hydroxyl substituents in the equatorial orientation has the electron pair on the nitrogen *trans* to two axial α-hydrogens in accord with the spectroscopic characteristics. Reaction of the base IV with 3,4,5-trimethoxybenzoyl chloride gave the corresponding 18-ester XVII in moderate yield.

It was evident at this point that to obtain the desired isomeric tetracyclic base III (epiallo configuration), an alternative approach had to be sought. More gratifying results are reported in an accompanying paper (5). Since 3-isoreserpine (allo configuration as in the base IV) is devoid of reserpine-like activity (1), the analog XVII would be expected to be also inactive. Dr. M. Pindell of Bristol Laboratories, Syracuse, has confirmed this expectation using a variety of standard tests.

EXPERIMENTAL

Melting points and boiling points are uncorrected. The infrared spectra were determined with an Infracord instrument or a Perkin-Elmer spectrometer model 112G using chloroform as the solvent unless otherwise

noted. The sentence "was worked up in the usual manner" signifies that the reaction mixture was extracted with ether or chloroform and, wherever appropriate, the extract was washed with dilute acid or dilute base followed by drying and evaporation *in vacuo*. Microanalyses by Midwest Microlab, Indianapolis, Indiana.

4-Hydroxy-5-iodo-cis-cyclohexane-1,2-dicarboxylic Acid γ-Lactone (VI)

To a stirred suspension of Δ^4-cyclohexene-*cis*-1,2-dicarboxylic acid in 500 ml of water, 29 g of sodium hydrogen carbonate was added, followed by the addition in portions of a solutions of 29 g of iodine in 200 ml of water containing 112 g of potassium hydroxide. After stirring for 1 h at room temperature some sodium thiosulfate was added until the solution became colorless, and the mixture was acidified with conc. hydrochloric acid. The solution was filtered without delay whereupon a crystalline mass separated from the filtrate. After 1 h at 0°, the solid was collected and recrystallized from ethanol–hexane; m.p. 158–160° (reported (7): 161–162°), yield: 74–80%.

Anal. Calcd. for $C_8H_9IO_4$: C, 32.45; H, 3.06; I, 42.86; Found: C, 32.67; H, 3.30; I, 44.00. Infrared: λ_{max} (Nujol mull) 3 100, 1 750, 1 710 cm^{-1}.

The iodolactone acid VI was further characterized as the crystalline *diethylamine salt*; after recrystallization from methanol – ethyl acetate, the m.p. was 122–124°.

Anal. Calcd. for $C_{12}H_{20}INO_4$: C, 39.04; H, 5.46; I, 34.38; Found: C, 39.02; H, 5.43; I, 35.04.

4-Hydroxy-cis-1,2-cyclohexanedicarboxylic Acid γ-Lactone (VII)

A solution of 25.3 g of the iodolactone acid in 190 ml of methanol containing 12.5 ml of diethylamine was hydrogenated at 85 p.s.i. of hydrogen over 25 g of freshly prepared Raney nickel. After a pressure drop of about 6.5 pounds, the reaction was stopped and the catalyst was removed by filtration. The filtrate was treated with 17.0 g of freshly precipitated silver carbonate, and the suspension was shaken for 20 min and filtered through Florex XXX. The colorless filtrate was evaporated *in vacuo* and the residue was dissolved in 50 ml of 3 *N* aqueous sulfuric acid; some insoluble silver sulfate was removed by filtration and the filtrate was extracted five times with 50 ml portions of ethyl acetate. The combined extracts were dried and evaporated *in vacuo*, and the residue was crystallized from 100 ml of dry ether. This first crop weighed 6.0 g and had m.p. 142–143°. The filtrate was taken to dryness and the residue was partitioned between equal volumes (100 ml) of ether and water. The distribution coefficients of the lactone acid VII and the diacid VIII in this solvent system were 0.1 and 2.0 respectively. After equilibration, the aqueous phase was twice extracted with 100 ml portions of ether. The aqueous phase was saturated with ammonium sulfate and extracted with five 50 ml portions of chloroform. The combined extracts were dried and evaporated, and the residue was crystallized from ethyl acetate – ether to give an additional 0.30 g of lactone acid VII m.p. 140–141°. Total yield: 6.3 g or 47% of the theoretical. After recrystallization from benzene, the m.p. was 143–144°.

Anal. Calcd. for $C_8H_{10}O_4$: C, 56.46; H, 5.92. Found: C, 56.61; H, 5.91. λ_{max}: 1 755, 1 700 cm^{-1}.

From the ether extracts and mother liquors there was isolated from 2 to 4 g of the *cis*-cyclohexane-1,2-dicarboxylic acid (VIII) which was characterized by mixture m.p. determination and comparison of its infrared spectrum with that of an authentic specimen.

Diazoketone IX from Lactone Acid VII

To a cooled solution of 6.78 g of the lactone acid VII in 220 ml of dry benzene containing 6.5 ml of triethylamine was added dropwise 8.6 ml of oxalyl chloride. After standing for 3.5 h, the suspension was filtered and the filtrate was treated with a freshly prepared ethereal solution of diazomethane (from 26 g of *N*-nitrosomethyl urea, 52 ml of 45% aqueous potassium hydroxide, and 370 ml of ether). After standing overnight, the mixture was filtered and the filtrate was evaporated *in vacuo*. The residue (7.4 g or 96% of theory) crystallized spontaneously. It was used as such without further purification.

λ_{max}: 2 140, 1 760, and 1 640 cm^{-1}.

(A) Wolff Rearrangement in Methanol

A quantity of diazoketone equivalent to 0.955 g of lactone acid VII was dissolved in boiling methanol and some freshly precipitated silver oxide was added. The mixture was boiled for 3 h, cooled, and filtered through Celite. The filtrate was evaporated *in vacuo* and the residue was distributed between 6 *N* aqueous sulfuric acid and ether. The ether extract was worked up in the usual manner to give 563 mg of semisolid residue. Repeated extraction of the aqueous layer with chloroform and isolation in the usual manner yielded an additional 110 mg of methyl ester. The total yield of crude ester X was 60%.

λ_{max}: 1 753, 1 725 cm^{-1}.

The *lactone homoacid* XI was obtained through saponification of the preceding crude ester X (542 mg) in boiling 5% methanolic potassium hydroxide. The solution was evaporated to dryness, the residue was taken up in 6 *N* aqueous sulfuric acid, and the resulting solution was saturated with ammonium sulfate and repeatedly extracted with chloroform. The extract was dried and evaporated to give an oil (390 mg or 77% of theory) which was dissolved in benzene and purified by chromatography on silicic acid (6 g). Ether eluted 333 mg of an oil which crystallized from benzene–pentane, m.p. 119–120°. Other crystalline forms of m.p. 111–116° exhibiting changes of crystal form at 100–110° were more frequently observed. These varied forms had superimposable infrared spectra in chloroform.

Anal. Calcd. for $C_9H_{12}O_4$: C, 58.69; H, 6.57. Found: C, 59.10; H, 6.53. λ_{max}: 1 750, 1 700 cm^{-1}.

Can. J. Chem. Downloaded from www.nrcresearchpress.com by 210.87.254.6 on 09/05/12
For personal use only.

N-(3',4'-dimethoxy-β-phenethyl)-cis-2-carboxy-4-hydroxy-cyclohexane-1-acetamide γ-Lactone (XII)

(A) From the Diazoketone IX

To a solution of 6.87 g of homoveratrylamine in 25 ml of pure dioxane, some freshly precipitated silver oxide was added and the suspension was heated to boiling. Heating was discontinued and a solution of 7.41 g of the crude diazoketone IX in 30 ml of dioxane was added dropwise whereupon a vigorous evolution of nitrogen ensued. At intervals, 13.4 g of silver oxide was added in portions over a period of 1 h. The suspension was then heated under reflux for 3 h, cooled, and filtered through a bed of Florex XXX. The precipitate was washed with acetone, and the washings and filtrate were combined and evaporated. The residue was taken up in chloroform; the solution was washed with dilute aqueous sulfuric acid and then with saturated sodium bicarbonate solution; the chloroform solution was finally filtered through a column of 100 g of aluminium oxide (Woelm, activity II) and the column was thoroughly washed with chloroform. Removal of the solvent *in vacuo* afforded 13.2 g of the crude homoamide lactone XII as an uncrystallizable oil. It was used as such in the next step.

λ_{max}: 2 125, 1 765, 1 640 cm^{-1}.

(B) From the Homoacid Lactone XI

The homoacid lactone acid chloride was prepared by treatment of the acid triethylamine salt in benzene with oxalyl chloride as described above in the case of the preparation of the diazoketone IX. The benzene solution of the acid chloride was treated with excess homoveratrylamine in the cold, and the mixture was worked up in the usual manner to give in high yield the oily homoamide lactone XII identical in the infrared with the amide obtained through the application of method A above.

1-[(cis-2'-Carboxy-4'-hydroxy)-1'-cyclohexylmethyl]-3,4-dihydro-6,7-dimethoxyisoquinoline γ-Lactone (XIII)

The preceeding homoamide lactone XII (13.0 g) was heated under reflux and under an oxygen-free nitrogen atmosphere in 100 ml of dry toluene containing 25 ml of freshly distilled phosphorous oxychloride. After 75 min, the solution was evaporated to dryness *in vacuo*. The residual syrup was taken up in chloroform and the solution was washed twice with saturated sodium bicarbonate, dried, and evaporated to give 12.1 g (97% of theory) of a clear deep-yellow oil.

λ_{max}: 1 750, 1 600, 1 555, 1 500 cm^{-1}.

The *picrate* crystallized from methanol; recrystallization from acetone – ethyl acetate gave yellow crystals m.p. 193–194°; recrystallization from acetone–chloroform gave another form m.p. 175–176°. The two forms are interconvertible.

Anal. Calcd. for $C_{25}H_{26}N_4O_{11}$: C, 53.76; H, 4.69. Found: C, 53.48; H, 4.92.

Ring Closure of XIII to the Tetracyclic Ene-lactam XIV

A solution of 12 g of the preceeding base XIII in 200 ml of dry xylene was heated under reflux for 24 h under an atmosphere of oxygen-free nitrogen. The hot mixture was decanted from some insoluble gum and the solvent was removed *in vacuo*. The residue was dissolved in chloroform and the solution was worked up in the usual manner to give an oil which crystallized from 70 ml of boiling toluene. The yield was 5.1 g (42% of theory). Recrystallization from benzene gave white crystals m.p. 195–196°.

Anal. Calcd. for $C_{19}H_{23}NO_4$: C, 69.28; H, 7.04; N, 4.25. Found: C, 69.83; H, 6.89; N, 4.40. λ_{max}: 3 400, 1 640, 1 500 cm^{-1}.

Catalytic Hydrogenation of XIV to the Decahydrodibenzo[a,g]quinolizinone XV

A solution of 1.41 g of the preceeding ene-lactam XIV in 20 ml of ethanol containing 0.5 ml of 75% aqueous perchloric acid was shaken in a hydrogen atmosphere at atmospheric pressure in the presence of 300 mg of Adam's catalyst. After 6 min, the theoretical amount of hydrogen was adsorbed; the catalyst was removed and the solvent was evaporated. The residue was dissolved in chloroform and the solution was worked up in the usual manner to give a solid which on recrystallization from benzene afforded 1.14 g (80% of theory) of the lactam XV, m.p. 217–219°. Depending on the rate of heating the m.p. varied from 213–216° to 217–219°. Additional recrystallizations did not alter the m.p. The product was homogeneous as ascertained by thin-layer chromatography (silicic acid; chloroform–methanol).

Anal. Calcd. for $C_{19}H_{25}NO_4$: C, 68.86; H, 7.60. Found: C, 68.81; H, 7.72. λ_{max}: 3 400, 1 620, 1 500 cm^{-1}.

Reduction of XV to the Tetracyclic Base IV

To a suspension of 1 g of lithium aluminium hydride in 30 ml of dry ether was added dropwise a solution of 1.44 g of the preceeding lactam XV in 100 ml of dry tetrahydrofuran. After 3 h of heating under reflux, the mixture was cooled and treated successively with 1 ml of water, 0.75 ml of 20% aqueous sodium hydroxide, and 3.5 ml of water. The salts were filtered off, the filtrate was evaporated, and the residue was partitioned between 16 ml of 3 *N* aqueous sulfuric acid and 50 ml of ether. The aqueous phase was made alkaline and extracted with ether. The ether was dried and evaporated and the residue was crystallized from acetone–water to give 1.22 g (89% of theory) of the base IV, m.p. 178–180°. Recrystallization from acetone did not change the m.p.

Anal. Calcd. for $C_{19}H_{27}NO_3$: C, 71.89; H, 8.57. Found: C, 71.92; H, 8.40. λ_{max}: 2 800, 2 760 cm^{-1} (Bohlmann bands); 3 400, 1 500 cm^{-1}.

Can. J. Chem. Downloaded from www.nrcresearchpress.com by 210.87.254.6 on 09/05/12
For personal use only.

Treatment of the base with a 10% excess of mercuric acetate in acetic acid at 60° gave an immediate precipitate of mercurous acetate. After working up the mixture in the usual manner (excess mercuric ions being removed with H_2S), the dehydrobase XVI was isolated as the chloride salt in the form of an uncrystallizable yellow oil identical in the infrared with a sample prepared as described below.

λ_{max}: 3 400, 1 720, 1 500 cm^{-1}.

Reduction of Ene-lactam XIV to the Dehydrobase XVI

The ene-lactam XIV (400 mg) was reduced with lithium aluminium hydride by the same method described above in the case of the reduction of XV to IV. After isolation in the usual manner, the free base (which is sensitive to air) was converted to the oily chloride XVI which was identical in the infrared with a sample obtained by mercuric acetate dehydrogenation of IV (see above).

Attempted reduction of this dehydrobase XVI by zinc in acetic acid led to unchanged starting material. Reduction with boiling hydrochloric acid and zinc gave in good yield the base IV (identity established by mixed m.p. determination and infrared); similar results were obtained using either lithium aluminium hydride or sodium borohydride (in aqueous ethanol). The reduced base was obtained in good yield (75–90%) in each instance.

Reduction with sodium – liquid ammonia – *t*-butanol (using the procedure of Stork and Hill (11)) also gave the base IV in high yield.

3,4,5-Trimethoxybenzoic Acid Ester XVII of the Base IV

The method of Lucas *et al.* (13) was applied. Thus, 317 mg of the base IV was treated in 15 ml of dry pyridine with 920 mg of 3,4,5-trimethoxybenzoyl chloride. After 4 days at room temperature, the mixture was poured onto ice-cold dilute ammonia and the precipitate was collected. After several recrystallizations from methanol, the pure ester XVII (100 mg) had m.p. 149–150°.

Anal. Calcd. for $C_{29}H_{37}NO_7$: C, 68.10; H, 7.24; N, 2.74. Found: C, 67.80; H, 7.24; N, 2.95. λ_{max}: 1 700, 1 590 cm^{-1}.

ACKNOWLEDGMENTS

The financial support of this work by the National Research Council of Canada is gratefully acknowledged.

REFERENCES

1. R. A. Lucas. The chemistry and pharmacology of the Rauwolfia alkaloids. *In* Progress in medicinal chemistry. Vol. III. *Edited by* G. P. Ellis and G. B. West. Butterworths, London. Chap. 4. 1963.
2. B. Belleau. Can. J. Biochem. **36**, 731 (1958).
3. A. Pletscher. Science, **126**, 507 (1957).
4. G. P. Quinn, P. A. Shore, and B. B. Brodie. J. Pharmacol. Exp. Therap. **127**, 103 (1959).
5. B. Belleau and J. Puranen. Can. J. Chem. In press. 1965.
6. E. E. van Tamelen and M. Shamma. J. Am. Chem. Soc. **76**, 2315 (1954).
7. F. V. Brutcher and D. D. Rosenfeld. J. Org. Chem. **29**, 3154 (1964).
8. B. Belleau and S. McLean. Determination of the stereochemistry of natural products by chemical methods. *In* Technique of organic chemistry. Vol. 11, Part 2. *Edited by* A. Weissberger and K. W. Bentley. Interscience Publishers, New York. 1963. Chap. 19. p. 1041.
9. J. F. Lane and E. S. Wallis. J. Am. Chem. Soc. **63**, 1674 (1941).
10. F. L. Weisenborn and P. A. Diassi. J. Am. Chem. Soc. **78**, 2022 (1956).
11. G. Stork and R. K. Hill. J. Am. Chem. Soc. **79**, 495 (1957).
12. F. Bohlmann and C. Arndt. Chem. Ber. **91**, 2167 (1958).
13. R. A. Lucas, R. J. Kiesel, and M. J. Ceglowski. J. Am. Chem. Soc. **82**, 493 (1960).

Can. J. Chem. Downloaded from www.nrcresearchpress.com by 210.87.254.6 on 09/05/12
For personal use only.

Can. J. Chem. Downloaded from www.nrcresearchpress.com by 210.87.254.40 on 09/05/12
For personal use only.

STEREOSELECTIVE SYNTHESIS OF A DIBENZO[*a*,*g*]QUINOLIZINE ANALOG OF 18-HYDROXYEPIALLOYOHIMBANE

B. BELLEAU AND J. PURANEN
Department of Chemistry, University of Ottawa, Ottawa, Ontario

Received April 7, 1965

ABSTRACT

Starting from *cis*-Δ^4-cyclohexenedicarboxylic acid anhydride, a stereoselective synthesis of *cis*-Δ^4-tetrahydrohomophthalic acid (IX) is described (Chart 1). The synthesis involves selective reduction to Δ^4-tetrahydrophthalide (III) and reaction of the latter with cyanide to give mainly the *cis*-nitrile acid V in good yield. Alkaline hydrolysis leads to the *cis*-homodiacid IX which was characterized as its corresponding anhydride. The nitrile acid intermediate could be transformed to stereoisomeric decahydroisoquinolines (VIII). Bromolactonization of the *cis*-diacid IX afforded the bromo-γ-lactone XIII (R = Br; Chart 2) which underwent hydrogenolysis to the already described γ-lactone homoacid intermediate XV in good yield. Transformation of the latter to the dihydroisoquinoline XVIII was uneventful. Reduction with sodium borohydride gave XIX which on heating gave the two isomeric lactams XX and XXII. The former was identical to a lactam already obtained by a different route (ref. 1). The latter was reduced to the tetracyclic base XXIII which is believed to exist in conformation XXIV*c*. The corresponding trimethoxybenzoic acid ester was prepared and tested for reserpine-like activity. It was found to be inactive. The significance of this result is briefly discussed.

In an accompanying paper (1), a rationale was presented which led to the suggestion that dibenzo[*a*,*g*]quinolizine analogs of certain indole alkaloids may be of physiological interest. In particular, attention was centered on the 18-hydroxyepialloyohimbane analog XXIII (Chart 2), a substance which is related both to the physiologically long-acting molecule of reserpine and the short-acting drug Tetrabenazine (2). If, as suggested by Quinn *et al.* (3), the same receptors are involved in the binding of the two drugs, it may be expected that the analog XXIII should produce protracted effects when interacting at the same level. Our initial attempts to obtain XXIII led instead to a stereospecific synthesis of the "allo"-epimer XXI which, however, is related to the physiologically ineffective 3-isoreserpine. It is the purpose of this communication to describe an alternative approach to the desired epimer XXIII (epiallo configuration). The new approach is based on the use of *cis*-Δ^4-tetrahydrohomophthalic acid (IX) as a key intermediate. The technical procedures provide for large scale preparations and are free of the hazards associated with the handling of large quantities of diazo compounds as was the case in our first approach (1). The ready availability of the *cis*-diacid intermediate IX suggests a number of applications in the field of the synthesis of indole alkaloids.

The preparation of intermediate IX was accomplished as shown in Chart 1. Its use in the synthesis of XXIII is described in Chart 2. A key finding is that 4-cyclohexene-*cis*-1,2-dicarboxylic anhydride (I) can be readily converted in 60–70% yields to Δ^4-*cis*-tetrahydrophthalide (III) by reduction with sodium borohydride in dry dimethyl formamide (DMF). The aldehydo-acid salt II is an obvious candidate as an unisolatable intermediate in this reaction. The phthalide III was characterized by its elemental composition, its equivalent molecular weight and its infrared spectrum. The same structure III was assigned by others (4) to a solid m.p. 100° (hydrazide m.p. 170°) obtained by a different and somewhat ambiguous route. Our preparation is liquid and no well defined crystalline hydrazide could be obtained. The discrepancy may be attributable to *cis–trans* isomerism. That our liquid phthalide III has the *cis* configuration was shown by its stability to potassium *t*-butoxide in *t*-butanol (5).

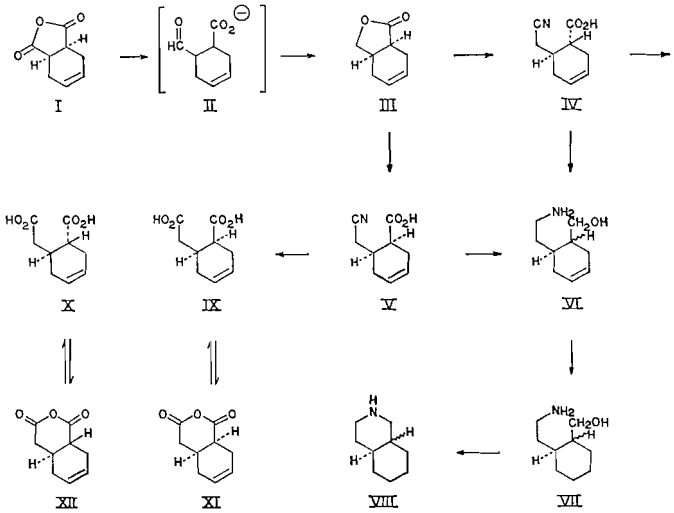

CHART 1.

On the basis of the known reactivity of γ-lactones in nucleophilic carbon–oxygen fission reactions (6), the phthalide III was reacted with cyanide ion using a variety of experimental conditions with a view to obtaining the nitrile-acid V. In the absence of a solvent, only tarry material was produced. In dimethylsulfoxide (DMSO) as the solvent the reaction proceeded smoothly and in good yield but extensive epimerization to the *trans*-nitrile acid IV occurred. Separation of the isomeric nitrile acids IV and V was not feasible on a preparative scale, but the corresponding diacids IX and X resulting from alkaline hydrolysis could be readily separated. In this way it could be established that the *trans*-nitrile acid IV accounted for 40–50% of the mixture when DMSO was used as the solvent. Reduction of the crystalline mixture of isomeric nitrile acids with lithium aluminium hydride gave VI which was converted to VII by catalytic hydrogenation and then to decahydroisoquinoline VIII after treatment with thionyl chloride followed by basification. The melting point behavior of the picrate and hydrochloride salts of VIII was consistent with that expected for a mixture of *cis* and *trans* isomers. Paper chromatography confirmed the presence of the isomeric bases thus pointing to the correctness of the assigned structures for the nitrile acids IV and V. It was eventually found that the proportion of *trans*-nitrile acid IV could be reduced to about 20% of the total yield of nitrile acid product by reacting the lactone III with sodium cyanide in DMF as the solvent. The mixture thus obtained (*cis*:*trans* ratio of 80:20) was hydrolyzed with boiling dilute sodium hydroxide to give a mixture of *cis*- and *trans*-Δ^4-tetrahydrohomophthalic acids (IX and X). The *cis* isomer IX crystallized in pure form from water in 60% yield. From the mother liquors, a mixture of *cis* and *trans* isomers was obtained. Recently, an alternative synthesis of the *cis*- and *trans*-homodiacids IX and X based on the Arndt–Eistert homologation reaction was described (7). The reported melting points for the isomers (7, 8) are in satisfactory agreement with our observations. It was essential at this point to establish the correctness of our configurational assignment to the *cis*-homodiacid IX. The melting points could hardly be relied upon to distinguish between the two isomers because, as was also noted by others (7), they are nearly identical. Recourse was made therefore to the corresponding anhydrides. Using a variety of conditions, Brutcher and Rosenfeld (7) were able to obtain only the *trans*-anhydride XII

Can. J. Chem. Downloaded from www.nrcresearchpress.com by 210.87.254.40 on 09/05/12
For personal use only.

either from the *cis*-diacid IX or the *trans* isomer X. However, under appropriate conditions, we have been successful in preparing in nearly quantitative yield the *cis*-anhydride XI, m.p. 67–68°. The two isomeric anhydrides exhibit a difference of 100° in their m.p. and have different infrared spectra. Hydrolysis with water regenerated the pure diacid precursor. A mixture of the two anhydrides can be readily separated by crystallization. It is obvious that the conditions applied by Brutcher and Rosenfeld (7) are too vigorous for the *cis*-anhydride to retain its configurational integrity. We found it expedient to isolate and purify the *cis*-diacid IX as its *cis*-anhydride prior to use in subsequent steps. Large scale preparations of this useful intermediate IX have been successfully carried out.

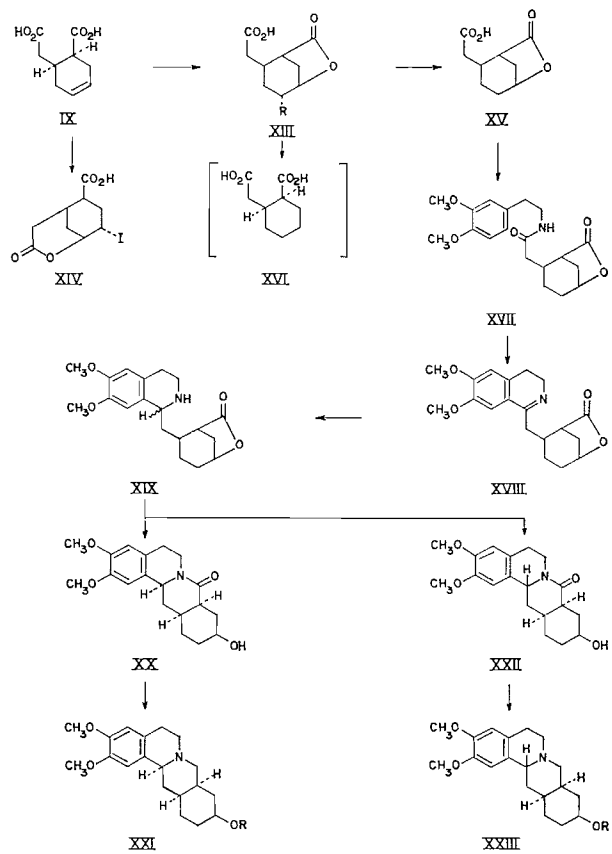

CHART 2.

The synthesis of XXIII from IX is summarized in Chart 2. As a means of introduction of the *cis*-hydroxyl function on ring D of XXIII, we initially submitted the *cis*-homodiacid IX to the Bougault iodolactonization reaction (9). Two likely reaction paths are available, one leading to the desired γ-lactone XIII, the other to the isomeric δ-lactone XIV. In practice, the γ-lactone XIII (R = I) was the major product of the reaction but was uniformly contaminated by small quantities of an isomeric lactone showing strong absorption at 1 720 cm^{-1} in the infrared. Although we have not established the structure of this minor product we suspect that it corresponds to the expected iodo-δ-lactone XIV. The iodo-γ-lactone XIII (R = I) had poor crystallization properties and was somewhat unstable. These difficulties were obviated when it was found that bromolactonization of

Can. J. Chem. Downloaded from www.nrcresearchpress.com by 210.87.254.40 on 09/05/12
For personal use only.

Can. J. Chem. Downloaded from www.nrcresearchpress.com by 210.87.254.40 on 09/05/12
For personal use only.

IX gave a well crystallized, stable bromo-γ-lactone XIII (R = Br) free of contaminating isomers. If any bromo-δ-lactone isomer was formed, its presence was not detectable by infrared. Hydrogenolysis of the carbon–bromine bond of XIII (R = Br) proceeded best using Raney nickel as the catalyst and afforded the already known lactone homoacid XV (1). A small amount of a by-product lacking the γ-lactone bond but absorbing strongly at 1 700 cm^{-1} was detected. It seems likely on the basis of previous experience (1) that this compound corresponds to *cis*-hexahydrohomophthalic acid (XVI) although no effort was made to characterize it further. The proportion of this contaminant in the hydrogenolysis mixture was found to be a function of the reaction time. Hydrogen uptake was initially very rapid and, if the reaction was stopped as soon as stoichiometry was attained, the amount of by-product (XVI?) was negligible thus suggesting that the homoacid lactone XV can suffer further attack by hydrogen albeit at a slow rate (see preceding paper (1)).

The homoacid lactone XV was next converted in high yield to the previously described (1) oily amide XVII by the mixed anhydride technique. The latter amide was ring closed the the dihydroisoquinoline lactone XVIII (1) which was purified as the crystalline hydrochloride. At this stage, our previous experience (1) suggested that reduction of the double bond of XVIII ought to be accomplished before the formation of ring C to provide for the formation of the two possible isomers at the position 1 of the tetrahydroisoquinoline ring. No stereoselectivity in the reduction of XVIII is to be expected and in agreement with theory, sodium borohydride reduction of XVIII afforded a mixture of epimers (XIX) which was used as such in the next step. Heating in boiling DMF caused smooth cyclization of XIX to two isomeric lactams which could be readily separated by crystallization. From benzene, a lactam m.p. 213–216° (XX) separated whereas a lactam m.p. 161–163° (XXII) was obtained from ethyl acetate. A rapid and quantitiative method of separation of these two isomers consists in digesting the mixture with tetrahydrofuran in which the high-melting isomer is insoluble in contrast to the low-melting one. The lactam m.p. 213–216° proved identical in every respect with the lactam previously obtained by another route (1) and consequently has the configuration XX. Moreover, lithium aluminium hydride reduction of this lactam gave the expected crystalline base (XXI, R = H) already described by Belleau and Dvornik (1). Similar treatment of the low-melting isomer XXII afforded the corresponding tetracyclic base XXIII (R = H) in high yield. In agreement with the configurational assignment, this latter base did not give rise to Bohlmann bands (10) in the infrared (in contrast to its isomer XXI (1)), an observation which might be taken to indicate that the dimethoxyphenyl substituent assumes the axial orientation with respect to ring C (as shown in XXIV*a*). However,

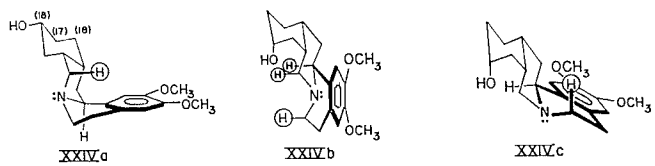

XXIV*a* XXIV*b* XXIV*c*

this is unlikely in view of the fact that the *A* value for a phenyl ring is from 3 to 6 times greater than that of a hydroxyl function (11). Of the alternative conformations XXIV*b* and XXIV*c* only the latter satisfies the criterion of thermodynamic stability (*A* values) and that of the infrared absorption characteristics (absence of Bohlmann bands). Conformation XXIV*b* places more than two axial hydrogens (circled atoms) *trans* to the α-electrons on the nitrogen. It follows that XXIII would not exist in a reserpine-like

conformation because of the absence of the 17 and 16 substituents which in reserpine stabilize conformation XXIV*a*. The possibility must be recognized that ring D of XXIV*c* may exist in a twisted boat conformation which would serve to relieve the 1,3-interactions introduced by the axial hydroxyl. The base XXIII was converted in moderate yield to the corresponding 3,4,5-trimethoxybenzoic acid ester for pharmacological evaluation.

Pharmacological results.—In a variety of standard tests Dr. M. Pindell, Bristol Laboratories, Syracuse, found that the analog XXIII (R = trimethoxybenzoyl) is devoid of reserpine-like activity. It could be argued that the absence in XXIII of the 16 and 17 substituents of reserpine may be responsible for the observed lack of activity either because these substituents participate in the binding of reserpine onto its physiological receptors or because they impose the proper conformation (equivalent to XXIV*a*) to the molecule. However, after our work was completed, we have learned from Dr. G. Muller (Roussel-Uclaf, Romainville, France) that the analog of XXIII in which both the 16 and 17 substituents of reserpine are present (synthesized by the Woodward method for reserpine (12) is also inactive. We are led to the conclusion that the indole ring of reserpine is critical for activity. These observations cast some doubt on the proposed identity of the receptors for Tetrabenazine and reserpine (3).

EXPERIMENTAL

Melting points and boiling points are uncorrected. Infrared spectra were recorded using a Perkin-Elmer Infracord instrument; chloroform solutions were used unless otherwise noted. Microanalyses were by Midwest Microlab, Indianapolis, and by Daessle Organic Microanalyses, Montreal. The sentence "worked up in the usual manner" signifies that the reaction mixture was extracted with ether or chloroform, and that the extract was washed successively with water and dilute base (or dilute acid when appropriate), dried over sodium sulfate, and evaporated to dryness *in vacuo*.

cis-6-Hydroxymethyl-3-cyclohexene-1-carboxylic Acid γ-Lactone (III)

A solution of 152 g of *cis*-Δ^4-tetrahydrophthalic acid anhydride (I) in 475 ml of dry DMF was added dropwise over a period of 1 h to a stirred, ice-cold solution of 30 g sodium borohydride in 475 ml of dry DMF. The temperature of the reaction was kept below 20°. The solvent was removed under reduced pressure and the residue was carefully treated with 2.1 l of 2 *N* aqueous sulfuric acid. After standing for 16 h the turbid solution was extracted with chloroform and the extract was processed in the usual manner. The residue was distilled *in vacuo* to give 71 to 83 g (52–60% yield) of colorless liquid, b.p. 128–130° at 2.8 mm, n^{22} 1.499. Yields as high as 73% were obtained when the starting anhydride I was purified before use. Solvents other than DMF such as diglyme gave inferior yields.

Anal. Calcd. for $C_8H_{10}O_2$: C, 69.54; H, 7.30; Sap. Equiv. 138. Found: C, 68.91; H, 7.27; Sap. Equiv. 140. Infrared: λ_{max} 1 770 cm^{-1}.

Attempts to prepare a crystalline hydrazide were unsuccessful (see ref. 4).

cis- and trans-Δ^4-Tetrahydrohomophthalonitrile (V and IV)

(A) DMF as Solvent

To a boiling suspension of 9.0 g sodium cyanide in 1.3 l of DMF was added in portions a solution of 25 g of the preceding tetrahydrophthalide III in 200 ml of DMF. The mixture was heated under reflux for 18 h, cooled, and filtered, and the filtrate was then evaporated under reduced pressure. The residue was dissolved in water, acidified to pH 3 with dilute sulfuric acid, and thoroughly extracted with chloroform. The extract was washed several times with aqueous sodium bicarbonate, and the combined washings were acidified and cooled in ice whereupon crystals separated. They were collected, the filtrate was extracted with chloroform, and the extract was worked up in the usual manner to give a crystalline mass. The combined solids were recrystallized from water to give 18.7 g (56% yield) of a mixture of *cis*- and *trans*-nitrile acid IV and V, m.p. 72–76°.

Anal. Calcd. for $C_9H_{11}NO_2$: C, 65.44; H, 6.71; N, 8.48. Found: C, 64.90; H, 6.90; N, 8.55. λ_{max} (Nujol mull): 2 240, 1 700 cm^{-1}.

(B) DMSO as Solvent

Using one fifth as much of this solvent as of DMF, the same reaction as described in (A) above was carried out. It was found that in DMSO the optimum reaction time (which minimizes epimerization to IV) is 4 h. The mixture was worked up as described above to give the nitrile acid mixture in 60–65% yield. However, the proportion of *trans* isomer IV in this mixture was increased by a factor of 2–3.

Can. J. Chem. Downloaded from www.nrcresearchpress.com by 210.87.254.40 on 09/05/12
For personal use only.

cis- and trans-Decahydroisoquinoline (VIII) from the cis- and trans-Nitrile Acids IV and V

The sequence of reactions followed conventional lines. Thus, the nitrile acid (IV + V) was reduced in hot tetrahydrofuran (THF) with excess lithium aluminium hydride for 6 h. The mixture was decomposed with water and aqueous sodium hydroxide, and the liberated amino alcohol VI was isolated in crude form in the usual manner. It was purified by a short path distillation (bath temp. 100° under reduced pressure (1.2 mm) to give a colorless oil which was catalytically hydrogenated over Adams' catalyst in ethanol under a pressure of 40 p.s.i. of hydrogen. The reduced base VII was isolated in the usual manner (no olifinic absorption in the infrared, converted to the oily hydrochloride, and treated in dry chloroform with a 10% excess of pure thionyl chloride. After boiling the mixture for 1 h, the solvent was evaporated and the residue was treated at 100° with an excess of 10% aqueous sodium hydroxide. The mixture was cooled and worked up in the usual manner to give a liquid which was purified by distillation to give a colorless liquid, b.p. 80° (bath temp.) at 0.2 mm. It was converted to a crystalline picrate and crystalline hydrochloride which had respective m.p. 151–160° and 165–188° after several recrystallizations from ethanol (reported (13) for the *cis* isomer, 150° and 175–178°). The liquid base gave rise to two distinct spots on paper chromatograms (pyridine–methanol–water).

Anal. Calcd. for the picrate $C_{15}H_{20}N_4O_7$: C, 48.91; H, 5.47. Found: C, 49.22; H, 5.53.

cis-Δ^4-Tetrahydrohomophthalic Acid (IX)

A solution of 33 g of the preceding mixture of nitrile acids IV and V in 600 ml of 1 *N* aqueous sodium hydroxide was heated under reflux until ammonia was no longer evolved (about 66 h). The solution was cooled in ice and acidified to pH 3 whereupon the *cis*-homodiacid IX separated as a white crystalline mass. It was collected, washed, and recrystallized from water to give 22 g (60% yield) of the pure *cis* isomer, m.p. 162–164° (reported (7): 155–157°). Extraction of the combined mother liquors with chloroform yielded 5.3 g of a mixture of *cis* and *trans* isomers (IX and X), m.p. 130–140° (reported for a 50:50 mixture, 130–144° (7). Separation of the *trans* isomer could be more readily accomplished by conversion to the anhydride.

Anal. Calcd. for $C_9H_{12}O_4$: C, 58.69; H, 6.57. Found: C, 58.83; H, 6.57. λ_{max} (Nujol): 2 600, 1 700 cm^{-1}.

cis-Δ^4-Tetrahydrohomophthalic Anhydride (XI)

A solution of 400 mg of the preceding *cis*-homodiacid IX in 4 ml of benzene containing 1 ml of acetic anhydride was heated under reflux for 2 h and the solution was taken to dryness *in vacuo*. The residue crystallized from ether–hexane to give 320 mg of crystals, m.p. 67–68° unchanged after recrystallization.

Anal. Calcd. for $C_9H_{10}O_3$: C, 65.05; H, 6.07. Found: C, 65.07; H, 6.15. λ_{max}: 1 795, 1 750, 1 022, 960 cm^{-1}.

Hydrolysis with cold water regenerated the *cis*-homodiacid precursor, m.p. and mixed m.p. 162–164°.

trans-Δ^4-Tetrahydrohomophthalic Anhydride (XII) from a Mixture of cis- and trans-Diacids

When the above mixture of *cis*- and *trans*-homodiacids IX and X (m.p. 130–140°) was treated as described in the preceding experiment, there was obtained a solid which when recrystallized from benzene gave in 50% yield the *trans*-anhydride XII, m.p. 166– 8° (reported (7, 8): 166– 7° and 167– 8°). λ_{max}: 1 798, 1 750, 1 070, 980 cm^{-1}. Hydrolysis of the pure anhydride XII with cold water gave *trans*-Δ^4-tetrahydrohomophthalic acid (X) m.p. 154–155° (reported (7): 154–156°). Mixed m.p. with the *cis* isomer IX, 130–140° (reported (7): 130–144°).

5-Iodo-cis-4-hydroxy-2-carboxy-cyclohexaneacetic Acid γ-Lactone (XIII, R = I)

The *cis*-homodiacid IX was submitted to the conditions of iodolactonization exactly as described for Δ^4-cyclohexene-*cis*-dicarboxylic acid in an accompanying paper (1). After the acidification step, however, the iodolactone did not separate spontaneously. It was extracted with ether and the extract was processed in the usual manner to give a solid which was recrystallized from ethanol–water. Repeated recrystallizations gave crystals of m.p. 133–135° (40% yield.

Anal. Calcd. for $C_9H_{11}IO_4$: C, 34.83; H, 3.54. Found: C, 35.11; H, 3.38. λ_{max}: 1 780, 1 705 cm^{-1}.

On standing, the mother liquors deposited some solid which after repeated recrystallizations from methanol had m.p. 185–188°. This material was tentatively assigned structure XIV on the basis of its infrared spectrum; λ_{max} (Nujol): 1 720, 1 695 cm^{-1}.

Anal. Calcd. for $C_9H_{11}IO_4$: C, 34.83; H, 3.54. Found: C, 34.70; H, 3.44.

5-Bromo-cis-4-hydroxy-2-carboxy-cyclohexaneacetic Acid γ-Lactone (XIII, R = Br)

A solution of 22 g of the *cis*-homodiacid IX in 300 ml of 0.8 *N* aqueous sodium hydroxide was prepared. To this was added a solution of 20.2 g of sodium hydrogen carbonate in 150 ml of water followed by the dropwise addition of 13.2 ml of bromine. Stirring was maintained during the addition and for 1 h at room temperature. Some solid sodium thiosulfate was added to remove some light-yellow color and the solution was acidified to Congo red. After chilling for 2 h, a crystalline mass was collected and recrystallized from methanol–water to give 20.2 g (64% yield) of colorless crystals, m.p. 127–129°, unchanged by further recrystallizations.

Anal. Calcd. $C_9H_{11}BrO_4$: C, 41.08; H, 4.21; Br, 30.37. Found: C, 41.48; H, 4.16; Br, 29.51. λ_{max}: 1 770, 1 700 cm^{-1}.

Can. J. Chem. Downloaded from www.nrcresearchpress.com by 210.87.254.40 on 09/05/12
For personal use only.

cis-4-Hydroxy-2-carboxy-cyclohexaneacetic Acid γ-Lactone (XV)

A solution of 13.15 g of the preceding bromolactone acid XIII (R = Br) in 150 ml of ethanol containing 3.65 g of pure diethylamine and 2 teaspoonfuls of freshly prepared Raney nickel was shaken in a hydrogen atmosphere under an initial pressure of 80 p.s.i. After a pressure drop of 4.5 p.s.i. the mixture was worked up in the usual manner and the residue was taken up in hot benzene. The diethylamine hydrobromide was filtered off and the filtrate was concentrated and set aside in the cold whereupon 7.5 g (80% yield) of crude lactone homoacid XV, m.p. 95–102°, was obtained. Recrystallization from benzene raised the m.p. to 111–116° (crystal change at 100–110°). Repeated recrystallizations did not alter the m.p. The crude material proved satisfactory for use in the next step. (Reported m.p. (1): 119–120°, 111–116°). This material proved identical as ascertained by mixed m.p. determination and infrared spectroscopy with a sample prepared by another route (1).

From the mother liquors a small amount of chloroform-insoluble material lacking the lactone band at 1 760 cm^{-1} but absorbing strongly at 1 700 cm^{-1} was obtained. It did not decolorize bromine in chloroform and behaved as an acid. It is tentatively assigned the structure XVI. No attempt was made to further characterize this minor component.

Lactone Homoamide XVII by the Mixed Anhydride Technique

A solution of 4.8 g of the preceding lactone homoacid XV in 150 ml of benzene containing 2.6 g triethylamine was cooled in ice and treated dropwise with 2.8 g of freshly distilled ethyl chloroformate. The insoluble salt was filtered; to the ice-cold filtrate 4.7 g of homoveratrylamine was added. After standing for 1 h, the solution was evaporated to dryness to give a viscous yellow oil which proved identical in the infrared with a sample prepared by another method (1). The yield was quantitative.

Cyclization to XVIII

This reaction has been described in an accompanying paper (1). The hydrochloride salt was obtained in crystalline form. It gave yellow crystals from toluene–chloroform, m.p. 175–176°.

Anal. Calcd. for $C_{19}H_{24}ClNO_4$: C, 62.37; H, 6.61; N, 3.83. Found: C, 61.86; H, 6.71; N, 3.69.

Reduction to the Tetrahydroisoquinoline Lactone XIX and Ring Closure to XX and XXII

To a solution of 5.5 g of the preceding hydrochloride salt of XVIII in 66% aqueous ethanol was added in portions 0.75 g of sodium borohydride. After 30 min at room temperature the reaction was complete as ascertained by the disappearance in the ultraviolet of the long-wavelength chromophore at 310 mμ. The solution was concentrated *in vacuo*, and was then saturated with carbon dioxide and thoroughly extracted with chloroform. The extract yielded 3.5 g (70% yield) of a solid absorbing strongly in the infrared at 1 760 cm^{-1} (γ-lactone band). This mixture of epimers (XIX) was used as such in the next step.

The solid thus obtained was heated under reflux in 100 ml of dry DMF for 3 h under an oxygen-free atmosphere of nitrogen. The solvent was removed *in vacuo* and the residue was taken up in benzene whereupon crystals m.p. 191–196° separated. Recrystallization from benzene–methanol raised the mp. to 213–216° (yield: 1.0 g). This lactam XX proved identical in every respect with the lactam previously obtained by Belleau and Dvornik (1).

From the benzene mother liquors there was obtained a crude crop of the isomer XXII which after recrystallization from ethyl acetate had m.p. 161–163°, unchanged after further recrystallizations (yield: 1.10 g).

Anal. Calcd. for $C_{19}H_{25}NO_4$: C, 68.86; H, 7.60; N, 4.23. Found: C, 68.25; H, 7.92; N, 4.25. λ_{max}: 3 400, 1 600 cm^{-1}.

The crude mixture of isomeric lactams XX and XXII could be readily separated by taking advantage of the insolubility in THF of the former isomer.

Reduction of XXII to the Tetracyclic Base XXIII (Epiallo Configuration)

A solution of 900 mg of the lactam XXII in 50 ml of dry THF was added dropwise to a stirred and cooled suspension of 1 g lithium aluminium hydride in 50 ml of dry ether. The mixture was heated under reflux for 20 h and carefully decomposed with 1.1 ml of water followed by the addition of 0.9 ml of 20% aqueous sodium hydroxide and 4.0 ml of water. The solids were filtered, the filtrate was evaporated and the residue was taken up in dilute sulfuric acid. The solution was washed with ether and then made strongly alkaline whereupon a solid separated. It was collected and recrystallized from acetone; m.p. 197–199°, unchanged after additional recrystallizations (yield: 450 mg).

Anal. Calcd. for $C_{19}H_{27}NO_3$: C, 71.89; H, 8.57; N, 4.41. Found: C, 71.97; H, 9.00; N, 4.44. λ_{max}: 3 600, 3 400 cm^{-1}.

In a similar way, the lactam XX gave the isomeric base XXI which proved identical in every respect with a sample prepared as described in an accompanying paper (1).

The *3,4,5-trimethoxybenzoic acid ester* of the epiallo base XXIII was prepared according to the method of Lucas *et al.* (14). After several recrystallizations from methanol it had m.p. 164–165°.

Anal. Calcd. for $C_{29}H_{37}NO_7$: C, 68.08; H, 7.29; N, 2.74. Found: C, 67.76; H, 7.24; N, 2.95. λ_{max}: 1 700, 1 580 cm^{-1}.

Can. J. Chem. Downloaded from www.nrcresearchpress.com by 210.87.254.40 on 09/05/12
For personal use only.

ACKNOWLEDGMENTS

The financial support of this work by Bristol Laboratories, Syracuse, was highly appreciated.

REFERENCES

1. B. BELLEAU and D. DVORNIK. Can. J. Chem. In press. 1965.
2. A. PLETSCHER. Science, **126**, 507 (1957).
3. G. P. QUINN, P. A. SHORE, and B. B. BRODIE. J. Pharmacol. Exp. Therap. **127**, 103 (1959).
4. D. L. HUFFORD, D. S. TARBELL, and T. R. KOSZALKA. J. Am. Chem. Soc. **74**, 3014 (1952).
5. B. BELLEAU and S. MCLEAN. Determination of the stereochemistry of natural products by chemical methods. *In* Technique of organic chemistry. Vol. 11, Part 2. *Edited by* A. Weissberger and K. W. Bentley. Interscience Publishers, New York. 1963. Chap. 19. p. 1053.
6. G. PARIS, R. GAUDRY, and L. BERLINQUET. Can. J. Chem. **33**, 1724 (1955).
7. F. V. BRUTCHER and D. D. ROSENFELD. J. Org. Chem. **29**, 3154 (1964).
8. S. HEŘMANEK and J. TROJÁNEK. Chem. Listy, **51**, 539 (1957).
9. E. E. VAN TAMELEN and M. SHAMMA. J. Am. Chem. Soc. **76**, 2315 (1954).
10. F. BOHLMANN and C. ARNDT. Chem. Ber. **91**, 2167 (1958).
11. E. ELIEL. Stereochemistry of carbon compounds. McGraw-Hill Book Co., New York. 1962. p. 236.
12. G. MULLER and A. ALLAIS. Naturwissenschaften, **47**, 82 (1960); R. B. WOODWARD, F. E. BADER, H. BICKEL, A. J. FREY, and R. W. KIERSTEAD. Tetrahedron, **2**, 1 (1958).
13. B. WITKOP. J. Am. Chem. Soc. **70**, 2617 (1948).
14. R. A. LUCAS, R. J. KIESEL, and M. J. CEGLOWSKI. J. Am. Chem. Soc. **82**, 493 (1960).

Can. J. Chem. Downloaded from www.nrcresearchpress.com by 210.87.254.40 on 09/05/12
For personal use only.

NUCLEAR MAGNETIC RESONANCE SPECTRA AND CONDUCTIVITIES OF SOME METAL ACETYLACETONATES

A. J. CARTY, D. G. TUCK
Department of Chemistry, The University, Nottingham, England

AND

E. BULLOCK
Department of Chemistry, Memorial University, St. John's, Newfoundland

Received March 18, 1965

ABSTRACT

Chemical shift data and conductivities of acetylacetonates of some group IA, IIA, and IIIA metals in dimethylsulfoxide are recorded. It is concluded that nuclear magnetic resonance spectra cannot give definite information on π-bonding in these complexes, though the results for the group III elements are consistent with the presence of such bonds, as is the evidence from related spectroscopic studies.

INTRODUCTION

Nuclear magnetic resonance spectroscopy (n.m.r.) has been used to a considerable extent in the study of inorganic complexes (see, for example, refs. 1 and 2). An early study (3) of diamagnetic acetylacetone complexes of several divalent and trivalent metals has been extended recently (4). Both of these investigations revealed small shifts in the proton spectra of the complexes relative to the enol form of acetylacetone. A much larger effect has been reported for a paramagnetic complex, vanadium (III) trisacetylacetonate (5). In a related study, Hester (6) concluded that the n.m.r. spectrum of silicon trisacetylacetonate chloride hydrochloride indicates the presence of π-orbital 'benzenoid' conjugation involving the ligand and silicon orbitals.

We have reinvestigated the proton n.m.r. spectra of the trisacetylacetonates of aluminium, gallium, and indium as part of a program of work on the coordination complexes of indium (7). We have also recorded the spectra of the salts of lithium, sodium, and potassium, and of the diacetylacetonates of beryllium, magnesium, and calcium in the basic solvent, d_6-dimethylsulfoxide. Conductivities of the compounds in dimethylsulfoxide have also been measured. Although the n.m.r. results agree well with those reported by previous workers (3, 4), our interpretation is somewhat different from that given by them. This is a consequence of our belief that the enol form of acetyl acetone is an unsuitable standard against which to compare the spectra of the complexes.

EXPERIMENTAL

Melting points were determined on a Kofler block.

Materials

The acetylacetone salts were prepared by literature methods.

(a) Group IIIA Metals (8)

Aluminium trisacetylacetonate formed colorless crystals from acetone/ethanol mixtures, m.p. 196°, lit. m.p. 192° (8).

Gallium trisacetylacetonate was crystallized as for the indium salt, m.p. 198°, lit. m.p. 196° (8).

Indium trisacetylacetonate formed colorless crystals from acetone, m.p. 189°, lit. m.p. 186° (8).

(b) Group IIA Metals

Beryllium bisacetylacetonate was crystallized from benzene or chloroform (with large losses, due to high solubility) to white crystals m.p. 108–109°, lit. m.p. 108–109° (9).

Can. J. Chem. Downloaded from www.nrcresearchpress.com by 210.87.254.42 on 09/05/12
For personal use only.

Magnesium bisacetylacetonate (9) was crystallized from ethanol, m.p. 265–267 °C.
Found: Mg, 11.1; C, 53.2. Calcd. for $C_{10}H_{14}MgO_4$: Mg, 10.9; C, 54.0.
Calcium bisacetylacetonate (10) formed white crystals from ethanol, m.p. 320° (decomp.).
Found: Ca, 15.8; C, 48.7. Calcd. for $C_{10}H_{14}CaO_4$: Ca, 16.8; C, 50.4.

(c) Group IA Metals (11)

Lithium acetylacetonate was prepared by dissolving clean lithium metal in freshly distilled acetylacetone. The product was recrystallized from ethanol/ether mixtures, and dried at $60°/10^{-2}$ mm.
Found: C, 56.8. Calcd. for $C_5H_7LiO_2$: C, 56.7.
Sodium acetylacetonate was crystallized from ethanol/ether mixtures and dried at $70°/10^{-2}$ mm.
Anal. Found: Na, 17.4; C, 46.9. Calcd. for $C_5H_7O_2Na$: Na, 18.9; C, 49.2.
Potassium acetylacetonate was crystallized as for the sodium salt.
Anal. Found: K, 25.0; C, 39.1. Calcd. for $C_5H_7KO_2$: K, 28.3; C, 43.2.

The compounds were analyzed for Na, K, and Ca by flame photometry, and for Mg by EDTA titration. Carbon was analyzed by van Slyke wet oxidation; equally poor results were obtained for some of these compounds by combustion analysis, both by us and by other workers (11). Nuclear magnetic resonance spectra of the sodium and potassium salts showed the presence of small amounts of ethanol, even in samples which had been dried at $70°/10^{-2}$ mm.

Dimethylsulfoxide (d.m.s.o.). Commercial material (B.D.H. laboratory reagent) was refluxed over predried calcium oxide for several hours. The material was fractionated at $10^{-2}-10^{-3}$ mm Hg through a 30 in. column of glass helices. A liberal head and tail fraction was rejected, and refractionation of the middle cut gave material with conductivity not greater than 10^{-7} ohm^{-1} cm^2. d_6-Dimethyl sulfoxide (d_6-d.m.s.o. Merck, Sharpe and Dohme of Canada) was used without further purification.

Conductivity Measurements

The salts were recrystallized immediately before use and dried for several hours *in vacuo*. Measurements were made on a Mullard bridge, type E7591/B using a cell of the type described by Groeneveld and Zuur (12). Exclusion of moisture was essential for reproducible measurements, and as a further precaution the solvents and solutions were kept under nitrogen. The measurements were made at 25 ± 0.2 °C. Nitrogen pressure was used to transfer solvents and to mix solutions during dilution studies (cf. ref. 13 for details of the method).

N.m.r. Measurements

Spectra were obtained on a Varian A-60 analytical spectrometer at a probe temperature of about 36 °C. The d_6-d.m.s.o. was saturated with tetramethylsilane to provide an internal reference. The compounds were examined in approximately 10% solutions and were diluted by volume (as indicated in the table). The results are given on the τ-scale.

RESULTS

Nuclear Magnetic Resonance

Chemical shifts for protons of the various salts in d_6-d.m.s.o. are recorded in the table. Results are also given for deuterochloroform solutions of those salts which were sufficiently soluble in that solvent. Some literature values (CCl_4 solution) are also included to show that the chemical shifts are relatively independent of solvent.

Conductivities

Figure 1 shows the concentration dependence of the conductivities of the Li, Na, and Ca acetylacetonates in dimethylsulfoxide. The curve for the potassium salt (Fig. 2) shows surprising deviations from the monotonic curves for the other salts. Repeat determinations with fresh samples of this salt gave similar curves, although the detailed features of the maxima and minima were not reproducible. This behavior may be related to the apparent instability of dimethylsulfoxide solutions of potassium acetylacetonate, evidenced by the fact that dilute solutions (10^{-2} *M* and below), although initially colorless, become yellowish brown over the course of a few days at room temperature. Fortunately, the more concentrated solutions used in the n.m.r. studies are above the region of apparent instability.

Can. J. Chem. Downloaded from www.nrcresearchpress.com by 210.87.254.42 on 09/05/12
For personal use only.

Can. J. Chem. Downloaded from www.nrcresearchpress.com by 210.87.254.42 on 09/05/12
For personal use only.

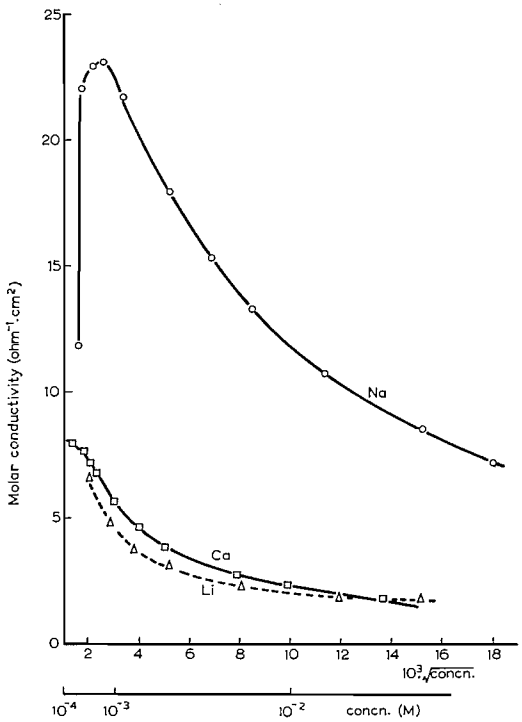

FIG. 1. Molar conductivities of sodium, calcium, and lithium acetylacetonates in dimethylsulfoxide as a function of concentration, and (concn.)$^{\frac{1}{2}}$.

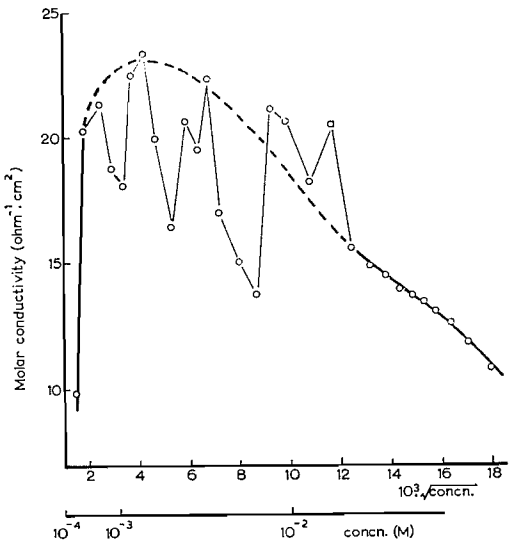

FIG. 2. Molar conductivity of potassium acetylacetonate in dimethylsulfoxide as a function of concentration, and (concn.)$^{\frac{1}{2}}$. The solid line joins the points in the order of measurement (starting with the pure solvent and progressively adding a concentrated solution of the salt); the broken line is drawn by rough analogy with the curves in Fig. 1.

The conductivities at 10^{-3} M of the acetylacetonates of the group IA and IIA salts are as follows.

Element	Li^{I}	Na^{I}	K^{I}	Be^{II}	Mg^{II}	Ca^{II}
Molar conductivity, $ohm^{-1}cm^{2}$	4.46	22.2	23	0.37	0.86	5.3

These show the predictable order K $\geqslant$ Na > Li, Ca > Mg > Be and group I > group II. The conductivities of the group III salts were not determined. The values given can be compared with the molar conductivities of 25–40 found for 1:1 electrolytes at concentrations of $\sim 10^{-3}$ M in dimethylsulfoxide by Sears, Lester, and Dawson (14).

TABLE I

Proton chemical shifts of some acetylacetonates

	Solvent					
	$CDCl_3$		d_6-d.m.s.o.		CCl_4(4)	
Metal	—CH	CH_3	—CH	CH_3	—CH	CH_3
Al	4.52	8.00	4.48	8.02	4.69	8.08
Ga	4.57	7.99	4.53	8.10	4.75	8.07
In	4.59	7.98	4.51	8.06		
Li			4.99	8.33		
			5.00*	8.33		
Na			5.14	8.35		
			5.17†	8.36		
K			5.28	8.28		
			5.33†	8.27		
Be			4.24	7.97	4.53	8.02
Mg			4.88	8.27		
Ca			4.82	8.25		

*After eightfold dilution.
†After fourfold dilution.

DISCUSSION

It is clear from the conductivity measurements that beryllium acetylacetonate is a non-electrolyte in d.m.s.o. and this is in keeping with its high solubility in benzene (9). The solubility evidence (9, 15) suggests that this is also true for the aluminium salt and it is assumed in the following discussion that the group III salts are essentially non-electrolytes.

The acetylacetonates of the remaining elements under study show significant conductivity in 10^{-3} M solution, and this is attributed to the presence, and dissociation, of ion pairs in solution. This dissociation may be aided by the basic nature of the solvent, since, although d.m.s.o. does not appear to form stable salts with group IA and IIA cations (16), it does coordinate to a number of other metal cations to give stable species (17). It is also known to form salts with certain mineral acids (18), presumably by bonding to the acidic proton.

The enol form of acetylacetone shows only one methyl proton peak in the n.m.r. spectrum, and this is ascribed (19) to rapid hydrogen exchange between the two oxygen atoms rather than to any orbital degeneracy in the molecule itself. Previous workers (3, 4, 6) have compared the spectra of acetylacetonate complexes with the enol, and find that the γ-proton signals of most of the complexes occur to high field of the corresponding enol proton. Thus, such comparisons cannot give any information about π-orbital delocalization which, by ring-current effects, would be expected to cause a low-field shift

Can. J. Chem. Downloaded from www.nrcresearchpress.com by 210.87.254.42 on 09/05/12
For personal use only.

of the γ-proton (4) in the complex. We considered that a more informative comparison should be possible with the free acetylacetonate anion in which orbital degeneracy of the type

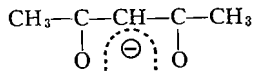

can be assumed to occur. The n.m.r. spectrum of this system can, in principle, be obtained from dilute solutions of the acetylacetonates of group IA metals in an ionizing solvent. The possibility that the *free* anion exists with the oxygen atoms *trans* to one another cannot be ignored, though in ion pairs the *cis* arrangement seems more plausible. Our results (table) show that the spectra of the sodium and potassium salts give concentration-dependent signals for the γ-proton, and that the chemical shifts of the methyl signals are virtually independent of concentration. No concentration dependence was observed for the lithium salt or any of the other compounds examined. The spectra of the highly covalent species (Al, Ga, In, Be, and Li) were characterized by very sharp resonance signals. In the remaining spectra, especially those of the sodium, potassium, and calcium salts, the peaks were rather broad, although the tetramethylsilane resonance suggested that the resolution of the instrument was as good as for the other solutions. This effect may be a function of the expected exchange process between ion pairs and free ions.

The chemical shifts of the methyl groups fall into two distinct groups. Beryllium and the group IIIA metal complexes give signals at τ 8.04 $\pm$ 0.07 whilst the remaining compounds show an absorption within the range τ 8.30 $\pm$ 0.06, but there is no obvious relationship of the detailed shifts to the ionization potential or electron-negativity of the metals. The conductivity and n.m.r. results are consistent with the presence of an equilibrium

$$[\text{ion pair} \rightleftharpoons \text{free anion} + \text{(solvated) cation}]$$

in solutions of the sodium and potassium salts in d.m.s.o. It follows, therefore, that the n.m.r. absorption of the γ-proton of the acetylacetonate anion is to high field of 5.33 τ (the signal of the weakest solution of the potassium salt which we were able to study). It would clearly be valuable to obtain the n.m.r. spectrum of a 10^{-3} M solution of this salt.

In the more concentrated solutions (approx. 0.5 M or above) where the salts of group IA metals would be expected to be essentially undissociated, the γ-protons occur to low field in the order Li < Na < K. Obviously, association of the anion and cation, whether by strong ion-pairing or by formation of metal oxygen bonds (as seems possible for the Li salt), causes some localization of the negative charge at the oxygen atoms of the ligand. This will deshield the γ-proton and cause a low-field shift relative to the free anion. This is important, since in the formation of acetylacetonate coordination complexes, some transfer of negative charge of this type must always occur and hence a low-field shift of the γ-proton relative to the anion is to be expected, irrespective of any other electronic effects which might be present. It may be significant that the order of shifts for the Li, Na, and K salts is that of decreasing ionization potential.

The magnesium and calcium salts are weak electrolytes in 10^{-3} M solution and by the argument above, the n.m.r. spectrum is probably that of the ion pair for each compound. Surprisingly the γ-proton of the Mg complex absorbs 0.06 p.p.m. to high field of the corresponding calcium salt proton. The beryllium bisacetylacetonate shows the largest low-field shift for the γ-proton, of the compounds investigated by us (or by Smith and

Can. J. Chem. Downloaded from www.nrcresearchpress.com by 210.87.254.42 on 09/05/12
For personal use only.

Can. J. Chem. Downloaded from www.nrcresearchpress.com by 210.87.254.42 on 09/05/12
For personal use only.

Thwaites (4)), implying a strong donation of charge from the anion in bonding to the central metal atom. This result illustrates the difficulty of investigating π-bonding in this type of compound by n.m.r. methods. As noted above, electron localization on the oxygen atom in ion pairs would cause deshielding of the 'olefinic' proton, and the formation of covalent bonds involving electron donation to the metal will have the same effect. There appears to be no quantitative way of estimating the extent of these effects when one is comparing complexes of the same anion with different metals. It follows that there is equally no way of estimating how much (if any) further deshielding of the γ-proton might have occurred through ring currents from 'aromatic' delocalization of π-electrons involving the anion and the central metal atom. In fact, the Be—O bonds in beryllium bisacetylacetonate must be essentially of the pure σ-type, since the only orbitals available for π-overlap with the p_π orbitals on the oxygen are the $3d_\pi$ of the beryllium (assuming a tetrahedral distribution of the oxygens around the metal) and these are probably of too high energy to be utilized. It is notable that the analogous BF_4^- anion, in which the central atom has the isoelectronic rare-gas configuration, is taken by Cotton and Leto (20) to be a pure σ-bonded system against which additional π-contributions to bonding can be compared. The observation of very sharp methyl resonance signals in the beryllium salt and the group III metal complexes suggest a symmetrical (probably planar) configuration for the metal–ligand ring system in agreement with X-ray structural determinations on Fe(III) and Mn(III) trisacetylacetonates (21).

The γ-proton signals of the acetylacetonate complexes of aluminium, gallium, and indium lie well to low field of the corresponding signal in the acetylacetone anion. A quantitative discussion of the origin of this shift is not possible for the reasons outlined above. Further, a precise comparison with the beryllium salt is precluded by the difference in coordination number and orbital hybridization between the group II and group III metals. The n.m.r. results, therefore, serve only to confirm that strong metal–oxygen bonding occurs in the group III complexes. However, the chemical shifts of the signals appear to be virtually independent of the metal (see table; note that the methyl resonances show a larger spread of chemical shifts than the γ-protons). This observation would be consistent with the existence of some effect (e.g. π-orbital delocalization) which effectively masks electronegativity differences of the metals in the various salts, and this is as much as we are able to deduce concerning the existence of π-bonding in these complexes, from this type of evidence.

Results of ultraviolet (3) and Raman (15) spectroscopic measurements are also consistent with a measure of π-bonding in the Al, Ga, and In complexes. Furthermore, the M—O force constant in Al $(acac)_3$ is significantly higher than that for the Cr(III), Co(III), and Fe(III) complexes (22), and the force constants in Al, Ga, and In compounds are very similar to each other (15). These two statements also imply a π-contribution to the M—O bond.

Holm and Cotton (3) have pointed out that since the available p_π orbitals on the oxygen atoms in the acetylacetone anion are filled, the π-donation must be in the sense $\overset{\curvearrowleft}{\underset{\curvearrowright}{M—O}}$, and it is perhaps rather surprising that donation of this type should occur into the nd orbitals of the group IIIA metals (the $(n-1)d^{10}$ shell being filled). It has been suggested (7) that in certain coordination complexes of indium, according to the theory of Craig and Doggett (23) for transition metal elements, strong σ-donation improves the chance of π-overlap with metal d-orbitals by reducing the charge on the metal, allowing the d-orbitals to expand towards the appropriate ligand π-orbitals. It would be very useful

to have some measure of the electronegativities of the oxygen atoms in the acetylacetone anion, to make a comparison of the likelihood of this effect (as against ligands such as H_2O, oxalate, etc.). One factor which might encourage σ-donation is that sp^2 hybridization of the oxygens (implied by the M—O—C bond angles) will place filled non-bonding sp^2 orbitals outside the ring, which may cause repulsion of the M—O bonding electrons towards the metal, with the consequences outlined above.

REFERENCES

1. E. L. Muetterties and W. D. Phillips. Advan. Inorg. Chem. Radiochem. **4**, 231 (1962).
2. Discussions Faraday Soc. **34**, (1962).
3. R. H. Holm and F. A. Cotton. J. Am. Chem. Soc. **80**, 5658 (1958).
4. J. A. S. Smith and J. D. Thwaites. Discussions Faraday Soc. **34**, 143 (1962).
5. A. Forman, J. N. Murrell, and L. E. Orgel. J. Chem. Phys. **31**, 1129 (1959).
6. R. E. Hester. Chem. Ind. London, 1397 (1963).
7. A. J. Carty and D. G. Tuck. J. Chem. Soc. In press.
8. C. J. Morgan and H. D. K. Drew. J. Chem. Soc. 1058 (1921).
9. L. F. Hatch and G. Sutherland. J. Org. Chem. **13**, 249 (1948).
10. R. West and R. Riley. J. Inorg. Nucl. Chem. **5**, 295 (1958).
11. C. J. Morgan and A. E. Rawson. J. Soc. Chem. Ind. London, **44**, 462 (1925).
12. W. L. Groeneveld and A. P. Zuur. Rec. Trav. Chim. **72**, 617 (1953).
13. B. F. G. Johnson. Ph.D. Thesis, University of Nottingham. 1963.
14. P. G. Sears, R. R. Lester, and L. R. Dawson. J. Phys. Chem. **60**, 1433 (1956).
15. R. E. Hester and R. A. Plane. Inorg. Chem. **3**, 513 (1954).
16. E. J. Corey and M. Chaykovsky. J. Am. Chem. Soc. **84**, 867 (1962).
17. F. A. Cotton and R. Francis. J. Am. Chem. Soc. **82**, 2986 (1960). D. W. Meek, D. K. Straub, and R. S. Drago. J. Am. Chem. Soc. **82**, 6013 (1960). J. Selbin, L. Bull, and L. H. Holmes, Jr. J. Inorg. Nucl. Chem. **16**, 219 (1961).
18. P. Nylen. Z. Anorg. Chem. **246**, 227 (1941). W. Steinkopf and S. Müller. Ber. **56**, 1926 (1923).
19. W. G. Schneider and L. W. Reeves. Ann. N.Y. Acad. Sci. **70**, 858 (1958).
20. F. A. Cotton and J. R. Leto. J. Chem. Phys. **30**, 993 (1959).
21. R. B. Roof, Jr. Acta Cryst. **9**, 781 (1956). B. Morosin and J. R. Brathovde. Acta Cryst. **17**, 705 (1964).
22. K. Nakamoto, P. J. McCarthy, A. Ruby, and A. E. Martell. J. Am. Chem. Soc. **83**, 1066, 1272 (1961).
23. D. P. Craig and G. Doggett. J. Chem. Soc. 4189 (1963).

Can. J. Chem. Downloaded from www.nrcresearchpress.com by 210.87.254.42 on 09/05/12
For personal use only.

FATTY ACIDS OF CATALPA BIGNONIOIDES AND OTHER BIGNONIACEAE SEED OILS[1,2]

MARY J. CHISHOLM AND C. Y. HOPKINS
Division of Pure Chemistry, National Research Council, Ottawa, Canada

Received May 11, 1965

ABSTRACT

Seed oils of 11 species of Bignoniaceae, representing four of the five tribes of the family, were analyzed by gas–liquid chromatography and other techniques. The fatty acids of *Catalpa bignonioides* oil had the following composition: *trans*-9,*trans*-12-octadecadienoic 5, *trans*-9,*trans*-11,*cis*-13-octadecatrienoic 31, palmitic 5, stearic 1, octadecenoic 8, linoleic 50%. One of the five samples of this species showed evidence of an appreciable amount of conjugated dienoic acid.

Jacaranda semiserrata had 33% of a *cis*,*trans*,*cis* trienoic acid. *Kigelia pinnata* had 57% of a non-conjugated trienoic acid. The other eight species had the ordinary palmitic–oleic–linoleic composition. The total fatty acid composition of the oils is reported.

The tribe Tecomeae yielded both conjugated and non-conjugated seed oils. Single species of each of the other three tribes gave non-conjugated oils.

INTRODUCTION

The seed oils of relatively few species of Bignoniaceae have been studied but it is already evident that very unusual fatty acids occur in this plant family. Recent investigations have disclosed the occurrence of acids with conjugated diene and triene unsaturation (1, 2, 3) and others with non-conjugated unsaturation but with *trans* double bonds (4, 5).

In the present work, the seed oil of *Catalpa bignonioides* and 10 additional species of the family have been examined and their fatty acid composition has been determined. Two of the uncommon acids were identified by orthodox chemical methods. The composition of the mixed acids of each oil was determined by gas–liquid chromatography (g.l.c.) of the methyl esters. In species yielding acids with conjugated double bonds, the content of conjugated acids was determined by ultraviolet absorption analysis and the amount of each non-conjugated acid was calculated as a percentage of the remainder.

RESULTS AND DISCUSSION

Preliminary data are given in Table I. The classification into tribes is that of Engler (6) and the species are named in accordance with Sandwith (7).

The oil content was relatively low in some species, apparently because a large part of the seed is made up of the fibrous wing which contains little or no oil. Most of the oils had refractive indices in the range 1.470–1.476 at 25°, indicating the presence of ordinary unsaturated acids and absence of those with conjugated unsaturation. The exceptions are discussed below.

Catalpa bignonioides

Five lots of seed of this species from different sources were examined. Four of them yielded oils in which the fatty acids contained 31–34% of conjugated triene acid, as shown by the ultraviolet spectra. The acid was concentrated by low-temperature crystallization and identified by means of its adduct with maleic anhydride as *trans*-9,*trans*-11,*cis*-13-octadecatrienoic acid. This acid was found previously in two species of *Catalpa* (2, 8) and in *Chilopsis linearis* (1).

[1]*Issued as N.R.C. No. 8565.*
[2]*Presented in part before the Australian and New Zealand Association for the Advancement of Science, Canberra, January, 1964.*

Can. J. Chem. Downloaded from www.nrcresearchpress.com by 210.87.254.5 on 09/05/12
For personal use only.

TABLE I

Seed oils of Bignoniaceae

Tribe and species	Oil in seed,* wt. %	Refractive index, 25°†	Iodine value‡
Bignonieae			
Bignonia capreolata L.	11.5	1.4752	137
Tecomeae			
Campsis grandiflora (Thunb.) K.Schum.	7.6	1.4755	126
Campsis radicans (L.) Seem.	14.3	1.4758	139
Catalpa bignonioides Walt.	23.0	1.4949	155
Jacaranda semiserrata Cham.	12.9	—	—
Pandorea jasminoides (Lindl.) K.Schum.	28.2	1.4735	131
Spathodea campanulata Beauv.	8.9	1.4730	117
Tabebuia rosea (Bertol.) DC.	23.1	1.4689	82
Incarvillea delvayi Bur. and Franch.	23.6	1.4751	138
Eccremocarpeae			
Eccremocarpus scaber Ruiz. and Pav.	27.5	1.4731	134
Crescentieae			
Kigelia pinnata (Jacq.) DC.	—	1.4800	185

*By extraction at 25°, air-dry basis.
†n_D^{25}.
‡Wijs (30 min).

The infrared spectrum of the oil showed stronger absorption in the region 960 cm^{-1} than would be expected from a *trans,trans,cis* conjugated acid, as judged by comparison with the intensity of the main peak at 985 cm^{-1}. Consequently, the presence of non-conjugated *trans* double bonds was suspected.

This was confirmed by fractional crystallization of the mixed acids, which resulted in a concentrate of the *trans* acid along with about 20% of conjugated triene acid. The latter was removed by adduction with maleic anhydride. The remainder of the concentrate yielded *trans*-9,*trans*-12-octadecadienoic acid on recrystallization. Its identity was confirmed by hydroxylation with alkaline permanganate, which gave di-*threo*-9,10,12,13-tetrahydroxystearic acid. *trans*-9,*trans*-12-Octadecadienoic acid was found previously in the seed oil of *Chilopsis linearis* (4).

One sample of seed of *Catalpa bignonioides* gave oil of a different composition. Its ultraviolet spectrum showed a content of only 12% of conjugated triene acid but there was also an absorption peak at 233 mμ, not observed in the oils from the previous seed samples. After allowance was made for the absorption at this wavelength caused by the triene, it was calculated that 7.9% of conjugated diene acid was present.

It appears, therefore, that some samples of this species contain a conjugated diene acid and that other samples do not. Markman and Bodnya (9) reported 4% of conjugated diene acid in their sample, based on ultraviolet absorption analysis, but Earle and coworkers (10) reported no conjugated diene acid. Occurrence of a conjugated diene acid in the oil of *Chilopsis linearis* has been demonstrated (1). It is possible that the diene acid is an intermediate in the formation of the conjugated triene acid in the seed.

In their work, Markman and Bodnya assumed, on the basis of the ultraviolet spectrum, that the conjugated triene acid was eleostearic acid. However, since the spectra of the two isomeric acids (*cis,trans,trans* and *trans,trans,cis*) are almost identical, it seems likely that their triene acid was *trans*-9,*trans*-11,*cis*-13-octadecatrienoic acid, as found in the present work. A comparison of the analyses is given in Table II.

Jacaranda semi-serrata

The small sample of seed (0.1 g) yielded an oil whose ultraviolet spectrum had maxima

Can. J. Chem. Downloaded from www.nrcresearchpress.com by 210.87.254.5 on 09/05/12
For personal use only.

TABLE II

Fatty acid composition of the seed oil of *Catalpa bignonioides* (%)

Acid	Present work	Markman and Bodnya (9)	Earle *et al.* (10)
Palmitic	5	}4.4	}18
Stearic	1		
Octadecenoic	8	10.1	14
Octadecadienoic	55*	48.8	36
Octadecatrienoic	Nil	Nil	Nil
Conjugated dienoic	Trace†	4.0	Nil
Conjugated trienoic	31‡	32.6	28

*Composed of 5% of *trans*-9,*trans*-12-octadecadienoic acid and 50% of linoleic acid.
†Higher in one sample.
‡Identified as *trans*-9,*trans*-11,*cis*-13-octadecatrienoic acid.

at 266, 275, and 286 mμ, characteristic of a *cis*,*trans*,*cis* trienoic acid. This is presumed to be the same acid as the one identified in *J. mimosifolia*, viz. *cis*-8,*trans*-10,*cis*-12-octadecatrienoic acid (3). The absorptivity was equivalent to a content of 33.1% of the acid.

Kigelia pinnata

The seeds yielded a small amount of oil with an iodine value of 185, the highest of any of the oils. The infrared spectrum had maxima at 1 650(w) and 3 000(s) cm^{-1}, indicating ordinary unsaturation. There were no peaks in the region of *trans* and conjugated unsaturation, i.e. 900–1 000 cm^{-1}. Similarly, the ultraviolet spectrum showed no evidence of conjugated double bonds. The g.l.c. curve denoted the presence of 57% of non-conjugated octadecatrienoic acid, judged from its emergence time to be linolenic acid.

TABLE III

Composition of the fatty acids

	Fatty acid, wt. % of total acids						
			Non-conjugated				
Tribe and species	Conjugated dienoic	Conjugated trienoic	16:0*	18:0	18:1	18:2	18:3
Bignonieae							
Bignonia capreolata	tr†	0	7	3	24	50	16
Tecomeae							
Campsis grandiflora	1.2	0.4	9	3	22	57	9
Campsis radicans	0	0.4	8	1	24	55	12
Catalpa bignonioides	tr	31.4	5	1	8	55	0
Jacaranda semiserrata	0	33.1	8	2	31	26	0
Pandorea jasminoides	0	0	12	2	27	46	13
Spathodea campanulata	0	0	18	2	15	65	0
Incarvillea delavayi	tr	tr	9	1	15	74	0
Tabebuia rosea‡	0	0	18	12	36	30	1
Eccremocarpeae							
Eccremocarpus scaber	0	0	10	1	19	70	0
Crescentieae							
Kigelia pinnata	0	0	7	1	10	25	57

*The figures indicate chain length and number of double bonds.
†tr = trace.
‡Also contains 3% of an unidentified acid.

Composition of the Fatty Acids

The total composition of the fatty acids of the oils is given in Table III. *Catalpa* and *Jacaranda*, the only species having appreciable amounts of conjugated trienoic acid,

Can. J. Chem. Downloaded from www.nrcresearchpress.com by 210.87.254.5 on 09/05/12
For personal use only.

contained no non-conjugated trienoic acid. *Kigelia* had a high content of non-conjugated trienoic acid but no other unusual features. The other species had essentially the ordinary palmitate–oleate–linoleate composition with little or no conjugated acid(s). Their content of non-conjugated octadecatrienoic acid (judged to be linolenic) varied from nil to 16%.

The two *Campsis* species were calculated to have a small but measurable amount of conjugated acid on the basis of ultraviolet absorption. *Tabebuia* oil was exceptional in having the highest content of saturated acids, including 12% of stearic acid. The content of hexadecenoic acid was quite low in all of the oils and was estimated to be less than 1%.

Taxonomy and Fatty Acid Composition

Four of the five tribes of Bignoniaceae are represented in the present study. All species found so far to contain conjugated polyenoic acids in the seed oils are from the tribe Tecomeae. They are species of *Catalpa*, *Jacaranda*, and *Chilopsis*. All of the examples of these genera that have been examined, including those in earlier work (1, 2, 3, 8), contain conjugated triene acids. However, it cannot be assumed that conjugated acids occur only in Tecomeae until more species of the other tribes have been studied.

Several species of Tecomeae yield non-conjugated oils (Table III) but, in general, it may be said that this tribe produces oils of unusually varied composition.

EXPERIMENTAL

Samples of some seeds were kindly supplied by the Director, Jardin Botanico, Buenos Aires, and by the Department of Forestry, Republic of South Africa. The remainder were purchased from established commercial suppliers.

Ultraviolet spectra were determined in cyclohexane solution with a Beckman DU spectrophotometer. Infrared spectra were determined in carbon disulfide in a Perkin–Elmer model 21 spectrophotometer with sodium chloride prism. Melting points were determined in capillary tubes and were corrected. The oils were obtained by extracting the finely ground sample with petroleum ether (b.p. 30–60°) at room temperature. Iodine values were determined by the Wijs method (30 min).

The oils were converted to methyl esters by transesterification in methanol with hydrogen chloride catalyst. The esters were examined by g.l.c. and their composition was estimated by measuring the peak areas. The g.l.c. analyses were made using a 1 meter copper column at 185° and a thermal conductivity detector. The liquid phase was a diethyleneglycol – succinic acid polyester (15% on diatomaceous earth).

Catalpa bignonioides

The oil was extracted and the solvent was removed in a current of nitrogen at 25–30°. A typical sample of the oil had infrared absorption maxima at 985(vs) and 958(m) cm^{-1}. Ultraviolet absorption maxima were at 262, 272, 283 mμ and the absorptivity was $E_{1\ cm}^{1\%}$ 556 at 272 mμ, equivalent to 31.4% of conjugated triene acid. There was some absorption but no peak in the 233 mμ region. Three other samples had 32.3, 34.4, and 33.0% of conjugated triene acid.

One sample of the seed gave an oil with absorptivity $E_{1\ cm}^{1\%}$ 211 at 271 mμ, equivalent to 12.0% of conjugated triene acid. The same oil had a peak at 233 mμ and absorptivity $E_{1\ cm}^{1\%}$ 102 at 233 mμ. The absorptivity at 233 mμ due to the content of conjugated triene was calculated to be 15. Hence the net absorptivity due to the diene was 102 − 15 = 87, equivalent to 7.9% of conjugated diene acid, if we employ the factor 0.091 (11). This sample was not investigated further.

The typical oil (35 g) was hydrolyzed by ethanolic 5% potassium hydroxide under nitrogen at 25°. Unsaponifiable matter was removed and the mixed acids were dissolved in acetone and cooled. Crystals were taken off at −5°, −40°, and −62°. The crystals collected at −62° (8.5 g) contained most of the conjugated triene acid. This portion was heated with maleic anhydride in benzene (2), yielding an adduct, m.p. 71–72°. This substance, when mixed with the adduct of maleic anhydride with *trans*-9,*trans*-11,*cis*-13-octadecatrienoic acid (2), did not lower its melting point.

The mixed acids from another portion of the oil (46 g) were crystallized fractionally from acetone by the procedure described previously (4), to concentrate the acid with isolated *trans* bonds. The fractionation was monitored by infrared absorption. The concentrate was treated with maleic anhydride to remove the conjugated triene acid and the rest was crystallized from pentane, giving 1.5 g of *trans*-9,*trans*-12-octadecadienoic acid, m.p. 24–25°. Upon oxidative splitting it gave azelaic and hexanoic acids.

The *trans*,*trans* diene acid (1.0 g) was hydroxylated by alkaline permanganate (12) for 20 min at 10° and the product was crystallized from ethanol. It gave the higher melting racemic form of di-*threo*-9,10,12,13-

Can. J. Chem. Downloaded from www.nrcresearchpress.com by 210.87.254.5 on 09/05/12
For personal use only.

tetrahydroxystearic acid, m.p. 147–148°. The melting point was unchanged in admixture with a sample prepared from pure linelaidic acid.

A solution of 0.4 g of the diene acid was treated with 2,4′-dibromoacetophenone by the method of Neish and Lemieux (13). The crude product (0.6 g) was crystallized from ethanol and then from acetone, giving 4-bromophenacyl *trans*-9,*trans*-12-octadecadienoate, m.p. 50.5–51.5°.

Anal. Calcd. for $C_{26}H_{37}O_3Br$: C, 65.39; H, 7.81. Found: C, 65.30; H, 7.80.

Linoleic acid was identified in the final filtrate from the crystallization of the total mixed acids. The acids (2 g) from the filtrate were hydroxylated by alkaline permanganate for 5 min at 10°. The product was crystallized from ethyl acetate and then from ethanol, giving the higher melting form of di-*erythro*-9,10,12,13-tetrahydroxystearic acid, m.p. and mixed m.p. 173–174°.

Other Bignoniaceae Oils

Infrared spectra of the oils of *Bignonia capreolata*, *Pandorea jasminoides*, *Tabebuia rosea*, *Eccremocarpus scaber*, and *Kigelia pinnata* were examined. None showed absorption that would indicate the presence of *trans* double bonds (ca. 960 cm^{-1}), conjugated double bonds (900–1 000 cm^{-1}), or hydroxyl groups (ca. 3 500 cm^{-1}).

All had a fairly strong peak at 3 023 cm^{-1}, denoting considerable unsaturation, except *Tabebuia rosea*, which had lower intensity than the others in agreement with the iodine value. *Kigelia pinnata* showed stronger unsaturation and the peak was at 3 000 cm^{-1}. Its peak of low intensity at 1 650 cm^{-1} also indicated considerable *cis* unsaturation. Absorption at this wave number was very slight for the other species.

Ultraviolet absorption spectra of *Catalpa* and *Jacaranda* oils had maxima attributed to conjugated trienes. The two species of *Campsis* had similar but weak triene absorption at 272 and 282 mμ and *Incarvillea* had a trace amount (Table III). The other oils had no appreciable absorption or maxima in this region.

Evidence of conjugated diene unsaturation was scanty except in the anomalous sample of *Catalpa bignonioides* described above. However, there was a little absorption at 232–233 mμ equivalent to 1.2% of conjugated dienoic acid in *Campsis grandiflora*, less than 1% in *Bignonia* and *Incarvillea*, and none in the other oils. The g.l.c. curve for *Tabebuia* esters included an unidentified peak representing 3% of the total acids.

ACKNOWLEDGMENTS

The authors are indebted to Mr. N. Y. Sandwith for helpful advice in identifying and naming of species, to Mr. R. Lauzon for determination of infrared spectra, and to Mr. H. Seguin for microanalysis.

REFERENCES

1. C. Y. Hopkins and M. J. Chisholm. J. Am. Oil Chemists' Soc. **41**, 42 (1964).
2. C. Y. Hopkins and M. J. Chisholm. J. Chem. Soc. 573 (1962).
3. M. J. Chisholm and C. Y. Hopkins. J. Org. Chem. **27**, 3137 (1962).
4. M. J. Chisholm and C. Y. Hopkins. Can. J. Chem. **41**, 1888 (1963).
5. C. Y. Hopkins and M. J. Chisholm. J. Chem. Soc. 907 (1965).
6. A. Engler. Syllabus der Pflanzenfamilien. Vol. 2. Gebrüder Borntraeger, Berlin. 1964. p. 453.
7. N. Y. Sandwith. Kew Bull. **8** (Pt. 4), 451 (1953); and references cited therein.
8. C. Y. Hopkins and M. J. Chisholm. Can. J. Chem. **40**, 2078 (1962).
9. A. L. Markman and M. D. Bodnya. J. Gen. Chem. USSR Engl. Transl. **27**, 2353 (1957).
10. F. R. Earle, C. A. Glass, G. C. Geisinger, and I. A. Wolff. J. Am. Oil Chemists' Soc. **37**, 440 (1960).
11. American Oil Chemists' Society. Official and tentative methods of analysis. 2nd ed., rev. to 1961. Chicago. 1961.
12. A. Lapworth and E. N. Mottram. J. Chem. Soc. **127**, 1628 (1925).
13. A. C. Neish and R. U. Lemieux. Can. J. Chem. **33**, 1701 (1955).

Can. J. Chem. Downloaded from www.nrcresearchpress.com by 210.87.254.5 on 09/05/12
For personal use only.

Can. J. Chem. Downloaded from www.nrcresearchpress.com by 210.87.254.6 on 09/05/12
For personal use only.

ALICYCLIC KETYLS

I. ANGULAR DEPENDENCE OF HYPERFINE COUPLING AND CONFORMATIONAL MOBILITY OF CYCLOHEXANONE KETYLS

J. W. LOWN

Department of Chemistry, University of Alberta, Edmonton, Alberta

Received April 14, 1965

ABSTRACT

The electron paramagnetic resonance (e.p.r.) spectra of ketyls derived from cyclopentanone and 4-*tert*-butyl, 4-methyl, 3-methyl, and unsubstituted cyclohexanone have been recorded in dimethoxymethane at room temperature. The proton hyperfine splittings (a_H) observed with rigid ketyls are consistent with a dihedral angular (θ) dependence of hyperfine coupling of the form, $a_H = 4.8 + 9.6 \cos^2 \theta$. Conformational averaging of the hyperfine coupling is observed with 4-methyl, 3-methyl, and unsubstituted cyclohexanone ketyls. The conformer populations calculated from the e.p.r. spectra are in accordance with A values for the methyl group derived from non-radical cyclohexane compounds.

Ketyls may be generated from ketones by the reducing action of alkali metals in ethereal solvents (1, 2, 3). They display well-resolved electron paramagnetic resonance (e.p.r.) spectra which show the unpaired spin to be concentrated largely on the carbonyl carbon (2), although hyperfine coupling occurs from protons on adjacent carbons. It has been postulated that the efficiency of hyperconjugative coupling to such adjacent protons is dependent on the dihedral angle subtended by the proton and the singly occupied 2p orbital centered on the carbonyl carbon (4). Recently the angular dependence of hyperfine coupling, and conformational mobility, in radicals derived from alicyclic alcohols has been examined (5). The radicals are generated in aqueous solution by hydrogen atom abstraction from the alcohols by primary radicals postulated to be OH·. This system suffers from a number of disadvantages. While hydrogen abstraction occurs mainly alpha to the hydroxyl group, other positions are also attacked leading to complex e.p.r. spectra arising from a mixture of free radicals. Also, many compounds which would provide interesting models are not sufficiently water soluble for the technique.

In view of the relationship of ketyls as conjugate bases of the radicals resulting from the abstraction of an alpha hydrogen in cyclic alcohols, and their specific generation from ketones, it appeared that suitably rigid ketones would serve as good models for testing the angular dependence of hyperfine coupling. The conformational mobility of less rigid ketyls could then be examined. It would then be possible to see if A values (conformational free energy differences) characteristic of substituents in non-radicals had validity when applied to the conformational analysis of nonrigid radicals.

Angular Dependence of Hyperfine Coupling in Ketyls

4-*tert*-Butylcyclohexanone was selected for the preparation of a suitably rigid model ketyl. The ketyl (as in the case of other free radicals discussed) could be generated by the action of potassium on a 5% degassed solution of the ketone in 1,2-dimethoxyethane, producing a yellow solution. The ketyl was quite stable under these conditions and gave a seven line e.p.r. spectrum (see Fig. 1) of overall splitting of 43.2 Oe and having an intensity pattern (1:2:3:4:3:2:1). This was interpreted as arising from coupling with two equivalent (axial) protons, ($a_{H_a} = 14.4$ Oe) and two equivalent (equatorial) protons ($a_{H_e} = 7.2$ Oe). No hyperfine coupling due to the associated potassium ion could be resolved. This is expected since such coupling is small (~ 0.12 Oe) (3). Since the axial

Can. J. Chem. Downloaded from www.nrcresearchpress.com by 210.87.254.6 on 09/05/12
For personal use only.

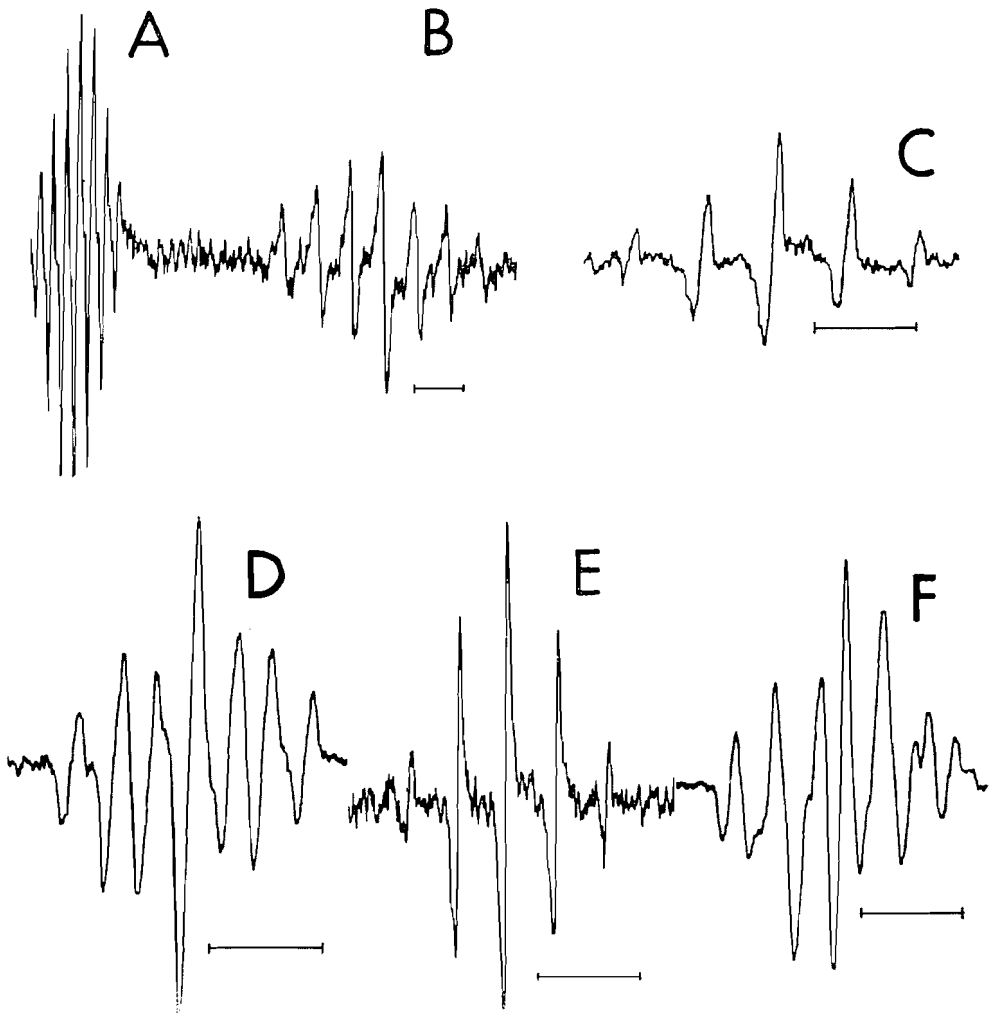

FIG. 1. First derivative e.p.r. spectra. A, 4-*tert*-butylcyclohexyl ketyl at rapid scan; B, 4-*tert*-butylcyclohexyl ketyl at slow scan; C, cyclopentyl ketyl; D, 4-methylcyclohexyl ketyl; E, cyclohexyl ketyl; F, 3-methylcyclohexyl ketyl. The bar in each case represents 20 Oe.

proton is aligned close to the plane of the $C_1 2p$ orbital, it shows more efficient hyperconjugative coupling, reflected in the larger hyperfine constant. Some distortion of the cyclohexane chair is to be expected to accommodate the sp^2 hybridized ketyl carbon, and as a result of the bulky 4-*tert*-butyl group. However, these should not be serious and examination of a Barton model* predicts values for the dihedral angles of $\theta_{a,p} = 0°$,

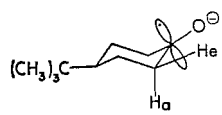

Scale 1 Å = 10 cm.

$\theta_{e,p} = 120°$ (where a and e subscripts refer to axial and equatorial respectively).

A relationship between dihedral angle and hyperfine coupling a_H of the following form has been proposed (6, 7).

[1] $$a_H = B_0 + B \cos^2 \theta$$

where B_0 and B are constants, characteristic of a given type of radical. In the chair to chair interconversion of the cyclohexyl radical in solid cyclohexane (8, 9), best agreement between theory and practice is obtained with $B_0 = 4.5$ and $B = 40.5$ Oe, while in the case of a radical derived from cyclopentylamine the following constants provide the best agreement, $B_0 = 3.5$ and $B = 45.6$ (5). In the present work substitution of observed hyperfine coupling and measured angles leads to a relationship of the form

[2] $$a_H = 4.8 + 9.6 \cos^2 \theta.$$

To test the application of eq. [2] to five-membered rings the ketyl generated from cyclopentanone was examined. An e.p.r. spectrum consisting of five equally spaced lines ($a_H = 13.8$ Oe) having an intensity pattern of (1:4:6:4:1) was obtained. Thus all four protons at the 2 and 5 positions are equivalent. Examination of a Barton model shows that little conformational freedom exists and that the ring is virtually planar. The dihedral angle is 30° from which eq. [2] predicts a hyperfine coupling of 12.0 Oe. The agreement is fair since no account has been taken of differences of spin density at the ketyl carbon. However, since much better agreement is obtained when eq. [2] is applied to other six-membered rings it is possible that such an equation may not be indiscriminately applied to ketyls of different ring sizes. Such has been the experience with the Karplus relationship when applied to nuclear magnetic resonance spin–spin coupling in five- and six-membered rings (10). Camphor which would have provided a further test of eq. [2] could not be induced to form a ketyl.

Conformational Mobility in Six-Membered Ketyls

Cyclohexyl ketyl afforded an e.p.r. spectrum consisting of five equidistant ($a_H = 10.4$ Oe) lines with an intensity pattern of (1:4:6:4:1). This clearly arises from rapid chair to chair conformational interconversion where two pairs of C_2 and C_6 axial and equatorial protons are expected to show a time-averaged equal hyperfine coupling. Since each conformational form is equally populated a coupling $a_{H_{av}}$ equal to the average of those characteristic of axial and equatorial protons in 4-*tert*-butylcyclohexyl ketyl is anticipated, provided eq. [2] is valid.

$$a_{H_{av}} = \tfrac{1}{2}(a_{Ha} + a_{He}) = \tfrac{1}{2}(14.4 + 7.2) = 10.8 \text{ Oe}.$$

Since the estimated accuracy of the hyperfine coupling constants is ±0.2 Oe and in view of possible distortion of the chair in the rigid ketyl, the agreement is good.

The observation of five equally sharp lines displaying the expected intensity pattern for four equivalent protons is essential to the above argument. This implies that the rate of chair to chair inversion is *not* comparable with the frequency difference of couplings of axial and equatorial protons (11). If such were the case then uncertainty broadening of the lines would result and the simple intensity pattern obtained here would not have been observed. Norman has observed this phenomenon in the case of radicals derived by hydrogen abstraction from piperidine, cyclohexanol, and dioxan (5). In such cases the frequency difference between axial and equatorial couplings corresponded to ~38 Oe, and therefore comparable to the rate of interconversion estimated to be ca. 5×10^8 s^{-1}.

Can. J. Chem. Downloaded from www.nrcresearchpress.com by 210.87.254.6 on 09/05/12
For personal use only.

That the axial–equatorial frequency difference observed in ketyls is much smaller (corresponding to 7.2 Oe) accounts for the lack of uncertainty broadening, since the rate of conformational inversion might be expected to be comparable with that found by Norman.

Effects of Ring Substitution on the Position of Conformational Equilibrium

4-Methylcyclohexyl ketyl gives a spectrum consisting of a (1:2:1) triplet of (1:2:1) triplets which overlap giving the appearance of seven lines and corresponding to two unequal couplings of 13.5 and 7.5 Oe resulting from conformational averaging between forms I and II.

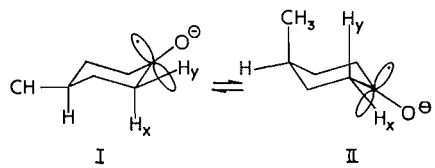

I II

Provided eq. [2] is valid it is possible to estimate the position of conformational equilibrium from the following relations

$$na_a + (1 - n)a_e = a_{av}(X) \quad [3]$$

$$na_e + (1 - n)a_a = a_{av}(Y) \quad [4]$$

where a_a and a_e are the hyperfine couplings characteristic of axial and equatorially oriented protons in the 4-*tert*-butylcyclohexanone ketyl, n is the proportion of I at equilibrium, and $a_{av}(X)$ and $a_{av}(Y)$ represent the time-averaged couplings observed for protons X and Y respectively. Substitution in eqs. [3] and [4] predicts a value of n between 0.88 and 0.96, representing a great preponderance of I at equilibrium.

Since the ketyl oxygen is held in the sp^2 plane of the ketyl group in both I and II, it will not affect the position of equilibrium. Therefore we may expect the 1,3 interactions of the 4-methyl group and the 2 and 6 axial hydrogens to control the position of equilibrium. The conformational free energy difference of the methyl group in cyclohexyl derivatives is 1.5 to 1.9 kcal/mole (12, 13, 14). Taking a standard free energy difference of 1.74 kcal/mole at 25° predicts an equilibrium constant $K = 19.00$, representing 95% of the more stable conformer at equilibrium (15), or a value for n of 0.95. This good agreement between the observed position of equilibrium and the predicted value gives one confidence in the validity of this approach to the conformational analysis of free radicals, and of the general applicability of A values in this regard. 3-Methylcyclohexyl ketyl similarly gives a basic seven line spectrum with unequal spacing, resolvable into a triplet of overlapping triplets and corresponding to two hyperfine couplings of 13.5 and 7.5 Oe respectively. Therefore in this case also we predict between 88 and 95% of the more stable conformer (placing the 3-methyl group equatorial) at equilibrium. This shows that the A value of the methyl group has equal validity at the 4 and 3 positions of the cyclohexane ring. An examination of ketyls derived from other ring systems and the thermodynamics of their conformational equilibria will be reported in a subsequent publication.

EXPERIMENTAL

Materials

All liquid ketones were fractionated and gave single peaks on gas–liquid chromatographic analysis. 4-*tert*-Butylcyclohexanone was prepared by oxidizing the corresponding alcohol with chromic acid according to

Can. J. Chem. Downloaded from www.nrcresearchpress.com by 210.87.254.6 on 09/05/12
For personal use only.

TABLE I

Observed hyperfine couplings in alicyclic ketyls*

Ketone	Intensity pattern	Hyperfine coupling (Oe)
4-*tert*-Butylcyclohexanone	1:2:3:4:3:2:1	$a_{H_a}=14.4$; $a_{H_e}=7.2$
Cyclopentanone	1:4:6:4:1	$a_H=13.8$
Cyclohexanone	1:4:6:4:1	$a_H=10.4$
4-Methylcyclohexanone	1:2:1 triplet of 1:2:1 triplets	$a_{H_1}=13.5$; $a_{H_2}=7.5$
3-Methylcyclohexanone	1:2:1 triplet of 1:2:1 triplets	$a_{H_1}=13.5$; $a_{H_2}=7.5$

*Solvent = 1,2-dimethoxyethane.

the method of Winstein and Holness (16). The ketyls were all generated by the following procedure. Freshly cut potassium was added to degassed 5% solutions of the ketones in dry 1,2-dimethoxyethane. The resulting yellow solutions were allowed to cool to room temperature and transferred to e.p.r. tubes and sealed. First derivative e.p.r. spectra were measured on a Varian V-2503 spectrometer fitted with a V-4532 dual cavity, operating at a nominal frequency of 9.5 Gc.p.s. The microwave power incident on the cavity was attenuated to 10 db below maximum. Hyperfine couplings were measured by comparison with a peroxylamine disulfonate solution in the audio cavity. The triplet spacing of the standard was taken to be 13.0 Oe (17). Reported hyperfine couplings are an average of several determinations with an estimated reproducibility of ±0.2 Oe.

ACKNOWLEDGMENT

This research was supported by a National Research Council of Canada grant-in-aid of research.

REFERENCES

1. N. HIROTA and S. I. WEISSMAN. J. Am. Chem. Soc. **82**, 4424 (1960).
2. N. HIROTA. J. Chem. Phys. **37**, 1884 (1962).
3. R. L. WARD. J. Chem. Phys. **36**, 2230 (1962).
4. M. C. R. SYMONS. Tetrahedron, **18**, 333 (1962).
5. W. T. DIXON and R. O. C. NORMAN. J. Chem. Soc. 4850 (1964).
6. A. HORSFIELD, J. R. MORTON, and D. H. WHIFFEN. Mol. Phys. **4**, 425 (1961).
7. M. C. R. SYMONS. *In* Advances in physical organic chemistry. Vol. I. *Edited by* V. Gold. Academic Press, New York. 1963. p. 284.
8. S. OGAWA and R. W. FESSENDEN. J. Chem. Phys. **41**, 994 (1964).
9. R. W. FESSENDEN and R. SCHULER. J. Chem. Phys. **39**, 2147 (1963).
10. R. U. LEMIEUX, J. D. STEVENS, and R. R. FRASER. Can. J. Chem. **40**, 1955 (1962).
11. J. A. POPLE, H. J. BERNSTEIN, and W. G. SCHNEIDER. High resolution nuclear magnetic resonance. McGraw-Hill Book Co., Inc., New York. 1959. p. 223.
12. C. W. BECKETT, K. S. PITZER, and R. SPITZER. J. Am. Chem. Soc. **69**, 2488 (1947).
13. E. L. ELIEL and M. N. RERICK. J. Am. Chem. Soc. **82**, 1367 (1960).
14. D. S. NOYCE and L. T. DOLBY. J. Org. Chem. **26**, 3619 (1961).
15. E. L. ELIEL. Stereochemistry of carbon compounds. McGraw-Hill Book Co., Inc., New York. 1962.
16. S. WINSTEIN and N. J. HOLNESS. J. Am. Chem. Soc. **77**, 5562 (1955).
17. J. Q. ADAMS and J. R. THOMAS. J. Chem. Phys. **39**, 1904 (1963).

Can. J. Chem. Downloaded from www.nrcresearchpress.com by 210.87.254.6 on 09/05/12
For personal use only.

A L.E.T. INDEPENDENT DOSIMETER BASED ON THE CHEMILUMINESCENT DETERMINATION OF H_2O_2[1]

W. A. ARMSTRONG AND W. G. HUMPHREYS

Defence Chemical Biological and Radiation Laboratories, Department of National Defence, Ottawa, Canada

Received April 21, 1965

ABSTRACT

A sensitive method for the determination of H_2O_2 based on the copper-catalyzed chemiluminescent reaction between luminol and H_2O_2 has been developed. The integral luminescence measured with a modified spectrophotofluorometer was found to increase linearly with concentration for 3×10^{-8} to 1.5×10^{-5} M H_2O_2 solutions. This method was applied to the determination of H_2O_2 formed in irradiated water and it was shown that this system may be used as a dosimeter in the range 30 to 3 000 rads. The following values were obtained for the initial H_2O_2 yields: $G(H_2O_2) = 1.22 \pm 0.07$ for ^{60}Co γ-radiation, 1.28 ± 0.09 for 250 kVcp (105 keV effective) X-radiation and 1.31 ± 0.04 for 14 MeV neutrons. These results and those of other workers demonstrate that the initial yield of H_2O_2 in aerated water increases only by about 15% for an increase in radiation l.e.t. of 0.02 to 14 eV/Å.

INTRODUCTION

Very few radiation-induced chemical reactions are independent of the energy and l.e.t. (linear energy transfer) of the incident radiation. Of the chemical dosimeters commonly used, only the ceric sulfate dosimeter has a response nearly independent of l.e.t. The use of it, however, is normally restricted to doses greater than 10 000 rads although a fluorometric method of Ce(III) analysis has extended its range to doses as low as 1 000 rads(1). Since it is the dose range below 1 000 rads that is of particular interest in the field of radiobiology, there is a requirement for a sensitive tissue-equivalent dosimeter whose response is the same for X, γ, and particle radiation.

The initial yield of H_2O_2 in aerated water has been shown to change little for radiations of a wide range of l.e.t. (2) but the method of analysis commonly used by radiation chemists (3, 4) is limited to concentrations produced by doses greater than 4 000 rads. One of the few methods cited in the literature for the determination of H_2O_2 concentrations less than 10^{-6} M is that developed by Andreae (5) and modified by Perschke and Broda (6). It is based on the observation that when H_2O_2 is decomposed by peroxidase in the presence of scopoletin, 1 mole of fluorescent scopoletin is destroyed for each mole of H_2O_2 decomposed. The chief disadvantage of this method is that in order to obtain an accurately measurable decrease in fluorescence, the concentration of H_2O_2 must not be less than 0.33 nor more than 0.84 times the concentration of scopoletin (6). This limits the usefulness of the technique in determining unknown H_2O_2 concentrations over a range of several orders of magnitude. The most sensitive method of analysis which has been applied to irradiated aqueous solutions is based on the chemiluminescent reaction of phthalic cyclic hydrazide with H_2O_2 and was developed by Mayneord (7). By the application of sensitive photomultiplier techniques involving a liquid nitrogen-cooled, nine-stage photomultiplier, he was able to determine H_2O_2 concentrations of the order of 10^{-7} M.

There are available now a number of commercial instruments for the measurement of fluorescence, phosphorescence, and luminescence which, although unable to quantitatively measure the weak luminescence of phthalic hydrazide, might be used to study more intense chemiluminescent reactions. One such reaction reported to be orders of magnitude brighter

[1]*Issued as DCBRL Report No. 461.*

than phthalic hydrazide is the luminol–H_2O_2 reaction (8). Babko has developed a photographic method based on this reaction but only H_2O_2 concentrations in the range 2×10^{-5} to 2×10^{-4} M could be analyzed (9). The investigation reported here was undertaken to develop an analytical technique based on the luminol–H_2O_2 chemiluminescent reaction as followed by either a commercial instrument or one with simple modifications, capable of determining H_2O_2 concentrations of 5×10^{-8} to 10^{-5} M and to apply this technique to the development of a chemical dosimeter with a response nearly independent of l.e.t. for a wide range of energies and capable of measuring doses of 30 to 3 000 rads.

EXPERIMENTAL

Materials

Samples of luminol (5-amino-2,3-dihydro-1,4-phthalazinedione) from Matheson, Coleman and Bell and from Mann Research Laboratories were used without purification after it had been established that recrystallization from dilute aqueous acetic acid did not affect the luminescent properties. All other materials were of reagent grade.

Stock hydrogen peroxide solutions, approximately 10^{-4} M, were prepared by irradiating thrice-distilled water with ^{60}Co γ-radiation to doses of about 100 000 rads. These were analyzed by the Ghormley method (3, 4) which is based on the measurement of the optical absorption of the triiodide ion formed by the reaction of H_2O_2 with KI catalyzed by molybdate ions. The molar extinction coefficient of the triiodide ion at 350 mμ was determined to be 2.44×10^4 by analyzing solutions 10^{-5} to 10^{-4} M in H_2O_2 prepared from a 0.2 M H_2O_2 solution which had been standardized by the standard arsenious acid method. The stock 10^{-4} M H_2O_2 solutions, if kept in the dark, were found to be stable for many weeks.

Water was purified in a manner similar to that described by Dainton (10). Laboratory distilled water was distilled from alkaline permanganate, then from dilute sulfuric acid, then irradiated with ^{60}Co γ-radiation to a dose of about 200 000 rads, and finally refluxed in a quartz still over alkaline permanganate for at least 24 h.

Irradiation vessels made from quartz standard-taper 19/38 joints (o.d. 1.5 cm, i.d. 1.3 cm) were rinsed with chromic acid, washed many times with once-, twice-, and thrice-distilled water, flushed with steam, filled with thrice-distilled water, irradiated to a dose of about 200 000 rads, and finally flushed with steam from the quartz still. Steam from the top of the still column was then condensed directly into the irradiation vessels which were capped immediately after the desired volume (5.0 ml) had been added.

Irradiations

Samples were irradiated with γ-rays from either a 200 curie (dose rate = 14 rad/min) or a 1 000 curie (dose rate = 146 rad/min) ^{60}Co source. A Muller constant-potential machine was used for X-irradiations at a dose rate of 19 rad/min. The beam was filtered with 0.9 g/cm^2 Cu and 0.13 g/cm^2 Al to give an effective energy of 105 keV when the machine was operated at 250 kVcp (kV constant potential). Dose rates were determined with the Fricke ferrous sulfate dosimeter using $G(\mathrm{Fe(III)}) = 15.5$ for ^{60}Co γ-radiation and 14.9 for the X-radiation. The ferric ion yield was determined by its absorption at either 224 mμ or 304 mμ using the extinction coefficients given by Scharf and Lee (11). The appropriate corrections were applied to obtain the dose rates in water.

Monoenergetic 14 MeV neutrons were obtained from a Cockroft–Walton accelerator by means of the $H^3(d,n)He^4$ reaction. Four sample tubes mounted on an aluminium turntable were rotated at 60 r.p.m. as close as possible to the target. The irradiations were monitored with a Tullamore BF_3 counter. The relationship between the output of the monitor and the dose received by the samples was determined by irradiating samples of 10^{-3} M ferrous sulfate – 0.8 M H_2SO_4, calculating the absorbed dose from the ferric ion yield, assuming $G(\mathrm{Fe(III)}) = 10.5$ (1), and comparing this dose with the monitor count. This calibration was repeated each time the tritium target was changed.

Measurement of Chemiluminescence

The chemiluminescence from the copper-catalyzed luminol–H_2O_2 reaction was measured with an Amino–Bowman spectrophotofluorometer (No. 4 8100) equipped with a IP 28 photomultiplier tube. In order to achieve high sensitivity the reaction was carried out in a quartz optical cell placed in the photomultiplier shutter compartment directly in front of the photomultiplier tube.

Preliminary investigations showed that the peak height registered by the microphotometer did not give a reproducible measurement of the luminescent reaction. Thus methods of measuring the total luminescence were investigated. The circuit developed is outlined in Fig. 1. The 50 ohms resistor (R_{14} in ref. 12) across the recorder outlet terminals of the microphotometer was removed and a Texas Instruments rectilinear recorder (coil resistance 1 500 ohms, full scale reading 1 mA) was plugged into the outlet. This put the meter mechanism of the recorder in series with the meter of the microphotometer and permitted the recording of light intensity vs. time curves. The output from the microphotometer was collected on a 33 000 μF capacitor and the voltage across the capacitor measured with a Keithley model 220 vacuum tube voltmeter. To prevent appreciable current leakage back through the microphotometer meter the voltage was limited to less than

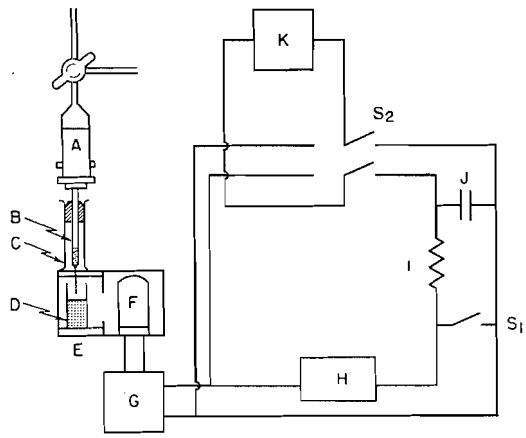

FIG. 1. Apparatus for measuring chemiluminescence. A, plunger activated by compressed air, B, syringe; C, blackened glass tube; D, reaction cell; E, shutter compartment and phototube housing of Aminco–Bowman spectrophotofluorometer; F, photomultiplier tube; G, microphotometer; H, recorder or 1 500 ohms resistor; I, 24 ohms resistor; J, 33 000 μF capacitor; K, vacuum tube voltmeter; S_1 and S_2, switches.

0.1 V. Since voltages as low as 0.01 V could be measured accurately and since the microphotometer was equipped with a seven-position switch to enable changes in sensitivity in fixed steps over the range of 1 000 to 1, accurate measurements could be made over a wide range of light intensities. After it had been demonstrated many times for various reactant concentrations that the voltage across the capacitor after the completion of the chemiluminescent reaction was directly proportional to the area under the light intensity vs. time curve, the integrated luminescence was measured as the voltage multiplied by the microphotometer sensitivity setting. The performance of the system was checked with a low intensity light source of constant output made from a plastic phosphor containing ^{14}C (13). Fluctuations of sensitivity during a day were negligible and over a period of some weeks changes of not more than 5% were observed.

The chemiluminescent reaction was carried out in the following manner. A 2.0 ml sample was pipetted into the optical cell, 0.2 ml of aqueous $CuCl_2$ (10^{-4} to 10^{-2} *M*) added, and the cell placed in position. The reaction was initiated by adding 0.1 ml alkaline luminol, usually 10^{-4} *M* luminol – 0.1 *M* NaOH, and lasted from 10 to 45 s depending upon the reaction conditions. The most satisfactory rate of addition of luminol was obtained when the plunger of the syringe was suddenly subjected to 4 p.s.i. pressure. Under these conditions the reactants were mixed thoroughly by the addition and results were more reproducible than those obtained when the samples were mixed by bubbling through compressed air.

The concentration of H_2O_2 in an irradiated sample was determined from a comparison of its integrated luminescence with the plot of luminescence vs. [H_2O_2] obtained from the analysis of known H_2O_2 solutions freshly prepared by the dilution of the standardized stock solution. Usually known H_2O_2 solutions were analyzed either before or after the irradiated samples although the luminescence vs. [H_2O_2] plot did not change significantly from day to day. Irradiated samples kept in the dark were stable for at least 24 h.

RESULTS

The Chemiluminescent Reaction

An investigation was made of the effects of luminol concentration, Cu^{++} ion concentration and pH on the integrated luminescence from 10^{-7} to 10^{-5} *M* H_2O_2 solutions with a view to finding conditions under which the integrated luminescence would be a linear function of the H_2O_2 concentration.

Preliminary results confirmed Mayneord's observation (7) of a luminescence due to the autooxidation of luminol in alkaline solution but it was found to decrease to a low constant value after the solution had been left to stand for several days in the dark. The solution could then be used for several months with only slight changes occurring in its luminescent properties.

Before each run the luminescence of a thrice-distilled water sample was determined with the same reagent concentrations as were to be used with the H_2O_2 samples. This blank luminescence, never greater than the chemiluminescence from a 3×10^{-8} *M* H_2O_2 sample, was subtracted from the measured luminescence of each H_2O_2 sample.

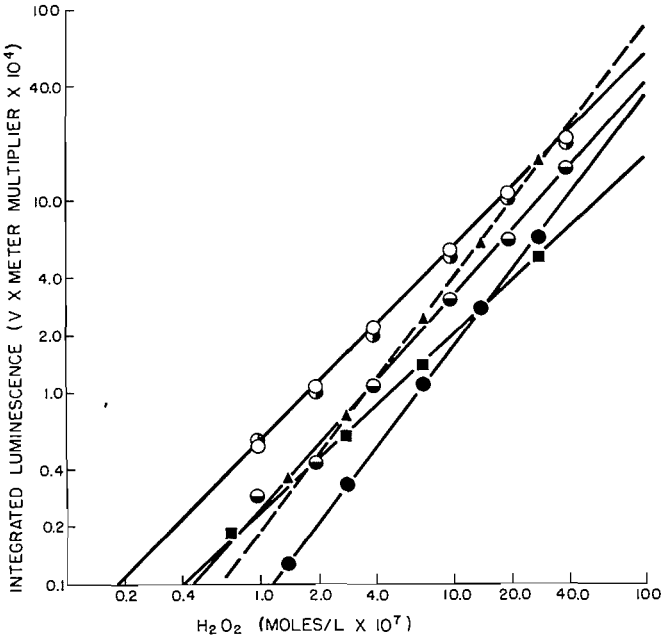

FIG. 2. The effect of luminol and Cu^{++} concentration on luminescence. Reaction mixture: 4.6×10^{-3} M NaOH. ○, 4.6 μM luminol, 460 μM Cu^{++}; ◑, 4.6 μM luminol, 230 μM Cu^{++}; ◒, 4.6 μM luminol, 46 μM Cu^{++} ●, 4.6 μM luminol, 4.6 μM Cu^{++}; ▲, 46.0 μM luminol, 46.0 μM Cu^{++}; ■, 0.46 μM luminol, 46.0 μM Cu^{++}.

TABLE I

The effect of luminol and Cu^{++} concentrations on luminescence

[Luminol] (moles/l $\times 10^6$)	[Cu^{++}] (moles/l $\times 10^6$)	[Cu^{++}]/[luminol]	n (Slope of log luminescence vs. log [H_2O_2])
46	46	1	1.33
4.6	4.6	1	1.33
4.6	46	10	1.12
4.6	230	50	1.01
4.6	460	100	1.01
0.46	46	100	0.94

The effects of the concentration of luminol and of $CuCl_2$ on the chemiluminescent reaction are illustrated in Fig. 2. It is evident that

$$\text{integrated luminescence} \propto [H_2O_2]^n$$

where n is the slope of the line obtained when the log of the integrated luminescence is plotted against the log of the H_2O_2 concentration. Values of n for different luminol–Cu^{++} mixtures are listed in Table I. It would appear that n is a function of the ratio [Cu^{++}]/[luminol] and decreases as this ratio increases. For the integrated luminescence to increase linearly with increasing H_2O_2 concentration, n must be 1.0. The reaction mixture which fulfilled this condition and had an acceptably low blank luminescence and high sensitivity was 4.6×10^{-6} M luminol, 4.6×10^{-3} M NaOH, and 4.6×10^{-4} M $CuCl_2$. As shown in Fig. 3 the pH of this system (11.7) was nearly optimal for chemiluminescence efficiency. To obtain these reagent concentrations, 0.1 ml of 10^{-2} M $CuCl_2$ was added to a 2.0 ml sample of H_2O_2 and the reaction initiated with 0.1 ml of 10^{-4} M luminol – 0.1 M NaOH. The

integrated luminescence was found to increase linearly up to H_2O_2 concentrations of about 1.5×10^{-5} M while at higher concentrations there was a decrease from linearity. H_2O_2 concentrations in the range of 3×10^{-8} to 1.5×10^{-5} M could be determined with an accuracy of about $\pm 5\%$.

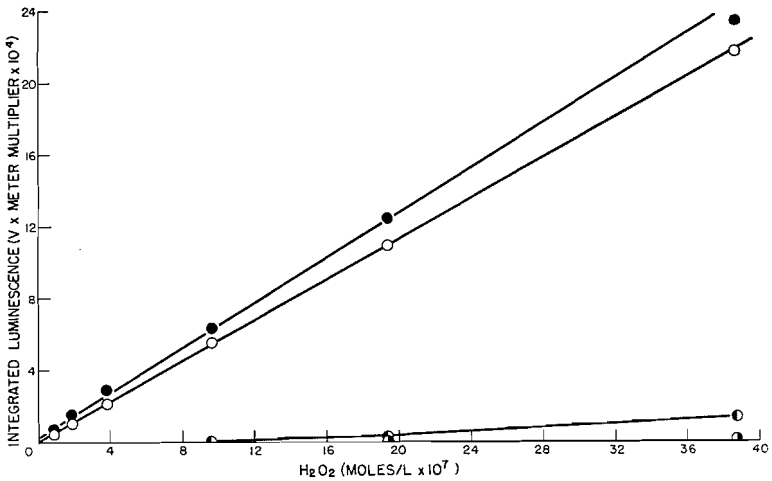

FIG. 3. The effect of pH on chemiluminescence. Reaction mixture: 4.6 μM luminol, 460 μM Cu^{++}. ◑, 0.46×10^{-3} M NaOH, pH 6.43; ◐, 2.3×10^{-3} M NaOH, pH 6.73; ○, 4.6×10^{-3} M NaOH, pH 11.62; ●, 9.6×10^{-3} M NaOH, pH 12.01.

H_2O_2 in Irradiated Aqueous Solutions

The yields of H_2O_2 were measured in aerated water samples which had been irradiated to doses of 28 to 3 500 rads with ^{60}Co γ-rays, 100 to 1 200 rads with 250 kVcp X-rays, or 100 to 2 200 rads with 14 MeV neutrons. For each type of radiation a plot of $[H_2O_2]$ vs. dose gave a straight line passing through the origin (Fig. 4) and $G(H_2O_2)$ values were determined from the slopes of these lines as calculated by the method of least squares.

The amounts of H_2O_2 formed in irradiated 0.5×10^{-5} M and 1.0×10^{-5} M KBr solutions were also measured for each type of radiation. Results were less reproducible than those obtained with aerated water and plots of $[H_2O_2]$ vs. dose gave small intercepts (0.02 to 0.05×10^{-6} M) on the H_2O_2 axis. For bromide solutions irradiated with γ-rays or X-rays G-values were calculated from the slopes of these plots as determined by the method of least squares while for neutron-irradiated samples they were determined by direct comparison with ferric ion yields in 10^{-3} M ferrous sulfate – 0.4 M H_2SO_4 solutions irradiated simultaneously.

The values of $G(H_2O_2)$ for each set of conditions along with the standard deviations and the number of measurements are listed in Table II. It is felt that for aerated water the G-values of 1.22 ± 0.07 for ^{60}Co γ-rays and 1.28 ± 0.09 for 250 kVcp X-rays are accurate to about $\pm 7\%$. With the neutron irradiated solutions the largest source of error lies in the value of G(Fe(III)). Recently Axtmann and Licari (14) have calculated that G(Fe(III)) for 14 MeV neutrons should be about 10 and have measured a value of 11.5 ± 1.8. We therefore believe that our previously determined value of 10.5 ± 0.2 is valid to about $\pm 10\%$. Hence $G(H_2O_2) = 1.31 \pm 0.04$ for aerated water irradiated with 14 MeV neutrons is accurate to about $\pm 15\%$.

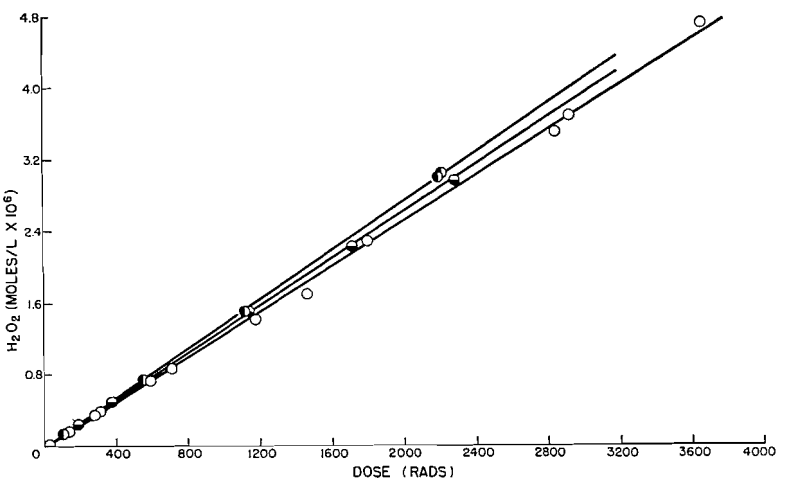

FIG. 4. The effect of radiation energy on the formation of H_2O_2 in aerated water. ○, 1.25 MeV ^{60}Co γ-rays; ◒, 250 kVcp (105 keV effective) X-rays; ◐, 14 MeV neutrons.

TABLE II

The effect of l.e.t. and KBr concentration on $G(H_2O_2)$

Radiation	Mean l.e.t. (eV/Å)	[KBr] (moles/l × 10^5)	$G(H_2O_2)$ (molecules/100 eV)	Number of measurements
^{60}Co γ-ray	0.02	0	1.22±0.07	24
^{60}Co γ-ray	0.02	0.5	1.00±0.11	17
^{60}Co γ-ray	0.02	1.0	0.89±0.08	8
250 kVcp X-ray	0.20	0	1.28±0.09	20
250 kVcp X-ray	0.20	0.5	1.12±0.08	12
250 kVcp X-ray	0.20	1.0	1.02±0.06	12
14 MeV neutron	1.2	0	1.31±0.04	18
14 MeV neutron	1.2	0.5	1.30±0.03	4
14 MeV neutron	1.2	1.0	1.25±0.02	4

DISCUSSION

The Chemiluminescent Reaction

Although the chemiluminescent reaction of luminol (I) has been investigated since 1928 (15), very few uncontested facts have been put forward and the identity of the emitting species is still in dispute. A number of mechanisms have been proposed and discussed by various authors (8, 15–19). The assumption that some form of luminol is the light emitter is based on the observation that about 70 moles of H_2O_2 are consumed per mole of luminol indicating that luminol may not be consumed in the chemiluminescent reaction (20) and on the similarity of the fluorescence spectrum of luminol in dilute acid solution with the chemiluminescence spectrum in basic solution (15). The opposing view that the 3-aminophthalate ion (III) is the emitter is supported by a close match between the fluorescence spectrum of this compound and the chemiluminescence of luminol and by the fact that the pH – fluorescence efficiency profile is the same as the pH – chemiluminescence efficiency profile (19, 21). The overall reaction based on this assumption is given by eq. [1].

Recently White and co-workers (22) identified nitrogen and sodium 3-aminophthalate as the reaction products of the luminol–O_2 chemiluminescent reaction in alkaline dimethylsulfoxide and also showed that the fluorescence spectrum of the total reaction products

[1]

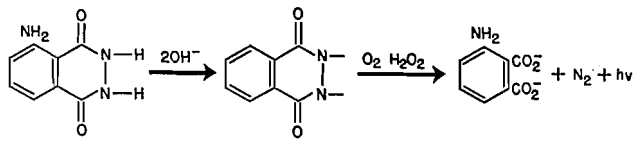

(I) (II) (III)

from the luminol, NH_3, H_2O_2, and Cu^{++} system was identical with that of the 3-aminophthalate ion (23). Although we did not attempt to identify the reaction products of our luminol, NaOH, H_2O_2, and Cu^{++} system, we did observe that the wavelength of maximum fluorescence of the reaction mixture was identical with that of a sodium 3-aminophthalate solution at the same pH and corresponded as well with the wavelength of the maximum chemiluminescence. A comparison of the increase in fluorescence of the reaction product vs. time with the chemiluminescence vs. time indicated that about one-half of this product was produced during the chemiluminescent reaction, which lasted approximately 10 s, and the rest was formed at a slower rate during the next 2 or 3 min.

This evidence supports the contention that the aminophthalate ion is the light emitter. However, if the chemiluminescence of the parent unsubstituted phthalic cyclic hydrazide is considered, there is no evidence to support hypotheses corresponding to those put forward to explain luminol chemiluminescence. The phthalic hydrazide chemiluminescence spectrum does not resemble its fluorescence spectrum in either acidic or basic solutions and the presumed reaction product, sodium phthalate, does not exhibit detectable fluorescence. Hence there is still some doubt as to the nature of the light emitter.

Our observed dependence of chemiluminescence on pH is similar to that reported by Seliger for the luminol, H_2O_2, and NaOCl system (21). This has been interpreted by White (18) and others as demonstrating that it is the dinegative ion of luminol (II) which takes part in the chemiluminescent reaction.

The effect of copper salts on the luminol reaction has been studied by Babko (24, 25). He explains the increase in the luminescence intensity in the presence of copper salts on the formation of a copper–luminol complex which affects the equilibrium between the neutral, mononegative, and dinegative forms of luminol in favor of the dinegative form and also catalyzes the decomposition of H_2O_2 (25). Under conditions where the concentration of Cu^{++} ions is equal to or greater than the concentration of luminol, the decrease in the slope of log luminescence vs. log $[H_2O_2]$ with increasing Cu^{++} concentration may be due to a quenching effect.

H_2O_2 in Irradiated Solutions

The radiolysis of aerated water may be described by the following equations which are similar to those given by Allen and Schwarz (26) but assume the formation of both hydrated electrons (e_{aq}^-) and H atoms in neutral solutions (27) as well as ionization of the HO_2 radical ($pK \sim 4.4$).

[2] $$H_2O \rightsquigarrow e_{aq}^-, H, OH, HO_2, H_2, H_2O_2$$

[3] $$e_{aq}^- + O_2 \rightarrow O_2^-$$

[4] $$H + O_2 \rightarrow HO_2$$

[5] $$HO_2 \rightarrow H^+ + O_2^-$$

[6] $$O_2^- + O_2^- + 2H_2O \rightarrow H_2O_2 + O_2 + 2OH^-$$

[7] $$OH + H_2O_2 \rightarrow H_2O + HO_2$$

Then for initial yields

[8] $$G(H_2O_2) = G_{H_2O_2} + \tfrac{1}{2}(G_{HO_2} + G_{e_{aq}^-} + G_H - G_{OH}).$$

Although $G_{H_2O_2}$ and G_{HO_2} increase with increasing l.e.t. while $G_{e_{aq}^-}$, G_H, and G_{OH} decrease, the measured initial value of $G(H_2O_2)$ changes very little over a wide range of l.e.t. (2).

As the radiation dose is increased and appreciable concentrations of H_2 and H_2O_2 are built up, reactions [9], [10], and [11] may affect the value of $G(H_2O_2)$.

[9] $$OH + H_2 \rightarrow H_2O + H$$

[10] $$H + H_2O_2 \rightarrow H_2O + OH$$

[11] $$e_{aq}^- + H_2O_2 \rightarrow H_2O + OH + OH^-$$

Sworski (28) and Allen (29) showed that the H_2 could be protected from OH attack by the addition of bromide ion.

[12] $$OH + Br^- \rightarrow Br + OH^-$$

However, with aerated bromide solutions the initial yield of H_2O_2 is dependent on the concentration of the bromide ion (28, 29) and the degree of this dependency is related to the l.e.t. of the radiation (30). The results in Table II are in agreement with this. The value of $G(H_2O_2)$ decreased with increasing bromide ion concentration to a much greater extent for solutions irradiated with ^{60}Co γ-rays than for neutron-irradiated solutions. Therefore the yields of H_2O_2 in irradiated bromide solutions are more dependent on l.e.t. than those in irradiated aerated water.

At high doses the concentration of dissolved oxygen is reduced and reactions [10] and [11] may compete with [3] and [4] resulting in a decrease in the yield of H_2O_2. Usually this falloff is not noticeable with solutions irradiated to doses of less than 10 000 rads. However, in this investigation, water was condensed directly from the still head into the sample tubes which were then immediately capped. The samples were, therefore, not air-saturated and a falloff in the yield of H_2O_2 was noticed at doses greater than 4 000 rads.

The value of $G(H_2O_2) = 1.22 \pm 0.07$ for ^{60}Co γ-radiation (l.e.t. ~ 0.02 eV/Å) is in good agreement with the figure 1.23 by Allen (29). The result with 14 MeV neutrons (l.e.t. ~ 1.2 eV/Å) of 1.31 ± 0.04 also corresponds with the values of 1.31 for 19 Mev deuterons (l.e.t. ~ 0.5 eV/Å) and 1.21 for 32 MeV helium ions (l.e.t. ~ 2.3 eV/Å) given by Schwarz (2). Recently Anta (31) has published $G(H_2O_2) = 1.41$ for aerated 0.4 M H_2SO_4 irradiated with ^{210}Po α-particles (l.e.t. ~ 14 eV/Å) but the value for neutral aerated water is probably somewhat lower since it has been shown that the initial yield of H_2O_2 increases with increasing acidity (2).

It should be emphasized that the values of $G(H_2O_2)$ for aerated water reported here are based on results obtained in a dose range not adequately covered by other workers. Extrapolation of Allen's H_2O_2 yields to zero dose (29) leads to an intercept on the H_2O_2 axis, the exact value of which depends upon the method of water purification. The smallest reported intercept of about 0.3×10^{-6} mole/l is equivalent to a dose of nearly 300 rads and indicates a very high initial yield. The only available results obtained with doses of less than 1 000 rads are those of Mayneord (7). His plot of H_2O_2 concentration vs. dose is linear from 200 to 1 250 rads and extrapolates to the origin but gives $G(H_2O_2) = 1.83$ for 140 kVp X-rays, a value about 50% higher than that obtained in the present investigation with 250 kVcp X-rays. High initial yields are usually attributed to traces of organic impurities (29). Various methods of purification may be used to destroy organic substances in water but it is extremely difficult to protect the purified water from airborne contaminants. In this investigation the problem was avoided by condensing the water directly

into the irradiation vessels and capping them as soon as the desired volume had been added. Reproducible initial H_2O_2 yields could only be obtained through the use of this procedure.

From the results mentioned above it is evident that the initial yield of H_2O_2 in aerated water increases only by about 15% for an increase in radiation l.e.t. of nearly three orders of magnitude. Thus the method of H_2O_2 analysis reported here enables the use of aerated water as a sensitive dosimeter which is nearly independent of the quality of the radiation over a wide range of l.e.t.'s.

ACKNOWLEDGMENTS

The authors wish to thank Dr. C. E. Clifford and Messrs. R. A. Facey and F. G. Strain for valuable advice and assistance.

REFERENCES

1. W. A. ARMSTRONG and W. G. HUMPHREYS. Can. J. Chem. **42**, 1092 (1964).
2. H. A. SCHWARZ, J. M. CAFFREY, and G. SCHOLES. J. Am. Chem. Soc. **81**, 1801 (1959).
3. A. O. ALLEN, C. J. HOCHANADEL, J. A. GHORMLEY, and T. W. DAVIS. J. Phys. Chem. **56**, 575 (1952).
4. C. J. HOCHANADEL. J. Phys. Chem. **56**, 587 (1952).
5. W. A. ANDREAE. Nature, **175**, 859 (1955).
6. H. PERSCHKE and E. BRODA. Nature, **190**, 257 (1961).
7. W. V. MAYNEORD, W. ANDERSON, H. D. EVANS, and D. ROSEN. Radiation Res. **3**, 379 (1955).
8. T. I. QUICKENDEN. J. New Zealand Inst. Chem. **28**, 10 (1964).
9. A. K. BABKO and N. M. LUKOVSKAYA. Zh. Analit. Khim. **17**, 50 (1962).
10. F. S. DAINTON and W. S. WATT. Proc. Royal Soc. London, Ser. A, **275**, 447 (1963).
11. K. SCHARF and R. M. LEE. Radiation Res. **16**, 115 (1962).
12. Aminco–Bowman Spectrophotofluorometer Instruction and Service Manual No. 657.
13. R. A. FACEY. To be published.
14. R. C. AXTMANN and J. A. LICARI. Radiation Res. **22**, 511 (1964).
15. H. O. ALBRECHT. Z. Physik. Chem. Leipzig, **136**, 321 (1928).
16. H. D. K. DREW. Trans. Faraday Soc. **35**, 207 (1939).
17. R. S. ANDERSON. Ann. N.Y. Acad. Sci. **49**, 337 (1948).
18. T. BREMER. Bull Soc. Chim. Belges, **62**, 569 (1953).
19. E. H. WHITE. *In* Light and life. *Edited by* W. D. McElroy and B. Glass. The Johns Hopkins Press, Baltimore. 1961. p. 183.
20. H. D. K. DREW and R. F. GARWOOD. J. Chem. Soc. 791 (1938).
21. H. H. SELIGER. *In* Light and life. *Edited by* W. D. McElroy and B. Glass. The Johns Hopkins Press, Baltimore. 1961. p. 200.
22. E. H. WHITE, O. ZAFIRIOU, H. H. KAGI, and J. H. M. HILL. J. Am. Chem. Soc. **86**, 940 (1964).
23. E. H. WHITE and M. M. BURNSEY. J. Am. Chem. Soc. **86**, 941 (1964).
24. A. K. BABKO and N. M. LUKOVSKAYA. Ukr. Khim. Zh. **28**, 968 (1962).
25. A. K. BABKO and L. I. DUBOVENKO. Z. Anal. Chem. **200**, 428 (1964).
26. A. O. ALLEN and H. A. SCHWARZ. Proc. Intern. Conf. Peaceful Uses of At. Energy, Geneva, **29**, 30 (1958).
27. A. O. ALLEN. Radiation Res. Suppl. **4**, 54 (1964).
28. T. J. SWORSKI. J. Am. Chem. Soc. **76**, 4687 (1954).
29. A. O. ALLEN and R. A. HOLROYD. J. Am. Chem. Soc. **77**, 5852 (1955).
30. M. BURTON and K. C. KURIEN. J. Phys. Chem. **63**, 899 (1959).
31. M. C. ANTA, M. H. MARIANO, and M. L. DE SANTOS. J. Chim. Phys. **61**, 577 (1964).

Can. J. Chem. Downloaded from www.nrcresearchpress.com by 210.87.254.40 on 09/05/12
For personal use only.

SOLVENT EFFECTS IN THE NUCLEAR MAGNETIC RESONANCE SPECTRA OF BENZALMALONONITRILES[1]

M. A. WEINBERGER, R. M. HEGGIE
Defence Chemical, Biological and Radiation Laboratories, Ottawa, Canada

AND

H. L. HOLMES
Suffield Experimental Station, Ralston, Alberta

Received April 15, 1965

ABSTRACT

The nuclear magnetic resonance spectra of a series of substituted benzalmalononitriles were examined in various solvents. The chemical shifts for the olefinic protons are susceptible to large solvent effects which are interpreted as arising from association of a solvent molecule with the olefinic proton (acetone) or a site in its vicinity (benzene). With acetone this leads to a downfield shift from values observed in chloroform. In benzene solution the association produces increased shielding and is present in addition to a second solvation complex, the arrangement of which is governed by the substituent. The difference in behavior of the ethylenic proton in benzalmalononitriles from the formyl proton in benzaldehyde is ascribed to its more highly acidic nature.

INTRODUCTION

In a series of papers (1, 2) Klinck and Stothers reported on studies of the solvent effects in the nuclear magnetic resonance (n.m.r.) spectra of substituted aromatic aldehydes which provided evidence for the occurrence of specific solvent–solute association. In benzene solutions, for example, the observed changes in the chemical shifts of the various protons in the molecule from their values in chloroform solution were interpreted in terms of a molecular complex in which a benzene molecule tends to lie over the electron-deficient portion of the solute, the aromatic rings being parallel to each other. The anisotropy of the benzene then leads to substantially increased shielding of those protons in the vicinity of the center of the solvent ring, and the effect decreases for the more distant protons. Similar "collisional" complexes had been proposed earlier by Hatton and Richards (3) for solutions of amides and other polar compounds in aromatic solvents. These solvents always associate with sites of the solute as far away from an electronegative portion as possible. The observed enhanced shielding by benzene of the formyl and adjacent ring protons in benzaldehydes with electron-withdrawing para-substitutents, and the smaller effect on these protons in the case of electron-donating substituents are thus explained by the association positions of the benzene molecule favored in the respective compounds.

With acetone as solvent the observed differential shifts from chloroform solutions are much smaller and did not allow as definite conclusions for the existence of solute–solvent complexes as with benzene, since part of the shift could be attributed to effects arising from the reaction field of the solvent.

In the present work we have investigated the effect of substituents and solvents on the chemical shift of the protons in benzalmalononitriles which formally resemble the benzaldehydes. The highly electronegative side-chain substituents, however, cause the olefinic protons to be more acidic than the corresponding protons in benzaldehydes. In an interesting synthesis based on this difference in acidity, Bastus (4) obtained acetophone in

[1]*Issued as DCBRL Report No. 462.*

excellent yield by methylation with diazomethane, not directly from benzaldehyde but via benzalmalononitrile and subsequent hydrolysis. It was therefore believed that in the benzalmalononitriles we might encounter more extreme solvent effects with electron-donating solvents. The study of the chemical shifts was simplified by referencing with respect to an internal standard. This eliminated effects due to bulk diamagnetic susceptibility, and the non-specific parts of solvent diamagnetic anisotropy and van der Waals interactions (5).

EXPERIMENTAL

Solutions (10% w/v, about 4–5 mole %) of the compounds in chloroform and acetone were studied at 30°. Deuterated solvents supplied by Merck, Sharp and Dohme of Canada Ltd., Montreal, Que., were used when necessary. In a few examples carbon tetrachloride solutions were also examined, and the spectra of a number of representative compounds were determined in d_6-benzene; 60 Mc/s n.m.r. spectra were recorded with a Varian 4300C spectrometer. The spectra were calibrated by the sideband technique using an electronic counter. The chemical shifts referenced with respect to internal tetramethylsilane are reported as τ values. These are the averages of at least five measurements and have standard deviations of 0.007 p.p.m. or better.

The benzalmalononitriles were obtained by the method of Corson and Stoughton (6) and recrystallized, usually from ethanol. Corrected melting points are given in Table I as well as analytical figures for new compounds.

RESULTS AND DISCUSSION

The chemical shifts of the ethylenic proton in the variously substituted benzalmalononitriles are given as τ values in Table II. This is arranged according to position of the substituent and then in order of increasing values of τ. For reasons to be discussed later the effect of structure on τ will be considered only for chloroform solutions. For the para-substituted compounds there is a qualitative correlation between the expected polarization of the CH bond and the τ value. The latter has a range of 0.45 p.p.m. between the extremes, *p*-nitro- and *p*-dimethylamino-benzalmalononitrile. Quantitatively the correlation between the observed shifts and the Hammett sigma parameters of the substituents as listed by McDaniel and Brown (15) and by Jaffe (16) is, however, not too satisfactory: $\tau = -0.259$ (± 0.035) $\sigma + 2.303$ (± 0.016), correlation coefficient (r) $= -0.93$, $n = 10$. The correlation is no better when the meta- and non-ortho-disubstituted compounds are included ($\tau = -0.244$ (± 0.036) $\sigma + 2.322$ (± 0.015), $r = -0.85$, $n = 20$). As was suggested for the formyl proton in benzaldehydes (1) the exposed nucleus of the ethylenic proton may be more susceptible to perturbing effects than a fluorine for the shift of which much better correlations with substituent constants have been obtained.

In the ortho-substituted benzalmalononitriles the τ values as shown in Table II are, in the main, little affected by the electronic nature of the substituents, and a quantitative correlation with Hammett's σ_r is very poor ($r = -0.22$). The electronic effect of the substituent on the τ values of the ethylenic proton is thus less marked in the ortho- than in the meta- and para-substituted compounds. In addition, the resonance occurs at lower field in each of the ortho-substituted compounds than in the parent compound. The similar behavior in benzaldehydes has been adequately discussed by Klinck and Stothers (1) and explained in terms of reduced side chain – ring conjugation resulting from non-coplanarity because of the presence of an ortho substituent. Since, even with the least bulky substituents, the ethylenic proton in ortho-substituted benzalmalononitriles gives peaks which are 0.3 p.p.m. to lower field than those in benzalmalononitrile or the corresponding para-substituted compounds, it is evident that the effects caused by decreased conjugation completely overshadow the opposite effects due to ring current changes. Calculations based on the model of Johnson and Bovey (17) show that, as the side-chain proton goes out of the plane of the ring, its shielding is increased by, at most, 0.11 p.p.m.

Can. J. Chem. Downloaded from www.nrcresearchpress.com by 210.87.254.40 on 09/05/12
For personal use only.

Further evidence for the isolation of the side chain from the ring in ortho-substituted compounds is afforded by ultraviolet spectra. The K band for 2-methylbenzalmalononitrile occurs at 312 mμ (ϵ = 16 500) and that for 4-methylbenzalmalononitrile at 323 mμ (ϵ = 25 800). Since the substituent in this case is non-functional, Braude's expression (18) for the extinction coefficient ratio in terms of the out-of-plane angle θ of the side chain may be applied with some confidence, giving $\cos^2\theta = 0.64$, and $\theta = 37°$. This may be regarded as a measure of the loss of through-conjugation in the ortho compound.

Solvent Effects

Most of the benzalmalononitriles are not soluble enough in interaction-free solvents such as *n*-hexane and, as a compromise, chloroform or deuterated chloroform was chosen as the standard solvent. Chloroform is an acceptor and very likely associates with the cyano groups. It can be seen from Table II that the τ values in carbon tetrachloride are about 0.1 p.p.m. higher than in chloroform. It is therefore inferred that the effect of association of chloroform with the compounds is relatively small. Use of the chloroform values as reference causes no appreciable error when one is discussing the large changes in benzene and it implies minimum values for the effects observed in acetone.

The dilution shift was checked in a few cases. 2-Nitrobenzalmalononitrile showed no change on fourfold dilution of a 3.5 mole % solution in chloroform and a decrease of 0.02 p.p.m. in acetone. The same change was also found on similar dilution of an acetone solution of the 4-nitro compound. It is therefore considered that "infinite dilution" conditions have been sufficiently approached in these experiments.

Before we consider the shifts in Table II in solvents other than chloroform, the effect of the reaction field of the solvent on the highly polar solute will be calculated in the case of 4-methylbenzalmalononitrile (μ = 4.1 D, by addition of group moments). Using the method of Buckingham (19) based on a spherical cavity model, with a calculated value of 1.93×10^{-23} cc for the polarizability of the solute, the contribution to the shielding of a proton is

$$\sigma_R = -0.104\,[(\epsilon - 1)/(2\epsilon + 2.5)]\,\mu\cos\theta \quad \text{p.p.m.}$$

in which ϵ is the solvent dielectric constant and θ the angle that the proton bond axis makes with the dipole μ (in D). The contribution turns out to be much too small to account for the variation of the shift of the olefinic, ortho, and meta protons[2] with solvent shown in Table III. For the solvent change from chloroform to acetone, for example, the calculated shifts caused by the reaction field are only 0.02 p.p.m. downfield on the ethylenic and meta protons and 0.02 p.p.m. upfield on the ortho proton.

The ellipsoidal cavity model of Diehl and Freeman (20) using ellipsoid semi-axes of 6.25, 3.75, and 1.95 Å, a shape factor of 0.144 as calculated by the method of Ross and Sack (21), and a refractive index of 1.5 leads to a contribution

$$\sigma_R = -0.0323\,[(\epsilon - 1)/(\epsilon + 0.378)]\,\mu\cos\theta \quad \text{p.p.m.}$$

This is even smaller than that calculated with the simpler model. Inspection of Table III indicates that the shift of the olefinic proton in fact depends more on the chemical nature of the solvent. In the relatively non-interacting solvents τ is 2.4, in ethers it is 2.1, and in solvents with carbonyl groups τ drops to 1.8.

To pinpoint the interactions in acetone and benzene solutions it is necessary to determine, as well, the solvent dependence of the shift of the aromatic protons in the benzalmalononitrile molecule. The shifts can be readily deduced only for the para-substituted

[2]*Here and subsequently ortho and meta refer to the ring position relative to the* —CR = $C(CN)_2$ *substituent.*

Can. J. Chem. Downloaded from www.nrcresearchpress.com by 210.87.254.40 on 09/05/12
For personal use only.

Can. J. Chem. Downloaded from www.nrcresearchpress.com by 210.87.254.40 on 09/05/12
For personal use only.

TABLE I

Melting points and analyses

Aromatic substituent	Melting point		Calcd. %			Found %			Ref.
	Obs.	Lit.	C	H	N	C	H	N	
			Benzalmalononitriles						
None	83.4– 84.0	83.5– 84							6
4-NO_2	161.0–161.4	159 –160				67.94	4.02	13.00	7
4-COOMe	163.0–163.8		67.71	3.79	13.30	67.62	3.84	13.18	
						69.77	3.12	16.01	
4-F	126.8–127.2		69.82	2.93	16.26	69.63	3.13	16.00	
4-Cl	161.0–162.0	162 –163				51.36	3.34	11.94	7
4-Br	161.8–162.5		51.53	2.16	12.02	51.63	2.53	11.73	
4-Me	134.0–135.0	134							8
4-OMe	113.6–114.2	114.5–115				72.66	5.08	13.76	6
4-OEt	138.0–138.4		72.71	5.08	14.13	72.43	4.93	13.55	
4-NMe_2	180.7–181.2	178	67.91	3.79	13.30	67.83	3.71	13.16	8
2-COOMe	85.0– 86.0								9
2-NO_2	138.8–139.2	143							9
2-OEt	79.0– 80.0	80				73.75	5.74	12.94	
2-OnPr	60.0– 60.6		73.55	5.70	13.20	73.62	5.83	13.04	
						73.70	5.83	13.09	
2-OiPr	102.4–102.8		73.55	5.70	13.20	73.61	5.83	12.86	
						74.26	6.35	11.83	
2-OnBu	69.8– 70.3		74.31	6.24	12.38	73.98	6.19	11.88	
2-OMe	84.0– 85.0	84 – 84.5							6
2-Cl	95.2– 95.8	95 – 96							6
2-Br	90.5– 91.0	90 – 90.5							7
									10

Can. J. Chem. Downloaded from www.nrcresearchpress.com by 210.87.254.40 on 09/05/12
For personal use only.

TABLE I (*Concluded*)

Melting points and analyses

Aromatic substituent	Melting point		Calcd. %			Found %			Ref.
	Obs.	Lit.	C	H	N	C	H	N	
			Benzalmalononitriles						
2-F	118.4–118.8	119							7
2-Me	106.0–106.6	104 –106							6
3-NO_2	106.6–107.0	104.5–105				69.88	3.09	15.90	
3-F	93.0– 93.4		69.82	2.93	16.26	69.85	3.10	15.84	
						71.57	4.34	15.20	
3-OMe	105.6–106.2		71.72	4.38	15.21	71.39	4.34	14.97	
3-Cl	115.5–116.0	116 –117				72.34	5.06	14.02	7
3-OEt	82.0– 82.6		72.71	5.08	14.13	72.37	5.16	13.96	
3-Br	110.0–110.8	109.5–110							7
2-OMe 5-OMe	107.4–108.2	110							11
2-Cl 5-NO_2	121.8–122.2	119 –120							7
2-Cl 4-Cl	150.0–151.0	150				50.14	2.74	—	8
2-OMe 5-Br	137.0–139.0		50.21	2.67		50.08	2.73	—	
						67.40	4.73	12.82	
2-OMe 4-OMe	142.2–142.6	144	67.28	4.70	13.08	67.15	4.77	12.89	12
2-Cl 6-Cl	88.0– 89.0	89– 90				53.76	2.09	12.46	7
3-Cl 4-Cl	151.0–151.6		53.83	1.80	12.56	53.99	2.17	12.55	
3-OMe 4-OMe	145.0–145.6	144							8
3-OEt 4-OEt	105.0–106.0	106							9
3,4-OCH_2O—	198.4–198.8	199 –200							6
2,3 $(CH)_4$	168.0–169.0	170 –171.5							7
3,4 $(CH)_4$	140.2–140.8	141							9
			1,1-Dicyano-2-phenyl-1-propenes						
4-Cl	95 – 96	96							13
4-Me	98 – 99	97							13
4-OMe	80 – 81	73 – 74	72.71	5.09	14.13	72.71	5.22	14.29	14

TABLE II

The τ values (p.p.m.) of the ethylenic proton in benzalmalononitriles in various solvents

Aromatic substituent	τ in $CHCl_3$	$\Delta\tau$*			Aromatic substituent	τ in $CHCl_3$	$\Delta\tau$*	
		CCl_4	Acetone	C_6D_6			Acetone	C_6D_6
None	2.23	0.07	−0.49	1.15	3-NO_2	2.04	−0.56	1.66
4-NO_2	2.13		−0.65	1.74	3-F	2.24	−0.58	
4-COOMe	2.15		−0.55		3-OMe	2.27	−0.50	
4-F	2.23	0.11	−0.53	1.33	3-Cl	2.28	−0.59	
4-Cl	2.28		−0.57	1.44	3-OEt	2.29	−0.51	
4-Br	2.28		−0.58		3-Br	2.30	−0.61	
4-Me	2.30		−0.49	1.11	2-OMe 5-OMe	1.74	−0.08	
4-OMe	2.36		−0.47	1.01	2-Cl 5-NO_2	1.76	−0.38	
4-OEt	2.37		−0.45		2-Cl 4-Cl	1.82	−0.30	
4-NMe_2	2.58		−0.39	0.75	2-OMe 5-Br	1.84	−0.18	
2-COOMe	1.28		−0.17	0.68	2-OMe 4-OMe	1.85	−0.06	
2-NO_2	1.56		−0.38	1.29	2-Cl 6-Cl	2.08	−0.57	1.21
2-OEt	1.70	0.15	−0.13		3-Cl 4-Cl	2.32	−0.64	
2-OnPr	1.70		−0.15		3-OMe 4-OMe	2.36	−0.42	
2-OiPr	1.71		−0.14		3-OEt 4-OEt	2.39	−0.42	
2-OnBu	1.71		−0.14		3,4-OCH_2O	2.41	−0.53	
2-OMe	1.73	0.13	−0.10	0.60	2,3 $(CH)_4$	1.38	−0.50	
2-Cl	1.75		−0.27	0.87	3,4 $(CH)_4$	2.18	−0.54	
2-Br	1.80		−0.26					
2-F	1.91		−0.31		$CH_3CH{:}C(CN)_2$	2.57	−0.34	1.47
2-Me	1.91	0.09	−0.44					

*$\Delta\tau = \tau$ (in solvent) − τ (in chloroform).

TABLE III

The τ values in various solvents of the olefinic and aromatic protons in 4-methylbenzalmalononitrile

Solvent	ϵ	Olefinic	Aromatic	
			Ortho	Meta
Cyclohexene	2.22	2.45	2.25	2.77
p-Dioxane	2.21	2.09	2.19	2.64
Ether	4.33	2.08	2.14	2.66
Chloroform	4.80	2.30	2.20	2.69
Methyl acetate	6.68	1.87	2.07	2.57
Acetone	20.7	1.81	2.08	2.57

compounds from the pseudo-AB-like part of the A_2B_2 spectrum (22). Analysis of these spectra also yield values for the sums of the ortho and para coupling constants of 8.5–9.3 c.p.s., which are almost independent of substituent and solvent.

Acetone Solutions

Table IV shows the results for para-substituted benzalmalononitriles and some 1,1-dicyano-2-phenyl-1-propenes. It is apparent that the chemical shift of the aromatic protons of para-substituted benzalmalononitriles is generally decreased in changing from chloroform to acetone solutions and by about the same amount (0.1–0.2 p.p.m.) as for benzaldehydes (2). The propylidene methyl and substituent protons are very little affected by this solvent change, but there is a larger effect on the olefinic proton shift. A large effect on the ethylenic proton shift is also noted in the meta-substituted compounds in Table II. When ortho substituents are present this "solvent shift" is much reduced in most of the examples and is then of the same order as that observed for the formyl proton in benzaldehyde. In the disubstituted benzalmalononitriles without an ortho substituent

Can. J. Chem. Downloaded from www.nrcresearchpress.com by 210.87.254.40 on 09/05/12
For personal use only.

TABLE IV

The τ values in chloroform and changes in these values in acetone solutions for the system

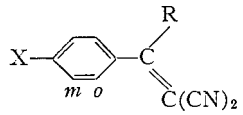

		Chloroform solution				Acetone solution			
X	R	τ_R	τ_o	τ_m	τ_X	$\Delta\tau_R$	$\Delta\tau_o$	$\Delta\tau_m$	$\Delta\tau_X$
H	H	2.23				−0.49			
NO_2	H	2.13	1.93	1.62		−0.65	−0.19	−0.06	
COOMe	H	2.15	2.03	1.82		−0.55	−0.18	+0.04	
F	H	2.23	2.03	2.77		−0.53	−0.16	−0.18	
Cl	H	2.28	2.15	2.49		−0.57	−0.18	−0.14	
Cl	CH_3	7.38	2.48	2.48		−0.06	−0.19	−0.08	
Br	H	2.28	2.28	2.28		−0.58	−0.23	−0.10	
Me	H	2.30	2.20	2.69	7.55	−0.49	−0.12	−0.12	0.01
Me	CH_3	7.39	2.52	2.71	7.58	−0.04	−0.12	−0.07	0.01
OMe	H	2.36	2.10	2.99	6.09	−0.47	−0.13	−0.13	−0.03
OMe	CH_3	7.39	2.38	3.01	6.13	−0.03	−0.11	−0.10	−0.02
OEt	H	2.37	2.12	3.01		−0.45	−0.11	−0.12	
NMe_2	H	2.58	2.21	3.31	6.86	−0.39	−0.11	−0.17	

the solvent shift is roughly the same, 0.5 p.p.m., as for the derivatives with a single meta or para substituent, whilst if an ortho substituent is present, it appears to govern the solvent effect. A notable exception is 2,6-dichlorobenzalmalononitrile where the solvent shift is more like that of a 3,4-disubstituted compound.

The small solvent effects on aromatic protons in both benzalmalononitriles and benzaldehydes are probably due to a vague solvation of a dipolar nature, but the large changes in τ value of the ethylenic proton are only explicable on the basis of a specific solvent interaction of the acetone carbonyl oxygen with the ethylenic proton. This is quite different from the behavior of the formyl proton in benzaldehydes, but since this ethylenic proton is more acidic, an interaction of the hydrogen bond type with acetone is not unreasonable, and a substantial downfield shift of the field position of the proton results in compounds without ortho substituents. As might be expected, compounds with electron-withdrawing groups in the para position show an enhanced shift, those with electron-donating groups a reduced one compared to the value for the parent compound. With ortho-substituted benzalmalononitriles the situation is complicated by the long-range shielding effects of the substituent and by the possibility of intramolecular hydrogen bonding of it with the olefinic proton. In those compounds where such bonding is unlikely, the "normal" acetone solvent shift of the corresponding para compound would be observed. This is the case with 2-methylbenzalmalononitrile where the solvent shift is nearly as large as that of the 4-methyl analogue and in 2,6-dichlorobenzalmalononitrile where, for steric reasons, intramolecular interaction is not possible. However, those substituents which may show intramolecular association are also most likely to have large magnetic anisotropic effects, and it is impossible at present to separate these factors. The effects can be discussed generally by considering the equilibrium

$$A + \text{acetone} \rightleftharpoons \text{solvent complex (B)},$$

where A is the ortho-substituted benzalmalononitrile, perhaps internally complexed. The solvent shift $\Delta\tau$ is then given by

$$\Delta\tau = \alpha(\tau_B - \tau_A),$$

Can. J. Chem. Downloaded from www.nrcresearchpress.com by 210.87.254.40 on 09/05/12
For personal use only.

where α is the mole fraction of solvent complex and the τ values are those of the extreme forms (A and B). Association with the solvent disrupts the influence of the magnetic anisotropy of the substituent and of any intramolecular hydrogen bond, both of which contribute to the net effect which is measured by $\tau_B - \tau_A$. In 2-nitrobenzalmalononitrile where formation of a six-membered ring would lend some stability to the intramolecular hydrogen bond which is also aided by a favorable electron distribution, one may expect a smaller α than in the 2-alkoxy compounds. The solvent shift for 2-nitrobenzalmalononitrile is, however, much bigger than that for the 2-methoxy analogue. Hence it appears that $(\tau_B - \tau_A)_{NO_2} > (\tau_B - \tau_A)_{OMe}$, i.e. on solvation with acetone the net change in shielding of the ethylenic proton is less in the methoxy than in the nitro compound.

Benzene Solutions

The solvent shifts are shown in Table V as well as their differences from the solvent shifts of the corresponding protons in benzaldehydes observed by Klinck and Stothers (2).

TABLE V

Solvent shifts (p.p.m.) in d_6-benzene solution (relative to chloroform values) in the system

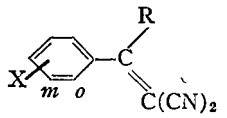

and differences from corresponding values for benzaldehydes and acetophenones

						Solvent shift differences* at:			
X	R	$\Delta\tau_R$	$\Delta\tau_o$	$\Delta\tau_m$	$\Delta\tau_X$	R	*o*	*m*	X
4-NO_2	H	1.74	1.27	0.96		0.94	0.34	0.24	
4-F	H	1.33	0.88	0.78		0.85	0.28	0.18	
4-Cl	H	1.44	0.95	0.79		0.92	0.34	0.23	
4-CH_3	H	1.11	0.59	0.65	0.57	0.88	0.33	0.18	0.10
4-OCH_3	H	1.01	0.57	0.62	0.76	0.83	0.30	0.22	0.08
4-$N(CH_3)_2$	H	0.75	0.46	0.66	0.97	0.86	0.42	0.26	0.27
H	H	1.15				0.81			
3-NO_2	H	1.66				0.81			
4-Cl	CH_3	0.94	†	†					
4-CH_3	CH_3	0.83	0.53	0.49	0.45	0.43	0.40	0.14	0.08
4-OCH_3	CH_3	0.78	0.52	0.44	0.63	0.40	0.39	0.17	0.04

*These differences are $\Delta\tau$(benzalmalononitrile) minus $\Delta\tau$(benzaldehyde) or $\Delta\tau$(1,1-dicyano-2-phenyl-1-propene) minus $\Delta\tau$(acetophenone).

†Solvent shifts of 0.81 and 0.60 p.p.m. were found for the aromatic protons but they could not be assigned.

The results for a few 1,1-dicyano-2-phenyl-1-propenes are also shown and compared differentially with the values for the acetophenones with the same substituent (2). These comparisons yield the striking result that the differences between the solvent shifts of the corresponding protons in benzalmalononitriles and benzaldehydes are quite large but relatively insensitive to substituent, the average values being 0.88 p.p.m. for the olefinic proton, 0.34 p.p.m. for the ortho proton, and 0.22 p.p.m. for the meta proton. To a good approximation therefore the benzene solvent shifts in benzalmalononitriles can be explained in terms of a complex in which two molecules of benzene participate, one whose substituent-dependent position is similar to that in the Klinck and Stothers model for benzaldehydes, and the other whose location over the side chain is independent of the substituent (Fig. 1). The association with the side chain is reminiscent of the complexing of toluene with acetonitrile (23). Ring current effect calculations (17) show that the above differential solvent shifts result for the ethylenic and ortho protons when the second benzene molecule is centered at about 2.5 ring radii over the carbon atom adjacent to the ring, its plane parallel

Can. J. Chem. Downloaded from www.nrcresearchpress.com by 210.87.254.40 on 09/05/12
For personal use only.

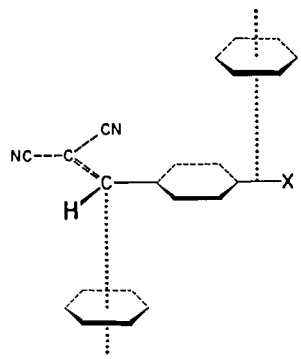

FIG. 1. Association of benzene with a para-substituted benzalmalononitrile. The substituent-dependent position of the benzene molecule at upper right is shown for an electron-donating substituent.

to that of the solute ring. The value calculated for the meta proton is, however, too small by 0.2 p.p.m. A similar model with the second benzene molecule having a position at about 2.5 ring radii over the middle of the bond between the aromatic and olefinic carbons accounts approximately for the observed solvent shifts in the 1,1-dicyano-2-phenyl-1-propenes.

CONCLUSIONS

The strongly electron-attracting cyano groups in benzalmalononitriles cause solvation of the olefinic proton or sites in its vicinity by the donor solvents acetone and benzene, in addition to the solvation normally encountered with these solvents and aromatic molecules. The solvent shifts observed in the n.m.r. spectra are relatively large, but are modified in ortho-substituted compounds.

ACKNOWLEDGMENTS

The authors thank Mr. K. Oikawa and Miss P. M. Lutley for assisting with the n.m.r. spectra. Mr. R. F. Silver, Miss P. D. Frandsen, and Miss S. J. Kelley assisted in the preparation of the compounds.

REFERENCES

1. R. E. KLINCK and J. B. STOTHERS. Can. J. Chem. **40**, 1071 (1962).
2. R. E. KLINCK and J. B. STOTHERS. Can. J. Chem. **40**, 2329 (1962).
3. J. V. HATTON and R. E. RICHARDS. Mol. Phys. **5**, 139, 153 (1962).
4. J. B. BASTUS. Tetrahedron Letters. No. 15, 955 (1963).
5. R. J. ABRAHAM. Mol. Phys. **4**, 369 (1961).
6. B. B. CORSON and R. W. STOUGHTON. J. Am. Chem. Soc. **50**, 2825 (1928).
7. H. G. STURZ and C. R. NOLLER. J. Am. Chem. Soc. **71**, 2949 (1949).
8. L. HORNER and K. KLÜPFEL. Ann. **591**, 69 (1955).
9. D. CRICHTON, M. A. P. HOGG, P. J. R. BRYANT, and G. J. LEWIS. British Ministry of Defence. Unpublished report.
10. P. J. R. BRYANT. British Ministry of Defence. Unpublished report.
11. H. KAUFFMANN. Ber. **49**, 1324 (1916).
12. H. KAUFFMANN. Ber. **52B**, 1422 (1919).
13. D. T. MOWRY. J. Am. Chem. Soc. **67**, 1050 (1945).
14. H. E. EDWARDS, F. P. DOYLE, and S. J. PALLING. U.S. Patent No. 2,839,402 (1958).
15. D. H. MCDANIEL and H. C. BROWN. J. Org. Chem. **23**, 420 (1958).
16. H. H. JAFFE. Chem. Rev. **53**, 191 (1953).
17. C. E. JOHNSON and F. A. BOVEY. J. Chem. Phys. **29**, 1012 (1958).
18. E. A. BRAUDE and F. C. NACHOD. Determination of organic structures by physical methods. Academic Press, Inc., New York, N.Y. 1955. pp. 173–174.
19. A. D. BUCKINGHAM. Can. J. Chem. **38**, 300 (1960).
20. P. DIEHL and R. FREEMAN. Mol. Phys. **4**, 39 (1961).
21. I. G. ROSS and R. A. SACK. Proc. Phys. Soc. London, B, **63**, 893 (1950).
22. R. E. RICHARDS and T. P. SCHAEFER. Trans. Faraday Soc. **54**, 1280 (1958).
23. J. V. HATTON and W. G. SCHNEIDER. Can. J. Chem. **40**, 1285 (1962).

Can. J. Chem. Downloaded from www.nrcresearchpress.com by 210.87.254.40 on 09/05/12
For personal use only.

Can. J. Chem. Downloaded from www.nrcresearchpress.com by 210.87.254.105 on 09/05/12
For personal use only.

CEANOTHUS ALKALOIDS

I. ISOLATION, SEPARATION, AND CHARACTERIZATION

E. W. WARNHOFF,[1] S. K. PRADHAN,[2] AND J. C. N. MA[3]
Department of Chemistry, University of Western Ontario, London, Ontario
Received April 13, 1965

ABSTRACT

Five pure alkaloids have been separated from the crude mixture of *Ceanothus americanus* (Rhamnaceae) bases by means of column and thick-layer chromatography. Their molecular formulas have been established as $C_{30}H_{40}O_4N_4$, $C_{29}H_{36}O_4N_4$, $C_{26}H_{38}O_4N_4$, and $C_{28}H_{44}O_3N_4$ (two compounds). One of these may be identical with the previously reported ceanothine. Evidence is presented for the functional groups and other features of the molecules.

Since colonial times various medicinal properties have been ascribed to the plant *Ceanothus americanus* (Rhamnaceae) (1). This shrub is indigenous to eastern and central North America, and other species grow in the western part of the continent (e.g. *Ceanothus velutinus*) and in Mexico (*Ceanothus azurea*) (2). Aside from the non-medical use of the leaves, known as New Jersey or Jersey tea, for a tea substitute during both the American Revolutionary and Civil wars (3), the plant is reputed to have been used for treatment of venereal disease, dysentery, and disorders of the spleen. Its coagulant properties have made it useful as a styptic and oral haemostatic agent (4, 5). Alcoholic extracts of the root bark were found to have hypotensive action (4, 6).

This medical history stimulated chemical investigation of *Ceanothus americanus*. In 1884 Clinch (7) obtained a positive test for alkaloids from the leaves, and shortly thereafter Gerlach (8) isolated alkaloidal material from the root and called it ceanothine. Subsequently Gordin (9) separated the alkaloidal material into two crystalline fractions, and Clark (10) demonstrated that a complex mixture of alkaloids was present. No elemental analytical data were reported in this early work. In 1933 Bertho and Liang (11) described the "first satisfactorily characterized ceanothus alkaloid" and named it ceanothine also. This base, m.p. 227–228°, $[\alpha]_D^{19}$ −309° (chloroform), was assigned the formula $C_{29}H_{36}O_4N_4$. It was found to be monobasic and to contain one N-methyl but no O-methyl group. From a different species, *C. velutinus*, Richards and Lynn (12) isolated a basic material whose analysis fitted the formula $C_{23}H_{26}O_4N_2$. Recently, more systematic, but not very successful, attempts have been made to separate pure alkaloids from the crude mixtures of *Ceanothus* bases by column chromatography monitored by paper chromatography (13, 14).

The foregoing summary emphasizes the difficulty of obtaining pure alkaloids from this plant, and as will become evident below, perhaps none of the compounds reported in the earlier work was completely pure. Indeed, further chemical progress on this problem would have been quite tedious without thin-layer chromatography (t.l.c.) and nuclear magnetic resonance and mass spectroscopy.

Our own interest in *Ceanothus* alkaloids was aroused both by their potential medical applications and by the possibility that they might belong to a new type of plant base. Bertho and Liang's ceanothine had the unusual feature of four nitrogen atoms, only one

[1]*Fellow of the Alfred P. Sloan Foundation.*
[2]*Department of Chemistry, Shivaji University, Kolhapur, India.*
[3]*Present address: National Heart Institute, National Institutes of Health, Bethesda, Maryland.*

Can. J. Chem. Downloaded from www.nrcresearchpress.com by 210.87.254.105 on 09/05/12
For personal use only.

of which was basic. Furthermore, at the outset of the present work there were no other Rhamnaceae alkaloids known (15), although recently there has been reported the isolation of two alkaloids from *Zizyphus oenoplia* Mill., an oriental member of the family (16*a*). The structure of one of these bases, zizyphine, has now been determined (16*b*). Originally it was even conceivable that the *Ceanothus* bases might be triterpenoid in origin since the triterpenes ceanothic acid (17) and ceanothenic acid (18) are found in *C. americanus*.

The isolation procedure used in the present work was adapted from previous procedures (13, 14) (see Experimental). Analytical thin-layer chromatography on silica gel developed with chloroform–methanol gave apparently good resolution of the crude alkaloid mixture into 8–10 circular spots. From this observation was developed a separation procedure involving column chromatography on silicic acid followed by further separation of fractions on thick-layer chromatograms. In this way the three least polar constituents, designated I (least polar), II, and III, were isolated in a state of purity according to thin-layer chromatography with chloroform:methanol solutions. Later, however, other t.l.c. solvent systems revealed each of these supposedly pure substances to be in fact mixtures of several components. Therefore, the separation process was further refined to include thick-layer chromatography of appropriate fractions in chloroform–acetone, chloroform–dioxane, chloroform–acetonitrile, and chloroform – ethyl acetate systems. Finally, five of the major alkaloids were obtained pure according to melting point, n.m.r. spectrum, t.l.c. behavior in four solvent systems (see Table IV in Experimental section), and, in the case of IIB, constancy of optical rotation. Their properties are summarized in Table I. The close correspondence in the properties of alkaloid IIB and Bertho and Liang's ceanothine (Table II) suggests that the two compounds are probably identical. Although a direct comparison was not possible,[4] the name ceanothine is now adopted for the II alkaloids since no more of the original German specimen exists.

From what is now known of their chemical and physical properties, the *Ceanothus* compounds are not of terpenoid derivation, but belong to the new class of basic polyamide alkaloids including pandamine (19), zizyphine (16), and the adouétines (20).

The molecular formulas are given with a high degree of confidence since the elemental analyses agree well with the molecular weights determined by mass spectrometer, and checked by titration or thermistor osmometer for some of the compounds. The alkaloids IIIA and IIIB (named ceanothamine-A and -B) are probably stereoisomers rather than structural isomers. All five compounds are monobasic secondary or tertiary amines (Table I). The ceanothines each have one N-methyl group, while the ceanothamines each have two such functions. All of these methylimino groups are attached to the *basic* nitrogen in the molecule as seen from the 0.79–1.05 p.p.m. downfield shift (Table I) of the N-methyl proton magnetic resonance peak in changing from deuterochloroform to perdeuteroacetic acid solution (21). This observation was confirmed in the case of ceanothine-A by the preparation of a neutral N-acetyl derivative with n.m.r. peaks at 2.85 p.p.m. (CH_3—N—C=O) and 2.00 p.p.m. (CH_3—C=O); ceanothine-B and -C did not react with acetic anhydride. Each base contains two to six C-methyl groups (Table I).

Although there are three neutral nitrogen atoms present per molecule, the ultraviolet spectrum (Fig. 1) of each alkaloid (unchanged in acidic or basic medium) is not that of a common neutral nitrogen heterocyclic compound. The infrared spectrum does not allow imide or nitrile functions; hydrogenation experiments exclude oxidized nitrogen functions. From these facts and semiquantitative measurements of the intensity of the

[4]*Professor Bertho has informed us that his ceanothine samples were unfortunately destroyed by fire in 1944, but he is of the opinion that the two compounds are the same.*

Can. J. Chem. Downloaded from www.nrcresearchpress.com by 210.87.254.105 on 09/05/12
For personal use only.

TABLE I

Properties of *Ceanothus* alkaloids

Alkaloid	Mol. formula	Mol. wt.	M.p.	$[\alpha]_D$ $CHCl_3$	Base peak of mass spec., *m/e*	Type of amine	No. N-Me groups*	N-Me n.m.r. position in p.p.m. from t.m.s.‡ = 0		No. C-Me groups
								$CDCl_3$	CD_3COOD	
Ceanothine-A (IIA)	$C_{30}H_{40}O_4N_4$	520	256–259°	−256°	134	2°	1	2.13	2.75	**4**
Ceanothine-B (IIB)	$C_{29}H_{36}O_4N_4$	504	238.5–240.5°	−293°	84	3°	1	1.97	3.02	**2**
Ceanothine-C (IIC)	$C_{26}H_{38}O_4N_4$	470	223–229°	−368°	84	3°	1	2.24	3.03	**4**
Ceanothamine-A (IIIA)†	$C_{28}H_{44}O_4N_4$	500	276–279°		114	3°	2	2.15	3.03	**6**
Ceanothamine-B (IIIB)	$C_{28}H_{44}O_4N_4$	500	279–280.5°	−370°	114	3°	2		3.03	**6**

*From integration of n.m.r. spectrum.
†Although ceanothamine-A has the same melting point and molecular formula as adouétine X (20), the latter compound is clearly different since it has no ultraviolet absorption above 210 mμ.
‡t.m.s. = tetramethylsilane.

TABLE II

Comparison of alkaloid IIB and ceanothine

	% C	% H	% O	% N	% NMe	M.p.	Mol. wt.	$[\alpha]_D(CHCl_3)$	M.p. HI salt
Bertho's ceanothine (11)	68.95 69.28	7.45 7.10	—	11.26 11.05	5.81	227–228°	500, 520*	−309°	189–190°
Alkaloid IIB	69.33	7.11	13.12	11.51	1 N-Me†	238.5–240.5°§	504‡	−293°	195–200°§
Calcd. for $C_{29}H_{36}O_4N_4$	69.02	7.19	12.68	11.10	5.77		504		

*Rast method.
†Integration of n.m.r. spectrum.
‡From mass spectrum.
§Microscope hot stage.

carbonyl infrared absorption at 1 580–1 800 cm^{-1}, there are three amide functions per molecule, and two —HNC=O groups can be clearly seen in the n.m.r. spectra of ceanothine-B and -C. Thus, all four nitrogen and three oxygen atoms are accounted for in the alkaloids. The fourth oxygen atom is as yet uncharacterized, but it is evidently not present as another type of carbonyl group (no infrared absorption in 2 000–1 685 cm^{-1} region; no reaction of IIA with sodium borohydride) or as a methoxyl group (negative Zeisel analyses; no n.m.r. peak).

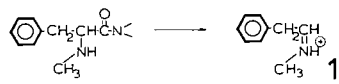

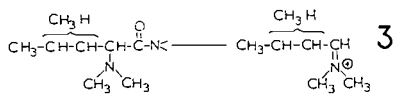

In the mass spectrum of each alkaloid there is one extremely intense peak (even *m/e*). On the reasonable assumption that in the fragmentation of these polyamides the strongest peak will be due to the N-terminal group (there is no C-terminal group) minus the C=O (22, 23, 24), the single nitrogen atom present in this even *m/e* base peak must be the basic nitrogen atom of the alkaloid. For ceanothine-A the base peak is at *m/e* 134 corresponding to $C_9H_{12}N^+$, which, in consideration of another peak at *m/e* 91 ($C_7H_7^+$) and the presence of an N_b-methyl group, must be **1** derived from an N-methylphenylalanyl residue. Ceanothine-B, being a tertiary amine with one N_b-methyl group, therefore contains the N-methylprolyl (hygryl) end group in order to have its base peak at *m/e* 84 ($C_5H_{10}N^+$) corresponding to **2**. For the same reasons ceanothine-C with its base peak at *m/e* 84 must also have the N-methylprolyl end group. Ceanothamine-A and -B both have their base peaks at *m/e* 114 ($C_7H_{16}N^+$), which is presumably due to an N,N-dimethylleucyl or -isoleucyl end group furnishing the ion (**3**).

The ultraviolet spectra of all five alkaloids are very similar (Fig. 1). Hydrogenation of each of the compounds in the presence of palladium results in the uptake of 1 mole equivalent of hydrogen and produces the same change in the ultraviolet absorption of each base (Fig. 1). The chromophore removed by reduction is revealed by the subtraction curve in Fig. 1 to have λ_{max} 250 mμ($\epsilon \sim 4\,000$), which fits very well the system 4 as in the model compounds **5** (25), **6** (26), **7** (27), and **8** (28). The similarities in the ultraviolet spectra and certain features of the n.m.r. spectra strongly suggest that there is a fundamental unit common to all of these alkaloids.

The results of hydrolytic studies and further work in progress will be reported in due course.

EXPERIMENTAL

General

Melting points: Reichert Microscope hotstage, corrected.

Optical rotations: Schmidt-Haensch or Rudolph model 80 polarimeter, chloroform solutions unless otherwise specified, 1-dm tube.

Ultraviolet spectra: Bausch and Lomb Spectronic 505 spectrometer.

Can. J. Chem. Downloaded from www.nrcresearchpress.com by 210.87.254.105 on 09/05/12
For personal use only.

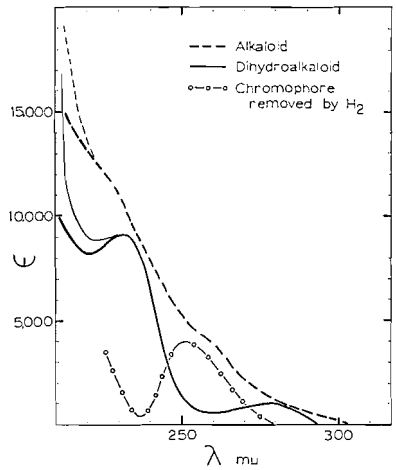

FIG. 1. Ultraviolet spectra of *Ceanothus* alkaloids. Where the curves for the alkaloids and dihydroalkaloids diverge at low wavelength, the lighter line is the absorption of IIA and IIB; the darker line is the absorption of IIC, IIIA, and IIIB.

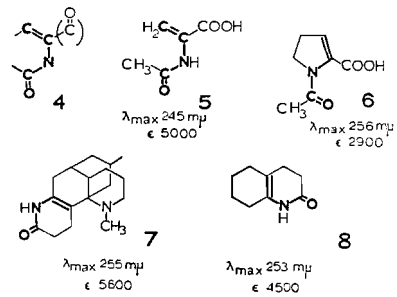

Infrared spectra: Beckman IR-5 or IR-7 spectrometer.

Nuclear magnetic resonance spectra: Varian A-60 spectrometer, cut-and-weigh integrations.

Mass spectra: Consolidated Electrodynamics Corp. model 103, or Associated Electrical Industries model MS-9. Ionization potential 70 V. Samples were introduced directly into the ion source.

Thin-layer chromatography: Camag Kieselgel DF-5 silica gel with calcium sulphate binder and fluorescent indicator. Chloroform refers to the commercial reagent grade containing 0.75% ethanol as a preservative.

Analyses: Dr. A. Bernhardt and associates, Mulheim, Germany; Dr. C. Daesslé and associates, Montreal, Quebec; Dr. J. F. Alicino, Metuchen, New Jersey.

Extraction and Column Chromatography

Ground root bark of *Ceanothus americanus* was supplied by Baxter Laboratories, Morton Grove, Illinois (formerly Flint, Eaton and Co., Decatur, Illinois) and by the S. B. Penick Co., Jersey City, New Jersey. The bark (4 kg) was exhaustively extracted with 60–80° petroleum ether in a Soxhlet type apparatus for 1 week to remove wax and triterpenoids (15.5 g). The defatted bark was dried and then exhaustively extracted with methanol for 2 weeks, the long period being necessitated by the slow solvent cycling rate. The solvent charge was changed after the first, fourth, and ninth days, the color of the extracts changing from a deep red to light tea color.

The methanol extract was diluted, 1 l at a time, with an equal amount of water and acidified with 400 ml of 0.4 *N* sulfuric acid in saturated sodium chloride solution. The acidified mixture was shaken with ether to remove brown neutral material (41 g from the entire methanol extract). The aqueous layer was then basified with 10% sodium hydroxide solution to pH 9–10 and extracted with chloroform. Evaporation of the dried chloroform solution from work up of all the methanol extracts left 9.1 g (0.23%) of crude amorphous alkaloid mixture, the usual yield being between 0.2 and 0.4%. Thin-layer chromatography in methanol:chloroform (7:93) gave 5 major spots: I (R_f 0.65, purplish color on short charring with 30% sulfuric acid), II (0.54, purplish), III (0.46, purplish), IV (0.37, grey), and V (0.33, yellowish); there were other less well-resolved spots closer to the origin. The relative proportions of components II and III varied considerably in different lots.

Can. J. Chem. Downloaded from www.nrcresearchpress.com by 210.87.254.105 on 09/05/12
For personal use only.

A 6 × 130-cm column containing chloroform was packed with 1 000 g of silicic acid (Fisher) in layers of gradually decreasing activity, the bottom layer (50 g) having been activated by heating at 120° overnight, the next layer (200 g) being an equal mixture of activated and unactivated silica gel, the next layer (500 g) being unactivated adsorbent, and the top layer (250 g) having been deactivated by addition of 5% by weight of water. The 9.1 g of crude alkaloid in chloroform solution were applied to the column which was then developed with chloroform. The progress of the separation was followed by fluorescence of various bands on the column under ultraviolet light. After 7 l of eluent had been collected, the column was allowed to "run dry". The wet silicic acid was extruded and immediately cut into sections under an ultraviolet lamp. Each section was extracted thoroughly by chloroform–methanol or methanol–ether and filtered. The composition of each fraction was determined by thin-layer chromatography in chloroform:methanol (95.5:4.5). From the figures in Table III and the relative intensities of the charred t.l.c. spots, the crude alkaloid mixture was estimated to consist of ~9% of I, ~25% of II, and ~12% of III. With some batches of crude base the alkaloids were eluted from the column, but extrusion saved time and solvent, and probably gave somewhat sharper separation.

TABLE III

Column chromatogram of alkaloids

Section	Wt., g	Cum. wt., g	Approx. comp.
10	0.258	0.258	(Bottom of column)
11	0.058	0.316	
12	0.063	0.379	
13	0.111	0.490	I>>II
14	0.693	1.183	I > II
15	0.729	1.912	I<<II
16	0.804	2.716	II
17	0.617	3.333	II
18	0.320	3.653	II>>III
19	0.408	4.061	III
20	0.394	4.455	III
21	0.603	5.058	III > IV
22	0.392	5.450	III ≈ IV
23	0.539	5.989	
24	0.521	6.510	
25	0.622	7.132	
26	2.130	9.262	(Top of column)

Separation by Thick-Layer Chromatography

Glass plates (20 × 20 cm) coated with 20 g of silica gel were used for thick-layer chromatography. Up to 150 mg of alkaloid mixture from the column chromatogram were applied per plate. Five solvent systems were used for development, some plates being developed two or three times. Chloroform containing 4–10% of methanol was used to separate alkaloid mixtures I, II, III, and IV cleanly from each other. Acetone:chloroform (15:85), dioxane:chloroform (25:75), and acetonitrile:chloroform (15:85) were used for separation of the I and II mixtures into their components. Ethyl acetate:chloroform (50:50) was used for separation of alkaloids III*a* and III*b*. Progress in the thick plate separations was followed by thin-layer chromatograms developed in these solvents and charred with 30% aqueous sulfuric acid at 140° for 10 min to note colors, and then often for a longer time to carbonize the spots. The best means of assessing the purity of the individual alkaloids was a combination of the n.m.r. spectrum (particularly the N-methyl and C-methyl regions), m.p. behavior and t.l.c. behavior in several solvent systems.

Ceanothine-A

The amount of this compound in the II zone is usually less than the ceanothine-B and -C content, and it has so far been obtained pure from only one lot of bark. Material from column chromatographic sections which contained the II spot was purified on thick plates (100 mg/plate) with methanol:chloroform (4:96) to get complete separation from I and then with methanol:chloroform (7:93) to effect complete separation from III. Molecular weight determination of this II by thermistor osmometer gave values of 498 and 511. Subsequent thick-layer chromatography in acetone:chloroform (15:85) gave five zones under ultraviolet light. The lowest zone was separated and further purified by chromatography in dioxane:chloroform (25:75). After several recrystallizations from methylene chloride – ether the colorless matted needles had m.p. 256–259°, $[\alpha]_D$ −256° (*c*, 0.50).

Anal. Calcd. for $C_{30}H_{40}O_4N_4$ (520.65): C, 69.20; H, 7.74; O, 12.29; N, 10.76. Found: C, 69.31, 69.12; H, 7.53, 7.62; O, 12.66; N, 10.78. Mol. wt. (mass spectrum), 520.

When 10 mg of ceanothine-A in 3 ml of *i*-propyl alcohol was treated with a large excess of sodium borohydride and the reaction mixture allowed to stand overnight, 8 mg of basic product was recovered by dilution

Can. J. Chem. Downloaded from www.nrcresearchpress.com by 210.87.254.105 on 09/05/12
For personal use only.

with water and extraction. The material was shown to be ceanothine-A by melting point, infrared spectrum, and t.l.c. comparison in methanol:chloroform (3.5:96.5).

Ceanothine-B

In most lots of the root bark this alkaloid was the major component of the II mixture. The II zone was first separated from I and III as described for ceanothine-A. Thick-layer chromatography in acetone:chloroform (15:85) gave a broad purple band under ultraviolet light, the *lower* portion of which band was nearly pure ceanothine-B. Several recrystallizations from chloroform–ether gave colorless matted needles, m.p. 238.5–240.5°, $[\alpha]_D^{25}$ −293° (*c*, 0.68), $[\alpha]_D^{23}$ −292° (*c*, 0.90), pK_a 5.85 [determined in methanol:water (95:5)].[5]

Anal. Calcd. for $C_{29}H_{36}O_4N_4$ (504.61): C, 69.02; H, 7.19; O, 12.68; N, 11.10; 2 (C)CH_3, 5.95; 1 (N)CH_3, 2.97, OCH_3, 6.11. Found: C, 69.33; H, 7.11; O, 13.12; N, 11.51; (C)CH_3, 5.75; (N)CH_3, 3.43, 3.93; OCH_3, 0.00. Neutral equivalent, 505. Mol. wt. (mass spectrum), 504.

The hydriodide salt was prepared from 4 mg of ceanothine-B as described by Bertho and Liang (11) for ceanothine. After two recrystallizations from aqueous acetic acid the white plates had m.p. 195–200°.

Ceanothine-C

This alkaloid was isolated from the *front* edge of the II zone after the thick-layer chromatography in acetone:chloroform (15:85) described for ceanothine-B. Ceanothine-C was further purified by a second thick-layer chromatography in the same solvent system. Several recrystallizations from chloroform:ether gave colorless matted needles, m.p. 223–229°, $[\alpha]_D^{25}$ −368° (*c*, 1.01).

Anal. Calcd. for $C_{28}H_{38}O_4N_4$ (470.60): C, 66.35; H, 8.14; O, 13.60; N, 11.91. Found: C, 66.27, 66.39; H, 8.04, 7.86; O, 13.57; N, 12.43. Neutral equivalent, 485. Mol. wt. (mass spectrum), 470.

Ceanothamine-A and -B

Column chromatogram fractions containing the zone III alkaloids were completely separated from the II and IV zones by thick-layer chromatography in methanol:chloroform (3:97) and (5:95). Zeisel analysis of the total III alkaloids gave 0.00% OCH_3. Thermistor osmometer molecular weight determination on total III gave a value of 492; neutral equivalent titration gave 490. The material from the III band was then chromatographed on thick layers (only 15 mg per plate because of low solubility) in ethyl acetate : chloroform (50:50) to give two main bands.

The upper band of ceanothamine-A crystallized from methylene chloride – ethyl acetate in the form of colorless matted needles, m.p. 276–279°, R_f 0.28 in pure ethyl acetate.

Anal. Calcd. for $C_{28}H_{44}O_4N_4$ (500.66): C, 67.17; H, 8.86; N, 11.19. Found: C, 67.34; H, 8.92; N, 10.94. Mol. wt. (mass spectrum), 500.

The lower band of ceanothamine-B crystallized from methylene chloride – ethyl acetate in colorless matted needles, m.p. 279–280.5°, $[\alpha]_D^{25}$ −370° (*c*, 0.205), R_f 0.16 in pure ethyl acetate on the same plate on which ceanothamine-A gave R_f 0.28. Ceanothamine-B did not noticeably depress the melting point of ceanothamine-A.

Anal. Calcd. for $C_{28}H_{44}O_4N_4$ (500.66): C, 67.17; H, 8.86; O, 12.78; N, 11.19. Found: C, 67.36; 67.43, H, 8.84, 8.97; O, 13.15; N, 11.46. Mol. wt. (mass spectrum), 500.

TABLE IV

R_f values of pure alkaloids in various solvent systems

	$MeOH:CHCl_3$ 4:96	$Me_2CO:CHCl_3$ 15:85	$EtOAc:CHCl_3$ 50:50	$MeCN:CHCl_3$ 15:85
IIA	0.55	0.18	0.10	0.11
IIB	0.55	0.17	0.11	0.09
IIC	0.55	0.21	0.15	0.12
IIIA	0.43	0.12	0.10	0.06
IIIB	0.43	0.10	0.05	0.05

NOTE: The values for a particular system are averages taken from a single t.l.c. plate (250 μ thick layer of silica gel) on which two 10–25 γ spots of each pure compound appeared.

Acetylation of Ceanothines

(*a*) A solution of 27 mg of ceanothine-A in 1 ml of a mixture of chloroform and benzene to which had been added 0.5 ml of acetic anhydride was allowed to stand at room temperature for 24 h. Dilution with sodium bicarbonate solution and extraction with chloroform yielded 27 mg of crude neutral product which was purified by thick-layer chromatography in acetone:chloroform (15:85) to give 19 mg of white crystals of the N-acetate, m.p. 281–282°. The infrared spectrum had no O-acetate carbonyl absorption. The n.m.r. spectrum (deuterochloroform) had unsplit methyl peaks at 2.85 p.p.m. (CH_3—NAc) and 2.00 p.p.m. (CH_3—C=O).

Anal. Calcd. for $C_{32}H_{42}O_5N_4$ (562.68): 1 CH_3C=O, 7.65. Found: CH_3C=O (basic hydrolysis), 7.59.

[5]*The base was not completely soluble in the usual methylcellosolve:water (80:20) system. In the methanol:water (95:5) solvent atropine gave pK_a 8.33, the same value found in methylcellosolve:water (80:20) (29).*

Can. J. Chem. Downloaded from www.nrcresearchpress.com by 210.87.254.105 on 09/05/12
For personal use only.

(*b*) A solution of 27 mg of ceanothine-B in 1 ml of chloroform to which had been added 0.2 ml of acetic anhydride was allowed to stand at room temperature for 34 h. Dilution with chloroform–ether and extraction with potassium bicarbonate solution and then with dilute hydrochloric acid left only 4 mg of neutral material (presumably from impurities in the ceanothine-B) in the chloroform–ether solution. Basification of the acid extract yielded 24 mg (90%) of recovered ceanothine-B which after recrystallization from chloroform–ether afforded 17 mg, m.p. 238–240°. T.l.c. comparison also confirmed its identity with starting material.

(*c*) A solution of 10 mg of ceanothine-C in 1 ml of chloroform to which had been added 0.2 ml of acetic anhydride was allowed to stand at room temperature for 62 h. Workup as for ceanothine-B in (*b*) gave no neutral material but 11 mg of basic white solid which after recrystallization from chloroform–ether gave 7.5 mg, m.p. 219–227°. The recovered alkaloid had the same R_f as ceanothine-C.

Hydrogenations

Each alkaloid was hydrogenated over 5% palladium-on-carbon catalyst (Matheson) in a Hösli microhydrogenation apparatus,[6] and the results are collected below. Each dihydrocompound was run on the same t.l.c. plate as the starting material.

Alkaloid	Wt., mg	Mg catalyst	Ml MeOH	Temp.	Atm. pressure, mm	Ml H_2 abs.	Eq of H_2/mole	R_f 2H product	R_f start. material
IIA	14.6	6	5	22°	730	0.85	1.03	0.22	0.43
IIB	48.4	40	20	22°	727	2.71	1.02	0.29	0.44
IIC	5.7	10	3	23°	735	0.34	1.00	0.38 0.27	0.63
IIIA	16.6	7	20	21°	742	0.85	0.90	0.10	0.26
IIIC	15.8	13	20	19°	745	0.90	1.01	0.14	0.28

The crude dihydroceanothine-B had $[\alpha]_D^{25}$ −81° (*c*, 1.01, methanol). Recrystallization from chloroform–ether gave a microcrystalline powder, m.p. 263–273°, $[\alpha]_D^{25}$ −91° (*c*, 0.38, methanol).

Recrystallization of the dihydroceanothamine-A from chloroform–ether gave white crystals, m.p. 305–309°.

Anal. Calcd. for $C_{28}H_{46}O_4N_4$ (502.67): C, 66.90; H, 9.22; O, 12.73; N, 11.15. Found: C, 66.75, 67.01; H, 9.28, 9.38; O, 12.65; N, 10.79.

ACKNOWLEDGMENT

The support of the U.S. National Heart Institute under Grant HE-07394 (formerly H-5762) is gratefully acknowledged. Baxter Laboratories, Morton Grove, Illinois (formerly Flint, Eaton and Company), generously furnished several lots of ground *Ceanothus americanus* root bark. Professors D. B. MacLean and K. Biemann were very helpful in obtaining some of the mass spectra. Dr. W. Simon, Zürich, kindly measured the pK_a values. Mrs. P. Stoessl was responsible for much of the alkaloid isolation.

REFERENCES

1. D. H. HUBBARD. Boston Med. Surg. J. **15**, 42 (1835).
2. A. ENGLER and K. PRANTL. Die naturlichen Pflanzenfamilien. III Teil, Abt. 5. 1st ed. W. Engelmann, Leipzig. 1897. pp. 412–414.
3. T. S. WIEGAND. Am. J. Pharm. **50**, 86 (1878).
4. J. T. GROOT. J. Pharmacol. Exptl. Therap. **30**, 275 (1927).
5. C. E. THARALDSEN and J. KRAWETZ. Am. J. Physiol. **79**, 545 (1927).
6. H. WASTL. Federation Proc. **7**, 131 (1948).
7. J. H. M. CLINCH. Am. J. Pharm. **56**, 131 (1884).
8. F. C. GERLACH. Am. J. Pharm. **63**, 332 (1891).
9. H. M. GORDIN. Pharm. Rev. **18**, 266 (1900).
10. A. H. CLARK. Am. J. Pharm. **98**, 147 (1926); **100**, 240 (1928).
11. A. BERTHO and W. S. LIANG. Arch. Pharm. **271**, 273 (1933).
12. L. W. RICHARDS and E. V. LYNN. J. Am. Pharm. Assoc. **23**, 332 (1934).
13. A. A. MANIAN. Ph.D. Thesis, Purdue University. 1954.
14. C. W. ROSCOE and N. A. HALL. J. Am. Pharm. Assoc. Sci. Ed. **49**, 108 (1960).
15. J. J. WILLAMAN and B. G. SCHUBERT. Alkaloid-bearing plants and their contained alkaloids. Tech. Bull. 1234, U.S. Dept. Agr. Washington, D.C. 1961. p. 186.
16. (*a*) E. L. MÉNARD, J. M. MÜLLER, A. F. THOMAS, S. S. BHATNAGAR, and N. J. DASTOOR. Helv. Chim. Acta, **46**, 1801 (1963). (*b*) E. ZBIRAL, E. L. MÉNARD, and J. M. MÜLLER. Helv. Chim. Acta, **48**, 404 (1965).

[6]*H. Hösli, Bischofszell, Switzerland.*

Can. J. Chem. Downloaded from www.nrcresearchpress.com by 210.87.254.105 on 09/05/12
For personal use only.

17. P. DE MAYO and A. N. STARRATT. Can. J. Chem. **40**, 788 (1962).
18. P. DE MAYO and A. N. STARRATT. Can. J. Chem. **40**, 1632 (1962).
19. M. PAÏS, X. MONSEUR, X. LUSINCHI, and R. GOUTAREL. Bull. Soc. Chim. France, 817 (1964).
20. M. PAÏS, J. MAINIL, and R. GOUTAREL. Ann. Pharm. Franc. **21**, 139 (1963).
21. J. C. N. MA and E. W. WARNHOFF. Can. J. Chem. **43**, 1849 (1965).
22. K. HEYNS and H.-F. GRÜTZMACHER. Ann. **669**, 189 (1963).
23. K. BIEMANN. Mass spectrometry, organic chemical applications. McGraw-Hill Co., New York. 1962. pp. 260–296.
24. H. J. SVEC and G. A. JUNK. J. Am. Chem. Soc. **86**, 2278 (1964).
25. J. A. KING and F. H. MCMILLAN. J. Am. Chem. Soc. **72**, 835 (1950).
26. K. HASSE and P. HOMANN. Biochem. Z. **335**, 474 (1962).
27. B. P. MOORE and L. MARION. Can. J. Chem. **31**, 952 (1953).
28. W. A. AYER, R. HAYATSU, P. DE MAYO, S. T. REID, and J. B. STOTHERS. Tetrahedron Letters, No. 18, 648 (1961).
29. W. SIMON, G. H. LYSSY, A. MÖRIKOFER, and E. HEILBRONNER. Zusammenstellung von Scheinbaren Dissoziationskonstanten. Juris-Verlag, Zürich. 1959. p. 59.

Can. J. Chem. Downloaded from www.nrcresearchpress.com by 210.87.254.105 on 09/05/12
For personal use only.

Can. J. Chem. Downloaded from www.nrcresearchpress.com by 210.87.254.42 on 09/05/12
For personal use only.

LIGHT ABSORPTION STUDIES

PART XXI. THE ULTRAVIOLET AND INFRARED ABSORPTION OF *o*-ALKYL- AND *o,o'*-DIALKYL-SUBSTITUTED ANISOLES[1]

A. BALASUBRAMANIAN,[2] J. C. DEARDEN,[3] W. F. FORBES,[2] AND (IN PART) N. F. CHEETHAM[4]

Department of Chemistry, University of Waterloo, Ontario;
Department of Pharmacy, College of Technology, Liverpool, England;
and Division of Protein Chemistry, C.S.I.R.O., Parkville, N.2., Victoria, Australia

Received January 21, 1965

ABSTRACT

Steric effects, previously reported by other workers in *o*- and *o,o'*-alkyl-substituted anisoles, were reinvestigated using compounds carefully purified by vapor phase chromatography. The ultraviolet spectral data indicate that the *o*-alkyl-substituted anisoles exist in one conformation, whereas the investigated *o,o'*-dialkyl-substituted anisoles exist in a different conformation. The conformations appear to be almost independent of the size of the substituent groups. Infrared, dipole moment, and other data are consistent with this interpretation.

INTRODUCTION

It is well known that steric hindrance in a conjugated molecule frequently causes a hypsochromic shift and a hypochromic effect in the ultraviolet absorption *B*-bands ($^1L_a \leftarrow {}^1A$ bands). Related, but by no means identical, effects are observed for *C*-bands ($^1L_b \leftarrow {}^1A$ bands). Generally, the bulkier the hindering group(s), the more pronounced are these steric effects, and particularly so the hypochromic effect; for aromatics, such spectral changes imply an increasing loss of uniplanarity with increasing size of the ortho-substituent(s). Steric effects in the anisoles have previously been investigated by Goodman and co-workers (1, 2). The purpose of the present paper is to extend such work to anisoles containing bulkier *o*-substituents. The spectra were found to be anomalous in that some ultraviolet and infrared spectral effects are observed on *o*-*t*-butyl and *o,o'*-di-*t*-butyl substitution, which are similar to those observed with *o*-methyl and *o,o'*-dimethyl substituents respectively.

EXPERIMENTAL

The ultraviolet absorption spectra were determined by standard methods in 1 cm cells using Beckman model DU and Cary model 14 spectrophotometers calibrated against solutions of potassium chromate and potassium nitrate. Wavelength readings obtained on the two instruments were found to be within 1 mμ of each other. The accuracy of λ_{max} values is estimated to be ± 1 mμ, and the precision of molar absorptivities $\pm 5\%$ or better. Most molar absorptivity values were reproducible to $\pm 2\%$. The oscillator strength, f, was calculated from

$$f = 4.319 \times 10^{-9} \int \epsilon \, d\nu,$$

where ϵ is the molecular extinction coefficient and ν the frequency in cm^{-1}. Each integration was carried out graphically over the entire band envelope.

Generally, our results were in good agreement with recent values reported elsewhere. However, Frolen and Goodman (1) obtained a considerably different spectrum from ours for *o,o'*-dimethylanisole (3); we have therefore redetermined the spectrum of this compound, and have confirmed our original ϵ values. A mass spectrometric analysis showed our compound to be 99.7% pure, the main impurity being 2,4,6-trimethylanisole. See also refs. 4, 5 where spectra similar to ours are reported.

The infrared spectra were determined on Beckman model IR7 and model IR9 spectrophotometers, calibrated against a polystyrene film, using a KBr prism and a diffraction grating. The frequency accuracy

[1]*Part XX: Can. J. Chem. 39, 2452 (1961).*
[2]*Present address: Department of Chemistry, University of Waterloo, Waterloo, Ontario, Canada.*
[3]*Present address: Department of Pharmacy, College of Technology, Liverpool 3, England.*
[4]*Present address: Department of Chemistry, Monash University, P.O. Box 92, Clayton, Victoria, Australia.*

in the 1 200 cm^{-1} region is believed to be ± 0.4 cm^{-1} and the frequency reproducibility is ± 0.1 cm^{-1}. Solutions were examined mainly in 0.1 mm and 1 mm cells fitted with sodium chloride or potassium bromide windows. The solute concentration was ca. 0.01–0.06 M (1 mm cells). The integrated absorption intensities (A_{RJ}) were calculated from the equation

$$A_{RJ} = K(1/cl) \times \log_{10}(T_0/T)_{max} \times \Delta\nu_{\frac{1}{2}}^{a} \times 2.303 \times 10^{-4},$$

where c is the molar concentration, l is the cell length in cm, $\log (T_0/T)_{max}$ is the absorbance at the absorption maximum, and $\Delta\nu_{\frac{1}{2}}^{a}$ the band width in cm^{-1} at half maximum intensity (cf. ref. 6 and refs. cited there); K was determined from Ramsay's Tables (7). The intensities were also recorded in terms of the new units, A_{IUPAC} (8). The accuracy of the A values is estimated to be $\pm 5\%$.

Two independent sets of observations were made for all the spectral results. All solvents, except the ethanol, were commercially available spectroanalyzed solvents (Fisher). The ethanol was best-grade undenatured absolute ethanol (Consolidated Alcohol, Toronto).

Most of the compounds were prepared by standard methods as described in the literature or were commercially available samples. The samples were purified by distillation. Final purifications were usually carried out by vapor phase chromatography using the Autoprep model A-700 with fraction collection system on a 10 ft × 3/8 in. column packed with 30% SE-30 silicone rubber on 60/80 mesh Chromosorb W, and sample purity was also checked on 30% Carbowax 20M 10 ft × 3/8 in. and 10% Carbowax 20 MD TPH 10 ft × 3/8 in. columns. For some anisoles, repeated purification using vapor phase chromatography with different columns was necessary before a chromatographically homogeneous sample could be obtained.

DISCUSSION

The ultraviolet spectra are listed in Table I.

Table I shows that the compounds studied fall into two groups, namely anisoles which possess two ortho-alkyl-substituents and anisoles which possess one or no ortho-alkyl-substituent. For the mono-substituted anisoles, not even *o*-*t*-butyl substitution causes

TABLE I

Main maxima of alkyl-substituted anisoles in cyclohexane solution (values in italics represent inflections)

Substituent		*B*-Band		*C*-Band		
o	*o'*	λ_{max} (mμ)	ϵ_{max}	λ_{max} (mμ)	ϵ_{max}	Oscillator strength $f \times 10^3$
H	H*	220	8 100	265	1 400	
		~224	*6 400*	271	2 100	23.0
				277.5	2 100	
CH_3	H*	211.5	7 100	*~265*	*1 500*	
		216	7 400	272.5	2 100	24.3
		220.5	7 200	278	2 100	
$CH(CH_3)_2$	H*	211	7 400	*~265*	*1 500*	
		217	7 800	272	2 150	24.0
		221	7 700	278	2 050	
$C(CH_3)_3$	H*	217.5	7 500	*~265*	*1 500*	
		222	7 400	270	2 000	22.9
				277	2 050	
2,3-Dimethylanisole		*~217*	*7 600*	270	1 355	
				274	1 355	17.8
				279	1 540	
CH_3	CH_3*	*~215*	*9 000*	268	390	5.5
				273	346	
C_2H_5	C_2H_5	*~215*	*9 700*	266.5	415	5.7
				273	380	
$CH(CH_3)_2$	$CH(CH_3)_2$*	*~212*	*10 500*	265	425	
				272.5	385	5.6
$C(CH_3)_3$	$C(CH_3)_3$	Submerged		270	340	
				~275	*320*	5.5
				~300	*35*	

*These values supersede the values reported in ref. 3.

Can. J. Chem. Downloaded from www.nrcresearchpress.com by 210.87.254.42 on 09/05/12
For personal use only.

any appreciable wavelength displacement nor is the intensity of the *B*- or *C*-band appreciably reduced. This absence of such typical steric effects may be attributed to the ability of the methoxy group to take up a position in which electronic interaction between the methoxy group and the benzene ring is not reduced appreciably. Considering actual conformations, seven possible forms of *o*-*t*-butylanisole may be obtained by twisting the aryl—O bond, and considering eclipsed and staggered forms in the usual way. These forms are schematically represented in Fig. 1 by structures 1 to 7. The diagrams, it should be noted, are qualitative and idealized since, for example, the bonds and lone-pair hybrids are assumed to make angles of 120° with each other when viewed along the aryl—O bond (cf. ref. 9).

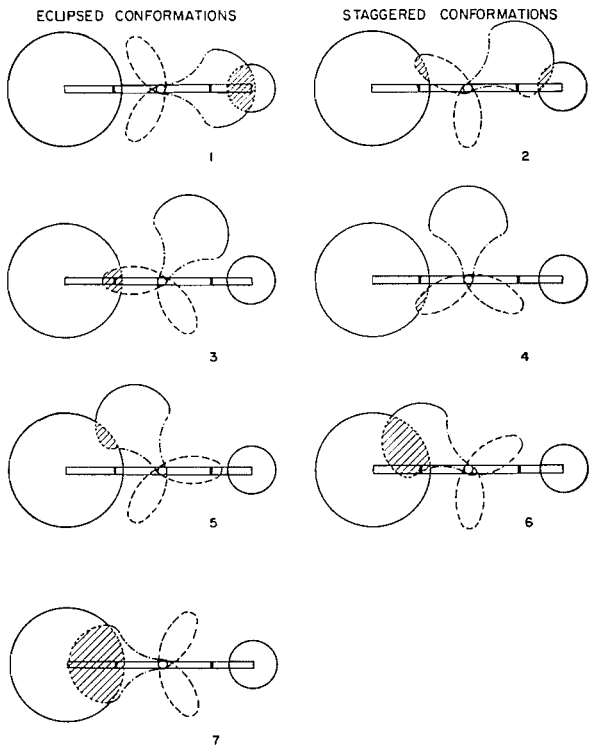

FIG. 1. Schematic diagram of *o*-*t*-butylanisole conformations as the methoxyl group undergoes successive 30° twisting displacements.

In the diagrams, the horizontal bars represent the side-on view of the plane of the benzene ring, attached to which are the ortho-substituents hydrogen and *t*-butyl. The center of each diagram represents the oxygen atom, attached to which are two lone pairs and the oxygen-linked CH_3 group; the former are indicated by dotted lines. Of the seven conformations obtained in this way, four (Nos. 1, 3, 5, and 7) are eclipsed structures in which the repulsive interactions between the bonds and the atomic dipoles are large. These forms will not therefore represent conformations of minimum energy (cf. the fact that ethane has a staggered conformation). Of the remaining three structures, Nos. 2 and 6 have the advantage over structure 4 inasmuch as one of the lone pairs of electrons is able to overlap effectively with the π-electrons of the benzene ring. In *o*-*t*-butylanisole, structure 2 would be preferred to structure 6 since in the latter the repulsive interactions between the *o*-*t*-butyl group and the oxygen-linked methyl group are likely to be considerable.

Can. J. Chem. Downloaded from www.nrcresearchpress.com by 210.87.254.42 on 09/05/12
For personal use only.

The above considerations suggest that structure 2 is preferred for *o*-alkyl-substituted anisoles. Incidentally, the data for *o*-iodoanisole (3) and for *o*-*t*-butyl-*N*-methylaniline (10) likewise show only slightly modified ultraviolet spectra compared with the spectra of the appropriate reference compounds, indicating that these compounds also may exist in a conformation similar to structure 2. *o*-Nitroanisole shows evidence of steric interactions in the nitrobenzene-type *B*-band of its ultraviolet absorption spectrum (11) but this may be because repulsive interactions between the lone pairs of the oxygen atom of the OCH_3 group and the nitro group displace the latter group from the plane of the benzene ring; the molecule may still exist in form 2.

On the other hand, in *o*,*o*′-dialkyl-substituted anisoles, structures corresponding to form 2 would be appreciably hindered since interactions in that conformation would now be comparable to those existing in form 6. Consequently, it seems probable that in *o*,*o*′-dialkyl-substituted anisoles, conformations analogous to structure 4 are preferred. In structure 4, repulsive interactions are relatively small, but overlap between the unpaired electrons of the oxygen atom and the benzene ring is now more difficult. By assuming this change of conformation, it is possible to explain the drastically reduced oscillator strength of the *C*-band in *o*,*o*′-dialkyl-substituted anisoles, which is approximately independent of the size of the alkyl substituent. A similar behavior, incidentally, is observed for the 2,4,6-trihaloanisoles, where the *C*-band of 2,4,6-triiodoanisole has about the same molar absorptivity as that of 2,4,6-trichloroanisole (12).

Alternative Explanations

The above discussion shows that the spectral data can be rationalized by assuming a different conformation for *o*,*o*′-dialkyl-substituted anisoles, which is preferred because of increased steric interactions in compounds of this type. However, 1,2-disubstituted benzenes may inherently absorb differently from 1,2,3-trisubstituted benzenes, even in the absence of steric interactions (13). There is some evidence for this, since *o*-dimethoxybenzene (veratrole) has an intense *C*-band centered around 275 mμ (ϵ = 2 550), while 1,2,3-trimethoxybenzene (in methanol solution) has a *C*-band centered around 267 mμ (ϵ = 660) (14). Moreover, 1,3,5-trimethoxybenzene has a maximal extinction coefficient of only 480 at λ_{max} 265 mμ (14), although steric interactions in this compound must be relatively small.

However, the present, and other, data cannot readily be rationalized in terms of substituent effects alone. This is well illustrated by the spectrum of 2,3-dimethylanisole, the ϵ value of which is almost as high as for 2-methylanisole, but unlike that for 2,6-dimethylanisole (see Table I).* We conclude therefore that the effect of *o*-alkyl substitution on the *C*-band spectra can best be rationalized in terms of mainly steric interactions affecting the conformations as outlined in this paper.

Infrared Spectra

The frequencies and intensities of the aryl—O stretching absorption of the anisoles, as 0.01–0.06 *M* solutions (1 mm cells) in carbon disulfide, are listed in Table II. Some of the results, are consistent with the conclusion drawn from the ultraviolet spectra, that *o*,*o*′-dialkyl substitution causes a change of conformation, since the results again fall into two groups; those for anisole and monoalkyl-substituted anisoles and those for *o*,*o*′-dialkyl-substituted anisoles. This division is most readily evident for the intensities of the aryl—O stretching band; *o*-alkyl substitution produces some intensity decrease relative to the absorption intensity of anisole, but *o*,*o*-dialkyl substitution produces a

**We are grateful to a referee for suggesting this compound as a test case.*

Can. J. Chem. Downloaded from www.nrcresearchpress.com by 210.87.254.42 on 09/05/12
For personal use only.

much greater decrease. Similar changes are observed for the frequency of the aryl—O band, which is lowered slightly by one *o*-alkyl substituent (3.5–10 cm^{-1}), but is lowered more significantly on *o,o'*-dialkyl substitution (28–45 cm^{-1}).

TABLE II

Aryl—O stretching vibrations of alkyl-substituted anisoles in carbon disulfide solution ($\Delta\nu$ = band width, A = integrated absorption intensity)

Substituent		Aryl—O stretching band				
o	*o'*	ν_{max} (cm^{-1})	ϵ_{max}	$\Delta\nu_{\frac{1}{2}}$ (cm^{-1})	A_{RJ} ($mole^{-1}$ l cm^{-2} $\times 10^{-4}$)	A_{IUPAC} practical
H	H	1 246.5	760	5.5	1.5	0.65
CH_3	H	1 243	515	11.6	2.16	0.93
$CH(CH_3)_2$	H	1 241	680	7	1.7	0.75
$C(CH_3)_3$	H	1 236.5	470	10	1.1	0.48
2,3-Dimethylanisole		1 259	655	6.5	1.55	0.67
CH_3	CH_3	1 215	230	8	0.66	0.30
C_2H_5	C_2H_5	1 208	120	10.5	0.45	0.20
$CH(CH_3)_2$	$CH(CH_3)_2$	1 201	100	8.5	0.30	0.13
$C(CH_3)_3$	$C(CH_3)_3$	1 218	285	12	1.24	0.54

Although this band near 1 200 cm^{-1} is clearly not a "pure" C—O stretching band and bands of this type are known to be affected on substitution (for example, by isotopic modification (15)) a possible explanation of the observed spectral changes is in terms of different conformations. That is, in conformation 2 (the preferred form for *o*-alkyl-substituted anisoles), but not in conformation 4 (the preferred form for *o,o'*-dialkyl-substituted anisoles), there may be in addition to the C—O dipole, a dipole caused by the interaction of the lone pair electrons with the π-electrons of the benzene ring which gives rise to a shortening of the aryl—O nuclear bond. This would therefore suggest that compounds which exist in form 2—i.e., compounds in which p–π conjugation occurs —should absorb at higher frequency. It has also been shown that a conjugated carbonyl group affords a more intense band (16), so that it is possible that the lower intensities in *o,o'*-dialkyl-substituted anisoles are due to steric inhibition of this p–π conjugation.

It may next be noted that the infrared stretching bands are generally symmetrical and show no pronounced fine structure, such as might be anticipated if the molecules existed in more than one conformation. A typical spectrum is shown in Fig. 2. The absorption observed at 1 039 cm^{-1} in anisole has been provisionally assigned to the O—methyl stretching vibration (17), although it is probable that this vibration actually occurs at 1 172 cm^{-1} (18). Since there is a closely spaced band at 1 182 cm^{-1} with only slightly lower intensity, the effects of *o*- and *o,o'*-alkyl substitution on this band were not investigated.

Dipole Moments

Additional indications that *o,o'*-dialkyl substitution in anisole can twist the methoxy group from the plane of the benzene ring may be obtained from dipole moment data. The dipole moment in benzene solution of anisole is 1.28 D (19) and that of dimethyl ether is 1.25 D (20). Since the dipoles of an unshared electron pair on an oxygen atom in the sp^3 hydridization state are approximately 1.4 D per electron (9), this indicates that the dipole moments of anisole and of dimethyl ether are caused by the dipole moment of the two lone electron pairs *less* the dipoles of the two bonded groups. The dipole moment of the aryl—O moiety will be made up of a number of components

Can. J. Chem. Downloaded from www.nrcresearchpress.com by 210.87.254.42 on 09/05/12
For personal use only.

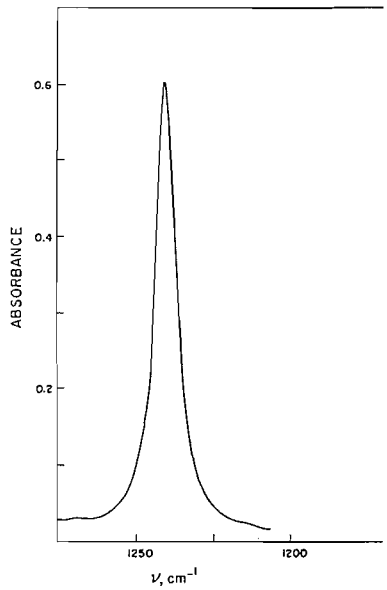

FIG. 2. Infrared aryl—O stretching band of *o*-isopropylanisole.

including an inductive component and a mesomeric component and it is this latter component which is likely to be absent in a substituted anisole existing in form 4. This latter component will tend to shorten the aryl—O nuclear bond, and its removal will therefore cause a reduction in the overall dipole moment. A dipole moment of 1.24 D in benzene solution is, in fact, observed for *o,o'*-dimethylanisole (19) and consequently the data may be regarded as consistent with the interpretation deduced from absorption spectra.

Other Data

Fong and Smyth (21) have recently shown, using microwave absorption techniques, that *o,o'*-dimethylanisole is highly sterically hindered. Le Fèvre *et al.* (22) conclude from a study of molecular polarizabilities that the C_{Ar}—O—C_{Me} plane in this compound is orthogonal with the benzene ring. These data are therefore again consistent with our evidence that *o,o'*-dialkyl-substituted anisoles exist in a different conformation from *o*-alkyl-substituted anisoles or anisole itself.

ACKNOWLEDGMENTS

The authors thank Professor N. Kornblum of Purdue University for a generous sample of *o,o'*-di-*t*-butylanisole. They are indebted to Miss M. A. Shadbolt for competent technical assistance. Financial assistance from the National Research Council of Canada is also gratefully acknowledged.

REFERENCES

1. L. J. FROLEN and L. GOODMAN. J. Am. Chem. Soc. **83**, 3405 (1961).
2. E. G. MCRAE and L. GOODMAN. J. Mol. Spectry. **2**, 464 (1958).
3. J. C. DEARDEN and W. F. FORBES. Can. J. Chem. **37**, 1305 (1959).
4. G. BADDELEY, N. H. P. SMITH, and M. A. VICKARS. J. Chem. Soc. 2455 (1956).
5. B. T. COMMINS and A. J. LINDSEY. Anal. Chim. Acta, **15**, 446 (1956).
6. R. N. JONES, W. F. FORBES, and W. A. MUELLER. Can. J. Chem. **35**, 504 (1957).
7. D. A. RAMSAY. J. Am. Chem. Soc. **74**, 72 (1952).

Can. J. Chem. Downloaded from www.nrcresearchpress.com by 210.87.254.42 on 09/05/12
For personal use only.

8. K. S. SESHADRI and R. N. JONES. Spectrochim. Acta. **19**, 1013 (1963).
9. W. J. ORVILLE-THOMAS. *In* Foundations of modern chemical theories. *Edited by* W. F. Forbes and W. J. Orville-Thomas. Elsevier Inc., New York. 1965.
10. B. M. WEPSTER. Rec. Trav. Chim. **76**, 357 (1957).
11. J. C. DEARDEN and W. F. FORBES. Can. J. Chem. **38**, 1837 (1960).
12. A. BURAWOY and J. T. CHAMBERLAIN. J. Chem. Soc. 2310 (1952).
13. A. L. SKLAR. Revs. Mod. Phys. **14**, 232 (1942); J. Chem. Phys. **10**, 135 (1942).
14. T. W. CAMPBELL and G. M. COPPINGER. J. Am. Chem. Soc. **73**, 2708 (1951).
15. A. C. ALBRECHT. J. Mol. Spectry. **5**, 236, 256 (1960).
16. G. M. BARROW. J. Chem. Phys. **21**, 2008 (1953).
17. K. W. F. KOHLRAUSCH. Monatsh. **76**, 231 (1947).
18. J. H. S. GREEN. Spectrochim. Acta. **18**, 39 (1962).
19. H. LUMBROSO and G. DUMAS. Bull. Soc. Chim. France, 651 (1955).
20. G. A. BARCLAY and R. J. W. LE FÈVRE. J. Chem. Soc. 1643 (1952).
21. F. K. FONG and C. P. SMYTH. J. Chem. Phys. **40**, 2404 (1964).
22. M. J. ARONEY, M. G. CORFIELD, and R. J. W. LE FÈVRE. J. Chem. Soc. 2954 (1964).

Can. J. Chem. Downloaded from www.nrcresearchpress.com by 210.87.254.42 on 09/05/12
For personal use only.

Can. J. Chem. Downloaded from www.nrcresearchpress.com by 210.87.254.105 on 09/05/12
For personal use only.

THE SYNTHESIS OF 2-AMINOBENZENETHIOL HYDROCHLORIDES

RALPH L. DANNLEY AND DIMITRI A. ZAZARIS

Representative 2-aminobenzenethiols were needed to synthesize a series of phosphothiazoles. Surprisingly few of the simple aminothiols are known, the yields are generally poor, and experimental details are often lacking. Much of the difficulty is due to the facile oxidation to disulfides, particularly in alkaline media. It was therefore decided to prepare the hydrochloride salts to obtain greater stability. The salts may be converted to the free aminothiols *in situ* either by treatment with a base or by thermal decomposition in an inert solvent (1). The previously unknown but typical 2-aminobenzenethiols which have been prepared are shown in Table I.

TABLE I

Yields, melting points, and analyses for 2-aminobenzenethiol hydrochlorides

2-Aminobenzenethiol hydrochloride	m.p.*	Yield†	Calcd.			Found‡		
			C	H	N	C	H	N
4-Methyl	189–191§	65	47.85	5.73	8.02	47.83	6.00	7.90
4-Trifluoromethyl	200–202‖	46	36.68	3.07	6.10	36.45	2.94	6.15
4-Carboxy	267–268‖	27	41.00	3.92	6.82	40.77	3.88	6.76
4-Carbomethoxy	198–201¶	59	43.72	4.59	6.37	42.91	4.57	6.22
4-Methoxy	210–211¶	35	44.06	5.25	7.37	44.13	4.82	7.48
5-Methoxy	208–209‖	20	43.80	5.22	7.32	43.60	5.28	7.25
4-Nitro	218–219‖	30	—	—	13.56	—**	—**	13.45**

*All melt with decomposition.
†Yields of crude products suitable for most purposes.
‡Analyses performed by Galbraith Laboratories, Knoxville, Tenn.
§From methanol – hydrochloric acid, 1:1.
‖From ethanol – hydrochloric acid (1:1).
¶From methanol saturated with dry hydrogen chloride.
**This hydrochloride salt was too unstable to survive mailing to an analytical laboratory. A Kjeldahl nitrogen analysis was performed on a fresh sample.

The reduction of *o*-nitrophenyl disulfides, a common route to aminothiols, was used in much of the present work. The required sulfides were obtained from *o*-nitrochlorobenzenes and sodium polysulfides. The mixture of di- and tri-sulfides which was thus formed usually was not separated since both yield the thiol on reduction.

Catalytic hydrogenation of the sulfides to the aminothiols was attempted unsuccessfully. Reduction with tin and hydrochloric acid produced the aminothiol hydrochlorides in good yield, however.

4-Carbomethoxy-2-aminobenzenethiol hydrochloride was not prepared directly from the chloro compound through the sulfide, for the ester would be saponified by the strongly alkaline polysulfides. Esterification of the corresponding carboxylic acid proceeded smoothly, however.

The direct replacement of a halogen by the thiol group (or its salt) is generally undesirable because of competitive diaryl sulfide formation. 4-Nitro-2-aminobenzenethiol was prepared in this way, however, to avoid a subsequent reduction of the nitro group.

An alternate route to the aminothiols is by cleavage of benzothiazoles. These hydrolyses

have conventionally been carried out in small quantities in sealed tubes. It has now been found that in a larger scale synthesis of 5-methoxy-2-aminobenzenethiol, hydrolysis of the thiazole in a refluxing aqueous alkaline solution is accomplished in 7 h.

The aminothiol hydrochlorides all exhibited peaks at 3.7 to 4.0 μ in their infrared spectra characteristic of the SH group.

EXPERIMENTAL

bis-(4-Methyl-2-nitrophenyl)trisulfide

Sodium tetrasulfide was obtained by dissolving sulfur (48 g, 1.5 g-atoms) in molten sodium sulfide enneahydrate (120 g, 0.5 mole). This hot liquid was added dropwise to 3-nitro-4-chlorotoluene (171 g, 1.0 mole) in 95% ethanol (700 ml). After the exothermic reaction had ceased, the mixture was refluxed (2 h) and filtered while hot, and the precipitate washed with water (200 ml) and ethanol (100 ml) to give 155 g (84%) of crude product suitable for reduction to the aminobenzenethiol. Recrystallization from glacial acetic acid gave pure bis-(4-methyl-2-nitrophenyl) trisulfide, m.p. 195.5°.

Anal. Calcd. for $C_{14}H_{12}N_2O_4S_3$: C, 45.62; H, 3.28; S, 26.0. Found: C, 45.52; H, 3.31; S, 25.77.

4-Methyl-2-aminobenzenethiol Hydrochloride (a Typical Reduction)

Concentrated hydrochloric acid (730 ml) was slowly added (4 h) at 70° to a well-stirred suspension of the trisulfide (200 g, 0.55 mole) just described, 95% ethanol (1 200 ml), and tin (520 g). After filtration of the hot solution, the filtrate was allowed to stand at room temperature overnight to precipitate a crude product containing tin salts. The precipitate was collected on a filter, washed with ethanol – hydrochloric acid (50:50), and dissolved in hot methanol – hydrochloric acid (50:50). Upon cooling of the methanol solution, tin salts precipitated immediately and were removed by filtration. The filtrate, after several hours, deposited white needles of 4-methyl-2-aminobenzenethiol hydrochloride (125 g, 65%) which were collected and washed with ice-cold methanol – hydrochloric acid. A second recrystallization gave the pure salt (25 g, 13%).

4-Trifluoromethyl-2-aminobenzenethiol Hydrochloride

This compound was obtained by an identical procedure except for the use of 2 000 ml of ethanol per mole of nitro compound.

4-Carboxy-2-aminobenzenethiol Hydrochloride

Sodium disulfide was obtained by adding sulfur (48 g, 1.5 g-atoms) to molten sodium sulfide enneahydrate (360 g, 1.5 moles). This molten mixture was added to a solution of 3-nitro-4-chlorobenzoic acid (300 g, 1.5 moles) in sodium hydroxide (40 g,), water (50 ml), and ethanol (900 ml). After the resultant mixture had been heated under reflux (4 h) and then cooled, the crude disulfide precipitated. The reduction was accomplished as described above.

4-Carbomethoxy-2-aminobenzenethiol Hydrochloride

A mixture of 4-carboxy-2-aminobenzenethiol hydrochloride (40 g, 0.2 mole) and absolute methanol (110 ml) saturated with dry hydrogen chloride was kept overnight at 50–60° and filtered while warm, and the filtrate cooled and saturated again with dry hydrogen chloride. The precipitated 4-carbomethoxy-2-aminobenzenethiol hydrochloride (16 g, 35%) m.p. 198–201°, was collected by filtration and washed with cold methanol saturated with hydrogen chloride. Evaporation of the mother liquor to 25 ml produced more product (10 g, 60% total yield) of m.p. 196–197°.

4-Methoxy-2-aminobenzenethiol Hydrochloride

The sluggish reactivity of the corresponding chloronitro compound in dilute solution necessitated the following procedure to yield the disulfide. A mixture of 3-nitro-4-chloroanisole (183 g, 1.0 mole) and molten sodium disulfide hydrate (272 g, 1.0 mole prepared as described above) was stirred and cooled to maintain a temperature of 105–110°. When the temperature dropped to 40°, the dark mass was extracted with five 200-ml portions of 95% ethanol. The combined ethanol extracts were passed through a column of neutral alumina which adsorbed at least three impurities (distinct bands). To the eluent was added tin (700 g) and hydrochloric acid (1 000 ml). After the spontaneous refluxing ceased, the mixture was heated to 70–80° for 1 h. The mixture was filtered and the filtrate evaporated to 700 ml, hydrochloric acid (500 ml) was added, and the acid solution cooled to precipitate a crude aminothiol hydrochloride contaminated with tin salts. The crude product was dissolved in 200 ml of hot ethanol, filtered to remove tin salts, and the hydrochloride crystallized (67 g, 35% yield) by adding hydrochloric acid (200 ml) and cooling. Recrystallization from methanol saturated with dry hydrogen chloride produced 4-methoxy-2-aminobenzenethiol hydrochloride, m.p. 210–211°.

5-Methoxy-2-aminobenzenethiol Hydrochloride

A mixture of 2-amino-6-methoxybenzothiazole (100 g, 0.55 mole), potassium hydroxide (170 g, 3.0 moles), and water (500 ml) was refluxed until ammonia (70% yield) was no longer evolved (7 h). The solution was cooled, neutralized with acetic acid, and filtered. The precipitate was washed with water, dissolved in hot

Can. J. Chem. Downloaded from www.nrcresearchpress.com by 210.87.254.105 on 09/05/12
For personal use only.

95% ethanol (200 ml), and filtered. The addition of concentrated hydrochloric acid (200 ml) followed by cooling of the solution yielded 5-methoxy-2-aminobenzenethiol hydrochloride (17 g, 20%), m.p. 208–209° (lit. (2) m.p. 210–211 decomp.) after recrystallization from ethanol – hydrochloric acid. A small portion was converted to the free aminothiol, m.p. 102–103° (lit. (3) m.p. 103–105°).

4-Nitro-2-aminobenzenethiol Hydrochloride

A hot solution of sodium sulfide enneahydrate (48 g, 0.20 mole, in a minimum amount of water) was added slowly to a boiling mixture of 5-nitro-2-bromoaniline (4) (54 g, 0.25 mole) and absolute ethanol (150 ml). After the exothermic reaction had subsided, the mixture was refluxed for 1 h and then cooled. The red crystalline precipitate was collected by filtration and treated with three 100-ml portions of water. From this point on the procedure was carried out under a nitrogen atmosphere. The aqueous extracts were acidified to litmus with 10% hydrochloric acid and the precipitated free aminothiol collected on a filter, then immediately dissolved in 95% ethanol (100 ml). The ethanolic solution was clarified by filtration, concentrated hydrochloric acid added (100 ml), and the mixture saturated with dry hydrogen chloride. Upon cooling, 4-nitro-2-aminobenzenethiol hydrochloride precipitated. Recrystallization from ethanol – hydrochloric acid gave crystals (15 g, 30%), m.p. 218–219°.

ACKNOWLEDGMENT

Grateful acknowledgement is made for financial support by Public Health Service Grant CY-04104 and by a Texaco Co. Fellowship.

1. R. L. DANNLEY and P. L. WAGNER. J. Org. Chem. **26**, 3995 (1961).
2. H. H. FOX and M. T. BOGERT. J. Am. Chem. Soc. **61**, 2013 (1939).
3. T. TAKAHASHI, J. SHIBASAKI, and J. OKADA. J. Pharm. Soc. Japan, **71**, 41 (1951).
4. H. L. WHEELER. Am. Chem. J. **17**, 697 (1895).

RECEIVED MARCH 1, 1965.
MORLEY CHEMICAL LABORATORY,
WESTERN RESERVE UNIVERSITY,
CLEVELAND 6, OHIO.

Can. J. Chem. Downloaded from www.nrcresearchpress.com by 210.87.254.105 on 09/05/12
For personal use only.

cis–trans ISOMERISM IN 2-ARYLIDENE-3,3-DIPHENYLINDAN-1-ONES[1]

J. A. BEVAN, P. E. GAGNON, AND I. D. RAE

INTRODUCTION

The condensation of aromatic aldehydes with 3,3-diphenylindan-1-one, reported by Gagnon and Charette (1), gave rise to pairs of compounds identified as belonging to the isomeric series I and II. The members of each pair could be separated by crystallization and gave rise to the same substituted indanone on hydrogenation of the benzylidene double bond.

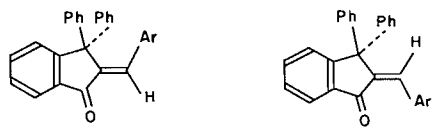

SERIES I — 474 – 496 c/s

SERIES II — 404 – 423 c/s

[1]*Issued as N.R.C. No. 8533.*

95% ethanol (200 ml), and filtered. The addition of concentrated hydrochloric acid (200 ml) followed by cooling of the solution yielded 5-methoxy-2-aminobenzenethiol hydrochloride (17 g, 20%), m.p. 208–209° (lit. (2) m.p. 210–211 decomp.) after recrystallization from ethanol – hydrochloric acid. A small portion was converted to the free aminothiol, m.p. 102–103° (lit. (3) m.p. 103–105°).

4-Nitro-2-aminobenzenethiol Hydrochloride

A hot solution of sodium sulfide enneahydrate (48 g, 0.20 mole, in a minimum amount of water) was added slowly to a boiling mixture of 5-nitro-2-bromoaniline (4) (54 g, 0.25 mole) and absolute ethanol (150 ml). After the exothermic reaction had subsided, the mixture was refluxed for 1 h and then cooled. The red crystalline precipitate was collected by filtration and treated with three 100-ml portions of water. From this point on the procedure was carried out under a nitrogen atmosphere. The aqueous extracts were acidified to litmus with 10% hydrochloric acid and the precipitated free aminothiol collected on a filter, then immediately dissolved in 95% ethanol (100 ml). The ethanolic solution was clarified by filtration, concentrated hydrochloric acid added (100 ml), and the mixture saturated with dry hydrogen chloride. Upon cooling, 4-nitro-2-aminobenzenethiol hydrochloride precipitated. Recrystallization from ethanol – hydrochloric acid gave crystals (15 g, 30%), m.p. 218–219°.

ACKNOWLEDGMENT

Grateful acknowledgement is made for financial support by Public Health Service Grant CY-04104 and by a Texaco Co. Fellowship.

1. R. L. DANNLEY and P. L. WAGNER. J. Org. Chem. **26**, 3995 (1961).
2. H. H. FOX and M. T. BOGERT. J. Am. Chem. Soc. **61**, 2013 (1939).
3. T. TAKAHASHI, J. SHIBASAKI, and J. OKADA. J. Pharm. Soc. Japan, **71**, 41 (1951).
4. H. L. WHEELER. Am. Chem. J. **17**, 697 (1895).

RECEIVED MARCH 1, 1965.
MORLEY CHEMICAL LABORATORY,
WESTERN RESERVE UNIVERSITY,
CLEVELAND 6, OHIO.

Can. J. Chem. Downloaded from www.nrcresearchpress.com by 210.87.254.42 on 09/05/12
For personal use only.

cis–trans ISOMERISM IN 2-ARYLIDENE-3,3-DIPHENYLINDAN-1-ONES[1]

J. A. BEVAN, P. E. GAGNON, AND I. D. RAE

INTRODUCTION

The condensation of aromatic aldehydes with 3,3-diphenylindan-1-one, reported by Gagnon and Charette (1), gave rise to pairs of compounds identified as belonging to the isomeric series I and II. The members of each pair could be separated by crystallization and gave rise to the same substituted indanone on hydrogenation of the benzylidene double bond.

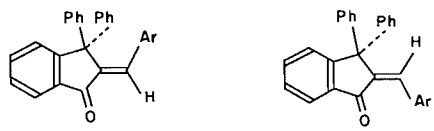

SERIES I — 474 – 496 c/s

SERIES II — 404 – 423 c/s

[1]*Issued as N.R.C. No. 8533.*

Throughout the series the lower melting isomer was also the more soluble and more labile, and was therefore assigned the "*cis*" configuration (I) by analogy with simple *cis–trans* systems (2). The compounds have now been re-examined using nuclear magnetic resonance spectroscopy and some revision of the original assignments has been necessary. It was anticipated that the benzylidene protons of series I would be strongly deshielded by the adjacent carbonyl while those of series II would be relatively unaffected (3). In fact both types of proton gave rise to sharp singlets which were well separated from the complex signals of the aromatic protons, and assignment of configuration presented little difficulty. The results are summarized in Table I.

TABLE I

Nuclear magnetic resonance spectra of 2-arylidene-3,3-diphenylindan-1-ones (cycles per second downfield from tetramethylsilane, at 60 Mc/s)

Group Ar—	M.p.	Earlier assignment	New assignment	Chemical shift (c/s) Benzylidene proton	Chemical shift (c/s) Ring substit.
C_6H_5—	172°	I	I	478	—
	192°	II	II	409.5	—
p-Cl—C_6H_4—	176°	I	II	404.5	—
	201°	II	I	474	—
p-MeO—C_6H_4—	133°	I	II	414	223
	163°	II	I	479	214.5
m-Me—C_6H_4—	104°	I	II	407	140
	175°	II	I	474.5	121
o-Cl—C_6H_4—	151°	I	I	477	—
	197°	II	II	423	—
o-Me—C_6H_4—	176°	I	I	474.5	95
	190°	II	II	418	120
o-MeO—C_6H_4—	182°.	I	II	414	222.5
	216°	II	I	492	212
o-EtO—C_6H_4—	153°	I	II	409	70, 230*
	161°	II	I	496	72, 224*

*Methyl and methylene protons respectively.

DISCUSSION OF SPECTRA

The relatively deshielded benzylidene protons of compounds in series I gave rise to sharp singlets in the narrow range 474–479 c/s except in the two cases where *o*-alkoxy substituents were present in the benzylidene ring, but the positions were more variable in series II. The proton magnetic resonance (p.m.r.) spectrum of the 2-benzylidene-indan-1-one analogous to series I has been reported (4) and a signal at 453 c/s assigned to the benzylidene proton. When bulky substituents are present in the 3-position of the indanone moiety the benzylidene substituent is probably forced closer to the carbonyl, resulting in the greater deshielding of the benzylidene proton (by 25 c/s), which was observed with 2-benzylidene-3,3-diphenylindan-1-ones.

Certain other differences in the spectra of isomeric pairs were attributable to the proximity of 3,3-diphenyl substituents and the benzylidene ring in series I. Thus in this series the protons of the two phenyl groups give rise to multiplets which merge with those of the other aromatic protons in the molecule, whereas in series II they give rise to 10-proton singlets at 435–438 c/s which are clearly distinguishable. Similarly in series I the substituents in the benzylidene ring are shielded by the nearer of the two phenyl groups,

Can. J. Chem. Downloaded from www.nrcresearchpress.com by 210.87.254.42 on 09/05/12
For personal use only.

and the chemical shifts of both methyl and methoxyl protons are considerably less than those of toluene (140 c/s) (5*a*) and anisole (226 c/s) (5*b*) respectively. In series II, however, the chemical shifts of protons in such substituents are quite normal, with the exception of those in the *o*-methyl group which are still shielded to the extent of 20 c/s. In this case steric interactions are best reduced by location of the methyl group out of the indanone plane where it could suffer shielding, for example, from the carbonyl group in some conformations.

EXPERIMENTAL

Proton magnetic resonance spectra were recorded on a Varian A-60 spectrometer for dilute solutions (ca. 5%) in deuterochloroform with tetramethylsilane as internal standard.

ACKNOWLEDGMENTS

The authors are grateful to Mr. M. Lesage, who recorded the p.m.r. spectra. This work was carried out during the tenure of Postdoctorate awards held by J. A. B. and I. D. R.

1. P. E. GAGNON and L. P. CHARETTE. Can. J. Res. B, **19**, 275 (1941).
2. E. L. ELIEL. Stereochemistry of carbon compounds. McGraw-Hill Book Company, Inc., New York. 1962. p. 326.
3. L. M. JACKMAN. Applications of nuclear magnetic resonance spectroscopy in organic chemistry. Pergamon Press, Oxford. 1959. Section 7.3, p. 119.
4. NMR spectra catalog. Vol. 2. Varian Associates, Palo Alto, California. 1963. Spectrum no. 649.
5. (*a*) NMR spectra catalog. Vol. 1. Varian Associates, Palo Alto, California. 1962. Spectrum no. 157. (*b*) NMR spectra catalog. Vol. 1. Varian Associates, Palo Alto, California. 1962. Spectrum no. 162.

RECEIVED MARCH 15, 1965.
DIVISION OF PURE CHEMISTRY,
NATIONAL RESEARCH COUNCIL,
OTTAWA, CANADA.

BASICITIES OF METHYLTHIO- AND PHENYLTHIO-ANILINES[1]

IAN D. RAE[2]

An extensive spectral study of aryl sulfides has led to the conclusion that electron-pair acceptance by the sulfur atom is not an important process in these molecules (1), and it is generally believed that such electron-accepting properties as sulfur does possess will only become prominent when the sulfur atom bears at least a partial positive charge (2). However, a recent study of the dissociation constants of arylthio-phenols has revealed effects which are best explained by proposing that the sulfur atom can accept an electron pair (3).

A bivalent sulfur atom attached to an aromatic ring may interact electronically with the ring in three main ways, by inductive withdrawal of electrons from the ring and by mesomeric donation and acceptance of electrons. In alkylthio- and arylthio-anilines, the inductive effect of the thio-substituent, operating both in the free amine and its conjugate cation, tends to reduce the basicity of the nitrogen atom. This effect falls off as the number of bonds between the sulfur and nitrogen atoms increases and the variation in effect with the position of the substituent should be $o > m > p$. The other electron-withdrawing mechanism available to sulfur, electron-pair acceptance, depends on the

[1]*Issued as N.R.C. No. 8532.*
[2]*Present address: Division of Pure Chemistry, National Research Council, Ottawa 2.*

Can. J. Chem. Downloaded from www.nrcresearchpress.com by 210.87.254.42 on 09/05/12
For personal use only.

and the chemical shifts of both methyl and methoxyl protons are considerably less than those of toluene (140 c/s) (5*a*) and anisole (226 c/s) (5*b*) respectively. In series II, however, the chemical shifts of protons in such substituents are quite normal, with the exception of those in the *o*-methyl group which are still shielded to the extent of 20 c/s. In this case steric interactions are best reduced by location of the methyl group out of the indanone plane where it could suffer shielding, for example, from the carbonyl group in some conformations.

EXPERIMENTAL

Proton magnetic resonance spectra were recorded on a Varian A-60 spectrometer for dilute solutions (ca. 5%) in deuterochloroform with tetramethylsilane as internal standard.

ACKNOWLEDGMENTS

The authors are grateful to Mr. M. Lesage, who recorded the p.m.r. spectra. This work was carried out during the tenure of Postdoctorate awards held by J. A. B. and I. D. R.

1. P. E. GAGNON and L. P. CHARETTE. Can. J. Res. B, **19**, 275 (1941).
2. E. L. ELIEL. Stereochemistry of carbon compounds. McGraw-Hill Book Company, Inc., New York. 1962. p. 326.
3. L. M. JACKMAN. Applications of nuclear magnetic resonance spectroscopy in organic chemistry. Pergamon Press, Oxford. 1959. Section 7.3, p. 119.
4. NMR spectra catalog. Vol. 2. Varian Associates, Palo Alto, California. 1963. Spectrum no. 649.
5. (*a*) NMR spectra catalog. Vol. 1. Varian Associates, Palo Alto, California. 1962. Spectrum no. 157. (*b*) NMR spectra catalog. Vol. 1. Varian Associates, Palo Alto, California. 1962. Spectrum no. 162.

RECEIVED MARCH 15, 1965.
DIVISION OF PURE CHEMISTRY,
NATIONAL RESEARCH COUNCIL,
OTTAWA, CANADA.

BASICITIES OF METHYLTHIO- AND PHENYLTHIO-ANILINES[1]

IAN D. RAE[2]

An extensive spectral study of aryl sulfides has led to the conclusion that electron-pair acceptance by the sulfur atom is not an important process in these molecules (1), and it is generally believed that such electron-accepting properties as sulfur does possess will only become prominent when the sulfur atom bears at least a partial positive charge (2). However, a recent study of the dissociation constants of arylthio-phenols has revealed effects which are best explained by proposing that the sulfur atom can accept an electron pair (3).

A bivalent sulfur atom attached to an aromatic ring may interact electronically with the ring in three main ways, by inductive withdrawal of electrons from the ring and by mesomeric donation and acceptance of electrons. In alkylthio- and arylthio-anilines, the inductive effect of the thio-substituent, operating both in the free amine and its conjugate cation, tends to reduce the basicity of the nitrogen atom. This effect falls off as the number of bonds between the sulfur and nitrogen atoms increases and the variation in effect with the position of the substituent should be $o > m > p$. The other electron-withdrawing mechanism available to sulfur, electron-pair acceptance, depends on the

[1]*Issued as N.R.C. No. 8532.*
[2]*Present address: Division of Pure Chemistry, National Research Council, Ottawa 2.*

Can. J. Chem. Downloaded from www.nrcresearchpress.com by 210.87.254.105 on 09/05/12
For personal use only.

participation of the sulfur *d*-orbitals either in a bonding or non-bonding capacity. Such electron acceptance might lead to conjugation between the nitrogen and sulfur atoms in the free amines (formulae I and II) but such interactions are not possible in *m*-isomers so the substituent effects should be in the order $o, p > m$. Because of the difference in primary quantum number between the sulfur lone-pair electrons (3p) and the aromatic π-electrons (2p) the third process, electron-pair donation to the aromatic ring, is less important for sulfur than it is for oxygen (4, 10).

All the substituted anilines recorded in Table I are less basic than aniline itself since electron-withdrawing effects predominate, and the variation of pK_a values with the position of the substituent relative to nitrogen shows that inductive effects outweigh mesomeric effects.

TABLE I

pK_a values of methylthio- and phenylthio-anilines in water at 25 °C

Substituent	pK_a	Substituent	pK_a
None	4.58 (10)	None	4.58 (10)
o-SCH_3	3.57	*o*-SC_6H_5	2.87, (2.5) (13)
m-SCH_3	4.05 (10)	*m*-SC_6H_5	3.69
p-SCH_3	4.40 (10)	*p*-SC_6H_5	3.91

EXPERIMENTAL

The pK_a values were measured spectrophotometrically using the technique described by Albert and Serjeant (5). The buffers employed had ionic strength 0.01 (6). Pure *o*-methylthioaniline was available commercially and the *o*- and *p*-phenylthioanilines were prepared by the method of Gilman and Broadbent (7). *m*-Phenylthioaniline was prepared by diazotization of *m*-acetamidoaniline and coupling of the diazonium salt with sodium thiophenoxide, followed by hydrolysis of the N-acetyl group; its properties agreed with those recorded in the literature (8).

DISCUSSION

The data presented by Taft (9) support the generalization that, for electron-withdrawing substituents which operate principally by induction, the pK_a values of *o*-, *m*-, and *p*-substituted anilines and aniline itself form a monotonically increasing series. For example, the chloroanilines (2.64, 3.34, 3.98, and 4.58) (10) and the second protonation of phenylenediamines (1.2, 2.8, 3.0, and 4.58).* Clearly the methylthio- and phenylthio-anilines form such series and it may be deduced that the inductive effect of the sulfur atom is the chief base-weakening factor. The greater inductive effect of the phenylthio-substituent is no doubt due to resonance involving structures III and IV which have been proposed to explain spectral (1) and kinetic findings (12). While the effect of both methylthio- and phenylthio-substituents is predominantly inductive, it is possible that the two mesomeric processes also operate, but, in opposite senses, to produce only a small net effect.

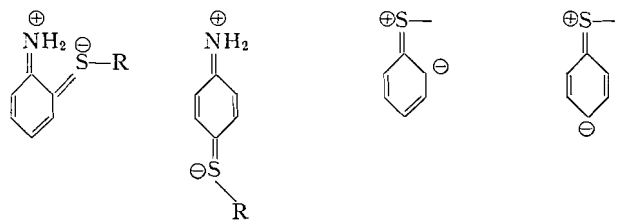

I II III IV

* *Values calculated from the data given in ref. 11.*

Can. J. Chem. Downloaded from www.nrcresearchpress.com by 210.87.254.105 on 09/05/12
For personal use only.

From the pK_a values presented here the σ_m and σ_p values for C_6H_5S are calculated to be 0.31 and 0.24 respectively. These should be compared with the values, 0.18 and 0.29, derived by Meyers (3) for the corresponding phenols.

ACKNOWLEDGMENT

The author acknowledges helpful discussion with Dr. R. F. C. Brown and Dr. J. M. Brown.

1. R. C. PASSERINI. *In* Organic sulfur compounds. Vol. I. *Edited by* N. Kharasch. Pergamon Press, London. 1961.
2. C. C. PRICE. Chem. Eng. News, **42**, No. 48, 58 (1964).
3. C. Y. MEYERS. Gazz. Chim. Ital. **93**, 1206 (1963).
4. C. C. PRICE and S. OAE. Sulfur bonding. The Ronald Press Company, New York. 1962. pp. 16, 26.
5. A. ALBERT and E. P. SERJEANT. Ionization constants of acids and bases. Methuen and Co., Ltd., London. 1962. Chap. 4.
6. D. D. PERRIN. Australian J. Chem. **16**, 572 (1963).
7. H. GILMAN and H. S. BROADBENT. J. Am. Chem. Soc. **69**, 2053 (1947).
8. A. MANGINI, R. PASSERINI, and S. SERRA. Gazz. Chim. Ital. **84**, 47 (1954).
9. R. W. TAFT, JR. *In* Steric effects in organic chemistry. *Edited by* M. S. Newman. John Wiley and Sons, Inc., New York. 1956. Chap. 13.
10. F. G. BORDWELL and G. D. COOPER. J. Am. Chem. Soc. **74**, 1058 (1952).
11. J. CLARK and D. D. PERRIN. Quart. Rev. London, **18**, 295 (1964).
12. C. C. PRICE and S. OAE. Sulfur bonding. The Ronald Press Company, New York. 1962. p. 10.
13. B. ROTH and J. F. BUNNETT. J. Am. Chem. Soc. **87**, 334 (1965).

RECEIVED APRIL 20, 1965.
CHEMISTRY DEPARTMENT,
SCHOOL OF GENERAL STUDIES,
AUSTRALIAN NATIONAL UNIVERSITY,
CANBERRA, AUSTRALIA.

Can. J. Chem. Downloaded from www.nrcresearchpress.com by 210.87.254.105 on 09/05/12
For personal use only.

SOME COMMENTS ON CRAIG'S RULES

R. A. ABRAMOVITCH AND K. L. MCEWEN

On the basis of valence bond (v.b.) and other calculations, Craig proposed some rules which would permit the prediction of whether or not a certain fully conjugated hydrocarbon would have a totally symmetric v.b. wave function and hence have aromatic character (1–3). The rule was applied to molecules having at least one twofold axis passing through two or more π-centers, an axis that converts one Kékulé structure into itself or into another of the same canonical set. The molecule is labelled with equal numbers of spin symbols α and β, giving different symbols to the two ends of all double bonds in one Kékulé structure such that as few as possible like spins adjoin. Upon performing the symmetry operation, if the sum of p, the number of interchanges of π-electron centers effected by the operation, and q, the number of interchanges of spin symbols required to restore the original labelling scheme from the transformed one, is even, one finds that the molecule will have a totally symmetric v.b. ground state and it should be aromatic. If $p + q$ is odd, the v.b. ground state is non-totally symmetric and the molecule should not have aromatic stability: it would be pseudoaromatic.

A case in which the application of Craig's rules gives ambiguous results has been reported (4). Structure I*a* can be labelled as shown, leading to $p + q = 7$. On the other

From the pK_a values presented here the σ_m and σ_p values for C_6H_5S are calculated to be 0.31 and 0.24 respectively. These should be compared with the values, 0.18 and 0.29, derived by Meyers (3) for the corresponding phenols.

ACKNOWLEDGMENT

The author acknowledges helpful discussion with Dr. R. F. C. Brown and Dr. J. M. Brown.

1. R. C. PASSERINI. *In* Organic sulfur compounds. Vol. I. *Edited by* N. Kharasch. Pergamon Press, London. 1961.
2. C. C. PRICE. Chem. Eng. News, **42**, No. 48, 58 (1964).
3. C. Y. MEYERS. Gazz. Chim. Ital. **93**, 1206 (1963).
4. C. C. PRICE and S. OAE. Sulfur bonding. The Ronald Press Company, New York. 1962. pp. 16, 26.
5. A. ALBERT and E. P. SERJEANT. Ionization constants of acids and bases. Methuen and Co., Ltd., London. 1962. Chap. 4.
6. D. D. PERRIN. Australian J. Chem. **16**, 572 (1963).
7. H. GILMAN and H. S. BROADBENT. J. Am. Chem. Soc. **69**, 2053 (1947).
8. A. MANGINI, R. PASSERINI, and S. SERRA. Gazz. Chim. Ital. **84**, 47 (1954).
9. R. W. TAFT, JR. *In* Steric effects in organic chemistry. *Edited by* M. S. Newman. John Wiley and Sons, Inc., New York. 1956. Chap. 13.
10. F. G. BORDWELL and G. D. COOPER. J. Am. Chem. Soc. **74**, 1058 (1952).
11. J. CLARK and D. D. PERRIN. Quart. Rev. London, **18**, 295 (1964).
12. C. C. PRICE and S. OAE. Sulfur bonding. The Ronald Press Company, New York. 1962. p. 10.
13. B. ROTH and J. F. BUNNETT. J. Am. Chem. Soc. **87**, 334 (1965).

RECEIVED APRIL 20, 1965.
CHEMISTRY DEPARTMENT,
SCHOOL OF GENERAL STUDIES,
AUSTRALIAN NATIONAL UNIVERSITY,
CANBERRA, AUSTRALIA.

Can. J. Chem. Downloaded from www.nrcresearchpress.com by 210.87.254.105 on 09/05/12
For personal use only.

SOME COMMENTS ON CRAIG'S RULES

R. A. ABRAMOVITCH AND K. L. MCEWEN

On the basis of valence bond (v.b.) and other calculations, Craig proposed some rules which would permit the prediction of whether or not a certain fully conjugated hydrocarbon would have a totally symmetric v.b. wave function and hence have aromatic character (1–3). The rule was applied to molecules having at least one twofold axis passing through two or more π-centers, an axis that converts one Kékulé structure into itself or into another of the same canonical set. The molecule is labelled with equal numbers of spin symbols α and β, giving different symbols to the two ends of all double bonds in one Kékulé structure such that as few as possible like spins adjoin. Upon performing the symmetry operation, if the sum of p, the number of interchanges of π-electron centers effected by the operation, and q, the number of interchanges of spin symbols required to restore the original labelling scheme from the transformed one, is even, one finds that the molecule will have a totally symmetric v.b. ground state and it should be aromatic. If $p + q$ is odd, the v.b. ground state is non-totally symmetric and the molecule should not have aromatic stability: it would be pseudoaromatic.

A case in which the application of Craig's rules gives ambiguous results has been reported (4). Structure I*a* can be labelled as shown, leading to $p + q = 7$. On the other

hand, I*b*, in which the axis of symmetry transforms one Kékulé structure into itself, gives rise to $p + q = 8$. I*a* and I*b* are stated to belong to different group representations and may not contribute to the same linear combination v.b. resonance hybrid (4). The

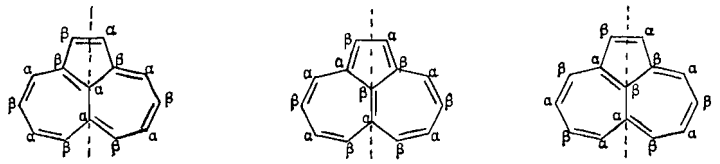

(I*a*) (I*b*) (I*c*)

rules are not clear, however, in that structure (I*c*), in which the double bonds are arranged exactly as in I*a*, appears to be labelled in an acceptable manner but gives $p + q = 12$. It has been pointed out (5), however, that this labelling is not acceptable since, upon performing the symmetry operation, one finds that the resulting Kékulé structure has similar spins at the ends of some double bonds (see also II*a*). This aspect of the rules can be made clearer by specifying that the labelling with equal numbers of spin symbols α and β should be carried out in such a way that they give different symbols to the ends of all double bonds in *both* Kékulé structures. In any event, I exhibits aromatic properties (6). A similar situation obtains with the hydrocarbon (II), the dimethyl derivative of which is reported to exhibit polyolefinic character (7).

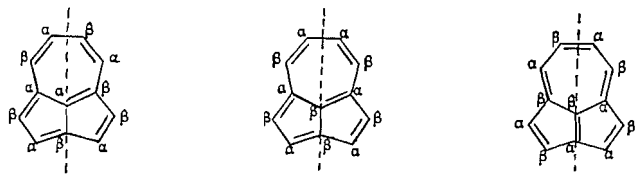

(II*a*) (II*b*) (II*c*)

$p + q = 8$ $p + q = 5$ $p + q = 10$

The rules were also applied to fulvene (III), and the results would indicate that this molecule should be aromatic (1–3). While (III) does exhibit weak aromatic properties

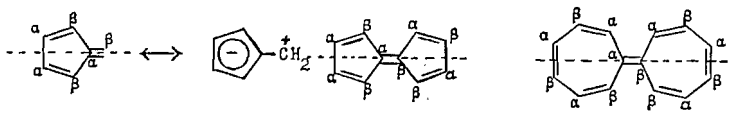

(III) (IV) (V) (VI)

$p + q = 6$ $p + q = 12$

(a measure of which is indicated by its dipole moment of 1·1D (8) caused by contributing structure IV) the rules do not predict the correct answer at all when they are applied to fulvalene (V), which is quite polyolefinic (9). Neither does it hold for heptafulvalene (VI), which does not behave as an aromatic compound (9). It may or may not be significant that in both of these only one uncharged conjugated structure may be written, in which the symmetry operation transforms the molecule into itself. The rules also indicate that the interesting systems VII and VIII (V and VI, respectively, with one extra C—C bond)

Can. J. Chem. Downloaded from www.nrcresearchpress.com by 210.87.254.105 on 09/05/12
For personal use only.

Magnetic Measurements

Magnetic susceptibilities were obtained with a Gouy magnetic balance. The Gouy tubes were calibrated with $Hg[Co(CNS)_4]$. The magnetic data are summarized in Table III. The magnetic moments reported in this table were corrected for diamagnetic contributions by the use of Pascal's constants as indicated by Figgis and Lewis (9).

TABLE III

Magnetic data of N-methyl-γ-butyrolactam complexes

Compound	$\chi_g \times 10^6$	χ_M(corr.) $\times 10^6$	T °K	μ_{eff}, B.M
$[MnL_6](ClO_4)_2$	16.60	14 520	302	5.95
$[FeL_6](ClO_4)_3$	15.56	15 230	303	6.10
$[CoL_6](ClO_4)_2$	13.07	11 570	302	5.31
$[NiL_6](ClO_4)_2$	5.01	4 700	303	3.39

Infrared Spectra

Infrared spectra of the complexes were obtained as chloroform solutions on a Beckman IR-10 recording spectrophotometer.

DISCUSSION

The analytical data of Table I indicate that, except for zinc, the complexes formed are six-coordinate. These might be expected to be octahedral species, a supposition indicated by the magnetic data.

Coordination of the lactam caused no major change in its infrared spectrum except for a shift of the carbonyl stretching vibration. In all cases the frequency of this vibration was lowered on complexation relative to the frequency of the free ligand. Thus the very intense C=O absorption band appearing at 1 680 cm^{-1} in the free lactam gave rise to a strong absorption band shifted of the order of 40 cm^{-1} to lower frequency in the metal ion complexes. Manganese and zinc exhibited the minimum and maximum effects, respectively. In the former case a strong band appeared at 1 645 cm^{-1}; this band appeared at 1 632 cm^{-1} for the latter metal ion. These results are in accord with earlier findings (2), and may be interpreted as evidence for bonding of the ligand to the metal ion through the carbonyl oxygen (3, 5, 10).

From the results of the conductivity measurements appearing in Table II, it can be inferred that the manganese, cobalt, nickel, and zinc complexes are of the 1:2 electrolyte type. These molar conductance values in nitromethane are in reasonable agreement with reference standards determined for this solvent at 20 °C by Gill and Nyholm (11). The iron complex exhibits the expected behavior of a 1:3 electrolyte type.

Finally, the magnetic moments calculated for this series of compounds fall in the range expected for spin-free octahedral complexes (9). The zinc compound, for which data do not appear in Table III, was found to be diamagnetic, as expected.

The above findings are in agreement with the work of Bright and co-workers (6), who found that the electronic spectra of nickel(II) and chromium(III) perchlorate-lactam systems indicated the presence of octahedral species.

ACKNOWLEDGMENTS

The authors gratefully acknowledge the aid of General Aniline and Film Corporation, who supplied the initial sample of lactam, Dr. D. W. Meek and associates of The Ohio State University, who made available a Gouy balance for our use, and the National Research Council of Canada, for financial support. Communication with Drs. D. M. Hart and S. K. Madan is also appreciated.

Can. J. Chem. Downloaded from www.nrcresearchpress.com by 210.87.254.105 on 09/05/12
For personal use only.

1. R. S. DRAGO, D. A. WENZ, and R. L. CARLSON. J. Am. Chem. Soc. **84**, 1106 (1962).
2. C. A. ROLLINSON and R. C. WHITE. Inorg. Chem. **1**, 281 (1962).
3. R. S. DRAGO, D. W. MEEK, M. D. JOESTEN, and L. LAROCHE. Inorg. Chem. **2**, 124 (1963).
4. W. E. BULL, S. K. MADAN, and J. E. WILLIS. Inorg. Chem. **2**, 303 (1963).
5. C. D. SCHMULBACH and D. M. HART. J. Org. Chem. **29**, 3122 (1964).
6. J. H. BRIGHT, R. S. DRAGO, D. M. HART, and S. K. MADAN. Inorg. Chem. 4, 18 (1965). D. M. HART. Personal communication. S. K. MADAN. Personal communication.
7. E. FISHER. J. Chem. Soc. 1382 (1955).
8. K. STARKE. J. Inorg. Nucl. Chem. **11**, 77 (1959).
9. B. N. FIGGIS and J. LEWIS. *In* Modern coordination chemistry. *Edited by* J. Lewis and R. G. Wilkins. Interscience Publishers, Inc., New York. 1960. p. 403.
10. C. D. SCHMULBACH and R. S. DRAGO. J. Am. Chem. Soc. **82**, 4484 (1960).
11. N. S. GILL and R. S. NYHOLM. J. Chem. Soc. 3997 (1959).

RECEIVED APRIL 26, 1965.
DEPARTMENT OF CHEMISTRY,
UNIVERSITY OF WINDSOR,
WINDSOR, ONTARIO.

CONCERNING THE PREPARATION OF *p*-ALLYLPHENOL FROM SAFROLE BY SODIUM – LIQUID AMMONIA REDUCTION

M. J. BALDWIN AND R. K. BROWN

During recent studies (1) of halogen elimination and of halogen and allyl group migration during the rearrangement of allyl 2,6-dichlorophenyl ether (2, 3), some 4-allyl-2-chlorophenol was required as reference material. One possible route for the synthesis of 4-allyl-2-chlorophenol required the precursor *p*-allylphenol. Of the methods available for the preparation of *p*-allylphenol (4–8), that developed by Birch (4), involving the sodium and liquid ammonia reduction of safrole, appeared to be the most convenient and productive.

A repetition of the published procedure with careful attention to Birch's directions, and using anhydrous ethanol with the liquid ammonia, gave a substance whose boiling point agreed with that reported (4, 5) and whose infrared spectrum (neat) supported the structure of *p*-allylphenol.

Gas–liquid chromatography of this substance on a column packing of 20% Apiezon L on Gas-Chrom P (60–80 mesh) with a helium flow rate of 100 ml/min gave only one peak with a shoulder, indicating the presence of two compounds of similar retention times. The ultraviolet spectrum in methanol showed adsorption at 202 μ and 224 μ along with slight absorption at 282 μ. No absorption was found at 244 μ, the region of strong absorption caused by the styrene chromophore (9), thus indicating the absence of *p*-propenylphenol, a product found by Birch (4) when safrole was reduced by sodium in liquid ammonia in the *absence* of alcohol.

The nuclear magnetic resonance (n.m.r.) spectrum of this substance (Fig. 1*a*), in carbon tetrachloride with tetramethylsilane as internal reference, clearly showed it to be a mixture of *p*-allylphenol and *p*-*n*-propylphenol in the molar ratio of 3:1. The boiling points of these two substances are quite similar and are reported to be respectively 236–238° at 760 mm pressure and 232.2–232.5 at 763 mm pressure (5, 10). The allyl group joined to carbon of the benzene ring shows a doublet at 6.75 τ, $J = 7.0$ c.p.s. for the methylene group attached directly to aromatic ring carbon, while the vinyl methylene protons show two characteristic, poorly resolved multiplets centered at 4.90 τ and 5.12 τ.

Can. J. Chem. Downloaded from www.nrcresearchpress.com by 210.87.254.105 on 09/05/12
For personal use only.

1. R. S. DRAGO, D. A. WENZ, and R. L. CARLSON. J. Am. Chem. Soc. **84**, 1106 (1962).
2. C. A. ROLLINSON and R. C. WHITE. Inorg. Chem. **1**, 281 (1962).
3. R. S. DRAGO, D. W. MEEK, M. D. JOESTEN, and L. LAROCHE. Inorg. Chem. **2**, 124 (1963).
4. W. E. BULL, S. K. MADAN, and J. E. WILLIS. Inorg. Chem. **2**, 303 (1963).
5. C. D. SCHMULBACH and D. M. HART. J. Org. Chem. **29**, 3122 (1964).
6. J. H. BRIGHT, R. S. DRAGO, D. M. HART, and S. K. MADAN. Inorg. Chem. 4, 18 (1965). D. M. HART. Personal communication. S. K. MADAN. Personal communication.
7. E. FISHER. J. Chem. Soc. 1382 (1955).
8. K. STARKE. J. Inorg. Nucl. Chem. **11**, 77 (1959).
9. B. N. FIGGIS and J. LEWIS. *In* Modern coordination chemistry. *Edited by* J. Lewis and R. G. Wilkins. Interscience Publishers, Inc., New York. 1960. p. 403.
10. C. D. SCHMULBACH and R. S. DRAGO. J. Am. Chem. Soc. **82**, 4484 (1960).
11. N. S. GILL and R. S. NYHOLM. J. Chem. Soc. 3997 (1959).

RECEIVED APRIL 26, 1965.
DEPARTMENT OF CHEMISTRY,
UNIVERSITY OF WINDSOR,
WINDSOR, ONTARIO.

Can. J. Chem. Downloaded from www.nrcresearchpress.com by 210.87.254.6 on 09/05/12
For personal use only.

CONCERNING THE PREPARATION OF *p*-ALLYLPHENOL FROM SAFROLE BY SODIUM – LIQUID AMMONIA REDUCTION

M. J. BALDWIN AND R. K. BROWN

During recent studies (1) of halogen elimination and of halogen and allyl group migration during the rearrangement of allyl 2,6-dichlorophenyl ether (2, 3), some 4-allyl-2-chlorophenol was required as reference material. One possible route for the synthesis of 4-allyl-2-chlorophenol required the precursor *p*-allylphenol. Of the methods available for the preparation of *p*-allylphenol (4–8), that developed by Birch (4), involving the sodium and liquid ammonia reduction of safrole, appeared to be the most convenient and productive.

A repetition of the published procedure with careful attention to Birch's directions, and using anhydrous ethanol with the liquid ammonia, gave a substance whose boiling point agreed with that reported (4, 5) and whose infrared spectrum (neat) supported the structure of *p*-allylphenol.

Gas–liquid chromatography of this substance on a column packing of 20% Apiezon L on Gas-Chrom P (60–80 mesh) with a helium flow rate of 100 ml/min gave only one peak with a shoulder, indicating the presence of two compounds of similar retention times. The ultraviolet spectrum in methanol showed adsorption at 202 μ and 224 μ along with slight absorption at 282 μ. No absorption was found at 244 μ, the region of strong absorption caused by the styrene chromophore (9), thus indicating the absence of *p*-propenylphenol, a product found by Birch (4) when safrole was reduced by sodium in liquid ammonia in the *absence* of alcohol.

The nuclear magnetic resonance (n.m.r.) spectrum of this substance (Fig. 1*a*), in carbon tetrachloride with tetramethylsilane as internal reference, clearly showed it to be a mixture of *p*-allylphenol and *p*-*n*-propylphenol in the molar ratio of 3:1. The boiling points of these two substances are quite similar and are reported to be respectively 236–238° at 760 mm pressure and 232.2–232.5 at 763 mm pressure (5, 10). The allyl group joined to carbon of the benzene ring shows a doublet at 6.75 τ, $J = 7.0$ c.p.s. for the methylene group attached directly to aromatic ring carbon, while the vinyl methylene protons show two characteristic, poorly resolved multiplets centered at 4.90 τ and 5.12 τ.

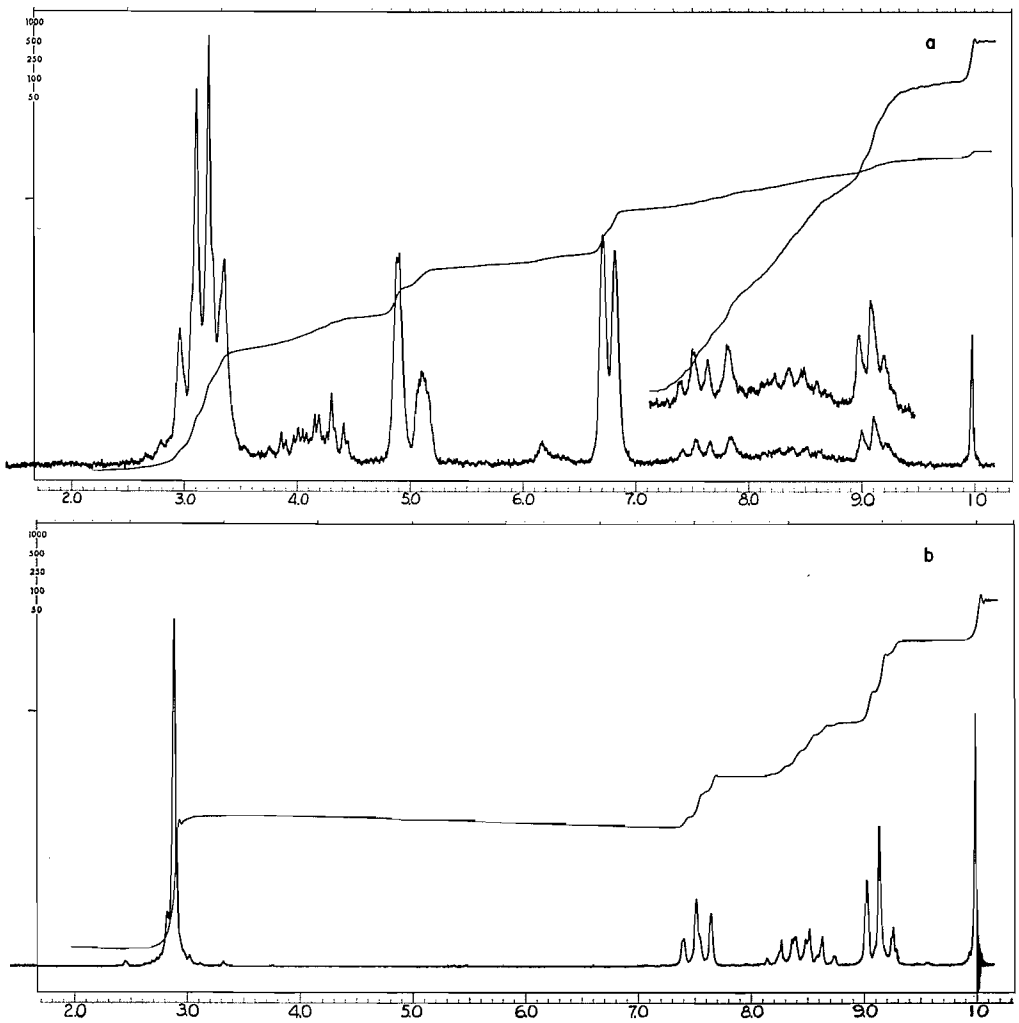

FIG. 1, *a* and *b*.

FIG. 1. Nuclear magnetic resonance spectra in carbon tetrachloride with tetramethylsilane as reference (*a*) product mixture from Birch reduction of safrole in the presence of ethanol, (*b*) *n*-propylbenzene, (*c*) product mixture from Birch reduction of safrole in the absence of ethanol.

The remaining vinyl proton gives a multiplet between 3.8 τ and 4.5 τ. Aromatic proton signals lie between 2.8 τ and 3.5 τ.

The appearance of signals at higher field, above 7.3 τ, characteristic for the *n*-propyl group attached to a benzene ring (ref. 11; see also the n.m.r. spectrum of *n*-propylbenzene in Fig. 1*b*) (triplet at 7.52 τ, $J = 7.0$ c.p.s. for the CH_2 group attached to ring carbon; multiplet between 8.15 τ and 8.75 τ for the other CH_2 group; and a multiplet centered at 9.10 τ for the methyl group) clearly supported the presence of an *n*-propyl group. That no *p*-propenylphenol was present in the mixture was supported also by the absence of a doublet for the methyl group of the propenyl moiety at 8.17 τ and 8.24 τ, $J = 5$ c.p.s. (12) and the sharp olefinic absorption at 4.2 τ. These signals are present in the n.m.r. spectrum (Fig. 1*c*) of the product obtained from the Birch reduction of safrole

Can. J. Chem. Downloaded from www.nrcresearchpress.com by 210.87.254.6 on 09/05/12
For personal use only.

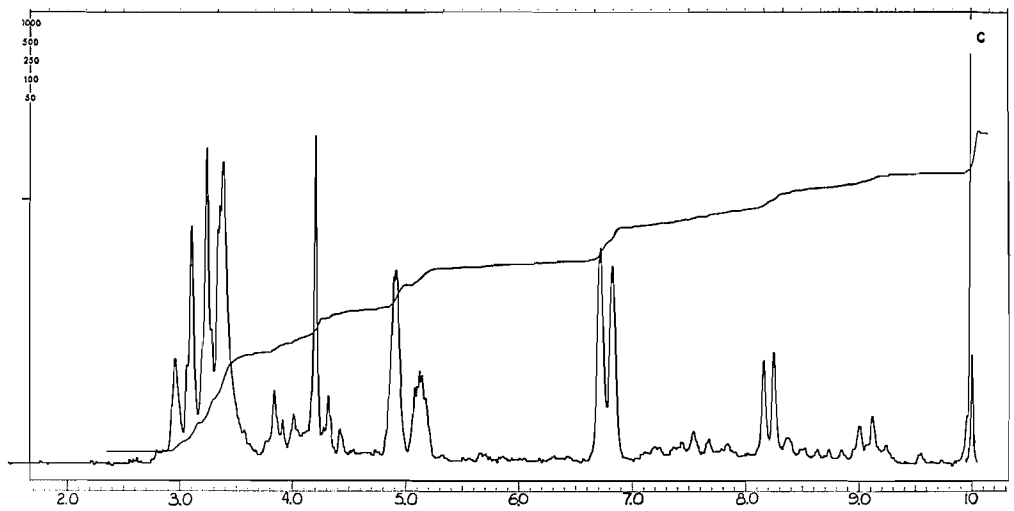

FIG. 1*c*.

in the absence of ethanol (4). The spectrum in Fig. 1*c* indicates that in this case all three of the compounds, *p*-allylphenol, *p*-propenylphenol, and *p*-*n*-propylphenol are present.

A comparison of the integrated areas of the signals for the ring-attached methylene group of both the allyl and *n*-propyl chains (Fig. 1*a*) provided an estimate of the relative amount of the two products. Calculated values for carbon and hydrogen, assuming a 3:1 mixture of *p*-allylphenol and *p*-*n*-propylphenol, are 80.3% and 7.8%, respectively, values quite similar to those calculated for pure *p*-allylphenol (C, 80.6% and H, 7.4%).

It is thus apparent that the reduction of safrole under the conditions employed is somewhat more extensive than originally realized.

ACKNOWLEDGMENT

The authors are grateful for the financial support given by the National Research Council of Canada.

1. M. J. BALDWIN and R. K. BROWN. Submitted for publication, 1965.
2. E. PIERS and R. K. BROWN. Can. J. Chem. **41**, 329 (1963).
3. E. PIERS and R. K. BROWN. Can. J. Chem. **41**, 2917 (1963).
4. A. J. BIRCH. J. Chem. Soc. 102 (1947).
5. NG. PH. BUU-HOÏ, B. ECKERT, and P. DEMERSEMAN. J. Org. Chem. **19**, 726 (1954).
6. M. S. KHARASCH, G. STAMPA, and W. NUDENBERG. Science, **116**, 309 (1952).
7. V. D. AZATYAN. Izv. Akad. Nauk Arm. SSR, Khim. Nauki, **13**, No. 2–3, 181 (1960); Chem. Abstr. **55**, 7323 (1961).
8. I. L. KOTLYAREVSKII and T. G. SHISHMAKOVA. Tr. Vost. Sibirsk. Filiala, Akad. Nauk SSSR, Ser. Khim. No. 4, 32 (1956); Chem. Abstr. **51**, 14594 (1957).
9. N. M. SILVERSTEIN and G. C. BASSLER. Spectroscopic identification of organic compounds. John Wiley and Sons, N.Y. 1963. p. 101.
10. E. BERLINER, F. BERLINER, and I. NELIDOW. J. Am. Chem. Soc. **76**, 507 (1954).
11. High resolution NMR spectra catalog. Vol. II. Varian Associates, Palo Alto, California, Instrument Division. 1963. Spectrum No. 682.
12. High resolution NMR spectra catalog. Vol. I. Varian Associates, Palo Alto, California, Instrument Division. 1962. Spectra Nos. 60 and 61.

RECEIVED APRIL 5, 1965.
DEPARTMENT OF CHEMISTRY,
UNIVERSITY OF ALBERTA,
EDMONTON, ALBERTA.

Can. J. Chem. Downloaded from www.nrcresearchpress.com by 210.87.254.6 on 09/05/12
For personal use only.

THE H_- FUNCTION IN AQUEOUS ALCOHOLS CONTAINING BASE

KEITH BOWDEN

INTRODUCTION

Recently a number of studies have been made on the application of H_- and $H_=$ acidity functions to a number of strongly basic systems (1–10). The indicators have been nitrogen (1) or carbon acids (2). A number of workers have made H_- measurements in alcoholic alkoxide solutions (4–12). This function measures the ability of a system to ionize an acid, HA, to form the anion, A^-, and is defined as (13)

[i] $$H_- = pK_a - \log([HA]/[A^-]) = -\log(a_{H^+}f_{A^-}/f_{HA}).$$

In dilute aqueous solution H_- becomes identical with pH.

The H_0 acidity function has already been determined in aqueous alcohols, dioxan, and acetone containing hydrochloric acid (13–15). The function is similarly defined as (13)

[ii] $$H_0 = pK_a - \log([BH^+]/[B]) = -\log(a_{H^+}f_B/f_{BH^+}).$$

As the nonaqueous component increases, the acidity of the system, at first, falls to a minimum. The acidity then increases to a value somewhat greater in the case of ethanol and acetone and somewhat smaller in the case of dioxan (containing *very* small quantities of water) than that of the purely aqueous system. These results have been interpreted as a "salting-in" of the uncharged base as the nonaqueous component increases, and this decreases the acidity, H_0 (13). Alternatives to this interpretation are a disturbance in the structure of the water (14, 15) and a change in the relative basicities of the aqueous and nonaqueous components with their concentrations (16–18). This is then followed by an increase in acidity caused by the presence of the strong acid, in the case of an alcohol ROH_2^+, in the more highly nonaqueous solutions.

In aqueous alcohols containing base the equilibrium [iii] exists as

[iii] $$H_2O + OR^- \rightleftharpoons OH^- + ROH$$

and thus the equilibrium constant, K, is given by

[iv] $$K = [OH^-]a_{ROH}f_{OH^-}/[OR^-]a_{H_2O}f_{OR^-}.$$

Caldin and Long have investigated this equilibria in aqueous ethanol using as an indicator, 2,4,6-trinitrotoluene (19). Hine and Hine have also made measurements for isopropyl alcohol containing small quantities of water using the indicator, 4-nitrodiphenylamine (11). Kinetic measurements have been made by Wells (16); Tommila and Murto (20, 21); and by Johnson, Nilawar, and Peters (22). The latter workers, also, have been unable to reproduce the results of Caldin and Long. However, the results on the aqueous ethanol system calculated from the kinetic results of Tommila and Murto (21, 23) do not agree with those of Peters.

The present studies report the extension of the H_- function to aqueous alcohols and aqueous dioxan containing base, using substituted anilines as indicators, to investigate their physicochemical behavior.

EXPERIMENTAL AND RESULTS

The measurements were made as previously described (1–3). A Bausch and Lomb Spectronic 505 spectrophotometer was used. The solvents were purified by standard

Can. J. Chem. Downloaded from www.nrcresearchpress.com by 210.87.254.6 on 09/05/12
For personal use only.

THE H_- FUNCTION IN AQUEOUS ALCOHOLS CONTAINING BASE

KEITH BOWDEN

INTRODUCTION

Recently a number of studies have been made on the application of H_- and $H_=$ acidity functions to a number of strongly basic systems (1–10). The indicators have been nitrogen (1) or carbon acids (2). A number of workers have made H_- measurements in alcoholic alkoxide solutions (4–12). This function measures the ability of a system to ionize an acid, HA, to form the anion, A^-, and is defined as (13)

[i] $$H_- = pK_a - \log([HA]/[A^-]) = -\log(a_{H^+}f_{A^-}/f_{HA}).$$

In dilute aqueous solution H_- becomes identical with pH.

The H_0 acidity function has already been determined in aqueous alcohols, dioxan, and acetone containing hydrochloric acid (13–15). The function is similarly defined as (13)

[ii] $$H_0 = pK_a - \log([BH^+]/[B]) = -\log(a_{H^+}f_B/f_{BH^+}).$$

As the nonaqueous component increases, the acidity of the system, at first, falls to a minimum. The acidity then increases to a value somewhat greater in the case of ethanol and acetone and somewhat smaller in the case of dioxan (containing *very* small quantities of water) than that of the purely aqueous system. These results have been interpreted as a "salting-in" of the uncharged base as the nonaqueous component increases, and this decreases the acidity, H_0 (13). Alternatives to this interpretation are a disturbance in the structure of the water (14, 15) and a change in the relative basicities of the aqueous and nonaqueous components with their concentrations (16–18). This is then followed by an increase in acidity caused by the presence of the strong acid, in the case of an alcohol ROH_2^+, in the more highly nonaqueous solutions.

In aqueous alcohols containing base the equilibrium [iii] exists as

[iii] $$H_2O + OR^- \rightleftharpoons OH^- + ROH$$

and thus the equilibrium constant, K, is given by

[iv] $$K = [OH^-]a_{ROH}f_{OH^-}/[OR^-]a_{H_2O}f_{OR^-}.$$

Caldin and Long have investigated this equilibria in aqueous ethanol using as an indicator, 2,4,6-trinitrotoluene (19). Hine and Hine have also made measurements for isopropyl alcohol containing small quantities of water using the indicator, 4-nitrodiphenylamine (11). Kinetic measurements have been made by Wells (16); Tommila and Murto (20, 21); and by Johnson, Nilawar, and Peters (22). The latter workers, also, have been unable to reproduce the results of Caldin and Long. However, the results on the aqueous ethanol system calculated from the kinetic results of Tommila and Murto (21, 23) do not agree with those of Peters.

The present studies report the extension of the H_- function to aqueous alcohols and aqueous dioxan containing base, using substituted anilines as indicators, to investigate their physicochemical behavior.

EXPERIMENTAL AND RESULTS

The measurements were made as previously described (1–3). A Bausch and Lomb Spectronic 505 spectrophotometer was used. The solvents were purified by standard

Can. J. Chem. Downloaded from www.nrcresearchpress.com by 210.87.254.6 on 09/05/12
For personal use only.

procedures. The alkoxide solutions were made by reaction of sodium and the alcohol under nitrogen, followed by filtration. Freshly prepared solutions were always used. The following indicators (1) were employed: 2,4,4′-trinitrodiphenylamine ($pK_a = 12.35$); 2,4-dinitrodiphenylamine ($pK_a = 13.84$); 2,4-dinitroaniline ($pK_a = 15.00$); 4-nitrodiphenylamine ($pK_a = 15.90$); and 2-nitrodiphenylamine ($pK_a = 17.57$).

The solvent dependence of the spectra over the ionization range was small. The measurements could usually be carried out at a wavelength where the acid did not absorb.

TABLE I

H_-* for systems studied

Mole % nonaqueous component	Nonaqueous component											
	Methanol		Ethanol		Isopropyl alcohol		*t*-Butyl alcohol		*t*-Pentyl alcohol		Dioxan	
	a	*b*	*a*	*b*	*a*	*b*	*a*	*b*	*a*	*b*	*a*	*b*
0	11.02	11.74	11.02	11.74	11.02	11.74	11.02	11.74	11.02	11.74	11.02	11.74
20	—	—	11.71	12.40	11.72	12.40	12.58	13.28	*c*	*c*	11.64	12.32
40	—	—	12.30	13.03	12.51	13.20	13.31	14.03	*c*	*c*	12.30	13.01
60	—	—	12.38	13.09	13.12	13.85	14.03	14.75	13.94	14.62	*c*	*c*
80	—	—	12.47	13.16	13.84	14.56	14.74	15.45	14.54	15.23	*c*	*c*
90	—	—	—	—	14.33	15.01	15.55	16.28	14.98	15.68	*c*	*c*
100	10.69	11.40	12.62	13.35	15.00	15.71	17.16	17.85	15.98	16.70	—	—

NOTE: (*a*) Containing 0.001 *M* base; (*b*) containing 0.005 *M* base; (*c*) immiscible solutions.
*The averaged H_- values are considered to be accurate to between ±0.05 and ±0.010 unit.

In Table I the H_- values for aqueous alcohol and aqueous dioxan solutions containing base are given. The results are average values and, for the pure alcohols, agree satisfactorily with those published and reviewed elsewhere (4–12, 24). The values obtained from different indicators agreed to within ±0.1 unit and the values, between H_- equal to 13 and 17, were obtained from at least two different indicators.

The variation between the basicity of the aqueous and methanolic systems is small ($\Delta H_- = -0.34$) and the changes were too small for effective measurement. They showed, however, the same regular change as observed for the other alcohols.

DISCUSSION

The discussion will be divided into two sections. First, the relative basicity of the purely alcoholic to the purely aqueous system is considered. For these dilute solutions (e.g. 0.001 *M* sodium alkoxide in the alcohol) there is an order of basicity rising from methanol ($H_- = 10.69$), ethanol ($H_- = 12.62$), isopropyl alcohol ($H_- = 15.00$), *t*-pentyl alcohol ($H_- = 15.98$), to *t*-butyl alcohol ($H_- = 17.16$). The basicity of the methanolic solution is comparable to that of an aqueous solution of the same base concentration. For all of these alcohols there is a direct relation between H_- and dilute base concentrations (up to about 0.1 *M* base) such that (20, 4–12)

$$H_- = B + \log [OR^-], \qquad [v]$$

where B is a constant dependent on the nature of the alcohol. Values are given in Table II. The basicity of an alcoholic solution appears to be a function of both the autoprotolysis constant and the proton affinity of the solvent.

The H_- function, as originally conceived (13), must be firmly anchored in the aqueous pH region. This has recently been effected (1). However, O'Ferrall and Ridd (5) have

Can. J. Chem. Downloaded from www.nrcresearchpress.com by 210.87.254.6 on 09/05/12
For personal use only.

TABLE II

Alcohol	B*	Autoprotolysis constant†, pK_H^{ROH} (25°)	Log γ^{ROH} Calcd.	Log γ^{ROH} Lit.‡	Dielectric constant§, D (25°)
Methanol	13.69	16.68	2.99	3.1–3.5	32.6
Ethanol	15.63	18.88	3.25	4.1–4.3	24.3
Isopropyl	18.00	20.80	2.80	—	18.3
t-Butyl	20.15	—	—	—	10.9¶
t-Pentyl	18.99	—	—	—	5.8
2-Aminoethanol	16.88	5.2‖	−11.18	—	37.7
2-Diethylaminoethanol	16.54	—	—	—	9.1
Water	14.03	14.00	−0.03	0.0	78.5
Dioxan	—	—	—	—	2.2

*Calculated from present results, and lit. data (4–12).
†See refs. 27–30.
‡See ref. 26.
§See refs. 31–33.
‖At 20°.
¶At 30°.

set up an acidity scale in methanolic methoxide solutions with methanol as the reference system. They should have, like Schaal (6), termed this a H_m scale. However, these workers clearly recognize the direct relation between their pK_a values obtained from methanolic solution and the aqueous pK_a values for these indicators.

The results can be examined by an adaptation of the ideas of Grunwald (25) and Izmailov (26). The ionization of an acid in an alcohol may be written as

[vi] $$HA + OR^- \rightleftharpoons A^- + HOR.$$

The negative logarithm of the equilibrium constant, pK_e^{HA}, can be defined as

[vii] $$pK_e^{HA} = \log [OR^-] + \log ([HA]/[A^-]).$$

The autoprotolysis constant K_H^{ROH} is related by

[viii] $$pK_H^{ROH} = -\log [OR^-] - \log [ROH_2^+].$$

The above relations and the earlier considerations (eq. [i]), assuming the indicator activity coefficient ratio is unity, gives

[ix] $$pK_a^{HA} - pK_e^{HA} - pK_H^{ROH} = \log [ROH_2^+] - \log a_{H^+}.$$

The degenerate activity coefficient, $\log \gamma^{ROH}$, proportional to the difference in chemical energy of solvation of the protons in water and the alcohol[1] (26), is then given by

[x] $$\log \gamma^{ROH} = \log a_{H^+} - \log [ROH_2^+],$$

or

[xi] $$\log \gamma^{ROH} = pK_e^{HA} + pK_H^{ROH} - pK_a^{HA}.$$

The values so obtained are shown in Table II and are in reasonable agreement with those calculated by other means (26). As the dielectric constant falls, the validity of the assumptions and, therefore, the derived values of $\log \gamma^{ROH}$ become less secure. In the dilute solutions, the acidity of an alcoholic solution is related to that of the same concentration of the base in water by the equation

[xii] $$H_-(\text{alcohol}) - H_-(\text{water}) = pK_H^{ROH} - pK_H^{H_2O} - \log \gamma^{ROH}.$$

[1]*The difference in chemical energy of solvation of the protons in water and the alcohol is equal to 2.303RT log* γ^{ROH} *kcal (26).*

Can. J. Chem. Downloaded from www.nrcresearchpress.com by 210.87.254.6 on 09/05/12
For personal use only.

Thus the relative basicity of the alcoholic alkoxide solution is determined by both the change in the autoprotolysis constant and the difference in the energy of the proton in alcohol relative to that in water.

Secondly, the change in basicity from an aqueous, via aqueous alcoholic, to an alcoholic solution will be considered. Irrespective of other effects, there is a gradual change in dielectric constant on progressively changing the medium from water (D = 78.5) to an alcohol (D = 32.6 to 5.8). To assess this factor, aqueous dioxan containing base was examined. Dioxan has a very low dielectric constant. Unfortunately dioxan has a narrow range of miscibility with aqueous sodium hydroxide. The limited results indicate that there is a definite increase in basicity with increasing dioxan content. Unlike the aprotic solvents studied previously (1–3), dioxan is not a strong hydrogen-bond acceptor for water (34). These aprotic solvents, such as dimethyl sulfoxide, compete with the hydroxide ion for the solvating specie, water. This causes very greatly increased activity of the hydroxide ion in these aqueous mixtures (24). The increase in basicity for the aqueous dioxan system could not be caused by the latter effect. Any "salting-in" effect on the uncharged acid, as postulated for the H_0 function, would have the opposite effect and decrease basicity. Thus, a lowering of the dielectric constant appears to increase the activity of the hydroxide ion, in excess of that expected for the simple effect of replacement of water by dioxan (35). A decrease in dielectric constant could also cause an increase in the autoprotolysis constant of water, $pK_H^{H_2O}$, which would cause an increase in the basicity of the system (see eq. [xii] and earlier discussion).

In all the aqueous alcohols studied a regular change in basicity is observed. This is quite unlike the previous data for H_0. Qualitatively a satisfactory explanation of the situation is the gradual change in the *effective* autoprotolysis constant and in the difference in energy of the proton relative to water.

A quantitative estimation of the species actually present has been suggested by Caldin and Long (19). With this method the results for K vary with the composition over quite a wide range and the value increases with increasing water content. The lack of activity corrections (for indicator, base, or solvent), therefore, appear to be important. It is very likely that the activity of the alkoxide and hydroxide vary with the solvent composition. However, the equilibrium constants, K, for any one molar composition are always in the order, t-BuOH > t-PeOH > i-PrOH > EtOH.

ACKNOWLEDGMENT

The author wishes to thank Dr. Ross Stewart for his interest and encouragement.

1. R. STEWART and J. P. O'DONNELL. J. Am. Chem. Soc. **84**, 493 (1962). Can. J. Chem. **42**, 1681, 1694 (1964).
2. K. BOWDEN and R. STEWART. Tetrahedron, **21**, 261 (1965).
3. R. STEWART, K. BOWDEN, and A. BUCKLEY. To be published.
4. R. SCHAAL and C. GADET. Bull. Soc. Chim. France, 2154 (1961).
5. R. A. MORE O'FERRALL and J. H. RIDD. J. Chem. Soc. 5030 (1963).
6. R. SCHAAL and G. LAMBERT. Bull. Soc. Chim. France, 2154 (1963). R. SCHAAL and G. LAMBERT. J. Chim. Phys. **59**, 1164 (1962).
7. C. JACQUINOT-VERMESSE, R. SCHAAL, and P. RUMPF. Bull. Soc. Chim. France, 2030 (1960).
8. C. JACQUINOT-VERMESSE, R. SCHAAL, and P. SOUCHAY. Bull. Soc. Chim. France, 141 (1960).
9. F. MASURE, R. SCHAAL, and P. SOUCHAY. Bull. Soc. Chim. France, 1143 (1956).
10. R. GABORIAUD, B. MONNAYE, and R. SCHAAL. Compt. Rend. **254**, 4027 (1961).
11. J. HINE and M. HINE. J. Am. Chem. Soc. **74**, 5266 (1952).
12. D. BETHELL. J. Chem. Soc. 666 (1963).
13. M. A. PAUL and F. A. LONG. Chem. Rev. **57**, 1 (1957).
14. E. A. BRAUDE. J. Chem. Soc. 1971 (1948).
15. E. A. BRAUDE and E. S. STERN. J. Chem. Soc. 1976 (1948).
16. C. F. WELLS. Discussions Faraday Soc. **29**, 219 (1960).

Can. J. Chem. Downloaded from www.nrcresearchpress.com by 210.87.254.6 on 09/05/12
For personal use only.

17. C. F. WELLS. Nature, **196**, 770 (1962).
18. G. D. GILES and C. F. WELLS. Nature, **201**, 606 (1964).
19. E. F. CALDIN and G. LONG. J. Chem. Soc. 3737 (1954).
20. E. TOMMILA and J. MURTO. Acta Chem. Scand. **16**, 53 (1962).
21. J. MURTO. Acta Chem. Scand. **18**, 1029, 1043 (1964).
22. A. JOHNSON, B. B. NILAWAR, and R. H. PETERS. Nature, **199**, 692 (1963).
23. R. SCHAAL and F. PEURE. Bull. Soc. Chim. France, 2638 (1963).
24. K. BOWDEN. To be published.
25. B. GUTBEZAHL and E. GRUNWALD. J. Am. Chem. Soc. **75**, 565 (1953). J. E. LEFFLER and E. GRUNWALD. Rates and equilibria of organic reactions. John Wiley and Sons, Inc., New York. 1963. Chap. 8.
26. N. A. IZMAILOV. Proc. Acad. Sci. USSR, Phys. Chem. Sect. English Transl. **127**, 501 (1959).
27. H. S. HARNED and R. A. ROBINSON. Trans. Faraday Soc. **36**, 973 (1949).
28. M. L. DONDON. J. Chim. Phys. 48 (1951).
29. F. MASURE and R. SCHAAL. Bull. Soc. Chim. France, 1141 (1956).
30. R. SCHAAL and A. TEZE. Bull. Soc. Chim. France, 1783 (1961).
31. A. A. MARYOTT and E. R. SMITH. Nat. Bur. Std. (U.S.), Circ. No. 514 (1951).
32. J. T. PINKSTON and H. T. BRISCOE. J. Phys. Chem. **46**, 469 (1942).
33. S. MOURONVAL, R. GABORIAUD, and R. SCHAAL. Compt. Rend. **255**, 2605 (1962).
34. J. R. HOLMES, D. KIVELSON, and W. C. DRINKARD. J. Am. Chem. Soc. **84**, 4677 (1962).
35. G. YAGIL and M. ANBAR. J. Am. Chem. Soc. **85**, 2376 (1963).

RECEIVED JANUARY 26, 1965.
DEPARTMENT OF PURE AND APPLIED CHEMISTRY,
ROYAL COLLEGE OF ADVANCED TECHNOLOGY,
SALFORD, LANCASHIRE, ENGLAND.

Can. J. Chem. Downloaded from www.nrcresearchpress.com by 210.87.254.6 on 09/05/12
For personal use only.

THE FEIST SYNTHESIS OF PYRROLE-3-CARBOXYLIC ESTERS

D. M. MCKINNON[1]

In connection with another investigation (1) which required some pyrrole derivatives, their preparation, particularly that of their N-substituted-3-carboxylic esters, was studied. The method of study was that of Feist (2), who condensed benzoin and ethyl β-aminocrotonate in potassium hydrogen sulfate at 170° to produce the N-unsubstituted-pyrrole-3-carboxylic ester (I*a*).

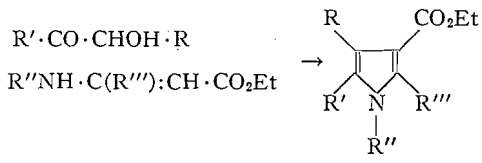

I

	R	R′	R″	R‴		R	R′	R″	R‴
I*a*	Ph	Ph	H	Me	I*i*	H	Ph	CH_2Ph	Me
b	"	"	Ph	"	*j*	"	"	$C_6H_4oNMe_2$	"
c	"	"	C_6H_4oMe	"	*k*	"	"	Me	"
d	"	"	C_6H_4pMe	"	*l*	"	"	H	"
e	"	"	CH_2Ph	"	*m*	Me	Me	Ph	"
f	H	"	Ph	"	*n*	"	"	Me	"
g	"	"	C_6H_4oMe	"	*o*	"	"	H	"
h	"	"	C_6H_4pMe	"	*p*	Ph	Ph	Ph	Ph

The severe conditions used were inapplicable to the preparation of N-aryl pyrroles, since β-arylaminocrotonic esters cyclize at high temperatures (3), or in strong acid (4), to produce quinolone derivatives (II).

[1]*Dalhousie University Postdoctorate Fellow.*

17. C. F. WELLS. Nature, **196**, 770 (1962).
18. G. D. GILES and C. F. WELLS. Nature, **201**, 606 (1964).
19. E. F. CALDIN and G. LONG. J. Chem. Soc. 3737 (1954).
20. E. TOMMILA and J. MURTO. Acta Chem. Scand. **16**, 53 (1962).
21. J. MURTO. Acta Chem. Scand. **18**, 1029, 1043 (1964).
22. A. JOHNSON, B. B. NILAWAR, and R. H. PETERS. Nature, **199**, 692 (1963).
23. R. SCHAAL and F. PEURE. Bull. Soc. Chim. France, 2638 (1963).
24. K. BOWDEN. To be published.
25. B. GUTBEZAHL and E. GRUNWALD. J. Am. Chem. Soc. **75**, 565 (1953). J. E. LEFFLER and E. GRUNWALD. Rates and equilibria of organic reactions. John Wiley and Sons, Inc., New York. 1963. Chap. 8.
26. N. A. IZMAILOV. Proc. Acad. Sci. USSR, Phys. Chem. Sect. English Transl. **127**, 501 (1959).
27. H. S. HARNED and R. A. ROBINSON. Trans. Faraday Soc. **36**, 973 (1949).
28. M. L. DONDON. J. Chim. Phys. 48 (1951).
29. F. MASURE and R. SCHAAL. Bull. Soc. Chim. France, 1141 (1956).
30. R. SCHAAL and A. TEZE. Bull. Soc. Chim. France, 1783 (1961).
31. A. A. MARYOTT and E. R. SMITH. Nat. Bur. Std. (U.S.), Circ. No. 514 (1951).
32. J. T. PINKSTON and H. T. BRISCOE. J. Phys. Chem. **46**, 469 (1942).
33. S. MOURONVAL, R. GABORIAUD, and R. SCHAAL. Compt. Rend. **255**, 2605 (1962).
34. J. R. HOLMES, D. KIVELSON, and W. C. DRINKARD. J. Am. Chem. Soc. **84**, 4677 (1962).
35. G. YAGIL and M. ANBAR. J. Am. Chem. Soc. **85**, 2376 (1963).

RECEIVED JANUARY 26, 1965.
DEPARTMENT OF PURE AND APPLIED CHEMISTRY,
ROYAL COLLEGE OF ADVANCED TECHNOLOGY,
SALFORD, LANCASHIRE, ENGLAND.

Can. J. Chem. Downloaded from www.nrcresearchpress.com by 210.87.254.40 on 09/05/12
For personal use only.

THE FEIST SYNTHESIS OF PYRROLE-3-CARBOXYLIC ESTERS

D. M. MCKINNON[1]

In connection with another investigation (1) which required some pyrrole derivatives, their preparation, particularly that of their N-substituted-3-carboxylic esters, was studied. The method of study was that of Feist (2), who condensed benzoin and ethyl β-aminocrotonate in potassium hydrogen sulfate at 170° to produce the N-unsubstituted-pyrrole-3-carboxylic ester (I*a*).

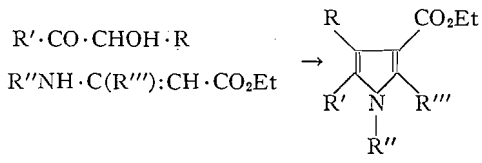

I

	R	R′	R″	R‴		R	R′	R″	R‴
I*a*	Ph	Ph	H	Me	I*i*	H	Ph	CH_2Ph	Me
b	"	"	Ph	"	*j*	"	"	$C_6H_4oNMe_2$	"
c	"	"	C_6H_4oMe	"	*k*	"	"	Me	"
d	"	"	C_6H_4pMe	"	*l*	"	"	H	"
e	"	"	CH_2Ph	"	*m*	Me	Me	Ph	"
f	H	"	Ph	"	*n*	"	"	Me	"
g	"	"	C_6H_4oMe	"	*o*	"	"	H	"
h	"	"	C_6H_4pMe	"	*p*	Ph	Ph	Ph	Ph

The severe conditions used were inapplicable to the preparation of N-aryl pyrroles, since β-arylaminocrotonic esters cyclize at high temperatures (3), or in strong acid (4), to produce quinolone derivatives (II).

[1]*Dalhousie University Postdoctorate Fellow.*

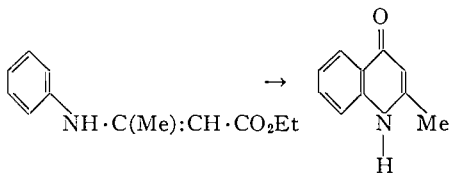

II

Boiling ethanolic zinc chloride, used previously to condense α-ketols with β-ketoesters, forming furan derivatives (III) (5), also condensed N-substituted and N-unsubstituted

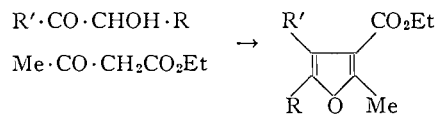

III

crotonic esters, prepared by the reaction of acetoacetic ester with the appropriate amines, with three α-ketols studied, benzoin, α-hydroxyacetophenone, and acetoin, From benzoin and acetoin, the 4,5-diphenyl- (I, *a–e*) and 4,5-dimethyl- (*m–o*) pyrrole-3-carboxylic esters respectively were obtained, while α-hydroxyacetophenone yielded the 4-unsubstituted esters (I, *f–l*) some of which (I, *f–h*, *l*) had been obtained previously (6) by the well-known Paal–Knorr synthesis.

Where it was found impossible to crystallize the pyrrole-3-carboxylic ester, the crude products were either distilled under reduced pressure, or hydrolyzed to the free acid.

Lederer and Paal (6*a*) reported that ethyl α-phenacylacetoacetate condensed with aqueous methylamine to give ethyl 1,2-dimethyl-5-phenylpyrrole-3-carboxylate (I*k*), m.p. 112°. The compound obtained from α-hydroxyacetophenone and ethyl β-aminocrotonate, which gave a satisfactory analysis, had m.p. 75°. Two compounds were obtained from a check of the original experiment. One was identical with that (m.p. 75°) obtained above, while a second, which softened above 85° and melted completely at 112°, was completely converted to the first by being heated at a temperature above its melting point for 5 min. On the basis of its analysis and properties, it is assumed to be an intermediate condensation product (IV), or a tautomer.

$$Ph\cdot CO\cdot CH_2CH(CO_2Et)\cdot C(Me):NMe_2$$

Ethyl β-phenylaminocinnamate also condensed with benzoin under the conditions described above. The tetraphenylpyrrole-3-carboxylic ester (I*p*) was obtained, but the major product was a white crystalline nitrogen-containing material whose infrared spectrum showed no carbonyl absorption. It did not give a satisfactory analysis for any simple product.

The results of the syntheses using α-hydroxyacetophenone show that the groups attached to the carbonyl and hydroxy functions of the α-ketol become pyrrole-5- and pyrrole-4- substituents respectively, and also that the β-aminocrotonic ester must react in that form, and not as its β-iminobutyrate tautomer. They are in contrast to the reactions of α-ketols with β-keto esters (5) where the positions of the substituents in the furans (III) produced are reversed.

These reactions are analogous to the similar Hantzsch (7) and Feist-Benary (8) syntheses of pyrroles and furans where the positions of the group adjacent to the carbonyl function become 5- and 4- substituents respectively.

Can. J. Chem. Downloaded from www.nrcresearchpress.com by 210.87.254.40 on 09/05/12
For personal use only.

Can. J. Chem. Downloaded from www.nrcresearchpress.com by 210.87.254.40 on 09/05/12
For personal use only.

EXPERIMENTAL

Ethyl β-(o-Dimethylaminophenyl) Aminocrotonate

Equimolar quantities of *o*-aminodimethylaniline and acetoacetic ester, with a trace of acetic acid, were heated under reflux in benzene until the calculated quantity of water, removed by continuous azeotropic distillation, had separated. The solvent was evaporated and the residue distilled under reduced pressure. The pale yellow fraction, b.p. 102° at 0.5 mm was collected (73%).

Found: C, 66.6; H, 7.8; N, 10.3. $C_{14}H_{20}N_2O_2$ requires C, 67.6; H, 8.0; N, 11.3.

2 Methylpyrrole-3-Carboxylic Esters (I, a–o)

Equimolar quantities of the ethyl β-aminocrotonic ester and the α-ketols (acetoin was used as the commercial 85% solution in water) were heated under reflux in ethanol with an approximately equal weight of zinc chloride for times varying between 4 and 24 h. The yellow oils obtained by diluting the ethanol were worked up by trituration under ethanol, distillation under reduced pressure, or hydrolysis to the parent acid. The results are presented in Table I. The products were crystallized from ethanol except where stated.

TABLE I

Preparation of pyrroles from β-aminocrotonic esters and α-ketols

Compound	Reaction time, hours	Yield, %	M.p.	Formula	Required, %			Found, %		
					C	H	N	C	H	N
I*a*	10	42	203–204*	$C_{20}H_{19}NO_2$						
I*b*	24	46	132–134	$C_{26}H_{23}NO_2$	81.8	6.03	3.67	81.5	6.13	3.70
I*c*	24	45†	273‡	$C_{25}H_{21}NO_2$	81.9	5.72	3.82	82.1	5.43	3.58
I*d*	24	68	134	$C_{27}H_{25}NO_2$	81.9	6.32	3.54	81.6	6.51	3.51
I*e*	24	51	126–127	$C_{27}H_{25}NO_2$	81.9	6.32	3.54	82.9	6.72	3.87
I*f*	24	43	92.5–93§	$C_{20}H_{19}NO_2$						
I*g*	24	32	199†,‖	$C_{19}H_{17}NO_2$						
I*h*	24	36	115¶	$C_{21}H_{21}NO_2$						
I*i*	24	54	164	$C_{19}H_{17}NO_2$	78.3	5.83	4.81	77.9	5.68	4.20
I*j*	24	26†	245‡	$C_{20}H_{20}N_2O_2$	75.0	6.25	8.75	74.3	6.69	8.30
I*k*	4	49	74–75**	$C_{15}H_{17}NO_2$	74.1	6.99	5.76	74.3	7.12	6.21
I*l*	4	38	115–116††	$C_{14}H_{15}NO_2$						
I*m*	8	44	—‡‡	$C_{16}H_{19}NO_2$	74.8	7.41	5.45	75.1	7.49	5.97
I*n*	4	38	72–73§§	$C_{11}H_{17}NO_2$						
I*o*	4	46	104–105‖‖	$C_{10}H_{15}NO_2$						

*Lit. (2) 203°.
†As free acid.
‡From acetic acid.
§Lit. (6*a*) 100°. Original experiment repeated gave m.p. 92.5° mixed m.p. 92.5°.
‖Lit. (6*a*) 199°.
¶Lit. (6*a*) 115°.
**Lit. (6*a*) 112°.
††Lit. (6*b*) 115–116°.
‡‡B.p. 142–146°, 0.5 mm.
§§Lit. (6*d*) 72–73°.
‖‖Lit. (6*c*) 104–105°.

Reaction of Ethyl α-Phenacylacetoacetate with Methylamine

The reaction, performed as described (7), afforded a solid precipitate, which was recrystallized from ethanol. It softened at 85° and completely melted at 112°.

Found: C, 68.8; H, 7.01; N, 5.74. $C_{15}H_{19}NO_3$ requires C, 68.9; H, 7.28; N, 5.57.

The mother liquors of the reaction, diluted with a large excess of water, gave a precipitate, m.p. 75° (from ethanol), which was identical with the pyrrole (I*k*) obtained above. The compound $C_{15}H_{19}NO_3$ obtained above was heated at 120° for 5 min. The cooled product, recrystallized from ethanol, deposited the pyrrole (I*k*), m.p. 75°.

Reaction of Ethyl β-Phenylaminocinnamate with Benzoin

Benzoin and ethyl β-phenylaminocinanmate were heated under reflux with zinc chloride as described above for the 2-methylpyrrole-3-carboxylic ester for 24 h. The mixture, worked up in the usual manner, gave a white solid which was separated into two components by chromatography on activated alumina in benzene. The course of the elution was followed under ultraviolet light. When the first pale fluorescent band had been eluted, the column was stripped with ether.

The first fraction on evaporation yielded a white solid, m.p. 175–176° from ethanol (17.5%).

Found: C, 83.5; H, 5.51; N, 3.29. $C_{31}H_{25}NO_2$ requires C, 83.8; H, 5.66; N, 3.16.

The second fraction on evaporation yielded a colorless crystalline compound, m.p. 212–220° from benzene.

Found: C, 85.5; H, 5.67; N, 6.13.

ACKNOWLEDGMENTS

This work was supported by the Dalhousie University Research and Development Fund for the Sciences.

1. K. T. LEFFEK and D. M. MCKINNON. Unpublished results.
2. F. FEIST. Ber. **35**, 1558 (1902).
3. M. CONRAD and L. LIMPACH. Ber. **20**, 944, 948 (1887).
4. R. G. GOULD and W. A. JACOBS. J. Am. Chem. Soc. **61**, 2890 (1939). C. C. PRICE and R. M. ROBERTS. J. Am. Chem. Soc. **68**, 1204 (1946).
5. F. GARCIA GONZALEZ, F. J. LOPEZ APARICIO, and F. SANCHEY-LAULHE. Anales real Soc. españ. fis. y quim. Madrid, Ser. B, **50B**, 407 (1954); Chem. Abstr. **49**, 13206 (1955). T. SZEKI and E. LASZLO. Ber. **73**, 924 (1940). J. K. N. JONES. J. Chem. Soc. 116 (1945).
6. (*a*) L. LEDERER and C. PAAL. Ber. **18**, 2594 (1885).
   (*b*) V. SPRIO and G. C. VACCARO. Ann. Chim. Rome, **49**, 2075 (1959). Chem. Abstr. **54**, 16443 (1960).
   (*c*) L. KNORR and K. HESS. Ber. **44**, 2762 (1911).
   (*d*) J. L. RAINEY and H. ADKINS. J. Am. Chem. Soc. **61**, 1104 (1939).
7. A. HANTZSCH. Ber. **23**, 1474 (1890). R. C. ELDERFIELD. Heterocyclic compounds. Vol. 1. John Wiley and Sons, Inc., New York. 1950. pp. 132, 290.
8. F. FEIST. Ber. **35**, 1537 (1902). E. BENARY. Ber. **44**, 493 (1911). R. C. ELDERFIELD. Heterocyclic compounds. Vol. 1. John Wiley and Sons, Inc., New York. 1950. p. 132.

RECEIVED OCTOBER 30, 1964.
CHEMISTRY DEPARTMENT,
DALHOUSIE UNIVERSITY,
HALIFAX, NOVA SCOTIA.

STEREOCHEMISTRY OF THE REDUCTION OF CYCLIC KETONES WITH THE PYRIDINE-*n*-BUTYLLITHIUM ADDUCT: STERIC APPROACH AND PRODUCT DEVELOPMENT CONTROLS

R. A. ABRAMOVITCH, W. C. MARSH, AND J. G. SAHA

The dihydropyridyllithium adduct formed from phenyllithium and pyridine has been shown to reduce ketones to the corresponding alcohols (1). While the yield from benzophenone was reasonable (64%), cyclohexanone gave a poor yield (6.5%) of cyclohexanol. It was, nevertheless, thought to be of interest to examine whether or not there was any stereoselectivity in the reduction of cyclic ketones with this reagent. The publication of a study of the stereochemistry of the reduction of cyclic ketones with lithium tri-*t*-butoxyaluminium hydride and the discussion of the factors controlling the geometry of the products formed (2) prompts the reporting of our results.

The reducing agent used here was the adduct (I) formed by the addition of *n*-butyllithium in ether in the cold to an excess of pyridine in dry ether. The ketone in ether was added at room temperature and, after the usual workup (1), the products were analyzed by gas-phase chromatography. In addition to recovered ketone, 2-*n*-butylpyridine was formed, together with the mixture of isomeric alcohols.

Reduction of 4-*t*-butylcyclohexanone in this way gave a mixture of isomeric alcohols of which 91–96% was the *trans*- and 9–4% was the *cis*-isomer. Very similar ratios were obtained when lithium aluminium hydride (3) and lithium tri-*t*-butoxyaluminium hydride (2) were used. It has been proposed (2) that the stereochemical results observed with

Can. J. Chem. Downloaded from www.nrcresearchpress.com by 210.87.254.40 on 09/05/12
For personal use only.

The second fraction on evaporation yielded a colorless crystalline compound, m.p. 212–220° from benzene.

Found: C, 85.5; H, 5.67; N, 6.13.

ACKNOWLEDGMENTS

This work was supported by the Dalhousie University Research and Development Fund for the Sciences.

1. K. T. LEFFEK and D. M. MCKINNON. Unpublished results.
2. F. FEIST. Ber. **35**, 1558 (1902).
3. M. CONRAD and L. LIMPACH. Ber. **20**, 944, 948 (1887).
4. R. G. GOULD and W. A. JACOBS. J. Am. Chem. Soc. **61**, 2890 (1939). C. C. PRICE and R. M. ROBERTS. J. Am. Chem. Soc. **68**, 1204 (1946).
5. F. GARCIA GONZALEZ, F. J. LOPEZ APARICIO, and F. SANCHEY-LAULHE. Anales real Soc. españ. fis. y quim. Madrid, Ser. B, **50B**, 407 (1954); Chem. Abstr. **49**, 13206 (1955). T. SZEKI and E. LASZLO. Ber. **73**, 924 (1940). J. K. N. JONES. J. Chem. Soc. 116 (1945).
6. (*a*) L. LEDERER and C. PAAL. Ber. **18**, 2594 (1885).
   (*b*) V. SPRIO and G. C. VACCARO. Ann. Chim. Rome, **49**, 2075 (1959). Chem. Abstr. **54**, 16443 (1960).
   (*c*) L. KNORR and K. HESS. Ber. **44**, 2762 (1911).
   (*d*) J. L. RAINEY and H. ADKINS. J. Am. Chem. Soc. **61**, 1104 (1939).
7. A. HANTZSCH. Ber. **23**, 1474 (1890). R. C. ELDERFIELD. Heterocyclic compounds. Vol. 1. John Wiley and Sons, Inc., New York. 1950. pp. 132, 290.
8. F. FEIST. Ber. **35**, 1537 (1902). E. BENARY. Ber. **44**, 493 (1911). R. C. ELDERFIELD. Heterocyclic compounds. Vol. 1. John Wiley and Sons, Inc., New York. 1950. p. 132.

RECEIVED OCTOBER 30, 1964.
CHEMISTRY DEPARTMENT,
DALHOUSIE UNIVERSITY,
HALIFAX, NOVA SCOTIA.

STEREOCHEMISTRY OF THE REDUCTION OF CYCLIC KETONES WITH THE PYRIDINE-*n*-BUTYLLITHIUM ADDUCT: STERIC APPROACH AND PRODUCT DEVELOPMENT CONTROLS

R. A. ABRAMOVITCH, W. C. MARSH, AND J. G. SAHA

The dihydropyridyllithium adduct formed from phenyllithium and pyridine has been shown to reduce ketones to the corresponding alcohols (1). While the yield from benzophenone was reasonable (64%), cyclohexanone gave a poor yield (6.5%) of cyclohexanol. It was, nevertheless, thought to be of interest to examine whether or not there was any stereoselectivity in the reduction of cyclic ketones with this reagent. The publication of a study of the stereochemistry of the reduction of cyclic ketones with lithium tri-*t*-butoxyaluminium hydride and the discussion of the factors controlling the geometry of the products formed (2) prompts the reporting of our results.

The reducing agent used here was the adduct (I) formed by the addition of *n*-butyllithium in ether in the cold to an excess of pyridine in dry ether. The ketone in ether was added at room temperature and, after the usual workup (1), the products were analyzed by gas-phase chromatography. In addition to recovered ketone, 2-*n*-butylpyridine was formed, together with the mixture of isomeric alcohols.

Reduction of 4-*t*-butylcyclohexanone in this way gave a mixture of isomeric alcohols of which 91–96% was the *trans*- and 9–4% was the *cis*-isomer. Very similar ratios were obtained when lithium aluminium hydride (3) and lithium tri-*t*-butoxyaluminium hydride (2) were used. It has been proposed (2) that the stereochemical results observed with

Can. J. Chem. Downloaded from www.nrcresearchpress.com by 210.87.254.105 on 09/05/12
For personal use only.

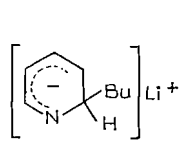

I

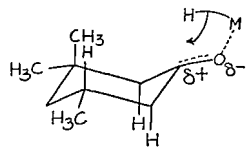

II

these two reagents can be accounted for on the basis of steric factors alone ("steric approach control") and not of "product development control" (4). If the attacking reagent is the hydride ion then approach would be easier from the axial side than from the equatorial side; in the latter case, the axial hydrogens at C-2 and C-6 would interfere with a species approaching the carbonyl group. With 3,3,5-trimethylcyclohexanone, however, the axial methyl group at C-3 would lead to a much larger steric hindrance to axial approach, and the main product formed (55–88%) with the complex metal hydrides is the less stable *trans* axial alcohol (2, 5). At first sight the present observation with 4-*t*-butylcyclohexanone would suggest that hydride ion may be the effective reducing agent with (I) as well, and that the direction of attack is governed by the ease of approach of the hydride ion. If this were so, then reduction of 3,3,5-trimethylcyclohexanone should lead to the *trans* alcohol, predominantly. This was not the case, however. Under conditions in which thermodynamic control is highly unlikely (thermodynamic control leads to 100% of the *cis*-isomer (5)) the mixture of alcohols obtained consisted of 79% of the *cis*- and 21% of the *trans*-isomer, i.e. the more stable alcohol predominated, in marked contrast to the complex hydride reductions. This result cannot be rationalized on the basis of ease of attack from the axial side and must indicate that product development control is involved when I is the reducing agent. It is felt that the generalization that it is possible to explain all the stereochemical results of the hydride reduction of cyclic ketones on the basis of steric factors alone is not always justified. The stereochemistry will also depend to a large extent upon how far the geometry of the transition state has progressed towards that of the product: with a powerful hydride ion donor, the geometry of the transition state will resemble that of starting ketone and steric approach control will operate. With a weak hydride donor, as I appears to be, however, the transition state will look more like the product alcohol and, with the oxygen atom probably complexed with the metal (II) so that it will prefer even more to adopt the least hindered configuration, transfer of hydrogen will take place to give mainly the equatorial alcohol. Adduct I may find some use in the reduction of ketones *under non-equilibrating conditions* in which the equatorial isomer is desired but in which axial approach is sterically difficult.

EXPERIMENTAL

The procedure used will be illustrated with the reduction of 3,3,5-trimethylcyclohexanone.

A solution of *n*-butyllithium (0.64 g, 0.01 mole in 4.5 ml of hexane) in dry ether (15 ml) was added slowly with stirring and under oxygen-free nitrogen to a cooled solution of pyridine (4.0 g) in dry ether (25 ml) at such a rate that no rise in temperature occurred. A solution of the ketone (0.7 g, 0.005 mole) in dry ether (25 ml) was now added slowly and the reaction mixture stirred at room temperature for a further 12 h. It was decomposed by the addition of 6 *N* hydrochloric acid (50 ml); the organic layer separated; and the acid layer was extracted with ether. The combined ether layers were dried (Na_2SO_4) and the solvent distilled through a fractionating column. The residue (3–5 ml) was transferred quantitatively to a 10 ml volumetric flask and the volume brought to the mark with acetone. Aliquots of the solution were then analyzed by gas-phase chromatography using a 5 ft × $\frac{1}{4}$ in. column packed with glycerol (20%) on Chromosorb W (80–100 mesh) operated at 100° and a helium inlet pressure of 30 p.s.i. (120 ml/min). Calibration curves using pure *cis* and *trans* alcohols were obtained for the quantitative

Can. J. Chem. Downloaded from www.nrcresearchpress.com by 210.87.254.105 on 09/05/12
For personal use only.

analyses. The response factors for the two alcohols (flame ionization detector) were found to be the same. The average overall yield of alcohols (duplicate runs) was 12.3%. The accuracy of the method was checked by analyzing a synthetic mixture of the two alcohols. The results are correct within ±0.4%.

The mixture of the isomeric 4-*t*-butylcyclohexanols was resolved on a 6 ft × ¼ in. column of 20% Carbowax 20 on Chromosorb W at 130°.

ACKNOWLEDGMENTS

We thank the National Research Council for financial assistance and Dr. E. L. Eliel for gifts of the authentic *cis*- and *trans*-3,3,5-trimethylcyclohexanols.

1. R. A. Abramovitch and B. Vig. Can. J. Chem. **41**, 1961 (1963).
2. J-C. Richer. J. Org. Chem. **30**, 324 (1965).
3. E. L. Eliel and R. S. Ro. J. Am. Chem. Soc. **79**, 5992 (1957).
4. W. G. Dauben, G. J. Fonken, and D. C. Noyce. J. Am. Chem. Soc. **78**, 2579 (1956).
5. H. Haubenstock and E. L. Eliel. J. Am. Chem. Soc. **84**, 2363, 2368 (1962).

Received March 25, 1965.
Department of Chemistry,
University of Saskatchewan,
Saskatoon, Saskatchewan.

Can. J. Chem. Downloaded from www.nrcresearchpress.com by 210.87.254.105 on 09/05/12
For personal use only.

HYDROGEN ATOM ABSTRACTION FROM ETHYLENEIMINE AND ETHYLENEIMINE-d_4[1]

R. F. Klemm

INTRODUCTION

As part of a more extensive investigation into the mercury photosensitized decomposition of ethyleneimine it was necessary to establish the rates at which methyl radicals abstract H attached to both carbon and nitrogen, and thereby subsequently to observe, if possible, the reactions of the ethyleneimino radical. Brinton and Volman (1) using di-*tert*-butyl peroxide as a thermal methyl source reported k_1 for the reaction

[1] $$CH_3 + \overline{CH_2CH_2NH} \rightarrow CH_4 + R\cdot$$

to be $k_1 = 3.2 \times 10^{10} \exp(-4800/RT)$ (mole/cc)$^{-1}$ s^{-1} in the interval 120–160°. Their original value has been adjusted by Shepp's (2) value for

[2] $$CH_3 + CH_3 \rightarrow C_2H_6$$

of $k_2 = 2.2 \times 10^{13}$ (mole/cc)$^{-1}$ s^{-1} independent of temperature. Since the value given by Brinton and Volman (1) is the only determination of k_1 to date, the opportunity was taken to reevaluate k_1 over a wider temperature range (100–260°) using the photolysis of acetone as an alternate methyl source.

EXPERIMENTAL

Ethyleneimine (Fisher reagent) was distilled on a 1 m pyrex helices-packed column with a vapor takeoff. Its purity was ascertained by gas chromatography and mass spectrometry. Acetone (Fisher reagent) was similarly processed. Ethyleneimine-d_4 (Merck, Sharpe & Dohme, Montreal) was 98.5 atom % deuterium, judged from its n.m.r. (nuclear magnetic resonance) spectrum by using known quantities of benzene as internal standard. Acetone-d_6 (Merck, Sharpe & Dohme, Montreal) was 99.5 atom % deuterium and used without additional purification.

The cylindrical quartz photolysis cell was 172 cc in volume and enclosed in a well-lagged, aluminium furnace. Radiation from a Hanovia SH medium pressure lamp was limited to predominantly 3 130 Å

[1]*Contribution No. 294 from The Research Council of Alberta, Edmonton, Alberta, Canada.*

analyses. The response factors for the two alcohols (flame ionization detector) were found to be the same. The average overall yield of alcohols (duplicate runs) was 12.3%. The accuracy of the method was checked by analyzing a synthetic mixture of the two alcohols. The results are correct within ±0.4%.

The mixture of the isomeric 4-*t*-butylcyclohexanols was resolved on a 6 ft × ¼ in. column of 20% Carbowax 20 on Chromosorb W at 130°.

ACKNOWLEDGMENTS

We thank the National Research Council for financial assistance and Dr. E. L. Eliel for gifts of the authentic *cis*- and *trans*-3,3,5-trimethylcyclohexanols.

1. R. A. Abramovitch and B. Vig. Can. J. Chem. **41**, 1961 (1963).
2. J-C. Richer. J. Org. Chem. **30**, 324 (1965).
3. E. L. Eliel and R. S. Ro. J. Am. Chem. Soc. **79**, 5992 (1957).
4. W. G. Dauben, G. J. Fonken, and D. C. Noyce. J. Am. Chem. Soc. **78**, 2579 (1956).
5. H. Haubenstock and E. L. Eliel. J. Am. Chem. Soc. **84**, 2363, 2368 (1962).

Received March 25, 1965.
Department of Chemistry,
University of Saskatchewan,
Saskatoon, Saskatchewan.

HYDROGEN ATOM ABSTRACTION FROM ETHYLENEIMINE AND ETHYLENEIMINE-d_4[1]

R. F. Klemm

INTRODUCTION

As part of a more extensive investigation into the mercury photosensitized decomposition of ethyleneimine it was necessary to establish the rates at which methyl radicals abstract H attached to both carbon and nitrogen, and thereby subsequently to observe, if possible, the reactions of the ethyleneimino radical. Brinton and Volman (1) using di-*tert*-butyl peroxide as a thermal methyl source reported k_1 for the reaction

[1] $$CH_3 + \overline{CH_2CH_2NH} \rightarrow CH_4 + R\cdot$$

to be $k_1 = 3.2 \times 10^{10} \exp(-4800/RT)$ (mole/cc)$^{-1}$ s^{-1} in the interval 120–160°. Their original value has been adjusted by Shepp's (2) value for

[2] $$CH_3 + CH_3 \rightarrow C_2H_6$$

of $k_2 = 2.2 \times 10^{13}$ (mole/cc)$^{-1}$ s^{-1} independent of temperature. Since the value given by Brinton and Volman (1) is the only determination of k_1 to date, the opportunity was taken to reevaluate k_1 over a wider temperature range (100–260°) using the photolysis of acetone as an alternate methyl source.

EXPERIMENTAL

Ethyleneimine (Fisher reagent) was distilled on a 1 m pyrex helices-packed column with a vapor takeoff. Its purity was ascertained by gas chromatography and mass spectrometry. Acetone (Fisher reagent) was similarly processed. Ethyleneimine-d_4 (Merck, Sharpe & Dohme, Montreal) was 98.5 atom % deuterium, judged from its n.m.r. (nuclear magnetic resonance) spectrum by using known quantities of benzene as internal standard. Acetone-d_6 (Merck, Sharpe & Dohme, Montreal) was 99.5 atom % deuterium and used without additional purification.

The cylindrical quartz photolysis cell was 172 cc in volume and enclosed in a well-lagged, aluminium furnace. Radiation from a Hanovia SH medium pressure lamp was limited to predominantly 3 130 Å

[1]*Contribution No. 294 from The Research Council of Alberta, Edmonton, Alberta, Canada.*

by a Corning 0–54 filter. Acetone and ethyleneimine were individually admitted to the cell and allowed to mix as the lamp equilibrated. No "dark" reaction between reactants was evident. Methane and ethane were resolved by gas chromatography using a temperature-programmed molecular sieve 13X column and a hot wire detector. The various deuterated methanes were determined by mass spectrometry.

RESULTS

With acetone (A) and acetone-d_6 (Ad_6) as methyl sources, data have been obtained according to Methods I and II as employed by Trotman-Dickenson and Steacie (3). Use is made of the relationship

$$[3] \qquad \frac{R(CH_4)}{R^{1/2}(C_2H_6)} = \frac{k_1[E]}{k_2^{1/2}} + \frac{k_4[A]}{k_2^{1/2}}$$

where E = ethyleneimine and k_4 refers to

$$[4] \qquad CH_3 + A \rightarrow CH_4 + CH_2COCH_3.$$

Thus $R(CH_4)/R^{1/2}(C_2H_6)$ should be a linear function of [E] at constant [A] with slope of $k_1/k_2^{1/2}$ and intercept of $k_4[A]/k_2^{1/2}$. Fig. 1 illustrates the validity of such a relationship. Values of $k_1/k_2^{1/2}$ obtained from Fig. 1 are used to obtain the Arrhenius plot, Fig. 2. From the least squares slope of Fig. 2 and Shepp's (2) value of k_2

$$[5] \qquad k_1 = 5.8 \times 10^{10} \exp(-5280/RT) \text{ (mole/cc)}^{-1}\text{ s}^{-1}.$$

The alternate method (Method II) of finding the rate constant for metathetical methyl reactions involves the use of acetone-d_6. Additionally, it circumvents the need for an

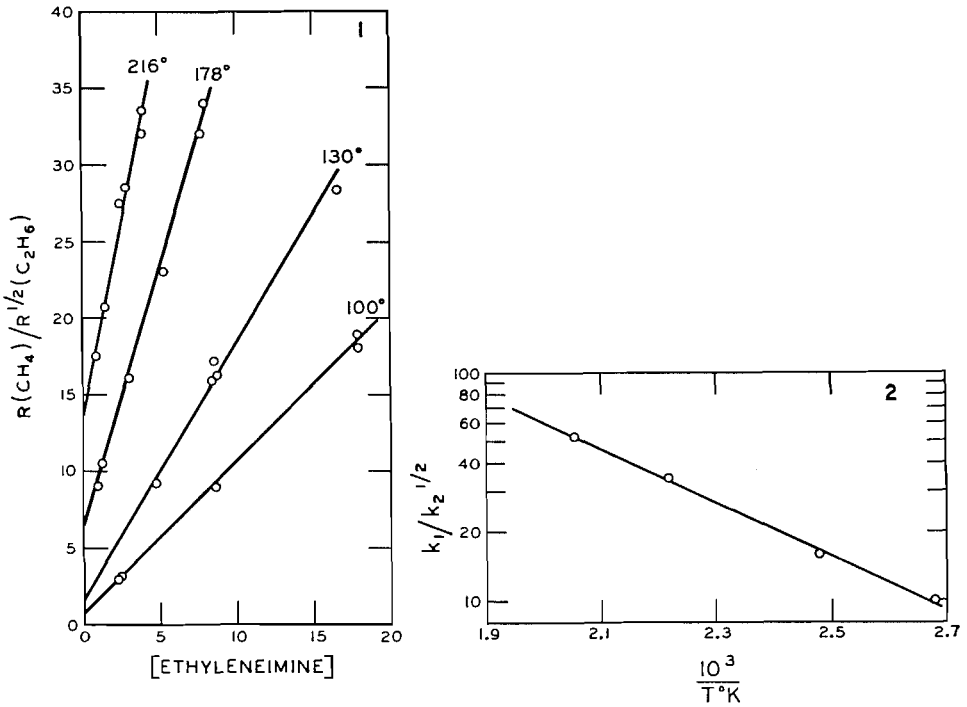

FIG. 1. Ratio of formation rates, $R(CH_4)/R^{1/2}(C_2H_6) \times 10^6$ (mole/cc)$^{1/2}$ s$^{-1/2}$ vs. ethyleneimine concentration $\times 10^7$ mole/cc.
FIG. 2. Ratio of rate constants, $k_1/k_2^{1/2}$ (mole/cc)$^{1/2}$ s$^{-1/2}$ vs. $1/T$ °K $\times 10^3$.

ethane measurement. When Ad_6 is photolyzed, the CD_3 radicals formed yield methane by the reactions

[6] $$CD_3 + Ad_6 \rightarrow CD_4 + \cdot CD_2COCD_3$$

[1] $$CD_3 + E \rightarrow CD_3H + R\cdot .$$

Based upon these reactions, the expression

$$\frac{k_1}{k_6} = \frac{R(CD_3H)}{R(CD_4)} \times \frac{[Ad_6]}{[E]}$$

is obtained. k_1/k_6 is derived from the appropriate pressure measurements and a mass spectrometric determination of CD_3H/CD_4. Figure 3 is a semilog plot of k_1/k_6, so derived, vs. $1/T$ over the range 120–260°; it conforms to the relationship $k_1/k_6 = 0.121 \exp(6000/RT)$. The value

$$k_6 = 7.25 \times 10^{11} \exp(-11400/RT) \text{ (mole/cc)}^{-1}\ \text{s}^{-1}$$

derived from the equations given by Creak, Dainton, and Ivin (4) affords

$$k_1 = 8.8 \times 10^{10} \exp(-5400/RT) \text{ (mole/cc)}^{-1}\ \text{s}^{-1}$$

in fair agreement with k_1 obtained from Method I when allowance is made for the experimental error in (k_1/k_6) and also that in the "best" value of k_6.

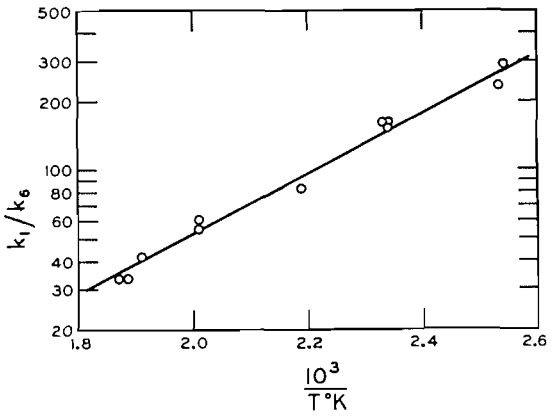

FIG. 3. Ratio of rate constants, k_1/k_6 vs. $1/T$ °K $\times 10^3$.

Up to this point the precise abstractive process to which k_1 refers has not been established (i.e. does k_1 refer to abstraction from nitrogen, carbon, or a combination of both?). To resolve this question acetone was photolyzed in the presence of ethyleneimine-d_4 (Ed_4). The pertinent reactions are

[7] $$CH_3 + Ed_4 \rightarrow CH_4 + \overline{CD_2CD_2N}\cdot$$

[4] $$CH_3 + A \rightarrow CH_4 + \cdot CH_2COCH_3$$

[8] $$CH_3 + Ed_4 \rightarrow CH_3D + \cdot\overline{CDCD_2NH}$$

from which the relationship

$$\frac{R(CH_4)}{R(CH_3D)} = \frac{k_7}{k_8} + \frac{k_4}{k_8}\frac{[A]}{[Ed_4]}$$

is developed. Again $R(CH_4)/R(CH_3D)$ should be a linear function of $[A]/[Ed_4]$. In fact, however, such an expression could not be applied with any reliability because the $m/e = 17$ peak due to CH_3D was less than 0.5% of the CH_4 peak under even the most favorable conditions of high temperature and large $[A]/[Ed_4]$.

The insignificance of reaction [8] compared to reaction [7] even at 200° implies that the only important metathetical process involving methyl radicals is abstraction of an amino hydrogen, thus supporting the assumption of Brinton and Voman (1) in this regard. Furthermore, a ratio $k_7/k_8 > 200$ suggests an activation energy difference between reactions [7] and [8] of roughly 5 kcal/mole, given comparable pre-exponential factors. This would represent an activation energy for reaction [8] of 5.3 + 5.0 = 10.3 kcal/mole. If, following McNesby (5), $E_D - D_H = 1.5$ kcal/mole, then the activation energy for

[9] $$CH_3 + \overline{CH_2CH_2NH} \rightarrow CH_4 + \cdot\overline{CHCH_2NH}$$

would be nearly 9 kcal/mole, in line with the values for similar metathetical processes in the isoelectronic species cyclopropane and ethylene oxide (6).

Since, as a result of the abstraction process, considerable amounts of $\overline{CH_2CH_2N}\cdot$ are formed, it is appropriate to consider reactions which have been proposed to account for their removal. In particular, the possible importance of the following have been investigated

[10] $$2\overline{CH_2CH_2N}\cdot \rightarrow N_2 + 2C_2H_4$$

[11] $$2\overline{CH_2CH_2N} \rightarrow (CH_2)_2NN(CH_2)_2$$

[12] $$\overline{CH_2CH_2N}\cdot \rightarrow CH_3 + HCN$$

Brinton and Volman (1) have proposed [10] on the basis of a mass spectrometric analysis of reactions run to completion, while the occurrence of [11] rests upon the appearance of a peak at $m/e = 84$.

In the present system repeated attempts in the interval 100–250° to observe ethylene by gas chromatographic analysis of the reaction products only established its absence. The unimportance of [10] was additionally confirmed by the absence of any excess N_2 over the small amount associated with residual air in the system. With reaction [11], it was possible to isolate by gas chromatography a sufficient amount of a particular fraction which indicated major responses in its mass spectrum at $m/e = 28, 42, 84$. This is partial evidence that the gas chromatographic peak may be attributed to the dimer, $(CH_2)_2NN(CH_2)_2$, which has been prepared and characterized by Graefe and Mayer (7).

Both HCN and CH_4 have been obtained as principal products of the low pressure reaction of H atoms with ethyleneimine (8). It was proposed that such products arose as a consequence of reaction [12]. Attempts to observe HCN under the present conditions proved futile as might be expected where an excess of amine is present. Evidence for the insignificance of [12] hinges on analyses of the mass spectra obtained in the determination of k_7 according to Method II. By applying experimentally established cracking patterns of CD_4, CD_3H, and CH_4 in the range $m/e = 12$ to $m/e = 21$, it was concluded that less than 0.5% of the methane formed could have arisen via reactions [12] and [7]. A low (0.01) quantum yield for methane production was also observed in the mercury-photosensitized decomposition of ethyleneimine (9).

With regard to the ethyleneimino radical, it can only be concluded that, while it is no doubt a principal product of the abstraction process (reaction [7]) among the reactions previously proposed ([10]–[12]) for this species only reaction [11] is of any consequence in the present system. Therefore it must be stated that the more interesting reactions [10] and [12] are still not definitely established.

1. R. K. Brinton and D. H. Volman. J. Chem. Phys. **20**, 25 (1952).
2. Allan Shepp. J. Chem. Phys. **24**, 939 (1956).
3. A. F. Trotman-Dickenson and E. W. R. Steacie. J. Chem. Phys. **19**, 329 (1951).
4. G. A. Creak, F. S. Dainton, and K. J. Ivin. Trans. Faraday Soc. **58**, 326 (1962).
5. J. R. McNesby. J. Phys. Chem. **64**, 1671 (1960).
6. A. F. Trotman-Dickenson. Gas kinetics. Butterworths, London, 1955. p. 200.
7. A. F. Graefe and R. E. Meyer. J. Am. Chem. Soc. **80**, 3939 (1958).
8. J. W. S. Jamieson and C. A. Winkler. J. Phys. Chem. **60**, 1542 (1956).
9. C. Luner and H. Gesser. J. Phys. Chem. **62**, 1148 (1957).

Received April 28, 1965.
Petroleum Research Division,
Research Council of Alberta,
Edmonton, Alberta.

THE PREPARATION AND HYDROLYSIS OF ALKYL HYDROGEN METHYLPHOSPHONATES

Leonard Keay[1]

Although the hydrolysis of secondary phosphate esters (I) has been extensively studied (1–4), the hydrolysis of phosphonate monoesters (II) has received little attention (5, 6), although several esters, mainly those of aromatic phosphonic acids, have been prepared by various means (7–12).

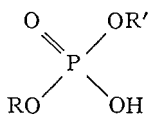

I

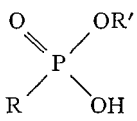

II

The phosphonate monoesters are similar to phosphate diesters, being hydrolyzed in strongly acid solution, very stable at neutral pH's, and very slowly hydrolyzed in alkaline solutions (3, 4). Studies on the phosphonate diesters (13, 14) have shown that, just as with the phosphate triesters (15, 16), hydrolysis of one ester group proceeds with P—O fission in alkali and C—O fission in acid solution. It was, therefore, of some interest to study accurately the rates of solvolysis of a series of phosphonate monoesters and see if the results corroborate the mechanisms postulated for dialkyl phosphates (3, 4). Preliminary experiments showed that the hydrolysis of phosphonate monoesters was too slow for accurate measurement in alkaline or neutral solution and detailed measurements were, therefore, only made in acid solution. The pK of ethyl hydrogen methylphosphonate was determined to be 2.00 at 25° and when the hydrolysis rate at 130.5° was determined at several pH's, the observed first-order rate constant increased as the pH decreased, suggesting that, at least over the pH range 1–5, the only substrate involved in hydrolysis

[1]*Present address: Central Research Department, Monsanto Company, St. Louis 66, Mo., U.S.A.*

With regard to the ethyleneimino radical, it can only be concluded that, while it is no doubt a principal product of the abstraction process (reaction [7]) among the reactions previously proposed ([10]–[12]) for this species only reaction [11] is of any consequence in the present system. Therefore it must be stated that the more interesting reactions [10] and [12] are still not definitely established.

1. R. K. Brinton and D. H. Volman. J. Chem. Phys. **20**, 25 (1952).
2. Allan Shepp. J. Chem. Phys. **24**, 939 (1956).
3. A. F. Trotman-Dickenson and E. W. R. Steacie. J. Chem. Phys. **19**, 329 (1951).
4. G. A. Creak, F. S. Dainton, and K. J. Ivin. Trans. Faraday Soc. **58**, 326 (1962).
5. J. R. McNesby. J. Phys. Chem. **64**, 1671 (1960).
6. A. F. Trotman-Dickenson. Gas kinetics. Butterworths, London, 1955. p. 200.
7. A. F. Graefe and R. E. Meyer. J. Am. Chem. Soc. **80**, 3939 (1958).
8. J. W. S. Jamieson and C. A. Winkler. J. Phys. Chem. **60**, 1542 (1956).
9. C. Luner and H. Gesser. J. Phys. Chem. **62**, 1148 (1957).

Received April 28, 1965.
Petroleum Research Division,
Research Council of Alberta,
Edmonton, Alberta.

THE PREPARATION AND HYDROLYSIS OF ALKYL HYDROGEN METHYLPHOSPHONATES

Leonard Keay[1]

Although the hydrolysis of secondary phosphate esters (I) has been extensively studied (1–4), the hydrolysis of phosphonate monoesters (II) has received little attention (5, 6), although several esters, mainly those of aromatic phosphonic acids, have been prepared by various means (7–12).

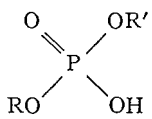

I

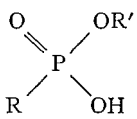

II

The phosphonate monoesters are similar to phosphate diesters, being hydrolyzed in strongly acid solution, very stable at neutral pH's, and very slowly hydrolyzed in alkaline solutions (3, 4). Studies on the phosphonate diesters (13, 14) have shown that, just as with the phosphate triesters (15, 16), hydrolysis of one ester group proceeds with P—O fission in alkali and C—O fission in acid solution. It was, therefore, of some interest to study accurately the rates of solvolysis of a series of phosphonate monoesters and see if the results corroborate the mechanisms postulated for dialkyl phosphates (3, 4). Preliminary experiments showed that the hydrolysis of phosphonate monoesters was too slow for accurate measurement in alkaline or neutral solution and detailed measurements were, therefore, only made in acid solution. The pK of ethyl hydrogen methylphosphonate was determined to be 2.00 at 25° and when the hydrolysis rate at 130.5° was determined at several pH's, the observed first-order rate constant increased as the pH decreased, suggesting that, at least over the pH range 1–5, the only substrate involved in hydrolysis

[1]*Present address: Central Research Department, Monsanto Company, St. Louis 66, Mo., U.S.A.*

Can. J. Chem. Downloaded from www.nrcresearchpress.com by 210.87.254.6 on 09/05/12
For personal use only.

is the neutral species. If this is so, then the specific rate constant is given by $k_N = k_1/$ [neutral ester], where k_1 is the observed rate constant at any pH and the [neutral ester] at that pH is calculated from the pK. The results (Table I) show that in view of the uncertainty of the pH and pK at 130.5°, the k_N is reasonably constant.

TABLE I

The effect of pH on hydrolysis of ethyl hydrogen methylphosphonate; temperature, 130.5°; ester, 0.10 N

pH*	5.00	2.48	2.41	2.00	1.65	0†
Fraction undissociated	0	0.25	0.28	0.50	0.69	1.00
10^2k_1, h^{-1}	0.00	2.02	2.30	4.24	4.32	11.2
k_N	—	8.1	8.2	8.5	6.3	11.2

*The ester was dissolved in $N/1$ benzene sulfonic acid solution, and 10 N sodium hydroxide added until the desired pH was attained (pH meter), then 5-ml aliquots were transferred to ampoules, sealed, placed in the constant temperature bath (time zero). Ampoules were removed at suitable time intervals, chilled to quench reaction, and the contents titrated with standard alkali.

†Rate in 1 N benzene sulfonic acid solution, the pH of a $N/1$ solution of strong acid assumed to be zero.

The larger positive deviation in 1 N benzene sulfonic acid might suggest that two processes occur, one an uncatalyzed hydrolysis of the undissociated hemiester and the other in strongly acid solutions an acid-catalyzed reaction as with the phosphate diesters. The rates of hydrolysis of a series of esters were determined (Table II) and the relative

TABLE II

The rates of hydrolysis of alkyl hydrogen methylphosphonates in N $PhSO_3H$

	[Ester], moles/liter	Temp., °C	k_1, h^{-1}
Methyl hydrogen methylphosphonate	0.30	112.5	0.0157
	0.20	130.5	0.057
Ethyl hydrogen methylphosphonate	0.20	112.5	0.0148
	0.20	130.5	0.112
Isopropyl hydrogen methylphosphonate	0.10	91.3	0.0401
	0.20	100.4	0.097
	0.30	102.7	0.175
	0.20	105.5	0.244
Neopentyl hydrogen methylphosphonate	0.10	130.0	0.130

rates of hydrolysis at 130.5° calculated to be methyl, 1.06; ethyl, 1.00; isopropyl, 40; neopentyl, 1.20. The order of reactivity is very close to that observed in the hydrolysis of the diesters (13) and it suggests that the main mechanism involves C—O fission, which has been suggested for the phosphate diesters (3, 4). The acid catalysis also suggests C—O fission since the hydrolysis of phenyl esters which cannot undergo C—O fission is not acid catalyzed (17). The reaction observed is probably a mixture of acid-catalyzed and uncatalyzed reactions. The acid-catalyzed reaction probably proceeds by carbonium ion formation from the protonated hemiester, as has been shown for the 2-ethylhexyl and neopentyl diesters (13, 14). The mechanism of the uncatalyzed reaction of the primary esters could be either C—O fission to form phosphonate anion and carbonium ion, or by an attack by a water molecule on either the carbon or phosphorus atom, although the effect of changing the alkyl group upon the rate makes either mechanism seem unlikely since steric effects are quite marked in substitution reactions at both neopentyl (18, 19) and phosphoryl groups (20, 21, 22).

Can. J. Chem. Downloaded from www.nrcresearchpress.com by 210.87.254.6 on 09/05/12
For personal use only.

EXPERIMENTAL

Materials

Phosphonate monoesters were generally prepared by the hydrolysis of the corresponding phosphonochloridate in an aqueous acetone medium. Kinetic studies and neutralization equivalents have shown the reaction to give quantitative yields (20). The same preparation has been carried out with aqueous formic acid and the hemiester demonstrated to have the correct neutralization equivalent (23). The neopentyl hydrogen methylphosphonate was obtained from neopentyl alcohol and methylphosphonic dichloride by mono substitution, followed by hydrolysis of the unisolated neopentyl methylphosphonochloridate.

Methyl hydrogen methylphosphonate.—6.4 g (0.05 mole) methyl methylphosphonochloridate was added slowly with external cooling by ice water. After 24 h, the solvent was removed under reduced pressure and the residual oil dried in a vacuum desiccator containing potassium hydroxide pellets and finally distilled *in vacuo* to yield 5.1 g (90% yield) colorless oil, b.p. 120° at 0.2 mm. Microanalysis: Found P, 28.3; C, 21.5; H, 6.51. $C_2H_7PO_3$ requires P, 27.7; C, 21.4; H, 6.25.

The following other compounds were prepared in a similar manner.

Ethyl hydrogen methylphosphonate.—86% yield, b.p. 120° at 0.3 mm. Microanalysis: Found P, 24.9; C, 29.4; H, 7.32. $C_3H_9PO_3$ requires P, 24.6; C, 28.6; H, 7.14.

Isopropyl hydrogen methylphosphonate.—81% yield, b.p. 123–125° at 0.2 mm. Microanalysis: Found P, 23.1; C, 35.0; H, 7.82. $C_4H_{11}PO_3$ requires P, 22.5; C, 34.8; H, 7.97.

Neopentyl hydrogen methylphosphonate.—44 g neopentyl alcohol and 67.5 triethylamine were dissolved in 200 ml ether and placed in a three-necked flask fitted with stirrer, dropping funnel, and drying tube; 33 g methyl phosphonic dichloride in 100 ml ether was slowly added with stirring and external ice cooling. The mixture was kept at room temperature overnight. The precipitated amine hydrochloride was removed by filtration, but as the filtrate became cloudy on standing, the ether was washed with dilute hydrochloric acid and then with water. The ether layer was dried, the solvent removed, and the residue distilled *in vacuo* to yield a colorless oil, acid to methyl red indicator. Yield 18 g (38%), b.p. 150° at 5 mm, 170° at 9 mm. Microanalysis: Found P, 17.9; C, 43.8; H, 9.07. $C_8H_{15}PO_3$ requires P, 18.7; C, 43.4; H, 9.04.

Evaluation of Rates of Hydrolysis

The hydrolysis of monoalkyl esters was determined by titration of the second acid group liberated upon hydrolysis. A solution of the ester in reaction medium (usually *N*/1 benzene sulfonic acid) was prepared and 5-ml aliquots pipetted into test tubes which were then sealed into vials. The vials were then immersed in a constant-temperature oil bath and at suitable time intervals a vial was removed, cooled, and opened and the contents titrated with standard sodium hydroxide solution using phenolphthalein indicator with a stream of CO_2-free nitrogen to exclude atmospheric CO_2 and prevent end-point fade. CO_2-free water was used for preparing all solutions and at all stages in the work.

The reactions were found to follow a first-order disappearance of reactant.

1. O. Bailly and J. Gaume. Bull. Soc. Chim. France, Ser. 5, **2**, 354 (1935); **3**, 1396 (1936).
2. R. H. A. Plimmer and W. J. N. Burch. J. Chem. Soc. 279, 292 (1929).
3. P. C. Haake and F. H. Westheimer. J. Am. Chem. Soc. **83**, 1102 (1961).
4. C. A. Bunton *et al.* J. Chem. Soc. 3574 (1958); 3293 (1960).
5. E. Cherbuliez, F. Hunkeler, and J. Rabinowitz. Helv. Chim. Acta, **44**, 1817 (1961).
6. P. Nylen. Svensk. Kem. Tidskr. **49**, 29, 79 (1937).
7. A. Michaelis. Ann. **181**, 265 (1876).
8. A. Michaelis and F. Kammerer. Ber. **8**, 1306 (1875).
9. H. H. Hatt. J. Chem. Soc. 2412 (1929); 776 (1933).
10. A. Burger and J. J. Anderson. J. Am. Chem. Soc. **79**, 3575 (1957).
11. A. Varon, F. Jakob, K. C. Park, and W. Riemann III. Talanta, **9**, 573 (1962).
12. E. Cherbuliez, F. Hunkeler, and J. Rabinowitz. Helv. Chim. Acta, **44**, 1802, 1810, 1812, 1815 (1961).
13. R. F. Hudson and L. Keay. J. Chem. Soc. 2463 (1956).
14. L. Keay. J. Org. Chem. **28**, 1426 (1963).
15. E. Blumenthal and J. B. M. Herbert. Trans. Faraday Soc. **41**, 611 (1945).
16. W. Gerrard, W. J. Green, and R. A. Nutkins. J. Chem. Soc. 4076 (1952).
17. C. A. Barnard, C. A. Bunton *et al.* Chem. Ind. 760 (1955).
18. I. Dostrovsky and E. D. Hughes. J. Chem. Soc. 157 (1946).
19. S. Winstein and H. Marshall. J. Am. Chem. Soc. **74**, 1120 (1952).
20. R. F. Hudson and L. Keay. J. Chem. Soc. 1859 (1960).
21. I. Dostrovsky and M. Halmann. J. Chem. Soc. 503, 508, 511, 517 (1953).
22. L. Keay. J. Org. Chem. **28**, 329 (1963).
23. R. F. Hudson and L. Keay. J. Chem. Soc. 1865 (1960).

Received March 4, 1965.
Queen Mary College,
London, E.1, England.

Can. J. Chem. Downloaded from www.nrcresearchpress.com by 210.87.254.6 on 09/05/12
For personal use only.

REACTION OF AMINES WITH DIMETHYLTHIOFORMAMIDE[1,2]

GEORGE R. PETTIT AND LORRIN R. GARSON

Formylation of aromatic amines has been accomplished by the use of dimethylformamide in the presence of sodium methoxide (1). The reaction was found to proceed in a comparable manner with sodium amide or hydride in place of sodium methoxide.[3] However, acylation was not observed employing dimethylformamide alone or in the presence of sodium hydroxide. Subsequently, it became of interest to determine whether substitution of dimethylformamide by a thioamide would provide a route to thioformanilides or follow a different reaction pathway. Thioamides are known (2) to react with amines yielding amidines and in special cases, for example, with 5-thioformamido-6-aminopyrimidines, to produce cyclic formamidines[4] characteristic of the imidazole (in the example cited a purine) ring system. Thus, reaction between an amine and dimethylthioformamide might be expected to yield an N-substituted-N′,N′-dimethylformamidine. The following experiments were undertaken to ascertain the course of reaction between primary amines and dimethylthioformamide in the presence of sodium methoxide.

Dimethylthioformamide, prepared essentially as described by Willstätter (4) in 1909 by treating dimethylformamide with phosphorus pentasulphide,[5] was allowed to react at reflux with 1-aminonaphthalene and sodium methoxide. After 1.5 h, the mixture was cooled, diluted with water, and separated into neutral and basic fractions. When the neutral fraction was found to represent only dimethylthioformamide, thereby eliminating 1-thioformamidonaphthalene from further consideration, the basic fraction was further characterized by conversion to a red crystalline 1,3,5-trinitrobenzene derivative. The base was also found to form bright yellow picrate and styphnate salts. A pure specimen of the basic product (I), m.p. 40–40.5°, was obtained by destroying the trinitrobenzene π-complex with dilute hydrochloric acid. Infrared spectra of both the π-complex and free base (I) displayed a strong absorption band at 1 630 cm^{-1} which was initially assigned and later found to represent a C=N stretching frequency. An infrared band at 1 706 cm^{-1}, reminiscent of carbonyl-type absorption, appeared in infrared spectra of both the picrate and styphnate salts and was eventually attributed to a protonated form of the amidine group.

Employing (7) mass spectral data and results of elemental microanalyses, the base (I) was assigned empirical formula $C_{13}H_{14}N_2$. Considering the composition, chemical properties, and infrared spectra of the base and three derivatives, the substance was readily assumed to be N-(1-naphthyl)-N′,N′-dimethylformamidine (I). Assignments for the positively charged fragments believed to result from simple C–N bond cleavage (8) of the formamidine sidechain have been suggested in structure II. As might be expected,

[1]*The present contribution may be considered Part XVI of our series on Antineoplastic agents. For Part XV, refer to a paper by G. R. Pettit, D. S. Blonda, and R. A. Upham, Can. J. Chem. 43, 1798 (1965).*

[2]*Abstracted in part from the Master of Science thesis submitted by L. R. Garson to the Graduate School, University of Maine, June, 1964.*

[3]*Later the acylation reaction was extended to certain aliphatic amines and to substitution of dimethylacetamide (found to yield acetamides) for dimethylformamide: unpublished experiments by G. R. Pettit and M. V. Kalnins.*

[4]*Cyclization of appropriately substituted 5-thioformamidopyrimidines has been shown (3) to occur readily in hot pyridine or quinoline solution or in methanol containing sodium methoxide. Synthesis of linear formamidines employing an analogous (but intermolecular) reaction between a thioformamide and amine does not appear to have been reported.*

[5]*Recently (5) dimethylthioformamide has been prepared from dimethyl-amine, chloroform, and sodium hydrogen sulfide. Several less convenient methods (6) have also been used in attempts to obtain dimethylthioformamide.*

Can. J. Chem. Downloaded from www.nrcresearchpress.com by 210.87.254.6 on 09/05/12
For personal use only.

REACTION OF AMINES WITH DIMETHYLTHIOFORMAMIDE[1,2]

GEORGE R. PETTIT AND LORRIN R. GARSON

Formylation of aromatic amines has been accomplished by the use of dimethylformamide in the presence of sodium methoxide (1). The reaction was found to proceed in a comparable manner with sodium amide or hydride in place of sodium methoxide.[3] However, acylation was not observed employing dimethylformamide alone or in the presence of sodium hydroxide. Subsequently, it became of interest to determine whether substitution of dimethylformamide by a thioamide would provide a route to thioformanilides or follow a different reaction pathway. Thioamides are known (2) to react with amines yielding amidines and in special cases, for example, with 5-thioformamido-6-aminopyrimidines, to produce cyclic formamidines[4] characteristic of the imidazole (in the example cited a purine) ring system. Thus, reaction between an amine and dimethylthioformamide might be expected to yield an N-substituted-N′,N′-dimethylformamidine. The following experiments were undertaken to ascertain the course of reaction between primary amines and dimethylthioformamide in the presence of sodium methoxide.

Dimethylthioformamide, prepared essentially as described by Willstätter (4) in 1909 by treating dimethylformamide with phosphorus pentasulphide,[5] was allowed to react at reflux with 1-aminonaphthalene and sodium methoxide. After 1.5 h, the mixture was cooled, diluted with water, and separated into neutral and basic fractions. When the neutral fraction was found to represent only dimethylthioformamide, thereby eliminating 1-thioformamidonaphthalene from further consideration, the basic fraction was further characterized by conversion to a red crystalline 1,3,5-trinitrobenzene derivative. The base was also found to form bright yellow picrate and styphnate salts. A pure specimen of the basic product (I), m.p. 40–40.5°, was obtained by destroying the trinitrobenzene π-complex with dilute hydrochloric acid. Infrared spectra of both the π-complex and free base (I) displayed a strong absorption band at 1 630 cm^{-1} which was initially assigned and later found to represent a C=N stretching frequency. An infrared band at 1 706 cm^{-1}, reminiscent of carbonyl-type absorption, appeared in infrared spectra of both the picrate and styphnate salts and was eventually attributed to a protonated form of the amidine group.

Employing (7) mass spectral data and results of elemental microanalyses, the base (I) was assigned empirical formula $C_{13}H_{14}N_2$. Considering the composition, chemical properties, and infrared spectra of the base and three derivatives, the substance was readily assumed to be N-(1-naphthyl)-N′,N′-dimethylformamidine (I). Assignments for the positively charged fragments believed to result from simple C–N bond cleavage (8) of the formamidine sidechain have been suggested in structure II. As might be expected,

[1]*The present contribution may be considered Part XVI of our series on Antineoplastic agents. For Part XV, refer to a paper by G. R. Pettit, D. S. Blonda, and R. A. Upham, Can. J. Chem. 43, 1798 (1965).*

[2]*Abstracted in part from the Master of Science thesis submitted by L. R. Garson to the Graduate School, University of Maine, June, 1964.*

[3]*Later the acylation reaction was extended to certain aliphatic amines and to substitution of dimethylacetamide (found to yield acetamides) for dimethylformamide: unpublished experiments by G. R. Pettit and M. V. Kalnins.*

[4]*Cyclization of appropriately substituted 5-thioformamidopyrimidines has been shown (3) to occur readily in hot pyridine or quinoline solution or in methanol containing sodium methoxide. Synthesis of linear formamidines employing an analogous (but intermolecular) reaction between a thioformamide and amine does not appear to have been reported.*

[5]*Recently (5) dimethylthioformamide has been prepared from dimethyl-amine, chloroform, and sodium hydrogen sulfide. Several less convenient methods (6) have also been used in attempts to obtain dimethylthioformamide.*

Can. J. Chem. Downloaded from www.nrcresearchpress.com by 210.87.254.42 on 09/05/12
For personal use only.

fragments corresponding to *m/e* 57 and 71 were found in relatively small abundance, in fact less than 10%, as a result of further fragmentation. Further support for the formamidine structure (I) was obtained by partially hydrolyzing (9*a*) the base to 1-formamidonaphthalene and the assignment was finally confirmed by direct comparison with an authentic sample (I) prepared (9*b*) from dimethylformamide and naphthyl isocyanate.[6]

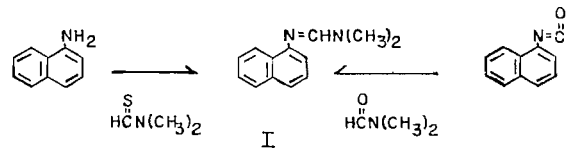

I

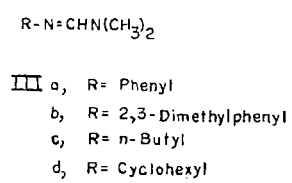

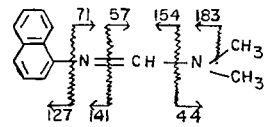

II

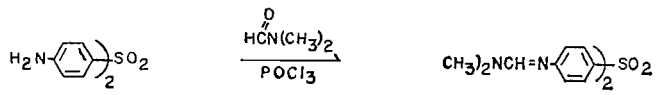

IV

Meanwhile, the dimethylthioformamide – sodium methoxide reaction sequence was applied to three aromatic and two aliphatic-type amines. Further study of the reaction was terminated when each amine was found to yield a formamidine (III*a*–III*d* and IV). Except for 2,3-dimethylaniline derivative III*b*, the structure of each formamidine was confirmed by comparison with an authentic sample prepared (9*a*, 10, or 11) employing either the dimethylformamide (cf. IV) or isocyanate route. Finally, reaction between dimethylthioformamide and 1-naphthylamine was studied in respect to base requirements. Substituting sodium hydroxide for the alkoxide led to a 90% yield of formamidine I (as the trinitrobenzene derivative). Under similar conditions, 1-aminonaphthalene and dimethylthioformamide alone provided a 97% yield of formamidine (I). At this point the investigation's original objectives had been satisfied and no further attempt was made to extend the scope of the reaction.

In view of the preceding experiments involving 1-aminonaphthalene and dimethylthioformamide, reaction between suitably constituted amines and thioformamides may provide a useful route to certain formamidines.

EXPERIMENTAL

All solvents were redistilled and both dimethylformamide, b.p. 36° (5.5 mm), and dimethylthioformamide were stored over molecular sieve (Fisher type 4A, see reference 1, footnote 9). Dry sodium methoxide was

[6]*Other trisubstituted formamidines have been prepared by this method or by allowing an amine to react with a formamide in the presence of phosphorous oxychloride (10), sulfonyl chloride (11), or phosphorous pentachloride (12). A variety of other methods (13) have been employed for synthesis of the parent system formamidine (14), symmetrically di-substituted formamidines (15), and unsymmetrically disubstituted formamidines (13, 16).*

Can. J. Chem. Downloaded from www.nrcresearchpress.com by 210.87.254.42 on 09/05/12
For personal use only.

prepared in this laboratory. The purity of each analytical specimen was assessed by thin-layer chromatography on silica gel G (E. Merck, AG., Darmstadt, Germany) containing calcium sulfate as binder. Thin-layer chromatograms of the 1,3,5-trinitrobenzene complexes and the picrate and styphnate salts were prepared using 15:85 water–tetrahydrofuran as mobile phase (and developed with iodine). Substituting, for example, 1:9 water–tetrahydrofuran or 1:1 chloroform–methanol as eluant led to considerable streaking of the chromatogram.

Melting points were observed employing a Kofler melting point apparatus and are corrected. The infrared spectra were recorded (using potassium bromide) by Dr. R. A. Hill of these laboratories. Microanalytical determinations were provided by Dr. A. Bernhardt, Max-Planck Institut, Mülheim, Germany.

Dimethylthioformamide

Quantities of dimethylformamide amounting to 500 ml (56% yield) were prepared from dimethylformamide (770 ml, 10 moles) and phosphorus pentasulfide (888 g, 4 moles) as described by Willstätter and Wirth (4). The thioformamide was distilled *in vacuo* through a 4-ft vacuum-jacketed column packed with glass helices. The fraction boiling at 77.0–77.6° (3.4 mm) was collected and stored over molecular sieve.

Anal. Calcd. for C_3H_7NS: C, 40.44; H, 7.92; N, 15.72; S, 35.92. Found: C, 40.25; H, 7.67; N, 15.99; S, 35.73.

Several new physical constants including a proton magnetic resonance spectrum of dimethylthioformamide have recently been recorded by Walter and Maerten (5).

N-(1-Naphthyl)-N′,N′-dimethylformamidine (I)

Procedure A

A mixture of dimethylthioformamide (10 ml), 1-aminonaphthalene (0.5 g), and sodium methoxide (0.38 g) was heated at reflux 1.5 h. After it had cooled, the mixture was poured into water (25 ml) and carefully acidified (litmus) with 12 *N* hydrochloric acid. The acidic solution was extracted with diethyl ether and next made basic (litmus) with 6 *N* sodium hydroxide and extracted with diethyl ether. The latter combined and dry (magnesium sulfate) ethereal extract was concentrated (*in vacuo*, steam bath) to a viscous oil. A solution of the product in absolute ethanol (30 ml) was treated with a saturated ethanolic solution of 1,3,5-trinitrobenzene. The solution turned red immediately and approximately 2 minutes later a red crystalline complex began to separate. The *trinitrobenzene complex* weighed 0.89 g (94%) and melted at 142–142.5°. Five recrystallizations from absolute ethanol caused no change in the melting point but produced a pure specimen as fibrous red needles; ν_{max} 1 630, 1 565, and 1 545 cm^{-1}.

Anal. Calcd. for $C_{19}H_{17}N_5O_6$: C, 55.45; H, 4.17; N, 17.02. Found: C, 55.25; H, 4.50; N, 17.09.

A specimen of the 1,3,5-trinitrobenzene complex was treated with 5% hydrochloric acid. The red coloration disappeared at once and the acidic solution was successively extracted with benzene, made basic with potassium hydroxide, and extracted with diethyl ether. The combined ethereal extract was dried (magnesium sulfate) and evaporated (steam bath) to a viscous oil. A specimen of *N-(1-naphthyl)-N′,N′-dimethylformamidine (I)*[7] crystallized from 2-propanol–water as colorless needles melting at 39.5–40.5° (lit. m.p. 40–40.5°, ref. 11); ν_{max} 3 000, 2 900, 1 630 (broad), 1 570, 1 500, 1 460, 1 440, 1 380, 1 270, 1 230, 1 110, 1 080, 1 043, 1 015, 970, 800, and 775 cm^{-1}; mass spectrometry: *m/e* 198 (M^+), 197, 183, 170, 156, 154, 153, 141, 129, 128, 127, 126, 99, 44, 42, 28.[8] Based on an isotope abundance of 15 at M + 1 (199) and 0.8 at M + 2 (200), the product was found consistent with empirical formula $C_{13}H_{14}N_2$.

The *picrate derivative* (prepared in absolute ethanol) of formamidine I recrystallized from absolute ethanol as bright yellow needles melting at 212–213°; ν_{max} 1 705, 1 625, and 1 610 cm^{-1}.

Anal. Calcd. for $C_{19}H_{17}N_5O_7$: C, 53.39; H, 4.00; N, 16.39. Found: C, 52.94; H, 4.04; N, 16.03.

Recrystallizing (3 times) the *styphnate derivative* (prepared in absolute ethanol employing styphnic acid) from absolute ethanol yielded a pure sample of fine yellow needles; m.p. 214–215°; ν_{max} 1 705, 1 635, and 1 565 cm^{-1}.

Anal. Calcd. for $C_{19}H_{17}N_5O_8$: C, 51.47; H, 3.86; N, 15.80. Found: C, 51.82; H, 4.12; N, 15.43.

When reaction between 1-aminonaphthalene and dimethylthioformamide was repeated as described above substituting sodium hydroxide (0.28 g) for sodium methoxide and the basic reaction product treated with 1,3,5-trinitrobenzene, a 1.3 g yield (90%), m.p. 142–143°, of the formamidine (I) complex was isolated. Repeating the same experiment using only 1-aminonaphthalene and dimethylthioformamide led to 1.4 g (97%) of the formamidine (I) 1,3,5-trinitrobenzene complex melting at 142–142.5°. In both cases the trinitrobenzene derivative was found to be identical[7] with the corresponding samples noted above and with that prepared below in Procedure B.

Procedure B

By the general method described by Jovtscheff and Falk (10) formamidine I was prepared (in 82% yield) from 1-naphthyl isocyanate (6.2 g) and dimethylformamide (15 ml). The product (6.4 g) was converted

[7]*Identity was established by mixture melting point determination and infrared spectral comparison with an authentic sample.*

[8]*All values less than 10% of the base peak (198) were omitted.*

Can. J. Chem. Downloaded from www.nrcresearchpress.com by 210.87.254.42 on 09/05/12
For personal use only.

to the 1,3,5-trinitrobenzene complex in ethanol solution. Two recrystallizations from ethanol gave a pure specimen melting at 142–142.5°.

N-Phenyl-N',N'-dimethylformamidine (IIIa)

The crude formamidine obtained by allowing aniline (0.65 g) to react with dimethylthioformamide (20 ml) as described in procedure A (for formamidine I) was treated with a saturated solution of styphnic acid in absolute ethanol. The yellow styphnate was collected, washed with ethanol, and dried; the yield was 0.61 g (18%). One recrystallization from ethanol led to bright yellow platelets melting at 169–170°. The same substance (III*a*, styphnate, m.p. 169–170°) was obtained as previously reported (10), using phenyl isocyanate and dimethylformamide. The styphnate salts were found to be mutually identical.[7]

N-(2,3-Dimethylphenyl)-N',N'-dimethylformamidine (IIIb)

Dimethylthioformamide (15 ml) was allowed to react with 2,3-dimethylaniline (5.0 g) as noted for preparation of formamidine I (procedure A). A solution of the crude oily formamidine in absolute ethanol was treated with a saturated ethanolic solution of picrate acid. The yellow solid which separated weighed 1.5 g (16%). Four recrystallizations from absolute ethanol gave bright yellow platelets melting at 177–178°.

Anal. Calcd. for $C_{17}H_{19}N_5O_7$: C, 50.37; H, 4.72; N, 17.28. Found: C, 50.32; H, 5.03; N, 17.54.

4,4-Bis(N',N'-dimethylguanyl)diphenyl Sulfone (IV)

A solution of phosphorous oxychloride (13.0 g) in tetrahydrofuran (30 ml) was added dropwise (during 0.5 h) to a solution composed of dimethylformamide (12.4 g) and tetrahydrofuran (50 ml). Stirring was continued at room temperature for 0.5 h and a solution of 4,4'-diaminodiphenyl sulfone (7.0 g) in tetrahydrofuran (50 ml) was next added dropwise to the reaction mixture. The solid hydrochloride salt which separated was collected and washed with diethyl ether. An aqueous solution of the hydrochloride was treated with potassium hydroxide until the solution became basic (litmus). The mixture was extracted with chloroform and the combined extract was dried and solvent removed *in vacuo*. The crystalline residue weighed 8.1 g. Two recrystallizations from tetrahydrofuran yielded a sample of colorless platelets melting at 146–148°. Additional recrystallization (3 times) from tetrahydrofuran – diethyl ether provided an analytical specimen melting at 149–150°.

Anal. Calcd. for $C_{18}H_{22}N_4O_2S$: C, 60.32; H, 6.19; N, 15.63; O, 8.93; S, 8.93. Found: C, 60.14; H, 6.07; N, 15.67; S, 9.11.

Reaction between dimethylthioformamide and 4,4'-diphenyl sulfone (3.0 g) as illustrated for the preparation of formamidine I proved less satisfactory for preparation of amidine IV. A thin-layer chromatogram (methanol as mobile phase with sulfuric acid development) indicated that less than 30% of the required formamidine (IV) was formed. When the same reaction was repeated in absence of sodium methoxide, only starting amine was isolated.

N-Butyl-N',N'-dimethylformamidine (IIIc)

Applying the general procedure described by Bredereck (11), for reaction between *n*-butylamine (13.2 g) and the dimethylformamide (41.0 g) – phosphorous oxychloride (34.6 g) reagent, afforded 7.1 g (31%) of formamidine III*c* boiling at 61–62° (15 mm). Conversion of 1-butylamine (10.0 g) to formamidine III*c* (2.1 g, 12%) was even less rewarding by use of the dimethylthioformamide (10 ml) route (see I, procedure A). Here, the reaction mixture was heated at reflux 48 h. The identical composition of both products was confirmed by infrared spectral comparison.

N-Cyclohexyl-N',N'-dimethylformamidine (IIId)

Both procedures summarized in the preceding experiment (see III*c*) were repeated with cyclohexylamine (10 g), and essentially analogous yields of oily cyclohexylformamidine III*d* were obtained. Both specimens (III*d*) were converted to styphnate salt derivatives (m.p. 186–187°, ref. 11 reports m.p. 186–187°) and the salts were found to be identical.[7]

ACKNOWLEDGMENTS

This investigation was aided by grant Nos. T-79D and T-79Ef rom the American Cancer Society. We are also grateful to John Occolowitz, Defence Standards Laboratories, Maribyrnong, Victoria, Australia, for determining the mass spectrum of formamidine I and to T. M. Liu for performing a number of introductory experiments.

1. G. R. Pettit, M. V. Kalnins, T. M. H. Liu, E. G. Thomas, and K. Parent. J. Org. Chem. **26**, 2563 (1961).
2. A. Bernthsen. Ann. **192**, 1 (1878); **184**, 321 (1876).
3. A. R. Todd, F. Bergel, and Karimullah. J. Chem. Soc. 1557 (1936). J. Baddiley, B. Lythgore, D. McNeil, and A. R. Todd. J. Chem. Soc. 383 (1943). J. H. Lister. Rev. Pure Appl. Chem. **11**, 178 (1961).
4. R. Willstätter and T. Wirth. Ber. **42**, 1920 (1909).

Can. J. Chem. Downloaded from www.nrcresearchpress.com by 210.87.254.42 on 09/05/12
For personal use only.

5. W. WALTER and G. MAERTEN. Ann. **669**, 66 (1963).
6. P. L. DE BENNEVILLE, J. S. STRONG, and V. T. ELKIND. J. Org. Chem. **21**, 772 (1956). J. WITTE and R. HUISGEN. Chem. Ber. **91**, 1129 (1958).
7. K. BIEMANN. Mass spectrometry. McGraw-Hill Book Co., Inc., New York. 1962. R. M. SILVERSTEIN and G. C. BASSLER. Spectrometric identification of organic compounds. John Wiley and Sons, Inc., New York. 1963.
8. H. BUDZIKIEWICZ, C. DJERASSI, and D. H. WILLIAMS. Interpretation of mass spectra of organic compounds. Holden-Day, Inc., San Francisco. 1964. p. 63.
9. (*a*) R. H. DE WOLFE. J. Am. Chem. Soc. **86**, 864 (1964). (*b*) M. L. WEINER. J. Org. Chem. **25**, 2245 (1960).
10. A. JOVTSCHEFF and F. FALK. J. Prakt. Chem. **13**, 265 (1961).
11. H. BREDERECK, R. GOMPPER, K. KLEMM, and H. REMPFER. Chem. Ber. **92**, 837 (1959). H. BREDERECK, F. EFFENBERGER, and G. SIMCHEN. Angew. Chem. **73**, 493 (1961).
12. H. PRIEWE and A. POLJAK. Chem. Ber. **93**, 2347 (1960). P. OXLEY, D. A. PEAK, and W. F. SHORT. J. Chem. Soc. 1618 (1948).
13. A. W. HOFMANN. Ann. **54**, 197 (1858).
14. P. OXLEY and W. F. SHORT. J. Chem. Soc. 1252 (1951). R. L. SHRINER and F. W. NEUMANN. Chem. Rev. **35**, 351 (1944).
15. K. ODO, E. ICHIKAWA, K. SHIRAI, and K. SUGINO. J. Org. Chem. **22**, 1715 (1957). C. GRUNDMANN and R. RÄTZ. J. Org. Chem. **21**, 1037 (1956). A. PINNER and F. KLEIN. Ber. **11**, 1475 (1878).
16. R. M. ROBERTS and P. J. VOGT. J. Am. Chem. Soc. **78**, 4778 (1956). C. GRUNDMANN and A. KREUTZBERGER. J. Am. Chem. Soc. **77**, 6559 (1955). G. G. NOVAS and M. CALBERT. Anales Real Soc. Españ. Fiś. Quīm. Madrid, Ser. B, **50**, 741 (1964); Chem. Abstr. **49**, 8106 (1955). E. C. TAYLOR and N. W. KALENDA. J. Am. Chem. Soc. **76**, 1699 (1954). R. KUHN and H. A. STAAB. Chem. Ber. **87**, 272 (1954). T. TAKAHASHI, K. SATAKE, and S. YASUI. Yakugaku Zasshi, **74**, 577 (1954); Chem. Abstr. **48**, 11412 (1954). E. B. KNOTT and R. A. JEFFREYS. J. Org. Chem. **14**, 879 (1949). R. ASHWORTH. J. Chem. Soc. 1716 (1948). W. B. WHALLEY. J. Chem. Soc. 1014 (1948). E. FERBER and G. SCHMOLKE. J. Prakt. Chem. **155**, 234 (1940). W. H. WARREN and F. E. WILSON. Ber. **68**, 957 (1935). A. W. HOFMANN. Ber. **2**, 116 (1869).

RECEIVED FEBRUARY 10, 1965.
DEPARTMENT OF CHEMISTRY,
UNIVERSITY OF MAINE,
ORONO, MAINE.

ERRATUM: THE SYNTHESIS AND REACTIONS OF DIVINYL CARBONIUM IONS

T. S. SORENSEN

(Ref. Can. J. Chem. 42, 2768 (1964))

The compound referred to as 4-methylene-2,6-dimethyl-2,5-heptatriene on page 2769, under Results and Discussion, line 3, should be 4-methylene-2,6-dimethyl-2,5-heptadiene.

DEPARTMENT OF CHEMISTRY,
UNIVERSITY OF ALBERTA,
CALGARY, ALBERTA.

Can. J. Chem. Downloaded from www.nrcresearchpress.com by 210.87.254.42 on 09/05/12
For personal use only.

Can. J. Chem. Downloaded from www.nrcresearchpress.com by 210.87.254.40 on 09/05/12
For personal use only.

Canadian Journal of Chemistry

Issued by THE NATIONAL RESEARCH COUNCIL OF CANADA

VOLUME 43 OCTOBER 1965 NUMBER 10

NUCLEAR MAGNETIC RESONANCE SPECTRAL OBSERVATIONS ON THE GLYCOL-SCISSION OF DEUTERATED D-GLUCOSE[1]

W. MACKIE[2] AND A. S. PERLIN

National Research Council of Canada, Prairie Regional Laboratory, Saskatoon, Saskatchewan

Received April 27, 1965

ABSTRACT

The positions of formyl ester groups in products obtained on oxidative glycol-scission of specifically deuterated D-glucose and its 3-*O*-methyl ether have been determined by n.m.r. spectroscopy. These structural assignments are based on the effect of deuteration on the signal given by the proton located α to the formyloxy group in the undeuterated compound. Thus, mono-*O*-formyl-2-*O*-methyl-D-arabinose-4-*d* (IV) produced by lead tetraacetate oxidation of 3-*O*-methyl-D-glucose-5-*d* (I) shows a modified resonance signal for this proton, whereas the signal is absent from the spectrum of the monoformate (III) obtained by periodate oxidation of I. Therefore, IV is a 3-formate and III a 4-formate. According to these findings a furanose form (II) of I is involved in the lead tetraacetate reaction, whereas periodate degrades the pyranose form of the sugar directly.

Oxidation of D-glucose-6,6′-d_2 with lead tetraacetate is shown in similar fashion to yield 2,3-di-*O*-formyl-D-erythrose-4,4′-d_2, evidence that this degradation involves two successive pyranose-to-furanose interconversions.

The preparation of I, and of some other derivatives of D-glucose-5-*d*, is described.

The properties of lead tetraacetate oxidation (1) of D-glucose in acetic acid are consistent with a reaction pathway involving the furanose, rather than pyranose, form of the sugar (2, 3). Most probably a 1,2-lead complex (4) of α-D-glucofuranose is produced and decomposes to 3-*O*-formyl-D-arabinose which, in turn, consumes a second mole of the oxidant and gives 2,3- or 2,4-di-*O*-formyl-D-erythrose. With periodate as oxidant a more complex series of reactions takes place (5–8), but the pyranose form of the sugar undoubtedly plays the dominant role. Probably, therefore, 4-*O*-formyl-D-arabinose is the major initial product, and 2-*O*-formyl-D-glycerose (6) the main end product. Satisfactory information about the structure of these various esters has not been readily accessible in the past because of the general need for reliable means for characterizing partially acylated polyols. With n.m.r. spectroscopy, however, structural problems of this type can now be examined with greater confidence. In the current study, n.m.r. spectral analysis together with the use of specifically deuterated compounds has made it possible to clearly define the structure of some formate esters produced in these glycol-scission oxidations.

The first step in the oxidation of D-glucose by either oxidant has been studied most conveniently with a derivative, i.e., the 3-*O*-methyl ether, that precludes degradation beyond the pentose formate stage (9, 10). Each reaction yields a syrupy product characterized as 2-*O*-methyl-D-arabinose monoformate (ref. 9 and Experimental section). It is pertinent that when the two products were examined at 60 Mc/s, their spectra were so

[1]*Issued as N.R.C. No. 8556.*

[2]*National Research Council Postdoctorate Fellow, 1964–1965.*

closely similar as to suggest that the same product is formed in both reactions. However, when the spectra were recorded at 100 Mc/s several distinct differences became apparent. For the present purpose, attention is restricted to the region at about 530–570 c.p.s. (5.3–5.7 p.p.m.) (Figs. 1*a* and 1*b*) that shows the signal attributable to the proton (A)

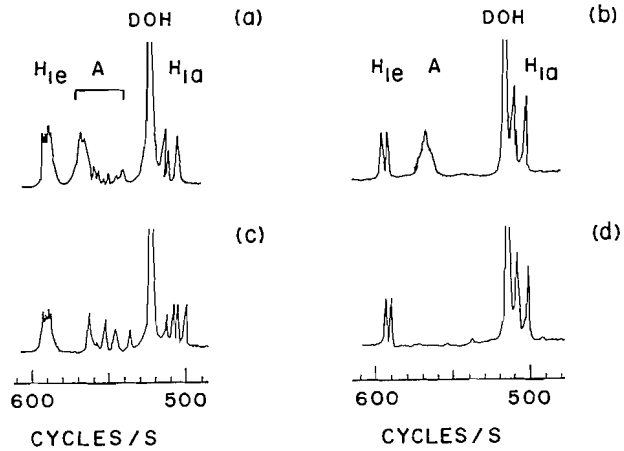

FIG. 1. Partial n.m.r. spectra at 100 Mc/s of oxidation products dissolved in deuterium oxide: (*a*) and (*c*) represent the products obtained by oxidation of 3-*O*-methyl-D-glucose and 3-*O*-methyl-D-glucose-5-*d*, respectively, in acetic acid with one molar proportion of lead tetraacetate; (*b*) and (*d*) represent the products obtained by oxidation of the same two compounds in water with one molar proportion of sodium meta-periodate. A is the signal attributed to the proton located α to the formyloxy group; H_{1e} and H_{1a} are signals attributed to the anomeric protons.

located α to the formyloxy group. This assignment is based on its occurrence at relatively low field and, more important, on the fact that it is displaced toward higher field by about 120 c.p.s. when the ester group is hydrolyzed. There is more splitting of the signal in Fig. 1*a* than in 1*b*, and this greater complexity appears to be reflected also in the signals ascribed to H_{1e} and H_{1a} (11), as well as in other portions of the spectrum that are not shown here. In neither instance, however, was analysis of the spectrum sufficiently complete for a structural assignment to be made.

A more direct approach to the problem was afforded by carrying out the oxidations with 3-*O*-methyl-D-glucose deuteriated at position-5. Degradation of this compound in the pyranose form (I) should give 4-*O*-formyl-2-*O*-methyl-D-arabinose-4-*d* (III), whereas a pathway involving the furanose form (II) should yield 3-*O*-formyl-2-*O*-methyl-D-arabinose-4-*d* (IV). From an inspection of formulae III and IV, it is seen that the resonance signal associated above with proton A can be produced only by the 3-formate, thus making possible a clear choice between the two structures.

It was found, in fact, that the product formed by oxidation with lead tetraacetate gives a signal corresponding in chemical shift to that of proton A (Fig. 1*c*), its intensity being equal to that of the formate proton signal. Also, the structure of this signal is simpler than that of A in Fig. 1*a*, as could be expected upon replacement of an adjacent proton by deuterium. In marked contrast, the periodate oxidation product shows no response in this region of the field (Fig. 1*d*). Therefore, it may be concluded that the lead tetraacetate scission of 3-*O*-methyl-D-glucose yields the 3-formate (IV) and hence that the oxidative attack on D-glucose involves a pyranose $\rightarrow$ furanose interconversion. Periodate oxidation gives the 4-formate (III). In that portion of the overall reaction of D-glucose itself in which the C1–C2 diol is split in the initial step (most evident with the α-anomer (8)) this reagent must oxidize only the pyranose sugar.

Can. J. Chem. Downloaded from www.nrcresearchpress.com by 210.87.254.40 on 09/05/12
For personal use only.

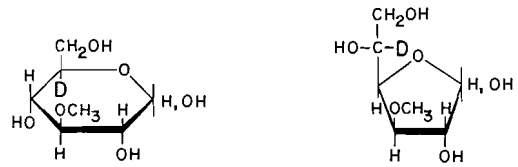

I

II

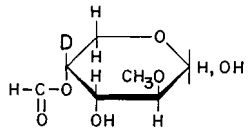

III

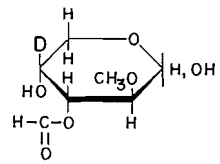

IV

The possibility that the formyl group of IV could have migrated to position-3 from -4 during lead tetraacetate cleavage (12) cannot be ignored, although such a pathway is at variance with results of recent experiments dealing with this question (3). One must also consider the possibility that the ester group migrates from the 4- to the 5-position of the intermediary *aldehydo*-D-arabinose derivative and that the product isolated is actually 2-*O*-methyl-D-arabinofuranose-5-formate. However, this alternative has been eliminated by examining the product obtained from 3-*O*-methyl-D-glucose-6,6′-d_2. Since its spectrum contains a resonance signal corresponding to that of proton A, the formyloxy group cannot have been located at the di-deuterated 5-position.

An additional point bearing on the n.m.r. spectral data may be noted. The 3-formate gives a more complex overall spectrum than does the 4-formate. This is evident from Fig. 1, and also in other parts of the total spectrum, notably in the signals for methoxy protons. Thus, III contains two nonequivalent methyl groups whereas IV shows two additional, weaker signals attributable to methoxyl protons. Undoubtedly two of these signals represent the two anomeric forms of the product since they are present in the spectra of equilibrated solutions of 2-*O*-methyl-D-arabinose itself and of its 3,4-*O*-isopropylidene derivative, as well as of other 2-*O*-methyl aldoses (unpublished observations). To account for these effects it is suggested that 3-*O*-formyl-2-*O*-methyl-D-arabinose (IV) exists partially in furanose forms.[3] The 4-formate (III) cannot adopt the smaller ring size and its simpler spectrum must be that of the $\alpha\beta$-pyranose mixture only.

Since periodate oxidation of D-glucose gives arabinose esterified at the 4-position, subsequent degradation can proceed to the triose level (6), resulting in an overall uptake of 3 moles of the reagent (5, 7, 8). However, only 2 moles of oxidant are consumed in the lead tetraacetate reaction, the second mole being used to convert arabinose-3-formate to di-*O*-formyl-D-erythrose. Depending upon whether this latter step involves the pyranose or furanose form of the pentose derivative, the final product would be the 2,4- or 2,3-diester. Di-*O*-formyl-D-erythrose obtained from D-glucose (12) gives a spectrum (Fig. 2*a*) that is not readily amenable to analysis. However, this difficulty has been obviated by using D-glucose deuteriated at the 6- and 6′-positions (V). Because of the characteristically large displacement of a proton signal towards lower field when the hydroxyl group α to the proton is formylated (as noted above) it was to be expected that H_2 of the 2,4-derivative (VI) would resonate at relatively low field, and H_3 at a much higher field. By contrast,

[3]*Perhaps this is caused by the same steric influence that leads to a dominance of furanoside in the equilibrium methanolysate of 2,3-di-O-methyl-arabinose (13).*

Can. J. Chem. Downloaded from www.nrcresearchpress.com by 210.87.254.40 on 09/05/12
For personal use only.

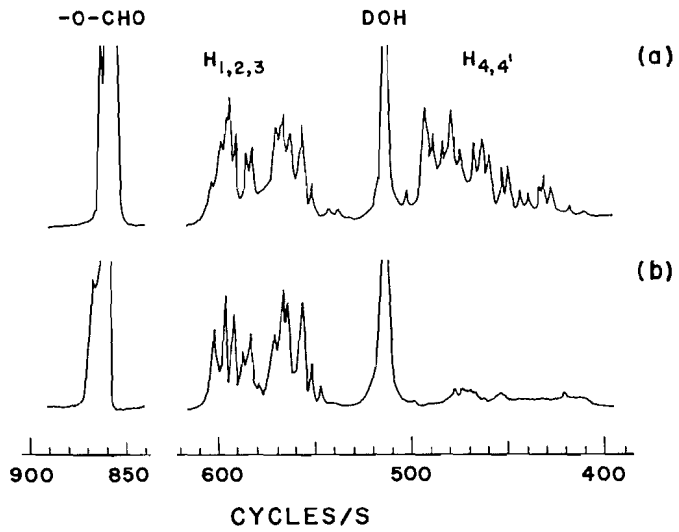

FIG. 2. N.m.r. spectra at 100 Mc/s of oxidation products dissolved in deuterium oxide: (*a*) and (*b*) represent the products obtained by oxidation of D-glucose and D-glucose-6,6′-d_2, respectively, in acetic acid with two molar proportions of lead tetraacetate.

2,3-di-*O*-formyl-D-erythrose-4,4′-d_2 (VII) should exhibit both of these signals at low field. This latter situation was found to apply almost completely for the product of the oxidation of V (Fig. 2*b*), showing that the tetrose formate is esterified predominantly at positions-2 and -3 (as in VII).

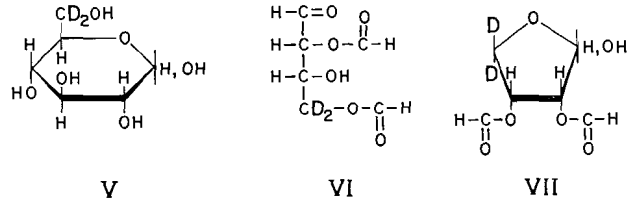

V VI VII

Results obtained in the lead tetraacetate oxidation both of 3-*O*-methyl-D-glucose-5-*d* and of D-glucose-6,6′-d_2 are thus consistent in requiring that the initial oxidation step involves D-glucofuranose. The oxidation of D-arabinose-3-formate, in turn, also undoubtedly involves a furanose pathway.

Although lead tetraacetate and periodate are commonly equated as glycol-scission agents, it is clear that they can differ markedly in their mode of attack on reducing sugars. Since tetravalent lead and the iodine atom in periodate have closely analogous properties (14), this difference likely arises mainly from the fact that the sugars can exist in diverse forms and that the two reactions take place in different solvents. Under such circumstances variations in the relative importance of glycol scission and structural change (mutarotation, pyranose–furanose interconversion, etc.) dominate the outcome of the reactions (see also ref. 8). Thus, for example, the rate of oxidation of 3-*O*-methyl-D-glucose by lead tetraacetate in acetic acid is regulated by the intervention of an unusually reactive species, such as a furanose form (3). However, a comparison of acetic acid and benzene as media shows that oxidation of the pyranose form of this sugar itself is sufficiently vigorous in

Can. J. Chem. Downloaded from www.nrcresearchpress.com by 210.87.254.40 on 09/05/12
For personal use only.

benzene to preclude the change in ring size (3). This latter situation appears to apply also for periodate oxidation in water, and since mutarotation can be relatively slow in this solvent some oxidation takes place also at positions other than at the more usually favored *cis*-α-hydroxyhemiacetal group (7, 8).

For the preparation of D-glucose-5-*d*, a compound that does not appear to have been reported previously, D-*xylo*-5-hexulosonic acid (VIII) (15, 16) was utilized as starting material. Hamilton and Smith (17) have reported that VIII is reduced by sodium borohydride to an equimolar mixture of D-gluconic and L-idonic acids. Hence, by using pure borodeuteride the 5-deuterio-hexonic acids were prepared. They were lactonized and a reduction was then carried out with sodium borohydride in the presence of a cation-exchange resin (18), to give a mixture of D-glucose- and L-idose-5-*d*. For as yet undetermined reasons, the overall yield of hexose obtained using these well established procedures was very low. The mixture of sugars was acetonated, and 1,2:5,6-di-*O*-isopropylidene-D-glucofuranose-5-*d* was isolated by fractional crystallization. 3-*O*-Methyl-D-glucose-5-*d* (I) was then prepared by methylation of the diacetone derivative, followed by acid hydrolysis.

D-Glucose-6,6′-d_2 (V) was prepared by reduction of 1,2-*O*-isopropylidene-D-glucofuranurono-6,3-lactone with sodium borodeuteride, followed by acid hydrolysis of the derived 1,2-*O*-isopropylidene-D-glucofuranose-6,6′-d_2, by analogy with the preparation of the di-tritiated sugar (19). 3-*O*-Methyl-D-glucose-6,6′-d_2 was obtained from V via the 1,2:5,6-di-*O*-isopropylidene derivative.

EXPERIMENTAL

Nuclear magnetic resonance spectra were recorded with a Varian HA-100 high resolution spectrometer using deuterium oxide as solvent and tetramethysilane, contained in a coaxial capillary, as reference.

Oxidation of 3-O-Methyl-D-glucose with Lead Tetraacetate or Sodium Periodate

(*a*) 3-*O*-Methyl-α-D-glucose (100 mg) was taken up in water (0.2 ml) and the solution was diluted with acetic acid (6 ml). Lead tetraacetate (220 mg; 0.97 molar equivalents) dissolved in acetic acid (12 ml) was added to the sugar solution, and 10 min later the solvent was evaporated off at 40°. The residue was triturated several times with ethyl acetate, and concentration of the extract afforded a colorless syrup (95 mg). This syrup absorbed strongly in the infrared region at 1 730 cm^{-1}, characteristic of a formate ester group; the intensity of the resonance signal attributable to the proton of this group (at 870 c.p.s.) showed that the product contained 0.94 formate groups.

An alternative isolation procedure, more convenient for oxidations on a smaller scale, was as follows: after removal of the acetic acid by distillation the residue was taken up in deuterium oxide and treated with the equivalent quantity of oxalic acid in deuterium oxide. The lead oxalate was filtered off and the filtrate concentrated *in vacuo* to a volume (about 0.5 ml) appropriate for use directly in the n.m.r. spectrometer sample tube.

(*b*) Sodium metaperiodate (55 mg) was added to a solution of 3-*O*-methyl-α-D-glucose (50 mg; 1 molar equivalent) in deuterium oxide (5 ml). After 10 min reaction time the solution was concentrated *in vacuo* to a volume appropriate for use directly in the n.m.r. spectrometer sample tube. In some experiments, this reaction was carried out in water, the solution was concentrated to dryness, and the oxidation product extracted into ethyl acetate, as described above under (*a*).

3,4-O-Isopropylidene-2-O-methyl-D-arabinopyranose

The syrupy formate ester prepared by lead tetraacetate oxidation[4] (0.35 g) was taken up in cold acetone (10 ml); concentrated hydrochloric acid (0.1 ml) was added, and the solution was stored at 3° for 72 h. Several volumes of acetone were added, and the solution was neutralized with lead carbonate and then concentrated to dryness. The residue (0.30 g) solidified; m.p. 114–117°. Several attempts to recrystallize the material from various solvents were unsuccessful and, as had been found for this same derivative by Barker and Smith (9), the carbon content was considerably lower than the theoretical value (by 1.0% C). However, after a portion of this crude sample had been sublimed it served as seed, thus enabling recrystallization of the pure compound from ether: m.p. 117–118°; $[\alpha]_D$ −108° (*c*, 2.5 in methanol, no mutarotation observed).

Anal. Calcd. for $C_9H_{16}O_5$: C, 52.9; H, 7.9. Found: C, 53.0; H, 8.0.

[4]*3,4-O-Isopropylidene-2-O-methyl-D-arabinose has already been prepared in this connection by Barker and Smith (9), in characterizing the product formed by the oxidation with periodate.*

Can. J. Chem. Downloaded from www.nrcresearchpress.com by 210.87.254.40 on 09/05/12
For personal use only.

Reduction of D-*Xylo-5-hexulosonic Acid with Sodium Borodeuteride*

An ice-cold aqueous solution (20 ml) of potassium D-xylo-5-hexulosonate[5] (5.0 g) was added dropwise with stirring to a cooled solution (5 ml) of aqueous sodium borodeuteride[6] (1.0 g). After 1 h at 3° and 18 h at room temperature, the reaction mixture was passed through a column (13 × 2.5 cm) of Amberlite IR-120 (H^+) and the resin was washed thoroughly. The total effluent was concentrated *in vacuo* to dryness, the residue was treated several times with methanol to remove borate, and the syrupy product (4.2 g) was warmed (50–60°) *in vacuo* to aid lactonization of the aldonic acids. Paper chromatographic examination of the syrup (1-butanol:ethanol:water 40:11:19) showed the presence of at least two components ($R_{glucose}$ 0.51 and 1.6) which, together with its infrared absorption characteristics, indicated the presence of a mixture of 1,5-lactone (strong band at 1 730 – 1 740 cm^{-1}), 1,4-lactone (shoulder at 1 775 cm^{-1}), and free acid. Saponification of a portion of the syrup with barium hydroxide caused all of these components to be retained at the starting line of the chromatogram.

Borohydride Reduction of D-*Glucono- and* L-*Idono-lactones in the Presence of Cation-Exchange Resin*

The syrupy mixture of acid and lactone (1.5 g) was dissolved in boric acid (0.05 *M*; 60 ml) and cooled in an ice bath. Excess of Amberlite IR-120 (H^+) was introduced (18), and a solution of potassium borohydride (1.5 g; 60 ml) was then added dropwise with vigorous stirring over a period of 15 min. Stirring was continued for an additional 15 min, the resin was filtered off, the solution was concentrated, and borate was removed from the residue by repeated addition and distillation of methanol. Paper chromatographic examination showed that the syrupy product contained glucose, idose, and probably some sorbitol, as well as the two components of the original syrup. The latter were largely removed by treating a solution of the mixture with Dowex-1 (bicarbonate form) for 1 h, the final yield of product recovered from 3.8 g of the crude reduction product being 0.8 g.

*1,2:5,6-Di-O-isopropylidene-α-*D-*glucofuranose-5-d*

The neutral syrup (0.75 g) was taken up in acetone (50 ml) containing concentrated sulfuric acid (0.4 ml). After 5 h at room temperature the reaction mixture was cooled, saturated with gaseous ammonia, filtered, and concentrated to dryness. The residue (0.95 g) was dissolved in chloroform, the solution was washed with water, and the chloroform-soluble material (0.64 g) was taken up in cyclohexane. An initial crystalline deposit recovered was found to contain a mixture of *gluco-* and *ido-*isomers, which was not separated by repeated recrystallization, but material obtained from the mother liquor consisted only of the *gluco-*isomer; m.p. 109°, its X-ray powder diagram was indistinguishable from that of 1,2:5,6-di-*O*-isopropylidene-α-D-glucofuranose.

*3-O-Methyl-α-*D-*glucose-5-d*

A solution of the deuteriated diacetone-glucose (0.14 g) in methyl iodide (10 ml) containing silver oxide (0.2 g) was heated under reflux for 18 h. The solids were filtered off and washed with chloroform, and the combined filtrate and washings were concentrated to a syrup (0.13 g). Hydrolysis of the latter with 0.1 *N* sulfuric acid furnished 3-*O*-methyl-D-glucose-5-*d*, crystallizing as the α-anomer from ethanol: m.p. 160–161°; identity confirmed by its X-ray powder diagram.

*1,2-O-Isopropylidene-α-*D-*glucofuranose-5-d*

1,2:5,6-Di-*O*-isopropylidene-α-D-glucofuranose-5-*d* (15 mg) was dissolved in methanol (1 ml) and 0.1 *N* sulfuric acid (1 ml) (20). After 20 h at room temperature, the solution was neutralized with barium carbonate and then concentrated to dryness.

The n.m.r. spectrum of this product was indistinguishable from that of 1,2-*O*-isopropylidene-D-glucofuranose-5-*d* prepared by a different procedure (21). This fact served to establish that the deuteration procedure had specifically labelled position-5 of the D-glucose moiety in a virtually quantitative manner. Thus the spectrum consists of six well resolved doublets that show coupling between H-1 and H-2, H-3 and H-4, and H-6 and H-6′, respectively. Such data are consistent only with the absence of hydrogen at the 5-position.

*1,2-O-Isopropylidene-α-*D-*glucofuranose-6,6′-d_2*

1,2-*O*-Isopropylidene-α-D-glucofuranurono-6,3-lactone (0.15 g) in water (1 ml) was added to a freshly prepared solution (0.5 ml) of sodium borodeuteride (0.10 g). The reaction mixture was stored overnight in the cold, deionized with a mixture of ion-exchange resins, and concentrated, and borate was then removed from the residue with methanol. The solid product (0.14 g) was recrystallized from methanol–ether: m.p. 156–158°. The n.m.r. spectrum of the product showed that deuteration had been effected only at the 6- and 6′-positions. Thus, signals given by H-6 and H-6′ of the undeuterated compound are absent, H-5 is a doublet (J = 3.5 c.p.s.) that is coupled with the H-4 quartet; the remainder of the spectrum is indistinguishable from that of 1,2-*O*-isopropylidene-D-glucofuranose.

Lead Tetraacetate Oxidation of D-*Glucose-6,6′-d_2*

Crystalline 1,2-*O*-isopropylidene-α-D-glucofuranose-6,6′-d_2 (60 mg) was hydrolyzed on the steam bath for

[5]*Supplied by Miles Chem. Co., Elkhart, Indiana, as the calcium salt; this compound was prepared by double decomposition using potassium oxalate.*

[6]*Supplied by Merck, Sharp and Dohme, Montreal, Quebec.*

Can. J. Chem. Downloaded from www.nrcresearchpress.com by 210.87.254.40 on 09/05/12
For personal use only.

3 h with 0.1 *N* sulfuric acid to give the free hexose (35 mg). The latter was taken up in water (0.1 ml) and acetic acid (4 ml), and was then treated with lead tetraacetate (175 mg; 2 molar equivalents) in acetic acid (8 ml). The syrupy product (28 mg) was recovered by extraction into ethyl acetate, as described for the undeuteriated material (12); its n.m.r. spectrum is reproduced in Fig. 2*b*.

*3-O-Methyl-α-*D*-glucose-6,6′-d_2*

The preparation of this compound was analogous to that of the 5-deuterio-3-*O*-methyl ether (above). Crystalline 1,2-*O*-isopropylidene-D-glucofuranose-6,6′-d_2 was acetonated further to give the 1,2:5,6-di-*O*-isopropylidene derivative: m.p. 109°. The latter was methylated with methyl iodide and silver oxide and the product hydrolyzed, giving 3-*O*-methyl-α-D-glucose-6,6′-d_2 by crystallization from ethanol: m.p. 158–160°.

ACKNOWLEDGMENTS

N.m.r. spectra were recorded by M. Mazurek. Microanalyses were performed by W. Haid, who also prepared X-ray powder diagrams.

REFERENCES

1. R. CRIEGEE. Ber. **64**, 260 (1931).
2. A. S. PERLIN. Advan. Carbohydrate Chem. **14**, 9 (1959).
3. A. S. PERLIN. Can. J. Chem. **42**, 2365 (1964).
4. R. CRIEGEE, L. KRAFT, and B. RANK. Ann. **507**, 159 (1933).
5. G. HUGHES and T. P. NEVELL. Trans. Faraday Soc. 44, 941 (1948).
6. C. SCHÖPF and H. WILD. Chem. Ber. **87**, 1571 (1954).
7. L. HOUGH, T. J. TAYLOR, G. H. S. THOMAS, and B. M. WOODS. J. Chem. Soc. 1212 (1958).
8. S. J. ANGYAL and J. E. KLAVINS. Australian J. Chem. **14**, 577 (1961).
9. G. R. BARKER and D. C. C. SMITH. Chem. Ind. 1035 (1952).
10. A. J. CHARLSON and A. S. PERLIN. Can. J. Chem. **34**, 1200 (1956).
11. R. U. LEMIEUX, R. K. KULLNIG, H. J. BERNSTEIN, and W. G. SCHNEIDER. J. Am. Chem. Soc. **80**, 6098 (1958).
12. A. S. PERLIN and C. BRICE. Can. J. Chem. **34**, 541 (1956).
13. C. T. BISHOP and F. P. COOPER. Can. J. Chem. **41**, 2743 (1963).
14. L. J. HEIDT, E. K. GLADDING, and C. B. PURVES. Paper Trade J. **121**, No. 9, 35 (1945).
15. M. L. BOUTROUX. Compt. Rend. **102**, 924 (1886).
16. L. B. LOCKWOOD. Methods in Carbohydrate Chem. **2**, 54 (1963).
17. J. K. HAMILTON and F. SMITH. J. Am. Chem. Soc. **76**, 3543 (1954).
18. H. L. FRUSH and H. S. ISBELL. J. Am. Chem. Soc. **78**, 2844 (1956).
19. H. S. ISBELL, H. L. FRUSH, and J. D. MOYER. J. Res. Natl. Bur. Std. A, **64**, 359 (1960).
20. F. BLINDENBACHER and T. REICHSTEIN. Helv. Chim. Acta, **31**, 1669 (1948).
21. W. MACKIE and A. S. PERLIN. Can. J. Chem. In press. 1965.

Can. J. Chem. Downloaded from www.nrcresearchpress.com by 210.87.254.40 on 09/05/12
For personal use only.

Can. J. Chem. Downloaded from www.nrcresearchpress.com by 210.87.254.40 on 09/05/12
For personal use only.

PROTON MAGNETIC RESONANCE SPECTRA OF D-GLUCOPYRANOSE POLYMERS[1]

C. A. GLASS

Northern Regional Research Laboratory,[2] U.S. Department of Agriculture, Peoria, Illinois

Received March 8, 1965

ABSTRACT

The proton magnetic resonance spectra of carbohydrates in deuterium oxide solution were obtained and considered with respect to probable conformation. The anomeric proton signal occurred at lowest field and was easily recognized. In the various glucose derivatives investigated, this signal occurred from 4.62 to 5.25 τ for equatorial protons and from 5.12 to 5.65 τ for axial protons. Within each of these ranges, the chemical shifts varied inversely with the electronegativity at the C_1 site, as calculated by the technique of Gordy (1). Variable electronegativity at C_1 accounts for the overlap of ranges for equatorial and axial protons, thereby bringing the n.m.r. data into agreement with assignment of the C1 chair form of the pyranose ring to the linear polymers of D-glucopyranose. The orientation of the glucopyranose rings in cyclodextrins is shown to preclude ring current effects, and the up-field chemical shifts of these materials are shown to be consistent with the C1 form.

Some solution properties of amylose, amylopectin, and dextran, such as solubility and changes of optical rotation with pH, may depend on the conformation of the anhydro-D-glucopyranose rings. Reeves (2) investigated the optical rotation of amylose and other carbohydrates in cuprammonium hydroxide solution and interpreted his results in terms of conformational differences between the eight Sachse strainless rings. He was able to show that only the C1 conformation would account for the results on all the substituted D-glucopyranose derivatives examined; although in a few cases the B1 and 3B conformations were not ruled out. Later Reeves (3) interpreted the decrease in rotation for amylose and methyl-β-maltoside with increase in sodium hydroxide concentration as resulting from a conformational change: B1 to 3B. According to Senti and Witnauer (4), X-ray diffraction data favor the C1 conformation for alkali amylose in the solid state. Greenwood and Rossotti (5) investigated the infrared spectra of some carbohydrates and found that their results were compatible with the C1 form for both neutral and alkaline material.

Lemieux, Kullnig, Bernstein, and Schneider (6) showed that in the proton magnetic resonance spectra of five isomeric 1,2,3,4,5,6-hexachlorocyclohexanes, the chemical shift could be correlated with orientation of protons relative to the plane of the ring. A proton equatorially oriented resonated at lower field than an axially oriented proton with the same environment, and this difference was about 0.5 p.p.m. Pople, Schneider, and Bernstein (7) reasoned that the bond-anisotropy contribution would be relatively small and postulated that ring current effects are responsible for the magnitude of the difference in chemical shift between axial and equatorial protons.

From molecular orbital considerations, Karplus (8) has derived this set of equations relating the dihedral angle and the coupling constant.

$$J_{H_1H_2} = A \cos^2\phi - 0.28$$
$$A = 8.5 \text{ when } 0° \leqslant \phi \leqslant 90°$$
$$\text{and } A = 9.5 \text{ when } 90° \leqslant \phi \leqslant 180°$$

[1]*Presented at the 15th Pittsburgh Conference on Analytical Chemistry and Applied Spectroscopy, Pittsburgh, Pennsylvania, March 2–6, 1964.*

[2]*A laboratory of the Northern Utilization Research and Development Division, Agricultural Research Service, U.S. Department of Agriculture. Article not copyrighted.*

In a more recent communication (9), he points out that coupling constants depend on factors other than the vicinal dihedral angle and that the relation should be taken only qualitatively. Lenz and Heeschen (10) determined the H_1H_2 dihedral angle of α- and β-D-glucopyranose, α- and β-D-mannopyranose, and some D-glucopyranose derivatives by n.m.r. using a modified Karplus equation. From the dihedral angles, together with the chemical shifts of the anomeric proton signals, they ascribed the C1 or a skewed chair form to these pyranoses. D-Glucose, cellobiose, and maltose were examined by van der Veen (11) and, assuming a C1 form, the alpha and beta configuration of the anomeric proton was correlated with its n.m.r. signal.

Proton magnetic resonance measurements of the anomeric proton signals cannot be completely definitive because conformations C1, B2, and 1B of the alpha anomer have H_1 equatorially oriented and a dihedral angle of 60° between H_1 and H_2. Furthermore, for the beta anomer, three conformations (C1, 1B, and B2) have H_1 axially oriented and at a 180° dihedral angle with H_2. In these ambiguous cases, the possibilities can be narrowed to the C1 conformation with reasonable assurance. The 1B and B2 conformations do not give rotational data consistent with Reeves' observations on cuprammonium complexes (2). Therefore only the C1 conformation appears possible.

Rao and Foster (12) examined methyl D-glucopyranosides, cellobiose, maltose, and the γ-Schardinger dextrin by n.m.r. and considered the pyranose rings to be in the C1 form. We have determined the n.m.r. spectra of some of the compounds studied by Lenz and Heeschen (10) and Rao and Foster (12) and have found good agreement. In addition, nine other carbohydrates were studied to confirm the C1 conformational assignment of pyranose rings in amylose, amylopectin, and dextran.

EXPERIMENTAL

All spectra were obtained on a Varian A-60 n.m.r. spectrometer[3] with a variable temperature probe. Spectra were obtained on solutions of 10 to 20% concentration in D_2O at room temperature with the HOD signal at 5.30 τ as an internal reference. Later the spectra were determined at about 80° and referenced to the prominent signals in the room temperature spectra. Chemical shifts are reported in parts per million (p.p.m.) in τ values with HOD (at room temperature) equal to 5.30 τ. Although the water signal is not the preferred reference, because it is not very sharp and highly subject to shift as a function of temperature, care was exercised to maintain the probe at the same temperature, and frequent checks were made with the addition of materials such as dioxane and acetone. Chemical shifts are reported to the hundredth with a probable uncertainty of ±0.03 p.p.m. Coupling constants are reported in cycles per second (c.p.s.) and are apparent coupling constants determined from the chart. These measured spacings do not give the true value of the coupling constant $J_{H_1H_2}$ since little is known about H_2. They do, however, serve to differentiate between di-axial and axial-equatorial orientations. For brevity these spacings are referred to in the text as J values. Dihedral angles are calculated from the following modified Karplus equation used by Lenz and Heeschen (10):

$$J_{H_1H_2} = F(A \cos^2 \phi - 0.28)$$

where $F = 1.09 \pm 0.05$ and the other constants are as in Karplus' original equation (8).

RESULTS AND DISCUSSION

Nuclear magnetic resonance measurements are given in Table I.

The alpha anomers have calculated dihedral angles between 49° and 58°, and the beta anomers have dihedral angles between 142° and 151°. In the light of Karplus' recommendation (9), since the coupling constants depend on properties other than the dihedral angle, the best interpretation here is that the alpha anomers have an axial-equatorial configuration while the beta anomers have a di-axial configuration.

Data for α- and β-D-glucopyranose, which are obtained simultaneously on the same equilibrated sample, agree well with those of Lenz and Heeschen (10). Any differences

[3]*The mention of trade names or products does not constitute endorsement by the Department of Agriculture over those not named.*

Can. J. Chem. Downloaded from www.nrcresearchpress.com by 210.87.254.40 on 09/05/12
For personal use only.

TABLE I

Nuclear magnetic resonance results

Material	Coupling constant $J_{H_1H_2}$ (c.p.s.)	Dihedral angle (degrees)	Chemical shifts (τ)				
			Anomeric protons		Other protons		
			H_e	H_a			
α-D-Glucopyranose	3.2	52	4.80		6.26	6.44	
β-D-Glucopyranose	6.8	146		5.42	6.26		6.62
Methyl α-D-glucopyranoside	3.3	52	5.25		6.27	6.47	(6.64)*
Methyl β-D-glucopyranoside	7.4	149		5.65	6.15	6.63	(6.48)*
Maltose	3.3	52 (3)†	4.80		6.02	6.21	
"	7.3	149 (2)†		5.35			
"	3.0	53 (5)†	4.62				
Methyl β-maltoside	3.2	52	4.62		6.28		(6.44)*
"	7.6	151		5.62			
Methyl α-isomaltoside	2.8	55	5.17		6.25	6.46	(6.63)*
"	3.0	53	5.10				
α-Schardinger dextrin	2.7	55	4.95		6.15	6.28	
γ-Schardinger dextrin	3.5	50	4.93		6.20	6.33(J=3.5)	
Maltotriose	3.7	49 (3)†	4.80		6.20	6.40	
"	7.3	149 (2)†		5.37			
"	3.5	50 (10)†	4.63				
Hydrolyzed starch	3.0	53	4.62		6.21	6.38	
Dextran B512E	2.3	58	5.09		6.21	6.44	
Dextran B1355	*‡	(2)†	5.07		6.37		
"	*‡	(1)†	4.73				
Laminarin	6.7	145		5.25	6.20	6.33	6.47
Crown gall polysaccharide	6.2	142		5.12	6.12	6.32	6.50

*Methyl signal.
†Signal area ratios.
‡Insufficient resolution but about 3 c.p.s.

are a matter of reference and sensitivity since the coupling constants cannot be determined with great accuracy.

Methyl α- and β-D-glucopyranosides, equilibrated maltose, and the γ-Schardinger dextrin gave results that agree well with those of Rao and Foster (12).

Methyl β-maltoside (methyl *O*-α-D-glucopyranosyl-(1→4)-β-D-glucopyranoside) gives a spectrum that resembles a composite of the corresponding structures in methyl β-D-glucopyranoside and equilibrated maltose. Thus the C_1 proton is axial and, like that of methyl β-D-glucoside, produces a doublet at 5.62 τ with a coupling constant of 7.6 c.p.s. This coupling constant is equivalent to an H_1H_2 dihedral angle of 151°. The anomeric proton of the α-linked nonreducing glucose unit is equatorial and, like the anomeric proton of the nonreducing glucose unit of maltose, has a chemical shift of 4.62 τ, with J = 3.2 c.p.s., corresponding to a dihedral angle of 52° in the nonreducing glucose unit. These findings, together with the cuprammonium work of Reeves (2), show both glucopyranose units to be in the C1 form.

The spectrum of maltotriose (*O*-α-D-glucopyranosyl-(1→4)-*O*-α-D-glucopyranosyl-(1→4)-D-glucopyranose) resembles that of maltose except for the signal area ratios reflecting the two fixed equatorial C_1 protons of the α-pyranosyl rings and the equilibrated mixture of equatorial and axial protons on the reducing end group. The chemical shifts and the coupling constants are about the same as for maltose.

The remaining materials may be considered as two series of glucopyranose carbohydrates: The alpha series consisting of acid-hydrolyzed starch, dextran B1355, dextran B512E, methyl α-isomaltoside (methyl *O*-α-D-glucopyranosyl-(1→6)-α-D-glucopyranoside),

Can. J. Chem. Downloaded from www.nrcresearchpress.com by 210.87.254.40 on 09/05/12
For personal use only.

Can. J. Chem. Downloaded from www.nrcresearchpress.com by 210.87.254.40 on 09/05/12
For personal use only.

and methyl α-D-glucopyranoside; the beta series consisting of crown gall polysaccharide (poly-*O*-β-(1→2)-D-glucopyranoside), laminarin (poly-*O*-β-(1→3)-D-glucopyranoside), and methyl β-D-glucopyranoside.

Acid-hydrolyzed starch, a commercial preparation from Corn Products Company, has only one signal in the region at 4.62 τ. Resolution was poor, but the coupling constant was about 3.0 c.p.s., indicating a dihedral angle of 53°. The equatorial proton, plus the dihedral angle, indicates the C1 form. Dextran B1355, which is known to contain about 30% α-(1→3)-linkages, in addition to the predominant α-(1→6)-linkages typical of dextrans, gives two signals in this region at 4.73 τ and 5.07 τ. The resolution is less than perfect, but both coupling constants are about 3 c.p.s. Dextran B512E, in which 95% of the linkages are α-(1→6), has a single signal in this region at 5.09 τ. Again, poor resolution precludes highly accurate determination of J, but it is about 2.3 c.p.s., indicating a dihedral angle of 58°. Methyl α-isomaltoside also has two signals in this region: 5.10 τ (J = 3.0 c.p.s.) and 5.17 τ (J = 2.8 c.p.s.).

A comparison of chemical shifts for the anomeric protons within the alpha-anomeric series reveals differences greater than that between the anomeric methyl-D-glucopyranosides. For example, the resonance of the anomeric proton of hydrolyzed starch occurs more than 0.6 p.p.m. downfield of that of methyl α-D-glucopyranoside, whereas that of methyl β-D-glucopyranoside is upfield of methyl α-D-glucopyranoside about 0.4 p.p.m. The occurrence of the signal for hydrolyzed starch so far downfield of that of methyl α-D-glucopyranoside can hardly be ascribed to an axial rather than an equatorial orientation of the anomeric proton of starch. It is reasonable to assume that members of the alpha-anomeric series are all in the same conformation.

A similar comparison of chemical shifts was made in the beta-anomeric series of carbohydrates. In this series, two members were investigated for the first time: Laminarin and crown gall polysaccharide. Crown gall polysaccharide has a signal at 5.12 τ, J = 6.2 c.p.s. An axially oriented H_1 and a dihedral angle of 142° are indicated with C1 as the most probable conformation. Laminarin exhibits a signal at 5.25 τ, J = 6.7 c.p.s. This condition indicates a dihedral angle of 145° and an axial orientation of H_1. Both conditions indicate the C1 conformation.

Also in the beta-anomeric series, there is a range of chemical shifts comparable to that in the alpha series. Crown gall polysaccharide exhibits a signal at 5.12 τ and laminarin at 5.25 τ, whereas methyl β-D-glucopyranoside has one at 5.65 τ. The anomeric protons of these three beta-linked glucopyranoses are certainly axial, and the range of chemical shifts might be related to some property other than pyranose ring conformation.

The variation in chemical shift within each series (Table I) leads to an overlapping of values that reflects either ambiguity in the assignment of axial and equatorial positions to the proton or an influence of other factors in the structure. We believe that differences in electronegativity of the group attached to the glycosidic oxygen (O_1) are the cause of the variations in chemical shift. An experimental relation between n.m.r. chemical shift and the nature of substituents has been developed by Shoolery (13) but without consideration of electronegativity. The property of electronegativity has been utilized, however, to explain differences in molecular dimension, dipole moment, molecular spectra, and reaction rates. Electronegativity of an atom cannot be directly measured so it has been based on various other properties: ionization potential, electron affinities (14), bond-stretching force constants (1), atomic radii (15), and bond energies (16).

In a study of some cyclohexyl derivatives, Neikam and Dailey (17) showed the dependence of chemical shifts of axial and equatorial protons on electronegativity. Eliel,

Gianni, and Williams (18) examined 36 substituted cyclohexanols and found an appreciable overlap of the ranges of chemical shift for axial and equatorial protons. Williamson (19) examined the n.m.r. spectrum of hexachlorobicyclo(2.2.1)heptenes and showed that the differences of internal chemical shift depend on the electronegativity of the substituent. The scale of electronegativities, most applicable in our study, is that of Gordy (1). He relates electronegativity of a nucleus with a bond-stretching constant, the bond length, and the bond order. In a study of a number of compounds, he gives electronegativity values for each element. Kagarise (20) demonstrated a technique of calculating electronegativity at a new site from Gordy values:

$$\chi_{ef} = \frac{\chi_C}{2} + \frac{1}{6}(\chi_x + \chi_y + \chi_z),$$

where χ_C is the electronegativity of the carbon nucleus and where x, y, and z refer to the substituents on the carbon being considered. In this manner, Forsen (21) calculated the infrared frequencies for a number of carbonyl compounds. Electronegativities of some groups are plotted against Pauling's electronegativity values, and a linear relation is obtained.

A typical calculation is this for hydrolyzed starch:

$$\chi_{O_6} = \frac{3.45a}{2} + \frac{2.13a}{2} = 2.79$$

$$\chi_{C_6} = \frac{2.55a}{2} + \frac{1}{6}(2.13a + 2.13a + 2.79\chi_{O_6}) = 2.45$$

$$\chi_{O_{ac}} = \frac{3.45a}{2} + \frac{2.55a}{2} = 3.00$$

$$\chi_{C_5} = \frac{2.55a}{2} + \frac{1}{6}(2.13a + 2.45\chi_{C_6} + 3.00\chi_{O_{ac}}) = 2.54$$

$$\chi_{C_2} = \frac{2.55a}{2} + \frac{1}{6}(2.55a + 2.13a + 2.79\chi_{O_2}) = 2.52$$

$$\chi_{C_3} = \frac{2.55a}{2} + \frac{1}{6}(2.13a + 2.52\chi_{C_2} + 2.79\chi_{O_3}) = 2.52$$

$$\chi_{C_4} = \frac{2.55a}{2} + \frac{1}{6}(2.13a + 2.52\chi_{C_3} + 2.54\chi_{C_5}) = 2.48$$

where a = electronegativity value of nucleus from Gordy (1).

Table II gives the chemical shifts and the electronegativities of the substituents for the materials making up the alpha- and the beta-anomeric series. If it is assumed that the alpha anomers are all C1 in form, then the only difference is in the substituent on O_1. The observed chemical shifts increase from 4.62 τ for hydrolyzed starch to 5.25 τ for methyl α-D-glucopyranoside, whereas the electronegativity of the O_1 substituent decreases from 2.48 for hydrolyzed starch to 2.34 for methyl α-D-glucopyranoside. Intermediate electronegativities produce intermediate chemical shifts. Interestingly, dextran B1355, which contains not only the main-chain α-(1→6)-linkage common to dextrans but also some α-(1→3)-linkage, has two signals: one at 5.07 τ similar to the signal of dextran B512E and one at 4.73 τ. Pasika and Cragg (22) report like signals in the spectrum of dextran B742, which also has some (1→3)-linkages. The O_1 substituent of a (1→3)-linked glucose

Can. J. Chem. Downloaded from www.nrcresearchpress.com by 210.87.254.40 on 09/05/12
For personal use only.

TABLE II

Comparison of chemical shift of the anomeric proton with electronegativity of O_1 substituent

Material	O_1 substituent	Chem. shift (τ) H_e	Chem. shift (τ) H_a	Electronegativity
Hydrolyzed starch (α-1→4)	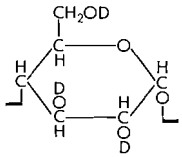	4.62		2.48
Dextran B1355 (α-1→3)	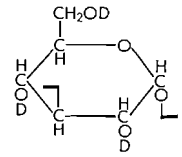	4.73		2.47
Dextran B1355 (α-1→6)	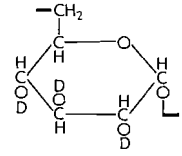	5.07		2.41
Dextran B512 (α-1→6)		5.09		2.41
Methyl α-D-glucopyranoside	$-CH_3$	5.25		2.34
Crown gall polysaccharide (β-1→2)	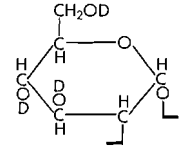		5.12	2.54
Laminarin (β-1→3)	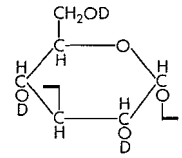		5.25	2.47
Methyl β-D-glucopyranoside	$-CH_3$		5.65	2.34
α-D-Glucopyranose	—D (?)	4.80		2.13
β-D-Glucopyranose	—D (?)		5.42	2.13

unit is more negative than the substituent of one that is (1→6)-linked, and the chemical shifts for the anomeric protons agree.

Similarly, the beta-anomers exhibit the same relationship. As the chemical shifts increase from 5.12 τ for crown gall polysaccharide to 5.65 τ for methyl β-D-glucopyranoside, the electronegativities decrease from 2.54 to 2.34.

The overlapping ranges of the equatorial and axial protons are explained in terms of the electronegativities of the O_1 substituents. N.m.r. evidence alone would allow either the

Can. J. Chem. Downloaded from www.nrcresearchpress.com by 210.87.254.40 on 09/05/12
For personal use only.

C1 or the 1B conformation for these materials. By using the cuprammonium complexing data of Reeves (2) where available to eliminate 1B, the conformations may be assigned as C1.

The discussion of the alpha- and beta-anomeric series has purposely avoided mention of the two anomers of D-glucose, although they are included in Table II. The relation between chemical shift and electronegativity is not maintained for these conpounds, presumably because we cannot be sure exactly what is being measured. The electronegativity given is that of the nonhydrogen-bonded sugar monomer in each case. Any form of hydrogen or deuterium bonding involving substituents on C_1 will make this site more negative and shift the resonance of the anomeric proton downfield. For example, if the C_1 hydroxyl of one glucose unit is bonded to the acetal oxygen of another, the electronegativity of the O_1 substituent would be 2.54 and the corresponding chemical shift would be about 4.5 τ. Likewise, hydrogen or deuterium bonding involving the D_2O solvent would increase the electronegativity of the substituent and bring about a downfield shift in the resonance of the anomeric proton. Probably hydrogen bonding has influenced the electronegativity of the substituent on O_1 and brought about a downfield shift in the resonance of the anomeric proton from about 5.6 τ to 4.80 τ for the alpha anomer. If the extent and kind of hydrogen bonding were known, the glucose anomers might fit in the proper place in each series. Hence, the chemical shifts of sugar protons might indicate the degree of hydrogen bonding.

In addition to these linear glucopyranose derivatives, two of the Schardinger dextrins were investigated. Although they have the same linkage and conformation as maltose, the anomeric proton signal occurs at a higher field. For the α-Schardinger dextrin, the anomeric proton signal is at 4.95 τ, $J = 2.7$ c.p.s., and for the γ-Schardinger dextrin, at 4.93 τ, $J = 3.5$ c.p.s. The linear counterpart, acid-hydrolyzed starch, which has the same α-(1→4)-linkage, has an anomeric proton signal at 4.62 τ, $J = 3.0$ c.p.s. The dihedral angles obtained from these coupling constants are about the same for all three materials so that the only observed difference is 0.3 p.p.m. chemical shift. Since the linkages in these materials are the same as those in hydrolyzed starch, the electronegativity of the substituents at O_1 is the same. This upfield shift from 4.62 τ for hydrolyzed starch to 4.95 τ for α-Schardinger dextrin is probably related to the ring current effect.

A single D-glucopyranose ring can orient itself with the magnetic field in such a way that ring currents associated with the pyranose ring shift the resonance of axial groups upfield and equatorial groups downfield. This movement is also true for linear materials since free rotation about the glucosidic linkage is possible, and on the average, the rings can orient themselves with the field. The methyl signal of methyl α-D-glucoside (6.64 τ), methyl β-D-glucoside (6.48 τ), methyl β-maltoside (6.44 τ), and methyl α-isomaltoside (6.63 τ) demonstrate this shift (Table I).

Schardinger dextrins, however, are semirigid rings of glucose units and little freedom exists for a glucopyranose ring to move with respect to the other units of the cyclodextrin. Any orientation that might occur must involve some favored orientation of the dextrin as a whole. Construction of cyclodextrins with molecular models, such as Stuart models, shows that the pyranose rings are nearly normal to the plane of the dextrin. As the cyclodextrin is rotated in space, one pyranose ring, favorably oriented, is opposed by another. The orientation that makes the pyranose rings magnetically equivalent is the one with the magnetic field directed normal to the plane of the cyclodextrin ring. Since this orientation places the pyranose rings edgewise to the field vector, no shift would be produced by ring currents.

Can. J. Chem. Downloaded from www.nrcresearchpress.com by 210.87.254.40 on 09/05/12
For personal use only.

This theory is supported by the observed chemical shifts for the C_1 proton, about 4.95 τ, which is intermediate between the chemical shifts of hydrolyzed starch (alpha anomer), 4.62 τ, and laminarin (beta anomer), 5.25 τ. The electronegativity of the O_1 substituent for all three materials is about the same, but the laminarin anomeric proton is axial, and that of hydrolyzed starch is equatorial. The resonance in the cyclodextrins occurs at a chemical shift such as would be observed for similar groups in the absence of ring current effects.

At the 1963 Starch Round Table, sponsored by the Corn Industries Research Foundation, Hybil of the University of Maryland described X-ray results that he and his co-workers, Williams and Rundle, has obtained showing glucose units in α-Schardinger dextrin to be C1 in the solid state. We can correlate our n.m.r. results with their X-ray results. The difference in chemical shift for the two Schardinger dextrins might be explainable when probable values for the angles which the glucose rings make with the cyclodextrin ring plane are known.

It has been demonstrated that the C1 pyranose form in solution can be assigned to D-glucose, methyl D-glucopyranosides, methyl β-maltoside, methyl α-isomaltoside, maltose, maltotriose, acid-hydrolyzed starch, α- and γ-Schardinger dextrins, dextrans, laminarin, and crown gall polysaccharide on the basis of n.m.r. data, sometimes combined with rotation data. Future plans call for a continuation of these studies with other carbohydrates and other solvent systems.

ACKNOWLEDGMENTS

We wish to express our sincere gratitude to the following who provided samples: Dr. G. G. Bartless, National Research Council, Saskatoon, Canada, for crown gall polysaccharide; Dr. Dexter French, Iowa State University, Ames, Iowa, for Schardinger dextrins; and co-workers in the Northern Laboratory Dr. C. L. Mehltretter for methyl α- and β-D-glucopyranosides, R. W. Jones for methyl α-isomaltoside, Dr. H. B. Sinclair for methyl β-maltoside, and Dr. A. R. Jeanes for dextrans.

REFERENCES

1. W. GORDY. J. Chem. Phys. **14**, 305 (1946).
2. R. E. REEVES. J. Am. Chem. Soc. **71**, 215 (1949).
3. R. E. REEVES. J. Am. Chem. Soc. **76**, 4595 (1954).
4. F. R. SENTI and L. P. WITNAUER. J. Am. Chem. Soc. **70**, 1438 (1948).
5. C. T. GREENWOOD and J. ROSSOTTI. J. Polymer Sci. **27**, 481 (1958).
6. R. U. LEMIEUX, R. K. KULLNIG, H. J. BERNSTEIN, and W. G. SCHNEIDER. J. Am. Chem. Soc. **80**, 6098 (1958).
7. J. A. POPLE, W. G. SCHNEIDER, and H. J. BERNSTEIN. High resolution nuclear magnetic resonance. McGraw-Hill Book Co., Inc., New York. 1959. p. 392.
8. M. J. KARPLUS. J. Chem. Phys. **30**, 11 (1959).
9. M. J. KARPLUS. J. Am. Chem. Soc. **85**, 2870 (1963).
10. R. W. LENZ and J. P. HEESCHEN. J. Polymer Sci. **51**, 247 (1961).
11. J. M. VAN DER VEEN. J. Org. Chem. **28**, 564 (1963).
12. V. S. R. RAO and J. F. FOSTER. J. Phys. Chem. **67**, 951 (1963).
13. J. N. SHOOLERY. Technical Information Bull. 2, No. 3, Varian Associates, Palo Alto, California. 1959. p. 4.
14. R. S. MULLIKEN. J. Chem. Phys. **2**, 782 (1935); **3**, 571 (1935).
15. R. T. SANDERSON. J. Am. Chem. Soc. **74**, 4792 (1952).
16. L. PAULING. The nature of the chemical bond. 2nd ed. Cornell University Press, N.Y. 1940. p. 58.
17. W. C. NEIKAM and B. P. DAILEY. J. Chem. Phys. **38**, 445 (1963).
18. E. L. ELIEL, M. H. GIANNI, and T. H. WILLIAMS. Tetrahedron Letters, 741 (1962).
19. K. L. WILLIAMSON. J. Am. Chem. Soc. **85**, 516 (1963).
20. R. E. KAGARISE. J. Am. Chem. Soc. **77**, 1377 (1955).
21. S. FORSEN. Spectrochim. Acta, **18**, 595 (1962).
22. W. M. PASIKA and L. H. CRAGG. Can. J. Chem. **41**, 293 (1963).

Can. J. Chem. Downloaded from www.nrcresearchpress.com by 210.87.254.40 on 09/05/12
For personal use only.

Can. J. Chem. Downloaded from www.nrcresearchpress.com by 210.87.254.105 on 09/05/12
For personal use only.

PERMANGANATE–PERIODATE OXIDATION

PART VII. THE OXIDATION OF SOME ACYCLIC MONOTERPENES[1]

E. VON RUDLOFF

National Research Council of Canada, Prairie Regional Laboratory, Saskatoon, Saskatchewan

Received May 17, 1965

ABSTRACT

The reaction of permanganate–periodate with 1-decene and 1-octadecene in aqueous suspension or media containing *tert*-butanol has been studied. C_{10}-compounds are oxidized almost quantitatively with the aqueous reagent. Myrcene, *cis*-ocimene, citronellol, citronellal, citronellic acid, geraniol, nerol, linalool, and linalyl acetate are all oxidized in high yield to the predicted products. These can serve conveniently for chemical identification of the aliphatic terpenes when isolated from mixtures by gas–liquid chromatography. The reaction may also be useful in locating the ^{14}C-label in tracer studies.

INTRODUCTION

Rapid progress in the analysis of essential oils and other complex mixtures of mono- and sesquiterpenes has been made with the advent of gas–liquid chromatography (g.l.c.). However, the chemical identification of such terpenes in milligram amounts has remained very difficult and usually physical data alone must be relied upon for characterization. Also, even the more efficient liquid phases developed (1–6) do not give complete resolution of all terpenes, and therefore a chemical means of identification for overlapping components is very desirable. Thus, the detection of small amounts of β-pinene in oils containing much sabinene was found to be impossible by physical data (7, 8), and many other such overlaps have been encountered by the author in the analysis of conifer leaf oils and other essential oils.

Since many terpenes have olefinic double bonds it was of interest to determine if these could be oxidized to predictable end products by means of the permanganate–periodate reagent. Earlier, we established that this reagent cleaves olefinic double bonds giving characteristic end products in almost quantitative yields (9–11) and this observation, together with the known behavior of oxygenated functional groups in a wide variety of aliphatic compounds towards the reagent (12), permits a reasonable prediction to be made of the mode of reaction of such groups in terpenes. This communication deals with the oxidation of the common aliphatic monoterpenes.

The permanganate–periodate reagent oxidizes isopropylidene groups almost quantitatively to acetone (11) and isopropenyl groups to varying amounts of formaldehyde (10). When commercial samples of citronellol, citronellal, and geraniol were analyzed by this technique it was confirmed that these exist essentially in the isopropylidene form. Chemical evidence for the predominance of this group in the aliphatic terpenes has been obtained by Caldwell and Jones (13, cf. also 14); Barnes *et al.* (15) have shown by means of infrared spectroscopy that in purified acyclic terpenes the isopropenyl form does not exceed 3%. In the present study the formation of acetone was confirmed by the iodoform reaction and that of formaldehyde by reaction with chromotropic acid.

Souček and Dolejš (16) have oxidized (−)-dihydrolavandulol to L(−)-isopropyl succinic acid by means of the permanganate–periodate reagent which is in full agreement with prediction. The isolation of this acid was useful in establishing the absolute configuration of (−)-lavandulol.

[1]*Issued as N.R.C. No. 8581. Presented in part at the 47th Annual Meeting of the Chemical Institute of Canada, Kingston, June 1–3, 1964.*

Can. J. Chem. Downloaded from www.nrcresearchpress.com by 210.87.254.105 on 09/05/12
For personal use only.

Since most terpenes are only very slightly soluble in water, the reaction of permanganate–periodate was first studied with 1-decene and 1-octadecene in the presence of 10 to 50% *tert*-butanol. This solvent was found to give good results in the oxidation of water-insoluble lipids (17). In subsequent experiments with terpenes it was found that the presence of *tert*-butanol is detrimental to the recovery and analysis of neutral oxidation products. Hence, particular attention has been paid to the reaction of 1-decene and 1-octadecene in aqueous suspension. Since this reaction is heterogeneous (at least in the early stages) two procedures were used. In procedure A aliquots of the olefin were shaken with the reagent in separate flasks. This procedure was also used when 30% or more *tert*-butanol was added since it had been found previously (17) that an insoluble periodate salt may be formed. In procedure B the olefin and oxidant were shaken vigorously until solution appeared to be complete and aliquots were withdrawn after various intervals for back-titration of unconsumed oxidant.

EXPERIMENTAL

Melting points were recorded on a Leitz hotstage microscope. Infrared spectra were recorded either as films between sodium chloride plates or as potassium bromide disks, using a Perkin–Elmer model 21 double-beam spectrophotometer. Analytical g.l.c. runs were carried out with an F & M model 500 (F & M Scientific Corp.) chromatograph having a thermal conductivity detector. The purity of starting materials and the composition of oxidation products were determined on 180 × 0.45 cm o.d. polyethylene glycol (Carbowax 20 M, 15% on Gaschrom P, 60–80 mesh) or Apiezon N (10%) columns. In standard runs temperature-programming from 55° to 210° at 4° per min was employed and the helium flow rate was 103–105 ml per min. The percentage composition was determined by measurement of the area under the peaks (triangulation methods) and no correction factor was employed for compounds of different molecular weight. Relative retention times (r.r.t.) were measured with respect to methyl octanoate. Preparative g.l.c. runs were carried out with an Aerograph model A700 instrument (Wilkins Instrument and Research Inc.). Optical rotations were measured either neat or in chloroform solution (3–5%) at room temperature (23–26 °C).

Purification of Starting Materials

All terpenes except linalool contained more than 1% impurities, most of which were removed by preparative g.l.c. on 2.5 to 5 m × 9 mm o.d. polyethylene glycol columns. In a typical experiment citronellol (73.5%) was injected repeatedly in 50 μl aliquots in 24 min cycles, using temperature-programming (non-linear, voltage regulator setting at 50) from 120° to 180°. The trip switch on the recorder was set to collect the upper two-thirds of the recorded citronellol peak. The purity of the collected material was found to be 98.5% and the identity with citronellol was confirmed by comparison of the infrared spectra and physical constants, including relative retention times (r.r.t.).

Several compounds could not be purified to better than 92–95% by preparative g.l.c. Purification by silver nitrate – silicic acid column chromatography (18) was tried, but only citronellol was purified satisfactorily by this method.

Oxidation Procedure

A. Water-Insoluble Compounds

1-Decene (3.55 mg, 0.025 mmoles) was weighed into a glass-stoppered Erlenmeyer flask (50 ml) and to this was added water and *tert*-butanol (8.0 ml), potassium carbonate (6.7 mg), and stock oxidant solution (2.0 ml). The latter consisted of an aqueous solution of sodium metaperiodate (97.5 mmoles/l) and potassium permanganate (2.5 mmoles/l) (12). The mixture was shaken for the required length of time; unconsumed oxidant was determined by addition of excess 0.1 *N* sodium arsenite solution (10.0 ml) and sodium bicarbonate (1 g) followed by back-titration (after 15 min) with standard iodine solution, using starch indicator (2%) for the end point. The values obtained were calculated as atoms of oxygen per mole of olefin (9, 12) (see Tables I and II).

When 30% or more *tert* butanol was used, an insoluble precipitate formed which reacted with arsenite only on heating (17). When more than the above amount of potassium carbonate was added, this precipitate formed more readily. Additional potassium carbonate is required when more than 1 equiv of acid is formed in the reaction.

B-1. Slightly Water-Soluble Compounds

Citronellol (39.06 mg, 0.25 mmole) was weighed into a 100 ml volumetric flask. Water (60–70 ml), potassium carbonate (67 mg), and stock oxidant solution (20.0 ml) were added and the mixture was shaken vigorously until the initial turbidity had disappeared. The solution was made up to volume and aliquots (10.0 ml) were withdrawn at the desired intervals. The amount of residual oxidant was determined as above.

B-2. Water-Soluble or Highly Reactive Compounds

Highly reactive compounds tend to reduce permanganate faster than the latter is reoxidized by periodate. To prevent this extensive reduction of permanganate, the compound to be oxidized was added to the oxidant (same proportions as above) (12). After mixing, the procedure in B-1 was followed.

Preparative Scale Oxidations

The olefin (1–2 mmoles) was added to the required amounts of water, potassium carbonate, and oxidant, and the mixture was shaken for the optimum length of time. The excess oxidant was reduced with a minimum of sodium bisulfite, and the weakly alkaline solution was extracted with ether to remove neutral products. If necessary, potassium carbonate was added to maintain a pH of 7 to 8. The ethereal solution was dried over anhydrous sodium sulfate and evaporated carefully to a small volume. The residue was analyzed by g.l.c. The aqueous portion was evaporated *in vacuo* (rotary evaporator) to a small volume. The aqueous distillate was used for qualitative acetone determination by the iodoform reaction (11) or for qualitative formaldehyde determination with chromotropic acid (10). The precipitated iodoform was filtered off, washed, and dried. The melting point (119–122°) was undepressed in admixture with authentic iodoform. The residue from the evaporation was completely reduced with bisulfite, acidified, and extracted continuously with ether. The ethereal solution was dried and evaporated to give the crude acidic oxidation products. An aliquot (5 to 10 mg) was methylated either with freshly prepared diazomethane or by the methanol – sulfuric acid method (19), and the derived methyl esters were analyzed by g.l.c. The balance of the acidic product was used for crystallization or preparation of crystalline derivatives.

TABLE I

Oxidant consumed (atoms oxygen per mole) by 1-decene and 1-octadecene at 0, 10, 20, 30, and 50% *tert*-butanol in the reaction mixture and using procedure A (continuous shaking) or procedure B-1 (1 h shaking)

	Time (h)	0%, proc. A	10%, proc. A	10%, proc. B-1	20%, proc. A	20%, proc. B-1	30%, proc. A	50%, proc. A
1-Decene	1	0.57	1.30	0.63	3.30	0.87	3.85	3.8
	3	1.42	2.20	1.25	3.65	1.85	3.90	3.85
	6	1.89	2.78	1.58	3.85	2.10	3.97	4.0
	24	3.65	3.35	1.78	3.90	2.38	4.02	4.1
	48	3.93	3.80	1.95	3.90	2.60	4.05	4.15
	72	3.95	3.90	2.25	3.95	3.05	4.10	4.15
	96	—	—	2.55	—	3.43	—	—
	144	—	—	—	—	4.10	4.10	4.15
1-Octadecene	3	—	0.20		0.15		3.90	4.0
	6	—	0.30		0.45		4.00	4.0
	24	0.30	0.80		2.20		4.00	3.95
	48	0.60	0.80		3.90		4.05	4.05
	72	0.88	0.85		4.10		—	—

1-Decene

The single impurity (5%; possibly 2-decene) could not be removed by preparative g.l.c. or by silver nitrate – silicic acid column chromatography. The rate of oxidation in aqueous suspension and in the presence of 10, 20, 30, and 50% *tert*-butanol was determined by procedure A (see Table I). An aliquot (300 mg) was oxidized in aqueous suspension for 24 h. No neutral product was recovered but the aqueous distillate gave a positive formaldehyde test. The acidic product (328 mg; 96%) showed three peaks on g.l.c. analysis (as methyl esters) with r.r.t. 0.70, 0.99, and 1.69 in 1.5, 5.0, and 93.5% amounts respectively; r.r.t. of methyl heptanoate = 0.71, methyl octanoate = 1.00, and methyl nonoate = 1.69. The derived hydrazide (19) was recrystallized twice from aqueous ethanol; m.p. 92.5–93.5° (undepressed by admixture of authentic *n*-nonanoic hydrazide, m.p. 94–95°).

Anal. Calcd. for $C_9H_{20}N_2O$: C, 62.74; H, 11.70; N, 16.26. Found: C, 62.48; H, 11.51; N, 16.08.

The oxidation was repeated using 20% *tert*-butanol solution. No neutral extract was obtained and the acidic product (96%) contained *n*-heptanoic (2%), *n*-octanoic (8.5%), and *n*-nonanoic (85%) acids as well as several unidentified minor components (g.l.c. analysis of methyl esters).

1-Octadecene

The single impurity (8%, possibly 2-octadecene) could not be removed by g.l.c. or column chromatography. The olefin was oxidized by procedure A and the rate of oxidation in aqueous suspension and media containing *tert*-butanol is shown in Table I. Because of the low solubility, duplicate runs gave values which differed by as much as 0.2 atoms oxygen per mole.

Preparative oxidation (24 h) of 1-octadecene (126.5 mg) in 30% *tert*-butanol gave a neutral extract

Can. J. Chem. Downloaded from www.nrcresearchpress.com by 210.87.254.105 on 09/05/12
For personal use only.

(2.8 mg) and a solid acidic fraction (133 mg, 98.5%); m.p. 54–58°. Recrystallization raised the m.p. to 59.7–61.3°; mixed m.p. with *n*-heptadecanoic acid undepressed.

Anal. Calcd. for $C_{17}H_{34}O_2$: C, 75.50; H, 12.67. Found: C, 75.42; H, 12.34.

Analysis by g.l.c. of the methyl esters derived from the total acidic fraction showed 4 peaks with r.r.t. (methyl octanoate = 1.00) 4.72, 5.10, 5.48, and 5.84 in 0.5, 2, 11.5, and 86% amount respectively. The r.r.t. values corresponded to those of the *n*-C_{14}, C_{15}, C_{16}, and C_{17} methyl esters.

TABLE II

Oxidant consumed (atoms oxygen per mole) by aliphatic monoterpenes

Compound	Time, hours								
	1	2	3	6	24	48	72	96	144
Myrcene	7.02	7.47	7.60	8.02	9.30	9.70	10.15	—	—
cis-Ocimene	8.31	8.85	9.57	9.67	10.90	11.15	11.50	—	—
cis-Ocimene*	9.26	9.78	10.18	10.73	11.27	11.55	11.60	—	—
Citronellal	2.74	2.89	2.95	3.02	3.40	3.64	3.70	—	—
Citronellal*	3.42	3.48	3.52	3.54	3.70	3.70	—	—	—
Citronellic acid	2.60	2.78	2.85	2.92	3.04	3.04	—	—	—
Citronellol	3.84	—	3.93	—	3.96	4.00	4.15	4.20	4.30
Geraniol	5.42	5.82	6.07	6.27	6.65	—	—	7.20	—
Nerol	5.67	5.96	6.22	6.44	6.83	7.11	7.29	—	7.53
Linalool	5.88	6.21	6.39	6.62	7.12	—	—	7.83	—
Linalyl acetate	5.52	—	5.78	6.07	6.32	6.44	6.59	—	—

*Mixture containing 10% *tert*-butanol.

Myrcene

Technical grade myrcene was purified by g.l.c. to give a product of 97% purity; n_D^{24} 1.4688, $[\alpha]_D$ +0.25°. The rate of oxidation with the aqueous reagent (procedure B-2) is shown in Table II. Preparative oxidation (150 mg; 48 h) gave acetone (as iodoform), formaldehyde (chromotropic acid color test) and succinic acid (91 mg, 72%); m.p. 185–188.5°. Recrystallization from acetone–chloroform raised the m.p. to 187–189° (undepressed by admixture of authentic succinic acid). Analysis by g.l.c. of the derived methyl esters gave only a single peak with r.r.t. (1.44) of methyl succinate.

cis-Ocimene

The sample, kindly donated by Messrs. International Flavors and Fragrances Inc., Union Beach, N.J., U.S.A., showed four minor impurities (2%) on g.l.c. analysis. The rate of oxidation in water and 10% *tert*-butanol (procedure B-2) is shown in Table II. Preparative oxidation gave acetone and formaldehyde. No ether-soluble acidic product was obtained.

Citronellol

The g.l.c. purified material (see above) had n_D^{23} 1.4552; $[\alpha]_D$ +4.18° (neat) and that obtained by column chromatography n_D^{25} 1.4535; $[\alpha]_D$ +3.52°. The rate of oxidation with the aqueous reagent (procedure B-1) is shown in Table II. Preparative oxidation (156 mg; 6 h) gave a neutral fraction (12 mg), acetone and an acidic extract (142.5 mg, 92.5%), which contained mainly an hydroxy acid (infrared spectrum). Analysis by g.l.c. of the derived methyl esters showed two peaks with r.r.t. 2.03 (4%) (3-methyl adipate = 2.04) and 2.52 (96%). Attempts to purify the expected 6-hydroxy-4-methyl hexanoic acid by distillation or column chromatography failed because of lactone formation and polymerization. The acid was characterized via the methyl ester, $[\alpha]_D$ +4.67° (*c*, 5.0); 3,5-dinitrobenzoate m.p. 145–147°.

Anal. Calcd. for $C_{15}H_{18}N_2O_8$: C, 50.85; H, 5.12; N, 7.91. Found: C, 50.78; H, 5.05; N, 7.75.

When the oxidation was allowed to continue for 4 d the amount of 6-hydroxy-4-methyl hexanoic acid dropped to about 58% and that of 3-methyl adipic acid increased to 28%. In addition at least 9 other acidic oxidation products were recorded in 0.5 to 3% amounts.

Geraniol

The g.l.c. purified material (98%) had n_D^{23} 1.4745 $[\alpha]_D$ −0.20° (neat). The rate of oxidation with the aqueous reagent (procedure B-1) is shown in Table II. Preparative oxidation (160 mg, 24 h) gave no neutral product, acetone and an acidic fraction (106 mg, 88%), n_D^{23} 1.4460, which consisted mainly of levulinic acid (g.l.c. methyl ester r.r.t. = 1.41); phenylhydrazone, m.p. 106.5–108° from benzene and aqueous ethanol (lit. 108° (20)); mixed m.p. undepressed. It is noteworthy that this phenylhydrazone (prepared in ethanolic solution) is in the form of the ethyl ester.

Anal. Calcd. for $C_{13}H_{18}N_2O_2$: C, 66.64; H, 7.74; N, 11.96. Found: C, 66.60; H, 7.76; N, 11.94.

Nerol

The g.l.c. purified material (97%) had n_D^{23} 1.4737, $[\alpha]_D$ −0.1°. The rate of oxidation with the aqueous reagent (procedure B-1) is shown in Table II. Preparative oxidation (152 mg, 24 h) gave acetone and levulinic acid (90%); phenylhydrazone m.p. 105–107°.

Can. J. Chem. Downloaded from www.nrcresearchpress.com by 210.87.254.105 on 09/05/12
For personal use only.

Linalool

The commercial sample (99%), n_D^{24} 1.4620, $[\alpha]_D$ +0.03° was oxidized as above (see Table II) and acetone and levulinic acid (88%) were identified as the major oxidation products.

Citronellal

The g.l.c. purified compound (96%) n_D^{25} 1.4572 $[\alpha]_D$ +9.39° was oxidized as above (see Table II). Preparative oxidation (308 mg, 48 h) gave acetone and an acidic fraction (270 mg, 90%), but no neutral extract. 3-Methyl adipic acid, m.p. 78–85°, $[\alpha]_D$ +0.1° crystallized from ether–hexane mixture (lit. m.p. 84.5–85° (21)). Purification via the methyl ester did not give a sharp melting compound. Analysis by g.l.c. of the crude methyl esters showed one major peak (95%) with r.r.t. 2.04.

Anal. Calcd. for $C_7H_{12}O_4$: C, 52.49; H, 7.55. Found: C, 52.72; H, 7.74.

Citronellic Acid

The commercial sample was purified via the methyl ester; n_D^{25} 1.4561, $[\alpha]_D$ +3.86°. The free acid was oxidized as above (see Table II). Preparative oxidation (212 mg, 6 h) gave acetone and an acidic fraction (184 mg, 93%) from which 3-methyl adipic acid, m.p. 79–85°, $[\alpha]_D$ +0.2°, was obtained; r.r.t. of derived methyl ester = 2.05.

Linalyl Acetate

The commercial sample (95%) could not be purified further owing to decomposition. The compound was oxidized as above (see Table II). Preparative oxidation (392 mg, 18 h) was carried out with the pH not exceeding 7.5 and yielded a neutral extract (7 mg), acetone, formaldehyde, and an acidic fraction (303.4 mg, 79%). The infrared spectrum of the latter showed it to be an acid containing an acetoxy group (1 250 cm^{-1}, strong).

RESULTS AND DISCUSSION

The rate of reaction of the permanganate–periodate reagent with 1-decene and 1-octadecene in aqueous suspension and media containing 10 to 50% *tert*-butanol is shown in Table I. The oxidation of 1-decene proceeded entirely satisfactorily in aqueous suspension (procedure A) and the assumed product, *n*-nonanoic acid, was isolated in 95% yield.[2] Although the rate of reaction was markedly increased by the addition of *tert*-butanol, no advantage was gained since the yield of *n*-nonanoic acid dropped and measurable amounts of the next lower homologue were formed. With 1-octadecene, at least 20% *tert*-butanol had to be added for a satisfactory rate of oxidation. Under these conditions the yield of the expected acidic oxidation product, *n*-heptadecanoic acid, was 92%.[2] Hence is was concluded that monoterpenes are best oxidized in aqueous suspension but that sesquiterpenes would in all probability require the presence of solvent.

The polyunsaturated monoterpene hydrocarbons myrcene (I) and *cis*-ocimene (IV) were oxidized very rapidly in aqueous suspension (see Table II). Both olefins gave acetone and formaldehyde as neutral products, but only myrcene was oxidized to an isolable acidic product.

Figure 1 shows the various steps of the permanganate–periodate oxidation of myrcene in detail. At pH 7.5 each double bond is hydroxylated by permanganate to a mixture of polyol (II) and isomeric acyloins (e.g. III) (9). These are cleaved by periodate to acetone, succinic semialdehyde, succinic acid, formaldehyde, and formic acid. Acetone and succinic acid are relatively stable towards the reagent (at pH 7.5), but succinic semialdehyde would be oxidized fairly rapidly to succinic acid, formic acid to carbon dioxide, and formaldehyde slowly to formic acid and carbon dioxide (10, 11, 12). Hence the expected products from myrcene would be acetone, formaldehyde, carbon dioxide, and succinic acid, which is in agreement with the experimental results. *cis*-Ocimene (IV) would be expected to yield acetone, formaldehyde, carbon dioxide, and acetic acid, the central fragment (malonic semi- and dialdehyde) being cleaved further (12, 16).

In g.l.c. analysis myrcene overlaps with camphene, sabinene, or β-pinene on non-polar columns, and with 3-carene or α-phellandrene on polar columns (3, 5, 7, 8). Hence the

[2]*Allowing for the impurity being the 2-isomer.*

Can. J. Chem. Downloaded from www.nrcresearchpress.com by 210.87.254.105 on 09/05/12
For personal use only.

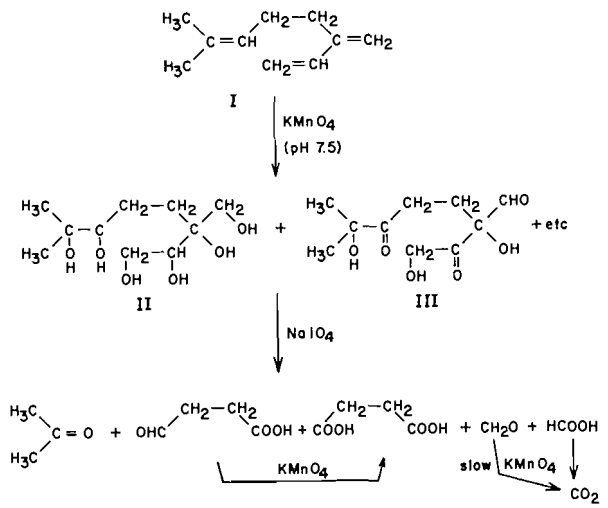

FIG. 1. Permanganate–periodate oxidation of myrcene.

formation of acetone and succinic acid by permanganate–periodate oxidation would confirm the presence of myrcene. Formaldehyde would also be expected from camphene, sabinene, and β-pinene and would have little diagnostic value. *cis*-Ocimene may overlap with limonene, *p*-cymene, 1,8-cineole, and α-terpinene, none of which would be expected to yield acetone in the oxidation. Thus, even qualitative detection of acetone in the oxidation product would have diagnostic value.

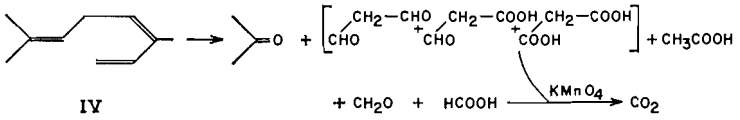

The oxygenated aliphatic monoterpenes citronellol, geraniol, nerol, linalool, citronellal, citronellic acid, and linalyl acetate all reacted at a satisfactory rate with the aqueous reagent (see Table II). The rate of reaction of the dienoid compounds was very rapid and precautions against too rapid reduction of permanganate (procedure B-2) was advisable. The amount of oxidant consumed by each of these compounds was in agreement with expected values and in each instance the presumed products were isolated in good yield. Thus geraniol (V*a*), nerol (V*b*) and linalool (VI) gave acetone and levulinic acid as

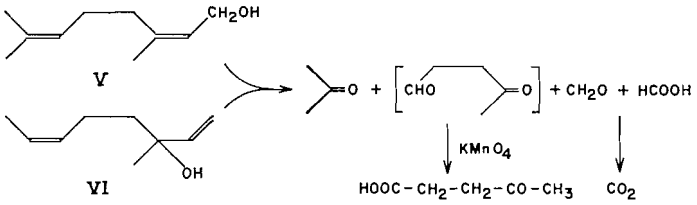

characteristic products. Since methyl ketones are relatively stable towards the oxidant (12), levulinic acid may be presumed to be fairly stable too and the duration of oxidation is not critical. It is noteworthy that the rates of oxidation of geraniol and nerol did not differ significantly. Hence it appears that the reagent does not differentiate between *cis*- and *trans*-isomers, unless steric hindrance is involved (12). In g.l.c. analysis geraniol

Can. J. Chem. Downloaded from www.nrcresearchpress.com by 210.87.254.105 on 09/05/12
For personal use only.

may overlap with bornyl and sabinyl acetate (non-polar columns), neither of which would be expected to yield acetone or an acidic product. Linalool has much lower retention characteristics and tends to overlap with either fenchone or camphor, neither of which is expected to react with the oxidant.

Citronellal (VII*a*) and citronellic acid (VII*b*) were oxidized smoothly to acetone and 3-methyl adipic acid in 6 to 48 h. When citronellol (VII*c*) was oxidized for 4 d, 3-methyl

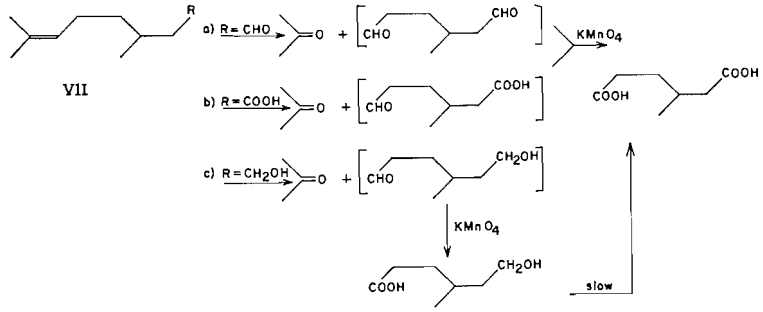

adipic acid was also obtained, but side reactions became apparent which may detract from the analytical value. Since it was shown previously (12) that primary alcohols reacted only very slowly with the reagent, citronellol was oxidized only for 6 h when 6-hydroxy-4-methyl hexanoic acid and acetone were obtained in excellent yield. 3-Methyl adipic acid was formed only in amounts of 3–5%. 6-Hydroxy-4-methyl hexanoic acid was not obtained previously from citronellol (22), nor does the acid seem to have been prepared by other means. This acid, together with acetone, could serve conveniently for differentiation from borneol, *p*-methan-8-ol, thujyl alcohol, and myrtenol, with which citronellol may overlap.

Finally, linalyl acetate was oxidized to determine if an allylic acetoxy group would be stable. It was already demonstrated that saturated esters were not attacked by the reagent provided the pH was kept at 7.5 or lower (12). The products after 24 h reaction were acetone, formaldehyde, and 2-acetoxy-2-methyl glutaric acid. Hence, this acetoxy group is unaffected by the reagent.

The above results demonstrate clearly that aliphatic terpenes are oxidized by the permanganate–periodate reagent in high yield to predictable end products. These may serve conveniently in the differentiation from the cyclic monoterpenes which may be present in fractions isolated by g.l.c. In this study millimole amounts of the terpenes were oxidized to permit isolation of crystalline derivatives of the characteristic oxidation products. However, the acidic products were also characterized readily by g.l.c. analysis of the methyl esters and acetone and formaldehyde may be detected colorimetrically in very small amounts. Hence for routine analysis of these terpenes milligram amounts will suffice for characterization by permanganate–periodate oxidation. Because of the high yield of characteristic fission products and little, if any, side reaction the method may also be of considerable value in locating the position of ^{14}C-labelled carbon atoms in studies with radioactive compounds. The study is being continued with cyclic terpenes to determine whether equally satisfactory results can be obtained with this group of compounds.

ACKNOWLEDGMENTS

The author wishes to thank Mr. M. Granat for technical assistance and Mr. W. C. Haid for microanalyses and recording of infrared spectra.

Can. J. Chem. Downloaded from www.nrcresearchpress.com by 210.87.254.105 on 09/05/12
For personal use only.

REFERENCES

1. R. A. BERNHARD. Food Res. **25**, 531 (1960).
2. D. M. SMITH, J. C. BARTLET, and L. LEVI. Anal. Chem. **32**, 568 (1960).
3. W. J. ZUBYK and A. Z. CONNER. Anal. Chem. **32**, 912 (1960).
4. E. VON RUDLOFF. Can. J. Chem. **39**, 1190 (1961).
5. M. H. KLOUWEN and R. TER HEIDE. J. Chromatog. **7**, 297 (1962).
6. R. A. BERNHARD. Anal. Chem. **34**, 1576 (1962).
7. E. VON RUDLOFF. Can. J. Chem. **41**, 2876 (1963).
8. E. VON RUDLOFF and F. M. COUCHMAN. Can. J. Chem. **42**, 1890 (1964).
9. R. U. LEMIEUX and E. VON RUDLOFF. Can. J. Chem. **33**, 1701 (1955).
10. R. U. LEMIEUX and E. VON RUDLOFF. Can. J. Chem. **33**, 1710 (1955).
11. E. VON RUDLOFF. Can. J. Chem. **33**, 1714 (1955).
12. A. S. PERLIN and E. VON RUDLOFF. Can. J. Chem. **43**, 2071 (1965).
13. A. G. CALDWELL and E. R. H. JONES. J. Chem. Soc. 599 (1946).
14. T. OLIVER. J. Chem. Soc. 2353 (1961).
15. D. BARNARD, L. BATEMAN, A. J. HARDING, H. P. KOCH, N. SHEPPARD, and G. B. B. M. SUTHERLAND. J. Chem. Soc. 915 (1950).
16. M. SOUČEK and L. DOLEJŠ. Collection Czech. Chem. Commun. **24**, 3802 (1959).
17. E. VON RUDLOFF. Can. J. Chem. **34**, 1413 (1956).
18. B. DE VRIES. Chem. Ind. London, 1049 (1962); J. Am. Oil Chemists' Soc. **40**, 784 (1963).
19. P. P. T. SAH. Rec. Trav. Chim. **59**, 1036 (1940).
20. F. TIEMANN and F. W. SEMMLER. Chem. Ber. **28**, 2126 (1895).
21. F. W. SEMMLER. Chem. Ber. **29**, 908 (1896).
22. J. L. SIMONSON. The terpenes. Vol. I. Cambridge University Press. 1947. p. 26ff.

Can. J. Chem. Downloaded from www.nrcresearchpress.com by 210.87.254.105 on 09/05/12
For personal use only.

Can. J. Chem. Downloaded from www.nrcresearchpress.com by 210.87.254.5 on 09/05/12
For personal use only.

THE AMINO PROTON SHIFTS OF SOME SUBSTITUTED ANILINES IN CYCLOHEXANE

T. YONEMOTO,[1] W. F. REYNOLDS,[2] H. M. HUTTON, AND T. SCHAEFER[3]
Department of Chemistry, University of Manitoba, Winnipeg, Manitoba

Received May 13, 1965

ABSTRACT

The amino proton shifts of 41 ortho, meta, and para substituted anilines at low concentrations in cyclohexane are reported. The shifts for meta and para substituents correlate with Hammett σ constants and it is shown that they are probably proportional to the π-electron density on the nitrogen atom. These shifts also correlate with the pK_a values of the corresponding anilinium ions in aqueous acid. The amino proton shifts for the ortho substituents, apart from methyl groups, follow a correlation line which lies about 0.5 p.p.m. to low field from that for the meta and para substituents. This negative deviation is discussed in terms of a weak hydrogen bonding interaction with the ortho substituents and the H—N—H bond angles as derived from infrared data.

INTRODUCTION

In recent years, correlations have been noted between Hammett σ constants and the chemical shift of the ring protons in *p*-substituted benzenes (1), formyl protons in *m*- and *p*-substituted benzaldehydes (2), hydroxyl protons in *m*- and *p*-substituted phenols (3), methoxy protons of substituted anisoles (4), and amino protons in *m*- and *p*-substituted anilines (5, 6). The anilines were measured in carbon tetrachloride (5, 6) and acetonitrile (6), where hydrogen bonding between solvent and amino protons is probable (see below).

The ring proton shifts at the para position of substituted benzenes are proportional to the calculated π-electron densities at the carbon atom (7). We report here the amino proton shifts of 41 *o*-, *m*-, and *p*-substituted anilines in cyclohexane solution, where interactions with the solvent are at a minimum, and discuss the results in terms of Hammett σ constants of the substituents, the π-electron density at the nitrogen atom, the pK_a values of the corresponding anilinium ions, and the H—N—H angles derived from high resolution infrared measurements. Low solubility in cyclohexane precluded measurements on a number of compounds, among them the nitroanilines, aminophenols, and *o*- and *p*-phenylenediamines.

EXPERIMENTAL

1. Sample Preparation

Solid anilines were sublimed before use, except for *o*-bromoaniline and *p*-iodoaniline which were recrystallized from cyclohexane. The liquid haloanilines were distilled in vacuum over fresh potassium hydroxide. Spectroscopy-grade cyclohexane was used as a solvent without further purification. As long as solubility allowed, samples of 5, 2, and 1 mole % concentration were prepared by weighing.

2. Spectra

The proton resonance spectrum of the amino group was recorded on a DP60 spectrometer. The solvent resonance peak provided a convenient reference signal, sidebands of which were used to find the shift of the amino proton resonance. The line width of the latter, a broad band due to exchange and relaxation phenomena involving the ^{14}N quadrupole, was usually about 3–5 c/s at 5 mole % and tended to increase with dilution. In some cases the linewidth approached 25 c/s. A dozen recordings were averaged for each solution. The reproducibility of the shifts was about 1 c/s in most cases but for very broad or weak signals it decreased to 3 c/s. The shifts obtained at the three concentrations were extrapolated to infinite dilution. Most of the solutions showed no significant dilution shift in this concentration range. Low solubility in some cases

[1]*National Research Council Postdoctorate Fellow, 1962–1964.*
[2]*National Research Council Studentship Holder, 1962–1963.*
[3]*National Research Council Senior Research Fellow, 1964–1965.*

demanded the use of the shift of the 1 mole % solution only. These are given the superscript *a* in Table I. In other cases large line widths at lower concentrations only allowed the measurement of 2 or 5 mole % solutions. These are given the superscript *b* in Table I.

3. Effect of Purification on Spectra

An investigation of the effect of impurity on the shift was made with aniline solutions. In Fig. 1, line 1 was obtained for aniline distilled in vacuum over potassium hydroxide. Line 2 shows the results for the distilled aniline if the solutions were prepared 1 d after opening the distillation vessel, while line 3 was obtained for undistilled deeply colored aniline. The resonance peaks obtained for the solutions prepared from unpurified aniline were narrower than for purified aniline, probably because of faster proton exchange catalyzed by water or other impurities. For this reason, the error in measurement was larger for the purified aniline solutions. Consequently, although the solutions of unpurified aniline appear to show both a smaller dilution shift and a high-field shift compared to the solutions of purified aniline, the experimental error is such that little was gained by purification.

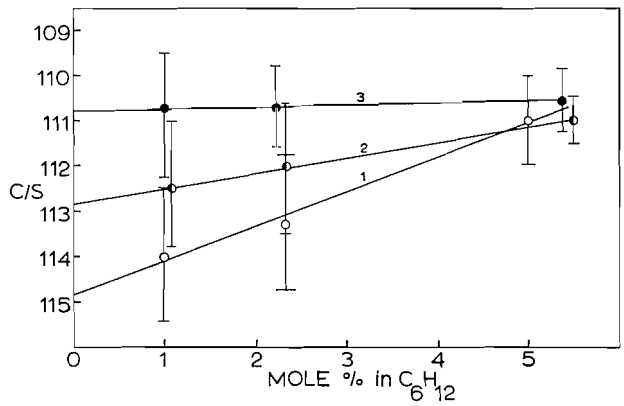

FIG. 1. Line 1 (open circles) shows the chemical shift in c/s to low field from cyclohexane of the amino protons of vacuum-distilled aniline at three concentrations in cyclohexane. Line 2 (half-filled circles) is for aniline which was used one day after vacuum distillation. Line 3 (filled circles) is for unpurified, deeply colored aniline.

RESULTS AND DISCUSSION

In Table I the amino proton shifts, $\Delta\nu$, of 41 *o*-, *m*-, and *p*-substituted anilines are given relative to aniline itself. Prior to the discussion of these shifts in terms of molecular parameters, the state of the aniline molecules in solution must be considered. If our $\Delta\nu$ values represented the true shift at infinite dilution, they would naturally be those of aniline molecules isolated from each other by solvent molecules. Because of signal-to-noise problems, however, the extrapolation to infinite dilution is probably somewhat unreliable.* There may be a substantial, at present undetectable, change in shift between 1 and 0 mole %, especially if self-association through hydrogen bonding occurs.

The intensity of the first overtone of the N—H stretching band of aniline in cyclohexane has been interpreted in terms of hydrogen-bonding association (8). A dimerization model is consistent with the data up to 0.2 *M*. The equilibrium constant for dimer formation is about 0.4 at room temperature (8). For a 0.2 *M* solution, which happens to be about 2 mole %, only about 5% of the aniline molecules are therefore in the form of dimers. On an n.m.r. time scale the dimers will break up and reform rapidly, so that the observed shift represents the weighted average of the monomer and dimer shifts. Unfortunately, the difference in shift between dimer and monomer is not known. However, if we assume

**The viable, if expensive, procedure to follow here would be the use of* ^{15}N *substituted compounds to eliminate quadrupole relaxation broadening and a computer of average transients to allow measurements on very dilute solutions.*

Can. J. Chem. Downloaded from www.nrcresearchpress.com by 210.87.254.5 on 09/05/12
For personal use only.

Can. J. Chem. Downloaded from www.nrcresearchpress.com by 210.87.254.5 on 09/05/12
For personal use only.

TABLE I

Chemical shifts, $\Delta\nu$, in p.p.m. of the amino-protons of some substituted anilines in cyclohexane solutions

No.	Substituent	$\Delta\nu$[c]	σ[d]	ΔpK_a[e]	No.	Substituent	$\Delta\nu$[c]	σ[d]	ΔpK_a[e]
1.	2-F[a]	−0.12	0.24	−1.62	22.	3,4-diCl	−0.02	0.60	—
2.	3-F[b]	−0.08	0.34	−1.20	23.	3,5-diCl[a]	−0.12	0.74	—
3.	4-F	0.12	0.06	−0.06	24.	2,4-diCl	−0.45	0.43	—
4.	2-Cl	−0.45	0.20	−1.96	25.	2,5-diCl	−0.53	0.57	—
5.	3-Cl	−0.02	0.37	−1.26	26.	2,6-diCl	−0.97	0.40	—
6.	4-Cl[a]	0.03	0.23	−0.77	27.	2,6-diBr	−1.10	0.42	—
7.	2-Br[b]	−0.52	0.21	−1.98	28.	2,4-diCH_3	0.20	−0.34	—
8.	3-Br	−0.03	0.39	−1.07	29.	2,3-diCH_3	0.13	−0.24	−0.01
9.	4-Br[a]	0	0.23	−0.67	30.	2,6-diCH_3	0.10	−0.34	—
10.	2-I[b]	−0.50	0.21	−1.98	31.	2,5-diCH_3	0.13	−0.24	—
11.	3-I	0	0.35	−0.97	32.	3,5-diCH_3[a]	0.20	−0.14	—
12.	2-CH_3	0.12	−0.17	−0.20	33.	3,4-diCH_3	0.22	−0.24	0.57
13.	3-CH_3	0.10	−0.07	−0.09	34.	2-Br-4-CH_3	−0.37	0.04	—
14.	4-CH_3	0.15	−0.17	0.49	35.	4-F-2-CH_3[b]	0.18	−0.11	—
15.	4-CH_2CH_3[b]	0.13	−0.17	—	36.	4-Cl-2-CH_3	0.07	0.06	—
16.	2-OCH_3[b]	−0.23	−0.39	−0.09	37.	2-Cl-6-CH_3	−0.47	0.03	—
17.	3-OCH_3[a]	0.07	0.12	−0.38	38.	4-Br-2-CH_3	0.05	0.06	—
18.	4-OCH_3[a]	0.28	−0.27	0.71	39.	2-CF_3	−0.60	0.54[f]	—
19.	2-OCH_2CH_3[b]	−0.22	−0.35	−0.11	40.	2-CN[a]	−0.97	0.64[f]	—
20.	4-OCH_2CH_3[a]	0.28	−0.24	0.67	41.	2-COC_6H_5-5-Cl	−2.65	—	—
21.	3-NH_2[a]	0.03	−0.16	0.30					

[a] [b]See experimental procedure.
[c]Relative to aniline.
[d]Hammett σ-constants. See discussion for choice of values.
[e]Taken from refs. 35 and 36.
[f]As recommended in ref. 14.

that the substituted anilines have very similar association constants to aniline then the discussions below should still be valid. Certainly, the absortivity–concentration relationships of *m*-methylaniline and *m*-chloroaniline are qualitatively similar to the ones for aniline, although they are somewhat different for *o*-chloroaniline (9). A reasonable expectation is that *o*-substituents would hinder self-association and that self-association through hydrogen bonding leads to low-field shifts. Therefore the observed large low-field shifts for *o*-substituents can also reasonably be discussed in terms of the properties of the isolated molecules, as is done below.

1. Correlation of $\Delta\nu$ with σ Constants

In Fig. 2, $\Delta\nu$ is plotted versus the Hammett σ constants. The effect of more than one substituent is taken as additive (10) and the recent σ values from the analysis of McDaniel and Brown (11) were used when available. For *o*-substituents the σ values derived by Taft (12) were used since these are on the same scale as the Hammett σ values for *m*- and *p*-substituents.

For solubility reasons, the range of σ is only 1.2 units as compared to 1.6 units available in acetonitrile solution (6). Disregarding the *o*-substituents, except for methyl groups, the range of $\Delta\nu$ is very small and we feel there is little to be gained from a least squares treatment. Instead, the dashed line has been drawn as shown in Fig. 2. As expected, the electron-withdrawing substituents (positive σ) lead to a low-field shift. The average deviation for *m*- and *p*-substituents (but including *o*-methyl) is just over 0.03 p.p.m. which is probably within experimental error.

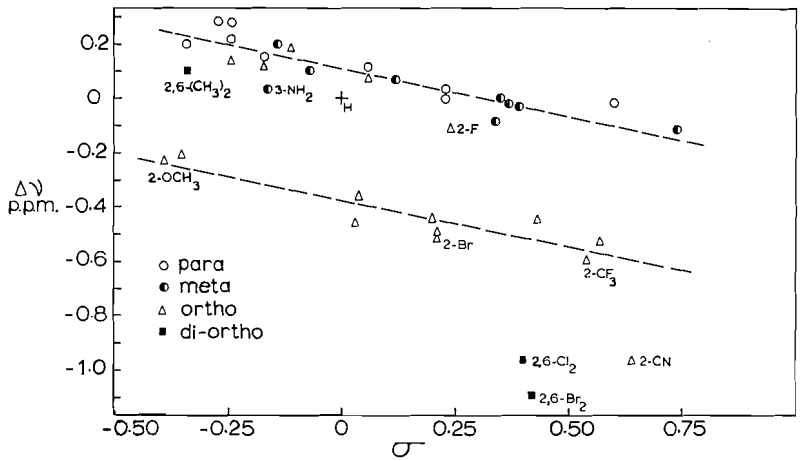

FIG. 2. The chemical shift in p.p.m. relative to aniline of the amino protons in substituted anilines is plotted versus the Hammett σ-constants of the substituents. The unidentified ortho points clustered about the top line are those with methyl groups in the ortho position.

Per unit change in σ, $\Delta\nu$ changes by 0.35 p.p.m. which compares with 0.53 p.p.m. in carbon tetrachloride and 0.97 p.p.m. in acetonitrile solutions (6). The larger values in the latter solutions can be understood in terms of hydrogen bonding to the solvent. As σ increases algebraically the N—H bond increases in acidity, and hydrogen bonding with an acceptor solvent is favored, causing larger shifts. That carbon tetrachloride should hydrogen bond to N—H is perhaps unexpected, yet there is evidence that it does so even to C—H bonds. As an example, proton shifts of many haloalkanes (13) in cyclohexane and carbon

Can. J. Chem. Downloaded from www.nrcresearchpress.com by 210.87.254.5 on 09/05/12
For personal use only.

tetrachloride solution indicate that the latter offers chlorine atoms for hydrogen bonding to the C—H bonds of the solute. Further, it is known that some substituted anilines react rapidly with carbon tetrachloride (14, 15). For the discussion in the next subsection, measurement of amino proton shifts in solvents like cyclohexane is therefore essential.

2. $\Delta\nu$ and π-Electron Density on the Nitrogen Atom

In *p*-substituted benzenes, the *p*-proton shift changes by 1 p.p.m. when the Hammett σ constant changes by 1.4 units (1). For this σ range, the calculated π-electron density on the *p*-carbon atom varies by 0.1 electron (7), indicating a proton shift of about 10 p.p.m./electron. The electron density on the nitrogen atom of substituted anilines is expected to be much less sensitive than the *p*-carbon atom to the influence of a substituent on the ring. Thus, the calculated π-density on the nitrogen atom in *N,N*-dimethylaniline is only 0.007 electrons less than in *N,N*-dimethyl-*p*-anisidine (16). This compares with 0.031 electron more at the *p*-carbon atom in anisole than in benzene (7) (these two calculations used the same bond and core parameters for the oxygen atom in the methoxy group). In this way an approximate estimate may be made of the expected change in $\Delta\nu$ of the amino protons for a change of one unit in σ in the substituted anilines. It is $\Delta\nu \approx 0.007/1.4 \times 0.031 = 0.16$ p.p.m., about half the observed value. However, the N—H bond is much more polarizable than the C—H bond. From chemical shift data, Musher (17) deduces that it is roughly 5/3 more polarizable, leading to a calculated $\Delta\nu$ of 0.27 p.p.m.

The electrostatic field of the excess charge on the nitrogen atom produces a potential difference between the two ends of the N—H bond which drives electrons into the hydrogen 1s orbital. However, the hybridization of the nitrogen atom changes when the ring is substituted (see below) and this will change the excitation energies of the orbitals involved and therefore change any assumed proportionality between π-density and proton shielding.

In view of the approximations and experimental errors involved, it seems reasonable to conclude that the amino proton shift in *m*- and *p*-substituted anilines is primarily dependent on the π-electron density at the nitrogen atom. In this connection, it is interesting to note a shift of the zero point of about 0.08 p.p.m. to high field in Fig. 2. Such a shift also occurs for the proton shifts in *p*-substituted benzenes and is evidence for an additional factor in determining the σ constants. The latter depend on the electronic structure of a reaction intermediate related to the substituted benzoic acids.

3. Correlation of $\Delta\nu$ with pK_a Values

In Fig. 3, $\Delta\nu$ is plotted versus ΔpK_a of the protonated anilines in aqueous acid. The average deviation from the straight line is less than 0.03 p.p.m. However, because of the slight slope of the line a measurement of the amino proton shift in cyclohexane allows the prediction of the pK_a of a substituted aniline with an accuracy of only about ± 0.25 units. For this purpose, it would be better to use a polar solvent like acetonitrile for which the correlation line has a much steeper slope. As in Fig. 2, there is a zero point shift of the correlation line. Also, the point for *m*-aminoaniline shows a rather large negative deviation, a possible result of increased hydrogen bonding for this compound in cyclohexane solution.

The points for *o*-substituted anilines (apart from *o*-fluoro and *o*-methyl anilines) show large negative deviations but they appear to parallel the correlation line for the *m*- and *p*-substituents. The reason for this will become clearer from the discussion below.

4. Ortho-Substituted Anilines

In Fig. 2, the *o*-substituted anilines fall, on an average, about 0.50 p.p.m. below the correlation line for the *m*- and *p*-substituted anilines. Although the scatter is considerable,

Can. J. Chem. Downloaded from www.nrcresearchpress.com by 210.87.254.5 on 09/05/12
For personal use only.

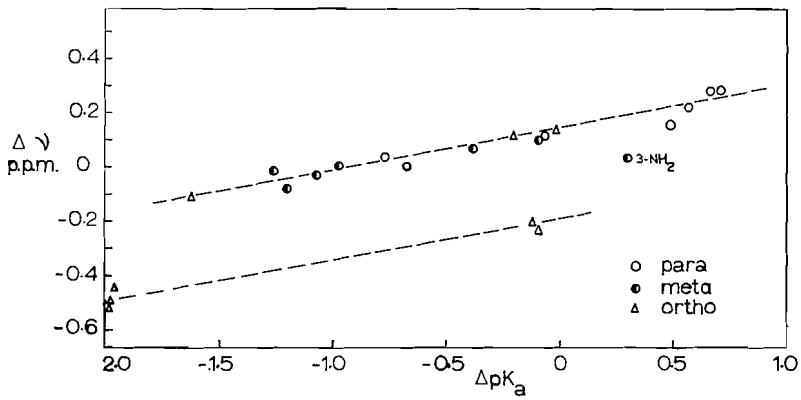

FIG. 3. The chemical shift in p.p.m. relative to aniline of the amino protons in substituted anilines is plotted versus the available ΔpK_a values of the corresponding anilinium ions in aqueous acid; ΔpK_a is relative to the pK_a value of anilinium ion.

we consider that two parallel lines can be drawn, one for *m*- and *p*-substituents and one for the *o*-substituents (with the exceptions of *o*-methyl and *o*-fluoro which are discussed later).

A number of possible reasons for this low-field shift suggest themselves. These are a steric hindrance to π-overlap of the amino group with the ring, the magnetic anisotropy of the substituent (18, 19), the electric field of the substituent dipole (20), and an intramolecular van der Waals or dispersion interaction (21). These will now be discussed in order.

(a) Steric Hindrance to π-Overlap

Electronic absorption spectra (22) and ^{13}C chemical shifts (23) of substituted anilines agree that even bulkier substituents than those under consideration do not cause steric hindrance to π-overlap of the amino group with the ring. In any event, steric hindrance of this nature would lead to high-field shifts of the amino protons since less charge would be delocalized from the amino group into the aromatic nucleus.

(b) Magnetic Anisotropy and Electric Field Effects

We have carried out calculations for both these effects, using the point dipole approximation. The geometry of the system was assumed to be planar with H—N—H angles of 120°, and the mean of the calculated shifts for the two protons was examined. Because of the unfavorable angle between the internuclear vector and the C—X bond, reasonable values of the magnetic anisotropy of the C—X bond lead to quite small shifts (but see the discussion of the cyano group below). In the dipole approximation, the electric field effect of the bond dipole moments (24) dominates. Using the recommended coefficients for the N—H bond (17) in Buckingham's equation (20), low-field shifts are calculated which decrease in the order F > Cl > Br > I, opposite to the observed order of shifts. This is so whether the dipole is placed midway along the C—X bond or on the atom X. We do not reproduce a table of the calculations here since they do not account for the observed shifts.

It is perhaps possible that a judicious choice of anisotropy and bond dipole moments, together with a variation in the location of the dipoles, would lead to agreement with the observed shifts for some of the substituents (see cyano group below). The significance of such an agreement is doubtful. Martin and Dailey (25) point out similar difficulties in accounting for the *o*-proton shifts in substituted benzenes. A further relevant point these

Can. J. Chem. Downloaded from www.nrcresearchpress.com by 210.87.254.5 on 09/05/12
For personal use only.

authors make is that the electric dipole field of the substituent does not contribute significantly to *m*- or *p*-proton chemical shifts in these molecules.

(c) Dispersion Interactions

There is considerable overlap of the van der Waals radii of the amino proton and the heavier halogen substituents. Such an overlap would be expected to lead to low-field shifts of the amino protons because of the fluctuating electric fields arising from the instantaneous dipoles in the halogen atoms (effect proportional to the mean square of these fields (26)). However, the methoxy group causes much the same effect as the heavier halogens and, furthermore, the latter cause nearly the same shift. The similar shielding for bromo and chloro substituents could possibly be rationalized as follows. The hydrogen–iodine distance is so small (about 2.5 Å compared to the sum of the van der Waals radii of $1.2 + 2.15 = 3.35$ Å) that a compensating high-field shift arises from the magnetic anisotropy of the iodine, just as the proton in hydrogen iodide is more shielded than in hydrogen bromide (27). This argument not only serves to show the unreliability of the point dipole approximation in calculating magnetic anisotropy effects at short distances, but also illustrates the tenuousness of any explanation of such low-field shifts in terms of long-range models of electric field and magnetic anisotropy; or dispersion effects. A recent paper from this laboratory (28) concerning the *o*-proton and *o*-fluorine shifts in ethylenes, propylenes, benzenes, and perfluorobenzenes throws some doubt on their explanation in terms of a single one of these effects.

(d) Weak Hydrogen Bonding

It is well known that hydrogen bonding causes a shift to low field of the proton involved. As originally suggested (27) it is probably a combination of the electric field and magnetic anisotropy effects of the proton acceptor. A recent calculation of the shift of the chloroform proton caused by weak hydrogen bonds to nitrogen bases illustrates the difficulties involved in the calculation (27*a*). It turns out that the nitrogen lone pair is responsible for at least 95% of the electric field at the proton in a linear intermolecular hydrogen bond. The point dipole approximation is therefore useless. The calculation also illustrates that the magnetic anisotropy effect is much less than the electric field effect, even for the cyano group.

In our compounds, we consider it most sensible to discuss the ortho shifts qualitatively in terms of an interaction of the N—H bond with the substituent lone pairs, which we prefer to call weak hydrogen bonding as opposed to the strong hydrogen bond found in 2-amino-5-chloro-benzophenone (see below). The plausibility of this approach is supported by the fact that the low-field shift for the *o*-substituents in Fig. 2 increases as σ becomes more positive, i.e., as the N—H bond becomes more acidic its interaction with the substituent increases; as would be expected for hydrogen bonding.

Further support comes from the H—N—H bond angles calculated from the frequencies of the symmetric and antisymmetric stretching bonds of these compounds (14). In Fig. 4, $\Delta\nu$ is plotted versus the H—N—H angle. With the exception of the *o*-trifluoromethyl and *o*-cyano groups (discussed below) there is a roughly parallel change in the expected direction of $\Delta\nu$ with the H—N—H angle. The enhanced H—N—H angle on ortho substitution has been attributed to intramolecular hydrogen bonding (14).

Finally, the splitting of the first overtone of the N—H symmetric stretching band in *o*-substituted anilines has been interpreted in terms of a double-minimum potential for the hydrogen bonded proton (29). This is further support for the above interpretation of the low-field shifts.

Can. J. Chem. Downloaded from www.nrcresearchpress.com by 210.87.254.5 on 09/05/12
For personal use only.

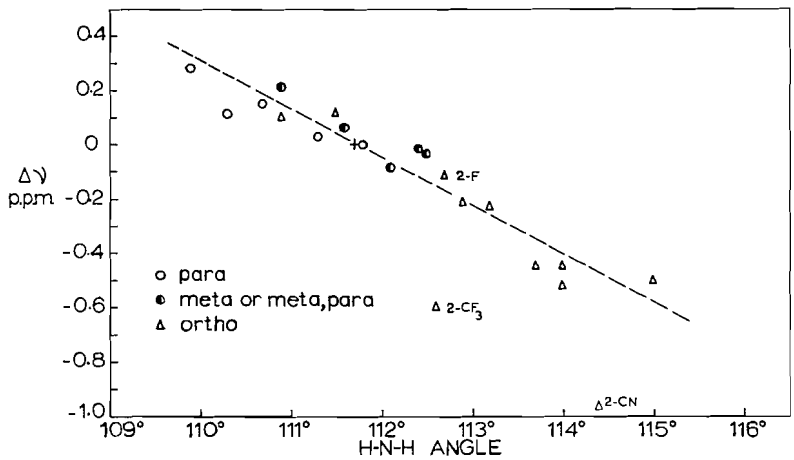

FIG. 4. The chemical shift in p.p.m. relative to aniline of the amino protons in substituted anilines is plotted versus the H—N—H angle derived from the symmetric and antisymmetric stretching frequencies in ref. 14.

From the viewpoint of π-electron density on the nitrogen atom it is important to realize that the range in $\Delta\nu$ of about 1 p.p.m. in Fig. 4 should not be taken as representing a proportionate change in the former. The electron density changes, as discussed above, would be reasonably expected to account only for about 0.3 p.p.m. in $\Delta\nu$. It is true that as the H—N—H angle increases towards 120° the π-overlap between the amino group and the ring will increase but not to the extent that a naive interpretation of the $\Delta\nu$ values would indicate. The *excess* low-field shift for the *o*-substituted anilines is probably caused by the perturbation of the electron density near the proton by the substituent lone pairs.

(e) The o-Fluoro and o-Methyl Substituents

In Fig. 2, the amino proton shift of *o*-fluoroaniline does not deviate far from the straight line. This is to be expected if, as indicated by infrared data (14), the small size of the fluorine atom prevents the close approach of the hydrogen atom to its lone pair orbitals. The amino proton shifts of the compounds containing an *o*-methyl group do not indicate a large anisotropy of the C—C bond (30), unless the anisotropy of the C—H bonds leads to a fortuitous cancellation of the C—C bond anisotropy.

(f) o-Cyanoaniline

In Figs. 2 and 4, the $\Delta\nu$ value deviates strongly to low field from all regular trends. In this particular case, the magnetic anisotropy of the C—X bond is rather large. If an experimental (31) and theoretical value (32) for the triple bond of about 20×10^{-6} cm^3/mole is used, one calculates a low-field shift of about 0.33 p.p.m. for the planar geometry assumed above. This agrees roughly with the excess low-field shifts in Figs. 2 and 4, i.e., from the lines drawn for *o*-substituents in Fig. 2 and the line in Fig. 4.

(g) o-Trifluoromethylaniline

The $\Delta\nu$ value falls roughly on the lower line in Fig. 2. This is not unexpected since the lone pairs of the fluorine atoms are now considerably closer to the hydrogen atom than in *o*-fluoroaniline. In Fig. 4, however, the $\Delta\nu$ value deviates strongly from the expected value. The deviation is easily rationalized in terms of the geometry of the molecule. The interaction of the hydrogen atom and the fluorine atom in the trifluoromethyl group, although stronger than in *o*-fluoroaniline, need not, because of their relative positions lead to an

Can. J. Chem. Downloaded from www.nrcresearchpress.com by 210.87.254.5 on 09/05/12
For personal use only.

enhancement of the H—N—H angle; but the interaction can lead to a considerably increased low-field shift because the lone pairs are now closer to the hydrogen atom.

(h) 2,6-Dichloro- and Dibromoanilines

The low-field shift in these two compounds is roughly twice that of the mono-substituted compounds. This is reasonable in that both amino protons now interact with the substituent, whereas proton exchange leads to an averaging of hydrogen bonded and unbonded shifts for the monosubstituted compounds.

5. Ring Current Shifts

As the H—N—H angle increases the possibility arises of a change in ring current contributions to the amino proton shift (33). To estimate this change we have calculated the ring current contributions to the N—H proton shift for two extreme orientations of the amino group with respect to the plane of the ring: planar, and N—H bonds perpendicular to the ring. Using the procedure recommended by Dailey (34) we find that, at most, the protons in the perpendicular form would be shifted -0.1 p.p.m. relative to protons in the planar form (the adverse angle is more than compensated for by the decrease in ring–proton distance). However, since the H—N—H angle appears to vary between 109° and 115° in our compounds the changes in ring current shifts will amount to less than 0.05 p.p.m., which can be disregarded in our discussion.

6. Strong Hydrogen Bonding

The one compound in Table I expected to form a strong intramolecular hydrogen bond is 2-amino-5-chlorobenzophenone. Here the hydrogen bond to the carbonyl group forms part of a six-membered ring and would be expected to be strong. In agreement, we find a $\Delta\nu$ of -2.65 p.p.m. The H—N—H angle in this compound has not been calculated from the vibrational bands (14), but the splitting of the overtone of the symmetric stretching band has been measured for 2-aminobenzophenone (29). From a plot of this splitting versus H—N—H angle in other compounds we deduce an approximate value of 127° for 2-amino-5-chlorobenzophenone.* From Fig. 4 a predicted shift of 2.50 ± 0.33 p.p.m. follows, assuming the linearity of the plot. It is, however, to be noted that the carbonyl bond and the other ring may contribute to this shift to an unknown extent.

CONCLUSIONS

The small range of the chemical shift of the amino protons of *m*- and *p*-substituted anilines in cyclohexane can be interpreted in terms of small changes in the π-electron density on the nitrogen atom. The much larger shifts in the *o*-substituted anilines are at present best interpreted in terms of weak hydrogen bonding of the amino protons to the substituent. The shifts can be used to predict pK_a values of the anilinium ions but for this purpose it is best to use a polar solvent.

ACKNOWLEDGMENTS

We are very grateful to the National Research Council for financial support.

REFERENCES

1. H. Spiesecke and W. G. Schneider. J. Chem. Phys. **35**, 731 (1961).
2. R. E. Klinck and J. B. Stothers. Can. J. Chem. **40**, 1071 (1962).
3. R. J. Ouellette. Can. J. Chem. **43**, 707 (1965).
4. C. Heathcote. Can. J. Chem. **40**, 1865 (1962).

**2-Aminoacetophenone has an* H—N—H *angle of 133° (14) and the splitting of its first overtone is greater than for 2-aminobenzophenone (29).*

Can. J. Chem. Downloaded from www.nrcresearchpress.com by 210.87.254.5 on 09/05/12
For personal use only.

5. W. F. REYNOLDS. Ph.D. thesis, University of Manitoba. 1963.
6. L. K. DYALL. Australian J. Chem. **17**, 419 (1964).
7. T. K. WU and B. P. DAILEY. J. Chem. Phys. **41**, 2796 (1964).
8. J. H. LADY and K. B. WHETSEL. J. Phys. Chem. **68**, 1001 (1964).
9. K. B. WHETSEL, W. E. ROBERTSON, and M. W. KRELL. Anal. Chem. **32**, 1281 (1960).
10. H. H. JAFFE. Chem. Rev. **53**, 191 (1953).
11. D. H. MCDANIEL and H. C. BROWN. J. Org. Chem. **23**, 420 (1958).
12. R. W. TAFT. *In* Steric effects in organic chemistry. *Edited by* M. S. Newman. John Wiley and Sons, New York. 1956. p. 618.
13. A. L. MCCLELLAN and S. W. NICKSIC. J. Phys. Chem. **69**, 446 (1965).
14. P. J. KRUEGER. Can. J. Chem. **40**, 2300 (1962).
15. Unpublished observations in this laboratory.
16. A. ZWEIG, J. E. LANCASTER, N. T. NEGLIA, and W. H. JURA. J. Am. Chem. Soc. **86**, 4130 (1964).
17. P. LASZLO and J. I. MUSHER. J. Chem. Phys. **41**, 3906 (1964).
18. J. A. POPLE. Proc. Roy. Soc. London, Ser. A, **239**, 541, 550 (1957).
19. H. M. MCCONNELL. J. Chem. Phys. **27**, 226 (1957).
20. A. D. BUCKINGHAM. Can. J. Chem. **38**, 300 (1960).
21. T. SCHAEFER, W. F. REYNOLDS, and T. YONEMOTO. Can. J. Chem. **41**, 2969 (1963).
22. B. M. WEPSTER. Rec. Trav. Chim. **76**, 357 (1957).
23. P. C. LAUTERBUR. J. Chem. Phys. **38**, 1415 (1962).
24. C. P. SMYTH. Dielectric behaviour and structure. McGraw-Hill Book Co., Inc., New York. 1955.
25. J. S. MARTIN and B. P. DAILEY. J. Chem. Phys. **39**, 1722 (1963).
26. W. T. RAYNES, A. D. BUCKINGHAM, and H. J. BERNSTEIN. J. Chem. Phys. **36**, 3481 (1962).
27. W. G. SCHNEIDER, H. J. BERNSTEIN, and J. A. POPLE. J. Chem. Phys. **28**, 601 (1958).
27*a*. P. J. BERKELEY and M. W. HANNA. J. Am. Chem. Soc. **86**, 2990 (1964).
28. F. HRUSKA, H. M. HUTTON, and T. SCHAEFER. Can. J. Chem. In press. 1965.
29. P. J. KRUEGER. Can. J. Chem. **42**, 201 (1964).
30. G. S. REDDY and J. H. GOLDSTEIN. J. Chem. Phys. **38**, 2736 (1963).
31. G. S. REDDY and J. H. GOLDSTEIN. J. Chem. Phys. **39**, 3509 (1963).
32. J. A. POPLE. J. Chem. Phys. **37**, 34 (1962).
33. J. A. POPLE. J. Chem. Phys. **24**, 111 (1956).
34. B. P. DAILEY. J. Chem. Phys. **41**, 2304 (1964).
35. H. C. BROWN, D. H. MCDANIEL, and O. HAEFLIGER. *In* Determination of organic structures by physical methods. Vol. I. *Edited by* E. A. Braude and F. C. Nachod. Academic Press, Inc., New York. 1955.
36. A. ALBERT and E. P. SERJEANT. Ionization constants of acids and bases. Methuen and Co., London. 1962.

Can. J. Chem. Downloaded from www.nrcresearchpress.com by 210.87.254.5 on 09/05/12
For personal use only.

Can. J. Chem. Downloaded from www.nrcresearchpress.com by 210.87.254.5 on 09/05/12
For personal use only.

THE PHOTOLYSIS AND THE MERCURY-PHOTOSENSITIZED DECOMPOSITION OF HYDROXYLAMINE VAPOR[1]

J. BETTS[2] AND R. A. BACK

Division of Pure Chemistry, National Research Council of Canada, Ottawa, Canada

Received April 30, 1965

ABSTRACT

The mercury-photosensitized decomposition (2 537 Å) and the direct photolysis of hydroxylamine vapor have been studied at a pressure of 0.27 Torr, at 25 °C. The mercury-sensitized decomposition followed closely the simple stoichiometry, $3NH_2OH \rightarrow N_2 + NH_3 + 3H_2O$, which strongly suggests an initial decomposition into NH_2 and OH. The direct photolysis was more complex, with N_2, H_2, and H_2O major products, and N_2O and NH_3 minor ones. The mechanism is uncertain, but it seems probable that the major primary process is $NH_2OH + h\nu \rightarrow NH_2O + H$. The absorption spectrum of hydroxylamine vapor was examined, and extinction coefficients determined from 2 250 to 1 600 Å. Absorption was continuous, starting about 2 250 Å, with no structure evident except a broad maximum at about 1 825 Å.

INTRODUCTION

The photolysis of hydroxylamine vapor was studied previously by Smith and Leighton (1) with somewhat inconclusive results, due in part to the accompanying thermal decomposition. The mercury-photosensitized decomposition has apparently never been studied. The present paper describes a re-examination of the photolysis and a first study of the mercury-photosensitized decomposition.

EXPERIMENTAL

Hydroxylamine, prepared by the method of Hurd and Brownstein (2), was stored in the vacuum line at −78 °C and purified as required by repeated sublimation *in vacuo* between traps at 0 and −60 °C until the saturation vapor pressure attained a minimum value. The measurement of the vapor pressure of solid hydroxylamine, and details of the piston pressure gauge used, have been described elsewhere (3).

All experiments were performed in a flow system. Hydroxylamine vapor was supplied from a trap containing the solid held at 0 °C. Flow of reagent and products out of the reaction vessel was controlled by an all-glass needle valve, and was always slow enough that the hydroxylamine vapor reached its saturation pressure at 0°, 0.27 Torr. The reaction vessel was a cylindrical annulus, about 12 cm long, 6 cm o.d. and 4 cm i.d., made of silica. Inside this was sealed another silica tube, forming a thin (5 mm) annular space through which cooling water was circulated, and in the center of this the light source was mounted coaxially. The whole assembly was immersed in a water thermostat at 25 °C. The purpose of this vessel design was to obtain a high light intensity in the reaction vessel so that a reasonable rate of photolysis could be attained even at low pressures of hydroxylamine vapor. Four light sources were used. These were, (*a*) a 200 W Hanovia medium-pressure mercury arc operated normally; (*b*) the same lamp, cooled by a stream of air at 0 °C; (*c*) a 25 W "Spectral" low-pressure zinc lamp (Phillips); and (*d*) a mercury-resonance lamp. Examination of the emission from the cooled medium-pressure arc showed it to consist almost entirely of the 2 537 Å mercury resonance line. The second resonance line at 1 850 Å was effectively removed by absorption by the cooling water. Reaction products were continuously pumped away through the glass needle value. Undecomposed hydroxylamine was trapped at −196 °C and later distilled into a removable trap held at −78 °C. It was estimated spectrophotometrically by oxidation to nitrous acid and formation of an azo dye (4, 5). Occasional attempts were made also to estimate hydrazine using *p*-dimethylaminobenzaldehyde (6) and hydrogen peroxide by complexing with tetravalent titanium (5). The more sensitive oxidation–reduction methods such as iodometry could not be used for hydrogen peroxide because of the large excess of hydroxylamine present (5).

All gaseous products were measured in a gas burette. Hydrogen and nitrogen mixtures were analyzed by combustion of the hydrogen over copper oxide; nitric oxide was isolated at −210°, and nitrous oxide and ammonia, originally trapped at −196°, were separated at −155° in a low-temperature still. It was confirmed by mass spectrometry that there were no other products noncondensable at −78°. No attempt was made to estimate water.

[1]*Issued as N.R.C. No. 8570.*

[2]*National Research Council Postdoctorate Fellow, 1962–1964. Present address: Department of Chemistry, Carleton University, Ottawa, Canada.*

In the mercury-photosensitized decomposition, no special provision was made for introducing mercury, since mercury cutoffs were used in place of greased traps throughout the vacuum system. The mercury-photosensitized reaction between hydrogen and hydroxylamine was also studied in the same apparatus. Hydrogen (Linde, 99.995% pure) was passed through a trap at −196° and allowed to equilibrate to 0° before passage over solid hydroxylamine at 0° and entry into the reaction vessel. Attempts were made to analyze for nitrogen in the large excess of hydrogen present, with rather uncertain results. In most experiments, nitrous oxide and ammonia only were measured.

The ultraviolet absorption spectrum of hydroxylamine vapor had been briefly examined by Smith and Leighton (1) at wavelengths above 2 000 Å; extinction coefficients were not reported. We therefore measured extinction coefficients for the vapor at wavelengths from 1 575 to 2 250 Å, using a silica cell, 22 cm long, attached to a McPherson 0.5 m vacuum grating monochromator equipped with a photomultiplier detector. A continuous flow of vapor through the cell was maintained during the measurement to prevent accumulation of decomposition products.

RESULTS

The Absorption Spectrum

The absorption spectrum of hydroxylamine vapor, measured at pressures of 0.254 and 1.1 Torr, is shown in Fig. 1. Data at the two pressures are in good agreement; the higher-pressure data are the more accurate at longer wavelengths. Absorption in the quartz windows of the cell prevented measurements much below 1 600 Å. No structure was evident at the resolution employed (~10 Å) other than the broad maximum around 1 825 Å, which probably corresponds to dissociative excitation of the lowest excited singlet state. A second dissociative process appears to be setting in at about 1 700 Å. The effective light in the present photolysis experiments was in the long-wavelength shoulder of the broad maximum. The effective emission of the zinc lamp consisted of three lines at 2 139, 2 062, and 2 025 Å, with relative intensities of 9, 1, and 1. These lines should have contributed to the photolysis approximately in the ratio 9/3/5, taking into account the absorption spectrum of the vapor. The effective light from the medium-pressure mercury arc was largely continuous emission with a few lines superimposed, extending from about 2 250 to 1 900 Å.

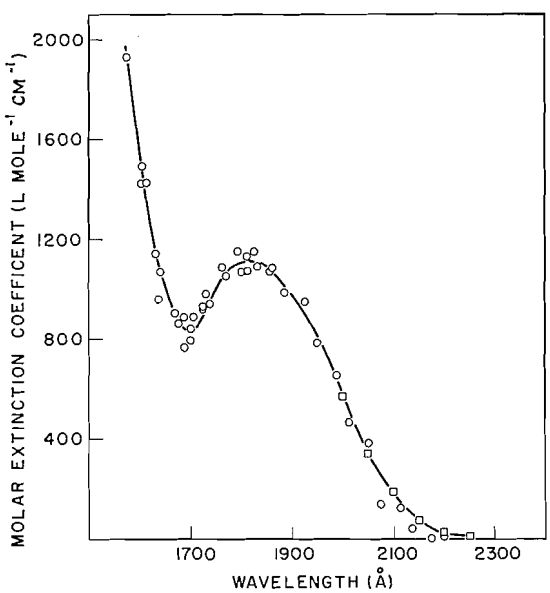

FIG. 1. The absorption spectrum of hydroxylamine vapor: ○ = 0.254 Torr, □ = 1.1 Torr.

Can. J. Chem. Downloaded from www.nrcresearchpress.com by 210.87.254.5 on 09/05/12
For personal use only.

The Thermal Decomposition

Some data for the thermal decomposition of hydroxylamine vapor at 0.27 Torr pressure and 25 °C, obtained over a period of 4 months, are shown in Table I. The hydrazine yields are too small to be reliable, and the yields of all products show considerable scatter and no particular trends with flowrate. The addition of nitrogen at atmospheric pressure reduced the combined yields of N_2O and NH_3 about threefold, but lowering the temperature to 5 °C had little effect. At higher hydroxylamine pressures the thermal decomposition was greatly enhanced, as observed previously (1). These observations point to a surface reaction.

TABLE I

Thermal decomposition of hydroxylamine vapor at 0.27 Torr and 25 °C

NH_2OH flowrate (μmoles/h)	Products (μmole/h)				
	N_2	NO	N_2O	NH_3	N_2H_4
314*	0.017	0.048	0.049	0.161	0.07
287	0.010	0.018	0.014	0.011	n.d.†
143‡	0.016	0.054	0.055	0.043	0.15
85	0.012	0.021	0.056	0.043	n.d.
68	0.003	0.021	0.036	0.008	n.d.
22§	0.008	0.029	0.027	0.008	n.d.
17§	0.005	0.028	0.020	0.003	n.d.

*Average of 5 experiments.
†n.d. = not determined.
‡Average of 3 experiments.
§Average of 2 experiments.

To minimize thermal decomposition, all photochemical experiments were carried out at low pressure, 0.27 Torr, and 25 °C, with the reservoir of solid hydroxylamine held at 0 °C. All photochemical product yields have been corrected for the thermal reaction by simple subtraction of yields from "blank" experiments done shortly before each photolysis. This is a small correction for major products, but a very large and uncertain one for minor ones; this accounts for the negative yields of NO in Table II.

The Direct Photolysis

Product yields and ratios for the direct photolysis are shown in Table II. All experiments were of 1 h duration; the % conversion was varied by varying the flowrate of hydroxylamine and products out of the reaction vessel. Some of the data of Smith and Leighton (1) are also shown for comparison.

The Mercury-Photosensitized Decomposition

Product yields from the mercury-photosensitized decomposition, studied under conditions similar to those of the direct photolysis, are shown in Table III. In both Tables II and III, the varying rates of consumption of NH_2OH (third column) reflect differences in the light intensity, which depended on the light source employed, its age, and its operating conditions.

DISCUSSION

The most notable feature of the present results is the marked difference between the direct photolysis (Table II) and the mercury-photosensitized decomposition (Table III). Hydrogen was a major product in the former, together with lesser amounts of N_2O and NH_3; in the mercury-sensitized decomposition, H_2 and N_2O were very minor products, and NH_3 a major one. From the elemental balance of the products in both systems, water was deduced to be a probable major product.

Can. J. Chem. Downloaded from www.nrcresearchpress.com by 210.87.254.5 on 09/05/12
For personal use only.

TABLE II

The photolysis of hydroxylamine vapor*

NH_2OH consumed†		H-Deficit‡ / O-Deficit	Product yields (% of NH_2OH consumed)§					
(%)	(μmoles/l h)		N_2	H_2	NO	N_2O	NH_3	H_2O‖
		This work, 25 °C, 0.7 Torr, Zn spectral lamp						
0.096	1.6	2.27	39	24	−2	4	12	108
0.179	3.0	2.29	38	20	−2	5	15	108
0.443	3.3	2.27	38	21	−10	5	14	108
0.940	3.4	2.50	43	24	0	5	4	119
1.71	3.5	2.56	42	21	+1	5	6	121
2.23	2.6	2.74	41	24	+3	6	−2	124
3.31	3.3	2.63	41	25	−2	7	1	122
		This work, Hg arc						
0.65	10.	2.36	34	21	+7	4	16	105
3.4	57.	2.06	33	25	+6	4	21	94
		From ref. 1, 1 Torr, room temp., Zn spark source						
15.4	28.	2.60	40	34	0	10	0	116
8.3	30.	2.38	37	31	0	9	7	109
10.5	68.	2.60	38	35	0	11	0	115
10.7	111.	2.41	36	37	0	12	4	106
13.5	217.	2.53	37	38	2	12	1	111
7.75	249.	2.35	37	38	0	11	5	105

*Some of the data from the present work represent averages of several experiments. All experiments of 1 h duration.
†NH_2OH consumed = $2N_2 + 2N_2O + NH_3$ (measurement based on NH_2OH recovery is much too inaccurate at low conversion).
‡H-deficit = (3 × NH_2OH consumed) − $2H_2$ − $3NH_3$; O-deficit = (NH_2OH consumed) − N_2O.
§Product yields rounded to nearest 1% of NH_2OH consumed.
‖H_2O yield calculated = ½ × H-deficit.

TABLE III*

The mercury-photosensitized decomposition of hydroxylamine vapor†

NH_2OH consumed		H-Deficit / O-Deficit	Product yields (% of NH_2OH consumed)					
(%)	(μmoles/l h)		N_2	H_2	NO	N_2O	NH_3	H_2O
		Medium pressure Hg arc, air cooled						
0.69	11.0	2.13	34	3	1	1	29	105
0.80	12.7	2.02	32	2	0	2	32	100
2.0	31	2.06	34	2	0	1	31	103
7.8	57	2.02	33	2	0	1	33	100
5.1	77	2.06	33	2	0	1	31	102
10.2	170	2.02	32	6	1	2	31	98
23.8	396	2.00	31	4	1	2	32	98
		Hg resonance lamp						
3.1	50	2.06	33	2	0	1	31	102
4.8	48	2.04	33	3	0	1	31	101
7.8	123	2.06	33	3	1	1	31	101
8.0	132	2.04	32	3	1	2	32	100
11.2	50	2.06	33	3	0	1	31	101
17.7	48	2.06	33	3	0	1	30	102
30.3	46	2.06	33	3	0	2	31	101
37.2	43	2.08	33	3	0	2	30	102

*Data treated as in Table II.
†All experiments of 1 h duration, at 0.27 Torr pressure and 25 °C.

Rates of decomposition, % conversion, and other conditions were similar in the two systems, and it may be argued rigorously that the different product distributions must reflect different modes of primary dissociation of NH_2OH. The mercury-photosensitized reaction followed to a good approximation the very simple stoichiometry,

[1] $$3NH_2OH \rightarrow N_2 + NH_3 + 3H_2O,$$

Can. J. Chem. Downloaded from www.nrcresearchpress.com by 210.87.254.5 on 09/05/12
For personal use only.

with no significant trends over a 36-fold change in the rate of decomposition and for conversions ranging from 0.7 to 37% (Table III). The following mechanism seems the most probable one.

[2] $$Hg\ 6(^3P_1) + NH_2OH \rightarrow NH_2 + OH + Hg\ 6(^1S_0)$$

[3] $$NH_2 + NH_2OH \rightarrow NH_3 + NHOH$$

[4] $$OH + NH_2OH \rightarrow H_2O + NHOH$$

[5] $$2NHOH \rightarrow N_2 + 2H_2O$$

Smith and Leighton (1) suggested that the direct photolysis proceeded by a primary dissociation into NH_2 and OH, followed by a complex sequence of reactions leading to the observed products. Our mechanism for the mercury-photosensitized decomposition, starting from the same primary dissociation, differs chiefly in the inclusion of the abstraction reactions [3] and [4] which Smith and Leighton apparently considered much too slow to be of importance, probably because they overestimated the strengths of the N—H and O—H bonds in NH_2OH (1). It is well established now that the N—H and O—H bonds in hydrazine, hydrogen peroxide, and probably thus in hydroxylamine, are relatively weak, and abstraction of hydrogen from these compounds is very fast (7, 8, 9). One might still question whether reactions [3] and [4] would have proceeded quantitatively in the present systems with the pressure of NH_2OH of 0.27 Torr. The lack of appreciable yields of N_2H_4 or H_2O_2 over a wide range of intensities and conversions suggests that these reactions were quantitative, although the sensitivity of the analysis for these products was not high.

In reactions [3] and [4], it is suggested that abstraction occurred from the nitrogen rather than from the oxygen atom, partly because the N—H bond is probably weaker, and partly because the resulting NHOH radicals seem more likely to combine simply to N_2 and $2H_2O$ (reaction [5]) as required.

The stoichiometry of the direct photoly : was considerably more complex than that of the mercury-sensitized reaction, with N_2, H_2, and H_2O major products, and appreciable yields of N_2O and NH_3 (Table II). Our results are in fair agreement with those of Smith and Leighton; their % yields of H_2 and N_2O were appreciably higher and that of ammonia lower, although the ammonia analysis was badly scattered, both in the earlier and the present work, reflecting the difficulty in analyzing small amounts of this product (Table II). The conversions attained by Smith and Leighton were much higher than in the present experiments, and it is possible that secondary photolysis of ammonia was occurring and could account for their lower yields of ammonia and higher yields of hydrogen, although there are no significant trends with conversion either in their work or ours. Light intensities employed by Smith and Leighton, reflected in column 2, Table II, were generally much higher than in the present work, although there is some overlap, and this may also have had some effect on the product distribution.

If reactions [2] to [5] represent the mercury photosensitized decomposition, the following mechanism would appear to account for the products observed in the direct photolysis and for the differences between the two systems,

[6] $$NH_2OH + h\nu \rightarrow NHOH + H$$

[7] $$H + NH_2OH \rightarrow NHOH + H_2,$$

followed by reaction [5.] To account for the production of ammonia, and the observation that $N_2 > H_2$, the simplest explanation is the occurrence to the extent of about 40% of a second primary process,

[8] $$NH_2OH + h\nu \rightarrow NH_2 + OH,$$

Can. J. Chem. Downloaded from www.nrcresearchpress.com by 210.87.254.5 on 09/05/12
For personal use only.

followed by reactions [3], [4], and [5]. The primary process in the photolysis of H_2O_2 vapor is almost certainly a split into 2OH (10, 11) while that of N_2H_4 is probably rupture of an N—H bond (12, 13, 14); it is not unreasonable that NH_2OH might show primary processes analogous to each of these modes of photolysis.

The source of the N_2O observed is not clear. Smith and Leighton suggested that it came from a reaction between H_2O_2 and NH_2OH which they showed to occur readily, with H_2O_2 arising from OH combination or by reaction of OH with NH_2OH. The lack of dependence of % N_2O on light intensity and other considerations indicate that this is not a likely source of N_2O in the photolysis. The reaction,

[9] $$2HNO \rightarrow H_2O + N_2O,$$

has been suggested as a source of N_2O in several systems (15, 16), and it is possible that HNO radicals could have arisen in the present experiments by disproportionation reactions such as

[10] $$2NHOH \rightarrow NH_2OH + HNO$$

Then, however, N_2O should have been formed equally in the direct photolysis and in the mercury-sensitized reaction, which it was not. This suggests that the primary photolysis reaction might have been

[11] $$NH_2OH + h\nu \rightarrow NH_2O + H$$

rather than reaction [6]. The NH_2O radical might be much more prone to disproportionate than NHOH,

[12] $$NH_2O + NH_2O \text{ (or NHOH)} \rightarrow HNO + NH_2OH,$$

and this would explain the production of much more N_2O in the direct photolysis than in the mercury-sensitized reaction. In considering the formation of HNO in a disproportionation reaction, it may be noted that NH_2O is isoelectronic with CH_3O, which disproportionates very readily.

Another possible source of HNO and hydrogen might be the primary process

[13] $$NH_2OH + h\nu \rightarrow HNO \text{ (or NOH)} + H_2$$

by analogy with the photolysis of ethane which yields ethylidene and H_2 (17); there is no proof for or against this possibility.

Evidence against the role of HNO as a precursor of nitrous oxide is the virtual absence of nitric oxide, which one might expect to arise from disproportionation of HNO with other radicals in the system:

[14] $$R + HNO \rightarrow RH + NO.$$

In view of this, direct formation of nitrous oxide from NH_2O radicals is perhaps more probable:

[15] $$NH_2O + NHOH \text{ (or } NH_2O) \rightarrow N_2O + H_2O + H_2.$$

The NH_2O radical would be more likely to undergo this reaction than would NHOH, and if it were formed by reaction [11] in the direct photolysis, the absence of N_2O (and H_2) in the mercury-sensitized reaction would be accounted for.

An alternative possible source of ammonia in the photolysis is the cracking reaction,

[16] $$H + HNOH \rightarrow [NH_2OH]^* \rightarrow NH_2 + OH,$$

followed by reactions [3] and [4]. Such a reaction would be favored at the low pressures used in the present experiments. If it occurred, it would be favored at high intensity at

Can. J. Chem. Downloaded from www.nrcresearchpress.com by 210.87.254.5 on 09/05/12
For personal use only.

the expense of reaction [7], so that H_2 would decrease and NH_3 increase with increasing intensity; this was not observed, and reaction [16] may probably be ruled out.

The mercury-photosensitized reaction of hydrogen with hydroxylamine vapor yielded NH_3, N_2O, and N_2 in amounts comparable to the sensitized decomposition of pure NH_2OH, with product ratios roughly independent of hydrogen pressure from 50 to 700 Torr. Nitrogen analysis in the large excess of hydrogen was very uncertain, while the N_2O and NH_3 yields were also considerably scattered. Quenching of Hg $6(^3P_1)$ should have been almost exclusively by hydrogen, generating hydrogen atoms, and the observed decomposition of hydroxylamine confirms that hydrogen atoms reacted rapidly with NH_2OH even at a pressure of the latter of 0.27 Torr. Incomplete and uncertain product analysis (H_2 could not be measured) and uncertainty about the efficiency of quenching of Hg $6(^3P_1)$ in pure hydroxylamine vapor prevent any firm conclusions about the mode of formation of the observed products.

In summary, it appears probable that the mercury-photosensitized decomposition of hydroxylamine vapor proceeds via reactions [2] to [5]. The mechanism of the direct photolysis is less certain, but probably includes primary processes [8] and [11] with secondary reactions [3], [4], [5], [7], and [15]. The thermal instability of the vapor even at low pressure is a formidable obstacle to the more precise kinetic studies that would be needed to confirm or disprove the suggested mechanisms.

REFERENCES

1. R. N. Smith and P. A. Leighton. J. Am. Chem. Soc. **66**, 172 (1944).
2. C. DeW. Hurd and H. J. Brownstein. J. Am. Chem. Soc. **47**, 67 (1925).
3. R. A. Back and J. Betts. Can. J. Chem. **43**, 2157 (1965).
4. M. Lefort and X. Tarrago. J. Inorg. Nucl. Chem. **16**, 169 (1961).
5. X. Tarrago. Ann. Chim. **5**, 5 (1960).
6. G. W. Watt and J. D. Crisp. Anal. Chem. **24**, 2006 (1952).
7. M. Schiavello and G. G. Volpi. J. Chem. Phys. **37**, 1510 (1962).
8. S. Foner and R. L. Hudson. J. Chem. Phys. **36**, 2681 (1962).
9. P. Gray and J. C. J. Thynne. Trans. Faraday Soc. **60**, 1047 (1964).
10. D. H. Volman. J. Chem. Phys. **17**, 947 (1949).
11. F. S. Stone and H. S. Taylor. J. Chem. Phys. **20**, 1339 (1952).
12. R. R. Wenner and A. O. Beckman. J. Am. Chem. Soc. **54**, 2787 (1932).
13. C. H. Bamford. Trans. Faraday Soc. **35**, 568 (1939).
14. A. N. Terenin, B. L. Kurbatov, and F. I. Vilesov. Tr. po Khim. i Khim. Tekhnol. **4**, 181 (1961).
15. A. Serewicz and W. A. Noyes, Jr. J. Phys. Chem. **63**, 843 (1959).
16. O. P. Strausz and H. E. Gunning. Trans. Faraday Soc. **60**, 347 (1964).
17. R. F. Hampson, J. R. McNesby, H. Akimoto, and I. Tanaka. J. Chem. Phys. **40**, 1099 (1964).

Can. J. Chem. Downloaded from www.nrcresearchpress.com by 210.87.254.5 on 09/05/12
For personal use only.

Can. J. Chem. Downloaded from www.nrcresearchpress.com by 210.87.254.40 on 09/05/12
For personal use only.

PYRIDINE N-OXIDE COMPLEX OF TITANYL PERCHLORATE

V. KRISHNAN AND C. C. PATEL
Department of Inorganic and Physical Chemistry, Indian Institute of Science, Bangalore, India
Received April 13, 1965

ABSTRACT

Pentakispyridine N-oxide oxotitanium(IV) perchlorate, $TiO.5C_5H_5NO.(ClO_4)_2$, has been prepared and its physicochemical properties investigated. The infrared and electronic spectra show that pyridine N-oxide is bonded to the metal ion through oxygen of the N—O. The complex explodes at 215 °C, a temperature slightly above the starting decomposition temperature of titanyl perchlorate, $TiO(ClO_4)_2.3H_2O$.

INTRODUCTION

Recently Ramamurthy and Patel (1, and references therein) prepared pyridine N-oxide complexes of zirconyl, thorium, and uranyl perchlorates and studied their infrared and electronic spectra. But the corresponding titanyl perchlorate complex has not been studied before. Pyridine N-oxide complex of titanyl perchlorate has therefore been prepared and its properties investigated and compared with those of zirconyl complex.

EXPERIMENTAL

Materials Employed

Pyridine N-oxide was prepared by the oxidation of pyridine with hydrogen peroxide in glacial acetic acid medium as described by Ochiai (2). Titanyl perchlorate hexahydrate, $TiO(ClO_4)_2.6H_2O$, was prepared by the reaction of titanium tetrachloride with perchloric acid (3).

Preparation of the Complex

When pyridine N-oxide (3 g) solution in anhydrous ethanol is added to an agitated ethanolic solution of titanyl perchlorate (1 g) at 25 °C a white complex is precipitated. The complex is washed free of pyridine N-oxide with anhydrous ethanol and dried in vacuum over phosphorus pentoxide. The complex was analyzed for titanium by decomposing it by boiling with concentrated nitric acid, precipitating the titanium as hydroxide, and igniting the precipitate to the dioxide. Perchlorate was estimated by the Kurz's method (4) and nitrogen by Duma's semimicro method. The experimental values for titanium, perchlorate, and nitrogen were 6.54, 26.72, and 9.02% while the corresponding values for $TiO.5C_5H_5NO.(ClO_4)_2$ are 6.46, 26.86, and 9.45% respectively.

Properties

The complex is slightly hygroscopic, soluble in water and acetonitrile, and insoluble in nonpolar solvents. The complex is found to explode at 215 °C.

Infrared and Electronic Absorption Spectral Studies

The infrared spectrum of the complex was taken in Nujol mull with a Perkin–Elmer single beam infrared spectrometer, model 112, equipped with sodium chloride optics. The spectrum is given in Fig. 1. The electronic absorption spectrum of the complex in pure dry acetonitrile was taken with a Hilger Uvispeck spectrophotometer, model H 700, using 1 cm matched pair quartz cells. The spectrum is given in Fig. 2.

DISCUSSION

The titanyl complex explodes at 215 °C whereas titanyl perchlorate (5) starts decomposing at 190 °C. This shows that the perchlorate is somewhat thermally stabilized on complex formation. The thermal stabilizing effect on complex formation is also found in pyridine N-oxide complexes of zirconyl and thorium perchlorates (1). Their explosion temperatures are 307 and 350 °C whereas the corresponding perchlorates start decomposing at 275 and 290 °C respectively (6).

The infrared spectrum of $TiO.5C_5H_5NO(ClO_4)_2$ is very similar to that of the zirconyl complex. In these complexes perchlorate retains its T_d symmetry as shown by the ν_3

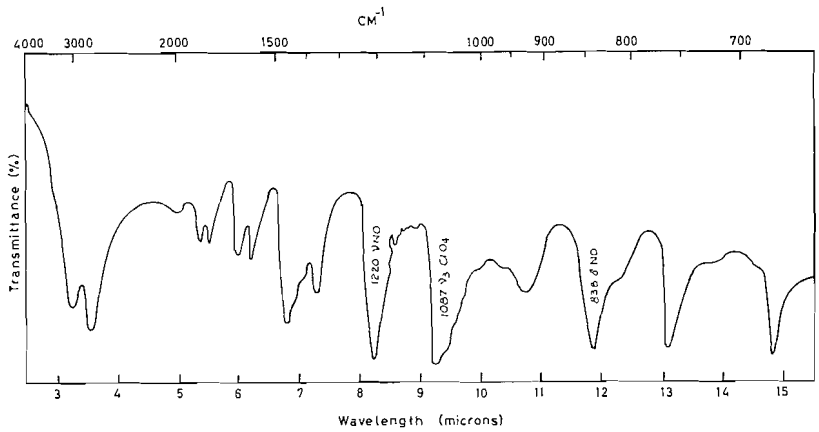

FIG. 1. Infrared absorption spectrum of $TiO.5(C_5H_5NO)(ClO_4)_2$.

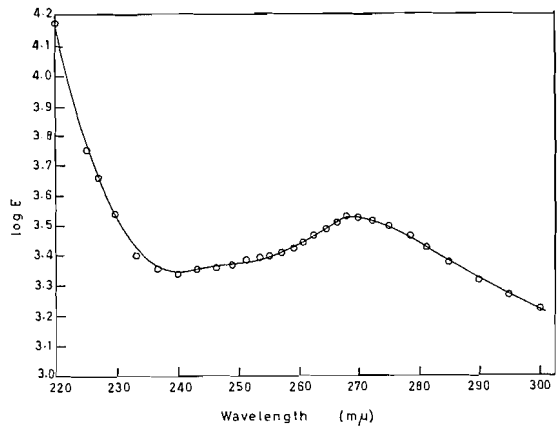

FIG. 2. Electronic absorption spectrum of $TiO.5(C_5H_5NO)(ClO_4)_2$ in acetonitrile.

band at 1 085 cm^{-1} and the nonappearance of the ν_1 band around 930 cm^{-1}. All the pyridine N-oxide vibrations also occur at more or less the same frequencies in the two complexes. The N—O stretching frequency which occurs at 1 265 cm^{-1} in pyridine N-oxide (7) has been lowered to 1 220 cm^{-1} in the titanyl complex. This lowering of the N—O stretching is due to the reduction in π-bond character of N—O as a result of complex formation by the donation of a lone pair of electrons from oxygen of N—O to the metal ion. In the zirconyl complex, the N—O stretching frequency occurs at 1 222 cm^{-1}. The NO frequency difference in these two complexes is so small that it is difficult to draw any conclusion on the bond strength between the metal and pyridine N-oxide in the two complexes. However, the small shift from 1 220 cm^{-1} in the titanyl complex to 1 222 cm^{-1} in the zirconyl complex may be due to the slight decrease in the bond strength of M—ON< from the titanium to the zirconium complex. The N—O bending in the titanyl and zirconyl complexes occurs around 840 cm^{-1}. Thus, practically there is no shift in N—O bending frequency (840 cm^{-1}) (7) on complex formation. This may be due to the two opposing effects: the coordination which raises the N—O bending frequency, and the lowering of the π-bond character which tends to lower the frequency almost to the same extent.

Can. J. Chem. Downloaded from www.nrcresearchpress.com by 210.87.254.40 on 09/05/12
For personal use only.

The electronic absorption spectrum of the complex gives a strong band at 268 mμ and also shows another band below 210 mμ, as indicated by the increasing absorption from 220 mμ to the lower wavelength. The electronic absorption spectrum of pyridine N-oxide gives two bands, one intense band at 280 mμ, arising from the $\pi-\pi^*$ transition and a weak band at 320 mμ arising from the $n-\pi^*$ transition of the N—O group (8). The $n-\pi^*$ band has disappeared in the complex due to the stabilization of the non-bonded p-electrons on complex formation. The $\pi-\pi^*$ band of pyridine N-oxide has shifted towards lower wavelength in the complex as a result of the complex formation. The zirconyl complex gives an absorption band at 276 mμ while titanyl complex gives a band at 268 mμ. Thus the hypsochromic shift of the $\pi-\pi^*$ band is greater in the titanyl complex showing stronger bond formation between oxo-titanium and oxygen of $\rangle$NO than that between oxo-zirconium and $\rangle$NO. This is expected considering the smaller cationic size of oxo-titanium ion as compared to the oxo-zirconium ion. This general trend is indicated by a very small shift of N—O stretching frequencies both in the titanyl and zirconyl complexes, where the N—O frequencies occur at 1 220 and 1 222 cm^{-1} respectively.

Titanyl takes five molecules of pyridine N-oxide ligands, thus giving six-coordination to titanium. This suggests d^2sp^3 hybridization with distorted octahedral configuration.

ACKNOWLEDGMENT

The authors' thanks are due to Prof. M. R. A. Rao for his keen interest in the work.

REFERENCES

1. P. Ramamurthy and C. C. Patel. Can. J. Chem. **42**, 856 (1964).
2. E. Ochiai. J. Org. Chem. **18**, 534 (1953).
3. V. Krishnan and C. C. Patel. Chem. Ind. London, 321 (1961).
4. E. Kurz, G. Kober, and M. Berl. Anal. Chem. **30**, 1983 (1958).
5. V. Krishnan and C. C. Patel. Indian J. Chem. **2**, 425 (1964).
6. P. Ramamurthy and C. C. Patel. Indian J. Chem. **3**, 134 (1965).
7. S. Kida, J. V. Quagliano, J. V. Walmsley, and S. Y. Tyree. Spectrochim. Acta, **19**, 189 (1963).
8. M. Ito and N. Hata. Bull. Chem. Soc. Japan, **28**, 260 (1955).

Can. J. Chem. Downloaded from www.nrcresearchpress.com by 210.87.254.40 on 09/05/12
For personal use only.

Can. J. Chem. Downloaded from www.nrcresearchpress.com by 210.87.254.40 on 09/05/12
For personal use only.

THERMODYNAMIC FUNCTIONS OF THE PARTIALLY DEUTERATED METHYL HALIDES AS ANHARMONIC OSCILLATORS

JOHN R. RITER, JR. AND MARVIN C. GOLDBERG[1]
Department of Chemistry, University of Denver, Denver, Colorado

Received May 4, 1965

ABSTRACT

By determination of the diagonal anharmonic constants x_{ii} in the expression for vibrational terms as a power series in the vibrational quantum numbers, the rigid-rotor anharmonic oscillator thermodynamic functions of the eight partially deuterated methyl halides (CH_2DX and CHD_2X, X = F, Cl, Br, I) have been computed. The effects of omission of the cross terms x_{ij} is discussed. From the computed x_{ii}, the calculated positions of 23 combination bands were found to have a mean deviation of 0.3% above the observed values, and the calculated positions of 11 first overtone bands had a mean deviation of 2.7% below the corresponding observed values. Tables of $-(F^0 - E_0^0)/RT$, $(H^0 - E_0^0)/RT$, S^0/R, and C_p^0/R for the anharmonic case and C_p^0/R for the harmonic case at 100 deg intervals between 100 and 1 500 °K, and thence in 500 deg intervals to 3 000 °K, have been made available. Tables of observed fundamental frequencies, anharmonicity constants x_{ii}, and moments of inertia for all molecules are included. A comparison of differences in each of the four thermodynamic functions for the anharmonic and harmonic cases is given for 1 000 and 3 000 °K. The maximum differences in C_p^0 and S^0 occur for CHD_2Cl and amount to 0.50 and 2.08 (C_p^0), and 0.10 and 0.36 (S^0) cal/mole deg at 1 000 and 3 000 °K respectively, with the anharmonic values always larger.

INTRODUCTION

Departures of real molecules from the rigid-rotor harmonic-oscillator model, used for thermodynamic function calculations, have long been of interest. One of the chief corrections to this model is the anharmonicity of the vibrational motion, i.e. the set of anharmonic constants x_{ij} defined by the equation for vibrational terms as a power series in the quantum numbers v_i

$$[1] \qquad \frac{W}{hc}(v_1, v_2, v_3, \ldots) = \sum_i \omega_i(v_i + \tfrac{1}{2}) + \sum_{i \geqslant j} \sum_j x_{ij}(v_i + \tfrac{1}{2})(v_j + \tfrac{1}{2}) + \ldots$$

with the ω_i the harmonic fundamental frequencies. The evaluation of these anharmonic constants from the vibrational spectra is of course a very formidable task. We have taken the known spectral assignments (1) of each of the partially deuterated methyl halides (PDMH), and from normal coordinate treatments for the series CH_3X, CH_2DX, CHD_2X, CD_3X (1) have deduced a relation for the quadratic constants x_{ii}. The cross term constants x_{ij}, as well as higher terms x_{ijk}, have been assumed to be zero. Using the formulation of Pennington and Kobe (2) we have computed thermodynamic functions for the eight PDMH as rigid-rotor anharmonic oscillators.

ANHARMONIC CONSTANTS x_{ij}

The "single mode" anharmonicity

$$[2] \qquad x_i = 1 - (\nu_i/\omega_i)$$

with ν_i the observed (anharmonic) fundamental, was introduced by Hansen and Dennison in work on the system C_2H_6–C_2D_6 (3). The x_i's for CH_3X and CD_3X were determined by King, Mills, and Crawford (4) and for the PDMH as a part of the above-mentioned normal coordinate analysis (5).

[1]*Present address: U.S. Geological Survey, Denver Federal Center, Denver, Colorado.*

Taking x_{ij} to be zero, which is surely an assumption of convenience (see also the discussion under Conclusions), we find

[3] $$x_{ii} = -\omega_i x_i/2.$$

In this approximation then the combination bands should have frequencies that are the sums of the fundamentals, while the frequency of the nth harmonic ($(n-1)$st overtone) should be given by

[4] $$\nu_i(n) = n\nu_i + (n^2 - n)x_{ii}.$$

That the implication of eq. [3] of strict additivity for sum bands is quite a good one is borne out by comparison of the observed positions of 23 assigned binary sums for the PDMH (1); the mean deviation is 0.3% with three-fourths of the calculated values higher than the observed. For the 11 first overtone bands assigned (1) the mean deviation is 2.7% with the calculated values too low in every case but one. Hence the above expression, eq. [4], overcorrects for overtone anharmonicity. Table I lists the observed fundamentals ν_i and anharmonicity constants x_{ii} for the PDMH.

TABLE I

Observed fundamentals ν_i and diagonal anharmonicity constants x_{ii}

	CH_2DF	CHD_2F	CH_2DCl	CHD_2Cl	CH_2DBr	CHD_2Br	CH_2DI	CHD_2I
ν_1*	2950†	2174	2990	2194	3001	2196	3002	2194
ν_2	1364	1321	1269	1249	1225	1036	1172	1018
ν_3	1052	1050	713	705	594	584	518	508
ν_4'	2197	2976	2224	3012	2244	3027	2241	3030
ν_5'	1466	1092	1436	1050	1425	1208	1416	1170
ν_6'	938	965	827	870	769	816	710	754
ν_4''	3016	2259	3035	2279	3052	2288	3057	2336
ν_5''	1299	1344	1260	1300	1240	1289	1240	1287
ν_6''	1160	897	986	768	930	717	862	659
x_{11}	−53†	−18	−65	−38	−56	−32	−61	−32
x_{22}	−23	−22	−16	−23	−5	−7	−10	−4
x_{33}	−14	−12	0	2	−2	−1	−1	0
$x_{4'4'}$	−30	−53	−54	−80	−40	−67	−95	−74
$x_{5'5'}$	−14	−6	−36	−20	−29	−38	−25	−38
$x_{6'6'}$	−2	−6	−17	−18	−14	−3	−16	−6
$x_{4''4''}$	−45	−23	−92	−58	−76	−52	−86	−32
$x_{5''5''}$	4	−2	−36	−32	−52	−20	−41	−16
$x_{6''6''}$	−2	−7	−21	−17	0	−12	−3	−8

*Fundamentals 1 through 6′ are species A′ and 4″, 5″, and 6″ are species A″. The doubly degenerate fundamentals in CH_3X and CD_3X are traced to the corresponding fundamentals in CH_2DX and CHD_2X through the L matrices. See ref. 5.
†Units of cm^{-1}.

CALCULATION OF THERMODYNAMIC FUNCTIONS

By the method of ref. 2, the partition function can be written as a product of translational, rigid-rotor, harmonic-oscillator, and anharmonic correction terms. See especially eqs. [1], [9], and [20]. The moments of inertia used are given in Table II. The calculation of the free energy and enthalpy functions, entropies, and heat capacities for both harmonic and anharmonic oscillators was performed on the IBM 709 at the University of Colorado. Thirty temperatures were chosen in the interval from 100 to 3 000 °K, plus 273 and 298 °K. The higher temperatures were not chosen to provide meaningful thermodynamic data, but rather to follow the deviations from the harmonic model caused by the introduction of anharmonicity. Condensed results for the anharmonic case together with C_p^0 for the

Can. J. Chem. Downloaded from www.nrcresearchpress.com by 210.87.254.40 on 09/05/12
For personal use only.

harmonic case are presented in Tables V–XII.* Comparison of the complete harmonic results with existing tables of functions for CH_2DBr and CHD_2Br (6) and CH_2DI and CHD_2I (7) showed very good agreement. The fundamental frequencies of refs. 6 and 7 were not all observed but rather inferred in part from normal coordinate treatments.

TABLE II

Principal moments of inertia

	I_a	I_b	I_c
CH_2DF	4.303†	21.396	22.397
CHD_2F	5.419	22.974	24.181
CH_2DCl	4.326	40.182	41.192
CHD_2Cl	5.438	42.927	44.116
CH_2DBr	4.287	56.219	57.222
CHD_2Br	5.388	60.330	61.505
CH_2DI	4.324	72.051	73.065
CHD_2I	5.433	77.368	78.550

†Units of AWU·Å² (atomic weight units·angstroms²).

TABLE III

Differences in thermodynamic functions for anharmonic and harmonic oscillators (columns 3 through 6 are the differences (anharmonic minus harmonic) between the corresponding dimensionless thermodynamic functions of Tables V–XII)

	T (°K)	$\frac{\Delta F}{RT}$	$\frac{\Delta H}{RT}$	$\frac{\Delta S}{R}$	$\frac{\Delta C_p}{R}$
CH_2DF	1000	0.01	0.02	0.01	0.08
CHD_2F	1000	0.01	0.03	0.02	0.11
CH_2DCl	1000	0.02	0.07	0.05	0.22
CHD_2Cl	1000	0.03	0.08	0.05	0.25
CH_2DBr	1000	0.02	0.06	0.04	0.19
CHD_2Br	1000	0.02	0.06	0.04	0.19
CH_2DI	1000	0.03	0.07	0.04	0.22
CHD_2I	1000	0.02	0.06	0.04	0.18
CH_2DF	3000	0.09	0.17	0.08	0.40
CHD_2F	3000	0.13	0.21	0.08	0.48
CH_2DCl	3000	0.26	0.44	0.18	1.00
CHD_2Cl	3000	0.29	0.47	0.18	1.04
CH_2DBr	3000	0.22	0.36	0.14	0.83
CHD_2Br	3000	0.22	0.36	0.14	0.81
CH_2DI	3000	0.26	0.42	0.16	0.97
CHD_2I	3000	0.21	0.33	0.12	0.76

CONCLUSIONS

Table III shows the difference in the dimensionless free energy and enthalpy functions, entropies, and heat capacities for anharmonic and harmonic oscillators at 1 000 and 3 000 °K. The heat capacity, which is essentially the second temperature derivative of the logarithm of the vibrational partition function, is the quantity most sensitive to anharmonic corrections. Note that even at 1 000 °K the anharmonic C_p^0 for CHD_2Cl exceeds the harmonic value by 0.50 cal/mole deg. The maximum deviation in S^0 at 1 000 °K is 0.10 e.u. (entropy units), also for CHD_2Cl.

**Tables V–XII have been placed in*
The Depository of Unpublished Data,
National Science Library,
National Research Council,
Ottawa, Canada,
and photocopies may be obtained upon request.

Can. J. Chem. Downloaded from www.nrcresearchpress.com by 210.87.254.40 on 09/05/12
For personal use only.

The neglect of quadratic cross terms x_{ij} is certainly suspect. For example Table IV presents the results of Arakawa and Nielsen (8) for anharmonicity factors in $^{14}NO_2$. Note that x_{11} and x_{12} are about the same size, with x_{13} bigger by a factor of three. Similarly, x_{23} is about five times as big as x_{22}. The consistently low predictions of the first overtone positions in the PDMH is additional evidence there are serious shortcomings in this method.

TABLE IV

Anharmonicity constants in $^{14}NO_2$ (data of ref. 8)

x_{11}	x_{12}	x_{13}	x_{22}	x_{23}	x_{33}
−9.0	−9.7	−28.7	−0.5	−2.7	−16.4

Yet with the number of overtone and sum bands available generally far less than the number required to fix all the x_{ij}, and lacking other information such as transferable constants from isotopic or other related molecules, one feels in general he is on the right track by giving first preference to the diagonal terms.

The method described herein is presented as an attempt to systematically apply meaningful anharmonicity corrections to thermodynamic function calculations for molecules of this size.

ACKNOWLEDGMENT

The authors wish to thank Dr. Walter Macintyre, director of the Computing Center at the University of Colorado, for a grant of computer time.

REFERENCES

1. J. R. RITER, JR. and D. F. EGGERS, JR. To be published.
2. R. E. PENNINGTON and K. A. KOBE. J. Chem. Phys. **22**, 1442 (1954).
3. G. E. HANSEN and D. M. DENNISON. J. Chem. Phys. **20**, 313 (1952).
4. W. T. KING, I. M. MILLS, and B. L. CRAWFORD. J. Chem. Phys. **27**, 455 (1957).
5. J. R. RITER, JR. Ph.D. Thesis. University of Washington, Seattle, Wash. 1962.
6. J. M. DOWLING. J. Chem. Phys. **23**, 700 (1955).
7. E. F. DITZEL *et al.* Can. J. Chem. **42**, 2841 (1964).
8. E. T. ARAKAWA and A. H. NIELSEN. J. Mol. Spectry. **2**, 413 (1958).

Can. J. Chem. Downloaded from www.nrcresearchpress.com by 210.87.254.40 on 09/05/12
For personal use only.

Can. J. Chem. Downloaded from www.nrcresearchpress.com by 210.87.254.5 on 09/05/12
For personal use only.

X-RAY STUDY OF LIQUID $AsBr_3$

R. HOGE AND J. TROTTER
Department of Chemistry, University of British Columbia, Vancouver, British Columbia
Received May 4, 1965

ABSTRACT

The structure of liquid arsenic tribromide has been investigated by deriving the radial distribution function from X-ray intensity data recorded with monochromatic Cu K_α radiation. The results are consistent with pyramidal molecules with dimensions similar to those in the vapor and solid states. Most of the intermolecular distances in the crystal are preserved in the liquid.

INTRODUCTION

Methods for examining the structures of liquids by X-ray diffraction are well established (1); the object of this investigation was to examine whether significant results could be obtained using counter intensity measurements, with monochromatization of the radiation by pulse height discrimination and balanced filters. Arsenic tribromide was chosen for the study since it has a suitably low melting point, and its structure is known in both solid and vapor states (2, 3).

EXPERIMENTAL

Arsenic tribromide is a colorless crystalline solid at room temperature, it is quite volatile, and is hydrolyzed by water. The molecular weight is 314.7, the melting point is 32.8 °C, and the density of the liquid is 3.54 g cm^{-3}. A sample was sealed in a thin-walled Lindemann glass capillary (diameter 0.5 mm, wall thickness 0.01 mm), and maintained at 75 °C in a stream of warm air.

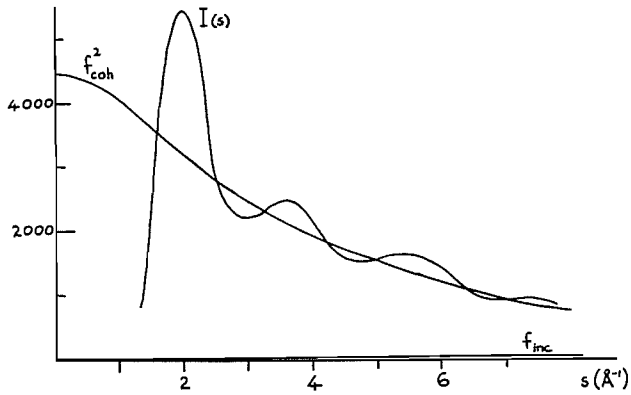

FIG. 1. Corrected and scaled experimental scattering, and independent coherent and incoherent scattering

The diffraction pattern was recorded on a General Electric XRD-5 Spectrogoniometer, with Cu K_α radiation and a scintillation counter. Partial monochromatization was achieved by use of a pulse height analyzer; since the scintillation counter has a rather wide pulse height distribution, further monochromatization was accomplished with Ross balanced filters (0.0100 mm nickel foil and 0.0108 mm cobalt foil (4)). The best experimental arrangement was one with the balanced filters between the X-ray source and the sample (to minimize fluorescence from the cobalt filter reaching the detector) and a nickel filter between the sample and the detector (to absorb fluorescence from the specimen). The pattern was recorded in the range $2° < 2\theta(\text{Cu } K_\alpha) < 148°$, corresponding to a maximum value of $s(= 4\pi \sin\theta/\lambda)$ of 7.8 $Å^{-1}$, with a scan speed of 2° per minute. The scattered intensity was corrected for diffraction by the glass container, for polarization, and for absorption (cylindrical specimen, $\mu R = 8.5$). The corrected experimental scattering, $I(s)$, was then brought to an absolute scale by equating $\sum s^2.I(s)$ and $\sum s^2(\sum f_{coh}^2 + \sum f_{inc})$ in the range $s = 3.0$ to 7.8. $\sum f_{coh}^2$ and $\sum f_{inc}$ are the independent atomic coherent and incoherent scattering

for one $AsBr_3$ molecule. The corrected and scaled experimental scattering is shown in Fig. 1. The function $s.i(s) = (I(s) - \sum f_{coh}^2 - \sum f_{inc})/\sum f_{coh}^2$ was then computed (Fig. 2) and the integral $\int_0^{17.8} s.i(s) \sin rs.ds$ was evaluated for $r = 0.0$ to 10.0 Å in steps of 0.1 Å, the integration being carried out numerically with an interval in s of 0.01 $Å^{-1}$. The resulting radial distribution function $4\pi r^2\rho(r) = 4\pi r^2\rho_o(\sum Z_j) + (\sum Z_j^2)(2r/\pi)$ (integral), is shown in Fig. 3.

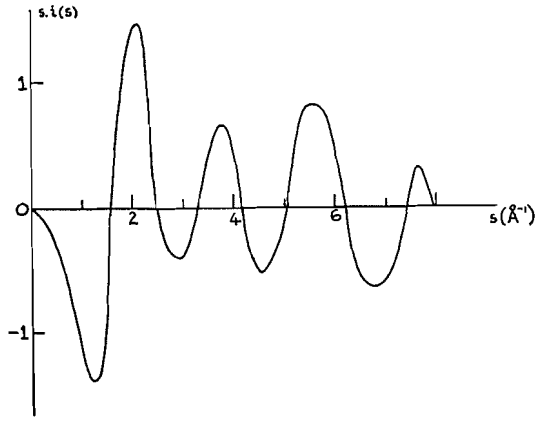

FIG. 2. $s.i(s)$ function.

The diffraction pattern was measured at s values up to 17.0 $Å^{-1}$ using Mo K_α radiation (zirconium/yttrium balanced filter pair). The less favorable peak-to-background of the molybdenum radiation resulted in poorer patterns than for Cu K_α radiation, and no significant fluctuations in the scattered intensity were found at the higher angles.

DISCUSSION

The radial distribution function for liquid arsenic tribromide (Fig. 3) exhibits two very small maxima at about 0.5 Å and 1.5 Å; the small size of these spurious fluctuations gives confidence that the experimental data is reasonably accurate, and the radial distribution function quite reliable. The remainder of the distribution can be interpreted in terms of the presence of pyramidal $AsBr_3$ molecules. The first significant feature is a well-defined maximum at 2.55 Å, corresponding to the As—Br intramolecular distance. A second peak at 3.7 Å probably contains the Br ··· Br intramolecular distances and the shorter intermolecular contacts, and a third peak at 4.4 Å corresponds to further intermolecular separations.

These conclusions can be verified by using the area under the radial distribution curve to calculate the number of distances responsible for each peak. The area under the first peak is 7 100 electrons². One As—Br pair within each molecule contributes $2K_{As}K_{Br}$ to the area, K being the effective number of electrons in an atom (approximately equal to the atomic number). This product is 2 310 electrons², so that the area under the peak at 2.55 Å is caused by 3.1 such pairs in each molecule, that is each arsenic atom is bonded to *three* bromine atoms.

The area under the peak at 3.7 Å (derived by making the maximum symmetrical about 3.7 Å, Fig. 3) is 41 300 electrons². The Br ··· Br intramolecular distances are certainly contained in this peak, and contribute $3 \times 2K_{Br}^2 = 7\,350$ electrons², leaving a further 34 000 electrons² due to intermolecular distances. Each of these intermolecular distances contributes K_mK_n (m, n = As, Br) ≈ 1 200 electrons². The 3.7 Å peak therefore corresponds to 34000/1200 ≈ 28 intermolecular separations. To evaluate the area under the peak at 4.4 Å, the 3.7 Å has to be substracted from the total distribution, giving a peak centered

Can. J. Chem. Downloaded from www.nrcresearchpress.com by 210.87.254.5 on 09/05/12
For personal use only.

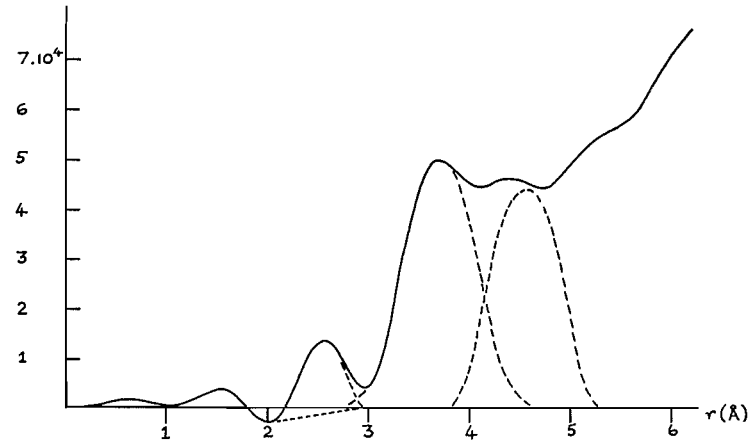

FIG. 3. Radial distribution function for liquid $AsBr_3$($4\pi r^2\rho(r)$, electrons²/Å).

at about 4.5 Å (Fig. 3) with area 34 600 electrons², corresponding to about 28 intermolecular distances.

A single-crystal X-ray study of solid arsenic tribromide (2) has shown that the crystal is built up from discrete pyramidal molecules, which have As—Br = 2.36 ± 0.01 Å, Br—As—Br = 97.7° ± 0.3°, Br ··· Br (intramolecular non-bonded) = 3.55 ± 0.01 Å. The dimensions in the vapor are reported as As—Br = 2.31–2.35 ± 0.02–0.04 Å, Br—As—Br = 100°–101.5° ± 2° (3), not significantly different from the crystal values. The present study of $AsBr_3$ liquid has again indicated pyramidal molecules; the As—Br distance obtained is 2.55 Å, and the difference between this value and those for the solid and vapor is probably not a real difference, but is an indication of the limited accuracy of the liquid study. The intramolecular Br ··· Br distance of 3.55 Å is part of the 3.7 Å peak in the liquid radial distribution function.

In the $AsBr_3$ crystal each molecule has 24 intermolecular As ··· Br and Br ··· Br contacts in the range 3.72–4.00 Å, and 18 distances in the range 4.12–4.33 Å. The number of distances in the shorter range is very similar to the number, 28, of intermolecular distances in the liquid 3.7 Å peak. Although it cannot be claimed that the liquid possesses any periodicity as in a crystal, the agreement between the number of closest contacts in the liquid and in the solid suggests that many of the intermolecular distances of the crystal are preserved over short ranges in the liquid. For the second range of intermolecular contacts, the agreement between number of distances is relatively good (18 in the solid, 28 in the liquid), especially since the liquid value has been determined from a peak which is not clearly resolved. The crystal has no intermolecular distances in the range 4.33–5.0 Å, and this is paralleled to some extent in the liquid, the radial distribution function exhibiting a minimum just below 5 Å, and then rising steeply with an inflection at about 5.2 Å, and no further structure.

The study appears to have been successful in the original purpose of obtaining significant results with the use of balanced filters for monochromatization. The use of only a nickel filter gave poor results, as evidenced by large spurious fluctuations in the radial distribution function at low r; this was a result of radiation other than Cu K_α reaching the counter, particularly fluorescent X-rays from the sample. The balanced filter method seems to compare reasonably well with crystal monochromatization. It has the disadvantage that

Can. J. Chem. Downloaded from www.nrcresearchpress.com by 210.87.254.5 on 09/05/12
For personal use only.

the measured intensity curve is a difference between two measurements (one with each filter of the balanced pair), but this is offset by the use of the counter measurements with a high-intensity primary X-ray beam, which are more accurate than the usual film measurements with the weaker monochromatized radiation.

The computations were carried out with our own programs on the IBM 7040 Computer, and we are indebted to the staff of the U.B.C. Computing Centre for assistance, and to the National Research Council of Canada for financial support.

REFERENCES

1. R. F. KRUH. Chem. Rev. **62**, 319 (1962).
2. J. TROTTER. Z. Krist. In press.
3. Tables of Interatomic Distances and Configuration in Molecules and Ions. Chem. Soc. Special Publ. No. 11. 1958.
4. International Tables for X-ray Crystallography. Vol. III. Kynoch Press, Birmingham. 1962.

Can. J. Chem. Downloaded from www.nrcresearchpress.com by 210.87.254.5 on 09/05/12
For personal use only.

Can. J. Chem. Downloaded from www.nrcresearchpress.com by 210.87.254.5 on 09/05/12
For personal use only.

PHOTOCHEMISTRY OF ELECTRONS TRAPPED IN GLASSES OF METHYLTETRAHYDROFURAN AT 77 °K[1]

P. J. Dyne and O. A. Miller
Research Chemistry Branch, Chalk River Nuclear Laboratories, Chalk River, Ontario

Received May 7, 1965

ABSTRACT

In the radiolysis of methyltetrahydrofuran glass at 77 °K electrons are produced with a high yield. These are immobilized in traps in the glass and do not recombine with positive ions. They can be released from their traps by illumination with visible and infrared light and may then diffuse to positive ions and be captured. The quantum efficiencies for bleaching have been measured as a function of wavelength. This quantum efficiency falls as bleaching proceeds and depends on the fraction of the electrons bleached and not on their concentrations. About half the electrons are trapped close to positive ions and, on release, have a high probability of diffusing to the positive ion. The remaining half are trapped homogeneously. On release from their traps, few of these electrons reach positive ions although they diffuse over long distances before being retrapped in the glass. This behavior is compared to that discussed by Samuel and Magee for the thermalization and capture of electrons in liquid water.

The rate of recombination of an electron and positive ion in a condensed phase is an almost unknown quantity and the uncertainties which remain about this process lie at the root of many fundamental problems of radiation chemistry. Important advances, permitting a direct study of the process under special conditions, have, however, recently been made by W. H. Hamill who has extended to radiolytic reactions the techniques of studying the photochemistry of organic glasses which were pioneered by G. N. Lewis (see for instance ref. 1).

In an organic glass at low temperature reactive intermediates formed in radiolytic or photolytic decomposition are held immobile in a rigid solvent cage. They have long lifetimes and can be observed, at leisure, by conventional optical techniques. Ronayne, Guarino, and Hamill (2) (henceforth R. G. and H.) found that, on radiolysis of glasses of 2-methyltetrahydrofuran (MTHF), a strong optical absorption is observed in the near infrared which is due to electrons trapped in the glass. In glasses containing biphenyl as a solute the intensity of the electron band is reduced and a new absorption due to the biphenyl anion ϕ_2^- appears.[3] The electron band is photosensitive, being bleached by visible and near infrared light. If biphenyl is present in a bleaching experiment the intensity of the biphenyl anion band increases as the intensity of the electron band is diminished. Electrons released from their traps in the the glass may be captured by positive ions or by biphenyl molecules.

In a sense this technique allows one to observe, in slow motion, the recombination of electrons and positive ions. This paper describes a study of the photochemistry of the bleaching of trapped electrons in MTHF glasses which shows that thermal electrons have a high mobility in the glass. While few electrons recombine with the positive ion before being trapped, they prefer trapping locations in the vicinity of positive ions.

EXPERIMENTAL

The experimental techniques for purifying MTHF, making optical cells from square drawn glass tubing, and preparing samples follow closely those described by Hamill and his co-workers, and are described in detail in ref. 3. For spectrophotometry a styrofoam optical dewar was used which is based on the design proposed by Nelson (4). Sealed optical cells were irradiated under liquid nitrogen with Co-60 γ-rays at dose

[1]*Issued as AECL No. 2326.*

rates of 3.7×10^{17} eV/min and 1.02×10^{18} eV/min per ml of glass. No effect of dose rate was observed in any of these experiments. After irradiation the cells were transferred to the optical dewar and their absorption recorded using a Beckman D.K.-2 spectrophotometer with an unirradiated cell filled with MTHF in the 'blank' optical path.

Considering that unmatched cells were used which were not optically perfect the precision of the spectrophotometry was good; at an optical density of 0.50 the reproducibility of an absorption peak was ±0.01 (i.e. 2%).

Bleaching was carried out in the optical dewar used for absorption measurements. Two light sources were used, a 500 W slide projector for wavelengths between 4 000 and 7 000 Å and a 100 W microscope illuminator for wavelengths from 8 000 to 18 000 Å. "Monochromatic" light was obtained using Spectracoat "Monopass" interference filters. In the visible region these have a full width at half intensity of ~ 30 Å. More than half the light transmitted by the 5 000 Å filter lies between 4 985 and 5 015 Å. In the near infrared, 10 000 Å or more, the full width at half intensity is ~ 250 Å. For experiments in which complete and rapid bleaching was required, a Corning Glass Filter No. 2600 and interference filters from a Spectracoat Variable band pass set were used.

In the determination of quantum efficiencies absolute light intensities were obtained with a calibrated Eppley 12 junction bismuth–silver thermopile. This was placed in a mock-up of the optical dewar so that the effects of internal reflection in the windows of the dewar were duplicated. Corrections were made for the reflection losses at glass–air interfaces. The thermocouple readings themselves were reproducible to better than 5%.

Two measurements of optical density (o.d.) are required in the calculation of the quantum efficiency: the change in the optical density at the peak of the electron band and the average optical density at the wavelength of the illumination. The measured change in optical density at the peak was about 0.1; the optical density at the wavelength of the illumination would be between 0.1 and 0.3 in many instances. The precision in these two measurements is at best ±10% so that the precision of the quantum efficiency measurements is about ±15%. It would be unrealistic to assume that the accuracy of the absolute intensity measurement was better than ±10% so that the uncertainty in the quantum efficiency must be at least ±25%.

There are further uncertainties in the absolute quantum efficiencies, as well as in the other data reported here, due to possible errors in values for the extinction coefficients of the biphenyl anion and two related quantities, the yield of electrons and the extinction coefficient of the electron band. In this paper we have consistently used the extinction coefficient of 3.7×10^4 l/mole cm at 410 mμ for the biphenyl anion in MTHF glass at 77 °K (2) and 1.6×10^4 l/mole cm for the electron band at 1 200 mμ (5).

Smith and Pieroni (6) have recently measured the yield of trapped electrons in MTHF by electron spin resonance (e.s.r.) methods which are independent of these extinction coefficients. Their yield, 2.6 electrons/100 eV, confirms R. G. and H.'s methods which gave a yield of 3 electrons/100 eV.

RESULTS AND DISCUSSION

Mechanistic Steps in Photobleaching

Before discussing our own data it is convenient to summarize R. G. and H.'s observations in terms of mechanistic steps.

In radiolysis, molecules of MTHF (M) are ionized giving an electron e_k^-, with some kinetic energy greater than thermal and a positive ion P^+.

[1] $$M \rightsquigarrow e_k^- + P^+$$

These free electrons lose energy, become thermalized (e_{th}^-) and may be trapped in the glass (e_{tr}^-).

[2] $$e_k^- \rightarrow e_{th}^- \rightarrow e_{tr}^-$$

In the presence of a solute with high electron affinity (such as biphenyl ϕ_2) a new trapping process may occur.

[3] $$e_{th}^- + \phi_2 \rightarrow \phi_2^-$$

R. G. and H. found that as the concentration of biphenyl solute was increased, the yield of trapped electrons fell to zero and the yield of biphenyl anions reached a plateau. At this concentration they concluded that every electron normally trapped as a result of processes [1] and [2] was now being trapped by [3]. Smith and Pieroni's e.s.r. measurements confirm the validity of this procedure. Since the extinction coefficient of the biphenyl anion is known, its limiting concentration allows one to deduce a value for the yield of

Can. J. Chem. Downloaded from www.nrcresearchpress.com by 210.87.254.5 on 09/05/12
For personal use only.

trapped electrons in steps [1] and [2] and hence to deduce an extinction coefficient for the absorption band of the electrons. The yield of trapped electrons (3 per 100 eV absorbed) is large. By comparison with values of W, the energy/ion pair in gases, which give $G(e^-)$ between 3 and 4, it follows that a greater part, if not all, of the electrons formed in the initial ionization are trapped in the glass and are not captured by the positive ion.

The first step in the bleaching process may be written

[4] $$e_{tr}^- + h\nu \rightarrow e_k^- \rightarrow e_{th}^-.$$

This mobile electron will have one of three fates; it may simply be retrapped in reaction [2], or be recaptured by the positive ion after thermalization

[5] $$e_{th}^- + P^+ \rightarrow \text{not-}e_{tr}^-,$$

or if biphenyl is present, it may be captured by the biphenyl to give ϕ_2^- (reaction [3]).

The Bleaching of the Electron Band

The quantum efficiency for bleaching trapped electrons is not constant but decreases continuously as the bleaching proceeds. This is shown in Fig. 1 for three samples of differing γ-ray dose. The optical density, measured at the peak of the electron band at 1 200 mμ is plotted against the amount of light absorbed. This light absorption is calculated from the product: average % absorption at the wavelength of the illumination $\times$ time of illumination. The slope of these curves at any electron concentration is proportional to the quantum efficiency for bleaching at that concentration. From these curves we see that one can produce samples with identical electron concentrations but which differ markedly in bleaching efficiency. This can be seen by comparing the initial slope of the sample irradiated for 2 min (o.d. 0.64) with the slope for the 4 min sample where bleaching has reduced the optical density to 0.64.

The quantum efficiencies at any electron concentration can be estimated graphically by drawing tangents to the curves shown in Fig. 1. These quantum efficiencies are shown in Fig. 2, where it is seen that they depend on the fraction of electrons bleached and not on their concentration in the sample. We conclude that the electron traps are not all alike. About half of the electrons are easily bleached and the other half has a quantum efficiency for bleaching about 1/20th that of the first group. The spectrum of quantum efficiencies may, of course, be more complex than this, but this simple distribution would give a linear decrease of quantum efficiency to a constant lower value as seen in Fig. 2.

The question then arises: How do these traps differ? What causes this difference in quantum efficiency? One might anticipate that the two (or more) groups of electrons might have different absorption spectra and this would be shown by a change in band shape as the bleaching progresses. R. G. and H. reported that the electron band bleaches as a whole. Our measurements show, however, that this is not exactly true. Fig. 3 compares two spectra, one before bleaching and one after 54% of the original concentration had been removed by illumination at 466 mμ. The partially bleached sample has weaker absorption on the short wavelength side. The electrons forming the more easily bleached fractions must, therefore, absorb more strongly at shorter wavelengths. This effect, however, is small.

The quantum efficiency for bleaching electrons is increased by adding biphenyl, the increase being due to the additional trapping to form ϕ_2^-. Figure 4 shows the quantum efficiency for bleaching electrons and forming biphenyl anions. This could only occur if, in the absence of biphenyl, there was a competition between capture by positive ions and retrapping in the glass (reaction [2]).

Can. J. Chem. Downloaded from www.nrcresearchpress.com by 210.87.254.5 on 09/05/12
For personal use only.

Can. J. Chem. Downloaded from www.nrcresearchpress.com by 210.87.254.5 on 09/05/12
For personal use only.

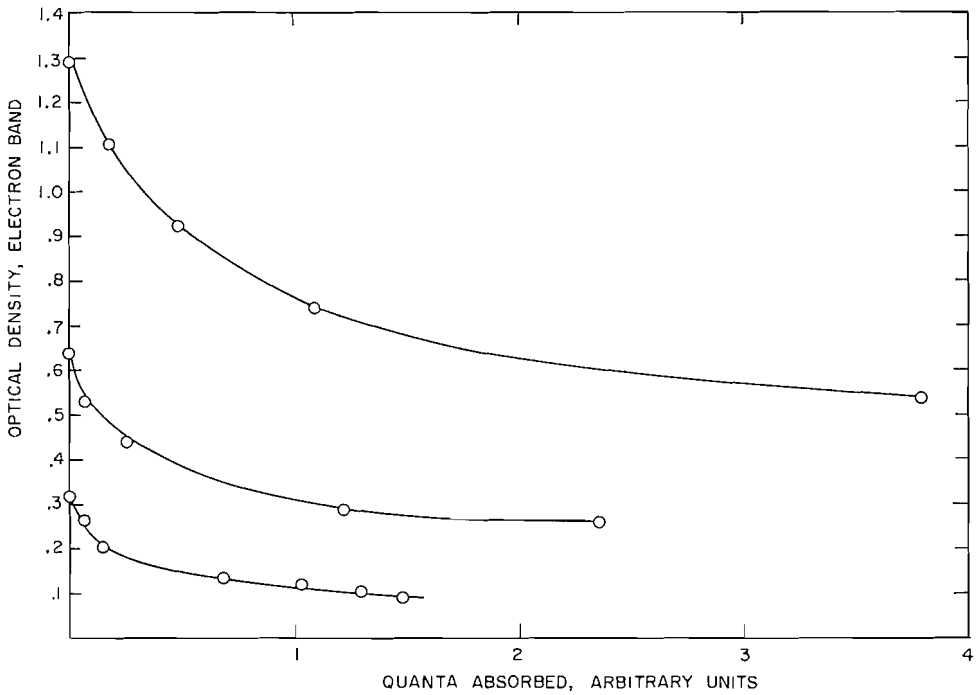

FIG. 1. Bleaching of the electron band in MTHF glasses. The three samples were irradiated for 1, 2, and 4 min at a dose rate of 3.7×10^{17} eV min/ml of MTHF glass.

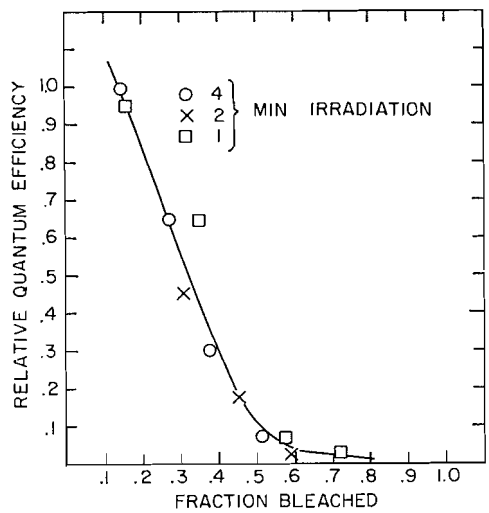

FIG. 2. Relative quantum efficiency for bleaching calculated from the data in Fig. 1.

Can. J. Chem. Downloaded from www.nrcresearchpress.com by 210.87.254.5 on 09/05/12
For personal use only.

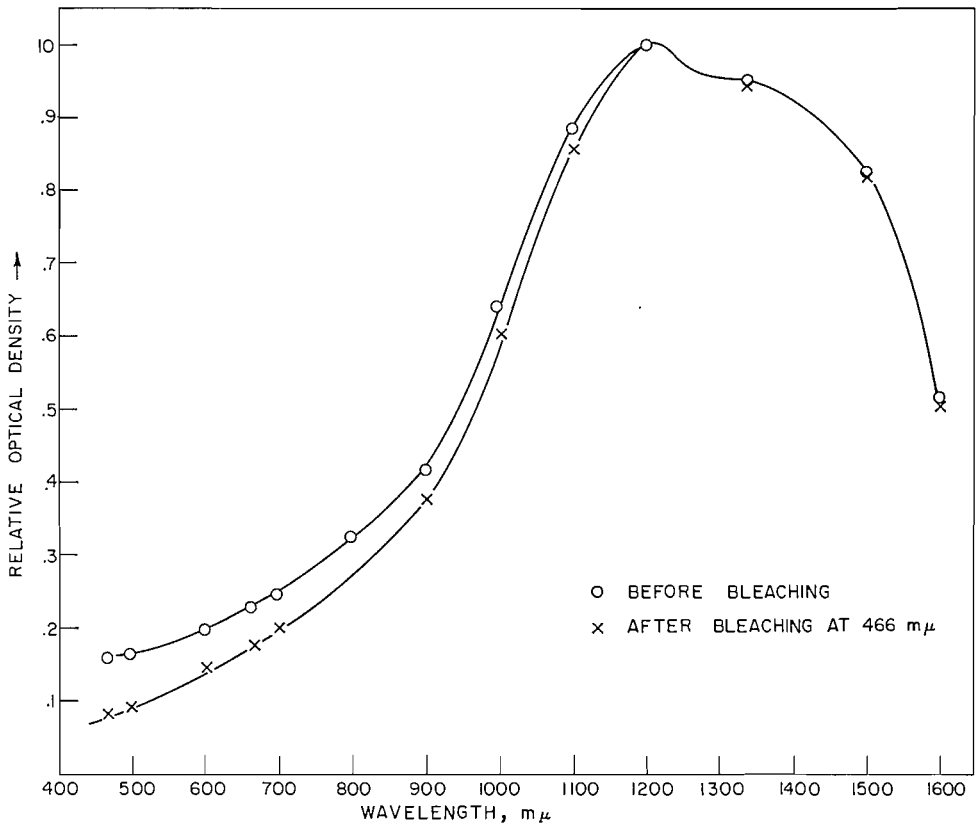

FIG. 3. Optical density of the electron band before bleaching and after bleaching at 466 mμ to 46% of the original optical density. The spectra have been normalized at 1 200 mμ to show the decreased absorption at shorter wavelengths.

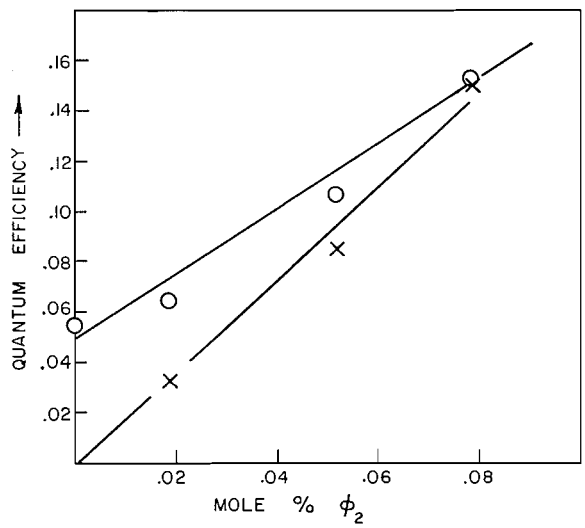

FIG. 4. Quantum efficiency for bleaching electrons (O) and for forming biphenyl anions (×) as a function of the biphenyl concentration. Bleaching carried out at 800 mμ.

If P_N and P_T are the probabilities of neutralizing and trapping, then the measured quantum efficiency for bleaching, Φ_B, is related to Φ_4, the quantum efficiency for initial release from the traps by the relation:

$$[6] \qquad \Phi_B = \Phi_4 \cdot \frac{P_N}{P_N + P_T}.$$

In the presence of biphenyl we have to include P_c, the probability of reaction [3] ($e_{th}^- + \phi_2 \rightarrow \phi_2^-$), and the measured quantum efficiency becomes:

$$[7] \qquad \Phi_B = \Phi_4 \cdot \frac{P_N + P_c}{P_N + P_c + P_T}.$$

Inspection of eq. [6] shows that the quantum efficiency will vary as the probability of recapture by the positive ion (P_N) varies and this provdes an explanation for the variation in the quantum efficiency of bleaching. Suppose that the trapped electrons differed simply in their proximity to a positive ion. Electrons released from traps which are close to positive ions are likely to be recaptured since for these electrons $P_N > P_T$; electrons which are released from traps which are far away from a positive ion are more likely to be retrapped since for these electrons $P_T > P_N$.

This conclusion is consistent with the e.s.r. measurements and the conclusions of Smith and Pieroni (7) on the thermal decay of electrons in MTHF glasses. The kinetics of this decay are complex following neither a first nor second order law. The decay curves for different initial concentrations of electrons can, however, be superimposed. This is analogous to the optical bleaching in that the rate of decay (bleaching for optical measurements) is determined by the fraction of the initial electron concentration which has been removed and that a residue of about half the electrons decay much more slowly than the rest.*

The absolute quantum efficiency of bleaching varies with wavelength as shown in Fig. 5. Two sets of values are shown: the absolute measurements were made using the Eppley thermopile as a standard; the relative measurements were made with a self-balancing bolometer lent to us by Dr. R. Banville. We have adjusted the readings from this instrument to coincide with the absolute measurements at 800 mμ. The agreement between the two measurements is satisfactory.

This variation in quantum efficiency with wavelength suggests that the absorption spectrum consists of two parts, a transition to a bound state giving a strong absorption band peaked at 1 200 mμ which is overlapped on the short wavelength side by the ionization continuum which starts at about 900 mμ and stretches out to the blue. On this interpretation the ionization potential of the trapped electron is $\simeq$ 1.4 eV and the first excited (bound) level is $\simeq$ 1 eV above the ground state.

The trapped electron in MTHF is, consequently, similar in several respects to the solvated electron in liquid ammonia and related solvents. Blades and Hodgins (8) proposed a similar interpretation for the optical absorption of electrons in methylamine. Their Fig. 9 shows a separation of the optical absorption into a band and a continuum identical to that suggested by our quantum efficiency measurements. This observation is supplemented by Jortner's calculation (9) showing that the electron in ammonia is in

Dainton and Salmon (Proc. Roy. Soc. London, Ser. A, 285, 319 (1965)) have recently published studies of the thermal decay of electrons in MTHF, over the temperature range 91 to 97 °K. This decay follows second order kinetics. In these experiments about half of the electrons in the sample, initially irradiated at 77 °K, have decayed before constant temperature is attained and the kinetics observed. This observation is, therefore, not necessarily in disagreement with Smith and Pieroni's observations at 77 °K in which the kinetics of decay of all the electrons was followed.

Can. J. Chem. Downloaded from www.nrcresearchpress.com by 210.87.254.5 on 09/05/12
For personal use only.

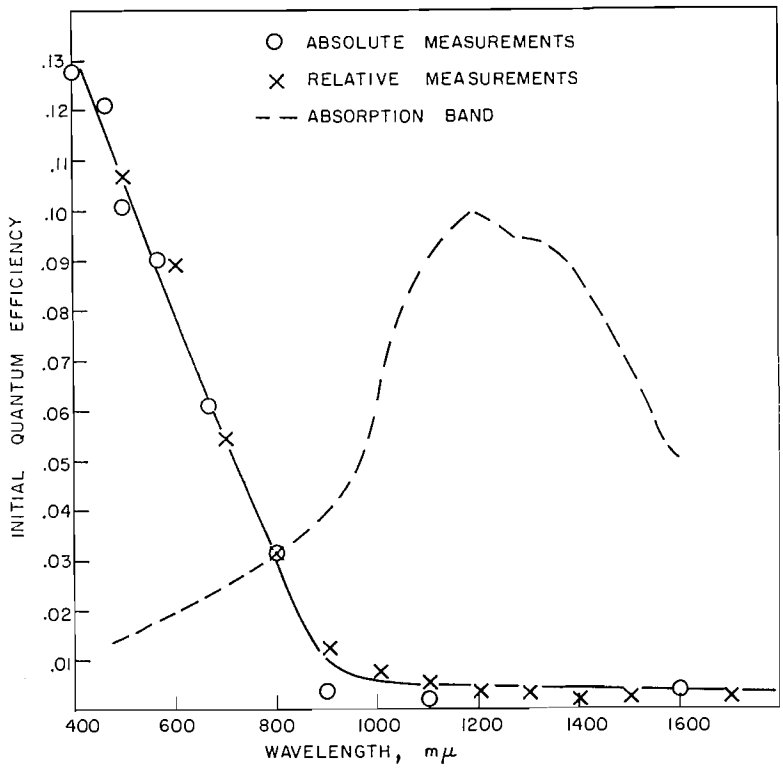

FIG. 5. Quantum efficiency for bleaching as a function of the wavelength of the bleaching light. The envelope of the electron band is shown on the same wavelength scale for comparison.

a trap whose ground state lies $\simeq 2$ eV below the continuum. The trapped electron has an excited bound state ~ 0.8 eV above the ground state.

According to this simple interpretation, the quantum efficiency should fall to zero at long wavelengths. However, while the quantum efficiency is small above 900 mμ, it is not zero. We suggest that some electrons are trapped sufficiently close to a positive ion that, in even the "bound" excited state they also have a finite probability of escape and of being captured by the positive ion. This would require that the quantum efficiency would fall to a very low value after this initial fraction of electrons is bleached out. Qualitatively this is observed: after about 10% of the electrons have been bleached out at longer wavelengths, the quantum efficiency (which is already low) is reduced to 1/10 or less of its initial value. However, bleaching at these wavelengths is so slow that the accurate data on quantum efficiencies required to substantiate this interpretation in detail are not readily obtained.

This conclusion also suggests an interpretation for the change in shape of the electron band. Electrons which are trapped closer to positive ions are moving in a field perturbed by the positive ion. We suggest that this perturbation leads to a stronger absorption in the blue end of the spectrum than is found for isolated, unperturbed, traps.

The Diffusion and Trapping of Electrons in MTHF Glasses

R. G. and H.'s observations on the radiolysis of MTHF glasses lead to two conclusions on the mobility of electrons in this medium:

1. Since the yield of electrons is high, primary recombination of the positive ion and electron is improbable.

Can. J. Chem. Downloaded from www.nrcresearchpress.com by 210.87.254.5 on 09/05/12
For personal use only.

Can. J. Chem. Downloaded from www.nrcresearchpress.com by 210.87.254.5 on 09/05/12
For personal use only.

2. Biphenyl competes with the traps in the glass for electrons at low concentrations (< 0.1 mole %) so that the electron must follow an extended path through the glass before it is trapped by the solvent or captured by solute, as the case may be.

The classical discussion of the motion of an electron in a condensed phase in the vicinity of a positive ion was given by Samuel and Magee (10). Following Onsager (11) they defined a critical escape distance r_c for the electron where its thermal energy (kT) was equal to its coulombic potential energy. The probability of an electron escaping from the field of a positive ion at a distance r is exp $(-r_c/r)$ and is large where $r_c > r$. The critical escape distance for an electron in MTHF with a high frequency dielectric constant of 2.0 (12) is $\sim 1\,200$ Å at 77 °K. These optical experiments were carried out at doses giving final concentrations of ions and electrons of $\sim 5 \times 10^{16}$/cm³. At this concentration the average separation of nearest neighbors of positive ions is ~ 300 Å so that an electron is never free of the coulombic field of a positive ion.

Let the number of trapping sites in the glass be T/cm³, the number of positive ions be P/cm³, and the number of solvent (MTHF) molecules be S/cm³. Let the cross section for electron capture by the trapping sites, positive ions, and biphenyl molecules be σ_T, σ_P, and σ_B (cm²) and the scattering cross section by the solvent molecules be σ_S (cm²).

The macroscopic trapping cross section Σ_T, is equal to $T\sigma_T$ cm^{-1}* and the mean free path for trapping is $1/\Sigma_T$.† We can estimate Σ_T from the experiments in which biphenyl competes with the glass for electrons. From Fig. 6 we see that the yield of electrons is reduced to half its initial value at 0.04 mole % biphenyl. At this concentration $G(e^-) = G(\phi_2^-)$ and, hence, $\Sigma_T = \Sigma_B$ where $\Sigma_B = B\sigma_B$. Since $B = 4 \times 10^{-4}S$ and $S = 7.2 \times 10^{21}$/cm³ we find $\Sigma_T = 2.9 \times 10^{18}\sigma_B$.

The mean square distance (crow's flight) between thermalization and trapping $\overline{r^2}$ is

$$\overline{r^2} = 6(D/\Sigma_T)$$

where Σ_T is the macroscopic trapping cross section and D, the diffusion constant is given by $D = 1/3\Sigma_S = 1/3S\sigma_S$ whence $\overline{r^2} = 2/S\sigma_S\Sigma_T$. This diffusion constant is related to the conventional diffusion constant D' by $D = D'/V$ where V is the velocity of the electron. Using the values of S and Σ_T given above we find

$$\sqrt{(\overline{r^2})} = \frac{10^{-20}}{(\sigma_S\sigma_B)^{1/2}}$$

This is essentially a phenomenological relation. Now σ_S, the scattering cross section, is likely to be of the order of molecular dimensions, i.e. $\sim 10^{-15}$ cm². (The cross section corresponding to the molecular volume of MTHF is 3×10^{-15} cm².) If the electron capture cross section of biphenyl is large it will also be of the same order. Asundi and Craggs (13) found the electron capture cross section at 0.1 eV to be 1.5×10^{-15}/cm² for SF_6. They reported "the highest known electron capture cross section" for perfluoro methylcyclohexane C_7F_{14} to be 7.5×10^{-15} cm².

With $\sigma_S = \sigma_B = 10^{-15}$ cm² we find $\sqrt{(\overline{r^2})} = 10^{-5}$ cm, (1 000 Å). To reduce this crow's flight distance to, say 100 Å, we would have to make both σ_S and σ_B 10 times larger ($\sim 10^{-14}$ cm²) and such values seem improbable. It follows that electrons in MTHF glasses can diffuse over distances which are at least comparable with the separation of positive ions at doses of 1×10^{18} eV/ml.

**The important quantity is Σ_T which can be defined as the reciprocal of the mean free path. The definitions of T and σ_T implying a definite concentration of trapping sites each with a capture cross section are a convenient mathematical formalism.*

†Details of this and other formulae used in this section can be found in "The Elements of Nuclear Reactor Theory" S. Glasstone and M. C. Edlund, D. Van Nostrand Company, New York, 1952.

These estimates can, of course, be criticized because they are based on gas phase data. It might be argued, for instance, that the interaction of thermal electrons with molecules in a condensed phase is very strong and the diffusion of an electron could be described by a very large scattering cross section which bore no real relation to molecular size. This would reduce, $\overline{r^2}$ but does not affect estimates of Σ_T and Σ_B since it simply increases the time which a diffusing electron takes to find a biphenyl molecule or a positive ion. In other words, while we could visualize circumstances in which an electron moves very slowly through the glass, this also means that the trapping process also takes place very slowly since the competition between biphenyl and trapping in the glass is still observed at low biphenyl concentrations.

Smith and Pieroni (7) found that $G(e^-)$ decreased slowly as the total dose increased. From their data $G(e^-)$ is reduced to 90% of its initial value when the final concentration of electrons is $2 \times 10^{17}/cm^3$. If this reduction in yield is due to the recombination of positive ions and electrons then we can say that, at the average positive ion concentration in the irradiation ($10^{17}/cm^3$) the macroscopic capture cross section of positive ions $\Sigma_P = P\sigma_P$ is one tenth Σ_T, i.e. $10^{17}\sigma_P = 1/10(\Sigma_T) = 2.9 \times 10^{17}\sigma_B$ so that $\sigma_P/\sigma_B \sim 3$. The capture cross section of an electron by a positive ion is only three times that for its capture by a neutral biphenyl molecule. This estimate gives an upper limit to σ_P since part of the decrease in yield may be due to the thermally induced recombination of electrons and positive ions which is beginning to occur at a significant rate at these doses.

We can use this estimate of σ_P/σ_B to estimate the bleaching quantum efficiency for electrons homogeneously distributed in the glass. Consider a sample with an average concentration of positive ions during irradiation of $2 \times 10^{16}/cm^3$. Then (putting $\sigma_P = 3\sigma_B$) $\Sigma_P = 6 \times 10^{16}\sigma_B$. If the quantum efficiency of release from the traps is given by equation [6] and P_N and P_T are proportional to Σ_P and Σ_T

$$\Phi_B \approx \Phi_4(\Sigma_P/\Sigma_T) = \phi_4 \left(\frac{6 \times 10^{16}}{2.9 \times 10^{18}}\right) \approx 0.02\ \Phi_4 .$$

If $\Phi_4 = 1$ the maximum value of Φ_B would be 0.02. Referring to the observed quantum efficiencies (Fig. 5) we see that the initial values at wavelengths shorter than 800 mμ are greater than this. It follows, in agreement with our earlier conclusions, that the electrons bleached in the first stages are not homogeneously distributed but are trapped preferentially close to the positive ion.

The quantum efficiencies for bleaching the residual half of the electrons are (Fig. 2) $\sim 1/20$ of the initial value, i.e. they have values of 0.005 or less depending on the wavelength of the light used. These quantum efficiencies are consistent with those to be expected for the diffusion of homogeneously distributed electrons if Φ_4 varies with wavelength, rising linearly from a small value at 900 mμ to a value close to unity at 400 mμ.

The Bleaching of the Biphenyl Anion Band

At wavelengths of 400 and 433 mμ the biphenyl anion band is bleached and the intensity of the electron band increases. We are observing the process

$$\phi_2^- + h\nu \rightarrow \phi_2 + e^-$$

followed by the trapping of the electron in the glass. The longer wavelength band of the biphenyl anion at 660 mμ is not photosensitive in MTHF glasses. A sample containing biphenyl can be bleached alternately with blue (400 mμ) and near infrared (800 mμ) light transferring the electrons from biphenyl molecules to the glass and back again. The results of such an experiment are shown in Fig. 7. The sample containing 0.006 mole %

Can. J. Chem. Downloaded from www.nrcresearchpress.com by 210.87.254.5 on 09/05/12
For personal use only.

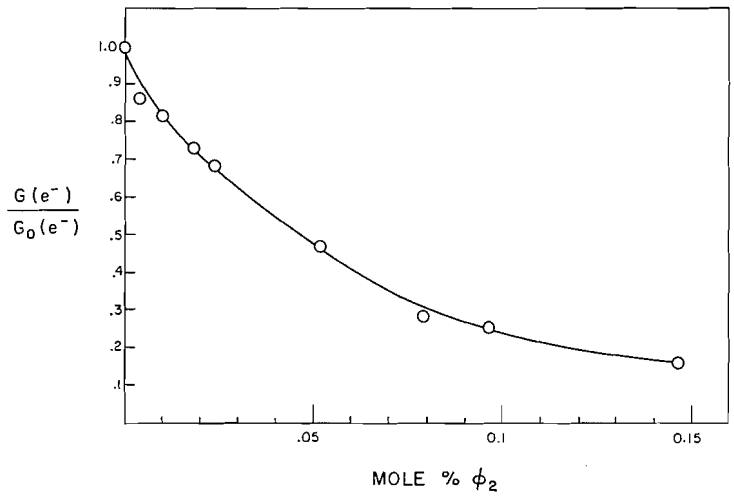

FIG. 6. Yield of trapped electrons as a function of the biphenyl concentration. The initial yield in the pure solvent is 3/100 eV.

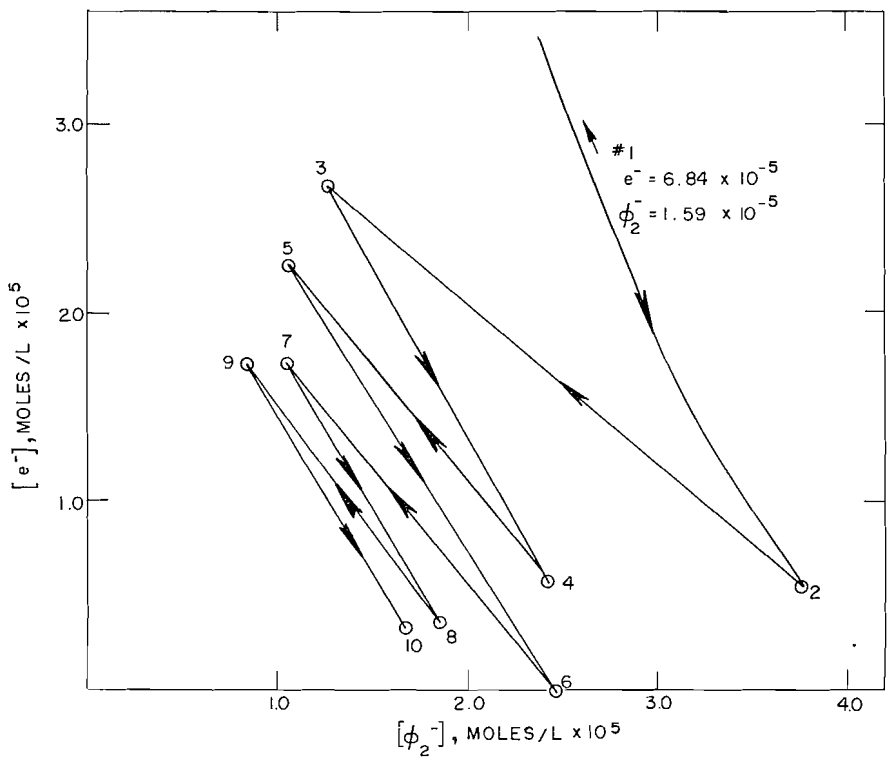

FIG. 7. Variation in the concentration of trapped electrons (e^-) and biphenyl anions ϕ_2^- after illuminating with red light at 800 mμ (steps 1–2, 3–4, etc.) and after illumination with blue light at 400 mμ (steps 2–3, 4–5, etc.).

Can. J. Chem. Downloaded from www.nrcresearchpress.com by 210.87.254.5 on 09/05/12
For personal use only.

biphenyl was irradiated giving initial concentrations of $e^- = 6.84 \times 10^{-5}$ moles/l and $\phi_2^- = 1.59 \times 10^{-5}$ moles/l. Prolonged bleaching with red light gave a sample with concentration #2. Irradiations with blue light were carried out in steps 2 to 3, 4 to 5, etc., and irradiations with red light were carried out in steps 3 to 4, 5 to 6, etc.

After the sample has been bleached to point 3 it can be seen that electrons can be transferred to and from the biphenyl molecules with little loss to neutralization of positive ions. In the latter steps (6 to 10) the sum of the electron and biphenyl anion concentration is nearly constant within the precision of the measurements and the accuracy of the extinction coefficients. In the initial bleaching process (1-2-3) more than half of the initial concentration was lost and, according to our interpretation, we have thus, at point 3, eliminated almost all the electrons which are trapped close to positive ions. The high efficiency of transfer of electrons between the glass and biphenyl at this low biphenyl concentration shows again that electrons can diffuse over significant distances in the glass without being strongly affected by the presence of the positive ions.

Electrons in MTHF and the Samuel Magee Model

In conclusion, we compare our observations on the motion of electrons in MTHF glasses with the theoretical conclusions of Samuel and Magee (10) on the motion of electrons in water. They argued that, in liquid water, electrons were thermalized at small distances (12–17 Å) from the positive ion and were, hence, quickly recaptured. The possibility of electron capture by water was regarded, on the basis of information then available (1953), to be improbable.

In MTHF glasses we find evidence that the electron travels considerable distances (100 to 1 000 Å) between thermalization and capture in the glass. The time taken for trapping is long, at least of the order of the dielectric relaxation time (14). Since we find that initial recombination of the positive ion and electron is improbable, it follows that the distance in which the electron is thermalized must be appreciable and certainly greater than the 17 Å distance suggested by Samuel and Magee for liquid water. A distance of at least 100 Å is reasonable. A thermalization distance of 100 Å for electrons in liquid cyclohexane has been suggested by Freeman (15) from conductivity observations. Comparable distances have been estimated by Ffrancon Williams on chemical evidence (16).

In MTHF glasses the effects of coulombic attraction between the positive ion and electron are not dominant. We suggest that instead of providing a compelling driving force for recombination, coulombic attraction produces a weaker effect, concentrating a fraction of the free electrons in traps close to the positive ion. At the end of an irradiation in one of our optical experiments, the average separation of positive ions is $\sim$ 300 Å and so electrons are at most 150 Å from a positive ion. Since we observe a factor of 20 between the bleaching efficiencies for the two groups of electrons, we can make the naive estimate that the closely spaced electron-positive ion pairs are, perhaps, only 1/20 of this distance apart, i.e. $<$ 10 Å. Smith and Pieroni's e.s.r. measurements give an upper limit to this distance. They found an average positive ion – electron separation for all electrons of 50 Å. The separation of the closely spaced group must be less than this and the other electrons must be trapped at greater distances than this from the positive ion. In summary, therefore, we conclude that the "closely spaced" electron-positive ion pairs (which bleach readily) are separated by a distance of 10 to 50 Å and the "homogeneously" trapped electrons lie more than 50 Å from a positive ion.

Can. J. Chem. Downloaded from www.nrcresearchpress.com by 210.87.254.5 on 09/05/12
For personal use only.

ACKNOWLEDGMENTS

Dr. W. H. Hamill, Dr. S. Z. Toma, and Father Bertin generously helped us by telling us many details of technique. We thank Dr. D. R. Smith, Dr. J. A. Stone, and Dr. E. Vogt for stimulating discussions during the preparation of this paper.

REFERENCES

1. G. N. Lewis, D. Lipkin, and T. T. Magel. J. Am. Chem. Soc. **63**, 3005 (1941).
2. M. R. Ronayne, J. P. Guarino, and W. H. Hamill. J. Am. Chem. Soc. **84**, 4230 (1962).
3. Farhataziz and P. J. Dyne. An anthology of experimental techniques in radiation chemistry. AECL-2113, Atomic Energy of Canada Limited. 1964.
4. L. S. Nelson. Rev. Sci. Instr. **27**, 655 (1956).
5. J. P. Guarino and W. H. Hamill. J. Am. Chem. Soc. **86**, 777 (1964).
6. D. R. Smith and J. Pieroni. Can. J. Chem. **43**, 2141 (1965).
7. D. R. Smith and J. Pieroni. Can. J. Chem. **43**, 876 (1965).
8. H. Blades and J. W. Hodgins. Can. J. Chem. **33**, 411 (1955).
9. J. Jortner. J. Chem. Phys. **30**, 839 (1959).
10. A. H. Samuel and J. L. Magee. J. Chem. Phys. **21**, 1080 (1953).
11. L. Onsager. Phys. Rev. **54**, 554 (1938).
12. N. E. Hill. Proc. Roy. Soc. London, Ser. A, **240**, 101 (1957).
13. R. K. Asundi and J. D. Craggs. Proc. Phys. Soc. London, **83**, 534, 611 (1964).
14. C. J. Hochanadel. *In* Comparative effects of radiation. *Edited by* M. Burton, J. S. Kirby Smith, and J. L. Magee. John Wiley and Sons, New York. 1960. p. 151.
15. G. R. Freeman. Discussions Faraday Soc. **36**, 248 (1963).
16. Ffrancon Williams. J. Am. Chem. Soc. **86**, 3954 (1964).

Can. J. Chem. Downloaded from www.nrcresearchpress.com by 210.87.254.5 on 09/05/12
For personal use only.

Can. J. Chem. Downloaded from www.nrcresearchpress.com by 210.87.254.40 on 09/05/12
For personal use only.

QUANTITATIVE PREPARATION OF CHLORO- AND BROMOPHTHALAZINES

A. HIRSCH AND D. ORPHANOS
Canadian Technical Tape Ltd., Montreal, Quebec
Received April 27, 1965

ABSTRACT

A new improved synthesis of 1,4-dichloro- and 1,4-dibromophthalazine has been effected by reaction of 1,4-dioxophthalazine with PX_5 (X = Cl, Br) in a sealed reaction flask. Halogenation of the dioxophthalazine has also been accomplished at atmospheric pressure in a halogenated solvent. The synthesis of 1-bromophthalazine is reported.

INTRODUCTION

1,4-Dichlorophthalazine has been synthesized by the reaction of 1,4-dioxophthalazine with either $POCl_3$ (1, 2) or PCl_5 (3–6). Repetition of the $POCl_3$ method gave unsatisfactory results. The use of PCl_5 gave rise to an impure product in 55% yield. The purification of the reaction mixture was quite laborious, and always accompanied by considerable amounts of 1-chloro-4-oxophthalazine, which could only be removed with difficulty.

A modification of this latter method has now been developed in which heating of 1,4-dioxophthalazine with PCl_5 in a sealed reaction vessel results in a quantitative yield of almost pure 1,4-dichlorophthalazine, without the need for further purification.

It has been earlier reported (3) that reaction of 1,4-dioxophthalazine with PBr_5 always affords a mixture of 1,4-dibromophthalazine and 1-oxo-4-bromophthalazine. No yields were mentioned. 1,4-Dibromophthalazine has now been readily obtained in a nearly quantitative yield by applying the modified procedure for the preparation of the analogous dichlorophthalazine.

It was later found that the preparation of 1,4-dibromophthalazine could also be achieved under atmospheric conditions by using CBr_4 as a solvent. In this alternative modification, the obtained yield was 78% and the CBr_4 solvent was easily recovered. No reference to the preparation of 1-bromophthalazine is available.

EXPERIMENTAL

1,4-Dichlorophthalazine

In a closed pressure bottle, a mixture of 1,4-dioxophthalazine (16.2 g, 0.1 mole and an excess of phosphorous pentachloride (85 g) was heated at 140–150° in an oil bath for 4 h. During the heating period the reaction mixture was agitated with the aid of a magnetic stirrer. After cooling to room temperature, the pressure bottle was placed in a refrigerator for a few hours and then carefully opened in a hood. HCl gas escaped vigorously. The solid orange-colored mass was crushed with a spatula and poured into 1 l of ice water. The whole mixture was stirred until all lumps were disintegrated. Then ammonium hydroxide was added to a basic reaction; care being taken to maintain the temperature below 10 °C. The solid was collected on a filter paper, washed with water, and dried. This crude material was redissolved in methylene chloride, shaken with charcoal, and filtered. The colorless filtrate was subjected to partial concentration until a thick paste was obtained. Upon addition of 100 ml diethyl ether, a white crystalline material melting at 161–162° separated. The yield was 19.2 g (96.5%).

1,4-Dichlorophthalazine was recrystallized from tetrahydrofuran in colorless long needles m.p. 164° (lit. m.p. 161–162°, 164°, 164–165°); see Fig. 1.

Infrared spectra were determined on Perkin-Elmer model 337 from Nujol mulls.

1,4-Dibromophthalazine

This compound was prepared in 97% yield by applying the reaction conditions for the preparation of the analogous 1,4-dichlorophthalazine. In this preparation, the halogenating agent was phosphorous pentabromide and a reaction temperature of 140° was more effective.

Can. J. Chem. Downloaded from www.nrcresearchpress.com by 210.87.254.40 on 09/05/12
For personal use only.

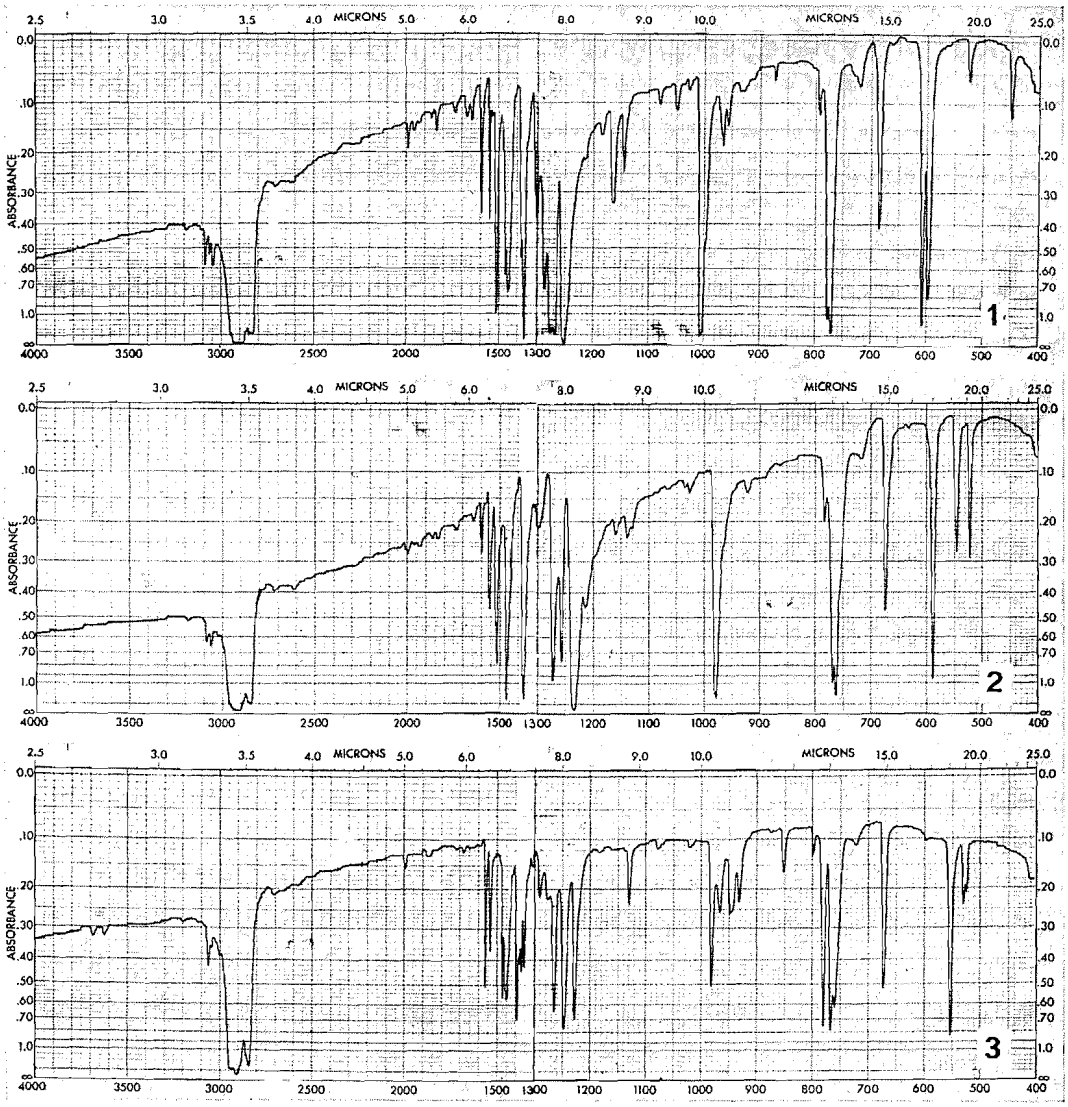

FIG. 1. Absorbance vs. frequency (cm^{-1}) for 1,4-dichlorophthalazine.
FIG. 2. Absorbance vs. frequency (cm^{-1}) for 1,4-dibromophthalazine.
FIG. 3. Absorbance vs. frequency (cm^{-1}) for 1-bromophthalazine.

1,4-Dibromophthalazine was crystallized from tetrahydrofuran in colorless long needles m.p. 160–161° (lit. m.p. 162°); see Fig. 2.

Preparation of 1,4-Dibromophthalazine in an Open Flask

A mixture of 1,4-dioxophthalazine (1.62 g, 0.01 mole), phosphorous pentabromide (9.5 g, 0.02 mole plus 10% excess), and carbon tetrabromide (50 g) were heated at 130° (temperature of oil bath) for 6 h. After cooling, the solid mass was treated with methylene chloride (25 ml) until all lumps had been disintegrated. This mixture, under vigorous stirring, was poured into ice water (100 ml) and stirring was continued for an additional 2 h. The yellow solid material was collected on a filter paper and washed thoroughly with water followed by petroleum ether. 1,4-Dibromophthalazine was crystallized from tetrahydrofuran in long pale-yellow needles melting at 160°, yield 2.2 g (78%).

1-Bromophthalazine

A mixture of phosphorous oxybromide (12 g), diethyl ether (25 ml), 2*H*-1-phthalazinone (2 g), and tetrahydrofuran (80 ml) was stirred at room temperature for 15 min. Then, under vigorous stirring, the mixture was heated for 3 h in an oil bath maintained at a temperature of 55–60°. After cooling, a pale-yellowish solid was collected on a filter paper, washed with diethyl ether, and dried in a vacuum desiccator. The product reacted acidic, and obviously was the hydrobromide salt of 1-bromophthalazine. On heating over 210°, it acquired a grey color and at 245° melted with decomposition, yield 3.5 g. This product was taken in water (no solution was achieved) and under vigorous stirring was carefully neutralized to a weakly basic reaction with ammonium hydroxide. The pale-yellow solid was collected on a filter paper, washed with distilled water until the washings were neutral, and finally washed with petroleum ether. It was dried in the dark in a vacuum desiccator. On heating, it became orange colored at about 100°, and at 175° melted with foaming; yield 2.52 g (88%); see Fig. 3.

Anal. Calcd. for $C_8H_5BrN_2$: C, 45.95; H, 2.41; N, 13.40; Br, 38.22. Found: C, 45.82; H, 2.55; N, 13.10; Br, 38.51.

ACKNOWLEDGMENT

The authors are indebted to the National Research Council of Canada whose financial assistance made this work possible.

REFERENCES

1. A. WOLFRAM. Ger. Patent No. 481,650 (July 17, 1925).
2. J. HARY and L. YALE. J. Am. Chem. Soc. **75**, 675 (1953).
3. R. STOLLÉ and H. STORCH. J. Prakt. Chem. **135**, 128 (1932).
4. H. DREW and H. HATT. J. Chem. Soc. 16 (1937).
5. R. HAWORTH and S. ROBINSON. J. Chem. Soc. 777 (1948).
6. S. BINIECKI *et al.* Acta Polon. Pharm. **15**, 421 (1957).

Can. J. Chem. Downloaded from www.nrcresearchpress.com by 210.87.254.40 on 09/05/12
For personal use only.

PHOTO-ADDITION OF *N*-NITROSODIALKYLAMINES TO CYCLOHEXENE

Y. L. CHOW
Department of Chemistry, University of Alberta, Edmonton, Alberta
Received May 28, 1965

ABSTRACT

Under the simultaneous influence of light and an acid, the nitrosamines derived from four heterocyclic amines readily form 1:1 photo-adducts with cyclohexene giving excellent yields of 2-*tert*-aminocyclohexanone oximes. While *N*-nitrosodi-*n*-butylamine, under similar conditions, gives a fair yield of the 1:1 photo-adduct, *N*-nitrosodicyclohexylamine and *N*-nitrosodi-isopropylamine do not. The conformations of these oximes are discussed in conjunction with the n.m.r. data.

INTRODUCTION

In spite of the stability of neutral *N*-nitrosodialkylamine solutions toward irradiation, these nitrosamines readily undergo photo-decomposition if an acid is present (1). Previous work (1) has shown that such photolysis resulted in rearrangement of the nitrosamines to amidoximes or elimination to give Schiff bases. Though the nature of this photo-decomposition is yet to be elucidated, the behavior of the nitrosamines under an influence of an acid and irradiation is sufficiently intriguing to warrant further scrutiny. In the following we report a novel photo-addition of nitrosamines across a carbon–carbon double bond. Cyclohexene was chosen as the model olefin to demonstrate the photo-addition of various nitrosamines.

RESULTS AND DISCUSSION

The irradiation of *N*-nitrosopiperidine (IA) in methanol containing at least 1 mole equivalent of hydrochloric acid was shown to give a similar result to that in the aqueous hydrochloric acid solution, 2-piperidonoxime and isotripiperidein being the products (1). When the photo-reaction was carried out in a presence of 1 mole equivalent or more of cyclohexene, none of these compounds was detected but instead an excellent yield of 1:1 adduct of the nitrosamine to cyclohexene was isolated. The addition did not take place in the absence of either irradiation or the acid catalysts demonstrating the requirement for both. The adduct is basic and conveniently isolated as the corresponding hydrochloride merely by triturating the residue with cold acetone. Alternatively, the nicely crystalline 1:1 adduct precipitated out on neutralization and was readily purified by recrystallization. The assignment of 2-piperidinocyclohexanone oxime (IIA) to the 1:1 adduct follows from the fact that thermal decomposition gave piperidine and Δ^2-cyclohexenone oxime. Further the adduct was found to be identical (infrared spectra and mixed melting point) with 2-piperidinocyclohexanone oxime synthesized according to the published method (2). Regardless of the mode of preparation only one oxime was obtained. Of the two possible geometric isomers, the *syn* configuration was considered to be more stable due to the probable intramolecular hydrogen bond formation and, therefore, structure III was assigned to the single adduct obtained. It should be mentioned that the crude basic fraction contained a small amount of 2-piperidinocyclohexanone as an impurity as indicated by the weak infrared peak at 1 710 cm^{-1}. Without attempting to isolate the cyclohexanone derivative, the crude basic fraction was oximated to give IIA as the only isolable product. The substituted cyclohexanone was probably formed by the hydrolysis of the oxime IIA during the working up.

Can. J. Chem. Downloaded from www.nrcresearchpress.com by 210.87.254.6 on 09/05/12
For personal use only.

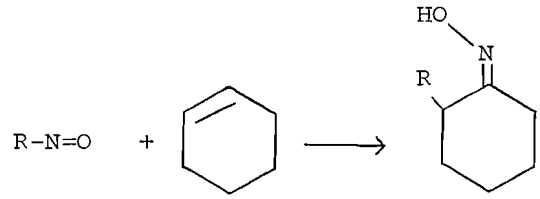

I II

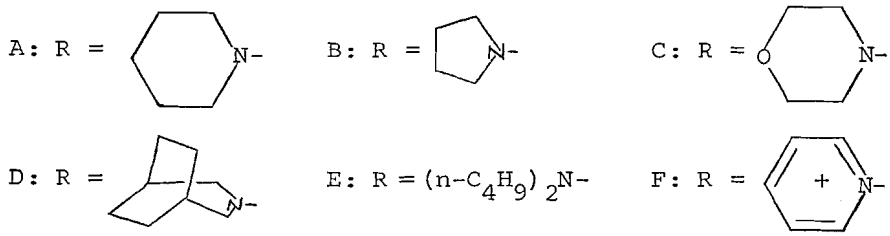

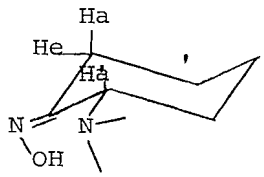

III

The net result of the photo-addition is represented by the addition of a molecule of *N*-nitrosopiperidine as nitroso and piperidino residues across the carbon–carbon double bond. Encouraged by the high yield as well as the simplicity of the photo-addition, several other nitrosamines were subjected to the same photo-addition conditions using cyclohexene as the model olefin in order to examine the scope of the reaction. *N*-Nitrosopyrrolidine (IB) and *N*-nitrosomorpholine (IC) underwent the addition smoothly to give the expected 1:1 photo-adducts, 2-pyrrolidino- and 2-morpholinocyclohexanone oximes (IIB and IIC), in total yield of 82 and 81% respectively. In both cases the presence of small amounts of the corresponding substituted cyclohexanones were detectable spectroscopically (1 710 cm^{-1}). The photo-addition of *N*-nitroso-3-azabicyclo[3,2,2]nonane (ID) to cyclohexene proceeded as expected giving the crystalline hydrochloride (39%) of IID, *N*-(2-oximinocyclohexyl)-3-azabicyclo[3,2,2]nonane, and the corresponding ketone of IID (46%). The ketone was oximated to IID directly. The facile hydrolysis of IID to the ketone was probably due to the steric acceleration associated with bulkiness of the amine group and will be a useful tool if an α-aminoketone is the desired product.

Under similar conditions *N*-nitrosodi-*n*-butylamine (IE) gave the unstable liquid adduct IIE, 2-di-*n*-butylaminocyclohexanone oxime, in only 38% yield and it did not yield a crystalline salt with perchloric, hydrochloric or picric acid. The balance of the starting nitrosamine was transformed to di-*n*-butylamine. On storage IIE decomposed rapidly to a tar but the infrared and n.m.r. spectra of the freshly distilled IIE possessed the absorptions required for the assigned structure. *N*-Nitrosodicyclohexylamine and *N*-nitrosodiisopropylamine did not give the expected adduct under the photolytic conditions. In the former case dicyclohexylamine was the major product and cyclohexylamine, cyclohexanone, and its oxime were the minor products identified in the photolysate. In these

Can. J. Chem. Downloaded from www.nrcresearchpress.com by 210.87.254.6 on 09/05/12
For personal use only.

photolytic reactions the disappearance of the nitroso absorption at 350–360 mμ proceeded much faster than that of the nitrosamine derived from the heterocyclic amines (IA–ID). This observation suggested that another photolytic pathway independent of the photo-addition was operating leading to the different results. Control experiments showed that these acyclic nitrosamines are stable under the conditions without irradiation. Simple hydrolysis is, therefore, not the pathway responsible for the formation of the parent dialkylamines. An investigation is underway presently to locate the end product derived from the nitroso residue of the nitrosamines which should provide a clue to this question.

It is interesting to point out that only those nitrosamines having methylene groups flanking the amino nitrogen undergo photo-addition while those with methine groups do not. Coincident with this observation, it has been shown that the former group of nitrosamines undergo the photo-rearrangement to give amidoximes while the latter undergo the photo-elimination to Schiff bases (1). The course of photo-addition of *N*-nitrosopiperidine is not altered by the presence of air and, therefore, a free radical mechanism is not likely. It is felt that proposal of a mechanism for the photo-addition should not be made until more data are available. The mild conditions required, the simplicity of the reaction, and the excellent yield obtained from heterocyclic nitrosamines all favor application of the photo-addition as a potential tool in the syntheses of α-aminoketoximes.

Discussion of N.m.r. Data

In connection with the conformation of these oximes (II) the spectral data merit a brief discussion. In the infrared region the usual absorptions as expected for an oxime are all present except that each of these oximes shows a complex pattern of several strong absorption peaks in 900 – 1 000 cm^{-1} (3). The bulky α-amino group in II is expected to occupy the equatorial position forcing the oximes to assume the conformation as shown in III. Partial overlap of some of the n.m.r. signals, however, hampered a complete analysis of these spectra. The n.m.r. data of II together with that of 2-pyridiniumcyclohexanone oxime chloride (IIF) are summarized in Table I. All of these oximes show one proton

TABLE I*

Chemical shifts and coupling constants of α-amino oximes

α-Amino oximes		τ for OH	H_e		H_a'		τ for H_a
No.	Amino group		τ	J_{ea} (c.p.s.)	τ	$w_{1/2}$ (c.p.s.)	
IIA	Piperidino	0.5	6.88, 7.11	13	7.28	10	
		0.6	6.97, 7.08	11	7.26	8	~8.10†§
IIA	Piperidino (hydrochloride)	—	6.75, 6.90	15	6.05	‖	~8.00‡§
IIB	Pyrrolidino	0.75	6.82, 7.05	13	7.25	8	
IIC	Morpholino	0.65	6.83, 7.06	13	7.22	7.5	7.95§
IID	3-Azabicyclo[3,2,2]nonano	1.06	6.74, 6.94	13	7.19	7	
IIE	Di-*n*-butylamino	0.5	6.85	—	—	—	
IIF	Pyridinium (chloride)	—	6.47, 6.70	13	4.41	‖	7.57‡¶

*The spectra were recorded in $CDCl_3$ solution with an internal TMS standard with a Varian A 60 spectrometer, unless specifie d otherwise.
†In CCl_4 solution.
‡In D_2O solution.
§The data obtained from decoupling experiment with Varian HR 100 spectrometer.
‖J_{aa} = 10 c.p.s. and J_{ae} = 4.5 c.p.s.
¶The width at half height is 23 c.p.s.

doublet centered at τ6.8 with a coupling constant of 12–13 c.p.s. Each doublet is further split to a poorly resolved triplet. Decoupling experiments with a Varian HR 100 spectrometer indicated that this proton is coupled to a proton at τ ca. 8.00, part of which is

Can. J. Chem. Downloaded from www.nrcresearchpress.com by 210.87.254.6 on 09/05/12
For personal use only.

submerged under the intense signal due to the other methylene protons. The former is, therefore, assigned to H_e and the latter to H_a in agreement with the large geminal coupling constant and the generally accepted fact that axial protons resonate at higher field than equatorial protons (4). The large chemical shift difference (ca. 1 p.p.m.) between H_e and H_a has its precedence in heterocyclic amines (5). The signal of H_a' appears at or around τ7.2 (except that of IIF) with the width at the half height ($w_{1/2}$) 7–8 c.p.s., which is too narrow for an axial proton signal. It is suggested that C—N bond may have been bent down in order to make intramolecular hydrogen bonding possible and thus to slightly flatten the conformation at this carbon center. Under these circumstances, the coupling pattern of H_a' may depart considerably from the axial character. Pertinent to this assignment is the fact that in the spectrum of IIA hydrochloride (in D_2O) H_a' is now shifted downfield and appears at τ6.05 while the double triplet of H_e remains at τ6.83 which is coupled with H_a at τ8.00. In compound IIF the proton H_a' appears further downfield at τ4.40 as a double doublet (J_{ae} = 4.5 and J_{aa} = 10 c.p.s.) in agreement with the pyridinium ring attached at the same carbon atom.

EXPERIMENTAL

The infrared spectra were recorded in Nujol mull with a Perkin-Elmer model 421 spectrophotometer. All melting points were uncorrected. The analyses were performed by the Microanalytical Laboratory of this Department.

N-Nitrosamines

The nitrosamines were prepared by nitrosation of the respective amines with sodium nitrite in aqueous hydrochloric acid solution. The boiling points are: *N*-nitrosopiperidine (6), 109° at 24 mm; *N*-nitrosopyrrolidine (7), 99–100° at 15 mm; *N*-nitrosodi-*n*-butylamine (8), 112–114° at 13 mm; *N*-nitrosomorpholine (9), 110° at 14 mm. The melting points are: *N*-nitrosodicyclohexylamine (10), 102–104°, and *N*-nitrosodiisopropylamine (11), 42–44°.

N-Nitroso-3-azabicyclo[3,2,2]nonane, prepared by the nitrosation of the parent amine, was recrystallized from methanol–water but turned to a sticky cake on filtration. The analytical sample was prepared by sublimation and has infrared peaks at 3 010, 1 425, 1 340, 1 140, and 912 cm^{-1} and n.m.r. signals at τ5.56 (2H, doublet) and 6.10 (2H, doublet).

Anal. Calcd. for $C_8H_{14}N_2O$: C, 62.30; H, 9.08; N, 18.17. Found: C, 62.38; H, 8.83; N, 18.37.

General Procedure of Photo-addition

In a pyrex photolysis vessel a nitrosamine (0.05 moles), 1 mole equivalent or more of cyclohexene, 1–2 mole equivalents of concentrated hydrochloric acid, and methanol (ca. 300 ml) were placed. The photolysis vessel was cooled with tap water and externally with an ice bath. The solution was agitated with a magnetic stirrer and a slow stream of nitrogen. A Hannovia ultraviolet lamp (type 54A36) situated at the center sleeve was used as the light source. The photolysis was continued until the absorption at 340–360 mμ region disappeared completely. The solvent was evaporated under vacuum. Generally, the hydrochloride of the adduct crystallized on triturating the residue with acetone or isopropanol and was recrystallized from isopropanol. The combined mother liquor was evaporated and the residue was taken up in water. Neutralization with sodium carbonate solution gave the basic fraction which was either ether extracted or filtered. The photo-adduct was then recrystallized or distilled. Each photo-addition was backed with a control experiment. A small portion of the above photolysis solution was kept in a dark icebox. The ultraviolet absorption spectrum was not changed at all over the entire period of photolysis.

Addition of N-Nitrosopiperidine

The nitroso compound (10.5 g) and cyclohexene (50 ml) were photolyzed according to the procedure as described. The residue obtained after evaporation of the solvent was treated with cold acetone to give the hydrochloride (11 g) of 2-piperidinocyclohexanone oxime (IIA). This was recrystallized from isopropanol to give white crystals, m.p. 203–205° (decomposition) and infrared peaks at 3 160, 2 620, 2 550, 1 662 (weak), 1 490, and 1 000 – 900 cm^{-1} (complex).

Anal. Calcd. for $C_{11}H_{21}N_2OCl$: C, 56.76; H, 9.09; N, 12.04; Cl, 15.23. Found: C, 56.73; H, 8.88; N, 12.33; Cl, 15.18.

The combined mother liquor was vacuum evaporated followed by the usual working up to furnish a basic fraction (7.4 g), the infrared spectrum of which showed the carbonyl peak at 1 710 cm^{-1}. The partially crystalline residue was purified by recrystallization from methanol–water and sublimation to give IIA, m.p. 118–120°. Alternatively IIA was synthesized from 2-pyridinium cyclohexanone oxime chloride (IIE)

Can. J. Chem. Downloaded from www.nrcresearchpress.com by 210.87.254.6 on 09/05/12
For personal use only.

according to Birch's method (2). The mixed m.p. of two substance was 118–120°. This substance shows the infrared peaks at 3 240, 2 810, 2 790, 1 665 (weak), 1 490, 890–990 (complex), and 780 cm^{-1}.

Anal. Calcd. for $C_{11}H_{20}N_2O$: C, 67.30; H, 10.27; N, 14.27. Found: C, 67.31; H, 10.24; N, 13.96.

The methanol–water mother liquor obtained from these recrystallizations contained IIA and the corresponding cyclohexanone derivative as shown by the medium intensity carbonyl peak at 1 710 cm^{-1}. Treatment of this mother liquor with hydroxylamine hydrochloride and sodium acetate gave a solid product in which the 1 710 cm^{-1} absorption was no longer present. Recrystallizations from methanol–water gave IIA as the only isolatable product, m.p. 118–120°.

An attempt to distill the partially crystalline residue lead to an extensive decomposition. Distillation of the decomposed products under atmospheric pressure gave piperidine identified as the hydrochloride by the superimposable infrared spectra. Further distillation under vacuum (12 mm) gave a fraction which crystallized and was recrystallized to give Δ^2-cyclohexenone oxime, m.p. and mixed m.p. with an authentic sample prepared from Δ^2-cyclohexenone 87–88°, reported m.p. 89–90° (12).

The photo-addition in the presence of only 20% excess of cyclohexene also gave IIA (36%) and the hydrochloride of IIA (42%). When the photo-addition was carried out under air bubble agitation instead of nitrogen, a yellowish solution was obtained. On working up in the usual manner it gave the hydrochloride (25%) of IIA and a basic fraction which contained mostly IIA and a minor amount of unidentified impurities. Either in the absence of hydrochloric acid or in dark, the intensity of the nitroso peak at 248 mμ did not decrease.

Addition of N-Nitrosopyrrolidine

The nitroso compound (5 g) and cyclohexene (15 ml) were photolyzed as described above. The free base IIB (7.5 g) crystallized immediately upon neutralization and was recrystallized from methanol–water to give white crystals, m.p. 123° and infrared peaks at 3 170, 3 050, 1 650 (weak), 1 490, and 1 000 – 900 (complex) cm^{-1}.

Anal. Calcd. for $C_{10}H_{18}N_2O$: C, 65.89; H, 9.96; N, 15.37. Found: C, 65.80; H, 9.73; N, 15.12.

Addition of N-Nitrosomorpholine

The nitroso compound (8.55 g) and cyclohexene (25 ml) were photolyzed as described above. Following the usual working up procedure, the hydrochloride (5.7 g) of 2-morpholinocyclohexanone oxime IIC and a basic fraction (6.9 g) were obtained. The basic fraction is partially crystalline and the oil and crystals had very similar infrared spectra. Recrystallization of this fraction from benzene – Skellysolve B and sublimation gave IIC, m.p. 113–114°, reported m.p. 118° (2). The same crystals were also obtained when the above hydrochloride was neutrallized with sodium carbonate in aqueous solution and the collected solid sublimed. This has infrared peaks at 3 300, 3 100, 1 650 (weak), 1 490, 1 115, 1 000 – 900 (complex), and 785 cm^{-1}. The n.m.r. spectrum of IIC shows, besides the signals listed in Table I, a triplet at τ6.27 (4H, J = 4.5) due to —CH_2—O—CH_2— protons and a multiplet centered at τ7.50 (4H) due to —CH_2—N—CH_2— protons.

Anal. Calcd. for $C_{10}H_{18}N_2O_2$: C, 60.58; H, 9.15; N, 14.13. Found: C, 60.39; H, 9.23; N, 14.21.

Addition of N-Nitroso-3-azabicyclo[3,2,2]nonane

The nitroso compound (3 g) and cyclohexene (25 ml) were photolyzed as described above. The residue obtained after evaporation of the solvent was treated with cold acetone to give white crystals (2 g) which were recrystallized from isopropanol to give the hydrochloride of *N*-(2-oximinocyclohexyl)-3-azabicyclo[3,2,2]-nonane IID, m.p. 183–185°, infrared peaks at 3 160, 3 085, 2 635, 2 600, 1 660 (weak), 1 485, 900 – 1 000 (complex), and 745 cm^{-1}.

Anal. Calcd. for $C_{14}H_{25}N_2OCl$: N, 10.27. Found: N, 10.13.

A part of the hydrochloride was taken up in water and neutralized to give the free base. Recrystallization of the solid precipitate from Skellysolve B and sublimation gave IID, m.p. 148–151° and infrared peaks at 3 120, 3 070, 2 780, 2 800, 1 180, 940 and 910 cm^{-1}.

Anal. Calcd. for $C_{14}H_{24}N_2O$: C, 71.14; H, 10.24; N, 11.85. Found: C, 71.09; H, 9.93; N, 11.89.

The acetone mother liquor was evaporated and the residue was taken up in water. The aqueous solution was neutralized with sodium carbonate and the precipitate was ether extracted to give the basic fraction. The infrared spectrum of this showed strong absorption at 1 710 cm^{-1} and weak peaks belonging to a small amount of the oxime IID. This fraction was oximated with hydroxylamine hydrochloride and potassium carbonate in methanol–water and purified to give IID exclusively as identified by mixed m.p. 147–150° and by superimposable infrared spectra.

Addition of N-Nitroso-di-n-butylamine

The nitroso compound (8.5 g) and cyclohexene (25 ml) was photolyzed as described and the solvent was vacuum distilled. Trituration of the residue with cold acetone gave a precipitate (3.4 g) which was recrystallized from isopropanol to give di-*n*-butylamine hydrochloride having an infrared spectrum superimposable with that of an authentic sample.

The acetone mother liquor was worked up in the usual manner to give a basic fraction (11.2 g). Distillation of this fraction gave di-*n*-butylamine as the forerun and II as the major fraction, b.p. 100–102° at 0.2 mm (7.6 g). This fraction decomposed gradually changing to a black tar and did not give a satisfactory analysis in

Can. J. Chem. Downloaded from www.nrcresearchpress.com by 210.87.254.6 on 09/05/12
For personal use only.

spite of repeated distillation. Freshly distilled sample of IIE was a faintly yellowish liquid showing infrared peaks at 3 200, 1 640 (medium), 1 180, 945 and 910 cm^{-1}.

Attempted Photo-addition of N-Nitrosodicyclohexylamine

The nitroso compound (3 g) and cyclohexene (25 ml) were photolyzed in ethanol (300 ml) containing concentrated hydrochloric acid (5 ml) under a similar condition as described. The photolysate was vacuum evaporated and the residue was triturated with water to give a precipitate (1.4 g). This precipitate was recrystallized from water to give dicyclohexylamine hydrochloride as shown by the superimposable infrared spectrum.

The aqueous solution was neutrallized with sodium carbonate solution and ether extracted to give a fraction (1.08 g). A portion of this was treated with Brady's reagent to give cyclohexanone 2,4-dinitrophenylhydrazone, m.p. and mixed m.p. 155–158°. The remainder was distilled under atmospheric pressure at a bath temperature 130–140°. This distillate contained cyclohexylamine as identified by a comparison of the infrared spectrum of its hydrochloride with that of an authentic sample. The residue was vacuum distilled at 10 mm. The crystalline distillate was recrystallized from water and sublimed to give cyclohexanone oxime, m.p. and mixed m.p. 85–87°.

Attempted Photo-addition of N-Nitrosodiisopropylamine

The nitroso compound (5.3 g) and cyclohexene (20 ml) were photolyzed as described above. The residue obtained after evaporation of solvent was triturated with cold acetone to give a white precipitate (3 g) which was identified as diisopropylamine hydrochloride. The aqueous mother liquor was neutralized with sodium carbonate followed by the usual work-up to furnish a basic fraction (850 mg). The infrared spectrum of this indicates that the fraction contains diisopropylamine as the major component but no cyclohexanone oxime.

ACKNOWLEDGMENT

The author is much indebted to Messrs. R. Swindlehurst and G. Bigam for recording spectra and Miss D. Roberts for performing analyses. It is a pleasure to acknowledge partial financial support by the National Research Council on this project.

REFERENCES

1. Y. L. CHOW. Tetrahedron Letters, 2333 (1964). E. M. BURGESS and E. M. LAVANISH. Tetrahedron Letters, 1221 (1964).
2. A. J. BIRCH. J. Chem. Soc. 314 (1944).
3. A. PALM and H. WERBIN. Can. J. Chem. **31**, 1004 (1953).
4. L. M. JACKMAN. Application of nuclear magnetic spectroscopy in organic chemistry. Pergamon Press, London. 1959. p. 115.
5. H. P. HAMLOW, S. OKUDA, and N. NAKAGAWA. Tetrahedron Letters, 2553 (1964).
6. F. B. AHRENS. Chem. Ber. **30**, 533 (1897).
7. F. C. PETERSEN. Chem. Ber. **21**, 290 (1888).
8. V. MEYER, J. BARBIERI, and FR. FORTER. Chem. Ber. **10**, 130 (1877).
9. L. KNORR. Ann. **301**, 1 (1898).
10. J. K. WOLFE and K. L. TEMPLE. J. Am. Chem. Soc. **70**, 1414 (1948).
11. J. BEWAD. Chem. Ber. **40**, 3065 (1907).
12. P. D. BARTLET and G. F. WOODS. J. Am. Chem. Soc. **62**, 2933 (1940).

Can. J. Chem. Downloaded from www.nrcresearchpress.com by 210.87.254.6 on 09/05/12
For personal use only.

Can. J. Chem. Downloaded from www.nrcresearchpress.com by 210.87.254.5 on 09/05/12
For personal use only.

STUDIES IN THE PYRROLINE SERIES

V.[1] 3,3-DIMETHYL-1-PYRROLINE-1-OXIDE

R. BONNETT, S. C. HO, AND J. A. RALEIGH
The Chemistry Department, University of British Columbia, Vancouver, British Columbia

Received March 8, 1965

ABSTRACT

The pyrolysis of 1-ethyl-3,3-dimethylpyrrolidine-1-oxide gives 1-hydroxy-3,3-dimethylpyrrolidine, which, on dehydrogenation, yields 3,3-dimethyl-1-pyrroline-1-oxide. The identification of the nitrone is described. The cyclo-additions of styrene to this nitrone and to 5,5-dimethyl-1-pyrroline-1-oxide were investigated, and the direction of addition was deduced from the n.m.r. spectra of the adducts.

In connection with other work (1) it was desired to prepare pyrroline ring systems with geminal substitution at a β-position, and to this end attempts were made to synthesize one or more of the dimethyl compounds I–IV.

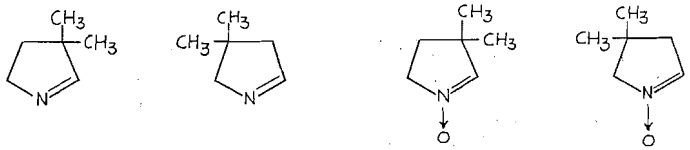

I II III IV

Three approaches were tried. The first followed the nitroalkane synthesis (2) and involved the attempted conjugate addition of nitromethane to senecialdehyde, this being the first step on the route to II and IV. Under a variety of reaction conditions, no absorption due to an unconjugated carbonyl group was found in the infrared spectrum of the product, and it was concluded that 1,4-addition had not occurred to an appreciable extent. This result is presumably due to the steric effect of the substituents at the β-position of the unsaturated aldehyde, and it is pertinent that, whereas nitromethane adds readily across the conjugated system of acrolein (3), in the reaction of crotonaldehyde with nitromethane, conjugate addition is not the main path.

The second approach, which suffered from the disadvantage that it would be expected to yield a mixture of isomers III and IV, was the direct oxidation of the corresponding secondary amine to the cyclic hydroxylamine (ref. 4, cf. 5) followed by dehydrogenation to the nitrone.

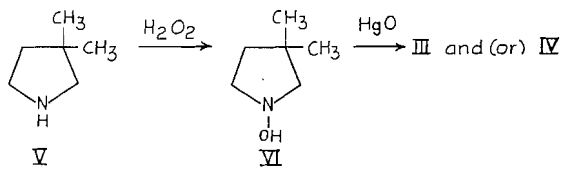

V VI

As others have recently reported (6, 7), some difficulty was experienced with the direct oxidation with hydrogen peroxide, a step which gave erratic and low yields. The best yield

[1]*For Part IV see R. Bonnett. J. Chem. Soc. 2313 (1965).*

of solid 1-hydroxypyrrolidine (from pyrrolidine itself in preliminary experiments) was 8%; and from 3,3-dimethylpyrrolidine the corresponding hydroxylamine could not be isolated, although a trace of the nitrone (III) was obtained.

The third approach did prove successful as a preparative method. 1-Ethyl-3,3-dimethylpyrrolidine (VII) (from the corresponding imide) was converted into the amine oxide (VIII). This, on pyrolysis, eliminated 1-hydroxy-3,3-dimethylpyrrolidine (VI) (cf. ref. 7), which was characterized as the hydrogen oxalate. Oxidation of the cyclic hydroxylamine with yellow mercuric oxide in chloroform or dichloromethane yielded a hygroscopic oil, b.p. 74–76° at 0.55 mm, which solidified on cooling and which was identified as 3,3-dimethyl-1-pyrroline-1-oxide on the basis of the following evidence.

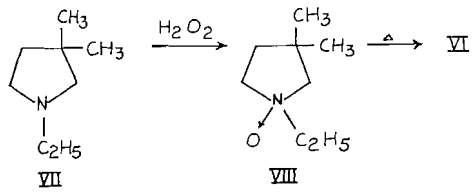

VII VIII

The product gave, not unexpectedly in view of its hygroscopic nature, rather poor analytical values itself, but these figures, and those for the picrate, indicated the molecular formula $C_6H_{11}NO$. Repeated fractionation of the picrate and its mother liquors did not furnish a second derivative. Reduction and hydrogenolysis of the product with lithium aluminium hydride/aluminium chloride gave 3,3-dimethyl pyrrolidine, which indicated that the ring system had remained intact. Both the infrared and ultraviolet spectra of the product were in accord with the nitrone formulation. In the infrared region a strong absorption at 1 580 cm^{-1} was assigned to the —CH=N → O system: 5,5-dimethyl-1-pyrroline-1-oxide shows a similar band at 1 573 cm^{-1} (8). The ultraviolet spectrum had λ_{max} 235 mμ (log ϵ 3.92) in ethanol and λ_{max} 248 mμ (log ϵ 3.98) in hexane. For comparison, 5,5-dimethyl-1-pyrroline-1-oxide has λ_{max} 234 mμ (log ϵ 3.89) in ethanol (8) and λ_{max} 247 mμ (log ϵ 3.94) in hexane. Ultraviolet irradiation produced a considerable decrease in absorption in all cases, presumably as a result of oxaziran formation (9). These results indicated that the base probably had structure III or IV, or could possibly be a mixture of the two. The double bond was located by a combination of chemical and physical methods. Reaction of the base with methyl magnesium iodide, followed by dehydrogenation of the product, furnished a trimethyl-1-pyrroline-1-oxide which (i) had the spectral characteristics of a ketonitrone rather than an aldonitrone (infrared band at ~1 610 cm^{-1} and not at ~1 580 cm^{-1}), (ii) appeared to be a single substance, and (iii) was not identical with 2,4,4-trimethyl-1-pyrroline-1-oxide. Hence it is formulated as IX. Furthermore, reaction of the original dimethyl nitrone with phenyl magnesium bromide, followed by dehydrogenation of the product (X), gave the phenyl nitrone (XI), which, when subjected to the oxygen transfer reaction (10) with triphenylphosphine, gave a volatile base that proved to be identical with an authentic sample (11) of 3,3-dimethyl-2-phenyl-1-pyrroline (XII). Alternatively, the hydroxylamine (X) could be directly converted into the pyrroline (XII) by melting it with potassium hydrogen sulfate. It may be noted that the ultraviolet spectrum of XI shows absorption at somewhat lower wavelength and intensity than that of 2-phenyl-1-pyrroline-1-oxide (12). This is attributed to a certain degree of steric inhibition of conjugation analogous to that which has been observed with a series of phenyl ketones (13).

Can. J. Chem. Downloaded from www.nrcresearchpress.com by 210.87.254.5 on 09/05/12
For personal use only.

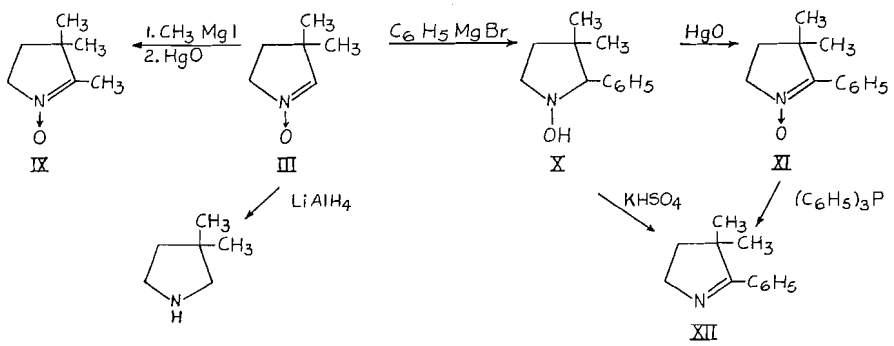

These chemical sequences suggest that the dimethyl nitrone has structure (III), and the proton magnetic resonance spectrum of the base supports this conclusion (1). The absence of the other isomer (IV), in which dehydrogenation has occurred on the least hindered side, is noteworthy. To detect small quantities of this isomer in the product, the sequence (III) → (IX) → trimethylpyrroline was followed, purification at the intermediate and final stages being deliberately avoided. The trimethylpyrroline resulting from this process was examined by vapor phase chromatography, and was shown to consist mainly of a base which had a retention volume different from that of 2,4,4-trimethyl-1-pyrroline, and which was characterized as 2,3,3-trimethyl-1-pyrroline. A small peak which had approximately the same retention volume as 2,4,4-trimethyl-1-pyrroline was indeed present, but amounted to less than 3% of the area of the main peak. It thus appears that dehydrogenation occurs predominantly on the more hindered side of the cyclic hydroxylamine. Two possible interpretations of this result have been considered. Firstly, it is apparent that the nitrone (IV) can undergo self-condensation of the aldol type, whereas III cannot. Hence it might be supposed that both isomers are formed extensively, but that IV is not isolated because it polymerizes. However, it is to be noted that the parent nitrone in this series, 1-pyrroline-1-oxide itself, has been prepared in good yield by this route (7). The second involves the steric effect of the *gem*-dimethyl group, an effect already manifested in certain of the ultraviolet spectra. On the basis of the analogy to the dehydrogenation of N,N-disubstituted hydrazines (14) it is likely that the oxygen function is involved in the initial stages of the reaction: although the process may be further complicated by conformational considerations it would appear reasonable that subsequent reaction proceeds in that direction which will relieve most effectively the non-bonded interactions of C-methyl and C—H bonds, leading to structure III in preference to IV.

The 1-pyrroline-1-oxides are known to undergo cyclo-addition reactions with suitably substituted olefins (15), the adducts possessing the novel 2-oxa-1-azabicyclo[3.3.0]octane ring system (XIII).

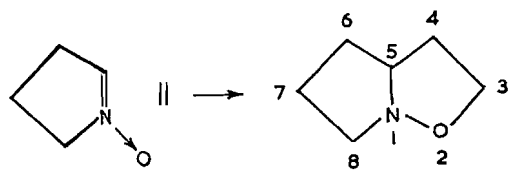

XIII

Can. J. Chem. Downloaded from www.nrcresearchpress.com by 210.87.254.5 on 09/05/12
For personal use only.

Thus, for the addition of ethyl acrylate to 5,5-dimethyl-1-pyrroline-1-oxide, evidence has been presented (16) which suggests that the adduct of structure XIV is rapidly formed but that the isomer XV is thermodynamically more stable.

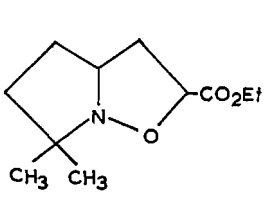

XIV

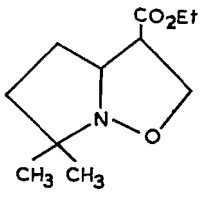

XV

It was of interest to determine whether the nitrone prepared in the present work was subject to this type of addition. Although the yields were only moderate in some instances the cyclo-addition reaction was shown to proceed satisfactorily at temperatures below 100°. The addition of styrene gave a colorless oil which could be satisfactorily purified by distillation under low pressure and which formed a picrate. The infrared and ultraviolet spectra of the adduct were in accord with the bicyclic structure (XVI). A decision between the positional isomers XVI*a* and XVI*b* could be made on the basis of the proton magnetic resonance spectrum, since in XVI*a* the proton at C3 is subject to two deshielding influences and would be expected to be brought into resonance at relatively low field (cf. $PhCH_2OH$ at 5.6 τ (17)), whereas in the isomer there is no similar compounding of deshielding effects. The spectrum of the base did, in fact, show a signal corresponding to one proton at 5.04 τ, and this was assigned to the proton at C3 in structure XVI*a*.

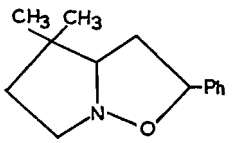

XVIa

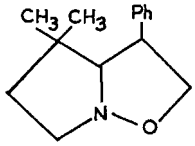

XVIb

Since this signal took the form of a triplet, the coupling constants between the C3 proton and the protons at C4 would appear to be fortuitously similar or to be subject to an averaging process (cf. the triplet assigned to the anomeric hydrogen in thymidine (18): the positions of the other signals supported structure XVI*a*, as did the ratios of their areas. That the steric effect of the *gem*-dimethyl group was not primarily responsible for the direction of addition observed to predominate was shown by examining the adduct of styrene and 5,5-dimethyl-1-pyrroline-1-oxide. Again the proton magnetic resonance spectrum showed a signal in the 5 τ region, and it was concluded that addition had occurred in the same sense as in the previous example. The same orientation has been observed in the addition of styrene to benzylidene aniline N-oxide (19).

When it arises the question of configuration at C3 (or C4) has not been settled for any of the 2-oxa-1-azabicyclo[3.3.0]octanes made in this way. Thus in the present examples the two possibilities are indicated in structures XVI*c* and XVI*d*, each being a racemate. The analogous problem in the Diels–Alder reaction has sustained a good deal of attention, and since the *cis* mode of addition has been demonstrated for several examples of 1,3-dipolar addition (19) it remains of particular interest to determine to what extent, if any, considerations analogous to the "rule" of endo-addition (leading to XVI*d*) also apply.

Can. J. Chem. Downloaded from www.nrcresearchpress.com by 210.87.254.5 on 09/05/12
For personal use only.

XVIc

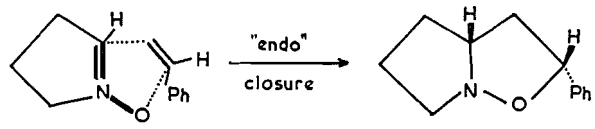

XVId

It is pertinent that electron-accommodating substituents at the alkene linkage are not strictly necessary for nitrone addition to proceed in satisfactory yield (15, 19, 20) and that the 1,3-dipolar group, being smaller in extent than the 1,3-diene system, will be less likely to interact directly with such a substituent in the transition state.

EXPERIMENTAL

The following equipment was used. Melting points: Fisher-Johns heated block. Infrared spectra: Perkin–Elmer Infracord or Model 21. Vapor phase chromatography: Aerograph model A-100-C. Proton magnetic resonance spectra: Varian A60; dilute solutions in carbon tetrachloride: tetramethylsilane internal reference. Analyses by Dr. A. Bernhardt, Mulheim.

1-Ethyl-3,3-dimethylpyrrolidine (VII)

$\alpha\alpha$-Dimethylsuccinic acid (257 g) (21) was treated with aqueous ethylamine (50%; 450 ml) and gradually heated to 200° under a short air condenser. After 15 min at this temperature the product, 1-ethyl-3,3-dimethylsuccinimide, was distilled as a colorless liquid, (207 g, 76%), b.p. 110° at 24 mm, η_D^{20} 1.4605.

Found: C, 61.5; H, 8.0; N, 9.4. $C_8H_{13}NO_2$ requires C, 61.9; H, 8.4; N, 9.0.

The imide was reduced in tetrahydrofuran with lithium aluminium hydride in the normal way (21) to give 1-ethyl-3,3-dimethylpyrrolidine (65%) b.p. 127° at 746 mm as a colorless liquid, η_D^{20} 1.4280. Infrared maxima (film) at 2 778, 1 372, and 1 359 cm^{-1}.

Picrate from ethanol, m.p. 165°. Found: C, 47.6; H, 5.7; N, 15.8. $C_{14}H_{20}N_4O_7$ requires C, 47.2; H, 5.7; N, 15.7.

1-Hydroxy-3,3-dimethylpyrrolidine (VI)

1-Ethyl-3,3-dimethylpyrrolidine (63.2 g) was carefully added, with stirring, to hydrogen peroxide (30%; 295 g) cooled in ice so that the internal temperature did not exceed 60°. The mixture was stirred for 24 h. A pinch of platinum black was added and the mixture stirred at room temperature for a further 24 h. Any unchanged amine was extracted with ether, and the resulting aqueous solution was concentrated to an oily liquid, the last traces of water being removed by codistillation with benzene. The picrate, m.p. 135°, of 1-ethyl-3,3-dimethylpyrrolidine-1-oxide was prepared in water and recrystallized from ethanol.

Found: C, 45.1; H, 5.3; N, 15.2. $C_{14}H_{20}N_4O_8$ requires C, 45.15; H, 5.4; N, 15.05.

The amine oxide was pyrolyzed in small portions (7) in an oil bath at 145° and at a pressure of approximately 10 mm. Under these conditions 1-hydroxy-3,3-dimethylpyrrolidine slowly distilled as a pale yellow liquid with an apparent b.p. of 71–74° and in an overall yield of 34–45% based on the tertiary amine. The infrared absorption spectrum (film) showed no band at 2 770 cm^{-1}, a very weak peak at 1 582 cm^{-1}, and a strong band at 3 226 cm^{-1}. The hydrogen oxalate, m.p. 125°, was prepared in acetone and recrystallized from methanol–water.

Found: C, 47.05; H, 7.2; N, 7.1. $C_8H_{15}NO_5$ requires C, 46.8; H, 7.4; N, 6.8.

3,3-Dimethyl-1-pyrroline-1-oxide (III)

The hydroxylamine (3.6 g) in anhydrous chloroform (85 ml) was treated with yellow mercuric oxide (13.5 g) and shaken for 2 h. Another portion of mercuric oxide (3.5 g) was then added, and, after 2 more hours of shaking, the grey-green mixture was filtered (Celite) and the pad washed with a little chloroform. The solvent was removed, and the residual oil was kept in the dark over phosphorus pentoxide for 72 h.

Can. J. Chem. Downloaded from www.nrcresearchpress.com by 210.87.254.5 on 09/05/12
For personal use only.

Distillation gave 3,3-dimethyl-1-pyrroline-1-oxide (2.2 g, 62%) as a hygroscopic oil, b.p. 74–76° at 0.55 mm. It solidified, on cooling, to a mass of long needles, m.p. ca. 25°, and was stored at −20°.

Found: C, 62.5; H, 9.4; N, 12.1. $C_6H_{11}NO$ requires C, 63.7; H, 9.8; N, 12.4.

The picrate, m.p. 105° from ethanol. Found: C, 42.2; H, 4.35; N, 16.4. $C_{12}H_{14}N_4O_8$ requires C, 42.1; H, 4.1; N, 16.4.

The infrared spectrum of the nitrone (film) showed peaks at 3 460 (broad) and 1 580 cm^{-1} (strong). The ultraviolet spectrum: in hexane λ_{max} 248 mμ (log ϵ 3.98); in ethanol λ_{max} 235 mμ (log ϵ 3.93). On continued irradiation with ultraviolet light these absorbancies fell sharply.

Methylation Experiments

3,3-Dimethyl-1-pyrroline-1-oxide (1.29 g) in dry ether (15 ml) was added to methyl magnesium iodide (from 0.35 g magnesium) in 25 ml dry ether and then heated under reflux for 1 h. After decomposition with aqueous ammonium chloride, the product was isolated in ether. The ether solution was dried and evaporated to yield 1-hydroxy-2,3,3-trimethylpyrrolidine as an oil. This was dissolved in dry dichloromethane (30 ml) and treated with yellow mercuric oxide (portions of 4.8 g and 1.2 g) as in the previous oxidation experiment. Isolation of the product gave 2,3,3-trimethyl-1-pyrroline-1-oxide (IX) (0.64 g, 44%) as an oil, b.p. 62° at 0.17 mm, which, on cooling, formed very hygroscopic needles. Infrared spectrum (film); 3 436 cm^{-1} (moisture), 1 610 cm^{-1} (C=N → O): ultraviolet spectrum; in methanol λ_{max} 229 mμ, (log ϵ 3.96).

The picrate, m.p. 174°, needles from ethanol.

Found: C, 43.8; H, 4.7; N, 15.6. $C_{13}H_{16}N_4O_8$ requires C, 43.8; H, 4.5; N, 15.7.

Repeated fractional crystallization of the total picrate preparation did not yield an isomeric picrate.

In a second series of experiments, the above steps were repeated starting with 0.4 g of the dimethyl nitrone, but the trimethyl nitrone was not purified by distillation. Instead the crude oily product was heated (free flame) with triphenylphosphine (1 g) for 5 min before the volatile base (0.15 ml) was distilled out. This basic liquid was submitted to purification by vapor phase chromatography (Aerograph instrument, 5 ft Ucon polar column at 95°, helium carrier gas at 100 ml/min). Under these conditions 2,4,4-trimethyl-1-pyrroline exhibited a retention volume of 590 ml. The product from the oxygen-transfer reaction showed a small response at retention volume 580 ml, and a major one at retention volume 750 ml. The ratio of the areas was 1:34. The 2,3,3-trimethyl-1-pyrroline represented by the second peak was collected. Infrared absorption (film) occurred at 1 637 cm^{-1}. The picrate, tiny prisms, m.p. 249–251° (decomp.), from ethanol was analyzed.

Found: C, 46.0; H, 4.5; N, 16.5. $C_{13}H_{16}N_4O_7$ requires C, 45.9; H, 4.7; N, 16.5.

3,3-Dimethyl-2-phenyl-1-pyrroline (XII) from 3,3-Dimethyl-1-pyrroline-1-oxide

(i) Addition of Phenyl Magnesium Bromide

3,3-Dimethyl-1-pyrroline-1-oxide (1 g) in ether (10 ml) was added to phenyl magnesium bromide (from 3 g phenyl bromide) in ether (20 ml), heated under reflux for 1 h and treated with aqueous ammonium chloride. The ether layer was washed with water, dried, and concentrated. Addition of hexane caused 1-hydroxy-3,3-dimethyl-2-phenylpyrrolidine (0.97 g, 57%) to crystallize out as small prisms, m.p. 129°. Recrystallization of a small sample from ether/hexane raised the melting point to 130°.

Found: N, 7.55. $C_{12}H_{17}ON$ requires N, 7.3.

(ii) Dehydrogenation

The hydroxylamine (0.9 g) was stirred in 25 ml dichloromethane with yellow mercuric oxide (5 g) for 3 h. Filtration, drying, and concentration gave an oil which crystallized on cooling (0.71 g, 79%). A small portion of the 3,3-dimethyl-2-phenyl-1-pyrroline-1-oxide was distilled (hot box, 115° at 0.2 mm) and showed a new band in the infrared (film) at 1 534 cm^{-1}. The ultraviolet spectrum (ethanol) had λ_{max} 283 mμ (log ϵ 3.83).

The picrate, m.p. 137°, light-sensitive prisms from ethanol.

Found: C, 51.6; H, 4.5; N, 13.2. $C_{18}H_{18}N_4O_8$ requires C, 51.7; H, 4.3; N, 13.4.

(iii) Oxygen Transfer

3,3-Dimethyl-2-phenyl-1-pyrroline-1-oxide (0.5 g) was heated with 1 g of triphenylphosphine (free flame) for 5 min. A volatile liquid was formed which was distilled off at 125–135° at 15 mm. The infrared spectrum of the liquid was essentially identical with that of authentic 3,3-dimethyl-2-phenyl-1-pyrroline (11). The picrate (0.46 g, 43%) was prepared in ether and recrystallized from ethanol.

M.p. and mixed m.p. 161° (lit. (11) 160°).

Found: C, 53.4; H, 4.5; N, 13.9. $C_{18}H_{18}N_4O_7$ requires C, 53.7; H, 4.5; N, 13.9.

(iv) The Direct Dehydration of the Hydroxylamine (X)

1-Hydroxy-3,3-dimethyl-2-phenylpyrrolidine (0.32 g from (i)) and potassium hydrogen sulfate (0.4 g) were mixed and heated for 1 h in a stoppered tube in an oil bath at 150–155°. Water was added to the warm dark-brown product, which was treated with aqueous sodium hydroxide, and extracted with ether. The ether was washed with water, heated under reflux with charcoal, filtered, and treated with picric acid in moist ether. This gave 0.19 g (28%) of 3,3-dimethyl-2-phenyl-1-pyrroline picrate, m.p. 158–159°, raised to 160–161° on one recrystallization from ethanol. Mixed m.p. 160–161°.

Can. J. Chem. Downloaded from www.nrcresearchpress.com by 210.87.254.5 on 09/05/12
For personal use only.

Reduction of 3,3-Dimethyl-1-pyrroline-1-oxide to 3,3-Dimethylpyrrolidine

To lithium aluminium hydride (1 g) in ether (70 ml) was added 3,3-dimethyl-1-pyrroline-1-oxide (0.5 g) in ether (10 ml). The mixture was refluxed for 1 h. Aluminium chloride (anhydrous, 1 g) was then added and the mixture heated under reflux for a further hour. Decomposition with 30% aqueous sodium hydroxide followed by treatment of the separated, washed ether layer with ethereal picric acid gave a precipitate of yellow needles (0.90 g, 62%) m.p. and mixed m.p. 160°.

Analytical sample from ethanol.

Found: C, 43.8; H, 4.8; N, 16.8. $C_{12}H_{16}N_4O_7$ requires C, 43.9; H, 4.9; N, 17.1.

Dipolar Addition Reactions

(i) 6,6-Dimethyl-3-phenyl-2-oxa-1-azabicyclo[3.3.0] octane (XVIa)

3,3-Dimethyl-1-pyrroline-1-oxide (0.5 g) was heated with styrene (2.5 ml) on the steam bath for 20 h. Distillation (hot box; 135° at 0.35 mm) gave the adduct (XVI*a*) as a colorless oil (0.7 g, 73%) with η_D^{20} 1.5345.

Found: C, 77.0; H, 8.6; N, 6.9. $C_{14}H_{19}NO$ requires C, 77.4; H, 8.8; N, 6.45.

λ_{max} (ethanol): 258 mμ, log ϵ 2.45. ν_{max} (film) at 1 595, 1 484, 1 377, 1 359 cm^{-1}. The n.m.r. spectrum (CCl_4 solution, τ values): 2.82 (Ph); 5.04 (Ph—C*H*—O); ~6.81 (NCH); and 7.62–8.57, 8.93 (CH_2 and CH_3) with relative areas of 5.0, 0.95, 3.09, and 10.6 respectively.

The picrate, recrystallized from ethanol, had m.p. 153°.

Found C, 53.9; H, 4.9; N, 12.8. $C_{20}H_{22}N_4O_8$ requires C, 53.8; H, 5.0; N, 12.55.

(ii) 8,8-Dimethyl-3-phenyl-2-oxa-1-azabicyclo[3.3.0] octane

5,5-Dimethyl-1-pyrroline-1-oxide (1 g) in styrene (5 ml) was heated on the steam bath for 8 h. Distillation gave 1.74 g (90%) of the adduct as a colorless liquid, b.p. 98–100° at 0.1 mm., η_D^{20} 1.5335.

Found: C, 77.3; H, 8.7; N, 6.6.

λ_{max} (ethanol): 258 mμ, log ϵ 2.44. ν_{max} (film) 1 603, 1 493, 1 379, 1 364 cm^{-1}. The n.m.r. spectrum (CCl_4 solution, τ values): 2.81 (Ph): 5.13 (Ph—C*H*—O); ~6.20 (NC*H*); and 7.65; 7.86–8.60; 8.69; 8.99 (CH_2 and CH_3) with relative areas of 5.0, 0.97, 1.08, and 12.4 respectively.

The picrate, from ethanol, had m.p. 175°. Found: C, 53.6; H, 4.9; N, 12.8.

ACKNOWLEDGMENTS

Dr. D. E. McGreer is thanked for the n.m.r. spectra, and Mr. K. S. Chan for repeating the preparation of the 3,3-dimethylnitrone. The financial support of the National Research Council of Canada is gratefully acknowledged.

REFERENCES

1. R. Bonnett and D. E. McGreer. Can. J. Chem. **40**, 177 (1962).
2. R. Bonnett, V. M. Clark, A. Giddey, and Sir Alexander Todd. J. Chem. Soc. 2087 (1959).
3. H. Schecter, D. E. Ley, and L. Zeldin. J. Am. Chem. Soc. **74**, 3664 (1952).
4. R. Wolffenstein. Ber. **25**, 2777 (1892). L. Mamlock and R. Wolffenstein. Ber. **33**, 159 (1900).
5. T. Kan and S. Nakajima. Chem. Abstr. **51**, 2734 (1957). R. Huisgen and F. Bayerlein. Ann. **630**, 138 (1960).
6. M. A. T. Rogers. J. Chem. Soc. 769 (1955).
7. J. Thesing and W. Sirrenberg. Ber. **92**, 1748 (1959).
8. R. Bonnett, R. F. C. Brown, V. M. Clark, I. O. Sutherland, and Sir Alexander Todd. J. Chem. Soc. 2094 (1959).
9. R. Bonnett, V. M. Clark, and Sir Alexander Todd. J. Chem. Soc. 2102 (1959).
10. F. Agolini and R. Bonnett. Can. J. Chem. **40**, 181 (1962).
11. A. P. Terentev, A. N. Kost, and A. M. Berlin. Zh. Obshch. Khim. **25**, 1613 (1955).
12. J. Thesing and W. Sirrenberg. Ber. **91**, 1978 (1958).
13. E. A. Braude and F. Sondheimer. J. Chem. Soc. 3754 (1955).
14. C. G. Overberger, J. G. Lombardino, and R. G. Hiskey. J. Am. Chem. Soc. **79**, 6430 (1957); and references therein.
15. C. W. Brown, K. Marsden, M. A. T. Rogers, C. M. B. Tylor, and R. Wright. Proc. Chem. Soc. 254 (1960).
16. G. R. Delpierre and M. Lamchen. Proc. Chem. Soc. 386 (1960); 118 (1962); J. Chem. Soc. 4693 (1963).
17. G. V. D. Tiers. Tables of τ-values for a variety of organic compounds. Minnesota Mining and Manufacturing Co.
18. R. U. Lemieux. Can. J. Chem. **39**, 116 (1961).
19. R. Grashey, R. Huisgen, and H. Leitermann. Tetrahedron Letters, **12**, 9 (1960). R. Huisgen. Angew. Chem. Intern. Ed. Engl. **2**, 633 (1963).
20. N. A. Lebel and J. J. Whang. J. Am. Chem. Soc. **81**, 6334 (1959).
21. R. F. Brown and N. M. Van Gulick. J. Am. Chem. Soc. **77**, 1083 (1955).

Can. J. Chem. Downloaded from www.nrcresearchpress.com by 210.87.254.5 on 09/05/12
For personal use only.

Can. J. Chem. Downloaded from www.nrcresearchpress.com by 210.87.254.6 on 09/05/12
For personal use only.

THE KINETICS OF THE INHIBITED AUTOXIDATION OF TETRALIN. II[1]

J. A. HOWARD AND K. U. INGOLD
Division of Applied Chemistry, National Research Council, Ottawa, Canada

Received May 10, 1965

ABSTRACT

The kinetics of the oxidation of tetralin inhibited by a number of phenols have been examined. The chain transfer reaction between phenoxy radicals and hydroperoxides is subject to both polar and steric effects. The rate of this reaction is increased by electron-attracting substituents on the phenol and is decreased both by ortho-alkyl groups on the phenol and by an increase in the size of the substituents on the hydroperoxides.

INTRODUCTION

In Part I (1) it was shown that the overall process for the inhibition of the autoxidation of tetralin by the highly hindered phenol, 2,6-di-*t*-butyl-4-methylphenol (BMP) can be represented by the following simplified reaction scheme

[1] $$I_2 \rightarrow 2I\cdot$$

[2] $$R\cdot(I\cdot) + O_2 \rightarrow RO_2\cdot$$

[3] $$RO_2\cdot + RH \rightarrow ROOH + R\cdot$$

[6] $$RO_2\cdot + AH \rightarrow ROOH + A\cdot$$

[7] $$RO_2\cdot + A\cdot \rightarrow ROOA$$

where I_2 represents α,α'-azo-bis-isobutyronitrile (AIBN) which initiated the oxidation. RH represents tetralin and AH the phenol. The inhibited rate (P) can be represented by

[I] $$P = \frac{ek_1k_3[RH][I_2]}{k_6[AH]}$$

where e is the efficiency with which the AIBN initiates reaction chains.

To represent the inhibition of tetralin oxidation by phenol two additional reactions are required.

[−6] $$A\cdot + ROOH \rightarrow AH + RO_2\cdot$$

[8] $$A\cdot + RH \rightarrow AH + R\cdot$$

The inhibited rate is proportional to the square root of the tetralin hydroperoxide (ROOH) concentration. It is given by

[II] $$P = \frac{ek_1k_3[RH][I_2]\alpha}{2k_6[AH]} + \frac{ek_1k_6k_8[RH][I_2][AH]\alpha}{2k_6[AH](k_{-6}[ROOH] + k_8[RH]) + ek_1k_7[I_2]\alpha}$$

where

$$\alpha = 1 + \left(1 + \frac{4k_6[AH](k_{-6}[ROOH] + k_8[RH])}{ek_1k_7[I_2]}\right)^{1/2}.$$

Inhibition with 4-methoxyphenol requires the additional reaction

[9] $$A\cdot + A\cdot \rightarrow A_2\cdot$$

[1]*Issued as N.R.C. No. 8571.*

The inhibited rate is independent of [AH] at high 4-methoxyphenol concentrations. Neglecting reactions [−6] and [7], it is given by

$$[III] \qquad P = \frac{2ek_1k_3[RH][I_2]}{k_6[AH]}\left(1 + \frac{k_8[RH]}{2(ek_1k_9[I_2])^{1/2}}\right) + k_8[RH]\left(\frac{ek_1[I_2]}{k_9}\right)^{1/2}.$$

The present work describes the inhibition of the oxidation of tetralin by a number of other phenols using the same experimental technique as in Part I (1). Further examples of all three types of kinetics have been found. The accelerating effect of hydroperoxides on inhibited rates has also been examined in detail.

RESULTS AND DISCUSSION

2,6-Di-t-butyl-4-substituted Phenols

Several of these highly hindered phenols were examined. In all cases, they followed the simple first order kinetics described by eq. [I] except that the inhibited rates were very slightly increased by the addition of tetralin hydroperoxide (see below). Values of k_6 at 65 °C calculated from eq. [I] are given in Table I. These results are based on $k_3 = 16.4$ l mole^{-1} s^{-1}, a value which has been calculated from a self-termination rate constant, $k_5 = 4 \times 10^6$ l mole^{-1} s^{-1} (average of some of our unpublished data from 13–50 °C) and a $k_3\sqrt{(2k_5)}$ value of 5.8×10^{-3} l$^{1/2}$ mole$^{-1/2}$ s$^{-1/2}$ at 65 °C. This table also includes values of k_6 for hydrogen abstraction from the same phenols by poly(peroxystyryl) peroxy radicals, these values having been recalculated from our previous data (3) using $k_3 = 178$ l mole^{-1} s^{-1} for styrene at 65 °C (2). The two sets of rate constants are in fair agreement as might be expected for two hydrocarbons which give secondary peroxy radicals since both the steric and the polar effects should be rather similar. The k_6 values in tetralin, like those in styrene (3), can be correlated with the σ^+ constants of the parasubstituents by means of the Hammett equation. The slope of the best straight line, i.e., the ρ factor is −1.36 (standard deviation 0.043*) which is in good agreement with the value of −1.12 found in styrene.

TABLE I

k_6 for 2,6-di-*t*-butylphenols at 65 °C

	$k_6 \times 10^{-3}$ (l mole^{-1} s^{-1})	
4-Substituent	Tetralin	Styrene (3)*
4-MeO	89	78
4-Me	24 (1)	17
4-Bu^t	28 (5)	16
None	7.7	4.9
4-Cl	8.5	6.8
4-CN	1.6	1.7
4-NO_2	0.6	1.0

*Recalculated using k_3(styrene) = 178 l mole^{-1} s^{-1}.

Unhindered and Weakly Hindered Phenols

A thorough study of inhibition kinetics was only attempted for two non-hindered phenols, para-cresol and 4-chlorophenol. Both compounds showed the same kinetic behavior as phenol (1), i.e., they appeared to follow eq. [II]. Our main interest in these simple phenols was to measure the accelerating effect of tetralin hydroperoxide on the

**A better correlation with a smaller ρ factor is obtained if we employ σ values of 0.227 for 4-Cl and the enhanced σ values (4) of 1.00 for 4-CN and 1.27 for 4-NO_2.*

Can. J. Chem. Downloaded from www.nrcresearchpress.com by 210.87.254.6 on 09/05/12
For personal use only.

inhibited rate. For this reason, substituents which were more strongly electron attracting than para-chloro were only cursorily examined since they gave such weak inhibition that the accelerating effect of added hydroperoxide was insignificant. For example, 4-nitro- and 4-cyano-phenol did not measurably inhibit the oxidation of tetralin under the standard conditions used to compare oxidation rates in Table II.

TABLE II

The inhibited oxidation of tetralin at 65 °C

Phenol substituents	Initial rate $\times 10^7$ (moles l^{-1} s^{-1})*	$k_{-6}/k_7 \times 10^7$†
4-MeO	1.3‡	10
4-Me	1.7	215
4-Bu^t	1.7	260
3-Me	7.1	370
None	9.0	515
3-MeO	2.8	230
4-Cl	7.6	285
2,6-Me_2	1.5‡	17
2,6-Me_2-4-CN	6.5	92
2-Me-6-Bu^t	1.2§	4.6
2,6-Bu_2^t	0.3	0.1
2,6-Bu_2^t-4-CN	1.5	4.9

*With [RH] = 6.61 moles/l, $[I_2] = 1.23 \times 10^{-3}$ mole/l, and [AH] = 6.12×10^{-3} mole/l, unless otherwise noted.
†With added tetralin hydroperoxide.
‡Limiting rate independent of [AH].
§With [AH] = 6.12×10^{-4} mole/l.

The kinetics were also carefully examined for 2,6-dimethylphenol since this compound is known to dimerize very readily in oxidizing hydrocarbons (6, 7, 8). It was expected that this phenol would show the same kinetics as 4-methoxyphenol (eq. [III]), i.e., kinetics which result from the rapid coupling of phenoxy radicals (reaction [9]). This was in fact observed, i.e., as the 2,6-dimethylphenol concentration was increased the rate decreased to a constant limiting value which depended on $[RH] \times [I_2]^{1/2}$ but was unaffected by the further addition of inhibitor. The limit was reached at a dimethylphenol concentration of about 2×10^{-3} mole/l. From this limiting rate, the ratio $k_8/k_9^{1/2}$ was found to be 2.0×10^{-4} $(l/mole\ s)^{1/2}$. This value is very similar to the value of 1.7×10^{-4} $(l/mole\ s)^{1/2}$ which can be calculated from our previous data (1) to be the ratio of $k_8/k_9^{1/2}$ for 4-methoxyphenol. If it is assumed that k_9 is similar to the recently determined value of $\sim 6 \times 10^9$ l $mole^{-1}$ s^{-1} for the dimerization of phenoxy and 4-methylphenoxy radicals in aqueous solution (9), then k_8 will be about 15 l $mole^{-1}$ s^{-1}.

In view of the complex kinetics exhibited by unhindered and weakly hindered phenols in tetralin, "relative inhibiting efficiencies" obtained by comparisons of initial inhibited rates or induction periods are *not* linearly related to the relative rates of reaction [6] (see e.g. ref. 10). Such a correlation only applies to those phenols for which eq. [I] is applicable, i.e., to the highly hindered 2,6-di-*t*-butylphenols.

A plot of the phenol-inhibited rate against the square root of the tetralin hydroperoxide concentration gives a straight line (1, 11). From the first term in eq. [II] the slope of this line is

$$[IV] \qquad \frac{P_1 - P_2}{[ROOH]^{1/2}} = k_3[RH]\left(\frac{ek_1[I_2]}{k_6[AH]}\right)^{1/2}\left(\frac{k_{-6}}{k_7}\right)^{1/2}$$

Since k_6 appears to be virtually the same in styrene and tetralin (Table I) the value obtained previously in styrene (3*) can be used to obtain k_{-6}/k_7 in tetralin. This data is

**Recalculated using k_3 = 178 l $mole^{-1}$ s^{-1} for styrene at 65 °C (2).*

Can. J. Chem. Downloaded from www.nrcresearchpress.com by 210.87.254.6 on 09/05/12
For personal use only.

given in Table II for several phenols. In calculating k_{-6}/k_7 the increased rate of chain initiation from the added hydroperoxide has been allowed for in all cases. Table II also includes the initial inhibited rates in the absence of added hydroperoxide under standard conditions ([RH] = 6.61 moles/l (10% by volume *o*-dichlorobenzene as diluent), $[I_2] = 1.23 \times 10^{-3}$ moles/l, and $[AH] = 6.12 \times 10^{-3}$ moles/l).

Equation [IV] was obeyed by phenol over a wide range in $[I_2]$ (10^{-2} to 10^{-4} mole/l), [AH] (5×10^{-2} to 5×10^{-4} mole/l), and [RH] (6.61 to 1.32 moles/l). The values of k_{-6}/k_7 for 4-methoxyphenol and 2,6-dimethylphenol were obtained at low inhibitor concentrations where the kinetics approximate that for phenol itself, i.e., where the inhibited rate is approximately proportional to $[AH]^{-1/2}$. The fact that tetralin hydroperoxide accelerates the inhibited rates for both these phenols implies that reaction [−6] should have been included in the derivation of eq. [III]. When this is done, an extremely complex expression is obtained which, however, still simplifies to $k_8[RH](ek_1[I_2]/k_9)^{1/2}$ at high inhibitor and low hydroperoxide concentrations. The accelerating effect of the hydroperoxide can, for all practical purposes, be neglected from the kinetic treatment when k_{-6}/k_7 is less than about 10^{-5}.

Although the values of k_{-6}/k_7 in Table II cannot be linearly related to the polar effects of the substituents they are significantly larger for electron-attracting than for electron-releasing groups (compare, e.g., 4-methoxyphenol with the other unhindered phenols, or 2,6-dimethylphenol, or 2,6-di-*t*-butylphenol with their 4-cyano derivatives). This polar effect might be due to a change in either rate constant.

Steric effects are both more regular and more pronounced than polar effects. That is, k_{-6}/k_7 decreases along the series phenol, 2,6-dimethylphenol, 2-methyl-6-*t*-butylphenol, and 2,6-di-*t*-butylphenol. The importance of polar effects in this series can be diminished by comparing phenol with 2,6-dimethyl-4-cyanophenol and 2,6-di-*t*-butyl-4-cyanophenol since electron attraction by the 4-cyano group will roughly compensate for electron release by the ortho-alkyl groups. This steric effect is probably due to a change in k_{-6} since the reverse process, i.e., reaction [6], is subject to a very similar steric effect (3). In both reactions [6] and [−6] the steric effect of two ortho-methyl groups is much smaller than the steric effect of two ortho-*t*-butyl groups. This result is in agreement with the conclusions derived from studies of the infrared spectra of ortho-alkyl phenols (12, 13).

TABLE III

Effect of hydroperoxide on $k_{-6}/k_7 \times 10^7$ in tetralin at 65 °C

Phenol substituents	Hydroperoxide			
	Tetralin	$(CH_3)_3C$-	$C_6H_5(CH_3)_2C$-	$(C_6H_5)_3C$-
None	515	225	225	20
2,6-Me_2-4-CN	92	20	20	3.4
2,6-Bu_2^t-4-CN	4.9	1.3	1.5	0.2

The importance of the steric effect in reaction [−6] was confirmed by comparing the acceleration of inhibited rates which was produced by added tetralin, *t*-butyl, cumyl, and triphenylmethyl hydroperoxides. The results in Table III show that increased steric protection of both the hydroperoxide and the phenol reduces k_{-6}/k_7. For each phenol the steric effect of the hydroperoxide can be attributed to reaction [−6] since the peroxy radicals involved in reaction [7] must come mainly from the tetralin, i.e., k_7 is constant for each phenol. The decrease in the rate of reaction [−6] along the series from tetralin to triphenylmethyl hydroperoxide implies that unhindered or partly hindered phenols

Can. J. Chem. Downloaded from www.nrcresearchpress.com by 210.87.254.6 on 09/05/12
For personal use only.

will be more likely to follow the simple kinetics of eq. [I] in a hydrocarbon yielding hindered tertiary peroxy radicals than in one yielding unhindered secondary radicals. Moreover, the inhibition efficiencies of unhindered phenols (relative to highly hindered phenols) should be improved in a hydrocarbon giving tertiary radicals since the unhindered phenoxy radicals will be more likely to end a second chain than to undergo reaction [−6].

ACKNOWLEDGMENT

The authors wish to acknowledge the assistance of Mr. D. V. Gardner in the early part of this work.

REFERENCES

1. J. A. HOWARD and K. U. INGOLD. Can. J. Chem. **42**, 2324 (1964).
2. J. A. HOWARD and K. U. INGOLD. Can. J. Chem. This issue.
3. J. A. HOWARD and K. U. INGOLD. Can. J. Chem. **41**, 1744, 2800 (1963).
4. H. H. JAFFE. Chem. Rev. **53**, 191 (1953).
5. D. V. GARDNER, J. A. HOWARD, and K. U. INGOLD. Can. J. Chem. **42**, 2847 (1964).
6. R. F. MOORE and W. A. WATERS. J. Chem. Soc. 2432 (1952); 243 (1954).
7. W. A. WATERS and C. WICKHAM-JONES. J. Chem. Soc. 2420 (1952).
8. J. R. DUNN, W. A. WATERS, and C. WICKHAM-JONES. J. Chem. Soc. 2427 (1952).
9. G. DOBSON and L. I. GROSSWEINER. Trans. Faraday Soc. **61**, 708 (1965).
10. D. S. DAVIES, H. L. GOLDSMITH, A. K. GUPTA, and G. R. LESTER. J. Chem. Soc. 4926 (1956).
11. J. R. THOMAS. J. Am. Chem. Soc. **86**, 4807 (1964).
12. K. U. INGOLD and D. R. TAYLOR. Can. J. Chem. **39**, 471 (1961).
13. W. HEINEN. Rec. Trav. Chim. **82**, 859 (1963).

Can. J. Chem. Downloaded from www.nrcresearchpress.com by 210.87.254.6 on 09/05/12
For personal use only.

Can. J. Chem. Downloaded from www.nrcresearchpress.com by 210.87.254.6 on 09/05/12
For personal use only.

ABSOLUTE RATE CONSTANTS FOR HYDROCARBON AUTOXIDATION

I. STYRENE[1]

J. A. HOWARD AND K. U. INGOLD
Division of Applied Chemistry, National Research Council, Ottawa, Canada

Received May 6, 1965

ABSTRACT

Absolute rate constants for the uninhibited oxidation of styrene have been obtained by the rotating sector technique. The rate constants for the propagation (k_p), bimolecular termination (k_t), and a kinetically first order termination (k_x) for 2 M styrene in chlorobenzene can be represented by

$$k_p = (4.7 \pm 0.2) \times 10^7 \exp(-8400 \pm 300/RT) \text{ l mole}^{-1} \text{ s}^{-1}$$

$$k_t = (5.1 \pm 3.4) \times 10^8 \exp(-1800 \pm 1200/RT) \text{ l mole}^{-1} \text{ s}^{-1}$$

$$k_x = (5.8 \pm 1.4) \times 10^7 \exp(-11600 \pm 2800/RT) \text{ s}^{-1}.$$

The rate constant for the reaction of poly(peroxystyryl) peroxy radicals with 2,6-di-*t*-butyl-4-methylphenol can be represented by

$$k_{inh} = 8.4 \times 10^7 \exp(-5600/RT) \text{ l mole}^{-1} \text{ s}^{-1}.$$

Chemically inert solvents can affect the rate of chain initiation and the rate of chain propagation but they do not appear to affect the rate of chain termination.

INTRODUCTION

Although the absolute rate constants for chain propagation and termination in the autoxidation of many hydrocarbons have been determined, these constants are not known for the oxidation of styrene. Our interest in these quantities arose from our studies of the phenolic inhibition process in which styrene was used as the oxidizing substrate (1). This paper reports the measurement of these constants by the rotating sector technique, the theory of which has recently been clearly reviewed by Burnett and Melville (2). The nomenclature of these authors has been generally followed in the brief résumé given below.

The separation of the rate constants for propagation (k_p) and bimolecular termination (k_t)* involves measurement of the lifetime (τ) of the reaction chains. The lifetime is defined by the equation

$$\tau = (2k_tR_i)^{-1/2}$$

where R_i is the rate of the photo-initiation. A sectored disc is rotated between the light and the reaction vessel and oxidation rates are measured at various rotation speeds. At fast speeds the rate is

$$R_f = K[I/(r+1)]^{1/2}$$

where $KI^{1/2}$ is the oxidation rate at a steady light intensity I (i.e., $R_{steady} = KI^{1/2}$), and r is the ratio of dark to light periods. At slow rotation speeds the rate is

$$R_s = KI^{1/2}/(r+1).$$

[1]*Issued as N.R.C. No. 8590.*

**The rate of the reaction*

$$RO_2\cdot + RO_2\cdot \rightarrow \textit{inactive products}$$

is defined as $2k_t[RO_2\cdot]^2$ in this paper rather than $k_t[RO_2\cdot]^2$ as was used by Burnett and Melville.

Rates intermediate between R_f and R_s are denoted by R_λ. They have a complicated dependence on the duration of the light flash (λ) and the lifetime of the chains. Values of the ratio R_λ/R_{steady} have been given in terms of λ/τ for various values of r in Table I of ref. 2. Since λ is known from the rotation speed, τ is readily obtained and this gives k_t once R_i has been measured. Under steady illumination the rate can be represented by

$$R_{steady} = k_p[RH]\left(\frac{R_i}{2k_t}\right)^{1/2}$$

where [RH] is the hydrocarbon concentration. Substitution of R_i and k_t into this expression yields k_p.*

In the oxidation of styrene a first order chain termination process occurs together with the usual second order process (1). Following Burnett and Melville (2), the first order process can be represented as

$$RO_2\cdot \rightarrow \text{inactive products; rate} = k_x[RO_2\cdot].$$

It produces a reduction in the value of R_f/R_{steady}. This ratio is used to obtain a quantity γ by means of the relation

$$\frac{R_f}{R_{steady}} = \frac{((\gamma^2 r + 1)/(r + 1))^{1/2} - \gamma}{1 - \gamma}$$

where γ is defined as $k_x/(k_x^2 + 8k_tR_i)^{1/2}$. Once γ has been determined the value of R_λ/R_{steady} yields a second quantity m defined as

$$(k_x^2 + 8k_tR_i)^{1/2}\lambda/2.\dagger$$

The rate constants k_x and k_t are readily calculated from γ and m. The propagation rate constant, k_p, is obtained from the equation

$$R_{steady} = k_p[RH]\frac{k_x(1 - \gamma)}{4k_t\gamma}.$$

EXPERIMENTAL

The reaction vessel, a 50 ml round-bottomed pyrex flask, was immersed in a water bath and was connected to a standard, constant pressure, oxygen absorption apparatus. It was irradiated through a Corning U.V. transmitting filter (C.S. No. 7-51, maximum transmittance at 365 mμ) with the light from a 200/250 V, 250 W ME/D B.T.H. ultraviolet lamp. The light was collimated by 3.5 in. diameter quartz lenses with a focal length of 6 in. The reaction vessel was shaken along the light beam at 30–120 cycles/min. Oxidation rates did not depend on the shaking speed nor upon the oxygen pressure in the range 50–760 mm.

Two 45° sectors (i.e., $r = 3$) were cut from a disc of blackened aluminium. This disc was driven by a 7.5 W, 10 r.p.m. Bodine synchronous motor through a series of gears which could be changed so as to give rotation speeds varying from 0.4 to 250 r.p.m. The light intensity was monitored by a photocell before and after each oxidation. The transmittance of screens used to decrease the light intensity was measured on a Cary model 14 recording spectrophotometer.

**In this analysis it has been assumed that there was no chain initiation from any thermal (dark) reaction. Such a process leads to a small increase in R_f and to a relatively larger increase in R_s, thereby decreasing the difference between these two rates. Provided the dark rate is less than 5% of the photochemical rate its effect on the estimated lifetimes can generally be neglected (2). Under the experimental conditions employed in this work the thermal rate of oxidation of styrene at 50 °C was only 3.6% of the rate at full light intensity.*

†Values of R_λ/R_{steady} have been tabulated in ref. 2 (Table III) as a function of m for five values of γ at $r = 3$. We have had a more complete table of these ratios calculated at $r = 3$ for values of γ increasing in steps of 0.01 from 0.00 to 0.60. Photocopies of this table may be obtained upon request to:

Depository of Unpublished Data,
National Science Library,
National Research Council,
Ottawa, Canada.

Can. J. Chem. Downloaded from www.nrcresearchpress.com by 210.87.254.6 on 09/05/12
For personal use only.

α,α'-Azo-bis-cyclohexylnitrile (ACHN) was chosen as the photo-initiator because of its high thermal stability. This compound has a maximum absorption at 348 mμ with a molar extinction coefficient of 19.6 in chlorobenzene. For most experiments 10 ml of chlorobenzene was used as a solvent for 3 ml of styrene with an ACHN concentration of 6.68×10^{-3} mole/l. The styrene polyperoxide formed in the oxidation acts as a rather weak photo-initiator.* To some extent, its formation must compensate for the destruction of styrene and ACHN during a reaction since the measured oxidation rates do not vary by more than 2% for a styrene consumption of up to 10%. The transmittance of the reactants at 365 mμ drops by nearly a factor of 3 at this extent of oxidation.

Previous workers have generally determined the chain lifetime by measuring R_λ over the range of flash times which gave rates varying all the way from R_f to R_s. Because R_λ values near R_f and R_s are of little use in estimating τ we found this procedure to be much less accurate than choosing a particular λ which gave a rate midway between R_f and R_s and then repeatedly measuring alternately R_{steady} and R_λ. Even with this procedure rather large errors creep into the calculated values of k_p, k_t, and k_x. That is, oxidation rates are not reproducible to much better than $\pm 2\%$ and there is possibly a variation of $\pm 5\%$ in the rate of chain initiation from one run to another. These relatively small experimental errors can lead to errors of up to 50% in k_p, 20% in k_t, and 30% in k_x. The measured rate of gas adsorption has been taken to equal the rate of oxidation in all calculations. That is, the corrections to the measured rates for nitrogen evolution by the initiator, oxygen absorption by the initiator radicals, and oxygen evolution in bimolecular chain termination were too small to be really significant in any experiment.

RESULTS AND DISCUSSION

When chain termination is bimolecular the oxidation rate must be proportional to $R_i^{1/2}$. Under ideal conditions, the rate should therefore be proportional to the square root of the initiator concentration and to the square root of the light intensity. This ideal, however, is not achieved with styrene. In the first place, at low ACHN concentrations (or in its absence) the oxidation rate is larger than would be expected and, moreover, the reaction is autocatalytic. This is due to photochemical initiation from the styrene polyperoxide formed in the oxidation. The degree of autocatalysis can be correlated with the square root of the polyperoxide concentration. Secondly, at high ACHN concentrations the rate is lower than expected. This is probably due to the absorption of a significant fraction of the light by the initiator so that the rate of chain initiation is no longer uniform throughout the reaction vessel. Under standard conditions with full light intensity the rate was only proportional to $[ACHN]^{1/2}$ in the range 2×10^{-3} to 2×10^{-2} mole/l ACHN. A concentration of 6.7×10^{-3} mole/l, near the middle of this range, was therefore used in most experiments. Finally, upon decreasing the light intensity at this initiator concentration, it was found that the rate was only proportional to the square root of the intensity at, or near, full intensity. At lower intensities the order increased as the intensity decreased, the deviation from a half order relationship becoming more pronounced as the temperature was raised (see Fig. 1). This deviation can be attributed to the occurrence of a first order chain termination process in addition to the normal bimolecular chain termination reaction (see ref. 1). The importance of the first order process naturally increases as the rate of initiation decreases, i.e., as the radical concentration decreases. Furthermore, it is obvious from Fig. 1 that the first order termination has a much higher activation energy than the second order termination.

The rate of chain initiation, R_i, was determined by the induction period method of Boozer *et al.* (ref. 3, see also refs. 1, 4, and 5) using 2,6 di-*t*-butyl-4-methylphenol (BMP), an inhibitor which is known to stop two oxidation chains per molecule (3, 6). The induction periods in equivalent photochemically and thermally initiated oxidations† at 40 °C were

**A concentration of 0.27 mole/l $C_8H_8O_2$ (molecular weight ~ 3 000) increases the rate under the standard conditions by only 15%.*

†The thermal oxidations were initiated with a quantity of α,α'-azo-bis-isobutyronitrile (AIBN) sufficient to give an oxidation rate equal to that produced photochemically. Under these conditions the rates of chain initiation from ACHN and AIBN must be equal (see e.g. refs. 7, 8, 9).

Can. J. Chem. Downloaded from www.nrcresearchpress.com by 210.87.254.6 on 09/05/12
For personal use only.

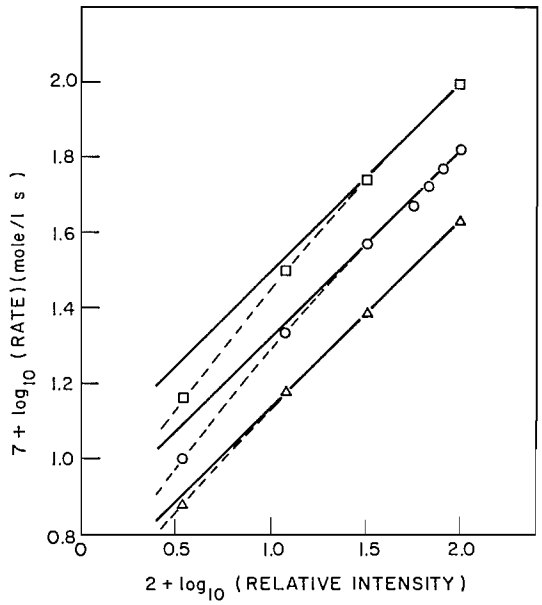

FIG. 1. Rate of oxidation of 2.01 moles/l of styrene in chlorobenzene (with 6.7×10^{-3} mole/l ACHN) as a function of the light intensity at 30° (△), 40° (○), and 50° (□). The solid lines have a slope of 0.5, i.e., only in the region where the experimental points lie on these lines is the oxidation rate proportional to the square root of the light intensity.

compared and were found to be approximately equal.* Similar results were obtained at 40 °C using hydroquinone as the inhibitor.

Our preliminary measurements from 13 to 50 °C suggested that the bimolecular chain termination process had an activation energy (E_t) of about 3 or 4 kcal/mole. This completely unexpected result led us to measure R_i as accurately as was possible over the same temperature range. Cumene was used in place of styrene as the oxidizing substrate in the

TABLE I

Effect of temperature on R_i, k_i, and e for the photochemically initiated oxidation of cumene (cumene 1.66 moles/l in chlorobenzene, ACHN 6.7×10^{-3} mole/l, BMP 5.44×10^{-4} mole/l)

Temp. (°C)	$R_i \times 10^7$ (moles/l s)	$k_i \times 10^5$ (s^{-1})	e
13	2.2	3.5_5	0.46
22	2.4	3.8	0.47
30	2.7	4.4	0.47
40	3.1	4.8	0.48
50	3.5	5.1	0.51

**This comparison was made because the photochemical induction periods might be affected by the photochemically induced decomposition of the BMP-peroxy radical addition product since these cyclohexadienone peroxides have a fairly strong absorption near 365 mμ (6). To check on this point two of these compounds were synthesized by the method of Bickel and Kooyman (6). The t-butyl peroxy and α-tetralyl peroxy derivatives of BMP both had a maximum in their absorption spectra at 370 mμ in chlorobenzene with molar extinction coefficients of 24.9 and 23.9, respectively. Both compounds were about twice as efficient photo-initiators as ACHN. However, in measuring the induction period the BMP concentration was only 0.6% of the ACHN concentration. Chain initiation from the BMP-radical addition products was therefore insignificant compared with initiation from the ACHN.*

Can. J. Chem. Downloaded from www.nrcresearchpress.com by 210.87.254.6 on 09/05/12
For personal use only.

Can. J. Chem. Downloaded from www.nrcresearchpress.com by 210.87.254.6 on 09/05/12
For personal use only.

chlorobenzene since it gives much sharper induction periods.* The results in Table I show that R_i increases with temperature. It has an apparent activation energy of about 2.4 kcal/mole. Measurements of the rate of nitrogen evolution in pure chlorobenzene (rate constant k_1) suggests that the change in R_i with temperature is due more to a change in the rate of decomposition of the ACHN than to a change in the efficiency (e) with which the cyclohexylnitrile radicals initiate oxidation. This result can be compared with the data of Kodama on the photolysis of azomethane over a wide temperature range in a variety of solvents (10). Kodama found that the rate of nitrogen evolution decreased as the temperature was lowered with an apparent activation energy of about 1 kcal/mole in solvents such as toluene or cyclohexane. This phenomenon was ascribed to the recombination of the initially formed radicals, $CH_3N_2^{\cdot}$ and $CH_3^{\cdot}$, in the solvent cage. Furthermore, Kodama showed that the yield of ethane relative to nitrogen increased as the temperature was decreased with an apparent activation energy of about 1.0–1.7 kcal/mole for the quantity $(1 - [C_2H_6]/[N_2])$. Since the ethane was formed entirely by the geminate recombination of methyl radicals this energy is probably related to the diffusion energy of the methyl radicals. That is, geminate recombination was enhanced by a temperature decrease because of the increase in solvent viscosity. By analogy, therefore, the chain-generating efficiency, e, with ACHN should decrease as the temperature decreases (see also ref. 11). The values of e in Table I show a smaller decrease than would be expected on the basis of Kodama's data, that is, there appears to be little or no geminate recombination between cyclohexylnitrile radicals. However, the overall activation energy for R_i is of about the expected order of magnitude, i.e., it is roughly equal to the sum of the activation energies for nitrogen evolution and for the diffusion of the geminate radical pairs.

TABLE II

Absolute rate constants for styrene oxidation at different light intensities

Temp. (°C)	Light intensity (%)	k_p ($l\,mole^{-1}\,s^{-1}$)	$k_t \times 10^7$ ($l\,mole^{-1}\,s^{-1}$)	k_x (s^{-1})
22	100	30	2.8	—*
	32	29 (41)	2.3 (5.3)	0.18
	12	30 (45)	2.4 (6.3)	0.11
40	100	75 (116)†	3.8 (10.3)†	0.45†
	32	86 (154)	4.5 (17.8)	0.46

*First order termination could not be detected at full intensity.
†Average of two separate experiments.

The absolute rate constants obtained in this work are given in Tables II–V. Within the limits of experimental accuracy these rate constants do not depend on the light intensity (Table II) although it should be noted that the first order chain termination process cannot be identified at temperatures of 22 °C or less under full light intensity (Tables II and IV). The k_p and k_t values which would be obtained if the first order process were neglected are given in parentheses in Table II. It can be seen that the error introduced by this simplification increases with decreasing light intensity and with increasing temperature. The fact that k_x does not depend on the styrene concentration (Table III) and is not significantly affected by added styrene polyperoxide indicates that the first order process

At 40 °C under the standard conditions with 3 ml of hydrocarbon in 10 ml of chlorobenzene both styrene and cumene give the same induction period. This similarity was assumed to exist at the other temperatures and in the other solvents. That is, it was assumed that the initiation rates measured with cumene as the substrate were also applicable to styrene.

TABLE III

Absolute rate constants at 40 °C for different styrene concentrations in chlorobenzene (R_i assumed to be the same at all styrene concentrations, including pure styrene (see ref. 5))

Styrene (moles l^{-1})	k_p ($l\ mole^{-1}\ s^{-1}$)	$k_t \times 10^{-7}$ ($l\ moles^{-1}\ s^{-1}$)	k_x (s^{-1})
0.67	75	4.6	0.50
1.34	65	2.7	0.52
2.01	70	3.6	0.45
2.01*	85	5.1	0.30
2.68	57	2.1	0.37
8.71†	61	2.1	0.30

*Containing 0.27 mole/l $C_8H_8O_2$ (molecular weight ~ 3 000).
†Pure styrene.

TABLE IV

Absolute rate constants for the oxidation of 2.01 M styrene in chlorobenzene at different temperatures

Temp. (°C)	k_p ($l\ mole^{-1}\ s^{-1}$)	$k_t \times 10^7$ ($l\ mole^{-1}\ s^{-1}$)	k_x (s^{-1})	$k_{inh} \times 10^{-3}$ ($l\ mole^{-1}\ s^{-1}$)
13	19	2.4	—*	4.7
22	30†	2.5†	0.15†	—
30	41	2.1	0.24	8.1
40	70‡	3.6‡	0.43‡	10.8
50	98	3.1	0.90	14.5

*First order termination could not be detected at full intensity.
†Average of values from Table II. At all the other temperatures the values given correspond to those obtained at full light intensity.
‡Average of first five values in Table III.

TABLE V

Absolute rate constants for styrene oxidation at 13 °C in different solvents (styrene concentration 2.01 moles/l)

Solvent	$R_i \times 10^7$* ($moles\ l^{-1}\ s^{-1}$)	k_p ($l\ mole^{-1}\ s^{-1}$)	$k_t \times 10^{-7}$ ($l\ mole^{-1}\ s^{-1}$)	Relative rates of oxidation†	
				Photochemical	Thermal (5)‡
n-Decane	1.3	10	3.3	0.38	0.45
t-Butylbenzene	1.6	15	2.2	0.74	0.67
Benzene	1.9	21	3.1	0.99	0.84
Chlorobenzene	2.2	19	2.4	1.00	1.00
Acetonitrile	2.7	23	3.6	1.17	1.58

*R_i measured with cumene as substrate.
†Rates are given relative to the rate in chlorobenzene.
‡Thermal rates are at 65 °C with 0.42 mole/l of styrene.

does not involve a reaction between a peroxy radical and a molecule of styrene or a molecule of styrene polyperoxide.

The data in Table IV can be represented by

$$k_p = (4.7 \pm 0.2) \times 10^7 \exp(-8400 \pm 300/RT)\ l\ mole^{-1}\ s^{-1}$$
$$k_t = (5.1 \pm 3.4) \times 10^8 \exp(-1800 \pm 1200/RT)\ l\ mole^{-1}\ s^{-1}$$
$$k_x = (5.8 \pm 1.4) \times 10^7 \exp(-11600 \pm 2800/RT)\ s^{-1}.$$

The limits of error represent standard deviations calculated by the method of least squares. After correction for the variation in the chain initiation rate with temperature, the overall activation energy is 7.20 ± 0.25 kcal/mole. This value is in fairly good agreement with our

Can. J. Chem. Downloaded from www.nrcresearchpress.com by 210.87.254.6 on 09/05/12
For personal use only.

previously reported value of 7.7 ± 0.5 kcal/mole which was obtained from the thermally initiated oxidation of styrene (1). The activation energy for propagation is in the range expected for a hydrocarbon which is fairly readily oxidized (7, 8, 9, 12, 13, 14). There is little or no activation energy for bimolecular chain termination (cf. ref. 15). It should perhaps be pointed out that if k_x were neglected the apparent activation energy for bimolecular termination would be about 10 kcal/mole. With regard to the activation energy of the first order process, the oxidation of styrene resembles the polymerization of vinyl chloride which also has a first order chain termination process with a fairly large activation energy, i.e., $k_x = 1.9 \times 10^5 \exp(-7800/RT)$ (16). First order chain termination processes with high activation energies are not confined to liquid phase polymerizations. For example, in the photolysis of acetaldehyde in the gas phase there is a first order termination on the walls with an activation energy of 7 800 kcal/mole (17). The nature of the first order termination in the oxidation of styrene is discussed in the following paper (15).

Under the standard experimental conditions the initial rates of oxidation of styrene inhibited with 1.3×10^{-3} to 1.3×10^{-2} mole/l BMP were measured at four temperatures. Rate constants for the hydrogen atom abstraction reaction from the phenol (i.e., k_{inh}) are included in Table IV. These results can be represented by

$$k_{inh} = 8.4 \times 10^7 \exp(-5600/RT) \text{ l mole}^{-1} \text{ s}^{-1}.$$

Although the absolute rate constants are in fairly good agreement with our previous estimates (1) this activation energy is much larger than the value of 1.7 kcal/mole which we have reported (1). The present value is in fair agreement with the value of about 5 kcal/mole for the reaction of cyclohexyl peroxy radicals with BMP (18) and with values of 6.8 and 7.3 kcal/mole for the reaction of α-phenethyl peroxy radicals with α- and β-naphthol, respectively (14).

In some previous work from this laboratory (5) on the AIBN thermally initiated oxidation of styrene at 65 °C it was shown that solvents affect the rate of chain generation (both k_i and e). After corrections for these changes in R_i were made, it was found that solvents of high dielectric constant increased the rate of oxidation of styrene relative to the rate for pure styrene and those of low dielectric constant decreased the rate. It was suggested that the solvent exerted its main effect on the propagation reaction (see also refs. 19, 20, and 21). This view is supported by the data in Table V since the changes in k_t from one solvent to another are too small to be significant. Similar results at 40 °C indicate that k_x also does not depend on the solvent. It should perhaps be pointed out that the effect of solvents on k_p is not the same as their effect on the polymerization of styrene (22) or on the hydrogen abstraction (23) and addition (24) reactions of chlorine atoms. The influence of the solvents on R_i can probably be mainly attributed to changes in viscosity from one solvent to another (10) since the position of the absorption maximum for ACHN and its extinction coefficient showed little variation with solvent. However, the possibility that the increase in R_i from *n*-decane to acetonitrile is actually an artifact which results from the method by which it is measured cannot be completely ruled out at the present time. That is, even a hindered phenol has a reduced reactivity towards peroxy radicals in polar solvents since the phenolic hydroxyl group forms hydrogen bonds with these solvents. If R_i does not, in fact, vary with the solvent then k_t must increase along the series of solvents from *n*-decane to acetonitrile. In this connection, if increased hydrogen bonding is responsible for an apparent increase in R_i then the measured values of e at the lower temperatures in Table I may be greater than their true values since hydrogen bonding becomes more important as the temperature is decreased. That is, there may, in fact, be a greater increase in e with temperature than the measured values suggest.

Can. J. Chem. Downloaded from www.nrcresearchpress.com by 210.87.254.6 on 09/05/12
For personal use only.

REFERENCES

1. J. A. HOWARD and K. U. INGOLD. Can. J. Chem. **40**, 1851 (1962).
2. G. M. BURNETT and H. W. MELVILLE. Investigation of rates and mechanisms of reactions. *In* Technique of organic chemistry. Vol. VIII. Part II. *Edited by* S. L. Friess, E. S. Lewis, and A. Weissberger. Interscience, New York. 1963. Chap. 20.
3. C. E. BOOZER, G. S. HAMMOND, C. E. HAMILTON, and J. N. SEN. J. Am. Chem. Soc. **77**, 3233 (1955).
4. G. S. HAMMOND, J. N. SEN, and C. E. BOOZER. J. Am. Chem. Soc. **77**, 3244 (1955).
5. J. A. HOWARD and K. U. INGOLD. Can. J. Chem. **42**, 1044 (1964).
6. A. F. BICKEL and E. C. KOOYMAN. J. Chem. Soc. 3211 (1953).
7. L. BATEMAN and G. GEE. Proc. Roy. Soc. London, Ser. A, **195**, 376, 391 (1948); Trans. Faraday Soc. **47**, 155 (1951).
8. L. BATEMAN, J. L. BOLLAND, and G. GEE. Trans. Faraday Soc. **47**, 274 (1951).
9. H. W. MELVILLE and S. RICHARDS. J. Chem. Soc. 944 (1954).
10. S. KODAMA. Bull. Soc. Chem. Japan, **35**, 652, 658, 824, 827 (1962).
11. G. S. HAMMOND and J. R. FOX. J. Am. Chem. Soc. **86**, 1918 (1964).
12. J. A. HOWARD and J. C. ROBB. Trans. Faraday Soc. **59**, 1590 (1963).
13. R. L. MCCARTHY and A. MACLACHLAN. J. Chem. Phys. **35**, 1625 (1961).
14. V. P. TSEPALOV and V. YA. SHLYAPINTOKH. Kinetika i Kataliz, **3**, 870 (1962).
15. J. A. HOWARD and K. U. INGOLD. Can. J. Chem. This issue.
16. G. M. BURNETT and W. W. WRIGHT. Proc. Roy. Soc. London, Ser. A, **221**, 41 (1954).
17. W. L. HADEN, Jr. and O. K. RICE. J. Chem. Phys. **10**, 445 (1942).
18. J. C. ROBB and M. SHAHIN. Trans. Faraday Soc. **55**, 1753 (1959).
19. D. G. HENDRY and G. A. RUSSELL. J. Am. Chem. Soc. **86**, 2368 (1964).
20. J. A. HOWARD and K. U. INGOLD. Can. J. Chem. **42**, 1250 (1964).
21. R. KERBER. Z. Electrochem. **61**, 1256 (1957); **63**, 296 (1959); Makromol. Chem. **40**, 25, 39 (1960).
22. G. HENRICI-OLIVÉ and S. OLIVÉ. Markromol. Chem. **68**, 219 (1963).
23. G. A. RUSSELL. J. Am. Chem. Soc. **80**, 4987, 4997 (1958).
24. M. L. POUTSMA and R. L. HINMAN. J. Am. Chem. Soc. **86**, 3807 (1964).

Can. J. Chem. Downloaded from www.nrcresearchpress.com by 210.87.254.6 on 09/05/12
For personal use only.

Can. J. Chem. Downloaded from www.nrcresearchpress.com by 210.87.254.40 on 09/05/12
For personal use only.

ABSOLUTE RATE CONSTANTS FOR HYDROCARBON AUTOXIDATION

II. DEUTERO STYRENES AND RING-SUBSTITUTED STYRENES[1]

J. A. HOWARD AND K. U. INGOLD
Division of Applied Chemistry, National Research Council, Ottawa, Canada

Received May 6, 1965

ABSTRACT

The effect of deuterium substitution on the absolute rate constants for the bimolecular chain termination process in the oxidation of styrene indicates that the α-hydrogen is abstracted in this reaction. The first order chain termination process is suppressed both by deuteration of styrene at the α-position and by the addition of heavy water. A possible mechanism for this termination is proposed. There appear to be small secondary deuterium isotope effects in the propagation reaction.

The overall oxidation rates and the propagation rate constants are increased by the addition to the aromatic ring of both electron-attracting and electron-releasing substituents. This is attributed in the former case to the increased stability of the resulting styryl radicals and in the latter case to the increased stability of a dipolar transition state. In hydrogen atom abstraction from 2,6-di-*t*-butyl-4-methylphenol, the peroxy radical from 3-chlorostyrene is more reactive than that from styrene which, in turn, is more reactive than the peroxy radical from 4-methoxystyrene.

INTRODUCTION

A cyclic transition state for the chain-ending interaction of secondary peroxy radicals with one another was first proposed in 1957 by G. A. Russell as a result of his work on the oxidation of ethylbenzene (1). A model of this transition state for two poly(peroxystyryl) peroxy radicals is shown below.

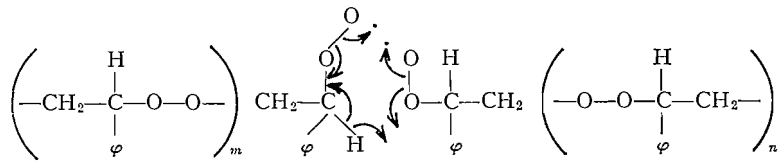

Russell's evidence favoring this mechanism was based on product studies at short kinetic chain lengths and, particularly, on the effects of deuterium substitution on oxidation rates. That is, provided it was assumed that the deuterium isotope effect on the propagation reaction was the same for ethylbenzene as for cumene then it could be calculated from the relative oxidation rates of ethylbenzene and ethylbenzene-α-d_1 that α-phenethyl peroxy radicals interacted to form non-radical products 1.9 times as rapidly as their α-deutero derivatives. This fairly large isotope effect has, so far, not been directly confirmed. We therefore decided to extend our measurements of the absolute rate constants for the autoxidation of styrene by the rotating sector technique (2) to four deuterostyrenes, α-d_1, β-d_2, α,β-d_3, and phenyl-d_5. We have also measured the propagation and termination rate constants for five ring-substituted styrenes (4-CH_3O, 4-CH_3, 4-Cl, 3-Cl, and 4-CN).

EXPERIMENTAL

The experimental conditions were the same as with styrene (2), i.e., 3 ml of hydrocarbon in 10 ml of chlorobenzene with α,α'-azo-bis-cyclohexylnitrile (6.7×10^{-3} mole/l) as the photo-initiator. The deuterostyrenes were obtained from Merck, Sharp and Dohme of Canada, Limited. Their deuterium content was not less than 98% of theory. The isotopic purities were confirmed by mass spectrometry and the positions of labelling were checked by nuclear magnetic resonance (n.m.r.) spectroscopy on the corresponding polystyrenes and polystyrene peroxides. 4-Methoxy-, 4-methyl-, 4-chloro-, and 3-chloro-styrene were obtained from the

[1]*Issued as N.R.C. No. 8591.*

Borden Chemical Company. 3-Nitrostyrene was obtained from the Aldrich Chemical Company. 4-Cyanostyrene was prepared from 4-cyanoacetophenone by the method of Marvel and Overberger (3) and 4-nitrostyrene was prepared from (2-bromoethyl) benzene by the method of Strassburg, Gregg, and Walling (4). All the styrenes were carefully purified before use.

RESULTS AND DISCUSSION

The Deuterostyrenes

Absolute rate constants for styrene and four deuterostyrenes at 40 °C and for styrene and two deuterostyrenes at 13 °C are given in Table I. The values for styrene itself differ somewhat from the values given in the previous paper (2) because they represent particular experiments (rather than the average of several experiments) which were done immediately before or after the deuterostyrene experiments under conditions which were as nearly identical as possible. Although the errors involved in determining k_t are considerable, the results support the occurrence of an α-deuterium isotope effect for bimolecular chain termination. From the data in Table I, the directly measured effect is found to be between 1.8 and 3.0 which is in good agreement with the value of 1.9 obtained indirectly by Russell (1). It provides additional support for the view that the α-hydrogen is abstracted in the bimolecular chain-terminating process for secondary peroxy radicals. This abstraction may occur directly (1) or it may, perhaps, involve the prior elimination of oxygen with the subsequent transfer of a hydrogen atom between the two resulting alkoxy radicals while they are still in the same solvent cage (5).

TABLE I

Absolute rate constants for deuterium-substituted styrenes (3 ml of styrene in 10 ml chlorobenzene)

Styrene	Relative rates of oxidation	k_p (l mole^{-1} s^{-1})	$k_t \times 10^{-7}$ (l mole^{-1} s^{-1})	k_x (s^{-1})
T = 40 °C				
$C_6H_5CH{:}CH_2$	1.00	65	2.7	0.52
$C_6H_5CD{:}CH_2$	1.18	57	1.5	—
$C_6H_5CH{:}CD_2$	1.14	78	2.1	0.50
$C_6H_5CD{:}CD_2$	1.43	55	1.0	—
$C_6D_5CH{:}CH_2$	1.01	69	3.0	0.40
T = 13 °C				
$C_6H_5CH{:}CH_2$	1.00	16	1.9	—
$C_6H_5CD{:}CH_2$	1.14	11	0.7	—
$C_6H_5CD{:}CD_2$	1.39	13	0.6	—

The propagation rate constants in Table I suggest that there are some secondary deuterium isotope effects in chain propagation. The enhanced value of k_p for the styrene-β-d_2 is probably due to the change in the configuration of the β-carbon atom from trigonal to tetrahedral (ref. 6; cf., however, refs. 7 and 8). The low values of k_p for styrene-α-d_1 and the styrene-α,β-d_3 are unexpected and might imply that k_t has been underestimated for these two styrenes, particularly in view of the fact that their actual oxidation rates are greater than for styrene itself. However, the fact that the propagation rate constant for styrene-α-d_1 is probably smaller than for styrene has been confirmed by n.m.r. analysis of the polymer produced by co-oxidizing equal concentrations of these two compounds at 40 °C. The polymer was prepared in a thermally initiated oxidation under conditions where the chain length was fairly long. It was purified by precipitation from a benzene solution with petroleum ether and n.m.r. analysis gave $(k_p)_{C_6H_5CHCH_2}/(k_p)_{C_6H_5CDCH_2} \approx 1.27$ with good agreement between the isotope effect calculated from the C_6H_5/CH ratio and from the CH_2/CH ratio. This value adds some support to the idea that there is a small positive secondary α-deuterium isotope effect in the propagation reaction.

Can. J. Chem. Downloaded from www.nrcresearchpress.com by 210.87.254.40 on 09/05/12
For personal use only.

The absolute rate constants for α-deuterostyrene were measured at four temperatures from 13 to 50 °C. They can be represented by

$$(k_p)_{C_6H_5CDCH_2} = (2.3 \pm 0.3) \times 10^8 \exp(-9500 \pm 1300/RT) \text{ l mole}^{-1} \text{ s}^{-1}$$

$$(k_t)_{C_6H_5CDCH_2} = (4.8 \pm 1.5) \times 10^9 \exp(-3700 \pm 1200/RT) \text{ l mole}^{-1} \text{ s}^{-1}.$$

The propagation activation energy is in fairly good agreement with the value found for styrene (2). The small activation energy for bimolecular termination is probably significant. However, if it is ignored an average value for k_t of $(1.2 \pm 0.3) \times 10^7$ l mole^{-1} s^{-1} is obtained. After correction for the variation in the chain initiation rate with temperature the overall activation energies for the oxidation of styrene (2), $C_6H_5CDCH_2$, $C_6H_5CHCD_2$, and $C_6D_5CHCH_2$ are all close to 7.2 kcal/mole.

Probably the most noticeable feature about Table I is that no first order termination could be detected under full illumination at 40 °C when the styrene contained a deuterium in the α-position. This was also true at 50 °C. These results indicate that k_x for styrene-α-d_1 is less than one-quarter of the value for styrene (2) and suggest that the α-hydrogen atom is abstracted in the rate-determining step of the first order termination process. Since this hydrogen is not abstracted from either monomer or polyperoxide (2) it must come either from a minor oxidation product or there must be an intramolecular abstraction in which the peroxy radical abstracts from one of the styrene units in its own chain. In the latter case, if abstraction occurred from the middle of the chain a benzyl radical would be produced and this radical should be able to continue the chain unless it was very deeply buried in the coiled up polymer. However, we were unable to detect any radicals by electron spin resonance (e.s.r.) in a sample of the polyperoxide polymer formed under conditions where first order termination was an important process. This suggests that if the first order process involves an intramolecular abstraction the hydrogen must come from the growing end of the polymer. This would give an unstable alkyl radical which should immediately decompose to a ketone and a hydroxyl radical. Alternatively, the benzyl radical formed by α-hydrogen atom abstraction from the middle of the chain may depolymerize to give formaldehyde, benzaldehyde, and, eventually, a hydroxyl radical (9). This radical could either initiate a new chain or add to an aromatic ring to give a cyclohexadienyl radical.

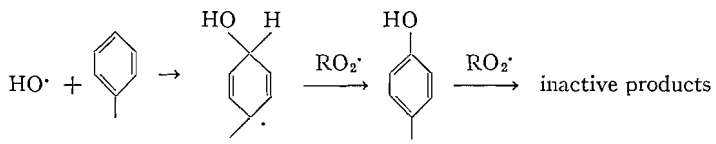

These radicals would not be expected to continue the chain but they could terminate additional chains by loss of hydrogen to give a phenol. The phenol would then react with more peroxy radicals in the usual way. This last reaction could perhaps be the actual process which shows the first order kinetics for chain termination.

The connection between compounds such as phenols, which contain readily exchangeable and abstractable hydrogen atoms, and the first order termination process is indicated by some experiments on the effect of H_2O and D_2O on the oxidation of styrene. That is, we have shown previously (10) that the addition of 10–20% by volume of H_2O increases the rate of oxidation of styrene by 12–15% and D_2O increases the rate by 30–50%. Some experiments on the rotating sector apparatus have now shown that the effect of H_2O can be entirely attributed to an increase in k_p, probably by a simple inert solvent effect (2).

Can. J. Chem. Downloaded from www.nrcresearchpress.com by 210.87.254.40 on 09/05/12
For personal use only.

In contrast, although D_2O has no effect on k_t and little effect on k_p, it entirely eliminates all measurable first order termination even at 50 °C (i.e., at 50 °C, k_x in the presence of D_2O is less than 0.2 s^{-1}). No deuterium could be detected by infrared spectroscopy in samples of styrene polyperoxide prepared in the presence of D_2O and therefore this isotope effect is not due to exchange of the α-hydrogen atom in the polymer. A possible explanation for these results is that the addition of D_2O causes those labile hydrogen atoms which are suitable for abstraction (e.g., phenolic hydrogens) to be replaced by much less readily abstractable deuterium atoms. These labile hydrogen atoms must therefore play an important role in the first order chain termination process just as does the α-hydrogen atom.

TABLE II

Absolute rate constants for substituted styrenes at 40 °C (3 ml in 10 ml of chlorobenzene)

Substituent	Relative rate of oxidation*		k_p (l $mole^{-1}$ s^{-1})	$k_t \times 10^{-7}$ (l $mole^{-1}$ s^{-1})	k_x (s^{-1})	$k_{inh} \times 10^{-3}$† (l $mole^{-1}$ s^{-1})
	Thermal‡	Photochemical				
$4CH_3O$	1.97	2.07	123	2.2	0.45	8.5
$4CH_3$	1.29	1.32	83	2.8	0.40	—
None	1.00	1.00	70§	3.6§	0.43§	10.8§
4Cl	1.37	1.48	123	4.9	0.32	—
3Cl	1.24	1.26	101	5.4	0.34	14.8
4CN	1.30	1.28	91	4.4	0.40	—
$3NO_2$	1.14	—	—	—	—	—
$4NO_2$	1.25	—	—	—	—	—

*At 2.01 moles/l. That is, these relative rates were calculated after correcting the measured rates to the values they would have at a concentration equal to that obtained with 3 ml of styrene in 10 ml of solvent. This correction produces the largest change with 4-methoxystyrene, the ratios obtained with the measured rates being 1.68 and 1.77, respectively.

†Rate constant for hydrogen abstraction from 2,6-di-*t*-butyl-4-methylphenol.

‡These oxidations were initiated thermally with 0.31 mole/l azo-bis-isobutyronitrile and were then compared with the rate obtained with styrene under these conditions.

§Average value from preceding paper (2).

The Substituted Styrenes

The absolute rate constants and thermal and photochemical rates of oxidation (relative to styrene at the same concentration) for five ring-substituted styrenes at 40 °C are given in Table II, the substituents being arranged in order of decreasing electron-donating power. This table also includes relative thermal rates of oxidation for meta- and para-nitrostyrene. Both these compounds are oxidized extremely slowly when the reaction is initiated photochemically. The slow photooxidations are not due to the low intrinsic oxidizability of the nitrostyrenes but, instead, result from their strong absorption of light at the initiating wavelength of 365 mμ. The rates of oxidation of all these styrenes were unaffected by decreasing the oxygen pressure from 760 mm to 50 mm.

The relative rates for 4-methoxystyrene and 4-nitrostyrene are in fairly good agreement with the values 1.56 and 0.99, respectively, obtained by Russell and Williamson (11) for the thermally initiated oxidations of 1.0 *M* styrene solutions in benzene at 60 °C.

Although the strongly electron-donating 4-methoxy group does produce a fairly large increase in the oxidation rate, there is no obvious correlation between the relative rates and the polar properties of the substituents. This result contrasts with the results obtained for the oxidation of substituted cumenes (11, 12) and toluenes (12) and for many other reactions involving hydrogen atom abstraction by radicals from substituted aromatic compounds (11, 13).

The absolute rate constants for first order termination do not vary appreciably from one substituent to another, but for second order termination there would appear to be an

Can. J. Chem. Downloaded from www.nrcresearchpress.com by 210.87.254.40 on 09/05/12
For personal use only.

increase in k_t as the substituents become more strongly electron attracting. However, it should be pointed out that Russell and Williamson's measurements of oxidation rates for mixtures of styrene with 4-methoxystyrene and with 4-nitrostyrene suggest that the rate constants for chain termination (k_t and k_x) are the same for all three styrenes (11).

The propagation rate constants cannot be correlated with the polar effects of the substituents. In this respect, therefore, the reactivity of substituted styrenes towards peroxy radicals differs from their reactivity towards the polystyryl radical (14) and the polystyrene anion (15). In these cases the reactivities can be approximately correlated with the σ constants of the substituents (see, however, ref. 16). The present results resemble instead those obtained for the reactivities of substituted styrenes towards methyl methacrylate and maleic anhydride, both of which give rise to strongly alternating systems as does styrene and oxygen (14). That is, with both these monomers electron-releasing groups enhance reactivity but electron-withdrawing groups either have little effect (maleic anhydride) or also enhance reactivity (methyl methacrylate) (14).

The results in Table II can be compared with the relative propagation rate constants obtained by Russell and Williamson by the competitive co-oxidation of styrene, 4-methoxystyrene, and 4-nitrostyrene with analysis for the unreacted styrenes (11). Solution of the "copolymerization" equation gave $(k_p)_{4MeO}/(k_p)_{styrene} = 1.2–1.8$ and $(k_p)_{4NO_2}/(k_p)_{styrene} = 0.2–0.6$. In a similar way, except that the styrene polyperoxide was analyzed, Dulog *et al.* (17) have obtained relative propagation rate constants for para-F, Cl, Br, I, and CH_3 styrenes at 50 °C. The relevant rate constants are $(k_p)_{4Me}/(k_p)_{styrene} = 1.4–1.5$ and $(k_p)_{4Cl}/(k_p)_{styrene} = 0.98–1.12$. The results obtained by both groups of workers suggest that the reactivity towards addition to styrene of para-substituted styryl peroxy radicals may depend on the para-substituent. It was, therefore, conceivable that a regular change in k_p with the polar properties of the substituents was disguised by a change in the reactivity of the attacking peroxy radicals. That is, the relatively large k_p's for electron-attracting substituents might be due to the greater reactivity of the corresponding peroxy radicals rather than to the enhanced reactivity of the substituted styrenes themselves.

With this point in mind, we measured the oxidation rates at 40 °C of 4-methoxy- and 3-chloro-styrene in the presence of several different concentrations of the inhibitor, 2,6-di-*t*-butyl-4-methylphenol. These inhibited rates yield k_p/k_{inh} where k_{inh} is the rate constant for abstraction of the phenolic hydrogen by peroxy radicals. The k_{inh} values obtained are compared with the value given previously for styrene at 40 °C (2) in Table II. The differences in k_{inh} are surprisingly large considering the distance separating the reaction site and the substituent. However, the changes in k_{inh} are in the expected direction. That is, hydrogen atom abstraction from phenols by peroxy radicals is known to involve a significant separation of charge in the transition state (13, 18). The radical with an electron-attracting substituent will tend to have a higher electron affinity than an unsubstituted radical or a radical with an electron-donating substituent. The transition state for this radical will therefore tend to be stabilized relative to the transition states for the other radicals and the rate constant for its reaction with the phenol will therefore be larger. However, the effect of substituents on the reactivity of peroxy radicals in hyrogen atom abstraction from phenols will be very much greater than their effect on reactivity for addition to styrene since the former reaction is so very much more sensitive to polar factors (e.g., 4-methoxyphenol is more than 80 times as reactive towards styryl peroxy radicals as is 3-chlorophenol (13)). Therefore, although the increased reactivity of styryl peroxy radicals containing electron-attracting substituents will tend to disguise the decreased reactivity of the substituted styrene itself, this effect should be relatively small.

Can. J. Chem. Downloaded from www.nrcresearchpress.com by 210.87.254.40 on 09/05/12
For personal use only.

The k_p values in Table II should therefore reflect mainly changes in the reactivity of the styrene molecule rather than its peroxy radical.* This means that polar effects are small in chain propagation and although they probably account for the small accelerating effect of the 4-methoxy and 4-methyl substituents their influence with electron-attracting substituents is more than outweighed by the effect these substituents have in increasing the stability of the resulting styryl radical. That is, electron-donating groups contribute little to radical stability, but radical stabilization by electron-attracting groups roughly parallels their electron-attracting ability in the para-position (14, 19). If we consider the transition state for propagation to consist of the three resonance forms

$$\underset{\text{I}}{XC_6H_4CH{=}CH_2\cdot OOR} \leftrightarrow \underset{\text{II}}{XC_6H_4\overset{\delta+}{C}H\text{---}\overset{\delta-}{C}H_2{:}OOR} \leftrightarrow \underset{\text{III}}{XC_6\dot{H}_4CH{-}CH_2{:}OOR}$$

then the present results suggest that structure III (which resembles the products) plays a more important role than structure II in stabilizing the transition state. This conclusion differs from the suggestion we made previously that structure II must make an important contribution to the transition state because of the fairly good correlation between the dielectric constant of a solvent and its effect on the rate of oxidation of styrene (20). That is, solvents with high dielectric constants increased the oxidation rate and this was attributed to their stabilizing influence on the dipolar structure II. The present results imply that in free radical reactions, solvent effects provide a more sensitive test than substituent effects for the occurrence of a contribution from structure II to the transition state.

TABLE III

Absolute rate constants for 4-methoxystyrene at different temperatures

Temp. (°C)	k_p (l mole^{-1} s^{-1})	$k_t \times 10^{-7}$ (l mole^{-1} s^{-1})	k_x (s^{-1})
22	55	1.7	0.20
30	81	1.8	0.30
40	123	2.2	0.45
50	159	1.7	0.77

The absolute rate constants for 4-methoxystyrene (Table III) give

$$k_p = (1.3 \pm 0.1) \times 10^7 \exp(-7200 \pm 500/RT) \text{ l mole}^{-1}\text{ s}^{-1}$$
$$k_t = (1.9 \pm 0.2) \times 10^7 \text{ l mole}^{-1}\text{ s}^{-1}$$
$$k_x = (8.5 \pm 0.4) \times 10^5 \exp(-8900 \pm 500/RT) \text{ s}^{-1}.$$

The propagation and first order termination activation energies are rather lower than the values found for styrene (2). The overall activation energy is 6.2 ± 0.4 kcal/mole.

ACKNOWLEDGMENT

We wish to thank Mr. M. Lesage for measuring the n.m.r. spectra of the styrene polyperoxide samples.

In calculating the absolute rate constants R_i was assumed to be the same for the substituted styrenes as for styrene itself. However, the referee has pointed out that the polar substituents (chloro, cyano, nitro) may have some effect on R_i at the substrate concentrations employed. If this is indeed the case, it might account for some of the "discrepancies" in k_p, e.g., it is hard to imagine the 3-chloro substituent having much stabilizing ability on a benzyl-type radical.

Can. J. Chem. Downloaded from www.nrcresearchpress.com by 210.87.254.40 on 09/05/12
For personal use only.

REFERENCES

1. G. A. RUSSELL. J. Am. Chem. Soc. **79**, 3871 (1957).
2. J. A. HOWARD and K. U. INGOLD. Can. J. Chem. This issue.
3. C. S. MARVEL and C. G. OVERBERGER. J. Am. Chem. Soc. **67**, 2250 (1945).
4. R. W. STRASSBURG, R. A. GREGG, and C. WALLING. J. Am. Chem. Soc. **69**, 2141 (1947).
5. S. W. BENSON. J. Am. Chem. Soc. **87**, 972 (1965).
6. M. MATSUOKA and M. SZWARC. J. Am. Chem. Soc. **83**, 1260 (1961).
7. G. S. HAMMOND and K. R. KOPECKY. J. Polymer Sci. **60**, S54 (1962).
8. I. M. BURKALOV, V. I. GOLDANSKII, and M. K. KUO. Dokl. Akad. Nauk SSSR, **155**, 883 (1964).
9. A. A. MILLER and F. R. MAYO. J. Am. Chem. Soc. **78**, 1017 (1956).
10. J. A. HOWARD and K. U. INGOLD. Can. J. Chem. **40**, 1851 (1962).
11. G. A. RUSSELL and R. C. WILLIAMSON, JR. J. Am. Chem. Soc. **86**, 2357, 2364 (1964).
12. G. A. RUSSELL. J. Am. Chem. Soc. **78**, 1047 (1956).
13. J. A. HOWARD and K. U. INGOLD. Can. J. Chem. **41**, 1744 (1963).
14. C. WALLING. Free radicals in solution. John Wiley & Sons, Inc., New York. 1957. Chap. 4.
15. M. SZWARC. Proc. Roy. Soc. London, Ser. A., **279**, 260 (1964).
16. R. M. WILEY, L. K. HEIDEMANN, and B. DAVIS. J. Polymer Sci. **B1**, 521 (1963).
17. L. DULOG, J. SZITA, and W. KERN. Fette Seifen Anstrichmittel, **65**, 108 (1963).
18. J. A. HOWARD and K. U. INGOLD. Can. J. Chem. **41**, 2800 (1963).
19. R. L. HUANG and S. SINGH. J. Chem. Soc. 3183 (1959).
20. J. A. HOWARD and K. U. INGOLD. Can. J. Chem. **42**, 1044 (1964).

Can. J. Chem. Downloaded from www.nrcresearchpress.com by 210.87.254.40 on 09/05/12
For personal use only.

Can. J. Chem. Downloaded from www.nrcresearchpress.com by 210.87.254.42 on 09/05/12
For personal use only.

THE PREPARATION OF A TRIVINYL CARBONIUM ION

T. S. SORENSEN
Department of Chemistry, University of Alberta at Calgary, Calgary, Alberta
Received April 13, 1965

ABSTRACT

The preparation of a stable trivinyl carbonium ion is described. A detailed evaluation and comparison of the n.m.r. spectrum of this ion with other stable carbonium ions, coupled with the use of ultraviolet spectroscopy, is used for the structure proof. The synthesis of the necessary tetraene precurser and the cyclization reactions of the above ion are also described. Comparisons of the cyclization rate of various stable carbonium ions are given and an attempt is made to evaluate the resonance stability of the trivinyl carbonium ion.

INTRODUCTION

Triphenyl carbonium ion is the classic of stable carbonium ions but examples of what might be called aliphatic analogs, trivinyl carbonium ions, have not been observed. In the last few years, however, many "enylic" carbonium ion solutions have been prepared, chiefly by Deno and his students; the structural confirmation of these ions being obtained mainly from the use of n.m.r. spectroscopy in quantitatively accounting for the hydrogen atoms. Sufficient results have now been obtained on carbonium ion proton positions in n.m.r. spectroscopy and the position of their maxima in ultraviolet spectroscopy that an analysis of the more complex behavior of trivinyl carbonium ions can be attempted.

Tricyclopropyl carbonium ion has been observed (1) and is a remarkably stable compound compared to the *t*-butyl cation, the obvious, though not so easily visualized, explanation being some sort of orbital overlap which delocalizes the positive charge. On this basis, a trivinyl carbonium ion might be expected to be even more stable. It is also of theoretical interest to observe to what extent the extra cross-conjugated —CH=C< group will stabilize this system over a divinyl carbonium ion.

Evidence is now presented to show that a trivinyl carbonium ion, I (R = R′ = CH_3), can be prepared at low temperatures, as a solution in neat fluorosulfonic acid. Attempts

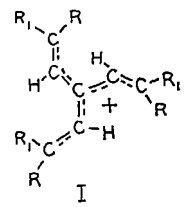

I

to prepare the analogs R = CH_3, R′ = H, and R = R′ = H have not been successful because the necessary carbonium ion precursors could not be obtained. Fluorosulfonic acid is even stronger than sulfuric acid and has a conveniently low melting point and viscosity. It has been previously used (2) as a protonating acid solvent in several instances as has the related chlorosulfonic acid (3).

One of the cyclized ions has been recovered from sulfuric acid solution by Deno and Pittman (4) and we believe that sufficient verification of the recoverability of these dienylic ions has been obtained in other similar systems (4, 9).

Can. J. Chem. Downloaded from www.nrcresearchpress.com by 210.87.254.42 on 09/05/12
For personal use only.

RESULTS

Synthesis of the Polyenes

Methallyl magnesium chloride can be added to phorone to yield the alcohol II which was obtained only in an impure form because of its very ready dehydration. The alcohol

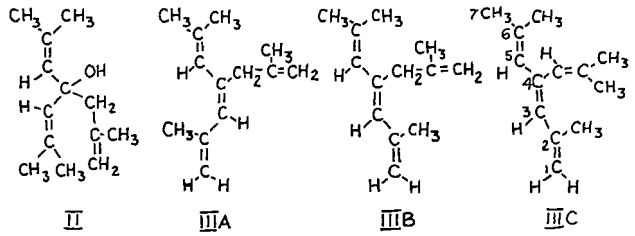

II IIIA IIIB IIIC

was easily dehydrated to yield a mixture containing principally (>95%) three compounds (labelled A, B, and C in the order of elution from a g.l.c. column). Compound A (52% of the total) could be separated in nearly pure form by careful fractional distillation at reduced pressure. Final purification was accomplished by preparative g.l.c. Compounds B (23%) and C (25%) could not be separated by distillation but could be separated in small amounts by the laborious application of preparative g.l.c. There are three possible unrearranged products of this simple dehydration III A and B, which are *cis* and *trans* isomers and a fully conjugated tetraene III C, for which there are no geometric isomers. Compound C is the fully conjugated tetraene as is quickly seen by the absence of $—CH_2—$ signals in the n.m.r. spectrum (Fig. 1C). The *cis* structure III A is assigned to the compound A and the *trans* to B based on experience obtained in the structural assignments of *cis*- and *trans*-2,4,6-trimethyl-1,3,5-heptatriene (5) which are similar to III A and III B (a methyl group instead of a methallyl group at C4). The significant feature in the n.m.r. spectrum of A (Fig. 1A) is a methyl group resonance at 8.44 τ which is absent in tetraene B (Fig. 1B). The presence of this same feature, at 8.40 τ, was in part used to assign the structures of the heptatrienes and a corresponding assignment is made in the case of the tetraenes. Also, the ultraviolet spectrum of tetraene A is similar to that of the *cis*-triene and that of tetraene B to the *trans*-triene (see Table I). The ultimate correctness of the geometry assigned to these two tetraenes rests therefore mainly on the validity of the original triene assignments.

Attempts to prepare III C by use of the Wittig reaction on phorone led to a mixture of two products (g.l.c.) neither of which had the correct retention time for III C. These compounds decomposed on attempted preparative separation at 150 °C and could not be characterized.

Attempts were made to prepare tripropenyl carbinol, as reported (6), from ethyl crotonate and 2 moles of propenyl magnesium bromide, with a view to dehydrating this to the corresponding conjugated tetraene. In our hands, the reaction leads mainly to ketonic material, presumably due to 1,4-addition. In another attempt, allyl magnesium chloride was added to hepta-2,5-dien-4-one. A small yield of a polyene mixture was obtained but the individual components could not be obtained pure. The material was very unstable and it should be noted that the system is favorable for Cope cyclizations (7). By adding allyl magnesium chloride to ethyl crotonate, there was obtained in 60% yield, 4-allylhepta-1,5-dien-4-ol. This was easily dehydrated to the corresponding tetraene IV which is a mixture of two isomers in about equal amount (the g.l.c. traces overlap

Can. J. Chem. Downloaded from www.nrcresearchpress.com by 210.87.254.42 on 09/05/12
For personal use only.

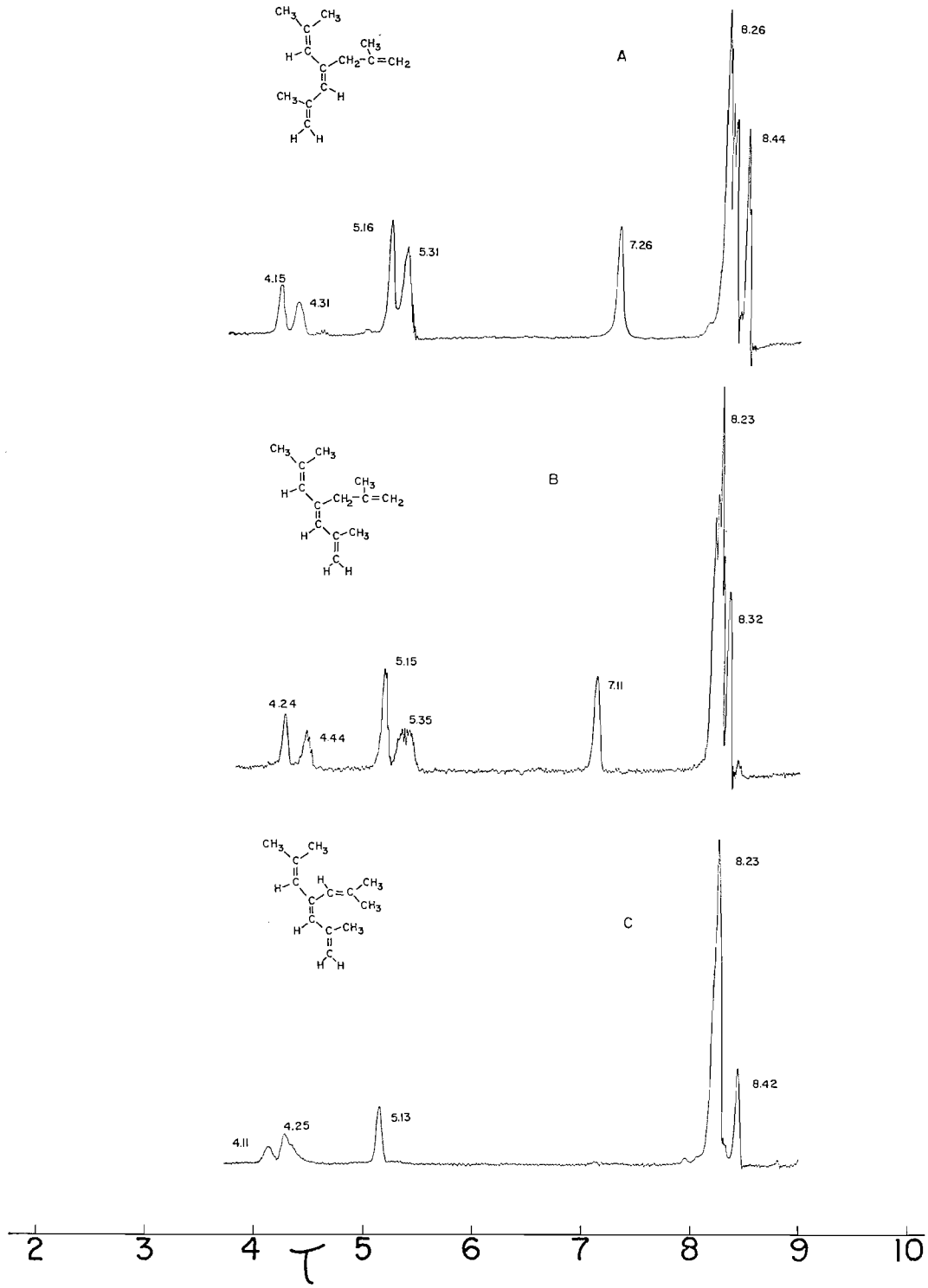

FIG. 1. The n.m.r. spectra of: A, the *cis*-tetraene (III A); B, the *trans*-tetraene (III B); and C, the completely conjugated tetraene (III C).

TABLE I
Ultraviolet spectra

Compound	Max (mμ)	ϵ_{max}	Solvent
III A	210(s)*		Isooctane
	241.8	12 200	
cis-2,4,6-Trimethyl-1,3,5-heptatriene	210(s)		Isooctane
	239.5	11 300	
III B	261.0	11 600	Isooctane
trans-2,4,6-Trimethyl-1,3,5-heptatriene	258.5	9 900	Isooctane
III C	225	10 430	Isooctane
	281.0	15 980	
IV (*cis–trans* mixture)	260(s)	28 900	Isooctane
	269.0	35 500	
	278.5	27 100	
I (R = R′ = CH_3)	402	~45 000†	FSO_3H
VII and VIII (mixture)	378	40 000	96% H_2SO_4
	373	—	FSO_3H
VI	396‡	45 000	96% H_2SO_4
XII	396	50 000	96% H_2SO_4
	395	—	FSO_3H

* Shoulder.
†Based on the ϵ_{max} of the VII and VIII mixture which was determined in 96% H_2SO_4 as 40 000 and which is assumed for these ions in FSO_3H. This value is likely low in view of the extraneous material appearing in the n.m.r. spectrum of I.
‡A similar result has been found by Deno and Pittman (4).

strongly). These are likely *cis* and *trans* isomers about the 3,4-double bond. Attempts to cause the isolated double bond to move into conjugation failed.

Attempts to prepare trivinyl carbinol by adding vinyl magnesium bromide to ethyl carbonate or ethyl acrylate yielded only polymeric material in both cases.

The Carbonium Ions

The chemical shifts of the carbonium ion protons in fluorosulfonic acid are consistently at 0.2–0.3 p.p.m. higher field than in 96% sulfuric acid, with reference to external tetramethylsilane. The trivinyl carbonium ion cannot be prepared in sulfuric acid solvent because of the high freezing point of the latter. However, one would still like to compare the τ values for the protons in this ion with those of similar ions, almost all of which have been obtained in sulfuric acid. This comparison is obtained by recording curves where the ion I (R = R′ = CH_3) has only partially cyclized and one can directly compare the proton positions of the original trivinyl ion relative to those of the cyclized ions. Since the cyclized ion positions are well known in 96% sulfuric acid, one can easily calculate theoretical τ values for the trivinyl carbonium ion protons in this solvent. All τ values referred to in the text are for (hypothetical) 96% sulfuric acid solution. It should be emphasized that this involved procedure is only valid because all the protons appear to be shifted a constant amount in the two solvents and is done only because direct comparisons are needed.

Fig. 2A shows the spectrum of III C obtained in fluorosulfonic acid at −55 °C. The two main peaks in their respective regions are at 3.11 τ and 7.65 τ with relative areas about 1:6 (depending to some extent on how one extends the line for the peak at 7.65 τ). These positions are at higher fields than those in divinyl carbonium ions (see Table II) and, coupled with the immediate disappearance of only these two peaks on warming, lead to the conclusion that one is observing the trivinyl carbonium ion I (R = R′ = CH_3). The ultraviolet spectrum shows a similar phenomena, a peak disappearing at 402 mμ and the resulting appearance of one at 373 mμ. The other n.m.r. peaks in the spectrum fit to some extent with those obtained by the protonation of the *cis* and *trans* unconjugated tetraenes III A and B. The conjugated tetraene sample used for this work contains no

Can. J. Chem. Downloaded from www.nrcresearchpress.com by 210.87.254.42 on 09/05/12
For personal use only.

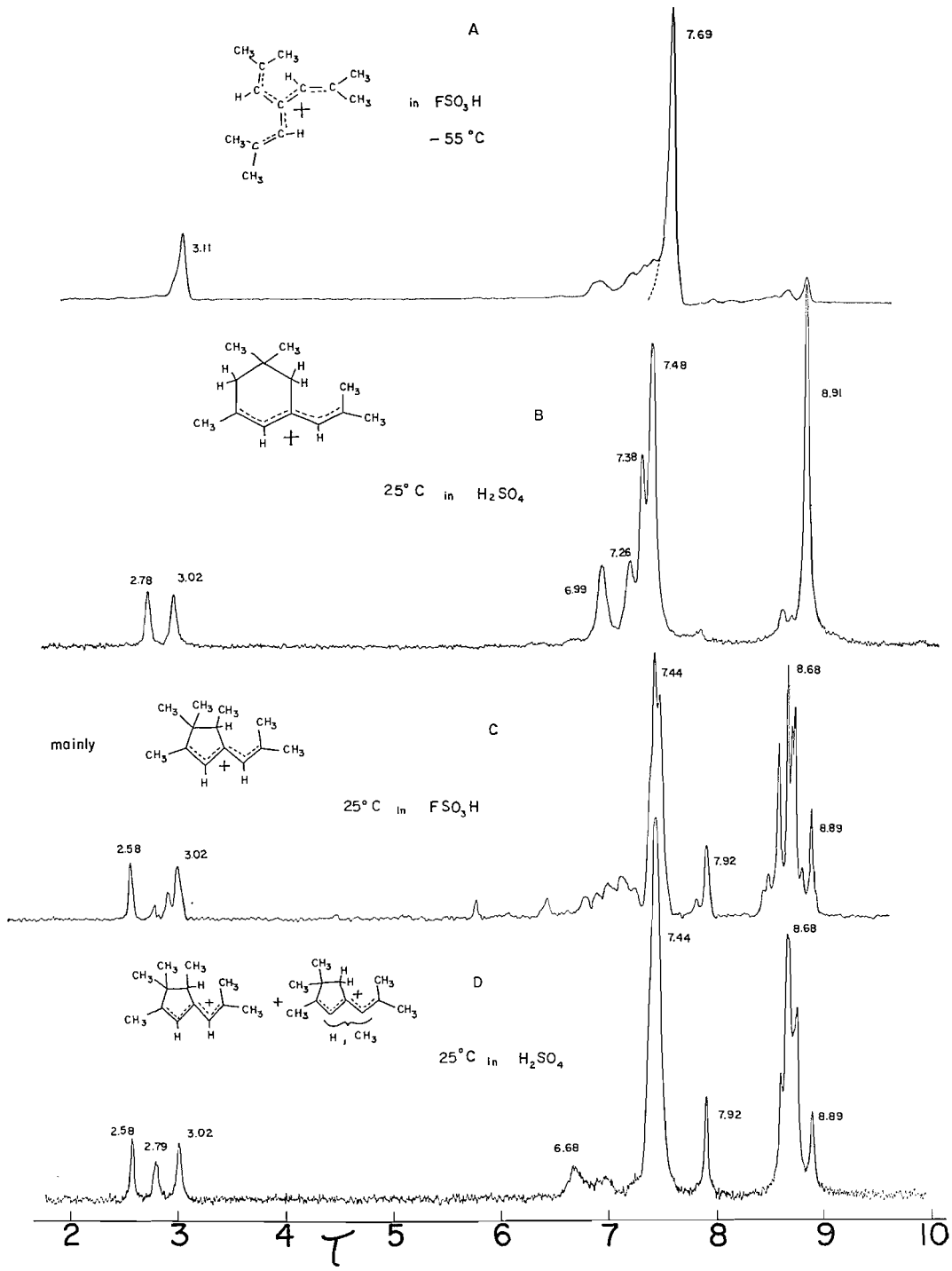

FIG. 2. The n.m.r. spectra of the pertinent carbonium ions.

Can. J. Chem. Downloaded from www.nrcresearchpress.com by 210.87.254.42 on 09/05/12
For personal use only.

TABLE II
Comparison of n.m.r. proton positions

Ion	Protons	Resonance position (τ)
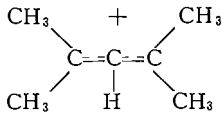	12 Methyl protons 1 Alkene proton	7.04* 2.26
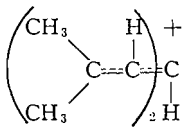	2 Methyl protons 12 Alkene protons	7.33 and 7.38 (av. 7.35) 2.79 and 3.01 (av. 2.90)
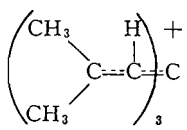	18 Methyl protons 3 Alkene protons	7.65 3.11

*Reported in ref. 8.

III A and no more than 1–2% of III B. There may be somewhat more than 1% of a higher retention product but the tetraene has approximately 97% purity and the bulk of the extraneous peaks are not due to impurities. There are two reasonable positions for the protonation of III C, at C1 or C3. Protonation at C3 leads to the same intermediate ion (V) that is presumed to be formed on protonation of III A or B.

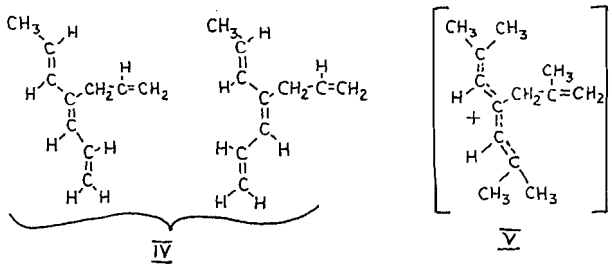

IV V

The relative affinity of C1 or C3 for a proton will ordinarily depend on the stability of the resulting ions. In the above case, however, the tetraene was added dropwise (a rapid addition) to the fluorosulfonic acid and the position of the addition might be kinetically controlled to some extent. Considering the method of addition, there is surprisingly little polymeric material (absorption background about 9 τ). Addition of the tetraene from the gas phase was not very satisfactory since fluorosulfonic acid is reasonably volatile and trace amounts will polymerize the incoming tetraene on the walls of the vacuum line.

Fig. 2B shows the spectrum of the sulfuric acid solution of either III A or B, for comparison purposes, in order to show the similar peak positions of this ion with the extraneous absorption discussed above. The structure of this ion (VI) has been previously proven by Deno and Pittman (4) who have prepared it from the alcohol II and independently by first synthesizing the corresponding cyclized triene. Fig. 2C shows the

Can. J. Chem. Downloaded from www.nrcresearchpress.com by 210.87.254.42 on 09/05/12
For personal use only.

spectrum resulting from the warming of the solution of Fig. 2A (Half-life of ion I ca. 1 h at −55 °C). This is compared with Fig. 2D which was obtained by adding the conjugated tetraene to 96% sulfuric acid. Even at −30 °C, this same spectrum was obtained. In general, there is reasonable agreement for the peaks which have appeared from warming the solution in Fig. 2A with those obtained in sulfuric acid solution, the former being somewhat sharper in the less viscous solvent. The spectrum shown in Fig. 3 D is assigned to a mixture of ion VII (ca. 60%) and ion VIII (ca. 40%), the relative amounts not changing on standing at 25 °C.

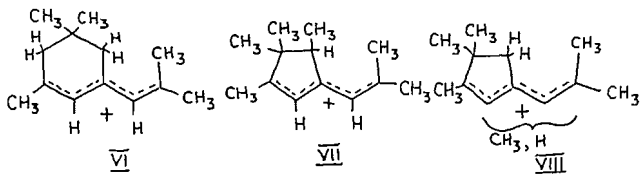

VI VII VIII

This assignment is based on (*a*) the presence of $^{+}C—CH_3$ methyl groups at 7.44 τ, in the region found for dienylic ions; (*b*) the presence of a sharp peak at 7.92 τ, very characteristic of a methyl group attached to carbon atoms between carbonium ion centers, but of an intensity indicating only 40% of the area expected if the solution contained pure VIII; (*c*) the presence of three peaks in the region where protons attached to carbon atoms between carbonium ion centers are found, two for ion VII and one for ion VIII; and (*d*) the *gem*-dimethyl protons found at 8.68 τ, indicating that they are one carbon removed from a carbonium ion center, i.e., compare with the higher signals found in ion VI and also with the extensive table of proton positions elaborated by Deno *et al.* (8). There is also a precedent for the formation of these two compounds. The cyclization of the ion IX at −30 °C leads to ions X and XI except that, in this case, the ion X quickly rearranges to ion XI (9).

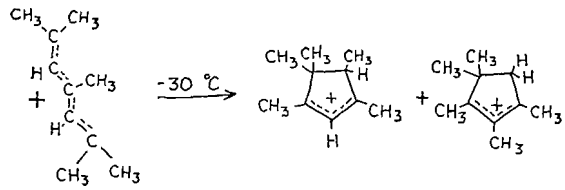

IX X XI

As additional evidence, the ultraviolet spectra of these ions have been determined (Table I). Ion VI has a λ_{max} 396 mμ, similar to acyclic dienylic ions (4, 9) while the mixture of ions VII and VIII have λ_{max} 378 mμ, at considerably shorter wavelengths but certainly still due to a dienylic ion. Cyclopentenyl ions are known (10) to absorb at appreciably shorter wavelengths than cyclohexenyl ions or acyclic analogs so that the ultraviolet evidence also supports the assignment of the structures VII and VIII.

Attempts to add the compound IV to sulfuric acid resulted only in polymer formation, but in very dilute solutions an ultraviolet spectrum was obtained, λ_{max} 356 mμ, ϵ_{max} 43 000. This ion would be expected to be analogous to ion VI without methyl groups at C3, C5, or C2′.

For comparisons of the rates of various cyclizations, ions IX and XII were prepared in fluorosulfonic acid. Ion IX has a half-life of only a few minutes at −55 °C; an n.m.r.

Can. J. Chem. Downloaded from www.nrcresearchpress.com by 210.87.254.42 on 09/05/12
For personal use only.

spectrum of the pure ion, uncontaminated with cyclized ion, was not obtained. Ion XII is more stable and, interestingly, one can observe the fleeting appearance of the intermediate ion XIII during the warming-up process.

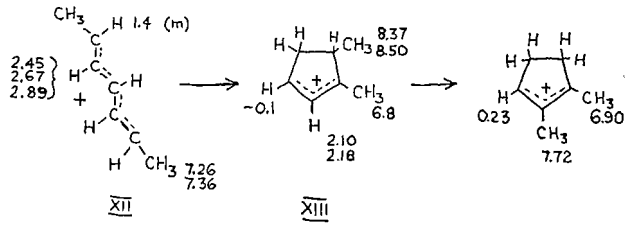

XII XIII

DISCUSSION

The trivinyl carbonium ion, I (R = R′ = CH_3), undergoes a cyclization reaction at least 10^5 times faster than the corresponding divinyl carbonium ion XIV, even allowing for a statistical factor favoring the cyclization in I, but its cyclization is slower than that of the ion IX. The rapidity of the cyclization of IX compared to XIV has been suggested (9) to be due to steric repulsion of methyl groups resulting in a non-planar ion and a lower transition state energy for IX. Molecular model studies of I, where R = R′ = CH_3, indicate that it is likewise prevented by steric repulsion from being completely planar. The above steric argument may be used to explain its fast cyclization reaction but an alternative rationalization can be envisaged. For cyclization to take place, the molecule must have two double bonds in an s-*cis*, s-*cis* arrangement. It is clearly impossible for these to be coplanar with the middle carbon and, in fact, molecular model studies indicate that at least one of the double bonds (and probably both) must be nearly orthogonal to this carbon. One is therefore comparing intermediates where the positive charge is localized on a secondary carbon or delocalized by an allylic system with resulting reduction in energy. This process is represented below.

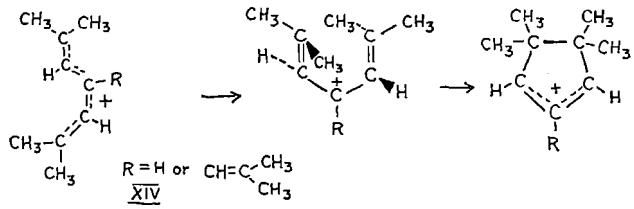

XIV

By analogy to the triphenyl carbonium ion, ion I might be expected to have a propeller shape. The actual position of the n.m.r. signals may be taken as evidence that the delocalization involves all three rings simultaneously (propeller shape), with concomitant reduction in the charge density at the individual positions and higher τ values. Alternatively, there may be a rapid interchange of non-equivalent groups leading to averaged τ values which could be higher than in divinyl carbonium ions.

There was some vague indication in the n.m.r. spectral results that the stability of ion I might not differ greatly from that of V. In comparing the stability of these two ions we can ignore the fact that ion V can cyclize readily since this process probably occurs subsequently. Hückel simple M.O. calculations (11) lead to values of 2 β for the stabilization energy of I and 1.464 β for V. The corresponding polyenes, III C and III A or B,

Can. J. Chem. Downloaded from www.nrcresearchpress.com by 210.87.254.42 on 09/05/12
For personal use only.

have stabilization energies of 1.441 and 0.988 β respectively. These calculations are, however, of limited value because of the steric effects involved, and it is not unreasonable to expect that because of deviations from maximum overlap in the trivinyl carbonium ion, its stabilization energy could be lowered to nearly that of the divinyl carbonium ion. An analogy for this can be found. Triphenyl carbonium ion has a pK_R^+ of -6.63 while the corresponding diphenyl carbonium ion value is -13.3 (12). However, this difference is attributed mainly to a steric effect favoring ionization in the triphenyl case and the resonance energy of these two ions is postulated to be nearly the same.

The ion I (R = H, R′ = CH_3) will not have any steric repulsions preventing coplanarity, but results with the corresponding divinyl carbonium ion XII lead us to believe that ion I will not be much more stable toward cyclization than is XII.

Ultraviolet Spectra

The trivinyl carbonium ion has a λ_{max} 402 mμ, ϵ_{max} ca. 45 000 in fluorosulfonic acid. This is not greatly different from that of divinyl carbonium ions and is in agreement with the results of Hückel simple LCAO calculations which predict a transition energy of β in both cases. The curve for the trivinyl carbonium ion, is however, somewhat broader than that of the divinyl carbonium ion.

EXPERIMENTAL

Ultraviolet spectra were measured using a Beckman DK-1 or DU with 0.1 cm cells and are listed in Table I. Infrared spectra have been obtained on all new compounds using a Perkin–Elmer model 337 spectrophotometer. The n.m.r. spectra were recorded using a Varian Assoc. A-60 spectrometer equipped with a variable temperature probe, using ca. 10% solutions in carbon tetrachloride and tetramethylsilane internal reference. For the carbonium ion spectra in FSO_3H or H_2SO_4, tetramethylammonium cation (8) or external tetramethylsilane was used as a reference. Areas were obtained by integration or by weighing the peaks. Gas chromatography separations were made using an Aerograph "Autoprep" model A-700 with a 12 ft × 3/8 in. column packed with 30% Carbowax 20M on 60/80 Chromosorb W, HMDS treated. Analytical results were obtained on an Aerograph "Hy-Fi" model 600 using a 6 ft × 1/8 in. column of 5% SE-30 on Chromosorb W.

The gas-phase addition of polyenes to sulfuric acid has been described previously (9). Addition of the polyenes to FSO_3H was made dropwise from a capillary tip at -80 °C. The fluorosulfonic acid was redistilled in the absence of moisture. The preparation of several of the trienes used in this work has been described previously (5).

4-Methallyl-2,6-dimethylhepta-2,5-dien-4-ol (II)

Methallyl magnesium chloride was prepared by adding 45.2 g (0.5 moles) of methallyl chloride in 100 ml of ether over a 3 h period to 182.4 g (7.5 moles) of magnesium suspended in 1 l of dry ether. Magnesium chloride precipitates out and the ether solution becomes very syrupy. Phorone, recrystallized from ether, m.p. 28 °C, 35 g (0.25 moles) in 100 ml of ether, was added over a 30 min period to this solution. After letting the mixture stand for several hours, most of the ether solution was decanted from the excess magnesium and then decomposed by adding 500 cc of water to it. The two layers were separated, and the aqueous layer was extracted with a further 200 ml of ether. The magnesium turnings were also washed with water and portions of ether; the combined ether layers were then dried over magnesium sulfate. The ether was removed under reduced pressure and the residue was distilled through a spinning band column, b.p. ~60 °C at 0.25 mm. Slight cloudiness in the product indicated that some dehydration had occurred. Yield 40.2 g (82%).

Dehydration of 4-Methallyl-2,6-dimethylhepta-2,5-dien-4-ol

The title alcohol (46.5 g, 0.24 moles) in 100 ml of benzene was treated with 100 mg of *p*-toluenesulfonic acid. The solution was then heated to reflux temperature and the water formed by azeotropic distillation was collected in a Dean–Stark trap. The residual benzene solution was washed with aqueous potassium hydroxide and several times with water before drying over anhydrous magnesium sulfate. Rapid distillation of the residue after removal of the benzene yielded 32.5 g (77%) of crude mixed tetraenes, b.p. 25–35 °C at 0.05–0.2 mm. This mixture was analyzed by g.l.c. and showed three main peaks (>95% of the total area). The remaining 5% consists of several longer retention peaks, one of which overlaps to some extent with the third of the three main peaks. The approximate amounts of each compound were determined by measuring the area under the peaks and are 52%, 23%, and 25% in the order of increasing retention time.

Can. J. Chem. Downloaded from www.nrcresearchpress.com by 210.87.254.42 on 09/05/12
For personal use only.

This mixture was fractionally distilled at 5–6 mm through a 1 m spinning band column, 12 fractions of nearly equal size being collected.

Fraction No.	Boiling range, °C	Refractive index, $n_D^{21.5}$
1.	57–68.5	1.4821
2.	68.5–69.5	1.4878
3.	69.5–70.5	1.4885
4.	70.5–71.0	1.4892
5.	71.0–72.0	1.4907
6.	72–75.0	1.4951
7.	75.0–76.0	1.4994
8.	76.0–76.5	1.5016
9.	76.5–77.0	1.5044
10.	77.0–78.0	1.5091
11.	78.0–78.5	1.5115
12.	78.5	1.5070

A significant amount of material polymerizes in the distillation pot during the course of the distillation (about 12 h). Each of the above fractions was analyzed by g.l.c. Fractions 2–5 were 98% compound A but the other fractions were mixtures. By using the best fractions for g.l.c. preparative separations, it proved possible to isolate each compound. For this purpose, fractions 2–5 were used to obtain A, 8 to obtain B, and 10–11 to obtain C. The column operating temperature was 125 °C, the helium flow rate was ca. 200 ml/min, and the size of the injection sample was 50 μl. The retention times were 11, 18, and 20.25 min respectively. The g.l.c. trace for compound A is completely separated but those for compounds B and C overlap to some extent. These could be obtained in about 98 and 97% purity respectively; the main impurity in C is not B but a higher retention product which could not be completely removed. Attempts to use longer columns necessitated higher temperatures, and 12 ft was picked as the maximum length possible without causing decomposition of the sample. The n.m.r. and ultraviolet spectra of these tetraenes are reported in Fig. 1 and Table I. The purity of the compounds separated by g.l.c. was checked by analytical g.l.c. These tetraenes were stored under nitrogen in the freezing compartment of a refrigerator. Before use, they were evaporated under high vacuum to remove any polymeric material.

Compound A. cis-2,6-dimethyl-4-(2-methyl-2-propenyl)-1,3,5-heptatriene (III A).—$n_D^{23.5}$ = 1.486. Anal. Calcd. for $C_{13}H_{20}$: C, 88.56; H, 11.44. Found: C, 88.31; H, 11.47.

Compound B. trans-2,6-dimethyl-4-(2-methyl-2-propenyl)-1,3,5-heptatriene (IIIB).—n_D^{25} = 1.496. Anal. Calcd. for $C_{13}H_{20}$: C, 88.56; H, 11.44. Found: C, 88.18; H, 11.44.

Compound C. 2,6-dimethyl-4-(2-methyl-1-propenyl)-1,3,5-heptatriene (III C).—$n_D^{22.5}$ = 1.516. Anal. Calcd. for $C_{13}H_{20}$: C, 88.56; H, 11.44. Found: C, 88.46; H, 11.73.

4-Allylhepta-2,5-dien-4-ol

Magnesium (60 g, 2.47 moles) and 500 ml of ether were placed in a 2 l three-neck flask. A solution of 20 g (0.26 moles) of allyl chloride in 100 ml of ether was added at such a rate that the solution maintained a gentle reflux. Then a solution of 55.5 g (0.49 moles) of ethyl crotonate and 133 g (1.74 moles) of allyl chloride in 400 ml of ether was added over a 2 h period. The solution was refluxed for 1 h and then decomposed with cold saturated ammonium chloride (500 ml). The two layers were separated, the aqueous layer was extracted with a further 250 ml of ether, and the combined ether fractions were dried over anhydrous potassium carbonate. Distillation of the residue after removal of the ether yielded 50 g (59%) of clear liquid, b.p. 63–63.2 °C at 5–6 mm, n_D^{22} = 1.4687. Reported (13) b.p. 93.5° at 35 mm, n_D^{20} = 1.4707. Anal. Calcd. for $C_{10}H_{16}0$: C, 78.89; H, 10.59. Found: C, 78.39; H, 10.02.

The n.m.r. spectrum is in good agreement with the expected structure. The spectrum also indicates the presence of only one (presumably *trans*) isomer.

Dehydration of 4-Allylhepta-2,5-dien-4-ol

A solution consisting of the above alcohol (20 g, 0.132 moles), dry benzene (100 ml), and *p*-toluenesulfonic acid dihydrate (100 mg) was heated under reflux (~1 h), about 2 ml. of water being collected in a Dean–Stark trap. The solution was then washed with potassium hydroxide solution and several times with water before being dried over potassium carbonate. Rapid distillation of the residue, after careful removal of the benzene, gave 11.8 g of product (67%), b.p. 53 °C at 5–6 mm. This was redistilled through a spinning band column to yield a constant refractive index product, b.p. 54.3–54.5 °C at 5–6 mm, n_D^{21} = 1.5365. This material shows two, nearly equal size, very strongly overlapping peaks on g.l.c. analysis. This result is also consistent with the n.m.r. spectrum of the material which shows two overlapping doublets for the split methyl protons. The integrated areas for the alkene, methylene, and methyl protons are in the expected ratio of 9:2:3. This product is therefore a mixture of *3,4-trans and 3,4-cis-4(2-propenyl)-1,3,5-heptatriene* (IV).

Anal. Calcd. for $C_{10}H_{14}$: C, 89.49; H, 10.51. Found: C, 89.79; H, 10.47.

Attempts to isomerize the double bond with acetic acid – sulfuric acid resulted in much polymerization and the recovery of only unchanged starting material.

Can. J. Chem. Downloaded from www.nrcresearchpress.com by 210.87.254.42 on 09/05/12
For personal use only.

Reaction of Phorone and 2-Methyl-2-propenylidenetriphenylphosphorane

A suspension of 19.39 g (0.055 moles) of methallyltriphenylphosphonium chloride in 150 ml of ether was treated with 1 equiv of butyl lithium (20 ml of a 2.83 *M* heptane solution). The resulting red solution was stirred an additional 30 min, and then 6.21 g of phorone (0.045 moles) in 100 ml of dry ether was added over a 30 min period. The resulting solution was refluxed in a N_2 atmosphere for 18 h. Water (200 ml) was added, the two layers were separated, and the aqueous layer was extracted with a further 100 ml of ether. The combined ether layers were dried over potassium carbonate. Removal of the ether left a residual paste from which 5.4 g (68% assuming $C_{13}H_{20}$) was distilled at about 0.1 mm. Analysis by g.l.c. indicates two main components in the ratio 3:5. Both have retention times slightly longer than that expected for III C. Spectral studies of the mixed material by n.m.r. and infrared tend to confirm the absence of the desired product. These two components appear to decompose on attempted preparative g.l.c. at 150 °C using the previously described column.

ACKNOWLEDGMENTS

The author wishes to thank the National Research Council of Canada for financial support. Acknowledgments are also due to Dr. Frank Adam for many helpful discussions, Mr. Kam. T. Wong for help in the low-temperature ultraviolet spectral measurements, and Miss V. Knutsen for the n.m.r. spectra.

REFERENCES

1. N. C. Deno, H. G. Richey, Jr., J. S. Liu, J. D. Hodge, J. J. Houser, and M. J. Wisotsky. J. Am. Chem. Soc. **84**, 2016 (1962).
2. T. Birchall and R. J. Gillespie. Can. J. Chem. **42**, 502 (1964).
3. D. G. Farnum. J. Am. Chem. Soc. **86**, 934 (1964).
4. N. C. Deno and C. U. Pittman, Jr. J. Am. Chem. Soc. **86**, 1871 (1964).
5. T. S. Sorensen. Can. J. Chem. **42**, 2781 (1964).
6. H. Normant and P. Maitte. Bull. Chim. Soc. France, 951 (1956).
7. E. N. Marvell, G. Caple, and B. Schatz. Tetrahedron Letters, **7**, 385 (1965). E. Vogel, W. Grimme, and E. Dinne. Tetrahedron Letters, **7**, 391 (1965).
8. N. C. Deno, H. G. Richey, Jr., N. Friedman, J. D. Hodge, J. J. Houser, and C. U. Pittman, Jr. J. Am. Chem. Soc. **85**, 2991 (1963).
9. T. S. Sorensen. Can. J. Chem. **42**, 2768 (1964).
10. N. C. Deno, J. Bollinger, N. Friedman, K. Hafer, J. C. Hodge, and J. J. Houser. J. Am. Chem. Soc. **85**, 2998 (1963).
11. A. Streitwieser. Molecular orbital theory for organic chemists. John Wiley and Sons, Inc., New York. 1961.
12. N. C. Deno and A. Schriesheim. J. Am. Chem. Soc. **77**, 3051 (1955).
13. J. Munch-Petersen, P. M. Joergensen, and S. Refn. Acta Chem. Scand. **13**, 1955 (1959).

Can. J. Chem. Downloaded from www.nrcresearchpress.com by 210.87.254.42 on 09/05/12
For personal use only.

Can. J. Chem. Downloaded from www.nrcresearchpress.com by 210.87.254.42 on 09/05/12
For personal use only.

THE MONO-OXALATO COMPLEXES OF IRON(III)

PART I. EQUILIBRIA

R. F. Bauer and W. MacF. Smith
Department of Chemistry, Queen's University, Kingston, Ontario

Received October 1, 1964

ABSTRACT

The formation of the mono-oxalato complexes of iron(III) has been examined spectrophotometrically at ionic strength 0.50, between 5 and 25 °C and hydrogen ion concentrations 0.2 to 0.5 *M*. Evidence is presented that the protonated complex $FeHC_2O_4^{++}$ is present in significant concentration in these solutions. The formation quotients of the species $FeC_2O_4^{+}$ and $FeHC_2O_4^{++}$ for temperatures 5, 15, and 25 °C have been determined and the extinction coefficients at 310 mμ have been estimated.

INTRODUCTION

The formation of the oxalato complexes of iron(III) has been studied by Badoz-Lambling (1, 2) and Babko and Dubovenko (3). Lambling established the existence of the complexes $Fe(C_2O_4)^+$, $Fe(C_2O_4)_2^-$, and $Fe(C_2O_4)_3^{3-}$ on the basis of neutralization curves and estimated values for the formation constants of these complexes. Using the method of continuous variation with solutions 5×10^{-4} *M* in iron(III) perchlorate and in oxalic acid Babko and Dubovenko found that at pH 1 the complex $Fe(C_2O_4)^+$ is the predominant species in aqueous solution. This is consistent with Lambling's values for the formation constants which indicate that the concentration of $Fe(C_2O_4)_2^-$ should be less than 0.5% of that of $Fe(C_2O_4)^+$ under these conditions.

There appears to be no published data indicating that the protonated mono-complex $Fe(HC_2O_4)^{++}$ is formed. However, in view of the fact that at pH 1 the ratio $[HC_2O_4^-]/[C_2O_4^=]$ is of the order of 1000/1, a relatively small formation constant could lead to such a complex being a significant species in solution. Before a study of the kinetics of the oxalate complexes of iron(III) was undertaken we obtained information about the formation constants of mono-oxalato iron(III) and the corresponding protonated complex at ionic strength 0.5.

EXPERIMENTAL

Apparatus

The formation of the complexes was examined spectrophotometrically using thermostated quartz cells of 10 mm and 1 mm path length and a Beckman DK1 extended range spectrophotometer. Optical densities at λ 310 mμ were used in assessing the formation quotients. At this wavelength the species $C_2O_4^=$, $HC_2O_4^-$, and $H_2C_2O_4$ are substantially transparent and the difference in the extinction coefficients of the oxalato complexes of iron(III) and the iron(III) not so complexed approaches a maximum. pH measurements were made with a Radiometer Number 4 pH meter.

Solutions

Solutions were prepared from triply distilled water, the second distillation being from alkaline permanganate solution. Solutions involving iron(III) perchlorate, perchloric acid, and sodium perchlorate were prepared and analyzed as previously described (4). Oxalic acid was reagent grade from Nichols Chemical Company.

DISCUSSION

Preliminary Considerations

The predominant reactions to consider are

$$Fe^{+++} + C_2O_4^= \rightleftharpoons Fe(C_2O_4)^+$$

$$Fe^{+++} + HC_2O_4^- \rightleftharpoons Fe(HC_2O_4)^{++}.$$

Can. J. Chem. Downloaded from www.nrcresearchpress.com by 210.87.254.42 on 09/05/12
For personal use only.

Other pertinent reactions which may occur are (*a*) the hydrolysis of Fe^{+++} to $Fe(OH)^{++}$, (*b*) the formation of polynuclear iron(III) species, (*c*) the photochemical oxidation of oxalic acid sensitized by ferric ion.

Reactions *a* and *b* have been studied by Mulay and Selwood (5), Milburn and Vosburgh (6), and Turner and Miles (7). Turner and Miles consider that the absorption spectrum of iron(III) solutions is interpretable in terms of $FeOH^{++}$ having absorption peaks at 205 mμ and 300 mμ and Fe^{+++} having one at 240 mμ. The dimer $Fe_2(OH)_2^{4+}$ is believed to absorb fairly markedly at 335 mμ and Milburn and Vosburgh suggest that this polynuclear iron(III) species contributes significantly to optical density at hydrogen ion concentrations of 0.2 *M* if the ferric ion concentration exceeds 10^{-3} *M*. Since the method described below of treating the experimental data is based on the assumption that the effective extinction coefficient of Fe(III), $\epsilon_{Fe\ eff}$ is constant at a given acidity it was necessary to determine the dependence of $\epsilon_{Fe\ eff}$ on the concentration of Fe(III). The values of $\epsilon_{Fe\ eff}$ will depend on the relative concentrations of Fe^{+++}, $FeOH^{++}$, and $Fe_2(OH)_2^{++}$. The ratio $[FeOH^{++}]/[Fe^{+++}]$ should remain constant but the ratio $[Fe_2(OH)_2^{4+}]/[FeOH^{++}]$ should rise with increase in concentration of total iron(III). This could lead to a significant dependence of extinction coefficient of iron(III) on its total concentration. To assess the magnitude of such an effect we have measured at λ 310 mμ the effective extinction coefficient of iron(III) in solutions containing ferric perchlorate (2×10^{-4} to 20×10^{-4} *M*) and perchloric acid (0.1 to 0.4 *M*) with ionic strength adjusted to 0.5 with sodium perchlorate. The results are given in Table I. Rabinowitch and Stockmayer (8) point out that in the absence of significant contribution from the dimer

$$\epsilon_{Fe\ eff} = \epsilon_{Fe^{+++}} + \epsilon_{FeOH^{++}} K_h/[H^+]$$

where $\epsilon_{Fe\ eff}$ is the effective extinction coefficient of iron(III) ion. $\epsilon_{Fe^{+++}}$ and $\epsilon_{FeOH^{++}}$ are the extinction coefficients of ferric ion and its first hydrolysis product, and K_h is the first hydrolysis quotient for ferric ion. Plots of $\epsilon_{Fe\ eff}$ against $1/[H^+]$ involving our data are linear but the data in Table I do indicate a significant dependence of $\epsilon_{Fe\ eff}$ on the iron(III) concentration at a given acidity. Our measurements (outlined below) relating to the formation of the protonated complexes were made in solutions with iron(III) concentrations in the range 2×10^{-4} to 6×10^{-4} *M* and over this range the variation in the value of $\epsilon_{Fe\ eff}$ is less than 11%. The quantity which is pertinent in assessing data bearing on complex formation is the change in optical density due to complex formation on the addition of oxalate. The contribution to the observed change in optical density (ΔD_{obs}) which is due to a change in $\epsilon_{Fe\ eff}$ will be $\Delta c'\ \Delta\epsilon_{eff}$ where $\Delta c'$ is the decrease in the concentration of iron(III) due to oxalate complexing and $\Delta\epsilon_{Fe\ eff}$ is the corresponding change in the effective extinction coefficient which must be substantially less than

TABLE I

The effective extinction coefficient ϵ of iron(III) in acidified aqueous solutions of ferric perchlorate at 25 °C and wavelength 310 mμ. All values for ϵ are in $mole^{-1}\ l\ cm^{-1}$

	Concentration of iron(III) perchlorate (moles l^{-1})		
$[H^+]$	2×10^{-4}	6×10^{-4}	20×10^{-4}
0.10	82.5	91.3	139
0.20	66.2	72.6	104
0.40	59.6	63.0	77.4

(91.3 − 82.5 =) 8.8 mole^{-1} l cm^{-1}. The overall observed change in optical density will be approximately $\Delta c'$ ($\bar{\epsilon}_{Fe\ ox} - \bar{\epsilon}_{Fe\ eff}$) where $\bar{\epsilon}_{Fe\ ox}$ is the effective extinction coefficient of the iron oxalate complexes and $\bar{\epsilon}_{Fe\ eff}$ that for the iron(III) not complexed with oxalate. As shown below ($\bar{\epsilon}_{Fe\ ox} - \bar{\epsilon}_{Fe\ eff}$) is greater than 1.1×10^3. Consequently the correction to be applied to the observed optical density will be less than $8.8/(1.1 \times 10^3)$ (= 0.008) of its value and we have neglected it.

Livingston (9) and Allmand and Webb (10) showed that carbon dioxide is formed when ferric oxalate solutions are irradiated in the presence of oxygen. Our experiments in which solutions were irradiated in the spectrophotometer with λ 310 mμ and the spectrophotometric character examined at intervals indicate that photochemical changes during our measurements were negligible.

Interpretation of Spectrophotometric Data

For λ 310 mμ the species $C_2O_4^=$, $HC_2O_4^-$, and $H_2C_2O_4$ do not contribute significantly to optical density and the difference in the optical densities of two solutions differing only in that one (s) contains oxalate and the other (ref.) does not is

$$[1] \qquad D_s - D_{ref} = \Delta D = \sum X_i(\epsilon_i - \epsilon_{Fe\ eff}) = \sum X_i \Delta\epsilon_i$$

where X_i is the concentration of a particular oxalate-iron complex and ϵ_i its extinction coefficient. It is assumed that any change in $\epsilon_{Fe\ eff}$ following upon the decrease in concentration of uncomplexed iron does not lead to significant change in $\Delta\epsilon_i$.

The data subjected to examination below were obtained with solutions where [H$^+$] was equal to or greater than 0.2 *M*. Connick and co-workers' (11) values for the hydrolysis constant for ferric ion indicate that under these conditions $FeOH^{++}$ constitutes less than 1% of the uncomplexed iron(III). Consequently

$$[2] \qquad a = [Fe^{+++}] + [FeC_2O_4^+] + [FeHC_2O_4^{++}]$$

where "*a*" represents the total concentration of iron(III).
Also

$$[3] \qquad b = [C_2O_4^=] + [HC_2O_4^-] + [H_2C_2O_4] + [FeC_2O_4^+] + [FeHC_2O_4^{++}]$$

where "*b*" is the total concentration of oxalate.
The concentrations of these species are interrelated by the formation quotients Q_1 and Q_2 for the complexes and the acid ionization quotients Q_{a_1} and Q_{a_2} for oxalic acid.

$$Q_1 = \frac{[FeC_2O_4^+]}{[Fe^{+++}][C_2O_4^=]} \qquad Q_2 = \frac{[FeHC_2O_4^{++}]}{[Fe^{+++}][HC_2O_4^-]}$$

$$Q_{a_1} = \frac{[H^+][HC_2O_4^-]}{[H_2C_2O_4]} \qquad Q_{a_2} = \frac{[H^+][C_2O_4^=]}{[HC_2O_4^-]}$$

It follows from these relations and eqs. [2] and [3] that

$$[4] \qquad b = [C_2O_4^=]\left(1 + \frac{[H^+]}{Q_{a_2}} + Q_1[Fe^{+++}] + \frac{Q_2[H^+][Fe^{+++}]}{Q_{a_2}} + \frac{[H^+]^2}{Q_{a_1}Q_{a_2}}\right).$$

If both $FeC_2O_4^+$ and $FeHC_2O_4^{++}$ are present eq. [1] becomes

$$[5] \qquad \Delta D = \Delta\epsilon_1[FeC_2O_4^+] + \Delta\epsilon_2[FeHC_2O_4^{++}]$$

Can. J. Chem. Downloaded from www.nrcresearchpress.com by 210.87.254.42 on 09/05/12
For personal use only.

which in terms of equilibrium quotients becomes

$$\Delta D = [Fe^{+++}][C_2O_4^{=}]\left(\Delta\epsilon_1 Q_1 + \frac{\Delta\epsilon_2 Q_2[H^+]}{Q_{a2}}\right)$$

and this with [4] yields

$$\frac{\Delta D}{[Fe^{+++}]}\left(1 + \frac{[H^+]}{Q_{a2}} + \frac{[H^+]^2}{Q_{a1}Q_{a2}}\right) = -\Delta D\left(Q_1 + \frac{Q_2[H^+]}{Q_{a2}}\right) + b\left(\Delta\epsilon_1 Q_1 + \frac{\Delta\epsilon_2 Q_2[H^+]}{Q_{a2}}\right).$$

In our experiments iron(III) was in substantial (from 5- to 30-fold) excess over total oxalate and complexing was incomplete. The values for the association constants derived from our data below indicate that more than 80% of total iron remains uncomplexed under conditions most favorable for its removal as oxalate complexes and that over 95% remains free for 90% of the measurements. Also, as indicated above, hydrolysis and dimer formation have negligible effects at the acidity and iron(III) concentrations of this work. We have consequently equated the concentration of ferric ion to "a". A plot of $\Delta D/a$ against ΔD for constant b and $[H^+]$ should yield a straight line with the negative slope S given by

[7] $$S = \frac{Q_1 + \frac{Q_2[H^+]}{Q_{a2}}}{1 + \frac{[H^+]}{Q_{a2}} + \frac{[H^+]^2}{Q_{a1}Q_{a2}}}.$$

[7] may be written

[8] $$S\left(\frac{Q_{a2}}{[H^+]} + \frac{[H^+]}{Q_{a1}} + 1\right) = \frac{Q_{a2}}{[H^+]}Q_1 + Q_2$$

If it be assumed that $FeHC_2O_4^{++}$ is not formed to an appreciable extent then eq. [8] becomes

[9] $$S\left(\frac{Q_{a2}}{[H^+]} + \frac{[H^+]}{Q_{a2}} + 1\right) = \frac{Q_{a2}}{[H^+]}Q_1$$

where S is still the negative slope of the plot of $\Delta D/a$ against ΔD.*

If the left side of eqs. [8] and [9] is plotted against $Q_{a2}/[H^+]$, a straight line should be obtained with slope Q_1, the formation quotient for $FeC_2O_4^+$. A significant magnitude for the intercept indicative of Q_2 would suggest formation of $FeHC_2O_4^{++}$.

Dissociation Quotients for Oxalic Acid

The first and second dissociation quotients of oxalic acid at ionic strength 0.50 and temperatures 5 to 25 °C were needed in the interpretation of our data. Two series of buffered solutions corresponding to mixtures of $H_2C_2O_4$ with $NaHC_2O_4$ and $NaHC_2O_4$ with $Na_2C_2O_4$ were prepared from solutions of sodium hydroxide and oxalic acid, and perchloric acid and sodium oxalate. The ionic strength was adjusted with sodium perchlorate. pH readings were made using Radiometer saturated calomel and G202B glass

As $[Fe^{+++}]$ is less than "a" our approximation will lead to estimates of $\Delta D/[Fe^{+++}]$ and of S which are somewhat low. However, variation in the value of $[Fe^{+++}]/a$ (and in the percentage error in S) with acidity should be slight. For example at the highest oxalate concentration used and an iron concentration of 4×10^{-4} M, calculations based on our values for Q_1 and Q_2 (obtained directly from plots based on [9]) indicate that the percentage of iron(III) in the uncomplexed form changes from 91.8 to 93.0 as the hydrogen ion concentration changes from 0.2 to 0.4 M. Consequently, while our estimate for Q_2 may be slightly high, the error in Q_1 associated with our approximation should be negligible compared with experimental errors.

Can. J. Chem. Downloaded from www.nrcresearchpress.com by 210.87.254.42 on 09/05/12
For personal use only.

electrodes. The hydrogen ion concentration in the oxalate solutions were estimated using the relationship

$$[H^+] = \frac{\text{antilog } (-\text{pH})}{\gamma_{H^+}'}$$

where γ_{H^+}' was determined empirically from pH readings on solutions containing known concentrations of perchloric acid and adjusted to ionic strength 0.5 with sodium perchlorate.* Concentrations of the various species in the oxalate solutions could be readily calculated from the known overall composition of the solutions and the hydrogen ion concentrations. The values for the ionization quotients Q_{a_1} and Q_{a_2} caculated from the data interpreted in this way are given in Table II. These vaues are fairly consistent with those of Dutt and Sur (12) of 7.586×10^{-2} for K_{a_1} and 2.089×10^{-4} for K_{a_2} for ionic strength of about 1.1 and temperature 32 °C.

TABLE II

The ionization quotients of oxalic acid at ionic strength 0.50

Temp. (°C)	Q_{a_1} (mole l^{-1})	Q_{a_2} (mole l^{-1})
5.0	$(4.77 \pm 0.06) \times 10^{-2}$	$(2.32 \pm 0.05) \times 10^{-4}$
15.0	$(5.90 \pm 0.07) \times 10^{-2}$	$(2.23 \pm 0.05) \times 10^{-4}$
25.0	$(6.25 \pm 0.08) \times 10^{-2}$	$(2.16 \pm 0.06) \times 10^{-4}$

Measurements Relating Directly to the Association Constants

The data bearing directly on the association constants were obtained with solutions containing oxalic acid concentrations of either 2×10^{-5} or 4×10^{-5} M, total iron(III) concentrations from 2×10^{-4} to 6×10^{-4} M, and perchloric acid concentrations between 0.2 and 0.5 M. All solutions were of ionic strength 0.5 and runs were made at 5, 15, and 25 °C with temperature control better than ±0.1 deg. Spectrophotometric absorption curves were obtained covering a wavelength range which included λ 310 mμ with the solution in the reference beam of the double beam spectrophotometer differing from the "sample" solutions only in that it did not contain oxalic acid. In consequence with 1 cm absorption cells the optical density corresponded to ΔD of the above equations. All solutions were prepared from available stock solutions and examined spectrophotometrically within 10 h of the time of preparation.

The plots of $\Delta D/a$ against ΔD for constant oxalate concentration yielded straight lines with negative slopes whose values (S) are given in Table III. Figure 1 shows plots of

$$S\left\{\frac{Q_{a_2}}{[H^+]} + \frac{[H^+]}{Q_{a_1}} + 1\right\} \text{ against } \frac{Q_{a_2}}{[H^+]}$$

suggested by eq. [8]. The data for 25 and 15 °C imply lines with positive intercepts and consequently the presence of significant concentrations of protonated complexes, although the uncertainties associated with the values of the slopes and intercepts and of Q_1 and Q_2 are considerable. The plot for the data for 5 °C shows two points (the lowest) falling markedly below an approximate linear grouping of the other six points. The figure shows lines of regression with that for the lowest temperature drawn ignoring the two lowest

γ_{H^+}' showed a significant dependence on acidity over the range of perchloric acid concentrations 5×10^{-5} to 3×10^{-1} M when estimated from data obtained with a glass electrode but was constant to within ±2% when a quinhydrone electrode was used. It should be noted that γ_{H^+}' is only a parameter for relating pH reading and hydrogen ion concentrations and is not to be identified necessarily with the activity coefficient of hydrogen ion.

Can. J. Chem. Downloaded from www.nrcresearchpress.com by 210.87.254.42 on 09/05/12
For personal use only.

TABLE III

Slopes of plots of $\Delta D/a$ against ΔD at various acidities and temperatures. Ionic strength 0.5. Range of iron(III) concentrations 2×10^{-4} to 6×10^{-4}. All concentrations are in moles l^{-1}

Temp. (°C)	Concentration of: Hydrogen ion	Concentration of: Total oxalate	Slope $S \times 10^{-3}$
5.0	0.2	2×10^{-5}	13.7
	0.3		7.6
	0.4		2.2
	0.5		1.9_5
	0.2	4×10^{-5}	16.2
	0.3		8.0_5
	0.4		4.7
	0.5		3.5
15.0	0.2	2×10^{-5}	17.3_5
	0.3		10.0
	0.4		6.4
	0.5		4.7
	0.2	4×10^{-5}	17.8
	0.3		10.8
	0.4		5.5
	0.5		4.7
25.0	0.2	2×10^{-5}	9.9
	0.3		6.9
	0.4		4.0
	0.5		3.5
	0.2	4×10^{-5}	13.0
	0.3		7.4
	0.4		5.5_5
	0.5		3.5

TABLE IV

The formation quotients of $FeC_2O_4^+$ (Q_1) and of $FeHC_2O_4^{++}$ (Q_2) at ionic strength 0.50

Temp. (°C)	Q_1 (mole^{-1} l)	Q_2 (mole^{-1} l)
5.0	5.6×10^7	1.27×10^4
15.0	5.06×10^7	2.17×10^4
25.0	2.45×10^7	2.22×10^4

points. Table IV contains the values of Q_1 and Q_2 obtained from the slopes and intercepts of these lines. The 95% confidence limit determined by standard methods and assigning equal weight to each point are better (less) than ±17% of the value given for Q_1 and ±30% of the value given for Q_2 for 25 and 15 °C.

We have obtained approximate values for $\Delta\epsilon_1$ and $\Delta\epsilon_2$ by solving eq. [6] simultaneously using a number of sets of experimental values at 25 °C. The arithmetic means are 1.22×10^3 mole^{-1} l cm^{-1} for $\Delta\epsilon_1$ and 1.41×10^3 mole^{-1} l cm^{-1} for $\Delta\epsilon_2$. Since the values for $\epsilon_{Fe\ eff}$ at wavelength 310 mμ are about 2% of these, $\Delta\epsilon_1$ and $\Delta\epsilon_2$ may be considered as approximate values for the extinction coefficients of the complexes $FeC_2O_4^+$ and $FeHC_2O_4^{++}$.

In Fig. 2 are shown the absorption curves of two solutions at 25 °C differing considerably in acidity and, on the basis of our values for ionization and formation quotients Q_{a_1}, Q_{a_2}, Q_1 and Q_2, in the relative concentrations of the protonated and unprotonated species. We estimate that in the solution indicated by the filled circles the concentrations of $FeC_2O_4^+$ and $FeHC_2O_4^{++}$ are 1.43×10^{-4} and 2.2×10^{-5} respectively while in that

Can. J. Chem. Downloaded from www.nrcresearchpress.com by 210.87.254.42 on 09/05/12
For personal use only.

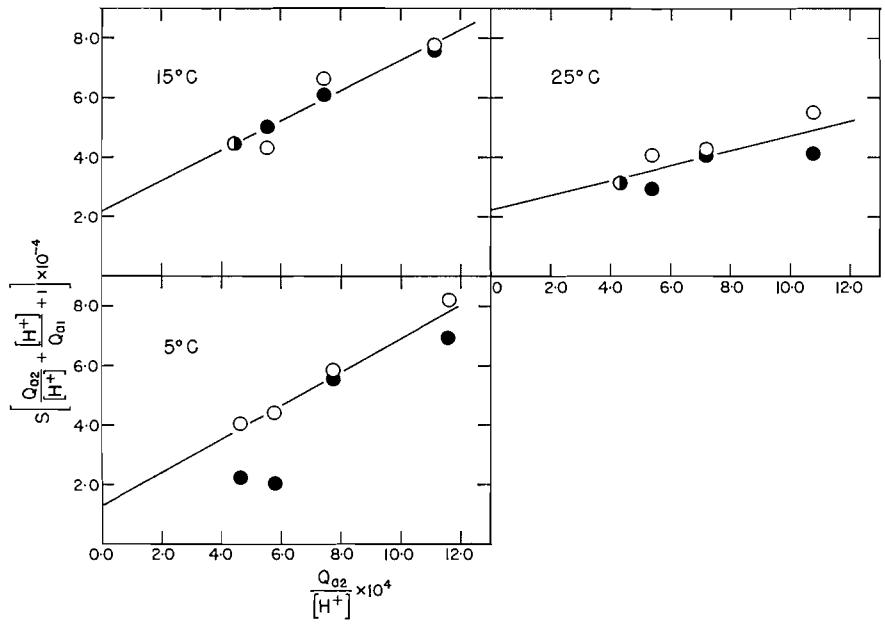

FIG. 1. Plots yielding the formation quotients of $FeC_2O_4^+$ (slope) and $FeHC_2O_4^{++}$ (intercept) at 5, 15, and 25 °C and ionic strength 0.5. Total concentration of oxalate: (●) 2.0×10^{-5} *M*; (○) 4.0×10^{-5} *M*; total concentration of iron(III): (●) 2.0×10^{-4} *M* to 6.0×10^{-4} *M*; (○) 2.0×10^{-4} *M* to 6×10^{-4} *M*.

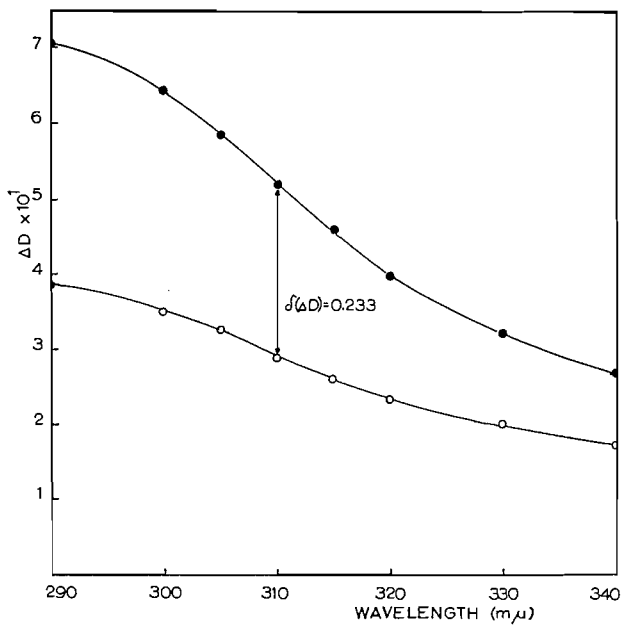

FIG. 2. Change of optical density ΔD occurring at various wavelengths on complexing iron(III) with oxalate. Total concentration of iron(III) in all forms: (●) 2.0×10^{-3} *M*, (○) 2.0×10^{-3} *M*; total concentration of oxalate in all forms: (●) 4.0×10^{-4} *M*, (○) 2.0×10^{-4} *M*; concentration of perchloric acid: (●) 0.40 *M*, (○) 0.10 *M*; ionic strength adjusted with sodium perchlorate to: (●) 0.50, (○) 0.50.

Can. J. Chem. Downloaded from www.nrcresearchpress.com by 210.87.254.42 on 09/05/12
For personal use only.

indicated by the open circles the corresponding concentrations are 1.43×10^{-4} and 5.52×10^{-5}. It is apparent that there are no marked differences in the forms of the absorption curves. The observed difference in the optical densities of these solutions agrees with that calculated on the basis of our quotients and extinction coefficients at λ 310 mμ to within 1%.

There is the possibility that the protonated monocomplex is monodentate or bidentate. It does not appear to be possible to assess definitely the alternatives on the basis of our data.

REFERENCES

1. J. LAMBLING. Bull. Soc. Chim. France, **16**, 495 (1949).
2. J. BADOZ-LAMBLING. Ann. Chim. Paris, **8**, 586 (1953).
3. A. K. BABKO and L. J. DUBOVENKO. J. Gen. Chem. USSR Eng. Transl. **26**, 757 (1956).
4. G. G. DAVIS and W. MACF. SMITH. Can. J. Chem. **40**, 1836 (1962).
5. L. N. MULAY and P. W. SELWOOD. J. Am. Chem. Soc. **77**, 2693 (1955).
6. R. M. MILBURN and W. C. VOSBURGH. J. Am. Chem. Soc. **77**, 1352 (1955).
7. R. C. TURNER and K. E. MILES. Can. J. Chem. **35**, 1002 (1957).
8. E. RABINOWITCH and W. H. STOCKMAYER. J. Am. Chem. Soc. **64**, 336 (1942).
9. R. LIVINGSTON. J. Phys. Chem. **44**, 601 (1940).
10. A. J. ALLMAND and W. W. WEBB. J. Chem. Soc. 1518 (1929).
11. R. E. CONNICK and C. P. COPPEL. J. Am. Chem. Soc. **81**, 6389 (1959).
12. N. K. DUTT and B. SUR. Z. Anorg. Allgem. Chem. **293**, 195 (1957).

Can. J. Chem. Downloaded from www.nrcresearchpress.com by 210.87.254.42 on 09/05/12
For personal use only.

Can. J. Chem. Downloaded from www.nrcresearchpress.com by 210.87.254.40 on 09/05/12
For personal use only.

THE MONO-OXALATO COMPLEXES OF IRON(III)

PART II. KINETICS OF FORMATION

R. F. Bauer and W. MacF. Smith
Department of Chemistry, Queen's University, Kingston, Ontario

Received October 1, 1964

ABSTRACT

The kinetics of the formation of the mono-oxalato complexes of iron(III) have been examined spectrophotometrically over the range of temperatures 5 to 25 °C in an aqueous medium of ionic strength 0.50 and the range of hydrogen ion concentrations 0.03 to 0.45 *M*. The kinetically significant paths under the conditions studied involve reactions first order in iron(III) and in bioxalate but there appears to be some decrease in the second order rate constant with increase in hydrogen ion concentration at the highest acidities and at the highest temperatures. Although there is no significant contribution to the rate by an acid-independent path first order in free oxalate under the experimental conditions, the possibility of the rate constant for such a path being greater than that first order in bioxalate is not precluded.

INTRODUCTION

The kinetics of the anation reaction of iron(III) ion with fluoride (1), chloride (2), bromide (3), thiocyanate (4), and sulfate (5) have been examined by techniques ranging from relaxation methods to stopwatch timing and show a fairly marked dependence of the second order rate constant on ligand type. Such behavior is in contrast to that exhibited by certain bivalent metal ions such as nickel(II) whose rate constants for corresponding anation reactions show little dependence on ligand type (6) and are presumably controlled by the rate of water loss from the metal ion.

This paper presents more information bearing on the influence of ligand type on the anation reactions of iron(III). The reaction studied, that of iron(III) with oxalate ion and its protonated forms, is convenient to examine because of its relative slowness in acid solution. It differs from the anation reaction of iron(III) with singly charged ligands which have been previously examined in that the principal complex formed is probably bidentate rather than monodentate.

EXPERIMENTAL

Materials

Solutions were prepared from triply distilled water, the second distillation being from alkaline permanganate. Ferric perchlorate (non-yellow), perchloric acid (double vacuum distilled 70%), sodium perchlorate (anhydrous), and oxalic acid were all reagent grade. The sodium perchlorate was dried at 110° for 2 h before weighing. Stock solutions ferric perchlorate and perchloric acid were analyzed for acid and iron content by the method previously discussed (1).

Method and Apparatus

The reaction was followed spectrophotometrically with a Beckman DK-1 spectrophotometer at λ 310 mμ using thermostated standard 1 cm silica cells as reaction vessels. Two solutions, one containing iron(III) perchlorate, the other oxalic acid, and both adjusted for ionic strength and acidity, were simultaneously injected into the reaction cell from thermostated 2 ml syringes fitted with polythene tips to ensure mixing. The solution in the cell in the reference beam had a composition identical with the reacting solution except that it contained no oxalic acid. At λ 310 mμ the uncomplexed oxalic acid and its ions do not contribute significantly to optical density and the difference in optical densities (ΔD) of reference and sample solutions is

$$[1] \qquad \Delta D = \{r\epsilon_{FeHC_2O_4} + (1 - r)\epsilon_{FeC_2O_4}\}x$$

where x is the total concentration of the complexes, r is the fraction of the complexes which is $FeHC_2O_4^{++}$, and ϵ is the extinction coefficient in $mole^{-1}\ l\ cm^{-1}$ of the species indicated by the subscript. If it is assumed that at a given acidity the ratio $[FeC_2O_4^{+}]/[FeHC_2O_4^{++}]$ remains at the equilibrium value, the change of

optical density is proportional to x, the concentration of complexed iron. Since as indicated in the preceding paper the extinction coefficients of the two complexed species differ by less than 20%, ΔD would remain nearly proportioned to x even if there were moderate deviations from the equilibrium value.

INTERPRETATION OF THE KINETIC DATA

In interpreting the experimental rate data we have used the integrated form of the relation

$$\frac{dx}{dt} = k_f''(a - x)(b - x) - k_b x \qquad [2]$$

where a is the total concentration of iron(III) in all species, b is the total concentration of oxalate, and x is the total concentration of iron(III) complexed as $FeC_2O_4^+$ and $FeHC_2O_4^{++}$.

k_f'' is a composite rate constant for the formation of the complexes and will depend on the rate constants of the various paths. It will involve factors for the fractions of uncomplexed oxalate in the protonated and unprotonated forms and will consequently depend on the concentration of hydrogen ions. k_b is a corresponding composite constant for the reactions involving breakup or aquation of the complexes and like k_f'' will be acid dependent.

The relation [2] will be valid for a variety of possible mechanisms, e.g. three parallel forward reactions opposed by back reactions if the ratio of the concentrations of the protonated and unprotonated complexes is maintained close to the equilibrium value.

$$Fe^{+++} + HC_2O_4^- \underset{k_{-1}}{\overset{k_1}{\rightleftharpoons}} FeC_2O_4^+ + H^+$$

$$Fe^{+++} + C_2O_4^{=} \underset{k_{-2}}{\overset{k_2}{\rightleftharpoons}} FeC_2O_4^+$$

$$Fe^{+++} + HC_2O_4^- \underset{k_{-3}}{\overset{k_3}{\rightleftharpoons}} FeHC_2O_4^{++}$$

$$FeC_2O_4^+ + H^+ \rightleftharpoons FeHC_2O_4^{++} \text{ (equilibrium)}*$$

In this case eq. [2] takes the form

$$\frac{dx}{dt} = (k_1 + k_3)[Fe^{+++}][HC_2O_4^-] + k_2[Fe^{+++}][C_2O_4^{=}] - (k_{-1}[H^+] + k_{-2})[FeC_2O_4^+] - k_{-3}[FeHC_2O_4^{++}]$$

which may be written

$$\frac{dx}{dt} = \left(\frac{k_1 + k_3}{Q_{a2}}[H^+] + k_2\right)s(a - x)(b - x) - ((k_{-1}[H^+] + k_{-2})(1 - r) + k_{-3}r)x$$

or

$$\frac{dx}{dt} = k_f s(a - x)(b - x) - k_b x \qquad [3]$$

*The transition state for this reaction would of course be different from that for reaction [1].

Can. J. Chem. Downloaded from www.nrcresearchpress.com by 210.87.254.40 on 09/05/12
For personal use only.

where Q_{a2} is the acid ionization quotient for $HC_2O_4^-$,

$$s = [C_2O_4^{=}]/([HC_2O_4^-] + [C_2O_4^{=}]),$$

$$r = [FeHC_2O_4^{++}]/([FeHC_2O_4^{++}] + FeC_2O_4^{+}]),$$

$$[4] \qquad k_f = \frac{k_1 + k_3}{Q_{a2}}[H^+] + k_2.$$

Equation [2] would of course also apply if the protonated complex were formed solely by protonation of $FeC_2O_4^+$ if the rates of protonation and deprotonation of the complexes were rapid compared to the rate of complex formation. In this event k_f would equal

$$\frac{k_1}{Q_{a2}}[H^+] + k_2$$

instead of

$$\frac{k_1 + k_3}{Q_{a2}}[H^+] + k_2.$$

There is the marked possibility that the protonated and unprotonated complexes are formed from a common intermediate. The rate expression [2] would then apply only if the rate-controlling steps involved solely the transformation of the initial reactants to the intermediate or if the intermediate occurred in the relatively small concentrations consistent with applicability of the stationary state approximations.

If x_e represents the total concentration of complexes at equilibrium

$$[5] \qquad \frac{k_b}{k_f} = \frac{(a - x_e)s(b - x_e)}{x_e}$$

Substitution of [5] into [3] with rearrangement yields

$$\frac{dx}{(ab - x_e x)(x_e - x)} = \frac{k_f s}{x_e}\,dt$$

which on integration and introduction of the condition that $x = 0$ when $t = 0$ yields

$$[6] \qquad \log\left(\frac{x_e - x}{x_e}\right) + \log\left(\frac{ab}{ab - x_e x}\right) = \frac{k_f s}{2.303 x_e}(x_e^2 - ab)t.$$

The second term on the left of [6] is negligible relative to the first. a is much greater than b under our experimental conditions and even when x approaches x_e the product $x_e x$ is rarely as great as 1% of ab.

It follows from [1] that

$$[7] \qquad \frac{x_e - x}{x_e} = 1 - \frac{\Delta D_t}{\Delta D_\infty}$$

where x_e and ΔD_∞ are corresponding values for equilibrium.

Substituting [7] into [6] and dropping the second term on the left of [6] yields

$$[8] \qquad \log\left(1 - \frac{\Delta D_t}{\Delta D_\infty}\right) = \frac{k_f s}{2.303 x_e}(x_e^2 - ab)t.$$

Can. J. Chem. Downloaded from www.nrcresearchpress.com by 210.87.254.40 on 09/05/12
For personal use only.

The slope S' of the plot of log $(1 - (\Delta D_t/\Delta D_\infty))$ against t should then be related to k by the relation

$$[9] \qquad k_f = \frac{2.303 x_e S'}{s(x_e^2 - ab)}.$$

x_e and s can be calculated from the values of the association quotients of the mono-oxalate complexes and the ionization quotients for oxalic acid given in the previous paper.

RESULTS OF THE KINETIC MEASUREMENTS AND DISCUSSION

The data from kinetic runs for all conditions investigated yielded linear plots for log $(1 - (\Delta D_t/\Delta D_\infty))$ against time. Rate constants k_f were calculated from the slopes of these plots using eq. [9] and showed no significant dependence on total concentration of iron(III) or oxalate at a given acidity over the range of concentrations investigated, i.e. 2×10^{-4} to 8×10^{-4} for iron(III), 2×10^{-5} to 12×10^{-5} for oxalate. Mean values for k_f for each acidity and temperature along with the standard deviations are given in Table I and plotted in Fig. 1 against the concentration of hydrogen ions.

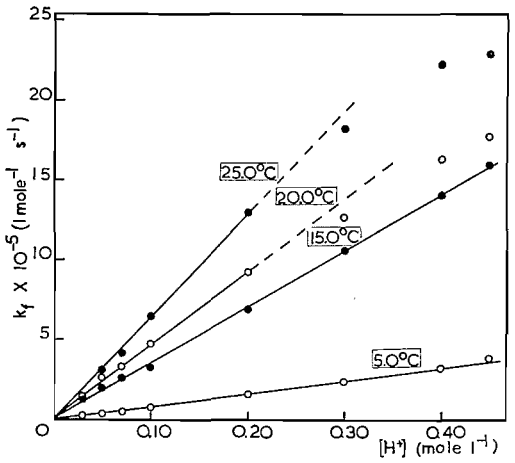

FIG. 1. Plots of observed forward rate constant k_f against hydrogen ion concentration.

As indicated above

$$k_f = \frac{k_1 + k_3}{Q_{a2}}[H^+] + k_2$$

if there are three parallel paths, one first order in oxalate and the other two first order in bioxalate.

Figure 1 indicates a linear relationship between k_f and $[H^+]$ (i.e. proportionality between rate and bioxalate ion concentration) over the range of acidities investigated for the two lowest temperatures and a significant falloff from first order dependence on hydrogen ion concentration for the highest acidities at the two highest temperatures. Lines of regression through the points at each temperature, ignoring those for concentrations of hydrogen ion in excess of 0.2 M at 20 and 25 °C, have slopes implying, through eq. [4], values for $k_1 + k_3$ listed in Table II. Cursory examination of Fig. 1 suggests that k_f approaches zero at zero hydrogen ion concentration and consequently that k_2 equals zero. However,

Can. J. Chem. Downloaded from www.nrcresearchpress.com by 210.87.254.40 on 09/05/12
For personal use only.

TABLE I

Average values for the forward rate constant (k_f) for reaction between iron(III) and oxalate at various temperatures and acidities. Ionic strength 0.50

Temp. (°C)	H^+ (mole l^{-1})	$k_f \times 10^{-5}$ (mole^{-1} l s^{-1})
5	0.03	0.241±0.035
	0.05	0.435±0.037
	0.07	0.554±0.026
	0.10	0.780±0.020
	0.20	1.68±0.03
	0.30	2.50±0.04
	0.40	3.35±0.10
	0.45	3.90±0.18
15	0.03	1.54±0.35
	0.05	2.08±0.15
	0.07	2.68±0.33
	0.10	3.31±0.28
	0.20	6.88±0.44
	0.30	10.63±1.68
	0.40	14.1±0.41
	0.45	16.0±1.2
20	0.03	1.47±0.54
	0.05	2.75±0.80
	0.07	3.21±0.69
	0.10	4.74±0.51
	0.20	9.19±0.84
	0.40	16.4±0.5
	0.45	17.8±0.1
25	0.05	3.11±1.12
	0.07	4.14±0.90
	0.10	6.59±0.56
	0.20	13.0±0.8
	0.30	18.2±1.8
	0.40	22.3±2.0
	0.45	22.8±0.5

statistical treatment of the data, implies values for k_2 of $(19 \pm 20^*) \times 10^3$ at 15 °C and $(30 \pm 32) \times 10^3$ mole^{-1} l s^{-1} at 25 °C. It is apparent that there is the possibility that k_2 is larger than $k_1 + k_3$. However, under all conditions investigated $k_2[C_2O_4^{=}]$ must be negligible compared with $(k_1 + k_3)[HC_2O_4^{-}]$ because of the very large value of the ratio $[HC_2O_4^{-}]/[C_2O_4^{=}]$ and consequently there will be negligible contributions to the overall rate by the path with first order dependance of rate on free oxalate ion concentration.

The plot of log $(k_1 + k_3)$ against $1/T$ implies effective values for $\Delta H^{\neq}$ and $\Delta S^{\neq}$ of 18 ± 4 kcal mole^{-1} and 16 ± 10 cal deg^{-1} mole^{-1} respectively. In the subsequent argument we tentatively identify the experimental $(k_1 + k_3)$ with k_1 and consequently imply that the values for $\Delta H^{\neq}$ and $\Delta S^{\neq}$ apply to the path with rate constant k_1. It is of interest that $\Delta H^{\neq}$ for other anation reactions of iron(III) range from 13 kcal (thiocyanate) to 22.8 kcal (fluoride) and $\Delta S^{\neq}$ from −5 cal deg^{-1} (thiocyanate) to +35 cal deg^{-1} (fluoride). However, the points in the plot of log k against $1/T$ for oxalate show considerable dispersion and do not rule out curvature. We do not therefore consider our values for $\Delta H^{\neq}$ and $\Delta S^{\neq}$ suitable for critical comparison with those for other anation reactions. It is possible that an extensive group of measurements obtained with a technique such as "stop flow" which would remove complications due to back reaction and permit an extension of the

*95% confidence limit.

Can. J. Chem. Downloaded from www.nrcresearchpress.com by 210.87.254.40 on 09/05/12
For personal use only.

TABLE II

Values for effective rate constant $(k_1 + k_3)$ for reactions forming mono-complexes with first order dependence on bioxalate ion concentration

Temp. (°C)	$(k_1 + k_3) \times 10^{-2}$ (mole^{-1} l s^{-1})
5	2.0±0.1
15	7.72±0.32
20	9.8±3.2
25	14.4±1.0

temperature range might help elucidate through the shape of the log k against $1/T$ plot whether $(k_1 + k_3)$ is indeed composite.

It is apparent that an acceptable mechanism for the reaction between iron(III) and oxalate must be in accord with a second order rate law, first order in iron(III) ion and first order in bioxalate for all conditions except the highest acidities at the two highest temperatures where there is some decrease in the magnitude of the second order rate constant with increase in acidity.

k_1 (and also k_3) could conceivably be composite and involve rate constants for steps in a series reaction leading to the formation of the final complex. For example, if the protonated complex could be ignored the reaction path might be

$$Fe^{+++} + HC_2O_4^- \underset{k_b}{\overset{k_a}{\rightleftharpoons}} FeC_2O_4^{+}\cdot + H^+$$

$$FeC_2O_4^{+}\cdot \xrightarrow{k_d} FeC_2O_4^{+} \qquad [10]$$

where $FeC_2O_4^{+}\cdot$ represents a monodentate intermediate. That the formation of a monodentate intermediate is rate controlling in the formation of the multidentate complexes of nickel(II) is suggested by the findings of Wilkins and co-workers (7) and of Margerum and co-workers (8).

If the stationary state approach is applicable, the following relation should apply for the forward rate of formation of the bidentate complex.

$$\frac{k_d k_a}{k_b[H^+] + k_d}[Fe^{+++}][HC_2O_4^-]$$

At any one hydrogen ion concentration the rate should be first order in iron(III) and in bioxalate with an effective rate constant k_1 equal to $k_d k_a/(k_b[H^+] + k_d$. If $k_b[H^+]$ is much less than k_d then the rate constant k_1 equals k_a (i.e. the first step is rate controlling) and the rate constant is independent of acidity. If $[H^+]$ is such that $k_b[H^+]$ becomes significant relative to k_d there will be a decrease in k_1. A corresponding mechanism involving a protonated monodentate intermediate would imply that k_1 should be independent of hydrogen ion concentration. In fact, in the range of higher acidities where there appears to be a falloff in the observed rate constant, the protonated complex is a significant species at equilibrium and should not be ignored. Identification of a protonated intermediate with the final protonated complex would imply a series reaction which in general would show a dependence of rate on concentration more involved than the second order dependence which is actually observed. The possibility of there being a reaction path parallel to that

Can. J. Chem. Downloaded from www.nrcresearchpress.com by 210.87.254.40 on 09/05/12
For personal use only.

summarized by eq. [10] and involving a protonated intermediate different from the final product cannot be definitely ruled out but we shall ignore this possibility and assume that the essential reaction path is that summarized by eq. [10] and that the final protonated and unprotonated species are in labile equilibrium. Such an assumption is in accord with our data and our method of interpreting them and implies values quoted for $k_1 + k_3$ above are those for k_1.

The work of Eigen and co-workers (6, 9, 10) and of Wendt and Strehlow (11) has led to general acceptance of a mechanism of ion association which emphasizes that there is a rate-determining exchange between ligand and the water of the first coordination shell of the metal ion within ion pairs where the partners are separated by one water molecule. The rate of water loss may be independent of or dependent on the nature of the potential ligand of the ion pair. In the latter case the reaction could approach in character that often designated by S_N2. Ion pair formation should be a labile process and an equilibrium concentration of ion pairs relative to reactant species may be expected. On this basis the concentration of ion pairs between iron(III) and bioxalate would be $K_{10}[Fe^{+++}][HC_2O_4^-]$ where K_{10} is an equilibrium quotient whose magnitude may be roughly estimated by the method of Hammes and Steinfeld (12, 13). For ions of opposite charge and valences three and one the value of the association quotient is about 14 $mole^{-1}$ l if the separation of centers is assumed to be 5 Å. The values for ion pairs between iron(III) and various singly charged anions may be expected to vary somewhat but not markedly and the value 14 may be considered to represent the order of magnitude of association quotients.

The rate constant k_1 for complex formation should on this picture be $K_{10}k_1^*$ where k_1^* is a first order rate constant. Also, if our value for $k_1(+ k_3)$ is indeed that for formation of the monodentate intermediate, $k_1(+ k_3)/K_{10}$ will represent the effective first order rate constant for transformation of the ion pairs into the intermediate and at 25 °C will be of the order of 1 440 $mole^{-1}$ l s^{-1}/14 $mole^{-1}$ l $\approx$ 100 s^{-1}. The rate constants at 25 °C for the anation reactions of iron(III) in aqueous solution are listed in Table III along with values for the reciprocal of the ionization constants (K_a) for the acids conjugate to the associating ligand. The ionic strengths to which the rate constants apply vary from 0.1 to 1.0 but the effect of such variation on the constants should be small. On the basis of the theory outlined above, the first order rate constants k_1^* for transformation of ion pair to complex should be roughly parallel to the rate constants listed for all singly charged ligands. The values listed for the ionization constants apply to zero ionic strengths but their reciprocals should give fair measure of the ability of the ligand in the ion pair to accept protons from water in the inner hydration sphere of the metal ion. It is apparent that there is a fairly marked increase in rate constant with increase in ligand basicity and that the value which we have determined for bioxalate is roughly in accord with there being a correlation between rate constant and ligand basicity for singly charged anions and monodentate complex formation.

Wendt and Strehlow (11) have suggested that the dependence of rate on ligand type is related to the ability of the potential ligand in an ion pair to accept a proton from one of the waters coordinated with the metal ion. In this picture such an inner hydrolysis leads to an increase in the rate of loss of one of the other water molecules coordinated with the metal ion. If it is assumed that the partially desolvated metal ion is the precursor to the complex, such an increase in the rate of water loss could lead to an increase in the first order rate constant for complex formation from the ion pair and in the second order rate constant with regard to the primary reactants.

Superficial assessment of the data of Table III suggests that they are in accord with such

Can. J. Chem. Downloaded from www.nrcresearchpress.com by 210.87.254.40 on 09/05/12
For personal use only.

TABLE III

Rate constants of anation reactions yielding mono-complexes of iron(III) at 25 °C and estimates of the basicities of the anions involved in the reactions

Anion involved	Rate constant	Ref.	$1/k_a$	Ref.
Br^-	20	3	10^{-9}	14
Cl^-	9.4	2	10^{-6}	15
SCN^-	127	4	7	16
$HC_2O_4^-$	1 440	This paper	17.5	17, 18
HF	12*	1		
F^-	4 000*	1	1.5×10^3	19
$SO_4^=$	6 370	5	10^2	20

*Obtained by extrapolation.

a view. However, we doubt the direct applicability of Wendt and Strehlow's hypothesis to the reactions of iron(III) mainly because the rate constant for water exchange from iron(III) is markedly in excess of the value of the rate constant for complex formation. The rate constant for the exchange of a water molecule from the first coordination sphere of hexahydrated iron(III) ion has been estimated by Connick and co-workers on the basis of nuclear magnetic resonance (n.m.r.) measurements to be in the range 2.4×10^4 to 1.1×10^6 s^{-1} (21, 22). The presence of a ligand in the ion pair could conceivably raise the value for water exchange of the hydrated metal ion through inner hydrolysis in the ion pair above this. We have implied that the first order rate constant for formation of the oxalate complex from the ion pair is approximately 100 s^{-1}, a value substantially less than that for water exchange. If it is assumed that the rate of water exchange measures the rate of formation of the pentahydrated iron(III) and that this is the precursor to complex formation it is apparent that very few of the partially desolvated ion pairs complete reaction to form the complex and that the reaction

$$(Fe(H_2O)_5^{+++} \ldots HC_2O_4^-)_{\text{ion pair}} \rightleftharpoons (Fe(H_2O)_5^{+++} \ldots HC_2O_4^-)_{\text{ion pair}}$$

is essentially in equilibrium. If the equilibrium constant for this reaction is represented by K^1 and the rate constant for transformation of the partially desolvated ion pair into mono-complex (presumably with proton transfer from the bioxalate ion to the water of the solvent) by k^1 then

$$k^* = K^1k^1$$
$$\text{or } k_1 = K_{10}K^1k^1$$

The associating ligand will then be influential via its effect on K^1 and k^1. Presumably there will be partial proton transfer from water coordinated with the metal to the associating ligand in both types of ion pairs and although such inner hydrolysis may well affect the lability of loss and gain of water it is difficult to see how there could be much influence on the equilibrium constant K^1. On the other hand the rate constant k^1 for the relatively slow nucleophilic attack by the ligand would doubtlessly be dependent on the nucleophilicity of the ligand. We suggest that the influence of ligand is through its nuc'eophilicity towards the metal ion rather than its basicity with regards to proton acceptance, and that the apparent parallelism of rate constant on the basicity is a reflection of the parallelism between basicity and nucleophilicity.

The behavior of iron(III) and nickel(II) in anation reactions seems to be in marked contrast. For nickel the rate of reaction is close to the rate of water loss and in terms of the above picture this implies that the probability of nucleophilic attack by ligand within the

Can. J. Chem. Downloaded from www.nrcresearchpress.com by 210.87.254.40 on 09/05/12
For personal use only.

partially desolvated ion pair is much greater than that for attack by water, whereas for iron(III) the converse applies. As the relative nucleophilicities of water and a given ligand (e.g. oxalate) should not be greatly different for the reactions involving nickel(II) and iron(III) perhaps the differences in behavior are to be explained in terms of availability of water for nucleophilic attack within the ion pairs.

REFERENCES

1. D. POULI and W. MACF. SMITH. Can. J. Chem. **38**, 567 (1960).
2. R. E. CONNICK and C. P. COPPELL. J. Am. Chem. Soc. **81**, 6389 (1959).
3. P. MATHIES and H. WENDT. Z. Physik. Chem. Frankfurt, **30**, 137 (1961).
4. J. F. BELOW, JR., R. E. CONNICK, and C. P. COPPEL. J. Am. Chem. Soc. **80**, 2961 (1958).
5. G. G. DAVIS and W. MACF. SMITH. Can. J. Chem. **40**, 1836 (1962).
6. M. EIGEN and K. TAMM. Z. Electrochem **66**, 107 (1962).
7. G. A. MELSON and R. G. WILKINS. J. Chem. Soc. 4208 (1962).
8. D. W. MARGERUM, D. B. RORABACHER, and J. F. G. CLARKE, Jr. Inorg. Chem. **2**, 667 (1963).
9. M. EIGEN. Proc. 7th Intern. Congr. Co-ord. Chem. Stockholm. 1962.
10. M. EIGEN. Z. Elektrochem. **64**, 119 (1960).
11. H. WENDT and H. STREHLOW. Z. Elecktrochem. **66**, 228 (1962).
12. G. G. HAMMES and J. I. STEINFELD. J. Am. Chem. Soc. **84**, 4639 (1962).
13. G. H. NANCOLLAS and N. SUTIN. Inorg. Chem. **3**, 360 (1964).
14. J. C. MCCOUBREY. Trans. Faraday Soc. **51**, 743 (1955).
15. A. M. POSNER. Nature, **171**, 519 (1953).
16. T. SUZUKI and H. HAGISAWA. Bull. Inst. Phys. Chem. Res. Tokyo, **21**, 601 (1942).
17. H. M. DAWSON, C. R. HOSKINS, and J. E. SMITH. J. Chem. Soc. 1884 (1929).
18. H. M. DAWSON and J. E. SMITH. J. Chem. Soc. 2530 (1929).
19. H. H. BROENE and T. DEVRIES. J. Am. Chem. Soc. **69**, 1644 (1947).
20. C. W. DAVIES, H. W. JONES, and C. B. MONK. Trans. Faraday Soc. **48**, 921 (1952).
21. R. E. CONNICK and R. E. POULSON. J. Chem. Phys. **30**, 759 (1959).
22. R. E. CONNICK and E. D. STOVER. J. Phys. Chem. **65**, 2075 (1961).

Can. J. Chem. Downloaded from www.nrcresearchpress.com by 210.87.254.40 on 09/05/12
For personal use only.

Can. J. Chem. Downloaded from www.nrcresearchpress.com by 210.87.254.105 on 09/05/12
For personal use only.

RADIATION-INDUCED CHANGES IN THE UNSATURATION OF POLYISOPRENE[1]

MORTON A. GOLUB AND JEANNE DANON[2]
Stanford Research Institute, Menlo Park, California
Received March 12, 1965

ABSTRACT

Polyisoprene in the solid state and in benzene solution undergoes radiation-induced *cis–trans* isomerization and loss of unsaturation. Starting with various *cis* or *trans* polymers, the isomerization approaches an equilibrium in which the *cis/trans* ratio is around 50/50 for polyisoprenes irradiated in solution or in the solid state. The *G*(isom.) values for either *cis* → *trans* or *trans* → *cis* isomerization, i.e., the number of *cis* (or *trans*) units isomerized initially per 100 eV absorbed by *both* polymer and solvent, in 1% solution, and by polymer alone, in the solid state, are about 1.0 and 10, respectively. The energy transfer mechanism proposed previously for polybutadiene and squalene isomerization is assumed to hold for polyisoprene as well. The loss of unsaturation in films irradiated with electrons under nitrogen is twice as rapid as in films γ-irradiated *in vacuo*, the *G*(-d.b.) (d.b. = double bond) values being 13.4 and 6.7, respectively. Correspondingly, *G*(-d.b.) for a γ-irradiated solution is 27, calculated in terms of energy absorbed directly by the polymer; intermolecular energy transfer is again indicated, although phenylation may also contribute to the loss of double bonds in solution. The large drop in unsaturation in solution and in the solid state is attributed to a chain process involving cyclization and some cross-linking, with the participation of both free radicals and carbonium ions. Work with polyisoprene-3-*d* confirmed the importance of isomerization and loss of unsaturation and gave an activation energy of 1.1 kcal/mole for the latter reaction.

INTRODUCTION

Considerable theoretical as well as practical interest has been shown in recent years in the radiation chemistry of polyisoprene, and a number of fundamental papers (1–8) and reviews (9–13) have appeared dealing with various microstructural changes produced in this polymer and with possible mechanisms to account for these changes. The principal change noted for polyisoprene, apart from cross-linking and evolution of hydrogen, is a more or less important decrease in the original isoprenic unsaturation (—$C(CH_3)$=CH— double bonds). Most of the published data on this latter effect are based on changes in the infrared absorption bands of irradiated polyisoprenes at 12 μ (C—H out-of-plane deformation vibration of the —$C(CH_3)$=CH— unit) and (or) at 6 μ (C=C stretching vibration of this same unit), but some unsaturation data have also been obtained by various chemical means.

The question of the loss of unsaturation in irradiated polyisoprene has met with much controversy, some workers taking the position that the effect is small but real, and others contending that the effect is very large. According to Turner and co-workers (3), the infrared spectrum of a degassed sample of natural rubber, irradiated *in vacuo* to a dose of 326 Mrads, showed only small changes in the 12 and 6 μ bands, while squalene, a hexaisoprene which can serve as an intermediate molecular weight model for polyisoprene, showed (4) about a 10% drop in chemical unsaturation when irradiated to a dose of 242 Mrads. A comparable result was obtained by Hayden (6) who reported a 10% decrease in the 6 μ band for a rubber film irradiated *in vacuo* to 410 Mrads. On the other hand, Heinze *et al.* (7) have observed as much as 25% reduction in the 12 μ band for carefully purified, but not degassed, samples of natural rubber irradiated with electrons under nitrogen to

[1]*Presented at the IUPAC Meeting, Moscow, USSR, July 1965.*
[2]*NATO Fellow, 1962–1963, from Laboratoire de Chimie Physique, Faculté des Sciences, Orsay (S. et O.), France.*

250 Mrads; after a dose of 1 400 Mrads the unsaturation was reduced to below 20% of the original value. Moreover, Kuzminsky *et al.* (14) claimed a decrease in unsaturation, determined by chemical titration and infrared analysis, of 50% after about 220 Mrads, and as much as 70% after 500 Mrads for unpurified natural rubber exposed to X-rays in air.

In sharp contrast to Heinze's rapid loss of unsaturation and even Turner's and Hayden's moderate reduction in unsaturation is the observation by Loughborough *et al.* (15) that a sulfur-based vulcanizate of natural rubber on irradiation in nitrogen showed a decrease of only about 2% after 100 Mrads and approximately 15% after about 1 000 Mrads.

However, it is not obvious how the different results obtained by these workers can be reconciled, and one of the aims of this research is to resolve the question of the actual consumption of double bonds in the irradiation of polyisoprene. In this connection, it is important to point out that a diminution of the 12 μ band (associated with the —C(CH_3)=CH— units, whether *cis* or *trans*) in the spectrum of *cis*-polyisoprene can represent not only a loss of the original double bonds but also some *cis* → *trans* isomerization, inasmuch as the absorption of the *trans* unit at 12 μ is approximately 70% of that of the corresponding *cis* unit (16). Since polybutadiene undergoes radiation-induced *cis–trans* isomerization in the solid state with a high $G(c \rightarrow t) \sim 8.0$ (17), and liquid squalene likewise undergoes this same type of reaction, although with a much lower yield ($G(t \rightarrow c) = 0.83$) (18), it is reasonable to expect polyisoprene to show this reaction too. Such a reaction had been suggested by Turner (3, 13), but there is no unambiguous evidence for it. Accordingly, a further aim of this study was to explore the possibility of a radiation-induced *cis–trans* isomerization of polyisoprene in the solid state. Moreover, since polybutadiene and squalene were found to isomerize with much greater yields in benzene than in the pure state, a related aim was to carry out complementary irradiations of polyisoprene solutions in order to seek an analogous benzene-sensitized isomerization of this polymer.

Apart from the observed decrease in original unsaturation, evidence was obtained for the radiation-induced formation of new double bonds in solid polyisoprene. Thus, a small increase in vinylidene units (>C=CH_2) was indicated (3) by a growth of the 11.3 μ infrared band coupled with the appearance of a shoulder near the 6 μ band. Also, the formation of *trans* —CH=CH— units was suggested by the development of a band at 10.4 μ, as noted by Hayden and as may be seen in the published spectra of Heinze *et al.* and of Turner and co-workers (3). Moreover the last-named workers, on the basis of ultraviolet spectroscopic analysis, concluded that a very small amount of conjugated diene groups and an even smaller amount of conjugated triene groups were also formed. The following processes were postulated to account for the new unsaturation.

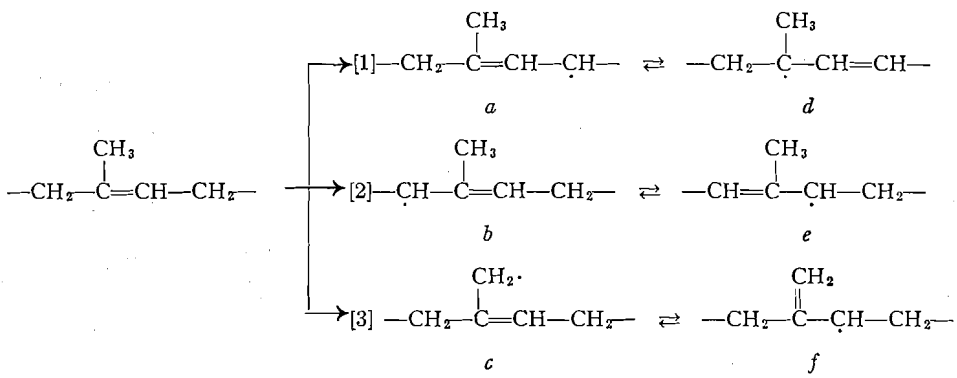

Can. J. Chem. Downloaded from www.nrcresearchpress.com by 210.87.254.105 on 09/05/12
For personal use only.

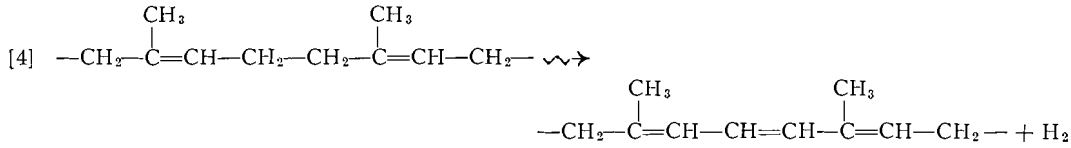

The diene groups were considered to arise through disproportionation reactions involving the mesomeric radicals *d*, *e*, and *f*, while the trienes were assumed to arise through disproportionation reactions involving the radicals *a* and *b* and to a negligible extent through reaction [4] (3). It should be noted that isoprenic double bonds formed according to reaction [2] cannot be distinguished from the original double bonds, except for possible *cis–trans* effects, so that this reaction can neither be proved nor disproved on the basis of ordinary polyisoprene. However, the use of a suitably deuterated polyisoprene, such as $(—CH_2—C(CH_3)=CD—CH_2—)_n$, should afford a direct test for this and other double bond shift reactions. Since, as demonstrated by Turner *et al.* and by Hayden, reactions [1] to [4] were not very important, it was not one of our main aims to study these reactions in detail, but rather to focus attention on the decrease in original unsaturation and the phenomenon of *cis–trans* isomerization both in the solid state and in solution. Nevertheless, the availability of the above deuterated polyisoprene prompted us to carry out some irradiation experiments with it and to examine briefly the various reactions mentioned above.

EXPERIMENTAL

Materials

Five different polyisoprenes were used in this work: naturally occurring all-*cis* (Hevea) and all-*trans* (Balata) polyisoprenes, obtained through the courtesy of the B. F. Goodrich Research Center, Brecksville, Ohio; two synthetic polyisoprenes with very high *cis*-1,4 structure but different 3,4 content (Ameripol SN, obtained from Goodrich-Gulf Chemicals, Inc., Cleveland, Ohio, and Shell isoprene rubber, obtained from Shell Chemical Company, Torrance, California); and a sample of *cis*-polyisoprene-3-*d*, specially prepared by the late Dr. David Craig and Mr. Harold Tucker of the Goodrich Research Center and kindly donated to us.

As analyzed by nuclear magnetic resonance (n.m.r.) methods (19, 20) and supported by infrared (see below), the microstructure of Ameripol SN consists of 97.3% *cis*-1,4, 2.0% *trans*-1,4, and 0.7% 3,4 units while that of the Shell rubber consists of 89.4% *cis*-1,4, 6.2% *trans*-1,4, and 4.4% 3,4 units. Since the 3,4 units are not involved in *cis–trans* isomerization, for purposes of following this reaction only the percentage of the total 1,4 polymerization units having the *cis* (or *trans*) configuration in the polymer before and after irradiation was significant. Accordingly, the initial *cis*-1,4 contents of Ameripol SN and Shell rubber were taken as 98 and 94% respectively, while those for Hevea and Balata were assumed (20) to be 100 and 0%, respectively. The detailed microstructure of the deuterated polyisoprene was not determined but its high *cis* —C(CH$_3$)=CD— content was confirmed by n.m.r. analysis.

Irradiations

For the solid state work, thin films were cast from dilute benzene solutions of the purified polymers onto rock salt plates and irradiated *in vacuo* to various doses at room temperature, using a 1 500 curie ^{60}Co γ-ray source. Some polyisoprene films were irradiated under a stream of cooled nitrogen, using 1 MeV electrons from a G.E. resonant transformer. Because of the heat generated in the course of the high intensity electron irradiation, the polymer films were kept close to room temperature during irradiation by placing them in contact with a surface cooled by a suitable coolant. In addition, some films of polyisoprene-3-*d* were irradiated with electrons at −15 and −50 °C as well as at room temperature. The various films were analyzed before and after irradiation by infrared spectroscopy.

For solution work, portions of the polyisoprene solutions, with and without antioxidant, were sealed in conventional n.m.r. tubes *in vacuo* or in air and then γ-irradiated. The isomerization and loss of unsaturation in the polymers were followed by analysis of the n.m.r. spectra obtained directly on the irradiated tubes. In several of the low dose runs, complementary infrared analysis was conducted on samples of polyisoprene recovered from the irradiated solutions; the results were in good accord with those obtained from n.m.r. Since the polyisoprene solutions became completely gelled invariably when irradiated *in vacuo*, and frequently even when irradiated in air, especially at high doses, it was not feasible to recover the polymers from those runs for purposes of infrared analysis; however, the gelation did not interfere with obtaining fully satisfactory n.m.r. spectra of highly irradiated solutions.

Can. J. Chem. Downloaded from www.nrcresearchpress.com by 210.87.254.105 on 09/05/12
For personal use only.

Infrared Analysis

As noted above, changes in the 12 μ band of polyisoprene can arise from either *cis–trans* isomerization or loss of original unsaturation, or both. Consequently, for a film irradiated to a dose D, the absorbance of the 12 μ band, relative to that of the 7.25 μ band (due to CH_3 groups) as an internal standard, designated $(R_{12})_D$, can be expressed by the relation

$$[5] \qquad (R_{12})_D = [R_{12}^{H} - (R_{12}^{H} - R_{12}^{B})(t_0 + x)](1 - y).$$

R_{12}^{H} and R_{12}^{B} are the corresponding relative absorbances of the 12 μ bands for pure *cis* (Hevea) and pure *trans* (Balata) polyisoprenes, respectively, t_0 is the initial *trans*-1,4 content in the polymer, x is the fraction of double bonds isomerized from *cis* → *trans* (or *trans* → *cis*, in which case x is negative, by definition), and y is the fraction of the original —C(CH_3)=CH— units destroyed. Dividing relation [5] by the corresponding expression for the relative absorbance of the 12 μ band in the unirradiated polyisoprene, we obtain the more convenient relation

$$[6] \qquad R_1 = (R_{12})_D/(R_{12})_0 = \frac{M - Nx}{M}(1 - y)$$

where R_1 can be measured directly, and the constants M and N are given by

$$[7] \qquad M = 1 - (1 - R_{12}^{B}/R_{12}^{H})t_0$$

$$[8] \qquad N = (1 - R_{12}^{B}/R_{12}^{H}).$$

Making the reasonable assumption that the extinction coefficient of the 7.25 μ band is the same in both Hevea and Balata, we further obtain[3]

$$R_{12}^{B}/R_{12}^{H} = \epsilon_{12}^{B}/\epsilon_{12}^{H} = 0.625$$

and hence the particular values for M and N given in Table I for various polyisoprenes studied. Thus by determining the extent of isomerization x, we can calculate directly from relation [6] the loss of unsaturation y.

TABLE I

Radiation-induced isomerization and decrease of unsaturation in various polyisoprenes in the solid state

Polymer	Dose, Mrads	R_2	t	x	R_1	$1 - y$
			γ-Rays at room temperature			
Shell polyisoprene*	0	2.22	0.06	0	1	1
	95.7	1.89	0.14	0.08	0.95	0.98
	193.3	1.76	0.17	0.11	0.83	0.86
	301.0	1.60	0.23	0.17	0.80	0.85
	398.8	1.53	0.25	0.19	0.77	0.82
Ameripol SN†	0	2.34	0.02	0	1	1
	104.0	2.12	0.07	0.05	0.94	0.96
	197.0	1.73	0.18	0.16	0.87	0.92
	382.2	1.60	0.23	0.21	0.75	0.81
Hevea‡	0	2.41	0	0	1	1
	109.0	2.00	0.10	0.10	0.93	0.97
	252.3	1.70	0.19	0.19	0.82	0.88
			Electrons at 25–30 °C			
Shell polyisoprene*	100	1.81	0.16	0.10	0.87	0.90
	200	1.58	0.23	0.17	0.76	0.82
	300	1.44	0.28	0.22	0.62	0.68
	400	1.23	0.37	0.31	0.54	0.61

*$M = 0.978$; $N = 0.375$.
†$M = 0.994$; $N = 0.375$.
‡$M = 1$; $N = 0.375$.

[3] *Assuming the ratio of extinction coefficients for the cis and trans bands to be 1.61 (21).*

Can. J. Chem. Downloaded from www.nrcresearchpress.com by 210.87.254.105 on 09/05/12
For personal use only.

To obtain x, the method of Cunneen *et al.* (22), developed for polyisoprene solutions, was adapted for polymer films. The Cunneen method is based on the fact that Hevea and Balata possess characteristic bands at 8.89 and 8.74 μ, respectively,[4] and that at 9.18 μ the absorption of both polymers is identical. Our method thus consists of deriving an expression for the *trans* content of isomerized polyisoprene as a function of the ratio of absorbances (relative to that of the 9.18 μ band as an internal standard) of the 8.89 and 8.74 μ bands. It may be seen that the method gives results which are independent of the loss of unsaturation. Expressions analogous to relation [5] can be written for these bands

$$[9] \qquad (R_{8.89})_D = [R_{8.89}{}^{H} - (R_{8.89}{}^{H} - R_{8.89}{}^{B})t](1 - y)$$

$$[10] \qquad (R_{8.74})_D = [R_{8.74}{}^{H} - (R_{8.74}{}^{H} - R_{8.74}{}^{B})t](1 - y)$$

where $R_{8.89}{}^{H}$ (or $_{8.74}$) and $R_{8.89}{}^{B}$ (or $_{8.74}$) are corresponding relative absorbances at the wavelengths indicated for Hevea and Balata, respectively, and $t = (t_0 + x)$ is the total *trans* content of the polymer. Dividing [9] by [10], and substituting for the empirical values of the various R^{H} and R^{B} terms, we obtain, finally

$$[11] \qquad t = \frac{2.53 - 1.05R_2}{R_2 + 2.16}$$

where $R_2 = (R_{8.89})_D/(R_{8.74})_D = A_{8.89}/A_{8.74}$, the A's being the measured absorbances at the given wavelengths. The validity of relation [11] was verified by measurements on the spectra of synthetic mixtures of these two polymers.

The infrared analysis employed here to follow *cis–trans* isomerization and loss of unsaturation thus consisted of determining x by means of relation [11] and then substituting its value in relation [6], from which y was obtained. The spectra of irradiated polyisoprene films as well as films cast from irradiated solutions were obtained from 2 to 15 μ with a Perkin–Elmer Model 221 infrared spectrophotometer.

Nuclear Magnetic Resonance Analysis

The n.m.r. spectra of irradiated polyisoprene solutions ($\sim$ 1% concentration in benzene) were obtained at room temperature with a Varian HR-60 spectrometer operated at both normal and slow magnetic field sweep rates; the procedure was essentially the same as that described for squalene solutions (18). The assignment of the significant peaks in the spectra of irradiated polyisoprene solutions (which contained no internal standard) was based on examination of the spectra of unirradiated solutions containing tetramethylsilane. The slow sweep spectra ($\sim$ 0.5 c.p.s./s) were employed to give the best possible resolution of the *cis* and *trans* methyl proton resonance peaks at 8.21 and 8.32 τ, according to the technique of Chen (19), while the normal magnetic sweep spectra ($\sim$ 2 c.p.s./s) were used to determine the olefinic proton content (—CH=$\dot{C}$—, at 4.90 τ). The combination of slow and normal sweep spectra, and planimetric integration of the appropriate peaks, thus provided data for estimating the extent of isomerization and loss of original double bonds in irradiated polyisoprene solutions.

RESULTS AND DISCUSSION

Solid State Irradiations

The infrared spectra of the various *cis*-polyisoprenes after γ-irradiation *in vacuo* to doses of 400-500 Mrads were similar to that published by Turner *et al.* (3), while those obtained for films irradiated to comparable doses with electrons in a nitrogen atmosphere were similar to those published by Heinze *et al.* (7). Hence, there was no need to present them here.

Typical data, based on infrared analysis, for the radiation-induced *cis–trans* isomerization and decrease of original unsaturation in the *cis*-polyisoprenes in the solid state are presented in Table I. These and other data were used to construct the kinetic plots shown in Figs. 1 and 2 from which G-values for these two important processes were obtained (see Table II). Because films of Balata (*trans*-polyisoprene) tend to undergo rapid post-irradiation oxidation, especially when heated for the purpose of obtaining spectra characteristics of the amorphous polymer, very little solid state work was done with this material.

The shapes of the kinetic plots presented in Fig. 1 for the radiation-induced isomerization of polyisoprene in the solid state conform to the known first order reversible character of such a process (17). Although these particular irradiations have not been carried to the

[4]*The 8.89 and 8.74 μ bands, as suggested by Sutherland and Jones (23) and recently demonstrated by Binder (24), are associated with the methyl vibration of the cis and trans* —C(CH_3)=CH— *units, respectively.*

Can. J. Chem. Downloaded from www.nrcresearchpress.com by 210.87.254.105 on 09/05/12
For personal use only.

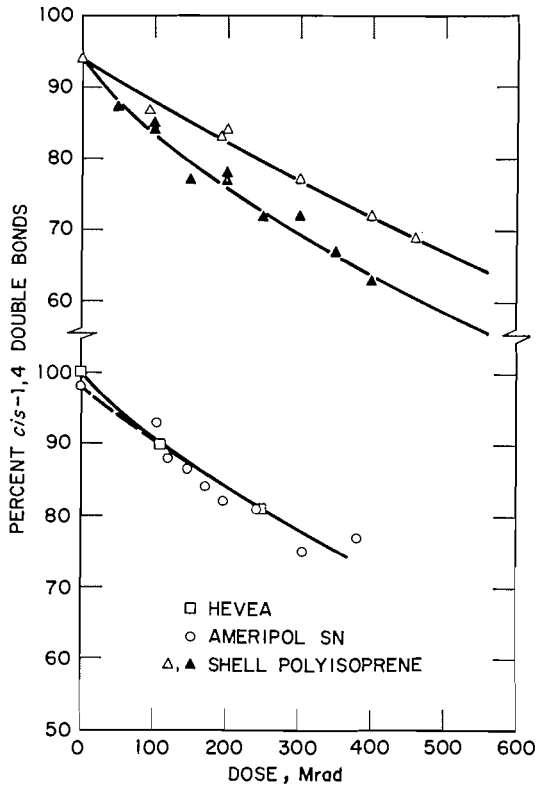

FIG. 1. Radiation-induced *cis–trans* isomerization of various polyisoprenes in the solid state. Open symbols represent γ-irradiations *in vacuo* and closed symbols represent irradiations with electrons under nitrogen at room temperature.

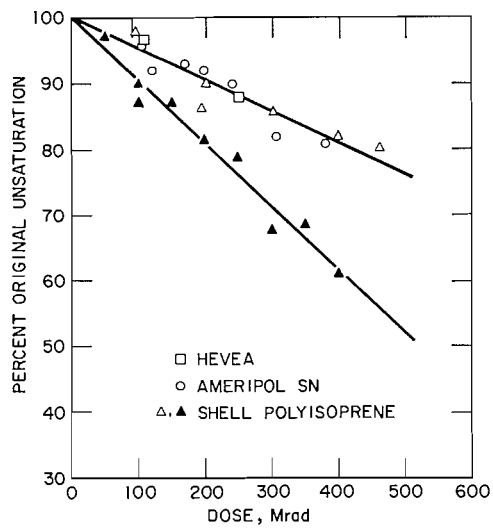

FIG. 2. Radiation-induced disappearance of original unsaturation in various polyisoprenes in the solid state. The ordinate corresponds to $100(1 - y)$, and the open and closed symbols have the same significance as in the previous figure.

Can. J. Chem. Downloaded from www.nrcresearchpress.com by 210.87.254.105 on 09/05/12
For personal use only.

point of equilibrium, in view of some measurements on γ-irradiated Balata films which reveal definite *trans* → *cis* isomerization, there is no doubt that an equilibrium does exist. Moreover, the radio-stationary *cis*/*trans* ratio for the solid state irradiations appears to be nearly the same as that obtained (~ 50/50) in the solution irradiations of *cis*- and *trans*-polyisoprenes (see Fig. 6). In this connection, it should be noted that the equilibrium *cis* content of the internal double bonds of squalene when isomerized in benzene is around 45–50% (as with Balata in solution), but the corresponding equilibrium in pure squalene was not determined (18). It is also noteworthy that the isomerization of natural rubber and Balata catalyzed by sulfur dioxide at 140 °C (22) leads to a similar equilibrium *cis* content (~ 55%).

TABLE II

G-values for changes in unsaturation of various irradiated polyisoprenes

Polymer	Irradiation temp., °C	*G*(-d.b.)	G_p(isom.)	G_s(isom.)
	γ-Irradiations			
Shell polyisoprene	25–30	6.7	9.0	1.0
Ameripol SN	25–30		10.9	
Hevea	25–30		14.1	0.5
Balata	25–30		10	1.1
	Electron irradiations			
Shell polyisoprene	25–30	13.4	14.4	
Polyisoprene-3-*d*	15	15.0		
	−15	10.7		
	−50	8.6		

Because of the nonlinearity of the isomerization plots in Fig. 1, the G_p(isom.) values given in Table II correspond to the number of *cis* or *trans* double bonds *initially* isomerized per 100 eV absorbed by the *pure* polymer. The value indicated for γ-irradiated Balata is only an estimate based on limited data. Partially reflecting the different initial *cis* contents of Hevea, Ameripol SN, and Shell polyisoprene, the G_p(isom.) values for the γ-irradiation of these polymers fall in the decreasing order, 14.1, 10.9, and 9.0, respectively. A somewhat higher G_p(isom.) of 14.4 is noted for the electron-irradiated Shell polymer. Undoubtedly the microstructural differences between these high *cis*-polyisoprenes involving, for example, 0, 0.7, and 4.4% 3,4 units, respectively, and their likely participation in competing intramolecular energy transfer processes, must be responsible for the larger spread in *G*-values than is expected solely on the basis of different initial *cis* contents in these polymers. Considering G_p(isom.) ~ 10 as representative for the solid state γ-ray-induced isomerization of either *cis*- or *trans*-polyisoprene, we note that it is of the same order of magnitude as that for the corresponding reaction in *cis*- and *trans*-polybutadienes (8.0 and 4.0 respectively) (17, 25). Thus the mechanism advanced to explain the isomerization in the latter polymers—involving direct as well as indirect excitation of the double bonds to a state where free rotation and hence geometric interconversion can take place—probably holds for the polyisoprenes as well. The comparative isomerizability of various small, medium, and high molecular weight olefinic compounds has been discussed recently (25) and treated more fully in our previous paper (18), so that there is no need to expand further on this topic here.

It can be seen from the straight line plots of Fig. 2 that polyisoprene undergoes also an important radiation-induced consumption of the original double bonds. This reaction proceeds twice as fast in the films irradiated with electrons under nitrogen as in those

Can. J. Chem. Downloaded from www.nrcresearchpress.com by 210.87.254.105 on 09/05/12
For personal use only.

irradiated with γ-rays *in vacuo*, the G(-d.b.) values being 13.4 and 6.7[5] respectively. From the G(-d.b.) values given in Table II for polyisoprene-3-*d* irradiated with electrons at several temperatures (based on the plots in Fig. 4), an activation energy of 1.1 kcal/mole was calculated for the loss of double bonds in that polymer. This value, which probably holds for ordinary polyisoprene too, compares very well with the activation energy of 0.53 kcal/mole reported previously for the same process in the model compound squalene (18). This additional result further emphasizes the similarities in the radiation chemistry of the various isoprenic compounds.

Apart from the decrease in relative intensities of the 12 and 6 μ bands (associated with consumption of the —C(CH_3)=CH— units), which was more pronounced in the case of electron irradiations than in the case of γ-irradiations, the infrared spectra of irradiated polyisoprenes also revealed subtle changes in both the 8.5–9.5 μ and 7.5–7.7 μ regions which were related to the *cis–trans* isomerization.

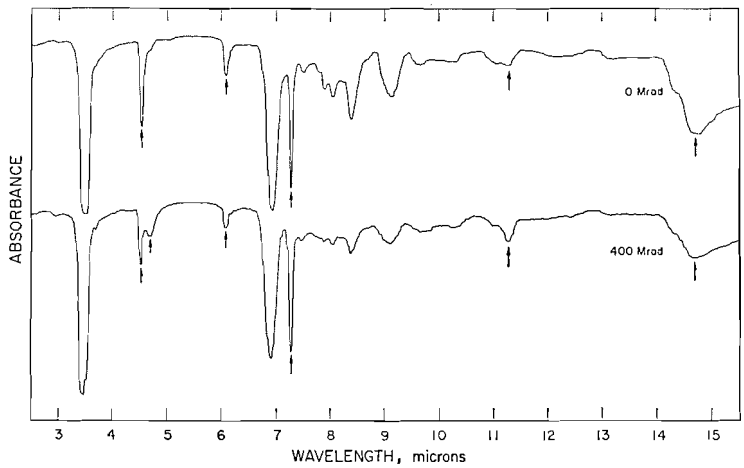

FIG. 3. Infrared spectra of *cis*-polyisoprene-3-*d* before and after irradiation with electrons.

Confirmation of the important loss of original unsaturation and occurrence of *cis–trans* isomerization in irradiated polyisoprene films is afforded by an examination of the infrared spectra of *cis*-polyisoprene-3-*d* before and after irradiation (Fig. 3). Thus the decrease in the 4.5 μ band (C—D stretching vibration for an olefinic carbon atom) and the growth of a band at 4.65 μ (C—D stretching vibration associated with a saturated carbon atom) provide unambiguous evidence for the transformation of the original —C(CH_3)=CD— units in the monodeuterio polyisoprene into the saturated structures $\rangle$C(CH_3)—CDH— and (or) $\rangle$C(CH_3)—CD$\langle$. Accompanying these spectral changes is a marked decrease in relative intensity of the 14.7 μ band (C—D out-of-plane deformation of the *cis* and *trans* —C(CH_3)=CD— units), analogous to the situation with the 12 μ band in ordinary polyisoprene. As shown in Fig. 4, the intensity of the 14.7 μ band diminishes faster than that of the 4.5 μ band, the intensities of both bands having been expressed relative to that of the 7.25 μ band as an internal standard. If, now, the ratio of absorption coefficients for the

[5]*Due to additional data acquired since the previous paper (18) was submitted, as well as to a re-examination of the earlier results, it was necessary to revise the G(-d.b.) for polyisoprene announced in that paper from 5.3 to the new value of 6.7. This change does not affect the earlier arguments, however.*

Can. J. Chem. Downloaded from www.nrcresearchpress.com by 210.87.254.105 on 09/05/12
For personal use only.

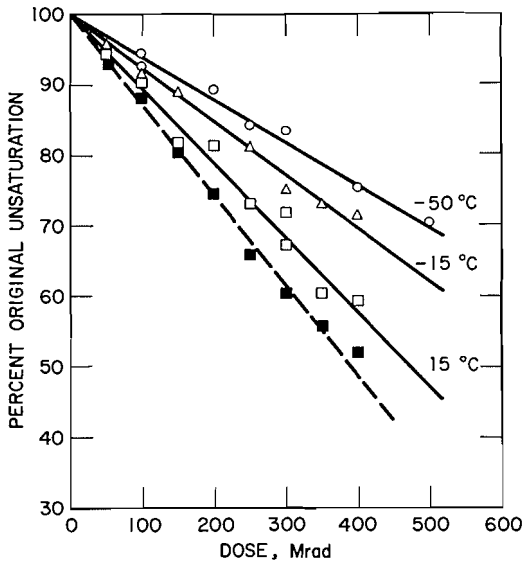

FIG. 4. Decrease of original unsaturation in *cis*-polyisoprene-3-*d* (based on changes in the 4.5 μ band) on irradiation of films with electrons under nitrogen at different temperatures. The dashed line (with closed squares) represents the decrease in relative intensity of the 14.7 μ band for the films irradiated at 15 °C.

cis and *trans* —C(CH$_3$)=CD— units is assumed to be comparable to that for the corresponding —C(CH$_3$)=CH— units, as is quite reasonable, it follows from Fig. 4 that *cis–trans* isomerization definitely occurs in polyisoprene-3-*d*. In fact, it may be calculated[3] that a film of this polymer irradiated to a dose of 400 Mrads with electrons at 15 °C has a *cis* content of 57% (of the remaining 58% original double bonds), which agrees rather well with the 63% *cis* content noted in Fig. 1 for the Shell polyisoprene which was similarly irradiated. This result clearly substantiates the infrared method used to assess the *cis–trans* isomerization and loss of unsaturation in the ordinary polyisoprenes.

The rates at which the double bonds are consumed in both ordinary and monodeuterio polyisoprenes when irradiated with electrons under nitrogen at around 15–25 °C (compare appropriate plots of Figs. 2 and 4) are not only approximately equal to each other but are also comparable to that observed by Heinze *et al.* (7) for electron-irradiated Hevea films. Thus, for example, after a dose of about 400 Mrads the unsaturation decreased by about 38% in Shell polyisoprene and by about 42% in polyisoprene-3-*d*, whereas the corresponding decrease in the Hevea studied by Heinze *et al.* can be estimated (from their Fig. 11) as around 30–35%.[6] The γ-irradiated polyisoprenes, on the other hand, showed a decrease in unsaturation of only about 9–10% after a dose of 200 Mrads. This rate of consumption of original double bonds, although somewhat higher than that reported by Hayden (6) for polyisoprene ($\sim$ 10% after 410 Mrads, based on the 6 μ band), is of the same order of magnitude as that in squalene observed by Turner (4) ($\sim$ 10% at 242 Mrads) and by ourselves (18) (7% at 200 Mrads, corresponding to a G(-d.b.) of 4.6).

On the basis of the detailed discussion presented in the previous paper (18), we are led to consider that cyclization and cross-linking involving some double bonds are responsible

[6]*For a more exact comparison of these two studies, it should be noted that the Hevea sample of Heinze et al., which was exposed to electrons for a dose of 400 Mrads, showed a diminution of about 40% in the intensity of the 12 μ band compared to a diminution of 46% in our simliarly irradiated Shell polyisoprene (see Table I).*

Can. J. Chem. Downloaded from www.nrcresearchpress.com by 210.87.254.105 on 09/05/12
For personal use only.

Can. J. Chem. Downloaded from www.nrcresearchpress.com by 210.87.254.105 on 09/05/12
For personal use only.

for the radiation-induced loss of unsaturation in polyisoprene, just as in squalene.[7] Both free radical and ionic mechanisms were invoked for these two processes. Such an interpretation, however, does not account for the surprising fact that the loss of double bonds occurs more rapidly with electrons than with γ-rays. It might be thought, of course, that the films irradiated under nitrogen, which were not outgassed in contrast to the films irradiated *in vacuo*, encountered sufficient residual oxygen to undergo an additional loss of double bonds through some radiation-induced oxidation. Certainly the drastic drop in unsaturation observed by Kuzminsky *et al.* (14) for polyisoprene irradiated in air can be explained in this way. But this argument probably does not apply to our electron-irradiated films since there was no infrared evidence to suggest that they were at all oxidized.

Whatever the particular mechanism(s) may be, the very high G(-d.b.) values of 7–13 obtained in the present work, combined with the very low activation energy for the loss of double bonds, are compatible with a carbonium ion chain mechanism for this process occurring in polyisoprene. On the other hand, a free radical chain mechanism is consistent with the fact, noted above, that sulfur, which apparently can act as a free radical scavenger (12, 13), lowers considerably the rate of disappearance of double bonds in a natural rubber vulcanizate exposed to γ-rays (15). At the present time, we cannot say for certain which of the two mechanisms is the dominant one, and future work involving other additives which act either as radical acceptors or electron sinks should help settle this point. But the evidence so far obtained prompts the view that the loss of double bonds consists of chain cyclization and cross-linking involving the participation of both free radicals and carbonium ions.

To conclude the discussion of the solid state work, we may comment on some other aspects of the spectra of irradiated polyisoprene and polyisoprene-3-*d*. In common with the spectra published by Turner *et al.* and by Heinze *et al.*, and as also reported by Hayden (6), our spectra for undeuterated polyisoprenes showed the development of a very small blip at 10.4 μ and in the case of Hevea and Ameripol SN, a slight increase in the 11.3 μ band indicative of new vinylidene unsaturation. With Shell polyisoprene, on the other hand, the latter band actually showed a small decrease in intensity. The changes in the 11.3 μ band thus observed for the various irradiated polyisoprenes are reminiscent of the growth or decay of this same band encountered incidentally in the course of the $TiCl_4$-catalyzed cyclization of these polymers (Fig. 8, ref. 21), and presumably has the same type of explanation: formation of vinylidene units through a process such as reaction [3] which is in equilibrium with the radiation-induced consumption of such double bonds.

Although the appearance of the 10.4 μ band in the spectra of irradiated polyisoprenes has been attributed by other workers (3, 6, 7) to the production of *trans* —CH=CH— units, it is more likely that this band is due to the presence of cyclic structures in the polymer backbone. Such an interpretation was invoked for the 10.4 μ band in the spectra of cyclized polyisoprenes, and it is significant that the relative intensity of this band in these polymers (see Figs. 1 and 2, ref. 21) is quite comparable to that of an extensively electron-irradiated polyisoprene (see Fig. 9, ref. 7, for example). Since both the CH_2 deformation vibrations of cyclohexyl rings and *trans* —CH=CH— units absorb fortuitously at around 10.3 μ, we require additional evidence to decide which of these structures is responsible for the observed absorption. If the —CH=CH— units were actually formed in polyisoprene, say, through reaction [1] or reaction [4], analogous reactions [1′] and (or) [4′] should take

[7]*The zero order consumption of double bonds observed in these two isoprenic compounds is difficult to explain on mechanistic grounds, unless the energy absorption is the only limiting factor here.*

place in polyisoprene-3-*d* to yield —CD=CH— units, which absorb at 11.2 μ (26), and new —CH=CH— units, respectively:

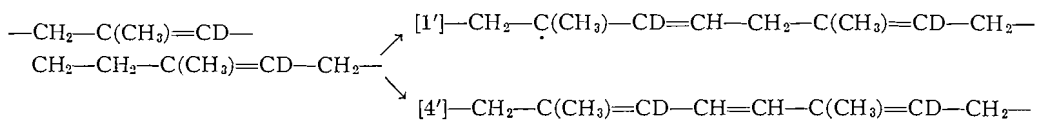

As may be seen from Fig. 3, there is no development of absorption at 10.3 μ to suggest that reaction [4′] occurs to any significant extent. On the other hand, although the figure does show an increase in absorption at 11.3 μ, in view of a similar increase at this wavelength in the spectra of irradiated Hevea and Ameripol SN (but not in Shell polyisoprene, which actually shows a decrease), this growth at 11.3 μ might simply be due to the formation of $\rangle C{=}CH_2$ units in monodeuterio polyisoprene (reaction [3′]) just as with ordinary polyisoprene, and not at all to —CD=CH— units through reaction [1′]. In addition, Fig. 3 shows no development of a band at 12 μ to support the occurrence of the "deuterio" analog of the other double bond shift reaction (2).[8] These observations with respect to reactions [1], [2], and [4] thus agree qualitatively with the findings of Turner *et al.* (3) based on ultraviolet spectra of irradiated Hevea, that diene and triene structures are formed in very low yields, the *G*-values being around 0.09 and 0.02, respectively.

Solution Irradiations

As in the solid state, polyisoprene in dilute benzene solution undergoes pronounced radiation-induced *cis–trans* isomerization and loss of original unsaturation. Unambiguous evidence for the former reaction is clearly indicated in Fig. 5 which shows representative

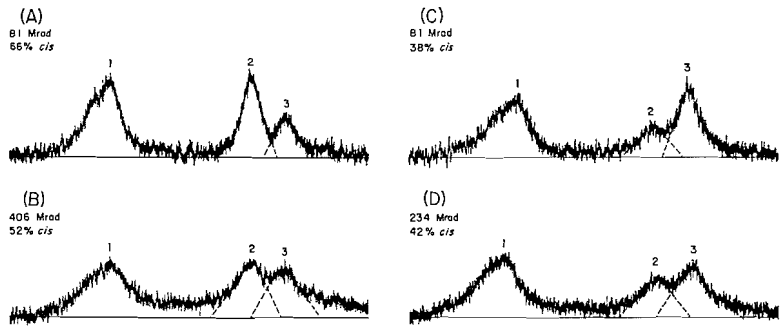

FIG. 5. Nuclear magnetic resonance spectra obtained at slow magnetic field sweep rate of Shell polyisoprene (A, B) and Balata (C, D) in benzene solution after γ-irradiation to various doses. Peak 1, $—CH_2—\dot{C}=$; peak 2, *cis* $—C(CH_3)=$; peak 3, *trans* $—C(CH_3)=$.

slow sweep n.m.r. spectra of solutions of both *cis*- and *trans*-polyisoprenes exposed to various γ-ray doses. Thus, the *cis* methyl proton resonance peak becomes progressively smaller and the *trans* peak progressively larger as the *cis* polymer (Shell polyisoprene) is irradiated to higher doses, while the reverse is the case with the *trans* polymer (Balata). Eventually, an equilibrium is attained in which the *cis/trans* ratio is about 50/50 (Fig. 6). To appreciate the important changes in these slow sweep spectra, it should be noted that peak 2 is completely absent in the spectrum of unirradiated Balata, whereas peak 3 is

[8]*It is worth noting also that the absence of a 12μ band in the spectrum of irradiated polyisoprene-3-d demonstrates that no discernible radiation-induced isotopic substitution occurs in this polymer.*

Can. J. Chem. Downloaded from www.nrcresearchpress.com by 210.87.254.105 on 09/05/12
For personal use only.

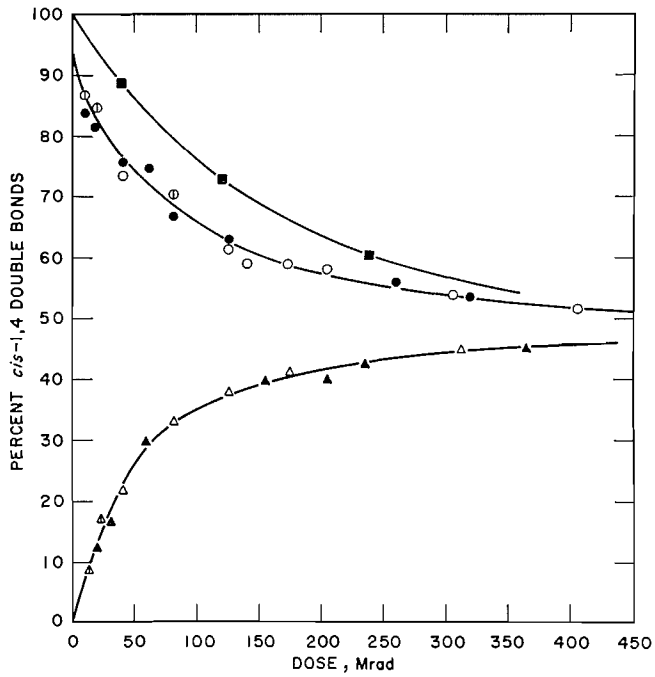

FIG. 6. Radiation-induced *cis–trans* isomerization of various polyisoprenes in benzene. Samples γ-irradiated *in vacuo*: Hevea with natural antioxidants (a.o.) (■); Shell polyiosprene with (●) and without (○) a.o.; Balata with (▲) and without (△) a.o. Samples γ-irradiated in air, with a.o.: Shell polyisoprene, ⊕; Balata, ⧋.

barely present in the spectrum of unirradiated Shell polyisoprene (corresponding to a *trans* content of about 6% of the 1,4 units).

The signal-to-noise ratio of these spectra is poor, owing to the high dilution of the polymer solution (~ 1% polyisoprene in benzene), but this offered no real difficulty in determining the *cis/trans* ratio in the irradiated polymers. In fact, in some related experiments carried out at the higher polymer concentrations, the signal-to-noise ratio improved to the point where the slow sweep spectra of polyisoprene were as well defined as the corresponding squalene spectra shown in the previous paper (18); except for yielding somewhat different kinetic data for the *cis* → *trans* and *trans* → *cis* isomerization, the spectra for the more concentrated solutions presented the same separation of *cis* and *trans* methyl peaks and the same equilibrium *cis/trans* ratio. We chose to concentrate on the 1% polyisoprene solutions in this study so as to have isomerization data which could be compared directly with corresponding data reported for polybutadiene (in 1% benzene solution) (17).

A more serious problem than the signal-to-noise situation in the spectra typified by Fig. 5 is the fact that the loss of unsaturation in polyisoprene, as in irradiated squalene, involving processes such as

$$-CH_2-C(CH_3)=CH-CH_2- \rightarrow -CH_2-\underset{|}{C}(CH_3)-\underset{|}{CH}-CH_2-$$

gives rise to "saturated" methylene groups which appear at higher field than the corresponding "unsaturated" methylene groups. The protons of the former groups, along with new tertiary protons, show up fortuitously in the *cis* and *trans* methyl proton region. This perturbation of the n.m.r. spectrum in the range of interest becomes more serious as

Can. J. Chem. Downloaded from www.nrcresearchpress.com by 210.87.254.105 on 09/05/12
For personal use only.

the dose and hence the loss of unsaturation increases, so that the determination of the *cis/trans* ratio in the highly irradiated solutions can be regarded as somewhat uncertain.

In Fig. 6 are plotted kinetically the isomerization data obtained from n.m.r. spectra for various polyisoprenes irradiated in benzene solution under different conditions. As may be seen, the presence or absence of oxygen or antioxidant has no perceptible effect on the rate of isomerization of Shell polyisoprene or of Balata. These two polymers isomerize in solution at roughly comparable rates and approach, at high doses, a common equilibrium structure with a *cis/trans* ratio of $\sim 50/50$. Surprisingly, Hevea in solution with antioxidant isomerizes at a lower rate than does Shell polyisoprene, which is just the reverse of the situation in the solid state case where the polymers are free of antioxidant. Evidently the natural antioxidants left in Hevea in the solution case exert some inhibiting effect on the isomerization reaction, which nevertheless approaches the same equilibrium as with the Shell polyisoprene or Balata.

From the initial slopes of the curved plots of Fig. 6, the G_s(isom.) values given in Table II were obtained. These values represent the number of *cis* or *trans* double bonds isomerized initially per 100 eV absorbed by both polymer and solvent. Taking a G_s(isom.) of ~ 1.0 as typical for *cis*- and *trans*-polyisoprenes in 1% solution in benzene, we see that, if no energy transfer occurred between solvent and polymer molecules, the effective isomerization yield would be ~ 100 double bonds per 100 eV absorbed by the polymer alone. Since, as we have seen, the pure polyisoprene isomerizes with a yield of about 10 double bonds per 100 eV, it follows that the polymer must receive some nine times as much energy from the solvent as it does directly. This efficiency of intermolecular energy transfer is practically the same as that encountered with polybutadiene (17). Since the topic of intermolecular energy transfer in benzene solutions of various *cis* and *trans* olefinic compounds has been discussed in detail in the previous paper (18) and elsewhere (25, 27), we shall not pursue the matter here. Suffice to say, we have shown definitely that *cis*- and *trans*-polyisoprenes, in common with polybutadiene, squalene, and butene-2, undergo radiation-induced *cis–trans* isomerization both in the pure (solid) state and in benzene solution. In the latter case, it has been assumed that much of the energy transfer from solvent to solute proceeds from the benzene triplet (3.6 eV) to the low-lying triplet state of the polymer double bond (3.2 eV).

Turning now to the radiation-induced loss of original unsaturation in polyisoprene in benzene, we note that this reaction was studied by following the sharp decrease in relative area of the olefinic proton peak in the normal sweep n.m.r. spectra with dose; since these spectra were substantially the same as the corresponding ones for irradiated squalenes (18), there was no need to present them here. From the straight line kinetic plots obtained for the loss of unsaturation, the G-value for this process was found to be 0.27 double bonds consumed per 100 eV of energy absorbed by the whole solution. This corresponds to a hypothetical yield of 27 double bonds per 100 eV absorbed by the polymer alone, as though there were no energy transfer between excited benzene and polyisoprene molecules. Since this yield is some four times that in the pure polymer (G(-d.b.) = 6.7), we again see the participation of intermolecular energy transfer, although some of the enhanced loss of double bonds in the solution case compared to that in the solid state may be due to phenylation of polyisoprene, just as in squalene (18). Interestingly, the latter compound, in a 10% solution in benzene, showed a loss of unsaturation (hypothetical yield of 9.8 double bonds consumed per 100 eV absorbed by solute alone) which is comparable to that of polyisoprene, taking into account the fact that the solutions of these two compounds were irradiated at different concentrations.

Can. J. Chem. Downloaded from www.nrcresearchpress.com by 210.87.254.105 on 09/05/12
For personal use only.

ACKNOWLEDGMENTS

This research was supported in part by Aeronautical Systems Division, U.S.A.F., and in part by Stanford Research Institute. The authors wish to record their appreciation to W. R. Anderson, Jr., for providing the n.m.r. spectra, and to L. F. Nye, who monitored the irradiations. Thanks are also extended to Professor P. J. Flory for helpful discussions.

REFERENCES

1. A. CHARLESBY. Rubber Chem. Technol. **28**, 1 (1955).
2. D. T. TURNER. J. Polymer Sci. **35**, 541 (1959).
3. M. B. EVANS, G. M. C. HIGGINS, and D. T. TURNER. J. Appl. Polymer Sci. **2**, 340 (1959).
4. D. T. TURNER. Polymer, **1**, 27 (1960).
5. L. MULLINS and D. T. TURNER. J. Polymer Sci. **43**, 35 (1960).
6. P. HAYDEN. Intern. J. Appl. Radiation Isotopes, **8**, 65 (1960).
7. H. D. HEINZE, K. SCHMIEDER, G. SCHNELL, and K. A. WOLF. Kautschuk Gummi, **14**, WT 208 (1961); Rubber Chem. Technol. **35**, 776 (1962).
8. D. T. TURNER. J. Polymer Sci. **B1**, 93, 97, 101 (1963).
9. F. A. BOVEY. The effects of ionizing radiation on natural and synthetic high polymers. Interscience Publishers, New York. 1958.
10. A. CHARLESBY. Atomic radiation and polymers. Pergamon Press, London. 1959.
11. S. D. GEHMAN and T. C. GREGSON. Rubber Chem. Technol. **33**, 1375 (1960).
12. A. CHAPIRO. Radiation chemistry of polymeric systems. Interscience Publishers, New York. 1962.
13. D. T. TURNER. *In* The chemistry and physics of rubber-like substances. *Edited by* L. Bateman. John Wiley & Sons, New York. 1963.
14. A. S. KUZMINSKY, T. S. NIKITINA, E. V. ZHURAVSKAYA, L. A. OXENTIEVICH, L. I. SUNITSA, and N. I. VITUSHKIN. Second United Nations International Conference on the Peaceful Uses of Atomic Energy. A/Conf. 15/P/2085. 1958.
15. D. L. LOUGHBOROUGH, A. E. JUVE, J. R. BEATTY, and J. W. BORN. WADC Tech. Rept. 55–58 (AD 97234). 1958.
16. W. S. RICHARDSON and A. SACHER. J. Polymer Sci. **10**, 353 (1953).
17. M. A. GOLUB. J. Am. Chem. Soc. **82**, 5093 (1960); J. Phys. Chem. **66**, 1202 (1962).
18. J. DANON and M. A. GOLUB. Can. J. Chem. **42**, 1577 (1964).
19. H. Y. CHEN. Anal. Chem. **34**, 1793 (1962).
20. M. A. GOLUB, S. A. FUQUA, and N. S. BHACCA. J. Am. Chem. Soc. **84**, 4981 (1962).
21. M. A. GOLUB and J. HELLER. Can. J. Chem. **41**, 937 (1963).
22. J. I. CUNNEEN, G. M. C. HIGGINS, and W. F. WATSON. J. Polymer Sci. **40**, 1 (1959).
23. G. B. B. M. SUTHERLAND and A. V. JONES. Discussions Faraday Soc. **9**, 281 (1950).
24. J. L. BINDER. J. Polymer Sci. **A1**, 37 (1963).
25. M. A. GOLUB. Discussions Faraday Soc. **36**, 264, 276 (1963).
26. M. A. GOLUB and J. J. SHIPMAN. Spectrochim. Acta, **16**, 1165 (1960).
27. R. B. CUNDALL and P. A. GRIFFITHS. Discussions Faraday Soc. **36**, 111 (1963).

Can. J. Chem. Downloaded from www.nrcresearchpress.com by 210.87.254.105 on 09/05/12
For personal use only.

Can. J. Chem. Downloaded from www.nrcresearchpress.com by 210.87.254.5 on 09/05/12
For personal use only.

STRUCTURES OF MERCURY MERCAPTIDES

PART II. X-RAY STRUCTURAL ANALYSIS OF MERCURY ETHYLMERCAPTIDE

D. C. BRADLEY[1] AND N. R. KUNCHUR[2]

Department of Chemistry, University of Western Ontario, London, Ontario

Received November 16, 1964

ABSTRACT

The unit cell parameters for $Hg(SC_2H_5)_2$ were determined by X-ray diffraction: $a = 7.54 \pm 0.02$; $b = 4.87 \pm 0.01$; $c = 23.80 \pm 0.04$ Å; $\beta = 85°$. The unit cell contains four formula units, and a complete structural analysis revealed a molecular lattice with insignificant intermolecular bonding involving mercury and sulfur. Interatomic distances (excluding C—H) were determined.

INTRODUCTION

This work forms a part of the programme of studying the coordination compounds of mercaptans with mercury. Recent work (1) showed that mercury methylmercaptide had an unusual structure and it seemed worthwhile to investigate the structure of mercury ethylmercaptide. The crystal structure $Hg(S \cdot C_2H_5)_2$ was partially solved by Wells (2) but his results were qualitative. The work described in the present paper was carried out to locate all atoms (except hydrogens) in order to establish the stereochemistry of mercury in this compound and to obtain reliable values for the dimensions of the molecule.

EXPERIMENTAL

Mercury ethylmercaptide $Hg(S \cdot C_2H_5)_2$ was prepared by Wertheim's method (3) and purified by crystallization from ethanol. It forms thin plates on (001) outlined by (110) faces. With Cu K_α radiation ($\lambda = 1.542$ Å) the compound had a high absorption coefficient of 421 cm^{-1}. Unfortunately the thinness and fragility of the crystals prevented them from being ground into spheres or cylinders to facilitate the absorption correction. The thin plates were cut into needles with square cross-section of 0.1 mm. Absorption corrections were applied assuming that the needles were cylinders of diameter 0.1 mm.

The cell parameters were $a = 7.54 \pm 0.02$ Å; $b = 4.87 \pm 0.01$ Å; $c = 23.80 \pm 0.04$ Å; $\beta = 85°$; $Z = 4$; $d_{calcd} = 2.45$ g cm^{-1}; $d_{obs} = 2.47$ g cm^{-1}; space group = Cc.

The intensity data on $h0l$ and $0kl$ reflections were collected using the multifilm technique and a range of exposure times on a Stoe Weissenberg camera. Intensities were estimated visually and corrected for Lorentz and polarization factors. The relative F_0 values were scaled by Wilson's method, and in the final stages the scaling was improved by comparison with the calculated structure amplitudes.

Structure Determination

Although the systematic absences correspond to the space groups Cc and $C2/c$, the latter space group was discarded on the basis of the intensities of the reflections hkl with l odd. The space group Cc has no special positions and so all atoms have to be placed in general positions. $h0l$ and $0kl$, being the best resolved projections, were considered for structure determination. Patterson syntheses computed for these projections gave the following coordinates for the mercury atom.

	x/a	y/b	z/c
Hg	0.000	0.218	0.000

The contribution of mercury to the structure amplitude is such that it has only a real component for hkl with l even and only an imaginary component for hkl with l odd. A mercury-phased Fourier has, therefore, a higher symmetry than the real symmetry with the result that for every peak in a $h0l$ Fourier map, another peak related to the first by a center of symmetry (which is at origin where mercury is placed) would be produced. So if the distribution of two sulfur atoms and four carbon atoms around mercury is acentric, four peaks for two sulfur atoms and eight peaks for four carbon atoms would be produced. Since the stereochemistry of the mercury mercaptide molecule was not known, the problem of locating the light sulfur and carbon atoms was solved by the following procedure.

[1]*Present address: Chemistry Department, Queen Mary College, London, England.*

[2]*Present address: Center for Crystallographic Research, Roswell Park Memorial Institute, Buffalo, N. Y. Correspondence regarding this communication should be sent to this address.*

Can. J. Chem. Downloaded from www.nrcresearchpress.com by 210.87.254.5 on 09/05/12
For personal use only.

The values for atomic scattering factors for all atoms were taken from ref. 4. A mean isotropic temperature factor $B = 2.8$ Å^2 was applied to the scattering curves of all atoms. F_{obs} were brought on the absolute scale by Wilson's method.

Both the $h0l$ and $0kl$ Patterson projections showed clearly peaks corresponding to mercury–sulfur interactions. Since the coordinates of mercury were known, the coordinates of sulfur were derived. Structure factors were calculated for mercury and one sulfur atom only. For the reflections hkl with l even, both mercury and sulfur contributed to the real part of the structure amplitude and only sulfur contributed to the imaginary part. Contribution of mercury was subtracted from the real part while the imaginary part was not changed since it did not have any contribution from mercury. Phase angles were calculated using the modified real component and the unmodified imaginary component. These phase angles were used for computing a mercury difference Fourier. The coefficients used in this Fourier were obtained by subtracting the contribution of mercury from the F_{obs} which were brought on an absolute scale. A similar procedure was carried out for reflection hkl with l odd. Only sulfur contributed to the real part and both sulfur and mercury contributed to the imaginary part of these reflections. The $h0l$ and $0kl$ mercury difference Fourier done in this manner revealed the positions of all sulfur and carbon atoms. New phase angles were calculated considering all light atoms in the structure factor calculations, and a second cycle of mercury difference Fourier syntheses was carried out. A third cycle was repeated so that the atomic coordinates of all atoms were further refined. The 'y' coordinate of mercury was also refined during these successive Fourier syntheses. The final agreement index for various groups of reflections is shown in Table I. The final mercury difference Fourier projections upon (010) and (001) are shown in Figs. 1 and 3.

The final coordinates are listed in Table II while the observed and calculated structure factors including the phase angles are listed in Table IV. The lowest value of F_0 which could be observed was 8, and hence unobserved reflections are indicated as < 8. The agreement index stated in Table I takes into account observed reflections as well as observed and unobserved reflections.

TABLE I

Type of reflections	No. of observed reflections	No. of observed and unobserved reflections	Agreement index for observed reflections only	Agreement index for observed and unobserved reflections
$h0l$	55	61	0.133	0.139
$\bar{h}0l$	32	38	0.164	0.169
$0kl$ $(= 2n)$	24	27	0.133	0.135
$0kl$ $(= 2n + 1)$	22	25	0.156	0.156

TABLE II

	x/a	y/b	z/c
Hg	0.000	0.211	0.000
S_1	0.216	0.211	0.071
S_2	0.784	0.200	0.929
C_1	0.100	0.211	0.133
C_2	0.200	0.166	0.185
C_3	0.900	0.205	0.867
C_4	0.800	0.250	0.800

TABLE III

Interatomic distances and bond angles

	Distance (Å)		Angles (°)
Hg_1—S_1	2.45	$Hg_1S_1C_1$	106
Hg_1—S_2	2.45	$Hg_1S_2C_3$	106
Hg_1—S_3	3.56	$S_1C_1C_2$	103
Hg_1—S_4	3.53	$S_2C_3C_4$	116
S_1—C_1	1.65	$Hg_1S_4Hg_2$	100
S_2—C_3	1.65	$Hg_1S_1Hg_2$	99
C_1—C_2	1.54	$S_4Hg_1S_1$	84
C_3—C_4	1.84	$S_4Hg_2S_1$	83
$Hg_1 \ldots Hg_1$	4.87±0.02		
$Hg_1 \ldots Hg_2$	4.65±0.02		

TABLE IV

h	k	l	F_0	F_c	Alpha[0]
0	0	2	79.0	86.8	0.5
0	0	4	53.0	59.1	359.8
0	0	6	53.0	53.9	358.5
0	0	8	41.0	43.8	3.5
0	0	10	44.0	55.6	357.5
0	0	12	50.0	56.9	1.0
0	0	14	59.0	62.3	0.8
0	0	16	44.0	53.4	357.9
0	0	18	40.0	30.1	3.7
0	0	20	24.0	22.5	357.2
0	0	22	23.0	21.1	359.6
0	0	24	26.0	20.8	2.9
0	0	26	24.0	21.6	356.7
0	0	28	<8.0	20.4	2.4
2	0	0	44.0	41.2	0.0
2	0	2	43.0	39.0	359.7
2	0	4	62.0	62.3	359.4
2	0	6	68.0	74.0	1.3
2	0	8	74.0	78.3	358.6
2	0	10	58.0	54.8	1.0
2	0	12	40.0	42.6	0.7
2	0	14	46.0	34.6	357.4
2	0	16	36.0	22.9	4.5
2	0	18	33.0	27.9	357.7
2	0	20	36.0	33.1	360.0
2	0	22	32.0	30.7	1.8
2	0	24	25.0	23.1	356.9
2	0	26	<8.0	14.7	3.5
2	0	28	<8.0	11.1	358.8
4	0	0	52.0	59.2	360.0
4	0	2	61.0	64.5	359.9
4	0	4	54.0	56.1	0.7
4	0	6	45.0	45.6	358.8
4	0	8	43.0	25.3	1.4
4	0	10	44.0	26.9	0.4
4	0	12	47.0	36.2	358.3
4	0	14	38.0	34.3	2.3
4	0	16	35.0	34.3	358.4
4	0	18	28.0	28.6	0.2
4	0	20	19.0	20.1	2.0
4	0	22	15.0	12.9	355.4
4	0	24	10.0	9.6	5.0
4	0	26	<8.0	12.3	358.6
6	0	0	35.0	29.4	0.0
6	0	2	38.0	23.1	0.5
6	0	4	28.0	26.8	359.1
6	0	6	28.0	24.9	0.9
6	0	8	42.0	31.7	0.1
6	0	10	42.0	35.8	359.1
6	0	12	38.0	26.3	1.9
6	0	14	22.0	18.6	357.8
6	0	16	12.0	12.9	0.7
6	0	18	10.0	12.5	2.0
6	0	20	10.0	13.6	356.7
6	0	22	<8.0	3.7	360.0
8	0	0	20.0	18.8	0.0
8	0	2	23.0	26.5	359.7
8	0	4	22.0	23.1	0.4
8	0	6	19.0	20.0	360.0
8	0	8	13.0	16.7	359.1
2	0	2	63.0	77.1	0.6
2	0	4	60.0	69.2	359.2
2	0	6	65.0	75.8	0.0
2	0	8	55.0	74.7	1.0
2	0	10	39.0	47.6	357.5
2	0	12	28.0	32.8	3.0
2	0	14	30.0	27.0	358.9
2	0	16	33.0	34.2	358.7
2	0	18	41.0	38.6	2.4

Can. J. Chem. Downloaded from www.nrcresearchpress.com by 210.87.254.5 on 09/05/12
For personal use only.

TABLE IV *(Continued)*

h	k	l	F_0	F_c	Alpha^0
2	0	20	42.0	32.1	357.3
2	0	22	28.0	28.1	1.5
2	0	24	17.0	20.3	0.7
2	0	26	<8.0	11.9	355.8
2	0	28	<8.0	9.3	6.0
4	0	2	48.0	46.1	359.6
4	0	4	50.0	41.2	1.0
4	0	6	34.0	26.8	358.7
4	0	8	33.0	35.9	359.9
4	0	10	35.0	48.6	1.1
4	0	12	28.0	43.0	358.2
4	0	14	30.0	36.0	1.7
4	0	16	30.0	25.5	359.4
4	0	18	20.0	18.6	358.0
4	0	20	16.0	15.5	4.1
4	0	22	<8.0	14.2	356.1
4	0	24	18.0	17.8	1.3
4	0	26	<8.0	17.2	0.8
6	0	2	44.0	37.8	0.1
6	0	4	44.0	40.5	359.4
6	0	6	44.0	38.1	0.9
6	0	8	30.0	23.4	359.0
6	0	10	16.0	18.2	359.6
6	0	12	17.0	19.1	2.0
6	0	14	18.0	17.4	357.1
6	0	16	19.0	20.7	1.7
6	0	18	20.0	21.1	359.8
6	0	20	18.0	17.5	358.4
6	0	22	8.0	0.6	180.0
0	2	1	39.0	40.5	92.6
0	2	3	30.0	24.9	85.2
0	2	5	30.0	21.2	85.2
0	2	7	18.0	17.7	96.8
0	2	9	16.0	17.7	86.6
0	2	11	22.0	22.2	92.9
0	2	13	18.0	23.4	92.9
0	2	15	18.0	23.8	86.6
0	2	17	15.0	16.9	90.7
0	2	19	10.0	8.7	86.9
0	2	21	9.0	8.3	86.7
0	2	23	<7.0	8.3	96.2
0	2	25	<7.0	8.1	89.3
0	2	27	<9.0	9.1	90.8
0	4	1	36.0	36.2	271.0
0	4	3	31.0	25.7	267.9
0	4	5	21.0	20.4	267.7
0	4	7	18.0	18.1	272.9
0	4	9	18.0	18.5	268.6
0	4	11	18.0	22.1	271.6
0	4	13	14.0	24.7	271.6
0	4	15	17.0	24.7	268.1
0	4	17	19.0	17.8	270.2
0	4	19	17.0	10.0	268.3
0	4	21	9.0	9.1	268.2
0	2	0	78.0	−79.0	−180.0
0	2	2	75.0	58.1	180.0
0	2	4	45.0	42.9	182.6
0	2	6	38.0	37.9	177.8
0	2	8	38.0	33.6	182.2
0	2	10	37.0	39.1	178.2
0	2	12	42.0	40.5	179.2
0	2	14	47.0	44.9	181.2
0	2	16	26.0	38.1	178.4
0	2	18	27.0	22.4	183.8
0	2	20	18.0	17.2	178.9
0	2	22	17.0	15.5	178.5
0	2	24	14.0	15.9	182.1
0	2	26	17.0	16.1	176.6
0	4	0	18.4	18.0	23.8

Can. J. Chem. Downloaded from www.nrcresearchpress.com by 210.87.254.5 on 09/05/12
For personal use only.

TABLE IV *(Concluded)*

h	k	l	F_0	F_c	Alpha^0
0	4	2	21.0	19.7	359.8
0	4	4	19.0	16.1	10.0
0	4	6	19.0	13.6	355.5
0	4	8	15.0	13.2	0.7
0	4	10	17.0	14.4	358.2
0	4	12	15.0	14.4	352.8
0	4	14	15.0	16.7	3.0
0	4	16	15.0	13.5	0.2
0	4	18	12.0	9.0	5.2
0	4	20	<7.0	7.5	3.9
0	4	22	<7.0	6.0	353.9
0	4	24	<8.0	1.0	223.9

Diffraction Effects and the Accuracy of Coordinates

The diffraction effects due to the presence of heavy mercury atom were eliminated by doing mercury difference Fourier syntheses. A rough estimate regarding the accuracy of the coordinates was obtained by comparing the common 'Z' coordinates of the atoms in the two projections. The deviations in the coordinates of mercury and sulfur are found to be 0.01 Å and 0.05 Å respectively. All carbon atoms excepting carbon C_4 correspond to reasonable bond lengths and bond angles within the molecule. The bond length C_3—C_4 of 1.84 Å is much longer than one would expect. On the whole one can state that all carbon atoms have been located and thus the stereochemistry of the mercury mercaptide molecule was defined.

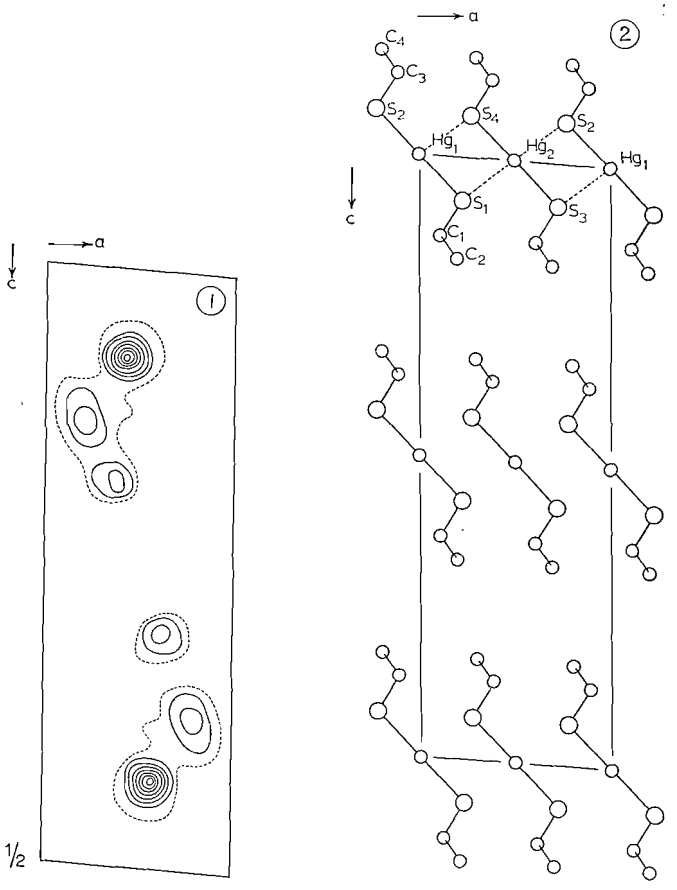

FIG. 1. Electron density projection along b axis. Contours are drawn at equal arbitrary intervals.
FIG. 2. Interpretation diagram for Fig. 1.

Can. J. Chem. Downloaded from www.nrcresearchpress.com by 210.87.254.5 on 09/05/12
For personal use only.

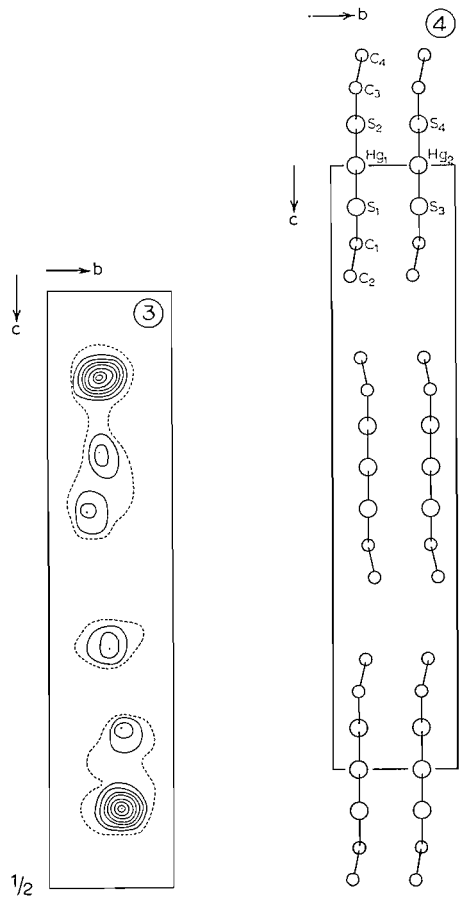

FIG. 3. Electron density projection along *a* axis. Contours are drawn at equal arbitrary intervals.
FIG. 4. Interpretation diagram for Fig. 3.

RESULTS AND DISCUSSION

The various bond lengths and bond angles obtained from the final coordinates are shown in Table III. The arrangement of the molecules in the (*h*0*l*) and (0*kl*) projections can be seen in Figs. 2 and 4 respectively. In the crystal structure a simple molecule C_2H_5S—Hg—SC_2H_5 contains two Hg—S bonds which are linear within the experimental errors, the Hg—S distance being 2.45 Å for both these bonds. There are four more sulfur atoms arranged at a distance of 3.54 Å from each mercury arranged in a square planar configuration. The short Hg—S bonds are perpendicular to this plane so that a mercury atom is surrounded by six sulfur atoms in a distorted octahedral arrangement. The low melting point of this compound (76 °C) suggests that the sulfur atoms at 3.53 Å and 3.56 Å from mercury do not give rise to strong intermolecular bonds. A comparison of this compound with mercury methylmercaptide (1) shows that the next longer Hg—S bond lengths of 3.25 Å in the latter are slightly shorter than in the former. The higher melting point of $Hg(SCH_3)_2$ (175°) suggests that the secondary interactions are of greater significance in this compound. Also the larger size of the ethylmercaptide group leads to a looser packing of the mercury ethylmercaptide molecules and hence the crystal structure is essentially molecular in type. It is noteworthy that the estimated sum of the Van der

Can. J. Chem. Downloaded from www.nrcresearchpress.com by 210.87.254.5 on 09/05/12
For personal use only.

Waal's radii of mercury sulfur of 3.35 Å is greater than the secondary Hg . . . S bond lengths in $Hg(SCH_3)_2$ but less than those in $Hg(SC_2H_5)_2$.

ACKNOWLEDGMENTS

We are indebted to the U.S. Office of Naval Research for supporting this research. We thank Mr. W. Wilson of the Computation Center for much help in writing the programs in Fortran IV for IBM 7040 computer and Dr. J. Hart for providing the computing facilities.

REFERENCES

1. D. C. Bradley and N. R. Kunchur. J. Chem. Phys. **40**, 2258 (1964).
2. A. F. Wells. Z. Krist. **96**, 435 (1937).
3. E. Wertheim. J. Am. Chem. Soc. **51**, 3661 (1929).
4. International Tables for X-ray Crystallography. Vol. III. Birmingham : Kynoch Press. 1962.

Can. J. Chem. Downloaded from www.nrcresearchpress.com by 210.87.254.5 on 09/05/12
For personal use only.

Can. J. Chem. Downloaded from www.nrcresearchpress.com by 210.87.254.6 on 09/05/12
For personal use only.

THE STEREOCHEMISTRY OF THE TETRAHYDROPIMARIC ACIDS[1]

J. W. ApSimon, P. V. Demarco, and J. Lemke
Department of Chemistry, Carleton University, Ottawa, Canada
Received June 3, 1965

ABSTRACT

Evidence is presented that the fully reduced derivatives of pimaric acid (I), sandaracopimaric acid (II), and isopimaric acid (III) have *trans–anti–trans* fused skeletons. The implications of this observation are discussed.

Extensive chemical evidence both degradative and synthetic has confirmed the structures of pimaric acid I (1), sandaracopimaric acid II (2), and isopimaric acid III (3). The vinyl groups in these acids readily absorb 1 mole of hydrogen using a palladium catalyst in ethanol yielding the corresponding dihydro-derivatives I, II, or III (ethyl group in place of vinyl at C-13); however, the nuclear double bonds require more vigorous conditions for reduction, hydrogenation occurring with Adams' catalyst in acetic acid for 24 h to give the tetrahydropimaric acids (IV*a* is tetrahydropimaric acid and IV*b* is tetrahydrosandaracopimaric or isopimaric acid).[2]

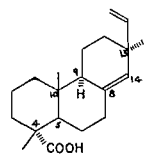

I

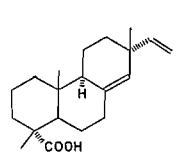

II

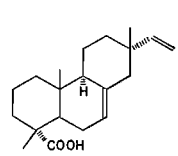

III

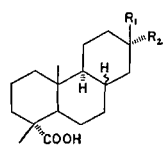

	R_1	R_2
IV*a*	Et	Me
IV*b*	Me	Et

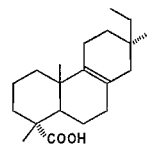

V

Edwards and Howe (1*a*) showed that, in the case of the hydrogenation of dihydropimaric acid, the nuclear double bond underwent migration to the $\Delta^{8,9}$ position giving V which was then reduced. This isomerization could be carried out by the action of acid on dihydropimaric acid I (Et for vinyl at C-13) giving V which, on hydrogenation, gave the fully reduced acid IV*a*. On the basis of the commonly accepted concept that the addition of hydrogen occurs from the less hindered side of an unsaturated molecule in a *cis* fashion (for reviews on the stereochemistry of hydrogenation see ref. 4) one would predict that the

[1]*The work described in this paper formed part of a thesis submitted by P. V. D. in partial fulfilment of the requirements for the degree of M.Sc., September 1964. It was presented to the Atlantic Section of the CIC during January 1965 and at the 48th Canadian Chemical Conference, May 31st, 1965.*
Issued as N.R.C. No. 8615.
[2]*As may be expected, the tetrahydro derivatives of IVb of sandaracopimaric acid and isopimaric acid were found to be identical.*

Can. J. Chem. Downloaded from www.nrcresearchpress.com by 210.87.254.6 on 09/05/12
For personal use only.

tetrahydropimaric acids IV*a* and IV*b* would have the *trans–anti–cis* fused backbones IV*a* or IV*b* (H-8 is α). We have shown that this is not the case and describe the work here. During the course of our studies Asselineau (5) described two tetrahydro derivatives from pimaric acid; one was identical to that obtained by earlier workers with m.p. 240°; however, if the hydrogenation was carried out under pressure at 60° another tetrahydro acid m.p. 168° was obtained. On the basis that this latter acid was formed very readily (4 h) Madame Asselineau applying the above generalization (4) assigned to it the *trans–anti–cis* configuration IV*a* (H-8 is α). She was unable to assign a configuration to the acid m.p. 240° which we show in the sequel to have the *trans–anti–trans* configuration.

The dihydro acids I, II, and III (Et for C-13 vinyl) were hydrogenated using Adams' catalyst in acetic acid using the conditions of Edwards and Howe (1*a*). Reduction proceeded slowly (up to 24 h) with uptake of 1 mole of hydrogen, and the tetrahydro acids IV*a* and IV*b* were isolated. The first crops from the crystallization of these products were pure compounds as shown by vapor phase chromatography (v.p.c.) of their methyl esters; however, the mother liquors contained up to 15% of another compound which had a longer retention time than the unreduced species or the major products. In the case of the reduction of dihydropimaric acid I (Et for vinyl at C-13), the methyl ester of this minor product had the same retention time on two columns as the methyl ester of the acid m.p. 168° kindly supplied by Madame Asselineau (5). We have been unable to isolate this compound in a pure state from the hydrogenation reaction mixture. If the French workers are correct in their assignment of configuration to the acid m.p. 168°, then the configuration of the tetrahydropimaric acid m.p. 240° is unknown, a fact which encouraged us in our studies.

The following sequence of reactions was performed in all three series starting from the dihydro acids I, II, or III (Et for C-13 vinyl). Reaction with excess diborane in tetrahydrofuran followed by alkaline peroxide work-up gave the corresponding diols VI*a*, VI*b*, and VII as major products.[3] The stereochemistries shown for these diols are assigned on the basis of the preferred mode of attack of diborane from the less hindered side of the double bond giving products resulting from *cis* addition of reagent (6). Our intention was to oxidize these alcohols to the corresponding keto aldehydes VIII*a*, VIII*b*, and IX, but even though Jones' reagent (7) has been reported to oxidize alcohols without affecting

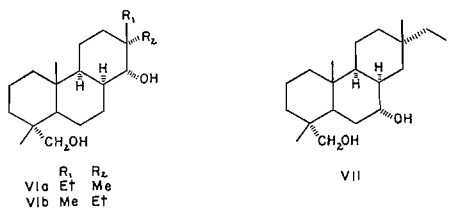

	R_1	R_2
VI*a*	Et	Me
VI*b*	Me	Et

VII

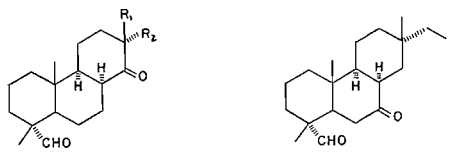

	R_1	R_2
VIII*a*	Et	Me
VIII*b*	Me	Et

IX

[3]*The other products from this reaction are a complex mixture which we have not as yet made any attempt to separate.*

the stereochemistry at α-carbons (1*c*, 8), we were unable to realize this aim and such oxidation of the diols VI*a*, VI*b*, and VII gave mixtures which could not be separated. On oxidation with an excess of Jones' reagent high yields of the keto acids X*a*, X*b*, and XI were obtained, which were unaffected by treatment with base and hence must have the most stable *trans–anti–trans* configuration (9). The n.m.r. spectra of the acids X*a* and X*b* supported this assignment; their C-10 methyl signals both appeared at 59 c.p.s. below tetramethylsilane, compared to 48 c.p.s. for dihydropimaric acid I (Et for C-13 vinyl and 49 c.p.s. for II (Et for C-13 vinyl). Thus in going from the corresponding dihydro acid to the keto acids X*a* and X*b* the C-10 methyl groups are deshielded.[4] If the configuration of X*a* and X*b* had been *trans–anti–cis*, then the C-10 methyl groups in the two keto acids would have been in the shielding cones of the carbonyl groups (10) and thus might have been expected to resonate at higher field than in the parent compounds. Such a prediction is supported by our earlier work on the perhydrophenanthrene acids derived from podo-

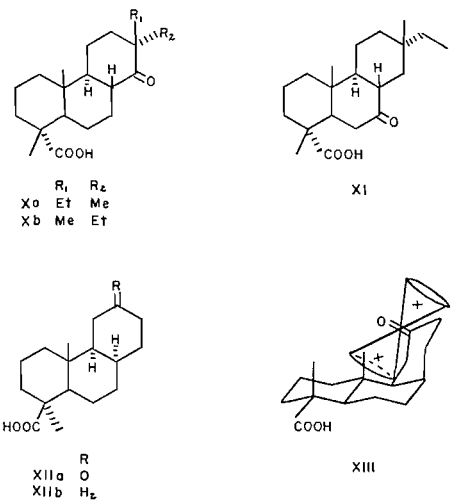

carpic acid (11). The acids XII*a* and XII*b* were synthesized from the natural product for model studies. The keto acid XII*a* showed C-10 methyl resonance at 40 c.p.s. below tetramethylsilane compared to 58 c.p.s. for the reduced acid XII*b*, the methyl group clearly lying in the shielding cone of the carbonyl group at C-11 as illustrated in XIII.

The keto acids X*a*, X*b*, and XI were next reduced, using the Wolff–Kishner technique, to the fully reduced acids IV*a* and IV*b* (H-8 is β). These two products were identical to the tetrahydropimaric acids obtained by hydrogenation. Although the ketoacids had the most stable configuration, there was a possibility that hydrazone formation in the Wolff–Kishner procedure was faster with the less stable epimer which could be present in low concentration at equilibrium (12). Decomposition of such a hydrazone would then give the less stable *trans–anti–cis* isomer. To test this possibility, we reduced ketopimaric acid X*a* by reduction of the dithioketal with Raney nickel, a method which has been demonstrated to proceed without affecting the stereochemistry at α-carbon atoms to carbonyl groups (13). The dithioketal was prepared by the method of Fieser (14) and was obtained as a high melting crystalline solid which, on refluxing with Raney nickel in ethanol overnight, yielded the same tetrahydropimaric acid IV*a* (H-8 is β) as obtained by the Wolff–Kishner reduction of X*a* or by hydrogenation of dihydropimaric acid I (Et for C-13 vinyl).

[4]*It may be argued that the double bond has a large effect in these spectra. This is not the case as the fully reduced acids show the same C-10 methyl resonance positions.*

Can. J. Chem. Downloaded from www.nrcresearchpress.com by 210.87.254.6 on 09/05/12
For personal use only.

We therefore assume that in all three cases Wolff–Kishner reduction proceeds in the expected manner to give the *trans–anti–trans* tetrahydro acids IV*a* and IV*b* (H-8 is β) and thus hydrogenation of the dihydroacids I, II, and III (Et for C-13 vinyl) also yields these compounds. It now remains to rationalize the formation of these *trans* products on catalytic hydrogenation.

The early work of Linstead (15) on the hydrogenation of phenanthrene and diphenic acids over platinum led to the postulate that reduction occurs from the less hindered side of an unsaturated molecule with simultaneous transfer of two or more hydrogen atoms from the catalyst to the adsorbed molecule. This concept has led to the commonly accepted generalization that catalytic hydrogenation of double bonds results in *cis* addition of hydrogen from the less hindered side of the unsaturated linkage. There are, however, many cases documented of *trans* products from hydrogenation, as illustrated by the studies of Siegel (16) and Hussey (17). These workers have used dialkyl cycloolefins as substrates to study the stereochemistry of catalytic hydrogenation over various catalysts. In all their cases mixtures of products have been observed, the amounts of each isomer depending on the reaction conditions: for instance, in the case of 1,2-dimethylcyclohexene about 80% of *cis* reduction product is obtained at atmospheric pressure over platinum, rising to over 95% at very high hydrogen pressures. To account for these observations Siegel and his co-workers (16) have suggested that *trans* isomers arise from an isomerization to 2,3-dimethylcyclohexene on the catalyst surface followed by desorption and readsorption on both sides of the new double bond in a random manner giving mixtures resulting from the formal *cis* and *trans* addition of hydrogen to the original double bond. Objections to this postulate have been advanced on two counts (18); firstly, the necessary isomerization is in a thermodynamically unfavorable direction (i.e. tetrasubstituted to trisubstituted double bond) and, secondly, if the isomerization did occur the olefin would be unlikely to desorb to the required extent. Regarding the first of these objections it may also be argued that the trisubstituted double bond isomer is the more reactive entity present in low concentration at equilibrium and hence reduces first displacing the equilibrium further in that direction (16*b*).

Hussey and his associates (17) believe that a "stereochemically symmetrical intermediate" is involved (XIV for the case in question) and the objection to this suggestion (18) is that it is difficult to account for the observed pressure dependences. The present

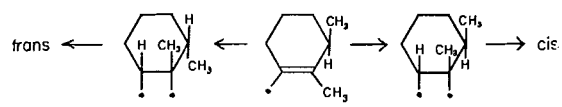

XIV

situation is thus somewhat unsettled. In our cases, we are dealing with cyclic olefins in a conformationally more rigid system which may therefore yield further information on this problem.

For the purpose of discussion we will consider $\Delta^{8,9}$-dihydropimaric acid V which appears to be the species which is reduced.[5,6] Why does one observe large yields of *trans* hydrogenation product in this case? The first explanation that comes to mind is an acid catalyzed

[5]*We assume that the species being reduced in the cases of dihydrosandaracopimaric acid and dihydroisopimaric acid is the* $\Delta^{8,9}$ *isomer also, though for reasons which will be developed later, it does not matter which double bond isomer is reduced.*

[6]*The same product ratios were observed by v.p.c. for the hydrogenation of both dihydropimaric acid and* $\Delta^{8,9}$*-dihydropimaric acid methyl esters.*

Can. J. Chem. Downloaded from www.nrcresearchpress.com by 210.87.254.6 on 09/05/12
For personal use only.

double bond isomerization prior to reduction so that the reactant is in fact the $\Delta^{7,8}$, $\Delta^{8,14}$, or $\Delta^{9,11}$ species. Our objection to this possibility is that, as in the case of 1,2-dimethylcyclohexane, it is thermodynamically unfavorable though the same counterargument may also be applied. We must, however, consider what would happen if such an isomerization did take place (16*b*) and was followed by transfer of hydrogen.[7] Double bond migration on catalyst surface is well known. It has been suggested that isomerization is accelerated by an allylic rearrangement (19, 20), the allylic hydrogen that is removed being available to the catalyst surface (Fig. 1) and, in the case of subsequent reduction, hydrogen transfer then being able to proceed without desorption. If this is the case then we would expect transfer of hydrogen to the same side of the molecule as the allylic hydrogen being

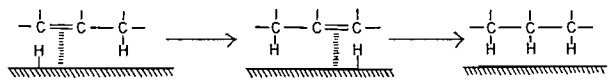

FIG. 1.

removed, and thus the product of hydrogenation would be expected to have a *cis* B–C ring junction. This is illustrated in XV and the allylic hydrogen atoms are shown in their approximate orientation to the catalyst surface. Formula XVI shows the situation if one considers that the dihydropimaric acid derivative with an 8,9-double bond could exist in the conformation XVI and here again, although it is difficult to see from models which side of the molecule is more available to the catalyst surface, either mode of adsorption on catalyst followed by allylic migration and reduction would still give a product with a *cis* B–C ring fusion. It is of course conceivable that desorption occurs after double bond migration as suggested by Siegel (16) and subsequent readsorption could occur from the other side of the molecule; however, we do not feel this would be a major pathway with such a large molecule where such a process would involve approach of catalyst from the highly hindered β-face. Likewise the "dissociatively adsorbed olefin" pathway (17) leads to a similar conclusion.

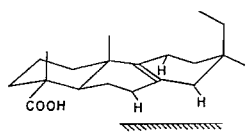

XV

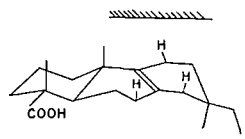

XVI

Our observations suggest the possibility of an alternative mechanism of catalytic hydrogenation in the case of inaccessible double bonds. It is well known that if a double bond is difficult to reduce then the use of acetic acid as solvent and a relatively large amount of catalyst is often advantageous, and in several cases traces of stronger acid have been used for the reduction of extremely unreactive double bonds (21). In our case, we have noted that reduction of $\Delta^{8,9}$-dihydropimaric acid is accelerated fivefold by the addition of a few drops of perchloric acid to the reaction mixture. This, plus observations that reduction in acid solution changes the steric course of reduction of steroidal olefins (22) and of

[7]*There are conflicting reports on such isomerizations. Siegel (16b) has shown that 1,2-dimethylcyclohexane is isomerized rapidly to 2,3-dimethylcyclohexane yet Burwell (28) was unable to detect any isomerization of* $\Delta^{1,9}$- *or* $\Delta^{9,10}$-*octalins. We are attempting to detect small amounts of double bond isomers by v.p.c. techniques but at the present time have been unsuccessful.*

Can. J. Chem. Downloaded from www.nrcresearchpress.com by 210.87.254.6 on 09/05/12
For personal use only.

cyclic ketones (23), suggests that hydrogen transfer from solvent as protons is a vital step in the reaction sequence[8] (24). To account for the observed products it is suggested that the first step of the reduction is protonation of the nuclear double bond, possibly whilst the olefin is associated with the catalyst surface, to yield a tertiary carbonium ion which then adds hydrogen as hydride ion from the catalyst surface (a similar proposal has been advanced by Augustine, ref. 26). Thus if the olefin is close to catalyst surface,

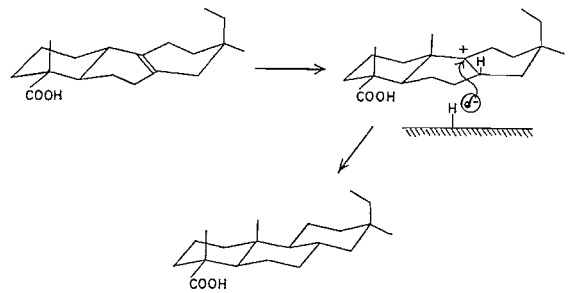

FIG. 2.

then the α-face of the molecule is effectively shielded giving an intermediate protonated from the β-side. That hydrogen adsorbed on catalyst can function as hydride ion receives support from the work of Pliskin and Eischens (27) who have examined the infrared spectrum of hydrogen adsorbed on platinum and observed bands associated with platinum hydrides. Such a mechanism needs to be tested and we have further work in progress to this end. An obvious approach would seem to be by catalytic deuteration studies (28), which we have started, but extensive deuterium exchange was encountered in our compounds (29); further studies are in progress.[9]

EXPERIMENTAL

Nuclear magnetic resonance spectra were determined on a Varian A-60 spectrometer, and chemical shifts are given in c.p.s. below tetramethylsilane used as an internal standard. Sample concentrations were approximately 10% (w/v) in deuterochloroform as solvent. All optical rotations were taken using absolute ethanol as solvent, and compound concentrations ranged from 1.0–1.5 g per 100 ml. Melting points are uncorrected and were determined on a Kofler hot stage. Infrared spectra were determined on a Perkin-Elmer 137 or 237 "Infracord" spectrophotometer in Nujol mulls. Hydrogen uptake is expressed as percentage of theory for one double bond.

Partial Hydrogenation of the Pimaric Acids

(i) Pimaric acid I (2.0 g), m.p. 216–218 °C, $[\alpha]_D$ +62.4°, and ν_{max} 1 698^{-1} (—COOH), 825 cm^{-1} (trisubstituted double bond), 913 and 994 cm^{-1} (vinyl group), was hydrogenated by the method of Edwards and Howe (1*a*). Hydrogen (98%) was absorbed yielding small needle-like crystals of dihydropimaric acid I (Et for C-13 vinyl) (1.8 g), m.p. 239–244 °C, $[\alpha]_D$ +23.0°, and ν_{max} 1 698 cm^{-1}, (—COOH), 825 cm^{-1} (trisubstituted double bond).

(ii) Sandaracopimaric acid II (1.9 g), m.p. 169–170 °C, $[\alpha]_D$ −20.1°, ν_{max} 1 698 cm^{-1}, 825 cm^{-1}, 913 and 994 cm^{-1} was hydrogenated as above. Hydrogen (100%) was absorbed yielding dihydrosandaracopimaric acid II (Et for C-13 vinyl) (1.75 g), m.p. 170–174 °C, $[\alpha]_D$ +20.8°, ν_{max} 1 698 cm^{-1}, 825 cm^{-1}.

(iii) Isopimaric acid III (950 mg), m.p. 160–161 °C, $[\alpha]_D$ 0°, ν_{max} 1 698 cm^{-1}, 825 cm^{-1}, 913 and 994 cm^{-1} was hydrogenated as above. Hydrogen (101%) was absorbed yielding dihydroisopimaric acid III (Et for C-13 vinyl) (910 mg), m.p. 172–175 °C, $[\alpha]_D$ −7.2°, ν_{max} 1 698 cm^{-1}, 825 cm^{-1}.

[8]*A referee has suggested that the acid may affect the properties of the catalyst (25); however, even if this is the case, it is still difficult to account for the observed stereochemistry of the hydrogenation products. We thank this referee for this and other suggestions.*

[9]*Dr. O. E. Edwards and his associates have concurrently observed large percentages of trans products in the catalytic hydrogenation of an acid derived from podocarpic acid, XIIb ($\Delta^{8,9}$). This work will be published independently, and we thank Dr. Edwards for keeping us informed of the progress of his studies.*

Can. J. Chem. Downloaded from www.nrcresearchpress.com by 210.87.254.6 on 09/05/12
For personal use only.

Hydrogenation of Dihydropimaric Acids

(i) Dihydropimaric acid (100 mg) was hydrogenated with Adams' catalyst by the method of Edwards and Howe (1*a*). Hydrogen (97.5%) was absorbed over a period of 24 h yielding tetrahydropimaric acid IV*a* (85 mg), m.p. 240–241 °C, $[\alpha]_D$ +18.4°, and ν_{max} 1 695 cm^{-1} (—COOH).

(ii) Dihydrosandaracopimaric acid (100 mg) was hydrogenated with Adams' catalyst as above. Hydrogen (99%) was absorbed over a period of 24 h, and crystallization from aqueous methanol gave tetrahydrosandaracopimaric acid IV*b* (90 mg), m.p. 172–174 °C, $[\alpha]_D$ +19.1°, and ν_{max} 1 695 cm^{-1}.

(iii) Dihydroisopimaric acid (100 mg) was hydrogenated as above. Hydrogen (97.5%) was absorbed over a period of 24 h. Crystallization from aqueous methanol yielded tetrahydroisopimaric acid IV*b* (85 mg), m.p. 173–174 °C, $[\alpha]_D$ +19.4°, and ν_{max} 1 695 cm^{-1}. Mixed melting point with tetrahydrosandaracopimaric acid was undepressed, and their infrared spectra were superimposable.

Hydroboration Procedure (ref. 9a)

Diborane (1.0 mole per mole of reactant) was added every 3 h for three consecutive additions to a stirring solution of the reactant in dry tetrahydrofuran maintained at room temperature over nitrogen. On the fourth addition, diborane (3.0 moles per mole of reactant) was added, and the solution was allowed to stir for a further 8 h before the destruction of the excess diborane by the addition of water. Sodium hydroxide (30 ml 3 *N*) and hydrogen peroxide (5 ml 30%) were then added to the resulting suspension and the mixture was refluxed for 2 h, after which time the mixture was concentrated on a rotary evaporator and ether-extracted to yield the crude product.

Hydroboration of Dihydropimaric Acids

(i) Dihydropimaric acid (4.23 g) was subjected to these conditions. Thin-layer chromatography of the reaction mixture, using benzene – ethyl acetate (4:1) on silical gel, illustrated the presence of six compounds. The product was then chromatographed on neutral alumina (90 g Woelm Gr. 1). Elution with ether produced a pale-yellow oil (1.59 g) which was shown by thin-layer chromatography to be a mixture of four compounds. Further elution with ether – ethyl acetate (4:1) yielded colorless needles (2.63 g). Recrystallization from ether–benzene gave fluffy needles (2.2 g, 50%) which proved to be the required diol V*a*. Sublimation at 130° and 10^{-4} mm yielded the diol, m.p. 174–175°, $[\alpha]_D$ −17.6°, ν_{max} 1 025 and 3 400 cm^{-1} (—OH).

Anal. Calcd. for $C_{20}H_{36}O_2$: C, 77.86; H, 11.76. Found: C, 77.80; H, 11.70.

(ii) Dihydrosandaracopimaric acid (2.1 g) was hydroborated as described above. Thin-layer chromatography of a sample of the reaction mixture indicated the presence of six compounds. The viscous semisolid reaction product was then washed twice with *n*-hexane leaving insoluble material (1.5 g), which was crystallized twice from aqueous methanol to yield stout prisms (1.1 g, 41%) which showed only one spot on thin-layer chromatography and proved to be the required diol V*b*. Sublimation at 130° at 10^{-4} mm yielded colorless plates of the diol, m.p. 183–184°, $[\alpha]_D$ −17°, ν_{max} 1 025 and 3 410 cm^{-1}.

Anal. Calcd. for $C_{20}H_{36}O_2$: C, 77.86; H, 11.76. Found: C, 78.66; H, 11.56.

(iii) Dihydroisopimaric acid (900 mg) was reduced as described. Thin-layer chromatography of a sample of the crude reaction mixture (910 mg) indicated the presence of two compounds. The semicrystalline product was then separated on thin-layer plates giving two fractions. The bottom fraction, on elution with ether, gave colorless needles (740 mg, 87%) which crystallized from aqueous methanol. They were sublimed at 130° at 10^{-4} mm to give the required diol VII, m.p. 183–184°, $[\alpha]_D$ +31.9°, ν_{max} 1 025 and 3 410 cm^{-1}.

Anal. Calcd. for $C_{20}H_{36}O_2$: C, 77.86; H, 11.76. Found: C, 77.33; H, 11.67.

*Oxidation of the Dihydropimaric Diols VI*a*, VI*b*, and VII*

(i) Dihydropimaric acid diol VI*a* (475 mg) was dissolved in acetone (50 ml), and Jones' reagent (7) was added dropwise with stirring until the reaction mixture no longer changed color (3 min). The mixture was allowed to stir for 10 min, after which time excess oxidant was decomposed with methanol, and the reaction mixture was concentrated on a rotary evaporator to a green oil which was shaken with water and ether-extracted. Drying and evaporation gave an oil (430 mg) with ν_{max} at 2 750 and 1 740 cm^{-1} (aldehyde) and 1 700 cm^{-1} (carbonyl). This product resisted all attempts at purification so was oxidized again with Jones' reagent for a further 10 min. Ether extraction after decomposition of excess oxidant gave ketoacid X*a* which crystallized as prisms from aqueous methanol (410 mg), m.p. 244–245°, $[\alpha]_D$ −48.7°. Infrared spectrum, ν_{max} at 3 400 – 3 000 cm^{-1} and 1 695 cm^{-1} (—COOH), 1 695 cm^{-1} (carbonyl).

Anal. Calcd. for $C_{20}H_{32}O_3$: C, 74.96; H, 10.06. Found: C, 75.10; H, 10.02.

In later oxidations the reaction mixture was stirred for 15 min without attempts at isolation of the ketoaldehyde.

(ii) Dihydrosandaracopimaric diol VI*b* (230 mg) was oxidized as described above without attempting to isolate the intermediate keto aldehyde. Isolation after 20 min reaction time gave the ketoacid X*b* (195 mg) as plates from aqueous methanol, m.p. 205–207°, $[\alpha]_D$ −30.6°. Infrared spectrum, ν_{max} 3 500 – 3 000 cm^{-1} and 1 695 cm^{-1}.

Anal. Calcd. for $C_{20}H_{32}O_3$: C, 74.96; H, 10.06. Found: C, 75.04; H, 9.86.

(iii) Diol VII (400 mg) was oxidized as described giving the keto acid XI (350 mg), m.p. 239°, $[\alpha]_D$ +2°, identical in all respects to a sample prepared by hydrolysis of the corresponding methyl ester (3).

Can. J. Chem. Downloaded from www.nrcresearchpress.com by 210.87.254.6 on 09/05/12
For personal use only.

Equilibrium Procedures

The keto acid was dissolved in aqueous methanol (20 ml) to which was added potassium hydroxide (100 mg), and the mixture was refluxed for 3 h. The mixture was then acidified with 2 *N* hydrochloric acid, and ether-extracted to yield the equilibrated keto acid.

(i) The keto acid X*a* (12 mg) was subjected to these conditions, and recovery of the equilibrated acid (10 mg) gave crystalline material with m.p. 242–245° and $[\alpha]_D$ −47.2°, identical in all respects (mixed m.p., infrared, n.m.r., and thin-layer chromatography) to starting material X*a*.

(ii) Ketodihydrosandaracopimaric acid X*b* (15 mg) was equilibrated to yield a white crystalline product (13 mg) with m.p. 207–208° and $[\alpha]_D$ −30.8°, identical to starting material X*b*.

(iii) Ketodihydroisopimaric acid XI (10 mg) was equilibrated and gave crystals (9 mg) with m.p. 238–240°, identical to XI.

Wolf–Kishner Reduction Procedure

The keto acid under consideration (100 mg), 95% hydrazine (2 ml which had stood for several days over molecular sieve), and triethylene glycol (7 ml freshly distilled over anhydrous magnesium sulfate), were refluxed at 140° overnight. Potassium hydroxide (1.2 g) was then added, and the temperature was gently raised to 200° ± 5° for a further 6 h, with distillation of hydrazine out of the reaction flask. The reaction mixture was cooled, acidified with 2 *N* sulfuric acid, and ether-extracted. The ether extract was washed well with water, dried, and evaporated to yield the crude reaction products.

(i) The keto acid X*a* (120 mg) was subjected to the conditions described above to yield a crude crystalline product (101 mg) which when crystallized twice from aqueous methanol and sublimed at 120° at 10^{-4} mm gave short needle-like crystals, m.p. 240–241°, $[\alpha]_D$ +19°, ν_{max} 3 300 – 3 000 cm^{-1} and 1 695 cm^{-1} (—COOH). Mixed melting with tetrahydropimaric acid IV*a* gave no depression of melting point, and their infrared spectra were superimposable.

(ii) The keto acid X*b* (110 mg) was reduced as described above, giving crystals (96 mg) which when recrystallized twice from aqueous methanol and sublimed at 130° and 10^{-4} mm gave needles (89 mg) with m.p. 174–175°, $[\alpha]_D$ +19.5°; ν_{max} 3 300 – 3 000 cm^{-1} and 1 695 cm^{-1}. Mixed melting point with tetrahydrosandaracopimaric acid IV*b* gave no depression, and their infrared spectra were superimposable.

(iii) Upon reduction of the keto acid XI (90 mg), crude tetrahydro acid (80 mg) was obtained which when recrystallized from aqueous methanol and sublimed at 130° and 10^{-4} mm gave long, white needles, m.p. 171–172°, $[\alpha]_D$ +19.0°, ν_{max} 3 300 – 3 000 cm^{-1} and 1 695 cm^{-1}. Mixed melting point with tetrahydrosandaracopimaric acid IV*b* gave no depression of melting point, and their infrared spectra were superimposable.

Reduction of the Dithioketal of Ketodihydropimaric Acid Xa

The keto acid X*a* (128 mg) in acetic acid (5 ml) was mixed with boron trifluoride etherate (0.5 ml) and ethanedithiol (0.5 ml) (14) and allowed to stand for 2 d at room temperature when a crystalline solid was precipitated. Filtration and washing with cold methanol gave the dithioketal as small needles, m.p. above 275° (110 mg); thin-layer chromatography demonstrated the absence of starting material in this product. The dithioketal (110 mg) was refluxed with W-2 Raney nickel (30) in ethanol for 15 h. Filtration and evaporation gave tetrahydropimaric acid (96 mg). After recrystallization from methanol, this was identical in all respects to the Wolff–Kishner or hydrogenation product IV*a* (H-8 is β).

ACKNOWLEDGMENTS

We wish to thank the National Research Council of Canada for financial aid and the Government of Ontario for a fellowship (to P. V. D.). We are indebted to Dr. O. E. Edwards for his encouragement and helpful discussions.

REFERENCES

1. (*a*) O. E. Edwards and R. Howe. Can. J. Chem. **37**, 760 (1959).
(*b*) E. Wenkert and J. Chamberlin. J. Am. Chem. Soc. **80**, 2912 (1958).
(*c*) R. E. Ireland and P. W. Schiess. J. Org. Chem. **28**, 6 (1963).
See also references in these papers.
2. O. E. Edwards, A. Nicolson, and M. N. Rodger. Can. J. Chem. **38**, 633 (1960). J. W. ApSimon, B. Green, and W. B. Whalley. J. Chem. Soc. 752 (1961). A. K. Bose and S. Harrison. Chem. Ind. London, 254 (1963). M. Fetizon and M. Golfier. Bull. Soc. Chim. France, 167 (1963).
3. W. Z. Antkowiak, O. E. Edwards, R. Howe, and J. W. ApSimon. Can. J. Chem. **43**, 1257 (1965). R. E. Ireland and J. Newbould. J. Org. Chem. **28**, 23 (1963).
4. E. L. Eliel. Stereochemistry of carbon compounds. McGraw-Hill Co., New York, N.Y. 1962. p. 350. H. O. House. Modern synthetic reactions. W. A. Benjamin Inc., New York, N.Y. 1965. p. 16. R. L. Burwell, Jr. Chem. Rev. **57**, 895 (1957).
5. C. Asselineau, S. Bory, and A. Diara. Bull. Soc. Chim. France, 1197 (1964).
6. H. C. Brown. Hydroboration. W. A. Benjamin, Inc., New York, N.Y. 1962.
7. K. Bowden, I. M. Heilbron, E. R. H. Jones, and B. C. L. Weedon. J. Chem. Soc. 39 (1946). C. Djerassi, R. R. Engle, and A. Bowers. J. Org. Chem. **21**, 1547 (1956).

Can. J. Chem. Downloaded from www.nrcresearchpress.com by 210.87.254.6 on 09/05/12
For personal use only.

8. W. F. ERMAN and T. J. FLAUTT. J. Org. Chem. **27**, 1526 (1962). J. A. MARSHALL, NOAL COHEN, and K. R. ARENSON. J. Org. Chem. **30**, 762 (1965).
9. (*a*) E. WENKERT, P. W. JEFFS, and J. R. MAHAJAN. J. Am. Chem. Soc. **86**, 2218 (1964).
(*b*) A. W. BURGHSTAHLER and J. N. MARX. Tetrahedron Letters, 3333 (1964).
10. L. M. JACKMAN. Applications of nuclear magnetic resonance spectroscopy in organic chemistry. Pergamon Press, Oxford. 1959. p. 124.
11. J. W. APSIMON, O. E. EDWARDS, and R. HOWE. Can. J. Chem. **40**, 630 (1962). J. W. APSIMON. Unpublished observations.
12. N. S. CROSSLEY and H. B. HENBEST. J. Chem. Soc. 4413 (1960). C. DJERASSI, T. T. GROSSNICKLE, and L. B. HIGH. J. Am. Chem. Soc. **78**, 3166 (1956). R. L. CLARKE. J. Am. Chem. Soc. **83**, 965 (1961).
13. R. E. IRELAND and J. A. MARSHALL. J. Org. Chem. **27**, 1620 (1962).
14. L. F. FIESER. J. Am. Chem. Soc. **76**, 1945 (1954).
15. R. P. LINSTEAD, W. E. DOERING, S. B. DAVIS, P. LEVINE, and R. W. WHETSTONE. J. Am. Chem. Soc. **64**, 1985 (1942) and following papers.
16. (*a*) S. SIEGEL and G. V. SMITH. J. Am. Chem. Soc. **82**, 6082, 6087 (1960).
(*b*) S. SIEGEL, P. A. THOMAS, and J. T. HOLT. J. Catalysis, 4, 73 (1965).
17. J. F. SAUVAGE, R. H. BAKER, and A. S. HUSSEY. J. Am. Chem. Soc. **82**, 6090 (1960); **83**, 3874 (1961).
18. G. C. BOND and P. B. WELLS. Advances in catalysis. Vol. 15. Academic Press Inc., New York, N.Y. 1964. p. 139.
19. J. B. BREAM, D. C. EATON, and H. B. HENBEST. J. Chem. Soc. 1974 (1957). F. G. GAULT, J. J. ROONEY, and C. KEMBALL. J. Catalysis, **1**, 255 (1962).
20. D. K. FUKUSHIMA and T. F. GALLAGHER. J. Am. Chem. Soc. **77**, 139 (1955).
21. E. B. HERSHBERG, E. OLIVETO, M. RUBIN, H. STAEUDLE, and L. KUHLON. J. Am. Chem. Soc. **73**, 1144 (1951). J. ELKS, R. M. EVANS, C. H. ROBINSON, G. H. THOMAS, and L. J. WYMAN. J. Chem. Soc. 2933 (1953). P. E. PETERSON and C. CASEY. J. Org. Chem. **29**, 2325 (1964). J. D. CHANLEY and T. MEZZETTI. J. Org. Chem. **29**, 228 (1964).
22. L. F. FIESER and M. FIESER. Steroids. Reinhold Publishing Corp., New York, N.Y. 1959. p. 272. J. R. LEWIS and C. W. SHOPPEE. Chem. Ind. London, 897 (1953). *See also* H. I. Hadler. Experientia **XI**, 175 (1955), and M. J. T. Robinson. Tetrahedron, **1**, 49 (1957).
23. J. H. BREWSTER. J. Am. Chem. Soc. **76**, 6361 (1954).
24. F. J. MCQUILLIN. Chem. Ind. London, 251 (1957). F. J. MCQUILLIN and W. O. ORD. J. Chem. Soc. 2902 (1959).
25. H. C. YAO and P. H. EMMETT. J. Am. Chem. Soc. **83**, 799 (1961).
26. R. L. AUGUSTINE. J. Org. Chem. **28**, 152 (1963).
27. W. A. PLISKIN and R. P. EISCHENS. Z. Physik. Chem. Frankfurt, **24**, 11 (1960). J. CHATT, L. DUNCANSON, and B. SHAW. Proc. Chem. Soc. 343 (1957).
28. G. V. SMITH and R. L. BURWELL, Jr. J. Am. Chem. Soc. **84**, 925 (1962).
29. J. W. CHAMBERLIN. Dissertation, Stanford University. 1964.
30. R. MOZINGO. Organic syntheses. Coll. Vol. III. John Wiley and Sons Inc., New York, N.Y. 1955. p. 181.

Can. J. Chem. Downloaded from www.nrcresearchpress.com by 210.87.254.6 on 09/05/12
For personal use only.

Can. J. Chem. Downloaded from www.nrcresearchpress.com by 210.87.254.5 on 09/05/12
For personal use only.

SULFUR ISOTOPE EFFECTS IN THE HYDROGEN ION DECOMPOSITION OF THIOSULFATE

U. AGARWALA, C. E. REES, AND H. G. THODE
McMaster University, Hamilton, Ontario
Received April 15, 1965

ABSTRACT

Sulfur isotope effects in the decomposition of thiosulfate have been studied. There are two distinct intermolecular isotope effects and these have been used to examine various mechanisms for the reaction. By use of the theory of competing isotope reactions the thiosulfate decomposition mechanisms of La Mer and Davis have been shown to predict isotope effects not in accord with experiment, while a simple bimolecular three-centered reaction has been shown to predict sulfur and sulfite isotope effects in good agreement with the experimentally determined values of 1.9% and 0.9%.

INTRODUCTION

The study of kinetic isotope effects in the course of a chemical reaction can give information regarding the mechanism by which the reaction proceeds and the nature of the activated complexes associated with rate-controlling steps in the reaction. The information derived from such experiments forms a valuable addition to that obtained in more conventional kinetic studies.

The hydrogen ion decomposition of thiosulfate has been extensively studied (1–11). Various kinetic investigations have been made (2, 3, 4, 9, 10, 11) but the results remain difficult to interpret on the basis of a reaction mechanism. Because of this, a study of the intermolecular isotope effects involving ^{32}S and ^{34}S in thiosulfate decomposition is likely to be of value. In addition, the thiosulfate ion is of special interest since it contains two non-equivalent sulfurs, so that the products of the decomposition, sulfite and sulfur, each show distinct intermolecular isotope effects. Thus the study of sulfur isotope fractionations provides a more than usually strong diagnostic tool for the determination of the reaction mechanism.

THEORETICAL

The theory of isotope fractionation in the course of chemical reactions is considered in terms of the theory of absolute rates and was first formulated by Bigeleisen (12). For the competing isotope reactions

$$A_1 + B + \ldots \rightarrow P_1 + \ldots .$$

$$A_2 + B + \ldots \rightarrow P_2 + \ldots .$$

the ratio of rate constants is given by:

$$\frac{k_1}{k_2} = \left(\frac{Q_2}{Q_1} \Big/ \frac{Q_2^{\ddagger}}{Q_1^{\ddagger}}\right) \frac{\nu_{1L}^{\ddagger}}{\nu_{2L}^{\ddagger}}.$$

This expression omits the transmission coefficient and Wigner tunnelling correction of absolute rate theory, the assumption being made that for heavy elements these terms will remain invariant under isotopic substitution. The terms Q_2/Q_1 and $Q_2^{\ddagger}/Q_1^{\ddagger}$ are ratios of

partition functions for the reactants and activated complexes respectively and each may be evaluated as

$$\prod_i^N \frac{u_{2i}}{u_{1i}} \left(\frac{e^{-u_{2i}/2}}{e^{-u_{1i}/2}} \right) \frac{1 - e^{-u_{1i}}}{1 - e^{-u_{2i}}}$$

where $u_i = h\nu_i/kT$ and ν_i is the ith fundamental vibrational frequency of the molecule. If n is the number of atoms in the molecule, then for the reactants N is $(3n - 6)$, and for the activated complexes it is $(3n - 7)$ since in an activated complex one of the vibrational degrees of freedom (ν_L) is non-genuine, corresponding to the cleavage of a bond, and is equivalent to a translation along the reaction coordinate.

According to Slater (13) the term $\nu_{1L}^{\ddagger}/\nu_{2L}^{\ddagger}$, the ratio of the two frequencies which become imaginary in the activated complexes, may be evaluated in terms of the effective masses of the activated complexes as they traverse the critical region of the reaction coordinate. So that:

$$\nu_{1L}^{\ddagger}/\nu_{2L}^{\ddagger} = \sqrt{(\mu_2^{\ddagger}/\mu_1^{\ddagger})}.$$

Bigeleisen and Wolfsberg (14) have considered the more complicated case where in the activated complex there is not merely a bond breaking but there is simultaneous bond rupture and formation, the case of the three center reaction.

If we consider the case of the tri-polar group ABC with a bond between B and C breaking while one between A and B forms, the mass term in the expression for rate constant ratios may be written:

$$\left(\frac{\frac{1}{M_{B1}} + \frac{1}{M_{C1}} + p\left(\frac{1}{M_{B1}} + \frac{1}{M_{A1}}\right) + 2p^{1/2}\frac{1}{M_{B1}}}{\frac{1}{M_{B2}} + \frac{1}{M_{C2}} + p\left(\frac{1}{M_{B2}} + \frac{1}{M_{A2}}\right) + 2p^{1/2}\frac{1}{M_{B2}}} \right)^{1/2}.$$

Here the parameter p represents the relative amounts of bond formation and bond extension. For $p = 0$, 1, and ∞ the formula represents pure bond rupture, equal rupture and formation, and pure bond formation respectively.

TABLE I

Fundamental vibrational frequencies for the three main isotopic species of thiosulfate ion

Molecule	Frequencies, cm^{-1}					
$^{32}S^{32}SO_3^=$	1 123 (2)*	541 (2)	335 (2)	995 (1)	435 (1)	669 (1)
$^{34}S^{32}SO_3^=$	1 123	541	333	995	423	666
$^{32}S^{34}SO_3^=$	1 107	538	335	983	430	664

*Figures in parentheses indicate degeneracy.

Calculations

To calculate partition function ratios it is necessary to know the fundamental frequencies of the three isotopic species of thiosulfate. The ion has the form XYZ_3 and is a tetrahedral molecule belonging to the point group C_{3v}. The method of Slawsky and Dennison (15) was used to determine the force constants for this molecule using the fundamental frequencies for $^{32}S^{32}SO_3^=$ reported by Siebert (16) and the crystal structure data of Taylor and Beevers (17). Five of the six distinct fundamental frequencies were used to calculate the five unknown force constants which were then used to calculate the sixth fundamental

Can. J. Chem. Downloaded from www.nrcresearchpress.com by 210.87.254.5 on 09/05/12
For personal use only.

frequency for a check of the method. The calculated values of force constants are: $k_1 = 6.64$, $k_2 = 0.88$, $k_3 = 0.53$, $k_4 = 0.013$, and $C = 3.95$ dyn/cm. These values were used to calculate the fundamental frequencies of $^{32}S^{34}SO_3^=$ and $^{34}S^{32}SO_3^=$ which values are shown in Table I.

EXPERIMENTAL

Partial decomposition of thiosulfate ($\sim 10\%$) was carried out by the following method: To 1 500 ml of 0.01 *M* sodium thiosulfate pentahydrate solution, 10 ml of 5.0 *N* HCl was added, followed by 250 ml of thiophene-free benzene at 25 °C. The whole mixture was stirred for 15–20 min. When the experiments were performed at 47 °C, the stirring was continued for 3–4 min only. To quench the reaction 0.1 *M* iodine solution was added, an amount slightly in excess of that required to convert $S_2O_3^=$ to $S_4O_6^=$ and sulfite to sulfate. The whole mixture was vigorously shaken for 20–30 more minutes and kept for some time so that the benzene and aqueous phases were separated. From the aqueous layer $SO_4^=$ was precipitated as $BaSO_4$. From the benzene layer sulfur was separated, by evaporating benzene on a water bath, and was then oxidized to sulfate and precipitated as $BaSO_4$. The sulfur from the benzene layer represents the outer sulfur of thiosulfate ion (the thio sulfur), whereas $BaSO_4$ precipitated from the aqueous layer represents the central sulfur (the sulfite sulfur). The weight of barium sulfate from sulfur was usually lower ($\sim 20\%$) than that precipitated from the aqueous layer.

Thiosulfate used in the above reactions was also decomposed completely by silver nitrate at 25 °C, according to the following equation:

$$S - SO_3^= + 2AgNO_3 + H_2O \rightarrow Ag_2S + SO_4^= + 2HNO_3.$$

The silver sulfide and the sulfate formed by this reaction contain respectively all the thio and sulfite sulfurs of the thiosulfate (18). These were converted to SO_2 and their isotopic ratios were measured. These isotopic ratios were compared separately with those of the corresponding sulfurs obtained by partial decomposition of thiosulfate.

All the samples were analyzed as sulfur dioxide (19) on a 90° simultaneous collection mass spectrometer whose design and operation have been described previously (20).

Under the experimental conditions there is the possibility of a side reaction, especially at 47 °C (21), which may be written:

$$10H_2O + S_4O_6^= + 7I_2 \rightarrow 4SO_4^= + 14I^- + 20H^+.$$

The isotopic ratio of sulfate formed in this reaction might produce an error in the isotopic ratio of the sulfate formed by the decomposition of thiosulfate. However, the rate of this reaction is dependent on the concentration of iodine and iodide (21). Excess of iodide will suppress the reaction. Under our experimental conditions, there is a very slight excess of iodine and a large excess of iodide. Therefore, the formation of the sulfate by this method should be very small. In one experiment a dilute solution of iodine was added to the tetrathionate solution and kept overnight. A small amount of sulfate formed due to the above reaction was precipitated as $BaSO_4$ and the isotopic ratio of sulfur was measured by the usual method. Sulfate sulfur was found to be depleted in ^{34}S by 10 parts per thousand (p.p.t.). As will be seen later in this paper, this value of depletion is approximately the same as was found in sulfite sulfur formed by the decomposition of thiosulfate into sulfur and sulfite. Thus, this very slow side reaction should not produce any serious error in the experimental results.

Many investigations (6) have reported the simultaneous production of various polythionates, the most likely of which is pentathionate formed by reaction [2] which competes with the main reaction [1]:

[1] $$H^+ + S_2O_3^= \rightarrow HSO_3^- + S$$

[2] $$6H^+ + 5S_2O_3^= \rightarrow 2S_5O_6^= + 3H_2O.$$

The extent of each of the two reactions may be evaluated separately, at any time, by titration. The method described by Zaiser and La Mer (6) uses simultaneous iodine and base titration. It was found that reaction [2] goes to the extent of 1–1.8%, while reaction [1] goes to the extent of 14% in about 30 min. This indicates that reaction [1] under our experimental conditions is predominant.

Willard (22) has shown that there is no possibility of isotope exchange between the thiosulfate and sulfite produced in reaction [1]. This exchange becomes appreciable only at temperatures in excess of 60 °C.

RESULTS

The experimental results are given in Tables II, III, and IV which represent thiosulfate decompositions using hydrochloric acid at 25 °C, hydrochloric acid at 47 °C, and acetic

Can. J. Chem. Downloaded from www.nrcresearchpress.com by 210.87.254.5 on 09/05/12
For personal use only.

acid at 47 °C respectively. In each table column 2 represents the $^{34}S:^{32}S$ ratios in the starting material, measured relative to a laboratory standard.

$$\delta = \frac{\left(\frac{^{34}S}{^{32}S}\right)_{sample} - \left(\frac{^{34}S}{^{32}S}\right)_{standard}}{\left(\frac{^{34}S}{^{32}S}\right)_{standard}} \times 1000 \text{ p.p.t.}$$

Column 3 represents the $^{34}S:^{32}S$ ratios in the products of the reaction, measured relative to the same standard, and column 4 is the net isotope effect between reactants and products. The isotope effects for sulfite sulfur and thio sulfur are designated $\delta(^{34}SO_3^{=})$ and $\delta(^{34}S)$ respectively.

TABLE II

Isotope effects in the decomposition of thiosulfate (temperature 25 °C, acid used HCl)

Products	$\delta^{34}S$ in 100% decomposition of thiosulfate, p.p.t.	$\delta^{34}S$ in 10% decomposition of thiosulfate, p.p.t.	Isotope effect, p.p.t.
Sulfur	−2.30	−21.50	−19.20
Sulfite	−0.81	−9.54	−8.73
Sulfur	−2.30	−21.80	−19.50
Sulfite	−0.81	−9.88	−9.07
Sulfur	+1.33	−16.20	−17.53
Sulfite	−0.65	−8.30	−7.65
Sulfur	+1.33	−17.43	−18.76
Sulfite	−0.65	−7.75	−7.10
Average $\delta(^{34}S)$			−18.8
Average $\delta(^{34}SO_3^{=})$			−8.1

TABLE III

Isotope effects in the decomposition of thiosulfate (temperature 47 °C, acid used HCl)

Products	$\delta^{34}S$ in 100% decomposition of thiosulfate, p.p.t.	$\delta^{34}S$ in 10% decomposition of thiosulfate, p.p.t.	Isotope effect, p.p.t.
Sulfur	+1.33	−17.60	−18.93
Sulfite	−0.65	—	—
Sulfur	+1.37	−18.99	−20.32
Sulfite	−0.65	−8.79	−8.14
Sulfur	+1.33	−19.20	−20.54
Sulfite	−0.65	−8.97	−8.32
Sulfur	+1.33	−18.77	−20.10
Sulfite	−0.65	−9.00	−8.35
Sulfur	−2.30	−22.74	−20.24
Sulfite	−0.81	−9.66	−8.85
Sulfur	−2.30	−22.10	−19.80
Sulfite	−0.81	−10.05	−9.24
Average $\delta(^{34}S)$			−20.0
Average $\delta(^{34}SO_3^{=})$			−8.6

The tables of results show the following points: (*a*) the isotope effects are appreciable so that S—S bonds must break in the rate-determining step of the reaction, (*b*) there are two isotope effects involved, one for each sulfur position in thiosulfate, (*c*) the isotope effect in the thio sulfur positions is greater than that in the sulfite sulfur position, and (*d*) there is no large temperature coefficient.

Can. J. Chem. Downloaded from www.nrcresearchpress.com by 210.87.254.5 on 09/05/12
For personal use only.

TABLE IV

Isotope effects in the decomposition of thiosulfate (temperature 47 °C, acid used acetic acid)

Products	$\delta^{34}S$ in 100% decomposition of thiosulfate, p.p.t.	$\delta^{34}S$ in 10% decomposition of thiosulfate, p.p.t.	Isotope effect, p.p.t.
Sulfur	+1.33	−14.77	−16.10
Sulfite	−0.65	−8.76	−8.11
Sulfur	+1.33	−16.45	−17.78
Sulfite	−0.65	−9.40	−8.75
Sulfur	−2.30	−18.99	−16.69
Sulfite	−0.81	−10.10	−9.29
Sulfur	−2.30	−19.66	−17.36
Sulfite	−0.81	−10.10	−9.29
Average $\delta(^{34}S)$			−17.0
Average $\delta(^{34}SO_3^{=})$			−8.9

NOTE: From Tables II, III, IV; average $\delta(^{34}S) = -18.6$ p.p.t., average $\delta(^{34}SO_3^{=}) = -8.5$ p.p.t.

DISCUSSION

Two mechanisms due to La Mer and his co-workers (9) and to Davis (11) have been suggested for the decomposition of thiosulfate.

The La Mer mechanism may be written

$$[3] \qquad H^+ + S_2O_3^{=} \overset{K}{\rightleftharpoons} HS_2O_3^-$$

$$[4] \qquad S_2O_3^{=} + HS_2O_3^- \overset{k_1}{\rightarrow} (HS_2O_3 \cdot S_2O_3)^{3-}$$

$$[5] \qquad (HS_2O_3 \cdot S_2O_3)^{3-} \overset{k_2}{\rightarrow} HSO_3^- + SO_3^{=} + S_2$$

where $k_1 \sim 2k_2$.

This reaction scheme shows the formation of bithiosulfate by a protonation process followed by bithiosulfate and thiosulfate ions coming together to form an addition compound. The addition compound then decomposes to form bisulfite, sulfite, and sulfur.

The mechanism proposed by Davis is as follows

$$H^+ + S_2O_3^{=} \overset{K}{\rightleftharpoons} HS_2O_3^-$$

$$HS_2O_3^- + S_2O_3^{=} \overset{k_1}{\rightarrow} HS_3O_3^- + SO_3^{=}$$

$$HS_3O_3^- + S_2O_3^{=} \overset{k_2}{\rightarrow} HS_4O_3^- + SO_3^{=}$$

$$\vdots \qquad\qquad \vdots \qquad\qquad \vdots$$

$$HS_8O_3^- + S_2O_3^{=} \overset{k_7}{\rightarrow} HS_9O_3^- + SO_3^{=}$$

$$HS_9O_3^- \overset{k}{\rightarrow} S_8 + HSO_3^-$$

After the initial protonation of thiosulfate, a series of unstable addition compounds are formed, each of which reacts with thiosulfate to form the next member of the series, until finally eight sulfurs break off the last member forming sulfur and bisulfite.

Calculations have been made, and are presented below, of the isotope effects to be expected in the decomposition of thiosulfate, the following models being considered: (i) Simple unimolecular mechanism, (ii) simple one step bimolecular mechanism, (iii) Davis mechanism, (iv) La Mer mechanism.

Can. J. Chem. Downloaded from www.nrcresearchpress.com by 210.87.254.5 on 09/05/12
For personal use only.

Can. J. Chem. Downloaded from www.nrcresearchpress.com by 210.87.254.5 on 09/05/12
For personal use only.

Calculations are made without taking into account any possible isotope effect in protonation of the reacting species. It is not to be expected that there will be any sulfur isotope effect in the process of protonation and the simple models considered for activated complexes will not be affected by the presence or absence of protons.

Simple Unimolecular Mechanism

If the decomposition of thiosulfate is unimolecular, with respect to sulfur isotope effects, then the three distinct isotopic cases may be written

$$S_2O_3^{=} \xrightarrow{k_1} SO_3^{=} + S$$

$$S^*SO_3^{=} \xrightarrow{k_2} SO_3^{=} + S^*$$

$$SS^*O_3^{=} \xrightarrow{k_3} S^*O_3^{=} + S$$

where S refers to ^{32}S and S* to ^{34}S.

For small fractions of reaction the sulfur and sulfite isotope effects, referred to the starting material, are given by:

$$-\delta(^{34}SO_3^{=}) = (k_1/k_3) - 1$$

$$-\delta(^{34}S) = (k_1/k_2) - 1.$$

For the unimolecular reaction, the activated complex is assumed to be the same as the starting material, except that the vibrational mode corresponding to the S—S bond extension has taken on an imaginary frequency. This frequency in the ion $S_2O_3^{=}$ is ~ 430 cm^{-1} and in the evaluation of partition functions for the activated complexes its contribution is omitted. The mass term is taken as the reduced mass of the dipolar species S—SO_3 and may be evaluated using either mass or atom fragments. The results of rate ratio calculations are shown in Table V.

TABLE V

Predicted isotope effects in the decomposition of thiosulfate: simple unimolecular model

	Mass fragments		Atom fragments	
Rate ratio	$T = 25$ °C	$T = \infty$	$T = 25$ °C	$T = \infty$
k_1/k_2	1.031	1.022	1.025	1.015
k_1/k_3	1.008	1.004	1.019	1.015

NOTE: Experimentally, $k_1/k_2 = 1.019$, $k_1/k_3 = 1.009$, assuming the above model (see Table IV).

It may be seen that the simple unimolecular model does not give rise to predicted isotope effects that are in accord with experiment either from the point of view of their absolute or their relative magnitudes.

Simple One Step Bimolecular Mechanism

If the decomposition of thiosulfate is bimolecular, there are three distinct isotopic cases each of which has two possible modes of reaction.

$$S_2O_3^{=} + S_2O_3^{=}\left[\rightleftharpoons O_3^{=}S\underset{b}{\cdots}S\underset{f}{\cdots}SSO_3^{=}\right] \xrightarrow{k_1} SO_3^{=} + SO_3^{=} + SS$$

$$S_2O_3^{=} + S_2O_3^{=}\left[\rightleftharpoons O_3^{=}SS\underset{f}{\cdots}S\underset{b}{\cdots}SO_3^{=}\right]\xrightarrow{k_1} SO_3^{=} + SO_3^{=} + SS$$

$$S_2O_3^{=} + S^*SO_3^{=}\left[\rightleftharpoons O_3^{=}S\underset{b}{\cdots}S\underset{f}{\cdots}S^*SO_3^{=}\right]\xrightarrow{k_2'} SO_3^{=} + SO_3^{=} + SS^*$$

$$S_2O_3^{=} + S^*SO_3^{=}\left[\rightleftharpoons O_3^{=}SS\underset{f}{\cdots}S^*\underset{b}{\cdots}SO_3^{=}\right]\xrightarrow{k_2''} SO_3^{=} + SO_3^{=} + SS^*$$

$$S_2O_3^{=} + SS^*O_3^{=}\left[\rightleftharpoons O_3^{=}S\underset{b}{\cdots}S\underset{f}{\cdots}SS^*O_3^{=}\right]\xrightarrow{k_3'} SO_3^{=} + S^*O_3^{=} + SS$$

$$S_2O_3^{=} + SS^*O_3^{=}\left[\rightleftharpoons O_3^{=}SS\underset{f}{\cdots}S\underset{b}{\cdots}S^*O_3^{=}\right]\xrightarrow{k_3''} SO_3^{=} + S^*O_3^{=} + SS$$

The equations above represent in each case the equilibrium between the reactants and the activated complex followed by the unidirectional steps to form the reaction products. The "b" and "f" in the activated complexes indicate the breaking and formation of bonds.

For small fractions of reaction the thio sulfur and sulfite sulfur isotope effects, referred to the starting material, are given by:

$$-\delta(^{34}SO_3^{=}) = \frac{2k_1}{k_3' + k_3''} - 1$$

$$-\delta(^{34}S) = \frac{2k_1}{k_2' + k_2''} - 1.$$

For the bimolecular three-centered reaction, the activated complex is assumed to be the same as the starting material, except that the S—S bond stretching frequency in each thiosulfate is imaginary. In physical terms this means that as the two thiosulfates come together, the thio sulfur breaks off one and becomes attached to the other thiosulfate group while at the same time the sulfite of this group is beginning to separate from the sulfur.

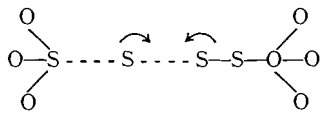

The partition function terms appropriate to k_1/k_2', k_1/k_2'', k_1/k_3', and k_1/k_3'' are 1.0094, 1.0094, 1.0040, and 1.0040 respectively. The results of calculations using this model are presented in Table VI.

The calculations indicate that this model gives good agreement with experiment, both from the point of view of the magnitude and of the isotope effects and their relative values, for atom fragments and a p value of about 0.1.

The Davis Mechanism

The Davis mechanism proceeds in seven distinct steps with isotope fractionation in each, the net sulfur and sulfite fractionations being the means of the fractionation in these steps.

Let us consider the nth step of the reaction: the reaction is three centered, and the activated complex may be schematized as:

$$O_3^{=}S\underset{b}{\cdots}S\underset{f}{\cdots}S_{n+1}O_3^{=}$$

Can. J. Chem. Downloaded from www.nrcresearchpress.com by 210.87.254.5 on 09/05/12
For personal use only.

Can. J. Chem. Downloaded from www.nrcresearchpress.com by 210.87.254.5 on 09/05/12
For personal use only.

TABLE VI

Predicted isotope effects in the decomposition of thiosulfate: simple bimolecular model

	p term							
	0	10^{-3}	10^{-2}	10^{-1}	1	10	10^{2}	10^{3}
	(A) Mass fragments (T = 25 °C)							
k_1/k_2'	1.0094	1.0094	1.0094	1.0095	1.0099	1.0106	1.0111	1.0113
k_1/k_2''	1.0313	1.0317	1.0324	1.0341	1.0357	1.0354	1.0342	1.0336
k_1/k_3'	1.0040	1.0040	1.0040	1.0041	1.0045	1.0052	1.0057	1.0059
k_1/k_3''	1.0075	1.0074	1.0071	1.0063	1.0050	1.0042	1.0040	1.0040
$2k_1/(k_2' + k_2'')$	1.0202	1.0204	1.0208	1.0216	1.0227	1.0228	1.0225	1.0223
$2k_1/(k_3' + k_3'')$	1.0058	1.0057	1.0055	1.0052	1.0048	1.0047	1.0049	1.0049
	(B) Atom fragments (T = 25 °C)							
k_1/k_2'	1.0094	1.0094	1.0095	1.0104	1.0144	1.0200	1.0230	1.0241
k_1/k_2''	1.0246	1.0251	1.0260	1.0281	1.0298	1.0281	1.0260	1.0251
k_1/k_3'	1.0040	1.0040	1.0040	1.0040	1.0040	1.0040	1.0040	1.0040
k_1/k_3''	1.0191	1.0186	1.0176	1.0146	1.0090	1.0050	1.0041	1.0040
$2k_1/(k_2' + k_2'')$	1.0169	1.0172	1.0177	1.0192	1.0220	1.0240	1.0245	1.0246
$2k_1/(k_3' + k_3'')$	1.0115	1.0113	1.0107	1.0093	1.0065	1.0045	1.0041	1.0040

NOTE: Experimentally, $2k_1/(k_2' + k_2'') = 1.0186$, $2k_1/(k_3' + k_3'') = 1.0085$, assuming the above model (see Table IV).

The isotopically distinct cases, with their corresponding rate constants are:

$$O_3S - - - S - - - S_{n+1}O_3 \quad (k_{1n})$$

$$O_3S - - - S^* - - - S_{n+1}O_3 \quad (k_{2n})$$

$$O_3S^* - - - S - - - S_{n+1}O_3 \quad (k_{3n})$$

$$O_3S - - - S - - - S..S^*..SO_3 \quad (k_{4n}).$$

The last of these may be neglected for small fractions of reaction, so that the overall thio sulfur and sulfite sulfur isotope fractionations are given by:

$$-\delta(^{34}S) = \frac{1}{7}\sum_{n=1}^{7}\left(\frac{k_{1n}}{k_{2n}} - 1\right)$$

$$-\delta(^{34}SO_3^{=}) = \frac{1}{7}\sum_{n=1}^{7}\left(\frac{k_{1n}}{k_{3n}} - 1\right).$$

If we consider the activated complex to be the same as the starting material except that the S—S stretching frequency in the thiosulfate becomes imaginary, the partition function ratios appropriate to k_{1n}/k_{2n} and k_{1n}/k_{3n} are 1.0094 and 1.0040 respectively. Table VII shows the results of calculations based on this model.

TABLE VII

Predicted isotope effects in the decomposition of thiosulfate: Davis mechanism

	p term							
	0	10^{-3}	10^{-2}	10^{-1}	1	10	10^{2}	10^{3}
	(A) Mass fragments (T = 25 °C)							
k_1/k_2 (average)	1.0313	1.0317	1.0325	1.0342	1.0365	1.0370	1.0364	1.0360
k_1/k_3 (average)	1.0076	1.0074	1.0071	1.0063	1.0051	1.0043	1.0040	1.0040
	(B) Atom fragments (T = 25 °C)							
k_1/k_2 (average)	1.0246	1.0251	1.0250	1.0281	1.0298	1.0281	1.0260	1.0251
k_1/k_3 (average)	1.0191	1.0186	1.0176	1.0146	1.0090	1.0050	1.0041	1.0040

NOTE: Experimentally, k_1/k_2 (average) = 1.0186, k_1/k_3 (average) = 1.0085, assuming the above mechanism (see Table IV).

It may be seen that the model chosen on the basis of the Davis mechanism does not give rise to predicted isotope effects that are in accord with experiment, either for mass or atom fragments or over the entire range of p values.

The La Mer Mechanism

It is assumed that there is no isotope fractionation in the initial protonation equilibrium between thiosulfate and bithiosulfate [3] and that further there will be no isotope effect in the formation of the addition compound [4]. Such isotope effects as are observed experimentally will then be the result of fractionation in the third stage of the reaction sequence in which the addition compound decomposes. Since the second and third stages of the sequence have rate constants of the same order of magnitude, the third stage is not completely rate controlling, so the experimentally observed fractionations should be lower than those predicted for the third stage alone.

From the point of view of isotope effect calculations the La Mer addition compound is very similar to the tetrathionate ion, so that the isotope fractionations to be expected in the third stage of the La Mer mechanism should be similar to those obtained in the decomposition of tetrathionate. From the experimental results on this decomposition (23) the thio sulfur and sulfite sulfur isotope effects in the decomposition of the La Mer addition compound should be ~ -8 p.p.t. and ~ -7 p.p.t. respectively.

Calculations may be made, assuming the rate-controlling step in the La Mer addition compound decomposition to be the breaking off of an $SO_3^=$ group. These are not presented here since they are formally the same as calculations made for the decomposition of tetrathionate (23). However, the results of such calculations confirm the arguments of the above paragraph in that they predict isotope effects which are smaller than those observed experimentally.

Thus the isotope effects are too small and do not have the correct relative magnitudes, also the dilution effect, caused by the preceding stage of the La Mer mechanism being partially rate controlling, will further reduce the net isotope effects.

CONCLUSIONS

The calculations and arguments in the preceding section show that it is difficult to explain the isotope effects observed experimentally in the decomposition of thiosulfate in terms of a unimolecular model or in terms of the Davis or La Mer mechanisms.

However, the second model considered, in which the decomposition of thiosulfate is considered to be a one step bimolecular process, can lead to predictions in accord with experiment. When the isotope effects for this model are calculated, using atomic masses rather than mass fragments and a p factor of 0.1, then good agreement is obtained, both for the absolute magnitude of the effects and their relative values. Considering the physical nature of the model chosen, it seems reasonable that atom rather than mass fragments should be significant and that the p value for the reaction should indicate that bond cleavage is somewhat more advanced than bond formation.

ACKNOWLEDGMENTS

The authors wish to express their thanks to the National Research Council of Canada whose financial assistance made possible the above study.

REFERENCES

1. G. FOUSSEREAU. Ann. Chim. et Phys. 6, **15**, 533 (1888).
2. J. SCHEFFER and P. BOHM. Z. Anorg. Allgem. Chem. **183**, 151 (1929).
3. H. BASSETT and R. G. DURRANT. J. Chem. Soc. 1401 (1927).

Can. J. Chem. Downloaded from www.nrcresearchpress.com by 210.87.254.5 on 09/05/12
For personal use only.

4. C. K. JABLCZYNSKI and Z. WARSZAWSKA-RYTEL. Bull. Soc. Chim. France, **39**, 409 (1926).
5. G. OSTER. J. Colloid Sci. **2**, 291 (1947).
6. E. M. ZAISER and V. K. LA MER. J. Colloid Sci. **3**, 571 (1948).
7. V. K. LA MER and A. S. KENYON. J. Colloid Sci. **2**, 257 (1947).
8. I. JOHNSON and V. K. LA MER. J. Am. Chem. Soc. **69**, 1184 (1947).
9. R. H. DINEGAR, R. H. SMELLIE, and V. K. LA MER. J. Am. Chem. Soc. **73**, 2050 (1951).
10. F. PRAKKE and E. STIASNY. Rec. Trav. Chim. **52**, 615 (1933).
11. R. E. DAVIS. J. Am. Chem. Soc. **80**, 3565 (1958).
12. J. BIGELEISEN. J. Chem. Phys. **17**, 344 (1949).
13. N. B. SLATER. Theory of unimolecular reactions. Cornell, Ithaca, N.Y. 1959.
14. J. BIGELEISEN and M. WOLFSBERG. J. Chem. Phys. **21**, 1972 (1953).
15. Z. I. SLAWSKY and D. M. DENNISON. J. Chem. Phys. **7**, 522 (1939).
16. H. SIEBERT. Z. Anorg. Allgem. Chem. **275**. 225 (1954).
17. P. C. TAYLOR and C. A. BEEVERS. Acta. Cryst. **5**, 341 (1952).
18. K. ANDERSON. Z. Physik. Chem. **B32**, 237 (1936).
19. A. G. HARRISON and H. G. THODE. Trans. Faraday Soc. **53**, 1648 (1953).
20. R. K. WANLESS and H. G. THODE. J. Sci. Instr. **30**, 395 (1953).
21. A. D. AWTREY and R. E. CONNICK. J. Am. Chem. Soc. **73**, 4546 (1951).
22. D. P. AMES and J. E. WILLARD. J. Am. Chem. Soc. **73**, 164 (1951).
23. U. AGARWALA, C. E. REES, and H. G. THODE. To be published.

Can. J. Chem. Downloaded from www.nrcresearchpress.com by 210.87.254.5 on 09/05/12
For personal use only.

Can. J. Chem. Downloaded from www.nrcresearchpress.com by 210.87.254.40 on 09/05/12
For personal use only.

DETERMINATION OF THE CRYSTAL STRUCTURE OF ERBIUM TITANATE, $Er_2Ti_2O_7$, BY X-RAY AND NEUTRON DIFFRACTION

OSVALD KNOP AND FRANÇOIS BRISSE
Department of Chemistry, Dalhousie University, Halifax, Nova Scotia

AND

LOTTE CASTELLIZ AND SUTARNO
Department of Chemical Engineering, Nova Scotia Technical College, Halifax, Nova Scotia

Received April 21, 1965

ABSTRACT

The crystal structure of erbium titanate, $Er_2Ti_2O_7$, has been shown by X-ray and neutron powder diffraction to be of the cubic pyrochlore type, with $a_o = 10.0762 \pm 6$ Å. Least-squares isotropic refinement based on resolved single reflections gave $x(O_2) = 0.4200 \pm 10$ and $R = 2.25\%$. Ionic and neutral X-ray scattering factors gave practically identical results. The six equal Ti—O_2 distances in the distorted coordination octahedron of the Ti atom are 1.955 ± 5 Å. The two short (apparent) Er—O distances are 2.1815 ± 5 Å (Er—O_1) and 2.471 ± 8 Å (Er—O_2). The infrared spectrum of the titanate in the region 1 600 to 250 cm^{-1} shows features similar to those encountered in the spectra of other simple oxygen compounds of titanium.

INTRODUCTION

Previously we had occasion to examine compounds of the type $Ln_2Ti_2O_7$ (La = La, Pr, Nd, Sm, Gd, Dy, Ho, Er, and Y) prepared by firing intimate mixtures of the corresponding sesquioxide (or Pr_6O_{11}) and rutile in air (1). Some of these compounds (La, Nd, Sm, Gd, Dy, Yb, and Y) had been investigated by Roth (2), who stated that the crystal structures of the Sm, Gd, Dy, Yb, and Y titanates were similar to that of pyrochlore, $NaCaNbTaO_6F$ (3–6), while the X-ray powder patterns of the La and Nd compounds strongly suggested distorted structures of the pyrochlore type. Our results confirmed this finding to the extent that the titanates of Sm, Gd, Dy, Ho, Er, and Y gave very similar patterns, indexable on a cubic unit cell of the pyrochlore symmetry, whereas the powder patterns of the La, Pr, and Nd compounds were different and much more complex. Very recently Brixner (7) prepared the complete series of these lanthanon titanates and reported the unit-cell dimensions of the cubic members, again in agreement with Roth's results.

To demonstrate the similarity of the cubic titanates with pyrochlore Roth calculated the intensities of the reflections 111, 222, 400, 331, and 333 + 511 for $Sm_2Ti_2O_7$. The atoms were assumed to be distributed in a unit cell of symmetry *Fd3m* as follows (origin taken at center (8)):

16 Sm in 16(*c*): 000 etc.
16 Ti in 16(*d*): $\frac{1}{2}\frac{1}{2}\frac{1}{2}$ etc.
8 O_1 in 8(*a*): $\pm$(1/8, 1/8, 1/8) etc.
48 O_2 in 48(*f*): *x*, 1/8, 1/8 etc.

Two values of *x*, 0.375 and 0.414, were used in the calculation. The latter value was reported by Byström (6) for the cubic pyrochlore $Cd_2Ta_2O_7$, while $x = 0.375 = 6/16$ applies to a double cell of the fluorite type, with eight oxygen atoms missing from the equipoint 8(*b*): $\pm$(3/8, 3/8, 3/8) etc.

The agreement between the diffractometer peak heights and the calculated intensities was poor for both parameter values, but similar calculations for $Nd_2Zr_2O_7$, $Y_2Zr_2O_7$, and

$Nd_2Sn_2O_7$ in the same paper gave a fair fit. The higher value gave better agreement in all four cases. Roth concluded that the parameter of the oxygen atom in $Sm_2Ti_2O_7$ was slightly different from that in $Cd_2Ta_2O_7$.

The evidence presented by Roth seems to indicate that it is reasonable to assume a pyrochlore-type structure for the four compounds, and that x is greater than 0.414. However, since the shape of the coordination figure of the Ti atom in the pyrochlore structure depends on x (for $x = 7/16 = 0.4375$ it is a regular octahedron of oxygen atoms), in the absence of an accurately determined value of the parameter an important feature of the structure remains unknown. Furthermore, the contribution of O_1 to the structure factor of $Sm_2Ti_2O_7$ is relatively small, and it is even less significant in the two zirconates and the stannate. Thus the possibility that the eight O_1 atoms are distributed statistically over 8(*a*) and 8(*b*), or that they are entirely in 8(*b*), may not be great, but it cannot be ruled out unless the observed intensities are shown beyond doubt to fit the pyrochlore structure better than any other reasonable model.

For this reason we carried out a more detailed investigation of the crystal structure of one of the cubic titanates. $Er_2Ti_2O_7$ seemed the best choice. It gave powder patterns of very good quality, and it was well suited for a neutron diffraction study, since the absorption cross-section of erbium is lower than that of Sm, Gd, or Dy, and at the same time the large quantities of material needed for neutron powder diffraction were more readily procurable.

EXPERIMENTAL

Erbium oxide of 99.9% purity (Lindsay Chemical Division, American Potash & Chemical Corporation, Code No. 1305; main impurities, Ho and Tm), which had been calcined at 600 °C, was thoroughly mixed with rutile (TiO_2, Fisher certified reagent) by grinding the fine powders together and brushing the resulting mixture repeatedly through a 200 mesh screen. Disks 1 in. diameter were then pressed at 10 000 p.s.i. without binder.

Two batches of $Er_2Ti_2O_7$ were prepared, one for exploratory and X-ray work, and another, totalling about 40 g, for neutron diffraction experiments. Green disks of the first batch were fired, on recrystallized alumina support in open air, for 1 h at 1 300 °C, cooled in furnace, transferred to another furnace, fired at 1 400 °C for 2 h, and again cooled in furnace. The first firing cycle took 1 day, the second, 2 days. Powder photographs of the titanate taken before and after the second firing were practically identical.

The second batch was fired, in a 2 day cycle, at 1 400 °C for 2 h and cooled in furnace. The fired disks were crushed and ground to pass a 325 mesh screen. The powder was pressed again and refired in a similar manner with a 4 h soaking. The final product obtained by crushing and grinding the sintered material was a pale-pink powder which passed easily a 325 mesh screen.

A thermogravimetric analysis (t.g.a.) run on a green pellet of about 2.6 g in a carefully adjusted Stanton HT-SM thermobalance, which was sensitive to ±1 mg (heating rate, 6 deg/min; Pt crucible in stagnant air), indicated no change in weight on heating from room temperature to 1 400 °C.

Well-exposed powder photographs of both batches still contained what appeared to be the residual 110 reflection of the rutile pattern, of an estimated intensity of about 0.4 (relative to the strongest line of intensity 100).

Integrated X-ray intensities were obtained by 2θ counting scans of the peaks at 1/8° (2θ) / min and subtracting appropriate background counts. Generous allowance was made for background on both sides of a peak. Three complete rounds, and additional counts wherever they appeared desirable, were taken. The shape of the $\sigma(\Delta N)$ vs. N curve followed reasonably closely $N^{-\frac{1}{2}}$ vs. N, the precision σ being 0.8–2% for I_o between 20 and 100, 0.2–3.3% for I_o between 5 and 20, and 1–25% for I_o less than 5. A Norelco diffractometer with a proportional counter, pulse-height analyzer, and rotating specimen holder were used both for counting and for survey charts. The generator was a Philips PW 1010 unit with additional external stabilization. Cu K_α radiation ($\lambda\alpha_1 = 1.54051$ Å) filtered with nickel, and 1° slits were employed throughout, except for the 111 and the correlation peaks, where ½° slits had to be substituted to obtain the correct intensities.

Special attention was paid to the preparation of the specimen. After preliminary experiments powder of batch 2 (325 mesh) was slightly moistened with a solution of polyvinyl alcohol in acetone and pressed to a circular disk 1 in. diameter and 3/16 in. thick. The disk had a completely smooth surface and could be inserted directly into the rotating specimen holder. Comparison with smear mounts showed good agreement between specimens prepared by the two methods, but the intensities from the pressed disk were much higher and more reproducible, especially in the low-angle range. There was no indication of preferential orientation, presumably because of the great fineness of the powder and the high crystal symmetry.

Can. J. Chem. Downloaded from www.nrcresearchpress.com by 210.87.254.40 on 09/05/12
For personal use only.

The lattice parameters were obtained from powder photographs taken with a 114.6 mm diameter camera of the Straumanis type. Nelson-Riley extrapolation and least-squares refinement gave final values of a_o with very small spreads. The correction for refraction fell within the limits of uncertainty of the determination.

The neutron diffraction experiments were performed at the NRX reactor of the Atomic Energy of Canada Ltd. at Chalk River, Ont. The erbium titanate powder was enclosed in a flat circular container 4 in. diameter and 1/8 in. thick, formed by 0.01 in. thick vanadium foil held in an aluminium ring mount. The neutron beam was monochromatized by reflection from the 111 plane of a germanium crystal (λ = 2.234 Å). The third-order content of the monochromatized beam was reduced to about 2% with a 5 in. thick quartz single-crystal filter, whose absorption had been calibrated in dependence on neutron energy, and by differential absorption in the specimen. A straight-through count was used to obtain the absorption correction. The 2θ transmission scan covered the angular range of 2θ from 20 to 91° in ¼° (2θ) increments. The counting time per point was 5–6 min. There was some contamination of the recorded pattern from the aluminium mount.

Because of accidental circumstances at the time the neutron diffraction patterns were not of a quality sufficient for a refinement of the oxygen parameter, but they were adequate for a confirmation of the results of the X-ray study.

Infrared spectra of $Er_2Ti_2O_7$ and of comparison compounds were recorded using KBr pellets on a Perkin–Elmer Model 521 spectrophotometer from 4 000 to 250 cm^{-1}.

Computations were performed on Royal McBee LGP-30 and IBM 1620 (40K) computers. The final refinement of the structure from X-ray data was carried out by Dr. F. R. Ahmed using programs described in ref. 9.

RESULTS OF THE X-RAY STUDY

The lattice parameter of the second batch of erbium titanate, a_o = 10.0762 ± 6 Å, differed remarkably little from that of the first batch, 10.0759 ± 10 Å. The high degree of compatibility of both a_o values with those of other $Ln_2Ti_2O_7$ phases will be discussed elsewhere, but it should be noted that they are higher than the value reported for $Er_2Ti_2O_7$ by Brixner (7), 10.069 ± 1 Å.

Preliminary intensity calculations based on the pyrochlore model (case I, Table III) and using neutral atomic scattering factors* corrected for dispersion (10) indicated that $x(O_2)$ was in the vicinity of 0.425. This value, together with assumed values of the individual isotropic temperature factors, $B(Å^2)$, was used as the initial value in a block diagonal least-squares refinement based on 20 $|F_o|$ from single, fully resolved reflections (Table II). A weighting scheme defined by $1/w = 1 + [(K|F_o| - b)/a]^2$ (a = 300, b = 400, K, scaling factor) was adopted (9). The refinement was repeated till the slowly converging unweighted R(neutral) was brought down to 2.42%; this was accomplished in 9 cycles (Table I). The initial values for the 5th cycle were estimated from the averages of the parameters obtained in the preceding cycles, and for cycles 6 to 8 the shifts were multiplied by 0.5 to avoid oscillation.†

For comparison, the pyrochlore structure was refined using the tabulated scattering factor for Ti^{3+} and graphically estimated factors for Er^{3+} and O^{2-}, all corrected for dispersion (10).‡ To prevent oscillation of the parameters the shifts were multiplied by 0.5 from the beginning. This procedure resulted in a substantial measure of agreement already in the 2nd cycle (Table I). The slowly converging R(ionic) was reduced after 7 cycles to 2.25%, which is a value only slightly lower than R_9(neutral).

Inspection of the differences between F_o and F_c suggested that the refinement might be improved further if the very weak reflections 931 and 953 were disregarded altogether, as with 931 and 953 omitted R_9(neutral) decreased to 1.88% and R_7(ionic), to 1.63%. This

*Er, *Thomas-Fermi-Dirac; oxygen and* Ti, *self-consistent field.*

†*At the beginning of the refinement* $|F_o|$ *(311) was by mistake taken to be 368.3 instead of 212.6. Although* $x(O_2)$ *refined, after 4 cycles, to 0.4188, and* B(Er), B(Ti), *and* $B(O_2)$ *to 0.644, 1.568, and 0.667 respectively, with R decreasing from 7.67 to 6.57%, the single wrong* $|F_o|$ *caused* $B(O_1)$ *to increase steadily to 18.90. A similar situation resulted with the ionic scattering factors. Considering that all atoms contribute to the intensity of 311, it is interesting to note the selectivity of the effect.*

‡Er^{3+}, *extrapolated, Thomas-Fermi-Dirac;* Ti^{3+}, *self-consistent field;* O^{2-}, *extrapolated, self-consistent field.*

Can. J. Chem. Downloaded from www.nrcresearchpress.com by 210.87.254.40 on 09/05/12
For personal use only.

TABLE I

Least-squares refinement of X-ray data*

	Neutral scattering factors					
	Cycle					
	1	5	7	8	9	σ_9, ±
B(Er)	0.150	0.300	0.413	0.437	0.454	0.043
B(Ti)	0.600	1.000	0.953	0.910	0.877	0.144
$B(O_1)$	1.500	2.000	0.927	0.855	0.613	0.765
$B(O_2)$	1.500	0.400	0.580	0.774	0.832	0.331
$x(O_2)$	0.4250	0.4162	0.4195	0.4200	0.4202	0.0010
Scale factor, K	1.000	1.024	1.017	1.013	1.013	0.004
R, %	6.23	2.92	2.44	2.41	2.42	
$[\sum w(\Delta F)^2/(n-m)]^{1/2}$	1.219	0.567	0.458	0.444	0.424	
	Ionic scattering factors					
	Cycle					
	1	2	5	6	7	σ_7, ±
B(Er)	0.150	0.325	0.416	0.439	0.461	0.037
B(Ti)	0.600	1.183	1.050	1.003	0.955	0.127
$B(O_1)$	1.500	2.607	0.734	0.511	0.320	0.610
$B(O_2)$	1.500	0.744	0.905	0.993	1.067	0.300
$x(O_2)$	0.4250	0.4221	0.4201	0.4200	0.4200	0.0009
Scale factor, K	1.000	1.015	1.009	1.008	1.007	0.001
R, %	5.95	2.65	2.33	2.28	2.25	
$[\sum w(\Delta F)^2/(n-m)]^{1/2}$	1.181	0.532	0.445	0.427	0.403	

*All 20 $|F_o|$ of Table II were used in the refinement. With $F_o(931)$ and $F_o(953)$ omitted the standard deviations for the last cycle were 0.385 for the neutral and 0.338 for the ionic scattering factors.

would leave 18 $|F_o|$, of which 14 contain contributions from both the metal and the oxygen atoms, and 4 (222, 622, 662, and 10.6.2) from the metal atoms only.*

Further refinement on this basis, using as initial parameter values those from cycles 9(neutral) and 7(ionic), did not improve R(neutral) and R(ionic) but made them progressively worse. At the same time the scale factor and $x(O_2)$ remained practically unchanged, while B(Er) increased somewhat, B(Ti) varied slightly, and $B(O_2)$ increased, after 3 cycles, by some 40%. However, $B(O_1)$ decreased and eventually assumed negative values. A somewhat worse but otherwise much the same result was obtained by omitting, in addition to 931 and 953, the "metal only" reflections 222, 622, 662, and 10.6.2.

Although in the first refinement, which included all 20 $|F_o|$, the final values of $B(O_2)$ were practically identical with B(Ti), and $B(O_1)$, compared with B(Er) and B(Ti), seemed far too low, the still smaller, and eventually negative, values of $B(O_1)$ resulting from the second refinement were clearly unreasonable. Since the scale factor and $x(O_2)$ remained practically constant further refinement using a reduced number of $|F_o|$ was considered unprofitable. In fact, it was felt that at this stage the uncertainties in the scattering factors and the dispersion corrections set a far more serious limit to further improvement of the accuracy. Moreover, the slow convergence of R seemed to indicate that the disparity of f(Er) and f(O), and the location of Er and Ti in special positions, were not favorable to further progress of the refinement.

The final values of the parameters are then those of cycle 9 for the neutral atoms and cycle 7 for the ionic atoms (Table I). In particular, $x(O_2)$ = 0.4202 and 0.4200 for the

The intensities of the reflections originating in the oxygen atoms only (cf. Table II) were too low to be measured with confidence.

Can. J. Chem. Downloaded from www.nrcresearchpress.com by 210.87.254.40 on 09/05/12
For personal use only.

Can. J. Chem. Downloaded from www.nrcresearchpress.com by 210.87.254.40 on 09/05/12
For personal use only.

TABLE II

Spacings, structure factors, and intensities (Cu K_α)

	Spacing, Å*		Neutral atoms				Ionic atoms			
hkl	*d*(obs.)	*d*(calcd.)	$\|F_o\|$	F_c	I_c†	I_o	$\|F_o\|$	F_c	I_c†	I_o
111 *a*	5.816	5.823	251.4	−254.0	26.90	25.28	250.0	−259.4	26.52	25.68
220 *b*	—	3.562		19.2	0.08	—		20.7	0.09	—
311 *a*	3.038	3.038	215.4	212.7	13.81	14.17	214.0	207.5	13.51	14.17
222 *a*	2.905	2.909	1038.0	1039.8	100	99.65	1031.8	1025.6	100	101.21
400 *a*	2.517	2.519	727.8	733.2	27.05	26.47	723.4	721.8	26.95	26.88
331 *a*	2.307	2.312	351.6	340.4	19.16	20.46	349.4	345.6	20.31	20.78
422 *b*	2.058	2.057		−56.9	0.41	—		−55.8	0.40	—
511	1.938	1.939		−278.0	8.49	8.34		−278.0	8.69	8.34
333				−87.5	0.28			−88.8	0.29	
440 *a*	1.781	1.781	1005.8	997.8	44.28	45.04	999.8	994.5	45.26	45.75
531 *a*	1.702	1.703	213.8	214.4	7.33	7.28	212.4	216.1	7.66	7.40
620 *b*	—	1.593		46.3	0.01	—		44.8	0.01	—
533 *a*	1.534	1.537	166.0	163.6	1.66	1.70	165.0	165.1	1.73	1.73
622 *a*	1.518	1.519	775.0	765.6	35.26	36.13	770.4	762.8	35.98	36.70
444 *a*	1.454	1.454	658.4	651.1	7.64	7.83	654.6	649.6	7.82	7.95
711	1.4110	1.4109		224.7	2.54	2.96		225.6	2.63	3.01
551				−133.1	0.89			−138.2	0.99	
642 *b*	—	1.3465		−10.5	0.01	—		−11.6	0.01	—
731	1.3114	1.3112		125.1	1.33	2.67		123.0	1.34	2.71
553				208.4	1.84			206.6	1.86	
800 *a*	1.2606	1.2595	746.0	745.0	5.38	5.39	741.6	739.3	5.44	5.47
733 *a*	1.2309	1.2310	250.0	−272.1	2.74	2.31	248.6	−259.8	2.57	2.35
822 *b*	‡	1.1917		71.7	0.18	—		64.2	0.15	—
660 *b*				−70.6	0.09			−66.6	0.08	
751	1.1627	1.1635		166.9	1.90	2.53		166.4	1.90	2.37
555				−237.4	0.63			−231.5	0.61	
662 *a*	1.1573	1.1558	618.6	618.9	12.64	12.57	614.8	616.3	12.88	12.76
840 *a*	1.1263	1.1266	556.0	556.1	9.83	9.83	552.6	555.0	10.06	9.98
911	1.1059	1.1060		−150.4	0.70	2.65		−153.6	0.75	2.67
753				195.4	2.37			195.0	2.43	
664 *b*	—	1.0741		41.1	0.05	—		39.7	0.05	—
931 *a*	1.0562	1.0563	131.0	147.8	1.30	1.02	130.4	148.1	1.34	1.04

Can. J. Chem. Downloaded from www.nrcresearchpress.com by 210.87.254.40 on 09/05/12
For personal use only.

TABLE II (*Concluded*)

	Spacing, Å*		Neutral atoms				Ionic atoms			
hkl	*d*(obs.)	*d*(calcd.)	$\|F_o\|$	F_c	I_c†	I_o	$\|F_o\|$	F_c	I_c†	I_o
844 *a*	1.0276	1.0284	586.8	573.8	9.71	10.15	583.2	571.7	9.91	10.31
933	1.0119	1.0126		185.4	1.01	2.39		184.9	1.04	2.43
771				198.5	1.16			197.4	1.18	
755				141.2	0.59			144.5	0.63	
10.2.0 *b*	‡	0.98805		−49.3	0.07	—		−47.3	0.07	—
862 *b*				−24.9	0.04			−20.6	0.03	
951	0.97359	0.97410		−174.7	1.83	12.31		−172.0	1.83	12.50
773				−83.7	0.21			−87.9	0.24	
10.2.2	0.96862	0.96958		520.4	8.17			517.3	8.30	
666				520.4	2.72			517.5	2.77	
953 *a*	0.93922	0.93961	116.0	138.2	1.20	0.85	115.4	140.8	1.28	0.86
10.4.2 *b*	‡	0.91983		28.6	0.05	—		28.6	0.06	—
11.1.1	0.91191	0.91226		138.9	0.65	0.75		137.8	0.66	0.76
775				113.1	0.43			114.3	0.45	
880 *a*	0.89040	0.89062	495.8	480.7	4.15	4.42	492.8	479.5	4.25	4.48
11.3.1	0.88016	0.88036		151.9	1.73	2.66		152.9	1.80	2.70
971				144.6	1.57			146.0	1.64	
955				−98.3	0.36			−103.7	0.41	
10.6.0 *b*	‡	0.86403		−64.4	0.17	—		−60.2	0.15	—
866 *b*				−3.8	0.00			−5.7	0.00	
11.3.3	0.85473	0.85465		−94.1	0.38	18.89		−96.2	0.41	19.12
973				101.0	0.88			102.8	0.93	
10.6.2 *a*	0.85147	0.85159	453.6 *c*	449.1	17.63		451.0	448.5	18.07	
12.0.0	0.83960	0.83968		404.9	1.95	11.38		402.7	1.98	11.56
884				449.5	9.61			442.5	9.57	
11.5.1	0.83093	0.83107		113.6	1.32	1.13		117.5	1.45	1.15
777				−178.7	0.54			−176.4	0.54	
12.2.2 *b*	‡	0.81729		−47.6	0.13	—		−40.5	0.10	—
10.6.4 *b*				−46.3	0.25			−43.9	0.23	
11.5.3	0.80931	0.80934		115.9	1.75	2.59		115.4	1.78	2.63
975				122.4	1.95			121.4	1.97	
12.4.0 *a*	0.79654	0.79659	435.4	434.5	15.23	15.33	432.8	431.2	15.43	15.56

NOTE: (*a*) Used in the least-squares refinement; (*b*) zero contribution from the metal atoms; (*c*) only a minor correction required to separate 10.6.2 from 11.3.3 + 973.
*From 844 on *d*(obs.) is based on α_1 only.
†Normalized to $I_c(222)$.
‡Barely visible in the films.

TABLE III

Comparison of the pyrochlore model with alternative structures

		I_c(ionic)			
hkl	I_o*	Case I	Case II	Case III	Case IV
111	25.68	26.52	10.33	17.49	17.49
220†	—	0.09	0.09	0.09	1.37
311	14.49	13.51	25.07	18.84	18.84
400	26.88	26.95	26.95	26.95	30.54
331	20.78	20.31	13.73	16.86	16.86
422†	—	0.40	0.40	0.40	1.17
511;333	8.47	8.98	13.02	10.90	10.90
440	45.75	45.26	45.26	45.26	45.26
531	7.40	7.66	4.77	6.13	6.13
620†	—	0.01	0.01	0.01	0.00
533	1.73	1.73	2.69	2.19	2.19
444	7.95	7.82	7.82	7.82	8.48
711;551	3.01	3.62	2.37	2.96	2.96
642†	—	0.01	0.01	0.01	0.00
731;553	2.71	3.20	4.68	3.92	3.92
800	5.47	5.44	5.44	5.44	5.12
733	2.35	2.57	2.00	2.27	2.27
822;660†	—	0.23	0.23	0.23	0.30
751;555	2.37	2.51	3.38	2.93	2.93
840	9.98	10.06	10.06	10.06	10.77
911;753	2.67	3.18	2.32	2.73	2.73
664†	—	0.05	0.05	0.05	0.01
931	1.04	1.34	1.85	1.58	1.58
844	10.31	9.91	9.91	9.91	9.32
$\Sigma\|\Delta I\|/\Sigma I_o$	‡	3.3%	23.9%	12.2%	15.0%
	§	5.6%	47.3%	24.2%	24.2%

*Scaled to I_c(case I). The I_c values are normalized to I_c(222). Reflections with zero contribution from the oxygen atoms have been omitted.
†Zero contribution from the metal atoms.
‡Includes all observed intensities up to 844.
§Includes 111, 311, 331, 511 + 333, 531, 533, 711 + 551, 731 + 553, 733, 751 + 555, 911 + 753, and 931.

neutral and ionic case respectively. These values were used to calculate the intensities of the observable reflections. The calculated intensities, I_c, were normalized to $I_c(222)$ and the absolute $|F_o|$ were converted to the I_o values listed in Table II. The agreement indices, $\Sigma|I_c - I_o|/\Sigma I_o$ and $\Sigma I_c/\Sigma I_o$, were 3.55% and 1.014 for the neutral and 3.67% and 1.014 for the ionic scattering factors. When intensities lower than 2 were rejected the corresponding values were 3.16%, 1.006, 3.03%, and 1.007 respectively.

The standard deviation $\sigma(x)$ was ± 0.0010 for the neutral and ± 0.0009 for the ionic model. These uncertainties are greater than the difference between x(neutral) and x(ionic). This circumstance, together with the consistently lower values of $\sigma(B)$ for the ionic scattering factors, seems to justify taking 0.4200 ± 10 as the final value of $x(O_2)$. No attempt has been made to attribute special significance to the low thermal parameters of both oxygen atoms.

ALTERNATIVE STRUCTURES

In view of the relatively small contribution of O_1 to the diffraction intensities the possibility of existence of alternative structures was examined. Intensities were calculated from the final parameter values (ionic) for the following distributions:

case II: 8 O_1 in 8(b), 8(a) unoccupied;

case III: 8 O_1 distributed at random over 8(a) and 8(b).

Can. J. Chem. Downloaded from www.nrcresearchpress.com by 210.87.254.40 on 09/05/12
For personal use only.

As a check of the sensitivity of the intensities to the location of O_1 a fourth alternative, case IV, was considered, in which the 8 O_1 atoms were omitted. The possibility of a statistical distribution of the Er and Ti atoms over 16(*c*) and 16(*d*) was disregarded because of the low *R* values for case I.

The alternative distributions did not give as good an agreement as case I for those reflections that involve both the metal and oxygen atoms (Table III). The differences between I_o and I_c were particularly noticeable for 111, 311, 331, and 511 + 333. At higher Bragg angles the differences were of the order of the experimental error for case I and could no longer be used to distinguish between the four alternatives.

Since the intensities of Table III have been normalized to $I_c(222)$, to which the oxygens do not contribute, the calculated intensities for cases I–IV can be compared directly. However, the temperature factors and $x(O_2)$ used in calculating I_c were in all four cases those of cycle 7(ionic), and the I_o were scaled with respect to case I. It may be objected that if case II or case III had been taken as models for the least-squares refinement, case I might have emerged less favorably in the comparison.

Calculation shows that $I_c(111)$ for case I changes, for small variations in x, by about $5.6\,\Delta x.I$, so that for $\Delta x = \pm 0.03$ the change in the intensity would be ca. ± 4.4. At the same time $I_c(840)$, $I_c(844)$, and $I_c(880)$, which change with x but not with the location of O_1 and for which the indices are sufficiently high to magnify the effect of Δx considerably, would change in the following manner:

	$I_c - I_c/I_o - F_c/\lvert F_o\rvert$		
hkl	$\Delta x = -0.03$	$\Delta x = 0$	$\Delta x = 0.03$
840	7.84 − 0.79 − 0.88	10.06 − 1.01 − 1.00	11.32 − 1.14 − 1.06
844	12.56 − 1.22 − 1.12	9.91 − 0.96 − 1.00	8.20 − 0.79 − 0.91
880	5.53 − 1.23 − 1.14	4.25 − 0.95 − 1.00	4.14 − 0.94 − 0.99

It is thus seen that in order for the ratios $I_c(840):I_c(844):I_c(880)$ and $F_c(840):F_c(844):F_c(880)$ to remain reasonably close to the observed ratios the value of Δx must be quite close to zero; and the same holds for other reflections of this type, and a fortiori for the "metal only" reflections.

Consequently the Δx-induced variation in $I(111)$ will be insignificant and the differences between $I_o(111)$ and $I_c(111)$ for cases I, II, and III will be produced almost entirely by the location of O_1; and similarly for the intensities of the other critical reflections. Inspection of the index $\sum|\Delta I|/\sum I_o$ (Table III) for the three physically meaningful cases then leaves no doubt that case I is the correct choice. This argument can of course be strengthened by taking into consideration other suitable reflections, such as 12.4.0, and by calling to attention the necessity of matching the observed and the calculated intensities of the "metal only" reflections 222, 622, 662, and 666 + 10.2.2, all of which are strong.

A more obvious demonstration of the correctness of the pyrochlore model was provided by the neutron diffraction pattern. With $b(O) = 0.577$, $b(Ti) = -0.34$, and $b(Er) = 0.79 \times 10^{-12}$ cm (natural isotopic contents) (10), the neutron scattering amplitudes are particularly favorable for locating the O_1 atom, since the non-zero contributions of Ti and Er to structure factors with h, k, l all even will now have opposite signs and thus counteract each other, and the oxygen contributions will be appreciable.

Neutron diffraction intensities were calculated from the final parameter values for the neutral atoms for first-order reflections up to 620 and for third-order reflections up to 19.1.1. Although third-order reflections with very high $h^2 + k^2 + l^2$ had to be taken into

Can. J. Chem. Downloaded from www.nrcresearchpress.com by 210.87.254.40 on 09/05/12
For personal use only.

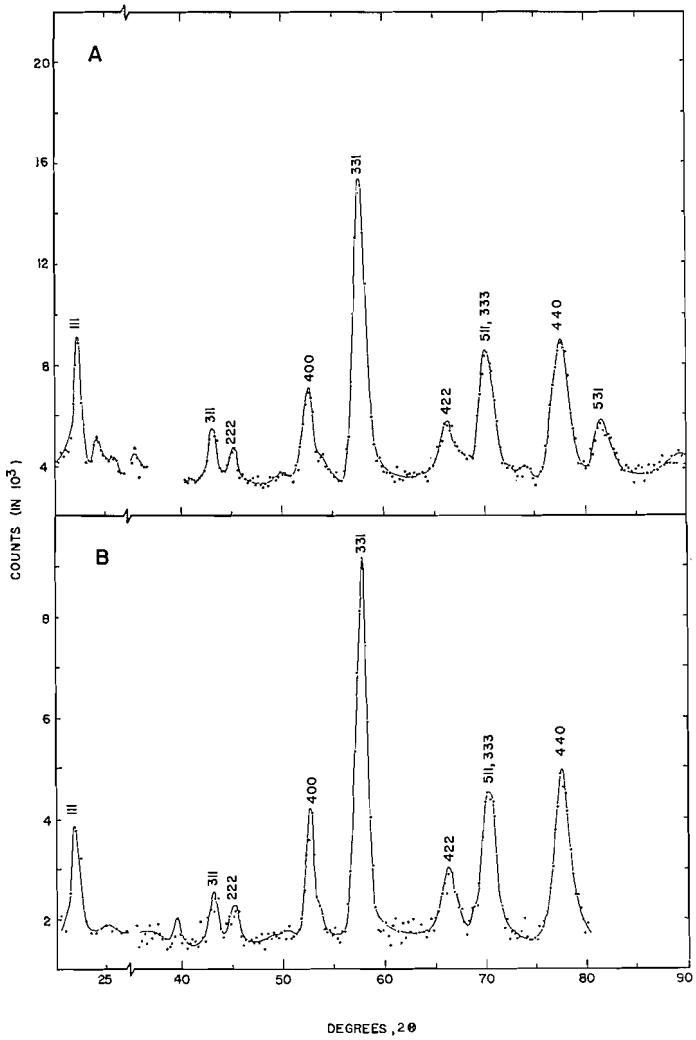

FIG. 1. Neutron powder diffraction patterns of erbium titanate. A, unfiltered beam; B, quartz filter in the beam.

account, it was found that the third-order contamination in the quartz-filtered spectrum amounted to only about 2% of the first-order intensity, so that only the strongest third-order reflections had a noticeable effect on the diffraction pattern.

The extent of agreement between the observed patterns and the intensities calculated for cases I–IV can be judged by comparing Fig. 1 and 2. In spite of the uncertainty in the amount of the third-order contamination there can be little doubt that the pyrochlore model is the only one that fits the observed patterns.

DESCRIPTION OF THE STRUCTURE

The principal features of the structure may be seen in Figs. 3–5. Figure 5 in particular shows the arrangement of the distorted TiO_6 octahedra (with the six O_2 atoms equidistant) about the erbium atoms, and the coordination scalenohedron of the six O_2 atoms (in

Can. J. Chem. Downloaded from www.nrcresearchpress.com by 210.87.254.40 on 09/05/12
For personal use only.

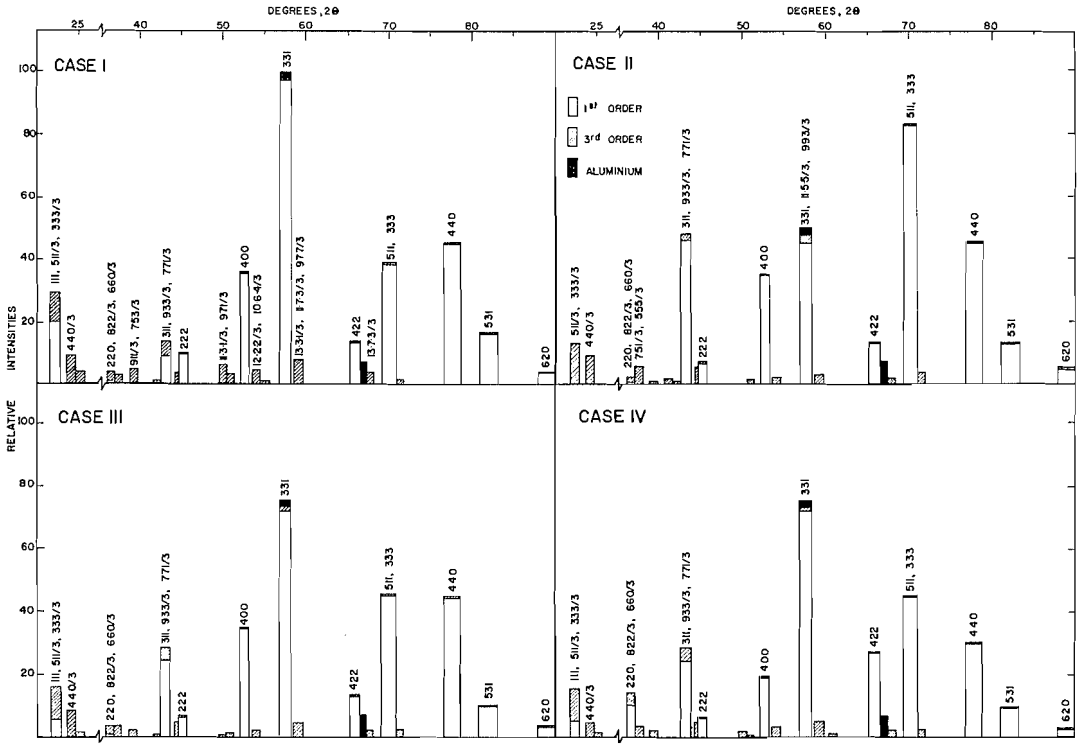

FIG. 2. Representation of the neutron diffraction intensities calculated for cases I–IV, with 2% of third-order contamination. The column heights for case I have been adjusted relative to the observed peak heights. The column heights for cases II–IV are on the same scale as those for case I. The two Al peaks are spurious first-order reflections from 111 and 200. Note the break in the angular range between 27 and 35° (2θ).

equatorial positions) and the two O_1 atoms (in polar positions) about each erbium atom. This scalenohedron is related, via a rhombohedron, to the coordination cube of a metal atom in the fluorite structure, the latter being, geometrically, the limiting case of the pyrochlore structure for $x = 3/8$.

Each O_1 atom is completely enclosed in a cage of four erbium atoms at the corners of a regular tetrahedron. This isolation from the TiO_6 framework may be expected to affect the vibrational freedom of the O_1 atoms. It might account for the low value of $B(O_1)$ if the temperature factor could be considered a physically meaningful quantity rather than an arithmetical parameter of the refinement process; and it might be helpful in the interpretation of the infrared spectrum.

Apparent interatomic distances and selected bond angles are listed in Table IV. The figures indicating precision refer to the last decimal. They are conservative estimates of σ obtained from the uncertainties in a_0 and x. In the absence of an anisotropic refinement of the thermal parameters no attempt has been made to take into account thermal motion in computing the distances. Obviously those distances that involve O_2 depend ultimately on the reliability of the scattering factors and dispersion corrections used in the refinement. That apparent interatomic distances in simple compounds should be viewed with caution even when based on single-crystal data and a large number of observed reflections has been demonstrated for $CaWO_4$ in a recent paper by Burbank (11), in which a set of 828 $|F_o|$'s obtained by a conventional single-crystal method, and a set of 54 $|F_o|$'s derived from

Can. J. Chem. Downloaded from www.nrcresearchpress.com by 210.87.254.40 on 09/05/12
For personal use only.

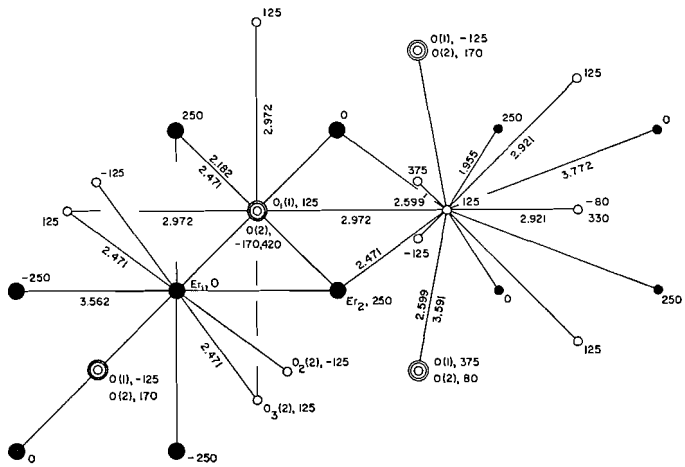

FIG. 3. Environment of the Er, O_1, and O_2 atoms. Interatomic distances up to 3.8 Å are shown. Small full circles, Ti; large full circles, Er; small open circles, O_2; double open circles, O_1. The fractional height coordinates have been multiplied by 1 000. Origin at Er_1.

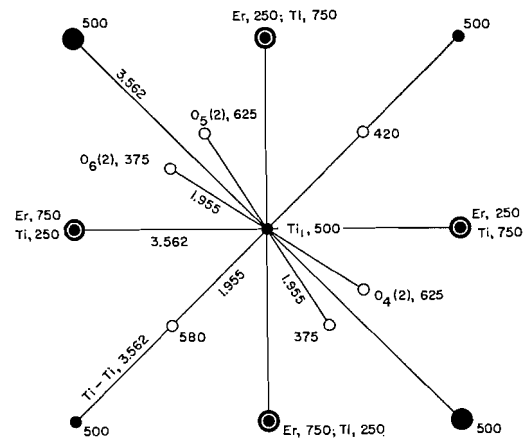

FIG. 4. Environment of the Ti atom. Interatomic distances up to 3.57 Å are shown. Coordinates of Ti_1: $\frac{1}{2}\frac{1}{2}\frac{1}{2}$.

neutron diffraction intensities, are compared with 104 $|F_o|$'s based on the author's absolute intensity measurements.

The only Er—O distances that were found in the literature were those for Er_2O_3 obtained from neutron diffraction (12). The shorter of the two Er—O distances in erbium titanate, Er—O_1, compares well with the shortest distance in the oxide, but the Er—O_2 separation is appreciably greater than any of the Er—O distances in Er_2O_3.

The shortest Ti—O distance, 1.955 Å, is seen to be very close to the average of the Ti—O distances in a variety of simple oxygen compounds of titanium (Table V), almost all of which contain Ti atoms in octahedral environment.

Each O_2 atom is surrounded by two Ti atoms at 1.955 Å, two Er atoms at 2.471 Å, four O_2 atoms at 2.599 Å, and another four O_2 atoms at 2.921 Å (Fig. 3). The symmetry of this coordination is *mm* (Fig. 5).

Can. J. Chem. Downloaded from www.nrcresearchpress.com by 210.87.254.40 on 09/05/12
For personal use only.

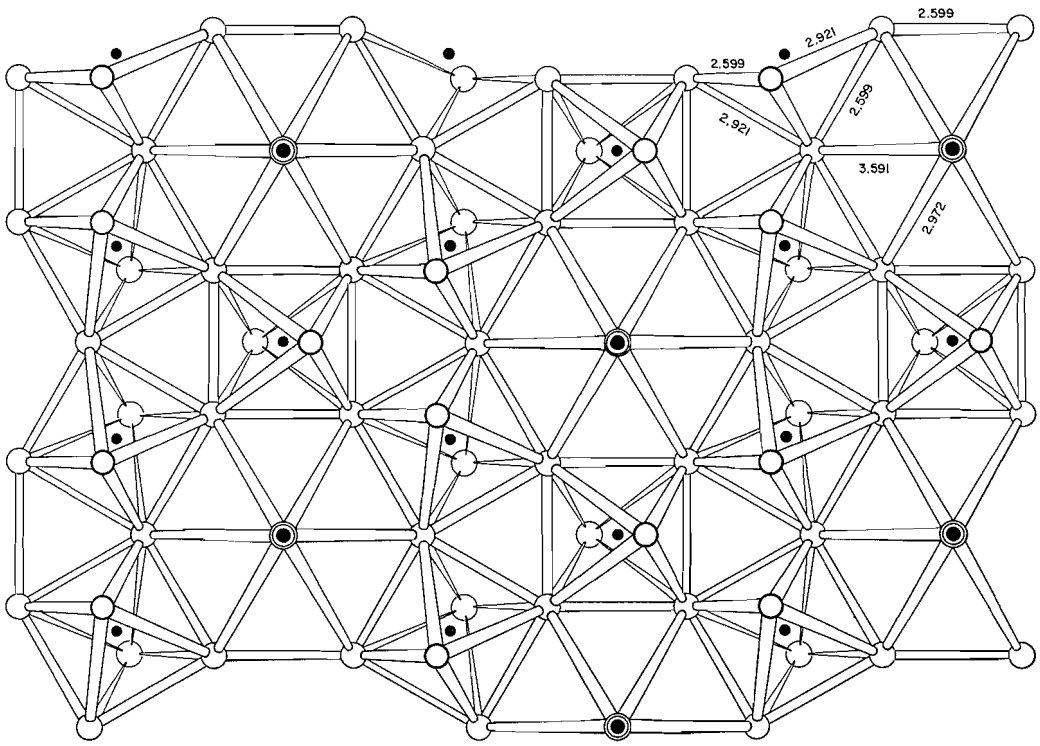

FIG. 5. Projection of a part of the erbium titanate structure along the threefold axis. The centers of the hexagons contain overlapping projections of one Er and two O_1 atoms.

TABLE IV

Apparent interatomic distances and bond angles*

Bond	Distance, Å	Bond	Bond angle,°
Ti—O(2)	1.955±8	$O_4(2)$—Ti_1—$O_5(2)$	96.68
Ti—O(2)	3.772±10	$O_5(2)$—Ti_1—$O_6(2)$	83.32
Er—O(1) = $a_o\sqrt{3}/8$	2.1815±5	$O_2(2)$—Er_1—$O_3(2)$	63.46
Er—O(2)	2.471±8	$O_1(1)$—Er_1—$O_3(2)$	79.13
$O_5(2)$—$O_6(2)$	2.599±6	$O_1(1)$—Er_1—$O_2(2)$	100.87
$O_4(2)$—$O_5(2)$	2.921±10	$O_2(2)$—$O_1(1)$—$O_3(2)$	45.46
$O_1(1)$—$O_3(2)$	2.972±10	Er_1—$O_1(1)$—Er_2	109.47†
$O_1(1)$—$O_2(2)$	3.591±6		
O(1)—O(1) = $a_o\sqrt{3}/4$	4.3630±5		
Ti–Ti, Er—Er, Ti—Er = $a_o\sqrt{2}/4$	3.5625±5		

*The distances are not corrected for thermal motion. For atomic positions see Figs. 3 and 4.
†Tetrahedral angle.

INFRARED SPECTRUM

The transmission spectra of erbium titanate and of Er_2O_3 (calcined at 600 °C; C type), rutile (calcined at 950 °C), and tetragonal $BaTiO_3$ of high purity (prepared by the double-oxalate method and calcined at 950 °C; loose unpoled powder) are shown in Fig. 6. The portions of the spectra between 4 000 and 1 600 cm^{-1} show no characteristic features and have been omitted.

Can. J. Chem. Downloaded from www.nrcresearchpress.com by 210.87.254.40 on 09/05/12
For personal use only.

TABLE V

Shortest metal–oxygen distances in Er_2O_3 and in some oxygen compounds of titanium

Compound	Distance, Å	Ref.
	Er—O distances	
Er_2O_3	2.20; 2.23; 2.28; 2.33	12
	Ti—O distances	
TiO	2.088	13
TiO_2 (rutile)	1.944±4; 1.988±6	14
	1.946; 1.983	15
TiO_2 (anatase)	1.937±3; 1.964±9	16
TiO_2 (brookite)	1.84; 1.94; 1.95; 1.99; 2.00; 2.03 (all ±5)	17
	1.87; 1.92; 1.94; 1.99; 2.00; 2.04 (all ±2)	18
Ti_2O_3	2.01 ± 1; $2.08\pm1_5$	19
Ti_5O_9	1.75–2.35	20
$SrTiO_3$ (25°)	1.953	21
$EuTiO_3$	1.948	21
$BaTiO_3$ (cubic)	2.0059±6 (201°); 2.0392±6 (1 372°)	22
$BaTiO_3$ (tetragonal)	1.86; 2.00; 2.17 (18°)	23
$BaTiO_3$ (orthorhombic)	1.90; 2.00; 2.11	24
$BaTiO_3$ (hexagonal)	1.96; 2.02	25
$K_2Ti_6O_{13}$	1.83; 1.84; 1.86; 1.95; 1.96; 1.98; 2.11; 2.22; 2.28	26

The spectrum of Er_2O_3 (A, 563; B, 505; C, 469; D, 414; E, 377; F, 332; G, 318; and H, 291 cm^{-1}) is better defined than the Nujol-mull spectrum published previously by Baun and McDevitt (27), for which the positions of the band maxima were reported as 563, 500–345 (broad band), 325, and 285 cm^{-1}.

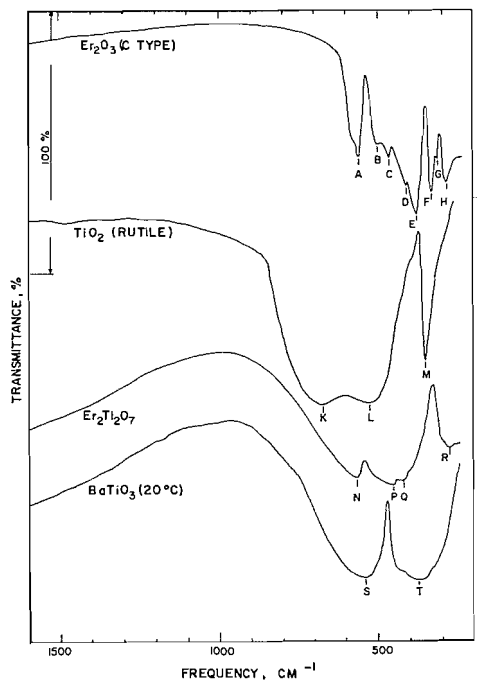

FIG. 6. Infrared spectra of erbium titanate and comparison substances. For positions of the absorption maxima see text.

Can. J. Chem. Downloaded from www.nrcresearchpress.com by 210.87.254.40 on 09/05/12
For personal use only.

The absorption maxima were at 675 (K), 515 (L), and 350 (M) cm^{-1} in the rutile spectrum, and at 535 (S) and 370 (T) cm^{-1} in the spectrum of $BaTiO_3$. Although standard KBr-pellet technique was used, the peak maxima were not in complete agreement with the band centers reported for $BaTiO_3$ in pressed KBr disks by Last (28), 540 (or 545?) and 400 cm^{-1}, and the bands were broader. This discrepancy may be real and may have originated in the physical state of the $BaTiO_3$ powder. Last powdered a small section of a single crystal to a particle size of about 1 micron, whereas we used polycrystalline powder obtained by calcining barium titanyl oxalate. The fine powder passed 325 mesh with ease and was subsequently ground with KBr. It is possible that a higher calcining temperature and a more careful reduction of the particle size may have produced a spectrum more closely similar to Last's, though the absorption maxima reported in Last's paper for transmission spectra obtained with a thin single crystal of $BaTiO_3$ and with polarized radiation were appreciably lower, 495 and 517 cm^{-1} for the electric vector parallel to the *a* axis and to the *c* axis respectively. They would be lowered further by correcting for surface reflectivity of the thin crystal plate.

The positions of the absorption maxima in the spectrum of erbium titanate were 560 (N), 450 (P), 425 (Q), and 280 (R) cm^{-1}. The gross features of the spectrum resemble those of rutile and, allowing for a shift towards higher frequencies, also those of $BaTiO_3$.

It seems to be generally agreed that Last's assignment of the highest-frequency band in $BaTiO_3$ to a Ti—O stretching vibration, ν_1, is correct. His assignemnt of the lower-frequency (T) band to a Ti—O—Ti bending mode, ν_2, has been the subject of some discussion (29, 30, 31), but recent detailed studies and *K–K* analyses of the spectra of titanate perovskites (32), and comparison of the spectra of $BaTiO_3$ and rutile with the spectra of the corresponding model structures $KMgF_3$ and MgF_2 (33, 34), indicate that neither ν_1 nor ν_2 are affected by the nature of the heavy cation and that ν_2 indeed is a bending mode of the TiO_6 octahedron. A similar situation exists in rutile.

It is tentatively suggested that while the main, broad absorption bands of the erbium titanate spectrum arise from Ti—O modes, the minor features of the spectrum (shoulders and subsidiary maxima in the PQ band) are probably associated with the oxygen environment of the erbium atoms. In view of the greater complexity of the erbium titanate structure and the different arrangement of the TiO_6 octahedra a more satisfactory interpretation of the spectrum will have to await a detailed comparative study of the spectra and dielectric characteristics of $Ln_2Ti_2O_7$ and related compounds.

CONCLUSION

The above results have established that $Er_2Ti_2O_7$ has the pyrochlore structure, with some distortion in the TiO_6 coordination octahedra. From the similarity of the diffraction patterns of erbium titanate with those of the other $Ln_2Ti_2O_7$ preparations it may be concluded that the titanates of the elements from Sm to Lu belong to the same structure type, as suggested previously (2, 1, 7).

For a more direct confirmation, and to determine if the parameters of the O_2 atom differ significantly from one lanthanon to another, the crystal structures of two other titanates are now being refined in similar manner. At the same time the examination of the infrared spectra is being extended to the other titanates.

ACKNOWLEDGMENTS

We are indebted to Dr. F. R. Ahmed of the Division of Pure Physics, National Research Council, Ottawa, for the refinement of the structure. We should also like to express

Can. J. Chem. Downloaded from www.nrcresearchpress.com by 210.87.254.40 on 09/05/12
For personal use only.

our gratitude to Dr. A. D. B. Woods and the staff of the Neutron Physics Branch for permission to use the neutron diffraction facilities of the Atomic Energy of Canada Ltd., and to Dr. M. Falk for placing at our disposal the infrared spectrophotometer at the Atlantic Regional Laboratories of the National Research Council.

Financial support of this investigation by the Defence Research Board and the National Research Council through grants in aid of research to the first-named author is hereby acknowledged. The preparative work and a part of the preliminary X-ray study were carried out under DRB Contract No. 800107/200024 and are reported in the present form with the permission of the Board.

REFERENCES

1. L. CASTELLIZ and O. KNOP. 13th Progress Rept. December 31st, 1963; 14th Progress Rept. June 30th, 1964. DRB Contract No. 200024. Nova Scotia Technical College, Halifax, Nova Scotia.
2. R. D. ROTH. J. Res. Nat. Bur. Std. **56**, 17 (1956).
3. H. R. GAERTNER. Neues Jahrb. Mineral. Abhand. **61**, 1 (1930).
4. F. MACHATSCHKI. Z. Krist. **73**, 159 (1930); Chem. Erde, **7**, 56 (1932).
5. O. ROSÉN and A. WESTGREN. Geol. Fören. Stockholm Förh. **60**, 226 (1938).
6. A. BYSTRÖM. Arkiv Kemi Mineral. Geol. **18A**, No. 21 (1944).
7. L. H. BRIXNER. Inorg. Chem. **3**, 1065 (1964).
8. International Tables for X-Ray Crystallography. Vol. 1. Kynoch Press, Birmingham. 1952.
9. F. R. AHMED, E. J. GABE, G. A. MAIR, and M. E. PIPPY. A unified set of crystallographic programs for the IBM 1620 computer. September 1963. Unpublished.
10. International Tables for X-Ray Crystallography. Vol. III. Kynoch Press, Birmingham. 1962.
11. R. D. BURBANK. Acta Cryst. **18**, 88 (1965).
12. A. FERT. Bull. Soc. Franc. Minéral. et Crist. **85**, 267 (1962).
13. M. E. STRAUMANIS and H. W. LI. Z. Anorg. Chem. **305**, 143 (1960).
14. W. H. BAUR. Acta Cryst. **9**, 515 (1956); Naturwissenschaften, **42**, 295 (1955).
15. M. E. STRAUMANIS, T. EJIMA, and W. J. JAMES. Acta Cryst. **14**, 493 (1961).
16. D. T. CROMER and K. HERRINGTON. J. Am. Chem. Soc. **77**, 4708 (1955).
17. R. WEYL. Z. Krist. **111**, 401 (1959).
18. W. H. BAUR. Acta Cryst. **14**, 214 (1961).
19. R. E. NEWNHAM and Y. M. DE HAAN. Z. Krist. **117**, 235 (1962).
20. S. ANDERSSON. Acta Chem. Scand. **14**, 1161 (1960).
21. J. BROUS, I. FANKUCHEN, and E. BANKS. Acta Cryst. **6**, 67 (1953).
22. J. W. EDWARDS, R. SPEISER, and H. L. JOHNSTON. J. Am. Chem. Soc. **73**, 2934 (1951).
23. F. JONA and G. SHIRANE. Ferroelectric crystals. Pergamon Press, New York. 1962. p. 155.
24. G. SHIRANE, H. DANNER, and R. PEPINSKY. Phys. Rev. **105**, 856 (1957).
25. R. D. BURBANK and H. T. EVANS, JR. Acta Cryst. **1**, 330 (1948). H. T. EVANS, JR. and R. D. BURBANK. J. Chem. Phys. **16**, 634 (1948).
26. H. CID-DRESDNER and M. J. BUERGER. Z. Krist. **117**, 411 (1962).
27. W. L. BAUN and N. T. MCDEVITT. J. Am. Ceram. Soc. **46**, 294 (1963).
28. J. T. LAST. Phys. Rev. **105**, 1740 (1957).
29. W. G. SPITZER, R. C. MILLER, D. A. KLEINMAN, and L. E. HOWART. Phys. Rev. **126**, 1710 (1962).
30. A. S. BARKER, JR. and M. TINKHAM. Phys. Rev. **125**, 1527 (1962).
31. R. I. JOSEPH and B. D. SILVERMAN. J. Phys. Chem. Solids, **24**, 1349 (1963); **25**, 1125 (1964).
32. C. H. PERRY, B. N. KHANNA, and G. RUPPRECHT. Phys. Rev. **135**, A408 (1964).
33. C. H. PERRY, G. R. HUNT, and J. FERGUSON. Quarterly Progress Rept. No. 72. Research Laboratory of Electronics, M.I.T. January 15th, 1964. pp. 31–38.
34. G. R. HUNT, C. H. PERRY, and J. FERGUSON. Phys. Rev. **134**, A688 (1964).

Can. J. Chem. Downloaded from www.nrcresearchpress.com by 210.87.254.40 on 09/05/12
For personal use only.

Can. J. Chem. Downloaded from www.nrcresearchpress.com by 210.87.254.42 on 09/05/12
For personal use only.

CORRELATION OF ETHYLENIC PROTON COUPLING CONSTANTS WITH THE ELECTRONEGATIVITY OF SUBSTITUENTS

INTERPRETATION OF THE DEVIATIONS OF BROMO AND IODO SUBSTITUENTS

F. HRUSKA,[1] G. KOTOWYCZ,[1] AND T. SCHAEFER[2]
Department of Chemistry, University of Manitoba, Winnipeg, Manitoba
Received May 7, 1965

ABSTRACT

It is shown that for the geminal, *cis* and *trans* proton coupling constants in vinyl bromide and vinyl iodide there exist significant deviations from an inverse linear relationship between coupling constants and the electronegativity of the substituent in monosubstituted ethylenes. By an adaptation of the box model of Juan and Gutowsky to the ^{13}C—H coupling constants in the system $CH_2{=}{=}^{13}CHX$, it is shown that there are related anomalies in the ^{13}C—H coupling constants in vinyl bromide and vinyl iodide. A comparison of the three types of ^{13}C—H coupling constants in some vinyl compounds suggests that there may be an interaction between the substituent and the C—H bond which affects the coupling constant but not the s-character of the carbon orbital in the bond.

INTRODUCTION

Following the suggestion of Banwell and Sheppard (1), an inverse proportionality between the three proton coupling constants in monosubstituted ethylenes ($J_g \equiv J_{gem}$, $J_c \equiv J_{cis}$, $J_t \equiv J_{trans}$) and the electronegativity, E_X, of the substituent, X, has been accepted (2–4). Theoretical support for such a relationship was provided by Karplus (5), who showed that substituent-induced changes in the hybridization of the carbon atoms in the fragment HCCH are the primary cause, as opposed to a direct inductive effect on the polarity of the C—H bonds (6, 7).

Some time ago, one of us noted that the coupling constants in vinyl bromide deviated consistently from the straight line relationship (3). Banwell and Sheppard indicated a similar, if smaller, deviation for vinyl chloride (1). In this paper we point out the extent of these deviations and discuss them in the light of present knowledge of spin–spin coupling in vinyl compounds.

Two papers by Goldstein *et al.* appeared on the proton spectra of the vinyl halides (8, 9). While they did not discuss electronegativity correlations, the very accurate values of the proton coupling constants given there will be used in our discussion.

Preferred Values of Coupling Constants and Electronegativity

The geminal proton coupling, J_g, in ethylenic compounds is often strongly solvent dependent (9, 10). According to Watts and Goldstein (9), it depends on the dielectric constant of the medium. They extrapolate the values of J_g for the vinyl halides and vinyl cyanide to a "zero-field" value, i.e., to a medium with unit dielectric constant. Since the error in this extrapolation is somewhat uncertain, we prefer to use the values of J_g, J_c, and J_t in cyclohexane at infinite dilution. In any case, our conclusions would not be changed by the use of the "zero-field" values of J_g. The solvent dependence of J_c and J_t is relatively small and certainly not large enough to cause ambiguities even if values in different solvents are used.

In addition to the vinyl halides and vinyl cyanide, Table I lists J values for other compounds. These were chosen for one or more of the following reasons: The J values

[1]*N.R.C. Studentship holder, 1964–1965.*
[2]*N.R.C. Senior Research Fellow, 1964–1965.*

TABLE I

Coupling constants in c/s and electronegativities of substituents in some vinyl compounds

Substituent	E_X	J_g(H—H)	J_c(H—H)	J_t(H—H)	J(^{13}C—H)*	Ref.
F†	3.90	−3.06±0.05	4.70±0.05	12.68±0.05	200.18	8, 9
O—R‡	3.40	−1.8±0.2	7.0±0.2	14.3±0.3	—	36
Cl†	3.15	−1.28±0.05	7.16±0.05	14.78±0.05	194.86	8, 9
Br†	2.87	−1.59±0.05	7.27±0.05	15.10±0.05	196.58	8, 9
I†	2.60	−0.88±0.05	7.83±0.05	15.82±0.05	190.85	8, 9
S—CH_3§	2.63	−0.3±0.2	10.3±0.2	16.5±0.2	—	36
C≡N†	2.50	1.20±0.05	11.65±0.05	17.89±0.05	176.74‖	9, 29
COOH‖	2.60	1.3±0.1	10.4±0.1	17.2±0.1	—	37
H¶	2.10	2.5±0.2	11.6±0.1	19.1±0.1	156.4	28
Hg—R‖	1.90	3.5±0.3	13.1±0.3	21.0±0.3	—	38
Sn—R_3‖	1.90	3.7±0.3	13.2±0.3	20.3±0.3	—	38
Si—R_3‖	1.85	3.63±0.05	14.63±0.05	20.36±0.05	140.28	30
Al—R_2**	1.5	6.3±0.3	15.3±0.3	21.4±0.3	—	38
Li††	1.0	7.1±0.5	19.3±0.5	23.9±0.5	—	39

*In the molecule CH_2=^{13}CHX.
†At infinite dilution in cyclohexane.
‡Coupling constants for three vinyl alkyl ethers in tetramethylsilane.
§In tetramethylsilane.
‖Pure compound.
¶Under pressure in carbon tetrachloride.
**As the etherate.
††In ethyl ether.

were accurately determined, preferably in solvents of low dielectric constant (e.g. the vinyl ethers were measured in tetramethylsilane); the J values were needed to cover the range 1 to 4 of E_X; the E_X values of the substituents were fairly reliable, i.e., the E_X values from different scales agreed fairly well.

E_X values from Pauling (11), Huggins (12), Gordy (13), Pritchard and Skinner (14), and

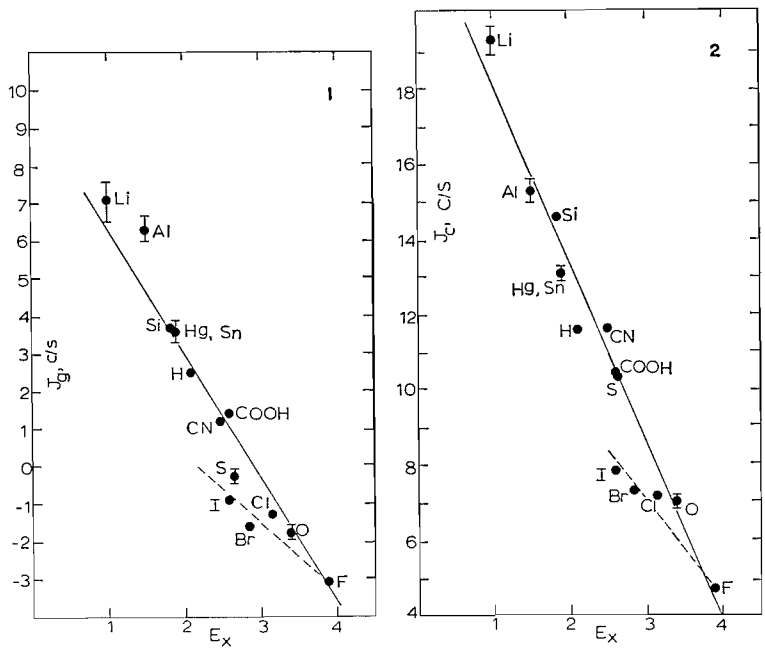

FIG. 1. The geminal proton coupling constant plotted versus the electronegativity of the substituent, E_X, in some vinyl compounds.
FIG. 2. A plot of the *cis* proton coupling constant versus E_X in some vinyl compounds.

Can. J. Chem. Downloaded from www.nrcresearchpress.com by 210.87.254.42 on 09/05/12
For personal use only.

from Cavanaugh and Dailey (15) were considered in arriving at the values in Table I. For substituent groups the E_X values of Cavanaugh and Dailey were favored since these derive from chemical shift measurements and have been used in a variety of coupling constant correlations (16, 17). In any case, the various E_X values do not deviate by more than about 0.1 unit from the set in Table I.

Linearity of the Correlation of J with E_X

In Figs. 1 to 4, the individual J_g, J_c, and J_t values and their sum are plotted versus E_X. The following features of these plots are noted. Within experimental error, with the *consistent* exception of I and Br, a change in E_X of 0.1 unit is sufficient to bring the J values on to the solid straight line. Two other exceptions are S, which deviates from the lines except for its J_c value, and Al where only J_g deviates outside of $\Delta E_X = 0.1$ limit.* A third exception is J_c for X = H. If I and Br are disregarded, 5 points out of 44 in Figs. 1 to 4 deviate outside the $\Delta E_X = 0.1$ limit. Out of these 5, S accounts for 3.

The points for I and Br, 8 in all, deviate negatively from the solid line. The extent of these deviations can best be measured from Fig. 4. The average deviation, including S but excluding I and Br, is 0.8 c/s in a range of about 36 c/s in $J_g + J_c + J_t$. The deviations of I and Br are −6.4 and −5.4 c/s, respectively; an average of −5.9 c/s. On the other hand, if S is excluded together with I and Br, an average deviation of 0.5 is found in 36 c/s and the average deviation of S, Br, and I is now −4.5 c/s.

It is suggested, therefore, that I and Br (and perhaps S) deviate significantly from the assumed straight line relationship. In other words, I and Br appear to be much more electronegative than the E_X values in Table I suggest. In fact, Br would appear to be more electronegative than Cl (see Fig. 4) and I about as electronegative as Cl. This anomaly is discussed below.

From the solid lines in Figs. 1 to 4, the dependence of the J values on E_X can be written

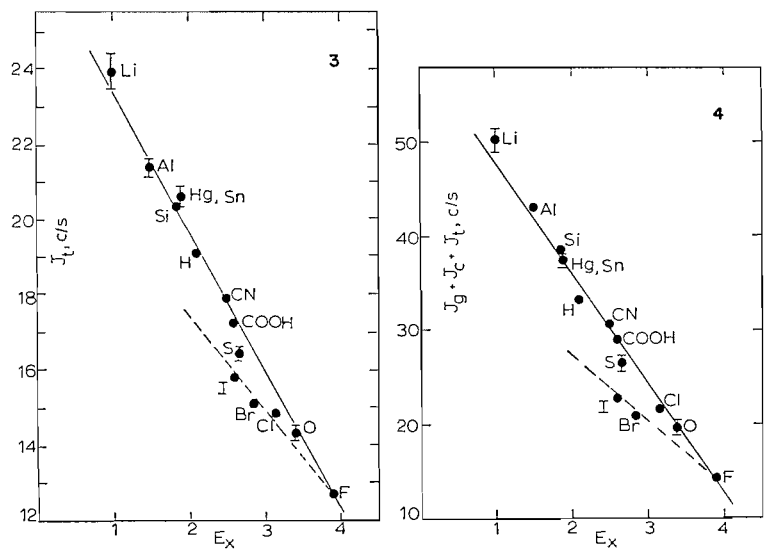

FIG. 3. A plot of the *trans* proton coupling constant versus E_X in some vinyl compounds.
FIG. 4. The sum of the geminal, *cis* and *trans* proton coupling constants plotted versus E_X in some vinyl compounds.

**The proton resonance spectrum is that of the etherate of trivinylaluminium and therefore there is an additional uncertainty in either J or E_X.*

Can. J. Chem. Downloaded from www.nrcresearchpress.com by 210.87.254.42 on 09/05/12
For personal use only.

as $\Delta J_c = -4.7\Delta E$, $\Delta J_t = -3.2\Delta E$, $\Delta J_g = -3.3\Delta E$, $\Delta(J_g + J_c + J_t) = -3.9\Delta E$. Karplus (5) predicts $\Delta J_c > \Delta J_t$. A recent review suggests $\Delta J_c = -4\Delta E$ and $\Delta J_t = -3.3\Delta E$ (4).

Discussion of the Deviations for I and Br

(a) J Dependence on Other Molecular Parameters

In addition to the E_X dependence, other factors which may affect the proton coupling constants in these compounds are changes in bond angle, C=C bond length, exchange integrals, bond excitation energies, π-bonding, and molecular vibrations (5). From the available structural data on the vinyl halides and ethylene (18–24) and from the estimates given by Karplus (5), it appears unlikely that changes in bond angle or C=C bond length are responsible for these deviations. Thus, the C=C bond length appears to vary by less than 0.01 Å and any bond angle changes are also too small. Theory predicts +1.5 c/s as the π-electron contribution to J_c and J_t in ethylene (25). Hence, any reasonable change in π-bonding in vinyl bromide and iodide is too small to account for the observed deviations. Whether the other three factors would account for them is not known.

(b) Relation of Deviations to a Hybridization Model

However, it is interesting to note that I and Br cause anomalies in other coupling constants as well. In their discussion of $J(^{13}C—H)$ in methane derivatives, Juan and Gutowsky (26, 27) define a quantity Δ_X. It is derived from the $J(^{13}C—H)$ values and expresses the affinity for s-character of the substituent X and is expected to follow E_X. For the halogens Δ_X is virtually the same in spite of the large range of E_X. More precisely, on the box model in which changes in $J(^{13}C—H)$ are caused solely by rehybridization of the C—H bond, the experimental $J(^{13}C—H)$ values lead to Δ_X values which follow the order Br > I > Cl > F. Br and I appear to be more electronegative than Cl or F.

Juan and Gutowsky extend their treatment to substituted ethylenes and calculate the s-character in the carbon orbital of the C—H bond in the system $=^{13}CHX$ by using the Δ_X values for the substituted methanes. By a variation of their procedure, we have calculated Δ_X values for the halogens, the cyano group, and silicon from the experimental $J(^{13}C—H)$ values in the system $=^{13}CHX$ as follows.* For substituted methanes Juan and Gutowsky (27) write

$$0.25\Delta_X J_0 = J_{CH}(CH_3X) - J_{CH}(CH_4) \quad [1]$$

$$J_{CH} = J_0\alpha_H^2 \quad [2]$$

where $J_0 = 500$ c/s and α_H^2 is the s-character of the carbon orbital in the C—H bond. For ethylene we write†

$$0.316\Delta_X J_0 = J_{CH}(CH_2{=}{}^{13}CHX) - J_{CH}(CH_2{=}CH_2) \quad [3]$$

$$J_{CH} = 156.4 \text{ c/s} = J_0\alpha_H^2 = (495 \text{ c/s})(0.316). \quad [4]$$

In these equations, account is taken of the actual structure of ethylene (22, 23) which has an HCH angle of 117.5°. Hence we use $\alpha_H^2 = 0.316$ for a C—H bond in ethylene and from the experimental $J(^{13}C—H)$ value in ethylene (28) the value $J_0 = 495$ c/s follows. This procedure normalizes to $\Delta_X = 0$ for H. From the available data (Table I) eq. [3] yields Δ_X values of F = 0.280, Cl = 0.240, Br = 0.257, I = 0.220, CN = 0.130, and Si = −0.097.

In Fig. 5 these Δ_X values are plotted versus E_X since they are expected to follow E_X,

*$J(^{13}C—H)$ values are not available for the other compounds in Table I.

†Contributions by π-electrons to $J(^{13}C—H)$ are expected to be ≈ 2 c/s (26, 31) and to vary little for the various substituents.

Can. J. Chem. Downloaded from www.nrcresearchpress.com by 210.87.254.42 on 09/05/12
For personal use only.

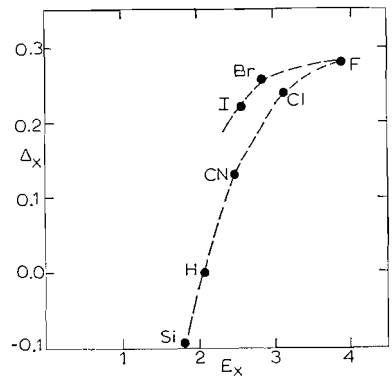

FIG. 5. The quantity Δ_X as defined and derived in the text for vinyl compounds plotted versus E_X.

although not necessarily linearly. F, Cl, H, CN, and Si appear to fall on a smooth curve, from which I and Br deviate considerably. Effective E_X values of I = 3.0 and Br = 3.4 bring them on to the curve. In Fig. 4, effective E_X values of I = 3.1 and Br = 3.3 bring them on to the straight line relating $J_g + J_c + J_t$ to E_X. In their effect both on $J(^{13}C—H)$ and on $J_g + J_c + J_t$, I and Br appear to be much more electronegative than is normally accepted.

It seems reasonable to conclude that the anomalies in $J(^{13}C—H)$ and $J_c + J_g + J_t$ have a common origin. This behavior is expected if rehybridization is the reason for the change in $J(^{13}C—H)$ on substitution, since Karplus (5) finds the reason for the decrease in J_c and J_t as E_X increases in the rehybridization of the carbon atoms in the fragment HCCH.

(c) Rehybridization at the β-Carbon

J_c and J_t will depend also on the rehybridization of the β-carbon in CH_2=CHX. From the available data (8, 29, 30) it appears, however, that this is much smaller at the β-carbon. In structure I the $J(^{13}C—H_2)$ and $J(^{13}C—H_3)$ values are given in c/s. Juan and Gutowsky

X	$^{13}C—H_2$	$^{13}C—H_3$		X	$^{13}C—H_2$	$^{13}C—H_3$
CN	165.42	163.20		Br	160.26	163.63
F	162.16	159.18		I	159.20	164.09
Cl	160.89	162.64		Si	156.45	156.13

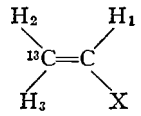

I

(27) suggest possible interactions between lone pairs on the substituent and the C—H bonds which affect $J(^{13}C—H)$ but not the s-character of the C—H bond. In that case, $J(^{13}C—H_2)$ would be least affected by such interactions. According to these authors, changes in the polarity of the C—H bond (ionic terms in the bond wave function) do not make an important contribution to $J(^{13}C—H)$.* Nevertheless, we note that $J(^{13}C—H_2)$ for H, I, Br, Cl, F, CN vary smoothly in the expected direction with the parameter μ/r, where μ is the substituent dipole moment and r is the C—X bond length. Thus, CN with $\mu \simeq 4$ D causes the largest change in $J(^{13}C—H_2)$, as would be expected if the C—H_2 bond is being polarized by electric fields to favor a contributing structure C^-H^+.

**The small deviations from addivity in polysubstituted halomethanes are in the wrong direction to be explained by polarity effects.*

Can. J. Chem. Downloaded from www.nrcresearchpress.com by 210.87.254.42 on 09/05/12
For personal use only.

The $J(^{13}C—H_3)$ values do not vary in this way, the largest values occurring for I and Br. An interaction between the lone pairs on I and Br and the C—H_3 bond is again possible here. How such interactions would affect J_c and J_t is not obvious but a detailed theory will have to account for the parallel deviations of J_c, J_t, and $J(^{13}C—H)$. J_g behaves like J_c and J_t (Figs. 1 to 4) but the HCCH fragment calculations (5) do not make any predictions on this matter.

(d) Objections to the Rehybridization Model

Ranft (31) accepts the rehybridization model and rationalizes the anomalies in $J(^{13}C—H)$ for the methyl halides by writing

$$[5] \qquad J(^{13}C—H) = 64 + 15.4r(C—X)E_X.$$

In this way the calculated E_X values for the halogens agree well with their normally accepted values. Support for eq. [5] comes from the work of Bent (32). The p-character of the carbon orbitals concentrates in the direction of the more electronegative substituent (hence the E_X dependence of $J(^{13}C—H)$); while increasing p-character in the carbon bond to a more distant substituent increases overlap and therefore the C—X bond energy (hence the dependence of $J(^{13}C—H)$ on $r(C—X)$).

A necessary consequence is the concept of bent bonds as pointed out originally by Muller and Pritchard (33). This is because the "interorbital" angles corresponding to the hybridization parameters obtained from $J(^{13}C—H)$ data are consistently smaller than the observed bond angles (26). There is conflicting evidence as to whether the maximum electron density of a σ-bond always lies along the internuclear line or not (34, 35). In view of the behavior of the three $^{13}C—H$ couplings discussed above, it may be best not to treat $J(^{13}C—H)$ data as support for the concept of bent bonds.

CONCLUSIONS

The geminal, *cis* and *trans* proton coupling constants in vinyl bromide and vinyl iodide (and perhaps vinyl sulfide) show significant deviations from the linear inverse relationship between coupling constants and the electronegativity of the substitutent in vinyl compounds. An adaptation of the box model to the $J(^{13}C—H)$ values in vinyl compounds suggests that these anomalies in proton coupling constants are closely related to anomalies in $J(^{13}C—H)$ in vinyl bromide and vinyl iodide.

ACKNOWLEDGMENTS

T. S. is grateful for hospitality received at the National Physical Laboratory, Teddington, where part of this paper was written. We gratefully acknowledge financial support from the National Research Council, Ottawa.

REFERENCES

1. C. N. Banwell and N. Sheppard. Mol. Phys. **3**, 351 (1960).
2. J. S. Waugh and S. Castellano. J. Chem. Phys. **35**, 1900 (1961).
3. T. Schaefer. Can. J. Chem. **40**, 1 (1962).
4. C. N. Banwell and N. Sheppard. Discussions Faraday Soc. **34**, 115 (1962).
5. M. Karplus. J. Am. Chem. Soc. **85**, 2870 (1963).
6. E. Hiroike. J. Phys. Soc. Japan, **15**, 270 (1960).
7. J. Ranft. Anal. Phys. **9**, 124 (1962).
8. R. E. Mayo and J. H. Goldstein. J. Mol. Spectry. **14**, 273 (1964).
9. V. S. Watts and J. H. Goldstein. J. Chem. Phys. **42**, 228 (1965).
10. P. Bates, S. Cawley, and S. S. Danyluk. J. Chem. Phys. **40**, 2415 (1964).
11. L. Pauling. Nature of the chemical bond. 3rd ed. Cornell University Press, Ithaca, N.Y. 1960.
12. M. L. Huggins. J. Am. Chem. Soc. **75**, 4123 (1953).
13. W. Gordy. J. Chem. Phys. **14**, 305 (1946).

Can. J. Chem. Downloaded from www.nrcresearchpress.com by 210.87.254.42 on 09/05/12
For personal use only.

14. H. O. PRITCHARD and H. A. SKINNER. Chem. Rev. **55**, 745 (1955).
15. J. R. CAVANAUGH and B. P. DAILEY. J. Chem. Phys. **34**, 1099 (1961).
16. K. L. WILLIAMSON, C. A. LANFORD, and C. R. NICHOLSON. J. Am. Chem. Soc. **86**, 762 (1964).
17. P. LASZLO and P. VON R. SCHLEYER. J. Am. Chem. Soc. **85**, 2709 (1963).
18. D. KIVELSON and E. B. WILSON. J. Chem. Phy. **32**, 205 (1960).
19. B. BAK, D. CHRISTENSON, L. HANSEN-NYGARD, and J. RASTRUP-ANDERSON. Spectrochim. Acta, **13**, 120 (1958).
20. H. W. MORGAN and J. H. GOLDSTEIN. J. Chem. Phys. **30**, 1025 (1959).
21. L. S. BARTELL and R. A. BONHAM. J. Chem. Phys. **27**, 1414 (1957).
22. H. C. ALLEN and E. K. PLYLER. J. Am. Chem. Soc. **80**, 2673, (1958).
23. J. M. DOWLING and B. P. STOICHEFF. Can. J. Phys. **37**, 703 (1959).
24. R. E. GOEDERTIER. J. Phys. Radium, **24**, 633 (1963).
25. M. KARPLUS. J. Chem. Phys. **33**, 1842 (1960).
26. C. JUAN and H. S. GUTOWSKY. J. Chem. Phys. **37**, 2198 (1962).
27. C. JUAN and H. S. GUTOWSKY. Discussions Faraday Soc. **34**, 52 (1962).
28. R. M. LYNDEN-BELL and N. SHEPPARD. Proc. Roy. Soc. London, Ser A, **269**, 385 (1962).
29. R. FREEMAN. J. Chem. Phys. **40**, 3571 (1964).
30. R. T. HOBGOOD, R. E. MAYO, and J. H. GOLDSTEIN. J. Chem. Phys. **39**, 2501 (1963).
31. J. RANFT. Anal. Phys. **10**, 399 (1963).
32. H. A. BENT. Chem. Rev. **61**, 275 (1961).
33. N. MULLER and D. PRITCHARD. J. Chem. Phys. **31**, 768, 1471 (1959).
34. W. H. FLYGARE. Science, **140**, 1179 (1963).
35. L. S. BARTELL, B. L. CARROLL, and J. P. GUILLORY. Tetrahedron Letters, **13**, 705 (1964).
36. R. T. HOBGOOD, G. S. REDDY, and J. H. GOLDSTEIN. J. Phys. Chem. **67**, 110 (1963).
37. J. S. WAUGH and S. CASTELLANO. J. Chem. Phys. **34**, 295 (1961).
38. D. W. MOORE and J. A. HAPPE. J. Phys. Chem. **65**, 224 (1961).
39. C. S. JOHNSON, M. A. WEINER, J. S. WAUGH, and D. SEYFERTH. J. Am. Chem. Soc. **83**, 1306 (1961).

Can. J. Chem. Downloaded from www.nrcresearchpress.com by 210.87.254.42 on 09/05/12
For personal use only.

Can. J. Chem. Downloaded from www.nrcresearchpress.com by 210.87.254.6 on 09/05/12
For personal use only.

THE DIFFUSE LAYER CORRECTION TO THE DISCRETE-ION EFFECT IN ELECTRIC DOUBLE LAYER THEORY

S. LEVINE
Department of Mathematics, University of Manchester, Manchester, England

J. MINGINS
Chemical Physics Division, Unilever Research Laboratory, Port Sunlight, Cheshire, England

AND

G. M. BELL
Department of Mathematics, Chelsea College of Science and Technology, London, England

Received December 6, 1963, and, as revised, May 25, 1965

ABSTRACT

The screening effect of the diffuse layer on the self-atmosphere (or discrete-ion) potential of a counter-ion adsorbed from aqueous electrolyte on to a plane charged interface is investigated. A theory based on Fourier–Bessel integrals and the approximate method of Loeb and Williams for treating the potential distribution in the diffuse layer is presented. The distribution of counter-ions in the adsorption plane surrounding a specified ion adsorbed in the plane is expressed in terms of a two-dimensional grand canonical ensemble and this is approximated by a 'revised cut-off model'. The 'Grahame cut-off model' is an approximation to the adsorbed counter-ion distribution based on a canonical ensemble and we present arguments to show that this interpretation is incorrect. We also show that the radius of the revised disc is, in general, smaller than that of the Grahame disc but approaches it at large charge densities (σ_β) of counter-ions in the Stern inner region. Comparison is made with an alternative approach to this discrete-ion effect by Buff and Stillinger, who also applied a Fourier–Bessel technique to the mercury – aqueous electrolyte system. Their results provide a lower estimate to the magnitude of the self-atmosphere potential, whereas our revised cut-off model gives an upper estimate. A third method, which assumes the adsorbed ions to be situated on a hexagonal lattice, is also discussed and is found to give a potential larger than the upper estimate of the revised cut-off approach.

It is shown that the effect of the diffuse layer is to diminish the discrete-ion potential at the adsorbed ion. When the electrolyte concentration tends to zero the results with the Grahame model reduce to those derived in an earlier paper from the method of multiple electrostatic images. Calculations on the discrete-ion potential at an adsorbed counter-ion are given for metallic and dielectric surfaces in contact with an aqueous 1–1 electrolyte solution and the parameters of the inner region are chosen to be consistent with known data on mercury and silver iodide systems. It is shown in both cases that on dilute salt solutions ($\lesssim M/100$) the diffuse layer screening is small compared to the unscreened term except at small charge densities of counter-ions in the inner region.

1. INTRODUCTION

The theory of the discrete-ion (or discreteness-of-charge) effect for adsorbed ions has recently been applied to a variety of charged interfaces in aqueous electrolyte systems and though still in its initial stages, it has explained, certainly in a qualitative manner, several phenomena quite inconsistent with the classical Gouy–Chapman–Stern double layer theory. The adequacy and applicability of the theory to the experimental situation has been the topic of a number of papers (1–12) and here we need only mention some results of the comparison with experiment. The discrete-ion effect was originally introduced to explain the Esin–Markov effect, which is concerned with the dependence on electrolyte concentration of the potential of the electrocapillary maximum for the mercury–electrolyte interface. Evidence has been obtained for the mercury–electrolyte interface (13), silver halide – electrolyte interfaces (see refs. 6, 7, 8, 14, 15), and fully ionized monolayers (11) that the potential at the inner boundary of the diffuse layer (the outer Helmholtz plane or O.H.P.) passes through a maximum when the primary charge at the interface

is increased at fixed ionic strength in the electrolyte medium. This behavior is accompanied by an apparent strong dependence of the Stern specific (chemical) adsorption energy of counter-ions on the electrical conditions at the interface (see ref. 11). Two anomalous stability properties found for example with silver halide sols are (i) a decrease in concentration of coagulating electrolyte (i.e. a decrease in stability) with increase in the surface density of potential-determining ions (6, 7, 8, 16), particularly with polyvalent coagulating ions and (ii) the phenomenon of mutual antagonism in the presence of mixed coagulating electrolytes (17). All these properties find a common explanation in the discrete-ion effect.

Three different approaches to the discrete-ion effect have been proposed. The earliest one is that of Soviet authors (1–4) who account for the discrete nature of the adsorbed ions by representing the distribution of these ions in the Stern layer (inner Helmholtz plane or I.H.P.) by a regular hexagonal array and this model has very recently been examined by Barlow and Macdonald (18) (see also Stigter (38)). In the second method, which has been developed by the present authors (6–12), the discrete-ion effect for the adsorbed counter-ions is described in terms of a lateral repulsion between neighboring counter-ions in the case where these are all of the same sign. Consequently in the adsorption plane each counter-ion is surrounded by an area in which the mean surface charge distribution is strongly depleted. This depletion causes a change in the potential at the adsorbed ion, and this change may be called the self-atmosphere or fluctuation potential. The resultant mean potential at the center of an adsorbed ion due to its Coulomb interaction with all the surrounding ions (minus the 'self-image' potential) has been called the micropotential, and the basis of the discrete-ion effect is that this potential differs from the mean electrostatic potential at the adsorption plane, which is called the macropotential. Following Grahame (19) we imagine that each (fully charged) adsorbed ion is situated at the center of a disc which is free of adsorbed charge and has an area equal to the average area per adsorbed counter-ion. This method, which we shall call the 'Grahame cut-off' approximation, has been used in the earlier papers by us (6–12). In this paper, investigations of this model by statistical mechanics show that the radius of the Grahame disc, which is to be free of adsorbed charge, is too large, particularly at small densities of adsorbed ions; we shall refer to the model of the appropriate smaller disc as the 'revised cut-off' approximation. The third method is that of Buff and Stillinger (20) who have recently applied cluster theory to the discrete-ion effect for adsorbed ions in the mercury–electrolyte system. Their key assumption is that the electrostatic forces between adsorbed ions are weak because of the proximity of the conducting mercury surface and they conclude that the pair distribution function of the adsorbed ions is mainly governed by the short-range forces between them. For the hard-sphere model this is equivalent to choosing a cut-off disc having as radius the distance of nearest approach between two adsorbed ions and thus their approach bears some resemblance to that used by us.

Buff and Stillinger criticize (at least for the mercury surface) the model of the plane hexagonal lattice of surface ions which has been used to account for the discrete-ion effect (1–5). The hexagonal lattice is the configuration minimizing the electrostatic interaction energy of the adsorbed ions and it might appear that this should be a reasonable model for the distribution of ions around a given ion in the adsorption plane, provided the electrostatic energy of the ion with its neighbors and their images in the planes of dielectric discontinuities at the interface is appreciably greater than $\mathbf{k}T$, where $\mathbf{k}$ is Boltzmann's constant and T the absolute temperature. However, the validity of a highly ordered two-dimensional structure is not only governed by the magnitude of this energy. A better criterion is probably the steepness of the potential well which characterizes the cell in

Can. J. Chem. Downloaded from www.nrcresearchpress.com by 210.87.254.6 on 09/05/12
For personal use only.

Can. J. Chem. Downloaded from www.nrcresearchpress.com by 210.87.254.6 on 09/05/12
For personal use only.

which the adsorbed ion is subjected to thermal motion. We have therefore recently investigated the effect of temperature on a hexagonal array of point charges at the mercury surface (21). Making use of the equipartition theorem in statistical mechanics the root mean square displacement $(\overline{r^2})^{1/2}$ of an adsorbed ion in the field of the surrounding lattice ions, which are all fixed in their lattice positions, is calculated. This displacement can be regarded as the mean radius of the 'blur' in the ion's position due to its thermal motion. When the radius of the blur exceeds half of the nearest neighbor distance ($s/2$) then the central ion has left its oxn hexagonal cell and this must mean that the lattice structure is breaking down. In the absence of diffuse layer screening at the mercury surface and for the double layer parameters given in Fig. 2, $(\overline{r^2})^{1/2} = s/2$ at an area per univalent surface ion of 85 Å^2, corresponding to a surface charge density of 19 μC/cm^2. If the effect of the diffuse layer is included, the repulsive forces between the adsorbed ions are reduced, so that the lattice would become unstable at lower areas. In the limiting case where the O.H.P. is assumed to be a perfect conductor, $(\overline{r^2})^{1/2} = s/2$ at an area of 70 Å^2 per adsorbed ion. In recent unpublished work we have found that the lattice structure breaks down at similar charge densities for the silver halide – water interface. This seems to bear out Buff and Stillinger's objection to the lattice model since the results indicate that the hexagonal lattice is not a good description of the relative positions of adsorbed ions except at high densities of adsorbed (univalent) ions. As a result of the breakdown of the hexagonal lattice at $\sigma_\beta < 15$–20 μC/cm^2, the probability of ions approaching to within distances appreciably closer than the nearest neighbor distance s in the hexagonal lattice is quite large. In our opinion, the adsorbed layer of counter-ions should behave more like a two-dimensional dense gas than like a solid, for such σ_β. Nevertheless, we shall show that all three methods of treating the discrete-ion effect give similar results for the self-atmosphere potential at an adsorbed ion at the mercury–water interface.

The hexagonal lattice and Grahame cut-off models may be regarded as similar approaches to the problem. The hexagonal lattice around a specified ion can be replaced by a smoothed-out charge having the mean surface charge density and giving the same potential as the lattice at the center of the ion. We find that this ion is now at the center of a circular 'hole' free of charge, which corresponds to the disc in the Grahame model, but has a different (larger) radius. Whereas the rigid lattice structure takes no account of thermal motion the Grahame model is superior in that it does allow for such motion, although to a rather arbitrary extent which is independent of temperature. If we assume no oscillations in the two-dimensional pair distribution function of adsorbed ions (i.e. we exclude high charge densities exceeding ~ 20 μC/cm^2), then we are able to show that, quite independently of the nature of the planes bounding the 'Stern' inner region, both the revised and Grahame cut-off approximations overestimate the absolute magnitude of the self-atmosphere potential. But it follows from the comparisons by Krylov (5) and Barlow and Macdonald (18) of the hexagonal lattice and Grahame models that the latter gives a smaller absolute value for the self-atmosphere potential and is therefore the more accurate. We shall show that the revised cut-off model is more accurate than the Grahame one, but the differences are small in the mercury case. Krylov (5) has applied the results of the hexagonal lattice and Grahame models to the experimental adsorption isotherms of HCl and HBr at the air–water interface and finds that the Grahame model gives the closer agreement between the calculated and experimental so-called Esin–Markov coefficients. One point in favor of the lattice model is that if the thermal motion is approximated by small (harmonic) oscillations about the lattice sites, then a term $\mathbf{k}T/z_\beta e_0$ is added to the micropotential (21) where e_0 is the proton charge and z_β the valency of the adsorbed ion.

Can. J. Chem. Downloaded from www.nrcresearchpress.com by 210.87.254.6 on 09/05/12
For personal use only.

Since this term is independent of the density of adsorbed ions it can be ignored in the discrete-ion theory and can be treated as part of the true specific adsorption energy.

We shall also show that again in the absence of oscillations in the pair distribution function the Buff–Stillinger hard-sphere model provides a lower estimate in the magnitude of the self-atmosphere potential. However, when the O.H.P. in the mercury system is assumed to be a perfect conductor, and is separated from the mercury wall by a distance less than the distance of nearest approach of two adsorbed ions, then this lower estimate from the hard-sphere model differs at the most by 10% from the upper estimate that can be obtained with the cut-off model. The reason for this good agreement is essentially the short-range character of the electrostatic interaction of two adsorbed ions situated between two metallic walls, as stressed by Buff and Stillinger. When the O.H.P. is replaced by an aqueous diffuse layer the short-range character is less marked but the above results are not greatly altered; since the exact value of the radius of the equivalent circular hole for the lattice model, as mentioned above, is likewise of secondary importance we can understand why all three models agree. Because of the short-range character of the electrostatic interaction between the surface ions at the mercury surface the self-atmosphere potentials calculated from both the hexagonal lattice and Grahame models may be quite good approximations even when neither model gives an accurate picture of the surface ion-pair distribution function. In the case of a dielectric – aqueous electrolyte interface, the interaction of two adsorbed ions is no longer of such short-range nature and hence we must expect a greater difference between Buff and Stillinger's theory and our two cut-off models.

Two problems which have so far been largely ignored are the effect of the thermal motion of the adsorbed ions and the screening effect of the diffuse layer on the self-atmosphere potential. The first, a more difficult problem will be considered in a later paper and here we shall only investigate the diffuse layer screening for the cut-off approximation. In their treatment of the discrete-ion effect for the head-group ions of an ionized monolayer, Bell, Levine, and Pethica (10) allowed for the diffuse layer by placing in the bulk solution at a depth equal to the Debye–Hückel thickness of the diffuse layer, an imaginary charged disc, similar to the one used in the cut-off approximation but oppositely charged. On 0.1 M 1–1 electrolyte solution this screening term amounted to a significant factor whose magnitude depended on the surface concentration of head-group ions, but on 0.001 M the effect was negligible compared with the unscreened term except at high areas per head-group ion. The diffuse layer correction tended to reduce the magnitude of the self-atmosphere potential and, as to be expected, assumed a greater proportion of this potential with increase in area per head-group ion. In the present paper we shall develop a more rigorous method of calculating the screening effect of the diffuse layer on the self-atmosphere potential at an adsorbed counter-ion. The method of multiple imaging used in previous papers (9, 11) to determine the self-atmosphere potential is replaced here by a more general technique involving the use of Fourier–Bessel integrals. (Throughout this paper ref. 9 will be designated I.) This approach was used over 30 years ago by Oka (22) and at a later date by Schmutzer (23) in the related problem of the surface tension of electrolyte solutions. The technique has been introduced recently into the double layer problem by Buff and Stillinger (20) but we had independently worked out the main details in the present paper prior to the publication of their work, and are indebted to Prof. F. J. Ursell for suggesting the general method. Fourier transforms have also been introduced by Hurst and Jordine (36) in the problem of the electrostatic interaction of montmorillonite plates. Recently Krylov and Levich (24) investigated the potential distribution in the diffuse layer in the presence of a discrete layer of adsorbed ions in the Stern layer.

However, their emphasis and method of treating the diffuse layer, which resembles that of Stillinger and Kirkwood (25), are different from those used in this paper.

2. THE CUT-OFF DISC MODEL AND THE CONDITION OF ELECTRICAL NEUTRALITY

We shall adopt the model of Grahame (13, 19) and Devanathan (26) for the electric double layer as shown in Fig. 1. The mean charge densities on the wall, the inner Helmholtz plane, and the diffuse layer are σ_0, σ_β, and σ_d respectively. The I.H.P. and O.H.P. are situated at distances β and $d(>\beta)$ from the wall. We assume that the inner region of thickness d is a uniform medium of dielectric constant ϵ_1 and take the dielectric constants of the diffuse layer (ϵ) and the wall-medium (ϵ_2) as equal to the bulk value of the aqueous and nonaqueous phases respectively. More elaborate models of the inner region have been introduced by Devanathan (26), Mott, Parsons, and Watts-Tobin (27), and more recently by Bockris, Devanathan, and Müller (28). Our analysis could be extended, for example, to the case where the two zones of the inner region separated by the I.H.P. have different dielectric constants but for simplicity we shall confine ourselves to a single dielectric constant which may be regarded as an appropriate mean. The mean electrostatic potentials at the wall, the I.H.P., and the O.H.P. are ψ_0, ψ_β, and ψ_d respectively. We wish to determine the mean electrostatic potential or micropotential at the center of an ion of charge $z_\beta e_0$ adsorbed on the I.H.P. This potential can be written as $\psi_\beta + \phi_\beta$, where ϕ_β is the self-atmosphere or fluctuation potential associated with the discrete character of the ionic charge. In order to calculate ϕ_β, the mean surface charge density surrounding the specified ion $z_\beta e_0$ is required.

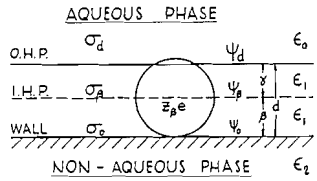

FIG. 1. Model of the electric double layer.

The use of an adsorption isotherm for counter-ions in electric double layer theory is meaningful provided the adsorbed layer is treated as a separate phase. In applying the methods of statistical mechanics we can choose a canonical ensemble (closed system) for the adsorbed phase so that the total number of adsorbed ions N is fixed. Thus we are working with a subspace of the entire configurational part of the phase space available to the ions and this is permissible for large enough N. The electrochemical potential of the adsorbed ions must be a function of their number N which is a thermodynamic variable, and hence, by definition, the fluctuation potential ϕ_β is calculated for specified N. If $g(\rho)$ is the two-dimensional pair distribution function for adsorbed ions at separation ρ in the I.H.P. and the adsorbed phase is treated as a two-dimensional fluid, then from statistical mechanics (see Hill, p. 185 (29)), we have the 'canonical normalization' condition,

$$[2.1] \qquad \frac{N}{A}\int_A g(\rho)\,\mathrm{d}A = N - 1,$$

where we integrate over the area A of the I.H.P. This relation amounts to the statement that the integral of the fluctuation surface density of ions is -1 and it is applicable to any

Can. J. Chem. Downloaded from www.nrcresearchpress.com by 210.87.254.6 on 09/05/12
For personal use only.

type of intermolecular force. The mean surface charge density in the I.H.P. at distance ρ from a specified ion $z_\beta e_0$ may be written as

$$z_\beta e_0 q(\rho) = \sigma_\beta + S(\rho), \qquad [2.2]$$

where $S(\rho)$ is the (canonical ensemble) fluctuation surface charge density due to the presence of this ion at position $\rho = 0$. By substitution of $\sigma_\beta = Nz_\beta e_0/A$, [2.1] becomes the electrical neutrality condition

$$\int_A S(\rho)\, dA = -z_\beta e_0. \qquad [2.3]$$

An important but difficult problem relevant to the accuracy of the cut-off approximation is the asymptotic behavior of $S(\rho)$ at large ρ. If the adsorbed phase is treated as open, i.e. we use a grand canonical ensemble for the adsorbed ions, then the fluctuation surface charge density becomes $S^*(\rho)$, such that $S^*(\rho) \to 0$ as $\rho \to \infty$ and

$$S(\rho) = S^*(\rho) - z_\beta e_0 k_A(\sigma_\beta)/A, \qquad [2.4]$$

where the form of $k_A(\sigma_\beta)$, which is a positive proper fraction, is discussed in Appendix A. Substituting [2.4] into [2.3], we may allow A to become infinite when integrating $S^*(\rho)$ and so

$$2\pi \int_0^\infty \rho S^*(\rho)\, d\rho = -z_\beta e_0[1 - k_A(\sigma_\beta)]. \qquad [2.5]$$

If $V(\rho)$ is the potential of the mean force between two adsorbed ions at separation ρ, averaged over all configurations of the other ions, in a grand canonical ensemble for the adsorbed phase, then $V(\rho) \to 0$ as $\rho \to \infty$ and

$$S^*(\rho) = \sigma_\beta[\exp(-V(\rho)/\mathbf{k}T) - 1]. \qquad [2.6]$$

We shall show below how [2.5] can be used to obtain qualitative information concerning $V(\rho)$ and the self-atmosphere potential ϕ_β.

It is convenient to introduce r_β defined by

$$\pi r_\beta^2 \sigma_\beta = z_\beta e_0[1 - k_A(\sigma_\beta)]. \qquad [2.7]$$

Then [2.5] and [2.6] will be satisfied by the hypothetical distribution function

$$V(\rho) = \infty,\ \rho < r_\beta; \qquad V(\rho) = 0,\ \rho > r_\beta, \qquad [2.8]$$

which describes the revised cut-off approximation. If $|k_A(\sigma_\beta)| \ll 1$, then r_β becomes the radius r_0 of the disc whose area is equal to the average area available to an adsorbed ion, and so

$$\pi r_0^2 \sigma_\beta = z_\beta e_0. \qquad [2.9]$$

This is the Grahame cut-off approximation, used in the previous papers by the authors (6–12). The following interpretation of $k_A(\sigma_\beta)$, which is proved in Appendix A, suggests that $k_A(\sigma_\beta)$ is small at large σ_β. Consider a grand canonical ensemble for the phase of adsorbed counter-ions and suppose that $z_\beta e_0$ is fixed in position at $\rho = 0$. This ion now becomes the center of an external force field and the total number of mobile adsorbed ions has been reduced by 1. To restore thermodynamic equilibrium, counter-ions will tend to cross the O.H.P. from the diffuse layer into the inner region. Since the charge density σ_β is unaltered at large ρ in a grand canonical ensemble, such a movement of ions can only

Can. J. Chem. Downloaded from www.nrcresearchpress.com by 210.87.254.6 on 09/05/12
For personal use only.

occur in the vicinity of the fixed ion at $\rho = 0$. The quantity $k_A(\sigma_\beta)$ is the 'mean fraction' of one ion that enters the adsorbed phase. Clearly, for high densities, the I.H.P. cannot accommodate this ion under the necessary condition of fixed σ_β at large ρ and so $k_A(\sigma_\beta)$ is small. From [2.7] and [2.9]

$$[2.10] \qquad r_\beta/r_0 = [1 - k_A(\sigma_\beta)]^{1/2} < 1.$$

By [2.5]–[2.7], we can also write

$$[2.11] \qquad r_\beta^2 = 2\int_0^\infty \rho[1 - \exp(-V(\rho)/\mathbf{k}T)]\,d\rho = a^2 + 2\int_a^\infty \rho[1 - \exp(-V(\rho)/\mathbf{k}T)]\,d\rho$$

and this is equivalent to

$$[2.12] \qquad k_A(\sigma_\beta) = 1 - \frac{a^2}{r_0^2} - \frac{2}{r_0^2}\int_a^\infty \rho[1 - \exp(-V(\rho)/\mathbf{k}T)]\,d\rho.$$

As $\sigma_\beta \to 0$, $r_0 \to \infty$, but provided the integral in [2.11] or [2.12] converges, $k_A(\sigma_\beta) \to 1$ and r_β tends to a finite upper limit. The more short-range the function $V(\rho)$, the larger is $k_A(\sigma_\beta)$ and the smaller is this limiting value of r_β.

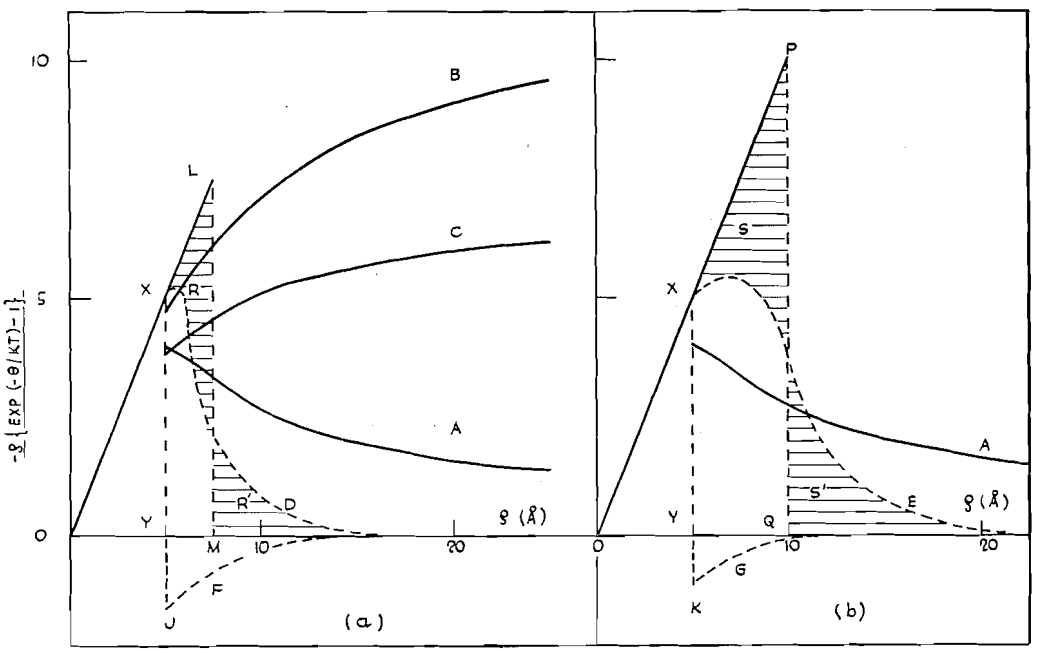

FIG. 2. Behavior of the pair distribution function $\exp(-\theta/\mathbf{k}T)$ where θ is $V(\rho)$ or $U(\rho)$. The quantity $2\pi\sigma_\beta \exp(-U(\rho)/\mathbf{k}T)$ is the mean charge in the I.H.P. lying between ρ and $\rho + d\rho$ when an adsorbed ion is situated at $\rho = 0$. The corresponding charge that would be present in the same area $(\rho, \rho + d\rho)$ in the absence of the adsorbed ion is $2\pi\sigma_\beta\rho\,d\rho$ and the function plotted in curves A, B, and C is proportional to the difference between these charges. Curves A, B, and C describe respectively mercury, silver iodide, and bulk electrolyte with the following parameters at 20°. A. Hg. $\epsilon = 80.1$, $\epsilon_1 = 10$, $\epsilon_2 = \infty$, $\beta = 3$, $\gamma = 2$. B. AgI. $\epsilon = 80.1$, $\epsilon_1 = 10$, $\epsilon_2 = 15$, $\beta = 3$, $\gamma = 1$. C. Bulk electrolyte. $\epsilon = 80.1$. Triangle OXY represents the Buff–Stillinger hard-sphere model, $a = 5$ Å.

The dashed curves D and E describe the hypothetical behavior of the pair distribution function $\exp(-V(\rho)/\mathbf{k}T)$ for the mercury–electrolyte system at ordinary values of σ_β. The radius r_β equals 7.5 Å in *a* and 10 Å in *b*. Curves D and E are so chosen that area $R = R'$ and $S = S'$ as required by the electrical neutrality condition. Curves F and G depict the general trend of the pair distribution function from the Helfand, Frisch, and Lebowitz model. The points J and K are calculated from [2.13] with $a = 5$ Å.

Can. J. Chem. Downloaded from www.nrcresearchpress.com by 210.87.254.6 on 09/05/12
For personal use only.

Can. J. Chem. Downloaded from www.nrcresearchpress.com by 210.87.254.6 on 09/05/12
For personal use only.

In Figs. 2*a* and 2*b*, which depict $\rho[1 - \exp(-V(\rho)/\mathbf{k}T)]$ as a function of ρ, the form [2.8] is represented by the triangles OLM and OPQ where $r_\beta = 7.5$ and 10 Å respectively. The two broken curves D and E illustrate possible forms of the true distribution function $V(\rho)$ satisfying [2.5]–[2.7] for the above values of r_β and these curves are obtained as follows. If a, the distance of nearest approach between two ions, equals 5 Å, then the condition [2.7] requires that the respective shaded areas be equal (i.e. $R = R'$ and $S = S'$). From our knowledge of the Debye–Hückel theory, we suggest that because of diffuse layer screening, $V(\rho)$ dies off exponentially with ρ at large ρ. The curves D and E are known for $\rho < a$ (the hard-sphere part where $V(\rho) = \infty$) and we have joined the two parts at large and small ρ by a continuously turning curve. Now according to Stillinger and Kirkwood (25), Krylov and Levich (24), and Martynov and Derjaguin (30) oscillations occur in the potential distribution in the diffuse layer at large electrolyte concentrations (> 0.6 M for the 1–1 valency type) because of ion size, although apparently these oscillations are weak. At low σ_β, similar oscillations in $S^*(\rho)$ are unlikely and we exclude their possibility or assume them unimportant in Fig. 2, i.e. we regard the adsorbed layer of counter-ions as a two-dimensional gas.

For the Buff–Stillinger hard-sphere model with small σ_β, $V(\rho) = \infty$, $\rho < a$, and $V(\rho) = 0$, $\rho > a$ and in Fig. 2, this model is represented by the triangular form OXY. At larger σ_β, one could use the theory of a two-dimensional fluid given by Helfand, Frisch, and Lebowitz (31). When two spheres of such a fluid are in contact (at separation a) their (canonical ensemble) distribution function reads in our notation

$$q(a) = \frac{1}{2}\left[\left\{1 - \left(\frac{a}{2r_0}\right)^2\right\}^{-1} + \left\{1 - \left(\frac{a}{2r_0}\right)^2\right\}^{-2}\right]. \qquad [2.13]$$

At $a = 5$ Å and $r_0 = 7.5$ and 10 Å, $q(a) = 1.20$ and 1.10 respectively. Curves F and G in Figs. 2*a* and 2*b* respectively show the expected form of $\rho(1 - q(\rho))$ for $r_0 = 7.5$ and 10 Å with this model. It might appear that the normalization condition [2.1] is not satisfied by the models of Buff and Stillinger and Helfand, Frisch, and Lebowitz. However, their hard-sphere models strictly apply to uncharged species in a canonical ensemble and this means that at large ρ, their function $q(\rho) = -k_A/A$, where the fraction k_A is of the order of 1. Hence, in Figs. 2*a* and 2*b*, the functions $\rho(1 - q(\rho))$ for hard-spheres have very long 'tails' (which are not shown in the diagrams) extending to the very edge of the interface and lying just above the ρ-axis at large ρ. These ensure that the condition [2.1] is satisfied. For example, in Fig. 2*a*, the area under this tail beyond the distance $\rho = r_0$ must compensate exactly the area bounded by the two ordinates $\rho = a$ and $\rho = r_0$, the line OL, and either the ρ-axis in the Buff–Stillinger theory or the curve JF in the Helfand–Frisch–Lebowitz theory. The contribution to the self-atmosphere potential from the distant parts of these tails is negligible and thus it would seem that since both r_0 and r_β differ from the hard-sphere a, there could be a considerable discrepancy between our value of the self-atmosphere potential and that of Buff and Stillinger. However, we show below that for the case where the inner region is bounded by two infinitely conducting walls, their expression for ϕ_β differs only slightly from that obtained with the cut-off models. At the same time, we believe that the curves JF and KG are on the wrong side of the ρ-axis, because the electrostatic repulsion between adsorbed ions is ignored.

The Grahame cut-off approximation, in which r_β is identified with r_0, may be described as follows. In the usual double layer theory we imagine a uniform sheet of charge density σ_β on the I.H.P. An area equal to $z_\beta e_0/\sigma_\beta$ is then available to each ion and if this charge is spread out uniformly over a disc, its radius r_0 is given by [2.9]. We suppose now that this

disc of charge is contracted to a point which becomes the center of the discrete ion $z_\beta e_0$. This is equivalent to choosing the potential distribution $V(\rho) = \infty$, $\rho < r_0$; $V(\rho) = 0$, $\rho > r_0$. In the corresponding description of the revised cut-off approximation [2.8], we contract a disc of radius r_β and charge density σ_β to a point. It is then necessary to augment the resulting charge $z_\beta e_0[1 - k_A(\sigma_\beta)]$ at the center of the disc by an amount $z_\beta e_0 k_A(\sigma_\beta)$, thereby attaining the charge $z_\beta e_0$ of a single ion at this center. The difference between the two approximations can be understood from the relation between the pair distribution functions in grand canonical and canonical ensembles. The two ensembles for the adsorbed phase should give the same thermodynamic properties of our system, such as the electrochemical potential of an adsorbed ion and therefore the micropotential and self-atmosphere potential. However, the eqs. [2.3] and [2.5], being essentially fluctuation relations, take different forms (cf. Hill, p. 236 (29)). In the grand canonical ensemble it follows from the discussion given above that the effect of fixing an ion $z_\beta e_0$ at $\rho = 0$ is to remove a fraction $1 - k_A(\sigma_\beta)$ of one ionic charge from the uniform charge distribution σ_β on the I.H.P. in the vicinity of $\rho = 0$; hence the eq. [2.5]. In the canonical ensemble, a whole unit $z_\beta e_0$ of ionic charge is removed from the I.H.P. and so we have eq. [2.3]. However, a fraction $k_A(\sigma_\beta)$ of this unit represents a diminution of amount $k_A(\sigma_\beta)/N$ in the surface density of counter-ions at large ρ. This is responsible for a 'long tail' similar to that described above for the hard-sphere model and again the contribution to the self-atmosphere of the fixed ion at $\rho = 0$ from the minute decrease in density is found to be negligible. This illustrates a characteristic of strong electrolyte theory that ionic atmospheres are governed by the pair distribution function of the grand canonical ensemble. It should be clearly understood that the term 'contraction' used here is simply a graphic way of representing the difference between the average ion density (or absolute probability distribution) on the plane and the ion density (or conditional probability distribution) when it is known that one surface ion has its center in a given position on the plane.

It is convenient to examine the limiting case of small σ_β and low electrolyte concentrations. If ρ is small compared to both the mean separation of two adjacent adsorbed ions and the thickness of the diffuse layer, then a good approximation to $V(\rho)$ is given by the interaction energy $U(\rho)$ of an isolated pair of adsorbed ions at separation ρ, in the absence of diffuse layer screening. We now introduce the functions

$$y(u) = (1 + 4u^2)^{-1/2} \qquad [2.14]$$

and

$$Y(t, w) = f_1 y(t) + \sum_{n=1}^{\infty} \sum_{m=n, n\pm 1} f_1^m f_2^n \{2 - (m - n)^2\} y(mt + nw), \qquad [2.15]$$

where

$$f_1 = (\epsilon_1 - \epsilon_2)/(\epsilon_1 + \epsilon_2), f_2 = (\epsilon_1 - \epsilon)/(\epsilon_1 + \epsilon). \qquad [2.16]$$

For the general case of different dielectric constants ϵ, ϵ_1, ϵ_2 the energy $U(\rho)$ may be expressed in the form

$$U(\rho) = \frac{(z_\beta e_0)^2}{\epsilon_1 \rho} [1 + Y(\beta/\rho, \gamma/\rho)], \qquad [2.17]$$

where $\gamma = d - \beta$. In the particular case where $\epsilon_1 = \epsilon_2$, this simplifies to

$$U(\rho) = \frac{(z_\beta e_0)^2}{\epsilon_1 \rho} [1 + f_2 y(\gamma/\rho)]. \qquad [2.18]$$

Can. J. Chem. Downloaded from www.nrcresearchpress.com by 210.87.254.6 on 09/05/12
For personal use only.

The series [2.15] represents the sum of an infinite array of electrostatic images due to multiple reflections in the plane of the wall and in the O.H.P. of the isolated pair of ions. In describing the discrete-ion effect the general sum [2.15] will appear again with different 'basic' functions $y(u)$. A closed expression in the form of a Fourier–Bessel integral, which is equivalent to [2.15] can also be used (2, 3, 4, 20).

For a perfectly conducting wall (e.g. mercury) where $\epsilon_2 = \infty$ and $f_1 = -1$ (and with $f_2 \neq -1$), $U(\rho)$ dies off as $1/\rho^3$ at large ρ. In Fig. 2*a*, this case is illustrated by curve A, which is a plot of the function $\rho\{1 - \exp(-U(\rho)/\mathbf{k}T)\}$ (see legend for double layer parameters). The electrical neutrality condition [2.3] or [2.5] is not satisfied by curve A. For the above double layer parameters, $U(\rho) = 1.6$, 0.6, and 0.3 $\mathbf{k}T$ at $\rho = 5$, 7.5, and 10 Å respectively at $T = 20°$, illustrating the short-range character of the Coulomb forces at the metallic wall. In the hexagonal lattice model the interaction energy of an adsorbed ion with its neighbors in the inner region exceeds $6U(s)$ and therefore at $s < 10$ Å (corresponding to an area per adsorbed ion $\lesssim 100$ Å^2) this energy is greater than 1.8 $\mathbf{k}T$ at the above mercury surface. However, we have already indicated that this is not a sufficient criterion for a stable hexagonal lattice. For a dielectric wall $U(\rho)$ decreases as $1/\rho$ at large ρ and so the integral in [2.11] or [2.12] diverges if $V(\rho)$ is replaced by $U(\rho)$. In Fig. 2*a*, curve B is a plot of $\rho\{1 - \exp(-U(\rho)/\mathbf{k}T)\}$ for a wall of low dielectric constant (see legend) and, for comparison, curve C depicts the case of two ions in bulk water of dielectric constant $\epsilon = 80$. The values of $U(\rho)$ at $\rho = 5$, 7.5, and 10 Å are respectively 2.8, 1.7, and 1.2 $\mathbf{k}T$ at $T = 20°$. However, diffuse layer screening will force convergence of the above integral.

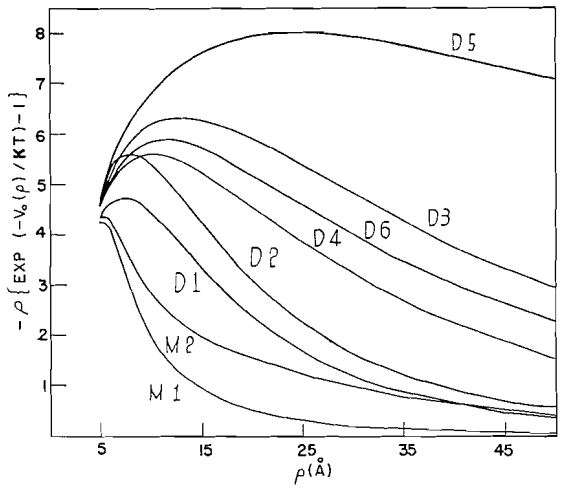

FIG. 3. Behavior of the pair distribution function exp $(-V_0(\rho)/\mathbf{k}T)$ for metallic and dielectric walls. $\epsilon = 80.1$, $T = 20°$.

Curve	ϵ_2	ϵ_1	β (Å)	γ (Å)	c (mole/l)	η_d
M1	∞	10	3	2	0.1	0
M2	∞	10	3	2	0.01	0
D1	15	15	—	1	0.1	0
D2	15	15	—	2	0.1	0
D3	15	15	—	1	0.01	0
D4	15	15	—	1	0.01	2
D5	15	15	—	1	0.001	0
D6	15	15	—	1	0.001	4

Can. J. Chem. Downloaded from www.nrcresearchpress.com by 210.87.254.6 on 09/05/12
For personal use only.

At small enough σ_β, $V(\rho)$ can be approximated by $V_0(\rho)$, the interaction energy of an isolated pair of adsorbed ions at separation ρ in the presence of a diffuse layer, provided ρ is small compared to the mean distance between two neighboring adsorbed ions. In the limiting case of zero electrolyte concentration, $V_0(\rho)$ reduces to $U(\rho)$. In Appendix D, we have obtained an expression for $V_0(\rho)$ in the form of a Fourier–Bessel integral and in Fig. 3 we have plotted $\rho\{1 - \exp(-V_0(\rho)/\mathbf{k}T)\}$ as a function of ρ for both metallic and dielectric walls with various parameters describing the double layer. In these curves we have chosen $a = 5$ Å and thus $V_0(\rho) = \infty$ for $\rho < 5$ Å; hence there is a discontinuity in the ordinate at $\rho = 5$ Å. Our results show that the higher the electrolyte concentration c or the potential ψ_d at the O.H.P., the smaller is $V_0(\rho)$, as is to be expected. For general σ_β, $V(\rho)$ should decay more rapidly than $V_0(\rho)$ with increase in ρ and hence substitution of $V_0(\rho)$ for $V(\rho)$ into [2.11] yields an upper limit to the value of r_β. In Table I we estimate this upper limit to r_β by numerical integration of [2.11]. In view of the long computing time required, only a limited number of cases have been considered.

TABLE I

Upper limits to radius r_β of the disc according to eq. [2.11] ($\epsilon = 80.1$, $T = 20°$)

ϵ_1	ϵ_2	β (Å)	γ (Å)	c (mole/l)	η_d	ψ_d (mV)	r_β (Å)
15	15	—	1	0.1	0	0	15.8
15	15	—	2	0.1	0	0	16.4
10	15	3	1	0.1	0	0	15.1
15	15	—	1	0.01	0	0	26.4
15	15	—	1	0.01	2	49	21.1
15	15	—	1	0.001	0	0	49.2
15	15	—	1	0.001	4	97	24.5
10	15	3	1	0.001	4	97	24.4
10	∞	3	1	0.1	0	0	9.5
10	∞	3	2	0.1	0	0	9.3
10	∞	3	2	0.01	0	0	11.0

In describing the discrete-ion effect it is convenient to introduce the following convention into our notation. As explained in Section 3, the 'self-image' contribution to ϕ_β will be ignored and therefore in Section 4 only the part of ϕ_β which depends directly on σ_β is determined. For both metallic and dielectric walls and for the general diffuse layer screening, we shall denote this part by $\phi_1(0, 0)$ and introduce the function $g_\phi(r_\beta)$ by writing

$$\phi_1(0, 0) = -\frac{4\pi\beta\gamma}{\epsilon_1 d}\sigma_\beta g_\phi(r_\beta). \qquad [2.19]$$

In the revised cut-off model used here, $\phi_1(0, 0)$ is the potential at the center of a disc of radius r_β on the I.H.P. due to a surface charge density $-\sigma_\beta$ uniformly distributed on this disc and screened by the diffuse layer.

A limiting case which has received considerable attention in the past is that of two conducting walls bounding the inner region and in this section we shall proceed to examine the form of $g_\phi(r_\beta)$ for this limiting case. In an earlier paper (ref. 7, eq. [7]) it was shown that $g_\phi(r_\beta) - 1$ is a measure of the deviation from Grahame's linear relation between the micropotential ψ_1 and the mean potential in the inner region for two such walls. This relation reads

$$\psi_1 - \psi_d = \frac{\gamma}{d}(\psi_0 - \psi_d) \qquad [2.20]$$

Can. J. Chem. Downloaded from www.nrcresearchpress.com by 210.87.254.6 on 09/05/12
For personal use only.

and is obtained when $g_\phi(r_\beta) = 1$. (The fact that we previously identified r_β with r_0 does not affect the present discussion.) Also, Calvert (32) has shown that for two conducting walls, the cut-off model yields

$$[2.21] \qquad g_\phi(r_\beta) = 1 - \frac{d^2}{\beta\gamma}\left[\tfrac{1}{4}f(\tau) + s_0^2 I_2(\tau) + s_0^4 I_4(\tau) + \ldots\right],$$

where $\tau = r_\beta/d$, $s_0 = (\beta - \gamma)/2d$ and if K_1 is the Bessel function of the second kind with imaginary argument and order 1,

$$[2.22] \qquad f(\tau) = \frac{8\tau}{\pi}\sum_{m=1}^{\infty}\frac{1}{(2m-1)}K_1(\overline{2m-1}\,\pi\tau)$$

and

$$[2.23] \qquad I_2(\tau) = 2\tau^2\sum_{m=1}^{\infty}\frac{1}{(\tau^2 + (2m-1)^2)^{3/2}} - 1,$$

$$[2.24] \qquad I_4(\tau) = 2\tau^2\sum_{m=1}^{\infty}\frac{\{4(2m-1)^2 + \tau^2\}}{\{\tau^2 + (2m-1)^2\}^{7/2}}.$$

The expansion [2.21], which reduces to the form derived in I when $\gamma = \beta$ ($s_0 = 0$), is valid for $|s_0| < 0.5$ if $\tau > \sqrt{2}$ and for $|s_0| < 0.36$ if $\tau > 1$. Some values of the coefficient in [2.20] for various τ and also of $1 - g_\phi(r_\beta)$ when $\gamma = 1$ or 2 Å and $\beta = 3$ Å are shown in Table II.

TABLE II

Two conducting walls bounding inner region with $\beta = 3$

r_β/d	1.0	1.2	1.4	1.6	1.8	2.0
$10f(\tau)/4$	0.2160	0.1242	0.0708	0.0400	0.0225	0.0126
$-I_2$	0.2013	0.1189	0.0687	0.0391	0.0221	0.0124
I_4	0.5553	0.3559	0.2148	0.1253	0.0716	0.0404
$1 - g_\phi$ $\gamma = 1$	0.0597	0.0340	0.0193	0.0109	0.0061	0.0034
$1 - g_\phi$ $\gamma = 2$	0.0818	0.0470	0.0267	0.0151	0.0085	0.0047

It is apparent from Fig. 2 that the cut-off approximation [2.8] overestimates the magnitude of $\phi_1(0, 0)$, since the net charge defined by the fluctuation charge density $S^*(\rho)$ in the shaded area R (or S) must equal the corresponding charge in R' (or S') and in the cut-off approximation the charge in R (or S) which replaces that in R' (or S') is now closer to the center of the adsorbed ion, $z_\beta e_0$. On the other hand an underestimate of $|\phi_1(0, 0)|$ is given by the formula

$$[2.25] \qquad \phi_1(0, 0) = -\frac{4\pi\beta\gamma}{\epsilon_1 d}\sigma_\beta g_\phi(a),$$

which follows from the Buff–Stillinger model. Now the analysis in the Appendix of I shows that if the restriction of [2.5] is removed then σ_β and r_β can be varied independently in the formula [2.19]. If we put $g_\phi = 1$, $\phi_1(0, 0)$ is proportional to σ_β and is independent of the radius r_β of the disc; this is the limiting form at $r_\beta = \infty$. On the other hand if we choose $r_\beta = d$ and assume $\gamma = \beta$, then $g_\phi = 1 - f(1)$, where from Table I, $f(1) \approx 0.09$. The function $f(r_\beta/d)$ rapidly diminishes with increase in r_β having, for example, a value 0.005 at $r_\beta/d = 2$. Thus for the model of an inner region sandwiched between two metallic walls the over- and under-estimates given above for $\phi_1(0, 0)$ differ at most by 9% for $r_\beta \geqslant d$. But from [2.11], $r_\beta > a$ and for simple inorganic ions a and d are of the same order. We

Can. J. Chem. Downloaded from www.nrcresearchpress.com by 210.87.254.6 on 09/05/12
For personal use only.

conclude that the error in $\phi_1(0, 0)$ at $\beta = \gamma$ with either the Grahame cut-off model (radius of disc $r_0 > r_\beta$) or the revised cut-off model (radius of disc r_β), should be less than 9%. When $\beta \neq \gamma$ these conclusions are still valid and indeed from Table I, the error is smaller because $I_2(\tau) < 0$. A cut-off radius r_c giving the correct $\phi_1(0, 0)$ lies between the distance of nearest approach a of two adsorbed ions and the cut-off radius r_β defined by [2.11]. Furthermore a simple way of obtaining the correct $\phi_1(0, 0)$ if r_c were known, whilst satisfying [2.5], would be to approximate to the true fluctuation charge density $S^*(\rho)$ beyond $\rho = r_c$ by placing an annulus of uniform charge density and total charge $z_\beta e_0[1 - k_A(\sigma_\beta)] - \pi\sigma_\beta r_c^2$ between $\rho = r_c$ and some $\rho \gg r_c$. The annulus makes a negligible contribution to $\phi_1(0, 0)$.

It follows from the above analysis that even though Buff and Stillinger's a is apparently fixed and practically independent of σ_β and our disc radius r_β exceeds a and increases somewhat with decrease of σ_β, the two approaches are in good agreement on the value of the self-atmosphere potential for two metallic walls. A more striking result is that although r_0 increases indefinitely with decrease in σ_β, the Grahame cut-off model yields values for $|\phi_1(0, 0)|$ which exceed only slightly those obtained with the revised cut-off model. Because of the short-range character of the electrostatic interaction of two adsorbed ions situated between two metallic walls, the contribution to $\phi_1(0, 0)$ from the distribution function $S^*(\rho)$ beyond a distance $\rho = d$ is small, so that when $\rho > d$ the exact form of $S^*(\rho)$ is not needed in a first order theory. In other words, the function $g_\phi(r_\beta)$ in [2.19] changes only slightly with r_β for $r_\beta > d$ and hence the radius of the disc carrying a specified σ_β is unimportant.

In their comparison of the hexagonal lattice and the Grahame cut-off model ($r_\beta = r_0$), Barlow and Macdonald (18) discuss the case where the wall and O.H.P. are perfect conductors and also assume $\psi_d = 0$. It can be shown from an earlier paper (7) that if the 'self-image' part of ϕ_β is again ignored, the micropotential then takes the form

$$[2.26] \qquad \psi_1 = \psi_\beta + \phi_1(0, 0) = \frac{\gamma}{d}\psi_0\left[1 + \frac{4\pi}{\epsilon_1}\{1 - g_\phi(r_0)\}\frac{\beta\sigma_\beta}{\psi_0}\right].$$

If $\sigma_0 = 0$, the electrostatic relations pertaining to the inner region yield $\psi_0 = \psi_\beta = 4\pi\gamma\sigma_\beta/\epsilon_1$ and, using the notation of Barlow and Macdonald, [2.20] becomes $\psi_1 = (\gamma/d)\psi_0(1 + \Delta_0)$, where

$$[2.27] \qquad \Delta_0 = \frac{\beta}{\gamma}[1 - g_\phi(r_0)].$$

The expansion [2.21] for $g_\phi(r_0)$ is valid when $r_0 > d$ (i.e. $\sigma_\beta < 16\ \mu C/cm^2$ for $d = 5$ Å) and then $\Delta_0 > 0$ in [2.27]. The following discussion is restricted therefore to this range of σ_β. To compare the micropotential ψ_1 derived from the hexagonal lattice and cut-off disc theories, it is sufficient to consider the self-atmosphere potential $\phi_1(0, 0)$ since the determination of ψ_β is identical in the two theories. Also, for two perfectly conducting walls $\phi_1(0, 0)$ is determined only by σ_β (and the dimensions and dielectric constant ϵ_1 of the inner region) and so is independent of σ_0 at constant ϵ_1. Barlow and Macdonald evaluate Δ_0 on the basis of the hexagonal model and for $\gamma = \beta$ and $\sigma_\beta < 10\ \mu C/cm^2$ (when $\Delta_0 > 0$), find Δ_0 to be considerably smaller than that given by [2.22] with the Grahame cut-off model (for example, by a factor of 12 at $\sigma_\beta = 10\ \mu C/cm^2$). This feature is also obtained by Krylov (5) and comparison of [2.21] with Barlow and Macdonald's values of Δ_0 for $\gamma \neq \beta$ again yields this difference. However, we have argued that the Grahame cut-off approximation to the magnitude of the self-atmosphere potential [2.19] is an overestimate and

Can. J. Chem. Downloaded from www.nrcresearchpress.com by 210.87.254.6 on 09/05/12
For personal use only.

this means that [2.27] is an underestimate. It follows that the Grahame cut-off model provides a lower estimate of $|\phi_1(0, 0)|$ than does the hexagonal model and is therefore the more accurate, contrary to comments by Barlow and Macdonald; the revised cut-off model in turn gives a somewhat better value than the Grahame model. It should be stressed that Δ_0 is a correction to the linear relation between ψ_1 and ψ_0 which is small except at large σ_β and so the discrepancy between the two values of Δ_0 quoted by Barlow and Macdonald does not affect the good agreement on $\phi_1(0, 0)$ for the two models. When $\sigma_\beta > 20$ μC/cm^2 we can no longer apply the argument developed above to predict which of the two theories is the more accurate, since the existence of a lattice structure can no longer be ruled out. It is significant that the hexagonal lattice model implies that σ_β is unchanged at large ρ, so that $k_A(\sigma_\beta) = 0$ and therefore $r_\beta = r_0$; this is consistent with our contention that the lattice model is justifiable only at large σ_β.

3. AN INTEGRAL FORM OF THE SELF-ATMOSPHERE POTENTIAL

Let the mean potential $\Psi(x)$ at distance x from the wall satisfy Laplace's equation both in the wall-medium, $x < -\beta$, and in the inner region $-\beta < x < \gamma$, where $\gamma = d - \beta$ is the distance between the I.H.P. and the O.H.P. In the diffuse layer $x > \gamma$, we assume the Poisson–Boltzmann (P.B.) equation to hold, and for a 1–1 electrolyte this reads

$$[3.1] \qquad d^2\Psi(x)/dx^2 = (8\pi n e_0/\epsilon) \sinh (e_0\Psi(x)/\mathbf{k}T),$$

where n is the number per unit volume of univalent ions of either type in the electrolyte interior. This has the solution

$$[3.2] \qquad \Psi(x) = 4\mathbf{k}T/e_0 \tanh^{-1}[\exp -(\kappa x') \tanh(\eta_d/4)],$$

where $x' = x - \gamma$ and $\eta_d = e_0\psi_d/\mathbf{k}T$ and κ is the characteristic Debye–Hückel parameter of the electrolyte defined by

$$[3.3] \qquad \kappa^2 = 8\pi n e_0^2/\epsilon\mathbf{k}T.$$

Many authors have investigated the limitations of the P.B. equation and have dealt, in particular, with the volume (ion size), dielectric, and self-atmosphere effects; the latter corrects for the correlation between ion positions in the diffuse layer. One important aspect of ion size, first considered by Buff and Stillinger (20) and more recently by us (33) is the correction to the potential at an ion from the diffuse layer 'cavity charge' that would be present inside the exclusion volume of the hydrated ion if the ion were absent. This 'cavity effect' has been ignored by previous authors and a more rigorous statistical approach (24, 25, 30) shows that it becomes important in 1–1 electrolytes at concentrations above 0.1 M. The uncorrected P.B. equation, however, should be a reasonable approximation for 1–1 electrolyte concentrations $\lesssim 0.01$ M if $\psi_d \lesssim 100$ mV and $\lesssim 0.1$ M if $\psi_d \lesssim 50$ mV. In this paper we shall be applying the discrete-ion theory to systems in electrolyte concentrations of 0.1 M or less and because we are concerned with the self-atmosphere potential of an adsorbed ion in the *inner region* and are *correcting* for diffuse layer screening, we feel justified in using the P.B. equation at the present stage of our first-order theory.

In Section 2 we explained how the (revised) cut-off model can be described in terms of a removal of charge $z_\beta e_0[1 - k_A(\sigma_\beta)]$, distributed uniformly with charge density σ_β over a disc of radius r_β, and also the placing of a point charge $z_\beta e_0$ at the center of the disc (for brevity, we shall refer to this as the contraction process). Our task is to calculate the change in potential (ϕ_β) at the center of the disc due to the contraction process and in

Can. J. Chem. Downloaded from www.nrcresearchpress.com by 210.87.254.6 on 09/05/12
For personal use only.

particular, to determine its dependence on σ_β. The uniform charge distribution σ_β outside the radius r_β is unchanged and therefore makes no contribution to ϕ_β. Prior to the contraction process the mean potential distribution was $\Psi(x)$, whereas after the contraction this distribution may be written as

$$\psi(x, \rho) = \Psi(x) + \phi(x, \rho), \qquad [3.4]$$

where $\phi(x, \rho)$ is the fluctuation potential distribution and x and ρ are the usual cylindrical polar coordinates with origin at the center of the disc in the I.H.P. It follows that $\phi_1(0, 0) = \phi_\beta$. Again $\psi(x, \rho)$ satisfies Laplace's equation in the two regions $x < -\beta$ and $-\beta < x < \gamma$ and the P.B. equation in the diffuse layer $x > \gamma$ namely

$$\nabla^2\psi(x, \rho) = (8\pi n e_0/\epsilon) \sinh (e_0\psi(x, \rho)/\mathbf{k}T). \qquad [3.5]$$

Adopting the method of Loeb (34) and Williams (35) we assume ϕ small and subtract [3.1] from [3.5] to obtain the approximate relation

$$\nabla^2\phi(x, \rho) = \kappa^2 \cosh (e_0\Psi(x)/\mathbf{k}T).\, \phi(x, \rho). \qquad [3.6]$$

The coefficient of $\phi(x, \rho)$ on the right can be interpreted as a local diffuse-layer κ^2 (or electrolyte concentration) which is a function of x. The solution of [3.6] is

$$\phi(x, \rho) = \int_0^\infty X(x, k) J_0(k\rho)\, \mathrm{d}k, \qquad [3.7]$$

where $J_n(k\rho)$ is the Bessel function of the first kind of order n and the function $X(x, k)$ is obtained in Appendix B.

The fluctuation potential $\phi(x, \rho)$ can be written as

$$\phi(x, \rho) = \phi_1(x, \rho) + \phi_2(x, \rho). \qquad [3.8]$$

Here $\phi_1(x, \rho)$ is *defined* as the potential change due only to the removal of the charge $z_\beta e_0(1 - k_A(\sigma_\beta))$ spread over the disc of radius r_β on the I.H.P. Then $\phi_2(x, \rho)$ is due to the creation of a point charge $z_\beta e_0$ at the center of the disc for fixed uniform σ_β on the I.H.P. beyond the radius r_β. Since $\phi(x, \rho)$ satisfies Laplace's equation when $x < \gamma$ and the linear eq. [3.6] is assumed when $x > \gamma$, the two potentials $\phi_1(x, \rho)$ and $\phi_2(x, \rho)$ can satisfy [3.6] separately and hence can be treated independently. As a result of the contraction process the uniform charge density σ_0 (e.g. of stabilizing or potential-determining ions) on the wall is replaced by a charge distribution $\sigma_0(\rho)$, the exact form of which is known in two limiting cases. One is that of a perfectly conducting wall, when the condition that the potential at this wall be constant implies that we can choose

$$\phi_1(-\beta, \rho) = \phi_2(-\beta, \rho) = 0 \qquad [3.9]$$

and these conditions automatically account for the change in charge distribution, $(\sigma_0(\rho) - \sigma_0)$ which accompanies the contraction process. The other is that of a perfect dielectric wall on which the charge density remains fixed i.e. $\sigma_0(\rho) = \sigma_0$, when we may assume continuity of the normal component of the 'perturbed' dielectric displacement across the wall. This yields the boundary condition

$$\epsilon_2(\partial\phi_1(x, \rho)/\partial x)_{x=-\beta-0} = \epsilon_1(\partial\phi(x, \rho)/\partial x)_{x=-\beta+0} \qquad [3.10]$$

and an identical relation for $\phi_2(x, \rho)$. In the classical case of AgI particles, the wall potential ψ_0 is assumed constant, implying complete mobility of the stabilizing ions on the wall, even though AgI is a dielectric medium. A distinction should be made, however, between

Can. J. Chem. Downloaded from www.nrcresearchpress.com by 210.87.254.6 on 09/05/12
For personal use only.

Can. J. Chem. Downloaded from www.nrcresearchpress.com by 210.87.254.6 on 09/05/12
For personal use only.

the potential of the mean force at the center of a stabilizing ion and the mean potential at the wall and it is the former potential which presumably is constant. We need to add to the right-hand side of [3.10] a term $4\pi(\sigma_0'(\rho) - \sigma_0)$, where $\sigma_0'(\rho)$ is the part of $\sigma_0(\rho)$ due to the removal of the charged disc. However, in the present paper we shall not pursue the difficult problem of the true form for $\sigma_0(\rho)$, but shall confine ourselves to the two limiting cases described by [3.9] and [3.10].

We denote the potentials $\phi_1(0, 0)$ and $\phi_2(0, 0)$ at the center of the disc by ϕ_1 and ϕ_2. The potential ϕ_1 depends directly on σ_β and, because we are interested in that part of the discrete-ion effect which varies with σ_β, we shall be concerned with ϕ_1. The 'self-image' potential ϕ_2 has been treated by other authors (2, 3, 20) and will only be briefly discussed here. It is convenient to write $\phi_2 = \phi_2' + \phi_2''$, where the main term ϕ_2' is obtained when $\sigma_\beta = 0$ for a specified electrolyte concentration. The term ϕ_2'' arises from the change in the diffuse layer local electrolyte concentration, due to the presence of a uniform σ_β at $\rho > r_\beta$. It will depend approximately on the sum $\Delta\sigma_0 + \sigma_\beta$ where $\Delta\sigma_0$ is the increment in σ_0 resulting from a change in σ_β at fixed electrolyte concentration. For a conducting wall at constant potential, $\Delta\sigma_0 + \sigma_\beta$ and therefore ϕ_2'' will be small. For the case $\sigma_0 =$ constant, $|\phi_2''|$ will increase with $|\sigma_\beta|$ but $|\phi_1|$ does likewise. Because ϕ_2 is the potential at the center of an empty circle of radius r_β due to placing an ion there, it seems unlikely that even in this case ϕ_2'' will be a significant fraction of ϕ_2. Thus in the light of the above discussion we attribute the dependence of the discrete-ion effect on σ_β mainly to ϕ_1, and shall not determine ϕ_2 in the present paper.

A limitation of our basic eq. [3.6] is that $\phi(x, \rho)$ is assumed small in the diffuse layer though it must be stressed that we used a linear theory only for $\phi(x, \rho)$ and not for the average potential $\Psi(x)$. However, the largest values of $\phi(x, \rho)$ and $\phi_2(x, \rho)$ will in fact occur near the central ion charge in the region $x < \gamma$ which is outside the diffuse layer and where $\phi(x, \rho)$ accurately satisfies Laplace's equation. (The remarks below about the magnitude of γ have some bearing here.) Also the two terms $\phi_1(x, \rho)$ and $\phi_2(x, \rho)$ in [3.8] have opposite signs which tend to reduce the magnitude of $\phi(x, \rho)$.

For some systems (e.g. AgI – electrolyte solution interface (7, 8, 21)) it seems possible that γ is very small and in our model this would have the effect of making ϕ_2' very large. However, it must be pointed out that in defining γ we have identified several different quantities to make mathematical treatment possible. As Buff and Stillinger (20) have remarked the plane of dielectric discontinuity and the mean (outer Helmholtz) plane of nearest approach of diffuse layer ions to the interface are not identical in principle and we may denote their distances from the adsorption plane ($x = 0$) by γ_1 and γ_2 respectively. For cations and anions of comparable size in the diffuse layer, one would certainly expect the counter-ions to be adsorbed closer to the wall than the distance of nearest approach of co-ions and therefore γ_2 will remain appreciable. If $\gamma_2 > \gamma_1$, the mean potential at the wall is given by

$$\psi_0 = \frac{4\pi\sigma_0\beta}{\epsilon_1} + 4\pi(\sigma_0 + \sigma_\beta)\left(\frac{\gamma_1}{\epsilon_1} + \frac{\gamma_2 - \gamma_1}{\epsilon}\right) + \psi_d, \qquad [3.11]$$

where ψ_d is the mean potential at $x = \gamma_2$. This is equivalent to an inner region of dielectric constant ϵ_1, with the plane of dielectric discontinuity and the diffuse layer boundary coincident, and of thickness γ_m for its 'outer zone' given by

$$\gamma_m = \gamma_1 + \epsilon_1/\epsilon(\gamma_2 - \gamma_1). \qquad [3.12]$$

Since $\epsilon_1/\epsilon \ll 1$, γ_m may appear small when γ_1 is small even if γ_2 is appreciable. In addition

to these 'mean γ's' there may also be a 'local γ' to consider as suggested by Barlow and Macdonald [18]. If the adsorbed ions retain the part of their hydration shell of radius b lying on the solution side, then each absorbed ion has its own local region of dielectric saturation and in general the potentials of different adsorbed ions are no longer additive. If, to avoid great mathematical difficulties, we retain the concept of a plane of dielectric discontinuity, then the appropriate values of γ for calculating ϕ_1 and ϕ_2 will both lie between γ_1 and b and it is interesting to note that if the major contribution to ϕ_1 comes from a portion of the disc of radius a then the γ's for ϕ_1 and ϕ_2 should be close together. Barlow and Macdonald (18) have suggested a value of b as much as 7 Å for the mercury – KI electrolyte solution interface, but this seems excessive and values of 2–3 Å for the local γ are perhaps more reasonable.

4. EVALUATION OF THE SELF-ATMOSPHERE POTENTIAL $\phi_1(x, \rho)$

We shall first consider the limiting case where the wall is a perfect dielectric. The function $\phi_1(x, \rho)$ satisfies Laplace's equation in the region of space $x < \gamma$ and the linear eq. [3.6] in the diffuse layer where $x > \gamma$. Also, $\phi_1(x, \rho)$ and the corresponding normal component of the dielectric displacement must be continuous at the wall and at the O.H.P. Thus in addition to [3.10] we have the boundary conditions

[4.1] $$\phi_1(x, \rho) \text{ continuous at } x = -\beta \text{ and } x = \gamma,$$

[4.2] $$\epsilon_1(\partial\phi_1(x, \rho)/\partial x)_{x=\gamma-0} = \epsilon(\partial\phi_1(x, \rho)/\partial x)_{x=\gamma+0}.$$

Since $\phi_1(x, \rho)$ is due to the removal of a disc of charge density σ_β and radius r_β, where r_β is defined by [2.7], $\phi_1(x, \rho)$ at $x = 0$ on the I.H.P. must satisfy the conditions

[4.3] $$\phi_1(x, \rho) \text{ continuous}$$

and

[4.4] $$\epsilon_1\left[\left(\frac{\partial\phi_1(x, \rho)}{\partial x}\right)_{x=-0} - \left(\frac{\partial\phi_1(x, \rho)}{\partial x}\right)_{x=+0}\right] = \begin{cases} 0 & , r > r_\beta \\ -4\pi\sigma_\beta & , r < r_\beta \end{cases}.$$

The solutions of Laplace's equation for $\phi_1(x, \rho)$ in the inner region and in the wall medium are given in Appendix C.

Case of Small Potential at the O.H.P.

In this particular case, the value of $\phi_1(x, \rho)$ at the center of the disc is expressed in integral form as

[4.5] $$\phi_1(x, \rho) = \frac{-2\pi\sigma_\beta r_\beta}{\epsilon_1} \int_0^\infty \frac{N(k)}{D(k)} \cdot J_1(kr_\beta) \frac{dk}{k},$$

where, introducing the notation

[4.6] $$f = \epsilon/\epsilon_1, f_p = \epsilon_2/\epsilon_1, f' = f(1 + \kappa^2/k^2)^{1/2}, f_2' = (1 - f')/(1 + f')$$

with f_1 defined in [2.16], then

[4.7] $$N(k) = (1 + f_1 e^{-2k\beta})(1 + f_2' e^{-2k\gamma}),$$

[4.8] $$D(k) = (1 - f_1 f_2' e^{-2k(\beta+\gamma)}).$$

When the electrolyte concentration is so small that we can put $\kappa = 0$ then f_2' tends to f_2 (also defined in [2.16]) and $\phi_1(0, 0)$ will be denoted by $\phi_1^*(0, 0)$. In Section 2 we found eq.

Can. J. Chem. Downloaded from www.nrcresearchpress.com by 210.87.254.6 on 09/05/12
For personal use only.

[2.19] to be a convenient way of expressing $\phi_1(0, 0)$ for the case of two conducting walls and we can write $\phi_1^*(0, 0)$ in a corresponding form with the appropriate $g_\phi(r_\beta)$ now denoted by $g_\phi^*(r_\beta)$, namely

$$[4.9] \qquad \phi_1^*(0, 0) = \frac{-2\pi\sigma_\beta}{(z_\beta e_0)^2} \int_0^{r_\beta} \rho U(\rho)\, d\rho = -\frac{4\pi\beta\gamma}{\epsilon_1 d}\, \sigma_\beta g_\phi^*(r_\beta),$$

where $g_\phi^*(r_\beta)$ is derived in Appendix C and is expressed as an infinite series having a form similar to [2.17] which represents multiple image reflection in the two boundaries of the inner region. The first relation of [4.9] is a direct consequence of the cut-off model, if [2.17] is substituted for $U(\rho)$ in the integral. In the second relation in [4.9], both $g_\phi^*(r_\beta)$ and $U(\rho)$ depend on distance only and therefore r_β and σ_β may be treated as independent variables. Differentiating [4.9] with respect to r_β we obtain

$$[4.10] \qquad U(r_\beta) = \frac{2\beta\gamma}{\epsilon_1 dr_\beta} (z_\beta e_0)^2 g_\phi^{*\prime}(r_\beta),$$

where the prime denotes differentiation with respect to r_β. The formulae [4.9] and [4.10] apply not only to the limiting case of zero electrolyte concentration ($\kappa = 0$) but also to the opposite limit of infinite concentration, when the conducting O.H.P. may be treated as a perfect conductor and $f_2 = -1$. The wall may be either a dielectric or a conductor ($f_1 = -1$). Thus the case of two conducting walls bounding the inner region as described by [2.19] and [2.21] is also included in the above relations.

Case of General Potential at the O.H.P.

For general η_d, the potential at the center of the disc $\phi_1(0, 0)$ can be expressed as

$$[4.11] \qquad \phi_1(0, 0) = \phi_1^*(0, 0) + \Delta\phi_1(0, 0),$$

where

$$[4.12] \qquad \Delta\phi_1(0, 0) = (2\pi\sigma_\beta r_\beta/\epsilon_1) I_1,$$

with I_1 given by [C.20].

If instead of a perfect dielectric, the wall is a perfect conductor, then [3.9] holds and we need only put $f_p = \infty$ and hence $f_1 = -1$ in the above formulae for $\phi_1^*(0, 0)$ and $\Delta\phi_1(0, 0)$.

In the limiting case where $r_\beta \gg d$ a simple expression is obtained for $\phi_1(0, 0)$. Let

$$[4.13] \qquad C_1 = \epsilon_1/4\pi d,\ C_1 = \epsilon_1/4\pi\beta,\ C_2 = \epsilon_1/4\pi\gamma$$

be the capacitances per unit area of the molecular condensers consisting of (i) the inner region, (ii) the part of this region of thickness β lying between the I.H.P. and the wall, and (iii) the part of thickness γ lying between I.H.P. and O.H.P., respectively. Suppose also that the diffuse layer can be regarded as a molecular condenser of capacitance per unit area

$$[4.14] \qquad C_d = \epsilon_1/4\pi(\kappa \cosh \tfrac{1}{2}\eta_d)^{-1}$$

in series with the condensers of the inner region. This means that the diffuse layer can be replaced by a conducting wall at a distance $(\kappa \cosh \frac{1}{2}\eta_d)^{-1}$ from the O.H.P. This distance is the Debye–Hückel length defined by an effective electrolyte concentration which would be found at a point in the diffuse layer where the potential is $\psi_d/2$. For a perfect dielectric wall, we show in Appendix C that for large r_β the discrete ion potential at the center of the disc is the potential drop across a molecular condenser of unit area which consists of C_2

Can. J. Chem. Downloaded from www.nrcresearchpress.com by 210.87.254.6 on 09/05/12
For personal use only.

and C_d in series and has the charge $-\sigma_\beta$ on the I.H.P. This potential is given by

$$\phi_1(0, 0) = -\sigma_\beta\left(\frac{1}{C_2} + \frac{1}{C_d}\right) \qquad [4.15]$$

which is independent of β and ϵ_2. For a perfectly conducting wall, the corresponding formula reads (Appendix C)

$$\phi_1(0, 0) = -\frac{\sigma_\beta}{C_1}\cdot\left(\frac{1}{C_2} + \frac{1}{C_d}\right)\Big/\left(\frac{1}{C_1} + \frac{1}{C_d}\right). \qquad [4.16]$$

Although the condition $r_\beta \gg d$ strictly applies only to a dielectric wall at low electrolyte concentration (see Table I) the formulae [4.15] and [4.16] are useful because they give simple upper bounds to $\phi_1(0, 0)$.

For a general interface with a diffuse layer beyond the O.H.P. and an arbitrary r_β it is again possible to write $\phi_1(0, 0)$ in the form [2.19] but now $g_\phi(r_\beta)$ will depend on η_d as well as on r_β. Since η_d will vary with σ_β we should really write $g_\phi(r_\beta, \eta_d(\sigma_\beta))$ but the explicit dependence of g_ϕ on η_d will be omitted. Comparison of [4.15] or [4.16] with [2.19] yields the limiting form $g_\phi(\infty)$. For a perfectly conducting O.H.P. ($\epsilon = \infty$), again adopting the convention $g_\phi(r_\beta) = g_\phi^*(r_\beta)$, we find that [4.15] yields $g_\phi^*(\infty) = d/\beta$ when the wall is a dielectric and either [2.21] or [4.16] gives $g_\phi^*((\infty) = 1$ when the wall is metallic. Simplified versions of the electrostatic arguments in I justifying these results are outlined in Appendix C.

For a dielectric wall in the limiting case of zero electrolyte concentration ($\kappa = 0$), $U(\rho)$ behaves as $1/\rho$ when $\rho \to \infty$ and it follows from [4.9] that at large r_β, $g_\phi^*(r_\beta)$ increases as r_β. In order that $g_\phi^*(r_\beta)$ remain finite, the screening by the diffuse layer is essential when applying the cut-off model at a dielectric wall and it should be remarked that the hexagonal lattice behaves similarly. This infinite limit to $g_\phi^*(r_\beta)$ is due to the model of an infinite sheet of like charges in the absence of equal and opposite charges which would produce screening; such a model is, of course, physically impossible. For either a conducting wall or a conducting O.H.P., $U(\rho)$ behaves as $1/\rho^3$ at large ρ and hence $g_\phi^*(\infty)$ is finite. The derivative on the right of [4.10] behaves as $1/r_\beta^2$ for large r_β and so $g_\phi^*(r_\beta) = g_\phi^*(\infty) - w/r_\beta$ where it will be seen that the constant $w > 0$. When $\gamma = \beta$, $s_0 = 0$ in the formula [2.21] for two infinitely conducting boundaries of the inner region and since $K_1(x)$ behaves as $\exp(-x)/\sqrt{x}$ at large x, we see that in this case $U(\rho)$ behaves as $\exp(-\pi\, d\rho)/\sqrt{\rho}$ at large ρ. We have not succeeded in transforming the more general case $\gamma \neq \beta$ ($s_0 \neq 0$) into a corresponding form but it seems likely that $U(\rho)$ displays a similar asymptotic behavior. This limiting case describes the most extreme form of screening, since it corresponds to infinite electrolyte concentration at a conducting wall.

5. NUMERICAL RESULTS AND DISCUSSION

In this paper we shall only consider the mean potential energy $z_\beta e_0 \phi_1(0, 0)$ and shall postpone the more difficult problem of the discrete-ion contribution to the electrochemical potential of an adsorbed ion to a future paper. If the function $g_\phi(r_\beta)$ (denoted g_ϕ in this section) could be assumed independent of the charge $z_\beta e_0$ on an adsorbed ion, then $z_\beta e_0 \phi_1(0, 0)$ would be identical with the discrete-ion part of the electrochemical potential. In calculating this energy it is necessary to assume some relation between r_β and σ_β and for simplicity we have chosen the Grahame relation [2.9] which overestimates $|\phi_1(0, 0)|$. We have calculated the unscreened term $e_0\phi_1^*(0, 0)/\mathbf{k}T$ from [4.9], (assuming $z_\beta = 1$) and in Fig. 4 have plotted this quantity as a function of r_β for both the metallic medium –

Can. J. Chem. Downloaded from www.nrcresearchpress.com by 210.87.254.6 on 09/05/12
For personal use only.

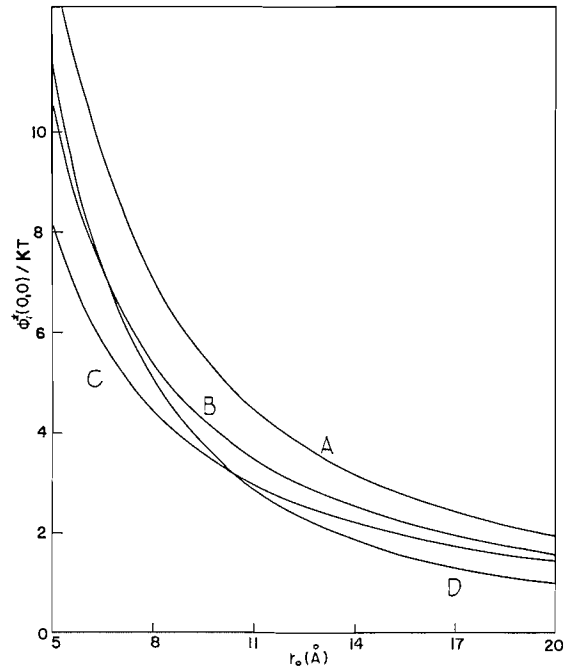

FIG. 4. Unscreened discrete-ion potential $\phi_1^*(0, 0)$. $\epsilon = 80.1$, $T = 20°$.

Curve	ϵ_2	ϵ_1	β (Å)	γ (Å)
A	15	10	3	2
B	15	10	3	1
C	15	15	—	1
D	∞	10	3	2

water and dielectric medium – water interfaces. [We are particularly interested in both mercury and silver iodide – water interfaces and in this section we have chosen values for the double layer parameters which are consistent with known data on these systems.] The parameters are given in the figure legend and, as to be expected, the curves show that the discrete-ion potential increases with an increase in γ or a decrease in ϵ_1. For the same values of the relevant parameters of the inner region the discrete-ion potential at the silver halide wall is greater than at the mercury wall and this is compatible with the greater screening by the image terms in the latter case. The effect of screening of the Grahame cut-off model by the diffuse layer of a 1–1 electrolyte is shown in Fig. 5 and Table III. In Fig. 5 we have plotted $e_0\Delta\phi_1(0, 0)/\mathbf{k}T$ for the silver iodide – water interface as a function of r_β over a range of $|\eta_d|$ and salt concentration. For the mercury surface it is more convenient to show this dependence as in Table III. These results confirm the conclusion drawn from the much simpler model introduced by Bell, Levine, and Pethica (10) that on dilute solutions ($< M/100$) the diffuse layer screening is small compared to the unscreened term except at large r_β. An increase in $|\eta_d|$ or salt concentration c increases $\Delta\phi_1(0, 0)$ but since $|\eta_d|$ decreases with c, the explicit dependence of $\phi_1(0, 0)$ on c is not immediately accessible unless σ_β and η_d are known. The plots in Figs. 4 and 5 and the results in Table III can only indicate qualitative trends in the behavior of $\phi_1(0, 0)$, because the distribution function $S^*(\rho)$ is not determined. We should expect that these results become more reliable the smaller r_β, i.e. the higher the surface charge density σ_β. The results in Table I show that

Can. J. Chem. Downloaded from www.nrcresearchpress.com by 210.87.254.6 on 09/05/12
For personal use only.

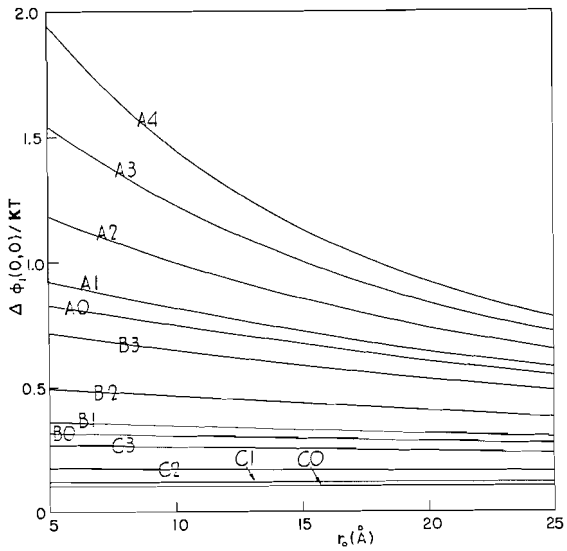

FIG. 5. Diffuse layer correction $(\Delta\phi_1\ (0, 0)/\mathbf{k}T)$ to the discrete-ion potential at a dielectric wall. $\epsilon = 80.1$, $T = 20°$, $\epsilon_2 = 15$, $\epsilon_1 = 10$, $\beta = 3$ Å, $\gamma = 1$ Å. A. $M/10$. B. $M/100$. C. $M/1000$. The numbers 4, 3, 2, 1, and 0 refer to the value of $|\eta_d|$.

the larger values of r_β plotted in the above curves (> 15 Å say) may be somewhat unrealistic in the case of strong screening e.g. at a mercury wall or in high electrolyte concentrations.

It was shown in Section 2 that for the idealized model of two conducting planes bounding the inner region, we were able to impose fairly narrow limits on the value $\phi_1(0, 0)$ even though the distribution function was unknown. To arrive at this result it was found convenient to express $\phi_1(0, 0)$ in the form [2.19] and then to examine the factor g_ϕ as a function of r_β. We found that g_ϕ varies only slightly with r_β, and this suggests that g_ϕ is a very useful quantity in describing the discrete-ion potential. In Figs. 6 and 7, we have plotted the term g_ϕ as a function of r_β with varying $|\eta_d|$ and c for the silver iodide – water interface. As expected, there is a much greater variation in g_ϕ at this interface than for the model of two conducting walls. It can be seen from Fig. 6 that $g_\phi(a)$, the smallest value of g_ϕ, lies in the range 1.25 to 1.54 when $\gamma = 1$ and $\beta = 3$, the actual value depending on $|\eta_d|$ and c; the corresponding range in $g_\phi(a)$ from Fig. 7 when $\gamma = 2$ and $\beta = 3$ is 1.13 to 1.26. We observe that $g_\phi(a)$ diminishes with increase in $|\eta_d|$ or c. From Table I, it appears that for a silver iodide wall the maximum value of r_β at low σ_β is of the order 15 Å in 0.1 M salt solution, about 20–25 Å in 0.01 M and in the range 25–50 Å in 0.001 M, depending on the value of $|\eta_d|$. Electrophoretic measurements indicate that the value of $|\eta_d|$ at coagulation is of the order of 2 for a number of common hydrophobic sols in 1–1 valent electrolyte. Thus assuming a maximum $r_\beta = 15$ Å and $|\eta_d| = 2$ in a 0.1 M solution g_ϕ will therefore lie between 1.36 and 1.92 when $\gamma = 1$. This is to be compared with the constant value of $g_\phi = d/\beta = 1.33$ assumed by the authors in earlier papers (7, 8, 17). For $\gamma = 2$, the corresponding increase in g_ϕ is from 1.17 to 1.75 whereas d/β is now 1.67. Thus for 1–1 electrolytes, the value $g_\phi = d/\beta$ was apparently an underestimate for $\gamma = 1$ and could possibly have been an overestimate for $\gamma = 2$. If we assume a maximum in r_β of 20 Å for the concentration 0.01 M and $|\eta_d| = 2$, then g_ϕ lies between 1.46 and 2.81 for $\gamma = 1$ and between 1.22 and 2.29 for $\gamma = 2$. In Table IV, we give g_ϕ for the mercury–water interface with

Can. J. Chem. Downloaded from www.nrcresearchpress.com by 210.87.254.6 on 09/05/12
For personal use only.

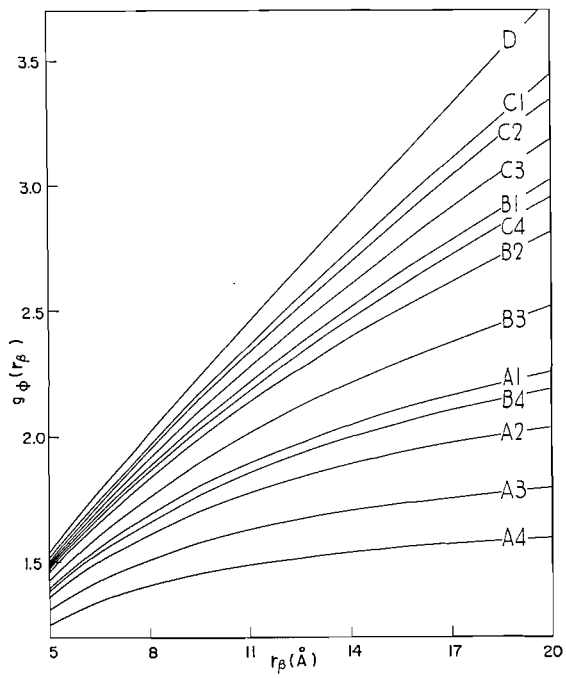

FIG. 6. The function $g_\phi(r_\beta)$ for a dielectric wall with $\gamma = 1$ Å, $\epsilon = 80.1$, $\epsilon_1 = 10$, $\epsilon_2 = 15$, $\beta = 3$ Å. A. $M/10$. B. $M/100$. C. $M/1000$. The numbers 4, 3, 2, and 1 refer to the value of $|\eta_d|$. D is the unscreened case.

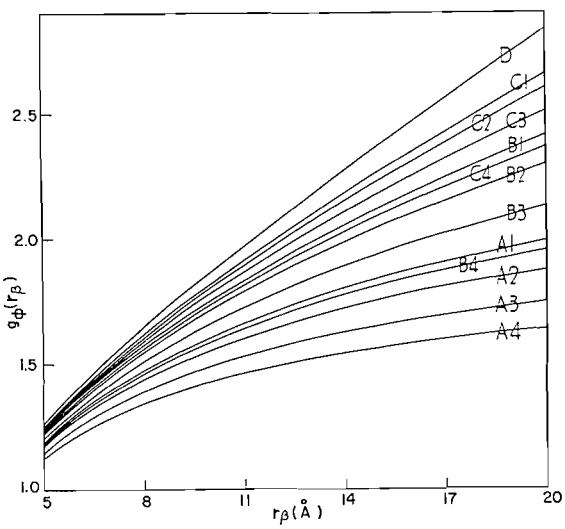

FIG. 7. The function $g_\phi(r_\beta)$ for a dielectric wall with $\gamma = 2$ Å, $\epsilon = 80.1$, $\epsilon_1 = 10$, $\epsilon_2 = 15$, $\beta = 3$ Å. A. $M/10$. B. $M/100$. C. $M/1000$. The numbers 4, 3, 2, and 1 refer to the value of $|\eta_d|$. D is the unscreened case.

various η_d, c, and r_β. These values should be compared with the underestimate $g_\phi = 1$ which was suggested in an earlier paper (9). The greater screening at this interface restricts the range of r_β (5 to 15 Å) over which g_ϕ can be applied. The explanation of the various phenomena described in the Introduction in terms of the discrete-ion effect requires that

Can. J. Chem. Downloaded from www.nrcresearchpress.com by 210.87.254.6 on 09/05/12
For personal use only.

$\phi_1(0, 0)$ be fairly large. This, in turn, requires that γ should not vanish and that g_ϕ should be of the order of 1. When the parameters of the inner region are chosen to be consistent with experimental data, values of g_ϕ result which lie in the range 1 to 2 for most experimental conditions at charged interfaces as shown by Table IV and Figs. 6 and 7. The earlier estimates of g_ϕ, namely $g_\phi = d/\beta$ for a silver iodide wall and $g_\phi = 1$ for a metallic wall, were thus not too greatly in error. The discussion in Section 3 would indicate that γ can hardly vanish.

To understand the significance of the above results in the stability theory of silver iodide sols we first point out that our calculations on a 1–1 electrolyte can be applied to a binary symmetrical electrolyte of valency type Z–Z. We need only replace e_0, κ, and η_d respectively by Ze_0, $Z\kappa$, and $Z\eta_d$ and also the Grahame relation [2.9] by

$$\pi r_\beta^2 \sigma_\beta = -Z z_\beta e_0, \qquad [5.1]$$

provided z_β is redefined as ± 1, according as the adsorbed counter-ion is positive or negative. In the previous papers (6–8) on the relation between the discrete-ion effect and colloid stability, we compared the coagulating powers of 1–1, 2–2, and 3–3 electrolytes and assume $g_\phi = d/\beta$ for all three valency types. Choosing the same value of g_ϕ we also treated a mixture of 1–1 and 2–2 electrolytes and showed that the phenomenon of mutual antagonism can be obtained on the basis of the discrete-ion effect. Because present-day electric double layer theory, for a variety of reasons (for example neglect of image terms in the diffuse layer (37)), is likely to be inadequate to give a quantitative account of the coagulating properties of trivalent ions, we shall confine our discussion to a comparison of 1–1 and 2–2 electrolytes.

The concentrations $c = 0.1$ and 0.01 M of 1–1 electrolyte correspond to $c/Z^2 = 0.1$ and 0.0025 M of 1–1 and 2–2 valency types respectively and these are typical flocculating concentrations for silver halide sols. The discrete-ion correction has a significant effect on stability when $|\sigma_\beta| > |\sigma_\beta^m|$, where $|\sigma_\beta^m|$ is the value of σ_β at the maximum in $|\psi_d|$ which is obtained when the wall potential is varied at fixed electrolyte concentration. In the examples given in earlier papers (6–8) σ_β^m was in the range 2 to 4 $\mu C/cm^2$ for the 1–1 case and 1 to 2 $\mu C/cm^2$ in the 2–2 case. According to [5.1] which gives an upper bound to r_β for a specified σ_β, $r_\beta = 13$ Å at $\sigma_\beta = 3$ $\mu C/cm^2$ in 1–1 electrolyte and $r_\beta = 26$ Å at $\sigma_\beta = 1.5$ $\mu C/cm^2$ in 2–2 electrolyte. It is shown elsewhere (17) that, in the case of 2–2 electrolyte in the range $|\sigma_\beta| > |\sigma_\beta^m|$, values of g_ϕ significantly greater than 1 are required to explain mutual antagonism for a 1–1 plus 2–2 electrolyte mixture in terms of the discrete-ion effect. If we assume $|\eta_d| = 2$ and a value of r_β as low as 10 Å for the case of 0.0025 M of 2–2 electrolyte, Figs. 6 and 7 show that such values of g_ϕ are readily attainable.

Some of the manifestations of the discrete-ion effect (such as those in colloid stability) should strictly be described in terms of a function, which we may call $g_\mu(r_\beta)$. This is the factor in the discrete-ion contribution to the electrochemical potential which corresponds to $g_\phi(r_\beta)$ in the potential $\phi_1(0, 0)$. It can be shown that $g_\mu(\infty) = g_\phi(\infty)$ and it is likely that for finite r_β, $g_\phi(a) < g_\mu(r_\beta) < g_\phi(r_\beta)$. Table IV and Figs. 6 and 7 show that $g_\phi(a)$ is nearly always greater than 1.

APPENDIX A

For a canonical ensemble the pair distribution function $g_{ij}(r)$ between two ions of types i and j, charges $z_i e_0$ and $z_j e_0$, at separation r in a volume V of a 1–1 electrolyte solution may be written as

$$\frac{N_t}{V}[g_{ij}(r) - 1] = f_{ij}^*(r) + k_{ij}/V = f_{ij}(r). \qquad [A.1]$$

Can. J. Chem. Downloaded from www.nrcresearchpress.com by 210.87.254.6 on 09/05/12
For personal use only.

Can. J. Chem. Downloaded from www.nrcresearchpress.com by 210.87.254.6 on 09/05/12
For personal use only.

TABLE III

Effect of diffuse layer screening on discrete-ion potential at mercury – electrolyte solution interface with the Grahame cut-off model ($\gamma = 2$, $\beta = 3$, $\epsilon_1 = 10$, $\epsilon = 80.1$, $\epsilon_2 = \infty$, $T = 20°$, $\psi_d = 24.36\eta_d$ in mV, c in mole/l). For $z_\beta = 1$, the charge density $\sigma_\beta = e_0/\pi r_\beta^2 = 510/r_\beta^2$ in $\mu C/cm^2$

		$\Delta\phi_1(0,0)/\mathbf{k}T$ ($c = 0.1$) with η_d equal to:					$\Delta\phi_1(0,0)/\mathbf{k}T$ ($c = 0.01$) with η_d equal to:					$10\Delta\phi_1(0,0)/\mathbf{k}T$ ($c = 0.001$) with η_d equal to:				
r_0 (Å)	$\phi_1^*(0,0)/\mathbf{k}T$	0	1	2	3	4	0	1	2	3	4	0	1	2	3	4
5	11.28	0.215	0.250	0.350	0.497	0.666	0.049	0.060	0.101	0.175	0.389	0.075	0.092	0.184	0.388	0.778
6	8.33	0.209	0.242	0.335	0.470	0.621	0.048	0.059	0.098	0.170	0.277	0.074	0.091	0.181	0.381	0.761
7	6.40	0.202	0.233	0.320	0.444	0.577	0.047	0.058	0.096	0.164	0.266	0.073	0.090	0.178	0.374	0.743
8	5.07	0.196	0.225	0.305	0.418	0.536	0.046	0.057	0.094	0.159	0.254	0.072	0.088	0.175	0.366	0.724
10	3.41	0.183	0.208	0.277	0.369	0.462	0.045	0.054	0.089	0.148	0.232	0.070	0.086	0.169	0.351	0.688
15	1.65	0.152	0.170	0.217	0.274	0.327	0.040	0.049	0.077	0.124	0.185	0.066	0.079	0.154	0.314	0.601
20	0.99	0.127	0.140	0.172	0.210	0.248	0.037	0.043	0.068	0.104	0.150	0.062	0.073	0.140	0.281	0.526

TABLE IV

Factor $g_\phi(r_\beta)$ in [2.19] at mercury – electrolyte solution interface with diffuse layer screening ($\gamma = 2$, $\beta = 3$, $\epsilon_1 = 10$, $\epsilon_2 = \infty$, $T = 20°$, $\psi_d = 24.36\eta_d$ in mV, c in mole/l)

	$g_\phi(r_\beta)$															
	$c = 0$ and $\eta_d = 0$	$c = 0.1$ and η_d equal to:					$c = 0.01$ and η_d equal to:					$c = 0.001$ and η_d equal to:				
r_β (Å)		0	1	2	3	4	0	1	2	3	4	0	1	2	3	4
5	1.03	1.01	1.01	1.00	0.98	0.97	1.03	1.02	1.02	1.01	1.00	1.03	1.03	1.03	1.03	1.02
6	1.09	1.07	1.06	1.05	1.03	1.01	1.09	1.09	1.08	1.07	1.06	1.09	1.09	1.09	1.09	1.08
7	1.14	1.11	1.10	1.09	1.07	1.04	1.14	1.13	1.13	1.12	1.10	1.14	1.14	1.14	1.14	1.13
8	1.18	1.14	1.13	1.11	1.09	1.06	1.17	1.17	1.16	1.15	1.12	1.18	1.18	1.18	1.18	1.17
9	1.22	1.16	1.15	1.13	1.10	1.07	1.20	1.20	1.19	1.17	1.14	1.21	1.21	1.21	1.21	1.20
10	1.25	1.18	1.17	1.14	1.11	1.08	1.23	1.23	1.21	1.19	1.16	1.24	1.24	1.24	1.23	1.22
15	1.36	1.23	1.22	1.18	1.13	1.09	1.32	1.32	1.29	1.26	1.20	1.35	1.35	1.34	1.33	1.31

Here N_t is the total number of ions of either type, k_{ij} is a constant, and $f_{ij}^*(r) \to 0$ as $r \to \infty$ in the sense that it becomes negligible outside the 'sphere of influence' or the 'region of the ionic atmosphere' of the fixed ion i. For a grand canonical ensemble, the term k_{ij}/V is absent. Assuming the limiting Debye–Hückel theory of electrolytes, we postulate that

$$[A.2] \qquad f_{ij}^*(r) \approx \frac{N_t}{V} z_j \frac{e_0 \varphi_i(r)}{\mathbf{k}T} \approx \frac{-N_t}{V} \cdot \frac{z_i z_j e_0^2}{\epsilon \mathbf{k} T} \frac{e^{-\kappa r}}{r},$$

where $\varphi_i(r)$ is the potential in the ionic atmosphere of ion i and κ is given by [3.3] if $N_t = nV$. Integrating over a large enough sphere with center at ion i (which can be taken equal to V)

$$[A.3] \qquad \int_V f_{ij}^*(r)\, dv = \frac{-4\pi N_t z_i z_j e_0^2}{\epsilon \mathbf{k} T V \kappa^2}.$$

Summing over the two ion types, we obtain the conditions of electrical neutrality

$$[A.4] \qquad e_0 \int_V (z_i f_{i1}^* + z_2 f_{i2}^*)\, dV = -z_i e_0,\ i = 1, 2.$$

For a canonical ensemble we have the 'normalization' condition

$$[A.5] \qquad \int_V f_{ij}(r)\, dv = -1,\ i = j;\ 0,\ i \neq j,$$

which leads to conditions identical in form to [A.4]. Integrating the second relation in [A.1] over V and making use of [A.3] and [A.5] the linear Debye–Hückel theory yields $k_{11} = k_{22} = k_{12} = -1/2$ and so we arrive at the important result

$$[A.6] \qquad e_0(z_1 k_{i1} + z_2 k_{i2}) = 0,\ i = 1, 2.$$

It follows that although the individual pair distribution functions $f_{ij}(r)$ do not tend to zero at large r, the charge density distribution functions for the canonical ensemble $e_0(z_1 f_{i1}(r) + z_2 f_{i2}(r))$, $i = 1, 2$ tend to zero, as in the case of the grand canonical ensemble. This is equivalent to the condition of 'local electrical neutrality' which is obeyed throughout the system for both canonical and grand canonical ensembles. A clearer picture of the physical significance of the term k_{ij}/V is obtained by writing [A.1] as

$$[A.7] \qquad f_{ij}(r) = \frac{(N_t - \frac{1}{2})}{V} [\bar{g}_{ij}(r) - 1] = f_{ij}^*(r) - \frac{1}{2V},\ \bar{g}_{ij}(r) = g_{ij}(r) + \frac{1}{2N_t},$$

where $\bar{g}_{ij}(r) \to 1$ as $r \to \infty$. By fixing an ion i we have prevented this ion from participating in the thermal motion, thereby reducing by 1 the total number of ions free to move in the volume. This causes an adjustment of the ion concentration at large r from $2N_t/V$ to $(2N_t - 1)/V$. Because of the condition of local electrical neutrality this can only be achieved by reducing the concentration of positive and negative ions by the same amount, which explains the factor $(N_t - 1/2)$ in [A.7].

Consider now the problem of an adsorbed ion $z_\beta e_0$ fixed at $x = \rho = 0$ on the I.H.P. Suppose that a grand canonical ensemble is chosen for the adsorbed layer of counter-ions in this plane and the electrolyte in the aqueous phase is again a 1–1 type. In the diffuse layer, the function $f_{ij}(r)$ of [A.1] is replaced by $f_{\beta j}(x, \rho)$, the fluctuation density distribution of ions of type j due to the presence of the fixed absorbed ion $z_\beta e_0$. We may expect $f_{\beta j}(x, \rho)$ to take the form

$$[A.8] \qquad f_{\beta j}(x, \rho) = f_{\beta j}^*(x, \rho) + k_{\beta j}/V,$$

Can. J. Chem. Downloaded from www.nrcresearchpress.com by 210.87.254.6 on 09/05/12
For personal use only.

where $f_{\beta j}^*(x, \rho)$ is zero outside the hemisphere of influence of the absorbed ion. As a result of the extremely small change in electrolyte concentration at large x when $z_\beta e_0$ is fixed in position, $k_{\beta j}$ varies very slightly with x in the region of the diffuse layer, but this may be ignored. Since no ions oppositely charged to $z_\beta e_0$, which we shall call type 1, are allowed to cross the O.H.P.,

$$\int_V f_{\beta 1}(x, \rho)\, \mathrm{d}V = 0, \qquad [A.9]$$

where V is the volume of the electrolyte phase. Substituting [A.8] with $j = 1$

$$k_{\beta 1} = -\int_V f_{\beta 1}^*(x, \rho)\, \mathrm{d}V. \qquad [A.10]$$

The grand canonical, two-dimensional, fluctuation distribution function for adsorbed ions $f_\beta^*(\rho)$ due to the fixed ion $z_\beta e_0$, is confined to the 'circle of influence', and thus $f_\beta^*(\rho) \to 0$ as $\rho \to \infty$. Since the system as a whole is treated as a canonical ensemble, the 'normalization condition' replacing the first equation in [A.5] is

$$\int_V f_{\beta 2}(x, \rho)\, \mathrm{d}V + \int_A f_\beta^*(\rho)\, \mathrm{d}A = 1, \qquad [A.11]$$

where ion type 2 has the charge $z_\beta e_0$. Local electrical neutrality in the electrolyte interior requires that $k_{\beta 1} = k_{\beta 2}$ and so, by [A.8] and [A.10], [A.11] yields

$$\int_A f_\beta^*(\rho)\, \mathrm{d}A + \int_V [f_{\beta 2}^*(x, \rho) - f_{\beta 1}^*(x, \rho)]\, \mathrm{d}V = -1. \qquad [A.12]$$

The eq. [3.8] for $\phi(x, \rho)$ should be interpreted as yielding the grand canonical functions $f_{\beta j}^*(x, \rho)$ in the diffuse layer in the same way as the Debye–Hückel theory gives $f_{ij}(r)$ in [A.2]. Because $z_2 = -z_1 = z_\beta$ we can write

$$f_{\beta j}^*(x, \rho) = n\mathrm{e}^{\pm z_\beta e_0 \Psi(x)/\mathbf{k}T}[\mathrm{e}^{\pm z_\beta e_0 \phi(x,\rho)/\mathbf{k}T} - 1] \approx \frac{\pm n z_\beta e_0 \phi(x, \rho)\mathrm{e}^{\pm z_\beta e_0 \Psi(x)/\mathbf{k}T}}{\mathbf{k}T}, \qquad [A.13]$$

where $j = 1$ or 2, according as the sign is plus or minus. The volume integral in [A.12] therefore reads

$$\int_V [f_{\beta 2}^*(x, \rho) - f_{\beta 1}^*(x, \rho)]\, \mathrm{d}V = \frac{-2nz_\beta e_0}{\mathbf{k}T} \int_V \phi(x, \rho) \cosh \frac{z_\beta e_0 \Psi(x)}{\mathbf{k}T}\, \mathrm{d}V \qquad [A.14]$$

$$= \frac{-2nz_\beta e_0}{\mathbf{k}T\kappa^2} \int_V \nabla^2 \phi\, \mathrm{d}V = \frac{2nz_\beta e_0}{\mathbf{k}T\kappa^2} \int_A \frac{\partial \phi}{\partial n} \cdot \mathrm{d}A = -q^*(\sigma_\beta)/z_\beta e_0,$$

where we denote differentiation along the normal to the O.H.P. drawn outward into the diffuse layer by $\partial/\partial n$. We have substituted [3.6] and then applied Green's theorem and Gauss's theorem in turn. Because $\phi(x, \rho)$ is the potential change in the hemisphere of influence as a result of fixing the adsorbed ion $z_\beta e_0$ on the O.H.P., $q^*(\sigma_\beta)$ is the total amount of charge that crosses the O.H.P. into the inner region during this process. Since a grand canonical ensemble is being used for the adsorbed phase (i.e. V is large) the surface charge density σ_β is unaltered at large ρ when $z_\beta e_0$ is fixed in position and consequently the movement of ions of type 2 across the O.H.P., which gives $q^*\sigma_\beta$ can only take place in the circle of influence. Substituting [A.14] into [A.12],

$$q^*(\sigma_\beta)/z_\beta e_0 = 1 + \int_A f_\beta^*(\rho)\, \mathrm{d}A. \qquad [A.15]$$

Can. J. Chem. Downloaded from www.nrcresearchpress.com by 210.87.254.6 on 09/05/12
For personal use only.

The quantity $z_\beta e_0 f_\beta^*(\rho)$ is identical with the fluctuation charge density $S^*(\rho)$ which is given by [2.6]. Substituting [2.6] into [A.15] and expressing σ_β in terms of r_0 by means of [2.9], we have

$$[A.16] \qquad q^*(\sigma_\beta)/z_\beta e_0 = 1 - \frac{2}{r_0^2}\int_0^\infty \rho[1 - \exp(-V(\rho)/\mathbf{k}T)]\,\mathrm{d}\rho.$$

Suppose we choose a canonical ensemble for the phase of adsorbed ions. When one ion $z_\beta e_0$ is fixed at $x = \rho = 0$ and thereby becomes the source of an external force field, no ions are permitted to cross the O.H.P. Corresponding to [A.7], the fluctuation distribution function for adsorbed ions $f_\beta(\rho)$ can be written as

$$[A.17] \qquad f_\beta(\rho) = \frac{N}{A}[q(\rho) - 1] = f_\beta^*(\rho) - k_A(\sigma_\beta)/A$$

and the condition of constant total number of adsorbed ions [2.1] yields

$$[A.18] \qquad \int_A f_\beta(\rho)\,\mathrm{d}A = -1.$$

It follows from [A.15], [A.17], and [A.18] that

$$[A.19] \qquad k_A(\sigma_\beta) = q^*(\sigma_\beta)/z_\beta e_0$$

and so [A.16] is identical with [2.12]. In place of [A.8] we postulate for the fluctuation density distribution in the electrolyte phase

$$[A.20] \qquad f_{\beta j}(x, \rho) = f_{\beta j}^*(x, \rho) + \bar{k}_{\beta j}(x)/V,$$

where certain properties of the function $\bar{k}_{\beta j}(x)$ can be obtained as follows. If we assume that $\phi(x, \rho)$ does not change sign in the hemisphere of influence then by [A.13], $f_{\beta 1}^*(x, \rho)$ and $f_{\beta 2}^*(x, \rho)$ are opposite in sign. Since a normalization condition of the type [A.9] will hold for $\bar{f}_{\beta 1}(x, \rho)$ and $\bar{f}_{\beta 2}(x, \rho)$, it follows from [A.20] that the integrals

$$\int_V \bar{k}_{\beta 1}(x)\,\mathrm{d}V \text{ and } \int_V \bar{k}_{\beta 2}(x)\,\mathrm{d}V$$

are also of opposite sign. Beyond the diffuse layer ($x \gg \kappa^{-1}$), however, the condition of local electrical neutrality requires that $\bar{k}_{\beta 1}(x) = \bar{k}_{\beta 2}(x)$ and since V is much larger than the volume occupied by the diffuse layer, these two integrals would have the same sign, unless $\bar{k}_{\beta 1}(x)$ and $\bar{k}_{\beta 2}(x)$ are both virtually zero for $x \gg \kappa^{-1}$. This means that the process of fixing ion $z_\beta e_0$ at $x = \rho = 0$ does not alter the concentration in the electrolyte interior for the canonical ensemble. From the normalization conditions for $\bar{f}_{\beta j}(x, \rho)$

$$[A.21] \qquad \int_V f_{\beta j}^*(\rho)\,\mathrm{d}V = \frac{-1}{V}\int_V \bar{k}_{\beta j}(x)\,\mathrm{d}V = \frac{-A}{V}\int_\gamma^\infty \bar{k}_{\beta j}(x)\,\mathrm{d}x,\ j = 1, 2,$$

since $\bar{k}_{\beta j}(x)$ differs from zero only near the O.H.P. in the range of x defined by the diffuse layer. Making use of [A.14] and [A.19], we therefore derive

$$[A.22] \qquad \frac{z_\beta e_0 k_A(\sigma_\beta)}{A} + \frac{e_0}{V}\int_\gamma^\infty [z_1\bar{k}_{\beta 1}(x) + z_2\bar{k}_{\beta 2}(x)]\,\mathrm{d}x = 0,$$

which may be interpreted as follows. Consider a prism of unit area in cross section, normal to the interface and including the I.H.P. and diffuse layer, at large distance ρ from the fixed ion $z_\beta e_0$. When the canonical ensemble is used, the process of fixing $z_\beta e_0$ at

Can. J. Chem. Downloaded from www.nrcresearchpress.com by 210.87.254.6 on 09/05/12
For personal use only.

$x = \rho = 0$ produces a change in charge equal to $z_\beta e_0 k_A(\sigma_\beta)/A$ on the part of the I.H.P. contained in the prism. The condition of local electrical neutrality requires an equal and opposite change in net charge in the diffuse layer part of the prism and this change is given by the integral term in [A.22]. We have chosen here the simplified model of fixed σ_0 on the wall. The analysis could be extended to allow for the presence in the electrolyte of the 'potential-determining' ion type which may constitute the charge σ_0, but this would involve additional normalization conditions and a more complicated form of the local electrical neutrality.

We need to comment on the use of the same 'local' functions $f_{\beta j}^*(x, \rho)$ and $f_\beta^*(\rho)$ in the grand canonical and canonical ensembles. The terms $k_{\beta j}/V$, $k_A(\sigma_\beta)/A$ and $\bar{k}_{\beta j}(x)/V$ contribute a negligible amount to the self-atmosphere potential $\phi_1(0, 0)$ and so common local distribution functions lead to the same expression for $\phi_1(0, 0)$ with the two ensembles. The differential equation satisfied by $\phi(x, \rho)$ in the two ensembles differ because of changes $k_{\beta 1}/V$ in the bulk concentration of electrolyte and $k_A(\sigma_\beta)/A$ in the surface concentration of adsorbed ions at points distant from the fixed ion. These differences are negligible at large enough V and A and hence $\phi(x, \rho)$ is virtually the same potential function in the two ensembles.

APPENDIX B

On substituting [3.2] into [3.6], we can write [3.6] in the form given by Williams (35)

$$[B.1] \qquad \frac{1}{\rho}\frac{\partial}{\partial \rho}\left(\frac{\rho \partial \phi(x, \rho)}{\partial \rho}\right) + \frac{\partial^2 \phi(x, \rho)}{\partial x^2} = \kappa^2\left[1 + \frac{8 \exp(-2\kappa x')\xi}{(1 - \exp(-2\kappa x')\xi)^2}\right]\phi(x, \rho)$$

where $\xi = \tanh^2 \frac{1}{4}\eta_d$. Separation of variables gives as the solution of [B.1] the integral

$$[B.2] \qquad \phi(x, \rho) = \int_0^\infty X(x, k) J_0(k\rho) k \, dk,$$

where $X(x, k)$ satisfies the equation

$$[B.3] \qquad \frac{d^2X}{dx^2} = \left[\kappa^2\left\{1 + \frac{8 \exp(-2\kappa x')\xi}{(1 - \exp(-2\kappa x')\xi)^2}\right\} + k^2\right]X.$$

If the substitution $y = \exp(-2\kappa x')$ is made then [B.3] becomes

$$[B.4] \qquad \frac{d^2X}{dy^2} + \frac{1}{y}\frac{dX}{dy} = \left[\frac{\alpha^2}{y^2} + \frac{2\xi}{y(1 - y\xi)^2}\right]X,$$

where $\alpha = (1 + k^2/\kappa^2)^{1/2}/2$. The solution of this equation which tends to zero as $x \to \infty$, can be expressed as

$$[B.5] \qquad X(x, k) = F(k) y^\alpha (1 - y\xi)^{-1}\left[1 - \left(\frac{2\alpha - 1}{2\alpha + 1}\right) y\xi\right] \exp(-\gamma \sqrt{(\kappa^2 + k^2)}),$$

where $F(k)$ is an arbitrary function of k. In the case where $\eta_d \to 0$, [3.6] reads $\nabla^2 \phi(x, \rho) = \kappa^2 \phi(x, \rho)$ and [B.3] simplifies to

$$[B.6] \qquad \frac{d^2X}{dx^2} = (\kappa^2 + k^2)X.$$

This equation has the solution

$$[B.7] \qquad X(x, k) = F(k) \exp(-x\sqrt{(\kappa^2 + k^2)}),$$

to which [B.5] reduces on putting $\eta_d = 0$.

Can. J. Chem. Downloaded from www.nrcresearchpress.com by 210.87.254.6 on 09/05/12
For personal use only.

Can. J. Chem. Downloaded from www.nrcresearchpress.com by 210.87.254.6 on 09/05/12
For personal use only.

APPENDIX C

The solution of Laplace's equation for $\phi_1(x, \rho)$ in the inner region and in the wall-medium can be expressed in the forms

$$[C.1] \qquad \phi_1(x, \rho) = \int_0^\infty kJ_0(k\rho)[A(k)e^{kx} + B(k)e^{-kx}]\,dk + \int_0^\infty kJ_0(k\rho)C(k)e^{-k|x|}\,dk, \; -\beta < x < \gamma,$$

$$[C.2] \qquad \phi_1(x, \rho) = \int_0^\infty kJ_0(k\rho)E(k)e^{kx}\,dk, \; x < -\beta.$$

On differentiating [C.1] and substituting into [4.4] we find that

$$[C.3] \qquad 2\int_0^\infty k^2C(k)J_0(k\rho)\,dk = \begin{cases} 0 & , \rho > r_\beta \\ -4\pi\sigma_\beta/\epsilon_1, & \rho < r_\beta \end{cases}.$$

The Fourier–Bessel inversion of [C.3] yields

$$[C.4] \qquad kC(k) = \frac{-2\pi\sigma_\beta}{\epsilon_1}\int_0^{r_\beta} \rho J_0(k\rho)\,d\rho = \frac{-2\pi\sigma_\beta}{\epsilon_1}\frac{r_\beta}{k}J_1(kr_\beta).$$

From [C.1], the value of $\phi_1(x, \rho)$ at the center of the disc reads

$$[C.5] \qquad \phi_1(0, 0) = \int_0^\infty [A(k) + B(k) + C(k)]k\,dk = \frac{-2\pi\sigma_\beta}{\epsilon_1}\int_0^\infty \frac{J_1(kr_\beta)}{k}[1 + a(k) + b(k)]\,dk$$

after having made use of [C.4] and introducing

$$[C.6] \qquad a(k) = A(k)/C(k), \; b(k) = B(k)/C(k).$$

In the case of small potentials (small η_d) at the O.H.P., the solution [B.7] applies in the diffuse layer region ($x > \gamma$) and $\phi_1(x, \rho)$ is given by the form [3.7] namely

$$[C.7] \qquad \phi_1(x, \rho) = \int_0^\infty F_1(k)e^{-x\sqrt{(\kappa^2+k^2)}}\,J_0(k\rho)\cdot k\,dk, \; x > \gamma.$$

The boundary conditions [3.10], [4.1], and [4.2] yield the four simultaneous equations

$$[C.8] \qquad a(k) + b(k)\,e^{-2k\gamma} - d(k) = -e^{-2k\gamma},$$

$$[C.9] \qquad a(k) + b(k)\,e^{2k\beta} - e(k) = -1,$$

$$[C.10] \qquad a(k) - b(k)\,e^{-2k\gamma} + f'd(k) = e^{-2k\gamma},$$

$$[C.11] \qquad a(k) - b(k)\,e^{2k\beta} - f_p e(k) = -1,$$

where

$$[C.12] \qquad d(k) = \frac{F_1(k)\,e^{-\gamma(\sqrt{(\kappa^2+k^2)}-k)}}{C(k)}, \; e(k) = E(k)/C(k).$$

Hence, solving for $a(k)$ and $b(k)$ and substituting into [C.5], we derive the expression [4.5] for the potential at the center of the disc $\phi_1(0, 0)$.

Can. J. Chem. Downloaded from www.nrcresearchpress.com by 210.87.254.6 on 09/05/12
For personal use only.

When $\kappa = 0$, we may expand in the form used by us (11)

$$[C.13] \qquad \frac{N(k)}{D(k)} = 1 + f_1 e^{-2k\beta} + \sum_{n=1}^{\infty} \sum_{m=n-1,n,n+1} f_1^m f_2^n \{2 - (m-n)^2\} e^{-2k(m\beta+n\gamma)},$$

which can be substituted into [4.5]. Introducing

$$[C.14] \qquad g\left(\frac{u}{v}\right) = \int_0^\infty \frac{1}{k} J_1(kv) e^{-2ku} dk = \left[1 + \left(\frac{2u}{v}\right)^2\right]^{1/2} - \frac{2u}{v},$$

the expression [4.5] for $\phi_1(0, 0)$ simplifies to the $\phi_1^*(0, 0)$ introduced in [4.9], where if G is the infinite series which is derived from the function g in the same way as Y is derived from y in [2.15], then

$$[C.15] \qquad g_\phi^*(r_\beta) = \frac{dr_\beta}{2\beta\gamma}[1 + G(\beta/r_\beta, \gamma/r_\beta)].$$

In the case of a general potential at the O.H.P., it is convenient to introduce the function

$$[C.16] \qquad Q(x) = \left[1 - \left(\frac{2\alpha - 1}{2\alpha + 1}\right) \cdot \xi e^{-2\kappa x}\right] \Big/ [1 - \xi e^{-2\kappa x}].$$

In place of [C.7], the potential in the diffuse layer is given by

$$[C.17] \qquad \phi_1(x, \rho) = \int_0^\infty F_1(k) e^{-x\sqrt{(\kappa^2+k^2)}} Q(x - \gamma) \cdot J_0(k\rho) k \, dk, \; x > \gamma.$$

The coefficients of $d(k)$ in eq. [C.8] and [C.10] become $-Q(0)$ and $hf'(dQ/dx)_{x=0}$ respectively, where

$$[C.18] \qquad h = 1 - \frac{1}{\sqrt{(\kappa^2 + k^2)}} \cdot \frac{(dQ/dx)_{x=0}}{Q(0)} = 1 + \frac{4\xi\kappa}{(1-\xi)(2\alpha + 1 - (2\alpha - 1)\xi)\sqrt{(\kappa^2 + k^2)}}.$$

Introducing

$$[C.19] \qquad f_2'' = (1 - hf')/(1 + hf'),$$

it can be verified that the effects of the diffuse layer is to add on to [4.9] the positive quantity $\Delta\phi_1(0, 0)$ in [4.12], where

$$[C.20] \qquad I_1 = \int_0^\infty \frac{J_1(kr_\beta)}{k} H(k) \, dk,$$

with

$$[C.21] \qquad H(k) = \frac{(f_2 - f_2'') e^{-2k\gamma}(1 + f_1 e^{-2k\beta})^2}{(1 - f_1 f_2 e^{-2k(\beta+\gamma)})(1 - f_1 f_2'' e^{-2k(\beta+\gamma)})}.$$

In the limiting case of $\eta_d = 0, h = 1$ and so f_2'' is replaced by f_2' in [C.21].

When $r_\beta \gg d$ we can neglect "edge effects" and assume $\partial\phi_1/\partial\rho = 0$. Thus $\phi_1(x, \rho)$ depends only on x and will be denoted by $\Phi_1(x)$. The equation [B.1], which is satisfied by $\phi_1(x, \rho)$ becomes an ordinary differential equation in $\Phi_1(x)$ which is identical with [B.3], provided $k = 0$. Since $\alpha = 1/2$ the eq. [B.5] yields

$$[C.22] \qquad \Phi_1(x) = A e^{-\kappa x}/(1 - \xi e^{-2\kappa(x-\gamma)}),$$

where A is a constant of integration. In determining $\Phi_1(x)$ for a perfect dielectric wall, the condition [3.10] implies that the wall is uncharged. For $x < 0$, $\Phi_1(x)$ is a constant which is zero since $\Phi_1(x) \to 0$ as $x \to \infty$. In the region $0 < x < \gamma$, $d\Phi_1/dx$ is constant and from [4.2] and [4.4]

$$[C.23] \qquad \epsilon_1(d\Phi_1/dx)_{x=+0} = -4\pi\sigma_\beta = \epsilon(d\Phi_1/dx)_{x=\gamma+0}.$$

Hence, applying [C.22]

$$[C.24] \qquad \Phi_1(x) = -\frac{4\pi\sigma_\beta}{\epsilon\kappa}\,\mathrm{sech}\,\tfrac{1}{2}\eta_d,$$

and at large r_β the potential at the center of the disc is given by

$$[C.25] \qquad \Phi_1(0, 0) = \Phi_1(0) = \Phi_1(\gamma) - \frac{4\pi\gamma}{\epsilon_1}\sigma_\beta,$$

which leads to [4.13].

For a perfectly conducting wall at $x = -\beta$, [3.9] applies and the constant A in [C.22] is different. If the potential drops from the I.H.P. to the wall and O.H.P. are $E_B\beta$ and $E_C\gamma$ where E_B and E_C are the corresponding field strengths, then

$$[C.26] \qquad \phi_1(0, 0) = \Phi_1(0) = E_B\beta = E_C\gamma + \psi(\gamma).$$

From [4.4]

$$[C.27] \qquad \frac{\epsilon_1}{4\pi}(E_B + E_C) = -\sigma_\beta,$$

and from [4.2] and [C.22]

$$[C.28] \qquad E_C = \frac{-\epsilon}{\epsilon_1}\left(\frac{d\Phi_1}{dx}\right)_{x=\gamma+0} = \frac{\epsilon\kappa}{\epsilon_1}\psi(\gamma)\cosh\tfrac{1}{2}\eta_d.$$

Eliminating E_B, E_C, and $\psi(\gamma)$ from the equations above we obtain $\phi_1(0, 0) = \Phi_1(0)$, which is given in [4.14]

To justify the results that $g_\phi^*(\infty) = 1$ or d/β according as the wall is metallic or dielectric we suppose that a sheet of charge density $-\sigma_\beta$ is situated in the I.H.P., which lies between two equipotential planes B and C at distances β and γ respectively. If the planes are metallic, their potentials are zero, the potential drops from the I.H.P. to B and C must be equal and so $E_B\beta = E_C\gamma$. By use of the electrostatic condition [C.27] if follows that

$$[C.29] \qquad E_B = \frac{4\pi\gamma}{\epsilon_1 d}\sigma_\beta,\ E_C = \frac{4\pi\beta}{\epsilon_1 d}\sigma_\beta.$$

The potential at the I.H.P. is now

$$[C.30] \qquad \phi_1(0, 0) = \Phi_1(0) = -E_B\beta = -E_C\gamma = \frac{-4\pi\sigma_\beta}{\epsilon_1}\frac{\beta\gamma}{d},$$

and thus $g_\phi^*(\infty) = 1$. For a dielectric wall at B and an infinitely conducting O.H.P. at C, we remove the boundary B and put $E_B = 0$ so that $\epsilon_1 E_C = 4\pi\sigma_B$. The potential at the I.H.P. is therefore

$$[C.31] \qquad \phi_1(0, 0) = -E_C\gamma = \frac{-4\pi\sigma_\beta}{\epsilon_1}\gamma,$$

Can. J. Chem. Downloaded from www.nrcresearchpress.com by 210.87.254.6 on 09/05/12
For personal use only.

which is independent of ϵ_2 and gives $g_\phi^*(\infty) = d/\beta$. If the electrolyte concentration is assumed so large that κ is virtually infinite, then [4.13] and [4.14] reduce respectively to [C.31] and [C.30].

APPENDIX D

It is a simple matter to determine $V_0(\rho)$ from the analysis in Appendix C. We need to find the potential, $\phi_0(0, \rho)$ say, due to a point charge $z_\beta e_0$, situated at the origin $x = \rho = 0$, at any point in the I.H.P. at distance ρ from the origin. Since the second integral in the right-hand member of [C.1] represents the potential distribution in an infinite medium of dielectric constant and

$$\int_0^\infty J_0(k\rho)\, e^{-k|x|}\, dx = (x^2 + \rho^2)^{-1/2}$$

it follows that the formula (C.4) for $kC(k)$ is replaced by

$$[D.1] \qquad kC_0(k) = \frac{z_\beta e_0}{\epsilon_1} J_0(k\rho).$$

The determination of the functions $A(k)$ and $B(k)$ in [C.1] proceeds exactly as before. In the case of small potentials at the O.H.P. we obtain

$$[D.2] \qquad V_0(\rho) = z_\beta e_0 \phi_0(0, \rho) = -\frac{(z_\beta e_0)^2}{\epsilon_1} \int_0^\infty \frac{N(k)}{D(k)} J_0(k\rho)\, dk.$$

When the electrolyte concentration (or κ) tends to zero, this reduces to the interaction energy in the absence of screening $U(\rho)$, defined by [2.17]. For arbitrary potential at the O.H.P., we obtain

$$[D.3] \qquad V_0(\rho) = U(\rho) - \frac{(z_\beta e_0)^2}{\epsilon_1} \int_0^\infty J_0(k\rho) H(k)\, dk.$$

REFERENCES

1. O. A. Esin and B. F. Markov. Zh. Fiz. Khim. **13**, 318 (1939). O. A. Esin and V. M. Shikov. Zh. Fiz. Khim. **17**, 236 (1943). B. V. Ershler. Zh. Fiz. Khim. **20**, 679 (1946). R. Parsons. *In* Modern aspects of electrochemistry. *Edited by* J. O'M Bockris. Butterworths, London. 1954.
2. V. G. Levich, V. A. Kiryanov, and V. S. Krylov. Dokl. Akad. Nauk SSSR, **135**, 1425 (1960).
3. V. G. Levich and V. S. Krylov. Dokl. Akad. Nauk SSSR **142**, 123 (1962).
4. V. S. Krylov. Dokl. Akad. Nauk SSSR, **144**, 155 (1962).
5. V. S. Krylov. Electrochim. Acta, **9**, 1247 (1964).
6. S. Levine, G. M. Bell, and D. Calvert. Nature, **191**, 699 (1961).
7. S. Levine and G. M. Bell. J. Colloid Sci. **17**, 838 (1962).
8. S. Levine and G. M. Bell. J. Phys. Chem. **67**, 1408 (1963).
9. S. Levine, G. M. Bell, and D. Calvert. Can. J. Chem. **40**, 518 (1962).
10. G. M. Bell, S. Levine, and B. A. Pethica. Trans. Faraday Soc. **58**, 904 (1962).
11. S. Levine, J. Mingins, and G. M. Bell. J. Phys. Chem. **67**, 2095 (1963).
12. S. Levine, J. Mingins, and G. M. Bell. IV International Congress on Surface Activity. Brussels. September 1964.
13. D. C. Grahame. Chem. Rev. **41**, 441 (1947). D. C. Grahame and B. A. Soderberg. J. Chem. Phys. **22**, 449 (1954). M. A. V. Devanathan and S. G. Canagaratna. Electrochim. Acta, **8**, 77 (1963).
14. J. Lyklema. Trans. Faraday Soc. **59**, 418 (1963).
15. A. L. Smith. Ph.D. Thesis, University of Nottingham, Nottingham, England. 1963. G. D. Parfitt and A. L. Smith. To be published.
16. B. Tezak, E. Matijevic, and K. Schulz. J. Phys. Chem. **55**, 1567 (1951). J. P. Kratohvil, M. Orhanovic, and E. Matijevic. J. Phys. Chem. **64**, 1216 (1960).
17. S. Levine and G. M. Bell. J. Colloid Sci. In press.
18. C. A. Barlow and J. R. Macdonald. J. Chem. Phys. **40**, 1535 (1964).
19. D. C. Grahame. Z. Elektrochem. **62**, 264 (1958).
20. F. P. Buff and F. H. Stillinger. J. Chem. Phys. **39**, 1911 (1963).
21. G. M. Bell, S. Levine, and J. Mingins. IV International Congress on Surface Activity. Brussels. September 1964.

Can. J. Chem. Downloaded from www.nrcresearchpress.com by 210.87.254.6 on 09/05/12
For personal use only.

22. S. OKA. Proc. Phys. Math. Soc. Japan, (3) **14**, 649 (1932).
23. E. SCHMUTZER. Z. Phys. Chem. **204**, 131 (1955).
24. V. S. KRYLOV and V. G. LEVICH. Zh. Fiz. Khim. **37**, 106 (1963).
25. F. H. STILLINGER and J. G. KIRKWOOD. J. Chem. Phys. **33**, 1282 (1960).
26. M. A. V. DEVANATHAN. Trans. Faraday Soc. **50**, 373 (1954). M. A. V. DEVANATHAN and P. PERIES. Trans. Faraday Soc. **50**, 1 (1954).
27. R. J. WATTS-TOBIN. Phil. Mag. **6**, 133 (1961). N. F. MOTT, R. PARSONS, and R. J. WATTS-TOBIN. Phil. Mag. **7**, 483 (1962).
28. J. O'M Bockris, M. A. V. DEVANATHAN, and K. MÜLLER. Proc. Roy. Soc. London, Ser. A, **247**, 55 (1963).
29. T. L. HILL. Statistical mechanics. McGraw-Hill, New York. 1956.
30. G. A. MARTYNOV and B. V. DERJAGUIN. Dokl. Akad. Nauk SSSR, **152**, 767 (1963).
31. E. HELFAND, H. L. FRISCH, and J. L. LEBOWITZ. J. Chem. Phys. **34**, 1073 (1961).
32. D. CALVERT. M.Sc. Thesis, University of Manchester, Manchester England. 1960.
33. G. M. BELL and S. LEVINE. 125th Meeting, Electrochemical Society, Toronto, Ont. May 1964.
34. A. L. LOEB. J. Colloid Sci. **6**, 75 (1951).
35. W. E. WILLIAMS. Proc. Phys. Soc. London, **A66**, 372 (1953).
36. C. A. HURST and E. ST. A. JORDINE. J. Chem. Phys. **41**, 2735 (1964).
37. P. G. ALI-ZADE, G. A. MARTYNOV, and V. G. MELAMED. Dokl. Akad. Nauk SSSR, **151**, 601 (1963).
38. D. STIGTER. J. Phys. Chem. **68**, 3603 (1964).

Can. J. Chem. Downloaded from www.nrcresearchpress.com by 210.87.254.6 on 09/05/12
For personal use only.

Can. J. Chem. Downloaded from www.nrcresearchpress.com by 210.87.254.105 on 09/05/12
For personal use only.

ULTRAVIOLET STUDY OF THE IONIZATION OF BISULFATE ION

J. T. EDWARD AND I. C. WANG
Department of Chemistry, McGill University, Montreal, Quebec
Received August 24, 1964, and, as revised, June 15, 1965

ABSTRACT

Studies of the ultraviolet absorption of dilute aqueous solutions of lithium, sodium, potassium, and ammonium sulfates show that the concentration of sulfate ion in the presence of univalent cations can be determined from the optical density of the solution at 190 mμ. The concentrations of sulfate ion thus determined in dilute solutions of sulfuric acid are in agreement with values reported previously from Raman spectral, conductivity, and other studies, which indicate a dissociation constant $K_2 = 0.01$ for the second stage in the ionization of sulfuric acid.

Sulfuric acid ionizes in water in two stages.

[1]* $$H_2SO_4 \rightleftarrows H^+ + HSO_4^-$$

[2]* $$HSO_4^- \rightleftarrows H^+ + SO_4^=$$

Estimates of the dissociation constant for the first stage vary, but it is known to be very large, so that dissociation to hydrogen ion and bisulfate ion is essentially complete in acid solutions more dilute than about 80% (3). The dissociation constant for the second stage has been estimated by several different methods to be about 0.01 (4 (p. 383), 5, 6), so that even in relatively dilute solution ionization of bisulfate ion is incomplete. In the present study we have shown that the ultraviolet absorption of dilute solutions of sulfuric acid confirms this value for the second dissociation constant. Ultraviolet absorption was used long ago to determine the dissociation constant of nitric acid (7).

EXPERIMENTAL

Solutions of reagent grade lithium, sodium, potassium, ammonium, and magnesium sulfates and of sulfuric acid were made up in distilled water free from carbon dioxide. The absorption of these solutions over the range 185–200 mμ was measured in quartz cells of 1.0 or 0.1 cm light path with a Unicam SP 500 spectrophotometer at 27.0 ± 1.5 °C against water as a blank. No attempt was made to purge this apparatus of oxygen, although it is known that absorption by oxygen becomes increasingly important at lower wavelengths (8) and can result in spurious absorption peaks because of scattered light (9). Spurious peaks of this nature at 186–188 mμ were observed in several cases, as exemplified in Fig. 1 (curve *a*) for sodium sulfate. These peaks were not observed when measurements were made down to 186 mμ with cells of 1.0 mm light path in a Perkin–Elmer 350 spectrophotometer purged with nitrogen (Fig. 1, curve *b*). No attempt was made to observe the spectrum at shorter wavelengths; recently Halmann and Platzner (10) have reported a peak at 185 mμ (ε, 200) for this solution. Our results with the Perkin–Elmer spectrophotometer are in fair agreement with those obtained in 1932 by Ley and Arends (11) (cf. Fig. 1).

Further evidence of scattered light in the unpurged Unicam spectrophotometer came from the failure to obtain linear Beer's law plots at wavelengths below 190 mμ; on the other hand, linear plots at these wavelengths were obtained with the purged Perkin–Elmer spectrophotometer. However, at 190 mμ scattering has become relatively unimportant in the Unicam, as shown by the linearity of Beer's law plots in Fig. 2 for low concentrations of salts. Consequently, all measurements were made at this wavelength with the Unicam spectrophotometer.

RESULTS AND DISCUSSION

Spectra of lithium, sodium, potassium, and ammonium sulfates down to 190 mμ were found to be essentially the same, and must be due to sulfate ion, since alkali and alkaline earth metals are transparent in this region of the spectrum (12). Recently Halmann and

**No account is taken in these equations of the degree of hydration of the ions, which varies with the concentration of acid (1, 2); this is discussed later in the paper.*

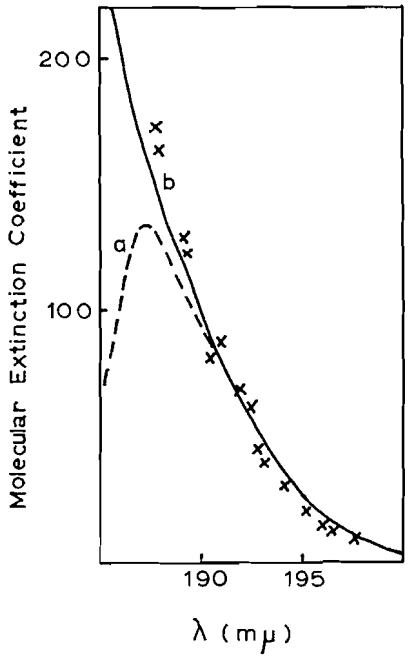

FIG. 1. Measurements of ultraviolet absorption of sodium sulfate: (*a*) 0.00998 *M* solution in Unicam SP 500 spectrophotometer; (*b*) 0.0277 *M* solution in Perkin–Elmer 350 spectrophotometer. (×) Values reported by Ley and Arends (11).

Platzner (10) have attributed a peak at 185 mμ in the spectrum of sodium sulfate in water to a "change-transfer-to-solvent" (c.t.t.s.) transition. Peaks due to these transitions are sensitive to the nature of the solvent, and are shifted to shorter wavelengths with increasing concentration of counterion (13), presumably because of ion association. This may explain the deviation from Beer's law for 1:1 electrolytes (curve *a*, Fig. 2) at concentrations above 0.1 M, and the lower absorbance for magnesium sulfate (curve *b*, Fig. 2) at all molar concentrations, since ion association is extensive at much lower concentrations for 1:2 electrolytes (4 (p. 416), 14).

The absorption of sulfuric acid (curve *c*, Fig. 2) is always much less than that of the sulfate salts and Beer's law is not obeyed even at low concentrations. This indicates that dissociation of bisulfate ion to hydrogen ion and sulfate ion is incomplete.

It seems likely that, as a first approximation, the effect of H_3O^+ and of NH_4^+ as counterions should be similar, so that curve *a* would give the absorbance of sulfuric acid at different molar concentrations if it were (like the salts) completely ionized to sulfate ion. The difference between curves *a* and *c* may accordingly be taken as a measure of the extent to which bisulfate ion is not ionized to sulfate ion.* The fraction α of bisulfate dissociated in different stoichiometric concentrations of sulfuric acid has been calculated from the equation

$$[3] \qquad \alpha = A_{H_2SO_4}/A_{M_2SO_4}$$

**This argument ignores the fact that at a given stoichiometric concentration, the ionic strength of a solution of alkali metal sulfate will be greater than that of a solution of sulfuric acid. This effect will become less important at lower concentrations, where effects of ionic strength become less important and curve a is linear.*

Can. J. Chem. Downloaded from www.nrcresearchpress.com by 210.87.254.105 on 09/05/12
For personal use only.

TABLE I

Fraction (α) of bisulfate ion dissociated in different molar concentrations of sulfuric acid

Concentration (M)	α	Concentration (M)	α
0.010	0.566	0.100	0.269
0.020	0.458	0.150	0.242
0.040	0.379	0.200	0.230
0.060	0.324	0.250	0.219
0.080	0.291	0.300	0.212

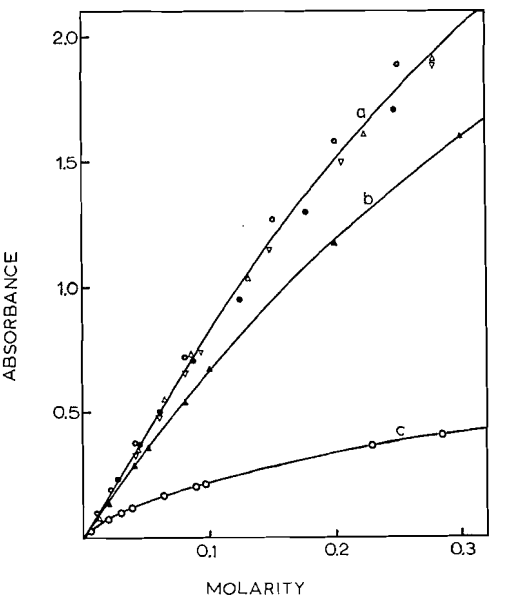

FIG. 2. Absorbance of 1 mm thickness of sulfate solutions at different concentrations: (*a*) lithium sulfate (○), sodium sulfate (△), potassium sulfate (▽), ammonium sulfate (●); (*b*) magnesium sulfate; (*c*) sulfuric acid.

where $A_{H_2SO_4}$ is the absorbance of the sulfuric acid solution (obtained from curve *c*) and $A_{M_2SO_4}$ is the absorbance of the same concentration of univalent cation sulfate (obtained from curve *a*). The results are given in Table I.

The concentration quotient K_2' for the equilibrium represented by eq. [2] may be calculated from the relation

$$K_2' = c\alpha(1 + \alpha)/(1 - \alpha) \qquad [4]$$

where c is the stoichiometric (molar) concentration of acid. In Fig. 3 $pK_2'(= -\log K_2')$ has been plotted against the square root of the ionic strength, μ, of solutions ranging in concentration from 0.01 to 0.30 M. Also shown in this figure are the values of pK_2' at 25° obtained from conductivity (5) and Raman spectral studies (3). The extrapolation to zero ionic strength shown in Fig. 3 gives the thermodynamic pK_2 of 1.99 ($K_2 = 0.0102$) already reported. It is evident that the pK_2' values obtained in the present study are in reasonable agreement with the earlier values, particularly at lower ionic strengths, where (for the reasons given above) they are likely to be more reliable.

Can. J. Chem. Downloaded from www.nrcresearchpress.com by 210.87.254.105 on 09/05/12
For personal use only.

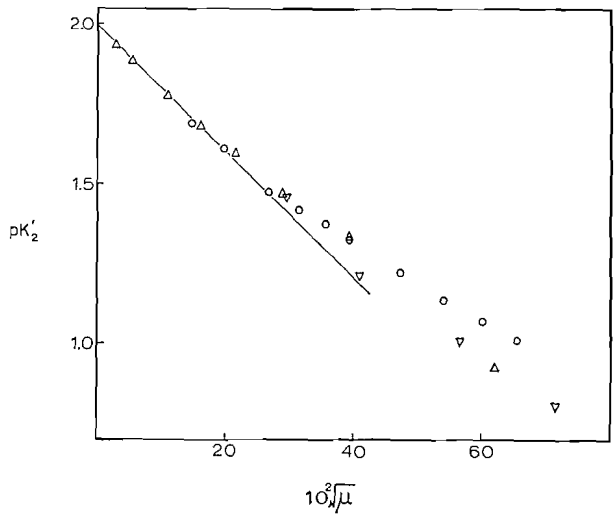

FIG. 3. Plot of pK_2' against the square root of the ionic strength (μ) of aqueous sulfuric acid. Experimental points: this paper (○); Sherrill and Noyes (given in ref. 5) (△); Smith (given in ref. 3) (▽).

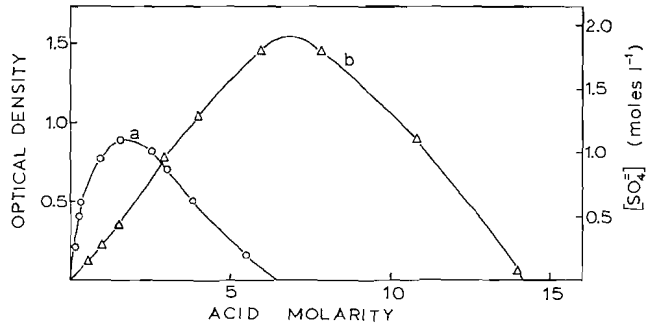

FIG. 4. Variation in absorbance at 190 mμ (curve *a*; left-hand scale) and in concentration of sulfate ion (curve *b*; right-hand scale) with concentration of aqueous sulfuric acid.

With cells of 1 mm light path, absorbance measurements at 190 mμ cannot be made with the Unicam SP 500 spectrophotometer on solutions of inorganic sulfates more concentrated than about 0.3 *M* (the absorbance then exceeding 2.0) (Fig. 2). However, absorbance measurements can be made for all concentrations of sulfuric acid. The results are shown in Fig. 4 (curve *a*). The absorbance of the acid solution increases with concentration up to a maximum in 1.75 *M* acid and thereafter decreases. However, the concentration of sulfate ion (as measured by Raman spectra (3)) increases with acid concentration up to a maximum in 7 *M* acid (Fig. 4, curve *b*) and thereafter decreases.* Evidently sulfate ion becomes progressively more transparent to radiation of 190 mμ wavelength as the acid concentration is increased. This may possibly be explained by the

**Equations [1] and [2] both ignore hydration of ions; the latter should be replaced by*

[2*a*] $$HSO_4^-(aq.) + nH_2O \rightleftarrows H^+(aq.) + SO_4^=(aq.),$$

the formulae of the equation now representing the hydrated ions. The activity of water in aqueous solutions of sulfuric acid decreases drastically with increase of molarity of acid (1); at acid strengths above 7 M this effect outweighs the increase in concentration of bisulfate ion with increasing acid concentration, so that the concentration of sulfate ion decreases.

Can. J. Chem. Downloaded from www.nrcresearchpress.com by 210.87.254.105 on 09/05/12
For personal use only.

formation of stable sulfate-oxonium ion-pairs or ion-triplets (such as I). In 7 *M* sulfuric acid there are approximately 1.9 moles of SO_4^-, 5.1 moles of HSO_4^-, 8.9 moles of H_3O^+, and 29.6 moles of H_2O (3). If each H_3O^+ binds 3 water molecules (1), very little water is left to hydrate the other ions, and ion association (e.g. to form I) should be strong. Such a drastic alteration in the environment of the sulfate ion from that found in water would be expected to lead to a corresponding alteration in the energy of the c.t.t.s. transition (13).

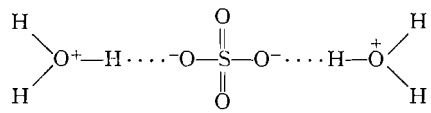

I

The results given in Fig. 4 are of some practical importance because they show that aqueous sulfuric acid at concentrations greater than about 6 *M* is reasonably transparent at 190 mμ, and hence this region of the spectrum may be used to study protonation phenomena in sulfuric acid.

ACKNOWLEDGMENTS

We are indebted to Professor G. C. B. Cave and Professor C. Sandorfy for the loan of equipment, and to Mr. K. C. Liu for experimental assistance. Grateful acknowledgment is made to the Petroleum Research Fund, administered by the American Chemical Society, and to the National Research Council for financial support.

REFERENCES

1. K. N. Bascombe and R. P. Bell. Discussions Faraday Soc. **24**, 158 (1957). R. W. Taft. J. Am. Chem. Soc. **82**, 2965 (1960).
2. P. A. H. Wyatt. Discussions Faraday Soc. **24**, 162 (1957).
3. T. F. Young, L. F. Maranville, and H. M. Smith. *In* The structure of electrolyte solutions. *Edited by* W. J. Hamer. John Wiley, New York. 1959. p. 35.
4. R. A. Robinson and R. H. Stokes. Electrolyte solutions. 2nd ed. Butterworths, London. 1959.
5. M. Kerker. J. Am. Chem. Soc. **79**, 3664 (1957).
6. T. F. Young and D. E. Irish. Ann. Rev. Phys. Chem. **13**, 435 (1962). M. H. Lietzke and R. W. Stoughton. J. Phys. Chem. **67**, 652 (1963). V. S. K. Nair and G. H. Nancollas. J. Chem. Soc. 4144 (1958).
7. H. von Halban and J. Eisenbrand. Z. Physik. Chem. **A132**, 401, 433 (1928). C. D. Coryell and L. S. Goldring. Quoted by C. D. Coryell and R. C. Fix. J. Inorg. Nucl. Chem. **1**, 119 (1955).
8. E. A. Johnson. Unicam Spectrovision. No. 8, 1 (1960).
9. P. Bladon, H. B. Henbest, and G. W. Wood. Chem. Ind. London, 866 (1951).
10. M. Halmann and I. Platzner. Proc. Chem. Soc. 261 (1964).
11. H. Ley and B. Arends. Z. Physik. Chem. **B15**, 311 (1932).
12. L. E. Orgel. Quart. Rev. London, **8**, 422 (1954).
13. M. Smith and M. C. R. Symons. Discussions Faraday Soc. **24**, 206 (1957); Trans. Faraday Soc. **54**, 338, 346 (1958).
14. D. A. L. Hope, R. J. Otter, and J. E. Prue. J. Chem. Soc. 5226 (1960).

Can. J. Chem. Downloaded from www.nrcresearchpress.com by 210.87.254.105 on 09/05/12
For personal use only.

Can. J. Chem. Downloaded from www.nrcresearchpress.com by 210.87.254.105 on 09/05/12
For personal use only.

STEROIDS AND RELATED NATURAL PRODUCTS. XXV

PHOTOCHEMICAL TRANSFORMATION OF 3β-NITRITO-5α-LANOSTANE[1]

GEORGE R. PETTIT,[2] RAYMOND E. KADUNCE,[3] PAUL SUNDER-PLASSMANN, AND JOHN OCCOLOWITZ[4]

Department of Chemistry, University of Maine, Orono, Maine

Received April 6, 1965

ABSTRACT

Ultraviolet irradiation of 3β-nitrito-5α-lanostane was found to follow an unusual reaction pathway and yield 2-oximo-3-oxo-3,4-seco-5α-lanostane (IV). The new aldehyde was easily converted to oxime and phenylhydrazone derivatives. Acetylating the photolysis product led to an oxime acetate (IX) which readily rearranged to 1-cyano-3,4-seco-5α-lanostane (III). Confirmation for the structural assignments was obtained from a series of proton magnetic resonance and mass spectral studies. Application of the new photochemical reaction was suggested to preparation of certain aldehydes otherwise accessible only with difficulty.

Chemical degradation of lanosterol to both 14α-methyl progesterone and 14α-methyl testosterone was previously accomplished, as part of an investigation concerned with evaluating the biological importance of 14α-methyl steroids (1). Reconstituting the triterpene-type ring A of lanosterol to one typical of the steroid hormones requires, at present, a somewhat lengthy series of synthetic steps. With eventual view to providing a greater selection of methods for reconstructing or otherwise transforming the 3β-hydroxy-4,4-dimethyl system of lanosterol, we decided to study photolytic decomposition[5] of 3β-nitrito-5α-lanostane (I*b*).

Preparation of 3β-hydroxy-5α-lanostane (I*a*) was performed essentially as previously reported (1*c*), and the required nitrite ester (I*b*) was prepared in good yield using nitrosyl chloride (5*a*) in pyridine. Although the ester proved relatively unstable (5*b*, 5*c*) rapid chromatographic purification on a Florisil column was found suitable for preparing a pure specimen. Irradiation (high-pressure mercury vapor arc lamp) of nitrite I*b* in benzene solution was performed under conditions commonly employed for the Barton reaction.[5] After approximately 40 min at 15°, spot tests (diphenylamine in concentrated hydrochloric acid) for the nitrite ester became negative. When a total of 45 min had elapsed, irradiation was terminated and the crude product was isolated. A thin-layer chromatogram of the product indicated that at least six substances were present. Partial separation of the viscous yellow oil on a column of basic alumina led to two readily predictable products in small yield: the substance expected from alkoxy radical decomposition with α-hydrogen fission (3-oxo-5α-lanostane, II) and the substance resulting from intermolecular hydrogen abstraction (alcohol I*a*). The ketone (II) was finally separated from an oily impurity (later assumed to be nitrile III) by preparative thin-layer chromatography. However, the

[1]*For Part XXIV refer to: G. R. Pettit, A. K. Das Gupta, H. Klinger, and J. Occolowitz. Experientia, 20, 545 (1964). Contribution XXV was abstracted in part from the Ph.D. dissertation submitted by R. E. Kadunce to the Graduate School, University of Maine, May 1964.*

[2]*Present address: Department of Chemistry, Arizona State University, Tempe, Arizona.*

[3]*NDEA Predoctoral Fellow, 1960–1963.*

[4]*Present address: Defence Standards Laboratories, Maribyrnong, Victoria, Australia.*

[5]*Stereoselective intramolecular hydrogen abstraction by alkoxy radicals formed during photolysis of nitrites and recombination of the resulting carbon radicals with nitric oxide to form nitroso monomers, dimers, or oximes has been designated the Barton reaction (2). An interesting review of the reaction has been prepared by Nussbaum and Robinson (2) and valuable extensions have recently been described by Barton and colleagues (3). A non-cage free-radical mechanism for the transformation has been proposed (4a) and other studies (4b, 4c) related in a general way to the mechanism of photochemical reactions have recently been summarized.*

major photolysis product (1.3 g from 3.6 g of I*b*) was eventually assigned structure IV. The vitreous-like aldehyde (IV) resisted attempts at crystallization, and was further purified by successive column and preparative thin-layer chromatography on silica gel. Aldehyde IV appears to have arisen by alkoxy radical decomposition with carbon–carbon bond cleavage followed by a novel series (I*b* → IV) of transformations. While the mechanistic pathway leading to aldehyde IV is only a tentative suggestion, experiments described below provide definitive support for the structural formulation.

At the outset, photolytic transformation of nitrite I*b* was not expected to follow a predictable reaction pathway and any firm assumption concerning composition of the product(s) seemed premature. Shortly after the photolysis product was found consistent with empirical formula $C_{30}H_{53}NO_2$, Robinson and colleagues (6) reported conversion of certain nitrite esters (adjacent to a tertiary-carbon atom) to the corresponding hydroxamic acids. Thus, it appeared that an initially formed alkoxy radical underwent ring fission to give a tertiary-carbon radical which then combined with nitric oxide yielding a tertiary-nitroso aldehyde (such as V) with eventual formation of hydroxamic acid VI (2). An infrared (neat) study of the photolysis product showed stretching absorption at 3 395, 1 710, and 1 670 cm^{-1} and on this basis hydroxamic acid structure VI did not appear likely[6]. Also, the product gave a negative iron(III) chloride test, and attempts to prepare a crystalline lactam derivative by reduction with a variety of reagents including zinc – acetic acid[7] and Raney nickel (9) were unsuccessful. Furthermore, an infrared examination of substance IV in chloroform solution revealed free hydroxyl stretching at 3 630 cm^{-1} and bonded hydroxyl absorption at 3 330 cm^{-1} characteristic of an oxime grouping (10). Absence[8] of infrared absorption in the 2 700 cm^{-1} region typical of aldehyde carbon–hydrogen stretching delayed recognition of this functional group until detection by a proton magnetic resonance (p.m.r.) investigation.

In carbon tetrachloride solution a p.m.r. spectrum of oxime IV exhibited, in addition to high-field skeletal responses, signals at 2.50 (two protons), 9.05 (one proton) and 9.63 (one proton) δ. The low-field response at 9.05 δ was undiminished by treating the solution with deuterium oxide (12*a*); however, the signal at 9.63 δ was absent. The oxime proton of androstane derivative VII*a* (prepared for comparison purposes), in the same solvent, emerged at 8.75 δ and also disappeared on exposure to deuterium oxide. Similar observations were noted in both cases using deuterochloroform as solvent. The signals at 9.05 and 9.63 δ were, therefore, assigned to aldehyde (12*b*) and oxime (12*c*) protons, respectively.

Presence of the aldehyde group was further substantiated by conversion of substance IV to dioxime VIII*a* using hydroxylamine in pyridine solution (13). Infrared carbonyl absorption was absent in the product and a p.m.r. signal for the oxime proton appeared at 7.54 δ. Treating the dioxime with nickel(II) chloride in ethanol gave a deep orange precipitate indicative of a vicinal *anti* dioxime (13*a*).

An attempt at confirming respective assignment of positions C-2 and C-3 for the oxime and aldehyde groups was next undertaken. Aldehyde IV was allowed to react with excess phenylhydrazine in ethanol (14) as the first step in a sequence directed at obtaining the corresponding osotriazole (15). The crystalline phenylhydrazone derivative, which separated from solution as the reaction progressed, was assigned structure VIII*b*. Results of elemental and mass spectral analyses were consistent with a monophenylhydrazone structure (VIII*b*). Interestingly, a p.m.r. spectrum of the hydrazone suggested two different

[6]*An infrared and ultraviolet study of hydroxamic acids has recently been reported (7).*

[7]*We are grateful to Dr. C. H. Robinson (6b) for providing us with unpublished details of his experience with the cyclic hydroxamic acid → lactam reduction reaction (8).*

[8]*The mono-2,4-dinitrophenylhydrazone derivative of glyoxal also lacks absorption in the aldehyde region (11).*

Can. J. Chem. Downloaded from www.nrcresearchpress.com by 210.87.254.105 on 09/05/12
For personal use only.

environments for the C-1 methylene group protons as two distinct signals corresponding to one proton each were evident[9] at 2.58 and 2.78 δ. The five aromatic-type protons emerged at 6.67–7.15 δ and signals corresponding to one proton each appeared at 7.61 (oxime or amino proton) and 7.78 (C-3 proton) δ. The signal at 7.61 δ disappeared in the presence of deuterium oxide. No further attempt at preparing a diphenylhydrazone derivative was made when a series of experiments (IV $\rightarrow$ III) beginning with acetylation of oxime IV were shown to reflect 2,3-positioning of the oxime and aldehyde groups.

Allowing oxime IV to react with acetic anhydride – pyridine at room temperature led to a crystalline monoacetyl derivative corresponding to empirical formula $C_{32}H_{55}NO_3$. An infrared spectrum of the acetate (IX) displayed carbonyl absorption at 1 790 (acetate) and 1 715 (aldehyde) cm^{-1}. Confirmation for assignment IX was obtained by evaluating the acetate's p.m.r. spectrum. In addition to responses expected for the hydrocarbon skeleton, three significant peaks were observed: three acetyl protons at 2.15, two methylene protons at 2.54, and one aldehyde proton at 9.31 δ. No change in the p.m.r. response occurred when the solution was treated with deuterium oxide. Nearly identical infrared and p.m.r. spectra were observed in the acetyl regions employing an authentic sample of oxime acetate VII*b*.[10]

Oxime acetate IX derived from photolysis product IV proved quite labile and purification required mild procedures. Recognition of the unusual stability properties of acetate IX opened a path to the most compelling structural evidence for aldehyde IV and its transformation products. When the acetate was chromatographed in hexane–benzene solution on silica gel and elution delayed until the following day, the product was nitrile III. The distinctive nitrile infrared stretching frequency at 2 350 cm^{-1} and absence of carbonyl-type absorption provided the first indication that oxime IX had been converted to a nitrile. In accordance with structure III the lowest-field signal in the nitriles p.m.r. spectrum appeared at 2.25 δ. Elemental analytical data for the nitrile corresponded to empirical formulas $C_{30}H_{53}N$ or $C_{29}H_{51}N$. Definite selection of the formula (III) representing loss of one carbon atom was possible when mass spectral examination of the nitrile yielded a molecular ion at m/e 413. Formation of the nitrile with loss of one carbon atom indicated a type of "second-order Beckmann" rearrangement (16) arising from an α-oximino aldehyde structure, thereby eliminating a ketone formulation for the photolysis product. In addition, facile formation of the nitrile[11] by simply absorbing oxime acetate IX on silica gel suggested an *anti* configuration for the photolysis product (IV). Basic hydrolysis of *syn* oxime acetates having an adjacent oxygen substituent results in saponification with relatively little rearrangement (17).

In summary, photochemical transformation of 3β-nitrito-5α-lanostane (I*b*) was found to follow a novel reaction pathway leading to aldehyde IV.[12] The preceding experiments suggest that the new photochemical reaction may provide a useful synthetic avenue to certain α-oximino aldehydes and derivatives, e.g. α-amino acids, otherwise accessible only with difficulty.

[9]*Appearance of a partially resolved or distinct C-1 methylene doublet in p.m.r. spectra of the photolysis product and derivatives may be due, in part, to asymmetry of the adjacent C-10 position (see e.g. ref. 12d).*

[10]*The oxime acetate signal of substance VII*b *appeared with a shoulder at approximately one-half height which may indicate a mixture of anti and syn isomers.*

[11]*Significant amounts of nitrile-containing products have been obtained by Beckmann rearrangement of unconjugated oximes using p-toluenesulfonyl chloride in pyridine (18).*

[12]*Although several examples of irradiation-induced cleavage of a triterpene ring A have been recorded (19), the presently described reaction appears to follow a unique course. The experimental results used in support of structure IV, however, do not necessarily exclude a reaction sequence involving ring B (cf. 20, p. 584). Final support for the structural assignments must now await correlation with a substance of established structure.*

Can. J. Chem. Downloaded from www.nrcresearchpress.com by 210.87.254.105 on 09/05/12
For personal use only.

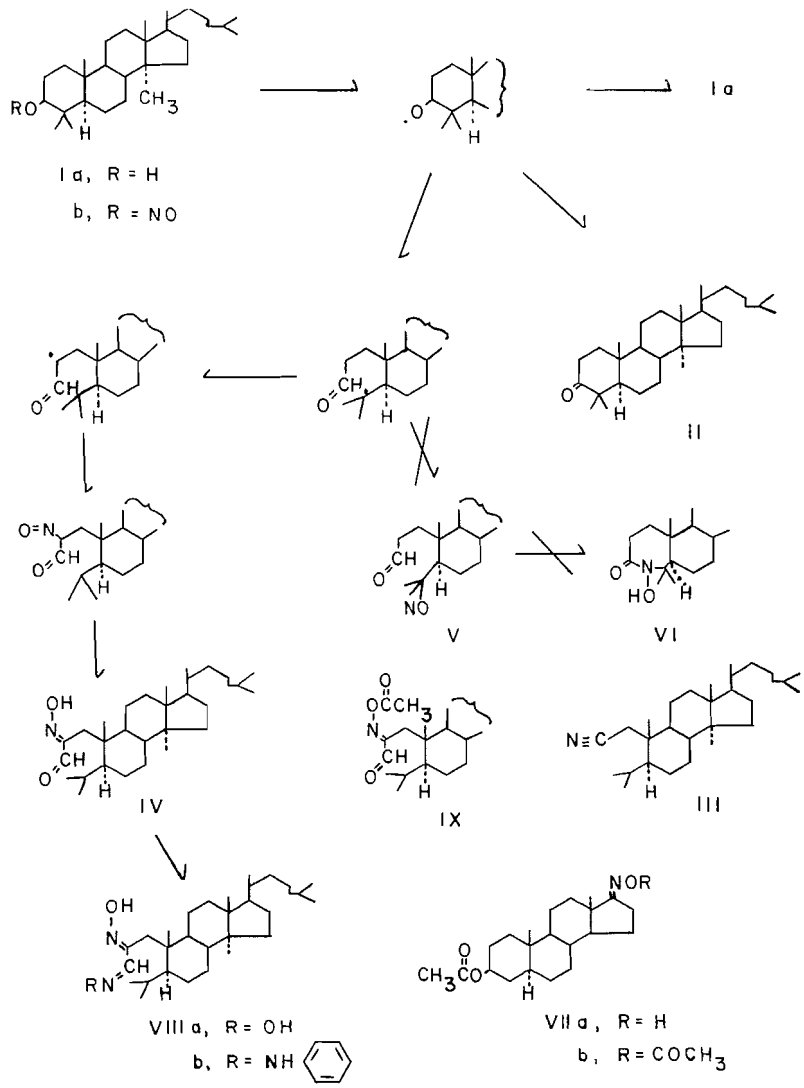

EXPERIMENTAL

Melting points were determined employing a Kofler melting point apparatus. Introduction to the experimental section of a previous contribution (1*c*) concerned with oxidation of 3β-acetoxy-5α-lanostane provides a brief description of several reagents and techniques (e.g. silica gel t.l.c.) employed below. The acetic anhydride, pyridine (from potassium hydroxide), and all solvents were redistilled. In addition, diethyl ether was further purified by filtration through a column of activated alumina. Acid-washed alumina (Merck, Rahway), neutral alumina (E. Merck, AG., Darmstadt, Germany), basic alumina (Aluminum Company of America F-20), silica gel (0.05–0.20 mm, E. Merck), and Florisil (100 mesh) were employed as column chromatographic adsorbents. Fluorescent silica gel (HF 254, average particle size 5–25 μ, E. Merck) was employed for one preparative thin-layer chromatogram, which contained a substance fluorescent under ultraviolet light. The photolysis experiments were performed using a Hanovia high-pressure mercury arc lamp (Englehard Hanovia, Inc., 200 W) with a Pyrex filter sleeve (E. H., Inc., No. 516-27-116). All new substances are colorless unless otherwise noted.

The p.m.r. spectra were obtained using a Varian Associates Model A-60 n.m.r. spectrometer. Each solvent contained approximately 10% w/v of sample and enough tetramethylsilane was added to standardize the instrument. The scanning rate (from low to high field) was 120 c.p.s./min and measurements are reported in

Can. J. Chem. Downloaded from www.nrcresearchpress.com by 210.87.254.105 on 09/05/12
For personal use only.

δ (p.p.m.) units with respect to TMS. The optical rotation (chloroform solution) and infrared measurements and elemental analyses were provided by Drs. Hill, Janssen, and Bernhardt (1*c*). Mass spectral determinations were performed using a direct inlet technique.

3β-Hydroxy-5α-lanostane (Ia).

A specimen (45 g) of 3β-acetoxy-7,11-dioxo-5α-lanostane was converted to 3β-hydroxy-5α-lanostane as previously described (1*c*). The crude product (37.4 g) was dissolved in 1:1 benzene–hexane and absorbed on 750 g of acid-washed alumina. Elution with the same solvent gave a sample (8.5 g) of alcohol I*a* melting at 172–175°. Further elution with benzene gave a pure sample (12.5 g) which after recrystallization from chloroform–methanol melted at 173–175°; $[\alpha]_D^{20}$ +34.8 (*c*, 1.1); reported (21) m.p. 171–172°, $[\alpha]_D$ +35°.

3β-Nitrito-5α-lanostane (Ib)

Method A

A solution of nitrosyl chloride (2 ml) in pyridine (20 ml) was added dropwise (over 1 h) to a solution of alcohol I*a* (4.0 g) in dry benzene (50 ml) and pyridine (25 ml). After stirring the mixture one additional hour, the brown solution was diluted with water and extracted with benzene. The combined benzene extract was washed with cold dilute hydrochloric acid, washed with water, dried, and concentrated *in vacuo*. A thin-layer chromatogram (3:17 ethyl ether – hexane mobile phase) indicated that the product contained a small quantity (less than 10%) of starting alcohol. A solution of the residue in petroleum ether was chromatographed on Florisil (90 g) and eluted with the same solvent to yield 3.6 g of nitrite ester I*b* melting at 122–126°. Two recrystallizations from hexane afforded an analytical sample melting at 123.5–126.5°; $[\alpha]_D^{20}$ +28.9° (*c*, 2.35); ν_{max}^{KBr} 1 640, 1 595, and 800 cm^{-1}.

Anal. Calcd. for $C_{30}H_{52}NO_2$: C, 78.40; H, 11.62; N, 3.05. Found: C, 78.02; H, 11.45; N, 3.16.

In later experiments, a 5-min addition period for the nitrosyl chloride (at ice-bath temperature) and a 1/2 h period at room temperature was found satisfactory. In general, the nitrite ester proved sensitive and rapid isolation and purification proved desirable.

Method B

Samples of the nitrite ester suitable for the photolysis reaction were prepared as follows. Nitrosyl chloride was passed into a pyridine (40 ml) solution of alcohol I*a* (4.0 g) at −10°. Stirring and addition of gaseous nitrosyl chloride was continued until the reaction mixture retained a pale-brown color. The solution was allowed to warm to room temperature and after 1/2 h was poured into ice water (200 ml) .The solid product was collected, washed with cold water, and dissolved in hexane, and the resulting solution was washed with cold dilute hydrochloric acid and water. Removal of solvent (*in vacuo* at room temperature) gave 3.7 g (87%) of the nitrite ester.

2-Oximo-3-oxo-3,4-seco-5α-lanostane (IV)

A solution of the nitrite ester (I*b*, 3.6 g) in dry benzene (250 ml under nitrogen) was cooled (10–15°) and irradiated for 45 min. Spot tests (diphenylamine in concentrated hydrochloric acid) for the nitrite group became negative after 40 min. The fluorescent green solution was concentrated *in vacuo* at room temperature to a viscous yellow oil. A hexane solution of the residue was chromatographed on basic alumina (70 g). One fraction eluted with hexane–benzene (1:1) afforded a viscous yellow oil (0.6 g). A 0.09-g sample of the oil was further purified using preparative thin-layer chromatography (8:1 hexane – ethyl ether mobile phase). By this means a 0.04-g specimen of *3-oxo-5α-lanostane* (II), m.p. 130–134°, was isolated.[13] The next most abundant component (0.02 g) was an oily nitrile (λ_{max}^{Nujol} 4.44 μ) later assumed to correspond with degradation product III. The fractions eluted with 3:2 to 1:4 hexane–benzene corresponded to the principal photolysis product. A thin-layer chromatogram (5:1 hexane – ethyl ether mobile phase) indicated that these fractions (IV, 1.3 g) represented a nearly pure substance. Continued elution with benzene gave an oily fraction (0.04 g) which was not investigated further, while the fractions eluted with benzene – ethyl ether and with ethyl ether afforded another 2.7 g of viscous oil. The latter fractions were combined and rechromatographed on acid-washed alumina (60 g). The fraction (0.64 g, m.p. 160–170°) eluted with hexane–benzene (3:1) was recrystallized from chloroform–methanol and identified[13] as *3β-hydroxy-5α-lanostane (21).*

When attempts to crystallize the principal photolysis product (1.3 g) proved unsuccessful, the photolysis reaction was repeated. As with the example noted above, a thin-layer chromatogram (9:1 hexane – ethyl acetate mobile phase) indicated that the crude product was composed of at least six components. Chromatographic separation of the viscous yellow oil was repeated employing neutral alumina with hexane, benzene, and chloroform solvent systems. Essentially the same observations were made. The following procedure, however, was used to obtain a pure specimen of oxime IV.

The reaction was again repeated and the product was chromatographed on 100 g of neutral alumina. Elution with 99:1 to 9:1 hexane – ethyl acetate yielded 1.6 g corresponding principally to 3-ketone II, lesser quantities of 3β-alcohol I*a*, and a small quantity of the nitrile (III) accompanied by a trace of nitrite ester (I*b*). Continued elution with 9:1 hexane – ethyl acetate to ethyl acetate gave 1.5 g of oxime IV. The oxime was rechromatographed on silica gel (45 g) and elution with 99:1 to 19:1 hexane – ethyl acetate removed

[13] *Identity was established by mixture melting point determination and infrared spectral comparison (in potassium bromide) with an authentic sample.*

Can. J. Chem. Downloaded from www.nrcresearchpress.com by 210.87.254.105 on 09/05/12
For personal use only.

approximately 0.1 g of less polar impurities. The next fraction eluted with 19:1 hexane – ethyl acetate weighed 1.15 g and was found by thin-layer chromatography (9:1 hexane – ethyl acetate mobile phase) to represent pure product (IV, 31% yield). However, attempts to crystallize the vitreous solid were unsuccessful. An analytical specimen was prepared by preparative thin-layer chromatography on silica gel HF 254 (4:1 cyclohexane – ethyl ether mobile phase), and the desired zone was identified using an ultraviolet lamp. In this case, the plate was first eluted with methanol (and reactivated at 110°) to remove some impurities. The oxime was eluted from the silica gel with chloroform, and the solution was filtered, concentrated to dryness *in vacuo*, treated with pentane, and finally evaporated in high vacuum to yield a colorless foam. Purity was reconfirmed by a thin-layer chromatogram but attempts to crystallize the product were again unsuccessful. A p.m.r. spectrum of the oxime in CCl_4 exhibited responses at 0.11, 0.74, 0.80, 0.84, 0.89, 1.15–1.47 (complex and broad), 2.50 (two methylene protons), 9.05 (one aldehyde proton) and 9.63 (one oxime proton) δ. After shaking the carbon tetrachloride solution with deuterium oxide for 15 min, the peak at 9.63 δ disappeared. The infrared spectrum displayed absorption at: ν_{max}^{KBr} 3 300 (broad), 1 700 (broad), 1 470, 1 450, 1 392, 1 370, and 1 200 cm^{-1}. Results of elemental analyses were consistent with the oxime structure.

Anal. Calcd. for $C_{30}H_{53}NO_2$: C, 78.37; H, 11.62; N, 3.05; O, 6.96. Found: C, 77.95; H, 11.48; N, 3.16; O, 7.35.

3-Oxo-5α-lanostane (II)

To a solution of 3β-hydroxy-5α-lanostane (2.0 g) in acetone (150 ml) at room temperature was added excess 8 *N* chromium trioxide reagent (22). When oxidation appeared complete, the remaining chromium trioxide was reduced with methyl alcohol and the mixture was filtered through Celite and concentrated to approximately 10 ml. After dilution with water, the product was collected and recrystallized from hexane to yield 1.43 g melting at 132–133°, $[\alpha]_D^{20}$ +25.4° (*c*, 7.29); reported (21) m.p. 127–128° and $[\alpha]_D$ +27°.

P.m.r. Chemical Shifts of 3β-Acetoxy-17-oximo-5α-androstane (VIIa) and 3β-Acetoxy-17-acetoximino-5α-androstane (VIIb)

Oxime VII*a* (23): p.m.r. in CCl_4 solution 0.80, 0.84, 1.19, 1.61, 1.88 (three acetate protons), 2.34 (broad, C-3 proton), and 8.75 (one oxime proton which disappears in the presence of deuterium oxide); in $CDCl_3$ solution 0.84, 0.88, 1.23–1.82 (complex), 1.97, 2.11 (three acetate protons), 2.44 (broad, C-3 proton), and 8.64 (one oxime proton which disappears in the presence of deuterium oxide). Oxime acetate VII*b* (16, 23): in CCl_4 solution 0.84, 0.94, 1.22–1.72 (broad and complex), 1.88 (3-acetate), 2.0–2.02 (oxime acetate), and 2.42 (broad, C-3 proton).

2,3-Dioximo-3,4-seco-5α-lanostane (VIIIa)

The dioxime derivative (VIII*a*, 0.06 g) obtained (0.08 g hydroxylamine hydrochloride, 1 ml pyridine, for 12 h at room temperature) from 0.08 g of the mono-oxime IV was purified by preparative thin-layer chromatography (3:1 hexane – ethyl ether mobile phase). Recrystallization from chloroform–hexane gave a pure sample melting at 168–171°: p.m.r. in $CDCl_3$ solution gave responses at 0.46, 0.78, 0.89, 0.99, 1.15–1.50 (complex and broad), 2.58 (two methylene protons) and 7.54 (broad, oxime proton, disappears in the presence of deuterium oxide) δ; ν_{max}^{Nujol} 3 570, 959, 935, and 885 cm^{-1}.

Anal. Calcd. for $C_{30}H_{54}N_2O_2$: C, 75.89; H, 11.47; N, 5.90. Found: C, 75.73; H, 11.49; N, 6.26.

2-Oximo-3-phenylhydrazono-3,4-seco-5α-lanostane (VIIIb)

Phenylhydrazine hydrochloride (0.53 g) in water (8 ml) was added to a stirred solution of oxime IV (0.75 g) in ethanol (30 ml). After approximately 3 h at room temperature, a crystalline product began to separate. Eighteen hours later, the mixture was cooled and the solid was collected and washed with methanol: yield 0.62 g (62%), m.p. 158–160°. An analytical specimen (pure as evidenced by thin-layer chromatography using 7:3 hexane – ethyl acetate as mobile phase) recrystallized from acetone–methanol as pale-yellow crystals, m.p. 169–170°; p.m.r. spectrum in $CDCl_3$ solution 0.65, 0.80, 0.90, 0.99, 1.18, 1.52, 2.58 (one proton), 2.78 (one proton), 6.67–7.15 (five aromatic protons), 7.61 (one proton which disappears in the presence of deuterium oxide) and 7.78 (one C-3 proton); ν_{max}^{KBr} 3 200, 1 600, 1 560, 1 510, 1 490, 1 470, 1 380, 1 250, 1 230, 1 160, 970, and 930 cm^{-1}. The mass spectral data (M^+ at 549 with a calculated mass of 549) and elemental analyses were also consistent with structure VIII*b*.

Anal. Calcd. for $C_{36}H_{59}N_3O$: C, 78.63; H, 10.82; N, 7.64; O, 2.91. Found: C, 78.74; H, 10.70; N, 7.78; O, 2.79.

2-[O-Acetyloximo]-3-oxo-3,4-seco-5α-lanostane (IX)

A solution of oxime IV (0.60 g) in acetic anhydride (4 ml) and pyridine (8 ml) was allowed to stand at room temperature 15 h. The mixture was poured into ice water containing excess sodium bicarbonate and allowed to stand 1 h. A hexane extract of the aqueous mixture was washed with water and concentrated *in vacuo* (after drying) at room temperature to a viscous yellow oil (0.52 g) which melted at 104–115°, following crystallization from hexane. Three recrystallizations from hexane – ethyl ether yielded a pure sample melting at 117–119°; $[\alpha]_D^{20}$ +37.5° (*c*, 0.48); p.m.r. spectrum in CCl_4 solution 0.71, 0.75, 0.80, 0.84, 1.14–1.45 (complex and broad), 2.15 (three acetyl protons), 2.54 (two methylene protons), and 9.31 (one aldehyde proton which remains unchanged in the presence of deuterium oxide) δ; ν_{max}^{KBr} 1 790, 1 715, 1 470, 1 370, 1 220, and 1 160 cm^{-1}.

Can. J. Chem. Downloaded from www.nrcresearchpress.com by 210.87.254.105 on 09/05/12
For personal use only.

Anal. Calcd. for $C_{32}H_{55}NO_3$: C, 76.59; H, 11.05; N, 2.79; O, 9.57. Found: C, 77.08; H, 11.18; N, 2.70; O, 9.12.

The oxime acetate was found sensitive and purification was achieved more easily by avoiding heat, light, and the atmosphere. In earlier experiments, an analytical sample prepared following four recrystallizations from hexane melted at 120–123° and exhibited $[\alpha]_D^{20}$ +35.8° (*c*, 0.36). Found: C, 76.74; H, 11.24; N, 2.33; O, 9.88.

1-Cyano-3,4-seco-5α-lanostane (III)

A solution of oxime acetate IX (0.14 g) in 4:1 hexane–benzene was added to a column of silica gel. After approximately 20 h the column was eluted with the same solvent. Removal of solvent *in vacuo* yielded an oil (0.09 g) which solidified, m.p. 83–87°, upon trituration with methanol. Recrystallization from methanol afforded pure needles melting at 85–87°; $[\alpha]_D^{20}$ +42.4° (*c*, 0.24); p.m.r. in CCl_4 solution gave signals at 0.15, 0.69, 0.72, 0.83, 1.05–1.55 (complex and broad) and 2.25 (partially masked doublet) δ; ν_{max}^{Nujol} 2 350 and 1 400 cm^{-1}.

Anal. Calcd. for $C_{29}H_{51}N$: C, 84.26; H, 12.35; N, 3.39. Found: C, 84.52; H, 12.21; N, 3.40.

A mass spectrum of the nitrile exhibited a molecular ion at 413 (calcd. mol. wt. 413).

ACKNOWLEDGMENTS

This investigation was supported by Public Health Service Research Grant No. CA-04074-06 and CA-04074-07 from the National Cancer Institute. One of us (G. R. P.) is indebted to Professor C. Djerassi and the Department of Chemistry, Stanford University for their hospitality during preparation of this manuscript. We also wish to acknowledge the assistance of P. A. Whitehouse with several accessory experiments.

REFERENCES

1. (*a*) G. R. Pettit and P. Hofer. Helv. Chim. Acta, **46**, 2142 (1963).
   (*b*) G. R. Pettit and P. Hofer. J. Chem. Soc. 4439 (1963).
   (*c*) G. R. Pettit, D. S. Alkalay, P. Hofer, and P. A. Whitehouse. Tetrahedron, **20**, 1745 (1964).
2. A. L. Nussbaum and C. H. Robinson. Tetrahedron, **17**, 35 (1962).
3. M. Akhtar *et al.* J. Am. Chem. Soc. **86**, 3394 (1964); **86**, 1528 (1964).
4. (*a*) M. Akhtar and M. M. Pechet. J. Am. Chem. Soc. **86**, 265 (1964).
   (*b*) H. E. Zimmerman and S. Somasekhara. J. Am. Chem. Soc. **85**, 922 (1963).
   (*c*) H. E. Zimmerman and D. I. Schuster. J. Am. Chem. Soc. **83**, 4486 (1961).
5. (*a*) L. J. Beckham, W. A. Fessler, and M. A. Kise. Chem. Rev. **48**, 319 (1951).
   (*b*) N. Kornblum and E. P. Oliveto. J. Am. Chem. Soc. **69**, 465 (1947).
   (*c*) K. Freudenberg and H. Biller. Ann. **510**, 230 (1934).
6. (*a*) P. Kabasakalian and E. R. Townley. J. Org. Chem. **27**, 3562 (1962).
   (*b*) C. H. Robinson *et al.* J. Am. Chem. Soc. **83**, 1771 (1961).
7. O. Exner and B. Kakáč. Collection Czech. Chem. Commun. **28**, 1656 (1963).
8. J. A. Moore and J. Binkert. J. Am. Chem. Soc. **81**, 6029 (1959).
9. R. M. Jipson, F. H. Pettit, C. G. Skinner, and W. Shive. J. Org. Chem. **28**, 1425 (1963).
10. A. Palm and H. Werbin. Can. J. Chem. **31**, 1004 (1953).
11. The Sadtler Standard Spectra. Sadtler Research Laboratories, Philadelphia. No. 8470. 1960.
12. (*a*) H. M. Fales and A. V. Robertson. Tetrahedron Letters, 111 (1962).
   (*b*) L. M. Jackman. Nuclear magnetic resonance spectroscopy. Pergamon Press, N.Y. 1959. p. 62.
   (*c*) G. J. Karabatsos, R. A. Taller, and F. M. Vane. J. Am. Chem. Soc. **85**, 2327 (1964).
   (*d*) G. M. Whitesides *et al.* J. Am. Chem. Soc. **87**, 1058 (1965).
13. (*a*) D. H. R. Barton and J. M. Beaton. J. Am. Chem. Soc. **83**, 4083 (1961).
   (*b*) C. V. Banks. Record Chem. Progr. **25**, 85 (1964).
14. S. P. Findlay. J. Org. Chem. **21**, 644 (1956).
15. L. Mester, E. Moczar, and J. Parello. Tetrahedron Letters, 3223 (1964). R. M. Hann and C. S. Hudson. J. Am. Chem. Soc. **66**, 735 (1944).
16. A. Hassner and I. H. Pomerantz. J. Org. Chem. **27**, 1760 (1962). A. R. Ferris, G. S. Johnson, and F. E. Gould. J. Org. Chem. **25**, 1813 (1960). A. H. Blatt. Chem. Rev. **12**, 215 (1933).
17. R. P. Barnes and A. H. Blatt. J. Am. Chem. Soc. **57**, 1330 (1935).
18. R. T. Conley and R. J. Lange. J. Org. Chem. **28**, 210 (1963). L. Mangoni and M. Belardini. Tetrahedron Letters, 921 (1963). G. H. Whitham. Proc. Chem. Soc. 271 (1959).
19. P. de Mayo and S. T. Reid. Quart. Rev. London, **15**, 393 (1961). D. H. R. Barton, J. F. McGhie, and M. Rosenberger. J. Chem. Soc. 1215 (1961). D. Arigoni *et al.* Proc. Chem. Soc. 306 (1959).
20. J. Karliner, H. Budzikiewicz, and C. Djerassi. J. Am. Chem. Soc. **87**, 580 (1965).
21. W. Voser *et al.* Helv. Chim. Acta, **33**, 1893 (1950).
22. K. Bowden, I. M. Heilbron, E. R. H. Jones, and B. C. L. Weedon. J. Chem. Soc. **39** (1946).
23. R. D. H. Heard, M. T. Ryan, and H. I. Bolker. J. Org. Chem. **24**, 172 (1959).

Can. J. Chem. Downloaded from www.nrcresearchpress.com by 210.87.254.105 on 09/05/12
For personal use only.

Can. J. Chem. Downloaded from www.nrcresearchpress.com by 210.87.254.6 on 09/05/12
For personal use only.

ON A PLATINUM–RHODIUM – OXYGEN ELECTRODE IN SILICATE MELTS

R. E. RANFORD[1] AND S. N. FLENGAS
Department of Metallurgy and Material Science, University of Toronto, Toronto, Ontario

Received March 22, 1965

ABSTRACT

The potential of the formation cell

$$\begin{array}{l} \text{Pt} - 10\%\ \text{Rh} \\ \quad\quad\quad\ \ \text{O}_2 \end{array} \Big| \begin{array}{c} \text{NiO} \\ \text{(silicate solvent)} \end{array} \Big| \ \text{Ni}$$

was studied in the temperature range 900 °C to 1 100 °C. The platinum–rhodium – oxygen electrode was found to behave reversibly in the pressure range 5×10^{-3} atm to 1 atm oxygen. The effects on the cell potential of oxygen pressure, nickelous oxide concentration, and temperature, were all found to follow an exact Nernst relationship.

INTRODUCTION

In spite of the established ionic nature of molten silicates (1–4), very few precise electrochemical measurements in these systems can be found in the literature. The concentration of oxygen anions in silicates has been shown (5) to be governed by an acid–base relationship of the type:

$$[O^{2-}] + [—O—] = 2[O—]$$

for which,

$$K_{eq} = \frac{[O—]^2}{[O^{2-}][—O—]}$$

The equilibrium constant represents the reaction between free oxygen anions O^{2-} in the slag and double-bonded oxygen —O— to form single-bonded oxygen O— species. The O— species are found at the end of a broken silicate chain as —Si—O, while the species —O— indicate oxygen shared between two silicon atoms as —Si—O—Si— in the inner structure of the silicate network. The concentration of the free oxygen anions in an oxide system of the type $MO—SiO_2$ is determined by the overall composition of the mixture, the basicity of the metal oxide component, and temperature.

Potentiometric determination of oxygen ion activities, or metal oxide activities, should therefore be possible by potential measurements using a suitable formation cell. The cell should include an oxygen electrode representing the reaction

$$O^{2-} = \tfrac{1}{2}O_2 + 2e^-$$

as well as a metal – metal ion electrode.

Didtschenko and Rochov (6) were the first to operate a platinum–oxygen concentration cell in solutions of various metal oxides in lead silicate. The results indicated a dependence of the potential on the type of metal oxide present. However, no attempt was made to investigate the quantitative response of this electrode to either oxygen pressure, temperature, or concentration of the metal oxide in the electrolyte. Flood, Forland, and Motzfeldt (7) carefully investigated the behavior of a platinum–oxygen electrode in molten carbonate and sulfate melts. Two oxygen electrodes were used in each cell, and the results indicated an exact Nernst relationship with respect to the mole % carbonate in these mixtures.

[1]*Present address: Dominion Foundries and Steel Co. Limited, Hamilton, Ontario, Canada.*

The reversibility of the oxygen electrode in silicate melts, and its exact response to either oxygen anion concentration in the melt, or to the oxygen pressure over the electrode, has not been shown in any previous work. In the present investigation, a systematic study was made using a simple formation cell of the type

Ni	NiO (X)	Pt – 10% Rh
(–)	(K_2O—Na_2O—SiO_2)	O_2 (+)

The experimental technique for operating oxygen electrodes in silicate melts has been developed. The potentials of the cell were measured as a function of oxygen pressure, of NiO concentration in the electrolyte, and temperature.

The Ni–NiO electrode was chosen because of the stability of the divalent oxide at high temperatures. Bogatskii (8) has shown that the higher oxide Ni_2O_3 totally decomposes at temperatures higher than 800 °C.

EXPERIMENTAL

The cell design is shown in Fig. 1.

The electrode assembly consisted of the oxygen and nickel electrodes. The nickel electrode was made by welding a spectrographically pure nickel rod of 1/8 in. diameter to a stainless steel wire. The oxygen electrode consisted of two concentric platinum – 10% rhodium alloy tubes of a total length of 20 in. To economize on this alloy, the upper halves of these tubes were made of silver welded to the alloy. The melt was contained in a platinum crucible.

Preliminary experiments indicated that stirring the melt made the measured potentials unstable. Therefore all measurements were made under absolutely static conditions. For this purpose, the oxygen–argon mixtures were introduced through the inner tube and then allowed to escape into the outer tube through an exit hole drilled at approximately 1/2 in. higher than the melt level. The inner tube was approximately 1/4 in. O.D., and was immersed in the melt to about 1/2 in. The outer tube of 1/2 in. diameter with a flared end was also immersed into the melt and simply separated the nickel electrode compartment from the oxygen in the inner tube. The nickel electrode was at all times under a slight positive pressure of purified argon.

To eliminate short circuits as well as electrode movements, the oxygen electrode assembly, the nickel electrode, and the slag containing crucible, were all firmly positioned by a boron nitride disc machined to hold both the electrodes and the crucible. A Pt – Pt, 13% Rh thermocouple was also led through this insulator with the bead placed about 1/4 in. above the melt.

The cell was carefully assembled outside the furnace, including the positioning of the electrodes, and the addition of the slag to the crucible. The assembled cell was then introduced into the furnace and was evacuated at about 300 °C for 12 h to remove any absorbed water from the slag. The temperature was then raised to that required for the experiment, and purified argon was fed into the nickel electrode compartment.

The furnace consisted of a single, tubular, silicon carbide element (Crusalite), connected in series to a power-stabilized variac. With this type of power source, and a fairly constant room temperature, the cell temperature could be controlled to ±2 deg, up to 1 400 °C.

The silicate solvent chosen for this work had the composition 54 mole % SiO_2, 28 mole % K_2O, and 18 mole % Na_2O, corresponding to a weight % of 46, 37, 16, respectively. The melting point of this slag is 750 °C. The melt was prepared by mixing stoichiometric amounts of reagent-grade potassium and sodium carbonates with silica at 900 °C. To control the rapid carbon dioxide evolution, silica was added gradually into the molten carbonates as quartz glass. The melt was finally evacuated to remove any residual carbon dioxide. A solute slag containing 0.75 weight % nickelous oxide was prepared by dissolving into the solvent melt the desired amount of nickelous oxide. This slag was then used for adding the solute to the cell to make the desired concentrations. Solute additions were made by removing the inner electrode and dropping weighed amounts of solute slag into the crucible.

At each concentration level, the equilibrium potentials were measured as a function of temperature on heating and cooling the cell in the temperature range 900 °C to 1 100 °C. The duration of a temperature cycle was about 12 h. At the end of every cycle run, the melt was sampled and analyzed for the nickel content.

The oxygen electrode was operated under a total pressure of 1 atm. Various mixtures of argon and oxygen were employed. The gas mixtures were made by metering known volumes of the two gases into the oxygen electrode. Calibrated rotameter type flowmeters were used, and the compositions of the mixtures at the higher oxygen concentrations were also verified by Orsat gas analysis.

The partial pressure of oxygen was varied stepwise from 5×10^{-3} atm to 1 atm. Potentials were measured at each oxygen-to-argon ratio, with the temperature and the metal ion concentration kept constant.

Can. J. Chem. Downloaded from www.nrcresearchpress.com by 210.87.254.6 on 09/05/12
For personal use only.

Can. J. Chem. Downloaded from www.nrcresearchpress.com by 210.87.254.6 on 09/05/12
For personal use only.

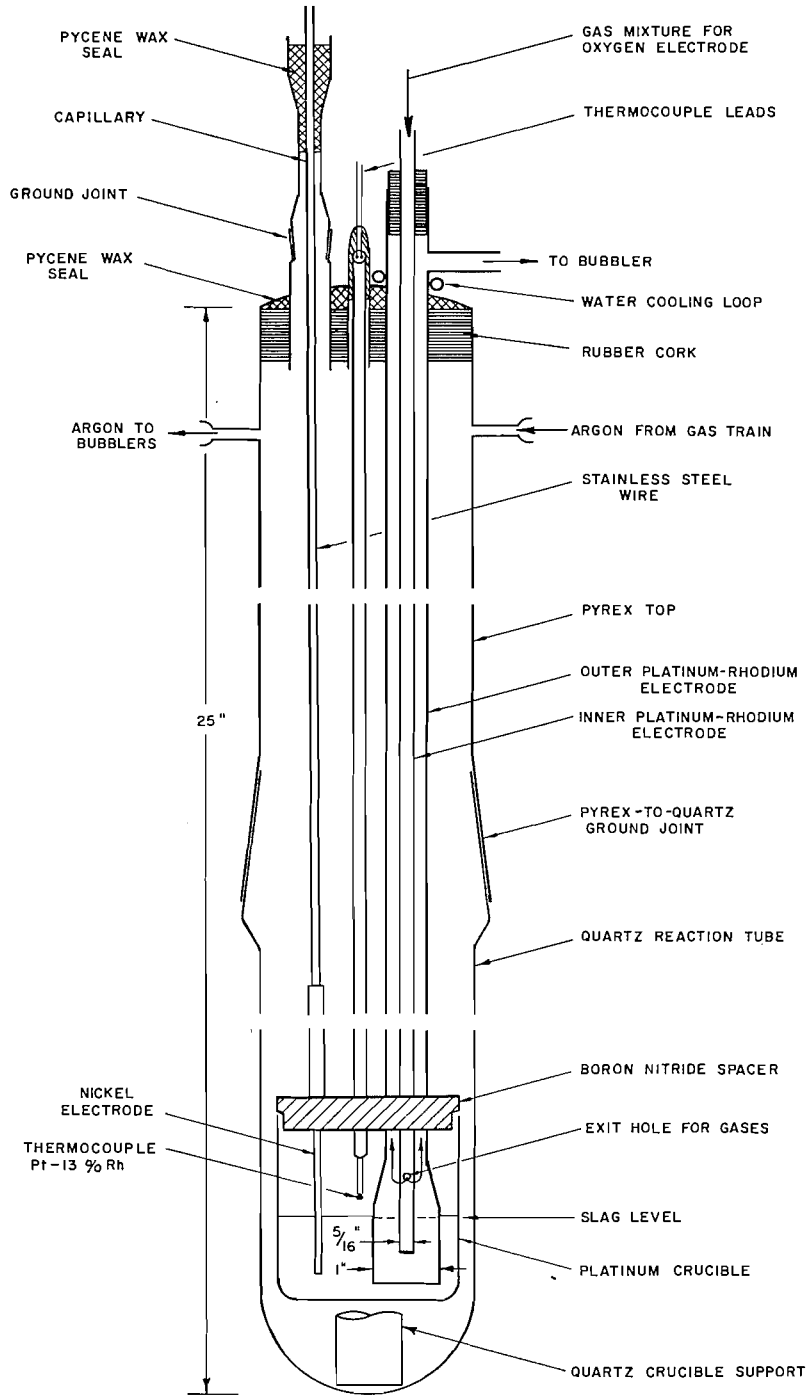

FIG. 1. Cell design.

One early difficulty experienced in this work was the uncontrollable oxidation of the nickel electrode, and the subsequent increase of the nickelous oxide concentration in the melt. This resulted in a continuous decrease in the cell potential with time at a given temperature. This effect was particularly evident when the oxygen electrode was operated at an oxygen pressure of 1 atm. Over a period of 24 h, the cell potential would decrease by as much as 20 mV. However, using a low oxygen pressure i.e., 5×10^{-2} atm, at the oxygen electrode, it was found that the potential decreased by about only 1 mV. Accordingly, in all experimental work reported here, the low oxygen pressure of 5×10^{-2} atm was used. In the investigation of the effect of pressure on the potential, the entire run lasted approximately 6 h, and the time spent at the high oxygen pressures was kept to a minimum.

The potentials were measured with a type K-2, Leeds and Northrup potentiometer.

Thermoelectric potentials were also measured at temperatures from 800 °C to 1 200 °C by short circuiting the Pt–Rh and nickel electrodes. In the temperature range of the experiments, these amounted to only 2 to 4 mV and were neglected in the calculations as negligibly small.

RESULTS

For the cell

Ni	NiO (X)	Pt – 10% Rh
(−)	K_2O:Na_2O:SiO_2	O_2 (+)
	28 18 54	(at P_{O_2} atm)

the corresponding cell reaction is given as:

$$Ni_{(s)} + \tfrac{1}{2}O_{2(\text{at } P_{O_2})} = NiO_{(\text{in solution})}$$

The relationship between the cell potential, the activity of NiO in the melt, and the oxygen pressure at the oxygen electrode, can be readily derived as:

$$[1] \qquad E_{\text{cell}} = E_{\text{NiO}}{}^{0} - \frac{2.303RT}{2F} \log \frac{a_{\text{NiO}}}{P_{O_2}{}^{1/2}}$$

where, $E_{\text{NiO}}{}^{0}$ is the standard formation potential of pure solid NiO at that temperature. This may be calculated from the standard free energy of formation of solid nickelous oxide (9) at that temperature, following the relationship: $\Delta G_f{}^{0} = -2E^{0}F$. Accordingly, the nickelous oxide activity, a_{NiO}, refers to pure solid NiO as the standard state.

For the study of the effect of pressure, the cell potential was measured as a function of the oxygen pressure at the platinum–rhodium electrode, at constant nickelous oxide content and constant temperature.

The results of two pressure runs are shown in Fig. 2.

The plot of the measured potential versus the log $P_{O_2}{}^{1/2}$ is linear, as expected from eq. [2]. The slopes of the straight lines are in good agreement with the theoretical slopes for a two-electron electrode process. These runs were done at two different temperatures and concentrations of nickelous oxide.

In Fig. 2, the two potential curves differ by 31 mV on the high oxygen pressure side and by 23 mV on the low pressure side. Assuming that the activity coefficient of NiO remains constant in the temperature and concentration range considered, the calculated difference from eq. [1] is only 20 mV.

The results shown in Fig. 2 were obtained over the pressure range from pure oxygen to 5×10^{-3} atm pressure. At the high oxygen pressures ($0.75 \sim 1$ atm), steady potentials were established within 10 min, while more time was required when changing the gas composition to lower pressures. This slower response of the electrode at the lower pressures may be explained by the time required to purge the preceding atmosphere in the apparatus and replace it with the new mixture.

During a run, the potentials were reproducible over a complete pressure cycle, indicating the reversibility of the oxygen electrode in these melts.

Can. J. Chem. Downloaded from www.nrcresearchpress.com by 210.87.254.6 on 09/05/12
For personal use only.

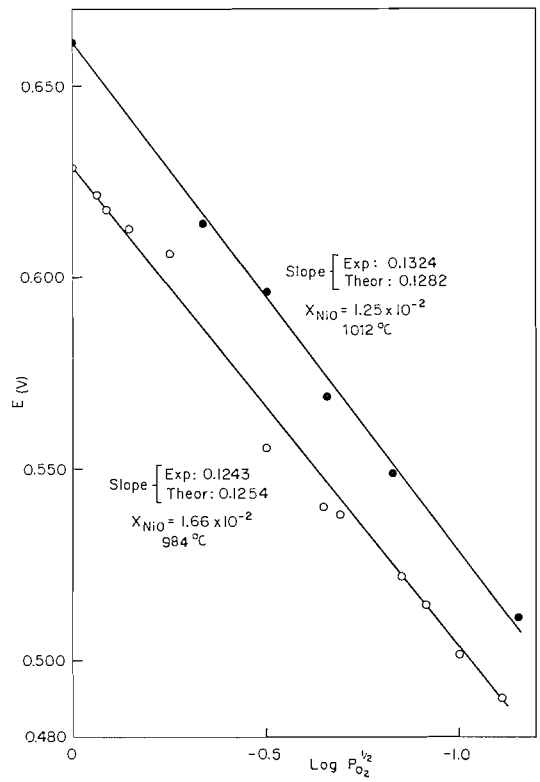

FIG. 2. Electromotive force of the cell

Ni	NiO (X)	Pt – 10% Rh
(–)	(K_2O:Na_2O:SiO_2)	O_2 (+)

as a function of log $P_{O_2}^{1/2}$.

Cell potentials were also measured as a function of temperature, at concentration levels from 7.5×10^{-4} to 1.5×10^{-2} mole fraction of NiO.

For these measurements, the oxygen pressure at the oxygen electrode was maintained at the low pressure of 5×10^{-2} atm.

The results are shown in Fig. 3.

Although scatter of the order of ± 5 mV is present, all curves are almost parallel, indicating the consistency of the results. From the data on Fig. 3, the cell potentials were obtained at the three selected temperatures of 900 °C, 1 000 °C, and 1 100 °C, and are plotted versus log X_{NiO} in Fig. 4.

By eq. [1], and on the assumption that the activity coefficients are constant at each of the temperatures, the theoretical slopes were calculated, and are shown by the dotted straight lines drawn through the experimental points. Since these lines closely approximate the data, it may be concluded that the activity coefficients are constant and therefore the system obeys Henry's law.

The arithmetic means of the activity coefficients, calculated from all the available experimental points, are given in Table I.

The plot of log γ_{NiO} versus the reciprocal of the absolute temperature is also linear. From the slope, the partial molar heat of mixing of solid nickelous oxide is found to be

Can. J. Chem. Downloaded from www.nrcresearchpress.com by 210.87.254.6 on 09/05/12
For personal use only.

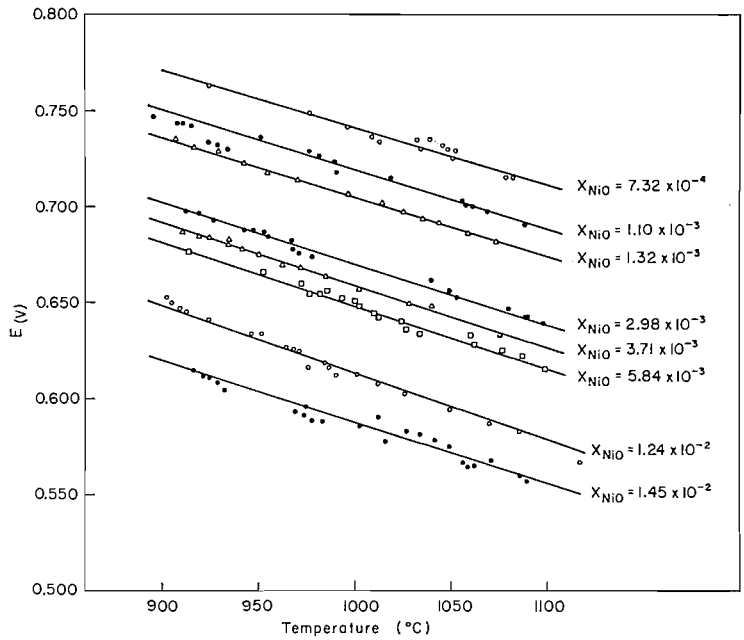

FIG. 3. Electromotive force of the cell

Ni	NiO	Pt – 10% Rh
(–)	(K_2O:Na_2O:SiO_2)	O_2 (+)

as a function of temperature, at various nickelous oxide mole fractions.

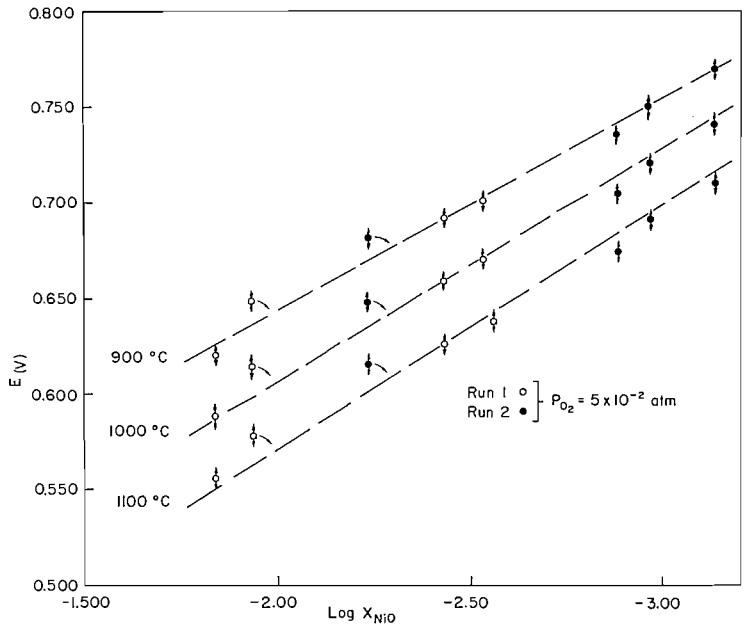

FIG. 4. Electromotive force of the cell

Ni	NiO	Pt – 10% Rh
(–)	(K_2O:Na_2O:SiO_2)	O_2 (+)

as a function of log X_{NiO}, at constant temperatures.

Can. J. Chem. Downloaded from www.nrcresearchpress.com by 210.87.254.6 on 09/05/12
For personal use only.

TABLE I
Thermodynamic properties of NiO in solution

Temp. (°C)	Experimental $(\gamma_{NiO})_S$	Experimental $(\overline{\Delta H_m})_{S,NiO}$ (cal/mole)	Calculated $(\gamma_{NiO})_L$*	Calculated $(\overline{\Delta H_m})_{L,NiO}$* (cal/mole)	Calculated $(\overline{\Delta S_m})_{L,NiO}^{xs}$* (e.u.)
900	35.3±5	5000±500	2.5	−7100	−8.25
1000	27.4±4	5000±500	3.6	−7100	−8.35
1100	21.8±4	5000±500	3.9	−7100	−8.05

*Approximate figures.

5 000 ± 500 cal/mole, in the temperature range 900 °C to 1 100 °C. The limits as shown correspond to the upper and lower values of the activity coefficients given in Table I.

DISCUSSION

The partial molar properties of nickelous oxide, calculated with respect to pure solid NiO as the state of reference, do not provide any information concerning the nickelous oxide species in solution.

In the partial molar properties shown in Table I, the experimental values include the thermal data for the fusion of nickelous oxide at these temperatures. Accordingly, the activity coefficients and the partial molar heats of mixing of nickelous oxide must be recalculated to represent the liquid state of reference.

The relationship between the heats of mixing of solid, $(\overline{\Delta H_m})_{S,NiO}$, and liquid nickelous oxide, $(\overline{\Delta H_m})_{L,NiO}$, is given by the expression:

$$[2] \qquad (\overline{\Delta H_m})_{S,NiO} = (\overline{\Delta H_m})_{L,NiO} + \Delta H_F$$

where, ΔH_F corresponds to the heat of fusion at the mixing temperature.

Similarly, the activity coefficients are related by the expression

$$[3] \qquad \Delta G_F = RT \ln \frac{(\gamma_{NiO})_S}{(\gamma_{NiO})_L}$$

where, ΔG_F is the free energy of fusion of nickelous oxide at the mixing temperature. $(\gamma_{NiO})_S$ and $(\gamma_{NiO})_L$ are activity coefficients referring to pure solid and pure liquid nickelous oxide, respectively, as the states of reference.

From eqs. [2] and [3], and the thermodynamic data for fusion given in the literature (10), the partial molar properties of liquid nickelous oxide were calculated and are also shown in Table I. These calculations are given without any limits of accuracy, as the heat of fusion of NiO, as well as the heat capacities are only approximate (10).

The activity coefficients of liquid nickelous oxide indicate positive deviations from ideality, increasing with increasing temperature. The partial molar heat of mixing is exothermic, and the excess entropy of mixing is also negative, indicating the formation of complex nicelo-silicate species in solution.

The calculation of activity coefficients in terms of an "ionic" model does not affect the positive deviations from ideality found in this system. Thus, the activity in the "molecular" model is given as

$$[4] \qquad a_{NiO} = \gamma_{NiO} X_{NiO} = \gamma_{NiO} \times \frac{n_{NiO}}{n_{NiO} + n_{K_2O} + n_{Na_2O} + n_{SiO_2}} = \gamma_{NiO} n_{NiO}$$

Can. J. Chem. Downloaded from www.nrcresearchpress.com by 210.87.254.6 on 09/05/12
For personal use only.

where n_{NiO} is the number of moles of NiO per gram-mole of solution. In the "ionic" model,

$$a_{NiO} = \gamma_{NiO}'(N_{Ni^{++}}N_{O^{--}}) = \gamma_{NiO}' \frac{n_{Ni^{++}}}{n_{K^+} + n_{Na^+} + n_{Ni^+}} \cdot N_{O^{--}}$$

$$= \gamma_{NiO}' \frac{n_{NiO}}{2n_{K_2O} + 2n_{Na_2O} + n_{NiO}} N_{O^{--}}$$

where $N_{Ni^{++}}$ and $N_{O^{--}}$ represent the ionic fractions of nickel and oxygen, and γ_{NiO}' is the "ionic" activity coefficient.

For the dilute solutions of nickelous oxide in a slag having the specified composition, this equation reduces to

[5] $$a_{NiO} = \gamma_{NiO}' \frac{n_{NiO}}{0.92} N_{O^{--}}.$$

The comparison of the two expressions [4] and [5] for the activity gives the following relationship between the "molecular" and the "ionic" activity coefficients.

[6] $$\frac{\gamma_{NiO(molecular)}}{\gamma_{NiO}'_{(ionic)}} = \frac{N_{O^{--}}}{0.92}$$

As the oxygen anion fraction $N_{O^{--}}$ is always less than unity, it is evident that the "ionic" activity coefficients show deviations from ideality, which are even more positive than those indicated by the "molecular" model. It should be noted that large positive deviations from ideality have also been found by Chipman *et al.* (11) in solutions of ferrous oxide in a basic slag containing calcium and magnesium oxides.

The properties of silicates are understood at present by the gradual breakdown of the silicate network upon the addition of oxygen ions from a more basic oxide. The simple ionic theory, however, is inadequate to account for the existence of free oxygen anions in any slag in which the MO/SiO_2 ratio is less than 2. To resolve this problem, several models have been proposed (12, 13) in which other ionic species besides the orthosilicate have been considered. Such calculations, however, are rather arbitrary and do not necessarily represent the true structure of the silicate. Furthermore, the various models cannot account for Henry's law behavior, as found in this work. The positive deviations from ideality in an acidic slag of this type indicate that the concentration of the free oxygen anions is relatively high. Their activity is expected to be governed by the more basic components K_2O and Na_2O that constitute the solvent slag. The positive temperature dependence of the activity coefficient is then indicative of the dissociation of the complex silicate network at the higher temperatures.

If these assumptions are correct, it may be predicted that for a given weak basic oxide, like nickelous oxide, the positive deviations from ideality should become more pronounced as the basicity, or the proportion of the more basic components in the solvent slag, is increased.

ACKNOWLEDGMENT

The authors are indebted to the National Research Council of Canada for a research grant in support of this work. The assistance of the Mines Branch of the Department of Mines and Technical Surveys, Ottawa, in the analysis of the silicate samples, is also gratefully acknowledged.

Can. J. Chem. Downloaded from www.nrcresearchpress.com by 210.87.254.6 on 09/05/12
For personal use only.

REFERENCES

1. J. CHIPMAN and LO-CHING-CHANG. Met. Trans. **2**, 191 (1949).
2. P. HERASYMENKO and G. E. SPEIGHT. J. Iron Steel Inst. **11**, 169 (1950).
3. M. G. FROHBERG. Arch. Esienhuettenw. **32**, 597 (1961).
4. H. FLOOD and T. FORLAND. Acta Chem. Scand. **1**, 592 (1947).
5. C. B. FINCHAM and F. D. RICHARDSON. Proc. Roy. Soc. London, Ser. A, **223**, 40 (1954).
6. R. DIDTSCHENKOV and E. C. ROCHOV. J. Am. Chem. Soc. **76**, 3291 (1954).
7. H. FLOOD, T. FORLAND, and K. MOTZFELDT. Acta Chem. Scand. **6**, 257 (1952).
8. D. P. BOGATSKII. J. Gen. Chem. USSR Eng. Transl. **21**, 3 (1951).
9. O. KUBASCHEWSKI and E. LL. EVANS. Metallurgical thermochemistry. Pergamon Press, New York. 1958.
10. A. GLASSNER. The thermodynamic properties of the oxides, fluorides and chlorides to 2500° K. Argonne National Laboratory. Circ. ANL 5750.
11. J. CHIPMAN and T. B. WINKLER. Trans. Am. Inst. Mining Met. Engrs. **167**, 111 (1946).
12. G. W. TOOP and C. S. SAMIS. Can. Met. Quart. **1**, 129 (1962).
13. J. O'M. BOCKRIS, J. W. TOMLINSON, and W. L. WHITE. Trans. Faraday Soc. **52**, 299 (1956).

Can. J. Chem. Downloaded from www.nrcresearchpress.com by 210.87.254.6 on 09/05/12
For personal use only.

Can. J. Chem. Downloaded from www.nrcresearchpress.com by 210.87.254.105 on 09/05/12
For personal use only.

SPECTROSCOPIC STUDIES OF ALCOHOLS

V. INTRAMOLECULAR HYDROGEN BONDS IN 2-CYANOETHANOL AND IN SOME NITROALCOHOLS[1]

P. J. KRUEGER AND H. D. METTEE
Department of Chemistry, University of Alberta, Calgary, Alberta
Received May 19, 1965

ABSTRACT

The enthalpy difference between the *trans* and the intramolecularly hydrogen bonded *gauche* conformation of 2-cyanoethanol in dilute CCl_4 solution is shown to be -0.14 ± 0.03 kcal/mole from the temperature dependence of the fundamental OH stretching bands. At higher concentrations cyclic dimers with double OH...O bonds form. The enthalpy change on dimerization is -6.1 ± 0.3 kcal/mole. A small percentage of dimers with acylic OH...O bonds are also present, but these are thermodynamically less stable than the cyclic dimers.

Intramolecular hydrogen bonds are found between OH and NO_2 groups in some 2-nitroalcohols, leading to stabilization of the *gauche* form with respect to the *trans* form. For 2-nitroethanol the *trans* conformer is in equilibrium with two intramolecularly hydrogen bonded conformers ($\Delta H = -0.40 \pm 0.10$ and -0.71 ± 0.09 kcal/mole respectively). 2,2-Dinitropropanol and 2-methyl-2-nitro-1,3-propanediol show complex ν_{OH} bands due to *trans* and intramolecularly hydrogen bonded *gauche* conformers. 2,2,2-Trinitroethanol has a relatively narrow symmetrical OH peak at temperatures up to 55 °C which is assigned to the exclusively populated intramolecularly hydrogen bonded conformation.

INTRODUCTION

High-resolution infrared spectra of 2-substituted ethanols in the 3 μ region give valuable information about the factors affecting intramolecular hydrogen bond strengths (particularly geometry), and about those governing frequency displacements of hydrogen bonded OH groups. As a continuation of previous studies on 2-mono-, 2,2-di-, and 2,2,2-trihalosubstituted ethanols (3), hydrogen bonding in 2-cyanoethanol (hydracrylonitrile) and in some nitroalcohols in dilute CCl_4 solution has been investigated.

Cyano Groups as Proton Acceptors

The cyano group is well known to be a moderately strong proton acceptor because of the directed lone pair orbital on the nitrogen atom (4). The linearity of the group prevents steric complications in intermolecular hydrogen bonding studies. Hydrogen bond strengths between nitriles and phenol ($\Delta H = -4$ kcal/mole) and methanol ($\Delta H = -2$ kcal/mole) have been measured (5)

In the formation of intramolecular hydrogen bonds to the cyano group in 2-cyanoethanol the geometry of the system plays a major role, prohibiting access of the proton donating group to the nitrogen lone pair orbital. The weaker hydrogen bonds which form involve the π-electrons of the triple bond. The OH stretching frequencies of representative hydroxynitriles and their acetylene analogues have been studied by Allerhand and Schleyer (4), and intramolecular NH...CN interaction has been noted in *o*-cyanoaniline (6). No thermodynamic investigation of the strength of intramolecular hydrogen bonds to nitrile groups appears to have been reported.

The gas phase electron diffraction results of Yamaha (7) on 2-cyanoethanol itself showed

[1]*While this work was in progress the authors were informed of other studies then in press on nitro groups as proton acceptors in hydrogen bonds by Schleyer et al. (1). Their work did not, however, include quantitative thermodynamic measurements on which this paper is based. Since this work was completed, H. E. Ungnade, E. M. Roberts, and L. W. Kissinger have also confirmed the existence of weak hydrogen bonds between nitro groups and alcoholic* OH *groups (2).*

no evidence of an intramolecularly hydrogen bonded *gauche* conformation, and the conclusion was reached that the molecule was exclusively in the *trans* form.

Nitro Groups as Proton Acceptors

Although chelation in *o*-nitrophenol is a well established fact (1, 8*a*) based on numerous investigations using a wide variety of techniques, intramolecular $OH\cdots O_2N$ hydrogen bonding in systems which do not involve direct resonance interaction of the OH and NO_2 groups (which is responsible for the unusual strength of the intramolecular hydrogen bond in *o*-nitrophenol and the large OH spectral shift) is subject to conflicting reports. In connection with other studies of intramolecular hydrogen bonds in simple systems (3), 2-nitroethanol is of particular interest since no quantitative thermodynamic data on the conformational mobility of this compound appear to be available.

Flett (9) found only a broad band at 3 588 cm^{-1} for 2-nitroethanol in CCl_4 solution, significantly lower than the OH stretching frequency of 3 636 cm^{-1} usually found for monomeric normal primary alcohols under the same conditions. Kuhn, Luettke, and Mecke (10) report a *trans* band at 3 623 cm^{-1} and a *gauche* band at 3 608 cm^{-1} for 2-nitroethanol, and conclude that the latter is more stable because of a weak intramolecular $OH\ldots O_2N$ hydrogen bond. For nitroalcohols with two β-hydroxyl groups Urbanski and co-workers (11) have interpreted shifts in both ultraviolet and infrared peaks associated with the NO_2 group in terms of intramolecular hydrogen bonding.

Recently intramolecular hydrogen bonding in 2-nitroalcohols, including 2-nitroethanol, has been refuted on the basis of infrared studies in the 3 μ region using a NaCl prism spectrophotometer of low resolution (12, 13).

Studies of intermolecular hydrogen bonding of various hydroxylic proton donors and nitro compounds as proton acceptors show that nitro groups uniformly form weak hydrogen bonds as reflected in very small spectral shifts of the OH vibrational band (1). Spectra obtained with high resolution are therefore essential for the complete interpretation of the role these weak hydrogen bonds play in conformational equilibria, and the investigation of the temperature dependence of such spectra is advisable since frequency displacements do not necessarily measure the strength of weak intramolecular hydrogen bonds.

EXPERIMENTAL

Spectroscopic measurements were made with a Beckman IR-7 infrared spectrophotometer operating at a calculated nominal slit width of about 1 cm^{-1}. Matched fused quartz absorption cells of 2 and 10 cm path length were used. Cell temperatures were controlled with a Lauda UK-70 DW Ultrakryostat. Other details concerning technique have been described previously (3). Carbon tetrachloride (reagent grade) was dried over P_2O_5 and fractionally distilled through a 50 theoretical plate spinning band column. Other solvents used were commercial products of spectroscopic quality.

Hydracrylonitrile (Eastman) was dried over anhydrous sodium sulfate and fractionally distilled through a 23 plate spinning band column, collecting colorless material with a b.p. 82.5 °C at 4 mm, n_D^{23} 1.4257 (lit. b.p. 82 °C at 4 mm, n_D^{25} 1.4374 (14)). 2-Nitroethanol was a commercial product (K & K Laboratories, Inc.) which was dried over anhydrous Na_2SO_4 and distilled under reduced pressure (n_D^{25} 1.4497; lit. 1.4383^{25} (15), 1.4403^{20} (16)). 2-Methyl-2-nitro-1,3-propanediol and 2,2-dinitropropanol were given by Dr. H. E. Ungnade, Los Alamos Scientific Laboratory, University of California. A small sample of 2,2,2-trinitroethanol (as an anhydrous CCl_4 solution) was obtained from Dr. T. N. Hall, U.S. Naval Ordnance Laboratory, White Oak, Silver Springs, Maryland, U.S.A. This was diluted further with dry CCl_4 and used directly.

RESULTS AND DISCUSSION

2-Cyanoethanol

Concentrations of the order of 10^{-4} *M* in CCl_4 were necessary to eliminate a broad concentration and temperature dependent absorption band centered at 3 500 cm^{-1}. At these low concentrations a concentration independent but temperature dependent doublet

Can. J. Chem. Downloaded from www.nrcresearchpress.com by 210.87.254.105 on 09/05/12
For personal use only.

remained in the 3 μ region. The more intense high frequency component (3 633.$_8$ cm^{-1}) must be due to the *trans* conformation, with the low frequency component (3 619.$_0$ cm^{-1}) due to the intramolecularly hydrogen bonded *gauche* conformation.[2] Figure 1(*a*) shows some typical spectra.

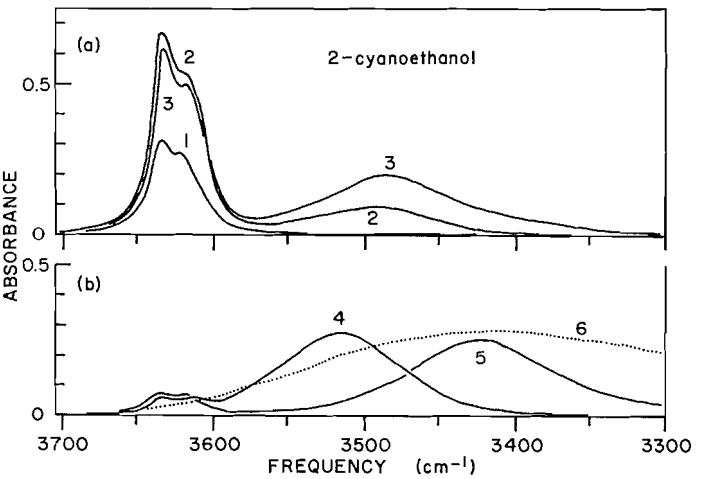

FIG. 1. Fundamental OH stretching bands of 2-cyanoethanol in dilute CCl_4 solution: (1) concentration 4×10^{-4} *M*, path length 10.0 cm, temperature 20 °C; (2) concentration 2.5×10^{-3} *M*, path length 2.00 cm, temperature 20 °C; (3) same as (2) but at 0 °C; (4) concentration 2.5×10^{-3} *M*, and 0.65 *M* with respect to acetonitrile in both sample and reference cell; (5) concentration 2.5×10^{-3} *M*, and 0.5 *M* with respect to diethyl ether in both sample and reference cell; (6) capillary film of pure 2-cyanoethanol.

The relative intensity of the *trans/gauche* doublet is increased slightly by intermolecular association which sets in at the higher concentrations ($\sim 10^{-3}$ *M*). The first associated species to appear with increasing concentration would be expected to be the dimer (*vide supra*) which could conceivably have one of the following structures.

$$N{\equiv}CCH_2CH_2OH\cdots OCH_2CH_2C{\equiv}N \quad (H)$$

I

$$N{\equiv}CCH_2CH_2O \quad (H) \quad OCH_2CH_2C{\equiv}N \quad (H)$$

II

$$N{\equiv}CCH_2CH_2OH\cdots N{\equiv}CCH_2CH_2OH$$

III

In I and III the proton acceptor molecule could also be in the intramolecularly hydrogen bonded gauche form.

Figure 1(*b*) shows comparative spectra of the 2-cyanoethanol–acetonitrile and the 2-cyanoethanol – diethyl ether complexes respectively in dilute CCl_4 solution, as well as a spectrum of a thin film of pure 2-cyanoethanol. It is known that the frequencies of bonded OH groups can show a marked dependence on the proton acceptor concentration (17) so that these band positions do not represent values extrapolated to infinite dilution, but they are useful in identifying the nature of the 2-cyanoethanol dimer. Since the *G* value (17) of diethyl ether ($G = 64$) is very close to that of CCl_4 ($G = 69$) little change

[2]*These bands have been reported at 3 625 and 3 610 cm*$^{-1}$ *(9) and at 3 632 and 3 617 cm*$^{-1}$ *(4) in very dilute* CCl_4 *solution.*

Can. J. Chem. Downloaded from www.nrcresearchpress.com by 210.87.254.105 on 09/05/12
For personal use only.

in the 2-cyanoethanol–Et_2O complex band is expected as the Et_2O concentration is altered, but the 2-cyanoethanol–acetonitrile complex band is expected to shift to somewhat higher frequency on extrapolation to infinite dilution (*G* for CH_3CN is 93). The basicity of the N atom in 2-cyanoethanol is expected to be less than that of the N atom in acetonitrile,[3] so that the frequency shift on intermolecular hydrogen bond formation as in III should be *less* than that in $N{\equiv}CCH_2CH_2OH\cdots N{\equiv}CCH_3$ hydrogen bond formation. This is not the case. On the other hand the electron-withdrawing nature of the $C{\equiv}N$ group would increase the acidity[3] of the OH but decrease the basicity of the hydroxyl oxygen atom in 2-cyanoethanol,[4] making it a poorer proton acceptor than the oxygen atom in diethyl ether. Therefore the frequency shift on intermolecular hydrogen bond formation as in I is expected to be *less* than that on $N{\equiv}CCH_2CH_2OH\ldots OEt_2$ hydrogen bond formation, and this is observed experimentally. A dimer like II is expected to have a bonded OH frequency like that of I, or perhaps a little higher.

The hydrogen bond strength of 6.1 kcal/mole in the 2-cyanoethanol dimer as determined in this work rules out III and favors II over I. Strengths of $OH\ldots N{\equiv}C$ hydrogen bonds involving phenol and methanol have been found to be only 4 and 2 kcal/mole respectively (5) whereas the ΔH values for dimerization of simple alcohols are 6–7 kcal/mole (20), in line with the 2-cyanoethanol value. There is considerable evidence favouring cyclic dimers with two non-linear $OH\cdots O$ hydrogen bonds for simple alcohols (*8b*), and this may also apply to the 2-cyanoethanol dimers. The capillary film shows extremely broad OH absorption, presumably due to a variety of molecular aggregates.

Figure 2(*b*) shows the temperature dependence of the *trans/gauche* absorbance ratio

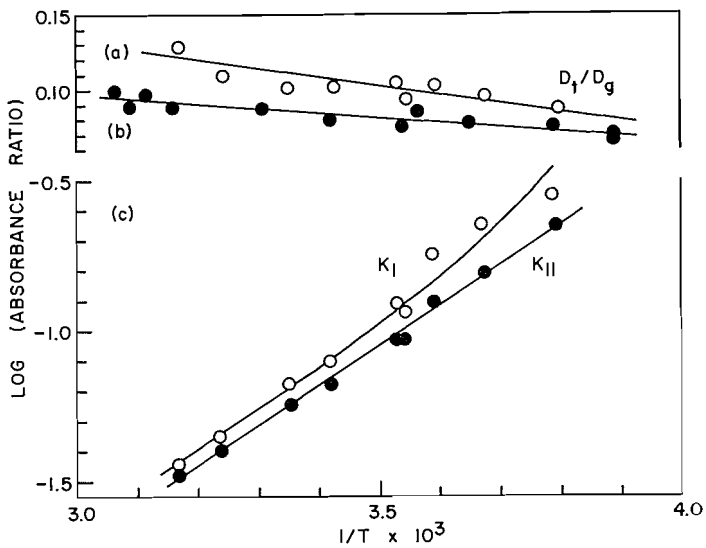

FIG. 2. (*a*) Temperature dependence of *trans/gauche* absorbance ratio of monomeric 2-cyanoethanol at concentrations where some dimerization occurs. (*b*) Temperature dependence of *trans/gauche* absorbance ratio in monomeric 2-cyanoethanol in very dilute CCl_4 solution ($\leqslant 4 \times 10^{-4}$ *M*). (*c*) Temperature dependence of dimerization constant for 2-cyanoethanol at higher concentrations in CCl_4 ($4 \times 10^{-4} <$ concentration $\leqslant 2.5 \times 10^{-3}$ *M*). Apparent equilibrium constants K_I and K_{II} calculated on the basis of open and cyclic dimers respectively. For convenience the factor 2 in the K_{II} expression is omitted.

[3]*The Taft* σ^* *values (18) for* $HOCH_2CH_2$— *and* $N{\equiv}CCH_2CH_2$— *groups are estimated to be +0.20 and +0.46 respectively relative to a value of zero for the* CH_3— *group. Electron-withdrawing groups on a nitrile decrease the frequency shift observed on intermolecular hydrogen bond formation with a given proton donor (4).*

[4]*It has been demonstrated that this is the case in 2,2,2-trifluoroethanol (19).*

Can. J. Chem. Downloaded from www.nrcresearchpress.com by 210.87.254.105 on 09/05/12
For personal use only.

at concentrations in CCl_4 where intermolecular association is absent. Evaluation of the slope of the $\log_{10}(D_t/D_g)$ vs. $1/T$ plot by the least squares method gives $\Delta H = -0.14 \pm 0.03$ kcal/mole for the process in which the hydrogen bond forms. Considering the interactions between non-bonded atoms on the adjacent carbon atoms in the *trans* and *gauche* forms (21), it follows that the *trans* → *gauche* process is accompanied by the gain of one weak repulsive interaction (H—H) and the loss of two stronger repulsive interactions (H—CN and H—OH) as well as the gain of the attractive OH—CN interaction. The observed $-\Delta H$ is therefore probably greater than would be expected on the basis of the intramolecular hydrogen bond alone because of the lost repulsive interactions, i.e. the hydrogen bond strength itself is less than 0.14 kcal/mole. The very weak nature of this interaction accounts for the fact that no bonded OH peak is observed for compounds of the type $HO—(CH_2)_n—CN$ when $n = 3$ or 4 (4).

From measurements at higher concentrations the enthalpy change on intermolecular association can be determined. Using absorbances at the maxima of the intermolecularly bonded peak (D_d), the *trans* peak (D_t) and the *gauche* peak (D_g) as estimates of the respective relative concentrations, the following approximate equilibrium expressions apply for the formation of I and II respectively.

$$K_{\mathrm{I}} = D_d/(D_t + D_g - D_d)^2$$

$$K_{\mathrm{II}} = D_d/2(D_t + D_g)^2$$

In the first expression the total monomer absorbance $(D_t + D_g)$ is corrected for the absorbance of "terminal" OH groups of open dimers, which probably contribute to the *trans* band (8*c*). Extinction coefficient differences for the bands are ignored since the behavior of K vs. $1/T$ will be affected little if $E_t \approx E_g$, which is reasonable for such a weak intramolecular hydrogen bond. Furthermore, the dimer concentration was always relatively small. Figure 2(*c*) shows the temperature dependence of K_{I} and K_{II}. The linearity of K_{II} vs. $1/T$ implies that cyclic dimerization is the dominant type of association in this concentration range, with $\Delta H = -6.1 \pm 0.3$ kcal/mole (least squares method, 90% confidence limits), which reflects the intermolecular hydrogen bond strength of the two angular OH···O bonds in the cyclic dimer. The plot of K_{I} vs. $1/T$ is linear at high temperatures where the dimer concentration is small, but curves upward at lower temperatures where dimer concentration is larger.

Figure 2(*a*) also shows the increase in D_t/D_g in solutions where dimerization occurs. This increase indicates the contribution of some 'terminal" OH absorption from a small amount of the acyclic dimer I to the *trans* band. At these low concentrations the monomeric conformational equilibrium should not be affected by the presence of a minute amount of dimer. Because the measurements were made at several concentrations these points are spread over a narrow belt, the edges of which can be extrapolated to meet line (*b*) in Fig. 2 at −35 °C, where all I would have reverted to the more stable II.

Acetone Cyanohydrin

Weak intramolecular OH interaction with a nitrile group leading to a formal four-membered ring also seems possible. Thus, for acetaldehyde cyanohydrin, only one OH band has been reported at 3 607 cm^{-1} (ref. 4, interpreted as "bonded" ν_{OH}) and 3 604 cm^{-1} (ref. 9, interpreted as "free" ν_{OH}). For acetone cyanohydrin we have found a single sharp symmetrical band at 3 600.$_4$ cm^{-1}, $\Delta\nu_{1/2}{}^a = 16.{}_6$ cm^{-1} at 28 °C, shifting to 3 602.$_6$ cm^{-1} with $\Delta\nu_{1/2}{}^a = 17.{}_3$ cm^{-1} at 55 °C, and becoming slightly asymmetric on the high frequency side. The low value of this OH frequency indicates that it belongs to a hydrogen bonded

Can. J. Chem. Downloaded from www.nrcresearchpress.com by 210.87.254.105 on 09/05/12
For personal use only.

group. Rotation about the C—O bond to move the hydroxyl proton from the *gauche* to the *trans* position with respect to the CN group would bring repulsive forces between the oxygen lone pair orbitals and the CN π-electrons into play, and this may help to stabilize the *gauche* form. Intramolecular hydrogen bonding involving OH···O=C interaction in four-membered rings is well known in carboxylic acids (22), and similar NH···O=C interaction in partially deuterated primary acid amides leads to *cis–trans* isomerism of the —NHD groups (23).

Nitroalcohols

Figure 3(*a*) shows the fundamental OH stretching bands of 2-nitroethanol (0.0038 *M* in CCl_4) obtained at room temperature. The maximum at 3 630 cm^{-1} is assigned to the *trans* conformer, and maxima at 3 620 and 3 612 cm^{-1} are assigned to two intramolecularly hydrogen bonded *gauche* conformers. These measurements agree well with those of Schleyer *et al.* (1).

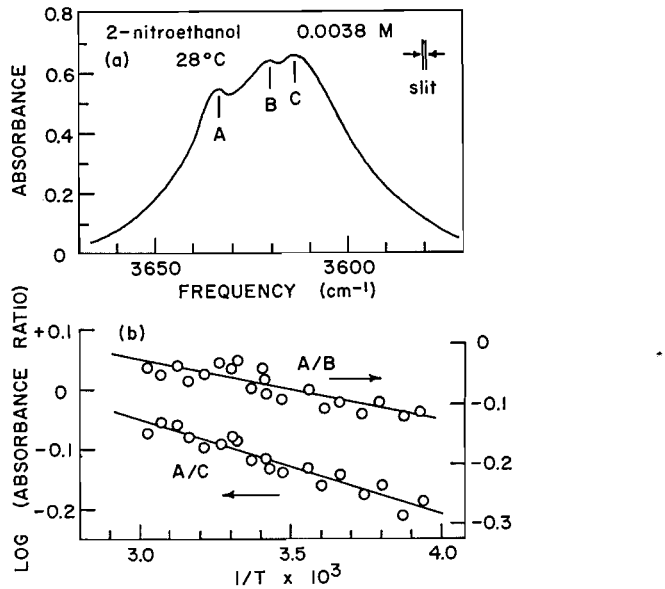

FIG. 3. (*a*) Fundamental OH stretching bands of 2-nitroethanol, 0.0038 *M* in CCl_4, path length 2.00 cm, temperature 28 °C. (*b*) Temperature dependence of OH absorbance ratios for 2-nitroethanol.

The temperature dependence of the spectra, shown in Fig. 3(b), indicates that bands B and C arise from conformers which are thermodynamically more stable than the *trans* conformer (band A) by -0.40 ± 0.10 and -0.71 ± 0.09 kcal/mole respectively (least squares method, 90% confidence limits). Since the barrier to rotation about a C—NO_2 bond is known to be insignificantly small (6 cal/mole, ref. 24), hydrogen bonded conformations involving one or both oxygen atoms of the nitro group have been suggested (1). In the conformer where the OH group bonds to one of the nitro group oxygen atoms, the proton may be imbedded in an oxygen p-orbital, forming a six-membered ring. It is doubtful whether more specific assignments of bands B and C can be made at the present time. The $-\Delta H$ values observed are probably larger than the hydrogen bond strengths themselves because of the loss of repulsive non-bonded interactions on going from the *trans* to the *gauche* form.

Can. J. Chem. Downloaded from www.nrcresearchpress.com by 210.87.254.105 on 09/05/12
For personal use only.

The present measurements on 2-methyl-2-nitro-1,3-propanediol (Fig. 4(*a*)) are in agreement with those of Schleyer *et al.* (1). The main maximum at 3 608.$_1$ cm^{-1} and the shoulder at ~3 591 cm^{-1} are attributed to OH intramolecularly bonded to NO_2 in two different ways, the pronounced high frequency shoulder at 3 633 cm^{-1} is due to "free" OH groups, whereas the very weak low frequency shoulder at ~3 553 cm^{-1} must be due to intramolecular OH...O bonding in a seven-membered ring. Although OH...O_2N interaction is weaker than OH...O interaction the former is favored because of the proximity of the two groups in the molecule.

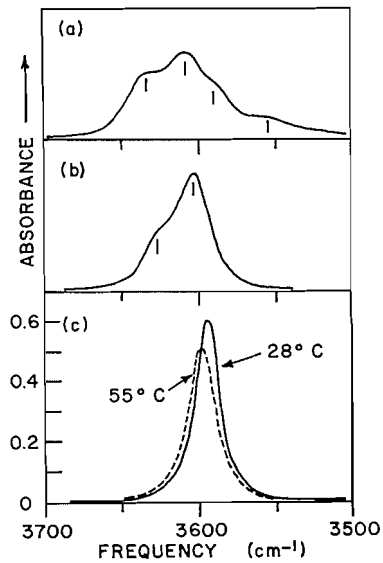

FIG. 4. Fundamental OH stretching bands of several nitroalcohols in dilute CCl_4 solution, path length 2.00 cm, temperature ambient unless indicated: (*a*) 2-methyl-2-nitro-1,3-propanediol (1.8×10^{-3} *M*); (*b*) 2,2-dinitropropanol (3.1×10^{-3} *M*); (*c*) 2,2,2-trinitroethanol (~6×10^{-3} *M*).

In 2,2-dinitropropanol (Fig. 4(*b*)) the relative intensity of the "free" OH shoulder (3 628 cm^{-1}) has diminished with respect to the intramolecularly hydrogen bonded band (3 602.$_7$ cm^{-1}) because of the enhanced acidity of the OH group due to the electron-withdrawing effect of two NO_2 groups, and the possibility of hydrogen bonding to two NO_2 groups. In the extreme case of 2,2,2-trinitroethanol a narrow ($\Delta\nu_{1/2}^{a} = 20$ cm^{-1}) symmetrical OH band is observed at 3 593.$_2$ cm^{-1} at room temperature (Fig. 4(*c*)). At 55 °C the peak has moved to 3 596.$_6$ cm^{-1}, but it is still symmetrical. The low frequency and narrow symmetrical nature of this band imply a single intramolecularly hydrogen bonded conformation. The acidity of the OH group would be enhanced by the electron-withdrawing effect of three NO_2 groups. Further, "free" OH groups can only arise by rotation about the C—O bond, bringing strong repulsive forces between the lone pair orbitals on the hydroxyl oxygen atom and the nitro groups into play. Thus even a weak OH...O_2N bond would be sufficient to keep all the OH groups hydrogen bonded.

Nitro groups are therefore capable of acting as proton acceptors in intramolecular hydrogen bond formation in aliphatic systems.

Can. J. Chem. Downloaded from www.nrcresearchpress.com by 210.87.254.105 on 09/05/12
For personal use only.

ACKNOWLEDGMENTS

The authors are greatly indebted to Drs. T. N. Hall and H. E. Ungnade for gifts of chemicals, and to Drs. P. von R. Schleyer and H. E. Ungnade for preprints of their manuscripts. This work was supported financially by the National Research Council of Canada.

REFERENCES

1. W. F. Baitinger, P. von R. Schleyer, T. S. S. R. Murty, and L. Robinson. Tetrahedron, **20**, 1635 (1964).
2. H. E. Ungnade, E. M. Roberts, and L. W. Kissinger. Unpublished results.
3. P. J. Krueger and H. D. Mettee. Can. J. Chem. **42**, 326 (1964) and other papers in this series.
4. A. Allerhand and P. von R. Schleyer. J. Am. Chem. Soc. **85**, 866 (1963).
5. S. S. Mitra. J. Chem. Phys. **36**, 3286 (1962).
6. P. J. Krueger. Can. J. Chem. **40**, 2300 (1962); **42**, 201 (1964).
7. M. Yamaha. Bull. Chem. Soc. Japan, **29**, 876 (1956).
8. G. C. Pimentel and A. L. McClellan. The hydrogen bond. W. H. Freeman and Co., San Francisco. 1960. (*a*) Chap. 5 (*b*) p. 99 (*c*) pp. 96–97.
9. M. St. C. Flett. Spectrochim. Acta, **10**, 21 (1957).
10. M. Kuhn, W. Luettke, and R. Mecke. Z. Anal. Chem. **170**, 106 (1959).
11. T. Urbanski. *In* Hydrogen bonding. *Edited by* D. Hadzi. Pergamon Press, N.Y. 1959. p. 143.
12. H. E. Ungnade and L. W. Kissinger. Tetrahedron, **19**, Suppl. 1, 121 (1963).
13. H. E. Ungnade, E. D. Loughran, and L. W. Kissinger. J. Phys. Chem. **66**, 2643 (1962).
14. E. F. Dupre. Anal. Chem. **27**, 1878 (1955).
15. W. E. Norland and P. J. Hartman. J. Am. Chem. Soc. **76**, 3227 (1954).
16. Z. Eckstein, P. Gluzinski, W. Sobotka, and T. Urbanski. J. Chem. Soc. 1370 (1961).
17. A. Allerhand and P. von R. Schleyer. J. Am. Chem. Soc. **85**, 371 (1963).
18. R. W. Taft, Jr. *In* Steric effects in organic chemistry. *Edited by* M. S. Newman. J. Wiley and Sons, Inc., New York. 1956. Chap. 13.
19. B. D. Nageswara Rao, Putcha Venkateswarlu, A. S. N. Muthy, and C. N. R. Rao. Can. J. Chem. **40**, 387 (1962). C. N. R. Rao, R. Venkataraghavan, K. R. Bhaskar, and A. Balasubramanian. *In* Proceedings of the Xth Colloquium Spectroscopicum Internationale. *Edited by* E. R. Lippincott and M. Margoshes. Spartan Books, Washington, D.C. 1963. p. 505.
20. U. Liddel and E. D. Becker. Spectrochim. Acta, **10**, 70 (1957).
21. L. P. Kuhn and R. A. Wires. J. Am. Chem. Soc. **86**, 2161 (1964).
22. M. Oki and M. Hirota. Bull. Chem. Soc. Japan, **34**, 374 (1961).
23. A. G. Moritz. Nature, **195**, 800 (1962).
24. E. Tannenbaum, R. D. Johnson, R. J. Myers, and W. D. Gwinn. J. Chem. Phys. **22**, 949 (1954). E. Tannenbaum, R. J. Myers, and W. D. Gwinn. J. Chem. Phys. **25**, 42 (1956).

Can. J. Chem. Downloaded from www.nrcresearchpress.com by 210.87.254.105 on 09/05/12
For personal use only.

Can. J. Chem. Downloaded from www.nrcresearchpress.com by 210.87.254.6 on 09/05/12
For personal use only.

COORDINATION COMPOUNDS OF OLEFINS WITH ANHYDROUS SILVER SALTS

II. AN INFRARED AND NUCLEAR MAGNETIC RESONANCE INVESTIGATION OF SILVER TETRAFLUOROBORATE – OLEFIN COMPLEXES[1]

H. W. QUINN, J. S. MCINTYRE, AND D. J. PETERSON
Exploratory Research Laboratory, Dow Chemical of Canada, Limited, Sarnia, Ontario
Received May 18, 1965

ABSTRACT

A determination has been made of the changes which occur in the infrared and proton magnetic resonance spectra of a number of olefins when they form $AgBF_4$.2 olefinates. The data obtained indicate that: (i) asymmetric substitution at a double bond results in nonsymmetric orientation of the silver ion relative to the trigonal carbon atoms and to the plane of the pi orbital; (ii) complexing may affect the rotation about the bond between a secondary or tertiary tetrahedral carbon and a trigonal carbon in order to reduce interaction between the two olefin molecules; (iii) in the solid state, lattice restrictions can result in interaction between the two olefin molecules.

INTRODUCTION

Numerous investigations of the nature of the interaction of aliphatic monoolefins with silver(I), palladium(II), and platinum(II) by study of the infrared (1–4), Raman (5), and nuclear magnetic resonance (n.m.r.) (2, 6, 7, 8) spectra have been reported.

These studies have established that, upon complexing, the olefinic character of the hydrocarbon molecule is retained although it is perturbed by withdrawal of pi electrons, presumably effected, as Dewar has suggested (9), by overlap of the pi molecular orbitals with the atomic orbitals of the metal ion. In the infrared, the perturbation results in a shift of the double bond stretch vibration to a lower frequency from that in the uncomplexed olefin by 50–70 cm^{-1} for Ag(I) and about 150 cm^{-1} for Pt(II) while in the n.m.r. the olefinic protons are somewhat deshielded producing a change in chemical shift of less than 1 p.p.m. The reported data, relating particularly to Ag(I) complexes, do not, however permit speculation regarding the positioning of the silver ion with respect to the double bond.

Some structural determinations of platinum(II) and palladium(II)–olefin complexes have revealed that, whereas the symmetric ethylene molecule is symmetrically oriented about the bond joining it to the metal atom (10–12), the styrene molecule, exhibiting nonsymmetric substitution at the double bond, is not symmetrically oriented, the bond to the metal atom making an angle of 74° with the double bond axis at a point closer to the β- than to the α-carbon of the vinyl group (13). No similar structural data exist for mono-olefin – silver ion complexes.

The present investigation of the infrared and n.m.r. spectra of a number of anhydrous silver tetrafluoroborate – olefin complexes deals primarily with the changes which occur in the olefin spectra when complex formation is effected and the dependence of the magnitude of the change upon the substitution at the double bond. The unsaturated hydrocarbons employed have included the methyl-substituted ethylenes from ethylene through 2,3-dimethyl-2-butene, some straight chain 1-olefins from C_3 to C_{18}, and several branched-chain olefins.

[1]*Contribution No. 132. Presented in part at the 8th International Conference on Coordination Chemistry, Vienna, Austria, September 1964.*

Can. J. Chem. Downloaded from www.nrcresearchpress.com by 210.87.254.6 on 09/05/12
For personal use only.

EXPERIMENTAL

Anhydrous silver tetrafluoroborate was prepared from silver fluoride and boron trifluoride according to the method of Olah and Quinn (14).

Ethylene and *cis*- and *trans*-2-butene were Matheson C.P. grade with a 99.5% minimum purity.

Propylene, 2-methylpropene, 1-butene, 1-pentene, 2-methyl-2-butene, 4-methyl-1-pentene, and 2,4,4-trimethyl-1-pentene were Phillips pure grade materials of 99% minimum purity.

The straight chain 1-olefins from C_6 to C_{18} with the exception of C_{13} were obtained from Humphrey-Wilkinson, Inc. and were purified by fractional distillation.

All of the remaining olefins employed were obtained in 95% minimum purity from Columbia Organic Chemicals.

The n.m.r. solvents were Merck reagent grade chloroform and 99.5% isotopically pure deuterochloroform purchased from Merck, Sharp and Dohme.

Preparation of Complexes

Earlier investigations (4) have established that, with the exception of ethylene, the most stable complexes exhibit a 1:2 silver tetrafluoroborate : olefin stoichiometry. Preparation of the solid complexes was accomplished by exposure of anhydrous $AgBF_4$ to gaseous olefin until the weight increase corresponded essentially to the 1:2 stoichiometry or contact of $AgBF_4$ with liquid olefin in a 1:2 mole ratio. With the straight-chain 1-olefins above C_3, and branched-chain 1-olefins above C_4 the complex has a melting point above 35 °C. The complexes of lower molecular weight olefins dissociate without melting at higher temperatures. The complexes with the lower olefins demonstrated a marked hygroscopicity which tends to decrease with increasing olefin molecular weight.

Chloroform or deuterochloroform solutions of the complexes were prepared by contact of a 10% solution of the olefin with anhydrous $AgBF_4$ in an amount slightly less than that necessary for preparation of the $AgBF_4$.2-olefinate. Although $AgBF_4$ was relatively insoluble in chloroform, the complex was readily soluble and a clear, colorless solution was obtained. A slow reaction between chloroform and $AgBF_4$ was observed resulting in precipitation of AgCl, upon standing at 25 °C for some time. This reaction appeared to proceed more rapidly in the presence of excess uncomplexed $AgBF_4$ and less rapidly in the presence of excess olefin, suggesting that uncomplexed silver salt was involved. At 0 °C, the reaction was much retarded and, at −80 °C, the complex could be kept frozen indefinitely without evidence of silver chloride precipitation. Precipitation of a small amount of AgCl during recording of the n.m.r. spectrum did not appear to affect at all the spectrum of the complex.

Infrared Spectra

The infrared spectra were recorded at 25 °C with a Perkin–Elmer 421 grating spectrophotometer. Nujol and fluorolube mulls of the crystalline complexes were prepared in a dry box and placed in cells with KBr windows. Chloroform solutions of the complexes were compensated by samples of the solvent in identical 0.1 mm cells with KBr windows.

Nuclear Magnetic Resonance Spectra

The n.m.r. spectra of chloroform or deuterochloroform solutions of the complexes were recorded with a Varian A60 proton resonance spectrometer. By a first-order treatment of the spectra, the chemical shifts were measured relative to internal tetramethylsilane (TMS) and the chemical shifts and coupling constants for the $AgBF_4$ complexes compared with those of the uncomplexed olefins at identical concentrations in the same solvent.

RESULTS

Stoichiometry of Complexes

From the infrared and n.m.r. spectra it was possible, except with ethylene, to establish that all olefins employed formed $AgBF_4$.2 olefinates as the most stable complexes, both in the crystalline form and in chloroform solution. Earlier investigations (4) have shown that, with ethylene, complexes of lower stoichiometry are formed and it is considered that the ethylene complex employed in this study has the stoichiometry, $AgBF_4.C_2H_4$. With other olefins, infrared bands of uncomplexed olefin were observed only after a 2:1 mole ratio of olefin : silver salt had been exceeded. Similarly, identical n.m.r. shifts were observed for systems of 1:1 and 2:1 olefin : silver salt stoichiometry but further addition of olefin resulted in decreasing shifts. With the chloroform solutions, a stoichiometry of less than 2:1 resulted also in incomplete solution of $AgBF_4$ while at the 2:1 mole ratio all of the salt was dissolved.

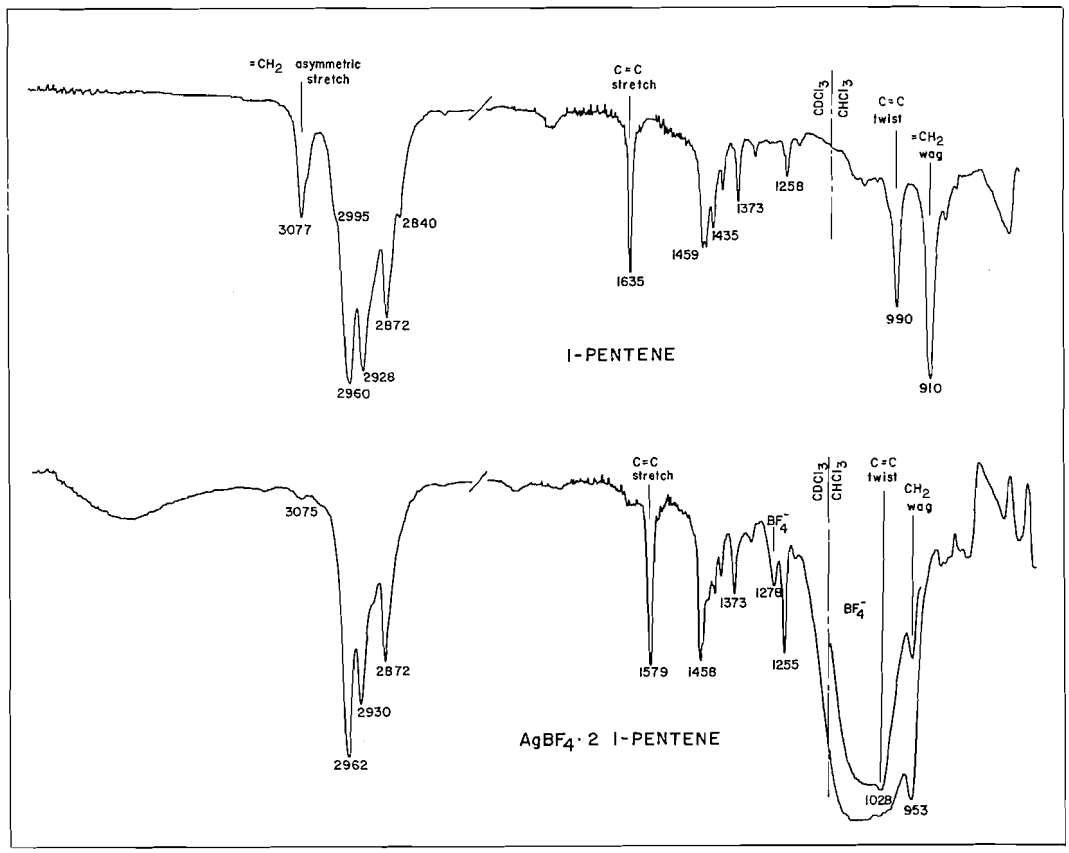

FIG. 1. Infrared spectra of 1-pentene and $AgBF_4$.2 1-pentene (10% in $CDCl_3$ and $CHCl_3$).

Infrared Spectra

Formation of the $AgBF_4$.2 olefinates results in some significant changes in the olefin spectrum. As may be seen from the comparison of the spectrum of $AgBF_4$.2 1-pentene with that of 1-pentene depicted in Fig. 1, complex formation results in a shift of the C=C stretch vibration frequency from 1 635 cm^{-1} to 1 579 cm^{-1}, a shift of the C=C twist out-of-plane deformation from 990 cm^{-1} to 1 028 cm^{-1}, and a shift of the CH_2 wag deformation from 910 cm^{-1} to 953 cm^{-1}. Similar shifts as observed with a variety of olefins are recorded in Table I.

With *trans*-2-butene and 2,3-dimethyl-2-butene, in which the C=C stretch vibration is infrared inactive, the shifts were obtained from the Raman spectra of nitromethane solutions. Chloroform solutions of the complexes were unsatisfactory for Raman because of the slow reaction of the solvent with $AgBF_4$ (*vide* Experimental, Preparation of Complexes). Complex formation does, however, introduce sufficient asymmetry to give an infrared active C=C stretch with these olefins.

In general, the magnitude of the shift to lower frequencies of the C=C stretch vibration is dependent upon substitution at the double bond, being about 55 cm^{-1}, 63 cm^{-1}, and 70 cm^{-1} for mono-, di-, and tri-alkyl substitution, respectively. These values reflect increasing interaction of the silver ion with the double bond, i.e. more extensive overlap

Can. J. Chem. Downloaded from www.nrcresearchpress.com by 210.87.254.6 on 09/05/12
For personal use only.

of the olefinic pi orbital with the Ag^+ orbitals, as a result of increasing pi basicity due to the $-I$ effect of the alkyl substituents. The shift is not, however, very dependent upon the extent of branching of the alkyl substituent being, for example, 56 cm^{-1} for 1-pentene, 57 cm^{-1} for 3-methyl-1-butene, and 56 cm^{-1} for 4,4-dimethyl-1-pentene.

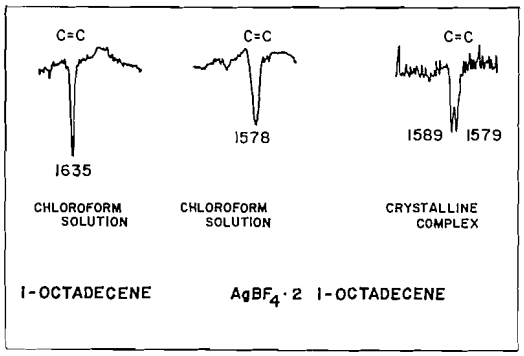

FIG. 2. Infrared bands for the C=C stretch vibration in 1-octadecene and $AgBF_4$.2 1-octadecene showing splitting in the crystalline complex.

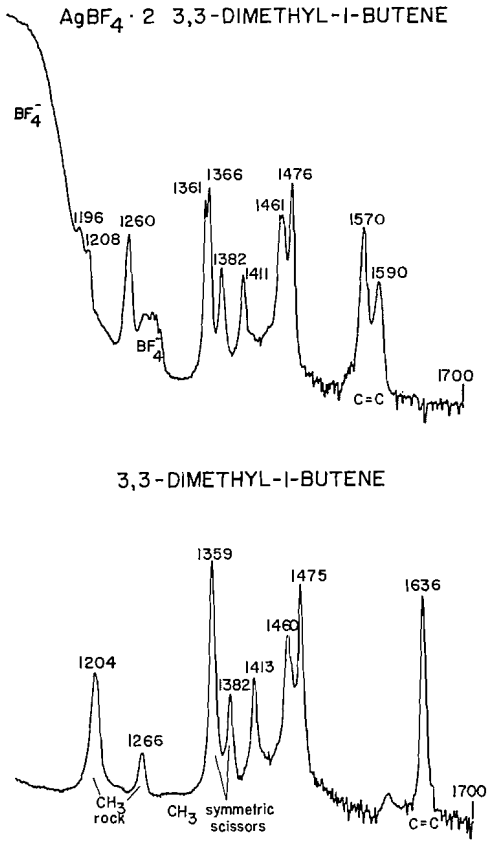

FIG. 3. A portion of the infrared spectra of 3,3-dimethyl-1-butene and $AgBF_4$.2 3,3-dimethyl-1-butene (10% in $CDCl_3$) showing the splittings observed in the complex.

Can. J. Chem. Downloaded from www.nrcresearchpress.com by 210.87.254.6 on 09/05/12
For personal use only.

Can. J. Chem. Downloaded from www.nrcresearchpress.com by 210.87.254.6 on 09/05/12
For personal use only.

TABLE I

Infrared frequency shifts in olefin spectra upon formation of $AgBF_4$.2 olefinates (cm^{-1})

Olefin	$\nu_{C=C}$			γ_{CH}			γ_{CH_2}		
	Olefin	Complex	$\Delta\nu^*_{C=C}$	Olefin	Complex	$\Delta\gamma_{CH}$	Olefin	Complex	$\Delta\gamma_{CH_2}$
(i) Spectrum of solid complex†									
Propene	1 648	1 595	−53						
1-Butene	1 645	1 590	−55						
1-Pentene	1 645	1 591	−54				908	952	44
4-Methyl-1-pentene	1 645	1 592	−53						
1-Hexene	1 643	1 590	−53						
1-Heptene	1 645	1 591	−54						
1-Octene	1 644	1 590	−54				903	950	47
1-Decene	1 644	1 590	−54						
1-Dodecene	1 645	1 591	−54				902	948	46
1-Tridecene	1 642	1 583	−59	990	1 023	33	907	952	45
		1 594	−48						
1-Tetradecene	1 645	1 588	−57						
		1 597	−48						
1-Hexadecene	1 644	1 588	−56				900	944	44
		1 597	−47						
1-Octadecene	1 645	1 586	−59						
		1 595	−50						
Isobutene	1 657	1 593	−64						

Can. J. Chem. Downloaded from www.nrcresearchpress.com by 210.87.254.6 on 09/05/12
For personal use only.

TABLE I (*Concluded*)

Olefin	$\nu_{C=C}$			γ_{CH}			γ_{CH_2}		
	Olefin	Complex	$\Delta\nu^*_{C=C}$	Olefin	Complex	$\Delta\gamma_{CH}$	Olefin	Complex	$\Delta\gamma_{CH_2}$
2-Methyl-1-butene	1 653	1 590	−63						
2-Methyl-1-pentene	1 648	1 585	−63						
cis-2-Butene	1 663	1 604	−59						
trans-2-Butene	1 673‡	1 615	−58						
2-Methyl-2-butene	1 680	1 610	−70						
(ii) Solution spectrum§									
Propene	1 635	1 580	−55	985	1 011	26	908	947	39
2-Methylpropene	1 647	1 587	−60				885	918	33
cis-2-Butene	1 653	1 595	−58	670‖	715‖	45			
trans-2-Butene	1 673‡	1 614‡	−59	967	996	29			
2-Methyl-2-butene	1 669	1 596	−73	800	839	39			
2,3-Dimethyl-2-butene	1 672‡	1 599‡	−73				503‡,¶	520‡,¶	17
1-Pentene	1 635	1 579	−56	990	1 028	38	910	953	43
3-Methyl-1-butene	1 636	1 579	−57	993					
3,3-Dimethyl-1-butene	1 636	1 570	−66	995	1 030	35	908	953	45
		1 590	−46						
4,4-Dimethyl-1-pentene	1 635	1 579	−56						
2,4,4-Trimethyl-1-pentene	1 633	1 571	−62				889	923	34
1-Octadecene	1 635	1 578	−57						

*$\Delta\nu = \nu_{complex} - \nu_{olefin}$.
†Fluorolube and Nujol mulls compared with 10% CCl_4 and CS_2 solution of olefin.
‡Raman spectrum of nitromethane solution.
§Chloroform or deuterochloroform solutions (10% olefin by volume).
‖Accuracy doubtful because of strong solvent absorption in this region.
¶Probably an out-of-plane bending mode, e.g. $C(CH_3)_2$ wag which is shifted to lesser extent than is th CH_2 wag.

In the crystalline complexes of straight-chain 1-olefins with 13 or more carbon atoms, the band representing the C=C stretch vibration appears as a doublet with a splitting of about 9 cm^{-1}, one member being at higher and one at lower frequency than the corresponding single band observed with the shorter chain 1-olefins. In solution or in the melt this splitting disappears, however (Fig. 2). No similar splitting is observed in solid 1-octadecene.

Only with $AgBF_4$.2 3,3-dimethyl-1-butene (*t*-butylethylene) has a splitting of the C=C stretch band been observed in chloroform solution, (Fig. 3). In this instance, the splitting amounts to 20 cm^{-1}, one member of the doublet being about 10 cm^{-1} lower and the other 10 cm^{-1} higher than the frequency of the corresponding single band observed for $AgBF_4$.2 3-methyl-1-butene (isopropylethylene). This same splitting is observed in the crystalline complex of 3,3-dimethyl-1-butene but not in that of crystalline $AgBF_4$.2 3-methyl-1-butene.

In addition, the spectrum of $AgBF_4$.2 3,3-trimethyl-1-butene shows a splitting, but no significant frequency shifts, of the bands attributed to a symmetric CH_3 scissors at $\sim$ 1 360 cm^{-1} and an in-plane CH_3 rock at about 1 200 cm^{-1}.

Accurate determination of the shifts to higher frequency of the C=C twist and CH_2 wag deformations effected by complexing was difficult because of superposition of these bands upon the very intense BF_4^- absorption band at about 1 065 cm^{-1}. With some of the complex spectra it was possible, however, to identify the bands and determine the shifts. Those olefins having vinyl substitution exhibit, upon complexing, a somewhat greater shift of the CH_2 wag frequency ($\sim$ 45 cm^{-1}) than of the C=C twist frequency ($\sim$ 35 cm^{-1}). No splitting of these bands was observed in complexes which demonstrated splitting of the C=C stretch vibration band. With *cis*-2-butene and 2-methyl-2-butene, the out-of-plane hydrogen deformation does not constitute a C=C twisting mode, occurring at lower frequencies than does the C=C twist band in *trans*-2-butene and undergoing a somewhat greater shift to higher frequencies upon formation of the silver salt complex. With propylene, the C=C twist deformation frequency is shifted to a lesser extent than with the other monoalkyl olefins. Similarly, the CH_2 wag deformation is shifted somewhat less for propylene, 39 cm^{-1}, than for the other monoalkyl olefins, $\sim$ 45 cm^{-1}. This shift is also lower for vinylidene, e.g. 2-methylpropene or 2,4,4-trimethyl-1-pentene, than for vinyl substitution.

An interesting feature of the $AgBF_4$.2 1-pentene spectrum (Fig. 1) and of all the complex spectra is the very marked decrease in intensity of the bands at about 3 075 cm^{-1} and 2 995 cm^{-1} which are attributed to the asymmetric CH_2 stretching and CH stretching modes respectively. Although the band at 2 995 cm^{-1} (which appears as a shoulder in the olefin spectrum) was not detectable in the complex, a very small band was always observed at 3 075 cm^{-1}. The absence of any evidence of these bands having been shifted to lower frequencies and superimposed upon the other CH stretch absorption bands (requiring a shift of more than 80 cm^{-1} for $=CH_2$) supports the suggestion that for these vibrations an intensity change only is involved.

Nuclear Magnetic Resonance Spectra

A comparison of the proton resonance spectrum of the $AgBF_4$.2 olefinate with that of the parent olefin has established that, although, in general, the pattern is the same for both, there is an increase in the downfield chemical shift of the protons relative to tetramethylsilane when the olefin is complexed. The magnitude of the increase in chemical shift is dependent upon the nature and extent of substitution at the double bond and is quite similar to that previously reported (2, 8).

Can. J. Chem. Downloaded from www.nrcresearchpress.com by 210.87.254.6 on 09/05/12
For personal use only.

Can. J. Chem. Downloaded from www.nrcresearchpress.com by 210.87.254.6 on 09/05/12
For personal use only.

In Table II are reported the chemical shifts for the olefins and $AgBF_4$.2 olefinates from ethylene, through the various methyl-substituted ethylenes, to 2,3-dimethyl-2-butene (tetramethylethylene). With the exception of those for the *trans*-2-butene system, all spectra were obtained at room temperature; the lower stability of the $AgBF_4$.2 *trans*-2-butene complex (4) required that the spectrum be obtained at reduced temperature (−40 °C) in order that the maximum chemical shifts could be observed. Lowering the temperature did not affect, however, the shifts observed with the other olefins. The presence of a single pattern (even at −40 °C) when uncomplexed olefin is known to be present in a system, indicates a rapid exchange between complexed and uncomplexed species.

While the chemical shifts of the olefinic protons are essentially identical in ethylene and *cis*- and *trans*-2-butene, upon complexing the change in the shift is twice as great for the butenes (45 c.p.s.) as for ethylene (21 c.p.s.). While the change in chemical shift of the methyl protons in propene (17 c.p.s.) is essentially the same as for those in *cis*- and *trans*-2-butene and 2,3-dimethyl-2-butene and in the methyl group (R_3) at the mono-substituted carbon atom of 2-methyl-2-butene, it is greater for the methyl protons in 2-methyl-propene (25 c.p.s.) and in the methyl groups (R_1 and R_4) at the disubstituted carbon of 2-methyl-2-butene (25 c.p.s.).

Approximate chemical shift and coupling constant data for a number of 1-alkenes of configuration

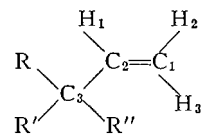

and their $AgBF_4$ complexes are reported in Tables III and IV and the chemical shift changes obtained therefrom are found in Table V. The data were obtained by a first-order treatment of the spectra and in the case of the olefins agree very well with literature data (15, 16). Since the object of this investigation was to establish the general dependence of spectral changes when the complex is formed upon the alkyl substitutent at the double bond rather than to obtain highly accurate n.m.r. data for the complexes, the first-order treatment was considered to be satisfactory.

The effect of complex formation upon the chemical shifts is a downfield change of order $\Delta\nu_1 > \Delta\nu_2 > \Delta\nu_3$ (where ν is the chemical shift of the proton in c.p.s. from TMS). Although the magnitude of the change of chemical shift is not markedly dependent upon the alkyl substitutent, there appears to be some increase in $\Delta\nu_1$ when there is a single proton in the 3-position.

From Table III it is apparent that, in the uncomplexed olefin, H_2 is slightly more shielded than H_3 but that, in the complex, H_3 is more shielded. The change of chemical shift of H_2 relative to H_3 which tends to increase as the alkyl substitutent becomes bulkier near the double bond is given in column 6 of Table V and is illustrated for 3,3-dimethyl-1-butene in Fig. 4.

Complex formation appears to result in a small decrease in the magnitude of $J_{1,2} + J_{1,3}$. While the change in the coupling constant $J_{2,3}$ is as small as to approach the experimental error, there is a suggestion of an increase in its magnitude upon complexing of the olefin.

With many of the olefins, complex formation results in very little change in the coupling constant, $J_{1,4}$, between the protons on C_2 and C_3. There is, however, a noticeable decrease (except with vinylcyclohexane) when there are two alkyl substituents on C_3. As one of those substituents becomes bulkier, there is a greater decrease in $J_{1,4}$, e.g. from 0.9 c.p.s. for methyl to 1.5 c.p.s. for neopentyl.

Can. J. Chem. Downloaded from www.nrcresearchpress.com by 210.87.254.6 on 09/05/12
For personal use only.

TABLE II

Change of proton chemical shifts* in n.m.r. spectra of olefins 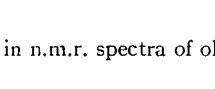 upon formation of $AgBF_4$.2-olefinates† (c.p.s.)

Olefin	R_1	R_2	R_3	R_4	ν_1 (c.p.s.)			ν_2 (c.p.s.)			ν_3 (c.p.s.)			ν_4 (c.p.s.)		
					ν_1^o	ν_1^c	Δ‡	ν_2^o	ν_2^c	Δ	ν_3^o	ν_3^c	Δ	ν_4^o	ν_4^c	Δ
Ethylene	H	H	H	H	323	344	21		$\equiv\nu_1$			$\equiv\nu_1$			$\equiv\nu_1$	
Propene	H	H	H	CH_3	352	400	48	295	324	29	300	319	19	104	121	17
2-Methylpropene	CH_3	H	H	CH_3		$\equiv\nu_4$		279	304	25		$\equiv\nu_2$		103	128	25
cis-2-Butene	H	H	CH_3	CH_3	328	373	45		$\equiv\nu_1$			$\equiv\nu_4$		96	115	19
trans-2-Butene	H	CH_3	H	CH_3	326	371	45		$\equiv\nu_4$			$\equiv\nu_1$		100	117	17
2-Methyl-2-butene	CH_3	H	CH_3	CH_3		$\equiv\nu_4$		311	350	39	90	107	17	95	120	25
2,3-Dimethyl-2-butene	CH_3	CH_3	CH_3	CH_3		$\equiv\nu_4$			$\equiv\nu_4$			$\equiv\nu_4$		97	116	19

*Chemical shifts expressed in c.p.s. ± 1 c.p.s. at 60 Mc/s downfield with respect to internal $Si(CH_3)_4$.
†Stoichiometry of ethylene complex in solution not established.
‡$\Delta = \nu^o - \nu^o$ where "c" and "o" designate complex and olefin respectively.

TABLE III

Chemical shifts* (c.p.s.) for the vinyl protons in 1-alkenes 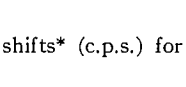 and the corresponding $AgBF_4$.2 1-alkenes

Olefin	ν_1		ν_2		ν_3	
	ν_1^o	ν_1^c	ν_2^o	ν_2^c	ν_3^o	ν_3^c
Propene	352	400	295	324	300	319
1-Butene	355	407	296	329	300	322
1-Pentene	351	401	293	329	297	321
1-Dodecene	349	399	293	325	297	317
1-Hexadecene	350	400	293	326	296	318
Allylcyclohexane	348	397	294	328	295	317
3-Methyl-1-butene	347	400	288	324	293	316
3-Methyl-1-pentene	343	402	294	332	296	320
3,5,5-Trimethyl-1-hexene	347	409	289	328	295	317
Vinylcyclohexane	349	404	293	329	297	319
3,3-Dimethyl-1-butene	352	406	288	325	293	313

*Chemical shifts are expressed in c.p.s. ± 1 c.p.s. at 60 Mc/s downfield with respect to internal $Si(CH_3)_4$.

TABLE IV

Approximate coupling constants (c.p.s.) for the vinyl protons in 1-alkenes and the corresponding $AgBF_4$.2 1-alkenes

Olefin	R	R′	R″	$J_{1,2}+J_{1,3}$		$J_{2,3}$		$J_{1,4}$	
				$\sum J^o$	$\sum J^c$	J^o	J^c	J^o	J^c
Propene	H	H	H	26.8	26.5	2.6	2.9	6.3	6.4
1-Butene	CH_3	H	H	27.4	26.8	2.5	2.7	6.0	6.0
1-Pentene	C_2H_5	H	H	26.7	26.3	2.5	2.8	6.2	6.4
1-Dodecene	C_9H_{19}	H	H	27.2	26.4	2.6	2.7	6.3	6.2
1-Hexadecene	$C_{13}H_{27}$	H	H	27.3	26.3	2.5	2.7	6.3	6.0
4,4-Dimethyl-1-pentene	$(CH_3)_3C$	H	H	27.1	26.3	2.8	3.1	7.4	7.3
Allylcyclohexane	c-C_6H_{11}	H	H	27.1	26.3	2.7	2.8	6.8	7.0
3-Methyl-1-butene	CH_3	CH_3	H	28.0	27.5	2.2	2.4	6.5	5.6
3-Methyl-1-pentene	C_2H_5	CH_3	H	27.5	26.9	2.6	2.6	7.0	6.2
3,5,5-Trimethyl-1-hexene	$(CH_3)_3CCH_2$	CH_3	H	27.4	27.1	2.3	2.5	7.9	6.4
Vinylcyclohexane	c-C_5H_{10}		H	27.9	27.0	2.2	2.4	6.0	5.8
3,3-Dimethyl-1-butene*	CH_3	CH_3	CH_3	28.4	27.5	1.8	2.1		

*The simplicity of the H_1 pattern (Fig. 4) permits estimation of $J_{1,2}$ to be 10.5 c.p.s. and 10.2 c.p.s. and of $J_{1,3}$ to be 17.9 c.p.s. and 17.2 c.p.s. for the olefin and complex respectively.

TABLE V

Change of chemical shift (c.p.s.) of the vinyl protons of 1-alkenes upon formation of $AgBF_4$.2 1-alkenes

Olefin	$\Delta\nu_1$	$\Delta\nu_2$	$\Delta\nu_3$	$\nu_2^o-\nu_3^o$*	$\nu_2^c-\nu_3^c$	$\Delta\nu_2-\Delta\nu_3$
Propene	48	29	19	−5.2	4.9	10.1
1-Butene	52	33	22	−4.3	6.9	11.2
1-Pentene	50	36	24	−3.4	8.0	11.4
1-Dodecene	50	32	20	−3.6	8.0	11.6
1-Hexadecene	50	33	22	−3.2	8.2	11.4
Allylcyclohexane	49	34	22	−1.0	10.5	11.5
3-Methyl-1-butene	53	36	23	−5.0	7.8	12.8
3-Methyl-1-pentene	59	38	24	−2.2	11.9	14.1
3,5,5-Trimethyl-1-hexene	62	39	22	−5.6	11.2	16.8
Vinylcyclohexane	55	36	22	−4.2	10.2	14.4
3,3-Dimethyl-1-butene	54	37	20	−5.1	11.3	16.4

*$\nu_2-\nu_3$ was obtained from an expanded trace of the H_2 and H_3 patterns with an accuracy of ±0.5 c.p.s.

Can. J. Chem. Downloaded from www.nrcresearchpress.com by 210.87.254.6 on 09/05/12
For personal use only.

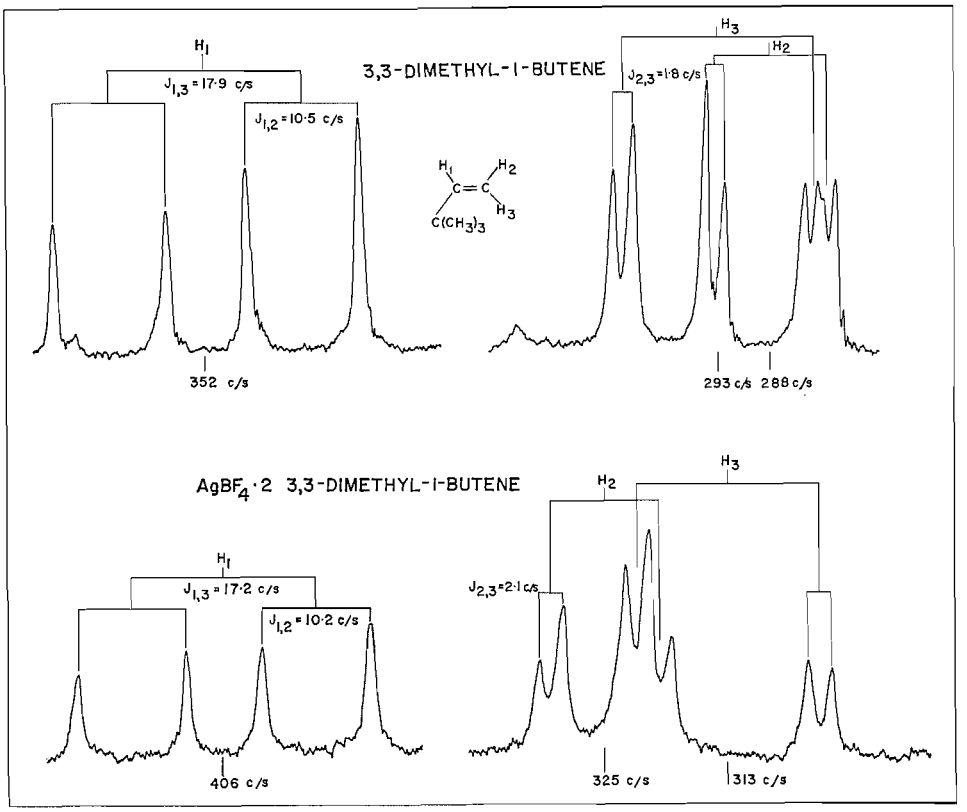

FIG. 4. Proton resonance spectra for the vinyl protons in 3,3-dimethyl-1-butene and $AgBF_4$.2 3,3-dimethyl-1-butene (10% in $CDCl_3$).

DISCUSSION

The splitting observed in the C=C stretch band for crystalline complexes of long chain 1-olefins which disappears upon melting or dissolving the complex is probably attributable to crystal lattice restrictions which require that the long alkyl chain assume a position resulting in interaction between the olefin molecules in the $AgBF_4$.2 olefinate. Such intermolecular interaction is known (17) to produce splitting of infrared bands, particularly those assigned to deformation modes in long chain paraffins and polymers. While it is tempting to interpret the splitting of the C=C stretch band as indicative of non-equivalent complexing of the two olefin molecules at the silver ion because of intermolecular interactions, this does not appear at present to be possible since one would expect to observe as well a splitting of the CH_2 wag and C=C twist deformation bands.

Similarly, the splitting observed in the C=C stretch band, as well as in some of the methyl deformation bands, for the complex of 3,3-dimethyl-1-butene in solution may arise from interaction between the olefin molecules introduced by the *t*-butyl group adjacent to the double bond. The observation (Table I) that removal of one of the methyl groups in the 3-position, as in 3-methyl-1-butene eliminates the splitting suggests that in this case there is a possibility of reduction of intermolecular interaction by rotation about the C_2C_3 bond.

This suggestion is further substantiated by the dependence of the change in the coupling

Can. J. Chem. Downloaded from www.nrcresearchpress.com by 210.87.254.6 on 09/05/12
For personal use only.

Can. J. Chem. Downloaded from www.nrcresearchpress.com by 210.87.254.6 on 09/05/12
For personal use only.

constant $J_{1,4}$, between the protons on C_2 and C_3, upon the substituents in the 3-position. The magnitude of $J_{1,4}$ in olefins has been related (16) to the population of the rotational conformers about C_2C_3, being greater when there is substitution at C_3 which tends to increase the population of the *trans* conformer, since $J_{1,4}$ *trans* is greater than $J_{1,4}$ *gauche*, while maintaining the staggered conformations. In general when there are two protons at C_3 and the alkyl substituent is linear, there appears to be no hindered rotation about C_2C_3 and $J_{1,4}$ has a value that is representative of one *trans* and two *gauche* conformers, i.e. 6–6.5 c.p.s. When, however, the alkyl group is branched near C_3 or if there is a single proton at C_3, there may be rotational hindrance, the population of *trans* conformer will be greater and $J_{1,4}$ will increase to about 7.5 c.p.s. if there are equivalent numbers of *trans* and *gauche* conformers and to about 11 c.p.s. if the *trans* conformer predominates.

If the observation that complexing of olefins having two protons at C_3 results in no significant change in $J_{1,4}$ can be interpreted to indicate that complex formation does not affect the rotation about C_2C_3 in those olefins, the decrease in $J_{1,4}$ upon complexing of olefins with only one proton at C_3 can then be interpreted to indicate that in the complex the proton is less frequently in the *trans* position. This situation could arise if, in order to reduce interaction between the two olefin molecules complexed at the silver ion, the favored rotational conformations have the proton closer to the silver ion (i.e. less often in the *trans* position) and the interfering alkyl groups directed away.

Such a change in populations of rotational conformers would also decrease the shielding at H_1 due to the contribution of the magnetic anisotropy in the bond C_3C_4 (18) and may explain the larger $\Delta\nu_1$ values observed when there is a single proton at C_3. When, however, there are no protons at C_3, the interaction cannot be eliminated by changing the rotation about C_2C_3 and the splittings in the spectrum of $AgBF_4$.2 3,3-dimethyl-1-butene result.

Since it is known that electron-withdrawing functional groups in a molecule markedly decrease the intensities of CH stretching bands (19) the observed very marked decrease in intensities of the 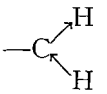 and $=C \rightarrow H$ stretch absorption bands when the olefin is complexed may be due to the decrease of pi electron density at the trigonal carbon atoms. There is also a possibility that the reduced intensities are indicative of smaller changes of dipole moment for these vibrations when the olefin is complexed.

The shifts observed in the out-of-plane hydrogen deformation frequencies upon complex formation are quite analogous to the frequency rise observed when the alkyl group is replaced by a more electropositive group (containing a metal atom), 20 cm^{-1} for the C=C twist and 50–65 cm^{-1} for the CH_2 wag deformation (20, 21) which has been explained in terms of electron inductive and mesomeric effects for the twist and wag respectively. While silver ion complexing is not equivalent to substitution of a metal atom for the α-carbon of an alkyl substituent, it does result in decrease of pi electron density at the trigonal carbon atoms and might be expected to produce shifts similar to those observed when the substituent metal atom can effect a similar decrease. A comparison of some of the infrared frequencies for trimethylvinylsilane and the $AgBF_4$ complex of the structurally similar olefin, 3,3-dimethyl-1-butene is given in Table V. It is observed in particular that the C=C stretch and CH_2 wag frequencies are very similar for these two compounds. The difference between the frequencies for the CH_2 wag in the silane and 3,3-dimethyl-1-butene has been attributed to decrease of pi electron density at the terminal carbon by d_π–P_π overlap with the silicon atom (21).

If an increase in the CH_2 wag frequency can be explained in terms of decreased electron

density at that carbon atom, the lesser shift observed upon complexing for vinylidene than for vinyl substitution would indicate a lesser decrease of electron density in the vinylidene compounds.

The small apparent decrease of $J_{1,2} + J_{1,3}$ upon complexing may result from a reduced contribution of the pi electrons to the coupling constants. Karplus (22) has calculated the pi electron contribution to approximate +1.5 c.p.s. for *cis* and *trans* coupling in olefins.

Since it is known that the magnetic shielding of protons at trigonal carbon atoms in aromatic and olefinic compounds increases with increasing pi electron density at the carbon (23–25), it is to be expected that decrease in pi density by overlap of the pi orbital with an atomic orbital of the silver ion might well result in a proton deshielding. It has been suggested (26) that if there is a paramagnetic contribution by the pi electrons to the proton shielding, pi bonding to a metal atom could result in increased shielding of olefinic protons. To date, however, no such increased shielding has been observed upon formation of complexes resulting in only slight perturbation of the olefin molecule (2, 8). Schug and Martin (8) have suggested that the proton deshielding observed upon complexing of unsaturated compounds with aqueous silver ion might be largely accounted for by polarization effects. This argument is not too convincing, however, since the observed deshielding changes much more markedly with increasing distance from the silver ion than would be calculated. While there may be then shielding effects attributable to factors other than change of pi electron density at the trigonal carbons, the latter effect may, in these complexes, predominate and the observed shifts will be discussed in the light of this possibility.

TABLE VI

Comparison of infrared data for trimethylvinylsilane with those for $AgBF_4$.2 3,3-dimethyl-1-butene

	Infrared (cm^{-1})		
	C=C	CH_2 wag	C=C twist
$(CH_3)_3CCH{=}CH_2$	1 636	908	995
$AgBF_4.2(CH_3)_3CCH{=}CH_2$	1 570 1 590	953	1 030
$(CH_3)_3SiCH{=}CH_2$	1 590	949	1 005

Employing the premise that the extent of perturbation of the olefin molecule when complexed is dependent upon the pi basicity of the olefin (as suggested by the infrared shifts), one might expect a continuously increasing pi electron withdrawal from the double bond with increasing methyl substitution resulting in increasingly greater olefinic proton deshielding. On this basis the observation that the methyl protons of 2,3-dimethyl-2-butene are not more deshielded than are those of the 2-butenes is rather surprising. If, however, the model of the silver ion – olefin complex postulated by Dewar (9) applies, one must consider not only the effect on proton shielding of electron withdrawal by overlap of the bonding pi orbital of the olefin with the vacant s or sp hybrid orbital of the ion (σ-bonding) but also of the electron donation effected by the overlap of an occupied d-orbital of the ion with the antibonding pi orbital (π-bonding). The result of stronger complexing will be then both more pi electron withdrawal from and more d-electron donation to the olefin and the change of proton shielding may not be markedly dependent upon the pi basicity of the olefin. The observed net deshielding, however, establishes that the pi electron density decrease at the trigonal carbons is not fully compensated by d-electron donation (i.e. the σ-bond is stronger than the π-bond).

Can. J. Chem. Downloaded from www.nrcresearchpress.com by 210.87.254.6 on 09/05/12
For personal use only.

The greater deshielding of the methyl protons in 2-methylpropene and of those at the disubstituted carbon of 2-methyl-2-butene may suggest non-equivalent d-orbital overlapping, i.e. non-equivalent reshielding by d-electrons, at the two trigonal carbon atoms, that at the disubstituted carbon being less. A similar suggestion derives from a consideration of the greater deshielding of the proton at the substituted than at the terminal trigonal carbon atom of monoalkyl substituted 1-alkenes (Table V) which in turn suggests that the silver ion is not symmetrically positioned with respect to the trigonal carbon atoms but is closer to the terminal carbon. Such a positioning is consistent with that observed for the palladium atom relative to the double bond of styrene in the palladium chloride – styrene dimer (13) and may also follow from the suggestion that Markownikoff double-bond additions (which perhaps involve π-complex intermediates (27)) indicate a higher electron density at the less-highly substituted carbon atom in asymmetrically substituted olefins.

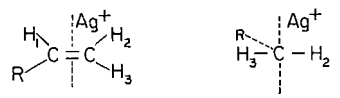

Electronic effect Steric effect

FIG. 5. Schematic representation of the effect of the alkyl substituent upon positioning of the silver ion at the double bond of a monoalkyl substituted 1-alkene.

Bothner-By and Naar-Colin have suggested (15) that the greater shielding of H_2 than of H_3 in a 1-alkene might be attributable to a field effect of the dipole which is directed somewhat toward H_2. A similar approach to explain the greater shielding of H_3 in the complex would require a field or electronic effect directed more toward H_3 than H_2. It appears reasonable to suggest that, if, as a result of a steric effect introduced by the alkyl substituent, the silver ion is somewhat displaced from the plane of the pi orbital away from the substituent, the direction of overlap of the occupied d-orbital with the antibonding pi orbital will be at an angle to that plane and any field effect due to the d-electrons will be directed more toward H_3 than H_2 resulting in a greater reshielding of H_3. With increasing steric effect of the alkyl substituent the silver ion would be located further out of the plane of the pi orbital and a greater difference in the reshielding of H_3 relative to H_2 would be expected (as observed in Table V, column 6). Increasing steric effect seemingly is introduced by increasing the extent of substitution at the tetrahedral carbon atom, C_3, and by branching of the substituent groups.

The positioning of the silver ion at the olefinic double bond might then be considered to be determined by a combination of an electronic effect and a steric effect of the alkyl substituent which position it with respect to the trigonal carbon atoms and the plane of the pi orbital respectively. This is schematically illustrated in Fig. 5.

The observation that in general the most stable complexes exhibit a 1:2 silver ion : olefin stoichiometry suggests that in order to achieve maximum orbital overlap, complexing probably involves sp digonal hybrid orbitals, e.g. sp_x, and the two associated d-orbitals, d_{xy} and d_{xz}, resulting in an orientation of the olefin molecules with their double bonds in perpendicular planes with the silver ion between them.

ACKNOWLEDGMENT

The authors wish to thank J. C. Evans (The Dow Chemical Company, Midland, Michigan) for providing Raman data and E. B. Baker and J. P. Heeschen (The Dow Chemical Company, Midland, Michigan) for helpful discussion relating to the n.m.r. study.

Can. J. Chem. Downloaded from www.nrcresearchpress.com by 210.87.254.6 on 09/05/12
For personal use only.

REFERENCES

1. J. CHATT and L. A. DUNCANSON. J. Chem. Soc. 2939 (1953).
2. D. B. POWELL and N. SHEPPARD. J. Chem. Soc. 2519 (1960).
3. D. M. ADAMS and J. CHATT. J. Chem. Soc. 2821 (1962).
4. H. W. QUINN and D. N. GLEW. Can. J. Chem. **40**, 1103 (1962).
5. H. J. TAUFER, M. J. MURRAY, and T. F. CLEVELAND. J. Am. Chem. Soc. **63**, 3500 (1961).
6. L. W. REEVES. Can. J. Chem. **38**, 736 (1960).
7. S. MARIČIĆ, C. R. REDPATH, and J. A. S. SMITH. J. Chem. Soc. 4905 (1963).
8. J. SCHUG and R. J. MARTIN. J. Phys. Chem. **66**, 1554 (1962).
9. M. J. S. DEWAR. Bull. Soc. Chim. France, **18**, C79 (1951).
10. J. A. WUNDERLICH and D. P. MELLOR. Acta Cryst. **7**, 130 (1954).
11. J. N. DEMPSEY and N. C. BAENZIGER. J. Am. Chem. Soc. **77**, 4984 (1955).
12. P. R. H. ALDERMAN, P. G. OWSTON, and J. M. ROWE. Acta Cryst. **13**, 149 (1960).
13. J. R. HOLDEN and N. C. BAENZIGER. J. Am. Chem. Soc. **77**, 4987 (1955).
14. G. A. OLAH and H. W. QUINN. J. Inorg. Nucl. Chem. **14**, 295 (1960).
15. A. A. BOTHNER-BY and C. NAAR-COLIN. J. Am. Chem. Soc. **83**, 231 (1961).
16. A. A. BOTHNER-BY, C. NAAR-COLIN, and H. GUNTHER. J. Am. Chem. Soc. **84**, 2748 (1962).
17. C. N. R. RAO. Chemical applications of infrared spectroscopy. Academic Press, New York. 1963. p. 23.
18. A. A. BOTHNER-BY and C. NAAR-COLIN. Ann. N.Y. Acad. Sc. **70**, 833 (1958).
19. T. L. BROWN. Chem. Rev. **58**, 581 (1958).
20. W. J. POTTS and R. A. NYQUIST. Spectrochim. Acta, **15**, 679 (1959).
21. J. J. EISCH and J. T. TRAINOR. J. Org. Chem. **28**, 487 (1963).
22. M. KARPLUS. J. Chem. Phys. **33**, 1842 (1960).
23. C. N. BANWELL and N. SHEPPARD. Mol. Phys. **3**, 351 (1960).
24. T. SCHAEFER and W. G. SCHNEIDER. Can. J. Chem. **41**, 966 (1963).
25. J. C. SCHUG and J. C. DECK. J. Chem. Phys. **37**, 2618 (1962).
26. M. L. H. GREEN, L. PRATT, and G. WILKINSON. J. Chem. Soc. 3753 (1959).
27. M. J. S. DEWAR. The electronic theory of organic chemistry. Oxford University Press, Toronto. 1949. p. 144.

Can. J. Chem. Downloaded from www.nrcresearchpress.com by 210.87.254.6 on 09/05/12
For personal use only.

Can. J. Chem. Downloaded from www.nrcresearchpress.com by 210.87.254.6 on 09/05/12
For personal use only.

CHLORIDE AND SULFATE ION ASSOCIATION WITH SOME LANTHANIDE AND ACTINIDE IONS

P. G. MANNING

A stepwise stability constant (b) for a metal (M) – ligand (L) ion association reaction in solution is defined as

$$[1] \qquad b_n = [ML_n][ML_{n-1}]/[L].$$

Bjerrum (1) proposed that the ratios of stepwise stability constants for two stages of ion association may be given by the equation

$$[2] \qquad P = b_1{:}b_2 = S \times T,$$

where S is a statistical factor readily calculable from a knowledge of the number of cation bonding sites and ligand groups, and T is a measure of the work done in bringing a second ligand from infinity to its equilibrium position in the ML_2 species against the repulsive force exerted by the already bound ligand. Thus, if the cation has N available sites and the anion is monodentate then $S = 2 \times N(N - 1)$. The factor 2 arises because the probability of a ligand's leaving the ML_2 species is twice that of leaving the ML. The T factor is electrostatic in nature and is independent of the ability of the metal ion to bind ligands (1). For the chloride complexes of Sn^{2+} and Hg^{2+} (cations of similar size to rare earths) $T = 2.0$ (1), and for the Zn–mandelate system (2) $T = 1.5$.

Bjerrum (3) has shown that

$$[3] \qquad \log T = \frac{1}{2.303} \times \frac{e^2}{Dr} \times \frac{1}{kK}$$

where e is the electronic charge, D the dielectric constant, r the separation of the charged ligands in the ML_2 species, k the Boltzmann constant, and K the absolute temperature. In an earlier work (4) it was shown that acetate hydrogen-bonded to the protons of the cation hydration sheath and that $T = 1.1$. It was also shown that if acetate ion binds to a proton of a given water molecule then the second proton of that same water becomes relatively unattractive to a second acetate. The ligand–ligand separation is greater in an ion pair than in a complex, and using simple Coulombic theory and $T = 1.1$ for an ion pair, then $T \simeq 1.4$ for rare-earth complexing with a singly charged ligand. Moreover, this T value ($= 1.4$) is likely to be a lower limit because $D \sim 78$ for an ion pair and $D \ll 78$ for a complex (5). A reasonable T value for rare-earth–chloride complexing would seem to be 1.5.

Table I presents P values determined experimentally for rare-earth chlorides, and Table II presents calculated S, T, and P values for 6- and 8-hydrated cations and for chloride complexing and ion pairing. The ion pair calculations were performed assuming that chloride binds at the octahedral (oct.) edge of a 6-hydrated cation (Brady's model, ref. 9) and at the corresponding dodecahedral (dodec.) edge of an 8-hydrated cation. Should chloride ion hydrogen-bond to the protons of the cation primary hydration

TABLE I

b_1:b_2 ratios for rare-earth chlorides

M	T (°C)	I*	b_1	b_2	P	Ref.
Eu	20	1.0	0.59	0.54	1.1	6
Eu	20	1.0	0.77	0.27	2.8	6
La	25	4.0	0.60	0.38	1.6	7
Eu	25	4.0	0.71	0.27	2.6	7
Lu	25	4.0	0.45	0.60	0.8	7
Ce	25	1.0	0.78	0.33	2.3	8
Ce	25	1.0	0.83	0.20	4.1	8
Eu	25	1.0	0.80	0.19	4.2	8
Eu	25	1.0	0.79	0.30	2.6	8
Eu	25	1.0	0.82	0.19	4.2	8
Eu†	25	1.0	0.58	0.35	1.6	8
Average P value = 2.6						

*Ionic strength = I.
†Bromide ion associate.

TABLE II

Calculation of P values for rare-earth chlorides

	6-Hydrated		8-Hydrated	
Factor	Complex	Ion pair	Complex	Ion pair
S	2.40	2.2	2.3	2.1
T	1.5	1.1	1.5	1.1
P	3.6	2.4	3.5	2.3

sheath, however, then S = 2.4 for a 6-hydrate and 2.3 for an 8-hydrate. The respective P values would be 2.6 and 2.5.

A comparison of experimentally and theoretically determined P values (Tables I and II and also text) strongly suggests that the rare-earth chlorides are ion pairs, the P values for complexing being outside experimental error.

TABLE III

S, T, and P values for M(III) sulfates

	6-Hydrated			8-Hydrated		
Orientation	S	T	P	S	T	P
Oct./dodec. edge	2.2	1.45	3.2	2.1	1.45	3.2
One proton	2.4	1.45	3.5	2.3	1.45	3.4
Complex	2.4	6.	14.	2.3	6.	14.

TABLE IV

Stability constants for M(III) sulfates (ref. 7)

M	Log b_1	Log b_2	P
La	1.45	1.01	2.7
Eu	1.54	1.15	2.5
Am	1.57	1.09	3.0

Now sulfate and acetate ions are similar in that both have oxygens that can interact with the protons of the cation hydration sheath. At the comparatively large ligand

Can. J. Chem. Downloaded from www.nrcresearchpress.com by 210.87.254.6 on 09/05/12
For personal use only.

separation in the ML_2 ion pairs, r(acetate) $\sim r$(sulfate), and from eq. [3] T(sulfate) = $(1.1)^4 = 1.45$. For sulfate complexing $T = (1.5)^4 = 6$. The relevant S, T, and P values are listed in Table III and may be compared with the experimental P values (Table IV). The rare-earth sulfates are clearly ion pairs. The experimental data and the theoretical treatment do not cast any light on whether the rare-earth ions are 6-hydrated or 8-hydrated.

1. J. BJERRUM. Metal ammine formation in aqueous solution. P. Haase and Son, Copenhagen. 1941.
2. R. LARSSON and B. FOLKESON. Acta Chem. Scand. **19**, 53 (1965).
3. N. BJERRUM. Z. Physik. Chem. Leipzig, **106**, 238 (1923).
4. P. G. MANNING. Rare-earth acetate ion association. In press.
5. R. A. ROBINSON and R. H. STOKES. Electrolyte solutions. Butterworths, London. 1959.
6. H. M. N. H. IRVING and P. K. KHOPKAR. J. Inorg. Nucl. Chem. **26**, 1561 (1964).
7. T. SEKINE. J. Inorg. Nucl. Chem. **26**, 1463 (1964).
8. I. GRENTHE. Acta Chem. Scand. **18**, 283 (1964).
9. G. W. BRADY. J. Chem. Phys. **33**, 1079 (1960).

RECEIVED FEBRUARY 2, 1965.
MINES BRANCH,
DEPARTMENT OF MINES AND TECHNICAL SURVEYS,
OTTAWA, CANADA.

NUCLEOPHILIC CATALYSIS IN THE HYDROLYSIS OF DICHROMATE[1]

BERTA PERLMUTTER-HAYMAN AND MICHAEL A. WOLFF

The hydrolysis of the dichromate ion, viz.

[1] $$Cr_2O_7^{2-} + H_2O \rightarrow 2HCrO_4^-,$$

has been found to be catalyzed by bases (1, 2, 3), the results suggesting a correlation between the base strength and the catalytic constant. The special case where the catalyzing base is CrO_4^{2-} has recently been investigated (4) by measuring the influence of the ratio $[CrO_4^{2-}]/[Cr_2O_7^{2-}]$ on the rate of exchange of ^{17}O between the bridging and terminal positions in $Cr_2O_7^{2-}$. The catalytic constant was found to be much higher than that of the strongest base, OH^-. It was concluded (4) that not only basic strength but other properties characteristic of good nucleophilic reagents play a role in the catalysis. Following Edwards (5), the authors used polarizability as the additional criterion for nucleophilic character, and obtained a reasonable correlation between the catalytic constants, basic strengths, and polarizabilities of OH^-, CO_3^{2-}, NH_3, and CrO_4^{2-}. Some of the catalytic constants employed are only approximate (1); in particular, those of negatively charged ions contain a certain arbitrariness (2), because they refer to different ionic environments. However, this does not seriously affect the correlation, and in any case CrO_4^{2-} has an abnormally high rate constant in comparison with its basic strength. This fact becomes even more striking when we consider the charge-type of the reaction.

Now, if this high reactivity of CrO_4^{2-} is indeed due to its nucleophilic character (as expressed by its high polarizability), and not to its special role in the reaction scheme, other typical nucleophiles should also accelerate the hydrolysis. In this note we wish to illustrate this point by two examples: thiourea and urea. Both these substances are very weak bases (the pK of the conjugate acid being 0.96 for thiourea and 0.18 for urea (6)); thiourea, however, is a good nucleophile in many substitution reactions (5).

[1]*This note forms part of a thesis to be submitted by M. A. Wolff to the Senate of the Hebrew University in partial fulfilment of the requirements for a Ph.D. degree.*

Can. J. Chem. Downloaded from www.nrcresearchpress.com by 210.87.254.6 on 09/05/12
For personal use only.

separation in the ML_2 ion pairs, r(acetate) $\sim r$(sulfate), and from eq. [3] T(sulfate) = $(1.1)^4 = 1.45$. For sulfate complexing $T = (1.5)^4 = 6$. The relevant S, T, and P values are listed in Table III and may be compared with the experimental P values (Table IV). The rare-earth sulfates are clearly ion pairs. The experimental data and the theoretical treatment do not cast any light on whether the rare-earth ions are 6-hydrated or 8-hydrated.

1. J. BJERRUM. Metal ammine formation in aqueous solution. P. Haase and Son, Copenhagen. 1941.
2. R. LARSSON and B. FOLKESON. Acta Chem. Scand. **19**, 53 (1965).
3. N. BJERRUM. Z. Physik. Chem. Leipzig, **106**, 238 (1923).
4. P. G. MANNING. Rare-earth acetate ion association. In press.
5. R. A. ROBINSON and R. H. STOKES. Electrolyte solutions. Butterworths, London. 1959.
6. H. M. N. H. IRVING and P. K. KHOPKAR. J. Inorg. Nucl. Chem. **26**, 1561 (1964).
7. T. SEKINE. J. Inorg. Nucl. Chem. **26**, 1463 (1964).
8. I. GRENTHE. Acta Chem. Scand. **18**, 283 (1964).
9. G. W. BRADY. J. Chem. Phys. **33**, 1079 (1960).

RECEIVED FEBRUARY 2, 1965.
MINES BRANCH,
DEPARTMENT OF MINES AND TECHNICAL SURVEYS,
OTTAWA, CANADA.

NUCLEOPHILIC CATALYSIS IN THE HYDROLYSIS OF DICHROMATE[1]

BERTA PERLMUTTER-HAYMAN AND MICHAEL A. WOLFF

The hydrolysis of the dichromate ion, viz.

[1] $$Cr_2O_7^{2-} + H_2O \rightarrow 2HCrO_4^-,$$

has been found to be catalyzed by bases (1, 2, 3), the results suggesting a correlation between the base strength and the catalytic constant. The special case where the catalyzing base is CrO_4^{2-} has recently been investigated (4) by measuring the influence of the ratio $[CrO_4^{2-}]/[Cr_2O_7^{2-}]$ on the rate of exchange of ^{17}O between the bridging and terminal positions in $Cr_2O_7^{2-}$. The catalytic constant was found to be much higher than that of the strongest base, OH^-. It was concluded (4) that not only basic strength but other properties characteristic of good nucleophilic reagents play a role in the catalysis. Following Edwards (5), the authors used polarizability as the additional criterion for nucleophilic character, and obtained a reasonable correlation between the catalytic constants, basic strengths, and polarizabilities of OH^-, CO_3^{2-}, NH_3, and CrO_4^{2-}. Some of the catalytic constants employed are only approximate (1); in particular, those of negatively charged ions contain a certain arbitrariness (2), because they refer to different ionic environments. However, this does not seriously affect the correlation, and in any case CrO_4^{2-} has an abnormally high rate constant in comparison with its basic strength. This fact becomes even more striking when we consider the charge-type of the reaction.

Now, if this high reactivity of CrO_4^{2-} is indeed due to its nucleophilic character (as expressed by its high polarizability), and not to its special role in the reaction scheme, other typical nucleophiles should also accelerate the hydrolysis. In this note we wish to illustrate this point by two examples: thiourea and urea. Both these substances are very weak bases (the pK of the conjugate acid being 0.96 for thiourea and 0.18 for urea (6)); thiourea, however, is a good nucleophile in many substitution reactions (5).

[1]*This note forms part of a thesis to be submitted by M. A. Wolff to the Senate of the Hebrew University in partial fulfilment of the requirements for a Ph.D. degree.*

Can. J. Chem. Downloaded from www.nrcresearchpress.com by 210.87.254.42 on 09/05/12
For personal use only.

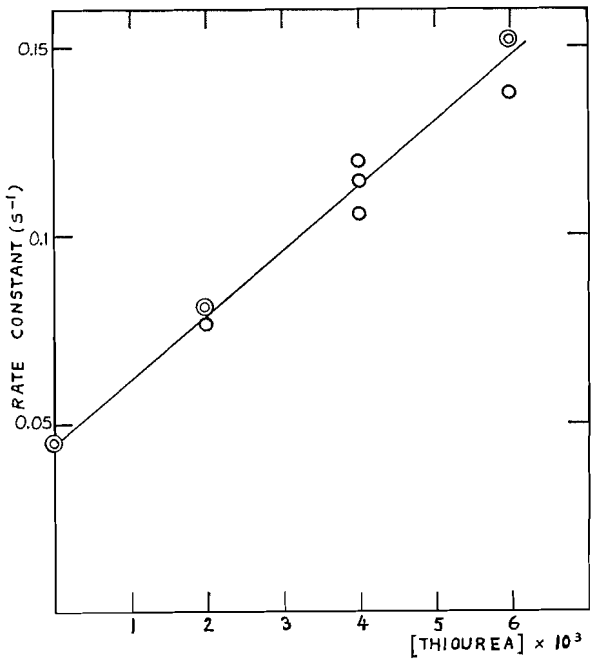

FIG. 1. The pseudo-first-order rate-constant as a function of thiourea concentration. (Coinciding results are designated by double circles.)

Our reaction mixtures contained 0.016 M sodium acetate and a trace of acetic acid in order to ensure a pH of ~ 7, where the contributions of both H^+ and OH^- to the observed rate are negligible (2). The measuring technique was the same as that described previously (2). Thiourea was employed in concentrations between (2 to 6) $\times 10^{-3}$ M. Figure 1 shows the pseudo-first-order rate-constant as a function of thiourea concentration. From the slope we calculate

$$k_{\text{thiourea}} = 17.2 \text{ mole}^{-1} \text{ l s}^{-1}.$$

The intercept represents a residual rate which is due to the solvent and the acetate (2).

On the other hand urea, up to a concentration of ~ 1 M, causes only a slight increase above this residual rate, which leads to $k_{\text{urea}} \sim 0.012$ mole^{-1} l s^{-1}. The catalytic effect of thiourea is therefore due almost entirely to nucleophilic properties other than basic strength. Further experiments are in progress, aiming at the determination of the factors governing the catalytic activity in this reaction (3).

We should like to thank S. de Groot for technical assistance.

1. A. LIFSHITZ and B. PERLMUTTER-HAYMAN. J. Phys. Chem. **65**, 2098 (1961).
2. B. PERLMUTTER-HAYMAN. J. Phys. Chem. **69**, 1736 (1965).
3. B. PERLMUTTER-HAYMAN and M. A. WOLFF. In preparation.
4. B. N. FIGGIS, R. G. KIDD, and R. S. NYHOLM. Can. J. Chem. **43**, 145 (1965).
5. J. O. EDWARDS. Inorganic reaction mechanisms. W. A. Benjamin Inc., Amsterdam. 1964. pp. 53–54.
6. Handbook of Chemistry and Physics. 42nd ed. Chemical Rubber Publishing Co., Cleveland. 1960. p. 1751.

RECEIVED MAY 13, 1965.
DEPARTMENT OF PHYSICAL CHEMISTRY,
THE HEBREW UNIVERSITY OF JERUSALEM,
JERUSALEM, ISRAEL.

Can. J. Chem. Downloaded from www.nrcresearchpress.com by 210.87.254.42 on 09/05/12
For personal use only.

THE YIELD OF SINGLET OXYGEN IN THE REACTION OF CHLORINE WITH HYDROGEN PEROXIDE

R. J. Browne and E. A. Ogryzlo

In a recent communication (1) it was shown that all the chemiluminescence from the reaction of chlorine with aqueous hydrogen peroxide could be attributed to the two singlet states of oxygen $a^1\Delta_g$ and $b^1\Sigma_g^+$. Emission from these two states has also been studied in the products of an electrical discharge (2, 3). In these gas phase studies it was shown that the visible emission at 6 340 Å arises from a simultaneous electronic transition in two colliding O_2 ($^1\Delta_g$) molecules and that the emission intensity in this band is proportional to the square of the O_2 ($^1\Delta_g$) concentration.

[1] $$\text{i.e. } I_{6340} = k' [O_2 (^1\Delta_g)]^2$$

Since the band at 12 700 Å is due to the emission from one O_2 ($^1\Delta_g$) molecule we can write

[2] $$I_{12700} = k''[O_2 (^1\Delta_g)]$$

the ratio of the emission intensities in these two bands is given by

[3] $$R = \frac{I_{6340}}{I_{12700}} = k[O_2 (^1\Delta_g)].$$

When O_2 ($^1\Delta_g$) is obtained from an electrical discharge both R and the absolute concentration of O_2 ($^1\Delta_g$) can be measured (see ref. 2). Hence the proportionality constant k in eq. [3] can be evaluated (for a particular detecting system). With this value of k it is possible to estimate the O_2 ($^1\Delta_g$) concentration in any system simply by measuring the ratio R for that system. In contrast to other methods of determining chemiluminescence yields, geometric factors and collisional quenching rates are of no consequence when eq. [3] is used.

Using an $f/4.5$ Hilger-Watts glass-prism spectrometer with a slit of 500 microns combined with an R.C.A. 7102 photomultiplier the following results were obtained when O_2 ($^1\Delta_g$) was measured in the products of an electrical discharge:

$$[O_2 (^1\Delta_g)] = 1.5 \times 10^{-5} \text{ mole/l}; R = 36; k = 2.4 \times 10^6 \text{ l/mole}.$$

When the emission from the chlorine – hydrogen peroxide reaction was observed with the same optical system, the maximum ratio R measured was 1.8×10^3. From eq. [3] it follows that the concentration of O_2 ($^1\Delta_g$) is 7.5×10^{-4} mole/l. If we assume the bubble temperature is 300 °K this corresponds to a partial pressure of 14 mm Hg. Since the total oxygen pressure in the bubbles is about 750 mm Hg, this corresponds to a minimum yield of 2% O_2 ($^1\Delta_g$) in the reaction.

There are a number of reasons for believing that the yield of O_2 ($^1\Delta_g$) is actually larger than this. Firstly, the temperature of the gas in the bubbles is probably somewhat above room temperature since the reaction is about 62 kcal exothermic. We have not found it possible to estimate the bubble temperature directly; however, the "vibrational temperature" of the emitting gas can be estimated from the relative intensity of the emission from vibrationally excited states. From the intensity of the O_2 ($^1\Delta_g$, $v = 1$ to $^3\Sigma g^-$, $v = 0$) transition at 10 670 Å we estimate a vibrational temperature somewhat less than 600 °K.

Can. J. Chem. Downloaded from www.nrcresearchpress.com by 210.87.254.40 on 09/05/12
For personal use only.

It is quite likely that the true temperature of the gas is less than this so that the yield reported is low by a factor of two at most.

Secondly, insofar as the reaction is not infinitely fast, dilution of the O_2 ($^1\Delta_g$) by Cl_2 and by H_2O vapor will give low values for the yield. We have attempted to minimize these effects by working with a cooled and very basic solution where the reaction is rapid, the vapor pressure of water is low, and the bubble temperature is nearer to 25 °C.

The question of the yield of O_2 ($^1\Sigma g^+$) will prove much more difficult to answer, because not only is it quenched on almost every collision by water molecules, but it is also rapidly formed from the reaction of two O_2 ($^1\Delta_g$) molecules (4). We have studied the reaction in nonaqueous solvents, but even less emission from O_2 ($^1\Sigma g^+$) was observed in these systems.

NOTE ADDED IN PROOF: Some recent work by R. M. Badger, A. C. Wright, and R. F. Whitlock (to be published) indicates that at a pressure of 1 atm only 1/5 of the 12 700 Å band intensity is due to the spontaneous emission process (the remaining portion being due to a pressure-induced transition). This means that the ratio R for the aqueous reaction is actually 5 times as great and therefore the yield of O_2 ($^1\Delta_g$) is at least 10% in this reaction.

ACKNOWLEDGMENTS

This work was supported by Air Force Office of Scientific Research Grant No. OSR 158–65 and by the Defence Research Board of Canada Grant No. 9530–31.

1. R. J. BROWNE and E. A. OGRYZLO. Proc. Chem. Soc. April (1964). p. 117.
2. L. W. BADER and E. A. OGRYZLO. Discussions Faraday Soc. **37**, 46 (1964).
3. S. J. ARNOLD, R. J. BROWNE, and E. A. OGRYZLO. To be published. J. Photochem. Photobiol. December (1965).
4. R. A. YOUNG and G. BLACK. To be published. J. Photochem. Photobiol. December (1965).

RECEIVED JUNE 22, 1965.
DEPARTMENT OF CHEMISTRY,
UNIVERSITY OF BRITISH COLUMBIA,
VANCOUVER, BRITISH COLUMBIA.

Can. J. Chem. Downloaded from www.nrcresearchpress.com by 210.87.254.40 on 09/05/12
For personal use only.

$J_{^{13}C-H}$ FOR SUBSTITUTED ALDEHYDES

R. M. HAMMAKER

Malinowski *et al.* (1) have proposed an empirical equation predicting $J_{^{13}C-H}$ for a substituted aldehyde XCHO from $J_{^{13}C-H}$ for CH_4 and CH_3X. The valence bond approach of Juan and Gutowsky (2) for an sp^2 carbon atom yields the following theoretical equation for $J_{^{13}C-H}$ for a substituted aldehyde:

$$[1] \qquad J_{^{13}C-H}(XCHO) = J_{^{13}C-H}(HCHO) + 4/3[J_{^{13}C-H}(CH_3X) - J_{^{13}C-H}(CH_4)].$$

Values of $J_{^{13}C-H}(XCHO)$ calculated from eq. [1] using the $J_{^{13}C-H}(CH_3X)$ data (3–10) listed in Table I deviate significantly from the experimental values listed in Table I. Plots of Δ, defined as observed $J_{^{13}C-H}(XCHO)$ less the value calculated from eq. [1], versus the observed $J_{^{13}C-H}$ value are linear. Least squares analysis for all the data in Table I except X = o-C_6H_4OH and OH gives the result:

$$[2] \qquad \Delta = 0.658\, J_{^{13}C-H}(XCHO); \text{ obs. } -113.3.$$

It is quite likely that the true temperature of the gas is less than this so that the yield reported is low by a factor of two at most.

Secondly, insofar as the reaction is not infinitely fast, dilution of the O_2 ($^1\Delta_g$) by Cl_2 and by H_2O vapor will give low values for the yield. We have attempted to minimize these effects by working with a cooled and very basic solution where the reaction is rapid, the vapor pressure of water is low, and the bubble temperature is nearer to 25 °C.

The question of the yield of O_2 ($^1\Sigma g^+$) will prove much more difficult to answer, because not only is it quenched on almost every collision by water molecules, but it is also rapidly formed from the reaction of two O_2 ($^1\Delta_g$) molecules (4). We have studied the reaction in nonaqueous solvents, but even less emission from O_2 ($^1\Sigma g^+$) was observed in these systems.

NOTE ADDED IN PROOF: Some recent work by R. M. Badger, A. C. Wright, and R. F. Whitlock (to be published) indicates that at a pressure of 1 atm only 1/5 of the 12 700 Å band intensity is due to the spontaneous emission process (the remaining portion being due to a pressure-induced transition). This means that the ratio R for the aqueous reaction is actually 5 times as great and therefore the yield of O_2 ($^1\Delta_g$) is at least 10% in this reaction.

ACKNOWLEDGMENTS

This work was supported by Air Force Office of Scientific Research Grant No. OSR 158–65 and by the Defence Research Board of Canada Grant No. 9530–31.

1. R. J. BROWNE and E. A. OGRYZLO. Proc. Chem. Soc. April (1964). p. 117.
2. L. W. BADER and E. A. OGRYZLO. Discussions Faraday Soc. **37**, 46 (1964).
3. S. J. ARNOLD, R. J. BROWNE, and E. A. OGRYZLO. To be published. J. Photochem. Photobiol. December (1965).
4. R. A. YOUNG and G. BLACK. To be published. J. Photochem. Photobiol. December (1965).

RECEIVED JUNE 22, 1965.
DEPARTMENT OF CHEMISTRY,
UNIVERSITY OF BRITISH COLUMBIA,
VANCOUVER, BRITISH COLUMBIA.

$J_{^{13}C-H}$ FOR SUBSTITUTED ALDEHYDES

R. M. HAMMAKER

Malinowski *et al.* (1) have proposed an empirical equation predicting $J_{^{13}C-H}$ for a substituted aldehyde XCHO from $J_{^{13}C-H}$ for CH_4 and CH_3X. The valence bond approach of Juan and Gutowsky (2) for an sp^2 carbon atom yields the following theoretical equation for $J_{^{13}C-H}$ for a substituted aldehyde:

$$[1] \qquad J_{^{13}C-H}(XCHO) = J_{^{13}C-H}(HCHO) + 4/3[J_{^{13}C-H}(CH_3X) - J_{^{13}C-H}(CH_4)].$$

Values of $J_{^{13}C-H}(XCHO)$ calculated from eq. [1] using the $J_{^{13}C-H}(CH_3X)$ data (3–10) listed in Table I deviate significantly from the experimental values listed in Table I. Plots of Δ, defined as observed $J_{^{13}C-H}(XCHO)$ less the value calculated from eq. [1], versus the observed $J_{^{13}C-H}$ value are linear. Least squares analysis for all the data in Table I except X = o-C_6H_4OH and OH gives the result:

$$[2] \qquad \Delta = 0.658\, J_{^{13}C-H}(XCHO);\ \text{obs.} -113.3.$$

Can. J. Chem. Downloaded from www.nrcresearchpress.com by 210.87.254.5 on 09/05/12
For personal use only.

TABLE I

Calculated and observed ^{13}C—H coupling constants of substituted aldehydes (XCHO)

	$J_{^{13}C-H}$, c.p.s.			
	Experimental		Calcd. from eqs.	
Substituent (X)	CH_3X	XCHO	[1] and [2]	[4]
—H	125 (3)	172 (6)	172	172.0
—$C(CH_3)_3$	124 (3)	168.6	168.3	168.1
—CH_2CH_3	124 (4)	170.6	169.7	168.1
—CH_3	124.9 (7)	172.4	172.0	171.6
—C_6H_5	126 (3)	173.7	174.3	175.8
—o-C_6H_4OH	124 (5)	177 (8)	173.9	168.1
—$N(CH_3)_2$	131 (3)	191.2	192.5	195.2
—O^-	130.8 (9)	194.8 (9)	194.6	194.4
—CCl_3	134 (3)	207.2	207.0	206.8
—OH	141.5 (9)	222 (8)	225.5	235.8
—OCH_3	139.6 (10)	226.2	227.0	228.5
—F	149.1 (10)	267 (8)	266.5	265.2

NOTE: Numbers in parentheses are references; data without such numbers are from ref. 1.

Addition of Δ calculated from eq. [2] to $J_{^{13}C-H}$(XCHO) calculated from eq. [1] yields $J_{^{13}C-H}$(XCHO) values in good agreement with observed values.

A plot of Δ versus $J_{^{13}C-H}$(XCHO) calculated from eq. [1] is also linear and least squares analysis for all data in Table I except X = o-C_6H_5OH and OH gives:

$$\Delta = 1.902\, J_{^{13}C-H}(\mathrm{XCHO}); \text{ calcd. } -327.7. \quad [3]$$

The addition of eqs. [1] and [3] and use of observed $J_{^{13}C-H}(CH_4)$ and $J_{^{13}C-H}$(HCHO) from Table I give the following Malinowski-type equation*

$$J_{^{13}C-H}(\mathrm{XCHO}) = 10.7 + 3.87\,[J_{^{13}C-H}(CH_3X) - 2/3\, J_{^{13}C-H}(CH_4)]. \quad [4]$$

This equation may also be obtained by least squares analysis of all data in Table I except X = o-C_6H_4OH and OH. The constants in eq. [4] are different from those in eq. [2] of ref. 1 because of the use of different data in the least squares analysis.

Table I lists $J_{^{13}C-H}$(XCHO) values calculated from the combination of eqs. [1] and [2] and from eq. [4] where the standard errors of estimate are 1.5 c.p.s. and 5.3 c.p.s., respectively. The fit of eq. [4] to the data in Table I is a mild improvement over the fit in ref. 1 for the nine data common to both. The calculation using the combination of eqs. [1] and [2] gives better overall fit as anticipated; however, this approach is not useful for predicting a value of $J_{^{13}C-H}$(XCHO) which has not been measured. In cases where $J_{^{13}C-H}$(XCHO) has been measured (1, 8, 11) but $J_{^{13}C-H}(CH_3X)$ is not known, the latter may be predicted from the combination of eqs. [1] and [2]. $J_{^{13}C-H}$ values for seven methane derivatives predicted in this way are listed in Table II.

An alternate way of writing eq. [4] is

$$J_{^{13}C-H}(\mathrm{XCHO}) = J_{^{13}C-H}(\mathrm{HCHO}) + 4/3\,[(2.902\, J_{^{13}C-H}(CH_3X) - 238.1) - J_{^{13}C-H}(CH_4)], \quad [5]$$

which is eq. [1] with $J_{^{13}C-H}(CH_3X)$ replaced by (2.902 $J_{^{13}C-H}(CH_3X)$ − 238.1). Thus, for eq. [1] to give a correct prediction, the term in $J_{^{13}C-H}(CH_3X)$ must be increased above

The quantity in parentheses in eq. [4] is φ_X in eq. [2] of ref. 1.

Can. J. Chem. Downloaded from www.nrcresearchpress.com by 210.87.254.5 on 09/05/12
For personal use only.

TABLE II

^{13}C—H coupling constants predicted for substituted methanes (CH_3X)

Substituent (X)	J_{CH}(XCHO) exptl., c.p.s.	J_{CH}(CH_3X) calcd., c.p.s.
—$CH(CH_3)_2$	168.9	124.3
—p-$C_6H_4OCH_3$	173 (*a*)	125.4
—p-C_6H_4Cl	175.2	126.0
—m-C_6H_4Cl	177.5	126.6
—o-C_6H_4Cl	182.8	127.9
—$CHCl_2$	196.5 (*b*)	131.4
—OCH_2CH_3	225.6	138.9

NOTE: All data from ref. 1 except as noted: (*a*) ref. 8; (*b*) ref. 11.

the observed $J_{^{13}C-H}(CH_3X)$ and the required increase is larger the greater the electronegativity of X. The Δ values from eq. [2] whose addition to eq. [1] is required for correct prediction increase linearly (within 0.1 electronegativity unit or better) with the electronegativity of the first atom of X (12) and with the group electronegativity of X (13).

The cause of this required correction to eq. [1], which appears to vary linearly with substituent electronegativity, remains uncertain. Eq. [1] assumes no π electron contribution to $J_{^{13}C-H}$. Juan and Gutowsky interpreted the fact that their equation for ethylene derivatives gave $J_{^{13}C-H}$ values consistently higher than observed values as a consequence of a negative π electron contribution to $J_{^{13}C-H}$ of 5–10 c.p.s. However, this effect showed no dependence on substituent. It seems reasonable that a π electron correction must be applied to eq. [1]; however, such a correction seems unlikely to show the observed dependence on substituent electronegativity. The sources in addition to π electron contributions to $J_{^{13}C-H}$ that determine the parameters for eq. [4] and its equivalent expressions may include significant spin-dipole and (or) electron orbital contributions to $J_{^{13}C-H}$ as suggested by Karabatsos and Orzech (14), who maintain that the Fermi contact term alone is not adequate to account for $J_{^{13}C-H}$ values for substituted aldehydes and that s characters calculated from $J_{^{13}C-H}$ are unreliable and misleading. On the other hand, observed $J_{^{13}C-H}$ values for substituted aldehydes appear (15) to vary linearly with the group orbital electronegativities (13), which themselves are linearly related to the amount of s character in the hybrid orbitals.

1. E. R. MALINOWSKI, L. Z. POLLARA, and J. P. LARMANN. J. Am. Chem. Soc. **84**, 2649 (1962).
2. C. S. JUAN and H. S. GUTOWSKY. J. Chem. Phys. **37**, 2198 (1962).
3. N. MULLER and D. E. PRITCHARD. J. Chem. Phys. **31**, 768, 1471 (1959).
4. N. SHEPPARD and J. J. TURNER. Mol. Phys. **3**, 168 (1960).
5. P. C. LAUTERBUR. J. Am. Chem. Soc. **83**, 1846 (1961).
6. P. C. LAUTERBUR. J. Phys. Chem. **26**, 217 (1957).
7. R. M. LYNDEN-BELL and N. SHEPPARD. Proc. Roy. Soc. **A269**, 385 (1962).
8. N. MULLER. J. Chem. Phys. **36**, 359 (1962).
9. R. M. HAMMAKER. J. Mol. Spectroscopy, **15**, 506 (1965).
10. S. G. FRANKISS. J. Phys. Chem. **67**, 752 (1963).
11. G. P. VANDERKELEN and Z. EECKHAUT. J. Mol. Spectroscopy, **10**, 141 (1963).
12. M. L. HUGGINS. J. Am. Chem. Soc. **75**, 4123 (1953).
13. J. HINZE and H. H. JAFFE. J. Am. Chem. Soc. **84**, 540 (1962); M. A. WHITEHEAD and H. H. JAFFE. J. Am. Chem. Soc. **85**, 148 (1963).
14. G. J. KARABATSOS and C. E. ORZECH. J. Am. Chem. Soc. **86**, 3574 (1964).
15. R. M. HAMMAKER. J. Chem. Phys. **43**, 0000 (1965).

RECEIVED MAY 25, 1965.
DEPARTMENT OF CHEMISTRY,
KANSAS STATE UNIVERSITY,
MANHATTAN, KANSAS 66504.

Can. J. Chem. Downloaded from www.nrcresearchpress.com by 210.87.254.5 on 09/05/12
For personal use only.

ALIPHATIC CHEMISTRY OF FLUORENE
PART X. 2-PHENYLINDOLENINE-3-SPIRO-9′-FLUORENE

P. M. G. Bavin

Wislicenus and Fehrle in 1915 (1) reported that 9-benzoylfluorene reacted rapidly with phenylhydrazine in hot acetic acid to give a substance $C_{26}H_{17}N$. The absence of an α-methylene group precludes formation of an indole, and it was of interest to establish the structure of this product. In addition to the structures I and II proposed earlier (1), we have considered III and eliminated it by synthesis. Physical methods have established that the unknown is the spiroindolenine (I).

The empirical formula $C_{26}H_{17}N$ has been confirmed. The ultraviolet spectrum is typical of 9-substituted fluorenes (e.g. 9,9-dimethylfluorene (2)), although less well resolved, and eliminates both II (9-benzylidenefluorene) and III (phenanthridine). The mass

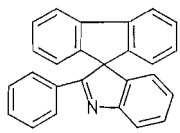

I

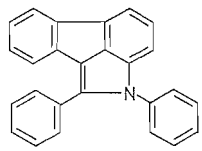

II

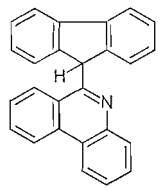

III

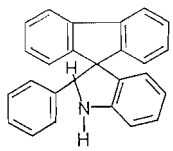

IV

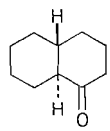

V

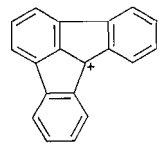

VI

spectrum confirms the molecular weight (343). Chemical confirmation of structure I has been difficult to obtain. The indolenine is resistant to alkalis, to oxidizing agents, and to dimethyl sulfate in boiling nitrobenzene (3, 4). Its stability towards strong acids is noteworthy and in marked contrast to the lability of 3,3-dimethylindolenines (5). The presence of the 2,3,3-trisubstituted indolenine system prevents acid-catalyzed rearrangement. However, hydrogenation gave the expected indoline (IV, cf. ref. 6) characterized by its infrared (very sharp N—H stretching band at 3 400 cm^{-1}), ultraviolet (typical fluorene spectrum), and mass spectra (parent ion at m/e 345).

Indolenines have only rarely been reported as the major products of the reaction of phenylhydrazine with ketones (methyl isopropyl ketone (7, 8); iosbutyraldehyde (9, 10); the decalone (V) (11); and methylated cyclohexanones (12)). Their formation as by-products of the Fischer indole synthesis is known to be favored by use of acetic acid as solvent (13). 9-Acetylfluorene forms a rather unstable phenylhydrazone and both 9-acetyl and 9-benzoylfluorene form 2,4-dinitrophenylhydrazones. Benzhydryl phenyl ketone was recovered unchanged after it was boiled with phenylhydrazine in acetic acid. This ketone does not enolize (13) and it may be the facile enolization (14, 15) of 9-benzoylfluorene which is responsible for the rapid formation of I (cf. the mechanism of the Fischer indole synthesis, generally held to involve initial tautomerism of the hydrazone (16)).

Can. J. Chem. Downloaded from www.nrcresearchpress.com by 210.87.254.5 on 09/05/12
For personal use only.

For comparison purposes 6-(9-fluorenyl)-phenanthridine (III) was synthesized by a general method (17). The ultraviolet spectrum closely resembled that of phenenthridine (18), confirming its structure.

EXPERIMENTAL

Melting points were recorded using a gas-heated block and thermometer calibrated for stem exposure. Microanalyses were carried out by Mr. M. Graham.

2-Phenylindolenine-3-spiro-9'-fluorene (I)

The crude product (1) was recrystallized several times from chloroform–cyclohexane to give pale yellow prisms, obtained colorless only after the impurities were oxidized with permanganate in acetone. As a result of solvation, the melting point was variable, in the range 219–229°. (Lit. m.p. 217–218° (1).) Analytical samples, prepared by drying at 120° and 0.01 mm, had m.p. 229–230°.

Found: C, 91.08; H, 5.02; N, 4.28; $C_{26}H_{17}N$ requires C, 90.93; H, 4.99; N, 4.08.

The ultraviolet spectrum in 95% ethanol showed the following peaks (λ (mμ)/log ϵ): 306/3.98; 295/3.72; 282/3.94; 267/4.19.

The indolenine was recovered unchanged from the following reaction conditions: alcohol – sulfuric acid (50–98%), alcohol – hydrochloric acid; potassium hydroxide and boiling ethanol or diethylene glycol; sodium borohydride (large excess) in methanol; dimethyl sulfate in boiling nitrobenzene; potassium permanganate in boiling aqueous acetone; sodium dichromate or chromium trioxide in hot acetic acid.

2-Phenylindoline-3-spiro-9'-fluorene, IV

A solution of the indolenine (1.4 g) in ethyl acetate (50 ml) containing 10% palladium-on-charcoal (0.1 g) was shaken in a hydrogen atmosphere. The uptake of hydrogen (115 ml at N.T.P., theory 91.5 ml) was complete in 1 h. The product separated from cyclohexane as colorless needles, m.p. 199°–200°, depressed to 155° by I.

Found: C, 90.23; H, 5.43; N, 3.86. $C_{26}H_{19}N$ requires C, 90.40; H, 5.54; N, 4.06.

The infrared spectrum of a Nujol mull showed a very sharp band at 3 400 cm^{-1}, attributed to the NH stretching mode.

9-Acetylfluorene Phenylhydrazone

This was prepared in hot acetic acid, crystallized from methanol as colorless slender needles, m.p. 140–142° with decomposition.

Found: C, 84.27; H, 6.19; N, 9.13; $C_{21}H_{18}N$ requires C, 84.53; H, 6.08; N, 9.39.

9-Acetylfluorene 2,4-Dinitrophenylhydrazone

This crystallized from heptane as orange needles, m.p. 202–203°.

Found C, 65.36; 65.47; H, 4.41, 4.31; N, 14.61. $C_{21}H_{16}N_4O_4$ requires C, 64.94; H, 4.15; N, 14.43.

9-Benzoylfluorene 2,4-Dinitrophenylhydrazone

This crystallized from benzene as orange blades, m.p. 207–209° with decomposition.

Found: C, 69.32; H, 3.98; N, 12.35. $C_{26}H_{18}N_4O_4$ requires C, 69.32; H, 4.03; N, 12.44.

Benzhydryl phenyl ketone was recovered unchanged after it was boiled under reflux for up to 12 h with an excess of phenylhydrazine in acetic acid.

6-(9-Fluorenyl)-phenanthridine (III)

9-(9-Fluorenyl)-9-fluorenol (0.8 g) was converted to the phenanthridine in the usual way (17). The basic product separated from heptane as small colorless prisms (0.07 g), m.p. 204–205°.

Found: N, 3.87. $C_{26}H_{17}N$ requires N, 4.09.

A solution in sulfuric acid was colorless, the starting alcohol giving an orange solution. The ultraviolet spectrum of a hexane solution showed the following peaks (μ/log ϵ_{max}): 344.7/3.49; 338.0/2.98; 322.7/3.13; 314.3/3.42; 301.2/4.05; 290/4.03; 279.4;* 273.3;* 267;* 261;* 255/4.70; 250.* (* Denotes shoulder.)

Mass Spectra

The main features of the spectra are as follows (*m/e* values).

For 2-phenylindolenine-3-spiro-9-fluorene, the parent ion is at 343, doubly charged ion at 171.5; the small number of fragmentations indicates a relatively stable molecule. The main fragmentations are 343 → 266, loss of 77, i.e. C_6H_5; 343 → 239, loss of 104, i.e. $C_6H_5 \cdot CH{=}\overset{\oplus}{N}$ or equivalent, easily the most important fragmentation.

For *2-phenylindoline-3-spiro-9'-fluorene*, the parent ion is at 345, doubly charged ion at 172.5; the larger number of ions indicates a less stable molecule. The three main fragmentations, of comparable importance, are 345 → 268, shown to occur directly by the presence of a metastable ion at 208.2 i.e. loss of 77, C_6H_5; 345 → 267, loss of 78, i.e. C_6H_6 (indications of a second metastable ion at 206.6 masked by 208.2 suggest

Can. J. Chem. Downloaded from www.nrcresearchpress.com by 210.87.254.5 on 09/05/12
For personal use only.

that 345 → 267 also occur directly); 345 → 239, loss of 106, i.e. $C_6H_5CH_2$—$\overset{\oplus}{N}H$ or equivalent; of lesser importance are ions at 329, loss of 16, i.e. NH_2 or equivalent, and 213, loss of 132.

The ion at 239 is common to both spectra. It probably represents a stable ion, for which structure VI is not unreasonable (cf. fluoradene).

ACKNOWLEDGMENT

The author is greatly indebted to Dr. J. S. E. Holker (Liverpool) for the mass spectra.

1. W. Wislicenus and A. Fehrle. Ber. **48**, 1320 (1915).
2. P. M. Everitt and E. E. Turner. J. Chem. Soc. 3477 (1957).
3. F. Ullmann and A. Marie. Ber. **34**, 4307 (1901).
4. G. T. Morgan and L. P. Walls. J. Chem. Soc. 2447 (1931).
5. F. E. King, M. Liguori, and R. Robinson. J. Chem. Soc. 1475 (1933).
6. B. Witkop and J. B. Patrick. J. Am. Chem. Soc. **73**, 2188 (1951).
7. G. Plancher. Ber. **31**, 1488 (1898).
8. G. Jenisch. Monatsh. **27**, 1223 (1906).
9. H. Brunner. Monatsh. **16**, 850 (1895); **21**, 179 (1900).
10. G. Plancher. Gazz. Chim. Ital. **28**, 374 (1898).
11. V. Georgian. Chem. Ind. (London), 1124 (1954).
12. G. Plancher, B. Cecchetti, and E. Ghigi. Gazz. Chim. Ital. **59**, 334 (1929).
13. K. H. Pausacker. J. Chem. Soc. 621 (1950).
14. K. H. Meyer and H. Gottlieb-Billroth. Ber. **54**, 575 (1921).
15. H. Ley and W. Manecke. Ber. **56**, 779 (1923).
16. C. F. H. Allen and C. V. Wilson. J. Am. Chem. Soc. **65**, 611 (1943).
17. C. L. Arcus and R. J. Mesley. J. Chem. Soc. 180 (1953).
18. G. M. Badger, R. S. Pearce, and R. Pettit. J. Chem. Soc. 3199 (1951).

Received April 20, 1965.
Smith Kline & French Laboratories Ltd.,
Mundells,
Welwyn Garden City,
Hertfordshire, England.

1,2-*O*-ISOPROPYLIDENE-α-D-GLUCOFURANOSE-5-*d* AND -5,6,6′-d_3[1]

W. Mackie[2] and A. S. Perlin

D-Glucose-5-*d* (I), required in a recent study on oxidative glycol-scission, has been prepared in low isotope yield via a series of reactions that involve initially the reduction of D-*xylo*-5-hexulosonic acid with sodium borodeuteride (1). Other means for preparing this labelled sugar have also been examined and one, which is more satisfactory for the purpose and, in addition, provides a ready route to D-glucose-5,6,6′-d_3 (II), is reported here.

The current method is based on the conversion of 1,2-*O*-isopropylidene-α-D-glucofuranurono-6,3-lactone (III) to the 5-keto derivative (IV). This oxidation step was carried out with chromium trioxide in acetic acid, ketone IV being isolated as a crystalline monohydrate. Coincidentally, the same compound was very recently prepared by oxidation of III with activated manganese dioxide (2), although details of this procedure have yet to be communicated. In accord with the structure ascribed to IV (2) the nuclear magnetic resonance (n.m.r.) spectrum of the compound consists of four doublets (Fig. 1*a*) (in addition to the *O*-isopropylidene methyl group signals), showing coupling between H_1 and H_2, H_3 and H_4. The latter two protons resonate at much lower frequencies than do their counterparts in the original D-glucurone derivative (III). One of these (probably H_4)

[1]*Issued as N.R.C. No. 8557.*
[2]*National Research Council of Canada Postdoctorate Fellow, 1964–65.*

Can. J. Chem. Downloaded from www.nrcresearchpress.com by 210.87.254.5 on 09/05/12
For personal use only.

that 345 → 267 also occur directly); 345 → 239, loss of 106, i.e. $C_6H_5CH_2$—$\overset{\oplus}{N}H$ or equivalent; of lesser importance are ions at 329, loss of 16, i.e. NH_2 or equivalent, and 213, loss of 132.

The ion at 239 is common to both spectra. It probably represents a stable ion, for which structure VI is not unreasonable (cf. fluoradene).

ACKNOWLEDGMENT

The author is greatly indebted to Dr. J. S. E. Holker (Liverpool) for the mass spectra.

1. W. Wislicenus and A. Fehrle. Ber. **48**, 1320 (1915).
2. P. M. Everitt and E. E. Turner. J. Chem. Soc. 3477 (1957).
3. F. Ullmann and A. Marie. Ber. **34**, 4307 (1901).
4. G. T. Morgan and L. P. Walls. J. Chem. Soc. 2447 (1931).
5. F. E. King, M. Liguori, and R. Robinson. J. Chem. Soc. 1475 (1933).
6. B. Witkop and J. B. Patrick. J. Am. Chem. Soc. **73**, 2188 (1951).
7. G. Plancher. Ber. **31**, 1488 (1898).
8. G. Jenisch. Monatsh. **27**, 1223 (1906).
9. H. Brunner. Monatsh. **16**, 850 (1895); **21**, 179 (1900).
10. G. Plancher. Gazz. Chim. Ital. **28**, 374 (1898).
11. V. Georgian. Chem. Ind. (London), 1124 (1954).
12. G. Plancher, B. Cecchetti, and E. Ghigi. Gazz. Chim. Ital. **59**, 334 (1929).
13. K. H. Pausacker. J. Chem. Soc. 621 (1950).
14. K. H. Meyer and H. Gottlieb-Billroth. Ber. **54**, 575 (1921).
15. H. Ley and W. Manecke. Ber. **56**, 779 (1923).
16. C. F. H. Allen and C. V. Wilson. J. Am. Chem. Soc. **65**, 611 (1943).
17. C. L. Arcus and R. J. Mesley. J. Chem. Soc. 180 (1953).
18. G. M. Badger, R. S. Pearce, and R. Pettit. J. Chem. Soc. 3199 (1951).

Received April 20, 1965.
Smith Kline & French Laboratories Ltd.,
Mundells,
Welwyn Garden City,
Hertfordshire, England.

1,2-*O*-ISOPROPYLIDENE-α-D-GLUCOFURANOSE-5-*d* AND -5,6,6′-d_3[1]

W. Mackie[2] and A. S. Perlin

D-Glucose-5-*d* (I), required in a recent study on oxidative glycol-scission, has been prepared in low isotope yield via a series of reactions that involve initially the reduction of D-*xylo*-5-hexulosonic acid with sodium borodeuteride (1). Other means for preparing this labelled sugar have also been examined and one, which is more satisfactory for the purpose and, in addition, provides a ready route to D-glucose-5,6,6′-d_3 (II), is reported here.

The current method is based on the conversion of 1,2-*O*-isopropylidene-α-D-glucofuranurono-6,3-lactone (III) to the 5-keto derivative (IV). This oxidation step was carried out with chromium trioxide in acetic acid, ketone IV being isolated as a crystalline monohydrate. Coincidentally, the same compound was very recently prepared by oxidation of III with activated manganese dioxide (2), although details of this procedure have yet to be communicated. In accord with the structure ascribed to IV (2) the nuclear magnetic resonance (n.m.r.) spectrum of the compound consists of four doublets (Fig. 1*a*) (in addition to the *O*-isopropylidene methyl group signals), showing coupling between H_1 and H_2, H_3 and H_4. The latter two protons resonate at much lower frequencies than do their counterparts in the original D-glucurone derivative (III). One of these (probably H_4)

[1]*Issued as N.R.C. No. 8557.*
[2]*National Research Council of Canada Postdoctorate Fellow, 1964–65.*

Can. J. Chem. Downloaded from www.nrcresearchpress.com by 210.87.254.6 on 09/05/12
For personal use only.

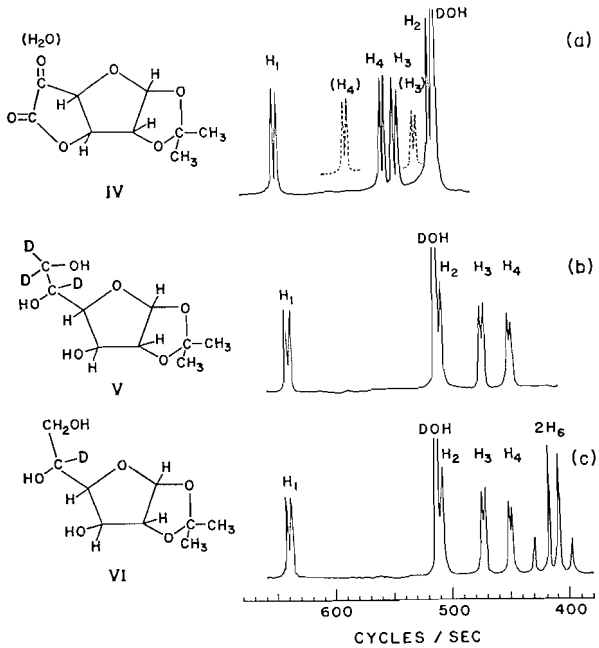

FIG. 1. Nuclear magnetic resonance spectra at 100 Mc/s in deuterium oxide of (*a*) 1,2-*O*-isopropylidene-α-D-xylohexofuranurono-6,3-lactone-5-ulose (IV); the broken line tracings show the location of the H_3 and H_4 signals after excess of potassium carbonate has been added to the solution; (*b*) 1,2-*O*-isopropylidene-α-D-glucofuranose-5,6,6′-d_3; (*c*) 1,2-*O*-isopropylidene-α-D-glucofuranose-5-*d*. Signals at relatively high field for protons of the isopropylidene groups are omitted.

gives its signal even further downfield (broken line) when the lactone structure is opened, whereas the other is affected slightly in the reverse fashion. The probability that the ketone group of IV is hydrated to give the *gem*-diol has already been pointed out (2). More direct evidence of this effect has been obtained by examining the resonance characteristics of the protons associated with the water of hydration, dimethyl sulfoxide being the solvent of choice for this purpose (3). Thus, the spectrum showed two singlets 149 and 133 c.p.s., respectively, downfield from the H_1 signal, both of which disappeared when deuterium oxide was added to the solution (3).[3] The non-equivalence of these signals, as well as their chemical shift (3), shows clearly that the protons responsible cannot be those of water itself but, rather, must be structural elements of the compound in solution.

Borohydride reduction of IV was found to yield 1,2-*O*-isopropylidene-α-D-glucofuranose and only a minor amount of the isomer having the L-ido configuration. Hence by using sodium borodeuteride, 1,2-*O*-isopropylidene-α-D-glucofuranose-5,6,6′-d_3 (V) was obtained in almost quantitative yield. Alternatively, the ketone (IV) was first converted to the sodium salt, and then reduced with the borodeuteride to produce a uronic acid deuteriated at position 5. The latter product was lactonized, and reduced with borohydride, giving a 2:1 mixture of 1,2-*O*-isopropylidene-α-D-glucofuranose-5-*d* (VI) and the corresponding L-ido derivative, from which VI was readily isolated by fractional crystallization.

The n.m.r. spectra of V and VI (Fig. 1) show clearly that the deuteriation steps were fully specific for the positions designated. Thus, in Fig. 1*b* signals attributable only to

[3]*The known gem-diol, chloral hydrate, gives a signal intermediate in chemical shift between those of the two singlets noted above. Because of the α-proton this signal is in the form of a doublet (J = 6.0 c.p.s.), and it has an intensity twice that of the α-proton triplet; on addition of deuterium oxide, the latter signal collapses to a singlet and the signals for the gem-diol protons disappear.*

Can. J. Chem. Downloaded from www.nrcresearchpress.com by 210.87.254.6 on 09/05/12
For personal use only.

protons 1 to 4 are found, and 1*c* contains the two extra doublets expected for the isolated 6- and 6′-protons. The high stereoselectivity of the reductions in yielding D-gluco isomers is particularly fortunate for the present purpose. However, this would not necessarily have been anticipated since borohydride reduction of 1,2-*O*-isopropylidene-α-D-xylo-hexofuranose-5-ulose gives the L-idose derivative predominantly (4), and with D-xylo-5-hexulosonic acid about equal proportions of the two isomeric aldonic acids are obtained (5).

EXPERIMENTAL

1,2-O-Isopropylidene-α-D-xylohexofuranurono-6,3-lactone-5-ulose (IV)

Chromium trioxide (1.25 g) was added to a stirred solution of 1,2-*O*-isopropylidene-α-D-glucofuranurono-6,3-lactone (III) (1.40 g) in acetic acid (25 ml). After 20 h, when a negative test with lead acetate showed that all of the oxidant had been consumed, the acetic acid was removed by lyophilization. Examination of the reaction mixture by thin-layer chromatography (benzene–methanol (9:1)) indicated the presence of a trace of unreacted III and two major products, one travelling faster than III (and later found to be IV), and the other being retained at the origin (as yet unidentified). The dark green residue was extracted with chloroform and the extract concentrated to a syrup (0.92 g), hot water was added, and, on cooling, the green aqueous solution deposited white needles. Two crops of the crystalline material were collected (total yield, 0.25 g) and, after recrystallization from water, the product had m.p. 128–130° (on a microscope melting block; dehydration appeared to take place at 115–125°); m.p. 145–148° (in a capillary tube). $[\alpha]_D$ +73° (*c*, 1.2 water) (ref. 2 gives m.p. 146–149°; $[\alpha]_D$ +76°).

Anal. Calcd. for $C_9H_{10}O_6.H_2O$: C, 46.5; H, 5.2. Found: C, 46.3; H, 5.3.

The compound absorbed strongly at 1 785 cm^{-1} (γ-lactone). A chromatographically pure, syrupy sample of IV obtained by countercurrent extraction (chloroform–water) of the crude oxidation product, showed absorption at 1 620 cm^{-1} (ascribed to the ketone group) and also at 1 780 cm^{-1} (γ-lactone).

The n.m.r. spectrum of the crystalline product is recorded in Fig. 1*a*. Presence of water of hydration was readily detected as an increase in the intensity of the DOH signal when the compound was dissolved in the deuterium oxide.

1,2-O-Isopropylidene-α-D-glucofuranose-5,6,6′-d_3 (V)

To a solution of sodium borodeuteride[4] (75 mg) in water (1 ml) was added an aqueous solution (2 ml) of the ketolactone (IV) (150 mg). The solution was stored at 3° overnight, treated with Amberlite-IR 120 (H^+), and concentrated to dryness, the residue being treated several times with methanol to remove borate. The product (142 mg) was crystalline, and acid hydrolysis followed by paper chromatographic examination ((ethyl acetate – pyridine – water (10:4:3)) showed that it was a derivative mainly of glucose, with idose ($R_{glucose}$ 1.4) present in low proportion. After several recrystallizations from ethyl acetate the product (103 mg) had m.p. 158–160°; its X-ray powder diagram was indistinguishable from that of 1,2-*O*-isopropylidene-α-D-glucofuranose. The n.m.r. spectrum is recorded in Fig. 1*b*.

1,2-O-Isopropylidene-α-D-glucofuranose-5-d (VI)

Sodium bicarbonate (95 mg) was added to a cold solution of the ketolactone (IV) (225 mg) in water (3 ml) and the solution left overnight at 3°. To this cooled solution sodium borodeuteride (170 mg) in water (1 ml) was added, and after 30 min the reaction mixture was allowed to warm to room temperature. One hour later the solution was deionized with mixed-bed ion exchange resins and concentrated to a syrup (237 mg). This product was dissolved in toluene (6) and heated under reflux for 3 h to promote lactonization, and the solvent was then evaporated off. Thin-layer chromatography of the residue showed the presence of two components having mobility close to that of III, with additional material at the origin. The residue (228 mg) was extracted with acetone, and the soluble material was taken up in water (2 ml) and treated at 3° overnight with potassium borohydride (120 mg in 1 ml of water). The final product (140 mg) was found by acid hydrolysis, followed by paper chromatographic examination, to consist of a mixture of gluco and ido-isomers in a ratio of about 2:1. Material obtained after several recrystallizations from ethyl acetate had m.p. 156–158°; its X-ray diffraction diagram was indistinguishable from that of 1,2-*O*-isopropylidene-α-D-glucofuranose. Its n.m.r. spectrum is recorded in Fig. 1*c*.

ACKNOWLEDGMENT

Nuclear magnetic resonance spectra were recorded by M. Mazurek. Microanalyses were performed by W. Haid, who also prepared X-ray powder diagrams and infrared spectra.

[4]*Supplied by Merck, Sharp and Dohme, Montreal, Quebec.*

Can. J. Chem. Downloaded from www.nrcresearchpress.com by 210.87.254.6 on 09/05/12
For personal use only.

1. W. MACKIE and A. S. PERLIN. Can. J. Chem. This issue.
2. H. WEIDMANN and G. OLBRICH. Tetrahedron Letters, No. 12, 725 (1965).
3. O. L. CHAPMAN and R. W. KING. J. Am. Chem. Soc. **86**, 1256 (1964).
4. O. THEANDER. Acta Chem. Scand. **17**, 1751 (1963).
5. J. K. HAMILTON and F. SMITH. J. Am. Chem. Soc. **76**, 3543 (1954).
6. J. SOWDEN. J. Am. Chem. Soc. **74**, 4377 (1952).

RECEIVED MAY 6, 1965.
PRAIRIE REGIONAL LABORATORY,
NATIONAL RESEARCH COUNCIL,
SASKATOON, SASKATCHEWAN.

Can. J. Chem. Downloaded from www.nrcresearchpress.com by 210.87.254.6 on 09/05/12
For personal use only.

THE ACTION OF FENTON'S REAGENT ON CYCLOPROPYLCARBINOL

C. C. LEE, A. J. CESSNA, AND MOIRA K. FROST

Fenton's reagent is well known as a source of OH radicals (1–3). In connection with some exploratory studies on the possibility of inducing rearrangements by γ-irradiation of cyclopropylcarbinol (I) in aqueous solution, which may involve OH radicals, the action of Fenton's reagent on I was investigated.

In the initial experiments, 2.0 *M* solutions of ferrous sulphate and hydrogen peroxide were added simultaneously to a dilute aqueous solution of I, and the resulting mixture was heated under reflux for 3 h. The products, identified by nuclear magnetic resonance and vapor phase chromatography analyses, were unchanged I, cyclobutanol (II), allylcarbinol (III), and cyclopropanecarboxaldehyde (IV). These results show the occurrence of rearrangements besides the expected oxidation of a primary alcohol to an aldehyde (4, 5). Facile interconversions among the cyclopropylcarbinyl, cyclobutyl, and allylcarbinyl systems are well known in carbonium ion types of reactions (6 and references given therein), whereas the free radical photochlorination of methyl-^{13}C-cyclopropane showed quite different results (7). It is thus of interest to ascertain whether the rearrangements accompanying the oxidation of I by Fenton's reagent is ionic or free radical in nature. To this end, compound I was subjected to treatment under various conditions, and the results are summarized in Table I.

From Table I, it may be noted that expts. 1–6 showed that oxidation of I to IV occurred within 2 minutes and that the observed rearrangements of I to II and III took place during the subsequent heating of the reaction mixture under reflux. This was further confirmed by expts. 7–10 when the two components on Fenton's reagent were first heated under reflux for 1 h before being added to I. The remaining expts. 11–20 showed that neither hydrogen peroxide nor ferrous sulfate alone could cause any reaction, and that the species responsible for the rearrangements was the ferric ion. These results demonstrated conclusively that the rearrangements observed under the present reaction conditions arose from a polar rather than a free radical mechanism. The findings are very similar to the aluminium alkoxide induced rearrangements found to accompany the Oppenauer oxidation of I (8). By analogy with the mechanism suggested by Kolthoff and Medalia (5), the oxidation of I by Fenton's reagent may be formulated as follows.

[1] $$Fe^{2+} + H_2O_2 \rightarrow Fe^{3+} + OH^- + HO\cdot$$

[2] $$Fe^{2+} + HO\cdot \rightarrow Fe^{3+} + OH^-$$

1. W. MACKIE and A. S. PERLIN. Can. J. Chem. This issue.
2. H. WEIDMANN and G. OLBRICH. Tetrahedron Letters, No. 12, 725 (1965).
3. O. L. CHAPMAN and R. W. KING. J. Am. Chem. Soc. **86**, 1256 (1964).
4. O. THEANDER. Acta Chem. Scand. **17**, 1751 (1963).
5. J. K. HAMILTON and F. SMITH. J. Am. Chem. Soc. **76**, 3543 (1954).
6. J. SOWDEN. J. Am. Chem. Soc. **74**, 4377 (1952).

RECEIVED MAY 6, 1965.
PRAIRIE REGIONAL LABORATORY,
NATIONAL RESEARCH COUNCIL,
SASKATOON, SASKATCHEWAN.

Can. J. Chem. Downloaded from www.nrcresearchpress.com by 210.87.254.5 on 09/05/12
For personal use only.

THE ACTION OF FENTON'S REAGENT ON CYCLOPROPYLCARBINOL

C. C. LEE, A. J. CESSNA, AND MOIRA K. FROST

Fenton's reagent is well known as a source of OH radicals (1–3). In connection with some exploratory studies on the possibility of inducing rearrangements by γ-irradiation of cyclopropylcarbinol (I) in aqueous solution, which may involve OH radicals, the action of Fenton's reagent on I was investigated.

In the initial experiments, 2.0 *M* solutions of ferrous sulphate and hydrogen peroxide were added simultaneously to a dilute aqueous solution of I, and the resulting mixture was heated under reflux for 3 h. The products, identified by nuclear magnetic resonance and vapor phase chromatography analyses, were unchanged I, cyclobutanol (II), allylcarbinol (III), and cyclopropanecarboxaldehyde (IV). These results show the occurrence of rearrangements besides the expected oxidation of a primary alcohol to an aldehyde (4, 5). Facile interconversions among the cyclopropylcarbinyl, cyclobutyl, and allylcarbinyl systems are well known in carbonium ion types of reactions (6 and references given therein), whereas the free radical photochlorination of methyl-^{13}C-cyclopropane showed quite different results (7). It is thus of interest to ascertain whether the rearrangements accompanying the oxidation of I by Fenton's reagent is ionic or free radical in nature. To this end, compound I was subjected to treatment under various conditions, and the results are summarized in Table I.

From Table I, it may be noted that expts. 1–6 showed that oxidation of I to IV occurred within 2 minutes and that the observed rearrangements of I to II and III took place during the subsequent heating of the reaction mixture under reflux. This was further confirmed by expts. 7–10 when the two components on Fenton's reagent were first heated under reflux for 1 h before being added to I. The remaining expts. 11–20 showed that neither hydrogen peroxide nor ferrous sulfate alone could cause any reaction, and that the species responsible for the rearrangements was the ferric ion. These results demonstrated conclusively that the rearrangements observed under the present reaction conditions arose from a polar rather than a free radical mechanism. The findings are very similar to the aluminium alkoxide induced rearrangements found to accompany the Oppenauer oxidation of I (8). By analogy with the mechanism suggested by Kolthoff and Medalia (5), the oxidation of I by Fenton's reagent may be formulated as follows.

[1] $$Fe^{2+} + H_2O_2 \rightarrow Fe^{3+} + OH^- + HO\cdot$$

[2] $$Fe^{2+} + HO\cdot \rightarrow Fe^{3+} + OH^-$$

[3] $$HO\cdot + \triangleright\!\!-CH_2OH \rightarrow \triangleright\!\!-\dot{C}HOH + H_2O$$

[4] $$\triangleright\!\!-\dot{C}HOH + Fe^{3+} \rightarrow \triangleright\!\!-CHO + H^+ + Fe^{2+}$$

The ferric ions produced according to eqs. [1] and [2], besides reacting as in eq. [4], could act as a Lewis acid to induce rearrangements typical of carbonium ion reactions involving the cyclopropylcarbinyl system.

TABLE I

Results from treatment of cyclopropylcarbinol in aqueous solution with various reagents

Expt.	Refluxing time (h)	Reagent used	Relative composition of products*			
			% I	% II	% III	% IV
1	3	Fenton's reagent	22.2	38.9	7.0	31.9
2	"	"	22.8	40.1	6.4	30.7
3	1	"	54.0	10.9	0.0	35.1
4	"	"	53.7	13.7	0.0	32.7
5	1/30	"	63.8	Trace	0.0	36.2
6	"	"	62.7	0.0	0.0	37.3
7	3	$FeSO_4$ and H_2O heated under	22.7	65.7	11.6	0.0
8	"	reflux 1 h "	22.0	68.7	9.7	0.0
9	1	"	64.4	29.4	6.2	0.0
10	"	"	63.0	32.7	4.3	0.0
11	3	H_2O_2	100.0	—	—	—
12	1	"	100.0	—	—	—
13	3	$FeSO_4$	100.0	—	—	—
14	1	"	100.0	—	—	—
15	3	$Fe_2(SO_4)_3$†	4.7	83.0	12.3	0.0
16	"	"	3.8	81.4	14.8	0.0
17	1	"	26.2	65.3	8.5	0.0
18	"	"	24.2	66.3	9.5	0.0
19	3	"	16.5	69.7	9.5	0.0
20	1	"	42.5	50.2	7.3	0.0

*Assayed by v.p.c. Compounds I, II, III, and IV are, respectively, cyclopropylcarbinol, cyclobutanol, allylcarbinol, and cyclopropanecarboxaldehyde.

†In expts. 15–18, the ratio of g-ions of Fe^{3+} to moles of I was 2:1; in expts. 19 and 20, this ratio was 1:1.

EXPERIMENTAL

Cyclopropylcarbinol (I), cyclobutanol (II), and cyclopropanecarboxaldehyde (IV) were obtained by methods mentioned previously (8). Allylcarbinol (III) was prepared by the lithium aluminium hydride reduction of vinylacetic acid (6). All of these compounds, I, II, III, and IV, were purified by preparative v.p.c. before their use either as reactant or as standards in v.p.c. calibrations.

For expts. 1–6, a typical run is as follows. In a three-necked flask fitted with reflux condenser and two dropping funnels was placed a solution of 0.25 g (3.5 mmole) of I in 12.5 ml of water. The vessel and its content were heated in an oil bath to maintain a gentle reflux. The Fenton's reagent, consisting of 2.0 *M* solutions of ferrous sulphate and hydrogen peroxide (9), were added simultaneously through the two dropping funnels, 3.5 ml (7.0 mmole) of each solution being used. The mixture was heated under reflux for the desired length of time, cooled in an ice bath, and extracted three times with 3-ml portions of absolute ether. After the extract was dried over anhydrous magnesium sulphate, it was analyzed by v.p.c., using a column packed with 30% β,β'-oxydipropionitrile on 30–60 mesh fire brick.

In a larger scale experiment with 3 h of refluxing time, the products, I, II, III, and IV, were recovered by preparative v.p.c. and identified by comparisons of their n.m.r. spectra and v.p.c. retention times with those of authentic samples.

For expts. 7–10, the two components (3.5 ml each) of Fenton's reagent were heated under reflux together for 1 h and then the mixture was added to the solution of I in the reaction vessel. In expts. 11–20, instead of Fenton's reagent, 3.5 ml of a solution containing the appropriate compound and 3.5 ml of water were used. The reaction mixtures from expts. 7–20 were worked up exactly as described for expts. 1–6.

ACKNOWLEDGMENT

The financial support given by The National Research Council of Canada is gratefully acknowledged.

Can. J. Chem. Downloaded from www.nrcresearchpress.com by 210.87.254.5 on 09/05/12
For personal use only.

1. F. HABER and J. WEISS. Proc. Roy. Soc. **A147**, 332 (1934).
2. J. H. BAXENDALE, M. G. EVANS, and G. S. PARK. Trans. Faraday Soc. **42**, 155 (1946).
3. W. A. WATERS. *In* Progress in organic chemistry. Vol. 5. *Edited by* J. W. Cook and W. Carruthers. Butterworths and Co., London. 1961. pp. 1–45.
4. J. H. MERZ and W. A. WATERS. J. Chem. Soc. 515 (1949).
5. I. M. KOLTHOFF and A. I. MEDALIA. J. Am. Chem. Soc. **73**, 2509 (1951).
6. K. L. SERVIS and J. D. ROBERTS. J. Am. Chem. Soc. **86**, 3773 (1964).
7. E. RENK, P. R. SHAFER, W. H. GRAHAM, R. H. MAZUR, and J. D. ROBERTS. J. Am. Chem. Soc. **83**, 1987 (1961).
8. C. C. LEE and I. S. BHARDWAJ. Can. J. Chem. **41**, 1031 (1963).
9. R. J. WOODS and J. W. T. SPINKS. Can. J. Chem. **35**, 1475 (1957).

RECEIVED MAY 25, 1965.
DEPARTMENT OF CHEMISTRY,
UNIVERSITY OF SASKATCHEWAN,
SASKATOON, SASKATCHEWAN.

Can. J. Chem. Downloaded from www.nrcresearchpress.com by 210.87.254.5 on 09/05/12
For personal use only.

ADDENDUM: EVIDENCE FOR $ZnF_2.2H_2O$

E. A. SECCO AND O. K. SRIVASTAVA

(Ref. Can. J. Chem. 43, 175 (1965))

More detailed data from weight loss, X-ray diffraction, and solubility studies on an unknown fluoride hydrate reveal that the earlier interpretation in terms of zinc fluoride dihydrate (1) is not valid. It is necessary, therefore, to present a reinterpretation of the previously reported data along with more recent results.

EXPERIMENTAL

Five grams of the unidentified fluoride hydrate supplied by A. D. MacKay Inc. were stirred in 200 ml of distilled water for 1 h and filtered. The filtrate, on slow evaporation at room temperature, produced crystals of zinc fluoride tetrahydrate. The insoluble residue was washed several times with distilled water and dried in air.

Weight loss studies were carried out and X-ray diffraction patterns obtained on three samples, viz., I the stock sample, II zinc fluoride tetrahydrate crystals obtained from the filtrate, and III the insoluble residue.

RESULTS AND DISCUSSION

The results of the weight loss studies are summarized in Table I.

TABLE I

Sample No.	T (°C)	Time (h)	% weight loss Obs.	% weight loss Calcd.
I	105	2	20.12	20.05*
I	105	2	20.12	
II	120	2	38.3	41.1†
II	100	2	39.1	
II	100	2	42.4	
III	Ignited‡	1/4	18.4	19.8§
III	Ignited‡	1/3	19.3	

*Calculated value for equimolar mixture of Zn(OH)F and $ZnF_2.4H_2O$.
†Calculated value for $ZnF_2.4H_2O$.
‡Sample ignited in platinum crucible to bright redness.
§Calculated value for Zn(OH)F.

The X-ray diffraction pattern of the stock fluoride was reported earlier (1). The insoluble residue gave an X-ray diffraction pattern very similar to that reported by Feitkneckt and Bucher (2) for zinc hydroxyfluoride which appeared in our earlier work

1. F. HABER and J. WEISS. Proc. Roy. Soc. **A147**, 332 (1934).
2. J. H. BAXENDALE, M. G. EVANS, and G. S. PARK. Trans. Faraday Soc. **42**, 155 (1946).
3. W. A. WATERS. *In* Progress in organic chemistry. Vol. 5. *Edited by* J. W. Cook and W. Carruthers. Butterworths and Co., London. 1961. pp. 1–45.
4. J. H. MERZ and W. A. WATERS. J. Chem. Soc. 515 (1949).
5. I. M. KOLTHOFF and A. I. MEDALIA. J. Am. Chem. Soc. **73**, 2509 (1951).
6. K. L. SERVIS and J. D. ROBERTS. J. Am. Chem. Soc. **86**, 3773 (1964).
7. E. RENK, P. R. SHAFER, W. H. GRAHAM, R. H. MAZUR, and J. D. ROBERTS. J. Am. Chem. Soc. **83**, 1987 (1961).
8. C. C. LEE and I. S. BHARDWAJ. Can. J. Chem. **41**, 1031 (1963).
9. R. J. WOODS and J. W. T. SPINKS. Can. J. Chem. **35**, 1475 (1957).

RECEIVED MAY 25, 1965.
DEPARTMENT OF CHEMISTRY,
UNIVERSITY OF SASKATCHEWAN,
SASKATOON, SASKATCHEWAN.

Can. J. Chem. Downloaded from www.nrcresearchpress.com by 210.87.254.5 on 09/05/12
For personal use only.

ADDENDUM: EVIDENCE FOR $ZnF_2.2H_2O$

E. A. SECCO AND O. K. SRIVASTAVA

(Ref. Can. J. Chem. 43, 175 (1965))

More detailed data from weight loss, X-ray diffraction, and solubility studies on an unknown fluoride hydrate reveal that the earlier interpretation in terms of zinc fluoride dihydrate (1) is not valid. It is necessary, therefore, to present a reinterpretation of the previously reported data along with more recent results.

EXPERIMENTAL

Five grams of the unidentified fluoride hydrate supplied by A. D. MacKay Inc. were stirred in 200 ml of distilled water for 1 h and filtered. The filtrate, on slow evaporation at room temperature, produced crystals of zinc fluoride tetrahydrate. The insoluble residue was washed several times with distilled water and dried in air.

Weight loss studies were carried out and X-ray diffraction patterns obtained on three samples, viz., I the stock sample, II zinc fluoride tetrahydrate crystals obtained from the filtrate, and III the insoluble residue.

RESULTS AND DISCUSSION

The results of the weight loss studies are summarized in Table I.

TABLE I

Sample No.	T (°C)	Time (h)	% weight loss Obs.	% weight loss Calcd.
I	105	2	20.12	20.05*
I	105	2	20.12	
II	120	2	38.3	41.1†
II	100	2	39.1	
II	100	2	42.4	
III	Ignited‡	1/4	18.4	19.8§
III	Ignited‡	1/3	19.3	

*Calculated value for equimolar mixture of Zn(OH)F and $ZnF_2.4H_2O$.
†Calculated value for $ZnF_2.4H_2O$.
‡Sample ignited in platinum crucible to bright redness.
§Calculated value for Zn(OH)F.

The X-ray diffraction pattern of the stock fluoride was reported earlier (1). The insoluble residue gave an X-ray diffraction pattern very similar to that reported by Feitkneckt and Bucher (2) for zinc hydroxyfluoride which appeared in our earlier work

as Fig. 4 and erroneously interpreted as the diffraction pattern for the hemihydrate. For comparison purposes the *d*-spacings corresponding to the observed peaks on the diffractogram and their relative intensities of the insoluble residue are given in Table II with those of zinc hydroxyfluoride. The zinc fluoride tetrahydrate diffractogram checked with the pattern for $ZnF_2.4H_2O$ recorded in the ASTM file index.

TABLE II

A. D. MacKay insoluble residue		Zn(OH)F (2)	
d	I/I_0	*d*	I/I_0
5.05	6	—	—
4.25	100	4.30	98
3.45	9	3.43	12
2.76	49	2.78	74
2.66	40	2.65	57
2.56	40	—	—
2.52	90	2.53	100
2.32	27	2.34	49
2.26	22	2.28	49
2.24	22	—	—
2.06	12	2.11	51
1.98	11	1.99	30
—	—	1.90	23
1.87	11	1.87	28
1.84	9	—	—
1.76	50	1.78	82
1.73	19	1.73	20
1.64	9	1.62	60
1.60	27	—	—
1.56	23	1.56	54
—	—	1.51	60
1.49	22	1.48	42

It is now concluded that the weight loss and solubility data along with the X-ray diffraction pattern of the unknown fluoride hydrate are compatible with an equimolar mixture of zinc fluoride tetrahydrate and zinc hydroxyfluoride. Unfortunately, the stoichiometric weight losses expected from the dehydration of a fluoride dihydrate via a hemihydrate is fortuitously quasi-identical to the equimolar mixture.

1. E. A. Secco and R. R. Martin. Can. J. Chem. **43**, 175 (1965).
2. W. Feitkneckt and H. Bucher. Helv. Chim. Acta, **26**, 2196 (1943).

Chemistry Department,
St. Francis Xavier University,
Antigonish, Nova Scotia.

Can. J. Chem. Downloaded from www.nrcresearchpress.com by 210.87.254.5 on 09/05/12
For personal use only.

Can. J. Chem. Downloaded from www.nrcresearchpress.com by 210.87.254.5 on 09/05/12
For personal use only.

Canadian Journal of Chemistry

Issued by THE NATIONAL RESEARCH COUNCIL OF CANADA

VOLUME 43 NOVEMBER 1965 NUMBER 11

STRUCTURAL FEATURES OF TWO EXTRACELLULAR POLYSACCHARIDES FROM SERRATIA MARCESCENS[1]

ROBERT YOUNG[2] AND G. A. ADAMS

Division of Biosciences, National Research Council, Ottawa, Canada

Received June 2, 1965

ABSTRACT

A polysaccharide insoluble in acidified ethanol solution has been isolated from a culture filtrate of *Serratia marcescens*. Fractionation by cetyltrimethylammonium bromide ("Cetavlon") and by diethylaminoethyl (DEAE) cellulose yielded a polysaccharide which was electrophoretically homogeneous and contained D-glucose, L-rhamnose, D-galactose, L-*glycero*-D-*manno*-heptose, D-*glycero*-D-*manno*-heptose, glucosamine, and galactosamine in an approximate molar ratio of 6.5:3.5:0.5:1.0:0.5:1.0:0.2. However, following methylation it was found that the fully methylated polysaccharide could be fractionated by organic solvents into a rhamnoglucan and a heptoglucan. Both polysaccharides contained lipid material consisting mainly of hydroxy myristic acid and hydroxy lauric acid. The main chain of the rhamnoglucan was composed of (1 → 3) linked L-rhamnopyranose units and (1 → 4) linked D-glucose units with the non reducing end groups being D-glucose; some branching occurred through D-glucose units. The heptoglucan was composed mainly of chains of (1 → 4) linked D-glucose units with smaller amounts of (1 → 6) linked D-glucose and (1 → 2) linked D-*glycero*-D-*manno*-heptose units; these chains were terminated by D-glucopyranose and L-*glycero*-D-*manno*-heptose end groups.

Although previous work (1, 2, 3) has indicated the presence of polysaccharides in the culture filtrates of *Serratia marcescens*, no attempt has been made to isolate them in homogeneous form and to examine their structural features. The preparation, fractionation, and preliminary examination of the extracellular polysaccharides produced by *Serratia marcescens*, grown on a sucrose medium, has been carried out in this laboratory and described in a previous communication (4). The crude polysaccharides were fractionated primarily on the basis of their solubility in acidic ethanol solution. In the present study, the acid–alcohol insoluble polysaccharides have been fractionated further and information on their main structural features has been obtained. The constitution of an acidic glucomannan isolated from the acid–alcohol soluble material will be reported in a later communication.

The acid–alcohol insoluble polysaccharide preparation, on examination by moving boundary electrophoresis (5) in borate buffer, was found to comprise one main component together with several other minor polysaccharide fractions. Cetavlon (6) precipitated a small amount of polysaccharide from aqueous solution, leaving a fraction in the supernatant which showed fewer minor fractions on electrophoresis. Further purification of this latter fraction was achieved by chromatography on diethylaminoethyl (DEAE) cellulose (7). Elution was effected with a gradient (0–0.5 *M*) phosphate buffer at pH 6,

[1]*Issued as N.R.C. No. 8632.*

[2]*National Research Council Postdoctorate Fellow 1963–1965.*

followed by a gradient (0–0.3 *M*) sodium hydroxide. The major polysaccharide component was eluted with the phosphate buffer. It contained 0.98% nitrogen, 7% ash, had $[\alpha]_D$ +62° (*c*, 1.0 in H_2O) and gave a sharp symmetrical peak ($\mu = -2.38 \times 10^{-5}$ cm^2 s^{-1} V^{-1}), on free boundary electrophoresis in borate buffer with only a trace of a faster moving component. This polysaccharide was considered pure enough to warrant structural studies.

The constituent neutral monosaccharides of the polysaccharide were determined quantitatively after acid hydrolysis by gas–liquid partition chromatography (g.l.p.c.) of the derived acetylated polyols (8). This procedure provided identification of the various sugars, which were D-glucose, L-rhamnose, D-*glycero*-D-*manno*-heptose, L-*glycero*-D-*manno*-heptose, and a trace of D-galactose. Configuration of the sugars was assigned by later determination of the specific rotation of crystalline derviatives. The presence of heptose was first indicated by positive color reactions with *p*-anisidine hydrochloride (9) and the specific periodate – acetyl acetone spray reagent (10). The acetylated polyols on g.l.p.c. gave two peaks in the heptitol region. These could have arisen from reduction of one heptulose or from reduction of two heptoses. However, authentic heptuloses were found to give a different color when sprayed with the orcinol reagent and do not give a positive reaction with the periodate – acetyl acetone reagent (10). Partition chromatographic procedures could not be employed to isolate the two heptoses as they had similar chromatographic mobility to glucose which was present in large excess. The polysaccharide hydrolysate was treated with glucose oxidase and the resulting gluconic acid removed with basic ion-exchange resin. The residual mixture of neutral monosaccharides was fractionated by cellulose column chromatography. A fraction was obtained containing both heptoses, mixed with a small amount of galactose. The latter was removed by conversion to the 1,6-dialdehyde with galactose oxidase (11) and subsequent preparative paper chromatography. A portion of the material containing the two heptoses was treated with 1 mole equivalent of periodate. This selectively cleaved the exocyclic C_6—C_7 bond and reduction of the resulting aldehyde gave the parent hexose (12). Paper and gas–liquid partition chromatographic evidence showed mannose to be the only hexose produced. The remainder of the heptose mixture was reduced and acetylated. The resulting heptitol acetates were separated by preparative g.l.p.c. and identified as D-*glycero*-D-*manno*-heptitol heptaacetate and L-*glycero*-D-*manno*-heptitol heptaacetate.

In a separate experiment, using cellulose column chromatography with a different eluant, the major heptose component L-*glycero*-D-*manno*-heptose was isolated and identified by its specific rotation and preparation of a crystalline derivative.

The presence of hexosamine in the polysaccharide was indicated initially by paper chromatography. This was confirmed by g.l.p.c. (13) of the trimethyl silyl derivatives of the polysaccharide hydrolysate; 8.1% glucosamine and 2.3% galactosamine were found to be present.

The polysaccharide was found to consume 0.58 moles of periodate per anhydro hexose unit. Most of the glucose residues were oxidized and all the rhamnose residues remained intact. Utilization of the Smith procedure (14) indicated no contiguous rhamnose residues in the molecule. The products were glycerol, erythritol, rhamnose, and glucose in a molecular ratio of 1.1:1.05:1.0:0.13.

Exhaustive methylation of the polysaccharide with dimethyl sulfate and sodium hydroxide, with methyl iodide and silver oxide, and also by Kuhn's procedure (15) did not raise the methoxyl content above 35.5%. Examination by infrared spectroscopy showed only a small amount of absorption in the hydroxyl region. The methylated

Can. J. Chem. Downloaded from www.nrcresearchpress.com by 210.87.254.5 on 09/05/12
For personal use only.

product was fractionally precipitated from chloroform solution with light petroleum to give an insoluble fraction (polysaccharide A) and a soluble fraction (polysaccharide B).

Methylated polysaccharide A was hydrolyzed, and demethylation of a sample of the products indicated glucose and rhamnose were the only constituent sugars. The mixture of *O*-methyl ethers was analyzed by a combination of gas–liquid, paper, and thin-layer chromatography. The relative amounts of *O*-methyl sugars in the mixtures were determined by g.l.p.c. using three different liquid phases. The quantitative results for methylated polysaccharide A are given in Table I; each of the methylated sugars was characterized by isolation of a crystalline derivative. Also present in the hydrolysate was an appreciable amount of lipid material, which was identified by chromatographic techniques as α-hydroxy fatty acids.

TABLE I

Hydrolysis products* from methylated polysaccharide A from *Serratia marcescens*

O-Methyl ether	Composition (mole %)
2,3,4,6-Tetra-*O*-methyl-D-glucose	7.4
2,4-Di-*O*-methyl-L-rhamnose	29.0
2,3,6-Tri-*O*-methyl-D-glucose	63.6

*Also found was a small amount of dimethyl- and monomethyl-glucoses.

Methylated polysaccharide B was found to contain a large proportion of free lipid material. This was separated from the methylated polysaccharide by column chromatography on silicic acid, and found to contain methoxy myristic acid, methoxy lauric acid, and two unidentified fatty acids. A methylated polysaccharide was obtained which appeared homogeneous on thin-layer chromatography, but infrared spectroscopic examination indicated the presence of some lipid moieties. Hydrolysis followed by demethylation of a small portion of the sugar ethers indicated the constituent monosacchrides to be glucose, L-*glycero*-D-*manno*-heptose, and D-*glycero*-D-*manno*-heptose. Insufficient material was available for separation and characterization of the *O*-methyl ethers, but gas–liquid and paper chromatography identified the main components as shown in Table II. Also obtained from the hydrolysis products of the methylated polysaccharide was a lipid component. This was not further investigated, as a comprehensive study of the bound lipids from *Serratia marcescens* polysaccharides is at present underway in this laboratory.

TABLE II

Hydrolysis products of the methylated heptoglucan

Component sugar	Molar ratio
2,3,4,6-Tetra-*O*-methyl-glucose	3.7
2,3,6-Tri-*O*-methyl-glucose	3.5
2,3,4-Tri-*O*-methyl-glucose	1.0
3,4,6,7-Tetra-*O*-methyl-D-*glycero*-D-*manno*-heptose	1.05
Fully methylated D-*glycero*-D-*manno*-heptose	0.3
Fully methylated L-*glycero*-D-*manno*-heptose	2.2

From the above results it is apparent that the polysaccharide product, which resulted from various fractionation procedures and appeared homogeneous on electrophoresis, contained two entirely different polysaccharides, a rhamnoglucan and a heptoglucan.

Can. J. Chem. Downloaded from www.nrcresearchpress.com by 210.87.254.5 on 09/05/12
For personal use only.

The possibility cannot be dismissed, however, that since the polysaccharide preparation before methylation appeared homogeneous on free boundary electrophoresis, the two polysaccharides may have been joined by some alkali-labile bond. The failure to find any galactose or hexosamine in the methylation products, both of which were present in the hydrolysis products of the original polysaccharide, indicates that other polymeric species may exist. This failure could also be attributed to the destruction of the hexosamine during the prolonged methylation with strong alkali.

A significant feature of the polysaccharide is the presence of an appreciable amount of lipid. The latter must have been firmly bound since any 'free' lipid would not have survived the purification procedures used and would almost certainly not have been precipitated with ethanol. During the Haworth methylation, treatment with 30% sodium hydroxide for a long period of time would have cleaved any amide or ester bound fatty acids. This explains why these substances were found in the light-petroleum soluble fraction which was obtained after methylation. However, infrared spectroscopy has indicated that a significant proportion of the lipids survived the alkali treatment and so it is possible that these were glycosidically linked. This is substantiated by the fact that the lipids found in the hydrolysate of methylated polysaccharide A have unmethylated hydroxyl groups which suggests that the lipids were bound to the polysaccharide through these groups. The indication supplied by infrared spectroscopy was confirmed by the finding of lipids in the acid hydrolysates of both methylated polysaccharides. The dilution effect introduced by these non-carbohydrate moieties in the polysaccharide accounts for the low methoxyl values of the methylated polysaccharide. The gradual increase in methoxyl content during prolonged Haworth methylation may be explained by slow cleavage of ester and amide bound fatty acids which would make additional hydroxyl groups available for methylation.

Although no unique structure can be postulated for the rhamnoglucan, from the methylation results the following deductions can be made. The main chain of the polysaccharide comprises (1 → 3) linked L-rhamnopyranose units and (1 → 4) linked D-glucopyranose units, the chain being terminated by D-glucopyranose residues. If the chain is unbranched, the amount of tetra-*O*-methyl-glucose indicates a chain length of 14. The molecular weight, however, gives a degree of polymerization of 35, and while this value represents the average for the mixture of polysaccharides the discrepancy is too great to be explained in this way. Consequently a certain amount of branching must occur, and this possibility is supported by the presence of small quantities of partially methylated glucose residues in the hydrolysis products of the methylated polysaccharide. On the other hand, some of the latter residues may have hydroxyl groups unsubstituted during methylation because of the presence of fatty acids, which were later cleaved off by acid hydrolysis. To establish unequivocally the sequence of glucose and rhamnose units in the chain, oligosaccharides formed by partial hydrolysis of the molecule would have to be isolated. Evidence accrued by periodate oxidation, however, shows that there are no contiguous rhamnose residues. Consequently since there are approximately twice as many (1 → 4) linked glucose residues as (1 → 3) linked rhamnose residues, it is possible that the following partial structure may be present.

$$\rightarrow 3)\text{L-Rha}p(1 \rightarrow 4)\text{D-G}p(1 \rightarrow 4)\text{D-G}p(1 \rightarrow 3)\text{L-Rha}p(1 \rightarrow 4)\text{D-G}p(1 \rightarrow 4)\text{D-G}p(1 \ldots$$

Definite conclusions from the results of periodate oxidation are limited since a significant proportion of hydroxyl groups in the polysaccharide are substituted by fatty acids and since the results were obtained on what is now known to have been a mixture of polysaccharides. The glycerol formed must have arisen from end groups of glucose and

Can. J. Chem. Downloaded from www.nrcresearchpress.com by 210.87.254.5 on 09/05/12
For personal use only.

L-*glycero*-D-*manno*-heptose together with any other residues which were chain-ending. Theoretically the ratio of erythritol to rhamnose in the oxidation products should be the same as the ratio of 2,3,6-tri-*O*-methyl-D-glucose to 2,4-di-*O*-methyl-L-rhamnose. The relatively low yield of erythritol can be attributed in part to the substitution of some glucose residues at positions C_2 and C_3 by fatty acids. This substitution would explain the presence of some unoxidized glucose residues in the products of periodate oxidation.

The results of the methylation study indicate that the heptoglucan is composed of main chains of $(1 \rightarrow 4)$ linked glucose residues with smaller amounts of $(1 \rightarrow 6)$ linked glucose and $(1 \rightarrow 2)$ linked D-*glycero*-D-*manno*-heptose moieties. These chains are terminated by D-glucopyranose and L-glycero-D-*manno*-heptose units. No prediction can be made as to whether or not branching occurs.

The occurrence of heptoses in polysaccharides of gram-negative bacteria is well known (16). L-*Glycero*-D-*manno*-heptose and D-*glycero*-D-*manno*-heptose have both been found in cell wall polysaccharides. As far as the authors are aware, however, this is the first report of two different heptoses occurring in the same molecule. Parikh and Jones (17) found D-*glycero*-D-*manno*-heptose linked $(1 \rightarrow 2)$ in an extracellular polysaccharide of *Azobacter indicum*. This heptose is linked in the same way in the heptoglucan described above. No other attempts have been made to find the mode of linkage of heptoses in polysaccharides.

It is obvious that the culture filtrate of *Serratia marcescens* contains several distinct polysaccharide entities, two of which, a rhamnoglucan and a heptoglucan, have been studied in some detail. The pattern of occurrence is very similar to that already found in the capsular polysaccharides from this bacteria (18). The conclusion, therefore, is that these extracellular polysaccharides have their origin in the capsular layer. From the cells of *Serratia marcescens* an entirely different polysaccharide containing glucose, mannose, and mannuronic acid has been isolated and its structure determined (19).

EXPERIMENTAL

All evaporations were carried out under diminished pressure below 40°.

Paper chromatograms were run by the descending method on Whatman No. 1 filter paper, using the following solvent systems (v/v).

(*a*) Ethyl acetate:pyridine:water (10:4:3).

(*b*) Butan-1-ol:ethanol:water (4:1:5, upper phase).

(*c*) Ethyl acetate:acetic acid:formic acid:water (18:3:1:4).

Sugars were detected on chromatograms by *p*-anisidine hydrochloride (9) or alkaline silver nitrate (20) spray reagents. Paper electrophoresis was done on Whatman 3 MM paper in 0.1 *M* sodium tetraborate at a potential gradient of 25 V/cm for 2 h. The rates of movement of the glycoses on the paper chromatograms are relative to that of D-glucose (R_{glu}) or 2,3,4,6-tetra-*O*-methyl-D-glucose (R_g), and relative to D-glucose (M_g) on the paper elctrophoretograms.

Gas–liquid partition chromatography (21) was done with a Pye argon chromatograph fitted with an ionization detector using straight glass columns (120 × 0.5 cm inside diameter) with the following packings:

(*a*) 10% (w/w) Carbowax 6,000 on 80–100 acid-washed Chromosorb W (Johns-Manville),

(*b*) 10% (w/w) neopentyl glycol succinate (Applied Science Laboratories) on 80–100 mesh non-acid-washed Chromosorb W (Johns-Manville),

(*c*) 15% (w/w) polyphenyl ether on Gas Chrom A, 100–200 mesh.

The retention times of the methylated glycoses are quoted relative to methyl 2,3,4,6-tetra-*O*-methyl-α-D-glucoside (T_g) and the polyols to hexa-*O*-acetyl-D-galactitol (T_{gal}). Preparative g.l.p.c. was carried out on an F and M model 500 chromatograph.

Thin-layer chromatography was carried out with silica gel G using benzene:acetone (1:1) as developing solvent (22) and the sugars were detected by spraying with 70% sulfuric acid. Preparative thin-layer chromatography was effected on 0.66 mm thicknesses of silica gel G on glass plates (20 × 20 cm). Sugar regions on the plates were detected by the following method.

After removal of solvent, the plates were sprayed heavily with methanol and guide strips (1 cm wide) of Whatman No. 1 filter paper, thoroughly soaked with water, were pressed against the plate and left for 10 min. The strips were removed and sprayed with *p*-anisidine hydrochloride, thus indicating the position of the sugar zones on the plate. These were marked and scraped from the plate, and the products were obtained by extraction with boiling butan-1-one.

Can. J. Chem. Downloaded from www.nrcresearchpress.com by 210.87.254.5 on 09/05/12
For personal use only.

A Tiselius-type, Spinco model H apparatus was used for moving boundary electrophoresis in 0.05 *M* borate buffer (5).

Melting points were determined on a Fisher-Johns apparatus and are corrected.

Isolation of the Acid–Alcohol Insoluble Polysaccharide from the Crude Extracellular Polysaccharide Material

Batches of the desired polysaccharide were obtained according to the following typical experiment. Crude extracellular polysaccharide (4) (200 g) containing 3.5% nitrogen and 42% ash was taken up in water (6 l); an insoluble residue was washed twice with water and the washings were added to the solubles. The aqueous solution (6 520 ml) was poured with vigorous stirring into ethanol (32.5 l) containing conc. hydrochloric acid (140 ml). The precipitate which formed was filtered off, washed twice with 80% aqueous ethanol, and freeze-dried to yield a polysaccharide (15 g) containing 5.8% nitrogen and 19% ash. Moving boundary electrophoresis showed at least three peaks, with one main one.

Fractionation and Purification of the Polysaccharide

(a) Fractionation by Cetavlon (6)

Polysaccharide material (35 g.) was slurried in water (1 500 ml), and a portion which remained insoluble was removed by centrifugation. To the combined supernatant and washings (2 300 ml), was added a 1% aqueous solution of cetyltrimethylammonium hydroxide (Cetavlon) (500 ml) and 0.5 *N* sodium hydroxide (40 ml). The precipitate obtained was dissolved in 10% acetic acid and dialyzed, and the solution was poured into ethanol (4 volumes). This gave fraction (i) (1.4 g), which had 4.4% nitrogen and 21% ash. Acid hydrolysis of fraction (i) afforded glucose, mannose, and uronic acid, in the ratio of 3:1:1 as assessed by visual examination of paper chromatograms. Subsequent additions of Cetavlon followed by boric acid (23) gave no further precipitates.

The supernatant (3 850 ml) was acidified to pH 4.5 with acetic acid, dialyzed overnight, and poured into ethanol (5 volumes) giving fraction (ii) (8.8 g). This polysaccharide had 1.7% nitrogen and 7% ash. Visual inspection of paper chromatograms of the acid hydrolysis products indicated glucose, rhamnose, heptose, hexosamine, and uronic acid in a ratio of 5:2:1:1:1. Moving boundary electrophoresis showed the presence of one major component with traces of two faster moving components.

(b) DEAE–Cellulose Chromatography (7)

Fraction (ii) (8.8 g) from the above Cetavlon fractionation was dissolved in water (100 ml), and the solution was poured onto a column (7.5 × 36 cm) of diethylaminoethyl cellulose (phosphate form) as described by Neukom *et al.* (7). The column was eluted with a gradient of sodium dihydrogen phosphate (pH 6) (0–0.5 *M*; 4 l) followed by a gradient of sodium hydroxide (0–0.3 *M*; 2 l). Fractions (ca. 20 ml) were collected and analyzed for sugars by the phenol – sulfuric acid method (24). Two polysaccharide fractions were eluted; one by the phosphate buffer (fraction A) and the other by alkali (fraction B). The polysaccharides were recovered by dialyzing for 48 h, stirring with mixed ion exchange resins, evaporating the eluate to a small volume, and pouring into ethanol (5 volumes).

Fraction A (6.9 g) had 0.98% nitrogen and 7% ash and on acid hydrolysis gave glucose, rhamnose, heptose, hexosamine, and a trace of fucose. Fraction B (0.54 g) gave glucose, uronic acid, and a trace of mannose on hydrolysis.

Fraction A was used for structural investigations and henceforth will be referred to as 'the polysaccharide'.

Properties of the Polysaccharide

The polysaccharide had $[\alpha]_D^{25}$ 62° (*c*, 1.0 in water). A portion (50 mg) was dissolved in formamide (2 ml) and acetylated with acetic anhydride (0.8 ml) after addition of pyridine (6 ml). Vapor pressure osmometry of the acetylated derivative using the Mechrolab osmometer indicated a minimum degree of polymerization of 35. Moving boundary electrophoresis gave a large symmetrical peak having $\mu = -2.38 \times 10^{-5}\ cm^2\ s^{-1}\ V^{-1}$, plus one small fast moving impurity.

Samples (10 mg) of the polysaccharide were hydrolyzed with *N* sulfuric acid for 12 h. Quantitative analysis by g.l.p.c. of reduced acetylated products of the hydrolysate, using the procedure of Gunner *et al.* (8) indicated the following neutral sugars: D-glucose, L-rhamnose, D-galactose, L-*glycero*-D-*manno*-heptose, and D-*glycero*-D-*manno*-heptose in a molar ratio of 6.5:3.5:0.5:1.0:0.5. (The configurations of glucose, rhamnose, and the heptoses was established later by the determination of the specific rotation of their derivatives. Since galactose oxidase is specific for the D enantiomorph, the above assigned configuration for galactose is correct).

The presence of heptose in the polysaccharide hydrolysate was indicated by the brown-black color of a spot, R_{glu} 0.91 in solvent A, on a chromatogram sprayed with *p*-anisidine hydrochloride. Orcinol reagent (25) gave a red spot, R_{glu} 0.91; all the available authentic heptoses gave a similar red color, while heptuloses gave a blue-green color. Periodate – acetyl acetone spray reagent (10) gave the characteristic yellow color of formaldehyde, providing further evidence that heptose was present. Examination by g.l.p.c. on column B of the alcohol acetates (8) derived from the hydrolyzed polysaccharide gave two peaks in the heptitol region, having T_{gal} 2.32 and 1.98.

Since the two heptoses had the same chromatographic mobility on paper and cellulose columns as galactose and also moved close to a large amount of glucose, it was impossible to isolate the heptoses by normal partition chromatographic procedures. Crude extracellular polysaccharide (10 g) was hydrolyzed

Can. J. Chem. Downloaded from www.nrcresearchpress.com by 210.87.254.5 on 09/05/12
For personal use only.

with N H_2SO_4 for 12 h. The recovered mixture of sugars was dissolved in water (250 ml) and stirred overnight, at room temperature, in an atmosphere of oxygen with glucose oxidase (1 g). The gluconic acid formed was removed by basic ion exchange resin and the aqueous eluate evaporated to a syrup (1.29 g). Investigation by g.l.p.c. of the alcohol acetates (8) prepared from a portion of the syrup showed the latter to contain 27% heptose. A partial separation of the sugars was obtained by fractionating the syrup on a cellulose column with *n*-propanol:ethyl acetate:water (7:2:1). The fraction (600 mg) containing the heptoses was further fractionated on filter paper sheets in solvent A. The recovered syrup (165 mg) was shown by g.l.p.c. (8) to contain galactose in addition to the two heptoses. The syrup was dissolved in 0.1 M phosphate buffer pH 7.0 (10 ml) and ethanol (5 ml). Galactose oxidase (11.5 mg) with a small amount of catalase was added, and the solution was stirred and aerated with oxygen at room temperature for 24 h. A further addition of galactose oxidase (2.2 mg) and catalase was then made and the digestion was continued for a further 24 h. The solution was evaporated to small volume and the components were separated on filter sheets. The galactose was quantitatively converted to *meso-galacto*-hexodialdose, R_{glu} 0.43 in solvent A. The heptose mixture (57 mg) could not be resolved by paper chromatography using the following solvent systems and gave a spot with R_{glu} 0.97 in solvent B, 0.96 in solvent C, and 0.94 in solvent A. Paper electrophoresis in borate buffer did not separate the sugars which both had M_g 0.8. The heptose mixture had $[\alpha]_D$ −4° (*c*, 1.0 in H_2O).

A portion (22 mg) of the syrupy material was selectively periodate oxidized according to the method of Perry (12). After treating with 2% methanolic hydrogen chloride to form the methyl glycosides, 1 mole equivalent of periodate was added to the syrup. The resulting aldehyde was reduced with sodium borohydride and the free sugar was obtained by acid hydrolysis. Paper chromatography and g.l.p.c. (8) showed the products to consist mainly of mannose with traces of unreacted heptoses and a trace of unknown pentose, R_{glu} 1.29.

The remainder (30 mg) of the fraction containing the two heptoses was reduced with sodium borohydride and acetylated with acetic anhydride and sulfuric acid. The resulting acetylated heptitols were isolated by preparative g.l.p.c.

D-*Glycero*-D-*manno*-heptitol heptaacetate had the same retention time, T_{gal} = 1.98, on column B at 210° as the same derivative of the authentic sugar. The acetylated heptitol had $[\alpha]_D$ +34° (*c*, 0.38 in $CHCl_3$). The reported value for D-*glycero*-D-*manno*-heptitol heptaacetate is +36.1° (in $CHCl_3$) (26). L-*Glycero*-D-*manno*-heptitol heptaacetate had the same T_{gal} = 2.32 as the corresponding derivative of the authentic sugar, using the same conditions as above. The crystals had $[\alpha]_D$ −11° (*c*, 1.1 in $CHCl_3$) and m.p. 116° compared with $[\alpha]_D$ −13.3° (*c*, 2 in $CHCl_3$) and m.p. 119° reported in the literature (26).

Isolation of L-*Glycero*-D-*manno*-*heptose*

Crude extracellular polysaccharide (14.2 g) was hydrolyzed with 2 N sulfuric acid for 12 h. The resulting monosaccharides were treated with glucose oxidase as described earlier. The gluconic acid was removed with basic ion-exchange resin, Duolite A4. The eluate was concentrated to a syrup and fractionated on a cellulose column, using butan-1-ol, 1/2 saturated with water as eluant to give two fractions (A and B).

Fraction A (100 mg) was shown by paper chromatography and by g.l.p.c. (8) to contain L-*glycero*-D-*manno*-heptose, together with traces of glucose and gluconic acid. Preparative paper chromatography in solvent A yielded the pure heptose (52 mg). The sugar had $[\alpha]_D$ +14° (*c*, 0.85 in H_2O); attempts to crystallize it failed. The literature value (27) for D-*glycero*-L-*manno*-heptose is $[\alpha]_D$ −15.3° (equil.). A portion of the heptose (20 mg) was treated with benzoyl chloride (200 mg) in pyridine (2.0 ml), and the resulting compound was recrystallised from ethanol – light petroleum, b.p. 30–60°. Hexa-*O*-benzoyl-L-*glycero*-D-*manno*-heptose had m.p. 100° and $[\alpha]_D$ −32° (*c*, 1.0 in $CHCl_3$). The reported values (28) of hexa-*O*-benzoyl-D-*glycero*-L-*manno*-heptose are m.p. 99° and $[\alpha]_D$ +30.8°.

Chromatographic procedures indicated that Fraction B (250 mg) comprised a mixture of both heptoses together with mannose, galactose, glucose, and a trace of gluconic acid. Preparative paper chromatography yielded a mixture (118 mg) of the two heptoses but these could not be further resolved by chromatographic procedures.

Hexosamine Determination

Paper chromatography of the hydrolysis products of the polysaccharide in solvent B, indicated a spot with the same R_{glu} 0.66 as glucosamine or galactosamine, which gave a blue spot with ninhydrin. The polysaccharide contained 0.98% nitrogen which was consistent with the presence of hexosamine in the polymer. This was confirmed as follows by using the method described by Perry (13).

An aliquot (52 mg) from the hydrolysis products of the polysaccharide was N-acetylated and converted to the trimethylsilyl ethers. Examination of the latter by g.l.p.c. on column B at 191° showed peaks with the same retention times as the trimethylsilyl derivatives of 2-acetamido-2-deoxy-D-glucose and 2-acetamido-2-deoxy-D-galactose, in the ratio 1:0.28. By incorporating an internal standard of galactosamine hydrochloride (4.80 mg) in a second aliquot (52 mg), the hexosamine content of the polysaccharide was calculated to be 10.4%, comprising 8.1% glucosamine and 2.3% galactosamine.

Periodate Oxidation of the Polysaccharide

A sample (101 mg) of the polysaccharide was dissolved in water (30 ml), 0.0375 M sodium metaperiodate (50 ml) was added, and the solution was made up to 100 ml with water. The flask was stored in the dark

Can. J. Chem. Downloaded from www.nrcresearchpress.com by 210.87.254.5 on 09/05/12
For personal use only.

at 15°, together with solutions of periodate and iodate of the same molarity. At intervals, aliquots (1.0 ml) were removed and diluted to 250 ml with water and periodate was determined spectrophotometrically (29). Periodate consumption reached a constant value of 0.58 moles per mole of anhydrohexose unit after 24 h.

After the oxidation was complete, excess periodate was destroyed by ethylene glycol and the solution was dialyzed. The non-dialyzable material was reduced with potassium borohydride. The resulting polyalcohol (92.5 mg) was hydrolyzed with N H_2SO_4 for 4 h at room temperature (14), and the products were examined by paper chromatography. No oligosaccharides could be detected. Total hydrolysis was then effected with N H_2SO_4 at 100° for 6 h. Paper chromatographic examination of the products indicated the presence of rhamnose, erythritol, glycerol, and a small amount of glucose. A portion of the hydrolysate was reduced with sodium borohydride, and the products were acetylated and examined by g.l.p.c. (8) on the three different columns (A, B, and C). Four peaks were obtained, corresponding to glycerol triacetate, erythritol tetraacetate, rhamnitol pentaacetate, and glucitol hexaacetate. By estimating the areas under the peaks given by the individual components, the following molecular ratio of the polyols was obtained: glycerol, erythritol, rhamnitol, glucitol (1.10:1.05:1.0:0.13).

Methylation of the Polysaccharide

The polysaccharide (5.0 g) was dissolved in water (100 ml) and treated with sodium borohydride (100 mg) for 2 h. Methylation was carried out by additions of dimethyl sulfate and 30% sodium hydroxide (30) on seven successive days. Extraction with chloroform furnished partly methylated polysaccharide (2.68 g). From the residual aqueous solution the remaining polysaccharide material (2.25 g) was recovered and methylated five times more with dimethyl sulfate and sodium hydroxide yielding chloroform soluble methylated polysaccharide (1.32 g).

The combined chloroform soluble material (4.00 g) was methylated four times with Purdie's reagents (31). The syrup obtained was dissolved in a minimum of chloroform and poured into a large excess of petroleum ether to yield a precipitated methylated polysaccharide having methoxyl 32.3%. Two more Purdie methylations did not increase this value. The syrup was dissolved in dimethyl formamide (40 ml) and methyl iodide (20 ml); silver oxide (10 g) was added at intervals, and methylation was conducted according to the method of Kuhn *et al.* (15). An additional Kuhn methylation did not increase the methoxyl content (35.5%) of the petroleum ether insoluble material. Examination by infrared spectroscopy indicated only a very small amount of hydroxyl absorption.

The syrup (3.59 g) obtained from methylation of the polysaccharide was fractionated by dissolving in chloroform and pouring into petroleum ether. The precipitate obtained was designated polysaccharide A (1.127 g). Evaporation of the supernatant gave a syrupy methylated polysaccharide B (1.25 g).

Hydrolysis of Methylated Polysaccharide A

Methylated polysaccharide A (1.127 g), $[\alpha]_D$ +97° (c, 0.49 in $CHCl_3$), OCH_3 35.5%, was hydrolyzed with 72% sulfuric acid (w/w) (30 ml) for 30 min at room temperature and with 12.5% (w/w) sulfuric acid at 100° for 4 h (32). The solution was neutralized and carefully evaporated to a syrup (892 mg). Paper chromatography of the syrup and g.l.p.c. of the derived methyl glycosides indicated 2,3,4,6-tetra-*O*-methyl-glucose, a dimethyl-rhamnose, and 2,3,6-tri-*O*-methyl-glucose as the major components. The methylated sugars were fractionated on cellulose (45 × 3 cm), (i) light petroleum (b.p. 85–100) – butan-1-ol (7:3), saturated with water, (ii) light petroleum – butan-1-ol (4:6) saturated with water, and (iii) butan-1-ol, half saturated with water, being used as eluants to give fractions I–VI. Table III shows the composition of fractions I–III. Composition of the individual fractions was calculated from g.l.p.c. data obtained from their methanolysis products. Since some of the peaks overlapped on certain columns, it was necessary to use mean values from all three columns to determine the molar ratio of each component; these are as follows: 2,3,4,6-tetra-*O*-methyl-D-glucose, 2,4-di-*O*-methyl-L-rhamnose, 2,3,6-tri-*O*-methyl-D-glucose (0.27:1.0:2.2). Almost identical values, 0.24:1.0:2.2, were obtained by g.l.p.c. of the methanolysis products of methylated polysaccharide A.

Isolation and Identification of the Methylated Sugars

Fraction I (123.4 mg) gave on demethylation with boron trichloride (33), glucose and rhamnose. The mixture was separated on thin-layer plates and three fractions were obtained. The fastest moving fraction (50 mg), gave only glucose on demethylation. It had R_g = 1.00 in solvent B and had $[\alpha]_D$ +82° (c, 0.71 in H_2O). The sugar was converted to its anilide which, on recrystallization from ethyl ether – light petroleum, gave white needles m.p. 136°; reported value 137° (34). The m.p. was not depressed on mixing with an authentic sample of *N*-phenyl-2,3,4,6-tetra-*O*-methyl-D-glucosylamine. The remainder of fraction I was combined with fraction II.

Fraction II (499.0 mg) on demethylation gave glucose and rhamnose and on paper chromatography gave two unresolved spots in solvent B, R_g 0.89 and R_g 0.84. Fractionation by preparative thin-layer chromatography gave two pure fractions. The faster moving component gave only rhamnose on demethylation. The sugar had R_g 0.89 in solvent B and had 30.0% methoxyl groups compared with a theoretical value of 32.3% for dimethyl-6-deoxy hexose. In borate buffer it had M_g 0.00 and it had $[\alpha]_D$ +12° (c 0.9 in H_2O). Spraying with *p*-anisidine hydrochloride gave a yellow-brown spot. A portion of the syrupy material was

Can. J. Chem. Downloaded from www.nrcresearchpress.com by 210.87.254.5 on 09/05/12
For personal use only.

Can. J. Chem. Downloaded from www.nrcresearchpress.com by 210.87.254.5 on 09/05/12
For personal use only.

TABLE III

Hydrolysis products from methylated polysaccharide A

Fraction No.	Yield (mg)	Components identified	G.l.p.c. retention times (T_g), sugars examined as methyl glycosides			Composition (mole %)	Relative amount (mg)
			Column A	Column B	Column C		
1	123.4	2,3,4,6-Tetra-*O*-methyl-D-glucose	0.71, 1.00*	0.73, 1.00	0.73, 1.00	45.1	59.4
		2,4-Di-*O*-methyl-L-rhamnose	0.84	0.73	0.50	25.4	27.5
		2,3,6-Tri-*O*-methyl-D-glucose	2.69, 3.64	1.96, 2.49	1.29, 1.68	24.4	30.3
2	499.0	2,4-Di-*O*-methyl-L-rhamnose	0.84	0.73	0.50	32.9	150
		2,3,6-Tri-*O*-methyl-D-glucose	2.69, 3.64	1.96, 2.49	1.29, 1.68	67.1	349
3	74.0	2,3,6-Tri-*O*-methyl-D-glucose	2.69, 3.64	1.96, 2.49	1.29, 1.68	98.0	72.5

*Where two values are given, they refer to the β and α anomers respectively.

converted to the anilide. After recrystallization from light petroleum (b.p. 30–60°), the crystals of *N*-phenyl-2,4-di-*O*-methyl-L-rhamnosylamine had m.p. 138–139° and $[\alpha]_D$ +134° → +4° (equil.) (*c*, 1.00 in ethanol), reported values (35) m.p. 141° and $[\alpha]_D$ +136° → +4° (equil.). The remainder of fraction II was combined with fraction III.

Fraction III weighed 72.5 mg. The syrupy product showed a single spot on paper chromatography, R_g 0.84 in solvent B. Demethylation gave only glucose. The sugar, $[\alpha]_D$ +70° (*c*, 2.28 in H_2O), gave a reddish-brown color with *p*-anisidine hydrochloride. On slow evaporation from ethanol, crystals of 2,3,6-tri-*O*-methyl-D-glucose were obtained, which on recrystallization from absolute ether had m.p. 119–121°, $[\alpha]_D$ +70°; reported values m.p. 121–123° and $[\alpha]_D$ +70° (36). Preparation of the 1,4-di-*p*-nitrobenzoate (36) yielded the crystalline derivative, m.p. 189° (after recrystallization from methanol) and $[\alpha]_D$ −31° (*c*, 1.0 in $CHCl_3$). Reported values are m.p. 189–190° and $[\alpha]_D$ −33° (36).

Fraction IV (54.2 mg) gave a single spot, R_g 0.74 on paper chromatographic examination in solvent B. Demethylation gave only glucose. A small portion was treated with 3% methanolic hydrogen chloride and the products were examined by g.l.p.c. on column B. A number of peaks indicative of lipids were observed; this finding was inconsistent with the paper chromatographic homogeneity of this fraction. The remainder of the fraction was extracted with 50% aqueous methanol, to remove methylated sugars from lipid material. The supernatant gave on evaporation a syrup (15.9 mg), which was shown by g.l.p.c. to contain only one component. From its paper chromatographic mobility and from the retention time of its methyl glycoside on g.l.p.c. this sugar was tentatively identified as 2,3-di-*O*-methyl-glucose.

Fraction V (33.6 mg) was extracted with 50% aqueous methanol giving a component (4.1 mg) which had R_g 0.58 in solvent B and gave a yellowish-brown color with *p*-anisidine hydrochloride (9). Demethylation yielded glucose.

Fraction VI (54.3 mg) after similar treatment gave a methylated sugar (3.4 mg) with chromatographic mobility R_g = 0.47, which yielded only glucose on demethylation.

Lipids from Methylated Polysaccharide A

The aqueous-methanol insoluble residues from fractions IV–VI were combined and found to be readily soluble in chloroform. From infrared spectroscopy and thin-layer chromatographic characteristics, the material was found to comprise a mixture of long-chain, methoxy carboxylic acids. Examination, as methyl esters, by g.l.p.c. (37) showed two isomeric C_{12} hydroxy fatty acids, together with a small amount of hydroxy myristic acid.

Purification of Methylated Polysaccharide B

Methylated polysaccharide B (1.25 g) was found to have a low methoxyl content (ca. 10%) and yet had little OH absorption in the infrared. The syrup was refluxed with methanol overnight, and on cooling an insoluble residue (340 mg) remained. The thin-layer chromatographic behavior of this latter material showed it to be non-polar, and since infrared spectroscopy indicated a mixture of hydrocarbons, it was concluded that it had originated from the light petroleum.

The methanol soluble material was fractionated on a column of silicic acid, using the following elution sequence; hexane, benzene, benzene:ether (1:1), and chloroform:methanol (1:1). The fractions obtained were shown by thin-layer chromatography to consist of two main groups of substances: (*a*) lipid material (325 g) and (*b*) methylated polysaccharide. Infrared spectroscopy of the lipid material indicated a long hydrocarbon chain (bands around 3 000, 1 450, 1 380, and 750 cm^{-1}) with carbalkoxy (1 725 and 1 280 cm^{-1}) and alkoxy (1 120 cm^{-1}) substituents. Examination by g.l.p.c. (37) indicated the presence of the following fatty acids: methoxy myristic, methoxy lauric, and two unidentified acids.

Constitution of Methylated Polysaccharide B

The methylated polysaccharide (326 mg) obtained from the silica column had methoxyl content of 37.25% and $[\alpha]_D$ +37° (*c*, 2.12 in $CHCl_3$). The molecular weight was 1 660 as assessed by vapor phase osmometry using the Mechrolab osmometer. The material moved as a single homogeneous spot on thin-layer chromatography in chloroform:methanol:water (80:20:2). Infrared spectroscopy showed only a small amount of free hydroxyl groups but showed a relatively large peak at 1 640 cm^{-1} and at 1 730 cm^{-1}. The latter are not consistent with a methylated neutral polysaccharide and appear to be due to non-carbohydrate moieties firmly bound to the molecule.

Methylated polysaccharide B (310 mg) was hydrolyzed with 72% sulfuric acid (8.7 ml) for 30 min at room temperature and with 12% acid at 100° for 4 h (32). During the hydrolysis, lipid material was precipitated. The supernatant aqueous solution was neutralized and carefully evaporated to a syrup (178 mg) of partially methylated monosaccharides. Demethylation gave glucose, L-*glycero*-D-*manno*-heptose, and D-*glycero*-D-*manno*-heptose. No rhamnose could be detected in the demethylation products. The methylated sugars were examined by paper chromatography in solvent B. Spots corresponding to 2,3,4,6-tetra-*O*-methyl-glucose (R_g 1.00), 3,4,6,7-tetra-*O*-methyl-D-*glycero*-D-*manno*-heptose (R_g 0.86), 2,3,6-tri-*O*-methyl-glucose (R_g 0.80), and unknown spots with R_g 0.91, 0.70, and 0.35 were obtained. The latter were brownish yellow with *p*-anisidine hydrochloride (9). The spot corresponding to 3,4,6,7-tetra-*O*-methyl-D-*glycero*-D-*manno*-heptose gave a red color with triphenyl tetrazolium spray reagent (38). This spray is specific for sugars with the C_2 position unsubstituted. The same component also moved (M_g 0.28) on paper electrophoresis

Can. J. Chem. Downloaded from www.nrcresearchpress.com by 210.87.254.5 on 09/05/12
For personal use only.

in borate buffer. Examination by g.l.p.c. (21) on columns A, B, and C of the methanolysis products from a small sample gave results shown in Table II. (The molar ratios were obtained from the mean values of the areas of the peaks.) Authentic samples of the fully methylated heptoses were obtained by treating a small portion of the heptose with methyl iodide and barium oxide in dimethyl formamide (39). After shaking at room temperature for 24 h, the mixture was extracted with light petroleum and the products were examined by g.l.p.c. in both instances only one peak was observed.

ACKNOWLEDGMENTS

The authors are indebted to Dr. J. K. N. Jones, Queen's University, for supplying 3,4,6,7-tetra-*O*-methyl-D-*glycero*-D-*manno*-heptose and to our colleagues Drs. M. Kates and B. Palameta for gas–liquid partition and thin-layer chromatography of fatty acids.

REFERENCES

1. J. L. Hartwell, M. J. Shear, and J. R. Adams, Jr. J. Natl. Cancer Inst. **4**, 107 (1943).
2. H. J. Creech, L. H. Koehler, H. F. Havas, R. M. Peck, and J. Andre. Cancer Res. **14**, 817 (1954).
3. P. Rathgeb and B. Sylven. J. Natl. Cancer Inst. **14**, 1099, 1109 (1954).
4. G. A. Adams and S. M. Martin. Can. J. Biochem. **42**, 1403 (1964).
5. D. H. Northcote. Biochem. J. **58**, 353 (1954).
6. J. E. Scott. Methods Biochem. Anal. **8**, 145 (1960).
7. H. Neukom, H. Deuel, W. J. Heri, and W. Kundig. Helv. Chim. Acta, **43**, 64 (1960).
8. S. W. Gunner, J. K. N. Jones, and M. B. Perry. Can. J. Chem. **39**, 1892 (1961).
9. L. Hough, J. K. N. Jones, and W. H. Wadman. J. Chem. Soc. 1702 (1950).
10. J. K. N. Jones, M. B. Perry, and W. Sowa. Can. J. Chem. **41**, 2712 (1963).
11. G. Avigad, D. Amaral, C. Asensio, and B. L. Horecker. J. Biol. Chem. **237**, 2736 (1962).
12. N. J. Antia and M. B. Perry. Can. J. Chem. **38**, 1917 (1960).
13. M. B. Perry. Can. J. Biochem. **42**, 451 (1964).
14. I. J. Goldstein, G. W. Hay, B. A. Lewis, and F. Smith. Abstracts Papers, Am. Chem. Soc. **135**, 3D (1959).
15. R. Kuhn, H. Trischmann, and I. Low. Angew. Chem. **67**, 32 (1955).
16. D. A. L. Davies. Advan. Carbohydrate Chem. **15**, 271 (1960).
17. V. M. Parikh and J. K. N. Jones. Can. J. Chem. **41**, 2826 (1963).
18. G. A. Adams and R. Young. Can. J. Biochem. In press. 1965.
19. H. C. Srivastava and G. A. Adams. Can. J. Chem. **40**, 1415 (1962).
20. W. E. Trevelyan, D. P. Procter, and J. S. Harrison. Nature, **166**, 444 (1950).
21. C. T. Bishop. Advan. Carbohydrate Chem. **19**, 95 (1964).
22. R. Tschesche and G. Balle. Tetrahedron, **19**, 2323 (1963).
23. H. O. Bouveng and B. Lindberg. Acta Chem. Scand. **12**, 1977 (1958).
24. M. Dubois, K. A. Gilles, J. K. Hamilton, P. A. Rebers, and F. Smith. Anal. Chem. **28**, 350 (1956).
25. A. Bevenue and K. T. Williams. Arch. Biochem. Biophys. **34**, 225 (1951).
26. C. S. Hudson. Advan. Carbohydrate Chem. **1**, 1 (1945).
27. R. A. Hann, A. T. Merrill, and C. S. Hudson. J. Am. Chem. Soc. **57**, 2100 (1935).
28. J. O. Deferrari and R. M. de Lederkremer. J. Org. Chem. **27**, 2558 (1962).
29. G. O. Aspinall and R. J. Ferrier. Chem. Ind. 1216 (1957).
30. W. N. Haworth. J. Chem. Soc. **107**, 8 (1915).
31. T. Purdie and J. C. Irvine. J. Chem. Soc. **83**, 1021 (1903).
32. I. Croon, G. Herrstrom, G. Kull, and B. Lindberg. Acta Chem. Scand. **14**, 1338 (1960).
33. T. G. Bonner, E. J. Bourne, and S. McNally. J. Chem. Soc. 2929 (1960).
34. J. C. Irvine and A. M. Moodie. J. Chem. Soc. **93**, 95 (1908).
35. K. Butler, P. F. Lloyd, and M. Stacey. J. Chem. Soc. 1531 (1955).
36. P. A. Rebers and F. Smith. J. Am. Chem. Soc. **76**, 6097 (1954).
37. A. T. James. Methods Biochem. Anal. **8**, 1 (1960).
38. K. Paech (*Editor*). Modern methods of plant analysis. Vol. II. Springer-Verlag, Berlin. 1955. p. 9.
39. R. Kuhn and H. Trischmann. Chem. Ber. **94**, 2258 (1961).

Can. J. Chem. Downloaded from www.nrcresearchpress.com by 210.87.254.5 on 09/05/12
For personal use only.

Can. J. Chem. Downloaded from www.nrcresearchpress.com by 210.87.254.105 on 09/05/12
For personal use only.

CONSTITUTION OF AN EXTRACELLULAR ACIDIC GLUCOMANNAN FROM SERRATIA MARCESCENS[1]

G. A. ADAMS AND ROBERT YOUNG[2]
Division of Biosciences, National Research Council, Ottawa, Canada
Received June 25, 1965

ABSTRACT

An acidic glucomannan isolated from culture filtrate of *Serratia marcescens* contained D-glucose and D-mannose (3.5:1), D-glucuronic acid (5.5%), and "bound" fatty acids (7.4%). The polysaccharide, on examination by moving boundary electrophoresis and by sedimentation in the ultracentrifuge, was homogeneous. Degree of polymerization was estimated to be ca. 20 by vapor pressure osmometry. Isolation of nigerose (3-*O*-α-D-glucopyranosyl-D-glucopyranose) established the glycosidic linkage between the D-glucose units as α (1 → 3). Methylation and periodate oxidation data showed that the D-glucose and D-mannose units were joined by (1 → 3) linkages in a straight chain structure terminated at the non-reducing end by a unit of D-glucuronic acid which was attached to C_3 of a D-mannose residue. The reducing end of the molecule was terminated by a D-glucose unit. The fatty acids, consisting mainly of hydroxymyristic acid and myristic acid, were attached to the molecule mainly by ester linkages.

Polysaccharides have been isolated from culture filtrates of *Serratia marcescens* and some preliminary studies have been made on their fractionation and composition (1, 2). In a previous study made in this laboratory, the crude polysaccharides were separated primarily on the basis of their solubility in acidified 80% aqueous ethanol solution (3). From the soluble portion, an acidic glucomannan was isolated and an investigation of its chemical structure is reported in this paper.

The acidic glucomannan was homogeneous on moving boundary electrophoresis and on ultracentrifugation. It was isolated in 3.1% yield from the crude extracellular polysaccharides of the culture filtrate and contained D-glucose and D-mannose (3.5:1), and D-glucuronic acid (5.5%). The composition and properties of the polysaccharide are given in Table I.

TABLE I
Composition and properties of polysaccharide

Electrophoretic mobility, u ($cm^2\ s^{-1}\ V^{-1}$)	-8.4×10^{-5}
$[\alpha]_D^{25}$	+60° (c, 1 in H_2O)
Degree of polymerization	20 ± 1
Monosaccharides*	D-Glucose 77.8% D-Mannose 22.2%
Uronic acid	5.5%
Glucosamine	Nil
Lipid	Bound 7.44% Free nil
Nitrogen	1.55%
Nitrogen (protein)	1.55%
Phosphate	Inorganic 0.10% Organic 0.09%

*Calculated as a percentage of the neutral sugar content.

Graded hydrolysis of the polysaccharide yielded three uronic acid components (A, B, and C) which were separated from the neutral sugars by ion-exchange chromatography

[1]*Issued as N.R.C. No. 8617.*
[2]*National Research Council Postdoctorate Fellow 1963–1965.*

Can. J. Chem. Downloaded from www.nrcresearchpress.com by 210.87.254.105 on 09/05/12
For personal use only.

and from each other by paper chromatography. Component A was identified as D-glucuronic acid by gas–liquid partition chromatography (g.l.p.c.) of the derived 2,3,5,6-tetra-*O*-trimethylsilyl-gulono-1,4-lactone (4) and by reduction to glucose. Component B was an aldobiouronic acid composed of D-glucuronic acid and D-mannose, as shown by the finding of equimolar amounts of D-glucose and D-mannose after reduction and hydrolysis of the methyl ester methyl glycoside of the aldobiouronic acid. Component C was an aldotriouronic acid comprising a glucuronic acid residue attached to two mannose units.

Methylation of the disaccharide glucoside derived from the aldobiouronic acid (component B) followed by methanolysis yielded methyl 2,3,4,6-tetra-*O*-methyl-α,β-D-glucosides and methyl 2,4,6-tri-*O*-methyl-α-D-mannoside. Therefore, component B was 3-*O*-(D-glucuronosyl)-D-mannose.

The polysaccharide proved highly refractory to methylation by the Haworth procedure; other methylation procedures were inapplicable because of lack of solubility of the partly methylated polysaccharide in the appropriate solvents. Gradual saponification of fatty acids attached to the polysaccharide by ester linkages may account in part for the slow methylation of the polysaccharide (5). Some fatty acids were found in the acid hydrolysate of the methylated polysaccharide, having apparently survived alkaline hydrolysis during the methylation procedures. Although repeated methylations could not raise the methoxyl content of the polysaccharide to theoretical value, no hydroxyl absorption was present in the infrared spectrum.

The methylated polysaccharide was hydrolyzed and the *O*-methyl sugars and *O*-methyluronic acid were separated by solvent extraction. The methylated sugars were separated quantitatively from each other by paper chromatography and the results are given in Table II. Identification of the individual *O*-methyl sugars was made by preparation of

TABLE II

Methylated sugars from methylated polysaccharide

Methylated sugar	Composition (mole %)
2,4,6-Tri-*O*-methyl-D-glucose	13.5
2,4,6-Tri-*O*-methyl-D-mannose	4.1
2,4-Di-*O*-methyl-D-glucose	1.0

crystalline derivatives and by comparison of retention times of their glycosides on g.l.p.c. with those of authentic samples. Isolation of 2,4,6-tri-*O*-methyl-D-glucose and 2,4,6-tri-*O*-methyl-D-mannose showed that the polysaccharide had a main chain of D-glucose and D-mannose units joined by $(1 \rightarrow 3)$ glycosidic bonds. The relatively high specific optical rotation of the polysaccharide (+60°) as well as that of its methyl ether (+57°) indicated that most of the glycosidic bonds were in the α configuration. Identification of nigerose, 3-*O*(α-D-glucopyranosyl)-D-glucopyranose, as the main product of partial acid hydrolysis proved the existence of an $\alpha(1 \rightarrow 3)$ linkage between the D-glucose units.

The hydrolysis products from the reduced aldobiouronic acid portion of the methylated polysaccharide were 2,4,6-tri-*O*-methyl-D-mannose and 2,3,4-tri-*O*-methyl-D-glucose. This finding confirmed the earlier conclusion that the D-glucuronic acid was linked to C_3 of a mannose residue in the main chain and also was in a terminal position.

The consumption of periodate (0.24 mole) per anhydrohexose unit showed that most of the hexose residues were resistant to periodate oxidation confirming the existence of

mainly (1 → 3) linkages in the molecule; only the reducing end groups and the D-glucuronic acid would be oxidized.

From the methylation data it is apparent that the polysaccharide consisted of D-glucose and D-mannose units joined in a straight chain to form a glucomannan. The acidic component was a unit of D-glucuronic acid constituting the non-reducing end group and attached to a D-mannose residue. The absence of any tetra-*O*-methyl sugars showed that there were no hexose units in non-reducing terminal positions. The reducing end of the molecule was a D-glucose unit as established by its reduction to sorbitol. The presence of 2,4-di-*O*-methyl-D-glucose in the hydrolysate of the methylated polysaccharide may have been due to incomplete methylation. It did not represent a branch point in the molecule as no corresponding methylated sugars forming end groups were found. The most likely explanation, however, was that some of the fatty acids were attached to the glucose units in the molecule through C_6 and were only removed by acid hydrolysis of the methylated polysaccharide.

Earlier data indicated that the polysaccharide had a degree of polymerization of ca. 20 units (3). Such a molecule, having the structure as described above, would consume 0.23 moles of periodate and yield 0.13 mole of formic acid per sugar unit if no hydrolysis of intermediary esters occurred; experimental values of 0.24 moles of periodate consumed and a yield of 0.11 moles of formic acid are in reasonable agreement with the theoretical values.

Previous studies of the polysaccharides in culture filtrates of *Serratia marcescens* have reported only the sugars found after acid hydrolysis, and little or no fractionation of polysaccharides was attempted (1, 2). Current studies in this laboratory have established the presence of a rhamnoglucan and a heptoglucan, in addition to the described acid glucomannan as extracellular polysaccharides of *Serratia marcescens* (5). Similar, but not identical polysaccharides have also been found as components of the capsular polysaccharides of *Serratia marcescens* (6).

EXPERIMENTAL

All specific rotations are equilibrium values unless otherwise stated, melting points are corrected, and all evaporations were done at 35 °C or less.

Chromatography

Paper chromatograms were run by the descending method on either Whatman No. 1 or No. 3 MM filter paper in the following solvent systems (v/v ratio).

(A) Butan-1-ol:ethanol:water (40:11:19)
(B) Pyridine:ethyl acetate:water (1:2.5:2.5)
(C) Pyridine:ethyl acetate:water (10:4:3)
(D) Ethanol:benzene:water:ammonia (47:200:14:1)
(E) Ethyl acetate:acetic acid:formic acid:water (18:3:1:4)

Neutral sugars were detected on papers by *p*-anisidine hydrochloride (7) or alkaline silver nitrate (8) spray reagents; amino sugars were detected by the Morgan–Elson reagent (9) and by ninhydrin (0.1% in chloroform) and the heptoses by detection of formaldehyde after periodate oxidation (10).

Gas–liquid partition chromatography (g.l.p.c.) was carried out with a Pye argon chromatograph fitted with an ionization detector (^{90}Sr 80 μc) using straight glass columns (120 × 0.5 cm inside diameter) containing the following packings:

(A) 10% w/w Carbowax 6000 on 80–100 mesh acid-washed Chromosorb W (Johns-Manville); operating temperature 155 °C,

(B) 10% w/w neopentyl-glycol sebacate polyester (Applied Science Laboratories) on 80–100 mesh non-acid-washed Chromosorb W (Johns Manville); operating temperature 175 °C,

(C) 15% polyphenyl ether on Gas Chrom A, 100–120 mesh; operating temperature 200 °C,

(D) Apiezon L, 10% on Gas Chrom P; operating temperature 190 °C,

Thin-layer chromatography (t.l.c.) was done on glass plates coated with silica gel G (0.25 mm thickness).

Can. J. Chem. Downloaded from www.nrcresearchpress.com by 210.87.254.105 on 09/05/12
For personal use only.

Developing solvents (v/v) were:
(A) benzene:acetone (1:1),
(B) benzene:methanol (96:4).

Electrophoresis

An aqueous solution of the polysaccharide (1%) was dialyzed against sodium borate solution, 0.05 *M*, pH 9.2 for 48 h at 5 °C. The solution was analyzed in a free boundary apparatus (Spinco model H). Paper electrophoreses were done on Whatman 3MM paper in 0.1 *M* sodium borate solution at a potential gradient of 25 V/cm for 2 h.

Sedimentation

The polysaccharide solutions used in the foregoing free boundary electrophoresis measurements were centrifuged in a Spinco model E ultracentrifuge at 58 780 r.p.m., and the sedimentation pattern was photographed at appropriate time intervals.

Isolation and Properties of Polysaccharides

The isolation procedure was essentially that previously described (3) with some minor refinements added. The starting material was culture filtrate solids (114.5 g ash-free basis), nitrogen 6.04%. The polysaccharide fraction which was soluble in acidified 80% aqueous ethanol solution was recovered by evaporation and dialyzed (28 h, tap water), weight 7.1 g, N 2.18%, and $[\alpha]_D^{25}$ +57° (*c*, 1.0 in water). Purification by a modified Cetavlon – boric acid procedure (11) yielded a main insoluble fraction 3.44 g, N 1.55%. On electrophoresis a single symmetrical peak was observed. Ultracentrifugation showed a main peak with a small faster moving peak ahead of it; the latter had sedimented in 2 h 15 min. The composition and properties of the polysaccharide are given in Table I. Analytical procedures were described in an earlier paper (3), except that for uronic acids which were determined as their 2,3,5,6-tetra-*O*-trimethylsilyl-aldono-1,4-lactone derivatives by gas–liquid chromatography on column B (4).

Isolation of Neutral Sugars and Uronic Acid Components

Polysaccharide (10 g) was heated in *N* sulfuric acid (200 ml) in a boiling water bath for 10 h. After neutralization, barium ions were removed by Amberlite IR-120 and the acidic components were adsorbed on a column of Dowex I (OH^- form). After the neutral sugars were washed off with water, the acids were eluted with *N* sodium hydroxide solution; passage over Amberlite IR-120 removed the sodium ions and the acid fraction (wt. 846 mg) was recovered. Chromatographic examination on paper in solvent E showed three spots: A had the same mobility as glucuronolactone, and the other two spots, B and C, had $R_{glucurone}$ values of 0.35 and 0.14 respectively. The acids were separated on Whatman No. 3 MM paper with solvent E to yield A 46 mg, B 362 mg, and C 15 mg. Component A had $[\alpha]_D^{25}$ +18.5° (*c*, 1 in water), and the sugar obtained by lithium aluminium hydride reduction (12) and acid hydrolysis of its methyl glycoside methyl ester was identified chromatographically (solvent B) as glucose. A portion of the reduced methyl ester methyl glycoside (3 mg) was methylated by the Kuhn procedure (13) and examined by g.l.p.c. on columns A and B. The only peaks observed corresponded to those of authentic methyl 2,3,4,6-tetra-*O*-methyl-α-D-glycoside and 2,3,4,6-tetra-*O*-methyl-β-D-glucoside. The methylated glycosides were subjected to methanolysis (5% methanolic hydrogen chloride, reflux for 6 h) and re-examined by g.l.p.c.; no change was observed, establishing the absence of any aldobiouronic acid in component A.

Component B, 20 mg, $[\alpha]_D^{25}$ +39° (*c*, 1% in water), was let stand in 2% methanolic hydrogen chloride (5 ml) for 48 h at room temperature. The methyl ester methyl glycoside was dissolved in tetrahydrofuran:ethyl ether (4:1) and reduced with lithium aluminium hydride (50 mg) (12). The recovered disaccharide glycoside (13 mg) was hydrolyzed with *N* sulfuric acid, and chromatographic examinations of the hydrolysate in solvents B and C showed glucose and mannose. An additional amount of the disaccharide glycoside (28 mg) was fully methylated (13) and the methylated product was extracted into chloroform. The solvent was removed and the syrup was heated with 4% metholic hydrogen chloride (3 ml) for 7 h at 100 °C. The glycosides were examined by g.l.p.c. on columns A and B. Three peaks were obtained corresponding to authentic samples of methyl 2,3,4,6-tetra-*O*-methyl-β-D-glucoside, methyl 2,3,4,6-tetra-*O*-methyl-α-D-glucoside, and methyl 2,4,6-tri-*O*-methyl-α-D-mannoside. Hence the original methylated disaccharide was 3-*O*-(2,3,4,6-tetra-*O*-methyl-D-glucosyl)-2,4,6-tri-*O*-methyl mannose. Component C (15 mg) was converted to its neutral glycoside as described above and the acid hydrolysate on chromatographic examination (solvents B and C) showed glucose and mannose in a ratio of approximately 1:2.

Methylation

The polysaccharide (5.02 g, N 1.55%) was methylated with dimethyl sulfate and 45% sodium hydroxide (14). After 12 methylations, the methoxyl content was only 17.6% and only 886 mg of the product were soluble in chloroform. Five additional methylations increased the methoxyl content to 21.4%. The methylated product was partly soluble in dimethyl sulfoxide and was methylated by Srivastava's procedure (15) without any appreciable gain in methoxyl content. Insolubility in dimethyl formamide precluded application of the Kuhn methylation method (13). Repeated methylations by the Haworth procedure (14) gave a product (2.72 g) whose methoxyl content could not be increased beyond 34.8%, $[\alpha]_D^{25}$ +53° (*c*, 0.6

Can. J. Chem. Downloaded from www.nrcresearchpress.com by 210.87.254.105 on 09/05/12
For personal use only.

in chloroform). There was no hydroxyl adsorption at 3 500 cm^{-1}. The methylated polysaccharide was dissolved in chloroform (50 ml) and precipitated by the addition of petroleum ether (b.p. 30–60°). One main fraction was recovered, 2.39 g, methoxyl 38.4%, $[\alpha]_D^{25}$ +58.2° (*c*, 1 in chloroform). Methylation by Purdie's procedure (16) did not increase the methoxyl content of this product.

Methanolysis of Methylated Polysaccharide

For preliminary examination of the constituent methyl glycosides by g.l.p.c. a small sample of the methylated polysaccharide was methanolyzed as follows: methylated polysaccharide (19 mg) was heated in a sealed tube with 7% methanolic hydrogen chloride for 12 h at 100 °C. After neutralization (Ag_2CO_3) the recovered glycosides were examined on columns A and B. The peaks were tentatively identified as (1) methyl 2,4,6-tri-*O*-methyl-β-D-glucoside, (2) methyl 2,4,6-tri-*O*-methyl-α-D-mannoside, (3) methyl 2,4,6-tri-*O*-methyl-α-D-glucoside, and (4) methyl di-*O*-methyl glucoside.

Acid Hydrolysis of Methylated Polysaccharide

The methylated polysaccharide (2.3 g) was dissolved by stirring for 60 min in 72% sulfuric acid at room temperature (17). The acid solution was then diluted with water to 12.5% and refluxed for 4 h. The solution was neutralized with barium carbonate and barium hydroxide and heated at 65 °C for 1 h. After filtration, the clear solution was extracted with ethyl acetate for 96 h to remove neutral methylated sugars (fraction I 0.5940 g). The aqueous solution was acidified with *N* sulfuric acid to pH 2.0, and extraction with ethyl acetate was continued for a further 96 h to give fraction II (0.5506 g). The aqueous solution was neutralized with barium hydroxide and filtered, and the solids were recovered by freeze-drying (fraction III 0.2667 g). Chromatographic examination (solvent D) showed that fraction I contained only methylated sugars; fraction II contained methylated sugars and methylated uronic acid components and fraction III contained methylated uronic acids and a trace of a dimethyl glucose. The components of fraction II and III were completely separated on sheets of Whatman 3 MM paper using solvent D into neutral methylated sugars and methylated uronic acids. Purified materials were combined to yield methylated sugars (912 mg) and methylated uronic acids (305 mg).

Separation of Neutral Sugars

The mixture (900 mg) was separated on Whatman No. 1 paper using solvent D. Three fractions were obtained (1) trimethyl glucose, (2) trimethyl mannose, and (3) dimethyl glucose. Since fractions 1 and 2 were not completely free of each other and also of debris from the filter paper they were further purified by t.l.c. using solvent A and three 40 min development periods. The appropriate pure sugars were combined to yield (1) trimethyl-glucose (390 mg), (2) trimethyl-mannose (121 mg), and dimethyl-glucose (28 mg).

Identification of Methylated Sugars

2,4,6-Tri-O-methyl-D-glucose

This sugar yielded only glucose on demethylation with boron trichloride (18). On paper chromatograms it gave the same bright red color with *p*-anisidine spray and the same R_g values (0.47 in solvent C and 0.86 in solvent A) as 2,4,6-tri-*O*-methyl-D-glucose. The syrup crystallized readily and after recrystallization from ethyl ether had m.p. and mixed m.p. 123–125 °C, $[\alpha]_D^{25}$ +71° (*c*, 1.0 in water). Anilide formation yielded *N*-phenyl-2,4,6-tri-*O*-methyl-D-glucosylamine, m.p. 162–165° C (19). Examination of the methyl glycoside of this sugar by g.l.p.c. on column B gave 2 peaks which had the same retention times as authentic samples of methyl 2,4,6-tri-*O*-methyl-β-D-glucoside and methyl 2,4,6-tri-*O*-methyl-α-D-glucoside.

2,4,6-Tri-O-methyl-D-mannose

On demethylation with boron trichloride this sugar gave only mannose. Its R_g 0.61 (solvent D) and M_g 0.0 in borate buffer were in agreement with those of an authentic sample of 2,4,6-tri-*O*-methyl-D-mannose. On seeding, the syrup crystallized and after recrystallization from ethyl ether had m.p. 62–65° and $[\alpha]_D^{25}$ +17° (*c*, 1 in water) (20). The anilide, after recrystallization from ethyl ether had m.p. and mixed m.p. 132 °C and $[\alpha]_D^{25}$ +7.6° (*c*, 0.5 in methanol) in good agreement with the reported values (21). Gas liquid chromatography of the methyl glycoside on column B and column C gave one peak corresponding to that of authentic methyl 2,4,6-tri-*O*-methyl-α-D-mannoside.

2,4-Di-O-methyl-D-glucose

This sugar (28 mg) gave only glucose on demethylation. On paper chromatograms it had the same R_g values in solvents A and D as 2,4-di-*O*-methyl-D-glucose. It had no mobility in borate buffer on electrophoresis and gave a negative reaction with triphenyltetrazolium chloride (22, 23) and periodate–benzidene spray (24). The sample was converted to its methyl glucoside by refluxing with 2% methanolic hydrogen chloride for 5 h. The glycosides were separated by g.l.p.c. on column C into 2 peaks which had the same retention times as authentic methyl 2,4-di-*O*-methyl-α-D-glucoside and methyl 2,4-di-*O*-methyl-β-D-glucoside.

Identification of Methylated Uronic Acids

A sample of the methylated uronic acid fraction (Ba salt) was examined on paper chromatograms using solvent E and showed four components having R_g values of 0.87, 0.67, 0.50, and 0.25 respectively. These were separated by filter paper chromatography using solvent E to yield fractions I (34 mg), II (28 mg), III (103 mg), and IV (80 mg). Small samples (10 mg) of each fraction were converted to their methyl ester

Can. J. Chem. Downloaded from www.nrcresearchpress.com by 210.87.254.105 on 09/05/12
For personal use only.

methyl glycosides by heating with 2% methanolic hydrogen chloride (1 ml) at 100 °C in a sealed tube for 6 h. Reduction with lithium aluminium hydride (25 mg) in tetrahydrofuran (30 ml) yielded methyl glycosides, portions of which were hydrolyzed by heating for 12 h at 100 °C with *N* sulfuric acid. Chromatographic examination of the sugars in solvent D showed one spot R_g 0.64 from fraction IV, and 2 spots R_g 0.64 and 0.61 respectively from fractions I, II, and III. These R_g values corresponded to those for 2,4,6-tri-*O*-methyl-D-mannose (R_g 0.61) and 2,3,4-tri-*O*-methyl-D-glucose (R_g 0.64). Portions of the methyl glycosides of these sugars were examined by g.l.p.c. on column B and column C. Methyl 2,4,6-tri-*O*-methyl-α-D-mannoside, methyl 2,3,4-tri-*O*-methyl-β-D-glucoside, and methyl 2,3,4-tri-*O*-methyl-α-D-glucoside were found and their identity confirmed by chromatography of authentic samples of these glycosides under the same conditions.

The remaining quantities of fractions III and IV were converted to their methyl ester methyl glycosides and reduced with lithium aluminium hydride to the corresponding disaccharide methyl glycoside and methyl glycoside respectively. The glycosides were hydrolyzed to their free sugars with *N* sulfuric acid. Fraction IV yielded only 2,3,4-tri-*O*-methyl-D-glucose and fraction III a mixture of 2,3,4-tri-*O*-methyl-D-glucose and 2,4,6-tri-*O*-methyl-D-mannose. The mixture was separated on paper sheets using solvent D and the sugar was identified as follows.

2,4,6-Tri-O-methyl-D-mannose

On paper chromatograms using solvents A and D, this sugar had the same R_g values as an authentic sample of 2,4,6-tri-*O*-methyl-D-mannose. Refluxing an ethanolic solution of the sugar with aniline yielded the crystalline anilide which on recrystallization from ethyl ether gave *N*-phenyl-2,4,6-tri-*O*-methyl-D-mannosylamine, m.p. 132 °C and $[\alpha]_D^{25}$ +7.3° (*c*, 0.4 in methanol) in good agreement with reported values (21).

2,3,4-Tri-O-methyl-D-glucose

This syrup gave the same color with *p*-anisidine hydrochloride and had the same mobility on paper chromatograms in solvents A and D as an authentic sample of 2,3,4-tri-*O*-methyl-D-glucose. The crystalline anilide, *N*-phenyl-2,3,4-tri-*O*-methyl-D-glucosylamine, had m.p. 145° C and $[\alpha]_D^{25}$ +72° (*c*, 1.0 in ethanol (25).

Partial Hydrolysis of Polysaccharide

The optimal conditions for maximum production of di- and tri-saccharides were found to be as follows: polysaccharide (1.0 g) was dissolved in *N* sulfuric acid and heated in a glass pressure bottle for 15 h at 70 °C. After neutralization with barium hydroxide and filtration of the solution, a syrup (674 mg) was recovered. Chromatographic examination on paper (solvent B and C) showed glucose, mannose, a spot having the same mobility as nigerose ($R_{maltose}$ 1.13) and several unidentified spots. Impure nigerose (80 mg) was recovered by preparative chromatography on sheets of Whatman No. 1 paper and after extraction with methanol yielded 69 mg of chromatographically pure product. Complete acid hydrolysis yielded only glucose.

Nigerose Octaacetate

A portion of the syrup (50 mg) was acetylated with acetic anhydride (2 ml) containing sodium acetate (30 mg) by refluxing for 1 h. The cooled solution was poured into ice water (100 ml) and extracted with chloroform (4 × 30 ml). The chloroform extract was washed with saturated sodium bicarbonate solution, dried with anhydrous sodium sulfate and concentrated to a syrup (28.1 mg). Preparative thin-layer chromatography (solvent B) yielded a pure sample of β-nigerose octaacetate (18 mg). Recrystallization from ethanol yielded β-nigerose octaacetate, m.p. 150–151 °C, $[\alpha]_D^{25}$ +77° (*c*, 0.9 in chloroform) in good agreement with reported values (26).

Periodate Oxidation

The polysaccharide (100.2, 100.1 mg) was dissolved in water (50 ml) and oxidized by 0.1 *M* sodium periodate at 5 °C in the dark; at intervals, aliquots were removed for estimation of periodate consumption (27) and formic acid production (28). The results expressed in moles per mole of anhydroglucose were as follows:

Time (hours)	Formic acid produced	Periodate consumed
48	0.07	0.22
69	0.07	0.24
92	0.09	0.24
121	0.10	0.245
144	0.11	0.26
168	0.12	0.28

Lipid Determination

"Free" lipids in the polysaccharide were extracted with water:chloroform:methanol as previously described (29). "Bound" lipids were determined in the residue by hydrolyzing for 2 h at 100 °C with 6 *N* hydrochloric acid followed by extraction of the released fatty acids with petroleum ether (b.p. 30–60):ethyl ether (1:1). The fatty acids were dried *in vacuo* to constant weight, converted to their methyl esters (16),

Can. J. Chem. Downloaded from www.nrcresearchpress.com by 210.87.254.105 on 09/05/12
For personal use only.

and identified by g.l.p.c. on column D. The fatty acids (7.44%) were identified as hydroxy myristic acid, myristic acid, lauric acid, hydroxy lauric acid, palmitic acid, palmitoleic acid, oleic acid, and stearic acid (in approximate order of amounts found).

Identity of Sugar Forming Reducing End of the Polysaccharide

Polysaccharide (10 mg) was dissolved in water (1 ml) and reduced with sodium borohydride (20 mg) over a period of 2 h. The solution was neutralized with acetic acid and passed over a column of Amberlite IR-120, and the borate was removed by repeated distillation with methanol. The reduced polysaccharide was hydrolyzed with *N* sulfuric acid for 12 h at 100 °C. After neutralization of the acid with barium carbonate, the sugars were oxidized by *N* iodine (4 ml) and *N* sodium hydroxide (6 ml) for 24 h at room temperature. The acidic components were removed with Amberlite IR-4B and the hexitol was recovered as a syrup. Chromatographic examination of the hexitol in solvent C with mannitol (R_{glu} 0.97) and sorbitol (R_{glu} 0.92) as references showed that it was sorbitol.

REFERENCES

1. J. L. Hartwell, M. J. Shear, and J. R. Adams, Jr. J. Natl. Cancer Inst. **4**, 107 (1943).
2. H. J. Creech, L. H. Koehler, H. F. Havas, R. M. Peck, and J. Andre. Cancer Res. **14**, 817 (1954).
3. G. A. Adams and S. M. Martin. Can. J. Biochem. **42**, 1403 (1964).
4. M. B. Perry and R. K. Hulyalkar. Can. J. Biochem. **43**, 573 (1965).
5. R. Young and G. A. Adams. Can. J. Chem. In press. 1965.
6. G. A. Adams and R. Young. Can. J. Biochem. In press. 1965.
7. L. Hough, J. K. N. Jones, and W. H. Wadman. J. Chem. Soc. 1703 (1950).
8. W. E. Trevelyan, D. P. Procter, and J. S. Harrison. Nature **166**, 44 (1950).
9. W. T. J. Morgan and L. A. Elson. Biochem. J. **28**, 988 (1934).
10. J. K. N. Jones, M. B. Perry, and W. Sowa. Can. J. Chem. **41**, 2712 (1963).
11. H. O. Bouveng and B. Lindberg. Acta Chem. Scand. **12**, 1977 (1958).
12. B. Lythgoe and S. Trippett. J. Chem. Soc. 1983 (1950).
13. R. Kuhn, H. Trischman, and I. Low. Angew. Chem. **67**, 32 (1955).
14. W. N. Haworth. J. Chem. Soc. **107**, 8 (1915).
15. H. C. Srivastava, S. N. Harshe, and Prem Pal Singh. Indian J. Chem. **1**, 304 (1963).
16. T. Purdie and J. C. Irvine. J. Chem. Soc. **83**, 1021 (1903).
17. I. Croon, G. Herrstrom, G. Kull, and B. Lindberg. Acta Chem. Scand. **14**, 1338 (1960).
18. S. Allen, T. G. Bonner, E. J. Bourne, and N. M. Saville. Chem. Ind. London, 630 (1958).
19. H. Granichstädten and E. G. V. Percival. J. Chem. Soc. 54 (1943).
20. N. Prentice, W. S. Guendet, and F. Smith. J. Am. Chem. Soc. **78**, 4439 (1956).
21. W. N. Haworth, R. L. Heath, and S. Peat. J. Chem. Soc. 833 (1941).
22. D. S. Feingold, L. Avigad, and S. Hestrin. Biochem. J. **64**, 351 (1956).
23. S. Haq and W. J. Whelan. Nature, **178**, 1221 (1956).
24. J. A. Cifonelli and F. Smith. Anal. Chem. **26**, 1132 (1954).
25. S. Peat, E. Schluchterer, and M. Stacey. J. Chem. Soc. 581 (1931).
26. S. Peat, W. J. Whelan, and K. A. Hinson. Chem. Ind. London, 385 (1955).
27. L. M. Malprade. Compt. Rend. **186**, 382 (1928).
28. A. Jeanes and C. A. Wilham. J. Am. Chem. Soc. **72**, 2657 (1950).
29. M. Kates, G. A. Adams, and S. M. Martin. Can. J. Biochem. **42**, 461 (1964).

Can. J. Chem. Downloaded from www.nrcresearchpress.com by 210.87.254.105 on 09/05/12
For personal use only.

Can. J. Chem. Downloaded from www.nrcresearchpress.com by 210.87.254.6 on 09/05/12
For personal use only.

ON THE RELATIONSHIP BETWEEN EQUILIBRIUM PRESSURES AND THE PHASE DIAGRAM OF A REACTIVE SYSTEM

THE SYSTEMS: $NaCl–Na_2ZrCl_6$, $KCl–K_2ZrCl_6$, $NaCl–KCl–ZrCl_4$

R. L. LISTER[1] AND S. N. FLENGAS

Department of Metallurgy and Materials Science, University of Toronto, Toronto, Ontario

Received February 5, 1965

ABSTRACT

The binary equilibrium phase diagrams for the systems $NaCl–Na_2ZrCl_6$ and $KCl–K_2ZrCl$ were established from the combined results of cooling curve and vapor pressure measurements. A portion of the ternary $NaCl–KCl–ZrCl_4$ has also been determined. Vapor pressure measurements on the two pure compounds, Na_2ZrCl_6 and K_2ZrCl_6, as well as on mixtures with the respective alkali metal chlorides, were taken. The vapor-producing reaction is given as

$$M_2ZrCl_6 = 2MCl + ZrCl_{4(v)}$$

where M represents, respectively, sodium and potassium.

Thermodynamic relationships relating the phase diagram to the measured equilibrium pressures have been developed. The classical shape of the pressure–temperature curves, even for the pure compound, as well as mixtures of the two components, indicates a dependency on liquidus and eutectic melting. Vapor pressure measurements were also carried out over that composition of the ternary which could be of interest for the recovery of zirconium metal by fused salt electrolysis. From these data, the activities and the other partial molar properties of the components in solution were calculated for both the M_2ZrCl_6 and $ZrCl_4$ species.

INTRODUCTION

Zirconium tetrachloride vapor has been found (1) to react directly with solid alkali metal chlorides and to form complex compounds of the general formula M_2ZrCl_6. These compounds represent stabilized forms of the highly volatile zirconium tetrachloride, and could be considered as potential electrolytes for the recovery of zirconium metal by fused salt electrolysis. The problem of solubility of $ZrCl_4$ in alkali chloride melts may be explained in terms of compound formation, and the thermal stability of these solutions may be directly related to the decomposition pressures of $ZrCl_4$ vapor. The complexes of the type M_2ZrCl_6 have also been shown to exist as congruently melting compounds in phase diagram studies by both Howell *et al.* (2) and Morozov and In'Chzhu (3). The former have determined the phase diagram between NaCl and Na_2ZrCl_6, while the latter have investigated the system $KCl–K_2ZrCl_6$. Morozov and In'Chzu (4) have also investigated the thermal stability of the pure compounds Na_2ZrCl_6, K_2ZrCl_6, and Cs_2ZrCl_6 by transportation vapor pressure measurements.

In the present study, the binary equilibrium phase diagrams for the systems $NaCl–Na_2ZrCl_6$ and $KCl–K_2ZrCl_6$ have been determined with accuracy by the cooling curve technique, as well as from vapor pressure measurements (1). The vapor pressures of $ZrCl_4$ in equilibrium with various compositions across the systems $NaCl–Na_2ZrCl_6$ and $KCl–K_2ZrCl_6$ were also investigated at various temperatures. A portion of the ternary diagram of the system $NaCl–KCl–ZrCl_4$ has been defined, and vapor pressure measurements over the low melting region, i.e., that concentration range which would be considered for electrodeposition of zirconium metal, have been made.

From the results, activities and other partial molar properties of the component salts in their molten solutions have been calculated. It is shown that the thermodynamic

[1]*Present address: National Lead Company, Research Laboratory, P.O. Box 58, South Amboy, New Jersey 08879, U.S.A.*

information obtained from reaction pressure measurements is severely restricted by eutectic and liquidus melting. Accordingly, such measurements can be interpreted only in relation to the phase diagram of the system.

THERMODYNAMIC RELATIONSHIPS

In a simple phase diagram representing the binary system MCl–M_2ZrCl_6, there are four temperature–composition zones of interest (shown in Fig. 1).

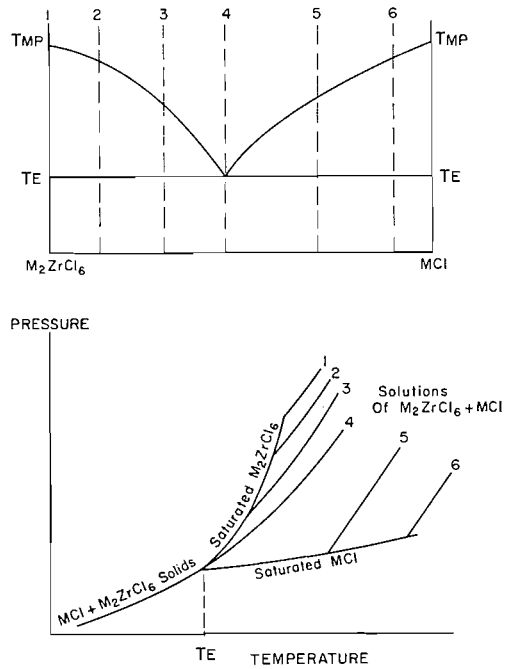

FIG. 1. Predicted pressure versus temperatures curves.

The first includes all compositions and temperatures below the eutectic tieline. In this area, the phases present are: pure solids M_2ZrCl_6 and MCl, and a vapor phase of $ZrCl_4$.

The decomposition reaction may be represented as

$$M_2ZrCl_{6(s)} = 2MCl_{(s)} + ZrCl_{4(v)}$$

and the equilibrium constant for this reaction is

[1] $$K_{eq} = \frac{a_{MCl}^2 f_{ZrCl_4}}{a_{M_2ZrCl_6}}$$

where a_{MCl} and $a_{M_2ZrCl_6}$ are the activities of MCl and M_2ZrCl_6, respectively, and f is the fugacity of $ZrCl_4$ vapor. For all practical purposes, the vapor may be considered as an ideal gas at low pressures, and therefore its fugacity may be taken equal to its pressure. The state of unit activity for the condensed phases shall be defined as the pure solid compounds at all temperatures. For the vapor phase, the standard state is chosen as zirconium tetrachloride vapor at 1 atm. Therefore, in this range,

[2] $$K_{eq} = P_{ZrCl_4}$$

since $a_{MCl} = 1$, and $a_{M_2ZrCl_6} = 1$.

Can. J. Chem. Downloaded from www.nrcresearchpress.com by 210.87.254.6 on 09/05/12
For personal use only.

The variation of the equilibrium constant with temperature is given by the well-known van't Hoff relationship

$$[3] \qquad \frac{\mathrm{d} \ln K_{eq}}{\mathrm{d}\left(\frac{1}{T}\right)} = \frac{-\Delta H_r^0}{R}$$

or by its equivalent

$$[4] \qquad \frac{\mathrm{d} \ln P_{ZrCl_4}}{\mathrm{d}\left(\frac{1}{T}\right)} = \frac{-\Delta H_r^0}{R}$$

where P_{ZrCl_4} is the measured reaction pressure of $ZrCl_4$ in equilibrium with the pure solids M_2ZrCl_6 and MCl at any temperature below the eutectic, and ΔH_r^0 is the standard heat of the decomposition reaction.

From eqs. [2] and [4] it can be seen that the pressure exerted over the system corresponds to the decomposition of pure solid M_2ZrCl_6 and will be equal to the thermodynamic equilibrium constant K_{eq}. Over a limited temperature range, the plot of log P (mm) vs. $1/T$ (°K) should therefore exist as a straight line relationship. Pressure measurements in this range are independent of the composition of the mixtures, and therefore all mixtures should be represented by a single vapor pressure curve. Equation [2] is valid only in the case of negligible or no solid-solubility of the pure materials. If, however, a degree of solid-solubility exists, the equilibrium constant would then include the activities of the solid components in their solutions.

The second zone of interest includes all compositions of the M_2ZrCl_6 side of the eutectic, defined by the corresponding eutectic and liquidus tielines. In this range, the solutions of MCl and M_2ZrCl_6 are saturated with respect to M_2ZrCl_6. The phases present are a solution of the liquidus composition, pure solid M_2ZrCl_6, and a vapor phase of $ZrCl_4$ in equilibrium, according to the reaction

$$M_2ZrCl_{6(s)} = 2MCl_{(sol)} + ZrCl_{4(v)}.$$

In this range, $M_2ZrCl_{6(s)} \rightleftharpoons M_2ZrCl_{6(\text{in sol})}$, and accordingly, $a_{M_2ZrCl_6} = 1$. Therefore,

$$[5] \qquad K_{eq} = P_{ZrCl_4} a_{MCl}^2$$

or,

$$[6] \qquad P_{ZrCl_4} = \frac{K_{eq}}{a_{MCl}^2}$$

where K_{eq} represents the equilibrium constant at that temperature. For calculations, the equilibrium constant obtained from measurements below the eutectic may be expressed as a function of temperature, and then extrapolated to the desired temperature.

From eq. [6], it may be seen that the temperature–pressure curve will change slope at the eutectic temperature because of the introduction of the activity of MCl, which is less than unit in these solutions. The predicted shape of the pressure–temperature curves is shown in Fig. 1. As the temperature is further increased beyond the eutectic temperature, the composition of the solution in equilibrium with the pure solid changes, following the liquid solubility line, and, therefore, the activity of MCl will be changing continuously. The activity of the MCl does not depend upon the composition of the mixture, but rather

Can. J. Chem. Downloaded from www.nrcresearchpress.com by 210.87.254.6 on 09/05/12
For personal use only.

on the composition of the saturated solution, which is temperature dependent. At any specific temperature in this composition range, the pressure of zirconium tetrachloride exerted by any two different compositions will be identical, and there should be one common pressure curve for all compositions.

This brings to light a rather important conclusion which has been neglected in the interpretation of reaction pressure measurements done in the past. Free energies of formation of pure compounds can be obtained only at temperatures below the corresponding eutectic temperature, as this is the only range where the thermodynamic equilibrium constant may be equated to a reaction pressure. For example: when measuring the reaction pressures of *pure* M_2ZrCl_6, some free alkali metal chloride will always be produced because of its decomposition. Measurements taken at temperatures higher than the corresponding eutectic of the MCl–M_2ZrCl_6 binary system would therefore represent saturated solutions of liquidus composition. It is evident that the thermodynamic properties of the *pure* compound cannot be obtained in this range; instead, the data may be used to calculate the partial molar properties of the solutions.

Differentiation of the logarithm of eq. [7] with respect to $1/T$ gives

$$[7] \qquad \frac{\mathrm{d} \ln P_{ZrCl_4}}{\mathrm{d}\left(\frac{1}{T}\right)} = \frac{\mathrm{d} \ln K_{eq}}{\mathrm{d}\left(\frac{1}{T}\right)} - \frac{2\,\mathrm{d} \ln a_{MCl}}{d\left(\frac{1}{T}\right)}$$

where the temperature dependence of the activity is given by

$$\frac{\mathrm{d} \ln a_{MCl}}{\mathrm{d}\left(\frac{1}{T}\right)} = \frac{(\overline{\Delta H}_m)_{MCl}}{R}.$$

Equation [7] may now be expressed as

$$[8] \qquad \frac{\mathrm{d} \ln P_{ZrCl_4}}{\mathrm{d}\left(\frac{1}{T}\right)} = -\frac{\Delta H_r^0 + 2(\overline{\Delta H}_m)_{MCl}}{R} = -\frac{\Delta H_r'}{R}, \text{ or}$$

$$[9] \qquad \Delta H_r' = \Delta H_r^0 + 2(\overline{\Delta H}_m)_{MCl}.$$

The latter represents the heat term obtained from the log P_{ZrCl_4} vs. $1/T$ plot and, therefore, the temperature dependence of the pressures in the temperature range previously defined. The heat term $\Delta H_r'$ shown in this equation depends upon the heat of the standard reaction at the given temperature, and the partial molar heat of mixing of the MCl in a solution of the liquidus composition. The ΔH_r^0 term is expected to be temperature dependent, while the partial molar heat of mixing is, in the general case, both temperature and composition dependent. If the temperature dependency over a small temperature range is neglected, then the slope of the log P_{ZrCl_4} vs. $1/T$ curve will change only as the $(\overline{\Delta H}_m)_{MCl}$ changes with composition.

If the solution is ideal, then the heat of mixing with respect to the solid standard state would be only the heat of fusion. Therefore, it would be expected that the log P_{ZrCl_4} vs. $1/T$ curve should change slope at the eutectic temperature, even when the solutions are ideal.

The third zone of interest is represented by the MCl-rich side of the eutectic, and all temperatures below the liquidus but above the eutectic. The equilibrium in this involves

Can. J. Chem. Downloaded from www.nrcresearchpress.com by 210.87.254.6 on 09/05/12
For personal use only.

the $ZrCl_4$ vapor phase and a solution of MCl and M_2ZrCl_6 saturated with respect to MCl. The equation governing the decomposition reaction in this range is

$$M_2ZrCl_{6(sol)} = 2MCl_{(s)} + ZrCl_{4(v)}$$

for which

$$K_{eq} = \frac{P_{ZrCl_4}}{a_{M_2ZrCl_6}}$$

and

$$[10] \qquad \frac{d \ln P_{ZrCl_4}}{d\left(\frac{1}{T}\right)} = -\frac{\Delta H_r^0 - (\overline{\Delta H}_m)_{M_2ZrCl_6}}{R} = -\frac{\Delta H_r'''}{R}$$

$$[11] \qquad \Delta H_r''' = \Delta H_r^0 - (\overline{\Delta H}_m)_{M_2ZrCl_6}.$$

For a given mixture of this composition, increasing the temperature to that above the eutectic would cause a change in slope of the log P vs. $1/T$ plot because of the introduction of the activity of the M_2ZrCl_6 component in solution. Again the predicted shape of the curves on this side of the phase diagram may be seen in Fig. 1. All compositions of this range are represented by a common vapor pressure curve, the curvature of which would depend upon the deviations of the solutions from ideality.

Finally, the fourth zone of interest includes all compositions at temperatures above the liquidus solubility lines. In this area, the system is described by homogeneous solutions of MCl and M_2ZrCl_6 and a vapor phase of $ZrCl_4$. The decomposition reaction is

$$M_2ZrCl_{6(sol)} = 2MCl_{(sol)} + ZrCl_{4(v)}$$

for which the equilibrium constant is given by

$$[12] \qquad K_{eq} = \frac{P_{ZrCl_4} a_{MCl}^2}{a_{M_2ZrCl_6}}$$

Following the same treatment as before, we obtain

$$[13] \qquad \frac{d \ln P_{ZrCl_4}}{d\left(\frac{1}{T}\right)} = -\frac{\Delta H_r^0 - (\overline{\Delta H}_m)_{M_2ZrCl_6} + 2(\overline{\Delta H}_m)_{MCl}}{R}$$

where

$$[14] \qquad \Delta H_r'' = \Delta H_r^0 + 2(\overline{\Delta H}_m)_{MCl} - (\overline{\Delta H}_m)_{M_2ZrCl_6}.$$

In the liquid region, the partial molar heat of mixing terms correspond to solutions of fixed composition, and their temperature dependence will be due only to a change of the heat capacities, which are either very small or give a negligible contribution over a limited temperature range. Therefore, the plot of log P vs. $1/T$ will again become linear, and the slope of the curve should give a heat term that includes all the heats in this equation. When crossing the liquid solubility line upon increasing temperature, the pressure curve will again undergo a change in slope because of the introduction of the activity of the other component, as may be seen in Fig. 1. It is seen that the pressure temperature curve should change slope at the eutectic and the liquidus temperatures; accordingly, it should be possible to construct the phase of the system from vapor pressure measurements.

Can. J. Chem. Downloaded from www.nrcresearchpress.com by 210.87.254.6 on 09/05/12
For personal use only.

Can. J. Chem. Downloaded from www.nrcresearchpress.com by 210.87.254.6 on 09/05/12
For personal use only.

EXPERIMENTAL

The sodium and potassium hexachlorozirconates were prepared by the direct reaction of the solid alkali metal chlorides with zirconium tetrachloride vapor at 1 atm (1). The sodium and potassium chlorides were of reagent grade and were vacuum degassed at about 400 °C to remove any traces of water. The zirconium tetrachloride was of reactor grade, purified by triple distillation in the presence of copper filings. A quantitative analysis on the hexachlorozirconates produced indicated a mole ratio of $MCl/ZrCl_4 = 2.00 \pm 0.01$ and further identification was made by the X-ray diffraction patterns (1).

The apparatus used for the phase diagram study consisted of a closed-end tube furnace, powered by a voltage-stabilized variac. The variac could be turned down by a variable speed eccentric drive, thus allowing for various uniform linear cooling rates. The furnace was wound noninductively to eliminate the possibility of induced currents in the thermocouples.

The temperature measurements were made using 22-gauge chromel–alumel thermocouples, calibrated against a platinum – platinum rhodium standard. The thermocouple tips were cut as small as possible to increase their response to the temperature fluctuations. When the furnace was at thermal equilibrium, the temperature was recorded with the current both on and off to determine if the net currents induced by the windings affected the thermocouple readings; no difference was observed. Temperature measurements were recorded continuously on a 1 mV full scale deflection recorder, and were intermittently checked by a potentiometer.

The mixture to be studied was introduced into a heart-shaped ampoule, and evacuated while being heated to 160 °C. The cell was then vacuum sealed, loaded into the furnace, and heated to the desired temperature. The initial cooling rate was rapid, usually about 2 deg per minute, and was of importance only to obtain the approximate positions of the inflections and plateaux which occurred for the material. This was followed by a series of cooling curves taken using rates of cooling of between 3/4 to $1\frac{1}{4}$ deg per minute. During the cooling cycle, the cells were periodically shaken to assure a uniform temperature in the melt and minimize supercooling.

A static method was used for the vapor pressure measurements, the apparatus for which is shown in Fig. 2. It consists of the following major sections: the furnace heating the reaction cell, the vacuum system, and the heated air bath. To obtain a constant temperature zone, a heavily insulated tubular furnace, 25 in. long with a 10 in. internal diameter, was used. The wiring consisted of one continuous coil over the whole length of the inner tube, and three equal resistance coils superimposed on this, each independently controlled by a variac. The power was supplied through a voltage stabilizer and with a fairly constant room temperature, a steady state heat flow gave an excellent temperature control of ±0.50 deg for long periods of time over the middle 6 in. of the furnace.

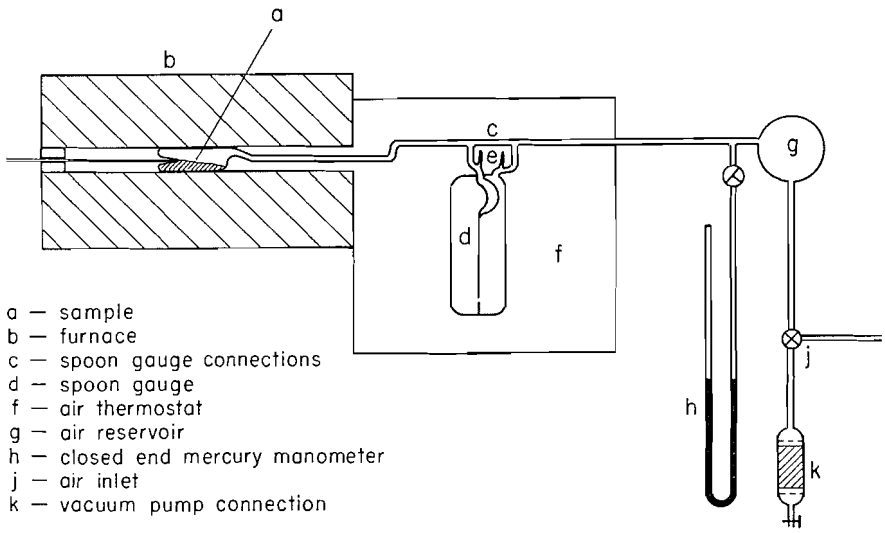

FIG. 2. Pressure measurements apparatus.

The reaction cell was constructed of quartz and was connected to a quartz spoon gauge. The external part of the gauge was connected to a manometer and two-way stopcock. To allow for evacuation of the system, a bypass of the spoon gauge was made which was later sealed under vacuum. The spoon gauge

was made totally of quartz and acted as a null point detector, while keeping the corrosive zirconium tetrachloride vapor separated from the mercury in the closed-end manometer. The sensitivity of the spoon gauge was such that pressure differences of better than $\frac{1}{2}$ mm could be easily detected.

To prevent condensation of zirconium tetrachloride vapor, the spoon gauge and cell connections were heated in an air furnace to a temperature above the dew point of zirconium tetrachloride. The air furnace was heavily insulated and thermally controlled at 390 ± 15 °C.

The approximate volume of the reaction cell, spoon, and connecting glass tubing was determined, and at all times this volume was maintained at a low level, so that with a large amount of material in the cell, only a small amount of $ZrCl_4$ vapor would be required to fill the cell volume. To determine the true compositions of the mixtures in the cell, approximate corrections were made to allow for the amount of $ZrCl_4$ in the vapor phase at the various temperatures.

Various compositions of alkali metal chlorides and hexachlorozirconates were transferred to the quartz cell in a dry box, and the cell was then flame sealed to the system. The system was evacuated while increasing the temperature to between 160 and 180 °C, and evacuation continued at this temperature for at least 3 h, so that all traces of water vapor in the apparatus could be removed.

The hot box was then cooled, the bypass constriction sealed, the hot box heated to the required temperature, and the vapor pressure measurements initiated. After the temperature had remained constant for the desired length of time, e.g. 5 h for vapor pressure readings of less than 400 mm and 3 h for readings above 400 mm, the spoon gauge pointer was adjusted to null by alternately evacuating and introducing air into the external part of the spoon gauge. To prevent breakage of the gauge, the pointer was kept at about the null position at all times. To determine the equilibrium pressure versus temperature curve, readings were taken on both increasing and decreasing temperature cycles.

Initially, the pressure runs were made on the pure hexachlorozirconates. This was followed by a series of runs using mixtures of the pure hexachlorozirconates and their respective alkali metal chlorides, so that the effect on the pressure curves due to the change of composition over the entire range from pure hexachlorozirconate to alkali metal chloride could be observed. These mixtures were made by weighing the reaction cell before and after the addition of each of the two components in a dry box. Similarly, a few runs were made in the ternary $NaCl–KCl–ZrCl_4$ system, for the purpose of determining the pressure at temperatures and compositions suitable for fused salt electrolysis.

Zirconium tetrachloride vapor has been shown to be unimolecular in the vapor phase by the work of Fisher and Rahlfs (5), and Spiridonov *et al.* (6). Therefore, the pressures measured represent the thermodynamic pressure of the $ZrCl_4$ species over the systems.

RESULTS

Phase Diagram Determination

Figure 3 represents the binary equilibrium phase diagram for the system $NaCl–Na_2ZrCl_6$. This diagram was compiled with the information obtained from cryoscopic measurements and supplemented by liquidus points obtained from the vapor pressure curves. It can be seen that the results for the liquidus obtained from the vapor pressure measurements agree quite well with those obtained by the cooling curve technique. In Fig. 3, the results obtained by Howell *et al.* (2) were recalculated to correspond to the $NaCl–Na_2ZrCl_6$ scale, and are included for comparison.

No accurate data for the NaCl side of the eutectic were given. The present work indicates the same eutectic temperature of 548 °C, but the liquid solubility lines are shifted slightly. The melting point of the Na_2ZrCl_6 in both cases was found to be 646 ± 1 °C. This work has shown the eutectic to be at 61.50 mole % Na_2ZrCl_6.

Figure 4 represents the binary equilibrium phase diagram for the system $KCl–K_2ZrCl_6$ obtained in the same manner. The results of Morozov and In'Chzhu (3) are also included for comparative purposes, and indicate a large discrepancy in the position of the liquid solubility lines. The latter found a eutectic which occurred at 47 mole % K_2ZrCl_6, and 594 °C. This work has shown the eutectic to be at the same temperature, but at 40.00 mole % K_2ZrCl_6. The melting point of K_2ZrCl_6 was determined at 799 ± 2 °C.

X-ray diffractometer measurements made on dilute solutions rapidly quenched from above the eutectic temperatures indicated no evidence of solid solubility in either system: $NaCl–Na_2ZrCl_6$ or $KCl-K_2ZrCl_6$.

Figure 5 represents the 600 °C and 540 °C isotherms for the system $NaCl–KCl–ZrCl_4$

Can. J. Chem. Downloaded from www.nrcresearchpress.com by 210.87.254.6 on 09/05/12
For personal use only.

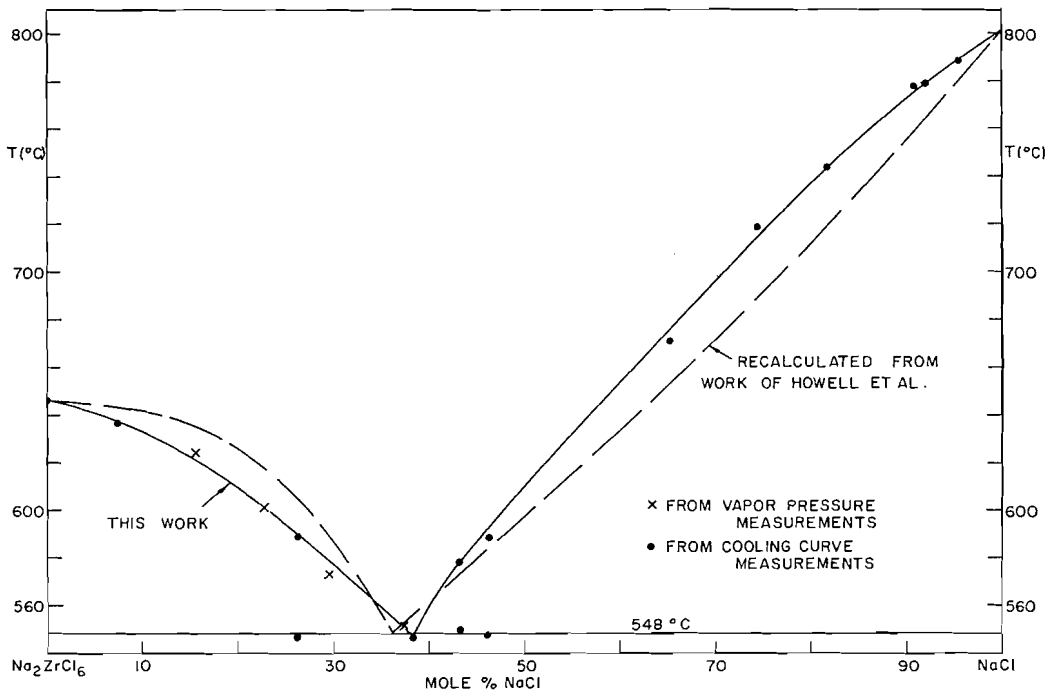

FIG. 3. Phase diagram of the Na_2ZrCl_6–NaCl system.

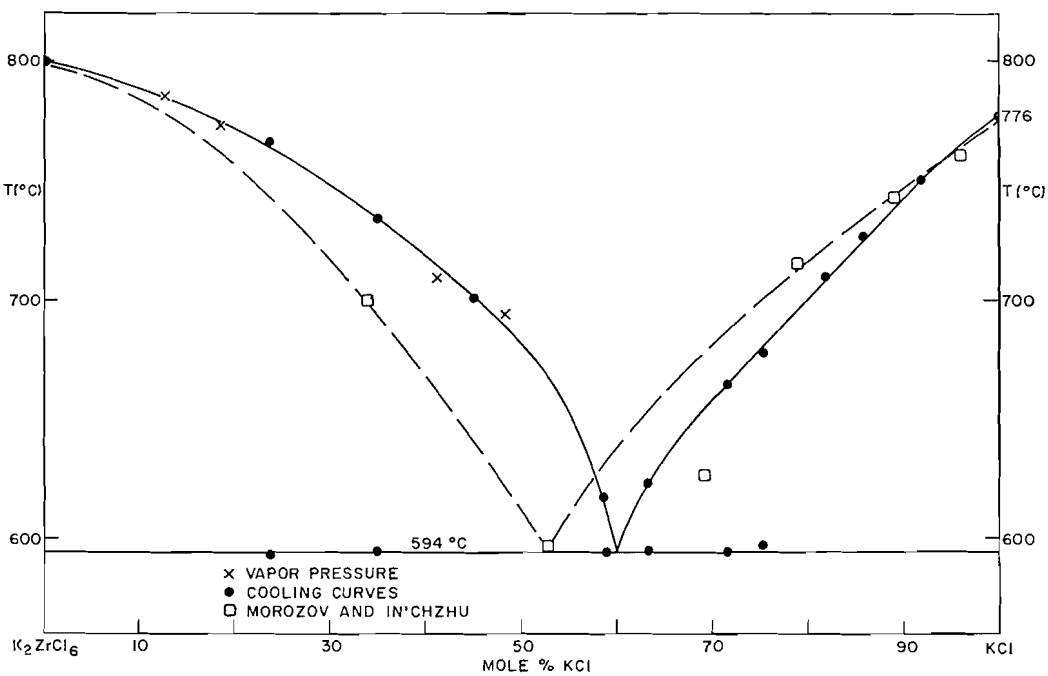

FIG. 4. Phase diagram of the K_2ZrCl_6–KCl system.

Can. J. Chem. Downloaded from www.nrcresearchpress.com by 210.87.254.6 on 09/05/12
For personal use only.

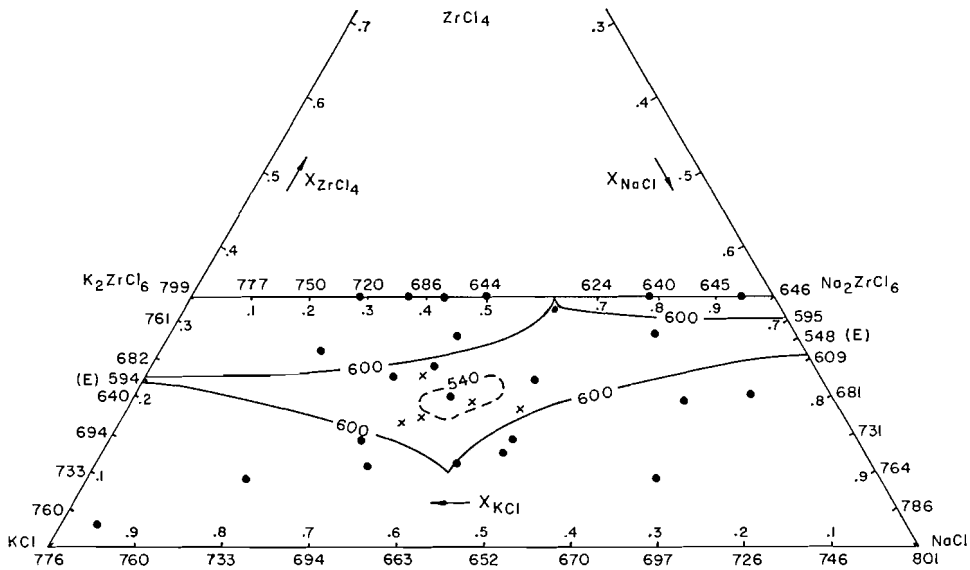

FIG. 5. The 540 °C and 600 °C isothermal surfaces in the KCl–NaCl–$ZrCl_4$ ternary system.

in the dilute $ZrCl_4$ range. It appears that the ternary eutectic occurs at 513 ± 3 °C, with the approximate composition 36 mole % NaCl, 20 mole % $ZrCl_4$, and 44 mole % KCl. The solid circles represent the points obtained, by cooling curves, while the ×'s represent the compositions where vapor pressure measurements have been made.

Vapor Pressure Measurements

The equilibrium vapor pressures of zirconium tetrachloride over the two pure components Na_2ZrCl_6 and K_2ZrCl_6, respectively, were measured. Various compositions of MCl and M_2ZrCl_6 were also investigated according to the decomposition reaction

$$M_2ZrCl_{6(s,l,sol)} = 2MCl_{(s,l,sol)} + ZrCl_{4(v)}$$

where the M_2ZrCl_6 and MCl are in the solid, liquid, or solution states, depending upon the composition and temperature at which the investigation was carried out.

Figure 6 represents the $\log P$ vs. $1/T$ plots for the various compositions over the system NaCl–Na_2ZrCl_6. Curve 1 represents the vapor pressure curve of solutions of NaCl and Na_2ZrCl_6 saturated with respect to Na_2ZrCl_6. The pressure curves for all systems follow curve 1, up to the liquidus temperature and then change slope; therefore, the intersections of curve 1 with the curves 2, 3, 4, and 5 occur at the liquid temperatures for the respective compositions, as shown in Fig. 6. These points have also been included in Fig. 3, as liquidus temperatures determined by vapor pressure measurements. Curves 2, 3, 4, and 5 represent the pressures of $ZrCl_4$ vapor in equilibrium with solutions of NaCl and Na_2ZrCl_6 on the Na_2ZrCl_6 side of the eutectic. Curve 6 represents the equilibrium pressures of $ZrCl_4$ vapor over solutions of NaCl and Na_2ZrCl_6 saturated with respect to NaCl. The curve is common for all compositions up to the corresponding liquidus temperatures, after which a change in slope occurs at the liquidus composition and temperature. Curves 7 to 12 inclusive represent the equilibrium pressures of $ZrCl_4$ vapor over the liquid solutions on the NaCl side of the eutectic. The vapor pressure measurements corresponding to all curves, with the exception of curve 6, were fully reproducible

Can. J. Chem. Downloaded from www.nrcresearchpress.com by 210.87.254.6 on 09/05/12
For personal use only.

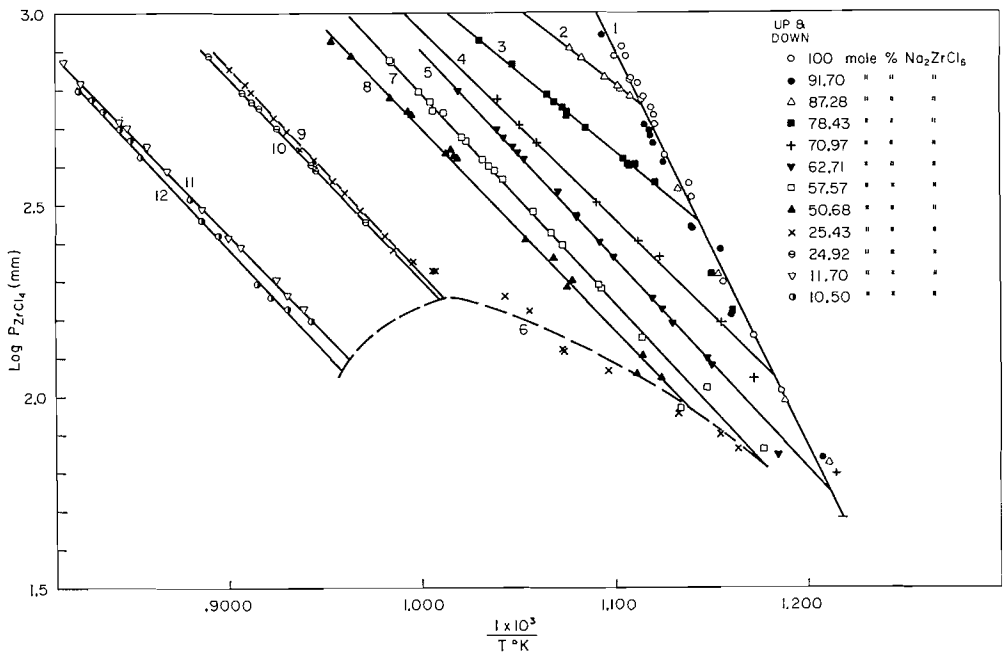

FIG. 6. Zirconium tetrachloride pressures in the Na_2ZrCl_6–NaCl system as a function of temperature at various compositions.

on both an increasing and decreasing temperature cycle. The pressures corresponding to solutions saturated with respect to sodium chloride (curve 6) are only approximate, and the curve was established by extrapolating the high temperature curves to the liquidus temperature indicated from the phase diagram for the specified composition. It may be seen that the experimentally obtained points approximate this curve. The magnitude of the pressures measured, as well as the observed irreversibility of the system at low pressures, did not permit vapor pressure measurements at temperatures below the eutectic. Accordingly, the effect of eutectic melting could not be observed in this system.

Figure 7 represents the log P vs. $1/T$ plots for the equilibrium pressures corresponding to various compositions of the binary system KCl–K_2ZrCl_6. Curve 1 represents the pressures of $ZrCl_4$ vapor in equilibrium with solutions of KCl and K_2ZrCl_6 saturated with respect to K_2ZrCl_6, and is common for all compositions up to the corresponding liquidus temperature. Liquidus melting is similarly shown by the change in slope at the liquidus temperature, and these temperatures have also been included in the corresponding phase diagram in Fig. 3. Curves 2, 3, 4, and 5 correspond to the completely liquid phase. Curves 6, 7, and 8 represent measurements on the potassium chloride side of the eutectic and could be obtained only at temperatures above the liquidus, as at lower temperatures, the system was too stable to produce a measurable vapor pressure. A detailed summary of the vapor pressure data is given in Table I for the system NaCl–Na_2ZrCl_4, and Table II for the system KCl–K_2ZrCl_6.

Vapor pressure measurements were also taken on selected compositions lying in the eutectic valley of the ternary NaCl–KCl–$ZrCl_4$ system, as shown in Fig. 5. The log P vs. $1/T$ curves for these specified compositions are given in Fig. 8, and the data for these curves may be found in Table III. The pressures correspond to the molten range only, as the pressures exerted over the saturated solution were again too small to be measured.

Can. J. Chem. Downloaded from www.nrcresearchpress.com by 210.87.254.6 on 09/05/12
For personal use only.

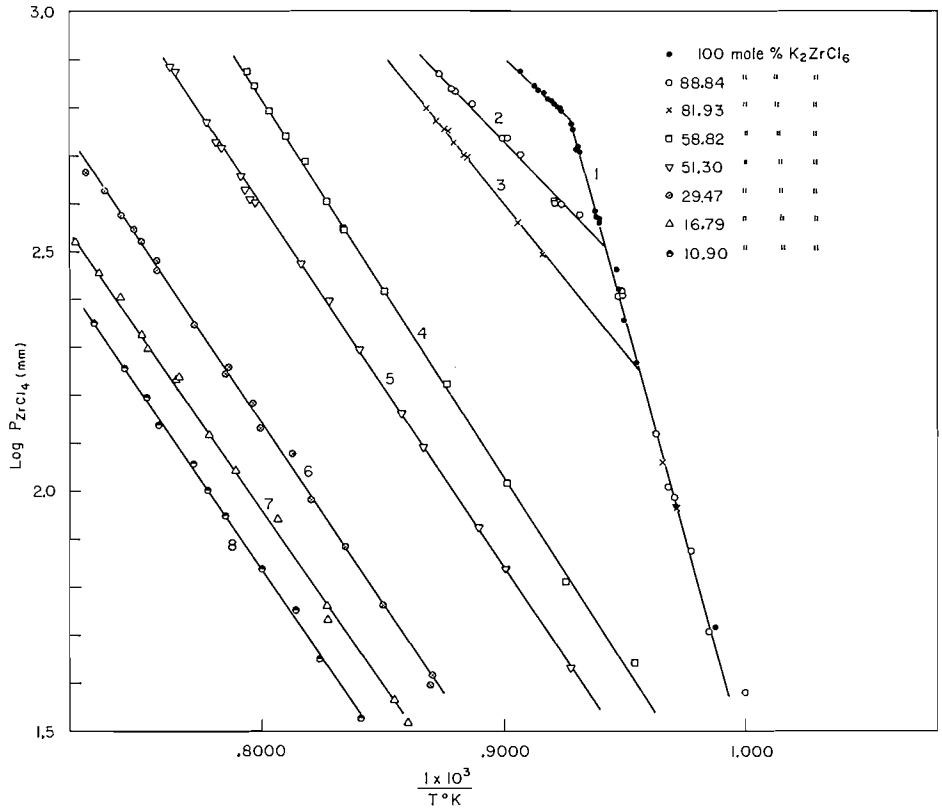

FIG. 7. Zirconium tetrachloride pressures in the K_2ZrCl_6–KCl system as a function of temperature at various compositions.

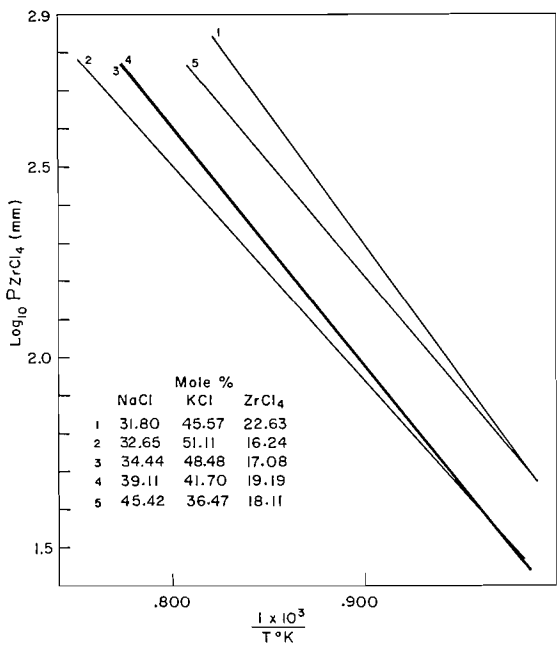

FIG. 8. Zirconium tetrachloride pressures in the KCl–NaCl–$ZrCl_4$ ternary system as a function of temperature at various compositions.

Can. J. Chem. Downloaded from www.nrcresearchpress.com by 210.87.254.6 on 09/05/12
For personal use only.

Tables I to III inclusive show the log P relationships determined by the least squares method over the temperature range specified, as well as the liquidus temperature, and the heats of reactions calculated from the slopes of the log P vs. $1/T$ curves, according to the previously derived relationships [9] and [14]. The partial molar heats of mixing of the M_2ZrCl_6 at various compositions may be determined from the difference

$$[15] \qquad \Delta H_r' - \Delta H_r'' = (\overline{\Delta H}_m)_{M_2ZrCl_6}$$

where the quantities $\Delta H_r'$, and $\Delta H_r''$ have been defined previously. These calculations are also shown in Tables I and II. The error limits applied to the heat terms were obtained from the standard deviations.

The partial molar properties correspond to the liquid compositions denoted as "corrected at the liquidus." This correction was found necessary because at higher pressures a small amount of zirconium tetrachloride was depleted from the initial mixture in order to fill the free volume of the pressure-measuring apparatus.

DISCUSSION OF RESULTS

The partial molar heats of mixing of K_2ZrCl_6 and Na_2ZrCl_6 for various compositions of the MCl–M_2ZrCl_6 mixtures are included in Tables I and II, and indicate that the solution processes are highly endothermic.

The linearity of the pressure curves shown in Figs. 6 and 7 indicates that the heats of mixing may be considered as constant in the temperature range of the pressure measurements. Heats of mixing calculated in this manner refer to the pure solids M_2ZrCl_6 as the state of reference, and include by definition the heats of fusion of the complex compounds. The relationship between the heat of fusion and the partial molar heats of mixing, referred to either pure solid or pure liquid M_2ZrCl_6, is given as

$$[16] \qquad (\overline{\Delta H}_m)_{s,M_2ZrCl_6} = (\overline{\Delta H}_m)_{l,M_2ZrCl_6} + \Delta H_f$$

where $(\overline{\Delta H}_m)_{s,M_2ZrCl_6}$ and $(\overline{\Delta H}_m)_{l,M_2ZrCl_6}$ are the heats of mixing of pure solid and liquid M_2ZrCl_6, respectively, and ΔH_f is the corresponding heat of fusion.

An estimate of the heat of fusion may be made only for the K_2ZrCl_6 compound, where pressure data could be obtained at temperatures higher than its melting temperature. From curve 1 in Fig. 7, it is seen that the pressure curve changes slope at about 798 °C, which corresponds to the liquidus temperature for the 99 mole % M_2ZrCl_6 mixture on the phase diagram. Such a concentrated solution is expected to obey Raoult's law and behave ideally. Accordingly,

$$(\overline{\Delta H}_m)_{l,K_2ZrCl_6} = 0$$

and

$$(\overline{\Delta H}_m)_{s,K_2ZrCl_6} = (\Delta H_f)_{K_2ZrCl_6} = 62.4 \text{ kcal/mole.}$$

This is an unusually high heat of fusion, indicative of a dissociating complex compound. From the results in Table II, it is seen that the heats of mixing of solid K_2ZrCl_6 become less endothermic as the solution becomes more concentrated in KCl, indicating that the dissociation of the $ZrCl_6^{--}$ anion in solution decreases with increasing chloride ion concentration.

If the dissociation reaction is represented by the general equation

$$ZrCl_6^{2-} \rightarrow ZrCl_{6-n}^{n-2} + nCl^-$$

then the decrease in dissociation may be accounted for by a common ion effect.

Can. J. Chem. Downloaded from www.nrcresearchpress.com by 210.87.254.6 on 09/05/12
For personal use only.

Can. J. Chem. Downloaded from www.nrcresearchpress.com by 210.87.254.6 on 09/05/12
For personal use only.

TABLE I

Thermodynamic properties of the binary system $NaCl–Na_2ZrCl_6$

Initial mole % Na_2ZrCl_4	$\log_{10} P$ (mm) $= (A/T) + B$		Temp. range (°C)	T_{liq} (°C)	Corrected mole % Na_2ZrCl_6 at T_{liq}	$\Delta H'$ (kcal/mole)	$\Delta H''$ (kcal/mole)	$(\overline{\Delta H}_m)_{Na_2ZrCl_6}$ (kcal/mole)
	A	B						
100	−10 394	14 339	548–640	*646		47.40±1.40		
91.70	−10 394	14 339	548–634	630		47.40±1.40		
87.28	−10 394	14 339	548–624			47.40±1.40		
				624	84.49			29.20±1.60
	−3 992	7 204	624–650				18.20±0.20	
78.43	−10 394	14 339	548–601			47.40±1.40		
				601	77.38			28.30±1.90
	−4 187	7 242	601–687				19.10±0.50	
70.97	−10 394	14 339	548–573			47.40±1.40		
				573	70.35			24.78±1.90
	−4 960	7 916	573–712				22.62±0.50	
62.71	−10 394	14 339	548–552.5			47.40±1.40		
				552.5	62.51			22.60±1.60
	−5 453	8 354	552.5–723				24.80±0.20	
57.57	−5 475	8 265	516–745	*516	57.40		24.97±0.20	
50.68	−5 282	7 980	605–762	*605	50.64		24.09±0.75	
25.43	−5 400	7 720	716–850	*716	25.28		24.62±0.50	
24.91	−5 285	7 588	718–850	*718	24.78		24.10±0.50	
11.70	−5 258	7 158	767–960	*767	11.59		23.98±0.50	
10.50	−5 417	7 261	770–960	*770	10.41		24.70±0.50	

*Liquidus temperature taken from phase diagram of Fig. 2.

Can. J. Chem. Downloaded from www.nrcresearchpress.com by 210.87.254.6 on 09/05/12
For personal use only.

TABLE II

Thermodynamic properties of the binary system $KCl–K_2ZrCl_6$

Initial mole % K_2ZrCl_6	$\log_{10} P$ (mm) $= (A/T) + B$		Temp. range (°C)	T_{liq} (°C)	Corrected mole % K_2ZrCl_6 at T_{liq}	$\Delta H'$ (kcal/mole)	$\Delta H''$ (kcal/mole)	$(\overline{\Delta H}_m)_{K_2ZrCl_6}$ (kcal/mole)
	A	B						
100	−18 380	19 826	735–804			83.81±2.00		
				804	98.90			62.43±2.50
	−4 689	7 124	804–831				21.38±0.50	
88.84	−18 380	19 826	735–785			83.81±2.00		
				785	87.63			59.87±2.50
	−5 250	7 455	785–875				23.94±0.50	
81.93	−18 380	19 826	735–773			83.81±2.00		
				773	81.51			55.38±2.50
	−6 234	8 213	773–896				28.43±0.50	
58.82	−18 380	19 826	*			83.81±2.00		
				708.5	58.81			48.00±2.50
	−7 853	9 100	708.5–990				35.81±0.50	
51.30	−18 380	19 826	*			83.81±2.00		
				695.5	51.29			49.49±2.50
	−7 527	8 620	695.5–1040				34.32±0.50	
29.47	−7 495	8 136	875–1080	659†	29.46		34.18±0.75	
16.47	−7 216	7 736	890–1100	714†	16.77		32.90±0.50	
10.90	−7 411	7 764	900–1080	739†	10.85		33.80±0.50	

*Extrapolated below measured range.
†Liquidus temperatures taken from phase diagram of Fig. 3.

TABLE III

Thermodynamic properties of the ternary system $NaCl–KCl–ZrCl_4$

Initial mole %			$\log_{10} P$ (mm) $= (A/T) + B$		Temp. range (°C)	ΔH reaction (kcal/mole)	T_{decomp} (°C)	Corrected mole % at T_{decomp}		
NaCl	KCl	$ZrCl_4$	A	B				NaCl	KCl	$ZrCl_4$
31.80	45.57	22.63	−6 897	8 504	700–960	31.45±0.1	954	31.91	45.72	22.3
32.65	51.11	16.24	−5 680	7 048	730–1100	25.90±0.8	1 090	32.73	51.25	16.0
34.44	48.48	17.08	−6 283	7 625	750–1050	28.65±0.8	1 051	34.53	48.60	16.8
39.11	41.70	19.19	−6 224	7 575	750–1050	28.38±1.0	1 053	39.22	41.83	18.9
45.52	36.47	18.11	−5 926	7 547	750–1000	27.02±0.50	997	45.64	36.56	17.9

Activity Calculation in the Binary Systems

The activity of the M_2ZrCl_6 in the totally liquid range may be calculated at any temperature, T, from the van't Hoff relationship

$$[17] \qquad \ln \frac{a_T}{a_{T_L}} = \frac{(\overline{\Delta H}_m)_{M_2ZrCl_6}}{R}\left[\frac{1}{T} - \frac{1}{T_L}\right]$$

where a_T is the activity of the M_2ZrCl_6 species at any temperature T; a_{T_L} is the activity at the liquidus temperature; and $(\overline{\Delta H}_m)_{M_2ZrCl_6}$ is the partial molar heat of mixing of M_2ZrCl_6 of the MCl–M_2ZrCl_6 solutions given in Tables I and II. For the calculation, the activity along a liquidus tieline is taken as equal to unity, thus defining the standard state as being that of the pure solids at all temperatures. Activity isotherms, calculated at selected temperatures by this method, are shown in Figs. 9 and 10 for the systems $NaCl$–Na_2ZrCl_6 and KCl–K_2ZrCl_6, respectively.

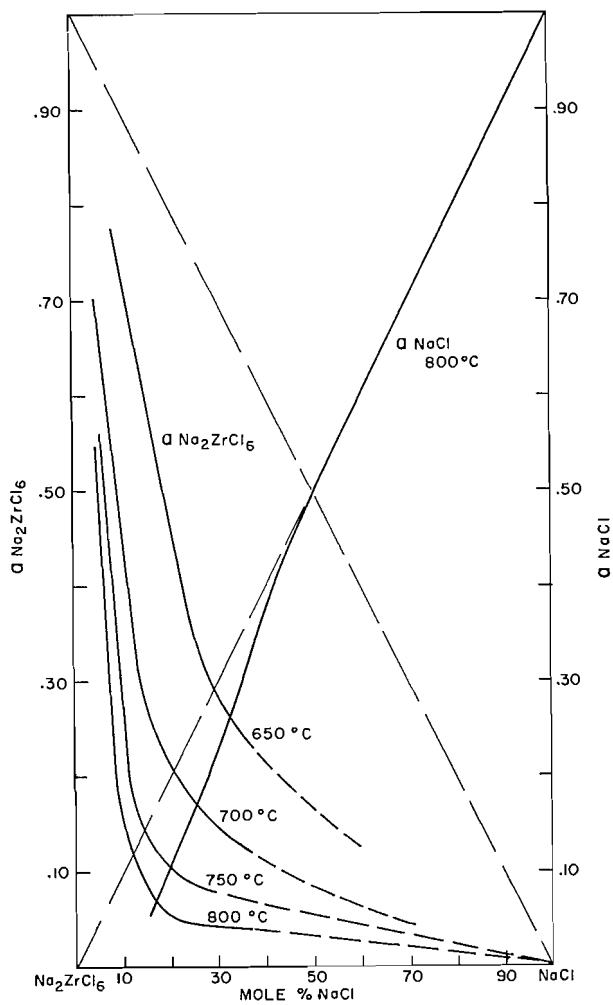

FIG. 9. Activity isotherms of Na_2ZrCl_6 and NaCl, in the Na_2ZrCl_6–NaCl binary system.

Can. J. Chem. Downloaded from www.nrcresearchpress.com by 210.87.254.6 on 09/05/12
For personal use only.

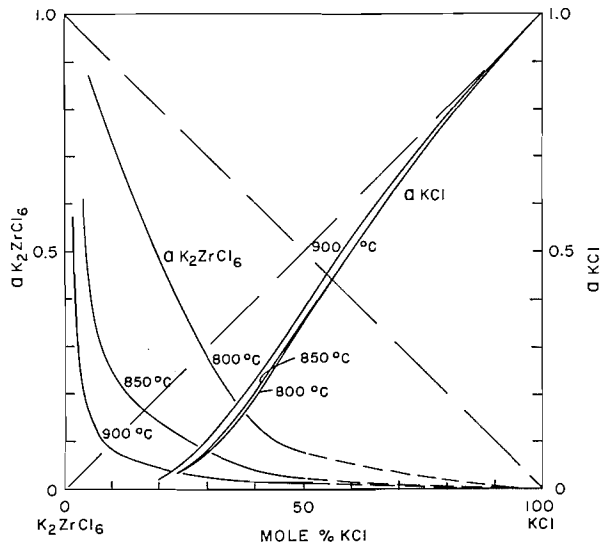

FIG. 10. Activity isotherms of K_2ZrCl_6 and KCl, in the K_2ZrCl_6–KCl binary system.

These data were obtained in the range of pure M_2ZrCl_6 to the eutectic composition and were then extrapolated to the infinite dilution range (indicated by the dotted lines). The activity coefficients of the MCl component have been determined by the Gibbs–Duhem equation in the form

$$[18] \qquad \log \gamma_1 = -\int_{N_1=1}^{N_1=N_1} \frac{N_2}{N_1} \, \mathrm{d} \ln \gamma_2.$$

Activities of MCl calculated from these results are also shown in Figs. 9 and 10. The activity isotherms indicate negative deviations from ideality for the two components. The activities of the M_2ZrCl_6 decrease with increasing temperature, indicating dissociation of the complex species at higher temperatures. This dissociation is also indicated by the large positive values of the partial molar heats of mixing shown in Tables I and II and discussed previously. With reference to the MCl component, the activities approach ideality in the concentrated MCl side, and are, for all practical purposes, temperature independent.

A solution containing m moles of MCl and n moles of M_2ZrCl_6 may be thought to be equivalent to one containing $m + 2n$ moles MCl, and n moles of $ZrCl_4$. Accordingly the activities of zirconium tetrachloride in the system MCl–$ZrCl_4$ have also been calculated with respect to the pure solid $ZrCl_4$ as the standard state. For the calculation the vapor pressure exerted by pure solid $ZrCl_4$ has been obtained from the relationship (7)

$$[19] \qquad \log_{10} P_{ZrCl}{}^{0} \text{ (mm)} = \frac{-5400}{T} + 11.766$$

and the activities were calculated as

$$[20] \qquad a_{ZrCl_4} = \frac{P_{ZrCl_4}}{P_{ZrCl_4}{}^{0}}$$

where P_{ZrCl_4} is the experimentally obtained pressure over the solutions in the liquid range.

Can. J. Chem. Downloaded from www.nrcresearchpress.com by 210.87.254.6 on 09/05/12
For personal use only.

The results of these calculations for the systems NaCl–$ZrCl_4$ and KCl–$ZrCl_4$ are given in Figs. 11 and 12. The activity isotherms show pronounced negative deviations from ideality, indicating the effect of the formation of the complex $ZrCl_6^{2-}$ species in solution.

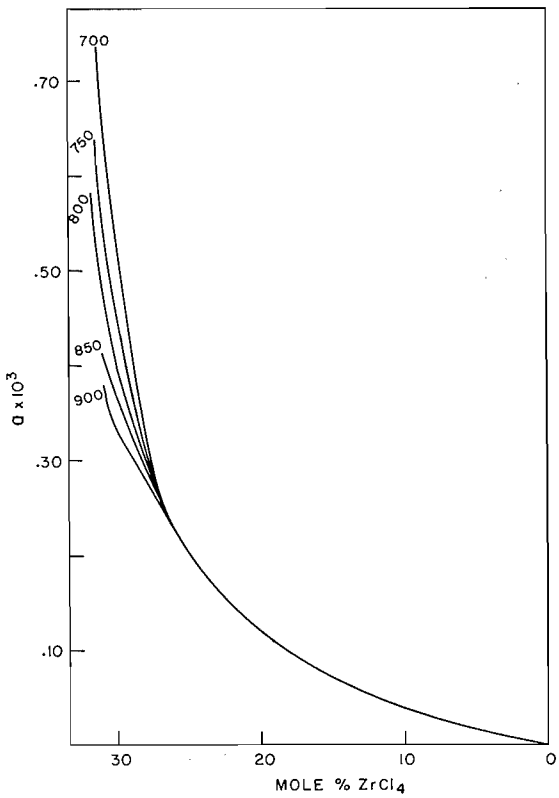

FIG. 11. Activity isotherms of $ZrCl_4$ in the NaCl–$ZrCl_4$ system.

The partial molar heats of mixing of zirconium tetrachloride have also been calculated from the temperature dependence of the activities, and are shown in Table IV.

The partial molar properties, calculated with respect to either M_2ZrCl_6 or $ZrCl_4$ solids as the states of reference, are related by the following thermodynamic cycle:

[a] $$2MCl_{(s)} + 2[(MCl)_{m+2n}\cdot(ZrCl_4)_n] = 2[(MCl)_{m+2n+i}\cdot(ZrCl_4)_n] \ldots . 2(\overline{\Delta H}_m)_{MCl}$$

[b] $$M_2ZrCl_{6(s)} = 2MCl_{(s)} + ZrCl_{4(v,\ 1\ atm)} \ldots . \Delta H_r^0$$

[c] $$M_2ZrCl_{6(s)} + [(MCl)_{m+2n}\cdot(ZrCl_4)_n] = [(MCl)_{m+2n+2}\cdot(ZrCl_4)_{n+1}] \ldots . (\overline{\Delta H}_m)_{M_2ZrCl_6}$$

[d] $$ZrCl_{4(s)} = ZrCl_{4(v,\ 1\ atm)} \ldots . \Delta H_s.$$

Reactions [a] and [c] represent the mixing of pure solids M_2ZrCl_6 and MCl, respectively, while reactions [b] and [d] correspond to the processes of the decomposition of solid M_2ZrCl_6 and to the sublimation of zirconium tetrachloride.

When these equations are added in the sequence [c] + [d] − [a] − [b], it is found that

[e] $$ZrCl_{4(s)} + [(MCl)_{m+2n}\cdot(ZrCl_4)_{n-1}] = [(MCl)_{m+2n}\cdot(\overline{ZrCl_4})_n] \ldots . (\Delta H_m)_{ZrCl_4}.$$

Reaction [e] is the process of mixing solid zirconium tetrachloride. Therefore, the various heat terms are related by the following expression:

[21] $$(\overline{\Delta H}_m)_{ZrCl_4} = (\overline{\Delta H}_m)_{M_2ZrCl_6} + \Delta H_s - \Delta H_r^0 - 2(\overline{\Delta H}_m)_{MCl}.$$

Can. J. Chem. Downloaded from www.nrcresearchpress.com by 210.87.254.6 on 09/05/12
For personal use only.

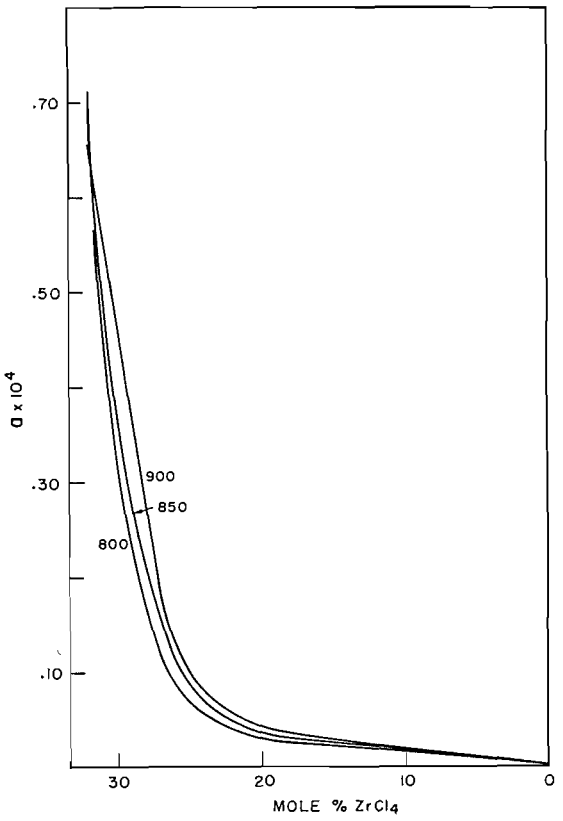

FIG. 12. Activity isotherms of $ZrCl_4$ in the KCl–$ZrCl_4$ system.

TABLE IV

The partial molar heats of mixing of $ZrCl_4$ in the systems NaCl–$ZrCl_4$ and KCl–$ZrCl_4$

NaCl–$ZrCl_4$ system		KCl–$ZrCl_4$ system	
Mole % $ZrCl_4$ corrected at liquidus	$(\overline{\Delta H}_m)_{ZrCl_4}$ (kcal)	Mole % $ZrCl_4$ corrected at liquidus	$(\overline{\Delta H}_m)_{ZrCl_4}$ (kcal)
31.41	6.27±0.1	33.21	2.60±0.1
30.37	5.74±0.1	31.84	0.73±0.1
29.23	1.89±0.1	30.99	−3.19±0.1
27.78	−0.22±0.1	27.02	−10.67±0.1
26.72	−0.50±0.1	23.52	−9.35±0.1
25.16	0.78±0.1	18.54	−9.80±0.1
16.79	0.00±0.1	12.56	−8.30±0.1
16.56	0.40±0.1	8.92	−10.18±0.1
9.41	0.24±0.1		
8.62	−0.18±0.1		

Equation [21] may also be used for the calculation of the heat of decomposition ΔH_r^0 of pure solid K_2ZrCl_6. Thus, from equation [19] the heat of sublimation of zirconium tetrachloride is calculated as 24 850 cal/mole; the partial molar heats of mixing of K_2ZrCl_6 and $ZrCl_4$, respectively, are given in Tables II and IV. The slight temperature dependence of the activities of potassium chloride indicates that the partial molar heat of mixing

Can. J. Chem. Downloaded from www.nrcresearchpress.com by 210.87.254.6 on 09/05/12
For personal use only.

of KCl should be negligibly small. For the 32.2 mole % $ZrCl_4$ composition, corresponding to almost pure K_2ZrCl_6, the approximate heat of decomposition is calculated as

$$\Delta H_r^0 = 84.7 \text{ kcal/mole.}$$

It is evident that the thermodynamic analysis of a system of the type $ZrCl_4$–MCl depends upon the choice of components. When choosing M_2ZrCl_6 as a component, the behavior of the pressure–temperature curves may be understood and predicted. Furthermore, some knowledge of the properties and structure of these liquids may be gained. Thus, it has been indicated that the $ZrCl_6^{--}$ anion dissociates in these solutions, and that the dissociation is promoted by higher temperatures and is suppressed by a higher chloride ion concentration. As the formation of the $ZrCl_6^{--}$ complex anion has already satisfied most of the bonding requirements of zirconium tetrachloride, the activities of M_2ZrCl_6 in solution indicate rather moderate deviations from ideality.

On the contrary, activities calculated with respect to zirconium tetrachloride as the component indicate pronounced negative deviations from ideality. Such deviations could be accounted for only by the tendency of zirconium tetrachloride to react with the alkali metal chlorides and form complex species in solution. From these results, however, the nature of the complexes could not be specified and the dissociation effect was not too apparent. Furthermore, the behavior of the pressure–temperature curves could not be predicted.

It is evident that the choice of M_2ZrCl_6 as a component is more useful in indicating the properties of these liquids. On the other hand, activities calculated with respect to zirconium tetrachloride are of practical value in indicating the thermal stability of the solutions.

Ternary System NaCl–KCl–$ZrCl_4$

As indicated previously, the vapor pressure measurements taken at compositions in the area of the ternary eutectic valley were of interest from the point of view of determining a low vapor pressure area over this system, which might be used in an electrodeposition process. The decomposition temperatures given in Table II correspond to the temperature at which the equilibrium pressure exerted by the system becomes 1 atm. These decomposition temperatures are all quite high, indicating a high degree of thermal stability of the system.

In the concentration range of the liquid corresponding to the 600 °C isothermal surface, the pressures of zirconium tetrachloride are less than 6 mm. The decomposition pressures over the binary systems, NaCl–$ZrCl_4$ and KCl–$ZrCl_4$, have also been calculated from the data as a function of composition, and the pressure isotherms are given in Figs. 13 and 14 for comparison.

It is seen that the decomposition pressures increase rapidly with increasing zirconium tetrachloride content, thus diminishing the usefulness of the more concentrated $ZrCl_4$ solutions for purposes of electrolysis.

A given solution of zirconium tetrachloride in the liquid range may be stablilized when subjected to an external pressure equal to the corresponding decomposition pressure indicated on the isotherms. Thus, the problem of solubility may be understood in terms of the thermal stability of the solutions.

In Table V, a comparison between the pressures measured over the ternary compositions and the pressures exerted over the corresponding MCl–$ZrCl_4$ binary systems, having the same $ZrCl_4$, is given. It may be seen that the pressures of the ternary are of the same

Can. J. Chem. Downloaded from www.nrcresearchpress.com by 210.87.254.6 on 09/05/12
For personal use only.

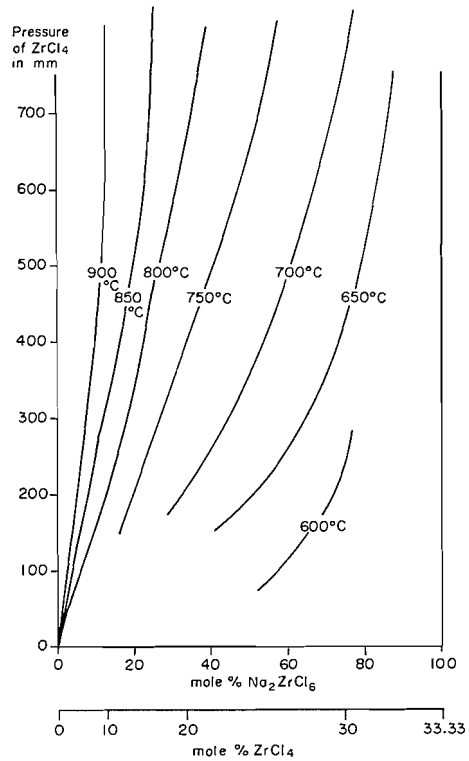

FIG. 13. Pressure isotherms of $ZrCl_4$ in the NaCl–$ZrCl_4$ system.

order of magnitude as for the corresponding binary solutions of the KCl–$ZrCl_4$ system; however, the NaCl–$ZrCl_4$ solutions exhibit pressures which are greater by one to two orders of magnitude. This may be understood by the following equilibria:

$$\begin{array}{ccc} K_2ZrCl_{6(sol)} + 2NaCl_{(sol)} & \overset{[1]}{\rightleftharpoons} & NaZrCl_{6(sol)} + 2KCl_{(sol)} \\ \downarrow\uparrow [2] & & \downarrow\uparrow [3] \\ 2KCl_{(sol)} + ZrCl_{4(v)} & & 2NaCl_{(sol)} + ZrCl_{4(v)} \end{array}$$

Reaction [1] represents an exchange reaction, while [2] and [3] represent the vapor-producing reactions. The equilibrium vapor over the solution can represent only one of the two possible decomposition reactions, the other being totally suppressed. The similarity between the pressures exerted by the ternary and by the binary KCl–$ZrCl_4$ systems appears to indicate that the latter is the vapor-producing reaction; accordingly, the equilibrium represented by reaction [1] is shifted to the left. If the Na_2ZrCl_6 complex exists in solution, it should be present in such small quantities that its equilibrium pressure should be very small and decomposition reaction [3] would be totally suppressed.

For the electrodeposition of zirconium in a fused salt bath containing NaCl–KCl–$ZrCl_4$, it may be said that the K_2ZrCl_6 is the prominent zirconium bearing species, while only a small amount of Na_2ZrCl_6 is present in the solution. The ternary offers the advantage of operating in a totally liquid phase at low temperatures ($\sim$ 600 °C) and pressures. Although a correspondingly low pressure could be achieved in the KCl–$ZrCl_4$ system at

Can. J. Chem. Downloaded from www.nrcresearchpress.com by 210.87.254.6 on 09/05/12
For personal use only.

Can. J. Chem. Downloaded from www.nrcresearchpress.com by 210.87.254.6 on 09/05/12
For personal use only.

TABLE V

Comparison between the pressures over the ternary and binary systems

Ternary composition (mole %)			Ternary pressures in liquid at T (°C):				Corresponding pressures in $NaCl–ZrCl_4$ solutions with same amount of $ZrCl_4$ as in ternary pressures at T (°C):					Corresponding pressures in $KCl–ZrCl_4$ solutions with same amount of $ZrCl_4$ as in ternary pressures at T (°C):				
NaCl	KCl	$ZrCl_4$	750	800	850	900	700	750	800	850	900	700	750	800	850	900
31.80	45.57	22.63	57	119	230	419	620	vh	vh	vh	vh	—	45	120	212	375
32.65	51.11	16.24	31	56	99	161	340	635	vh	vh	vh	4	16	35	76	155
34.44	48.48	17.08	31	60	108	186	370	675	vh	vh	vh	5	20	41	87	175
39.11	41.70	19.19	31	60	108	186	450	822	vh	vh	vh	—	26	65	125	240
45.52	36.47	18.11	56	105	186	316	385	740	vh	vh	vh	5	24	53	105	205

Abbreviation: vh represents pressures too high to be measured.

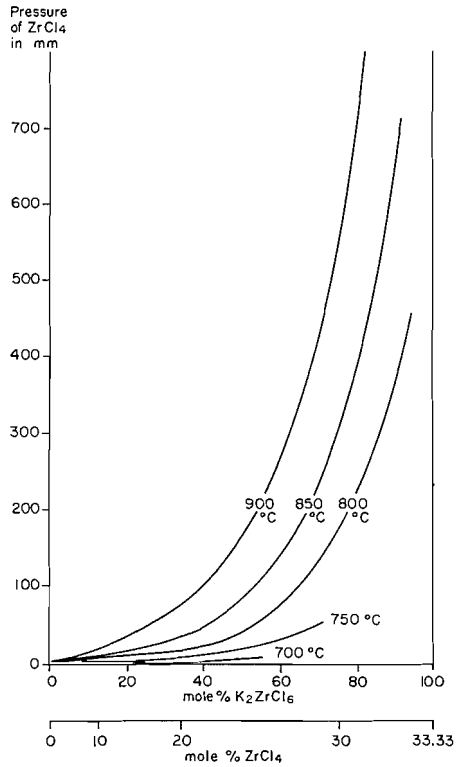

FIG. 14. Pressure isotherms of $ZrCl_4$ in the KCl–$ZrCl_4$ system.

such low temperatures, the phases present would always be solid and liquid according to the phase diagram. It appears, therefore, that the use of a ternary solution should be beneficial for electrolytic purposes.

CONCLUSIONS

It has been shown that the solubilities of zirconium tetrachloride in alkali chloride melts may be explained by formation of compounds of the general formula M_2ZrCl_6. The thermal stability of the solutions increases with increasing ionic size of the alkali metal cation.

The possibility of using the ternary NaCl–KCl–$ZrCl_4$ as a fused salt medium for the electrodeposition of zirconium metal appears quite promising. If we consider the 600 °C isotherm as a reasonable working temperature, it has been shown that the pressure exerted over the ternary system in this temperature and concentration range is less than 6 mm. The K_2ZrCl_6 complex appears to be present in the ternary in preference to the Na_2ZrCl_6 species and imposes its equilibrium pressure. The dissociation of this complex to smaller ionic species indicates that the solution could possess favorable ionic mobilities.

Equilibrium vapor pressures of zirconium tetrachloride have been obtained over the entire composition range for the binary systems NaCl–Na_2ZrCl_6 and KCl–K_2ZrCl_6. The pressure data have been used to calculate activities and to support the phase diagram determinations. The thermodynamic properties of the *pure* solid compounds M_2ZrCl_6 may be obtained from equilibrium pressure measurements at temperatures up to only the eutectic of the binary system M_2ZrCl_6 and MCl and not, as is commonly assumed,

Can. J. Chem. Downloaded from www.nrcresearchpress.com by 210.87.254.6 on 09/05/12
For personal use only.

to the melting point of the pure compound. The vapor pressure curves for the decomposition of the compound undergo a change in slope at the eutectic and the liquidus temperatures, and from these, the phase diagram for any system of this type can be predicted. Thus, the interpretation of thermodynamic data derived from reaction pressure measurements is restricted by eutectic and liquidus melting in the system. When these two effects are accounted for, a far more complete thermodynamic analysis of the system may be derived, and the partial molar properties of the components in the solutions may be calculated.

It should be emphasized that the conclusions drawn from this treatment would be equally applicable to any reactive system, such as sulfates, carbides, silicides, etc., where a congruently melting compound exists, which will decompose upon heating, producing a vapor phase.

ACKNOWLEDGMENTS

Acknowledgment is made to the Defence Research Board of Canada for its support of this work, and to the National Research Council for a Fellowship to one of the authors (R. L. L.).

REFERENCES

1. R. L. Lister and S. N. Flengas. Can. J. Chem. **42**, 1102 (1964).
2. L. J. Howell, R. C. Sommer, and H. H. Kellogg. J. Metals, **209**, 1, 193 (1957).
3. I. S. Morozov and Sun In'Chzhu. Russ. J. Inorg. Chem. English Transl. **4**, 3, 307 (1959).
4. I. S. Morozov and Sun In'Chzhu. Russ. J. Inorg. Chem. English Transl. **4**, 11, 1179 (1959).
5. W. Fischer and O. Rahlfs. Z. Anorg. Chem. **211**, 349 (1933).
6. V. P. Spiridonov, P. A. Akishin, and V. I. Tsirel'nikov. Zh. Strukt. Khim. **3**(3), 329 (1962).
7. A. A. Palko, A. D. Ryon, and D. W. Kuhn. J. Phys. Chem. **62**, 319 (1958).

Can. J. Chem. Downloaded from www.nrcresearchpress.com by 210.87.254.6 on 09/05/12
For personal use only.

Can. J. Chem. Downloaded from www.nrcresearchpress.com by 210.87.254.105 on 09/05/12
For personal use only.

SPECTROSCOPIC STUDIES OF ALCOHOLS

VI. INTRAMOLECULAR HYDROGEN BONDS IN ETHANOLAMINE AND ITS *O*- AND *N*-METHYL DERIVATIVES

P. J. KRUEGER AND H. D. METTEE
Department of Chemistry, University of Alberta, Calgary, Alberta
Received May 19, 1965

ABSTRACT

The competitive intramolecular OH · · · N and NH · · · O hydrogen bonding in ethanolamine and *N*-methylethanolamine has been studied in dilute C_2Cl_4 solution by means of the temperature dependence of the fundamental OH and NH stretching bands. Of the three conformers identified for each of these compounds, the least stable shows a distinct band which is assigned to a "terminal" OH group involved in an intramolecular NH · · · OH hydrogen bond. Enthalpy differences between conformers are reported and discussed, and compared with those found for the conformational equilibria in 2-methoxyethylamine and *N*,*N*-dimethylethanolamine.

INTRODUCTION

Hydrogen bonding studies involving both NH groups and OH groups as proton donors and both N atoms and O atoms as proton acceptors are of interest since such multiplicity of proton donor and acceptor sites is prevalent in many biological systems. Both intra- and intermolecular OH · · · N and NH · · · O bonds may form, leading to a number of complexes in simultaneous equilibrium. This paper reports some infrared absorption studies of a simple model compound ethanolamine in a relatively inert solvent under conditions where only intramolecular hydrogen bonds can form.

Bergmann, Gil-Av, and Pinchas (1) first reported a downward shift of the OH stretching frequency on intramolecular OH · · · N hydrogen bond formation in *N*-mono- and *N*,*N*-disubstituted 2-aminoethanols in dilute CCl_4 solution. More recently Flett (2) has compared OH stretching frequencies in a number of substituted alcohols in dilute CCl_4 solution. The downward frequency displacements from the normal monomeric "free" OH position on intramolecular hydrogen bonding are much greater in *N*,*N*-dialkyl-2-aminoethanols than in 2-alkoxyethanols. Freedman (3) has reviewed the frequency shift data pertaining to inter- and intramolecular OH · · · O and OH · · · N hydrogen bonds, concluding that in simple compounds (or binary systems) containing similar OH · · · O and OH · · · N bonds the latter are stronger. Mean energies of intermolecular OH · · · N, OH · · · O, and NH · · · O hydrogen bonds have been estimated to be about 7, 6, and 2–3 kcal/mole respectively (4*a*).

Kanzawa (5) have investigated OH · · · N bonding in the diasteroisomeric ephedrines and related compounds, but the interpretation of these spectra is complicated by the presence of the phenyl and methyl groups on the 2-*N*-methylaminoethanol skeleton.* The conclusion that the —$NHCH_3$ group in ephedrine plays almost no role as a proton donor in intramolecular hydrogen bond formation is probably not justified in the light of the results on alkanolamines reported in this paper.

Kuhn, Luettke, and Mecke (8) concluded that strong intramolecular OH · · · N hydrogen bonds form in ethanolamine and its *N*-methyl derivatives, but no thermodynamic

**Intramolecular OH · · · π-electron hydrogen bonding occurs in benzyl alcohol (6) and in 2-phenylethanol ($\Delta H = -1.04 \pm 0.02$ kcal/mole for the trans–gauche equilibrium (7)). The methyl group exerts its steric influence in the conformational equilibrium.*

investigation of these compounds appears to have been reported to date. Although the magnitude of OH (or NH) frequency shifts on hydrogen bond formation are conventionally considered to be measures of the hydrogen bond strength, following the work of Badger and Bauer (9), caution must be exercised in the application of this rule if (*a*) experimental measurements of frequency shifts are not made at very low base concentration (10), (*b*) small enthalpy differences (small frequency displacements) are involved, (*c*) comparisons are made between systems involving radical changes in the nature of the base (11), and (*d*) intramolecular hydrogen bonds are formed (where the AH···B distance and geometry are largely dictated by the system). In such cases ΔH reflects a change in molecular conformation in which all the nonbonded interactions in the two conformations are balanced against each other. The attractive force between two groups which engage in hydrogen bonding is just one of these interactions. The hydrogen bond also involves a repulsive interaction between A and B which ultimately decides the minimum A···B distance.

EXPERIMENTAL

A Beckman IR-7 infrared spectrophotometer was employed under the conditions described previously (12). Matched fused quartz absorption cells with a path length of 2.0 cm were used. Cell temperatures were regulated with a Lauda UK70D Ultrakryostat. All the aminoalcohols and their *O*- and *N*-methyl derivatives were commercial products which were dried and fractionally distilled through a 23-theoretical-plate spinning band column. Boiling points and refractive indices of the fractions collected for use agreed well with literature values. Reagent grade tetrachloroethylene was dried over P_2O_5 and distilled through a 50-theoretical-plate spinning band column. This was used as a solvent instead of carbon tetrachloride, which is known to be a poor solvent for aminoalcohols and alkyl amines (13, 14, 15). Alkanolamine concentrations were of the order of 0.01 *M* or less, while amine concentrations were about 0.02 *M*. No concentration dependent bands due to intermolecular association were found. For ethanolamine in CCl_4 (concentration range 0.11–1.00%) such a band has been reported at 3 340 cm^{-1} (16).

RESULTS AND DISCUSSION

The high resolution infrared spectra in the 3 μ region obtained at room temperature for dilute C_2Cl_4 solutions of ethanolamine and 3-aminopropanol and some of their *O*- and *N*-methyl derivatives are shown in Fig. 1. The OH and NH frequencies are recorded in Table I, which also includes some comparative values from the literature.

The spectra of *N*,*N*-dimethylethanolamine and 2-methoxyethylamine are simply interpreted in terms of an equilibrium between "free" and "bonded" OH and NH_2 groups respectively, arising from *trans* and *gauche* conformers.* In *N*,*N*-dimethylethanolamine the ν_{OH} shift on intramolecular OH···N hydrogen bond formation is 132 cm^{-1}. For 2-methoxyethylamine, where weaker intramolecular NH···O hydrogen bonds form, "free" and "bonded" NH_2 groups exhibit the antisymmetric vibrational mode at 3 398 and 3 387.$_5$ cm^{-1} respectively (ν_{NH} shift = 10.$_5$ cm^{-1}). The *trans* population greatly exceeds the *gauche* population. Since the symmetric vibrational mode in aliphatic amines in C_2Cl_4 solution has a low intensity (14), the two components due to "free" and "bonded" NH_2 groups were only observed as a broad weak band at about 3 331 cm^{-1}, with asymmetry on the low frequency side.

The spectra of ethanolamine and *N*-methylethanolamine are similarly composed of "free" OH and NH bands as well as the characteristically broad OH···N band and the "bonded" NH bands which have undergone only a small displacement. A broad very weak absorption is found in the region where the symmetric NH_2 stretching vibration of "free" and "bonded" NH_2 groups is expected. In addition, a distinct band is found

**The gauche form may deviate from the perfectly staggered conformation, according to n.m.r. data on the ephedrines (19).*

Can. J. Chem. Downloaded from www.nrcresearchpress.com by 210.87.254.105 on 09/05/12
For personal use only.

Can. J. Chem. Downloaded from www.nrcresearchpress.com by 210.87.254.105 on 09/05/12
For personal use only.

TABLE I

Fundamental OH and NH stretching frequencies in alkanolamines (temperature ~25 °C, dilute C_2Cl_4 solution; (as) = antisymmetric mode, (s) = symmetric mode)

Compound	ν_{OH} (cm^{-1})			ν_{NH} (cm^{-1})		
	ν_{OH}"free"	$\nu_{NH\cdots OH}$	$\nu_{OH\cdots N}$	ν_{NH}"free"		$\nu_{NH\cdots O}$
$HOCH_2CH_2NH_2$[a]	3 640.8	3 624.5	3 526		3 411(as)[b] ~3 340(s)[b] weak	
$HOCH_2CH_2CH_2NH_2$	3 638	3 626	3 395		[c]	
$CH_3CH(OH)CH(NH_2)CH_3$[d]						
Erythro	3 627	?	3 510		3 398(as)[b,e]	
Threo	3 627	?	3 486		3 396(as)[b,e]	
$HOCH_2CH_2NHCH_3$[f]	3 641.2	3 622.4	3 515.0	3 378.5		3 350.5
$HOCH_2CH_2N(CH_3)_2$[g]	3 638.6	—	3 506.4	—		—
$HOCH_2CH_2N(CH_2CH_3)_2$[h]	3 630	—	3 472	—		—
$HOCH_2CH_2CH_2N(CH_2CH_3)_2$[h]	3 628	—	3 288	—		—
$CH_3OCH_2CH_2NH_2$	—	—	—	3 398.1(as) ~3 335(s)[b]		3 387.5(as)
$CH_3OCH_2CH_2CH_2NH_2$	—	—	—		3 395(as) 3 331(s)[b]	
$CH_3CH_2CH_2NH_2$[i]	—	—	—	3 393(as) 3 326(s)		—
$CH_3CH_2CH_2OH$[j]	3 638.5	—	—	—		—

[a] "Free" and "bonded" ν_{OH} also reported at 3 610 and 3 509 cm^{-1} respectively (5), and at 3 634 and 3 513 cm^{-1} respectively, with ν_{NH} at 3 400 and 3 336 cm^{-1} (8), all in dilute CCl_4 solution.
[b] "Free" and "bonded" NH bands not resolved, but the observed band is asymmetric on the low frequency side.
[c] NH frequencies masked by broad OH $\cdots$ N band.
[d] Measurements by Sicher, Horak, and Svoboda (13).
[e] Symmetric mode not reported, presumably because of its low intensity.
[f] "Free" and "bonded" ν_{OH} also reported at 3 641 and 3 517 cm^{-1} respectively (17), and at 3 629 and 3 496 cm^{-1} respectively, with ν_{NH} at 3 370 and 3 336 cm^{-1} (8), all in dilute CCl_4 solution.
[g] "Free" and "bonded" ν_{OH} also reported at 3 632 and 3 491 cm^{-1} respectively (8).
[h] Measurements by Flett (2).
[i] Measurements by Smith (14).
[j] In CCl_4; main OH band (18) at 15 °C.

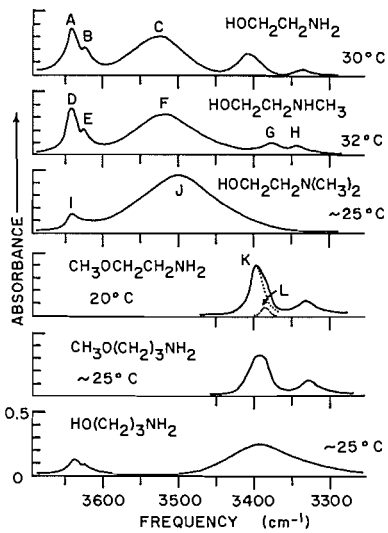

FIG. 1.

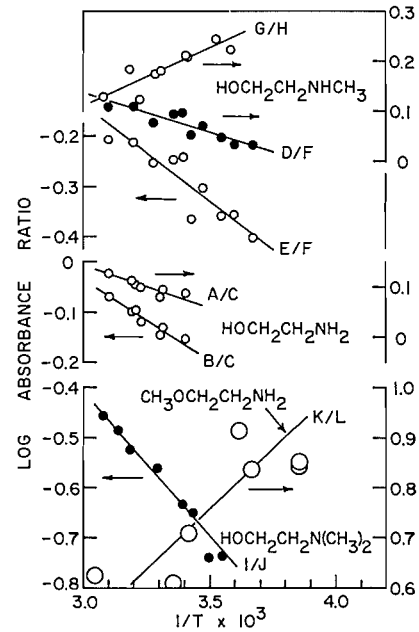

FIG. 2.

FIG. 1. Fundamental OH and NH stretching bands in ethanolamine and 3-aminopropanol and some of their *O*- and *N*-methyl derivatives in dilute C_2Cl_4 solution. Path length = 2.0 cm.

FIG. 2. Temperature dependence of peak absorbance ratios in ethanolamine spectra in dilute C_2Cl_4 solution. Letters refer to bands in Fig. 1.

about 15 cm^{-1} below the "free" OH band in each of these spectra (bands B and E, Fig. 1). The identification of this band follows from the observed temperature dependence of these spectra.

Figure 2 shows some of the changes in relative band intensities as a function of temperature (log absorbance ratios vs. $1/T$). From the slopes the enthalpy differences (ΔH) between conformers involved in the equilibria may be determined, fitting lines to the experimental points by the least-squares method. For ethanolamine and *N*-methylethanolamine there is a competition between intramolecular OH···N and NH···O hydrogen bonds. The experimentally determined ΔH values are fitted to postulated

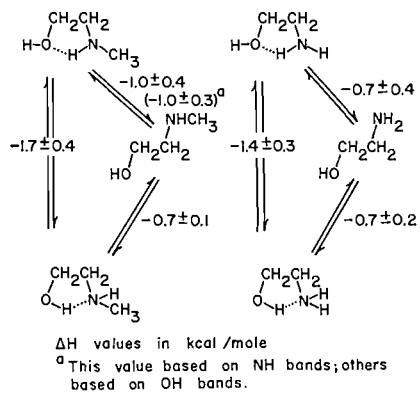

FIG. 3. Conformational equilibria for ethanolamine and *N*-methylethanolamine in dilute C_2Cl_4 solution, together with experimental ΔH values (with calculated 90% confidence limits). For each system, stability increases in the downward direction.

Can. J. Chem. Downloaded from www.nrcresearchpress.com by 210.87.254.105 on 09/05/12
For personal use only.

equilibria in Fig. 3. The intramolecularly hydrogen bonded species would presumably take up quasi-*gauche* conformations in which the proton donor and acceptor groups are in relative positions consistent with the strongest hydrogen bond permitted by the restrictive geometry of the system and the other nonbonded forces involved.

Bands B and E in the spectra of ethanolamine and *N*-methylethanolamine are assigned to the "terminal" OH group of conformers with angular NH···OH hydrogen bonds. On lowering the temperature of the *N*-methylethanolamine solution band E ("terminal" OH in NH···OH bond) decreases with respect to the "free" OH band ($\Delta H = -1.0 \pm 0.4$ kcal/mole) and more rapidly with respect to the OH···N band ($\Delta H = -1.7 \pm 0.4$ kcal/mole), while the "free" NH band increases with respect to the "bonded" NH band ($\Delta H = 1.0 \pm 0.3$ kcal/mole), and the "free" OH band decreases with respect to the OH···N band ($\Delta H = -0.7 \pm 0.1$ kcal/mole). These ΔH values are self-consistent and fit the scheme outlined in Fig. 3 if the conformer with the NH···O bond has the lowest stability, and if the "terminal" NH group (in the conformer bonded OH···NH) absorbs at the same frequency as the "free" NH and with about the same extinction coefficient. The data for ethanolamine can be interpreted in a similar way.

The temperature dependence of the "free" and "bonded" antisymmetric NH_2 bands of 2-methoxyethylamine shows that here too the *trans* conformer appears to be more stable than the *gauche* conformer with the NH···O bond, in this case by 1.6 ± 0.9 kcal/mole (Fig. 2). These two bands are badly overlapped and since the *trans* conformer predominates, the high frequency side of this band was reflected across the ordinate at the band maximum and the resulting symmetrical band subtracted from the experimental envelope to obtain the "bonded" band. The electron-donating methyl group in 2-methoxyethylamine would be expected to increase the NH···O hydrogen bond strength over what it is in ethanolamine, but it would at the same time increase the repulsion between the O and N atoms in the *gauche* conformation. The latter factor, which dominates over the weak NH···O bond in ethanolamine, becomes even more important in 2-methoxyethylamine. The angular nature of the NH···O bond removes the screening effect of the H atom between the N and O atoms and also weakens the attractive interaction.

Although the early work of Smith and Creitz (20) on association of simple alcohols in CCl_4 solution gave some evidence for a characteristic "terminal" OH group frequency of an acyclic dimer at 3 636 cm^{-1} for a monomeric "free" OH group (21), an analysis of all the more recent work suggests that the terminal OH group of the open dimer absorbs at the same frequency as the monomer (22). This is also considered to be the case in intramolecular OH···OH hydrogen bonds in various diols (23, 24, 25).

The question as to why a terminal OH in an intramolecular NH···OH system absorbs at a slightly lower frequency than a "free" OH, whereas a terminal OH in an intramolecular OH···OH system with similar geometry does not, remains to be answered. A possible explanation lies in the relative polarizabilities of the proton donating group and the proton accepting group. For the NH···OH system, the OH dipole fluctuation during vibration would be accompanied by changes in the oxygen lone pair dipole, which may induce charge fluctuation in the more mobile N lone pair orbital and thus exercise a damping effect on the vibration of the terminal OH, thereby lowering its frequency. Non-linearity of the hydrogen bond would augment interactions of this nature.

Following this argument further, the terminal NH frequency in an intramolecular OH···NH system would not be expected to differ from the corresponding "free" NH frequency because dipole oscillations during an NH vibration are smaller than in an OH vibration, and because the polarizability of the O atom is not as great as that of the N atom.

Can. J. Chem. Downloaded from www.nrcresearchpress.com by 210.87.254.105 on 09/05/12
For personal use only.

Can. J. Chem. Downloaded from www.nrcresearchpress.com by 210.87.254.105 on 09/05/12
For personal use only.

Previous infrared investigations of 1,2-aminoalcohols do not deal with the 3 625 cm^{-1} "terminal" OH band. Sicher, Horak, and Svoboda (13) obtained spectra of some 2-aminocyclanols using a LiF prism spectrophotometer but note only one NH_2 band (presumably a composite of the antisymmetric vibrations of "free" and "bonded" NH_2 groups) without discussing NH···O bonding. It is not possible to draw any conclusions concerning the "terminal" OH band from the spectra of *cis*- and *trans*-2-aminocycloundecanol published in their paper. Drefahl and Heublein (26) show shoulders on the low frequency side of the "free" OH bands in *trans*-2-aminocyclohexanol, *cis*-2-aminocyclohexanol, and 1-amino-2-hydroxytetraline, but do not comment on them. Burford, Hewgill, and Jeffries (27) report low resolution data for some 2- and 3-aminocyclohexanols. Kuhn, Luettke, and Mecke (8) do not discuss intramolecular NH···OH hydrogen bonding and its effect on the OH group which is acting as a base.

In 3-aminopropanol the OH···N interaction is much greater than it is in ethanolamine, as measured by comparison of the bonded/free intensity ratios and the ν_{OH} shifts which are 243 and 115 cm^{-1} respectively. This can be accounted for by more favourable geometry for intramolecular hydrogen bonding in the six-membered ring. The large ν_{OH} shift in 3-aminopropanol masks the NH bands completely, but the "terminal" OH band is present 12 cm^{-1} lower than the "free" OH band. In 3-methoxypropylamine the antisymmetric NH_2 stretching band is wide ($\Delta\nu_{\frac{1}{2}}^{a} \sim 25.5$ cm^{-1} compared to 20.5 cm^{-1} in 2-methoxyethylamine) and has a flattened maximum, suggesting that it is composed of two closely spaced bands of equal intensity. On going from a five- to a six-membered ring the net NH···O attraction has also been increased.

The enthalpy difference between *trans* and OH···N hydrogen bonded *gauche* forms of *N*,*N*-dimethylethanolamine ($\Delta H = -2.8 \pm 0.2$ kcal/mole) is much greater than the corresponding difference for ethanolamine itself and for *N*-methylethanolamine ($\Delta H = -0.7 \pm 0.1$ and -0.7 ± 0.2 kcal/mole respectively). Within the uncertainty of these measurements there is no detectable increase in the relative stability of the *gauche* conformer in going from ethanolamine to the *N*-methyl derivative, although there is a large increase in the relative stability of the *gauche* conformer for *N*,*N*-dimethylethanolamine. This can be ascribed to the change in basicity of the N atom which is in the order $RNH_2 < R_2NH \ll R_3N$ for the base strengths of *n*-alkyl amines towards protonic acids in non-aqueous solvents (*4b*). The usual pK_b values determined in aqueous solution are altered by solvation effects to lead to an apparent basicity order $R_2NH > RNH_2 > R_3N$ towards a small acid (where F- and B-strain are absent). These values therefore do not measure the nitrogen lone pair electron density, which is increased by the substitution of methyl groups. Another factor which may contribute to the large increase in $-\Delta H$ on going from $HOCH_2CH_2NHCH_3$ to $HOCH_2CH_2N(CH_3)_2$ is the "Thorpe–Ingold effect" (28). Crowding of the two methyl groups on the nitrogen may increase the $H_3C—N—CH_3$ angle, with an accompanying decrease in the angle the N lone pair orbital makes with the C—N bond. This would favor OH···N interaction in the five-membered ring.

Using infrared techniques, Zeegers-Huyskens, Lamberts, and Huyskens (29) have investigated intermolecular OH···N hydrogen bonding in alcohol–amine systems in CCl_4 using low ($\sim$0.015 *M*) alcohol concentrations and amine concentrations 3–30 times as high. No competitive intermolecular OH···N and NH···O hydrogen bonding studies have been reported, and such investigations would be difficult because of the large ν_{OH} shift which would mask the NH bands. The high rate of proton exchange in alcohol–amine solutions as deduced from n.m.r. measurements has been attributed to coordinated migration of the protons in complexes involving two non-linear hydrogen bonds of the following type (30).

It is not known whether such hydrogen bonding interaction is possible if the N and O atoms are tied together by a two carbon chain as in ethanolamine. A cyclic complex involving three non-linear hydrogen bonds has been suggested (31) for primary amine – alcohol mixtures in an inert solvent.

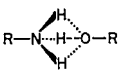

The hydrogen bond enthalpies determined calorimetrically (32) for the systems ROH + n-$BuNH_2$ = −7.48 kcal/mole, ROH + Et_2NH = −5.28 kcal/mole, and ROH + Et_3N = −4.89 kcal/mole have been interpreted in terms of triply, doubly, and singly hydrogen bonded complexes respectively.

The main contributions of this paper are (*a*) the characterization of a "terminal" OH vibration in intramolecular NH···OH hydrogen bonds, and (*b*) the presentation of spectral data which indicate that in ethanolamine, N-methylethanolamine, and 2-methoxyethylamine the *gauche* conformer with an intramolecular NH···O hydrogen bond appears to be thermodynamically less stable than the corresponding *trans* conformer. This focuses attention on the delicate balance between the exothermic contributions (electrostatic, delocalization, and dispersion forces) and the endothermic contribution (repulsive force between O and N) to the overall NH···O interaction energy (33) in these systems.

ACKNOWLEDGMENTS

The financial assistance of the National Research Council of Canada is gratefully acknowledged.

REFERENCES

1. E. D. Bergmann, E. Gil-Av, and S. Pinchas. J. Am. Chem. Soc. **75**, 68 (1953).
2. M. St. C. Flett. Spectrochim. Acta, **10**, 21 (1957).
3. H. H. Freedman. J. Am. Chem. Soc. **83**, 2900 (1961).
4. L. N. Ferguson. The modern structural theory of organic chemistry. Prentice-Hall, Inc., Englewood Cliffs, New Jersey. 1963. (*a*) p. 128 (*b*) p. 291.
5. T. Kanzawa. Bull. Chem. Soc. Japan, **29**, 398, 479, 604 (1956).
6. J. J. Fox and A. E. Martin. Trans. Faraday Soc. **36**, 897 (1940).
7. H. D. Mettee. Ph.D. Thesis, University of Alberta, Calgary. 1964.
8. M. Kuhn, W. Luettke, and R. Mecke. Z. Anal. Chem. **170**, 106 (1959).
9. R. M. Badger and S. H. Bauer. J. Chem. Phys. **5**, 839 (1937).
10. A. Allerhand and P. von R. Schleyer. J. Am. Chem. Soc. **85**, 371 (1963).
11. H. J. Bernstein. *Cited in* R. West, D. L. Powell, L. S. Whatley, M. K. T. Lee, and P. von R. Schleyer. J. Am. Chem. Soc. **84**, 3221 (1962).
12. P. J. Krueger and H. D. Mettee. Can. J. Chem. **42**, 326 (1964).
13. J. Sicher, M. Horak, and M. Svoboda. Collection Czech. Chem. Commun. **24**, 950 (1959).
14. D. W. Smith. Unpublished results, this laboratory.
15. T. G. Bonner and R. A. Hancock. Chem. Ind. London, 267 (1965).
16. A. M. de Roos and G. A. Bakker. Rec. Trav. Chim. **81**, 219 (1962).
17. J. Pitha. *Reported by* M. Tichy. Chem. Listy, **54**, 536 (1960).
18. P. J. Krueger and H. D. Mettee. Can. J. Chem. **42**, 347 (1964).
19. J. B. Hyne. Can. J. Chem. **39**, 2536 (1961).
20. F. A. Smith and E. C. Creitz. J. Res. Natl. Bur. Std. **46**, 145 (1951).
21. R. N. Jones and C. Sandorfy. *In* Chemical applications of spectroscopy. Technique of Organic Chemistry Series. Vol. IX. *Edited by* A. Weissberger. Interscience Publishers, Inc., N.Y. 1956. pp. 419–420.
22. G. C. Pimentel and A. L. McClellan. The hydrogen bond. W. H. Freeman and Co., San Francisco. 1960. pp. 96–98.
23. L. P. Kuhn. J. Am. Chem. Soc. **74**, 2492 (1952).

Can. J. Chem. Downloaded from www.nrcresearchpress.com by 210.87.254.105 on 09/05/12
For personal use only.

24. L. L. INGRAHAM, J. CORSE, G. F. BAILEY, and F. STITT. J. Am. Chem. Soc. **74**, 2297 (1952).
25. L. P. KUHN, P. VON R. SCHLEYER, W. F. BAITINGER, JR., and L. EBERSON. J. Am. Chem. Soc. **86**, 650 (1964).
26. G. DREFAHL and G. HEUBLEIN. Chem. Ber. **94**, 915 (1961).
27. R. R. BURFORD, F. R. HEWGILL, and R. R. JEFFRIES. J. Chem. Soc. 2937 (1957).
28. P. VON R. SCHLEYER. J. Am. Chem. Soc. **83**, 1368 (1961).
29. T. ZEEGERS-HUYSKENS, L. LAMBERTS, and P. HUYSKENS. J. Chim. Phys. 521 (1962).
30. T. ZEEGERS-HUYSKENS, P. HUYSKENS, and P. VAN TIGGELEN. Bull. Soc. Chim. Belges, **70**, 386 (1961). P. HUYSKENS and T. ZEEGERS-HUYSKENS. Bull. Soc. Chim. Belges, **70**, 511 (1961).
31. P. HUYSKENS and T. ZEEGERS-HUYSKENS. Bull. Soc. Chim. Belges, **69**, 267 (1960).
32. L. LAMBERTS and T. ZEEGERS-HUYSKENS. J. Chim. Phys. 435 (1963).
33. C. A. COULSON. *In* Hydrogen bonding. *Edited by* D. Hadzi. Pergamon Press, N.Y. 1959. pp. 339–360.

Can. J. Chem. Downloaded from www.nrcresearchpress.com by 210.87.254.105 on 09/05/12
For personal use only.

Can. J. Chem. Downloaded from www.nrcresearchpress.com by 210.87.254.40 on 09/05/12
For personal use only.

FORMATION OF CYCLIC *O*-2′-HYDROXYETHYLIDENE ACETALS FROM POLYALCOHOLS OF 4-*O*-LINKED POLYSACCHARIDES[1]

P. A. J. GORIN AND J. F. T. SPENCER
National Research Council of Canada, Prairie Regional Laboratory, Saskatoon, Saskatchewan
Received June 3, 1965

ABSTRACT

Partial acid hydrolysis of polyalcohols derived from some 1,4-*O*-linked polysaccharides gave cyclic *O*-2′-hydroxyethylidene derivatives as by-products in yields of 6–18%. Polysaccharides containing β-links such as *Rhodotorula glutinis* mannan and cellulose gave rise to 6-membered ring acetals with lesser amounts of the 5-membered ring form. On the other hand, two α-linked polyalcohols, obtained following partial and complete oxidation of starch with sodium periodate, were converted to 5-membered *O*-2′-hydroxyethylidene acetals.

In a previous publication oxidation of the exocellular mannan from *Rhodotorula glutinis* with periodic acid and reduction with sodium borohydride to a polyalcohol was described (1). Partial hydrolysis of the polyalcohol gave as the main product 2-*O*-β-D-mannopyranosyl-D-erythritol which arose from alternate 3-*O*- and 4-*O*-β-D-mannopyranosyl units in the mannan. Paper chromatographic examination showed two minor products running at 1.7 (A) and 2.1 (B) times the rate of 2-*O*-β-D-mannopyranosyl-D-erythritol (1). To obtain good yields of A and B for characterization purposes, various hydrolysis conditions have now been investigated and the most suitable appeared to be hydrolysis for 1 h at 100° in an aqueous solution adjusted to pH 2 with hydrochloric acid. Coincidentally, these experimental conditions gave an optimum yield of 2-*O*-β-D-mannopyranosyl-D-erythritol. More prolonged heating caused further hydrolysis to mannose and erythritol. These hydrolysis conditions differ from those of Smith and co-workers (2) who used 0.5 *N* hydrochloric acid at room temperature for 8 h to degrade oat glucan polyalcohol to 2-*O*-β-D-glucopyranosyl-D-erythritol, its 1,3-*O*-(2′-hydroxyethylidene) derivative (3) and other related products. Oat glucan is similar to the above mannan in that it has 1,3-β- and 1,4-β-pyranosyl units distributed along a polymer chain.

In a larger scale experiment the mannan polyalcohol hydrolysate was fractionated on cellulose, and A and B were isolated in yields of 15% and 3% respectively based on polyalcohol. Compound A was crystalline and, based on the observed molecular weight of 316, consumed 2 moles of sodium periodate with concomitant release of 1 mole of acid. Methylation gave a crystalline hexa-*O*-methyl ether which was hydrolyzed to two products detectable on a paper chromatogram. One of these was obtained by extraction of the aqueous hydrolysate with chloroform and was tentatively identified as 2,3,4,6-tetra-*O*-methyl-D-mannose. The other remained in the aqueous phase and was shown to be 4-*O*-methyl-D-erythritol which was characterized as its crystalline tris-*p*-nitrobenzoate. Partial hydrolysis of A gave 2-*O*-β-D-mannopyranosyl-D-erythritol which was isolable only in low yield since the stability of the *O*-2′-hydroxyethylidene group was close to that of the glycosidic link. The above information indicates that A is 1,3-*O*-(2′-hydroxyethylidene)-2-*O*-β-D-mannopyranosyl-D-erythritol (III; R = β-D-Manp), similar to 1,3-*O*-(2′-hydroxyethylidene)-2-*O*-β-D-glucopyranosyl-D-erythritol obtained from oat glucan polyalcohol (3), via an acid-catalyzed acetal migration reaction.

[1]*Issued as N.R.C. No. 8628.*

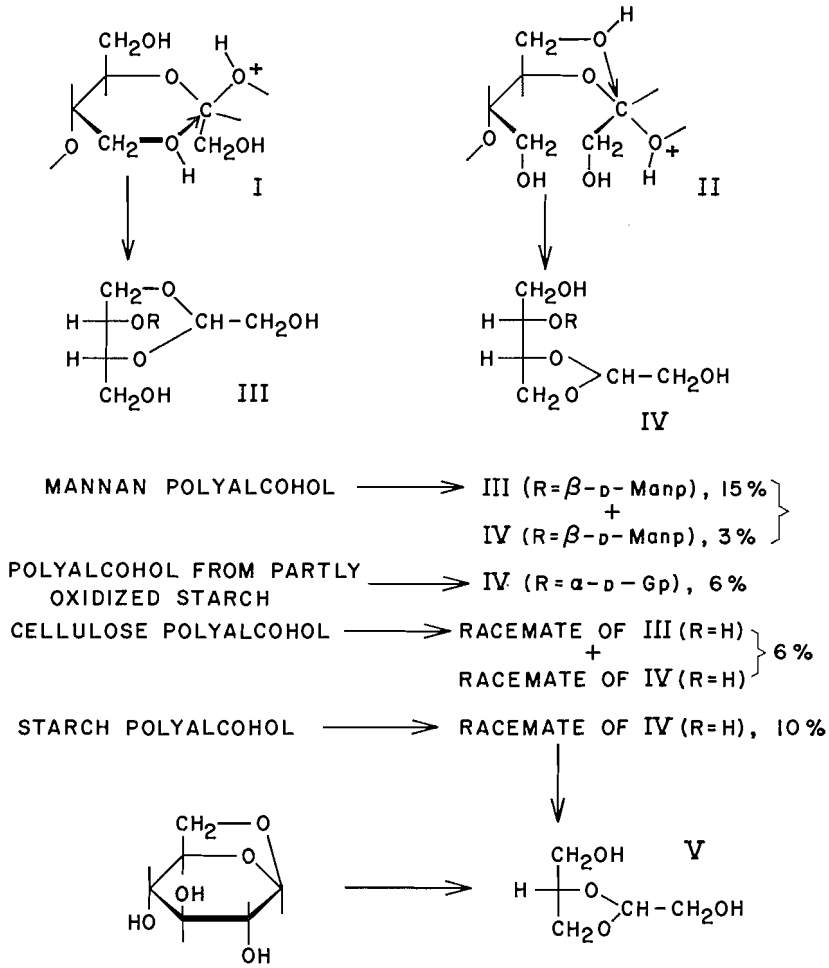

The amorphous minor product B consumed 1.8 moles of periodate with formation of 0.9 moles of acid, and on partial hydrolysis gave 2-*O*-β-D-mannopyranosyl-D-erythritol and a compound corresponding to glycolaldehyde on thin-layer chromatography (t.l.c.) using silica gel plates. Methylation of B followed by hydrolysis provided 1-*O*-methyl-D-erythritol characterized as its tris-*p*-nitrobenzoate and a sugar corresponding to 2,3,4,6-tetra-*O*-methyl mannose on a paper chromatogram. Compound B is therefore in all likelihood 3,4-*O*-(2′-hydroxyethylidene)-2-*O*-β-D-mannopyranosyl-D-erythritol (IV; R = β-D-Manp).

To obtain further information on the acetal migration reaction, a polysaccharide containing 1,4-α-hexopyranosyl units was used as starting material. Accordingly starch was oxidized with 0.4 moles of sodium periodate per anhydroglucose unit, and the product was isolated and reduced with sodium borohydride. Partial hydrolysis of the polyalcohol gave a complex mixture including compound C which ran at 1.6 times the rate of 2-*O*-α-D-glucopyranosyl-D-erythritol on a paper chromatogram. Chromatography of the mixture on cellulose provided compound C in 6% yield. Partial hydrolysis of this product gave 2-*O*-α-D-glucopyranosyl-D-erythritol and glycolaldehyde, the latter being characterized by conversion to glyoxal bis-2,4-dinitrophenylhydrazone. Methylation of C followed by

Can. J. Chem. Downloaded from www.nrcresearchpress.com by 210.87.254.40 on 09/05/12
For personal use only.

hydrolysis of the resulting hexa-*O*-methyl ether provided 2,3,4,6-tetra-*O*-methyl-D-glucose and sirupy 1-*O*-methyl-D-erythritol, which was converted to its tribenzoate. These data show that C has the 3,4-*O*-(2′-hydroxyethylidene)-2-*O*-α-D-glucopyranosyl-D-erythritol (IV; R = α-D-Gp) structure.

Other polyalcohols from polysaccharides containing 1,4-α- and 1,4-β-glucopyranosyl units were partially hydrolyzed and gave rise to 5- and 6-membered *O*-2′-hydroxyethylidene acetal rings, respectively.

Cellulose was oxidized in the presence of excess sodium periodate and the product was reduced with sodium borohydride. The resulting cellulose polyalcohol was partially hydrolyzed and resulting glycolaldehyde was destroyed with hot aqueous barium hydroxide. The reaction product was examined on paper chromatograms, and erythritol and two faster moving minor components were detected. These by-products (racemates of III (R = H) and IV (R = H)) were isolated as a mixture by cellulose chromatography in 6% yield and converted to their *p*-nitrobenzoates which were separated by fractional crystallization. The minor product crystallized initially and was identical with 3,4-*O*-(2′-hydroxyethylidene)-DL-erythritol tris-*p*-nitrobenzoate, described later. The mother liquors provided a tris-*p*-nitrobenzoate which was deesterified to the racemate of III (R = H). This was hydrolyzable to erythritol and since it was not oxidized with sodium periodate the erythritol residue was substituted in the 1,3 or 2,3 positions. The n.m.r. (nuclear magnetic resonance) spectrum of the derivative was indistinguishable from that of 1,3-*O*-(2′-hydroxyethylidene)-L-erythritol tris-*p*-nitrobenzoate and differed from that of the 2,3-*O*-isomer. The derivative had zero specific rotation and was therefore racemic. Authentic specimens, kindly supplied by Dr. N. K. Richtmyer, were obtained by oxidation of anhydroheptosans with sodium periodate and subsequent hydrogenation (4, 5).

Fully oxidized starch, on treatment in the above manner, was converted to the polyalcohol which was partially hydrolyzed to give sirupy 3,4-*O*-(2′-hydroxyethylidene)-DL-erythritol (racemate of IV (R = H)) in 10% yield. On periodate oxidation followed by sodium borohydride reduction and hydrolysis, this was converted to glycerol, which contained a trace of erythritol. Compound IV (R = H) was purified via its crystalline tris-*p*-nitrobenzoate which was characterized as follows. Deesterification and oxidation of the product with periodic acid followed by sodium borohydride reduction of the resulting glyceraldehyde derivative yielded 2,3-*O*-(2′-hydroxyethylidene)-DL-glyceritol (racemate of V), which was converted to its optically inactive bis-*p*-nitrobenzoate. The n.m.r. spectrum of this compound was identical with the bis-*p*-nitrobenzoate of the D-isomer (V), obtained following oxidation of levoglucosan with periodic acid and reduction of the product by sodium borohydride. Although inversion at C-2′ of the D-isomer during its preparation seems likely, by analogy with the acid-catalyzed conversion of the thermodynamically unstable methyl 4,6-*O*-benzylidene 2,3-di-*O*-methyl α-D-glucoside to the stable form (6), definite proof of this is lacking.

Formation of 5-membered *O*-2′-hydroxyethylidene acetal rings from a polysaccharide containing 1,4-α-hexopyranosyl units occurs. This contrasts with preferential formation of 6-membered acetal rings from the polysaccharides with 1,4-β-hexopyranosyl units. Simultaneous protonation of the oxygen originally involved in the glycosidic link (before periodate oxidation) and nucleophilic attack at C-1 by a primary hydroxyl group of the erythritol moiety appears to take place (as in I and II) resulting in formation of cyclic acetals (III and IV). Since the acetal migration reaction appears to be controlled by kinetic factors the size of the resulting ring should depend on the relative proximity to C-1 of the two available primary hydroxyl groups in the erythritol residue(s).

Can. J. Chem. Downloaded from www.nrcresearchpress.com by 210.87.254.40 on 09/05/12
For personal use only.

Formation of small amounts of *O*-2′-hydroxyethylidene acetals from a variety of polyalcohols shows that care should be exercised in using the Smith degradation for structural analysis of polysaccharides. Conclusions drawn from paper chromatographic evidence should be checked by isolation and characterization of the reaction products.

EXPERIMENTAL

Specific rotations were measured at 25°. Nuclear magnetic resonance measurements were carried out with a Varian HA 100 n.m.r. spectrometer with tetramethyl silane as standard. *n*-Butanol–ethanol–water (40:11:19 v/v) was used as solvent for paper chromatography and chloroform–methanol–water (90:10:1 v/v) for t.l.c.

Formation of 1,3-O- and 3,4-O-(2′-Hydroxyethylidene)-2-O-β-D-mannopyranosyl-D-erythritol (A and B respectively) from Rhodotorula glutinis Mannan Polyalcohol

A 1% aqueous solution of mannan polyalcohol was adjusted to pH 2 with hydrochloric acid and then heated at 100°. Aliquots were taken out at intervals and neutralized (Ag_2CO_3), and the products were examined on paper chromatograms (spray: ammoniacal silver nitrate). 2-*O*-β-D-Mannopyranosyl-D-erythritol and spots running at 1.7 (A) and 2.1 (B) times the rate of the above polyol were detected. (No spots were detected initially using the *p*-anisidine hydrochloride spray). During the first 3 h only these three components were detected, but thereafter mannose and erythritol were formed, in trace amounts at first, but in high proportion after 24 h. The spot intensities of A and B decreased after 1–3 h, the latter more rapidly.

Characterization of A (III; R = β-D-Manp)

The mannan polyalcohol (3.5 g) was hydrolyzed at 100° for 1 h in water (250 ml) adjusted to pH 2 with hydrochloric acid. After neutralization (Ag_2CO_3), the mixture was fractionated on a cellulose column using *n*-butanol one-half saturated with water as solvent, and A (0.42 g), B (0.09 g), and 2-*O*-β-D-mannopyranosyl-D-erythritol (1.67 g) were eluted. Two recrystallizations from ethanol gave compound A with m.p. 168–170° and $[\alpha]_D$ −3° (*c*, 1.0 MeOH). It consumed 2 moles of sodium periodate with concomitant release of 1 mole of acid.

Anal. Calcd. for $C_{12}H_{22}O_{10}$: C, 44.17; H, 6.80; mol. wt., 326. Found: C, 44.3; H, 6.8; mol. wt. in H_2O, 316.

Its n.m.r. spectrum in D_2O precluded a methyl orthoformate group which is possible from the analytical figures.

Hydrolysis of A for 20 h at 100° with 0.01 *N* hydrochloric acid gave 2-*O*-β-D-mannopyranosyl-D-erythritol, which was isolated in 30% yield by cellulose chromatography (solvent: *n*-butanol one-half saturated with water). It was crystallized from methanol–ethanol and had m.p. 82–86° and $[\alpha]_D$ −36° (*c*, 0.9 MeOH) and its X-ray diffraction pattern was identical with that of an authentic specimen. Gorin and Spencer (1) reported m.p. 87–90° (from EtOH) and $[\alpha]_D$ −36° (*c*, 1.1 H_2O). Another hydrolysis product, glycolaldehyde, was detected with Bredig's reagent as a yellow spot R_f 0.4, on an orange background, or as a brown spot with the 50% sulfuric acid spray.

Compound A (0.30 g) was methylated at room temperature using the sodium hydroxide – dimethyl sulfate procedure of Haworth (7). Dimethyl sulfate was destroyed by heating the solution at 100°, and following neutralization the product was isolated by continuous chloroform extraction. The extract was methylated to completion with silver oxide in refluxing methyl iodide (8). The resulting hexa-*O*-methyl ether was recrystallized twice from *n*-hexane to give material (0.20 g) with m.p. 63–64° and $[\alpha]_D$ −8° (*c*, 1.0 EtOH).

Anal. Calcd. for $C_{18}H_{34}O_{10}$: C, 52.67; H, 8.35; mol. wt., 410. Found: C, 52.4; H, 8.2; mol. wt. in Me_2CO, 418.

A portion (0.10 g) of the ether was hydrolyzed with *N* sulfuric acid (5 ml) at 100° for 18 h. Neutralization ($BaCO_3$), filtration, and five extractions with chloroform removed tetra-*O*-methyl mannose (63 mg) which gave a red spot on a paper chromatogram with the *p*-anisidine hydrochloride spray. The remaining sirupy 4-*O*-methyl-D-erythritol (32 mg) ran at 1.2 times the rate of glycerol on a paper chromatogram (ammoniacal silver nitrate spray), had $[\alpha]_D$ +13° (*c*, 2.0 EtOH), and was characterized by conversion to its tris-*p*-nitrobenzoate; m.p. 154–157° (from EtOAc) and $[\alpha]_D$ −72° (*c*, 0.9 $CHCl_3$).

Anal. Calcd. for $C_{26}H_{21}O_{13}N_3$: C, 53.52; H, 3.63. Found: C, 53.4; H, 3.65.

This material gave an X-ray diffraction pattern identical with authentic material prepared in the following manner.

Charlson and Perlin (9) have shown that in acetic acid 6-*O*-methyl-D-glucose consumes 2 moles of lead tetraacetate in forming di-*O*-formyl-4-*O*-methyl-D-erythrose. Accordingly, a solution of 6-*O*-methyl-D-glucose (0.18 g) in acetic acid (50 ml) containing water (2 ml) was treated with 2.0 moles of 1% lead tetraacetate in acetic acid. After 30 min 1.85 moles of oxalic acid in acetic acid was added, the precipitate of lead oxalate was filtered off, and the filtrate was evaporated to dryness. To the residue sodium borohydride (0.20 g) in water (20 ml) was added, and after 1 h excess reagent was destroyed with acetic acid. The solution was evaporated and boric acid was removed by repeated evaporation from methanol. Extraction of the residue

Can. J. Chem. Downloaded from www.nrcresearchpress.com by 210.87.254.40 on 09/05/12
For personal use only.

with ethyl acetate gave 4-*O*-methyl-D-erythritol with $[\alpha]_D$ +9° (*c*, 2.5 EtOH). Its tris-*p*-nitrobenzoate had m.p. 151–154° and $[\alpha]_D$ −72° (*c*, 1 $CHCl_3$).

Anal. Calcd. for $C_{26}H_{21}O_{13}N_3$: C, 53.52; H, 3.63. Found: C, 53.6; H, 3.35.

Smith *et al.* (10) reported m.p. 162.5–164° (from Me_2CO–EtOH) and $[\alpha]_D^{22}$ +80° (*c*, 1 $CHCl_3$) for the tris-*p*-nitrobenzoate of the enantiomer.

Characterization of B (IV; R = β-D-Manp)

Using the same procedure as in the partial hydrolysis of A, a sample of B (30 mg) was converted to 2-*O*-β-D-mannopyranosyl-D-erythritol, which after crystallization from methanol–ethanol had m.p. and mixed m.p. 81–84° and gave an X-ray diffraction pattern identical with that of authentic material. Glycolaldehyde appeared to be formed also, as shown by t.l.c. Periodate oxidation of B for 24 h resulted in consumption of 1.8 moles of oxidant with release of 0.9 moles of acid.

Methylation of B (93 mg) gave a derivative (87 mg) which was shown to be fully methylated since it gave after hydrolysis two spots on t.l.c. (spray: 50% sulfuric acid) which corresponded to 2,3,4,6-tetra-*O*-methyl-D-mannose and 4-*O*-methyl-D-erythritol (or its enantiomer). The mobilities and color reactions of the products on paper chromatograms with *p*-anisidine hydrochloride and ammoniacal silver nitrate sprays were identical with authentic specimens. 1-*O*-Methyl-D-erythritol was isolated by the previously described procedure and converted to its tris-*p*-nitrobenzoate which had m.p. 150–153° (from EtOAc) and $[\alpha]_D$ +75° (*c*, 1.0 $CHCl_3$).

Anal. Calcd. for $C_{26}H_{21}O_{13}N_3$: C, 53.52; H, 3.63. Found: C, 53.5; H, 3.4.

Its X-ray diffraction pattern was identical with that of 4-*O*-methyl-D-erythritol tris-*p*-nitrobenzoate. Since the compound derived from B had a specific rotation which was equal and opposite to the 4-*O*-methyl derivative, the 1-*O*-methyl-D-erythritol tris-*p*-nitrobenzoate structure is indicated.

3,4-O-(2′-Hydroxyethylidene)-2-O-α-D-glucopyranosyl-D-erythritol (C or IV (R = α-D-Gp)) from Starch Modified with Sodium Periodate (0.4 Mole) and Sodium Borohydride

Soluble starch (22.8 g) was oxidized with aqueous sodium periodate (12.2 g in 500 ml) for 10 d. The resulting dialdehyde starch was precipitated by addition of acetic acid (2.5 l), filtered off, and washed with acetic acid. The dried isolated product was added with stirring to a solution of sodium borohydride (5.0 g) in water (1 l). After 24 h the solution was adjusted to pH 7 and evaporated to dryness and boric acid was removed by repeated evaporation from methanol. The product was dissolved in water (500 ml) and isolated after precipitation with 4 volumes of methanol. Yield, 16.0 g.

The resulting starch polyalcohol (9.5 g) was partially hydrolyzed in a similar manner to the mannan polyalcohol. The product was refluxed in methanol and 6.7 g of soluble material was isolated. On a paper chromatogram the mixture gave spots corresponding to erythritol, 2-*O*-α-D-glucopyranosyl-D-erythritol, and many slower moving materials. In addition compound C running at 1.6 times the rate of 2-*O*-α-D-glucopyranosyl-D-erythritol was detected. Chromatography of the hydrolysate on cellulose using *n*-butanol one-half saturated with water as solvent gave compound C as a sirup (0.54 g) with $[\alpha]_D$ +107° (*c*, 1.0 MeOH).

Compound C (200 mg) was methylated by the previously described procedure to give its hexa-*O*-methyl ether (236 mg). Hydrolysis of a portion (200 mg) gave two detectable products corresponding to tetra-*O*-methyl-glucose and 1-*O*-methyl-erythritol when examined by paper chromatography and t.l.c. Fractionation of the hydrolysate by the previously described method (methylation of A) gave 2,3,4,6-tetra-*O*-methyl-D-glucose (109 mg) which was recrystallized twice from *n*-hexane to give material with m.p. and mixed m.p. 81°. The other component, 1-*O*-methyl-D-erythritol (46 mg), was converted to its tribenzoate which had m.p. 99–100° (from ethyl acetate – *n*-hexane) and $[\alpha]_D$ +44° (*c*, 1.0 $CHCl_3$).

Anal. Calcd. for $C_{26}H_{24}O_{17}$: C, 69.63; H, 5.39. Found: C, 69.4; H, 5.5.

The derivative gave an X-ray diffraction pattern identical with that of 4-*O*-methyl-D-erythritol tribenzoate (m.p. 98–100°, $[\alpha]_D$ −38° (*c*, 0.8 $CHCl_3$). Found: C, 70.0; H, 5.3). The specific rotations therefore show that the two tribenzoates were enantiomers.

Compound C (76 mg) was partially hydrolyzed with 0.01 *N* sulfuric acid (10 ml) at 100° for 24 h. The solution was neutralized ($BaCO_3$), filtered, and evaporated to a mixture which was examined by t.l.c. (sprays: 50% sulfuric acid and Bredig's reagent). One of the spots co-chromatographed with glycolaldehyde. Chromatography of the remainder on cellulose (solvent: *n*-butanol one-half saturated with water) gave 2-*O*-α-D-glucopyranosyl-D-erythritol (43 mg) which was recrystallized three times from methanol–ethanol. It had m.p. 134–135° and $[\alpha]_D$ +136° (*c*, 0.6 H_2O) and gave an X-ray diffraction pattern identical with that of an authentic specimen. Charlson and Perlin (9) report a higher melting point of 147–148° and $[\alpha]_D$ +130° (*c*, 1.8 H_2O) for this material.

Compound C (100 mg) was partially hydrolyzed as described above and extraction of the hydrolysate with refluxing ethyl acetate gave a product (7 mg) containing glycolaldehyde (t.l.c.). This was treated with an ethanolic solution (5 ml) of 2,4-dinitrophenylhydrazine (45 mg) and acetic acid (1 ml) for 24 h under reflux. The solution was seeded with the expected product and left in the refrigerator for 1 week. A few crystals of glyoxal bis-2,4-dinitrophenylhydrazone were formed which had m.p. and mixed m.p. 308–312° and gave an X-ray diffraction pattern identical with that of an authentic specimen.

3,4-O-(2′-Hydroxyethylidene)-DL-erythritol (Racemate of IV (R = H)) from Starch Polyalcohol

Starch polyalcohol (7.5 g) prepared from completely oxidized soluble starch was partially hydrolyzed

Can. J. Chem. Downloaded from www.nrcresearchpress.com by 210.87.254.40 on 09/05/12
For personal use only.

according to the previously described conditions. Erythritol (2.35 g), m.p. and mixed m.p. 107–109°, was isolated by crystallization from ethanol (30 ml) and the mother liquors were evaporated to a syrup (4.32 g). One-half of the sirup was heated at 100° for 1 h in aqueous barium hydroxide (5.0 g in 100 ml) to destroy glycolaldehyde. Carbon dioxide was then bubbled through to remove alkali and the precipitate of barium carbonate was removed. Fractionation of the product on a cellulose column using benzene–ethanol–water (300:50:1 v/v) as solvent gave a fraction (0.76 g), which moved at 1.2 times the speed of glycerol on a paper chromatogram. It consumed 1.0 mole of sodium periodate after 24 h, and reduction of the product with sodium borohydride and acid hydrolysis gave glycerol and a trace of erythritol (paper chromatogram).

A portion (90 mg) of IV (R = H) was converted to 3,4-*O*-(2′-hydroxyethylidene)-DL-erythritol tris-*p*-nitrobenzoate (0.31 g) with m.p. 125–127° (from EtOAc) and $[\alpha]_D$ 0° (*c*, 1.2 $CHCl_3$).

Anal. Calcd. for $C_{27}H_{21}O_{14}N_3$: C, 53.03; H, 3.46. Found: C, 53.15; H, 3.6.

3,4-*O*-(2′-Hydroxyethylidene)-DL-erythritol (200 mg), obtained on deesterification of the tris-*p*-nitrobenzoate with 0.1 *N* sodium methoxide (0.3 mole) in methanol, was oxidized overnight by periodic acid (0.40 g) in water (10 ml). The solution was neutralized ($BaCO_3$) and filtered, and the filtrate was treated with sodium borohydride (0.20 g). After 24 h the solution was neutralized with acetic acid and evaporated to dryness, and boric acid was removed from the residue by repeated evaporation from methanol. Dissolution in water followed by continuous extraction with chloroform gave the racemate of V (0.12 g) which had $[\alpha]_D$ 0° (*c*, 3.2 EtOH) and gave glycerol (paper chromatogram) on acid hydrolysis. It was converted to 2,3-*O*-(2′-hydroxyethylidene)-DL-glyceritol bis-*p*-nitrobenzoate with m.p. 90–92° (from EtOAc–*n*-hexane) and $[\alpha]_D$ 0° (*c*, 2 $CHCl_3$).

Anal. Calcd. for $C_{19}H_{16}O_{10}N_2$: C, 52.78; H, 3.73. Found: C, 52.4; H, 3.68.

The derivative gave a complex n.m.r. spectrum in chloroform which was identical with that of 2,3-*O*-(2′-hydroxyethylidene)-D-glyceritol tris-*p*-nitrobenzoate, obtained from levoglucosan following successive periodic acid and sodium borohydride treatments. The polyol V obtained in this way had $[\alpha]_D$ +8.5° (*c*, 3.6 EtOH), and its derived bis-*p*-nitrobenzoate (from EtOAc) had m.p. 100–101° and $[\alpha]_D$ −17° (*c*, 1.1 $CHCl_3$).

Anal. Calcd. for $C_{19}H_{16}O_{10}N_2$: C, 52.78; H, 3.73. Found: C, 52.6; H, 3.8.

2,3-*O*-(2′-Hydroxyethylidene)-D-glyceritol prepared by periodic acid and sodium borohydride treatment of levoglucosan gave an n.m.r. spectrum in D_2O which was identical with that of a specimen prepared using sodium periodate and sodium borohydride as reagents. In the latter experiment the pH of the reaction solutions was kept above 7.

O-(2′-Hydroxyethylidene)-erythritols (Racemates of III (R = H) and IV (R = H)) from Cellulose Polyalcohol

Cellulose polyalcohol (11.0 g) prepared from fully oxidized cellulose, according to the previously described method, was partially hydrolyzed. The solution was neutralized (Ag_2CO_3), filtered, and evaporated to a sirup which was dissolved in hot ethanol (50 ml). On cooling, crystallization of erythritol (4.68 g), m.p. and mixed m.p. 108–111° took place and after filtration the mother liquor was evaporated to a sirup (5.0 g). Half of the sirup was treated with barium hydroxide as described previously and then fractionated on a cellulose column (solvent: benzene–ethanol–water 300:50:1 v/v) to give a mixture of *O*-(2′-hydroxyethylidene)-erythritols (0.70 g) which gave rise on acid hydrolysis to erythritol. On paper chromatography two spots were detected moving at 1.2 and 1.4 times the rate of glycerol (spray: ammoniacal silver nitrate) and corresponded to the 3,4-*O*- and 1,3-*O*-isomers, respectively. The latter was the major component since successive treatments of the fraction with sodium periodate, sodium borohydride, and acid gave erythritol and a small proportion of glycerol.

A portion (0.14 g) was converted to mixed tris-*p*-nitrobenzoates which were fractionally crystallized from ethyl acetate (10 ml) to give 3,4-*O*-(2′-hydroxyethylidene)-DL-erythritol tris-*p*-nitrobenzoate (37 mg) with m.p. and mixed m.p. 125–126° and $[\alpha]_D$ 0° (*c*, 2 $CHCl_3$).

Anal. Calcd. for $C_{27}H_{21}O_{14}N_3$: C, 53.03; H, 3.46. Found: C, 52.8; H, 3.7.

Its X-ray diffraction pattern was identical with that of authentic material isolated from starch polyalcohol. Addition of a little *n*-hexane to the mother liquor gave 1,3-*O*-(2′-hydroxyethylidene)-DL-erythritol tris-*p*-nitrobenzoate (170 mg) with m.p. 131–133° and $[\alpha]_D$ 0° (*c*, 2 $CHCl_3$).

Anal. Calcd. for $C_{27}H_{21}O_{14}N_3$: C, 53.03; H, 3.46. Found: C, 53.0; H, 3.5.

The product obtained on deesterification of this tris-*p*-nitrobenzoate was not oxidized by aqueous sodium periodate. The complex n.m.r. spectrum of the tris-*p*-nitrobenzoate in chloroform was identical with the spectrum of authentic 1,3-*O*-(2′-hydroxyethylidene)-DL-erythritol (4). It differed from that of 2,3-*O*-(2′-hydroxyethylidene)-erythritol (5).

ACKNOWLEDGMENTS

The authors would like to thank Dr. N. K. Richtmyer for samples of 1,3-*O*- and 2,3-*O*-(2′-hydroxyethylidene)-erythritols. Preparation of X-ray diffraction patterns and microanalytical determinations were carried out by Mr. W. Haid, and n.m.r. spectra were obtained by Mr. M. Mazurek.

Can. J. Chem. Downloaded from www.nrcresearchpress.com by 210.87.254.40 on 09/05/12
For personal use only.

REFERENCES

1. P. A. J. GORIN and J. F. T. SPENCER. Can. J. Chem. **43**, 950 (1965).
2. I. J. GOLDSTEIN, G. W. HAY, B. A. LEWIS, and F. SMITH. Methods in carbohydrate chemistry. Vol. 5. Academic Press, N.Y. 1965. p. 361.
3. B. A. LEWIS and F. SMITH. Abstracts Papers Am. Chem. Soc. 144, 8D (1963).
4. L. C. STEWART and N. K. RICHTMYER. J. Am. Chem. Soc. **77**, 424 (1953).
5. J. W. PRATT, N. K. RICHTMYER, and C. S. HUDSON. J. Am. Chem. Soc. **75**, 4503 (1953).
6. N. BAGGETT, J. M. DUXBURY, A. B. FOSTER, and J. W. WEBBER. Chem. Ind. London, 1832 (1964).
7. W. N. HAWORTH. J. Chem. Soc. 8 (1915).
8. T. PURDIE and J. C. IRVINE. J. Chem. Soc. 1021 (1903).
9. A. J. CHARLSON and A. S. PERLIN. Can. J. Chem. **34**, 1200 (1956).
10. I. J. GOLDSTEIN, J. K. HAMILTON, and F. SMITH. J. Am. Chem. Soc. **81**, 6252 (1959).

Can. J. Chem. Downloaded from www.nrcresearchpress.com by 210.87.254.40 on 09/05/12
For personal use only.

Can. J. Chem. Downloaded from www.nrcresearchpress.com by 210.87.254.40 on 09/05/12
For personal use only.

THERMAL STABILITY OF AN ADSORBED ARRAY OF CHARGES IN THE EINSTEIN APPROXIMATION

J. Ross Macdonald and C. A. Barlow, Jr.
Texas Instruments Incorporated, Dallas, Texas
Received December 28, 1964

ABSTRACT

For an infinite hexagonal array of ions adsorbed on a conducting plane of infinite extent, the thermal fluctuation from strict lattice ordering in the neighborhood of a given adion is considered. The ions are imaged in the uniform, conducting adsorbent and are assumed to move freely in the plane; they thus arrange themselves in a perfect hexagonal array at absolute zero temperature. By use of the accurate planar potential seen by one adion moving in the field arising from an infinite number of fixed hexagonally arrayed surrounding ions, the root-mean-square (r.m.s.) amplitude of planar vibration of the ion relative to its neighbors is approximately determined for several values of nearest neighbor distances between ions, r_1. On the basis of these results, we find, for example, that for a distance, β, between the center of charge of an ion and the imaging plane of 3 Å, an ionic valence z_v of unity, and an effective dielectric constant of ϵ, a hexagonal array with $r_1 = 15$ Å is stable up to a temperature, T_0, of approximately $1760/\epsilon$ °K while one with $r_1 = 21$ Å is stable up to about $760/\epsilon$ °K. Results apply to adsorption from either a gas or liquid phase and, as well, to an array of real dipoles adsorbed on a non-conducting surface. The appropriate values for ϵ are of the order of 2 and 6, respectively, for adsorption from gas or from aqueous electrolytes. For various r_1's, explicit expressions for T_0 are obtained which depend on ϵ, β, and z_v.

INTRODUCTION

In many treatments (1–7) of the adsorption of ions from a gas phase onto a conducting plane adsorbent, it is assumed that the adions are strongly bound to the surface by physical or chemisorption forces but are free to move in the plane. If the adsorbent surface is relatively uniform and without many discrete, strongly preferred adsorption sites, then the mutual repulsion between adions will tend to make each such ion move as far away from every other ion as possible, leading, at absolute zero temperature and for surface coverage of a monolayer or less, to the establishment of a fixed hexagonal array of discrete charges, the configuration that minimizes the electrostatic energy of interaction in the plane. As the concentration of adions is quasi-statically increased, a hexagonal array will be maintained but with decreasing nearest-neighbor distance, r_1. Finally, a full hexagonally arranged monolayer of adsorbed ions will be reached when steric forces prohibit the addition of further adions in the first adsorbed layer.

At non-zero temperature, planar thermal vibrations of adsorbed ions will tend to destroy the long range order of the fixed hexagonal array. As the coverage is decreased, mutual repulsion between adions weakens because r_1 increases and, at a given non-zero temperature, a coverage will be reached where thermal energy and interaction energy are comparable and the order represented by the hexagonal array substantially disappears. Alternatively, at fixed coverage, increasing temperature will eventually lead to "melting" of the two-dimensional adsorbed structure and again the order will degrade.

This paper is concerned with establishing approximate but reasonably quantitative conditions for the loss of quasi long range order (defined later), primarily in the case of ions electrically imaged in a conducting adsorbent surface. Such imaging leads to the formation of nonideal discrete dipoles which can again form ordered hexagonal arrays at low temperatures or sufficiently high coverages. This situation of ordered dipolar arrays

has received much attention in treatments of adsorption from a gas phase, although the dipoles are usually approximated as ideal (1–6). Elsewhere, we (see ref. 8, hereafter referred to as II) have treated the situation of hexagonally arrayed, nonideal dipoles in considerable detail and have also discussed the error to be expected from using the classical electrostatic image potential. For most cases of interest, the error is small, and the classical imaging formula was used there and will also be employed herein since we shall make use here of planar potentials calculated by the methods of II.

The question of thermal stability of a hexagonal array of adions is also of importance in adsorption of ions from a liquid phase. In a number of treatments of the electrolyte double layer (9–13), it has again been assumed that at least above some minimum surface coverage, the ions adsorbed on the electrode (usually a mercury drop) arrange themselves in a fixed hexagonal array. In this situation, there is the possibility of imaging of adions in the diffuse double layer as well as in the electrode (10–13). Such imaging leads to an infinite array of image charges perpendicular to the adsorbent surface and has been termed infinite imaging (13). When the imaging in the diffuse layer is assumed to be incomplete, the situation is termed partial imaging, whose limit is the present single-imaging situation (8) when imaging in the diffuse layer (if it exists) is absent or negligible. Bell, Levine, and Mingins (14) have considered the thermal stability problem for a partial-imaging situation nearly approximating infinite imaging. Their results and method, which is based on more approximate planar potentials and calculations than those used herein, will be discussed later.

The results of the present treatment, which apply to adsorption from a gas phase and, perhaps to a somewhat lesser extent, to adsorption from an electrolyte, may be used to show under what conditions the single-imaging, hexagonal-array treatment of nonideal dipoles referred to earlier (8) is a good representation of the actual situation for an adsorbed layer of ions. Buff and Stillinger (15) have constructed a cluster integral theory of the double layer in which in treating the adsorbed ionic layer they properly account for short range forces. Hence, in their treatment the tendency of the adsorbed ions to form a lattice under conditions approaching close packing, as a result of the steric effects arising from such short range forces, is a natural consequence of the theory. It is important to recognize that the long range forces between the ions will also play a part in creating array structures. These arrays have nothing to do with steric effects and so are quite different from any arrays consistent with the Buff and Stillinger treatment. In the present work, we are concerned with the long range interaction type of array and ignore short range forces entirely. Our interest is to determine under what conditions such arrays are essentially undestroyed by thermal motion and therefore under what conditions arrays are adequate as models for the adsorbed layer. It should be pointed out that in those circumstances where the long range forces lead to array structures, the Buff and Stillinger theory loses validity: The reason for this is that in their theory (eqs. [33] *et seq.*) the long range forces are treated as a small perturbation—all Mayer f-bonds are linearized in the long range interaction and, consistent with this, contributions from the long range forces to clusters higher than first order are ignored. It is precisely in the regime where long range forces lead to array structures that such approximations become poor, however. Clearly, the treatments of Buff and Stillinger and those which assume an array model *ab initio* are complementary, but one should know where the crossover occurs, and this question, while not considered by Buff and Stillinger, is approximately answered by this paper. As we shall see, even for infinite imaging (13), where adsorbed concentrations must be somewhat

Can. J. Chem. Downloaded from www.nrcresearchpress.com by 210.87.254.40 on 09/05/12
For personal use only.

higher than for single-imaging situations in order that a hexagonal array will be formed and maintained at the usual experimental temperatures, there is an appreciable range of surface concentration less than the maximum experimentally observed concentration over which the hexagonal array seems to be a good model. The Buff and Stillinger approach seems more appropriate only at rather small adsorbed concentrations where quasi long range order has completely disappeared and where the effect of adsorption itself on measured quantities such as double-layer differential capacitance is still small.

THERMAL AVERAGING CALCULATION

Before actually attempting to estimate the degree of thermal disorder present in a lattice, it is desirable to present a physical picture of the system as the temperature is raised from absolute zero. Consider the surroundings of a given particle: At any finite temperature, the correlation between the position of that particle, taken to define the origin, and the position of any other particle is a steadily decreasing function of distance. In fact, for sufficiently large arrays there will be a distance beyond which the fluctuations of particle positions relative to the particle at the origin will be comparable to or greater than the zero-temperature lattice separation between nearest neighbors. It is consequently only within such distances that the lattice structure is a good concept. Within this distance, the environment of a particle is that of a two-dimensional "microcrystal"; beyond this distance are other particles in motion, essentially uncorrelated with the given particle and belonging to their own microcrystals. As a particle moves over the surface, some particles remote from the given one gradually leave this microcrystal and are replaced by other particles. Thus, after a sufficiently long time the original microcrystal will disappear and new microcrystals will have formed. In this respect, our two-dimensional system is different from the usual concept of a solid, three-dimensional lattice and resembles more the case of liquid crystals. Nonetheless, it is important to recognize that at any time the environment of any particle may be considered as a crystal of possibly very many lattice spacings in size. Now as the temperature is increased, the correlations between particle positions decrease and accordingly the sizes of the microcrystals decrease. Of course, provided the interaction potential between particles asymptotically falls off faster than the inverse square of the distance, all particles sufficiently remote from a given one will play an arbitrarily minor role in influencing that particle or its immediate surroundings. Accordingly, we shall say that quasi long range order exists provided the size of the microcrystals is sufficient that negligible change would result in the neighborhood of a given particle by taking the size of the microcrystals as infinite. In the present work, we shall, in fact, use the potential appropriate for an infinite array in carrying out thermal averaging.

As the temperature is raised further, quasi long range order begins to deteriorate and the particles become so agitated that eventually even the short range order, correlations between the positions of near neighbors, has dropped to a point where fluctuations play a significant role in determining even the local environment of a given particle. When the microcrystals have become only a few lattice spacings in linear dimension, a further raising of the temperature will finally destroy the obvious lattice structure and the n-body correlations remaining will become sufficiently small to be considered as mere perturbations upon a highly randomized system, as in Buff and Stillinger's (15) treatment of long range forces.

As has already been pointed out, the transition between the phase possessing indefinitely long range order and that described by microcrystals takes place at absolute zero. The

Can. J. Chem. Downloaded from www.nrcresearchpress.com by 210.87.254.40 on 09/05/12
For personal use only.

transition which concerns us here, however, is the one wherein the neighborhood of a particle ceases to resemble a lattice at all, that is, the melting of the microcrystals. It is this melting which truly affects the appropriateness of a lattice model of a particle array for practical purposes. We shall be concerned, therefore, with the regime in which this gradual phase transition takes place and shall use the term "quasi long range order" to indicate the order of a microcrystal having a minimum linear dimension sufficiently greater than r_1. Note that our treatment involves a gradual diminution of order and is not relevant to first order phase transitions which may possibly occur.

In describing melting phenomena of three-dimensional crystals, two types of criteria have been used: One of these involves macroscopic thermodynamic quantities such as chemical potentials and pressures of the two phases; the other approach (which should lead to the same results, of course) is the microscopic statistical method exemplified by the melting criterion of Lindemann. This criterion which provides that melting takes place when the root-mean-square (r.m.s.) displacement of a particle relative to its neighbors is of the order of the lattice spacing or thereabouts seems appropriate for the type of gradual loss-of-ordering transition considered here. In applying such a criterion to the present situation, the "critical" r.m.s. displacement is determined by the maximum amount of disorder deemed consistent with an array model. Thus, the value actually used amounts to a choice for which the ions fluctuate so strongly as to be somewhat weakly associated with their lattice sites but not so strongly as to destroy the appropriateness of such sites as estimates of particle positions, and hence of local potentials. Finally, some discussion is necessary regarding the basis for calculating the r.m.s. thermal motion of a given particle relative to its neighbors.

Let us consider a fixed hexagonal array of ions of charge e and their images in the plane, conducting adsorbent. Let β be the distance between the center of charge of an adion and the conducting plane and r_1 the nearest-neighbor distance for adsorbed ions. Take the origin of a rectangular coordinate system on the adsorbent surface between a given adion and its image, let x and y be in the plane, and take z positive along the outward perpendicular to the plane. For convenience define the normalized quantities $R_1 \equiv r_1/\beta$, $X \equiv x/\beta$, $Y \equiv y/\beta$, and $Z \equiv z/\beta$. Then $Z = 1$ will define the plane in which the centers of charge of the adions lie. There will be a charge at $(X, Y, Z) = (0, 0, 1)$, $(R_1, 0, 1)$, $(R_1/2, \sqrt{(3)}R_1/2, 1)$, etc.

An accurate treatment of thermal averaging should involve averaging in the plane with all adions subject to thermal motion. Since even the problem of determining the accurate potential at a given point in the $Z = 1$ plane arising from an infinite number of fixed, hexagonally arranged surrounding ions is itself quite difficult (8, 13), we shall consider the simpler problem in which the ion originally at (0, 0, 1) is allowed to move, under thermal perturbation, in the potential arising from all other ions and their images, taken to be substantially at the regular lattice sites. The solution of this problem will approximate closer and closer to the full vibration problem above as the planar r.m.s. distance of vibration from the equilibrium position at (0, 0, 1) decreases. For consistency as well as stability, of course, we demand that this r.m.s. vibration distance be sufficiently small. Since the criterion we shall use for melting of two-dimensional quasi long range order is not very precise, the accuracy and applicability of the solution of the simplified problem will be adequate for our purpose. This simplification was also made by Bell, Levine, and Mingins (14). In further support of the reasonableness of this approximation, we remark that the very same replacement of coupled particles by a system of individual particles, each

Can. J. Chem. Downloaded from www.nrcresearchpress.com by 210.87.254.40 on 09/05/12
For personal use only.

Can. J. Chem. Downloaded from www.nrcresearchpress.com by 210.87.254.40 on 09/05/12
For personal use only.

vibrating in the constant potential well representing the average interaction (calculated here as though at absolute zero) with its neighbors, was introduced by Einstein to calculate the vibrational energy of a solid (16) (see ref. 17 for an application of the Einstein model to adsorption). When Debye subsequently removed this approximation, it was seen that in spite of the introduction of coupled vibrations the Einstein and Debye theories predicted almost identical behavior except at temperatures very close to absolute zero. When we realize that except for a multiplicative constant these thermal energies predicted so accurately by the Einstein model are identical to the mean-square-displacement of the particles relative to their neighbors, we gain some optimism regarding the usefulness of our approach.

To carry out two-dimensional averaging conveniently, we need an analytic expression for the potential $\psi_a(X, Y, 1) \equiv \psi_a$ at the point $(X, Y, 1)$ arising from all charges but that originally at (0, 0, 1). Although such an expression was obtained in II, it is too complicated to lend itself readily to the weighted double integration needed in two-dimensional averaging. Thus, here we shall initially consider one-dimensional averaging along certain selected lines in the plane, then apply these results to consideration of two-dimensional motion.

Bell, Levine, and Mingins (14) have carried out their thermal stability, partial-imaging treatment using a fixed-array planar potential arrived at by two distinct types of approximation. First, only terms in the potential quadratic in x and y have been kept. Second, the doubly infinite sums remaining in the expression for the potential have been approximated by finite sums: only contributions from ions and their images lying relatively near the origin have been included. The quadratic approximation allows the integrals arising in the averaging problem to be carried out analytically. Another consequence of retaining only terms through quadratic is that to this order of approximation the potential becomes circularly symmetric. This is very convenient in determining the r.m.s. thermal displacement from the origin in the two dimensions of the planar array inasmuch as each degree of freedom contributes equally, reducing the complexity of the problem to that of one dimension. In the present calculation, however, higher order terms destroy the circular symmetry and present us with an essentially two-dimensional problem which is not so easily reduced to one dimension. Thus, we have been led to the method of studying motion along selected lines. As it turns out, the potential for single imaging in the neighborhood of the origin ($r \equiv (x^2 + y^2)^{1/2} \lesssim 0.3r_1$) is fairly well approximated by the circularly symmetric form when a hexagonal array itself is a good approximation. We shall later see in the present single-imaging case how much difference is obtained between results calculated with the quadratic approximation and the results obtained when this approximation is not made.

Figure 1 shows the potential difference $\xi \equiv \psi_a(X, Y, 1) - \psi_a(0, 0, 1)$ plotted versus the normalized distance l for several values of R_1 and several specific lines in the plane indicated by the heavy lines and arrows in the diagrams. These curves were calculated by the method described in II using $\beta = 3$ Å, $\epsilon = 1$, and positive adions of unit valence. Here ϵ is the dielectric constant in the neighborhood of adsorbed charges and l is the distance from an assumed center of one-dimensional vibration normalized by the basic triangle height $h \equiv (\sqrt{(3)}/2)r_1$. Thus for the line to which the solid curves apply, $l \equiv 2r/\sqrt{(3)}r_1 \equiv 2R/\sqrt{(3)}R_1 \equiv 4x/3r_1$, where $R \equiv r/\beta$. This particular line, a binary axis (and its five other half-line equivalents under the symmetry of the hexagonal lattice), is that along which vibration can occur most readily because the potential increases most slowly along

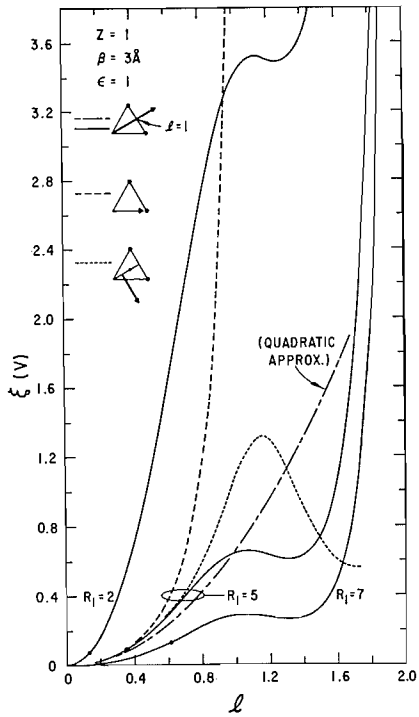

FIG. 1. The quantity $\xi \equiv \psi_a(X, Y, 1) - \psi_a(0, 0, 1)$ versus normalized distance: $l = |4X/3R_1|$, $l = (\sqrt{(3)}/2)|X/R_1|$, and $l = (1/\sqrt{3})|(4X/R_1) - 1|$, respectively, for the three directions indicated. The distance l is measured along the heavy directed lines in the diagrams.

this line. Thus, it is of the most immediate interest to obtain the r.m.s. distance, $\overline{(r^2)}^{\frac{1}{2}}$, of vibration along this line. It will be termed line 1.

Let us define $L \equiv \overline{(r^2)}^{\frac{1}{2}}/h$ as the normalized r.m.s. vibration amplitude. Then

[1]
$$L^2 = \frac{\int_0^\infty l^2 \rho(\xi) \exp(-e\xi/\epsilon kT)\, d\xi}{\int_0^\infty \rho(\xi) \exp(-e\xi/\epsilon kT)\, d\xi} = \frac{\int_0^{l\max} l^2 \exp(-e\xi/\epsilon kT)\, dl}{\int_0^{l\max} \exp(-e\xi/\epsilon kT)\, dl}.$$

The second form follows because the weighting factor $\rho(\xi) \propto (d\xi/dl)^{-1}$. The quantity l_{max} is the value of l for which $\xi = \infty$ provided such an l exists, and is infinite otherwise; $l_{max} = 2$ for line 1. The dielectric constant enters (1) because ξ was calculated with $\epsilon = 1$.

The introduction of ϵ is itself an approximation; it has been discussed at length elsewhere (6, 8, 13). For adsorption from a gas phase, there will be no material between adions and ϵ can arise only from adion polarizability itself. Therefore, in this case ϵ will vary with coverage and will lie between approximately 1 and 3 or 4 at most. In the single-imaging

Can. J. Chem. Downloaded from www.nrcresearchpress.com by 210.87.254.40 on 09/05/12
For personal use only.

Can. J. Chem. Downloaded from www.nrcresearchpress.com by 210.87.254.40 on 09/05/12
For personal use only.

electrolyte case, it has been found (8) that there is a very high field in the inner region of the double layer where ions are adsorbed and this field (for constant ϵ) varies only slightly with adsorbed ion concentration (itself a function of electrode charge). The field is large enough to produce almost entire dielectric saturation of the dipolar contribution of water molecules between adions. Thus, in this case the appropriate dielectric constant is probably 6 or less (8, 18) and will not vary much with coverage until the contribution from ionic polarizability outweighs that from water-molecule polarizability when the coverage approaches that of a monolayer. There is a feedback mechanism at work here which tends to ensure complete saturation. If the field is large enough to produce some dielectric saturation, the consequent reduction in ϵ will increase the effective field, reducing ϵ further and so on. The final self-consistent value of field and dielectric constant may not be that for complete saturation—this depends on the details of the dielectric constant-field dependence—but in the electrolyte single-imaging case, saturation is apparently virtually complete (8). In the present calculations, we shall use $\epsilon = 6$; remember, however, that ϵ and T enter the equations together. Thus, the lower ϵ appropriate for gas phase adsorption can be associated with a higher temperature than the 20 °C we shall use in the electrolyte situation.

Since the potential is an even function of l, it must involve l^{2n}, $n = 1, 2, 3 \ldots$, not l^n. To carry out the integrations in [1] numerically, we found it convenient to fit $\xi(l^2)$ by rational approximations of the form

$$[2] \qquad \xi \cong [l^2/f(l^2)] \sum_{i=0}^{3} \alpha_i l^{2i} \Big/ \sum_{i=0}^{3} \beta_i l^{2i},$$

where $f(l^2)$ varies in form with the line considered. For line 1, $f(l^2) = l^2 - 4$; for line 2, a bisectrix axis (associated with the dashed curve in Fig. 1), $f(l^2) = l^2 - 4/3$, $l_{max} = \sqrt{(4/3)}$; and for line 3 (associated with the dotted curve in Fig. 1), $f(l^2) = 1$, $l_{max} = \infty$. The constants α_i and β_i were determined for given β and R_1 from numerical values of $\xi(l^2)$ calculated by the methods of II. A Chebyshev type of rational fitting* was used in finding best values for α_i and β_i. This is an equi-ripple method which minimizes the absolute error between the original (or transformed) data and the approximation. Typical values obtained for $\beta = 3$ Å and $R_1 = 5$ were, for line 1, $\alpha_0 = 121.2885$, $\alpha_1 = -29.07516$, $\alpha_2 = -25.75952$, $\alpha_3 = 12.05564$, $\beta_0 = -45.52907$, $\beta_1 = 33.67155$, $\beta_2 = -29.53773$, and $\beta_3 = 1$. With ξ available to very high accuracy in the form of eq. [2], the integrals of [1] could be readily evaluated numerically.

It is of interest to note that when $\xi(l^2) \cong \chi l^2$, where χ is a constant, the integrals can be evaluated analytically and yield

$$[3] \qquad L_0 = (\epsilon kT/2e\chi)^{1/2} \equiv (\phi_1/\chi)^{1/2},$$

where $\phi_1 \equiv \epsilon kT/2e$. This quadratic approximation has been evaluated in several cases using χ values obtained from an accurate fit of $\xi(l^2)$ near the origin. The dash–dot curve of Fig. 1 is the result for $R_1 = 5$ and line 1. For the quadratic approximation, as pointed out by Bell, Levine, and Mingins (14), who used only this approximation with $2\phi_1$ rather than ϕ_1 since two-dimensional vibrations were envisaged, the average value $\bar{\xi} = \epsilon kT/2e = \phi_1$. Since the original ξ was defined with $\epsilon = 1$, we must divide the above result by ϵ to obtain the average potential difference appropriate to a non-unity value of ϵ.

Programmed for computer by E. L. Jones of this laboratory.

Can. J. Chem. Downloaded from www.nrcresearchpress.com by 210.87.254.40 on 09/05/12
For personal use only.

RESULTS OF CALCULATIONS

The single-imaging curves of Fig. 2 were calculated for line 1 using eqs. [1] and [3]. Clearly, terms in ξ higher than l^2 cause L to be less than L_0 provided the peak and valley parts of the ξ curves have negligible effect in the averaging. When they do become important, for $R_1 > 4.5$, the moving ion can vibrate further, on the average, and $L > L_0$. The dotted curve in Fig. 2 has been derived from the results of Levine, Mingins, and Bell (14) by transforming from the value $\epsilon = 10$ they used to $\epsilon = 6$, more appropriate for the electrolyte situation, by changing the normalization to agree with our convention, and by dividing their results by $\sqrt{2}$ to change (within the framework of the quadratic approximation) from two-dimensional to one-dimensional motion and averaging. It is evident that the ion can vibrate considerably more freely in the nearly infinite-imaging case than in the single-imaging case. For $\epsilon = 2$, more appropriate for adsorption from a gas phase, the curves of Fig. 2 apply to a temperature of about 790 °K.

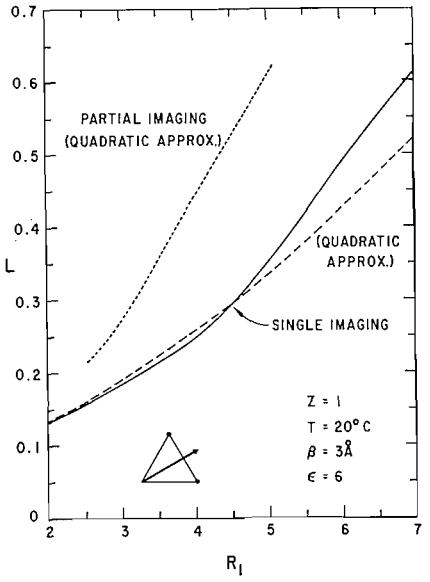

FIG. 2. The normalized r.m.s. vibration amplitude $L \equiv [3(\overline{X^2 + Y^2})/4R_1^2]^{1/2}$ versus normalized nearest-neighbor distance $R_1 \equiv r_1/\beta$.

The superiority of two-dimensional over one-dimensional averaging depends on the ratio of the normalized distance l_0, over which circular symmetry is a good approximation, to L. If both these numbers are small enough that a hexagonal array is well maintained, two-dimensional averaging using the quadratic approximation will be the more appropriate provided $l_0/L \lesssim 1$. When vibration along a particular line, such as line 1, is greatly favored over all other directions of vibration, l_0/L will be much less than unity and the assumption of circular symmetry will be very poor.

Figures 1 and 2 show that $l_0/L \approx 1$ for $R_1 = 5$. The ratio will be even larger for smaller R_1. Thus, for the input parameters shown in Fig. 2, two-dimensional averaging will be a somewhat better approximation than one dimensional for $R_1 \gtrsim 5$. If a criterion is established for the maximum one-dimensional L for which we may expect maintenance of a hexagonal array, then the criterion is divided by $\sqrt{2}$ to obtain that appropriate for

Can. J. Chem. Downloaded from www.nrcresearchpress.com by 210.87.254.40 on 09/05/12
For personal use only.

circular symmetry and two-dimensional averaging. It seems to us reasonable to pick $L \lesssim 0.5$ as a rough criterion for hexagonal array (microcrystal) stability. This is somewhat more stringent than that used by Bell, Levine, and Mingins (14) when transformed to the same basis for comparison. The two-dimensional criterion is thus $L_2 \lesssim 0.35$. It is of interest to compare this figure with the corresponding one for the melting of single-crystal solids: In the latter case the value ~ 0.1 has been found to be appropriate (19); however, it is important to realize that the case considered here is actually quite different from that of solids insofar as first order phase transitions are not treated and the forces are the long range repulsions of the similarly charged adions and their images rather than the crystal-binding fields of an ionic crystal or the short range forces found in metals and covalent crystals. We should accordingly not expect the analogous values to carry over from one situation to the other. Although we have here used the stability criterion $L_2 \lesssim 0.35$, Fig. 2 may be used in conjunction with any other reasonable value to obtain the limiting value of R_1 appropriate to the new criterion.

Since $L \simeq 0.35$ from Fig. 2 for $R_1 = 5$, this value of R_1 seems, according to the above criterion, to be at or near the limit of hexagonal stability for the choices $\beta = 3$ Å, $z_v = 1$, $\epsilon = 6$, and 20 °C. Further, Fig. 1 shows that for $l \lesssim 0.35$, circular symmetry is a fair approximation for $R_1 = 5$. In fact, the values of L obtained for lines 1, 2, and 3 were 0.351, 0.268, and 0.344, respectively, for $R_1 = 5$. The fair correspondence of these figures indicates the approximate validity of the circular symmetry assumption for $R_1 \lesssim 5$ under the conditions of Fig. 2. The quadratic approximation for $R_1 = 5$ leads to $L_0 \simeq 0.336$, again showing that this further approximation is also not too bad for this value of R_1. Note that the heavy solid circles on the curves of Fig. 1 indicate the calculated values of L for the conditions of Fig. 2. It is worth noting that these conditions lead for $R_1 = 5$ to an adsorbed charge density, q_1, of 8.22 μC/cm^2, a nearest-neighbor distance of 15 Å, and an area per adsorbed ion of about 195 Å^2.

When the present two-dimensional averaging stability criterion is applied to the partial-imaging curve of Fig. 2, one obtains a limiting R_1 of about 3.5. In turn, this leads to a limiting area per ion of about 106 Å^2, almost exactly the criterion for loss of hexagonal order derived by Bell, Levine, and Mingins for the partial-imaging case. This agreement is somewhat fortuitous since the effect of our more stringent criteria for loss of quasi long range order is offset by the present use of $\epsilon = 6$ rather than 10. Comparison of the present results for partial and single imaging shows that the hexagonal array is appreciably more rigid for single imaging, and quasi long range order is not lost until ionic nearest-neighbor distance is appreciably greater in the single-imaging case than for partial imaging. Note especially that since the circular symmetry assumption is not very well met for $R_1 = 5$, the criteria for melting should actually lie between the two values 0.35 and 0.5, leading to a larger limiting R_1 than 5 (and accordingly even poorer applicability of the assumption of circular symmetry) for stability calculations at 20 °C.

Finally, Fig. 3 shows how L depends on ϕ_1 for several values of R_1. The temperature scale shown at the top is appropriate for $\epsilon = 6$; its values should be multiplied by 3 for the choice $\epsilon = 2$ more appropriate in the gas adsorption situation. In this case, we see that even the array with $R_1 = 7$ will be stable at room temperature. For $\epsilon = 3$, it will be stable only below about −20 °C. We may write the temperature at which stability tends to disappear according to the present two-dimensional criterion as $T_0 \sim 1760/\epsilon$ or $760/\epsilon$ °K for $r_1 = 15$ Å or 21 Å, respectively, when $\beta = 3$ Å. Note that since the $R_1 = 2$ curve is exactly proportional to $\sqrt{\phi_1}$, the circular symmetry and quadratic approximations are completely valid for this curve.

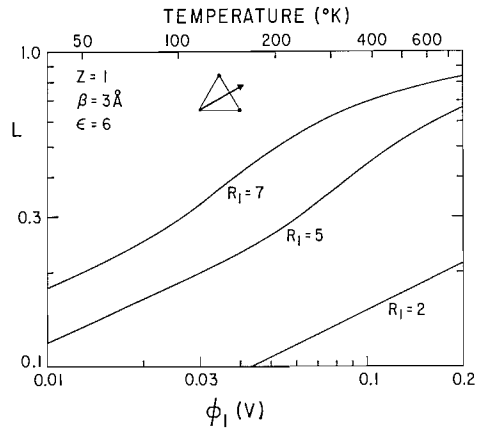

FIG. 3. The normalized r.m.s. amplitude L versus $\phi_1 \equiv \epsilon kT/2e$. The temperature scale at the top applies for $\epsilon = 6$.

Thus far, we have considered only adions of valence $z_v = 1$. When z_v is different from unity, our ϕ_1 becomes ϕ_1/z_v^2. Thus, for adions of valence 2, for example, the instability temperature is four times greater than that for $z_v = 1$. Further, when $R_1 \gtrsim 5$, it turns out (8) that $\psi_a(0, 0, 1)$, for example, may be well approximated by β times the field at (0, 0, 1) derived by replacing all nonideal dipoles by ideal dipoles (6). In this case, ξ will be proportional to β^2, and our present L curves, derived with $\beta = 3$ Å, may be transformed to apply to arbitrary β by replacing a given ϕ_1 by ϕ_1/β^2. In the present work we have used $\beta = 3$ Å since this value seems most appropriate for most electrolyte double layer situations of interest. In adsorption from a gas phase, β may frequently be somewhat smaller even when the imaging plane is taken ≈ 0.5 Å behind the "physical" surface of the conducting adsorbent (8, 16). When $R_1 \gtrsim 5$, the effective ϵ appropriate for adsorption from a gas phase is probably (6) appreciably less than 2. For $r_1 = 15$ Å, we may finally write $T_0 \sim 1760(z_v\beta/3\text{ Å})^2/\epsilon$ °K. A similar expression for $r_1 = 21$ Å is $T_0 \sim 760(z_v\beta/3\text{ Å})^2/\epsilon$ °K.

No information seems currently available concerning the sharpness of melting of two-dimensional order with temperature increase or increase in nearest-neighbor distance. It is clear, however, that if quasi long range order has disappeared by the time R_1 has reached a certain value, say R_{10}, R_1 must be somewhat smaller than R_{10} before the order will reestablish itself. Further, R_1 must be larger than R_{10} before the cluster theory of Buff and Stillinger (15) is a good approximation. If $R_{10} = 5$, for example, corresponding to a q_1 of 8.22 μC/cm², a q_1 of 10 or 12 μC/cm² might be required before hexagonal order were regained, and a value of q_1 as small as 5 or 6 μC/cm² might be required before the Buff–Stillinger approach would be applicable. As an example, for 1.0 N KI ($z_v = -1$), the results of Grahame (20) indicate that the charge on the electrode, q, might have to be less than ~ -9 μC/cm² for the Buff–Stillinger approach to apply and greater than ~ -6 μC/cm² for the hexagonal lattice model to apply. Between -9 and -6 μC/cm² neither model would theoretically apply well but the gap might be bridged reasonably accurately by extrapolation between the results of the two approaches. Grahame's data extends to $q_{max} = 18$ μC/cm² and $|q_{1(max)}| \cong 42.61$ μC/cm², indicating that the hexagonal model applies, at 20 °C, $\epsilon = 6$, and $z_v = \pm 1$, over a much greater and more important part of the $|q_1|$ range than does the Buff–Stillinger approach.

Can. J. Chem. Downloaded from www.nrcresearchpress.com by 210.87.254.40 on 09/05/12
For personal use only.

REFERENCES

1. J. TOPPING. Proc. Roy. Soc. London, Ser. A, **114**, 67 (1927).
2. I. LANGMUIR. J. Am. Chem. Soc. **54**, 2798 (1932).
3. J. K. ROBERTS. Some problems of adsorption. Cambridge University Press, London. 1939.
4. A. R. MILLER. (*a*) Proc. Cambridge Phil. Soc. **42**, 292 (1946). (*b*) The adsorption of gases on solids. Cambridge University Press, London. 1949.
5. J. H. DE BOER. (*a*) Electron emission and adsorption phenomena. Cambridge University Press, London. 1935. (*b*) Advan. Catalysis, **8**, 118 (1956).
6. J. R. MACDONALD and C. A. BARLOW, JR. J. Chem. Phys. **39**, 412 (1963). **40**, 237 (1964). J Chem. Phys. To be published.
7. R. GOMER. J. Chem. Phys. **21**, 1869 (1953).
8. C. A. BARLOW, JR. and J. R. MACDONALD. J. Chem. Phys. In press.
9. O. ESIN and V. SHIKOV. Zh. Fiz. Khim. **17**, 236 (1943).
10. B. V. ERSHLER. Zh. Fiz. Khim. **20**, 679 (1946).
11. D. C. GRAHAME. Z. Elektrochem. **62**, 264 (1958).
12. V. G. LEVICH, V. A. KIR'YANOV, and V. S. KRYLOV. Dokl. Akad. Nauk SSSR, **135**, 1193 (1960). V. S. KRYLOV. Dokl. Akad. Nauk SSSR, **144**, 356 (1962); Electrochim. Acta, **9**, 1247 (1964).
13. C. A. BARLOW, JR. and J. R. MACDONALD. J. Chem. Phys. **40**, 1535 (1964).
14. G. M. BELL, S. LEVINE, and J. MINGINS. To be published.
15. F. P. BUFF and F. H. STILLINGER. J. Chem. Phys. **39**, 1911 (1963).
16. M. BORN. Atomic physics. 5th ed. Hafner Publishing Company, New York. 1952. pp. 241–247.
17. J. J. MCALPIN and R. A. PIEROTTI. J. Chem. Phys. **41**, 68 (1964).
18. J. R. MACDONALD and C. A. BARLOW, JR. J. Chem. Phys. **36**, 3062 (1962).
19. L. CARTZ. Proc. Phys. Soc. London, **B68**, 957 (1955).
20. D. C. GRAHAME. J. Am. Chem. Soc. **80**, 4201 (1958).

Can. J. Chem. Downloaded from www.nrcresearchpress.com by 210.87.254.40 on 09/05/12
For personal use only.

Can. J. Chem. Downloaded from www.nrcresearchpress.com by 210.87.254.5 on 09/05/12
For personal use only.

TERPENOIDS

XII. THE STRUCTURE OF CHAPARRIN[1]

T. A. DAVIDSON, T. R. HOLLANDS, P. DE MAYO, AND M. NISBET
Department of Chemistry, University of Western Ontario, London, Ontario

Received June 23, 1965

ABSTRACT

Chaparrin, the bitter principle from *Castela nicholsonii* may be dehydrated in two stages to give the partially aromatized substance chaparrol. By further stepwise degradation the latter has been converted to the dihydrophenanthrene (XIII) which allows the assignment of structures XVII and I to chaparrol and chaparrin respectively.

In 1922 Bosman (2) reported the isolation, from *Castela nicholsonii* Hook (Chaparro amargosa), of two bitter substances, castelin and castelamarin. In view of the improbable nature of the structure (the lactone of 2-hydroxy-3-methoxycyclohexaneacetic acid) proposed for one of these, a reinvestigation seemed called for. However, an attempt to isolate either of these substances failed. Instead, a new and apparently unrelated compound was obtained and characterized. While it was under investigation the isolation of the same substance was reported by Geissman and Chandorkar (3). Although there were originally minor differences in the characterization, essentially similar conclusions had been reached. Further degradative work was then continued with exchanges of information between the two groups resulting, by different means, in the same gross structural conclusions (1, 4).

It is the purpose of this report to present our results leading to the selection of formula I as the representation of the constitution of chaparrin. Our results leading to the elucidation of the stereochemistry and absolute stereochemistry of this substance together with those of chaparrol and its isomers neochaparrol and isochaparrol will be presented in the following paper in this series.

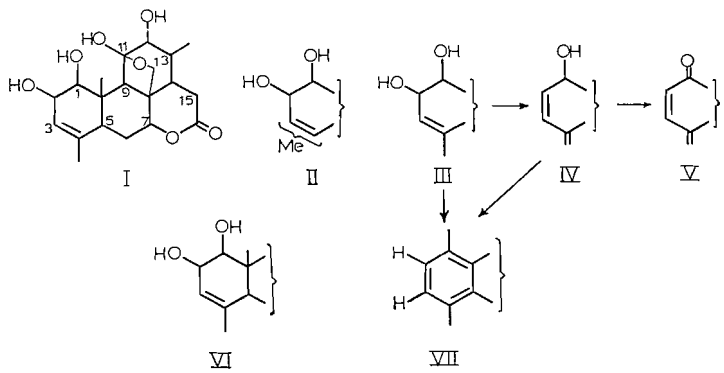

Chaparrin, best isolated (see Experimental) as the acetate mixture, forms a tri- and a tetraacetate from which chaparrin can be recovered on alkaline hydrolysis. Since chaparrin has the formula $C_{20}H_{28}O_7$ three oxygen atoms remain to be accounted for.

Of these, two must be present in a lactone. Thus, although chaparrin will dissolve in aqueous alkali and is precipitated from the alkaline solution on acidification it shows, itself,

[1]*Part of the material here described was first presented in preliminary form (1).*

Can. J. Chem. Downloaded from www.nrcresearchpress.com by 210.87.254.5 on 09/05/12
For personal use only.

no acidic properties: it is, for instance, recovered unchanged on brief diazomethane treatment. Since the infrared spectrum of the acetate shows no absorption higher than 1740 cm^{-1}, and the lack of strong maximal absorption in the ultraviolet precludes the possibility of α,β-unsaturation, the presence of γ-lactone could be excluded. The ready re-lactonization on acidification rendered a large ring lactone improbable, leaving only a δ-lactone for serious consideration.

The remaining oxygen atom is assigned to a carbonyl function (masked in chaparrin itself) for the following reasons. Chaparrin triacetate-A and chaparrin tetraacetate both show the low intensity $n \rightarrow \pi^*$ absorption in the ultraviolet associated with saturated ketones and aldehydes. Chaparrin does not, however, have absorption here nor does it show a Cotton effect in its optical rotatory dispersion (o.r.d.) curve. The sodium salt, on the other hand, shows carbonyl absorption near 1 730 cm^{-1} (Nujol mull). These facts, and others to be described below and in the following paper establish that chaparrin is a hemi-ketal. Since this is so, the absorption at 1 720 cm^{-1} shown by chaparrin must be attributed to the δ-lactone alone and supports the assignment of ring size.

Chaparrin shows only end-absorption in the ultraviolet (ϵ_{203} = 5 600) and so is devoid of conjugation. On bromination of the tetraacetate a crystalline tetraacetate dibromide was obtained. Since chaparrin and its acetates showed no indication of further unsaturation, with the functional groups already enumerated, chaparrin must be tricarbocyclic.

Chaparrin tetraacetate contains three methyl groups. One (at τ 8.57, singlet) is attached to quaternary carbon while a singlet at τ 8.32 indicated the presence of a vinylic methyl group. The third methyl group appeared as a doublet centred at τ 9.00 ($J \sim 6.6$ c.p.s.) (see also Table I) and was assigned to a methyl group attached to carbon bearing one hydrogen atom.

Some indication as to the environment of the ethylenic linkage was obtained by periodic acid titration of chaparrin. There was a rapid consumption of 1 mole of oxidant, and the crude product showed maximal absorption at 244 mμ ($\epsilon \sim 4\,500$). Since there is both a single ethylenic linkage and vinyl methyl group, this suggested the presence in chaparrin of the system indicated in II. This was more clearly shown by the following sequence of transformations.

On heating in 0.1 *N* hydrochloric acid chaparrin loses one molecule of water to give, amongst other products, a diene, characterized as the triacetate. This diene shows maximal absorption of 228 mμ (ϵ = 13 400) and so is heteroannular and very lightly substituted. In the n.m.r. spectrum it could be observed that the vinyl methyl absorption was now absent, and that absorption (two protons) had appeared at τ ca. 5.00 (multiplet in the triacetate) which could be attributed to an exocyclic methylene group. This compound, anhydrochaparrin-A, on hydrogenation, absorbed two molecules of hydrogen giving a crystalline tetrahydroanhydro derivative which was optically transparent in the ultraviolet. These observations are compatible with the conversion of the part-structure shown in III to that shown in IV.

Oxidation of anhydrochaparrin-A with 2,3-dichloro-4,5-dicyanobenzoquinone (DDQ) gave, by conversion of an alcohol to a ketone, a dienone with maximal absorption at 276 mμ (ϵ = 10 000). This is compatible with expectation for a substance with structure V.

On prolonged treatment with dilute mineral acid chaparrin may be induced to lose a second molecule of water (4). This may also be achieved by passage of anhydrochaparrin-A in ether–benzene solution through a column of alumina or, better, by dissolution of chaparrin in cold concentrated hydrochloric acid. The product, chaparrol, $C_{20}H_{24}O_5$, is aromatic. It shows benzenoid absorption in the ultraviolet (ϵ_{268} = 400) and inspection of the n.m.r.

Can. J. Chem. Downloaded from www.nrcresearchpress.com by 210.87.254.5 on 09/05/12
For personal use only.

TABLE I

Nuclear magnetic resonance data of chaparrin derivatives ($CDCl_3$ solution)

COMPOUND	C-7 H τ	C-9 H τ	C-12 H τ	C-4 CH_3 τ	C-10 CH_3 τ	C-13 CH_3 τ; J	$-CH_2-OR$ τ J_{AB}; δ_A δ_B	Aromatic H τ	Aromatic $-CH_3$ τ	Acetate $-CH_3$ τ	Methoxyl τ	Others τ
Chaparrin*	5.45	6.93	ca.6.0	8.38	8.32	8.90; 8.4	5.98 9.0; 25.5	—	—	—	—	—
Chaparrin triacetate-A	5.52	6.28	ca. 6.18	8.30	8.56	8.87; 7.2	5.75 12.6; 43.2	—	—	7.92 7.99 8.03	—	—
Chaparrin tetra acetate	5.47	6.71	ca.4.92	8.32	8.57	9.00; 6.6	5.75 12.6; 44.2	—	—	7.80 7.90 8.01 8.17	—	—
Chaparrin triacetate-B	5.62	7.43	ca.5.35	8.28	8.63	9.14; 7.8	6.18 10.0; 20.9	—	—	7.88 8.00(6)	—	—
Anhydro chaparrin-A triacetate		6.66	ca.5.45	—	8.72	8.97; 6.0	5.81 14.4; 45.1	—	—	7.81 7.92 8.08	—	Vinyl H ca.3.60 (1) ca.5.00 (3)
Chaparrol	5.47 5.53	7.04	6.09 6.29	—	—	8.95; 7.8	6.25 8.4; 17.3	3.02(2)	7.74 7.79	—	—	—
Chaparrol monoacetate	ca.5.2	7.01	ca.5.2	—	—	8.89; 7.2	6.01 12.0; 22.8	3.05(2)	7.84 7.96	8.09	—	—
Chaparrol triacetate	ca.5.4	—	4.35 4.48	—	—	8.93; 9.0	6.09 12.0; 35.8	3.00(2)	7.76 7.86	7.97 8.01 8.26	—	—
Dihydro chaparrol triacetate		—	4.29 4.38	—	—	8.94; 7.2	6.11 9.0; 25.4	3.04(2)	7.73 7.85	7.97 8.09 8.26	—	C-16 H ca.4.70
Chaparrol-enol ether alcohol*	ca.5.33	—	—	—	—	8.77; 6.0	6.00 9.6; 31.1		7.63 7.77	—	6.44	—
Chaparrol-enol acetate acetate bromide	ca.5.50	—	—	—	—	7.73(s)	5.52 12.0; 61.8	2.88(2)	7.73 7.94	7.94 8.00	—	—
Chaparrol-enol acetate acetate	ca.5.45	—	—	—	—	8.83; 6.3	5.84 12.0; 32.0	2.90(2)	7.70 7.80	7.95 7.98	—	—
Dihydro phenanthrene	ca.7.0 to 8.0	—	—	—	—	—	—	2.97(2)	7.66 7.74 7.90	—	6.81	α-H(COOH) 6.20(2)

*Spectrum done in pyridine.

Can. J. Chem. Downloaded from www.nrcresearchpress.com by 210.87.254.5 on 09/05/12
For personal use only.

spectrum confirmed this conclusion since the presence of two aromatic protons, as a singlet (at τ 3.02), could be observed. Two aromatic methyl groups at τ 7.74 and 7.79 were also present, the chaparrin singlet near τ 8.57 now being absent. Taking into consideration the requirements expressed in the part-formula III, the part-structures VII and VI for chaparrol and chaparrin follow, the conversion of IV to VII being, essentially, a dienol–benzene rearrangement (5). Chaparrol proved a useful starting point for further structural investigation into the remaining rings of the chaparrin framework.

Under a variety of conditions chaparrol could be oxidized by hexavalent bismuth to give enolic material. In acetic acid a monoacetate was obtained which on methylation with diazomethane gave a methyl ether monoacetate. The methyl ether itself was obtained with bismuth triacetate in ethylene glycol again followed by treatment with diazomethane. Oxidation in acetic acid followed by acetylation gave the enol acetate monoacetate. The ultraviolet absorption of these compounds clearly indicated the conjugation of the enolic system with the aromatic ring.

Bromination of the enol acetate gave a monobromo derivative in which this extended chromophore was untouched. The position of entrance of the bromine atom was revealed by changes in the signal for the remaining non-aromatic methyl group. This absorption, originally present (Table I) as a doublet near τ 9.0 was now displaced to 7.73 and had become a singlet. This permitted the part-structure VIII, X = Br to be written for the bromoenol acetate and VIII, X = H for the enol acetate itself. At this point the alternative IX for the enol acetate could not be strictly excluded, but was unlikely in view of the tetracyclic nature of the substance and the restrictions implied by Bredt's Rule. The size of ring C (VIII, X = H) was suggested by the position of absorption (at 1 697 cm^{-1}) of the ketonic carbonyl group.

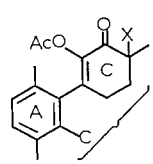

VIII

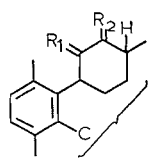

X a R_1 = O
R_2 = H,OH
b R_1 = H,OH
R_2 = O

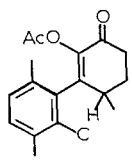

IX

These facts required that the part-structure VII for chaparrol be expanded to X*a* or X*b*.

In the n.m.r. spectrum of a number of chaparrin and chaparrol derivatives there appeared a two-proton nonequivalence quartet. Chaparrin tetraacetate, for instance, shows these signals at τ 5.75 (2H, AB; J_{AB} = 12.6; $\delta_B - \delta_A$ = 44.2 c.p.s.). The presence of these signals was suggestive of a $-CH_2OR$ (R = H or Ac) grouping in these compounds, where the point of attachment was a quaternary carbon. The correctness of this view is shown by the following sequence of reactions which also revealed the disposition of the atoms constituting rings B and D.

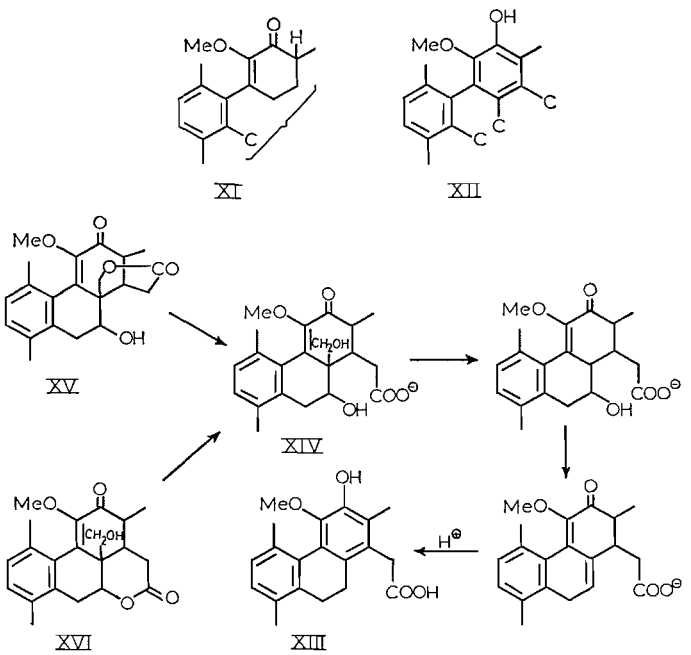

The enol methyl ether (XI) was treated with dilute alcoholic alkali: conditions suitable for the induction of dealdolisation. After standing, the solution was acidified and a crystalline product obtained. Its analysis indicated that in the overall process the elements of formaldehyde had been lost. This substance evidently contained an enolic acidic function because of the spectral shift observed in the ultraviolet in neutral and alkaline solution. Further information was contained in the n.m.r. spectrum (Fig. 1). In this spectrum signals for three aromatic or vinylic methyl groups were apparent. Since two were necessarily to be attributed to ring A the previously secondary methyl group in ring C (in XI) must now be attached to a double bond. The methyl ether remained intact, and there were still only two aromatic protons. The original nonmethylated oxygen adjacent to the ether must, therefore, still be present, and must be the new enolic (and therefore phenolic since the enol required stabilisation) function. Part-structure XII may then be written in which two carbon atoms are lacking. One of these is the carbonyl group of the original lactone, while the other was represented in chaparrin and chaparrol by the $—CH_2OH$ grouping. In a supposed reverse aldol reaction this would be eliminated as formaldehyde (6). That this was so was confirmed by treatment of VIII (X = H) with sulfuric acid and estimation of the formaldehyde (15%) by the chromotropic acid procedure (10).

A singlet (2H) at τ 6.20 in the n.m.r. spectrum of the phenol remained to be attributed. This is in the position expected of a phenylacetic acid, and so permitted the final representation of the structure of the dihydrophenanthrene derivative as XIII. The ultraviolet absorption spectrum may be compared with those of certain diphenyls (Fig. 2): more exact models are not available.

Its genesis from the anion XIV allows of two structures for the ether itself (and therefore of chaparrol), depending on the position of lactonization (XV and XVI). The n.m.r. spectrum of chaparrol shows a multiplet (1H) near τ 5.5 which moves very slightly (to 5.2) in a monoacetate prepared from chaparrol by heating in acetic anhydride in the absence of base. However, in this derivative a nonequivalence quartet (2H) is visible at τ 6.01

Can. J. Chem. Downloaded from www.nrcresearchpress.com by 210.87.254.5 on 09/05/12
For personal use only.

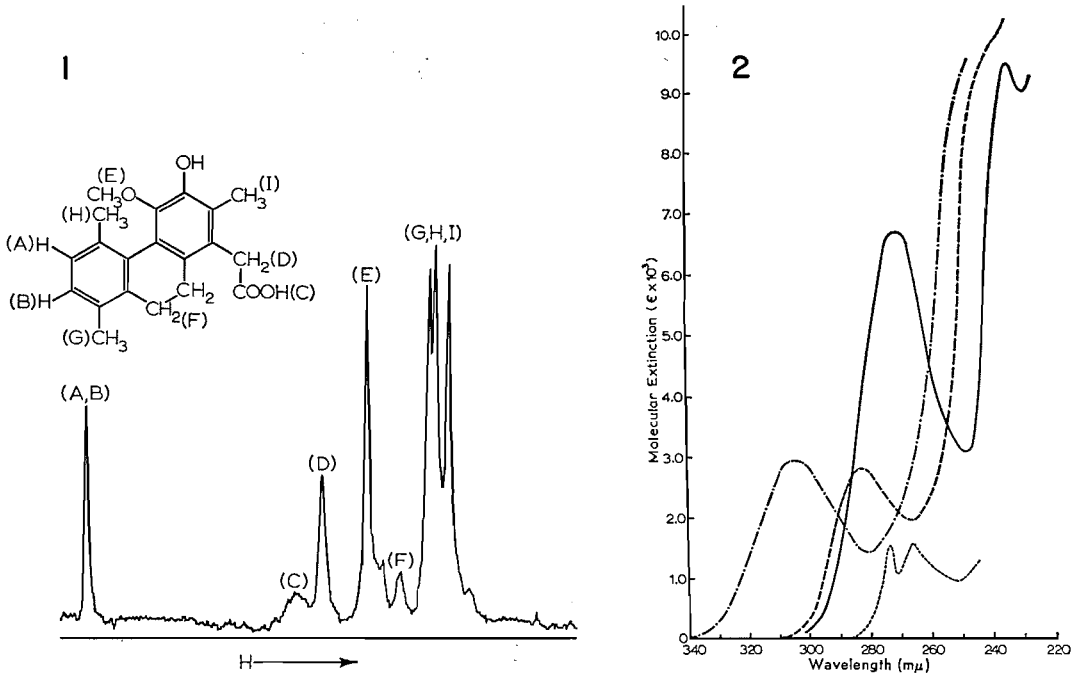

FIG. 1. Nuclear magnetic resonance spectrum of dihydrophenanthrene (XIII).
FIG. 2. Ultraviolet spectra of – – – neutral and —·—·— alkaline dihydrophenanthrene (XIII); of —— 2-hydroxy-2′-methoxybiphenyl (ref. 12, λ_{max} corrected for solvent); and of – – – – 2,2′,5,5′-tetramethyl biphenyl (ref. 13, λ_{max} corrected for solvent).

(2H, AB; J_{AB} = 12.0; $\delta_B - \delta_A$ = 22.8 c.p.s.) in an area quite clear of absorption in chaparrol, itself requiring that the primary hydroxyl group be that function acetylated. The single hydrogen must accordingly be attributed to the lactonic methine hydrogen, both facts requiring that the primary hydroxyl group not be involved in lactone formation: structure XV for the ether must therefore be excluded.

With the main structure of chaparrol completed only the specific positions of the oxygen in the masked ketol in ring C remained to be ascertained. In a large number of derivatives of chaparrin and chaparrol there appears a singlet (1H) whose position fluctuates about τ 7.0. In chaparrin tetraacetate and chaparrol monoacetate it is at 6.71 and 6.93 respectively. Deuterium exchange studies (to be reported later) indicate that this proton is adjacent to a (masked or potential) carbonyl. Since, in all compounds (including those derivatives where C_9 is inverted) the band, attributed to the proton at C_9, remains a singlet, then there are no protons on carbon atoms adjacent to C_9. Hence C_{11} must be the location of the (masked) carbonyl. The singularity of the absorption also provides confirmatory evidence for the position of the —CH_2OH grouping. The correctness of XVII as the representation of chaparrol was demonstrated by the nature of an acetate obtained from chaparrol by acetylation with acetic anhydride and pyridine. This substance (XVIII) was a triacetate, as shown by analysis and by the presence of three singlets in the n.m.r. spectrum to be attributed to acetyl groups. It was thus an enol acetate. This was confirmed by the ultraviolet spectrum which exhibited intense maximal absorption at 244 mμ. In this substance the absorption attributed to the proton at C_9 is lacking.

A combination of the part-structure VI with that part of XVII which is relevant to chaparrin leads to two possible formulations for the latter, XIX and I. That represented by XIX may be rejected because the proton at C_9, as already mentioned, is a singlet.

Can. J. Chem. Downloaded from www.nrcresearchpress.com by 210.87.254.5 on 09/05/12
For personal use only.

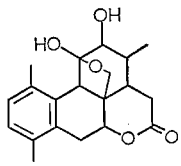

XVII

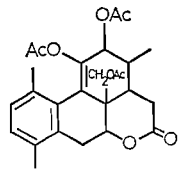

XVIII

With the structure of chaparrin and chaparrol established it is possible to discuss the nature of some reduction products of these compounds.

Reduction of chaparrol with sodium borohydride gave a dihydro compound showing no carbonyl absorption in the infrared spectrum. Oxidation with chromium trioxide in pyridine gave back some chaparrol. That reduction of the (masked) carbonyl had not taken

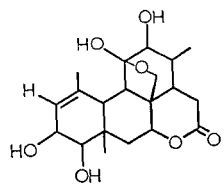

XIX

place was shown by the ultraviolet spectrum of the triacetate obtained by acetylation (acetic anhydride – pyridine) of this dihydrochaparrol. This showed the same maximal absorption (at 244 mμ) in the ultraviolet as did chaparrol triacetate. Furthermore acetylation of the dihydrochaparrol gave a triacetate which could be oxidized with manganese dioxide overnight to regenerate chaparrol triacetate.

It is, therefore, the lactone which has been reduced by the sodium borohydride treatment. The initially observed formation of only a triacetate under the acetylation conditions was not surprising since the hydrolysis of a labile hemiacetal acetate could be expected during the working up. Under modified conditions the tetraacetate could be isolated. The sequence of reactions can be represented as in XVII $\rightarrow$ XXI.

Reduction of chaparrin tetraacetate in a similar manner gave an acetal triacetate in which one of the four original acetoxyl functions had also been hydrogenolyzed. Under acetylation conditions the relevant hydroxyl group was reacetylated with the formation of the hemiacetal tetraacetate. Oxidation of this with chromic acid in acetic acid regenerated chaparrin tetraacetate. Oxidation of the hemiacetal in the hemiacetal triacetate with sodium dichromate in acetic acid or with manganese dioxide, gave a triacetate of chaparrin (chaparrin triacetate B) different from that previously obtained by the acetylation of chaparrin. The resistance to further oxidation with manganese dioxide probably excludes C_2 as the site of hydrogenolysis and the position of the free hydroxyl group, while the presence of the nonequivalence quartet at τ 6.17 (2H, A.B; $J_{AB} = 9.0$; $\delta_B - \delta_A = 20.9$ c.p.s.) implies that the primary hydroxyl group is not acetylated. Hydrogenolysis must therefore have occurred at this position.

More prolonged exposure of chaparrin tetraacetate to the action of sodium borohydride gave a substance lacking carbonyl absorption in the infrared spectrum. This substance, which had the empirical formula $C_{20}H_{30}O_7$, most probably has the structure XXII corresponding to a dihydrochaparrin.

Can. J. Chem. Downloaded from www.nrcresearchpress.com by 210.87.254.5 on 09/05/12
For personal use only.

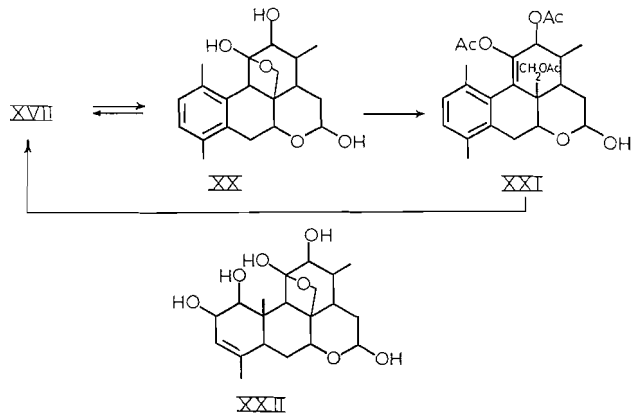

The structure of chaparrin so arrived at has many features in common with that of quassin (7, 8) the bitter from *Quassia amara*. Since the first presentation of this work in preliminary form, Polonsky and her collaborators, in the course of an impressive and detailed study of Simaroubacea constituents, have elucidated the structure and stereochemistry of glaucarubol (9) the bitter from *Simaruba glauca* and their deductions have been confirmed by X-ray analysis (11). This substance they showed, stereochemistry aside, to be a 15-hydroxychaparrin. Further comment on this relationship will be made in the following paper.

EXPERIMENTAL

Infrared spectra and rotations were determined in chloroform solution, ultraviolet spectra in 95% ethanol and "light petroleum" refers to the fraction of b.p. 60–80°. Melting points were determined on the Köfler hot stage.

Thin-layer chromatography (t.l.c.) was done using Camag silica gel DF-5 with fluorescent indicator. Elution of fractions from preparative t.l.c. was done with ethyl acetate.

The n.m.r. spectra were determined in deuteriochloroform using 1% tetramethylsilane as internal standard using a Varian D.P. 60 spectrometer. The peak positions were determined using an audio oscillator calibrated with a Hewlett Packard 522-B frequency counter. Band positions are in tau (τ) units.

Isolation of Chaparrin Tri- and Tetraacetates

The ground branches (3 kg) supplied by S. B. Penick and Co. were soaked in ethanol (95%, 8 l) for 24 h. After draining, fresh alcohol was replaced and the procedure repeated a total of five times. Evaporation of the combined extracts to 4 l under reduced pressure led to the separation of a green greasy solid which was collected and defatted by extraction in a soxhlet with benzene. The resultant powdery solid (40 g) was acetylated (acetic anhydride – pyridine, room temperature overnight) and the acetylated material was evaporated to dryness under reduced pressure.

The residue in benzene was added to a column of alumina (Brockmann Grade III, 530 g). Elution with ether–benzene (1:19) gave chaparrin tetraacetate (3.7 g) which after recrystallization from ethyl acetate – light petroleum had m.p. 229–231°, $[\alpha]_D$ +33° (*c*, 1.29 in pyridine), $\lambda_{max}^{CHCl_3}$ 308 mμ (ϵ = 38).

Anal. Calcd. for $C_{28}H_{36}O_{11}$: C, 61.22; H, 6.64. Found: C, 61.19; H, 6.46.

Further elution with ether–benzene (1:9) gave chaparrin triacetate-A (8.5 g) which after recrystallization from ethyl acetate – light petroleum had m.p. 125–135° (solvated), $[\alpha]_D$ −4° (*c*, 0.91 in pyridine) and +70° (*c*, 1.01), $\lambda_{max}^{CHCl_3}$ 315 mμ (ϵ = 25). The analytical specimen was dried at 140° (0.1 mm).

Anal. Calcd. for $C_{26}H_{34}O_{10}$: C, 61.65; H, 6.77. Found: C, 61.94; H, 6.82.

Preparation of Chaparrin

The hydrolysis of either acetate, or a mixture of the two as isolated by partial chromatographic separation may be performed as follows: The acetate (~40 mg) in alcoholic potassium hydroxide (1 *N*; 3 ml) was heated on the steam bath for 90 min. The alcohol was removed under reduced pressure, water (5 ml) was added, and the mixture was acidified. The resultant precipitate was collected, washed with water, and dried (m.p. 299–301°). Recrystallization from methanol gave material of m.p. 306–308°, $[\alpha]_D$ +14° (*c*, 0.81 in pyridine). The material showed no maximum in the ultraviolet between 300–320 mμ in methanol or in dimethylformamide λ_{max} 203 (ϵ = 5 600).

Anal. Calcd. for $C_{20}H_{28}O_7$: C, 63.14; H, 7.42. Found: C, 62.84; H, 7.22.

Can. J. Chem. Downloaded from www.nrcresearchpress.com by 210.87.254.5 on 09/05/12
For personal use only.

Chaparrin (18.3 mg) in aqueous methanol was treated with excess periodic acid. The consumption was 1.01 atoms of oxygen. After 100 h this had increased to 1.55 atoms. Extraction of the residue gave material having absorption at 244 mμ ($\epsilon \sim 4\,500$).

Acetylation of Chaparrin Triacetate-A

The triacetate (54 mg) in pyridine (4 ml) and acetic anhydride (2 ml) was heated at 110° for 4 h. The reagents were removed *in vacuo* and the residue crystallized from ethyl acetate – light petroleum to give the tetraacetate, m.p. 218–232°. Recrystallization gave material (44 mg) m.p. 228–230°, $[\alpha]_D$ +35° (*c*, 0.99 in pyridine).

Bromination of Chaparrin Tetraacetate

The tetraacetate (50 mg) in chloroform (1 ml) was added to a solution of bromine in chloroform (0.2%, 10 ml). The mixture was allowed to stand for 8 h, excess bromine was removed with aqueous sodium thiosulfate, and the product separated by t.l.c. (solvent: diethyl ether). After crystallization from methanol at low temperature the dibromide was obtained, m.p. 158–160°, $[\alpha]_D$ +119° (*c*, 0.6).

Anal. Calcd. for $C_{28}H_{36}O_{11}Br_2$: C, 47.45; H, 5.08. Found: C, 47.92; H, 5.14.

Anhydrochaparrin-A

Chaparrin (92 mg) was dissolved in methanol (100 ml); water (80 ml) and hydrochloric acid (*N*, 20 ml) were then added, and the solution was heated for 4 h (until there was little further change in the absorption near 225 mμ). After isolation with chloroform the product was crystallized from ethanol to give anhydrochaparrin-A, m.p. 258–260°, $[\alpha]_D$ +40° (*c*, 0.77 in ethanol), λ_{max} 230 mμ (ϵ = 17 500).

Anal. Calcd. for $C_{20}H_{26}O_6$: C, 66.28; H, 7.23. Found: C, 66.05; H, 6.99.

Anhydrochaparrin-A Triacetate

(*a*) Anhydrochaparrin-A (35 mg) in pyridine (4 ml) and acetic anhydride (2 ml) was allowed to stand overnight. Evaporation and crystallization from ethyl acetate – light petroleum gave the triacetate, m.p. 178–180°, $[\alpha]_D$ +61° (*c*, 1.5). The compound showed no absorption in the hydroxyl region (3 600 – 3 400 cm^{-1}) of the infrared spectrum.

Anal. Calcd. for $C_{26}H_{32}O_9$: C, 63.92; H, 6.60. Found: C, 64.36; H, 6.75.

(*b*) Chaparrin tetraacetate (50 mg) was refluxed in acetic acid (2 ml) for 6 h. Evaporation and crystallization of the residue from ethanol gave the triacetate (23 mg), m.p. 178–180°, $[\alpha]_D$ +58° (*c*, 0.51), λ_{max} 223, 230, 239 (ϵ = 16 300, 17 700, and 11 000) respectively.

Hydrogenation of Anhydrochaparrin-A

The compound (42 mg) was hydrogenated in ethanol over palladized charcoal (5%, 60 mg). The uptake was 2 mole equivalents. After 100 min the solution was filtered and evaporated, and the product was crystallized from ethyl acetate – diethyl ether and from chloroform – diethyl ether to give the tetrahydro compound, m.p. 140–142°. There was no absorption in the ultraviolet above 200 mμ.

Anal. Calcd. for $C_{20}H_{30}O_6.H_2O$: C, 62.48; H, 8.39. Found: C, 62.41; 62.40; H, 8.43, 8.08.

Dehydroanhydrochaparrin

Anhydrochaparrin-A (45 mg) and 2,3-dichloro-4,5-dicyanobenzoquinone (39 mg) were dissolved in dry dioxan (3 ml) and heated in a sealed tube at 85° for 15 h. A precipitate of quinol formed slowly. Chloroform was added to the cooled solution and the organic phase was washed with water until the washings were colorless. Evaporation and crystallization from ethanol gave the dienone, m.p. 245–247°, $[\alpha]_D$ +278° (*c*, 0.97 in ethanol), λ_{max} 276 mμ (ϵ = 10 000 in dioxan).

Anal. Calcd. for $C_{20}H_{24}O_6$: C, 66.65; H, 6.71. Found: C, 66.75; H, 6.90.

Chaparrol

(a) From Chaparrin

Chaparrin (1.5 g) was added to hydrochloric acid (conc., 15 ml) and the mixture was allowed to stand at room temperature for 45 min. After dilution with water the product was isolated with chloroform. After evaporation the residue was crystallized from ethyl acetate to give chaparrol, m.p. 220–223°, $[\alpha]_D$+107° (*c*, 1.22 in pyridine), λ_{max} 268 mμ (ϵ = 400).

Anal. Calcd. for $C_{20}H_{24}O_5$: C, 69.75; H, 7.02. Found: C, 69.35; H, 6.69.

(b) Through Anhydrochaparrin-A

Chaparrin (437 mg) as a slurry in hydrochloric acid (0.1 *N*, 50 ml) was refluxed for 2 h. The product (containing crude anhydrochaparrin-A) was then filtered in chloroform through a column of alumina (11 g, Grade III). The chloroform eluate gave, from ethyl acetate, chaparrol m.p. 199–205° (177 mg).

Hydrogenation of chaparrol in acetic acid over platinum oxide catalyst resulted in the uptake of 1 mole equivalent of hydrogen.

Chaparrol from Anhydrochaparrin-A

Anhydrochaparrin-A (40 mg) was chromatogramed on alumina (Woelm neutral Grade III, 1 g). The crystals were dissolved into ethanol and evaporated to dryness, and the gum was put on the column with benzene. The material (25 mg) eluted with 10% ether–benzene was crystallized from ethyl acetate – light petroleum, UV_{max} 268 mμ (ϵ = 400), m.p. 211–215°, and so it is chaparrol.

Can. J. Chem. Downloaded from www.nrcresearchpress.com by 210.87.254.5 on 09/05/12
For personal use only.

Chaparrol Monoacetate

A solution of chaparrol (160 mg) in acetic anhydride (10 ml) containing acetic acid (ca. 0.5 ml) was heated on the steam bath for 4 h. After dilution with methanol the product was evaporated to dryness (165 mg). The product containing some chaparrol was separated by thin-layer chromatography by development with ether when the monoacetate had an R_f of ca. 0.7. Elution of the band with chloroform and crystallization from ethyl acetate – light petroleum gave the pure monoacetate, m.p. 194–196°, $[\alpha]_D$ +116° (*c*, 0.42), λ_{max} 270, 278 mμ (ϵ = 460, 410).

Anal. Calcd. for $C_{22}H_{26}O_6$: C, 68.38; H, 6.78. Found: C, 68.55; H, 7.15.

Chaparrol Triacetate

Chaparrol (110 mg) was added to a mixture of acetic anhydride (3 ml) and pyridine (6 ml) and the solution was allowed to stand for 72 h at room temperature. After evaporation of the reagents under reduced pressure the product was filtered, in benzene solution, through a short column of alumina. After five crystallizations from ethyl acetate – light petroleum the triacetate (25 mg) was obtained, m.p. 176–178°, $[\alpha]_D$ +120° (*c*, 1.15 in chloroform), λ_{max} 244, 276 mμ (ϵ = 12 500 and 1 025 respectively).

Anal. Calcd. for $C_{26}H_{30}O_8$: C, 66.37; H, 6.43. Found: C, 66.09; H, 6.34.

Bismuth Trioxide Oxidation of Chaparrol

(*a*) Bismuth trioxide (250 mg) was added to a solution of chaparrol (200 mg) in acetic acid (15 ml) and the mixture was heated under reflux for 5 h. The cooled supernatant was poured into chloroform, and the organic medium was washed with water. Evaporation afforded a gum giving a dark green coloration with alcoholic ferric chloride solution and which showed λ_{max} 247, 300 mμ (ϵ = 5 200 and 11 700 respectively) in neutral and λ_{max} 350 mμ (ϵ = 7 200) in alkaline solution.

Methylation of the gum (diazomethane) afforded, after crystallization from ethanol, the methyl ether acetate (XVI; —CH_2OH becomes —CH_2OAc) m.p. 189–199° (65 mg). Recrystallization from chloroform–ether raised the m.p. to 198–202°, $[\alpha]_D$ +144° (*c*, 0.46), λ_{max} 247, 302 mμ (ϵ = 3 200 and 10 400 respectively).

Anal. Calcd. for $C_{23}H_{26}O_6$: C, 69.33; H, 6.78; OMe, 7.79. Found: C, 69.06; H, 6.78; OMe, 7.89.

(*b*) Bismuth triacetate (44 mg) and chaparrol (30 mg) were added to ethylene glycol (60 ml) and heated to 150°. After 3 h the absorption at 298 (neutral) and 350 (alkaline) mμ reached maxima ($\epsilon \sim$ 8 000 and 6 000 respectively). The mixture was then cooled, diluted with water, and extracted with chloroform. After evaporation the residual gum was methylated (diazomethane) and chromatographed on silica gel. Elution with ether–benzene (1:19) gave the methyl ether (XVI), m.p. 273–275°, $[\alpha]_D$ +203° (*c*, 0.77 in pyridine), λ_{max} 244, 300 mμ (ϵ = 3 400 and 10 200 respectively).

Anal. Calcd. for $C_{21}H_{24}O_5$: C, 70.76; H, 6.79. Found: C, 70.50; H, 6.82.

(*c*) Chaparrol (500 mg) in refluxing acetic acid (40 ml) was treated with bismuth trioxide (500 mg) and heated for 5 h. The product was isolated in the usual way and acetylated (acetic anhydride – pyridine at room temperature for 16 h). The resulting material, isolated with chloroform, after crystallization from ethanol and from chloroform – diethyl ether gave the enol acetate acetate (part structure VIII; X = H), m.p. 183–185°, $[\alpha]_D$ +111° (*c*, 1.28), λ_{max} 288 mμ (ϵ = 9 800), ν_{max} 1 750, 1 697 cm^{-1}.

Anal. Calcd. for $C_{24}H_{26}O_7$: C, 67.59; H, 6.15. Found: C, 67.38; H, 5.87.

Bromination of Chaparrol Enol Acetate Acetate

The enol acetate (100 mg) in acetic acid (50 ml) containing bromine ($\sim$75 mg) and a drop of hydrobromic acid in acetic acid was allowed to stand. After 22 h, uptake had ceased at 1.14 atoms of bromine. Dilution of the remainder, isolation with chloroform, washing of the organic phase with sodium bisulphite, and evaporation gave crystals (98 mg) m.p. 209–211°, $[\alpha]_D$ +108° (*c*, 0.95), λ_{max} 304 mμ (ϵ = 9 000).

Anal. Calcd. for $C_{24}H_{25}BrO_7$: C, 57.03; H, 4.99. Found: C, 57.10; H, 4.99.

Dihydrophenanthrene (XIII) Formation

The enol ether alcohol (XVI) (46 mg) was dissolved in ethanol (20 ml) and aqueous potassium hydroxide (1 *N*, 20 ml) was added. After standing overnight the now yellow solution was acidified, and the product was isolated with chloroform and crystallized from ethyl acetate – light petroleum, m.p. 200–202°, $[\alpha]_D$ +79° (*c*, 0.98), λ_{max} 250, 294 mμ (ϵ = 9 600 and 2 800 respectively), λ_{max} (alkaline) 250, 310 mμ (ϵ = 12 100 and 3 000 respectively).

Formaldehyde Estimation

The enol acetate (part structure VIII; X = H) of chaparrol (2.79 mg) was dissolved in sulfuric acid (conc., 0.5 ml), and chromotropic acid (10 mg) and water (0.1 ml) were added. The mixture was heated at 100° for 20 min and diluted to 10 ml, and the optical density was measured at 570 mμ. Comparison with a standard and controls gave 15% as the amount of formaldehyde liberated.

Reduction of Chaparrin Tetraacetate

(*a*) Chaparrin tetraacetate (1 g) and sodium borohydride (5 g) were dissolved in ethanol (100 ml) and the solution was left for 30 min. After dilution with water the hemiacetal triacetate (XXIII; OAc's C_1, C_2, and C_{12}) was isolated with chloroform and crystallized from ethyl acetate – light petroleum (530 mg) m.p. 223–224°, $[\alpha]_D$ +56° (*c*, 0.68).

Anal. Calcd. for $C_{26}H_{36}O_{10}$: C, 61.40; H, 7.14. Found: C, 61.49; H, 7.15.

Can. J. Chem. Downloaded from www.nrcresearchpress.com by 210.87.254.5 on 09/05/12
For personal use only.

Acetylation of the reduction product (75 mg) (pyridine – acetic anhydride at room temperature, 16 h) followed by decomposition of the acylating medium with ice water and hydrochloric acid gave, after isolation with ethyl acetate and crystallization from light petroleum, the hemiacetal tetraacetate (XXIII; OAc's at C_1, C_2, C_{12}, and $—CH_2O$), m.p. 189–191°, $[\alpha]_D$ +95° (*c*, 0.78).

Anal. Calcd. for $C_{28}H_{38}O_{11}$: C, 61.10; H, 6.91. Found: C, 61.41; H, 6.66.

(*b*) Chaparrin tetraacetate (160 mg) in ethanol (5 ml) was treated with a solution of sodium borohydride (160 mg) in water (2 ml), and the mixture was set aside for 30 h. After the addition of excess hydrochloric acid the ethanol was removed by evaporation, water (20 ml) was added, and the product was isolated with chloroform. Crystallization from acetone gave the product, m.p. 250–252°, $[\alpha]_D$ 67° (*c*, 0.6 in methanol).

Anal. Calcd. for $C_{20}H_{30}O_7$: C, 62.81; H, 7.91. Found: C, 62.62; H, 7.78.

Oxidation of the Acetal Tetraacetate

The tetraacetate (XXIII; OAc's at C_1, C_2, C_{12}, and $—CH_2O$) (15.7 mg) was dissolved in chromic acid – acetic acid (0.02 *N*, 10 ml). After 4 h oxidation had ceased with the consumption of 1.1 atoms of oxygen. Isolation of the product with chloroform, and crystallization from ethyl acetate – light petroleum gave chaparrin tetraacetate, m.p. and mixed m.p. 231–233°, $[\alpha]_D$ +34° (*c*, 0.46 in pyridine).

Oxidation of the Acetal Triacetate

(*a*) The triacetate (XXIII; OAc's at C_1, C_2, and C_{12}) (155 mg) in chloroform (5 ml) was shaken with active manganese dioxide for 3 d. Filtration gave a gum. This was separated by thin-layer chromatography (solvent: diethyl ether). Material with R_f near 0.35 was eluted with ethyl acetate (30 mg) and the triacetate-B (XIX; OAc's at C_1, C_2, and C_{12}) crystallized from ethyl acetate – light petroleum, m.p. 245–247°, $[\alpha]_D$ +18° (*c*, 0.87).

Anal. Calcd. for $C_{20}H_{34}O_{10}$: C, 61.65; H, 6.77. Found: C, 61.85; H, 6.72.

Chaparrin triacetate was unaffected by this reagent.

(*b*) The triacetate (25.9 mg) was dissolved in sodium dichromate – acetic acid solution (0.02 *N*, 10 ml). After 6 h, uptake of oxygen had ceased at 1.15 atoms. Isolation of the product with chloroform and crystallization from benzene gave the same triacetate obtained as described in (*a*), m.p. 248–250°, $[\alpha]_D$ +17° (*c*, 0.65).

This same compound was obtained by hydrolysis of chaparrin tetraacetate using a mole per mole ratio of potassium hydroxide in ethanol at room temperature for 2 h.

Dihydrochaparrol

Sodium borohydride (ca. 100 mg) was added to a solution of chaparrol (265 mg) in ethanol (8 ml). After 3 h the solution was diluted with water and extracted with chloroform. The product (140 mg) crystallized from ethyl acetate – light petroleum, m.p. 198–200° and 228–232°, $[\alpha]_D$ +63° (*c*, 0.71 in methanol), λ_{max} 270 (ϵ = 440).

Anal. Calcd. for $C_{20}H_{26}O_5.H_2O$: C, 65.91; H, 7.74. Found: C, 65.57; H, 7.66.

Oxidation of Dihydrochaparrol

Dihydrochaparrol (31 mg) was added to a mixture of chromium trioxide (35 mg) and pyridine (0.5 ml) and shaken for 2.5 h. Dilution of the mixture with aqueous acid and isolation with chloroform gave a gum which on t.l.c. gave a fraction having the same R_f as chaparrol. The eluted product had m.p. 215–220° undepressed on admixture with chaparrol of m.p. 218–222°, $[\alpha]_D$ +104° (*c*, 0.62 in pyridine).

Acetylation of Dihydrochaparrol

Dihydrochaparrol (25 mg) in pyridine (2 ml) and acetic anhydride (1 ml) was heated overnight on the steam bath. After removal of the solvents under reduced pressure the residue was filtered through a short column of Woelm acid alumina. Separation by t.l.c. gave the triacetate XXII which crystallized from ether – light petroleum (15 mg) (m.p. 152–156°) and which on further crystallization from the same solvent melted at 153–156, $[\alpha]_D$ +184° (*c*, 0.63), λ_{max} 244 mμ (ϵ = 13 400).

Anal. Calcd. for $C_{26}H_{32}O_8$: C, 66.08; H, 6.83. Found: C, 66.12; H, 6.82.

Dihydrochaparrol Tetraacetate

Dihydrochaparrol (96 mg) was heated on the steam bath for 17 h in acetic anhydride (5 ml) and pyridine (0.5 ml). It was then diluted with water and neutralized with sodium bicarbonate. The solution was extracted with chloroform to yield 140 mg crude product, separated by thin-layer chromatography (solvent: diethyl ether). The fraction (100 mg R_f near 0.7) was again separated (solvent: diethyl ether – benzene (1:3). The tetraacetate had m.p. 138–189°, $[\alpha]_D$ +218° (*c*, 0.76), λ_{max} 244, 276 (ϵ = 13 000 and 1 030 respectively).

Anal. Calcd. for $C_{28}H_{32}O_9$: C, 65.61; H, 6.29. Found: C, 65.33; H, 6.73.

Oxidation of the Triacetate (XXI)

The triacetate (XXI) (22 mg) in acetone (10 ml) was stirred with active manganese dioxide (200 mg) overnight. After filtration the solvent was evaporated separation by preparative thin-layer chromatography (solvent: diethyl ether) gave material which after crystallization from ethyl acetate – light petroleum (7 mg) had m.p. 176–178°, $[\alpha]_D$ +121° (*c*, 0.44). The melting point was undepressed on admixture with chaparrol triacetate (XVIII).

Can. J. Chem. Downloaded from www.nrcresearchpress.com by 210.87.254.5 on 09/05/12
For personal use only.

ACKNOWLEDGMENTS

The authors would like to thank Dr. W. Ayer for the o.r.d. measurements, and R. E. Klinck for the n.m.r. spectra. They are indebted to the Eli Lilly Co. and the National Research Council of Canada for financial support.

The would also like to express their appreciation to Professor T. A. Geissman (U.C.L.A.) for exchanges of views.

REFERENCES

1. T. A. DAVIDSON, T. R. HOLLANDS, and P. DE MAYO. Tetrahedron Letters, 1089 (1962).
2. L. P. BOSMAN. J. Chem. Soc. **121**, 969 (1922); **123**, 207 (1923).
3. T. A. GEISSMAN and K. R. CHANDORKAR. J. Org. Chem. **26**, 1217 (1960).
4. T. A. GEISSMAN and G. A. ELLESTAD. Tetrahedron Letters, 1083 (1962).
5. N. L. WENDLER. *In* Molecular rearrangements. *Edited by* P. de Mayo. Interscience Publ. Co. 1964. p. 1033.
6. D. H. R. BARTON and P. DE MAYO. J. Chem. Soc. 887 (1954).
7. Z. VALENTA, A. H. GRAY, D. E. ORR, S. PAPADOPOULOS, and C. PODESVA. Tetrahedron, **18**, 1433 (1962).
8. R. M. CARMAN and A. D. WARD. Austral. J. Chem. **15**, 807 (1962).
9. J. POLONSKY, C. FOUQUEY, and A. GAUDEMER. Bull. Soc. Chim. France, 1818, 1827 (1964).
10. R. L. STRONG and K. O. KUTSCHKE. Can. J. Chem. **37**, 1456 (1959).
11. G. KARTHA and D. J. HAAS. J. Am. Chem. Soc. **86**, 3630 (1964).
12. G. AULIN-ERDTMAN and R. SANDEN. Acta Chim. Scand. **17**, 1998 (1963).
13. G. H. BEAVEN and E. A. JOHNSON. *In* Conference on molecular spectroscopy. *Edited by* E. Thornton and H. W. Thompson. Pergammon Press. 1959. p. 85.

Can. J. Chem. Downloaded from www.nrcresearchpress.com by 210.87.254.5 on 09/05/12
For personal use only.

Can. J. Chem. Downloaded from www.nrcresearchpress.com by 210.87.254.6 on 09/05/12
For personal use only.

TERPENOIDS

XIII. THE STEREOCHEMISTRY OF CHAPARRIN, CHAPARROL, AND RELATED COMPOUNDS

T. R. HOLLANDS, P. DE MAYO, M. NISBET
Department of Chemistry, University of Western Ontario, London, Ontario

AND

P. CRABBÉ
Syntex S.A., Apartado Postal 2679, México, D.F.

Received June 23, 1965

ABSTRACT

Evidence is presented which leads to the absolute stereostructures XX, X, XI, and XII for chaparrin, chaparrol, isochaparrol, and neochaparrol respectively. The absolute configuration is arrived at by conversion to an optically active biphenyl (dihydrophenanthrene).

In our preceding papers (1, 2) we showed that the gross structures I and II were to be attributed to chaparrin, the bitter principle extracted from *Castela nicholsonii* (chaparro amargosa) and to chaparrol, its degradation product, respectively. Similar conclusions were simultaneously reached by Geissman and Ellestad (3). It is the purpose of this paper to discuss the stereochemistry of these and related compounds.

On the assumption that the absolute stereochemistry of the molecule requires that the primary hydroxyl be β, nine asymmetric centers remain in chaparrin giving a total of 512 possible isomers. Although a tenth center at C_{11} is introduced by the hemiketal formation, the stereochemistry of this center is rigidly defined with respect to the primary hydroxyl group and so does not increase the total number of isomers.

Chaparrol (II), derived from chaparrin by the acid-catalyzed loss of two molecules of water, has, aside from C_8 and C_{11}, five centers of asymmetry (32 isomers) and appeared a suitable starting point for investigations.

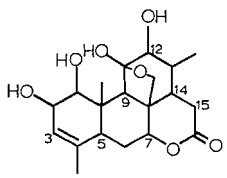

I

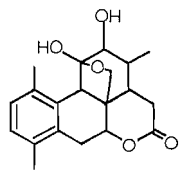

II

Whereas chaparrin (I) is stable to the action of mild alkali, and may be recovered from its acetate by alkaline hydrolysis, chaparrol (II) is not stable. Merely its solution in aqueous ethanolic alkali at room temperature for 30 min is sufficient to isomerize it to a new compound, isochaparrol. However, the transformation is not instantaneous because after 7 min some chaparrol can be recovered from a solution in which it has been present as an anion. Some slow step, other than lactone opening, is therefore involved.

The formation of isochaparrol could in principle involve isomerization at C_9, C_{12}, C_{13} (the last, through ketol equilibration), with, in addition, a possible change in the position of lactonization; or a combination of these. The substance is still a hemiketal since it shows no

Can. J. Chem. Downloaded from www.nrcresearchpress.com by 210.87.254.6 on 09/05/12
For personal use only.

Cotton effect in the 300 mμ region. Reduction with sodium borohydride gives a dihydroisochaparrol which, having no carbonyl absorption in the infrared, is evidently a hemiacetal hemiketal analogous to that formed from chaparrol (1).

Acetylation of isochaparrol gives a monoacetate, which also shows a plain optical rotatory dispersion curve above 280 mμ, and in which a secondary alcoholic function (with methine proton at τ 5.00; $J \sim 8.4$ c.p.s.) has been acetylated. Acetylation under forcing conditions (acetic anhydride – perchloric acid) results in further acetylation to give a diacetate. The second function to be acetylated is also a secondary alcohol (methine proton at τ 4.43), but the product, isochaparrol diacetate, now exhibits a positive Cotton effect curve.* A secondary hydroxyl group is therefore involved in ketal formation in isochaparrol, and in the formation of this substance hydrolysis and relactonization on to the primary hydroxyl group must have occurred since it is now no longer available for acetylation. This could not be the only change, however, since formation of the carboxylate anion had been shown, as stated, to be a necessary but insufficient requirement for isochaparrol formation. At least one slower process, presumably an epimerization, was hence required.

Acetylation of isochaparrol under different conditions, analogous to those used by Polonsky and her collaborators in the acetylation of isoglaucanol A (4), that is, with sodium acetate and acetic anhydride, gave a different product. This is most probably to be represented as in (IV).† The difference in behavior may be attributed to the high energy of the strained oxonium ion (V) which would be an intermediate in the acid-catalyzed formation of IV. The alternative acetylation at C_7 therefore occurs. Base-catalyzed acetylation, on the other hand, might well be expected to occur under these conditions at the more acidic (though more hindered) 11-hydroxyl group (17).

The proton at C_{12} in isochaparrol is a doublet (τ 6.56; $J \sim 8.4$ c.p.s.) whose large spin–spin coupling with the adjacent C_{13} methine proton indicates a *trans* diaxial relationship of these protons. Because of the requirements of the hemiketal system, isochaparrol must thus be represented as in the *cis*-fused B/C system (III) where only C_{14} remains undefined.

The stereochemical assignments in III are not all, however, transferable to the equivalent centers in chaparrol. Isomerization of chaparrol to isochaparrol under deuterating conditions and comparison of n.m.r. spectra of deuterated and non-deuterated material clearly indicated that, by their disappearance from the deuterated proton spectrum, the protons at C_9 and C_{12} had been exchanged. In addition, the C_{13} methyl group, which was a clear doublet in chaparrol and a broad singlet in isochaparrol (18), was distinctly narrower and taller in deuterated isochaparrol. The proton at C_{13} must, through ketol equilibration, have exchanged. Since such exchange at these centers implies the opportunity of epimerization, only the configuration at C_7 must necessarily be the same in chaparrol as in isochaparrol.

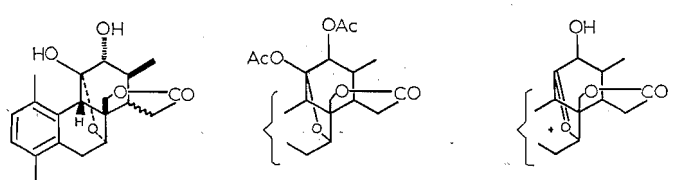

III IV V

We are indebted to Dr. W. A. Ayer for these determinations.

†*We understand from Mme. Polonsky that she has now reached a similar conclusion, and that isoglaucanol A is attributed the structure 15-hydroxyisochaparrol.*

The stereochemistry at C_{12} in chaparrol may be deduced as follows. In chaparrin the C_{12} hydroxyl is axial, firstly because the low intensity $n \rightarrow \pi^*$ absorption in chaparrin triacetate-A ($\lambda_{max}^{CHCl_3}$ 315 mμ, $\epsilon = 25$) moves to shorter wavelength ($\lambda_{max}^{CHCl_3}$ 308 mμ, $\epsilon = 38$) on acetylation to give the tetraacetate. This parallels the equivalent acetylation of methyl 3α,12α-dihydroxy-11-oxocholanoate (λ_{max} 313 $\rightarrow$ λ_{max} 308 mμ, ref. 19). Secondly, the difficulty of acetylation of this function is in keeping with an axial disposition. Because chaparrin is a hemiketal, ring C may be represented as in VI and so, with the previously made assumption that the primary hydroxyl group is β, the axial 12-hydroxyl group is then necessarily α.

The transference of this conclusion to the equivalent center in chaparrol is only permissable if, in the conversion of chaparrin to this substance, no inversion takes place at C_9; that is, that no conformational change in ring C has occurred. This was demonstrated by conducting the acid-catalyzed dehydration in deuterium chloride: the proton at C_9 was not exchanged.

Treatment of chaparrol with boiling pyridine—conditions under which the lactone is not opened—isomerizes it to a new substance termed neochaparrol. This differs from chaparrol in the configuration at C_9. Thus, preparation in pyridine containing 2% D_2O gives neochaparrol in which the C_9 proton, as judged from the relevant n.m.r. spectra, (see Table I) has been exchanged. In addition, acetylation of neochaparrol under conditions suitable for converting chaparrol into its triacetate (VII) gives, in fact, the same substance.

TABLE I

N.m.r. data from neochaparrol and some isochaparrol derivatives

Compound	C_7 H τ	C_9 H τ	C_{12} H τ (J)	C_{13} Me τ (J)	—CH_2—OR τ	Aromatic H, τ	Aromatic Me, τ	Acetate Me, τ
Neochaparrol*	~4.95	5.68	5.47 (3.0)	8.64 (7.2)	6.90		7.89	—
Isochaparrol	5.58	7.20	6.56 (4.2)	8.80 (6.0)	5.97	3.00	7.77	
Isochaparrol monoacetate	5.53	7.11	5.00 (4.0)	8.95 (7.2)	5.98	2.98	7.76 7.81	7.91
Isochaparrol diacetate I								7.94 8.32
Isochaparrol diacetate II	4.43	6.64	4.93 (4.8)	8.91 (6.0)	5.93	2.98	7.85	7.94 8.09

*Spectrum done in pyridine.

One significant feature readily observed was the fact that neochaparrol did not form a hemiketal. The infrared spectrum showed clearly resolved peaks at 1 715 and 1 750 cm^{-1} (KBr) for the ketonic and lactonic carbonyl functions respectively, and the optical rotatory dispersion curve showed a strongly positive Cotton effect ($a = +250$), in agreement with the stereochemistry proposed for this homoconjugated π-system (21).

It may be presumed that since the B/C ring junction in chaparrin is stable, that it is *trans* fused. From a consideration of models, this was probable, and since there is no inversion in the conversion to chaparrol, this is required to have a *trans* fusion also. The same conclusion may be reached by an alternative route.

Clearly, since stereochemically chaparrol and neochaparrol differ only at C_9 it is this

Can. J. Chem. Downloaded from www.nrcresearchpress.com by 210.87.254.6 on 09/05/12
For personal use only.

Can. J. Chem. Downloaded from www.nrcresearchpress.com by 210.87.254.6 on 09/05/12
For personal use only.

inversion at this point which has discouraged hemiketal formation. Since no assumption with regard to the stereochemistry at C_{14} has been made, four possibilities [9α,14α; 9β,14α; 9α,14β; 9β,14β] exist for the B/C/D ring systems in these two substances.

Inspection of models makes it evident that the two cases wherein the C_9 proton is β, hemiketal formation will not occur. In this pair the model with 14β proton the distance is, in the most favorable arrangement, too great to be spanned by the ethereal oxygen, and in this and the model with 14α proton hemiketal formation increases severely the non-bonded interaction between the oxygen function at C_{11} and the C_1 methyl group. On the other hand the two models with the C_9 proton in the α configuration are well oriented for hemiketal formation, and such formation rather decreases the interaction of the C_{11} oxygen function with the C_1 methyl group. This, with the favorable bond energy changes, rationalizes the hemiketal formation.

Hence, irrespective of the configuration at C_{14}, it can be concluded that in chaparrol (and hence chaparrin) the C_9 proton is α, and that in neochaparrol it is β. This conclusion is supported by the optical rotatory dispersion curve of chaparrol. A Cotton effect appears in the 270–280 mμ region and is due to an optically active aromatic B-band: its sign (positive) is in agreement with the 9αH-stereochemistry in chaparrol (see ref. 21, p. 293).

With the configuration at C_9 established in chaparrin, since chaparrin prefers to lactonize at C_7 rather than at the primary hydroxyl, it follows that the side chain at C_{14} is α. Were it β, inspection of models clearly indicates that, the occasion provided, the carboxyl group should prefer the less strained closure on to the primary hydroxyl group.

The following observations are compatible with this conclusion. The enol acetate previously described (1, 2), prepared by the bismuth oxide oxidation of chaparrol followed by acetylation, may, with the stereochemistry now assigned, be represented as in VIII, or

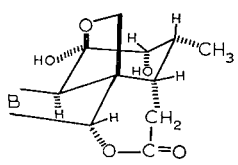

VI

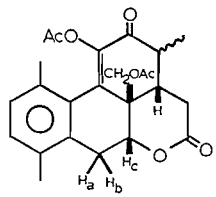

VIII

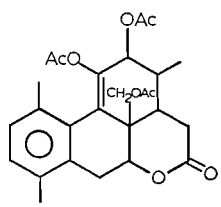

VII

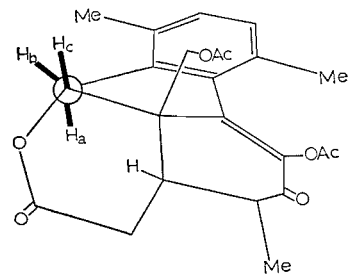

IX

as IX in the most favorable conformation. H_a and H_c are then coplanar and *trans*, and a large spin–spin coupling constant between them would be expected. There is, in addition, a smaller coupling to be expected between H_b and H_c. The proton H_c is partly overlain by the methylene protons of the primary acetate (Fig. 1), but a doublet of doublets may be observed, one of the coupling constants of which is large (near 10 c.p.s.).

All the asymmetric centres of chaparrol have therefore been defined with the exception of C_{13}. The coupling between the protons at C_{12} and C_{13} is small ($J \sim 3$ c.p.s.) but since

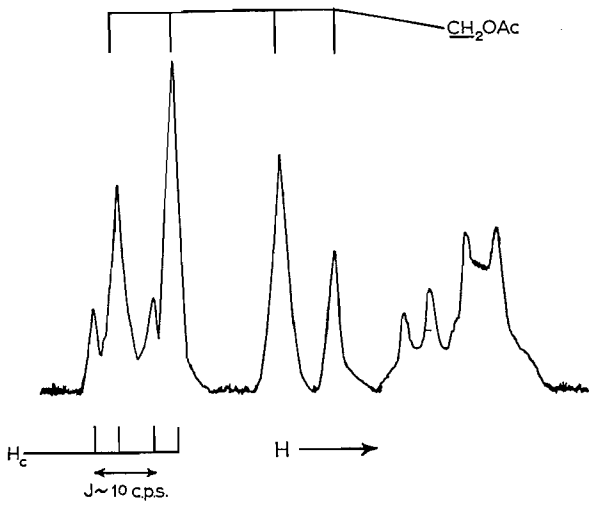

FIG. 1. Nuclear magnetic resonance spectrum of IX in region showing H_c and —CH_2OAc.

the C_{12} proton is equatorial* this is not informative since axial–equatorial and equatorial–equatorial couplings are comparable. Although compelling evidence is not available the following argument suggests that the methyl group is α (equatorial), and that it is therefore inverted in isochaparrol formation. That this was a possibility has already been demonstrated by the deuteration experiments reported.

Chaparrol shows no Cotton effect above 290 mμ, but as already mentioned, presents a peak at 283 mμ. In contrast the corresponding monoacetate (2) exhibits a negative Cotton effect around 300 mμ ($a = -56$). No change in structure occurs during acetylation since acid hydrolysis regenerates chaparrol. It is therefore the primary hydroxyl which has been acetylated. (See Table I, ref. 1.)

In such a configuration (and with the previously made assumption that the absolute configuration at C_8 is as shown) the 13-methyl group of chaparrol monoacetate, irrespective of configuration, falls into a positive octant (22). Ring A roughly lies in a nodal plane. The positive effect of the 13-methyl group is counterbalanced by carbon atoms 6 and 7, the 8,14-lactone and the 12α-hydroxyl group all falling into negative octants. Moreover, the negative Cotton effect is still enhanced, and probably largely attributable to the 8β-CH_2OAc function also in a negative octant. If the 13-methyl group were axial, it would be expected that the strong non-bonded diaxial interactions, occuring between the 8β-acetoxy-methyl and the 13β-methyl groupings, would lead to conformational changes, with ring C becoming a boat or twisted. A stronger negative Cotton effect might then be expected.

Accepting these conclusions the stereostructures of chaparrol, isochaparrol, and neochaparrol may be represented as in X, XI, and XII, respectively.

Five of the asymmetric centers in chaparrin are thus defined.

The configurations of the two hydroxyl groups in ring A of chaparrin follow from the study of the n.m.r. spectra of certain derivatives. Chaparrin triacetate-A shows a doublet ($J \sim 8$ c.p.s.) at τ 5.0. This doublet, which is due to the methine proton at C_1, is obscured

**The configuration at C_{12} does not change in the conversion of chaparrol to isochaparrol but the ring conformation does, and hence the C_{12} proton becomes axial, as already noted.*

Can. J. Chem. Downloaded from www.nrcresearchpress.com by 210.87.254.6 on 09/05/12
For personal use only.

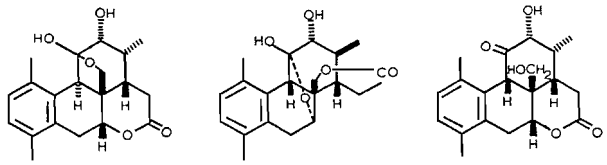

X XI XII

in the tetraacetate by the C_{12} methine proton which moves from ca. 6.18 to 4.92. This same doublet may be discerned in the isomeric triacetate-B (1) of chaparrin in which the primary hydroxyl group is unacetylated.

The magnitude of the coupling between the C_1 and C_2 protons requires, in the fused system, that these protons be coplanar and diaxial.

The manganese dioxide treatment of chaparrin gives chaparrinone, an α,β-unsaturated ketone, by oxidation at C_2. Hydrogenation then gives, with the uptake of one molecule of hydrogen, the saturated ketone dihydrochaparrinone. Aside from the stereochemistry at C_4 the complete molecule may be represented in four ways. In two of these, indicated by the partial structures XIII and XIV, a positive Cotton effect would be predicted, irrespective of the configuration at C_4 while in the other two a negative Cotton effect would very probably be expected. The observation of a weak positive Cotton effect ($a = +16$) restricts the possibilities to XIII and XIV. Usually 2-oxo-steroids exhibit rather strong positive rotatory dispersion curves ($a \approx +120$), but in the present substance this positive effect is counterbalanced by the 1-hydroxyl group (5, 6) and the 4-(probably β)-methyl group; moreover, this grouping seems to have induced a conformational change of ring A in XIII in order to release 1,3-diaxial interactions with the 10-methyl substituent. From this it is reasonable to conclude that the methyl group at C_{10} is β in chaparrin.

XIII XIV

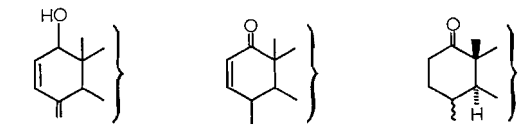

XV XVI XVII

The acid-catalyzed dehydration of chaparrin gives, aside from anhydrochaparrin-A (XV) (2), an isomeric substance which is an unsaturated ketone (XVI) (3). This compound, anhydrochaparrin-B, may be hydrogenated to the saturated ketone hemiketal (XVII), or which three other stereochemical representations are possible, depending on the nature of the A/B ring fusion.

The rotatory dispersion curve of this substance shows a rather strong positive Cotton effect ($a = +94$). An examination of the four molecular models of this ketone permits an interpretation of the positive Cotton effect which is observed, in terms of XVII. The angular methyl at C_{10}, ring C and its substituents, the hemi-ketal bridge between the

Can. J. Chem. Downloaded from www.nrcresearchpress.com by 210.87.254.6 on 09/05/12
For personal use only.

8-hydroxymethylene and C_{11}, all fall into positive octants. This strong positive contribution effect is only partly counterbalanced by carbon atoms C_6 and C_7 of ring B and very slightly by the δ-lactone grouping (far away from the carbonyl) falling into negative octants. With this evidence the stereochemistry of chaparrin may be represented in its entirety as shown in XX.

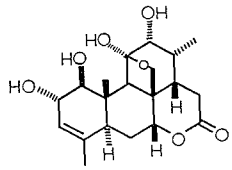

XX

These arguments have been based on the assumption that the absolute configuration of the C_8 center has the primary hydroxyl group β. This may be justified in the following way.

The Cotton effects exhibited by several of the above mentioned compounds have been related to those shown by corresponding compounds from the steroid series. Since the absolute configuration of natural steroids has been established, the absolute configuration of chaparrin may be ascertained. A further, and independent, argument also leads to the same conclusion.

A degradation product of chaparrol, instrumental in arriving at the gross structure of this substance, was attributed the structure represented in XXI. This substance has, of course, no asymmetric centre and accordingly might be expected to have no optical activity. However, the considerable amount of steric interference between the methoxyl group and the aromatic methyl group at C_1 could prohibit their mutual crossing, despite the aromatization of ring C, under the mild condition for the genesis of XXI.

The dihydrophenanthrene is in fact optically active. Its optical rotatory dispersion curve exhibited three successive Cotton effects of increasing amplitudes towards shorter wavelengths, in agreement with the inherently dissymmetric nature of the chromophore (see Experimental). The shape of the dispersion curve from 600 mμ to about 300 mμ appeared to be very similar to, and of the same sign as, that of the 2,2′-dimethyl dihydrophenanthrene (XXII) reported by Mislow and Hopps (7) which has been attributed the (R)-configuration. The change of —OMe for —CH_3 in an unchanged stereochemical situation gives the (S)-configuration for the absolute stereochemistry of the dihydrophenanthrene from chaparrol which is that represented in XXI.

If it be assumed that in the aromatization of chaparrin the angular methyl group migrates and retains its position relative to the substituent at C_{11} in going from I to II then, if the angular methyl group be β, the dihydrophenanthrene CXXI) will have the (S)-configuration, as observed. Since it has been demonstrated that the angular methyl group and the hydroxyl methyl group at C_8 are on the same side of the molecule the absolute stereochemistry of chaparrin is as represented in XX.

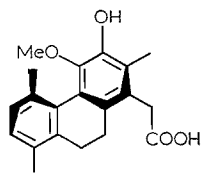

XXI

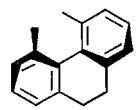

XXII

Can. J. Chem. Downloaded from www.nrcresearchpress.com by 210.87.254.6 on 09/05/12
For personal use only.

Subsequent to the description of the gross structure of the chaparrin and that of the earlier reported quassin (8, 9) a number of other members of this chemical family have been investigated, largely because of the efforts of Polonsky and her school (ref. 10 and earlier papers in this series). The structure of simarolide (XXIII) (11) confirmed by X-ray studies (12) is of special relevance. It has the absolute configuration shown, which is that of the triterpenoids, and its relationship to butyrospermol (XXIV), as has been pointed out (13–15), is obvious. The loss of the side chain has clear association in the chemistry of limonin with the conversion of limonol to merolimonol (XXV) (20). Since this has been amply discussed elsewhere (13–16) further elaborations, in the absence of additional evidence, would be supererogatory. It is sufficient to note that the structure and stereochemistry deduced for chaparrin conforms with the general pattern.

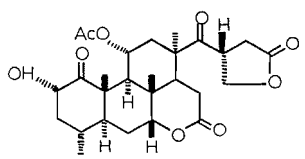

XXIII

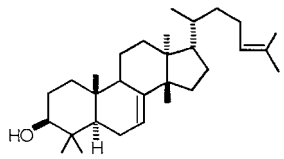

XXIV

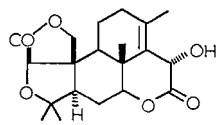

XXV

EXPERIMENTAL*

Neochaparrol (XII)

A solution of chaparrol (60 mg) in pyridine (4 ml) was refluxed for 2 h. The pyridine was removed under reduced pressure and the gummy residue was dissolved in chloroform. The solution was washed with dilute hydrochloric acid and water. Removal of the solvent afforded a glass which was crystallized from ethyl acetate (37 mg) m.p. 225–230 °C. Further recrystallization from ethanol raised the melting point to 233–237 °C, $[\alpha]_D$ +150° (*c*, 0.6, methanol); o.r.d. (*c*, 0.1, dioxane): $[\Phi]_{600}$ +385°, $[\Phi]_{500}$ +771°; $[\Phi]_{400}$ +1 768°; $[\Phi]_{318}$ +11 252°; $[\Phi]_{279}$ −13 739°; $[\Phi]_{246}$ −6 622°; $[\Phi]_{228}$ −17 217°.

Anal. Calcd. for $C_{20}H_{24}O_5$: C, 69.75; H, 7.02. Found: C, 69.70; H, 6.77.

The deuterated material was prepared as follows: chaparrol (88 mg) was refluxed in pyridine containing 2% D_2O for 2 h. After evaporation to dryness the product was crystallized from ethyl acetate – light petroleum and from ethanol – light petroleum.

Preparation of Chaparrol with Deuterium Chloride

Chaparrin (113 mg) was dissolved in deuteriochloric acid (1.5 ml) and allowed to stand for 45 min. The reaction mixture was poured into heavy water (5 ml) and the product isolated with chloroform. Crystallization from ethyl acetate – light petroleum gave chaparrol, m.p. 215–216°. Chaparrol (X) o.r.d. (*c*, 0.1, dioxane): $[\Phi]_{600}$ +502°; $[\Phi]_{500}$ +626°; $[\Phi]_{400}$ +1 128°; $[\Phi]_{300}$ +2 821°; $[\Phi]_{283}$ +4 792°; $[\Phi]_{278}$ +3 196°; $[\Phi]_{276}$ +3 385°; $[\Phi]_{270}$ +2 442°; $[\Phi]_{232}$ +20 977°; $[\Phi]_{226}$ +3 550°; $[\Phi]_{222}$ +16 457. Chaparrol monoacetate o.r.d. (*c*, 0.13, dioxane): $[\Phi]_{600}$ +216°; $[\Phi]_{500}$ +397°; $[\Phi]_{400}$ +995°; $[\Phi]_{348}$ +1 070°; $[\Phi]_{324}$ +408°; $[\Phi]_{288}$ +6 080°; $[\Phi]_{274}$ +5 130°; $[\Phi]_{256}$ +3 880°.

Isochaparrol

A solution of chaparrol (93 mg) in methanol (10 ml) containing potassium hydroxide (0.5 g) was refluxed under nitrogen for 4 h. After evaporation of the methanol, water was added and the mixture was acidified and extracted with chloroform. The product was crystallized from ethyl acetate – light petroleum and was

**For general indications, see Part XII (1). The optical rotatory dispersion (o.r.d.) curves, obtained through the courtesy of Dr. L. Throop, were measured with an automatic spectropolarimeter of the Japan Spectroscopic Co. Ltd. (JASCO), model ORD-UV-5.*

Can. J. Chem. Downloaded from www.nrcresearchpress.com by 210.87.254.6 on 09/05/12
For personal use only.

homogeneous on thin-layer chromatography (solvent: diethyl ether, R_f 0.24) and had constant rotation $[\alpha]_D$ −48° (*c*, 0.7). The m.p. varied with the rate of heating in the region 135–138° to 156–158°.

Anal. Calcd. for $C_{20}H_{24}O_5$: C, 69.75; H, 7.02. Found: C, 69.35; H, 7.12.

The deuterated material was prepared as follows: potassium deuteroxide (from potassium hydroxide and heavy water, evaporation, re-dissolution in heavy water and evaporation) (0.5 g) was added to heavy water (10 ml) and chaparrol (92 mg). The mixture was refluxed for 6 h under nitrogen. Acidification with deuteriochloric acid, extraction with chloroform, and crystallization from ethyl acetate – light petroleum then gave deuterated isochaparrol. Deuterated isochaparrol was obtained in a similar manner from neochaparrol.

Isochaparrol was also obtained under the following conditions.

(*a*) Solution of chaparrol in 5% (w/v) aqueous ethanolic potassium hydroxide at room temperature for 30 min. After 7 min, crystallization yielded chaparrol.

(*b*) Solution of neochaparrol in ~1% (w/v) aqueous ethanolic potassium hydroxide at room temperature for 6 min.

Equilibration of isochaparrol in alkali gave no detectable amount of neochaparrol as indicated by thin-layer chromatography (t.l.c.).

Isochaparrol Monoacetate

Isochaparrol (40 mg) in pyridine (1 ml) and acetic anhydride (0.5 ml) was heated for 4 h on a steam bath, then set aside overnight. Evaporation of the reagents and filtration of the residue through a short column of alumina gave material which was crystallized from ethyl acetate – light petroleum to give the monoacetate, m.p. 237–239°, $[\alpha]_D$ +17° (*c*, 0.58).

Anal. Calcd. for $C_{22}H_{26}O_6$: C, 68.38; H, 6.78. Found: C, 67.91; H, 6.94.

Isochaparrol Diacetate

(*a*) Isochaparrol (20 mg) was dissolved in a mixture of acetic acid (1 ml) and acetic anhydride (0.5 ml). Perchloric acid (5 *N* in acetic acid, 5 drops) was added, care being taken to keep the temperature below 35 °C. After 35 min the mixture was diluted with diethyl ether (30 ml) and the ethereal solution was washed with 3% aqueous sodium bicarbonate. Removal of the ether afforded a solid which was crystallized from chloroform – light petroleum to m.p. 308–310°.

Anal. Calcd. for $C_{24}H_{28}O_7.\frac{1}{2}H_2O$: C, 65.87; H, 6.60. Found: C, 65.99; H, 6.48.

(*b*) Isochaparrol (9 mg) and sodium acetate (16 mg) were refluxed in acetic anhydride (1.5 ml) for 2 h. The solution was evaporated to dryness with methanol. A mixture ca. 1:1 was obtained of two compounds, as shown by t.l.c. (solvent: diethyl ether).

The second spot was the same as obtained in part (*a*) m.p. 308–310° and mixed m.p. 308–310°, $[\alpha]_D$ −20° (*c*, 0.71).

Anal. Found: C, 66.27; H, 6.45.

The first spot was a new diacetate crystallized from ethyl acetate – light petroleum m.p. 188–191°.

Anal. Calcd. for $C_{24}H_{28}O_7$: C, 67.27; H, 6.59. Found: C, 66.89; H, 6.60.

Acid Hydrolysis of Chaparrol Triacetate

The triacetate (48 mg) was added to a mixture of dioxane (3 ml) and hydrochloric acid (3 ml, 3 *N*) and the mixture allowed to stand at room temperature for 5 days. The product after isolation was complex, but thin-layer chromatography (solvent: ether) gave material which after crystallization from ethyl acetate – light petroleum was identified by melting point and rotation as neochaparrol.

Chaparrinone

A mixture of chaparrin (80 mg), manganese dioxide (800 mg), and dioxane (100 ml) was stirred overnight at room temperature for 13 h. The product remaining after filtration and evaporation was separated by thin-layer chromatography (solvent: 5% methanol in chloroform). The fraction of R_f 0.18 was crystallized from ethanol – ethyl acetate to give chaparrinone, m.p. 230–232°, $[\alpha]_D$ −47° (*c*, 0.88, pyridine), λ_{max} 241 mμ (ϵ = 5 700).

Anal. Calcd. for $C_{20}H_{26}O_7$: C, 63.48; H, 6.93. Found: C, 63.16; H, 6.57.

Dihydrochaparrinone

Chaparrinone (45 mg) in ethanol (10 ml) was hydrogenated over palladized charcoal (5%, 10 mg). The product (uptake 0.9 mole) was crystallized from ethanol – ethyl acetate to give the saturated ketone, m.p. 258–260°, $[\alpha]_D$ −3° (*c*, 0.78, EtOH).

Dihydrochaparrinone (XIII) o.r.d. (*c*, 0.1, dioxane): $[\Phi]_{600}$ +180°; $[\Phi]_{500}$ +340°; $[\Phi]_{400}$ +520°; $[\Phi]_{313}$ +2 000°; $[\Phi]_{307}$ +1 900°; $[\Phi]_{302}$ +1 950°; $[\Phi]_{267}$ +860°; $[\Phi]_{250}$ +980°.

Anal. Calcd. for $C_{20}H_{28}O_7$: C, 63.14; H, 7.42. Found: C, 63.10; H, 6.96.

Anhydrochaparrin-B (XVI)

Chaparrin (700 mg) was added to hydrochloric acid (*N*, 50 ml) and the mixture refluxed for $1\frac{3}{4}$ h in an oil bath (ca. 120°). The isolated material was separated by thin-layer chromatography (solvent: 5% MeOH in $CHCl_3$). Chaparrol and anhydrochaparrin-B ran close together ($R_f \sim 0.4$). Anhydrochaparrin-A (XV) runs more slowly in this system. The mixture of chaparrol and anhydrochaparrin-B was applied to thin-layer

Can. J. Chem. Downloaded from www.nrcresearchpress.com by 210.87.254.6 on 09/05/12
For personal use only.

plates again (solvent: diethyl ether) in which chaparrol had R_f 0.38 (152 mg) and anhydrochaparrin-B R_f 0.12 (158 mg).

Crystallization from ethanol – ethyl acetate gave the ketone, m.p. 258–260°, $[\alpha]_D$ +38° (*c*, 1.98, EtOH), λ_{max} 232 mμ (ϵ = 10 100).

Anal. Calcd. for $C_{20}H_{26}O_6$: C, 66.28; H, 7.23. Found: C, 66.22; H, 7.16.

Dihydroanhydrochaparrin-B

Anhydrochaparrin-B (34 mg) was hydrogenated in ethanol solution (10 ml) over palladized charcoal. The uptake of hydrogen ceased at 1 mole equivalent, and the product, after crystallization from ethanol – ethyl acetate – light petroleum, had m.p. 228–230°, $[\alpha]_D$ +54° (*c*, 1.02).

Dihydroanhydrochaparrin-B (XVII) o.r.d. (*c*, 0.12, dioxane): $[\Phi]_{600}$ +210°; $[\Phi]_{500}$ +255°; $[\Phi]_{400}$ +470°; $[\Phi]_{303}$ +4 400°; $[\Phi]_{260}$ −5 020°; $[\Phi]_{246}$ −4 450°.

Anal. Calcd. for $C_{20}H_{28}O_6$: C, 65.91; H, 7.74. Found: C, 65.56; H, 7.4.

Acetylation of Neochaparrol

Neochaparrol (20 mg) in pyridine (3 ml) containing acetic anhydride (1.5 ml) was heated overnight on the steam bath. After removal of the reagents under reduced pressure, filtration of the residue in benzene solution through a short column of alumina and crystallization from ethyl acetate – light petroleum gave chaparrol triacetate identified by m.p. and mixed m.p., $[\alpha]_D$ +121° (*c*, 0.53).

Dihydroisochaparrol

Sodium borohydride (20 mg) in aqueous ethanol (2 ml, 1:1) was added to a solution of isochaparrol (29 mg) in ethanol (0.5 ml). After 1 h the excess reagent was decomposed with acid, water was added, and the product was isolated with chloroform. After crystallization it had m.p. 254–256°, $[\alpha]_D$ −65° (*c*, 0.65, MeOH).

Anal. Calcd. for $C_{20}H_{26}O_5$: C, 69.34; H, 7.57. Found: C, 68.88; H, 7.86.

Hydrolysis of Chaparrol Monoacetate

The monoacetate (9 mg) was dissolved in dioxane (0.8 ml) containing hydrochloric acid (3 *N*, 0.8 ml) and the mixture was allowed to stand at room temperature for 25 h. After dilution and isolation with chloroform the product was crystallized from ethyl acetate – light petroleum. It had m.p. 210–215° undepressed on admixture with an authentic specimen of chaparrol.

Dihydrophenanthrene (XXI) o.r.d. (*c*, 0.08, dioxane): $[\Phi]_{600}$ 0°; $[\Phi]_{500}$ +236°; $[\Phi]_{400}$ +945°; $[\Phi]_{304}$ +19 162°; $[\Phi]_{286}$ −15 915°; $[\Phi]_{265}$ +46 977°; $[\Phi]_{241}$ −48 597°; $[\Phi]_{224}$ +132 829°; $[\Phi]_{222}$ +105 291°; $[\Phi]_{217}$ +140 930°.

REFERENCES

1. T. A. DAVIDSON, T. R. HOLLANDS, P. DE MAYO, and M. NISBET. Can. J. Chem. In press. 1965.
2. T. A. DAVIDSON, T. R. HOLLANDS, and P. DE MAYO. Tetrahedron Letters, 1089 (1962).
3. T. A. GEISSMAN and G. A. ELLESTAD. Tetrahedron Letters, 1083 (1962).
4. J. POLONSKY, C. FOUQUEY, and A. GAUDEMER. Bull. Soc. Chim. France, 1818 (1964).

5*a*. C. DJERASSI, P. A. HART, and E. J. WARAWA. J. Am. Chem. Soc. **86**, 78 (1964).

5*b*. C. DJERASSI, P. A. HART, and C. BEARD. J. Am. Chem. Soc. **86**, 85 (1964).

6. C. BEARD, C. DJERASSI, J. SICHER, F. SIPOS, and M. TICHY. Tetrahedron, **19**, 919 (1963).
7. K. MISLOW and H. B. HOPPS. J. Am. Chem. Soc. **84**, 3018 (1962).
8. Z. VALENTA, A. H. GRAY, D. E. ORR, S. PAPADOPOULOS, and C. PODESVA. Tetrahedron, **18**, 1433 (1962).
9. R. M. CARMAN and A. D. WARD. Australian J. Chem. **15**, 807 (1962).
10. J. POLONSKY and J. L. FOURREY. Tetrahedron Letters, 3983 (1964).
11. J. POLONSKY. Proc. Chem. Soc. 292 (1964).
12. W. A. C. BROWN and G. A. SIM. Proc. Chem. Soc. 293 (1964).
13. J. B-SON BREDENBERG. Chem. Ind. London, 73 (1964).
14. D. L. DREYER. Experientia, **20**, 297 (1964).
15. S. K. PRADHAN. Private communication. 1963.
16. J. POLONSKY, C. FOUQEY, and A. GAUDEMER. Bull. Soc. Chim. France, 1827 (1964).
17. D. H. R. BARTON, C. J. W. BROOKS, and J. S. FAWCETT. J. Chem. Soc. 2137 (1954).
18. F. A. L. ANET. Can. J. Chem. **39**, 1608 (1961).
19. R. C. COOKSON and S. H. DANDEGAONKER. J. Chem. Soc. 352 (1955).
20. D. ARIGONI, D. H. R. BARTON, E. J. COREY, and O. JEGER. Experientia, **16**, 41 (1960).
21. P. CRABBÉ. Optical rotatory dispersion and circular dichroism in organic chemistry. Holden-Day Publ. Inc., San Francisco. 1965. p. 238.
22. W. Moffitt, R. B. WOODWARD, A. MOSCOWITZ, W. KLYNE, and C. DJERASSI. J. Am. Chem. Soc. **83**, 4013 (1961).

Can. J. Chem. Downloaded from www.nrcresearchpress.com by 210.87.254.6 on 09/05/12
For personal use only.

Can. J. Chem. Downloaded from www.nrcresearchpress.com by 210.87.254.6 on 09/05/12
For personal use only.

REACTIONS OF SUGAR CHLOROSULFATES

PART VI. THE STRUCTURE OF UNSATURATED CHLORODEOXY SUGARS

H. J. JENNINGS[1] AND J. K. N. JONES
Department of Chemistry, Queen's University, Kingston, Ontario and The University of Bristol, England

Received May 20, 1965

ABSTRACT

Methyl α- and β-L-arabinopyranosides when treated with sulfuryl chloride yielded methyl 4-chloro-4-deoxy-α-D-xylopyranoside 2,3-dichlorosulfate and methyl 3,4-dichloro-3,4-dideoxy-β-D-ribopyranoside 2-chlorosulfate respectively. L-Arabinose gave, in addition to 4-chloro-4-deoxy-D-xylosyl chloride 2,3-dichlorosulfate, an unsaturated tetrachloro–tetradeoxy dimer. The structure and mode of formation of these compounds is discussed.

DISCUSSION

L-Arabinose when treated with sulfuryl chloride gave a syrupy mixture of chloroform-soluble products, one of which was shown to be 4-chloro-4-deoxy-D-xylosyl chloride 2,3-dichlorosulfate.* Methanolysis of the syrupy mixture yielded crystalline methyl 4-chloro-4-deoxy-α-D-xylopyranoside 2,3-dichlorosulfate (I) the structure of which was proved by the following series of reactions. An identical crystalline compound was obtained by the reaction of methyl β-L-arabinopyranoside with sulfuryl chloride thus establishing the configuration of the methyl glycosidic group and the pyranose ring structure of I. When treated with pyridine I gave a crystalline cyclic sulfate ester derivative, thus indicating the presence of vicinal chlorosulfate ester groups in I (1), and dechlorosulfation of I with sodium iodide (1)† gave a crystalline methyl chlorodeoxypentopyranoside. Hydrolysis of the methyl chlorodeoxypentopyranoside required drastic conditions (25% sulfuric acid) and gave a crystalline chlorodeoxypentose the periodate oxidation of which (2 moles periodate uptake, 1 mole formic acid liberated) was consistent with presence of the chlorodeoxy group on position C-4. The chlorodeoxypentose was proved to be of the D-*xylo*-configuration because the less likely alternative structure (the result of 4-chloro-substitution with retention of configuration) 4-chloro-4-deoxy-L-arabinose had been synthesised previously and was shown to have different physical constants (2).‡

The reaction of L-arabinose with sulfuryl chloride gave in addition to the chloroform-soluble products another highly crystalline compound (II) which separated from the acid wash of the reaction mixture. Compound II originated from the carbohydrate component of the reactants because the corresponding reaction with D-arabinose yielded the crystalline L-enantiomer of II. In comparison with similar reactions of other reducing sugars with sulfuryl chloride (2, 3) this appears to be a unique property of arabinose. A tentative structure (II) was proposed (2) based on elemental analysis, infrared spectroscopy (unconjugated ethylenic bond, 1 655 cm^{-1}) and approximate molecular weight determination (ca. 300). It was a trehalo-type dimer because it was non-reducing and the presence of vinylic chlorine was inferred because II was stable when subjected to ozonolysis (4)

[1]*Present address: Department of Chemistry, The University of Bristol, England.*

**In one reaction a crystalline compound was obtained the elemental analysis of which was consistent with this structure. However, the structure could not be proved as the crystals decomposed and could not be isolated from subsequent reactions.*

†*Part IV in this series.*

‡*Part III in this series.*

and lead tetraacetate oxidation (5). The structure of II, 4-deoxy-3,4-dichloro-α-D-*glycero*-pent-2-enopyranosyl 4′-deoxy-3′,4′-dichloro-α-D-*glycero*-pent-2′-enopyranoside, was finally confirmed by methanolysis of the dimer (II) to give III, methyl 4-deoxy-3,4-dichloro-β-D-*glycero*-pent-2-enopyranoside, which was also obtained from methyl α-L-arabinopyranoside by an independent synthesis.

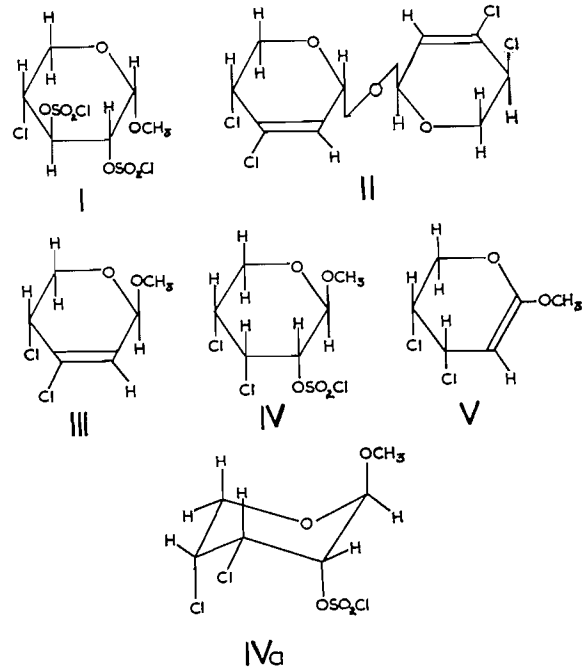

Methyl α-L-arabinopyranoside was treated with sulfuryl chloride to give a syrupy product, which was further heated with pyridine hydrochloride in chloroform solution to ensure chlorodeoxy-substitution and replacement of as many chlorosulfate groups as possible. A crystalline compound (IV) was isolated from the reaction mixture which was shown to be methyl 3,4-dichloro-3,4-dideoxy-β-D-ribopyranoside 2-chlorosulfate in the following way. Dechlorosulfation of IV with sodium iodide (1) gave a syrupy methyl dichlorodideoxypentopyranoside which was shown to be homogeneous by thin layer chromatography (t.l.c.) and which gave an elemental analysis consistent with this formulation. Prolonged hydrolysis of the syrupy methyl glycoside afforded a crystalline dichlorodideoxypentose in small yield. The presence of hydroxyl groups on adjacent carbon atoms and thus of chlorodeoxy groups on C-3 and C-4 of the dichlorodideoxypentose was proved by its considerable electrophoretic mobility in borate buffer (M_g = 0.68). This precludes the possibility of C-5 chlorodeoxy-substitution (3). Also a crystalline dichlorodideoxy-1,2-*O*-isopropylidene derivative was obtained from the mother liquors of the above hydrolysis products which were shown to contain only the 3,4-dichlorodideoxypentose and the unhydrolyzed methyl 3,4-dichlorodideoxypentopyranoside (t.l.c.). It was argued that 3,4-dichloro-3,4-dideoxy groups were both formed with inversion of configuration to give the D-*ribo* derivative on the following evidence. Inversion of configuration at C-4 would be expected as both methyl β-L-arabinopyranoside and L-arabinose gave 4-chloro-4-deoxy-D-*xylo* derivatives when treated with sulfuryl chloride. Methyl β-L-arabinopyranoside on treatment with sulfuryl chloride gave only a 4-chloro-4-deoxy-*xylo* derivative

Can. J. Chem. Downloaded from www.nrcresearchpress.com by 210.87.254.6 on 09/05/12
For personal use only.

Can. J. Chem. Downloaded from www.nrcresearchpress.com by 210.87.254.6 on 09/05/12
For personal use only.

(I) (axial anomeric methoxyl groups in the *CI* conformation) resistant to further chloro-substitution whereas methyl α-L-arabinopyranoside (equatorial anomeric methoxyl group in the *CI* conformation) gave a 3,4-dichloro-substituted derivative (IV). This observation is consistent with a mechanism of chloro-substitution with inversion of configuration at C-3 in the latter case. This has been demonstrated previously, when it was found that only the β-D-anomer (equatorial anomeric methoxyl group in the *CI* conformation) of the analogous methyl α- and β-D-galactopyranosides gave a 3,4,6-trichloro-D-*allo* derivative using similar reaction conditions. Chloro-substitution at C-3 in this case was shown to be dependent on the removal of the 1:3-diaxial interaction to the approach of chloride ion (3). A further example of a similar effect has also been reported (6).

Treatment of IV with pyridine gave compound III previously obtained by the methanolysis of the unsaturated dimer (II), and the structure of III was ascertained as follows. The elemental analysis and infrared spectrum (unconjugated ethylenic bond 1 657 cm^{-1}) of III indicated that it (III) was a product of elimination from IV and that it still contained two chlorodeoxy groups. Although structure III is the preferred elimination product as it involves a 2,3-*trans* elimination from IV, structure V is the alternative possibility the formation of which would involve a 1,2-*cis* elimination from IV. The n.m.r. spectrum of the elimination product (in carbon tetrachloride) contained two doublets (1 proton each) at 5.88 and 4.87 p.p.m. which could be assigned unambiguously to the vinylic and the anomeric proton of III respectively. Although the alternative structure V also has a vinylic proton it is unlikely that the C-3 proton of V would give a simple doublet. The remaining signals in the spectrum were a singlet assigned to the anomeric methoxyl group (3 protons, 3.34 p.p.m.) and a complex group of signals (3 protons) which were assigned to the remaining protons on C-4 and C-5 of III. A comparison of the n.m.r. spectra of II with III (in hot pyridine solution because of the insolubility of II in most solvents) was made and the spectra are shown in Fig. 1. Except for the anomeric methoxyl protons (3 protons, 2.59 p.p.m.) of III the remaining three groups of peaks in the spectra of II and III were similar in appearance and had the same proton ratios. The principal difference in the remaining groups of peaks was the difference in chemical shift of the signal assigned to the anomeric protons of II (two protons, 4.88 p.p.m.) and III (one proton, 4.33 p.p.m.). This could be attributed to the difference of configuration of the anomeric protons of II and III (α and β respectively) and provides tentative evidence that II is a symmetrical α,α′-linked dimer. Some support for this is also found in the high positive rotation of II.

In the formation of III from IV it is likely that 2,3-*trans*-diaxial elimination from the *1C* conformation of IV (IV*a*) had taken place, as this has previously been demonstrated to be the preferred mode of elimination of chlorosulfate groups under these conditions (1). This supports the fact that chloro-substitution had taken place on C-3 of IV with inversion of configuration as the alternative product (C-3-chlorodeoxy-substitution with retention of configuration) would require a 2,3-*cis* elimination to give III. Also this *trans*-diaxial elimination process provides a possible explanation of the formation of the monomeric unit of the dimer (II). It might be expected that 4-chloro-4-deoxy-D-xylosyl chloride, previously obtained in the reaction of sulfuryl chloride with L-arabinose, would be further substituted at C-3 to give 3,4-dichloro-3,4-dideoxy-D-ribosyl chloride 2-chlorosulfate (VI) which could undergo an analogous elimination to give compound VIII. Thus VI and VIII would be the precursors of the dimer II although it is difficult to see how either of these highly substituted compounds is extracted from chloroform solution by aqueous sulfuric acid to become the water-soluble precursor. Perhaps this is achieved

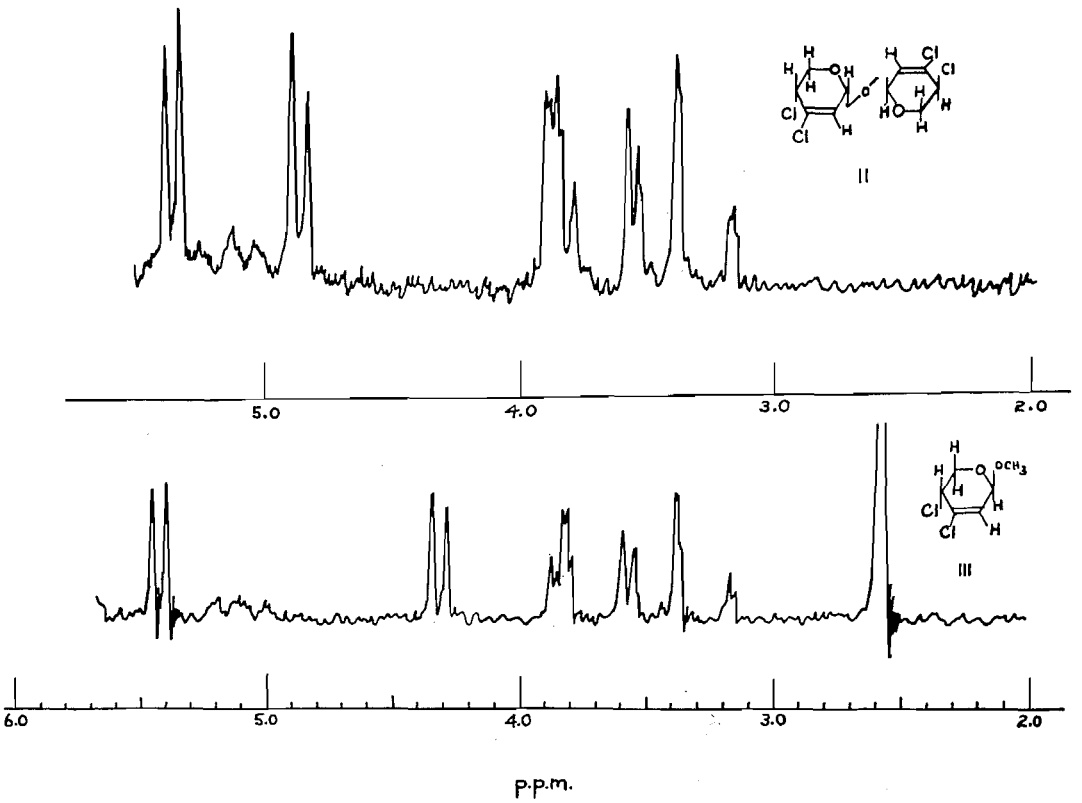

FIG. 1. Spectra of II and III both run in pyridine.

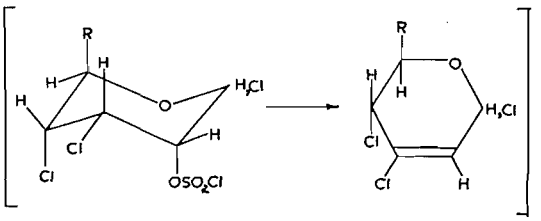

VI R=H
VII R=CH_2Cl

VIII R=H
IX R=CH_2Cl

through the agency of C-1 quaternary pyridinium salts which are known to form from acetohalo sugars (7). This still leaves the basic problem of the mechanism of the aqueous dimerization process which at present is not understood.

It is interesting to note that although reaction of sulfuryl chloride with D-galactose gave a fairly good yield of 3,4,6-trichloro-3,4,6-trideoxy-D-allosyl chloride 2-chlorosulfate (configurational analogue of VI) it does not appear to yield any analogous aqueous insoluble dimeric product from the acid wash of the reaction mixture (3). This might be explained by the inability of the allosyl chloride derivative to attain its *1C* conformation (VII) under these conditions, thus preventing the attainment of the favored *trans*-diaxial arrangement of the groups on C-2 and C-3 for elimination to give intermediate IX. This

Can. J. Chem. Downloaded from www.nrcresearchpress.com by 210.87.254.6 on 09/05/12
For personal use only.

could be attributed to the higher energy state of the *1C* conformation of the allosyl chloride derivative (VII) in comparison with VI due to the larger —CH_2Cl group at C-5 of VII. Some corroborating evidence for this is that methyl 3,4,6-trichloro-3,4,6-trideoxy-α-D-allopyranoside 2-chlorosulfate when treated with pyridine gave only the product of hydrolysis of the 2-chlorosulfate ester whereas the analogous compound IV (minus the large —CH_2Cl group at C-5) gave the 2,3-*trans* elimination product III. 3,4,6-Trichloro-3,4,6-trideoxy-D-allose gave a syrupy 1,2-*O*-isopropylidene derivative after a prolonged reaction time using the same vigorous conditions as applied in the formation of the corresponding 3,4-dichloro-3,4-dideoxy-D-ribose derivative. A previous attempt to make this 1,2-*O*-isopropylidene derivative had been unsuccessful (3).

EXPERIMENTAL

Optical rotations were measured at 21 ± 3°. Melting points were determined on a Kofler hot stage and are uncorrected. All solutions were concentrated under reduced pressure below 50°. Thin layer chromatographic analysis was carried out on prepared silica gel G plates. Infrared spectra were determined using a Perkin-Elmer model 21 instrument on samples dissolved in chloroform (6% w/v) unless otherwise stated. The n.m.r. spectra were determined at 60 Mc/s using a Varian M.60 n.m.r. spectrometer and trimethyl silane was used as an internal indicator.

4-Chloro-4-deoxy-D-xylosyl Chloride 2,3-Dichlorosulfate

L-Arabinose (10 g) was treated with sulfuryl chloride (21 ml) and pyridine (40 ml) in chloroform solution (2), and the reaction mixture was allowed to stand at room temperature for 4 h. The chloroform solution was then filtered and washed with 10% sulfuric acid, saturated sodium bicarbonate solution, and distilled water. Concentration of the chloroform extract afforded a syrup (7 g) which was shown to be a mixture containing at least 2 components (t.l.c.). The syrup partially crystallized on standing and the crystals (1 g) were removed from the syrup by washing them with chloroform–petrol (b.p. 40–60°). They had m.p. 84° and $[\alpha]_D$ +80° (*c*, 0.6 in chloroform).

Anal. Calcd. for $C_5H_6Cl_4O_7S_2$: C, 15.7; H, 1.6; Cl, 37.0; S, 16.7. Found: C, 16.0; H, 1.7; Cl, 36.4; S, 16.0.

This crystalline product could not be isolated again in subsequent reactions, and as it decomposed on standing, further reactions were carried out on the syrupy mixture of products.

Methyl 4-Chloro-4-deoxy-α-D-xylopyranoside 2,3-Dichlorosulfate

The syrupy mixture of products from above (7 g) was refluxed with anhydrous methanol for 8 h. Concentration of the methanol solution to a small volume produced a crystalline compound which was removed from the solution by filtration. Successive recrystallizations from methanol–water and chloroform–petrol (b.p. 40–60°) gave colorless needles (1 g) of $[\alpha]_D$ +49° (*c*, 1.0 in chloroform) and m.p. 89° undepressed on admixture with an authentic sample synthesised by another route (see below).

4-Deoxy-3,4-dichloro-α-D-glycero-pent-2-enopyranosyl 4′-Deoxy-3,4-dichloro-α-D-glycero-pent-2′-enopyranoside (II)

The 10% sulfuric acid wash from the above described reaction was left to stand in a beaker open to the atmosphere, and after 24 h fine colorless needles began to appear, the yield of which increased on further standing. The acid wash was allowed to stand for a further 48 h before the crystals were removed by filtration. Recrystallization from acetone–water gave colorless needles (0.8 g) of m.p. 223° and $[\alpha]_D$ +190° (*c*, 1.1 in doxane).

Anal. Calcd. for $C_{10}H_{10}Cl_4O_3$: C, 37.4; H, 3.1; Cl, 44.3. Found: C, 37.3; H, 3.5; Cl, 43.3.

The infrared spectrum of the crystals (0.8% in KBr) indicated no hydroxyl absorption and the presence of an unconjugated ethylenic bond (1 655 cm^{-1}). The crystals did not reduce Fehlings' solution and had an approximate molecular weight of 300 as determined by the Rast method (8). It was found that the yield of this crystalline product could be improved considerably (1.5 g) by allowing the L-arabinose–sulfuryl chloride reaction mixture to stand for 24 h before working up the products. The yield of chloroform-soluble product decreased correspondingly. The crystals were unaffected by ozonolysis (4) and by lead tetraacetate oxidation (5) of the chloroform solution.

The acid wash from the reaction between D-arabinose and sulfuryl chloride also gave a similar non-reducing crystalline product which when recrystallized from acetone–water gave needles of m.p. 223° and $[\alpha]_D$ −186° (*c*, 0.7 in dioxane).

Methyl 4-Deoxy-3,4-dichloro-β-D-glycero-pent-2-enopyranoside (III)

The crystals of the D-enantiomer above (0.6 g) were refluxed with 100 ml of anhydrous methanol and 0.6 ml of concentrated sulfuric acid for 24 h. The solution was concentrated to a small volume and partitioned between chloroform and water. The chloroform solution was washed with saturated sodium bicarbonate

Can. J. Chem. Downloaded from www.nrcresearchpress.com by 210.87.254.6 on 09/05/12
For personal use only.

solution, dried (anhydrous sodium sulfate), and concentrated to a syrup which crystallized. Recrystallization from methanol–water gave colorless plates (0.4 g, 58%) of $[\alpha]_D$ +53° (*c*, 0.8 in methanol) and m.p. 72–73° undepressed on admixture with the authentic compound synthesised by another route (see below). The crystals also gave an infrared spectrum indistinguishable from that of the authentic compound.

Methyl 4-Chloro-4-deoxy-α-D-xylopyranoside 2,3-Dichlorosulfate

Methyl β-L-arabinopyranoside (5 g) was treated with sulfuryl chloride (11 ml) and pyridine (20 ml) in chloroform solution (2). The washed chloroform extracts gave on concentration a syrup which crystallized. Recrystallization from methanol–water gave colorless needles (4 g, 29%) of m.p. 88–90° and $[\alpha]_D$ +49° (*c*, 1.0 in chloroform).

Anal. Calcd. for $C_6H_9Cl_3O_8S_2$: C, 19.0; H, 2.4; Cl, 28.1; S, 16.9. Found: C, 19.0; H, 2.3; Cl, 28.3; S, 16.6.

No further chloro-substitution was obtained when the crystals were heated with pyridine hydrochloride in chloroform solution (3) and the original crystalline compound was obtained in good yield (80%).

Methyl 4-Chloro-4-deoxy-α-D-xylopyranoside 2,3-Cyclic Sulfate

The above crystals (2 g) were dissolved in anhydrous pyridine and the solution was left at room temperature for 16 h. The solution was poured into ice water and the aqueous solution was extracted with chloroform. The chloroform solution was washed with 5% sulfuric acid, saturated sodium bicarbonate solution, and distilled water. The chloroform solution was dried (anhydrous sodium sulfate), filtered, and concentrated to a syrup which rapidly crystallized (0.6 g, 56%). Recrystallization from ether–petrol (b.p. 40–60°) gave colorless crystals of m.p. 106–107° and $[\alpha]_D$ +100° (*c*, 1.0 in methanol).

Anal. Calcd. for $C_6H_9ClO_6S$: C, 29.5; H, 3.7; Cl, 14.5; S, 13.1. Found: C, 29.7; H, 3.6; Cl, 14.2; S, 12.8.

Methyl 4-Chloro-4-deoxy-α-D-xylopyranoside

The crystals of the dichlorosulfate ester derivative described above (5 g) were dechlorosulfated in methanol solution by sodium iodide in the presence of barium carbonate (1). The solution was filtered and the filtrate was concentrated to a small volume. Water was added and the aqueous solution was continuously extracted with chloroform. Concentration of the chloroform solution gave a syrup which crystallized, and recrystallization of the product from ethyl acetate gave colorless needles (0.8 g, 37%) of m.p. 102–103° and $[\alpha]_D$ +135° (*c*, 0.9 in methanol).

Anal. Calcd. for $C_6H_{10}ClO_4$: C, 39.4; H, 6.1; Cl, 19.5. Found: C, 39.8; H, 6.1; Cl, 19.2.

4-Chloro-4-deoxy-D-xylopyranose

The crystals of the methyl glycoside above were unaffected by boiling *N* sulfuric acid; therefore, more drastic conditions were tried.

The methyl glycoside (0.6 g) was dissolved in 25% sulfuric acid and the solution was heated at 100° for 5 h. The solution was diluted with water, neutralized with barium carbonate, filtered, deionized by passage through Amberlite IR120 (H form) and Duolite A4 (OH form) ion exchange resins, and concentrated to a syrup which crystallized. Recrystallizations from acetone–ether gave colorless crystals (0.3 g, 55%) of m.p. 145° and $[\alpha]_D$ −45.5° (5 min) → +9° (equilibrium, 24 h) (*c*, 1.1 in methanol).

Anal. Calcd. for $C_5H_9ClO_4$: C, 35.6; H, 5.4; Cl, 21.1. Found: C, 36.1; H, 5.3; Cl, 21.3.

Periodate Oxidation of 4-Chloro-4-deoxy-D-xylopyranose

The oxidation was carried out in the dark at 25° using a small sample (10 mg) of the compound in distilled water (25 ml) containing 0.3 *M* sodium metaperiodate (1 ml). Aliquots (2 ml) were removed at intervals and the consumption of periodate (9) and the production of formic acid (10) were measured and were respectively as follows: 1.66, 0.77 (1.30 h); 1.88, 0.89 (6.30 h); 2.00, 1.02 (24 h); 2.14, 1.18 (48 h).

Methyl 3,4-Dichloro-3,4-dideoxy-β-D-ribopyranoside 2-Chlorosulfate

Methyl α-L-arabinopyranoside (5 g) was treated with sulfuryl chloride (11 ml) and pyridine (20 ml) in chloroform solution (2). The chloroform-soluble product was isolated as in previous reactions and was a syrup (6 g). To ensure maximum chloro-substitution the syrup was further heated with pyridine hydrochloride in chloroform at 50° for 10 h (3). The chloroform solution was washed with water and saturated sodium bicarbonate solution, dried (anhydrous sodium sulfate), filtered, and concentrated to a syrup which crystallized. Recrystallization from chloroform–*n*-hexane gave large colorless crystals (2.5 g, 30%) of m.p. 74° and $[\alpha]_D$ −102° (*c*, 1.3 in chloroform).

Anal. Calcd. for $C_6H_9Cl_3O_5S$: C, 24.0; H, 3.0; Cl, 35.6; S, 10.7. Found: C, 23.6; H, 2.9; Cl, 35.3; S, 10.6.

Methyl 3,4-Dichloro-3,4-dideoxy-β-D-ribopyranoside

The crystals above (2.5 g) were dechlorosulfated in methanol solution using sodium iodide in the presence of barium carbonate (1). The filtered solution was concentrated to small volume and partitioned between chloroform and water. The chloroform extract was dried (anhydrous sodium sulfate), filtered, and concentrated to a syrup (1.7 g, 100%) which did not crystallize but which was shown to be homogeneous by thin layer chromatography. A small quantity of the syrup was distilled under reduced pressure and had $[\alpha]_D$ −55° (*c*, 0.8 in methanol).

Anal. Calcd. for $C_6H_{10}Cl_2O_3$: C, 35.8; H, 5.0. Found: C, 35.7; H, 5.0.

Can. J. Chem. Downloaded from www.nrcresearchpress.com by 210.87.254.6 on 09/05/12
For personal use only.

3,4-Dichloro-3,4-dideoxy-β-D-ribopyranose

The syrup above (1.5 g) was refluxed in a *N* sulfuric acid solution of dioxane–water and the hydrolysis was followed by thin layer chromatography. The hydrolysis was extremely slow and was stopped after 3 days, when not completely hydrolyzed, because substantial decomposition had taken place. The solution was neutralized with barium carbonate, filtered, and the filtrate was deionized by passage through Amberlite 1R120 (H form) and Duolite A4 (OH form) ion exchange resins. The solution was then concentrated to a syrup (1 g) which slowly crystallized. Recrystallization from chloroform–petrol (b.p. 40–60°) gave needles (0.1 g, 7%) of m.p. 107–108° and $[\alpha]_D$ −9.5° (15 min) → −3.2° (24 h equilibrium) (*c*, 0.6 in methanol).

Anal. Calcd. for $C_5H_{10}Cl_2O_3$: C, 31.8; H, 5.3; Cl, 37.6. Found, C, 31.9; H, 5.3; Cl, 37.9.

Paper electrophoretograms of the crystals run in 0.05 *M* borate solution (3) and sprayed with alkaline silver nitrate (11) indicated one component at M_g = 0.68.

3,4-Dichloro-3,4-dideoxy-1,2-O-isopropylidene-α-D-ribopyranose

The mother liquors from the recrystallization from above were concentrated to a syrup (0.9 g). The syrup (0.9 g) was shaken with anhydrous acetone (40 ml), concentrated sulfuric acid (0.3 ml), and anhydrous copper sulfate (4 g) for 4 days. The solution was neutralized with concentrated ammonia solution, filtered, and concentrated to a syrup which rapidly crystallized. Recrystallization from chloroform–petrol (b.p. 40–60°) gave colorless needles (0.3 g) of m.p. 171° and $[\alpha]_D$ −52° (*c*, 0.7 in chloroform).

Anal. Calcd. for $C_8H_{12}Cl_2O_3$: C, 42.3; H, 5.3; Cl, 31.3. Found: C, 42.4; H, 5.4; Cl, 31.2.

1,2-O-Isopropylidene-3,4,6-trichloro-3,4,6-trideoxy-α-D-allopyranose

3,4,6-Trichloro-3,4,6-trideoxy-D-allose (0.5 g) (3) was shaken for 6 days with anhydrous acetone, concentrated sulfuric acid, and anhydrous copper sulfate and the product isolated as described previously. The product was a syrup which partially crystallized. Recrystallization from chloroform gave needles (0.15 g) of m.p. 170° undepressed on admixture with the starting compound. The mother liquors were washed with water (×3) and the chloroform solution was concentrated to a syrup (0.3 g, 51%) which was shown to be homogeneous except for a small quantity of the starting compound (t.l.c.). The syrup was purified by distillation under reduced pressure and had $[\alpha]_D$ −25° (*c*, 0.6 in chloroform).

Anal. Calcd. for $C_9H_{13}Cl_3O_3$: C, 39.2; H, 4.7. Found: C, 39.4; H, 4.7.

Methyl 4-Deoxy-3,4-dichloro-β-D-glycero-pent-2-enopyranoside

Crystalline methyl 3,4-dichloro-3,4-dideoxy-β-D-ribopyranoside 2-chlorosulfate (1.2 g) obtained previously was dissolved in pyridine (6 ml) and the reaction mixture was allowed to stand for 24 h. The reaction mixture was then partitioned between chloroform and water and the chloroform extract, after treatment with charcoal, was filtered and concentrated to a syrup (0.52 g, 71%) which crystallized. The crystalline product was purified by sublimation to give colorless plates of m.p. 70–71° and $[\alpha]_D$ +52° (*c*, 1.0 in methanol).

Anal. Calcd. for $C_6H_8Cl_2O_2$: C, 39.4; H, 4.4; Cl, 38.8. Found: C, 39.9; H, 4.8; Cl, 38.7.

The infrared spectrum of the crystals indicated no hydroxyl absorption and the presence of an unconjugated ethylenic bond (1 657 cm^{-1})

Methyl 3,4,6-Trichloro-3,4,6-trideoxy-α-D-allopyranoside 2-Chlorosulfate

Methyl 3,4,6-trichloro-3,4,6-trideoxy-α-D-allopyranoside (3) (2 g) was treated with sulfuryl chloride (6.5 ml) and pyridine (10 ml) in chloroform solution (2). The chloroform-soluble product was a syrup which rapidly crystallized. Recrystallization from chloroform–petrol (b.p. 40–60°) gave crystals (2.4 g, 90%) of m.p. 95° and $[\alpha]_D$ +81° (*c*, 1.1 in chloroform).

Anal. Calcd. for $C_7H_{10}Cl_4O_5S$: C, 24.2; H, 2.9; Cl, 40.8; S, 9.2. Found: C, 24.4; H, 2.8; Cl, 41.0; S, 9.2.

The crystals above (2 g) were treated with pyridine as in the previous reaction with methyl 3,4-dichloro-β-D-ribopyranoside 2-chlorosulfate and after 48 h the only isolable chloroform-soluble product was crystalline methyl 3,4,6-trichloro-3,4,6-trideoxy-α-D-allopyranoside as confirmed by a mixed melting point with the authentic compound (3).

ACKNOWLEDGMENTS

This work was supported by the National Research Council (N.R.C. T.19) and in part by the Department of Scientific and Industrial Research, London, England by the award of a N.A.T.O. postdoctoral fellowship to one of us (H. J. J.). The authors would like to thank Dr. W. Szarek for assistance with the n.m.r. spectroscopy and Dr. L. Hough for his interest.

REFERENCES

1. H. J. Jennings and J. K. N. Jones. Can. J. Chem. **41**, 1151 (1963).
2. H. J. Jennings and J. K. N. Jones. Can. J. Chem. **40**, 1408 (1962).
3. H. J. Jennings and J. K. N. Jones. Can. J. Chem. In press. 1965.

Can. J. Chem. Downloaded from www.nrcresearchpress.com by 210.87.254.6 on 09/05/12
For personal use only.

4. J. A. Sousa and A. Bluhr. J. Org. Chem. **25**, 108 (1960).
5. L. Zervas. Ber. **73**, 174 (1940).
6. N. A. Hughes and P. R. H. Speakman. J. Chem. Soc. 398 (1965).
7. L. J. Haynes and A. R. Todd. J. Chem. Soc. 303 (1950).
8. A. I. Vogel. A textbook of practical organic chemistry. Longmans Green and Co., London. 1954.
9. G. Neumüller and E. Vasseur. Arkiv. Kemi, **5**, 235 (1953).
10. D. M. W. Anderson, C. T. Greenwood, and E. L. Hirst. J. Chem. Soc. 225 (1955).
11. W. E. Trevelyan, D. D. Proctor, and J. S. Harrison. Nature, **166**, 444 (1950).

Can. J. Chem. Downloaded from www.nrcresearchpress.com by 210.87.254.6 on 09/05/12
For personal use only.

Can. J. Chem. Downloaded from www.nrcresearchpress.com by 210.87.254.40 on 09/05/12
For personal use only.

SEMIEMPIRICAL SCF CALCULATIONS ON AZULENE AND ITS SINGLY CHARGED IONS[1]

J. E. BLOOR[2]
Chemistry Division, Franklin Institute Research Laboratories, Philadelphia, Pennsylvania
Received May 18, 1965

ABSTRACT

SCF MOs for azulene have been obtained by the semiempirical Pariser, Parr, Pople procedure using the Nishimoto–Mataga method of calculating repulsion integrals and the assumption that nearest neighbor resonance integrals are independent of interatomic distance. Excited states calculated from these MOs by a CI calculation are in very good agreement with experiment. Ground state charge densities, bond orders, and the dipole moment are similar to other SCFMO calculations and reveal no disadvantage in adopting a constant resonance integral for all bonds. It is shown that estimates of the π-electron charge density by n.m.r. methods are not compatible with direct dipole moment measurements and it is suggested that the interpretation of the n.m.r. measurements suffers from inaccuracies in estimating ring currents. Doubt is also thrown on the use of simple relationships between calculated π-bond orders and bond lengths obtained by X-ray crystallographic measurements on the solid state, particularly since all the bond lengths in azulene are predicted to be longer than in benzene whereas experiment shows some to be shorter. Calculations on spin densities and charge densities of the singly charged azulene anion and cation have been performed by a restricted Hartree–Fock perturbation method in which the matrix elements for the interaction between singly excited states and the ground state are calculated using the closed shell SCFMOs of azulene as the basis set. Agreement with experiment for the anion is fairly good. For the cation our results are in severe disagreement with recent VB calculations, but there are no experimental results available to decide between the two methods.

I. INTRODUCTION

The assumptions usually employed in semiempirical self-consistent field (SCF) calculations of the type associated with the names of Pariser (4), Parr, and Pople (1–3) are so sweeping that, although they can be justified to some extent theoretically (1, 4), their adoption can only ultimately be condoned by their success, as has been achieved in the case of many polycyclic alternant hydrocarbons (1–7), in explaining experimental work, in predicting new effects, and as a guide to the design of new experiments.

However, the polycyclic alternant hydrocarbons are not the ideal class of molecules for parameter evaluation. As has been shown by Ruedenberg (4) the results of calculations on this class of molecule are more strongly dependent on their topological matrix than on the choice of repulsion or resonance integrals.

Two classes of conjugated hydrocarbons which are more sensitive to parameter choice are (*a*) the alternant hydrocarbons such as styrene, stilbene, and diphenyl, which possess one or more bonds with lengths considerably different from the bond length of benzene and (*l*) non-alternant hydrocarbons such as azulene. In a companion paper (7) to the present one we will present results of semiempirical calculations of styrene, stilbene, and diphenyl in which we demonstrate that the assumption that the nearest neighbor resonance integral β_{pq} is independent of the band distance r_{pq} is quite a good assumption to be used in calculating excited state ionization potentials and electron affinities (7).

In the present paper we examine the suitability of this assumption in calculating the excited states, ionization potential, electron affinity, charge densities, bond orders, and dipole moment of a typical non-alternant hydrocarbon, azulene. Since it is well known

[1]*Presented at the Symposium for Molecular Structure and Spectroscopy held at the Ohio State University, Columbus, Ohio, June 14–18, 1964.*
[2]*Address after September 1, 1965—Cobb Chemical Laboratory, University of Virginia, Charlottesville, Va.*

that the 9:10 bond (numbering system in Fig. 1) is considerably longer than the other bonds in azulene we would expect any weakness in our assumption of a distant independent β_{pq} to be revealed by calculations on such a molecule.

In addition to the results for azulene we have extended the calculations to the calculation of the charge densities and spin densities of the azulene singly charged positive and negative ions.

The computation of pi electron spin densities and their relationship to experimental hyperfine splitting constants is of very great interest and importance. At the present time it has not been clearly established whether any of several ways of calculating spin densities gives any better agreement with experiment than any other.

For the azulene negative ion several experimental determinations of hyperfine splitting constants have been made (33, 34) and the results of calculations using unrestricted Hartree–Fock (UHF) techniques (33, 36) and the valence bond (VB) method (35) have recently been reported for both the negative ion and the positive ion of azulene.

For the purpose of comparison with these earlier results we have carried out calculations of the spin and charge densities of these two ions using a restricted Hartree–Fock (RHF) perturbation method which uses the semiempirical self-consistent field molecular orbitals (SCFMOs) as the basis set for carrying out a configuration interaction (CI) calculation. The CI calculation is carried out by allowing the singly excited states to interact with the ground state (10). We have previously used this method (10) for a number of ions of alternant hydrocarbons and found it to be very satisfactory.

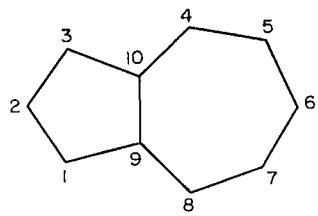

FIG. 1. Carbon skeleton of azulene.

II. METHOD OF CALCULATION

For the azulene molecule, we have used the standard SCF MO method described previously (8). In calculating the repulsion integrals, we have used the method proposed by Nishimoto and Mataga (9) i.e. for the one-center integrals we use $\gamma_{11} = 10.85$ eV and for the two-center integrals between two atoms p and q a distance r_{pq} Å apart we use the formula

$$\gamma_{pq} = \frac{14.397}{a_{cc} + r_{pq}} \text{ eV},$$

where $a_{cc} = 1.328$.

We have used one value $\beta_{pq} = -2.39$ eV for the resonance integral between neighboring atoms. All non-nearest neighbor β_{pq} are put equal to zero. By contrast to this present assumption it has, in recent years, become the custom to assume a very strong distance dependence of β_{pq} on r_{pq} e.g. by assuming β_{pq} is proportional to the overlap S_{pq} or is an exponential function of r_{pq}. However, our previous theoretical work on styrene and similar molecules (7) shows that such assumptions underestimate the interaction of vinyl and ethynyl groups with aromatic rings, because, in choosing β_{pq} from a curve of β_{pq} against r_{pq}, the steep slope of the curve gives very high values for β_{pq} at short r_{pq} distances and

Can. J. Chem. Downloaded from www.nrcresearchpress.com by 210.87.254.40 on 09/05/12
For personal use only.

low values for long bonds—both factors leading to small interactions between the separate fragments joined by the bonds in question. The calculations in the present paper are carried out with the same assumption to verify or disprove whether it is applicable to non-alternant hydrocarbons. For the MOs used to obtain the excited states of col. 4 (Table I) we diagonalized the F matrix (Table III, method 1, ref. 15) reported by Brown and Heffernan as being the final result of a variable electronegativity self-consistent field (VESCF) MO calculation (8).

In obtaining the excited states from our SCFMOs (Table I col. 3) and from the VESCFMOs (Table I col. 4) we carried out CI calculations (8) for both singlet and triplet states using the six lowest A-type and the six lowest B-type configurations. For the VESCF CI calculation we used repulsion integrals taken from ref. 15. The spin densities were calculated by a restricted Hartree–Fock LCAO perturbation procedure, the details of which have been described elsewhere (10). In this procedure, the correct expressions (10) for a radical ion with one unpaired electron are used to calculate the energies of the excited configuration and the matrix elements for the interaction of the excited configuration with the ground configuration, but the actual MOs used in the calculation are the SCF MOs of the neutral molecule. In the present work we used our closed-shell SCF MOs for azulene in the perturbation calculations for the azulene anion and cation.

III. AZULENE MOLECULE

1. Excited States

The existence of five singlet excited states with transition energies below 55 000 cm^{-1} has been established experimentally (5, 11) although the symmetry of only one of these (ν_{00} = 28 400 cm^{-1}) has been established by vibrational analysis (12). In Table I we have compared the calculated frequency values with experimental values for ν_{max} measured in cyclohexane solution. These may differ from the true values of the isolated molecule by up to 500 cm^{-1} because of solute–solvent interactions. For comparison, we have also included in Table I the results of three other calculations (13, 14) besides the new results reported in cols. 3 and 4.

Comparison of the MO calculations of Table I shows that they all predict the first transition to be a $^1A_1 \rightarrow {}^1B_1$ transition (short axis polarized) and the second one to be a $^1A_1 \rightarrow {}^1A_1$ transition. However, whereas our SCF result and the non-iterative antisymmetrical molecular orbitals with configuration interaction (ASMOCI) procedures* of Pariser (13), of Simmons (16), and of Koutecky (17) agree quite well with experiment. The method of Brown and Heffernan (15) and the non-iterative ASMO CI calculation of Hummel and Ruedenberg (14) yield very low values for the first transition. The reason for this, in the latter case (14), is probably because, even though they used topological MOs rather than SCFMOs, they did not include interaction of the singly excited configurations with the ground configuration. Similar calculations (13, 16, 17) show that such interactions are very important for azulene since they lower the ground configuration energy by 0.2–0.3 eV. The reason for the lack of agreement in the case of Brown and Hefferman's VESCF calculation is not clear since in other systems the method has apparently worked well (18). In another SCF calculation (19) Julg, using his LCAO "improved method", which includes the variation of parameters with the effective

**The calculations on azulene described in refs. 17 and 18 are substantially the same as those of Pariser, ref. 13, and so are not reported in Table I. The ASMOCI work of ref. 18 uses the same repulsion integrals as those employed in the present paper. The good agreement between our work and that of ref. 18 shows that, at least for azulene, the inclusion of interactions of only singly excited states with the ground state is sufficient CI to make up for not using SCF MOs.*

Can. J. Chem. Downloaded from www.nrcresearchpress.com by 210.87.254.40 on 09/05/12
For personal use only.

nuclear charge in a different way than the VESCF method of ref. 15, reaches good agreement between experiment and theory for the first excited state although no CI was included. In our calculation, the first transition was lowered 0.14 eV (1 130 cm^{-1}) by CI with the other five B-type configurations.

For the second transition, our calculation is in better agreement with experiment than the non-iterative ASMOCI calculations of Pariser (13) or Simmons (16) and of Koutekcy *et al.* (17), as is also the VESCF calculation of Brown and Heffernan (15). The oscillator strength of this ^1A excited state is predicted to be lower than for the first transition for all the calculations although experimentally it is found to be much higher:

$$(f_{II}/f_I)_{expt} = 9.0$$

However, it has recently been shown (20) that the band origin of this second transition is weak, and that it is quite possible for 80% of the total intensity of the band envelope to be due to intensity stealing brought about by vibrations in higher A-type transitions.

It has recently been established experimentally that there is a weak transition at 36 100 cm^{-1} almost overlapped by a strong broad transition at 36 470 cm^{-1}. All the theoretical calculations summarized in Table I except the VESCF method predict two bands in this region. Our SCFMO calculation predicts a weak transition to ^1B state at 36 230 cm^{-1} in excellent agreement with experiment. The ASMOCI calculations predict this transition 3 000 cm^{-1} lower than the observed one.

Both our SCFMOCI calculation and the ASMOCI calculation of Pariser are in good agreement with experiment in predicting two fairly strong transitions in the 36 000 to 45 000 cm^{-1} region. No transition is predicted in this region in the VESCF CI calculation while the transition energies of the Ruedenberg calculation are all, as expected, lower by about 3 000 cm^{-1} than the observed spectra.

There is no experimental information on the triplets of azulene. However, it is interesting to note that our calculation and those of Pariser (13) and of Simmons (16) agree in predicting the lowest triplet to be of ^3A symmetry and to be in the 12 000 cm^{-1} region. The VESCF method, however, predicts it to be very low at 2 600 cm^{-1} due to a large depression of the first triplet ($5 \rightarrow 6$) by the configuration ($3 \rightarrow 6$). (The MOs are numbered in order of ascending energy.) In our calculation the latter configuration interacts very little with the former configuration.

2. Ionization Potential and Electron Affinity

The ionization potential of azulene has not been measured directly, but recently (21) an indirect estimate of 7.4–7.5 eV has been obtained from the study of the spectra of charge-transfer complexes of azulene with different acceptors. We have shown elsewhere (7) that the ionization potentials of a number of hydrocarbons are given by

$$I = -(E_{HO}^{SCF} + 1.33)\ eV$$

where E_{HO}^{SCF} is the orbital energy of the highest occupied MO.

Using this equation, we obtain 7.43 eV in good agreement with experiment. Our previous contention (7) that Koopman's theorem, with a correction term, is a satisfactory way of calculating ionization potentials without carrying out separate corrective calculations for the molecule and its positive ion (22) is supported by the fact that our parameters give orbital energies which, when used together with *one* correction factor of 1.33 eV, predict successfully the ionization potentials of alternant polycyclic hydrocarbons, hydrocarbons such as stilbene and biphenyl, and also a non-alternant hydrocarbon, azulene.

Can. J. Chem. Downloaded from www.nrcresearchpress.com by 210.87.254.40 on 09/05/12
For personal use only.

Can. J. Chem. Downloaded from www.nrcresearchpress.com by 210.87.254.40 on 09/05/12
For personal use only.

TABLE I

Excited states of azulene

State symmetry	Expt.*		SCF† MO + CI		VESCF‡ + CI		ASHMO§ + CI		TBM‖ + CI	
	E (cm^{-1})	f	E	f	E	f	E	f	E	f
$^1B_1$	14 440 (0–0) 15 800 (max.)	0.009	15 810	0.03	10 700		13 980	0.02	10 950	0.01
$^1A_1$	28 200 (0–0) 29 500 (max.)	0.08	28 100	0.01	28 450		24 890	0.002	21 770	0.01
$^1B_1$	36 100 (max.)		36 230	0.13	29 540		33 180	0.12	30 310	0.05
$^1A_1$	36 470 (max.)	1.10	38 180	1.13			37 860	1.24	32 350	1.13
$^1B_1$	42 300 (max.)	0.38	41 880	0.54			45 220	0.37	39 260	0.54
$^3B_1$			12 340		2 580		11 840			
$^3A_1$			16 380		8 230		14 850			

*Based on data in refs. 5, 13, and 20.
†This work $\beta_{pq} = -2.39$ for nearest neighbors.
‡VESCF MOs reported in ref. 15 were used to carry out the CI calculation.
§Pariser's calculation, ref. 13; similar results have been obtained by Koutecky *et al.*, ref. 17, using the Mataga method of calculating repulsion integrals.
‖CI calculation using topological MOs and neglecting CI of singly excited states with ground state, ref. 14.

TABLE II

Bond orders and bond distances for azulene

Bond order positions	Expt. lengths* (Å)	Expt.† bond orders	SCF MO bond orders			VESCF¶	ASMO** CI	Huckel†† bond orders
			‡	§	‖			
9:10	1.483±0.004	0.2006	0.3101	0.2908	0.2737	0.196	0.288	0.331
1:9, 3:10	1.413±0.015	0.5801	0.6135	0.6184	0.6158	0.632	0.610	0.613
4:5, 7:8	1.401±0.018	0.6452	0.6540	0.6735	0.6473	0.656	0.651	0.659
1:2, 2:3	1.391±0.021	0.6994	0.6550	0.6526	0.6526	0.650	0.660	0.653
5:6, 6:7	1.385±0.021	0.7320	0.6450	0.6437	0.6473	0.648	0.648	0.642
4:10, 8:9	1.383±0.004	0.7430	0.6101	0.6145	0.6210	0.617	0.611	0.606

*Weighted average lengths, assuming C_{2v} structure, from X-ray data.
†Calculated from $p_{rs} = 5.422\,(1.52 - r_{rs})$ gives $p = 0.667$ for $r = 1.397$ Å i.e. benzene.
‡Our work, all resonance integrals β_{pq} equal.
§Hoyland and Goodman ref. 22.
‖A. Julg. Semiempirical SCF "improved" MO method. ref. 19.
¶R. D. Brown and M. L. Hefferman, ref. 15.
**R. Pariser, ASMO CI method, ref. 13.
††Huckel LCAO method assuming $\beta_{9,10} = 0.8\beta$. E. Heilbronner, ref. 5.

For the electron affinity as measured by $\epsilon_{1/2}$, the halfwave reduction potential measured in 75% aqueous dioxane, we have found for alternant hydrocarbons (7) that we can write

$$\epsilon_{1/2} = -(E_{LO}^{SCF} + 4.77)\ \text{eV}$$

where E_{LU}^{SCF} is the energy of the lowest unoccupied MO in eV. For azulene, our calculation gives an orbital energy E_L^{SCF} of -3.15 eV giving $\epsilon_{1/2} = -1.62$ eV, in good agreement with the experimental value of -1.64 eV. It is interesting to note that, if the energy values obtained from Huckel LCAO calculations are used to establish a linear relationship between E_{LU}^{H} and $\epsilon_{1/2}$, then the point for azulene is considerably off the least-squares correlation line (23); whereas, using SCF energy values, E_{LU}^{SCF} for azulene fits the line for alternant hydrocarbons (7).

3. Bond Orders and Bond Distances

The bond distances for azulene in the solid state have been measured in a thorough X-ray crystallographic study (24) and have been reported to be in the order of decreasing distance (Table II, column 2)

$$9\text{–}10 > 1\text{–}9 > 4\text{–}5 > 1.397\ \text{Å} > 1\text{–}2 > 5\text{–}6 > 4\text{–}10.$$

Most of the MO calculations summarized in Table II give this order except for the 4–10 bond, which is predicted to be one of the longer bonds rather than the shortest, as is observed. However, a much more serious discrepancy between experiment and theory is that whereas the measurements show the presence of three bonds shorter than the bond length of benzene (1.397 Å), the MO calculations, with only one exception, predict that all the bonds in azulene should have π-bond orders less than the π-bond order of benzene (0.667) and hence should have longer lengths than those of benzene. This discrepancy is clearly brought out in Table II where we compare experimental bond orders p_{pq} calculated from the experimental bond distance R_{pq} using the equation, calculated for polycyclic alternant hydrocarbons (6)

$$R_{pq} = (1.52 - 0.184p_{pq})\ \text{Å} \qquad [1]$$

with theoretical bond orders calculated by Coulson's definition of the π-bond order

$$p_{pq} = 2 \sum_{\substack{i \\ \text{doubly occupied orbitals}}}^{\text{Nocc}} C_{ip}\, C_{iq}$$

where C_{ip} is the AO coefficient for atom p in the ith MO and Nocc is the number of occupied MOs. The one calculation which predicts a bond order greater than 0.667 is the VESCF calculation of Hoyland and Goodman (22). However, in this case, only the 4–5 bond is predicted to be shorter than the one in benzene and then the difference is slight, i.e. $R_{4,5} = 1.396$ Å. The discovery of this difference between experiment and theory raises doubts on whether we are justified in using simple relationships between π-bond order and bond length, and whether we should use measurements on the solid state to test out theoretical calculations carried out on an isolated molecule. Measurements on the bond lengths of isolated molecules in the vapor phase by techniques such as electron diffraction on substances, chosen because considerable deviations from the standard aromatic bond length might be expected, are badly needed. For azulene it has been stated (5) that measurements of this type yielded a distance of 1.45 Å for the 9–10 bond, i.e. considerably shorter than that found by X-ray crystallographic measurements. However, no experimental details were given.

Can. J. Chem. Downloaded from www.nrcresearchpress.com by 210.87.254.40 on 09/05/12
For personal use only.

Can. J. Chem. Downloaded from www.nrcresearchpress.com by 210.87.254.40 on 09/05/12
For personal use only.

We might expect our bond order for the long 9–10 bond to be considerably higher than that calculated by methods in which the resonance integral $\beta_{9,10}$ was allowed to be lower than the other resonance integrals. The results of Table II show that this is not so and that except for the VESCF study of Brown and Heffernan (15), the other MO calculations gave a bond order similar to ours. Using our value of 0.3101 in eq. [1] gives a bond length for the 9–10 bond of 1.46 Å, in good agreement with the electron diffraction measurement reported by Heilbronner (5), but significantly lower than the X-ray value of 1.483 ± 0.004 Å (24). Examination of MO calculations for other molecules containing long bonds shows that this tendency to predict distances shorter than the observed is widespread. For example, when use is made of Coulson and Golebiewski's (25) technique of allowing the resonance integral to be a function of the bond order and iterating until the resulting bond orders do not change, then for the long bonds in tetracene and pentacene, Hutchison (26) found that the calculated values are 1.434 Å and 1.436 Å respectively, compared to experimental values of 1.46 Å and 1.45 Å. For biphenylene, Ali and Coulson (27) using a similar method calculated 1.467 Å for the longest bond, whereas the experimental value is 1.52 Å. In a recent SCF calculation (28), this same bond was predicted to be 1.48 Å, the extra .04 Å being attributed to hybridization changes.

On the basis of these findings we conclude that, in the case of azulene, the use of a constant resonance integral does not lead to predicted bond distances that are any less reliable than those for other MO calculations. However, the validity of the whole procedure of relating π-bond order to bond distances determined by X-ray analysis, especially for molecules with bond distances differing considerably from the standard benzene C—C length, is questionable, because of the results of all the calculations reported in Table II and the other examples cited above.

4. Dipole Moment

The dipole moment of azulene determined by conventional methods is 1.0 D (5). This is much lower than that calculated by the simple Huckel method; i.e., 6.4 D (5). SCF methods and the ASMOCI method, however, give lower values, and our SCF result is compatible with other calculations (Table III last row) in giving a value of 3.18 D.

This high value, compared to the experimental value, is not unexpected, since we have found, in SCF calculations on polar molecules (8), that, by choosing parameters giving agreement with ionization potentials, electron affinities, and electronic excited states,

TABLE III

Charge densities for azulene

	Expt. values			Theoretical values			
Position	(*a*)	(*b*)	(*c*)	(*d*)	(*e*)	(*f*)	(*g*)
1, 3	1.036	1.05	1.067	1.1072	1.117	1.061	1.068
2, 3	0.957	1.97	0.937	1.0043	0.9911	1.004	0.986
4, 8	0.964	0.96	0.967	0.8923	0.8710	0.937	0.922
5, 7	1.066	1.04	1.041	1.0193	1.0352	1.009	1.012
6	1.014	0.99	0.962	0.9238	0.9248	0.961	0.948
9, 10	(0.9485)	(0.97)	0.9845	1.0171	1.0105	1.0105	1.0310
Dipole moment (D)	−1.47	0.03	0.17	3.19	3.05	1.85	1.7

(*a*) Proton magnetic resonance measurements, ref. 31.
(*b*) Proton magnetic resonance measurements, ref. 29.
(*c*) ^{13}C magnetic resonance measurements, ref. 30.
(*d*) SCF method, this paper β_{pq} all equal.
(*e*) Calculated from SCF MOs supplied by Hoyland and Goodman, ref. 22.
(*f*) VESCF method (1), ref. 10.
(*g*) "Better MO" method, ref. 19. Value of 0.7 reported for the dipole moment in this paper does not correlate with the charge densities reported there, and is apparently in error.

the π dipole moment is calculated to be too high compared to the normal experimental result. At present, we cannot state whether the high value is due to a deficiency in our model, e.g., in neglecting effects such as CI of the ground state with doubly excited states, or in neglecting penetration integrals, or is due to a contribution to the dipole moment from polarization of the core electrons in the opposite direction to the π-electron dipole moment.

A possible way to arrive at the dipole moment of the π electrons, which does not appear to have been explored previously, is to use the π-electron charge density estimates obtained from n.m.r. studies (29, 30, 31). Using the bond distances and angles suggested by Brown and Heffernan (15), we have calculated μ_π values using the experimental charge densities reported in Table III. Extremely low μ_π values of 0.18 D for the C^{13} results (29), and of 0.02 D for Schaeffer and Schneider's proton chemical shift results were obtained (30). For Dailey's (31) estimate using proton chemical shifts we arrived at the quite reasonable value of 1.47 D; however, this value is in the opposite direction to that usually assumed for the azulene molecule (5) and supported by studies on the effect of solvents on the excited states (32); i.e., Dailey's results predict the negative end of the dipole to lie in the seven-membered ring. This reversal of sign in the dipole moment is due to Dailey's (31) estimate of quite large excess charge densities at the 5, 7, and 6 positions. The estimates of Schneider (29, 30) assign a deficiency of charge ($q < 1$) at the 6-position. The main difference between Dailey's and Schneider's interpretations of the measured azulene proton chemical shifts is in the method of estimating the magnitude of the ring current. Schneider's estimate of the ring-current corrections for the atoms in the five-membered ring are larger than Dailey's, but for those in the seven-membered ring, they are smaller. This difference is sufficient to lead to the charge reversal of the dipole moment for Dailey's charge density distribution. Thus, until more reliable procedures for the calculation of ring-current effects have been developed, the estimation of charge densities from proton magnetic resonance spectra is a very uncertain procedure, full of ambiguities in sign and uncertainties of magnitude—a conclusion reached by Dailey on other grounds.

5. Charge Densities

In view of our comments in the last section, conclusions obtained by comparison of theoretical π-electron densities with estimates from n.m.r. data must be regarded with caution. We have compiled, in Table III, charge densities from n.m.r. measurements and from the more recent MO calculations including our SCF calculation. The general similarity of the results of Table III calculated by different MO techniques shows that the charge density is rather insensitive to parameter variation. In general, the theoretical calculations give better rough qualitative agreement with Schneider's (29, 30) experimental estimates than with Dailey's (31). For example, the MO calculations predict excess charge density ($q > 1$) at the 6-position in agreement with Schneider whereas Dailey favors an electron density less than one for this position.

IV. CALCULATIONS ON THE IONS

1. Azulene Anion Spin Densities

Experimental measurements on the hyperfine splitting constants of the azulene anion have been reported by several workers (33, 34, 35), and these have recently been compared with calculations carried out by both valence bond (VB) calculations (35) and unrestricted Hartree–Fock calculations (36). However, in comparing the results of

Can. J. Chem. Downloaded from www.nrcresearchpress.com by 210.87.254.40 on 09/05/12
For personal use only.

Can. J. Chem. Downloaded from www.nrcresearchpress.com by 210.87.254.40 on 09/05/12
For personal use only.

TABLE IV

Electron spin densities and Q values for the azulene anion

	ρ values						Q values					
Position	SCF*	SCF* + CI	VB†	Unrestricted‡ HF	McLachlan§ HF	a_H(expt.)‖	Expt.¶ Q_{CH}	SCF*	SCF* + CI	VB†	Unrestricted‡ HF	McLachlan HF
1, 3	0.0015	−0.0238	0.1300	0.012	−0.0269	0.2740	23.3	18.27	11.51	2.108	22.83	11.12
2	0.1024	0.1064	0.1464	0.088	0.1195	3.948	25.9	38.55	37.11	26.97	44.86	65.80
4, 8	0.1912	0.2396	0.3060	0.306	0.2924	6.219	22.4	32.51	25.96	20.32	20.32	23.51
5, 7	0.0163	−0.0690	−0.1585	−0.154	−0.0807	1.338	22.8	7.77	19.39	8.44	8.69	18.64
6	0.2529	0.3617	0.3513	0.416	0.3681	8.829	22.4	34.77	24.41	25.13	21.22	26.67
9, 10	0.1136	0.0942	−0.0295	0.084	0.0714							

*This paper, all β_{pq} values equal.
†Valence bond calculation, ref. 35.
‡Unrestricted Hartree–Fock method with approx. projection of spin eigenfunction (ref. 36).
§Huckel MOs, $\lambda = 1.2$ using McLachlan's method (ref. 37). Reported in ref. 33.
‖Reference 33.
¶From n.m.r. coupling constants (refs. 35 and 38).

previous MO calculations (36, 37) with his own VB calculations, Brown (35) used the wrong sign for the calculated spin densities at the 1-position (designated *B* in Table II of ref. 35). For comparison we have summarized the results of other calculations and those of our RHF perturbation calculations in Table IV together with the effective $(Q_{CH})_p$ values defined by

$$[2] \qquad (Q_{CH})_p = \frac{a_H(\text{expt.})_p}{\rho_H(\text{calcd.})_p}$$

for atom p. The experimental values Q_{CH} (expt.) were obtained by Brown (35) from the nuclear magnetic resonance coupling constants ($J_{^{13}C-H}$) of azulene (36).

The results of Table IV show that two of the MO calculations which include electron correlation (columns 3, 6) yield negative spin densities in the 1, 3, 5, and 7 positions. By contrast the VB method of Brown (35) (Table IV col. 4) gives negative spin densities only in the 5 and 7 positions with a substantial positive spin density in the 1 and 3 positions. Considering the fact that the VB results were calibrated by varying three parameters to give the best overall fit for the three largest hyperfine splitting constants corresponding to positions 2, 4, and 6, and the MO calculations in cols. 4, 6, and 7 were not scaled in any way to fit e.s.r. data, the more sophisticated MO treatments must be regarded as preferable to use for the interpretation of e.s.r. results rather than the VB method.

None of the results of the calculations can be claimed to be completely satisfactory as is shown by the large variation in the Q_{CH} values (Table IV). It is noteworthy that the Q_{CH} values obtained using our SCF calculation (cols. 3 and 4) are much improved by carrying out the CI, and it would be of very great interest to know whether the use of open-shell MOs would improve the agreement still further especially for the 1-position. Calculations of this type raise the problem of whether the variation of the empirical parameters with the charge should be taken into account, as was done for positive ions by Hoyland and Goodman (22), and, if so, what is the best method to do this. Such calculations are in progress for a number of hydrocarbon ions.

2. Azulene Negative Ion Charge Densities

There are no experimental estimates of the charge densities for the azulene anion. We have compared our calculations of these quantities with those of others in Table V. Comparison between columns 2 and 3 show that the effect of CI is to transfer a considerable amount of electronic charge from the five-membered ring into the seven-membered ring. The results of the unrestricted Hartree–Fock calculation of Amos (36) are quite similar to our charge densities after CI. The VB calculation of Brown (35) predicts

TABLE V

Calculated charge densities for the azulene anion

Position	SCF*	SCF + CI*	Unrestricted† HF	VB‡
1, 3	1.1089	1.1546	1.165	1.1080
2	1.1067	1.1605	1.157	1.3953
4, 8	1.0836	1.0627	1.027	1.0419
5, 7	1.037	1.0340	1.065	1.0126
6	1.1747	1.1340	1.139	1.0280
9, 10	1.1301	1.0899	1.095	1.1259

*This work. β_{pq} all equal. CI perturbation of singly excited states on ground states using closed shell SCF MOs of neutral molecule as basis set.
†Reference 36.
‡Valence bond calcd. (ref. 35).

Can. J. Chem. Downloaded from www.nrcresearchpress.com by 210.87.254.40 on 09/05/12
For personal use only.

Can. J. Chem. Downloaded from www.nrcresearchpress.com by 210.87.254.40 on 09/05/12
For personal use only.

TABLE VI

Spin and charge densities for the azulene cation

	Spin densities				Charge densities				
Position	SCF*	SCF + CI*	Unrestricted† HF	VB†	SCF*	SCF + CI*	Open shell§ SCF	Unrestricted† HF	VB‡
1, 3	0.2745	0.4880	0.398	0.2101	0.1185	0.1387	0.1222	0.126	0.0707
2	0.0000	−0.0773	−0.133	−0.0113	−0.004	−0.019	0.0232	0.017	0.1721
4, 8	0.0232	−0.1209	−0.042	0.3333	0.120	0.1053	0.1390	0.150	0.0411
5, 7	0.1229	−0.0478	0.149	−0.1855	0.0913	0.1453	0.0187	0.113	0.0109
6	0.0000	−0.0518	−0.075	0.3740	0.0762	0.0137	0.1386	0.137	0.0119
9, 10	0.09910	0.2458	0.099	−0.0392	0.0815	0.1091	0.0392	0.032	0.2857

*This work. β_{pq} all equal. CI perturbation of singly excited states on ground state using closed shell SCFMOs of neutral molecule as basis set.
†Unrestricted HF method with approximate projection of spin eigenfunction (ref. 36).
‡Valence bond method (ref. 35).
§Reference 22.

quite a different charge distribution from those indicated by any of the MO calculations, particularly in the prediction of a very high charge density at the 2-position and a very low one at the 6-position. It is unfortunate that at the moment we have no direct method of distinguishing between these different predictions by experiment.

3. Azulene Positive Ion Spin Densities

There are at present no experimental results available for the hyperfine splitting constants of the azulene positive ion. However, our theoretical results for spin and charge densities are compared with other recorded theoretical calculations in Table VI. It is found that there are substantial differences between the VB method and the MO methods. This is particularly evident for position 1 for which both our work and that of Amos (36) predict a large positive spin density whereas the VB method (35) predicts a sizable negative spin density at this position. The fairly large differences in predictions by the various methods evident in Table V make it very important that a serious attempt be made to obtain the experimental hyperfine splitting constants for the azulene positive ion.

4. Azulene Positive Ion Charge Densities

A comparison of the charge densities of the positive ion calculated by different methods is made in Table VI. Columns 6 and 7 show that CI has a considerable effect on the charge densities in our SCFMO calculation. In col. 8 we report charge densities obtained for the azulene positive ion by an open-shell VESCF technique (22). The results of this calculation, and the UHF calculation of Amos (35) (col. 9), and our SCF + CI calculation are very similar. They differ from our calculation in positions 5 and 7, for which we predict a much lower charge density than the other methods. As we found for the spin densities there is also considerable difference between the HF and the VB calculations. At the present time, there are no experimental results to compare with the theoretical predictions.

V. CONCLUSIONS

Our SCF calculations on azulene, using the Mataga and Nishimoto (9) approximation for two-center integrals and a constant resonance integral for all nearest neighbors, are justified by the very good agreement we obtain with experiment for transition energies, the ionization potential, and the electron affinity. For ground-state properties, such as the bond lengths, the charge density, and the dipole moment, our method gives very similar results to other methods, all of which are in only poor agreement with experiment. Whether this disagreement is because of deficiencies in MO techniques, or in interpreting the experimental data directly in terms of such theoretical concepts as π-bond orders and π-charge densities, is not clear at present.

Our SCFMO calculations on the singly charged ions of azulene are in considerable disagreement with similar calculations using the VB technique. In the case of the negative ion, the spin densities are in fair agreement with experiment. Corresponding experimental data on the positive ion would help resolve the question of whether MO calculations are superior to the VB method for calculating spin densities. We believe that the SCFMO + CI procedure used in the present paper are to be preferred to other methods such as the VB and the unrestricted Hartree–Fock method because of its capabilities of calculating several unrelated physical properties with the same parameters.

VI. ACKNOWLEDGMENTS

The financial aid given by the National Research Council of Canada and the British Columbia Research Council for carrying out part of this work is gratefully acknowledged.

Can. J. Chem. Downloaded from www.nrcresearchpress.com by 210.87.254.40 on 09/05/12
For personal use only.

Thanks are also given to the staff of the Computing Center of The Franklin Institute for much friendly and helpful cooperation, and for the use of their Honeywell 1400 computer. The computer programs used in this paper are available for use at the computing center of The Franklin Institute.

REFERENCES

1. R. G. PARR. Quantum theory of molecular structure. W. A. Benjamin, Inc., New York. 1963.
2. R. PARISER. J. Chem. Phys. **24**, 250 (1956) or ref. 1, p. 324.
3. J. A. POPLE. Trans. Faraday Soc. **49**, 1375 (1953) or ref. 1, p. 257.
4. K. RUEDENBERG. J. Chem. Phys. **34**, 1861 (1961) or ref. 1, p. 391.
5. E. HEILBRONNER. *In* Non-benzenoid aromatic compounds. *Edited by* D. Ginsburg. Interscience Publishers, Inc., New York. 1959. p. 196.
6. J. E. BLOOR and N. BREARLEY. Can. J. Chem. In press (1965).
7. J. E. BLOOR and N. BREARLEY. To be published,
8. J. E. BLOOR, P. N. DAYKIN, and P. BOLTWOOD. Can. J. Chem. **42**, 121 (1964).
9. K. NISHIMOTO and N. MATAGA. Z. Physik. Chem. Frankfurt, **12**, 335 (1957); **13**, 140 (1957).
10. J. E. BLOOR and P. N. DAYKIN. Submitted for publication. J. Chem. Phys. 1964. W. D. HOBEY. Mol. Phys. **7**, 325 (1964). H. BEN JEMIA and R. LEFEBVRE. J. Chim. Phys. **68**, 755 (1962).
11. W. W. ROBERTSON and A. D. KING, JR. J. Chem. Phys. **34**, 2190 (1961).
12. J. W. SIDMAN and D. S. MCCLURE. J. Chem. Phys. **24**, 757 (1956).
13. R. PARISER. J. Chem. Phys. **25**, 1112 (1956) or ref. 1, p. 343.
14. R. L. HUMMEL and K. RUEDENBERG. J. Phys. Chem. **66**, 2334 (1962).
15. R. D. BROWN and M. L. HEFFERNAN. Australian J. Chem. **12**, 38 (1960).
16. H. E. SIMMONS. J. Chem. Phys. **40**, 3554 (1964).
17. J. KOUTECKY, P. HOCHMAN, and J. MICHL. J. Chem. Phys. **40**, 2439 (1964).
18. R. D. BROWN and M. L. HEFFERNAN. Australian J. Chem. **12**, 319, 330, 543, 554 (1959).
19. A. JULG and P. FRANCOIS. J. Chim. Phys. **59**, 339 (1962).
20. G. R. HUNT and I. G. ROSS. J. Mol. Spectry. **9**, 50 (1962).
21. A. C. M. FINCH. J. Chem. Soc. 1964, 2272.
22. J. R. HOYLAND and L. GOODMAN. J. Chem. Phys. **36**, 21 (1962) and private communication of MOs and energy levels.
23. A. STREITWEISER, JR. Molecular orbital theory for organic chemists. John Wiley & Sons, Inc., New York. 1961. Chap. 7.
24. J. M. ROBERTSON, H. M. M. SHEARER, G. A. SIM, and D. G. WATSON. Acta Cryst. **15**, 1 (1962).
25. C. A. COULSON and A. GOLEBIEWSKI. Proc. Phys. Soc. **78**, 1310 (1961).
26. D. A. HUTCHISON. Acta. Cryst. **15**, 949 (1962).
27. M. ALI and C. A. C. COULSON. Tetrahedron, **10**, 41 (1960).
28. P. N. SKANCKE. Acta. Chem. Scand. **18**, 1671 (1964).
29. H. SPIESECKE and W. G. SCHNEIDER. Tetrahedron Letters, No. 14, 468 (1961).
30. T. SCHAEFER and W. G. SCHNEIDER. Can. J. Chem. **41**, 966 (1963).
31. B. P. DAILEY, A. GOWER, and W. C. NEIKAM. Discussions Faraday Soc. **34**, 18 (1962).
32. A. G. ANDERSON, JR. and B. M. STECKLER. J. Am. Chem. Soc. **81**, 4941 (1959).
33. I. BERNAL, P. H. RIEGER, and G. K. FRAENKEL. J. Chem. Phys. **37**, 1489 (1962).
34. A. H. REDDOCK. J. Chem. Phys. **41**, 444 (1964).
35. T. H. BROWN. J. Chem. Phys. **41**, 2223 (1964).
36. A. T. AMOS. Mol. Phys. **5**, 91 (1962).
37. A. D. MCLACHLAN. Mol. Phys. **3**, 233 (1960).
38. R. A. BERNHEIM and T. P. DAS. J. Chem. Phys. **33**, 1813 (1960).

Can. J. Chem. Downloaded from www.nrcresearchpress.com by 210.87.254.40 on 09/05/12
For personal use only.

Can. J. Chem. Downloaded from www.nrcresearchpress.com by 210.87.254.5 on 09/05/12
For personal use only.

SPECTROSCOPIC STUDIES OF THE REVERSIBLE REACTION BETWEEN 2,2-DIPHENYL-1-PICRYLHYDRAZYL AND 2,4,6-TRI-*t*-BUTYLPHENOL

P. B. AYSCOUGH
Department of Physical Chemistry, University of Leeds, Leeds, England

AND

K. E. RUSSELL
Department of Chemistry, Queen's University, Kingston, Ontario

Received May 20, 1965

ABSTRACT

The reaction between 2,2-diphenyl-1-picrylhydrazyl (DPPH) and 2,4,6-tri-*t*-butylphenol in benzene solution has been studied by optical and electron spin resonance methods. In the absence of oxygen, equilibrium is reached with the products 2,2-diphenyl-1-picrylhydrazine and the tri-*t*-butylphenoxy radical. The equilibrium constant for the reaction is 0.10 ± 0.03 at 20 °C and from its variation with temperature the heat of reaction is estimated to be 1.6 ± 0.3 kcal/mole. The entropy change in the reaction is small.

The rate constants for the forward reactions with tri-*t*-butylphenol and deuterated tri-*t*-butylphenol are 0.12 ± 0.02 l/(mole s) and 0.010 ± 0.002 l/(mole s) respectively at 20 °C. The corresponding activation energies are 6.5 ± 0.8 kcal/mole and 7.7 ± 0.7 kcal/mole. The rate constant for the reverse reaction is approximately 2 l/(mole s) at 20 °C and the activation energy is 4.8 ± 1 kcal/mole.

INTRODUCTION

2,2-Diphenyl-1-picrylhydrazyl (DPPH) reacts with a wide range of hydrogen donors including aliphatic thiols (1), aromatic amines (2, 3), hydroaromatic compounds (4, 5), and phenols (6, 7, 8). The major product of these reactions is 2,2-diphenyl-1-picrylhydrazine (DPPH-H) and kinetic studies have shown that in reactions with phenols the rate-determining step involves hydrogen abstraction from the OH group (7, 8). Since DPPH is a free radical and the solvent e.g. benzene, is of low polarity, it is probable that the rate-determining step can be represented by eq. [1].

$$\text{DPPH} + \text{XH} \rightarrow \text{DPPH-H} + \text{X}\cdot \qquad [1]$$

The reactions with phenols are, however, quite sensitive to inductive effects of meta-substituents, and changes in para-substituents can alter the rate constants at 30 °C by factors as great as 20 000. McGowan, Powell, and Raw (6) have compared the effect of substituents on the rate of hydrogen abstraction by DPPH from phenols with their effect on the rates of solvolysis of dimethylbenzyl chlorides and have suggested that DPPH may abstract hydride ions rather than hydrogen atoms from phenols.

The reactions of DPPH with aromatic amines (3), phenols (7), and acetic acid and ethanol (9) are retarded by the product DPPH-H. The retardation of the reactions with amines and phenols has been explained in terms of the reversibility of the rate-determining step [1]. Proll and Sutcliffe (9) argue that the hydrogen abstraction process is not reversible when acetic acid and ethanol act as donors, and state that retardation is due solely to complex formation between DPPH and DPPH-H. If their explanation is correct it should also apply to the reactions of DPPH with amines and phenols.

The radical nature of the reaction between DPPH and phenols and the reversibility of the primary step can be most simply studied if a stable free radical X· is produced in

reaction [1]. This paper describes a study of the reaction between DPPH and 2,4,6-tri-*t*-butylphenol to give DPPH-H and the stable tri-*t*-butylphenoxy radical. The disappearance of DPPH was followed by visible spectrometry and the formation of tri-*t*-butylphenoxyl by electron spin resonance (e.s.r.). Forward and reverse reactions were investigated in addition to equilibria between 20 °C and 60 °C.

EXPERIMENTAL

Materials

DPPH-H was prepared by the reaction of picryl chloride with 1,1-diphenylhydrazine (10, 11). Melting point 170–171 °C. DPPH was prepared by lead dioxide oxidation of DPPH-H and was recrystallized from a benzene–ether mixture. It was heated *in vacuo* to remove complexed benzene (12). Melting point 137.5–138.5 °C. 2,4,6-Tri-*t*-butylphenol was recrystallized from ethanol in an atmosphere of nitrogen. Melting point 131–132 °C. Tri-*t*-butylphenoxyl was prepared by oxidation of tri-*t*-butylphenol using an alkaline ferricyanide solution (13). It was stored in an atmosphere of nitrogen. Deuterated tri-*t*-butylphenol was prepared in benzene solution by shaking a 0.01 *M* solution of the normal phenol with heavy water. Equilibrium is rapidly attained (8) and from the relative amounts of phenol and heavy water used it was estimated that the phenol was approximately 96% deuterated at the OH group.

Procedure

A preliminary spectroscopic study of the reaction was made using a Bausch and Lomb 'Spectronic 20' spectrometer. Solutions containing approximately 5×10^{-4} *M* DPPH and 10^{-3} to 5×10^{-2} *M* tri-*t*-butylphenol were prepared under nitrogen or *in vacuo* and their spectra after various times were compared with those of solutions of DPPH, DPPH-H, and tri-*t*-butylphenoxyl. The reverse reaction between tri-*t*-butylphenoxyl and DPPH-H was investigated using mixtures of approximately 10^{-4} *M* DPPH-H and tri-*t*-butylphenoxyl prepared under nitrogen.

Initial rates of reaction were determined using a modified Fisher electrophotometer, the 1 cm reaction tubes being placed in a jacket through which water at constant temperature was circulated (3). The absorbance at 525 mμ was measured at ½ min intervals and, after correction for the DPPH-H and tri-*t*-butylphenoxyl present, was used as a measure of the DPPH concentration. Initial rates of reaction of DPPH with tri-*t*-butylphenol are almost unaffected by oxygen and most of the early measurements were performed with air present. More accurate rate constants were obtained from data for reactions which proceeded to equilibrium, but these required thoroughly degassed solutions as tri-*t*-butylphenoxyl reacts with oxygen. Solutions of the reactants were preferably degassed separately since a considerable amount of reaction occurs during the degassing of a reaction mixture. Phenol concentrations ranged from 4 to 80×10^{-4} *M* and DPPH concentrations from 2 to 50×10^{-5} *M*. For reactions involving the higher concentrations of DPPH, absorbance measurements were made using a Unicam SP500 spectrophotometer at a wavelength of 700 mμ.

Initial rates of the reverse reaction between 2,4,6-tri-*t*-butylphenoxyl and DPPH-H were determined using the Fisher electrophotometer. The reactant solutions were prepared in an atmosphere of nitrogen and the concentration range of each reactant was approximately 5 to 15×10^{-5} *M*.

Electron spin resonance spectra of reaction mixtures were obtained using a Varian V-4500 EPR spectrometer, operating at 9 400 Mc/s, with a Mullard 10 in. electromagnet (14). It was established that microwave power saturation of the free radicals in benzene solution was negligible. The spectra of the two free radicals overlap but the narrow line spectrum of the tri-*t*-butylphenoxyl was readily observed at low gain and the broad line spectrum of DPPH at high gain. Relative concentrations of tri-*t*-butylphenoxyl during a reaction were obtained from peak heights of the first derivative curves. The ratio of concentrations of DPPH and tri-*t*-butylphenoxyl at equilibrium was obtained by double integration of the first derivative functions to give the areas under the absorption curves; the absolute concentration of each radical was derived on the assumption that the total radical concentration did not change during the establishment of equilibrium. Temperature control (±1 °C) for experiments conducted in the 20 °C to 60 °C temperature range was obtained using a stream of heated nitrogen. The initial concentrations of phenol varied from 8 to 150×10^{-4} *M* and the initial concentration of DPPH was 5×10^{-4} *M*.

RESULTS

When DPPH reacts with 2,4,6-tri-*t*-butylphenol in the presence of air the violet color of the DPPH gives way to the light brown of DPPH-H. In the absence of air an equilibrium is reached and a solution initially containing 5×10^{-4} *M* DPPH and 10^{-2} *M* tri-*t*-butylphenol remains violet because of the presence of DPPH. At higher concentrations (0.1 *M* to 1 *M*) the equilibrium DPPH concentration is reduced to a very low value and the visible spectrum of the equilibrium mixture shows a weak maximum at 625 mμ; on admission of air this maximum disappears. If the absorbance is due primarily to the tri-*t*-butylphenoxy

Can. J. Chem. Downloaded from www.nrcresearchpress.com by 210.87.254.5 on 09/05/12
For personal use only.

radical a rough calculation of its concentration using an extinction coefficient of 400 l/(mole cm) (15) gives a value of $5 \pm 1 \times 10^{-4}$ M, compared with 5×10^{-4} M if 1 mole tri-*t*-butylphenoxyl is formed from 1 mole DPPH.

Stronger evidence for the formation of tri-*t*-butylphenoxyl is obtained from the electron spin resonance spectrum of a reacting solution. At low gain the spectrum consists of a triplet with a peak to peak separation of 1.8 G, characteristic of the 2,4,6-tri-*t*-butylphenoxy radical under conditions when the hyperfine structure due to the *t*-butyl groups remains unresolved (16). At high gain the observed spectrum is principally the broad line spectrum of DPPH except that the central region is obscured by the phenoxy radical. If a g factor of 2.0036 is assumed for DPPH, the g factor of 2,4,6-tri-*t*-butylphenoxyl is estimated to be 2.0045 ± 0.0002 (cf. 2.0052 (17)).

The identification of the tri-*t*-butylphenoxy radical as a major product and the approach to a position of equilibrium are expressed in eq. [2].

[2] 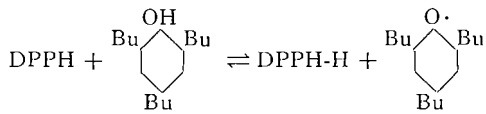

The reversibility was confirmed by mixing dilute solutions of DPPH-H and tri-*t*-butylphenoxyl in an atmosphere of nitrogen. The solution became violet and the visible spectrum was almost identical with that of DPPH. In separate experiments it was shown that DPPH and tri-*t*-butylphenoxyl do not react at an appreciable rate in benzene solution under the conditions of this work.

The Equilibrium Constant

The results of the equilibrium constant measurements are given in Table I. In optical determinations the equilibrium concentration of DPPH was estimated from absorbance measurements at 525 mμ or 700 mμ. Concentrations of DPPH-H and tri-*t*-butylphenoxyl are derived on the assumption that the reaction proceeds quantitatively according to eq. [2]. The concurrent hydrogen exchange reactions between tri-*t*-butylphenol and tri-*t*-butylphenoxyl (18) and between DPPH-H and DPPH should not affect the validity of this assumption. The mean value of the equilibrium constant from optical measurements is 0.12 ± 0.04, at 20 °C. The electron spin resonance results are probably of slightly higher accuracy because the ratio of the concentrations of the two radicals is obtained from the experimental observations. They yield an average value of 0.10 ± 0.03 for the equilibrium constant at 20 °C, in good agreement with the results of optical measurements.

TABLE I

Equilibrium constants for the reaction between DPPH and tri-*t*-butylphenol at 20 °C

Equilibrium constant	Phenol concentration (M)	Method
0.09	8×10^{-4}	e.s.r.
0.12	1.7×10^{-3}	e.s.r.
0.09	1.8×10^{-3}	e.s.r.
0.10	3.9×10^{-3}	e.s.r.
0.085	3.9×10^{-3}	e.s.r.
0.09	7.3×10^{-3}	e.s.r.
0.105	1.53×10^{-2}	e.s.r.
0.11	2.2×10^{-3}	Optical
0.12	3.9×10^{-3}	Optical
0.12	7.6×10^{-3}	Optical
0.14	5×10^{-2}	Optical

Can. J. Chem. Downloaded from www.nrcresearchpress.com by 210.87.254.5 on 09/05/12
For personal use only.

When the temperature of an equilibrium mixture was raised from 30 °C to 60 °C there was a decrease in absorbance at 525 mμ due (*a*) to a decrease in density of the solution (*b*) to a movement of the equilibrium in favor of the products; the absorbance slowly regained its former value on cooling to 30 °C. The enthalpy change in the reaction, estimated from the variation of equilibrium constant with temperature, was found to be 1.0 ± 0.5 kcal/mole. Values of the equilibrium constant were also determined from electron spin resonance studies at 30 °C, 40 °C, 50 °C, and 60 °C and these lead to an enthalpy change of 1.6 ± 0.3 kcal/mole. Since the free energy change in the reaction at 20 °C is 1.4 ± 0.2 kcal/mole, the entropy change for the reaction in benzene solution is small.

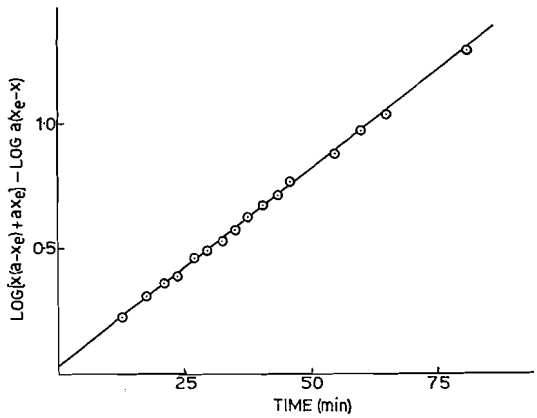

FIG. 1. Plot of kinetic data derived from electron spin resonance measurements at 20 °C.

The Rate Constants

In studies of the forward reaction carried out *in vacuo* the phenol concentration remained almost constant during any single experiment. First order velocity constants were derived using the integrated rate expression for a reaction of the type $A \rightleftharpoons C + D$. Fig. 1 is a plot of $\log [ax_e + x(a - x_e)] - \log a(x_e - x)$ vs. time t, where a, $a - x$, and $a - x_e$ are the concentrations of DPPH at times 0, t, and at equilibrium respectively. In this experiment the initial phenol concentration was 1.5×10^{-3} M, and the DPPH concentration was derived from electron spin resonance measurements of the tri-*t*-butylphenoxyl concentration assuming that the stoichiometry of the reaction is correctly expressed by eq. [2]. Straight lines obtained in the graphical treatment showed that the reaction is of first order with respect to DPPH. On dividing the first order constants by the phenol concentrations, the second order constants for the forward reaction were obtained. These are independent of phenol concentration in the range 1 to 7×10^{-3} M showing that under these conditions the reaction is of first order with respect to the phenol. Rate constants at 20 °C derived from optical measurements of the DPPH concentration and from electron spin resonance measurements of the tri-*t*-butylphenoxyl concentration are given in Table II. The mean value of the rate constant is 0.12 ± 0.02 l/(mole s) at 20 °C. Rate constants have also been derived from initial rates of reaction and the results agree with those in Table II provided that similar concentrations of reactants are used. However, for DPPH concentrations in the range 2 to 6×10^{-5} M and phenol concentrations in the range 2 to 20×10^{-4} M, the order with respect to phenol drops to 0.7–0.8. Initial rates are not significantly affected by degassing so that the change in order is not caused by oxygen in the system. The apparent second order 'rate constant' rises to 0.16–0.19 l/(mole s) at 20 °C.

Can. J. Chem. Downloaded from www.nrcresearchpress.com by 210.87.254.5 on 09/05/12
For personal use only.

TABLE II

Rate constants for the reaction between DPPH and tri-*t*-butylphenol at 20 °C

Rate constant (l/(mole s))	Phenol concentration (M)	Method
0.11	8.4×10^{-4}	e.s.r.
0.12	1.5×10^{-3}	e.s.r.
0.125	3.8×10^{-3}	e.s.r.
0.115	7×10^{-3}	e.s.r.
0.13	2.2×10^{-3}	Optical
0.115	3.9×10^{-3}	Optical
0.12	7.6×10^{-3}	Optical

The activation energy for the forward reaction is 6.5 ± 0.8 kcal/mole. With 2,4,6-tri-*t*-butylphenol approximately 96% deuterated at the OH group, the rate constant at 20 °C is 0.010 ± 0.002 l/(mole s) and the activation energy is 7.7 ± 0.7 kcal/mole.

The reverse reaction between DPPH-H and the tri-*t*-butylphenoxy radical is much faster than the forward reaction and reactant concentrations not greater than 1.5×10^{-4} M are required for measurable rates of reaction. Analysis of the initial rates of formation of DPPH shows that, over small concentration ranges, the reverse reaction appears to be of first order with respect to the tri-*t*-butylphenoxyl but only about half order with respect to DPPH-H. The second order 'rate constant' for a DPPH-H concentration of 10^{-4} M is 2.2 ± 0.4 l/(mole s) at 20 °C and the activation energy is 4.8 ± 1 kcal/mole. The difference between the activation energies of the forward and reverse reactions is 1.7 ± 1.3 kcal/mole compared with an enthalpy change derived from equilibrium constants of 1.6 ± 0.3 kcal/mole.

DISCUSSION

The reaction between DPPH and 2,4,6-tri-*t*-butylphenol in benzene solution gives DPPH-H and the stable 2,4,6-tri-*t*-butylphenoxy radical. Deuteration of the phenol at the OH group reduces the rate constant of the forward reaction by a factor of the order of 12, showing that abstraction of hydrogen occurs almost exclusively at the OH group. The equilibrium constant for the reaction of DPPH with the deuterated phenol is 0.11 ± 0.03, i.e. within experimental error it is unaffected by deuteration of the phenol. It may be inferred that the reverse reaction is subject to a primary kinetic isotope effect of comparable magnitude to that observed for the forward reaction.

At relatively high concentrations of DPPH and tri-*t*-butylphenol the reaction is of first order with respect to each reactant but at low concentrations the order with respect to phenol drops to 0.7–0.8. The reason for this divergence from simple kinetic behavior is not understood; a similar dependence of rate constant upon phenol concentration has been observed in reactions of styrylperoxy radicals with unhindered phenols (19). At low concentrations of reactants the reverse reaction is of first order with respect to tri-*t*-butylphenoxyl but of about 0.5 order with respect to DPPH-H. The second order 'rate constant' is therefore a function of concentration under these conditions and the ratio of the rate constants at 20 °C for the forward and reverse reactions, 0.12/2.2 = 0.055, is lower than the value of the equilibrium constant observed directly, 0.10 ± 0.03.

The reaction between DPPH and tri-*t*-butylphenol gives rise to a stable phenoxy radical and experiments in progress show that phenoxy radicals are intermediates when other hindered phenols are attacked by DPPH. While it remains possible that hydride ions are abstracted, to be followed by electron transfer, it appears more likely that hydrogen atoms

Can. J. Chem. Downloaded from www.nrcresearchpress.com by 210.87.254.5 on 09/05/12
For personal use only.

are directly transferred to the DPPH. The very great sensitivity of DPPH–phenol reactions to substituents in the phenol (6, 7) is then ascribed to the importance of polar contributions of the form $\overset{+}{X}OH\ \overset{-}{D}PPH$ to the transition state.

In the reversible reaction between DPPH and tri-*t*-butylphenol the rate constant for the reverse reaction is an order of magnitude greater than that for the forward reaction, and it is probable that addition of DPPH-H causes retardation of the overall reaction with other phenols by reducing the concentrations of reactive phenoxy intermediates. Reversibility of the primary step is likely to be quite general in hydrogen abstraction reactions of DPPH, and retardation of the reactions between DPPH and acetic acid and ethanol (9) may well be caused by this reversibility. DPPH forms complexes with solvents (12) and its reactions may in some cases be influenced by such complex formation, but retardation of DPPH hydrogen abstraction reactions by DPPH-H is not likely to be due to the formation of complexes between DPPH and DPPH-H at the concentrations used in these experiments.

In this work, electron spin resonance has been applied to the measurement of concentrations of the stable 2,4,6-tri-*t*-butylphenoxy radical in benzene solution and the derived rate and equilibrium constants are in excellent agreement with those obtained from optical studies. The success of the method depends upon the phenoxy radical having a narrow line spectrum compared with that of DPPH. In general, reactions of DPPH with phenols and other donors produce reactive intermediates at lower concentrations than those observed here but in many cases their stationary concentrations may be determined by similar methods. The kinetics of the secondary reactions of the reactive intermediates may then be studied directly.

ACKNOWLEDGMENTS

We are grateful to Janet Smith, Queen's University, for making the preliminary optical studies of this problem. This work was supported by an operating grant from the National Research Council. K. E. R.'s visit to the Department of Physical Chemistry, University of Leeds, was supported by grants from the Nuffield Foundation and the National Research Council.

REFERENCES

1. K. E. Russell. J. Phys. Chem. **58**, 437 (1954).
2. A. S. Kuz'minskiĭ and L. G. Angert. Dokl. Akad. Nauk SSSR, **96**, 1187 (1954).
3. J. E. Hazell and K. E. Russell. Can. J. Chem. **36**, 1729 (1958).
4. E. A. Braude, A. G. Brook, and R. P. Linstead. J. Chem. Soc. 3574 (1954).
5. J. S. Hogg, D. H. Lohmann, and K. E. Russell. Can. J. Chem. **39**, 1394 (1961).
6. J. C. McGowan, T. Powell, and R. Raw. J. Chem. Soc. 3103 (1959).
7. J. S. Hogg, D. H. Lohmann, and K. E. Russell. Can. J. Chem. **39**, 1588 (1961).
8. R. A. Bird, G. A. Harpell, and K. E. Russell. Can. J. Chem. **40**, 701 (1962).
9. P. J. Proll and L. H. Sutcliffe. Trans. Faraday Soc. **59**, 2090 (1963).
10. S. Goldschmidt and K. Renn. Ber. **55**, 628 (1922).
11. R. H. Poirier, E. J. Kahler, and F. Benington. J. Org. Chem. **17**, 1439 (1952).
12. J. A. Lyons and W. F. Watson. J. Polymer Sci. **18**, 141 (1955).
13. E. Muller and K. Ley. Ber. **87**, 922 (1954).
14. P. B. Ayscough, A. P. McCann, C. Thomson, and D. C. Walker. Trans. Faraday Soc. **57**, 1487 (1961).
15. C. D. Cook, C. B. Depatie, and E. S. English. J. Org. Chem. **24**, 1356 (1959).
16. J. K. Becconsall, S. Clough, and G. Scott. Trans. Faraday Soc. **56**, 459 (1960).
17. J. E. Wertz, C. F. Koelsch, and J. L. Vivo. J. Chem. Phys. **23**, 2194 (1955).
18. R. W. Kreilick and S. I. Weissman. J. Am. Chem. Soc. **84**, 306 (1962).
19. J. A. Howard and K. U. Ingold. Can. J. Chem. **41**, 1744 (1963).

Can. J. Chem. Downloaded from www.nrcresearchpress.com by 210.87.254.5 on 09/05/12
For personal use only.

Can. J. Chem. Downloaded from www.nrcresearchpress.com by 210.87.254.105 on 09/05/12
For personal use only.

THE ARSENIDES OF TUNGSTEN AND MOLYBDENUM

WAs_2, W_2As_3, $MoAs_2$, Mo_2As_3, AND Mo_5As_4[1]

J. B. TAYLOR, L. D. CALVERT, AND M. R. HUNT[2]
Division of Applied Chemistry, National Research Council, Ottawa, Canada

Received June 2, 1965

ABSTRACT

Binary alloys in the systems tungsten–arsenic and molybdenum–arsenic have been annealed at temperatures between 600 and 1 000 °C and, after quenching, examined by X-ray diffraction techniques. The only intermediate phases observed are WAs_2, W_2As_3, $MoAs_2$, Mo_2As_3, and Mo_5As_4. No solid solubility was detected in the elements or the compounds. The diarsenides are monoclinic, $C2$, and have the $NbAs_2$ structure. WAs_2, $a = 9.085 \pm 0.002$ Å, $b = 3.318 \pm 0.002$ Å, $c = 7.690 \pm 0.002$ Å, $\beta = 119° 31' \pm 2'$, $MoAs_2$, $a = 9.07$ Å, $b = 3.30$ Å, $c = 7.73$ Å, $\beta = 119° 20'$. The X_2As_3 compounds are monoclinic, condensed diffraction symbol $C*/*$; W_2As_3, $a = 13.346 \pm 0.002$ Å, $b = 3.278 \pm 0.002$ Å, $c = 9.599 \pm 0.002$ Å, $\beta = 124° 48' \pm 2'$; Mo_2As_3, $a = 13.339 \pm 0.002$ Å, $b = 3.240 \pm 0.002$ Å, $c = 9.628 \pm 0.002$ Å, $\beta = 124° 31' \pm 2'$. Mo_5As_4 is tetragonal, $I4/m$, with the Ti_5Te_4 structure, $a = 9.595 \pm 0.001$ Å, $c = 3.284 \pm 0.002$ Å. Data for $MoAs_2$ and Mo_5As_4 confirm or amplify previous reports. In contrast to other reports, MoAs and W_2As were not observed. W_4As_5 and Mo_4As_5, which have been mentioned briefly elsewhere, are here identified as W_2As_3 and Mo_2As_3.

During an investigation of crystal growth by vapor transport methods the phase relationships in the tungsten–arsenic and molybdenum–arsenic systems were studied over the full range of composition using powder diffraction and single crystal X-ray diffraction methods.

Both $MoAs_2$ and WAs_2 were prepared by Heinerth and Biltz (1). Boller and Nowotny (2) reported WAs_2, W_4As_5, and W_2As as the only phases occurring in the tungsten-arsenic system. W_4As_5 was examined by Weissenberg methods and assigned monoclinic cell parameters $a = 7.99$ Å, $b = 3.28$ Å, $c = 6.88$ Å, $\beta = 99° 12'$. No further information on the other phases was given except that WAs_2 is not stable at high temperatures. The same authors reported the existence of $MoAs_2$, Mo_4As_5, MoAs, and Mo_5As_4. On the basis of diffractometer powder patterns and intensity comparisons they assigned the MnP structure type to MoAs ($a = 5.98_9$ Å, $b = 3.36_8$ Å, $c = 6.41_7$ Å) and the Ti_5Te_4 structure type (3) to Mo_5As_4 ($a = 9.60_0$ Å, $c = 3.27_8$ Å). $MoAs_2$ was claimed to be orthorhombic and Mo_4As_5 to have the same structure as W_4As_5 but no further details were given. Jensen and Kjekshus (4) have concluded that $MoAs_2$ has the $NbAs_2$ structure type, $a = 9.069$ Å, $b = 3.2996$ Å, $c = 7.717$ Å, $\beta = 119.36°$. They reported the existence of $MoAs_{1.4}$ and $MoAs_{0.8}$ but did not stipulate that these are the only additional phases in the molybdenum–arsenic system.

We have been prompted to publish the results of our phase analytical and crystallographic work because of discrepancies which exist between our results and those of Boller and Nowotny.

EXPERIMENTAL

Materials

Tungsten powder (−200 mesh) was supplied by A. D. Mackay. It contained less than 100 p.p.m. Mo; between 5 and 50 p.p.m. each of Mg, Si, Fe, and Ni; and between 1 and 10 p.p.m. each of Cu and Ca. Molybdenum powder (−200 mesh) was donated by the U.S. Fansteel Corporation. It contained between 40 and 100 p.p.m. each of W, Fe, Ni, and Cu; between 5 and 50 p.p.m. each of Mg, Si, Ca, and Cr; and between 1 and 10 p.p.m. of Ag. Arsenic was obtained from Cominco as "high purity arsenic" which was

[1]*Issued as N.R.C. No. 8611.*
[2]*N.R.C. Postdoctorate Fellow.*

claimed to be spectroscopically better than 99.999%. It was fractionally sublimed *in vacuo* at 450 °C to reduce oxide contaminant not accounted for in the analysis.

Phase Analysis

Samples were prepared in the usual way by sealing under vacuum (10^{-5} mm Hg) weighed quantities of arsenic and tungsten or molybdenum in fused silica ampoules. Care was taken to ensure that the ampoules and charges were thoroughly outgassed before sealing. In the tungsten–arsenic system, samples having the following compositions were prepared: WAs_3; WAs_2; $WAs_{1.8}$; $WAs_{1.6}$; $WAs_{1.4}$; $WAs_{1.2}$; WAs; $W_{1.2}As$; $W_{1.4}As$; $W_{1.6}As$; $W_{1.8}As$; W_2As; W_3As; W_4As. In the molybdenum–arsenic system the following samples were prepared: $MoAs_4$; $MoAs_3$; $MoAs_2$; $MoAs_{1.8}$; $MoAs_{1.6}$; $MoAs_{1.4}$; $MoAs_{1.2}$; MoAs; $Mo_{1.2}As$; $Mo_{1.4}As$; $Mo_{1.6}As$; $Mo_{1.8}As$; Mo_2As; Mo_3As; Mo_4As; Mo_5As. Both series of samples were reacted at 850 °C for 40 days and then quenched in water. Each sample was divided into five parts, sealed in fused silica tubes under vacuum, and annealed at 600, 700, 800, 900, and 1 000 °C for periods of not less than 18 days. In addition, samples of composition WAs_6; WAs_5; $WAs_{4.5}$; WAs_4; WAs_3; $WAs_{2.6}$; $WAs_{2.4}$ were sealed in heavy-walled fused silica ampoules and annealed at 850 °C for 30 days.

Another set of samples WAs_2; $WAs_{1.8}$; $WAs_{1.6}$; $WAs_{1.4}$; $WAs_{1.2}$; WAs; $W_{1.2}As$; $W_{1.4}As$; $W_{1.6}As$; $W_{1.8}As$ was prepared by reaction for 20 days at 600 °C instead of 850 °C. Only one molybdenum arsenide, MoAs was prepared at 600 °C. As required, samples were quenched in water and Debye–Sherrer patterns obtained on 11.46 cm Norelco cameras using nickel-filtered copper radiation. Guinier focussing camera patterns were obtained on an 11.46 cm camera with monochromatic Cu K_α radiation ($\lambda = 1.5405$ Å).

The attack on the silica tubes was assessed by visual examination of the used ampoules coupled with spectrographic analysis of the reacted charges. Only in the case of samples richer in arsenic than XAs_2 was there any marked attack of the tubes. In these samples, silicon contents rose to 1 000 p.p.m. In all other samples analyzed, the silicon contaminant remained below 100 p.p.m. and very little attack of the silica was detected by visual examination.

Assignment of a particular molecular formula to a phase was based initially on careful examination of 16 h exposure Guinier photographs of a series of samples covering the composition range in question. The composition of the samples was calculated from the weighed quantities of each component prior to reaction.

Single Crystal Preparation

Single crystals of W_2As_3 were obtained using a bromide vapor transport reaction. The growth tube was fused silica, 9 mm i.d., 12 cms long. About 1 g of WAs_2 was placed at one end. Two sidearms about 8 cm long were attached to the tube and one contained 58 mg $PtBr_2$. The system was evacuated to 10^{-5} mm of mercury and sealed off. Bromine was generated by thermal decomposition of the $PtBr_2$ (about 500 °C) and trapped at liquid nitrogen temperature in the second side limb. The limb which had contained the $PtBr_2$ was sealed off and the bromine transferred by distillation into the growth tube. The growth tube was sealed off and placed in a furnace for 24 h with the end containing WAs_2 maintained at 1 075 °C and the other end at 900 °C. W_2As_3 crystals grew at the cooler end and to a lesser extent on the charge also.

Single crystals of $MoAs_2$ were obtained by chloride vapor transport reaction. The growth tube was of a similar size to that used for W_2As_3. The charge consisted of 0.8455 g of molybdenum and 1.5205 g of arsenic. Chlorine was obtained from a fused chloride electrolytic generator and 0.1025 g metered coulometrically. The tube was heated for 2 days with the charge held at 914 °C and the opposite end at 938 °C. Needles of $MoAs_2$ grew on the substrate at the hotter end of the tube. The relevant parameters are recorded for each case although they may not define unique conditions necessary for crystal growth.

RESULTS

In the tungsten–arsenic system, the only compound observed above 800 °C is W_2As_3 but below this temperature, WAs_2 is also stable. There is no indication of any binary phase richer in tungsten than W_2As_3. Guinier patterns obtained from $WAs_{1.4}$ showed W_2As_3 and tungsten reflections only.

In the molybdenum–arsenic system, the only intermediate phases obtained were $MoAs_2$, Mo_2As_3, and Mo_5As_4. They are all stable between 600 and 1 000 °C. No evidence was found to confirm the existence of MoAs. Thus in patterns obtained from samples of $MoAs_{1.4}$, there were reflections attributable to Mo_5As_4 and Mo_2As_3 only.

The intermediate phases have no detectable range of composition as judged from the constancy of their back reflection Debye–Scherrer patterns. There is little or no solid solubility of arsenic in tungsten or molybdenum. Thus the lattice parameter of tungsten is 3.1650 Å in a sample containing W_2As_3 and W annealed at 600 °C. The molybdenum parameter is 3.1468 Å in a sample containing Mo_5As_4 and Mo annealed at 700 °C. (Both

Can. J. Chem. Downloaded from www.nrcresearchpress.com by 210.87.254.105 on 09/05/12
For personal use only.

TABLE I

Powder diffraction pattern of WAs_2. (Monoclinic $a = 9.085 \pm 0.002$ Å, $b = 3.318 \pm 0.002$ Å, $c = 7.690 \pm 0.002$ Å, $\beta = 119° 31' \pm 2'$. Monochromatic Cu K_α radiation $\lambda_{\alpha 1} = 1.5405$ Å; Guinier focussing camera, diameter 11.46 cm; temp. 24 °C; internal standard As_2O_3 ($a = 11.075_5$ Å); low angle cut off 40 Å; high angle cut off 1.27 Å)

I/I_1	d_{obs} (Å)	d_{calcd} (Å)	hkl	I/I_1	d_{obs} (Å)	d_{calcd} (Å)	hkl
7	6.651	6.691	001	4.4	1.646	1.647	$31\bar{4}$
33	4.507	4.512	$20\bar{1}$	11	1.631	1.629	$20\bar{3}$
0.4	4.156	4.191	101	0.5	1.609	1.612	$50\bar{4}$
5.5	3.952	3.952	200			1.610	$02\bar{1}$
1.0	3.857	3.834	$10\bar{2}$	0.5	1.604	1.602	$11\bar{4}$
11	3.528	3.562	$20\bar{2}$	7	1.592	1.593	$51\bar{2}$
7	3.343	3.346	002	7	1.557	1.557	$51\bar{3}$
		3.319	010			1.557	$22\bar{1}$
13	3.060	3.060	110	1.8	1.541	1.543	$51\bar{1}$
13	3.003	3.009	$30\bar{1}$			1.542	121
		3.007	$11\bar{1}$	0.9	1.531	1.529	220
4.4	2.846	2.846	201	<0.4	1.523	1.522	122
0.7	2.680	2.673	$21\bar{1}$	2.8	1.514	1.515	$20\bar{5}$
0.4	2.629	2.648	102			1.515	$31\bar{2}$
		2.635	300	5.5	1.503	1.505	$60\bar{3}$
100	2.603	2.600	111			1.504	$60\bar{2}$
13	2.554	2.554	$20\bar{3}$			1.504	$40\bar{5}$
11	2.510	2.509	$11\bar{2}$			1.504	$22\bar{2}$
4.4	2.256	2.256	$40\bar{2}$			1.501	411
41	2.232	2.231	$00\bar{3}$	<0.4	1.494	1.494	104
		2.229	$31\bar{1}$			1.494	014
11	2.214	2.215	$40\bar{1}$	0.9	1.487	1.486	$02\bar{2}$
4.4	2.168	2.169	$31\bar{2}$	0.5	1.4483	1.4499	$51\bar{4}$
2.8	2.114	2.121	301	4.4	1.4328	1.4339	$60\bar{4}$
80	2.067	2.070	$11\bar{2}$			1.4336	$60\bar{1}$
		2.070	$40\bar{3}$			1.4332	$22\bar{1}$
		2.063	310	1.8	1.4246	1.4246	$50\bar{5}$
11	1.994	1.992	$11\bar{3}$	8.2	1.3937	1.3930	501
11	1.975	1.976	400	<0.4	1.3703	1.3703	$61\bar{3}$
13	1.929	1.931	$31\bar{3}$			1.3700	$61\bar{2}$
11	1.917	1.916	$20\bar{4}$			1.3700	$41\bar{5}$
		1.914	$10\bar{3}$	5.5	1.3640	1.3630	114
<0.4	1.824	1.829	$10\bar{4}$	7	1.3329	1.3310	$02\bar{3}$
<0.4	1.816	1.816	$50\bar{2}$	1.1	1.3280	1.3277	$42\bar{1}$
2.2	1.789	1.787	311	4.4	1.3174	1.3177	600
<0.4	1.752	1.756	$41\bar{3}$	7	1.2946	1.2943	$42\bar{3}$
4.4	1.683	1.683	401	4.4	1.2898	1.2873	313
13	1.659	1.659	$21\bar{4}$	7	1.2852	1.2843	511
		1.659	020	7	1.2711	1.2705	420
		1.658	113			1.2702	$70\bar{4}$

samples had a nominal composition X_2As.) The solid solubility of the metals in arsenic cannot be extensive but back reflection Debye–Scherrer lines of arsenic were not sharp enough to permit accurate measurement of its parameters.

CRYSTALLOGRAPHIC DATA

The Tungsten Arsenides

WAs_2.—Formula weight 333.69. Monoclinic, $NbAs_2$ structure type (5). The powder pattern, Table I, was indexed with the lattice parameters $a = 9.085 \pm 0.002$ Å, $b = 3.318 \pm 0.002$ Å, $c = 7.690 \pm 0.002$ Å, $\beta = 119° 31' \pm 2'$. $U = 201.7$ Å^3, $D_m = 10.46$ g cm^{-3} (pycnometrically in water), $Z = 4$, $D_x = 10.99$ g cm^{-3}. Cu K_α radiation, $\lambda_{\alpha 1} = 1.5405$ Å. Guinier focussing camera.

W_2As_3.—Single crystals obtained by bromide vapor transport between 1 075 °C and 900 °C were needles elongated along b with diameters 0.01 to 0.03 mm and lengths 0.1 to 0.3 mm. They were twinned, twin axis [001], and, under the microscope, appeared

Can. J. Chem. Downloaded from www.nrcresearchpress.com by 210.87.254.105 on 09/05/12
For personal use only.

notched parallel to their length. Goniometric measurements although not very accurate, indicated the possibility of twinning. One fragment, consisting largely of a single individual, was obtained by cleaving the longest needle found. Three crystals were examined. Monoclinic, $a = 13.31$ Å, $b = 3.27$ Å, $c = 9.58$ Å, $\beta = 124° 35'$. Precession photographs Mo K_α, $\lambda = 0.7107$. Condensed diffraction symbol $C^*/^*$. The body-centered cell, related by the transformation matrix 101/010/001 has $a = 11.11$ Å, $b = 3.27$ Å, $c = 9.58$ Å, $\beta = 100° 25'$, symbol $I\ ^*/^*$ and $c < a$.

Table II is an indexed powder pattern of W_2As_3. Formula weight 592.46. $a = 13.346 \pm 0.002$ Å, $b = 3.278 \pm 0.002$ Å, $c = 9.599 \pm 0.002$ Å, $\beta = 124° 48' \pm 2'$. $U = 344.8$ Å^3, $D_m = 11.28$ g cm^{-3} (pycnometrically in water), $Z = 4$, $D_x = 11.41$ g cm^{-3}. Cu K_α radiation, $\lambda_{\alpha 1} = 1.5405$ Å, Guinier focussing camera.

TABLE II

Powder diffraction pattern of W_2As_3. (Monoclinic $a = 13.346 \pm 0.002$ Å, $b = 3.278 \pm 0.002$ Å, $c = 9.599 \pm 0.002$ Å, $\beta = 124° 48' \pm 2'$. Monochromatic Cu K_α radiation $\lambda_{\alpha 1} = 1.5405$ Å; Guinier focussing camera, diameter 11.46 cm; temp. 24 °C; internal standard As_2O_3 ($a = 11.075_5$ Å); low angle cut off 40 Å; high angle cut off 1.41 Å)

I/I_1	d_{obs} (Å)	d_{calcd} (Å)	hkl	I/I_1	d_{obs} (Å)	d_{calcd} (Å)	hkl
0.7	7.865	7.879	001	7	1.872	1.870	113
1.8	6.592	6.592	201	1.1	1.825	1.827	600
26	5.480	5.480	200			1.822	510
11	4.721	4.721	202	1.1	1.816	1.816	402
11	3.630	3.630	201			1.815	205
2.8	3.297	3.297	402	8.2	1.806	1.808	605
11	3.222	3.220	401			1.807	114
11	3.209	3.206	203	33	1.792	1.791	312
4.4	3.144	3.140	110	1.8	1.646	1.647	713
41	3.095	3.097	111	21	1.639	1.639	315
5.5	2.890	2.893	403			1.639	020
100	2.766	2.766	111	2.8	1.620	1.621	712
8.2	2.739	2.739	400	2.8	1.599	1.604	714
26	2.677	2.679	112			1.604	021
26	2.627	2.632	311	7	1.589	1.591	601
		2.627	003			1.590	406
1.8	2.580	2.580	202			1.588	204
41	2.553	2.556	312	4.4	1.570	1.574	606
4.4	2.438	2.439	310	2.2	1.564	1.570	220
0.6	2.361	2.361	404	0.6	1.5575	1.5580	114
21	2.322	2.324	204	2.2	1.5470	1.5480	222
21	2.268	2.270	313	0.7	1.5331	1.5345	711
17	2.224	2.224	401	0.5	1.5226	1.5217	313
64	2.199	2.199	603	0.5	1.5127	1.5131	022
		2.199	113			1.5114	115
33	2.115	2.114	311	0.7	1.4999	1.5056	715
51	2.067	2.070	512	1.4	1.4933	1.4938	221
21	2.053	2.056	601	0.9	1.4839	1.4839	206
0.9	1.993	1.995	511	0.5	1.4671	1.4675	422
17	1.971	1.971	004	2.8	1.4568	1.4605	421
		1.971	203	7	1.4359	1.4367	516
21	1.936	1.936	314	0.7	1.4250	1.4257	423
1.8	1.920	1.920	405	4.4	1.4173	1.4173	512

The Molybdenum Arsenides

$MoAs_2$.—Monoclinic, $NbAs_2$ structure. Single crystals were needles (0.1 to 0.2 mm diameter, 1 to 2 mm long). $a = 9.07$ Å, $b = 3.30$ Å, $c = 7.73$ Å, $\beta = 119° 20'$. These results confirm Jensen and Kjekshus (4).

Mo_2As_3.—Formula weight 416.6. Monoclinic, isostructural with W_2As_3. The powder pattern in Table III was indexed with the lattice parameters $a = 13.339 \pm 0.002$ Å, $b = 3.240 \pm 0.002$ Å, $c = 9.628 \pm 0.002$ Å, $\beta = 124° 31' \pm 2'$. $U = 342.9$ Å^3, $D_m = 7.43$

Can. J. Chem. Downloaded from www.nrcresearchpress.com by 210.87.254.105 on 09/05/12
For personal use only.

g cm^{-3} (pycnometrically in water), $Z = 4$, $D_x = 8.07$ g cm^{-3}. Cu K_α radiation, $\lambda_{\alpha 1} = 1.5405$ Å, Guinier focussing camera. The alternative body-centered cell with $c < a$ is related by the transformation matrix 101/010/001.

Mo_5As_4.—Formula weight 779.38. Tetragonal, Ti_5Te_4 structure (2, 3). Lattice parameters (Debye–Scherrer patterns, Nelson–Riley extrapolation of back reflection lines) are $a = 9.595 \pm 0.001$ Å, $c = 3.284 \pm 0.002$ Å, $U = 302.3$ Å^3, $Z = 2$, $D_x = 8.56$ g cm^{-3}. Ni-filtered Cu radiation. = 1.5405 Å.

TABLE III

Powder diffraction pattern of Mo_2As_3. (Monoclinic $a = 13.339 \pm 0.002$ Å, $b = 3.240 \pm 0.002$ Å, $c = 9.628 \pm 0.002$ Å, $\beta = 124° 31' \pm 2'$. Monochromatic Cu K_α radiation $\lambda_{\alpha 1} = 1.5405$ Å; Guinier focussing camera, diameter 11.46 cm; temp. 24 °C; internal standard As_2O_3 ($a = 11.075_5$ Å); low angle cut off 40 Å; high angle cut off 1.37 Å)

I/I_1	d_{obs} (Å)	d_{calcd} (Å)	hkl	I/I_1	d_{obs} (Å)	d_{calcd} (Å)	hkl
2.2	7.922	7.936	001	8.2	1.812	1.819	510
5.5	6.622	6.592	20$\bar{1}$			1.810	60$\bar{5}$
17	5.494	5.494	200			1.808	11$\bar{4}$
11	4.731	4.731	20$\bar{2}$	64	1.792	1.792	312
0.6	3.973	3.966	002	3.5	1.669	1.665	80$\bar{3}$
11	3.654	3.651	201	7	1.650	1.648	80$\bar{4}$
0.9	3.559	3.560	40$\bar{2}$	11	1.6407	1.6417	71$\bar{3}$
8.2	3.225	3.222	40$\bar{1}$			1.6396	31$\bar{5}$
8.2	3.193	3.193	20$\bar{3}$	11	1.6342	1.6337	51$\bar{5}$
17	3.064	3.064	11$\bar{1}$	21	1.6179	1.6200	020
0.4	2.893	2.893	40$\bar{3}$			1.6168	71$\bar{2}$
41	2.748	2.748	400			1.6158	511
		2.748	111	17	1.5983	1.5983	204
51	2.659	2.662	11$\bar{2}$			1.5980	71$\bar{4}$
21	2.644	2.644	003			1.5973	601
26	2.608	2.593	202			1.5958	40$\bar{6}$
100	2.536	2.538	31$\bar{2}$	2.8	1.5783	1.5769	60$\bar{6}$
3.5	2.367	2.366	40$\bar{4}$	8.6	1.5690	1.5729	22$\bar{1}$
26	2.337	2.335	20$\bar{4}$	3.5	1.5508	1.5537	220
26	2.260	2.260	31$\bar{3}$	4.4	1.5248	1.5253	313
21	2.236	2.234	401			1.5226	403
21	2.198	2.206	60$\bar{2}$	4.4	1.5140	1.5145	11$\bar{5}$
21	2.194	2.197	60$\bar{3}$	3.5	1.5034	1.5047	80$\bar{1}$
		2.195	113			1.5021	71$\bar{5}$
26	2.110	2.110	311	3.5	1.4796	1.4809	22$\bar{1}$
100	2.060	2.059	60$\bar{1}$	4.4	1.4487	1.4475	42$\bar{1}$
1.8	1.999	1.999	51$\bar{3}$	21	1.4363	1.4367	51$\bar{6}$
17	1.986	1.988	51$\bar{1}$	8.6	1.4200	1.4203	512
		1.984	004	0.7	1.4029	1.4033	31$\bar{6}$
		1.984	203	7	1.3948	1.3955	420
11	1.932	1.932	31$\bar{4}$	8.6	1.3757	1.3774	71$\bar{6}$
5.5	1.871	1.871	113	5.5	1.3739	1.3739	222
4.4	1.834	1.836	51$\bar{4}$			1.3739	800
		1.832	600				
4.4	1.826	1.826	402				
		1.825	205				

DISCUSSION

X_2As_3 Phases

The formula assigned to these phases is based initially on a comparison of Guinier patterns of specimens with compositions $XAs_{1.4}$ (58 at. % As) and $XAs_{1.6}$ (62 at. % As). $WAs_{1.4}$ is a mixture of W_2As_3 and W; $WAs_{1.6}$, a mixture of W_2As_3 and WAs_2 when annealed below 800 °C. $MoAs_{1.4}$ is a mixture of Mo_5As_4 and Mo_2As_3; $MoAs_{1.6}$, a mixture of Mo_2As_3 and $MoAs_2$. The observed densities of the powders, within the limits of the accuracy, are consistent with X_2As_3 but the formulae X_8As_{11} and X_8As_{13} are not completely excluded by the density measurements.

Can. J. Chem. Downloaded from www.nrcresearchpress.com by 210.87.254.105 on 09/05/12
For personal use only.

A possible structural classification for these X_2As_3 phases can be derived by considering the alternative body-centered cell for which the cell parameters are simply related to the NiAs (*B*8) structure. Thus $a_{b.c} \approx 2c_{NiAs}$, $b_{b.c} \approx a_{NiAs}$, $c_{b.c} \approx 3a_{NiAs}$. Furthermore the powder patterns of W_2As_3 and Mo_2As_3 have certain specific resemblances to those for Ni_3Se_4 (6), Ni_3Sn_4 (7), Cr_3S_4 (8) which have monoclinic structures based on ordering of vacancies in the NiAs structure. The possibility of vacancies in the structure makes it unwise to place too much reliance on a specific stoichiometry in the absence of a complete structure determination.

The phase of approximate composition W_4As_5 reported by Boller and Nowotny has been assigned the formula W_2As_3 here, because their "monoclinic" cell with $a = 7.99$ Å, $b = 3.28$ Å, $c = 6.88$ Å, $\beta = 99° 12'$ can be transformed to the *c*-face-centered cell used here (transformation matrix $00\bar{2}/010/101$). It should be noted that the smaller cell is not a true unit cell and does not account for all the reflections on our powder patterns or single crystal photographs. Mo_4As_5, reported by Boller and Nowotny to be analogous, is also probably Mo_2As_3.

XAs_2 Phases

WAs_2 and $MoAs_2$ undoubtedly have the $NbAs_2$ structure as is shown by the very close similarity of the three powder patterns. It may be noted that this structure can be derived from the *C*18 marcasite structure in the setting *Pnnm* by the transformation $110/001/1\bar{1}0$ followed by relatively small shifts of the atoms (i.e. the monoclinic *a* and *c* axes are the face-diagonals of the *ab*-face of the *C*18 cell). The other family of diarsenides and related dipnictides typified for example by $CoAs_2$ (9), can also be derived from the *C*18 unit cell by the analogous transformation $\bar{1}01/010/101$ (i.e. the *a* and *c* monoclinic axes are derived from the diagonals of the *ac*-face of the *C*18 cell).

MoAs and W_2As

MoAs and W_2As were not observed in our experiments, contrary to Boller and Nowotny's report. We can offer no positive explanation for this discrepancy but we have given a full statement of our experimental procedures. Patterns from all samples richer in tungsten than W_2As_3 contained only W and W_2As_3 reflections. Similarly patterns obtained from samples richer in molybdenum than Mo_2As_3 contained reflections from Mo_5As_4 and Mo_2As_3.

Addendum

A paper by A. Brown (Nature, 206, 503 (1965)) has come to hand since this manuscript was submitted. His data for $MoAs_2$ independently confirm the data given here and in addition, the structure is determined. A phase of composition $Mo_{0.4}As_2$ is described and reported to have a defect *C*18 structure (*Pnnm*, $a = 5.299$ Å, $b = 5.983$ Å, $c = 2.885$ Å). This compound was not observed in the present work. In the absence of details of the preparative techniques used by Brown, it is not possible to offer any explanations for this discrepancy. Our own techniques are described in full and are based on a reaction temperature of 850 °C and subsequent annealing and quenching. It may be that this is another example of the surprisingly different results obtained from different conditions of sample preparation. A. Kjekshus and W. B. Pearson have recently commented on this (Progr. in Solid State Chem. 1, 83 (1964), pp. 86, 106, and 107) in discussing systems having the NiAs and closely related structures.

ACKNOWLEDGMENTS

The authors are indebted to Mr. G. J. G. Despault, who prepared the samples, and to Miss F. Hui, who obtained the powder patterns.

Can. J. Chem. Downloaded from www.nrcresearchpress.com by 210.87.254.105 on 09/05/12
For personal use only.

REFERENCES

1. E. HEINERTH and W. BILTZ. Z. Anorg. Allgem. Chem. **198**, 171, 173 (1931).
2. H. BOLLER and H. NOWOTNY. Monatsh. Chem. **95**, 1272 (1964).
3. F. GRØNVOLD, A. KJEKSHUS, and F. RAAUM. Acta Cryst. **14**, 930 (1961).
4. P. JENSEN and A. KJEKSHUS. Acta. Chem. Scand. **18**, 1798, (1964).
5. S. FURUSETH and A. KJEKSHUS. Acta. Cryst. **18**, 320 (1965).
6. F. GRØNVOLD and E. JACOBSEN. Acta. Chem. Scand. **10**, 1440 (1956).
7. H. NOWOTNY and K. SCHUBERT. Z. Metallk. **37**, 23 (1946).
8. F. JELLINEK. Acta. Cryst. **10**, 620 (1957).
9. J. CLAIRE QUESNEL and R. D. HEYDING. Can. J. Chem. **40**, 814 (1962).

Can. J. Chem. Downloaded from www.nrcresearchpress.com by 210.87.254.105 on 09/05/12
For personal use only.

Can. J. Chem. Downloaded from www.nrcresearchpress.com by 210.87.254.5 on 09/05/12
For personal use only.

THE UNIMOLECULAR DECOMPOSITION OF METHYL CHLORIDE

W. FORST AND P. ST. LAURENT[1]
Department of Chemistry, Université Laval, Québec, Québec
Received May 18, 1965

ABSTRACT

The second-order rate constant for the unimolecular decomposition of methyl chloride

$$CH_3Cl \rightarrow CH_3 + Cl$$

has been calculated on a computer by the quantum version of the Marcus–Rice theory assuming no active rotations and using the experimental activation energy. With a harmonic energy level density count the calculated rate constant is 32 times smaller than the experimental value. When correction for anharmonicity is applied, the agreement is somewhat improved but the calculated rate constant is still some 20 times too small. These results are discussed in the light of the assumptions made in the course of the calculations. It is concluded that the quantum statistical collision theory, to which the Marcus–Rice theory reduces at low pressure, is a good deal more successful than Slater's, which is in error by a factor of 10^5–10^6.

RÉSUMÉ

La constante de vitesse de la réaction du deuxième ordre pour la décomposition monomoléculaire du chlorure de méthyle

$$CH_3Cl \rightarrow CH_3 + Cl$$

a été calculée au moyen d'un ordinateur électronique suivant le modèle quantique de la théorie de Marcus–Rice en utilisant la valeur expérimentale de l'énergie d'activation, et dans l'hypothèse qu'aucune rotation n'est active. La constante ainsi calculée est plus petite que la valeur expérimentale d'un facteur 32. On peut augmenter la valeur de la constante calculée de 50% en corrigeant la densité des niveaux de vibrations pour l'anharmonicité. A la lumière des hypothèses posées pour ces calculs, on arrive à la conclusion que la théorie de Marcus–Rice, qui représente à basse pression le modèle quantique de la théorie statistique des collisions moléculaires, reproduit beaucoup mieux les données expérimentales de la vitesse de réaction que la théorie de Slater qui conduit à des valeurs trop faibles d'un facteur de 10^5 à 10^6.

INTRODUCTION

The thermal decomposition of methyl chloride has been studied experimentally by Shilov and Sabirova (1). Holbrook (2) analyzed the Russian workers' data and concluded that the rate of formation of HCl affords a measure of the unimolecular reaction

$$CH_3Cl \rightarrow CH_3 + Cl,$$

and that between 10 to 35 mm Hg this reaction is in its second-order region, the rate constant having the value $k_0 = 1.86 \pm 0.21 \times 10^4$ cc mole^{-1} s^{-1} at 1 116.7 °K. Holbrook then proceeded to compare the experimental value of k_0 with k_0 calculated according to Slater's theory of unimolecular reactions (3). Using the symmetrical C—Cl stretch as the reaction coordinate, he calculated $k_0 = 3.29 \times 10^{-2}$ or 1.03×10^{-1} cc mole^{-1} s^{-1}, depending on the force constant used; for a critical coordinate composed of an equally weighted combination of C—Cl stretching and symmetrical methyl deformation he obtained $k_0 = 3.99 \times 10^{-1}$ cc mole^{-1} s^{-1}. Slater's theory thus predicts a second-order rate constant that is too small by a factor of 10^5–10^6, which Holbrook ascribed (assuming the basic reaction mechanism is valid) to rapid vibrational energy redistribution among the vibrational modes, a redistribution the Slater theory does not permit. It seemed therefore interesting to calculate k_0 according to the quantum version of the theory of

[1]*Abstracted from a B.Sc. Thesis submitted to the Faculty of Science by P. St. Laurent, May 1965.*

Marcus and Rice (4, 5), since this theory is based on the explicit assumption of rapid energy flow among vibrational degrees of freedom, and see if better agreement between theory and experiment could be obtained.

THE METHYL CHLORIDE MOLECULE

The molecule belongs to symmetry C_{3v}; there are three totally symmetric vibrational modes and three doubly degenerate ones, with frequencies (6) in cm^{-1}: $\nu_1 = 2\,879$, $\nu_2 = 1\,355$, $\nu_3 = 732$, $\nu_4 = 3\,048$ (2), $\nu_5 = 1\,460$ (2), $\nu_6 = 1\,020$ (2). For the purpose of the calculations, ν_2 and ν_5 were grouped together and their geometric mean (1 424 cm^{-1}) used to represent the group. The molecular vibrational partition function Q_v in the harmonic oscillator approximation was calculated from the free energy function corresponding to these frequencies, as given in tables (7); $\log_e Q_v = -\sum_1^9 (F^0 - E_0^0)/RT$. In a similar fashion, the mean vibrational energy $\langle E_v \rangle$ was calculated from the enthalpy function; $\langle E_v \rangle = RT \sum_1^9 (H^0 - E_0^0)/RT$. The entropy of methyl chloride has been calculated by Herzberg (8) who showed that the experimental entropy is adequately accounted for by translations, vibrations, and overall rotations, so that there are no internal degrees of freedom of rotation. It will be assumed in the following that there are no rotational degrees of freedom active in intramolecular energy transfer. The collision diameter of methyl chloride has been calculated to be 4.3 Å (9).

THE RATE CONSTANT INTEGRAL

For no active rotations in the molecule, the Marcus–Rice expression for the limiting second-order rate constant k_0 is (5)

$$[I] \qquad k_0 = \frac{k_2 \exp(-E_a/kT)}{Q_v} \int_0^\infty N^*(E_a + E^+) \exp(-E^+/kT)\, dE^+,$$

where k_2 is the collision frequency, E_a is the critical energy and $N^*(E_a + E^+)$ is the number of vibrational energy states per unit energy at the energy $(E_a + E^+)$. It should be noted that the expression does not involve the properties of the activated complex, only those of the active molecule. The experimental low-pressure activation energy is $E_0 = 85.5$ kcal/mole (1) and E_a will be of the same order of magnitude. At such high energies, $N^*(E_a + E^+)$ can be adequately approximated by the semiclassical expression (4)

$$[II] \qquad N^*(E_a + E^+) = \frac{(E_a + E^+ + E_z)^{s-1}}{\Gamma(s) \prod_s h\nu_i}$$

where E_z = zero-point energy, s = number of vibrational degrees of freedom, Γ = gamma function. Substituting [II] in [I] allows the latter to be integrated after binomial expansion. Since by definition $E_0 = kT^2 (d \log k_0/dT)$, it can be shown (10) that for measurements at constant concentration the derivation yields

$$[III] \qquad E_0 = E_a + 3/2kT - \langle E_v \rangle$$

where $\langle E_v \rangle$ is the mean vibrational energy of the molecule. This result is valid for $(E_a + E_z) \gg (s - 1)kT$. For methyl chloride, eq. [III] yields $E_a = 30\,951$ cm^{-1}; furthermore, $E_z = 8\,009$ cm^{-1}, $s = 9$, and RT at 1 116.7 °K is 776 cm^{-1}, so that the inequality is satisfied.

Can. J. Chem. Downloaded from www.nrcresearchpress.com by 210.87.254.5 on 09/05/12
For personal use only.

For the purpose of evaluating the integral in eq. [I], $N^*(E_a + E^+)$ was calculated from an approximation formula of Whitten and Rabinovitch (11)

$$[IV] \qquad \sum_{E_V=0}^{E} P(E_V) = \frac{[E + (1 - \beta w)E_z]^s}{\Gamma(s+1)\prod_s h\nu_i}$$

$\beta = v(s-1)/s$, $\log w = -1.0506(\epsilon)^{0.25}$, $v = \langle \sum_s (h\nu_i)^2 \rangle / \langle \sum_s h\nu_i \rangle^2$, where $\epsilon = E/E_z$ and the other symbols have their usual meaning. $\sum_{E_V=0}^{E_V=E} P(E_V)$ is the total number of vibrational states at the energy E; $N^*(E)$, the number of states per unit energy at E, is then the derivative of $\sum P(E_V)$ with respect to E. At the high energies involved here this formula gives results that are within a few percent of the exact count, and is thus somewhat superior to the semiclassical formula [II], of which it is in fact a modification.

Equation [IV] was programmed on an IBM 1410 computer and the vibrational energy sums computed at 200 cm^{-1} intervals starting at $E = E_a = 31\,000$ cm^{-1} up to $E = 46\,000$ cm^{-1}; a derivative was then computed at each point and the results inserted into a program for the computation of the intergral in eq. [I] by the trapezoidal rule, likewise at 200 cm^{-1} intervals. It was found that at 46 000 cm^{-1} the integral has converged to virtually 100% of its value. The result of the integration is $k_0 = 5.82 \times 10^2$ cc $mole^{-1}$ s^{-1}, which is a considerably better value than the one calculated by Slater's theory but still some 32 times smaller than the experimental value.

ANHARMONICITY

Up to this point, all vibrations have been considered as strictly harmonic. If anharmonicity of vibrations is taken into account, the density of vibrational energy levels is increased, particularly at high energies. Since potential functions for polyatomic molecules other than linear triatomic are not available at present, one way of accounting for anharmonicity of molecular vibrations in cases like methyl chloride is to consider the molecule as a system of independent Morse oscillators. A convenient correction factor has been developed by Haarhoff (12) from considerations of the inverse Laplace transform of the vibrational partition function

$$[V] \qquad \frac{N^*(E)\,(\text{anharmonic})}{N^*(E)\,(\text{harmonic})} = \left\{\left(1 + \frac{2}{\epsilon}\right)^{\frac{\epsilon}{2}\left[1+\frac{\epsilon}{2}\right]} \exp\left[-\frac{v-1}{3(1+\epsilon)}\right]\right\}^{E_z/D} \times \exp\left[\frac{(1+\epsilon)^2}{2(s+1)}\left(\frac{E_z}{D}\right)^2 + \frac{(1+\epsilon)^3}{(s+1)(s+2)}\left(\frac{E_z}{D}\right)^3\right]$$

where $1/D = \langle 1/D_m \rangle$, D_m = dissociation energy of the mth Morse oscillator; the other symbols have their usual significance. Now for a Morse oscillator $D_m = (F_{2m})^3/2(F_{3m})^2$, where F_{2m} and F_{3m} are the quadratic and cubic force constants, respectively, of a stretching vibration. For polyatomic molecules, Herschbach and Laurie (13) have proposed a simple exponential function for the quadratic and higher bond-stretching force constants,

$$(-1)^n F_n = 10^{-(r_e - a_{ij})/b_{ij}} \qquad n = 2, 3$$

where r_e is the equilibrium bond length and a_{ij} and b_{ij} are empirical constants for bonds between atoms from row i and j of the periodic table. Thus for ν_1 and ν_4 (C—H stretch), taking a bond length of 1.09 Å as in methane (8), one obtains D_1 or $D_4 = 83.9$ kcal/mole; for ν_3 (C—Cl stretch), taking a bond length of 1.71 Å (8), one obtains $D_3 = 96.9$ kcal/mole. The assignment of a dissociation energy for ν_2 and ν_5 (CH_3 deformation) is difficult;

Can. J. Chem. Downloaded from www.nrcresearchpress.com by 210.87.254.5 on 09/05/12
For personal use only.

it was taken from Schneider and Rabinovitch (14) who used as an educated guess a dissociation energy of 500 kcal/mole in the case of CH_3NC. The assignment of D_6 (ν_6, $H_3{\equiv}C{-}Cl$ bending) is equally difficult; a frankly arbitrary assignment of 600 kcal/mole was made, which might be too high but is not very critical since D is only moderately sensitive to any particular D_m. This assignment corresponds to a Morse anharmonic constant of $-1.4\ cm^{-1}$. With the above values of the various D_m, D = 163.3 kcal/mole. Equation [V] was programmed on an IBM 1410 computer and the $N^*(E)$ (harmonic), calculated previously, corrected for anharmonicity, point by point; the $N^*(E)$ (anharmonic) thus obtained was then substituted in eq. [I] and the integration performed as before. The result is $k_0 = 8.4 \times 10^2$ cc mole^{-1} s^{-1}, i.e. some 50% higher than the k_0 calculated previously, but still some 22 times smaller than the experimental result.

CONCLUSIONS

The theoretical value of k_0 calculated on the harmonic model depends a good deal on the experimental activation energy, which affects E_a directly and through it $N^*(E_a+E^+)$, but in an opposite direction. For example, if the activation energy were 3.5 kcal/mole lower (a possible error in a complicated reaction), the factor multiplying the integral in eq. [I] would be 5 times larger; this would be offset somewhat by a decrease in the value of the integral, so that the net increase in k_0 would still be a factor of 3 or 4, leaving only a discrepancy between experiment and theory of about a factor of 10.

Nothing has been said so far about active rotations, beyond stating it as a pure assumption that no rotations are active. If any of the overall rotations were taken as active, the results would be an appreciable increase in k_0, but in the absence of any guiding principle the number of active rotations would merely take the character of an adjustable parameter. Another uncertainty enters into k_2 in the form of the assumption of unit collisional deactivation efficiency; an efficiency of less than unity would decrease the calculated value of k_0. There is also a relatively minor uncertainty in the collision diameter.

The same considerations apply to k_0 calculated on the anharmonic model. In addition, if we assume that eq. [V] is not significantly in error, the anharmonic correction factor used here can be described only as minimal, since an assignment of lower dissociation energies to CH_3 rocking and deformation frequencies would tend to increase the correction factor. This increase, however, would not be very large. For example, using D_2 or D_5 = 300 kcal/mole (three times the dissociation energy of a C—H bond), D_6 = 106 kcal/mole, and the same values as before for the remaining D_m's, calculation gives $k_0 = 9.7 \times 10^2$ cc mole^{-1} s^{-1}. Until the appropriate force constants are available for polyatomic molecules, it will be difficult to make very accurate predictions on the effects of anharmonicity. From the present results it would appear that anharmonicity increases k_0 only moderately, so that CH_3Cl behaves in this respect like a "large" molecule. In any event, considering a molecule as an assembly of independent Morse oscillators is a rather crude assumption. The effect of anharmonicity on the vibrational partition function Q_v has been neglected, since anharmonicity becomes appreciable only at the higher vibrational energies and here the exponential becomes predominant and wipes out most of the increase in the energy level density.

These calculations show that, on the whole, the Marcus–Rice theory is much more successful than Slater's theory in accounting for the low pressure rate of the methyl chloride decomposition, and would probably yield even better quantitative agreement

Can. J. Chem. Downloaded from www.nrcresearchpress.com by 210.87.254.5 on 09/05/12
For personal use only.

if a rational criterion could be found for the inclusion of active rotations. Additional work on the experimental aspects of the reaction would also be desirable to provide evidence in support of the mechanism and of the published values of E_0 and k_0.

ACKNOWLEDGMENT

The authors are indebted to Mr. P. Ardouin of the Centre de Traitement de l'Information de l'Université Laval for the programming and execution of the machine computations reported here, and to the National Research Council of Canada for financial assistance.

REFERENCES

1. A. E. SHILOV and R. D. SABIROVA. Zh. Fiz. Khim. **33**, 1365 (1959).
2. K. A. HOLBROOK. Trans. Faraday Soc. **57**, 2151 (1961).
3. N. B. SLATER. Theory of unimolecular reactions. Cornell University Press, Ithaca. 1954.
4. R. A. MARCUS and O. K. RICE. J. Phys. Colloid Chem. **55**, 894 (1951).
5. G. M. WIEDER and R. A. MARCUS. J. Chem. Phys. **37**, 1835 (1962).
6. T. Y. WU. Vibrational spectra and structure of polyatomic molecules. Edwards Brothers, Ann Arbor. 1946.
7. J. HILSENRATH and G. G. ZIEGLER. Tables of Einstein functions. Natl. Bur. Standards Monograph 49, Washington. 1962.
8. G. HERZBERG. Molecular spectra and molecular structure. II. Infrared and Raman spectra of polyatomic molecules. D. Van Nostrand, New York. 1945.
9. P. G. T. FOGG, P. A. HANKS, and J. D. LAMBERT. Proc. Roy. Soc. London, Ser. A, **219**, 490 (1953).
10. G. M. WIEDER. Ph.D. Thesis. Polytechnic Institute of Brooklyn, Brooklyn, N.Y. 1961.
11. G. Z. WHITTEN and B. S. RABINOVITCH. J. Chem. Phys. **38**, 2466 (1963).
12. P. C. HAARHOFF. Mol. Phys. **7**, 101 (1963).
13. D. R. HERSCHBACH and V. W. LAURIE. J. Chem. Phys. **35**, 458 (1961).
14. F. W. SCHNEIDER and B. S. RABINOVITCH. J. Am. Chem. Soc. **84**, 4215 (1962).

Can. J. Chem. Downloaded from www.nrcresearchpress.com by 210.87.254.5 on 09/05/12
For personal use only.

Can. J. Chem. Downloaded from www.nrcresearchpress.com by 210.87.254.42 on 09/05/12
For personal use only.

A STUDY OF TAUTOMERISM IN CYCLIC β-DIKETONES BY PROTON MAGNETIC RESONANCE

NATSUKO CYR AND LEONARD W. REEVES
Chemistry Department, University of British Columbia, Vancouver, British Columbia

Received May 25, 1965

ABSTRACT

The keto–enol equilibrium of cyclohexane-1,3-dione in chloroform is best interpreted from proton resonance measurements as

$$\text{enol dimer} \overset{K_1}{\rightleftharpoons} \text{2-enol monomer} \overset{K_2}{\rightleftharpoons} \text{2-keto monomer.}$$

K_1 and K_2 may be separately determined from chemical shift measurements of the enol-OH proton and intensity measurements of peaks assigned to keto and enol forms. K_1 and K_2 are satisfactorily independent of concentrations except in very dilute solutions where intensity measurements become unreliable. The overall equilibrium constant $K = K_1 \times K_2^2$ can be obtained for the same molecule in acetonitrile solutions where the enol monomer form is in very low concentration. 5,5′-Dimethylcyclohexane-1,3-dione in chloroform has less enol form than the unsubstituted molecule. The enthalpy change associated with 'K' for cyclohexane-1,3-dione in chloroform is 2.05 ± 0.5 kcal mole^{-1}.

INTRODUCTION

It is well known that β-diketones form enol isomers and that the extent of enolization is controlled mainly by the conjugation of C=O and C=C double bonds and the strong intramolecular hydrogen bond formed (1, 2). The equilibrium keto $\rightleftharpoons$ enol is affected by concentration and solvents as well as temperature (3). Proton magnetic resonance studies of such tautomeric systems generally reveal separate peaks for each tautomer thus enabling a simple intensity measurement to give the equilibrium constant (3, 4). There are several interesting features of proton magnetic resonance studies of tautomeric systems (5–13) including spin–spin coupling to the enol-OH proton (11) and multi-site proton exchange processes which can be determined by double resonance methods (14, 15).

The present study is directed towards the six-membered cyclic β-diketones where the formation of an intramolecular hydrogen bond is excluded. Cyclohexane-1,3-dione and 5,5′-dimethylcyclohexane-1,3-dione exist both in the solid state and concentrated solutions mostly as enolic molecules (16–18). A large dimer unit has been suggested (16) to provide the strong hydrogen bond which stabilizes the enol form. The study of the tautomeric equilibrium in these molecules is confined to chloroform and acetonitrile solutions where the solubility is appreciable.

EXPERIMENTAL

Commercially available samples (L. Light and Co. and Eastman Kodak Co.) of cyclohexane-1,3-dione and 5,5′-dimethylcyclohexane-1,3-dione were purified by recrystallization from benzene. Spectroscopic grade chloroform was shaken with concentrated sulfuric acid, washed with distilled water, and fractionally distilled to remove added ethanol. It was stored over calcium chloride in a dark place. Reagent grade acetonitrile was fractionally distilled and kept over calcium chloride. All concentrations were obtained by weighing solute and solution. The solutions were sealed in vacuum in nuclear magnetic resonance (n.m.r.) sample tubes after degassing by successive freeze, pump, thaw procedures. A small amount of magnesium perchlorate for the chloroform solutions and sodium sulfate for the acetonitrile solutions was added to each n.m.r. sample tube to keep solutions dry throughout measurements. A Varian A60 spectrometer was used for measurements with accurate calibrations provided by a Hewlett-Packard Wide Range Audio oscillator standardized at each measurement by a model 522B electronic frequency counter. Higher temperatures in the A60 spectrometer were obtained by using a V6057 variable temperature attachment and temperature measurement achieved with the calibrated separation of methylene and —OH proton resonances in ethylene

glycol. A small amount of tetramethylsilane (TMS) served as an internal reference for chemical shifts. The intensities of respective peaks in enol and keto forms were measured at the slowest sweep rate: 500 s on the narrowest sweep width, 50 c.p.s., and with the spectrum amplitude not exceeding the linear response region of the instrument. The absorption signals were carefully traced onto good quality bond paper and the cutouts weighed.

The signals used for intensity measurements are:

Cyclohexane-1,3-dione in $CHCl_3$

enol-OH (7 in structure I)

keto-CH_2 between the carbonyls (2 in structure II).

Cyclohexane-1,3-dione in CH_3CN

enol-olefinic proton (2 in structure I)

keto-CH_2 between the carbonyls (2 in structure II).

5,5′-Dimethylcyclohexane-1,3-dione

4 and 6 signals for both the keto and the enol.

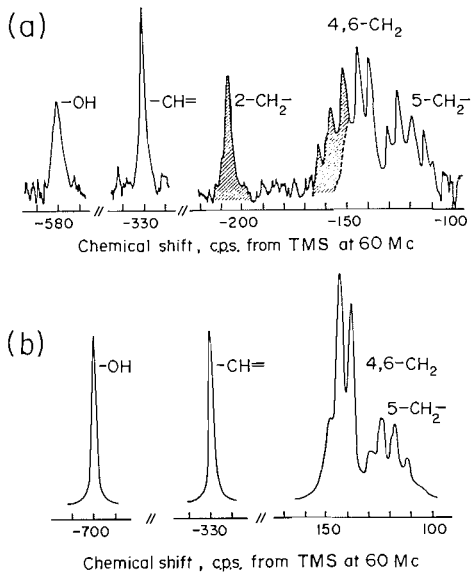

FIG. 1. (*a*) Spectrum of cyclohexane-1,3-dione in chloroform 16.0 mole %. (*b*) Spectrum of cyclohexane-1,3-dione in chloroform 1.05 mole %.

RESULTS AND DISCUSSION

A. Equilibrium Constants

The spectrum of cyclohexane-1,3-dione at the solubility limit of 16.0 mole % in chloroform is shown as Fig. 1*a*. The peaks can all be reliably assigned to the enol form.

As in structure I we have enolic-OH at −700 c.p.s. (−11.67 p.p.m.), olefinic C—H at position C2 −330 c.p.s. (−5.5 p.p.m.), aliphatic —CH_2— protons giving a complex spectrum of which peaks centered at −120 c.p.s. (−2 p.p.m.) can be attributed to 5C

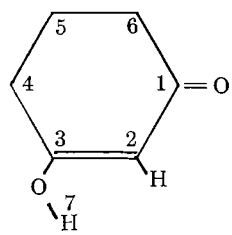

I

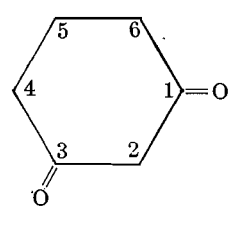

II

Can. J. Chem. Downloaded from www.nrcresearchpress.com by 210.87.254.42 on 09/05/12
For personal use only.

protons. In Fig. 1*b* at 1.05 mole % in $CHCl_3$ signals due to the keto form (structure II) appear. These have been shaded to make them more distinct in the figure.

Peaks at −207 c.p.s. (−3.45 p.p.m.) are assigned to the C2 methylene protons and the C4, C5, and C6 protons of II are in a region −155 c.p.s. (−2.58 p.p.m.). A noticeable feature of Fig. 1*b* is the change in chemical shift of the enol-OH proton to −580 c.p.s. (−9.66 p.p.m.) from Fig. 1*a*. The large change in chemical shift of the enol-OH proton with concentration is indicative of the rupture of hydrogen bonds (19) as the enol form is diluted. The chemical shift of the enol-OH proton has been measured accurately at all available concentrations and the variation can be described by a linear dependence on $1/\sqrt{C}$. Figure 2 shows a plot of chemical shift from TMS versus the inverse square root of concentration in (moles l)$^{-1/2}$. The chemical shift at infinite concentration is −740 c.p.s. (−12.32 p.p.m.) and must correspond to the completely hydrogen-bonded enol species, most reasonably represented as a dimer. (Structure III.)*

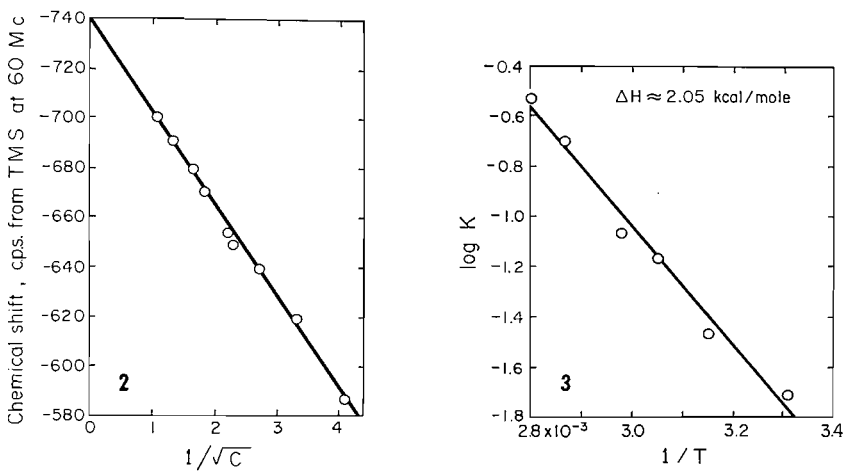

FIG. 2. Chemical shift of enol-OH proton as a function of $C^{-1/2}$ (C = concentration in moles/l).
FIG. 3. Dependence of log K for cyclohexane-1,3-dione in chloroform on inverse absolute temperature.

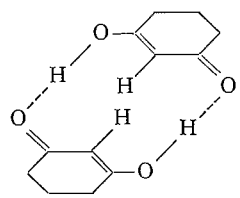

III

This dimer would account for the very low field shift of the —OH proton and is typical of the shifts observed for intramolecular hydrogen-bonded enols (4, 5). The large concentration dependence of the enolic-OH chemical shift must result from dissociation of

**The O—H · · · · O lines are approximately in the plane of the cyclohexane ring because the lone pairs on the oxygen determines the strongest hydrogen bonds in this direction. The olefinic hydrogens at C2 are not close enough to interact with each other.*

Can. J. Chem. Downloaded from www.nrcresearchpress.com by 210.87.254.42 on 09/05/12
For personal use only.

these dimers and the appearance of monomeric enol molecules in solution. The equilibria in chloroform solutions can therefore be described by

$$\underset{C_D(1-\alpha)}{\text{enol dimer}} \overset{K_1}{\rightleftharpoons} \underset{2\alpha C_D}{\text{enol monomer}} \overset{K_2}{\rightleftharpoons} \underset{2(C-C_D).}{\text{keto monomer}}$$

Concentrations at equilibirum in terms of initial concentrations of undissociated forms are given below the equation above. C = total concentration of cyclohexane-1,3-dione expressed in units of dimer (moles l^{-1}); C_D = concentration of enol form considered completely as dimeric form (moles l^{-1}); α = degree of dissociation of the enol form into monomers.

Two equilibrium constants can be defined as above in terms of these concentrations.

[1] $$K_1 = 4\alpha^2 C_D/(1-\alpha)$$

[2] $$K_2 = (C - C_D)/\alpha C_D$$

The value of C_D is determined from a knowledge of the signal areas for enol and keto forms

[3] $$C_D = C/(1 + (1/2R))$$

where R = [enol]/[keto].

The degree of dissociation 'α' will be obtained from the observed hydroxyl proton chemical shift

[4] $$\delta_{obs} = X_D\delta_D + X_M\delta_M.$$

X_D and X_M are the respective fractions of enol molecules in dimer and monomer form. δ_D and δ_M are chemical shifts associated with the enol-OH proton in dimer and monomer forms of the enol molecule. δ_{obs} is the observed chemical shift at some arbitrary concentration. From Fig. 2 the value of δ_D may be taken as -740 c.p.s. Thus

[5] $$\alpha = 740 - \delta_{obs}/(740 - \delta_M).$$

The only unknown is 'δ_M' which may be chosen so as to give constant values of K_1 and K_2 at all concentrations. The best value is -300 c.p.s. (-5 p.p.m.) giving a change in chemical shift due to hydrogen bond formation of 7.32 p.p.m. This is in close agreement with previous values suggested for a strong —O—H --- O hydrogen bond (20, 21). The equilibrium constants obtained are listed in columns 8 and 9 of Table I. The values of K_1 are satisfactorily constant for all concentrations but values of K_2 vary between 1.13 and 0.42 over the concentration range studied. There is a reasonably constant value of $K_2 = 0.55 \pm 0.01$ at the higher concentrations of cyclohexane-1,3-dione. The possible factors likely to cause errors are: (*a*) Impurities contained in the chloroform which contain —OH groups and enhance the enol-OH peak intensity at low concentration. (*b*) Low signal to noise and possible saturation of the resonances at low concentrations. This would cause broadening of signals and loss of intensity in the noise. If relaxation times for the resonances chosen for intensity measurements are different there could be a differential factor (22). (*c*) The solubility of magnesium perchlorate in chloroform is small at room temperature. However, in ketonic solvents such as acetone it is quite large. In the presence of a large quantity of cyclohexane-1,3-dione the increase of the solubility of the salt could cause some small error as well.

Can. J. Chem. Downloaded from www.nrcresearchpress.com by 210.87.254.42 on 09/05/12
For personal use only.

TABLE I

Equilibrium constant data for cyclohexane-1,3-dione in chloroform (C = concentration in moles l^{-1}, $-\delta_{obs}$ = chemical shift of —OH proton from TMS in c.p.s., C_M = concentration of monomer enol form moles l^{-1}. All other symbols are defined in equations in the text)

C (× 10)	R	C_D (× 10)	$-\delta_{obs}$	α	C_M (× 10^2)	$2(C - C_D)$ (× 10^2)	K_1 (× 10^2)	K_2
0.75	0.905	0.494	602	0.460	4.54	5.1	7.80	1.1
0.77	0.800	0.473	605	0.450	4.25	5.9	7.00	1.4
0.92	1.10	0.632	616	0.414	5.24	6.0	7.44	1.1
1.18	1.42	0.870	631	0.363	6.31	6.2	7.24	1.0
1.34	1.96	1.05	635	0.350	7.35	6.0	7.88	0.8
1.40	2.02	1.12	640	0.333	7.47	5.6	7.44	0.8
1.85	2.81	1.57	654	0.286	8.98	5.6	7.28	0.6
2.05	3.90	1.82	657	0.277	10.1	4.6	7.72	0.5
2.71	4.05	2.39	669	0.237	11.3	6.4	7.04	0.6
3.03	4.69	2.74	673	0.224	12.3	5.8	7.04	0.5
3.10	4.53	2.79	675	0.217	12.1	6.2	6.76	0.5
3.72	5.86	3.43	679	0.203	13.9	5.8	7.12	0.4
							Average 7.31×10^{-2}	

The purified chloroform was run as a blank sample and no impurities were found at the highest sensitivity of the spectrometer. The effect of (*b*) above would be most serious in measurements of K_2 at low concentration where the ratio 'R' occurs in both numerator and denominator of eq. [2]. It is reasonable thus to neglect values of K_2 below 1.4 moles/l.

The equilibrium constants obtained for acetonitrile solutions of cyclohexane-1,3-dione are obtained from direct measurements of intensities of keto and enol peaks assuming negligible monomer enol form is present. The equilibrium constant 'K' may be defined

$$[6] \qquad K = K_1 \times K_2^2 = 4(C - C_D)^2/(1 - \alpha)C_D \simeq 4(C - C_D)/C_D.$$

The values obtained for K over a threefold increase in concentration are satisfactorily constant as shown in Table II. Corresponding values of $K = K_1 \times K_2^2$ for 5,5′-dimethylcyclohexane in chloroform solutions were necessarily limited to the concentration range 0.67 to 0.87 moles/l by the solubility and spectrometer sensitivity. A constant value of $K = 5.5 \pm 0.4 \times 10^{-2}$ was, however, found in this limited range. This compares with $K = 2.21 \pm 0.2 \times 10^{-2}$ for the cyclohexane-1,3-dione itself in the same solvent from Table I. The keto form is thus favored slightly by the 5,5′-dimethyl substitution.

TABLE II

Overall equilibrium constant K for keto/enol system cyclohexane-1,3-dione in acetonitrile solutions (symbols as defined in the text)

C (× 10)	R	C_M (× 10)	C_D (× 10)	K (× 10)
0.62	0.568	0.29	0.33	1.0
0.95	0.699	0.38	0.57	1.0
1.37	0.951	0.47	0.90	1.0
1.56	0.944	0.54	1.02	1.1
2.11	1.062	0.68	1.43	1.3

B. Temperature Dependence of 'K'

The overall equilibrium constant 'K' for cyclohexane-1,3-dione in chloroform at a concentration of 0.47 mole/l was measured as a function of temperature. At this concentration, dissociation into monomer enol molecules is small and 'K' can be measured from peak intensities alone. The enthalpy change associated with 'K' is derived as 2.05 ±

Can. J. Chem. Downloaded from www.nrcresearchpress.com by 210.87.254.42 on 09/05/12
For personal use only.

0.5 kcal mole^{-1}, from the slope of Fig. 3. This can be compared with the value 2.7 kcal mole^{-1} obtained by Reeves (3) for pure acetylacetone.

ACKNOWLEDGMENTS

One of us (L. W. R.) is grateful to the National Research Council of Canada and the Petroleum Research Fund of the American Chemical Society for the financial support of this work.

REFERENCES

1. J. Powling and H. J. Bernstein. J. Am. Chem. Soc. **73**, 4353 (1951).
2. P. D. Bartlett and G. F. Woods. J. Am. Chem. Soc. **62**, 2933 (1940).
2*a*. R. S. Rasmussen, D. D. Tunnicliff, and R. R. Brattain. J. Am. Chem. Soc. **71**, 1068 (1949).
3. L. W. Reeves. Can. J. Chem. **35**, 1351 (1957).
4. H. S. Jarrett, M. S. Sadler, and J. N. Shoolery. J. Chem. Phys. **21**, 2092 (1953).
5. L. W. Reeves and W. G. Schneider. Can. J. Chem. **36**, 793 (1958).
6. S. Forsen and M. Nilsson. Acta Chem. Scand. **13**, 1383 (1959).
7. S. Forsen and M. Nilsson. Acta Chem. Scand. **14**, 1333 (1960).
8. S. Forsen and M. Nilsson. Arkiv Kemi, **17**, 523 (1960).
9. S. Forsen, M. Nilsson, and C. A. Wachtneister. Acta Chem. Scand. **16**, 583 (1962).
10. G. O. Dudek and R. M. Holm. J. Am. Chem. Soc. **84**, 2691 (1962).
11. S. Forsen and M. Nilsson. Arkiv Kemi, **19**, 569 (1962).
12. G. O. Dudek. J. Am. Chem. Soc. **85**, 694 (1963).
14. S. Forsen and R. A. Hoffman. J. Chem. Phys. **39**, 2892 (1963).
15. S. Forsen and R. A. Hoffmann. J. Chem. Phys. **40**, 1189 (1964).
16. K. Kodera. Yakugaku Zasshi, **80**, 1267 (1960).
17. C. Deval and J. Lecompte. Compt. Rend. **254**, 36 (1962).
18. C. L. Angell and R. L. Werner. Australian J. Chem. **6**, 294 (1953).
19. L. W. Reeves and W. G. Schneider. Trans. Faraday Soc. **54**, 314 (1958).
20. L. W. Reeves, E. A. Allan, and K. O. Strømme. Can. J. Chem. **38**, 1249 (1960).
21. E. A. Allan and L. W. Reeves. J. Phys. Chem. **67**, 591 (1963).
22. N.M.R. and E.P.R. Spectroscopy. Varian Associates. Pergamon Press, London. 1960. Chap. 8.

Can. J. Chem. Downloaded from www.nrcresearchpress.com by 210.87.254.42 on 09/05/12
For personal use only.

Can. J. Chem. Downloaded from www.nrcresearchpress.com by 210.87.254.40 on 09/05/12
For personal use only.

THE REACTION OF HEXAFLUOROACETONE WITH SOME SILANES

A. F. JANZEN AND C. J. WILLIS
Department of Chemistry, University of Western Ontario, London, Ontario
Received May 7, 1965

ABSTRACT

The reaction of hexafluoroacetone with various methyl- and chloro-silanes has been studied. It has been found that ready addition occurs to give a variety of fluorinated alkoxy-silanes, containing the grouping Si—O—$CH(CF_3)_2$. Some properties of these new compounds are given.

It has been known for some years (1) that ketones will add across the Si—H bond in various silanes, the addition occurring in an "abnormal" direction (as judged by analogous reactions of carbon compounds) to give alkoxy-silanes, rather than silyl alcohols, i.e.

$$R_3SiH + R_2'CO \rightarrow R_3SiOCHR_2'.$$

This reaction, although it proceeds in good yield with a variety of substituted silanes, is of limited synthetic value in conventional silicon chemistry, since the alkoxy-silanes produced are usually available from other routes involving the parent alcohols. In the field of highly fluorinated derivatives, however, the corresponding fluorinated alcohols are not readily available, due in many cases to their lack of stability. The fluorinated ketones are more accessible and very stable, and it would therefore seem that, if the direction of addition of fluorinated ketones across the Si—H bond is also "abnormal", this would represent a useful route to highly fluorinated alkoxides.

We have therefore investigated the addition of hexafluoroacetone to a variety of methyl-silanes and to trichlorosilane, and find that reaction does occur readily to give a variety of highly fluorinated, stable alkoxy-silanes. In most cases the reaction proceeded under the influence of ultraviolet irradiation in the gas phase. The compounds resulting from the addition of hexafluoroacetone to methyl-, dimethyl-, trimethyl-, and trichloro-silane are summarized in Table I. Yields quoted are based on silane present and are for typical reactions; no attempt was made to establish optimum conditions.

TABLE I
Products of reaction of hexafluoroacetone with silanes

Silane	Moles HFA per mole silane	Irradiation time, h	Products	Yield, based on silane, %
CH_3SiH_3	1.0	9	$CH_3SiH_2OCH(CF_3)_2$ +	52
			$CH_3SiH[OCH(CF_3)_2]_2$	11
CH_3SiH_3	2.5	12	$CH_3SiH[OCH(CF_3)_2]_2$	90
$(CH_3)_2SiH_2$	1.2	9.5	$(CH_3)_2SiHOCH(CF_3)_2$ +	80
			$(CH_3)_2Si[OCH(CF_3)_2]_2$	4
$(CH_3)_2SiH_2$	3.5	23	$(CH_3)_2Si[OCH(CF_3)_2]_2$	77
$(CH_3)_3SiH$	2.6	15	$(CH_3)_3SiOCH(CF_3)_2$†	68
$(CH_3)_3SiH$	1.3	33*	$(CH_3)_3SiOCH(CF_3)_2$ +	80
			$(CH_3)_3SiOC(CF_3)_2OCH(CF_3)_2$	9
Cl_3SiH	1.3	13	$Cl_3SiOCH(CF_3)_2$	68

*Reactants held in dark at −78°, not irradiated.
†NOTE ADDED IN PROOF. Since this work was completed, we have learned of the simultaneous preparation of this compound by other workers. (W. R. Cullen and G. E. Styan. Inorg. Chem. In press.) We thank Dr. Cullen for communication of his results in advance of publication.

The reaction of hexafluoroacetone with trimethylsilane was the only one which proceeded readily in the absence of irradiation. A reasonable intermediate in this reaction would be a molecular adduct involving coordination from oxygen to silicon, which could then rearrange to give the 1:1 product (I) (route A).

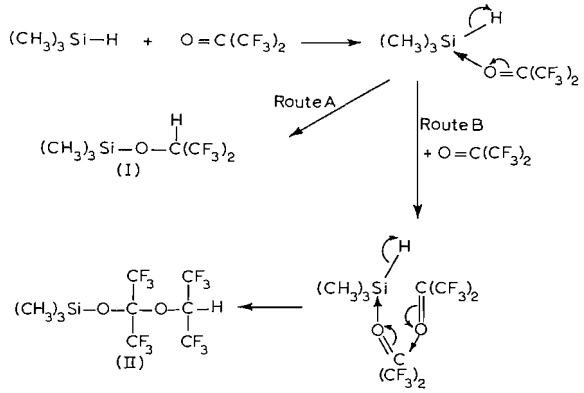

Compound (II), formed by the addition of two molecules of hexafluoroacetone to one of trimethylsilane, is presumably the result of attack by hexafluoroacetone on the above intermediate (route B) rather than by further reaction with the product (I), since it was found in a separate experiment that no reaction occurred between hexafluoroacetone and compound (I) under similar conditions.

The ready reaction of hexafluoroacetone with trimethylsilane at $-78°$ is presumably associated with the presence of three methyl groups on the silicon atom. The electron-releasing nature of these groups, as compared with the hydrogen or chlorine atoms present in the other silanes studied, would facilitate the migration of a hydrogen atom in the above schemes. The addition to trimethylsilane of a second molecule of hexafluoroacetone, a feature not found with other silanes studied, is presumably a result of the reaction occurring in the liquid phase in the presence of excess ketone, whereas all other reactions occurred in the gas phase.

Reaction with the remaining silanes in Table I proceeded under the influence of ultraviolet irradiation. It is noticeable that the presence of two hexafluoroisopropoxy groups on a silicon atom prevents addition of a further molecule of ketone. Thus, irradiation of methylsilane with an excess of hexafluoroacetone gave the 1:2 adduct, $CH_3SiH[OCH(CF_3)_2]_2$ in high yield, but no compound corresponding to the 1:3 adduct, $CH_3Si[OCH(CF_3)_2]_3$, could be found. Apart from the obvious steric effect of isopropoxy groups on the silicon atom, this result might be expected from considerations of charge distribution. Since these reactions must all involve at some stage the attachment of oxygen to silicon, they will be favored if the silicon is able to accept electrons. As isopropoxy groups are attached to silicon, there will be p_π–d_π back bonding from oxygen to silicon within the molecule, thus markedly lessening the acceptor tendencies of the silicon towards other species. It is not surprising, therefore, that it did not prove possible to attach more than two hexafluoroisopropoxy groups to the same silicon atom by this method.

Since a tetravalent carbon atom is unable to increase its coordination with the same readiness that silicon does, it would not be possible to invoke intermediates held together by coordination from oxygen to carbon in the analogous reactions of ketones with carbon–hydrogen bonds. This may be one reason why the addition of ketones across silicon–hydrogen bonds occurs in a direction opposite to that across carbon–hydrogen bonds.

Can. J. Chem. Downloaded from www.nrcresearchpress.com by 210.87.254.40 on 09/05/12
For personal use only.

Can. J. Chem. Downloaded from www.nrcresearchpress.com by 210.87.254.40 on 09/05/12
For personal use only.

The various silicon hexafluoroisopropoxides showed no sign of decomposition when handled in a moist atmosphere (with the exception of the trichloro compound). However, treatment with water at 110° in a sealed tube caused cleavage of the silicon–oxygen bond, giving 1,1,1,3,3,3-hexafluoroisopropanol. When the compounds were treated with concentrated sulfuric acid, the alcohol was evolved immediately at 20°.

Reduction of the hexafluoroisopropoxides with lithium tetrahydridoaluminate proceeded readily, either in absence of solvent or in dioxane. The corresponding methyl-silanes were produced in high yield.

The thermal stability of some of the new compounds produced was briefly investigated, and was found to be very high. No sign of decomposition was found below 400°, at which temperature slight (~ 3%) breakdown occurred in 10–12 h. At higher temperatures, above 500°, complete breakdown to give silicon tetrafluoride, fluoroform, carbon dioxide, etc., occurred in a few minutes.

Nuclear Magnetic Resonance Spectra

Proton nuclear magnetic resonance (n.m.r.) spectra were used extensively to provide confirmation of structure and, in some cases, to distinguish between possible isomers. Essential features of the spectra are given in Fig. 1.

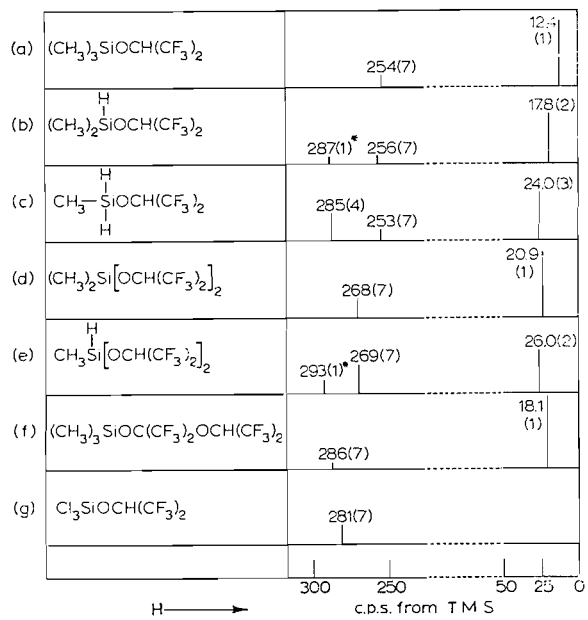

FIG. 1. Nuclear magnetic resonance spectra of hexafluoroisopropoxysilanes. Height proportional to area of peak; numbers in parenthesis indicate multiplicity. (*Peak broad, not clearly resolved.)

All absorption peaks occurred on the low field side of tetramethylsilane. Methyl groups attached to silicon showed small chemical shifts (12–26 c.p.s.) and showed coupling with protons on silicon, where present. Every spectrum contained a septet with chemical shift in the range 253–286 c.p.s. and coupling constant 5.4–5.9 c.p.s.; this is attributed to the proton of the hexafluoroisopropoxy group, which would be coupled equally with the six adjacent fluorine atoms. The only remaining peaks occurred in the range 285–293 c.p.s. in spectra *b*, *c*, and *e*. These are attributed to protons attached to silicon in those compounds,

and showed the expected interaction with the adjacent methyl groups, seen as a quartet in *c* (J = 3.5 c.p.s.) and as unresolved broadening in *b* and *e*.

Fluorine n.m.r. spectra were also recorded for some of these compounds. In all cases except *f*, all fluorine atoms in the molecule are equivalent and, typically, a single doublet was found (chemical shift for *a* is −69.9 c.p.s. from trifluoroacetic acid (TFA)) the splitting being due to the adjacent proton (J = 5.7 c.p.s.). For compound *f*, two fluorine resonances were observed, at −270 and +102 c.p.s. from TFA. Both were broad absorptions, that at −270 c.p.s. being a poorly resolved doublet. The broad doublet is attributed to the fluorine atoms adjacent to the proton of the hexafluoroisopropoxy group, where one would expect a doublet of septets from coupling with the proton and other fluorine atoms in the side chain. The second fluorine resonance is then attributed to the six remaining fluorine atoms, where one would expect a septet which is not resolved due to the considerable separation of the interacting nuclei.

Integration of all proton n.m.r. spectra was carried out, and the relative peak areas were in complete accordance with those expected from the structures in Fig. 1. In particular, the spectra eliminate the possibility that structures *d* or *e* might have been the isomers $(CH_3)_2SiH.OC(CF_3)_2OCH(CF_3)_2$ or $CH_3SiH_2.OC(CF_3)_2OCH(CF_3)_2$ respectively.

EXPERIMENTAL

General

Volatile materials were handled in a conventional vacuum system and separated by fractional condensation. Molecular weights were determined by Regnault's method. Hexafluoroacetone was a redistilled commercial sample* whose purity was checked by molecular weight measurement and infrared examination. Methyl-, dimethyl-, and trimethyl-silane were prepared by reduction of the corresponding chlorosilanes with lithium tetrahydridoaluminate (2). Irradiation was provided by a 400 W G.E. mercury arc lamp at a distance of 60 cm from the reaction tubes (clear silica, 100 ml volume), which were arranged so that only the gaseous phase was irradiated. Microanalyses were performed by Dr. Alfred Bernhardt. Analysis for fluorine was attempted in some cases but the presence of silicon in the molecule made it impossible to obtain reliable results. Nuclear magnetic resonance spectra were recorded on Varian model A-60 and DP-60 instruments, using 60 Mc/s and 56.4 Mc/s for proton and fluorine resonance respectively.

Infrared spectra of all new compounds were recorded, using Beckman IR-5A instruments (NaCl and CsBr), and were fully consistent with the assigned structures, showing absorption around 3 000 cm^{-1} (C—H), 2 200 – 2 300 cm^{-1} (Si—H), 1 150 – 1 400 cm^{-1} (C—F), and 1 100 – 1 120 cm^{-1} (Si—O—C). Essential features of the spectra are shown in Fig. 2.

Reaction of Hexafluoroacetone with Methylsilane

(i) Methylsilane (0.66 g, 14.3 mmoles) and hexafluoroacetone (2.50 g, 15.1 mmoles) in a sealed tube were irradiated for 9 h, the lower 10 cm of the tube being shielded and kept at 20°. Fractionation gave unreacted methylsilane (0.065 g, 1.41 mmoles), a trace of hexafluoroacetone, and 1,1,1,3,3,3-hexafluoroisopropoxymethylsilane (1.44 g, 6.84 mmoles, b.p. 50° at 737 mm).

Anal. Calcd. for $C_4H_6F_6OSi$: C, 22.6; H, 2.85. Found: C, 22.8; H, 2.71.

Also formed was a small amount (0.55 g, 1.45 mmoles) of bis(1,1,1,3,3,3-hexafluoroisopropoxy)methylsilane. The yield of this compound was markedly increased when the tube was not cooled, as in (ii) below, since the purpose of cooling was to remove the less volatile products from the reaction zone.

(ii) Methylsilane (0.454 g, 9.87 mmoles) and hexafluoroacetone (4.00 g, 24.1 mmoles) in a sealed tube were irradiated for 12 h. Fractionation gave bis(1,1,1,3,3,3-hexafluoroisopropoxy)methylsilane (3.37 g, 8.91 mmoles, b.p. 110–111° at 737 mm).

Anal. Calcd. for $C_7H_6F_{12}O_2Si$: C, 22.2; H, 1.60. Found: C, 22.3; H, 1.79.

(iii) In attempts to prepare tris(1,1,1,3,3,3-hexafluoroisopropoxy)methylsilane, the above reaction was repeated several times under various conditions. The molar ratio of hexafluoroacetone to methylsilane was increased up to 4:1 and irradiation was carried out for longer periods with the reaction tube maintained at 130° to keep reactants in the vapor phase, but no evidence of the desired compound was found.

Reaction of Hexafluoroacetone with Dimethylsilane

(i) Dimethylsilane (1.20 g, 20.0 mmoles) and hexafluoroacetone (4.02 g, 24.2 mmoles) in a sealed tube were irradiated for 9.5 h, the lower 10 cm of the tube being shielded and maintained at 20°. Fractionation gave unreacted dimethylsilane (0.084 g, 1.4 mmoles) and hexafluoroacetone (0.23 g, 1.4 mmoles) and 1,1,1,3,3,3-hexafluoroisopropoxydimethylsilane (3.37 g, 14.9 mmole, b.p. 72–73° at 743 mm).

Anal. Calcd. for $C_5H_8F_6OSi$: C, 26.5; H, 3.65. Found: C, 26.5; H, 3.53.

**Supplied by Allied Chemical Company, General Chemical Division.*

Can. J. Chem. Downloaded from www.nrcresearchpress.com by 210.87.254.40 on 09/05/12
For personal use only.

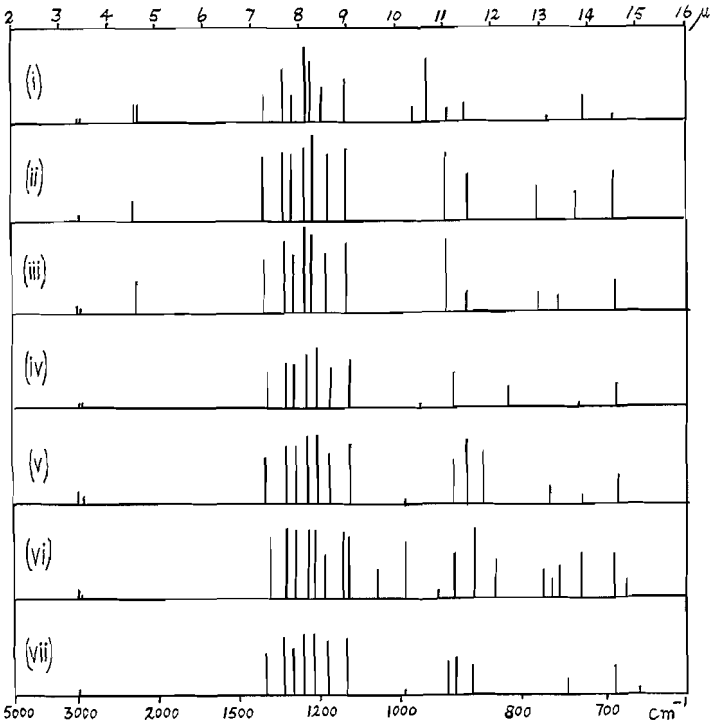

FIG. 2. Infrared spectra of hexafluoroisopropoxysilanes. Liquid films, except (i) and (iii) (gaseous). (i) $CH_3SiH_2OCH(CF_3)_2$, (ii) $CH_3SiH[OCH(CF_3)_2]_2$, (iii) $(CH_3)_2SiHOCH(CF_3)_2$, (iv) $(CH_3)_2Si[OCH(CF_3)_2]_2$, (v) $(CH_3)_3SiOCH(CF_3)_2$, (vi) $(CH_3)_3SiOC(CF_3)_2OCH(CF_3)_2$, (vii) $Cl_3SiOCH(CF_3)_2$.

The 1:2 adduct, bis(1,1,1,3,3,3-hexafluoroisopropoxy)dimethylsilane, was also produced in low yield (0.30 g, 0.8 mmole).

(ii) Dimethylsilane (0.636 g, 10.6 mmoles) and hexafluoroacetone (6.40 g, 38.5 mmoles) in a sealed tube (uncooled) were irradiated for 23 h. Fractionation gave unreacted hexafluoroacetone (0.63 g, 3.79 mmoles) and bis(1,1,1,3,3,3-hexafluoroisopropoxy)dimethylsilane (3.21 g, 8.19 mmoles, b.p. 127–128° at 732 mm).

Anal. Calcd. for $C_8H_8F_{12}O_2Si$: C, 24.5; H, 2.06. Found: C, 24.8; H, 1.99.

Reaction of Hexafluoroacetone with Trimethylsilane

(i) Trimethylsilane (0.65 g, 8.8 mmoles) and hexafluoroacetone (3.8 g, 23 mmoles) in a sealed tube were irradiated for 15 h. Fractionation gave traces of fluoroform and hexafluoroethane, unreacted hexafluoroacetone (1.8 g, 11 mmoles), and 1,1,1,3,3,3-hexafluoroisopropoxytrimethylsilane (1.43 g, 6.0 mmoles, b.p. 90° at 748 mm).

Anal. Calcd. for $C_6H_{10}F_6OSi$: C, 30.0; H, 4.20. Found: C, 29.7; H, 4.24.

(ii) Trimethylsilane (1.47 g, 19.9 mmoles), hexafluoroacetone (4.21 g, 25.4 mmoles) and trimethylchlorosilane (0.2 g) were kept in a sealed tube in the dark at −78° for 33 h. The products were warmed to 20° and subsequently separated by fractionation to give unreacted trimethylsilane (0.13 g, 1.8 mmoles) and hexafluoroacetone (0.25 g, 1.5 mmoles), 1,1,1,3,3,3-hexafluoroisopropoxytrimethylsilane (3.45 g, 14.4 mmoles), and 2-(1,1,1,3,3,3-hexafluoroisopropoxy)-hexafluoroisopropoxytrimethylsilane (0.71 g, 1.8 mmoles, b.p. 135–136°).

Anal. Calcd. for $C_9H_{10}F_{12}O_2Si$: C, 26.6; H, 2.48. Found: C, 27.2; H, 2.58.

Reaction of Hexafluoroacetone with Trichlorosilane

Trichlorosilane (2.99 g, 22.1 mmoles) and hexafluoroacetone (4.65 g, 28.0 mmoles) in a sealed tube were irradiated for 13 h. Fractionation gave traces of fluoroform, hexafluoroethane, some unidentified noncondensable gas (presumably carbon monoxide), unreacted hexafluoroacetone (0.72 g, 4.3 mmoles), and 1,1,1,3,3,3-hexafluoroisopropoxytrichlorosilane (4.52 g, 15.0 mmoles, b.p. 89° (743 mm).

Anal. Calcd. for $C_3HCl_3F_6OSi$: C, 12.0; H, 0.33; Cl, 35.3. Found: C, 12.1; H, 0.53; Cl, 35.1.

Hydrolysis

1,1,1,3,3,3-Hexafluoroisopropoxytrimethylsilane (0.5 g) was heated in a sealed tube with water (2 ml) for 8 days at 110°. Fractionation gave 1,1,1,3,3,3-hexafluoroisopropanol, but it was not possible to separate it

Can. J. Chem. Downloaded from www.nrcresearchpress.com by 210.87.254.40 on 09/05/12
For personal use only.

completely from water and an accurate estimate of yield could not be made. The alcohol produced in this and subsequent reactions was identified by infrared spectroscopic comparison with a known sample, prepared by the reduction of hexafluoroacetone with lithium tetrahydridoaluminate (3).

Acid Cleavage

1,1,1,3,3,3-Hexafluoroisopropoxytrimethylsilane (0.21 g, 0.88 mmole) was added to concentrated sulfuric acid (2 ml) at 20°. After the solution was mixed, volatile materials were pumped off and found to be solely 1,1,1,3,3,3-hexafluoroisopropanol (0.06 g, 0.36 mmole, 41%). A similar reaction with 1,1,1,3,3,3-hexafluoroisopropoxydimethylsilane gave the same alcohol in 81% yield.

Reduction

The various silanes were condensed onto a 10% molar excess of lithium tetrahydridoaluminate in an evacuated tube, which was sealed and kept at 110° for 2 h (4). Fractionation gave the following results.

Silane	Product	Yield, %
$CH_3SiH[OCH(CF_3)_2]_2$	CH_3SiH_3	81
$(CH_3)_2SiHOCH(CF_3)_2$	$(CH_3)_2SiH_2$	70
$(CH_3)_2Si[OCH(CF_3)_2]_2$	$(CH_3)_2SiH_2$	83
$(CH_3)_3SiOCH(CF_3)_2$	$(CH_3)_3SiH$	1.5
$(CH_3)_3SiOCH(CF_3)_2$	$(CH_3)_3SiH$	74 (with dioxane added)

Upon cautious treatment with sulfuric acid of the solid residues produced in the above reductions, 1,1,1,3,3,3-hexafluoroisopropanol was produced in yields up to 50%.

Thermal Decomposition

1,1,1,3,3,3-Hexafluoroisopropoxytrimethylsilane (0.29 g) in a heavy-walled pyrex tube (8 ml) was heated at 400° for 10 h, by which time a slight yellow coloration was apparent. Fractionation showed that the bulk of the silane was unchanged, with traces ($\sim$ 3%) of more volatile decomposition products.

When a similar reaction tube was heated from 100° to 500° over a period of 2 h, no change was noticed until 450°, when slight darkening began. The darkening rapidly increased above 500°. After the reaction tube was kept at 550° for 13 h, decomposition was complete, and fractionation gave fluoroform, silicon tetrafluoride, carbon dioxide, and other material, with a black residue remaining in the tube.

The decomposition of the silanes $(CH_3)_2Si[OCH(CF_3)_2]_2$ and $(CH_3)_2SiHOCH(CF_3)_2$ followed a very similar course, the presence of the hydrogen atom directly attached to silicon in the last compound apparently making little difference.

ACKNOWLEDGMENTS

The research for this paper was supported (in part) by the Defence Research Board of Canada, Grant number 7583-05. We also gratefully acknowledge the award of an Ontario Graduate Fellowship (to A. F. J.).

REFERENCES

1. R. Calas and N. Duffaut. Compt. Rend. **245**, 906 (1957). R. Calas, N. Duffaut, and C. Bardot. Compt. Rend. **249**, 1682 (1959). R. Calas, E. Frainnet, and J. Bonastre. Compt. Rend. **251**, 2987 (1960). H. Gilman and D. Wittenberg. J. Org. Chem. **23**, 501 (1958).
2. S. Tannenbaum, S. Kaye, and G. F. Lewenz. J. Am. Chem. Soc. **75**, 3753 (1953).
3. W. J. Middleton and R. V. Lindsey. J. Am. Chem. Soc. **86**, 4948 (1964).
4. H. Westermark. Acta Chem. Scand. **8**, 1830 (1954).

Can. J. Chem. Downloaded from www.nrcresearchpress.com by 210.87.254.40 on 09/05/12
For personal use only.

Can. J. Chem. Downloaded from www.nrcresearchpress.com by 210.87.254.105 on 09/05/12
For personal use only.

THE REACTION OF OZONE WITH DIMETHYLLAURYLAMINE[1]

GARSON P. SHULMAN[2]
Research Laboratories, Archer-Daniels-Midland Co., Minneapolis, Minnesota

Received April 13, 1965

ABSTRACT

In the oxidation of dimethyllaurylamine in chloroform solution by ozone, increase in temperature results in decreased yields of amine oxide and amine hydrochloride and increased yields of amide and carboxylic acid. The reaction is first order in amine and first order in ozone and is not affected by light. These data are consistent with a mechanism involving oxidation of an amine–chloroform charge transfer complex stable at low temperatures.

INTRODUCTION

The reaction of tertiary amines with ozone leads almost exclusively to amine oxides when conducted in chloroform solution below −50° (1, 2, 3). At somewhat higher temperatures (−45° to 0°) or in other polar solvents (specifically in methanol), somewhat lower yields, and isolation of amides, aldehydes, acids, and other products of oxidative attack on the alpha carbon have been reported (4, 5, 6). In nonpolar solvents (pentane, cyclohexane, 1-chlorobutane, carbon tetrachloride), amine oxide yields are very low, regardless of temperature.

Maggiolo and Niegowski (4) suggested a mechanism for the reaction involving electrophilic attack on the amine nitrogen by ozone, followed by decomposition of the intermediate zwitterion (I). This mechanism is postulated by analogy with the Criegee mechanism for reaction of olefins with ozone. No experimental data to support the mechanism are presented. Henbest and Stratford (5, 6) have presented a detailed scheme accounting for production of aldehydes, secondary amines, acids, and amides as a result of oxidation at the alpha carbon atom. This investigation was carried out in an attempt to establish experimentally a mechanism for oxidation at the nitrogen atom.

A systematic study covering a temperature range of −75° to 61° in chloroform solution was selected as the approach most likely to lead to better understanding of the reaction. After the observation that oxidation at the alpha carbon atom was negligible at dry ice temperature, experiments to determine the effects of some other variables were conducted. A preliminary kinetic study was also performed.

EXPERIMENTAL

Reaction at Various Temperatures

Vigorously stirred chloroform solutions of dimethyllaurylamine in a micro-reaction apparatus (7) were maintained at the desired temperature while ozone was introduced at a rate of 65 ± 10 mg/min (in a 0.02 c.f.m. oxygen stream). At intervals, titrations for unreacted ozone were performed. The reaction was terminated when a 10% excess of ozone had been absorbed, as determined from the area under the absorption vs. time graph. Solvent was removed by evaporation under vacuum at room temperature. The product was analyzed by titration for amine oxide, amine, amide, and acid, and qualitatively by infrared spectrometry and thin-layer chromatography. Assignment of acids as carboxylic or trialkyl ammonium chloride was based on presence of characteristic N—H or C=O absorption bands in the infrared spectrum. Details are given in Table I.

Effect of Other Variables

A 500-ml flask was fitted with a Tru-Bore stirrer, a gas inlet tube, and an outlet connected at regular intervals to a potassium iodide trap. After the initial reaction, the flask was wrapped to exclude light. Reaction in a dry ice bath (−75°) was continued until the desired amount of ozone had been introduced. Nearly quantitative uptake was observed. Results are summarized in Table II.

[1]*Presented at the Ozone Symposium, American Chemical Society Southwest Regional Meeting, Houston Texas, December 1963.*

[2]*Present address: Martin Company, Baltimore, Maryland.*

TABLE I

Effect of temperature on dimethyllaurylamine ozonization

Temp. (°C)	Concentration (g/100 ml)	Yield[a] (%)	Analysis (% of product) Amine oxide	Amine salt	Amide	Acid	Amine
61	5[b]	40	18	[c]	[c]	[c,d]	[c]
25	20	95	28	[c]	38	[c,d]	[c]
0	10	95	38	[e]	32	[e]	15
−15	10	—	42	17	25	0	16[f]
−75	10	91	65	22	[e]	0	13[f]

[a]100 × Weight of product/theoretical weight of amine oxide.
[b]Extensive evaporation of solvent during reaction.
[c]Not determined.
[d]Strong carboxyl band in infrared spectrum.
[e]Trace (weak infrared absorption).
[f]By difference.

TABLE II

Oxidation of dimethyllaurylamine at −75°

Concentration (g/100 ml)	Ozone excess (%)	Additive (g/100 ml)	Analysis (% of product) Amine oxide	Amine hydrochloride	Amine[a]
5	10	Light	48	27	25
10	10	None	64	23	
10	10	NaOMe (10)	45[b]	36	
5	10	$CaCO_3$ (10)	82	16	
5	10	Na_2CO_3 (10)	64	0[c]	36
10	35	Na_2CO_3 (10)	77	10	13
10	60	Na_2CO_3 (10)	47	16	
5[d]	10	None	44[b,e]		
5[f]	10	None	50[b]		

[a]By difference when t.l.c. and infrared show no other component.
[b]Strong amide carbonyl band in infrared.
[c]No N—H bands in infrared.
[d]MeOH solvent.
[e]Acid carbonyl band in infrared.
[f]EtOAc solvent.

Kinetic Studies

Solutions of 10.0 g of dimethyllaurylamine in 50.0 ml of chloroform were prepared. Using an oxygen flow rate of 0.05 c.f.m., each solution, in a gas-washing tower, cooled to −75° in a dry ice bath, was treated with a different concentration of ozone with vigorous stirring. The rate of the reaction, expressed as mg/min of ozone consumed, was initially constant. A straight line graph of rate vs. ozone concentration was obtained (see Table III).

Solutions of 1.00 to 4.00 g of amine in 50.0 ml of chloroform were prepared. Each was placed in a 100 ml, three-necked flask with ground glass sealed stirrer, cooled to −75°[3] and ozonized with a stream of 0.02 c.f.m. containing 65.4 mg/min of ozone. Figure 1 shows typical curves at low and high amine concentrations. A graph of initial rate (extrapolated linearly at high amine concentrations) vs. initial amine concentration was linear.

Amide Analysis[4]

A weighed sample (1–2 g) was placed in a Florence flask with 25 ml of 6 *N* sodium hydroxide. The mixture was distilled into 10.0 ml of standardized 0.5 *N* hydrochloric acid until most of the water had been removed.[5] The distillate was titrated with base, to a methyl red end point, giving the amount of

[3]*Pure chloroform freezes at −63.5°. The technical grade of chloroform used in these experiments froze when a solution containing only 10 g/l was employed, but the freezing point was lowered enough by higher concentrations of amine that no difficulty was encountered.*

[4]*The amides formed are all secondary products of alpha carbon oxidation to carbinolamine. Therefore, total amide, amine oxide, and amine salt are the significant analyses for determining the mechanism of the primary oxidation step.*

[5]*The decomposition of aliphatic amine oxides in aqueous solution is extremely slow, even in strong base. The analysis is essentially a Kjeldahl determination without a reduction step (8).*

Can. J. Chem. Downloaded from www.nrcresearchpress.com by 210.87.254.105 on 09/05/12
For personal use only.

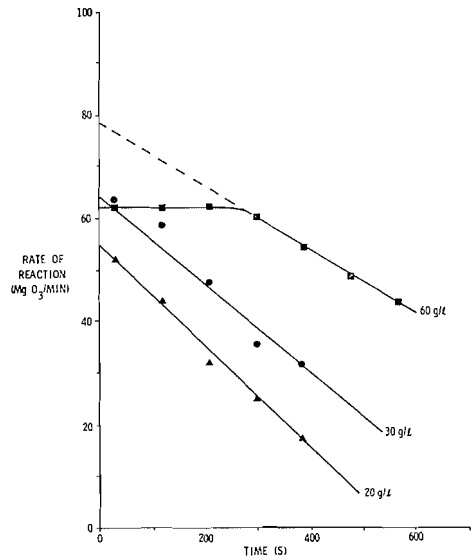

FIG. 1. Typical rates of ozonization.

TABLE III

Rates of dimethyllaurylamine oxidation

Ozone input (mg/min)	Initial amine concentration (g/l)	Initial ozone consumption (mg/min)
48.4	166.7	47.2
68.0	166.7	65.6
98.5	166.7	94.0
105	166.7	101.2
65.4	19.6	54.4
65.4	29.1	64.2
65.4	38.5	67.0
65.4	56.6	77.5[a]
65.4	74.1	86.0[a]

[a]Extrapolated.

dimethylamine (from dimethyllauramide and dimethylformamide). The residue was extracted three times with 25 ml of chloroform, then the combined extracts were washed twice with 150 ml of water, mixed with toluene – isopropyl alcohol – bromphenol blue solution, and titrated to determine methyllaurylamine (from *N*-methyl-*N*-laurylformamide) and unreacted dimethyllaurylamine.[6] A second sample was titrated without prior treatment, determining the dimethyllaurylamine, which was then subtracted from the sum of the other titrations.

Amine Hydrochloride Analysis

A standard titrimetric method[7] for determination of acids or ammonium salts was employed.

Amine and Amine Oxide Analysis

A nonaqueous acidimetric titration was used for determination of amine and amine oxide (9). Details of the thin-layer chromatography method have also been described previously.

Purification of Dimethyllaurylamine Oxide

The mixture obtained from reaction of 50 g of amine in 1 l of chloroform in the presence of 50 g of calcium carbonate at −75° was recrystallized from benzene, yielding 9 g of white powder, m.p. 108–112°.

[6]*American Oil Chemists' Society Standard Method Nb 2-62.*
[7]*American Oil Chemists' Society Standard Method Nc 1-62.*

Can. J. Chem. Downloaded from www.nrcresearchpress.com by 210.87.254.105 on 09/05/12
For personal use only.

Analysis showed that it contained no amine hydrochloride and 89.4% amine oxide. A second recrystallization of a small portion gave anhydrous dimethyllaurylamine oxide, m.p. 117–120° (reported m.p. 117–123°) (10).

Oxidation of Dimethyllaurylammonium Chloride

A solution of 2.0 g, m.p. 190–194°, in 200 ml of methanol was cooled to −30° and treated with 520 mg of ozone, absorbing 211 mg. Solvent was removed under vacuum. The product, m.p. 146°, contained 7.2% of amine oxide.

DISCUSSION

Synthetic Studies

Conversion of dimethyllaurylamine to the oxide increases as the temperature is lowered, while amide formation (Fig. 2) diminishes, until at −75° amide formation is negligible.

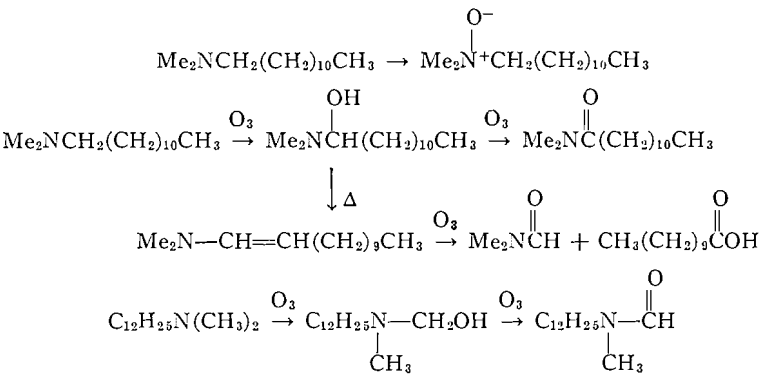

FIG. 2. Reactions of dimethyllaurylamine with ozone.

No improvement can be expected at temperatures below −75°, since conversion to the hydrochloride competes, and dimethyllaurylammonium chloride does not react rapidly with ozone.[8] By adding calcium or sodium carbonate, amine hydrochloride formation is minimized (0–10%), and higher yields (64–82%) of amine oxide are attained. Addition of sodium methoxide resulted in a markedly lower yield of amine oxide and extensive formation of by-products. A large (60%) excess of ozone gave a poorer conversion to amine oxide than either 10% or 35% excess. This is probably the result of oxidation of the amine oxide at the alpha carbon. Use of ethyl acetate and methanol as solvents normally leads to slightly lower yields (44 and 50%) of amine oxide than in chloroform carbonate mixtures (74 ± 10%) but amide formation becomes significant at −75°.

Kinetic Studies

The method employed by Wibaut (11) was used in this investigation. By keeping the oxygen–ozone flow constant and varying discharge voltage, one can measure the dependence of rate on ozone concentration. Absorption of the stream in a potassium iodide trap for 60 s leads to an expression of ozone concentration in mg/min. Similar titration of the off-gas and subtraction from input then gives ozone absorption in mg/min, and is a direct measurement of the rate. Similarly, with constant ozone input and varying concentration of amine, the dependence of rate on amine concentration may be determined. Since the reaction is essentially heterogeneous, no significant rate constants can be obtained.

[8]*Generally, salt formation stabilizes an amine toward ozone. Because of the marked solvent effects on this reaction, it would have been desirable to verify that reaction of the salt is slow in chloroform, but the amine salt is not appreciably soluble at low temperatures.*

Can. J. Chem. Downloaded from www.nrcresearchpress.com by 210.87.254.105 on 09/05/12
For personal use only.

Oxidation of dimethyllaurylamine to the oxide is first order in ozone and first order in amine at −75°,

$$d[O_3]/dt = K[O_3][R_3N].$$

Mechanism of Reaction

There are four likely mechanisms for amine oxide formation: (A) electrophilic attack of ozone [I] (4); (B) preliminary formation of an amine–solvent complex followed by displacement of solvent [II]; (C) formation and decomposition of a trialkylammonium ozonide [III and IV]; and (D) oxidation by a free radical process. Amine hydrochloride (or hydrogen chloride) formation must result from decomposition of chloroform, either free [V] or in an amine–solvent complex [VI].

[I] $$R_3N + O_3 \rightarrow R_3N^+—O—O—O^- \rightarrow R_3NO + O_2$$

[II] $$R_3N + CHCl_3 \rightleftharpoons R_3N.....CHCl_3 \xrightarrow{O_3} R_3N \rightarrow O + CHCl_3 + O_2$$

[III] $$H_2O + 3R_3N + 2O_3 \rightarrow 2(R_3NH^+O_3^-) + R_3NO$$

[IV] $$2(R_3NH^+O_3^-) \rightarrow R_3NO + H_2O + R_3N + 2O_2$$

[V] $$R_3N + CHCl_3 \xrightarrow{O_3} R_3NH^+Cl^- + COCl_2$$

[VI] $$R_3N.....CHCl_3 \xrightarrow{O_3} R_3NH^+Cl^- + COCl_2$$

While it might be possible to propose stepwise mechanisms for oxidation via free radical or trialkylammonium ozonide intermediates which would obey the observed rate expression, the kinetic data strongly suggest either I or II as the actual mechanism. The parallel decrease in conversion to amine oxide and to amine hydrochloride with increasing temperature is consistent with reaction of a low-temperature stable amine–solvent complex, but not with oxidative degradation of chloroform, which would be favored at higher temperatures. The remarkable ability of chloroform to suppress alpha carbon oxidation could be explained if alpha oxidation involves a free radical mechanism. Chloroform would function better as an inhibitor than the other solvents which have been employed.

Spectral evidence for amine–halomethane interaction has been presented (12). The evidence did not clearly differentiate between charge-transfer complexes and contact charge-transfer spectra, but it was suggested that charge-transfer complexes might be the species involved in photochemical reactions leading to amine hydrohalides or enamines (12). Since exclusion of light from the dimethyllaurylamine–chloroform–ozone system did not suppress amine hydrochloride formation, one must conclude that the reaction of ozone with an amine–chloroform complex is the principal source of hydrogen chloride. It has also been proposed that the superior yields of amine oxide in chloroform and methanol are due to the hydrogen bonding ability of these solvents (5). Additional work to determine the nature of the amine–solvent complex is needed.

REFERENCES

1. W. Strecker and H. Thienemann. Ber. **53**, 2096 (1920).
2. W. Strecker and M. Baltes. Ber. **54B**, 2693 (1921).
3. L. Horner, H. Schaefer, and W. Ludwig. Ber. **91**, 75 (1958).
4. A. Maggiolo and S. Niegowski. Advan. Chem. Ser. **21**, 202 (1959).
5. H. B. Henbest and M. J. W. Stratford. J. Chem. Soc. 711 (1964).
6. M. J. W. Stratford and H. B. Henbest. Chem. Ind. London, 1170 (1961).
7. A. Maggiolo. Organic ozone reactions and techniques. The Welsbach Corp., Philadelphia, Pa. p. 21.
8. E. H. Swift. Introductory quantitative analysis. Prentice-Hall, Inc., New York. 1950. p. 277.
9. G. P. Shulman and W. E. Link. J. Am. Oil Chemists' Soc. **41**, 329 (1964).
10. G. L. K. Hoh, D. O. Barlow, A. F. Chadwick, D. B. Lake, and S. R. Sheeran. J. Am. Oil Chemists' Soc. **40**, 268 (1963).
11. J. P. Wibaut *et al.* Rec. Trav. Chim. **69**, 1355 (1950).
12. D. P. Stevenson and G. M. Coppinger. J. Am. Chem. Soc. **84**, 149 (1962).

Can. J. Chem. Downloaded from www.nrcresearchpress.com by 210.87.254.105 on 09/05/12
For personal use only.

Can. J. Chem. Downloaded from www.nrcresearchpress.com by 210.87.254.6 on 09/05/12
For personal use only.

SYNTHESIS OF 3-AMINO-2,3-DIDEOXY-D-*lyxo*-HEXOSE

HANS H. BAER AND FRANK KIENZLE
Department of Chemistry, University of Ottawa, Ottawa, Canada

Received June 2, 1965

ABSTRACT

Catalytic hydrogenation of methyl 4,6-*O*-benzylidene-2,3-dideoxy-3-nitro-β-D-*threo*-hexopyranos-2-enide (I) afforded methyl 4,6-*O*-benzylidene-2,3-dideoxy-3-nitro-β-D-*lyxo*-hexopyranoside (II). Acid debenzylidenation and further hydrogenation gave in turn methyl 2,3-dideoxy-3-nitro-β-D-*lyxo*-hexopyranoside (III) and the corresponding amine hydrochloride (IV). Several crystalline derivatives of IV were prepared, and the configuration at C-3 was proved by degradation of the *N*-benzoate (VII) to *N*-benzoyl-D-aspartic acid. The title compound (V) was obtained as a chromatographically homogeneous sirup.

Some methyl 3-deoxy-3-nitro-β-L-hexopyranosides were prepared for potential use as starting materials in analogous syntheses in the L-series.

In the course of work directed at the synthesis of rare amino sugars a route was recently elaborated that led to 3-amino-2,3-dideoxy-D-*arabino*-hexose (1). We have now prepared 3-amino-2,3-dideoxy-D-*lyxo*-hexose in similar fashion. Sugars of this type are of interest as they are related to certain carbohydrate components of anthracycline antibiotics (2), namely to rhodosamine (3-dimethylamino-2,3,6-trideoxy-L-*lyxo*-hexose (3)) and daunosamine (3-amino-2,3,6-trideoxy-L-*lyxo*-hexose (4)). It may be anticipated that the principle presented in this paper can be utilized for the synthesis of these natural products, especially since 3-deoxy-3-nitro-hexopyranosides of the L-series have become accessible (see below).

Methyl 4,6-*O*-benzylidene-2,3-dideoxy-3-nitro-β-D-*threo*-hexopyranos-2-enide (I) which is available (5) starting from methyl 3-deoxy-3-nitro-β-D-galactopyranoside, was hydrogenated over palladium on charcoal to give in good yield methyl 4,6-*O*-benzylidene-2,3-dideoxy-3-nitro-β-D-*lyxo*-hexopyranoside (II). Debenzylidenation of II readily afforded methyl 2,3-dideoxy-3-nitro-β-D-*lyxo*-hexopyranoside (III) which by catalytic reduction over platinum in the presence of 1 equiv of dilute hydrochloric acid gave the corresponding amine, methyl 3-amino-2,3-dideoxy-β-D-*lyxo*-hexopyranoside hydrochloride (IV). Whereas all compounds up to this point crystallized well, the reducing sugar (V) produced upon acid hydrolysis has thus far failed to do so; it was characterized by paper chromatography.

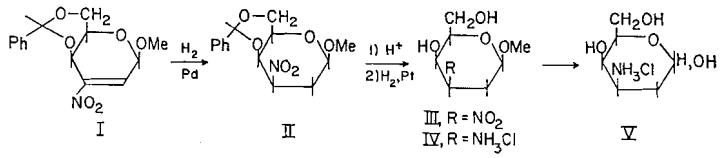

I II III, R = NO_2 IV, R = NH_3Cl V

It was presumed that hydrogen addition to the olefinic double bond in I would place the nitro group chiefly into equatorial disposition as has been the case with the analogous β-D-*erythro* nitroolefin (1). To prove this point, i.e., the D-*lyxo* configuration of II and the products derived from it, the *N*-acetate (VI), *N*-benzoate (VII), di-*O*-acetyl-*N*-acetate (VIII), and di-*O*-methanesulfonyl-*N*-acetate (IX) were prepared by standard procedures from the aminoglycoside IV and were dealt with as follows.

The triacetate VIII gave a 60 Mc n.m.r. spectrum[1] exhibiting methyl resonances of

[1]*In deuterochloroform solution with tetramethylsilane as internal standard; a Varian V-4302 high-resolution instrument was used.*

equal intensities at 8.07, 7.96, and 7.86 τ, consistent with one equatorial acetamido group, one equatorial acetoxy group, and one axial acetoxy group (6). The signal at 8.07 τ, in particular, can only be attributed to an equatorial *N*-acetyl (7). The OCH_3 signal appeared at 6.50 τ in line (8) with equatorial orientation of the glycosidic group. The spectrum, therefore, was indicative of the conformational formula VIII*a* (cf. also the data obtained (1) for the isomeric D-*arabino* compound).

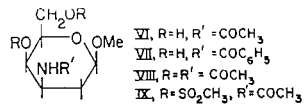

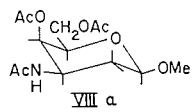

It was hoped that solvolysis of the dimesylate IX would provide further evidence as to the geometrical relationship between the C-3 acetamido group and the C-4 acetoxy group, the stereochemistry of the latter being known. This approach had proved fruitful in the D-*arabino* series, although the reaction had taken an unexpected course there (1). In the present case the solvolysis indeed proceeded with much greater difficulty than in the earlier case. Only 1 mole of sodium methanesulfonate was isolated and the solvolyzed product according to its infrared spectrum still contained mesyloxy. This fact suggested that the substituents at C-3 and C-4 were *cis*, i.e., unfavorably disposed for neighboring group participation. However, no crystalline sugar derivative could be elaborated in these experiments, neither directly nor upon acetylation or remesylation, so that the evidence furnished can be regarded only as circumstantial.

Unambiguous chemical proof of the configuration at C-3 came from another experiment, however. When the benzoylamino glycoside VII was partially hydrolyzed (0.1 *N* hydrochloric acid at 98° for 30 min) and the hydrolysate that was presumed to contain the reducing benzoylamino sugar (X) was oxidized, first with periodate and then with bromine water, crystalline levorotatory D-benzoylaspartic acid (XI) was isolated. Its identity was established by comparison with an authentic sample of dextrorotatory L-benzoylaspartic acid (9).[2]

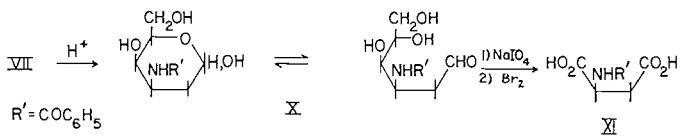

The key starting materials for the syntheses of 3-amino-2,3-dideoxy-D-hexoses as exemplified above and earlier (1) are methyl 3-deoxy-3-nitro-β-D-hexopyranosides from which nitroolefins of type I can be obtained (1, 5). In order that these syntheses may be performed also in the L-hexose series, the preparation of the requisite methyl 3-deoxy-3-nitro-β-L-hexopyranosides was undertaken by use of the nitromethane cyclization method (10). To this end the dialdehyde XII, D'-methoxy-L-hydroxymethyldiglycolic aldehyde, was needed. It is obvious from Jackson and Hudson's work (11) that this compound can be made, theoretically, by periodate oxidation of any methyl β-L-hexopyranoside or of any methyl β-L-pentofuranoside, although those authors did not in fact prepare it. L-Hexoses being difficult to provide, we chose to generate XII from methyl β-L-arabinofuranoside, which can be prepared with a reasonable outlay in time and materials (12). The dialdehyde was then subjected to a nitromethane cyclization according to the directions given (13, 14)

[2]*A similar degradation was employed (4) with daunosamine proving its* C-3 *to possess the opposite configuration.*

Can. J. Chem. Downloaded from www.nrcresearchpress.com by 210.87.254.6 on 09/05/12
For personal use only.

for its enantiomorph. In this way methyl 3-deoxy-3-nitro-β-L-glucopyranoside (XIII) was obtained, and by benzylidenation of the material contained in the mother liquor there was isolated methyl 4,6-*O*-benzylidene-3-deoxy-3-nitro-β-L-galactopyranoside (XIV) and -mannopyranoside (XV). The L-compounds were identical with their known enantiomorphs in all respects except for an opposite sign of rotation. The conversion in this manner of a pentofuranoside into hexopyranoside derivatives represents another example of lengthening of sugar chains "from within" (15, 13), a principle that has been fruitfully adopted recently in the nucleoside field (16).

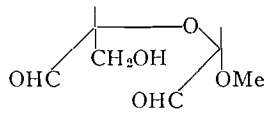

XII

EXPERIMENTAL

Methyl 4,6-O-Benzylidene-2,3-dideoxy-3-nitro-β-D-lyxo-hexopyranoside (II)

Methyl 4,6-*O*-benzylidene-2,3-dideoxy-3-nitro-β-D-*threo*-hexopyranos-2-enide (I, 2.70 g) was dissolved in 100 ml of ethyl acetate and hydrogenated at ordinary temperature and pressure in the presence of 300 mg of palladium on charcoal (10%). Within 15 min there was consumed 225 ml (s.t.p.) of hydrogen, corresponding to 1.08 molar equivalents. A very sharp decrease in the rate was noticed after that time. The catalyst was filtered off immediately and the solution was brought to dryness giving a crystalline residue. Recrystallization from ethyl acetate – petroleum ether (30–60°) afforded a first crop of needles (1.03 g; m.p. 169–172° (decomp.)) and a second crop (0.71 g; m.p. 166–168° (decomp.)) upon evaporating the mother liquor and taking up the residue in a small amount of absolute ethanol. Thus, the total yield of (slightly yellowish) crude product was 1.74 g (64%); this material was suitable for use in the next step. An analytical sample was obtained by one recrystallization from ethyl acetate – petroleum ether which raised the m.p. to 176° (decomp.) and by a second recrystallization which caused no further change in the melting point; $[\alpha]_D^{23}$ +15.2° (*c*, 0.8 in dimethylformamide).

Anal. Calcd. for $C_{14}H_{17}NO_6$ (295.3): C, 56.94; H, 5.83; N, 4.74. Found: C, 57.05; H, 6.00; N, 4.62.

Methyl 2,3-Dideoxy-3-nitro-β-D-lyxo-hexopyranoside (III)

Benzylidene compound II (1.9 g) in 50 ml of 70% acetic acid was heated on the steam bath for 30 min (but no longer). The acid was removed *in vacuo* and the residue was thrice evaporated with water. The resulting solid was taken up in 10 ml of water, whereby 30 mg of material remained undissolved and was discarded. The solution was treated with decolorizing carbon, evaporated, and dried by two evaporations with absolute ethanol. The residue was crystallized (at 4°, overnight) from 5 ml of ethanol with the addition of a few drops of petroleum ether. The yield was 720 mg of III melting at 139–140°; another 70 mg was obtained from the mother liquor (m.p. 128–136°), the combined yields being 59.4%. For analysis, a sample was recrystallized from ethyl acetate – petroleum ether; m.p. 141°, $[\alpha]_D^{23}$ +28.8° (*c*, 1 in water).

Anal. Calcd. for $C_7H_{13}NO_6$ (207.2): C, 40.58; H, 6.33; N, 6.76. Found: C, 40.64; H, 6.50; N, 6.80.

Debenzylidenations using the ion-exchange method (1) were also performed and gave the same product, but the yields were generally lower, the best being 39%.

Methyl 3-Amino-2,3-dideoxy-β-D-lyxo-hexopyranoside Hydrochloride (IV)

Nitro glycoside III (880 mg) was hydrogenated at ordinary temperature and pressure in 45 ml *N*/10 hydrochloric acid in the presence of 250 mg of prehydrogenated platinum dioxide catalyst. The hydrogen uptake was quantitative (3 molar equivalents); the time required was found in various similar runs to be 1–2.5 h depending on the efficiency of shaking. The filtrate from the catalyst was evaporated, with two additions of water toward the end. The crystalline residue was taken up in a small amount of ethanol, a few drops of ethyl acetate were added, and crystallization was allowed to take place overnight in a refrigerator. The yield of colorless crystals was 734 mg (81%); $[\alpha]_D^{23}$ −13.0° (*c*, 1 in water). Chromatography (17) showed only one spot (blue-violet with ninhydrin), $R_{glucosamine}$ 1.31. On heating, the compound decomposed slowly without showing a narrow decomposition range.

Anal. Calcd. for $C_7H_{16}ClNO_4$ (213.7): C, 39.35; H, 7.56; N, 6.56. Found: C, 39.26; H, 7.68; N, 6.61.

Methyl 3-Acetamido-2,3-dideoxy-β-D-lyxo-hexopyranoside (VI)

Aminoglycoside hydrochloride IV (500 mg) in 14 ml of water and 1.8 ml of methanol was stirred in an ice bath with 16 ml of Dowex-1-X2 (CO_3^{2-}). Acetic anhydride (0.4 ml) was added and the stirring was continued for 90 min. The resin was removed and the solution was evaporated giving a colorless sirup that was twice evaporated with ethanol. The material was crystallized from ethanol – ethyl acetate (15 h at 4°).

Can. J. Chem. Downloaded from www.nrcresearchpress.com by 210.87.254.6 on 09/05/12
For personal use only.

The yield was 465 mg (90.5%) of long prisms with m.p. 213° and $[\alpha]_D^{23}$ +41.8° (*c*, 0.9 in water). In a parallel run the m.p. was 210–212° and was raised to 213° by one recrystallization. The material gave a negative ninhydrin test.

Anal. Calcd. for $C_9H_{17}NO_5$ (219.2): C, 49.30; H, 7.82; N, 6.39. Found: C, 49.38; H, 7.65; N, 6.60.

A sample of *N*-acetate VI (2 mg) was heated in a sealed tube with 1 ml of *N* hydrochloric acid for 1 h at 110°. The acid was then removed by evaporation *in vacuo* with the addition of water. The solution reduced hot Fehling solution, was ninhydrin-positive, and on paper chromatography (17) gave virtually one spot of $R_{glucosamine}$ 1.06, attributed to 3-amino-2,3-dideoxy-D-*lyxo*-hexose hydrochloride (V). A number of larger-scale hydrolyses using VI as well as IV failed to produce V in crystalline condition.

Methyl 3-Acetamido-4,6-di-O-acetyl-2,3-dideoxy-β-D-lyxo-hexopyranoside (VIII)

Acetamido derivative VI (65 mg) was acetylated using pyridine (2.5 ml) and acetic anhydride (0.6 ml) at room temperature (15 h). The reaction mixture was worked up according to standard procedures (ice water; chloroform extraction) giving 52 mg of needles, m.p. 197–198° (from ethyl acetate – petroleum ether, 30–60°), $[\alpha]_D$ +66.0° (*c*, 0.9 in ethanol). The infrared spectrum indicated absence of hydroxyl and presence of *O*-acetyl and *N*-acetyl groups.

Anal. Calcd. for $C_{13}H_{21}NO_7$ (303.3): C, 51.47; H, 6.98; N, 4.62. Found: C, 51.49; H, 7.01; N, 4.43.

Methyl 3-Acetamido-2,3-dideoxy-4,6-di-O-mesyl-β-D-lyxo-hexopyranoside (IX)

Methanesulfonyl chloride (0.28 ml) was added dropwise with stirring to an ice-cold solution of acetamido derivative VI (200 mg) in pyridine (25 ml). The mixture was stirred for 30 min, then left overnight in a refrigerator. Water was added (20 ml) and the mixture stirred for 30 min, whereby a first crop of IX (45 mg) separated. The filtrate thereform was evaporated and the residue treated with 5 ml of water, which afforded a second (main) crop of IX (231 mg). The combined yield was 83%. Recrystallization from methanol–ethanol (1:1) furnished needles (240 mg) of m.p. 175° (decomp.), raised to 176° (decomp.) by a second recrystallization; $[\alpha]_D^{23}$ +13.3° (*c*, 0.6 in dimethylformamide).

Anal. Calcd. for $C_{11}H_{21}NO_9S_2$ (375.4): C, 35.19; H, 5.64; N, 3.73; S, 17.08. Found: C, 35.22; H, 5.98; N, 3.83; S, 16.93.

Methyl 3-Benzamido-2,3-dideoxy-β-D-lyxo-hexopyranoside (VII)

Amino glycoside hydrochloride (IV, 150 mg) and sodium bicarbonate (150 mg) were dissolved in 4 ml of water, and a solution of benzoylchloride (105 mg) in tetrahydrofuran (2 ml) was added dropwise with magnetic stirring. The stirring was continued for 30 min. Tests with indicator paper showed that the solution remained weakly alkaline throughout. The reaction mixture was then diluted with about 20 ml of water, deionized by stirring for 10 min with 2 ml of Dowex-50-X12 (H^+) and 5 ml of Amberlite IR-45 (OH^-) and filtered, the resins being washed well with water. The filtrate (pH about 4) was extracted twice with $\frac{1}{4}$ volume of ether to remove residual benzoic acid, and was then brought to dryness leaving 139 mg (70%) of white crystals of VII, m.p. 185–186°. Recrystallization from about 10 ml of boiling ethyl acetate containing a few drops of ethanol gave fine needles of m.p. 193–194°, raised to 194–195.5° (196–197° in a sealed capillary) by a further recrystallization, $[\alpha]_D^{23}$ +36° (*c*, 2 in water). The infrared spectrum showed hydroxyl, amide-I, and amide-II bands as expected.

Anal. Calcd. for $C_{14}H_{19}NO_5$ (281.3): C, 59.77; H, 6.81; N, 4.98. Found: C, 59.93; H, 6.92; N, 5.18.

Degradation of VII to N-Benzoyl-D-aspartic Acid

N-Benzoyl glycoside VII (145 mg) was hydrolyzed in 7 ml of *N*/10 hydrochloric acid for 1 h on a steam bath. After cooling, the solution was neutralized (to pH 4–5) by treatment with 3 ml of Amberlite IR-45 (OH^-) and concentrated *in vacuo*. Thin-layer chromatography on silica gel with benzene–methanol (4:1) gave only one spot; its rate of movement as compared with VII was 0.67. A ninhydrin test was negative. The product in solution was presumed to be X. Sodium metaperiodate (350 mg) in 4 ml of water was now added and the solution was stored in the dark at room temperature for 20 h. In the course of the oxidation 0.5 ml of a 0.5 *M* sodium bicarbonate solution was added in small portions maintaining the pH at 5–6. The solution was then evaporated nearly to dryness, the residue was triturated with 5 ml of ethanol, and the insoluble, inorganic material was discarded. The ethanol extract was evaporated and the residue again treated with a small amount of ethanol, whereby further inorganic material was removed. Finally, the ethanol was removed by two evaporations with methanol, and the remaining solid was taken up in about 10 ml of water in which it was sparingly soluble. Calcium carbonate (1 g) and an excess of bromine water were added and the mixture was stored in the dark at room temperature for 20 h, with occasional swirling. The solution was filtered, freed from excess bromine by aeration, shaken for 5 min with 1 g of silver carbonate, and filtered again. The filtrate was freed from cations by treatment with 5 ml of Rexyn RG-50 (H^+) and the resulting solution which was acidic and slightly yellow was cleared with activated carbon and evaporated *in vacuo*. *N*-Benzoyl-D-aspartic acid (XI) separated as colorless, small crystals of m.p. 163–164°. Recrystallization from water by slow evaporation in the air gave long needles with m.p. 170–171° (sealed capillary); the yield was 35 mg. The product (XI) showed $[\alpha]_D^{23}$ −22.3° (*c*, 1.03 in water containing 2 equiv of KOH).

A sample of the L-enantiomorph of XI was prepared (9) by *N*-benzoylation of authentic L-aspartic acid. It also was obtained as small crystals (m.p. 163–164°) or as long needles (m.p. 170–171°, sealed capillary),

Can. J. Chem. Downloaded from www.nrcresearchpress.com by 210.87.254.6 on 09/05/12
For personal use only.

depending on the mode of crystallization. The reported (9) m.p. of 180–181° was not observed. The two enantiomorphs moved at the same rate on a thin-layer plate and gave superimposable infrared spectra.

The L-enantiomorph exhibited $[\alpha]_D^{23}$ +34.5° (reported, +33° (4); +37.4° (9); all in water in the presence of 2 equiv of KOH). When a sample was treated in aqueous solution with silver carbonate and recovered by cation exchange and evaporation (as in the work-up procedure of XI), the rotation value decreased to +25.5°.

Solvolysis of Dimesylate IX

Dimesylate IX (190 mg) and anhydrous sodium acetate (230 mg) were refluxed for 48 h in 20 ml of 95% ethanol. Upon cooling, only starting material crystallized out. The solvent was therefore replaced by 20 ml of 95% 2-methoxyethanol, and another 150 mg of sodium acetate was added. After being refluxed for a further 48 h and concentrated *in vacuo* to 15 ml the brownish solution, on standing overnight at 4°, deposited 61 mg of sodium mesylate (calcd. for 1 molar equiv, 59.7 mg) which was identified by its infrared spectrum. Attempts to obtain a crystalline sugar derivative from the mother liquor either directly or by acetylation or remesylation were unsuccessful.

Preparation of the Deoxynitro L-*Hexopyranoside Derivatives XIII, XIV, and XV*

Glycosidation of L-arabinose was performed in 7 g batches using methanol containing 0.036% of hydrogen chloride according to Augestad and Berner's directions (12). The sirupy glycoside mixture was separated in 2 g batches on a column (3.5 × 60 cm) of powdered cellulose with ethylmethylketone saturated with water. The fractions (12 ml) were checked polarimetrically. In one such chromatography, for example, fractions No. 70–90 (levorotatory) were combined, fractions No. 91–99 were returned to a later chromatography, and fractions No. 100–120 (dextrorotatory) were combined. Both the combined levorotatory and the combined dextrorotatory fractions upon evaporation yielded colorless sirups that crystallized without difficulty when triturated with small amounts of ethyl acetate and when allowed to stand in a refrigerator overnight. The glycosides, which were very hygroscopic, had to be filtered and washed quickly and with the least possible exposure to moist air. Recrystallization from ethyl acetate of the dextrorotary material gave *methyl β-*L*-arabinofuranoside*, m.p. 56°, $[\alpha]_D^{23}$ +117° (*c*, 1 in water), in excellent agreement with the literature (12). The levorotatory material, which after one recrystallization showed m.p. 52° and $[\alpha]_D$ −111° (*c*, 1 in water), was methyl α-L-arabinofuranoside although it was, apparently, not quite pure (reported data: m.p. 64–66°; 65–67°; $[\alpha]_D$ −123° (12)).

The periodate oxidation of methyl β-L-arabinofuranoside and the nitromethane condensation of the resulting dialdehyde XII were performed as previously described for the analogous experiments relating to the D-series (13, 14).

*Methyl 3-deoxy-3-nitro-β-*L*-glucopyranoside (XIII).*—The crude product obtained melted at 194 ± 3°. The product recrystallized from ethyl acetate – ethanol showed m.p. 204–205° (decomp.) and $[\alpha]_D^{23}$ +12.1° (*c*, 1 in water). Reported (13) for the D-enantiomorph: m.p. 204–205° (decomp.), $[\alpha]_D$ −12.0°, −12.8° (*c*, 2 in water). The infrared spectra of the D- and L-forms were identical. Benzylidenation of the material that remained in the mother liquor of XIII was done, and the benzylidene derivatives were separated by fractional crystallization, as described (1, 5) for the D-series.

*Methyl 4,6-O-benzylidene-3-deoxy-3-nitro-β-*L*-galactopyranoside (XIV).*—The product showed m.p. 231° (decomp.) and $[\alpha]_D^{23}$ −26.2° (*c*, 1 in dimethylformamide). Reported (5) for the D-enantiomorph: m.p. 230–231° (decomp.); $[\alpha]_D^{23}$ +24.8°. The infrared spectra of the D- and L-compounds were identical.

*Methyl 4,6-O-benzylidene-3-deoxy-3-nitro-β-*L*-mannopyranoside (XV).*—The product had m.p. 197–199°; $[\alpha]_D^{23}$ +101.5° (*c*, 1.8 in dimethylformamide). Reported (5) for the D-enantiomorph: m.p. 198–199°; $[\alpha]_D^{23}$ −105°. The infrared spectra of the D- and L-compounds were identical.

ACKNOWLEDGMENT

This work was supported by research grants AI 4697 from the National Institute of Allergy and Infectious Diseases, United States Public Health Service, and A 1350 from the National Research Council of Canada.

REFERENCES

1. H. H. Baer and T. Neilson. Can. J. Chem. **43**, 840 (1965).
2. H. Brockman. Fortschr. Chem. Org. Naturstoffe, **21**, 121 (1963).
3. H. Brockman and E. Spohler. Naturwiss. **42**, 154 (1955). H. Brockmann, E. Spohler, and T. Waehneldt. Ber. **96**, 2925 (1963).
4. F. Arcamone, G. Cassinelli, P. Orezzi, G. Franceschi, and R. Mondelli. J. Am. Chem. Soc. **86**, 5335 (1964).
5. H. H. Baer, F. Kienzle, and T. Neilson. Can. J. Chem. **43**, 1829 (1965).
6. L. D. Hall. Advan. Carbohydrate Chem. **19**, 51 (1964).
7. F. W. Lichtenthaler. Ber. **96**, 2047 (1963). M. Nakajima, A. Hasegawa, and F. Lichtenthaler. Ann. **669**, 75 (1963); **680**, 21 (1964).
8. R. U. Lemieux and B. Fraser-Reid. Can. J. Chem. **42**, 532 (1964).

Can. J. Chem. Downloaded from www.nrcresearchpress.com by 210.87.254.6 on 09/05/12
For personal use only.

9. E. FISCHER. Ber. **32**, 2451 (1899).
10. H. H. BAER. *In* Nitro compounds. Proc. Intern. Symp., Warsaw, 1963. *Edited by* T. Urbánski. Pergamon Press, Oxford and New York. 1964. pp. 263–273.
11. C. S. HUDSON. Collected papers. Academic Press, Inc., New York. 1948. Vol. II, pp. 1125–1185. R. D. Guthrie. Advan. Carbohydrate Chem. **16**, 105 (1961).
12. I. AUGESTAD and E. BERNER. Acta Chem. Scand. **8**, 251 (1954). C. T. Bishop and F. P. Cooper. Can. J. Chem. **41**, 2743 (1963).
13. H. H. BAER. Ber. **93**, 2865 (1960).
14. H. H. BAER and F. KIENZLE. Can. J. Chem. **41**, 1606 (1963).
15. H. H. BAER and H. O. L. FISCHER. J. Am. Chem. Soc. **81**, 5184 (1959).
16. K. A. WATANABE and J. J. FOX. Chem. Pharm. Bull. Tokyo, **12**, 975 (1964). K. A. WATANABE, J. BERÁNEK, H. A. FRIEDMAN, and J. J. FOX. J. Org. Chem. **30**, 2735 (1965). F. W. LICHTENTHALER, H. P. ALBRECHT, and G. OLFERMANN. Angew. Chem. **77**, 131 (1965).
17. F. G. FISCHER and H. DÖRFEL. Z. Physiol. Chem. **301**, 224 (1955). F. G. FISCHER and H. J. NEBEL. Z. Physiol. Chem. **302**, 10 (1955).

Can. J. Chem. Downloaded from www.nrcresearchpress.com by 210.87.254.6 on 09/05/12
For personal use only.

Can. J. Chem. Downloaded from www.nrcresearchpress.com by 210.87.254.40 on 09/05/12
For personal use only.

EFFECT OF CHANGING pH UPON THE RATE AND MECHANISM OF DECARBOXYLATION OF SUBSTITUTED ANTHRANILIC ACIDS

G. E. DUNN, P. LEGGATE,[1] AND I. E. SCHEFFLER[2]
Department of Chemistry, University of Manitoba, Winnipeg, Manitoba

Received May 7, 1965

ABSTRACT

The ionization constants of 4-methoxyanthranilic acid have been determined spectrophotometrically in water at 60 °C and ionic strength 0.10. The variation in rate of decarboxylation with varying pH at constant ionic strength has been measured at 90 °C with 4-methylanthranilic acid and at 60 °C with 4-methoxyanthranilic acid. With each acid the maximum rate occurs at a pH about 2 units less than the isoelectric pH. To account for these results it is necessary to postulate an equilibrium between at least two intermediates formed by protonation of the 1-position of the aromatic ring. One of these must be formed from the anion and the other(s) by protonation of neutral acid and (or) zwitterion.

A number of aromatic amino acids have been observed to undergo decarboxylation under relatively mild conditions (1).

$$NH_2ArCOOH \rightarrow ArNH_2 + CO_2$$

Mechanistic investigations have been concentrated upon anthranilic (2, 3), *p*-aminobenzoic (2, 4), and *p*-aminosalicylic acids (5, 6, 7) in aqueous solution and upon anthranilic acid in the melt (3, 8) or in nitrobenzene solution (9).

Kinetic studies in aqueous solution are complicated by the fact that the amino acid may be present as neutral molecule, zwitterion, cation, or anion, any one or more of which may decarboxylate. Although the ratio of neutral molecule to zwitterion is independent of pH, the proportions of the other species present in solution will vary with the acidity of the solution. Consequently, the rates of decarboxylation of amino acids in solution may vary with the acidity of the solution, and the manner in which they vary may be expected to yield information about the nature of the species undergoing decarboxylation.

In aqueous solutions of an amino acid there are assumed to be four organic species in equilibrium with hydronium ion (10). These may be represented in general by $H_3N^+ArCOOH$ (abbreviated H_2A^+), $H_2NArCOOH$ (HA), $H_3N^+ArCOO^-$ (Z), and $H_2NArCOO^-$ (A^-). These will be referred to hereafter as the Bjerrum species. The equilibria are shown below with the accompanying hydronium ions omitted.

[1]

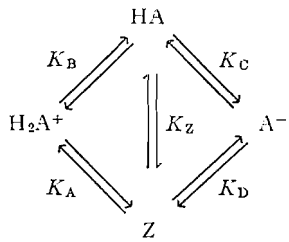

If the concentrations (or, at high ionic strengths, the activities) of HA and Z are represented by [HA] and [Z], then the concentration of total ampholyte is [N] = [HA] + [Z]. For most purposes N can be treated as a single species, since the ratio [Z]/[HA] = K_Z is independent of pH. The experimental ionization constants K_1 and K_2 define the equilibria

[1]*National Research Council Postdoctorate Fellow, 1960–1962.*
[2]*Holder of a N.R.C. Bursary, 1963–1964.*

$$H_2A^+ \overset{K_1}{\rightleftarrows} H^+ + N$$

$$N \overset{K_2}{\rightleftarrows} H^+ + A^-$$

and are related to the individual ionization constants of eq. [1] as follows.

$$K_1 = K_A + K_B$$

$$1/K_2 = 1/K_C + 1/K_D$$

From these relationships it follows that when the total concentration of amino acid is [C] the concentrations of the individual Bjerrum species are given by the equations below.

$$[H_2A^+] = \frac{[C]}{K_1K_2/[H^+]^2 + K_1/[H^+] + 1} \quad [2]$$

$$[N] = \frac{[C]}{[H^+]/K_1 + 1 + K_2/[H^+]} \quad [3]$$

$$[A^-] = \frac{[C]}{[H^+]^2/K_1K_2 + [H^+]/K_2 + 1} \quad [4]$$

These equations show that $[H_2A^+]$ approaches [C] at high hydronium ion concentrations, $[A^-]$ approaches [C] at low hydronium ion concentrations, and that [N] reaches a maximum when $[H^+]$ lies between K_1 and K_2. By setting $d[N]/d[H^+] = 0$ it is found that [N] reaches a maximum when $[H^+] = \sqrt{K_1K_2}$; that is, at the isoelectric point, where $pH = \frac{1}{2}(pK_1 + pK_2)$. Since [Z] and [HA] are both proportional to [N] and the proportionality is independent of pH it follows that both [HA] and [Z] will also have their maximum values at the isoelectric point. The variations with pH of the concentrations of the various species is shown schematically in Fig. 1.

If the rate-controlling step in the decarboxylation of an amino acid is the first-order or pseudo-first-order decomposition of any of the Bjerrum species, a plot of the rate constant against pH should show the same inflections as the concentration vs. pH plot for the corresponding species in Fig. 1. The same will be true, of course, for any other (non-Bjerrum) species in equilibrium with one of the Bjerrum species, or with one of these and water, so long as the equilibrium does not involve gain or loss of protons.

Furthermore, if the rate of decarboxylation is determined by the rate of formation or decomposition of any intermediate formed by protonation (or deprotonation) of one of the Bjerrum species, the rate constant vs. pH profile should follow the concentration vs. pH profile of the Bjerrum species next to the left (or next to the right) in eq. [1]. For example, suppose A^- can be protonated to give an intermediate AH* (non-Bjerrum) which then decarboxylates.

$$A^- + H^+ \underset{k_2}{\overset{k_1}{\rightleftarrows}} AH^*$$

$$AH^* \overset{k_3}{\rightarrow} CO_2 + P$$

The steady-state concentration of AH* will be given by

$$[AH^*] = \frac{k_1}{k_2 + k_3}[A^-][H^+]$$

and the rate of decarboxylation by

$$\frac{-d[C]}{dt} = k_3[AH^*] = \frac{k_1k_3}{k_2 + k_3}[A^-][H^+] = \frac{k_1k_3K_2}{k_2 + k_3}[N]. \quad [5]$$

Can. J. Chem. Downloaded from www.nrcresearchpress.com by 210.87.254.40 on 09/05/12
For personal use only.

Hence the observation of a maximum in the rate of decarboxylation at the pH where no maximum occurs in the concentration vs. pH curves could not be accounted for by first-order decarboxylation of any of the Bjerrum species nor of any other species formed from a Bjerrum species by simple protonation or deprotonation.

The aromatic amino acid for which the effect of pH upon rate of decarboxylation in aqueous solution has been most thoroughly examined is *p*-aminosalicylic acid. Willi and Stocker (5) found that the rate reaches a maximum at the isoelectric point and concluded that the rate-controlling step involves the protonation of *p*-aminosalicylate anion, A^-, at the 1-position of the aromatic ring. However, they found that, although the rate decreases as the pH is decreased below the isoelectric point, it does not decrease as fast as does the calculated value of $[H^+][A^-]$. They concluded, therefore, that the zwitterion is also subject to decarboxylation by proton attack at the 1-carbon, so that the overall rate expression becomes

$$[6] \qquad -\frac{d[C]}{dt} = k'[H^+][A^-] + k''[H^+][N]$$

with k' larger than k'' by a factor of about 10.

Rekker and Nauta (6) also observed a maximum in the rate of decarboxylation of *p*-aminosalicylic acid in aqueous solution at the isoelectric point, but they found no decarboxylation in strong acid where Willi's kinetic expression shows it should be appreciable. They concluded that the reaction is a first-order decarboxylation of the zwitterion.

The decarboxylation of *p*-aminosalicylic acid in aqueous solution was also investigated by Liquori and Ripamonte (7). They too, observed the rate-maximum at the isoelectric point at 25 °C, but concluded that the rate-controlling step is a first-order decomposition of the molecular acid, HA. The most interesting aspect of their work, however, is their observation that as the temperature of the reaction is increased the rate-maximum shifts towards lower pH, until at 97.4 °C the maximum occurs at a pH more than one unit less than the isoelectric pH.

The effect of acidity upon the rate of decarboxylation of anthranilic acid in aqueous solution was investigated briefly by Stevens and co-workers (3) as part of a study in which they showed that there is no carboxyl–carbon isotope effect in the reaction. They studied the rate of decarboxylation in varying concentrations of sulfuric acid at 100 °C without using buffered solutions or constant ionic strength and found a maximum rate at about 0.75 *N* sulfuric acid. Here again the rate-maximum appears to be at lower pH than the isoelectric point (3.5 at 25 °C). However, they concluded that the rate-controlling step is protonation of the zwitterion at the 1-carbon.

The most recent and most careful investigation of the pH dependence of rate of decarboxylation is that by Willi (4) using *p*-aminobenzoic acid. He found that the rate of decarboxylation increases with increasing hydrogen-ion concentration but does not reach a maximum at the isoelectric point (pH = 3) nor even at pH = 1.7, the highest acidity studied. He showed that, as with *p*-aminosalicylic acid, his data can be accommodated by eq. [6] with $k'' = 25k'$. However, since rates were not measured at high acidity this conclusion is open to the same objection raised by Rekker and Nauta regarding *p*-aminosalicylic acid (6).

In summary, there seems to be good reason to believe that the occurrence of a rate-maximum at the isoelectric point of *p*-aminosalicylic acid at temperatures in the vicinity of 20 °C is only a special case, and that for another amino acid and (or) another temperature the maximum rate may occur at a pH other than the isoelectric point. If this is true,

Can. J. Chem. Downloaded from www.nrcresearchpress.com by 210.87.254.40 on 09/05/12
For personal use only.

the mechanism of decarboxylation must be considerably more complex than any suggested by previous authors or any of those outlined in the discussion above. It is the purpose of the present investigation to test this hypothesis by determining the effect of changing pH upon the rate of decarboxylation of substituted anthranilic acid in buffered aqueous solutions of constant ionic strength. Decarboxylation of anthranilic acid is inconveniently slow, but 4-methylanthranilic acid decarboxylates at convenient rates at 90 °C and preliminary studies were made with this acid. However, measurement of the ionization constants at 90° proved difficult, so the main investigation used 4-methoxyanthranilic acid, for which both rates and ionization constants can be conveniently measured at 60°.

EXPERIMENTAL

Materials

The preparation and purification of 4-methyl and 4-methoxy anthranilic acids were reported in an earlier paper (11).

Buffer Solutions

Buffer solutions were prepared as suggested by Bates (12) using acetate in the pH region 5.6–5, formate in the region 5–3.5, chloroacetate in the region 3.5–2.5, and hydrochloric acid for pH's less than 2. Each buffer was adjusted to ionic strength 0.10 or 0.50 with potassium chloride.

pH Measurements

All pH measurements were made with a Radiometer model 4C pH meter with shielded glass and calomel electrodes in cells thermostatted to ±0.1 °C. At 25° the electrodes were Radiometer G202B (glass) and K100 (calomel); at 60° they were Radiometer G302BH (glass) and K4016 (calomel). The meter was calibrated against N.B.S. tetroxalate and hydrogen phthalate buffers at the appropriate temperatures. Measured pH's were reproducible to ±0.003 pH unit and are assumed to be accurate to ±0.01 unit.

pH measurements were made at both 25° and 60° on the same series of buffer solutions covering the range of each buffer compound and having the same composition as those used for ionization and rate determinations. By plotting pH at 60° against pH at 25° linear calibration curves were obtained which could be used to calculate from measurements made at 25° the pH of solutions to be used for equilibrium constant or rate determinations at 60°. Differences in pH at the two temperatures were usually less than 0.1 pH unit.

Absorbance

Measurements of absorbance were made in 1 cm cells thermostatted within ±1 °C using a Beckman model DK-1 spectrophotometer and the procedure previously described (11). Measurements were reproducible within ±0.01 unit of absorbance.

Determination of Ionization Constants

Determination of the ionization constants of 4-methyl- and 4-methoxyanthranilic acids at 25° by a spectrophotometric method was reported in an earlier paper (11). Attempts to use the same method at 90° were hampered by instability of the electrodes used for pH measurements at the high temperature and by difficulties encountered in thermostatting the cell compartment of the spectrophotometer at 90°. However, these difficulties were greatly reduced at 60°. The spectrophotometer cell compartment could be thermostatted to ±1° and pH readings on a particular buffer solution were constant and reproducible within ±0.004 unit over a period of 3 to 4 h. Consequently, the previously described method (11) was used to determine the ionization constants of 4-methoxyanthranilic acid at 60°. At pH's less than 2, absorbance readings at 60° decreased slightly with time because of decarboxylation. In these cases the readings were recorded over a period of about 10 min and back-extrapolated to zero time. Absorbance measurements were made at 330 mμ where the absorbance vs. pH curve shows a maximum at the isoelectric point.

Rate Measurements

The change in concentration of substituted anthranilic acid with time was followed spectrophotometrically by measurements made in alkaline solution where all the acid is in the anionic form, and at wavelengths where the absorbance of the reaction product is negligible. These were 322 mμ for 4-methylanthranilic acid and 315 mμ for 4-methoxyanthranilic acid.

A 250 ml round-bottom flask immersed to the neck in an oil bath at 60.0 ± 0.1° or 90.0 ± 0.1° served as the reaction vessel. The flask with 200 ml of buffer solution was allowed to come to the bath temperature, then 130 mg of the substituted anthranilic acid dissolved in 3 ml of 0.25 *N* sodium hydroxide solution were added. The flask was shaken and, after 10 min, 30 ml of solution were withdrawn and cooled to 25° for pH measurement. Two more 30 ml samples were withdrawn for pH measurement, one at the middle and one at the end of the run. The three samples had the same pH within 0.005 unit in all the runs reported below. Some attempted runs with chloroacetate buffers at 90° had to be abandoned because of pH changes during the run

Can. J. Chem. Downloaded from www.nrcresearchpress.com by 210.87.254.40 on 09/05/12
For personal use only.

caused, probably, by hydrolysis of the halogen. At approximately equal time intervals 2 ml aliquots were withdrawn for absorbance measurement and immediately injected into weighed 25 ml volumetric flasks containing about 15 ml of 0.1 *N* sodium hydroxide solution each. The volumetric flasks were reweighed, then filled to the mark with 0.1 *N* sodium hydroxide and set aside for spectrophotometric measurement at 25°. Absorbances were corrected to correspond to a constant weight of aliquot. First-order plots of the logarithm of absorbance against time gave excellent fits up to more than 90% conversion.

RESULTS

Ionization Constants

Determinations were made on two different samples of 4-methoxyanthranilic acid at 60° and ionic strength 0.10. Table I reports for each sample the resulting K's and pK's with their standard deviations and the two values for the absorbance, D_N, of the ampholyte, N, which are obtained, one in the calculation of K_1 and the other in the calculation of K_2. Details of the calculations are given in ref. 11.

The weighted means for the two samples are $K_1 = (1.15 \pm 0.10) \times 10^{-2}$, $K_2 = (1.97 \pm 0.09) \times 10^{-5}$ and $pK_1 = 1.94 \pm 0.05$, $pK_2 = 4.71 \pm 0.02$. These may be compared with the corresponding values obtained (11) by the same method at 25°: $K_1 = (8.74 \pm 0.94) \times 10^{-3}$, $K_2 = (1.33 \pm 0.07) \times 10^{-5}$ and $pK_1 = 2.06 \pm 0.05$, $pK_2 = 4.88 \pm 0.02$. From these values the pH at the isoelectric point is found to be 3.33 ± 0.03 at 60° and 3.47 ± 0.04 at 25°.

Rates of Decarboxylation

The best values of the specific rate constants, k, and their standard deviations were obtained by fitting the data to the equation $[C] = [C]_0 e^{-kt}$ by the least squares method and assuming a constant experimental uncertainty in [C] and t.

TABLE I

Dissociation constants of 4-methoxyanthranilic acid at 60 °C, $\mu = 0.10$

Sample	$K_1 \times 10^2$ (pK_1)	$K_2 \times 10^5$ (pK_2)	D_N From K_1	D_N From K_2
1	1.175±0.124 (1.93±0.05)	2.030±0.139 (4.69±0.03)	0.878±0.039	0.870±0.010
2	0.813±0.412 (2.09±0.30)	1.861±0.193 (4.73±0.05)	1.130±0.180	1.058±0.010

TABLE II

Rates of decarboxylation of 4-methylanthranilic acid at 90 °C, $\mu = 0.10$

Buffer	pH at 25 °C	$k \times 10^3$, s^{-1}
Formate	3.57	2.02±0.06
Formate	3.52	2.07±0.04
Formate	3.22	2.23±0.06
Formate	3.21	2.23±0.04
Formate	3.08	2.39±0.04
Formate	3.05	2.41±0.04
Formate	3.00	2.40±0.05
HCl	1.54	8.50±0.05
HCl	1.54	8.31±0.05
HCl	1.54	7.91±0.11
HCl	1.25	9.42±0.05
HCl	1.25	9.37±0.04
HCl	1.25	9.36±0.06
HCl	1.10	9.69±0.04
HCl	1.10	9.73±0.06
HCl	1.09	9.73±0.04
HCl	1 *N*	4.26±0.11

Can. J. Chem. Downloaded from www.nrcresearchpress.com by 210.87.254.40 on 09/05/12
For personal use only.

Can. J. Chem. Downloaded from www.nrcresearchpress.com by 210.87.254.40 on 09/05/12
For personal use only.

Table II records the rates obtained in some preliminary experiments on the decarboxylation of 4-methylanthranilic acid at 90° in buffered solutions with pH measured at 25°. The data are fragmentary because the difficulty in determining the ionization constants of the acid at 90° forced the discontinuation of experiments with the 4-methyl acid. However, enough data are available to show the reproducibility of the method and that the rate is a maximum at an intermediate pH and decreases at both high and low pH. The pH at the maximum can not be determined precisely because of the lack of data at low pH and because the pH's were measured at 25° instead of 90°. However, the pH's of buffers similar to these were found to increase in pH by less than 0.1 unit on changing temperature from 25° to 60°, so it is safe to say that the maximum rate occurs at a pH less than 1. The pH at the isoelectric point of 4-methylanthranilic acid at 25° is 3.71 (11) and, since the isoelectric pH of 4-methoxyanthranilic acid was shown above to increase by 0.14 unit on changing from 25° to 60°, it is probable that the isoelectric pH of 4-methylanthranilic acid at 90° is slightly greater than 3.7. Hence, it may be concluded that the rate of decarboxylation of 4-methylanthranilic acid is a maximum at a pH nearly three units less than the isoelectric pH.

Table III shows the variation with pH in the rate of decarboxylation of 4-methoxyanthranilic acid at 60° in buffers of ionic strength 0.10. The minimum pH attainable at this ionic strength is about 1.1 but within this limit it is seen that the rate increases as pH decreases.

TABLE III

Rates of decarboxylation of 4-methoxyanthranilic acid at 60 °C, $\mu = 0.10$

Buffer*	pH of the solution†		$k \times 10^4$, s^{-1}
	At 25 °C	At 60 °C	
HCl	1.14	1.18	1.77±0.02
HCl	1.39	1.44	1.70±0.02
HCl	1.60	1.65	1.52±0.02
HCl	1.73	1.78	1.39±0.01
HCl	2.00	2.06	1.05±0.02
ACl (0.04)	1.98	2.07	1.05±0.02
ACl (0.04)	2.11	2.21	1.02±0.04
ACl (0.04)	2.19	2.29	0.818±0.004
ACl (0.04)	2.42	2.52	0.609±0.006
ACl (0.04)	2.44	2.54	0.593±0.006
ACl (0.03)	2.17	2.27	0.859±0.006
ACl (0.03)	2.21	2.31	0.781±0.013
ACl (0.03)	2.44	2.54	0.573±0.016 0.585±0.006
ACl (0.03)	2.77	2.87	0.392±0.007
F (0.04)	2.93	3.00	0.338±0.005
F (0.04)	3.13	3.20	0.279±0.014
A	4.9		Very small

*The symbols A, ACl, and F refer to acetate, chloroacetate, and formate buffers, respectively. The numbers in parentheses represent the total molarity of buffer acid and buffer salt.
†A constant uncertainty of 0.01 in pH at 60 °C is assumed.

To reach lower pH values it is necessary to increase the ionic strength of the buffers, and Table IV shows the variation in rate of decarboxylation of 4-methoxyanthranilic acid at 60° in solutions of ionic strength 0.50. The data of both Tables III and IV are plotted in Fig. 1, where a definite peak in the rate is observed in the vicinity of pH = 1.3 at ionic strength 0.50, and it becomes evident that the curve for ionic strength 0.10 must have a maximum at about pH = 1. Since pH = 3.3 at the isoelectric point of this acid at this

TABLE IV

Rates of decarboxylation of 4-methoxyanthranilic acid at 60 °C, $\mu = 0.50$

Buffer*	pH of the solution† At 25 °C	At 60 °C	$k \times 10^4$, s^{-1}
F (0.2)	3.78	3.80	0.305±0.005
F (0.04)	3.76	3.77	0.242±0.001
F (0.2)	3.57	3.58	0.321±0.002
F (0.2)	3.38	3.40	0.337±0.003
F (0.04)	3.38	3.40	0.285±0.006
ACl (0.2)	3.38	3.48	0.305±0.003
ACl (0.2)	3.10	3.19	0.349±0.003
			0.360±0.004
ACl (0.05)	3.08	3.17	0.325±0.004
ACl (0.2)	2.95	3.04	0.359±0.006
F (0.2)	2.99	3.03	0.417±0.001
F (0.2)	2.92	2.96	0.427±0.004
ACl (0.2)	2.87	2.95	0.407±0.005
ACl (0.04)	2.53	2.61	0.601±0.002
ACl (0.2)	2.39	2.47	0.749±0.005
ACl (0.04)	2.28	2.39	0.803±0.012
ACl (0.2)	2.20	2.30	0.907±0.004
ACl (0.2)	1.99	2.09	1.20±0.007
ACl (0.2)	1.95	2.05	1.13±0.006
HCl	1.59	1.62	1.65±0.008
HCl	1.55	1.58	1.70±0.007
HCl	1.38	1.40	1.77±0.01
HCl	1.11	1.14	1.79±0.01
HCl	1.11	1.13	1.77±0.01
HCl	0.94	0.96	1.58±0.02
HCl	0.84	0.86	1.51±0.008
HCl	0.80	0.83	1.46±0.007
HCl	0.62	0.64	1.13±0.01
HCl	0.50	0.52	1.00±0.01
HCl	0.49	0.51	1.04±0.01
HCl	0.42	0.44	0.865±0.012
HCl	0.41	0.43	0.843±0.005
HCl	1 *N*		0.502±0.012
HCl	2 *N*		0.216±0.010

*The symbols ACl and F refer to chloroacetate and formate buffers, respectively. The numbers in parentheses represent the total molarity of buffer acid and buffer salt.
†A constant uncertainty of 0.01 in pH at 60 °C is assumed.

temperature and ionic strength, it is clear that the rate vs. pH profile does not fit any of the concentration vs. pH relationships described in the introduction.

Figure 1 also shows that on the high pH side of the peak, where rates were measured at two ionic strengths, the rate of decarboxylation at a given pH is greater at the higher ionic strength. The data do not permit a definite conclusion, but the shape of the curves suggests that the effect of decreasing ionic strength is to shift the position of the rate-maximum toward lower pH, and consequently, that on the low pH side of the peak rates would be greater at the lower ionic strength.

Figure 2 shows the results of an attempt to estimate the importance of general acid catalysis in the decarboxylation. Rate constants obtained in the same pH region using buffers of the same ionic strength but different buffer capacity are plotted against pH. To minimize errors in rate caused by errors in pH, measurements are made in the high pH region where the rate of change of rate constant with respect to pH is small. It is seen that the rate does vary with the nature of the buffering acid and with the concentration of a single buffer. The effect is small, however, and difficult to evaluate quantitatively. It was also demonstrated that general acid catalysis is very small at a pH near the peak in the rate vs. pH curve by measuring the rate of decarboxylation in a buffer made up of 0.05 *N*

Can. J. Chem. Downloaded from www.nrcresearchpress.com by 210.87.254.40 on 09/05/12
For personal use only.

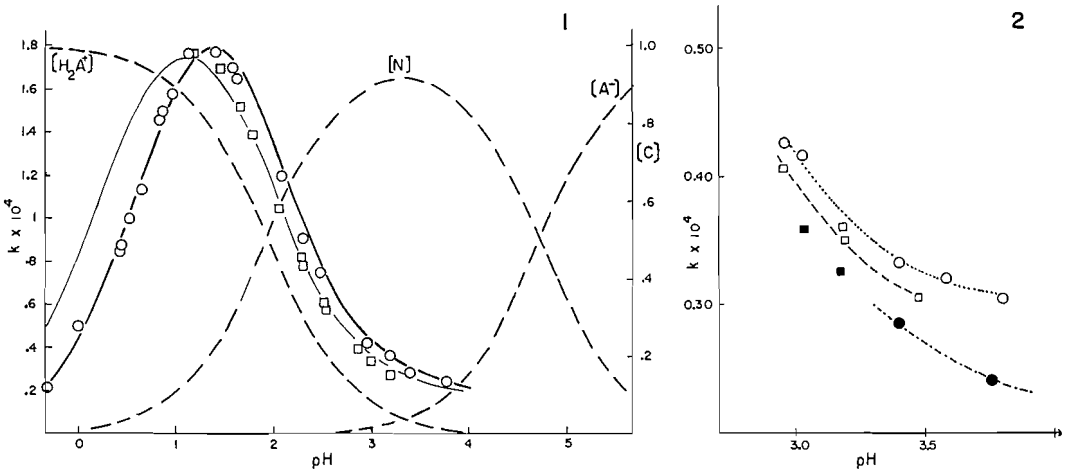

FIG. 1. Comparison between pH dependence of substrate concentration and pH dependence of rate constant for decarboxylation of 4-methoxyanthranilic acid at 60 °C. ○ Experimental rate constants at ionic strength 0.50; □ rate constants at ionic strength 0.10; ——— concentration of Bjerrum species; ▬▬ rate constants calculated from eq. [14], at $\mu = 0.50$; ——— rates constants calculated from eq. [14], at $\mu = 0.10$.

FIG. 2. Dependence of rate constant for decarboxylation of 4-methoxyanthranilic acid at 60 °C upon buffer acid and buffer capacity. ○ 0.20 *N* formate buffer; ● 0.04 *N* formate buffer; □ 0.20 *N* chloroacetate buffer; ■ 0.05 *N* chloroacetate buffer.

HCl and 0.05 *N* chloroacetic acid ($\mu = 0.10$, pH = 1.41 at 60°). The rate constant, $(1.77 \pm 0.02) \times 10^{-4}$ s^{-1}, obtained in this buffer may be compared with the value of 1.70×10^{-4} s^{-1} obtained by interpolation in the curve for a HCl buffer of the same pH and ionic strength. The effect of the chloroacetic acid (undissociated at this pH) is seen to be very small.

DISCUSSION

It will be noted that the shape of the rate vs. pH curve is very similar to that of the [N] vs. pH curve. Each has a maximum at intermediate pH and approaches zero at either end of the pH scale, but the rate curve is displaced toward lower pH. There are three obvious possibilities which might account for this discrepancy.

1. The reaction involves simultaneous decarboxylation of two or more Bjerrum species.
2. Decarboxylation results from a reaction between different Bjerrum species.
3. A fifth Bjerrum species is formed by further protonation of the cation.

The first possibility is the one suggested by Willi (4, 5) and requires a rate expression of the form:

$$[6] \qquad \frac{-\mathrm{d[C]}}{\mathrm{d}t} = k[\mathrm{C}] = k_1[\mathrm{H_2A^+}] + k_2[\mathrm{N}]$$

or its kinetic equivalent. Substituting eq. [2] and [3] into this gives:

$$k = \frac{k_1}{1 + K_1/[\mathrm{H^+}] + K_1K_2/[\mathrm{H^+}]^2} + \frac{k_2}{[\mathrm{H^+}]/K_1 + 1 + K_2/[\mathrm{H^+}]}.$$

In the region of the maximum rate $[\mathrm{H^+}] = 0.1$ approximately. Since K_2 is about 2×10^{-5}, the terms involving $K_2/[\mathrm{H^+}]$ are not important in this region and

$$k = \frac{k_1[\mathrm{H^+}] + k_2K_1}{[\mathrm{H^+}] + K_1}.$$

The slope of the plot of k against $[\mathrm{H^+}]$ is given by:

$$\frac{\mathrm{d}k}{\mathrm{d}[\mathrm{H^+}]} = \frac{K_1(k_1 - k_2)}{([\mathrm{H^+}] + K_1)^2}.$$

Can. J. Chem. Downloaded from www.nrcresearchpress.com by 210.87.254.40 on 09/05/12
For personal use only.

That is, the slope is zero only when $k_1 = k_2$, and when this is true the slope is zero at all pH values where the approximation is valid. Hence, the concurrent decarboxylation of two Bjerrum species cannot account for the observed pH at the rate maximum.

The second possibility suggests a rate expression of the form:

$$\frac{-\mathrm{d}[\mathrm{C}]}{\mathrm{d}t} = k[\mathrm{H_2A^+}][\mathrm{N}].$$

Since $[H_2A^+]$ approaches zero at high pH and [N] approaches zero at low pH, this equation predicts a maximum rate at a pH intermediate between those where $[H_2A^+]$ and [N] are maximum, but it also predicts that the rate at a given pH will be second order with respect to [C]. Since the reaction is distinctly first order, a reaction between two Bjerrum species cannot account for the observed kinetics.

The third of the possible interpretations suggests that the species undergoing decarboxylation is the cation, H_2A^+, but that at low pH this is further protonated to a doubly charged cation, H_3A^{2+}, which does not decarboxylate. The concentration of H_2A^+ would then reach a maximum at a pH between pK_1 and the pK of the new protonation. The possible sites for the new protonation are the carboxyl group or the substituent. However, carboxyl groups of aromatic acids are not appreciably protonated in the pH range under consideration here (13). Furthermore, the rate maximum at low pH is observed with 4-methyl as well as with 4-methoxy substituents, and the former is certainly not subject to protonation on the substituent. Hence, the position of the rate maximum cannot be explained by the appearance of a fifth Bjerrum species.

Since the pH at the rate maximum cannot be accounted for by reaction of any combination of Bjerrum species, decarboxylation must take place by way of an intermediate not part of the Bjerrum system. It was shown in the introduction that decarboxylation of a non-Bjerrum intermediate formed by protonation of a Bjerrum species would have a rate profile corresponding to the concentration profile of the next Bjerrum species. However, it will be noted that if either (but not both) of the terms in the denominator of eq. [5] contained $[H^+]$ the rate vs. pH profile would differ from the concentration profile of any of the Bjerrum species. This would require that the decomposition of the non-Bjerrum intermediate, AH*, involve two competing processes, one (but not both) of which must involve attack by proton upon the intermediate. The question then arises whether or not such a mechanism can be accommodated to the other known characteristics of the decarboxylation and structure of anthranilic acids.

The ease of decarboxylation increases in the order anthranilic < 4-methylanthranilic < 4-methoxyanthranilic acid, showing that the reaction is facilitated by a high electron density on the aromatic ring.[3] Decarboxylation involves the breaking of C—C and O—H bonds and the making of a C—H bond at the 1-carbon of the aromatic ring. Of these, only the last is facilitated by a high electron density on the aromatic ring. This suggests that the non-Bjerrum intermediate, HA*, is formed by protonation of a Bjerrum species at the 1-carbon.

After the ring is protonated two competing reactions will be loss of ring-proton and loss of carbon dioxide. One of these, but not both, must be brought about by a second proton attack. Thus, one of the competing reactions involves two successive protonations of a Bjerrum species. Obviously, the species most likely to play this role is the anion, A^-, but in principle either the neutral acid, HA, or the zwitterion, Z, could serve. Equation [7] below

[3]*Another possible interpretation would be that the order of increasing rates reflects an increase or decrease in percent zwitterion. However, eq. [20] of ref. 11 and the ρ values given there may be used to show that the order of increasing percent zwitterion is 4-methyl- > 4-methoxy- > anthranilic acid.*

Can. J. Chem. Downloaded from www.nrcresearchpress.com by 210.87.254.40 on 09/05/12
For personal use only.

[7]

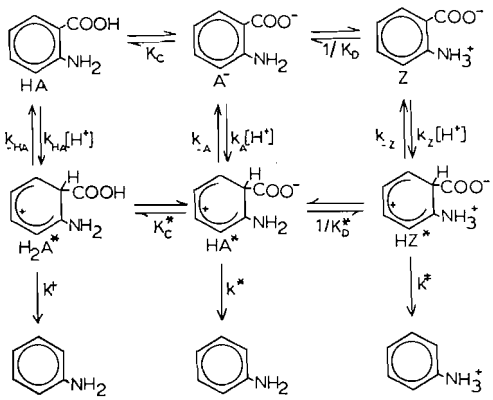

shows the structures of the non-Bjerrum intermediates, H_2A^*, HA*, and HZ*, which would be formed by ring-protonation of each of the species HA, A^-, and Z, respectively. Obviously the non-Bjerrum species are directly interconvertable by gain or loss of proton from the carboxyl groups of H_2A^* and HA* or the amino groups of HZ* and HA*. This interconversion constitutes the second protonation reaction which was postulated above in order to account for the shift in pH of the rate maximum. It should be rapid compared to the ring protonations, so it has been represented in eq. [7] as a pair of equilibria, K_C^* and K_D^*.

In the most general case we may suppose that all three intermediates decarboxylate. The overall rate expression may then be arrived at by calculating the total concentration of all three intermediates in the steady state.

Let $$[H_2A^*] + [HA^*] + [HZ^*] = [X].$$

Introducing the constants for equilibrium between intermediates from eq. [7] gives

$$[HA^*]\,([H^+]/K_C^* + 1 + [H^+]/K_D^*) = [X].$$

Letting the expression in parentheses $= Q$ leads to

$$[HA^*] = [X]/Q,$$

$$[H_2A^*] = [H^+][X]/K_C^*Q,$$

$$[HZ^*] = [H^+][X]/K_D^*Q.$$

The steady-state assumption for [X] is

$$\frac{d[X]}{dt} = k_{HA}[HA][H^+] + k_A[A^-][H^+] + k_Z[Z][H^+] - (k^+ + k_{-HA})[H_2A^*] - (k^* + k_{-A})[HA^*] - (k^{\mp} + k_{-Z})[HZ^*] = 0$$

which has as its solution

$$[X] = Q \times \frac{k_{HA}[HA][H^+] + k_A[A^-][H^+] + k_Z[Z][H^+]}{(k^+ + k_{-HA})[H^+]/K_C^* + (k^* + k_{-A}) + (k^{\mp} + k_{-Z})[H^+]/K_D^*}$$

$$= Q[N]\frac{k_AK_2 + (k_{HA}K_B/K_1 + k_ZK_A/K_1)[H^+]}{k^* + k_{-A} + \{(k^+ + k_{-HA})/K_C^* + (k^{\mp} + k_{-Z})/K_D^*\}[H^+]}.$$

Can. J. Chem. Downloaded from www.nrcresearchpress.com by 210.87.254.40 on 09/05/12
For personal use only.

Can. J. Chem. Downloaded from www.nrcresearchpress.com by 210.87.254.40 on 09/05/12
For personal use only.

The rate of decarboxylation is then

$$[8]\qquad \frac{-d[C]}{dt} = k^*[HA^*] + k^+[H_2A^*] + k^{\mp}[HZ^*]$$

$$= \frac{[X]}{Q}\{k^* + (k^+/K_C^* + k^{\mp}/K_D^*)[H^+]\}$$

$$= [N]\{k_A K_2 + (k_{HA}K_B/K_1 + k_Z K_A/K_1)[H^+]\} \times \frac{k^* + (k^+/K_C^* + k^{\mp}/K_D^*)[H^+]}{k^* + k_{-A} + \{(k^+ + k_{-HA})/K_C^* + (k^{\mp} + k_{-Z})/K_D^*\}[H^+]}.$$

This general expression for the rate of decarboxylation via non-Bjerrum intermediates reduces to the equivalent of eq. [6] in either of two special cases: first, if the rate of decarboxylation greatly exceeds the rate of deprotonation for all three intermediates (i.e. $k^+ \gg k_{-HA}$, $k^* \gg k_{-A}$, $k^{\mp} \gg k_{-Z}$); second, if the rate of deprotonation greatly exceeds the rate of decarboxylation for all three (i.e. $K_C^* k_{HA}/k_{-HA} = K_C k_A/k_{-A}$, $K_D^* k_Z/k_{-Z} = K_D k_A/k_{-A}$). Since eq. [6] does not fit the data, evidently neither of these conditions is met.

As it stands, eq. [8] does not fit the data either, because the $[H^+]^2$ terms of the numerator prevent the rate from becoming small at low pH. For the rate to decrease at low pH will require either that k_{HA} and $K_Z = 0$ or that k^+ and $k^{\mp} = 0$, but not both. That is, in order for eq. [7] to represent the mechanism one or both of H_2A^* and HZ^* must participate, but either they are not formed directly by protonation of HA and Z or they do not decarboxylate. In the former case the mechanism becomes

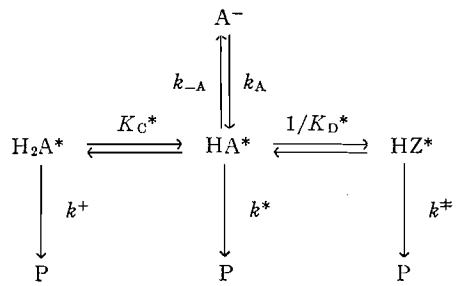

$$[9]\qquad \frac{-d[C]}{dt} = [N]k_A K_2 \frac{k^* + (k^+/K_C^* + k^{\mp}/K_D^*)[H^+]}{k^* + k_{-A} + \{(k^+ + k_{-HA})/K_C^* + (k^{\mp} + k_{-Z})/K_D^*\}[H^+]}$$

and in the latter case it is

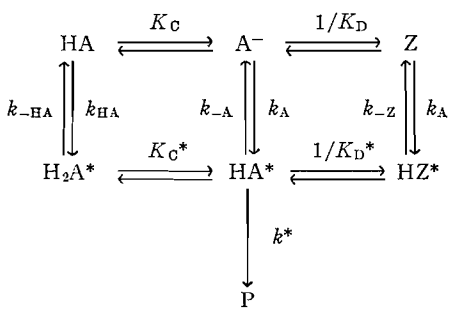

$$[10]\qquad \frac{-d[C]}{dt} = [N]k^* \frac{k_A K_2 + (k_{HA}K_B/K_1 + k_Z K_A/K_1)[H^+]}{k^* + k_{-A} + (k_{-HA}/K_C^* + k_{-Z}/K_D^*)[H^+]}.$$

Can. J. Chem. Downloaded from www.nrcresearchpress.com by 210.87.254.40 on 09/05/12
For personal use only.

It is difficult to decide which is the more likely. H_2A^* should be more stable than HZ^* because the amino group can help to distribute the positive charge in H_2A^* but not in HZ^*. That is, H_2A^* should be more easily formed but less easily decarboxylated, so that the former alternative (eq. [9]) would seem more reasonable for HZ^* but the latter (eq. [10]) would be more likely for H_2A^*. These considerations can be accommodated as special cases of the general mechanism if only one of HZ^* or H_2A^* is formed in significant concentration.

If only HZ^* is involved, eq. [9] reduces to

$$[11] \qquad \frac{-d[C]}{dt} = [N]k_A K_2 \frac{k^* + (k^{\ddagger}/K_D^*)[H^+]}{k^* + k_{-A} + (k^{\ddagger}/K_D^*)[H^+]}$$

and if only H_2A^* participates, eq. [10] becomes

$$[12] \qquad \frac{-d[C]}{dt} = [N]k^* \frac{k_A K_2 + (k_{HA}K_B)/K_1)[H^+]}{k^* + k_{-A} + (k_{-HA}/K_C^*)[H^+]}.$$

All four equations [9–12] are of the general form

$$[13] \qquad \frac{-d[C]}{dt} = [N]\frac{a + b[H^+]}{c + d[H^+]}$$

which, with suitable values of the constants, can be fitted to the data.

In order to estimate a, b, c, and d for 4-methoxyanthranilic acid it is necessary to expand eq. [13]. Substituting into it the value of [N] from eq. [3] gives:

$$\frac{-d[C]}{dt} = k[C] = \frac{a + b[H^+]}{c + d[H^+]} \times \frac{[C]}{[H^+]/K_1 + 1 + K_2/[H^+]}$$

or

$$[14] \qquad k = \frac{b}{d} \times \frac{a/b + [H^+]}{c/d + [H^+]} \times \frac{1}{[H^+]/K_1 + 1 + K_2/[H^+]}.$$

Since $K_2 \cong 2 \times 10^{-5}$, the last term in the denominator will be negligible compared to 1 when $[H^+]$ is larger than 2×10^{-3} M (or pH is less than 2.7) which includes almost the whole pH range over which rates were measured. Equation [14] can therefore be simplified to:

$$[15] \qquad k = \frac{b}{d} \times \frac{a/b + [H^+]}{c/d + [H^+]} \times \frac{K_1}{[H^+] + K_1}.$$

Setting $dk/d[H^+] = 0$ gives:

$$[16] \qquad \frac{a}{b} = \frac{K_1 c/d - [H^+]_{max}^2}{c/d + 2[H^+]_{max} + K_1},$$

where $[H^+]_{max}$ is the hydrogen ion activity at the maximum rate. Since a/b is a ratio of sums of rate constants it can not be negative; therefore, c/d must be larger than $[H^+]_{max}^2/K_1$. From Fig. 1 the pH at the rate-maximum may be estimated to be 1.1 at $\mu = 0.10$, which makes $[H^+]_{max} = 0.794$ M; K_1 at this ionic strength is 1.15×10^{-2}, so that c/d must be larger than 0.548. Since $[H^+]$ is much less than 0.548 over the whole range of rates studied at $\mu = 0.10$, $(c/d + H^+)$ may be set equal to c/d, so that eq. [15] becomes:

$$k = \frac{bK_1}{c} \times \frac{a/b + [H^+]}{K_1 + [H^+]}$$

which can be rearranged to

$$[17] \qquad k\frac{K_1 + [H^+]}{K_1} = \frac{a}{c} + \frac{b}{c}[H^+].$$

Fig. 3 shows a plot of the left-hand side of eq. [17] against $[H^+]$, using the data of Table III, from the slope and intercept of which $b/c = 1.90 \times 10^{-2}$ and $a/c = 2.03 \times 10^{-5}$, respectively. Dividing one by the other gives $a/b = 1.07 \times 10^{-3}$. Substituting this value of a/b

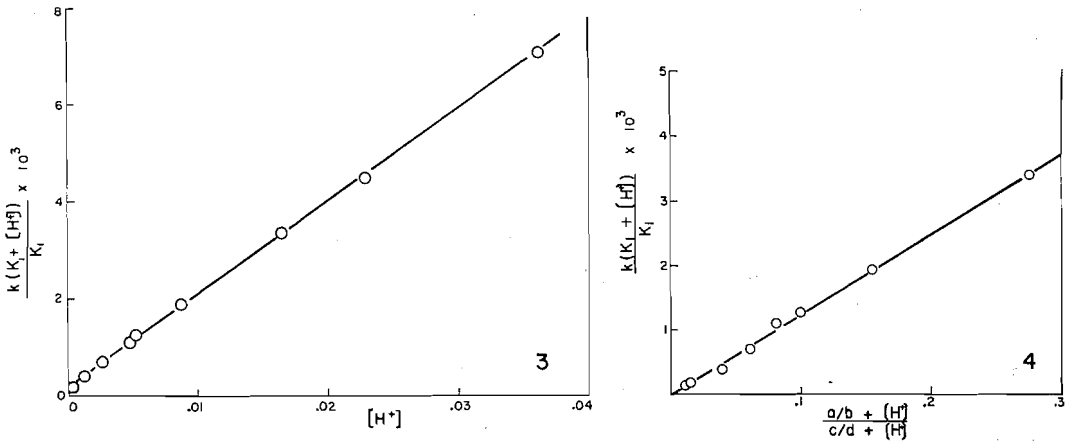

FIG. 3. Test of eq. [17]. Slope = b/c; intercept = a/c.
FIG. 4. Test of eq. [15]. Slope = b/d.

into eq. [16] gives $c/d = 0.622$, and using these values of a/b and c/d in a plot of eq. [15] (Fig. 4) gives a straight line with slope $b/d = 1.23 \times 10^{-2}$. Figure 1 compares the experimental points with the curve k vs. pH calculated from eq. [14] using the above values of a/b, c/d, and b/d. The fit is good but because experimental points are available only on one side of the peak, it is not possible to say whether eq. [14] adequately represents the data.

An adequate test of eq. [14] would require that the above calculations be repeated at $\mu = 0.50$ where rates are available on both sides of the peak. Since K_1 and K_2 were not measured at $\mu = 0.50$, it will be necessary to estimate them by an extrapolation of the Debye–Hückel theory to this range of ionic strengths. If it is assumed that the glass electrode measures hydrogen-ion activity and that ionic strength will have little effect on the activity of the neutral species, HA, then it follows that:

$$(K_1)_{0.5} = (K_1)_{0.1}\frac{(f_{H_2A^+})_{0.5}}{(f_{H_2A^+})_{0.1}} \quad \text{and} \quad (K_2)_{0.5} = (K_2)_{0.1}\frac{(f_{A^-})_{0.1}}{(f_{A^-})_{0.5}}$$

where K represents observed ionization constant, f represents activity coefficient, and the subscripts outside parentheses refer to ionic strengths. Introducing the simple Debye–Hückel relationship for activity coefficient in aqueous solution

$$-\log f = \frac{\sqrt{0.5\mu}}{1 + 1.6\sqrt{\mu}}$$

gives $(K_1)_{0.5} = 1.00 \times 10^{-2}$ and $(K_2)_{0.5} = 2.27 \times 10^{-5}$.

These small changes in equilibrium constant with ionic strength have a very small effect on the calculated values of a/b, c/d, and b/d, but the observed change in the pH at the rate-maximum has a much larger effect. Taking the rate-maximum when $\mu = 0.50$ to lie at pH = 1.38 (from Fig. 1) eq. [16] requires that c/d must be larger than 0.174, which shows that eq. [17] applies at all $[H^+]$ less than 0.01 M. A plot of eq. [17] using the data of Table IV for pH's greater than 2 gives a straight line from which $a/b = 0.9 \times 10^{-3}$.

Can. J. Chem. Downloaded from www.nrcresearchpress.com by 210.87.254.40 on 09/05/12
For personal use only.

Equation [16] then gives $c/d = 0.200$ and eq. [15] gives $b/d = 5.26 \times 10^{-3}$. Figure 1 shows that the experimental data fit this calculated curve satisfactorily over the whole range of rate measurements. Hence, all of eqs. [9–12] represent variants of the general mechanism which satisfactorily account for the pH dependence of the rate of decarboxylation of 4-methoxyanthranilic acid and probably of other aromatic amino acids as well.

At high pH these rate expressions are greatly simplified. Introducing the values of a/b, c/d, and b/d at $\mu = 0.50$ into eq. [14] gives:

$$[18] \qquad k[C] = \frac{b}{d}\frac{a/b + [H^+]}{c/d + [H^+]}[N] = 0.00506\frac{0.001 + [H^+]}{0.205 + [H^+]}[N].$$

At pH's greater than 4 (i.e. $[H^+]$ less than 0.0001) the $[H^+]$ becomes negligible and the rate expression is

$$[19] \qquad k[C] = \frac{a}{c}[N] = \frac{k^*K_AK_2}{k^* + k_{-A}}[N]$$

for all of eqs. [9–12]. This involves the rate constants for only one non-Bjerrum intermediate, HA*, so that at high pH the main route of decarboxylation is simply

$$H^+ + A^- \underset{k_{-A}}{\overset{k_A}{\rightleftharpoons}} HA^* \xrightarrow{k^*} \text{products.}$$

On the other hand, at pH's less than -0.3 (i.e. $[H^+]$ greater than 2) the fraction containing the sums disappears from eq. [18] and the rate expression becomes

$$k[C] = \frac{b}{d}[N].$$

However, this expression does not correspond to any simple mechanism except in the case of eq. [11] where it reduces to

$$k[C] = k_AK_2[N] = k_A[H^+][A^-]$$

which implies that the rate of decarboxylation at high acidities is determined by the rate of protonation of A^-.

The proposed mechanisms also permit some predictions concerning the possibility of a carboxyl–carbon isotope effect. At pH's greater than 4 all four mechanisms obey eq. [19] which contains k^*, the rate of carbon–carbon bond breaking, so that there will be an isotope effect unless the rate of decarboxylation, k^*, greatly exceeds the rate of deprotonation, k_{-A}. This is possible for eqs. [10] and [12] so that these mechanisms can accommodate an isotope effect or none. However, for eq. [9]

$$\frac{a/b}{c/d} = \frac{k^*}{k^* + k_{-A}}\left(1 + \frac{k_{-HA}K_D^* + k_{-Z}K_C^*}{k^+K_D^* + k^{\mp}K_C^*}\right) = 1.8 \times 10^{-3}.$$

Since the quantity in parentheses cannot be less than 1, k^* must be considerably smaller than k_{-A}. Therefore mechanism [9] and its special case [11] require a carboxyl–carbon isotope effect at pH 4 or greater.

At pH -0.3 or less eq. [9] reduces to

$$\frac{-d[C]}{dt} = [N]k_AK_2\frac{k^+/K_C^* + k^{\mp}/K_D^*}{(k^+ + k_{-HA})/K_C^* + (k^{\mp} + k_{-Z})/K_D^*}$$

Can. J. Chem. Downloaded from www.nrcresearchpress.com by 210.87.254.40 on 09/05/12
For personal use only.

so that there will be an isotope effect unless $k^+ \gg k_{-HA}$, and $k^{\pm} \gg k_{-Z}$, but if this were the case eq. [9] would become equivalent to eq. [5] which does not fit the data. Equation [10] also requires an isotope effect since k^* cannot be eliminated from the equation in this pH range. In summary, then, eqs. [9] and [11] require an isotope effect at all pH's, but eqs. [10] and [12] need not have one except at very low pH.

Stevens, Pepper, and Lounsbury (3) showed that the carboxyl–carbon isotope effect for the decarboxylation of anthranilic acid is very small in sulfuric acid concentrations up to 1 *N*. There did seem to be a tendency for the isotope effect to increase slightly at the highest acidity studied. Should this observation hold for 4-methoxy as well as for unsubstituted anthranilic acid this would be strong support for a mechanism corresponding to eq. [10] or [12]; that is, one in which HA* and H_2A^* (and (or), less probably, HZ*) are formed but only HA* decarboxylates. Of course, the pH at which the isotope effect should appear depends upon the value of c/d and this may well be different for anthranilic acid than for 4-methoxyanthranilic acid. In fact, we have shown c/d for a single acid to be fairly sensitive to ionic strength, so that the observance or non-observance of an isotope effect may well depend upon the substitutent, the pH, the ionic strength, the temperature and the solvent. Further work is planned to investigate the influence of these factors on the isotope effect.

ACKNOWLEDGMENT

The authors are grateful to Miss Paula Van Buren for assistance with some of the experimental work, and to a referee for valuable suggestions concerning the presentation of the kinetics.

REFERENCES

1. B. R. Brown. Quart. Rev. **5**, 131 (1951).
2. L. McMaster and R. L. Shriner. J. Am. Chem. Soc. **45**, 751 (1923).
3. W. H. Stevens, J. M. Pepper, and M. Lounsbury. Can. J. Chem. **30**, 529 (1952).
4. A. V. Willi. Z. Physik Chem. Frankfurt, **27**, 221 (1961).
5. A. V. Willi and J. F. Stocker. Helv. Chim. Acta, **37**, 1113 (1954).
6. R. F. Rekker and W. T. Nauta. J. Med. Pharm. Chem. **2**, 281 (1960).
7. A. M. Liquori and A. Ripamonte. Gazz. Chim. Ital. **85**, 578 (1955).
8. B. Pawlewski. Ber. **37**, 592 (1904).
9. G. E. Dunn and R. Prysiasniuk. Can. J. Chem. **39**, 285 (1961).
10. N. Bjerrum. Z. Physik Chem. **104**, 147 (1923).
11. P. Leggate and G. E. Dunn. Can. J. Chem. **43**, 1158 (1965).
12. R. G. Bates. Electrometric pH determinations. J. Wiley & Sons, New York. 1954.
13. W. M. Schubert, J. Donohue, and J. D. Gardner. J. Am. Chem. Soc. **76**, 9 (1954). R. Stewart and K. Yates. J. Am. Chem. Soc. **82**, 4059 (1960).

Can. J. Chem. Downloaded from www.nrcresearchpress.com by 210.87.254.40 on 09/05/12
For personal use only.

Can. J. Chem. Downloaded from www.nrcresearchpress.com by 210.87.254.6 on 09/05/12
For personal use only.

NOTES

DIRECT OBSERVATION OF $A^3\Sigma_u^+$ NITROGEN MOLECULES IN THE N–I_2 FLAME

D. I. WALTON, M. J. MCEWAN, AND L. F. PHILLIPS

Previous studies (1, 2) of the reaction of iodine with active nitrogen have shown that an energetic metastable species is produced by the reaction, and have made it appear very likely that the metastable species is a nitrogen molecule in the A-state. In the present work direct evidence for the presence of this species as a product of the reaction has been obtained by observing absorption of the nitrogen first positive bands by the reaction flame.

From the postulated mechanism (1) one can conclude that a maximum concentration of the excited species should be obtained when the N-atom concentration is large and when the rate of destruction of NI at the walls of the reaction vessel is small. Therefore we have used a condensed discharge as a source of nitrogen atoms, and a reaction vessel of large internal diameter (52 mm).

Up to 10% absorption of the (0,0) and (1,0) first positive bands could be produced by introducing iodine into the reaction vessel with the condensed discharge turned on. No absorption was found (*a*) on addition of the argon carrier gas alone, (*b*) on addition of iodine plus carrier gas with the condensed discharge turned off, (*c*) when argon replaced nitrogen in the microwave discharge which was used as a light source, or (*d*) for bands other than those with $v'' = 0$ (upper limit for other bands, 1% absorption). We have not observed any Vegard–Kaplan bands in emission, using a microwave discharge to produce N atoms, but have yet to try this experiment with the condensed discharge.

Oldenberg, Bills, and Carleton (3) observed 0.9% absorption of the (1,0) band in a 5 ft discharge tube with a calculated A-state molecule concentration of 6.5×10^{10} per cm^3. Assuming that the rotational temperatures in our experiments were not too different from theirs, this would indicate that in our reaction vessel, with a light path of 80 cm, there was a mean concentration of 1.4×10^{12} A-state molecules per cm^3. The maximum concentration, assuming exponential decay, would therefore have been 10^{13}–10^{14} per cm^3, since the lack of blue iodine emission at the exit to the reaction vessel showed that the A-state concentration was zero at this point. This is much less than the maximum N-atom concentration (10^{16} per cm^3 at least). Neglecting NI destruction at the walls, the steady state concentration of A-state molecules is approximately [N]/3, if the A-state is produced every time that N reacts with NI (2). In our experiments the N-atom concentration would have fallen somewhat by the time the steady state was reached; however, the results indicate that the production of an A-state molecule is a rather infrequent occurrence, and so diminish the prospect of using this reaction system as a convenient source of the metastable species.

EXPERIMENTAL

The light from a 100 W microwave discharge in a 14 mm quartz tube was chopped at 80 cycles/s before entering the 16 cm long, 52 mm i.d., reaction vessel. The end windows of the vessel were silvered externally, and the light entered through one small window at one end and left through a diagonally opposite one at the other end. Typically five traverses were used, for a total light path of 80 cm. From the exit window

the light was focussed on the entrance slit of a Hilger D2853 quartz monochromator. A lead sulfide photoconductor (Kodak Ektron, N2, uncooled) was placed at the exit slit of the monochromator, and the signal from this was taken to a Tektronix type 122 low-level preamplifier, a phase-sensitive detector, and a chart recorder. Very careful shielding was necessary to eliminate pickup from the condensed discharge. The nitrogen pressure was in the range 5–10 Torr, and the velocity of flow through the reaction tube was estimated to be about 80 cm/s. Nitrogen, argon, and iodine were as previously described (1). Once the apparatus was turned on an experiment consisted simply of repeatedly opening and closing a stopcock between a heated iodine saturator and the reaction vessel. The stability of the system was such that 1% absorption of the light beam could just be detected with certainty.

ACKNOWLEDGMENTS

We are indebted to Dr. W. S. Metcalf for the loan of the Hilger monochromator, and to Mr. K. S. Raxworthy for incidental assistance. This work was supported by grants from the New Zealand Universities Research Committee and the United States Air Force Office of Scientific Research.

1. C. G. Freeman and L. F. Phillips. J. Phys. Chem. **68**, 362 (1964).
2. L. F. Phillips. Can. J. Chem. **43**, 369 (1965).
3. O. Oldenberg, D. G. Bills, and N. P. Carleton. J. Opt. Soc. Am. **51**, 526 (1961).

Received May 3, 1965.
Chemistry Department,
University of Canterbury,
Christchurch, New Zealand.

Can. J. Chem. Downloaded from www.nrcresearchpress.com by 210.87.254.6 on 09/05/12
For personal use only.

AN APPARATUS FOR STUDYING HYDROGEN SULFIDE OXIDATION KINETICS

A. E. Werner

INTRODUCTION

The oxidation of hydrogen sulfide by dissolved oxygen is of importance in some water pollution problems (1). While the half-life of H_2S in sea water was recently found to be of the order of 17 min (2), there are indications that in polluted waters, coexistence of the dissolved gases is possible over prolonged periods.

A study was undertaken to investigate this reaction under a variety of conditions by an apparatus designed for measuring the rate constant involved and the influence on it of temperature, catalysts, and inhibitors. The effects of the latter were compared by a null method.

The oxidation involved is a complicated process because the primary reaction products tend to progressive further oxidation (3, 4, 5). In the gas phase a minimum of $1\frac{1}{2}$ volumes disappear for each volume of hydrogen sulfide oxidized.

[1] $$2H_2S_{(g)} + O_{2(g)} \rightarrow 2H_2O_{(l)} + 2S_{(s)}$$

At room temperature and in the absence of catalysts, oxidation is much faster in solution than in the gas phase. This can be deduced theoretically because at low pressures the specific rate constant in solution ($k_{(l)}$) and its counterpart in the gas phase $k_{(g)}$ are related by

[2] $$k_{(l)} = k_{(g)} \frac{\gamma_{H_2S}\,\gamma_{O_2}}{\gamma_{\neq}}$$

where γ denotes the activity coefficient in solution of the gas given by the subscript and $\gamma_{\neq}$ refers to that of the activated complex (6). In many relations the activity coefficient factor $= (\gamma_1\gamma_2)/\gamma_{\neq}$ has values around 100, although exceptions are known (7).

the light was focussed on the entrance slit of a Hilger D2853 quartz monochromator. A lead sulfide photoconductor (Kodak Ektron, N2, uncooled) was placed at the exit slit of the monochromator, and the signal from this was taken to a Tektronix type 122 low-level preamplifier, a phase-sensitive detector, and a chart recorder. Very careful shielding was necessary to eliminate pickup from the condensed discharge. The nitrogen pressure was in the range 5–10 Torr, and the velocity of flow through the reaction tube was estimated to be about 80 cm/s. Nitrogen, argon, and iodine were as previously described (1). Once the apparatus was turned on an experiment consisted simply of repeatedly opening and closing a stopcock between a heated iodine saturator and the reaction vessel. The stability of the system was such that 1% absorption of the light beam could just be detected with certainty.

ACKNOWLEDGMENTS

We are indebted to Dr. W. S. Metcalf for the loan of the Hilger monochromator, and to Mr. K. S. Raxworthy for incidental assistance. This work was supported by grants from the New Zealand Universities Research Committee and the United States Air Force Office of Scientific Research.

1. C. G. Freeman and L. F. Phillips. J. Phys. Chem. **68**, 362 (1964).
2. L. F. Phillips. Can. J. Chem. **43**, 369 (1965).
3. O. Oldenberg, D. G. Bills, and N. P. Carleton. J. Opt. Soc. Am. **51**, 526 (1961).

Received May 3, 1965.
Chemistry Department,
University of Canterbury,
Christchurch, New Zealand.

Can. J. Chem. Downloaded from www.nrcresearchpress.com by 210.87.254.105 on 09/05/12
For personal use only.

AN APPARATUS FOR STUDYING HYDROGEN SULFIDE OXIDATION KINETICS

A. E. Werner

INTRODUCTION

The oxidation of hydrogen sulfide by dissolved oxygen is of importance in some water pollution problems (1). While the half-life of H_2S in sea water was recently found to be of the order of 17 min (2), there are indications that in polluted waters, coexistence of the dissolved gases is possible over prolonged periods.

A study was undertaken to investigate this reaction under a variety of conditions by an apparatus designed for measuring the rate constant involved and the influence on it of temperature, catalysts, and inhibitors. The effects of the latter were compared by a null method.

The oxidation involved is a complicated process because the primary reaction products tend to progressive further oxidation (3, 4, 5). In the gas phase a minimum of $1\frac{1}{2}$ volumes disappear for each volume of hydrogen sulfide oxidized.

[1] $$2H_2S_{(g)} + O_{2(g)} \rightarrow 2H_2O_{(l)} + 2S_{(s)}$$

At room temperature and in the absence of catalysts, oxidation is much faster in solution than in the gas phase. This can be deduced theoretically because at low pressures the specific rate constant in solution ($k_{(l)}$) and its counterpart in the gas phase $k_{(g)}$ are related by

[2] $$k_{(l)} = k_{(g)} \frac{\gamma_{H_2S}\,\gamma_{O_2}}{\gamma_{\neq}}$$

where γ denotes the activity coefficient in solution of the gas given by the subscript and $\gamma_{\neq}$ refers to that of the activated complex (6). In many relations the activity coefficient factor $= (\gamma_1\gamma_2)/\gamma_{\neq}$ has values around 100, although exceptions are known (7).

In a heterogeneous system consisting of an aqueous and a gaseous phase, the reacting components, H_2S and O_2, are distributed between the phases. The equilibrium condition is characterized by the distribution coefficients α_{H_2S} and α_{O_2}. The latter are expressed by the ratio of the activities of the particular component in the respective phases.

$$[3] \qquad \alpha = \frac{(f_1[C_1])_{(g)}}{(f_2[C_2])_{(l)}}$$

The symbols f_1 and f_2 refer to the activity coefficients and $[C_1]$ and $[C_2]$ represent the concentrations.

When oxidation takes place preferentially in one phase, the concentrations $[H_2S]$ and $[O_2]$ decrease in that phase and the system tends to restore equilibrium by transferring the relevant species from the other phase.

This results (at constant temperature and pressure) in a measurable decrease of the gas volume. Alternatively, a pressure drop is experienced at constant volume. Inasmuch as $\Delta p \ll p$ under prevailing conditions the reaction rate is not noticeably influenced.

METHOD

To water, saturated with oxygen and in contact with a gaseous phase initially consisting of oxygen, a dilute, aqueous solution of hydrogen sulfide is added. The reaction is followed through the pressure change at constant volume (or the volume change at constant pressure) of the gaseous phase in contact with the solution.

In an apparatus of V_T ml capacity, an initial amount of oxygen (expressed as ml at S.T.P.) is present, partly as free gas and partly dissolved in x ml of water. When y ml of hydrogen sulfide solution is added, an equal volume of oxygen gas is vented. The volume of oxygen available for the reaction is therefore

$$[4] \qquad V_0 = V_T - (1 - 0.031)x - y \quad \text{(ml at S.T.P.)}.$$

Two volumes of hydrogen sulfide gas require at least 1 volume of oxygen (cf. eq. [1]) and the solubility of oxygen and hydrogen sulfide in water at 20 °C is 31.1 and 2 160 ml per liter (reduced to S.T.P.), respectively. The volumes of the saturated solutions which are to be mixed can be calculated as follows:

$$[5] \qquad 2(V_T - 0.969x - y) = 2.61y$$

$$[6] \qquad 2.305y + 0.969x = V_T.$$

It would be impossible to determine oxidation kinetics by this method if the rate of transfer across the phase boundary were the rate-determining step. Rapid mechanical agitation proved a suitable way of avoiding restriction at this point because the rate of transfer is proportional *inter alia* to the gas liquid interface A. The shaking not only increases A but it assists absorption by replacing slow diffusion by faster convectional processes (8).

APPARATUS

The assembly was constructed almost entirely of borosilicate glass, but stopcock plugs and leak-preventing "sleeves" between the standard tapers consisted of "Teflon". The temperature was controlled by immersion in a thermostatted water bath. Two almost identical parts which were joined by a differential manometer M (Fig. 1) made up the

Can. J. Chem. Downloaded from www.nrcresearchpress.com by 210.87.254.105 on 09/05/12
For personal use only.

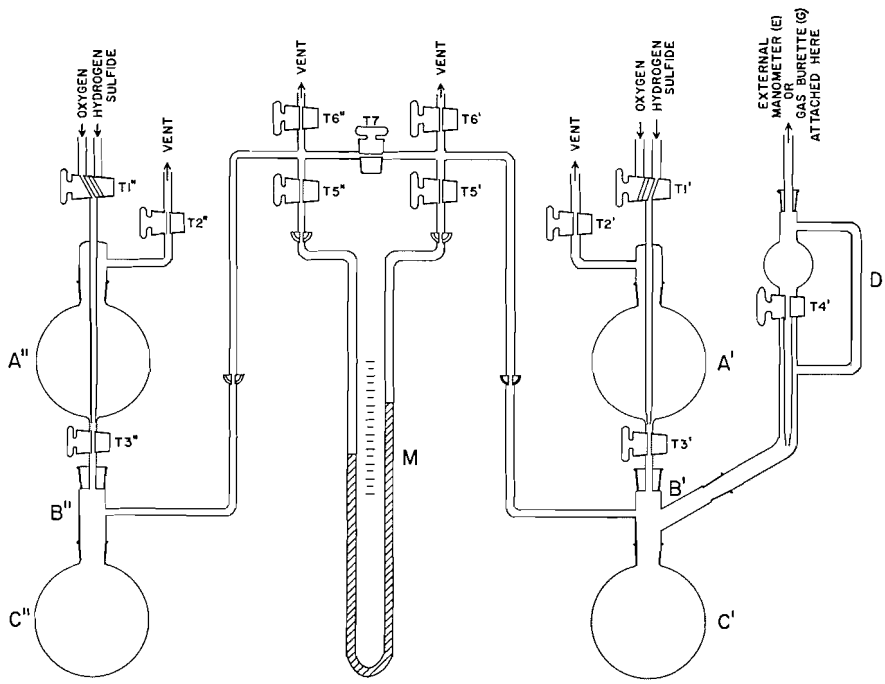

FIG. 1. Apparatus for the study of hydrogen sulfide oxidation kinetics. Legend: (A′, A″) saturators for preparing the solutions; (B′, B″) manifolds; (C′, C″) reaction flasks; (D) dropping funnel for adding catalysts and (or) inhibitors; (E) external manometer (not shown); (G) gas burette (not shown); (M) differential manometer; (T1′, T1″) stopcocks for controlling gas flow to saturators; (T2′, T2″) stopcocks for venting saturators; (T3′, T3″) stopcocks for dropping saturated solutions into reaction flasks; (T4′) stopcock for dropping catalysts or inhibitors into reaction flasks; (T5′, T5″) stopcocks for isolating differential manometer; (T6′, T6″) stopcocks for venting reaction flasks; (T7) stopcock for separating control side of apparatus.

unit. These left and right sides were used separately for finding pressure or volume changes or jointly for measuring relative pressure drops in catalyst or inhibitor studies.

In the volumetric technique the gas burette G was used. The whole apparatus was filled with oxygen at atmospheric pressure, then the sides were separated by closing the appropriate tap. The reaction mixture was prepared in one half of the apparatus and the contraction measured with the gas burette in conjunction with the manometer M.

The null method was applicable whenever it was desirable to compare directly the rates of catalyzed and non-catalyzed reactions. This was possible by letting them proceed side by side simultaneously in the two halves of the apparatus and measuring the time function of the pressure difference. Errors caused by small changes in temperature, illumination, etc. were thus minimized. Tap T7 remained open until the absolutely synchronous descent of the H_2S–water into the reactors was completed. Catalysts or inhibitors were placed into the reactor flasks C′ and (or) C″. In case they had to be added after the start of the reaction, they were put into D′. Duplicate runs were carried out as follows:

	LEFT SIDE	RIGHT SIDE
1st run	Catalyst A	Inhibitor B
2nd run	Inhibitor B	Catalyst A

Can. J. Chem. Downloaded from www.nrcresearchpress.com by 210.87.254.105 on 09/05/12
For personal use only.

Can. J. Chem. Downloaded from www.nrcresearchpress.com by 210.87.254.105 on 09/05/12
For personal use only.

PERFORMANCE

The two sides were made exactly equal in capacity (169.9 ml) by adding a small piece of glass rod to the larger of them. Leakage was so small that the pressure in the evacuated apparatus rose at the rate of 1.06×10^{-4} mm/min.

(a) Reaction in the Gas Phase

Oxygen (x ml) and hydrogen sulfide ($2x$ ml) were dosed in from the gas burette and a series of pressure readings was taken for calculating average pressure-drop coefficients. At 25 °C they were: (i) at 1 atm initial pressure, 8.99×10^{-2} mm Hg/min; (ii) at 0.5 atm initial pressure, 4.01×10^{-2} mm Hg/min. Their small rate of change with pressure (9.96×10^{-2} mm Hg/atm) justified the statement made above that pressure instead of volume measurement may be made whenever this is convenient.

(b) Transfer Across Phase Boundary

Only the right half of the apparatus was used. The system was filled with oxygen at atmospheric pressure, then a measured volume of degassed water was placed into C′. The shaker was started and manometer readings were taken.

The results are shown in Table I. The measured gas volumes, reduced to S.T.P., are presented as concentrations expressed in ml/l of water per minute. The last column shows the average % of oxygen which is transferred per minute in the particular time interval. It is based on the total average amount of oxygen transferred.

TABLE I

Transfer across phase boundary at 25 °C

Time interval, min	O_2 transported during time interval, ml/l min			Average transport (based on average total oxygen transported), % per min
	1*	2†	3‡	
0–1	7.1	6.6	3.2	47.5
1–2	3.8	3.1	2.1	23.1
2–3	2.6	1.5	1.3	15.4
3–4	0.8	0.5	0.8	5.9
4–6	0.4	0.1	0.5	2.8
6–8	0.1	0.1	0.1	0.8
8–12	0.0	0.0	0.0	0.0

*Total O_2 transferred 15.4 ml/l, total H_2O advanced 85.0 ml, total gas space 85.0 ml.
†Total O_2 transferred 12.1 ml/l, total H_2O advanced 75.0 ml, total gas space 95.0 ml.
‡Total O_2 transferred 8.5 ml/l, total H_2O advanced 50.0 ml, total gas space 120.0 ml.

Table I shows that the half-life constant of the transfer reaction is of the order of 1 min, amply adequate to prevent starvation of the H_2S oxidation reaction in solution.

1. A. B. Wheatland. Intern. Ver. Theoret. Angew. Limnol. Verhand. **12**, 772 (1955).
2. H. G. Ostlund and J. Alexander. J. Geophys. Res. **68** (13), 3995 (1963).
3. L. Meunier and M. Kapp. Chim. Ind. Paris (special number), 718 (1932).
4. H. Stamm. FIAT Rev. Ger. Sci. 1939–1946. Inorg. Chem. Pt. 1, 175 (1948).
5. A. Swinarski and F. Kroll. Chem. Stosowana, **6**, 409 (1962).
6. J. F. Kincaid, H. Eyring, and A. F. Stearn. Chem. Rev. **28**, 301 (1941).
7. R. P. Bell. Ann. Rept. Progr. Chem. Chem. Soc. London, **36**, 82 (1939).
8. W. G. Whitman. Chem. Met. Eng. **29**, 147 (1923).

Received April 6, 1965.
Fisheries Research Board of Canada,
Biological Station,
Nanaimo, British Columbia.

SOME HEATS OF SOLUTION IN LIGHT AND HEAVY WATER[1]

D. H. DAVIES[2] AND G. C. BENSON

Can. J. Chem. Downloaded from www.nrcresearchpress.com by 210.87.254.6 on 09/05/12
For personal use only.

The heats of solution of sodium chloride, sodium fluoride, sodium methane sulfonate ($MeSO_3Na$), sodium benzene sulfonate (ϕSO_3Na), and sodium *p*-toluenesulfonate (TOSNa) have been determined at several concentrations in light and heavy water at 25 °C.

Baker and Adamson reagent grade NaCl was recrystallized three times from equilibrium water and dried at 100 °C. The NaF was Baker and Adamson reagent grade dried at 120 °C. Eastman Kodak reagent grade TOSNa was recrystallized once from methanol and dried under vacuum at 80 °C. The samples of $MeSO_3Na$ and ϕSO_3Na were kindly supplied by Dr. R. E. Robertson (N.R.C.) and were recrystallized and dried by him. Infrared analyses of samples of the heavy water carried out by Dr. W. H. Stevens (Atomic Energy of Canada Ltd.) indicated a D_2O content of 99.8 weight %. The H_2O employed was equilibrium conductivity water. No attempt was made to remove dissolved gases from either of the solvents.

The sample to be dissolved was contained in a thin-walled glass bulb closed with a Teflon stopper. These bulbs were constructed from precision bore tubing to ensure a uniform fit of the stoppers. The calorimeter vessel (1), the adiabatic shield (2), and the control system (3) have been described previously.

TABLE I

Heats of solution in H_2O

Compound	Mole fraction	Temp. (°C)	ΔH (J mole^{-1})	ΔH (25 °C) (J mole^{-1})
NaCl	0.008927	24.961	4110	4106
	0.008927	24.992	4106	4105
	0.008927	24.941	4108	4102
	0.008927			Mean 4104±2
	0.004483	24.976	4229±7	4226±7
NaF	0.004481	24.999	1484±6	
$MeSO_3Na$	0.002495	24.961	7022±13	
	0.001249	25.058	6920±25	
ϕSO_3Na	0.002494	24.995	7492±13	
	0.001249	24.999	7387±41	
TOSNa	0.002495	25.004	9695±12	
	0.001248	25.004	9534±24	
	0.001249	25.068	9507±24	

Tables I and II report the results obtained for the heats of solution in light and heavy water respectively. The weights of all the components were corrected to *vacuo*. Concentrations are stated as mole fractions of the solute, and ΔH is expressed in joules per mole of solute.

The results for the solution of NaCl in H_2O were corrected to 25 °C by employing temperature coefficients of -102 J mole^{-1} deg^{-1} at $x = 0.0089$ and of -115 J mole^{-1}

[1]*Issued as N.R.C. No. 8613.*

[2]*National Research Council of Canada Postdoctorate Fellow, 1963–1965. Present address: Department of Chemistry, Dalhousie University, Halifax, Nova Scotia.*

deg^{-1} at $x = 0.0045$. These coefficients were calculated from heat capacity data determined for NaCl solutions by Lipsett, Johnson, and Maass (4). The temperature coefficient for the heat of solution of NaCl in D_2O at $x = 0.0045$ was estimated to be -143 ± 7 J $mole^{-1}$ deg^{-1} from the data in Table II. A temperature coefficient of -128 J $mole^{-1}$ deg^{-1} was calculated for the heat of solution of NaCl in D_2O at $x = 0.0089$ by assuming a concentration dependence proportional to that for the NaCl–H_2O system.

TABLE II

Heats of solution in D_2O

Compound	Mole fraction	Temp. (°C)	ΔH (J $mole^{-1}$)	ΔH (25 °C) (J $mole^{-1}$)
NaCl	0.008927	25.007	6297±3	6298±3
	0.004483	24.930	6529	6519
	0.004478	24.985	6509	6507
	0.004480	25.001	6492	6492
	0.004481	23.367	6739	6505
	0.00448		Mean	6506±10
NaF	0.004479	25.001	1484±6	
$MeSO_3Na$	0.002495	25.015	8259±13	
	0.001249	25.051	8163±27	
ϕSO_3Na	0.002495	25.007	8664±14	
	0.002495	24.989	8706±14	
	0.001249	25.002	8554±50	
TOSNa	0.002494	25.011	10904±13	
	0.001249	24.999	10656±26	

On the basis of the reproducibility of the results for the two NaCl systems, it was concluded that the calorimetric technique was precise to ±0.28 J in the total heat measured. This value was used to estimate the precisions indicated for the other systems in Tables I and II.

TABLE III

Isotope effect

Compound	Mole fraction	$\Delta H_{D_2O} - \Delta H_{H_2O}$ (J $mole^{-1}$)	$\overline{(\Delta H_{D_2O} - \Delta H_{H_2O})}$ (J $mole^{-1}$)
NaCl	0.00893	2194±4	
	0.00448	2280±12	
NaF	0.00448	0±8	
$MeSO_3Na$	0.00250	1237±18	1238
	0.00125	1243±37	
ϕSO_3Na	0.00250	1193±19	1191
	0.00125	1167±65	
TOSNa	0.00250	1209±18	1194
	0.00125	1136±35	

Table III reports the values obtained for the isotope effect ($\Delta H_{D_2O} - \Delta H_{H_2O}$). Since within the precision of the measurements at these low concentrations there is no significant dependence of the isotope effect for the sulfonates on concentration, average values were computed by assigning to each result a weight inversely proportional to the square of its precision.

Previous determinations of the heat of solution of NaCl in H_2O carried out in this laboratory (1) yielded values of 4117 ± 4 and 4245 ± 8 J $mole^{-1}$ at mole fractions of 0.0089 and 0.0045 respectively. A redetermination (2) at $x = 0.0089$ using the same

Can. J. Chem. Downloaded from www.nrcresearchpress.com by 210.87.254.6 on 09/05/12
For personal use only.

adiabatic shield assembly employed in the present work produced a value of 4116 J mole^{-1}. The heats of solution of NaCl in H_2O reported in Table I are in reasonable agreement with these earlier results, since the samples used in the previous investigations had been pumped under vacuum at 300 °C for 12 h and sealed in evacuated bulbs. Our results also agree with Lange and Martin's (5) experimental value of 2343 ± 84 J mole^{-1} for the isotope effect with NaCl at a mole fraction of 0.0045 and with their calculated value of 21 ± 84 J mole^{-1} for the isotope effect with NaF.

When an ionic compound is dissolved to form a very dilute solution, the thermodynamic properties for the process can be calculated as the resultant of contributions associated with the steps of an alternative path between the same initial and final states. The first step along this path is the dissociation of the crystal lattice to produce an ionic gas in some standard state. This is followed by the solution of the ionic gas in the solvent. The first step depends only on the solute, whereas the second, which corresponds to the hydration of the ions, is a function of both the solute and the solvent.

Discussions of the hydration of ions generally divide the process into two sub-steps, the creation of a cavity in the solvent and the insertion of the ion into this cavity. In principle the thermodynamic properties for the creation of a cavity can be calculated from the properties for the vaporization of the solvent plus a contribution from the formation of a new liquid surface; the ionic contribution to the solute–solvent interaction can be calculated from the Born equation (6, 7) and, if necessary, a contribution from the dispersion forces can be included. Unfortunately there is a marked lack of unanimity regarding the proper choice of an ionic radius (cavity size) and of an effective value for the dielectric constant in the neighborhood of the solvated ion, and thus the detailed application of the model varies from author to author (5, 7). The isotope effect arises from the difference between the solvation process in light and heavy water, and the thermodynamic properties associated with it are those for the transfer of an ion from light to heavy water.

Swain and Bader (8) have investigated the structures of light and heavy water by treating the librational motion (restricted rotation) of each solvent molecule as a three dimensional harmonic oscillator. They found that the isotope effect could be attributed almost entirely to the change in librational frequency of the water molecules in the first hydration shell of the ions. As the librational frequencies in light and heavy water are related to each other by a constant factor, only one frequency need be considered for each ion. Infrared absorption spectra of solutions of fluoride ions in light water exhibit a fairly well-defined librational band centered at 698 cm^{-1}. Using this value together with an assignment of 667 cm^{-1} for the librational frequency of pure H_2O, they calculated the isotope effect on the heat of hydration of the fluoride ion to be −732 J mole^{-1}. The isotope effects for other ions were obtained by combining this result with experimental heats of solution in light and heavy water. These effects were then used to calculate the librational frequency of the water molecules in the hydration shell, and the results compared with experimental infrared spectra. Unfortunately the librational bands observed were too broad to allow an unequivocal assignment of the frequency; but in all cases a fairly satisfactory correlation was possible.

The isotope effect on the heat capacities of hydration can be calculated (8) from the librational frequencies. For NaCl such a calculation predicts a difference of −2 J mole^{-1} deg^{-1} between the heat capacities of hydration in light and heavy water. This result is obtained whether the frequencies quoted by Swain and Bader or those calculated from our experimental heats are employed. This value is not in agreement with the experimentally determined value of −28 J mole^{-1} deg^{-1} at $x = 0.0045$ since the uncertainty in

Can. J. Chem. Downloaded from www.nrcresearchpress.com by 210.87.254.6 on 09/05/12
For personal use only.

the experimental value is only about 10 J mole^{-1} deg^{-1}. However, since the configurational integrals were equated in deriving the formula, this lack of agreement is not unexpected.

If one accepts Swain and Bader's value for the isotope effect on the heat of solution of the fluoride ion, the data in Table III lead to values of +732, +1548, +506, +459, and +462 J mole^{-1} for the Na^+, Cl^-, $MeSO_3^-$, ϕSO_3^-, and TOS^- ions respectively.

The fluoride ion is the only singly charged ion for which a negative contribution to the isotope effect has been observed, and hence is the only such ion for which the librational frequency of the solution is greater than that of pure water. This singular behavior of the fluoride ion does not imply that there is any discontinuity in the properties of the halogens, since plots of the ionic contributions to the thermodynamic properties against the ionic radius or its reciprocal are smooth curves (7).

It is interesting to note that the isotope effect on the heats of hydration of the sulfonates does not vary much with the size of the anion. We have not calculated the corresponding change in librational frequency for the sulfonates since in order to have done so we would have had to introduce further assumptions regarding the extent of coordination. However, it does appear that in all cases these ions tend to decrease the amount of water structure, the disruptive effect being greater in D_2O than in H_2O. This is in line with the positive entropies of transfer (H_2O to D_2O) deduced by Greyson from measurements of the ion exchange membrane potentials for a number of chlorides (9).

Provided that the solute–solvent interaction in the transition state for the solvolysis of alkyl halides and sulfonates in water is proportional to that in the final state, the isotope effects reported in this paper support the hypothesis (10) that it is the initial state solvation shell rather than that in the transition state which is the major factor in determining kinetic solvent isotope effects since the latter do not vary in the same manner as do the enthalpy changes.

1. G. C. Benson and G. W. Benson, Rev. Sci. Instr. **26**, 477 (1955).
2. G. C. Benson, E. D. Goddard, and C. A. J. Hoeve. Rev. Sci. Instr. **27**, 725 (1956).
3. J. E. Bennett and G. C. Benson. Can. J. Chem. **43**, 1912 (1965).
4. S. G. Lipsett, F. M. G. Johnson, and O. Maass. J. Am. Chem. Soc. **49**, 1940 (1927).
5. E. Lange and W. Martin. Z. Physik. Chem. Leipzig, **A180**, 233 (1937).
6. M. Born. Z. Physik. **1**, 45 (1920).
7. R. M. Noyes. J. Am. Chem. Soc. **84**, 513 (1962); **86**, 971 (1964). R. H. Stokes. J. Am. Chem. Soc. **86**, 979 (1964).
8. C. G. Swain and R. F. W. Bader. Tetrahedron, **10**, 182 (1960).
9. J. Greyson. J. Phys. Chem. **66**, 2218 (1962).
10. R. E. Robertson. Can. J. Chem. **42**, 1707 (1964). P. M. Laughton and R. E. Robertson. Can. J. Chem. **43**, 154 (1965).

Received May 25, 1965.
Division of Pure Chemistry,
National Research Council,
Ottawa, Canada.

ACYLGUANIDINES AS INTERMEDIATES IN PEPTIDE SYNTHESES

Eliahu Hoffmann and Dov Diller

In our investigation of new peptide syntheses we considered the properties of guanidine as a carboxyl-activating group.

Acylguanidines (I), according to the literature (1, 2), can be prepared by the action of guanidine (liberated from its salt by sodium alkoxide) on the esters of carboxylic

Can. J. Chem. Downloaded from www.nrcresearchpress.com by 210.87.254.6 on 09/05/12
For personal use only.

the experimental value is only about 10 J mole^{-1} deg^{-1}. However, since the configurational integrals were equated in deriving the formula, this lack of agreement is not unexpected.

If one accepts Swain and Bader's value for the isotope effect on the heat of solution of the fluoride ion, the data in Table III lead to values of +732, +1548, +506, +459, and +462 J mole^{-1} for the Na^+, Cl^-, $MeSO_3^-$, ϕSO_3^-, and TOS^- ions respectively.

The fluoride ion is the only singly charged ion for which a negative contribution to the isotope effect has been observed, and hence is the only such ion for which the librational frequency of the solution is greater than that of pure water. This singular behavior of the fluoride ion does not imply that there is any discontinuity in the properties of the halogens, since plots of the ionic contributions to the thermodynamic properties against the ionic radius or its reciprocal are smooth curves (7).

It is interesting to note that the isotope effect on the heats of hydration of the sulfonates does not vary much with the size of the anion. We have not calculated the corresponding change in librational frequency for the sulfonates since in order to have done so we would have had to introduce further assumptions regarding the extent of coordination. However, it does appear that in all cases these ions tend to decrease the amount of water structure, the disruptive effect being greater in D_2O than in H_2O. This is in line with the positive entropies of transfer (H_2O to D_2O) deduced by Greyson from measurements of the ion exchange membrane potentials for a number of chlorides (9).

Provided that the solute–solvent interaction in the transition state for the solvolysis of alkyl halides and sulfonates in water is proportional to that in the final state, the isotope effects reported in this paper support the hypothesis (10) that it is the initial state solvation shell rather than that in the transition state which is the major factor in determining kinetic solvent isotope effects since the latter do not vary in the same manner as do the enthalpy changes.

1. G. C. Benson and G. W. Benson, Rev. Sci. Instr. **26**, 477 (1955).
2. G. C. Benson, E. D. Goddard, and C. A. J. Hoeve. Rev. Sci. Instr. **27**, 725 (1956).
3. J. E. Bennett and G. C. Benson. Can. J. Chem. **43**, 1912 (1965).
4. S. G. Lipsett, F. M. G. Johnson, and O. Maass. J. Am. Chem. Soc. **49**, 1940 (1927).
5. E. Lange and W. Martin. Z. Physik. Chem. Leipzig, **A180**, 233 (1937).
6. M. Born. Z. Physik. **1**, 45 (1920).
7. R. M. Noyes. J. Am. Chem. Soc. **84**, 513 (1962); **86**, 971 (1964). R. H. Stokes. J. Am. Chem. Soc. **86**, 979 (1964).
8. C. G. Swain and R. F. W. Bader. Tetrahedron, **10**, 182 (1960).
9. J. Greyson. J. Phys. Chem. **66**, 2218 (1962).
10. R. E. Robertson. Can. J. Chem. **42**, 1707 (1964). P. M. Laughton and R. E. Robertson. Can. J. Chem. **43**, 154 (1965).

Received May 25, 1965.
Division of Pure Chemistry,
National Research Council,
Ottawa, Canada.

ACYLGUANIDINES AS INTERMEDIATES IN PEPTIDE SYNTHESES

Eliahu Hoffmann and Dov Diller

In our investigation of new peptide syntheses we considered the properties of guanidine as a carboxyl-activating group.

Acylguanidines (I), according to the literature (1, 2), can be prepared by the action of guanidine (liberated from its salt by sodium alkoxide) on the esters of carboxylic

Can. J. Chem. Downloaded from www.nrcresearchpress.com by 210.87.254.40 on 09/05/12
For personal use only.

acids. It seemed to us that these compounds should be very prone to proton-catalyzed aminolysis as outlined in eq. [1], since they have, indeed, distinctly basic properties (3).

[1] $$\underset{\text{(I)}}{RCNHCNH_2} \xrightarrow{H^+} \underset{\text{(II)}}{\left[RCNHCNH_2\right]^+} \xrightarrow{NH_2R'} RCNHR' + \left[NH_2CNH_2\right]^+$$

The positively charged intermediate (II) should then suffer nucleophilic attack by amines to yield the expected amide. The reaction could conceivably be carried out in aqueous or mixed aqueous–organic solvents. Furthermore, the trend of the reaction should be towards the formation of the resonance-stabilized guanidinium ion, thus facilitating the formation of the amide bond.

In a preliminary attempt to verify these assumptions we were successful in preparing acylguanidines of hippuric acid, benzyloxycarbonylglycine, benzyloxycarbonyl-DL-alanylglycine, formyl-L-valine, formyl-L-phenylalanine, and tosyl-L-proline from their corresponding ethyl or methyl esters. The yields in these reactions were fair to good and the substances could be obtained in crystalline form.

These guanidine compounds were then caused to react with either ethyl or benzyl glycinate in water or water–dimethylformamide solution at pH 8 to give ethyl hippurylglycinate, benzyl benzyloxycarbonylglycylglycinate, ethyl benzyloxycarbonyl-DL-alanylglycylglycinate, ethyl formyl-L-valylglycinate, ethyl formyl-L-phenylalanylglycinate, and ethyl tosyl-L-prolylglycinate, respectively, with fairly good yields.

It therefore seems that this is a feasible method for the synthesis of peptides and that optical activity can be retained in these reactions. The scope and limitation of this method are at present under investigation.

EXPERIMENTAL

All melting points were taken on a Fisher–Jones apparatus and are uncorrected.

Benzyloxycarbonylglycylguanidine

Methyl benzyloxycarbonylglycinate (6.1 g; 0.0274 mole) was treated with a solution of 0.0435 mole of free guanidine in 20 ml of absolute ethanol. The ester dissolved and the solution was left to stand at room temperature for several hours. After precipitation was complete, the material was filtered off and dried. The yield was 5.5 g (80.4%); the compound could be recrystallized from either nitromethane or ethanol – ethyl acetate and it melted at 152°.

Anal. Calcd. for $C_{11}H_{14}N_4O_3$: C, 52.8; H, 5.6. Found: C, 52.9; H, 5.9.

Similarly prepared were the following.

Hippurylguanidine

This compound was obtained in 87.6% yield. It was recrystallized from dioxane and melted at 182°.

Anal. Calcd. for $C_{10}H_{12}N_4O_2$: C, 54.5; H, 5.4. Found: C, 54.6; H, 5.6.

Benzyloxycarbonyl-DL-alanylglycylguanidine

This compound was obtained in 51% yield. It was recrystallized from ethanol and melted at 175–176°.

Anal. Calcd. for $C_{14}H_{19}N_5O_4$: C, 52.4; H, 5.9. Found: C, 52.6; H, 5.9.

Formyl-L-valylguanidine

This compound was obtained in 74% yield. It was recrystallized from *n*-butanol and melted at 162–164°; $[\alpha]_D^{25}$ +2.8° (*c*, 1.8 in absolute ethanol).

Anal. Calcd. for $C_7H_{14}N_4O_2$: C, 45.1; H, 7.5; N, 30.1. Found: C, 45.3; H, 7.8; N, 29.9.

Formyl-L-phenylalanylguanidine

This compound was obtained in 69% yield. It was recrystallized from *n*-butanol and melted at 153°; $[\alpha]_D^{25}$ +27.2° (*c*, 1.6 in absolute ethanol).

Anal. Calcd. for $C_{11}H_{14}N_4O_2$: C, 56.4; H, 6.0; N, 23.9. Found: C, 56.1; H, 6.3; N, 23.9.

Tosyl-L-prolylguanidine

This compound was obtained in 79% yield. It was recrystallized from absolute ethanol and melted at 187–188°; $[\alpha]_D^{25}$ −174° (*c*, 0.8 in absolute ethanol).

Anal. Calcd. for $C_{13}H_{18}N_4O_3S$: C, 50.4; H, 5.8; N, 18.0. Found: C, 50.5; H, 6.1; N, 18.3.

Can. J. Chem. Downloaded from www.nrcresearchpress.com by 210.87.254.40 on 09/05/12
For personal use only.

Ethyl Benzyloxycarbonylglycylglycinate

A solution of 1.25 g (0.005 mole) of benzyloxycarbonylglycylguanidine in 5 ml of dimethylformamide was added to an aqueous solution of 0.7 g (0.005 mole) of ethyl glycinate hydrochloride, the pH of which was adjusted to 8 with alkali. The resultant clear solution was stirred at room temperature overnight and then evaporated on a water bath (40°) under reduced pressure (0.4 mm Hg). The residue was treated with water until crystallization occurred, then filtered, and air dried to yield 1.35 g (90%) of white solid which was recrystallized from ethyl acetate and melted at 80° (lit. m.p. 80° (4)).

Anal. Calcd. for $C_{14}H_{18}N_2O_5$: C, 57.1; H, 6.1. Found: C, 57.0; H, 6.2.

Similarly prepared were the following.

Ethyl Hippurylglycinate

This was obtained in 76% yield. It was recrystallized from water and melted at 117° (lit. m.p. 117° (5)).

Anal. Calcd. for $C_{13}H_{16}N_2O_4$: C, 59.1; H, 6.1. Found: C, 59.0; H, 6.2.

*Ethyl Benzyloxycarbonyl-*DL*-alanylglycylglycinate*

This was obtained in 50% yield. It was recrystallized from ethanol–water and melted at 110° (lit. m.p. 113° (6)).

Anal. Calcd. for $C_{17}H_{23}N_3O_6$: C, 55.9; H, 6.3. Found: C, 56.0; H, 6.4.

*Ethyl Formyl-*L*-valylglycinate*

This was obtained in 71% yield. It was recrystallized from ethyl acetate – petroleum ether and melted at 155° (lit. m.p. 156–157° (7)).

Anal. Calcd. for $C_{10}H_{18}N_2O_4$: C, 52.2; H, 7.8; N, 12.2. Found: C, 52.1; H, 7.9; N, 12.4.

*Ethyl Formyl-*L*-phenylalanylglycinate*

This was obtained in 82% yield. It was recrystallized from water and melted at 132°; $[\alpha]_D^{25}$ +4.6° (*c*, 1.6 in absolute ethanol) (lit. m.p. 131–132°; $[\alpha]_D^{26}$ +4.4° (7)).

Anal. Calcd. for $C_{14}H_{18}N_2O_4$: C, 60.5; H, 6.5; N, 10.1. Found: C, 60.3; H, 6.6; N, 10.6.

*Ethyl Tosyl-*L*-prolylglycinate*

This was obtained in 68% yield. It was recrystallized from hexane – ethyl acetate (2:1) and melted at 84–86°; $[\alpha]_D^{25}$ −115.8° (*c*, 4.5 in absolute ethanol).

Anal. Calcd. for $C_{16}H_{22}N_2O_5S$: C, 54.3; H, 6.2; N, 7.9. Found: C, 54.4; H, 6.1; N, 8.0.

ACKNOWLEDGMENT

We are indebted to Mrs. M. Goldstein and her analytical group for the microanalyses.

1. W. Traube. Chem. Ber. **43**, 3586 (1910).
2. Cyanamid's Nitrogen Chemicals Digest. Vol. IV. American Cyanamid Co., New York. 1950. p. 15.
3. A. Albert, R. Goldacre, and J. Philips. J. Chem. Soc. 2241 (1948).
4. O. Süs. Ann. **572**, 96 (1951).
5. T. Curtius and R. Wustenfeld. J. Prakt. Chem. **70**, 78 (1904).
6. G. Schramm and H. Wissmann. Chem. Ber. **91**, 1073 (1958).
7. J. C. Sheehan and D.-D. H. Yang. J. Am. Chem. Soc. **80**, 1154 (1958).

Received September 17, 1964.
Department of Organic Chemistry,
Hebrew University,
Jerusalem, Israel.

SYNTHESIS OF 5-BENZAMIDO-5-DEOXY-D-XYLOPYRANOSE

M. S. Patel and J. K. N. Jones

The synthesis of the *N*-acetyl (1, 2) (I, R = $COCH_3$) and the *N*-benzyl (3) (I, R = CH_2Ph) derivatives of 5-amino-5-deoxy-D-xylopyranose (4) (I, R = H) and of the corresponding furanose compounds has been described (1–4). Recently we attempted the preparation by reported procedures of the acetobromo derivative of 5-acetamido-5-deoxy-D-xylopyranose (I, R = $COCH_3$) but were unsuccessful. The synthesis of the benzamido derivative of 5-amino-5-deoxy-D-xylopyranose (I, R = COPh) was therefore undertaken in the hope that this would yield, after *O*-benzoylation, a benzoylbromo sugar.

Can. J. Chem. Downloaded from www.nrcresearchpress.com by 210.87.254.40 on 09/05/12
For personal use only.

Ethyl Benzyloxycarbonylglycylglycinate

A solution of 1.25 g (0.005 mole) of benzyloxycarbonylglycylguanidine in 5 ml of dimethylformamide was added to an aqueous solution of 0.7 g (0.005 mole) of ethyl glycinate hydrochloride, the pH of which was adjusted to 8 with alkali. The resultant clear solution was stirred at room temperature overnight and then evaporated on a water bath (40°) under reduced pressure (0.4 mm Hg). The residue was treated with water until crystallization occurred, then filtered, and air dried to yield 1.35 g (90%) of white solid which was recrystallized from ethyl acetate and melted at 80° (lit. m.p. 80° (4)).

Anal. Calcd. for $C_{14}H_{18}N_2O_5$: C, 57.1; H, 6.1. Found: C, 57.0; H, 6.2.

Similarly prepared were the following.

Ethyl Hippurylglycinate

This was obtained in 76% yield. It was recrystallized from water and melted at 117° (lit. m.p. 117° (5)).

Anal. Calcd. for $C_{13}H_{16}N_2O_4$: C, 59.1; H, 6.1. Found: C, 59.0; H, 6.2.

*Ethyl Benzyloxycarbonyl-*DL*-alanylglycylglycinate*

This was obtained in 50% yield. It was recrystallized from ethanol–water and melted at 110° (lit. m.p. 113° (6)).

Anal. Calcd. for $C_{17}H_{23}N_3O_6$: C, 55.9; H, 6.3. Found: C, 56.0; H, 6.4.

*Ethyl Formyl-*L*-valylglycinate*

This was obtained in 71% yield. It was recrystallized from ethyl acetate – petroleum ether and melted at 155° (lit. m.p. 156–157° (7)).

Anal. Calcd. for $C_{10}H_{18}N_2O_4$: C, 52.2; H, 7.8; N, 12.2. Found: C, 52.1; H, 7.9; N, 12.4.

*Ethyl Formyl-*L*-phenylalanylglycinate*

This was obtained in 82% yield. It was recrystallized from water and melted at 132°; $[\alpha]_D^{25}$ +4.6° (*c*, 1.6 in absolute ethanol) (lit. m.p. 131–132°; $[\alpha]_D^{26}$ +4.4° (7)).

Anal. Calcd. for $C_{14}H_{18}N_2O_4$: C, 60.5; H, 6.5; N, 10.1. Found: C, 60.3; H, 6.6; N, 10.6.

*Ethyl Tosyl-*L*-prolylglycinate*

This was obtained in 68% yield. It was recrystallized from hexane – ethyl acetate (2:1) and melted at 84–86°; $[\alpha]_D^{25}$ −115.8° (*c*, 4.5 in absolute ethanol).

Anal. Calcd. for $C_{16}H_{22}N_2O_5S$: C, 54.3; H, 6.2; N, 7.9. Found: C, 54.4; H, 6.1; N, 8.0.

ACKNOWLEDGMENT

We are indebted to Mrs. M. Goldstein and her analytical group for the microanalyses.

1. W. Traube. Chem. Ber. **43**, 3586 (1910).
2. Cyanamid's Nitrogen Chemicals Digest. Vol. IV. American Cyanamid Co., New York. 1950. p. 15.
3. A. Albert, R. Goldacre, and J. Philips. J. Chem. Soc. 2241 (1948).
4. O. Süs. Ann. **572**, 96 (1951).
5. T. Curtius and R. Wustenfeld. J. Prakt. Chem. **70**, 78 (1904).
6. G. Schramm and H. Wissmann. Chem. Ber. **91**, 1073 (1958).
7. J. C. Sheehan and D.-D. H. Yang. J. Am. Chem. Soc. **80**, 1154 (1958).

Received September 17, 1964.
Department of Organic Chemistry,
Hebrew University,
Jerusalem, Israel.

SYNTHESIS OF 5-BENZAMIDO-5-DEOXY-D-XYLOPYRANOSE

M. S. Patel and J. K. N. Jones

The synthesis of the *N*-acetyl (1, 2) (I, R = $COCH_3$) and the *N*-benzyl (3) (I, R = CH_2Ph) derivatives of 5-amino-5-deoxy-D-xylopyranose (4) (I, R = H) and of the corresponding furanose compounds has been described (1–4). Recently we attempted the preparation by reported procedures of the acetobromo derivative of 5-acetamido-5-deoxy-D-xylopyranose (I, R = $COCH_3$) but were unsuccessful. The synthesis of the benzamido derivative of 5-amino-5-deoxy-D-xylopyranose (I, R = COPh) was therefore undertaken in the hope that this would yield, after *O*-benzoylation, a benzoylbromo sugar.

Can. J. Chem. Downloaded from www.nrcresearchpress.com by 210.87.254.5 on 09/05/12
For personal use only.

Also, it was of interest to compare the effect of the presence of a *N*-benzoyl group in 5-amino-5-deoxy-D-xylopyranose on the ratio of the pyranose and furanose forms of I, R = COPh.

5-Amino-5-deoxy-1,2-*O*-isopropylidene-D-xylofuranose (II) was prepared from D-xylose by an improved procedure (5). On treatment with an excess of benzoyl chloride in 10% aqueous sodium hydroxide it readily yielded crystalline 5-benzamido-3-*O*-benzoyl-5-deoxy-1,2-*O*-isopropylidene-D-xylofuranose (III) in 92% yield. The latter, on treatment with a catalytic amount of sodium methoxide in methanol, yielded 5-benzamido-5-deoxy-1,2-*O*-isopropylidene-D-xylofuranose (IV) in 82.5% yield (based on compound II). On treatment with benzoyl chloride (1.1 moles) in pyridine, compound IV gave III in 25% yield. Hydrolysis of IV with an acidic ion-exchange resin yielded 5-benzamido-5-deoxy-D-xylopyranose (I, R = COPh) (51% yield) as the major product in equilibrium with 5-benzamido-5-deoxy-D-xylofuranose (V). No other product was detected by chromatography (8).

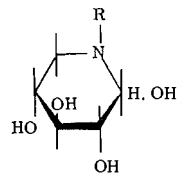

(I)

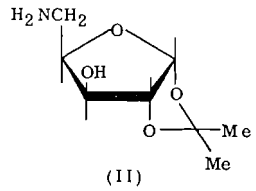

(II)

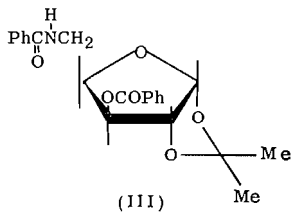

(III)

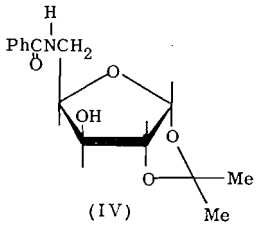

(IV)

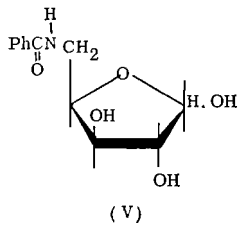

(V)

Cellulose column chromatography of the above mixture gave compounds V and I, R = COPh. One of these (I, R = COPh) was obtained in a crystalline form, and the other was obtained as a pale yellow chromatographically uniform syrup which could not be crystallized. The infrared spectrum of this syrup showed characteristic absorption caused by the presence of OH, NH, and an aromatic ring. The results of periodate oxidation in unbuffered aqueous solution also indicated that the compound possessed the structure V. The compound was, therefore, 5-benzamido-5-deoxy-D-xylofuranose. The crystalline compound (I, R = COPh) showed no NH band in its infrared spectrum and the results of periodate oxidation in unbuffered aqueous solution were consistent with the pyranose structure.

Can. J. Chem. Downloaded from www.nrcresearchpress.com by 210.87.254.5 on 09/05/12
For personal use only.

Can. J. Chem. Downloaded from www.nrcresearchpress.com by 210.87.254.5 on 09/05/12
For personal use only.

EXPERIMENTAL

Apparatus, Methods, and Material

Solutions were concentrated under reduced pressure below 40° with a rotatory vacuum-type evaporator. Melting points were determined on a Fisher–Johns melting point apparatus. Optical rotations were measured at 20 ± 3° with a Hilger standard polarimeter. Infrared spectra were measured with a Perkin–Elmer model 21 spectrophotometer. Paper chromatography was performed by the descending method at room temperature on Whatman No. 1 filter paper in the following solvent system (v/v/v): 1-butanol – ethanol – water (3:1:1). Sugars were detected on paper chromatograms by the following spray reagents: (*i*) alkaline silver nitrate (6); (*ii*) *p*-anisidine hydrochloride (7); (*iii*) modified ceric ammonium nitrate reagent (8); (*iv*) orcinol – trichloroacetic acid (ketose spray) (9).

Rates of movement of the sugars on paper chromatograms are given relative to that of L-rhamnose. Thin-layer chromatography was carried out on silica gel G supplied by Research Specialities Company, Richmond, California. Benzene–isopropanol (2:1) was used as eluent. The developed plates were dried in air, sprayed with concentrated sulfuric acid, and then heated in an oven at about 150°. Organic microanalyses were performed by Dr. C. Daessle, Montreal.

Periodate Oxidation

The compound under examination (10–15 mg) was dissolved in water containing 0.3 *M* sodium metaperiodate solution (1 ml). The total volume was made up to 25 ml with additional water. A blank was prepared with 0.3 *M* sodium metaperiodate (1 ml), which was made up to 25 ml with water. The solutions were stored in the dark at room temperature. Aliquots (2 ml) were removed at intervals from each of the two solutions for the determination of periodate uptake (11). Formic acid production was determined by addition of ethylene glycol (3 ml) to an aliquot portion (2 ml), followed by titration after 10 min with 0.01 *N* sodium hydroxide, with phenolphthalein as indicator. The results are summarized in Table I. (No formaldehyde was detected in either *a* or *b* by the chromotropic acid method (12).)

TABLE I

(*a*) 5-Benzamido-5-deoxy-D-xylofuranose (V)						
Time (h)	0.55	1.35	7.0	14.00	28.00	48.00
Periodate (moles/mole)	1.18	1.64	1.68	1.70	1.82	1.88
Formic acid (moles/mole)	0.48	0.96	1.22	1.31	1.5	1.53
(*b*) 5-Benzamido-5-deoxy-D-xylopyranose (I, R = COPh)						
Time (h)	1.00	6.00	8.00	24.00	48.00	
Periodate (moles/mole)	1.50	2.48	2.71	2.81	2.84	
Formic acid (moles/mole)	1.00	1.65	1.85	2.20	2.40	

5-Amino-5-deoxy-1,2-O-isopropylidene-D-xylofuranose (II) (Modified Procedure of Szarek and Jones (5))

Raney nickel (10) (10 g) was added to a solution of 5-azido-5-deoxy-1,2-*O*-isopropylidene-D-xylofuranose (10.0 g) (3) in methanol (250 ml) and the mixture was shaken overnight. Fresh catalyst (15 g) was then introduced, and after being shaken for an additional 6.0 h the solution was filtered and concentrated to give a crystalline product (5.0 g). This material could be recrystallized readily from ether, yielding crystals of m.p. 102–110°. The substance is highly hygroscopic, and satisfactory analytical results were not obtained. The infrared spectrum in chloroform showed absorption at 3 350 cm^{-1} (OH and NH) and absorption at 1 382 and 1 392 cm^{-1} (the isopropylidene group), but was devoid of azide absorption.

5-Benzamido-3-O-benzoyl-5-deoxy-1,2-O-isopropylidene-D-xylofuranose

To a solution of 5-amino-5-deoxy-1,2-*O*-isopropylidene-D-xylofuranose (3.5 g) in 10% aqueous sodium hydroxide (50 ml) was added excess benzoyl chloride (7 ml). After a few minutes of vigorous shaking a solid product separated; this was dissolved in chloroform (25 ml) and the solution was washed successively with aqueous sodium hydrogen carbonate and with water, and then dried ($MgSO_4$). Concentration of the filtered solution gave a solid (6.8 g, 92%), which was crystallized from benzene–petrol (b.p. 40–60°) as fine needles of m.p. 148–149° and $[\alpha]_D$ −64° (*c*, 1.2 in chloroform). The infrared spectrum in chloroform showed absorptions at 1 665 cm^{-1} (the amide-I band) and 1 730 cm^{-1} (ester carbonyl stretching), absorptions at 1 460 and 1 495 cm^{-1}, 1 590 and 1 610 cm^{-1} attributable to the aromatic ring, and a doublet at 1 382 and 1 390 cm^{-1} (the isopropylidene group), but was devoid of OH absorption.

Anal. Calcd. for $C_{22}H_{23}NO_6$: C, 66.5; H, 5.8; N, 3.5. Found: C, 66.8; H, 6.0; N, 3.45.

5-Benzamido-5-deoxy-1,2-O-isopropylidene-D-xylose (IV)

To a solution of 5-benzamido-3-*O*-benzoyl-5-deoxy-1,2-*O*-isopropylidene-D-xylofuranose (0.33 g) in absolute methanol (15 ml) was added a catalytic amount of metallic sodium. The reaction solution was allowed to stand at room temperature for 2 h with occasional shaking. It was then poured onto ice, and after the ice had melted the solution was concentrated to one-half the initial volume and then extracted

with chloroform. The combined chloroform extracts were washed with water, dried ($MgSO_4$), and filtered, and the filtrate was concentrated to a syrup (0.255 g) which crystallized immediately. Recrystallization from benzene–petrol (b.p. 40–60°) gave needles (0.225 g, 98.4%) of m.p. 163–163.5° and $[\alpha]_D$ +15° (*c*, 1.23 in CH_3OH). The infrared spectrum in chloroform showed absorptions at 3 485 cm^{-1} attributable to OH, at 3 400 cm^{-1} attributable to NH, at 1 650 cm^{-1} (the amide-I band), at 1 530 cm^{-1} (the amide-II band), aromatic absorption at 1 610, 1 585, 1 495, and 1 460 cm^{-1}, a doublet at 1 380 and 1 385 cm^{-1} (isopropylidene group, and showed the absence of an ester.

Anal. Calcd. for $C_{15}H_{19}NO_5$: C, 61.4; H, 6.5; N, 4.8. Found: C, 61.4; H, 6.4; N, 5.0.

Benzoylation of IV

5-Benzamido-5-deoxy-1,2-*O*-isopropylidene-D-xylofuranose (3.4 g) in pyridine (10 ml) was treated with benzoyl chloride (1.1 moles) and the mixture was left at room temperature overnight. Water was then added to the solution and the mixture was extracted with chloroform (3 × 30 ml). The solution was washed successively with dilute sulfuric acid, with sodium bicarbonate solution, and with water. The dried chloroform solution was evaporated and the product recrystallized from benzene–petrol (40–60°). The yield of purified product was 1.95 g. It had m.p. 148°, identical with the product (III) described above.

Hydrolysis of 5-Benzamido-5-deoxy-1,2-O-isopropylidene-D-xylofuranose (IV)

To an aqueous suspension (100 ml) of 5-benzamido-5-deoxy-1,2-*O*-isopropylidene-D-xylofuranose (1.345 g) was added Rexyn 50 (H form) (Fisher Scientific Company) (ca. 5.0 g). The reaction mixture was stirred at 75° until all the solid had dissolved (ca. 3 h). Rexyn 50 was removed by filtration and the filtrate was stirred with a small quantity of Duolite A-4 (OH form) to remove acidity. The filtered solution was concentrated to yield a colorless syrup (1.109 g) which was examined on paper chromatograms as well as by thin-layer chromatography. Sprays *i* and *ii* both showed the presence of components on paper chromatograms at R_{rh} 1.4 (I, R = COPh) and 2.0 (V). No unchanged starting material was detected either on paper chromatograms (spray *iii*) or by thin-layer chromatography. The syrup was placed on a cellulose column (54 × 2.5 cm) and irrigated with pure 1-butanol. Fractions (3 ml) were collected automatically. Chromatographic examination of the fractions showed that a partial separation of the two components (0.14 g of V and 0.20 g of I, R = COPh) had been achieved. The unresolved mixture was refractionated using the same experimental conditions. Complete separation was then obtained. The two components (I, R = COPh and V) of the hydrolysate were obtained in a chromatographically pure state.

(a) 5-Benzamido-5-deoxy-D-xylofuranose (V)

This component was obtained from the eluate as a yellow syrup (0.218 g) which could not be crystallized. The compound had $[\alpha]_D^{20}$ +19.2° (*c*, 0.8 in methanol) and R_{rh} 2.0. The infrared spectrum (thin film on KBr) showed characteristic absorption caused by OH at 3 310 cm^{-1}, by NH at 1 557 cm^{-1}, and by the aromatic ring at 1 460, 1 495, 1 590, and 1 610 cm^{-1}.

(b) 5-Benzamido-5-deoxy-D-xylopyranose (I, R = COPh)

This component was obtained from the eluent above as a white crystalline solid (0.6 g, 51.7%). It crystallized from methanol–ether with 1 molecule of methanol as a solvent of crystallization and had an indefinite melting point (m.p. 94–102°), $[\alpha]_D^{20}$ −11.5° (*c*, 0.69 in methanol), and R_{rh} 1.4. The infrared spectrum of this material (0.8% in KBr) showed strong absorption at 3 310 cm^{-1} attributable to OH, strong absorption at 1 625 cm^{-1} caused by *N*-benzoyl (amide-I), aromatic absorption at 1 475, 1 495, and 1 590 cm^{-1}, but no absorption caused by NH.

Anal. Calcd. for $C_{12}H_{15}NO_5 \cdot CH_3OH$: C, 55.7; H, 1.9; N, 5.0. Found: C, 55.6; H, 7.1; N, 5.1.

ACKNOWLEDGMENT

The authors thank the National Cancer Institute of Canada for financial assistance.

1. W. A. Szarek and J. K. N. Jones. Can. J. Chem. **41**, 637 (1963).
2. H. Paulsen. Ann. **670**, 121 (1963).
3. H. Paulsen, K. Todt, and K. Heyns. Ann. **679**, 168 (1964).
4. H. Paulsen. Ann. **683**, 187 (1965).
5. W. A. Szarek. Ph.D. Thesis, Queen's University, Kingston, Ontario. 1964.
6. W. E. Trevelyan, D. P. Proctor, and J. S. Harrison. Nature, **166**, 444 (1950).
7. L. Hough, J. K. N. Jones, and W. H. Wadman. J. Chem. Soc. 1702 (1950).
8. J. W. Bird. Can. J. Chem. **40**, 1716 (1962).
9. R. Klevstrand and A. Nordal. Acta Chem. Scand. **4**, 1320 (1950).
10. A. I. Vogel. Practical organic chemistry. 3rd ed. Longmans, Green & Co., Ltd., London. 1961. p. 870.
11. G. Neumüller and E. Vasseur. Arkiv Kemi, **5**, 235 (1953).
12. J. F. O'Dea and R. A. Gibbons. Biochem. J. **55**, 580 (1953).

Received July 9, 1965.
Department of Chemistry,
Queen's University,
Kingston, Ontario.

Can. J. Chem. Downloaded from www.nrcresearchpress.com by 210.87.254.5 on 09/05/12
For personal use only.

GLYCOSIDATION OF SUGARS
III. GAS–LIQUID CHROMATOGRAPHY OF THE METHYL GLYCOSIDES OF D-GALACTOSE, D-GLUCOSE, AND D-MANNOSE AS THEIR TRIMETHYLSILYL ETHERS[1]

V. SMIRNYAGIN,[2] C. T. BISHOP, AND F. P. COOPER

The previous paper (1) in this series described a study of the kinetics of methanolysis of the four D-pentoses. As a prelude to extending this work to the hexoses it was necessary to find methods for analyzing the methyl hexosides by gas–liquid chromatography. The present communication describes the gas–liquid chromatographic separation of the four methyl glycosides of each of the three aldohexoses, D-galactose, D-glucose, and D-mannose.

Unsubstituted methyl glycosides are considerably less volatile than many other derivatives in which some of the hydroxyl groups of the sugar ring are substituted by ester or ether groups. Nevertheless, gas–liquid chromatography of a number of unsubstituted methyl glycosides has been described (2, 3). However, the conditions required for these separations were not sufficiently selective to resolve the four isomeric glycosides of a single monosaccharide. In the previous studies in this series (1, 4) the methyl glycosides were *O*-methylated or *O*-acetylated to make them sufficiently volatile for analysis by gas–liquid chromatography. In the present study it was found that the *O*-trimethylsilyl derivatives of the methyl hexosides could be resolved better than either the *O*-acetyl or the *O*-methyl derivatives. The use of *O*-trimethylsilyl derivatives has the advantage of ease of preparation and simple recovery of the original compound by a very mild hydrolysis (5). The separations described here may therefore also be used on a preparative scale to provide pure samples of individual methyl glycosides for spectroscopic examination or studies of kinetics of hydrolysis.

The retention times of the methyl tetra-*O*-trimethylsilyl hexosides and of the trimethylsilyl tetra-*O*-trimethylsilyl hexosides, relative to the fastest moving component in each series, are shown in Table I. Three column packings were used and each required a different column temperature for optimum resolution. The crystalline hexoses each gave only one peak after trimethylsilylation; it is not known whether these single peaks contained more than one anomer or ring form. However, it is likely that the hexoses underwent trimethylsilylation before equilibration in the pyridine solution. If this was so, then the single peaks for each hexose must represent the anomeric species present in the common crystalline form of the sugar. This is in agreement with the results of Sweeley *et al.* (6), who found that "the products obtained from pure single anomers of pentoses and hexoses generally show a single peak on gas chromatography though, in some cases, small amounts of another anomeric form may be apparent. In general, anomerizations occurring in pyridine during preparation of the trimethylsilyl derivative are remarkably minimal."

The four methyl D-mannosides were well resolved on columns *a* or *b*, with the latter providing slightly better separation. Similarly, the four methyl D-glucosides were resolved on columns *b* or *c* but the separation was significantly improved on the latter column. The four methyl D-galactosides could not be completely resolved on a single column. Thus, on columns *a* and *b* methyl α-D-galactopyranoside and methyl α-D-galactofuranoside run together. On column *c* it is the methyl β-D-galactofuranoside and methyl α-D-galactopyranoside that are not separated. Successive separations on columns *a* and *c* or *b* and *c*

[1]*Issued as N.R.C. No. 8636.*

[2]*Exchange Scientist, 1965. Permanent address: Institute of Organic Chemistry, Academy of Sciences, Moscow, U.S.S.R.*

Can. J. Chem. Downloaded from www.nrcresearchpress.com by 210.87.254.5 on 09/05/12
For personal use only.

TABLE I

Relative retention times of *O*-trimethylsilyl derivatives of methyl D-hexosides and of hexoses

Methyl glycoside and hexose	Column:*		
	a	*b*	*c*
β-D-Galactofuranoside	*1.00*	1.16	*1.00*
D-Galactose	1.10	*1.00*	1.13
α-D-Galactopyranoside	1.22	1.42	1.05
α-D-Galactofuranoside	1.28	1.44	1.16
β-D-Galactopyranoside	1.65	1.80	1.43
β-D-Glucofuranoside	—	*1.00*	*1.00*
α-D-Glucofuranoside	—	1.09	1.10
D-Glucose	—	1.16	1.32
α-D-Glucopyranoside	—	1.79	1.52
β-D-Glucopyranoside	—	1.81	1.71
D-Mannose	*1.00*	*1.00*	—
α-D-Mannopyranoside	1.16	1.41	—
β-D-Mannopyranoside	1.51	1.74	—
α-D-Mannofuranoside	1.89	2.25	—
β-D-Mannofuranoside	2.29	2.69	—

*Carrier gas was argon at a flow rate of 100 ml/min; β-ionization detector. Columns were straight glass tubes (120 × 0.5 cm) and were packed with—*a*: 10% (w/w) of neopentylglycolsebacate polyester on acid-washed Chromosorb W (100–120 mesh) (temp. 150 °C); *b*: 15% (w/w) of polyphenyl ether (*m*-bis-(*m*-phenoxyphenoxy) benzene) on acid-washed Chromosorb W (100–120 mesh) (temp. 175 °C); *c*: 10% (w/w) of Carbowax 6000 on acid-washed Chromosorb W (100–120 mesh) (temp. 140 °C).

are therefore required for the analysis of each component. Figure 1, A–D, shows the separations obtained. Individual glycosides, prepared and characterized as described below, were used to establish the identities of the peaks. There was no evidence of anomerization or change in ring size during trimethylsilylation or during gas–liquid chromatography.

EXPERIMENTAL

A Pye Argon chromatograph was used for gas–liquid chromatography. Methyl glycosides were prepared by standard methods (7) and had physical constants in agreement with the literature values.

(*a*) Methyl α-D-galactofuranoside, m.p. 92–93 °C, $[\alpha]_D^{24}$ +104° (*c*, 2 in water). Reported (8), m.p. 91–92 °C, $[\alpha]_D^{20}$ +104° (*c*, 1 in water).

(*b*) Methyl β-D-galactofuranoside, m.p. 66–67 °C, $[\alpha]_D^{24}$ −113.5° (*c*, 3 in water). Reported (8), m.p. 69 °C, $[\alpha]_D^{20}$ −112° (*c*, 3 in water).

(*c*) Methyl α-D-galactopyranoside, m.p. 115–117 °C, $[\alpha]_D^{24}$ +192° (*c*, 2 in water). Reported (9), m.p. 114–116 °C, $[\alpha]_D^{20}$ +196° (in water).

(*d*) Methyl β-D-galactopyranoside, m.p. 176–179 °C, $[\alpha]_D^{20}$ ±0° (*c*, 2 in water). Reported (9), m.p. 178 °C, $[\alpha]_D^{20}$ ±0° (in water).

(*e*) Methyl α-D-glucofuranoside; this compound was prepared by borohydride reduction of methyl α-D-glucofuranosidurono-6,3-lactone, m.p. 145–147 °C, $[\alpha]_D^{24}$ +145° (*c*, 0.5 in water). Reported (10), m.p. 148 °C, $[\alpha]_D$ +147° (in water). The reduced product, after trimethylsilylation, showed only one peak on gas–liquid chromatography; the single peak had the same retention time as the second fastest peak of the four products obtained by methanolysis of D-glucose.

(*f*) Methyl β-D-glucofuranoside; this compound was prepared by borohydride reduction of methyl β-D-glucofuranosidurono-6,3-lactone, m.p. 138–139 °C, $[\alpha]_D^{24}$ −59° (*c*, 2.4 in water). Reported (10), m.p. 140–141 °C, $[\alpha]_D$ −58° (in water). The reduced, trimethylsilylated product gave a single peak on gas–liquid chromatography; the single peak corresponded to the fastest moving peak of the four components obtained by methanolysis of D-glucose.

(*g*) Methyl α-D-glucopyranoside, m.p. 166–167 °C, $[\alpha]_D^{27}$ +159° (*c*, 2.0 in water). Reported (11), m.p. 165–166 °C, $[\alpha]_D^{20}$ +158° (in water).

(*h*) Methyl β-D-glucopyranoside, m.p. 107–110 °C, $[\alpha]_D^{24}$ −33.7° (*c*, 2.1 in water). Reported (12), m.p. 108–110 °C, $[\alpha]_D^{20}$ −34.2° (in water).

(*i*) Methyl α-D-mannofuranoside, m.p. 120–121 °C, $[\alpha]_D^{24}$ +111° (*c*, 1.3 in water). Reported (13), m.p. 118–119 °C, $[\alpha]_D^{20}$ +113° (*c*, 1 in water).

Can. J. Chem. Downloaded from www.nrcresearchpress.com by 210.87.254.5 on 09/05/12
For personal use only.

Can. J. Chem. Downloaded from www.nrcresearchpress.com by 210.87.254.5 on 09/05/12
For personal use only.

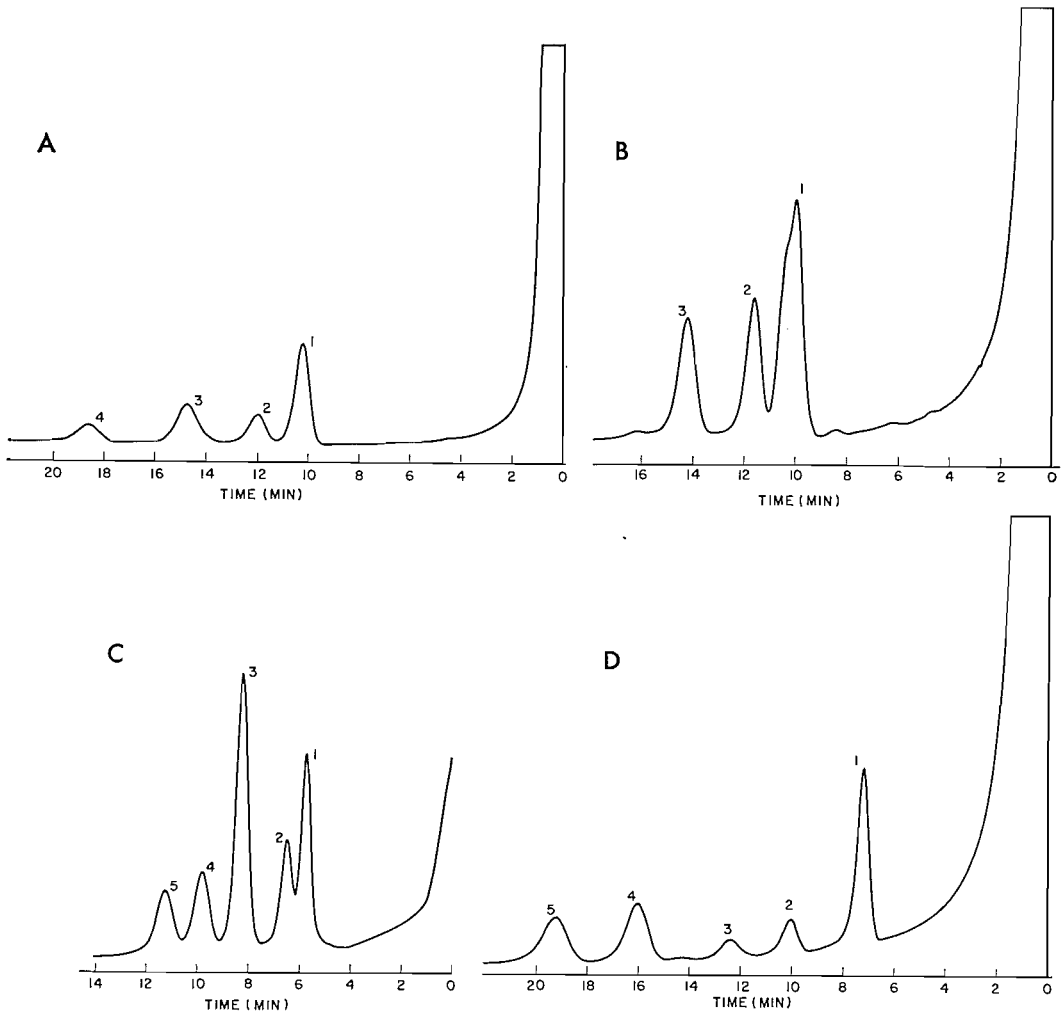

FIG. 1. Gas–liquid chromatograms of methyl tetra-*O*-trimethylsilyl-D-hexosides. A: Methyl D-galactosides and D-galactose on column *b*. Peaks: 1, D-galactose; 2, methyl β-D-galactofuranoside; 3, methyl α-D-galactopyranoside and methyl α-D-galactofuranoside; 4, methyl β-D-galactopyranoside. B: Methyl D-galactosides on column *c*. Peaks: 1, methyl β-D-galactofuranoside and methyl α-D-galactopyranoside; 2, methyl α-D-galactofuranoside; 3, methyl β-D-galactopyranoside. C: Methyl D-glucosides on column *c*. Peaks: 1, methyl β-D-glucofuranoside; 2, methyl α-D-glucofuranoside; 3, D-glucose; 4, methyl α-D-glucopyranoside; 5, methyl β-D-glucopyranoside. D: Methyl D-mannosides on column *b*. Peaks: 1, D-mannose; 2, methyl α-D-mannopyranoside; 3, methyl β-D-mannopyranoside; 4, methyl α-D-mannofuranoside; 5, methyl β-D-mannofuranoside.

(*j*) Methyl β-D-mannofuranoside; this compound could not be obtained in a crystalline form. Gas–liquid chromatography of its trimethylsilyl ether showed the presence of only one component which differed in retention time from the other three methyl D-mannosides; $[\alpha]_D^{24}$ −110° (*c*, 1 in water). Reported (14), m.p. 47°, $[\alpha]_D^{20}$ −107° (in water).

(*k*) Methyl α-D-mannopyranoside, m.p. 192–193 °C, $[\alpha]_D^{24}$ +80° (*c*, 5 in water). Reported (15), m.p. 193–194 °C, $[\alpha]_D^{20}$ +79.2° (in water).

(*l*) Methyl β-D-mannopyranoside isopropyl alcoholate, m.p. 74–76 °C, $[\alpha]_D^{24}$ −60° (*c*, 1.0 in water). Reported (16), m.p. 74–75 °C, $[\alpha]_D^{20}$ −53.3° (*c*, 4 in water).

Trimethylsilyl derivatives were prepared by the method of Sweeley *et al.* (6); reagents (pyridine, 1 ml; hexamethyldisilazane, 0.2 ml; and trimethylchlorosilane, 0.1 ml) were added to the crystalline hexoses (10 mg) successively and with a minimum of delay so that there was little time for anomerization.

1. C. T. Bishop and F. P. Cooper. Can. J. Chem. **41**, 2743 (1963).
2. J. N. Baxter and A. S. Perlin. Can. J. Chem. **38**, 2217 (1960).
3. H. G. Jones and M. B. Perry. Can. J. Chem. **40**, 1339 (1962).
4. C. T. Bishop and F. P. Cooper. Can. J. Chem. **40**, 224 (1962).
5. E. J. Hedgley and W. G. Overend. Chem. Ind. London, 378 (1960).
6. C. C. Sweeley, R. Bentley, M. Makita, and W. W. Wells. J. Am. Chem. Soc. **85**, 2497 (1963).
7. J. Conchie, G. A. Levvy, and C. A. Marsh. Advan. Carbohydrate Chem. **12**, 157 (1957).
8. I. Augestad and E. Berner. Acta Chem. Scand. **8**, 251 (1954).
9. E. Bourquelot. Ann. Chim. Paris, **7**, 218 (1917).
10. J. E. Cadotte, F. Smith, and D. Spriestersbach. J. Am. Chem. Soc. **74**, 1501 (1952).
11. E. Fischer. Ber. **26**, 2406 (1893).
12. W. Koenigs and E. Knorr. Ber. **34**, 957 (1901).
13. W. N. Haworth and C. R. Porter. J. Chem. Soc. 649 (1930).
14. E. Pacsu and A. Scattergood. J. Am. Chem. Soc. **61**, 534 (1939).
15. E. Fischer and L. Beensch. Ber. **29**, 2927 (1896).
16. H. S. Isbell and H. L. Frush. J. Res. Natl. Bur. Std. **24**, 125 (1940).

Received June 21, 1965.
Division of Biosciences,
National Research Council,
Ottawa, Canada.

Can. J. Chem. Downloaded from www.nrcresearchpress.com by 210.87.254.5 on 09/05/12
For personal use only.

3-MERCAPTOQUINUCLIDINE[1]

K. B. Shaw

This note describes the preparation of 3-mercaptoquinuclidine (I), which was required in connection with another problem. The usual methods (1) for the synthesis of thiols involving the reaction of a halide with a sulfur-containing compound, e.g. potassium thiolacetate, sodium hydrosulfide, or thiourea, failed in the present case, since 3-chloroquinuclidine was quite inert towards nucleophilic substitution by these reagents under a variety of conditions. Inspection of a model of 3-chloroquinuclidine indicated that attainment of the transition state in a S_N2 reaction is sterically improbable (similar to the situation in bicyclo[2.2.2]octane compounds (2)). The failure of reactions under conditions which would be expected to promote a S_N1 reaction can be attributed to the rigid structure of the quinuclidine molecule, which prevents the intermediate carbonium ion that would be formed from becoming planar.

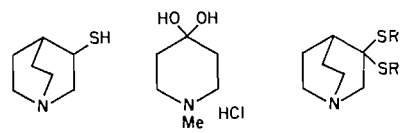

I II III, R = H
IV, R = COMe

Hence a route to I not involving displacement of a substituent in the 3-position of the quinuclidine ring was required, and the method used (3) for the preparation of 1-methyl-4-mercaptopiperidine seemed most promising.

It was shown by Lyle *et al.* (4) that, when 1-methyl-4-piperidone was dissolved in dilute hydrochloric acid and the solution evaporated to dryness, the salt crystallized with 1 molecule of water. The infrared spectrum of the hydrate proved that the structure

[1]*Issued as D.C.B.R.L. Report No. 455A.*

1. C. T. Bishop and F. P. Cooper. Can. J. Chem. **41**, 2743 (1963).
2. J. N. Baxter and A. S. Perlin. Can. J. Chem. **38**, 2217 (1960).
3. H. G. Jones and M. B. Perry. Can. J. Chem. **40**, 1339 (1962).
4. C. T. Bishop and F. P. Cooper. Can. J. Chem. **40**, 224 (1962).
5. E. J. Hedgley and W. G. Overend. Chem. Ind. London, 378 (1960).
6. C. C. Sweeley, R. Bentley, M. Makita, and W. W. Wells. J. Am. Chem. Soc. **85**, 2497 (1963).
7. J. Conchie, G. A. Levvy, and C. A. Marsh. Advan. Carbohydrate Chem. **12**, 157 (1957).
8. I. Augestad and E. Berner. Acta Chem. Scand. **8**, 251 (1954).
9. E. Bourquelot. Ann. Chim. Paris, **7**, 218 (1917).
10. J. E. Cadotte, F. Smith, and D. Spriestersbach. J. Am. Chem. Soc. **74**, 1501 (1952).
11. E. Fischer. Ber. **26**, 2406 (1893).
12. W. Koenigs and E. Knorr. Ber. **34**, 957 (1901).
13. W. N. Haworth and C. R. Porter. J. Chem. Soc. 649 (1930).
14. E. Pacsu and A. Scattergood. J. Am. Chem. Soc. **61**, 534 (1939).
15. E. Fischer and L. Beensch. Ber. **29**, 2927 (1896).
16. H. S. Isbell and H. L. Frush. J. Res. Natl. Bur. Std. **24**, 125 (1940).

Received June 21, 1965.
Division of Biosciences,
National Research Council,
Ottawa, Canada.

Can. J. Chem. Downloaded from www.nrcresearchpress.com by 210.87.254.6 on 09/05/12
For personal use only.

3-MERCAPTOQUINUCLIDINE[1]

K. B. Shaw

This note describes the preparation of 3-mercaptoquinuclidine (I), which was required in connection with another problem. The usual methods (1) for the synthesis of thiols involving the reaction of a halide with a sulfur-containing compound, e.g. potassium thiolacetate, sodium hydrosulfide, or thiourea, failed in the present case, since 3-chloroquinuclidine was quite inert towards nucleophilic substitution by these reagents under a variety of conditions. Inspection of a model of 3-chloroquinuclidine indicated that attainment of the transition state in a S_N2 reaction is sterically improbable (similar to the situation in bicyclo[2.2.2]octane compounds (2)). The failure of reactions under conditions which would be expected to promote a S_N1 reaction can be attributed to the rigid structure of the quinuclidine molecule, which prevents the intermediate carbonium ion that would be formed from becoming planar.

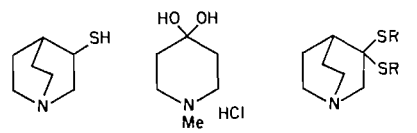

I II III, R = H
IV, R = COMe

Hence a route to I not involving displacement of a substituent in the 3-position of the quinuclidine ring was required, and the method used (3) for the preparation of 1-methyl-4-mercaptopiperidine seemed most promising.

It was shown by Lyle *et al.* (4) that, when 1-methyl-4-piperidone was dissolved in dilute hydrochloric acid and the solution evaporated to dryness, the salt crystallized with 1 molecule of water. The infrared spectrum of the hydrate proved that the structure

[1]*Issued as D.C.B.R.L. Report No. 455A.*

is as shown in II. Similar behavior was observed with 1-methyl-3-piperidone. The formation of the *gem*-diol (II) led Barrera and Lyle (3) to believe that hydrogen sulfide might add similarly to the carbonyl group of 1-methyl-4-piperidone to give a *gem*-dithiol, which could be reduced to the thiol; this was shown to be the case. However, it has been stated more recently by Lyle *et al.* (5) that a similar route to 1-methyl-3-mercaptopiperidine was unsuccessful.

3-Quinuclidinone was not available to us and its preparation from the available 3-quinuclidinol was investigated. Although chromic acid is the preferred reagent for the oxidation of secondary alcohols to ketones, the method proved impracticable in this case, primarily because of difficulties in separating the product from inorganic material; the oxidation was achieved finally with potassium permanganate in acetone solution. It was found that 3-quinuclidinone did not form a stable hydrate under the same conditions that the piperidones did; the salt showed no hydroxyl band in the infrared but did show a strong carbonyl band at 1 748 cm^{-1}. However, hydrogen sulfide did react with 3-quinuclidinone in isopropanol solution to give 3,3-dimercaptoquinuclidine (III). Clearly, the success or failure of a ketone to form a stable dithiol does not depend upon whether or not the ketone forms a stable hydrate by addition of water to the carbonyl group. Other examples of this are available; acetone, 3-pentanone, and cyclohexanone, for instance, form stable dithiols (6) but their hydrates are not isolable.

The reaction of hydrogen sulfide with 3-quinuclidinone in isopropanol solution was much slower than that with 1-methyl-4-piperidone, and it was necessary to increase the reaction time from about 6 h to 40 h to obtain a similar yield (65%) of product. The reaction was not accelerated by variations in solvent or temperature. The dithiol, a white solid which separated from solution as the reaction proceeded, had an onion-like odor (6), liberated hydrogen sulfide in water, and with alcoholic lead acetate solution gave a yellow color which darkened rapidly (6). It was not a hydrate (infrared), as was the case with 1-methyl-4,4-dimercaptopiperidine, and could not be recrystallized; however, the presence of two sulfhydryl groups was shown by reaction with acetic anhydride to give a diacetate (IV) (characterized as the picrate), and the two groups were shown to be on the same carbon atom (6) by reaction with 2,4-dinitrophenylhydrazine in hydrochloric acid to give 3-quinuclidinone 2,4-dinitrophenylhydrazone hydrochloride (identical (infrared) with an authentic sample prepared from 3-quinuclidinone). The free bases of these two derivatives were also identical.

Reduction of 3,3-dimercaptoquinuclidine with sodium borohydride in isopropanol solution, as in the preparation of 1-methyl-4-mercaptopiperidine from 1-methyl-4,4-dimercaptopiperidine (3), gave no identifiable product but, with a modified work-up, 3-mercaptoquinuclidine was obtained in about 50% yield. A by-product of the reaction was probably the corresponding disulfide (but see ref. 7) formed by the oxidation of the thiol in the alkaline medium, although the reaction had been worked up under nitrogen as far as possible.

EXPERIMENTAL

3-Quinuclidinone

Acetone (250 ml) containing finely ground potassium permanganate (110 g) was heated under reflux beneath a thimble containing 3-quinuclidinol (25.4 g). The extraction was complete in ca. 30 min and the mixture was heated under reflux for a further 2 h. The solid was separated (Celite) and the acetone removed *in vacuo*, leaving a white crystalline solid (10–13 g; 40–52%), m.p. 145–147.5° (sealed tube) (lit. 147–148° (8)).

The 2,4-dinitrophenylhydrazone hydrochloride, prepared in 95% ethanol containing concentrated hydrochloric acid, was crystallized several times from aqueous ethanol and was obtained as yellow needles, m.p. >250°, but a satisfactory elemental analysis was not obtained. The hydrochloride was dissolved in hot water and the solution made alkaline with sodium carbonate. The copious precipitate was filtered off,

Can. J. Chem. Downloaded from www.nrcresearchpress.com by 210.87.254.6 on 09/05/12
For personal use only.

dried, and crystallized several times from ethanol to give 3-quinuclidinone 2,4-dinitrophenylhydrazone as orange needles, m.p. 244–245°.

Anal. Calcd. for $C_{13}H_{15}N_5O_4$: C, 51.14; H, 4.95; N, 22.94. Found: C, 51.36; H, 5.04; N, 23.13.

3,3-Dimercaptoquinuclidine

3-Quinuclidinone (36 g) in dry isopropanol (85 ml) was stirred, and hydrogen sulfide was bubbled into the solution for 20 h. The solid was filtered off and dried (23 g), and the filtrate was treated with hydrogen sulfide for a further 20 h to yield an additional 9.3 g (64% total) of white solid, m.p. 94–99° decomp., after reddening from 60° (sealed tube).

3,3-Dimercaptoquinuclidine Diacetate

A solution of the foregoing dithiol (3.5 g) in pyridine (20 ml) containing acetic anhydride (4 ml) was left at room temperature for 6 days and then concentrated to yield a deep red, viscous liquid. This was dissolved in ether (150 ml) and passed twice (air pressure) through a column (4.5 × 1.2 cm) of activated charcoal. Removal of the ether left a pale yellow liquid which soon began to darken. The picrate, after several crystallizations from ethanol, was obtained as yellow plates, m.p. 145–146°.

Anal. Calcd. for $C_{17}H_{20}N_4O_9S_2$: C, 41.80; H, 4.13; N, 11.47; S, 13.13; mol. wt. 488.5. Found: C, 41.76; H, 4.25; N, 11.38; S, 13.29; mol. wt. (ultraviolet) 497.

3-Quinuclidinone 2,4-Dinitrophenylhydrazone from 3,3-Dimercaptoquinuclidine

3,3-Dimercaptoquinuclidine (1.3 g) and 2,4-dinitrophenylhydrazine (1.48 g) in 95% ethanol (100 ml) containing concentrated hydrochloric acid (10 ml) were heated under reflux for 5 h and then left overnight. The yellow crystalline solid was separated, dried (2.28 g; 89%), and after several crystallizations from aqueous ethanol was obtained as yellow needles, m.p. >250°. As was the case with the hydrochloride prepared from 3-quinuclidinone, a satisfactory elemental analysis was not obtained. The free base, prepared from the hydrochloride as described above, was crystallized several times from ethanol and obtained as orange rods, m.p. and mixed m.p. with above sample 244–245°.

Anal. Calcd. for $C_{13}H_{15}N_5O_4$: C, 51.14; H, 4.95; N, 22.94. Found: C, 51.29; H, 5.14; N, 22.44.

3-Mercaptoquinuclidine

(*a*) 3,3-Dimercaptoquinuclidine (30 g) was added in portions to a stirred suspension of sodium borohydride (10 g) in isopropanol (200 ml). When the addition was complete the temperature was raised to 65° and maintained there for 2.5 h. The mixture was cooled, diluted with water (100 ml), acidified with concentrated hydrochloric acid (40 ml), and then taken to dryness, the resulting white solid being finally dried over calcium chloride *in vacuo* to constant weight (56 g). A portion of this solid was stirred at room temperature with absolute ethanol and filtered, and the ethanol removed, leaving a white solid which was then similarly treated with dry chloroform. The resulting white solid was crystallized 3 times from ethanol, giving white prisms of 3-mercaptoquinuclidine hydrochloride, m.p. 242–244.5° (sealed tube, heated from 180°), 97% thiol by iodine titration.

Anal. Calcd. for $C_7H_{14}ClNS$: C, 46.79; H, 7.85; N, 7.80; Cl, 19.73; S, 17.84. Found: C, 46.80; H, 7.63; N, 7.70; Cl, 19.78; S, 17.87.

The rest of the original solid (40 g) in water (100 ml) was stirred under nitrogen, made alkaline with sodium carbonate, and extracted with chloroform (7 × 50 ml). The combined extracts were dried ($MgSO_4$), the chloroform removed, and the residue distilled to give 3-mercaptoquinuclidine (7.1 g, 40% based on 40 g of solid used), b.p. 97–98° at 8 mm, 96% thiol by iodine titration, equiv. wt. 150 (calcd. 143). The picrate was crystallized from ethanol as yellow needles, m.p. 171–174°.

Anal. Calcd. for $C_{13}H_{16}N_4O_7S$: C, 41.93; H, 4.33; N, 15.05. Found: C, 41.80; H, 4.60; N, 15.05.

(*b*) 3,3-Dimercaptoquinuclidine (60 g) was reduced with sodium borohydride (20 g) in isopropanol (350 ml) as described above. After 2 h at 70° the isopropanol was removed, the partially solid residue dissolved in water (200 ml), and the cooled solution acidified with concentrated hydrochloric acid. The solution, under nitrogen, was then adjusted to pH 8.5–9 with sodium carbonate, more water (200 ml) was added to dissolve the solid that was present, and the solution was extracted with chloroform (6 × 100 ml). The combined extracts were dried ($MgSO_4$), the chloroform removed, and the residue distilled to give 3-mercaptoquinuclidine (22.9 g, 47%), b.p. 97–98° at 8 mm, 98% thiol by iodine titration. The product eventually solidified, m.p. 48–50°, thiol titration unchanged.

Anal. Calcd. for $C_7H_{13}NS$: C, 58.72; H, 9.15; N, 9.78; S, 22.35. Found: C, 58.60; H, 9.25; N, 9.74; S, 22.26; equiv. wt. 146.

ACKNOWLEDGMENTS

A gift of 3-quinuclidinol from the U.S. Army Chemical Research and Development Laboratories is gratefully acknowledged. Analyses were performed by Mr. J. G. Helie of these laboratories.

Can. J. Chem. Downloaded from www.nrcresearchpress.com by 210.87.254.6 on 09/05/12
For personal use only.

1. L. F. FIESER and M. FIESER. Advanced organic chemistry. Rheinhold Publishing Corp., New York. 1961. p. 312.
2. L. G. HUMBER, G. MYERS, L. HAWKINS, C. SCHMIDT, and M. BOULERICE. Can. J. Chem. **42**, 2852 (1964).
3. H. BARRERA and R. E. LYLE. J. Org. Chem. **27**, 641 (1962).
4. R. E. LYLE, R. E. ADEL, and G. G. LYLE. J. Org. Chem. **24**, 342 (1959).
5. R. E. LYLE, R. MUNK, and L. LADD. J. Org. Chem. **30**, 293 (1965).
6. T. L. CAIRNS, G. L. EVANS, A. W. LARCHAR, and B. C. MCKUSIK. J. Am. Chem. Soc. **74**, 3982 (1952).
7. M. R. V. SAHYUN. Can. J. Chem. **42**, 2925 (1964).
8. L. H. STERNBACH. U.S. Patent No. 2,648,667 (August, 1953); Chem. Abstr. **49**, 1109 (1955).

RECEIVED JUNE 24, 1965.
DEFENCE CHEMICAL, BIOLOGICAL AND RADIATION LABORATORIES,
OTTAWA, CANADA.

Can. J. Chem. Downloaded from www.nrcresearchpress.com by 210.87.254.6 on 09/05/12
For personal use only.

ON THE FORMATION OF A PYRAZOLINE FROM ACETONE TOLUENESULFONYL HYDRAZONE[1]

Y.-C. LIN AND G. JUST

When the tosylhydrazone of acetone, m.p. 136°, was heated to 160°, a vigorous reaction occurred. Chloroform extraction of the reaction product and crystallization gave, in about 10% yield, a crystalline, colorless compound, m.p. 162–163°. Analysis indicated that the elemental composition was $C_{13}H_{18}N_2O_2S$. The infrared spectrum showed absorption at 1 650 cm^{-1} (C=N), 1 605 cm^{-1} (aromatic), and 1 170 cm^{-1} (*p*-toluenesulfonyl group). The nuclear magnetic resonance spectrum[2] showed an A_2B_2 quartet centered at 7.73 p.p.m., and singlets at 2.63 (2H), 2.42 (3H), 1.95 (3H), and 1.45 (6H) p.p.m. The only structure compatible with these data is represented by II.

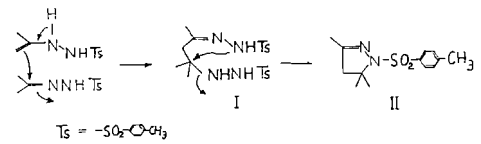

The same compound was also obtained by heating the *p*-toluenesulfonyl hydrazone of acetone, mesityl oxide, or ethyl acetoacetate in glacial acetic acid containing hydrochloric acid for 3–4 h at 90–100°.

A pyrazoline is known to be formed when the hydrazone of mesityl oxide is refluxed in acetic acid (1).

The reaction is not general. The *p*-toluenesulfonyl hydrazones of cyclopentanone, acetophenone, and acetaldehyde did not undergo the reaction. In the case of cyclohexanone, some pyrazoline was formed, but the yield was very low and the product that was obtained was impure.

EXPERIMENTAL

1-p-Toluenesulfonyl-3,5,5-trimethyl-2-pyrazoline (II)

(a) From Thermal Decomposition of Acetone Toluenesulfonyl Hydrazone

Acetone toluenesulfonyl hydrazone (1 g) was heated to 150–160°, at which temperature it decomposed spontaneously to a brownish sirup. After cooling, the mixture was extracted with ether and dioxane to

[1]*This work was supported by Bristol Laboratories, Syracuse, New York.*
[2]*The spectra were taken in deuterochloroform, with tetramethylsilane = 0 p.p.m.*

1. L. F. FIESER and M. FIESER. Advanced organic chemistry. Rheinhold Publishing Corp., New York. 1961. p. 312.
2. L. G. HUMBER, G. MYERS, L. HAWKINS, C. SCHMIDT, and M. BOULERICE. Can. J. Chem. **42**, 2852 (1964).
3. H. BARRERA and R. E. LYLE. J. Org. Chem. **27**, 641 (1962).
4. R. E. LYLE, R. E. ADEL, and G. G. LYLE. J. Org. Chem. **24**, 342 (1959).
5. R. E. LYLE, R. MUNK, and L. LADD. J. Org. Chem. **30**, 293 (1965).
6. T. L. CAIRNS, G. L. EVANS, A. W. LARCHAR, and B. C. MCKUSIK. J. Am. Chem. Soc. **74**, 3982 (1952).
7. M. R. V. SAHYUN. Can. J. Chem. **42**, 2925 (1964).
8. L. H. STERNBACH. U.S. Patent No. 2,648,667 (August, 1953); Chem. Abstr. **49**, 1109 (1955).

RECEIVED JUNE 24, 1965.
DEFENCE CHEMICAL, BIOLOGICAL AND RADIATION LABORATORIES,
OTTAWA, CANADA.

Can. J. Chem. Downloaded from www.nrcresearchpress.com by 210.87.254.40 on 09/05/12
For personal use only.

ON THE FORMATION OF A PYRAZOLINE FROM ACETONE TOLUENESULFONYL HYDRAZONE[1]

Y.-C. LIN AND G. JUST

When the tosylhydrazone of acetone, m.p. 136°, was heated to 160°, a vigorous reaction occurred. Chloroform extraction of the reaction product and crystallization gave, in about 10% yield, a crystalline, colorless compound, m.p. 162–163°. Analysis indicated that the elemental composition was $C_{13}H_{18}N_2O_2S$. The infrared spectrum showed absorption at 1 650 cm^{-1} (C=N), 1 605 cm^{-1} (aromatic), and 1 170 cm^{-1} (*p*-toluenesulfonyl group). The nuclear magnetic resonance spectrum[2] showed an A_2B_2 quartet centered at 7.73 p.p.m., and singlets at 2.63 (2H), 2.42 (3H), 1.95 (3H), and 1.45 (6H) p.p.m. The only structure compatible with these data is represented by II.

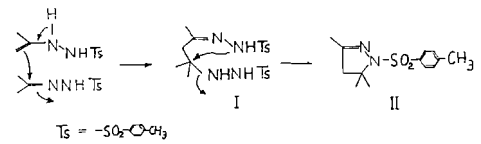

The same compound was also obtained by heating the *p*-toluenesulfonyl hydrazone of acetone, mesityl oxide, or ethyl acetoacetate in glacial acetic acid containing hydrochloric acid for 3–4 h at 90–100°.

A pyrazoline is known to be formed when the hydrazone of mesityl oxide is refluxed in acetic acid (1).

The reaction is not general. The *p*-toluenesulfonyl hydrazones of cyclopentanone, acetophenone, and acetaldehyde did not undergo the reaction. In the case of cyclohexanone, some pyrazoline was formed, but the yield was very low and the product that was obtained was impure.

EXPERIMENTAL

1-p-Toluenesulfonyl-3,5,5-trimethyl-2-pyrazoline (II)

(a) From Thermal Decomposition of Acetone Toluenesulfonyl Hydrazone

Acetone toluenesulfonyl hydrazone (1 g) was heated to 150–160°, at which temperature it decomposed spontaneously to a brownish sirup. After cooling, the mixture was extracted with ether and dioxane to

[1]*This work was supported by Bristol Laboratories, Syracuse, New York.*
[2]*The spectra were taken in deuterochloroform, with tetramethylsilane = 0 p.p.m.*

remove part of the colored impurities. Recrystallization of the residue from cyclohexane gave 130 mg (11%) of colorless crystals, m.p. 162–163°.

Anal. Calcd. for $C_{13}H_{18}N_2O_2S$: C, 58.63; H, 6.81; N, 10.52; S, 12.25. Found: C, 58.87; H, 6.74; N, 10.76; S, 12.20.

(b) From Mesityl Oxide p-Toluenesulfonyl Hydrazone

Mesityl oxide *p*-toluenesulfonyl hydrazone, m.p. 143–144° (1 g), prepared by the procedure described (2), was heated in 10 ml of glacial acetic acid and 0.5 ml of hydrochloric acid for 4 h at 90–100°. The mixture was allowed to stand for 5 h at room temperature and was then diluted with water until crystals precipitated. Recrystallization from chloroform–cyclohexane gave 0.22 g of II (24.7%), m.p. 161–162.5°, identical with II obtained as described under method *a* (mixed melting point, infrared spectrum).

(c) From Ethyl Acetoacetate p-Toluenesulfonyl Hydrazone

Ethyl acetoacetate *p*-toluenesulfonyl hydrazone (1 g) (2), m.p. 105–106°, was dissolved in 10 ml of glacial acetic acid and 1 ml of hydrochloric acid. It was heated for 3 h at 90°. The solvent was removed *in vacuo* at 25° and the residue was extracted several times with hot cyclohexane. Evaporation of the cyclohexane gave 0.258 g (28.9%) of II, m.p. 160–162°, identified by mixed melting point and comparison of the infrared spectrum.

(d) From Acid Treatment of Acetone Toluenesulfonyl Hydrazone

Acetone toluenesulfonyl hydrazone (0.1 g) was heated in 5 ml of glacial acetic acid and 0.5 ml of hydrochloric acid for 10 h at 100°. After evaporation of the solvent *in vacuo* at 25°, the residue was crystallized from ethanol–chloroform, and 15 mg of II, m.p. 160–162°, was obtained.

1. R. C. Elderfield (*Editor*). Heterocyclic compounds. Vol. 5. John Wiley & Sons, Inc., New York. 1957. p. 57.
2. W. R. Bamford and T. S. Stevens. J. Chem. Soc. 4735 (1952).

Received June 11, 1965.
Department of Chemistry,
McGill University,
Montreal, Quebec.

SOLVENT DEPENDENCE OF CHEMICAL SHIFT AND COUPLING CONSTANTS IN *p*-NITROANISOLE

H. M. Hutton and T. Schaefer

A solvent dependence of geminal proton coupling constants has been found in a number of compounds (1–5). For example, in the vinyl halides they vary by as much as 100% and are roughly proportional to the reaction field of the medium (5). A 2% variation is found for the vicinal coupling constants in the vinyl halides (5) but a 30% variation is found in 1-chloro-2-ethoxyethylene (6)

For the following reasons, a solvent dependence of the proton coupling constants in substituted benzenes may be observable. Valence bond calculations (7) predict π-contributions of $+0.5$, -0.2, and $+0.2$ c/s to the ortho, meta, and para coupling constants, respectively, in the benzene molecule. If benzene were substituted with a strong electron acceptor, A, and a strong electron donor, D, then the quinoid structure

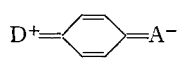

may contribute substantially to the ground state of the molecule. If so, the π-contribution to J_o (ortho coupling) would increase, and since J_o is probably positive (8), it would increase in magnitude. Similarly, the π-contribution to J_m (meta coupling) would decrease

Can. J. Chem. Downloaded from www.nrcresearchpress.com by 210.87.254.40 on 09/05/12
For personal use only.

remove part of the colored impurities. Recrystallization of the residue from cyclohexane gave 130 mg (11%) of colorless crystals, m.p. 162–163°.

Anal. Calcd. for $C_{13}H_{18}N_2O_2S$: C, 58.63; H, 6.81; N, 10.52; S, 12.25. Found: C, 58.87; H, 6.74; N, 10.76; S, 12.20.

(b) From Mesityl Oxide p-Toluenesulfonyl Hydrazone

Mesityl oxide *p*-toluenesulfonyl hydrazone, m.p. 143–144° (1 g), prepared by the procedure described (2), was heated in 10 ml of glacial acetic acid and 0.5 ml of hydrochloric acid for 4 h at 90–100°. The mixture was allowed to stand for 5 h at room temperature and was then diluted with water until crystals precipitated. Recrystallization from chloroform–cyclohexane gave 0.22 g of II (24.7%), m.p. 161–162.5°, identical with II obtained as described under method *a* (mixed melting point, infrared spectrum).

(c) From Ethyl Acetoacetate p-Toluenesulfonyl Hydrazone

Ethyl acetoacetate *p*-toluenesulfonyl hydrazone (1 g) (2), m.p. 105–106°, was dissolved in 10 ml of glacial acetic acid and 1 ml of hydrochloric acid. It was heated for 3 h at 90°. The solvent was removed *in vacuo* at 25° and the residue was extracted several times with hot cyclohexane. Evaporation of the cyclohexane gave 0.258 g (28.9%) of II, m.p. 160–162°, identified by mixed melting point and comparison of the infrared spectrum.

(d) From Acid Treatment of Acetone Toluenesulfonyl Hydrazone

Acetone toluenesulfonyl hydrazone (0.1 g) was heated in 5 ml of glacial acetic acid and 0.5 ml of hydrochloric acid for 10 h at 100°. After evaporation of the solvent *in vacuo* at 25°, the residue was crystallized from ethanol–chloroform, and 15 mg of II, m.p. 160–162°, was obtained.

1. R. C. Elderfield (*Editor*). Heterocyclic compounds. Vol. 5. John Wiley & Sons, Inc., New York. 1957. p. 57.
2. W. R. Bamford and T. S. Stevens. J. Chem. Soc. 4735 (1952).

Received June 11, 1965.
Department of Chemistry,
McGill University,
Montreal, Quebec.

SOLVENT DEPENDENCE OF CHEMICAL SHIFT AND COUPLING CONSTANTS IN *p*-NITROANISOLE

H. M. Hutton and T. Schaefer

A solvent dependence of geminal proton coupling constants has been found in a number of compounds (1–5). For example, in the vinyl halides they vary by as much as 100% and are roughly proportional to the reaction field of the medium (5). A 2% variation is found for the vicinal coupling constants in the vinyl halides (5) but a 30% variation is found in 1-chloro-2-ethoxyethylene (6)

For the following reasons, a solvent dependence of the proton coupling constants in substituted benzenes may be observable. Valence bond calculations (7) predict π-contributions of $+0.5$, -0.2, and $+0.2$ c/s to the ortho, meta, and para coupling constants, respectively, in the benzene molecule. If benzene were substituted with a strong electron acceptor, A, and a strong electron donor, D, then the quinoid structure

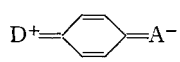

may contribute substantially to the ground state of the molecule. If so, the π-contribution to J_o (ortho coupling) would increase, and since J_o is probably positive (8), it would increase in magnitude. Similarly, the π-contribution to J_m (meta coupling) would decrease

Can. J. Chem. Downloaded from www.nrcresearchpress.com by 210.87.254.5 on 09/05/12
For personal use only.

and J_m, being positive (9), should increase. Finally, J_p (para coupling) will probably decrease.

Now it is true that coupling constants also depend on the energy of excitation to triplet states, which the quinoid structure, or intramolecular charge-transfer state (10), is not. Nevertheless, it is possible that the energy of the triplet states will also be lowered on substitution and that stabilization of the quinoid structure by polar solvents could therefore also lead to a change in coupling constants.*

We chose *p*-nitroanisole (I), which is soluble in nonpolar as well as polar solvents and

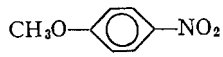

I

contains strong acceptor and donor groups (12). The parameter most easily obtained from the loosely coupled A_2B_2 proton resonance spectrum of *p*-nitroanisole is $|J_o + J_p|$, which is equal to the separation of the two intense lines in either half of the symmetrical spectrum (13).† To obtain individual values of all three coupling constants, solution of fourth-order secular equations is necessary. Fitting the calculated and observed spectra introduces an additional error into the values of the individual coupling constants, i.e. while $|J_o + J_p|$ can be determined to an accuracy of, say, 0.05 c/s, the derived values of J_o and J_p will also have an accuracy of 0.05 c/s. $J_p = 0.23 \pm 0.05$ c/s for *p*-nitroanisole in cyclohexane (14). Since any variation of J_o is expected to be larger than that of J_p, we have at this stage determined only $|J_o + J_p|$.

TABLE I

Chemical shifts and coupling constants in c/s at 60 Mc/s of 5 mole % *p*-nitroanisole in various solvents

Solvent	ϵ*	Chemical shifts				$\lvert J_o + J_p \rvert$§
		Ortho†	Meta†	Ortho‡	Meta‡	
Cyclohexane‖	2.0	409.9	485.8	0	0	9.21±0.04
Carbon tetrachloride	2.2	414.4	487.1	−4.5	−1.3	9.25±0.06
Benzene	2.3	380.3	473.3	+29.6	+12.5	9.26±0.06
Carbon disulfide	2.6	412.8	482.7	−2.9	+3.1	9.27±0.07
Acetone	21	427.2	492.4	−17.3	−6.6	9.28±0.08
Methanol	33	420.6	488.4	−10.7	−2.6	9.31±0.07
Acetronitrile	37	421.1	489.3	−11.2	−3.5	9.35±0.06 9.37±0.05¶

*Dielectric constant.
†To low field from internal tetramethylsilane.
‡Relative to shift in cyclohexane.
§Standard deviation of a minimum of 10 recordings is given.
‖Saturated solution, less than 5 mole %.
¶At 100 Mc/s.

In Table I are listed $|J_o + J_p|$ and the chemical shift, with respect to internal tetramethylsilane, of the ortho and meta protons of 5 mole % solutions of *p*-nitroanisole in a number of solvents with dielectric constants ranging from 2 to 37.‡ The high-field shift

The quinoid structure of p-nitrotoluene is stabilized by 15 kcal/mole in water as compared with the vapor (11).

†*It is true that the two major peaks in the half spectrum are multiple. In this molecule, however, the two meta couplings are equal (15) and J_p is among the smallest known (14). Under these circumstances it appears that the changes in internal shift with solvent will not account for the observed variation in the splitting. To check this point, the splitting of the major peaks in acetonitrile solution was measured independently at 100 Mc/s. The agreement with the results at 60 Mc/s is excellent (see Table I). We are grateful to a referee for stressing this point, of which we were aware. It may be that there are still grounds for doubt, but we hope that further work will dispel them.*

‡*The very high dielectric constants of some solvents (like hydrogen cyanide) are probably due to the internal arrangement of the solvent molecules and will probably not be reflected in the internal electric fields acting on the solute.*

Can. J. Chem. Downloaded from www.nrcresearchpress.com by 210.87.254.5 on 09/05/12
For personal use only.

was taken to be that of the ortho protons. This agrees with the substituent parameters (15) and also with the 0.1 to 0.2 c/s broadening of these resonance peaks, which is attributed to the coupling to the methoxy protons (15).

$|J_o + J_p|$ appears to be larger in acetonitrile and methanol than in cyclohexane. Thus, the difference between cyclohexane and acetonitrile solutions is 0.14 ± 0.10 c/s (0.16 ± 0.09 c/s if the 100 Mc/s result in acetonitrile is accepted). The increase in J_o may be somewhat offset by a smaller decrease in J_p. The larger values of $|J_o + J_p|$ tend to be associated with larger values of the dielectric constant of the medium, but it may well be true that the molecular properties of the solvent are as important as, or more important than, the dielectric constant, which is a bulk property. We are now improving the frequency–field stabilization of our spectrometer and intend to extend the measurements to other substituted benzenes and other solvents.

In Table I, it is seen that the solvent shifts of the protons meta to the nitro group are greater than those of the protons ortho to the nitro group. Since the dipole moment of the molecule is determined mainly by the nitro group (the dipole moment of nitrobenzene is 4.01 D while that of anisole is 1.30 D), the relative solvent shifts can be *qualitatively* understood in terms of the reaction field model (16). However, quantitatively, there are many discrepancies. For example, the solvent shift in acetone is larger than that in acetonitrile, yet the dielectric constant of the former is smaller. The solvent shift in benzene is presumably to be understood as a result of preferred orientations of solvent and solute molecules, such that the ring current effect is to high field. The benzene molecule appears to avoid the electron-rich region of the solute molecule (17). Further measurement of solvent shifts in substituted benzenes is in progress.

ACKNOWLEDGMENTS

We thank Dr. A. D. Cohen for valuable discussions and gratefully acknowledge financial support from the National Research Council. T. S. thanks the Basic Physics Division, National Physical Laboratory, Teddington, for the use of a 100 Mc/s spectrometer.

1. V. S. Watts, G. S. Reddy, and J. H. Goldstein. J. Mol. Specty. **11**, 325 (1963).
2. B. L. Shapiro, S. J. Ebersole, and R. M. Kopchik. J. Mol. Specty. **11**, 326 (1963); J. Chem. Phys. **39**, 3154 (1963).
3. S. G. Frankiss. J. Phys. Chem. **67**, 752 (1963).
4. P. Bates, S. Cawley, and S. S. Danyluk. J. Chem. Phys. **40**, 2415 (1964).
5. V. S. Watts and J. H. Goldstein. J. Chem. Phys. **42**, 228 (1965).
6. P. Laszlo and H. J. T. Bos. Tetrahedron Letters, **18**, 1325 (1965).
7. H. M. McConnell. J. Chem. Phys. **30**, 126 (1959).
8. A. D. Buckingham and K. A. McLaughlan. Proc. Chem. Soc. 144 (1963).
9. L. C. Snyder and E. W. Anderson. J. Am. Chem. Soc. **86**, 5023 (1964).
10. S. Nagakura and J. Tanaka. J. Chem. Phys. **22**, 236 (1954).
11. H. H. Jaffe and N. Orchin. Theory and applications of ultraviolet spectroscopy. John Wiley & Sons, Inc., New York. 1962. p. 267.
12. P. E. Stevenson. J. Mol. Specty. **15**, 220 (1965).
13. J. A. Pople, W. G. Schneider, and H. J. Bernstein. High resolution nuclear magnetic resonance. McGraw-Hill Book Co., Inc., New York. 1959. p. 138.
14. P. F. Cox. J. Am. Chem. Soc. **85**, 380 (1963).
15. J. Martin and B. P. Dailey. J. Chem. Phys. **37**, 2594 (1962).
16. A. D. Buckingham. Can. J. Chem. **38**, 300 (1960).
17. T. Schaefer. Can. J. Chem. **39**, 1864 (1961).

Received May 17, 1965.
Department of Chemistry,
University of Manitoba,
Winnipeg, Manitoba.

Can. J. Chem. Downloaded from www.nrcresearchpress.com by 210.87.254.5 on 09/05/12
For personal use only.

PREPARATION OF ANTIDOTES FOR ANTICHOLINESTERASE POISONING III. ESTERS OF 1-ARYLCYCLOALKANECARBOXYLIC ACIDS[1]

J. H. PARKKARI, R. A. B. BANNARD, AND I. W. COLEMAN

In preceding papers of this series (1, 2) the preparation of several analogues of 2′-diethylaminoethyl 1-phenylcyclopentanecarboxylate hydrochloride (Parpanit) and certain of their quaternary salts was described. These compounds were required for evaluation of their efficacy as substitutes for, or adjuncts to, atropine in the treatment of sarin poisoning (3–5). The preparation of fifteen additional analogues of Parpanit and four N-methyl-4′-piperidyl 1-arylcycloalkanecarboxylate hydrochlorides required for extension of these studies is reported herein. The compounds prepared and their properties are listed in Tables I to VI, and representative preparations are described in the Experimental section.

The majority of the Parpanit analogues (Table IV) was prepared by the interaction of potassium 1-phenylcyclopentanecarboxylate with the appropriate dialkylaminoalkyl chloride, followed by treatment with dry hydrogen chloride (method F) in ethanol (1, 6, 7). This was the most useful synthetic method when the requisite intermediate dialkylaminoalkyl chloride hydrochloride could be readily prepared, or when prepared, could be brought into reaction. 3′-Diethylaminopropyl 1-phenylcyclopentanecarboxylate hydrochloride, for example, was obtained in 62% yield from 3-diethylaminopropyl chloride and potassium 1-phenylcyclopentanecarboxylate, whereas the interaction of 3′-chloropropyl 1-phenylcyclopentanecarboxylate with diethylamine according to the general method of Weston (8) furnished only a 30% yield (method H).

The potassium salt method proved impractical for the synthesis of 3′-quinuclidinyl 1-phenylcyclopentanecarboxylate hydrochloride. 3-Quinuclidinyl chloride hydrochloride is readily prepared by the action of thionyl chloride upon 3-quinuclidinol (9). 3-Quinuclidinyl chloride (10), however, could not be induced to react with potassium 1-phenylcyclopentanecarboxylate, presumably because the rigidity of the ring system prevents the S_N1 reaction by inhibiting carbonium ion formation and also shields the 3-position from S_N2 attack. This compound was therefore prepared by interaction of 1-phenylcyclopentanecarbonyl chloride and 3-quinuclidinol in anhydrous benzene (cf. refs. 1, 8, 11–15; method K), or by transesterification of methyl 1-phenylcyclopentanecarboxylate with 3-quinuclidinol in toluene using a catalytic amount of sodium, followed by treatment with dry hydrogen chloride (cf. refs. 13, 14, 16; method J). Transesterification of 3-quinuclidinol with ethyl 1-phenylcyclopentanecarboxylate (17) was unsuccessful. 2′-*t*-Butylmethylaminoethyl 1-phenylcyclopentanecarboxylate hydrochloride was prepared by the interaction of 2′-*t*-butylaminoethyl 1-phenylcyclopentanecarboxylate with ethyl iodide in benzene, followed by ion exchange (method G).

The N-methyl-4-piperidyl hydrochloride esters of 1-phenylcyclopentanecarboxylic, 1-phenylcyclobutanecarboxylic, 1-*p*-methylphenylcyclobutanecarboxylic, and 1-*p*-methoxyphenylcyclobutanecarboxylic acids were prepared by treatment of the appropriate acid chloride with N-methyl-4-piperidinol in anhydrous benzene (1, 8, 11–15; method K).

The alkylamino- and dialkylamino-ethanols required as intermediates (Table II) were prepared by the interaction of an amine and ethylene oxide (18–20; method B) or 2-chloroethanol (21, 22; method C), by the action of an alkyl halide on a 2-alkylaminoethanol

[1]*Issued as D.C.B.R.L. Report No. 470.*

Can. J. Chem. Downloaded from www.nrcresearchpress.com by 210.87.254.5 on 09/05/12
For personal use only.

Can. J. Chem. Downloaded from www.nrcresearchpress.com by 210.87.254.5 on 09/05/12
For personal use only.

TABLE I

1-Arylcyclobutanecarbonyl chlorides*

Aryl group	Empirical formula	Yield (%)	b.p. (°C)	n_D^{25}	m.p. (°C)	Analysis (%)			
							C	H	Cl
1-*p*-Methoxyphenyl	$C_{12}H_{13}O_2Cl$	92	114 at 0.4 mm		42–44	Calcd.	64.14	5.83	15.79
						Found	64.40	5.70	15.68
1-*p*-Methylphenyl	$C_{12}H_{13}OCl$	88	84 at 0.25 mm	1.5377	10–15	Calcd.	69.06	6.28	16.99
						Found	69.29	6.30	16.70
1-Phenyl	$C_{11}H_{11}OCl$	83	66 at 0.15 mm	1.5395		Calcd.	67.87	5.70	18.21
						Found	68.06	5.53	18.25

*All compounds were prepared by method A.

TABLE II

2-Alkylamino- and 2-dialkylamino-ethanols

Compound	Method	b.p. (°C)	n_D^{25}	Yield (%)
2-*t*-Butylaminoethanol*	B	80 at 12 mm		78
2-*t*-Butylethylaminoethanol	D	76 at 13 mm	1.4441	60
2-Diisobutylaminoethanol†	C	100 at 18 mm	1.4334	53
2-Di(2′-butyl)aminoethanol‡	C	100 at 11 mm	1.4456	32
2-Dicyclohexylaminoethanol§	B	177 at 11 mm	1.4976	95
2-Di-*n*-propylaminoethanol‖	C, B	75 at 10 mm	1.4373	66, 77
2-Ethylmethylaminoethanol¶	D, E	46 at 11 mm	1.4355	41, 20
2-Isopropylpropylaminoethanol**	D	79 at 14 mm	1.4377	66

*Bortnick *et al.* (18) report b.p. 90–92° at 25 mm.
†Hannig and Haendler (21) report b.p. 70–73° at 4 mm; n_D^{20} 1.4373. Senkus (27) reports b.p. 89° at 10 mm; n_D^{20} 1.4355.
‡Adams and co-workers (22) report b.p. 225–226° at 750 mm. Heating period 16 h at 110°.
§Pratesi *et al.* (19) report b.p. 135° at 2 mm. Heating period 48 h at 110°.
‖Cadogan (20) reports b.p. 90–92° at 20 mm; n_D^{25} 1.4375.
¶Halverstadt *et al.* (28) report b.p. 145–150°. From methylaminoethanol and ethyl bromide.
**Wright *et al.* (24) report b.p. 80.5–81° at 17 mm. From 2-isopropylaminoethanol (23) and *n*-propyl bromide.

(1, 23, 24; method D), or by the reductive methylation of 2-ethylaminoethanol with formaldehyde and formic acid (24–26; method E). Salts of these aminoalcohols were prepared by standard methods for characterization purposes (Table III). The alkylamino- and dialkylamino-ethanols were converted into the corresponding chloride hydrochlorides by the action of thionyl chloride in benzene (1), from which the free bases were obtained by neutralization with aqueous potassium hydroxide and extraction (1) with ether.

The 1-arylcycloalkanecarbonyl chlorides (Table I) were prepared from the corresponding acids by treatment with thionyl chloride in anhydrous benzene (1; method A). Methyl and ethyl 1-phenylcyclopentanecarboxylates were prepared by interaction of the appropriate alcohol and 1-phenylcyclopentanecarbonyl chloride.

EXPERIMENTAL[2,3]

Method A: 1-Phenylcyclobutanecarbonyl Chloride

A solution of thionyl chloride (8 ml, 13.1 g, 0.11 mole) in sodium-dried benzene (15 ml) was added dropwise, with stirring, to a slurry of 1-phenylcyclobutanecarboxylic acid (7.05 g, 0.04 mole) in sodium-dried benzene (40 ml). The reaction mixture was heated under reflux, with stirring, for 4 h. Benzene and thionyl chloride were removed by distillation and the residue was fractionated, yielding 1-phenylcyclobutanecarbonyl chloride as a colorless, mobile oil; b.p. 66° at 0.15 mm; n_D^{25} 1.5395; 6.48 g (83%).

Preparation of 2-Alkylamino- and 2-Dialkylamino-ethanols

Method B: 2-t-Butylaminoethanol

2-*t*-Butylaminoethanol (b.p. 80° at 12 mm) was prepared in 78% yield by the method of Bortnick *et al.* (18).

Method C: 2-Diisobutylaminoethanol

A mixture of diisobutylamine (64.6 g, 0.50 mole) and 2-chloroethanol (40.3 g, 0.50 mole) was heated in a stainless steel bomb for 8 h at 110°. The cooled reaction mixture was dissolved in water, basified with 20% sodium hydroxide, and extracted with ether (3 × 100 ml). The extract was dried over anhydrous magnesium sulfate, and the ether was removed by distillation. Fractionation yielded a forerun consisting of unreacted starting materials, b.p. 51–57° at 28 mm, and 2-diisobutylaminoethanol, b.p. 100–101° at 18 mm; n_D^{25} 1.4334. Yield, 46.0 g (53%, 75% based upon reacted starting material).

Method D: 2-t-Butylethylaminoethanol

A solution of 2-*t*-butylaminoethanol (11.7 g, 0.10 mole) and ethyl iodide (46.8 g, 0.30 mole) in benzene (40 ml) was heated under reflux with stirring for 20 h. Massive precipitation occurred within the first hour. The precipitate was collected by filtration, washed with anhydrous ether, and dried *in vacuo*. Recrystallization from absolute ethanol – ether furnished N-*t*-butylethylaminoethanol hydriodide as colorless prisms, m.p. 162.5–163°. Yield, 23.1 g (85%). The hydriodide (20 g, 0.073 mole) was dissolved in water (100 ml), neutralized with solid sodium carbonate (to pH 9), and extracted with ether (1 × 50 ml; 3 × 25 ml). The

[2]*All melting and boiling points are uncorrected.*
[3]*Microanalyses were performed by J. G. Helie of these laboratories.*

Can. J. Chem. Downloaded from www.nrcresearchpress.com by 210.87.254.5 on 09/05/12
For personal use only.

Can. J. Chem. Downloaded from www.nrcresearchpress.com by 210.87.254.5 on 09/05/12
For personal use only.

TABLE III

Salts of alkylamino- and dialkylamino-ethanols

Compound	Empirical formula	Solvent for recrystallization	m.p. (°C)		Analysis (%) C	H	N	Cl
2-*t*-Butylaminoethanol hydrochloride	$C_6H_{16}NOCl$	Ethanol–ether	152–153	Calcd.	46.91	10.49	9.12	23.08
				Found	46.78	10.47	9.14	22.98
2-*t*-Butylethylaminoethanol hydriodide	$C_8H_{20}NOI$	Ethanol–ether	162.5–163	Calcd.	35.17	7.38	5.13	46.46
				Found	35.40	7.58	5.13	46.20
2-Diisobutylaminoethanol picrate	$C_{16}H_{26}N_4O_8$	Acetone–ether	117–118.5	Calcd.	47.75	6.51	13.92	
				Found	47.56	6.50	13.94	
2-Di(2′-butyl)aminoethanol hydrochloride	$C_{10}H_{24}NOCl$	Acetone–ether	107.5–108.5	Calcd.	57.26	11.53	6.68	16.90
				Found	57.18	11.60	6.71	16.76
2-Dicyclohexylaminoethanol hydrochloride	$C_{14}H_{28}NOCl$	Methanol–ether	156.5–157.5	Calcd.	64.22	10.78	5.35	13.54
				Found	64.32	10.95	5.46	13.69
2-Di-*n*-propylaminoethanol hydrochloride	$C_8H_{20}NOCl$	Acetone–ether	86.5–87.5	Calcd.	52.88	11.09	7.71	19.51
				Found	52.87	10.9	7.88	19.50
2-Ethylmethylaminoethanol methobromide*	$C_6H_{16}NOBr$	Ethanol–ether	282–284	Calcd.	36.37	8.14	7.07	40.34
				Found	36.27	8.13	6.79	40.09
2-Isopropylpropylaminoethanol methobromide*	$C_9H_{22}NOBr$	Acetone–ether	156–157	Calcd.	45.00	9.23	5.83	33.27
				Found	44.77	9.36	5.71	33.45

*Very hygroscopic.

Can. J. Chem. Downloaded from www.nrcresearchpress.com by 210.87.254.5 on 09/05/12
For personal use only.

TABLE IV

Alkylamino- and dialkylamino-alkyl chloride hydrochlorides

Aminoalkyl group	Empirical formula	Yield (%)	Solvent for recrystallization	m.p. (°C)	Analysis (%)				
						C	H	N	Cl
2-*t*-Butylaminoethyl	$C_6H_{15}NCl_2$	82	Ethanol–acetone	201.5–202.5	Calcd.	41.87	8.78	8.14	41.20
					Found	41.95	8.63	7.93	41.08
2-*t*-Butylethylaminoethyl	$C_8H_{19}NCl_2$	50	Methanol–ether	162–164	Calcd.	48.00	9.57	7.00	35.43
					Found	47.97	9.69	6.89	35.35
2-Dibenzylaminoethyl*,†	$C_{16}H_{19}NCl_2$	93	Ethanol–ether	186–187	Calcd.	64.87	6.46	4.73	23.94
					Found	64.77	6.35	4.72	23.84
2-Dibutylaminoethyl‡	$C_{10}H_{23}NCl_2$	62	Acetone–ether	85.5–86	Calcd.	52.63	10.16	6.14	31.07
					Found	52.78	10.12	5.96	31.45
2-Diisobutylaminoethyl	$C_{10}H_{23}NCl_2$	64	Acetone–ether	109.5–110.5	Calcd.	52.63	10.16	6.14	31.07
					Found	52.85	10.1	6.07	31.03
2-Di(2′-butyl)aminoethyl	$C_{10}H_{23}NCl_2$	56	Acetone–ether	115.5–117	Calcd.	52.63	10.16	6.14	31.07
					Found	52.60	10.00	6.14	30.96
2-Dicyclohexylaminoethyl§	$C_{14}H_{27}NCl_2$	85	Methanol–ether	184.5–185.5	Calcd.	59.99	9.71	5.00	25.30
					Found	60.09	9.81	5.09	25.28
3-Diethylaminopropyl‖	$C_7H_{17}NCl_2$	43	Acetone–ether	84–85	Calcd.	45.17	9.21	7.53	38.10
					Found	44.47	9.20	7.58	37.97
2-Dipropylaminoethyl¶	$C_8H_{19}NCl_2$	88	Acetone–ether	121–122	Calcd.	48.00	9.57	7.00	35.43
					Found	48.21	9.43	6.85	35.32
2-Ethylaminoethyl**	$C_4H_{11}NCl_2$	67	Ethanol–ether	218–219	Calcd.	33.35	7.70	9.72	49.23
					Found	33.44	7.73	9.82	49.37
2-Ethylmethylaminoethyl††	$C_5H_{13}NCl_2$	80	Methanol–ether	171–172	Calcd.	37.98	8.29	8.86	44.86
					Found	37.81	8.45	8.58	44.90
2-Isopropylpropylaminoethyl	$C_8H_{19}NCl_2$	83	Methanol–acetone–ether	170.5–171.5	Calcd.	48.00	9.57	7.00	35.43
					Found	48.08	9.55	6.90	35.29
2-Methylaminoethyl	$C_3H_9NCl_2$	57	Ethanol–ether	114–115	Calcd.	27.71	6.98	10.77	54.54
					Found	27.81	7.19	10.97	54.66

*Gump and Nikawitz (29) report m.p. 194–195°.
†Merck Index (30) reports m.p. 192° and m.p. 180–181°.
‡Klein and Kaye (31) report m.p. 86–88°.
§Ger. Patent No. 556,324 (32) reports m.p. 186°.
‖Hass and Huffman (33) report m.p. 85.8–86.2°.
¶Wright and co-workers (24) report m.p. 123–124°.
**Lasselle and Sundet (34) report m.p. 223°.
††Wright and co-workers (35) report m.p. 171–172°.

Can. J. Chem. Downloaded from www.nrcresearchpress.com by 210.87.254.5 on 09/05/12
For personal use only.

TABLE V

Aminoalkyl 1-phenylcyclopentanecarboxylate hydrochlorides

Aminoalkyl group	Empirical formula	Method	Yield (%)	Solvent for recrystallization	m.p. (°C)	Analysis (%)				
							C	H	N	Cl
2′-*t*-Butylaminoethyl	$C_{18}H_{28}NO_2Cl$	F	75	Methanol–ether	198–199	Calcd.	66.34	8.66	4.30	10.88
						Found	66.54	8.82	4.38	10.96
2′-*t*-Butylethylaminoethyl	$C_{20}H_{32}NO_2Cl$	F	73	Acetone–ether	163.5–164	Calcd.	67.87	9.11	3.96	10.02
						Found	67.89	8.99	4.15	10.02
2′-*t*-Butylmethylaminoethyl	$C_{19}H_{30}NO_2Cl$	G	23	Methanol–ether	149–149.5	Calcd.	67.14	8.90	4.12	10.43
						Found	67.22	8.76	4.01	10.23
2′-Dibenzylaminoethyl	$C_{28}H_{32}NO_2Cl$	F	67	Acetone–ether	161–161.5	Calcd.	74.73	7.17	3.11	7.88
						Found	74.80	7.43	3.21	7.88
2′-Dibutylaminoethyl	$C_{22}H_{36}NO_2Cl$	F	85	Acetone–ether	101.5–102.5	Calcd.	69.17	9.50	3.67	9.28
						Found	68.98	9.63	3.80	9.26
2′-Diisobutylaminoethyl	$C_{22}H_{36}NO_2Cl$	F	83	Acetone–ether	138–139	Calcd.	69.17	9.50	3.67	9.28
						Found	69.05	9.59	3.70	9.30
2′-Di(2″-butyl)aminoethyl	$C_{22}H_{36}NO_2Cl$	F	75	Acetone–ether	144–144.5	Calcd.	69.17	9.50	3.67	9.28
						Found	69.10	9.40	3.73	9.29
2′-Dicyclohexylaminoethyl	$C_{26}H_{40}NO_2Cl$	F	65	Acetone–ether	160–160.5	Calcd.	71.94	9.29	3.23	8.17
						Found	71.82	9.20	3.10	8.19
3′-Diethylaminopropyl	$C_{19}H_{30}NO_2Cl$	F	62	Ethanol–ether	140–141.5	Calcd.	67.14	8.90	4.12	10.43
		H	30			Found	67.11	8.87	4.30	10.48
2′-Di-*n*-propylaminoethyl	$C_{20}H_{32}NO_2Cl$	F	76	Acetone–ether	120–120.5	Calcd.	67.87	9.11	3.96	10.02
						Found	67.64	8.89	4.08	10.03
2′-Ethylaminoethyl	$C_{16}H_{24}NO_2Cl$	F	60	Acetone–ether	147–148	Calcd.	64.52	8.12	4.70	11.91
						Found	64.36	8.21	4.73	12.04
2′-Ethylmethylaminoethyl	$C_{17}H_{26}NO_2Cl$	F	59	Methanol–ether	128–128.5	Calcd.	65.47	8.40	4.49	11.37
						Found	65.55	8.56	4.36	11.36
2′-Isopropylpropylaminoethyl	$C_{20}H_{32}NO_2Cl$	F	84	Acetone–ether	98–99	Calcd.	67.87	9.11	3.96	10.02
						Found	67.71	9.08	3.81	9.97
2′-Methylaminoethyl	$C_{15}H_{22}NO_2Cl$	F	47	Methanol–ether	145–146	Calcd.	63.48	7.81	4.94	12.49
						Found	63.40	8.03	5.01	12.46
3′-Quinuclidinyl	$C_{19}H_{26}NO_2Cl$	J	28	Methanol–ether	207–208	Calcd.	67.94	7.80	4.17	10.56
		K	32			Found	67.65	7.67	3.96	10.59

Can. J. Chem. Downloaded from www.nrcresearchpress.com by 210.87.254.5 on 09/05/12
For personal use only.

TABLE VI

Esters of 4-hydroxy-N-methylpiperidine hydrochloride*

Acid moiety	Empirical formula	Yield (%)	Solvent for recrystallization	m.p. (°C)	Analysis (%)				
						C	H	N	Cl
1-*p*-Methoxyphenylcyclobutanecarboxylate	$C_{18}H_{26}NO_3Cl$	75	Methanol–ether	191.5–192	Calcd.	63.61	7.71	4.12	10.43
					Found	63.35	7.66	3.96	10.22
1-*p*-Methylphenylcyclobutanecarboxylate	$C_{18}H_{26}NO_2Cl$	77	Methanol–ether	206.5–207.5	Calcd.	66.75	8.09	4.33	10.95
					Found	66.55	8.03	4.39	10.70
1-Phenylcyclobutanecarboxylate	$C_{17}H_{24}NO_2Cl$	72	Methanol–ether	213–214	Calcd.	65.90	7.81	4.52	11.44
					Found	66.12	8.01	4.51	11.68
1-Phenylcyclopentanecarboxylate	$C_{18}H_{26}NO_2Cl$	60	Methanol–ether	177.5–178.5	Calcd.	66.75	8.09	4.33	10.95
					Found	66.86	8.24	4.31	10.74

*All compounds were prepared by method K.

extract was concentrated, and dried over anhydrous magnesium sulfate, and the ether was removed by distillation. Fractionation of the residue gave 2-*t*-butylethylaminoethanol; b.p. 75–76° at 13 mm; n_D^{25} 1.4441. Yield, 6.40 g (60%).

Method E: 2-Ethylmethylaminoethanol

2-Ethylaminoethanol (35.7 g, 0.40 mole) was added dropwise, with stirring, to 88% formic acid (51.2 g, 1.00 mole) at 0°. Formaldehyde solution (37%; 45 ml, 0.60 mole) was added dropwise at room temperature and the solution was heated to 90° when vigorous ebullition occurred. Heating was discontinued until the reaction subsided and was then resumed at 95–98° for 8 h. Hydrochloric acid (4 *N*, 100 ml) was added to the cooled solution, which was then evaporated to dryness *in vacuo*. The viscous residue was dissolved in water (60 ml), basified with sodium hydroxide (18 *N*, 50 ml), and extracted with benzene (4 × 30 ml). The extract was dried over anhydrous potassium carbonate, then heated under reflux with acetic anhydride (75 ml), poured into 5% hydrochloric acid (500 ml), and extracted with ether (1 × 100 ml; 3 × 50 ml) to remove the unreacted secondary amine as the N-acetyl derivative. The aqueous layer was basified by careful addition of solid sodium carbonate in portions and extracted with ether (1 × 100 ml; 3 × 50 ml). The ether was removed *in vacuo* and the residue was heated under reflux with 25% sodium hydroxide (200 ml) for 18 h. The two layers were separated and the aqueous layer was extracted with ether (4 × 50 ml). After the solution had been dried over anhydrous magnesium sulfate, the ether was removed *in vacuo* and the residue was fractionated, yielding 8.2 g (20%) of 2-ethylmethylaminoethanol as a heavy, colorless oil; b.p. 49° at 13 mm; n_D^{25} 1.4357 (cf. Leonard and Simet (25), Icke and Wisegarver (26), and Wright *et al.* (24)).

Alkylamino- and Dialkylamino-alkyl Chloride Hydrochlorides

The compounds shown in Table IV were prepared by treatment of the appropriate freshly distilled amino-alcohol with a good grade of thionyl chloride in chloroform, using the general method described by Bannard and co-workers (1). The thionyl chloride solution should be added as quickly as possible, without allowing the reaction temperature to rise above −10°. The reaction mixture is brought to room temperature and then heated under reflux with stirring until the mixture begins to darken, usually from 1½ to 4 h. Excessive heating frequently complicates the purification of the product, and should be avoided.

Alkylamino- and Dialkylamino-alkyl Chlorides

These compounds were prepared from the corresponding alkylaminoalkyl chloride hydrochlorides (Table IV) by neutralization and extraction, using the method previously described (1). Yields were generally over 90%. These compounds were not characterized, but were used immediately in reaction with potassium 1-phenylcyclopentanecarboxylate.

Preparation of Alkylamino- and Dialkylamino-alkyl 1-Phenylcyclopentanecarboxylate Hydrochlorides

Modifications to the method of interaction between potassium 1-phenylcyclopentanecarboxylate and a dialkylaminoalkyl chloride, which was described previously (1), have been made. The preparations of 2′-*t*-butylaminoethyl and 2′-*t*-butylmethylaminoethyl 1-phenylcyclopentanecarboxylate hydrochlorides are typical and are described below.

Method F: 2′-t-Butylaminoethyl 1-Phenylcyclopentanecarboxylate Hydrochloride

2-*t*-Butylaminoethyl chloride (4.39 g, 0.032 mole) in absolute ethanol (20 ml) was added dropwise to a warm, stirred solution of potassium 1-phenylcyclopentanecarboxylate (6.84 g, 0.03 mole) (1) in absolute ethanol (30 ml) and the resultant mixture was heated under reflux, with stirring, for 16 h. The reaction mixture was taken to dryness *in vacuo*, shaken with water (50 ml), and extracted with ether (4 × 50 ml). The extract was dried, filtered, and taken to dryness *in vacuo*. The residue, a colorless, mobile oil, was dissolved in methanol (60 ml), saturated with dry hydrogen chloride, and again taken to dryness *in vacuo*. Two recrystallizations from absolute methanol – ether yielded colorless needles, m.p. 198–199°. Yield, 7.37 g (75%).

Method G: 2′-t-Butylmethylaminoethyl 1-Phenylcyclopentanecarboxylate Hydrochloride

A warm, stirred solution of 1-phenylcyclopentanecarboxylic acid (11.4 g, 0.06 mole) in ethanol (50 ml) was neutralized with 10% ethanolic potassium hydroxide, with phenolphthalein as the external indicator. The reaction mixture was taken to dryness *in vacuo*, dissolved in absolute ethanol (100 ml), and added dropwise, with stirring, to 2-*t*-butylaminoethyl chloride, which was obtained by neutralization of 2-*t*-butylaminoethyl chloride hydrochloride (17.2 g, 0.10 mole). The mixture was heated under reflux, with stirring, for 18 h, and was taken to dryness *in vacuo*. The residue was shaken with water (100 ml) and ether (100 ml) for 2 h. The layers were separated and the ether layer was dried over anhydrous magnesium sulfate and taken to dryness *in vacuo*. The residue was dissolved in benzene (50 ml), methyl iodide (25 ml) was added dropwise, with stirring, and the reaction mixture was heated under reflux, with stirring, for 1 h. Ether (200 ml) was added and the precipitate was collected, washed with ether, and dried. Yield, 18.1 g (66% as the hydriodide). This compound was dissolved in 25% ethanol (900 ml) and passed through Amberlite IRA-400 resin in the chloride form, followed by 25% ethanol (1 000 ml). The eluate was taken to dryness *in vacuo* and recrystallized from absolute methanol – ether, yielding 4.42 g (32%) of the hydrochloride as colorless needles, m.p. 146–147°.

Can. J. Chem. Downloaded from www.nrcresearchpress.com by 210.87.254.5 on 09/05/12
For personal use only.

Method H: 3′-Diethylaminopropyl 1-Phenylcyclopentanecarboxylate Hydrochloride

(a) 3′-Chloropropyl 1-phenylcyclopentanecarboxylate.—A solution of 1-phenylcyclopentanecarbonyl chloride (4.17 g, 0.02 mole) in sodium-dried benzene (20 ml) was added dropwise, with stirring, to a solution of freshly distilled 3-chloropropanol (4.73 g, 0.05 mole) in dry benzene (25 ml). The reaction mixture was heated under gentle reflux, with stirring, for 1 h, and evaporated to dryness *in vacuo*. The residue was dissolved in ether and the solution was dried over anhydrous magnesium sulfate. After removal of the ether by distillation, the residue was fractionated *in vacuo*, yielding 3.98 g (76%) of 3′-chloropropyl 1-phenylcyclopentanecarboxylate; b.p. 178–180° at 10 mm; n_D^{25} 1.5218.

Anal. Calcd. for $C_{15}H_{19}O_2Cl$: C, 67.53; H, 7.18; Cl, 13.29. Found: C, 67.61; H, 7.12; Cl, 13.22.

(b) 3′-Diethylaminopropyl 1-phenylcyclopentanecarboxylate hydrochloride.—3′-Chloropropyl 1-phenylcyclopentanecarboxylate (2.27 g, 0.01 mole) was dissolved in freshly distilled diethylamine (20 ml) and heated in a stainless steel bomb at 110° for 16 h. The dark reaction mixture was decanted and the reaction vessel was washed several times with small portions of methanol. The combined reaction mixture and washings were heated with charcoal, filtered through a pad of Celite, and taken to dryness *in vacuo*. The residue was basified with 10% aqueous potassium hydroxide, and diluted with water (40 ml), and the dark, cloudy mixture was extracted with ether (4 × 15 ml). The extract was dried over anhydrous magnesium sulfate, and taken to dryness *in vacuo*. The dark, heavy residue was dissolved in ethanol (20 ml), saturated with dry hydrogen chloride, and again taken to dryness *in vacuo*. Recrystallization from absolute ethanol – ether gave colorless needles, m.p. 139.5–140°. Yield, 1.03 g (30%).

Method J: 3′-Quinuclidinyl 1-Phenylcyclopentanecarboxylate Hydrochloride

(a) Ethyl 1-phenylcyclopentanecarboxylate.—1-Phenylcyclopentanecarbonyl chloride (4.17 g, 0.02 mole) (1) dissolved in sodium-dried benzene (20 ml) was added dropwise, with stirring, to absolute ethanol (50 ml). The reaction mixture was heated under reflux for 2 h. Excess ethanol and benzene were removed by distillation, and the residue was fractionated. Ethyl 1-phenylcyclopentanecarboxylate, a heavy colorless liquid, was collected; b.p. 138–139° at 9 mm; n_D^{25} 1.5116. Yield, 3.66 g (84%). Laüger *et al.* (17) report b.p. 142–144° at 10 mm; n_D^{20} 1.5145.

Anal. Calcd. for $C_{14}H_{18}O_2$: C, 77.03; H, 8.32. Found: C, 76.97; H, 8.24.

(b) Methyl 1-phenylcyclopentanecarboxylate.—1-Phenylcyclopentanecarbonyl chloride (8.34 g, 0.04 mole) in anhydrous methanol (50 ml) was heated at 40°, with stirring, for 16 h. After the excess methanol had been removed by distillation, the residue was shaken with water (20 ml) and extracted with ether (2 × 15 ml). The extract was dried over anhydrous magnesium sulfate, the ether was removed, and fractionation gave methyl 1-phenylcyclopentanecarboxylate; b.p. 131–133° at 9 mm; n_D^{25} 1.5216. Yield, 7.26 g (90%).

Anal. Calcd. for $C_{13}H_{16}O_2$: C, 76.44; H, 7.89. Found: C, 76.22; H, 7.97.

(c) 3′-Quinuclidinyl 1-phenylcyclopentanecarboxylate hydrochloride.—A mixture of methyl 1-phenylcyclopentanecarboxylate (6.06 g, 0.30 mole), 3-quinuclidinol (4.45 g, 0.035 mole), and sodium (0.12 g, 0.005 mole) in toluene (100 ml) was heated under reflux, with stirring, for 20 h, during which massive precipitation occurred. The solid was collected, washed with benzene, dried, and dissolved in water. The filtrate was acidified with 10% hydrochloric acid (100 ml) and the layers were separated. The aqueous layer was basified by addition of sodium carbonate in portions, then combined with the aqueous solution of the precipitate, and extracted with ether (4 × 25 ml). The extract was dried over anhydrous magnesium sulfate and taken to dryness *in vacuo*. The residue was dissolved in ethanol (20 ml), saturated with dry hydrogen chloride, and again taken to dryness *in vacuo*. Recrystallization from ethanol–ether yielded colorless flakes, m.p. 206–207°. Yield, 2.80 g (28%).

N-Methyl-4′-piperidyl 1-Arylcycloalkanecarboxylate Hydrochlorides

Method K: N-Methyl-4′-piperidyl 1-p-Methoxyphenylcyclobutanecarboxylate Hydrochloride

A solution of 1-*p*-methoxyphenylcyclobutanecarbonyl chloride (2.25 g, 0.01 mole) in sodium-dried benzene (15 ml) was added dropwise, with stirring, to 4-hydroxy-N-methylpiperidine (2.90 g, 0.025 mole) in sodium-dried benzene (40 ml). The reaction mixture was heated under reflux, with vigorous stirring, for 2 h, and then chilled. Anhydrous ether was added and the precipitate was collected. The filtrate was taken to dryness *in vacuo*, shaken with water (50 ml), and extracted with ether (2 × 25 ml). The extract was dried over anhydrous magnesium sulfate and taken to dryness *in vacuo*, yielding 2.89 g (95%) of dark yellow oil. This material was dissolved in methanol (25 ml), and saturated with anhydrous hydrogen chloride, and the solution was evaporated to dryness *in vacuo*. Methanol (20 ml) was added, and the solution was boiled with charcoal, filtered through Celite, and again taken to dryness *in vacuo*. Recrystallization from methanol–ether gave N-methyl-4′-piperidyl 1-*p*-methoxyphenylcyclobutanecarboxylate hydrochloride as colorless flakes, m.p. 191.5–192.5°. Yield, 2.55 g (75%).

ACKNOWLEDGMENT

We are indebted to Geigy Pharmaceuticals for providing us with generous amounts of the 1-arylcycloalkanecarboxylic acids used herein.

Can. J. Chem. Downloaded from www.nrcresearchpress.com by 210.87.254.5 on 09/05/12
For personal use only.

1. R. A. B. BANNARD, J. H. PARKKARI, and I. W. COLEMAN. Can. J. Chem. **40**, 1909 (1962).
2. R. A. B. BANNARD, J. H. PARKKARI, and I. W. COLEMAN. Can. J. Chem. **41**, 2108 (1963).
3. I. W. COLEMAN, P. E. LITTLE, and R. A. B. BANNARD. Can. J. Biochem. Physiol. **40**, 815 (1962).
4. I. W. COLEMAN, P. E. LITTLE, and R. A. B. BANNARD. Can. J. Biochem. Physiol. **40**, 827 (1962).
5. I. W. COLEMAN, P. E. LITTLE, and R. A. B. BANNARD. Can. J. Biochem. Physiol. **41**, 2479 (1963).
6. J. R. GEIGY A-G. Swiss Patent No. 240,169 (May 16, 1946); Chem. Abstr. **43**, 6656*a* (1949).
7. W. A. LOTT and J. KRAPCHO. U.S. Patent No. 2,688,025 (August 31, 1954); Chem. Abstr. **49**, 11698*d* (1955).
8. A. W. WESTON. U.S. Patent No. 2,704,284 (March 15, 1955); Chem. Abstr. **50**, 1903*i* (1956).
9. C. V. GROB, A. KAISER, and E. RENK. Helv. Chim. Acta, **40**, 2170 (1957).
10. K. B. SHAW. Private communication.
11. H. MARTIN and F. HÄFLIGER. U.S. Patent No. 2,437,545 (March 9, 1948); Chem. Abstr. **42**, 46406*i* (1948).
12. J. R. GEIGY A-G. Swiss Patent No. 240,160 (November 30, 1945); Chem. Abstr. **43**, 6655*h* (1949).
13. H. MARTIN and F. HÄFLIGER. U.S. Patent No. 2,404,588 (July 23, 1946); Chem. Abstr. **40**, 6501 (1946).
14. M. G. VAN CAMPEN, JR. and C. H. TILFORD. U.S. Patent No. 2,474,796 (June 28, 1949); Chem. Abstr. **44**, 3018*b* (1950).
15. A. W. WESTON. J. Am. Chem. Soc. **68**, 2345 (1946).
16. H. G. MORREN. Brit. Patent No. 753,779 (August 1, 1956); Chem. Abstr. **51**, 7443*c* (1957).
17. P. LAÜGER, M. FROST, and R. CHARLIER. Helv. Chim. Acta, **42**, 2379 (1959).
18. N. BORTNICK, L. S. LUSKIN, M. D. HURWITZ, W. E. CRAIG, L. J. EXNER, and J. MIRZA. J. Am. Chem. Soc. **78**, 4039 (1956).
19. P. PRATESI, E. GRANA, L. LILLA, L. VILLA, and G. CASTORINA. Farmaco Pavia Ed. Sci. **15**, 821 (1960); Chem. Abstr. **55**, 23519*i* (1961).
20. I. G. CADOGAN. J. Chem. Soc. 2971 (1955).
21. E. HANNIG and F. HAENDLER. Arch. Pharm. **290**, 131 (1957).
22. R. ADAMS, E. H. VOLWILER, and R. L. JENKINS. U.S. Patent No. 1,513,730 (November 4, 1924); Chem. Abstr. **19**, 1536 (1925).
23. J. H. BIEL. J. Am. Chem. Soc. **71**, 1306 (1949).
24. J. B. WRIGHT, E. H. LINCOLN, R. V. HEINZELMANN, and J. H. HUNTER. J. Am. Chem. Soc. **72**, 3536 (1950).
25. F. LEONARD and L. SIMET. J. Am. Chem. Soc. **77**, 2855 (1955).
26. N. ICKE and B. B. WISEGARVER. Org. Syn. **25**, 89 (1945).
27. M. SENKUS. J. Am. Chem. Soc. **67**, 1515 (1945).
28. J. F. HALVERSTADT, W. R. HARDIE, and A. R. WILLIAMS. J. Am. Chem. Soc. **81**, 3618 (1959).
29. W. S. GUMP and E. J. NIKAWITZ. J. Am. Chem. Soc. **72**, 1309 (1950).
30. Merck Index. 7th ed. Merck and Co., Rahway, New Jersey. 1960. p. 242.
31. H. C. KLEIN and I. A. KAYE. J. Am. Chem. Soc. **70**, 1283 (1948).
32. Soc. Anon. pour l'Ind. Chim. à Bâle. Ger. Patent No. 556,324 (February 23, 1930); Chem. Abstr. **26**, 5573*6* (1932).
33. H. B. HASS and H. C. HUFFMAN. J. Am. Chem. Soc. **63**, 1233 (1941).
34. P. A. LASSELLE and S. A. SUNDET. J. Am. Chem. Soc. **63**, 2374 (1941).
35. W. B. WRIGHT, H. J. BRABANDER, and R. A. HARDY. J. Org. Chem. **26**, 2120 (1961).

RECEIVED JUNE 16, 1965.
DEFENCE CHEMICAL, BIOLOGICAL AND RADIATION LABORATORIES,
OTTAWA, CANADA.

ADDENDUM: THE CHROMIC ACID OXIDATION OF ARYL TRIFLUOROMETHYL ALCOHOLS: ISOTOPE AND SUBSTITUENT EFFECTS

ROSS STEWART AND DONALD G. LEE

(Ref. Can. J. Chem. 42, 439 (1964))

The unidentified compound (m.p. 70–71°) (see page 445) has been shown to be 2,4-dinitrobromobenzene. This compound is formed by the nitration of bromobenzene, an impurity (21%) in the α,α,α-trifluoroacetophenone used in the preparation of 3,5-dinitrophenyltrifluoromethyl ketone. (We thank Mr. J. M. McAndless for this work.)

DEPARTMENT OF CHEMISTRY,
UNIVERSITY OF BRITISH COLUMBIA,
VANCOUVER, BRITISH COLUMBIA.

Can. J. Chem. Downloaded from www.nrcresearchpress.com by 210.87.254.5 on 09/05/12
For personal use only.

Can. J. Chem. Downloaded from www.nrcresearchpress.com by 210.87.254.42 on 09/05/12
For personal use only.

Canadian Journal of Chemistry

Issued by THE NATIONAL RESEARCH COUNCIL OF CANADA

VOLUME 43 DECEMBER 1965 NUMBER 12

HIGH ENERGY MODIFICATIONS OF THE HYDRATES OF ZINC SULFATE

J. W. S. JAMIESON, R. A. LAMONTAGNE, BARBARA A. PATTERN, AND G. R. BROWN

Department of Chemistry, St. John's College, University of Manitoba, Winnipeg, Manitoba

Received May 31, 1965

ABSTRACT

Much higher heats of solution than have previously been observed for hydrates of zinc sulfate have been measured for various new vacuum dehydration products. It is suggested that the maximum heat of transition to normal crystalline form of 82.8 cal/g, 23.8 kcal per mole of heptahydrate, or 8.3×10^3 cm^{-1} is a satisfactory measure of the ligand field splitting energy for the hexaaquozinc(II) ion.

INTRODUCTION

Recently it has been postulated (1) that high energy vacuum dehydration products can be obtained for any salt hydrate for which the heat of solution of the normal anhydride is higher than would be expected from extrapolation of the data for higher normal crystalline hydrates.

For several hydrated salts, linear relations similar to those shown in Fig. 1 have been obtained by plotting the heats of solution in cal/g of solute against the % water in various samples. Maximum possible heats of solution for the vacuum dehydration products of a hydrated salt have then been estimated (1) by constructing a line CE through the point C for the heptahydrate and parallel to the line AB between the normal anhydride and the crystalline monohydrate.

Such maxima, however, are not always attained since lower heats of solution may result if the method of dehydration allows formation of one of the lower crystalline hydrates before high energy modifications are produced. This apparently was the case in the previous study of the hydrates of zinc sulfate by Frost, Moon, and Tompkins (2) who measured heats of solution for various crystalline hydrates and vacuum dehydration products. Similar results have been obtained (1) by vacuum dehydration of $CoSO_4.7H_2O$, although points on a maximum line such as CE were obtained when barium oxide was present as desiccant during the vacuum dehydration.

The possibility that modifications of lower hydrates of zinc sulfate having maximum heats of solution (on the line CE of Fig. 1) could also be obtained by alteration of the method of vacuum dehydration initiated the present investigation.

EXPERIMENTAL

Samples of $ZnSO_4.7H_2O$, 'Baker Analyzed' reagent, which was obtained from Canadian Laboratory Supplies Limited, were ground in a mortar and dehydrated under vacuum for sufficient time to give products of approximately the composition desired. An ordinary vacuum line with a mechanical pump, a liquid

nitrogen trap, and a McLeod gauge was used in all experiments. Each sample to be dehydrated was placed in a porcelain boat in either a Pyrex tube, 28 mm o.d. and about 30 cm long, or a vacuum oven of about 12 l volume, both of which were connected to the vacuum line. In most experiments a second porcelain boat containing barium oxide was present in the vessel containing the sample being dehydrated.

Heats of solution were measured at 29 °C, as cal/g of solute, in a simple calorimeter which has previously been described (1). After solution of a sample the concentration was 0.02 *m* or less.

RESULTS AND DISCUSSION

In accordance with the method used in a recent investigation in this laboratory of the hydrates of the divalent sulfates of manganese, iron, cobalt, and nickel (1) the data of Frost, Moon, and Tompkins (2) have been recalculated. In Fig. 1, the line BI with the equation

$$y = -2.06x + 82.6$$

represents their results for the normal crystalline hydrates of zinc sulfate. In this and the other linear equations given x is the % water in the sample and y is the heat of solution in cal/g of solute. The line FG denotes the data of Frost, Moon, and Tompkins (2) for the modifications obtained by vacuum dehydration, and has the equation

$$y = -4.51x + 148.5.$$

The heat of solution of the heptahydrate (−7.86 cal/g) obtained by extrapolation of the line BI to the point C (at 43.86% water) is thought to be more exact than the value (about −8 cal/g) estimated by direct measurement in the present calorimeter, since it is difficult to determine values close to zero accurately with this apparatus.

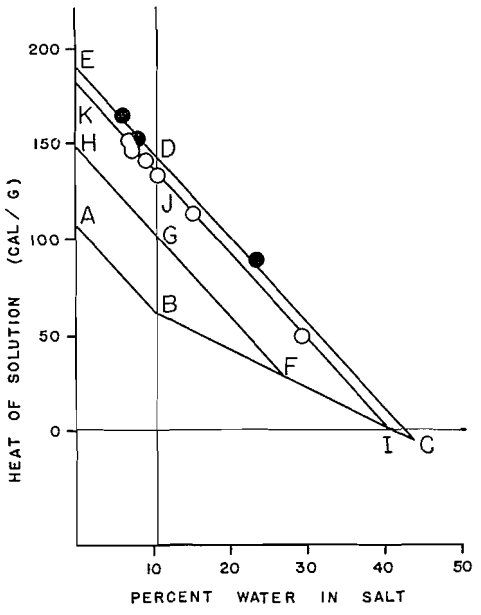

FIG. 1. Heats of solution for the hydrates of zinc(II) sulfate.

It appears that the line CE, passing through the point C for the heptahydrate and having the same slope as the line FG, which has the equation

$$y = -4.51x + 190.0,$$

Can. J. Chem. Downloaded from www.nrcresearchpress.com by 210.87.254.42 on 09/05/12
For personal use only.

represents the maximum possible heats of solution for high energy modifications of the hydrates of zinc sulfate.

Preliminary experiments in which the vacuum dehydration was done in the Pyrex tube without barium oxide have given results on the line FG in agreement with the work of Frost, Moon, and Tompkins (2). When barium oxide was present during vacuum dehydration in the Pyrex vessel, the results plotted in Fig. 1 along the line IK were obtained. This line has essentially the same slope as the lines FG and CE and passes through the point I at the hexahydrate composition (40.10% water). Furthermore, as shown in Fig. 1, dehydration in the vacuum oven gave results on the predicted maximum line CE, whether or not barium oxide was present. Data for the present results on the lines IK and CE are also given in Table I.

TABLE I

Heat of solution data

% water in sample	Heat of solution (cal/g)	Method of dehydration
6.96	151.9	Pyrex tube with BaO*
7.44	146.0	
9.22	140.8	
10.66	133.1	
15.31	112.5	
29.39	48.2	
6.08	164.4	Vacuum oven with BaO†
8.11	152.1	Vacuum oven, no BaO
23.35	88.4	Vacuum oven, no BaO

*This set of results falls on the line IK which meets the line BC for normal crystalline hydrates at the hexahydrate composition.
†This set of results falls on the maximum possible line CE which extrapolates to the point for the normal crystalline heptahydrate.

It appears that the different sets of results are due to differences in pressure, particularly at the start of dehydration. It is known (3, 4) that a liquid nitrogen trap is a better desiccant than barium oxide, while dehydration in a vacuum oven would surely begin long before the oven was fully evacuated. Thus it seems that dehydration at higher pressures gives products of higher energy. Dependence of rate of dehydration on water vapor pressure has been observed by Topley and Smith (5), Volmer and Seydel (6), and Frost and Campbell (7), all of whom found, as the pressure increased from zero, that the rate fell rapidly to a minimum, then rose to pass through a maximum, and finally decreased slowly at higher pressures. An apparent dependence of formation of energy-rich product on water vapor pressure, during the dehydration of $CuSO_4.5H_2O$ and $ZnSO_4.6H_2O$, has also been reported by Frost, Moon, and Tompkins (2). It may be that the present results on the maximum line CE were obtained because the initial pressure of water vapor was at or higher than the Topley–Smith minimum (5) for zinc sulfate. Unfortunately a McLeod gauge, as used in the present investigation, is unsuitable for the measurement of water vapor pressure.

The maximum heat of solution of the monohydrate (shown in Fig. 1 as a vertical line at 10.04% water) at the point D is found from the equation of the line CE to be

$$y_D = 144.7 \text{ cal/g}$$

while the heat of solution of the normal crystalline monohydrate at point B, calculated from the line BI is

$$y_B = 61.9 \text{ cal/g}.$$

Can. J. Chem. Downloaded from www.nrcresearchpress.com by 210.87.254.42 on 09/05/12
For personal use only.

The difference DB gives a maximum heat of transition of 82.8 cal/g or 23.8 kcal/mole of $ZnSO_4.7H_2O$.

Since it has recently been observed empirically (1) that the maximum heats of transition in kcal/mole of $MnSO_4.7H_2O$, $FeSO_4.7H_2O$, $CoSO_4.7H_2O$, and $NiSO_4.7H_2O$ are equal to the ligand field splitting energies for the hexaaquo divalent cations of manganese, iron, cobalt, and nickel, it is probable that the ligand field splitting energy for $[Zn(H_2O)_6]^{2+}$ is 23.8 kcal or 8.3×10^3 cm^{-1}, although it appears that a spectroscopic value for comparison is not available.

ACKNOWLEDGMENT

Financial assistance from the National Research Council is gratefully acknowledged.

REFERENCES

1. J. W. S. JAMIESON, G. R. BROWN, D. W. GRUENER, R. V. PEILUCK, and R. A. LAMONTAGNE. Can. J. Chem. **43**, 2148 (1965).
2. G. B. FROST, K. A. MOON, and E. H. TOMPKINS. Can. J. Chem. **29**, 604 (1951).
3. F. TRUSELL and H. DIEHL. Anal. Chem. **35**, 674 (1963).
4. W. L. JOLLY. Synthetic inorganic chemistry. Prentice-Hall, Englewood Cliffs, N.J. 1960.
5. B. TOPLEY and M. L. SMITH. J. Chem. Soc. 321 (1933).
6. M. VOLMER and G. SEYDEL. Z. Physik. Chem. Leipzig, **A179**, 153 (1937).
7. G. B. FROST and R. A. CAMPBELL. Can. J. Chem. **31**, 107 (1953).

Can. J. Chem. Downloaded from www.nrcresearchpress.com by 210.87.254.42 on 09/05/12
For personal use only.

Can. J. Chem. Downloaded from www.nrcresearchpress.com by 210.87.254.6 on 09/05/12
For personal use only.

STRUCTURE VIBRATIONNELLE DES SPECTRES D'ABSORPTION DANS L'ULTRAVIOLET DE QUELQUES DÉRIVÉS HALOGÉNÉS DU BENZÈNE

P. PESTEIL, H. F. SHURVELL[1] ET L. PESTEIL
Laboratoire de Physique P.C.B. 1, Faculté des Sciences, Marseille, France

Reçu le 11 mai 1965

SOMMAIRE

Les spectres d'absorption dans l'ultraviolet des cristaux purs suivants ont été étudiés à basse température: hexachlorobenzène, *o*, *m* et *p*-dichlorobenzènes, *o*, *m* et *p*-dibromobenzènes, trichloro 1,2,3-benzène et tétrachloro 1,2,4,5-benzène. Il s'agit, dans tous les cas, des premières bandes d'absorption correspondant à la transition $^1B_{2u}$–$^1A_{1g}$ du benzène. Pour six de ces composés, la résolution des spectres était suffisante pour permettre des analyses complètes de la structure vibrationnelle des bandes électroniques. Les résultats montrent que les vibrations totalement symétriques sont seules à apparaître dans le cas des transitions électroniques observées. Nous en concluons que quelques changements doivent être apportés à de précédentes attributions vibrationnelles.

ABSTRACT

Ultraviolet absorption spectra have been recorded, at low temperatures, for pure crystals of the following compounds: hexachlorobenzene, *o*, *m*, and *p*-dichlorobenzenes, *o*, *m*, and *p*-dibromobenzenes, 1,2,3-trichlorobenzene, and 1,2,4,5-tetrachlorobenzene. In all cases, the first electronic transition corresponding to the $^1B_{2u}$–$^1A_{1g}$ transition of benzene has been studied. For six of these compounds the spectra were sufficiently well resolved to permit complete analyses of the vibrational fine structure of the electronic bands. The results indicate that only totally symmetrical vibrations appear in conjunction with the observed electronic transitions. Several changes in published vibrational assignments are proposed, in the light of present results.

INTRODUCTION

Après l'étude des vibrations du benzène sur lesquelles la plupart des auteurs semblent maintenant d'accord (1, 2, 3), l'intérêt des chercheurs s'est porté sur les dérivés substitués. Ces recherches, basées généralement sur les résultats de spectroscopie Raman ou infrarouge, concernent la substance soit à l'état de vapeur, soit à l'état liquide, soit à l'état cristallisé. Il est possible de déterminer sur les spectres obtenus les différents types de vibrations et de confronter ces résultats avec les prévisions théoriques. L'adoption de constantes de force de tension et de flexion permet également de calculer les vibrations. On trouve enfin, dans de nombreux articles, des tableaux de vibrations classées en types de symétrie (4, 5, 6).

La structure des spectres électroniques en absorption ou en émission permet également de déterminer les différents types de vibrations. Les spectres d'absorption, obtenus lors du passage de l'électron du niveau fondamental à un niveau excité, fournissent les vibrations de la molécule à l'état excité, c'est-à-dire, en ce qui concerne notamment le benzène et ses dérivés, de la molécule dilatée par rapport à son état fondamental; les fréquences obtenues seront donc plus faibles que celles données par la diffusion Raman et l'absorption infrarouge. Les spectres de fluorescence, correspondant au passage de l'électron du niveau excité au niveau fondamental, permettent d'obtenir les vibrations de la molécule à l'état fondamental et de retrouver certaines vibrations Raman ou infrarouge.

Cette méthode expérimentale peut donc servir de complément utile pour vérifier des attributions; elle ne permet cependant pas de retrouver toutes les vibrations, mais seulement celles qui sont permises ou favorisées par le passage de la molécule d'un état à un autre. Lorsque la transition est permise par les règles de sélection, il est plus probable de

[1]*Adresse actuelle: Department of Chemistry, Queen's University, Kingston, Ontario.*

voir apparaître les vibrations totalement symétriques par rapport au groupe de point de la molécule (7); mais, dans certains cas, une vibration peut rendre la transition électronique permise en lui conférant la même symétrie que celle d'une translation: ainsi, pour le benzène, une vibration E_{2g} transforme la transition électronique interdite B_{2u} en symétrie E_{1u} de même type de symétrie que les translations T_x et T_y; la transition devient donc permise.

D'autre part, parmi les vibrations permises, certaines apparaissent avec une intensité accrue; ce sont les vibrations qui font passer la molécule de sa forme normale à sa configuration dans l'état électronique excité. Par exemple, la vibration 613 cm^{-1} de la molécule d'acétylène étudiée par Ingold et King (8) amène la molécule linéaire dans son état fondamental à une forme quasi-éthylénique *trans* dans l'état excité et donne naissance à des groupes de bandes que l'on observe dans le spectre d'absorption ultraviolet.

Cette méthode d'analyse a déjà été utilisée dans ce laboratoire; l'étude de la structure vibrationnelle des spectres d'absorption et de luminescence a permis de dresser des tableaux de vibrations totalement symétriques à l'état excité ou à l'état fondamental pour de nombreuses molécules aromatiques: naphtalène, acénaphtène, phénanthrène, fluoranthène, acénaphtylène et dérivés du naphtalène (9–15). L'étude simultanée des spectres d'absorption et de fluorescence permet même d'établir des correspondances entre vibrations des états fondamental et excité. On trouve généralement un nombre de vibrations actives en bon accord avec celui prévu par le dénombrement théorique, mais la complexité des molécules étudiés précédemment rend difficile l'attribution d'une vibration donnée à un type de mouvement prévu en utilisant les coordonnées de symétrie. C'est pourquoi il nous a paru préférable d'étudier des molécules plus simples et en particulier les dérivés halogénés du benzène, afin de baser nos recherches sur les résultats universellement admis pour le benzène.

On peut étudier, soit la vapeur, soit, à basse température, une solution ou un cristal pur; ces méthodes ont chacune des avantages et des inconvénients.

Les spectres d'absorption ou de luminescence des vapeurs de dérivés aromatiques sont généralement bien résolus en raies fines, mais leur étude se faisant à température élevée, leur complexité est extrême; on trouve, sur le même spectre, des vibrations de l'état fondamental et des vibrations de l'état excité. Cette méthode a cependant permis à Ingold d'expliquer la structure vibrationnelle du benzène.

L'état condensé peut être étudié, soit sur des solutions dans les paraffines (Shpol'skii a montré que, dans ce cas, les spectres sont remarquablement bien résolus (16, 9–15)), soit sur des échantillons de substances pures qui donnent également de bons résultats. Dans ces deux derniers cas, les spectres d'absorption ne fournissent que les vibrations de l'état excité, les spectres de luminescence, les vibrations de l'état fondamental; d'où une simplification notable par rapport aux spectres des vapeurs. En contrepartie, les interactions entre molécules de solvant et de soluté jouent un rôle non négligeable pour compliquer la structure des spectres par apparition des phénomènes excitoniques dont on trouvera l'étude dans les références suivantes (17, 18).

Le présent article rend compte des résultats obtenus à basse température sur les substances pures cristallisées suivantes: *o*, *m* et *p*-dichlorobenzènes, *o*, *m* et *p*-dibromobenzènes, trichloro 1,2,3-benzène, tétrachloro 1,2,4,5-benzène et hexachlorobenzène. Ces substances, faciles à obtenir dans le commerce, présentent un intérêt théorique certain et leur étude, aussi limitée soit-elle, peut apporter de nouveaux éléments à la connaissance des vibrations des dérivés halogénés du benzène.

Toutes les molécules étudiées ici ont donné lieu à de nombreuses publications tant en

Can. J. Chem. Downloaded from www.nrcresearchpress.com by 210.87.254.6 on 09/05/12
For personal use only.

Raman qu'en infrarouge; on trouvera dans l'article de Scherer et Evans (5) des tableaux très complets où les auteurs établissent des listes de vibrations classées en types de symétrie pour tous les dérivés chlorés étudiés dans le présent article; le *p*-dibromobenzène a été étudié par Whiffen (6). Ce sont principalement ces deux articles qui nous ont servi de base pour la discussion de nos résultats expérimentaux.

Certains de ces dérivés ont également donné lieu à des études dans l'ultraviolet, c'est le cas des *o* et *p*-dichlorobenzènes (19), du tétrachlorobenzène (20) et de l'hexachlorobenzène (21).

MÉTHODE EXPÉRIMENTALE

Les produits ont été trouvés dans le commerce à l'état purum ou purissimum; nous avons recristallisé les purum dans l'alcool; les *p*-dichlorobenzène, *p*-dibromobenzène et tétrachloro 1, 2,4,5-benzène ont été purifiés par fusion de zone (40 à 80 passages selon les cas); mais aucune modification du spectre n'a été observée entre les produits purissimum et les produits purifiés par fusion de zone. Les résultats expérimentaux montreront d'ailleurs que les spectres peuvent être expliqués en ne faisant intervenir que des vibrations de la substance étudiée, ce qui élimine l'influence des impuretés.

Les échantillons sont obtenus cristallisés par refroidissement lent de la substance entre deux disques de silice et l'épaisseur contrôlée au microscope polarissant; l'épaisseur convenable correspondant pour la plupart des substances à des couleurs vives entre nicols croisés. Dans le cas des liquides, le contrôle n'est plus possible; une goutte est alors déposée entre les deux disques de silice et l'ensemble plongé directement dans le cryostat; on recommence l'opération jusqu'à ce que la lame soit d'épaisseur convenable et sans trou.

Le cryostat utilisé est le même que celui qui a été décrit à plusieurs reprises (22, 9–15); le système dispersif est un spectrographe ultraviolet 120 de Huet (60 cm^{-1}/mm vers 2 700 Å); la source une lampe à xenon Osram de 500 W et les plaques des Superfulgur de Guilleminot; le temps de pose varie de quelques secondes à quelques minutes, selon l'épaisseur des lames. Le rayonnement infrarouge important de la lampe est arrêté au moyen d'une solution diluée de sulfate de nickel et de sulfate de cobalt; l'absorption de cette solution dans le proche ultraviolet ne nous a jamais gênés, car les spectres étudiés se situent toujours plus loin dans l'ultraviolet. Les fréquences ont été déterminées au microscope de mesure Beaudouin et au microphotomètre de Chalonge et Laffineur.

DÉNOMBREMENT DES VIBRATIONS ACTIVES

Pour le choix des axes de symétrie des différentes molécules, nous nous sommes conformés à la standardisation proposée en 1955 (23). Nous avons conservé les mêmes axes pour le benzène (symétrie D_{6h}) et pour les dérivés para et tétra halogénés (symétrie D_{2h}): l'axe z est perpendiculaire au plan de la molécule, l'axe y passe par un atome de carbone et l'axe x est perpendiculaire à une liaison C—C. Pour les autres dérivés, la molécule est dans le plan yz, l'axe z étant toujours l'axe binaire de symétrie.

Nous pensons qu'il n'y a pas lieu de s'étendre sur le dénombrement des vibrations de chaque molécule, puisque cela a été fait à maintes reprises et ne présente aucune difficulté. Nous avons résumé les résultats dans le Tableau I.

En tête du tableau, on trouvera le nom de la molécule, son schéma avec indication des axes et l'orientation du dipole d, correspondant à la transition électronique permise (issue de la transition interdite $^1B_{2u}$–$^1A_{1g}$ du benzène), ainsi que le groupe de symétrie (notation de Schoenflies) auquel appartient la molécule.

On trouvera dans les colonnes les types de symétrie des vibrations correspondant à des mouvements totalement symétriques ou qui sont susceptibles de faire tourner le dipole de $\pi/2$ dans le plan de la molécule (mouvements correspondant à une rotation autour de l'axe perpendiculaire à la molécule); les premières sont notées A_g ou A_1, les secondes B_{1g} ou B_2, selon le groupe de symétrie. Nous pensons que le Tableau I est suffisamment clair pour faire ressortir la correspondance entre les vibrations du benzène et les vibrations de ses dérivés. Dans chaque cas, nous avons également indiqué le nombre de vibrations attendues. Enfin au bas du tableau, nous avons fait la somme des vibrations totalement symétriques d'une part et des vibrations qui donnent une autre orientation au dipole, d'autre part. Il

Can. J. Chem. Downloaded from www.nrcresearchpress.com by 210.87.254.6 on 09/05/12
For personal use only.

TABLEAU I

Dénombrement des vibrations utilés dans le présent travail

C_6H_6		$p.C_6H_4Cl_2$ $p.C_6H_4Br_2$		$1,2,4,5.C_6H_2Cl_4$	$m.C_6H_4Cl_2$ $m.C_6H_4Br_2$ $1,2,3.C_6H_3Cl_3$		$O.C_6H_4Cl_2$ $O.C_6H_4Br_2$	
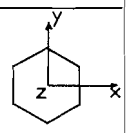		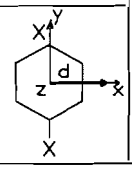		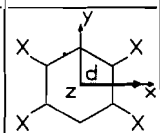	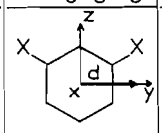		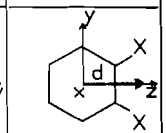	
D6h		D2h			C2v		C2v*	
A_{1g}	2	A_g	2		A_1	2	A_1	2
A_{2g}	1	B_{1g}	1		B_2	1	B_2	1
B_{1u}	2				A_1	2	B_2	2
B_{2u}	2	B_{3u}			B_2	2	A_1	2
E_{1u}	3				A_1	3	B_2	3
					B_2	3	A_1	3
E_{2g}	4	A_g	4		A_1	4	A_1	4
		B_{1g}	4		B_2	4	B_2	4
Total		A_g	6		A_1	11	A_1	11
		B_{1g}	5		B_2	10	B_2	10

est évident que l'hexachlorobenzène, qui ne figure pas nommément dans le tableau, a les mêmes propriétés que le benzène. Ajoutons enfin que ce tableau n'a de valeur que si les molécules conservent dans le cristal la même symétrie qu'à l'état libre.

La correspondance entre symétries du benzène et de ses dérivés est également encore valable pour la symétrie de chacune des transitions électroniques; le Tableau I donne également l'orientation du dipole correspondant à la transition électronique; elle est permise dans tous les cas, puisque $B_{2u}(D_{6h})$ devient: $B_{3u}(D_{2h})$, $B_2(C_{2v})$ et $A_1(C_{2v}{}^*)$; les groupes C_{2v} et $C_{2v}{}^*$ diffèrent par la position de leur axe de symétrie z.

Les spectres des dérivés halogénés (sauf celui de l'hexachlorobenzène) seront donc en principe assez différents de celui du benzène, puisque dans ce dernier cas, la transition interdite était rendue permise, comme nous l'avons déjà dit, par une vibration de symétrie E_{2g} (520 cm^{-1}) qui servait d'origine à une série de raies fortes dont les fréquences étaient données par une relation de la forme: $\nu' = (0''\text{–}0') + 520 + n.923$. Dans le cristal, à cause des interactions moléculaires, une autre série de raies plus faibles apparait cependant (24): $\nu' = (0''\text{–}0') + p.923$.

L'objet principal du présent article est de vérifier si la structure des spectres d'absorption peut s'expliquer avec les seules vibrations totalement symétriques; c'est pour cela qu'il est nécessaire de dresser maintenant un tableau des résultats obtenus en Raman et en infrarouge (Tableau II).

Can. J. Chem. Downloaded from www.nrcresearchpress.com by 210.87.254.6 on 09/05/12
For personal use only.

TABLEAU II

Frèquences de vibrations d'apres les réfs. 5 et 6

C_6Cl_6 (5)	p-$C_6H_4Cl_2$ (5)	p-$C_6H_4Br_2$ (6)	1,2,4,5-$C_6H_2Cl_4$ (5)	1,2,3-$C_6H_3Cl_3$ (5)	o-$C_6H_4Cl_2$ (5)
A_{1g} 372	A_g 328	A_g 218	A_g 190	A_1 212	A_1 203
1 210	747	708	352	352	480
E_{2g} 219	1 096	1 067	684	516	660
323	1 169	1 170	1 165	738	1 041
870	1 574	1 570	1 549	1 050	1 130
1 512	3 070	3 068	3 070	1 088	1 162
	B_{1g} 350	B_{1g} 307	B_{1g} 312	1 161	1 276
	626	623	511	1 416	1 468
	1 290	1 289	868	1 566	1 575
	1 574	1 570	1 240	3 072	3 070
	3 065	3 068	1 566	3 072	3 070
				B_2 212	B_2 334
				400	429
				492	740
				791	1 038
				1 156 (?)	1 130
				1 192	1 252
				1 261	1 438
				1 436	1 575
				1 566	3 070
				3 072	3 070

RÉSULTATS EXPÉRIMENTAUX ET ANALYSE VIBRATIONNELLE

Dans l'exposé qui suit, nous étudierons successivement les molécules précédemment citées dans l'ordre suivant: C_6Cl_6, p-$C_6H_4Cl_2$, p-$C_6H_4Br_2$, 1,2,4,5-$C_6H_2Cl_4$, 1,2,3-$C_6H_3Cl_3$, o-$C_6H_4Cl_2$, o-$C_6H_4Br_2$, m-$C_6H_4Cl_2$, m-$C_6H_4Br_2$.

On trouvera, pour chaque substance, une photographie du spectre d'absorption à 20 °K (Figs. 1, *a*, *b*, *c*, ...) et un microphotogramme (Figs. 2, *a*, *b*, *c*, ...).

Précisions que l'objet du présent article est l'étude de la structure vibrationnelle; nous ne chercherons donc pas à expliquer la structure de la transition électronique (0″–0′) (exciton), même si nous sommes souvent amenés à tenir compte de cette structure qui sert d'origine aux vibrations. Nous rappellerons simplement, pour mémoire, qu'il existe actuellement deux méthodes concurrentes pour expliquer, cette structure excitonique; la première, proposée par Davydov en 1948 (25), est admise par la plupart des chercheurs; elle considère que la structure provient de la séparation du niveau en composantes polarisées parallèlement aux axes ou plans de symétrie du cristal. L'autre a été proposée plus récemment par l'un de nous (17), puis développée par Benarroche (18); elle fait intervenir une structure quasi-hydrogénoïde qui rappelle l'exciton de Wannier (26); cette structure a été également trouvée dans les solutions cristallisées (27); elle semble avoir été confirmée récemment par la découverte d'un effet photoélectrique (28).

(a) Hexachlorobenzène, $C_6Cl_6(D_{6h})$

Ce cristal a déjà donné lieu à une étude extrèment soignée de Schnepp et Kopelman (21) à 4 °K; la structure étant suffisamment fine à 20 °K, nous n'avons pas jugé nécessaire d'utiliser l'hélium liquide.

Le spectre est reproduit sur la Fig. 1*a*; le microphotogramme correspondant se trouve sur la Fig. 2*a*; la Fig. 2*a*′ est le microphotogramme de la transition (0″–0′); on notera son extrême complexité. Enfin, dans le Tableau III, nous avons indiqué la position des raies d'absorption que l'on peut également reconnaître sur la Fig. 2*a*.

Can. J. Chem. Downloaded from www.nrcresearchpress.com by 210.87.254.6 on 09/05/12
For personal use only.

Can. J. Chem. Downloaded from www.nrcresearchpress.com by 210.87.254.6 on 09/05/12
For personal use only.

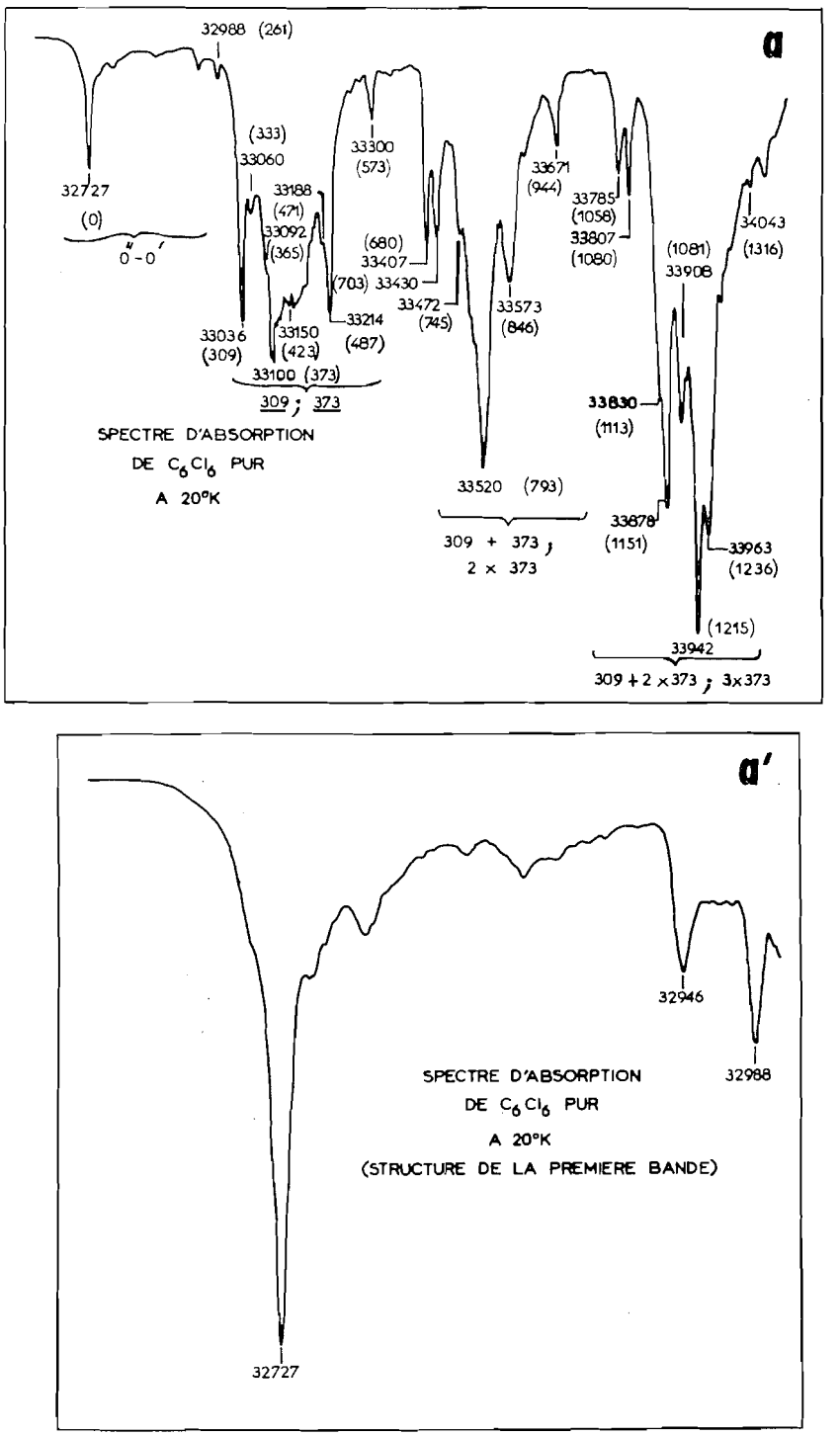

FIGS. 2*a* and 2*a'*.

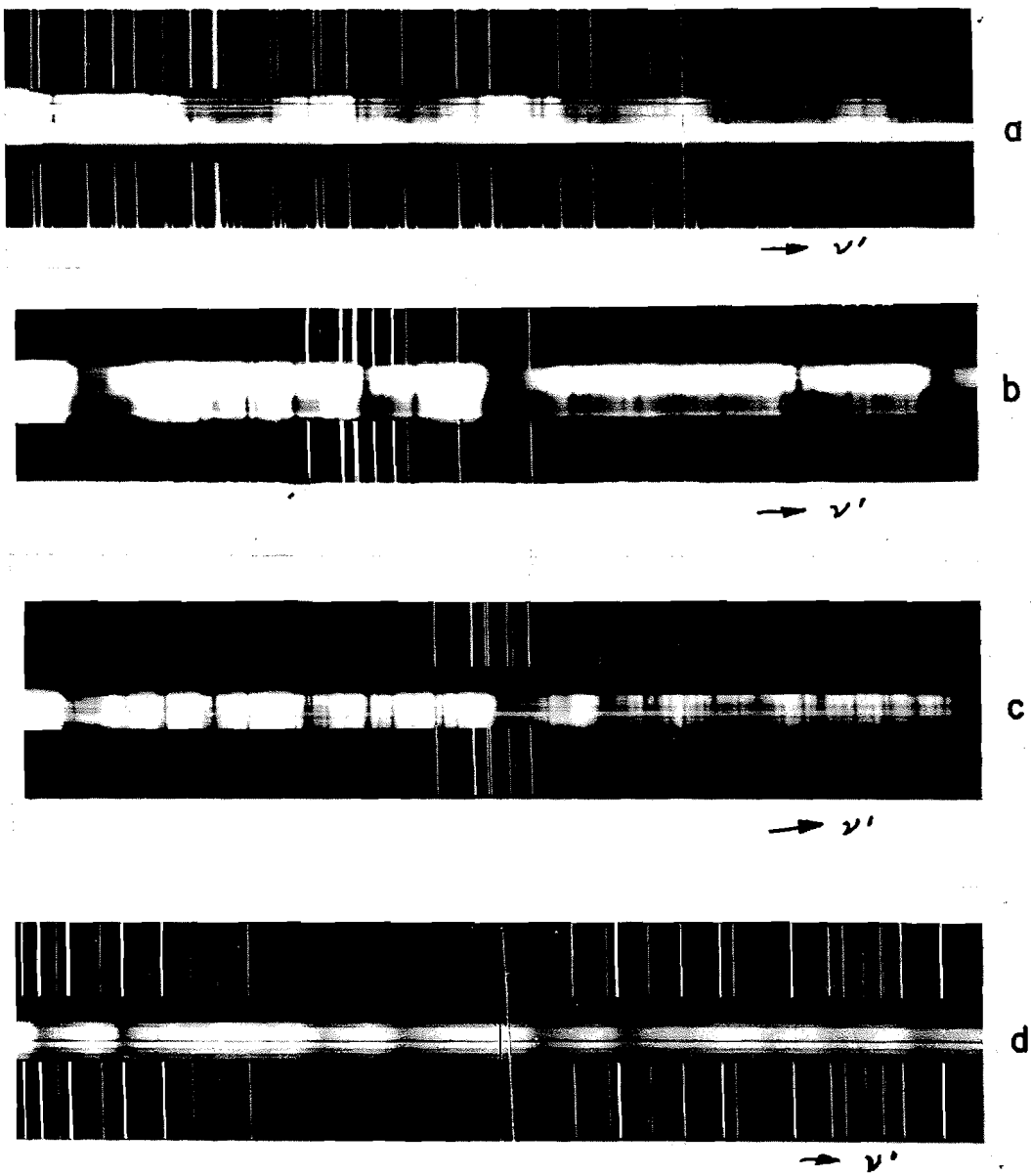

FIG. 1. (*a*) Spectre d'absorption du cristal d'hexachlorobenzène pur à 20 °K. (*b*) Spectre d'absorption du cristal de *p*-dichlorobenzène pur à 20 °K; les vibrations parallèles à chacune des lignes neutres de la lame cristalline ont été séparées par un prisme de Wollaston. (*c*) Spectre d'absorption du cristal de *p*-dibromobenzène pur à 20 °K. (*d*) Spectre d'absorption du cristal de tétrachloro 1,2,4,5-benzène pur à 4 °K.

Can. J. Chem. Downloaded from www.nrcresearchpress.com by 210.87.254.6 on 09/05/12
For personal use only.

Ces fréquences, précisons le bien, résultent de notre présentation du spectre avec une seule origine et non d'une séparation des vibrations en plusieurs composantes. Chacune des X_i, par exemple, est distante de 309 cm^{-1} d'une raie située dans la bande (0''–0'). Nous donnons, dans le Tableau IV, la liste des différences de fréquences calculées en utilisant les formules α et β.

TABLEAU IV

309	333	365	423	471	573	$(n = 0)$	
682	706	738	796	844	946	$(n = 1)$	(α)
1 055	1 079	1 111	(1 169)	1 217	1 319	$(n = 2)$	
1 428	1 452	1 484	1 542	1 590	1 692	$(n = 3)$	
373	746	1 119	1 492			$(q = 0)$	(β)
487	860	1 233	1 606			$(q = 1)$	

Si l'on compare les fréquences données par le Tableau IV et les $D\nu'$ du Tableau III et de la Fig. 2*a*, on voit que l'accord est très satisfaisant; on retrouve en effet toutes les raies du spectre d'absorption, exception faite des deux raies fortes 1 151 et 1 181.

Pour les expliquer, remarquons que la deuxième vibration A_{1g} doit également intervenir pour donner un motif de bandes analogue aux motifs α et β. Or, la fréquence de cette vibration à l'état électronique fondamental étant 1 210 cm^{-1} (voir sur le Tableau II), on doit la trouver vers 1 150 cm^{-1} dans l'état excité. Nous proposons donc de la situer à 1 169 cm^{-1} où elle serait en résonance de Fermi avec la fréquence de même symétrie située à la même place, pour donner les deux raies trouvées expérimentalement à 1 151 et à 1 181 cm^{-1}.

En conclusion de cette étude, on voit que tout le spectre peut être expliqué en n'utilisant que 3 vibrations qui sont, dans l'état électronique excité, de fréquence: 309 cm^{-1}, de symétrie E_{2g} (520 pour le benzène); 373 cm^{-1}, de symétrie A_{1g}; vibration C—Cl de tension (3 130 pour le benzène); 1 169 cm^{-1}, de symétrie A_{1g}; vibration C—C (923 pour le benzène).

Ces résultats sont conformes aux propositions du Tableau II et aux prévisions théoriques si l'on suppose que la molécule conserve sa symétrie D_{6h} dans le cristal. Un essai d'interprétation de la structure excitonique sera publié ultérieurement.

(b) Paradichlorobenzène, $C_6H_4Cl_2(D_{2h}$ ou $V_h)$

La substitution des halogènes en para supprime l'axe d'ordre 6 normal au plan de la molécule, mais lui conserve 3 axes binaires. La symétrie relativement élevée de la molécule explique le nombre réduit de vibrations A_{1g} (six) et de vibrations B_{1g} (cinq) susceptibles de faire tourner le dipole de $\pi/2$ (Tableau I).

La transition interdite, B_{2u}, du benzène devient B_{3u}, permise, avec un moment dipolaire vibrant parallèlement à l'axe x. L'aspect du spectre doit être très différent de celui du benzène (ou de C_6Cl_6) et sa structure vibrationnelle constituée par un seul motif de bandes. On peut cependant se demander si les deux vibrations de symétries A_g et B_{1g} issues de la vibration E_{2g} (521 cm^{-1}) du benzène n'interviennent pas ensemble pour donner deux transitions de polarisations différentes dans le plan de la molécule. C'est une possibilité dont il nous faudra tenir compte dans notre analyse.

L'utilisation des coordonnées de symétrie permet d'avoir une représentation simple des mouvements correspondant aux 6 vibrations A_g issues des 2 vibrations A_{1g} (923 et 3 130) et des 4 vibrations E_{2g} (521, 1 130, 1 470 et 3 080) du benzène.

Nous proposons, dans le Tableau V, une telle représentation qui a l'avantage de séparer nettement les vibrations C—H des vibrations C—Cl (ou C—Br). Nous nous sommes servis, pour le dresser, du tableau de vibrations reproduit par Brodersen et Langseth (3) et nous

Can. J. Chem. Downloaded from www.nrcresearchpress.com by 210.87.254.6 on 09/05/12
For personal use only.

avons conservé la numérotation des vibrations adoptée par ces auteurs. Il ne s'agit là, évidemment, que d'une représentation qualitative des mouvements des atomes.

Il n'y a aucune difficulté pour les vibrations 8 et 9 pour lesquelles les mouvements des atomes sont les mêmes que pour le benzène; pour les 4 autres vibrations, elles doivent être couplées deux à deux, en phase ou en opposition de phase, pour obtenir les schémas (1, 6)′ et (1, 6)″ d'une part et (2, 7)′ et (2, 7)″ d'autre part. (2, 7)′ est une vibration de tension purement C—H, alors que (2, 7)″ est une vibration de tension purement C—Cl.

Nous avons également porté sur ce tableau les résultats relatifs au *p*-$C_6H_4Br_2$ et au 1,2,4,5-$C_6H_2Cl_4$ que nous étudierons ensuite.

TABLEAU V

Schémas et fréquences des vibrations totalement symétriques des molécules appartenant au groupe de symétrie D_{2h}

9	8 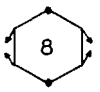
p.$C_6H_4Cl_2$: 1053 (1096) p.$C_6H_4Br_2$: 1010 (1067) 1,2,4,5.$C_6H_2Cl_4$: 195 (190)	p.$C_6H_4Cl_2$: 1479 (1573) p.$C_6H_4Br_2$: 1476 (1570) 1,2,4,5.$C_6H_2Cl_4$: 1455 (1549)
(2,7)′ 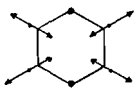	(2,7)″ 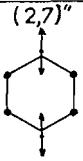
p.$C_6H_4Cl_2$: 3171 (3072) p.$C_6H_4Br_2$: 3170 (3068) 1,2,4,5.$C_6H_2Cl_4$: 330 (352)	p.$C_6H_4Cl_2$: 309 (330) p.$C_6H_4Br_2$: 217 (218) 1,2,4,5.$C_6H_2Cl_4$: 3085 (3070)
(1,6)′	(1,6)″ 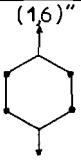
p.$C_6H_4Cl_2$: 551 (628) p.$C_6H_4Br_2$: 542 (623) 1,2,4,5.$C_6H_2Cl_4$: 645 (684)	p.$C_6H_4Cl_2$: 725 (747) p.$C_6H_4Br_2$: 693 (708) 1,2,4,5.$C_6H_2Cl_4$: 1135 (1165)

Le spectre d'absorption du *p*-dichlorobenzène a fait l'objet d'une étude à l'état de vapeur (19); Anno et Matubara ont expliqué sa structure par les fréquences de vibrations suivantes de l'état excité: 331, 528, 725, 1 051, 1 061, 1 089, 1 461 et 3 081 cm^{-1}, c'est-à-dire

Can. J. Chem. Downloaded from www.nrcresearchpress.com by 210.87.254.6 on 09/05/12
For personal use only.

par 8 vibrations alors qu'il n'y a que 6 vibrations totalement symétriques; mais, selon ces auteurs, la vibration 528 cm^{-1} serait la composante B_{1g} issue de la vibration 521 cm^{-1} (E_{2g}) du benzène, la fréquence 330 en étant la composante A_g. Cela évidemment est possible, mais on ne saurait plus où situer la vibration de tension C—Cl qui doit être voisine de 300 cm^{-1}.

On trouvera dans le Tableau II, les vibrations proposées par Scherer et Evans (5) et par Stojiljkovic et Whiffen (6). On constate que la vibration de fréquence 626 (528 à l'état excité) est proposée avec une symétrie B_{1g}; cette classification concorde donc avec les résultats d'Anno, tout au moins en ce qui concerne cette vibration.

Le spectre d'absorption à 20 °K est représenté sur la Fig. 1*b*; le microphotogramme du spectre est reproduit en Fig. 2*b*.

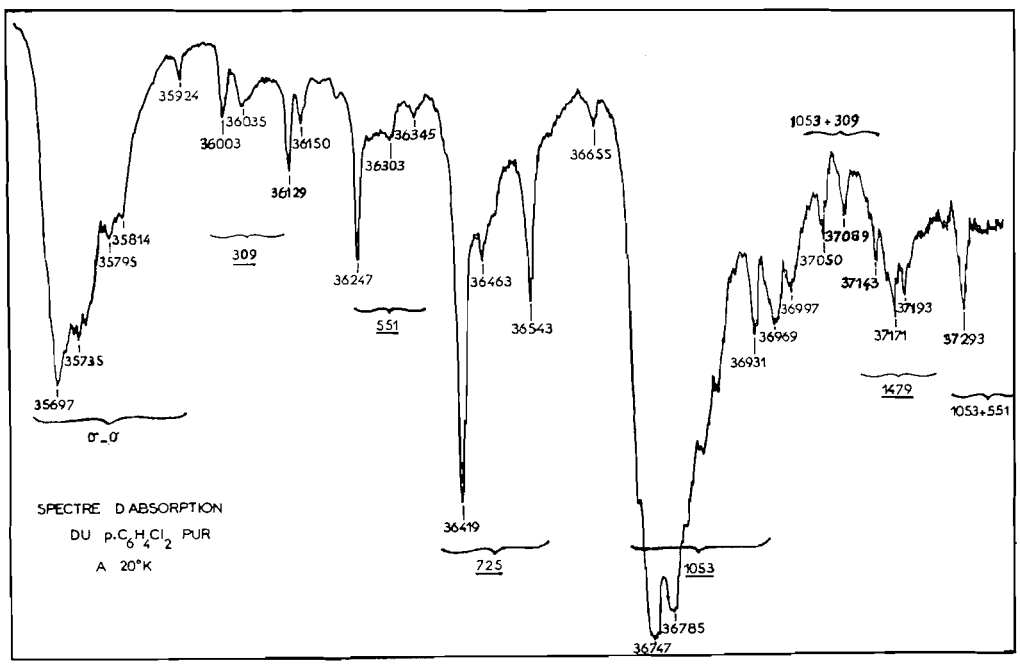

FIG. 2*b*.

Afin de trouver d'éventuelles variations d'orientation du dipole, nous avons étudié la polarisation du spectre et séparé les deux composantes vibrant suivant les lignes neutres de la lame cristalline. On peut voir, sur la Fig. 1*b*, que la vibration 551 cm^{-1}, repérée par un point (nous n'avons pas retrouvé la fréquence 528 proposé par Anno) a la même polarisation que l'ensemble du spectre. On peut interpréter ce résultat de deux manières; soit parce que la vibration 551 est totalement symétrique (ce que nous pensons), soit par une orientation convenable des molécules par rapport aux lignes neutres.

La fréquence des principales bandes a été indiquée sur la Fig. 2*b*; nous utiliserons cette figure pour étudier la structure vibrationnelle du spectre. L'étude détaillée, faite au microscope de mesure, montre que tout le spectre peut être expliqué en ne faisant intervenir que les 6 vibrations suivantes: 309, 551, 725, 1 053, 1 479 et 3 171 cm^{-1} (cette dernière vibration n'apparait pas sur la Fig. 2*b* qui ne va pas au delà de 37 500 cm^{-1}; la raie d'absorption correspondante se trouve à 38 868 cm^{-1}).

Can. J. Chem. Downloaded from www.nrcresearchpress.com by 210.87.254.6 on 09/05/12
For personal use only.

Ces résultats sont conformes aux prévisions théoriques qui nous donnaient 6 vibrations totalement symétriques (Tableau I); les fréquences des vibrations correspondantes de l'état fondamental sont incontestablement les suivantes, d'après le Tableau II: 330, 626, 747, 1 096, 1 574 et 3 070 cm^{-1}, alors que les vibrations A_g admises par Evans se situent à: 330, 747, 1 096, 1 169, 1 574 et 3 070 cm^{-1}.

La différence porte sur deux vibrations: 626, classée parmi les B_{1g}, et 1 169, sans équivalent dans notre spectre.

Nous avons porté, sur le Tableau V, à côté du schéma de chaque vibration, la fréquence que nous proposons pour l'état excité et, entre parenthèses, pour l'état fondamental.

(c) Paradibromobenzène, $C_6H_4Br_2(D_{2h})$

Afin de contrôler les résultats qui viennent d'être exposés, nous avons entrepris l'étude du *p*-$C_6H_4Br_2$ dont les fréquences de vibration sont connues également (6); par contre, nous n'avons trouvé aucune référence sur une éventuelle tentative d'analyse du spectre d'absorption ultraviolet.

Il est évident que les modes de vibrations proposés sur le Tableau V pour le dérivé chloré sont encore valables pour le paradibromobenzène.

Le spectre est reproduit sur la Fig. 1*c*; les Figs. 2*c* et 2*c'* représentent respectivement les microphotogrammes d'une portion étendue du spectre et de la structure de la transition électronique (0''–0'); cette structure est compliquée et fera l'objet d'une étude ultérieure.

Sur la Fig. 2*c*, nous avons indiqué les fréquences des principales raies d'absorption ainsi que les fréquences des vibrations responsables de la structure.

Nous avons trouvé les fréquences suivantes: 217, 542, 693, 1 010, 1 476 et 3 170 cm^{-1}; nous leur proposons les correspondantes suivantes dans l'état fondamental (6) (Tableau II): 218, 623, 708, 1 067, 1 570 et 3 068 cm^{-1}.

Le dérivé bromé nous donne donc des résultats comparables à ceux du dérivé chloré: la vibration 623 est classée parmi les B_{1g} par Whiffen et nous ne retrouvons pas la vibration de l'état excité correspondant à 1 170 cm^{-1}.

Notons encore, pour terminer, qu'il y a concordance parfaite entre le nombre de vibrations totalement symétriques prévues et le nombre de fréquences qui composent le motif vibrationnel.

(d) Tetrachloro 1,2,4,5-benzène, $C_6H_2Cl_4(D_{2h})$

L'intérêt de cette molécule vient de ce qu'elle a même symétrie que les deux précédentes et qu'elle est, en quelque sorte, le complément du *p*-$C_6H_4Cl_2$, les vibrations C—H de l'une étant remplacées par des vibrations C—Cl de l'autre (Tableau V).

Le spectre d'absorption ultraviolet à l'état de vapeur a été étudié par Anno (20) qui propose une structure expliquée par des vibrations de fréquences: 85, 155, 636 et 1 134 cm^{-1}; il est difficile de trouver leurs correspondantes dans l'état fondamental dont les vibrations totalement symétriques sont de fréquences: 190, 352, 684, 1 165, 1 549 et 3 070 cm^{-1} (Tableau II).

Nous avons reproduit, sur la Fig. 1*d*, la photographie du spectre à 4 °K et sur la Fig. 2*d*, le microphotogramme correspondant.

On notera d'abord que la résolution des bandes est moins bonne que dans le cas des molécules précédentes; les bandes sont cependant suffisamment fines pour permettre un pointé convenable. Tout le spectre peut être expliqué par la combinaison des fréquences suivantes de vibrations de l'état excité: 195, 330, 645, 1 135, 1 455 et 3 085 cm^{-1} qui correspondent aux vibrations totalement symétriques de l'état fondamental qui viennent d'être énumérées.

Can. J. Chem. Downloaded from www.nrcresearchpress.com by 210.87.254.6 on 09/05/12
For personal use only.

Can. J. Chem. Downloaded from www.nrcresearchpress.com by 210.87.254.6 on 09/05/12
For personal use only.

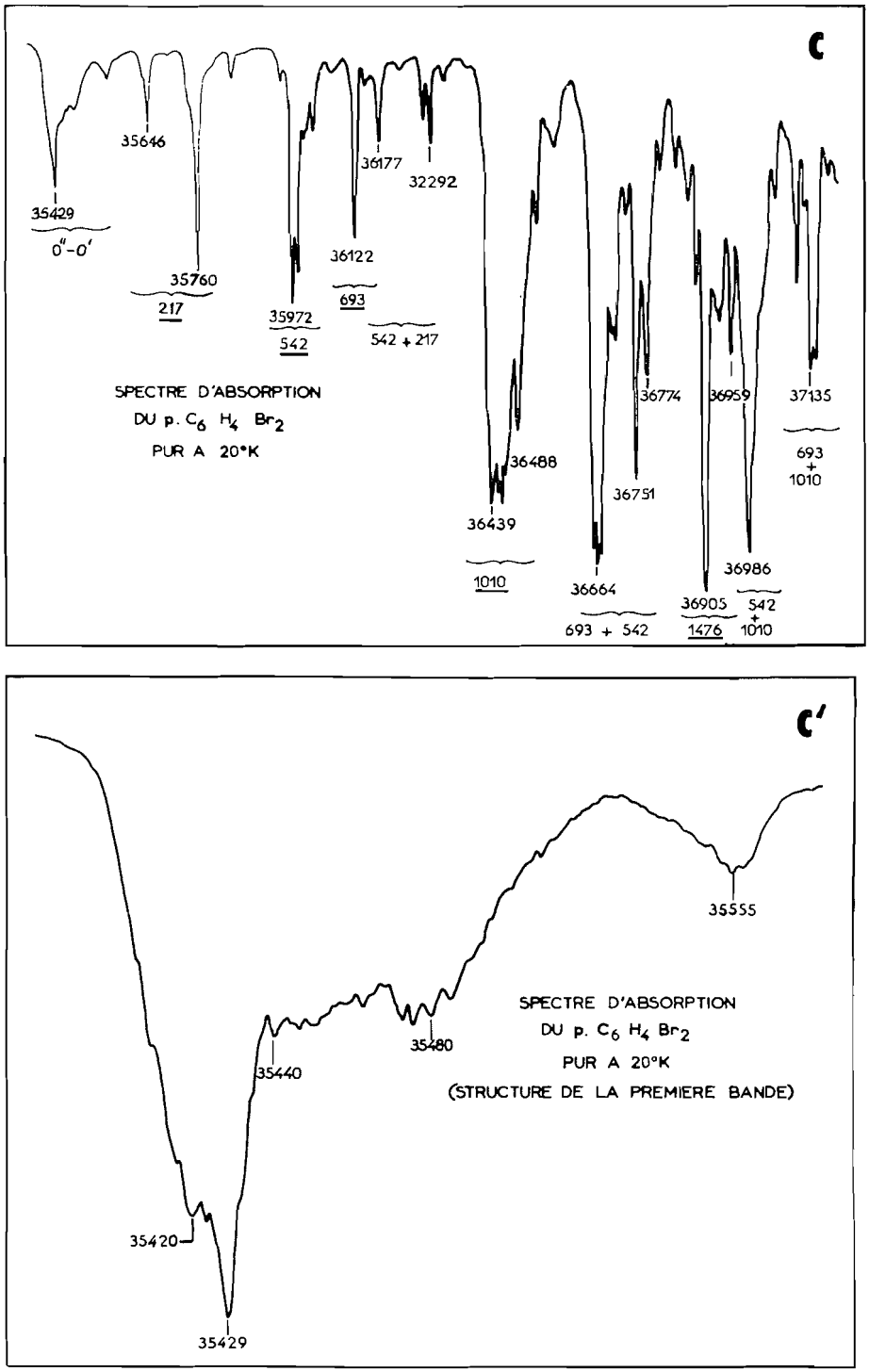

FIGS. 2*c* and 2*c'*.

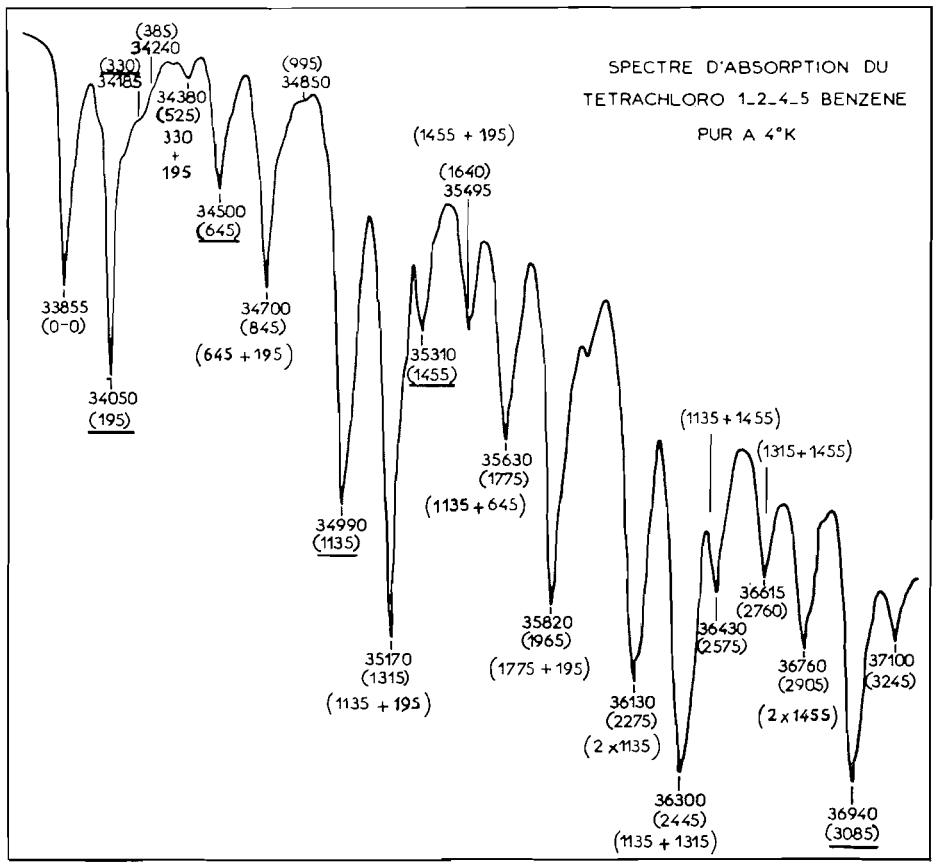

FIG. 2*d*.

Il y a donc, encore ici, une bonne concordance entre les prévisions théoriques et nos résultats expérimentaux.

(e) Trichloro 1,2,3-benzène, $C_6H_3Cl_3(C_{2v})$

Cette molécule n'a plus qu'un axe binaire et deux plans de symétrie; elle appartient donc au groupe C_{2v}; les vibrations A_1 et les vibrations B_2 sont en plus grand nombre que dans les cas précédents (11 A_1 et 10 B_2 dont on trouvera les fréquences de l'état fondamental dans le Tableau II).

Le spectre d'absorption à 20 °K est mieux résolu que celui du tétrachlorobenzène et permet un pointé plus précis des fréquences.

La Fig 1*e*, reproduit la photographie du spectre; le microphotogramme correspondant se trouve en 2*e*. Sur ce microphotogramme est indiquée la fréquence de chaque bande ainsi que l'attribution vibrationnelle que nous proposons. On voit que tout le spectre visible sur la figure peut être expliqué en tenant compte des vibrations suivantes: 215, 326, 383, 460, 502, 714, 1 126, 1 374, 1 490, 3 081 et 3 101 cm^{-1}, soit en tout 11 vibrations comme prévu si l'on suppose que seules les vibrations totalement symétriques interviennent.

La comparaison de ces fréquences avec celles du Tableau II permet de faire correspondre à ces vibrations de l'état excité, respectivement, les 11 fréquences suivantes de l'état fondamental: 212, 352, 400, 492, 516, 738, 1 161, 1 416, 1 566, 3 072 et 3 072 cm^{-1}.

Can. J. Chem. Downloaded from www.nrcresearchpress.com by 210.87.254.6 on 09/05/12
For personal use only.

Can. J. Chem. Downloaded from www.nrcresearchpress.com by 210.87.254.6 on 09/05/12
For personal use only.

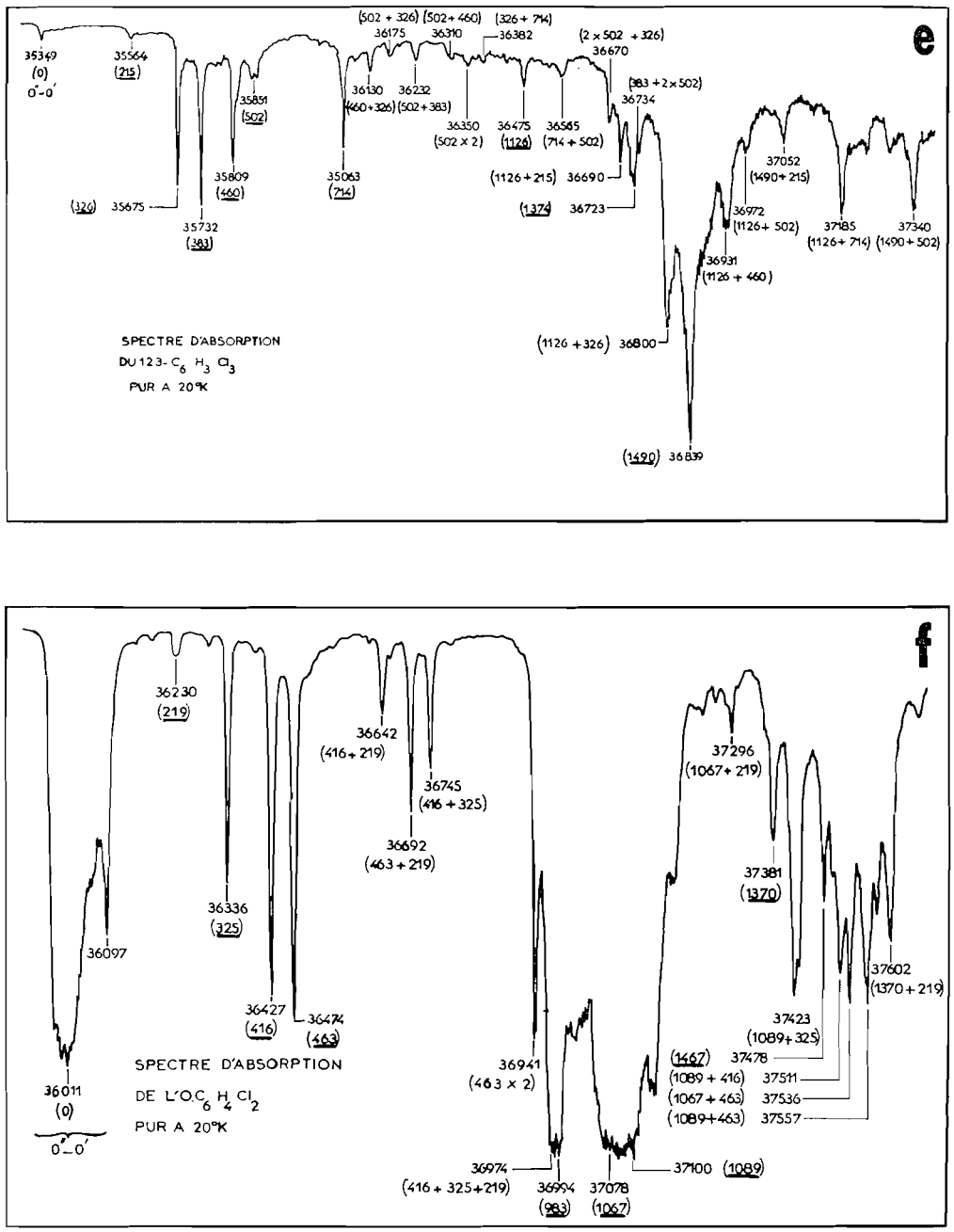

FIGS. 2*e* and 2*f*.

Deux de ces vibrations (400 et 492) sont classées par Evans parmi les B_2; toutes les autres sont données comme A_1.

Il est difficile de trancher définitivement cette question, mais nous pensons que le fait de trouver le même nombre de vibrations actives et de vibrations totalement symétriques

soit un argument en faveur de l'attribution de la symétrie A_1 aux fréquences 400 et 492 de l'état fondamental (383 et 460 à l'état excité).

Ajoutons enfin qu'il est difficile de proposer pour cette molécule des schémas de vibrations comme il a été fait pour les dérivés para et tétra substitués pour lesquels nous avions pu séparer nettement les vibrations C—Cl des vibrations C—H.

(f) Orthodichlorobenzène, $C_6H_4Cl_2(C_{2v}*)$

L'*o*-dichlorobenzène appartient également au groupe de symétrie C_{2v}; l'astérisque qui suit le symbole du groupe indique seulement que l'axe de symétrie est différent (ici, cet axe est perpendiculaire à une liaison C—C du benzène, alors qu'il passe par un atome de carbone dans le cas des dérivés méta et 1,2,3-$C_6H_3Cl_3$).

Le spectre d'absorption à l'état de vapeur a été également étudié par Anno (19) qui propose une structure vibrationnelle faisant intervenir les fréquences de vibrations suivantes: 151, 307, 437, 610, 1 089 et 1 486 cm^{-1}; il est difficile de trouver sur le Tableau II les fréquences correspondantes de l'état fondamental.

Le spectre est bien résolu à 20 °K, comme on peut le constater sur la Fig. 1*f*; le microphotogramme (Fig. 2*f*) permet également d'effectuer un pointé convenable des raies d'absorption.

Nous avons relevé les fréquences suivantes qui permettent d'expliquer la structure vibrationnelle: 219, 325, 416, 463, 983, 1 067, 1 089, 1 370, 1 467, 3 130 et 3 130 cm^{-1}.

D'après le Tableau II, les fréquences correspondantes dans l'état fondamental seraient, respectivement: 203, 334, 429, 480, 1 041, 1 130, 1 162, 1 468, 1 575, 3 070 et 3 070 cm^{-1}.

Toutes ces vibrations ont été classées dans le type A_1, sauf 334 et 429 que Evans pense être de symétrie B_2.

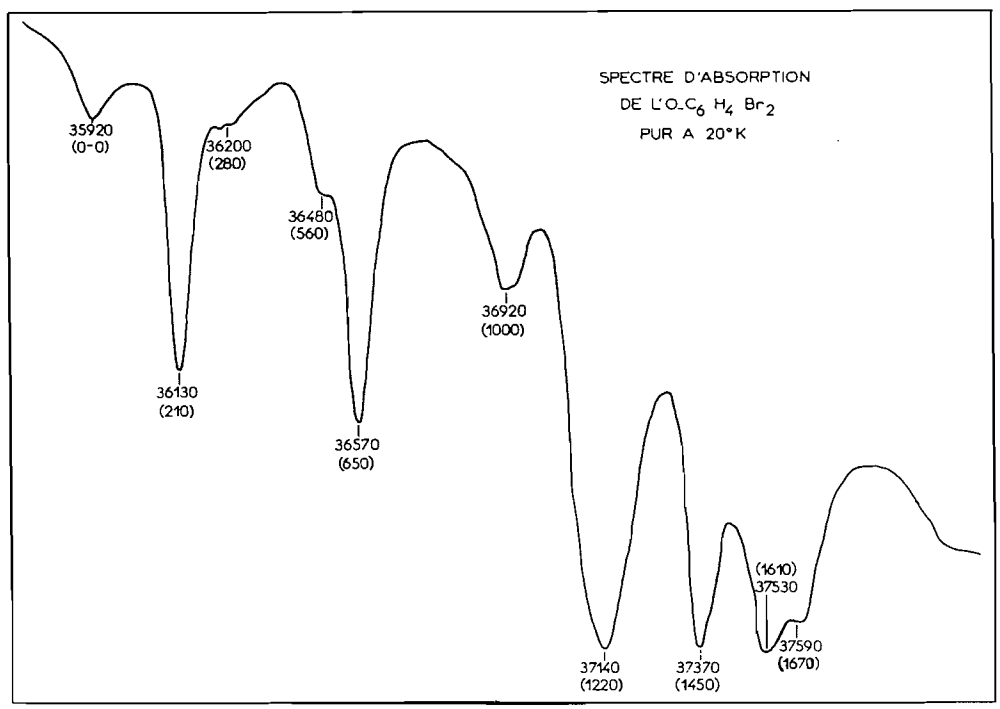

FIG. 2*g*.

Can. J. Chem. Downloaded from www.nrcresearchpress.com by 210.87.254.6 on 09/05/12
For personal use only.

Can. J. Chem. Downloaded from www.nrcresearchpress.com by 210.87.254.6 on 09/05/12
For personal use only.

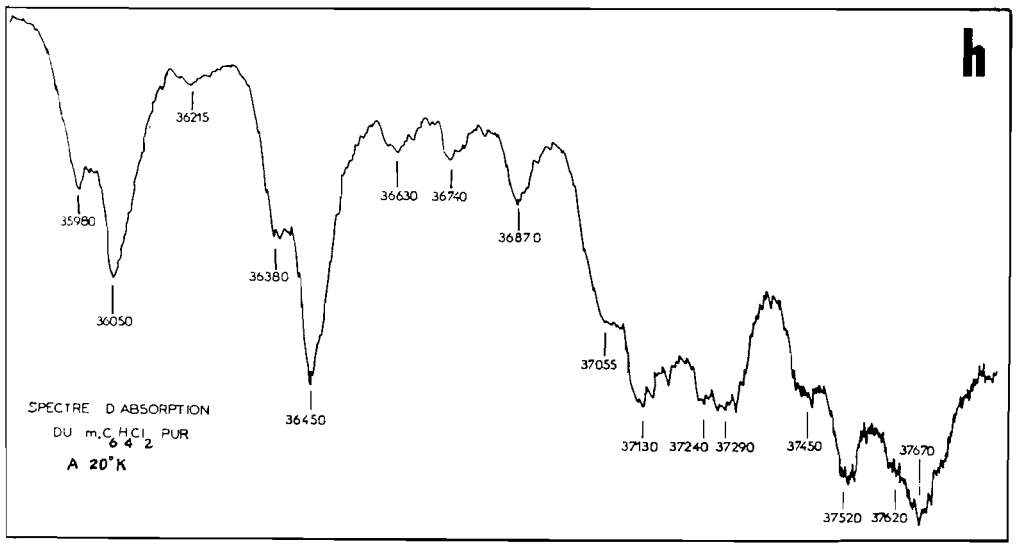

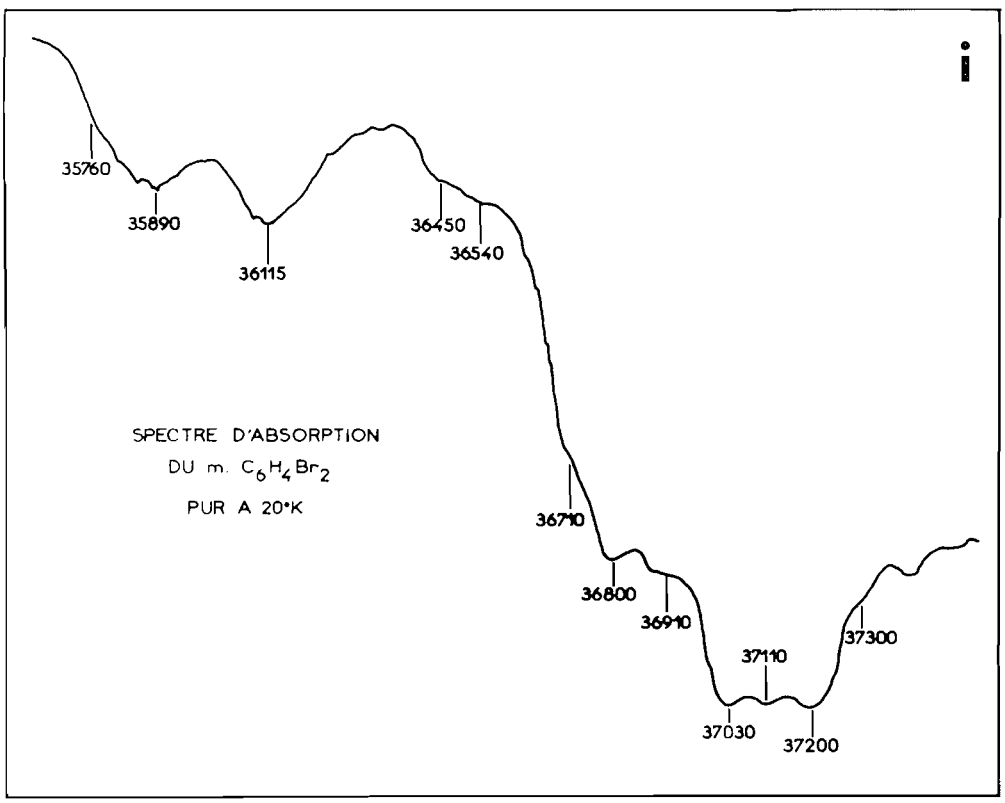

FIGS. 2*h* and 2*i*.

Can. J. Chem. Downloaded from www.nrcresearchpress.com by 210.87.254.6 on 09/05/12
For personal use only.

TABLEAU VI

Tableau des vibrations actives dans le spectre d'absorption (à l'état excité) d'aprés le présent travail et des vibrations correspondantes de l'état fondamental

C_6Cl_6		p-$C_6H_4Cl_2$		p-$C_6H_4Br_2$		1,2,4,5-$C_6H_2Cl_4$		1,2,3-$C_6H_3Cl_3$		o-$C_6H_4Cl_2$	
Exc.	Fond.	Exc.	Fond.	Exc.	Fond.	Exc.	Fond.	Exc.	Fond.	Exc.	Fond.
309	323	309	330	217	218	195	190	215	212	219	203
373	372	551	626*	542	623*	330	352	326	352	325	334*
1 169	1 210	725	747	693	708	645	684	383	400*	416	429*
		1 053	1 096	1 010	1 067	1 135	1 165	460	492*	463	480
		1 479	1 573	1 476	1 570	1 455	1 549	502	516	983	1 041
		3 171	3 072	3 170	3 068	3 085	3 070	714	738	1 067	1 130
								1 126	1 161	1 089	1 162
								1 374	1 416	1 370	1 468
								1 490	1 566	1 467	1 575
								3 081	3 072	3 130	3 070
								3 101	3 072	3 130	3 070

En ce qui nous concerne, nous proposons de classer toutes ces vibrations dans le type A_1, puisque leur nombre correspond exactement à celui des vibrations totalement symétriques.

(g) Orthodibromobenzène, $C_6H_4Br_2(C_{2v}*)$, métadibromobenzène, $C_6H_4Br_2(C_{2v})$ et métadichlorobenzène, $C_6H_4Cl_2(C_{2v})$

Ces 3 dernières substances ont été également étudiées à 20 °K mais, pour des raisons qui nous échappent, leurs spectres sont très mal résolus; les bandes sont trop larges pour permettre un pointé précis et une analyse vibrationnelle fructueuse.

Nous nous contenterons donc de reproduire, sans commentaires inutiles, les photographies des spectres sur les Figs. 1*g*, 1*h*, 1*i*, et les microphotogrammes correspondants sur les Figs. 2*g*, 2*h*, 2*i*.

CONCLUSION

Tous les résultats obtenus ont été résumés dans le Tableau VI; dans ce tableau, nous avons donné la liste des vibrations actives dans les spectres d'absorption, ainsi que les vibrations de l'état fondamental qui leur correspondent d'après les travaux antérieurs en diffusion Raman et en absorption infrarouge (5, 6).

Lorsque la transition est permise, le nombre de vibrations trouvées est rigoureusement égal à celui des vibrations totalement symétriques; cela nous conduit naturellement à la conclusion suivante: les vibrations totalement symétriques sont les seules actives en absorption ultraviolet. Cette conclusion nous oblige à corriger des résultats, obtenus en Raman et en infrarouge, qui attribuaient à certaines des vibrations reconnues sur nos spectres des mouvements non totalement symétriques. Ces vibrations sont suivies d'un astérisque sur le Tableau VI.

BIBLIOGRAPHIE

1. C. K. Ingold. J. Chem. Soc. 912 (1936); 222 (1946).
2. R. D. Mair et D. F. Hornig. J. Chem. Phys. **17**, 1236 (1949).
3. S. Brodersen et A. Langseth. Kgl. Danske Videnskab. Selskab Mat. Fys. Skrifter, **1**, 1 (1956).
4. C. Garrigou-Lagrange, B. Dupuy et G. Sourisseau. J. Chim. Phys. **62**, 261 (1965).
5. J. R. Scherer et J. C. Evans. Spectrochim. Acta, **19**, 1739 (1963).
6. A. Stojiljkovic et D. H. Whiffen. Spectrochim. Acta, **12**, 47 (1958).
7. H. Sponer et E. Teller. Rev. Mod. Phys. **13**, 75 (1941).
8. C. K. Ingold et G. W. King. J. Chem. Soc. 2702 (1953).
9. L. Pesteil. Compt. Rend. **250**, 497 (1960).
10. L. Pesteil et M. Rabaud. J. Chim. Phys. **59**, 167 (1962).
11. L. Pesteil, J. Vergnes et P. Pesteil. J. Chim. Phys. **60**, 492 (1963).
12. M. Benarroche. Compt. Rend. **254**, 3520 (1962).
13. L. Pesteil, R. Troisplis et P. Pesteil. J. Chim. Phys. **60**, 1294 (1963).
14. M. Benarroche. Compt. Rend. **257**, 1249 (1963).
15. L. Pesteil, P. Pesteil et F. Laurent. Can. J. Chem. **42**, 2601 (1964).
16. E. V. Shpol'skii et A. A. Il'ina. Dokl. Akad. Nauk SSSR, **87**, 945 (1952).
17. P. Pesteil. J. Chim. Phys. **58**, 661 (1961).
18. M. Benarroche. Acta Phys. Polon. **26**, 355 (1964); J. Chem. Phys. **42**, 2973 (1965).
19. T. Anno et I. Matubara. J. Chem. Phys. **23**, 796 (1955).
20. I. Matubara et T. Anno. J. Chem. Phys. **24**, 595 (1956).
21. O. Schnepp et R. Kopelman. J. Chem. Phys. **30**, 868 (1959).
22. P. Pesteil et R. Philip. Cryogenics, **1**, 49 (1960).
23. J. Chem. Phys. **23**, 1997 (1955).
24. M. Benarroche. Compt. Rend. **257**, 876 (1963).
25. A. S. Davydov. Zh. Eksperim. i Teor. Fiz. **18**, 210 (1948).
26. G. H. Wannier. Phys. Rev. **52**, 191 (1937).
27. A. Ciais. Compt. Rend. **260**, 1145 (1965).
28. M. Benarroche. Compt. Rend. **260**, 1606 (1965).

Can. J. Chem. Downloaded from www.nrcresearchpress.com by 210.87.254.6 on 09/05/12
For personal use only.

Can. J. Chem. Downloaded from www.nrcresearchpress.com by 210.87.254.40 on 09/05/12
For personal use only.

THE ULTRAVIOLET SPECTRA OF RIBONUCLEIC ACIDS IN SOLID STATE AND IN SOLUTION[1]

MICHAEL FALK
Atlantic Regional Laboratory, National Research Council, Halifax, Nova Scotia
Received July 14, 1965

ABSTRACT

The ultraviolet absorption spectra of nine samples of soluble, ribosomal, and viral ribonucleic acid (RNA) were studied over the range 3 500 to 1 830 Å. The spectra and the spectral changes which occur upon denaturation were the same for all types of RNA examined, which suggests that their secondary structure is comparable. Dehydration of solid films of RNA at room temperature caused spectral changes resembling those which occur when RNA is heated in aqueous solution. This indicates that the dehydration of RNA, like the dehydration of deoxyribonucleic acid (DNA), causes some loss of the regular stacking and pairing of the nucleotide bases in the helical regions. In contrast to DNA, the rehydration of RNA was not always complete at 98% relative humidity. The decrease of absorbance in the 2 900 Å region upon denaturation, previously reported by Rich and Kasha, was not confirmed with any of the RNA samples studied.

INTRODUCTION

Because of the great sensitivity of the ultraviolet spectra to conformational changes of nucleic acids, ultraviolet spectroscopy continues to be one of the most commonly employed techniques in the study of these compounds. Ultraviolet spectra of various types of ribonucleic acid (RNA) have been frequently measured in the past. However, the previous measurements have been limited to the spectra of solutions, mainly in the region of 2 600 Å. The purpose of the present study was to examine systematically the spectra of various types of RNA (soluble, ribosomal, viral), in solid films as well as in solution, throughout the spectral range of 3 500 to 1 830 Å and under a variety of experimental conditions. In addition, the effect of drying on the spectrum and structure of RNA was investigated.

EXPERIMENTAL

Ten samples of RNA were used. The following samples of soluble RNA from yeast were obtained: (i) one from Professor R. W. Holley, Cornell University; (ii) two from Dr. G. L. Brown, King's College, London; (iii) one from the Sigma Chemical Company, St. Louis; and (iv) one from the Nutritional Biochemicals Corporation, Cleveland. Samples of ribosomal RNA, (v) one from *Escherichia coli* and (vi) one from rat liver, were obtained respectively from Dr. R. A. Cox, Mill Hill Hospital, London, and Dr. S. L. Liu, Chester Beatty Institute, London. Three samples (vii) from tobacco mosaic virus were supplied by Professor H. Fraenkel-Conrat, University of California, Berkeley. The samples designated i, ii, v, vi, and vii were prepared by published methods in the order shown (1, 2, 3, 4, 5). All of the samples were in the form of the sodium salt. The spectra were recorded on a Beckman DK-2 far-ultraviolet spectrophotometer (6). The necessary precautions were observed in flushing the instrument and the sample and reference cells with purified nitrogen, and in rejecting that part of each spectrum at short wavelengths in which the proportion of stray light was above 0.5%. The experimental procedures used in previous work (7) were followed with only a few modifications.

Solutions of approximately 0.001% RNA were prepared in H_2O or D_2O containing 0.15 mole of sodium fluoride per liter. Fluoride rather than chloride was used because it does not have measurable far-ultraviolet absorption above 1 800 Å and does not shift the absorption of water (8). The solutions were stored at 1 °C and their pH was about 6.0.

Solid films of RNA were prepared by the slow evaporation at room temperature of a drop of concentrated aqueous solution spread on the inside surface of a standard 1-cm fused silica cell. The first spectrum was usually recorded before the film had dried completely. A small reservoir, which contained either a drying agent or a saturated solution of an appropriate salt in H_2O or in D_2O, was fitted into the cell. The sample could thus be exposed to a particular vapor pressure of H_2O or D_2O even while the spectrum was being

[1]*Issued as N.R.C. No. 8659.*

recorded. Overnight equilibration was found to be sufficient to bring the specimen to equilibrium at any selected value of relative humidity, as indicated by the lack of further spectral changes. The highest relative humidity which could be reproducibly attained was 98%. Higher humidities caused swelling and distortion of the RNA films.

RESULTS

Comparison of Spectra of the Three Types of RNA

Table I shows the wavelengths of the absorption maximum (λ_{max}) near 2 580 Å, and of the absorption minimum (λ_{min}) near 2 300 Å, averaged from a large number of spectra recorded under various experimental conditions. The centers of these broad maxima and minima can be reproducibly estimated to about 2 Å, but the absolute accuracy is only about ±4 Å. The values of λ_{max} and λ_{min}, the values of the wavelength maximum near 1 830 Å, and the values of several ratios of absorbances at different wavelengths, which together characterize the shape of the absorption spectrum, showed no systematic differences between the three types of RNA under study or between the various specimens of one type of RNA.

Spectra of RNA in Solution and the Effect of Heating

The spectra of RNA dissolved in H_2O and in D_2O were found to be identical. The spectral changes which occurred when the solutions were heated were also found to be identical in H_2O and in D_2O, in agreement with the findings of Mahler, Dutton, and Mehrotra (9). The spectra in D_2O are presented here, as they extend down to about 1 880 Å, some 30 Å further than the spectra in H_2O (7). A typical spectrum of a solution of approximately 0.001% of soluble RNA in D_2O containing 0.15 *M* sodium fluoride is shown in Fig. 1. It can be seen that, in the wavelength region studied, the absorption spectrum consists of the well-known band with a maximum near 2 570 Å and of a second, more intense band, with a maximum below 1 900 Å at room temperature. The shape of these RNA bands is essentially the same as that of the DNA bands (7), and, as in the spectrum of DNA, it can be seen that there are very weak shoulders at about 2 820 Å, 2 120 Å, and possibly also at about 1 950 Å.

The effect of heating to 95° on the spectrum of RNA in solution is also shown in Fig. 1. Thermal denaturation* caused an increase of the absorbance of RNA throughout the accessible region of the spectrum. The average increase of absorbance at 2 570 Å for the 10 RNA samples investigated was 26 ±3%, with allowance for the increase of the volume of solution by nearly 3% in the temperature interval studied. Thermal denaturation also caused an upward shift of the lower wavelength band of RNA by at least 50 Å. At 90° the maximum of this band is at about 1 915 Å, just within the region of spectrum observed at this temperature in aqueous solution. A similar shift has been observed for DNA (7). The changes of absorbance of this band upon denaturation of RNA are somewhat uncertain, because only about a half of the band is accessible to the present observations. The integrated intensity of this band may either increase or decrease upon denaturation. The spectra of native and denatured RNA suggest a crossing point just below the observable region, as for DNA.

The ultraviolet spectra of RNA in solution, recorded in the present work, and the spectral changes observed on heating, agree with the spectrum at 25° and 90° of a solution of soluble RNA reported by Voet *et al.* (10).

**The terms "native" and "denatured", applied here to RNA by analogy with DNA, denote simply the presence or absence of ordered double-helical regions and do not imply any relation to the actual structure of various types of RNA in vivo. "Denaturation" denotes the total or partial disappearance of such ordered regions.*

Can. J. Chem. Downloaded from www.nrcresearchpress.com by 210.87.254.40 on 09/05/12
For personal use only.

Can. J. Chem. Downloaded from www.nrcresearchpress.com by 210.87.254.40 on 09/05/12
For personal use only.

TABLE I

Average values of λ_{max} and λ_{min} (in Å)

		Soluble RNA (4 samples)	Ribosomal RNA (2 samples)	Viral RNA (3 samples)	RNA, average	DNA (from ref. 7)
Solution, 7°	λ_{max}	2573±3	2569±5	2567±2	2570±2	2579±2
	λ_{min}	2297±2	2299±11	2307±7	2301±4	2315±5
Solution, 95°	λ_{max}	2574±6	2572±4	2572±2	2573±1	2591±2
	λ_{min}	2279±2	2281±9	2282±10	2281±2	2310±5
Solid, 98% relative humidity	λ_{max}	2581±3	2584±4	2578±0	2581±2	2589±2
	λ_{min}	2309±4	2321±4	2307±3	2312±6	2310±5
Solid, 0% relative humidity	λ_{max}	2585±3	2588±1	2585±2	2586±1	2605±2
	λ_{min}	2311±3	2327±2	2308±3	2315±8	2310±5

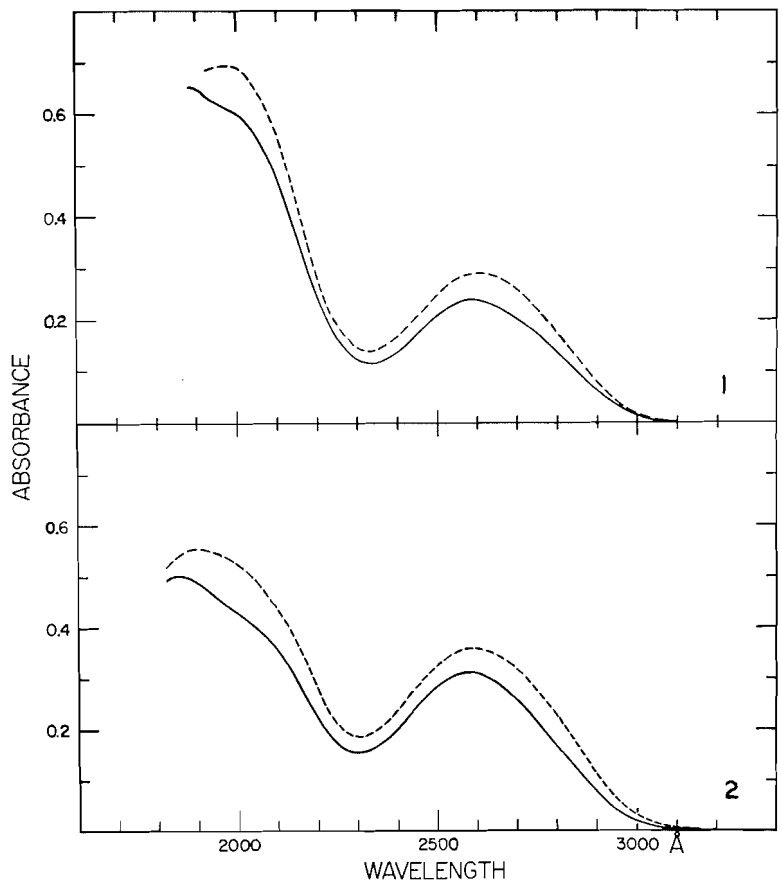

FIG. 1. Full line: spectrum of a solution of 0.001% RNA in D_2O containing 0.15 *M* NaF at 15° in a 1 cm cell. Broken line: spectrum of the same solution at 99°, uncorrected for the decrease in density with temperature.

FIG. 2. Full line: spectrum of a solid film of RNA exposed to 98% relative humidity (D_2O). Broken line: spectrum of the same film at 0% relative humidity (both at 22°).

Spectra of Solid Films and the Effect of Drying

The spectra of solid films of RNA hydrated by H_2O or D_2O were found to be nearly identical. Figure 2 shows a typical spectrum of a solid film of RNA in both the anhydrous and hydrated state. It is shown that the spectra of *highly hydrated* films of RNA differ only slightly from those of RNA in solution; for example the band maximum at 2 570 Å in solution is shifted to about 2 581 Å in the hydrated film. A similar upward shift of about 10 Å has been observed for DNA (Table I). Drying (Fig. 2) caused an absorbance increase throughout the spectral region investigated, similar to that which occurs upon thermal denaturation (Fig. 1). Drying and thermal denaturation also caused similar minor changes in the shape of the RNA absorption bands. The spectral changes which occurred when solid films of RNA were dried were largely but not completely reversible when the films were rehydrated. The initial increase of absorbance in the first drying cycle equalled 20–25% for most RNA samples. This approaches the absorbance increase of 26 ±3% which occurred upon heating of the RNA in solution. Subsequent rehydration at 98% relative humidity caused an absorbance decrease which occasionally equalled the original

Can. J. Chem. Downloaded from www.nrcresearchpress.com by 210.87.254.40 on 09/05/12
For personal use only.

decrease, but often fell considerably short of it. In a typical series of 17 consecutive hydration–dehydration cycles a film of soluble RNA showed the following percentage increases in absorbance: 21.2, 16.0, 12.0, 14.7, 6.4, 8.0, 8.8, 9.6, 10.8, 14.5, 13.8, 27.0, 21.8, 26.0, 26.8, 16.5, 17.5. The lack of reproducibility indicates failure of the RNA films to return to their original state of hydration when exposed to 98% relative humidity. This behavior of RNA contrasts with the complete rehydration of DNA at relative humidity as low as 92% (7, 11). Unlike the rather sharp spectral changes in DNA, which occur largely in the relative humidity range of 59 to 75%, the corresponding spectral changes in RNA appear to occur much more gradually, over the whole relative humidity range of 0 to 100%.

The absorption maximum of RNA at lower wavelengths is seen more clearly in the spectra of solid films, as these are observable down to 1 830 Å, which is about 70 Å farther than the spectra of solutions. Denaturation of RNA by drying clearly shifts the band maximum to higher wavelengths as it does for DNA. Because they extend to somewhat lower wavelengths, spectra of the solid films suggest more strongly than do those of solutions that the absorbances of native and denatured RNA cross just below 1 830 Å.

Effect of Temperature on Spectrum of Dry RNA

The effect of temperature on the spectrum of a typical dry film of RNA is shown in Fig. 3. It is shown that the spectral changes corresponding to an increase of temperature of 148°C are very slight, and consist of a very small broadening of the bands and of a shift of the band at 2 580 Å to higher wavelengths by about 5 Å. There is almost no change in the absorbance at 2 580 Å. It is shown in Fig. 4 that the effect of temperature on the spectrum of a mixture of nucleosides in aqueous solution is also very slight, especially if a correction for the 3% expansion in volume is applied, and that it is similar to the effect of temperature on the spectrum of the dry RNA films.

Light Scattering in Spectra of Films

The contribution of light scattering to the absorption spectrum of the solid samples was probably small and was neglected. The agreement between the spectra of solid films of varying thickness was good. The films were optically clear and generally showed no transmittance changes above 3 100 Å, that is, outside of the region of RNA absorption. Any contribution of increased scattering to the spectrum at shorter wavelengths would be expected to be largely independent of temperature and degree of hydration, and thus would not affect the present results.

DISCUSSION

Comparison of Various Types of RNA

The similarity of the ultraviolet absorption spectra and of spectral changes on denaturation of soluble, ribosomal, and viral RNA, which differ widely in molecular weight, suggests that the secondary structure of various types of RNA is comparable. This is in agreement with conclusions from X-ray diffraction studies summarized by Fuller (12), and from a variety of other investigations (13). The ultraviolet spectrum of RNA resembles closely that of DNA (cf. Table I) and previous discussion on this subject (7) largely applies also to RNA.

Thermal Denaturation of RNA

The spectral changes that occur during thermal denaturation of RNA are qualitatively similar to those for DNA. However, the increase of absorbance near 2 600 Å is about 42%

Can. J. Chem. Downloaded from www.nrcresearchpress.com by 210.87.254.40 on 09/05/12
For personal use only.

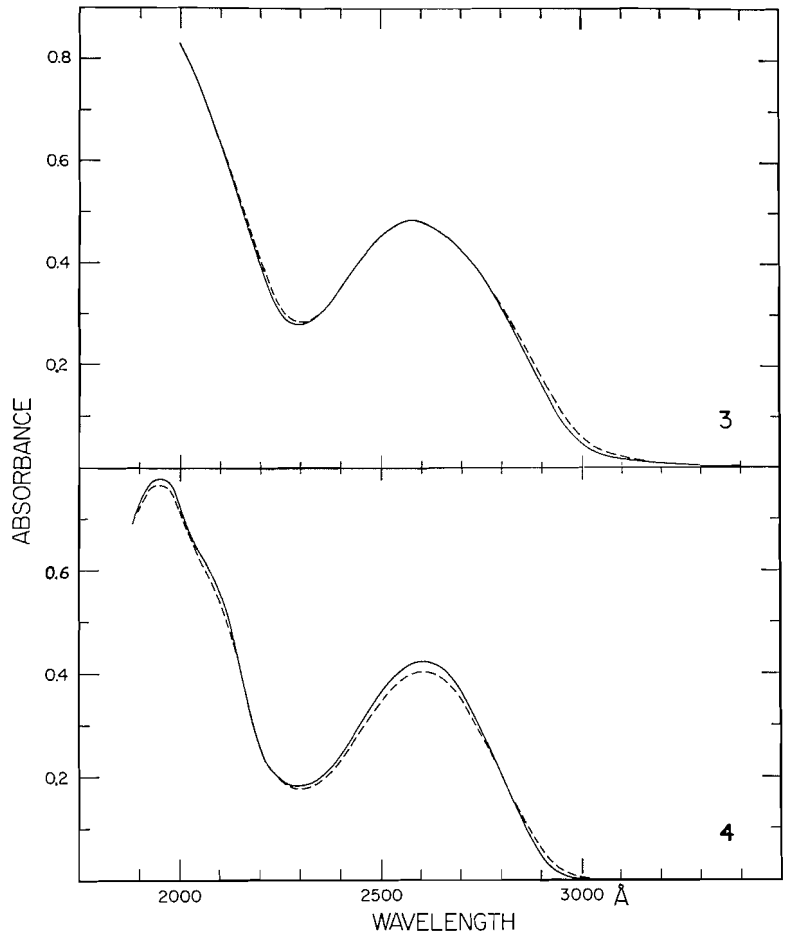

FIG. 3. Full line: spectrum of a thoroughly dry film of RNA at −45°. Broken line: spectrum of the same film at +103°.

FIG. 4. Full line: spectrum of a solution of a mixture of adenosine, guanosine, uridine, and cytidine (in proportions 4:3:4:3) in D_2O at pD 6 and 8°. Broken line: spectrum of the same solution at 94°, uncorrected for the decrease of density with temperature.

for DNA (7), and only about 26% for RNA. The smaller increase for RNA *may* be partly due to its incomplete helical structure. However, the structure of the helical parts of RNA has not been established and may differ from the DNA helix. Since hypochromism of polynucleotides (that is, a decrease of ultraviolet absorption intensity that accompanies transition from a disordered form to a helix) can be expected to be highly sensitive to the exact geometry of the helix (14), the hypochromism of helical RNA may be different from that of DNA. The increase of absorbance at 2 600 Å for fully double-stranded viral RNA has recently been measured by Gomatos and Tamm and found to be 27 to 36% for wound tumor virus RNA (15) and 30% for reovirus RNA (16), significantly lower than the value of about 39% for DNA under similar conditions.

A tacit assumption has often been made that the spectral changes which occur when RNA or other polynucleotides are heated in solution are *entirely* due to thermal denaturation. This assumption has now been tested by the study of the effect of heating on dry films of RNA. The negligible effect of temperature on the absorbance of dry RNA (Fig. 3)

Can. J. Chem. Downloaded from www.nrcresearchpress.com by 210.87.254.40 on 09/05/12
For personal use only.

Can. J. Chem. Downloaded from www.nrcresearchpress.com by 210.87.254.40 on 09/05/12
For personal use only.

or on the absorbance of a mixture of nucleotides in solution (Fig. 4), *under conditions where no structural changes occur*, shows that the large spectral changes which occur upon heating RNA in solution *are* in fact due almost entirely to thermal denaturation.

Comparison of the Effect of Drying on DNA and RNA

The reversible changes in the structure of the DNA helix, which are caused by the variation of relative humidity, are now known in considerable detail (17). At high values of relative humidity, DNA exists in either the B or the A configuration. The B configuration, usually stable at 92% relative humidity, is stabilized by hydrophobic forces between the nucleotide base pairs, which are stacked 3.4 Å apart with their planes normal to the axis of the helix. At a somewhat lower relative humidity (about 75%), most samples of the sodium salt of DNA transform to the A configuration, in which the base pairs are inclined by about 20° from normal to the axis of the helix. This results in somewhat looser base-stacking than in the B configuration and a slight increase in the ultraviolet absorbance at 2 600 Å (7). At relative humidities below about 65%, DNA undergoes a transition to a disordered form, characterized by a broadening or disappearance of the X-ray diffraction pattern (18), a broadening of the infrared absorption bands (19–21), almost complete loss of infrared and ultraviolet dichroism (11), and an increase of the ultraviolet absorbance at 2 600 Å identical with that which occurs upon thermal denaturation (7, 11). These observations imply that the "dry configuration" involves an irregular collapse of the DNA helix and loss of the stacking and of the pairing of the nucleotide bases. The transition at low relative humidity occurs because the hydrophobic forces disappear in the absence of water and the stacking of the base pairs is no longer energetically advantageous. The helix is then free to adopt the new configuration of minimum energy, which does not involve the stacking of bases. The A configuration, which is stable at an intermediate degree of hydration, may correspond to a state when the hydrophobic forces between the base pairs have decreased somewhat but have not disappeared.

The spectral changes observed in the present work prove that the dehydration of RNA causes reversible structural changes similar, at least qualitatively, to those that occur in DNA. The increase of absorbance near 2 600 Å indicates that these structural changes must involve a loss of stacking and of pairing of the nucleotide bases.* Heating of the dehydrated films to temperatures above 100° has no further effect on the structure. Additional evidence that drying produces structural changes in RNA similar to those produced in DNA is provided by infrared spectra of RNA (20, 22), which upon drying show changes similar to those observed for DNA (19–21). The infrared spectral changes indicate the complete or partial disappearance of the specific base pairing (23) and a diminution of the degree of molecular order (21). The diminution of order upon drying agrees with the observed broadening of the X-ray diffraction patterns of RNA upon drying (24, 25). Some samples of RNA, including RNA of intact ribosomes and viruses, show complete disappearance of the diffraction pattern upon drying (25–27), which is indicative of collapse of order. Such disappearance of the nucleic acid diffraction pattern is also characteristic of DNA–protein complexes (28, 29). On the other hand, recent studies of highly oriented and nearly 100% double-stranded RNA from reovirus (30), from wound tumor virus (31), and of crystalline RNA of low molecular weight (32, 33) indicate only minor changes in the X-ray diffraction pattern on drying. The present finding that rehydration of RNA is not always complete at 98% relative humidity may

**The present discussion is independent of whether base-pairing or base-stacking is the main cause of the hypochromism in polynucleotides, since in the solid films of nucleic acids any loss of pairing is likely to be accompanied by a loss of stacking, and vice versa (11).*

have some bearing on the behavior of these exceptional RNA samples. It would be of interest to study more thoroughly the effect of hydration on the structure of these samples in the difficult region above 98% relative humidity. This might also help to establish whether at high relative humidity (and thus also in vivo) RNA occurs in a form corresponding to the A or B configuration of DNA. The X-ray diffraction studies so far are divided on this point (25, 26, 30–32) and molecular model building shows that RNA helix can be accommodated in either form (12). The present optical study cannot clearly distinguish between the A- or the B-type configuration at high relative humidity, since all attempts at the preparation of highly oriented RNA films have so far failed and thus the ultraviolet (or infrared) dichroism could not be measured, as had been done earlier for DNA (11). However, the spectral changes which are occurring near 98% relative humidity in RNA could be analogous to those which occur near 85% relative humidity in DNA and which accompany the A $\rightleftarrows$ B transition.

The $n \rightarrow \pi^*$ Transitions

It may be expected that the $n \rightarrow \pi^*$ transitions of the nucleotide bases will contribute to the absorption spectrum of nucleic acids (34). Some evidence for such a contribution in the 2 900 Å region has been presented (34–39). Since the $n \rightarrow \pi^*$ transitions may exhibit *hyperchromism* (that is, an *increase* of their absorption intensity with transition from a disordered form to a helix) at long wavelengths, they should be distinguishable from the $\pi \rightarrow \pi^*$ transitions of the nucleotide bases, which are responsible for the bulk of the ultraviolet absorption of nucleic acids and which are known to be *hypochromic* (35, 40). Careful examination of the RNA spectra recorded in the present work shows that thermal denaturation as well as drying causes, invariably, an *absorbance increase* throughout the 2 570 Å band. The *decrease* of absorbance near 2 900 Å when RNA is heated to 90°, as reported by Rich and Kasha (34, 35), was not confirmed with any of the RNA samples studied. In fact the increase of absorbance in this region was somewhat greater than near the maximum at 2 570 Å. Thus, if the $n \rightarrow \pi^*$ transitions are assumed to be hyperchromic, they cannot contribute more than a small fraction of the absorption in the region of 2 900 Å of either DNA or RNA with the usual nucleotide content. Hyperchromism above 2 800 Å has been observed for the double-stranded helix of polyadenylic + polyuridylic acid (10, 35, 41), and nucleic acids that are particularly rich in adenine-uracil pairs may also be hyperchromic in that region (41). There is still some doubt, however, whether such hyperchromism is due to the contribution from $n \rightarrow \pi^*$ transitions (42).

A treatment of RNA with hot aqueous alkali or with ribonuclease does cause a decrease of absorbance in the 2 900 Å region (43, 44). Such treatment, however, results in the breakdown of the primary as well as of secondary structure of RNA; hence more complex spectral changes may be expected than those which occur upon simple denaturation.

ACKNOWLEDGMENTS

I thank Miss P. J. Baird for her skillful technical assistance throughout most of this work, and Drs. R. W. Holley, G. L. Brown, R. A. Cox, S. L. Liu, and H. Fraenkel–Conrat for their kindness in supplying samples of RNA. Dr. W. B. Gratzer offered several helpful comments on the manuscript.

REFERENCES

1. R. W. Holley. Biochem. Biophys. Res. Commun. **10**, 186 (1963).
2. G. L. Brown, Z. Cosinski, and C. A. Carr. Colloq. Intern. Centre Natl. Rech. Sci. Paris, **106**, 183 (1962).
3. U. Z. Littauer and H. Eisenberg. Biochim. Biophys. Acta, **32**, 320 (1959).

Can. J. Chem. Downloaded from www.nrcresearchpress.com by 210.87.254.40 on 09/05/12
For personal use only.

4. K. S. KIRBY. Biochem. Biophys. Acta, **55**, 545 (1962).
5. H. FRAENKEL-CONRAT, B. SINGER, and A. TSUGITA. Virology, **14**, 54 (1961).
6. W. I. KAYE. Appl. Spectry. **15**, 89 (1961).
7. M. FALK. J. Am. Chem. Soc. **86**, 1226 (1964).
8. M. FALK. Unpublished results.
9. H. R. MAHLER, G. DUTTON, and B. D. MEHROTRA. Biochem. Biophys. Acta, **68**, 199 (1963).
10. D. VOET, W. B. GRATZER, R. A. COX, and P. DOTY. Biopolymers, **1**, 193 (1963).
11. M. FALK, K. A. HARTMAN, JR., and R. C. LORD. J. Am. Chem. Soc. **85**, 391 (1963).
12. W. FULLER. J. Mol. Biol. **3**, 175 (1961). Sci. Progr. London, **52**, 26 (1964).
13. A. S. SPIRIN. Progr. Nucleic Acid Res. **1**, 301 (1963).
14. I. TINOCO. J. Am. Chem. Soc. **82**, 4785 (1960). H. DEVOE and I. TINOCO. J. Mol. Biol. **4**, 500 (1962).
15. P. J. GOMATOS and I. TAMM. Proc. Natl. Acad. Sci. U.S. **50**, 878 (1963).
16. P. J. GOMATOS and I. TAMM. Proc. Natl. Acad. Sci. U.S. **49**, 707 (1963).
17. M. H. F. WILKINS. Science, **140**, 941 (1963).
18. R. E. FRANKLIN and R. G. GOSLING. Acta Cryst. **6**, 673 (1953).
19. H. LENORMANT and C. DE LOZE. Bull. Soc. Chim. France, 1501 (1955).
20. G. B. B. M. SUTHERLAND and M. TSUBOI. Proc. Roy. Soc. London, Ser. A, **239**, 446 (1957).
21. M. FALK, K. A. HARTMAN, JR., and R. C. LORD. J. Am. Chem. Soc. **85**, 387 (1963).
22. M. FALK. To be published.
23. Y. KYOGOKU, M. TSUBOI, T. SHIMANOUCHI, and I. WATANABE. Nature, **189**, 120 (1961).
24. A. RICH and J. D. WATSON. Nature, **173**, 995 (1954).
25. G. L. BROWN and G. ZUBAY. J. Mol. Biol. **2**, 287 (1960).
26. G. ZUBAY and M. H. F. WILKINS. J. Mol. Biol. **2**, 105 (1960).
27. A. KLUG, K. C. HOLMES, and J. T. FINCH. J. Mol. Biol. **3**, 87 (1961).
28. G. ZUBAY and M. H. F. WILKINS. J. Mol. Biol. **4**, 444 (1962).
29. G. ZUBAY, M. H. F. WILKINS, and E. R. BLOUT. J. Mol. Biol. 4, 69 (1962).
30. R. LANGRIDGE and P. J. GOMATOS. Science, **141**, 694 (1963).
31. K. I. TOMITA and A. RICH. Nature, **201**, 1160 (1964).
32. M. SPENCER, W. FULLER, M. H. F. WILKINS, and G. L. BROWN. Nature, **194**, 1014 (1962).
33. M. SPENCER and F. POOLE. J. Mol. Biol. **11**, 314 (1965).
34. A. RICH and M. KASHA. J. Am. Chem. Soc. **82**, 6197 (1960).
35. M. KASHA. *In* Light and life. *Edited by* W. D. McElroy and B. Glass. Johns Hopkins Press, Baltimore, Md. 1961. p. 31.
36. J. BRAHMS and W. F. H. M. MOMMAERTS. J. Mol. Biol. **10**, 73 (1964).
37. J. R. FRESCO, A. M. LESK, R. GORN, and P. DOTY. J. Am. Chem. Soc. **83**, 3155 (1961).
38. J. R. FRESCO. Tetrahedron, **13**, 185 (1961).
39. T. SAMEJIMA and J. T. YANG. Biochemistry, **3**, 613 (1964).
40. B. H. ZIMM and N. R. KALLENBACH. Ann. Rev. Phys. Chem. **13**, 171 (1962).
41. J. R. FRESCO, L. C. KLOTZ, and E. G. RICHARDS. Cold Spring Harbor Symp. Quant. Biol. **28**, 83 (1963).
42. M. GELLERT. J. Am. Chem. Soc. **83**, 4664 (1961).
43. M. KUNITZ. J. Biol. Chem. **164**, 563 (1946).
44. J. STOCKX. Biochem. Biophys. Acta, **68**, 535 (1963).

Can. J. Chem. Downloaded from www.nrcresearchpress.com by 210.87.254.40 on 09/05/12
For personal use only.

Can. J. Chem. Downloaded from www.nrcresearchpress.com by 210.87.254.105 on 09/05/12
For personal use only.

OCCURRENCE IN SEED OILS OF SOME FATTY ACIDS WITH CONJUGATED UNSATURATION[1]

C. Y. Hopkins and Mary J. Chisholm
Division of Pure Chemistry, National Research Council, Ottawa, Canada

Received July 23, 1965

ABSTRACT

The following fatty acids were identified in the respective seed oils; α-eleostearic in *Kentranthus macrosiphon*; *trans*-8,*trans*-10,*cis*-12-octadecatrienoic in *Osteospermum hyoseroides*; 9-hydroxy-10,12- and 13-hydroxy-9,11-octadecadienoic in *Tagetes erecta*. Dimorphecolic acid was obtained from *Osteospermum ecklonis* in pure crystalline form. It gave 9-D-hydroxystearic acid on hydrogenation, thus establishing the D-configuration of the parent acid. Dehydration of dimorphecolic acid gave a mixture of all-*trans*-8,10,12- and all-*trans*-9,11,13-octadecatrienoic acids.

INTRODUCTION

Fatty acids with conjugated unsaturation were not known to occur in seed oils of species of Compositae until 1956, when McLean and Clark found a large amount of conjugated trienoic acid in the oil of the common calendula (1). Since then, the family Compositae has been shown to produce, in its seed oils, a surprising number of unusual fatty acids with such components as hydroxy and epoxy groups, *trans* double bonds, and conjugated olefinic and acetylenic linkages.

The present work consists of a study of three species of Compositae containing four different fatty acids with conjugated olefinic unsaturation, and one species of the related family Valerianaceae. The species and their distinctive acids are listed in Table I.

TABLE I

Identification of conjugated fatty acids

Family and species	Oil content of seed, % (air-dry basis)	Conjugated acid	
		Identity	Amount in total acids, %
Valerianaceae			
Kentranthus macrosiphon Boiss.	26.2	α-Eleostearic	50.4
Compositae			
Osteospermum hyoseroides (DC.) Norlindh	15.4	*trans*-8,*trans*-10,*cis*-12-octadecatrienoic	36.3
Osteospermum ecklonis (DC.) Norlindh	16.4	Dimorphecolic (9-hydroxy-*trans*-10, *trans*-12-octadecadienoic)	54.1
Tagetes erecta L.	18.5	9-Hydroxy-10,12-octadecadienoic\ 13-Hydroxy-9,11-octadecadienoic/	8.9

The acids were examined by spectrometric methods to show the number of double bonds in conjugation and to determine whether they were all-*trans* or mixed *cis* and *trans*. Chemical methods were employed to determine the chain length, the position of the double bonds, and their configuration.

RESULTS AND DISCUSSION

Seed oil of *Kentranthus macrosiphon* was examined. The fatty acids contained 50.4% of a conjugated trienoic acid which was isolated and identified as α-eleostearic acid. The

[1]*Issued as N.R.C. No. 8658.*

content of α-eleostearic acid compares with 43% in the related species *K. ruber* (2). The plant is an annual and can be grown in north temperate regions so that it is a potential source of eleostearic-type oil in northern countries. These two species of *Kentranthus* are the only members of the Valerianaceae family from which a conjugated fatty acid has been isolated.

The seed oil of *Osteospermum hyoseroides* was reported by Earle and co-workers to contain a conjugated triene component (3). In the present study, the acid was isolated and identified as *trans*-8,*trans*-10,*cis*-12-octadecatrienoic acid by its melting point and by mixed melting point of its maleic anhydride adduct with an authentic sample. The tetracyanoethylene adduct was also prepared. The acid has been shown previously to be a constituent of *Calendula officinalis* (1, 4).

Osteospermum ecklonis

The oil of *O. ecklonis* (syn. *Dimorphotheca ecklonis*) showed strong ultraviolet absorption at 233 mμ, corresponding to 54.1% of conjugated dienoic acid. Earle and co-workers reported a somewhat higher diene absorption in this species (3), and Smith and co-workers identified the substance as dimorphecolic acid by converting it to 10,12-octadecadiene-1,9-diol (5). The acid was isolated and characterized in the present work as follows.

The mixed acids were partitioned between methanol and petroleum ether. The methanol-soluble portion yielded, on fractional crystallization, a small amount of crystalline acid, m.p. 66.5–67.5° and a larger amount with m.p. 36–37°. The 36–37° acid showed by its infrared spectrum the presence of an OH group (3 600 cm^{-1}) and of *trans* double bonds (983 cm^{-1} but no maximum near 943 cm^{-1}). The intensity at 983 cm^{-1} was twice that of methyl elaidate; thus the acid had two *trans* linkages. Its optical rotation was positive.

The ultraviolet spectrum verified the presence of two double bonds in conjugation (λ_{max} 231 mμ). There was no absorption in the region of 275 mμ. Hydrogenation gave 9-hydroxystearic acid, m.p. 82.5–83.5°, that was not depressed in admixture with an authentic sample of the D-form of the acid of m.p. 83–84° (6*a*). Thus the hydrogenated acid is judged to have the D-configuration. (The racemic form of 9-hydroxystearic acid melts at 75.5° (6).) The original unsaturated acid must have a straight chain of 18 carbon atoms with an OH group at the 9-position. It is also judged to have the D-configuration since catalytic hydrogenation does not cause inversion.

The location of the OH group in the hydrogenated acid was confirmed by cleavage with solid potassium permanganate in acetic acid, which gave the expected fragments (nonanoic, decanoic, suberic, and azelaic acids). There were no fragments corresponding to 13-hydroxystearic acid.

The original dienoic acid was oxidized by von Rudloff's procedure, giving hexanoic acid, thus placing the conjugated double bonds at Δ^{10} and Δ^{12}. The acid was therefore (+)-9-D-hydroxy-*trans*-10,*trans*-12-octadecadienoic (dimorphecolic) acid.

Properties of Dimorphecolic Acid

The nuclear magnetic resonance (n.m.r.) spectrum confirmed the structure of the acid (Table II). The hydroxyl and carboxyl protons gave a combined peak as in other hydroxy acids (7), and it was extinguished by the addition of deuterium oxide. The peak for protons adjacent to double-bonded carbons had an area equivalent to two protons only, showing that the OH substituent was attached to the other allylic carbon. Furthermore, the —CHO— proton gave a band at 5.85 τ, instead of the usual 6.4 τ, because of the de-shielding effect of the adjacent double-bond linkage.

The acid has not been reported previously in crystalline form, although Lohmar and

Can. J. Chem. Downloaded from www.nrcresearchpress.com by 210.87.254.105 on 09/05/12
For personal use only.

TABLE II

Nuclear magnetic resonance spectral data for dimorphecolic acid

Chemical shift, τ	Multiplicity	No. protons	Assignment
	$CH_3(CH_2)_4CH{=}CHCH{=}CHCH(CH_2)_7COOH$		
		OH	
3.25	Broad singlet	2	OH + COOH
3.6–4.6	Multiplet	4	$(CH{=}CH)_2$
5.85	Apparent doublet	1	CH—OH
7.65–7.75	—	2	CH_2COO
7.85–7.95	Multiplet	2	$CH_2CH{=}$
8.65	Broad peak	18	Isolated $(CH_2)_n$
9.1	Irregular triplet	3	CH_3
		32	

co-workers (8) isolated a sample that was semisolid. The present sample had m.p. 36–37°, $E_{1\ cm}^{1\%}$ 1 170 at 231 mμ (in MeOH), ϵ = 34 700. Binder and co-workers (9) reported ϵ = 33 600 although the melting point and other properties were not given. The present sample had $[\alpha]_D^{25}$ +15.2° (*c* 5.2, MeOH). The optical properties of the acid have not been recorded previously, but Diamond and co-workers (10) found $[\alpha]_D^{25}$ +14.0° for the methyl ester.

The small fraction of melting point 66.5–67.5°, obtained during the fractional crystallization, may have been an isomorphic crystalline form of the same acid. Its n.m.r. spectrum was identical and its infrared spectrum virtually identical with the spectra of dimorphecolic acid of m.p. 36–37°.

Dehydration of Dimorphecolic Acid

Dimorphecolic acid is dehydrated by heating with acetic acid to give a product having conjugated triene absorption, as observed by Smith and co-workers (11). The product (not characterized by Smith) was found in our experiments to consist only partly of the expected $\Delta^{8,10,12}$ trienoic acid. The infrared spectrum showed that the double bonds were all *trans*. Hydrogenation gave stearic acid. However, the melting point of the substance could not be raised above 58–61° by recrystallization (all-*trans*-8,10,12-octadecatrienoic acid melts at 77–78° (1)). Oxidative cleavage gave approximately equal amounts of valeric and hexanoic acids, and of suberic and azelaic acids. Thus the dehydration product was a mixture of all-*trans*-8,10,12- and all-*trans*-9,11,13-octadecatrienoic acids. Possibly dehydration is preceded by rearrangement of a portion of the dienoic acid to 13-hydroxy-9,11-octadecadienoic acid.

The occurrence of a hydroxy-dienoic acid and a conjugated trienoic acid in different species of the same genus (*O. ecklonis* and *O. hyoseroides*) suggests that there is a biogenetic relationship between the two acids. They may arise from the same precursor. It is unlikely that the trienoic acid (*trans*-8,*trans*-10,*cis*-12-) is formed from the hydroxy acid since the Δ^{12} double bond is *trans* in the hydroxy acid of *O. ecklonis* but *cis* in the trienoic acid of *O. hyoseroides*. It is more likely that the trienoic acid arises from 9-hydroxy-*trans*-10,*cis*-12-octadecadienoic acid, which is considered to be one of the isomers present in some species of Compositae (12).

Tagetes erecta

Two samples of seed of *Tagetes erecta* were examined, but only one gave an oil with an

Can. J. Chem. Downloaded from www.nrcresearchpress.com by 210.87.254.105 on 09/05/12
For personal use only.

Can. J. Chem. Downloaded from www.nrcresearchpress.com by 210.87.254.105 on 09/05/12
For personal use only.

appreciable amount of conjugated diene absorption in the ultraviolet. Earle and co-workers (13) found only 2% of conjugated diene in their sample of this species. The present sample yielded an oil containing 8.9% of conjugated dienoic acid.

The total fatty acids were partitioned between methanol and petroleum ether. The methanol-soluble portion was purified by crystallization from acetone at low temperature, followed by a second partitioning. The product was a concentrate consisting mainly of conjugated dienoic acid (λ_{max} 233 mμ). It had infrared absorption at 3 620 cm^{-1}, indicating an OH group, and two peaks of nearly equal intensity at 945 and 980 cm^{-1}, characteristic of a conjugated *cis,trans* or *trans,cis* diene. The substance was identified by oxidative cleavage, before and after hydrogenation, as a mixture of 9-hydroxy-10,12- and 13-hydroxy-9,11-octadecadienoic acids. The procedure and results were similar to those described previously for the identification of these two acids in the oil of another species of the Compositae, *Tragopogon porrifolius* (4). The ratio of 9-hydroxy- to 13-hydroxy-acid was estimated to be about 60:40.

Occurrence of such acids in some but not all samples of a species indicates that they are probably intermediates and not end-products in fatty acid biosynthesis. On the basis of the theory recently advanced by Gunstone (14) it is likely that they are intermediates in the formation of conjugated trienoic acids in the seed. However, the possibility that they are secondary products formed under special climatic or cultural conditions is not excluded.

EXPERIMENTAL

Methods

Seeds were purchased from reliable commercial sources.

Infrared spectra were obtained in carbon disulfide solution; ultraviolet measurements were made in cyclohexane unless otherwise noted; n.m.r. spectra were obtained in deuterochloroform with tetramethylsilane as internal reference. Petroleum ether refers to the fraction of b.p. 30–60°. Hydrolysis of the oils was carried out at 25° for 16 hours in ethanolic 1 *N* potassium hydroxide.

Kentranthus macrosiphon

The oil had λ_{max} 262, 272, 283 and $E_{1\ cm}^{1\%}$ 891 at 272 mμ. There was little absorption and no peak in the region of 233 mμ. The mixed acids (6.1 g) were crystallized fractionally from 54 ml of acetone. Crystals collected at −15° (2.0 g) and −28° (1.3 g) contained 75% and 78% of conjugated trienoic acid respectively. Crystallization of the second fraction from acetone at −20° gave α-eleostearic acid, m.p. 48–49°. Its adduct with maleic anhydride, prepared by the usual method (15), had m.p. and mixed m.p. 63–64°.

Osteospermum hyoseroides

The oil had λ_{max} 263, 272, 283.5 mμ and $E_{1\ cm}^{1\%}$ 642 at 272 mμ. There was no peak in the region of 233 mμ. The infrared spectrum had ν_{max} 957 (w) and 987 (vs) cm^{-1}. There was a trace of absorption at 3 620 cm^{-1}.

The fatty acids were crystallized from acetone at low temperatures. Saturated acids were removed at −20°. The crystals obtained at −30° were recrystallized, first from pentane and then from acetone, yielding the trienoic acid, m.p. 38–39°. Its melting point was not depressed in admixture with *trans*-8,*trans*-10,*cis*-12-octadecatrienoic acid (m.p. 40–40.5°) prepared from calendula seed oil (4). The acid gave an adduct with maleic anhydride which melted at 72–73°, alone and in admixture with the authentic adduct prepared from the calendula acid.

The trienoic acid was treated with tetracyanoethylene in benzene solution by the method described previously (15). The adduct, 3–6′-carboxyhexyl-4,4,5,5-tetracyano-6-*cis*-1′-heptenylcyclohexene, was crystallized from ether – petroleum ether. It melted at 112.5–113.5°.

Anal. Calcd. for $C_{24}H_{30}N_4O_2$: N, 13.8. Found: N, 13.8.

Osteospermum ecklonis

The oil had $E_{1\ cm}^{1\%}$ 595 at 233 mμ (conjugated diene). There was weak absorption at 270 mμ, equivalent to 1.7% of conjugated trienoic acid. The infrared spectrum had ν_{max} 983 (vs) (*trans* double bonds in conjugation) and 3 600 (m) (OH) but no peak in the region 900–975 cm^{-1}.

The oil (12 g) was hydrolyzed for 16 h at 25°, unsaponifiable matter was removed, and the mixed acids were partitioned between petroleum ether and methanol–water (4:1). The methanolic portion yielded 6.8 g of solid acids. Two grams of this product was crystallized from acetone at −20°. The crystals, 0.2 g, m.p. 66.5–67.5°, were removed. When the filtrate was cooled to −50° crystals of dimorphecolic acid formed (1.6 g, m.p. 36–37°, λ_{max} 231 mμ, $E_{1\ cm}^{1\%}$ 1 170, ϵ 34 700).

Anal. Calcd. for $C_{18}H_{32}O_3$: C, 72.92; H, 10.88. Found: C, 72.71; H, 11.01.

A portion (0.15 g) was oxidized by permanganate–periodate (16). The fragments were identified by gas–liquid chromatography (g.l.c.) as hexanoic and azelaic acids.

A portion of the acid (0.7 g, m.p. 36–37°) was hydrogenated in ethanol with Adams' catalyst. The product, after crystallization from ethanol at 0°, had m.p. 82.5–83.5 °C, alone and mixed with 9-D-hydroxystearic acid. The hydroxy acid was oxidized by solid potassium permanganate in glacial acetic acid and the fragments were identified by g.l.c. as nonanoic, decanoic, suberic, and azelaic acids. There were minor amounts of octanoic and pimelic but no valeric or hexanoic acids.

A portion of the dienoic acid was dehydrated by being heated under reflux for 2 h in glacial acetic acid. The product, after crystallization from acetone, had m.p. 58–61° and infrared maximum 990 cm^{-1}, but no peaks in the region 945–975 cm^{-1}. Ultraviolet maxima were at 260, 269, 280 mμ. The substance was treated with iodine in pentane solution but there was no change in melting point or ultraviolet absorption. It was oxidized by permanganate–periodate and the resulting products were identified by g.l.c. as valeric, hexanoic, suberic, and azelaic acids.

Tagetes erecta

Two samples of seed from different sources yielded 22.5% and 18.5% of oil respectively. The first oil had negligible ultraviolet absorption in the regions of conjugated unsaturation. The second had n_D^{25} 1.4760, acid value 4.1, and $E_{1\ cm}^{1\%}$ 98 at 234 mμ. There was no appreciable absorption in the conjugated triene region. The infrared spectrum had ν_{max} 943, 975 (conjugated *cis,trans* diene) and 3 570 (OH), all of low intensity.

The mixed acids (20 g) were partitioned between petroleum ether and methanol–water ($4CH_3OH:1H_2O$). The methanolic fraction (3.1 g) had ultraviolet absorption at 233 mμ equivalent to 48% of conjugated dienoic acid. It was concentrated further by crystallization from acetone at −45° and then by solvent partition as before. The concentrate had ν_{max} 3 620 (OH) and 945 (m), 980 (m) cm^{-1} (*cis,trans* or *trans,cis* conjugated double bonds). A portion (0.7 g) was hydrogenated, giving a product of m.p. 57–59°. It was oxidized by solid potassium permanganate in acetic acid and the main products were identified by g.l.c. as valeric, hexanoic, nonanoic, decanoic, suberic, azelaic, dodecanedioic, and tridecanedioic acids.

ACKNOWLEDGMENTS

The authors are indebted to Dr. F. D. Gunstone for comparing the 9-hydroxystearic acid with his synthetic sample, to Mr. H. Seguin for n.m.r. spectra, and to Mr. R. Lauzon for infrared spectra.

REFERENCES

1. J. McLean and A. H. Clark. J. Chem. Soc. 777 (1956).
2. C. Y. Hopkins and M. J. Chisholm. Can. J. Chem. **40**, 2078 (1962).
3. F. R. Earle, K. L. Mikolajczak, I. A. Wolff, and A. S. Barclay. J. Am. Oil Chemists' Soc. **41**, 345 (1964).
4. M. J. Chisholm and C. Y. Hopkins. Can. J. Chem. **38**, 2500 (1960).
5. C. R. Smith, Jr., M. C. Burnett, T. L. Wilson, R. L. Lohmar, and I. A. Wolff. J. Am. Oil Chemists' Soc. **37**, 320 (1960).
6. (*a*) C. D. Baker and F. D. Gunstone. J. Chem. Soc. 759 (1963).
   (*b*) D. E. Ames and R. E. Bowman. J. Chem. Soc. 2752 (1951).
7. N. S. Bhacca, D. P. Hollis, L. F. Johnson, and E. A. Pier. Nuclear Magnetic Resonance Spectra Catalog. Vol. 2. Varian Associates, Palo Alto, California. 1963. Spectrum 499.
8. R. L. Lohmar, C. R. Smith, Jr., and T. L. Wilson. J. Org. Chem. **25**, 2034 (1960).
9. R. G. Binder, T. H. Applewhite, M. J. Diamond, and L. A. Goldblatt. J. Am. Oil Chemists' Soc. **41**, 108 (1964).
10. M. J. Diamond, R. E. Knowles, R. G. Binder, and L. A. Goldblatt. J. Am. Oil Chemists' Soc. **41**, 430 (1964).
11. C. R. Smith, Jr., T. L. Wilson, E. H. Melvin, and I. A. Wolff. J. Am. Chem. Soc. **82**, 1417 (1960).
12. L. J. Morris, R. T. Holman, and K. Fontell. J. Am. Oil Chemists' Soc. **37**, 323 (1960).
13. F. R. Earle, I. A. Wolff, C. A. Glass, and Q. Jones. J. Am. Oil Chemists' Soc. **39**, 381 (1962).
14. F. D. Gunstone. Chem. Ind. London, 1033 (1965).
15. C. Y. Hopkins and M. J. Chisholm. J. Chem. Soc. 573 (1962).
16. R. U. Lemieux and E. von Rudloff. Can. J. Chem. **33**, 1701 (1955).

Can. J. Chem. Downloaded from www.nrcresearchpress.com by 210.87.254.105 on 09/05/12
For personal use only.

Can. J. Chem. Downloaded from www.nrcresearchpress.com by 210.87.254.6 on 09/05/12
For personal use only.

INFRARED STUDY OF THE PHOTOCHEMISTRY OF TETRAMETHYLCYCLOBUTAN-1,3-DIONE

IVAN HALLER AND R. SRINIVASAN
IBM Watson Research Center, Yorktown Heights, New York

Received June 14, 1965

ABSTRACT

The photolysis of tetramethylcyclobutan-1,3-dione was investigated in a nitrogen matrix at 4 °K and in solution in cyclohexane at room temperature. Infrared spectra of the reactant after irradiation showed the formation of carbon monoxide, dimethylketene, tetramethylethylene, and a compound with an intense absorption at 1 840 cm^{-1} which has been identified as tetramethylcyclopropanone. Since the dimethylketene that was formed was also capable of undergoing secondary photolysis, the effect of light (mainly 2 537 Å) on dimethylketene in solution or in a nitrogen matrix, was also studied. It has been found that in solution 0.2 of the molecules of tetramethylcyclobutandione which decompose, do so to give two molecules of dimethylketene, while approximately the same number of molecules decompose to tetramethylcyclopropanone and carbon monoxide. The remainder of the molecules seem to give tetramethylethylene and carbon monoxide in a concerted process.

INTRODUCTION

The photochemical decomposition of tetramethylcyclobutan-1,3-dione (I) in solution has been the subject of three recent reports (1–3). In benzene solution at 3 660 Å the

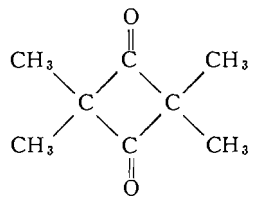

I

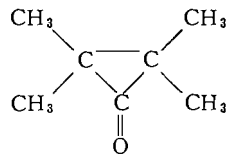

II

products that were observed were dimethylketene, $(CH_3)_2C{=}C{=}O$, carbon monoxide, tetramethylethylene, and an unstable material which was identified as tetramethylcyclopropanone (II) on the basis of its decomposition products. In hydroxylic solvents, a hemiketal of tetramethylcyclopropanone was isolated which also seemed to lend support to the idea that a primary photoproduct of tetramethylcyclobutandione is tetramethylcyclopropanone.

The present study[1] was undertaken to establish the formation of tetramethylcyclopropanone in this system by direct infrared observation of its presence. The use of infrared spectral analysis to look for transient intermediates in photochemical systems is by no means new (4). Fortunately, in this instance it has been possible to use infrared analysis not only for the purpose of identification, but also for a kinetic study so that a fairly detailed understanding of the photochemistry has been developed.

EXPERIMENTAL

Materials

Tetramethylcyclobutandione (Eastman practical grade), cyclohexane (Eastman spectrograde), ether (Mallinckrodt analytical reagent), and nitrogen (Linde, assayed reagent grade) for the matrix experiments were used as obtained. Dimethylketene was prepared by the pyrolysis of its dimer (5), purified by several bulb-to-bulb distillations *in vacuo*, and stored under its own vapor pressure at −78 °C.

[1] *A preliminary account of this work has appeared in J. Am. Chem. Soc. 87, 1144 (1965).*

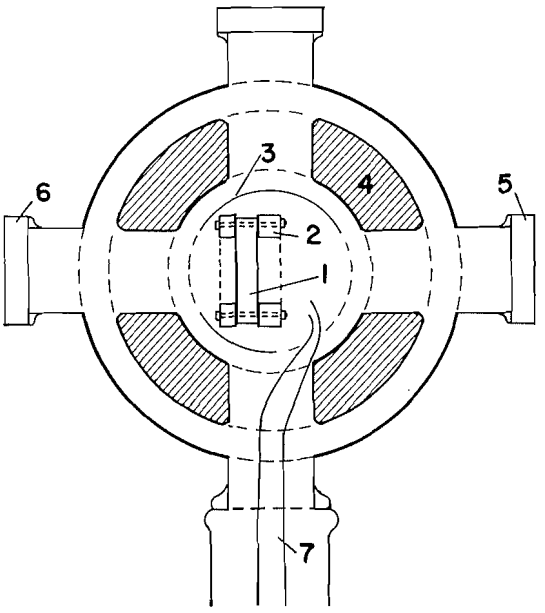

FIG. 1. Section of the low temperature cell. 1, CsBr plate; 2, copper cold finger; 3, copper radiation shield connected to liquid helium container; 4, liquid nitrogen container; 5 and 6, KBr windows; 7, gas inlet tube. The irradiation was affected through window 5.

Apparatus

The optical cell that was used in the matrix experiments was a modified, all-glass double dewar (H. S. Martin Co.) as shown in Fig. 1. Photolyses in solution were carried out in infrared cells with KBr windows which were 1 mm apart.

The light source was a medium pressure mercury arc (Hanovia type 73A10 or type SH) which was used in conjunction with a filter which consisted of a 2 cm layer of water to remove much of the infrared radiation. In some experiments a chlorine gas filter (3.2 cm long, $p = 1$ atm) or a grating monochromator (Bausch & Lomb type ZB3104) was also used to isolate the 2 537 Å radiation.

Infrared spectra were recorded on a Cary-White Model 90 spectrophotometer. The frequency accuracy is ± 3 cm^{-1} in survey spectra and ± 1 cm^{-1} in the regions that were observed in detail. Spectral slit-widths are indicated in the reproductions of the spectra.

Procedure

The mixture of nitrogen and tetramethylcyclobutandione vapor was prepared continuously during deposition by passing the former at a pressure of 20 mm through a glass coil which contained crystals of the latter. The vapor pressure of the diketone at room temperature is of the order of 0.2 mm. Mixtures of dimethylketene and nitrogen were prepared by standard methods (6).

Solutions of dimethylketene in hexane, which were used for the measurement of absorption coefficients, were prepared with particular care to exclude oxygen from the solvent (before the addition of dimethylketene) and from the solution (during transfer or measurements).

RESULTS

Matrix Studies

Tetramethylcyclobutandione was photolyzed in a nitrogen matrix in two separate experiments for 20 min and 2 h, respectively. The infrared spectra that were obtained in the second experiment are shown in Fig. 2. Absorption peaks belonging to the products of photolysis were observed at 2 138, 2 124, 2 103, 1 843, 1 824, 1 675, 1 414, 1 009, 972, 902 (?), 793, and 728 cm^{-1}. In addition, the band at 1 176 cm^{-1} in the spectrum of tetramethylcyclobutandione increased slightly after photolysis and shifted to lower frequencies, probably by the superposition of a product peak.

Can. J. Chem. Downloaded from www.nrcresearchpress.com by 210.87.254.6 on 09/05/12
For personal use only.

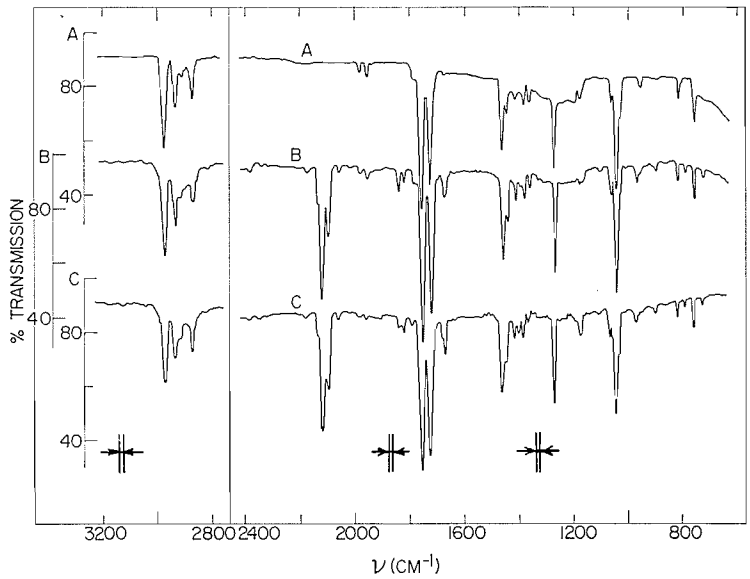

FIG. 2. Infrared spectra of tetramethylcyclobutandione in nitrogen matrix. A, before irradiation; B, after 120 min irradiation; C, after a warm-up cool-down cycle.

The intensity behavior of the stronger absorption peaks, due to the products, is shown in the first three colums of Table I. The spectra, from which these numbers were obtained, were recorded with a spectral slit-width which was less than the half-widths. Allowing the sample to warm to 35 °K, followed by recooling to 4 °K, did not result in the loss of any of the product bands or in the formation of new ones, even though extensive diffusion was indicated by the broadening and shifts in the maxima. When the CsBr plate in the cell was slowly warmed to 77 °K, a substantial part of the products remained as a solid deposit which gave rise to broad absorption bands corresponding to each of the bands observed in the matrix, with the exception of the one at 2 138 cm^{-1}.

Dimethylketene was deposited in a nitrogen matrix at a mole ratio of 1:80, in an amount comparable to that found in the previous experiments. Infrared bands were observed at 2 985, 2 944, 2 921, 2 899, 2 885, 2 866, 2 123.6, 2 104.0, 2 067, 2 061 (?), 1 911 (?), 1 905 (?), 1 450, 1 417, 1 401, 1 388, 1 332, 1 012, 913, and 729 cm^{-1}. None of these peaks changed in intensity, nor did any new peaks appear upon irradiation for 1 h under conditions that were identical to the photolysis of tetramethylcyclobutandione.

Solution Studies

A solution of tetramethylcyclobutandione in cyclohexane (1.22 mole %) was photolyzed at room temperature at 2 537 Å. Infrared bands of the photoproducts appeared at approximately the same frequencies as in the matrix isolation experiments. Figures 3A and 3B show the part of the spectrum from 2 200 cm^{-1} to 1 790 cm^{-1} before and after photolysis. Figure 3C shows the changes in the spectrum on bubbling a few milliliters of oxygen gas through the solution after photolysis.

In a different set of experiments a solution was photolyzed with 3 130 Å radiation. Infrared spectra were recorded after 8, 16, 32, 64, and 128 min of photolysis and after allowing the irradiated solution to stand in the dark for 38 h. Figures 3D and 3E present the regions of interest in the last two spectra. The observed intensities of the product bands are summarized in Table I.

Can. J. Chem. Downloaded from www.nrcresearchpress.com by 210.87.254.6 on 09/05/12
For personal use only.

Can. J. Chem. Downloaded from www.nrcresearchpress.com by 210.87.254.6 on 09/05/12
For personal use only.

TABLE I

Infrared absorption bands observed on photolysis of tetramethylcyclobutan-1,3-dione

		Conditions										
		N_2 matrix, 4 °K			Cyclohexane solution, 24 °C, 3 130 Å						Cyclohexane solution, 24 °C, 2 537 Å	
		Time (min)			Time (min)						Time (min)	
Assignment		20	120*	Warm-up	8	16	32	64	128	2 280 in dark	20	Oxygenation
CO	ν (cm^{-1})	2 138	2 138	2 137	—	—	—	—	—	—	—	—
	A†	0.02	0.06	0.06	—	—	—	—	—	—	—	—
	B (cm^{-1})	sh	sh	sh	—	—	—	—	—	—	—	—
Dimethylketene	ν (cm^{-1})	2 124	2 124	2 119	2 123	2 123	2 123	2 123	2 123	2 123	2 123	2 123
	A	0.13	0.36	0.33	0.02	0.04	0.06	0.18	0.40	0.28	0.49	0.14
	B (cm^{-1})	1.7	5.5	4.6	0.3	0.7	1.1	3.1	6.9	5.0	9.0	2.5
Tetramethylcyclopropanone	ν (cm^{-1})	2 101	2 103	2 097	2 101	2 101	2 101	2 101	2 101	2 101	2 101	2 101
	A	0.03	0.15	0.19	0.01	0.02	0.03	0.08	0.21	0.15	0.29	0.07
	B (cm^{-1})	0.6	2.1	3.1	sh	sh	sh	sh	sh	sh	sh	sh
	ν (cm^{-1})	1 843	1 843	1 840	1 840	1 840	1 840	1 840	1 840	1 840	1 840	1 840
	A	0.03	0.07	0.05	0.03	0.05	0.12	0.20	0.45	0.06	0.69	0.44
	B (cm^{-1})	0.2	0.5	0.3	0.3	0.5	1.2	2.0	4.5	0.7	6.7	4.9
	ν (cm^{-1})	1 824	1 824	1 823	1 820	1 820	1 820	1 820	1 820	1 820	1 820	1 820
	A	0.03	0.04	0.06	?	0.01	0.03	0.05	0.14	0.01	0.21	0.14
	B (cm^{-1})	0.1	0.2	0.4	—	sh	sh	sh	sh	sh	sh	sh

*Not a continuation of the preceding experiment.
†Intensity is reported as both optical density (o.d.) at the maximum, A, and integrated area (o.d. times half-width), B. "sh" refers to shoulder so that integration of the area under the absorption peak was not possible.

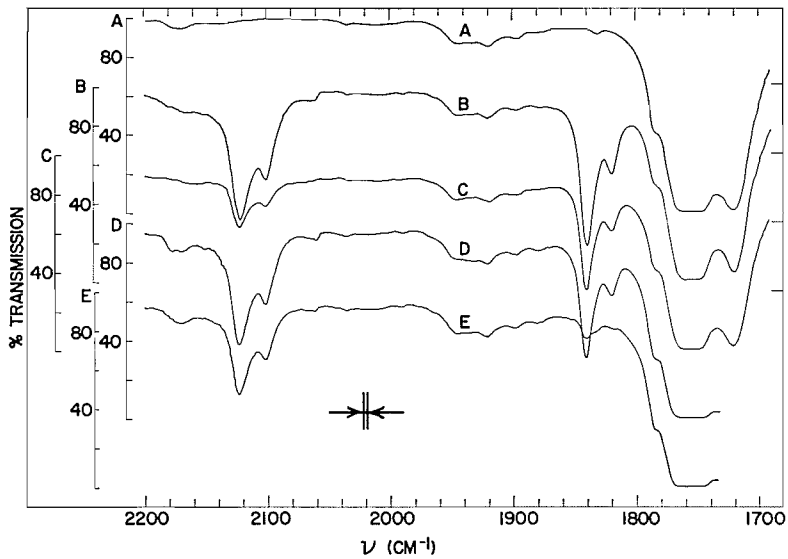

FIG. 3. Tetramethylcyclobutandione in cyclohexane solution. A, before photolysis; B, 20 min irradiation at 2 537 Å; C, after oxygenation; D, after 128 min irradiation at 3 130 Å (new sample); E, after 38 h standing in dark.

In the spectral regions in which the interference from the absorption due to the solvent was not a serious problem, weak bands due to products were observed at 1 415 cm^{-1} and 962 cm^{-1}. On allowing the solution to stand in the dark, and on oxygenation, the former band behaved similarly to the band at 2 123 cm^{-1}, the latter to the band at 1 840 cm^{-1}. A weak product band also appeared at 2 336 cm^{-1}. It underwent tremendous intensification upon oxygenation and was identified as due to carbon dioxide by comparison with the spectrum of a solution of dry ice in cyclohexane.

DISCUSSION

Interpretation of the Spectra

The behavior of the product bands in the warm-up cool-down cycle in the matrix experiments, and the fact that the similar absorption frequencies are observed in the cyclohexane solutions, lead to the conclusion that none of the observed bands belong to an unstable species such as a free radical. The effect of oxygenation and standing at room temperature in the dark indicates the presence of at least two compounds which have different chemical properties.

By direct comparison with the spectrum of dimethylketene the product bands at 2 124, 2 103, 1 414, 1 009, and 728 cm^{-1} were assigned to this compound. The two remaining strong bands, at 1 840 and 1 820 cm^{-1}, apparently belong to one compound as their intensities vary in a similar fashion. An assignment to tetramethylcyclopropanone is strongly favored by the near coincidence with the $\rangle$CO stretching frequency of cyclopropanone in a nitrogen matrix (7), and by the observed chemical behavior. The weak band at 2 138 cm^{-1} was obviously due to carbon monoxide (8).

The formation of dimethylketene as a product had already been shown by earlier work, (1, 3) but the production of tetramethylcyclopropanone was deduced indirectly from the formation of carbon monoxide. The present work thus offers the most direct evidence for the decarbonylation reaction [1].

Can. J. Chem. Downloaded from www.nrcresearchpress.com by 210.87.254.6 on 09/05/12
For personal use only.

[1] 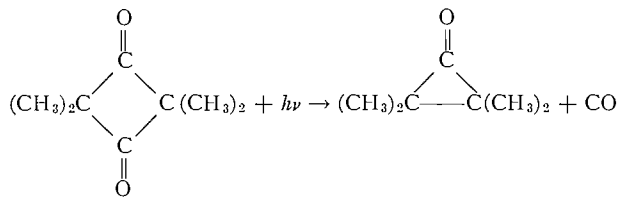

Early work had also shown that tetramethylethylene was an important product of photolysis. In this study efforts were made to look for this product in the infrared spectra. The increase in absorption at 1 176 cm^{-1} in the matrix experiments may be due to this product (9). However, it was best to look for this compound in the ultraviolet spectrum where it shows very intense end absorption rather than in the infrared spectrum where its absorption coefficient is low.

The ultraviolet spectrum of a solution of tetramethylcyclobutandione in cyclohexane did show an intense increase in absorption in the region from 2 400 to 2 000 Å on photolysis to low conversion in a quartz cell. This increased absorption could not be accounted for by the presence of dimethylketene or tetramethylcyclopropanone, an upper limit for the concentrations of these two species being available from the $n \rightarrow \pi^*$ absorption. In a typical photolysis, in which the extinction coefficient of the absorption due to the dione decreased from 0.22 to 0.21 at 3 075 Å, the optical density at 2 160 Å increased by more than 0.8. The contribution due to dimethylketene could not have been more than 0.01 at this wavelength, while the contribution due to tetramethylcyclopropanone can be estimated to be even less.

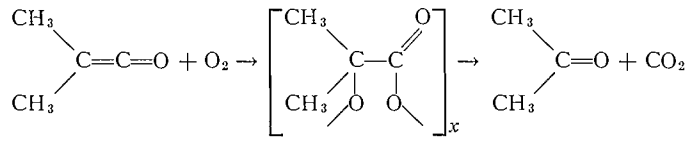

It was also found that bubbling oxygen through a solution of dimethylketene in cyclohexane resulted in no infrared bands belonging to the ketene peroxide (10, 11), only bands at 2 336 cm^{-1} and 1 720 cm^{-1} assignable to its decomposition products, namely, carbon dioxide and acetone. Isobutyric acid anhydride, formed by reacting small quantities of water with dimethylketene, exhibits infrared bands of equal intensity at 1 820 and 1 760 cm^{-1}.

$$H_2O + 2(CH_3)_2C{=}C{=}O \rightarrow [(CH_3)_2CHCO]_2O$$

Photochemical Primary Processes

Since discussions of the photochemistry of tetramethylcyclobutandione have already been published, (1, 3)[1] it is adequate to consider here the modifications which are suggested by the infrared spectral data that were obtained in the present study.

In addition to the photochemical primary process [1] there is undoubtedly a second primary process which gives rise to dimethylketene.

[2] 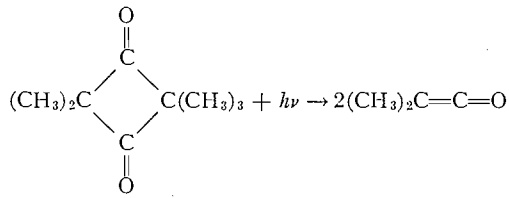

Can. J. Chem. Downloaded from www.nrcresearchpress.com by 210.87.254.6 on 09/05/12
For personal use only.

Direct measurement of the concentration of dimethylketene in both the ultraviolet and the infrared spectra of the solution has indicated that at least 2/10 of the molecules of tetramethylcyclobutandione that decompose follow reaction [2]. Whether all of the remaining molecules follow reaction [1] is one of the important questions that can be answered by the present studies. Since tetramethylcyclopropanone appears to be stable enough (half-life of several hours) to build up in solution during photolysis, its concentration can be estimated from the intensity of its carbonyl absorption provided that photolysis is not taken to conversions over a few per cent. The fact that the intensity of the carbonyl absorption due to tetramethylcyclopropanone is considerably less than the carbonyl absorption due to dimethylketene suggests that reaction [1] probably accounts for a smaller fraction of the dione than reaction [2].[2] Since one molecule of the dione gives rise to two molecules of dimethylketene but only one molecule of tetramethylcyclopropanone, an upper limit for the fraction of molecules of the reactant that take part in reaction [1] appears to be 0.4.[3]

The formation of tetramethylethylene was accounted for by the earlier workers (1, 3) through the formation and subsequent decomposition of tetramethylcyclopropanone. While this may be true if the reaction is carried to a point at which secondary photolysis does occur, the presence of tetramethylethylene from the early stages of the photolysis requires a third primary process. This process may very well account for the remaining

[3] 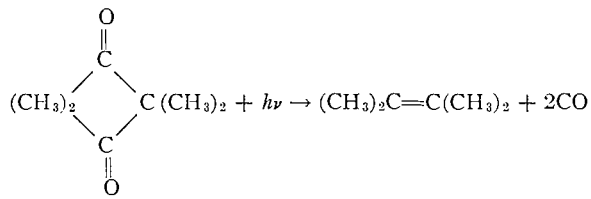

$$(CH_3)_2C(CO)C(CH_3)_2 + h\nu \rightarrow (CH_3)_2C{=}C(CH_3)_2 + 2CO$$

4/10 of the dione molecules which undergo decomposition. It is known (15) that tetramethylcyclobutandione in its $n \rightarrow \pi^*$ excited state showed an interaction and weak bonding between the carbonyl groups.[4] The effect of such an interaction would be to decrease the distance between the remaining two carbon atoms in the cyclobutane ring so that a concerted process such as that required in reaction [3] may well be possible.

REFERENCES

1. N. J. TURRO, G. W. BYERS, and P. A. LEERMAKERS. J. Am. Chem. Soc. **86**, 955 (1964).
2. H. G. RICHEY, JR., J. M. RICHEY, and D. C. CLAGETT. J. Am. Chem. Soc. **86**, 3906 (1964).
3. P. A. LEERMAKERS, G. F. VESLEY, N. J. TURRO, and D. C. NECKERS. J. Am. Chem. Soc. **86**, 4213 (1964).
4. G. C. PIMENTEL. Pure Appl. Chem. **4**, 61 (1962).
5. W. E. HANFORD and J. C. SAUER. *In* Organic reactions. *Edited by* R. Adams. Vol. III. John Wiley & Sons, Inc., New York. 1946. p. 136.

[2]*The integrated intensities of the carbonyl bands of cyclic ketones fall between 1.6 and 2.9 in units of 10^4 moles^{-1} l cm^{-2}, smaller rings being at the higher end of this range (12, 13). For tetramethylcyclopropanone 2.0 may then be taken as a lower limit. The measured integrated intensity for the 2 123 cm^{-1} band of dimethylketene in cyclohexane is 1.9 ± 0.3 in the same units.*

[3]*In earlier work (1, 3), the importance of primary process [1] has been estimated from the scavenging action of oxygen on the system. These estimates assume that tetramethylcyclopropanone reacts rapidly with oxygen, an assumption which is not borne out by the present work. It is wholly possible that an excited state which is the precursor for tetramethylcyclopropanone does react with oxygen, but the same excited state may lead to other products as well. Hence, the estimate is probably too high. The recent report that tetramethylcyclopropanone reacts with oxygen (14) points out the need for careful rate studies on this reaction.*

[4]*Reference 15 also presents data to show that in polar solvents the ultraviolet spectrum of tetramethylcyclobutandione shows marked shifts which are indicative of an interaction between the excited states of the dione and the solvent. As a result it is not possible to draw any conclusions regarding primary process [3] from data that were obtained during photolysis in a polar solvent.*

Can. J. Chem. Downloaded from www.nrcresearchpress.com by 210.87.254.6 on 09/05/12
For personal use only.

6. E. D. BECKER and G. C. PIMENTEL. J. Chem. Phys. **25**, 224 (1956).
7. W. B. DEMORE, H. O. PRITCHARD, and N. DAVIDSON. J. Am. Chem. Soc. **81**, 5878 (1959).
8. A. G. MAKI. J. Chem. Phys. **35**, 932 (1961).
9. INFRARED SPECTRAL DATA. American Petroleum Institute Research Project 44. Pittsburgh. 1955. Serial #128 and #129.
10. H. STAUDINGER, K. DYCKERHOFF, H. W. KLEVER, and L. RUZICKA. Ber. Deut. Chem. Ges. **58**, 1079 (1925).
11. L. J. BELLAMY. The infrared spectra of complex molecules. John Wiley & Sons, Inc., New York. 1958. p. 129.
12. R. N. JONES and C. SANDORFFY. *In* Techniques of organic chemistry. Vol. IX. *Edited by* A. Weissberger. Interscience Publishers, Inc., New York. 1956. p. 469.
13. T. BÜRER and Hs. H. GÜNTHARD. Helv. Chim. Acta, **39**, 356 (1956).
14. N. J. TURRO, W. B. HAMMOND, and P. A. LEERMAKERS. J. Am. Chem. Soc. **87**, 2774 (1965).
15. E. M. KOSOWER. J. Chem. Phys. **38**, 2813 (1963).

Can. J. Chem. Downloaded from www.nrcresearchpress.com by 210.87.254.6 on 09/05/12
For personal use only.

Can. J. Chem. Downloaded from www.nrcresearchpress.com by 210.87.254.5 on 09/05/12
For personal use only.

A NEW SYNTHESIS OF ALKYL FLUORIDES

THE PYROLYSIS OF 2-ALKYLPSEUDOURONIUM FLUORIDES AND FLUOROBORATES[1]

J. H. AMIN, J. NEWTON,[2] AND F. L. M. PATTISON
Department of Chemistry, University of Western Ontario, London, Ontario

Received August 16, 1965

ABSTRACT

The pyrolysis of 2-alkylpseudouronium fluorides and fluoroborates at approximately 185° gave alkyl fluorides in yields of up to 77%. The method is most useful for the preparation of primary alkyl fluorides; attempts to prepare secondary fluorides, such as cyclohexyl fluoride, gave the corresponding alkenes.

In the general investigation of new methods of forming the C—F bond, we have examined the pyrolysis of 2-alkylpseudouronium fluorides and fluoroborates. The reaction is analogous to the decomposition of 2-alkylpseudouronium chlorides (1).

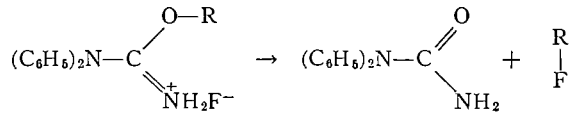

The pseudouronium salts were most conveniently prepared from diphenylcyanamide and the appropriate alcohols in the presence of potassium *tert*-butoxide (1–3). The reaction is readily followed by infrared spectroscopy: the C≡N stretching band at 2 250 cm^{-1} gives way to the new C=N band at 1 640 cm^{-1}. Maximum yields are obtained when the alcohols are freshly distilled and when moisture is rigorously excluded. The fluoride salts were prepared by mixing a dried ethereal solution of the resultant free base with an ethereal solution of hydrogen fluoride; the fluoroborates were obtained with 48% aqueous fluoroboric acid. The fluorides usually had the approximate composition $B \cdot 3HF$ whereas the fluoroborates had the expected stoichiometrical composition $B \cdot HBF_4$. (These ratios were used in the calculation of yields.) Occasionally other methods of preparation were used (3), but were generally less satisfactory. Some yields of pseudouronium salts are shown in Table I.

TABLE I

2-Alkylpseudouronium fluorides and fluoroborates

	$(C_6H_5)_2NC(OR)=\overset{+}{N}H_2F^-$		$(C_6H_5)_2NC(OR)=\overset{+}{N}H_2BF_4^-$	
R	Yield (%)	Melting point (°C)	Yield (%)	Melting point (°C)
$CH_3(CH_2)_4$	92	124–125	72	97–98
$CH_3(CH_2)_5$	88	118–121	83	98–99
$CH_3(CH_2)_7$	88	127–128	76	97–98
$CH_3(CH_2)_9$	89	123–125	75	86–87
$CH_3(CH_2)_{11}$	88	128–130	—	—
$C_6H_5CH_2$	80	119–120	90	128–129
C_6H_{11}	85	180–185	—	—
$Cl(CH_2)_6$	93	115–120	—	—
$F(CH_2)_6$	83	118–120	—	—

[1]*This paper was presented in part at the Third International Symposium on Fluorine Chemistry, Munich, Germany, August 30 – September 2, 1965.*

[2]*Present address: Chemical Abstracts Service, The Ohio State University, Columbus 10, Ohio 43210, U.S.A.*

The best yields of alkyl fluorides were obtained when the pyrolysis of the salts was carried out at a temperature of about 185°. The residue contained diphenylamine (92% yield); this product is consistent with the well-known decomposition of 1,1-diphenylurea to diphenylamine and cyanic acid. The amine can readily be reconverted into diphenylcyanamide by common synthetic procedures in 90% yield or better. The overall reaction may thus be considered as the reaction of an alcohol with hydrogen fluoride to give an alkyl fluoride; the diphenylcyanamide is alternately consumed and reformed.

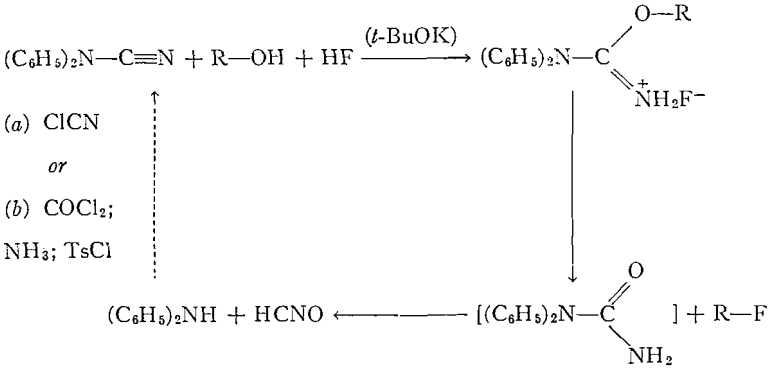

The pyrolysis may be carried out with or without solvents (Table II). The following high-boiling solvents were examined: mesitylene, octadecane, paraffin wax, diethylene glycol, and triethylene glycol, but in no case was the yield improved. The nonpolar solvents gave results comparable with those obtained by straight pyrolysis, whereas the

TABLE II
Some percentage yields of alkyl fluorides

R—F	Method of pyrolysis*	Via F^- salt	Via BF_4^- salt
$CH_3(CH_2)_4F$	Alone	42	—
	KHF_2;† no solvent	44	—
	KHF_2; octadecane	44	52
	KHF_2; mesitylene	44	57
$CH_3(CH_2)_5F$	KHF_2; no solvent	52	—
	KHF_2; octadecane	56	58
$CH_3(CH_2)_7F$	KHF_2; no solvent	70	47
	KHF_2; octadecane	76	55
	KHF_2; diethylene glycol	30	—
	KHF_2; triethylene glycol	23	—
$CH_3(CH_2)_9F$	Alone	53	0‡
	KHF_2; no solvent	77	53
	KHF_2; octadecane	69	55
$CH_3(CH_2)_{11}F$	KHF_2; no solvent	70	—
	KHF_2; wax	61	—
$C_6H_5CH_2F$	KHF_2; no solvent	34	0
	KHF_2; wax	21	—
$C_6H_{11}F$	KHF_2; wax	0§	—
$Cl(CH_2)_6F$	KHF_2; no solvent	48	—
$F(CH_2)_6F$	KHF_2; no solvent	51‖	—

*All pyrolyses were carried out by heating the reaction flask in an air bath.
†The molar ratio of KHF_2 to salt was usually 2 in the case of the fluorides and 4 in the case of the fluoroborates.
‡1-Decene (45% yield) was obtained.
§Cyclohexene (50% yield) was obtained.
‖From $F(CH_2)_6OH$.

Can. J. Chem. Downloaded from www.nrcresearchpress.com by 210.87.254.5 on 09/05/12
For personal use only.

polar solvents were usually less effective. Some yields were improved by adding potassium bifluoride to the pseudouronium salt before pyrolysis; this is necessary, in the case of the fluoroborates, to suppress alkene formation. Isolation and purification of the alkyl fluorides followed standard patterns.

Some variations in the procedure were examined briefly. Free 2-alkylpseudourea bases, on pyrolysis with an excess of potassium bifluoride, gave no alkyl fluorides. 2-Alkylpseudouronium fluorides, on pyrolysis with an excess of ammonium chloride, gave a mixture of alkyl chlorides and alkyl fluorides (RCl:RF = 3:1). 2-Alkylpseudouronium chlorides, on pyrolysis with an excess of potassium bifluoride, gave only alkyl chlorides.

As the work proceeded, it became apparent that, for two reasons, the method is mainly of value in the preparation of *primary* alkyl fluorides. Firstly, primary alcohols form the pseudouronium salts far more readily than do secondary and tertiary alcohols. Secondly, secondary and tertiary alkyl groups, under the conditions of pyrolysis, tend to form the corresponding alkene rather than the alkyl fluoride; thus, 2-cyclohexyl-3,3-diphenylpseudouronium fluoride gave cyclohexene exclusively (56%).

It was hoped that the method could be simplified by using imidate hydrofluorides or fluoroborates in place of the pseudouronium salts. So far, however, we have not been successful in forming the necessary salts, although we have examined a number of routes and techniques. Another alternative, involving the pyrolysis of a mixture of a carbamate and potassium bifluoride, was also unsuccessful.

It is probable that the mechanism of pyrolysis parallels that of the decomposition of imidate hydrochlorides. Kinetic results (4) in chloroform or *tert*-butyl alcohol at 60° (first-order disappearance of halide ion) were consistent with two routes, which, when applied to the pseudouronium fluorides, may be represented as follows:

[i] Intramolecular: $(C_6H_5)_2N-C(=O-R)(=NH_2\cdots F^-) \rightarrow (C_6H_5)_2N-C(=O)-NH_2 + R-F$

[ii] S_N2: $(C_6H_5)_2N-C(=O-R)(=NH_2F^-) \rightarrow (C_6H_5)_2N-C(=O-R\ F^-)(=NH_2) \rightarrow (C_6H_5)_2N-C(=O)-NH_2 + R-F$

For compounds in which R is optically active, the first of these would be expected to result in retention of configuration (S_Ni), and the second in inversion (S_N2). The fact that Walden inversion, in the pyrolysis of crystalline *sec*-butyl acetimidate hydrochloride, has now been observed (5) and that the rates of decomposition of imidate salts are of the same order as those of other recognized S_N2 reactions (4) makes *ii* the mechanism of choice. It is uncertain (but likely) that this conclusion can be applied to the pyrolysis of pseudouronium salts in the solid phase; studies involving optically active pseudouronium salts derived from RCHDOH (6) would clarify this point.

EXPERIMENTAL

The preparations described below represent a typical example of each procedure; obvious variations for obtaining different members have not been included. Melting points (uncorrected) were determined on a Kofler hot stage, and infrared spectra with Beckman IR-7 and IR-5 infrared spectrophotometers. Analyses were performed by the Schwarzkopf Microanalytical Laboratory, Woodside, New York 77. Fractionations were carried out with a 23-plate platinum-plated spinning-band column.

Can. J. Chem. Downloaded from www.nrcresearchpress.com by 210.87.254.5 on 09/05/12
For personal use only.

2-Decyl-3,3-diphenylpseudouronium Fluoride

Freshly distilled 1-decanol (150 g), diphenylcyanamide (38.8 g, 0.2 mole), and potassium *tert*-butoxide (0.5 g) were heated under reflux overnight on a steam bath with mechanical stirring. The infrared spectrum of an aliquot in chloroform indicated the complete disappearance of the C≡N band at 2 250 cm^{-1} and the presence of a C=N band at 1 640 cm^{-1}. The unreacted excess of 1-decanol was recovered by distillation under reduced pressure (b.p. 73–74° at 0.4 mm) and the viscous residue was dissolved in anhydrous ether (250 ml). Anhydrous hydrogen fluoride (15 g) (NOTE: *Use rubber gloves*) in cold ether (100 ml) was then added to the ethereal solution of the pseudourea base, which was contained in a polythene beaker. The mixture was stirred and cooled to −50°. The resultant salt was filtered off, washed several times with cold ether, and dried in a desiccator over potassium hydroxide pellets; yield: 73.0 g, 89%. Recrystallization from chloroform – petroleum ether (35–60°) gave colorless needles, m.p. 123–125°.

Titrimetric analysis, using 0.01 *N* sodium hydroxide, indicated that the product usually contained the elements of 3HF, but some variation in fluorine content was observed. This is consistent with the well-known tendency of hydrogen fluoride to form double molecules, complexes, and hydrofluorides of crystallization (7); with weak bases, for example, the molar ratio of HF to base varies between 1 and 4. For purposes of calculation in this work, the composition was taken to be B·3HF.

Melting points of the fluoride salts are listed in Table I. Two analyses follow.

2-Pentyl-3,3-diphenylpseudouronium Fluoride

Anal. Calcd. for $C_{18}H_{25}F_3N_2O$: C, 63.16; H, 7.36; N, 8.18; F, 16.64. Found: C, 62.90; H, 7.25; N, 8.29; F, 16.85.

2-Octyl-3,3-diphenylpseudouronium Fluoride

Anal. Calcd. for $C_{21}H_{31}F_3N_2O$: C, 65.60; H, 8.13; N, 7.29; F, 14.83. Found: C, 65.97; H, 7.76; N, 7.30; F, 15.37.

2-Decyl-3,3-diphenylpseudouronium Fluoroborate

The free pseudourea base was prepared as in the above procedure, with diphenylcyanamide (29.1 g, 0.15 mole), freshly distilled 1-decanol (100 g), and potassium *tert*-butoxide (0.5 g). After recovery of the excess 1-decanol by distillation under reduced pressure, the residue was dissolved in ether (200 ml) and to it was added 48% aqueous fluoroboric acid (50 ml). The ether was allowed to evaporate overnight at room temperature. The oily residue was dissolved in chloroform (250 ml), and the resultant solution was washed with water, dried over anhydrous sodium sulfate, and concentrated to about 100 ml. On careful dilution with petroleum ether (35–60°), the fluoroborate salt crystallized as colorless needles (49.5 g, 75%), m.p. 86–87°. It may be recrystallized from chloroform – petroleum ether (35–60°) and should be stored in a desiccator over potassium hydroxide pellets.

Titrimetric analysis, using 0.01 *N* sodium hydroxide, indicated the composition B·HBF_4. Two analyses follow.

2-Pentyl-3,3-diphenylpseudouronium Fluoroborate

Anal. Calcd. for $C_{18}H_{23}BF_4N_2O$: C, 58.41; H, 6.26; N, 7.57; F, 20.52. Found: C, 58.35; H, 6.44; N, 7.73; F, 20.37.

2-Octyl-3,3-diphenylpseudouronium Fluoroborate

Anal. Calcd. for $C_{21}H_{29}BF_4N_2O$: C, 61.18; H, 7.09; N, 6.79; F, 18.43. Found: C, 61.37; H, 7.24; N, 6.71; F, 18.60.

1-Fluorodecane (from Fluoride Salt)

A 500 ml round-bottomed flask, fitted with an 8 inch vertical air condenser carrying a Claisen-type distillation head leading to appropriate condensers and traps, was charged with a finely ground mixture of 2-decyl-3,3-diphenylpseudouronium fluoride (41.2 g, 0.1 mole) and potassium bifluoride (15.6 g, 0.2 mole). The flask was gradually heated in an air bath until decomposition started (ca. 185°). The temperature was then maintained at about 250° until distillation ceased; thereafter, the temperature was raised to about 300° and the pressure was reduced to ensure complete isolation of the product (15.3 g). The distillate was dissolved in ether (50 ml), and the ethereal solution was washed with 2% aqueous sodium bicarbonate and with water. After this solution was dried over anhydrous sodium sulfate and after removal of the ether, fractionation of the residue gave 1-fluorodecane (12.3 g, 77%), b.p. 187–190°, n_D^{25} 1.4087 (lit. (8) b.p. 74–75° at 13 mm, n_D^{25} 1.4080). The identity of the product was further confirmed by gas–liquid chromatographic analysis and infrared spectroscopy.

The residue, after pyrolysis, was treated with hot water (200 ml) and transferred to a beaker. The oily suspension solidified on the addition of aqueous sodium hydroxide, and cooling. The product was filtered, washed with water, dried in a desiccator, and recrystallized from aqueous methanol; yield: 15.6 g, 92%. It was proved to be identical with diphenylamine by the usual physical and chemical methods.

1-Fluorodecane (from Fluoroborate Salt)

The pyrolysis was carried out in the same equipment and by the same method as in the previous procedure, with 2-decyl-3,3-diphenylpseudouronium fluoroborate (44.0 g, 0.1 mole) and potassium bifluoride (31.2 g, 0.4 mole) in octadecane (100 g). The decomposition started at 225° and the temperature was maintained at

Can. J. Chem. Downloaded from www.nrcresearchpress.com by 210.87.254.5 on 09/05/12
For personal use only.

300° until distillation had ceased. The distillate (12 g) was washed, dried, and purified as before, yielding pure 1-fluorodecane (8.8 g, 55%), b.p. 184–187°, n_D^{25} 1.4084 (lit. (8) b.p. 74–75° at 13 mm, n_D^{25} 1.4080). The identity of the product was further confirmed by the usual methods.

1-Chloro-6-fluorohexane and *1,6-difluorohexane* were prepared by the above procedures (Table II); their identities were confirmed by reference to authentic samples (9).

ACKNOWLEDGMENTS

We express our indebtedness to the National Research Council for financial support, and to Dr. J. R. Robinson, Agricultural Research Institute, London, Ontario, for several valuable discussions.

REFERENCES

1. R. H. McKee. Am. Chem. J. **42**, 1 (1909).
2. J. R. Robinson and W. H. Brown. Can. J. Chem. **29**, 1069 (1951).
3. S. E. Forman, C. A. Erickson, and H. Adelman. J. Org. Chem. **28**, 2653 (1963).
4. S. M. McElvain and B. E. Tate. J. Am. Chem. Soc. **73**, 2233 (1951).
5. C. L. Stevens, D. Morrow, and J. Lawson. J. Am. Chem. Soc. **77**, 2341 (1955).
6. A. Streitwieser, Jr. J. Am. Chem. Soc. **75**, 5014 (1953).
7. J. H. Simons. *In* Fluorine chemistry. Vol. I. *Edited by* J. H. Simons. Academic Press Inc., New York. 1950. p. 246.
8. F. L. M. Pattison and J. E. Millington. Can. J. Chem. **34**, 757 (1956).
9. F. L. M. Pattison and W. C. Howell. J. Org. Chem. **21**, 748 (1956).

Can. J. Chem. Downloaded from www.nrcresearchpress.com by 210.87.254.5 on 09/05/12
For personal use only.

Can. J. Chem. Downloaded from www.nrcresearchpress.com by 210.87.254.105 on 09/05/12
For personal use only.

ORTHO PARTICIPATION IN THE CONVERSION OF *syn*-BENZALDOXIME ESTERS TO NITRILES

ROBERT J. CRAWFORD AND CHARLES WOO
Department of Chemistry, University of Alberta, Edmonton, Alberta
Received June 11, 1965

ABSTRACT

Substituted *syn*-benzaldoxime esters are transformed, in an alcoholic solution, to the corresponding nitriles according to first-order kinetics. All ortho substituents were observed to accelerate the rate of nitrile formation relative to the corresponding para derivative. While the k_o/k_p ratios for the bromo, chloro, fluoro, methoxy, and methyl substituents fall within the range of 2 to 9, the iodo and methylthio substituents are 119 and 11 000 respectively. Isotopic replacement of the aldoximino hydrogen by deuterium gives rise to a kinetic isotope effect, k_H/k_D being 5.21 for *syn*-*o*-chlorobenzaldoxime *p*-toluenesulfonate, 1.22 for *syn*-*o*-iodobenzaldoxime *p*-toluenesulfonate, and 1.23 for *syn*-*o*-methylthiobenzaldoxime *o*-iodobenzoate. The marked enhancement of rate and the absence of an appreciable isotope effect are considered to be associated with sulfur and iodine participation in the rate-determining step. A mechanism which is capable of explaining the results observed is suggested.

INTRODUCTION

In a recent study of the conversion of *syn*-aldoxime arenesulfonates to nitriles we found that the reaction could be characterized as a concerted elimination (1) having a transition state resembling I. However the possibility that the rate-determining step was proton loss to the solvent from an imidonium species II could not be dismissed. We have undertaken the work reported herein in an attempt to resolve this problem.

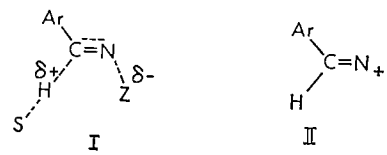

I II

We decided to approach this by trying to use an "internal trap" in the ortho position, i.e. if the imidonium species II is formed then a suitable substituent X in the ortho position may trap this species faster than the return to starting material or conversion to product may occur, as per Scheme I. The results from a study of the ortho substituted aromatic ketoximes by von Auwers and co-workers (2) suggests that the ortho substituted acetophenone oximes undergo the Beckmann rearrangement at a faster rate than the similarly substituted para derivatives. This point was confirmed by Pearson and Cole (3), by comparison of the rates of rearrangement of ortho and para acetophenone oximes in sulfuric acid. The acceleration was attributed to a steric force whereby the ortho substituent displaces the α-oximinoethyl group out of the plane of the benzene ring. The rates in concentrated sulfuric acid are complicated by the fact the protonation may occur on oxygen and nitrogen (4); thus we have used arenesulfonate leaving groups.

Some ortho substituents, particularly those in which the substituent can function as a nucleophile, have been observed to anchimerically accelerate the reaction rate. Thus the ionization of *o*-methoxyneophyl *p*-toluenesulfonate and *o*-iodophenylethyl *p*-bromobenzenesulfonate is assisted by the *o*-methoxy and *o*-iodo substituents respectively (5).

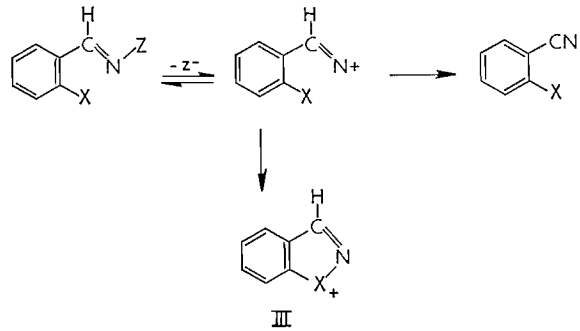

III

SCHEME I.

RESULTS AND DISCUSSION

Configuration of Aldoximes

In order that we may be confident of the configuration of the oximes the nuclear magnetic resonance (n.m.r.) spectrum of known oximes are compared in Table I with those not yet assigned, the *o*-iodo and *o*-thiomethylbenzaldoximes. The configurations of phenylhydrazones, semicarbazones, and thiosemicarbazones of the general structure IV

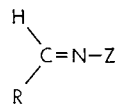

IV

have been determined by Karabatsos *et al.* (6) by n.m.r. Aldoximes are observed to follow a similar pattern (7). The OH and CH protons in the *syn* configuration appear as two singlets in the region τ 0.0 to 2.0 and are usually well separated. This is well distinguished from the corresponding protons in the *anti* isomer which appear at higher fields and closer together. The fact that these protons in the *o*-iodobenzaldoxime melting at 110° appear at τ 1.27 and 1.54 indicates that it has the *syn* configuration. The same is true for the *o*-methylthiobenzaldoxime melting at 88–90°.

Rate Comparisons

The rate constants were obtained as described in the previous paper (1). A comparison of reaction rates of para and ortho substituted *syn*-benzaldoxime *p*-toluenesulfonates is

TABLE I

N.m.r. data for some substituted benzaldoximes in deuterochloroform

	syn		*anti*	
Benzaldoxime	O—H* (τ)	C—H (τ)	O—H* (τ)	C—H (τ)
o-Cl	0.55	1.38		
p-Cl	0.87	1.81		
p-CH_3	0.39	1.81	2.59	2.72
p-OCH_3	0.77	1.83	2.63	2.69
o-OCH_3	0.14	1.49		
2,4,6-Trimethyl	0.92	1.54	2.35	2.71
o-I (m.p. 110°)	1.27	1.54		
o-SCH_3 (m.p. 88–90°)	0.61	1.31		

*Identified by D_2O exchange.

Can. J. Chem. Downloaded from www.nrcresearchpress.com by 210.87.254.105 on 09/05/12
For personal use only.

listed in Table II. The *p*-toluenesulfonate of *syn-o*-methylthiobenzaldoxime is very reactive and unstable; it cannot be isolated. Thus a slower leaving group was used. Table III presents, for comparison, the extrapolated value at 92° of the rate constants of *syn-o*-methylthiobenzaldoxime *o*-iodobenzoate in 50% dioxane. The reaction of *syn-p*-methylthiobenzaldoxime *o*-iodobenzoate was so slow at 92° that the rate was measured to only 40% completion.

An examination of the ortho and para (k_o/k_p) rate constants from Tables II and III clearly shows that all ortho substituents, irrespective of their resonance or inductive effect, increase the rate of nitrile formation when compared with their para isomer (3). However, it is interesting to note that in the seven pairs of isomeric structures studied, the k_o/k_p ratio of the bromo, chloro, fluoro, methoxy, and methyl substituents fall within the range of 2 to 9, while that for the iodo and methylthio substituents is 119 and 11 000, respectively. Thus substantial rate enhancements are involved in the latter two cases.

TABLE II

Rate constants for the reaction of substituted *syn*-benzaldoxime *p*-toluenesulfonates in 95% ethanol at 50.00 ± 0.02°

Run No.	Substituents	10^5k (s^{-1})	k_o/k_p
41	*o*-I	714	
48	*p*-I	6.10	119
42	*o*-Br	19.5	
49	*p*-Br	7.40	2.64
43	*o*-Cl	15.9	
39	*p*-Cl	6.14	2.59
44	*o*-F	12.6	
50	*p*-F	6.80	1.86
45	H	10.9	
46	*o*-OCH_3	95.5	
15	*p*-OCH_3	23.5	4.06
47	*o*-CH_3	102	
51	*p*-CH_3	12.1	8.44
52	*p*-SCH_3	12.4	

TABLE III

Rate constants for the reaction of substituted *syn*-benzaldoxime *o*-iodobenzoates in 50% dioxane

Run No.	Substituent	Temp. ±0.02°	10^5k (s^{-1})	k_o/k_p
53	*o*-SCH_3	30.00	18.2	
54	"	40.00	55.7	
55	"	50.00	141	
	"	92.00	5 390*	
				11 000
56	*p*-SCH_3	92.00	0.49	
57	2,4,6-Trimethyl	92.00	49.7	

*Extrapolated rate constant.

The mechanism of the thermal conversion of substituted *syn*-benzaldoxime esters to nitriles in methanol has been proposed (1) to involve a concerted *cis* elimination, as represented by I. The increase in rate by ortho substituents can be attributed to an increase in potential energy of the reactant in the ground state by virtue of steric inhibition

Can. J. Chem. Downloaded from www.nrcresearchpress.com by 210.87.254.105 on 09/05/12
For personal use only.

of resonance. This steric acceleration has been suggested by Pearson and Cole (3) to be one of the factors responsible for the enhanced rearrangement rate of the ortho substituted acetophenone oximes in sulfuric acid. While steric facilitation may contribute appreciably to the enhancement of rate by a factor up to 9 in the bromo, chloro, fluoro, methoxy, and methyl series, it does not as readily account for the factor of 119 in the iodo, and particularly, 11 000 in the methylthio substituents. The exceptional reactivity of the *o*-iodo and *o*-methylthio substituents is too great to be attributed to resonance, inductive, or steric effects, but suggests that the reaction may proceed through a heterocyclic "onium" ion III, where the *o*-iodo and *o*-methylthio groups contribute to the transition state by release of electrons to the nitrogen atom, thus producing an intermediate wherein the stereochemistry is favorable for the more rapid *trans* elimination to form the nitrile.

The activation parameters in Table IV indicate that the large enhancement of rate by the *o*-iodo substituent is associated with a lowering in $\Delta H^{\ddagger}$ of approximately 2 kcal mole^{-1} when compared with the other ortho substituents. From the rate constants of *syn-o-* and *syn-p*-methylthiobenzaldoxime *o*-iodobenzoates, an estimation of the change of free energy of activation can be made by the following relation.

$$\Delta\Delta F^{\ddagger} = -RT \ln \frac{k_o}{k_p}$$

This gives rise to a decrease in $\Delta F^{\ddagger}$ of 6.7 kcal mole^{-1} for the *o*-methylthio substituent when compared with the corresponding *p*-isomer.

TABLE IV

Activation parameters for *o*-substituted *syn*-benzaldoxime *p*-toluenesulfonates in 95% ethanol at 50.00 ± 0.02 °C

Substituent	$\Delta H^{\ddagger}$ (kcal mole^{-1})	$\Delta S^{\ddagger}$ e.u. mole^{-1}
I	18.7	−10.8
Br	21.3	−9.93
Cl	20.8	−12.8
F	20.5	−13.3
H	20.9	−12.3
OCH_3	22.1	−4.47
CH_3	20.7	−8.46
SCH_3*	19.7	−10.9

*o-Iodobenzoate in 50% dioxane.

TABLE V

Isotope effects in the reaction of ortho substituted *syn*-benzaldoxime *p*-toluenesulfonates

Run No.	Substituent	Solvent	Temp. ±0.02°	10^5k (s^{-1})	k_H/k_D
58	Cl—H	95% EtOH	65.00	67.2	
61	Cl—D	"	"	12.9	5.21
59	I—H	"	35.00	183	
62	I—D	"	"	150	1.22
46	OCH_3—H	"	50.00	95.5	
63	OCH_3—D	"	"	37.9	2.52
60	SCH_3—H*	80% MeOH	50.00	205	
64	SCH_3—D*	"	"	167	1.23

*o-Iodobenzoates.

Can. J. Chem. Downloaded from www.nrcresearchpress.com by 210.87.254.105 on 09/05/12
For personal use only.

Isotope Effects

Such an intermediate as III would be ideally set up for the elimination process and one would expect the second step, k_2 in Scheme II, to be very rapid. This point can be tested experimentally. It has been shown (1) that a k_H/k_D value of 4.51 was observed in the elimination of the para substituted compounds. With ortho participation, however, k_2 may be faster than k_{-1}, and k_H/k_D would approach unity. Table V shows that *syn-o*-chlorobenzaldoxime *p*-toluenesulfonate, which is not expected to participate, has a k_H/k_D value of 5.21. The k_H/k_D values for *syn-o*-methoxybenzaldoxime *p*-toluenesulfonate is 2.51, *syn-o*-iodobenzaldoxime *p*-toluenesulfonate is 1.22, and *syn-o*-methylthiobenzaldoxime *o*-iodobenzoate is 1.23. Thus the large enhancement in rate and the absence of appreciable kinetic isotope effect in the latter two cases suggest strongly that ortho participation is a major contributing factor, and that the reaction proceeds by at least a two step process.

The evidence does not, however, indicate how the participation occurs and two possibilities readily come to mind.

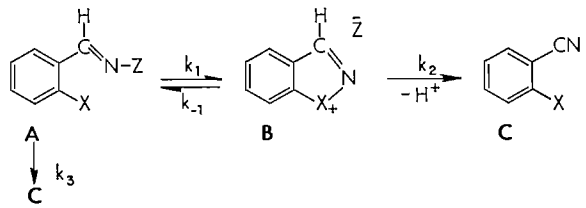

SCHEME II.

The ortho substituent may be affecting a nucleophilic displacement on the oximino nitrogen as in (*a*), or the participating group may act as an internal trap for the imidonium species V as in (*b*).

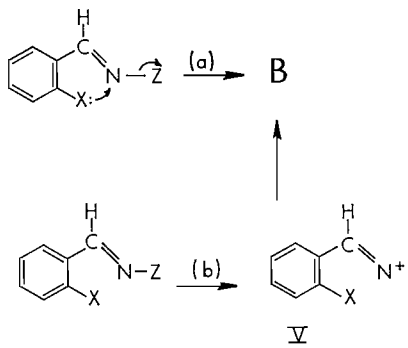

Route (*a*) implies a nucleophilic displacement by the participating group on sp^2 nitrogen, a process which is not well documented, whereas route (*b*) involves an ionic intermediate. By analogy with known properties of internal return from ^{18}O labeling of *p*-nitrobenzoate esters (8) as well as the rearrangement of sulfinates to sulfones (9) and and thiobenzoates to thiolbenzoates (10), one would expect the enhancement of k_1 due to the prevention of the step k_{-1} in Scheme II to be less than a factor of 5.

If the formation of the "onium" species B proceeds by route (*b*) then k_{-1} in Scheme II would approach zero for the *o*-methylthio substituent based on the assumption that it is an efficient trapping agent. From the relative rates of the ortho and para isomers, and

Can. J. Chem. Downloaded from www.nrcresearchpress.com by 210.87.254.105 on 09/05/12
For personal use only.

assuming a value of $k_{obs}^{o} = 8k_4$ (i.e. approximately the magnitude for the methyl substituent), the amount of ion-pair return, k_{-4} for the para isomer can be estimated from

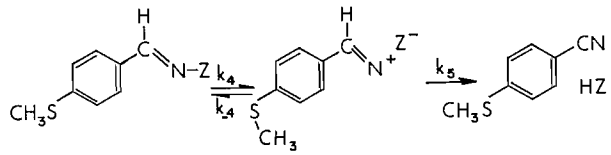

VI

SCHEME II

the observed rate constant for the ortho (k_{obs}^{o}) and para (k_{obs}^{p}) isomers. Then from the steady-state treatment for the para isomer we obtain, from Scheme II,

$$k_{obs}^{p} = \frac{k_5}{(k_4 + k_5)} k_4.$$

Thus

$$\frac{k_{obs}^{o}}{k_{obs}^{p}} = \frac{8k_4}{\left(\frac{k_5}{k_{-4} + k_5}\right)k_4} = 11\,000, \text{ and } k_{-4} \simeq 1\,400\, k_5.$$

This implies that if the electronic factors for ortho and para positions are the same and if the para species is going by the imidonium ion VI, then for every time that it formed it must return to starting material 1 400 times more frequently than it went on to product. Such a scheme would imply a much higher degree of internal return of the initially formed ion-pair than has been previously observed (8–10) and indeed what we conclude is that the *o*-thiomethyl group is not acting as an efficient trap, but must be bringing about reactions as per route (*a*), and that the transition state for the *o*-thiomethyl (and *o*-iodo) derivative may be best represented by VII. On this basis we may also rule out the deprotonation of the imidonium species II as the rate-determining step in the previously observed elimination (1).

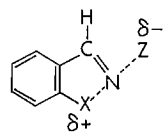

VII

syn-o-Methoxybenzaldoxime *p*-toluenesulfonate presents an interesting case. Its small k_o/k_p value of 4.06 shows no indication of anchimeric assistance, but the kinetic isotope effect of 2.51 is about half of that expected for a concerted *cis* elimination. However, it has been pointed out (5) that *syn-p*-methoxybenzaldoxime *p*-toluenesulfonate reacts unusually fast because of direct resonance interaction of the methoxy group with the reaction center, thus resulting in a smaller k_o/k_p value. The intermediate value of k_H/k_D of 2.51 may arise in two ways (*a*) that k_{-1} in Scheme II has become competitive with k_2 or (*b*) that k_3 is competitive with the participation route. If one assumes that k_{2H}/k_{2D} has a value of 5.2 (that of *o*-chlorobenzaldoxime), one finds that a ratio of $k_{-1}/k_2 = 0.56$ for

Can. J. Chem. Downloaded from www.nrcresearchpress.com by 210.87.254.105 on 09/05/12
For personal use only.

the *o*-methoxy compound would give rise to an isotope effect of 2.5. Using the steady-state treatment or B in Scheme II then

$$\frac{k_H}{k_D} = \frac{k_{2H}k_1(k_{-1} + k_{2D})}{k_{2D}k_1(k_{-1} + k_{2H})} = \frac{k_{2H}\left(\frac{k_{-1}}{k_{2H}} + \frac{k_{2D}}{k_{2H}}\right)}{k_{2D}\left(\frac{k_{-1}}{k_{2H}} + \frac{k_{2H}}{k_{2H}}\right)}$$

and making the appropriate substitution one can solve for k_{-1}/k_2. Similarly if k_{-1} is small and k_3 is competitive with k_1 then a value of $k_1/k_3 = 0.47$ would give rise to an isotope effect of 2.5.

The rate constant of *syn*-2,4,6-trimethylbenzaldoxime *o*-iodobenzoate at 92° in 50% dioxane shown in Table III is about 100 times that of *syn-p*-methylthiobenzaldoxime *o*-iodobenzoate under the same conditions. From Table II, the rate constant of *syn-p*-methylbenzaldoxime *p*-toluenesulfonate is about the same as that of *syn-p*-methylthiobenzaldoxime *p*-toluenesulfonate. Then the *syn*-2,4,6-trimethylbenzaldoxime derivative reacts about 100 times faster than the corresponding *p*-methylbenzaldoxime derivative. Since *syn-o*-methylbenzaldoxime *p*-toluenesulfonate reacts 8.4 times faster than its para isomer, therefore the *syn*-2,4,6-trimethylbenzaldoxime derivative reacts 12 times faster than the corresponding *syn-o*-methylbenzaldoxime derivative.

A factor of 12 between the rate constants of the *syn*-2,4,6-trimethylbenzaldoxime derivative and the *syn-o*-methylbenzaldoxime derivative is not surprising because a single ortho group will still allow some resonance in a confirmation such as VIII, whereas two

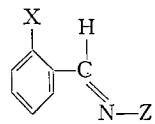

VIII

ortho substituents would remove this possibility and give rise to an even greater rate enhancement. Furthermore, the inductive effect of the two additional methyl groups in the trimethyl compound would also tend to increase the reaction rate relative to the *o*-methyl compound.

EXPERIMENTAL

A. Preparation of Materials

Aldehydes

The following substituted benzaldehydes were prepared in this laboratory. All the other aldehydes were obtained commercially.

o-Iodobenzaldehyde

The compound was prepared by the method of Sonn and Muller (11). *o*-Iodobenzanilide was converted to an imido chloride by reaction with phosphorus pentachloride, the imido chloride was reduced with stannous chloride, and the anil so formed was hydrolyzed to the aldehyde, m.p. 37°, in a yield of 50%. Reported m.p. 37° (12).

o-Methylbenzaldehyde

The compound was prepared by the Sonn and Muller method. *o*-Toluanilide was reacted with phosphorus pentachloride. Reduction of the imido chloride with anhydrous stannous chloride and dry hydrogen chloride in ether followed by acid hydrolysis and steam distillation gave the aldehyde, b.p. 94° at 16 mm, in a yield of 60%. Reported b.p. 90–93° at 16 mm (12).

o-Methylthiobenzaldehyde

The compound was prepared by essentially the method of Weygand and co-workers (13). A solution of thiosalicylic acid (58 g, 0.38 moles) and sodium hydroxide (32 g, 0.40 moles) in 200 ml of water was cooled

Can. J. Chem. Downloaded from www.nrcresearchpress.com by 210.87.254.105 on 09/05/12
For personal use only.

to 10°, and dimethyl sulfate (19 g, 0.20 moles) was added slowly with stirring. The mixture was refluxed for 3 h, cooled, and acidified with hydrochloric acid. The precipitate was filtered, washed with water, and recrystallized from hot water. The yield of *o*-methylthiobenzoic acid, m.p. 169–171°, was almost quantitative (reported 169–171°) (12).

A mixture of *o*-methylthiobenzoic acid (30 g, 0.18 moles) and thionyl chloride (30 g, 0.25 moles) was heated gently for 2 h, whereupon 80 ml of benzene was added. The mixture was cooled, and a solution of *N*-methylaniline (30 g, 0.28 moles) in 200 ml of benzene was added slowly with stirring. The mixture was then heated on a steam bath for 30 min, cooled, and washed with water, 5% hydrochloric acid, 5% sodium hydroxide, and water, respectively. The solution was dried and the solvent evaporated. The *N*-methyl *o*-methylthiobenzanilide was recrystallized from Skelly B. The yield was 42 g (91%) m.p. 103°.

Anal. Calcd. for $C_{15}H_{15}NOS$: C, 70.0; H, 5.84; N, 5.45. Found: C, 69.9; H, 5.98; N, 5.15.

A solution of the anilide (39 g, 0.15 moles) in 240 ml of redistilled tetrahydrofuran was cooled to 0° and lithium aluminium hydride (3.0 g, 0.08 moles) was added. The mixture was kept at 0° with stirring overnight, then 500 ml of 10% hydrochloric acid was added. The solvent was evaporated and the residue steam-distilled. The distillate was extracted with ether, the ethereal solution dried, the solvent removed, and the residue distilled under reduced pressure. *o*-Methylthiobenzaldehyde (13 g, 57%) b.p. 89–91° at 0.4 mm was isolated.

Anal. Calcd. for C_8H_8OS: C, 63.1; H, 5.26. Found: C, 63.2; H, 5.58.

Deuterated Aldehydes

The deuterated benzaldehydes were made by the same procedure as described for the synthesis of *o*-methylthiobenzaldehyde. Lithium aluminium deuteride reduction of the corresponding *N*-methyl benzanilides in tetrahydrofuran followed by acid hydrolysis and steam distillation gave rise to the isotopic compounds. They are characterized by the shift in the vibrational frequency of the C—H bond at 2 837 cm^{-1} to the C—D bond at 2 112 cm^{-1} in the infrared spectra in chloroform solution. Further, their n.m.r. spectra in carbon tetrachloride show that the deuterated isomers have no signal about τ 0.44 attributable to aldehydic C—H proton.

N-Methyl o-iodobenzanilide.—M.p. 69–71°, yield 84%. Anal. Calcd. for $C_{14}H_{12}INO$: C, 49.8; H, 3.56; N, 4.16. Found: C, 49.5; H, 3.82; N, 3.92.

o-Iodobenzaldehyde-d.—M.p. 37°, yield 21%.

N-Methyl o-chlorobenzanilide.—M.p. 55°, yield 92%. Anal. Calcd. for $C_{14}H_{12}ClNO$: C, 68.5; H, 4.89; N, 5.71. Found: C, 68.1; H, 4.88; N, 5.45.

o-Chlorobenzaldehyde-d.—B.p. 202°, yield 45%.

o-Methylthiobenzaldehyde.—B.p. 90–93° at 0.4 mm, yield 59%.

N-Methyl o-methoxybenzanilide.—M.p. 76–78°, yield 87%. Anal. Calcd. for $C_{15}H_{15}NO_2$: C, 74.6; H, 6.22; N, 5.81. Found: C, 74.8; H, 6.13; N, 5.71.

o-Methoxybenzaldehyde-d.—B.p. 196°, yield 34%.

Substituted Benzaldoximes

syn-Aldoximes

The substituted *syn*-benzaldoximes were prepared as described previously (1). Reaction of hydroxylamine hydrochloride with the aldehyde in dilute sodium hydroxide solution produces the *syn*-aldoximes in yields between 75 and 90%. The melting point of the *syn*-aldoximes together with that reported (12) are: *syn-o*-iodobenzaldoxime m.p. 110 (reported 107–108); *syn-o*-iodobenzaldoxime-*d* m.p. 108; *syn-p*-iodobenzaldoxime m.p. 123 (reported 122); *syn-o*-bromobenzaldoxime m.p. 103 (reported 102); *syn-p*-bromobenzaldoxime m.p. 110–111 (reported 110–111); *syn-o*-chlorobenzaldoxime m.p. 75 (reported 75–76); *syn-o*-chlorobenzaldoxime-*d* m.p. 74–75; *syn-o*-fluorobenzaldoxime m.p. 63 (reported 63); *syn-o*-methoxybenzaldoxime m.p. 93–95 (reported 92); *syn-o*-methoxybenzaldoxime-*d* m.p. 94–96; *syn-o*-methylthiobenzaldoxime m.p. 88–89.

Anal. Calcd. for C_8H_9NOS: C, 57.5; H, 5.39; N, 8.39. Found: C, 57.4; H, 5.37; N, 8.22;

syn-o-Methylthiobenzaldoxime-*d* m.p. 93; *syn-p*-methylthiobenzaldoxime m.p. 111 (reported 111); *syn-o*-methylbenzaldoxime m.p. 49 (reported 49); *syn*-2,4,6-trimethylbenzaldoxime m.p. 129 (reported 124).

anti-Aldoximes

The substituted *anti*-benzaldoximes were prepared as before (1). They were obtained by conversion of the corresponding *syn* isomers through the hydrochloride. The melting point together with that reported (12) are: *anti-p*-chlorobenzaldoxime m.p. 151 (reported 146); *anti-p*-methylbenzaldoxime m.p. 122–124 (reported 108–111); *anti-p*-methoxybenzaldoxime m.p. 132–133 (reported 133); *anti*-2,4,6-trimethylbenzaldoxime m.p. 179–180 (reported 178–180).

syn-Aldoxime Esters

The *syn*-aldoxime esters were prepared as described previously (1), by reacting the sodium salt of the aldoxime with the acid chloride in absolute ether. The aldoxime *p*-toluenesulfonates of *syn-p*-chloro-, *syn-p*-methoxy-, *syn-p*-fluoro-, and *syn*-benzaldoxime were the same samples used before (1). The data for the new esters are tabulated in Table VI.

Can. J. Chem. Downloaded from www.nrcresearchpress.com by 210.87.254.105 on 09/05/12
For personal use only.

Can. J. Chem. Downloaded from www.nrcresearchpress.com by 210.87.254.105 on 09/05/12
For personal use only.

TABLE VI

Summary of data for 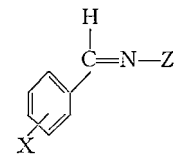

Substituent	M.p.* (°C)	Max. (mμ)	Molecular formula	Anal. Calcd. C	Anal. Calcd. H	Anal. Calcd. N	Anal. Found C	Anal. Found H	Anal. Found N
For Z = $O_3SC_7H_7$ (*p*-toluenesulfonate)									
o-I	81	257.5	$C_{14}H_{12}INO_3S$	41.9	3.01	3.49	42.0	3.24	3.25
o-I—D	79	255.5	$C_{14}H_{11}DINO_3S$						
p-I	109–110	271.0	$C_{14}H_{12}INO_3S$	41.9	3.01	3.49	42.0	3.37	3.26
o-Br	98–99	257.0	$C_{14}H_{12}BrNO_3S$	47.5	3.41	3.95	47.6	3.39	3.87
p-Br	106–107	263.0	$C_{14}H_{12}BrNO_3S$	47.5	3.41	3.95	47.7	3.65	3.86
o-Cl	100–101	256.5	$C_{14}H_{12}ClNO_3S$	53.3	3.90	4.52	54.0	3.88	4.71
o-Cl—D	101–102	254.5	$C_{14}H_{11}DClNO_3S$						
o-F	91–92	250.0	$C_{14}H_{12}FNO_3S$	57.3	4.12	4.78	57.5	4.19	4.61
o-OCH_3	90–91	257.0	$C_{15}H_{15}NO_4S$	59.0	4.91	4.59	58.7	4.82	4.30
o-OCH_3—D	88	255.0	$C_{15}H_{14}DNO_4S$						
o-CH_3	83–84	255.5	$C_{15}H_{15}NO_3S$	62.3	5.19	4.84	62.4	5.02	4.84
p-SCH_3	99–100	313.0	$C_{15}H_{15}NO_3S_2$	56.1	4.68	4.37	55.9	4.82	4.37
For Z = $O_2C_7H_4I$ (*o*-iodobenzoate)									
o-SCH_3	86–87	247.0	$C_{15}H_{12}INO_2S$	45.4	3.03	3.54	45.5	3.36	3.69
o-SCH_3—D	85–86	246.0	$C_{15}H_{11}DINO_2S$						
p-SCH_3	94–96	315.5	$C_{15}H_{12}INO_2S$	45.4	3.03	3.54	45.4	3.40	3.56
2,4,6-Trimethyl	105–107	271.0	$C_{17}H_{16}INO_2$	52.0	4.08	3.57	51.9	4.16	3.83

*Melted with decomposition.

B. Product Analysis

A mixture of the ester (0.50 g) and 10 ml of 95% ethanol was refluxed overnight. The solvent was evaporated at reduced pressure and 10 ml of 5% sodium hydroxide was added to the residue. The mixture was then extracted with 10 ml of ether and the ethereal solution washed with water, dried, and the solvent evaporated. The nitrile was recrystallized from Skelly B. Thus *o*-iodobenzonitrile, m.p. 53°, reported m.p. 54–55° (12), was obtained from *syn*-*o*-iodobenzaldoxime *p*-toluenesulfonate in 78% yield; *o*-chlorobenzonitrile, m.p. 43°, reported m.p. 42–43° (12), was isolated from *syn*-*o*-chlorobenzaldoxime *p*-toluenesulfonate in 83% yield; and 2,4,6-trimethylbenzonitrile, m.p. 55°, reported m.p. 55° (12), was obtained from *syn*-2,4,6-trimethylbenzaldoxime *o*-iodobenzoate in a yield of 80%.

C. Kinetic Measurements

Kinetic measurements were carried out as described in the previous paper (1). The reaction was studied by following the disappearance of the band at the wavelength of maximum absorption of the corresponding *syn*-aldoxime ester. The small absorption due to the products at this wavelength was corrected for in the rate equation.

REFERENCES

1. R. J. Crawford and C. Woo. Can. J. Chem. **43**, 1534 (1965).
2. K. von Auwers, M. Lechner, and H. Bundesmann. Ber. **58**, 36 (1925).
3. D. E. Pearson and W. E. Cole. J. Org. Chem. **20**, 488 (1955).
4. Y. Ogata, M. Ohuno, and K. Matsumoto. J. Am. Chem. Soc. **77**, 4643 (1955).
5. S. Winstein. Experientia, Suppl. II, 154 (1955).
6. G. J. Karabatsos, F. M. Vane, R. A. Taller, and N. Hsi. J. Am. Chem. Soc. **86**, 3351 (1964).
7. W. R. Benson and A. E. Pohland. J. Org. Chem. **30**, 1126 (1965). E. Lustig. J. Phys. Chem. **65**, 494 (1961).
8. H. L. Goering and J. F. Levy. J. Am. Chem. Soc. **84**, 3853 (1962).
9. D. Darwish and R. McLaren. Tetrahedron Letters, 1231 (1962).
10. S. G. Smith. Tetrahedron Letters, 979 (1962).
11. A. Sonn and E. Muller. Ber. **52**, 1927 (1917).
12. I. Heilbron and H. M. Bunbury. Dictionary of organic compounds. Eyre and Spottiswoode Ltd., London. 1953.
13. F. Weygand, G. Eberhardt, H. Linden, F. Schafter, and L. Eigen. Angew. Chem. **65**, 525 (1953).

Can. J. Chem. Downloaded from www.nrcresearchpress.com by 210.87.254.105 on 09/05/12
For personal use only.

Can. J. Chem. Downloaded from www.nrcresearchpress.com by 210.87.254.6 on 09/05/12
For personal use only.

A LINEAR CORRELATION OF PROTON CHEMICAL SHIFTS IN SOME ALKYL CHLORIDES AND HYDROCARBONS WITH THE OCCUPATION NUMBER OF THE HYDROGEN ORBITALS

F. HRUSKA,[1] G. KOTOWYCZ,[1] AND T. SCHAEFER[2]
Department of Chemistry, University of Manitoba, Winnipeg, Manitoba
Received July 16, 1965

ABSTRACT

A linear correlation exists between the proton shifts of some alkyl chlorides and some hydrocarbons and the occupation numbers of the hydrogen 1s orbitals in the C—H bonds. The occupation numbers are those given by the self-consistent group orbital and bond electronegativity method. The application of this correlation to the prediction of starting values for occupation numbers, to the derivation of bond anisotropies in ethylene and acetylene, and to the prediction of hydrogen-bonded shifts of C—H protons is discussed.

INTRODUCTION

It was originally hoped that the proton chemical shift in a molecule would be a direct measure of the electron density at the hydrogen atom. The paramagnetic term in Ramsey's equation (1), evaluated for electrons centered on the proton, is small because of the large electronic excitation energies for hydrogen, leaving the diamagnetic term to represent the effect of the electron density on the chemical shift. Experimentally, the protons in methyl compounds are indeed less shielded as the electronegativity of the substituent increases (2) and some success has been obtained in relating proton shifts in aromatic systems to π-electron densities on bonded carbon atoms (3; 4 and references therein).

However, there are many discrepancies in correlations of this sort (2; 4 and references therein) and they have been variously attributed to the magnetic anisotropies of neighboring bonds or atoms (5, 6), to electric fields arising from bond dipoles (7), to reaction fields from the solvent (8), and to intramolecular dispersion interactions (9).

Conversely, some attempts have been made to derive the anisotropies of bonds and substituents from the experimental shifts (10–13). One method is to use the coupling constant and the proton shift in the ^{13}C—H bond to determine irregularities in the shifts, which are then attributed to anisotropy effects (10). The underlying assumption that the ^{13}C—H coupling constant is a direct measure of the s-character of the bonding carbon orbital (14) has been questioned (15).

Recently, the self-consistent group orbital and bond electronegativity method has been employed to calculate the orbital charge distributions in some hydrocarbons and aliphatic chlorides (16). This method defines an effective occupation number, designated charge, of an atomic orbital. In particular, the occupation number or charge of the hydrogen 1s orbitals is given (16). In this paper we note a linear correlation between the proton shifts and the occupation numbers of the hydrogen orbitals and discuss briefly its application to some current topics in proton resonance. A linear correlation between the charge on the carbon atom and the ^{13}C shift in the chloromethanes has already been pointed out (16).

[1]*Holder of a N.R.C. Studentship, 1964–1965.*
[2]*N.R.C. Senior Research Fellow, 1964–1965.*

Can. J. Chem. Downloaded from www.nrcresearchpress.com by 210.87.254.6 on 09/05/12
For personal use only.

DISCUSSION

1. General

In Table I the occupation numbers, n, of the hydrogen orbitals in a number of hydrocarbons and aliphatic chlorides are presented, as are the proton shifts relative to internal tetramethylsilane for 5% solutions in carbon tetrachloride and cyclohexane. In a few cases the solvent was chloroform or tetramethylsilane. Ideally, the proton shifts in the gas phase are required to eliminate solvent effects (8) but these are not available for most of the compounds in Table I. The most extensive data are for carbon tetrachloride solutions although cyclohexane is preferable as a solvent.

2. Correlation of Proton Shift and Occupation Number

In Fig. 1 the proton shifts in carbon tetrachloride are plotted versus n. For the alkyl chlorides there is a linear correlation and the shielding decreases with the occupation number of the hydrogen 1s orbital. The proportionality constant is 46 ± 1 p.p.m. per electron, as compared to 27 p.p.m. calculated for the shielding in the hydrogen molecule (17). In the alkyl chlorides the hydrogen orbital is probably much less diffuse and this would lead to a higher value for the proportionality constant. However, the matter may be more complex.

TABLE I

Hydrogen orbital occupation numbers and proton shifts for some hydrocarbons and alkyl chlorides

Compound*	n†	Chemical shift in: CCl_4‡	Chemical shift in: C_6H_{12}‡	Hydrogen bond shift‡ at 27 °C
CH_3Cl	0.936	186	172	—
CH_2Cl_2	0.888	318	309	—
$CHCl_3$	0.843	436	426	516
CH_3CH_2Cl	0.968	90	83	—
$CH_3\mathit{CH}_2Cl$	0.926	211	205	—
$CH_3\mathit{CH}Cl_2$	0.890	352	346	—
CH_3CHCl_2	0.955	134	118	—
CH_2ClCH_2Cl	0.923	222	215	—
CH_3CCl_3	0.943	165	158	—
$\mathit{CH}_2ClCHCl_2$	—	236	229	262
$CH_2Cl\mathit{CH}Cl_2$	—	344	337	409
CH_2ClCCl_3	—	257	250	—
$CHCl_2CHCl_2$	0.870	356	347	416
$CHCl_2CCl_3$	—	367	359	—
CH_4	0.985	—	15§	—
$\mathit{CH}_3CH_2CH_3$	0.981	55‖	—	—
$(CH_3)_4C$	0.980	56¶	—	—
C_2H_2	0.881	110**	96††	—
C_2H_4	0.931	320**	318‡‡	—

*Protons in question are italicized.
†Occupation numbers are from ref. 16.
‡Chemical shift is in c/s at 60 Mc/s to low field from internal tetramethylsilane; ref. 20.
§Tetramethylsilane solvent; ref. 18.
‖$CDCl_3$ solvent; ref. 22.
¶Reference 23.
**Reference 24.
††Tetramethylsilane solvent; ref. 19.
‡‡Reference 10.

The shifts of the methyl protons in propane and neopentane also fall very near the correlation line in Fig. 1. Reliable data for methane and ethane are not yet available but it would appear that the former deviates considerably from this line. In the absence of further data on occupation numbers and (or) proton shifts we postpone to a later paper the question of separate correlation lines for various classes of compounds (but see below).

In Fig. 2, the proton shifts in cyclohexane are plotted versus n. Again a linear correlation is noted for the alkyl chlorides. The slope of the line is nearly the same as that in Fig. 1, but is slightly displaced to high field. Here the methane shift (measured in tetramethylsilane) deviates strongly to high field from the extended correlation line. If the correlation line held it would indicate $n = 0.996$ for the hydrogen orbital in methane and $n = 1.002$ for the hydrogen orbital in tetramethylsilane.

3. Application of the Linear Correlation

(a) Prediction of n from Proton Shift

For three chlorinated ethanes in Table I the occupation numbers are not yet calculated but they can be obtained from Figs. 1 and 2. The predicted n values from the two plots agree to within 0.001 units and are $n(CHCl_2—CH_2Cl) = 0.916$; $n(CHCl_2CH_2Cl) = 0.876$; $n(CCl_3CH_2Cl) = 0.909$; $n(CCl_3CHCl_2) = 0.868$. The calculation of charge distributions (16) begins with a chemically reasonable value of n for one of the orbitals and then

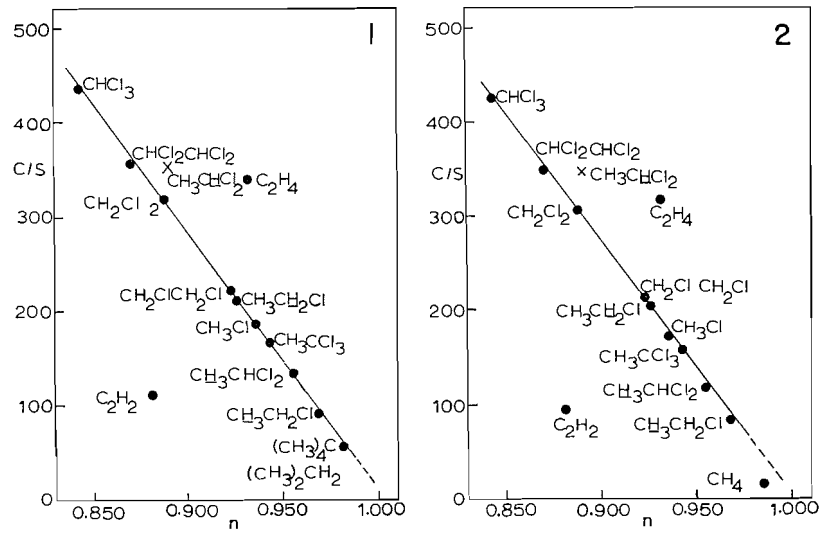

FIG. 1. The proton shifts in c/s at 60 Mc/s of some alkyl chlorides and hydrocarbons in carbon tetrachloride solution are plotted versus the occupation number of the hydrogen 1s orbital. The point marked as a cross is discussed in the text.

FIG. 2. As in Fig. 1 with cyclohexane as solvent.

iterates to a self-consistent charge distribution. The proton shift would seem to present a reasonable value for n and also serves as a check on the calculation. As an example, the proton shift of the methane proton in 1,1-dichloroethane indicates $n = 0.871$ instead of the calculated $n = 0.890$. The latter is marked as a cross in Figs. 1 and 2 and is the only 1 out of 10 that deviates significantly from the correlation line.

(b) Estimates of Bond Anisotropies

In view of the considerable anisotropies attributed to the C—C and C—Cl bonds in the literature (12, 18) the linear correlation in Figs. 1 and 2 is perhaps unexpected, unless they happen to be equivalent to C—H bonds in this respect. Whatever the explanation of this apparent contradiction, it is instructive to consider the ethylene and acetylene proton shifts. On the assumption that the deviations of these shifts from the lines in Figs. 1 and 2 are a measure of the anisotropy contribution of the double and triple bonds, one

Can. J. Chem. Downloaded from www.nrcresearchpress.com by 210.87.254.6 on 09/05/12
For personal use only.

calculates $\Delta\chi = 3.8$ p.p.m. for acetylene and $\Delta\chi = -2.1$ p.p.m. for ethylene. These contributions are of the right sign and compare with $\Delta\chi = 4.0 \pm 0.5$ p.p.m. for acetylene derived by the method discussed in the introduction (19). The ratio of the $\Delta\chi$ values for the two compounds is -1.9, in rough agreement with that calculated from molecular orbital theory (5).

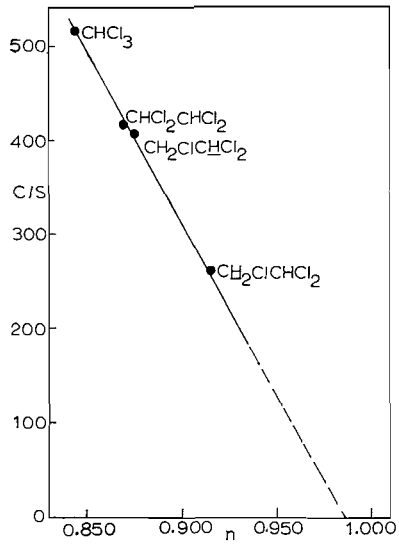

FIG. 3. The hydrogen-bonded shifts of four alkyl chlorides in dimethylsulfoxide are plotted versus the occupation number of the hydrogen 1s orbital.

(c) Hydrogen Bond Shifts

As n decreases the C—H bond becomes more polar and is expected to hydrogen bond more strongly with a proton acceptor. In Fig. 3 the four known hydrogen-bonded proton shifts (20) in dimethyl sulfoxide are plotted versus the occupation number of the hydrogen orbital in the C—H bond. The shifts were obtained by the method of Huggins, Pimentel, and Shoolery (21). There appears to be a linear correlation for this restricted number of values. For two of the points in Fig. 3 the n values were obtained from the plots in Figs. 1 and 2. The extended correlation line predicts a zero hydrogen-bonded shift for methane and this suggests that correlations of this sort will be useful in hydrogen bond studies by proton resonance.

CONCLUSIONS

The linear correlation between the proton shift in alkyl chlorides and some saturated hydrocarbons and the occupation number of the hydrogen orbital in C—H bond suggests its application in predicting starting values for occupation numbers in the iterative process for the calculation of charge distributions in molecules; in deriving bond anisotropies in some cases while, at the same time, casting doubt on some current values for others; and in predicting hydrogen-bonded shifts in equilibrium studies by proton magnetic resonance. There is a need for further data on both shifts and occupation numbers and such data are being gathered.

ACKNOWLEDGMENTS

We are grateful to the National Research Council for financial support. T. S. thanks members of the Basic Physics Division, National Physical Laboratory, Leddington, England, for their hospitality.

Can. J. Chem. Downloaded from www.nrcresearchpress.com by 210.87.254.6 on 09/05/12
For personal use only.

REFERENCES

1. N. F. RAMSEY. Phys. Rev. **78**, 699 (1950); **86**, 243 (1952); **91**, 303 (1953).
2. H. SPIESECKE and W. G. SCHNEIDER. J. Chem. Phys. **35**, 722 (1961).
3. T. SCHAEFER and W. G. SCHNEIDER. Can. J. Chem. **41**, 966 (1963).
4. A. H. GAWER and B. P. DAILEY. J. Chem. Phys. **42**, 2658 (1965).
5. J. A. POPLE. J. Chem. Phys. **37**, 53, 60 (1962).
6. H. M. MCCONNELL. J. Chem. Phys. **27**, 226 (1957).
7. A. D. BUCKINGHAM. Can. J. Chem. **38**, 300 (1960).
8. A. D. BUCKINGHAM, T. SCHAEFER, and W. G. SCHNEIDER. J. Chem. Phys. **32**, 1227 (1960).
9. T. SCHAEFER, W. F. REYNOLDS, and T. YONEMOTO. Can. J. Chem. **41**, 2969 (1963).
10. J. H. GOLDSTEIN and G. S. REDDY. J. Chem. Phys. **36**, 2644 (1962).
11. A. A. BOTHNER-BY and C. NAAR-COLIN. Ann. N. Y. Acad. Sci. **70**, 833 (1958).
12. J. I. MUSHER. J. Chem. Phys. **35**, 1159 (1961).
13. A. G. MORITZ and N. SHEPPARD. Mol. Phys. **5**, 361 (1962).
14. C. JUAN and H. S. GUTOWSKY. J. Chem. Phys. **37**, 2198 (1962).
15. W. J. CONSIDINE. J. Chem. Phys. **42**, 1130 (1965).
16. M. A. WHITEHEAD, N. C. BAIRD, and M. KAPLANSKY. Theoret. Chim. Acta, **3**, 135 (1965).
17. G. F. NEWELL. Phys. Rev. **80**, 476 (1950).
18. G. S. REDDY and J. H. GOLDSTEIN. J. Chem. Phys. **38**, 2736 (1963).
19. G. S. REDDY and J. H. GOLDSTEIN. J. Chem. Phys. **39**, 3509 (1963).
20. A. L. MCCLELLAN and S. W. NICKSIC. J. Phys. Chem. **69**, 446 (1965).
21. C. M. HUGGINS, G. C. PIMENTEL, and J. N. SHOOLERY. J. Chem. Phys. **23**, 1244 (1955).
22. R. C. FERGUSON and D. W. MARQUARDT. J. Chem. Phys. **41**, 2087 (1964).
23. G. VAN DYKE TIERS. Characteristic nuclear magnetic resonance shielding values. Minnesota Mining and Manufacturing Company. Project 737602. March 28, 1958.
24. R. M. LYNDEN-BELL and N. SHEPPARD. Proc. Roy. Soc. London, Ser. A, **269**, 385 (1962).

Can. J. Chem. Downloaded from www.nrcresearchpress.com by 210.87.254.6 on 09/05/12
For personal use only.

Can. J. Chem. Downloaded from www.nrcresearchpress.com by 210.87.254.6 on 09/05/12
For personal use only.

VIBRATIONAL SPECTRA OF SOME ALKYLARSONIUM COMPOUNDS

W. R. CULLEN
Chemistry Department, University of British Columbia, Vancouver, British Columbia
G. B. DEACON
William Ramsay and Ralph Forster Laboratories, University College, London, England
AND
J. H. S. GREEN
Chemical Standards Division, National Physical Laboratory, Teddington, Middlesex, England
Received June 15, 1965

ABSTRACT

The infrared spectra of some tetramethyl-, tetraethyl-, and triethylmethyl-arsonium salts, and that of tetramethylstibonium triiodomercurate(II) have been recorded in the region 4 000 to 200 cm^{-1}. Vibrational assignments are given for the quarternary 'onium cations, and comparisons are made with the spectra of alkylorganometallic compounds of germanium and tin.

The Raman spectra of aqueous solutions of tetramethylarsonium chloride and of tetramethylstibonium chloride have been measured and assigned (1), but infrared data on these and other alkylarsonium salts are lacking. In the present work, the infrared spectra of a number of tetramethyl-, tetraethyl-, and triethylmethyl-arsonium salts, and of tetramethylstibonium triiodomercurate(II) have been recorded in the range 4 000 to 200 cm^{-1} and assignments made for the fundamental frequencies.

RESULTS AND DISCUSSION

Tetramethylarsonium and Tetramethylstibonium Salts

The observed frequencies are given in Table I, together with the present assignments and the reported Raman frequencies (1). The fundamentals are numbered as by Shimizu and Murata (2). The 45 fundamentals of a tetrahedral $(CH_3)_4M$ molecule comprise $3a_1 + 4e + 7f_2 + a_2 + 4f_1$, the last two species being Raman and infrared inactive. All the remaining modes are Raman active, the a_1 class being polarized, but only the f_2 modes are infrared active. The active fundamental frequencies are compared with these of the isoelectronic group IV molecules in Table II. The frequencies of the infrared active modes of $(CH_3)_4As^+$ listed in Table II are average values for the compounds in Table I: where the observed bands are split, either the value of the most intense component or that of the band center has been used in averaging.

The results are in general accord with the expected tetrahedral symmetry of the 'onium cations, although the a_1 methyl symmetric deformation is observed as a weak or very weak band in the infrared spectra of two arsonium salts, and the a_1 skeletal stretch as a very weak absorption for the stibonium salt. As with the group IV tetramethyls (4), the position of the e methyl rocking mode (ν_6) cannot be located with certainty. Although there are weak Raman lines available as possibilities, it seems most likely that ν_6 is coincident with ν_{13}. The e and f_2 skeletal deformation modes are probably close together but not coincident, the latter being at higher frequencies than the former, as with $(CH_3)_4Ge$ and $(CH_3)_4Sn$ (3, 4). The infrared active mode is not observed above 220 cm^{-1},

Can. J. Chem. Downloaded from www.nrcresearchpress.com by 210.87.254.6 on 09/05/12
For personal use only.

TABLE I

Vibrational frequencies and assignments for tetramethylarsonium and tetramethylstibonium compounds*

Compounds						Assignments	
Me_4AsI (Infrared)	Me_4AsI_3 (Infrared)	Me_4AsHgI_3 (Infrared)	Me_4AsCl (Raman)	Me_4SbHgI_3 (Infrared)	Me_4SbCl (Raman)	Description	Mode (class)
			3 022 (5*b*)		3 028 (3*sb*)	ν(CH) asym.	ν_4 (e)
2 986 m	3 000 w	3 002 w		3 005 vw		"	ν_8 (f_2)
			2 935 (6*b*)		2 936 (4)	ν(CH) sym.	ν_1 (a_1)
2 908 m	2 915 w	2 917 vw		2 914 vw		"	ν_9 (f_2)
1 426 m	1 414 m, br 1 403 sh	1 416 m 1 404 w	1 418 (3*b*)	1 401 w, br	1 414 (4*b*)	CH_3 asym. def.	ν_5 (e) + ν_{10} (f_2)
				1 359 vw			
	1 298 w 1 287 w	1 303 vw 1 291 vw	1 304 (1*b*)	1 247 vw 1 242 sh	1 247 (4*b*)	CH_3 sym. def.	ν_2 (a_1)
1 270 1 265 m	1 273 w	1 274 w	1 275 (1*b*)	1 227 sh 1 218 vw	1 228 (4*b*)	"	ν_{11} (f_2)
				1 168 vw			
				1 090 vw			
			1 036 (00)		1 009 (1?)		
946 s 941 sh 937 s 931 sh 923 s	924 s, br	919 s, br	929 (0)	865 s, br	873 (0*b*)	CH_3 rock	ν_{13} (f_2)
			876 (0?)		851 (0*b*)		
657 651 m 647	649 m	652 m	652 (8*b*)	572 s	574 (8*b*)	ν(C—M)† asym.	ν_{12} (f_2)
			590 (10)	529 vw	535 (10*b*)	" sym.	ν_3 (a_1)
			217 (6*sb*)		178 (6*sb*)	δ(CMC) asym.	ν_{14} (f_2)

*Intensities (infrared spectra): s, strong, m, medium; w, weak; br, broad; v, very, sh, shoulder. Raman intensities and frequencies: ref. 1.
†M is As or Sb.

TABLE II

Fundamental frequencies of tetramethylarsonium and tetramethylstibonium ions and of tetramethylgermane and tetramethyltin

Class	Mode (description)	Me_4As^+	Me_4Ge*	Me_4Sb^+	Me_4Sn†
a_1	$\nu_1(\nu(CH)$ sym.)	2 935	2 907	2 936	2 912
	$\nu_2(\delta(CH_3)$ sym.)	1 304	1 247	1 247	1 205
	$\nu_3(\nu(C—M)$ sym.)	590	558	535	507
e	$\nu_4(\nu(CH)$ asym.)	3 022	2 978	3 028	2 988
	$\nu_5(\delta(CH_3)$ asym.)	1 418	1 400	1 414	1 400
	$\nu_6(CH_3$ rock)	927	825	865	772
	$\nu_7(\delta(CMC)$ sym.)	(217)	175	(178)	145
f_2	$\nu_8(\nu(CH)$ asym.)	2 996	2 981	3 005	3 000
	$\nu_9(\nu(CH)$ sym.)	2 913	2 920	2 914	2 920
	$\nu_{10}(\delta(CH_3)$ asym.)	1 418	1 435 1 428	1 401	1 443
	$\nu_{11}(\delta(CH_3)$ sym.)	1 272	1 240	1 218	1 198
	$\nu_{12}(\nu(C—M$ asym.)	651	602	572	530
	$\nu_{13}(CH_3$ rock)	927	828	865	770
	$\nu_{14}(\delta(CMC)$ asym.)	217	195	178	160

NOTE: M is As, Ge, Sb, or Sn.
*Reference 3.
†References 3, 4.

and, owing to the rising background absorption, no band could be established in the spectra of the arsonium compounds between 220 and 200 cm^{-1}. Probably the Raman lines of $(CH_3)_4AsCl$ and $(CH_3)_4SbCl$ at 217 and 178 cm^{-1}, respectively, are due to the f_2 mode.

The spectra of the two isoelectronic pairs $(CH_3)_4As^+$ and $(CH_3)_4Ge$, and $(CH_3)_4Sb^+$ and $(CH_3)_4Sn$ may be compared with those of trimethylarsine and trimethylstibine respectively. For trimethylarsine, the Raman data (5) have been assigned and the carbon–arsenic stretching frequencies are at 572 (a_1) and 584 cm^{-1} (e). (These are both infrared active and have apparently been observed, but the values for the frequenices are not given (6).) The CH_3 rocking modes are probably both very close to the Raman line at 884 cm^{-1}; the infrared values are not available. The methyl symmetric and antisymmetric deformation modes are at 1 263 (a_1), 1 242 (e), and 1 417 cm^{-1} (a_1 and e) respectively. For trimethylstibine both Raman (7) and infrared data (8) are available, and we assign the carbon–antimony stretch to 510 cm^{-1} (a_1 and e), CH_3 rocking to the strong infrared band at 813 cm^{-1}, the CH_3 symmetric deformations to 1 210 (a_1) and 1 193 (e), and the antisymmetric deformations to 1 380 cm^{-1} (a_1 and e). (An assignment (9) of the carbon–antimony stretch to 591 cm^{-1} must be in error, since there is no absorption band in that region (8).) Assignments for these modes have also been given (9) for trimethylantimony dihalides.

From these facts and the data in Table II, it follows that the carbon–metal stretching frequencies increase $(CH_3)_4Ge \sim (CH_3)_3As < (CH_3)_4As^+$ and $(CH_3)_4Sn \sim (CH_3)_3Sb < (CH_3)_4Sb^+$. The carbon–metal stretching force constants are approximately the same (1) for the first two compounds of each series. Evidently the charge on or higher oxidation state of the group V atoms in the ions gives stronger carbon–metal bonding. The methyl rocking frequencies (and therefore probably the H—C—M deformation force constant (1)) increase along each series. The changes in the methyl deformation frequencies are smaller, but certainly for the symmetric frequencies $(CH_3)_4Ge \sim (CH_3)_3As < (CH_3)_4As^+$ and $(CH_3)_4Sn \sim (CH_3)_3Sb < (CH_3)_4Sb^+$. The f_2 antisymmetric deformation is significantly higher for the group IV compounds than for the corresponding group V ions

Can. J. Chem. Downloaded from www.nrcresearchpress.com by 210.87.254.6 on 09/05/12
For personal use only.

and the *e* mode slightly lower; calculations (1) based on Raman data alone suggests the H—C—H deformation force constant is lower for the ions. The stronger carbon–metal bonding in the 'onium cations leads to stronger carbon–hydrogen bonding in the ions than in the corresponding group IV compounds. This is shown by the frequencies of the C—H stretching modes and, further, a calculation of the C—H stretching force constants from the data of Table I gives values 2–3% higher for $(CH_3)_4As^+$ and $(CH_3)_4Sb^+$ than those (1) for the corresponding group IV compounds.

Tetraethylarsonium Salts

The observed frequencies and assignments are shown in Table III together with those for the isoelectronic tetraethylgermane, assigned by one of us (10) from the literature data (11). Assignments for the ethyl group frequencies are based on those (12) for several ethyl compounds, and only a few points require comment.

The spectra are consistent with tetrahedral symmetry of the C_4As skeleton, although the a_1 skeletal stretching mode appears very weakly for one salt. The position of the C—C—As skeletal bending mode is clear since there is no corresponding absorption in the spectra of the tetramethyl compounds. The CH_2 twisting mode is assigned to the bands at 1 169 to 1 177 cm^{-1}, which are not readily explained as overtone or combination bands. In tetraethylgermane such alternatives do exist, as indicated in Table III, and there are observed Raman lines at 1 299 and 1 328 cm^{-1} which have no ready alternative explanation and may be due to the CH_2 twisting vibration. However, calculations place this at a lower frequency than the wagging mode (12, 13), the position of which is clear. The methylene wagging and rocking modes of the arsonium compounds are at higher frequencies than in tetraethylgermane, paralleling the methyl rocking modes of the corresponding tetramethyl compounds, and probably again reflect a greater H—C—M bending force constant in the cation.

The basis for assignments of the carbon–hydrogen stretching frequencies to methylene and methyl groups is provided by considerations of the spectra of tetraethylmethane, tetraethylsilane, and related compounds (10, 14). For the present molecules it shows that while the methyl frequencies are almost unchanged from those of *n*-butane (2 878 (sym.) and 2 939, 2 956 cm^{-1} (asym.)), the methylene frequencies are markedly higher than those in *n*-butane (2 861 (sym.) and 2 910 cm^{-1} (asym.), Raman values throughout). Again the ν(C—M) frequencies are higher in the arsonium compounds than in tetraethylgermane, reflecting stronger carbon–metal bonding in the cation. Further, the carbon–hydrogen stretching frequencies suggest that the stronger carbon–metal bonding in the cation may again lead to stronger carbon–hydrogen bonding in the cation.

Triethylmethylarsonium Salts

The observed frequencies and assignments are given in Table IV together with the data (11) and assignments (10) for triethylmethylgermane. The skeletal symmetry is effectively C_{3v} with the carbon-metal stretching modes comprising $2a_1 + e$ modes, all infrared active, though the a_1 mode derived from the a_1 mode of $(C_2H_5)_4M$ may be weak. The results are in agreement with this. The $\nu(CH_3—As)$ frequency corresponds closely to $\nu(CH_3—As)$ asym. of $(CH_3)_4As^+$, and all carbon–arsenic stretching frequencies are higher than the corresponding carbon–germanium frequencies.

Additional absorptions in the triethylmethylarsonium salts, compared with the tetraethylarsonium salts, are clear at ca. 880 cm^{-1}, ca. 1 290 cm^{-1}, and ca. 3 000 cm^{-1}, and, from the data for $(CH_3)_4As^+$, must be methyl rocking, methyl symmetric deformation, and ν(CH) asym. modes of Me(—As), respectively. (In triethymethylgermane the

Can. J. Chem. Downloaded from www.nrcresearchpress.com by 210.87.254.6 on 09/05/12
For personal use only.

TABLE III

Vibrational frequencies and assignments for tetraethylarsonium salts and tetraethylgermane

Et_4AsI (Infrared)	$[Et_4As]_2HgI_4$ (Infrared)	Et_4Ge Infrared	Et_4Ge Raman	Assignment
2 967 s	2 970 s	2 954 vs	2 954 (8)	ν(CH) asym. of CH_2
2 944 s	2 955 s, 2 935 s		2 930 (7)	ν(CH) asym. of CH_3
2 917 s	2 922 s	2 910 vs	2 905 (10)	ν(CH) sym. of CH_2
2 882 s	2 877 s	2 876 s	2 874 (9)	ν(CH) sym. of CH_3
1 465 s, br, 1 455 sh	1 462 s, 1 449 s	1 461 m	1 463 (7)	CH_3 asym. def.
1 417 s	1 403 s	1 426 m	1 430 (3)	CH_2 bending
1 392 s	1 389 s	1 378 m	1 381 (2)	CH_3 sym. def.
			1 328 (2)	
			1 299 (1)	
1 279 sh, 1 257 s, br	1 253 m, br	1 234 m	1 223 (8)	CH_2 wag
1 171 vw	1 177 vw, 1 169 vw			CH_2 twist
1 155 vw	1 155 vw			612+548=1160
			1 138 (1*b*), 1 104 (1)	CH_2 twist or $2\times572=1144$, $572+532=1104$
1 047 s, 1 033 s	1 049 sh, 1 042 m, 1 031 sh	1 019 m	1 025 (3*b*)	CH_3 rock
982 m	978 w	968 m	976 (5)	ν(C—C)
756 s, br, 740 sh, 726 sh	742 s, br, 724 sh	700 s		CH_2 rock
613 m	611 m	575 s	572 (8*b*)	ν(C—M) (f_2)
548 vw			532 (10)	ν(C—M) (a_1)
349 m, 327 vw, 312 vw			332 (1*b*)	δ(CCM)
			286 (4*b*), 252 (0)	C_2H_5 torsions
			153 (3*b*)	δ(CGeC)

Raman line at 1 239 cm^{-1} appears additionally compared with $(C_2H_5)_4Ge$ and the infrared absorption at this frequency is evidently slightly stronger in the former than in the latter compound, so that CH_2 wagging and CH_3(—Ge) symmetric deformation modes are probably virtually coincident.) The assignments for the carbon–hydrogen stretching modes are based on those for $(CH_3)_4As^+$ and $(C_2H_5)_4As^+$ and are consistent with them; again the evidence indicates stronger C—H bonding in the arsonium compounds than in the germanium derivative.

EXPERIMENTAL

The compounds investigated were obtained during previous studies (15–19) of the reactions of arsines and related compounds, and the preparations have been reported as follows: $(CH_3)_4AsI$ (15), $(CH_3)_4AsI_3$ (16), $(CH_3)_4AsHgI_3$ (17), $(CH_3)_4SbHgI_3$ (18), $(C_2H_5)_4AsI$ (17), $[(C_2H_5)_4As]_2HgI_4$ (17), $(C_2H_5)_3CH_3AsI$ (19), $(C_2H_5)_3CH_3AsHgI_3$ (19), and $[(C_2H_5)_3CH_3As]_2HgI_4$ (19).

Infrared Spectra

The compounds were examined as mulls (Nujol and hexachlorobutadiene) or in KCl discs, using Unicam SP100/130 and Grubb-Parsons DM2 instruments for 4 000 to 400 cm^{-1} and 400 to 200 cm^{-1} respectively. Some compounds were examined both as mulls and discs, and good agreement was observed, though the disc spectra sometimes showed more splitting.

ACKNOWLEDGMENT

One of us (G. B. D.) thanks Imperial Chemical Industries Limited for a Fellowship.

Can. J. Chem. Downloaded from www.nrcresearchpress.com by 210.87.254.6 on 09/05/12
For personal use only.

Can. J. Chem. Downloaded from www.nrcresearchpress.com by 210.87.254.6 on 09/05/12
For personal use only.

TABLE IV

Vibrational frequencies and assignments for triethylmethylarsonium salts and triethylmethylgermane

Et_3MeAsI (Infrared)	$Et_3MeAsHgI_3$ (Infrared)	$[Et_3MeAs]_2HgI_4$ (Infrared)	Et_3MeGe		Assignments
			Infrared	Raman	
	3 004 vw	2 994 m		2 975 (2)	ν(CH) asym. of $CH_3(-M)$
2 976 m	2 975 sh 2 967 w	2 977 sh 2 962 m	2 958 vs	2 951 (8)	ν(CH) asym. of CH_2
2 944 m	2 955 sh 2 935 w	2 955 m 2 935 m		2 928 (2)	ν(CH) asym. of $CH_3(-C)$
2 907 sh 2 900 w	2 920 w 2 907 sh	2 922 m 2 912 sh	2 901 vs	2 906 (10)	ν(CH) sym. of CH_2 + ν(CH) sym. of $CH_3(-M)$
2 880 w	2 877 vw	2 875 m	2 872 s	2 875 (7)	ν(CH) sym. of $CH_3(-C)$
1 464 sh 1 451 m	1 457 m 1 449 sh	1 462 m 1 448 m 1 443 m	1 460 m	1 460 (4*b*)	CH_3(—C) asym. def.
1 419 m	1 413 m	1 409 m	1 420 m	1 427 (3)	CH_2 bending + CH_3(—M) asym. def.
1 389 m	1 388 m	1 387 m	1 378 m	1 382 (1*b*)	CH_3(—C) sym. def.
				1 325 (0)	
1 291 w	1 291 vw	1 289 w			CH_3(—As) sym. def.
		1 259 m			
1 245 m, br	1 246 m 1 235 m	1 255 m 1 243 sh 1 234 sh	1 239 m	1 239 (2) 1 222 (5)	CH_2 wag + CH_3(—Ge) sym. def.
1 165 vw, br	1 169 vw, br	1 172 vw 1 164 vw		1 164 (0)	CH_2 twist + (or) 612+556=1168 (As), 592+573=1165 (Ge)

Can. J. Chem. Downloaded from www.nrcresearchpress.com by 210.87.254.6 on 09/05/12
For personal use only.

TABLE IV (*Concluded*)

Et_3MeAsI (Infrared)	$Et_3MeAsHgI_3$ (Infrared)	$[Et_3MeAs]_2HgI_4$ (Infrared)	Et_3MeGe Infrared	Et_3MeGe Raman	Assignments
1 043 sh 1 029 1 024 s, br 1 017	1 049 sh 1 044 vw 1 021 m 1 016 m	1 051 m 1 044 m 1 018 m 1 008 m	1 020 s	1 020 (3*b*)	CH_3(—C) rock
999 sh 987 sh	988 vw, br 977 vw, br	983 m	965 m	973 (3)	ν(C—C)
894 s, br	879 sh 873 m	880 s			CH_3(—As) rock
			852 w 783 s		CH_3(—Ge) rock
756 s 745 sh 726 sh	738 s	741 s 730 sh 708 s	705 s		CH_2 rock
			675 w		
641 m	642 m	636 m	593 s	592 (8)	$\nu(CH_3—M)$ (a_1)
611 m	616 m 606 w	610 m	580 vs	573 (8)	$\nu(C_2H_5—M)$ (e)
558 vw	558 vw	552 vw		536 (10)	$\nu(C_2H_5—M)$ (a_1)
342 s 306 m		335 m 332 sh 300 w		319 (0)	δ(CCM)
				287 (2*b*) 263 (1)	C_2H_5 torsions
				174 (3*b*)	δ(CGeC)

REFERENCES

1. H. SIEBERT. Z. Anorg. Allgem. Chem. **273**, 161, 170 (1953).
2. K. SHIMIZU and H. MURATA. Bull. Chem. Soc. Japan, **30**, 487 (1957).
3. E. R. LIPPINCOTT and M. C. TOBIN. J. Am. Chem. Soc. **75**, 4141 (1953).
4. W. F. EDGELL and C. H. WARD. J. Am. Chem. Soc. **77**, 6486 (1955).
5. E. J. ROSENBAUM, D. J. RUBIN, and C. R. SANDBERG. J. Chem. Phys. **8**, 366 (1940).
6. R. A. ZINGARO, R. E. MCGLOTHIN, and R. M. HEDGES. Trans. Faraday Soc. **59**, 798 (1963).
7. E. J. ROSENBAUM and T. A. ASHFORD. J. Chem. Phys. **7**, 554 (1939).
8. F. OSWALD. Z. Anal. Chem. **197**, 309 (1963).
9. G. G. LONG, G. O. DOAK, and L. D. FREEDMAN. J. Am. Chem. Soc. **86**, 209 (1964).
10. J. H. S. GREEN. In press.
11. L. A. LEITES, YU. P. EGOROV, J. YA. ZUEVA, and V. A. PONOMARENKO. Izv. Akad. Nauk SSSR Otd, Khim. Nauk, 2132 (1961).
12. I. NAKAGAWA. J. Chem. Soc. Japan, **77**, 602 (1956).
13. I. NAKAGAWA and S. I. MIZUSHIMA. Bull. Chem. Soc. Japan, **28**, 589 (1955).
14. N. I. BATUEVA, A. D. PETROV, V. A. PONOMARENKO, and A. D. MATVEEVA. Izv. Akad. Nauk SSSR Otd. Khim. Nauk, 1070 (1956).
15. W. R. CULLEN. Can. J. Chem. **40**, 426 (1962).
16. W. R. CULLEN. Can. J. Chem. **38**, 439 (1960).
17. M. M. BAIG and W. R. CULLEN. Can. J. Chem. **39**, 420 (1961).
18. M. M. BAIG and W. R. CULLEN. Can. J. Chem. **40**, 161 (1962).
19. M. M. BAIG, W. R. CULLEN, and D. S. DAWSON. Can. J. Chem. **40**, 46 (1962).

Can. J. Chem. Downloaded from www.nrcresearchpress.com by 210.87.254.6 on 09/05/12
For personal use only.

Can. J. Chem. Downloaded from www.nrcresearchpress.com by 210.87.254.5 on 09/05/12
For personal use only.

THE INFRARED SPECTRA OF SOME TITANIUM(IV) COMPLEXES WITH PRIMARY DIAMINES

D. HORLEY[1] AND E. G. TORRIBLE
Chemistry Department, Queen's University, Kingston, Ontario
Received July 5, 1965

ABSTRACT

A series of titanium(IV) halide – diamine complexes have been prepared and their infrared spectra measured in the solid state between 4 000 and 300 cm^{-1}. The configuration of the ligand and extent of aminolysis of the titanium–halide bond are discussed in relation to the spectra. Some assignments are proposed in the 600–300 cm^{-1} region for the ethylenediamine complexes.

INTRODUCTION

An extensive study of the reaction between titanium(IV) halides and primary monoamines has shown that the primary amines solvolyze the metal—halogen bond (1). By comparison, little is known of the reaction with primary diamines. Fowles and McGregor (2) reported an ethylenediamine (en) complex, $TiCl_2[HN(CH_2)_2NH_2]_2(en)_2$, and suggested that the ligands were chelated to the metal. More recently Sumarokova and Sakenova (3, 4) claimed no aminolysis of the Ti—Cl bond occurred in the complexes $TiCl_4.2en$, $TiCl_4.3en$, and $TiCl_4.4en$. However, there was evidence for aminolysis in the reaction with hexamethylenediamine (HMD), and the compounds $TiCl_3[HN(CH_2)_6NH_2].n$HMD, where n = 1, 2, and 3, were reported (4). No spectroscopic examination of these compounds has been offered to date. In this paper we describe the preparation of a number of titanium(IV) halide – diamine complexes including a series of 1:1 adducts. The infrared data for these compounds in the range 4 000 to 300 cm^{-1} is given in Table I.

EXPERIMENTAL

Materials and Manipulation

Special precautions were taken to exclude water from the apparatus and chemicals, and all reactions were conducted in an atmosphere of dry nitrogen. The amines and solvents were dried by refluxing over sodium and then fractionally distilled. The titanium halides were distilled or sublimed into the reaction vessels immediately before use.

The complexes were all prepared by the same general method. Solutions of the reactants in benzene were mixed in known molar ratios. Reaction was generally immediate and heat was evolved. The resulting mixture was stirred and occasionally heated for a period of time. The products, which were all insoluble, were filtered, washed with hot benzene, and dried *in vacuo*. All the products reacted vigorously with water and were hydrolyzed rapidly in air. The complexes were nonvolatile and insoluble in any solvent with which they did not react.

The infrared spectra were all determined as mulls in Nujol and hexachlorobutadiene-1,3 between NaCl or KRS-5 plates on a Beckman I.R. 10 grating instrument.

Analyses were obtained as previously described (5) and the data is presented in Table II.

RESULTS AND DISCUSSION

A number of questions remain to be answered with regard to the titanium(IV) halide – diamine complexes so far reported in the literature: (*a*) the extent to which aminolysis of the Ti—X bond (X = Cl, Br, or I) occurs; (*b*) whether the diamine is acting as a chelate or as a *trans* bridging unit between two different metal atoms thus forming polymeric chains; and (*c*) at what value of n in the chain $H_2N(CH_2)_nNH_2$ would there be a possible change from a chelate to a bridged system?

[1]*Present address: Polymer Corporation, Sarnia, Ontario.*

Can. J. Chem. Downloaded from www.nrcresearchpress.com by 210.87.254.5 on 09/05/12
For personal use only.

The infrared spectra of ethylenediamine complexes have been reviewed (6), and the spectra of some tris-ethylenediamine complexes of ruthenium(II) have been analyzed in detail (7). The data indicates that ethylenediamine has the *gauche* configuration when acting as a chelating ligand. When the ligand acts as a bridging unit between two metal atoms its configuration must be *trans*. Powell *et al.* (8, 9, 10) have concluded, on the basis of infrared spectra, that a number of mono-ethylenediamine complexes are long chain polymers with the ligand in the *trans* configuration. Brodersen (11) arrived at a similar conclusion and confirmed it by an X-ray study. Generally the chelate structure shows 14–16 peaks in 1 600 to 600 cm^{-1} region, e.g. the $Co(en)_3Cl_3$ complex exhibits 15 peaks. The bridged complexes, because of their higher symmetry, show only 6–9 peaks. The $Ti(en)X_4$ complexes show 15 and 14 peaks for the chloride and bromide respectively. Thus we assume that in the mono-ethylenediamine titanium(IV) complexes the ligand will be chelated and in the *gauche* form. However, the doublet near 840 cm^{-1} which is generally typical of chelated ethylenediamine complexes (10) is absent from the spectra of the $Ti(en)X_4$ complexes. The ruthenium complexes reported by Allen show the doublet very clearly (7).

TABLE I

Infrared data for 1:1 adducts, 4 000 to 300 cm^{-1}

Complex	
$Ti(en)Cl_4$	3 310 (sh), 3 270 (s), 3 130 (s), 2 970 (m), 1 565 (m), 1 548 (sh), 1 460 (m), 1 370 (w), 1 315 (w), 1 285 (w), 1 265 (w), 1 230 (w), 1 155 (m), 1 107 (s), 1 088 (w), 1 053 (s), 1 020 (sh, w), 1 004 (m), 981 (m), 880 (w), 680 (s), 520 (s), 442 (s), 390 (s), 372 (s), 350 (s), 315 (s)
$Ti(en)Br_4$	3 300 (sh), 3 230 (s), 2 970 (sh), 1 550 (w), 1 450 (m), 1 385 (w), 1 370 (w), 1 330 (w), 1 310 (w), 1 285 (w), 1 270 (w), 1 150 (w), 1 105 (w), 1 040 (s), 1 005 (w), 978 (w), 678 (w), 515 (s), 435 (s), 365 (s), 330 (s)
$Ti(Butdiam)Cl_4$*	3 230 (sh), 3 180 (s, b), 2 970 (sh), 1 600 (s), 1 500 (sh), 1 475 (m), 1 392 (w), 1 372 (w), 1 360 (w), 1 260 (m), 1 095 (m), 1 020 (m), 800 (m), 745 (m), 665 (m), 520 (w), 510 (w), 480 (w), 380 (s), 365 (sh, s)
$Ti(HMD)Cl_4$	3 220 (s), 2 970 (s), 2 900 (sh), 1 580 (m), 1 480 (m), 1 395 (w), 1 330 (w), 1 260 (w), 1 220 (w), 1 022 (w), 968 (w), 810 (w), 715 (w), 680 (w), 560 (w), 370 (sh), 310 (s)
$Ti(HMD)Br_4$	3 225 (s), 3 170 (sh), 2 960 (s), 2 875 (sh), 1 575 (m), 1 470 (m), 1 438 (w), 1 390 (w), 1 320 (w), 1 290 (w), 1 260 (w), 1 230 (w), 980 (w), 855 (w), 810 (w), 793 (w), 718 (w), 653 (w)

ABBREVIATIONS: sh = shoulder, s = sharp, m = medium, b = broad, w = weak.
*Butdiam = 1,4-butanediamine.

If aminolysis has occurred then absorption associated with the $-NH_3^+$ group is to be expected, i.e. a very strong broad band ranging approximately from 3 300 cm^{-1} to 2 500 cm^{-1} and in the process overlapping the $-CH_2-$ stretching bands (12). The spectra of the 1:1 ethylenediamine adducts did not show this type of absorption indicating the absence of aminolysis in the mono-complexes.

With the titanium(IV) halide – hexamethylenediamine complexes there are fewer data available for comparison. If a chelate is formed the chelate ring would contain nine members. Chelate rings of this size are rare but Pfeiffer (13) concluded that the compound $Cu(HMD)_2.(ClO_4)_2$ contained the diamine chelated to the metal. More recently Caglioti *et al.* (14) prepared a series of copper(II)–diamine complexes and suggested that the mono-complexes of the long chain ligands are polymeric. We have prepared the complexes $Cu(HMD)_2.Cl_2$ and $Cu(HMD).Cl_2.2H_2O$, both from ethanol. The analytical and infrared data (4 000 to 300 cm^{-1}) are given in Table III. By analogy with the argument used by Powell and Sheppard (8), the complexes in which the hexamethylenediamine is chelated should exhibit more complex spectra than those in which the ligand is *trans* and

TABLE II
Analytical results

Complex	Color	Found			Theoretical		
		M	X	N	M	X	N
$Ti(en)Cl_4$	Light brown	19.0	53.3	10.9	19.2	56.8	11.2
$Ti(en)Br_4$	Brown	11.0	73.4	6.5	11.2	74.8	6.6
$Ti(Butdiam)Cl_4$*	Yellow	16.6	49.5	8.3	17.3	51.1	9.4
$Ti(HMD)Cl_4$	Red	15.1	44.7	—	15.7	46.4	—
$Ti(HMD)Br_4$	Brown	9.9	64.6	—	9.9	66.1	—
$Ti(en)_2Cl_4$	Red brown	15.2	45.4	—	15.5	45.8	—
$Ti(en)_2I_4$	Black	7.2	74.6	—	7.1	75.1	—
$Ti(en)_3Cl_4$	Red brown	12.3	36.7	—	12.9	38.3	—
$Ti(HMD)_3Cl_4$	Orange	8.9	25.8	—	8.9	26.4	—
$Ti(en)_4Cl_4$	Pink	11.3	32.2	—	11.1	33.0	—
$Ti(HMD)_4Br_4$	Light brown	5.8	38.2	—	5.8	38.4	—

*Butdiam = 1,4-butanediamine.

bridging between two metal atoms. If the spectra in the range 1 600 to 600 cm^{-1} are considered, the bis complex is seen to exhibit 24 peaks as opposed to 16 for the mono-complex. Also, in this region at least two bands of the mono-complex can be assigned to vibrational modes of the coordinated water (15). Thus we conclude that the infrared spectra support the structures originally postulated for these copper(II) complexes. By comparison, the spectra of the mono-hexamethylenediamine titanium(IV) chloride and bromide in the region 1 600 to 600 cm^{-1} show 11 and 14 peaks respectively (Table I). Hence it is probable that these complexes are long chain polymers with the ligand in the *trans* form and bridging between two titanium atoms. Such a structure gives titanium its expected coordination number of six. The spectra between 3 500 to 2 200 cm^{-1} give no indication that aminolysis has occurred.

TABLE III
Analytical and infrared data for Cu(II)—HMD complexes

Compound	Color	Analysis	Infrared spectra (4 000 to 300 cm^{-1})
$Cu(HMD)_2Cl_2$	Purple	Found: Cu, 17.5; C, 38.6; H, 9.3	3 300 (s), 3 270 (s), 3 190 (s), 3 105 (s), 2 920 (s), 2 840 (s), 1 595 (s), 1 460 (s), 1 440 (sh),
		Theor.: Cu, 17.5; C, 39.3; H, 8.7	1 365 (m), 1 350 (m), 1 270 (w), 1 250 (w), 1 230 (m), 1 150 (s), 1 115 (s), 1 070 (sh), 1 050 (s), 1 005 (sh), 990 (s), 975 (s), 947 (m), 915 (m), 870 (w), 850 (w), 835 (w), 760 (w), 715 (m), 690 (s), 610 (s), 555 (m), 520 (m), 440 (m)
$Cu(HMD).Cl_2.2H_2O$	Green	Found: Cu, 22.5; C, 25.1; H, 7.0	3 270 (m), 3 240 (m), 3 140 (s), 3 080 (sh), 2 960 (w), 2 900 (m), 2 850 (m), 1 595 (sh), 1 585 (s), 1 475 (s)
		Theor.: Cu, 22.3; C, 25.1; H, 7.0	1 390 (w), 1 375 (w), 1 335 (w), 1 310 (w), 1 230 (m), 1 155 (s), 1 100 (w), 1 050 (w), 1 010 (w), 995 (m), 920 (w), 720 (m), 620 (s), 550 (w), 445 (w), 350 (sh)

ABBREVIATIONS: sh = shoulder, s = sharp, m = medium, b = broad, w = weak.

No clear-cut decision could be made about the configuration of the ligand in the mono-1,4-butanediamine titanium(IV) chloride. The infrared spectrum in the 1 600 to 600 cm^{-1} region showed 12 absorption peaks but no other data was available for comparison. Also the absorption in the 3 300 to 2 500 cm^{-1} region could be interpreted as indicating the presence of the $—NH_3^+$ group. This was unexpected since no evidence for

Can. J. Chem. Downloaded from www.nrcresearchpress.com by 210.87.254.5 on 09/05/12
For personal use only.

aminolysis was obtained for the mono-ethylenediamine and mono-hexamethylenediamine complexes.

The complexes of the type Ti(diamine)$_n$.X_4 where n = 2, 3, 4, all showed spectral evidence of aminolysis. This result is in accord with the results reported by Fowles *et al.* (16) for the analogous primary monoamine complexes. The extent of solvolysis could not be determined since it was not possible to separate the amine hydrochloride from the titanium complex. Attempts to wash out the amine hydrochloride with either the parent amine or a solution of the amine in benzene (16) were not successful, and in general there was further reaction between amine and the titanium complex. However, complete solvolysis of the titanium–halogen bond did not occur, at least in the chlorides, as an absorption band in the region 360–390 cm^{-1} could be assigned to the Ti—Cl stretching mode (5).

Thus the products shown as multiple addition complexes are more probably mixtures of the type $TiCl_2[(CH_2)_n(NH)_2].(CH_2)_n(NH_3)_2^{2+}$ or, $[(CH_2)_n(NH_3)_2]^{2+}.[TiCl_4(CH_2)_2(NH)_2]^{2-}$. A similar conclusion has been reached for the products of the reaction between hydrazines and titanium(IV) halides (17). Because of the presence of the amine hydrochloride it is not possible to arrive at any decision regarding the configuration of the ligand bound to the titanium.

The 600–300 cm^{-1} regions of the spectra are interesting. We have found that liquid ethylenediamine between KBr discs shows peaks at 500 and 465 cm^{-1}, and these can be attributed to N—C—C—N bending modes of the free amine possibly in the *gauche* configuration (18). If, as is probable, the amine is *gauche* in the mono-complexes of titanium(IV) then it seems reasonable that the bands at 520 and 442 cm^{-1} and 515 and 435 cm^{-1} for the chloride and bromide respectively (Table I) can be assigned to the N—C—C—N bending modes. We have found that the complex $Cu(en)_2Cl_2$ also shows peaks at 520 and 455 cm^{-1}.

On complex formation the Ti—X stretching frequency is expected to decrease. In a series of complexes of titanium(IV) halides with cyclic ethers and thioethers the Ti—Cl stretching frequency is decreased to 360–385 cm^{-1}, and the Ti—Br stretching frequency to 300 cm^{-1} or less (5). Hence the peak at 372 cm^{-1} in the chloride complex could be assigned to the Ti—Cl stretching mode. The corresponding Ti—Br frequency is beyond the limit of our instrument. The remaining bands are probably associated with metal–nitrogen vibrational modes. A recent review (19) shows that most assignments for the M—N stretching frequency are in the range 300–500 cm^{-1}. No data for the Ti—N bond were included although Fowles *et al.* (16) have made a tentative assignment of 540 cm^{-1} for the stretching frequency. This seems rather high in view of the other M—N assignments; also Fowles *et al.* were restricted to a lower limit of 400 cm^{-1} by their KBr prism. We are tentatively suggesting that the bands at 390 and 350 cm^{-1} in the chloride complex and at 365 and 330 cm^{-1} in the bromide are the Ti—N stretching frequencies. The band at 315 cm^{-1} in the chloride could be assigned to the N—M—N bending mode (19); the bending frequency in the bromide would be displaced to lower than 300 cm^{-1}. The Ti—N stretching frequencies in the mono-butanediamine and mono-hexamethylenediamine chloride complexes would be 365 cm^{-1} and 310 cm^{-1} respectively. Further work is in progress which it is hoped will confirm these assignments.

ACKNOWLEDGMENTS

Grateful acknowledgment is made to the National Research Council of Canada for financial support and to the Government of the Province of Ontario for a Fellowship (to D. H.).

Can. J. Chem. Downloaded from www.nrcresearchpress.com by 210.87.254.5 on 09/05/12
For personal use only.

REFERENCES

1. G. W. A. FOWLES. Proc. Symp. Chem. Co-ord. Compounds, Agra, India, 1959. 1960.
2. G. W. A. FOWLES and W. R. MCGREGOR. J. Chem. Soc. 136 (1958).
3. T. N. SUMAROKOVA and D. S. SAKENOVA. Zh. Obshch. Khim. **32**, 3 (1962).
4. T. N. SUMAROKOVA and D. S. SAKENOVA. Zh. Obshch. Khim. **34**, 2696 (1964).
5. E. C. ALYEA and E. G. TORRIBLE. Unpublished data.
6. K. NAKAMOTO. Infrared spectra of inorganic and coordination compounds. John Wiley, New York. 1963. p. 186.
7. A. D. ALLEN and C. V. SENOFF. Can. J. Chem. **43**, 888 (1965).
8. D. B. POWELL and N. SHEPPARD. J. Chem. Soc. 3089 (1959).
9. G. NEWMAN and D. B. POWELL. J. Chem. Soc. 477 (1961).
10. G. NEWMAN and D. B. POWELL. J. Chem. Soc. 3447 (1962).
11. K. BRODERSEN. Z. Anorg. Allgem. Chem. **298**, 142 (1959).
12. K. NAKANISHI. Infra-red absorption spectroscopy. Holden-Day Inc., San Francisco. 1962. p. 39.
13. P. PFEIFFER. Naturwissenschaften, **35**, 190 (1948).
14. V. CAGLIOTI, C. FURLANI, G. DESSEY, and C. IBARRA. Gazz. Chim. Ital. **92**, 1276 (1962).
15. K. NAKAMOTO. Infrared spectra of inorganic and coordination compounds. John Wiley, New York. 1963. p. 156.
16. R. T. COWDELL, G. W. A. FOWLES, and R. A. WALTON. J. Less-Common Metals, **5**, 386 (1963).
17. D. NICHOLLS and R. SWINDALLS. J. Chem. Soc. 4204 (1964).
18. A. SABATINI and S. CALIFANO. Spectrochim. Acta, **16**, 677 (1960).
19. K. NAKAMOTO. Infrared spectra of inorganic and coordination compounds. John Wiley, New York. 1963. p. 146.

Can. J. Chem. Downloaded from www.nrcresearchpress.com by 210.87.254.5 on 09/05/12
For personal use only.

Can. J. Chem. Downloaded from www.nrcresearchpress.com by 210.87.254.5 on 09/05/12
For personal use only.

FRACTIONATION OF PECTINS FROM SUNFLOWERS, SUGAR BEETS, APPLES, AND CITRUS FRUITS[1]

V. ZITKO[2] AND C. T. BISHOP
Division of Biosciences, National Research Council, Ottawa, Canada
Received July 28, 1965

ABSTRACT

Pectins from sunflower heads, sugar beet, apple, and citrus fruits were separated into acid-insoluble pectic acids and acid-soluble polysaccharides. The acid-soluble polysaccharides were shown by moving-boundary electrophoresis to be complex mixtures of four or five polysaccharides. The pectic acids were fractionated by precipitation with sodium acetate from aqueous solution. The fractions were examined for galacturonic acid content, specific rotation, limiting viscosity number, behavior on moving-boundary electrophoresis, and presence of neutral sugars. The results showed that each of the pectic acids contained two acidic components, one a galacturonan free of neutral sugars, the other a galacturonan to which neutral sugars were attached, probably as side chains.

The composition and constitution of pectic substances have been studied extensively and the early literature on the subject has been reviewed by Hirst and Jones (1). Pectins from all sources contain D-galacturonic acid, D-galactose, L-arabinose, and L-rhamnose but it has not been clear whether these components are joined together in a single polysaccharide or whether a group of polysaccharides is present. Early evidence (1) indicated that the pectic substances were mixtures of three polysaccharides, a galacturonan, a galactan, and an araban. However, subsequent attempts to isolate homoglycans by fractionation of various pectins have not confirmed this interpretation (2–8). For example, chromatography on diethylaminoethyl cellulose resolved pectin into a neutral fraction and several acidic fractions (7, 8), but each of these fractions still contained units of the same monosaccharides that were present in the original preparation. It has been known for some time that the predominant structural feature of pectin is a chain of $1 \rightarrow 4$ linked α-D-galacturonic acid residues (9, 10). There is chemical evidence that in some pectic acids neutral monosaccharides are linked to the basic chain of D-galacturonic acid units (3–6, 11, 12), but the homogeneity of those pectic acids was not established. There have been only two reports of the isolation of homoglycans from pectins. Both were galacturonans which yielded only D-galacturonic acid on hydrolysis; one was isolated from sunflower heads (13), the other from the bark of amabilis fir (12). The galacturonan from sunflower heads was obtained by extraction with ammonium oxalate:oxalic acid and reprecipitation in 60% ethanol. The galacturonan from the bark of amabilis fir was separated from another polysaccharide which contained D-galacturonic acid, D-galactose, and L-arabinose by ultracentrifugation of an acidified aqueous solution of the pectin.

Precipitation of acidic polysaccharides by electrolytes has been studied extensively with varying results in the fractionations obtained. Fractional precipitation of alginic acid with solutions of potassium chloride and manganous sulphate yielded fractions with different ratios of D-mannuronic and L-guluronic acids (14, 15). Most studies of the fractionation of pectins by this method have involved the use of electrolytes with polyvalent cations (2, 16, 17). Good separations of neutral from acidic polysaccharides were obtained in this

[1]*Issued as N.R.C. No. 8675. Presented at the 150th Meeting of the American Chemical Society, Atlantic City, Sept. 1965.*
[2]*National Research Council Postdoctorate Fellow 1964–1965.*

Can. J. Chem. Downloaded from www.nrcresearchpress.com by 210.87.254.5 on 09/05/12
For personal use only.

way, but there was no fractionation of acidic polysaccharides, probably because of the high precipitating power of the polyvalent ions.

In connection with a project to obtain an analytically pure galacturonan for structural studies (18) it was found that pectic acids could be fractionated by precipitation from aqueous solution with sodium acetate. In view of the varying results described above for the composition of pectic substances it was of interest to try this fractionation procedure on pectins from a number of sources. The present paper describes the fractionation of pectins from sunflower heads, sugar beets, apples, and citrus fruits. While this work was in progress it was reported that a galacturonan from amabilis fir pectin could be precipitated from aqueous solution by sodium chloride (12); however, in contrast to the present work, ultracentrifugation was required to separate the galacturonan.

The properties of the crude pectins are shown in Table I. Apple pectin was much higher than the others in galacturonic acid content and the sunflower pectin had a much lower

TABLE I
Properties of crude pectins

	Gal.A.*(%)	D.e.†(%)	$[\alpha]_D$	$[\eta]$	$\mu \times 10^{-5}$
Sunflower	71.7	38.7	+227°	340	12.6
Sugar beet	68.5	54.8	+215°	174	7.95
Apple	87.1	62.5	+253°	600	7.70
Citrus	72.9	67.0	+215°	500	6.70

*Galacturonic acid.
†Degree of esterification.

degree of esterification. The highest specific rotation ($[\alpha]_D$) was associated with the highest galacturonic acid content. The sunflower and sugar beet pectins showed considerably lower limiting viscosity numbers ($[\eta]$) than the pectins from apple and citrus fruits. Each pectin showed a very broad diffuse peak on moving boundary electrophoresis, indicative of heterogeneity; the electrophoretic mobilities (μ) were in the same order of magnitude and decreased with increasing degree of esterification. Obviously, those molecules with a lower degree of esterification had a higher charge:mass ratio because of free carboxyl groups and hence had a greater mobility on electrophoresis. The pectic acids, precipitated from the deesterified pectins by acid (19) were not analyzed before the sodium acetate fractionation described below. After removal of the pectic acids, polysaccharides which remained in solution were precipitated by ethanol. Table II shows some of the properties of these fractions. Each fraction still contained a considerable amount of galacturonic acid and made up only a small percentage of the crude pectin. A number of components were revealed by electrophoresis, as many as five being detected in this fraction from apple pectin. The ratios of neutral sugars were not determined but from visual examination of paper chromatograms of hydrolyzates the relative amounts of rhamnose, arabinose, and galactose were the same in each fraction. In addition to those three monosaccharides the fraction from sunflower pectin contained glucose, and the one from apple pectin contained glucose and xylose. The results showed that the acid-soluble polysaccharides from each of the four pectins were very similar and were extremely complex mixtures of a number of polysaccharides. The degree of complexity of this material is shown by the electrophoresis pattern given by the acid-soluble polysaccharides from citrus pectin (Fig. 1). As shown below in the results of the sodium acetate fractionation, a galacturonan was responsible for the peak of greatest mobility ($\mu = (11 - 13) \times 10^{-5}$).

Can. J. Chem. Downloaded from www.nrcresearchpress.com by 210.87.254.5 on 09/05/12
For personal use only.

TABLE II

Acid-soluble polysaccharides from pectins

	Gal.A.*(%)	% of crude pectin	Peaks on electrophoresis ($\mu \times 10^{-5}$)	Rhamnose	Arabinose	Galactose	Glucose	Xylose
Sunflower	63.7	4.7	12.5, 10.3, 7.5	+	+	+	+	−
Sugar beet	52.0	11.7	—	+	+	+	−	−
Apple	49.8	3.8	11.6, 8.2, 6.1, 3.3, 2.2	+	+	+	+	+
Citrus	37.2	5.7	12.5, 5.8, 3.7, 2.4	+	+	+	−	−

*Galacturonic acid.

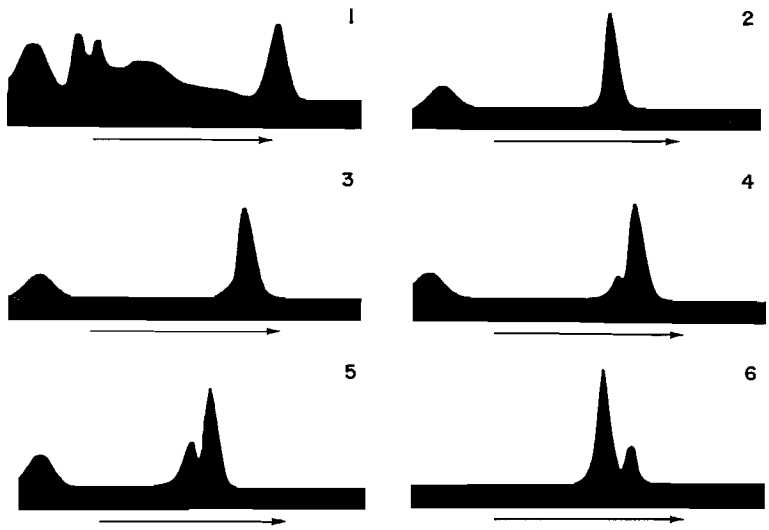

FIG. 1. Electrophoretic pattern of acid-soluble polysaccharides from citrus pectin. Buffer, 0.05 *M* sodium tetraborate; 750 V, 10 mA, 200 min.
FIG. 2. Electrophoretic pattern of sunflower pectic acid; fraction precipitated by 0.14 *N* sodium acetate (94.2% galacturonic acid). Buffer, 0.05 *M* sodium tetraborate; 750 V, 10 mA, 157 min.
FIG. 3. Electrophoretic pattern of sunflower pectic acid; fraction precipitated by 0.14 *N* sodium acetate (92.6% galacturonic acid). Buffer, 0.05 *M* sodium tetraborate; 750 V, 10 mA, 199 min.
FIG. 4. Electrophoretic pattern of sunflower pectic acid; fraction precipitated by 0.22 *N* sodium acetate (87.7% galacturonic acid). Buffer, 0.05 *M* sodium tetraborate; 750 V, 10 mA, 205 min.
FIG. 5. Electrophoretic pattern of sugar beet pectic acid, fraction precipitated by 0.18 *N* sodium acetate (76.5% galacturonic acid). Buffer, 0.05 *M* sodium tetraborate; 750 V, 10 mA, 174 min.
FIG. 6. Electrophoretic pattern of sugar beet pectic acid; fraction soluble in sodium acetate, precipitated by ethanol (62.3% galacturonic acid). Buffer, 0.05 *M* sodium tetraborate; 750 V, 10 mA, 167 min.

Pectic acids, isolated from crude deesterified pectins by precipitation with acid, were fractionally precipitated from 1% aqueous solutions by addition of 2 *M* aqueous sodium acetate. Polysaccharide material not precipitated by this procedure was recovered by precipitation with ethanol. The results are shown in Table III. The fractions obtained at sodium acetate concentrations shown in column 1 were refractionated giving precipitates at the sodium acetate concentrations shown in column 2. Each fraction was then examined for galacturonic acid content, specific rotation ($[\alpha]_D$), limiting viscosity number ($[\eta]$), peaks on electrophoresis, presence of neutral sugars, and yield. The fractions that precipitated earliest contained the most galacturonic acid, which amounted to more than 90% in all except the pectic acid from sugar beet. The galacturonic acid contents decreased with increasing sodium acetate concentration and were markedly lower in the fractions precipitated by ethanol. The specific rotations were directly related to galacturonic acid content and, in the purest fractions, were considerably higher than those which have been reported for pectins or pectic acids (2, 12, 16). The limiting viscosity numbers increased with increasing sodium acetate concentration except for apple pectic acid, in which the first fraction had the highest limiting viscosity number and subsequent fractions a lower and nearly constant value. Except for citrus pectic acid, plots of η_{sp}/c (η_{sp} is specific viscosity, c is concentration) against c were linear for all fractions in the range 0.07–0.20 g/100 ml. The slopes of these plots were nearly the same for the fractions from sugar beet pectic acids. However, with the fractions from apple and from sunflower pectic acids the slopes of η_{sp}/c against c increased with increasing sodium acetate concentrations required for

Can. J. Chem. Downloaded from www.nrcresearchpress.com by 210.87.254.5 on 09/05/12
For personal use only.

Can. J. Chem. Downloaded from www.nrcresearchpress.com by 210.87.254.5 on 09/05/12
For personal use only.

TABLE III

Sodium acetate fractionation of pectic acids

Concn. of sodium acetate, N*		Gal.A.** (%)	$[\alpha]_D$	$[\eta]$	Peaks on electrophoresis ($\mu \times 10^{-5}$) $cm^2 V^{-1} s^{-1}$	Neutral sugars†	Yield % of crude pectin
			A. Sunflower pectic acid				
0.12	0.12	99.2	+308°	189	12.4	—	5.8
	0.14	94.2	+300°	215	12.2	—	13.6
0.14	0.12	91.4	+291°	200	12.4	—	51.5
	0.14	92.6	+296°	222	12.3	—	12.0
	0.22	87.7	+282°	234	11.3, 10.6	Trace	3.4
Ethanol		75.6	—	—	12.5, 11.1	++	8.9
			B. Sugar beet pectic acid				
0.12	0.12	82.5	+277°	138		+	2.7
	0.14	77.4	+251°	176		+	3.3
0.14	0.14	87.5	+247°	152	12.1, 10.3	+	8.4
0.16	0.12	84.0	+274°	164	10.9, 9.9	+	6.8
	0.14	79.3	+267°	171	12.7, 10.8	+	28.8
	0.16	84.0	+254°	180	10.9, 10.0	+	8.4
0.18	0.18	76.5	+239°	170	11.4, 10.7	+	15.3
Ethanol		62.3	—	—	11.3, 9.8	++	11.1

Can. J. Chem. Downloaded from www.nrcresearchpress.com by 210.87.254.5 on 09/05/12
For personal use only.

TABLE III (*Concluded*)

Concn. of sodium acetate, *N**		Gal.A.‡ (%)	$[\alpha]_D$	$[\eta]$	Peaks on electrophoresis ($\mu \times 10^{-5}$) $cm^2 V^{-1} s^{-1}$	Neutral sugars†	Yield % of crude pectin
			C. Apple pectic acid				
0.12	0.06	91.3	+295°	270	11.9	Trace	3.7
	0.08	95.5	+300°	240	11.7	Trace	6.1
	0.10	92.7	+311°	248	12.2	Trace	70.5
	0.22	88.2	+281°	246	11.8, 10.8	+	12.6
Ethanol		65.0	—	—	12.1, 11.1	++	3.4
			D. Citrus pectic acid				
0.12	0.12	92.5	+277°	244	12.7	Trace	28.8
0.14	0.14	85.0	+264°	256	13.0	+	60.4
Ethanol		54.8	—	—	12.5, 9.6	++	5.2

*Column 1 shows sodium acetate concentrations at which precipitates were obtained in the first fractionation. Each precipitate was then refractionated giving precipitates at the sodium acetate concentrations in column 2.
†The sugars were rhamnose, arabinose, and galactose; apple pectic acid fractions contained xylose in addition.
‡Galacturonic acid.

precipitation. The values for this increase in slope, calculated as k_1 in the Huggins equation (20), were 0.042, 0.107, 0.500, 0.657, and 0.513 (100 ml/g) for the fractions from sunflower pectic acid in order of precipitation. It has been claimed that k_1 increases with an increase in degree of branching in a polymer (21) and the present data may therefore indicate structural differences between the various fractions from a single pectic acid. Certainly, if the pectic acids were linear polymers, it would be expected that the larger molecules would be precipitated first and have the higher viscosities. The reverse trend, increasing viscosities in order of precipitation (Table III), may therefore indicate that the fractions obtained at low sodium acetate concentrations were linear and those precipitated by higher concentrations of sodium acetate were branched. Further structural studies are required to confirm this interpretation.

The electrophoretic patterns gave some idea of the homogeneity of the pectic acid fractions. In all pectic acids except that from sugar beet the fractions precipitated at low sodium acetate concentrations showed a single symmetrical peak on electrophoresis. Figure 2 shows an electrophoretic pattern that was typical of these fractions. The broad peak at the origin in all electrophoretic patterns shown is a false boundary caused by salt gradients. Since these early fractions were very high in galacturonic acid and contained only traces of neutral sugars (apple and citrus) or none at all (sunflower), this single peak of $\mu = (12\text{–}13) \times 10^{-5}$ cm^2 V^{-1} s^{-1} must have represented a galacturonan. It may be noted that every fraction described in Table III contains a component with this electrophoretic mobility and the same component was present in the acid-soluble polysaccharide (Table II). It seems likely that every fraction from the pectins contains the same galacturonan, and the failure to resolve it completely from the other components was probably caused by a broad molecular weight distribution. The sugar beet pectin may be an exception as far as the presence of a galacturonan is concerned. The fractions from sugar beet pectic acid (Table III) had lower specific rotations and contained more than trace amounts of neutral sugars. The first two fractions from sugar beet pectic acid were not obtained in sufficient quantities to permit examination of them by electrophoresis.

Fractions of pectic acids with lower amounts of galacturonic acid showed a second component which appeared first as a shoulder on the main peak and then as a second peak in the electrophoretic patterns. Thus Fig. 3 shows the electrophoretic pattern given by the sunflower pectic acid fraction, which contained 92.6% galacturonic acid. The shoulder on the trailing edge of the peak is readily apparent when compared with the peak in Fig. 2. Figure 4 shows the electrophoretic pattern given by the next succeeding fraction from sunflower pectic acid. This fraction contained 87.7% of galacturonic acid and the appearance of a second component, $\mu = 10.6 \times 10^{-5}$ cm^2 V^{-1} s^{-1}, is quite distinct.

The difference between fractions precipitated by sodium acetate and those which were soluble in sodium acetate is shown by comparison of Figs. 5 and 6. Figure 5 shows the electrophoretic pattern of the last fraction precipitated from sugar beet pectic acid by sodium acetate. Figure 6 shows the electrophoretic pattern of the fraction from sugar beet pectic acid that was soluble in sodium acetate and had to be recovered by precipitation with ethanol. The same two components were present in each fraction but in different amounts; the major component in Fig. 5 was the one with greater mobility, the major component in Fig. 6 being the one with lower mobility. Thus, the addition of sodium acetate raised the ionic strength of the solution and diminished the repulsive forces between galacturonan chains. A linear galacturonan with the greater mobility would therefore aggregate first; and a galacturonan with side chains of neutral sugars and hence a lower charge:mass ratio and lower mobility, would tend to stay in solution.

Can. J. Chem. Downloaded from www.nrcresearchpress.com by 210.87.254.5 on 09/05/12
For personal use only.

Can. J. Chem. Downloaded from www.nrcresearchpress.com by 210.87.254.5 on 09/05/12
For personal use only.

It is apparent that sodium acetate preferentially precipitates the component of greater electrophoretic mobility in all of the fractionations shown in Table III. It is also clear that the pectic acids contained two components, all other polysaccharides in the crude pectins remaining in solution when the pectic acids were precipitated by acid. From the evidence presented in Table III and discussed above it is very likely that the two components in pectic acids are a linear galacturonan free of neutral sugars and a linear galacturonan to which neutral sugars are attached as side chains. This conclusion fully confirms the results of a study of pectin from the bark of amabilis fir (12) and supports the conclusion, based on a study of sisal pectic acid (3), that the pectic acid consisted of "a mixture of acidic polysaccharides, one composed solely of D-galacturonic acid residues and the other or others containing both neutral sugar and D-galacturonic acid residues". Barrett and Northcote (22) have shown that apple pectin is degraded when heated in buffer at pH 6.8 to give a galacturonan and an acidic polysaccharide which contains neutral sugars. It is possible that such a degradation, by β-elimination, occurred in the present work during the deesterification procedure. However, this is considered unlikely because the products were still of high molecular weight (38 000–49 000) and showed no absorption that was due to unsaturation in their ultraviolet spectra.

EXPERIMENTAL

Analyses

Galacturonic acid contents were determined by potentiometric titration with 0.1 *N* sodium hydroxide. Solutions of pectins and pectic acids in 0.155 *M* sodium chloride at pH 6.0 and 25 °C in the concentration range 0.07–0.2 g/100 ml were used for viscosity measurements; a Cannon-Fenske viscometer with a flow time for water of 52.52 s was used. Specific rotations were measured on 0.45–0.50% solutions at pH 6.0 in a 0.5-dm tube. A Tiselius-type, spinco Model H apparatus was used for moving-boundary electrophoresis, with 0.05 *M* sodium tetraborate as the buffer solution (23). Samples were hydrolyzed by 1 *N* sulphuric acid in sealed tubes at 100 °C for 15 h. Paper chromatograms were run by the descending method with ethyl acetate:pyridine:water in the proportions 10:4:3 (v/v), and sugars were detected on the papers by the *p*-anisidine hydrochloride spray reagent (24). All analytical results are expressed on a dry weight basis determined by drying samples at 105 °C for 12 h.

Pectins

Sunflower pectin was prepared by extraction of sunflower seed heads with a solution of ammonium oxalate:oxalic acid (13). Dr. R. M. McCready kindly supplied the sugar beet pectin, which had been prepared by extraction of sugar beet pulp with 0.5% calgon solution at pH 2.2. Apple pectin was a commercial preparation obtained from the Mann Research Laboratories. Citrus pectin was a commercial preparation from oranges and lemons obtained from Eastman Kodak. All pectins were washed with acidified 60% ethanol to yield the pectinic acids (2). Pectic acids were prepared as described previously (19).

Fractionation

One example of a typical fractionation procedure is given.

Sunflower pectinic acid (20 g) was dissolved in water (1 000 ml) containing 80 ml of 1 *N* sodium hydroxide. The solution was allowed to stand at room temperature for 2 h and was then centrifuged at 20 000 × *g*. Hydrochloric acid (18%) was then added dropwise to the clear solution with vigorous stirring. When precipitation was complete the gel of pectic acid was squeezed through a linen cloth and was washed thoroughly, twice with 60% acidified ethanol (5 ml of concentrated hydrochloric acid per liter), then successively with 60% ethanol, ethanol, and ether. The air-dried product was obtained in a yield of 15.7 g, 78.5% of the pectinic acids. The acid-soluble polysaccharides in the filtrate from the pectic acid precipitation were recovered by complete precipitation with ethanol, yield 0.6 g, 3% of pectinic acids.

The pectic acid (15 g) was dissolved in water (1 500 ml) containing 60 ml of 1 *N* sodium hydroxide to give a solution of pH 6.5. This solution was filtered through medium porosity sintered glass, 2.0 *M* sodium acetate (90 ml) was added with vigorous stirring, and the solution was kept at 5 °C for 18 h. The precipitate was then centrifuged off and dried by solvent exchange; yield, 2.75 g. A second fraction (11.7 g) was obtained by addition of a further 15 ml of 2.0 *M* sodium acetate to the mother liquors from the first fraction. No further precipitates were obtained by the addition of more sodium acetate. The residual polysaccharides in solution were recovered by precipitation with ethanol. The two fractions precipitated by sodium acetate were then refractionated separately by the same procedure. Concentrations of sodium acetate at which precipitates were obtained are shown in Table III, which also includes a record of the analyses of the various fractions.

ACKNOWLEDGMENTS

We are grateful to Dr. R. M. McCready, Western Regional Research Laboratory, U.S. Department of Agriculture, Albany, Calif., U.S.A., for a generous sample of sugar beet pectin.

REFERENCES

1. E. L. HIRST and J. K. N. JONES. Advan. Carbohydrate Chem. **2**, 235 (1946).
2. Z. I. KERTESZ. The pectic substances. Interscience Publishers, New York. 1951.
3. G. O. ASPINALL and A. CANAS-RODRIGUEZ. J. Chem. Soc. 4020 (1958).
4. G. O. ASPINALL and R. S. FANSHAWE. J. Chem. Soc. 4215 (1961).
5. T. E. TIMELL and A. JABBAR MIAN. Tappi, **44**, 788 (1961).
6. R. M. MCCREADY and M. GEE. J. Agr. Food Chem. **8**, 510 (1960).
7. H. NEUKOM, H. DEUEL, W. J. HERI, and W. KUNDIG. Helv. Chim. Acta. **43**, 64 (1960).
8. J. ROSÍK, V. ZITKO, and J. VAŠÁTKO. Collection Czech. Chem. Commun. **27**, 1346 (1962).
9. G. H. BEAVEN and J. K. N. JONES. Chem. Ind. London, 363 (1939).
10. F. SMITH. Chem. Ind. London, 363 (1939).
11. V. ZITKO, J. ROSÍK, and J. KUBALA. Collection Czech. Chem. Commun. In press.
12. S. S. BHATTACHARJEE and T. E. TIMELL. Can. J. Chem. **43**, 758 (1965).
13. C. T. BISHOP. Can. J. Chem. **33**, 1521 (1955).
14. A. HAUG. Acta Chem. Scand. **13**, 601 (1959).
15. A. HAUG. *In* Methods in carbohydrate chem. Vol. V. *Edited by* R. L. Whistler. Academic Press, Inc., New York. 1965. p. 69.
16. H. DEUEL and E. STUTZ. Advan. Enzymol. **20**, 341 (1958).
17. G. WUNSCH. Makromol. Chem. **8**, 124 (1952).
18. V. ZITKO and C. T. BISHOP. In preparation.
19. R. M. MCCREADY. *In* Methods in carbohydrate chem. Vol. V. *Edited by* R. L. Whistler. Academic Press, Inc., New York. 1965. p. 167.
20. P. F. ONYON. *In* Techniques of polymer characterization. *Edited by* P. W. Allen. Butterworths Scientific Publications, London. 1959. p. 171.
21. L. H. CRAGG and J. A. MANSON. J. Polymer Sci. **9**, 265 (1952).
22. A. J. BARRETT and D. H. NORTHCOTE. Biochem. J. **94**, 617 (1965).
23. D. H. NORTHCOTE. Biochem. J. **58**, 353 (1954).
24. L. HOUGH, J. K. N. JONES, and W. H. WADMAN. J. Chem. Soc. 1702 (1950).

Can. J. Chem. Downloaded from www.nrcresearchpress.com by 210.87.254.5 on 09/05/12
For personal use only.

Can. J. Chem. Downloaded from www.nrcresearchpress.com by 210.87.254.6 on 09/05/12
For personal use only.

PHOTOLYSIS OF HEXAFLUOROAZOMETHANE NEAR ROOM TEMPERATURE

J. R. DACEY, R. F. MANN, AND G. O. PRITCHARD[1]
Department of Chemistry and Chemical Engineering, Royal Military College, Kingston, Ontario
Received June 15, 1965

ABSTRACT

The mechanism for the formation of perfluorohexamethyl tetrazine in the photolysis of the title compound is found to occur via dimerization of two perfluorotrimethyl hydrazo radicals. Quantum yield data at 3 660 Å are presented, and compared with the azoethane system.

INTRODUCTION

Our previous work (1, 2, 3) on the photolysis of hexafluoroazomethane in the spectral regions at 2 537 Å and 3 660 Å has demonstrated that the primary step is

$$CF_3N_2CF_3 \xrightarrow{h\nu} N_2 + 2CF_3.$$

The CF_3 radicals either recombine

[1] $$2CF_3 \rightarrow C_2F_6$$

or add easily to the —N=N— double bond

[2] $$CF_3 + CF_3N{=}NCF_3 \rightarrow (CF_3)_2N{-}NCF_3$$

producing hydrazo radicals, with the eventual production of perfluorotetramethyl hydrazine (I) and perfluorohexamethyl tetrazine (II). Product I is formed by the radical–radical interaction

[3] $$CF_3 + (CF_3)_2N{-}NCF_3 \rightarrow (CF_3)_2N_2(CF_3)_2$$

but it is not certain (2) whether product II is formed predominantly by dimerization of two hydrazo radicals

[4] $$2(CF_3)_2N{-}NCF_3 \rightarrow (CF_3)_6N_4$$

or by hydrazo radical addition to hexafluoroazomethane

[5] $$(CF_3)_2N{-}NCF_3 + CF_3NN{=}CF_3 \rightarrow (CF_3)_5N_4$$

followed by the tetrazo radical combining with a CF_3 radical

[6] $$(CF_3)_5N_4 + CF_3 \rightarrow (CF_3)_6N_4.$$

This investigation attempts to distinguish between the two possible mechanisms; also some quantum yield determinations at 3 660 Å are reported.

EXPERIMENTAL

The cylindrical pyrex reaction cell (5 cm diam., 10 cm long, volume 192 cc) was part of a closed loop of total volume = 622 cc. The reacting gas was continually circulated by a magnetically operated all-glass pump. A trap was also included in the loop to freeze out condensables. Pressures were recorded on a constant volume Hg manometer. The light source was a high pressure Hg arc, and the incident light on the reaction space was 5.4×10^{16} quanta/s in the 3 660 Å spectral region, fully illuminating the cell. Conventional solution filters and actinometry were employed.

The circulating system was connected to a calibrated volume equipped with a manometer, which could be

[1]*Department of Chemistry, University of California, Santa Barbara, California.*

included in the carrier gas line to a chromatograph (Perkin–Elmer Model 154). Analysis was carried out in the majority of the experiments for N_2, C_2F_6, and unreacted hexafluoroazomethane, using a 50 cm silica-gel column, maintained at 55 °C with a carrier gas (H_2) flow rate of 18 cc/min. Respective retention times were $1\frac{3}{4}$, $3\frac{1}{2}$, and 17 min. As the reaction products are well established (1, 2, 3), the heavy products (I and II) were obtained by mass balance. Usually three analyses were performed on the products of each run and the results averaged.

Denoting the overall reactions by

$$A \rightarrow N_2 + C_2F_6$$

$$2A \rightarrow N_2 + \text{product I}$$

$$3A \rightarrow N_2 + \text{product II}$$

we have

$$C_2F_6 + I + II = N_2$$

$$\text{product I} = 3N_2 - A \text{ consumed} - 2C_2F_6$$

$$\text{product II} = A \text{ consumed} + C_2F_6 - 2N_2.$$

In some experiments products I and II were identified chromatographically. They did not pass through the silica-gel column in a finite time, but they were resolved and identified on a Dow Corning 200 silicone oil column. The only other substance in the reaction mixtures detectable by chromatography was CF_3I; this occurs as an impurity in the preparation of hexafluoroazomethane (3) and was not removed completely (4).

RESULTS AND DISCUSSION

Mechanism

Experiments were carried out at 5, 25, and 37 °C, and some results for the rates of formation of N_2, C_2F_6, and products I and II are recorded in Table I. If product II is formed via the reaction sequence [5] and [6], and reaction [5] is rate determining in the formation of product II (all the tetrazo radicals formed are rapidly consumed by CF_3 radicals) we may write $R_{II} = k_5$[Hyd.][A], where R is the mean rate of formation, [Hyd.] is the hydrazo radical concentration, and [A] is the hexafluoroazomethane concentration. As hydrazo radicals are consumed only in reactions [3] and [5], for the steady state, we have $R_{(I+II)} = k_2$[CF_3][A], and $R_I = k_3$[CF_3][Hyd.], so that

$$\frac{R_{(I+II)}R_{II}}{R_I} = \frac{k_2k_5[A]^2}{k_3}.$$

Plots of this function versus $[A]^2$ should be linear, passing through the origin. Although the experimental data is scattered at low pressures, distinct curvature is obtained at higher pressures.

Alternatively, if reaction [4] predominates in the formation of product II, we have

$$\frac{R_I}{R_{C_2F_6}^{1/2}R_{II}^{1/2}} = \frac{k_3}{k_1^{1/2}k_4^{1/2}}.$$

The values for this function are recorded in Table I. The data is again scattered, but the average value for the 17 experiments is 1.8. Similar cross-combination values for a great variety of alkyl radicals are reported in the literature (5). According to the simple collision theory of chemical kinetics the ratio should be 2 for reactions with no activation energy and steric factors close to unity, conditions which are assumed to prevail in many radical–radical interactions. Deviations may be expected when one of the radicals involved is strongly polar (6), but if both radicals are of similar polarity (conditions which may well apply in perfluororadical interactions), a value for the cross-combination ratio close to 2 is to be expected. In our previous study (7) of the system $CF_3 + C_3F_7$, a ratio equal to 1.77 ± 0.1 over a 107° temperature range was obtained. Gordon (8) has recently found the ratio 2.07 ± 0.08 for $CF_3 + C_2F_5$ from 50–300 °C. Although we cannot assume that

Can. J. Chem. Downloaded from www.nrcresearchpress.com by 210.87.254.6 on 09/05/12
For personal use only.

TABLE I*

Temp. (°C)	Pressure (A) (mm Hg)	Products (mole × 10^6)				$R_I/(R_{C_2F_6}{}^{\frac{1}{2}}R_{II}{}^{\frac{1}{2}})$	Φ_{N_2}	Run time (min)
		N_2	C_2F_6	I	II			
5	14.6	39.3	7.8	24.4	7.2	1.9	0.85	240
	11.0	26.0	7.7	8.6	9.7	0.6	0.74	240
	4.0	13.2	3.4	7.3	2.5	1.5	1.03	240
	32.9	78.9	11.9	44.9	22.1	1.7	0.75	240
	9.9	24.5	4.8	14.9	4.8	2.1	1.07	180
	8.4	18.2	4.5	11.6	2.1	2.6	0.95	180
	12.0	23.9	5.8	12.1	6.0	1.4	0.84	180
	7.0	17.5	5.2	7.1	5.2	0.9	1.06	180
	9.2	19.4	5.1	9.0	5.3	1.2	0.92	180
	5.2	13.6	3.9	5.9	3.7	1.1	1.08	180
	19.0	31.2	5.1	20.4	5.7	2.6	0.69	180
25	39.5	46.5	3.9	22.7	19.9	2.2	0.74	120
	18.0	62.2	8.3	48.0	5.9	3.6	0.87	300
37	21.7	61.8	8.6	46.2	7.0	3.2	0.76	300
	10.0	35.7	4.8	22.5	8.4	1.9	0.96	300
	4.5	17.1	3.0	11.3	2.8	2.1	0.95	300
	12.4	30.6	3.2	9.4	18.0	0.7	0.86	241

*The lack of precision in the cross-combination ratios is due to the fact that small errors in the measurements of the initial and final hexafluoroazomethane concentrations can reflect a large error in the hexafluoroazomethane consumed (10–15% conversion), leading to a large error in the rates of formation of products I and II, as determined by mass balance.

CF_3 and $(CF_3)_2NNCF_3$ are of equal polarity, the cross combination ratio obtained indicates that reaction [4] is the predominant mode of formation of product II, rather than reaction [5], followed by [6].

In some present studies (9) on the photolysis of $C_2F_5N{=}NC_2F_5$, ratios of $C_4F_{10}/N_2 \simeq 0.7$ were obtained at 100, 140 and 200 °C, at about 5 cm pressure. For a similar pressure of $CF_3N{=}NCF_3$ at room temperature and comparable intensity (1) $C_2F_6/N_2 = 0.2$. Assuming similar activation energies for the $R_fN{=}NR_f$ addition by the respective radicals, it is seen that the C_2F_5 radical addition process is less favored sterically (assuming that the perfluoro groups (R_f) attached to the N atoms are not rate controlling, sterically). This represents some corroborative evidence that the hydrazo radical addition in reaction [5] will be unlikely from steric considerations.

A few experiments were carried out with CO_2 added to the system, using 10 mm initial pressure of hexafluoroazomethane at 5 °C, and from 0–21 mm pressure of CO_2. The C_2F_6 yield was found to be independent of diluent gas pressure, indicating the homogeneous second-order recombination of CF_3 radicals. In experiments on the photolysis of CF_3CHO it has been shown that CF_3 radical combination only approaches the third-body dependence region at pressures <0.5 mm (10).

Quantum Yields

Quantum yields of the products arising from radical interactions are given in Fig. 1. (The data are not necessarily derived from those presented in Table I.) The quantum yield of product I increases with temperature as would be expected from the known temperature dependence (3) of reaction [2].

The quantum yield data on N_2 give a value of $\Phi_{N_2} = 1$ at low pressures ($\sim$ 5 mm), dropping to a value of $\Phi_{N_2} \simeq 0.75$ at $\sim$ 30 mm pressure. Although the quantum yield of N_2 does not fall below unity at pressures under 1 atm in the photolysis of azomethane (11), the substitution of fluorine for hydrogen increases the number of effective normal modes of vibration (12) so that we should expect collisional deactivation processes to be more evident at lower pressures with hexafluoroazomethane. Similarly the importance of collisional deactivation has been shown in the photolysis of azoethane because of the

Can. J. Chem. Downloaded from www.nrcresearchpress.com by 210.87.254.6 on 09/05/12
For personal use only.

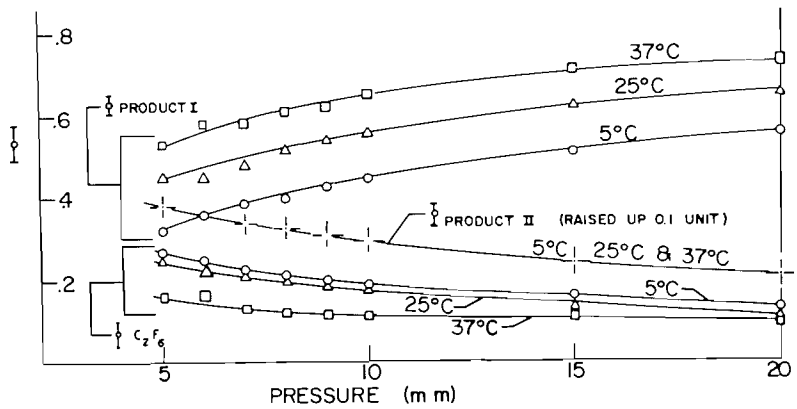

FIG. 1. Overall quantum yield, Φ, for hexafluoroethane (C_2F_6), perfluorotetramethyl hydrazine (product I), and perfluorohexamethyl tetrazine (product II) plotted against temperature and pressure.

larger number of degrees of vibrational freedom (13). At 28 °C and 3 660 Å values of Φ_{N_2} decrease from 0.85 to 0.59 in the pressure range 12 to 134 mm (13). A large pressure effect on Φ_{N_2} is also evident in the photolysis of $C_2F_5N_2C_2F_5$ (9).

From the simple deactivation mechanism

$$A + h\nu \rightarrow A^*$$

$$A^* \xrightarrow{k_a} \text{products}$$

$$A + A^* \xrightarrow{k_b} 2A$$

where A* represents an excited $CF_3N_2CF_3$ with sufficient energy to decompose, we have, in the steady state

$$1/\Phi = 1 + (k_b/k_a)[A].$$

A plot of our data in this form ($1/\Phi$ versus [A]) showed some scatter, but a least-squares treatment gave an intercept of 0.98, which is close to the theoretical value of unity. Similar intercepts were found in the azoethane system (13), in the temperature range 28 to 150 °C, although they were slightly high at lower temperatures (1.1 at 28 °C), probably due to internal conversion to an electronic state which is incapable of dissociation, or to a wall reaction (13). A flash photolysis study of azoethane (14) over the pressure range 20 to 80 mm also gave a unity intercept (for Φ_{N_2} measured at room temperature).

A value of $k_b = 1.6 \times 10^{14}$ mole^{-1} cc s^{-1} may be calculated at 25 °C from collision theory, assuming that $E_b = 0$, a collision efficiency factor of unity, and collision diameters of A and A* = 6.0 Å (based on (15) $(CF_3)_2CO$ = 6.0 Å). Taking this value in conjunction with the experimental slope ($k_b/k_a = 2.3 \times 10^5$ cc mole^{-1}) we obtain $k_a = 0.8 \times 10^9$ s^{-1}. The value for $k_b = 3.6 \times 10^{14}$ mole^{-1} cc s^{-1} for azoethane (assuming collision diameters for A and A* of 7.0 Å (13)); taking an average value for $k_b/k_a = 0.9 \times 10^5$ cc mole^{-1}, calculated from values of 0.81×10^5 and 1.04×10^5 cc mole^{-1} (13, 14), we find that $k_a = 4.0 \times 10^9$ s^{-1} for azoethane, indicating a factor of about 5 in the decomposition rates of the excited states at room temperature.[2] The ratios of k_b/k_a in the two systems indicate a factor of

[2]*Cerfontain and Kutschke (13) give $k_b = 1.8 \times 10^{14}$ mole^{-1} cc s^{-1} which is presumably obtained by dividing the collision number by 2. We have regarded A and A* as unlike species in both calculations. It is also assumed that the translational energy of A* is the same as that for A.*

Can. J. Chem. Downloaded from www.nrcresearchpress.com by 210.87.254.6 on 09/05/12
For personal use only.

Can. J. Chem. Downloaded from www.nrcresearchpress.com by 210.87.254.6 on 09/05/12
For personal use only.

2.5 in the respective rates, and with allowance for the differences in the reduced masses, the factor becomes 3.6. The remainder of the calculation then depends upon the values assigned to the collision diameters.

It is interesting to note that the rate of thermal decomposition of azoethane is appreciably faster than the rate for hexafluoroazomethane, which is attributable to a difference of ~ 7 kcal mole^{-1} in the respective activation energies for pyrolysis (12). (Using the Arrhenius parameters given (12) we may compute that azoethane decomposes 5 times faster than hexafluoroazomethane at 1 220 °K.)

In proposing the simple deactivation mechanism for azoethane Weininger and Rice (16) emphasized that although some of the excitation energy in photochemical decomposition is initially electronic, conversion into vibrational energy occurs, leading to cleavage of a critical bond(s) if sufficient energy is available. This picture has been retained by subsequent workers (11, 13) and by us. Most recent work (17) places an upper limit of about 30 kcal/mole for the quantum of vibrational energy that is transferred per collision, a figure which is consistent with the simple deactivation mechanism of Weininger and Rice (16), and the initial photochemical energy involved. It is difficult to explain the pressure dependence of the quantum yields in any other way. The energy taken up at 3 660 Å is equivalent to ~ 80 kcal mole^{-1}, which is well above the activation energies required for C—N bond fission[3] in the two compounds: 55.2 and 48.5 kcal mole^{-1} in hexafluoroazomethane and azoethane respectively (12). Although the differences in activation energy are in the right direction, as 10–20 kcal mole^{-1} of excess vibrational energy is transferred at each collision (17), the determining factor in the decomposition rate of the photochemically activated species is dependent upon the probability of it attaining the critical configuration which leads to decomposition, while deactivating collisions are occurring. This probability is a function of the number of available degrees of freedom in the molecule throughout which the excess energy can be distributed, decreasing with increasing degrees of freedom. In terms of the Kassel model the number of effective oscillators, S, is ~ 23 in hexafluoroazomethane (12), while $S = 18$ for azoethane (18), which is in accord with the differences in the decomposition rates and the pressure dependencies of the quantum yields that we have observed.

Implicit in the preceding comparison is the assumption that the collision efficiency factors (Q) are identical for the two systems at room temperature. Since relative deactivating efficiencies vary according to the species being deactivated, a direct comparison is difficult, but we have presumed that they are not markedly different.

In the azoethane photolysis Cerfontain and Kutschke (13) further observed decreasing slopes (k_b/k_a) with increasing temperature, from which they calculated increasing values of k_a. Although the increased vibrational energy content of A*, caused by raising the temperature, cannot be ignored, we may suggest that as energy transfer is less efficient at higher temperatures, the collision efficiency factor (Q) decreases, so that smaller values of k_b should be employed, yielding smaller values of k_a[4]. The increased quantum yields found with increasing temperature may then be largely correlated with a decreasing rate in energy transfer, an identical picture to that which accounts for the pressure dependence of the quantum yield. We are conducting (9) additional experiments with perfluoroazoethane to investigate this possibility.

[3]*The second* C—N *bond cleavage is spontaneous, requiring very little energy, see M. Page, H. O. Pritchard, and A. F. Trotman-Dickenson. J. Chem. Soc. 3878 (1953).*

[4]*If* $Q = 1.0$ *at 28° and 0.3 at 152°C,* k_a *has the same value at both temperatures.*

ACKNOWLEDGMENTS

The generous financial assistance of the Defence Research Board of Canada, under Grant 9530/13 is gratefully acknowledged. One of us (R. F. M.) would like to thank Professor W. M. Smith for his helpful guidance, and one of us (G. O. P.) thanks the National Science Foundation for assistance. We also thank Dr. A. S. Gordon for helpful discussion, and communication of results prior to publication.

REFERENCES

1. G. O. PRITCHARD, H. O. PRITCHARD, and A. F. TROTMAN-DICKENSON. Chem. Ind. London, 564 (1955).
2. J. R. DACEY and D. M. YOUNG. J. Chem. Phys. **23**, 1302 (1955).
3. G. O. PRITCHARD, H. O. PRITCHARD, H. I. SCHIFF, and A. F. TROTMAN-DICKENSON. Trans. Faraday Soc. **52**, 849 (1956).
4. A. H. DINWOODIE and R. N. HASZELDINE. J. Chem. Soc. 2266 (1965).
5. J. A. KERR and A. F. TROTMAN-DICKENSON. Progr. Reaction Kinetics. **1**, 107 (1961).
6. J. G. CALVERT. Ann. Rev. Phys. Chem. **11**, 41 (1960).
7. G. O. PRITCHARD, G. H. MILLER, and J. R. DACEY. Can. J. Chem. **39**, 1968 (1961).
8. A. S. GORDON. Can. J. Chem. In press.
9. J. R. DACEY, G. O. PRITCHARD, and C. R. SIMONDS. Unpublished data.
10. R. E. DODD and J. W. SMITH. J. Chem. Soc. 1465 (1957).
11. R. E. REBBERT and P. AUSLOOS. J. Am. Chem. Soc. **87**, 1847 (1965).
12. E. LEVENTHAL, C. R. SIMONDS, and C. STEEL. Can. J. Chem. **40**, 930 (1962).
13. H. CERFONTAIN and K. O. KUTSCHKE. Can. J. Chem. **36**, 344 (1958).
14. J. O. TERRY. M.Sc. Thesis, Air University, Wright-Patterson Air Force Base, Ohio. 1964.
15. P. B. AYSCOUGH and E. W. R. STEACIE. Proc. Roy. Soc. London, Ser. A, **243**, 476 (1956).
16. J. L. WEININGER and O. K. RICE. J. Am. Chem. Soc. **74**, 6216 (1952).
17. B. S. RABINOVITCH and M. C. FLOWERS. Quart. Rev. **18**, 122 (1964). D. W. SETSER, B. S. RABINOVITCH, and J. W. SIMONS. J. Chem. Phys. **40**, 1751 (1964). I. HALLER and R. SRINIVASAN. J. Chem. Phys. **42**, 2977 (1965).
18. C. STEEL and K. J. LAIDLER. J. Chem Phys. **34**, 1827 (1961).

Can. J. Chem. Downloaded from www.nrcresearchpress.com by 210.87.254.6 on 09/05/12
For personal use only.

Can. J. Chem. Downloaded from www.nrcresearchpress.com by 210.87.254.40 on 09/05/12
For personal use only.

ORGANIC SULFUR COMPOUNDS

PART I. BENZOTHIAZINE HYDROXAMIC ACIDS AND RELATED COMPOUNDS

R. T. COUTTS, H. W. PEEL, AND ELIZABETH M. SMITH
College of Pharmacy, University of Saskatchewan, Saskatoon, Saskatchewan

Received June 18, 1965

ABSTRACT

2*H*-1,4-Benzothiazine hydroxamic acids of type V (see Table I) are readily prepared by reducing suitably substituted (*o*-nitrophenylthio)acetates (II, R″ = Me or Et) by means of sodium borohydride and palladium–charcoal. The ester precursors can be prepared by the interaction of *o*-nitrothiophenols and α-bromoesters, but such a method is limited in scope. Diethyl bromomalonate, for example, reacts atypically with *o*-nitrothiophenol. The ester precursors are better prepared by Fischer–Speier esterification of the corresponding acids (II, R″ = H) which, in turn, are the products of nucleophilic attack by α-mercaptoacids on suitable *o*-chloro- (or bromo-) nitrobenzenes. This general preparative method failed in two instances. When *o*-chloronitrobenzene or 4-chloro-3-nitrotoluene was reacted with α-mercaptoisobutyric acid, the only acidic product obtained was α,α′-dithiodiisobutyric acid.

Reduction of methyl 2-(*o*-nitrophenylthio)benzoate (VI) with sodium borohydride and palladium–charcoal gave an azoxy compound, namely 2,2′-bis((*o*-methoxycarbonyl)phenylthio)azoxybenzene (VII).

When suitably substituted aromatic *o*-nitroesters are reduced with sodium borohydride and palladium–charcoal, the nitro group is converted into a hydroxylamino group which then cyclizes with the ester group, and cyclic hydroxamic acids are the result. Using this method of reduction, we have prepared a variety of such compounds (1, 2) including 3,4-dihydro-4-hydroxy-3-oxo-2*H*-1,4-benzothiazine (I*a*), the related sulfone (I*b*) and the corresponding benzoxazine (I*c*). Many cyclic hydroxamic acids possess antibacterial properties (2, 3, 4); Dimboa (3,4-dihydro-2,4-dihydroxy-7-methoxy-3-oxo-2*H*-1,4-benzoxazine) exhibits antimetabolic activity (5) and benzothiazines related to I have been shown to possess anthelmintic properties (6, 7). For these reasons, it was of interest to prepare simple derivatives of I*a* and test them initially for antibacterial activity and for their

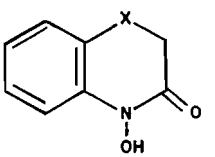

I

(*a*) X = S
(*b*) X = SO_2
(*c*) X = O

action on selected enzymes. This investigation also offered an opportunity to study further the reducing properties of sodium borohydride in the presence of palladium–charcoal.

For the preparation of the precursors (II) required for reduction to 2-substituted 3,4-dihydro-4-hydroxy-3-oxo-2*H*-1,4-benzothiazines, the initial method chosen was to condense the appropriate sodium *o*-nitrothiophenolate with suitable α-bromoesters (Scheme 1). This reaction, however, proved to be unsatisfactory. In the first place, the yields of pure *o*-nitrothiophenol obtained by mild reduction of bis(*o*-nitrophenyl) disulfide (III*a*) according to the methods of Claass (8, 9) and Mills and Whitworth (10) were poor, as were the yields of products; in addition, the scope of the reaction was limited by the

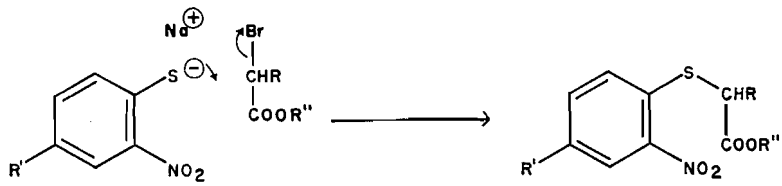

SCHEME 1.

nature of the substituent R on the α-carbon of the bromoester. Using this method, 2-(*o*-nitrophenylthio)propionic acid, its ethyl ester (II*a*), ethyl 2-(*o*-nitrophenylthio)butyrate (II*b*), and methyl (2,4-dinitrophenylthio)acetate (II*c*) were prepared from either the disulfides (III*a* or III*b*) or from sodium *o*-nitrothiophenolate. An unsuccessful attempt to extend this reaction to the preparation of the compound in which R was an ethoxycarbonyl group (II*d*) is described in detail later in this paper.

Numerous attempts were made to prepare (4-trifluoromethyl-2-nitrophenylthio)acetic acid (II*e*) from bis(4-trifluoromethyl-2-nitrophenyl) disulfide (III*c*). Using Claass' method of converting disulfides to thiophenols, the disulfide (III*c*) was reduced to 4-trifluoromethyl-2-nitrothiophenol, which was not isolated before being reacted with chloroacetic acid. By this method, very poor yields of II*e* were obtained. The presence of the trifluoromethyl group and its effect on the solubility in water of the product contributed to the poor yield (11). An attempt to isolate 4-trifluoromethyl-2-nitrothiophenol in pure form, prior to condensing with chloroacetic acid, was unsuccessful.

o-Chloronitrobenzene is an alternative starting material for the preparation of compounds of type II. This substance and its simple derivatives are known to react with thioglycollic acid and give (*o*-nitrophenylthio)acetic acids in good yields (12, 13, 14). Using this method, (4-trifluoromethyl-2-nitrophenylthio)acetic acid (II*e*) was prepared from 4-chloro-α,α,α-trifluoro-3-nitrotoluene and was isolated in a yield vastly superior to that obtained as described above. The related 4-bromo and 4-methyl derivatives of (*o*-nitrophenylthio)acetic acid (II*f* and II*g*) were also obtained by this method from 2,5-dibromonitrobenzene and 4-chloro-3-nitrotoluene respectively. This approach to the syntheses of precursors of benzothiazine hydroxamic acids is capable of extension to give the starting materials necessary for the preparation of products substituted in the 2-position of the benzothiazine ring. These starting materials were readily obtained by reacting various *o*-chloro- (or bromo-) nitrobenzenes with α-mercapto acids in the presence of sodium bicarbonate (Scheme 2). Generally, longer reaction times were necessary than when thioglycollic acid was employed in the reaction. Thus, when α-mercaptosuccinic acid and α-mercaptopropionic acid were each condensed with *o*-chloronitrobenzene, 4-chloro-α,α,α-trifluoro-3-nitrotoluene, 2,5-dibromonitrobenzene, and 4-chloro-3-nitrotoluene, a further selection of compounds of type II (II*h*–II*o*) were obtained, usually in good yield. The deactivating effect of the methyl group on the reactivity of 4-chloro-3-nitrotoluene to nucleophilic substitution was clearly illustrated by the fact that the yields of products obtained using this compound were appreciably lower than when the other *o*-nitrochloro (or bromo) compounds were employed in the reactions with α-mercapto acids. The major limitation, however, to this preparative method would seem to be the availability of α-mercapto acids, although the nature of the other substituents on the α-carbon of the mercapto acid and their effect on the reactivity of the thiol group also limits its scope. When, for example, α-mercaptoisobutyric acid is condensed with 4-chloro-α,α,α-trifluoro-3-nitrotoluene or with 2,5-dibromonitrobenzene, the nucleophilic reaction is typical and

Can. J. Chem. Downloaded from www.nrcresearchpress.com by 210.87.254.40 on 09/05/12
For personal use only.

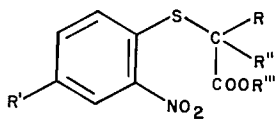

II

Compound	R	R′	R″	R‴	Compound	R	R′	R″	R‴
a	Me	H	H	Et	*l*	Me	H	H	H
b	Et	H	H	Et	*m*	Me	CF_3	H	H
c	H	NO_2	H	Me	*n*	Me	Br	H	H
d	COOEt	H	H	Et	*o*	Me	Me	H	H
e	H	CF_3	H	H	*p*	Me	CF_3	Me	H
f	H	Br	H	H	*q*	Me	Br	Me	H
g	H	Me	H	H	*r*	Me	H	Me	H
h	CH_2COOH	H	H	H	*s*	Me	Me	Me	H
i	CH_2COOH	CF_3	H	H	*t**	Me	H	H	Me
j	CH_2COOH	Br	H	H	*u*	Me	H	H	Me
k	CH_2COOH	Me	H	H					

*SO_2 replaces S in II.

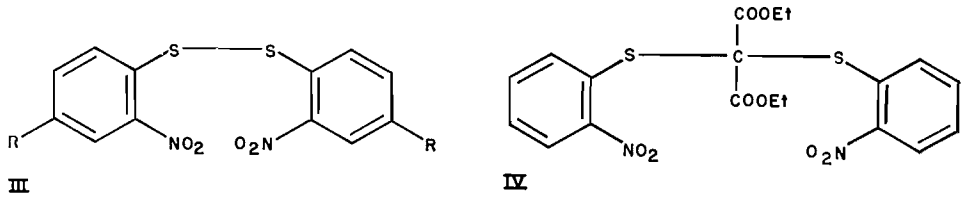

III IV

a, R = H; *b*, R = NO_2; *c*, R = CF_3.

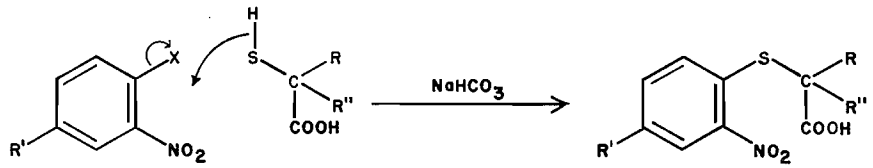

SCHEME 2.

α-(4-trifluoromethyl-2-nitrophenylthio)isobutyric acid (II*p*) and α-(4-bromo-2-nitrophenylthio)isobutyric acid (II*q*) are readily obtained in good yield. No α-(*o*-nitrophenylthio)isobutyric acids were obtained, however, when *o*-chloronitrobenzene and 4-chloro-3-nitrotoluene were reacted with α-mercaptoisobutyric acid. Under the conditions used, neither the thiol group of the α-mercapto acid nor the ortho-chlorine atom of the nitrobenzene employed in the reaction were sufficiently activated to promote a nucleophilic substitution reaction, and, in both cases, the same product, α,α′-dithiodiisobutyric acid, was the only acidic material isolable.

The acids II*e*–II*q* were readily esterified using Fischer–Speier conditions, before being reduced. Reductive cyclization of the esters of type II by means of sodium borohydride and palladium–charcoal produced good yields of cyclic hydroxamic acids (Table I) in most cases. Two attempts to reduce methyl (4-methyl-2-nitrophenylthio)acetate, however, resulted in poor yields of the expected hydroxamic acid (V*g*); the main product of this atypical reaction was the acid (II*g*) of the starting material. Reduction of methyl (2,4-dinitrophenylthio)acetate (II*c*) was also unsatisfactory. A dark brown amphoteric oil was obtained in an amount insufficient for characterization. It gave the color tests expected of

Can. J. Chem. Downloaded from www.nrcresearchpress.com by 210.87.254.40 on 09/05/12
For personal use only.

both a primary aromatic amine and a hydroxamic acid which suggested that the isolated nitro group (R′ in formula II) had, as expected, reduced beyond the hydroxylamino stage (15).

Condensation of methyl *o*-mercaptobenzoate with *o*-chloronitrobenzene produced methyl 2-(*o*-nitrophenylthio)benzoate (VI). This compound was reduced with sodium borohydride and palladium–charcoal in an attempt to prepare a cyclic hydroxamic acid with a seven-membered ring system. Hitherto, reduction of nitro groups with this reagent has produced either primary amines (15) or, as a result of cyclization at the hydroxylamino stage of reduction, cyclic *N*-oxy or *N*-hydroxy compounds (1, 2). In the present case, reduction did occur but the product was neither a primary amine nor a cyclic hydroxamic acid. Instead, an azoxy compound (VII) was obtained. In a different series of reactions, we have found that the yield and the nature of the product obtained in sodium borohydride/palladium–charcoal reductions is greatly influenced by the choice of solvent and the rate of addition of the nitro compound to the reducing medium (16). This is also true in the reduction of VI. When dioxane was employed as solvent and the rate of addition of the

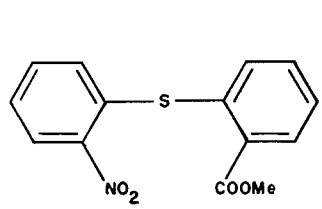

VI

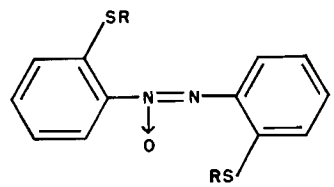

VII

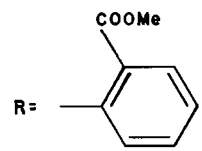

nitro compound was extended to 1 h, a good yield of azoxy compound resulted. A more rapid reduction of VI using ethanol as solvent gave the same product (VII) in much poorer yield. Reduction of the ester (VI) with zinc and ammonium chloride also gave the same azoxy compound, again in poor yield. The structure of the azoxy compound was inferred from its elemental analysis, its color, and the fact that such compounds can be prepared by reducing nitro compounds with zinc and ammonium chloride. Corroboration was obtained from infrared studies. The infrared spectrum of the starting material (VI) showed typical strong absorption in the nitro group regions which was absent in the reduced compound (VII), having been replaced by a strong absorption peak at 1 474 cm^{-1}. This absorption may be attributed to the azoxy group for the reasons which follow. The infrared spectra of 4,4′-dichloroazobenzene, 4,4′-diphenylazobenzene, and 4-chloro-4′-phenylazobenzene were compared with 4,4′-dichloroazoxybenzene, 4,4′-diphenylazoxybenzene, and 4-chloro-4′-phenylazoxybenzene (mixture of isomers) respectively, in the 1 450 – 1 500 cm^{-1} region (17). In the case of each pair of azo and azoxy compounds, the azoxy compound possessed a strong additional absorption peak at 1 473 cm^{-1} (4,4′-dichloroazoxybenzene), 1 469 cm^{-1} (4,4′-diphenylazoxybenzene), and 1 475 cm^{-1} (4-chloro-4′-phenylazoxybenzene mixture). One of the two strong peaks at 1 255 and 1 270 cm^{-1} in the infrared spectrum of compound VII may also be attributed to N—O stretching of an azoxy group (18).

Can. J. Chem. Downloaded from www.nrcresearchpress.com by 210.87.254.40 on 09/05/12
For personal use only.

Can. J. Chem. Downloaded from www.nrcresearchpress.com by 210.87.254.40 on 09/05/12
For personal use only.

TABLE I

3,4-Dihydro-4-hydroxy-3-oxo-2*H*-1,4-benzothiazine hydroxamic acids (V)

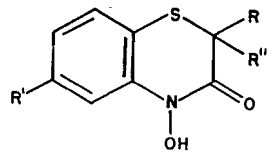

V

Compound	R	R′	R″	M.p.	Yield (%)	Calcd.				Found			
						C	H	N	S	C	H	N	S
V*a*	Me	H	H	149–150	43	55.37	4.65	7.17	16.42	55.30	4.47	7.12	16.24
V*b*	Et	H	H	104–106	41	57.39	5.30	6.70	15.32	56.77	5.44	6.60	15.26
V*e*	H	CF_3	H	137–139	87	43.38	2.43	5.62	12.78	43.48	2.62	5.48	12.67
V*f*	H	Br	H	169–170	42	36.94	2.33	5.39	12.33	37.00	2.33	5.39	12.33
V*g*	H	Me	H	105–107	21	55.37	4.65	7.17	16.42	55.36	4.61	7.18	16.35
V*h*	CH_2COOMe	H	H	122–124	71	52.16	4.40	5.53	12.61	52.08	4.57	5.42	12.72
V*i*	CH_2COOMe	CF_3	H	123–125	30	44.86	3.14	4.36	9.98	45.07	3.30	4.47	9.96
V*j*	CH_2COOMe	Br	H	165–167	83	39.77	3.03	4.22	9.65	39.43	2.92	4.36	9.66
V*k*	CH_2COOMe	Me	H	96–97	40	53.92	4.90	5.24	12.00	54.08	4.95	5.53	12.21
V*m*	Me	CF_3	H	126–128	83	45.63	3.06	5.32	12.18	45.77	3.22	5.11	12.45
V*n*	Me	Br	H	157–158	41	39.43	2.94	5.11	11.70	39.44	2.96	4.72	11.50
V*o*	Me	Me	H	135–137	73	57.39	5.30	6.69	15.32	57.25	5.31	7.24	15.45
V*p*	Me	CF_3	Me	100–101	72	47.65	3.64	5.05	11.56	47.58	3.66	5.15	11.77
V*q*	Me	Br	Me	116–118	93	41.68	3.50	4.86	11.13	41.90	3.76	5.15	10.96
V*i**	Me	H	H	186–188	89	47.57	3.99	6.16	14.11	47.32	4.13	6.39	14.15

*SO_2 replaces S in structure V.

One example of a substituted benzothiazine-1,1-dioxide was also prepared during this study. 3,4-Dihydro-4-hydroxy-2-methyl-3-oxo-2*H*-1,4-benzothiazine-1,1-dioxide (V*t*) was readily obtained by sodium borohydride/palladium–charcoal reduction of methyl 2-(*o*-nitrophenylsulfonyl)propionate (II*t*) which was, in turn, the product of oxidizing the related sulfide (II*u*) with potassium permanganate. Presumably the sulfones of the benzothiazines listed in Table I could be prepared in a similar manner.

Reduction by means of hydrazine hydrate and palladium–charcoal is also a suitable method of preparing cyclic hydroxamic acids (19) but when this method was applied to methyl (*o*-nitrophenylthio)acetate, no reduction occurred and the only product isolated was the hydrazide of the starting material. This preparative method was therefore not investigated further.

All the hydroxamic acids listed in Table I gave the expected violet color when ethanolic ferric chloride solution was added to an ethanolic solution of the acid. Addition of water to this solution usually resulted in the precipitation of a brown colored ferric chelate.

As previously mentioned, condensation of sodium *o*-nitrothiophenolate with diethyl bromomalonate gave no diethyl (*o*-nitrophenylthio)malonate (II*d*). Instead, a very good yield of bis(*o*-nitrophenyl) disulfide (III*a*) immediately resulted on the addition of the bromomalonate to an aqueous ethanolic solution of sodium *o*-nitrothiophenolate. The filtrate from this reaction, on concentration and standing, deposited a small amount of diethyl bis(*o*-nitrophenylthio)malonate (IV). Such a structure is suggested by elemental analysis, infrared spectrum, and the fact that the same compound is obtained when diethyl dibromomalonate is reacted with sodium *o*-nitrothiophenolate. The isolation of IV, however, is not due to the presence of diethyl dibromomalonate as an impurity in the monobromomalonate. When the dibromomalonate was condensed with sodium *o*-nitrothiophenolate in aqueous ethanol, a yield in excess of 80% of bis(*o*-nitrophenyl) disulfide was immediately formed and only a small quantity of IV was isolated. This reaction requires further investigation and will be the subject of a later communication. The formation of IV is reminiscent of the findings of Honkanen and Virtanen (20) who interacted sodium *o*-nitrophenolate and diethyl bromomalonate and obtained as a minor product of the reaction, a substance which was apparently diethyl bis(*o*-nitrophenoxy)malonate (IV, O replacing S).

A selection of the compounds of types I and II are at present being tested for antibacterial activity and for their action on selected enzymes. Preliminary results in the latter case are encouraging and will be reported elsewhere.

EXPERIMENTAL

Melting points and boiling points are uncorrected. Equivalent weights were determined in aqueous ethanol by direct titration with standard alkali. Infrared spectra were recorded on a Beckmann I.R. 8 spectrophotometer except where stated otherwise, and microanalyses were carried out by Dr. F. Pascher and E. Pascher, Bonn, who determined the molecular weight values by measurement of vapor pressure. Palladium–charcoal refers to 10% palladium-on-charcoal. Ether solutions were dried over Na_2SO_4.

o-Nitrothiophenol

Using Claass' method (8) except that aqueous acetic acid was employed instead of mineral acid to finally liberate the phenol, apparently good yields of *o*-nitrothiophenol (20–24 g) are obtained from bis(*o*-nitrophenyl) disulfide (30 g). The green precipitate, m.p. 48–52°, is impure, however, only approximately half of it being soluble in light petroleum from which the thiophenol is obtained as yellow crystals, m.p. 59–60°, lit. (10) m.p. 61°.

Ethyl 2-(o-Nitrophenylthio)propionate (IIa)

Bis(*o*-nitrophenyl) disulfide (10 g) was converted to sodium *o*-nitrothiophenolate using Claass' method (9), and to the aqueous solution of the salt was added ethyl 2-bromopropionate (8.8 ml). The mixture was stirred until the red solution became much lighter in color, and the oil which separated was extracted into ether.

Can. J. Chem. Downloaded from www.nrcresearchpress.com by 210.87.254.40 on 09/05/12
For personal use only.

The dried ether solution was distilled, and the fraction boiling at 184–188° at 10–15 mm Hg (4.41 g) was collected. The oil solidified when triturated with a little methanol and gave ethyl 2-(*o*-nitrophenylthio)propionate (3.71 g) as yellow crystals, m.p. 47–48°.

Anal. Calcd. for $C_{11}H_{13}NO_4S$: C, 51.71; H, 5.13; N, 5.52; S, 12.55. Found: C, 51.82; H, 4.86; N, 5.67; S, 12.38.

Methyl (2,4-Dinitrophenylthio)acetate (IIc)

This was prepared by the method used for II*a*, from the disulfide (20 g) and methyl bromoacetate (10 ml). The compound was a yellow solid (11.2 g), m.p. 92–93°, lit. (12) m.p. 93–94°.

Ethyl 2-(o-Nitrophenylthio)butyrate (IIb)

o-Nitrothiophenol (3.88 g) was dissolved in a solution of sodium hydroxide (1 g) in water, (4 ml) and ethanol (80 ml). To the red solution was added ethyl 2-bromobutyrate (5.09 g). A precipitate of crude disulfide (III*a*, 0.71 g) was removed and the filtrate was evaporated to 20 ml, flooded with water, and extracted with ether. The washed and dried ether layer was distilled. The yellow oil, b.p. 200–205° at 23 mm Hg, (2.49 g) was ethyl 2-(*o*-nitrophenylthio)butyrate.

Anal. Calcd. for $C_{12}H_{15}NO_4S$: C, 53.51; H, 5.61; N, 5.20; S, 11.91. Found: C, 53.21; H, 5.89; N, 4.96; S, 12.07.

(4-Trifluoromethyl-2-nitrophenylthio)acetic Acid (IIe)

Method (a)

Bis(4-trifluoromethyl-2-nitrophenyl) disulfide (25 g) was heated under reflux with ethanol (200 ml). To the refluxing solution was added successive small portions of a concentrated aqueous solution of sodium sulfide nonahydrate (11.7 g) and sodium hydroxide (6.7 g). The dark red solution of the mercaptide was diluted with water (500 ml), cooled, and filtered. To the filtrate was added a solution of chloracetic acid (16.7 g) and anhydrous sodium carbonate (10 g) in water (100 ml) and the whole was heated gently for 2 h. The cooled solution was then extracted with ether, and the aqueous layer was acidified with dilute hydrochloric acid and yielded an almost black solid (10.3 g), m.p. 90–95°. The crude product was purified by repeated dissolution in sodium bicarbonate solution, followed by reprecipitation with acetic acid and crystallization from benzene. This gave 3.22 g of yellow acid (II*e*), m.p. 158°, lit. (14) m.p. 154–155°.

Method (b)

The acid (II*e*) was obtained in 68% yield from 4-chloro-α,α,α-trifluoro-3-nitrotoluene and thioglycollic acid using the general method of preparing 2-(*o*-nitrophenylthio) acids, which is described below. Reflux time time was 5 h. Crystallization from benzene gave yellow crystals, m.p. 158°.

Anal. Calcd. for $C_9H_6F_3NO_4S$: C, 38.44; H, 2.15; N, 4.98; S, 11.40. Found: C, 38.48; H, 2.04; N, 5.17; S, 11.57.

General Method of Preparing 2-(o-Nitrophenylthio) Acids and Esters of Type II

The substituted *o*-nitrochloro or *o*-nitrobromobenzene (0.05 mole) and the α-mercaptoacid (0.05 mole) were refluxed for the stated time in 50% aqueous ethanol (100 ml), in which was suspended a slight excess of sodium bicarbonate (0.11 or 0.16 mole, for monobasic or dibasic acids respectively). The solution was then concentrated to approximately 50 ml, diluted with water, and extracted with ether. The ether layer was rejected. The *o*-nitrophenylthio acid was obtained in the stated yield from the aqueous solution by acidifying with dilute hydrochloric acid.

The acids listed in Table II were obtained by this method. All were yellow solids, except II*i* and II*p* which were pale brown in color, and all had characteristic infrared spectra (KBr discs) which showed the expected carbonyl, hydroxyl, and nitro group absorption peaks. The corresponding methyl esters were prepared in excellent yield by refluxing the acid (5 g) in methanol (50 ml) containing concentrated sulfuric acid (5 ml) for 18–24 h, and the products were isolated in the normal way. The esters were not analyzed before reduction but were characterized by infrared spectrum and m.p. only (see Table II).

Attempted Preparation of α-(2-Nitrophenylthio)isobutyric Acid (IIr)

o-Chloronitrobenzene (3.15 g), α-mercaptoisobutyric acid (2.48 g) and sodium bicarbonate (7.51 g) were refluxed in 50% aqueous ethanol (50 ml) for 48 h. The resulting pale yellow solution was diluted with water and extracted with ether. The ether layer was rejected. The aqueous solution was acidified and extracted with ether which was washed, dried, and evaporated to give an oily solid. Trituration with benzene gave a nitrogen-free cream solid (0.857 g), m.p. 195–197°. Lit. (21) m.p. of α,α'-dithiodiisobutyric acid is 196°.

Attempted Preparation of α-(4-Methyl-2-nitrophenylthio)isobutyric acid (IIs)

By a similar method to that reported immediately above, the interaction of 4-chloro-3-nitrotoluene (3.456 g) and α-mercaptoisobutyric acid (2.425 g) yielded α,α'-dithiodiisobutyric acid (0.905 g), the infrared spectrum and m.p. of which were identical to those of the compound reported above.

General Method of Preparing Cyclic Hydroxamic Acids by Reducing Esters of Type II with Sodium Borohydride and Palladium–Charcoal

Sodium borohydride (0.8 g) was dissolved in water (5 ml) or in some cases 2% aqueous sodium hydroxide (5 ml), and palladium–charcoal (0.1 g) suspended in water (3 ml) was carefully added. The suspension was

Can. J. Chem. Downloaded from www.nrcresearchpress.com by 210.87.254.40 on 09/05/12
For personal use only.

Can. J. Chem. Downloaded from www.nrcresearchpress.com by 210.87.254.40 on 09/05/12
For personal use only.

TABLE II

Substituted (*o*-nitrophenylthio)acetic acids (II)

Acid	Yield (%)	M.p.	S*	*t*† (h)	Calcd. C	Calcd. H	Calcd. Eq. wt.	Found C	Found H	Found Eq. wt.	Yield, form, and m.p. of methyl ester
(4-Bromo-2-nitrophenylthio)-acetic (II*f*)‡	63	216–218§	ae	4	—	—	—	—	—	—	91%, yellow solid, 109–110°
(4-Methyl-2-nitrophenylthio)-acetic (II*g*)	51	185–186‖	m	8	—	—	227.2	—	—	225	83%, yellow solid, 105–107°
α-(*o*-Nitrophenylthio)succinic (II*h*)¶	64	187–189	w	24	44.28	3.34	—	44.21	3.39	—	89%, orange oil
α-(4-Trifluoromethyl-2-nitrophenylthio)succinic (II*i*)	60	196–198	ae	24	38.94	2.38	169.6	39.23	2.38	172	92%, brown oil
α-(4-Bromo-2-nitrophenylthio)succinic (II*j*)	69	218–220	e	24	34.30	2.30	175.1	34.62	2.47	176	89%, yellow solid, 70–72°**
α-(4-Methyl-2-nitrophenylthio)succinic (II*k*)	35	215–218	e	24	46.31	3.86	142.6	46.32	3.86	144.5	70%, orange oil
α-(*o*-Nitrophenylthio)propionic (II*l*)	76	107–109	ae	18	47.56	3.99	227.3	47.71	4.12	224	83%, yellow solid, 54°
α-(4-Trifluoromethyl-2-nitrophenylthio)propionic (II*m*)	78	151–152	e	18	40.68	2.73	295.3	40.82	2.93	292	93%, yellow solid, 79–80°
α-(4-Bromo-2-nitrophenylthio)propionic (II*n*)	65	149–150	ae	18	35.31	2.35	305.9	35.56	2.53	310	95%, yellow solid, 62–64°
α-(4-Methyl-2-nitrophenylthio)propionic (II*o*)	47	141–142	ae	18	49.78	4.60	241.3	49.71	4.78	244	90%, yellow solid, 42–43°
α-(4-Trifluoromethyl-2-nitrophenylthio)isobutyric (II*p*)	86	125–126	w	20	42.72	3.26	309.3	42.88	3.34	308	84%, yellow solid, 58–60°
α-(4-Bromo-2-nitrophenylthio)isobutyric (II*q*)	71	137–139	w	18	37.52	3.15	320.2	37.55	3.04	320	62%, yellow solid, 44–46°

*S = Solvent of crystallization, where w = water, e = ethanol, ae = aqueous ethanol, and m = methanol.
†*t* = Reflux time.
‡Sodium salt precipitated during the reaction.
§Lit. (7) m.p. 216–217°.
‖Lit. (7) m.p. 182–183°.
¶Anal. Calcd.: N, 5.16; S, 11.82. Found: N, 5.27; S, 11.66.
**Calcd. for $C_{12}H_{12}NO_6SBr$: S, 8.48; Br, 21.13. Found: S, 8.35; Br, 20.97.

Can. J. Chem. Downloaded from www.nrcresearchpress.com by 210.87.254.40 on 09/05/12
For personal use only.

diluted with dioxane (10 ml) and nitrogen was passed through the mixture while the ester (2 g) in dioxane (10–20 ml) was added dropwise over a period of 30 min. The passage of nitrogen was continued for 15 min after the ester had been added. The mixture was then filtered, acidified with dilute hydrochloric acid, and diluted with water. In some cases the hydroxamic acid precipitated and was filtered off. In other cases, the solution was concentrated and extracted with ether. Extraction of the ether solution with sodium carbonate solution or sodium hydroxide solution, acidification of the aqueous layer with dilute hydrochloric acid, reextraction with ether, and evaporation of the ether gave the hydroxamic acid.

Using this general method of reduction, compounds II*a* and II*b*, the methyl esters of compounds II*e* to II*k*, and the methyl esters of compounds II*m* to II*q* gave rise respectively to 3,4-dihydro-4-hydroxy-2-methyl-3-oxo-2*H*-1,4-benzothiazine (V*a*), the corresponding 2-ethyl derivative (V*b*); 6-trifluoromethyl-3,4-dihydro-4-hydroxy-3-oxo-2*H*-1,4-benzothiazine (V*e*), the corresponding 6-bromo derivative (V*f*), the corresponding 6-methyl derivative (V*g*); methyl 2-(3,4-dihydro-4-hydroxy-3-oxo-2*H*-1,4-benzothiazinyl)acetate (V*h*); methyl 2-(6-trifluoromethyl-3,4-dihydro-4-hydroxy-3-oxo-2*H*-1,4-benzothiazinyl)acetate (V*i*), the corresponding 6-bromo derivative (V*j*), the corresponding 6-methyl derivative (V*k*); 6-trifluoromethyl-3,4-dihydro-4-hydroxy-2-methyl-3-oxo-2*H*-1,4-benzothiazine (V*m*), the corresponding 6-bromo derivative (V*n*); 3,4-dihydro-4-hydroxy-2,6-dimethyl-3-oxo-2*H*-1,4-benzothiazine (V*o*); 6-trifluoromethyl-3,4-dihydro-4-hydroxy-2,2-dimethyl-3-oxo-2*H*-1,4-benzothiazine (V*p*) and the corresponding 6-bromo derivative (V*q*), in the yields stated (see Table I).

All the hydroxamic acids listed in Table I were white solids and, with the exception of compound V*t* for which ethyl acetate was employed, all were crystallized from ethanol or aqueous ethanol. A solution of each hydroxamic acid in ethanol turned deep violet on the addition of ethanolic ferric chloride solution. The infrared spectrum of each compound in KBr showed typical broad hydroxyl absorption in the 3 000 – 3 400 cm^{-1} region, the position of the peak varying from 3 090 to 3 280 cm^{-1}. Carbonyl absorption within the range 1 635 to 1 655 cm^{-1} was observed in all cases except compounds V*h*, V*i*, V*j*, and V*k* which had two carbonyl peaks, one in the 1 640 to 1 665 cm^{-1} region (hydroxamate carbonyl) and a second within the range 1 720 to 1 730 cm^{-1} (ester carbonyl).

Reduction of Methyl (4-Methyl-2-nitrophenylthio)acetate

This ester (2.408 g) was reduced by the general method. An ether extraction of the acidified filtrate yielded a yellow solid (1.562 g) which was dissolved in sodium carbonate solution (5%) and extracted with ether. The ether extract was rejected. The aqueous layer was again acidified (dilute hydrochloric acid) and (4-methyl-2-nitrophenylthio)acetic acid (II*g*) (0.948 g) was obtained (m.p. and infrared spectrum were identical to those of an authentic sample). The filtrate was extracted with ether which, on drying and evaporation, yielded 3,4-dihydro-4-hydroxy-6-methyl-3-oxo-2*H*-1,4-benzothiazine (V*g*) (0.229 g), m.p. 98–102°, raised to 105–107° on recrystallizing from ethanol.

In a repeat reduction, the ester (1.641 g) yielded II*g* (0.766 g) and V*g* (0.282 g).

Reduction of Methyl (2,4-Dinitrophenylthio)acetate

This acetate (2 g) was reduced by the general method except that methanol was used as solvent, and 2 g of sodium borohydride and 0.2 g of catalyst were employed in the reaction. The acidified filtrate was made slightly basic with ammonia solution, the excess ammonia was boiled off, and the resulting solution was diluted with water and extracted with ether. From the ether solution, a brown oil (0.25 g) was obtained on evaporation. It gave a violet color with alcoholic ferric chloride solution; it could also be diazotized and coupled with β-naphthol and thus gave an orange-red dye.

Methyl o-Mercaptobenzoate

o-Mercaptobenzoic acid (18.4 g) was refluxed for 15 h in methanol (150 ml) containing concentrated sulfuric acid (15 ml) and the ester was isolated as an oil in the usual way. The oil was distilled and the fraction boiling at 154° at 24 mm Hg (15.8 g) was collected and used in the following reaction. Lit. (22) b.p. 252°.

Methyl 2-(Nitrophenylthio)benzoate (VI)

Methyl *o*-mercaptobenzoate (4.21 g) was dissolved in a solution of sodium hydroxide (1 g) in water (2 ml) and methanol (50 ml). To the resulting red solution was added *o*-chloronitrobenzene (4.75 g) dissolved in methanol (20 ml). The mixture was allowed to stand for 4 days at room temperature then it was concentrated to half volume and flooded with water. A yellow precipitate (5.1 g, m.p. 89–93°) was obtained. After crystallizing from ethanol, the m.p. was 93°, lit. (23) m.p. 92–93°. Infrared spectrum (KBr disc): 1 725 (s) (C=O); 1 560 (s), 1 330 (s), 850 (m) (NO_2) cm^{-1}.

Reduction of Methyl 2-(o-Nitrophenylthio)benzoate

Method (a)

Methyl 2-(*o*-nitrophenylthio)benzoate (1.1 g) in dioxane (15 ml) was reduced by the general method described for the preparation of cyclic hydroxamic acids, except that the solution of the benzoate was added over a longer period (1 h) to the sodium borohydride (0.4 g) and palladium–charcoal (0.05 g) in aqueous dioxane. The filtrate was acidified with dilute hydrochloric acid, concentrated, flooded with water, and finally

extracted with ether. The ether extract was shaken with 5% sodium hydroxide solution, shaken with water, dried, and then evaporated to give a yellow neutral oil (1.01 g). This oil solidified when triturated with methanol and yielded, after recrystallization from ethanol, yellow crystals (0.71 g), m.p. 148–149° of 2,2′-bis((*o*-methoxycarbonyl)phenylthio)azoxybenzene (VII). Infrared spectrum (KBr disc): 1 710 (s) (C=O), 1 474 (s), 1 270 (s) or 1 255 (s) (azoxy) cm^{-1} (determined on a Perkin-Elmer model 21 spectrophotometer).

Anal. Calcd. for $C_{28}H_{22}N_2O_5S_2$: C, 63.38; H, 4.18; N, 5.28; S, 12.09; mol. wt. 530.6. Found: C, 63.12; H, 4.24; N, 5.23; S, 12.16; mol. wt. 511.

Method (b)

The ester (2 g) dissolved in a mixture of ethanol:methanol (3:1) (40 ml) was reduced as described in the general method for the preparation of cyclic hydroxamic acids, except that dioxane was replaced with the mixed solvent. The acidified filtrate yielded a viscous orange neutral oil (1.3 g) when treated as described in the experiment immediately above. On standing, followed by trituration with ethanol, the azoxybenzene (VII) was isolated from this oil as orange crystals (0.19 g), m.p. 145–149°.

Method (c)

A solution of ammonium chloride (2 g) in water (20 ml) was added to a solution of methyl 2-(*o*-nitrophenylthio)benzoate (2 g) in ethanol (50 ml). The mixture was stirred, zinc dust (2 g) was added in small portions over 15 min, and stirring was continued for a further 2 h at room temperature. The colorless filtrate was acidified with dilute hydrochloric acid and extracted with ether. The ether extract was shaken successively with 5% sodium carbonate solution and water, dried, and evaporated to give a neutral viscous red oil (1.62 g) which, on standing, gave a yellow solid (0.15 g), m.p. 145–148°; the infrared spectrum of this solid was superimposable on that of the product obtained by methods (*a*) and (*b*).

Anal. Found: C, 63.79; H, 3.87; N, 4.90; S, 11.60.

Methyl α-(o-Nitrophenylthio)propionate (IIu)

Bis(*o*-nitrophenyl) disulfide (30 g) was converted to sodium *o*-nitrothiophenolate using Claass' method (9). The resulting red solution was filtered, and to the filtrate was added a solution of α-chloropropionic acid (18.8 ml) and anhydrous sodium carbonate (12 g) in water (100 ml). The solution was heated for 2 h, cooled, acidified, and extracted with ether. Re-extraction of the ether layer with sodium carbonate solution, followed by acidification (dilute hydrochloric acid) of the aqueous layer gave α-(*o*-nitrophenylthio)propionic acid (III) (22.2 g) as a brown solid; m.p. 76–81°, raised to 106–108° on crystallization from aqueous ethanol. (Compare yield of III by alternative method of preparation—see Table II). Fischer–Speier esterification of the acid gave an almost quantitative yield of the ester (II*u*) as an orange oil which quickly solidified. On crystallization from methanol, a yellow solid, m.p. 54°, was obtained which was not analyzed before oxidation.

Methyl α-(o-Nitrophenylsulfonyl)propionate (IIt)

The sulfide (II*u*) (3.25 g) was dissolved in glacial acetic acid (50 ml). To this solution, a 5% aqueous solution of potassium permanganate (90 ml) was added in small quantities, with stirring, over 1 h; stirring was then continued for an additional hour. Hydrogen peroxide solution was added dropwise to decolorize the solution and the pale brown sulfone crystals which had separated during the reaction (3.09 g, m.p. 77–81°) were filtered off. Crystallization from ethanol gave white rods, m.p. 87–88°.

Anal. Calcd. for $C_{10}H_{11}NO_6S$: C, 43.95; H, 4.06; N, 5.13; S, 11.73. Found: C, 43.79; H, 3.88; N, 5.09; S, 11.68.

3,4-Dihydro-4-hydroxy-2-methyl-3-oxo-2H-1,4-benzothiazine-1,1-dioxide (Vt)

This hydroxamic acid was prepared by reducing methyl α-(*o*-nitrophenylsulfonyl)propionate with sodium borohydride and palladium–charcoal, using the general method previously described. The yield, m.p., and analytical data are recorded in Table I.

Attempted Reduction of Methyl (o-Nitrophenylthio)acetate with Hydrazine Hydrate and Palladium–Charcoal

The ester (prepared in excellent yield by Fischer–Speier esterification of the corresponding acid, ref. 8) (1.923 g) was dissolved in methanol (25 ml), and palladium–charcoal (0.1 g) was added followed by hydrazine hydrate (2 ml). The mixture was refluxed for ½ h, a further 2 ml of hydrazine hydrate were added, and refluxing was continued for another ½ h. The solution was filtered and the filtrate was evaporated to dryness giving a brown oil which was dissolved in hot methanol. On cooling, yellow crystals of (*o*-nitrophenylthio)-acetic acid hydrazide separated (0.625 g), m.p. 164°. Infrared spectrum (KBr disc): 1 646 (s) (C=O); 1 536 (s), 1 342 (s), 856 (m) (NO_2) cm^{-1} when determined on a Perkin-Elmer model 21 spectrophotometer.

Anal. Calcd. for $C_8H_9N_3O_3S$: C, 42.28; H, 3.99. Found: C, 42.08; H, 3.97.

Treatment of o-Nitrothiophenol with Diethyl Bromomalonate

A solution of *o*-nitrothiophenol (3.89 g) was prepared as before (see II*b*). On the addition of diethyl bromomalonate (4.3 ml) with stirring, an immediate precipitate of bis(*o*-nitrophenyl) disulfide (2.703 g, m.p. 196°) resulted. The infrared spectrum was identical with that of an authentic sample. The red colored filtrate was cooled overnight and a second product, diethyl bis(*o*-nitrophenylthio)malonate (IV), separated (0.591 g, m.p. 98–101°). Crystallization from methanol gave yellow needles, m.p. 101–102°; the infrared spectrum displayed the expected bands at 1 775 (C=O); 1 555, 1 355, 855 (NO_2) cm^{-1}.

Can. J. Chem. Downloaded from www.nrcresearchpress.com by 210.87.254.40 on 09/05/12
For personal use only.

Anal. Calcd. for $C_{19}H_{18}N_2O_8S_2$: C, 48.92; H, 3.86; N, 6.01; S, 13.73; mol. wt. 466.5. Found: C, 48.72; H, 4.05; N, 5.84; S, 13.69; mol. wt. 464.

Treatment of o-Nitrothiophenol with Diethyl Dibromomalonate

Using the method described in the preparation immediately above, *o*-nitrothiophenol (3.88 g) and diethyl dibromomalonate (3.975 g) gave the disulfide (III*a*, 3.526 g, m.p. 192–196°), and from the concentrated and cooled filtrate, diethyl bis(*o*-nitrophenylthio)malonate (0.165 g) precipitated, m.p. 94–97°, raised to 101–102° on crystallizing from methanol.

ACKNOWLEDGMENTS

We are indebted to Dr. R. A. Abramovitch of the Chemistry Department for helpful discussion and for his and Mr. B. A. Davis's permission to quote their unpublished findings. The technical assistance of Mr. D. Barton is also acknowledged, as is the generosity of the National Research Council of Canada whose financial assistance is greatly appreciated.

REFERENCES

1. R. T. Coutts and D. G. Wibberley. J. Chem. Soc. 4610 (1963).
2. R. T. Coutts, D. Noble, and D. G. Wibberley. J. Pharm. Pharmacol. **16**, 773 (1964).
3. R. T. Coutts. Can. Pharm. J. (Scientific Section), **97** (6), 32 (1964). See refs. 2–8 contained therein.
4. R. T. Coutts, W. N. Pitkethly, and D. G. Wibberley. J. Pharm. Sci. **54**, 792 (1965).
5. J. E. Reimann and R. U. Byerrum. Tetrahedron Letters, No. 4, 211 (1964).
6. J. Raeburn and A. Mackie. J. Chem. Soc. 787 (1952).
7. A. A. Cutler and A. Mackie. J. Chem. Soc. 3716 (1953).
8. M. Claass. Chem. Ber. **45**, 2424 (1912).
9. M. Claass. Chem. Ber. **45**, 747 (1912).
10. W. H. Mills and J. B. Whitworth. J. Chem. Soc. 2738 (1927).
11. W. T. Caldwell and A. N. Sayin. J. Am. Chem. Soc. **73**, 5125 (1951).
12. P. Friedlander, A. Chwala, and Z. Slubek. Monatsh. **28**, 247 (1907).
13. G. M. Badger, D. J. Clark, W. Davies, K. T. H. Farrer, and N. P. Kefford. J. Chem. Soc. 2624 (1957).
14. Y. E. Gerasimenko, S. M. Shein, G. G. Bakulina, A. P. Cherepivskaya, G. V. Semenyuk, and L. M. Yagupolskii. Zh. Obshch. Khim. **32**, 1870 (1962); Chem. Abstr. **58**, 2524*g* (1963).
15. T. Neilson, H. C. S. Wood, and A. G. Wylie. J. Chem. Soc. 371 (1962).
16. R. T. Coutts and K. W. Hindmarsh. Unpublished results.
17. R. A. Abramovitch and B. A. Davis. Unpublished results.
18. K. Nakanishi. Infrared absorption spectroscopy (practical). Holden-Day, Inc., San Francisco. 1962. p. 51.
19. R. T. Coutts, M. Hooper, and D. G. Wibberley. J. Chem. Soc. 5058 (1961).
20. E. Honkanen and A. I. Virtanen. Acta Chem. Scand. **14**, 1214 (1960).
21. Y. Iskander and Y. Riad. J. Chem. Soc. 2397 (1961).
22. L. Gattermann. Chem. Ber. **32**, 1136 (1899).
23. V. Hach and M. Protiva. Chem. Listy, **51**, 1909 (1957); Chem. Abstr. **52**, 4652*e* (1958).

Can. J. Chem. Downloaded from www.nrcresearchpress.com by 210.87.254.40 on 09/05/12
For personal use only.

Can. J. Chem. Downloaded from www.nrcresearchpress.com by 210.87.254.40 on 09/05/12
For personal use only.

SALTING-IN BY QUATERNARY AMMONIUM SALTS

J. E. Desnoyers, G. E. Pelletier, and C. Jolicoeur
Département de Chimie, Université de Sherbrooke, Sherbrooke, Québec
Received July 2, 1965

ABSTRACT

The solubility of benzene in substituted quaternary ammonium bromide solutions has been measured by ultraviolet absorption. The solubility is found to increase in the presence of such salts as $R_{4-n}H_nN^+Br^-$ where R is an alkyl group and n varies between 0 and 3; a smooth transition in behavior is observed when passing from simple salts to long-chained micellar salts. This salting-in can be explained in terms of an association between the nonelectrolyte and the quaternary ammonium ion, which is induced by the increase in the structure of water near large nonpolar groups of the organic ions.

INTRODUCTION

Much interest has been shown recently in the physicochemical properties of tetraalkyl ammonium salt solutions. From the size and the symmetry of these large cations, very little primary hydration would be expected; this hypothesis was used by Robinson and Stokes (1) and by Nightingale (2) in attempts to correct Stokes radii in order to obtain radii of hydrated ions from mobility data. Also, since many of the limitations of the interionic theories do not apply in the case of these large ions, the dependance on concentration of their thermodynamic and electrochemical properties would also be expected to be normal. However, a close examination of these properties indicate numerous anomalies: the entropy of hydration (3), the partial molal heat capacities (4), the variation with concentration of the viscosity (5), osmotic coefficient (6), and partial molal volume (7) are all peculiar. Frank (3, 4) has offered an explanation for these unexpected behaviors in terms of an increase in the structure of water near these large ions. Water is known to be a largely associated liquid. The presence of nonelectrolytes or large organic ions tends to strengthen the hydrogen bonds between the water molecules near the large solute, and a cage or "iceberg" is effectively formed around them. Strong evidence for the correctness of this model was given by Jeffrey (8) when he succeeded in determining the structure of a clathrate hydrate of the salt $(Bu)_4NBr$ containing on the average 32.8 molecules of water.

Another property of these salts which requires further investigation is their ability to salt-in nonelectrolytes in water. While the presence of most salts tends to decrease the solubility of nonelectrolytes, tetraalkyl ammonium salts cause a significant increase in the solubility of nonelectrolytes (9, 10, 11).

The relation between the solubility of the nonelectrolyte and salt concentration can be expressed in two ways;

$$\ln (S_0/S) = k_{so}c \qquad [1a]$$

or

$$(S_0 - S)/S_0 = k_{so}'c \qquad [1b]$$

where S_0 and S are the solubilities of the nonelectrolyte in water and in the salt solution of concentration c. It can be shown by expansion of the logarithm into a power series that the two salting-out constants k_{so} and k_{so}', are identical at low concentration provided natural logarithms are used in [1*a*].

It has been shown recently (12) that salting-out arises from: (i) hydration of ions and (ii) the difference in polarization of the water and the nonelectrolyte molecules. Both these effects cause salting-out of nonpolar nonelectrolytes and cannot be responsible for the salting-in observed with large ions. A tentative explanation of salting-in was put forward by Bockris, Bowler-Reed, and Kitchener (10) in terms of van der Waals attractive forces between large ions and large nonelectrolytes. It will be shown later that these forces could be involved in salting-in but not in the sense implied by these authors, since salting-in occurs even with very small nonelectrolytes such as rare gases (13).

McDevit and Long (14) have derived a general theory based on the internal pressure concept where k_{so} is related to the extent of electrostriction of the salt in solution ($V_s - \bar{V}_s^0$) and to the partial molal volume of the nonelectrolyte, $\bar{V}_n$, by the relation,

$$[2] \qquad k_{so} = \frac{\bar{V}_n(V_s - \bar{V}_s^0)}{\beta_0 RT}$$

where V_s is the intrinsic or actual volume occupied by the salt in solution, $\bar{V}_s^0$ is the partial molal volume at infinite dilution, and β_0 is the compressibility of pure water. Deno and Spink (11) have shown that eq. [2] can account for the salting-in by quaternary ammonium salts since they find a negative electrostriction with these salts. They, however, offer no explanation as to the origin of this negative electrostriction. Both of these theories are therefore incomplete, and it was felt that more experimental data was required for a better understanding of the nature of this salting-in.

EXPERIMENTAL

In this work benzene was chosen as the nonelectrolyte because of the large amount of data already in existence in the literature on this system, and because of the ease of measurement of its solubility by ultraviolet absorption. The benzene used was purified by fractional distillation.

The five salts NH_4Br, $(Me)_4NBr$, $(Et)_4NBr$, $(n\text{-}Pr)_4NBr$, and $(n\text{-}Bu)_4NBr$ were purchased from Eastman Organic Chemicals and, with the exception of $(n\text{-}Bu)_4NBr$, were used without further purification. $(n\text{-}Bu)_4NBr$ was dissolved in CCl_4 and precipitated by addition of an excess of diethyl ether.

All other quaternary salts were prepared by bubbling pure HBr gas in a solution of the corresponding amine (Fisher's Highest Purity) in ethanol. When the salts produced were sufficiently pure, they were not recrystallized but thoroughly washed with diethyl ether. Otherwise they were dissolved in a minimum of ethanol and precipitated by addition of an excess of diethyl ether.

Solubility Measurements

The salt solutions were saturated with benzene at 25 °C by vigorously agitating these solutions for 20 h with an excess of benzene in a constant temperature bath (±0.1 °C) using an automatic shaker. After equilibrium had been reached, the agitation was stopped, and the saturated solutions were left in the bath for at least another 4 h to allow complete separation of the excess benzene and saturated solution. Aliquots (10 ml) of the saturated solutions were then transferred to 250 ml volumetric flasks containing approximately 225 ml of cold water (5 to 10 °C), care being taken to submerge the tip of the pipette under the surface of water during the delivery and maintaining minimum liquid surface exposure in all operations. These precautions were taken to prevent loss of benzene by evaporation during the dilution. The solutions were then warmed to 25 °C before completing the 1:25 dilution. Samples of these well-mixed dilute solutions were transferred to 50 mm stoppered cylindrical cells, and analyzed by ultraviolet absorption using a Perkin–Elmer Spectracord model 4,000. Check runs were also made on a Cary 14 Spectrometer. Water was used in the reference cell except with the larger quaternary salts where it was found necessary to use a salt solution of the same concentration as that containing the benzene. With the other salts absorption was negligible at the concentrations used.

The relative solubility of benzene in the salt solution and in water was obtained from the ratio of maximum absorption at 254 mμ. We have verified that the Beer–Lambert law holds at these low concentrations of benzene in water. The solubility of benzene in pure water was obtained by interpolation on a graph giving the absorbance of benzene as a function of the known concentration of the solutions. By this method, a value of 1.80 ± 0.02 g/l was obtained, which is in excellent agreement with the values obtained by other workers (15–19).

Can. J. Chem. Downloaded from www.nrcresearchpress.com by 210.87.254.40 on 09/05/12
For personal use only.

The salting-out of benzene by KCl and by NaCl was determined as a further check; the salting-out constants k_{so} obtained, 0.37 with KCl and 0.44 ± 0.01 with NaCl, agree within experimental error with the values of Saylor *et al.* (20), 0.38 and 0.45, and with those of Long and McDevit (9), 0.39 and 0.46.

RESULTS AND DISCUSSION

The salting-in results obtained are summarized in Table I, where the salting-in constant is defined as the negative salting-out constant.

$$k_{si} = \lim_{c \to 0} \frac{1}{c} \ln \frac{S}{S_0}$$

Each salting-in constant is based on an average of 8 to 12 solubility measurements in the concentration range 0.1 to 1.4 *M*. The values of k_{si} were compared with those of Deno and Spink (11) whenever possible, and good agreement was obtained.

TABLE I

Salting-in of benzene by quaternary ammonium bromides at 25 °C

Salt	k_{si} (l mole^{-1})	Salt	k_{si} (l mole^{-1})
NH_4Br	−0.115	*n*-$PrNH_3Br$	0.065
$(Me)_4NBr$	0.35 (0.35)*	*n*-$BuNH_3Br$	0.13
$(Et)_4NBr$	0.56 (0.58)	*n*-$PeNH_3Br$	0.20
$(n\text{-}Pr)_4NBr$	0.91 (0.94)	*n*-$HeNH_3Br$	0.27
$(n\text{-}Bu)_4NBr$	1.23	$(n\text{-}Pr)_2NH_2Br$	0.135
$(EtOH)_3NH\ Br$	0.25	$(n\text{-}Pr)_3NHBr$	0.50

*Values in parenthesis are those of Deno and Spink.

The dependance of salting-in on the number and size of the alkyl groups is shown in Fig. 1, where k_{si} is plotted as a function of the total number of carbon atoms in the different salts. With the symmetrical quaternary ammonium salts, the salting-in appears to be a linear function of the number of carbon atoms of the cations, while with the salts containing less than four alkyl groups, k_{si} depends also on the symmetry of the large ion. The difference between these two behaviors can be explained by the possibility of a certain amount of salting-out near the charge-bearing nitrogen atom when the large ions are not symmetrical. This would then indicate that the salting-in is caused principally by the organic part of the ion. Further evidence for this is given in Fig. 2 where $\ln(S/S_0)$ is plotted as a function of concentration of the RNH_3Br salts, and where the alkyl group R is varied in length. The limiting slopes are all regular and increase by about 0.07 l mole^{-1} for each additional methylene group (see Table I). However, while $\ln(S/S_0)$ increases linearly with concentration for the lower members of this homologous series, for the higher members, the solubility increases very rapidly with concentration. The same kind of behavior has also been observed by Durand (21) in his study of the solubility of benzene in carboxylic acid salts.

This abnormal dependance of solubility on concentration can be explained through micelle formation of these long-chain salts. The solubility of benzene inside a micelle is large (23), and the critical micelle concentration decreases with increasing length of the organic chain. On this basis, *n*-hexyl ammonium bromide probably forms a micellar complex with benzene at a concentration near 1 *M*. If the extreme case of salting-in, which is often called hydrotropism, can readily be understood through micelle formation, the normal salting-in could well be due to some similar effect since there is no sudden transition between these different cases of salting-in.

Can. J. Chem. Downloaded from www.nrcresearchpress.com by 210.87.254.40 on 09/05/12
For personal use only.

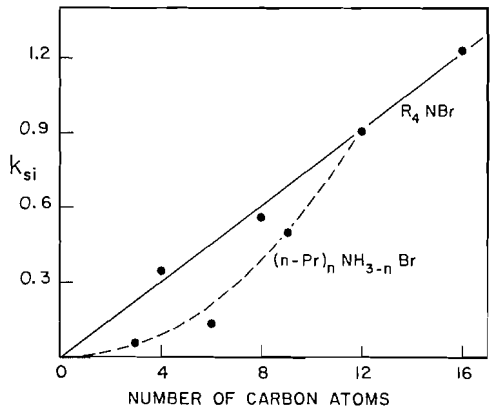

FIG. 1. Salting-in constants of benzene at 25 °C as a function of the number of carbon atoms in the quarternary ammonium bromides.

Diamond (6) has suggested that salting-in may be caused by the formation of an association complex between the large ion and the nonelectrolyte induced by the structure of water. The present work tends to confirm this explanation. In the Frank and Wen (4) model, liquid water consists of hydrogen-bonded ice-like clusters of H_2O molecules in equilibrium with non-hydrogen-bonded molecules. These clusters are unstable and melt by local energy fluctuation. Nemethy and Scheraga (22) have shown that such a model can account quantitatively for most of the physical properties of liquid water. The presence of a neutral molecule or the nonpolar part of a molecule protects the cluster from local attack, and consequently lengthens the average life of the clusters in the immediate vicinity of the neutral molecule. Therefore the presence of neutral molecules increases the ice-like structure of water. This corresponds to a decrease in entropy or increase in the free energy of water. In a system of tetraalkyl ammonium ions, benzene, and water, both the benzene and the large ion will tend to increase the water structure. The system will therefore tend to minimize the increase in free energy through association, the surface area of this association complex being smaller than that of the two particles separately. As the length of the organic chain increases the number of molecules forming the association complex probably increases, and at the limit, micelles containing benzene molecules in their center are formed. The solubility of a nonelectrolyte in water is limited to a large extent by the increase in structure of water. The presence of structure-inducing ions will therefore facilitate the dissolution of the neutral molecule since less work needs to be done by the nonelectrolyte against the structure of water.

The role of van der Waals forces in salting-in is now clearer. The structure of water forces two structure-enhancing particles to associate, and the strength of this association will depend to some extent on the van der Waals forces between the large ion and the nonelectrolyte. Therefore, as the size of either particle increases, both the structure of water and van der Waals interactions will increase, and the larger will be the salting-in. Specific interactions may also affect the strength of this association complex. For example, it is known that tetraethanol ammonium bromide has little influence on the structure of water (24). Similarly, triethanolamine hydrobromide should have little effect on water since the hydroxy groups can fit into the water structure. However, this salt also causes salting-in as seen from Table I. This behavior could possibly be explained by assuming

Can. J. Chem. Downloaded from www.nrcresearchpress.com by 210.87.254.40 on 09/05/12
For personal use only.

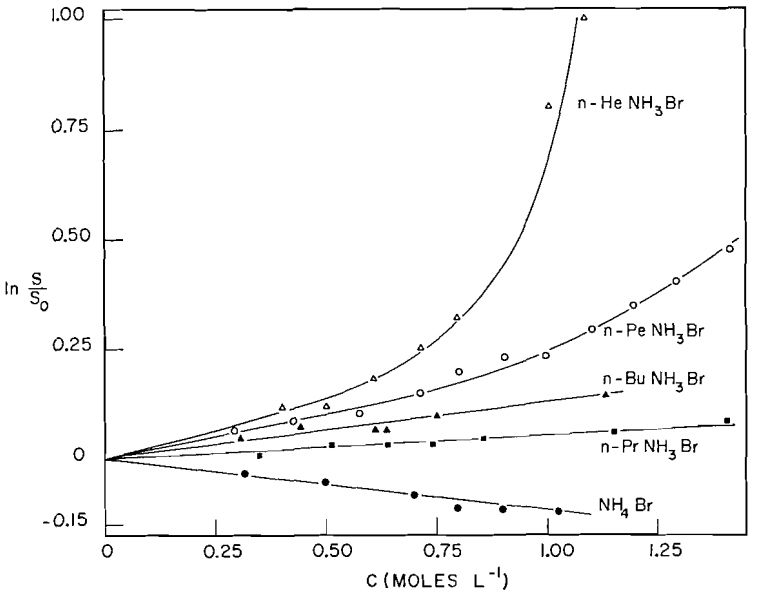

FIG. 2. Salting-in of benzene at 25 °C by monoalkyl quaternary ammonium bromides.

that an association complex is formed in this case as a result of specific interactions between the π bonds of benzene and the hydroxy groups of the salt.

The above explanation of salting-in, proposing association between the nonelectrolyte and the large ion due to the increase in the structure of water, can also account for the success of the McDevit and Long equation in predicting salting-in. Deno and Spink (11) found excellent agreement with the experimental salting-in or salting-out constants of benzene if the McDevit and Long relation, eq. [2], was multiplied by an empirical factor 0.3. On this basis, the negative electrostriction required to explain the observed salting-in of $(Bu)_4NBr$ would be 52.6 ml. Wen (25) and McMullan and Jeffrey (8) have found that this salt forms a polyhedral clathrate hydrate containing on the average 32.8 water molecules. From partial molal volume considerations, Wen and Saito (7) suggested that this same hydrate also exists on a time-average basis in solution. Since it is reasonable to assume that the volume of these large ions changes little upon dissolution (26), most of the electrostriction would result from changes in volume of water molecules surrounding the ions. The molar volume of water in a polyhedral cluster has been estimated by Nemethy and Scheraga (22) as 19.66 ml at 25 °C. The corresponding volume of ordinary water is 18.07 ml. Therefore the total electrostriction would be

$$\Delta V = n(v_w - v_{cl}) = 32.8(18.07 - 19.66) = 52.2 \text{ ml}$$

which is in excellent agreement with that estimated from salting-in data. Although the agreement between the negative electrostriction predicted from the increase in structure of water around the large ions and that obtained from salting-in is probably fortuitous to some extent, it can still be considered as supporting evidence for the dependance of salting-in on the increase in water structure near large ions.

Can. J. Chem. Downloaded from www.nrcresearchpress.com by 210.87.254.40 on 09/05/12
For personal use only.

CONCLUSION

The solubility of benzene in quaternary ammonium bromide solutions was studied systematically; the salting-in is shown to be a function of both the length of the alkyl chain and the number of alkyl groups on the nitrogen atom. These results indicate that the increase in structure of water in the vicinity of the large ions plays an important role in salting-in by promoting the formation of an association complex between the non-electrolyte and the organic ion as previously suggested by Diamond. This explanation can account for the partial success of the theories of Bockris, Bowler-Reed, and Kitchener and of McDevit and Long in predicting salting-in. It therefore appears that any successful theory of salting-in will have to consider, at least implicitly, the influence of large ions on the structure of water.

ACKNOWLEDGMENT

Grateful acknowledgment is made to the National Research Council for financial support of this project.

REFERENCES

1. R. A. Robinson and R. H. Stokes. Electrolyte solutions. Butterworths, London. 1959. Chap. 6.
2. E. R. Nightingale, Jr. J. Phys. Chem. **63**, 1381 (1959).
3. H. S. Frank and M. W. Evans. J. Chem. Phys. **13**, 507 (1945).
4. H. S. Frank and W.-Y. Wen. Discussions Faraday Soc. **24**, 133 (1957).
5. E. R. Nightingale, Jr. J. Phys. Chem. **66**, 894 (1962).
6. R. M. Diamond. J. Phys. Chem. **67**, 2513 (1963).
7. W.-Y. Wen and S. Saito. J. Phys. Chem. **68**, 2639 (1964).
8. R. McMullan and G. A. Jeffrey. J. Chem. Phys. **31**, 1231 (1959).
9. F. A. Long and W. F. McDevit. Chem. Rev. **51**, 119 (1952).
10. J. O'M Bockris, J. Bowler-Reed, and J. A. Kitchener. Trans. Faraday Soc. **47**, 184 (1951).
11. N. C. Deno and C. H. Spink. J. Phys. Chem. **67**, 1347 (1963).
12. B. E. Conway, J. E. Desnoyers, and A. C. Smith. Phil. Trans. Roy. Soc. London, Ser. A, **256**, 389 (1964).
13. T. J. Morrison and N. B. B. Johnstone. J. Chem. Soc. 3655 (1955).
14. W. F. McDevit and F. A. Long. J. Am. Chem. Soc. **74**, 1773 (1952).
15. D. M. Alexander. J. Phys. Chem. **63**, 1021 (1959).
16. R. L. Bohon and W. F. Claussen. J. Am. Chem. Soc. **73**, 1571 (1951).
17. (*a*) D. S. Arnold, C. A. Plank, E. E. Erickson, and F. P. Pike. Chem. Eng. Data Ser. **3**, 253 (1958). (*b*) F. Franks, M. Gent, and H. H. Johnson. J. Chem. Soc. 2716 (1963).
18. A. P. Brady and H. Huff. J. Phys. Chem. **62**, 644 (1958).
19. H. Stephen and T. Stephen. Solubilities of inorganic and organic compounds. Vol. I. MacMillan, Toronto. 1963.
20. J. H. Saylor, A. I. Whitten, I. Clairborne, and P. M. Gross. J. Am. Chem. Soc. **74**, 1778 (1952).
21. R. Durand. Compt. Rend. **223**, 878 (1946).
22. G. Nemethy and H. A. Scheraga. J. Chem. Phys. **36**, 3382, 3401 (1962).
23. H. B. Klevens. Chem. Rev. **47**, 1 (1950).
24. W.-Y. Wen. Unpublished work.
25. W.-Y. Wen. Ph.D. Thesis, University of Pittsburgh, Pittsburgh, Pa. 1957. (Microfilm No. 24753.)
26. J. E. Desnoyers, R. E. Verrall, and B. E. Conway. J. Chem. Phys. **43**, 243 (1965).

Can. J. Chem. Downloaded from www.nrcresearchpress.com by 210.87.254.40 on 09/05/12
For personal use only.

Can. J. Chem. Downloaded from www.nrcresearchpress.com by 210.87.254.42 on 09/05/12
For personal use only.

IODINE-CATALYZED RECOMBINATION OF ATOMIC NITROGEN

ROBERT A. YOUNG

Stanford Research Institute, Menlo Park, California

Received April 2, 1965

ABSTRACT

Recent conclusions of Phillips on the excitation of I_2 by $N_2(A^3\Sigma_u^+)$ formed as a product of iodine-catalyzed atomic nitrogen recombination are criticized. Spectroscopic experiments are performed which indicate that $[N_2(A^3\Sigma_u^+)] < 10^9$ molecules/cm^3 which is $\approx 10^{-5}$ of that implied by Phillips.

INTRODUCTION

Recently measurements of the decay of I_2 radiation excited by active nitrogen were interpreted by Phillips (1) to yield the radiative lifetime of the $N_2(A^3\Sigma_u^+)$ state. He supposes that

[1*a*] $$N + I_2 \rightarrow NI + N$$

[1*b*] $$NI + N \rightarrow N_2(A^3\Sigma_u^+) + I$$

produce $N_2(A^3\Sigma_u^+)$ and that

[2] $$N_2(A^3\Sigma_u^+) + I_2 \rightarrow N_2 + I_2^*$$

is followed by emission from I_2.

In this note we wish to point out errors in the interpretation of Phillips' data and present spectroscopic evidence that $N_2(A^3\Sigma_u^+)$ is much lower in the N, I_2 system than is consistent with Phillips' conclusions.

ANALYSIS

The differential equations determining the evolution of the N, I_2 system based on the assumption that only reactions [1*a*], [1*b*], and [2] are important and that [1*a*] controls the decay of [N], are

[3] $$\frac{d[N]}{dt} = -2k_1[N][I_2]$$

[4] $$\frac{d[N_2^*]}{dt} = k_1[N][I_2] - k_2[I_2][N_2^*]$$

[5] $$\frac{d[I_2^*]}{dt} = k_2[I_2][N_2^*] - \frac{1}{\tau}[I_2^*]$$

which have the following solutions:

[6] $$[N] = [N]_0 \exp -2k_1[I_2]t$$

[7] $$[N_2^*] = \frac{k_1}{k_2 - 2k_1}[N]_0 \exp -2k_1[I_2]t + \left([N_2^*]_0 - \frac{k_1[N]_0}{k_2 - 2k_1}\right) \exp -k_2[I_2]t$$

[8] $$[I_2^*] = \tau k_2[I_2][N_2^*]$$

where $1/\tau$ has been assumed so large that I_2 has reached a pseudo-steady-state with N_2^*, and that $[N_2^*]_0$ and $[N]_0$ are the initial concentrations of these species.

Can. J. Chem. Downloaded from www.nrcresearchpress.com by 210.87.254.42 on 09/05/12
For personal use only.

The data presented by Phillips for the exponential decay of the nitrogen 1st positive bands (his Table I—$d(\log_{10}I)/dt$) if plotted on his Fig. 3 coincide with the data representing the decay of I_2 emission for different amounts of I_2 added to discharged nitrogen. To convert this plot from $d(\log_{10}I)/dt$ to $k_1[I_2]$, the ordinate must be multiplied by $\log_{10} e = 2.3$ and divided by 2, since the intensity of the first positive bands of N_2 is proportional to $[N]^2$. These factors approximately cancel. Hence the rate at which I_2^* decays is essentially the same as the rate at which N decays and no measurement of k_2 has been made. There is also no evidence in Phillips' data to support the assumed reaction sequence although Rayleigh (2) did find that no compound of iodine and nitrogen was formed that could be collected in a liquid nitrogen trap. This old observation does strongly support the supposed general reaction sequence [1] and [2] without regard to the excited state of N_2.

If in eqs. [3], [4], and [5] k_1I_2 and k_2I_2 are replaced by $k_1I_2 + k_0$ and $k_2I_2 + k_0'$ where k_0 and k_0' represent a unimolecular loss of N and N_2^* then the exponentials in eqs. [6] and [7] become similarly modified. The observed values of k_0 from Fig. 3 of Phillips' paper are $\simeq 1\ s^{-1}$. If this is due to wall loss of N, then γ (the catalytic efficiency) is $\simeq 10^{-5}$ which is quite reasonable. Although no observed change in k_0 was found by Phillips when the surface to volume ratio was altered by $\simeq 2$ (by inserting a central glass rod in the flow stream) only a few measurements were made. If the added surface was less catalytic than the older tube walls, such an effect could occur.

In short, the data presented by Phillips do not indicate anything about the decay or the state of N_2^* formed in reaction [1*b*].

If process [2] is slow there should be an *increase* in the emission from I_2 with distance unless $[N_2^*]$ is large leaving the discharge. Dunford *et al.* (3) could not detect any emission from $N_2(A^3\Sigma_u^+)$ as pure nitrogen leaves the discharge, nor have we, with even more sensitive tests. Thus using the data in Phillips (4) earlier paper (with $[I_2]$ increased by 4 (1)), assuming $[N_2^*]_0$ is negligible, setting the first derivative of eq. [7] with respect to time to zero, and substituting $y = 2k_1/k_2$, one finds the condition for a maximum to be

$$y = \exp -k_2(1 - y)[I_2]t \text{ for } y \neq 1.$$

Upon substituting $t = 0.03$ s (the travel time from the discharge to the I_2 intensity max.) and $[I_2] \simeq 10^{14}/cm^3$ (the smallest value recorded by Phillips) one finds that $k_2 \simeq 10^{-13}$ cm^3/molecule s, using $k_1 = 3 \times 10^{-14}$ cm^3/molecule s (after correcting Phillips' calculation).

Because of the rapidity of process [2], N_2^* is probably in a pseudo-steady-state, i.e.,

$$[9] \qquad k_1[N][I_2] = k_2[I_2][N_2^*]$$

or

$$[10] \qquad [N_2^*] = k_1[N]/k_2 \simeq 0.3\,[N].$$

If $[N] \simeq 10^{15}$ cm^{-3}, $[N_2^*] \simeq 3 \times 10^{14}$ cm^{-3} and emission from the Vegard–Kaplan bands should be at least 10^{14} photons/cm^3 s which would be easily detectable.

EXPERIMENT AND RESULTS

A flow system composed of a 10 cm diameter × 100 cm long quartz observation tube (5) was set up and nitrogen discharged in a 10 mm quartz tube which flared into a 25 mm tube running parallel with the observation tube. The distance from the discharge to the observation tube including two right angle bends with light trap was $\simeq 1$ m (equivalent

to ≈ 0.5 s travel time). Prepurified nitrogen was discharged at ≈ 2 mm Hg and I_2 was added in an N_2 carrier from a trap-type saturator at 0 °C.

Two spectrographs were used to detect the Vegard–Kaplan bands ($A^3\Sigma_u^+ - X^1\Sigma_g^+$) of F 1.0 aperture but having dispersions (in the 2 500 to 3 000 Å region) of 44 Å/mm and 6 Å/mm. (The highest dispersion was obtained with a crossed grating echelle spectrograph having a concentric all reflective camera; the lower dispersion spectrograph used a 2 160 line/mm grating and a Muksutov camera with a LiF corrector lens.)

The strongest Vegard–Kaplan band (6) is the (0,5) at 2 603.8 Å where the overlapping I_2 continuum is weak. No structured band was observed at this location for $[I_2]$ concentrations from 4×10^{13} molecules/cm^3 to 4×10^{14} molecules/cm^3 and $[N] = 4 \times 10^{15}$ atoms/cm^3 with exposures of up to 1.2×10^3 min (20 h). Easily identifiable spectra of the NO bands (in particular the $\gamma(0,3)$ band with double heads at 2 595.7 Å and 2 587.5 Å (6)) were obtained in 1 min for $[N] = [O] = 2 \times 10^{15}$/cm^3. These bands are excited by atomic association

$$N + O + (M) \rightarrow NO + (M) + h\nu.$$

With previous measurements (7) of the rate coefficients of this reaction it was found that the emission rate of the $\gamma(0,3)$ band was 4×10^{11} photons/cm^3.

DISCUSSION

If reciprocity failure of the photographic emulsion (Kodak 103 a-O) did not occur, the (0,5) Vegard–Kaplan band emission rate must be less than 3×10^8 photons/cm^3 or, if the lifetime of this state is ≈ 1 s, the density of $N_2(A^3\Sigma_u^+)$ is less than 3×10^8 molecules/cm^3. Reciprocity effects increase this lower bound to $\approx 10^9$ molecules/cm^3. These results are incompatible with Phillips' analysis of his experiments and with our modifications to this analysis. This conclusion is consistent with Rayleigh's (8) early results.

REFERENCES

1. L. F. Phillips. Can. J. Chem. **43**, 369 (1965).
2. Lord Rayleigh. Proc. Roy. Soc. London, Ser. A, **85**, 219 (1911).
3. H. B. Dunford, E. R. V. Milton, and D. L. Walen. Can. J. Chem. **42**, 2504 (1964).
4. C. G. Freeman and L. F. Phillips. J. Phys. Chem. **68**, 362 (1964).
5. R. A. Young and R. L. Sharpless. Discussions Faraday Soc. **33**, 228 (1962).
6. R. W. B. Pearse and A. G. Gaydon. The identification of molecular spectra. John Wiley and Sons, Inc., New York. 1950.
7. R. A. Young and R. L. Sharpless. J. Chem. Phys. **39**, 1071 (1963).
8. Lord Rayleigh. Proc. Roy. Soc. London, Ser. A, **86**, 105 (1911).

Can. J. Chem. Downloaded from www.nrcresearchpress.com by 210.87.254.42 on 09/05/12
For personal use only.

Can. J. Chem. Downloaded from www.nrcresearchpress.com by 210.87.254.105 on 09/05/12
For personal use only.

THE PREPARATION OF L-LYXURONIC ACID, L-LYXOSE, AND 5-DEOXY-L-LYXOSE[1]

R. K. HULYALKAR[2] AND M. B. PERRY
Division of Biosciences, National Research Council, Ottawa, Canada

Received June 23, 1965

ABSTRACT

D-Galactono-1,4-lactone (I) was oxidized by 1 mole of periodate to give L-lyxuronic acid isolated as methyl L-lyxuronate (II). The methyl L-lyxuronate was converted into methyl (methyl α-L-lyxofuranosid)uronate (III) which on reduction by borohydride afforded methyl α-L-lyxofuranoside (IV) from which L-lyxose (V) was obtained by mild acid hydrolysis.

5-Deoxy-L-lyxose was prepared from the methyl (methyl α-L-lyxofuranosid)uronate (III) by the following sequence of reactions: (III) → methyl (methyl 2,3-*O*-isopropylidene-α-L-lyxofuranosid)uronate (VI) → methyl 2,3-*O*-isopropylidene-α-L-lyxofuranoside (VII) → methyl 2,3-*O*-isopropylidene-5-*O*-(*p*-tolylsulfonyl)-α-L-lyxofuranoside (VIII) → methyl 5-deoxy-5-iodo-2,3-*O*-isopropylidene-α-L-lyxofuranoside (IX) → methyl 5-deoxy-2,3-*O*-isopropylidene-α-L-lyxofuranoside (X) → 5-deoxy-L-lyxose (XI).

DISCUSSION

Glycol-cleaving reagents have proved particulary useful in synthetic carbohydrate chemistry for the preparation of sugars from both substituted and unsubstituted sugar precursors. Perlin (1, 2) has shown that lead tetraacetate is especially suitable for differentiating between various kinds of glycol groups and has successfully used the reagent for the synthesis of a wide variety of sugars using this selective property. Periodate is less specific in its glycol-cleaving properties than lead tetraacetate and, in general, its use in synthetic work (3) has been limited to its action on suitably protected carbohydrates in which the cleavage of the glycol systems can be predicted. Some exceptions are found in the selective oxidation with one molar portion of periodate of the exocyclic glycol systems (C_5—C_6) in methyl D-gluco- and D-galacto-furanosides to give methyl D-xylo- and L-arabino-furanosides respectively after reduction of the products (4) and similarly the cleavage of the exocyclic glycol system (C_6—C_7) of methyl D-*glycero*-D-*gulo*-heptopyranoside in the synthesis of D-gulose (5). In the present work the selective cleavage of the exocyclic glycol system (C_5—C_6) in D-galactono-1,4-lactone by 1 mole of periodate to yield L-lyxuronic acid has been used as the first step in the synthesis of the acid which was subsequently used in the synthesis of the rare sugars L-lyxose and 5-deoxy-L-lyxose.[3]

Trial experiments showed that D-galactono-1,4-lactone was oxidized by 1 mole of periodate with the release of 0.98 moles of formaldehyde indicating that the glycol cleavage occurred almost exclusively at the C_5—C_6 bond. An aqueous solution of D-galactono-1,4-lactone (I) was oxidized by the addition of one molar portion of periodic acid, and after removal of the inorganic ions, the resulting solution of L-lyxuronic acid was converted into crystalline methyl L-lyxuronate (II) by repeated evaporation with dry methanol. The methyl L-lyxuronate had equivalent weight, molecular weight, and elemental analysis in agreement with the theoretically expected values, and on borohydride reduction (6) it was converted into L-arabinitol. Treatment of the methyl L-lyxuronate

[1]*Issued as N.R.C. No. 8640.*
[2]*National Research Council Postdoctorate Fellow, 1963–1965.*
[3]*Dr. A. S. Perlin has independently studied the periodate oxidation of D-galactono-1,4-lactone and has prepared L-lyxuronic acid and related derivatives. The results of this work together with structural studies will be published by Dr. Perlin in due course.*

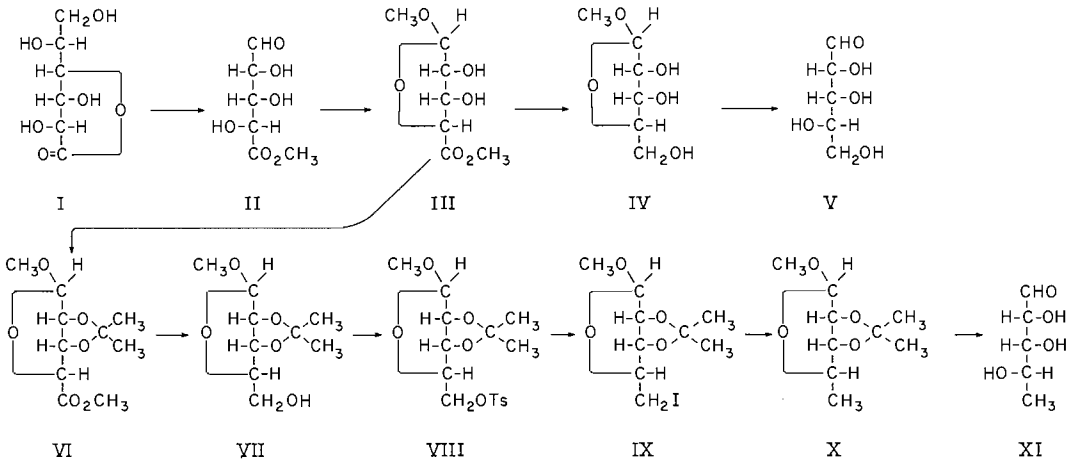

with 1 equiv of sodium hydroxide gave sodium L-lyxuronate. On borohydride reduction the sodium L-lyxuronate gave the expected L-arabonic acid which was identified by gas chromatography as its 2,3,5-tri-*O*-trimethylsilyl-aldono-1,4-lactone derivative (7). Removal of the sodium ions from the sodium L-lyxuronate by ion-exchange resin afforded L-lyxuronic acid as a syrup, which is probably a mixture of the free acid and its lactone.

Treatment of the methyl L-lyxuronate (II) with methanolic hydrogen chloride afforded crystalline methyl (methyl α-L-lyxofuranosid)uronate (III). Gas chromatographic analysis of the methanolysate indicated the presence of about 15% of the β-methyl glycoside; successive treatment with methanolic hydrogen chloride of the residues remaining after the removal of the crystalline α-anomer re-equilibrated the mixture and allowed increased yields of the methyl (methyl α-L-lyxofuranosid)uronate (total yield, 61%) to be obtained. Reduction of the methyl (methyl α-L-lyxofuranosid)uronate by sodium borohydride (6) in ethanol solution afforded crystalline methyl α-L-lyxofuranoside (IV). On mild acid hydrolysis compound IV gave crystalline α-L-lyxose (V), whose physical and chromatographic properties agreed with those recorded in the literature. The 2,4-dinitrophenylhydrazone and toluene-*p*-sulfonylhydrazone derivatives of the synthesized L-lyxose had melting points and infrared spectra identical with those of the corresponding derivatives prepared from authentic D-lyxose.

The above sequence of reactions, repeated without purification of the intermediates, showed that L-lyxose could be prepared from D-galactono-1,4-lactone in 87% overall yield.

5-Deoxy-L-lyxose was prepared in the following manner. On treatment with acetone in the presence of anhydrous copper sulfate catalyst, the methyl (methyl α-L-lyxofuranosid)uronate (III) afforded methyl (methyl 2,3-*O*-isopropylidene-α-L-lyxofuranosid)uronate (VI) which, on reduction with lithium aluminium hydride (8), was converted into methyl 2,3-*O*-isopropylidene-α-L-lyxofuranoside (VII). Treatment of this compound with *p*-toluenesulfonyl chloride in pyridine solution afforded crystalline methyl 2,3-*O*-isopropylidene-5-*O*-(*p*-tolylsulfonyl)-α-L-lyxofuranoside (VIII) which, on heating with sodium iodide in acetone solution, gave methyl 5-deoxy-5-iodo-2,3-*O*-isopropylidene-α-L-lyxofuranoside (IX). Reduction of IX with hydrogen in the presence of Raney nickel afforded methyl 5-deoxy-2,3-*O*-isopropylidene-α-L-lyxofuranoside (X) which on mild acid hydrolysis gave 5-deoxy-L-lyxose (XI). At all stages in the above sequence of reactions the

Can. J. Chem. Downloaded from www.nrcresearchpress.com by 210.87.254.105 on 09/05/12
For personal use only.

Can. J. Chem. Downloaded from www.nrcresearchpress.com by 210.87.254.105 on 09/05/12
For personal use only.

purity of the products was established by gas chromatographic analysis of the compounds or their *O*-trimethylsilyl derivatives.

The 5-deoxy-L-lyxose, obtained as a syrup, had the physical and chromatographic properties expected from those recorded in the literature for 5-deoxy-D-lyxose (9). The *p*-bromophenylosazone and 2,5-dichlorophenylhydrazone derivatives of the 5-deoxy-L-lyxose were obtained in a crystalline form.

L-Lyxose is reported to occur in the hydrolysis products of yeast nucleic acid (10) and of curamycin, an antibiotic produced by *Streptomyces curacoi* (11). L-Lyxose has been prepared from calcium L-galactonate using the Ruff degradation procedure (40% yield) (9, 12), and by the periodate oxidation of 2,3,4-tri-*O*-benzyl-D-galactitol prepared from allyl 6-*O*-allyl-2,3,4-tri-*O*-benzyl-α-D-galactopyranoside (13).

L-Lyxuronic acid has not been found in nature but D-lyxuronic acid is reported to be produced from D-glucose by *Acetobacter melanogenum* (14). 5-Deoxy-L-lyxose has not been found in nature but the related compounds 5-deoxy-3-*C*-formyl-L-lyxose (streptose) and 4-*O*-methyl-5,5-dimethyl-L-lyxose (noviose) are of considerable interest.

EXPERIMENTAL

Paper chromatography was performed by the descending method (15) on Whatman No. 1 filter paper using the following solvent systems: (A) butan-1-ol – acetic acid – water (4:1:5 v/v, top layer), and (B) pyridine – ethyl acetate – water (2:5:5 v/v, top layer). Detection of the sugars was made using the spray reagents: (*a*) 1% silver nitrate in acetone followed by 2% sodium hydroxide in ethanol (16), and (*b*) 2% *p*-anisidine hydrochloride in butan-1-ol (17). The rates of movement of the sugars on the chromatograms are quoted relative to D-galactose (R_{gal} = 1.0).

Gas–liquid chromatography was carried out using a Pye argon chromatograph fitted with an ionization detector (^{90}Sr 20 μcuries) and employing a straight glass column (120 × 0.5 cm. i.d.) packed with 10% (w/w) neopentylglycol sebacate polyester on 100–120 mesh acid washed Chromosorb W. The column was maintained at 170° and development was made with dry argon at a flow rate of 120 ml/min. Chloroform solutions of the sugars were analyzed directly or were converted to their *O*-trimethylsilyl derivatives by treatment with hexamethyldisilazane and trimethylchlorosilane in pyridine solution (18). The retention times of the compounds are quoted relative to methyl 2,3,4,6-tetra-*O*-methyl-α-D-glucoside (T_g = 1.00).

Melting points were determined on a hot stage and are corrected. Optical rotations were measured at 22°. Solutions were concentrated in a rotary evaporator under reduced pressure below 50°.

1. *Preparation of* L-*Lyxuronic Acid*

(*a*) *Methyl* L-*Lyxuronate*

A solution of D-galactono-1,4-lactone (89 g) in water (600 ml) was cooled to 5° and a solution of periodic acid (H_5IO_6, 114 g) in water (600 ml) was added dropwise with stirring over 1 h. After keeping the reaction mixture for a further 4 h at room temperature, barium acetate (64 g) in water (200 ml) was added and the insoluble precipitate of barium iodate was removed by filtration. The filtrate was passed down columns of Amberlite IR-120(H^+) and IR-45(OAc^-) ion-exchange resins and the eluate and washings were concentrated to a syrup (68 g, 96%). The product was evaporated to dryness with dry methanol (5 × 500 ml), and the resulting syrup was dissolved in methanol (50 ml) and kept overnight at 5°. The crude crystalline methyl L-lyxuronate (61 g) having m.p. 136–138° was collected and was found after two recrystallizations from methanol to have m.p. 140° and $[\alpha]_D$ −37.7° → −23° (*c*, 1.8 in water) and $[\alpha]_D$ −68° → −45° (*c*, 1.6 in methanol).

Anal. Found: C, 40.32; H, 5.54. $C_6H_{10}O_6$ requires C, 40.45; H, 5.66.

The trimethylsilyl derivative of the methyl L-lyxuronate on gas chromatographic analysis gave a single peak, T_g 1.440.

Methyl L-lyxuronate had a neutralization equivalent, determined by titration with 0.02 *N* sodium hydroxide, of 178 (calcd. equiv. wt. 178) and a molecular weight, determined by hypoiodite oxidation (19), of 176 (calcd. mol. wt. 178). Methyl L-lyxuronate (0.1 g) in water (5 ml) was reduced by the addition of sodium borohydride (58 mg) to give crystalline L-arabinitol (70 mg) having m.p. and mixed m.p. 103° and giving an acetate derivative which had the same gas chromatographic retention time as penta-*O*-acetyl-L-arabinitol (20).

(*b*) *Sodium* L-*Lyxuronate*

Methyl L-lyxuronate (1.78 g) in water (10 ml) was neutralized by the slow addition of *N* sodium hydroxide solution (10 ml); after 1 h ethanol (120 ml) was added to the stirred solution and the precipitated sodium L-lyxuronate (1.8 g) was collected. The product had $[\alpha]_D$ +8.1° (*c*, 3.5 in water).

Anal. Found: C, 32.8; H, 4.0. $C_5H_7O_6Na$ requires C, 32.3; H, 3.78.

Paper chromatographic examination of the sodium L-lyxuronate showed a single spot R_{gal} 0.93 (solvent A) which gave a yellow color with the *p*-anisidine hydrochloride spray. Sodium L-lyxuronate (10 mg) was reduced with sodium borohydride (6 mg) to give L-arabonic acid, which gave an *O*-trimethylsilyl derivative having the same gas chromatographic retention time as authentic 2,3,5-tri-*O*-trimethylsilyl-L-arabono-1,4-lactone (7).

(c) L-Lyxuronic Acid (and Lactone)

Sodium L-lyxuronate (0.93 g) in water (10 ml) was passed down a column of Amberlite IR-120(H^+) ion-exchange resin, and the eluate and washings were concentrated to a syrup (0.78 g) which was dried over phosphorus pentoxide under high vacuum for 3 d. Paper chromatographic examination of the product (solvent A) showed two spots having R_{gal} 0.92 (acid) and R_{gal} 1.61 (lactone) with considerable tailing between them. The preparation had $[\alpha]_D$ −10° (*c*, 2 in water).

Anal. Found: C, 34.8; H, 4.99. $C_5H_8O_6.\frac{1}{2}H_2O$ requires C, 34.7; H, 5.17.

2. Preparation of L-Lyxose

(a) Methyl (Methyl α-L-Lyxofuranosid)uronate

Methyl L-lyxuronate (53 g) was boiled under reflux for 1 h with 1% methanolic hydrogen chloride (1.5 l), and the cooled solution was neutralized with silver carbonate and filtered. After treatment with hydrogen sulfide and refiltration, the filtrate was concentrated to a syrup (58 g). The syrup was dissolved in chloroform and ether was added to incipient turbidity; on keeping at 5°, crystals of methyl (methyl α-L-lyxofuranosid)-uronate (16 g) were collected. The mother liquors were concentrated and again treated with methanolic hydrogen chloride and worked up as described above. The procedure was repeated twice to give a total yield of product of 35 g (61%), m.p. 85°, $[\alpha]_D$ −94° (*c*, 2 in methanol).

Anal. Found: C, 43.72; H, 6.30. $C_7H_{12}O_6$ requires C, 43.75; H, 6.29.

The trimethylsilyl derivative of methyl (methyl α-L-lyxofuranosid)uronate on gas chromatographic analysis gave a single peak, T_g 1.250. The trimethylsilylated product of the original methanolyzate gave two peaks having T_g 1.250 (85%) and T_g 1.781 (15%); the minor peak is probably the β-anomer.

(b) Methyl α-L-Lyxofuranoside

Methyl (methyl α-L-lyxofuranosid)uronate (30 g) in ethanol (400 ml) kept at 0° was reduced by the addition of sodium borohydride (12 g) in ethanol (150 ml). The mixture was kept at 0° for 5 h and then at room temperature for 60 h. The reaction mixture was treated with Amberlite IR-120(H^+) ion-exchange resin to destroy the excess of borohydride and remove sodium ions, and the filtered solution was then evaporated with dry methanol (6 × 250 ml) to remove boric acid. When the product was kept in the presence of a small quantity of methanol it gave crystals (22.8 g, 89%) which were collected after trituration with a chloroform–ether mixture. After recrystallization from ethyl acetate, the methyl α-L-lyxofuranoside had m.p. 93°, $[\alpha]_D$ −125° (*c*, 3 in water) and $[\alpha]_D$ −160° (*c*, 2 in methanol) (lit. $[\alpha]_D$ − 160° (methanol) and m.p. 93° (21)) and had an infrared spectrum identical with authentic methyl α-D-lyxofuranoside.

Anal. Calcd. $C_6H_{12}O_5$: C, 43.90; H, 7.37. Found: C, 43.70; H, 7.34.

Gas chromatographic analysis of the *O*-trimethylsilyl derivative of the methyl α-L-lyxofuranoside gave a single peak T_g 0.582 having the same retention time as the trimethysilyl derivative prepared from authentic methyl α-D-lyxofuranoside. When the methyl α-L-lyxofuranoside (0.1 g) was heated with 0.5 *N* sulfuric acid (10 ml) on a boiling water bath for 20 min, the optical rotation changed from $[\alpha]_D$ −123° to +12.4°.

Paper chromatographic examination of the methyl α-L-lyxofuranoside showed a single red spot with the *p*-anisidine hydrochloride spray having R_{gal} 3.18 (solvent A) and R_{gal} 4.40 (solvent B).

(c) L-Lyxose

Methyl α-L-lyxofuranoside (10 g) in 0.5 *N* sulfuric acid (100 ml) was heated on a boiling water bath for 25 min, and the cooled solution was neutralized ($BaCO_3$) and filtered. The filtrate was passed through small columns of Amberlite IR–120(H^+) and Duolite A4(OH^-) ion-exchange resins, and the eluate was concentrated to a syrup (9 g). The syrup was dissolved in hot ethanol (10 ml); on standing, crystals of α-L-lyxose (7.8 g) were obtained, m.p. 104° and $[\alpha]_D$ +13.9° (*c*, 3 in water, equilibrium value) (lit. m.p. 105° and $[\alpha]_D$ +13.5° (9, 12)).

Anal. Calcd. $C_5H_{10}O_5$: C, 40.00; H, 6.71. Found: C, 40.11; H, 6.64.

On paper chromatograms the L-lyxose gave a red spot with the *p*-anisidine hydrochloride spray having R_{gal} 1.57 (solvent A) and R_{gal} 2.06 (solvent B) corresponding in mobility with authentic D-lyxose. The trimethylsilyl derivative prepared from the crystalline α-L-lyxose on gas chromatographic analysis gave a single peak with T_g 0.41, whereas the product prepared from a sample of the α-L-lyxose equilibrated in aqueous solution showed two peaks, T_g 0.41 and 0.58, which corresponded to the trimethylsilyl derivatives prepared from authentic samples of crystalline α-D-lyxopyranose and β-D-lyxopyranose respectively.

The α-L-lyxose gave a crystalline 2,4-dinitrophenylhydrazone derivative having m.p. 171–172° (lit. m.p. 171–172° for D-lyxose 2,4-dinitrophenylhydrazone (12)) and a toluene-*p*-sulfonylhydrazone derivative having m.p. 142° (lit. m.p. 141° for D-lyxose toluene-*p*-sulfonylhydrazone (22)). The infrared spectra of the two derivatives were identical with the corresponding derivatives of D-lyxose.

Can. J. Chem. Downloaded from www.nrcresearchpress.com by 210.87.254.105 on 09/05/12
For personal use only.

3. Preparation of 5-Deoxy-L-lyxose

(a) Methyl (Methyl 2,3-O-Isopropylidene-α-L-lyxofuranosid)uronate

Methyl (methyl α-L-lyxofuranosid)uronate (43 g) and anydrous copper sulfate (95 g) in acetone (800 ml) were boiled under reflux for 16 h. The filtered reaction mixture was concentrated to a syrup which was then extracted with hot light petroleum (b.p. 60–100°), and after concentration of the extract, the methyl (methyl 2,3-*O*-isopropylidene-α-L-lyxofuranosid)uronate (45 g, 87%) was obtained as a syrup. This syrup had $[\alpha]_D$ −47.6° (*c*, 5 in methanol) and $[\alpha]_D$ −2.6 (*c*, 2.6 in chloroform), and on gas chromatography it gave a single peak T_g 0.932.

Anal. Found: C, 51.78; H, 6.88. $C_{10}H_{16}O_6$ requires C, 51.72; H, 6.94.

A distilled sample of the product (bath temperature 130° at 0.4 mm) had the same physical properties as those given above.

(b) Methyl 2,3-O-Isopropylidene-α-L-lyxofuranoside

Methyl (methyl 2,3-*O*-isopropylidene-α-L-lyxofuranosid)uronate (30 g) in dry ether (375 ml) was added dropwise with stirring to a cooled mixture of lithium aluminium hydride (15 g) in ether (600 ml). On completion of the addition, the stirred reaction mixture was heated under reflux for 6 h, and the reduction was then allowed to proceed at room temperature for 16 h. Moist ethyl acetate (220 ml) was added dropwise to the stirred, cooled reaction mixture followed by water (200 ml). The ether layer was separated and combined with the ether washings of the precipitated material, dried (anhyd. Na_2SO_4), and filtered. The filtrate was then concentrated to a syrup (25.5 g, 96%); $[\alpha]_D$ −51° (*c*, 3 in chloroform); η_D^{22} 1.4506; g.l.c. single peak with T_g 0.832.

Anal. Found: C, 53.2; H, 8.1. $C_9H_{16}O_5$ requires C, 52.9; H, 7.9.

(c) Methyl 2,3-O-Isopropylidene-5-O-(p-tolylsulfonyl)-α-L-lyxofuranoside

Methyl 2,3-*O*-isopropylidene-α-L-lyxofuranoside (21.4 g) in dry pyridine (80 ml) was cooled to 0° and treated with *p*-toluenesulfonyl chloride (27.8 g), and after 2 h at ice-bath temperature the mixture was kept at room temperature for 15 h. The reaction mixture was poured onto crushed ice and after 30 min the crude crystalline methyl 2,3-*O*-isopropylidene-5-*O*-(*p*-tolylsulfonyl)-α-L-lyxofuranoside (34.8 g, 92%) m.p. 62–68°, was collected. After recrystallization from aqueous ethanol, the pure product (29 g) was found to have m.p. 76–77° and $[\alpha]_D$ −41.7° (*c*, 3.2 in methanol).

Anal. Found: C, 53.64; H, 6.15. $C_{16}H_{22}O_7S$ requires C, 53.63; H, 6.19.

(d) Methyl 5-Deoxy-5-iodo-2,3-O-isopropylidene-α-L-lyxofuranoside

Methyl 2,3-*O*-isopropylidene-5-*O*-(*p*-tolylsulfonyl)-α-L-lyxofuranoside (26.1 g) and sodium iodide (15 g) dissolved in dry acetone (180 ml) was heated in sealed glass tubes at 115° for 60 h. After cooling, the insoluble sodium *p*-toluenesulfonate was removed by filtration and the filtrate was concentrated to a syrup. The syrup was dissolved in chloroform (250 ml) and the solution was washed with water (2 × 100 ml), dried (anhydrous Na_2SO_4), and concentrated to a syrup (22.9 g, 100%). The product was distilled (80–85° at 0.05 mm) and the methyl 5-deoxy-5-iodo-2,3-*O*-isopropylidene-α-L-lyxofuranoside (21 g) was obtained as a colorless oil, $[\alpha]_D$ −70.4° (*c*, 2 in methanol), η_D^{22} 1.4975.

Anal. Found: C, 34.33; H, 4.69. $C_9H_{15}O_4I$ requires C, 34.4; H, 4.8.

On gas chromatography the product gave a single peak with T_g 1.07.

(e) Methyl 5-Deoxy-2,3-O-isopropylidene-α-L-lyxofuranoside

Methyl 5-deoxy-5-iodo-2,3-*O*-isopropylidene-α-L-lyxofuranoside (14 g) in methanol (200 ml) containing 2.2 *N* methanolic potassium hydroxide (23 ml) and Raney nickel (10 g) was shaken for 5 h at room temperature in a Parr low-pressure shaker-type catalytic apparatus under 50 lb pressure of hydrogen. The nickel catalyst was removed by centrifugation and the supernatant and methanol washings of the catalyst were concentrated to a syrup (6.88 g, 82%) which was distilled (50–55° at 0.05 mm) to yield methyl 5-deoxy-2,3-*O*-isopropylidene-α-L-lyxofuranoside (6.2 g) as a colorless oil. The product on gas chromatographic analysis gave a single peak with T_g 0.128 and had $[\alpha]_D$ −92.7° (*c*, 4.7 in methanol) and η_D^{22} 1.4280.

Anal. Found: C, 57.31; H, 8.50. $C_9H_{16}O_4$ requires C, 57.43; H, 8.57.

(f) 5-Deoxy-L-lyxose

Methyl 5-deoxy-2,3-*O*-isopropylidene-α-L-lyxofuranoside (6 g) was heated for 2 h on a boiling water bath with 0.5 *N* sulfuric acid (50 ml). After cooling, the mixture was neutralized ($BaCO_3$) and filtered. The filtrate was passed through a small column of mixed Amberlite IR-120(H^+) and IR-45(OH^-) ion exchange resins and was concentrated to a syrup (4.05 g, 95%). The 5-deoxy-L-lyxose had $[\alpha]_D$ −30.0° (*c*, 2.5 in water) (lit. $[\alpha]_D$ +32.4° for 5-deoxy-D-lyxose (23)).

Anal. Found: C, 44.54; H, 7.26. $C_5H_{10}O_4$ requires C, 44.77; H, 7.51.

Paper chromatographic examination of the 5-deoxy-L-lyxose showed a single spot R_{gal} 2.74 (solvent A) and R_{gal} 3.33 (solvent B). The trimethylsilyl derivative on gas chromatographic analysis showed two peaks T_g 0.226 (major) and T_g 0.286 (minor).

A portion of the 5-deoxy-L-lyxose (0.1 g) was converted into 5-deoxy-L-lyxose *p*-bromophenylosazone (0.11 g) which had m.p. 153–154° (lit. m.p. 143–144° for 5-deoxy-D-lyxose *p*-bromophenylosazone (23)).

Anal. Found: C, 43.35; H, 3.81; N, 11.7. $C_{17}H_{18}O_2N_4Br_2$ requires C, 43.43; H, 3.86; N, 11.92.

Can. J. Chem. Downloaded from www.nrcresearchpress.com by 210.87.254.105 on 09/05/12
For personal use only.

5-Deoxy-L-lyxose (0.22 g) in methanol (15 ml) containing 2,5-dichlorophenylhydrazine (0.28 g) was boiled under reflux for 2 h; the mixture was then concentrated to dryness and the residue was extracted with ethyl acetate. The extract was concentrated and the residue was taken up in hot ether–petroleum mixture (b.p. 40–60°). When this solution cooled, 5-deoxy-L-lyxose 2,5-dichlorophenylhydrazone crystallized, (0.15 g), m.p. 113–114°.

Anal. Found: C, 44.7; H, 4.6. $C_{11}H_{14}O_3N_2Cl_2$ requires C, 45.0; H, 4.8.

ACKNOWLEDGMENTS

We thank Mr. J. G. Mignault for technical assistance and Mr. A. E. Castagne for the microanalyses.

REFERENCES

1. A. S. PERLIN. Advan. Carbohydrate Chem. **14**, 9 (1959).
2. A. S. PERLIN. Methods in carbohydrate chemistry. *Edited by* R. L. Whistler and M. L. Wolfrom. Vol. 1. Academic Press, N.Y. 1962. pp. 61–70.
3. J. M. BOBBITT. Advan. Carbohydrate Chem. **11**, 1 (1956).
4. O. KJØLBERG. Acta Chem. Scand. **14**, 1118 (1960).
5. N. J. ANTIA and M. B. PERRY. Can. J. Chem. **38**, 1917 (1960).
6. M. L. WOLFROM and K. ANNO. J. Am. Chem. Soc. **74**, 5583 (1952).
7. M. B. PERRY and R. K. HULYALKAR. Can. J. Biochem. **43**, 573 (1965).
8. R. K. NESS, H. G. FLETCHER, and C. S. HUDSON. J. Am. Chem. Soc. **73**, 4759 (1951).
9. W. A. VAN EKENSTEIN and J. J. BLANKSMA. Chem. Weekblad, **11**, 189 (1914).
10. J. M. GULLAND and G. R. BARKER. J. Chem. Soc. 625 (1943).
11. O. L. GALMARINI and V. DEULOFEU. Tetrahedron, **15**, 76 (1961).
12. R. L. WHISTLER and J. N. BEMILLER. Methods in carbohydrate chemistry. *Edited by* R. L. Whistler and M. L. Wolfrom. Vol. 1. Academic Press, N.Y. 1962. p. 79.
13. R. GIGG and C. D. WARREN. J. Chem. Soc. 2205 (1965).
14. M. AMEYAMA and K. KONDO. Bull. Agr. Chem. Soc. Japan, **22**, 271, 380 (1958).
15. S. M. PARTRIDGE. Biochem. J. London, **42**, 238 (1948).
16. W. E. TREVELYAN, D. P. PROCTER, and J. S. HARRISON. Nature, **166**, 444 (1950).
17. L. HOUGH, J. K. N. JONES, and W. H. WADMAN. J. Chem. Soc. 1702 (1950).
18. C. C. SWEELEY, R. BENTLEY, M. MAKITA, and W. W. WELLS. J. Am. Chem. Soc. **85**, 2497 (1963).
19. S. K. CHANDA, E. L. HIRST, J. K. N. JONES, and E. G. V. PERCIVAL. J. Chem. Soc. 1289 (1950).
20. S. W. GUNNER, J. K. N. JONES, and M. B. PERRY. Can. J. Chem. **39**, 1892 (1961).
21. C. T. BISHOP and F. P. COOPER. Can. J. Chem. **41**, 2743 (1963).
22. D. G. EASTERBY, L. HOUGH, and J. K. N. JONES. J. Chem. Soc. 3416 (1951).
23. E. VOTOČEK and F. VALENTIN. Collection Trav. Chim. Czech. **2**, 36 (1930).

Can. J. Chem. Downloaded from www.nrcresearchpress.com by 210.87.254.105 on 09/05/12
For personal use only.

Can. J. Chem. Downloaded from www.nrcresearchpress.com by 210.87.254.6 on 09/05/12
For personal use only.

HIGHER HOMOLOGUES FROM PYRROLES AND DIPYRRYLMETHENES[1]

S. F. MacDonald and A. Markovac[2]
Division of Pure Chemistry, National Research Council, Ottawa, Canada
Received July 20, 1965

ABSTRACT

Higher alkyl derivatives were obtained from bromomethyl-pyrroles or -dipyrrylmethenes with the use of Grignard reagents.

INTRODUCTION

The synthesis of pyrro- and δ-phyllo-porphyrins related to the *Chlorobium* chlorophylls (1) required I*a* and its homologues, I*c* and I*d*. These were obtained conventionally as the need for them arose:

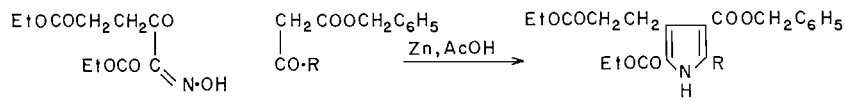

followed by

$$COOCH_2C_6H_5 \rightarrow COOH \rightarrow H \rightarrow CHO \rightarrow CH_3$$

The desirability of a general method for conversions such as that of I*a* into I*c* and I*d*, to obtain all three from common intermediates and avoid the use of propionyl- or butyryl-acetic esters, was clear in retrospect. A sequence of established reactions was available for this: 2-$CH_3 \rightarrow$ COOH $\rightarrow$ H $\rightarrow$ CO·R $\rightarrow$ CH_2R, and we have applied it to III*a* (see below). Modifications also reverse the β-substituents: 4-methyl-pyrrole-3-propionic acid (from II*a*), is acylated in the 5-position (2), and a general method follows from the conversion of III*a* into III (CHO for COOEt, R = COOEt) (1).

The well-known reactivity of bromomethyl-pyrroles suggested the shorter sequence now described: $CH_3 \rightarrow CH_2Br$ (+ RMgBr) $\rightarrow CH_2R$. The bromomethyl-pyrroles I*b*, II*b*, and III*b* reacted with methyl- or ethyl-magnesium iodide to form the homologues I (*c* or *d*), II (*c* or *d*), and III (*c* or *d*). By a standardized procedure yields of 55–70% were obtained. We have recorded the preparation of III*b* because, as noted by Fischer (3), earlier references (4) are to its hydrobromide. The less reactive pyrrole V did not react in the desired way, and 30% of it was recovered unchanged. The pyrrole IV*a* (5) (now prepared in double the reported yield) gave IV (*b*, *c*, *d*, and *e*) with the appropriate Grignard reagents. As expected, the pyrroles VI and VII did not react and were recovered in good yield.

Of these homologues, I*c* (1), I*d* (1), IV*b* (6), and IV*c* (5, 7) were known, and II*c* could be hydrolyzed to the known half-ester (free propionic acid) (6, 8). The structures of III*c* and III*d* were confirmed by comparison with the products of the alternative sequence mentioned above, III ($a \rightarrow e \rightarrow f \rightarrow$ (*g* or *h*) $\rightarrow$ (*c* or *d*)). As all these Grignard reactions had taken the expected course, the structures of the remaining products, II*d*, IV*d*, and IV*e*, could be inferred.

Two moles of Grignard reagent were required for 55–70% yields; with 1 mole the yield was less than 30% and the products were difficult to purify. Presumably the Grignard

[1]*Issued as N.R.C. No. 8681.*
[2]*National Research Council Postdoctorate Fellow, 1963–1965.*

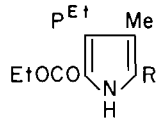

I

(a) R = CH_3
(b) R = CH_2Br
(c) R = Et

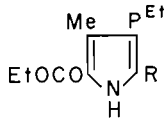

II

(d) R = CH_2Et
(e) R = COOH
(f) R = H

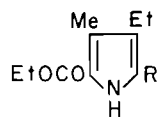

III

(g) R = $CO{\cdot}CH_3$
(h) R = CO·Et
P^{Et} = CH_2CH_2COOEt

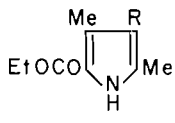

IV

(a) R = CH_2Cl
(b) R = Et ≡ IIIa
(c) R = CH_2Et

(d) R = $(CH_2)_5CH_3$
(e) R = $(CH_2)_6CH_3$

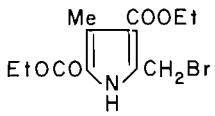

V

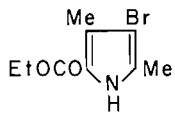

VI

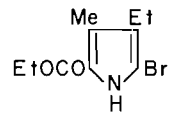

VII

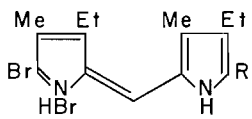

VIII

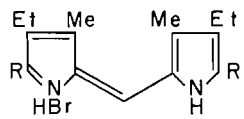

IX

(a) R = CH_3 (b) R = CH_2Br (c) R = Et

reagent reacts also with the active hydrogen of the pyrrole. The formally analogous reaction of pyrryl magnesium bromides with III*b* required only 1.3 moles of the former for a >70% yield of dipyrrylmethane (3). Like the acylation of N-ethyl pyrryl magnesium bromide (9), the latter may be condensations rather than Grignard reactions, because pyrroles such as III*b* and even V readily undergo acid-catalyzed condensation with reactive pyrroles to dipyrrylmethanes (10).

Although dipyrrylmethenes without 5-hydroxy groups are amenable to few general reactions, their 5-bromomethyl derivatives, when these can be obtained, are very reactive. Thus the hydrobromides of the dipyrrylmethenes VIII*b* and IX*b* reacted with an excess of methyl magnesium iodide to give VIII*c* and IX*c* respectively, both of which were identified by comparison with the products of conventional syntheses. Nucleophiles, including Grignard reagents (11), frequently attack the bridge of negatively substituted dipyrrylmethenes. No such addition was observed here, and furthermore, VIII*a* and IX*a* were recovered as the free bases but otherwise unchanged after the same treatment.

Can. J. Chem. Downloaded from www.nrcresearchpress.com by 210.87.254.6 on 09/05/12
For personal use only.

Can. J. Chem. Downloaded from www.nrcresearchpress.com by 210.87.254.6 on 09/05/12
For personal use only.

EXPERIMENTAL

2-Bromomethyl-3-ethyl-4-methyl-5-carbethoxy-pyrrole (IIIb)

Bromine (8 ml) in 50 ml of carbon tetrachloride was slowly dropped into a stirred and water-cooled solution of 16 g of 2,4-dimethyl-3-ethyl-5-carbethoxy-pyrrole (III*a* (12)) in 100 ml of carbon tetrachloride. After 2 h, the yellow crystals of the hydrobromide (22 g, m.p. 128–134°; lit. (4):128–132°) were separated, washed with ether, and dried. This was treated by reflux with benzene (120 ml) until solution was complete and no more HBr was evolved. Colorless needles of the product (16.5 g, 73%, m.p. 144°) were separated from the cooled solution and washed with *n*-hexane.

For analysis it was recrystallized from benzene–*n*-hexane, m.p. 145°.

Calcd. for $C_{11}H_{16}NO_2Br$: C, 48.16; H, 5.87; N, 5.11; Br, 29.16. Found: C, 48.31; H, 5.78; N, 5.31; Br, 29.06.

2,3-Di-ethyl-4-methyl-5-carbethoxy-pyrrole (IIIc)

(a) General Procedure

2-Bromomethyl-3-ethyl-4-methyl-5-carbethoxy-pyrrole (III*b*, 3.4 g, 0.0125 mole) in 70 ml of dry tetrahydrofuran was added dropwise to the Grignard reagent from 0.65 g (0.027 g-atom) of magnesium, 3.54 g (0.025 mole) of methyl iodide and 100 ml of dry ether. The yellow suspension was stirred and heated under reflux for 4 h. Half of the solvent was removed *in vacuo* and ether (50 ml), then aqueous ammonium chloride, were added to the remainder. The aqueous layer was separated off and washed with ether. The combined ether layers were washed with water and dried (Na_2SO_4), and the ether was evaporated *in vacuo*. The crystalline residue was recrystallized from 70% ethanol, and yielded 1.8 g (69%) of colorless prisms, m.p. 68°.

The analytical sample was thrice recrystallized, m.p. 73–74°, which was unchanged when it was mixed with the product of (*b*) below.

Calcd. for $C_{12}H_{19}NO_2$: C, 68.86; H, 9.15; N, 6.69. Found: C, 68.98; H, 9.29; N, 6.83.

(b) The pyrrole III*a* was converted successively into III*e* (13), III*f* (14), and III*g* (8). This last was hydrogenated in ethanol with Raney nickel (1200 p.s.i., 120°, 40 h). The filtrate from the catalyst was concentrated and then cooled to give the crystalline product (90%), m.p. 72°.

The analytical sample was thrice recrystallized from 70% ethanol as colorless prisms, m.p. 73–74°. Found: C, 68.71; H, 9.13; N, 6.83.

2-n-Propyl-3-ethyl-4-methyl-5-carbethoxy-pyrrole (IIId)

(a) By the general procedure, III*b* and ethyl magnesium iodide gave an oily crude product which was distilled (170°, 1×10^{-4} mm). The distillate (58%, m.p. 77°) was recrystallized from 80% ethanol as long colorless prismatic rods, m.p. 82°, which was unchanged when it was mixed with the product of (*b*) below.

Calcd. for $C_{13}H_{21}NO_2$: C, 69.92; H, 9.48; N, 6.27. Found: C, 70.05; H, 9.58; N, 6.48.

(b) 2-Propionyl-3-ethyl-4-methyl-5-carbethoxy-pyrrole (III*h*, see below) was reduced in ethanol over Raney nickel (120°, 1200 p.s.i., 40 h). The filtrate from the catalyst was concentrated and cooled to give the colorless crystalline product (95%), m.p. 80°. When recrystallized from 80% ethanol it formed prismatic rods m.p. 82°.

2-Propionyl-3-ethyl-4-methyl-5-carbethoxy-pyrrole (IIIh)

The acylation of III*f* with propionyl chloride was analogous to that with acetyl chloride (8). A colorless product (57%), m.p. 78°, was obtained by recrystallizing the crude material from petroleum ether (30–60°).

The analytical sample was thrice recrystallized from petroleum ether as prismatic rods, m.p. 80°.

Calcd. for $C_{13}H_{19}NO_3$: C, 65.80; H, 8.07; N, 5.90. Found: C, 65.80; H, 8.08; N, 5.72.

2-Ethyl-3-methyl-5-carboxy-pyrrole-4-propionic Acid Di-ethyl Ester (Ic)

The oily crude product of the above general Grignard procedure applied to I*b* (15) and methyl magnesium iodide was distilled (140–150°, 1×10^{-4} mm), after which it solidified as colorless crystals (65%), m.p. 76°.

The analytical sample was recrystallized four times from 60% ethanol as colorless needles, m.p. 79–80°, which was undepressed by authentic material of m.p. 81–82° (1).

Calcd. for $C_{15}H_{23}NO_4$: C, 64.03, H, 8.24; N, 4.98. Found: C, 63.91; H, 8.42; N, 5.10.

2-n-Propyl-3-methyl-5-carboxy-pyrrole-4-propionic Acid Di-ethyl Ester (Id)

A reaction between ethyl magnesium iodide and I*b* was carried out in the same way, and the oily crude product was distilled (1×10^{-4} mm). For analysis it (57%, m.p. 74°) was recrystallized four times from 60% ethanol as colorless needles, m.p. 77–78°, which was undepressed when it was mixed with authentic material of m.p. 77–79° (1).

Calcd. for $C_{16}H_{25}NO_4$: C, 65.06; H, 8.53; N, 4.74. Found: C, 65.13; H, 8.69; N, 4.77.

2-Ethyl-4-methyl-5-carboxy-pyrrole-3-propionic Acid Di-ethyl Ester (IIc)

Methyl magnesium iodide and II*b* (15) similarly gave an oily crude product, which was distilled (160–170°, 1×10^{-4} mm). For analysis the colorless distillate (60%, m.p. 49–50°) was thrice recrystallized from petrol (20–40°) as colorless prisms, m.p. 52°.

Calcd. for $C_{15}H_{23}NO_4$: C, 64.03; H, 8.24; N, 4.98. Found: C, 64.12; H, 8.21; N, 5.16.

2-Ethyl-4-methyl-5-carbethoxy-pyrrole-3-propionic Acid

The above di-ester was heated under reflux with 1 equivalent of potassium hydroxide in ethanol, and the solvent was then evaporated. The product was precipitated with acid from a solution of the residue in water, then recrystallized from benzene – petrol ether as colorless prisms, m.p. 140° (lit. (6): 138°).

Calcd. for $C_{13}H_{19}NO_4$: C, 61.64; H, 7.56; N, 5.53. Found: C, 61.54; H, 7.54; N, 5.70.

2-n-Propyl-4-methyl-5-carbethoxy-pyrrole-3-propionic Acid Di-ethyl Ester (IId)

The oily crude product from the reaction between II*b* and ethyl mganesium iodide was distilled (150°, 1×10^{-4} mm) and the product (56%, m.p. 57°) was recrystallized thrice from 80% ethanol as long colorless needles, m.p. 63–64°.

Calcd. for $C_{16}H_{25}NO_4$: C, 65.06; H, 8.53; N, 4.74. Found: C, 64.99; H, 8.57; N, 4.96.

2,4-Dimethyl-3-chloromethyl-5-carbethoxy-pyrrole (IVa) (5)

A slurry of paraformaldehyde (6 g) in 75 ml of acetic acid was cooled in ice and stirred while a rapid current of dry hydrogen chloride was passed through. A solution of 31 g of 2,4-dimethyl-5-carbethoxy-pyrrole in 200 ml of acetic acid was then dropped in over a period of 15 min. Passage of the gas stream was continued for 2 h. The mixture was poured into 1 liter of dry ether and refrigerated overnight. The crude product (30 g, m.p. 160° after washing with ether) was recrystallized from benzene as colorless needles (24 g, 60%), m.p. 164–165° (lit. (5): 164–166°).

2,4-Dimethyl-3-ethyl-5-carbethoxy-pyrrole (IVb)

The crude light yellow product of the reaction between IV*a* and methyl magnesium iodide was recrystallized from 95% ethanol as colorless crystals (72%), m.p. 90°. For analysis it was thrice recrystallized as colorless needles, m.p. 94° (lit. (6): 96°), which was unchanged when it was mixed with authentic material.

Calcd. for $C_{11}H_{17}NO_2$: C, 67.66; H, 8.78; N, 7.17. Found: C, 67.79; H, 8.96; N, 7.33.

2,4-Dimethyl-3-n-propyl-5-carbethoxy-pyrrole (IVc)

The crude product of the reaction between IV*a* and ethyl magnesium iodide was crystallized from 95% ethanol as colorless crystals (67%, m.p. 98°). For analysis it was thrice recrystallized as prisms, m.p. 97.5–98.5° (lit. (7): 98°).

Calcd. for $C_{12}H_{19}NO_2$: C, 68.86; H, 9.15; N, 6.69. Found: C, 68.57; H, 8.96; N, 6.81.

2,4-Dimethyl-3-n-hexyl-5-carbethoxy-pyrrole (IVd)

The oily crude product of the reaction between IV*a* and *n*-pentyl magnesium bromide was distilled (140–150°, 1×10^{-4} mm). The distillate solidified into colorless plates (70%), m.p. 59°. For analysis it was recrystallized thrice from 85% ethanol as colorless plates, m.p. 61–62°.

Calcd. for $C_{15}H_{25}NO_2$: C, 71.67; H, 10.03; N, 5.57. Found: C, 71.73; H, 10.13; N, 5.75.

2,4-Dimethyl-3-n-heptyl-5-carbethoxy-pyrrole (IVe)

The oily crude product of the reaction between IV*a* and *n*-hexyl magnesium bromide was distilled (140–150°, 1×10^{-4} mm). The crystalline distillate was recrystallized from 80% ethanol as colorless plates (61%), m.p. 52°. For analysis, it was thrice recrystallized, m.p. 54–55°.

Calcd. for $C_{16}H_{27}NO_2$: C, 72.41; H, 10.26; N,5.28. Found: C, 72.60; H, 10.41; N, 5.41.

2-Formyl-3-ethyl-4-methyl-5-bromo-pyrrole (16)

The corresponding 5-carboxy pyrrole (17) (1 g) was dissolved in 3 ml of acetic acid, a solution of bromine (0.3 ml) in acetic acid (1 ml) was added, and the mixture was heated for 1 h on a steam bath. The solvent was then removed *in vacuo* and the product extracted from the residue into hot petrol (40–60°), leaving the insoluble by-product. The petrol solution was washed with 5% ammonium hydroxide, then with water, and dried with sodium sulfate. The petrol was evaporated, and the residue was crystallized from petroleum ether as colorless prisms (0.4 g, 33%), m.p. 114–115° (lit. (16): 115°).

2,3-Di-ethyl-4-methyl-pyrrole (8)

The 5-carbethoxy derivative (III*c*, 1.5 g) was heated for 20 h at 180° with 10 ml of 15% sodium hydroxide in a Teflon lined screw-capped brass tube. After it was cooled, the product was extracted with ether and the solution was dried with potassium carbonate. The ether was evaporated, and the product distilled (110°, 15 mm) as a colorless oil (100 mg).

4,5,3'-Tri-ethyl-3,4'-dimethyl-5'-bromo-dipyrrylmethene Hydrobromide (VIIIc)

(a) The dipyrrylmethene hydrobromide (VIII*b*, 481 mg (3)), suspended in 80 ml of tetrahydrofuran, was dropped into a solution of Grignard reagent (4 moles, from 98 mg of magnesium, 567 mg of methyl iodide, and 50 ml of ether). The mixture was stirred under reflux for 2 h, then left for 2 h at 20°. Half the solvent was removed *in vacuo*, fresh ether was added, and the product was hydrolyzed with aqueous ammonium chloride. The ether layer and washings were washed with water, dried with sodium sulfate, and the solvent evaporated. The residue was treated by reflux with 3 ml of ethanol. An insoluble by-product separated out, after which the ethanol was evaporated. The residue was converted into the hydrobromide by dissolving it

Can. J. Chem. Downloaded from www.nrcresearchpress.com by 210.87.254.6 on 09/05/12
For personal use only.

in 32% hydrogen bromide in acetic acid. The latter was evaporated, and a crystalline product was left which was recrystallized from ethanol–ether as brown prisms (200 mg, 48%), m.p. 185° (dec.). The X-ray powder photograph of this product and of that of (*b*) below were identical.

For analysis, it was recrystallized thrice from chloroform–ether as red–brown prisms, m.p. 204–205° (dec.).

Calcd. for $C_{17}H_{24}N_2Br_2$: C, 49.04; H, 5.81; N, 6.73; Br, 38.42. Found: C, 48.87; H, 5.63; N, 6.89; Br, 38.24.

The hydrobromide (50 mg) was dissolved in ethanol, a drop of 5% aqueous sodium hydroxide was added, and the solution was cooled. The free base which separated was recrystallized from ethanol as orange–brown prisms, melting point and mixed melting point with the free base prepared by method (*b*) below, 85°.

(b) 2-Formyl-3-ethyl-4-methyl-5-bromo-pyrrole (55 mg), 2,3-di-ethyl-4-methyl-pyrrole (35 mg), and 0.2 ml of acetic acid were well mixed in a small beaker cooled in an ice bath. Hydrobromic acid (0.2 ml of 48%) was added and the mixture stirred for about 30 min. The crystalline hydrobromide was separated out, washed with ether then with acetic acid, and recrystallized from ethanol–ether as red–brown prisms, m.p. 190° (dec.).

For analysis, it was thrice recrystallized from chloroform–ether as red–brown prisms, m.p. 202–203° dec.). Found: C, 49.13; H, 5.76; N, 6.91.

The free base was obtained as under (*a*) above as orange–brown prisms, m.p. 85–86°.

3,5,3′,5′-Tetramethyl-4,4′-di-ethyl-dipyrrylmethene Hydrobromide (IXa) (18)

As in analogous cases, the 5-carbethoxy derivative is now more easily available than 2,4-dimethyl-3-ethyl-pyrrole itself, and the dipyrrylmethene can be more conveniently prepared directly from the former (19) by a general method devised by Fischer (20).

The hydrobromide was converted to the free base, m.p. 150° (lit. (18): 151°), which was unchanged when it was mixed with authentic material.

3,3′-Dimethyl-4,4′-di-ethyl-5,5′-di-bromomethyl-dipyrrylmethene Hydrobromide (IXb) (21)

The dipyrrylmethene hydrobromide (IX*a*, 3.5 g) was dissolved in 60 ml of acetic acid with warming, 4.5 g of bromine was added, and the mixture was heated for 2 h on a steam bath. After it was cooled, the crystals were separated out, washed with acetic acid, then with ether, and recrystallized from chloroform–ether as red–brown prisms (4 g, 78%).

4,5,4′,5′-Tetra-ethyl-3,3′-dimethyl-dipyrrylmethene Hydrobromide (IXc)

(a) The di-bromomethyl dipyrrylmethene hydrobromide (IX*b*, 496 mg), suspended in 80 ml of tetrahydrofuran, was dropped into a solution of Grignard reagent (4 moles, from 96 mg of magnesium, 567 mg of methyl iodide, and 50 ml of ether). The mixture was stirred under reflux for 1 h, then left for 2 h at 20°. Half the solvent was removed *in vacuo*, 10 ml of cold water was added, and the mixture was stirred for 10 min. Chloroform (50 ml) and hydrobromic acid (10 ml of 10%) were added and the mixture was well shaken. The chloroform layer and washings were washed with water and dried with sodium sulfate. The chloroform was evaporated and the residue crystallized from acetic acid as brown–red rods (150 mg, 41%), m.p. 180–184°, (lit. 180° (dec.) (8); 190° (21)). After it was recrystallized again from acetic acid, this product, m.p. 186°, and that obtained as under (*b*) below gave identical X-ray powder photographs.

The hydrobromide (100 mg) was dissolved in 3 ml of ethanol, a drop of ammonium hydroxide was added, the mixture was cooled, and the free base separated. It was recrystallized from aqueous ethanol as orange–brown needles, m.p. 116° (lit. 116° (8)), which was undepressed when it was mixed with the base obtained as under (*b*) below.

Calcd. for $C_{19}H_{28}N_2$: C, 80.23; H, 9.92; N, 9.85. Found: C, 80.33; H, 10.03; N, 10.09.

(b) 2,3-Di-ethyl-4-methyl-5-carbethoxy-pyrrole (III*c*, 300 mg), 3 ml of 98% formic acid, and 2 ml of 48% hydrobromic acid were heated for 1 h on a steam bath. After the mixture had stood overnight at 20°, the product was separated out and recrystallized from acetic acid as prismatic crystals (180 mg, 88%), m.p. 185–186°.

The free base, obtained as under (*a*) above, was thrice recrystallized from 95% ethanol as orange–brown needles, m.p. 116–117°. Found: C, 80.01; H, 9.74; N, 10.03.

VIIIa and IXa with the Grignard Reagent

The chloroform-insoluble perbromide of VIII*a* was treated under reflux for 10 min with 9 parts of acetone, then the mixture was refrigerated. On the next day orange–red prisms of the hydrobromide, VIII*a* (98%), were separated off and washed with ether, m.p. 215–217° (dec.) (lit. (3): 215°).

The dipyrrylmethene hydrobromides VIII*a* and IX*a*, suspended in tetrahydrofuran, were added to ethereal methyl magnesium iodide (3 and 4 moles respectively), heated under reflux, and worked up as in the preparation of VIII*c* by method *a*. When the ethanol was removed and the residues crystallized from aqueous ethanol, the starting methenes VIII*a* and IX*a* were obtained as the corresponding free bases.

The free base from VIII*a* (75%) had a melting point and mixed melting point with authentic material of 102° (lit. 103° (3)).

Calcd. for $C_{16}H_{21}N_2Br$: Br, 24.90. Found: Br, 25.02.

The free base from IX*a* (60%) had m.p. 152°, 151° when mixed with authentic material (lit. 151° (18)).

Can. J. Chem. Downloaded from www.nrcresearchpress.com by 210.87.254.6 on 09/05/12
For personal use only.

REFERENCES

1. J. L. ARCHIBALD, D. M. WALKER, K. B. SHAW, A. MARKOVAC, and S. F. MACDONALD. In preparation. J. L. ARCHIBALD, S. F. MACDONALD, and K. B. SHAW. J. Am. Chem. Soc. **85**, 644 (1963).
2. H. FISCHER and Z. CSUKAS. Ann. **508**, 167 (1934).
3. H. FISCHER, E. BAUMANN, and H. J. RIEDL. Ann. **475**, 205 (1929).
4. H. FISCHER and P. ERNST. Ann. **447**, 139 (1926). H. FISCHER and H. ORTH. Chemie des pyrrols. Vol. I. Akademische Verlagsgesellschaft, Leipzig. 1934. p. 95.
5. T. H. CURRY. Dissertation. Ohio State University 1953.
6. H. FISCHER and J. KLARER. Ann. **447**, 48 (1926).
7. H. FISCHER, M. GOLDSCHMIDT, and W. NÜSSLER. Ann. **486**, 1 (1931).
8. H. FISCHER and H. K. WEICHMANN. Ann. **492**, 35 (1932).
9. W. HERZ. J. Org. Chem. **22**, 1260 (1957).
10. H. FISCHER and P. HALBIG. Ann. **447**, 123 (1926).
11. J. H. PADEN, A. H. CORWIN, and W. A. BAILEY, JR. J. Am. Chem. Soc. **62** 418 (1940). K. J. BRUNINGS and A. H. CORWIN. J. Am. Chem. Soc. **66**, 337 (1944). H. BOOTH, A. W. JOHNSON, F. JOHNSON, and R. A. LANGDALE-SMITH. J. Chem. Soc. 650 (1963).
12. F. K. SIGNAIGO and H. ADKINS. J. Am. Chem. Soc. **58**, 709 (1936).
13. H. FISCHER and H. ORTH. Chemie des pyrrols. Vol. I. Akademische Verlagsgesellschaft, Leipzig. 1934. p. 252.
14. H. FISCHER and H. ORTH. Chemie des pyrrols. Vol. I. Akademische Verlagsgesellschaft, Leipzig. 1934. p. 241.
15. F. MORSINGH and S. F. MACDONALD. J. Am. Chem. Soc. **82**, 4377 (1960).
16. W. SIEDEL and H. FISCHER. Z. Physiol. Chem. **214**, 145 (1933).
17. H. FISCHER, E. STURM, and H. FRIEDRICH. Ann. **461**, 270 (1928).
18. H. FISCHER, P. HALBIG, and B. WALACH. Ann. **452**, 296 (1927).
19. A. W. JOHNSON, I. T. KAY, E. MARKHAM, R. PRICE, and K. B. SHAW. J. Chem. Soc. 3416 (1959).
20. H. FISCHER, H. FRIEDRICH, W. LAMATSCH, and K. MORGENROTH. Ann. **466**, 165 (1928).
21. H. FISCHER and A. KÜRZINGER. Z. Physiol. Chem. **196**, 213 (1931).

Can. J. Chem. Downloaded from www.nrcresearchpress.com by 210.87.254.6 on 09/05/12
For personal use only.

Can. J. Chem. Downloaded from www.nrcresearchpress.com by 210.87.254.105 on 09/05/12
For personal use only.

DIFFUSENESS IN ELECTRONIC SPECTRA

THE VAPOR SPECTRUM OF ANTHRACENE

J. P. Byrne and I. G. Ross
Chemistry Department, University of Sydney, Sydney, Australia

Received May 12, 1965

ABSTRACT

Approximate calculations of the number of rovibronic transitions per unit wavenumber are given for benzene, naphthalene, anthracene, and tetracene. Primarily because of the density of sequence structure all transitions in tetracene vapor should be irresolvably crowded, and hence apparently diffuse, at practical temperatures. Anthracene, whose spectrum has hitherto been described as wholly diffuse, is predicted to be capable of showing resolvable structure at room temperature. At 60 °C and 40 m path a short region of fine sharp structure has been observed. The origin of the first singlet transition is located at 27 688.3 cm^{-1} (27 757.6 cm^{-1} in anthracene-d_{10}).

INTRODUCTION

Congestion as a Cause of Spectral Diffuseness

The spectra of polyatomic molecules, when studied in the vapor phase under high resolution, are only occasionally found to be sharp and detailed. Most transitions are relatively or wholly diffuse. The reasons for this are not always clear. Predissociation is a recognized cause but implies a photolability which is commonly not observed. A second possible cause is a sufficiently strong interaction between the low vibronic levels of one electronic state with a quasi-continuum of high vibronic levels of a state below (1, 2); this interaction may be connected with radiationless transitions (3)—a point we are trying to establish. A third cause of diffuseness is sheer congestion: the rovibronic transitions may be too numerous to be resolved. This last is obvious, but to our knowledge has not been discussed quantitatively.

SPECTRAL CONGESTION

Table I presents the results of some simple approximate calculations of the density of spectral lines in a series of aromatic hydrocarbons.

TABLE I

Spectral congestion in the electronic spectra of some aromatic molecules (300 °K)

	Benzene	Naphthalene*	Anthracene	Tetracene
Doppler width at 2 500 Å (cm^{-1})	0.028	0.022	0.018	0.016
Rotational features†				
Asymmetry, κ	1	−0.68	−0.91	−0.97
Highest observed J	90	145	200	240
Corresponding P–R branch separation (cm^{-1})	55	35	25	20
Lines per Doppler width	15	50	100	170
Vibrational features				
No. of vibrations‡	2+18	9+39	12+54	15+69
Sequence length (cm^{-1})	400	300	200	ca. 150
Average sequence spacing (cm^{-1})	130	5	0.7	ca. 0.1
Other data				
Temp. (°K) for vapor pressure = 1 mm	240	330	420	530
% isotopic impurities (^{13}C)	7	11	15	21

*Predictions for the isomeric molecule azulene are closely similar.
†Calculated assuming that all levels with given J are degenerate and located at the center of gravity, e.g., for prolate tops, at $(A + 2B)J(J + 1)/3$; that all such J levels with populations > 3% of the most populated level will give rise to observable lines, and that the number of observable P, Q, and R lines originating from each J level is $8J$. Moments of inertia are assumed to be the same in initial and final states.
‡Given as the number of totally symmetric frequencies plus the number of all other frequencies.

Can. J. Chem. Downloaded from www.nrcresearchpress.com by 210.87.254.105 on 09/05/12
For personal use only.

Individual rotational lines, it is clear, will be quite unobservable in any molecules of the series, though analyzable structure is sometimes seen if the inertial constants are such that the lines cluster in dense clumps (4).

Vibrational detail becomes more complex along the series for two reasons. First, increase in the number of totally symmetric modes causes a few long progressions (as in benzene (5)) to be replaced by a more elaborate, and generally more compressed, vibrational structure in which most bands are combination tones. But more important still is the proliferation of sequence structure. That is, associated with every vibronic band originating from the zero point level of the initial state are many others originating from vibrationally excited levels, which quanta are retained after the transition. In spectra observed at or near room temperature vibrational levels up to 800 cm^{-1} are observably populated (6, 7). Table I shows the number of such levels, calculated from assigned vibrational spectra (benzene (8), naphthalene (9), anthracene (10)) or roughly estimated (tetracene). The spread of the sequence structure has been calculated according to the pattern which appears in the best resolved transitions of benzene (5), naphthalene (6), and azulene (7), wherein there is one particularly long sequence due to a low-frequency out-of-plane mode whose frequency decreases drastically on excitation (1, 5, 6). Estimates for anthracene (subsequently confirmed: see below) and tetracene were obtained by extrapolation. It is, of course, not necessary that every transition in the one molecule should have the same spread of sequence structure; the estimates given are probably upper limits and therefore represent lower limits to the average interval between sequence bands.

All spectra become more congested as the temperature is raised; thus even the sharp 2 500 Å system of benzene is structureless at 500 °C (11). The limitations of vapor pressure, cited in the table (12), may make low temperature measurements difficult.

Spectral congestion is also caused by the presence of 1.1% of ^{13}C in natural carbon. The total percentages of molecules other than the pure ^{12}C species are included in Table I. In benzene the impurity is almost entirely a single species $^{12}C_5{}^{13}CH_6$; the expected consequence in the 2 500 Å transition is a weak sharp system slightly blue-shifted with respect to the principal spectrum. These bands have not yet been identified. In the larger hydrocarbons, the most likely consequence is a substantial unresolved contribution to the diffuse background.

From Table I it appears certain that tetracene vapor, even at room temperature, should show a spectrum crowded to the point of unresolvability. Benzene, naphthalene, and azulene are known each to have at least one sharp transition; individual vibrational features are well resolved, with rotational envelopes of characteristic profile. Indeed, azulene even shows a rich array of sharp features within the rotational envelope (13). Anthracene emerges as a marginal case. The figure quoted for the sequence spacing is an average; given a transition in which the bulk of the sequence structure is developed to one side of the origin, the intervals near the origin (the least crowded region) could be observable.

SPECTRUM OF ANTHRACENE

Platt (14) has correlated the lower excited states of conjugated acenes. In benzene and naphthalene the first two transitions, in order, are to states designated ^1L_b (weak sharp) and ^1L_a (stronger, diffuse). In anthracene the order of these states is reversed and ^1L_a is lowest. The diffuseness seen in the smaller molecules was offered as a diagnostic criterion for these ^1L_a bands, but there is no clear reason why diffuseness should be a general characteristic in the way that intensity is. The alternative point of view (1) suggests that the ability of a state to fluoresce is a surer guide to whether or not the corresponding absorption spectrum will be sharp.

Can. J. Chem. Downloaded from www.nrcresearchpress.com by 210.87.254.105 on 09/05/12
For personal use only.

PLATE I

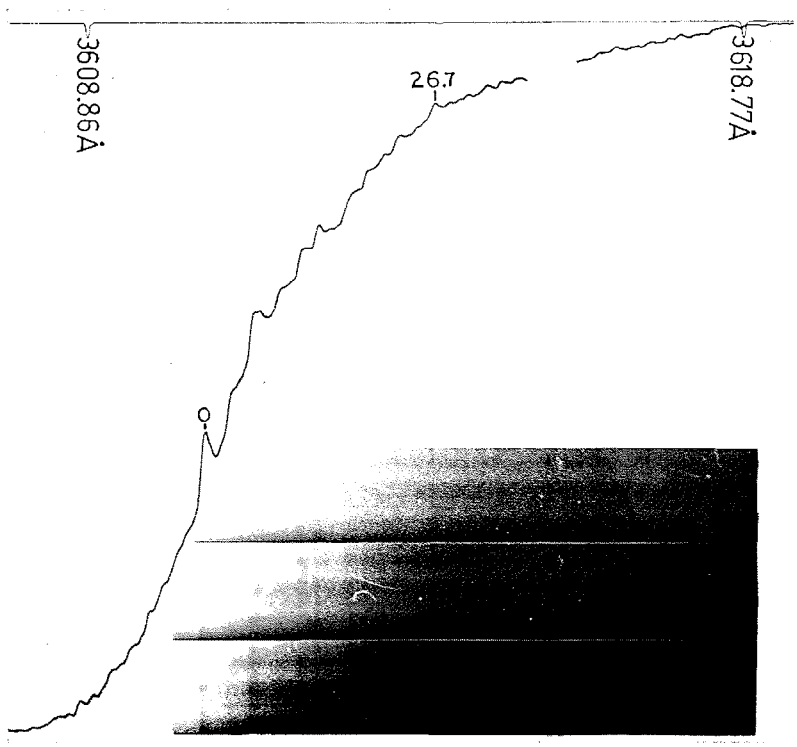

FIG. 1. Vapor absorption spectrum of anthracene (perprotonated). Values of $\Delta\nu$ (Table II) are indicated on two bands. The calibration trace shows two iron arc lines.

Can. J. Chem. Downloaded from www.nrcresearchpress.com by 210.87.254.105 on 09/05/12
For personal use only.

The first transition to ^1L_a in anthracene therefore assumes particular significance in this context, since anthracene fluoresces from the ^1L_a state with high efficiency. If then the temperature is low enough, and the ability to fluoresce (i.e., the absence of rapid radiationless transitions) is relevant, the absorption spectrum might be expected to show structure.

Previous measurements of the vapor spectrum have all been made at temperatures above 125 °C because the vapor pressure of anthracene is so low (Table I). Such spectra are diffuse (15). To search for the expected sharp structure we have now remeasured this spectrum, at a lower vapor temperature and at higher resolution.

RESULTS AND ANALYSIS

Using a multiple reflection cell, we find that the spectrum of anthracene can be measured at 60 °C (70 °C for the perdeuterated compound) at a path length of 40 m. With moderately high resolving power (about 100 000), this spectrum (Fig. 1) shows a short region of very sharp structure. This structured region coincides with the origin band of the solution spectrum. Another region with only hints of structure is found $\sim$ 380 cm^{-1} to the blue, this spacing being a progression interval (399 cm^{-1} in mixed crystals (16)). The rest of the spectrum is wholly diffuse.

The region with structure is a more crowded, but no less sharp, version of the kind of development seen in the 3 200 Å system of naphthalene (6) and the 3 500 Å system of azulene (1, 7). The region starts with a strong band at the high frequency end. This band is the most intense of the system, when background absorption, composed of accumulated rotational wings, is subtracted. This can only occur if the highest energy band of the system is the origin, and if the frequencies of all sequence-active vibrations are lower in the excited state than in the ground state. This is so in azulene also (7). Thus we identify the highest frequency band as the origin. Upon this origin is developed a closely packed sequence structure, initially with an average spacing of 2.5 cm^{-1}, but as the sequences progress and overlap and individual bands become weaker, the structure is no longer resolved. The known polarization (in plane, shorter axis) of this transition might be expected to produce double-headed bands as in similarly polarized transitions of naphthalene (6), but such doubling is not seen at all in perprotonated anthracene. In anthracene-d_{10} all the sequence bands except, probably, the origin occur in pairs spaced at 0.9 $\pm$ 0.2 cm^{-1}, but whether this is accidental or not cannot yet be decided.

Failure to see similar sequence structure in higher vibronic band groups could be due either to overlapping of progression members (there are 9 totally symmetric skeletal bending and stretching and CH in-plane bending vibrations, most of which are likely to be Franck–Condon active), or to mixing with the submerged ^1L_b transition which Pariser's calculations (17) place just above ^1L_a.

Table II lists the sequence members observed in anthracene and anthracene-d_{10}. The sequence interval 26.7 cm^{-1} in anthracene may well, on intensity grounds, be the expected large interval associated with the sensitive, low frequency, out-of-plane mode and which would be presumably responsible for the overall sequence length of $\sim$ 200 cm^{-1}. However, a detailed analysis of the sequence structure is not possible because of the large number of modes which are expected to be active.

DISCUSSION

The observation of structure in anthracene supports the general considerations of congestion, due to sequence structure, as a source of apparent spectral diffuseness. Another series of compounds in which the same considerations are clearly operative are the fluorobenzenes (18) wherein progressive substitution of fluorine for hydrogen systematically

Can. J. Chem. Downloaded from www.nrcresearchpress.com by 210.87.254.105 on 09/05/12
For personal use only.

TABLE II

Sequence structure in the origin band group in anthracene

Anthracene			Anthracene-d_{10}		
λ (Å)	ν (cm^{-1})	$\Delta\nu$ (cm^{-1})*	λ (Å)	ν (cm^{-1})	$\Delta\nu$ (cm^{-1})*
3 610.61 S†	27 688.3	0	3 601.59 S	27 757.6	0
0.97	85.5	2.8	2.10	53.7	3.9
1.32	82.8	5.5	2.25	52.5	5.1
1.71	79.8	8.5	2.98 S	46.9	10.7
2.09 S	76.9	11.4	3.09 S	46.1	11.5
2.31 S	75.3	13.0	3.64 S	41.8	15.8
2.84	71.2	17.1	3.77 S	41.0	16.6
3.09	69.3	19.0	4.04	38.8	18.8
3.33	67.4	20.9	4.18	37.8	19.8
3.54 S	65.8	22.5	4.50 S	35.2	22.4
4.09 S	61.6	26.7	4.60 S	34.4	23.2
4.56	58.0	30.3	5.07	30.8	26.8
4.85	55.8	32.5	5.18	29.9	27.7
5.07	54.1	34.2			
5.58	50.2	38.1			
5.87	48.0	40.3			

*Separation from the shortest wavelength band, assigned as the origin in each case.
†S: stronger bands.

lowers all vibrational frequencies. The hypothesis that rapid radiationless transitions may be associated with spectral diffuseness, though not yet conclusively demonstrated, is supported to the extent that this particular transition, leading to a radiative state, is now found to be intrinsically sharp.

The possibility of testing other apparently diffuse transitions in other molecules, by lowering the temperature to reduce the sequence structure, is obviously limited by vapor pressure considerations. However, noting that the spectrum of anthracene, as an impurity in naphthalene or phenanthrene, is also sharp (16) it now seems likely that such mixed crystal spectra may reliably indicate the intrinsic sharpness or diffuseness of electronic transitions in free molecules.

EXPERIMENTAL

The spectra were photographed in the 4th order of a Jarrell–Ash 3.4 m Ebert spectrograph using a 4½ in., 15 000 line/in. grating blazed for 4 000 Å in the first order. The dispersion was 1.15 Å/mm and the practical resolving power at the critical slit width was estimated at about 100 000. Exposure times with a 120 W xenon arc source and Kodak B4 plates were of the order of 4 h, during which time the temperature of the spectrograph was regulated to ±0.2 °C. Plates were microphotometered with a Joyce–Loebl Mark IIIC instrument. Because of the expected crowding and diffuse rotational background the contrast in the spectrum is not easily shown; at the available instrumental dispersion the microphotometer trace makes the features look less sharp than do the original photographs.

The multiple reflection cell was of glass, 2 m long, with brass end fittings connected by neoprene O-rings; the cell was enclosed in an oven for the high temperature measurements. Between fillings with the two anthracenes it was necessary to boil the end fittings in ether and to replace the O-rings.

ACKNOWLEDGMENTS

Acknowledgment is made to Mr. Alexander Boden, Sydney, and to the Petroleum Research Fund, administered by the American Chemical Society, for partial support of this work. J. P. B. acknowledges the award of a C.S.I.R.O. postgraduate studentship.

REFERENCES

1. G. R. Hunt and I. G. Ross. J. Mol. Spectry. **9**, 50 (1962).
2. G. R. Hunt, E. F. McCoy, and I. G. Ross. Australian J. Chem. **15**, 591 (1963).
3. J. P. Byrne, E. F. McCoy, and I. G. Ross. Australian J. Chem. In press.

Can. J. Chem. Downloaded from www.nrcresearchpress.com by 210.87.254.105 on 09/05/12
For personal use only.

4. J. M. HOLLAS. Spectrochim. Acta, **20**, 1563 (1964).
5. F. M. GARFORTH and C. K. INGOLD. J. Chem. Soc. 417 (1948).
6. D. P. CRAIG, J. M. HOLLAS, M. F. REDIES, and S. C. WAIT. Phil. Trans. Roy. Soc. London, Ser. A, **253**, 543 (1961).
7. E. F. MCCOY. Ph.D. Thesis, University of Sydney, Sydney, Australia. 1964.
8. D. H. WHIFFEN. Phil. Trans. Roy. Soc. London, Ser. A, **248**, 131 (1955).
9. J. R. SCHERER. J. Chem. Phys. **36**, 3308 (1962).
10. E. P. KRAINOV. Opt. Spectry. USSR English Transl. **16**, 532 (1964).
11. F. ALMASY and H. LAEMMEL. Helv. Chim. Acta, **34**, 462 (1951).
12. H. INOKUCHI, S. SHIBA, T. HANDA, and H. AKAMATU. Bull. Chem. Soc. Japan, **25**, 299 (1952).
13. A. J. MCHUGH, D. A. RAMSAY, and I. G. ROSS. Unpublished work.
14. J. R. PLATT. J. Chem. Phys. **17**, 484 (1949).
15. G. KORTÜM and B. FINCKH. Z. Physik. Chem. Leipzig, **B52**, 263 (1942). J. FERGUSON, L. W. REEVES, and W. G. SCHNEIDER. Can. J. Chem. **35**, 1117 (1957). O. P. KHARITONOVA. Opt. Spectry. **5**, 29 (1958).
16. J. W. SIDMAN. J. Chem. Phys. **25**, 115 (1956).
17. R. PARISER. J. Chem. Phys. **24**, 250 (1956).
18. S. H. BAUER and C. F. ATEN. J. Chem. Phys. **39**, 1253 (1963).

Can. J. Chem. Downloaded from www.nrcresearchpress.com by 210.87.254.105 on 09/05/12
For personal use only.

Can. J. Chem. Downloaded from www.nrcresearchpress.com by 210.87.254.105 on 09/05/12
For personal use only.

THE RATIOS OF STEPWISE STABILITY CONSTANTS

III. THE RARE-EARTH α-HYDROXYMONOCARBOXYLATES

P. G. MANNING
Mines Branch, Department of Mines and Technical Surveys, Ottawa, Canada
Received February 2, 1965

ABSTRACT

The magnitudes of stepwise stability constant ratios indicate that the α-hydroxymonocarboxylic acids, in their association reactions with the rare-earth cations, function as monodentate ligands.

INTRODUCTION

The α-hydroxymonocarboxylic acids (e.g., glycolate, lactate, and α-hydroxyisobutyrate) are normally accepted as being bidentate ligands, since they are stronger acids than acetic and form more stable ion associates with metals. It was shown (1) that the rare-earth acetates are ion pairs in which the acetate ion binds electrostatically to the cation primary hydration sheath, and a direct comparison of the stabilities of the rare-earth acetates and α-hydroxymonocarboxylates offers no proof of bidentate character in these glycolate-type ligands.

The determination of the N-dentate nature of these ligands is of interest because they form 1:4 (rare earth:ligand) species (2–6), and the formation of such complexes is evidence in favor of the contention that rare-earth ions have coordination numbers of eight.

In the present paper, the ratios of stepwise stability constants for some lanthanide – α-hydroxymonocarboxylate complexes have been examined statistically.

DISCUSSION

The stepwise stability constant is defined as

$$b_n = [ML_n]/[ML_{n-1}][L],$$

where M and L are metal and ligand ions respectively. Let $P = b_1:b_2$. The P factor is composed of both statistical and ligand effects, and is a measure of the relative ease with which the first two ligands bind to the central cation (7).

Published data on rare-earth – monocarboxylate complexing are abundant, but, unfortunately, do not pertain to standard aqueous conditions. The range in ionic strength is 0.1–2.0, and in temperature 20–25 °C. The P values are largely unaffected by changes in temperature and ionic strength, since activity and dielectric effects cancel out when two stages of ion association are considered (1). The absolute magnitudes of the stability constants are not important in subsequent discussions.

Let us consider, initially, the factors that can influence the magnitude of P. Bjerrum (7) has shown that P is dependent on three factors, the statistical (S), the ligand repulsion (T), the rest (R) effects. The relationship between these factors is

$$P = S \times T \times R.$$

The statistical factor.—S can be estimated from the number of cation association sites and ligand bonding groups. The α-hydroxymonocarboxylates are potentially bidentate,

Can. J. Chem. Downloaded from www.nrcresearchpress.com by 210.87.254.105 on 09/05/12
For personal use only.

while the number of cation association sites depends on whether the association species is an ion pair or a complex (1, 8). The magnitude of $S > 1$. For example, let us consider a simple monodentate ligand associating with a D-hydrated cation species. Then, if the ligand associates through the displacement of a single coordinated water molecule, it is evident that the first ligand to associate has D coordination sites from which to choose. A second ligand approaching the 1:1 (metal:ligand) species will then have $D - 1$ possible sites for coordination. Since there is twice the probability of a ligand departing from the 1:2 species as there is from the 1:1 species, then $S = 2 \times D/(D - 1)$, i.e., $S > 1$ (more correctly, $S > 2$). If we consider a bidentate ligand associating with a hexahydrated rare-earth ion (1), then the 1:3 species will be octahedral. The first ligand to associate can displace two bound water molecules in 12 different ways, the second can displace two water molecules in 5 ways, and the third in 1 way. Since the relative probabilities of a ligand leaving the 1:1 and 1:2 species is 1:2, then $S = 2 \times 12/5 = 4.8$.

The ligand repulsion effect.—A ligand that is about to associate with a 1:1 or 1:2 species will be repelled electrostatically by the bound ligands, since all ligands are charged or possess dipoles. Of necessity, $T > 1.0$.

The rest effect.—In a 1:2 association species, the two bound ligands will have an equal probability of escape from the cation. It is possible that on the escape of one ligand the remaining ligand in the 1:1 species will be held on more strongly to the cation, i.e. bound ligands can influence the binding power of the metal ion (7). In the case described, $R > 1.0$, but cases are known where $R < 1$. In the α-hydroxymonocarboxylate systems, the rest effect is likely to be small and $R \sim 1$ (7).

For carboxylic acids that associate electrostatically with the primary hydration sheath of a rare-earth ion, a plot of b_1 against Z (the atomic number) has a characteristic sinusoidal shape (5), the significance of which has been explained theoretically (1). Plots of b_1 against Z for the rare-earth α-hydroxymonocarboxylates differ considerably from the analogous acetate curves, indicating that the lanthanide α-hydroxymonocarboxylates are not ion pairs (9). Furthermore, pK values for the parent ligand acids increase in the order glycolate < lactate < α-hydroxyisobutyrate, and this is also the order of stability of the 1:1 metal associates (4, 9). The rare-earth α-hydroxymonocarboxylates are, therefore, complexes.

For complexing between a hexahydrated cation and a bidentate ligand, $S = 4.8$. The P values shown in Figs. 1 and 2 are smaller than 4.8, which suggests that this model is incorrect. Moreover, the T factor will inflate the calculated P value, and from chloride complexing with similarly sized cations (Hg^{2+}, Sn^{2+}) an approximate value of $T = 2.0$ (7).

For monodentate ligands displacing one water molecule from the cation hydration sheath, $S = 2 \times 6/5 = 2.40$. If $T = 1.5$, then the calculated P value is consistent with the experimentally derived P values (Figs. 1 and 2, refs. 2, 3, 5). It is possible that glycolate, for example, is bidentate in the first association stage and monodentate in the second, whence $S = 2 \times 12/4 = 6.0$. This P value is again too large.

If rare-earth ions are eight-hydrated (dodecahedral structure), then for a bidentate ligand $S = 2 \times 12/9 = 3.5$. This S value is in excellent agreement with the experimental P value if $T = 1.0$. If the ligands are monodentate $S = 2.3$ and $T = 1.6$. However, $T = 1.1$ for rare-earth acetate ion pairs. Since the average ligand separation is much greater in the acetate system than in the α-hydroxymonocarboxylate, T(acetate) < T(α-hydroxymonocarboxylate), and from simple Coulombic theory and T(acetate) = 1.1 then T(α-hydroxymonocarboxylate) = 1.3–1.4. This T value would favor a monodentate α-hydroxymonocarboxylate.

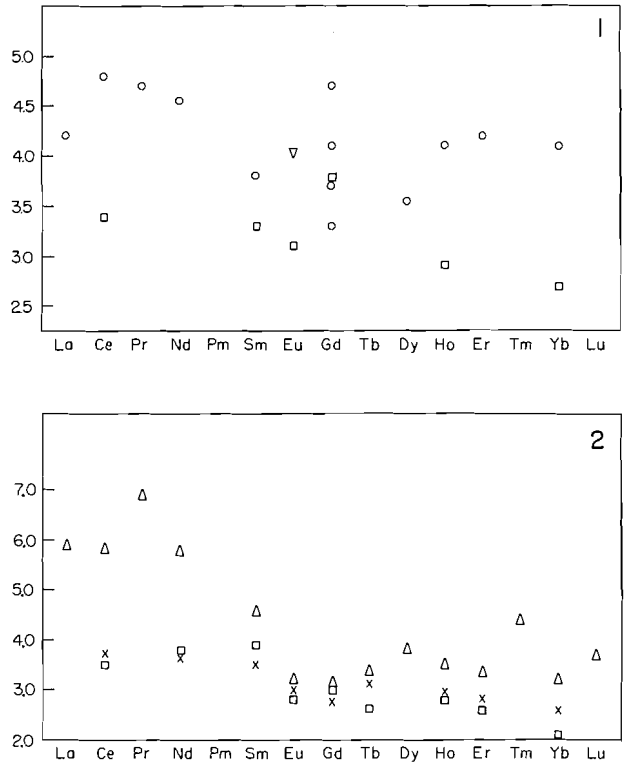

FIG. 1. P values for rare-earth glycolates. ○ Data of Sonesson (2, 3). □ Data of Choppin and Chopoorian (4). ▽ Data of Grenthe (6).

FIG. 2. P values for rare-earth lactates (×) and α-hydroxyisobutyrates (△, □). △ Data of Stagg and Powell (5). □ Data of Choppin and Chopoorian (4). × Data of Choppin and Chopoorian (4).

TABLE I

P values for Cu^{2+} acetates

Worker	Method	P	P'*	Ref.
Lundquist	Ion exchange	>3.8	4.8	10
Archer	Glass electrode	6.7		11
Pedesen	Glass electrode	13.6		12
Fronaeus	Potentiometry	4.9	3.7	13
Fronaeus	Ion exchange	4.5	4.4	13
Fronaeus	Spectrophotometry	4.4		13
Kolat and Powell	Glass electrode	4.9		14

*Where $P' = b_2:b_3$.

TABLE II

P values for Cu^{2+} glycolates

Worker	Method	P	P'	Ref.
Lundquist	Ion exchange		13	10
Fronaeus	Electromotive force	9.6	11.5	13
Fronaeus	Spectrophotometry	14.5		13

Can. J. Chem. Downloaded from www.nrcresearchpress.com by 210.87.254.105 on 09/05/12
For personal use only.

Can. J. Chem. Downloaded from www.nrcresearchpress.com by 210.87.254.105 on 09/05/12
For personal use only.

Accurate P values have been determined for cupric acetate and glycolate ion association (Tables I and II). Cupric and rare-earth ions are of similar size, and it would be expected that the average ligand separation in 1:2 rare-earth α-hydroxymonocarboxylate complexes and 1:2 cupric acetates and glycolates would be very similar, i.e., the T values would be approximately equal. The b_1 values for the transition metal acetates follow closely the Irving–Williams (15) rule, indicating the cupric acetates are complexes. The greater stability of the cupric glycolate associate relative to the acetate suggests that acetate is monodentate and glycolate bidentate. The cupric ion is six-hydrated, four waters being bound in a square plane and the other two perpendicular to the square plane, i.e., tetragonal configuration. In an analysis of the stepwise stability constants, therefore, the facility with which acetate and glycolate can displace the strongly and loosely bound waters must be considered.

In the cupric acetate system the P value = 13.6 may clearly be rejected (Table I). If we use Chauvenet's criterion of rejection (16) of doubtful data, then P = 6.7 may also be rejected with a 90% confidence limit. Therefore, with 90% confidence P(cupric acetate) = 4.7 ± 0.2. In Table III calculated S and T values for cupric acetates and glycolates and also for 4 and 6 available cation sites are given. Table IV presents the best T values for the rare-earth α-hydroxymonocarboxylates and cupric acetates and glycolates; clearly, for singly-charged ligands that bind to cations of the size of rare earths or Cu^{2+}, $T \sim 1.6$. These T values confirm that the α-hydroxymonocarboxylates associate with rare earths as monodentate ligands and also that a Jahn–Teller effect is operative in cupric acetate and glycolate systems (4 available coordination sites). In the cupric glycolate system, however, the ligand–ligand separation in the 1:2 species is greater than the average ligand separation in the corresponding rare-earth system. The difference in T values for the two systems would be expected to be ~ 0.1. This value is less, however, than the deviations quoted for the individual T values.

TABLE III

P, S, and T values for Cu^{2+} complexes

	Ligand			
	Acetate		Glycolate	
Available sites	6	4	6	4
P	4.7±0.2	4.7±0.2	12.0±2.5	12.0±2.5
S	2.40	2.67	4.8	8.0
T	1.95±0.1	1.75±0.1	2.5±0.5	1.5±0.3

TABLE IV

T values for metal complexes

System	Rare earth	Cu acetate	Cu glycolate
T	1.5±0.25	1.75±0.1	1.5±0.3

We may also calculate $P' = b_2{:}b_3$ for the cupric acetates. Thus $P' = 3/2 \times 3/2 \times 1.75 = 3.9$. The average experimental value is 4.3 (Table I).

Let us consider the mechanism of the reaction

$$M(OH_2)_6 + L = M(OH_2)_5L + H_2O.$$

Can. J. Chem. Downloaded from www.nrcresearchpress.com by 210.87.254.105 on 09/05/12
For personal use only.

The major cation species in solution is $M(OH_2)_6$, and concentrations of $M(OH_2)_5$ and $M(OH_2)_4$ are negligible (1, 17, 18). The metal–water bonds will make-and-break, and waters of the primary hydration sheath will exchange with other water molecules of the bulk medium or with ligands. While the (monodentate) α-hydroxymonocarboxylate is coordinated to the cation in the 1:1 complex, there is a probability that an adjacent water molecule will vacate its position in the primary hydration layer, and, because of the favorable orientation of the free OH group, chelation will occur. Therefore, the greater the pK value of the parent ligand acid the greater the time spent by the ligand coordinated to the metal and the greater its bidentate character. It would be expected from such a theory that P(α-hydroxyisobutyrate, pK = 3.76) > P(lactate, pK = 3.63) > P(glycolate, pK = 3.57). The data of Choppin and Chopoorian (4) indicate that P values for rare-earth complexing with three pertinent ligands are equal. Also, Sonesson's P values for the glycolates (2, 3) are of almost equal magnitude to those of Stagg and Powell for the α-hydroxyisobutyrates (5). The P values for the glycolates are also indicative of purely monodentate ligand bonding.

Since each monodentate ligand will have four adjacent water molecules in the 1:1 complex, it is clear that the α-hydroxymonocarboxylate ligand spends little time coordinated to the cation (relative to a water molecule). This suggests that the rare-earth hydration sheath is an extremely strong one. It was suggested, from an analysis of the acetate data (1), that the heavier rare-earth ions were hydrated through true coordination, and that water molecules were oriented beyond the first hydration layer so that the second layer acted as a cage preventing the escape of labile waters of the primary hydration sheath. The α-hydroxymonocarboxylate results would be in keeping with this hypothesis. There is infrared evidence that the water structure around La is highly ordered (19).

If the α-hydroxymonocarboxylates were bidentate ligands, then glyoxylic acid (dihydroxyacetic acid) should be a more powerful chelating agent than any of the three above-mentioned ligands, because of the greater number of possible binding groups (9). However, according to the present hypothesis, the stabilities of the rare-earth glyoxylates will depend on the pK value of the acid (pK = 3.17, ref. 9), and, in theory, the glyoxylates should be weaker complexes than glycolate, and P values should be approximately 4. The experimental results of Powell and Suzuki (9) confirm this.

This paper brings out an interesting point. Because pK(acetic acid) > pK(glycolic acid, e.g.) it would be expected that if glycolate bound directly to the cation then acetate would also do so. It is conceivable that in the rare-earth glycolate system the —COO group binds directly to the metal and that the —OH group binds to a neighboring water molecule of the cation hydration sheath, i.e., chelation occurs. This conclusion would be in agreement with that reached by Grenthe (20) on the basis of ΔH and ΔS data. On the basis of the number of water molecules of the rare-earth primary hydration sheath that are displaced, the α-hydroxymonocarboxylates are monodentate.

A recent study by Larsson and Folkeson (21) of the Zn–mandelate system shows that T = 1.5 and that mandelate is monodentate. These conclusions are similar to ours for the rare-earth α-hydroxymonocarboxylates.

We feel that we can justify the value of R = 1.0 used here. For the rare-earth acetates, by definition, R = 1.0 and T = 1.1. Using this latter T value, a T value = 1.3–1.4 was derived for α-hydroxymonocarboxylate complexing. Moreover, the T values listed in Table IV are largely independent of the cation and of the ligand. In the Cu systems, e.g., acetate and glycolate would be expected to give different R values. The T values in Table IV confirm that the R effect must be small.

CONCLUSION

The ratios of stepwise stability constants suggest that the α-hydroxymonocarboxylates are monodentate ligands in their reactions with rare-earth ions. The formation of 1:4 metal:ligand ion associates is not proof of eight-coordination in rare-earth complexes.

REFERENCES

1. P. G. MANNING. Ratios of stepwise stability constants. Part II. Submitted for publication.
2. A. SONESSON. Acta Chem. Scand. **13**, 998 (1959).
3. A. SONESSON. Acta Chem. Scand. **15**, 1 (1961).
4. G. R. CHOPPIN and J. A. CHOPOORIAN. J. Inorg. Nucl. Chem. **22**, 97 (1961).
5. W. R. STAGG and J. E. POWELL. Inorg. Chem. **3**, 242 (1964).
6. I. GRENTHE. Acta Chem. Scand. **16**, 1695 (1962).
7. J. BJERRUM. Metal ammine formation in aqueous solution. P. Haase and Son, Copenhagen. 1941.
8. J. M. SMITHSON and R. J. P. WILLIAMS. J. Chem. Soc. 457 (1958).
9. J. E. POWELL and Y. SUZUKI. Inorg. Chem. **3**, 690 (1964).
10. I. LUNDQUIST. Acta Chem. Scand. **18**, 858 (1963).
11. D. W. ARCHER and C. B. MONK. J. Chem. Soc. 3117 (1964).
12. K. J. PEDESEN. Kgl. Danske Videnskab. Selskab Mat. Fys. Medd. **22**, No. 12 (1945).
13. S. FRONAEUS. Ph.D. Thesis, Gleerupska University, Lund, Sweden. 1948.
14. R. S. KOLAT and J. E. POWELL. Inorg. Chem. **1**, 293 (1962).
15. H. IRVING and R. J. P. WILLIAMS. Nature, **162**, 746 (1948).
16. L. TUTTLE and J. SATTERLY. The theory of measurements. Longmans, London. 1925.
17. G. W. BRADY. J. Chem. Phys. **33**, 1079 (1960).
18. E. V. SAYRE, D. C. MILLER, and S. FREED. J. Chem. Phys. **26**, 109 (1957).
19. G. R. CHOPPIN and K. BUIJS. J. Chem. Phys. **39**, 2042 (1963).
20. I. GRENTHE. Acta Chem. Scand. **18**, 283 (1964).
21. R. LARSSON and B. FOLKESON. Acta Chem. Scand. **19**, 53 (1965).

Can. J. Chem. Downloaded from www.nrcresearchpress.com by 210.87.254.105 on 09/05/12
For personal use only.

Can. J. Chem. Downloaded from www.nrcresearchpress.com by 210.87.254.42 on 09/05/12
For personal use only.

THE INTERACTION OF THE ACETATES AND CARBAMATES OF SOME HETEROCYCLIC ALCOHOLS WITH ACETYLCHOLINESTERASE[1]

K. B. SHAW
Defence Chemical, Biological and Radiation Laboratories, Ottawa, Canada
Received June 24, 1965

ABSTRACT

The *N,N*-dimethylcarbamates of 3-quinuclidinol, 1-methyl-3-piperidinol, and 1-methyl-4-piperidinol have been prepared and found to be weak inhibitors of acetylcholinesterase. The acetates of the above alcohols were also prepared and found to be moderately good substrates for this enzyme.

The elucidation of the structure (1) of the carbamate physostigmine (eserine), a potent anticholinesterase, led to a search for simpler analogues and a large number of alkyl- and dialkylcarbamates have been prepared and tested for anticholinesterase activity (2). Physostigmine contains a methylcarbamate group attached to an aromatic ring, and perhaps for this reason, the vast majority of the synthetic compounds also contain a carbamate group attached to an aromatic nucleus. An additional structural feature which seems to be necessary for high activity is another nitrogen atom (usually quaternized), which may be incorporated in the aromatic ring as in pyridostigmine (I), or directly attached to it as in neostigmine (II). Since there appears to be very little information in the literature concerning aliphatic carbamates (2), the anticholinesterase activities of the *N,N*-dimethylcarbamates of the saturated alcohols 3-quinuclidinol, 1-methyl-3-piperidinol, and 1-methyl-4-piperidinol have been assessed by measurement of their pI_{50}

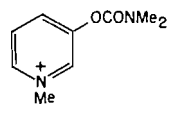

I

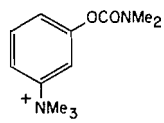

II

values on bovine acetylcholinesterase (the pI_{50} is the negative logarithm of the molar concentration of inhibitor which causes 50% inhibition of the enzyme activity in the system used). In addition, some experiments were performed to investigate the nature of the carbamate inhibition. The acetates of the above alcohols were also prepared and their effectiveness as substrates for acetylcholinesterase determined (by measurement of their Michaelis constants) to provide a comparison with the effectiveness of the carbamates as inhibitors of this enzyme.

1-Methyl-3-piperidyl *N,N*-dimethylcarbamate (III) was prepared from 1-methyl-3-piperidinol and dimethylcarbamyl chloride in pyridine solution (3) and this method proved satisfactory for the preparation of the corresponding 4-isomer (V). Both compounds discolored on storage and were further purified through their picrates, but V still turned slowly brown, even when stored in the freezer. Although some properties of 3-quinuclidinyl *N,N*-dimethylcarbamate (VII) (and its methiodide) have been discussed (4), its preparation does not appear to have been described in the literature. Repetition of the above reaction using 3-quinuclidinol gave a poor yield of impure carbamate and much

[1]*Issued as DCBRL Report No. 455B.*

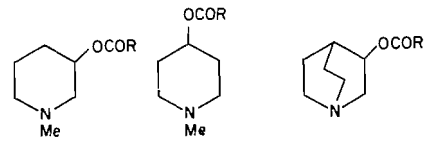

III R = NMe_2 V R = NMe_2 VII R = NMe_2
IV R = Me VI R = Me VIII R = Me

starting material remained. Separation of the mixture proved to be difficult and after a number of experiments it was apparent that pyridine was not a suitable solvent for this reaction. The required carbamate was eventually obtained in good yield using 2 moles of 3-quinuclidinol and 1.15 moles of dimethylcarbamyl chloride in chloroform solution, either at reflux temperature for 3 h or preferably at room temperature for 20 h. The distilled product showed strong absorption in the infrared at about the expected frequency (1 700 cm^{-1}) for a carbamate carbonyl group (5) and also weaker carbonyl absorption at about 1 760 cm^{-1}, and was conveniently purified, leading to material showing only a single carbonyl peak (1 702 cm^{-1}) through the picrate. The compound absorbing at 1 760 cm^{-1} appeared, albeit in very small yield, in all preparations of the carbamate; the compound was not separable from the carbamate by distillation, although it was separated by chromatography on alumina; it showed two carbonyl peaks in the infrared at 1 760 and 1 705 cm^{-1}, the latter more intense, and the spectrum differed in other respects from that of VII. Titration with hydrochloric acid indicated a pK_a (in aqueous ethanol) very similar to that (8.5) of VII and an equivalent weight of 280, and nitrogen analysis indicated a molecular weight of 288 for three nitrogen atoms. A structure for this compound has not been deduced from the available data.

The acetates (IV, VI, VIII) were prepared from the appropriate alcohol and acetic anhydride (6). Like the corresponding carbamate, 1-methyl-4-acetoxypiperidine (VI) discolored at room temperature, but after two months its infrared spectrum had not changed significantly. Although all three acetates were sufficiently stable at the pH (7.4) at which the kinetic measurements were made, they were unstable in aqueous solution at pH 9–10 and gave erratic equivalent weights on titration with hydrochloric acid. For example VIII (equiv. wt. 169) on rapid titration in 0.1 *N* saline solution gave an apparent equivalent weight of 210 and after standing for 5 h in the same solvent, a value of 338. Satisfactory equivalent weights were obtained in acetonitrile solution.

The pI_{50} values (25°, 2 min incubation time) obtained for the three carbamates, together with the Michaelis constants (K_m) and the V_{max} values, relative to acetylcholine = 1.00, for the corresponding acetates are given in Table I. The acetates are moderately good substrates for acetylcholinesterase, (the K_m for the acetylcholine–acetylcholinesterase system is 4.5×10^{-4} *M* (7)) but the carbamates are poor inhibitors and the pI_{50}

TABLE I

Values of pI_{50} for the inhibitors ($ROCONMe_2$) as well as Michaelis constants and V_{max} (relative to acetylcholine = 1.00) for the substrates (ROCOMe)

R	$ROCONMe_2$ pI_{50}	ROCOMe K_m (*M*)	ROCOMe V_{max}
3-Quinuclidinyl	2.75	$2.52 \pm 0.4 \times 10^{-3}$	0.69
1-Methyl-3-piperidyl	2.51	$2.44 \pm 0.27 \times 10^{-3}$	0.59
1-Methyl-4-piperidyl	2.40	$1.59 \pm 0.27 \times 10^{-3}$	0.42

Can. J. Chem. Downloaded from www.nrcresearchpress.com by 210.87.254.42 on 09/05/12
For personal use only.

values are considerably lower than that of physostigmine sulfate, which under the same conditions was found to be 6.26. It has been shown (8) that the inhibition of acetylcholinesterase by carbamates leads to a carbamylated enzyme, but the inhibition produced by the carbamates in the present work is weak enough to suggest that the heterocyclic nitrogen atom and not the carbamate group is almost wholly responsible. Support for this argument was obtained when under the same conditions the pI_{50} of 1-methylpiperidine was found to be 2.50.

In contrast to the physostigmine analogues referred to above, the carbamates described here do not contain a quaternary nitrogen atom. However, since at pH 7.4 these tertiary amine carbamates are predominantly cationic (approximate pK_a values determined by titration in saline were found to be 8.7, 9.1, and 9.5 for III, V, and VII respectively), conversion to the methiodide would not be expected to increase the inhibition (9), hence their weakness as inhibitors cannot be due to this. An example of an aliphatic carbamate with anticholinesterase activity is dimethylcarbamyl choline, but it is less potent than I, and especially II (8). Since the stereochemistry of dimethylcarbamyl choline must be favorable for reaction with the enzyme, its comparatively weak inhibitory power is probably caused by the carbonyl carbon atom being less electrophilic than that in I or II. The carbamates described here also contain a similar weakly electrophilic carbon atom, and in addition their stereochemistry is less favorable than that of dimethylcarbamyl choline since the acetates are weaker substrates than acetylcholine; hence the weakness of the carbamates as inhibitors is perhaps not surprising.

A limited number of experiments was performed with the present carbamates to investigate whether the inhibition was competitive or non-competitive. The rate of hydrolysis of acetylcholine was measured in the absence and presence of carbamate and the results fitted to a Lineweaver and Burk plot (10). Although in every case both the slopes and $1/v$ intercepts of the lines for the uninhibited and inhibited reactions were different, implying non-competitive inhibition, extrapolation of the lines to the $1/S$ axis showed that the K_m of the reaction was changed in the presence of inhibitor, indicating that the inhibition was neither completely competitive nor non-competitive (11).

EXPERIMENTAL

3-Quinuclidinyl N,N-Dimethylcarbamate

Dimethylcarbamyl chloride (24.6 g, 0.23 mole) was added to a solution of 3-quinuclidinol (50.8 g, 0.4 mole) in dry chloroform (250 ml), and the mixture was stirred at room temperature for 20 h. The 3-quinuclidinol hydrochloride was filtered off and dried (32.7 g, 0.2 mole) and the chloroform solution was washed with water (2 × 50 ml) and dried ($MgSO_4$). After removal of the chloroform the product was distilled to give a colorless liquid (27 g, 68%), b.p. 64–67° at 0.003–0.005 mm, n_D^{25} 1.4859. The picrate was prepared from the carbamate (8.6 g) in 50% ethanol–acetone (v/v). After two crystallizations from the same solvent mixture, there were obtained 10.2 g (52%) of yellow prisms, m.p. 174–177°.

Anal. Found: C, 45.13; H, 5.05; N, 16.30. $C_{16}H_{21}N_5O_9$ requires C, 44.97; H, 4.95; N, 16.30.

The picrate (10.5 g) was dissolved in cold saturated lithium hydroxide solution (50 ml) and the solution was extracted with chloroform (5 × 25 ml). The combined extracts were washed with water (50 ml) and dried ($MgSO_4$), the solvent was removed, and the residue was distilled to give 3-quinuclidinyl *N,N*-dimethylcarbamate (2.89 g, 62%) b.p. 75–78° at 0.05 mm, n_D^{25} 1.4481.

Anal. Found: C, 60.72; H, 9.25; N, 14.08; equiv. wt. 201. $C_{10}H_{18}N_2O_2$ requires C, 60.58; H, 9.15; N, 14.13; equiv. wt. 198.

1-Methyl-3-piperidyl N,N-Dimethylcarbamate

The method of Biel *et al.* (3) was used and the product was further purified through the picrate. The picrate was prepared from the carbamate (11.8 g) in 50% ethanol–acetone (v/v) and after one crystallization was obtained as yellow prisms (18.15 g, 69%) m.p. 162–164° (unchanged on recrystallization).

Anal. Found: C, 43.61; H, 5.36; N, 16.88. $C_{15}H_{21}N_5O_9$ requires C, 43.37; H, 5.10; N, 16.86.

The picrate (11.8 g) was converted to the free base as above. The crude product was distilled to give

Can. J. Chem. Downloaded from www.nrcresearchpress.com by 210.87.254.42 on 09/05/12
For personal use only.

1-methyl-3-piperidyl *N,N*-dimethylcarbamate (6.75 g, 81%), b.p. 83–84° at 1.1 mm, n_D^{25} 1.4640 (lit. b.p. 101–103 at 3 mm (3)).

Anal. Found: C, 57.99; H, 9.94; N, 15.20; equiv. wt. 191. $C_9H_{18}N_2O_2$ requires C, 58.03; H, 9.74; N, 15.04; equiv. wt. 186.

1-Methyl-4-piperidyl N,N-Dimethylcarbamate

This compound was prepared (65%) from 1-methyl-4-piperidinol and dimethylcarbamyl chloride following Biel *et al.* (3) and was further purified through the picrate. The picrate was prepared from the carbamate (5.6 g) in 50% ethanol–acetone (v/v) and after one crystallization was obtained as yellow needles (7.7 g, 58%), m.p. 198–200°, raised to 201–203° after two recrystallizations.

Anal. Found: C, 43.63; H, 5.19; N, 16.66. $C_{15}H_{21}N_9O_9$ requires C, 43.37; H, 5.10; N, 16.86.

The picrate (7.7 g) was converted to the free base in the usual way. The crude product was distilled to give 1-methyl-4-piperidyl *N,N*-dimethylcarbamate (2.53 g, 73%), b.p. 52–53° at 0.05 mm, n_D^{25} 1.4637.

Anal. Found: C, 57.88; H, 9.67; N, 15.13; equiv. wt. 191. $C_9H_{18}N_2O_2$ requires C, 58.03; H, 9.74; N, 15.04; equiv. wt. 186.

3-Acetoxyquinuclidine

The method of Grob *et al.* (6) was used. The product had b.p. 81–83° at 2.2 mm, n_D^{25} 1.4770 (lit. b.p. 113–115 at 11 mm, n_D^{25} 1.4675 (6)).

Anal. Found: C, 63.56; H, 9.05; N, 8.08; equiv. wt. 175. $C_9H_{15}NO_2$ requires C, 63.88; H, 9.05; N, 8.08, equiv. wt. 169.

1-Methyl-3-acetoxypiperidine

This compound (12, 13) was made by the method of Grob *et al.* (6) from 1-methyl-3-piperidinol and acetic anhydride; b.p. 76–78° at 11 mm; n_D^{25} 1.4470; equiv. wt. 160, calcd. 157 (lit. b.p. 32–40° at 0.2 mm; n_D^{25} 1.4471 (13); b.p. 72° at 11 mm, n_D^{20} 1.4512 (12)).

1-Methyl-4-acetoxypiperidine

The reaction of 1-methyl-4-piperidinol and acetic anhydride, following Grob *et al.* (6) gave the required compound (60%), b.p. 77–79° at 11 mm, n_D^{25} 1.4480.

Anal. Found: C, 61.09; H, 9.71; N, 8.65; equiv. wt. 160. $C_8H_{15}NO_2$ requires C, 61.12; H, 9.62; N, 8.91; equiv. wt. 157.

After several crystallizations from ethanol–acetone, the picrate was obtained as pale yellow needles, m.p. 170–171°.

Anal. Found: C, 43.20; H, 4.65; N, 14.66. $C_{14}H_{18}N_4O_9$ requires C, 43.52; H, 4.70; N, 14.50.

Kinetics

Kinetic measurements were made with a Polarad automatic recording titrator, model AT-2A at pH 7.4 and 25 ± 0.1 °C. The enzyme used was bovine erythrocyte acetylcholinesterase obtained from Winthrop Laboratories, New York. A stock solution, prepared by dissolving in water (5 ml) the material contained in one vial (20 000 units), was suitably diluted as required. The solvent used was water, 0.15 *M* in sodium chloride and 0.04 *M* in magnesium chloride, and the titrant was 0.018 *M* sodium hydroxide.

Determination of Michaelis Constants (K_m)

The acetates, made up in dilute hydrochloric acid and then brought to pH 7.4, were used in the following concentration ranges: IV, 2.0–6.0 × 10^{-3} *M*; VI, 3.0–14.0 × 10^{-3} *M*; VIII, 1.0–10.0 × 10^{-3} *M*. Initial rates of hydrolysis (v) were measured at a number of substrate concentrations (S) using enough dilute enzyme solution to ensure hydrolysis rates of about 0.010–0.015 ml sodium hydroxide/min. The volume of the reaction mixture was 10.2–10.6 ml depending upon the volume of substrate solution used. The Michaelis constant was calculated from a Lineweaver and Burk (10) plot ($1/v$ vs. $1/S$) using the method of least squares to obtain the best line.

Determination of pI_{50} Values

The three carbamates and 1-methylpiperidine were made up in dilute hydrochloric acid, and physostigmine sulfate was made up in water; the solutions were then adjusted to pH 7.4. Concentration ranges for the various inhibitors were: III, 0.95–4.55 × 10^{-3} *M*; V, 1.50–5.30 × 10^{-3} *M*; VII, 0.90–4.0 × 10^{-3} *M*; 1-methylpiperidine, 1.70–6.75 × 10^{-3} *M*; physostigmine sulfate, 4.0–8.0 × 10^{-7} *M*. Acetylcholine bromide (initial concentration approximately 8.3 × 10^{-4} *M*) was used as substrate, and the initial rate of hydrolysis was measured using enough dilute enzyme solution to produce a sodium hydroxide uptake of about 0.05 ml/min. The initial rate of hydrolysis was then measured after incubating the enzyme for 2 min with different concentrations of inhibitor before addition of the substrate. Concentrations of inhibitor and substrate were corrected for the total volume of water in the cell (10–11 ml). Inhibitor concentrations were then plotted against sodium hydroxide uptake and the inhibitor concentration at one half the sodium hydroxide uptake for the uninhibited reaction was read off.

Nature of Carbamate Inhibition

The carbamates were made up in dilute hydrochloric acid as before and the following concentrations were used: III, 1.7 × 10^{-3} *M*; V, 4.3 × 10^{-3} *M*; VII, 1.6 × 10^{-3} *M*. The substrate was acetylcholine bromide

Can. J. Chem. Downloaded from www.nrcresearchpress.com by 210.87.254.42 on 09/05/12
For personal use only.

which was used in the concentration range 2.0–10.0 $\times$ 10^{-4} M. Initial rates of hydrolysis were determined at a number of substrate concentrations, and then determined again after the enzyme had been incubated for 2 min with inhibitor. To determine the nature of the inhibition, $1/v$ was plotted against $1/S$ for both the inhibited and uninhibited reactions.

ACKNOWLEDGMENTS

Thanks are offered to Mr. J. Helie for the microanalyses, Mr. R. Miller for technical assistance, and the U.S. Army Chemical Research and Development Laboratories for a gift of the 3-quinuclidinol used in this work.

REFERENCES

1. E. Stedman and G. Barger. J. Chem. Soc. 247 (1925).
2. J. P. Long. Handbuch der experimentallen Pharmakologie. Vol. XV, Cholinesterases and anticholinesterase agents. Chap. 8. *Edited by* G. B. Koelle. Springer Verlag, Berlin. 1963.
3. J. H. Biel, E. P. Sprengeler, H. A. Leiser, J. Horner, A. Drukker, and H. L. Friedman. J. Am. Chem. Soc. **77**, 2250 (1955).
4. M. D. Mashkovsky. Modern concepts in the relationship between structure and pharmacological activity. Proceedings of the First International Pharmacological Meeting. Vol. 7. *Edited by* K. J. Brownings. The MacMillan Co., New York. 1963. p. 359.
5. A. D. Cross. Introduction to practical infrared spectroscopy. Butterworth Scientific Publications, London. 1960.
6. C. A. Grob, A. Kaiser, and E. Renk. Helv. Chim. Acta, **40**, 2170 (1957).
7. J. A. Cohen and R. A. Oosterbaan. Handbuch der experimentallen Pharmakologie. Vol. XV, Chap. 7. *Edited by* G. B. Koelle. Springer Verlag, Berlin. 1963.
8. I. B. Wilson, M. A. Harrison, and S. Ginsburg. J. Biol. Chem. **236**, 1498 (1961).
9. F. Bergmann, I. B. Wilson, and D. Nachmansohn. J. Biol. Chem. **186**, 693 (1950).
10. H. Lineweaver and D. Burk. J. Am. Chem. Soc. **56**, 658 (1934).
11. M. Dixon and E. C. Webb. Enzymes. 2nd ed. Longmans, London. 1964. Chap. 8.
12. E. G. Brain, F. P. Doyle, and M. D. Mehta. J. Chem. Soc. 633 (1961).
13. S. B. Kadin and J. G. Cannon. J. Org. Chem. **27**, 240 (1962).

Can. J. Chem. Downloaded from www.nrcresearchpress.com by 210.87.254.42 on 09/05/12
For personal use only.

Can. J. Chem. Downloaded from www.nrcresearchpress.com by 210.87.254.6 on 09/05/12
For personal use only.

ARYLATION OF AROMATIC COMPOUNDS WITH BENZENEDIAZONIUM BOROFLUORIDE

NATURE OF THE ARYLATING SPECIES[1]

R. A. ABRAMOVITCH AND J. G. SAHA
Department of Chemistry, University of Saskatchewan, Saskatoon, Saskatchewan

Received May 19, 1965

ABSTRACT

The decomposition of benzenediazonium borofluoride in a number of aromatic solvents has been studied. The main product is fluorobenzene but some substituted biphenyls are formed. The isomer ratios and apparent total rate ratios for these phenylations have been determined. The results are discussed and it is suggested that the reactive intermediate in the arylations is the phenyl diradical cation.

A large body of evidence has been accumulated in support of an S_N1 mechanism for the heterolytic dissociation of diazonium salts, both in aqueous and non-aqueous media. This included kinetic studies indicating that the first-order rate constant is independent of the nature of the anion present (1) and of acidity over a wide range (2), and has very low solvent sensitivity (3). The formation of phenols in aqueous solution and of aryl chlorides in the presence of chloride ions are readily explained on the basis of the formation of aryl cations (4). Evidence has also been presented (4, 5) for the reversibility of the slow heterolysis of the C—N bond.

$$\mathrm{Ar}\text{-}\overset{\text{slow}}{\underset{}{\rightleftharpoons}}\ [\mathrm{Ar^+N_2}] \rightarrow \mathrm{Ar^+} + \mathrm{N_2}$$

$$\mathrm{Ar^+} + \mathrm{H_2O} \xrightarrow{\text{fast}} \mathrm{ArOH} + \mathrm{H^+}$$

$$\mathrm{Ar^+} + \mathrm{Cl^-} \xrightarrow{\text{fast}} \mathrm{ArCl}$$

The formation of onium salts, such as the diphenylbromonium ion from bromobenzene, can also be understood as a reaction of the aryl cation with the lone pair of electrons on bromine (5).

The aryl cation so produced is reported to be highly reactive and unselective (7). The decomposition of benzenediazonium borofluoride in various benzoate esters, in benzotrifluoride and in nitrobenzene, for example, was said to give mainly, if not exclusively, the meta-substituted biphenyls, a result taken to support the intermediacy of phenyl cations as the active species (in some cases a small amount of the para isomer was obtained but the ortho isomer was never isolated) (6). The latter observation would, however, point to a highly selective substituting species. In a preliminary communication (8) the uncatalyzed thermal decomposition of solid benzenediazonium borofluoride in toluene and in nitrobenzene was reported and it was shown that the attacking species was highly reactive *but positionally selective*. Some degree of selectivity was also indicated in the molecular rearrangement of the aryl cation from 1-(*o*-aminophenyl)-1-(substituted aryl)ethanols to give benzophenone derivatives, when a strongly electron-donating substituent in the migrating aryl group increased the yield of ketone appreciably (9).

[1]*The present paper is Part X of the series on aromatic substitution. For Part IX see Can. J. Chem. 43, 940 (1965).*

A systematic study has been undertaken of the thermal decomposition of solid benzenediazonium borofluoride in various aromatic solvents. We now report a quantitative study of the decomposition in toluene, bromobenzene, anisole, and nitrobenzene, including the isomer distributions obtained in these reactions and apparent total rate ratios relative to benzene (obtained from competitive runs).

The gas chromatogram of the reaction mixture obtained from the decomposition of benzenediazonium borofluoride in toluene gave, in addition to peaks corresponding to the isomeric methylbiphenyls, a peak whose retention time was different from those of the latter and from that of bibenzyl. This proved to be due to a mixture of the fluorobiphenyls (microanalysis, infrared, and direct comparison with authentic samples) which is not resolved into the three components under the conditions used. Fluorobiphenyls were also formed in the decomposition in bromobenzene and in anisole, but were absent when nitrobenzene was used as the substrate. (It should be noted that nitrobenzene is the only one of these solvents which dissolves the diazonium borofluoride.) No bibenzyl was detected in the reaction mixture from toluene. The main product formed in all cases (>90%) was fluorobenzene, the normal Schiemann reaction product.

EXPERIMENTAL

Reagents

AnalaR thiophene-free benzene was dried, distilled, and kept over sodium wire. Toluene, bromobenzene, anisole, nitrobenzene, and aniline were purified by standard procedures and had the boiling points reported in the literature.

Reference Compounds

The isomeric methylbiphenyls, bromobiphenyls, nitrobiphenyls, and bibenzyl were obtained from commercial sources and purified by distillation or crystallization; they had the boiling points or melting points reported in the literature. The three isomeric methoxybiphenyls were prepared from the appropriate diazotized anisidine and benzene by the Gomberg–Hey reaction. The products were purified by chromatography on alumina and elution with light petroleum (b.p. 40–60°), when the biaryls were obtained in the first 100 ml of eluent and the by-products remained adsorbed on the column. The chromatographed products were further purified by distillation or recrystallization, as appropriate. The three isomeric fluorobiphenyls were prepared by the thermal decomposition of the corresponding solid diazonium borofluoride (from the appropriate aminobiphenyl) and purified by column chromatography followed by distillation or crystallization. The purity of each of the reference compounds was checked by gas chromatography and only a single peak was observed for each of them.

Benzenediazonium borofluoride was prepared from repurified aniline following the general method described by Roe (10), taking special precautions to avoid the intrusion of metal contaminants. Only freshly prepared and well-dried samples of benzenediazonium borofluoride were used.

All the solvents were degassed by passing oxygen-free nitrogen through them before the addition of the diazonium borofluoride.

General Procedure for the Decomposition

A suspension of benzenediazonium borofluoride (1.6 g, 0.0083 mole) in an excess of the dry solvent was heated with vigorous stirring in a thermostat at 60 ± 0.1°. Stirring was continued for 8 h by which time the evolution of nitrogen and of boron trifluoride had ceased. The reaction mixture was distilled through a 30 cm long fractionating column packed with glass helices to remove most of the solvent and fluorobenzene. The residue (2–5 ml) was analyzed directly by gas chromatography.

Quantitative Analyses

The products formed in the phenylation reactions were resolved gas chromatographically and the compounds corresponding to the individual peaks were identified (i) by comparing their retention times with those of authentic samples, and (ii) by collecting each compound and comparing its infrared spectrum with that of the authentic sample.

The molar thermal response of each compound was determined by the internal standard method of Chang and Karr (11). In those cases where the molar thermal responses of the components of a reaction mixture were found to be identical, the areas of the peaks were taken to be proportional to the relative concentrations of the compounds representing them. Where the thermal responses were found to be different a known amount of the internal standard was introduced into the reaction mixture, and the actual amount of each component was calculated from the areas of the peaks and the weight of the internal standard. The yields of the various products were always determined by introducing the internal standard into the reaction mixture.

Can. J. Chem. Downloaded from www.nrcresearchpress.com by 210.87.254.6 on 09/05/12
For personal use only.

Phenylation of Toluene; Isomer Ratios

The benzenediazonium borofluoride:toluene molar ratio was 1:56. The reaction mixtures were best resolved on a 6 ft × 1/4 in. column packed with asphalt (15%) on Chromosorb W (60–80 mesh) operated at 166° and a helium inlet pressure of 40 p.s.i. Under these conditions, the retention times of the three fluorobiphenyls, 2-methylbiphenyl, biphenyl, 3-methylbiphenyl, and 4-methylbiphenyl were 10.2, 11.4, 13.6, 19.6, and 21.3 min, respectively. The compounds corresponding to the first peak, retention time 10.2 min, from the reaction mixture gave the following analytical results.

Anal. Calcd. for $C_{12}H_9F$: C, 83.70; H, 5.26. Found: C, 83.79; H, 5.28.

2-Bromobiphenyl, retention time 17.5 min, was used as the internal standard. No bibenzyl was detected in any of the reaction mixtures, nor was any biphenyl.

Using the above gas–liquid chromatography conditions bibenzyl and 4-methylbiphenyl had identical retention times. However, all three isomeric methylbiphenyls and bibenzyl were well resolved on a 20 ft × 1/4 in. column packed with SE-30 (0.5%) on glass beads, using a column temperature of 162°. Under these conditions 4-methylbiphenyl and bibenzyl had retention times of 41.25 and 46.0 min, respectively.

Phenylation of Bromobenzene; Isomer Ratios

The borofluoride:bromobenzene molar ratio used was 1:35. The analyses were carried out on a 10 ft × 1/4 in. column packed with Apiezon L (25%) on Chromosorb W (45–60 mesh) operated at 215° and a helium inlet pressure of 40 p.s.i. The retention times of fluorobiphenyls, biphenyl, 2-, 3-, and 4-bromobiphenyl were 11.0, 15.3, 31.0, 49.0, and 52.0 min, respectively. Bibenzyl (retention time 26.0 min) was used as the internal standard.

Phenylation of Anisole; Isomer Ratios

The reactions were carried out with a benzenediazonium borofluoride:anisole molar ratio of 1:30. The same column was used as in the bromobenzene runs but was operated at 230°. The retention times of fluorobiphenyls, biphenyl, 2-methoxybiphenyl, 3-methoxybiphenyl, and 4-methoxybiphenyl were 8.5, 13.5, 25.0, 37.0, and 42.0 min, respectively. Bibenzyl (retention time 22.0 min) was used as the internal standard.

Phenylation of Nitrobenzene; Isomer Ratios

The borofluoride:nitrobenzene ratio was 1:50. The reaction mixture turned dark brown immediately upon addition of the benzenediazonium borofluoride to the nitrobenzene and the solid went into solution, while a considerable amount of tar separated during the reaction, unlike what happened in the other three substrates. The concentrated reaction mixture was analyzed on a 5 ft × 1/4 in. column packed with GE-SF-96 silicone fluid (20%) on Gas-Chrom P (60–80 mesh), operated at 182° and a helium inlet pressure of 40 p.s.i. The retention times of biphenyl, 2-, 3-, and 4-nitrobiphenyls were 7.0, 17.0, 25.0, and 29.0 min, respectively. Bibenzyl (retention time 11.6 min) was used as the internal standard. No fluorobiphenyls could be detected in these reactions.

Competitive Reactions

These were carried out with benzenediazonium borofluoride; total substrate ratios of 1:100 to 1:150. Equimolar proportions of the competing aromatic substrates were used for the determination of the total rate ratios for bromobenzene, anisole, and nitrobenzene. Various proportions of toluene:benzene were used in the determination of ${}^{CH_3}_{H}K$.* The latter are summarized in Table V. The reaction mixtures were analyzed gas chromatographically using the same conditions as were used in the determination of the isomer ratios.

Estimation of Total Yields

The overall yields of the various reaction products were determined by gas chromatography using the same conditions as for the isomer ratio determinations, after a known weight of internal standard had been added to the reaction mixture before work-up. The yield of fluorobenzene was determined on a 6 ft × 1/4 in. column packed with asphalt (25%) on Chromosorb W (60–80 mesh) operated at 70° and a helium inlet pressure of 40 p.s.i. Fluorobenzene had a retention time of 7.5 min under these conditions. *n*-Heptane (retention time 10.0 min) was used as internal standard.

DISCUSSION

The relative abundances of the different products obtained in the decomposition of benzenediazonium borofluoride in three of the four substituted benzene derivatives are given in Table I. No fluorobiphenyls were formed with nitrobenzene, and the overall yield of nitrobiphenyls in this case was at most 5% but was not estimated accurately because of the large quantities of tarry materials that were formed.

Products arising from nuclear aromatic substitution account for only about 5% of the total, the main product being the normal Schiemann reaction product, fluorobenzene.

*${}^{X}_{H}K$ *is the ratio of the total rate of attack on* C_6H_5X *compared with the rate of attack on* C_6H_6 *(12).*

Can. J. Chem. Downloaded from www.nrcresearchpress.com by 210.87.254.6 on 09/05/12
For personal use only.

TABLE I

Relative yields of products from decomposition of $C_6H_5N_2^+BF_4^-$ in C_6H_5X

	Product (%)		
C_6H_5X	C_6H_5F	r-$C_6H_5C_6H_4F$	r-$C_6H_5C_6H_4X$
$C_6H_5CH_3$	94–95	0.5–0.8	4–5
C_6H_5Br	93–95	0.6–0.8	3–4
$C_6H_5OCH_3$	85–90	0.5–0.8	3–5

The phenyl cation formed can, apparently, react in one of three ways, namely: (i) it can combine with a fluoride ion ($BF_4^- \rightarrow BF_3 + F^-$) to give fluorobenzene; (ii) it can substitute the latter to give fluorobiphenyls; or (iii) it can attack the aromatic substrate to give the substituted biaryls. Reactions (i) and (ii) are most probably taking place within the solid matrix, while the reactive species must diffuse out of the solid matrix to take part in the third mode of reaction. Had the reactive phenyl cations and the fluoride ions diffused out of the solid matrix there would have been much less chance of their recombination (even taking into account relative nucleophilicities of the various substrates) since the aromatic substrate was present in such large excess (30- to 150-fold) and appreciably larger amounts of biaryls would have been formed. Some of the fluorobenzene remains "trapped" in the solid matrix and is attacked by the cationic species to form the fluorobiphenyls and hydrogen fluoride. If reaction (ii) had to occur in the main bulk of the solvent this would require fluorobenzene to be about 1 300 times as reactive as toluene towards the attacking species, which is to be compared with $k_{Cl^-/H_2O} = 2.5$ (7).

It may be seen from Table I that the three products isolated in these reactions account for almost 100% of the phenyl groups present in the benzenediazonium borofluoride used. If any triphenyls are formed, e.g. from the further phenylation of the fluorobiphenyls or of the biphenyls derived from the reactions with the solvent, these will constitute a very minor proportion of the total products and are not likely to have any appreciable significance on the validity of the isomer ratios observed here. If there were any selective removal of one or more of the isomers by triphenyl formation it would have to be taking place to a very small extent only. Thus, less than 0.05% of products would be expected to arise from the attack of the phenyl cations upon the three fluorobiphenyls (ratio of PhF to r-$C_6H_5C_6H_4F$ = 1:120 – 1:180). Similar, and even more powerful, arguments could be raised against the formation of appreciable quantities of triaryls from solvent-derived biaryls since the latter are formed and are present in the bulk of the solvent. In the event, no peaks were observed in the gas chromatograms of the reaction mixtures after the biaryls had appeared.

Table II summarizes the isomer ratios obtained in the phenylation, and compares them with those obtained in the homolytic phenylations when benzoyl peroxide was used as the source of phenyl radicals (12, 13). The salient feature of the data is the non-statistical isomer distribution in the present case together with the formation of an appreciable amount of the meta isomer with toluene, bromobenzene, and anisole and a predominance of the meta isomer with nitrobenzene. The reaction mixtures were analysed directly by gas–liquid chromatography after concentration and no attempt was made to isolate any bromonium salt that might have been formed with bromobenzene, since it would not be eluted from the column. Also, no onium salt formation was reported from a similar reaction with fluorobenzene (14). In the latter case no *m*-fluorobiphenyl was said to have been formed (14), whereas in our experiments the formation of this isomer was proved by

Can. J. Chem. Downloaded from www.nrcresearchpress.com by 210.87.254.6 on 09/05/12
For personal use only.

TABLE II

Ratio of isomers formed in the phenylation of C_6H_5X

Compound	Position	% isomer formed with $C_6H_5N_2^+BF_4^-$	% isomer formed with $(C_6H_5CO_2)_2$ (12, 13)
$PhCH_3$	*o*	57.5	66.5
	m	20.0	19.3
	p	22.3	14.2
PhBr	*o*	56.1	56.2
	m	19.8	27.3
	p	24.1	16.5
$PhOCH_3$	*o*	57.5	69.8
	m	10.0	15.8
	p	32.5	15.8
$PhNO_2$	*o*	19.6	63.2
	m	80.4	9.7
	p	—	27.1

infrared spectroscopy on the mixture of isomers in those cases where this was formed. The isomer ratios obtained in the phenylation of toluene with benzenediazonium borofluoride are not out of line with those obtained, say, in the Friedel–Crafts alkylation of toluene under various conditions (15). The available data for the alkylation of bromobenzene and for some alkylations of toluene as well (15) indicate a much lower ortho/para ratio than is obtained here. No data are available on the isomer ratios obtained in the alkylation of anisole. Nitration, however, gives no meta isomer (16), but it must be appreciated that the nitronium ion is a much weaker electrophile, and hence a more selective one, than the alkyl cation. It should be pointed out, however, that even with very powerful and unselective electrophiles such as $NO_2^+AsF_6^-$ in tetramethylene sulphone or in nitromethane, toluene gives only a small amount (2–3%) of meta substitution product (17). Friedel–Crafts alkylation of nitrobenzene has not been achieved: in fact nitrobenzene may be used as a solvent in such reactions. Contrary to what was reported (6, 18), *m*-nitrobiphenyl is not the only isomer formed in the phenylation of nitrobenzene with benzenediazonium borofluoride, and appreciable amounts of *o*-nitrobiphenyl (but not of the para isomer) are formed ($F_o/F_m = 0.25$).* Such behavior is consistent with an electrophilic attack but not by a "classical" phenyl cation. This point is further emphasized later.

TABLE III

Total rate ratios for the substitution of C_6H_5X

Compound	${}^{C_6H_5X}_{C_6H_6}K$ for substitution using $C_6H_5N_2^+BF_4^-$	${}^{C_6H_5X}_{C_6H_6}K$ for substitution using Nitration (12)	${}^{C_6H_5X}_{C_6H_6}K$ for substitution using $(PhCO_2)_2$ (13, 19)
$C_6H_5CH_3$	0.72	23.0	1.23
C_6H_5Br	0.31	0.03	1.14
$C_6H_5OCH_3$	1.445	—	2.0
$C_6H_5NO_2$	0.35	$\sim 10^{-6}$	2.94

The apparent reactivities of substituted benzenes towards the cationic species relative to that of benzene were examined next using the competitive technique. The total rate ratios thus found are given in Table III, which also includes the corresponding values for nitration (12) and homolytic phenylation using benzoyl peroxide (13, 19).

*F_r *is the partial rate factor for substitution at position r in a substituted benzene compared with a position in benzene itself.*

Can. J. Chem. Downloaded from www.nrcresearchpress.com by 210.87.254.6 on 09/05/12
For personal use only.

Can. J. Chem. Downloaded from www.nrcresearchpress.com by 210.87.254.6 on 09/05/12
For personal use only.

The partial rate factors (the meaningfulness of which will be discussed later), calculated from isomer and total rate ratios, are given in Table IV and compared with the data for nitration and homolytic phenylation.

In an earlier communication (8) the total rate ratio for the phenylation of toluene with benzenediazonium borofluoride was reported to be slightly greater than unity. This may be caused by differences in the experimental procedures used: in the earlier work nitrogen was passed through the reaction mixture while it was kept at 60° and this could well have led to some losses of benzene (which has a higher vapor pressure than toluene) and thus to higher values for ${}^{CH_3}_{H}K$. In the present work the benzene and toluene were first degassed separately and then introduced into the reaction flask, and no nitrogen was bubbled through the mixture during the reaction. The possibility of preferential solvation of the cationic species was examined by carrying out the competitive reactions using different proportions of the competing solvents. The results are presented in Table V from which it can be seen that a fourfold increase in the relative amount of toluene to benzene leaves the total rate ratio unchanged.

TABLE IV

Partial rate factors for substitution of C_6H_5X by various reagents

Compound	Position	Partial rate factor F_r for reaction with		
		$C_6H_5N_2^+BF_4^-$	HNO_3 (12)	$(C_6H_5CO_2)_2$ (13, 19)
$C_6H_5CH_3$	*o*	1.24	40	2.5
	m	0.43	3	0.71
	p	0.96	51	1.0
C_6H_5Br	*o*	0.52	0.037	1.9
	m	0.18	0.000	0.93
	p	0.45	0.106	1.13
$C_6H_5OCH_3$	*o*	2.49	—	4.19
	m	0.43	—	0.87
	p	2.81	—	1.90
$C_6H_5NO_2$	*o*	0.21	0.24×10^{-6}	5.60
	m	0.84	2.75×10^{-6}	0.86
	p	0	0.03×10^{-6}	4.80

TABLE V

Effect of changing the relative proportions of toluene and benzene upon the total rate ratio ${}^{CH_3}_{H}K$ for the phenylation of toluene

$[C_6H_5CH_3]/[C_6H_6]$	$[C_6H_5N_2^+]/[\text{Total solvent}]$	${}^{CH_3}_{H}K^*$
1:1	1:150	0.70
1:1	1:150	0.70
2:1	1:150	0.73
2:1	1:150	0.75
4:1	1:100	0.72
4:1	1:100	0.72

*Values of ${}^{CH_3}_{H}K$ calculated after taking into account the ratio of the concentrations of the competing solvents.

The results given in the second column of Table III confirm the relatively indiscriminate character of the reactive entity from the thermal decomposition of benzenediazonium borofluoride. The electrical effects of the bromo, methoxyl, and nitro substituents are evident, the first ($-I > +M$) and the third being electron-attracting and deactivating, and the second ($+M > -I$) being electron-donating. These effects are very small,

however, and it is noteworthy that the bromo and nitro substituents are about equally deactivating. The possibility of some complexing of the cation with the substituent prior to substitution cannot be eliminated at this stage, but this does not seem very likely, particularly when one looks at the isomer ratios obtained: a much higher proportion of ortho isomer might have perhaps resulted from an intramolecular rearrangement of a complexed species. Also, complexing with the substituent by an electrophilic species should have led to values of ${}^{X}_{H}K$ of greater than unity. Unfortunately, no firm statement can be made one way or the other at this stage in view of the heterogeneous character of three of the reactions. In any event, the reactivity of nitrobenzene is much higher than one would expect for an attack by a normal cationic species (I), even a highly reactive one. The results are very reminiscent of those obtained in free radical arylations, particularly with electrophilic radicals. For example, ${}^{NO_2}_{H}K$ in the *o*-nitrophenylation of nitrobenzene is 0.26, ${}^{Cl}_{H}K$ in the *o*-nitrophenylation of chlorobenzene is 0.83 (20). Also ${}^{benz}_{py}K$ for the *o*-nitrophenylation of pyridine was found to be 0.47 (21); interestingly, in this last case, the 3-substituted compound (corresponding to the *m*-isomer) is the main product formed ($F_\beta = 0.71$), as is 3-nitrobiphenyl in the present case (see Table II) (${}^{NO_2}F_m = 0.84$). The results for the phenylation of C_6H_5X (where X = Br, OCH_3, and NO_2) with benzenediazonium borofluoride are then consistent with an attack by a highly electrophilic free radical intermediate. This view is also consistent with the absence of bibenzyl in the products obtained in the phenylation of toluene by benzenediazonium borofluoride. Thus no bibenzyl was obtained in the homolytic phenylation of toluene with *p*-nitrophenyl radical whereas 12.0% of bibenzyl was obtained with the phenyl radical itself (34).

Formation of phenyl radicals according to

$$PhN_2^+BF_4^- \rightarrow Ph + N_2^+ + BF_4^-$$

under the conditions of the reactions can be eliminated as being energetically unlikely (22) and as not being in accord with the results. Expanding a proposal made by Taft (23) it has been suggested (8, 23) that the phenyl cation (I) initially formed in the thermal decomposition of diazonium salts may isomerize to a diradical cation (II) with concerted uncoupling of a pair of π-electrons, one of which falls into the vacant sp^2 σ-orbital. The resulting species would be expected to behave like a highly electrophilic free radical in aromatic substitution reactions. Canonical structure II*a* would give the species some of the properties of a triplet carbene, whereas if a second π-electron fell into the σ-orbital, thus filling it, the species III might behave as a singlet carbene (II*a* and III could well take part in insertions into and hydrogen abstractions from aliphatic C—H groups and account for the demethylations and deaminations, as well as insertions observed in certain attempted Pschorr cyclizations (24, 25). The existence of equilibria I $\rightleftarrows$ II $\rightleftarrows$ III would account for all the reported properties of the phenyl cation. In fact, it might be expected that, provided the intermediate formed from the thermolysis could persist long enough, II and III would be formed. Preliminary M.O. calculations (26) indicate the order of stabilities II > III > I, the triplet diradical cation II being the ground state. Direct evidence for the formation of radicals in these reactions has been obtained from electron spin resonance spectroscopic measurements (8). These radicals are apparently trapped in the solid matrix and, as such, appear to be quite stable. An electron spin resonance spectrum was also observed when benzenediazonium borofluoride in nitrobenzene *solution* was heated at 42° for 10 min (8). *p*-Bromobenzenediazonium borofluoride in aqueous solution at 50° apparently produces free radicals in small concentrations which are sufficient to initiate the polymerization of acrylonitrile, styrene, methyl methacrylate, and methyl acrylate (27). A

Can. J. Chem. Downloaded from www.nrcresearchpress.com by 210.87.254.6 on 09/05/12
For personal use only.

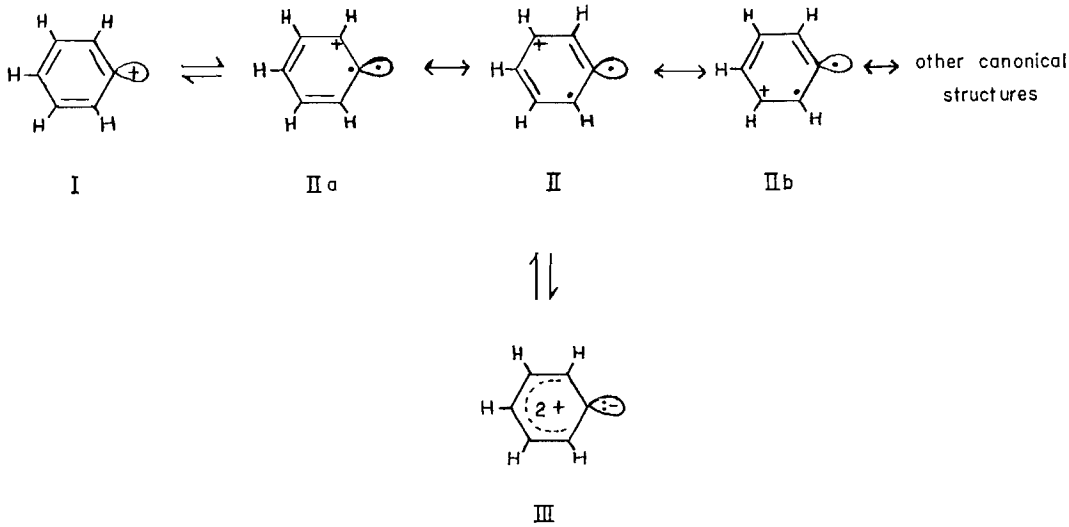

I IIa II IIb

III

study of the copolymerization of styrene and methyl methacrylate by benzenediazonium borofluoride has suggested that a cationic species is the initiator (28). These results can be reconciled if the intermediate is a diradical cation II in equilibrium with I (from which fluorobenzene, and phenol in aqueous solutions, is undoubtedly formed) and perhaps III.

The total rate and isomer ratios for the phenylation of bromobenzene, nitrobenzene, and anisole are readily explained if the attacking entity is the relatively non-discriminating (towards the nucleus as a whole) highly reactive, but apparently positionally selective, electrophilic diradical cation. Very comparable total rate ratios to those obtained here were reported by Dewar and Narayanaswami (29) for the arylation of substituted benzenes using benzene-1,4-diazo oxides. This reaction is thought to involve the carbene (IV) (29, 30) which attacks the aromatic substrate in the rate-determining step of the substitution process to form a π-complex or a spiran (V), the latter opening up to give the biphenyl derivative.

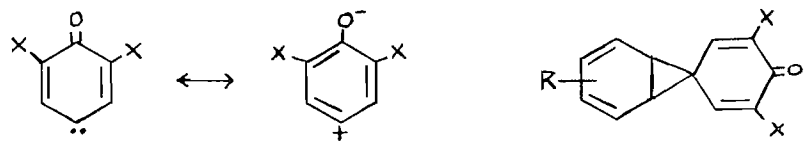

IV V

The formation of appreciable amounts of meta isomer, particularly with toluene and anisole, in the present work rules out a product-determining spiran ring opening and suggests a direct substitution process in our case. The value of ${}^{CH_3}_{H}K < 1$ is, however, disturbing and the effect of the substituent is very difficult to account for on any mechanism, since attack by a nucleophilic reagent must definitely be ruled out. A number of possible explanations were considered. An amount of boron trifluoride equivalent to the fluorobenzene formed is liberated and this could form a π-complex with the aromatic solvent. Toluene forms a complex more readily than does benzene, so that one could visualize more toluene than benzene molecules being complexed in the vicinity of the reactive species; and since the complex should be less susceptible to electrophilic attack

Can. J. Chem. Downloaded from www.nrcresearchpress.com by 210.87.254.6 on 09/05/12
For personal use only.

Can. J. Chem. Downloaded from www.nrcresearchpress.com by 210.87.254.6 on 09/05/12
For personal use only.

than would be the uncomplexed species, this would lead to a statistical advantage of the benzene over the toluene, though the amount of BF_3 formed relative to the amounts of solvent is small. Such a situation might be more likely if the phenylation reaction took place within the solvent cage and if there was a statistical distribution of substrate molecules around the reactive intermediate. If this were so, however, one might expect that increasing the proportion of toluene would then lead to larger values of ${}^{CH_3}_{H}K$, which was not the case (Table V). The most likely explanation at the moment is that the phenylation is a cage process and that the solvent shell around the reactive species does not contain an equivalent number of benzene and toluene molecules (when equimolar quantities of the two substrates are used), but that since toluene is a larger molecule than is benzene a larger number of molecules of the latter will always be present around the diradical cation, irrespective (within certain limits, probably) of the toluene:benzene ratio in the bulk of the system. This non-statistical distribution of solvent molecules in the immediate vicinity of the decomposing diazonium ion would lead to the low values of ${}^{CH_3}_{H}K$ observed and, in fact, would invalidate the use of the product ratios as a measure of the relative reactivities of the various aromatic substrates. A similar low value of ${}^{CH_3}_{H}K$ has been reported for the isopropylation of toluene via the isopropyl cation from isopropyl amine (31). In this case, however, the value of the total rate ratio *decreases* with increasing toluene:benzene molar ratio. The contamination of the cumene fraction by a product with the same retention time on gas chromatography invalidates these results (32).

It is clear, therefore, that too much importance cannot be attached at the moment to the *exact* values of the total rate ratios and hence of the partial rate factors determined in the present work, though these are reproducible from run to run and, apart from those for toluene, are probably of the correct general order of magnitude and in the right direction. This difficulty undoubtedly arises because, *except in the nitrobenzene reaction* (both under competitive and non-competitive conditions), *which is of key importance in the discussion of mechanism*, the reactions are heterogeneous in nature and there is an absence of kinetic control in the substitution process. The limitations of the competitive technique for the determination of relative reactivities in those cases where kinetic control is absent has been discussed recently by Tolgyesi (33). It becomes, therefore, very important to study this process in homogeneous solution with suitable agitation; such work is in progress and will be reported at a later date.

ACKNOWLEDGMENTS

This work was supported by a grant from the National Research Council. We wish to thank Dr. D. E. Pearson for communicating unpublished results to us.

REFERENCES

1. J. C. Cain. Chem. Ber. **38**, 2511 (1905).
2. H. Euler. Ann. **325**, 292 (1902).
3. H. A. H. Prey. J. Phys. Chem. **30**, 1477 (1926).
4. E. S. Lewis and J. E. Cooper. J. Am. Chem. Soc. **84**, 3847 (1962).
5. J. M. Insole and E. S. Lewis. J. Am. Chem. Soc. **85**, 122 (1963).
6. A. N. Nesmeyanov, L. G. Makarova, and T. P. Tolstaya. Tetrahedron, **1**, 145 (1957).
7. E. S. Lewis. J. Am. Chem. Soc. **80**, 1371 (1958).
8. R. A. Abramovitch, W. A. Hymers, J. B. Rajan, and R. Wilson. Tetrahedron Letters, 1507 (1963).
9. R. L. Cohen and A. J. Sisti. Can. J. Chem. **42**, 1388 (1964).
10. A. Roe. Org. Reactions, **5**, 203 (1949).
11. T. C. Chang and C. Karr, Jr. Anal. Chem. Acta, **21**, 474 (1959).
12. G. H. Williams. Homolytic aromatic substitution. Pergamon Press, London. 1960.
13. R. T. Morrison, J. Cazes, N. Samkoff, and C. A. Howe. J. Am. Chem. Soc. **84**, 4152 (1962).
14. G. A. Olah, S. J. Kuhn, and S. H. Flood. J. Am. Chem. Soc. **83**, 4571 (1961).

15. L. M. STOCK and H. C. BROWN. *In* Advances in physical organic chemistry. *Edited by* V. Gold. Academic Press, New York. 1963. p. 35.
16. C. A. BUNTON, B. J. MINKOFF, and R. I. REED. J. Chem. Soc. 1416 (1947).
17. G. A. OLAH and S. J. KUHN. J. Am. Chem. Soc. **84**, 3684 (1962).
18. L. G. MAKAROVA and M. K. MATVEEVA. Bull. Acad. Sci. U.S.S.R., Div. Chem. Sci. 1838 (1960); 1772 (1961).
19. G. H. WILLIAMS. Chem. Ind. London, 1285 (1961).
20. D. H. HEY, H. N. MOULDEN, and G. H. WILLIAMS. J. Chem. Soc. 3769 (1960).
21. R. A. ABRAMOVITCH and J. G. SAHA. J. Chem. Soc. 2175 (1964).
22. K. G. RUTHERFORD and W. A. REDMOND. J. Org. Chem. **28**, 568 (1963).
23. R. A. ABRAMOVITCH and G. TERTZAKIAN. Can. J. Chem. **43**, 940 (1965). R. W. TAFT. J. Am. Chem. Soc. **83**, 3350 (1961).
24. T. COHEN, A. H. DINWOODIE, and L. D. MCKEEVER. J. Org. Chem. **27**, 3385 (1962).
25. T. COHEN and J. LIPOWITZ. J. Am. Chem. Soc. **86**, 2515 (1964).
26. I. ABSAR and K. L. MCEWEN. Private communication.
27. C. S. MARVEL, H. Z. FRIEDLANDER, S. SWANN, JR., and H. K. INSKIP. J. Am. Chem. Soc. **75**, 3846 (1953).
28. R. L. DANNLEY and M. ESAYIAN. J. Polymer Sci. **45**, 105 (1960).
29. M. J. S. DEWAR and K. NARAYANASWAMI. J. Am. Chem. Soc. **86**, 2422 (1964).
30. E. WASSERMAN and R. W. MURRAY. J. Am. Chem. Soc. **86**, 4203 (1964).
31. D. E. PEARSON, C. V. BREDER, and J. C. CRAIG. J. Am. Chem. Soc. **86**, 5054 (1964).
32. D. E. PEARSON. Private communication.
33. W. S. TOLGYESI. Can. J. Chem. **43**, 343 (1965).
34. J. K. HAMBLING, D. H. HEY, S. ORMAN, and G. H. WILLIAMS. J. Chem. Soc. 3108 (1961).

Can. J. Chem. Downloaded from www.nrcresearchpress.com by 210.87.254.6 on 09/05/12
For personal use only.

Can. J. Chem. Downloaded from www.nrcresearchpress.com by 210.87.254.40 on 09/05/12
For personal use only.

REMARKS ON THE NITRONIUM SALT NITRATION OF TOLUENE AND BENZENE

G. A. OLAH[1] AND N. A. OVERCHUK
The Dow Chemical Company, Eastern Research Laboratory, Wayland, Massachusetts
Received February 22, 1965

ABSTRACT

The nitronium salt nitration of toluene and benzene in tetramethylene sulfone and nitromethane solution was critically reinvestigated.

Stable nitronium salts were introduced as new nitrating agents by Olah *et al.* (1, 2). They were found useful both in preparative nitrations (3) and in the investigation of certain mechanistic aspects of aromatic nitration (4–8). In the course of these investigations the competitive nitration of benzene and toluene, besides other systems, was carried out in tetramethylene sulfone (tetrahydrothiophene-1,1-dioxide) and nitromethane solutions.

Under most conditions toluene reacts about 20 times more rapidly than benzene in the nitration reaction. With stable nitronium salts toluene reacts only about twice as fast as benzene (4). This observation would be readily accommodated in terms of a decreased selectivity of the highly electrophilic nitronium ion. This interpretation is unsatisfactory, however, since the para:meta ratio for substitution in toluene is unaltered. The unusual result is that with reactive nitronium salts the intermolecular (substrate) selectivity is decreased appreciably but the intramolecular (positional) selectivity is not significantly altered (9).

It was pointed out that the low selectivity could have been caused by the very high reactivity of the reagent, reacting indiscriminantly with substrates present. Thus statistical or diffusion controlled reaction conditions and not kinetically controlled competition would be observed with highly reactive electrophilic agents (10).

For the ultimate electrophilic reagent not capable of selecting between two molecules or between available sites in a substituted benzene, like toluene, the relative rate, k(toluene)/k(benzene), k_t/k_b, would be 5/6 and the product ratio would be 40% ortho, 40% meta, and 20% para isomer.

In all of the investigated nitronium salt nitrations of alkylbenzenes (or halobenzenes) the meta:para ratio is extremely low. The amount of meta isomer in the nitration of toluene is generally less than 3%. Thus the observation of high intramolecular (positional) selectivity in reactions showing low intermolecular (substrate) selectivity in itself should invalidate the argument for statistical or diffusion controlled reactivity. For data on statistically controlled isomer distribution in free radical nitration of toluene see subsequent results. The question was however further examined by different methods including changing the ratio of concentration of the aromatic components in competitive experiments from the usual 1:1 to 4:1 and 1:0.25. The results showed that the relative rate ratio remains almost unchanged if a first-order dependence on the aromatic concentration is accepted (Table I).

[1]*Author to whom inquiries should be addressed at the Department of chemistry, Western Reserve University, Cleveland, Ohio.*

TABLE I

Concentration variation of toluene and benzene in competitive nitrations with $NO_2^+BF_4^-$ in tetramethylene sulfone solution at 25°

Toluene:benzene	Observed relative reactivity	k_t/k_b
4:1	6.40	1.60
3:1	5.13	1.71
2:1	3.40	1.70
1:1	1.67	1.67
1:1.5	1.11	1.66
1:2	0.81	1.62
1:3	0.62	1.86
1:4	0.45	1.80
		Av. 1.70

The experimental data obtained pointed to the fact that the observed relative reactivities are due to competition of NO_2^+ with the aromatic substrates, the reactions being first order in aromatic substrates. Statistical distribution which takes place in a fast reaction without any selectivity cannot explain the above data, although it is necessary to state that the reactions are indeed very fast even in high dilutions.

One of the major difficulties in investigating fast reactions is whether complete mixing of the reagents can be achieved before reaction with the reactive reagent takes place. The use of competitive experiments to determine the relative reactivity of substrates helps to overcome the difficulties involved in absolute rate determinations, but nevertheless this method can also have limitations in fast reactions. Should one of the reaction partners (e.g. toluene) in the competitive nitration react much faster than the other competing partner (e.g. benzene), the former would become impoverished in the immediate surroundings of the reagent. This would mean that the competitors appear more closely related in their speed of reaction, without necessarily showing the effects of statistical distribution (12). Our previous experiments carried out to show the effect of mixing on the reaction using various types of conventional stirrers were mostly negative. Nevertheless we continued the investigation of this aspect with more advanced methods, including high-speed flow systems (11, 12).

Reflecting recent interest in the nitronium tetrafluoroborate nitrations, two papers were published reinvestigating the competitive rate data of Olah, Kuhn, and Flood (4). Ritchie and Win carried out competitive nitrations of benzene and toluene (as well as chloro and fluorobenzene) by adding dropwise 0.30 ml of a 0.67 *M* solution of nitronium tetrafluoroborate in tetramethylene sulfone to a solution containing 100 μl of each of the aromatic compounds dissolved in 20 ml of tetramethylene sulfone, while maintaining rapid stirring. These conditions were similar to those used in our previous work concerning the ratio of the reagents and the concentration of the nitronium salt solution, but represented substantially more dilute solutions of the aromatic substrates (about 0.05 *M* solution of each of the aromatics, as compared with about 4.8 *M* solutions used by us). The work of Ritchie and Win fully substantiates our previous data in binary competing systems, even with a nearly 50-fold dilution of the substrate aromatic solution. Quaternary competition using two fast (toluene and benzene) and two slow (chlorobenzene and fluorobenzene) substrates shows some deviation of the relative rate data, but in the same order of magnitude (See Table II). The spread is scattered in both directions; therefore, we feel that these data also support, even if with some limitation, the binary competition data.

Can. J. Chem. Downloaded from www.nrcresearchpress.com by 210.87.254.40 on 09/05/12
For personal use only.

TABLE II

Competitive nitrations with nitronium tetrafluoroborate in 0.67 *M* tetramethylene sulfone solution at 25° according to Ritchie and Win (13)

	Rate ratio		
	Binary value* 0.1 *M* aromatic solution	Quaternary value†	Binary value* (Olah *et al.* (4))
Toluene–benzene	1.68 1.74	2.60	1.67
Toluene–fluorobenzene	6.72	3.80	(3.71)‡
Toluene–chlorobenzene	11.2	8.44	(11.8)
Benzene–fluorobenzene	1.89 2.08	1.50	2.22
Benzene–chlorobenzene	7.6	3.32	7.1
Fluorobenzene–chlorobenzene	3.20	2.22	(3.21)
Chlorobenzene–bromobenzene	1.08		(1.17)

*Nitration of a mixture of the two aromatics whose rate ratios are given.
†Nitration of a mixture of benzene, toluene, fluorobenzene, and chlorobenzene.
‡Values in parentheses were calculated from the rates relative to benzene.

Would the nitration indeed be diffusion controlled, changes of such extreme proportion in the reaction condition should have shown substantial changes. This was not the case.

Tolgyesi (14) on the other hand made the claim, that "the relative rates (of toluene/benzene competitive nitrations with nitronium tetrafluoroborate in tetramethylene sulfone) under certain conditions attained a range (25–30) which is considered to represent the range of relative reactivity and it corresponds to the known reactivity of toluene–benzene in nitric acid nitrations. On the basis of these results, there seems to be no reason to suppose that nitronium salt nitration involves a mechanism different from that of nitric acid nitration" (11).

In his work, competitive experiments were carried out by the addition of a solution of the nitronium salt in tetramethylene sulfone to a solution of toluene and benzene in the same solvent. It was found that the efficiency of the stirring, using a magnetic stirrer and expressed in the volt setting of a Powerstat attached to the stirrer, causes only very small differences in the toluene:benzene reactivity ratio, ranging from 1.4 to 2.2. In view of the experimental conditions and analytical method used, this spread is considered well in the limit of previous data. Somewhat larger changes were observed if the used nitronium salt solution was diluted (from 0.74 to 0.15 *M*). Even so, the toluene:benzene ratio showed an average value of 2.5–2.8 (with one extreme value of 5.1 noted) that is in the limit of previous data.

Replacing previously used conventional stirring methods with a claimed new and highly efficient method by the combined use of a vibrator stirrer and syringe addition of the nitrating agent, a spread of 3 to 7 for the toluene:benzene reactivity ratio was reported maintaining conditions otherwise similar to previous experiments. It was found, however, that significant dilution of the solution of the nitronium salt with simultaneous application of the new stirring system causes substantial changes of the toluene:benzene reactivity ratio, ranging from 25 to 30, thus equating it with the known order of nitric acid nitrations. These data were interpreted that having achieved good mixing of the reagents before reaction of a higher substrate selectivity was obtained. This was taken as evidence that previous low substrate selectivity data were obtained under conditions where the competing partners (benzene and toluene) were interacting more through statistical distribution than through real competition.

Can. J. Chem. Downloaded from www.nrcresearchpress.com by 210.87.254.40 on 09/05/12
For personal use only.

In view of our continued interest in nitronium salt nitrations and the fact that the claimed equivalence of nitronium salt nitrations with nitric acid nitration is in contradiction to our previous findings and our investigations comparing mixed acid nitrations with nitronium salt nitrations (7), we felt it of interest to report on additional work relating nitronium salt nitrations, including reinvestigation of the conditions used in the quoted paper (14).

RESULTS AND DISCUSSION

A. Substrate (Intermolecular) Selectivity

Comparison of the experimental data of Ritchie and Win (13), with those of Tolgyesi (14) shows that the change in the relative toluene:benzene reactivity ratio was observed only when *the concentration of the solution of the nitronium salt was decreased, but not when the aromatic substrates,* to which the nitrating agent was added, *were diluted.* This finding is extremely surprising. If indeed mixing of the reagents before reaction is the major factor in the differences observed and the higher substrate selectivity data indicate better mixing, then it is difficult to understand that only dilution of the solution of the nitrating agent (A) has any effect, but not dilution of the solution of the competing substrates (B). The two solutions once mixed should give the same overall concentration, regardless whether A or B were first diluted (assuming that the same amount of diluent is used).

The effect of dilution on the relative reactivity ratio can be interpreted in terms that in more dilute solution the number of active, reaction-producing collisions decrease. Having used this argument in one respect (e.g. dilution of the solution of the nitrating agent), Tolgyesi claims on the other hand, that dilute solutions of the substrates effectively show lower reactivity ratios, than those of more concentrated solutions (14). This claim is in direct contradiction with our previous data and our interpretation of the data of Ritchie and Win (13) who found that a nearly 50-fold dilution of the substrate solution had no effect on the toluene:benzene reactivity ratio. The offered explanation (14), e.g. that product ratios decrease with decreasing concentration of the aromatic solution because the extent of the selective depletion of the more reactive competitor in the diffusion layer around the droplet of the entering nitronium reagent is higher when the concentration of the aromatic compound is low, is unacceptable. We should keep in mind, that all the competitive experiments were carried out by adding a solution of the nitrating agent to a substantial (generally 10-fold) excess of the aromatics. The ratios of nitronium salt concentration compared with aromatic concentration are in themselves, however, meaningless, as during the whole reaction the ratios constantly change the nitronium salt is being added into the aromatic solution. The added nitronium reagent encounters in the early stages of the reaction a very large excess of the aromatic substrates and only if all the nitrating agent is added do we reach the 10:1 ratio. Using gas–liquid chromatography (g.l.c.) as the analytical method, 1:100, 1:1000 or an even smaller ratio of the nitronium salt to the aromatics is sufficient to carry out the competitive experiments. Ritchie and Win, having used 50-fold dilution of the substrate as compared to our previous work, maintained at the end of the reaction at least 10-fold excess of aromatics. We, in repeating some of the dilution work, added only 1/10 and 1/100 of the amount of nitronium salt, thus drastically eliminating the possibility of any depletion of the substrate, and still observed practically unchanged substrate reactivity. If we would accept the argument that the bulk concentration of the reaction mixtures is irrelevant since only the concentration in the diffusion layer surrounding the nitronium reagent droplet is important, Tolgyesi's experimental data would be even more inexplicable, since he himself reported

Can. J. Chem. Downloaded from www.nrcresearchpress.com by 210.87.254.40 on 09/05/12
For personal use only.

with the same stirring method a change in relative reactivity changing from 2.3 *M* to 0.3 *M* aromatic solutions.

The data so far discussed indicate that in the competitive experiments carried out by adding a solution of the nitronium salt to a solution of the competing substrate, only dilution of the nitronium salt solution had major effect on the substrate selectivities, but not the dilution of the aromatic substrate solution. This observation calls attention to the nature of the nitronium salt solution and its fate under dilution. According to the data of Tolgyesi in solutions of highest dilution (0.04 and 0.07 *M* solutions) the observed toluene:benzene reactivities were independent of the speed of stirring. Rechecking these systems under the experimental conditions reported, we found that "conventional" stirring gave the same results. Thus in these high-dilution solutions there is no effect whatsoever of stirring. However, we also found that these solutions *do not contain any more detectable nitronium salt!* Vacuum concentration of the solutions and subsequent spectroscopic (infrared and Raman) investigation revealed no 2 300 or 1 400 cm^{-1} bands, characteristic of nitronium ion. Recovery experiments resulted also in entirely negative results. The solutions, however, are still capable of nitrating. Thus all indications are that the *nitronium salt as such was lost during high dilution in tetramethylene sulfone solution.* The explanation was in our view already found in the experimental part of the quoted paper (14): "The solutions (e.g. NO_2BF_4 in tetramethylene sulfone) had a pale-yellow color probably originating from some impurity of the solvent. In one case a colorless solution was obtained using freshly distilled tetramethylene sulfone." (There was, however, no data given as to the behavior of this specific solution.)

In view of the essential need of high purity of the solvent and strictly anhydrous conditions using increasingly dilute solutions, the experimental techniques used were unsuitable. No vacuum line or dry box technique was used. The handling of highly hygroscopic materials, both during weighing solid nitronium salts on a balance and the treatment of equally hygroscopic tetramethylene sulfone solutions, in the reported experimental conditions seems highly inadequate. The quoted paper (14) further reports that "the purity of the solvent was checked by the freezing point and specific conductivity". The data when compared with those of Arnett (15), Burwell (16), and Olah (3) reported in the literature and summarized in Table III, clearly indicate that the solvent used was impure.

TABLE III

Freezing point and conductivity of tetramethylene sulfone of various purity

	Ref. 15	Ref. 16	Ref. 3	Ref. 14
Freezing point (°C)	28.4	28.8	27.6	26.7
Specific conductivity (mho/cm)		2×10^{-8}	1.35×10^{-7}	6.5×10^{-6}

Comparison of the purification methods described in the literature and particularly that of E. M. Arnett and C. F. Douty (15) with the purification via a simple distillation described by Tolgyesi makes it highly improbable that the latter used tetramethylene sulfone of sufficient purity. However, in view of the claims made in dilute tetramethylene sulfone solutions, we felt it necessary to reinvestigate the nature of impurities and their effects.

The effect of water present in tetramethylene sulfone could be followed by depression of the freezing point and increase of conductivity. Tetramethylene sulfone is extremely hygroscopic, and picks up water readily as shown by the freezing point depression and by increase of its conductivity. Triple distilled tetramethylene sulfone (from sodium

Can. J. Chem. Downloaded from www.nrcresearchpress.com by 210.87.254.40 on 09/05/12
For personal use only.

hydroxide pellets) when redistilled from calcium hydride to remove traces of water which it holds tenaciously had a freezing point of 28.35°. After venting the solvent to air the freezing point was depressed to 28.16° within 30 min. If purified tetramethylene sulfone was vented to the air while stirred with a vibrator mixer, the freezing point depressed to 27.21° in 15 min. (The thermometer used could be estimated at 0.01°). The specific conductivity of the solvent changed at the same time from 1.52×10^{-8} to 9.6×10^{-6} mho/cm. The Karl Fischer water determination in tetramethylene sulfone was found unreliable and irreproducible when checked on samples to which known amounts of water was added. One of the reasons for this behavior may be the presence of other impurities in the solvent. Tetramethylene sulfone is made commercially from the Diels–Alder reaction of 1,3-butadiene with sulfur dioxide, giving 2,5-dihydrothiophene-1, 1-dioxide which is then hydrogenated.

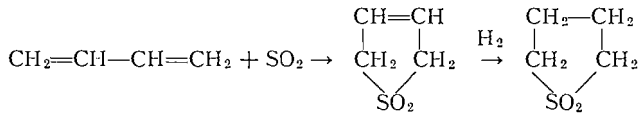

Commercial tetramethylene sulfone contains, according to our observations, besides varying amounts of water and some unidentified impurities, up to 2% 2,5-dihydrothiophene-1,1-dioxide (isolated by gas chromatography and identified by its infrared and n.m.r. spectra). Tetramethylene sulfone cannot be separated by a simple vacuum distillation from dihydrothiophene-1,1-dioxide or its cleavage products. Its presence is responsible for the formation of SO_2 during distillation or heating the solvent, thus reversing the Diels–Alder addition of butadiene and sulfur dioxide. Strong acids, like sulfuric acid, give coloration with tetramethylene sulfone containing the olefinic sulfone and a similar coloration indicating complex formation with the nitronium salts! It was indeed found suitable to purify tetramethylene sulfone for nitration experiments by distillation from nitronium tetrafluoroborate.

The effect of impurity moisture on nitronium tetrafluoroborate is not entirely yet clarified. Nitronium tetrafluoroborate reacts in all probability with water to give a more selective nitrating agent, e.g. nitracidium tetrafluoroborate (protonated nitric acid).

$$NO_2^+BF_4^- + H_2O \rightleftharpoons H_2NO_3^+BF_4^-$$

With excess water nitric acid formation takes place.

$$H_2NO_3^+BF_4^- + H_2O \rightarrow HNO_3 + HBF_4 \cdot H_2O$$

In our view nitronium tetrafluoroborate is not identical with nitric acid, even in the presence of small amounts of water. However, the "activity" of nitronium tetrafluoroborate is substantially affected by the presence of water.

We determined the effect of water and 2,5-dihydrothiophene-1,1-dioxide on the nitronium tetrafluoroborate nitrations by adding (in separate experiments) known amounts of them to a 0.5 *M* tetramethylene sulfone solution of nitronium tetrafluoroborate. In these experiments it was possible to reproduce what happens when the impurities are present in concentrations approximating those used in highly diluted solutions. Data obtained are summarized in Tables IV and V.

The experimental facts need little explanation. Using dilute solutions the impurity (in all probability both 2,5-dihydrothiophene-1,1-dioxide and water) can easily reach levels approximating the amount of $NO_2^+BF_4^-$ claimed to be present. A 0.04 *M* solution of the nitronium salt used in ref. 14 means that an equivalent of 0.72 g H_2O in 1 000 ml (1 261 g)

Can. J. Chem. Downloaded from www.nrcresearchpress.com by 210.87.254.40 on 09/05/12
For personal use only.

TABLE IV

Effect of addition of water to nitronium tetrafluoroborate in tetramethylene sulfone solution on the nitration of benzene and toluene

% equivalent H_2O related to NO_2BF_4	$k_t:k_b$
0	1.8
25	4.96
50	7.53
75	8.27
84	18.2
100	29.1

TABLE V

Effect of addition of 2,5-dihydrothiophene-1,1-dioxide to nitronium tetrafluoroborate in tetramethylene sulfone solution on the nitration of benzene and toluene

Equivalent dihydrothiophene-1,1-dioxide related to NO_2BF_4	$k_t:k_b$
0	1.8
10	2.95
20	3.6
50	7.97
100	37.3

tetramethylene sulfone thus a <0.06 wt. % amount of impurity moisture will completely bind all nitronium salt. In view of the demonstrated effect of water on the relative rate even a much smaller amount can have substantial influence. Similarly a 0.38% dihydrothiophene-1,1-dioxide impurity means a 0.04 *M* solution.

We must conclude based on our experimental data that the nitrations observed in increasing dilutions (14) were *not* pure nitronium salt solutions. In high dilutions it is even questionable that there was any free nitronium salt present. Mixing itself thus had no major effect on the competitive reactions besides distributing the nitrating agent better in the solution of the substrates before reaction, thus making it more susceptible to the effect of all impurities in the system.

Next we turned our attention to the problem of obtaining relative reactivity data of toluene:benzene in competitive nitration experiments using nitronium tetrafluoroborate in highly purified tetramethylene sulfone solution (see Experimental) and using the described new vibrator stirrer – syringe injection system (14). It must be emphasized that otherwise the reaction conditions were not suited to claim absolute anhydrous conditions, as no vacuum line technique was used. Data obtained in nitrating 0.5 *M* benzene and 0.5 *M* toluene solution with 0.67, 0.4, and 0.2 *M* nitronium tetrafluoroborate in tetramethylene sulfone solutions are shown in Table VI. Voltage of the vibrator motor was kept constant at 115 V. An all-glass vibrating stirrer was used instead of a metal one (used in the ref. 14) to avoid any interaction with or surface catalysis on the metal.

It was observed in our experiments too, that with decreasing concentration of the used nitronium salt solution the substrate selectivity increased. In the concentration range investigated the variation of the toluene:benzene reactivity ratio was, however, definitely

Can. J. Chem. Downloaded from www.nrcresearchpress.com by 210.87.254.40 on 09/05/12
For personal use only.

TABLE VI

Competitive nitration of toluene and benzene with NO_2BF_4 in tetramethylene sulfone solution at 25° using vibrator stirrer and syringe injection of reagent

		% nitrotoluene		
	$k_t:k_b$	ortho	meta	para
$[NO_2^+BF_4^-] = 0.67$	2.70	65.8	2.6	31.6
	3.50	65.0	2.5	32.5
	2.42	64.6	2.3	33.1
	4.31	66.1	1.9	32.0
	3.12	65.8	2.1	32.1
$[NO_2^+BF_4^-] = 0.4$	5.62	65.0	2.7	32.3
	5.03	64.4	2.1	33.5
	3.74	65.8	2.3	31.9
	4.41	65.0	1.8	33.2
	4.50	64.9	2.0	33.1
$[NO_2^+BF_4^-] = 0.2$	6.54	63.1	2.0	34.9
	4.41	64.8	1.7	33.5
	3.34	64.4	2.3	33.3
	6.77	64.0	1.8	34.2
	4.92	63.4	2.3	34.3

in a different order of magnitude than that of nitric acid nitration in the same solvent, and the spread of the experimental data is considerable and the reproducibility poor. All this indicates a mixed nitration system involving more than one nitrating agent. It would also seem that many factors not defined previously have an effect (position of injection, size, material, etc. of vibrator disc, its position in the reaction vessel).

In view of the difficulty of purification of tetramethylene sulfone and its hygroscopic nature, we felt it useful to extend the investigation of the vibrator stirrer – syringe injection system to another solvent system. Nitromethane was selected, the purification of which was previously described (17). Carrying out competitive nitration of toluene and benzene with 0.5 *M* and 0.2 *M* nitronium hexafluorophosphate (nitroniumtetrafluoroborate is not sufficiently soluble) solutions under conditions identical with those used previously, the change of the reactivity ratio with dilution of the solution of the nitrating agent and the use of the new stirring method was found very small (Table VII).

To compare the behavior of the toluene:benzene competitive nitrations with reaction

TABLE VII

Competitive nitration of toluene and benzene at 25° with $NO_2^+PF_6^-$ in nitromethane solution using vibrator stirrer and syringe injection of the reagent

		% nitrotoluene		
	$k_t:k_b$	ortho	meta	para
$[NO_2^+PF_6^-] = 0.5$	1.64	68.2	1.5	30.3
	1.70	67.2	2.3	30.5
	1.58	69.0	1.5	29.5
	1.54	67.0	2.1	30.9
	1.64	67.7	2.0	30.3
$[NO_2^+PF_6^-] = 0.2$	2.52	69.0	1.5	29.5
	2.97	67.7	2.0	30.3
	2.76	68.2	1.5	30.3
	1.98	68.6	1.5	29.9

Can. J. Chem. Downloaded from www.nrcresearchpress.com by 210.87.254.40 on 09/05/12
For personal use only.

conditions where, due to an extremely reactive substituting agent, predominantly statistical factors determine both substrate and positional selectivity, we carried out free radical type nitration of the substrates. Toluene and benzene (under competitive reaction conditions in 1:1 ratio) were reacted at the reflux temperature of the mixture with nitrogen dioxide in the presence of benzoyl peroxide catalyst while irradiating the reaction mixture with ultraviolet light (the reaction being carried out in a fused quartz reaction vessel).

TABLE VIII

Competitive nitration of benzene and toluene with nitrogen dioxide at reflux temperature of the mixture in ultraviolet light

		% nitrotoluene		
	$k_t:k_b$	ortho	meta	para
Benzene	1.0			
Toluene	2.6	37.2	38.1	24.7

Data obtained are summarized in Table VIII. From the data of Table VIII it is evident that low substrate selectivity is obtained with simultaneous low positional selectivity, approximating the statistical 40% ortho, 40% meta, 20% para isomer distribution. The high positional selectivity observed in nitronium salt and other electrophilic aromatic nitrations is in sharp contrast with the low positional selectivity observed under free radical nitration conditions.

The possible effect of diffusion control or incomplete mixing was also further investigated by the use of high-speed flow systems. The reaction time in these experiments was cut to 0.01 s. Solutions of the nitronium salt and the competing aromatics were sent through a capillary mixing chamber in concentration similar to those used in previous dropwise addition procedure (~0.7 *M* nitronium salt and also in dilution till 0.25 *M* solution). The reactor was a modified and improved version (with controlled-speed syringe-type addition system) of that used by H. C. Brown and H. Jungk (18) in Friedel–Crafts type reactions. Data of competitive nitration of toluene and benzene in the flow system are summarized in Table IX.

TABLE IX

Competitive nitration of benzene and methylbenzenes in flow reactor (average reaction time 0.01 s)

Aromatic	Nitrating agent	Solvent	$k_{aromatic}:k_{benzene}$
Benzene	$NO_2^+BF_4^-$	Tetramethylene sulfone	1.0
Toluene			2.07
m-Xylene			2.68
Mesitylene			3.50
Benzene	$NO_2^+PF_6^-$	Nitromethane	1.0
Toluene			2.56
m-Xylene			6.54
Mesitylene			10.38

Attempts were also made to measure the absolute rates of the nitration of toluene and benzene respectively in flow systems. Using an internal standard method to enable analysis after quenching of the reaction mixtures by the previously detailed g.l.c. method, measurements were carried out, but no reliable data could be obtained because of the fact that the reactions are fast enough that quenching could become the limiting factor. There was also

Can. J. Chem. Downloaded from www.nrcresearchpress.com by 210.87.254.40 on 09/05/12
For personal use only.

Can. J. Chem. Downloaded from www.nrcresearchpress.com by 210.87.254.40 on 09/05/12
For personal use only.

no evidence to prove complete mixing of the reagents as no ideal turbulent flow conditions with suitable Reynolds' numbers were obtainable in tetramethylene sulfone solutions. Using the less viscous nitromethane as solvent, turbulent flow conditions were easily obtained.

The high-speed flow system in competitive experiments gave only a slight increase in the relative reactivity ratio values compared with the previous dropwise addition method. The fact that there is any change in the relative rate indicates that mixing does have some effect on the reactions. Imperfect mixing is also demonstrated by the fact that high-temperature gas-chromatographic methods indicate the formation of small amounts (generally substantially less than 1%) of dinitro products in the nitration of alkylbenzenes (19). Dinitro products could not be formed in the kinetically controlled nitration of alkylbenzenes (in the presence of a large excess of the alkylbenzene), but originate from the fact that the mononitro product is not uniformly distributed in the nitration media and that some dinitration takes place in the immediate surroundings of the nitrating agent. The very small amount of dinitration, however, again indicates that in competitive experiments the effect of imperfect mixing is only a minor one.

The question of mixed acid nitration of benzene and toluene in tetramethylene sulfone and nitromethane solution was previously discussed by Olah, Kuhn, Flood, and Evans (7). It was shown that the concentration of nitronium ion (as monitored by infrared and Raman spectroscopy) decreases with increasing dilution of the acid in the solvent. In dilute solution (not containing spectroscopically detectable amounts of NO_2^+ concentration) the toluene:benzene reactivity ratio was found to be 28, whereas with more concentrated solutions (containing substantial NO_2^+ concentration) it was 1.6.

Nitric acid in organic solutions (acetic anhydride, acetic acid, nitromethane tetramethylene sulfone) shows substantial substrate selectivity ($k_t:k_b = >25$). These solutions according to spectroscopic evidence do not contain detectable amounts of NO_2^+. The observation (14), that using neat nitric acid as nitrating agent and adding it to a dilute tetramethylene sulfone solution of the aromatics gives a toluene:benzene ratio of 3.4 is in our view in accordance with the fact that neat nitric acid according to Raman spectroscopic data is about 0.2 *M* in $NO_2^+NO_3^-$. Thus its use represents the use of a dilute nitronium nitrate solution as nitrating agent. In our hands the competitive nitration of toluene and benzene with dilute (1 *M*) solution of nitric acid in tetramethylene sulfone gave $k_t:k_b = 37$ (% ortho 64.9, % meta 5.6, % para-nitrotoluene 29.5). In contrast neat nitric acid as nitrating agent gave $k_t:k_b = 1.65$ (% ortho 57.5, % meta 4.6, % para 37.9 nitrotoluene).

We are in disagreement with conclusions concerning the supposed equivalence of nitronium tetrafluoroborate nitration with nitric acid nitration (14). Similarly nitric acid in dilute organic (or aqueous) solution cannot be equated with strong proton acid solutions or the neat acid. Nitric acid itself is not an electrophilic nitrating agent. It must first form according to Ingold an electrophile and the formation of this species can be rate determining.

$$HNO_3^+ + H^+ \rightleftharpoons H_2NO_3^+$$

$$H_2NO_3^+ \rightleftharpoons NO_2^+ + H_2O$$

In contrast if we use prepared NO_2^+ salts the formation step is excluded and therefore the rate-determining step can be nothing else than interaction with the substrate. However, we agree that the reported nitronium fluoroborate nitrations in high dilutions (14) indeed do approximate nitric acid nitrations. This in all probability was due to the fact that in

high dilutions it was impossible to keep the system pure enough to carry out any more nitronium salt nitrations and the impure systems resulted in mixed nitrations indicated by the fact that practically any toluene:benzene reactivity value between 1.4 and 40 could be obtained.

B. Positional (Intramolecular) Selectivity

The classical nitration of toluene shows a remarkable constancy of the mononitrotoluene isomer distribution, regardless of the reagents employed. The many references relating to the nitration of toluene report only slight variation in the ortho:para ratio (from 1.41 to 1.66). In all the systems investigated, the *m*-nitrotoluene content also remained relatively constant fluctuating between 1.6 and 5%.

The constancy of the isomer distribution in the nitration of toluene remained unchallenged until our work on nitronium salt nitrations (4), which showed that the ortho:para ratio can be substantially increased (Table X).

Increasing solvation in nitronium salt and related electrophilic nitrations generally decreases the ortho:para ratio without, however, altering the meta isomer content. Mixed acid ($HNO_3 + H_2SO_4$) at $-15°$ gives an ortho:para ratio of 0.92 (4). Neopentyl nitrate in polyphosphoric acid gave a ratio of 0.49, amyl nitrate under similar conditions 0.64, and absolute nitric acid in polyphosphoric acid 0.86 (20).

The amount of meta isomer is generally so small (2–3%) that the analytical methods used do not allow significant differentiation. The ortho:para isomer ratio however is more easy to follow. It is observed that the low substrate selectivity nitrations show generally a higher ortho:para ratio than the higher selectivity reactions, indicating at least a partial change in the nature of the nitrating agent (NO_2^+ versus a bulkier precursor).

Mechanical factors, like efficiency of stirring, should have no effect on the isomer distributions. It was, however, reported (14) that the isomer distributions show changes depending on the efficiency of stirring used. Although the changes were relatively small, it must be remembered, as discussed previously, that the electrophilic nitration of toluene is remarkably insensitive to the nature of the nitrating agent employed.

It is our view that simultaneous changes in *both* substrate and positional selectivity indicate some change in the nature of the nitrating agent, because mechanical factors (efficiency of mixing) could not account for isomer distribution changes. Only if a statistically controlled indiscriminate nitration (giving a distribution of 40% ortho, 40% meta, and 20% para isomer) were superimposed onto a selective nitration (with high ortho:para ratio) could stirring (e.g. better distribution of the reagent before reaction) affect the isomer distribution. There are, however, no data available to substantiate this latter case as the amount of meta-nitrotoluene shows no significant variation.

The isomer distribution data of the nitration of toluene fully substantiate the view that stable nitronium salt nitrations in organic media are different from nitric acid nitrations. The nitronium salt nitrations gave the highest reported ortho:para ratios with the lowest meta isomer content. The isomer distributions are constant under purely mechanical changes in the nitration systems, but vary if the nature of the nitrating agent is affected.

In conclusion it is our belief that the competitive rate determination method for determination of the relative reactivity of toluene and benzene can be applied for the nitronium salt nitrations in tetramethylene sulfone and nitromethane solution. The data indicate low substrate (intermolecular) but high positional (intramolecular) selectivity. It was indicated by us from the very first publication on the topic (4) that the high reactivity of

Can. J. Chem. Downloaded from www.nrcresearchpress.com by 210.87.254.40 on 09/05/12
For personal use only.

Can. J. Chem. Downloaded from www.nrcresearchpress.com by 210.87.254.40 on 09/05/12
For personal use only.

TABLE X

Isomer distributions in mononitration of toluene

Nitrating agent	Solvent	Temp., °C	Isomer			Ratio ortho:para	Analytical method	Ref.
			ortho	meta	para			
94% HNO_3	None	0	60.3	2.5	37.2	1.62	Freezing point	(22)
HNO_3	Acetic anhydride	0	61.4	1.6	37.0	1.66	G.l.c.	(23)
HNO_3	Acetic anhydride	0	58.11	3.7	38.2	1.52	Freezing point	(24)
HNO_3	Acetic anhydride	30	58.4	4.4	37.2	1.57	Freezing point	(24)
HNO_3	Acetic anhydride	30	58.5	4.4	37.1	1.58	Freezing point	(25)
HNO_3	Nitromethane	30	58.5	4.4	37.1	1.58	Freezing point	(24)
HNO_3	H_2SO_4	25–50	62	5.0	33	1.88		(26)
HNO_3	H_2SO_4		58.45	4.4	37.15	1.57	Distillation	(27)
HNO_3	90% acetic acid	45	56.5	3.5	40.0	1.41	Infrared	(28)
$C_6H_5COONO_2$	CH_3CN	0	59	5	37	1.59	Infrared	(29)
NO_2BF_4	Tetramethylene sulfone	25	65.4	2.8	31.8	2.05	G.l.c.	(4)
NO_2BF_4	Nitromethane	25	65.7	3.2	31.1	2.11	G.l.c.	(4)
NO_2PF_6	Tetramethylene sulfone	25	67.6	1.4	31.0	2.18	G.l.c.	(4)
NO_2ClO_4	Tetramethylene sulfone	25	66.2	3.4	30.4	2.18	G.l.c.	(4)
N_2O_5	Tetramethylene sulfone	25	65.1	3.1	31.8	2.04	G.l.c.	(4)

the nitronium salt may cause experimental problems, but we think we have sufficiently proven that these are only minor ones under conditions of competitive rate determinations using large excess of the substrates. No selective depletion of the more reactive reaction partner (toluene) was observed, neither was evidence obtained indicating statistically (diffusion) controlled reaction conditions.

The claimed variation of the toluene:benzene reactivity ratio with the efficiency of stirring (14) was shown to a large degree to be a consequence of simultaneous high dilution of the system containing impurities affecting the reactivity of the nitrating agent. The final answer as to the possible effect of non-kinetic factors on competitive rate determinations should come from absolute rate determination of toluene and benzene in separate systems. Although attempts were made to this effect the reactions were found so far too fast for reliable measuring even in fast flow systems. We are, however, continuing our efforts to achieve this goal.

EXPERIMENTAL

Due to the extremely hygroscopic nature of nitronium salts and anhydrous tetramethylene sulfone, the preparation and handling of the reagents and their solutions was carried out in a good dry box (Kewaunee Co., Adrian, Michigan) purged with dry nitrogen and desiccated by phosphorus pentoxide. No claim for absolutely anhydrous conditions can, however, be made as no vacuumline techniques were employed in present investigations.

Reagents

Aromatic hydrocarbons (benzene, toluene, *m*-xylene, mesitylene) were highest purity materials dried and distilled from calcium hydride.

Nitronium tetrafluoroborate was prepared as described previously (3, 21). It should be emphasized that the preparation of Kuhn and Olah (3) which is extremely well suited to obtain nitronium tetrafluoroborate of 90–95% purity, applicable to most purposes, does not provide the quality of reagent needed for high dilution work. For this purpose the preparation of Cook, Kuhn, and Olah (21) from nitryl fluoride and boron trifluoride in a vacuum system was found necessary.

Tetramethylene sulfone, commercial material (Phillips Petroleum Company, Bartlesville, Oklahoma or Shell Development Co., Emeryville, California), was purified essentially as described by Arnett and Douty (15). The purification consisted of repeated vacuum distillation from sodium hydroxide pellets until a 1-ml sample in a small test tube did not show development of visible color within 5 min after the addition of an equal volume of 100% sulfuric acid. This usually required two or three distillations. It was then distilled again from calcium hydride to remove traces of water, which it holds extremely tenaciously. Storing the material under vacuum or nitrogen for brief periods of time was possible. It was, however, observed that tetramethylene sulfone is sufficiently hygroscopic to pick up moisture under prolonged storage even under careful conditions and much more so when vented to the atmosphere, even for brief periods of time. Purified tetramethylene sulfone had a freezing point of $28.5 \pm 0.1°$ and a specific conductivity 1×10^{-8} mho/cm. Fresh solutions of pure nitronium tetrafluoroborate in tetramethylene sulfone purified by described procedure were colorless. Coloration was observed when exposed to moisture or on prolonged standing. It was necessary to make up the solutions, to carry out the weighing of the nitronium salt and dilutions in the dry box.

Nitromethane was purified as reported previously (17).

Competitive Nitrations

Magnetic stirrer.—Nitrations using conventional magnetic stirrer were carried out as described (4). Addition of the nitronium salt solution was, however, carried out by running the solution below the level of the substrate solution stirred in the reaction vessel or by addition of the solution of the nitrating agent from a hypodermic syringe. In the concentrations reported in previous work (4), data were well reproducible and the mode of addition of the nitrating agent had little effect.

Vibrator stirrer and syringe addition of the nitronium salt solution.—Reactions were carried out under conditions suggested (14) to achieve maximum mixing. The reaction vessel was a jacketed test tube through which water was circulated at $25 \pm 0.1°$. The reaction vessel had a side arm closed with a serum cap. Generally 60 ml of the solution of the competing aromatic hydrocarbons was measured into the vessel which was agitated with a laboratory Vibro mixer using a perforated 23 mm diameter all-glass vibrating disc. Voltage of the vibrator motor was kept constant at 115 V. The solution of the nitrating agent was added from a hypodermic needle through the serum cap of the side arm of the reaction vessel. If not stated otherwise, the overall amount of nitronium salt was less than 1/100 mole equivalent of that of the combined aromatic substrates.

Can. J. Chem. Downloaded from www.nrcresearchpress.com by 210.87.254.40 on 09/05/12
For personal use only.

The addition of the nitronium salt was generally carried out in 3–4 min. The mixture was stirred for another 5 min. It was then poured into 150 ml water, extracted three times with ether using 50 ml each time, dried, and analyzed by capillary gas chromatography.

Flow Reactor

The reactor used was a modified and improved version of the flow system used by Brown and Jungk (18) in the investigation of Friedel–Crafts type reactions. Glass capillary mixing chambers of 1 mm diameter with volumes of 0.21, 0.12, and 0.07 ml were used. The solutions of the reagents (benzene, toluene, as well as the nitronium salt) were added from syringes, whose plungers were driven by synchronized motors. The quenching of the reaction mixture was effected with aqueous methanol. The work-up of the quenched mixture was effected by extraction with ether. Analyses were carried out under identical conditions as previous reaction mixtures.

Using tetramethylene sulfone as solvent, maximum flow rates of 3.30 ml/s were achieved. The critical velocity for turbulent flow, u_c, as given by the Reynolds' formula for tetramethylene sulfone (d^{30} 1.2615 g/s, viscosity at 30° 0.0987 g/cm s)

$$u_c = \frac{1\,000 \times \eta(\text{viscosity in poises})}{\rho(\text{density}) \times r(\text{radius of tube in cm})}$$

at 30° for a tube of 1 mm bore is 1 656 cm/s. The corresponding volume rate is 13 ml/s. Thus with the fairly viscous tetramethylene sulfone as solvent, no flow rates assuring turbulent flow conditions were possible. In the case of the substantially less viscous nitromethane (viscosity at 25° 0.00627 g/cm s, d^{25} 1.13149 g/s) the critical velocity for turbulent flow is only about 110 cm/s, the corresponding volume rate is 0.86 ml/s. With nitromethane solutions, flow rates of 8.1 ml/s could be obtained, and thus the Reynolds' number was high enough to assure turbulent flow conditions.

Analysis

All analyses were carried out on a Perkin–Elmer model 226 gas chromatograph equipped with flame ionization detector, 150 ft R-column (polypropylene glycol coated Golay column). Resolution of nitrobenzene and the three isomeric nitrotoluenes is seen in Fig. 1 of a representative analysis. Relative peak areas were determined by the use of a fast electronic integrator (Infatronics model CRS-1).

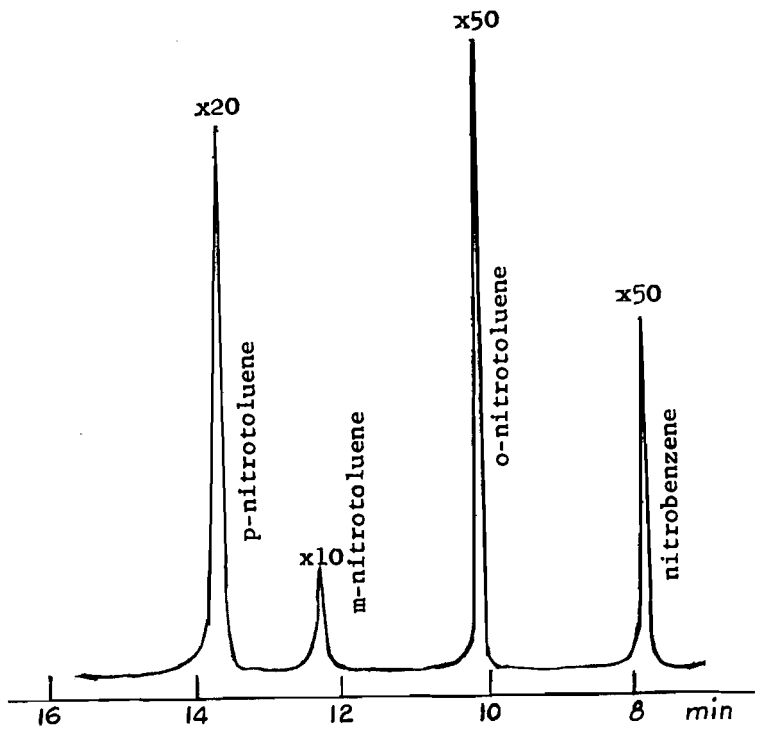

FIG. 1. Analysis of nitrobenzene–nitrotoluene reaction mixture on Perkin–Elmer model 226 gas chromatograph (150 ft R-column, 125°, 30 p.s.i.g. He pressure): k_t/k_b = 3.08; 65% ortho, 2.8% meta, 31% para nitrotoluene.

Can. J. Chem. Downloaded from www.nrcresearchpress.com by 210.87.254.40 on 09/05/12
For personal use only.

REFERENCES

1. G. OLAH and S. KUHN. Chem. Ind. London, 98 (1956).
2. G. OLAH, S. KUHN, and A. MLINKO. J. Chem. Soc. 4257 (1956).
3. S. J. KUHN and G. A. OLAH. J. Am. Chem. Soc. **83**, 4564 (1961).
4. G. A. OLAH, S. J. KUHN, and S. H. FLOOD. J. Am. Chem. Soc. **83**, 4571 (1961).
5. G. A. OLAH, S. J. KUHN, and S. H. FLOOD. J. Am. Chem. Soc. **83**, 4581 (1961).
6. G. A. OLAH and S. J. KUHN. J. Am. Chem. Soc. **84**, 3684 (1962).
7. G. A. OLAH, S. J. KUHN, S. H. FLOOD, and J. C. EVANS. J. Am. Chem. Soc. **84**, 3687 (1962).
8. G. A. OLAH and S. J. KUHN. J. Am. Chem. Soc. **86**, 1067 (1964).
9. L. STOCK and H. C. BROWN. *In* Advances in physical organic chemistry. Vol. I. *Edited by* V. Gold. p. 54.
10. Footnote 15 of ref. 4 referring to discussion with Professor H. C. Brown.
11. G. A. OLAH, S. J. KUHN, and C. G. CARLSON. XIX International Congress of Pure and Applied Chemistry, London. 1963. Abstr. of Papers A1–81.
12. G. A. OLAH and S. J. KUHN. *In* Friedel–Crafts and related reactions. Vol. III. *Edited by* G. A. Olah. Wiley-Interscience Publishers, New York and London. 1964. p. 1450 ff.
13. C. P. RITCHIE and H. WIN. J. Org. Chem. **29**, 3093 (1964).
14. W. S. TOLYGESI. Can. J. Chem. **43**, 343 (1965).
15. E. M. ARNETT and C. F. DOUTY. J. Am. Chem. Soc. **86**, 409 (1964).
16. R. L. BURWELL and C. H. LANGFORD. J. Am. Chem. Soc. **81**, 3799 (1959); **82**, 1503 (1960).
17. G. A. OLAH, S. J. KUHN, S. H. FLOOD, and B. A. HARDIE. J. Am. Chem. Soc. **86**, 1039 (1964).
18. H. C. BROWN and H. JUNGK. J. Am. Chem. Soc. **77**, 5583 (1955).
19. Ref. 12, p. 1450.
20. S. M. TSANG, A. P. PAUL, and M. P. DIGIAIMS. J. Org. Chem. **29**, 3387 (1964).
21. D. COOK, S. J. KUHN, and G. A. OLAH. J. Chem. Phys. **33**, 1669 (1960).
22. W. H. GIBSON, R. DUCKHAM, and R. F. FAIRBRAIN. J. Am. Chem. Soc. 270 (1922).
23. J. R. KNOWLES, R. O. C. NORMAN, and G. K. RADDA. J. Chem. Soc. 4885 (1960).
24. C. K. INGOLD *et al.* J. Chem. Soc. 1959 (1931).
25. A. F. HOLLEMAN *et al.* Rec. Trav. Chim. **33**, 11 (1914).
26. P. B. D. DE LA MARE and J. H. RIDD. Aromatic substitution: nitration and halogenation. Academic Press, Inc., New York, N.Y. 1959. p. 50.
27. K. L. NELSON and H. C. BROWN. J. Am. Chem. Soc. **73**, 5605 (1951).
28. J. H. COHN, E. D. HUGHES, M. H. JONES, and M. A. PEELING. Nature, **169**, 291 (1951).
29. R. HALVARSON and L. MELANDER. Arkiv. Kemi, **11**, 77 (1957).

Can. J. Chem. Downloaded from www.nrcresearchpress.com by 210.87.254.40 on 09/05/12
For personal use only.

ALICYCLIC KETYLS

II. TEMPERATURE DEPENDENCE OF THE CONFORMATIONAL MOBILITY OF MEDIUM-SIZED RINGS[1]

J. W. Lown

Department of Chemistry, University of Alberta, Edmonton, Alberta

Received July 28, 1965

ABSTRACT

The electron paramagnetic resonance spectra of ketyls derived from alicyclic ketones containing from 6 to 12 carbons have been recorded in 1,2-dimethoxyethane or dimethoxymethane at temperatures from −96 to +87 °C. At −96° individual conformers of the cyclohexyl ketyl are observed with hyperfine couplings in close agreement with that of the conformationally 'frozen' 4-*tert*-butyl analogue at room temperature. The cycloheptyl ketyl conformational equilibrium between forms which have a plane of symmetry through the C—O bond axis is 'frozen' with respect to the spectrometer frequency at temperatures from −40 to +88 °C. Cyclooctyl ketyl equilibrates at ordinary temperatures between two conformers lacking a plane of symmetry through the C—O bond axis. The electron paramagnetic resonance spectra of the ketyls derived from 10- and 12-membered rings show dramatic temperature dependence, which is interpreted in terms of two or more simultaneous conformational equilibria. Values for the dihedral angles of the alpha protons and for the spin density on the sp^2 carbon are derived.

We recently demonstrated (1) that a study of the electron paramagnetic resonance (e.p.r.) spectra of alicyclic ketyls in 1,2-dimethoxyethane can give valuable information about the conformations adopted by these radical anions in solution. It was found that the predicted (2) angular dependence of hyperfine coupling from protons alpha to the carbonyl group was confirmed and that it could be used to deduce dihedral angles. Within a given ring system, A values (conformational free energy differences) determined from neutral molecules were found to have validity when applied to the conformational analysis of such ketyls. In view of increasing interest in the shapes of medium-sized rings (7 to 12 carbons (3–8)) it was decided to examine the e.p.r. of the corresponding ketyls. A study of the temperature dependence of the e.p.r. spectra afforded valuable information concerning the individual conformers in each case.

Six-Membered Rings

Cyclohexyl ketyl had been shown (1) to give a sharp quintet of lines (1:4:6:4:1; a_H = 10.4 oersteds (Oe)) when generated from the ketone by potassium in dimethoxyethane at room temperature.

The conformationally 'frozen' 4-*tert*-butylcyclohexyl ketyl gave a seven-line spectrum ($a_{H_{ax}}$ = 14.4 and $a_{H_{eq}}$ = 7.2 Oe). Because of the conformational freedom of the unsubstituted six-membered ring, one would anticipate very little change in the e.p.r. spectrum except at low temperatures. A solution of the ketyl in dimethoxymethane (m.p. −104°) gave a quintet at room temperature, but as the temperature was lowered broadening of alternate lines occurred as the rate of inversion became comparable with the difference in the hyperfine frequencies between the two conformers, in accordance with prediction (9), until at −96° seven distinct lines were observed (Fig. 1B). At this temperature the lines are still broad, and accurate intensity computation is not possible. If it were possible to achieve lower temperatures with another solvent, presumably the lines would become

[1]*This research was supported by a National Research Council of Canada grant in aid of research.*

Can. J. Chem. Downloaded from www.nrcresearchpress.com by 210.87.254.5 on 09/05/12
For personal use only.

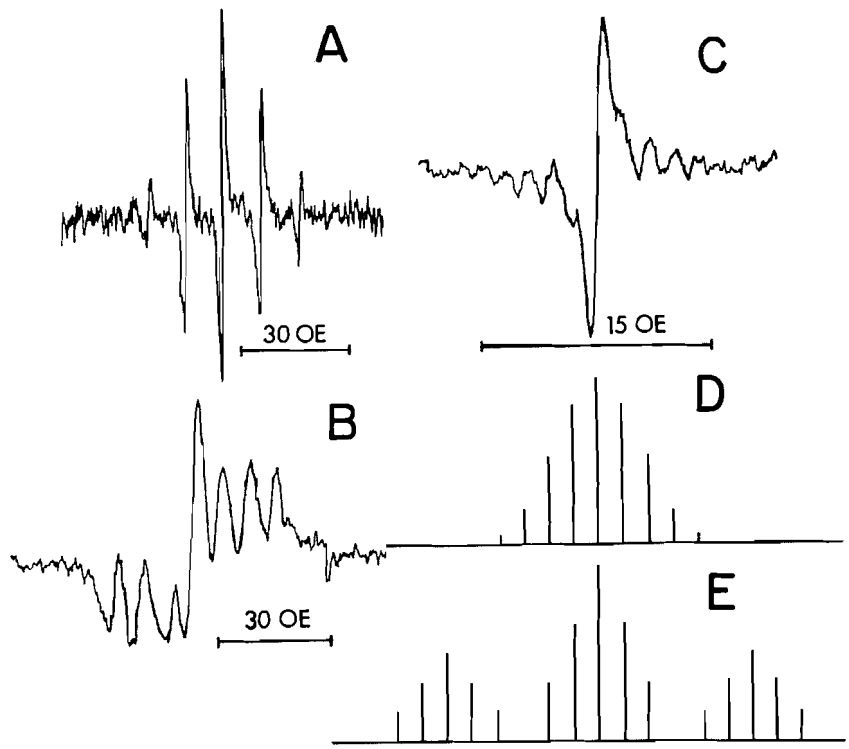

FIG. 1. First derivative e.p.r. spectra. LEGEND: A, cyclohexyl ketyl in 1,2-dimethoxyethane at +20°; B, cyclohexyl ketyl in dimethoxymethane at −96°; C, 2,2,6,6-tetradeuteriocyclohexyl ketyl in 1,2-dimethoxymethane at +20°; D, spectrum of C reconstructed from four equivalent deuterons (a_D = 1.6 Oe); E, spectrum of C reconstructed from one pair of equivalent deuterons (a_D = 1.6 Oe) and a pair of equivalent protons (a_H = 10.4 Oe).

sharp. However, the complete reversibility of the spectrum when the temperature is raised and lowered gives one confidence in assigning the seven-line spectrum to the conformationally 'frozen' ketyl. The fair agreement of the coupling constants 14.20 and 6.90 Oe with those of the 4-*tert*-butyl analogue is gratifying and confirms our previous prediction that distortion of the chair in the latter molecule is not serious (1).

Introduction of a ring substituent might be expected to slow down the rate of interconversion to the point where some temperature dependence could be observed at moderate temperatures. The e.p.r. spectra of the 3-methyl- and 4-methyl-cyclohexyl ketyls reported previously, while being well resolved, had lines appreciably broader than those of the unsubstituted ketyl, indicating some uncertainty broadening. Raising the temperature moderately (+60°) resulted in well-resolved spectra with accurate intensity distribution (Fig. 2A), whereas at temperatures of −35° extensive uncertainty broadening occurred.

The spectra retained their appearance up to +85°, a temperature approaching the boiling point of the solvent. This is consistent with our previous interpretation that inversion is rapid but that the equilibrium population favors the conformer which places the CH_3 group equatorial, so that complete averaging of the hyperfine couplings does not take place.

The increased resolution thus obtained allowed a more accurate determination of the coupling constants for these ketyls.

Can. J. Chem. Downloaded from www.nrcresearchpress.com by 210.87.254.5 on 09/05/12
For personal use only.

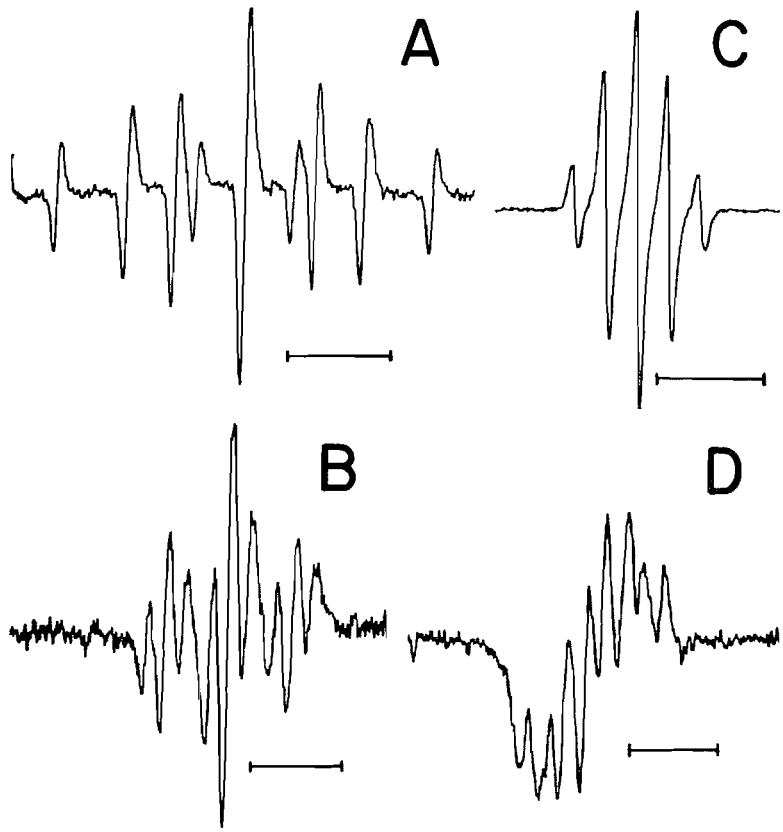

FIG. 2. First derivative e.p.r. spectra in 1,2-dimethoxyethane. LEGEND: A, 4-methylcyclohexyl ketyl at +61°; B, cycloheptyl ketyl at +72°; C, cyclooctyl ketyl at +24°; D, cyclooctyl ketyl at −35°. The bar in each case represents 10 Oe.

Care was taken to use excess potassium in the preparation of the samples to effect complete conversion of the ketone into the ketyl, so as to prevent broadening of the lines resulting from the electron exchange between ketyl and ketone (10). This more pronounced temperature dependence of the e.p.r. spectra of the substituted cyclohexyl ketyls indicates an appreciably larger energy barrier to inversion than exists in cyclohexyl ketyl itself.

Seven-Membered Ring

Cycloheptyl ketyl gives a well-resolved spectrum consisting of 1:2:1 triplets of 1:2:1 triplets at room temperature with a_H = 7.02 and 2.08 Oe (Fig. 2B). This shows that the conformation of the radical ion is 'frozen' with respect to the difference in the hyperfine frequencies between the two conformers and indicates a lower frequency of conformational inversion than that which obtains in analogues having six-membered rings. The shape of the spectrum is unaltered when the temperature is lowered to −40°, showing that a conformational equilibration between only two forms is involved (see later discussion on 10- and 12-membered rings). The spectrum is unchanged up to +86°, at which temperature decomposition appears to take place. Clearly, the cycloheptyl ketyl interconverts between two conformational forms which have a plane of symmetry through the C—O

Can. J. Chem. Downloaded from www.nrcresearchpress.com by 210.87.254.5 on 09/05/12
For personal use only.

bond axis at a rate much slower than that corresponding to the frequency difference of the two couplings (approximately 6×10^7 s^{-1}) up to a temperature of $+86°$.

The most detailed calculation of the conformational energies of cycloheptane yet reported (3) predicts the 'chair' form to be more stable than the 'boat' form. (These conformers are analogues to the cyclohexane forms.) A particular arrangement of the cycloheptane chair, the 'twist-chair' (I), was considerably preferred over other alternatives.

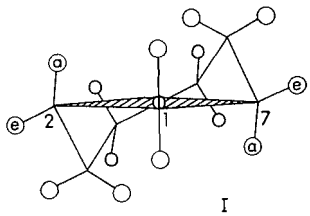

I

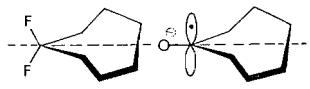

II

III

The most comfortable positions for the carbonyl group in cycloheptanone have been predicted to be at C-1, C-2, or C-7 (11) of the 'twist-chair' form of cycloheptanone (I). Since placing the $C—O^{\ominus}$ group only at the C-1 position in I yields a molecular form with a plane of symmetry, we may speculate that III is the preferred conformation of the ketyl. Coupling from two pairs of equivalent protons at the C-2 and C-7 positions would be expected to give rise to couplings of the order of those observed, since the dihedral angles are substantially different. It is interesting to note that recent nuclear magnetic resonance studies (12) of 1,1-difluorocycloheptane (II) show that this molecule interconverts between two 'twist-chair' conformations which have a similar plane of symmetry through the C-1 position.

Eight-Membered Rings

In rings of more than seven carbons transannular interactions become increasingly important in conformational considerations until one reaches rings which are large enough to approximate open chain compounds. At room temperature the spectrum of cyclooctyl ketyl consists of five lines (1:4:6:4:1; $a_H = 3.45$ Oe) clearly arising from four equivalent protons (Fig. 2C). This form of the spectrum is retained up to a temperature of $+88°$. At temperatures below $+14°$ an additional fine structure makes its appearance until, at $-35°$, eight clearly resolved lines with an intensity pattern close to 1:1:3:3:3:3:1:1, $a_{H_1} = 4.47$, $a_{H_2} = 2.35$ Oe, are observed (Fig. 2D). This spectrum arises from coupling of the unpaired electron to *three* equivalent protons and a single proton, and represents a 'freezing out' of the conformation, i.e. rate $\ll 3 \times 10^7$ s^{-1}. These interesting observations show that at room temperature the eight-membered ketyl is inverting more rapidly than the seven-membered analogue, that as a result of its marked temperature dependence the energy barrier to inversion is greater than that for the six-membered ring, and that inversion takes place between two conformers which do *not* possess a plane of symmetry through the C—O bond.

These dramatic changes, with temperature, of e.p.r. spectra from common intermediates show that consideration of conformational phenomena should be made in the interpretation of all e.p.r. spectra of cyclic radical species.

Ten- and Twelve-Membered Rings

Larger rings would be expected to show greater conformational freedom than six- or seven-membered rings. Consequently, the simple assumption of interconversion between

Can. J. Chem. Downloaded from www.nrcresearchpress.com by 210.87.254.5 on 09/05/12
For personal use only.

only two conformational forms is no longer valid. The existence of two or more equilibria between different conformational forms, which do not necessarily occur at the same rate, is therefore to be anticipated. Such considerations apply in the cases of the 10- and 12-membered rings.

The room temperature spectrum of cyclododecyl ketyl consists of three lines (a_H = 9.25 Oe), with the central line appreciably broader and less intense than the outer lines (Fig. 3C). Raising the temperature causes a marked sharpening of the central resonance

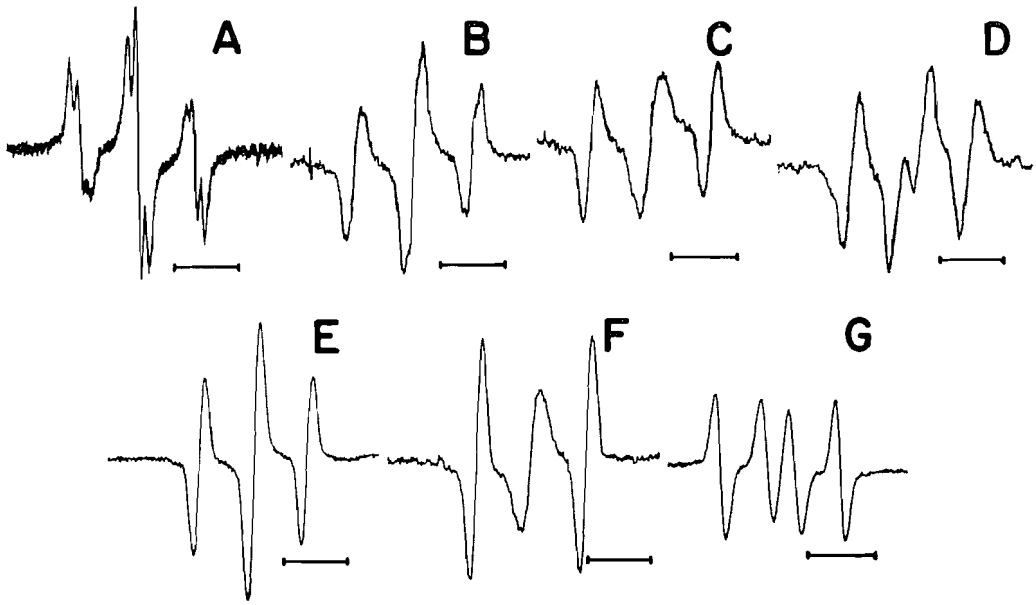

FIG. 3. First derivative e.p.r. spectra in 1,2-dimethoxyethane. LEGEND: A, cyclododecyl ketyl at +83°; B, cyclododecyl ketyl at +62°; C, cyclododecyl ketyl at +20°; D, cyclododecyl ketyl at −35°; E, cyclodecyl ketyl at +90°; F, cyclodecyl ketyl at +20°; G, cyclodecyl ketyl at −32°. The bar in each case represents 10 Oe.

until, at +61°, a 1:2:1 triplet is observed (Fig. 3B). At +83° further splitting of each line can be seen and the spectrum consists of a 1:2:1 triplet of 1:2:1 triplets (a_{H_1} = 9.02, a_{H_2} = 1.67 Oe) showing coupling to two pairs of equivalent protons (Fig. 3A). As the temperature is lowered below 0° the central line becomes increasingly broad, until at −35° four distinct lines are observed, corresponding to coupling to *two* non-equivalent protons, a_H = 11.0 and 7.3 Oe, respectively (Fig. 3D). It is noteworthy that the overall splitting remains constant at ~18.3 Oe and that these dramatic changes are completely reversible, confirming that we are dealing with conformational forms. We interpreted these observations in terms of simultaneous conformational equilibria.

At −35° interconversion occurs between pairs of conformers (which have no plane of symmetry through the C—O bond axis) at a rate much slower than that corresponding to the difference in the hyperfine frequencies. At this temperature in these equivalent conformations, coupling of 11.0 and 7.3 Oe occurs with two protons at the C-2 and (or) C-12 positions, the remaining two protons having couplings close to 0. At room temperature the interconversion between these conformers takes place at a rate now comparable with the hyperfine frequency difference, thus accounting for the broadening of the central line of the triplet. The appearance of the spectrum under these conditions (~+20°) can

Can. J. Chem. Downloaded from www.nrcresearchpress.com by 210.87.254.5 on 09/05/12
For personal use only.

be explained by an argument similar to that used by Dixon and Norman (13) to interpret the e.p.r. spectra of radicals derived from hydrogen abstraction from dioxane, cyclohexanol, and cyclohexylamine at room temperature.

TABLE I

Nuclear spin orientations in conformer A		Total spin interaction in:			
x	y	Conformer A	Conformer B	Difference	Average
+	+	$x+y$	$x+y$	0	$x+y$
+	−	$x-y$	$-x+y$	$+2x-2y$	0
−	+	$-x+y$	$x-y$	$-2x+2y$	0
−	−	$-x-y$	$-x-y$	0	$-x-y$

Since two of the protons at the C-2 and C-12 positions have 0 hyperfine couplings under these conditions, one need not consider their spin orientations in this discussion. x and y represent the positions adopted by the remaining (coupled) protons, analogous to axial and equatorial protons in cyclohexane. If an x proton changes places with a y proton of different spin in the conformational equilibria, a change in total nuclear spin interaction will result. Table I shows the difference and average spin interactions which result from the equilibration. The 'difference' column predicts that the two outer lines are not subject to change and therefore remain sharp, whereas there are two ways in which the central resonance will be changed, so that a broadened line equal to twice the intensity of the flanking lines is predicted. Examination of Fig. 3C shows that these predictions are confirmed.

As the temperature is raised to $\sim+62°$, interconversion is sufficiently rapid to produce an accurate 1:2:1 triplet (a_H = 9.25 Oe), indicating complete averaging of the two coupling constants 11.0 and 7.30 Oe. At this temperature the individual lines of the triplet are still broad enough to prevent resolution of the additional hyperfine splitting observed at +83°, thus revealing the presence of another conformational equilibration. At +62° this latter equilibration clearly takes place at a rate comparable with the hyperfine frequency difference, but at +83° is sufficiently rapid for clear resolution of the two hyperfine couplings of 9.02 and 1.67 Oe from two pairs of protons at the C-2 and C-12 positions in a conformer of cyclododecyl ketyl which possesses a plane of symmetry through the C—O bond axis. This latter conformational equilibrium does not make a significant contribution at −35°, as shown by the fact that couplings of 9.02 and 1.67 Oe are not involved at this temperature. This type of 'locking out' of a particular conformational equilibrium at low temperatures for energetic reasons has been postulated to account for the temperature variation of the nuclear magnetic resonance spectra of fluorinated cyclooctanes (12).

The spectrum at +87° resembles that of cycloheptyl ketyl, and presumably at a still higher temperature (provided the radical did not decompose) complete averaging of the couplings of the four equivalent protons would produce a 1:4:6:4:1 spectrum. In practice, the radical begins to disappear at $\sim+98°$.

Cyclodecyl ketyl exhibits similar behavior (cf. Fig. 3). The room temperature spectrum consists of three lines spacing 8.52 Oe, with the central line much broader and less intense than the outer lines (Fig. 3F). At lower temperatures the broadening of the central line increases until at −32° four lines (1:1:1:1; a_{H_1} = 10.77, a_{H_2} = 6.50 Oe) are observed,

Can. J. Chem. Downloaded from www.nrcresearchpress.com by 210.87.254.5 on 09/05/12
For personal use only.

arising from coupling to *two* non-equivalent protons (Fig. 3G). As the temperature is raised above +20° the central line is seen to sharpen, until at +61° an accurate 1:2:1 triplet is obtained (a_H = 8.52 Oe) consistent with the rapid conformational averaging of the two couplings observed at lower temperatures. The lines are still noticeably broad, however, up to +89°, at which temperature the radical is unstable (Fig. 3E). Consequently, further splitting, which was anticipated in view of the results obtained with cyclododecanone, could not be obtained.

These phenomena can be explained in a similar way in terms of the existence of two or more simultaneous conformational equilibria.

Angular Dependence of Hyperfine Couplings in Medium-Sized Ketyls

The coupling of protons attached to a carbon atom adjacent to a carbon bearing a free electron has been predicted (2) to satisfy an equation of the type

$$a_H = B\rho \cos^2 \theta, \quad [1]$$

where θ is the dihedral angle between the H—C_α—C_π and the C_α—C_π—$2p_\pi$ orbital planes, and ρ is the spin density on C_π.

Refinements of eq. [1] have been attempted by including a second parameter (13–15)

$$a_H = B_0 + B\rho \cos^2 \theta. \quad [2]$$

We derived (1) an equation of the form shown in eq. [2] which satisfactorily interpreted the observed couplings and conformational averaging for six-membered rings. It was found, not unexpectedly, that the derived equation could not be applied indiscriminately to different ring systems, because of substantial differences in unpaired spin density at the ketyl carbon in different rings.

In the discussion of the geometry of the wide range of ring sizes examined here it is preferable to use the simpler original McConnell equation because of uncertainty in the magnitude and signs (15) of the parameters required by eq. [2]. This approach, requiring the minimum of assumptions, has been employed recently in a discussion of the geometry of alicyclic semiquinones (16).

A value of B = 58.5 Oe derived from the $CH_3CH_2\cdot$ radical is used, and substitution in two equations of the type shown in eq. [1] for the two observed couplings (related by $\theta_{equat.\ H} = \theta_{axial\ H} + 120°$ for tetrahedral alpha carbon) allows derivation of the values for the angles and spin density shown in Table II.

The solution of equations of the type shown in eq. [2] lead to two values of $B\rho$ and of θ (except where $\cos^2 \theta_{equat.\ H} = 0$). In accordance with previous practice (16), unrealistic solutions ($B\rho > 58.5/2$) have not been listed.

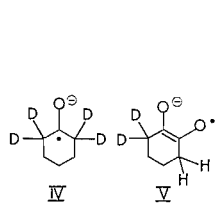

IV V

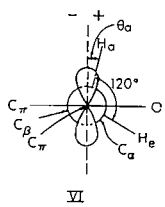

VI

The relationship of the dihedral angles considered is illustrated in VI. This type of analysis could not be carried out on the cyclodecyl ketyl at −35°, or the cyclododecyl ketyl at −32°, since coupling from only two protons was observed in both these cases. Therefore it is impossible to decide if these couplings arise from protons on the same carbon or not, and the relationship $\theta_{equat.\ H} = \theta_{axial\ H} + 120°$ cannot be applied in these cases.

Can. J. Chem. Downloaded from www.nrcresearchpress.com by 210.87.254.5 on 09/05/12
For personal use only.

Can. J. Chem. Downloaded from www.nrcresearchpress.com by 210.87.254.5 on 09/05/12
For personal use only.

TABLE II

Conformation of cycloalkyl ketyls*

Ketyl radical anion	Temp. (°C)	Hyperfine coupling ($a_{\text{axial H}}$ (Oe))† Axial	Equatorial	$\theta_{\text{axial H}}$	$B\rho$	ρ‡	$\theta_{\text{axial H}}$§	$B\rho$§	ρ§
Cyclohexyl	+20	10.40 (4)		+34°	15.0	0.25	(+43°)	13.8	0.24
	−96‖	14.20 (2)	6.90 (2)	+13°	15.0	0.25			
4-Methylcyclohexyl	+60	13.20 (2)	7.60 (2)	+17°	14.4	0.25			
3-Methylcyclohexyl	+58	13.20 (2)	7.60 (2)	+17°	14.4	0.25			
Cycloheptyl	+51	7.02 (2)	2.08 (2)	+3° or −50°	7.04 or 17.2	0.12 or 0.29	+3° or −50°	6.7 or 16.7	0.11 or 0.29
Cyclooctyl	+26	3.45 (4)		+31° or −60°	4.77 or 13.4	0.08 or 0.23	+30° or −60°	4.4 or 13.3	0.08 or 0.23
	−35	4.47 (3)	2.35 (1)	+15° or −55°	4.77 or 13.4	0.08 or 0.23			
Cyclodecyl	−35	10.78 (1) 6.30 (1)		¶					
	+84	8.52 (2)	~0 (2)	−30°	11.4	0.19	−30°	11.1	0.19
Clododecyl	−32	11.02 (1) 7.30 (4)		¶					
	+61	9.27 (2)					−30°	10.5	0.18
	+87	9.02 (2)	1.63 (2)	+5° or −47°	9.11 or 19.3	0.16 or 0.33			

*Except where otherwise stated, the solvent was 1,2-dimethoxyethane.
†The number of equivalent protons is shown in parentheses in each case.
‡B = 58.5 Oe.
§Values for the cycloalkanedione radical anions (see ref. 16) in dimethylsulfoxide (80%) – *tert*-butyl alcohol (20%) at room temperature.
‖Solvent was dimethoxymethane.
¶Angles cannot be assigned; see text.

However, since further resolution is obtained at higher temperatures, as has been noted, values for dihedral angles and parameters $B\rho$ and ρ could be obtained.

The results obtained are in good general agreement with the studies reported on the cycloalkyldione radical anions (16), which were, however, restricted to observations at room temperature. The close parallel with these latter results, also tabulated in Table II for comparison, necessitates a proof of the structure of our cycloalkyl ketyls to eliminate the possibility that our method of generation inadvertently has produced the cycloalkyldione radical anions. 2,2,6,6-Tetradeuteriocyclohexanone was prepared and treated with potassium in 1,2-dimethoxyethane, and the e.p.r. spectrum is shown in Fig. 1C. If oxidation to the radical anion V accounted for the signal, one would anticipate a nine-line spectrum similar to that shown in Fig. 1E. The much closer resemblance to that predicted for IV in Fig. 1D confirms the structure of the ketyls.

Some exchange of the deuterium is to be anticipated under the strongly basic conditions used to generate the ketyl, thereby accounting for the weak outer lines caused by traces of partially exchanged ketyl. The reduction in hyperfine coupling on deuteration equals the theoretically predicted value of 6.5.

In view of the complexity of the possible conformational forms of the medium-sized ring (3–5), it is idle to speculate about the actual shapes at this stage. An examination of the behavior of suitably substituted ketyls could, however, be expected to yield more precise information about ring geometry. Work along these lines is continuing.

In principle, it is possible to deduce conformational energy barriers from a consideration of line broadening of the e.p.r. spectra of the ketyls at different temperatures. This is very similar to problems encountered in the theory of nuclear resonance line widths when the environment of the nucleus is undergoing rapid fluctuations which change the resonance frequency. Such treatments based on the Bloch equations are commonly used (17–20). The same principles apply to e.p.r. line-width phenomena, and a theory accounting for the alternation in line widths as a result of rapid isomerization effects in the e.p.r. of radicals has been described (9). It is hoped that a computer program based on this theory will allow the derivation of energy barrier values by a comparison of observed and predicted e.p.r. line shapes.

EXPERIMENTAL

Materials

All liquid ketones, which were commercially available, were fractionated and gave single peaks on gas–liquid chromatographic analysis. The solvents used, 1,2-dimethoxyethane, dimethoxymethane, and bis-(2-methoxyethyl) ether, were refluxed over sodium metal for 12 h and fractionated.

The procedures used for the generation of the ketyls, and the recording and calibration of their e.p.r. spectra, have been described previously (1).

Temperature Control and Measurements

The temperature of the samples in the V-4532 dual cavity was controlled by passing cold dry nitrogen gas through the temperature variable unit of the Varian V-2503 spectrometer. The temperature inside the sample cavity was measured with a copper constantan thermocouple with the reference junction cooled to 0 °C. Temperature readings are estimated to have an accuracy of ±2°.

2,2,6,6-Tetradeuteriocyclohexanone

A solution of 5.06 g of cyclohexanone and 0.333 g of anhydrous potassium carbonate in 7 ml of 99.7% deuterium oxide and 10 ml of sodium-dried dioxane was refluxed for 12 h, cooled, and extracted with light petroleum (b.p. 30–60°). The extract was evaporated to a small volume *in vacuo* and the residual oil subjected to a second similar exchange. The 2,2,6,6-tetradeuteriocyclohexanone was isolated by extraction with light petroleum and fractionation *in vacuo* (b.p. 55° at 20 mm), yield 4.3 g. The nuclear magnetic resonance spectrum of the product showed removal of a band at 7.5 to 7.9 τ characteristic of the four protons alpha to the carbonyl group, with the required reduction in intensity.

The corresponding ketyl was generated with clean potassium and freshly dried, distilled 1,2-dimethoxyethane, and the e.p.r. spectrum was examined as rapidly as possible to minimize exchange.

Can. J. Chem. Downloaded from www.nrcresearchpress.com by 210.87.254.5 on 09/05/12
For personal use only.

REFERENCES

1. J. W. LOWN. Can. J. Chem. **43**, 2571 (1965).
2. C. HELLER and H. M. MCCONNELL. J. Chem. Phys. **32**, 1535 (1960).
3. J. B. HENDRICKSON. J. Am. Chem. Soc. **83**, 4537 (1961).
4. J. B. HENDRICKSON. J. Am. Chem. Soc. **84**, 3355 (1962).
5. J. B. HENDRICKSON. J. Am. Chem. Soc. **86**, 4854 (1964).
6. J. D. DUNITZ and V. PRELOG. Angew. Chem. **72**, 896 (1960).
7. H. C. BROWN and K. ICHIKAWA. Tetrahedron, **1**, 221 (1957).
8. R. A. RAPHAEL. Proc. Chem. Soc. 97 (1962).
9. A. CARRINGTON. Mol. Phys. **5**, 425 (1962).
10. F. C. ADAM and S. I. WEISSMAN. J. Am. Chem. Soc. **80**, 1518 (1958).
11. E. L. ELIEL, N. L. ALLINGER, S. J. ANGYAL, and G. A. MORRISON. Conformational analysis. Interscience Publishers, Inc., New York. 1965. p. 210.
12. J. R. ROBERTS. R. B. Sandin Lectures delivered at the Department of Chemistry, University of Alberta, Edmonton, June 28–30, 1965.
13. W. T. DIXON and R. O. C. NORMAN. J. Chem. Soc. 4850 (1964).
14. A. HORSFIELD, J. R. MORTON, and D. H. WHIFFEN. Mol. Phys. **4**, 425 (1961).
15. M. C. R. SYMONS. Advan. Phys. Org. Chem. **1**, 284 (1963).
16. G. A. RUSSELL and E. T. STROM. J. Am. Chem. Soc. **86**, 744 (1964).
17. H. S. GUTOWSKY, D. W. MCCALL, and C. P. SLICHTER. J. Chem. Phys. **21**, 279 (1953).
18. H. M. MCCONNELL. J. Chem. Phys. **28**, 430 (1958).
19. E. GRUNWALD, A. LOEWENSTEIN, and S. MEIBOOM. J. Chem. Phys. **27**, 630 (1957).
20. A. LOEWENSTEIN and S. MEIBOOM. J. Chem. Phys. **27**, 1067 (1957).

Can. J. Chem. Downloaded from www.nrcresearchpress.com by 210.87.254.5 on 09/05/12
For personal use only.

Can. J. Chem. Downloaded from www.nrcresearchpress.com by 210.87.254.6 on 09/05/12
For personal use only.

THE DEPENDENCE OF CONCENTRATION GRADIENT ON CURRENT DENSITY AT WORKING ELECTRODES

R. N. O'Brien,[1] C. A. Rosenfield,[2] K. Kinoshita,[3] W. F. Yakymyshyn,[4] and J. Leja[5]
Inorganic Materials Research Division, University of California, Berkeley, California
Received May 11, 1965

ABSTRACT

An interferometric study of working electrodes in a cell holding less than 1 ml of solution enabled the effects of cell depth, orientation, electrolyte concentration, and temperature on the concentration gradient to be evaluated. The concentration gradient (obtained from the perturbations of a parallel fringe pattern) is an error function of current density, but every factor studied produced deviation from this relationship. The electrodeposition of the following ions has been studied: Cu^{++}, Zn^{++}, Ni^{++}, Ag^{+}, in a wide variety of electrolytes.

INTRODUCTION

There are two optical techniques which give *directly* the concentration gradient in the electrolyte at working electrodes, with no disturbing perturbation. Schlieren optical techniques (1) give a solution density contour which depends in a complicated way on the local refractive index gradient; however, it must be noted that the density of the photographic image used in the evaluation of concentration gradient is also dependent on the photographic technique.

The other technique is interferometry for which the mathematical treatment giving the location of fringes as a function of path length difference, wavelength, and refractive index is well established. The quantitative method of conversion of fringe shift to concentration change, with some examples, has been published (2, 3). An attempt to calculate complete concentration contours has also been made (4).

When electrolysis conditions are ideal, the concentration change (encountered perpendicular to the faces of parallel horizontal electrodes in the cathode-over-anode orientation) follows the expression found by integrating the differential equation $\partial c/\partial x = D(\partial^2 c/\partial x^2)$ (Fick's second law of diffusion) between appropriate boundary conditions. The expression

$$\Delta C(x, t) = \frac{2\sqrt{(Dt/l^2)}\, Ilt_-}{nFD}\ \text{ierfc}\ \frac{(1-x)/l}{2\sqrt{(Dt/l^2)}}$$

is the solution of this equation and has been found to fit recorded interferograms (4). In this expression ΔC is the change in concentration at any point at any time, D is the molar diffusion coefficient, t is time in seconds, l is 1/2 the distance between the two electrodes, I is the current density, t_- is the anion transference number (since the electroactive species is the cation in these cases) and ierfc is the complement of the integrated error function (4). Every variable considered here influences the fringes (which are concentration contours) so that the above expression does not predict the concentration gradient under normal, nonideal conditions.

[1]*Chemistry Department, University of Alberta, on leave to the Inorganic Materials Research Division of the Lawrence Radiation Laboratory, University of California, Berkeley, California.*
[2]*Dow Chemical Company, Midland, Michigan.*
[3]*College of Chemistry, University of California, Berkeley, California.*
[4]*Canadian Chemicals Limited, Edmonton, Alberta, Canada.*
[5]*Department of Mining and Metallurgy, University of Alberta, on leave to Metallurgy Department, University of California, Berkeley, California.*

EXPERIMENTAL

Figure 1 gives an exploded view of one modification of a microcell formed by the parallel faces of the metallic half-discs (electrodes), which in turn are contained between two optical flats, clamped in a holder to give a slight wedge with its axis parallel to the length of the cell. The concentration polarization was always recorded photographically, either by still or motion picture camera, as perturbations to a system of parallel, equi-spaced, wedge-type fringes oriented at 90° to the working faces of the electrodes.

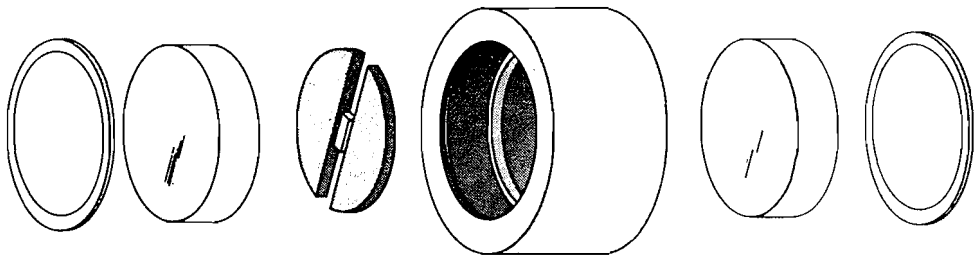

FIG. 1. The cell, exploded view, without the thermostating clamp.

When the cell is oriented in such a way that the working face of the electrode is vertical, natural convection always sets in once a certain current density (c.d.) (about 0.3 mA/cm²) is exceeded; about 15 s after the start of electrolysis its effects become noticeable. Since a quasi-steady-state is established in about 1 min, 3 min or more of electrolysis was allowed before recording any interferogram with a still camera. The concentration polarization was evaluated in two ways. In the first, a value of the concentration gradient which should be very little affected by convection was found by taking the slope of the fringes as close to the electrode as the optical resolution of the instrument would allow and converting this to $\partial c/\partial x$ (where x is the distance in cm measured perpendicularly to the electrode and c is concentration in moles/l). In the second, the total concentration change at an electrode may be found by noting the total displacement of any typical individual fringe (at vertical electrodes, except when they are closer than about 0.75 mm, there always remains a central portion uneffected by concentration changes which may be used as a reference). A knowledge of refractive index change with concentration of the electroactive species and of some cell parameters is required for this method (2).

When the electrode working faces are *horizontal* two distinctly different modes of transport of charge exist. If the anode is above the cathode, although there is always a diffusion layer, convection is the main transport mechanism; moreover it is turbulent convection with consequent unpredictably deep penetrations into the diffusion layer. Although the process is an interesting one and has been investigated it will be mentioned only briefly when the effect of orientation is discussed.

When the cathode is over the anode, diffusion is the principal transport mechanism and no steady-state develops until the gradient extends completely across the cell, but the gradient $\partial c/\partial x$ does not change appreciably during the process and this has been used as a usefully accurate parameter in comparison with vertical electrodes. Interferograms in this orientation were usually recorded with a motion picture camera.

Monochromatic collimated light (either the Na_D line or a continuous, uniphase output C.W. gas laser giving a wavelength of 6 328 Å) is passed through the cell. The coatings on the flats split the amplitude forming two beams (Fig. 2), one passing through, the other reflected back and forth until coherent, parallel, superimposed beams emerge and interfere to produce wedge fringes or fringes of equal thickness. Fringes, light or dark, appear at those places on the wedge where the thickness of the wedge is an integral number of half wavelengths; or, if the refractive index of a solution is varying, at $n\lambda = 2\mu l \cos\phi$. λ is the wavelength,

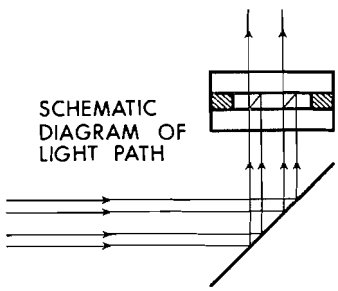

FIG. 2. Schematic diagram of the light path showing how the coated flats split the amplitude of the collimated light into two beams that interfere. No further optics are needed except a recording camera.

Can. J. Chem. Downloaded from www.nrcresearchpress.com by 210.87.254.6 on 09/05/12
For personal use only.

n is an integer known as the order of interference, μ the refractive index, t the thickness, ϕ the angle of incidence of the light with $\cos\phi = 1$ usually. The necessary wedge angle was produced by tightening screws in a massive brass clamp. The clamp was drilled appropriately to act as a thermostat and achieved a constant temperature to ± 0.1 °C. The principal cell used was $Cu/CuSO_4/Cu$ and all data reported pertain to it except where noted. The metals Cu, Zn, Ag, and Ni were of highest purity and polycrystalline. Electrodes were first cut out as discs polished flat on 400 or finer emery paper; then the discs were halved and the edges polished. The halved discs were washed in distilled water, immersed in an appropriate acid until the grain boundaries were visible, then washed again in distilled water, dried, and quickly assembled into the cell with a minimum of handling. When precautions were taken to eliminate contamination, no noticeable differences were observed; a trial run, in which all parts of the cell and all auxiliary vessels (which the electrolyte comes in contact with) were refluxed in a soxlet extractor with acetone and handled only with rubber gloves, showed no variation in specific conductivity. It is thought that this lack of sensitivity to purification procedures is due to the high electrode surface – electrolyte volume ratio, about 2 cm^2 and 0.2 ml (compared to 10 cm^2 and 200 ml in the usual cells, i.e. a ratio about 200 times greater).

A variety of cameras have been used. The basic requirement is that the lens opening be of a diameter 2 to 3 times greater than the distance between the electrodes. It is also desirable to have the best optics and the possibility of taking several pictures in quick succession. A 16 mm motion picture camera has been used successfully (4, 5).

All electrolyte solutions were made with highest purity reagents and conductivity water, and their concentrations were checked by appropriate titrations.

A large body of auxiliary information (6) such as refractive indices, (for a variety of ions in water at various pH's, concentrations, and temperatures) trial runs in different solvents (alcohols) and with different anions, etc. has been collected. Some work has also been done on the dependence of refractive index on frequency.

The interferograms (several thousands of them) have been measured using a variety of devices, such as a mm graticule, photographic prints, and a light box; then by draughting instruments after projection onto a ground-glass-topped table. A travelling photosensitive cell has been used but found to be unsatisfactory. A digitalized measuring microscope which produces five significant figure measurements on computer cards is the most recent system used.

RESULTS

The Effect of Current Density and Concentration

Figures 3 and 4 show total concentration change in the diffusion layer at various current densities and concentrations in the cell $Cu/CuSO_4/Cu$ with shallow (1.92 mm) vertical electrodes for the anode and the cathode. A wide range of concentrations of electrolyte was used. Precipitation of copper sulfate crystals was observed in the saturated solution at the anode; in Fig. 4 the vertical straight line at 1 g/l concentration change for the 1 g/l solution shows that no secondary reaction is occurring. No bubbles were observed in this solution at the cathode but some optical effects interpreted as increased convection velocity were noted.

The Effect of Depth of Cell with Vertical Electrodes

Since Ibl (7) has shown that the velocity of the electrolyte in a convective whorl is proportional to the 3/5 power of the height of the electrode and the 2/5 power of the current density, one would expect that both the depth of the cell and the current density would have some effect on the maximum concentration polarization attained for a set of given conditions.

Figure 5 shows the effect of depth (height) of electrodes. The best-fit curve to all points is drawn but the shallower electrodes have the least total concentration change per unit current density (c.d.). This slight influence of depth of solution will again be pointed out when plots of $\partial c/\partial x$ vs c.d. are considered. It has been shown that it is the height of the electrode not the depth of the electrolyte that controls the convective effects (8).

Effect of Temperature

Figure 6 shows the effect of temperature on concentration change at constant current density. The total concentration developed according to Keulegan (9) and others is

$$\frac{\partial n_j}{\partial t} = AD_j \frac{\partial c_j}{\partial x} + AU_j C_j Z_j e \frac{\partial v}{\partial x}$$

Can. J. Chem. Downloaded from www.nrcresearchpress.com by 210.87.254.6 on 09/05/12
For personal use only.

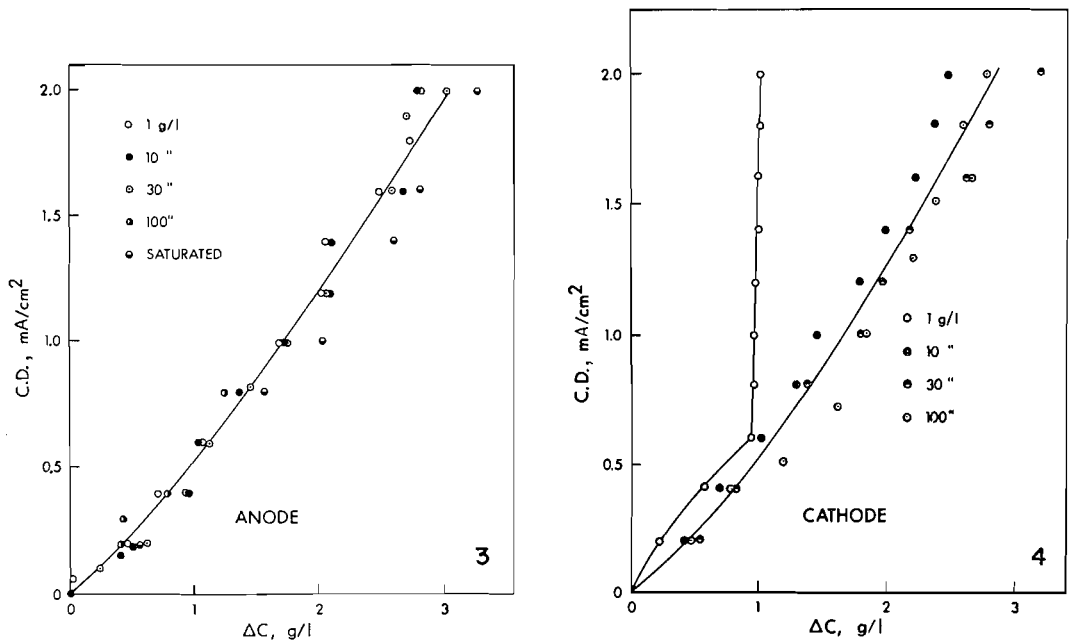

FIG. 3. Dependence of total concentration change on current density at various concentrations in the system $Cu/CuSO_4/Cu$ at 7.5 °C at the anode.
FIG. 4. Dependence of total concentration change on current density at various concentrations in the system $Cu/CuSO_4/Cu$ at 7.5 °C at the cathode.

where $\partial n_j/\partial t$ is the number of ions of the jth kind passing a cross-sectional reference frame per second, A is the reference frame area, D is the Fick diffusion constant, C the concentration, U the mobility of the ion, Z its valence, V the applied potential, and X the distance perpendicular to the electrode. The second term describes the effect of electromigration.

Only the diffusion constant and the mobility should be affected by temperature. The mobility and the diffusivity are connected through the Einstein relation $D = UkT$ where k is Boltzmann's constant and T is the absolute temperature. Thus only the diffusion coefficient need be considered. If the Einstein–Stokes equation is valid for the system then $D = kT/6\pi\eta r$ where η is the viscosity and r the effective radius of the hydrated ion. Both η and r should be affected by temperature exponentially; r in an unpredictable, exponential way.

The curves obtained are obviously a family of curves but they are not simple exponentials.

The Effect of Electrode Orientation

The orientation of the electrodes in the earth's gravitational field determines the dominant transport (3) process type. In all orientations electromigration occurs, but in the a/c (horizontal, anode above cathode) position only a small amount of transport of charge occurs by diffusion, whereas convection of a turbulent nature accounts for most, as illustrated in the interferogram in Fig. 7*a*. In the cathode over anode (c/a) position convection is absent and diffusion is the dominant process (Fig. 7*b*).

Hydrodynamic theory postulates a stationary film at the electrode surface of sufficient thickness to be observed interferometrically. On the strength of this, it is generally assumed that convection-perturbed systems should have a film next to the electrode where the

Can. J. Chem. Downloaded from www.nrcresearchpress.com by 210.87.254.6 on 09/05/12
For personal use only.

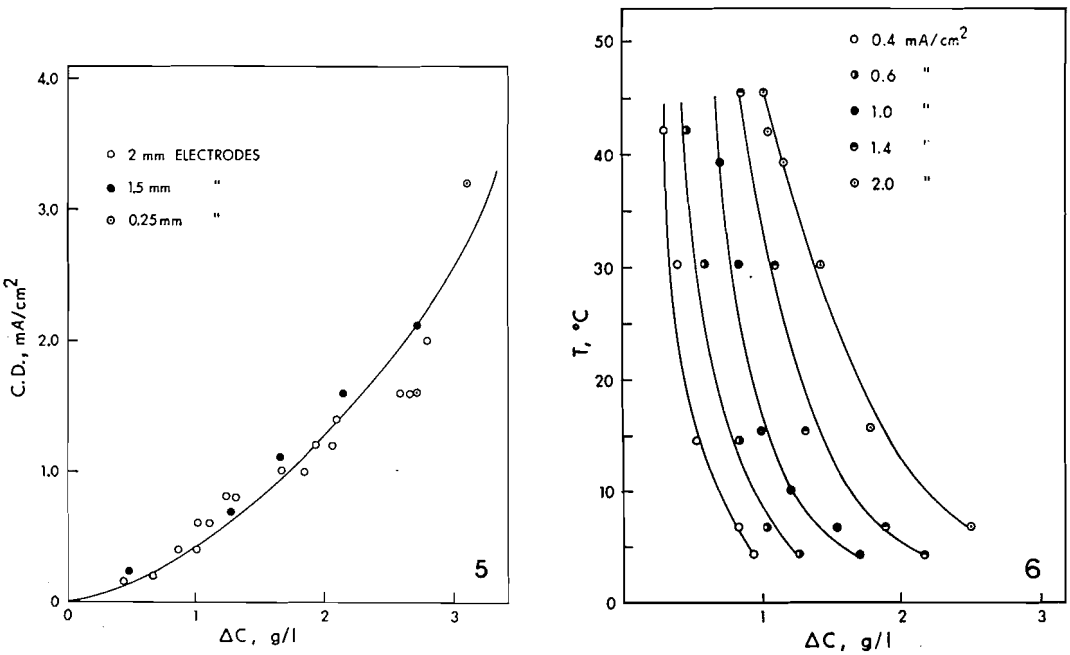

FIG. 5. The effect of depth in shallow vertical electrodes on total concentration change ($Cu/CuSO_4/Cu$ system) at 7.5 °C at the anode.

FIG. 6. The effect of temperature on total concentration change at constant current density ($Cu/CuSO_4/Cu$).

concentration gradient $(\partial c/\partial x)_{x=0}$ should approximate that of a convectionless system, and hence the gradient at $x = 0$ should be independent of electrode orientation. Figure 7 shows that this is not true. Thermodynamically, since $\partial \Delta G/\partial x$ (in each orientation at the same current density) is different for $x = 0$, the concentration gradient at $x = 0$ should also be different. This effect and others which occur close to electrodes has been extensively studied (13).

Figure 8 shows $\partial c/\partial x$ for various c.d.'s in 0.1 N $CuSO_4$, anode and cathode. The relationships are shown for two vertical electrode depths 2 mm (s.v.), shallow vertical, and 38 mm (d.v.), deep vertical, and also for the cathode over anode position. The nearly straight line of the 38 mm deep vertical electrodes suggests that considerable depth of electrode makes for less complicated concentration contour slopes. It also prevents large pH changes at the electrodes as the c.d. and time of electrolysis are increased.

Cell Geometry

A proper design of the cell ensures minimum pH change between the two electrodes (10). It has been observed in this laboratory that when the electrodes are separated by a distance which is more than about 1/3 of the height of the electrode, two convective whorls (with overflow and underflow) (3) tend to form; this appears to be the most efficient configuration to minimize pH gradients at the electrodes. Significantly, such a configuration does not yield the highest c.d. per applied voltage (11). A systematic investigation now underway suggests that whenever there is no chemical reaction either in solution or at the electrode, pH changes do not affect the dependence of concentration change on c.d. (12). Similarly the addition of inert salt as supporting electrolyte has little effect (6).

Can. J. Chem. Downloaded from www.nrcresearchpress.com by 210.87.254.6 on 09/05/12
For personal use only.

Can. J. Chem. Downloaded from www.nrcresearchpress.com by 210.87.254.6 on 09/05/12
For personal use only.

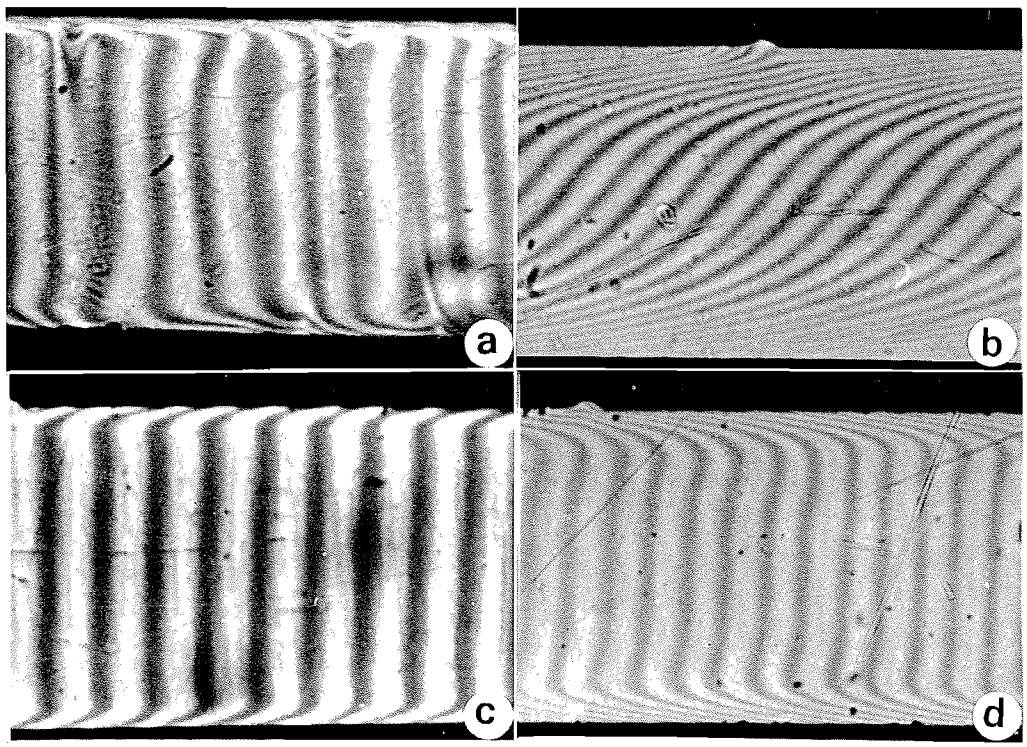

FIG. 7. Interferograms showing the effect of electrode orientation. The orientations are (*a*) horizontal, anode-over-cathode (a/c); (*b*) horizontal, cathode-over-anode (c/a); (*c*) shallow vertical (s.v.), 0.2 cm deep; (*d*) deep vertical (d.v.), 3.8 cm deep, 25 °C.

Can. J. Chem. Downloaded from www.nrcresearchpress.com by 210.87.254.6 on 09/05/12
For personal use only.

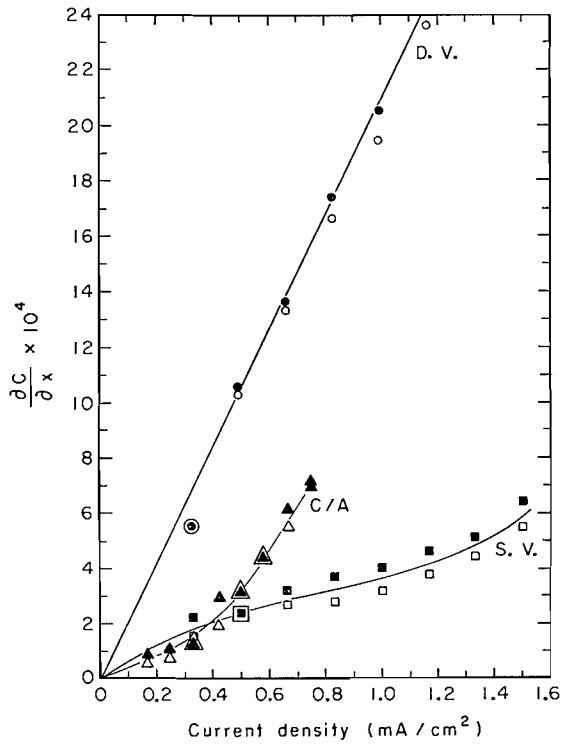

FIG. 8. The effect of electrode orientation on the concentration gradient, for $Cu/CuSO_4/Cu$. The open symbols are anode values, the solid symbols cathode values, 25 °C, 0.1 *N* $CuSO_4$.

Concentration Change with Current Density in Other Electrolyte Systems

Exploratory work in Fe^{3+}/Fe^{2+} solution, Ag^+, Ni^{2+}, and Zn^{2+} suggests that the same general dependence of concentration polarization on current density obtains in other systems.

In the case of the $Zn/ZnSO_4/Zn$ system (3*a*) the deep vertical electrodes gave $\partial c/\partial x$ values nearly identical with the c/a values, whereas the values for the shallow vertical electrodes coincided with those for $Cu/CuSO_4/Cu$ (Fig. 8).

Some exploratory work, carried out in buffered and chelated solutions, suggests that there are no general qualitative variations in results.

CONCLUSIONS

Although the results show that the concentration gradient at an electrode is proportional to the c.d., the proportionality factor depends on practically every conceivable variable; accordingly, if $\partial c/\partial x$ or just ΔC is to be used as a measure of the c.d., a calibration curve must first be obtained. When all variables are kept constant except for the electrochemical activity of the various portions of the electrode surface, then, from the average c.d., the true local c.d. can be obtained.

ACKNOWLEDGMENTS

The authors wish to acknowledge the partial support of this project by the National Research Council of Canada, the Defense Research Board of Canada, and the Inorganic Materials Research Division of the Lawrence Radiation Laboratory of the University of California.

Can. J. Chem. Downloaded from www.nrcresearchpress.com by 210.87.254.6 on 09/05/12
For personal use only.

REFERENCES

1. R. S. COOPER. J. Electrochem. Soc. **105**, 506 (1958).
2. R. N. O'BRIEN. Rev. Sci. Instr. **35**, 803 (1964).
3. (*a*) R. N. O'BRIEN, W. F. YAKYMYSHYN, and J. LEJA. J. Electrochem. Soc. **110**, 820 (1963). (*b*) R. G. HICKMAN. Ph.D. Thesis, University of California, Berkeley, California. 1958.
4. R. N. O'BRIEN. J. Electrochem. Soc. In press.
5. R. N. O'BRIEN. J. Electrochem. Soc. **111**, 1300 (1964).
6. W. F. YAKYMYSHYN. M.Sc. Thesis, University of Alberta, Edmonton, Alberta. 1962. C. A. ROSENFIELD. Ph.D. Thesis, University of Alberta, Edmonton, Alberta. 1960. R. N. O'BRIEN. To be published.
7. N. IBL and R. MULLER. J. Electrochem. Soc. **105**, 346 (1958).
8. (*a*) R. N. O'BRIEN and L. M. MUKHERJEE. J. Electrochem. Soc. **111**, 1358 (1964). (*b*) C. R. WILKE, M. EISENBERG, and C. W. TOBIAS. J. Electrochem. Soc. **100**, 513 (1953).
9. G. H. KEULEGAN. J. Res. Nat. Bur. Std. **47**, 156 (1951).
10. M. N. POLUKARPOV. Zh. Obshch. Khim. **18**, 1249 (1958).
11. R. N. O'BRIEN and C. ROSENFIELD. Nature, **187**, 935 (1960). R. N. O'BRIEN. Nature, **201**, 74 (1964).
12. R. N. O'BRIEN and K. KINOSHITA. To be published.
13. R. N. O'BRIEN and K. KINOSHITA. J. Electrochem. Soc. In press.

Can. J. Chem. Downloaded from www.nrcresearchpress.com by 210.87.254.6 on 09/05/12
For personal use only.

Can. J. Chem. Downloaded from www.nrcresearchpress.com by 210.87.254.6 on 09/05/12
For personal use only.

DESERT PLANT CONSTITUENTS

II.[1] OCOTILLOL: AN INTERMEDIATE IN THE OXIDATION OF HYDROXY ISOÖCTENYL SIDE CHAINS[1]

E. W. WARNHOFF[2] AND C. M. M. HALLS
Department of Chemistry, University of Western Ontario, London, Ontario
Received July 20, 1965

ABSTRACT

Ocotillol, $C_{30}H_{52}O_3$, a triterpene isolated from *Fouquieria splendens* Engelm., has been found to have structure I containing a new side chain modification. Confirmation was provided by a partial synthesis from dammarenediol-II monoacetate VII*a*. Ocotillol has been found to be an intermediate in one path for the chromic acid oxidation of the hydroxy isoöctenyl side chain XVI, a common feature of several triterpenes, to the tris nor γ-lactone XIX.

In parts of the Sonoran Desert of southwestern North America the most conspicuous form of vegetation is the ocotillo (2).[3] This singular plant (*Fouquieria splendens* Engelm.) (Fig. 1) belongs to a small family (Fouquieriaceae) which has not previously been investigated chemically.[4] Its long branches are covered with a resinous bark and formidable spines. During the wet season the branches also bear leaves (Fig. 1*a*, 1*b*) which drop off at the onset of dry periods (Fig. 1*c*). However, even after the leaves have fallen, the plant is apparently able to synthesize food, for underneath the tough laminated bark there is a chlorophyll layer. Light which reaches this layer could only do so by passing through the translucent bark. Any organic compounds in this resinous bark have thus been subjected to intense desert sunlight for many years, and it would be suprising if some photochemical transformation products had not been formed during this long irradiation period. With the hope of finding such products, a chemical investigation of the plant was initiated.

Isolation and Determination of Structure

Continuous ether extraction of ocotillo bark gave 10% of clear amber resin which was a mixture of 10 or more compounds. Attempts to separate this mixture by alumina chromatography afforded small amounts of two crystalline compounds, m.p. 260.5° and m.p. 200°. Greater success was attained when the resin was first saponified with methanolic potassium hydroxide. When the base-insoluble saponification fraction (60% of the resin weight) was chromatographed on alumina, thin-layer chromatography (t.l.c.) indicated the presence of three major components. One of these (16% of the unsaponified resin) could be purified by recrystallization to give a new compound, ocotillol, $C_{30}H_{52}O_3$, m.p. 198–200°, $[\alpha]_D$ +28°, which was identical with the compound of m.p. 200° that was obtained from the unsaponified resin. However, ocotillol was more conveniently isolated by direct crystallization of its high-melting monoacetate from the acetylation product of the base-insoluble saponification fraction. The infrared spectrum of ocotillol showed the presence of hydroxyl absorption at 3 622 cm^{-1} (secondary OH) and 3 580 cm^{-1} (intramolecularly hydrogen-bonded OH) (5), but no carbonyl peaks. The ultraviolet spectrum

[1]*Part I is considered to be reference 1 in which a preliminary account of some of this work appeared. Presented in part at the 47th Annual Conference of the Chemical Institute of Canada, Kingston, June 1964.*
[2]*Fellow of the Alfred P. Sloan Foundation.*
[3]*Spanish diminutive derivative of the Nahuatl word ocotl, a certain species of pine tree.*
[4]*The results of two earlier general examinations are given in references 3 and 4.*

revealed a complete absence of double bonds, an uncommon feature which temporarily encouraged thoughts of a photochemically transformed triterpene. In agreement, the nuclear magnetic resonance (n.m.r.) spectrum had no vinyl hydrogen peaks, but did have two multiplets (1H each) at δ 3.73 and 3.18 p.p.m. from protons bonded to carbon atoms bearing oxygen functions. Of the eight methyl groups visible in the spectrum, three were at appreciably lower field (δ 1.12–1.21 p.p.m.) than the others. The only structural feature present that could be capable of such deshielding action was oxygen substitution on the carbon atoms bearing these methyl groups.

Reaction with acetic anhydride – pyridine at room temperature gave as the only product a monoacetate, $C_{32}H_{54}O_4$, m.p. 260–261.5°, which proved to be identical with the second crystalline compound from chromatography of the unsaponified resin. The infrared spectrum had an ester carbonyl peak at 1 734 cm^{-1} and only one hydroxyl peak at 3 580 cm^{-1} (intramolecularly hydrogen-bonded OH) (5). An acetate methyl peak appeared at δ 2.03 p.p.m. in the n.m.r. spectrum, and the H—C—O multiplet formerly at δ 3.18 p.p.m. was now shifted to δ 4.50 p.p.m., as expected of the hydrogen on a carbon atom bearing a secondary hydroxyl group (6). More vigorous reaction of the monoacetate with acetic anhydride – pyridine at reflux furnished a diacetate, $C_{34}H_{56}O_5$, which had no hydroxyl infrared absorption. Its n.m.r. spectrum had two acetate methyl peaks at δ 1.96 and 2.03 p.p.m. However, the H—C—O multiplet at δ 3.73 p.p.m. in ocotillol and ocotillol monoacetate had moved only to δ 3.95 p.p.m. Saponification of both acetates regenerated ocotillol. From the facts just presented, ocotillol must be a saturated tetracarbocyclic triterpene with a secondary hydroxyl group, an intramolecularly hydrogen-bonded tertiary hydroxyl group, and an oxide ring with a single hydrogen atom on an α-carbon.[5] The hydroxyl groups were not vicinal since ocotillol was unaffected by sodium metaperiodate.

Oxidation of ocotillol by chromium trioxide in acetic acid at room temperature produced acetone, isolated as the 2,4-dinitrophenylhydrazone, and a keto γ-lactone, $C_{27}H_{42}O_3$, m.p. 182.5–184.5°, $[\alpha]_D$ +71°, as the only products. In like manner ocotillol monoacetate was rapidly oxidized at room temperature with the consumption of 1.37 moles of chromium trioxide per mole of acetate. The only non-volatile product formed in almost quantitative yield was an acetate γ-lactone, $C_{29}H_{46}O_4$. These facile oxidations with loss of three carbon atoms were reminiscent of the oxidation of the dammarenediols VII*b* (7), dipterocarpol VI (8), folientriol (9), and methyl dammarenolate (10). In fact the physical constants for the keto lactone were the same as those reported, m.p. 183–185°, $[\alpha]_D$ +69° to +71°, by three different groups (7, 8, 11) for the keto lactone IV from dammarenediol-II (VII*b*). The methyl peaks in the n.m.r. spectra of the keto γ-lactone and the acetate γ-lactone also corresponded to those reported (12) for IV and V*a*. A direct comparison of the two pairs of compounds revealed them to be identical, thus establishing the structure of the fused ring system of ocotillol. The oxide ring and the other hydroxyl group of the molecule were therefore restricted to the side chain.

Of the four conceivable side chain formulations A, B, C, and D with oxygen at some or all of carbon atoms C-20, C-24, and C-25 as required by the chromic acid oxidation products, three of these can be eliminated. While there are reasonable mechanisms by

[5]*A triol formula, $C_{30}H_{54}O_3$, for ocotillol is not excluded by the analytical data, but it is excluded by the absence of hydroxyl absorption in the infrared spectrum of the diacetate as well as by the amount of chromium VI consumed on oxidation of the monoacetate to the acetate lactone; a triol would have required 2.00 moles of chromium trioxide per mole of monoacetate as compared with the 1.37 moles actually found. After this work was concluded, the mass spectrum of ocotillol was taken by Dr. G. Snatzke in connection with his work on gratiogenin. The molecular ion at m/e 460 confirmed the molecular formula.*

Can. J. Chem. Downloaded from www.nrcresearchpress.com by 210.87.254.6 on 09/05/12
For personal use only.

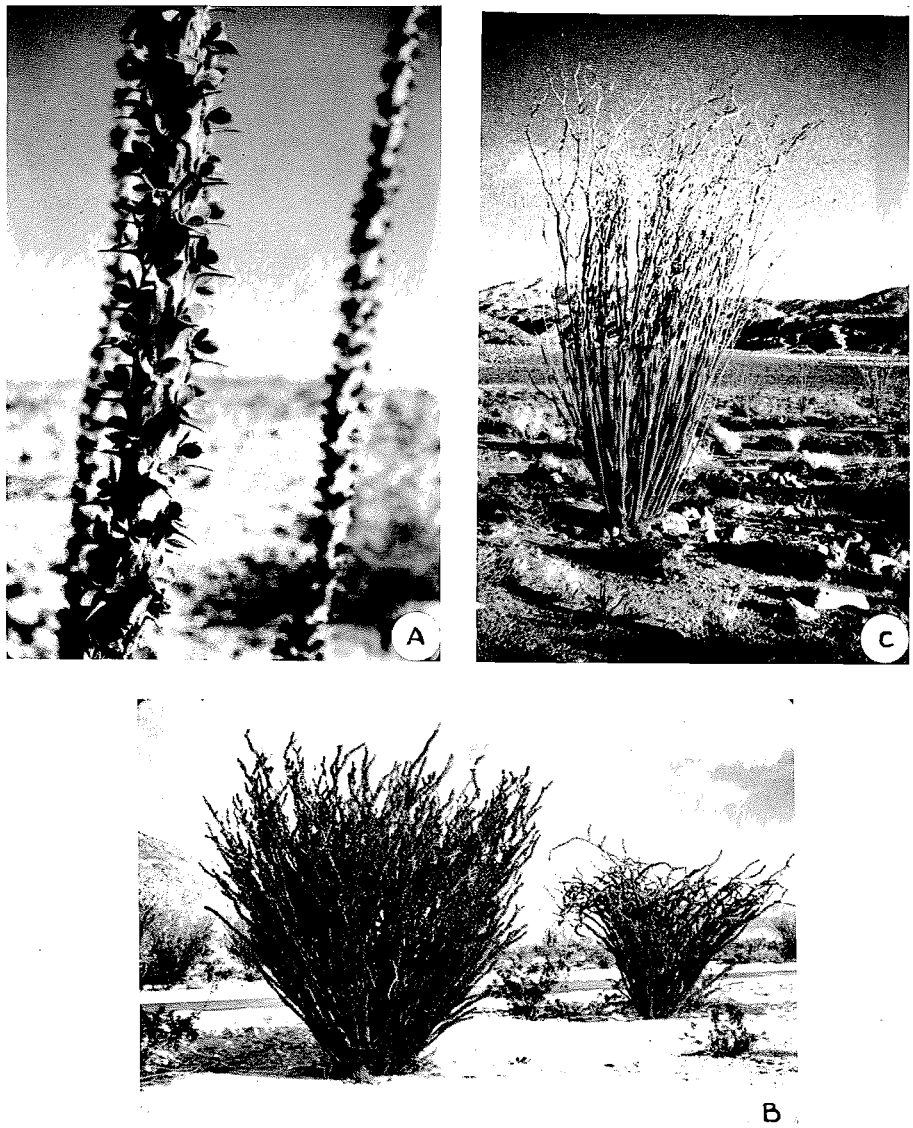

FIG. 1. Ocotillo (*Fouquieria splendens* Engelm.): (*a*) close up of branch, (*b*) in leaf, (*c*) in leafless dry stage.

Can. J. Chem. Downloaded from www.nrcresearchpress.com by 210.87.254.6 on 09/05/12
For personal use only.

Can. J. Chem. Downloaded from www.nrcresearchpress.com by 210.87.254.6 on 09/05/12
For personal use only.

Can. J. Chem. Downloaded from www.nrcresearchpress.com by 210.87.254.6 on 09/05/12
For personal use only.

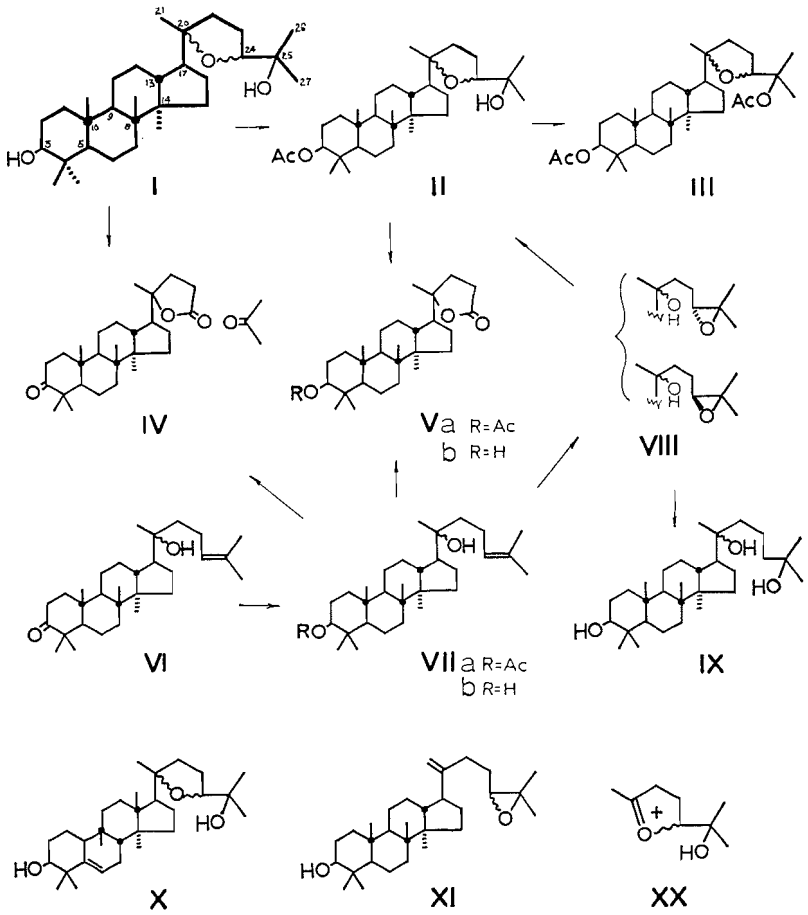

which each could be oxidized in acid solution to a γ-lactone and acetone with the consumption of 1.33 moles of chromium^{VI} per mole of compound, only A is consistent with *all* of the following observations: ocotillol (*a*) forms only a monoacetate at room temperature, (*b*) has three CH_3—C—O and two H—C—O groups, (*c*) is unchanged by anhydrous hydrogen chloride at room temperature, (*d*) is not affected by boiling methanolic potassium hydroxide, (*e*) is recovered from reflux with lithium aluminium hydride in ether or dioxane, and (*f*) is not oxidized by the chromium trioxide – pyridine reagent after monoacetylation. If ocotillol had a tetrahydropyran side chain B, (i) it would have formed the diacetate at room temperature, (ii) *both* H—C—O groups would have been strongly shifted to lower field in the n.m.r. spectrum of the diacetate, and (iii) ocotillol acetate would have been oxidized to a keto acetate by the chromic acid – pyridine reagent since the closely related linalool derivative XV is oxidized to a ketone by this reagent (13, 14).

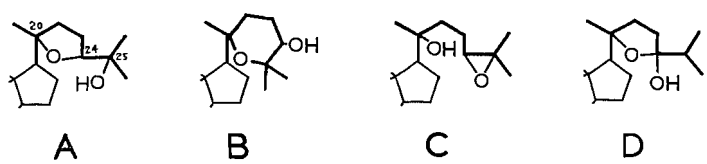

Therefore, ocotillol has the structure I, its monoacetate formula II, and the diacetate formula III. When this structure was originally proposed (1), the hydroxy tetrahydrofuran appendage was a new terpenoid side chain modification. At about the same time it was recognized in gratiogenin X (15).[6]

Partial Synthesis

The structure I banished consideration of a photochemical origin for ocotillol and suggested that it was probably formed in the plant from a dammarenediol derivative by the biogenetic equivalent of 1,2-epoxidation at C_{24}=C_{25} with subsequent oxide opening at C-24 by the C-20 hydroxyl group. This possibility was later rendered more likely by the discovery in Thailand of a closely related naturally occurring C_{24}—C_{25} oxide, aglaiol XI (16). Although oxide ring opening might occur at C-25, particularly in acid medium, five-membered rings are usually formed more rapidly than six-membered rings. Moreover, there is an excellent analogy for this course of events in the careful work on the so-called linalool oxide (13). Oxidation of R(—) linalool XII with one equivalent of monoperphthalic acid gives as the *primary* product a pair of very sensitive diastereoisomeric 1,2-epoxides XIII and not a mixture of two pairs of diastereoisomeric 1,4- and 1,5-oxides XIV and XV as previously claimed (17). The 1,2-epoxides XIII are very easily converted by acid or heat into a mixture of XIV and XV in the ratio of about 9:1, respectively, the five-membered ring being formed more rapidly even in acidic medium. Consequently, a partial synthesis of ocotillol monoacetate from dammarenediol-II monoacetate VII*a* was undertaken to confirm the structure I.

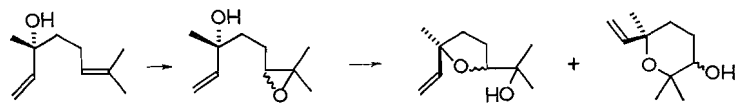

XII XIII XIV XV

Oxidation of VII*a* under the conditions that produced the true linalool oxide XIII did not permit isolation of the C_{24}—C_{25} epoxides VIII, which are apparently even more easily opened than XIII. Attempts to prepare VIII at lower temperatures or in solution buffered with triethylamine oxide were also unsuccessful. The presence of some 1,2-epoxide could be detected by t.l.c. and was further corroborated by dividing one oxidation product into two fractions, one of which was heated to 100° and the other reduced with lithium aluminium hydride. The thin-layer spot presumed to be epoxides VIII had disappeared in the heated portion with intensification of the spot corresponding to ocotillol monoacetate II, whereas the hydride reduction product contained a new component much more polar than dammarenediol-II (VII*b*) or ocotillol I, which could reasonably be only the triol IX. However, if the epoxidation of VII*a* was allowed to go to completion and worked up as usual, the product gave a single spot corresponding to II on t.l.c. Ocotillol monoacetate was crystallized directly from this product in 35% yield and shown to be identical with the natural material.

The optical rotation and n.m.r. spectrum of the residue from the filtrate betrayed the presence of a second component as well as of II in about equal amounts. From the n.m.r. spectrum and the single t.l.c. spot, the second compound is most probably the C-24 epimer of ocotillol monoacetate, but attempts to crystallize or separate it by chromatography were unsuccessful.

[6]*Dr. Snatzke has informed us that both gratiogenin and ocotillol have as the base peak in their mass spectra the ion m/e 143,* $C_8H_{15}O_2$, *from cleavage of the side chain to XX.*

Can. J. Chem. Downloaded from www.nrcresearchpress.com by 210.87.254.6 on 09/05/12
For personal use only.

Stereochemistry

The absolute configurations on the fused ring system of ocotillol at C-3, C-5, C-8, C-9, C-10, and C-14 are fixed by relation to the dammarane skeleton (8, 18), which has in turn been related (18) to *iso*euphol and *iso*tirucallol (19). The β-orientation of the C-13 hydrogen atom follows from the demonstration that the C-13 configuration of the dammarane system is the less stable one. Dammarane derivatives with a carbonyl group at C-17 (20) or at C-12 (21) are epimerized almost completely to the 13-*iso* compounds. The less stable C-13 configuration is β (rings C and D *trans* fused), and molecular rotation differences and conformational analysis support this assignment (20). On the other hand, C-17 has the more stable β-arrangement as witnessed by the stability to base of several C-20 keto derivatives (9, 18, 20). In agreement the coupling constant (10 c.p.s.) between the C-13 and C-17 protons in derivatives with a C-12 keto group is that expected for a *trans* relationship with a dihedral angle of ca. 150° (12). Of the two asymmetric centers in the side chain, the β-configuration of the C-20 hydroxyl has been assigned (21) to folientriol, folientetrol, and the II-series of dammarane compounds, but the grounds on which the assignment was made are erroneous.[7] Thus the stereochemistry at C-20 and C-24 is as yet unknown.

Hydroxy Isoöctenyl Side Chain Oxidation

The quantitative oxidation of the ocotillol side chain to a γ-lactone is merely a special case of the general oxidation of mono ethers of 1,2-diols which Chang and Westheimer (22) have studied with pinacol monomethyl ether. The rapidity of the oxidation suggested that the ocotillol side chain might be an intermediate in the earlier mentioned chromic acid oxidation of the hydroxy *iso*öctenyl side chain XVI of various triterpenes to tris nor γ-lactones XIX. This possibility was tested by oxidation of dammarenediol-II monoacetate (VII*a*) with just the amount of chromium trioxide stoichiometrically required for oxidation to II. From the reaction mixture there was isolated, in addition to lactone V*a* and recovered VII*a*, 6–13% of ocotillol monoacetate II. In view of this result, ocotillol must be an intermediate in one path for the oxidation of VII*a* to V*a*. The hydroxy *iso*öctenyl side chain XVI could produce the hydroxy tetrahydrofuran either by oxidation first to the 1,2-epoxides VIII followed by the rapid oxide opening previously noted, or by oxidation of the double bond to some such cationic intermediate as XVII which is then attacked at C-24 by the C-20 hydroxyl group (XVII → XVIII). Alternatively, the oxidation of the double bond might be an intramolecular process involving a chromate ester of the tertiary C-20 hydroxyl group. The details of this side chain oxidation are being examined further.

EXPERIMENTAL

General

Melting points: Reichert microscope hot stage, corrected.

Optical rotations: Schmidt–Haensch polarimeter, chloroform solutions, 1-dm tube.

Infrared spectra: Beckman IR-5 or IR-7 spectrometer.

Ultraviolet spectra: Bausch and Lomb Spectronic 505 or a Beckman DK spectrometer.

Nuclear magnetic resonance spectra: Varian HR-60 or A-60 spectrometer, 10–20% (g/ml) concentration in deuterochloroform with tetramethylsilane (=O) as internal reference. Integrations by the cut-and-weigh method.

Chromatography: Woelm neutral alumina graded according to the Brockman scale.

Thin-layer chromatography: Camag Kieselgel silica gel with calcium sulphate binder, methanol:chloroform (1.5:98.5) for development, sulphuric acid (33%) for charring. Reported R_f values are taken from one plate on which all compounds were present.

Microanalyses: Dr. A. Bernhardt and associates, Mülheim, Germany.

Petroleum ether refers to the fraction boiling at 60–80°.

[7]*The assignment was based on a molecular rotation difference between a 20-hydroxydammarane (C-13α?) of unknown C-20 configuration and a dammarane also of unknown C-20 configuration, which had been crystallized from a mixture of dammarane isomers.*

Can. J. Chem. Downloaded from www.nrcresearchpress.com by 210.87.254.6 on 09/05/12
For personal use only.

Can. J. Chem. Downloaded from www.nrcresearchpress.com by 210.87.254.6 on 09/05/12
For personal use only.

TABLE I

Nuclear magnetic resonance absorption of ocotillol derivatives*

Compound		4α Me	4β Me	10β Me	8β Me	14α Me	21 Me	25 *gem* diMe	3α H	24 H	3β MeCOO	25 MeCOO
Ocotillol	I	0.78	0.85	0.97	0.97	0.87	1.21	1.12	3.18	3.73	—	—
Ocotillol monoacetate	II	0.87	0.87	0.87	0.96	0.87	1.21	1.12	4.50 dd	3.73 dd	2.03	—
Ocotillol diacetate	III	0.85–0.87	0.85–0.87	0.85–0.87	0.96	0.85–0.87	1.11	1.45	4.49 dd	3.95 dd	2.03	1.96
Keto lactone	IV†	0.95	1.04	1.08	1.02	0.92	1.38	—	—	—	—	—
Acetate lactone	Va†	0.85–0.87	0.85–0.87	0.85–0.87	0.96	0.85–0.87	1.37	—	4.49 dd	—	2.04	—

*Chemical shifts are given in p.p.m. from tetramethylsilane (=0) for deuterochloroform solutions.
†The values for these compounds are the same (±0.01 p.p.m.) as those in ref. 12.

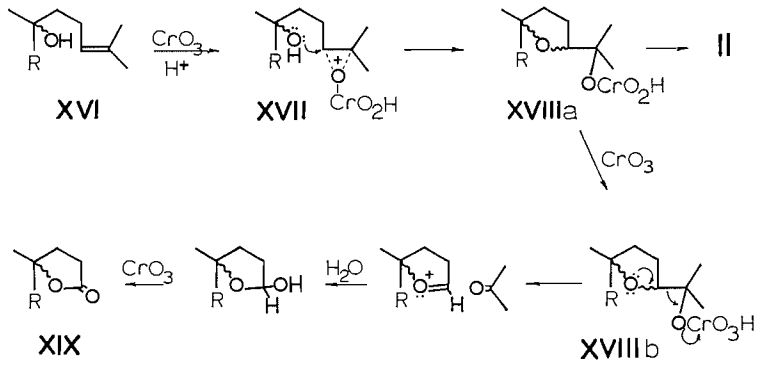

Isolation of Ocotillo Resin

Ocotillo bark was collected in Borrego Valley, California, in January, 1962. The loose sandy soil of the region and the shallow root system of the plant make the ocotillo vulnerable to toppling by wind or rain. Since the bark of the fallen and partially dried plants was more easily stripped than that of a freshly cut branch of a living plant, most of the bark was gathered from fallen specimens. The highly resinous bark could not be ground in a Wiley or a hand mill, and instead was cut into small bits with a pair of shears. These pieces, in batches of 20–40 g, were extracted exhaustively with ether in a Soxhlet apparatus. The yield of ether-soluble material per batch varied from 10% to 15% of the weight of the bark. The resin is concentrated in the inner bark, because extraction of the yellow translucent laminated inner bark after separation from the darker outer bark gave 15% of ether-soluble resin, whereas extraction of the whole bark with ether gave only 10–11% of ether-soluble resin. From 6.15 kg of whole bark a total of 618 g (10%) of clear amber resin was obtained. Further extraction of ~~the root~~ bark with methanol gave a small amount of a dark gummy material which was not investigated further. The resin had λ_{max} 269 mμ ($E_{1cm}^{1\%}$ 34), 329 mμ ($E_{1cm}^{1\%}$ 30); $\nu_{max}^{CHCl_3}$ 3 600 and 3 400 cm^{-1} (OH), and 1 725 cm^{-1} (broad, C=O).

The absence of alkaloids in the resin was demonstrated by extraction of an ethyl acetate – chloroform solution of it with dilute hydrochloric acid. The aqueous acid solution gave no precipitate with silicotungstic acid. Basification with sodium hydroxide and extraction with chloroform gave only a trace of residue on evaporation of the dried chloroform solution.

Isolation of Ocotillol Acetate II from Unsaponified Resin (with Mr. J. F. Sollors)

A sample (889 mg) of the unsaponified resin was chromatographed on 30 g of activity I Merck alumina. Only the fractions (58 mg, 6.5%) eluted with ether:benzene (1:3 and 1:1) could be induced to crystallize. These were recrystallized five times from ethyl acetate to give colorless blades, m.p. 260–260.5°, ϵ_{204} 0, ν_{max}^{KBr} 1 724 cm^{-1} (C=O), and 1 250 cm^{-1} (C—O—C). The compound gave a single t.l.c. spot, R_f 0.63, corresponding to ocotillol acetate. The melting point of a mixture with a specimen of the compound from acetylation of ocotillol (see below) (m.p. 257.5–260°) was 257.5–260°, undepressed. There was enough material for only one analysis.

Anal. Calcd. for $C_{32}H_{54}O_4$ (502.75): C, 76.44; H, 10.83. Found: C, 74.99; H, 11.30. Mol. wt. (osmometer, chloroform solution), 513, 517.

A 10-mg sample of the compound was treated under reflux overnight with methanolic potassium hydroxide. Dilution of the reaction mixture with water precipitated a white solid which was recrystallized from 95% ethanol to yield colorless prisms, m.p. 199° (m.p. of ocotillol 198–200°). The infrared spectrum no longer showed carbonyl absorption.

From chromatography of 2.33 g of a different lot of resin there was isolated a few milligrams of I, m.p. 197–200°.

Isolation of Ocotillol I from Saponified Resin

A solution of 10.46 g of ocotillo resin in 350 ml of methanol was heated under reflux with 8 g of potassium hydroxide for 5 h. The reaction mixture was diluted with 1 liter of water and extracted with several portions of ether. The combined ethereal solutions were washed with saturated sodium chloride solution, dried over magnesium sulphate, and filtered. Evaporation of solvents left 6.119 g (ca. 60%) of amber-colored neutral saponification product. Examination by thin-layer chromatography indicated the presence of at least seven compounds of which three were present in considerable amount. Attempts to crystallize the saponification product failed.

The neutral fraction in benzene was poured onto a column of 180 g of grade II alumina, and chromatographed. Benzene:ether (75:25) eluted two fractions weighing 928 mg (15% of the neutral fraction), which crystallized spontaneously and were essentially pure (t.l.c.). Two other fractions weighing 843 mg (13% of

Can. J. Chem. Downloaded from www.nrcresearchpress.com by 210.87.254.6 on 09/05/12
For personal use only.

the neutral fraction) crystallized on trituration with ether; these contained a small amount of two contaminants. The total yield of almost pure ocotillol was about 28% of the neutral fraction or approximately 16% of the unsaponified resin. Several recrystallizations of the 928-mg fraction from benzene – petroleum ether or ethyl acetate – petroleum ether gave colorless thin prisms of pure ocotillol I, m.p. 198–200°, $[\alpha]_D^{25}$ +28.3° (*c*, 2.42), $[\alpha]_D^{25}$ +25.7° (*c*, 2.29), R_f 0.36, ϵ_{205}^{EtOH} 228, $\nu_{max}^{CCl_4}$ (IR-7) 3 622 cm^{-1} and 3 580 cm^{-1} (OH) (conc. 0.005 *M*).[8] Integration of the n.m.r. spectrum gave a total of 52–54 hydrogen atoms.

Anal. Calcd. for $C_{30}H_{52}O_3$ (460.72): C, 78.20; H, 11.38; O, 10.42. Found: C, 78.17; H, 11.02; O, 10.90. Mol. wt. (mass spectrum), 460.

From the following experiments ocotillol was recovered almost quantitatively. In each case t.l.c. examination showed I to be the only product.

(*a*) A solution of 19 mg of I and 19 mg of sodium metaperiodate in 3.25 ml of water:dioxane (5:8) was allowed to stand for 140 min at room temperature.

(*b*) A solution of 10 mg of I in 3 ml of chloroform was saturated with anhydrous hydrogen chloride and allowed to stand overnight at room temperature.

(*c*) A solution of 11.2 mg of I in 8 ml of ether was treated by reflux with 87 mg of lithium aluminium hydride for 3.5 h.

(*d*) A solution of 11.4 mg of II in 20 ml of dioxane was treated by reflux with 191 mg of lithium aluminium hydride for 8 h (yield: 6 mg of I).

Ocotillol Monoacetate II

From Pure Ocotillol

A solution of 286 mg (0.62 mmole) of ocotillol in 3 ml of dry pyridine and 0.2 ml of acetic anhydride was allowed to stand for 24 h at room temperature. The reaction mixture was diluted with water and extracted with chloroform and ether. The combined chloroform–ether extracts were washed successively with dilute sulphuric acid, water, sodium bicarbonate solution, and water. The dried (sodium sulphate) and filtered solution was evaporated, to leave 284 mg (91%) of crystalline residue, which t.l.c. showed to be almost pure monoacetate. Four recrystallizations from ethyl acetate – petroleum ether or chloroform – petroleum ether gave colorless prisms of ocotillol monoacetate II, m.p. 260–261.5°, $[\alpha]_D^{25}$ +41° (*c*, 1.13), $[\alpha]_D^{22}$ +39.5° (*c*, 2.52) and +40.5° (*c*, 2.55), R_f 0.63; $\nu_{max}^{CCl_4}$ (IR-7) 3 580 cm^{-1} (OH), 1 734 cm^{-1} (ester C=O) (conc. 0.005 *M*); $\nu_{max}^{CHCl_3}$ 3 546 cm^{-1} (OH), 1 718 cm^{-1} (ester C=O), and 1 256 cm^{-1} (C—O—C).

Anal. Calcd. for $C_{32}H_{54}O_4$ (502.74): C, 76.44; H, 10.83. Found: C, 76.85; H, 10.99.

From Neutral Saponification Product

A solution of 10 g of the neutral fraction of the resin saponification product in 80 ml of dry pyridine and 8 ml of acetic anhydride was allowed to stand for 24 h at room temperature. The reaction mixture was worked up as in the preparation of the monoacetate from pure ocotillol, except that 10% potassium hydroxide solution was used in place of sodium bicarbonate solution. The acetylated product (9.7 g) was dissolved in ethyl acetate – petroleum ether, concentrated to about 200 ml, and seeded with pure II. After several days of slow crystallization first at room temperature and then at 3°, filtration gave 953 mg (ca. 8.7%) of colorless thin prisms (almost pure II), m.p. 222–243°, in three crops. Two recrystallizations from ethyl acetate – petroleum ether gave pure ocotillol monoacetate identical with that prepared as above from pure ocotillol.

Saponification

A solution of 71 mg of ocotillol monoacetate II and 0.4 g of potassium hydroxide in 20 ml of methanol was heated under reflux for 27.5 h. Dilution with water and extraction with ether gave 51 mg (78%) of ocotillol, m.p. 193.5–197°, which gave a single t.l.c. spot. One recrystallization from benzene – petroleum ether raised the melting point to 198–198.5°, undepressed on admixture with authentic ocotillol. The infrared spectrum was identical with that of ocotillol.

Ocotillol Diacetate III

Preparation

Ocotillol monoacetate (252 mg, 0.50 mmole) was treated by reflux for 48 h in 5 ml of pyridine with 0.5 ml of acetic anhydride. The reaction mixture was diluted with water, extracted with ether, and worked up as for the monoacetylation of pure ocotillol. The crude dark brown product (278 mg) was chromatographed on 10 g of activity II alumina. Benzene – petroleum ether (50:50) eluted 193 mg (70%) of colorless crystals which gave a single t.l.c. spot, R_f 0.74. Three recrystallizations from methanol – methylene chloride gave colorless flakes of ocotillol diacetate III, m.p. 199–202°, $[\alpha]_D^{21}$ +38° (*c*, 2.60), $\nu_{max}^{CCl_4}$ 1 736 (ester C=O) and 1 250 cm^{-1} (C—O—C).

Anal. Calcd. for $C_{34}H_{56}O_5$ (544.79): C, 74.95; H, 10.36. Found: C, 75.23; H, 10.49.

An attempted acetylation in pyridine – acetic anhydride at 90° for 24 h (conditions used for diacetylation of gratiogenin X (15)) gave back monoacetate containing only a small amount of diacetate.

Saponification

A 22-mg sample of the diacetate was treated by reflux for 48 h with 88 mg of potassium hydroxide in 15 ml of methanol. Dilution with water and extraction with ether gave 19 mg of a solid, which was recrystallized

[8]*For comparison, a 0.005 M solution of 3β-cholestanol had* $\nu_{max}^{CCl_4}$ *(IR-7) 3 620* cm^{-1}.

Can. J. Chem. Downloaded from www.nrcresearchpress.com by 210.87.254.6 on 09/05/12
For personal use only.

from benzene – petroleum ether to yield 12.4 mg of ocotillol, m.p. 197–198°, undepressed on admixture with an authentic specimen.

Oxidation of Ocotillol Monoacetate II

Chromic Acid – Acetic Acid

A solution of 303 mg (0.61 mmole) of II in 41 ml of glacial acetic acid was added to 91 mg (0.91 mmole) of chromium trioxide in 5 drops of water and 2 ml of glacial acetic acid. The reaction mixture was almost green after 1 h. After 24 h the emerald-green solution was treated with potassium iodide. Titration of the iodine liberated by excess chromium trioxide required 2.39 ml of 0.100 *N* sodium thiosulphate (corresponding to 7.9 mg of chromium trioxide). The 83.1 mg (0.83 mmole of chromium ^{VI} consumed in the oxidation was 102% of the theoretical amount required for oxidation of II to the lactone V*a* and acetone.

The titrated reaction mixture was diluted with water and extracted with ether. The ether extracts were washed with thiosulphate solution, water, sodium bicarbonate solution, saturated sodium chloride solution, and then dried over sodium sulphate. Evaporation of the filtered solution left 347 mg of crystalline product, which retained some solvent and gave a single t.l.c. spot, R_f 0.71. One recrystallization from methanol – methylene chloride gave 211 mg (75%) of prisms of acetate lactone V*a* (3β-hydroxy tris nor dammarane 24:20 ξ_2-olide acetate), m.p. 242–245.5° unchanged on further recrystallization, $[\alpha]_D$ +42° (*c*, 2.24); $\nu_{max}^{CHCl_3}$ 1 761 cm^{-1} (γ-lactone C=O), 1 721 cm^{-1} (ester C=O), and 1 253 cm^{-1} (C—O—C) (lit. (8): m.p. 237–238°, $[\alpha]_D$ +50°). The melting point was undepressed on admixture with V*a* from dipterocarpol (8).

Anal. Calcd. for $C_{29}H_{46}O_4$ (458.66): C, 75.94; H, 10.11. Found: C, 75.66; H, 10.04.

From another reaction in which 150 mg of II was oxidized the yield of crude acetate lactone (one t.l.c. spot) was 136 mg (99%).

A solution of 136 mg of acetate lactone in 30 ml of methanol was saponified by reflux with 564 mg of potassium hydroxide. Acidification with dilute sulphuric acid and extraction with ether gave 123 mg of hydroxy lactone V*b* (single t.l.c. spot), which after four recrystallizations from methanol–water had m.p. 208.5–210°, $[\alpha]_D$ +25° (*c*, 1.42, chloroform containing 5% of 95% ethanol) (lit. (8): m.p. 205–206°, $[\alpha]_D$ +39°).

Chromium Trioxide – Pyridine

To the oxidizing agent prepared from 14.3 mg (0.143 mmole) of chromium trioxide and 0.5 ml of pyridine was added a solution of 100 mg (0.207 mmole) of II in 9 ml of pyridine. After 4.7 h at room temperature the reaction mixture was diluted with 40 ml of methylene chloride and poured onto a column of 3 g of activity III alumina. Further elution with 160 ml of methylene chloride gave a colorless eluate which was washed successively with dilute sulphuric acid, water, sodium bicarbonate solution, water, and saturated sodium chloride solution. The dried solution (sodium sulphate) was concentrated, and left 99 mg (99%) of recovered ocotillol monoacetate, m.p. 250.5–254°, $[\alpha]_D^{25}$ +36° (*c*, 2.50), which gave a single t.l.c. spot. The melting point was undepressed on admixture with the starting material, and the n.m.r. spectrum was identical with that of the starting material.

Oxidation of Ocotillol I

A mixture of 202 mg (0.44 mmole) of I, 98 mg (0.98 mmole) of chromium trioxide, and 7 drops of water in 17 ml of glacial acetic acid was allowed to react at room temperature for 24 h. Then a solution of 11 mg of sodium bisulphite in 50 ml of water was added and the reaction mixture was steam distilled. The distillate (25 ml) was treated with acidic 2,4-dinitrophenylhydrazine solution and the resulting orange precipitate (30 mg, 28%) was collected on a filter. Two recrystallizations from ethanol gave 14 mg of prisms of acetone 2,4-dinitrophenylhydrazone, m.p. 125–126°. On admixture with an authentic sample, m.p. 125–126.5°, the melting point was 124.5–125.5°. The infrared spectra of both samples in chloroform were identical.

The residue from the steam distillation was extracted with three portions of ether. The combined ethereal solutions were washed in sequence with water, sodium bicarbonate solution, water, and saturated sodium chloride solution before being dried over anhydrous sodium sulphate. Evaporation of the ether left 181 mg (99%) of crystalline residue, m.p. 173.5–181.5°, which gave a single t.l.c. spot. Three recrystallizations from absolute ethanol – petroleum ether gave 101 mg of colorless prisms of the keto lactone IV, m.p. 182.5–184.5°, $[\alpha]_D^{25}$ +71° (*c*, 2.51), ϵ_{210}^{EtOH} 55; $\nu_{max}^{CHCl_3}$ 1 757 cm^{-1} (γ-lactone), 1 698 cm^{-1} (6-ring C=O), 1 421 cm^{-1} (CH_2 C=O); $\nu_{max}^{CCl_4}$ 1 775 cm^{-1} (γ-lactone) and 1 706 cm^{-1} (6-ring C=O). On admixture with a sample of the tris nor lactone from dipterocarpol VI (≡tris nor keto lactone from dammarenediol-II), the melting point was undepressed. The infrared spectra in chloroform solution were identical. Both samples had the same R_f 0.67 on t.l.c.

Anal. Calcd. for $C_{27}H_{42}O_3$ (414.61): C, 78.21; H, 10.21; O, 11.58. Found: C, 77.84; H, 10.13; O, 11.76. Mol. wt. (mass spectrum), 414.

A blank oxidation with the same reagents but with the omission of I, followed by distillation and addition of 2,4-dinitrophenylhydrazine gave no precipitate. However, extraction of the treated distillate and chromatography on silica gel did give 12 mg of a mixture of dinitrophenylhydrazones of which the acetone derivative constituted about 6 mg. Since this is much less than the *precipitate* collected in the ocotillol oxidation, acetone is one of the products of oxidation of ocotillol.

Dammarenediol-II Monoacetate VIIa from Dipterocarpol VI

A solution of 727 mg of sodium borohydride in 40 ml of dioxane–water (1:1) was added to a solution of

Can. J. Chem. Downloaded from www.nrcresearchpress.com by 210.87.254.6 on 09/05/12
For personal use only.

1.781 g of dipterocarpol VI (≡20-hydroxydammarenone-II), R_f 0.73, m.p. 124–134°, $[\alpha]_D^{25}$ +62° (*c*, 3.47) (lit. (8): m.p. 127° and 135–136°, $[\alpha]_D$ +65°) in 60 ml of dioxane. Work-up gave 1.732 g of crude product, which was recrystallized from methanol. There was obtained 1.482 g (85%) of colorless flakes of dammarenediol-II (VII*b*), m.p. 78.5–82° (lit. (7): m.p. 131–133°), R_f 0.44, which were either solvated or polymorphic.

Acetic anhydride (1.2 ml) was added to a solution of 1.48 g of VII*b* in 12 ml of pyridine, and the reaction mixture was allowed to stand at room temperature for 26 h. Work-up as for the monoacetylation of ocotillol gave 1.571 g of yellow resin. Recrystallization from methanol yielded 1.351 g (83%) of dammarenediol-II monoacetate VII*a*, m.p. 130–134°, $[\alpha]_D^{25}$ +38° (*c*, 2.68) (lit. (7): m.p. 135–137°, $[\alpha]_D$ +37°), R_f 0.73.

Epoxidation of Dammarenediol-II Monoacetate VIIa

To a solution of 299 mg (0.615 mmole) of VII*a* in 15 ml of ether chilled in a bath of Dry Ice and acetone, 1.5 ml of an ethereal solution of monoperphthalic acid (0.687 mmole) was added. The reaction mixture was stored at −10° for 210 h, then diluted with chloroform and washed successively with sodium bicarbonate solution, water, and saturated sodium chloride solution. Evaporation of the dried ether solution (water bath temperature = 90°) left 263 mg of colorless solid, which was recrystallized from ethyl acetate – petroleum ether. Seeding with a crystal of ocotillol acetate produced 110 mg (35%) of prisms, m.p. 247–248°, $[\alpha]_D^{25}$ +37° (*c*, 2.46). Three more recrystallizations from the same solvent gave 65 mg of pure ocotillol monoacetate (II), m.p. 260–260.5°, $[\alpha]_D^{25}$ +40° (*c*, 2.50), R_f 0.63. The melting point was undepressed on admixture with an authentic sample prepared as described above. The infrared and n.m.r. spectra were identical with those of authentic II.

Anal. Calcd. for $C_{32}H_{54}O_4$ (502.74): C, 76.44; H, 10.83. Found: C, 76.58; H, 10.95.

In an attempt to isolate the C-24 epimer of ocotillol monoacetate, the mother liquors from the first crop of crystals were combined with those from another reaction and chromatographed on activity II alumina. Various fractions which gave a single t.l.c. spot corresponding in R_f to II had optical rotations ranging from $[\alpha]_D$ +31° to $[\alpha]_D$ +34°, significantly lower than II or VII*a*. The n.m.r. spectrum of this material differed from that of ocotillol monoacetate in that there were two short methyl peaks at 1.11 and 1.13 p.p.m. instead of one tall methyl peak at ~1.12 p.p.m. The material was apparently a mixture of II and its C-24 epimer in about equal amounts; however, the C-24 epimer could not be crystallized from the mixture. A calculation based on the optical rotations of pure II and the estimated composition of the mixture gives a value of $[\alpha]_D$ ca. +24° for the C-24 epimer of ocotillol monoacetate.

Chromic Acid Oxidation of Dammarenediol-II Monoacetate VIIa

Dammarenediol-II monoacetate (249 mg, 0.51 mmole) shown by t.l.c. to be free of I and II in 6 ml of glacial acetic acid containing 10 drops of water was oxidized with 33.5 mg (0.33 mmole, the theoretical amount for oxidation of VII*a* to II) of chromium trioxide at room temperature. After 14 h the reaction mixture was diluted with water and worked up as for the oxidation of ocotillol monoacetate. Thin-layer chromatography of the 237 mg of crude product indicated the presence of the acetate lactone and ocotillol monoacetate as well as unreacted starting material. To remove the lactone the product was treated by reflux in a mixture of 15 ml of methanol, 5 ml of water, and 175 mg of potassium hydroxide for about 4 h. Dilution with water and extraction of the basic solution with chloroform and ether gave 159 mg of neutral material, which was mainly a mixture of I and VII*b*. Acidification of the basic aqueous layer with dilute sulphuric acid and extraction with ether yielded 46 mg (21%) of hydroxy lactone V*b*. Acetylation of this with pyridine – acetic anhydride at room temperature gave 50 mg of acetate lactone V*a* which after two recrystallizations from methylene chloride – methanol had m.p. 241–244.5°, undepressed on admixture with an authentic sample.

The 159 mg of neutral product was dissolved in benzene – petroleum ether and chromatographed on 5 g of grade III alumina. Benzene and benzene:ether (98:2) eluted 55 mg (24%) of dammarenediol-II (VII*b*), which was identified by t.l.c. and conversion to the acetate VII*a*. Benzene:ether (98:2 to 90:10) eluted 58 mg, which t.l.c. showed to be about half II (~13% yield). Five recrystallizations from benzene – petroleum ether gave ocotillol of m.p. 195–196°, undepressed on admixture with authentic I. Acetylation of the recrystallization mother liquors gave 53 mg, which was estimated by t.l.c. to contain ca. 14 mg (~6% yield from VII*a*) of II. Three recrystallizations from ethyl acetate – petroleum ether gave 4 mg of pure II, m.p. 254–255°, undepressed on admixture with an authentic sample.

Dammarenediol-II monoacetate gave little or no ocotillol monoacetate II on oxidation with the chromic acid – pyridine reagent.

ACKNOWLEDGMENTS

The authors would like to thank the National Research Council for support, Professor G. Ourisson for the authentic specimens of IV and V*a*, and Dr. G. Snatzke, Bonn, for the mass spectra and a copy of his manuscript in advance of publication. They are also indebted to Mr. J. F. Sollors for the experiment indicated.

Can. J. Chem. Downloaded from www.nrcresearchpress.com by 210.87.254.6 on 09/05/12
For personal use only.

REFERENCES

1. C. M. M. HALLS and E. W. WARNHOFF. Chem. Ind. London, 1986 (1963).
2. L. BENSON and R. A. DARROW. The trees and shrubs of the southwestern deserts. 2nd ed. University of Arizona Press, Tucson, Arizona. 1954. pp. 270–271.
3. H. C. DE S. ABBOTT. Am. J. Pharm. **57**, 81 (1885).
4. E. SCHAER. Arch. Pharm. **236**, 1 (1898).
5. A. R. H. COLE. *In* Elucidation of structures by physical and chemical methods. Part I. *Edited by* K. W. Bentley. Interscience Publishers, New York, N.Y. 1963. pp. 144–151.
6. J. N. SHOOLERY and M. T. ROGERS. J. Am. Chem. Soc. **80**, 5133 (1958).
7. J. S. MILLS and A. E. A. WERNER. J. Chem. Soc. 3132 (1955).
8. P. CRABBÉ, G. OURISSON, and T. TAKAHASHI. Tetrahedron, **3**, 279 (1958).
9. F. G. FISCHER and N. SEILER. Ann. **626**, 185 (1959).
10. D. ARIGONI, D. H. R. BARTON, R. BERNASCONI, C. DJERASSI, J. S. MILLS, and R. E. WOLFF. J. Chem. Soc. 1900 (1960).
11. L. VAN ITALLIE. Arch. Pharm. **250**, 204 (1912).
12. J.-M. LEHN. Bull. Soc. Chim. France, 1832 (1962).
13. D. FELIX, A. MELERA, J. SEIBL, and E. sz. KOVÁTS. Helv. Chim. Acta, **46**, 1513 (1963).
14. E. KLEIN, H. FARNOW, and W. ROJAHN. Tetrahedron Letters, **17**, 1109 (1963). E. KLEIN, H. FARNOW, and W. ROJAHN. Ann. **675**, 73 (1964).
15. R. TSCHESCHE, G. BIERNOTH, and G. SNATZKE. Ann. **674**, 196 (1964).
16. D. SHIENGTHONG, A. VERASARN, P. NANONGGAI-SUWANRATH, and E. W. WARNHOFF. Tetrahedron, **21**, 917 (1965).
17. M. MOUSSERON-CANET, C. LEVALLOIS, and J. WYLDE. Tetrahedron Letters, **17**, 769 (1962).
18. J. S. MILLS. J. Chem. Soc. 2196 (1956).
19. (*a*) D. ARIGONI, R. VITERBO, M. DÜNNENBERGER, O. JEGER, and L. RUZICKA. Helv. Chim. Acta, **37**, 2306 (1954). (*b*) D. ARIGONI, O. JEGER, and L. RUZICHA. Helv. Chim. Acta, **38**, 222 (1955). (*c*) D. H. R. BARTON, J. F. MCGHIE, M. K. PRADHAN, and S. A. KNIGHT. J. Chem. Soc. 876 (1955)
20. J.-F. BIELLMANN, P. CRABBÉ, and G. OURISSON. Tetrahedron, **3**, 303 (1958).
21. F. G. FISCHER and N. SEILER. Ann. **644**, 146 (1961).
22. Y. W. CHANG and F. H. WESTHEIMER. J. Am. Chem. Soc. **82**, 1401 (1960).

Can. J. Chem. Downloaded from www.nrcresearchpress.com by 210.87.254.6 on 09/05/12
For personal use only.

Can. J. Chem. Downloaded from www.nrcresearchpress.com by 210.87.254.40 on 09/05/12
For personal use only.

THE STRUCTURE OF AMINOPYRINE SALTS

DENYS COOK
Department of National Health and Welfare, Food and Drug Directorate, Ottawa, Canada
Received June 28, 1965

ABSTRACT

The infrared spectra of aminopyrine salts can be interpreted on the basis of protonation of the 4-dimethylamino group nitrogen atom. In the hydrohalides the normal N^+—H···Y^- hydrogen bond occurs, but in salts with complex anions an intramolecular N^+—H···O=C hydrogen bond is probable, though an intermolecular one between the same partners cannot be ruled out.

INTRODUCTION

Salts of antipyrine, a substituted pyrazolone having analgesic and antipyretic properties, have recently been studied (1) to determine the site of protonation. Satisfactory evidence was presented to demonstrate unequivocally that the carbonyl group was the basic site. In aminopyrine, a chemical differing only in the addition of a 4-dimethylamino group, the possibility of protonation at the substituent nitrogen atom arises.

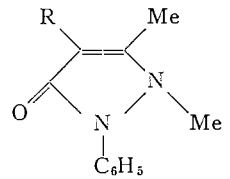

R = H for antipyrine

R = NH_2 for 4-aminoantipyrine

R = $N(CH_3)_2$ for aminopyrine

R = $N(CH_3)CH_2SO_3Na$ for dipyrone

The configuration of the $N(CH_3)_2$ group in the free base is not known. However, the basicity of such nitrogen atoms is much reduced when they are attached to aromatic ring systems: aniline for example has a pK_a of 4.58 while cytosine ($pK_a \sim 4.6$) protonates at the unsubstituted heterocyclic nitrogen (2), not the 4-amino group. The determination of protonation site is of intrinsic interest, and of possible metabolic application. It may also have some bearing on a problem associated with 4-amino substituted antipyrines (aminopyrine, dipyrone, and 4-aminoantipyrine) namely the generation of blood dyscrasias such as agranulocytosis (3).

RESULTS

Tables I and II list the complete frequencies found in the spectra of the salts. Those due to the protonated group are summarized in Table III.

DISCUSSION

Site of Protonation

The protonation site in organic bases has been determined from the deformation frequency, δ_{XH}, of the salt (4). Tertiary (sp^3) amine salts have δ_{NH} near 1 402 cm^{-1}, while protonated carbonyl groups absorb near 1 257 cm^{-1}. The prominent band near 1 400 cm^{-1} in aminopyrine salts, shifting to ~980 cm^{-1} in the deuterated salts, at once suggests that a tertiary (sp^3) nitrogen atom is protonated, and not a carbonyl group. Since no case of N protonation of an amide group has been proved* it is most unlikely that N_1 is protonated. The carbonyl frequency at ~ 1 660 cm^{-1} is also incompatible with N_1 protonation,

**2,2-Dimethylquinuclid-6-one, which protonates at the nitrogen atom (6), contains the amide grouping but not the planar amide configuration.*

TABLE I

Absorption bands in spectra of aminopyrine salts (type III)

	HCl	DCl	HI	DI	H_2TiF_6	H_2SiF_6
					3 060 m	3 070 m, sh
			3 052 w		3 050 m	
			2 975 m		2 930 m	2 930 m
			2 860 m, sh	2 176 m		
			2 850 m	2 108 m		
			2 806 m	2 064 m		
ν_{NH}	2 290 m, b	1 860 m	2 672 vs	2 048 m	3 025 m, b	3 030 m, b
			2 427 m	1 945 w	2 850 m, b	2 850 m
ν_{CO}	1 680 m, sh	1 680 m, sh	1 668 vs, sh		1 686 m, sh	1 688 m, sh
	1 670 m	1 650 m	1 660 vs	1 660 vs	1 677 vs	1 675 s
	1 655 m, sh		1 655 vs, sh	1 656 vs, sh	1 672 vs, sh	1 665 s, sh
	1 650 m, sh		1 650 m, sh	1 650 m, sh	1 652 m, sh	1 658 m, sh
			1 640 m, sh	1 638 m, sh	1 631 m	1 632 m
			1 602 m, sh	1 599 m, sh	1 596 m	1 598 m
	1 590 m	1 590 m	1 596 m	1 584 m		
	1 480 w, sh		1 500 m, sh	1 492 m, sh	1 496 m, sh	1 500 m, sh
	1 460 m, sh		1 488 m	1 488 m	1 482 m	1 482 m
			1 469 m	1 468 m	1 458 m	1 450 m
	1 430 m		1 455 m	1 452 m	1 422 m	1 425 m
				1 410 m, sh	1 412 m	1 412 m, sh
δ_{NH}	1 402 m	983 m	1 383 m	985 m	1 395 m	1 396 m
	1 390 m	1 395 m	1 410 m	1 402 m		
	1 368 m	1 370 m, sh	1 370 m, sh	1 370 m, sh	1 370 m	1 373 m
	1 335 m	1 335 m, sh	1 342 w	1 340 w	1 334 m	1 334 m
	1 300 m, sh					
	1 288 m	1 300 m	1 308 m	1 304 m	1 299 m	1 295 m
			1 260 w, sh	1 260 w, sh	1 238 w	1 230 w, sh
	1 225 m	1 228 w	1 230 w	1 229 w	1 221 m	1 218 m
				1 205 vw		
	1 174 m, sh		1 176 m, sh	1 180 b, w	1 182 m	1 178 w
	1 162 m, sh	1 162 m, sh	1 170 m	1 165 w	1 170 m	1 168 w
	1 148 m, sh		1 148 m, sh		1 158 m	1 155 w
	1 132 m, sh	1 138 m, sh	1 132 m, sh		1 138 m	1 134 m
	1 115 m	1 130 m	1 119 m	1 120 m	1 126 m	1 122 m
				1 112 m, sh		
	1 073 m	1 072 m	1 075 m	1 070 m	1 073 m	1 070 m
	1 055 m		1 061 m		1 054 m	1 052 m
	1 035 m	1 022 m	1 042 m	1 030 m	1 035 m	1 035 m
			1 035 m	1 025 m, sh	1 022 w	
	980 m		978 m	976 m	985 m	984 m
	930 w	919 m	940 vw	930 w	930 m	928 m
	905 w	904 m	920 w	900 w	902 w	900 w
	872 vw	866 w	876 w	862 w	873 vw	871 vw
	828 vw	825 m	840 m	822 m	830 w	832 vw
	825 vw		830 w, sh	830 w, sh		828 vw
	767 m	768 m	770 s	765 s	764 s	762 vs
	756 m	758 m, sh	755 m	750 m	750 s	750 vs
	720 m	725 m	726 m	722 w	722 m	722 vs
	693 s	700 m	686 m	682 m	690 s	688 vs
					680 m	

since the value of $\sim 1\,800$ cm^{-1} is usually associated with a positively charged nitrogen atom adjacent to a carbonyl group (5–7). There is in fact a small lowering of ν_{CO} on salt formation which will be examined in greater detail later; but in the present context it indicates the unlikelihood of N_2 protonation. Where such N_2 protonation does occur, as in N-methylphthalazone, which has a similar O=C—N—N— grouping, there is a rise of $\sim$38 cm^{-1} in ν_{CO} on protonation. Such an increase in ν_{CO} is quite common for heterocyclic compounds having one atom between the C=O group and the protonation site (8).

Can. J. Chem. Downloaded from www.nrcresearchpress.com by 210.87.254.40 on 09/05/12
For personal use only.

Can. J. Chem. Downloaded from www.nrcresearchpress.com by 210.87.254.40 on 09/05/12
For personal use only.

TABLE II

Absorption bands in spectra of aminopyrine salts (type I)

	HBF_4	DBF_4	$HClO_4$	$DClO_4$	HPF_6	DPF_6	$HAsF_6$	$DAsF_6$
	3 100 w		3 095 w	3 095 w				
	3 051 w		3 048 w	3 048 w	3 052 w		3 050 w	3 060 w
	2 950 w				2 968 m		2 950 w	2 928 m
					2 680 m, sh	2 200 m	2 680 m, sh	2 185 m
	2 585 m	2 030 m	2 580 m, b	2 026 m, b	2 645 m, b	2 140 m, b	2 635 m, b	2 120 m
					2 600 m, sh	2 045 m	2 600 m, sh	2 043 m, b
ν_{NH}	2 508 m	1 965 m	2 505 m, b	1 970 m, b	2 508 m	1 972 m	2 508 m	1 961 m
	2 460 m	1 903 m	2 450 m, b	1 905 m, b	2 460 m	1 902 m	2 462 m	1 900 m
	1 640 m, sh	1 640 m, sh	1 640 m, sh	1 640 m, sh	1 640 m, sh	1 640 m, sh	1 640 m, sh	1 639 m, sh
	1 630 s, sh	1 630 s, sh	1 635 m, sh	1 632 s, sh	1 632 s, sh	1 630 s, sh	1 630 s, sh	
	1 628 s, sh	1 620 s, sh	1 626 s, sh	1 628 s, sh	1 628 vs, sh	1 626 vs, sh	1 628 vs, sh	1 628 s, sh
				1 620 vs, sh				
ν_{CO}	1 619 vs	1 610 vs	1 620 vs	1 612 vs	1 621 vs	1 610 vs	1 620 vs	1 609 s
	1 580 m	1 572 s	1 578 m	1 572 s	1 582 m	1 579 m	1 582 m	1 582 s
	1 560 m, sh	1 560 m, sh	1 560 m	1 562 s, sh	1 560 m, sh	1 560 m	1 560 m, sh	1 560 m, sh
		1 540 m, sh						1 500 m, sh
	1 495 m	1 492 m	1 492 m	1 493 m	1 495 m, sh	1 495 m	1 490 m, sh	1 491 m
	1 485 m, sh	1 375 m	1 482 m	1 375 m	1 483 m	1 365 m, sh	1 482 m	1 369 m
			1 452 m	1 452 w	1 452 m	1 456 m	1 453 m	1 440 m

Can. J. Chem. Downloaded from www.nrcresearchpress.com by 210.87.254.40 on 09/05/12
For personal use only.

TABLE II (*Concluded*)

	HBF_4	DBF_4	$HClO_4$	$DClO_4$	HPF_6	DPF_6	$HAsF_6$	$DAsF_6$
δ_{NH}	1 426 m	994 s, sh	1 422 m	998 m	1 425 m	994 m	1 423 m	985 m, sh
	1 414 m	1 410 m	1 410 m	1 414 m	1 412 m, sh	1 410 m, sh	1 412 m, sh	1 410 w, sh
					1 404 m, sh		1 402 m, sh	
					1 382 m, sh	1 382 m, sh	1 385 m, sh	1 385 m, sh
	1 369 m	1 369 m, sh	1 360 w	1 375 m			1 366 m	1 360 m, sh
							1 325 m, sh	
	1 319 m	1 319 m	1 312 m	1 316 m	1 312 m	1 312 m	1 311 m	1 327 m
	1 280 m	1 287 m	1 298 m, sh	1 288 m, sh		1 290 m, sh		
	1 270 w, sh		1 265 w	1 258 m	1 256 w	1 255 m, sh	1 260 m	1 260 w
	1 230 vw	1 212 w	1 228 vw	1 215 w	1 229 w	1 229 w	1 229 w	
	1 182 m	1 198 w	1 178 m	1 200 w	1 180 m	1 180 m	1 180 m	1 180 m
	1 169 m				1 168 w	1 169 m	1 168 m	
	1 148 m	1 150 m, sh			1 146 m	1 140 m, sh	1 148 m	1 146 m
	1 128 m	1 138 m	1 122 m, sh		1 128 m	1 129 m	1 128 m	1 130 m, sh
					1 072 m, sh	1 072 m, sh		
					1 068 m	1 070 m	1 064 m	1 080 m
	1 038 s, sh		1 035 m, sh	1 040 m, sh	1 040 w	1 025 m	1 041 w	1 022 w
					1 024 w			
	987 m	982 m, sh	984 m	975 m, sh	984 m	982 m	982 m	981 m
	950 w							
	927 m	911 m	924 m	912 m	923 w	924 w	922 m	918 m
	888 w	877 w	885 w	878 w	883 m	880 s, sh	882 w	862 w
	835 w	830 w	833 vw	830 w			838 w	822 w
	780 s	778 s	777 m	778 s	776 m	772 s	775 s	764 s
	751 m	750 m	750 m	750 m	751 m	750 m	750 m	741 m
	725 w	721 m	720 w	720 m	722 w	722 m		
	705 s	704 s	703 s	705 s	704 m	702 s	704 vs, sh	704 vs, sh

TABLE III
Absorption bands due to NH group

	HCl	HI	HBF_4	$HClO_4$	$HAsF_6$	HPF_6	H_2TiF_6	H_2SiF_6
ν_{NH}		2 860			2 680	2 680		
		2 850	2 585	2 580	2 635	2 645		
		2 806			2 600	2 600		
	2 290	2 672	2 508	2 505	2 508	2 508	3 025	3 030
		2 427	2 460	2 450	2 462	2 460	2 850	2 850
ν_{ND}		2 176			2 185	2 200		
		2 108	2 030	2 026	2 120	2 140		
		2 064			2 043	2 045		
	1 860	2 048	1 965	1 970	1 961	1 972		
		1 945	1 903	1 905	1 900	1 902		
δ_{NH}	1 402	1 383	1 426	1 422	1 423	1 429	1 395	1 396
δ_{ND}		985	994	998	985	994		

Stereochemical Arrangement at the Protonation Site

In the absence of other functional donor groups, a hydrogen-bonded NH group in a salt will usually involve the anion X^- of the acid HX used to make the salt. When another good donor atom D is present, two factors are involved in determining whether $N^+—H\cdots D$ or $N^+—H\cdots X^-$ hydrogen bonding will occur. These are the relative basicities of D and X^- and the steric requirements of the salt. Three principal configurations can be considered for aminopyrine salts. These are depicted in I, intramolecular hydrogen bond; II, inter-

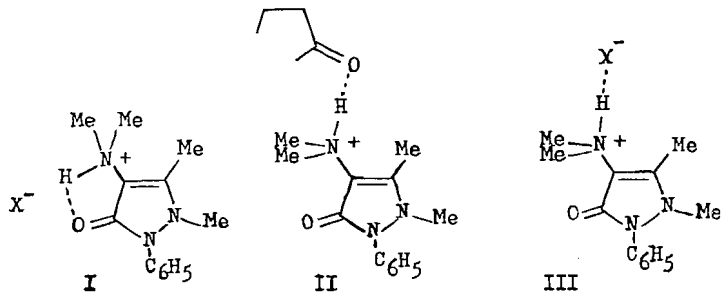

molecular hydrogen bond to a carbonyl group; and III, the conventional $N^+—H\cdots X^-$ hydrogen bond.

It will be obvious from the structural arrangements in I, II, and III that the position of the NH stretching frequency should be useful in deciding which structure is correct. One would expect III to show an increase in ν_{NH} as the anionic size increased and the effect of its force field decreased, i.e. an increase in the series $Cl^- < I^- < ClO_4^-$ etc. In II, where the structure consists of chains of protonated bases with repeated $N^+—H\cdots O$ hydrogen bonds, the anion not being intimately associated with them, there should be a reasonably constant value of ν_{NH} in different salts, unless a large difference in anionic size forced a changeover to a new lattice with an abrupt change in $N^+—H\cdots O$ distance. Structure I should show a remarkably constant value of ν_{NH} since the 5-membered ring would be almost insensitive to the influence of X^-.

The value of ν_{NH} in the hydrohalides show an increase from 2 290 cm^{-1} to 2 672 cm^{-1} from the HCl salt to the HI salt. Apart from the $N^+—H\cdots X^-$ stretching vibration absorption band, the spectra are all very similar. Structure III is therefore assigned to them, and is determined by the strong $N^+—H\cdots X^-$ hydrogen bonds usually associated

Can. J. Chem. Downloaded from www.nrcresearchpress.com by 210.87.254.40 on 09/05/12
For personal use only.

with halide ions. When the anionic size reaches a certain value, however, and the peripheral force gets weaker, a marked change takes place in the spectrum. Normally, in the sequence $Cl^- < Br^- < I^- < ClO_4^-$, the NH stretching frequency would still increase after the iodide. In aminopyrine perchlorate, however, ν_{NH} is 222 cm^{-1} lower than the iodide showing a change in the crystallographic arrangement. Moreover, salts of HBF_4, $HAsF_6$, and HPF_6 etc., show a value of ν_{NH} very similar to the perchlorate. This constancy in ν_{NH} means a similarity in environment, and points to either the structure I or II. At the same time distinct changes take place in the absorption band due to the carbonyl stretching vibration. From a position near 1 665 cm^{-1} in the hydrohalides it moves to near 1 620 cm^{-1} in the other salts. This is quite consistent with a change in structural type from III to I or II and the lowering in frequency ($\sim$40 cm^{-1}) is quite acceptable for either situation. These changes would not be consistent with a change in protonation site, for example, to the carbonyl group, since then the new carbonyl band (1) would be near 1 500 cm^{-1}, and the OH in-plane deformation mode (4) near 1 260 cm^{-1}.

These salts of complex monovalent acids have a higher deformation frequency, δ_{NH}, near 1 425 cm^{-1}, compared with salts of type III, where it is near 1 400 cm^{-1}. The higher frequency is compatible with the lowered stretching frequency, ν_{NH}, in the salts, and consistent with the view expressed previously that there is an inverse relationship between ν_{XH} and δ_{XH} in strong hydrogen bonds (1, 9).

In salts with complex divalent anions the behavior again reverts to that shown by the hydrohalides. The NH stretching frequency appears near 3 000 cm^{-1} in the hexafluorotitanate and hexafluorosilicate but otherwise the spectra of these salts are quite similar to the spectra of the hydrohalides. In particular, the carbonyl frequency is at its characteristic value near 1 665 cm^{-1}. There are two factors operating in this reversion to the hydrohalide structure. These are the slightly enhanced basicity of the divalent hexafluoro anions compared to the monovalent ones, and the altered stoichiometry. The size factor is of lesser importance since the SiF_6^{2-} and PF_6^- ions have similar dimensions.

X-Ray Powder Diffraction Patterns

While conclusions based on melting point variations may be misleading, a constant value throughout a series such as the $HClO_4$, HBF_4, $HAsF_6$, and HPF_6 salts of aminopyrine in the range 218 to 247° seems informative. It strengthens the conclusion that the organic portion of the salt determines the structure and the anion fits into a conveniently shaped hole of constant influence on lattice energy and melting point. This conclusion is reinforced by X-ray powder diffraction photographs showing that although the pattern of the hexafluorosilicate is unlike any of the others, the perchlorate and the tetrafluoroborate are isomorphous, and the hexafluoroarsenate and the hexafluorophosphate are isomorphous. The last two groups however are not isomorphous. This was unexpected, as the spectra suggest that all the salts shown in Table II would be isomorphous, although small changes in crystallographic arrangement could give rise to different powder diffraction patterns without altering the infrared spectrum appreciably.

The anionic sizes shown in Table IV reveal the cause of this unexpected situation. The BF_4^- and ClO_4^- anions are quite similar in size, effective radius 2.15 and 2.20 Å respectively (arbitrarily using the covalent radius of the peripheral atom) while the PF_6^- and AsF_6^- ions are a good deal larger, though comparable between themselves. In keeping with these differences in powder diffraction pattern, and anionic size, it is possible to detect slight differences in the spectra of these two groups. Table III shows the NH stretching band to be made up of two distinct groups of peaks: the first group contains

Can. J. Chem. Downloaded from www.nrcresearchpress.com by 210.87.254.40 on 09/05/12
For personal use only.

TABLE IV
Anionic dimensions (Å)

Anion	d_{MX}	r_X	$(d_{MX}+r_X)$	$(d_{MX}+r_X)^3$
BF_4^-	1.43	0.72	2.15	9.91
ClO_4^-	1.46	0.74	2.20	10.65
PF_6^-	1.73	0.72	2.45	14.70
AsF_6^-	1.85	0.72	2.57	16.96
SiF_6^{2-}	1.71	0.72	2.43	14.25

the broad band near 2 505 cm^{-1}, quite constant in position; the second group has its main band near 2 580 cm^{-1} in the HBF_4 and $HClO_4$ salts and at a slightly higher frequency, $\sim$ 2 640 cm^{-1}, in the HPF_6 and $HAsF_6$ salts. The precise assignment of these bands remains shrouded in the general uncertainty surrounding the breadth and structure of absorption bands due to hydrogen bonds. But it may be, if the salts of the monoacidic fluoro acids are in the internally hydrogen-bonded form, that some slight interaction between X^- and the protonating hydrogen atom exists and causes the spectroscopic differences referred to between the two groups.

The evidence given above slightly favors the structural type I with the internal hydrogen bond, since this would have the required small interaction with the environment. The hydrogen-bonded chain structure II might show more sign of perturbation of the hydrogen bond and therefore of ν_{NH} for small changes in crystallographic arrangement.

Finally, on steric grounds the intermolecular hydrogen bond II seems less favorable than I because of the hindering effects of the 1-phenyl group and the methyl groups of the 4-dimethylamino group. Rotation of the phenyl group might ease this, at the expense of some resonance energy, but even large rotations fo the NMe_2 group would not lessen the hindrance.

EXPERIMENTAL

Spectra

These were recorded as previously described (1).

Materials

Aminopyrine was obtained from the Aldrich Chemical Co. and was used without further purification. The salts were made in the following ways.

HCl

An ether solution of the base deposited a white precipitate of the salt on treatment with dry HCl m.p. 144–145°.

HI

Base (1.16 g) in 25 ml H_2O was mixed with 1.12 g aq. (57%) acid giving a white solid; m.p. 208–209°.

HBF_4

Base (2.31 g) in 83 ml H_2O and 1.76 g HBF_4 gave long needles on standing; m.p. 223–224°.

Anal. Calcd. $C_{13}H_{17}N_3O.HBF_4$: C, 48.92; H, 5.69; N, 13.17. Found: C, 49.25; H, 5.76; N, 13.11.

$HClO_4$

Addition of aq. (70%) $HClO_4$ to an aqueous solution of the base gave needles on standing; m.p. 228–229°.

Anal. Calcd. $C_{13}H_{17}N_3O.HClO_4$: C, 47.06; H, 5.47; N, 12.67. Found: C, 47.22; H, 5.54; N, 12.90.

HPF_6

Mixing concentrated aqueous solutions of acid and base gave a white solid after evaporation of excess water; m.p. 218–220°.

Anal. Calcd. $C_{13}H_{17}N_3O.HPF_6$: C, 41.38; H, 4.81; N, 11.14. Found: C, 40.36; H, 4.43; N, 11.04.

$HAsF_6$

Mixing of aqueous solutions of each component gave a white solid; m.p. 246–247°.

Anal. Calcd. $C_{13}H_{17}N_3O.HAsF_6$: C, 37.07; H, 4.31; N, 9.98. Found: C, 37.34; H, 4.38; N, 9.88.

H_2TiF_6

A solution of TiF_4 in aq. HF was added to the base dissolved in water, precipitating a white solid; m.p. 197–199°.

Anal. Calcd. $(C_{13}H_{17}N_3O)_2.H_2TiF_6$: C, 49.84; H, 5.79; N, 13.42. Found: C, 50.03; H, 5.60; N, 13.37.

Can. J. Chem. Downloaded from www.nrcresearchpress.com by 210.87.254.40 on 09/05/12
For personal use only.

H_2SiF_6

Aminopyrine (1.16 g) in 20 ml H_2O was treated with 2.32 g aq. H_2SiF_6. After evaporation of solvent long needles began to form; m.p. 176–178°.

Anal. Calcd. $(C_{13}H_{17}N_3O)_2.H_2SiF_6$: C, 51.47; H, 5.98; N, 13.86. Found: C, 51.24; H, 5.98; N, 14.11.

ACKNOWLEDGMENTS

Most of the work reported here was done in the laboratories of Dow Chemical of Canada, Limited, Sarnia, Ontario. The assistance of Mrs. R. H. Veach in preparing some of the salts and recording their spectra is gratefully acknowledged. The microanalytical data were obtained through the courtesy of Mr. L. E. Swim and his associates of The Dow Chemical Co., Midland, Michigan, U.S.A., and Mr. H. W. Rinn of the Chemical Physics Research Laboratory in that company kindly prepared the diffraction patterns and gave valuable advice on their interpretation.

REFERENCES

1. D. Cook. Can. J. Chem. **41**, 2794 (1963).
2. A. R. Katritzy and A. J. Waring. J. Chem. Soc. 3046 (1963).
3. Anonymous. J. Oral Ther. Pharm. **1**, 579 (1965).
4. D. Cook. Can. J. Chem. **42**, 2292 (1964).
5. R. Gompper and P. Altreuther. Z. Anal. Chem. **170**, 205 (1959).
6. H. Pracejus. Chem. Ber. **92**, 988 (1959).
7. D. Cook. Can. J. Chem. **40**, 2362 (1962).
8. D. Cook. Unpublished results.
9. G. C. Pimentel and A. L. McLellan. The hydrogen-bond. W. H. Freeman and Co., San Francisco. 1960. p. 118.

Can. J. Chem. Downloaded from www.nrcresearchpress.com by 210.87.254.40 on 09/05/12
For personal use only.

Can. J. Chem. Downloaded from www.nrcresearchpress.com by 210.87.254.6 on 09/05/12
For personal use only.

REACTIONS OF NITRO SUGARS

II.[1] THE CONVERSION OF METHYL 6-DEOXY-6-NITRO-HEXOPYRANOSIDES INTO DEOXYNITROINOSITOLS BY ALKALINE GLYCOSIDE CLEAVAGE

HANS H. BAER AND WERNER RANK
Department of Chemistry, University of Ottawa, Ottawa, Canada
Received July 2, 1965

ABSTRACT

Methyl 6-deoxy-6-nitro-D-glucopyranoside and methyl 6-deoxy-6-nitro-L-idopyranoside under mild alkaline conditions undergo fission of the pyranoside ring followed by loss of the aglycon and cyclization of the resulting nitro sugars to a mixture of *scyllo* and *myo-1* deoxynitroinositols. A mechanism for the alkaline glycoside cleavage is proposed in which a 5,6-dideoxy-6-nitro-aldos-5-ene is an intermediate. The susceptibility to attack by base of such nitroolefins has been studied using 3-*O*-acetyl-5,6-dideoxy-1,2-*O*-isopropylidene-6-nitro-α-D-*xylo*-hexofuranos-5-ene. It has been shown that this compound, when treated with methanolic sodium hydroxide, is methoxylated in position 5 and that this methoxylation occurs more rapidly than de-*O*-acetylation. The significance of this reaction with regard to alkaline acetal and ketal cleavages in the nitro sugar series is discussed.

INTRODUCTION

Lability towards alkali of acetals and ketals that bear a primary or secondary nitro group in the β-position has been observed on several occasions. Thus, Helferich and Hase (1) found that the base-catalyzed deacetylation of 2-nitroethyl β-D-glucopyranoside tetraacetate (I) was attended by fission of the glycosidic linkage; Fischer and Baer (2) observed a facile, alkaline removal of the 3,5-*O*-isopropylidene group in 6-deoxy-1,2:3,5-di-*O*-isopropylidene-6-nitro-α-D-glucofuranose (II)[2]; similarly, methyl 4,6-*O*-benzylidene-3-deoxy-3-nitro-β-D-glucopyranoside (III) readily loses benzaldehyde upon treatment with alkali (4); and finally, bis(2-nitrobutoxy)methane is cleaved by aqueous sodium hydroxide at 38° to 2-nitro-1-butanol and formaldehyde (5).

In view of these facts it appeared conceivable that alkyl hexopyranosides bearing a nitro group in the 6-position, e.g. IV, might represent a novel class of alkali-sensitive glycosides (cf. ref. 6), which would differ from Helferich and Hase's labile glycoside in that the activating substituent is located in the sugar moiety rather than the aglycon. If fission occurs it would be expected to take place between the ring oxygen and C-5 rather than between the lactol oxygen and aglycon. Compounds of this type were therefore prepared, and their predicted alkali cleavage was verified.

MATERIALS

Heating of 6-deoxy-1,2-*O*-isopropylidene-6-nitro-α-D-glucofuranose (V) under reflux in methanol containing 1% of hydrogen chloride produced a syrupy α,β mixture of methyl 6-deoxy-6-nitro-D-glucopyranosides (IV). Acetylation of this material produced a crystalline mixture of the 2,3,4-tri-*O*-acetates (VI) from which the pure α-anomer was obtained after lengthy recrystallizations. Since the anomeric configuration was not regarded as being of prime relevance to an initial study of the present problem, the mixtures IV and

[1] *For Part I, see ref. 8.*
[2] *Under the conditions employed (action of dilute methanolic sodium hydroxide for 30 min at room temperature) the 5-epimeric, L-idose analog of II (VIII) appeared more stable. However, recent investigations have shown that in this case complete loss of the 3,5 acetone group occurs within 3 h at 50° (3).*

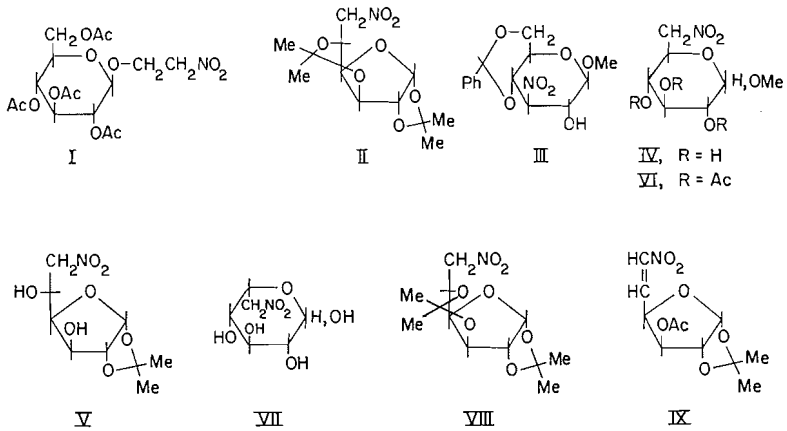

Formula VII should have OMe instead of OH at position 1.

VI were used in the subsequent work. Similarly, α,β mixtures of methyl 6-deoxy-6-nitro-L-idopyranoside (VII) were prepared. This was done best by methanolysis of crystalline 6-deoxy-1,2:3,5-di-*O*-isopropylidene-6-nitro-β-L-idofuranose (VIII). Glycosidation of free 6-deoxy-6-nitro-L-idose was also possible although some difficulty arose here because of an interesting instability of that sugar, which will be dealt with in an accompanying communication. Finally, it was convenient to subject to methanolysis the readily available, crystalline mixture of V and its 5-epimer, 6-deoxy-1,2-*O*-isopropylidene-6-nitro-β-L-idofuranose. The D-*gluco*-L-*ido* glycoside mixture so obtained (IV + VII) consumed 2 moles of periodate as required for hexopyranosides.

In the course of the studies described below it became desirable to prepare, as a model compound, 3-*O*-acetyl-5,6-dideoxy-1,2-*O*-isopropylidene-6-nitro-α-D-*xylo*-hexofuranos-5-ene (IX). Acetylation of V gave a syrup that was considered to be largely the 3,5-di-*O*-acetate. The infrared spectrum revealed, however, that the acetylation was accompanied to some extent by the generation of a nitroolefin grouping. Since the nitroolefin (IX) rather than a pure diacetate of V was the goal, the crude acetylation product was subjected to a Schmidt–Rutz reaction which produced crystalline IX in 56% yield.[3]

RESULTS AND DISCUSSION

The Alkaline Conversion of the Nitro Glycosides into Nitro Inositols

When the *gluco-ido* glycoside mixture IV + VII was heated for 20 min at 98° in 1.1 equivalents of aqueous $N/100$ sodium hydroxide, the methoxyl content decreased by 90%. Paper chromatography revealed the disappearance of the fast-traveling methyl glycosides and the formation of two slow-moving products. These products also appeared, in the course of several days, when a similar reaction was run at 20°. Treatment of the L-idosides (VII) and of the D-glucoside triacetates (VI) with 1 and 4 equivalents, respectively, of $N/100$ sodium hydroxide for 7 h at 60° resulted in their complete conversion into the same slow-moving products whose chromatographic spot intensities were all approximately equal.

The two reaction products were identified, by co-chromatography with authentic samples, as *scyllo*-deoxynitroinositol (X) (R_{rh} 0.70) and D,L-*myo*-1-deoxynitroinositol (XI) (R_{rh} 0.65). The *scyllo* isomer was isolated in crystalline form.

[3]*The analogous 1,2-O-cyclohexylidene derivative has recently been obtained in amorphous condition (7). Partial olefin formation in the acetylation step is not surprising in view of what has been found in similar systems (cf. ref. 8).*

Can. J. Chem. Downloaded from www.nrcresearchpress.com by 210.87.254.6 on 09/05/12
For personal use only.

Can. J. Chem. Downloaded from www.nrcresearchpress.com by 210.87.254.6 on 09/05/12
For personal use only.

The conversion of methyl 6-deoxy-6-nitro-α,β-D-glucopyranoside (IV) into deoxynitroinositols at 25° was followed by ultraviolet spectroscopy. This was possible by virtue of a change in absorbance of the nitronate peak that is associated with the reaction. The nitro glycoside (IV), in a buffer solution of pH 10,[4] has an initial ϵ value of 10 000 at λ_{max} 242.5 mμ, whereas nitro inositol (X) shows ϵ 3 000 at λ_{max} 250 mμ under the same conditions and attains an extinction comparable to that of IV only at increased pH (with λ_{max} shifting to 248 mμ) (Fig. 1). This difference evidently reflects a lower acidity of X as compared to IV, which causes a smaller proportion of the absorbing species, the nitronate ion, to exist in equilibrium with undissociated nitro compound at pH 10. In Fig. 2 is depicted the decrease in absorbance that occurred in a 0.004 *M* solution of IV at pH 10 in the course of 11 days, after which time ϵ had reached a value (4 000) close to that of X-nitronate. As with the latter, addition thereafter of sodium hydroxide to pH 12 produced a peak of λ_{max} 247 mμ and ϵ 10 000. The half-life of IV under the conditions employed was about 28 h.

When a similar reaction was carried out at pH 12.6 the picture was similar in the early stages (Fig. 3). Later on a broad, relatively weak absorption developed gradually in the near ultraviolet, which must have arisen from the formation of products other than nitro inositols.[5]

It has been demonstrated by Grosheintz and Fischer (9) that 6-deoxy-6-nitro-D-glucose and -L-idose undergo base-catalyzed cyclizations in which both yield three stereoisomeric deoxynitroinositols later shown (10, 11) to possess *scyllo* (X), D,L-*myo-1* (XI), and *muco-3*

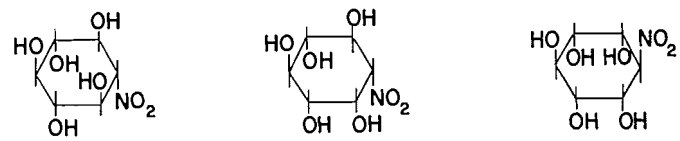

X XI XII

(XII) configurations. Lichtenthaler's (11) detailed studies established that the *muco* isomer arises by kinetic control; when allowed to remain in an alkaline medium it epimerizes to a thermodynamically more stable equilibrium mixture of the *scyllo* and *myo* compounds. It is obvious from our findings, therefore, that the methyl pyranosides of 6-deoxy-6-nitro hexoses readily undergo base-catalyzed deglycosidation to the free sugars, which do not accumulate but cyclize rapidly to inositol derivatives. The process is visualized to proceed via a nitroolefin hemiacetal (XIII) which instantly loses methoxide ion to furnish a nitroolefin aldose (XIV). The latter is attacked by hydroxyl ion, giving hexose nitronate (XV) predisposed to Fischer cyclization.

As far as the β-elimination of an acetal oxygen and the formation of a nitroolefin intermediate are concerned, the mechanism suggested here is the same as that proposed (2) in the alkaline removal of the 3,5-*O*-isopropylidene group from 6-deoxy-1,2:3,5-di-*O*-isopropylidene-6-nitro-α-D-glucofuranose (II). In this latter case the nitroolefin presumed to be primarily engendered was the 1,2-acetone derivative of XIV; it evidently added methoxide ion producing two stable, stereoisomeric methyl ethers.[6]

To assess the susceptibility of the hypothetical nitroolefin intermediates to nucleophile

[4]*The actual pH of an unbuffered M/10 sodium IV-nitronate solution was found to be 9.8.*

[5]*The spectral measurements were taken at pH 10 to ensure comparability with the reaction illustrated in Fig. 2. After 11 days no peak in the 247 mμ region was brought forth by measuring at pH 12, but only a slight intensity increase in the long wavelength area.*

[6]*The reaction was carried out in methanol solution (2). Cyclization of the products to inositol derivatives was, of course, prevented by the 1,2-acetone group that is alkali-stable under the conditions employed.*

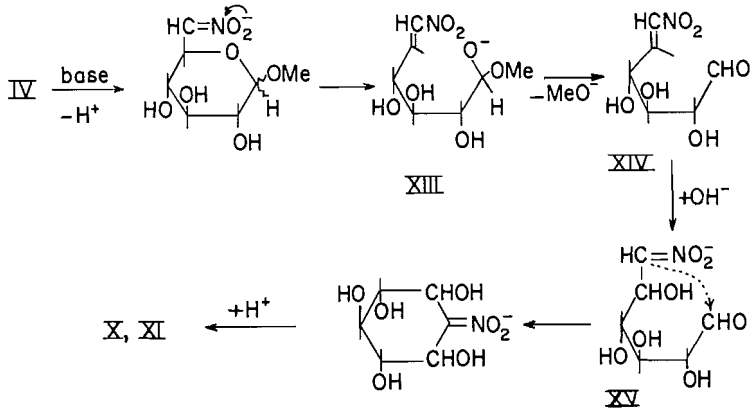

attack, the behavior toward methanolic sodium hydroxide of crystalline 3-*O*-acetyl-5,6-dideoxy-1,2-isopropylidene-6-nitro-α-D-*xylo*-hexofuranos-5-ene (IX) was studied. These experiments, which are described in the next section, clearly proved the extreme ease with which such olefins are liable to add base. As will be seen, the results are in full accord with the mechanism discussed above and earlier (2), and they suggest in addition that in the sequence IV → XIV → XV the ring cleavage is the rate-determining step.

The Action of Base upon Nitroolefin IX

3-*O*-Acetyl-5,6-dideoxy-1,2-*O*-isopropylidene-6-nitro-α-D-*xylo*-hexofuranos-5-ene (IX), owing to its nitroolefin structure, exhibits high-intensity absorption in neutral and acidic solution: λ_{max} 230 mμ (ε 10 500) in cyclohexane; and λ_{max} 234 mμ (ε 11 500) in methanol with and without addition of sulfuric acid. The addition of *excess* sodium hydroxide to a 10^{-4} *M*, methanolic solution caused an instantaneous bathochromic shift to 244–245 mμ (Fig. 4). When the amount of alkali added was limited to two equivalents,[7] however, the 234 mμ peak disappeared in the course of 90 min with a half-life of ca. 12 min (at 26°). Addition of excess hydroxide after 90 min then produced a new peak at 245 mμ (ε 9 500) (Fig. 5). Now the experiment was repeated over an extended period of time with aliquots being withdrawn at intervals. When the reaction was arrested in the aliquots by acidification with acetic acid or by cation exchange the absorption ceased to decrease, thus providing a measure for the amount of remnant nitroolefin. Thin-layer chromatography revealed the nature of the reaction (Fig. 6). Paralleling the decrease in ultraviolet absorbance, the spot of starting material IX (R_f 0.73) disappeared with concomitant appearance of a spot (R_f 0.65) attributable to 3-*O*-acetyl-6-deoxy-1,2-*O*-isopropylidene-5-*O*-methyl-6-nitro-D-glucofuranose (XVI) and -L-idofuranose (XVII), which were not separated. As the reaction continued the new spot gave way to one of R_f 0.53 that could be resolved into two spots by use of a different solvent system. These spots were indistinguishable from those given by 6-deoxy-1,2-*O*-isopropylidene-5-*O*-methyl-6-nitro-D-glucofuranose (XVIII) and -L-idofuranose (XIX) that had been obtained (2) by treatment with methanolic alkali of the diacetone compound II, and the ratio of XVIII and XIX, roughly estimated at 4:1, was found to be the same in both cases. This can be regarded as proof for the nitroolefin structure being an intermediate in the ketal fission and methoxylation of II as earlier proposed.

From an inspection of Figs. 5 and 6 it follows, moreover, that methoxylation of the

[7]*One equivalent to be consumed by saponification of the acetyl group.*

Can. J. Chem. Downloaded from www.nrcresearchpress.com by 210.87.254.6 on 09/05/12
For personal use only.

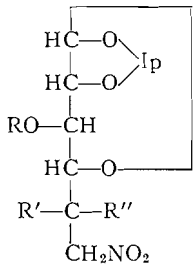

XVI, R = Ac, R′ = H, R″ = OMe
XVII, R = Ac, R′ = OMe, R″ = H
XVIII, R = R′ = H, R″ = OMe
XIX, R = R″ = H, R′ = OMe

olefinic bond in IX occurred at a rate markedly faster than the de-*O*-acetylation which was quite incomplete when, after 1 h, virtually all of IX had reacted. This conclusion was supported by the results of infrared spectroscopy, confirming the ultraviolet and chromatographic data. When the reaction was done at a higher initial concentration of IX (3.65×10^{-2} *M*), the ultraviolet and thin-layer patterns were fully analogous to those in Figs. 5 and 6, although the speed of reaction was considerably greater: after only 20 and 90 s, respectively, the 234 mμ-peak had decreased by 45 and 90%, while on the chromatograms (Fig. 7) a slow spot corresponding to deacetylated material was already visible after 90 s and became the sole spot within 1 h. The infrared spectra also indicate the rapid conversion of the nitroolefin IX into the nitroalkane acetates (XVI + XVII) and the deacetylation of the latter to XVIII and XIX. Figure 7*b* (20 s) shows a reduction by about half, of the (weak) C=C absorption at 1 680 cm^{-1} and, more significantly, the emergence of a nitroalkane peak (1 555 cm^{-1}) in addition to the olefinic nitro peak (1 530 cm^{-1}). Figure 7*c* (90 s) indicates a far-reaching though incomplete replacement of IX by XVI + XVII, since the C=C frequency has now vanished and the originally strong olefinic NO_2 peak is reduced to a shoulder of the newly generated nitroalkane peak. The change in the intensity ratio of the carbonyl and nitro absorptions and the occurrence of a (yet small) hydroxyl band in Fig. 7*c* bears out the beginning of the deacetylation which progresses (Fig. 7*d*,*e*), and after 1 h (Fig. 7*f*) appears to be complete.

EXPERIMENTAL

Paper Chromatography

Paper chromatography was performed using the descending technique on Whatman No. 1 paper with 1-butanol – acetic acid – water (4:1:5 (v/v), upper layer; the lower layer was placed in the bottom of the tank). The spots were made visible by spraying the chromatogram with ammoniacal silver reagent (0.1 *N* $AgNO_3$, 5 *N* NH_3, 2 *N* NaOH, 1:1:2) and heating it over steam. L-Rhamnose served as a reference standard (R_{rh} = 1). Authentic deoxynitroinositols X (R_{rh} 0.70), XI (R_{rh} 0.65), and XII (R_{rh} 1.04) were prepared according to Lichtenthaler (11; cf. also ref. 13).

Thin-Layer Chromatography

Thin-layer chromatography was done on Silica Gel G (E. Merck AG, Darmstadt) activated for 1 h at 110°, with cyclohexane – ether (1:6) (solvent A) and chloroform – acetone (4:1) (solvent B) as irrigating systems. The spots were detected with 1% ceric sulfate in 10% sulfuric acid.

Spectroscopy

Infrared spectra were taken using a Perkin–Elmer Infracord instrument.

Ultraviolet spectra were recorded with a Perkin–Elmer spectrophotometer Model 202.

Methyl 6-Deoxy-6-nitro-α,β-D-glucopyranosides (IV)

A solution of 500 mg of 6-deoxy-1,2-*O*-isopropylidene-6-nitro-α-D-glucofuranose (V) (12) in 50 ml of methanol containing 1% by weight of hydrogen chloride was refluxed for 4 h. Upon cooling of the solution to 25° the hydrogen chloride was removed by anion exchange with Dowex-1-X8 resin (carbonate form) and the filtrate was evaporated *in vacuo*, with 2 portions of methanol being added near the end. There was obtained 425 mg of a colorless syrup (IV) which, on paper chromatography, showed two spots (R_{rh} 1.48 and 1.62) and was free from starting material (R_{rh} 1.88).

Can. J. Chem. Downloaded from www.nrcresearchpress.com by 210.87.254.6 on 09/05/12
For personal use only.

Methyl 6-Deoxy-6-nitro-2,3,4-tri-O-acetyl-α,β-D-glucopyranosides (VI)

Glycoside mixture IV (340 mg) and anhydrous sodium acetate (340 mg) in 7 ml of acetic anhydride were heated for 1 h on a steam bath. The mixture was allowed to cool and then stirred into 70 ml of ice water, whereby an ochra-colored, crystalline product separated out. The crude product was exhaustively washed with water and dried; yield 448 mg. After one recrystallization from ethanol the acetate mixture (VI) was obtained as colorless needles melting at 148–151° and giving a correct elemental analysis.

Anal. Calcd. for $C_{13}H_{19}NO_{10}$ (349.3): C, 44.70; H, 5.48; N, 4.01. Found: C, 44.87; H, 5.62; N, 4.20.

A part of the acetate mixture VI (200 mg) was recrystallized eight more times. The melting point was 173–175° ($[\alpha]_D^{23}$ + 103.6° in chloroform) after the fifth, and 179–180° after the eighth and ninth recrystallizations. The final rotation was $[\alpha]_D^{23}$ +145° (*c*, 1 in chloroform). This product (21 mg) was considered to be the pure α-anomer. Its infrared spectrum was in agreement with the assigned structure: no hydroxyl absorption; 1 740 cm^{-1} (acetyl C=O); 1 550 and 1 370 cm^{-1} (asym. and sym. C—NO_2).

Methyl 6-Deoxy-6-nitro-α,β-L-idopyranosides (VII)

A solution of 200 mg of 6-deoxy-1,2:3,5-di-*O*-isopropylidene-6-nitro-β-L-idofuranose (VIII) (12) in 20 ml of methanol containing 1% by weight of hydrogen chloride was heated under reflux for 5 h. The reaction mixture was worked up as described above for IV. A colorless syrup of VII (150 mg; 97%) was obtained which gave two chromatographic spots (R_{rh} 1.50 and 1.65); no starting material and no slow-moving by-products (deoxynitroinositols, cf. ref. 13) were detectable. The product (VII) had a methoxyl content of 13.0% (calcd. 13.9).

Mixture of IV and VII

A crystalline mixture (2 g) of monoacetone compound V and its β-L-*ido* isomer (12) was methanolyzed for 4 h under reflux with 200 ml of 1% methanolic hydrogen chloride. Work-up as described above for IV afforded 1.7 g (95%) of a colorless syrup showing a methoxyl content of 13.15% (calcd. 13.9). Paper chromatography gave the same pattern as the glycosides IV and the glycosides VII.

A sample of the mixture IV + VII (22.3 mg; 0.1 mmole) was oxidized with sodium periodate, and the consumption of oxidant was followed by titration (14). The consumption, in molar equivalents of $NaIO_4$, was 0.93 (5 min) → 1.32 (10 min) → 1.48 (30 min) → 1.75 (70 min) → 2.02 (130 min), and did not increase further.

3-O-Acetyl-5,6-dideoxy-1,2-O-isopropylidene-6-nitro-α-D-xylo-hexofuranos-5-ene (IX)

To a suspension in anhydrous ether (15 ml) of 400 mg of monoacetone compound V (12) was added pyridine (2.4 ml) and acetic anhydride (0.9 ml). The reaction mixture was kept in a refrigerator for 18 h and then extracted three times with 3 ml of water, twice with 2 ml of 10% acetic acid, and twice with 2 ml of water. Finally, the solution was dried over anhydrous sodium sulfate and evaporated with several additions of xylene to give a colorless syrup (390 mg). The infrared spectrum of this syrup exhibited in addition to the expected characteristics of a V-diacetate (acetyl C=O at 1 755 cm^{-1}; C—NO_2 at 1 560 cm^{-1}), bands attributable to the olefin IX (olefinic NO_2 at 1 535 cm^{-1} and C=C at 1 670 cm^{-1}).

The above syrup was dissolved in 6 ml of dry benzene and the solution was heated under reflux for 5 h in the presence of sodium bicarbonate (600 mg). After it had been cooled and filtered the solution was evaporated, leaving a yellow syrup in which according to an infrared spectrum the nitroolefin predominated, but some nitroalkane was still present. The syrup was extracted twice with 10 ml of hot cyclohexane which upon evaporation gave a partly crystalline residue. This residue was taken up in a small amount of ether from which on standing IX crystallized in long prisms, and these were isolated and washed with ice-cold ether. The yield was 179 mg (56%); m.p. 106–107°. The melting point was raised to 109–110° by one recrystallization from ether and then remained constant. $[\alpha]_D^{23}$ +6.5° (*c*, 1 in chloroform). Ultraviolet absorption: λ_{max} 230 mμ (ε 10 500) in cyclohexane; 234 mμ (ε 11 500) in methanol, unchanged on addition of *N*/10 sulfuric acid (1 drop per milliliter). A 60-Mc nuclear magnetic resonance spectrum in deuterochloroform exhibited peaks corresponding to 3 protons each at 8.65 τ and 8.46τ (the two isopropylidene methyls) and at 7.95τ (acetoxy). A signal at 2.79τ that corresponded to two protons was assigned to the olefinic H-5 and H-6. The H-1, H-2, H-3, and H-4 protons gave doublets in the 4–5.3τ region.

Anal. Calcd. for $C_{11}H_{15}NO_7$ (273.3): C, 48.35; H, 5.53; N, 5.13. Found: C, 48.60; H, 5.63; N, 5.15.

Action of Base upon the Nitro Glycosides

An accurately weighed sample (4.70 mg) of the glycoside mixture IV + VII was introduced in the disconnected reaction flask of a micro methoxyl determination apparatus. *N*/100 sodium hydroxide (2.32 ml, 1.1 molar equivalent) was added and the loosely stoppered flask was heated in a steam bath for 20 min. Upon cooling of the solution, carbon dioxide was passed through the inlet tube for 10 min, and the solution was then freeze-dried. Water (1 ml) was added and the freeze-drying was repeated. Methoxyl determination gave 1.34% of OCH_3 corresponding to 9.65% of the theoretical value (and to 10.4% of the value found) for the starting glycoside.

In a similar experiment 12 mg of glycoside was heated for 20 min at 98° in an equivalent amount of *N*/100 sodium hydroxide; the solution was then deionized with Rexyn RG-50 (H^+), concentrated *in vacuo*, and chromatographed. It gave strong spots at R_{rh} 0.66 and R_{rh} 0.71, but no spots in the glycoside area of R_{rh} 1.5–1.65.

Can. J. Chem. Downloaded from www.nrcresearchpress.com by 210.87.254.6 on 09/05/12
For personal use only.

A sample of methyl L-idosides VII was dissolved in 1 molar equivalent of $N/100$ sodium hydroxide and heated in a closed vessel for 7 h at 60°. After deionization, chromatography gave spots of approximately equal intensity of X and XI; the glycoside spots had disappeared.

A 10-mg sample of the methyl D-glucoside triacetates VI was treated in the same way but with 4 molar equivalents of base. The material, which was difficultly soluble in the cold, dissolved within a few minutes at 60° as deacetylation proceeded. The results of chromatography were the same as with VII. From a 100-mg sample of VI that was treated analogously a syrup was obtained upon deionization and repeated evaporation with water and then with ethanol. When allowed to stand at 4°, a concentrated solution of the syrup in ethanol deposited crystals of *scyllo* deoxynitroinositol (X). The identity of the product was supported by paper chromatography and infrared spectrum. The melting point was 210–220°; reported: 215° decomp. (9); 224–225° for recrystallized product (11).

Ultraviolet Spectroscopic Observations

Nitroglycoside IV (4.46 mg, 0.02 mmole) was dissolved in 5.0 ml of buffer (pH 10) giving a 4×10^{-3} M

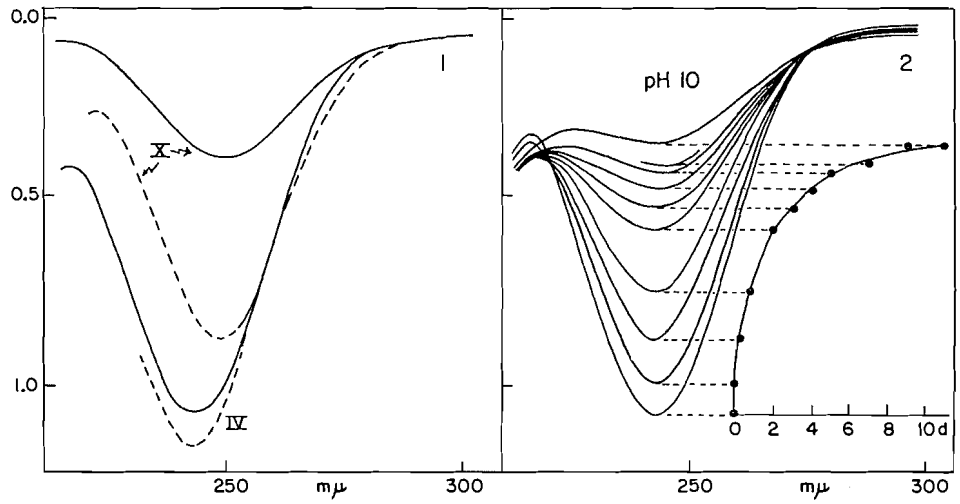

FIG. 1. Ultraviolet spectra of nitroglucoside IV and nitroinositol X at pH 10 (solid lines) and at pH 12 (broken lines); 10^{-4} M solutions in aqueous buffer (cf. Experimental).

FIG. 2. Decrease in absorbance in nitroglucoside IV at pH 10 and room temperature during 11 days. The three lower curves correspond to reaction times of 5 min, 3 h, and 10 h, respectively.

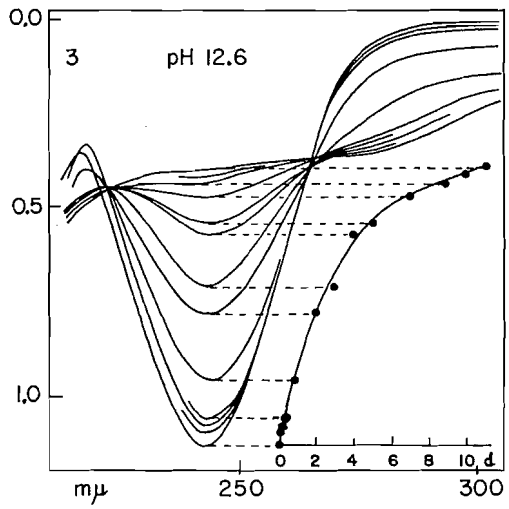

FIG. 3. Decrease in absorbance in nitroglucoside IV at pH 12.6 and room temperature during 11 days.

Can. J. Chem. Downloaded from www.nrcresearchpress.com by 210.87.254.6 on 09/05/12
For personal use only.

solution which was allowed to stand at room temperature. The buffer was composed of boric acid, potassium chloride, and sodium hydroxide according to Clark and Lubs (15). For the measurements recorded in Fig. 2, 0.08-ml aliquots of the solution were mixed in the photometer cell with 3 ml of buffer, the concentration in nitro compound thus becoming close to 10^{-4} *M*. The reference cell contained blank buffer. To record also the extinction at pH 12, 0.1 ml of *N* sodium hydroxide was added to the above, 3 ml of buffer. (The pH thus attained was found potentiometrically.)

The data shown in Fig. 3 were obtained analogously, except that IV was dissolved in *N*/10 sodium hydroxide. Again, pH 10 buffer was used as diluent for the measurements.

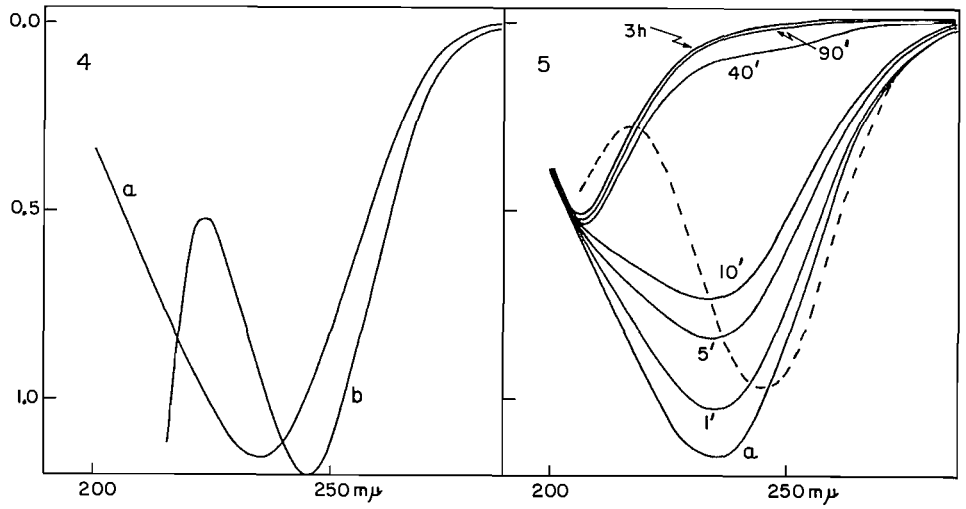

FIG. 4. Nitroolefin IX, 10^{-4} *M* solution in methanol (curve *a*; unchanged upon addition of sulfuric acid); curve *b*, the same after addition of excess sodium hydroxide (0.1 ml *N* NaOH per 3 ml of solution).

FIG. 5. Decrease in absorbance in a 10^{-4} *M* methanolic solution of nitroolefin IX in the presence of 2 equivalents of sodium hydroxide. Curve *a*, IX before the addition of alkali. Broken curve, reaction product at 3 h upon addition of excess alkali (0.1 ml of *N* NaOH per 3 ml of solution).

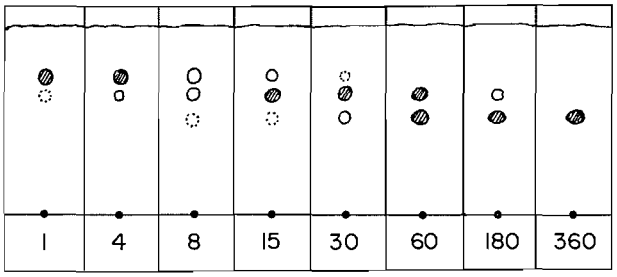

FIG. 6. Thin-layer chromatograms showing the conversion of IX via XVI + XVII into XVIII + XIX (solvent system A). The numbers indicate reaction time in minutes. Strong spots are shaded, medium spots are given as solid circles, trace spots as broken circles.

Action of Base upon Nitroolefin IX

To a 10^{-4} *M* solution of IX in methanol (50 ml) was added 0.1 ml *N*/10 sodium hydroxide solution (2 molar equivalents) and the changes in the ultraviolet spectrum were followed (Fig. 5).

The experiment was repeated with aliquots of 5 ml being withdrawn periodically. The aliquots were deionized by shaking them briefly with a small quantity of Rexyn RG-50 (H^+) that had been washed with methanol and dried in a desiccator. The spectra of the deionized aliquots indicated that the decrease in absorption was arrested. The solutions were then evaporated *in vacuo* and the residues (approximately 0.1 mg) taken up in a few drops of chloroform and applied to thin-layer plates (2.5 × 7.5 cm). Development with solvent A gave the patterns depicted in Fig. 6. The slow-moving spot (R_f 0.53) that occurred as the end product of the reaction was resolved into two spots of R_f 0.46 and 0.39 when larger plates (5 × 20 cm) and solvent B were employed. The following reference compounds were used: XVIII (2) with R_f 0.46 (solvent B)

Can. J. Chem. Downloaded from www.nrcresearchpress.com by 210.87.254.6 on 09/05/12
For personal use only.

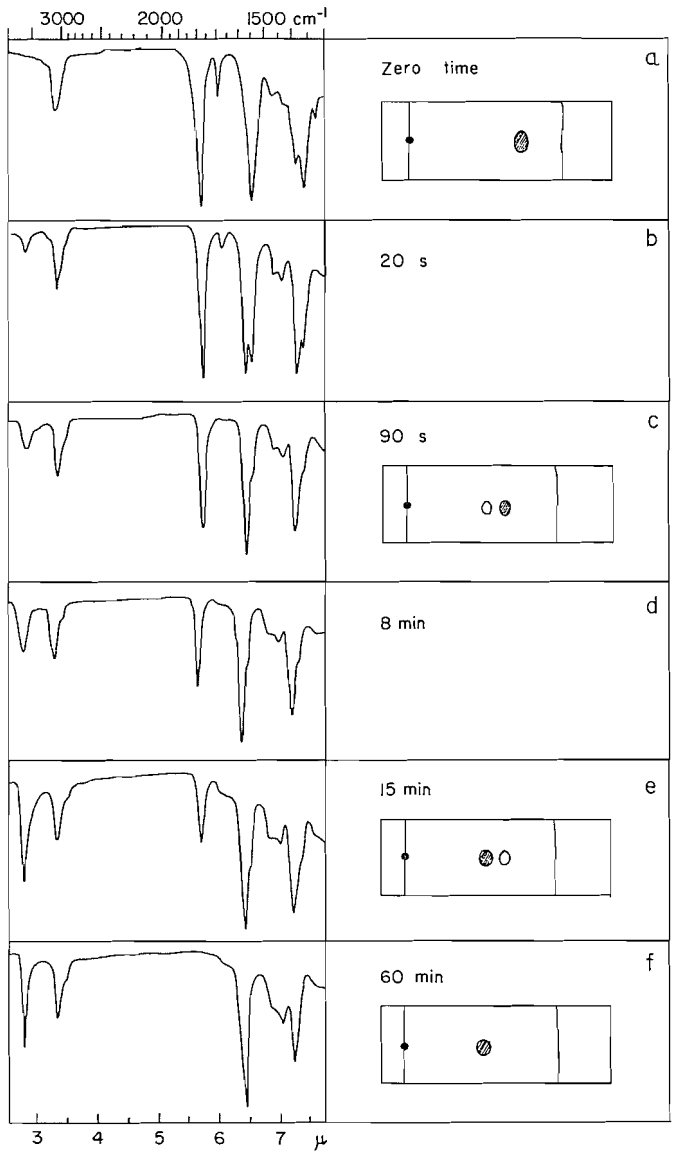

FIG. 7. Infrared spectra and thin-layer chromatograms (solvent A) showing the action of methanolic alkali upon nitroolefin IX.

and 0.53 (solvent A); XIX (2) with R_f 0.39 (solvent B) and 0.53 (solvent A); the product (R_f 0.65 in solvent A) that was obtained by acetylation of XIX (sodium acetate – acetic anhydride; 3 min at 130°).

For the experiments represented by Fig. 7, a solution was made of IX (20 mg) in methanol (20 ml) to which 0.15 ml of *N* NaOH was added. This corresponded to an initial concentration of 3.65×10^{-2} *M* in IX. Aliquots of 2 ml were taken at given intervals and neutralized using *N*/10 hydrochloric acid. From the aliquots withdrawn after 20 s to 60 min ultraviolet spectra were obtained, 0.1 ml of each aliquot having been diluted with 3 ml of methanol. The optical densities at 234 mμ were 55% (20 s), 10% (90 s) and almost 0% (60 min) of that given by a sample of IX of equal concentration but free of alkali. The aliquots were then evaporated to dryness *in vacuo* and the residues were taken up in dry chloroform. Thin-layer chromatograms (solvent A) were obtained (Fig. 7) and infrared spectra were taken of films produced by evaporation of the solvent chloroform on warmed sodium chloride plates (Fig. 7).

Can. J. Chem. Downloaded from www.nrcresearchpress.com by 210.87.254.6 on 09/05/12
For personal use only.

ACKNOWLEDGMENT

This work was supported by the National Research Council of Canada and by the Ontario Research Foundation.

REFERENCES

1. B. HELFERICH and M. HASE. Ann. **554**, 261 (1943).
2. H. O. L. FISCHER and H. H. BAER. Ann. **619**, 53 (1958).
3. H. H. BAER and W. RANK. In preparation.
4. H. H. BAER and F. KIENZLE. In preparation.
5. H. FEUER and S. MARKOFSKY. J. Org. Chem. **29**, 929 (1964).
6. C. E. BALLOU. Advan. Carbohydrate Chem. **9**, 59 (1954).
7. H. PAULSEN. Ann. **665**, 166 (1963).
8. H. H. BAER, F. KIENZLE, and T. NEILSON. Can. J. Chem. **43**, 1829 (1965).
9. J. M. GROSHEINTZ and H. O. L. FISCHER. J. Am. Chem. Soc. **70**, 1479 (1948)
10. T. POSTERNAK. Helv. Chim. Acta, **33**, 1957 (1950). T. POSTERNAK, W. H. SCHOPPER, and R. HUGUENIN. Helv. Chim. Acta, **40**, 1875 (1957).
11. F. W. LICHTENTHALER. Ber. **94**, 3071 (1961).
12. J. M. GROSHEINTZ and H. O. L. FISCHER. J. Am. Chem. Soc. **70**, 1476 (1948).
13. H. H. BAER and W. RANK. Can. J. Chem. This issue.
14. R. KUHN, A. GAUHE, and H. H. BAER. Ber. **87**, 289 (1954).
15. J. D'ANS and E. LAX. Taschenbuch für Chemiker und Physiker. Springer–Verlag, Berlin. 1949. p. 1592

Can. J. Chem. Downloaded from www.nrcresearchpress.com by 210.87.254.6 on 09/05/12
For personal use only.

Can. J. Chem. Downloaded from www.nrcresearchpress.com by 210.87.254.6 on 09/05/12
For personal use only.

NUCLEAR MAGNETIC RESONANCE AND INFRARED STUDIES OF ACYLATED IMIDAZOLIDINONES AND IMIDAZOLIDINETHIONES[1,2]

R. GREENHALGH AND M. A. WEINBERGER
Defence Chemical Biological and Radiation Laboratories, Ottawa, Canada

Received July 2, 1965

ABSTRACT

The infrared and nuclear magnetic resonance spectra of 1-acyl and 1,3-diacyl derivatives of 2-imidazolidinones and 2-imidazolidinethiones were determined, where the acyl groups were acetyl, benzoyl, or trifluoroacetyl. The frequency of the ring carbonyl stretching vibration increases with the degree of acylation and the electron-withdrawing power of the acyl group. The methylene protons of the diacylated derivatives show a single peak, the paramagnetic shift of which is similarly dependent on these parameters when the ring current effects are allowed for. This correlation between the $\nu_{C=O}$ and τ_{CH_2} favors the conclusion that the anisotropy of the acyl carbonyl group does not affect the relative methylene proton shift in these compounds and hence they all have the same preferred configuration. This was deduced to be the planar *trans,trans* structure with respect to the carbonyls. In the unsymmetrical 1,3-diacyl compounds the methylene protons are also nearly equivalent, the τ-value being the average of those for the symmetrical diacyl derivatives. This, together with the changes in the $\nu_{C=O}$ (acyl), is explained by mesomeric equalization of the electronic environment of nitrogen atoms 1 and 3. The C=S bond is found to have a strong deshielding influence on all protons.

INTRODUCTION

The potentialities of nuclear magnetic resonance (n.m.r.) spectroscopy for assigning structures and conformations in acylated 2-oxo-, 2-thio-, and 2-imino-imidazolidines have not in the past been fully exploited. We have used it to differentiate between the several structures suggested for triacetyl-2-imino-imidazolidine on the basis of its infrared spectrum (1). More recently Roberts (2) has also used n.m.r. to assign a symmetrical structure to diacetyl-2-imidazolidinone. Further aspects of the n.m.r. and infrared spectra of acylated 2-oxo- and 2-thio-imidazolidines will now be discussed.

Mecke *et al.* (3) have examined the infrared spectra of 1,3-dihetero-2-oxo-(or 2-thio-)-cyclopentanes and, in particular, investigated the ring carbonyl stretching vibration. They found that the carbonyl frequency is dependent on the nature of the adjacent atoms by virtue of their mass and their inductive and mesomeric effects, as well as on the ring angle at the carbonyl group. The mesomeric effect leads to an increase in the contribution of the canonical dipolar form $\overset{+}{C}—O^-$ and an increase in the angle, which favor a decrease in the carbonyl frequency. In the present work with compounds where the adjacent atoms are nitrogen, their nature is changed by acylation, thus complementing the work with compounds in which the atoms themselves were varied.

EXPERIMENTAL

The n.m.r. spectra were recorded with a Varian 4300–C spectrometer operating at 60 mc/s. Calibrations were made by the standard side band procedure. Chemical shifts with respect to tetramethylsilane are accurate to better than ±.01 p.p.m. The concentration of the compounds was normally 10% w/v.

A Perkin–Elmer Model 221 spectrophotometer was used to determine the infrared spectra. Solutions were 2% w/v in both chloroform and acetonitrile.

The compounds were prepared as specified below. All commercial samples were purified before use. Melting points are corrected.

[1]*Issued as DCBRL Report No. 472.*
[2]*Presented in part at the 46th C.I.C. Conference, Edmonton, June 1962.*

2-Imidazolidinone

A commercial sample obtained from du Pont de Nemour, U.S.A., was recrystallized from alcohol, m.p. 129–131°.

1-Acetyl-2-imidazolidinone

This compound was prepared by warming 2-imidazolidinone with acetic anhydride, m.p. 173–175° (lit. (4) 171.5–173°). The n.m.r. spectrum (D_2O) was analyzed as an A_2B_2 system and gave approximate τ-values of 6.6 and 6.2 for the 4- and 5-methylene protons respectively.

1,3-Diacetyl-2-imidazolidinone

1-Acetyl-2-imidazolidinone was refluxed for 1 h with acetic anhydride to give the diacetyl derivative, m.p. 126–127° (lit.(5) 126.7–127.5°).

1-Trifluoroacetyl-2-imidazolidinone

2-Imidazolidinone (400 mg) was heated under reflux with trifluoroacetic anhydride (2 ml) for 1 h, taken to dryness, and recrystallized from acetone in the form of white prisms, m.p. 166–168°, in 74% yield.

Anal. Calcd. for $C_5H_5O_2N_2F_3$: C, 32.96; H, 2.75; N, 15.38. Found: C, 33.13; H, 2.65; N, 15.46.

1,3-Ditrifluoroacetyl-2-imidazolidinone

2-Imidazolidinone (500 mg) was heated under reflux with trifluoroacetic anhydride (3 ml) for 24 h. Evaporation to dryness and recrystallization from chloroform/acetone gave white prisms, m.p. 123–124°, in 67% yield.

Anal. Calcd. for $C_7H_6O_3N_2F_6$: C, 29.10; H, 1.30; N, 9.72. Found: C, 29.29; H, 1.25; N, 10.03.

1-Acetyl-3-trifluoroacetyl-2-imidazolidinone

1-Acetyl-2-imidazolidinone (350 mg) was heated under reflux for 24 h with trifluoroacetic anhydride (1 ml). After the solution was concentrated, recrystallization of the product twice from ether gave white plates, m.p. 88–89°, in 81% yield.

Anal. Calcd. for $C_7H_7O_3N_2F_3$: C, 37.50; H, 3.12; N, 12.50. Found: C, 37.79; H, 3.15; N, 12.62 (Kjeldahl).

1,3-Dibenzoyl-2-imidazolidinone

2-Imidazolidinone (500 mg) and benzoyl chloride (2.5 ml) were dissolved in pyridine (5 ml) and heated on a steam bath for 30 min. The solid residue from evaporation was extracted with benzene, and removal of the benzene gave a crystalline residue. The product was finally recrystallized from chloroform to give white needles, m.p. 238–239°, in 42% yield.

Anal. Calcd. for $C_{17}H_{14}O_3N_2$: C, 69.40; H, 4.76; N, 9.52. Found: C, 69.80; H, 4.84; N, 9.57.

1-Acetyl-3-benzoyl-2-imidazolidinone

1-Acetyl-2-imidazolidinone (750 mg) and benzoyl chloride (2 ml) were dissolved in pyridine (5 ml) and heated for 45 min on a steam bath. The material that was left after evaporation to dryness was extracted with hot benzene, which was then removed, and the product was recrystallized from ethanol as white needles (61% yield) m.p. 182–184°.

Anal. Calcd. for $C_{12}H_{12}O_3N_2$: C, 62.00; H, 5.17; N, 12.05. Found: C, 62.20; H, 5.16; N, 11.97.

2-Imidazolidinethione

This material was obtained from the Matheson, Coleman, and Bell Co. U.S.A., and was recrystallized from alcohol, m.p. 202–203°.

1-Acetyl-2-imidazolidinethione

This substance was prepared by treating 2-imidazolidinethione with acetyl chloride in glacial acetic acid, m.p. 165–167° (lit. (6) 161–163°). The n.m.r. spectrum ($CHCl_3$) was analyzed as an A_2B_2 system and gave approximate τ values of 6.4 and 5.8 for the 4- and 5-methylene protons respectively.

1,3-Diacetyl-2-imidazolidinethione

2-Imidazolidinethione was refluxed with acetic anhydride, m.p. 87–89° (lit. (6) 85–87°).

1,3-Ditrifluoroacetyl-2-imidazolidinethione

2-Imidazolidinethione (500 mg) was heated under reflux for 5 h with trifluoroacetic anhydride (10 ml). When the solution was cooled crystals appeared, which were recrystallized from benzene to give red prisms, m.p. 142–144°, in 53% yield.

Anal. Calcd. for $C_7H_4O_2N_2SF_6$: C, 28.55; H, 1.36; N, 9.54; S, 10.88. Found: C, 28.68; H, 1.43; N, 9.58; S, 10.63.

RESULTS AND DISCUSSION

A list of the compounds studied in this investigation together with the main absorption bands in the 1 850–1 600 cm^{-1} region of the infrared is given in Table I.

The values found for 2-imidazolidinone and its acylated derivatives differ from those

Can. J. Chem. Downloaded from www.nrcresearchpress.com by 210.87.254.6 on 09/05/12
For personal use only.

Can. J. Chem. Downloaded from www.nrcresearchpress.com by 210.87.254.6 on 09/05/12
For personal use only.

TABLE I

The infrared absorption of solutions of acylated 2-imidazolidinones and 2-imidazolidinethiones in the region 1 850–1 600 cm^{-1}

	Frequency (cm^{-1})					
	$CHCl_3$			CH_3CN		
2-Imidazolidinone	1 703			1 712		
1-Acetyl-2-imidazolidinone	1 739 (VS)		1 680 (S)	1 741 (VS)		1 680 (S)
1,3-Diacetyl-2-imidazolidinone	1 759 (S)		1 698 (VS)	1 760 (S)		1 702 (VS)
1-Trifluoroacetyl-2-imidazolidinone	1 774 (VS)		1 710 (S)	1 774 (VS)		1 707 (S)
1,3-Ditrifluoroacetyl-2-imidazolidinone	1 810 (S)		1 739 (VS)	1 813 (S)		1 737 (VS)
1-Acetyl-3-trifluoroacetyl-2-imidazolidinone	1 781 (S)	1 722 (VS)	1 710 (Sh)	1 782 (S)	1 724 (VS)	1 709 (S)
1,3-Dibenzoyl-2-imidazolidinone	1 768 (S)		1 679 (VS)			
1-Acetyl-3-benzoyl-2-imidazolidinone	1 765 (S)	1 695 (Sh)	1 685 (VS)			
2-Imidazolidinethione	—	—	—	—	—	—
1-Acetyl-2-imidazolidinethione			1 677			1 681
1,3-Diacetyl-2-imidazolidinethione			1 695			1 692
1,3-Ditrifluoroacetyl-2-imidazolidinethione	1 780 (W)		1 740 (S)			1 720

quoted by Mecke *et al.* (3) and Roberts (2). This is attributed to the fact that the present values were obtained from solution spectra, whereas the other workers used potassium bromide pellets. A similar effect has been noted in this series by Hall and Zbinden (7).

The assignment of the acyl carbonyl vibration, by comparison of the acylated 2-imidazolidinethiones with the acylated 2-imidazolidinones (2), to the lower frequency band is confirmed by the fact that the relative intensity of this band with respect to the one at higher frequency is greater for diacyl than for monoacyl 2-imidazolidinone. The similarity in the frequency of the acyl carbonyl vibration for the acylated imidazolidinones and imidazolidinethiones also excludes the interpretation that the two carbonyl bands in the series of acylated imidazolidinones are due to coupled vibrations, as was suggested for N,N-diacylamines (8) and anhydrides (9). It may be seen from Table I that the frequency of the ring carbonyl is always higher than that of the acyl carbonyl, which agrees with the results obtained from a study of solid phase spectra.

The infrared spectra of 1-acetyl-3-trifluoroacetyl-2-imidazolidinone and 1-acetyl-3-benzoyl-2-imidazolidinone show three carbonyl peaks, which are attributed to the ring carbonyl and the two different acyl carbonyl bonds. It can be seen that the carbonyl frequency of the acetyl group in 1,3-diacetyl-2-imidazolidinone is 1 698 cm^{-1}, and that of the trifluoroacetyl group in 1,3-ditrifluoroacetyl-2-imidazolidinone is 1 739 cm^{-1}. In the mixed derivative, 1-acetyl-3-trifluoroacetyl-2-imidazolidinone, the two acyl carbonyls appear at 1 710 cm^{-1} and 1 722 cm^{-1}. The decrease in the difference between the acetyl and the trifluoroacetyl carbonyl absorption in going from the symmetrical to the mixed diacyl compounds indicates some form of mutual interaction in which there is an equalization of the electron densities on the nitrogen atoms by mesomerism through the ring.

The frequency assigned to the ring carbonyl is seen to increase with the degree of acylation of the molecule and with the electron-withdrawing power of the acyl group. Acylation reduces the availability of the electrons on the nitrogen atom, thus decreasing the mesomeric effect with the ring carbonyl, which results in a higher carbonyl frequency. This is in accord with the conclusions of Mecke *et al.*, who found that as the hetero-atoms in the series of 1,3-dihetero-2-cyclopentanones are changed from oxygen to nitrogen to sulphur, the frequency decreases with increasing mesomeric effect.

These considerations involving electronic effects may be applied to the interpretation of the n.m.r. results which are shown in Table II.

TABLE II

The τ-values of the methylene and acetyl protons in 2-imidazolidinone, 2-imidazolidinethione, and some of their acyl derivatives

Compound	Solvent	τ —CH_2—	τ —CH_3
2-Imidazolidinone	D_2O	6.50	
1,3-Diacetyl-2-imidazolidinone	D_2O	6.26	7.62
	$CHCl_3$	6.17	7.47
1-Acetyl-3-trifluoroacetyl-2-imidazolidinone	$CHCl_3$	6.05	7.32
	CCl_4	6.10	7.51
1,3-Ditrifluoroacetyl-2-imidazolidinone	$CHCl_3$	5.93	
1-Acetyl-3-benzoyl-2-imidazolidinone	$CHCl_3$	6.05	7.55
1,3-Dibenzoyl-2-imidazolidinone	$CHCl_3$	5.93	
2-Imidazolidinethione	D_2O	6.32	
1,3-Diacetyl-2-imidazolidinethione	$CHCl_3$	6.00	7.18
1,3-Ditrifluoroacetyl-2-imidazolidinethione	$CHCl_3$	5.74	

Can. J. Chem. Downloaded from www.nrcresearchpress.com by 210.87.254.6 on 09/05/12
For personal use only.

Can. J. Chem. Downloaded from www.nrcresearchpress.com by 210.87.254.6 on 09/05/12
For personal use only.

The spectra of the methylene protons in the series of diacylated-2-imidazolidinones are singlets, and this is consistent with acylation of the nitrogens. The τ-values decrease in the order, unacylated >1,3-diacetyl > 1,3-dibenzoyl = 1,3-ditrifluoroacetyl. The similarity of the last two compounds was unexpected, since the τ-value for the benzoyl derivative would be expected to be nearer that of the acetyl because of the relative strengths of the respective acids. Other factors, however, notably the magnetic anisotropy of the C=O group and the aromatic ring current, affect these τ-values. Following the method of calculation and the suggested values of the anisotropies given by Narasimhan and Rogers (10) for the carbonyl bond, and using interatomic distances from related compounds (11), we calculated that, for the planar configuration I, the side-chain carbonyls decrease the screening of the methylenic protons by about 0.24 p.p.m., and that for configuration II the decrease is 0.10 p.p.m. The ring carbonyl further descreens by 0.04 p.p.m. Because of the partial double bond character of the exocyclic C—N bond,

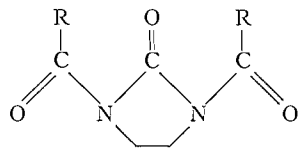

I

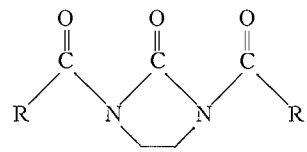

II

only configurations I and II would be expected to make significant contributions. As the π-electron distribution varies in the series there will, no doubt, be a concomitant variation of the location of the equivalent C=O dipole, but the resultant changes in anisotropy are very likely small. If it is assumed that the compounds in the above series have similar configurations, the carbonyl anisotropy is not then a factor in determining the relative shifts of the methylene protons. For the benzoyl derivatives, however, the contribution from the ring current must also be considered. This was calculated from the unsubstituted benzene model by the method of Johnson and Bovey (12) to be −0.29 p.p.m. for configuration I, a value which may produce an overcorrection, but the amended τ-values are now more as expected from electronic effects. Some evidence in support of these assumptions is provided by a correlation which is seen to exist between the τ-value of the methylene protons and the ring carbonyl frequency, which is shown in Table III. This

TABLE III

Correlation between τ of methylene protons and ring carbonyl frequency in 2-imidazolidinones

	τ	ν (cm^{-1})
2-Imidazolidinone	6.50	1 703
1,3-Diacetyl-2-imidazolidinone	6.17	1 759
1,3-Dibenzoyl-2-imidazolidinone	6.22*	1 768
1-Acetyl-3-trifluoroacetyl-2-imidazolidinone	6.05	1 781
1,3-Ditrifluoroacetyl-2-imidazolidinone	5.93	1 810

*Corrected for ring current effects from aromatic rings.

correlation would be expected only if the carbonyl anisotropic contributions are constant and τ and $\nu_{C=O}$ are similarly dependent on electronegativity.

For 1,3-dibenzoyl-2-imidazolidinone it is possible to utilize the ring current calculations to determine the preferred configuration. In configuration II, the ring current effect (−0.7 p.p.m.), when deducted, would increase the τ of the methylenes to a value higher

Can. J. Chem. Downloaded from www.nrcresearchpress.com by 210.87.254.6 on 09/05/12
For personal use only.

than that for 2-imidazolidinone. On the other hand, in configuration I the maximum correction (all rings coplanar) is only 0.29 p.p.m., and thus 1,3-dibenzoyl-2-imidazolidinone is mainly in this configuration.

The mixed 1,3-diacyl compounds give methylene proton spectra which are, surprisingly, almost A_4 ($J/\delta \sim 10$) and have τ-values which are the means of those of the respective unmixed diacyl compounds. Assuming certain configurations in the unmixed derivatives, the approximation to A_4 character can be calculated for a number of configurations of the mixed derivatives. The averaging of the τ-values indicates, however, that the overriding effect operating here is the equalization of the electron densities on the nitrogens via the urea moiety of the ring. Evidence for this effect has already been mentioned in connection with the infrared results. This equalization of the electron density allows an independent means of deducing the configuration of the acyl groups. If it is assumed that there is complete equalization of the shift contribution from the electron density, then, because the methylene protons are virtually an A_4 system, it follows that the anisotropy contributions are also equal, and that consequently the acyl groups have the same configuration.

A residual inequality of 0.12 p.p.m. (from the ring current effect) in the shift of the methylene protons is calculated for 1-acetyl-3-benzoyl-2-imidazolidinone when the simple model is used. This model treats the carbonyl and the benzene ring as independent systems and assumes a planar molecule. Although this is probably incorrect in the present case, these crude ring current calculations show that the benzoyl group has a preference for the *trans*- rather than the *cis*-configuration with respect to the ring carbonyl, since in the *cis*-structure the calculated methylenic proton non-equivalence is 0.3 p.p.m., which is unlikely to disappear even in an improved model. In addition the planar *trans*-configuration I exhibits some steric interaction between the ring carbonyl oxygen and an ortho aromatic proton.* This will most likely result in a twisting of the benzene ring out of the plane of the imidazolidine ring. Hence the ring current effect and the residual inequality will now be decreased. The preference of the *trans*-configuration might be expected, since in the *cis*-configuration there would be considerable carbonyl dipole–dipole interaction, which is virtually absent in the *trans*-form. This argument, which supports the conclusions from the dibenzoyl derivative, implies that all the other diacyl compounds will assume preferentially the *trans*-configuration since no steric factors are involved.

A striking result, which is apparent from Table II, is that in all the 2-imidazolidinethiones the methylene protons are deshielded by approximately the same amount, 0.18 p.p.m., from their counterparts in the 2-imidazolidinones. The acetyl protons are also quite strongly deshielded. This would not be expected on the basis of electronegativity considerations although similar descreening effects have been observed before when C=S replaces C=O (13). The reason for this behavior probably lies in the utilization of the sulphur d-orbitals in the C=S bond. This would markedly change the pattern and values of the magnetic anisotropy from that of the C=O bond. Since the ring carbonyl anisotropy only descreens the methylene protons by 0.04 p.p.m.,† a quite large effect is necessary to explain 0.18 p.p.m. The even larger effect on the methyl protons may be considered as supporting evidence for the supposition that the acetyl C=O group is located in the *trans*-configuration relative to the ring C=O or C=S, as this would reduce the distance of the methyl group from the anisotropic center.

In conclusion it may be pointed out that unlike the diacylated imidazolidinones, the

*The authors thank the referees for drawing this point to their attention.

†*This value may be different if the magnetic anisotropies given in the recent paper by Hooper and Kaiser (14) are used. However, the argument remains unaffected.*

monoacyl-imidazolidinones and imidazolidinethiones give well pronounced but not quite symmetrical A_2B_2-like spectra for the methylene protons. Although this is in agreement with the N-acyl structure, it is not conclusive evidence for it.

ACKNOWLEDGMENTS

The authors thank Mr. K. Oikawa for running some of the n.m.r. spectra and Mr. R. A. Gravelle for determining the infrared spectra. We are also grateful to Mr. J. G. Helie for the analytical work, and to Dr. R. M. Heggie for helpful discussion.

REFERENCES

1. R. GREENHALGH and R. A. B. BANNARD. Can. J. Chem. **39**, 1017 (1961).
2. J. G. ROBERTS. J. Chem. Soc. 176 (1964).
3. R. MECKE, R. MECKE, and A. LÜTTRINGHAUS. Chem. Ber. **90**, 975 (1957).
4. H. K. HALL and A. K. SCHNEIDER. J. Am. Chem. Soc. **80**, 6409 (1958).
5. M. N. KIRKWOOD and G. F. WRIGHT. J. Am. Chem. Soc. **76**, 1836 (1954).
6. J. E. BAER and R. G. LOCKWOOD. J. Am. Chem. Soc. **76**, 1162 (1954).
7. H. K. HALL and R. ZBINDEN. J. Am. Chem. Soc. **80**, 6428 (1958).
8. R. A. ABRAMOVITCH. J. Chem. Soc. 1413 (1957).
9. L. J. BELLAMY, B. R. CONNELLY, A. R. PHILPOTTS, and R. L. WILLIAMS. Z. Elektrochem. **64**, 563 (1960).
10. P. T. NARASIMHAN and M. T. ROGERS. J. Phys. Chem. **63**, 1388 (1959).
11. Chemical Society. Interatomic distances. Special Publication. No. 11. London. 1958.
12. C. E. JOHNSON and F. A. BOVEY. J. Chem. Phys. **29**, 1012 (1958).
13. I. D. RAE. Private communication.
14. D. L. HOOPER and R. KAISER. Can. J. Chem. **43**, 2363 (1965).

Can. J. Chem. Downloaded from www.nrcresearchpress.com by 210.87.254.6 on 09/05/12
For personal use only.

Can. J. Chem. Downloaded from www.nrcresearchpress.com by 210.87.254.40 on 09/05/12
For personal use only.

STRUCTURES OF CHLOROBIUM CHLOROPHYLLS (650)[1]

J. W. PURDIE[2] AND A. S. HOLT
Division of Biosciences, National Research Council, Ottawa, Canada

Received June 2, 1965

ABSTRACT

The structures of six *Chlorobium* chlorophylls (650) have been determined. The pheophorbides are derivatives of 2-desvinyl-2-α-hydroxyethyl pyropheophorbide *a*. Variation of the substituents at C_4 (isobutyl, *n*-propyl, or ethyl) and C_5 (ethyl or methyl) accounts for the six different compounds.

DISCUSSION

It was concluded on the basis of an earlier investigation that the pheophorbides of *Chlorobium* chlorophylls (650) were homologues of 2-desvinyl-2-α-hydroxyethyl pyropheophorbide *a* (1) ("homologues" in this case means compounds with different alkyl side chains). Hughes and Holt (2) separated the pheophorbides by liquid–liquid partition chromatography between ether and hydrochloric acid. The six fractions obtained, which were numbered 1 to 6 in order of decreasing acid numbers (order of elution), had almost identical visible absorption spectra. Each fraction was oxidized with chromic acid and the imides obtained were identified by comparison with synthetic imides, except for the neutral imide from fraction 1.

The pheophorbides (650) used in the present work were obtained from *Chlorobium thiosulfatophilum* (strain L) grown and harvested as described by Hughes and Holt (2) and stored at -10 °C. The chlorophylls were extracted and hydrolyzed, and the pheophorbides separated as described previously (2). Each fraction had to be re-chromatographed several times to obtain chromatographically pure pigment. Fraction 3, so obtained, when oxidized with chromic acid, yielded the same neutral imide as fraction 1 and not methyl-*n*-propylmaleimide as found previously. The neutral imide from fractions 1 and 3 has now been identified as methylisobutylmaleimide (3). It was first thought that it might be ethyl-*n*-propylmaleimide; ethyl and propyl groups could possibly arise more readily from uroporphyrin III, an intermediate in the biosynthesis of chlorophyll *a* (4). Also, the retention time of the imide on gas–liquid partition chromatography on polyphenyl ether (2) was greater than that of methyl-*n*-propylmaleimide but less than that which would be expected for methyl-*n*-butylmaleimide. Ethyl-*n*-propylmaleimide was synthesized and compared with the neutral imide from fractions 1 and 3; the retention times were identical on a polyphenyl ether column but differed significantly on a butanediol succinate column.

The nuclear magnetic resonance spectra of the methyl esters of the pheophorbides were measured in $CDCl_3$. Fractions 1 and 3 both showed peaks at $\tau = 8.85$ and 8.95 characteristic of a terminal isopropyl group. Thus these fractions possessed a pyrrole ring with either ethyl and isopropyl groups or methyl and isobutyl groups as substituents. The ratio of the intensities of the peaks at $\tau = 8.85$ and 8.95 was 1.31:1 for fraction 1 and 1.44:1 for fraction 3. This indicated that the substituent was an isobutyl group, since the methyl groups of isopropyl substituents in a similar environment give rise to signals which have

[1]*Issued as N.R.C. No. 8669.*
[2]*N.R.C. Postdoctorate Fellow, 1961–1963. Present address: Defence Chemical, Biological and Radiation Laboratories, Defence Research Board, Ottawa, Canada.*

Can. J. Chem. Downloaded from www.nrcresearchpress.com by 210.87.254.40 on 09/05/12
For personal use only.

intensity ratios of about 1.2:1 (5). Methylisobutylmaleimide was synthesized, and examined by gas–liquid partition chromatography. It had exactly the same retention time as the neutral imide from fractions 1 and 3 when run on columns with different characteristics, namely, polyphenyl ether, Carbowax, and butanediol succinate. The neutral imide from *Chlorobium* chlorophylls (660), fractions 1 and 2, also matched methylisobutylmaleimide (6, 7). The nuclear magnetic resonance spectrum of methylisobutylmaleimide, which is described in more detail below, had peaks at $\tau = 9.02$ and 9.12 (ratio of intensities 1.35:1), in good agreement with the spectra of fractions 1 and 3. Rapoport and co-workers (8) also obtained evidence for the presence of a butyl side chain in *Chlorobium* chlorophylls but did not show that it was an isobutyl group.

The pheophorbides were converted into "meso" derivatives by dehydrating the hydroxyethyl group to a vinyl group and hydrogenating the latter to give an ethyl substituent as described below. The "meso" derivatives of fractions 1 to 4 were converted into pyrroporphyrins, i.e. ring V was removed by oxidation and decarboxylation. Pyrroporphyrin XV, prepared from mesopyropheophorbide *a* by the same method, was oxidized with chromic acid in sulfuric acid and found to yield only methylethylmaleimide in the neutral fraction. However, milder oxidation, chromium trioxide in acetic acid, yielded a small amount of citraconimide from ring III in addition to methylethylmaleimide, and this method was used to oxidize the pyrrophorphyrins derived from the (650) pheophorbides. The products were examined by gas–liquid partition chromatography with a column of polyphenyl ether; this was the only column which was found to separate ethylmaleimide and methylethylmaleimide efficiently.

Each pyrroporphyrin yielded the neutral imide that was obtained previously from the corresponding pheophorbide. In addition, fractions 1 to 3 yielded methylethylmaleimide, which confirmed that these fractions all possessed a hydroxyethyl group. Since fraction 4 pyrroporphyrin, in which ring II would give methylethylmaleimide, did not give rise to a larger imide, it must have had a hydroxyethyl group also. Ethylmaleimide was obtained from the pyrroporphyrins of fractions 1, 2, and 4, indicating that each of these fractions had a C_5 ethyl substituent. Citraconimide was not obtained from the pyrroporphyrin of fraction 3, because insufficient material was used for the oxidation (yields from ring III were always very small) and paucity of sample prevented repetition of the oxidation. However, the acid number and the chromatographic properties of fraction 3 indicated that it was smaller than fraction 1 by a CH_2 unit. The results of the oxidative degradation of the pheophorbides and derivatives are summarized in Table I.

The data contained in Table I enabled all the β substituents to be determined, except those on ring I of fraction 6 and ring III of fractions 3, 5, and 6. However, the rate of elution during liquid–liquid partition chromatography of these fractions and their vinyl and meso derivatives indicated that they probably had methyl substituents on ring III. The visible absorption spectra indicated that all fractions were homologues of 2-desvinyl-2-α-hydroxyethyl pyropheophorbide *a* as follows. (*i*) After the hydroxyethyl group was converted into a vinyl group, all fractions had the same spectrum as pyropheophorbide *a*. (*ii*) After the vinyl group was reduced to an ethyl group, the spectrum of each fraction was identical with that of mesopyropheophorbide *a*. (*iii*) When the hydroxyethyl group of fraction 2* was oxidized to an acetyl group, the spectrum was the same as that of 2-desvinyl-2-acetyl pheophorbide *a* but differed from that of pheophorbide *b* (1). Therefore, the hydroxyethyl group had been on ring I, if one assumes that the cyclopentanone

**Main component of a fraction studied earlier (1, 9).*

TABLE I

Products* of oxidative degradation of pheophorbides (650) and derivatives

	Source pyrrole ring	Pheophorbide (2)	"Meso" pheophorbide (9)	Pyrroporphyrin
Pheophorbide *a*	I	Decomp.	MeEt	MeEt
	II	MeEt	MeEt	MeEt
	III	Decomp.	Decomp.	Me
	IV	DihydroH	—	—
Fraction 1	I	Decomp.	—	MeEt
	II	MeIsobu	—	MeIsobu
	III	Decomp.	—	Et
	IV	DihydroH	—	—
Fraction 2	I	Decomp.	MeEt	MeEt
	II	Me-*n*-Pr	Me-*n*-Pr	Me-*n*-Pr
	III	Decomp.	Decomp.	Et
	IV	DihydroH	—	—
Fraction 3	I	Decomp.	—	MeEt
	II	MeIsobu	—	MeIsobu
	III	Decomp.	—	Not found
	IV	DihydroH	—	—
Fraction 4	I	Decomp.	—	MeEt
	II	MeEt	—	MeEt
	III	Decomp.	—	Et
	IV	DihydroH	—	—
Fraction 5	I	Decomp.	MeEt	—
	II	Me-*n*-Pr	Me-*n*-Pr	—
	III	Decomp.	Decomp.	—
	IV	DihydroH	—	—
Fraction 6	I	Decomp.	—	—
	II	MeEt	—	—
	III	Decomp.	—	—
	IV	DihydroH	—	—

*Me = citraconimide; MeIsobu = methylisobutylmaleimide; Et = ethylmaleimide; DihydroH = dihydrohematinic acid; MeEt = methylethylmaleimide; Decomp. = destroyed during oxidation; Me-*n*-Pr = methyl-*n*-propylmaleimide; — = not investigated.

ring was attached to ring III. Hence, if one assumes that the arrangement of the β substituents on the rings was analogous to that of chlorophyll *a*, it was possible to write the structures as illustrated in Fig. 1.

On the basis of these structures it appeared that fraction 6 should be related closely to pyropheophorbide *a*. Consequently, fraction 6 was dehydrated to the 2-vinyl derivative, and this compound was found to co-chromatograph exactly with pyropheophorbide *a* by using the liquid–liquid partition technique which had been used to separate the pheophorbides (650) (2). The 2-vinyl derivative of fraction 5, on the other hand, separated readily from pyropheophorbide *a* when chromatographed similarly. The "meso" derivative of fraction 6 (2-ethyl compound) co-chromatographed with mesopyropheophorbide *a*. The X-ray powder photograph of fraction 6 (2-vinyl derivative) was identical with that of pyropheophorbide *a*; the methyl ester had melting point 222–225 °C alone and 220–225 °C in admixture with pyropheophorbide *a* methyl ester (m.p. 222–225 °C). Fraction 6 was therefore 2-desvinyl-2-α-hydroxyethyl pyropheophorbide *a*. This confirmed the nature of the substituents at C_2 and C_5. Furthermore, it established that the cyclopentanone ring was present as illustrated and showed that the configuration of the substituents on ring IV was the same as that in pyropheophorbide *a*. According to Linstead and co-workers (10), the hydrogen atoms on ring IV of chlorophyll *a* are in the

Can. J. Chem. Downloaded from www.nrcresearchpress.com by 210.87.254.40 on 09/05/12
For personal use only.

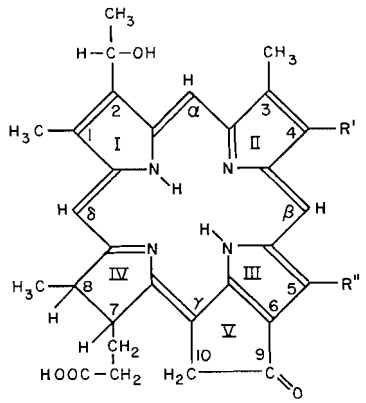

Fraction	R′	R″
1	$CH_2CH(CH_3)_2$	CH_2CH_3
2	$CH_2CH_2CH_3$	CH_2CH_3
3	$CH_2CH(CH_3)_2$	CH_3
4	CH_2CH_3	CH_2CH_3
5	$CH_2CH_2CH_3$	CH_3
6	CH_2CH_3	CH_3

FIG. 1. Structures of the pheophorbides from *Chlorobium* chlorophylls (650).

trans positions. The structures of the other fractions were subsequently confirmed by comparing porphyrin derivatives with synthetic porphyrins.

Fractions 1 to 4 were confirmed by comparing the pyrroporphyrin derivatives with synthetic pyrroporphyrins prepared by MacDonald and co-workers (11, 12). Thus, the methyl ester of fraction 1 pyrroporphyrin was identical with synthetic 1,3,8-trimethyl-2,5-diethyl-4-isobutylporphin-7-propionic acid methyl ester. Similarly, fraction 2 pyrroporphyrin methyl ester was identical with synthetic 1,3,8-trimethyl-2,5-diethyl-4-*n*-propylporphin-7-propionic acid methyl ester. Fraction 3 pyrroporphyrin methyl ester was identical with synthetic 1,3,5,8-tetramethyl-2-ethyl-4-isobutylporphin-7-propionic acid methyl ester. As previously reported by Archibald *et al.* (12), fraction 4 pyrroporphyrin methyl ester was identical with synthetic 1,3,8-trimethyl-2,4,5-triethylporphin-7-propionic acid methyl ester. The structure of fraction 5 was confirmed by MacDonald and co-workers (11, 12) as follows. The "meso" derivative was converted into the desoxo-phylloerythrin derivative, the methyl ester of which was identical with synthetic 4-*n*-propyl-4-desethyl-desoxo-phylloerythrin methyl ester.

The pheophorbides were obtained from *Chlorobium* chlorophylls (650) by alkaline hydrolysis. Only one alcohol resulted from this hydrolysis, and it was found to be farnesol (9, 13). Rapoport and Hamlow (13) concluded that it was *trans,trans*-farnesol on the basis of its proton magnetic resonance spectrum. Thus the *Chlorobium* chlorophylls (650) are farnesol esters of the magnesium complexes of the pheophorbides illustrated in Fig. 1.

It is now of interest to comment on the method which was used to separate the pheophorbides (650), i.e. liquid–liquid partition chromatography with hydrochloric acid on Celite as the stationary phase and ether as the mobile phase (2). In the initial separation of the mixture of pheophorbides, four bands were usually obtained on the column. Band I, which was eluted first from the column, contained fraction 1; band II contained fractions 2 and 3; band III contained fractions 4 and 5; and band IV contained fraction 6. Thus the compounds in each band differed from the compounds in the adjacent bands by one

Can. J. Chem. Downloaded from www.nrcresearchpress.com by 210.87.254.40 on 09/05/12
For personal use only.

CH_2. Bands II and III occasionally split into component fractions on the initial column but were normally resolved by further chromatography with hydrochloric acid of a slightly higher concentration.

The initial bands I to IV probably correspond to the four fractions obtained by countercurrent distribution between hydrochloric acid and ether (2).

EXPERIMENTAL

Synthesis of Imides

Ethylmaleimide

This imide was obtained by oxidation of 2-methyl-4-ethylpyrrole with chromium trioxide in sulfuric acid as described by Fischer *et al.* (14, 15). The ethyl propionylacetate used to prepare the pyrrole was kindly supplied by Dr. S. F. MacDonald. The imide was purified by sublimation in a vacuum at 80 °C, gas–liquid partition chromatography, and re-sublimation. The white crystalline product had m.p. 80 °C.

Anal. Found: C, 57.62; H, 5.84; N, 11.32. $C_6H_7O_2N$ requires C, 57.59; H, 5.64; N, 11.20.

Methylisobutylmaleimide

The general method followed was that used by Küster for the preparation of methylethylmaleimide (16). Ethyl isobutylacetoacetate was prepared in 55% yield from ethyl acetoacetate and isobutylbromide (1-bromo-2-methylpropane) as described by Renfrow (17). The product was purified by vacuum distillation with a 10 cm fractionating column; b.p. 105–110 °C at 20 mm. The ester (31 g) was dissolved in 100 ml ether and potassium cyanide (21 g) added. The mixture was cooled to −5 °C and concentrated HCl (3 ml) added. The flask was stoppered, shaken for 1 h, and cooled to −5 °C for 30 min, and then a further 3 ml of HCl added. The shaking, cooling, and addition procedure was repeated until 25 ml of HCl had been added. When the addition was complete the mixture was shaken for 12 h and the ether evaporated off. Concentrated HCl (100 ml) was added and the solution was refluxed for 8 h. The solution was concentrated by distillation and then heated slowly on a "Woods metal" bath. Between 174 and 230 °C (bath temperature) water distilled out, and at 260 to 270 °C the product distilled out; methylisobutylmaleic anhydride, b.p. 230–238 °C, pale yellow liquid, yield 4.44 g (16%).

The anhydride was converted into the imide as follows: 1 g was dissolved in anhydrous ethanol (8 ml) saturated with ammonia at 0 °C and heated at 140 °C for 3 h in a Teflon-lined brass bomb. After the ethanol had been evaporated off the product crystallized. Sublimation in a vacuum at 95 °C yielded a white product; yield 1.0 g from 3 g of anhydride (33%). The imide crystallized from petroleum ether as flat needles and plates, m.p. 92–93 °C.

Anal. Found: C, 64.40; H, 7.65; N, 8.51. $C_9H_{13}NO_2$ requires C, 64.65; H, 7.89; N, 8.38.

The infrared spectrum resembled that of methylethylmaleimide; in particular, it had peaks at 3 410 cm^{-1}, 1 770 cm^{-1}, and 1 720 cm^{-1}. The nuclear magnetic resonance spectrum of the imide was measured in $CDCl_3$ on a Varian A-60 high-resolution spectrometer. The spectrum had sharp peaks at $\tau = 9.02$ and 9.12 which were assigned to the methyl groups in the isobutyl chain, and a peak at $\tau = 8.05$ which was attributed to the other methyl group. Peaks at $\tau = 7.68$ and $\tau = 7.78$ (two protons) were assigned to the isobutyl CH_2 protons. The isobutyl CH proton showed up as a band centered approximately at $\tau = 8.3$ but split many times. The remaining proton attached to the nitrogen atom gave a broad band at $\tau = 1.8$.

Ethyl-n-propylmaleimide

This compound was prepared from ethyl *n*-propylpropionylacetate by the same general method as was used to prepare methylisobutylmaleimide. Ethyl *n*-propylpropionylacetate was prepared from commercial ethyl propionylacetate by a procedure analogous to that described for the preparation of ethyl ethylacetoacetate (18).

Ethyl *n*-propylpropionylacetate (30 g) was treated with HCN and hydrolyzed with HCl, and the crude product, ethyl-*n*-propylmaleic acid, extracted with ethyl acetate. This product was heated slowly on a "Woods metal" bath. At a bath temperature of 150 to 240 °C a clear distillate was obtained (mainly water); at a bath temperature of 255 °C ethyl-*n*-propylmaleic anhydride distilled out as a pale yellow oil with a boiling range of 220–230 °C, yield 4 g (15%). Ethyl-*n*-propylmaleimide was obtained by heating the anhydride in ethanol containing ammonia. After evaporation of the ethanol the crude product was purified by gas–liquid partition chromatography, yielding a colorless syrup which did not crystallize even on standing.

Anal. Found: C, 64.22; H, 7.56; N, 8.40. $C_9H_{13}NO_2$ requires C, 64.65; H, 7.87; N, 8.38.

Examination of the Neutral Imide from Fractions 1 and 3

For gas–liquid partition chromatography, a Pye argon chromatograph and columns (0.4 × 117 cm) of polyphenyl ether (17%), Carbowax (10%), or butanediol succinate polymer (10%) on Celite were used. The column temperature was 175 °C in each case. The neutral imides from pheophorbide (650) fractions 1 and 3 and pheophorbide (660) fractions 1 and 2 all had a retention time of 1.76 relative to that of quinoline on the polyphenyl ether column. Methylisobutylmaleimide had exactly the same retention time when run under identical conditions. The neutral imide from pheophorbide (650) fraction 1 also had the same retention

Can. J. Chem. Downloaded from www.nrcresearchpress.com by 210.87.254.40 on 09/05/12
For personal use only.

times as methylisobutylmaleimide: on the Carbowax column, 1.10 relative to methyl-*n*-propylmaleimide; on the butanediol succinate column, 3.74 relative to quinoline. The ethyl-*n*-propylmaleimide had retention times of 1.76 relative to quinoline on the polyphenyl ether column, 3.50 relative to quinoline on the butanediol succinate column, and 1.07 relative to methyl-*n*-propylmaleimide on the Carbowax column.

Preparation of "Meso" Derivatives of Pheophorbides (650)

General Procedure

The pheophorbide (50 mg) was dissolved in 100% phosphoric acid (20 ml) and maintained at 60 °C for 30 min with vigorous stirring. The pigment was extracted with ether and separated by partition chromatography between ether and hydrochloric acid on Celite. This separated the vinyl derivative, lower band, from the unchanged material, which could again be treated with phosphoric acid to produce more of the vinyl derivative. The vinyl derivatives of bands 1 to 6 were purified with 15.5, 15, 15, 14.5, 14.5, and 14% hydrochloric acid solutions, respectively. The vinyl derivative was hydrogenated (H_2 – palladium black) in acetone and the "meso" derivative that was obtained was purified by partition chromatography with hydrochloric acid which was 0.5% weaker than that required for the corresponding vinyl derivative.

Preparation of Pyrroporphyrins

Mesopyropheophorbide *a* (100 mg) was oxidized by oxygen in dimethylformamide (100 ml solution saturated with oxygen, plus 3 ml aqueous KOH) to a dicarbonyl compound (10-oxo-mesopyropheophorbide *a*) (19). It was immediately oxidized further by adding hydrogen peroxide (30%, 3 ml) to the dimethylformamide solution, shaking for 1 min, and extracting the product (mesochlorin p_6) with ether. The ether solution was washed well with water and evaporated to dryness. The mesochlorin p_6 was dissolved in glacial acetic acid (2–3 ml) and transferred to four Carius tubes. Hydrochloric acid (1%) was added to each tube and the mixture frozen at −80 °C. The tubes were sealed under vacuum and heated at 185 °C for 4 h. In some experiments stronger hydrochloric acid or more acetic acid was used, in an amount sufficient to keep the chlorin in solution after addition of the hydrochloric acid. This was better, as there was less black residue after the solution was heated. The solutions from the tubes were filtered and the pyrroporphyrin was extracted with ether and then crystallized from ether; yield 45 mg (50%). The methyl ester crystallized from tetrahydrofuran–methanol as needles, m.p. 238–241 °C. The mesochlorin p_6 and the pyrroporphyrin had visible absorption spectra identical with those in the literature (20, 21).

The pyrroporphyrins of the pheophorbides (650), fractions 1 to 4, were prepared from the pure "meso" derivatives in the same way, except that smaller quantities were used. The pyrroporphyrins were purified by crystallization from ether or by liquid–liquid partition chromatography (ether – hydrochloric acid on acid-washed Celite) (2). The samples for comparison with the synthetic pyrroporphyrins were chromatographed with 5.0, 4.5, 4.0, and 3.5% hydrochloric acid for fractions 1, 2, 3, and 4, respectively. The pure porphyrins were methylated by diazomethane in ether, crystallized, and examined: fraction 1 pyrroporphyrin methyl ester—fine needles from ether, m.p. 229.5–231 °C; fraction 2 pyrroporphyrin methyl ester—needles from ether or chloroform–methanol, m.p. 207–210 °C; fraction 4 pyrroporphyrin methyl ester—small plates from chloroform–methanol, m.p. 210–215 °C (phase change at 180 °C; plates melted and needles formed); fraction 3 pyrroporphyrin methyl ester—needles from ether, m.p. 220–222 °C (a different crystalline form was obtained from chloroform-methanol).

Anal. Found: C, 76.38; H, 7.67. $C_{34}H_{40}O_2N_4$ requires C, 76.09; H, 7.51.

The pyrroporphyrins all had visible absorption spectra identical with that of the pyrroporphyrin from mesopyropheophorbide *a*.

TABLE II

Gas–liquid partition chromatography of the neutral imides from the oxidation of the pyrroporphyrins (polyphenyl ether column; 175 °C; 100 ml per min)

Source of pyrroporphyrin	Retention times relative to methylethylmaleimide
Mesopyropheophorbide *a*	0.535, 1.00
(650) fraction 1	0.81, 1.00, 1.68
(650) fraction 2	0.81, 1.00, 1.44
(650) fraction 3	1.00, 1.69
(650) fraction 4	0.81, 1.00
Synthetic imides	
Citraconimide	0.53
Ethylmaleimide	0.81
Methylethylmaleimide	1.00
Methyl-*n*-propylmaleimide	1.44
Methylisobutylmaleimide	1.69

Can. J. Chem. Downloaded from www.nrcresearchpress.com by 210.87.254.40 on 09/05/12
For personal use only.

Oxidation of Pyrroporphins and Examination of Products

The pyrroporphin to be oxidized (5 mg) was dissolved in glacial acetic acid (2 ml) and the solution was cooled to 0 °C. Aqueous chromium trioxide solution (0.25 ml, 6.7% w/v) was added with stirring and the reaction mixture was allowed to warm up to room temperature. When the chromic acid had been used up (green solution) the pH was raised to 10 with sodium carbonate and the neutral imides were extracted with ethyl acetate in the usual way (2).

By this method the pyrroporphins were oxidized, and the neutral imides were examined by gas–liquid partition chromatography; the results are shown in Table II. It was found that all fractions yielded methylethylmaleimide; thus it was used as an internal reference compound.

ACKNOWLEDGMENTS

The authors are grateful to Dr. S. F. MacDonald of the Division of Pure Chemistry for generous assistance and cooperation throughout. Thanks are also due to Dr. H. J. Bernstein for assistance in nuclear magnetic resonance spectroscopy, and to Dr. Maria Przybylska for X-ray powder photographs and critical interpretation. We also thank Dr. M. Kates and Mr. F. P. Cooper of the Division of Biosciences for advice on gas–liquid partition chromatography.

REFERENCES

1. A. S. Holt and D. W. Hughes. J. Am. Chem. Soc. **83**, 499 (1961).
2. D. W. Hughes and A. S. Holt. Can. J. Chem. **40**, 171 (1962).
3. A. S. Holt, D. W. Hughes, H. J. Kende, and J. W. Purdie. Plant Cell Physiol. Tokyo, 4, 49 (1963).
4. S. Granick. J. Biol. Chem. **172**, 717 (1948); **236**, 1168 (1961).
5. Am. Petrol. Inst. Res. Proj. 44. Nuclear Magnetic Resonance Spectral Data, Nos. 176, 224, 225, 250, 253. October 1963.
6. H. V. Morley and A. S. Holt. Can. J. Chem. **39**, 755 (1961).
7. A. S. Holt, D. W. Hughes, H. J. Kende, and J. W. Purdie. J. Am. Chem. Soc. **84**, 2835 (1962).
8. J. W. Mathewson, W. R. Richards, and H. Rapoport. J. Am. Chem. Soc. **85**, 365 (1963).
9. A. S. Holt and D. W. Hughes. Unpublished results.
10. G. E. Ficken, R. B. Johns, and R. P. Linstead. J. Chem. Soc. 2272 (1956).
11. S. F. MacDonald *et al.* To be published.
12. J. L. Archibald, S. F. MacDonald, and K. B. Shaw. J. Am. Chem. Soc. **85**, 644 (1963).
13. H. Rapoport and H. P. Hamlow. Biochem. Biophys. Res. Commun. **6**, 134 (1961).
14. H. Fischer and G. Stangler. Ann. **459**, 81 (1927).
15. H. Fischer, G. Hummel, and A. Treibs. Z. Physiol. Chem. **185**, 33 (1929).
16. W. Küster. Ann. **345**, 10 (1906).
17. W. B. Renfrow. J. Am. Chem. Soc. **66**, 144 (1944).
18. C. S. Marvel and F. D. Hager. Org. Syn. Collective Vol. **1**, 248 (1941).
19. A. S. Holt and H. J. Kende. In preparation.
20. H. Fischer and H. Orth. Chemie des pyrroles. Vol. II. Akademische Verlagsgesellschaft, Leipzig. 1937. Part 1. p. 341.
21. H. Fischer and H. Orth. Chemie des pyrroles. Vol. II. Akademische Verlagsgesellschaft, Leipzig. 1940. Part 2. p. 123.

Can. J. Chem. Downloaded from www.nrcresearchpress.com by 210.87.254.40 on 09/05/12
For personal use only.

Can. J. Chem. Downloaded from www.nrcresearchpress.com by 210.87.254.5 on 09/05/12
For personal use only.

THE TRANSMISSION OF POLAR EFFECTS

PART II.[1] THE KINETICS OF ESTERIFICATION WITH DIAZODIPHENYLMETHANE AND THE IONIZATION OF 3-SUBSTITUTED ACRYLIC ACIDS

KEITH BOWDEN[2]

Department of Pure and Applied Chemistry, Royal College of Advanced Technology, Salford, Lancashire, England

Received July 20, 1965

ABSTRACT

The rate coefficients for the reaction with diazodiphenylmethane in ethanol, *t*-butyl alcohol, and ethyl acetate at 30° and the pK_a values in water at 25° of fourteen 3-substituted acrylic acids have been determined. The effect of substitution is assessed by use of linear free energy relations. A definite incremental acid-strengthening effect solely due to *cis*-substitution is confirmed. This is not a "bulk" steric effect and is due solely to the orientation of substitution. The polar effect of a substituent is found to be approximately the same from the *cis*- or *trans*-position. An attempt is made to test the suggested mechanisms for the transmission of the polar effect. In the reactions studied the transmission of the polar effect in 3-substituted acrylic acid and ortho-substituted benzoic acids is approximately twice that of the meta- or para-substituted benzoic acids. This appears to be reasonably accommodated by a significant field effect.

INTRODUCTION

In Part I (1), a review of the available data concerning the transmission of polar effects through various systems was given. The present studies have been undertaken to assess suitable models of known geometry. Previously, Hine and Bailey (2) had studied the reaction of certain *trans*-3-substituted acrylic acids with diazodiphenylmethane in ethanol at 30°. Charton and Meislich (3) have also assessed the efficiency of the transmission by the ethylenic system. Both these groups report good correlations with Hammett para σ values. A study of the reactivity of both *cis*- and *trans*-3-substituted acrylic acids in their reaction with diazodiphenylmethane in three solvents and their ionization in water has been undertaken in the present studies and is reported here.

EXPERIMENTAL

Materials

Acrylic, *trans*-crotonic, and 3,3-dimethylacrylic acids were obtained commercially. *cis*-Crotonic acid was prepared by the method of Rappe (4) and stored below 0°. The *trans*- and *cis*-3-halogenoacrylic acids were prepared by the addition of the hydrogen halide to propiolic acid (5, 6, 7). The *trans*- and *cis*-3-chlorocrotonic acids were synthesized by the reaction of phosphorous pentachloride with ethyl acetoacetate (8, 9). *trans*-3-Nitroacrylic (10) and *trans*-3-methoxyacrylic acids (11) were prepared by the known procedures. Acrylic acid was freshly distilled before use (12). The other acids were recrystallized to constant melting point and had melting points identical or very close to those in the literature (4–11). Neutralization equivalents were determined for all acids and were within 1% of the theoretical values. Proton magnetic resonance measurements also showed no evidence of impurities.

The stereochemistry of the 3-substituted acrylic acids was confirmed or determined by the proton magnetic resonance spectra (13). The results were definite in terms of stereochemistry (e.g. *trans*-coupling constants of the vicinal hydrogens greater than *cis*), but showed some interesting features (14). The stereochemical nature of the 3-chlorocrotonic acids has been recently confirmed (15).

Diazodiphenylmethane was prepared as before (16). Solutions were stored in a refrigerator. Pure ethanol, b.p. 78.5° (lit. 78.3°) (17), was prepared by Smith's method (18). *t*-Butyl alcohol, b.p. 82.5° (lit. 82.4°), was dried by fractional distillation from sodium and then by crystallization from its own melt (17). Ethyl acetate, b.p. 77.0° (lit. 77.1°) (17), was dried over freshly ignited potassium carbonate, filtered, and fractionally distilled (17). Karl Fischer titrations (19) showed water contents of $< 0.02\%$ by weight. The solvents were stored with careful exclusion of atmospheric moisture.

[1]*Part I; see Can. J. Chem. 41, 2781 (1963).*

[2]*Present address: Department of Chemistry, University of Essex, Wivenhoe Park, Colchester, Essex, England.*

Measurements

Rate Coefficients for Diazodiphenylmethane Reaction

These have been determined, at 30 (± 0.05)°, spectrophotometrically as described previously (20, 21), using a Unicam S.P. 600 spectrophotometer. An approximately 10-fold excess of the acid was used (0.03 *M*) and the reaction was studied as a first-order process, using the following equation

[i] $$k = k_1/[HA]$$

where k is the observed second-order rate coefficient, k_1 is the observed first-order rate coefficient and [HA] is the acid concentration. In accord with recent mechanistic studies (22), the observed second-order rate coefficient in alcoholic solvents is not corrected to give the "true" rate coefficient for esterification, which is accompanied by a competing etherification. Diazodiphenylmethane is stable in the alcoholic solvents at 30°. In ethyl acetate, the diazodiphenylmethane appears to be less stable. The decreased precision of the slower rate coefficients in ethyl acetate is probably due to this fact, though the rate of disappearance of the diazodiphenylmethane in ethyl acetate at 30° in the absence of acid is much slower than the first-order rate coefficients observed. The rate coefficients, k, are shown in Table I.

TABLE I

Esterification of the carboxylic acids

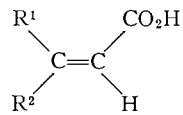

with diazodiphenylmethane at 30°

R^1	R^2	k in ethanol*	k in *t*-butanol*	k in ethyl acetate*
H	H	1.32†	0.447	0.230‡
H	Me	0.587†	0.181	0.0573‡
Me	H	0.437	0.125	0.0401‡
H	Cl	2.68 †	1.11	0.933
Cl	H	2.32	0.920	0.646
H	Br	3.31	1.49	1.13
Br	H	3.09	1.31	0.976
H	I	3.20	1.44	1.06
I	H	2.68	1.14	0.909
H	OMe	0.450	—	—
H	NO_2	21.5	—	—
Cl	Me	2.15	0.729	—
Me	Cl	1.51	0.510	—
Me	Me	0.261	0.0624	—
(Benzoic acid 0.998†)				

*The rate coefficients, k (l mole^{-1} min^{-1}), are reproducible to ±2% or better and are the mean of at least two determinations.

†Hine and Bailey (2) found k for acrylic (1.27), *trans*-crotonic (0.61), *trans*-3-chloroacrylic (2.48), *trans*-3-nitroacrylic (21.8), and benzoic acids (1.00).

‡Rate coefficients are ±5%.

pK_a Values of the Carboxylic Acids

These were determined, at 25 (± 0.1)°, by potentiometric titration of the acids (0.01 *M*) in water with aqueous sodium hydroxide (0.1 *M*), using a direct-reading pH-meter (Electronic Instruments Limited, model 23A) and glass and calomel electrodes. The instrument was calibrated by using phthalate (pH, 4.01) and phosphate (pH, 6.96) buffers (23).

Values of pK_a were calculated in a similar manner to that of Albert and Serjeant (24) from the following equation

[ii] $$pK_a = pH + \log ([HA] - [H^+])/([A^-] + [H^+]) + 0.51I^{1/2}$$

in which [HA] is the concentration of the acid, [A^-] is the concentration of the salt, [H^+] is the concentration of the hydrogen ion, and I is the ionic strength. A stream of nitrogen was played on the solution (50.0 ml) in the thermostatted vessel and carbon-dioxide-free reagents were used, solutions being protected with sode-lime tubes. The pK_a values are shown in Table II.

Can. J. Chem. Downloaded from www.nrcresearchpress.com by 210.87.254.5 on 09/05/12
For personal use only.

TABLE II

pK_a values of the carboxylic acids

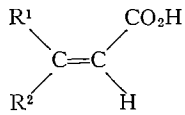

in water at 25°

R^1	R^2	pK_a*	Lit. pK_a	Ref.
H	H	4.25	4.26	25
H	Me	4.70	4.69	25
Me	H	4.42	4.44†	26
H	Cl	3.79	[3.65]‡	5
Cl	H	3.45	[3.32]‡	5
H	Br	3.71	—	—
Br	H	3.32	—	—
H	I	3.74	—	—
I	H	3.42	—	—
H	OMe	4.85	—	—
H	NO_2	2.58	—	—
Cl	Me	3.95	3.93†	26
Me	Cl	4.10	4.09†	26
Me	Me	5.12	5.12	25

*Mean of at least two determinations, accurate to ±0.01 unit.
†At 23°.
‡pK_0 at 18°.

DISCUSSION

Effect of Substitution on the Esterification Reaction

The effect of the substituents, shown in Table I, is in the usual order for the esterification of the acids with diazodiphenylmethane. However, a striking aspect is that the rate coefficients for the *cis*- and *trans*-isomers are almost the same. This effect is also *independent* of the solvent. The transmission of the polar effect from these substituents to the reactive group must be nearly independent of the *cis*- and *trans*-nature of the substitution. Primary steric effects appear to be unimportant in this reaction (20) and the substituents studied are all of moderate steric bulk.

TABLE III

Hammett equation analysis*

Reaction	ρ	Log k_0	n	r
1. Esterification with DDM at 30.0°				
trans-Acids in ethanol	1.617	0.086	7	0.998
	1.682	0.081	5†	0.992
cis-Acids in ethanol	1.772	0.011	5†	0.979
trans-Acids in *t*-butanol	2.065	0.625	5†	0.993
cis-Acids in *t*-butanol	2.160	0.536	5†	0.977
trans-Acids in ethyl acetate	2.960	1.303	5†	0.994
cis-Acids in ethyl acetate	3.042	1.211	5†	0.983
2. Aqueous pK_a values at 25.0°				
trans-Acids	2.187	4.279	7	0.999
	2.249	4.290	5†	0.994
cis-Acids	2.452	3.995	4‡	0.988

*n is number of substituents studied; r is the correlation coefficient.
†Substituents are H, Me, Cl, Br, and I.
‡Substituents are Me, Cl, Br, and I.

The substituent effect can be analyzed by use of linear free energy relations. The Hammett equation (eq. [iii]) (27)

[iii] $$\log (k/k_0) = \rho\sigma$$

Can. J. Chem. Downloaded from www.nrcresearchpress.com by 210.87.254.5 on 09/05/12
For personal use only.

Can. J. Chem. Downloaded from www.nrcresearchpress.com by 210.87.254.5 on 09/05/12
For personal use only.

can be applied to either the *cis*- or the *trans*-substituents, using the known σ values for substituents in the para-position. In Table III, the results are shown. The values used are those suggested by McDaniel and Brown (28), except for the para-iodo substituent. The latter value has been taken as 0.270 (29). The use of σ^n values (30) does not effect any significant improvement in the correlation and, in any case, their application can not be justified in this case. The transmission of the polar effect from the *cis*- or from the *trans*-position is, within the uncertainty of the relations, the same. However, the ρ value for the *cis*-position is, in all cases, slightly greater than that of the *trans*-position. Charton (3*b*) has found a similar effect. The reaction constants, ρ, for the *cis*- or *trans*-substituents show a linear response to the reciprocal of the dielectric constant, as shown in Fig. 1. This relation is given below.

[iv] $$\rho = \rho_c + \rho_s/D.$$

The reaction constant is composed of two parts. The first expresses transmission independent of the medium, ρ_c equal to 1.24 for the *trans*- and 1.34 for the *cis*-substituents; the second expresses transmission controlled by the medium, ρ_s equal to 10.3 for the *trans*- and 10.2 for the *cis*-substituents. However, although it seems likely that the mechanistic path remains the same, this correlation must be treated with reserve.

A treatment similar to that of Dewar and Grisdale (31, see also ref. 32) can be used to analyze the results. If exalted resonance effects are not important in the reaction under study, the relative rates can be assessed in terms of a field effect (F) and a π-inductive-resonance effect (M) such that,

[v] $$\log (k/k_0) = \rho_D(F/r_{ij} + Mq_{ij}),$$

where r_{ij} is the distance between the carbon atom bonded to the reactive group (measured in units of the benzene carbon–carbon bond distance) and q_{ij} is the formal charge at the site produced by the substituent. Only r_{ij} can be calculated, for our systems, and is assumed to be equal to unity. ρ_D and q_{ij} are thus disposable parameters and are given on finding the best fit of the correlation. The important factor is that in the case of the *cis*- and *trans*-3-substituted acrylic acids it would predict, in the absence of steric effect on the conjugation between the carboxyl and ethylenic groups, the *same* effect caused by *cis*- or *trans*-substituents. This is in fact the pattern of reactivity found in the diazodiphenylmethane reaction. The results of the analysis are given in Table IV and result in a very satisfactory

TABLE IV

Dewar–Grisdale analysis*

Reaction	ρ_D	q_{12}	Log k_0	n	r
1. Esterification with DDM at 30.0° in ethanol					
trans-Acids	0.818	0.267	0.082	7	1.000
	0.849	0.320	0.097	5†	1.000
cis-Acids	0.895	0.404	0.066	5†	0.999
2. Aqueous pK_a values at 25.0°					
trans-Acids	1.120	0.270	−4.295	7	1.000
	1.135	0.289	−4.286	5†	1.000

*ρ_D is the reaction constant obtained from the Dewar–Grisdale analysis. r_{12} is taken as 1 (see text). q_{12} is the formal charge term. n is the number of substituents. r is the correlation coefficient.
†Substituents are H, Me, Cl, Br, and I.

correlation. However, it will be realized that as the Hammett para-substituent constants correlate the system satisfactorily, the Dewar and Grisdale treatment must correlate the

system with the field and π-inductive-resonance effects having the same *relative* importance as existing at the para-position in substituted benzene derivatives.

The reaction constant, ρ_D, will be the same as that for the Hammett equation correlation for meta- or para-substituted benzene derivatives. For other systems, ρ_D should remain the same while the effect of change of substitution should be accommodation by r_{ij} and q_{ij}. In this case the reaction constant found, ρ_D equal to 0.85, is in reasonable agreement with the Hammett equation value of 0.94.

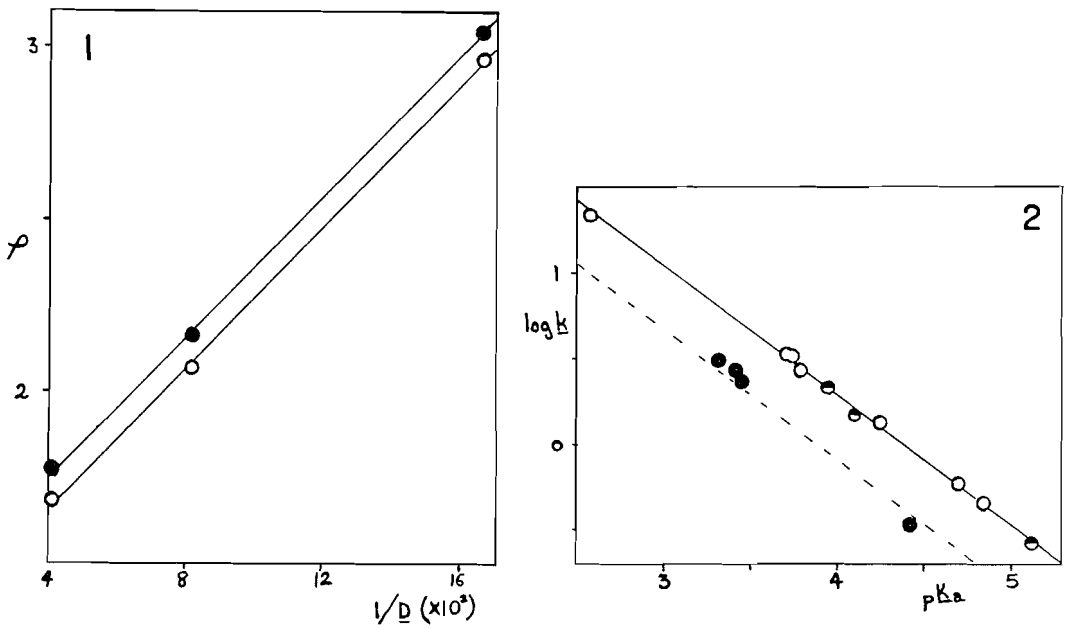

FIG. 1. Relation between the Hammett reaction constants, ρ, and the reciprocal of the dielectric constant of the medium (○, *trans*-; ●, *cis*-acids).

FIG. 2. Relation between the aqueous pK_a values of the acids and the rates of esterification with diazodiphenylmethane in ethanol (○, *trans*-; ●, *cis*-; ◓, di-3-substituted acids).

Relation between the Rate of Esterification with Diazodiphenylmethane and the Aqueous pK_a Values

The relation between the rate of esterification in ethanol and the aqueous pK_a values is shown in Fig. 2. A linear relation is shown by the *trans*-substituents and also includes the three disubstituted acids. The *cis*-substituents form a less delineated regression which can be regarded as parallel. The difference is equivalent to about 0.3 pK_a units. A similar relation has been previously found for benzoic acids (33). The *cis*-substituents correspond to ortho-substituted benzoic acids; while the *trans*-substituents correspond to meta- and para-substituted benzoic acids. The *cis*-substituents of moderate steric bulk (i.e. as large as the methyl or iodo groups) have this acid-strengthening effect due *solely* to their position. This effect is not due to a secondary steric effect causing de-conjugation of the carboxyl group. The cause of this effect has been tentatively suggested as being due to a specific water-bridge solvation effect (33). This is possible but the effect of a definite increment caused by the proximate substituent seems a more general phenomenon (34–36). This effect is difficult to understand in terms of the present evidence and an explanation must await the full analysis of a number of related systems. The correlation of the disubstituted

Can. J. Chem. Downloaded from www.nrcresearchpress.com by 210.87.254.5 on 09/05/12
For personal use only.

acids by the *trans*-acid regression line is thus quite unexpected and does not appear to be fortuitous. It would have been expected that these 3,3-disubstituted acids would respond in a similar manner to the *cis*-acids and no simple explanation for both facts appears obvious.

The application of the Hammett and the Dewar and Grisdale equations to the aqueous pK_a values are shown in Tables III and IV. The correlations are very good and the conclusions drawn are the same as those in the previous section. The *cis*-acids demonstrate in fact almost the same transmission of the substituent polar effect as the *trans*-acids.

The Transmission of the Polar Effects

This model system, like most others (37), is not completely ideal as a means of testing the likelihood of the various suggested modes of transmission of the polar effect. However, it is possible to make a number of tests and come to certain useful conclusions.

A purely inductive transmission could satisfy this system. The similarity of the effect of a substituent at either the *cis*- or the *trans*-position is thus simply accommodated, as no difference would be theoretically expected (1, 37). However, the dependence of the reaction constant on the medium is difficult to explain. It is possible that the susceptibility of the reaction constant to changes in the medium is controlled by the solvating power of the medium (38), which parallels to some extent the dielectric constant of the medium (39). Previously, this dependence has been mainly attributed to that portion of the polar effect transmitted by the medium itself.[2] Nevertheless, the objections previously raised to purely inductive transmission are still valid (37).

Recently, further studies (40, 41) have been made using the field effect calculations based on the method of Kirkwood and Westheimer (42). The application of these calculations to our system is made difficult by the conjugated π-electron system present, i.e. the possible occurrence of resonance and π-inductive effects. Westheimer applied his theoretical model to para-substituted benzoic acids (43). Sarmousakis (44) showed that the theory can be applied with reasonable success to meta-substituted benzoic acids, though the same model was not similarly successful for the para-substituted isomers due to the resonance effect at the latter position. However, it remains useful to attempt to compare the relative transmission by a field effect. Any absolute value of ΔpK_a, obtained from the known dipole moment, will not be a useful estimate.

The field effect model has been treated in two ways; by considering the molecular cavity as a sphere (42*a*) or as a prolate ellipsoid (42*b*). The second model seems more realistic for our system. The dipolar substituent can be treated as a point dipole or two point charges. Kirkwood and Westheimer have presented equations which allow both models to be tested for the *trans*-acrylic acids. In the case of the *cis*-acrylic acids, where the dipolar substituent is not situated on the main molecular axis, it is only possible to use the spherical model with the substituent as two point charges.

$$\log K/K_0 = \frac{e\mu \cos\theta}{2.303kTD_eR^2} \quad \text{for point dipolar substituents} \qquad [vi]$$

$$\log K/K_0 = \frac{e}{2.303kTD_eR} \quad \text{for charged substituents} \qquad [vii]$$

The eqs. [vi] and [vii] have been proposed by Kirkwood and Westheimer (42) to calculate the electrostatic field effect of a substituent group on ionization constants and the

[2]*A model system to test these points is under consideration.*

Can. J. Chem. Downloaded from www.nrcresearchpress.com by 210.87.254.5 on 09/05/12
For personal use only.

relative rates of reaction, where μ is the dipole moment, e the electronic charge, k the Boltzmann constant, T the absolute temperature, and R the distance between the dipole or charge and the reaction center, and D_e the effective dielectric constant. θ is the angle between the line joining the reaction center and the center of the dipole and the axis of the dipole. The molecule is considered to be a low dielectric cavity ($D = 2.0$) embedded in the solvent medium, water ($D = 78.5$) or ethanol ($D = 24.3$). The relative transmission, ϕ, is thus governed by the calculable factors as in equation [viii], for a point dipole substituent.

[viii] $$\phi = \rho/\rho_0 = (R_0^2 D_{e0} \cos\theta)/(R^2 D_e \cos\theta_0)$$

The reaction center is sited as before (1) and the molecular dimensions were calculated from the known molecular geometries (45). The important distance is that from the center of the dipole to the surface of the molecular cavity. This is taken as 1.5 Å in accordance with the suggestion of Tanford (46).

TABLE V

Field effect calculation (point dipole approximation)

			Spherical model		Ellipsoidal model	Spherical model		Ellipsoidal model
X	θ	R	D_e (in water)	D_e (in ethanol)	D_e (in water)	ϕ (in water)*	ϕ (in ethanol)*	ϕ (in water)*
3-X-substituted acrylic acid								
trans-H	18	3.76	3.26	3.10	4.0	2.9	2.8	3.9
cis-H	90	3.21	—	—	—	—	—	—
trans-Me	17	3.97	3.38	3.19	4.3	2.8	2.7	3.7
cis-Me	86	3.22	—	—	—	—	—	—
trans-Cl	16	4.08	3.43	3.24	4.4	2.7	2.6	3.7
cis-Cl	84	3.23	—	—	—	—	—	—
trans-Br	16	4.16	3.47	3.27	4.5	2.7	2.6	3.7
cis-Br	82	3.24	—	—	—	—	—	—
trans-I	16	4.25	3.51	3.31	4.6	2.7	2.5	3.6
cis-I	81	3.26	—	—	—	—	—	—
trans-NO_2	16	4.22	3.50	3.30	4.6	2.7	2.6	3.6
trans-OMe	16	4.21	3.50	3.30	4.6	2.7	2.6	3.6
p-X-substituted benzoic								
H	0	5.70	4.27	3.91	7.1	—	—	—
Me	0	5.91	4.39	4.00	7.5	—	—	—
Cl	0	6.02	4.44	4.03	7.8	—	—	—
Br	0	3.10	4.48	4.08	8.0	—	—	—
I	0	6.20	4.53	4.11	8.2	—	—	—
NO_2	0	6.17	4.51	4.10	8.1	—	—	—
OMe	0	6.16	4.51	4.10	8.1	—	—	—

*Calcd. $\phi = [\cos\theta(R \times D_e)^{-1}]_{\text{acrylic}} / [\cos\theta(R \times D_e)^{-1}]_{p\text{-benzoic}}$.

In Table V, the results for a point dipole substituent approximation and in Table VI, the results for a two point charge dipole substituent approximation are shown. The ratio of the reaction constants, ϕ, for the *trans*-acrylic acid to the para-substituted benzoic acids is given as 2.7 (point dipole approx.) or 2.4 (two point charges dipole approx.) for spherical model molecules in water. The ratio is 3.7 (point dipole approx.) or 3.3 (two point charges dipole approx.) for ellipsoidal model molecules in water. The two point charges model is less of an approximation than the point dipole. The calculated ratio, ϕ, falls to 2.6 in ethanol from 2.7 in water. The model also predicts a linear relation between the reaction constant for a particular system, e.g. the reaction of *trans*-substituted acrylic acids and diazodiphenylmethane, and the reciprocal of the dielectric constant.

The experimentally found ratio, ϕ, for this system is 2.2 (ionization in water). This is in

Can. J. Chem. Downloaded from www.nrcresearchpress.com by 210.87.254.5 on 09/05/12
For personal use only.

TABLE VI

Field effect calculation (two point charges dipole approximation)

X	R_1	R_2	Spherical model H_1 (in water)*	Spherical model H_2 (in water)*	Spherical model ϕ (in water)†	Ellipsoidal model D_{e1} (in water)	Ellipsoidal model D_{e2} (in water)	Ellipsoidal model ϕ (in water)‡
3-X-substituted acrylic acid								
trans-H	3.25	4.28	0.0256	0.0107	2.4	10.0	27.0	3.3
cis-H	3.25	3.25	0.0256	0.0207	0.8	—	—	—
trans-Me	3.25	4.70	0.0305	0.0090	2.4	9.0	38.0	3.4
cis-Me	3.25	3.36	0.0305	0.0204	1.1	—	—	—
trans-Cl	3.25	4.93	0.0331	0.0080	2.4	8.6	44.6	3.3
cis-Cl	3.25	3.44	0.0331	0.0196	1.3	—	—	—
trans-Br	3.25	5.07	0.0347	0.0074	2.4	8.5	49.0	3.3
cis-Br	3.25	3.51	0.0347	0.0183	1.5	—	—	—
trans-I	3.25	5.27	0.0369	0.0070	2.4	8.2	55.3	3.3
cis-I	3.25	3.59	0.0369	0.0169	1.6	—	—	—
trans-NO_2	3.25	5.20	0.0361	0.0074	2.4	8.3	52.9	3.3
trans-OMe	3.25	5.17	0.0356	0.0075	2.4	8.3	52.0	3.3
p-X-substituted benzoic								
H	5.15	6.24	0.0110	0.0049	—	20.1	52.8	—
Me	5.15	6.67	0.0131	0.0042	—	18.0	66.2	—
Cl	5.15	6.89	0.0142	0.0038	—	17.1	72.2	—
Br	5.15	7.04	0.0148	0.0036	—	16.6	75.4	—
I	5.15	7.24	0.0158	0.0031	—	16.0	79.6	—
NO_2	5.15	7.19	0.0156	0.0032	—	16.2	78.9	—
OMe	5.15	7.16	0.0154	0.0034	—	16.2	77.9	—

*H_1 or H_2 are simple functions of the reciprocal of dielectric and distance (see eq. [17] of ref. 42*a*).
†Calcd. $\phi = (H_1 - H_2)_{\text{acrylic}}/(H_1 - H_2)_{p\text{-benzoic}}$.
‡Calcd. $\phi = [(D_{e1} \times R_1)^{-1} - (D_{e2} \times R_2)^{-1}]_{t\text{-acrylic}}/[(D_{e1} \times R_1)^{-1} - (D_{e2} \times R_1)^{-1}]_{p\text{-benzoic}}$.

good agreement with the first results, considering the uncertainties. The ratio found in ethanol is 1.8 (diazodiphenylmethane reaction) compared to ratio for water of 2.2 (ionization in water). Thus, the correct qualitative decrease is shown. If the factors determining ρ_c and ρ_s (see eq. [iv]), which are dependent on the type of reaction studied, are the same, the ratio ρ_s/ρ_c should be constant for a given system, e.g. *trans*-acrylic acids. The ratio found experimentally is 8.3 for esterification reaction. Though no data exist to check its constancy, the calculated ratio for a two point charges / spherical model is about 8.0 (see Table VI).

Unfortunately the calculated values found for the *cis*-acids in Table VI, are quite unacceptable with regard to the experimental results (see Tables I and II). The "distant" end of the dipole has a large "neutralizing" effect on the field of the "proximate" end. The lack of reality of this model is probably significantly at fault here. The transmitting cavities are similar for the *cis*- and *trans*-acrylic acids and yet the "distant" end of the dipole has such a dissimilar effect. It seems likely that a reasonable transmitting cavity will enclose the whole molecule, whether or not *cis*- or *trans*-substituted, and the "distant" poles will have a comparable effect.

It seems that the Kirkwood–Westheimer models are not completely satisfactory. The best model indicated is one in which we consider the dipole to be embedded in the low dielectric molecular cavity such that the important influence is the "proximate" end of the dipole attached to the molecule. The polar effect is then transmitted by a field effect from the effectively "mono-pole" substituent through both the low dielectric cavity of the molecule and the solvent sheath. The latter effect is accompanied by, in this case, a π-inductive-resonance effect. This is essentially the model proposed by Dewar (31).

As in a previous study (21), the ρ/ρ_0 interpretation offered can be applied in a similar

Can. J. Chem. Downloaded from www.nrcresearchpress.com by 210.87.254.5 on 09/05/12
For personal use only.

manner. The value of ρ/ρ_0 for "unconjugated" benzoic acids, i.e. exclusion of π-electron effect, can be estimated to be 0.70. The π-electron effects contribute a factor of 0.30. Thus for the 3-substituted acrylic acids the field effect calculations allows us to calculate the "unconjugated" transmission as ρ/ρ_0 equal to 2.22 ("mono-pole" – ellipsoidal model) or 1.61 ("mono-pole" – spherical model) (see Table VI). The effect of using a dipole model for the *trans*-isomers gives similar results. The π-electron effect contribution can be calculated by assuming the effect to vary inversely with distance, as 0.48 or, by using the relative q_{ij} factors, as 0.57. The calculated values for ϕ are thus 2.70 or 2.79 (ellipsoidal model) and 2.09 or 2.18 (spherical model). The experimental ϕ is 2.2 in water.

TABLE VII

Hammett reaction constants*

Reaction	ρ	Log k_0	n	r	Ref.
1. Esterification with DDM at 30.0°					
trans-3-Subst. acrylic acids	1.617	0.086	7	0.998	This work
cis-3-Subst. acrylic acids	1.772	0.011	5	0.979	This work
Ortho-subst. benzoic acids	1.889	0.322	6†	0.997	33
Meta- and para- subst. benzoic acids	0.944	−0.002	7	0.998	47
2. Aqueous pK_a values at 25.0°					
trans-3-Subst. acrylic acids	2.187	−4.279	7	0.999	This work
cis-3-Subst. acrylic acids	2.452	−3.995	4	0.988	This work
Ortho-subst. benzoic acids	2.392	−4.946	7‡	0.997	25
Meta- and para-subst. benzoic acids	1.000	−4.200	—	—	28

*n is the number of substituents studied. r is the correlation coefficient.
†Substituents are Me, Et, F, Cl, Br, and I.
‡Substituents are Me, Et, F, Cl, Br, I, and OMe.

The Value of the Reaction Constants

The values of the reaction constants for a number of systems are shown in Table VII. These were obtained using the para σ values, except for meta-substituted benzoic acids. The reaction constants for the ortho-substituted benzoic acids were obtained by studying only those substituents of moderate steric bulk, i.e. absence of secondary steric effect causing de-conjugation of carboxyl and aromatic ring. The latter values are *very* similar to those obtained for the *cis*- or *trans*-3-substituted acrylic acids. The reaction constants for meta- and para-substituted benzoic acids are considerably smaller. It is very important to point out that 3-substituted acrylic acids (I and II) and ortho-substituted benzoic acids (III) in the reactions shown have a susceptibility to the polar effects of substituents of about twice that of meta- and para-substituted benzoic acids (IV). The cited examples

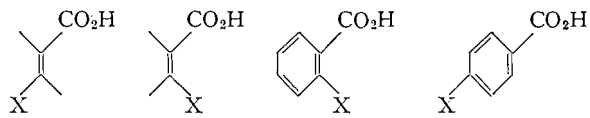

I II III IV

are two particular cases of a more complex situation which we intend to investigate in subsequent publications.

REFERENCES

1. K. BOWDEN. Can. J. Chem. **41**, 2781 (1963).
2. J. HINE and W. C. BAILEY. J. Am. Chem. Soc. **81**, 2075 (1959).
3. (*a*) M. CHARTON and H. MEISLICH. J. Am. Chem. Soc. **80**, 5940 (1958). (*b*) M. CHARTON. J. Org. Chem. **30**, 552, 557, 974 (1965).
4. C. RAPPE. Acta Chem. Scand. **17**, 2766 (1963).
5. H. J. BACKER and A. E. BEUTE. Rec. Trav. Chim. **54**, 167 (1935).

Can. J. Chem. Downloaded from www.nrcresearchpress.com by 210.87.254.5 on 09/05/12
For personal use only.

6. K. ALDER, F. BROCHHAGEN, C. KAISER, and W. ROTH. Ann. Chem. **593**, 1 (1955).
7. F. STOLZ. Ber. **19**, 536 (1886).
8. D. E. JONES, R. O. MORRIS, C. A. VERNON, and R. F. M. WHITE. J. Chem. Soc. 2349 (1960).
9. H. SCHEIBLER and J. VOSS. Ber. **53**, 382 (1920).
10. I. HEILBRON and H. M. BUNBURY. Dictionary of organic compounds. 3rd ed. Eyre and Spottiswoode, London. 1953.
11. H. SCHECHTER, F. CONRAD, A. L. DOULTON, and R. B. KAPLAN. J. Am. Chem. Soc. **74**, 3052 (1952).
12. L. N. OWEN and H. M. BABATUNDE SOMADE. J. Chem. Soc. 1030 (1947).
13. J. A. POPLE, W. G. SCHNEIDER, and H. J. BERNSTEIN. High resolution nuclear magnetic resonance. McGraw-Hill Book Co., Inc., New York. 1959. p. 238.
14. K. BOWDEN. To be published.
15. J. S. PIZEY and W. E. TRUCE. J. Chem. Soc. 865 (1964).
16. A. BUCKLEY, N. B. CHAPMAN, and J. SHORTER. J. Chem. Soc. 178 (1963).
17. A. WEISBERGER. Techniques of organic chemistry. Vol. VII. 2nd ed. Interscience Publishers. Inc., New York. 1955.
18. A. I. VOGEL. Practical organic chemistry. 3rd ed. Longmans, London. 1956. p. 168.
19. W. SEAMAN, W. H. MCCOMAS, and G. A. ALLEN. Anal. Chem. **21**, 510 (1949).
20. K. BOWDEN, N. B. CHAPMAN, and J. SHORTER. J. Chem. Soc. 5239 (1963).
21. K. BOWDEN, N. B. CHAPMAN, and J. SHORTER. Can. J. Chem. **42**, 1979 (1964).
22. K. BOWDEN, A. BUCKLEY, N. B. CHAPMAN, and J. SHORTER. J. Chem. Soc. 3380 (1964).
23. R. G. BATES and E. A. GUGGENHEIM. Pure Appl. Chem. **1**, 163 (1960).
24. A. ALBERT and E. P. SERJEANT. Ionisation constants of acids and bases. Methuen & Co. Ltd., London. 1962.
25. G. KORTUM, W. VOGEL, and K. ANDRUSSOW. Pure Appl. Chem. **1**, 190 (1960).
26. M. L. DONDON and M. T. PARIS. J. Chim. Phys. **58**, 222 (1961).
27. H. H. JAFFE. Chem. Rev. **53**, 191 (1953).
28. D. H. MCDANIEL and H. C. BROWN. J. Org. Chem. **23**, 420 (1958).
29. R. A. ROBINSON and K. P. ANG. J. Chem. Soc. 2314 (1959).
30. H. VAN BEKKUM, P. E. VERKADE, and B. M. WEPSTER. Rec. Trav. Chim. **78**, 815 (1959).
31. M. J. S. DEWAR and P. J. GRISDALE. J. Am. Chem. Soc. **84**, 3539, 3548 (1962).
32. J. D. S. RITTER and S. I. MILLER. J. Am. Chem. Soc. **86**, 1507 (1964).
33. N. B. CHAPMAN, J. SHORTER, and J. H. P. UTLEY. J. Chem. Soc. 1824 (1962).
34. R. W. TAFT. *In* Steric effects in organic chemistry. *Edited by* M. S. Newman. John Wiley and Sons Inc., New York. 1956. Chap. 13.
35. A. C. FARTHING and B. NAM. *In* Steric effects in conjugated systems. *Edited by* G. W. Gray. Butterworths, London. 1958. Chap. 11.
36. K. BOWDEN and D. C. PARKIN. To be published.
37. S. EHRENSON. *In* Progress in physical organic chemistry Vol. II. *Edited by* S. G. Cohen, A. Streitwieser, Jr., and R. W. Taft. Interscience Publishers, New York. 1964. p. 195.
38. C. REICHARDT. Angew. Chem. Intern. Ed. Engl. **4**, 29 (1965).
39. B. GUTBEZAHL and E. GRUNWALD. J. Am. Chem. Soc. **75**, 559 (1953). E. GRUNWALD and B. J. BERKOWITZ. J. Am. Chem. Soc. **73**, 4939 (1951).
40. H. D. HOLTZ and L. M. STOCK. J. Am. Chem. Soc. **86**, 5188 (1964).
41. C. F. WILCOX and J. S. MCINTYRE. J. Org. Chem. **30**, 777 (1965).
42. (*a*) J. G. KIRKWOOD and F. H. WESTHEIMER. J. Chem. Phys. **6**, 506 (1938). (*b*) F. H. WESTHEIMER and J. G. KIRKWOOD. J. Chem. Phys. **6**, 513 (1938).
43. F. H. WESTHEIMER. J. Am. Chem. Soc. **61**, 1977 (1939).
44. J. N. SARMOUSAKIS. J. Chem. Phys. **12**, 277 (1944).
45. H. J. M. BOWEN *et al.* (*Compilers*). Tables of interatomic distances and configurations in molecules and ions. The Chemical Society, London. 1958. Special Publication No. 11.
46. C. TANFORD. J. Am. Chem. Soc. **79**, 5348 (1957).

Can. J. Chem. Downloaded from www.nrcresearchpress.com by 210.87.254.5 on 09/05/12
For personal use only.

Can. J. Chem. Downloaded from www.nrcresearchpress.com by 210.87.254.40 on 09/05/12
For personal use only.

SYNTHESES WITH 5-DIBROMOMETHYL- AND 5-FORMYL-PYRROMETHENES[1]

A. MARKOVAC[2] AND S. F. MACDONALD
Division of Pure Chemistry, National Research Council, Ottawa, Canada

Received July 20, 1965

ABSTRACT

With many 5,5′-dimethyl- and 5-bromo-5′-methyl-pyrromethenes the sequence $CH_3 \rightarrow CH_2Br \rightarrow CH_2OMe$ had been possible. With two such pyrromethenes the following new sequences have been developed: (1) $CH_3 \rightarrow CHBr_2 \rightarrow CH(OMe)_2$ or CHO (cf. III*e* and IV*e*), (2) $CH(OMe)_2$, CHO, or $CH_2OMe \rightarrow Br$ (cf. III*f* and IV*f*), (3) (dimethoxy-methyl-)pyrromethene → formyl-dipyrrylmethane (cf. IX and VII). These provide new intermediates for new porphyrin syntheses and alternative or improved routes to established intermediates.

INTRODUCTION

The pyrrole I*a* is readily converted to III*a* by bromine in acetic acid, or to IV*a* by formic and hydrobromic acids, and its analogues behave likewise. The halogenation of

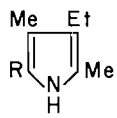

I a ; R = H
I b ; R = COOEt

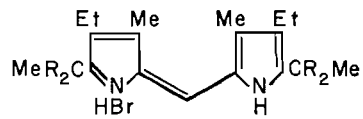

II a ; $R_2 = H_2$
II b ; $R_2 = HBr$
II c ; $R_2 = Br_2$

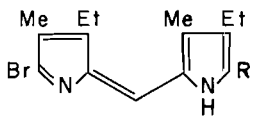

III

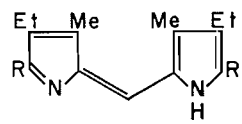

IV

(a) R = CH_3
(b) R = CH_2Br
(c) R = $CHBr_2$
(d) R = CHO
(e) R = $CH(OMe)_2$
(f) R = Br
(g) R = CH_2OMe

such 5,5′-dimethyl- and 5-bromo-5′-methyl-pyrromethenes to the corresponding bromomethyl derivatives is quite general when the other substituents are purely alkyl, and a 5-carbethoxy-5′-methyl-pyrromethene behaved likewise (1). Further, the bromomethyl-derivatives are readily converted into methoxymethyl-pyrromethenes. When, however, there are other halogen substituents or when the alkyl substituents are carboxylated, the halogenation frequently fails; therefore dihalomethyl- or trihalomethyl-pyrromethenes were unknown. In particular, we have not been able to halogenate 5-bromo-5′-methyl-pyrromethenes with acetic acid and propionic acid residues in the 3(3′) and 4(4′) positions to obtain desired intermediates.

[1]*Issued as N.R.C. No. 8682.*
[2]*National Research Council of Canada Postdoctorate Fellow, 1963–65.*

Hans Fischer had reported that an excess of undiluted bromine converted II*a* to a product containing five atoms of bromine but no perbromide (2, 3*a*). It seemed reasonable to assume that his product was not II*b* as provisionally formulated, but II*c*, and that this method of bromination might lead to hitherto unaccessible halogenated pyrromethenes.

This halogenation was also interesting in another connection. Pyrromethenes with acyl groups (formyl or keto) in the 3(3′) and 4(4′) positions were known (3*b*) but 5-acyl-pyrromethenes were only known as their 5′-hydroxy-derivatives (3*c*). This would be expected from the low reactivity of 2-free-5-acyl pyrroles and the exceptional reactivity of 5-free-5′-hydroxy-pyrromethenes. Further, we have failed to convert 5-bromomethyl- to 5-formyl-pyrromethenes in trials with 2-nitropropane, dimethyl–sulfoxide, or selenium dioxide. Recently, however, 4,3′,5′-trimethyl-3,4′-diacetyl-5-formyl-pyrromethene has been obtained from the corresponding 5-free-dipyrrylmethane by reaction with zinc cyanide and hydrogen chloride (4).

We first studied the bromination of the hydrobromides of III*b* and IV*b*. These were presumably favorable cases because the hydrobromides of III*a* and IV*a* are readily halogenated (to those of III*b* and IV*b*) by bromine in acetic acid. An excess of undiluted bromine at room temperature converted the hydrobromides of III*b* and IV*b* into those of III*c* and IV*c*. Later these were obtained directly under more vigorous conditions from the hydrobromides of III*a* and IV*a* but in equally good yield.

Treatment with methanol followed by alkali converted III*c* and IV*c* into the acetals III*e* and IV*e*. Here the 5-bromo group in the acetal III*e* remained intact, whereas that in 5-*bromo*-4,4′-dimethyl-5′-*carbethoxy*-pyrromethene-3,3′-dipropionic acid hydrobromide is reportedly converted into hydroxyl by cold methanolic hydrogen chloride (5). Although the aldehyde III*d* was obtained from III*c* by treatment with sodium acetate, this reaction failed with IV*c*. Possibly 5,5′-diformyl-, like 5,5′-dicarbethoxy-pyrromethenes (6), exist as carbinols rather than as pyrromethene bases, and unprotected 5,5′-diacyl-pyrromethenes may be generally less stable than the corresponding dipyrrylmethanes.

In the same way as 5,5′-diformyl-dipyrrylmethanes condense with 5,5′-free-dipyrrylmethanes at room temperature to form porphyrins (7), the pyrromethene IV*e* condensed with V to form the porphyrin VI (see also below). The yield was low (17%), perhaps because of the rigidity of an open-chain intermediate, and this new method has no obvious advantage over that using analogues of IV*b* (7) at 100°.

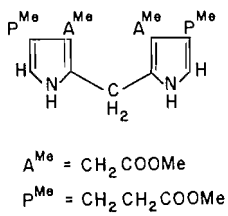

V

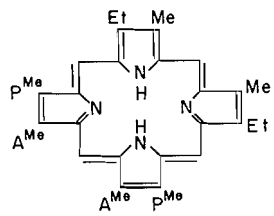

VI

Bromine in acetic acid converted the aldehyde III*d* or its acetal III*e* into the new unsymmetrical 5,5′-dibromo-pyrromethene III*f*. The two previously known unsymmetrical 5,5′-dibromo-pyromethenes had been obtained from dipyrrylmethanes (8, 9). Bromine also converted IV*e* into the symmetrical IV*f*. The full sequence now permits the conversion of a 5-methyl- to a 5-bromo-pyrromethene. A more convenient equivalent was later found

Can. J. Chem. Downloaded from www.nrcresearchpress.com by 210.87.254.40 on 09/05/12
For personal use only.

in the bromination of the methoxymethyl derivatives, III*g* and IV*g* also being converted to III*f* and IV*f*.

Fischer's methods permitted a single pyrrole (e.g. I*a* or I*b*) to be converted unambiguously into pyrromethenes leading to porphyrins (e.g. etioporphyrins) of types 1 and 4. The synthesis of pyrromethenes leading to type 2 and 3 porphyrins required, in addition, the isomeric pyrrole (e.g. 2,3-dimethyl-4-ethyl-pyrrole) (10), which might be much less accessible. However, when extended by the above sequence replacing methyl by bromine, the same methods would also give types 2 and 3 porphyrins from the one pyrrole (Chart I).

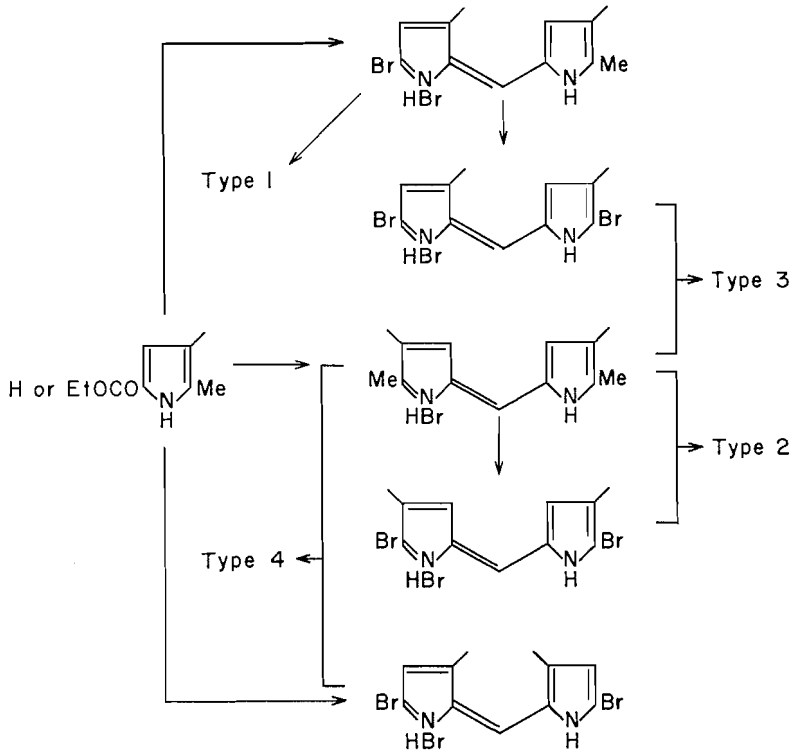

CHART I.

To illustrate this, etioporphyrin 3 (XI) was prepared from III*f* and IV*b*, which required a total of 8 steps compared to the 16 of Fischer's unmodified methods. There are less direct methods by which four isomeric porphyrins could be obtained unambiguously from one pyrrole: one pyrrole could be converted into its isomer (11), or types 2 (7, 12) and 3 (12) porphyrins could be obtained by unrelated methods.

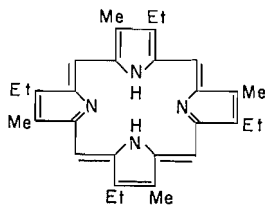

X

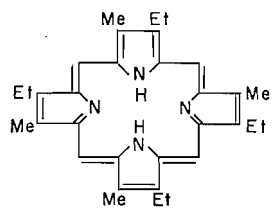

XI

Can. J. Chem. Downloaded from www.nrcresearchpress.com by 210.87.254.40 on 09/05/12
For personal use only.

The pyrromethene acetal IV*e* was reduced to the diformyl-dipyrrylmethane VII. This sequence, too, complements an established one, which proceeds over inherently less stable dipyrrylmethanes to convert, for example, *Ib* into VIII (13), the symmetrical isomer of VII. The condensation of VII with V led to the same porphyrin (VI) that was obtained from IV*e* and V (above), but the yield was better (36%). This porphyrin was further identified by degradation to the known mesoporphyrin 4.

This synthesis of porphyrins from a 5,5′-free- and a 5,5′-diformyl-dipyrrylmethane, like that from a 5,5′-dibromo- and a 5,5′-dimethyl-pyrromethene, requires that one component be symmetrically substituted to avoid an inseparable mixture of two isomers (7). It is thus not applicable to type 1 porphyrins. It suggests, however, a second porphyrin synthesis from two identical or different 5-free-5′-formyl-dipyrrylmethanes which, like the synthesis from two 5-bromo-5′-methyl-pyrromethenes (3*d*, 14), has different symmetry requirements. Accordingly III*d* was reduced but the unstable product, evidently IX, has not been isolated. However, this product did condense to etioporphyrin 1 (X, 44%), which was identified by comparison with authentic material.

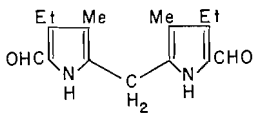

VII

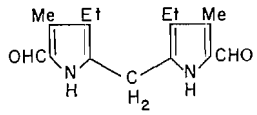

VIII

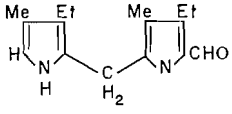

IX

It will be noted that the methoxymethyl- and formyl-pyrromethenes are for some purposes equivalent. However, we have assumed that the reduction of the latter would lead to more stable dipyrrylmethanes. A 5-carboxy-5′-formyl-dipyrrylmethane is reported elsewhere (15).

The nuclear magnetic resonance spectra of all the pyrromethenes and of the diformyl-dipyrrylmethane (Table I) were unambiguous and confirmed the structures assigned.

EXPERIMENTAL

5-Bromo-4,3′-dimethyl-3,4′-di-ethyl-5′-bromomethyl-pyrromethene Hydrobromide (Hydrobromide of IIIb) (3e)

The corresponding 5′-methyl-pyrromethene hydrobromide (III*a*, 2 g (3*f*, 16)) was dissolved in 50 ml of hot acetic acid, bromine (1.2 g) in acetic acid (15 ml) was added, and the solution was heated for 4 h on a steam bath. After the mixture had stood overnight at 20°, the crystalline product was separated out and treated under reflux with acetone for 10 min. The product which separated from the cooled solution was recrystallized from chloroform–hexane as red prismatic crystals (1.8 g, 75%) that decomposed above 250°.

5-Bromo-4,3′-dimethyl-3,4′-di-ethyl-5′-methoxymethyl-pyrromethene (IIIg) (3e)

The corresponding 5′-bromomethyl-pyrromethene hydrobromide (III*b*, 500 mg, prepared as above or, if prepared according to Fischer (3*e*), recrystallized twice from chloroform–hexane) was dissolved in 10 ml of methanol and boiled under reflux for 2 min. Then the solution was cooled and neutralized with 10% sodium hydroxide. The product was recrystallized from methanol as orange–brown needles (290 mg, 79%), m.p. 92–94°.

Unless precautions are taken to ensure that the starting material contains no 5′-methyl-pyrromethene (III*a*), the product has the lower melting point (84°) that has been previously recorded (3*e*).

5-Bromo-4,3′-dimethyl-3,4′-di-ethyl-5′-(dibromomethyl)-pyrromethene Hydrobromide (Hydrobromide of IIIc)

(*a*) The corresponding 5′-bromomethyl-pyrromethene hydrobromide (III*b* (3*e*), 500 mg, twice recrystallized from chloroform–petrol) in 3 ml of bromine was stirred at 20° for 1 h. Excess bromine was then completely removed *in vacuo* and the residue was treated under reflux for 30 min with 10 ml of acetone to dissociate any perbromide. After it had cooled the crystalline product was separated off and recrystallized from chloroform as red-brown prisms (450 mg, 77%) that decomposed above 200°, λ_{max} mμ (ϵ) in chloroform: 504 (112 000). The analytical sample was recrystallized once.

Calcd. for $C_{16}H_{20}N_2Br_4$: C, 34.31; H, 3.60; N, 5.00; Br, 57.09. Found: C, 34.49; H, 3.78; N, 5.24; Br, 56.89.

Can. J. Chem. Downloaded from www.nrcresearchpress.com by 210.87.254.40 on 09/05/12
For personal use only.

Can. J. Chem. Downloaded from www.nrcresearchpress.com by 210.87.254.40 on 09/05/12
For personal use only.

TABLE I

Chemical shifts of pyrromethenes and a dipyrrylmethane (p.p.m., τ-scale)

		—CH_2CH_3	—CH_2CH_3	—OCH_3		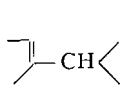	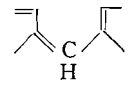	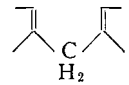	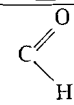	Solvent
III*a*	7.97; 7.66	8.82; 8.93	7.33; 7.44				2.95			$CDCl_3$
HBr	7.34									
III*b*	7.92; 7.63	8.77; 8.80	7.19; 7.35		5.05		2.73			$CDCl_3$
HBr										
III*c*	7.59; 7.84	8.70; 8.70	7.15; 7.15			2.82	2.58			$CDCl_3$ + CF_3COOH
HBr										
III*d*	7.85; 8.05	8.86; 8.82	7.46; 7.27				3.37		0.25	$CDCl_3$
III*e*	7.79; 8.01	8.90; 8.85	7.49; 7.41	6.60; 6.60		4.37	3.17			$CDCl_3$
III*f*	7.55; 7.96	8.81; 8.79	7.28; 7.30				2.75			$CDCl_3$
HBr										
III*g*	7.83; 8.03	8.91; 8.86	7.56; 7.44	6.62	5.53		3.25			$CDCl_3$
IV*a*	7.69; 7.69	8.92; 8.92	7.56; 7.56				2.83			$CDCl_3$
HBr	7.33; 7.33									
IV*b*	7.55; 7.55	8.56; 8.56	7.36; 7.36		5.17; 5.17		2.42			$CDCl_3$ + CF_3COOH
HBr										
IV*c*	7.54; 7.54	8.69; 8.69	7.12; 7.12			2.83	2.32			$CDCl_3$ + CF_3COOH
HBr										
IV*e*	7.82; 7.82	8.90; 8.90	7.50; 7.50	6.54; 6.54 6.54; 6.54		4.53; 4.53	3.15			$CDCl_3$
IV*f*	7.81; 7.81	8.87; 8.87	7.55; 7.55				3.27			$CDCl_3$
IV*g*	7.83; 7.83	8.81; 8.81	7.54; 7.54	6.57; 6.57	5.52; 5.52		3.23			$CDCl_3$
VII	7.93; 7.93	8.80; 8.80	7.77; 7.77					6.04	0.44; 0.44	$CDCl_3$

(*b*) The corresponding 5′-methyl-pyrromethene hydrobromide (III*a* (3*f*), 300 mg) and 3 ml of bromine were held under reflux for 1 h on a steam bath, then left at 20° for 1 h. The product was isolated as above. It formed red-brown prisms from chloroform (310 mg, 74%) that decomposed above 200°.

Its identity with the product of (*a*) above was established from their conversion to the same 5′-formyl-pyrromethene (see below).

5-Bromo-4,3′-dimethyl-3,4′-di-ethyl-5′-formyl-pyrromethene (IIId)

The corresponding 5′-(dibromo-methyl)-pyrromethene hydrobromide (III*c*, 560 mg, prepared by method (*a*) above) in 20 ml of chloroform, and saturated aqueous sodium acetate (10 ml, warmed to 60°) were stirred together for 1 h. The chloroform layer was washed with water, dried, and the solvent removed *in vacuo*. The residue was recrystallized from methanol as brown prisms (300 mg, 89%), m.p. 135–138° (dec.). Recrystallized for analysis, it melted at 138–140° (dec.), λ_{max} mμ (ϵ) in 95% ethanol: 270 (9 800); 434 (30 500).

Calcd. for $C_{16}H_{19}N_2OBr$: C, 57.32; H, 5.71; N, 8.36; Br, 23.84. Found: C, 57.16; H, 5.67; N, 8.21; Br, 24.00.

When the starting material was prepared by method (*b*) above, the product (84%) had m.p. 136–139° (dec.), and mixed melting point unchanged.

5-Bromo-4,3′-dimethyl-3,4′-di-ethyl-5′-formyl-pyrromethene Dimethyl Acetal (IIIe)

The corresponding 5′-(dibromo-methyl)-pyrromethene hydrobromide III*c* (200 mg) was treated under reflux with 2.5 ml of methanol for 5 min, cooled, and neutralized with 5% sodium hydroxide. The product, which crystallized after the container was scratched and refrigerated, was recrystallized from methanol as brown needles (100 mg, 84%), m.p. 99–100°, 100–101° after recrystallization for analysis. λ_{max} mμ (ϵ) in 95% ethanol: 271 (7 600); 432 (25 000).

Calcd. for $C_{18}H_{25}N_2O_2Br$: C, 56.70; H, 6.61; N, 7.35; Br, 20.95. Found: C, 56.72; H, 6.45; N, 7.52; Br, 21.08.

5,5′-Dibromo-4,3′-dimethyl-3,4′-di-ethyl-pyrromethene Hydrobromide (Hydrobromide of IIIf)

(*a*) Bromine (0.1 ml in 1 ml of acetic acid) was added to a solution of the aldehyde III*d* (100 mg) in 2 ml of acetic acid. The solution was stirred at 20° for 30 min; then the solvent was removed *in vacuo*. The residue was treated under reflux for 10 min with 5 ml of acetone. The crystalline product (100 mg, 71%) separated from the refrigerated solution. For analysis, it was recrystallized from chloroform–ether as red prisms that decomposed above 140°, λ_{max} mμ (ϵ) in 95% ethanol: 230 (22 000); 452 (76 000).

Calcd. for $C_{15}H_{19}N_2Br_3$: C, 38.57; H, 4.10; N, 6.00; Br, 51.33. Found: C, 38.73; H, 4.22; N, 5.89; Br, 51.08.

(*b*) The acetal III*e* was treated as in (*a*) above to give the product (69%) as red prisms that decomposed above 140°. Found: Br, 51.20.

(*c*) The 5′-methoxymethyl-pyrromethene (III*g*, m.p. 92–94°, 200 mg) dissolved in 4 ml of acetic acid was treated with bromine (0.2 ml) in acetic acid (4 ml). The mixture was heated for 2 h on a steam bath, the product was isolated as in (*a*) above, and washed with ether before it was recrystallized from chloroform–ether. It formed red prisms (160 mg, 61%) that decomposed above 140°.

The nuclear magnetic resonance spectra of the product obtained as under (*a*), (*b*), and (*c*) were identical.

Etioporphyrin 1 (X)

(*a*) The aldehyde III*d* (50 mg) was hydrogenated (6 h, 20°, 1 atmosphere) in 10 ml of 95% ethanol containing 0.2 ml of triethylamine, over 20 mg of palladium black (uptake 6.9 ml, calcd. for $2H_2$:7.2 ml). The catalyst was separated by decantation and the solvent was evaporated *in vacuo* from the initially pale yellow solution. The residue, evidently IX, was dissolved in 10 ml of acetic acid containing 0.2 ml of hydroiodic acid (56%, decolorized with hypophosphorous acid). After 1 h, 1 g of anhydrous sodium acetate in 15 ml of acetic acid was added, and air was passed through for 24 h while the mixture was kept in the dark. The crude product was precipitated with 25 ml of water, separated out, treated under reflux with 5 ml of methanol, separated out again, and crystallized from chloroform–methanol (yield: 15.5 mg, 44%). For analysis it was recrystallized as well-formed red prisms that decomposed above 380° (17) (evacuated capillary), λ_{max} mμ (relative density) in chloroform: 497 (1); 533 (0.73); 567 (0.49); 620 (0.36).

Calcd. for $C_{32}H_{38}N_4$: C, 80.29; H, 8.00. Found: C, 80.50; H, 8.28.

Both the aldehyde III*d* and its acetal III*e* were reduced as above to nearly colorless solutions (dark red in the absence of triethylamine) but they darkened rapidly, and the product has not been isolated.

(*b*) Authentic etioporphyrin 1 was prepared from the mixed hydrobromides (3*e*) of III*a* and III*b* in formic acid (3 *g*), in the form of red prisms (from chloroform–methanol) that decomposed above 380°.

X-ray powder photographs indicated the identity of the two specimens and showed that both existed in two forms. The analytical specimen obtained as under (*a*) was the first form, which was converted by one recrystallization into a mixture of the first and second forms. The specimen obtained as under (*b*) was the second form, and it was converted by one recrystallization into the first form. The X-ray powder photographs of the first forms were identical.

Etioporphyrin 3 (XI)

The hydrobromides of the pyrromethenes III*f* (40 mg) and IV*b* (40 mg) were heated for 1 h with 400 mg of succinic acid, and the product was isolated as in an analogous synthesis (3 *h*). From chloroform–methanol it separated as elongated prisms (4.8 mg, 12%) that decomposed above 355° (17) (evacuated capillary), λ_{max} mμ (relative density) in chloroform: 500 (1); 535 (0.72); 569 (0.49); 623 (0.36).

Can. J. Chem. Downloaded from www.nrcresearchpress.com by 210.87.254.40 on 09/05/12
For personal use only.

5,5′-Di-(dibromo-methyl)-3,3′-dimethyl-4,4′-di-ethyl-pyrromethene Hydrobromide (Hydrobromide of IVc)

(*a*) The corresponding 5,5′-di-(bromomethyl)-pyrromethene hydrobromide (IV*b* (16, 18), 1.5 g) was stirred for 1 h at 20° with 10 ml of bromine, the bromine was then removed *in vacuo*, and the residue was boiled under reflux for 30 min with 20 ml of acetone. The crystals were separated from the cooled mixture, washed with cold acetone, and recrystallized from chloroform as orange–red needles (1.2 g, 61%) that decomposed above 200°, λ_{max} mμ (ϵ) in chloroform: 252 (12 100); 519 (126 000). The analytical sample was recrystallized once.

Calcd. for $C_{17}H_{21}N_2Br_5$: C, 31.27; H, 3.25; N, 4.29; Br, 61.19. Found: C, 31.42; H, 3.37; N, 4.27; Br, 61.02.

(*b*) The 5,5′-dimethyl-pyrromethene hydrobromide (IV*a*, 300 mg) was brominated on a steam bath, and the product was isolated exactly as in the direct conversion of III*a* to III*c* (see above). The product crystallized from chloroform as orange-red needles (340 mg, 59%) that decomposed above 200°.

The identity of the products as obtained under (*a*) and (*b*) was established by the identity of their nuclear magnetic resonance spectra and by their conversion to the same acetal (see below).

5,5′-Diformyl-3,3′-dimethyl-4,4′-di-ethyl-pyrromethene Tetramethyl Acetal (IVe)

The corresponding 5,5′-di-(dibromo-methyl)-pyrromethene hydrobromide (IV*c*, 1 g, prepared by method (*a*) above) was boiled under reflux for 5 min in 10 ml of methanol. The solution was neutralized with 5% sodium hydroxide and refrigerated. The crystalline product was separated out and recrystallized from methanol as brown needles (450 mg, 77%), m.p. 63–64°. The analytical sample had been recrystallized as orange–brown needles, m.p. 65°, λ_{max} mμ (ϵ) in chloroform: 443 (24 700).

Calcd. for $C_{21}H_{32}N_2O_4$: C, 66.99; H, 8.57; N, 7.44. Found: C, 66.83; H, 8.45; N, 7.61.

When the starting material was prepared by method (*b*), above, the product (71%) had a melting point of 64–65°, and mixed melting point unchanged.

When IV*c* in chloroform was stirred with aqueous sodium acetate, the black product showed no bands in its visible spectrum.

5,5′-Dibromo-3,3′-dimethyl-4,4′-di-ethyl-pyrromethene Hydrobromide (Hydrobromide of IVf)

(*a*) Bromine (0.2 ml) in 2 ml of acetic acid was added to the acetal IV*e* (100 mg) dissolved in 2 ml of acetic acid. The solution was stirred for 30 min, then concentrated to one-half volume *in vacuo*. The crystalline product which separated out was treated under reflux with 2 ml of acetone for 5 min. The product (80 mg, 65%) was separated as red crystals that decomposed at 200°. The analytical sample was recrystallized from chloroform–ether as red prisms that decomposed at 200° (lit. (3*i*): dec. at 200°, as prepared from 2,3-dimethyl-4-ethyl-5-carbethoxy-pyrrole, the isomer of I*b*), λ_{max} mμ (ϵ) in 95% ethanol: 271 (20 600); 443 (79 000).

Calcd. for $C_{15}H_{19}N_2Br_3$: C, 38.57; H, 4.10; N, 6.00; Br, 51.33. Found: C, 38.54; H, 3.94; N, 5.88; Br, 51.21.

(*b*) The 5,5′-di-(methoxymethyl)-pyrromethene (IV*g* (3*j*), free base, m.p. 85°, 200 mg) dissolved in 4 ml of acetic acid was treated with 0.2 ml of bromine in 2 ml of acetic acid, the solution was heated in a steam bath for 2 h, then concentrated *in vacuo* to one-half volume. The crystals which separated were treated by reflux with 3 ml of acetone for 5 min. When the solution cooled, red prisms separated (160 mg, 54%) that decomposed above 200°. The product was recrystallized from chloroform–ether.

The identity of the products obtained as under (*a*) and (*b*) was established by comparing their free bases: 100 mg of the hydrobromides were dissolved in 2 ml of ethanol, the solutions were neutralized with 5% sodium hydroxide, and then refrigerated. The products which separated were recrystallized from 95% ethanol as orange needles (60 mg, 72%) m.p. 176°, mixed melting point unchanged (lit. (3*i*): 175–176°). Their nuclear magnetic resonance spectra were identical.

5,5′-Diformyl-3,3′-dimethyl-4,4′-di-ethyl-dipyrrylmethane (VII)

The acetal IV*e* (250 mg) was hydrogenated (20°, 1 atmosphere) in 15 ml of 95% ethanol over 70 mg of palladium black for 16 h (uptake 15.6 ml, calcd. for 1 mole:16.1 ml). After the catalyst was removed the solvent was evaporated *in vacuo*, and the crystalline residue was recrystallized from tetrahydrofuran-*n*-hexane as pale yellow prisms (170 mg, 89%), m.p. 245–247°. Recrystallization gave the colorless analytical sample, m.p. 250°, λ_{max} mμ (ϵ) in chloroform 301 (29 100); 320 (27 800).

Calcd. for $C_{17}H_{22}N_2O_2$: C, 71.30; H, 7.74; N, 9.78. Found: C, 71.42; H, 7.91; N, 9.95.

The hydrogenation (16 h) was prolonged to allow complete hydrolysis of the acetal; otherwise the product contained methoxy.

2,3-Dimethyl-1,4-di-ethyl-porphin-6,7-di-acetic acid-5,8-dipropionic acid Tetramethyl Ester VI

(*a*) The diformyl-dipyrrylmethane VII (14 mg) and dipyrrylmethane-3,3′-di-acetic acid-4,4′-dipropionic acid tetramethyl ester (V (7), 23 mg) were separately dissolved in warm acetic acid. The cooled solutions were combined, diluted to 10 ml with acetic acid, and 5 ml of acetic acid containing 0.2 ml of 56% hydroiodic acid was added. After 1 h, 1 g of anhydrous sodium acetate in 15 ml of acetic acid was put in, and the solution was aerated in the dark for 24 h. The precipitate was separated out, washed with acetic acid then with methanol, and left overnight in 5% methanolic hydrogen chloride. The solution was mixed with chloroform and ice water. The chloroform layer was well washed with water, dried with sodium sulfate, then passed through Grade IV alumina, which was eluted with 5% methanol in chloroform. The eluate was filtered and concentrated, and the chloroform finally displaced with methanol. The product (13 mg, 36%) separated as curly hairlike needles, m.p. 219–220°. For analysis it was recrystallized as above from chloroform–methanol as

Can. J. Chem. Downloaded from www.nrcresearchpress.com by 210.87.254.40 on 09/05/12
For personal use only.

red-brown hairlike needles, m.p. 220–222°, λ_{max} mμ (relative density) in chloroform: 501 (1); 537.5 (0.66); 572 (0.46); 626.5 (0.30).

Calcd. for $C_{40}H_{46}N_4O_8$: C, 67.59; H, 6.52; N, 7.88. Found: C, 67.78; H, 6.70; N, 7.71.

It was tested for scrambled products (etioporphyrins) by shaking an ethereal solution of the porphyrin-free acid with aqueous sodium hydroxide; the ether layer then showed no visible absorption. Further, the diformyldipyrrylmethane (VII) under the conditions of the synthesis but in the absence of V gave no porphyrin.

(*b*) The diformyl-pyrromethene tetramethyl acetal (IV*e*) was condensed with V as in (*a*) above to give a product (17%) with m.p. 218–220°, from chloroform–methanol. It was recrystallized as red-brown hairlike needles, m.p. 220–222°, which was unchanged when it was mixed with the product of (*a*) above. The X-ray powder photographs of the products of (*a*) and (*b*) were identical.

The porphyrin as obtained by method (*a*) above was degraded at 190° to mesoporphyrin 4, (VI, Me for A^{Me}) by the method used to degrade uroporphyrin 2 to coproporphyrin 2 (7). The methyl ester of the product (69%) crystallized from chloroform–methanol as prisms, m.p. 235° (lit. (3*k*): 233°; 238° corr.), λ_{max} mμ (relative density) in chloroform: 502 (1); 536.5 (0.72); 569 (0.48); 623 (0.35).

ACKNOWLEDGMENT

The authors thank Dr. R. E. Reavill for helpful discussions of the nuclear magnetic resonance spectra.

REFERENCES

1. H. FISCHER and H. J. RIEDL. Z. Physiol. Chem. **207**, 193 (1932).
2. H. FISCHER and H. K. WEICHMANN. Ann. **492**, 53 (1931).
3. H. FISCHER and H. ORTH. Chemie des pyrrols. Part 1. Vol. II. Akademische Verlagsgesell-Shaft, Leipzig. 1937. (*a*) p. 105. (*b*) pp. 25ff, 75 ff. (*c*) p. 136. (*d*) pp. 160 ff. (*e*) p. 106. (*f*) p. 73. (*g*) p. 193. (*h*) p. 200 (method (*b*)). (*i*) p. 92. (*j*) p. 147. (*k*) p. 438.
4. A. F. MIRONOV, R. P. EVSTIGNEEVA, A. V. CHUMACHENKO, and N. A. PREOBRAZHENSKII. J. Gen. Chem. U.S.S.R. Eng. Transl. **34**, 1493 (1964).
5. H. FISCHER and J. ASCHENBRENNER. Z. Physiol. Chem. **229**, 71 (1934).
6. K. J. BRUNINGS and A. H. CORWIN. J. Am. Chem. Soc. **66**, 337 (1944).
7. G. P. ARSENAULT, E. BULLOCK, and S. F. MACDONALD. J. Am. Chem. Soc. **82**, 4384 (1960).
8. F. MORSINGH and S. F. MACDONALD. J. Am. Chem. Soc. **82**, 4377 (1960).
9. E. J. TARLTON, S. F. MACDONALD, and E. BALTAZZI. J. Am. Chem. Soc. **82**, 4389 (1960).
10. S. F. MACDONALD. J. Chem. Soc. 4176 (1952).
11. J. L. ARCHIBALD, D. M. WALKER, K. B. SHAW, A. MARKOVAC, and S. F. MACDONALD. In preparation.
12. A. H. JACKSON, G. W. KENNER, G. MCGILLIVRAY, and G. S. SACH. J. Am. Chem. Soc. **87**, 676 (1965).
13. A. H. JACKSON, G. W. KENNER, and D. WARBURTON. J. Chem. Soc. 1328 (1965).
14. H. FISCHER and A. ROTHHAAS. Ann. **484**, 85 (1930).
15. J. PLUŠČEC, J. M. OSGERBY, K. B. SHAW, and S. F. MACDONALD. In preparation.
16. S. F. MACDONALD and A. MARKOVAC. Can. J. Chem. This issue.
17. H. FISCHER and G. STANGLER. Ann. **459**, 59 (1927).
18. H. FISCHER and A. KÜRZINGER. Z. Physiol. Chem. **196**, 213 (1931).

Can. J. Chem. Downloaded from www.nrcresearchpress.com by 210.87.254.40 on 09/05/12
For personal use only.

Can. J. Chem. Downloaded from www.nrcresearchpress.com by 210.87.254.40 on 09/05/12
For personal use only.

ESSENTIAL OILS AND THEIR CONSTITUENTS

XXIX.[1] THE ESSENTIAL OIL OF MARIHUANA: COMPOSITION OF GENUINE INDIAN CANNABIS SATIVA L.

M. C. NIGAM,[2,4] K. L. HANDA,[3,4] I. C. NIGAM, AND LEO LEVI
Pharmaceutical Chemistry Division, Food and Drug Directorate, Ottawa, Canada
Received July 2, 1965

ABSTRACT

The essential oil obtained by hydrodistillation of freshly harvested Indian *Cannabis sativa* L. was found to contain the following constituents that have not previously been reported: α-pinene, camphene, β-pinene, α-terpinene, β-phellandrene, γ-terpinene, linalool, *trans*-linalool oxide, sabinene hydrate, α-bergamotene, terpinene-4-ol, β-farnesene, α-terpineol, α-selinene, curcumene, and caryophyllene oxide. The presence of trace amounts of two alcohols and of an α,β-unsaturated ketone, for which gas chromatographic and spectral characteristics are recorded, was also detected.

INTRODUCTION

Marihuana, *Cannabis sativa* Linn., is, like opium, an important drug-bearing plant that grows wild and is also cultivated in many parts of the world. In 1896 Wood, Spivey, and Easterfield (1) examined volatile fractions obtained from plants grown in India, and reported the isolation of a terpene ($C_{10}H_{16}$, b.p. 170–175 °C) and a sesquiterpene ($C_{15}H_{24}$, b.p. 258–259 °C). About half a century later Simonsen and Todd (2) studied the essential oil obtained from Egyptian hashish. They found that its lower boiling fraction consisted mainly of *p*-cymene in admixture with small amounts of 1-methyl-4-isopropenyl-benzene and an unidentified optically active material. The higher boiling fraction of the oil was found to be largely composed of humulene. These authors failed to isolate any myrcene, a hydrocarbon that they assumed Wood *et al.* (1) had obtained, suggesting that it was polymerized in their product "prepared years ago from hashish of uncertain age". Dutt (3) subsequently established the presence in Indian *C. sativa* L. of *p*-cymene, myrcene, dipentene (limonene), and caryophyllene, along with unidentified sesquiterpenes and sesquiterpene alcohols. He reported also the presence of a compound designated as *p*-cymedene (b.p. 179–180 °C; 2-bromodibromide, m.p. 187–189 °C). Martin, Smith, and Farmilo (4) have recently confirmed that some of these are constituents of the essential oil distilled from plants that grow wild in Ontario and Quebec, Canada.

This paper presents the results of a more detailed investigation of the composition of the essential oil obtained from male plants of *C. sativa* L.

EXPERIMENTAL

Samples

Male and female plants of authentic wild *C. sativa* L. from the province of Jammu-Tawi, Kashmir State, India, were collected separately during their flowering period in the month of May. Two light yellow oils with similar characteristic odours were obtained from them in yields of 0.1% by hydrodistillation. Some physicochemical constants for the oil from male plants were d_{20}^{20} 0.9012, n_D^{20} 1.495, α_D^{20} −11.8°, acid value 1.24; and for that from female plants, d_{20}^{20} 0.9012, n_D^{20} 1.494, α_D^{20} −11.6°, acid value 1.48. The gas chromatograms that were obtained for both products under the same experimental conditions were almost identical. For this reason only the essential oil from male plants was analyzed in detail.

[1]*Paper XXVIII: J. Pharm. Sci. 54, 799 (1965).*
[2]*National Research Council of Canada Postdoctorate Fellow, 1964.*
[3]*Colombo Plan Research Associate, Food and Drug Directorate, 1962.*
[4]*Present address, Regional Research Laboratory, Jammu-Tawi, India.*

Fractional Distillation of Crude Isolate

The essential oil obtained by hydrodistillation (60 g) was fractionated under reduced pressure in a Towers column. Five cuts were collected, which are described in Table I.

TABLE I

Fractional distillation of essential oil of *Cannabis sativa* L.

Fraction	Yield (%)	Pressure (mm)	Temp. (°C)	n_D^{20}
1	10.2	23	62–70	1.468
2	6.2	10	82–84	1.484
3	66.0	7	98–104	1.498
4	2.0	7	104–107	1.499
5	10.0	7	107–115	1.501

Chromatography of Fraction 5

On gas chromatographic analysis, fraction 5 appeared to be composed of sesquiterpene hydrocarbons and oxygenated derivatives. It was therefore chromatographed on 120 g of Woelm, neutral grade I alumina, and eluted successively with petroleum ether, benzene, ether, and alcohol. Elution with petroleum ether yielded 3.63 g of product (fraction 5-A) and with benzene led to 1.86 g (fraction 5-B), which were further analyzed. Recoveries from elution with ether and alcohol were negligible.

Examination of Fractions 3, 4, and 5-A

These fractions consisted primarily of sesquiterpene hydrocarbons, and were very similar in composition. They were therefore combined, and a 5 g aliquot of the mixture was subjected to column chromatography over 500 g of Woelm, neutral grade I alumina, with petroleum ether (b.p. 60-80 °C) as eluant. Effluent fractions of 20 ml each were collected, the solvent was evaporated, and the isolation and characterization of the constituents of the products that were thus obtained were accomplished by gas chromatography and physicochemical analyses, respectively.

Gas Chromatographic Techniques

For gas chromatography, the apparatus and general procedures that have been described previously (5) were used.

Identification and Determination of Essential Oil Constituents

Gas chromatographic effluents were identified by the serial dilution technique and by comparison of the infrared spectra of eluates (collected in carbon tetrachloride and purified by re-chromatography under optimal conditions of temperature and flow rate) with those of authentic reference standards available in the authors' collection or with published data (6). Quantitative results were obtained from measurements of peak areas, as previously reported (7, 8).

RESULTS AND DISCUSSION

The complex composition of the essential oil is illustrated in Fig. 1. All materials collected during the course of this study, including crude products, isolates obtained by distillation, and fractions recovered by column chromatography, were subjected to gas chromatographic analysis to determine the composition of the essential oil, which is given in Table II.

α-Pinene, β-pinene, and myrcene.—These monoterpenes were found almost exclusively in fraction 1. Trace amounts only occurred in fraction 2.

Camphene and α-terpinene.—Minute amounts of these hydrocarbons were found in fraction 1.

Limonene, β-phellandrene, γ-terpinene, and p-cymene.—Limonene and β-phellandrene formed the major portion of fraction 1. Small amounts only were found in fraction 2. γ-Terpinene and *p*-cymene were identified as minor constituents of fraction 1, and trace amounts of them were detected in fraction 2. Neither of these fractions contained any 1-methyl-4-*iso*propenylbenzene, a hydrocarbon that Simonsen and Todd (2) reported to

Can. J. Chem. Downloaded from www.nrcresearchpress.com by 210.87.254.40 on 09/05/12
For personal use only.

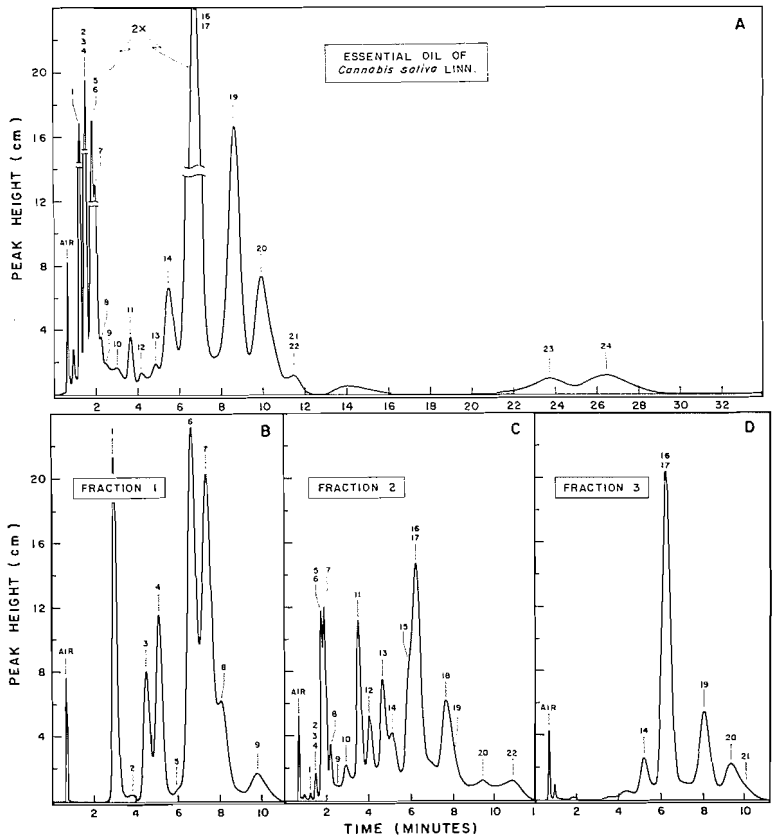

FIG. 1. The result of gas chromatography of oil of *Cannabis sativa* L. Column: Reoplex 400 (20%) on acid-washed chromosorb W. Temperature: A, C, and D,170 °C; B,110 °C. Sample volume: A, 5 λ; B and C, 1.5 λ; D, 1 λ. Helium flow: 75 ml/min.

be a constituent of Egyptian hashish. Its presence in the essential oil was questioned recently by Naves (9).

Linalool and trans-linalool oxide.—These terpenoids were found in fraction 2. *cis*-Linalool oxide, which usually is present with the *trans*-isomer in essential oils, was not detected.

Sabinene hydrate.—This alcohol was identified as a constituent of fraction 2. Its re-chromatography for the purpose of further purification was accompanied by marked decomposition to α- and β-phellandrene and α- and γ-terpinene (10). Hence, some of the β-phellandrene and some α- and γ-terpinene that are reported as constituents of the essential oil (Table II) must be considered as artefacts produced during analysis. Because of the presence of only a small amount of sabinene hydrate (0.4%), no α-phellandrene could be isolated.

Terpinene-4-ol and α-terpineol.—These alcohols were isolated from fraction 2 after repeated gas chromatographic purification.

α-Bergamotene, caryophyllene, β-farnesene, β-humulene, α-selinene, and curcumene.—These sesquiterpenes were identified as components of fraction 3, 4, and 5-A. They also occurred as trace constituents of fraction 2. Caryophyllene and β-farnesene were not resolved by gas

Can. J. Chem. Downloaded from www.nrcresearchpress.com by 210.87.254.40 on 09/05/12
For personal use only.

TABLE II

Composition of oil of *Cannabis sativa L.*

Peak No.	Constituent	Relative retention time: Temp., 110 °C, Reference Limonene	Relative retention time: Temp., 170 °C, Reference Caryophyllene	%
1	α-Pinene	0.45	0.18	1.3
2	Camphene	0.56	0.23	0.1
3	β-Pinene	0.67	0.23	0.8
4	Myrcene	0.76	0.23	1.3
5	α-Terpinene*	0.92	0.30	0.1
6	Limonene	1.00	0.30	2.8
7	β-Phellandrene*	1.10	0.32	2.7
8	γ-Terpinene*	1.21	0.35	1.3
9	*p*-Cymene	1.46	0.40	0.4
10	Alcohol A		0.46	0.2
11	Linalool oxide		0.55	0.8
12	Linalool		0.63	0.2
13	Sabinene hydrate		0.74	0.4‡
14	α-Bergamotene		0.81	5.0
15	Terpinene-4-ol		0.93	0.4
16	Caryophyllene		1.00	45.7
17	β-Farnesene		1.00	5.1
18	α-Terpineol		1.22	0.6
19	β-Humulene		1.30	16.0
20	α-Selinene		1.48	8.6
21	Curcumene		1.72	1.4
22	α,β-Unsaturated Ketone		1.72	0.2
23	Alcohol B		3.64	1.6
	Caryophyllene oxide†			1.7
	Unidentified			1.5

*Partial artefact resulting from degradation of sabinene hydrate under experimental conditions.
†Determined by gas chromatography of essential oil using a column of Reoplex 400 (10%) deposited on acid-base washed Chromosorb W (11).
‡Percentage based on the sabinene hydrate that remained unchanged during gas chromatography.

chromatography under the experimental conditions but they were effectively separated by column chromatography, and cyclic sesquiterpene was eluted more rapidly than the aliphatic hydrocarbon. Gas chromatographic analysis of the column chromatographic fractions permitted quantitative determinations.

Caryophyllene Oxide.—The presence of this terpenoid in *C. sativa* L. was deduced from the characterization of peak No. 24 on the gas chromatograph (see Fig. 1) as that of an aldehyde identical with one that is formed by rearrangement of caryophyllene oxide during gas chromatography (11). Its occurrence in the essential oil was established unequivocally by gas chromatographic analysis of fraction 5-B and of a pure reference standard with a column of Reoplex 400 (10%) on acid-base washed Chromosorb W, from which the epoxide was recovered unchanged.

Unidentified compounds.—These included two alcohols (peak No. 10, alcohol A; peak No. 23, alcohol B) and an α,β-unsaturated ketone (peak No. 22). Alcohol A and the α,β-unsaturated ketone occurred in fraction 2, whereas alcohol B was isolated from fraction 5-B. Alcohol A displayed characteristic infrared absorption at 1 280, 1 252, 1 180, 1 127, 1 070, 933, 930, and 840 cm^{-1}; alcohol B exhibited distinct bands at 1 298, 1 242, 1 162, 1 098, 988, and 918 cm^{-1}; and the unsaturated ketone showed marked absorption at 1 677, 1 645, 1 445, 1 428, 1 370, 1 265, 1 236, 1 180, 1 168, 1 137, 1 110, 1 057, 1 045, 1 018, 930, 891, and 840 cm^{-1}.

Can. J. Chem. Downloaded from www.nrcresearchpress.com by 210.87.254.40 on 09/05/12
For personal use only.

Composition of the Essential Oil

Data on the quantitative composition of the essential oil of *C. sativa* L. were obtained by correlating the results of fractional distillation with those of column and gas chromatography. They are summarized in Table II.

Value of the Experimental Findings

Previous work by the authors has shown that the geographical and botanical origin of medicinal plants can be determined with a high degree of accuracy by microanalysis of their essential oils (8, 12–16). Studies that will present such data for oil of marihuana will be the subject of a forthcoming publication.

REFERENCES

1. T. B. Wood, W. T. N. Spivey, and T. H. Easterfield. J. Chem. Soc. **69**, 539 (1896).
2. J. L. Simonsen and A. R. Todd. J. Chem. Soc. 188 (1942).
3. S. Dutt. Indian Soap J. **22**, 242 (1957).
4. L. Martin, D. M. Smith, and C. G. Farmilo. Nature, **191**, 774 (1961).
5. I. C. Nigam and L. Levi. Can. J. Chem. **40**, 2083 (1962).
6. J. Pliva, M. Horak, V. Herout, and F. Sörm. Die Terpene. Sammlung der Spektren und Physikalischen Konstanten. Teil I. Verlag, Berlin. 1960.
7. J. C. Bartlet and D. M. Smith. Can. J. Chem. **38**, 2057 (1960).
8. D. M. Smith and L. Levi. J. Agr. Food Chem. **9**, 230 (1961).
9. Y. R. Naves. Parfum. Cosmet. Savons, **5**, 1 (1962).
10. I. C. Nigam and L. Levi. J. Agr. Food Chem. **11**, 276 (1963).
11. I. C. Nigam and L. Levi. J. Org. Chem. **30**, 653 (1965).
12. J. M. Airth, B. Stringer, W. Skakum, and L. Levi. J. Assoc. Offic. Agr. Chemists, **45**, 475 (1962).
13. K. Rao, I. C. Nigam, J. C. Bartlet, and L. Levi. Proc. Sci. Sect. Toilet Goods Assoc. **38**, 5 (1962).
14. D. M. Smith, W. Skakum, and L. Levi. J. Agr. Food Chem. **11**, 268 (1963).
15. K. L. Handa, I. C. Nigam, D. M. Smith, and L. Levi. J. Pharm. Sci. **53**, 1407 (1964).
16. M. C. Nigam, I. C. Nigam, and L. Levi. J. Soc. Cosmetic Chemists, **16**, 155 (1965).

Can. J. Chem. Downloaded from www.nrcresearchpress.com by 210.87.254.40 on 09/05/12
For personal use only.

Can. J. Chem. Downloaded from www.nrcresearchpress.com by 210.87.254.40 on 09/05/12
For personal use only.

THE CONDENSATION OF PHOSPHONOTHIOIC AND PHOSPHONIC DICHLORIDES WITH *o*-DIAMINES[1]

RALPH L. DANNLEY AND ARTURS GRAVA
Department of Chemistry, Western Reserve University, Cleveland, Ohio

Received June 8, 1965

ABSTRACT

A series of 2,3-dihydro-1*H*-1,3,2-benzodiazaphosphole 2-sulfides and 2-oxides have been prepared, most commonly by the condensation of a diamine with a phosphonothioic or phosphonic dichloride in a refluxing inert solvent. The phosphonothioic dichlorides react more slowly than the corresponding phosphonic dichlorides, and phenylenediamines containing electron-donating substituents are more reactive than those containing electron-withdrawing substituents. The diazaphosphole 2-oxides undergo hydrolysis or alcoholysis of only one of the amide groups under mild conditions. The 2-sulfides are much more resistant to hydrolysis than the 2-oxides. The 2-sulfides are converted to the *N*-methyl derivatives by dimethyl sulfate and alkali. The 2-oxides are hydrolyzed under these conditions. The 2-sulfides are invariably lower melting and more soluble in nonpolar solvents than their 2-oxide analogues.

INTRODUCTION

In a previous paper (1) the reaction of phosphonic dichlorides with *o*-diamines has been found to give high yields of 1,3,2-diazaphosphole 2-oxides. The analogous 1,3,2-diazaphosphole 2-sulfides would be of interest as antimetabolites, not only because the sulfur atom would affect the physiological properties but also because the solubility and hydrolytic stability might be more favorable.

The only 1,3,2-diazaphosphole 2-sulfides previously reported were 2,3-dihydro-2-phenoxy-1*H*-1,3,2-benzodiazaphosphole 2-sulfide (2) and its 2-tolyloxy analogue (3) prepared by Autenrieth and his co-workers and the 2-phenyl compound synthesized by Wagner (4).

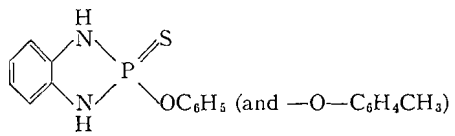

The present work was therefore undertaken to develop a general method of synthesis of the 1,3,2-benzodiazaphosphole 2-sulfides and by the preparation of a number of representative compounds to establish the factors influencing both their formation and stability.

EXPERIMENTAL

Reagents

Ethylphosphonous dichloride (5) was converted to ethylphosphonothionic dichloride, b.p. 178.6° at 760 mm (lit. b.p. 80–82° at 50 mm (6)). Ethylphosphonic dichloride, b.p. 177–179° (lit. b.p. 171–175° (7)), was prepared by the method of Kinnear and Perren (8).

4,N-Dimethyl-2-nitroaniline

This type of *N*-methyl amine has been conventionally prepared from the corresponding chloronitro compound and methylamine in a sealed tube. The following procedure at atmospheric pressure is more convenient for a larger scale synthesis. A solution of 4-chloro-3-nitrotoluene (34.3 g, 0.2 mole), ethanol (100 ml), 40% aqueous methylamine (40 g), and pyridine (20 ml added to provide a homogeneous reaction) was heated to incipient boiling (4 days). Each day methylamine (20 ml of 20% ethanolic solution) was added to compensate for any losses. After 4 days the excess amine and ethanol were removed by distillation. The oil phase was

[1]*Presented in part at the 139th National Meeting of the American Chemical Society, Chicago, Illinois, September 1961.*

separated from the residue and washed with three 200 ml portions of water; 30 ml of hexane was added to the semisolid mass, and the product was collected by filtration. Recrystallization from hexane gave 4,*N*-dimethyl-2-nitroaniline (15.5 g, 46%), m.p. 84.5–86° (lit. m.p. 84–85° (9)).

o-Phenylenediamines

In addition to the commercially available compounds, a number of diamines were prepared by reduction of the corresponding nitroanilines. The reduction of 4-ethoxy-2-nitroaniline is given as a typical example. Tin was added in small portions to a suspension of 4-ethoxy-2-nitroaniline (46 g, 0.25 mole) in 25% hydrochloric acid (400 ml) kept at 50°. When addition of a drop of the reaction mixture to aqueous sodium hydroxide gave no orange color, the reduction was judged complete (60 g of tin added). The solution was kept below 50° while being made alkaline and then filtered. The filtrate was extracted with seven 200 ml portions of benzene, and the combined extracts after filtration were saturated with dry hydrogen chloride to precipitate 4-ethoxy-*o*-phenylenediamine dihydrochloride. The dihydrochloride darkened above 230° and decomposed completely above 340°. Titration of a sample to the phenolphthalein endpoint gave 223.2 as a molecular weight (calcd. for $C_8H_{14}Cl_2N_2O$, 225.1). When free amines were desired, the benzene solutions were diluted with pentane and cooled to give crystals. If the parent nitro compounds were not commercially available they were synthesized from their chloronitro analogues by the method of Ashton and Suschitzky (10) unless otherwise indicated in Table I.

TABLE I

Melting points of *o*-diamines (or dihydrochlorides) obtained by reducing 2-nitroanilines

2-Nitroaniline	M.p. diamine		M.p. diaminedihydrochloride	
	Lit.	Found	Lit.	Found
4-Ethoxy	—	—	—	340 decomp.
4-Methoxy	—	—	188 decomp. (11)	222–225 decomp.
4-Trifluoromethyl	58 (12)	54.5–56	—	—
3,5-Dimethyl	77–78 (13)	76–78	—	—
N-Methyl[a]	—	—	191 (14)	193–194
4,*N*-Dimethyl	43–44 (9)	42.5–44	—	—
N-(*n*-Butyl)	35 (10)	35.8–36.2	—	—
N-Cyclohexyl	51 (10)	53–54.5	—	—
4-Methoxy-*N*-methyl[b]	78.3–78.8 (15)	74–76	—	—
(*N*,*N*′-Dimethyl-*o*-phenylenediamine)[c]	31.5 (16)	32–33	—	—

[a]Synthesis analagous to preparation of 4,*N*-dimethyl-2-nitroaniline described here.
[b]From methylation of the sulfonamide (14).
[c]This diamine prepared (16) by methylation of *N*,*N*′-di-*p*-toluenesulfonyl-*o*-phenylenediamide (17).

Condensation of a Phosphonothioic Dichloride with an o-Diamine in the Presence of a Tertiary Amine

Phenylphosphonothioic dichloride (5.28 g, 0.025 mole) in toluene (10 ml) was added dropwise with stirring to 4-carbomethoxy-*o*-phenylenediamine (4.15 g, 0.025 mole) in toluene (200 ml). The reaction mixture was maintained at 60° during the addition and for 15 min thereafter. Triethylamine (5.5 g, 0.054 mole) in toluene (10 ml) was added, and the mixture was refluxed for 2 h, cooled, and filtered. A solution of the precipitate in chloroform (15 ml) was poured into 150 ml of boiling toluene. Chloroform was distilled from this mixture while toluene was added to keep the volume at 150 ml. Filtration of the hot toluene solution removed triethylamine hydrochloride, and evaporation of the filtrate to 50 ml and cooling to 5° gave a semisolid precipitate. The decanted mother liquor when evaporated to 25 ml and cooled to −80° gave more product. Recrystallization of these solids from chloroform gave pure 5-carbomethoxy-2,3-dihydro-2-phenyl-1*H*-1,3,2-benzodiazaphosphole 2-sulfide.

Synthesis of Diazaphosphole 2-Sulfides and 2-Oxides in a Refluxing Solvent

The procedure for the reaction of a phosphonic dichloride with a diamine in bromobenzene was described in a previous paper (1). In using phosphonothioic dichlorides, several minor modifications were employed. Passing the exit gases through a cadmium acetate solution permitted measurement of the hydrogen sulfide evolved (max. yield 2%). With reactions which proceeded with difficulty, *o*-dichlorobenzene was often used as a solvent because of its higher boiling point. Some of the diazaphosphole 2-sulfides were quite soluble in aromatic solvents and it was necessary to reduce the volume of the reaction mixture and (or) add pentane to precipitate the product. The details are given in Tables II and III.

The melting point of every diazaphosphole 2-sulfide is lower than that of its 2-oxide analogue. When both amidic nitrogens are replaced by methyl groups a large decrease in melting point is observed for the 2-oxide structure, a small change for the 2-sulfide. These data reflect the weak hydrogen-bonding tendency of sulfur as compared to oxygen. As expected, this also leads to higher solubility in non-polar solvents for the 2-sulfides

Can. J. Chem. Downloaded from www.nrcresearchpress.com by 210.87.254.40 on 09/05/12
For personal use only.

as compared to the 2-oxides. Also, in both series the *N*-alkyl derivatives are more soluble in non-polar solvents. Both series of compounds are soluble in polar solvents such as methanol and ethanol but as traces of acid or base catalyze solvolysis, these solvents are seldom useful.

Hydrolysis of 2,3-Dihydro-2-phenyl-1H-1,3,2-benzodiazaphosphole 2-Oxide

When this benzodiazaphosphole 2-oxide (4.6 g, 0.02 mole) was added to 1 *N* sodium hydroxide (20 ml) at room temperature, an exothermic reaction occurred (the temperature rising to 38°) and the benzodiazaphosphole dissolved while a sodium salt precipitated. After cooling to 20°, the reaction mixture was filtered and the precipitate washed with absolute alcohol (three 5 ml portions) and dried. Additional product was obtained by partially evaporating the mother liquor and chilling. The sodium salt (2 g) was placed in water (20 ml) and acidification with 1 *N* hydrochloric acid to pH 5 gave 2-aminoanilido-phenylphosphonic acid (1.32 g), m.p. 240–247° decomp.

Anal. Calcd. for $C_{12}H_{13}N_2O_2P$: C, 58.06; H, 5.28; N, 11.29. Found: C, 57.56; H, 5.35; N, 11.38.

This product dissolved in aqueous sodium hydroxide and could be precipitated from the alkaline solution by careful acidification. It also dissolved in aqueous hydrochloric acid but underwent hydrolysis and could not be recovered by addition of alkali. When an aqueous acid solution of the 2-aminoanilidophenylphosphonic acid was boiled to remove most of the liquid, cooling produced the *o*-phenylenediamine salt of phenylphosphonic acid; m.p. 224–228°. This salt has been incorrectly reported as the amide (1).

Anal. Calcd. as 2-aminoanilido-phenylphosphonic acid, $C_{12}H_{13}N_2O_2P$: N, 11.29. Anal. Calcd. as the salt of *o*-phenylenediamine and phenylphosphonic acid, $C_{12}H_{15}N_2O_3P$: N, 11.05. Found (1): N, 11.02.

The salt was synthesized independently by heating to 80° a solution of phenylphosphonic acid (1.58 g, 0.01 mole) and *o*-phenylenediamine (1.08 g, 0.01 mole) in water (10 ml) and then cooling. The precipitate was collected, washed with alcohol, and dried, m.p. 226–230°. Its infrared spectrum was identical to that of the hydrolysis product described above.

Alcoholysis of 2,3-Dihydro-2-phenyl-1H-1,3,2-benzodiazaphosphole 2-Oxide

Dry hydrogen chloride was bubbled into a suspension of 2,3-dihydro-2-phenyl-1*H*-1,3,2-benzodiazaphosphole 2-oxide (1.15 g, 0.005 mole) in 10 ml of methanol until the solid dissolved. The mixture was heated just to boiling, cooled to room temperature, and made slightly alkaline with 1 *N* sodium hydroxide, and water was added to precipitate *O*-methyl-2-aminoanilido-phenylphosphonate (1.0 g, 76%), m.p. 149–150° (from methanol–water).

Anal. Calcd. for $C_{13}H_{15}N_2O_2P$: C, 59.53; H, 5.77; N, 10.68. Found: C, 59.49; H, 5.79; N, 10.59.

The same product was isolated when the diazaphosphole (2.3 g) in methanol (10 ml) was heated with sodium methoxide (0.1 g).

Hydrolysis of 2,3-Dihydro-2-phenyl-1H-1,3,2-benzodiazaphosphole 2-Sulfide

The 2-sulfide apparently does not react with 1 *N* sodium hydroxide at room temperature but slowly dissolves when the mixture is heated to 70°. Hydrogen sulfide is evolved when this solution is made acid.

Hydrolysis of 1,3-Dimethyl-2,3-dihydro-2-phenyl-1H-1,3,2-benzodiazaphosphole 2-Oxides and 2-Sulfides

The 2-oxide was recovered in 60% yield from a solution of 1 *N* sodium hydroxide refluxed for 1 min, but no recovery was possible after 3 min of refluxing. In contrast, the 2-sulfide in 1 *N* sodium hydroxide was recovered in 80% yield after 5 min of refluxing.

Methylation of 1-Methyl-2,3-dihydro-2-phenyl-1H-1,3,2-benzodiazaphosphole 2-Sulfide

Sodium hydroxide (6 ml, 25%) was added to the benzodiazaphosphole 2-sulfide (0.52 g, 0.002 mole) in dimethyl sulfate (1.3 g, 0.001 mole), and the mixture was stirred rapidly for 1 h at room temperature. The viscous liquid which separated from the reaction mixture was recrystallized twice from methanol–water to give a crude product, m.p. 91–92° (4.9 g, 89%). Recrystallization from *n*-hexane gave pure 1,3-dimethyl-2,3-dihydro-2-phenyl-1*H*-1,3,2-benzodiazaphosphole 2-sulfide, m.p. 100.5–101.5°, which did not depress the m.p. of an authentic sample obtained from *N,N'*-dimethyl-*o*-phenylenediamine and phenylphosphonothioic dichloride. The infrared spectra of the two samples were identical.

Methylation of 2,3-Dihydro-2-phenyl-1H-1,3,2-benzodiazaphosphole 2-Sulfide

Using identical quantities of materials to those above except for acetone (5 ml) and solid sodium hydroxide (ca. 0.4 g), this 2-sulfide was converted to the dimethyl derivative in 87% yield. The acetone was removed by distillation, and water (10 ml) was added to isolate the crude product.

Methylation of 2,3-Dihydro-2-ethyl-1H-1,3,2-benzodiazaphosphole 2-Sulfide

By the dimethylation procedure, this diazaphosphole produced 1,3-dimethyl-2,3-dihydro-2-ethyl-1*H*-1,3,2-benzodiazaphosphole 2-sulfide (88%), m.p. 70–71° from methanol–water.

Anal. Calcd. for $C_{10}H_{15}N_2PS$: C, 53.07; H, 6.68; N, 12.38. Found: C, 52.32; H, 6.91; N, 12.42.

Methylation of 1,2-Diphenyl-2,3-dihydro-1H-1,3,2-benzodiazaphosphole 2-Sulfide

By the monomethylation procedure, this diazaphosphole produced 1-methyl-2,3-diphenyl-2,3-dihydro-1*H*-1,3,2-benzodiazaphosphole 2-sulfide (93%), m.p. 115–116° from *n*-hexane.

Anal. Calcd. for $C_9H_{17}N_2PS$: C, 67.83; H, 5.09; N, 8.33. Found: C, 68.00; H, 5.12; N, 8.32.

Can. J. Chem. Downloaded from www.nrcresearchpress.com by 210.87.254.40 on 09/05/12
For personal use only.

Can. J. Chem. Downloaded from www.nrcresearchpress.com by 210.87.254.40 on 09/05/12
For personal use only.

TABLE II

Benzodiazaphosphole 2-sulfide syntheses

Diamine	Yield (%)[a]	Half-life (h)[b]	M.p. (°C)	Calcd. C	Calcd. H	Calcd. N	Found C	Found H	Found N
With phenylphosphonothioic dichloride									
o-Phenylenediamine	83[c]	17	152–153.5[d]			11.38			11.41
4-Methyl-*o*-phenylenediamine	71[e]	—	128–130[f]	59.98	5.03	10.76	59.61	5.03	10.82
4-Chloro-*o*-phenylenediamine	40[c]	—	114.5–116[g]	51.34	3.59	9.98	51.43	3.66	10.04
4-Methoxy-*o*-phenylenediamine.2HCl	99[c]	5	186–188[h]	56.53	4.74	10.14	56.39	4.66	10.31
4-Ethoxy-*o*-phenylenediamine.2HCl	63[i]	1.5	113–114[j]	57.88	5.21	9.65	58.29	5.16	9.69
4-Carbomethoxy-*o*-phenylenediamine	41[k]	—	219–222[d]	55.25	4.31	9.27	55.36	4.37	9.34
4-Nitro-*o*-phenylenediamine	24[l]	—	230–231.5[m]	49.48	3.43	14.43	49.74	3.53	14.42
4-Trifluoromethyl-*o*-phenylenediamine	89[e]	13	140–145[n]	49.68	3.27	8.91	49.63	3.16	8.81
3,5-Dimethyl-*o*-phenylenediamine	73[p]	1.5	208–210[j]	61.30	5.51	10.21	61.11	5.47	10.09
4,5-Dimethyl-*o*-phenylenediamine.2HCl	34[c]	—	198–199[j]	61.30	5.51	10.21	61.43	5.50	10.21
4,5-Dichloro-*o*-phenylenediamine	48[q]	2.8	184–186[r]	45.73	2.83	8.89	45.52	2.91	8.87
3-Nitro-5-chloro-*o*-phenylenediamine	49[p]	2.7	234–236[h]	44.22	2.78	12.90	44.05	2.77	12.78
N-Methyl-*o*-phenylenediamine	75[s]	1.2	114–115[t]	59.98	5.03	10.77	59.78	4.94	10.78
4,*N*-Dimethyl-*o*-phenylenediamine	72[e]	1.7	113–114.5[u]	61.30	5.51	10.21	61.06	5.48	10.32
4-Methoxy-*N*-methyl-*o*-phenylenediamine	79[c]	1.5	161.5–162.5[v]	57.92	5.21	9.65	57.58	5.17	9.75
N,*N*′-Dimethyl-*o*-phenylenediamine	71[e]	1.7	101–102[w]	61.30	5.51	10.21	61.38	5.53	10.23
N-(*n*-Butyl)-*o*-phenylenediamine.2HCl	45[e]	3	110.5–111.5[w]	63.55	6.33	9.26	63.77	6.45	9.44

Can. J. Chem. Downloaded from www.nrcresearchpress.com by 210.87.254.40 on 09/05/12
For personal use only.

TABLE II (*Concluded*)

Diamine	Yield (%)[a]	Half-life (h)[b]	M.p. (°C)	Calcd. C	Calcd. H	Calcd. N	Found C	Found H	Found N
N-Cyclohexyl-*o*-phenylenediamine.HCl	68[e]	4	158.5–159.5[z]	65.83	6.45	8.53	65.59	6.48	8.39
N-Phenyl-*o*-phenylenediamine	80[p]	0.2	188–189[d]	67.06	4.69	8.69	66.91	4.82	8.58
2,3-Diaminonaphthalene	6[v]	—	223–227[z]	64.85	4.42	9.46	64.97	4.49	9.52
1,2-Diaminonaphthalene.2HCl	63[i]	~10	180–181[aa]	64.85	4.42	9.46	65.00	4.48	9.55
2,3-Diaminopyridine	76[p]	2	234–236[bb]	53.43	4.08	16.99	53.83	4.41	16.94
With ethylphosphonothioic dichloride									
o-Phenylenediamine	84[e]	0.3	135.5–137[cc]	48.47	5.59	14.13	48.14	5.54	14.12
N-Methyl-*o*-phenylenediamine.2HCl	67[e]	3.7	92–93[g]	50.92	6.17	13.20	50.59	6.09	13.30

[a] Crude product suitable for most purposes.
[b] Approximate, for reagents were mixed at room temperature then heated to reflux. Also, the boiling points of the solvents used determine the temperature at which the reaction was run so that all of the figures are not comparable. Where an amine salt is the reagent, the half-life listed is for 50% evolution of hydrogen chloride beyond that calculated for the amine salt decomposition.
[c] In refluxing bromobenzene.
[d] From $CHCl_3$, dried in vacuum.
[e] In refluxing bromobenzene, pentane added to precipitate the product.
[f] From trichloroethylene.
[g] From CCl_4, then heptane.
[h] From a $CHCl_3$ solution passed through alumina.
[i] In refluxing bromobenzene, the reaction mixture reduced in volume, CCl_4 added to precipitate the product.
[j] From $CHCl_3$–CCl_4.
[k] In refluxing toluene containing triethylamine, see experimental section.
[l] In refluxing xylene–dioxane (1:2) containing tri-*n*-propylamine. The solvent was distilled, and the residue was dissolved in C_2H_5OH and poured into H_2O to precipitate the product.
[m] From C_2H_5OH–H_2O, then $CHCl_3$–CCl_4, then C_2H_5OH–H_2O.
[n] Recrystallized from chlorobenzene–CCl_4.
[p] In refluxing *o*-dichlorobenzene.
[q] In refluxing bromobenzene. The entire reaction mixture (0.0125 mole) was chromatographed on alumina (60 g), and eluted with $CHCl_3$; then CCl_4 was added to the eluent to produce crystals.
[r] Chromatographed on alumina from $CHCl_3$ solution, eluted with $CHCl_3$–CCl_4 (1:1).
[s] In refluxing bromobenzene. The product (0.05 mole) was adsorbed on alumina and eluted with CCl_4, then precipitated by adding hexane.
[t] From CCl_4.
[u] Chromatographed on alumina and eluted with $CHCl_3$; CCl_4 added to precipitate the product.
[v] A benzene solution passed through alumina, then cooled to give crystals from $CHCl_3$–CCl_4.
[w] A $CHCl_3$ solution chromatographed on alumina. The product was eluted with CCl_4, the volume of the eluent was reduced, and pentane was added.
[x] A CCl_4 solution chromatographed on alumina. The product was eluted with CCl_4, the eluent was reduced in volume, and hexane was added.
[y] In refluxing CCl_4 containing triethylamine. The product isolation was similar to that given in experimental section except that a $CHCl_3$ solution of the crude product was poured into ether to precipitate triethylamine hydrochloride.
[z] Recrystallized from benzene.
[aa] From $CHCl_3$–CCl_4, then benzene, then again from $CHCl_3$–CCl_4.
[bb] Chromatographed on alumina and eluted with dioxane.
[cc] A $CHCl_3$ solution passed through alumina; the eluent was evaporated and CCl_4 was added.

Can. J. Chem. Downloaded from www.nrcresearchpress.com by 210.87.254.40 on 09/05/12
For personal use only.

TABLE III

Benzodiazaphosphole 2-oxide syntheses

Diamine	Yield (%)[a]	Half-life (h)[b]	M.p. (°C)	Calcd.			Found		
				C	H	N	C	H	N
With phenylphosphonic dichloride									
4-Methoxy-*o*-phenylenediamine.2HCl	97[c]	0.15	227.5–229[d]	60.00	5.03	10.77	59.98	4.98	10.71
4-Ethoxy-*o*-phenylenediamine.2HCl	77[e]	0.9	189–190.5[f]	61.31	5.51	10.21	61.47	5.38	10.23
4-Trifluoromethyl-*o*-phenylenediamine	100[g]	1.2	154–157[h]	52.38	3.38	9.40	52.09	3.50	9.00
3,5-Dimethyl-*o*-phenylenediamine	98[c]	0.08	311–313[i]	65.11	5.85	10.85	64.88	5.76	10.89
4,5-Dimethyl-*o*-phenylenediamine.2HCl	98[g]	0.4	322–324[d]	65.11	5.85	10.85	64.98	5.76	10.84
4,5-Dichloro-*o*-phenylenediamine	95[c]	0.06	300–301[j]	48.18	3.03	9.37	48.06	3.11	9.37
3-Nitro-5-chloro-*o*-phenylenediamine	91[k]	0.04	283–286[l]	46.54	2.93	13.57	46.46	3.20	13.87
N-Methyl-*o*-phenylenediamine.2HCl	98[c]	0.25	263–265[m]	63.93	5.36	11.46	64.05	5.49	11.43
4,*N*-Dimethyl-*o*-phenylenediamine	93[g]	0.06	196–197[n]	65.11	5.84	10.85	64.79	5.86	10.74
4-Methoxy-*N*-phenyl-*o*-phenylenediamine.2HCl	96[c]	0.3	213–214.5[p]	61.31	5.51	10.21	61.08	5.53	10.14

Can. J. Chem. Downloaded from www.nrcresearchpress.com by 210.87.254.40 on 09/05/12
For personal use only.

TABLE III (*Concluded*)

Diamine	Yield (%)[a]	Half-life (h)[b]	M.p. (°C)	Calcd. C	Calcd. H	Calcd. N	Found C	Found H	Found N
N,N'-Dimethyl-*o*-phenylenediamine	81[c]	0.12	132.5–133.5[q]	65.11	5.85	10.85	64.75	5.83	10.76
N-(*n*-Butyl)-*o*-phenylenediamine.2HCl	88[g]	0.06	178–179[d]	67.12	6.68	9.79	67.10	6.94	9.71
N-Cyclohexyl-*o*-phenylenediamine	99[e]	0.08	260.5–262[d]	69.21	6.78	8.97	68.96	6.90	8.91
With ethylphosphonic dichloride									
o-Phenylenediamine	9.5[c]	0.16	193–194	52.76	6.09	15.38	52.02	6.18	15.49
N-Methyl-*o*-phenylenediamine.2HCl	20[g]	0.4	107.5–108[r]	55.08	6.68	14.28	54.88	6.97	14.50

[a]Crude product suitable for most purposes.
[b]Approximate, for the reagents were mixed at room temperature, then heated to reflux. The figures are not all comparable, for the boiling points of the solvents used determined the reaction temperatures.
[c]In refluxing bromobenzene.
[d]From $CHCl_3$–CCl_4.
[e]In refluxing chlorobenzene, pentane added to precipitate the product.
[f]From a $CHCl_3$ solution passed through alumina.
[g]In refluxing bromobenzene, pentane added to precipitate the product.
[h]The crude product contained solvent which could not be removed by heating in vacuum. The pure product crystallized after several days from a dilute bromobenzene–pentane solution.
[i]From $CHCl_3$–CH_3OH (9:1).
[j]From tetrahydrofuran.
[k]In refluxing *o*-dichlorobenzene.
[l]From bromobenzene.
[m]From $CHCl_3$.
[n]From CCl_4.
[p]A $CHCl_3$ solution was chromatographed on alumina and eluted with $CHCl_3$, and the eluent was evaporated and cooled.
[q]From CH_3OH.
[r]A CCl_4 solution was passed through alumina, then pentane was added.

Can. J. Chem. Downloaded from www.nrcresearchpress.com by 210.87.254.40 on 09/05/12
For personal use only.

RESULTS AND DISCUSSION

Cyclization Reactions

A series of 1,3,2-benzodiazaphosphole 2-sulfides (Table II) as well as some 2-oxides (Table III) have been prepared, most commonly by the condensation of a diamine with a phosphonothioic or phosphonic dichloride in a refluxing inert solvent. When these reagents are mixed at room temperature a precipitate usually forms immediately. In a previous paper (1), it was suggested that with phenylphosphonic dichloride the initial precipitate consisted of the non-cyclic intermediate I.

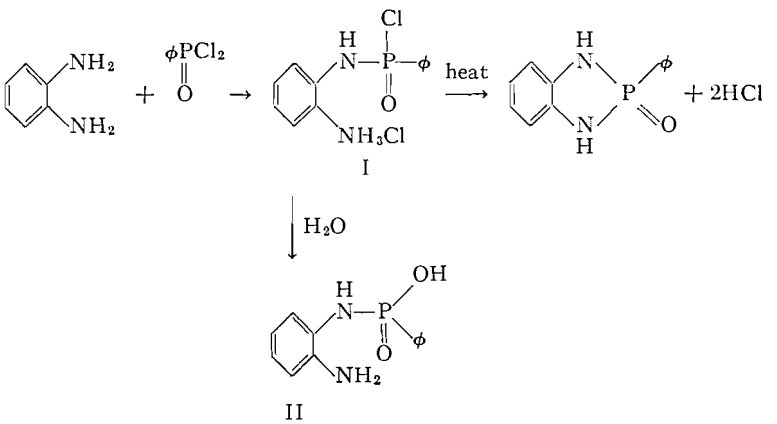

I

II

A halogen analysis of the precipitate corresponded very roughly to I and treatment with water produced a white solid thought to be II. In the present work, from the initial precipitate it has been possible to isolate only diazaphosphole 2-oxide and *o*-phenylenediamine hydrochloride. The hydrolysis product, originally thought to be II, now has been proved to be not the amide but instead the salt of *o*-phenylenediamine and phenylphosphonic acid. The inability to isolate a non-cyclic intermediate or its hydrolysis product indicates that the cyclization step proceeds with comparable rapidity, if not with greater rapidity, than the half-amide I formation.

To accomplish the cyclizations the hydrogen chloride formed was either removed physically by its insolubility in a refluxing solvent or removed chemically by combination with a tertiary amine. When a phosphonothioic dichloride reacts with an *o*-diamine in a refluxing solvent some hydrogen sulfide is evolved. Since it is evolved in less than 2% yield, the quantity of diazaphosphole 2-sulfide obtained is not appreciably affected. In the initial phases of the present work the hydrogen sulfide formation was thought to be more significant and, to avoid it, some of the desired heterocycles were obtained at room temperature by adding tertiary amines. However, the reactions in refluxing bromobenzene usually give better yields with greater convenience because the products are much more easily isolated.

In the thermal condensations, as the diazaphosphole is initially formed the hydrogen chloride liberated reacts with unchanged diamine to form a salt. This salt must be decomposed to the free base to permit its utilization in additional diazaphosphole formation. This salt dissociation is not merely the shift of a simple equilibrium process controlled by diffusion of the hydrogen chloride to the surface of the solution, for condensations of both phosphonic and phosphonothioic dichlorides with *o*-phenylenediamine in refluxing bromobenzene were found to proceed more rapidly than the decomposition of *o*-phenylenediamine hydrochloride alone under the same conditions.

Can. J. Chem. Downloaded from www.nrcresearchpress.com by 210.87.254.40 on 09/05/12
For personal use only.

Invariably the condensations of a diamine with a phosphonothioic dichloride required a much longer time than with a phosphonic dichloride. This lower reactivity of the phosphonothioic dichlorides is not unexpected for it has been firmly established in other investigations (18). The course of each reaction was followed by titrating the evolved hydrogen chloride. Despite the lack of temperature control other than that of a refluxing solvent medium, frequently (but not regularly) good first-order rate constants were obtained from these titrations. Thus with *N,N'*-dimethyl-*o*-phenylenediamine in refluxing bromobenzene both phenylphosphonic dichloride ($k = 95 \times 10^{-5}$ s^{-1}) and phenylphosphonothioic dichloride ($k = 2.9 \times 10^{-5}$ s^{-1}) gave first-order constants.

With phosphonothioic dichlorides the condensations with diamines containing electron-withdrawing substituents in the ring were invariably slower than with *o*-phenylenediamine itself. Much faster reactions occurred with amines containing electron-donating substituents. The presence of alkyl groups on the amino-nitrogen facilitated condensation while *N*-phenyl-*o*-phenylenediamine reacted sluggishly. All these data, as well as the lower reactivity of the phosphonothioic dichloride as compared to the phosphonic dichloride, are consistent with the rate-determining step being the nucleophilic displacement on phosphorus.

Using phosphonic dichlorides the condensations do not follow as clear a kinetic pattern. The reactions are so much faster that not only are the observed differences in time less significant but in addition the amine salt decomposition may be a factor in determing the overall rate.

Chemical Properties

The hydrolysis and alcoholysis of the benzodiazaphosphole 2-oxides have been briefly studied. Cleavage of only one amide linkage is possible under mild conditions.

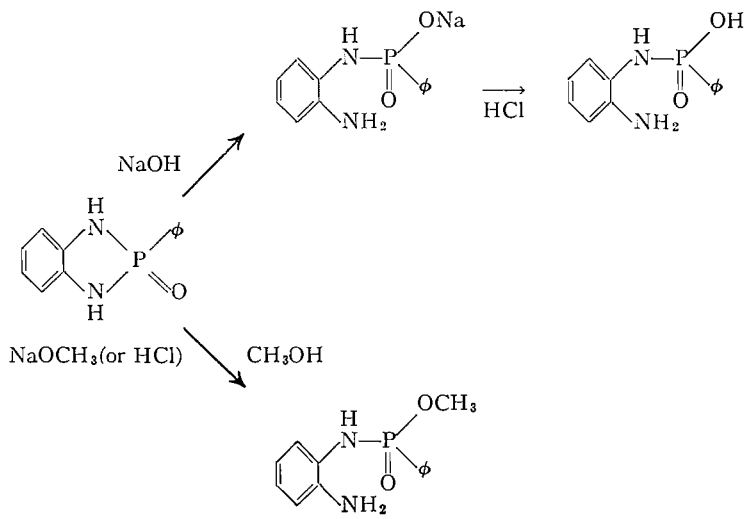

Under more drastic conditions (e.g. refluxing sodium hydroxide) complete hydrolysis to the diamine is obtained. The 2-sulfide analogue was somewhat more resistant to hydrolysis than the 2-oxide compound. The *N,N'*-dimethyl derivatives of the 2-phenyldiazaphosphole 2-oxide and 2-sulfide were much more resistant to hydrolysis than their unsubstituted counterparts. This hydrolytic stability is essential to any potential pharmaceutical use of the heterocycles.

Methylation of the diazaphosphole 2-sulfides was achieved with dimethyl sulfate and sodium hydroxide. These successful methylations offer encouragement for a future attachment of a sugar moiety to the diazaphosphole 2-sulfide to prepare a nucleoside analogue. The diazaphosphole 2-oxides hydrolyzed when subjected to the alkylation procedure and methylated products could not be isolated.

ACKNOWLEDGMENTS

Grateful acknowledgement is made to the U.S. Public Health Service for financial support by Grant No. CY-04104 and to Leonard T. Capell and Kurt L. Loening of Chemical Abstracts Service for aid in the nomenclature.

REFERENCES

1. R. L. DANNLEY and P. L. WAGNER. J. Org. Chem. **26**, 3995 (1961).
2. W. AUTENRIETH and O. HILDEBRAND. Ber. **31**, 1111 (1898).
3. W. AUTENRIETH and W. MEYER. Ber. **58**, 848 (1925).
4. P. L. WAGNER. Ph.D. Thesis, Western Reserve University. 1961.
5. M. S. KHARASCH, E. V. JENSEN, and S. J. WEINHOUSE. J. Org. Chem. **14**, 429 (1949).
6. F. GUTCHARD. Ber. **32**, 1572 (1899).
7. H. JEAN. Bull. Soc. Chim. France, 569 (1956).
8. A. M. KINNEAR and E. A. PERREN. J. Chem. Soc. 3437 (1952).
9. L. GATTERMAN. Ber. **18**, 1487 (1885).
10. B. W. ASHTON and H. SUSCHITZKY. J. Chem. Soc. 4559 (1957).
11. J. H. BERGEIM, K. LOSEE, and W. A. LOTT. J. Am. Chem. Soc. **69**, 586 (1947).
12. W. B. WHALLEY. J. Chem. Soc. 2792 (1950).
13. E. NOELTING and S. FOREL. Ber. **18**, 2683 (1885).
14. O. FISCHER. Ber. **25**, 2842 (1892).
15. A. M. SIMONOV and P. A. UGLOV. J. Gen. Chem. USSR **21**, 884 (1951). Chem. Abstr. **46**, 498^e (1952).
16. G. W. H. CHEESEMAN. J. Chem. Soc. 3308 (1955).
17. H. STETTER. Ber. **86**, 161 (1953).
18. D. J. HEATH. J. Chem. Soc. 3796 (1956).

Can. J. Chem. Downloaded from www.nrcresearchpress.com by 210.87.254.40 on 09/05/12
For personal use only.

REARRANGEMENT STUDIES WITH ^{14}C

XXIV. SOLVOLYSES OF 2-(α-NAPHTHYL)-1-^{14}C-ETHYL *p*-TOLUENESULFONATE

C. C. LEE AND A. G. FORMAN

Department of Chemistry, University of Saskatchewan, Saskatoon, Saskatchewan

Received June 28, 1965

ABSTRACT

Acetolysis and formolysis of 2-(α-naphthyl)-1-^{14}C-ethyl *p*-toluenesulfonate (I-OTs) were interrupted after 50% completion and the products, 2-(α-naphthyl)ethyl acetate and formate (I-OAc and I-OCHO), and the "unreacted" I-OTs were recovered. Rearrangements of the ^{14}C-label from C-1 to C-2 were found to be about 46% and 50%, respectively, in the I-OAc and I-OCHO. A similar rearrangement amounting to about 38% was observed in the I-OTs recovered from the acetolysis, while the I-OTs recovered from formolysis showed less than 1% ^{14}C rearrangement. Titrimetric rates for these reactions were determined and compared with known rates of solvolyses of 2-phenylethyl and ethyl *p*-toluenesulfonates. Small rate enhancements were indicated. The mechanistic implications of these results in relation to current carbonium ion theory are discussed.

INTRODUCTION

In current discussions on carbonium ion structure, Brown has emphatically suggested that rapidly equilibrating classical carbonium ions may be considered as an alternative to bridged or nonclassical ions (1, 2). Considering only β-phenylethyl systems which could give rise to symmetrical bridged ions, Brown (2) has pointed to the lack of significant enhancement in titrimetric rates for the β-phenyl substituted systems in comparison with the unsubstituted analogs as important evidence against the phenonium ion as a reaction intermediate. On the other hand, Cram (3) has strongly stated the case for the phenonium ion. The present paper reports the results from solvolyses of 2-(α-naphthyl)-1-^{14}C-ethyl *p*-toluenesulfonate (I-OTs) which may be of pertinence to the phenonium ion problem, especially when considered in conjunction with data from solvolyses of 2-phenyl-1-^{14}C-ethyl *p*-toluenesulfonate (II) (4, 5, 6) and 1-^{14}C-ethyl *p*-toluenesulfonate (III) (7).

RESULTS AND DISCUSSION

I-OTs was prepared from 2-(α-naphthyl)-1-^{14}C-ethanol (I-OH) which, in turn, was obtained from carbonation of the Grignard reagent with ^{14}C-carbon dioxide to give α-naphthyl-1-^{14}C-acetic acid, followed by lithium aluminium hydride reduction. Solutions of I-OTs in anhydrous acetic acid (0.350 *M*) and in anhydrous formic acid (0.060 *M*) were heated at 110.6 °C and 56.5 °C, respectively, until the reactions were 50% complete. The products, 2-(α-naphthyl)ethyl acetate or formate (I-OAc or I-OCHO) and the "unreacted" I-OTs were recovered by procedures as used in analogous studies with II (5). The recovered I-OTs was converted to I-OAc by treatment with fused sodium acetate in anhydrous ethanol (8); I-OAc from recovered I-OTs and the product, I-OAc or I-OCHO, were treated with lithium aluminium hydride to give I-OH which was oxidized by alkaline potassium permanganate to α-naphthoic acid (IV) (9). The activity of IV measured the extent of rearrangement of the ^{14}C-label from C-1 to C-2. The results are summarized in Table I. Titrimetric rates for acetolysis and formolysis of I-OTs were determined at convenient temperatures and then extrapolated to 75 °C for comparison with 2-phenylethyl and ethyl *p*-toluenesulfonates (II and III). The data are given in Table II.

Can. J. Chem. Downloaded from www.nrcresearchpress.com by 210.87.254.40 on 09/05/12
For personal use only.

Can. J. Chem. Downloaded from www.nrcresearchpress.com by 210.87.254.40 on 09/05/12
For personal use only.

TABLE I

Rearrangements in solvolyses of 2-(α-naphthyl)-1-^{14}C-ethyl tosylate

Reaction	Compound assayed	Reaction product				Recovered tosylate			
		Activity* (c.p.m./mmole)		% rearrangement		Activity* (c.p.m./mmole)		% rearrangement	
		Run 1	Run 2	Run 1	Run 2	Run 1	Run 2	Run 1	Run 2
Acetolysis	α-$C_{10}H_7CH_2CH_2OH$	684	341			303	232		
	α-$C_{10}H_7COOH$	318	156	46.5	45.7	116	89	38.3	38.4
Formolysis	α-$C_{10}H_7CH_2CH_2OH$	368	386			136	164		
	α-$C_{10}H_7COOH$	184	196	50.0	50.7	1.5	0.9	0.7	0.9

*Measured by a liquid scintillation counter.

TABLE II

Specific rate constants at 75 °C

Reaction	10^6k (s^{-1})		
	CH_3CH_2OTs (III)*	$C_6H_5CH_2CH_2OTs$ (II)*	α-$C_{10}H_7CH_2CH_2OTs$ (I-OTs)
Acetolysis	0.772	0.288	0.528
Formolysis	18.9	39.4	169

*From ref. 2.

From Table I, it may be noted that the ^{14}C rearrangement observed in the acetolysis of I-OTs is in complete agreement with the 46% rearrangement reported by Cram and Dalton (10) in their study with 2-(α-naphthyl)-1,1-dideuterioethyl p-toluenesulfonate. Data in Table I also indicate that complete equivalence of C-1 and C-2 has been achieved in the formolysis of I-OTs. These results may be compared with ^{14}C rearrangements of about 5% and 45%, respectively, for acetolysis and formolysis of II (4, 5, 6), and with the total absence of rearrangement in the solvolysis of III (7). The isotopic rearrangement observed in the recovered I-OTs (Table I) may be attributed to the process of return from ionic intermediate to covalent bonding. The extent of return accompanying acetolysis of I-OTs is relatively large ($\sim$38% rearranged), while the rearrangement in the recovered I-OTs from formolysis is almost negligible. These results are consistent with classic concepts regarding the effects of the reaction medium on internal return (11, 12). Returns to isotopically rearranged II have also been observed to accompany solvolyses of II (4, 5, 6); in formolysis such return is chiefly external (6). A decision as to whether the isotopically rearranged I-OTs recorded in Table I arose from intramolecular internal return or from intermolecular external return will require further investigation.

Acetolysis of III is faster than that of II by a factor of 2.7 (1, 2, 3). Cram (3) has attributed this partially to the negative inductive effect of phenyl and also to the unhindered back side of the incipient carbonium ion allowing the solvent to compete successfully with phenyl in this medium, as evidenced by only 5% ^{14}C rearrangement in the acetolysis of II. In the acetolysis of I-OTs, ^{14}C rearrangement rises to 46%, but the titrimetric rate is faster than that for acetolysis of II by only a factor of 1.8 (Table II). If relative rates were to be a true indication of anchimeric assistance, where internal return plays a role, polarimetric rather than titrimetric rates should be used (13). However, in the absence of optical activity for β-arylethyl systems, polarimetric data are not available. Where anchimeric assistance by the β-aryl group is to be considered, at least the basis for comparison should be a reaction involving ethyl cation without assistance. Since acetolysis of II or III entails extensive solvent participation, comparisons of rates of acetolysis among I-OTs, II, and III possibly will reflect only the difference between solvent assistance and aryl assistance rather than the true aryl assistance. Thus besides the influence of inductive effects, a predominance of solvent assistance in the acetolysis of II or III may be an important factor in giving rise to the small overall differences in relative acetolysis rates for I-OTs, II, and III.

Kinetic data (14) and the absence of ^{14}C rearrangement (7) suggest that even in formic acid, a less nucleophilic solvent, solvolysis of III is still not "limiting." The formolysis of II gave about 45% ^{14}C rearrangement and its titrimetric rate is faster than that for the formolysis of III by a factor of 2.1 after overcoming the negative inductive effect of phenyl and possibly also the more favorable solvent assistance for III. In the formolysis of I-OTs, 50% ^{14}C rearrangement is observed, and the titrimetric rate is greater than those for III

Can. J. Chem. Downloaded from www.nrcresearchpress.com by 210.87.254.40 on 09/05/12
For personal use only.

and II, respectively, by factors of 8.9 and 4.3 (Table II). It may also be noted that the negative inductive effect of α-naphthyl is believed to be greater than that of phenyl (15). Thus considering all the factors involved, the data do indicate some enhancement in rate as well as a complete equivalence of C-1 and C-2 in the formolysis of I-OTs. Such results would be consistent with the formulation of an ethylene-α-naphthonium ion (V, drawn by analogy with the structure of phenonium ion recommended by Brown (2)) as an intermediate (3, 10). The results from the formolysis of I-OTs are also analogous to those obtained in the acetolysis and formolysis of 2-(p-anisyl)-1-^{14}C-ethyl p-toluenesulfonate which showed rate enhancement as well as essential equivalence of C-1 and C-2, and for which a bridged ion has been proposed as reaction intermediate (16). On the other hand, where the rate enhancement is small as in the present case, Brown (2, 17) has suggested that the complete scrambling of the ^{14}C in C-1 and C-2 may be the result of rapid equilibration of "π-bridged" ions, VI, involving interaction between the π-cloud of the aromatic ring and the cationic center, instead of the truly bridged "nonclassical" ion V. It is not possible to differentiate V and VI from the present data.

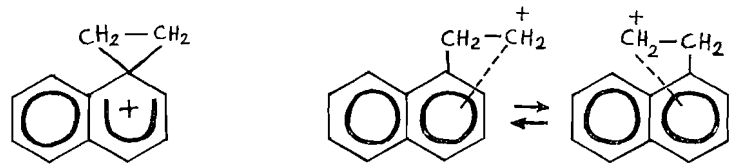

V VI

EXPERIMENTAL

2-(α-Naphthyl)-1-^{14}C-ethyl p-Toluenesulfonate (I-OTs)

Treatment of the Grignard reagent prepared from α-chloromethylnaphthalene with ^{14}C-carbon dioxide gave carboxyl-labeled α-naphthylacetic acid, m.p. 130–131 °C (lit. (18) m.p. 131 °C). Reduction of this acid with lithium aluminium hydride yielded 2-(α-naphthyl)-1-^{14}C-ethanol (I-OH), m.p. 61–62 °C (lit. (9) m.p. 61–62 °C), which was converted to I-OTs by reaction with p-toluenesulfonyl chloride in pyridine (19). Yields of I-OTs, m.p. 59–60 °C (lit. (10) m.p. 56.5–58.0 °C), based on the alcohol, were about 85%.

Anal. Calcd. for $C_{19}H_{18}O_3S$: C, 69.91; H, 5.56; S, 9.82. Found: C, 70.09; H, 5.62; S, 9.64.

Acetolysis of I-OTs

A solution of 5.712 g (0.0175 moles) of I-OTs in 50 ml of anhydrous acetic acid was heated at 110.6 °C for a period of one half-life (740 min). The resulting mixture was poured onto crushed ice and then worked up for "unreacted" I-OTs and for the product, 2-(α-naphthyl)ethyl acetate (I-OAc), by procedures previously described for analogous studies with 2-phenyl-1-^{14}C-ethyl p-toluenesulfonate (II) (5). The recoveries of I-OTs were about 80% of theoretical based on 50% reaction. For duplicate runs, yields of I-OAc, b.p. 144–148 °C at 1 mm, were 1.33 g and 1.73 g (71% and 92% based on 50% reaction).

Anal. Calcd. for $C_{14}H_{14}O_2$: C, 78.48; H, 6.59. Found: C, 78.07; H, 6.71.

Formolysis of I-OTs

Because of the lower solubility of I-OTs in formic acid, the reaction was carried out in more dilute solution than in the case of acetolysis. A solution of 4.896 g (0.0150 moles) of I-OTs in 250 ml of anhydrous formic acid was heated at 56.5 °C for one half-life (510 min), poured onto crushed ice, and worked up as before. For duplicate runs, recovered I-OTs amounted to 1.7 g and 1.9 g (70% and 78% based on 50% reaction) and the yields of product, 2-(α-naphthyl)ethyl formate (I-OCHO), b.p. 137–142 °C at 1 mm, were 1.05 g and 1.20 g (67% and 77% based on 50% reaction).

Anal. Calcd. for $C_{13}H_{12}O_2$: C, 77.98; H, 6.04. Found: C, 77.92; H, 6.05.

I-OAc from Recovered I-OTs

Each sample of recovered I-OTs was diluted with inactive carrier to give a total of 5.0 g of starting material and then dissolved in 50 ml of absolute ethanol. Freshly fused sodium acetate (2.9 g) was added and the mixture was refluxed for 24 h. It was then cooled, poured into water, and extracted with petroleum ether. The extract was dried over anhydrous magnesium sulfate and then fractionated to give about 2.0 g of the desired acetate, I-OAc.

Can. J. Chem. Downloaded from www.nrcresearchpress.com by 210.87.254.40 on 09/05/12
For personal use only.

Degradation

Each sample of the products, I-OAc and I-OCHO, and of the I-OAc from the recovered I-OTs, was treated with lithium aluminium hydride to give I-OH. The alcohol was oxidized by alkaline potassium permanganate to α-naphthoic acid (9), whose activity measured the extents of rearrangement. As a control experiment, I-OTs, before being subjected to solvolysis, was converted to I-OAc which, in turn, was degraded to give non-radioactive α-naphthoic acid, indicating that the conversion of recovered I-OTs to I-OAc and the degradation procedures would cause no rearrangement.

Kinetic Measurement

The kinetics of acetolysis and formolysis of I-OTs were followed titrimetrically by known methods already mentioned in earlier publications (20, 21). For acetolysis, specific rate constants at 110.6 °C and 100.0 °C, respectively, were found to be 1.37×10^{-5} and 5.53×10^{-6} s^{-1}. For formolysis, k values at 56.5 °C and 40.1 °C were, respectively, 2.18×10^{-5} and 2.90×10^{-6} s^{-1}. Specific rate constants at 75 °C (Table II) were obtained by extrapolation.

ACKNOWLEDGMENT

The financial assistance given by the National Research Council of Canada is gratefully acknowledged.

REFERENCES

1. H. C. Brown. *In* The transition state. Chem. Soc. London Spec. Publ. No. 16. 1962. pp. 140–158.
2. H. C. Brown, K. J. Morgan, and F. J. Chloupek. J. Am. Chem. Soc. **87**, 2137 (1965).
3. D. J. Cram. J. Am. Chem. Soc. **86**, 3767 (1964).
4. C. C. Lee, G. P. Slater, and J. W. T. Spinks. Can. J. Chem. **35**, 1417 (1957).
5. C. C. Lee, R. Tkachuk, and G. P. Slater. Tetrahedron, **7**, 206 (1959).
6. J. W. Clayton and C. C. Lee. Can. J. Chem. **39**, 1510 (1961).
7. C. C. Lee and M. K. Frost. Can. J. Chem. **43**, 526 (1965).
8. D. J. Cram. J. Am. Chem. Soc. **71**, 3863 (1949).
9. A. G. Forman and C. C. Lee. Can. J. Chem. **40**, 1130 (1962).
10. D. J. Cram and C. K. Dalton. J. Am. Chem. Soc. **85**, 1268 (1963).
11. W. G. Young, S. Winstein, and H. L. Goering. J. Am. Chem. Soc. **73**, 1958 (1951).
12. A. Streitwieser, Jr. Solvolytic displacement reactions. McGraw-Hill Book Co., New York. 1962. pp. 86–91.
13. S. Winstein, E. Clippinger, R. Howe, and E. Vogelfanger. J. Am. Chem. Soc. **87**, 376 (1965).
14. S. Winstein and H. Marshall. J. Am. Chem. Soc. **74**, 1120 (1952).
15. J. F. Dippy, S. R. C. Hughes, and J. W. Laxton. J. Chem. Soc. 4102 (1954).
16. E. F. Jenny and S. Winstein. Helv. Chim. Acta, **41**, 807 (1958).
17. H. C. Brown. Private communications.
18. I. Heilbron and H. M. Bunbury. Dictionary of organic compounds. Vol. III. Eyre and Spottiswoode, London. 1953. p. 571.
19. R. S. Tipson. J. Org. Chem. **9**, 235 (1944).
20. C. C. Lee and E. W. C. Wong. Tetrahedron, **21**, 539 (1965).
21. C. C. Lee and E. W. C. Wong. Can. J. Chem. **43**, 2254 (1965).

Can. J. Chem. Downloaded from www.nrcresearchpress.com by 210.87.254.40 on 09/05/12
For personal use only.

Can. J. Chem. Downloaded from www.nrcresearchpress.com by 210.87.254.6 on 09/05/12
For personal use only.

ADDITION OF FLUOROACETYLENES TO GROUP V HYDRIDES

W. R. CULLEN, D. S. DAWSON, AND G. E. STYAN
Chemistry Department, University of British Columbia, Vancouver, British Columbia
Received July 19, 1965

ABSTRACT

Compounds of the type R_2EH react readily with $CF_3C{\equiv}CCF_3$ to give $R_2EC(CF_3){=}C(CF_3)H$ (E = N, P, As), and with $CF_3C{\equiv}CH$ to give $R_2ECH{=}CHCF_3$ (E = N, As) and $R_2EC(CF_3){=}CH_2$ (E = As). The isomer distribution of the products is obtained from their n.m.r. spectra and the mechanism of the addition reaction is discussed.

INTRODUCTION

Although it was known that the fluoroacetylenes hexafluorobut-2-yne, $CF_3C{\equiv}CCF_3$ (I) and 1,1,1-trifluoropropyne $CF_3C{\equiv}CH$ (II), react with compounds such as $(C_2H_5)_2NH$ (1) and H_2S (2) to give adducts of the type $HSC(CF_3){=}C(CF_3)H$, very little information was available concerning the isomer distribution of the products. Because of our interest in the reactions of fluoroacetylenes (3, 4) and because little is known about the addition of compounds containing E—H bonds (E = N, P, As) to acetylenes, we have studied the products obtained by reacting hydrides of the type R_2EH (R = CH_3, C_6H_5, CF_3) with I and II.

Recently Stone and co-workers (5, 6) have found that I adds to transition metal hydrides to yield predominantly the *trans*-adduct, e.g.

$$(CO)_5ReH + CF_3C{\equiv}CCF_3 \rightarrow \begin{matrix} (CO)_5Re & & CF_3 \\ & C{=}C & \\ CF_3 & & H \end{matrix}$$

DISCUSSION AND RESULTS

The reactions investigated can be described by the following equations.

$$\begin{matrix} & & CF_3C{\equiv}CCF_3\ (I) & \rightarrow & RR'EC(CF_3){=}C(CF_3)H\ (IV) \\ RR'EH\ (III) & \longrightarrow & & & \\ & & CF_3C{\equiv}CH\ (II) & \rightarrow & RR'ECH{=}C(CF_3)H\ (V) + RR'EC(CF_3){=}CH_2\ (VI) \end{matrix}$$

The products isolated from these reactions will be described first.

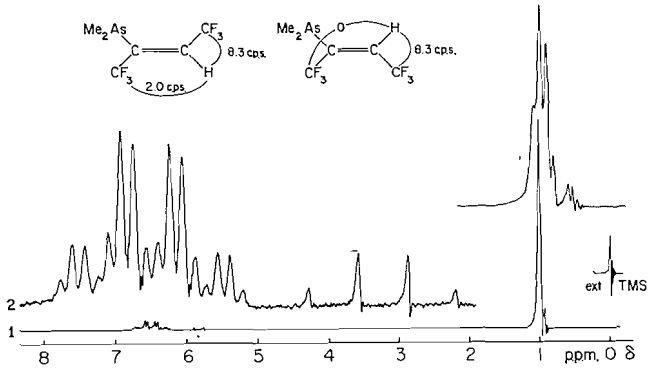

FIG. 1. ^1H n.m.r. spectrum of $(CH_3)_2AsC(CF_3){=}C(CF_3)H$.

Can. J. Chem. Downloaded from www.nrcresearchpress.com by 210.87.254.6 on 09/05/12
For personal use only.

Reaction Products

Dimethylarsine (III, R = R′ = CH_3, E = As) and I give the 1:1 adduct IV, a colorless liquid, b.p. 109–110°. The ^1H nuclear magnetic resonance (n.m.r.) spectrum of this product, before distillation, is shown in Fig. 1. The coupling constants indicated in the figure are consistent with the quartet of quartets being associated with the *trans*-isomer and the slightly higher field quartet with the *cis*-compound, the relative abundance of the two isomers being 15:1. In the high field region the areas of the two peaks are also in the ratio 15:1 indicating that they too are associated with the two isomers. These peaks which are due to the methyl groups on the arsenic atoms are split into quartets with J = 1.2 c.p.s. Splittings of this sort have been observed previously for the related compounds $(CH_3)RAsC(CF_3)=C(CF_3)Cl$ (R = CH_3, Br) (3) and $(CH_3)_2AsC(CF_3)=C(CF_3)As(CH_3)_2$. In the latter case the *cis*-compound (4) has an ill-defined quartet at 1.22 p.p.m. ($J \approx 0.5$ c.p.s.) and the *trans*-isomer a similar quartet at 1.18 p.p.m. ($J \approx 1.0$ c.p.s.). It has been suggested (3) that these splittings could be due to "through space" coupling of the arsenic methyl protons with the fluorine atoms of the geminal trifluoromethyl group since arsines of the type $(CH_3)RAsRf$, where Rf is any other type of fluorocarbon group, have only a single sharp methyl peak in their n.m.r. spectra. It is, however, possible to have the $CH_3AsC(CF_3)=$ group present without observing this splitting as in the compound $(CH_3)_2AsC(CF_3)=CHCl$ (7) where the methyl peak is split ($J \approx 1$ c.p.s.) when the arsenic atom is *cis* to the chlorine but is unsplit in the other isomer. Evidently bulky groups are necessary for splitting to occur. The ^{19}F n.m.r. spectrum of a sample of IV (R = R′ = CH_3, E = As) which was at least 90% *trans*-isomer shows two peaks. The downfield peak which consists of a doublet (J = 8.4 c.p.s.) of quartets (J = 1.9 c.p.s.) is assigned to the fluorine atoms of the $=C(CF_3)H$ group. Fig. 1 shows that $J_{CF_3\text{--}H} = 8.4$ c.p.s. and thus the 1.9 c.p.s. splitting must be due to the *trans*-CF_3 groups. These coupling constants are in agreement with those previously reported (6). The high field peak in the ^{19}F spectrum of the arsine is very broad and this is assigned to the fluorine atoms of the $(CH_3)_2AsC(CF_3)=$ group, the broadening being due to the combined effects of the weak CF_3--CF_3, CF_3--CH_3, and *cis*-CF_3--H interactions.

A predominantly *trans*-configuration is also found in the product of the reaction of methylphenylarsine (III, R = CH_3, R′ = C_6H_5, E = As) with I. The mixture of isomers of IV (R = CH_3, R′ = C_6H_5, E = As) obtained after distillation at 54° (10^{-3} mm) contained 92% *trans*-compound. This assignment can be made on the basis of the ^1H n.m.r. spectrum which is very similar to that described for the dimethylarsine adduct (IV, R = R′ = CH_3, E = As). Here again the methyl peak of each isomer has a different chemical shift and is split into a quartet by weak CF_3--CH_3 interactions. Bistrifluoromethylarsine and I give a product IV (R = R′ = CF_3, E = As) b.p. 99–100° which consists only of the *trans*-isomer as characterized by the quartet of quartets in its ^1H n.m.r. spectrum.

The product of the interaction of diphenylphosphine and I is the 1:1 adduct IV (R = R′ = C_6H_5, E = P) b.p. 127° (10^{-3} mm). The ^1H n.m.r. spectrum of this product shows the presence of aromatic and olefinic protons and the relative areas of the peaks indicate that some absorption due to the olefinic protons lies underneath the broad aromatic proton peak. The ^{31}P--H coupling for trivinylphosphine is given as 30 c.p.s. for the *trans*-hydrogen and 14 c.p.s. for the *cis* (8). Thus the diphenylphosphino compound would be expected to show some ^{31}P--H coupling also. Among the peaks associated with the olefinic protons is an isolated quartet (J = 9 c.p.s.) which shows some sign of secondary splitting and which can be assigned to a single proton or to half a proton in the group $=C(CF_3)H$ depending on

whether $J_{^{31}P\text{--}H} \simeq 0$ or $\geqslant 50$ c.p.s. The latter possibility is more likely, but the coupling can not be given more precisely because of overlap of peaks. If the trends found for the arsenic compounds are maintained for phosphorus, then the upfield position and slight secondary splittings of the quartet indicate that it is due to the *cis*-isomer. However, the secondary splitting criterion is not reliable as is seen for the nitrogen compounds described below. The area of this quartet indicates that there is a significant amount of this supposed *cis*-isomer in the mixture (ca. 40% if the ^{31}P--H coupling $\geqslant 50$ c.p.s.).

Dimethylamine and I afford the dimethylaminobutene (IV, R = R′ = CH_3, E = N) b.p. 96–97°. The initial reaction product, undistilled, consists of two isomers in the ratio 6:1 (trans:*cis*, *quod vide*), each isomer having a ^1H n.m.r. spectrum of a downfield quartet (J = 9 c.p.s., showing *slight* secondary splitting) and an upfield singlet which also shows the presence of weak coupling. By analogy with the arsenic compounds the downfield quartet is assigned to the *trans*-isomer and this is substantiated by the ^{19}F n.m.r. spectrum of the pure isomer which contains only two regions of absorption both of which show only very weak F--F coupling resulting in a broadening of the peaks. The ^{19}F spectrum of a mixture of isomers shows a quartet (J = 12.6 c.p.s.) due to the other isomer. It has been found that *trans*-CF_3--CF_3 coupling is much weaker than *cis*-CF_3--CF_3, the former having values of 1.1, 2.3 (5), and 2.5 c.p.s. (6), the latter being of the order of 11.5 c.p.s. (5). Thus in the present example the weak coupling can be assigned to the *trans*-isomer. The ^{19}F spectrum also shows the expected doublet associated with the $=C(CF_3)H$ group but unexpectedly each doublet is split into a septet presumably because of coupling with the methyl groups on the nitrogen. The slight splittings on the methyl peaks in the ^1H spectrum are a further manifestation of this interaction. This long-range coupling (J = 1.7 c.p.s.) is of similar magnitude to the 6-bond H--F coupling in *o*-fluoro-N-cyclohexyl-N-methylbenzamide (9).

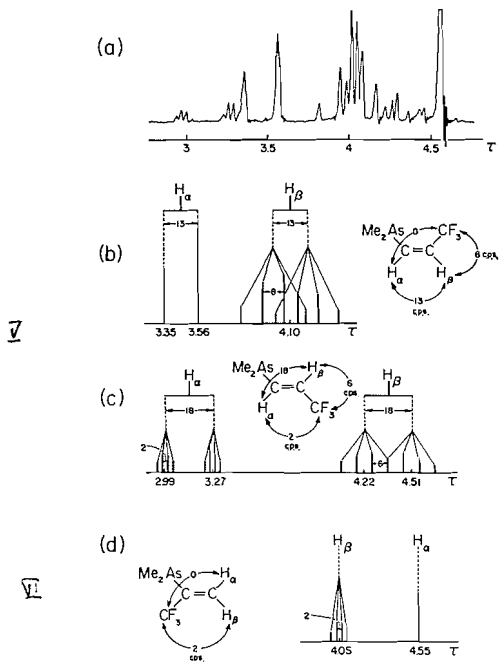

V

VI

FIG. 2. Down field region of the ^1H n.m.r. spectrum of the reaction products from $(CH_3)_2AsH$ and $CF_3C{\equiv}CH$.

Can. J. Chem. Downloaded from www.nrcresearchpress.com by 210.87.254.6 on 09/05/12
For personal use only.

Can. J. Chem. Downloaded from www.nrcresearchpress.com by 210.87.254.6 on 09/05/12
For personal use only.

Trifluoropropyne (II) and dimethylarsine give a product b.p. 109–110° whose low field n.m.r. spectrum is given in Fig. 2. Analysis of this spectrum resulted in the assignments given in the figure. The assignments were based on the possibility of obtaining three isomers and the expectation that $J_{H\alpha-H\beta}$ for the *cis*-compound would be less than for the *trans*-isomer as is found in related hydrocarbon systems (10). Subsequently the pure *cis*-compound was isolated by vapor phase chromatography (v.p.c.) and converted to the *trans*-form and the n.m.r. spectra of these proved to be identical with those derived (Fig. 2). Confirmation of the *trans*-isomer comes from the infrared spectrum which shows a highly characteristic band of medium intensity at 970 cm^{-1} (11). The *cis*-isomer is transparent in this region. The iso-compound (VI, R = R′ = CH_3, E = As) has an unsplit methyl peak with the same chemical shift found for the *cis*-compound. The ratio of isomers in the original reaction product, after distillation, is *cis*:*trans*:iso = 3:3:2.

Dimethylamine and II give only the *trans*-dimethylamino derivative (V, R = R′ = CH_3, E = N) b.p. 118°. The ^1H n.m.r. spectrum is almost identical with that of the analogous *trans*-dimethylarsino compound. Confirmation of the *trans*-configuration comes from its infrared spectrum which, like the arsenic analogue, contains a strong band in the *trans* —HC=CH— "out-of-plane" bending region at 960 cm^{-1}. The H_α--H_β coupling in the *trans*-amino compound is 13 c.p.s. which is to be compared with 18 and 13 c.p.s. for the *trans*- and *cis*-arsino derivatives respectively.

Isomerization of the Products

A limited amount of information regarding isomerization of the olefinic products has been obtained in the present investigation. Thus the *cis*-isomer of 2-dimethylarsino-1,1,1,4,4,4-hexafluorobutene (IV, R = R′ = CH_3, E = As) is isomerized to the *trans*-compound on heating ($T \geqslant 140°$) although the methylphenylarsinobutene is unaffected at 140°. Isomerization of the dimethylaminobutene (IV, R = R′ = CH_3, E = N) is apparently catalyzed by oxygen since leaving a *trans*-rich mixture exposed to the air at 20° results in an increase in the *cis*-isomer content and distilling the mixture in nitrogen results in an increase in the *trans*-isomer content. (Inevitably some oxygen would be present during the distillation.) However, if a mixture of the isomers is heated in the absence of air then no isomerization takes place below 160° even though other reactions, possibly polymerization, start to become significant at the higher temperatures.

The *cis*-isomer of 1-dimethylarsino-3,3,3-trifluoropropene (V, R = R′ = CH_3, E = As) is converted to the *trans*-isomer both on ultraviolet irradiation and on heating. This provides a convenient method of obtaining the *trans*-compound since the *cis*-isomer can be isolated by v.p.c. The thermal isomerization does not take place in the absence of air below 150°, but at 175° it is almost complete after 12 days.

Mechanism of the Addition Reactions

Haszeldine (1) found that nucleophilic attack by alkoxide ion occurs readily on hexafluorobut-2-yne but less readily on 1,1,1-trifluoropropyne. Since his work was reported, a number of studies have been made on the sterochemistry of nucleophilic attack on more commonly available acetylenes which have resulted in the generalization that nucleophilic attack results in *trans*-addition (12), although a few exceptions have been noted (13). More recently *trans*-addition of alkoxide to ethynylsulfur pentafluoride to give predominantly *cis*-$SF_5CH{=}CHOCH_3$ has been found (14). Thus it seems likely that Haszeldines' products $ROC(CF_3){=}C(CF_3)H$ and $ROCH{=}CHCF_3$ will have predominantly the configuration to be expected from *trans*-addition.

Can. J. Chem. Downloaded from www.nrcresearchpress.com by 210.87.254.6 on 09/05/12
For personal use only.

The mechanism of the addition of the compounds R_2EH to the acetylenes is less certain. In the hydrocarbon field it has been found that, in the absence of catalysts, amines add only to activated triple bonds (15, 16). It has been assumed that these additions involve nucleophilic attack by the amine (15, 16), but the geometry of the products has not been investigated.

The addition of arsines to I also appears to involve nucleophilic attack, presumably by the arsenic lone pair, since the ease of reaction of the arsines RR′AsH with I decreases in order $(CH_3)_2AsH > CH_3(C_6H_5)AsH > (CF_3)_2AsH$. This order reflects the decreasing availability of the arsenic lone pair for nucleophilic attack owing to the presence of electron-withdrawing groups on the arsenic atom (17). Similarly the reaction of dimethylamine with I probably involves nucleophilic attack. The nature of the reaction of diphenylphosphine with I is less certain because of the high proportion of what is probably the *cis*-isomer in the product. The transition state leading to *trans*-addition by nucleophilic attack can be represented by VII; hyperconjugation could result in VIII which in turn could result in some *cis*-isomer being produced, but it is difficult to see why VIII should be more stable when E = P.

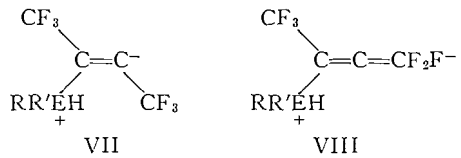

VII VIII

Haszeldine found that nucleophilic attack by alkoxide on the propyne (II) leads to the formation of only $ROCH{=}CHCF_3$, no $CF_3C(OR){=}CH_2$ being produced. Dimethylamine is now found to add in a similar way to give only *trans*-$(CH_3)_2NCH{=}C(CF_3)H$ but it seems unlikely that the product arises by *cis*-addition and consequently it is believed that *trans*-addition first takes place followed by isomerization. In the corresponding arsenic system it is the *trans*-compound which is more thermodynamically stable. Dimethylarsine and II give the three isomers shown in Fig. 2. The *cis*-compound could arise from nucleophilic attack by the arsine but the amount of the *trans*-compound, which is equal to that of the *cis*, seems to be too much to have resulted from isomerization of the initially formed *cis*-isomer unless the isomerization is catalyzed by unreacted arsine. The mechanism of the formation of the iso-compound VI (R = R′ = CH_3, E = As) is also of interest since electrophilic attack by the hydrogen of the arsine should proceed through intermediates such as IX and X.

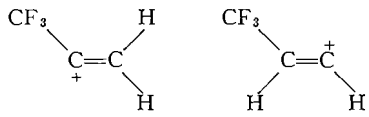

IX X

Of the two rather unlikely species X would be expected to be more stable and consequently electrophilic attack should also lead to the *cis*-isomer, Burnelle having recently calculated (18) that a *trans*-distortion of the alkyne is to be expected on the approach of an electrophile. Thus, although Haszeldine (1) found no evidence for nucleophilic attack by alkoxide at the center carbon atom of the propyne it seems likely that this is occurring in the arsine reaction. However, a concurrent free radical addition could be taking place giving rise to all three isomers.

One very important feature of these hydride addition reactions yet to be settled is the question of inter- or intra-molecular hydrogen transfer and it is hoped that competitive experiments with deuterated arsines will provide an answer.

EXPERIMENTAL

All reactions were carried out in sealed thick-walled pyrex tubes. Nuclear magnetic resonance spectra were obtained using Varian A-60 and HR-60 spectrometers and chemical shifts are reported in parts per million (p.p.m.) downfield from external tetramethylsilane (^{1}H spectra) and from external trifluoroacetic acid (^{19}F spectra). Infrared spectra were recorded using a Perkin–Elmer Model 21 instrument. Microanalyses were carried out by Dr. Alfred Bernhardt, Mulheim, Germany.

Reaction of Hexafluorobut-2-yne with Dimethylarsine

The arsine and the acetylene did not react in the gas phase at 20°. However, there was a vigorous reaction when the arsine (3.1 g) and the butyne (10.1 g) were condensed together and allowed to warm slowly to 20°. Trap-to-trap distillation gave 7.4 g of unreacted acetylene and 7.7 g of *2-dimethylarsino-1,1,1,4,4,4-hexafluorobutene* which condensed in a trap cooled to −78°. Vapor phase chromatography (dinonyl phthalate at 100°) showed the fraction to be at least 99% pure. It distilled in nitrogen at 109–110° (Found: C, 26.7; H, 2.8; As, 28.1; F, 42.3. Calcd. for $C_6H_7AsF_6$: C, 26.8; H, 2.7; As, 28.0; F, 42.6). Infrared spectrum (liquid film): 3 020(w), 2 940(w), 2 340(vw), 1 643(w), 1 430(sh,m), 1 424(m), 1 366(w), 1 331(vs), 1 257(vs), 1 160(vs), 1 140 (vs), 940(vw), 900(m), 870(sh,s), 859(s), 850(s), 722(w) cm^{-1}. Spectra (n.m.r.): ^{1}H spectrum (Fig. 1) methyl peaks at 1.03 and 0.94 p.p.m. each split into a multiplet of 4 (J = 1.2 c.p.s.), area ratio = 15.1:1. Two olefinic protons, one consisting of a quartet of quartets centered at 6.5 p.p.m. (J = 8.3 and 2.0 c.p.s.) and the other a quartet centered at 5.83 p.p.m. (J = 8.3 c.p.s.), of relative area 15.1:1. ^{19}F spectrum: two peaks of equal area at 13.6 and 11.1 p.p.m. The low field peak is a doublet (J = 8.4 c.p.s.) each doublet being further split into a quartet (J = 1.9 c.p.s .). The peak at 11.1 p.p.m. is broad being of the order of 8 c.p.s. at half height and is a multiplet of 13.

A sample of the adduct after distillation showed an isomer distribution of 95% *trans*:5% *cis*, and after 36 h at 140° even less of the *cis*-isomer remained. After 36 h at 160° the isomer composition was 98% *trans* and 2% *cis*.

The arsine (*trans*: *cis* = 95:5) and 10 ml of 10% aqueous sodium hydroxide were heated to 100° for 3 days to give 0.043 g (15% yield) of *trans*-1,1,1,4,4,4-hexafluorobutene of known infrared spectrum.

Reaction of Hexafluorobut-2-yne with Methylphenylarsine

The arsine (5.6 g) and the butyne (13.3 g) reacted slowly at 20° to give a single phase after 30 min. The less volatile product which distilled at 54° (10^{-3} mm) was identified as *2-methylphenylarsino-1,1,1,4,4,4-hexafluorobutene* (Found: C, 40.0; H, 2.9; As, 22.6; F, 34.7. Calcd. for $C_{11}H_9AsF_6$: C, 40.0; H, 2.7; As, 22.7; F, 34.6). Infrared spectrum (liquid film): 3 070(w), 2 930(vw), 2 280(vw), 1 641(w), 1 582(w), 1 485(w), 1 438(m), 1 363(w), 1 330(s), 1 283(m), 1 255(vs), 1 143(vs), 1 077(w), 1 069(vw), 1 023(w), 998(w), 870(w), 850(m), 844(m), 737(s), 721(vw), 693(s), 641(s) cm^{-1}. ^{1}H n.m.r. spectrum: two high field peaks at 1.06 and 0.93 p.p.m. of relative area 11:1, the larger one being a distorted quartet ($J \approx$ 1 c.p.s.). In the downfield region are two quartets (J = 8.5 c.p.s.) centered at 6.36 and 5.40 p.p.m. (area ratio = 11:1), each peak of the larger quartet at 6.36 p.p.m. is further split into a quartet (J = 2.0 c.p.s.). The aromatic protons appear as a complex system centered at 6.9 p.p.m. This same n.m.r. spectrum was obtained from a sample that had been heated at 140° for 3 days.

Reaction of Hexafluorobut-2-yne with Bistrifluoromethylarsine

Bistrifluoromethylarsine (2.9 g) and excess acetylene (11.0 g) did not react at 20° (2 days), and after 24 h at 130° only partial reaction had occurred. The reactants and products were then heated to 210° (24 h) to give hexafluorobut-2-yne (8.2 g) containing a little silicon tetrafluoride and fluoroform, and a fraction which condensed at −46° (5.0 g). This last fraction distilled at 99–100° in a nitrogen atmosphere and was identified as *2-bis(trifluoromethyl)arsino-1,1,1,4,4,4-hexafluorobutene*. An analytical sample was obtained by v.p.c. (dinonyl phthalate at 100°) (Found: C, 19.3; H, 0.27; As, 19.9; F, 60.5. Calcd. for C_6HAsF_{12}: C, 19.2; H, 0.27; As, 19.9; F, 60.6). Infrared spectrum (vapor): 3 100(vw), 2 302(vw), 1 793(vw), 1 649(vw), 1 385(m), 1 360(m), 1 331(vs), 1 265(vs), 1 215(s), 1 173(vs), 1 131(s), 1 099(s), 1 067(m), 1 029(m), 1 003(w), 949(vs), 887(m), 855(m), 820(vw), 735(s), 719(s) cm^{-1}. The ^{1}H spectrum consisted of a quartet of quartets centered at 6.93 p.p.m. (J = 7.5 and 1.5 c.p.s.).

Reaction of 1,1,1-Trifluoropropyne with Dimethylarsine

The propyne (6.0 g) and dimethylarsine (4.0 g) were left at 20° for 5 days. The excess alkyne was recovered by trap-to-trap distillation and the less volatile fraction was distilled in a nitrogen atmosphere to give 3.0 g of a product of formula $(CH_3)_2AsC_3F_3H_2$, b.p. 100° (Found: C, 30.2; H, 4.19; As, 37.4, F, 28.7. Calcd. for $C_5H_8AsF_3$: C, 30.0; H, 4.0; As, 37.5; F, 28.5). The ^{1}H n.m.r. spectrum of this product indicated it to be a mixture of isomers, the low field region and the assignments are shown in Fig. 2. The high field spectrum

Can. J. Chem. Downloaded from www.nrcresearchpress.com by 210.87.254.6 on 09/05/12
For personal use only.

showed peaks at 0.83 p.p.m. (*trans*) and 0.75 p.p.m. (*cis* and iso). The fraction was separated into two components by v.p.c. (dinonyl phthalate at 120°) the first being a mixture of the *trans*- and iso-compounds, the second being the *cis*-isomer. Infrared spectrum of the *cis*-isomer (vapor): 3 000(w), 2 915(w), 1 622(m), 1 424(w), 1 355(s), 1 280(vs), 1 192(vs), 1 146(vs), 1 125(vs), 892(w), 855(m), 714(m) cm^{-1}. The ^1H n.m.r. spectrum was as derived in Fig. 2 except that at high resolution $J_{H\text{--}CF_3}$ is 0.6 c.p.s. A sample of the *cis*-isomer was heated for 3 days at 110°, 3 days at 135°, and 1 day at 150° without change. However, at 175° the *trans*-isomer was slowly formed and after 12 days at this temperature almost complete isomerization had occurred. Infrared spectrum of the *trans*-isomer (vapor): 3 025(w), 2 940(w), 1 642(m), 1 435(w), 1 357(vw), 1 308(vs), 1 283(vs), 1 230(vs), 1 197(vs), 1 145(vs), 970(m), 895(w), 864(m), 722(m) cm^{-1}. The ^1H n.m.r. spectrum was as derived. A sample of the *cis*-isomer was also converted almost completely to the *trans*-compound by ultraviolet irradiation for 1 week (10 cm from 100 watt G.E. lamp).

Comparison of the infrared spectra of the *cis*- and *trans*-compounds with that of the original reaction product showed that the main bands associated with the iso-compound occur at 1 410(m), 1 220(w), 1 170(vs), 1 100(vs), 950(m) cm^{-1}.

Reaction of Hexafluorobut-2-yne with Diphenylphosphine

The phosphine (6.1 g, 32.8 mmoles) reacted immediately at 20° with hexafluorobut-2-yne (8.6 g, 53.0 mmoles) to give a viscous dark-brown material. All the butyne was consumed. The product was extracted with chloroform and distilled at 10^{-3} mm to give *2-diphenylphosphino-1,1,1,4,4,4-hexafluorobutene* b.p. 127° (Found: C, 55.1; H, 2.9; F, 32.9; P, 8.74; mol. wt. (Rast), 353. Calcd. for $C_{16}H_{11}F_6P$: C, 55.2; H, 3.2; F, 32.8; P, 8.91; mol. wt. 348). Infrared spectrum (liquid film): 3 100(w), 1 641(vw), 1 596(vw), 1 488(w), 1 445(m), 1 367(m), 1 334(m), 1 282(sh,s), 1 263(vs), 1 237(vs), 1 202(sh,s), 1 167(vs), 1 137(sh,w), 1 119(sh,w), 1 091(m), 1 072(w), 1 026(w), 1 000(w), 874(w), 841(sh,vw), 742(s), 733(sh,w), 694(s) cm^{-1}. ^1H n.m.r. spectrum: broad peak at 6.86 p.p.m. mainly due to aromatic protons, and a quartet (J = 9 c.p.s.) centered at 5.24 p.p.m. Between these lies a multiplet of 6 peaks (J = 8–9 c.p.s.) centered at 6.2 p.p.m. Both the quartet and the multiplet show secondary splittings (J = 1–2 c.p.s.).

Reaction of Dimethylamine with Hexafluorobut-2-yne

The acetylene (19.3 g) and amine (1.4 g) reacted immediately on melting. The recovered butyne weighed 13.4 g. The reaction product, which condensed in a trap cooled to −78°, distilled at 96–97° in a nitrogen atmosphere. An analytical sample of *2-dimethylamino-1,1,1,4,4,4-hexafluorobutene* was obtained by v.p.c. (dinonyl phthalate at 82°) (Found: C, 34.5; H, 3.5; N, 7.25. Calcd. for $C_6H_7F_6N$: C, 34.8; H, 3.4; N, 6.8). One small impurity was also isolated by v.p.c. from the reaction mixture and it proved to be 1,1,1,4,4,4-hexafluoropropanone (Found: C, 26.8; H, 1.31; F, 63.1. Calcd. for $C_4H_2F_6O$: C, 26.7; H, 1.12; F, 63.3. ^1H n.m.r. spectrum: quartet at 3.04 p.p.m. (J = 9 c.p.s.); infrared spectrum: carbonyl absorption at 1 790 cm^{-1}). When the reaction was done in an n.m.r. tube using excess acetylene as solvent, all the amine was used up immediately on mixing and the ^1H n.m.r. spectrum of the product showed quartets at 4.62 and 4.16 p.p.m. (J = 9.1 and 9.1 c.p.s. respectively) and slightly split methyl peaks at 2.41 and 2.24 p.p.m. The relative area of the downfield quartet to the downfield methyl peak (the *trans*-isomer) was 1:6. The other peaks are associated with the *cis*-isomer (relative area 1:6). The initial reaction product contains both isomers in the ratio of *trans*:*cis* = 6.2:1. Distillation of the isolated product mixture gave a fraction containing predominantly (>98%) the *trans*-isomer. However, if the initial reaction product is left exposed to air at 20° the proportion of *cis*-isomer increases as follows.

Time of exposure to air	*cis*:*trans*
10 min	1:6.5
25 min	1:1.9
2 days	1:1.7
12 days	1:1.6

The 1:1.6 (*cis*:*trans*) mixture was sealed and heated in the absence of air for 1 h at a variety of temperatures up to 140°. Slight darkening occurred at the higher temperatures but no change in isomer distribution was detected even though a second phase began to appear.

The infrared spectrum of the *trans*-isomer (98%) showed the following absorption bands (vapor): 2 915(m), 2 845(m), 1 710(w), 1 660(vs), 1 514(m), 1 476(m), 1 434(s), 1 310(vs), 1 274(vs), 1 239(vs), 1 195(vs), 1 156(vs), 1 127(vs), 1 069(s), 939(m), 859(s), 771(m), 730(w), 696(w), 654(s) cm^{-1}. The ^{19}F spectrum of the same sample showed a doublet (J = 9.4 c.p.s.) of septets (J = 1.7 c.p.s.) at 24.8 p.p.m. and a broad singlet at 11.4 p.p.m. Heteronuclear decoupling experiments showed that the doublet and septet splittings were due to coupling with hydrogen. Removal of hydrogen coupling still left broad fluorine peaks. The ^{19}F spectrum of a *cis–trans* mixture (ca. 1:1.5) showed a complex multiplet at 24.8 p.p.m. due to both isomers, a quartet (J = 12.6 c.p.s.) at 15.3 p.p.m. (*cis*-isomer), and a broad singlet at 11.0 p.p.m. (*trans*-isomer).

Reaction of Dimethylamine with 1,1,1-Trifluoropropyne

The amine (1.2 g) and the propyne (6.0 g) reacted violently well below room temperature. Propyne (4.1 g) was recovered and 2.1 g of a 1:1 adduct was produced. The adduct distilled with decomposition at 118° in a

Can. J. Chem. Downloaded from www.nrcresearchpress.com by 210.87.254.6 on 09/05/12
For personal use only.

nitrogen atmosphere and only 0.5 g of distillate were collected. Analysis indicated that the formula of the distillate was $(CH_3)_2NC_3H_2F_3$ (Found: C, 43.0; H, 5.7; F, 41.0; N, 10.3. Calcd. for $C_5H_8F_3N$: C, 43.2; H, 5.8; F, 41.0, N, 10.1). Infrared spectrum (vapor): 2 915(m), 2 820(w), 1 736(w), 1 660(vs), 1 488(w), 1 447(m), 1 362(s), 1 307(s), 1 258(s), 1 229(s), 1 154(sh,vw), 1 102(w), 1 076(vs), 960(s), 888(s), 845(m), 739(m), 678(s) cm^{-1}. ^1H n.m.r. spectrum peaks at 2.29 (CH_3—), 6.17 (H_α) and 3.66 (H_β) p.p.m. with $J_{CF_3\text{--}H\alpha} = 1.5$ c.p.s., $J_{H\alpha\text{--}H\beta} = 13$ c.p.s., and $J_{CF_3\text{--}H\beta} = 6.5$ c.p.s. $H_\alpha H_\beta$ are defined as in Fig. 2.

ACKNOWLEDGMENTS

The authors are grateful to the National Research Council and Defence Research Board of Canada for financial assistance. They also wish to thank Dr. L. D. Hall for assistance in obtaining the ^{19}F n.m.r. spectra, Mr. Peter Brierley for experimental assistance, and the Ansul Chemical Company for gifts of dimethylarsinic and methylarsonic acids.

REFERENCES

1. R. N. Haszeldine. J. Chem. Soc. 3490 (1952).
2. F. W. Stacey and J. F. Harris. J. Am. Chem. Soc. **85**, 963 (1963).
3. W. R. Cullen, D. S. Dawson, and G. E. Styan. J. Organometal. Chem. **3**, 406 (1965).
4. W. R. Cullen and G. E. Styan. J. Organometal. Chem. In press.
5. P. M. Treichel, E. Pitcher, and F. G. A. Stone. Inorg. Chem. **1**, 511 (1962).
6. J. B. Wilford and F. G. A. Stone. Inorg. Chem. **4**, 93 (1965).
7. W. R. Cullen. Unpublished results.
8. W. A. Anderson, R. Freeman, and C. A. Reilly. J. Chem. Phys. **39**, 1518 (1963).
9. A. H. Lewin. J. Am. Chem. Soc. **86**, 2303 (1964).
10. D. Seyferth and L. G. Vaughan. J. Organometal. Chem. **1**, 138 (1963).
11. L. J. Bellamy. Infrared spectra of complex molecules. 2nd ed. Methuen, London. 1958.
12. W. E. Truce and D. L. Goldhamer. J. Am. Chem. Soc. **81**, 5798 (1959).
13. W. E. Truce and D. L. Goldhamer. J. Am. Chem. Soc. **81**, 5795 (1959).
14. F. W. Hoover and D. D. Coffman. J. Org. Chem. **29**, 3567 (1964).
15. R. A. Raphael. Acetylenic compounds in organic synthesis. Butterworths, London. 1955.
16. J. F. Arens. *In* Advances in organic chemistry. Vol II. *Edited by* R. A. Raphael, E. C. Taylor, and H. Wynberg. Interscience, New York. 1960.
17. W. R. Cullen and D. C. Frost. Can. J. Chem. **40**, 390 (1962).
18. L. Burnelle. Tetrahedron, **20**, 2403 (1964).

Can. J. Chem. Downloaded from www.nrcresearchpress.com by 210.87.254.6 on 09/05/12
For personal use only.

Can. J. Chem. Downloaded from www.nrcresearchpress.com by 210.87.254.6 on 09/05/12
For personal use only.

THE ELECTRON SPIN RESONANCE SPECTRA OF DINITRONAPHTHALENE ANION RADICALS

P. H. H. FISCHER[1] AND C. A. MCDOWELL
Department of Chemistry, University of British Columbia, Vancouver, British Columbia

Received July 23, 1965

ABSTRACT

The radical anions of 1,4-dinitronaphthalene, 1,5-dinitronaphthalene, and 1,8-dinitronaphthalene have been generated by electrolytic means, and their e.s.r. spectra recorded. The spectra consist of 61, 111, and 85 lines respectively, and can be analyzed in terms of one nitrogen and three proton coupling constants, consistent with the full symmetry of the species giving rise to them. These constants are, for 1,4-dinitronaphthalene: $a_N = 0.97$ G, $a_{H2} = 1.69$ G, $a_{H5} = 0.53$ G, and $a_{H6} = 0.41$ G; for 1,5-dinitronaphthalene: $a_N = 2.30$ G, $a_{H2} = 2.42$ G, $a_{H3} = 0.44$ G, and $a_{H4} = 2.82$ G; for 1,8-dinitronaphthalene: $a_N = 3.03$ G, $a_{H2} = 3.63$ G, $a_{H3} = 0.95$ G, and $a_{H4} = 3.73$ G. Whereas the nitrogen coupling constants can be unambiguously assigned, this, in the absence of deuteration studies say, is not the case for the three sets of equivalent protons. As an aid in the assignment of proton coupling constants, Hückel LCAO calculations and simplified SCFMO calculations by the method of McLachlan have been performed. The first mentioned of the above proton constants could thus be assigned with reasonable certainty, the remaining two a_{Hi} remain ambiguous.

INTRODUCTION

The electron spin resonance (e.s.r.) spectra of paramagnetic species formed by reduction of nitro-substituted aromatic systems have been investigated by several groups of workers. Paramagnetic species have been formed by several processes: by the chemical reduction with alkali metals (1–4), a procedure yielding results which are not without ambiguity, by the more elegant electrolytic method (5–13), and more recently by photolytic methods (14, 15). In the course of our studies of radical anions produced by electrolytic means, we have been able to obtain, amongst many already known ones, the e.s.r. spectra of the anions of the 1,4-, 1,5-, and 1,8-isomers of dinitronaphthalene. Constructed theoretical spectra show good agreement with experimental spectra and it furthermore appears as if no gross anomalies in the linewidths and intensities exist, a search for these being the primary reason for an investigation of the above radical anions. Expecially the 1,8-isomer, also the 1,5-isomer, might be thought to give rise to such anomalies, since the structural arrangement of the nitro groups is similar to the 1,3-dinitrobenzene, where such anomalies have been observed (16, 17), and since no quinonoid structures can be formulated to indicate an inhibition of rotational freedom of the nitro groups. The oxygen atoms of adjacent nitro groups in the 1,8-dinitronaphthalene anion will, however, be in closer proximity than in the 1,3-dinitrobenzene anion, such that a steric effect may prevent free rotation of the nitro groups.

EXPERIMENTAL

Aldrich Chem. Co. 1,4-dinitronaphthalene was recrystallized from chloroform and sublimed under vacuum, to yield pale yellowish crystals of m.p. 130.5–131.5° C (lit. 131–132 °C). 1,5-Dinitronaphthalene was recrystallized from benzene and sublimed to give yellowish plates of m.p. 217–218 °C (lit. 217.5 °C). Flucka AG 80% technical grade 1,8-dinitronaphthalene was repeatedly sublimed and recrystallized until yellowish plates of m.p. 173–175 °C (lit. 173–173.5 °C) were obtained.

Solvents employed were of spectroscopic grade, distilled from P_2O_5 (excepting DMF), and degassed by freezing, pumping, and melting several times. The solvents were stored on a vacuum system and distilled directly into the electrolysis cell described elsewhere (13). Tetra-*n*-propylammonium perchlorate was used as supporting electrolyte and prepared by the method of Geske and Maki (5).

[1]*Present address: Max-Planck Institut f. mediz. Forschung, Institut f. Chemie, Heidelberg/Germany Jahnstrasse 29.*

The spectrometer employed was a Varian X-band spectrometer using 100 kc field modulation. The magnetic field was supplied by a Varian V4012B 12 in. magnet, and monitored using a proton resonance magnetometer.

RESULTS AND DISCUSSION

A. Experimental Results

1,4-Dinitronaphthalene.—When a 10^{-4} *M* solution of 1,4-dinitronaphthalene, with dimethylformamide (DMF) as solvent, was electrolyzed at −0.5 V vs. saturated calomel electrode (s.c.e.), a brown solution resulted exhibiting the hyperfine pattern shown in Fig. 1. The spectrum consists of 61 lines (theoretically 135 lines are possible) and has an overall splitting of only 9.15 G. This is a remarkably small total splitting, as total splittings of nitro-substituted aromatic systems are generally in the range 20 to 30 G. For 1,4-dinitrobenzene anion, the measured overall splitting is, however, also only 10.7 G. Linewidths of perfectly resolved lines towards the edge of the spectrum are 80 mG between points of maximum slope. The spectrum can be quite well reproduced by the following set of coupling constants $a_N = 0.97$ G, $a_{Hx} = 1.69$ G, $a_{Hy} = 0.53$ G, and $a_{Hz} = 0.41$ G, and is also shown in Fig. 1. The overall splitting of this spectrum is 9.14 G, in excellent agreement with the experimentally determined value. In a mixture of 80% dimethoxyethane (DME) and 20% acetonitrile, an identical spectrum was obtained, while in pure acetonitrile a remarkable drop in the degree of resolution occurred.

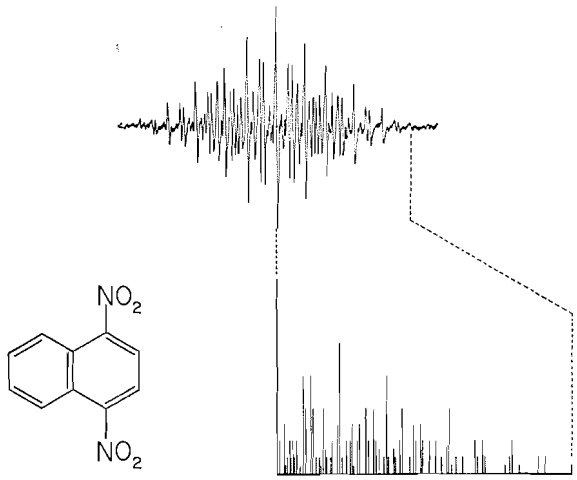

FIG. 1. Electron spin resonance and theoretical spectrum of 1,4-dinitronaphthalene anion radical.

1,5-Dinitronaphthalene.—Electrolysis at −0.62 V vs. s.c.e. of a 10^{-4} *M* solution of 1,5-dinitronaphthalene in DMF resulted in a reddish brown solution, which exhibited the spectrum shown in Fig. 2. This spectrum, under very low modulation and slow scanning conditions, exhibits 111 of the 135 possible lines, and has an overall splitting of 20.70 G. The linewidths of well-resolved hyperfine components are 70 mG, close to the limiting linewidth of the spectrometer employed. The spectrum showed little solvent and temperature dependence and can be analyzed in terms of four coupling constants: $a_N = 2.30$ G, $a_{Hx} = 2.82$ G, $a_{Hy} = 2.42$ G, and $a_{Hz} = 0.44$ G. The theoretical spectrum, of total width 20.56 G, again shows good agreement with the experimental one, and is also given in Fig. 2.

Can. J. Chem. Downloaded from www.nrcresearchpress.com by 210.87.254.6 on 09/05/12
For personal use only.

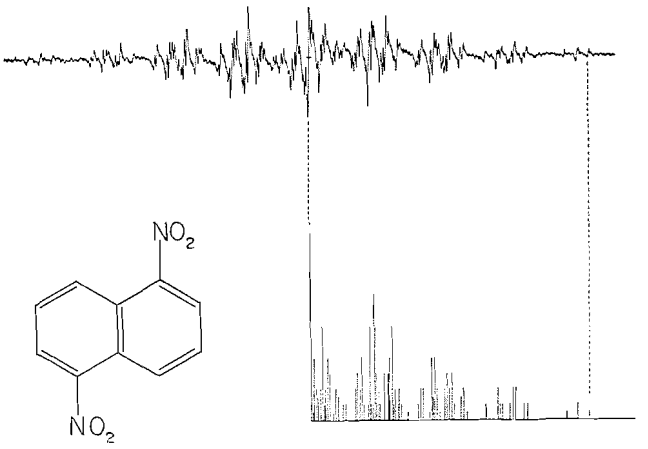

FIG. 2. Electron spin resonance and theoretical spectrum of 1,5-dinitronaphthalene anion radical.

1,8-Dinitronaphthalene.—When a 5×10^{-4} *M* solution of 1,8-dinitronaphthalene in DMF was subjected to reduction at -0.6 V vs s.c.e., a green-yellow solution resulted, showing the hyperfine pattern of Fig. 3. It consists of 85 lines spread over 29.38 G, and linewidths of well-resolved components are 140 mG between points of maximum slope. This is somewhat higher than for the other isomeric species and many other nitroaromatic anions. The spectrum can be reproduced by the following coupling constants: $a_N = 3.03$ G, $a_{Hx} = 3.73$ G, $a_{Hy} = 3.63$ G, and $a_{Hz} = 0.95$ G. The spectrum is shown in Fig. 3.

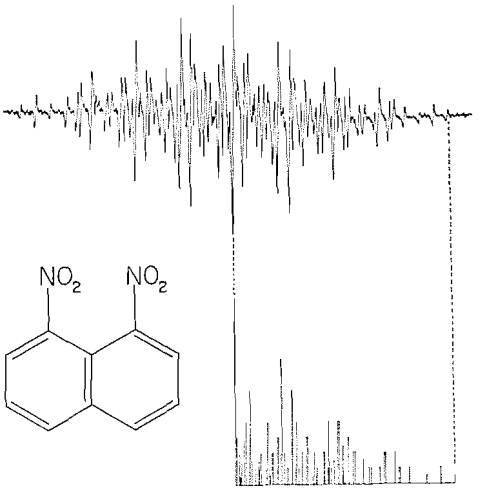

FIG. 3. Electron spin resonance and theoretical spectrum of 1,8-dinitronaphthalene anion radical.

B. Molecular Orbital Calculations

The Hückel LCAO calculations which were performed as an aid in assignment of proton coupling constants employed the Coulomb and exchange parameters suggested by Rieger and Fraenkel (11) namely

$$\alpha_O = \alpha_C + 1.4\beta_{cc},\ \alpha_N = \alpha_C + 2.2\beta_{cc},\ \beta_{CN} = 1.2\beta_{cc},\ \beta_{NO} = 1.67\beta_{cc}$$

Can. J. Chem. Downloaded from www.nrcresearchpress.com by 210.87.254.6 on 09/05/12
For personal use only.

Can. J. Chem. Downloaded from www.nrcresearchpress.com by 210.87.254.6 on 09/05/12
For personal use only.

these parameters having been found to give reasonable agreement with a substantial body of experimental results. Introduction of what amounts to an approximation of configuration interaction has been done via McLachlan's (20) method. For the McLachlan-type calculations Hückel orbitals for β-spin electrons were employed, while a set of orbitals for α-spin electrons is calculated with the exchange integrals β_{rs} unchanged, but with the Coulomb integral modified to $\alpha_r = \alpha + 2\lambda|C_{or}|^2\beta$. Here α is the Hückel-type Coulomb integral, C_{or} is the LCAO coefficient of atom r in the Hückel odd electron orbital, and λ is a constant, here taken as 1.2. The spin density ρ_r at atom r is now given by

$$\rho_r = |C_{or}|^2 + \sum_i (|C_{ir}|^2 - |C_{ir}'|^2)$$

where the primed and unprimed coefficients refer to orbitals of β and α spin, respectively. The summation occurs over all filled orbitals. If the dinitronaphthalenes are labelled as follows

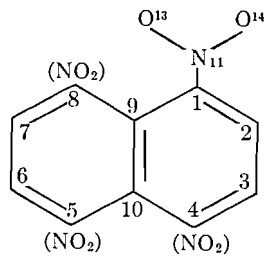

then column 3 of Table I reproduces the calculated Hückel spin densities and column 4 the corresponding McLachlan spin densities, while column 5 shows the experimentally determined values using the McConnel equation (18) and a value of $Q_{CH}^{H} = -23.7$ G (19). The experimentally determined coupling constants are given in the last column.

TABLE I

Calculated and experimental spin densities of isomeric dinitronaphthalene anion radicals

Radical anion	Position	Hückel	McLachlan	Expt.	a_i
1,4-Dinitronaphthalene	1	.0923	.1024	—	—
	2	.0707	.0711	.0713	1.69
	5	.0274	.0288	(.0224)	(0.53)
	6	.0209	.0146	(.0173)	(0.41)
	9	.0147	.0016	—	—
	11	.0820	.0811	—	0.97
	13	.0961	.1002	—	—
1,5-Dinitronaphthalene	1	.0540	.0485	—	—
	2	.0757	.0903	(.1021)	(2.42)
	3	.0296	.0067	.0186	0.44
	4	.0979	.1290	(.1190)	(2.82)
	9	.0106	−.0087	—	—
	11	.0743	.0741	—	2.30
	13	.0790	.0801	—	—
1,8-Dinitronaphthalene	1	.0356	.0028	—	—
	2	.1228	.1763	(.1532)	(3.63)
	3	.0095	−.0455	(−).0401	0.95
	4	.1412	.2152	(.1574)	(3.73)
	9	0	−.0095	—	—
	10	0	−.0431	—	—
	11	.0631	.0618	—	3.03
	13	.0639	.0579	—	—

Can. J. Chem. Downloaded from www.nrcresearchpress.com by 210.87.254.6 on 09/05/12
For personal use only.

Some of the above values of the calculated and experimental spin densities correspond quite closely, others show rather large discrepancies. As is usual, the first question to be posed is whether a different value of $Q_{CH}{}^{H}$ might yield better results, but only a rather arbitrary choice of Q_{CH} is possible. Values ranging from -22.5 to -30 G have, of course, been employed. For nitro compounds, many calculations of the Hückel and McLachlan type have been performed by Fraenkel and collaborators, yielding in some cases excellent, in other very poor, agreement. The chief advantage of the McLachlan and more elaborate SCF methods, is that of providing estimates of the negative spin densities at certain nuclei.

For the first mentioned of the anion radicals one set of proton coupling constants is approximately 3 to 4 times larger than the remaining two, as is also the case for the calculated spin densities of one set of carbon atoms contiguous to protons, so that one of the assignments can be made with reasonable certainty. This assignment places the 1.69 G splitting as arising from the 2 and 3 protons, the protons situated on the same ring as the nitro groups. Intuitively this assignment seems correct. The other two calculated coupling constants differ by only 80 mG and remain ambiguous. They are consequently bracketed, as are the spin densities derived from them. For the 1,5-dinitronaphthalene anion, a very similar situation is found, one coupling constant being approximately 1/6 the value of the remaining two. An inspection of Table I shows that this coupling constant must be assigned to position 3 and 7 protons. The McLachlan spin densities show improved agreement with experimentally determined ones. For the last isomeric species, the same considerations apply, placing the 0.95 G splitting as arising from positions 3 and 6 protons. Here agreement between McLachlan and experimental spin density is remarkably good, although the sign of the latter is not a result of our measurements and is bracketed. A further comment is with regard to the zero spin density at carbon atoms 9 and 10 of the last species, this being a consequence of the type of calculation employed. Since the Hückel wave function has a node at the twofold symmetry axis, spin density at C_9 and C_{10} is expected to be zero or very small. Since no protons are attached here, and no splitting can be observed as a consequence, it cannot be as clearly demonstrated, as for the 1,3-dinitrobenzene anion radical say, that negative spin densities occur at these positions. It is a well-known fact, however, that at positions for which a Hückel calculation shows zero or small spin densities, one often finds sites of negative spin when more elaborate calculations are employed. It is hence quite likely that at these positions negative spin densities occur, a statement supported by the considerably larger overall splitting of this isomer. McLachlan-type calculations bear this out. The overall splitting is $\sim$30 G, a value to be compared with the 10–20 G range of the other two isomers and certain other dinitro anion radicals. In the 10–20 G category, the lower value is often found when quinonoid-type structures may be drawn, indicative of greater coplanarity of nitro groups and aromatic ring system.

C. Nitrogen Coupling Constants

The nitrogen coupling constants for the isomeric dinitronaphthalenes show a variation from 0.97 G in the 1,4-isomer to 3.03 G in the 1,8-isomer. This variation in the coupling constants of isomeric species has been observed for other systems. For mononitro aromatic anions, nitrogen coupling constants between 5 and 15 G are generally observed. Comparing the present results with those for the isomeric dinitrobenzenes, we find for the 1,4-isomer a value for an a_N of 1.56 G, for the sterically hindered 1,2-isomer a value of 2.82 G to be compared with 3.03 G of 1,8-dinitronaphthalene, and a value of $\sim$4 G for the 1,3-dinitrobenzene anion. It thus appears in the dinitronaphthalenes, also, that the smallest a_N is observed whenever quinonoid resonance indicates a higher degree of planarity, while

otherwise larger constants are found. The dinitronaphthalene results are qualitatively in agreement with calculations by Rieger and Fraenkel (11), who performed MO calculations, employing a variation of the overlap integral β to indicate variation in the benzene ring/nitro group angle, and whose results indicate a larger splitting constant for nitrogen nuclei of nitro groups rotated out of the carbon skeleton plane.

Rieger and Fraenkel (11) have derived an equation, which defines the nitrogen coupling constant a_N in terms of various parameters S^N and Q_{xy}, and the spin density on the surrounding atoms and N nucleus. Their relation was derived employing McLachlan spin densities and is

$$a_N = K_N\rho_N{}^\pi + 2Q_{ON}{}^N\rho_O{}^\pi + Q_{CN}{}^N\rho_C{}^\pi$$

where all symbols have their usual meaning and the constants have the best values $K_N = (S_N + Q_{NC}{}^N + 2Q_{NO}{}^N) = \pm 99.0$ G, $Q_{ON}{}^N = \mp 35.8$ G, with $Q_{CN}{}^N$ negligibly small. With these values, nitrogen hyperfine coupling constants of 0.86, 1.60, and 1.97 G are calculated for the 1,4-, 1,5-, and 1,8-dinitronaphthalene anion radicals, respectively. These constants will not be of value employing Hückel spin densities, as their magnitude could be quite different. We have as a consequence derived by a least squares method on eight experimental results, a set of constants to be used with Hückel spin densities, so that the above relation takes the form

$$a_N = \pm 179\rho_N{}^\pi \mp 149.2\rho_O{}^\pi \pm 8.06\rho_C{}^\pi$$

that is, the above constants are: $K_N = (S^N + Q_{NC}{}^N + 2Q_{NO}{}^N) = \pm 179$ G, $Q_{ON}{}^N = \mp 74.6$ G, and $Q_{CN}{}^N = \pm 8.06$ G. The ratio of the two constants, as well as the relative sign, is similar to that derived by Rieger and Fraenkel, with $Q_{CN}{}^N$ also quite small. With these constants excellent agreement between calculated and experimented results can be found for some systems, poorer agreement for others. In general the agreement between calculated and experimental nitrogen coupling constants in nitro aromatic radicals is not as good as the remarkable agreement which has been found for nitrile anions (21), even when McLachlan spin densities are employed. For the dinitronaphthalene the agreement is not so impressive.

	a_N (G)	Hückel a_N (calcd.) (G)	McLachlan a_N (calcd.) (G)
1,4-Dinitronaphthalene	0.97	1.08	0.86
1,5-Dinitronaphthalene	2.30	1.96	1.60
1,8-Dinitronaphthalene	3.03	2.50	1.97

Now it has been found that large discrepancies occur when steric factors are operative (as in the 1,8-dinitronaphthalene anion), or when quinonoid resonance is possible (1,4-dinitronaphthalene radical falls into this category.) A more fundamental reason for the not overly impressive agreement is the fact that Hückel spin densities are employed. It is almost certain that these do not represent a true picture of the spin density distribution, as is likewise the case for McLachlan spin densities in such highly substituted aromatic systems. Secondly, it has become apparent that specific effects, such as steric and solvent influences, must be accounted for individually. This is evidenced by a solvent dependence of many observed coupling constants, and it is felt that even comparison of results obtained in the same solvent, need not necessarily be meaningful.

ACKNOWLEDGMENT

We wish to thank the National Research Council of Canada for grants in aid of this work. One of us (P. H. H. F.) thanks the same body for studentships from 1960 to 1963.

Can. J. Chem. Downloaded from www.nrcresearchpress.com by 210.87.254.6 on 09/05/12
For personal use only.

Can. J. Chem. Downloaded from www.nrcresearchpress.com by 210.87.254.6 on 09/05/12
For personal use only.

REFERENCES

1. T. L. CHU, G. E. PAKE, D. E. PAUL, J. TOWNSEND, and S. I. WEISSMAN. J. Phys. Chem. **57**, 504 (1953).
2. R. L. WARD and M. P. KLEIN. J. Chem. Phys. **26**, 518 (1958).
3. R. L. WARD. J. Chem. Phys. **32**, 410 (1960).
4. R. L. WARD. J. Am. Chem. Soc. **83**, 1297 (1961).
5. D. H. GESKE and A. H. MAKI. J. Am. Chem. Soc. **82**, 2671 (1960).
6. A. H. MAKI and D. H. GESKE. J. Chem. Phys. **33**, 825 (1960).
7. A. H. MAKI and D. H. GESKE. J. Am. Chem. Soc. **83**, 1852 (1961).
8. M. T. MELCHIOR and A. H. MAKI. J. Chem. Phys. **34**, 471 (1961).
9. L. H. PIETTE, P. LUDWIG, and R. N. ADAMS. J. Am. Chem. Soc. **83**, 3909 (1961); **84**, 4212 (1962).
10. J. H. FREED and G. K. FRAENKEL. J. Chem. Phys. **37**, 1156 (1962).
11. P. H. RIEGER and G. K. FRAENKEL. J. Chem. Phys. **39**, 609 (1963).
12. P. H. FISCHER. Thesis, University of British Columbia, Vancouver, B.C. (1963).
13. P. H. FISCHER and C. A. MCDOWELL. Mol. Phys. **8**, (1964).
14. C. LAGERCRANTZ and M. YHLAND. Acta Chem. Scand. **16**, 1043 (1962); **16**, 1799 (1962).
15. R. L. WARD. J. Chem. Phys. **38**, 2588 (1963).
16. J. H. FREED, P. H. RIEGER, and G. K. FRAENKEL. J. Chem. Phys. **37**, 1881 (1962).
17. P. H. FISCHER and C. A. MCDOWELL (unpublished); see also C. A. MCDOWELL. Rev. Mod. Phys. **35**, 528 (1963).
18. H. M. MCCONNELL. J. Chem. Phys. **24**, 633 (1956) and other publications.
19. M. KARPLUS and G. K. FRAENKEL. J. Chem. Phys. **35**, 1312 (1961).
20. A. D. MCLACHLAN. Mol. Phys. **3**, 233 (1960).
21. P. H. RIEGER and G. K. FRAENKEL. J. Chem. Phys. **37**, 2795 (1962).

Can. J. Chem. Downloaded from www.nrcresearchpress.com by 210.87.254.6 on 09/05/12
For personal use only.

THE REACTION OF SULFONYLIMIDO INTERMEDIATES WITH AROMATIC COMPOUNDS[1]

R. A. ABRAMOVITCH, J. ROY,[2] AND V. UMA
Department of Chemistry, University of Saskatchewan, Saskatoon, Saskatchewan

Received June 14, 1965

ABSTRACT

Thermolysis of methanesulfonyl azide in aromatic solvents gives methanesulfonamide and the isomeric methanesulfonanilides. The orientation of the latter and the relative reactivities of the aromatic substrate towards attack by the methylsulfonylimido intermediate have been studied quantitatively. The high reactivity and also great selectivity of the attacking species are interpreted in terms of a rate-determining addition process to give a sulfonylaziridine derivative followed by a product-determining ring opening and rearrangement to the substituted anilides. Partial rate factors are discussed, as are possible mechanisms for the formation of the methanesulfonamide. The methanesulfonylimido intermediate must be abstracting *two* hydrogen atoms synchronously from the aromatic substrate.

The thermal decomposition of sulfonyl azides in aromatic solvents was first studied by Curtius and Schmidt (1). The products obtained from the thermal decomposition of benzenesulfonyl azide in various substituted benzenes were shown to be the corresponding benzenesulfonanilides together with benzenesulfonamide (2, 3). The available evidence points to the intermediacy of a sulfonylimido intermediate (sulfonyl nitrene) (II) in both the thermal and photochemically induced reactions of sulfonyl azides (I), except in those cases where an assisted stepwise addition to olefinic double bonds followed by elimination

$$\underset{\text{I}}{R{-}SO_2N_3} \xrightarrow[\text{or } \Delta]{h\nu} \underset{\text{II}}{RSO_2{-}N} + N_2$$

of nitrogen can take place (4). Thus, the thermal decomposition of benzenesulfonyl azide and *t*-butyl hydroperoxide exhibits mutually induced decomposition of both reagents (5). Whereas sulfonyl azides and dimethyl sulfoxide do not react in the dark, photolysis or thermolysis of the azide gives nitrogen and the sulfonylimido intermediate (II) which is trapped by reaction with dimethyl sulfoxide. Thioethers are even more efficient trapping agents (6). *p*-Toluenesulfonyl azide initiates the copolymerization of mixtures of styrene and methyl methacrylate at 60–120° by a free-radical mechanism, but the activity is extremely low (7), suggesting that the intermediate exists mainly in the singlet electrophilic species (II*b*) rather than in the triplet diradical form (II*a*). More recently, the

$$\underset{\text{II}a}{RSO_2{-}\dot{\ddot{N}}\cdot} \rightleftarrows \underset{\text{II}b}{RSO_2{-}\ddot{\ddot{N}}}$$

thermal decomposition of aliphatic and aromatic sulfonyl azides in cyclohexane under pressure at 175° has been investigated (8). C—H insertion products were mainly obtained; *very little hydrogen abstraction was observed* in all cases. With the aliphatic azides a radical chain process resulting in the evolution of sulfur dioxide was found to compete with the

[1]*The present paper is Part XI of the series on aromatic substitution. Part X: Can. J. Chem. In press. 1965. Part of this work was embodied in a lecture given at the Symposium on Reactive Intermediates held at the Université Laval, Québec, in August 1964.*

[2]*National Research Council Postdoctorate Fellow.*

unimolecular decomposition of the azide, though the radical initiator R· could not be identified.

$$C_5H_{11}SO_2N_3 \rightarrow C_5H_{11}SO_2\dot{\underset{\cdot\cdot}{N}} + N_2$$

$$R\cdot + C_5H_{11}SO_2N_3 \rightarrow C_5H_{11}SO_2\cdot + RN_3$$

$$C_5H_{11}SO_2\cdot \rightarrow C_5H_{11}\cdot + SO_2$$

$$C_5H_{11}\cdot + R{-}H \rightarrow C_5H_{12} + R\cdot$$

The radical chain process could be inhibited to a certain extent by the addition of sulfur or of hydroquinone. Good first-order kinetics were observed in the decomposition of *p*-toluenesulfonyl azide.

The behavior of the imido intermediate after its formation will also depend upon the nature of the solvent used. While in aromatic or aliphatic non-polar solvents sulfonyl azides behave as "rigid" azides i.e. they do not undergo a Curtius-type rearrangement, irradiation of a solution of benzenesulfonyl azide in methanol followed by hydrolysis gave a 28% yield of aniline, presumably formed via $C_6H_5NSO_2$ and $C_6H_5NHSO_2OCH_3$ (9).

The orientation and partial and total rate factors in the substitution of benzene derivatives by the benzenesulfonylimido intermediate produced by thermolysis of the azide have been studied (2, 3). The decompositions were carried out at 105–120° and the products analyzed after preliminary hydrolysis of the anilides formed (2) or as the amides but after appreciable pretreatment (3). Of the aromatic compounds studied, most of those with meta-directing substituents did not react to produce the expected substitution products. With the other substituents, the total rate ratios and partial rate factors were said to be consistent with an attack of the aromatic nucleus by the electrophilic free radical $C_6H_5SO_2\dot{\underset{\cdot\cdot}{N}}\cdot$ (3). The failure of compounds with meta-directing substituents to produce the expected substitution products was attributed to complexing of the radical with the electron-rich substituent group (3). Benzoyl chloride gave a 7% yield of products, 90% of which was benzene-sulfonamide, the rest being exclusively the meta product of substitution. A number of observations remain unexplained by the postulated mechanism (10*a*). (i) The total rate ratios (10*b*) (from competitive reactions between C_6H_6 and C_6H_5X with $C_6H_5SO_2N_3$ at 105–120°) were not much different from unity, as expected for a homolytic substitution. However, the values of the total rate ratios ${}^{CH_3}_{H}K = 1.0$, ${}^{CH_3O}_{H}K = 0.96$, ${}^{OH}_{H}K = 0.80$ are unexpected, since such electron-donating substituents should facilitate attack by an electrophilic free radical (11) and lead to total rate ratios greater than unity. (ii) The partial rate factor calculated for attack at the meta position of toluene is unusually low ($F_m = 0.03$) and it is hard to see why F_m should be less than 1 in toluene, either for a free radical or for an electrophilic substitution process. (iii) Isomer ratios differed somewhat according to whether they were determined under competitive conditions or not.

It was felt that these observations needed careful reinvestigation and that, particularly, a more convenient and reliable analytical technique which would involve a minimum amount of manipulation before the actual analysis was carried out would be desirable. Gas-chromatographic analysis was the obvious choice and, in order to facilitate the elution of the reaction products from the column, it was decided to use methanesulfonyl azide* instead of benzenesulfonyl azide as the source for the imido intermediate. The

**A referee has pointed out that methanesulfonyl azide is, apparently, as sensitive to shock and impact as is nitroglycerine. No trouble was experienced in the present work except in the odd cases where reaction mixtures containing large amounts of undecomposed azide were introduced into the heated injector of the gas chromatograph, when explosions resulted which blew out the Teflon dams. Consequently, caution should be used in the handling of this compound.*

Can. J. Chem. Downloaded from www.nrcresearchpress.com by 210.87.254.6 on 09/05/12
For personal use only.

products expected would then be methanesulfonamide $CH_3SO_2NH_2$ (III) and the substituted mesylanilines (IV).

$$CH_3SO_2N_3 \xrightarrow[\text{or } \Delta]{h\nu} CH_3SO_2N$$

$$CH_3SO_2N + RC_6H_5 \rightarrow CH_3SO_2NHC_6H_4R$$

IV

The reaction mixtures were filtered from any tars formed, concentrated, and analyzed directly by gas–liquid chromatography, thus avoiding the possibility of the selective loss of some quantity of one or more of the isomers. All reactions were carried out at 120° under pressure with stirring. Preliminary experiments indicated that similar products were obtained on photolysis of the azides in solution in an excess of the aromatic solvent.

EXPERIMENTAL

Melting points are uncorrected.

Reagents

Reagent thiophene-free benzene and toluene were dried, distilled, and kept over sodium wire. Reagent chlorobenzene and anisole were dried, distilled, and kept over anhydrous sodium sulfate.

Methanesulfonyl Azide

Prepared by the procedure of Horner and Christmann (6), this product was purified by fractional distillation; it had b.p. 71° at 4.5 mm, n_D^{25} 1.4653, and was obtained in 73% yield.

Methanesulfonamide

This was obtained from mesyl chloride and dry ammonia as described by Field and Grunwald (12) and had m.p. 92–93°.

Preparation of Authentic Methanesulfonylanilides

The general procedure described by Marvel, Helfrick, and Belsley (13) was used. A benzene solution of 2 molar equiv of the amine was mixed with 1 equiv of methanesulfonyl chloride in benzene at room temperature. The stirred solution was boiled under reflux from 3 to 12 h. The amine hydrochloride was filtered, the benzene was evaporated *in vacuo*, and the amide was recrystallized from dilute ethanol.

Methanesulphonylanilide had m.p. 101–102°.

o-Methanesulphonyltoluidide had m.p. 106°.

m-Methanesulfonyltoluidide

This compound, prepared by the above method, had m.p. 92–92.5°.

Anal. Calcd. for $C_8H_{11}NO_2S$: C, 51.87; H, 5.99. Found: C, 51.80; H, 6.03.

p-Methanesulfonyltoluidide had m.p. 104.5–105°.

c-Methanesulfonamidochlorobenzene had m.p. 92–93°.

m-Methanesulfonamidochlorobenzene

This compound had m.p. 98–98.5°.

Anal. Calcd. for $C_7H_8ClNO_2S$: C, 40.88; H, 3.92. Found: C, 40.93; H, 4.00.

p-Methanesulfonamidochlorobenzene had m.p. 155–156°.

p-Methanesulfonylanisidide had m.p. 116°.

m-Methanesulfonylanisidide

The compound was obtained as a brown oil which gave a colorless liquid (38%), b.p. 160° at 2.7 mm. The liquid solidified on cooling and could be recrystallized from benzene – light petroleum (b.p. 60–80°) to give colorless crystals, m.p. 67.5°.

Anal. Calcd. for $C_8H_{11}NO_3S$: C, 47.77; H, 5.50. Found: C, 47.90; H, 5.52.

c-Methanesulfonylanisidide, prepared in the usual method, was obtained in 95% yield and had m.p. 69°. Since the reported m.p. is 115.5° (13), the amide was prepared by an alternate method. *o*-Anisidine (3.07 g), dry pyridine (2.23 g), and methanesulfonyl chloride (2.8 g) in benzene (50 ml) were boiled under reflux with stirring for 6 h. A brown gummy solid separated; this was filtered and washed with benzene. The combined filtrates were washed with 15 ml portions of 10% hydrochloric acid and then with water. Evaporation of the solvent gave the amide, which was recrystallized from 95% ethanol (charcoal) and had m.p. 69–69.5°.

Anal. Calcd. for $C_8H_{11}NO_3S$: C, 47.77; H, 5.50. Found: C, 48.05; H, 5.55.

1,2-Diphenoxyethane was prepared by boiling under reflux a mixture of phenol (9.4 g), sodium hydroxide (4 g), and ethylene bromide (9.4 g) for 16 h. The cooled reaction mixture was filtered; the solid was washed with 10% sodium hydroxide solution, washed with water, and recrystallized from 95% ethanol. The product (9.7 g) had m.p. 97.5–98.5°. Simons (14) gives m.p. 97° for this compound.

Can. J. Chem. Downloaded from www.nrcresearchpress.com by 210.87.254.6 on 09/05/12
For personal use only.

Methanesulfonylamidation of Aromatic Nuclei Using Methanesulfonyl Azide

General Procedure

Methanesulfonyl azide was dissolved in an excess of the aromatic substrate (molar ratio of azide to aromatic compound 1:25 – 1:50) and the solution was placed in the reaction bottle of a specially designed apparatus which permitted reactions to be carried out under pressure in a glass vessel at constant temperature while being stirred continuously. A description of this apparatus has been published elsewhere (15). The reaction vessels were immersed in a thermostatted oil bath maintained at 120° and stirred for 48 h. The apparatus consisted of three reaction vessels so that all runs could be carried out in triplicate. The cooled glass vessels were opened very carefully to release the nitrogen which had evolved, and the solutions were filtered from small quantities of black precipitate, the amount of which appeared to depend on the nature of the aromatic substrate. The solutions were then transferred quantitatively to a round-bottomed flask, the last traces being washed out with acetone, and concentrated by distillation from a fractionating column.

The products formed were analyzed qualitatively and quantitatively by gas chromatography. Identification was effected by comparing relative retention times with those of authentic samples and then by direct comparison of melting points and infrared spectra of collected material with those of authentic compounds. The internal standard method (16) was adapted for the quantitative analyses and the reliability of the method checked using authentic mixtures of the isomers. The results are accurate to within ±1%.

Methanesulfonylamidation of Benzene

The reaction of methanesulfonyl azide (0.3 g) with a 25 molar excess of benzene was carried out as described above. The reaction products (methanesulfonamide and mesylaniline) were best analyzed on a 6 ft × 1/4 in. column packed with precipitated asphalt on Chromosorb W (60–80 mesh) (25%). (Asphalt, as supplied by the Wilkens Instrument Co., was dissolved in the minimum amount of hot benzene to which was then added *n*-hexane. The precipitated asphalt was filtered and washed with light petroleum (b.p. 60–80°) until the filtrate was colorless). The column temperature was 220° and the helium inlet pressure 50 p.s.i. (flow rate of 55 ml/min). Under these conditions methanesulfonamide had a retention time of 2.3 min, mesylaniline a retention time of 14.1 min, and coumarin (which was used as the internal standard) a retention time of 10.9 min. No biphenyl (retention time 4.6 min) could be detected in the reaction mixtures. The results are summarized in Table I.

TABLE I

Products of reaction of methanesulfonyl azide with benzene

	Methanesulfonamide (%)	Mesylaniline (%)	Total yield (%)
Synthetic mixture 1	19.1(19.7)*	80.9(80.3)	—
Synthetic mixture 2	18.1(18.2)	81.9(81.8)	—
Expt. No. 1†	13.9	55.7	69.6
Expt. No. 2†	16.2	55.8	72.0
Expt. No. 3†	13.2	52.4	65.6
Mean	14.4	54.6	69.0

*Figures in parentheses refer to known percentage composition.
†Average of triplicate readings.

Methanesulfonylamidation of Toluene

The azide:toluene molar ratio was 1:50. The same column as was used above was also used here to resolve the reaction mixture into its components except that it was operated at 230° and a helium inlet pressure of 40 p.s.i. (flow rate 60 ml/min). Five peaks corresponding to methanesulfonamide, dibenzyl, and the *o*-, *m*-, and *p*-methanesulfonyltoluidides having retention times of 2.05, 5.8, 13.6, 16.2, and 18.35 min, respectively, were observed. Coumarin (retention time 10.1 min) was used as the internal standard. The results (mean of three experiments) were as follows. Total yield of methanesulfonyltoluidide (based on methanesulfonyl azide), 76.8%; methanesulphonamide, 22.7%; dibenzyl, 0.5% (assuming that each molecule of methanesulfonylimido intermediate abstracts one proton from each of two toluene molecules). Isomer ratio: *o*, 65.4%; *m*, 2.4%; *p*, 32.2%. Overall amount of azide accounted for: 99.5%.

The reaction was repeated by using a solution of azide in toluene which had been deaerated by passing nitrogen through it and carrying out the reaction under nitrogen. Under these conditions the yield of mesyltoluidides was 72.2% (*o* 65.1%, *m* 3.0%, *p* 31.8%), that of methanesulphonamide was 24.3%, and that of dibenzyl was 0.4%.

Methanesulfonamidation of Chlorobenzene

The azide:chlorobenzene molar ratio used was 1:50. The same column as above was operated at 240° and a helium inlet pressure of 41 p.s.i. (flow rate 68 ml/min). Four peaks corresponding to methanesulfonamide and the *o*-, *m*-, and *p*-methanesulfonylamidochlorobenzenes, having retention times of 1.3, 7.1, 17.8, and

Can. J. Chem. Downloaded from www.nrcresearchpress.com by 210.87.254.6 on 09/05/12
For personal use only.

20.15 min, respectively, were observed. *p*-Methanesulfonyltoluidide, retention time 10.15 min, was used as internal standard. The results (mean of three experiments) are summarized below.

Yield of methanesulfonylamido chlorobenzene (%)	Yield of methanesulfonamide (%)	Overall yield based on azide (%)	Yield of isomers (%)		
			o	*m*	*p*
65.1	13.1	78.2	57.4	0.9	41.7

Appreciably more tarry matter appeared to be formed in this reaction compared with the toluene one.

Methanesulfonamidation of Anisole

(*a*) The reaction was carried out as above using methanesulfonylazide (0.15 g) in anisole (6.7 ml) (molar ratio 1:50). Analysis on the same column as before, operated at 225° and 50 p.s.i. inlet pressure of helium (60 ml/min flow rate) gave the following retention times: methanesulfonamide, 1.5 min; coumarin (internal standard), 8.5 min; *o*-methanesulfonylanisidide, 16.5 min; *m*-methanesulfonylanisidide, 28.5 min; *p*-methanesulfonylanisidide, 34.0 min; 1,2-diphenoxyethane, 14.0 min. On a 9 ft × 1/4 in. column of 25% Apiezon N on Chromosorb W at 225°, 1,2-diphenoxyethane had a retention time of 30 min while *p*-methanesulfonylanisidide had a retention time of 25 min. The results of the quantitative analyses are summarized in Table II (expts. 4–6).

TABLE II

Products of reaction of methanesulfonylazide with anisole

	Methanesulfonamide (%)	Mesylanisidides (%)	Mesylanisidide (% of total)			Total yield (%)
			o	*m*	*p*	
Synthetic mixture 3	6.9(6.7)†	—	43.3(44.1)	8.3(9.0)	41.5(40.2)	—
Synthetic mixture 4	5.9(6.5)	—	43.5(43.6)	11.9(11.6)	38.7(38.3)	—
Expt. No. 4‡	4.1	67.3	54.9	1.2	43.9	71.4
Expt. No. 5‡	3.6	66.0	55.5	1.2	43.3	69.6
Expt. No. 6‡	3.7	67.4	56.2	1.1	42.7	71.1
Mean	3.8	66.9	55.5	1.2	43.3	70.7
Expt. No. 7‡	8.7	82.4	57.1	1.1	41.8	91.1
Expt. No. 8‡	9.5	82.2	56.0	1.1	42.9	91.7
Expt. No. 9‡	9.0	79.3	56.4	1.2	42.4	88.3
Mean	9.1	81.3	56.5	1.1	42.4	90.4

*Based on azide.
†Figures in parentheses refer to known percentage composition.
‡Average of triplicate determinations.

Some tars were also formed in this reaction and probably account for the balance of the azide. No 1,2-diphenoxyethane could be detected in any of the reaction products.

(*b*) The reaction was carried out as above except that the molar ratio of azide to anisole was 1:25. The results are summarized in Table II (expts. 7–9).

Competitive Reactions

A large excess (100- to 150-fold) of an equimolar mixture of the substituted benzene and benzene over the azide was heated in the sealed glass vessels at 120° as in the case of the non-competitive reactions, and the mixtures were worked up in the same way as before.

Determination of $^{CH_3}_{H}K$

The methanesulfonyl azide to solvent ratios used were 1:100 and 1:150. The gas chromatographic analyses were carried out with an 8 ft × 3/16 in. column packed with 30% Apiezon L on firebrick (60–80 mesh) operated at 220° and a helium inlet pressure of 50 p.s.i. (flow rate 46 ml/min); *o*-, *m*-, and *p*-methanesulfonyltoluidide and mesylaniline had retention times of 10.0, 13.3, 14.9, and 11.7 min, respectively. *o*-Methanesulfonamidochlorobenzene was used as the internal standard and had a retention time of 7.2 min. The results (mean of two experiments each) are summarized below.

Methanesulfonyl azide: solvent molar ratio	$^{CH_3}_{H}K$
1:100	1.84
1:150	1.88
Mean	1.86

Can. J. Chem. Downloaded from www.nrcresearchpress.com by 210.87.254.6 on 09/05/12
For personal use only.

Determination of ${}^{Cl}_{H}K$

The methanesulfonyl azide to mixed solvent ratio was 1:100. The reaction products were analyzed on an 8 ft × 3/16 in. column packed with 30% Apiezon L on firebrick operated at 225° and a flow rate of 46 ml/min. *o*-Methanesulfonamidochlorobenzene, methanesulfonylanilide, and an unresolved mixture of *m*- and *p*-methanesulfonamidochlorobenzenes had retention times of 5.6, 8.7, and 22.9 min, respectively. *p*-Methanesulfonyltoluidide (retention time 11.0 min) was used as the internal standard. The calibration factor for the mixed meta and para isomers was obtained by using a standard solution of these isomers in the same proportion as had been found in the non-competitive studies. The total rate ratio thus determined (mean of three experiments) was ${}^{Cl}_{H}K = 0.44$.

Determination of ${}^{CH_3O}_{H}K$

The analyses were carried out as described in the case of the non-competitive reaction with anisole. The azide to mixed solvents molar ratio employed was 1:100, three experiments being carried out. The total rate ratio found was ${}^{CH_3O}_{H}K = 2.54$. Standard mixtures were run to confirm the accuracy of the determinations.

DISCUSSION

The isomer ratios formed in the mesylamidation of the monosubstituted benzene derivatives studied are collected in Table III. These are to be compared with the corresponding results obtained in the benzenesulfonamidations previously reported (3) (Table IV).

TABLE III

Products obtained on decomposition of $CH_3SO_2N_3$ in C_6H_5X

Substrate	Average yield (%) based on azide	Yield (%) of $CH_3SO_2NH_2$	Yield (%) of $CH_3SO_2NHC_6H_4X$	Isomer ratios		
				o	*m*	*p*
C_6H_6	69.0*	14.4	54.6	—	—	—
$C_6H_5CH_3$	99.5†	22.7	76.8	65.4	2.4	32.2
	96.5‡	24.3	72.2	65.1	3.0	31.8
C_6H_5Cl	78.2	13.1	65.1	57.4	0.9	41.7
$C_6H_5OCH_3$	70.7§	3.8	66.9	55.5	1.2	43.3
	90.4‖	9.1	81.3	56.5	1.1	42.4

*No biphenyl was detected in this reaction.
†An 0.5% yield of dibenzyl was formed in this reaction.
‡Reaction carried out using degassed solvent and under a nitrogen atmosphere; yield of dibenzyl formed = 0.4%.
§Azide:anisole molar ratio was 1:50.
‖Azide:anisole molar ratio was 1:25.

TABLE IV

Composition of products isolated in thermolysis of $C_6H_5SO_2N_3$ in C_6H_5X (3)

Substrate	Average overall yield (%) based on $C_6H_5SO_2N_3$	Yield (%) of $C_6H_5SO_2NH_2$	Yield (%) of $C_6H_5SO_2NHC_6H_4X$	Isomer ratios		
				o	*m*	*p*
C_6H_6	30.2	18	12.2	—	—	—
$C_6H_5CH_3$*	55.3	11	44.3	61	1	38
C_6H_5Cl	38.2	5	33.2	46	2	52
$C_6H_5OCH_3$	36.0	0	36.0	71	2	27

*No dibenzyl formation reported.

The relative reactivities of the substituted benzenes compared with benzene itself were determined using the competitive technique. The total rate ratios are collected in Table V and compared with the total rate ratios reported for benzenesulfonamidation (3). On the basis of these results, apparent partial rate factors can be calculated and are given in Table VI.

The values of the total rate ratios reported here are in accord with the concept of a highly reactive electrophilic species as the reactive attacking reagent. The value for the

Can. J. Chem. Downloaded from www.nrcresearchpress.com by 210.87.254.6 on 09/05/12
For personal use only.

TABLE V

Total rate ratios for sulfonamidation of C_6H_5X

Substrate	Total rate ratio ${}^{X}_{H}K$ using	
	$CH_3SO_2N_3$	$C_6H_5SO_2N_3$ (3)
Toluene	1.86	1.00
Chlorobenzene	0.44	0.69
Anisole	2.54	0.96

TABLE VI

Apparent partial rate factors for sulfonamidation of C_6H_5X

C_6H_5X	Methanesulfonamidation			Benzenesulfonamidation (3)		
	F_o	F_m	F_p	F_o	F_m	F_p
$C_6H_5CH_3$	3.65	0.13	3.59	1.8	0.03	2.3
C_6H_5Cl	0.76	0.01	1.10	0.95	0.04	2.2
$C_6H_5OCH_3$	4.23	0.09	6.6	2.0	0.06	1.6

total rate ratio for toluene, for example, is somewhat more reasonable than the reported (3) value of ${}^{CH_3}_{H}K = 1.0$ for the corresponding benzenesulfonamidation. Also, it is clear that the methoxyl group is activating, as expected for an electrophilic attack, and that the value of ${}^{CH_3O}_{H}K$ of 0.96 reported for the benzenesulfonamidation is suspect. Again, in accord with the concept of a highly reactive electrophilic attacking reagent, chlorobenzene is somewhat deactivated compared with benzene. The chlorine atom has $-I > +M$, and with the highly reactive reagent the $+E$ effect due to the polarizability of the substituent is not called in play to any appreciable extent. A value of ${}_{C_6H_6}{}^{Xy}K = 2$ has been reported recently for the reactivity of *p*-xylene (8), which is of the correct order of magnitude that would be expected from the results described here.

These values of the total rate ratios would, if taken on their own, suggest that the methanesulfonylimido intermediate was behaving as a highly electrophilic free radical, and hence that it was in the diradical triplet state. The corresponding values of ${}^{X}_{H}K$ for substitution by the electrophilic *o*-nitrophenyl free radical are: ${}^{CH_3}_{H}K = 1.16$, ${}^{Cl}_{H}K = 0.83$ (17), while the apparent values for the phenylation of some C_6H_5X using benzenediazonium borofluoride, a reaction in which the reactive species has been postulated to be the phenyl diradical cation (18), are: ${}^{Br}_{H}K = 0.31$, ${}^{CH_3O}_{H}K = 1.45$ (18). The small amount of side-chain hydrogen abstraction, indicated by the yield of dibenzyl formed in the reaction with toluene (Table III), could also be taken in support of the intervention of an electrophilic free radical (17). On the other hand, application of the Wigner spin conservation rule would suggest that the thermal decomposition of the azides should lead *initially* to a singlet imido intermediate, which could subsequently drop to the triplet ground state (the e.s.r. spectrum of $C_6H_5SO_2N$ obtained by photolysis of the azide at 77 °K in a fluorolube matrix has suggested that the ground state, or a state just above the ground state, is the triplet $C_6H_5SO_2\dot{N}\cdot$ (19)). The small amount of side-chain hydrogen abstraction observed in the decomposition in toluene might also be consistent with a singlet imido intermediate. This minor percentage of hydrogen abstraction by sulfonylimido intermediates has also been commented on in a comparative study of the behaviors of azidoformates and sulfonyl azides (8); similarly, when sulfonyl azides are decomposed

Can. J. Chem. Downloaded from www.nrcresearchpress.com by 210.87.254.6 on 09/05/12
For personal use only.

in cyclohexane, less than 5% of the amide RSO_2NH_2 resulting from hydrogen abstraction is obtained (20). No 1,2-diphenoxyethane, which might have been expected to arise by dimerization of $C_6H_5OCH_2\cdot$ had any been formed by hydrogen abstraction, was detected in the present study. The most convincing evidence against a mechanism involving a straightforward aromatic substitution process by an electrophilic free radical comes from the values of the apparent partial rate factors that can be calculated from the total rate and isomer ratios (Table VI). In all cases, the values calculated for ${}^{x}F_m$ are very low indeed. While values of ${}^{x}F_m$ of slightly less than unity have been reported for the free radical phenylation of toluene and anisole, for example (11, 21), the deactivation observed here cannot be explained at all on the basis of an attack by an electrophilic free radical, nor, indeed, can most of these F values if a direct substitution is taking place. We are clearly dealing here with an attack by a highly *reactive* species, but one that *appears* to be highly selective as well. The values are consistent, however, with a two-step process, the first of which is a rate- (but not product-) determining addition step to form a sulfonylaziridine intermediate (V), and the second of which is the product-determining opening and rearrangement of V to give the substituted sulfonylaniline derivative (VI). The influence of the substituent upon the rate-determining step would be rather minor in view of the high reactivity of attacking sulfonylimidogen; its influence would be large, however, in the determination of the direction of ring opening of the various possible three-membered ring intermediates (V) since this process would involve a separation of charges and give rise to the opportunity for the substituent to stabilize the positive

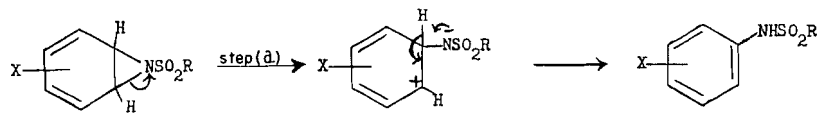

V VI

charge in the nucleus by delocalization. The direction of the ring-opening process (*a*) would then be governed by the relative stabilities of the various dipolar intermediates formed (Scheme 1).

A likely potential energy diagram for this process would be as illustrated in Fig. 1. Transition state 1 (T.S.1) would be the rate-determining one leading to aziridine formation, shown here as a highly exothermic process with a low energy of activation so that substituents will only exert a minor influence upon this energy of activation. Transition state 2 leading to the opening of the aziridine ring has a lower energy than T.S.1 so that formation of V is still rate controlling, though ring opening has a large activation energy and substituents will exert a large effect upon the *direction* of ring opening. The final proton transfer is expected to be faster than ring opening, hence transition state 3 with the lowest energy of the three. A partly concerted mechanism for the ring opening and hydrogen migration could also be visualized such that appreciable charge separation developed in the transition state. In that case, there would be no third maximum (T.S.3) in Fig. 1. Formation of an aziridine by addition to the benzene "double bond" rather than direct substitution has also been suggested to explain the predominant formation of 1-substituted, rather than 9-substituted, product when benzenesulfonyl azide was boiled under reflux with a solution of anthracene (22). In fact, the formation of four very interesting products of unknown structure when sulfonyl azide was heated with *p*-xylene was thought to involve an addition of NSO_2N to two molecules of *p*-xylene (1). Recently, Dewar and Narayanaswami (23) have suggested a mechanism very similar to the one proposed here

Can. J. Chem. Downloaded from www.nrcresearchpress.com by 210.87.254.6 on 09/05/12
For personal use only.

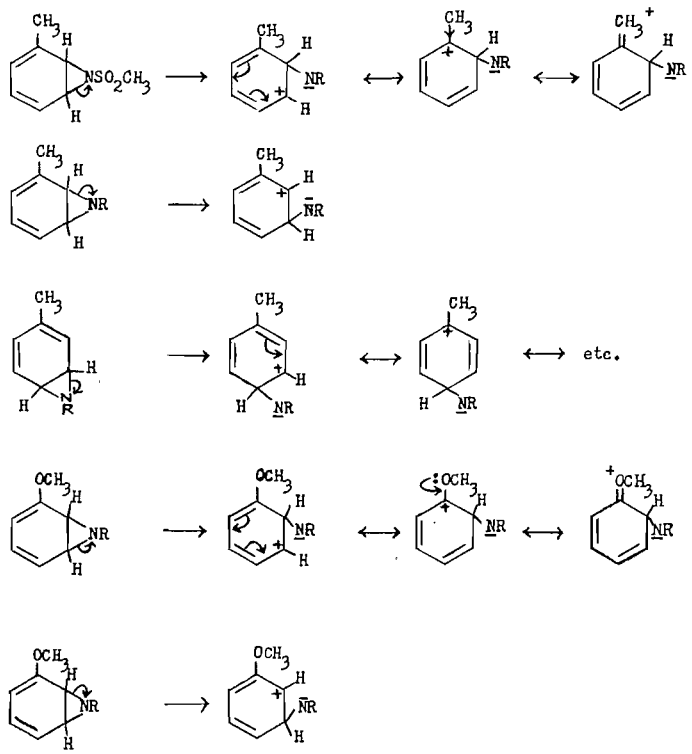

SCHEME I.

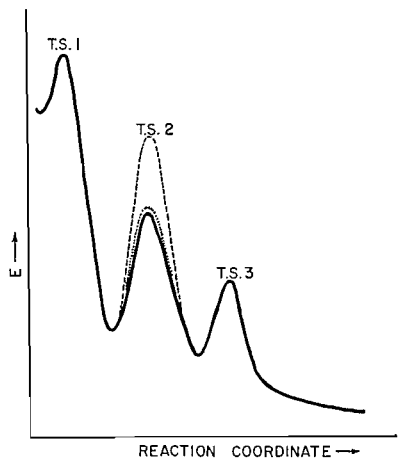

FIG. 1. Potential energy diagram for the reaction of $CH_3SO_2N_3$ with C_6H_5X (where X has a $+M$ effect); (———) opening leading to *p*-isomer, (.....) opening leading to *o*-isomer, (– – –) opening leading to *m*-isomer.

to account for the orientation and relative reactivities observed in the reaction of benzene-1,4-diazooxides with substituted benzenes to give derivatives of 4-hydroxybiphenyl. This behavior of the methanesulfonylimido intermediate is best explained if it is assumed that the thermal decomposition of the azide gives the highly reactive electrophilic singlet species $CH_3SO_2\ddot{N}$ which then reacts as such by adding to an aromatic "double bond".

Can. J. Chem. Downloaded from www.nrcresearchpress.com by 210.87.254.6 on 09/05/12
For personal use only.

The amount of dibenzyl formation observed with toluene may then be a measure of the amount of triplet diradicals present under these conditions.

An important point to be made at this stage concerns the meaning of partial rate factors in reactions of this type. The usual significance of a partial rate factor as a measure of the reactivity of a given position in a substituted benzene derivative compared with a position in benzene itself does not apply here since the product-determining step is not the rate-determining one and the various nuclear positions in the substituted benzene are not competing with those in benzene for the attacking reagent. This same point has been emphasized by Olah in connection with his studies of various electrophilic substitution reactions (24) using highly reactive electrophiles. Brown's "selectivity rule" (25) does not apply in such cases, the reagent being highly reactive but *apparently* selective. The selectivity here arises because of the relative energies of transition state 2 (Fig. 1) for the ortho, meta, and para positions. The use of partial rate factors is not justified in this case and they have no more meaning than do the isomer ratios; hence, they have been referred to as "apparent" partial rate factors in the preceding discussion.

One very interesting aspect of our results needs to be discussed now, and that is the amount and source of methanesulfonamide formed in these reactions (Table III). Two sets of reactions are particularly revealing, namely the decompositions in benzene and in toluene. In the latter solvent yields of 23–24% of methanesulfonamide were obtained, only 0.5% of which could have arisen by hydrogen abstraction from the alkyl side chain. It is also important to note that in this reaction 97–100% of the azide can be accounted for in the form of methanesulfonamide (III) and of the three mesyltoluidines. These considerations show that III is not formed in any important way according to equations [i] and [ii], or related types of reactions.

[i] $$CH_3SO_2\dot{\ddot{N}}\cdot + C_6H_5CH_3 \rightarrow CH_3SO_2NH\cdot + C_6H_5CH_2\cdot$$
$$CH_3SO_2NH\cdot + C_6H_5CH_3 \rightarrow CH_3SO_2NH_2 + C_6H_5CH_2\cdot$$

[ii] $$CH_3SO_2\dot{\ddot{N}}\cdot + CH_3C_6H_4NHSO_2CH_3 \rightarrow CH_3SO_2NH\cdot + CH_3C_6H_4\dot{N}SO_2CH_3$$

No biphenyl could be detected in the decomposition of the azide in benzene, though a careful search was made for this compound in the reaction mixture. Nor were any substituted biphenyls detected in the reactions with the other solvents. In benzene and chlorobenzene, the only source of hydrogen atoms (other than from methanesulfonyl azide itself, which has to be eliminated as a source in view of the fact that all the starting azide can be accounted for in the toluene reaction) is the aromatic nucleus. Had the methanesulfonylimido intermediate abstracted a *single* hydrogen atom from the benzene nucleus a phenyl radical would have resulted (see eq. [iii]). This, in the presence of excess benzene, would have given rise to biphenyl according to well known pathways (10*b*). The imidogen must, therefore, be abstracting *two* hydrogen atoms from the aromatic

[iii] $$CH_3SO_2N + C_6H_6 \rightarrow CH_3SO_2NH\cdot + C_6H_5\cdot$$
$$C_6H_5\cdot + C_6H_6 \rightarrow [C_6H_5C_6H_6\cdot] \xrightarrow{CH_3SO_2NH\cdot} (C_6H_5)_2 + CH_3SO_2NH_2$$

nucleus in a concerted, or very nearly concerted, process so that no aryl free radical is formed at any time. One possibility is that V may give rise directly to III and a benzyne intermediate which then undergoes polymerization. This might account for some of the tars formed in this reaction. No evidence is available at the moment that benzynes are formed under the conditions used here but experiments are under way to try and determine the origin of the methanesulfonamide (III) and to trap a benzyne intermediate if one is

Can. J. Chem. Downloaded from www.nrcresearchpress.com by 210.87.254.6 on 09/05/12
For personal use only.

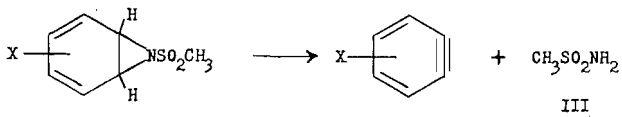

III

formed. A mechanism involving the simultaneous abstraction of two neighboring hydrogen atoms has been suggested in the carbene field (26).

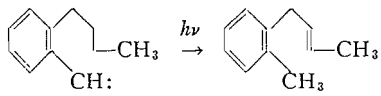

A very interesting concentration effect was observed in one case, namely the decomposition in anisole (Table III). At the usual azide:substrate molar ratio of 1:50 used with other solvents the overall yield of product was 70.7%, based on the amount of starting azide, and the total yield of mesylanisidines was 66.9%. The balance of azide must have been involved in some by-product and tar formation since no co-distillation of the anisidides with anisole could be detected by gas–liquid chromatography. When a higher azide concentration was used, however, the overall yield of product rose to 90.4% and the yield of mesylanisidides was 81.3%. It is interesting to note that though the yields of III and mesylanisidides both increased, they did so in different proportions so that the increase in the amount of amide (III) is probably not a direct consequence of the greater quantity of anisidides formed. One possible explanation of this observation comes to mind. As mentioned before, aliphatic sulfonyl azides have been shown to undergo a radical chain decomposition to give SO_2 and by-products to a certain extent, this reaction accompanying the more usual dissociation to the sulfonylimido intermediate and nitrogen (8). This might account for some or all of the starting azide not otherwise accounted for by the amounts of III and mesylanisidides formed in the 1:50 molar ratio reaction. At higher azide concentrations the induced decomposition to give the sulfonylimido intermediate at the expense of by-products may well be accelerated (5) leading to the increased yields of products in fact observed.

No products of Curtius-type rearrangements were ever observed under the conditions (aprotic solvents) used here (see also ref. 9). This does not exclude their formation, however, since some of the tars formed in a few cases might arise by the polymerization of $CH_3N{=}SO_2$ in the absence of a solvent capable of trapping the monomer. It seems more likely, however, that hydrogen bonding by a suitable solvent is necessary before the imido intermediate or its precursor will undergo the intramolecular 1,2-shift.

ACKNOWLEDGMENTS

Financial assistance for this work was kindly provided by the National Research Council. The award of a University of Saskatchewan Research Demonstratorship (to V. U.) is also acknowledged.

REFERENCES

1. A. Bertho, T. Curtius, and F. Schmidt. Chem. Ber. **60**, 1717 (1927). T. Curtius and F. Schmidt. Chem. Ber. **55**, 1571 (1922). A. Bertho. J. Prakt. Chem. **120**, 89 (1928).
2. O. C. Dermer and M. T. Edmison. J. Am. Chem. Soc. **77**, 70 (1955).
3. J. F. Heacock and M. T. Edmison. J. Am. Chem. Soc. **82**, 3460 (1960).
4. L. H. Zalkow and A. C. Oehlschlager. J. Org. Chem. **28**, 3303 (1963).
5. J. E. Leffler and Y. Tsuno. J. Org. Chem. **28**, 190 (1963).
6. L. Horner and A. Christmann. Chem. Ber. **96**, 388 (1963).
7. R. L. Dannley and M. Esayian. J. Polymer Sci. **45**, 105 (1960).
8. M. F. Sloan, T. J. Prosser, N. R. Newburg, and D. S. Breslow. Tetrahedron Letters, 2945 (1964).

Can. J. Chem. Downloaded from www.nrcresearchpress.com by 210.87.254.6 on 09/05/12
For personal use only.

9. W. LWOWSKI, R. DEMAURIAC, T. W. MATTINGLY, JR., and E. SCHEIFFELE. Tetrahedron Letters, 3285 (1964).
10. (*a*) R. A. ABRAMOVITCH and B. A. DAVIS. Chem. Rev. **64**, 149 (1964).
(*b*) G. H. WILLIAMS. Homolytic aromatic substitution. Pergamon Press, New York. 1960.
11. G. H. WILLIAMS. Chem. Ind. London, 1285 (1961).
12. L. FIELD and F. A. GRUNWALD. J. Am. Chem. Soc. **75**, 934 (1953).
13. C. S. MARVEL, M. D. HELFRICK, and J. P. BELSLEY. J. Am. Chem. Soc. **51**, 1272 (1929).
14. J. K. SIMONS. U. S. Patent No. 2,396,893 (1946); Chem. Abstr. **40**, 3780^2 (1946).
15. R. A. ABRAMOVITCH and J. S. WILLIAMS. Chem. Ind. London. In press.
16. T. C. CHANG and C. KARR, JR. Anal. Chem. Acta, **21**, 474 (1959).
17. D. H. HEY, H. N. MOULDEN, and G. H. WILLIAMS. J. Chem. Soc. 3769 (1960).
18. R. A. ABRAMOVITCH and J. G. SAHA. Part X. Can. J. Chem. In press. 1965.
19. G. SMOLINSKY, E. WASSERMAN, and W. A. YAGER. J. Am. Chem. Soc. **84**, 3220 (1962).
20. M. F. SLOAN, D. S. BRESLOW, and W. B. RENFROW. Tetrahedron Letters, 2905 (1964).
21. R. A. ABRAMOVITCH and J. G. SAHA. Tetrahedron. In press. 1965.
22. J. F. TILNEY-BASSETT. J. Chem. Soc. 2517 (1962).
23. M. J. S. DEWAR and K. NARAYANASWAMI. J. Am. Chem. Soc. **86**, 2422 (1964).
24. G. A. OLAH, S. J. KUHN, and S. H. FLOOD. J. Am. Chem. Soc. **83**, 4571, 4581 (1961). E. BERLINER. *In* Progress in physical organic chemistry. Vol. 2. *Edited by* Cohen, Streitwieser, and Taft. Interscience Publishers, New York. 1964. p. 253. G. A. OLAH. International Symposium on Organic Reaction Mechanisms. Cork, Ireland. 1964.
25. H. C. BROWN and K. L. NELSON. J. Am. Chem. Soc. **75**, 6293 (1953).
26. C. D. GUTSCHE, G. L. BACHMAN, and R. S. COFFEY. Tetrahedron, **18**, 617 (1962).

Can. J. Chem. Downloaded from www.nrcresearchpress.com by 210.87.254.6 on 09/05/12
For personal use only.

Can. J. Chem. Downloaded from www.nrcresearchpress.com by 210.87.254.6 on 09/05/12
For personal use only.

ÉTUDES CONFORMATIONNELLES EN SÉRIE CYCLOPENTANIQUE

I. LA *TERT*-BUTYL-3 CYCLOPENTANONE ET SES DÉRIVÉS

JEAN-CLAUDE RICHER ET CLAUDE GILARDEAU
Département de Chimie, Université de Montréal, Montréal, Qué.

Reçu le 10 juin 1965

RÉSUMÉ

La stéréochimie des réductions de la *tert*-butyl-3 cyclopentanone a été établie. Les alcools épimères qui en dérivent ont été préparés et leur structure déterminée.

INTRODUCTION

La publication du travail original de Winstein et Holness (1) sur l'utilisation du groupe *tert*-butyle pour fixer la conformation des cyclohexanes substitués, a provoqué une avalanche de travaux (2) sur l'analyse conformationnelle des cyclohexanes. Toutefois peu de travaux se rapportant à la série cyclopentanique ont été publiés. Nous rapportons dans le présent travail quelques études conformationnelles effectuées à l'aide des alcools dérivés de la *tert*-butyl-3 cyclopentanone.

RÉSULTATS

La synthèse de la *tert*-butyl-3 cyclopentanone (III) suivant le schéma A a déjà été rapportée par Pines et Ipatieff (3); une modification de cette méthode, décrite récemment (4), a été utilisée pour préparer la cétone III.

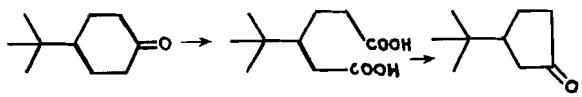

I II III

La réduction de III par divers agents réducteurs a été effectuée et les résultats obtenus sont rapportés dans le tableau I; la réduction de III par l'isopropylate d'aluminium dans des conditions équilibrantes est rapportée au tableau II aux côtés des résultats des équilibrations des alcools épimères dérivés de la cétone III.

TABLEAU I

Réduction de la *tert*-butyl-3 cyclopentanone par divers agents réducteurs

	% isomère *cis*
$LiAlH_4$/éther	60
$LiAl(OisoPr)_3H$/THF	66
$NaBH_4$/alcool isopropylique	58
Na/éthanol	56
Na/éther–eau	54
Hydrogénation/PtO_2/acide acétique/H	75
Isopropylate d'aluminium/conditions cinétiques	59

Le produit de l'hydrogénation catalytique de la cétone III peut être transformé en 3,5-dinitrobenzoate (5) qui est cristallisé jusqu'à point de fusion constant de 69–70°. La saponification de ce dérivé livre le *tert*-butyl-3 cyclopentanol cis (IV), $n_D^{21.5}$ 1.4561, chromatographiquement pur.

TABLEAU II

Equilibrations	% d'alcool *trans*
tert-Butyl-3 cyclopentanone	53
tert-Butyl-3 cyclopentanol *cis*	52
tert-Butyl-3 cyclopentanol *trans*	52
Moyenne	52

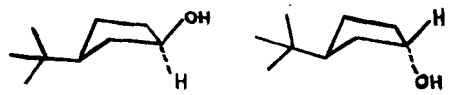

IV V

Le *tert*-butyl-3 cyclopentanol *trans* (V) pur ne peut toutefois pas être obtenu d'une manière aussi directe et l'on doit avoir recours à la méthode proposée dans le schéma B pour y arriver. La déshydratation d'un mélange des *tert*-butyl-3 cyclopentanols épimères (IV et V) à l'aide de sulfate acide de potassium (6) conduit à un mélange 50–50 de *tert*-butyl-3 cyclopentène (VI) et de *tert*-butyl-4 cyclopentène (VII). Ce dernier hydrocarbure (VII) est purifié par chromatographie en phase gazeuse préparative et identifié par un spectre de résonance magnétique nucléaire symétrique avec bandes à 0.85 p.p.m. (9 protons du groupe *tert*-butyle), 2.18 p.p.m. (4 protons allytiques), et 5.67 p.p.m. (2 protons vinyliques). L'hydrocarbure VII réagit avec l'acide méta-chloroperbenzoique (VIII) et conduit à un mélange d'époxydes (IX et X) qui est réduit par l'hydrure double de

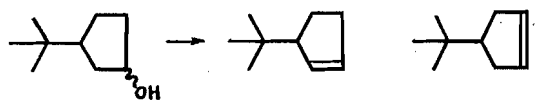

IV et V VI VII

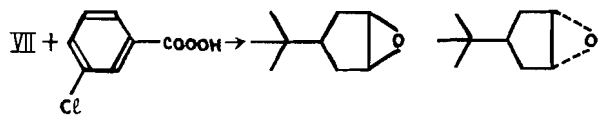

VIII IX X

lithium et d'aluminium (7). On obtient ainsi un mélange d'alcools où l'isomère *trans* (V) représente 75% du total. Le *tert*-butyl-3 cyclopentanol *trans*, $n_D^{21.5}$ 1.4550, peut être obtenu chromatographiquement pur par une combinaison de chromatographie en phase gazeuse préparative et de cristallisations fractionnées jusqu'à point fusion constant de 65° du *p*-nitrobenzoate de l'alcool correspondant.

La configuration relative des alcools IV et V est attribuée en partie grâce à une comparaison des spectres infrarouges de ces alcools à ceux des méthyl-3 cyclopentanols (8) et des iso-propyl-3 cyclopentanols correspondants (9). Cette comparaison est résumée dans le tableau III.

Les vitesses d'oxydation chromique du cyclopentanol et des alcools IV et V ont été déterminées et sont résumées au tableau IV. Pour fins de comparaison les vitesses d'oxydation des methyl-3 cyclopentanols correspondants sont aussi rapportées dans le tableau IV.

Can. J. Chem. Downloaded from www.nrcresearchpress.com by 210.87.254.6 on 09/05/12
For personal use only.

TABLEAU III

Fréquence de la vibration C—O dans les cyclopentanols

Cyclopentanols	*cis*	*trans*
Méthyl-3	996 cm^{-1}	1012/1000 épaulement
Isopropyl-3	993	1015/998 épaulement
tert-Butyl-3	990	1006/985 épaulement

TABLEAU IV

Vitesses d'oxydation chromique*

Cyclopentanol	0.150
tert-Butyl-3 cyclopentanol *trans*	0.218
tert-Butyl-3 cyclopentanol *cis*	0.256
Methyl-3 cyclopentanol *trans*	0.392
Methyl-3 cyclopentanol *cis*	0.513

*Mesures effectuées dans l'acide acétique 89.5%, à 25°.

DISCUSSION

Stéréochimie des réductions de la tert-butyl-3 cyclopentanone

Une cyclopentanone est à toutes fins pratiques planaire. Les hydrogènes qui y sont attachés sont donc distribués d'une manière symétrique au-dessous et au-dessus du plan de la molécule. A l'aide de la théorie complètement stérique proposée récemment (10) pour expliquer la stéréochimie des réductions des cétones cycliques par les hydrures complexes, on peut donc prévoir que l'attaque devrait être favorisée également d'un côté ou de l'autre, du groupement carbonyle. L'introduction d'un groupe *tert*-butyle en position 3 du centre réactionnel aura toutefois comme effet de masquer légèrement une face de la molécule. En se basant sur les concepts stériques proposés, on peut donc prévoir qu'une attaque du groupement carbonyle dans une telle molécule se ferait par la face opposée au groupe *tert*-butyle et conduirait à une formation légèrement prépondérante de l'alcool *cis*. Les résultats rapportés dans le tableau I sont en parfait accord avec cette hypothèse et de ce fait supportent la théorie complètement stérique proposée récemment (10).

Il est à noter que l'environnement stérique du *tert*-butyl-4 cyclopentène (VII) est similaire à celle de la cétone III et que théoriquement l'époxidation de cet hydrocarbure devrait conduire à la formation prépondérante de l'époxyde *trans*. Les résultats expérimentaux rapportés dans le présent travail, ainsi que dans le travail de Henbest (11) sur l'époxidation du méthyl-4 cyclopentène démontrent bien la véracité de cette prédiction.

Stabilité relative des alcools épimères

Les équilibrations directes des *tert*-butyl-3 cyclopentanols à l'aide de l'isopropylate d'aluminium montrent que la différence d'énergie libre entre ces deux alcools est faible, 90 cal/mole; l'isomère *trans* est plus stable que l'isomère *cis*. Les vitesses relatives d'oxydation chromique des alcools IV et V indiqueraient aussi que l'alcool *trans* est le plus stable. En utilisant la relation proposée par Sipos *et al.* (12) il est possible d'évaluer la différence d'énergie libre entre ces deux alcools à 130 cal/mole. Il est intéressant de noter à nouveau que les équilibrations directes et les vitesses relatives d'oxydation chromique conduisent à des conclusions très similaires sur la stabilité relative des alcools épimères.

Can. J. Chem. Downloaded from www.nrcresearchpress.com by 210.87.254.6 on 09/05/12
For personal use only.

La stabilité des alcools épimères telle qu'établie dans le présent travail est en parfait accord avec les valeurs déterminées pour les méthyl-3 cyclopentanols (8); dans les deux cas l'énergie libre semble favoriser l'isomère *trans*. Il est à noter que, par chaleur de combustion, Johnson, Prosen et Rossini (13) ont établi que l'enthalpie du diméthyl-1,3 cyclopentane *cis* est plus faible que celle du dérivé *trans*. Quoique ces deux séries de résultats puissent paraître contradictoires, les différences absolues qui les séparent sont tellement faibles que des facteurs entropiques tels que ceux provenant de la symétrie dans un diméthyl-1,3 cyclopentane, pourraient pratiquement concilier les deux séries de résultats.

Sur l'utilisation du groupe tert-butyle pour fixer la conformation

L'examen des vitesses d'oxydation chromique rapportées dans le tableau IV fait ressortir un fait troublant, à savoir que la vitesse d'oxydation du cyclopentanol n'est pas intermédiaire entre les vitesses d'oxydation des *tert*-butyl-3 cyclopentanols *cis* et *trans*. Une observation semblable peut être faite en examinant les vitesses de solvolyse des tosylates correspondants (14).

Ces résultats indiquent que le groupement *tert*-butyle a des revendications stériques telles qu'il force le cyclopentane à occuper une conformation qui n'est pas favorisée dans le cyclopentanol non substitué.

Cette remarque laisse prévoir que l'introduction d'un groupe *tert*-butyle sur un noyau cyclopentanique ne sera pas d'une très grande utilité dans l'analyse conformationnelle de ces cycles. De plus, sans nous joindre à Kwart et Takeshita (15) dans la critique de l'utilisation du groupe *tert*-butyle comme méthode de "fixer" la conformation d'un cyclohexane mobile, nous suggérons qu'il est possible que l'introduction d'un groupe *tert*-butyle puisse déformer légèrement même un cyclohexane.

PARTIE EXPÉRIMENTALE

Les points de fusion ont été déterminés sur un bloc Kofler et ne sont pas corrigés.

Les spectres infrarouges ont été pris sur un spectrophotomètre Perkin–Elmer modèle 21, à double faisceau, entre deux plaques de chlorure de sodium.

Les chromatographies en phase gazeuses analytiques ont été faites à l'aide d'un appareil Kromo–Tog, modèle K-2, de la compagnie Burrel.

Une colonne de 5 mètres contenant de l'hyprose à 10% sur Kromat FB et maintenue à 120° a été utilisé pour l'analyse des alcools. Une colonne de 2 mètres contenant du nitrate d'argent à 15% sur Kromat FB a été utilisé à la température de la pièce pour l'analyse des hydrocarbures.

Les séparations par chromatographie en phase gazeuse préparative ont été faites à l'aide d'un appareil Fisher Prep–Partitionner en employant 8 colonnes de 50 cm contenant de l'hyprose 10% sur Kromat FB (purification des alcools) ou du β,β'-oxydipropionitrile sur chromosorb P (purification des hydrocarbures).

Les spectres résonances magnétiques nucléaires ont été mesurés sur un appareil A-60 en utilisant le tétraméthylsilane comme standard interne. Les déplacements chimiques (δ) sont exprimés en p.p.m. du champ total.

Des analyses élémentaires satisfaisantes ont été obtenues par C. Daesslé, Organic Microanalysis, Montréal, pour les dérivés des tert-butyl-3 cyclopentanols.

Les vitesses d'oxydation chromiques ont été déterminées de la manière décrite précédemment (16).

REMERCIEMENTS

Les auteurs remercient vivement le Conseil National de Recherches du Canada pour une subvention de recherches qui a permis la réalisation de ce travail, la compagnie C.I.L. pour une bourse d'études à l'un d'entre nous (C.G.), et la compagnie Dow Canada pour un généreux échantillon de tert-butyl-4 cyclohexanone. Les auteurs remercient de plus les Dr. B. Fuchs et R. Haber qui leur ont fourni les méthyl-3 cyclopentanols isomères utilisés pour fins de comparaison.

Can. J. Chem. Downloaded from www.nrcresearchpress.com by 210.87.254.6 on 09/05/12
For personal use only.

REFERENCES

1. S. WINSTEIN et N. J. HOLNESS. J. Am. Chem. Soc. **77**, 5562 (1955).
2. E. L. ELIEL, N. L. ALLINGER, S. J. ANGYAL et G. A. MORRISON. Conformational analysis. Interscience Publishers, Inc., New York. 1965.
3. H. PINES et V. N. IPATIEFF. J. Am. Chem. Soc. **61**, 2728 (1939).
4. J. C. RICHER et P. BÉLANGER. Can. J. Chem. **42**, 2398 (1964).
5. R. L. SHRINER, R. C. FUSON et D. Y. CURTIN. The systematic identification of organic compounds. John Wiley and Sons, Inc., New York. 1964.
6. C. S. MARVEL et JACK L. R. WILLIAMS. J. Am. Chem. Soc. **70**, 3842 (1948).
7. B. RICHBORN et J. QUARTUCCI. J. Org. Chem. **29**, 2476 (1964).
8. B. FUCHS. Thèse de Doctorat, Institut de Technologie Technion-Israël, Haïfa. 1963.
9. W. HÜCKEL et R. BROSS. Liebigs Ann. Chem. **664**, 1 (1963).
10. J. C. RICHER. J. Org. Chem. **30**, 324 (1965).
11. H. B. HENBEST. Proc. Chem. Soc. 159 (1963).
12. F. SIPOS, J. KRUPICKA, M. TICHY et J. SICHER. Collection Czech. Chem. Commun. **27**, 2079 (1962
13. W. H. JOHNSON, E. J. PROSEN et F. D. ROSSINI. J. Res. Nat. Bur. Std. **42**, 251 (1949) R.P. 1966.
14. I. LILLIEN et K. KHALEELUDDIN. Chem. Ind. London, **24**, 1028 (1964).
15. H. KWART et T. TAKESHITA. J. Am. Chem. Soc. **86**, 1161 (1964).
16. J. C. RICHER et C. GILARDEAU. Can. J. Chem. **43**, 538 (1964).

Can. J. Chem. Downloaded from www.nrcresearchpress.com by 210.87.254.6 on 09/05/12
For personal use only.

Can. J. Chem. Downloaded from www.nrcresearchpress.com by 210.87.254.42 on 09/05/12
For personal use only.

QUINOXALINE DERIVATIVES

VIII. THE EFFECT OF ELECTRON-DONATING GROUPS ON THE FORMATION OF CERTAIN QUINOXALINECARBOXYANILIDE N-OXIDES AND THEIR REARRANGEMENT[1]

YUSUF AHMAD, M. S. HABIB[2], M. IQBAL, M. IKRAM QURESHI, AND ZIAUDDIN

Chemical Research Division, Central Laboratories, Pakistan Council of Scientific and Industrial Research, Karachi, Pakistan

Received June 28, 1965

ABSTRACT

Introduction of methyl or methoxy groups into the benzene ring of quinoxalinecarboxyanilide (I*d*), makes the resulting anilides less prone to "abnormal" oxidation (1). Normal N-oxides (II*f* and II*j*) were obtained from the anilides I*f* and I*j* in which the cyclic >NH was unprotected. The methyl-substituted anilides I*g* and I*h*, however, on oxidation with peracetic acid gave the hydroxy derivatives (V*g* and V*h*) instead of the N-oxides (II*g* and II*h*). The methoxy-substituted anilides I*k* and I*l* did not give the hydroxy derivatives V*k* and V*l* nor the expected *N*-oxides II*k* and II*l*. All the *N*-oxides (II*e*, II*f*, II*i*, and II*j*) on rearrangement with sulfuric acid yielded the corresponding amines IV*e*, IV*f*, IV*i*, and IV*j*. In spite of the slow rate of rearrangement of these N-oxides, attempts to isolate the intermediate hydroxyaminospirolactams (III) were unsuccessful.

The novel conversion of quinoxalinecarboxyanilide N-oxide (II*a*) in cold sulphuric acid to the amine (IV*a*) has been postulated (2) to proceed by intramolecular electrophilic substitution of the anilide ring by C-2 of the quinoxaline moiety. The N-oxide group intensifies the electrophilic property of C-2 and seems to be necessary for subsequent decarboxylation and dehydration by a cyclic mechanism (2). In the absence of the N-oxide function the anilide (I*a*) has been shown (3) to rearrange to the spirolactam (VI*a*), which unlike the postulated but unstable intermediate (III*a*) in the conversion of II*a* to IV*a*, is quite stable and has been isolated in quantitative yield. These rearrangements are comparatively slower in ethanolic hydrogen chloride than in concentrated sulphuric acid, and it has been possible to isolate (3) the hydroxyamino-spirolactam (VIII*a*) in the rearrangement of the pyrazine N-oxide (VII*a*). The strongly electrophilic character of C-2 in the quinoxaline N-oxide (II*a*) and its derivatives is probably responsible for the marked instability of its hydroxyamino-spirolactam intermediate (III*a*) and the impossibility of isolating this compound.

This is further borne out in the preparation of the N-oxides. It has been observed (1) that if both or either of the cyclic or acyclic NH groups in the anilide (I*d*) are not protected by methyl groups, I*b*, I*c*, and I*d* on oxidation with hydrogen peroxide in acetic acid, instead of giving the corresponding N-oxides (II*b*, II*c*, and II*d*) give the corresponding hydroxy derivatives (V*b*, V*c*, and V*d*), i.e. the anilide side-chain in each case is replaced by an OH group. However, the anilide (I*a*), in which both the NH groups are protected by methyl groups, or I*b* (R″ = Ac), in which the anilide NH is methylated and a mild protection is afforded to the heterocyclic NH, each give the corresponding normal N-oxides II*a* and II*b* (R″ = Ac). In the corresponding pyrazine analogues, the carboxyanilide (VII*b* without oxygen on N_1), which bears no protection on its cyclic amide-nitrogen, on oxidation gives the normal N-oxide (VII*b*). The marked electrophilic nature of the 2-position in 3-hydroxyquinoxaline-2-carboxyanilides has been considered (1) to be

[1]For Part VII see ref. 6.
[2]Present address: Burroughs Wellcome & Co. (Pakistan) Ltd., D/43 S.I.T.E., Karachi.

responsible for these "abnormal" oxidations. This hypothesis is further supported by the fact that in analogous quinoxaline anilide (I*f*), in which two electron-donating methyl groups at position 6 and 7 somewhat decrease the strongly electrophilic nature of C-2, the protection of the cyclic amide-nitrogen became unnecessary, and normal N-oxide (II*f*) could be obtained from the semiprotected anilide (I*f*) with peracetic acid. The fully protected anilide (I*e*), of course, gave the normal N-oxide (II*e*). However, the protection of the anilide NH was still necessary, as both of the anilides (I*g* and I*h*) underwent "abnormal" oxidation with peracetic acid and gave the hydroxy compounds (V*g* and V*h*).

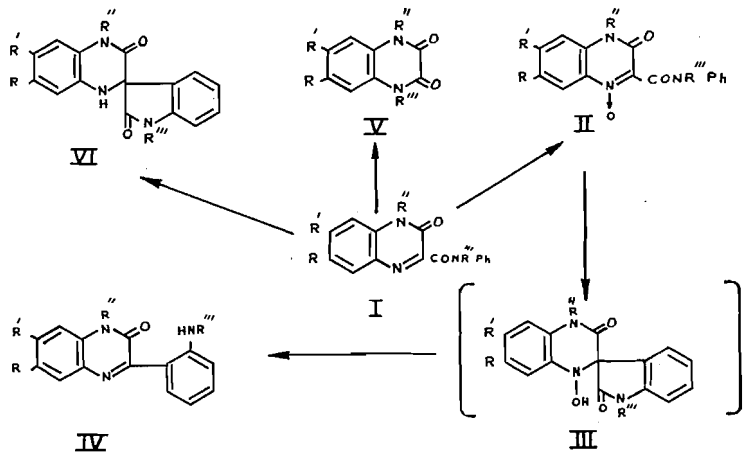

	R	R′	R″	R‴		R	R′	R″	R‴
(*a*)	H	H	Me	Me	(*h*)	Me	Me	H	H
(*b*)	H	H	H	Me	(*i*)	MeO	MeO	Me	Me
(*c*)	H	H	Me	H	(*j*)	MeO	MeO	H	Me
(*d*)	H	H	H	H	(*k*)	MeO	MeO	Me	H
(*e*)	Me	Me	Me	Me	(*l*)	MeO	MeO	H	H
(*f*)	Me	Me	H	Me	(*m*)	H	Cl	Me	Me
(*g*)	Me	Me	Me	H	(*n*)	Cl	H	Me	Me

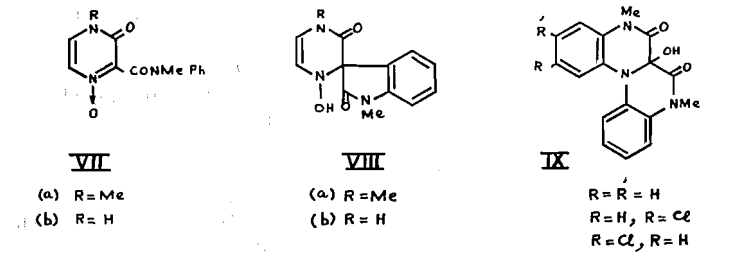

Under IX lower right column should be, R′ = Cl, R′ = H.

In place of the methyl groups at positions 6 and 7 in the above quinoxaline anilides, introduction of two methoxy groups, which are even stronger electron donators, would have further reduced the electrophilic nature of the C-2 in the molecule, and this was shown. The anilide (I*k*) in which the acyclic NH group is unprotected, and the anilide (I*l*) in which both the acyclic and cyclic NH groups are unprotected, on oxidation with peracetic acid did not give the corresponding hydroxy derivatives (V*k* and V*l*), which for

Can. J. Chem. Downloaded from www.nrcresearchpress.com by 210.87.254.42 on 09/05/12
For personal use only.

the purpose of comparison were synthesized through an unambiguous route. However, the compounds that were obtained by this oxidation were not even the N-oxides (II*k* and II*l*), since they did not undergo the usual decomposition even in warm concentrated sulphuric acid, and were recovered unchanged. The constitution of these new compounds, which were isolated in poor yields, is under further investigation. The fully protected anilide (I*i*) and the other semiprotected anilide (I*j*), as expected, gave the normal N-oxides (II*i* and II*j*).

The unsubstituted quinoxalinecarboxyanilide N-oxide (II*a*) in concentrated sulphuric acid at 0° has been reported (2, 4, 5) to undergo rearrangement to give the amine (IV*a*) and also an insoluble compound, for which the quinoxalinoquinoxaline structure (IX*a*) has been proposed (4, 5). The derivatives (II*m* and II*n*) of this N-oxide which bear chlorine atoms at positions 6 and 7, undergo this transformation at 0° even faster, and a larger amount of quinoxalinoquinoxaline type of compound (IX*b* or IX*c*) is formed in each case. On the other hand the N-oxides (II*e*, II*f*, II*i*, II*j*) are recovered unchanged from cold concentrated sulphuric acid, and to effect their rearrangement and conversion to the corresponding amines (IV*e*, IV*f*, IV*i*, and IV*j*) it is necessary to heat the mixture at 75° for about an hour, during which process there is virtually no formation of quinoxalino-quinoxaline-type compounds. This can also be attributed to a decrease of the electrophilic character of the C-2 in these quinoxaline N-oxides caused by the introduction of electron-releasing groups in their benzene rings.

Attempts to isolate the intermediate hydroxyamino-spirolactams (III*e*, III*f*, III*i*, and III*j*) by heating the corresponding N-oxides (II*e*, II*f*, II*i*, and II*j*) with ethanolic hydrogen chloride were unsuccessful, because the rearrangement rate of these N-oxides is even slower than that of the pyrazine N-oxide (VII*a*). All four quinoxaline N-oxides were recovered unchanged after they were heated for 8 h with ethanolic hydrogen chloride on a water bath.

EXPERIMENTAL

Infrared spectra were measured in Nujol mull.

General Procedure for the Preparation of N-Oxides

The appropriate quinoxalinecarboxyanilide (1 g), acetic acid (10 ml), and 30% hydrogen peroxide (1 ml) were heated together at 55° and two further quantities of hydrogen peroxide (0.5 ml each) were added after intervals of 24 and 48 h. After a total 72 h of heating (6), the acetic acid was removed under reduced pressure and the residue was crystallized to give the N-oxide.

3-Hydroxy-6,7-dimethyl-2-(N-methyl-N-phenylcarbamoyl) quinoxaline 1-Oxide (II*f*)

3-Hydroxy-6,7-dimethyl-2-(*N*-methyl-*N*-phenylcarbamoyl) quinoxaline (I*f*) (7), when treated with acetic acid and hydrogen peroxide as described above, gave yellow plates (from ethanol) of the *1-oxide* (II*f*), yield 55%, m.p. 266–267° (decomp.).

Anal. Calcd. for $C_{18}H_{17}N_3O_3$: N, 13.0. Found: N, 12.8.

3,4-Dihydro-4,6,7-trimethyl-2-(N-methyl-N-phenylcarbamoyl)-3-oxoquinoxaline 1-Oxide (II*e*)

(*a*) 3,4-Dihydro-4,6,7-trimethyl-2-(*N*-methyl-*N*-phenylcarbamoyl)-3-oxoquinoxaline (I*e*) (7), when similarly treated, gave yellow plates (from ethanol) of the *4-methyl 1-oxide* (II*e*), yield 40%, m.p. 263–264° (decomp.).

Anal. Calcd. for $C_{19}H_{19}N_3O_3$: C, 67.6; H, 5.7; N, 12.5. Found: C, 67.6; H, 5.7; N, 12.2.

(*b*) The 1-oxide (II*f*), when treated with methyl sulphate in the presence of anhydrous potassium carbonate in acetone, gave the 4-methyl 1-oxide (II*e*), m.p. 263° (decomp.), in good yield, identical (mixed melting point and infrared spectrum) with a sample obtained as described in (*a*).

3-Hydroxy-6,7-dimethoxy-2-(N-methyl-N-phenylcarbamoyl) quinoxaline 1-Oxide (II*j*)

3-Hydroxy-6,7-dimethoxy-2-(*N*-methyl-*N*-phenylcarbamoyl) quinoxaline (I*j*) (7), when similarly treated, gave yellow needles (from ethanol) of the *1-oxide* (II*j*), yield 30%, m.p. 272–273° (decomp.).

Anal. Calcd. for $C_{18}H_{17}N_3O_5$: C, 60.8; H, 4.8; N, 11.8. Found: C, 60.5; H, 4.5; N, 11.7.

3,4-Dihydro-6,7-dimethoxy-4-methyl-2-(N-methyl-N-phenylcarbamoyl)-3-oxoquinoxaline 1-Oxide (II*i*)

(*a*) 3,4-Dihydro-6,7-dimethoxy-4-methyl-2-(*N*-methyl-*N*-phenyl-carbamoyl)-3-oxoquinoxaline (I*i*) (7),

Can. J. Chem. Downloaded from www.nrcresearchpress.com by 210.87.254.42 on 09/05/12
For personal use only.

when similarly treated, gave, in 45% yield, yellow needles (from ethanol) of the *4-methyl 1-oxide* (II*i*), m.p. 250–251°.

Anal. Calcd. for $C_{19}H_{19}N_3O_5.H_2O$: C, 58.9; H, 4.9; N, 10.85. Found: C, 59.1; H, 4.9; N, 11.1.

(*b*) The 1-oxide (II*j*) on being treated with methyl sulphate in the presence of anhydrous potassium carbonate in acetone gave in good yield yellow needles (from ethanol) of the 4-methyl 1-oxide (II*i*), m.p. 250–251°, identical (mixed melting point and infrared spectrum) with a sample obtained as described in (*a*).

General Procedure for the Decomposition of N-Oxides in Concentrated Sulphuric Acid

Finely powdered N-oxide (1 g) in concentrated sulphuric acid (5 ml) was vigorously stirred while being heated at 75° till the evolution of CO_2 was complete (about 1 h). The cooled mixture was poured on ice, then neutralized with aqueous sodium hydroxide. The precipitate was collected and crystallized from ethanol as orange needles. Yield 50–80%.

3-Hydroxy-6,7-dimethyl-2-(o-methylaminophenyl) Quinoxaline (IV*f*)

The 1-oxide (II*f*), when treated as above, gave the *amine* (IV*f*), m.p. 238–240°.

Anal. Calcd. for $C_{17}H_{17}N_3O$: N, 15.1. Found: N, 15.1.

3,4-Dihydro-4,6,7-trimethyl-2-(o-methylaminophenyl)-3-oxoquinoxaline (IV*e*)

The 1-oxide (II*e*), when similarly treated, gave the *4-methylamine* (IV*e*), m.p. 163–164°.

Anal. Calcd. for $C_{18}H_{19}N_3O$: C, 73.7; H, 6.5; N, 14.3. Found: C, 73.4; H, 6.4; N, 13.9.

3-Hydroxy-6,7-dimethoxy-2-(o-methylaminophenyl) Quinoxaline (IV*j*)

The 1-oxide (II*j*), when similarly treated, gave the *amine* (IV*j*), m.p. 230–231° (decomp.).

Anal. Calcd. for $C_{17}H_{17}N_3O_3$: C, 65.6; H, 5.5; N, 13.5. Found: C, 65.9; H, 5.7; N, 13.6.

3,4-Dihydro-6,7-dimethoxy-4-methyl-2-(o-methylaminophenyl)-3-oxoquinoxaline (IV*i*)

The 1-oxide (II*i*), when similarly treated, gave the *4-methylamine* (IV*i*), m.p. 159–161°.

Anal. Calcd. for $C_{18}H_{19}N_3O_3$: C, 66.5; H, 5.9; N, 12.9. Found: C, 66.9; H, 6.5; N, 13.0.

3,4-Dihydro-4,6,7-trimethyl-2-(N-phenylcarbamoyl)-3-oxoquinoxaline (I*g*)

3,4-Dihydro-4,6,7-trimethyl-3-oxoquinoxaline-2-carboxylic acid (1.5 g), thionyl chloride (20 ml), and benzene (20 ml) were heated under reflux for 1 h. The solid that was obtained after the thionyl chloride and benzene were removed under reduced pressure, was suspended in dry benzene and a solution of aniline (6 ml) in benzene (10 ml) was added drop by drop. The mixture was shaken for 10 min and washed with dilute hydrochloric acid. The *anilide* (I*g*) that was thus separated was crystallized from ethanol as yellow needles, yield 100%, m.p. 210–212°.

Anal. Calcd. for $C_{18}H_{17}N_3O_2$: C, 70.3; H, 5.6; N, 13.7. Found: C, 70.3; H, 5.5; N, 13.2.

2,3-Dihydroxy-6,7-dimethyl Quinoxaline (V*h*)

(*a*) An attempted preparation of the 1-oxide of 3-hydroxy-6,7-dimethyl-2-(*N*-phenylcarbamoyl) quinoxaline (I*h*) by the general procedure described above for the preparation of N-oxides, led to the formation of *dihydroxyquinoxaline* (V*h*) (colorless needles from acetic acid), yield 80%, m.p. >325°, identical (infrared spectrum) with the synthetic sample obtained as described in (*b*).

(*b*) 4,5-Dimethyl-*o*-phenylenediamine, prepared by the hydrogenation of 4,5-dimethyl-2-nitroaniline (4 g) in ethanol (100 ml) over Pd–C, and without separation from ethanolic solution, was heated with ethyl oxalate (15 g) under reflux for 3 h. When the mixture was cooled a solid separated out, and was crystallized from acetic acid (charcoal) as colorless microneedles of the dihydroxyquinoxaline (V*h*), m.p. >325°.

Anal. Calcd. for $C_{10}H_{10}N_2O_2$: C, 63.2; H, 5.3. Found: C, 62.8; H, 5.1.

3,4-Dihydro-2-hydroxy-4,6,7-trimethyl-3-oxoquinoxaline (V*g*)

In a similar way the attempted preparation of the 1-oxide of the anilide (I*g*) afforded in good yield *4-methyl hydroxyquinoxaline* (V*g*) (colorless needles from ethanol), m.p. >325°.

Anal. Calcd. for $C_{11}H_{12}N_2O_2$: C, 64.7; N, 5.9; N, 13.7. Found: C, 65.4; H, 6.2; N, 13.4.

When this compound (V*g*) was treated with methyl sulphate in the presence of anhydrous potassium carbonate in acetone, it gave, in good yield, colorless needles (from acetone) of *1,2,3,4-tetrahydro-1,4,6,7-tetramethyl-2,3-dioxoquinoxaline* (V*e*), m.p. 305°, identical with the product obtained by methylation of the authentic V*h* described above under (*b*) (infrared spectrum and mixed m.p. 305°).

Anal. Calcd. for $C_{12}H_{14}N_2O_2$: C, 66.0; H, 6.5. Found: C, 66.4; H, 6.4.

Attempted Preparation of the 1-Oxides of 3,4-Dihydro-6,7-dimethoxy-2-(N-phenylcarbamoyl)-3-oxoquinoxaline (I*l*) *and 3,4-Dihydro-6,7-dimethoxy-4-methyl-2-(N-phenylcarbamoyl)-3-oxoquinoxaline* (I*k*)

Both of the anilides (I*l* and I*k*), when they were treated as above (and under various other experimental conditions) with hydrogen peroxide and acetic acid, yielded some unidentifiable compounds. The anilide (I*l*) gave a colorless compound, m.p. 245–247°, which was different (m.p. and infrared spectrum) from the expected *2,3-dihydroxy-6,7-dimethoxy quinoxaline* (V*l*) (colorless needles from acetic acid, m.p. >325°.

Anal. Calcd. for $C_{10}H_{10}N_2O_4$: C, 54.05; H, 4.5; N, 12.6. Found: C, 54.32; H, 4.25; N, 12.6.) prepared by heating together 4,5-dimethoxy-*o*-phenylenediamine and ethyl oxalate under reflux for 3 h. The anilide (I*k*) gave a yellow solid (crystallized from ethanol), m.p. 170° (decomp.), which also did not show the properties of an N-oxide, and was not the other expected compound V*k*.

Can. J. Chem. Downloaded from www.nrcresearchpress.com by 210.87.254.42 on 09/05/12
For personal use only.

ACKNOWLEDGMENT

We thank Dr. S. Siddiqui, Chairman of this Council, for his interest and encouragement. We also extend thanks to Dr. H. T. Openshaw and the Wellcome Research Laboratories, Kent (U.K.), through whose courtesy the analyses reported above were carried out in England; and to Miss M. Quadeem for help in experimental work.

REFERENCES

1. M. S. HABIB and C. W. REES. J. Chem. Soc. 3386 (1960).
2. M. S. HABIB and C. W. REES. J. Chem. Soc. 3371 (1960).
3. M. S. HABIB and C. W. REES. J. Chem. Soc. 123 (1962).
4. J. W. CLARK-LEWIS and G. F. KATEKAR. J. Chem. Soc. 2825 (1959).
5. E. H. USHEWOOD and M. A. WHITELEY. J. Chem. Soc. **123**, 1069 (1923).
6. Y. AHMAD, M. S. HABIB, M. IQBAL, M. I. QURESHI, and ZIAUDDIN. Bull. Chem. Soc. Japan. In press.
7. Y. AHMAD, M. S. HABIB, M. IQBAL, M. I. QURESHI. J. Chem. Soc. 4053 (1964).

Can. J. Chem. Downloaded from www.nrcresearchpress.com by 210.87.254.42 on 09/05/12
For personal use only.

Can. J. Chem. Downloaded from www.nrcresearchpress.com by 210.87.254.5 on 09/05/12
For personal use only.

THE SOLUBILITY OF ALUMINIUM IN $NaF–AlF_3–Al_2O_3$ MELTS

JOMAR THONSTAD

Royal Norwegian Council for Scientific and Industrial Research, Metallurgical Committee, The Technical University of Norway, Trondheim, Norway

Received June 25, 1965

ABSTRACT

The solubility of aluminium in $NaF–AlF_3$ melts saturated with alumina has been investigated by analyzing quenched samples of the melts to determine the contents of metallic sodium and aluminium. The total solubility at 1 000 °C given as wt. % Al decreases with decreasing NaF/AlF_3 molar ratio from 0.33 wt. % Al at $NaF/AlF_3 = 6.70$ to 0.10 wt. % Al in cryolite ($NaF/AlF_3 = 3$) and 0.075 wt. % Al at $NaF/AlF_3 = 1.70$. The change in the solubility is primarily due to a change in the sodium content, while the aluminium content remains almost constant over the range investigated. The solubility in cryolite increases with increasing temperature from 0.10 wt. % Al at 1 000 °C to 0.14 wt. % Al at 1 060 °C. In cryolite at 1 000 °C the dissolved metal was found to consist of 0.065 wt. % Al and 0.090 wt. % Na. The fraction of the dissolved metal represented by sodium increases with increasing temperature.

INTRODUCTION

The solubility of aluminium in $NaF–AlF_3–Al_2O_3$ melts is of interest in relation to the electrolytic production of aluminium, as the loss in current efficiency in that process is caused by oxidation of the dissolved metal by the anode gas. The solubility of aluminium in melts close to the cryolite composition (molar ratio $NaF/AlF_3 = 3$) has been measured by several workers. The results are somewhat controversial, particularly regarding the influence of the NaF/AlF_3 ratio. As will be shown subsequently the dissolved metal consists of sodium as well as aluminium. This fact has been disregarded by most workers and the solubilities are normally given as wt. % Al, which then includes both the sodium and the aluminium contents.

Zhurin (1) found solubilities in the range of 0.10–0.15 wt. % Al at 1 060 °C in cryolite–alumina melts, and 0.21 wt. % Al at $NaF/AlF_3 = 1.67$ and 0.062 wt. % Al at $NaF/AlF_3 = 4$. Pruvot (2) found the solubility in cryolite at 1 000 °C to be 0.02–0.04 wt. % Al. Mashovets and Svoboda (3) measured the solubilities in AlF_3-rich melts where it increased from approximately 0.12 wt. % Al at $NaF/AlF_3 = 2.70$ to 0.40 wt. % Al at $NaF/AlF_3 = 1.80$. Haupin (4) found the solubility at 980 °C to be 0.10 wt. % Al in cryolite, 0.11 wt. % Al at $NaF/AlF_3 = 3.70$, and 0.09 wt. % Al at $NaF/AlF_3 = 2.70$. Haupin also tried to analyze separately the sodium and the aluminium contents of the dissolved metal. In cryolite ($NaF/AlF_3 = 3$) the contents were found to be 0.16 wt. % Na and 0.05 wt. % Al and at $NaF/AlF_3 = 2.6$, 0.10 wt. % Na and 0.05 wt. % Al.

Condensates from $NaF–AlF_3–Al_2O_3$ melts in contact with aluminium contain metallic sodium and aluminium, as well as various fluoride compounds (3, 4). The evaporating species responsible for the metal loss from the melts are probably aluminium monofluoride (AlF) and sodium metal. Sodium has been found spectrographically in the vapor phase (5).

The nature of the dissolved metal in the melt has not been established. It is customary to assume (6) that aluminium occurs as monovalent ions, i.e.

$$[1] \qquad Al^{3+} + 2Al \rightleftarrows 3Al^{+},$$

and that sodium occurs as uncharged metal atoms or ions like Na_2^+, i.e.

$$[2] \qquad 6Na^{+} + Al \rightleftarrows 3Na_2^{+} + Al^{3+}.$$

The ionic nature of the dissolved metal is supported by electrochemical measurements (7).

It is apparent that the available data on the solubility of aluminium in $NaF–AlF_3–Al_2O_3$ melts are partly in conflict and furthermore that the role played by sodium has mostly been neglected. The present investigation has been carried out to determine the excess sodium and aluminium contents in melts having molar ratios from $NaF/AlF_3 = 6.70$ to 1.50.

EXPERIMENTAL

The materials used were Alcan super purity aluminium, hand-picked Greenland cryolite, and reagent grade anhydrous sodium fluoride, aluminium fluoride, and alumina.

The melts were contained in recrystallized alumina crucibles of 20 ml capacity covered by close-fitting lids made of boron nitride or graphite. The composition of the melts was determined from the weighed-in amounts, as the composition changed very little during a run. The melts had to be saturated with alumina to prevent attack on the crucibles. Enough aluminium was added to cover the bottom of the crucible. The equilibration was carried out in a vertical Kanthal furnace where the tube and the radiation shields were made of Inconel. Inert nitrogen gas was passed through the furnace. An equilibration time of 2 h was found to be sufficient. Samples of the melts were taken with a small thick-walled nickel ladle that was lowered from the cold part of the furnace into the melt and then quickly withdrawn. The ladle and the lid of the crucible could be manipulated from the outside by thin rods without admitting air to the furnace.

After cooling the samples were taken to a drybox with inert nitrogen atmosphere. The samples were crushed to −20 mesh, weighed, and transferred to the analyzing apparatus to determine the excess metal content. To this purpose each sample was treated with absolute ethyl alcohol and dilute hydrochloric acid. The metal would react with the alcohol and the hydrochloric acid and evolve hydrogen. The hydrogen was first led through a liquid air trap and then passed over cupric oxide at 350 °C in a tubular furnace, where it was converted to water vapor which was determined gravimetrically by absorption. The carrier gas for this determination was nitrogen.

By the addition of alcohol to the sample a reaction accompanied by gas evolution could be observed. The gas proved to be hydrogen. The reaction would last only for a few minutes, and even prolonged treatment would not produce any more hydrogen. When hydrochloric acid was added the reaction would recommence and normally reach completion after about 20 min.

Blank runs with samples from melts that had not been in contact with aluminium gave no reaction and no weight increase of the absorption tube. These samples were white while samples containing metal had a distinctive grayish tinge.

When the samples were quenched any dissolved metal in the form of subvalent compounds would become unstable. It was assumed that the aluminium was converted to metallic aluminium, e.g., by reversal of reaction [1], while the sodium was converted to metallic sodium. Both sodium and aluminium are expected to react with alcohol giving hydrogen and aluminium and sodium ethoxide respectively. The reaction with aluminium is known to be very slow, however, and the presence of catalyzers like chlorine or mercuric chloride are needed in order to initiate the reaction (8). In order to test this information, a piece of the aluminium used in these experiments was immersed in absolute alcohol and filed to remove the oxide layer. Even after heating no visible reaction occurred. A piece of sodium, on the other hand, reacted readily with the alcohol.

The assumption was then made that alcohol would react only with the sodium in the sample, while it would not react to any measurable extent with the aluminium. Since the metal present in the quenched samples was in a state of fine dispersion and therefore presumably very reactive, the justification of this assumption may be disputed. The shape of the experimental curve (Fig. 1) indicates, however, that the aluminium did not interfere with the determination of sodium.

RESULTS AND DISCUSSION

Figure 1 shows the results obtained at 1 000 °C with melts of varying NaF/AlF_3 ratio, saturated with Al_2O_3. The results at the highest NaF/AlF_3 ratio are somewhat uncertain, because the NaF-rich melts severely attacked the alumina crucibles. The high viscosity of these melts also made sampling difficult. Curve I shows the total solubility given in the customary way as wt. % metallic aluminium. Curve II shows the part of the total solubility found in the alcohol treatment, i.e., the sodium content, given as wt. % metallic sodium. Because the reducing power per mole aluminium is three times greater than that of sodium, the numerical values for the sodium content will for some compositions be higher than the total solubility as given by curve I. Curve III shows the aluminium content of the melt in wt. % Al. Results obtained with cryolite melts at various tem-

Can. J. Chem. Downloaded from www.nrcresearchpress.com by 210.87.254.5 on 09/05/12
For personal use only.

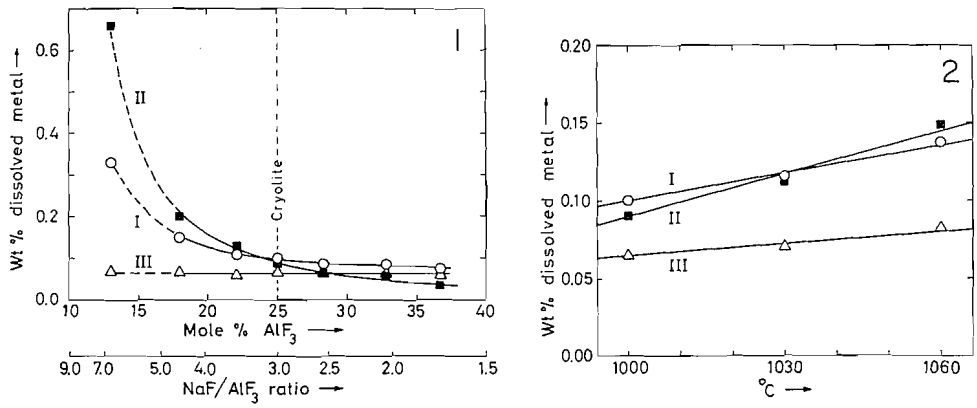

FIG. 1. The solubility of metal in $NaF-AlF_3-Al_2O_3$ melts. Curve I: Total solubility of sodium and aluminium as wt. % Al. Curve II: Sodium content in wt. % Na. Curve III: Aluminium content in wt. % Al.

FIG. 2. The solubility of metal in cryolite–alumina melts versus temperature. Curve I: Total solubility of sodium and aluminium as wt. % Al. Curve II: Sodium content in wt. % Na. Curve III: Aluminium content in wt. % Al.

peratures are presented in Fig. 2. Curves I, II, and III give the total solubility, the sodium content, and the aluminium content respectively.

The precision of the measurements is about ±5% for the total solubility and ±10% for the sodium and aluminium contents. Methods involving slow cooling of the samples gave low and irreproducible results. This was probably due to metal loss by evaporation during sampling. The vapor pressures of sodium over the melts are considerable, e.g., 0.1–0.3 atm in cryolite at 1 000 °C (5, 6, 9). The reproducibility of the results indicate, however, that the rapid quenching that was performed in these experiments permitted effective "freezing" of the existing equilibria in the melts so that possible evaporation losses were negligible.

The total solubility of sodium and aluminium in cryolite at 1 000 °C is 0.10 wt. % Al. The results for melts close to the cryolite composition are in good agreement with the data of Haupin (4). The results for AlF_3-rich melts disagree with those given by Zhurin (1) and by Mashovets and Svoboda (3), as these authors found the solubility to increase with increasing AlF_3 content. The observed total solubility in cryolite at 1 060 °C is slightly lower than that given by Zhurin (1). The results for the sodium content are lower than those found by Haupin (4) for melts with molar ratios $NaF/AlF_3 = 3$ and 2.6. Accordingly the results for the aluminium contents are higher, i.e., 0.065 wt. % Al in the present investigation as against 0.05 wt. % Al found by Haupin for both compositions.

In a previous investigation (10) the reactivity of the dissolved metal versus CO_2 was found to decrease with decreasing NaF/AlF_3 ratio as would be expected from the solubility data presented here. On the other hand, the metal loss due to evaporation (11) increases with decreasing NaF/AlF_3 ratio for melts with $NaF/AlF_3 < 2.7$. This is probably due to kinetic effects governing the evaporation.

The existing equilibrium between the sodium and aluminium contents of the melt may tentatively be described by a reaction as follows

[3] $$Al^{3+} + 2Na_2^+ \rightleftarrows Al^+ + 4Na^+$$

providing the dissolved species are Al^+ and Na_2^+. As long as the activities of the various constituents of these melts are virtually unknown, the Al^+/Na_2^+ ratio cannot be estimated from thermodynamic data. If eqs. [1], [2], and [3] are considered, however, the aluminium

Can. J. Chem. Downloaded from www.nrcresearchpress.com by 210.87.254.5 on 09/05/12
For personal use only.

content would be expected to increase and the sodium content to decrease with decreasing NaF/AlF_3 ratio.

The apparent constancy of the aluminium content as given by curve III in Fig. 1 is therefore somewhat surprising. However, for melts with $NaF/AlF_3 < 3$ saturated with alumina at 1 000 °C, it can be shown that the cation fraction of Al^{3+} (regardless of the structural entities in which it occurs) changes very little with decreasing NaF/AlF_3 ratio, e.g., from 0.36 at $NaF/AlF_3 = 3$ to 0.42 at $NaF/AlF_3 = 1.85$. This is due to the decreasing solubility of alumina in this range. The saturation concentrations of alumina at 1 000 °C are about 13 wt. % Al_2O_3 for melts in the range $NaF/AlF_3 = 3$ to 4.2 and decreases to 7 wt. % Al_2O_3 at $NaF/Alf_3 = 6.4$ (12) and 9.7 wt. % Al_2O_3 at $NaF/AlF_3 = 1.85$ (13).

From the sodium content of pig aluminium, Grjotheim (6) estimated the sodium pressure of a cryolite melt at 1 000 °C to be about 0.1 atm, while Feinleib and Porter (9) from measurements with Pb–Na cathodes found it to be about 0.15 atm. The sodium pressure above the melt has been measured spectroscopically by Stokes and Frank (5) and was found to be 0.3 atm at 1 000 °C, and 0.5 atm at 1 050 °C. Measurements by Jander and Hermann (14) and Grube and Hantelmann (15) indicate that the sodium pressure reaches 1 atm in the range 1–6 mole % AlF_3 in NaF at 1 000 °C.

The sodium content of the melts as given by curve II in Fig. 1 increases rapidly with increasing NaF/AlF_3 ratio as would be expected from the vapor pressure data. This is also in excellent agreement with the data presented by Pearson and Waddington (16) for the sodium content of aluminium in equilibrium with $NaF–AlF_3$ melts at 1 000 °C. The sodium content of the metal thus decreases from 0.031 wt. % Na at $NaF/AlF_3 = 4.25$ to 0.005 wt. % Na at $NaF/AlF_3 = 1.85$, while the sodium content of the melt, as determined in the present work, varies from 0.25 to 0.04 wt. % Na within the same range. It is readily seen that the relative changes in sodium content are the same in the metal and the melt.

The temperature dependence of the sodium solubility shown in Fig. 2 is in agreement with that of the vapor pressures found by Stokes and Frank (5). From Fig. 2 it can also be seen that the fraction of the total solubility represented by sodium increases with increasing temperature. This seems to agree with the fact (9) that the chemical potential of sodium approaches that of aluminium as the temperature increases.

REFERENCES

1. A. Zhurin *in* Y. K. Delimarskii and B. F. Markov. Electrochemistry of fused salts. The Sigma Press, Washington. 1961. p. 212.
2. E. Pruvot. Alluminio, **22**, 699 (1953).
3. V. P. Mashovets and R. V. Svoboda. J. Appl. Chem. USSR Eng. Transl. **32**, 2210 (1959).
4. W. E. Haupin. J. Electrochem. Soc. **107**, 232 (1960).
5. J. J. Stokes and W. B. Frank. Extractive metallurgy of aluminium. Vol. II. Interscience Publishers, New York. 1963. p. 3.
6. K. Grjotheim. Kgl. Norske Videnskab. Selskabs Skrifter, 1956. No. 5. pp. 65–80.
7. L. A. Firsanova. Sb. Nauchn. Tr. Inst. Tsvetn. Metal. **35**, 68 (1963).
8. E. Müller. Metoden der organischen Chemie. Vol. IV. Georg Thieme Verlag, Stuttgart. 1955. p. 234.
9. M. Feinleib and B. Porter. J. Electrochem. Soc. **103**, 231 (1956).
10. J. Thonstad. J. Electrochem. Soc. **111**, 959 (1964).
11. A. I. Beljajev, M. B. Rapoport, and L. A. Firsanova. Metallurgie des aluminiums. Vol. I. VEB Verlag Technik, Berlin. 1956. p. 114.
12. P. A. Foster, Jr. J. Chem. and Eng. Data, **9**, 200 (1964).
13. A. Fenerty and E. A. Hollingshead. J. Electrochem. Soc. **107**, 993 (1960).
14. W. Jander and H. Hermann. Z. Anorg. Allgem. Chem. **239**, 65 (1938).
15. G. Grube and P. Hantelmann. The reactions of Al with melts of the system $NaF–AlF_3$ and $NaF–AlF_3–Al_2O_3$. Kaiser Wilhelm Institut für Metallforschung. Feb. 1945.
16. T. G. Pearson and J. Waddington. Discussions Faraday Soc. **1**, 307 (1947).

Can. J. Chem. Downloaded from www.nrcresearchpress.com by 210.87.254.5 on 09/05/12
For personal use only.

Can. J. Chem. Downloaded from www.nrcresearchpress.com by 210.87.254.42 on 09/05/12
For personal use only.

NOTES

DEMJANOV REARRANGEMENT OF 9-XANTHENEMETHYLAMINE

S. N. Alam and D. B. MacLean

The ring expansion of xanthene derivatives to dibenz[*b*,*f*]oxepin is already known. Thus Anet and Bavin (1) have reported the synthesis of dibenz[*b*,*f*]oxepin and 10-methyldibenz[*b*,*f*]oxepin by Wagner–Meerwein rearrangement of 9-xanthenemethanol and 9-hydroxymethyl-9-methylxanthene. More recently, Whitlock (2) has reported the formation of dibenz[*b*,*f*]oxepin in 61% yield when xanthylium perchlorate is treated with ethereal diazomethane. We wish to report on the reaction of 9-xanthenemethylamine under the conditions of the Demjanov rearrangement (3), in which ring expansion has also been observed.

9-Xanthenemethylamine (4, 5) was prepared from 9-xantheneacetic acid (6) in the following manner. The acid was converted into its acid chloride with thionyl chloride and this in turn into the azide, which underwent Curtius rearrangement (7) to the isocyanate. Treatment of the isocyanate with alkali, however, gave N,N′-di(9-xanthenemethyl)urea instead of the amine. The formation of the urea was avoided by conversion of the crude isocyanate into the ethylurethane followed by hydrolysis of the urethane to 9-xanthenemethylamine, which was isolated as the hydrochloride salt, in a yield of 41.5% based on 9-xantheneacetic acid. The yield was improved to 52.5% by treatment of the crude isocyanate with benzyl alcohol followed by reduction of the benzylurethane to the amine.

9-Xanthenemethylamine was treated with nitrous acid in acetate buffer under experimental conditions normally employed in the Demjanov rearrangement. The crude product was worked up as described in the Experimental section and separated into an olefinic and an alcoholic fraction by column chromatography on alumina. The alcoholic fraction, comprising 96% of the product, was shown to be a mixture of 9-xanthenemethanol and 10,11-dihydrodibenz[*b*,*f*]oxepin-10(11,H)-ol in a ratio of 1:4. The ring-expanded alcohol is formed in an overall yield of 65% based on the amine. The composition of the mixture was established by nuclear magnetic resonance (n.m.r.) analysis of the mixture of the two alcohols and by partition chromatography on a silica gel column. To carry out the analysis it was necessary to synthesize the two alcohols by established procedures and to examine their physical properties. 9-Xanthenemethanol was prepared by the method of Anet and Bavin (1) and 10,11-dihydrodibenz[*b*,*f*]oxepin-10(11,H)-ol by borohydride reduction of the corresponding oxepinone, which was prepared by the method of Manske and Ledingham (8). The isomeric tertiary alcohol, 9-methyl-9-xanthenol, a possible product of this reaction, was also prepared (9), but its properties were such that its presence in the alcoholic fraction from the Demjanov reaction is precluded. We found that, when the tertiary alcohol was placed on an alumina column and chloroform applied to the column, the recovered product was not the alcohol. The product showed no hydroxyl absorption in the infrared, and was not further examined.

The foregoing results show that the Demjanov rearrangement may be applied successfully to the synthesis of 10,11-dihydrodibenz[*b*,*f*]oxepin-10(11,H)-ol and of dibenz[*b*,*f*]-oxepin itself. Manske and Ledingham have shown (8), and we have confirmed, that the alcohol may be converted quantitatively into the olefin.

Can. J. Chem. Downloaded from www.nrcresearchpress.com by 210.87.254.42 on 09/05/12
For personal use only.

EXPERIMENTAL

Apparatus, Methods, and Materials

Melting points were recorded on a Kofler micro hot stage melting point apparatus and are uncorrected.

The infrared spectra were recorded on a Beckman model IR-5 recording spectrophotometer in Nujol mull unless otherwise stated.

The n.m.r. spectra were measured in deuterochloroform solutions, with tetramethylsilane as an internal standard, on a Varian V-4300B high resolution spectrometer at a frequency of 60 Mc/s.

9-Xantheneacetyl Chloride

Purified thionyl chloride (4 ml) was cooled in an ice bath and 9-xantheneacetic acid (6) (4 g) was added slowly with mechanical stirring, at which time a semisolid green mass formed. Additional thionyl chloride (4 ml) was added and the mixture boiled gently under reflux for 25 min. The excess thionyl chloride was then removed under reduced pressure and the residual green solid crystallized from benzene to give 9-xantheneacetyl chloride (3.5 g, 82%), m.p. 95–96°. The reported melting point for the acid chloride is 98 °C (6).

9-Xantheneacetyl Azide

A solution of sodium azide (1.0 g) in water (2 ml) was added dropwise to a stirred ice-cooled solution of 9-xantheneacetyl chloride (1.0 g) in acetone (15 ml) and the mixture allowed to stand for 15 min. The resulting oily mixture was diluted with water (30 ml) and the crystalline azide filtered and dried at room temperature under reduced pressure. The azide was used in subsequent experiments without further purification. The yield was 0.92 g (90.2%). The infrared spectrum of the azide showed a strong peak at 2 120 cm^{-1} (azide) and 1 730 cm^{-1} ($\rangle C{=}O$).

N,N'-Di(9-xanthenemethyl)urea

The azide prepared above was dissolved in dry benzene (5 ml) and heated under reflux for 2 h (or until nitrogen evolution had ceased). Removal of solvent on a rotary evaporator gave the isocyanate as a brownish solid. The crude isocyanate was dissolved in benzene (10 ml), treated with 10 ml of 50% potassium hydroxide solution, and heated on a steam bath for 1 h. Removal of benzene on a rotary evaporator followed by cooling of the aqueous layer gave a crystalline solid which was separated and washed with water. Crystallization from methanol gave N,N'-di(9-xanthenemethyl)urea which melted at 222–223°. The infrared spectrum showed an absorption peak at 3 330 cm^{-1} (—NH absorption) and a peak at 1 627 cm^{-1} which was attributed to the carbonyl group of the urea linkage.

Anal. Calcd. for $C_{29}H_{24}O_3N_2$: C, 77.90; H, 5.36; N, 6.27. Found: C, 78.31; H, 5.18; N, 6.34.

9-Xanthenemethyl Isocyanate

9-Xantheneacetyl azide (0.9 g) was dissolved in dry benzene (5 ml) and heated under reflux for 2.5 h, at which time the evolution of nitrogen had ceased. Upon evaporation of the benzene a brownish solid (0.8 g) was obtained. The infrared spectrum showed that the azide and the carbonyl peak had disappeared and that a new peak at 2 265 cm^{-1} (—N=C=O) had appeared. The yield of the isocyanate was quantitative.

9-Xanthenemethylamine

Method A

The crude isocyanate (0.6 g) was dissolved in absolute ethanol (20 ml) containing potassium hydroxide (4 g) and boiled under reflux for 15 h, during which time a small amount of a reddish precipitate formed. Additional absolute ethanol (15 ml) was added to dissolve the precipitate and the mixture was boiled under reflux for a further 30 min. The mixture was filtered, and the filtrate acidified with dilute hydrochloric acid and filtered free of potassium chloride. The filtrate was then refluxed for 1 h, cooled, and basified with ammonia, and most of the ethanol removed on a rotary evaporator. Water was added to the residue and the mixture extracted with ether. The ether extract, dried over anhydrous sodium sulfate, was saturated with dry hydrogen chloride gas, whereupon white crystals separated which, after they were dried, weighed 0.26 g (41.5% based on the acid chloride) and melted at 225–230°. Recrystallization from ethanol (95%) gave 9-xanthenemethylamine hydrochloride, which melted at 235–236°. The melting point reported for this compound is 235–236° (5).

Method B

The crude azide (2 g), prepared by the method described previously, was heated under reflux with benzyl alcohol (5 ml) and dry toluene (5 ml) for 3 h. The mixture was poured into a porcelain evaporating dish and the toluene was allowed to evaporate slowly. The crystalline residue was transferred to a Buchner funnel, washed with a little absolute ethanol, and dissolved in a mixture of methanol (15 ml) and glacial acetic acid (5 ml). This solution was hydrogenated at 50 p.s.i.g. in the presence of palladium black catalyst (0.5 g) for 6 h, filtered, concentrated under reduced pressure, and poured into cold water (200 ml). The aqueous solution was treated with 10% hydrochloric acid solution (50 ml) and the mixture was extracted twice with ether to remove non-basic impurities. Basification with ice-cold 10% sodium hydroxide solution gave a white residue, which was extracted with ether. The ether extract, dried over anhydrous sodium sulfate, was saturated with

dry hydrogen chloride gas, after which 1.0 g (53.8% based on acid chloride) of crystalline 9-xanthenemethylamine hydrochloride which melted at 230–231° was obtained. A sample recrystallized from ethanol (95%) melted at 235–237°. The infrared spectrum showed a continuous series of bands between 3 030 cm^{-1} and 2 500 cm^{-1} characteristic of NH_3^+ absorption, and absorption peaks at 1 600 and 1 570 cm^{-1} characteristic of aromatic absorption of xanthene derivatives, but no absorption in the carbonyl region. The mass spectrum of the free base showed a molecular ion peak at m/e 211.

Anal. Calcd. for $C_{14}H_{13}ON \cdot HCl$: C, 68.00; H, 5.65. Found: C, 67.88; H, 5.70.

Demjanov Rearrangement of 9-Xanthenemethylamine

9-Xanthenemethylamine hydrochloride (1.0 g, 0.004 mole) was dissolved in acetic acid – sodium acetate buffer (pH 5.8, 20 ml) and cooled to 0 °C in an ice bath, and the stirred solution was treated with a solution of sodium nitrite (0.4 g) in water (2 ml). When the addition was complete the reaction mixture was allowed to warm up slowly to room temperature and was kept there for 6 h. The mixture was then heated on a steam bath until nitrogen evolution had ceased (approximately 45 min). The cooled reaction mixture was then extracted with ether, and the ether extract washed with water and dried over anhydrous sodium sulfate. Evaporation of the ether gave a yellow oil (0.8 g). This oil was heated under reflux for 1 h with methanolic potassium hydroxide solution (5%, 50 ml) to hydrolyze the acetates to the corresponding alcohols. The reaction mixture was cooled, the methanol removed under reduced pressure, more water added, and the reaction mixture extracted with ether. The ether extract was washed with water and dried over anhydrous sodium sulfate. On removal of the ether a yellow oil (0.74 g) which could not be induced to crystallize was obtained.

Vapor phase chromatography on a 2.5% silicone gum rubber on a Celite column showed that approximately 96% of this material was a mixture of isomeric alcohols, the rest being olefin. However, no separation of the alcohol mixture was achieved by vapor phase chromatography. The peak assigned to the alcohol mixture was established by comparison with the peak of a mixture of synthetic alcohols. A mixture of the synthetic primary and secondary alcohols showed a single peak with the same retention time as the alcohol fraction obtained from the Demjanov reaction.

This oil was adsorbed on an alumina column (non-basic alumina, Woelm, Germany) and eluted successively with petroleum ether (b.p. 30–60°), ether, and chloroform. The ether fraction, after evaporation, gave yellow crystals (0.02 g) which melted over a wide range and which were not further investigated.

The chloroform fraction, after removal of solvent, gave a yellow oil (0.71 g). The infrared spectrum showed an absorption of medium intensity at 1 645 cm^{-1} and 1 610 cm^{-1}, a strong peak at 1 570 cm^{-1}, and a strong peak in the OH region at 3 400 cm^{-1}. The ultraviolet spectrum showed absorption at λ_{max} 337, 270, and 260 mμ and continuous absorption beyond 241 mμ. Vapor phase chromatography on the column described above showed only one peak, with a trace of another peak corresponding to that of dibenz[*b,f*]oxepin. The composition of the mixture was estimated from its n.m.r. spectrum by comparison with that of a synthetic mixture of the 9-xanthenemethanol and 10,11-dihydrodibenz[*b,f*]oxepin-10(11,H)-ol. It was found that the ratio of the rearranged alcohol to the unrearranged primary alcohol was approximately 4:1. Thus it may be calculated that the rearranged product is obtained in 65% yield, based on the weight of the free amine.

The alcohol fraction (0.5 g) obtained from alumina chromatography was chromatographed on a silica gel column (12% water) (w/w), elution being performed with ether, benzene–chloroform mixture (1:1), and finally chloroform. There was no material in the ether fraction. The 1:1 benzene fraction, after evaporation, yielded a viscous oil (0.09 g) which would not crystallize but which had an infrared spectrum similar to that of 9-xanthenemethanol. The chloroform fraction gave a viscous oil (0.4 g), the infrared spectrum of which was identical with that of synthetic 10,11-dihydrodibenz[*b,f*]oxepin-10(11,H)-ol.

10,11-Dihydrodibenz[b,f]oxepin-10(11,H)-one

This compound was prepared by the method of Manske and Ledingham (8). It melted at 55–56° (reported m.p. 56° (8)). The infrared spectrum showed carbonyl absorption at 1 675 cm^{-1} and peaks at 1 600 and 1 510 cm^{-1}. The mass spectrum showed a molecular weight of 210.

The n.m.r. spectrum showed a two-proton singlet at $\tau = 6.02$ (methylene protons), a multiplet centered at $\tau = 2.8$ (aromatic protons), and a doublet (one proton) at $\tau = 2.1$ and 1.95. The doublet may be assigned to the aromatic proton adjacent to the carbonyl group. This signal is shifted downfield as a result of diamagnetic anisotropy of the adjacent carbonyl group (10). The splitting into a doublet may be attributed to spin–spin coupling with the adjacent aromatic proton. The other half of the AB system is probably embedded in the general aromatic resonance multiplet.

10,11-Dihydrodibenz[b,f]oxepin-10(11,H)-ol

The oxepinone (1 g) was dissolved in absolute ethanol (15 ml), and sodium borohydride (2 g) was added to it in portions. The mixture was allowed to stand overnight, and the excess borohydride destroyed by adding acetone in portions. The clear solution was then acidified with dilute hydrochloric acid and filtered. The solution was extracted with chloroform, and the extract washed with water and dried over anhydrous sodium sulfate. The removal of solvent gave a viscous oil (0.8 g) which would not crystallize. This oil was

Can. J. Chem. Downloaded from www.nrcresearchpress.com by 210.87.254.42 on 09/05/12
For personal use only.

chromatographed on an alumina column (Woelm, non-basic), elution being performed with ether and chloroform. A small amount of gummy material was eluted with ether. The chloroform fraction, after removal of solvent, gave a viscous oil which would not crystallize. Thin-layer chromatography showed only a single spot. The infrared spectrum showed a peak at 3 400 cm^{-1} (OH) and peaks at 1 605 and 1 575 cm^{-1} (aromatic ring). The mass spectrum of this alcohol showed a molecular weight of 212. The ultraviolet spectrum showed absorption maxima at λ_{max} 300, 270, and 264 mμ, with a shoulder at 275 mμ and intense absorption below 228 mμ.

The n.m.r. spectrum of 10,11-dihydrodibenz[*b*,*f*]oxepin-10(11,H)-ol shows a symmetrical quartet at τ = 5.17 (one proton), a one-proton signal at τ = 7.38 which may be assigned to the hydroxyl proton, and a multiplet of eight signals between τ values 7.26 and 6.62 (two protons). This spectrum is reminiscent of an ABX type (10). Because of the rigidity enforced upon the system by the ether linkage, it can be seen from a Dreiding model of this molecule that the electronic environments around the two methylene protons are not identical. Furthermore, the chemical shift of the proton on the tertiary carbon atom will be different from that of the methylene protons because of the attached hydroxyl group. Consequently, the expected spectrum would be of the ABX type. Thus the quartet may be assigned to the —C*H*OH proton and the multiplet to the methylene protons.

Dibenz[b,f]oxepin

A portion of the alcohol (0.4 g) described above, in toluene (10 ml), was heated under reflux for 15 min with *p*-toluenesulfonic acid (0.5 g). The reaction mixture was poured onto crushed ice, and the toluene layer separated and washed with water. Evaporation of the toluene under reduced pressure yielded dark-colored crystals (0.35 g). The crystals were purified by eluting with ether through an alumina column. The eluted material was crystallized from methanol and melted at 110–111°. The melting point reported in the literature is 111° (8). The infrared spectrum showed two peaks of medium intensity at 1 600 and 1 575 cm^{-1} and a series of strong peaks in the low-frequency region. The mass spectrum showed a molecular weight of 194. The ultraviolet spectrum was identical with that reported by Anet and Bavin (1) for dibenz[*b*,*f*]oxepin. The n.m.r. spectrum of dibenz[*b*,*f*]oxepin is composed of two signals, as expected. There is a two-proton signal at τ = 3.25 (singlet) due to the olefinic protons, and an eight-proton multiplet centered at τ = 2.75 due to the aromatic protons.

9-Xanthenemethanol

This compound was prepared by the method of Anet and Bavin (1). The infrared spectrum showed peaks at 3 600, 3 450, 1 600, 1 570, 1 120, 1 098, and 895 cm^{-1}. The mass spectrum showed a molecular weight of 212. The n.m.r. spectrum of 9-xanthenemethanol shows a one-proton signal at τ = 7.72 (OH proton), a doublet centered at τ = 6.52 (two protons), and a triplet centered at τ = 6.12 (one proton). We have assigned the triplet to the tertiary —C—H proton and the doublet to the methylene protons (10). The coupling constant is found to be 6.6 c.p.s. The line positions and intensities are typical of an AB_2 spectrum with equal AB coupling constants (10), which is expected for such a system.

9-Methyl-9-xanthenol

9-Xanthenone (5 g) was treated with methylmagnesium iodide (2.16 g magnesium plus 11.84 g methyl iodide) in dry ether in a Soxhlet apparatus. A yellow solid separated during the course of the reaction. The whole was boiled under reflux for 1 h, after which the solid was filtered, washed with ether, and decomposed with cold 3% ammonium chloride solution. The mixture was extracted with ether and the ether extract dried over anhydrous sodium sulfate. Removal of the ether gave a crystalline product (3.9 g, 71%) which melted over a wide range. Repeated recrystallizations from a petroleum ether – ether mixture raised the melting point to 95–99° (capillary). The reported melting point for 9-methyl-9-xanthenol is 96–99° (9). The infrared spectrum of 9-methyl-9-xanthenol showed absorption peaks at 3 300, 1 600, 1 570, and 930 cm^{-1}. The mass spectrum did not show the molecular ion peak; instead, the strongest peak in the spectrum was at *m/e* 194 (M-18), which corresponds to a loss of water from the molecular ion.

ACKNOWLEDGMENTS

Financial assistance to S. N. Alam from the Canadian Commonwealth Scholarship Committee during the period 1960–1963 is gratefully acknowledged. This work was supported by a grant from the National Research Council of Canada.

1. F. A. L. Anet and P. M. G. Bavin. Can. J. Chem. **35**, 1084 (1957).
2. H. W. Whitlock. Tetrahedron Letters, **17**, 593 (1961).
3. P. A. S. Smith and D. R. Baer. Organic reactions. Vol. XI. John Wiley & Sons, Inc., New York. 1960. p. 157.
4. E. Sawicke and V. T. Oliverio. J. Org. Chem. **21**, 183 (1956).

Can. J. Chem. Downloaded from www.nrcresearchpress.com by 210.87.254.42 on 09/05/12
For personal use only.

5. V. EVDOKIMOFF and A. CALO. Ann. Chim. Rome, **49**, 1321 (1959).
6. A. A. GOLDBERG and A. H. WRAGG. J. Chem. Soc. 4823 (1957).
7. P. A. S. SMITH. Organic reactions. Vol. III. John Wiley & Sons, Inc., New York. 1946. p. 337.
8. R. H. F. MANSKE and A. E. LEDINGHAM. J. Am. Chem. Soc. **72**, 4797 (1950).
9. H. DECKER. Ber. **38**, 2507 (1905).
10. L. M. JACKMAN. Nuclear magnetic resonance spectroscopy. Pergamon Press, New York. 1962.

RECEIVED JULY 15, 1965.
DEPARTMENT OF CHEMISTRY,
MCMASTER UNIVERSITY,
HAMILTON, ONTARIO.

Can. J. Chem. Downloaded from www.nrcresearchpress.com by 210.87.254.42 on 09/05/12
For personal use only.

SYNTHESIS OF THE TRIMETHOXYPHENYLPROPENES

ALEXANDER T. SHULGIN

In the reaction shown in eq. [1] eighteen compounds are represented, of which four (elemicin (1), I*a*; isoelemicin (2), III*a*; asarone (3), III*b*; and β-asarone (4), II*b*), as well as an undesignated "calamol" (5), have been observed as constituents of essential oils, and another four have, in addition, been encountered synthetically as chemical intermediates (6). The syntheses and physical properties of these and of the ten remaining

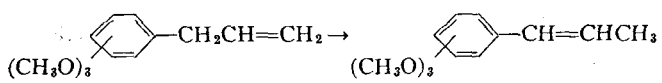

I*a* 3,4,5-Trimethoxy
I*b* 2,4,5-Trimethoxy
I*c* 2,3,4-Trimethoxy
I*d* 2,3,5-Trimethoxy
I*e* 2,3,6-Trimethoxy
I*f* 2,4,6-Trimethoxy

II (*cis*)
III (*trans*)

isomers are described in this note. The methylation of the Claisen rearrangement product of allyl 2,6-dimethoxyphenyl ether yielded elemicin (I*a*) which was identical with that isolated from nutmeg oil (7), and the 2,4,6 counterpart (I*f*) has been synthesized (6*a*) by methylation of the rearrangement product of allyl 3,5-dimethoxyphenyl ether. The synthesis of 2,3,4-trimethoxyallylbenzene (I*c*) was achieved through the corresponding rearrangement of allyl 2,3-dimethoxyphenyl ether (6*b*), but it has been neither isolated nor characterized.

The three remaining isomers, I*b*, I*d*, and I*e*, were obtained by the thermal rearrangement of the appropriate allyl dimethoxyphenyl ethers, followed by methylation of the potassium salts of the resulting phenols with methyl iodide. In the first of these, the rearrangement of allyl 3,4-dimethoxyphenyl ether to the phenolic precursor of I*b*, there are two ortho positions available. Rearrangement occurred preferentially (7:1) to the side nonadjacent to the methoxyl group, as shown by eventual conversion into asarone (III*b*) which was identical with that obtained from parsley oil. In the latter two required rearrangements (those of allyl 2,4-dimethoxyphenyl ether and allyl 2,5-dimethoxyphenyl ether to yield the phenolic precursors to I*d* and I*e* respectively), only a single ortho position is available for the migrating allyl group. The first of these ethers, indeed, rearranged exclusively (>95%) to the available ortho position, but the second underwent appreciable para rearrangement (57% ortho, 43% para) as well as diallylation through some intermolecular phenomenon (see Experimental).

5. V. EVDOKIMOFF and A. CALO. Ann. Chim. Rome, **49**, 1321 (1959).
6. A. A. GOLDBERG and A. H. WRAGG. J. Chem. Soc. 4823 (1957).
7. P. A. S. SMITH. Organic reactions. Vol. III. John Wiley & Sons, Inc., New York. 1946. p. 337.
8. R. H. F. MANSKE and A. E. LEDINGHAM. J. Am. Chem. Soc. **72**, 4797 (1950).
9. H. DECKER. Ber. **38**, 2507 (1905).
10. L. M. JACKMAN. Nuclear magnetic resonance spectroscopy. Pergamon Press, New York. 1962.

RECEIVED JULY 15, 1965.
DEPARTMENT OF CHEMISTRY,
MCMASTER UNIVERSITY,
HAMILTON, ONTARIO.

Can. J. Chem. Downloaded from www.nrcresearchpress.com by 210.87.254.6 on 09/05/12
For personal use only.

SYNTHESIS OF THE TRIMETHOXYPHENYLPROPENES

ALEXANDER T. SHULGIN

In the reaction shown in eq. [1] eighteen compounds are represented, of which four (elemicin (1), I*a*; isoelemicin (2), III*a*; asarone (3), III*b*; and β-asarone (4), II*b*), as well as an undesignated "calamol" (5), have been observed as constituents of essential oils, and another four have, in addition, been encountered synthetically as chemical intermediates (6). The syntheses and physical properties of these and of the ten remaining

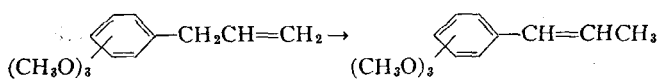

I*a* 3,4,5-Trimethoxy
I*b* 2,4,5-Trimethoxy
I*c* 2,3,4-Trimethoxy
I*d* 2,3,5-Trimethoxy
I*e* 2,3,6-Trimethoxy
I*f* 2,4,6-Trimethoxy

II (*cis*)
III (*trans*)

isomers are described in this note. The methylation of the Claisen rearrangement product of allyl 2,6-dimethoxyphenyl ether yielded elemicin (I*a*) which was identical with that isolated from nutmeg oil (7), and the 2,4,6 counterpart (I*f*) has been synthesized (6*a*) by methylation of the rearrangement product of allyl 3,5-dimethoxyphenyl ether. The synthesis of 2,3,4-trimethoxyallylbenzene (I*c*) was achieved through the corresponding rearrangement of allyl 2,3-dimethoxyphenyl ether (6*b*), but it has been neither isolated nor characterized.

The three remaining isomers, I*b*, I*d*, and I*e*, were obtained by the thermal rearrangement of the appropriate allyl dimethoxyphenyl ethers, followed by methylation of the potassium salts of the resulting phenols with methyl iodide. In the first of these, the rearrangement of allyl 3,4-dimethoxyphenyl ether to the phenolic precursor of I*b*, there are two ortho positions available. Rearrangement occurred preferentially (7:1) to the side nonadjacent to the methoxyl group, as shown by eventual conversion into asarone (III*b*) which was identical with that obtained from parsley oil. In the latter two required rearrangements (those of allyl 2,4-dimethoxyphenyl ether and allyl 2,5-dimethoxyphenyl ether to yield the phenolic precursors to I*d* and I*e* respectively), only a single ortho position is available for the migrating allyl group. The first of these ethers, indeed, rearranged exclusively (>95%) to the available ortho position, but the second underwent appreciable para rearrangement (57% ortho, 43% para) as well as diallylation through some intermolecular phenomenon (see Experimental).

Twelve isomers (II*a*–II*f*; III*a*–III*f*) can result from the base-catalyzed isomerization of the six trimethoxyallylbenzenes, I*a*–I*f*. II*b*, III*a*, and III*b* have been mentioned above as natural products, and both III*c* and III*f* have been prepared synthetically (6). The six allyl isomers described above have each been isomerized in ethanolic potassium hydroxide to mixtures of their *cis*- and *trans*-propenyl counterparts. The ratio of isomers that are formed invariably favored the *trans* form, which further was found to be the slower moving component in gas–liquid chromatography (g.l.c.) separations (8) and to be, in all cases except one, a crystalline solid at or near room temperature. The isomers were purified by preparative g.l.c., and only materials so obtained were utilized for the physical data recorded in Table I.

TABLE I

Physical characteristics of the eighteen trimethoxyphenylpropenes

Methoxy position	Alkyl group	Refractive index*	Melting point (°C)†	Retention time (min)‡	Isomer ratio, *trans*/*cis*§
3,4,5	Allyl	1.5308		2.38	11.4
	cis-Propenyl	1.5487		2.78	
	trans-Propenyl	1.5572	17–18	3.94	
2,4,5	Allyl	1.5317		2.59	11.5
	cis-Propenyl	1.5559		3.27	
	trans-Propenyl	1.5652	57–58	4.70	
2,3,4	Allyl	1.5174		1.37	5.4
	cis-Propenyl	1.5345		1.69	
	trans-Propenyl	1.5460	25–26	2.28	
2,3,5	Allyl	1.5240		2.24	13.4
	cis-Propenyl	1.5394		2.53	
	trans-Propenyl	1.5495	44–45	3.68	
2,3,6	Allyl	1.5238		1.73‖	12.2
	cis-Propenyl	1.5340		1.78‖	
	trans-Propenyl	1.5529		2.81	
2,4,6	Allyl	1.5306		2.62	5.8
	cis-Propenyl	1.5342		3.86	
	trans-Propenyl	1.5638	72–73	5.32	

*All values measured with the sodium D line at 24.5 °C. Solids were supercooled.
†Uncorrected.
‡Determined on a 20M polyethylene glycol column, described in the Experimental. 1,2,3-Trimethoxybenzene was added to the test mixtures, and its retention time taken as 1.00.
§Determined from the areas of the appropriate peaks, as measured by a rolling-disk planimeter.
‖Complete separation is obtained when a SE-30 silicone substrate is employed.

EXPERIMENTAL

The g.l.c. separations were achieved on a Wilkens Instrument Company Autoprep A-700. The principal column employed was an aluminium column, 5 ft by $\frac{3}{8}$ inch diameter, loaded to 10% with 20M polyethylene glycol on 60/80 mesh Chromosorb W. At an air bath temperature of about 180 °C and with a helium flow of about 500 ml/min, the standard internal reference chemical, 1,2,3-trimethoxybenzene, required about 4 min to emerge. The retention times of materials summarized in this report may thus be estimated from the values in Table I. Other substrates employed in the work will be described as they are mentioned. Samples for microanalytical evaluation were obtained from the g.l.c. separation directly in sealable capillaries. The members of this series all carry the empirical formula $C_{12}H_{16}O_3$, and all analyses were acceptable.

All infrared spectra were recorded on a Beckman IR-5A spectrophotometer. With the exception of the three higher melting *trans*-propenyl isomers, all samples were recorded as films between salt plates. These eighteen spectra have been placed in The Depository of Unpublished Data.* The physical data are given in Table I.

All materials described in this report were synthesized by the general sequence of reactions: dimethoxyphenol → allyl dimethoxyphenyl ether → allyldimethoxyphenol → trimethoxyallylbenzene (I) → trimethoxypropenylbenzene (II and III). As it would be unnecessarily repetitious to describe all six parallel processes,

**Photocopies may be obtained upon request to: The Depository of Unpublished Data, National Science Library, National Research Council, Ottawa, Canada.*

Can. J. Chem. Downloaded from www.nrcresearchpress.com by 210.87.254.6 on 09/05/12
For personal use only.

only one will be presented in detail. Any significant deviations required in the other isomeric syntheses will be mentioned briefly.

2,4-Dimethoxyphenol

A solution of 68 g of 2,4-dimethoxybenzaldehyde (K and K Laboratories) in 250 g glacial acetic acid was brought to 25° and treated dropwise, over 1 h, with 86 g of a 40% solution of peracetic acid in acetic acid. The reaction mixture was diluted with three volumes of water, and then neutralized cautiously with 283 g of anhydrous potassium carbonate. Extensive extraction with ether yielded, after removal of the solvent, 66 g of the formate of 2,4-dimethoxyphenol. This was hydrolyzed with 10% base for 1 h at steam bath temperatures. The resulting solution was extracted once with methylene chloride (discarded), acidified with aqueous hydrochloric acid, and re-extracted several times with methylene chloride. These latter extracts were washed once with an aqueous solution of sodium bicarbonate (which removed much of the color), dried, and concentrated by evaporation on the steam bath. The resulting product, which crystallized when the concentrate was cooled below room temperature, weighed 34.4 g (54% yield) and yielded a benzoate (with benzoyl chloride in pyridine, recrystallized from cyclohexane) which melted at 89–90 °C (literature values: phenol, m.p. 28°; benzoate, m.p. 90° (9)). The 2,3-, 3,4-, and 2,5-dimethoxybenzaldehydes were oxidized similarly to the phenols, in similar yields. 3,5-Dimethoxybenzaldehyde gave no phenolic product with peracetic acid, and the corresponding phenol was synthesized from phloroglucinol (10). 2,6-Dimethoxyphenol was obtained commercially from Eastman Kodak Company.

Allyl 2,4-Dimethoxyphenyl Ether

A solution of 31.0 g of the above crude phenol in 60 ml absolute ethanol was combined with another containing 11.25 g potassium hydroxide in 90 ml anhydrous ethanol. Allyl bromide was immediately added (28 g) and the resulting solution refluxed on the steam bath for 2 h. A precipitate of potassium bromide formed within a minute of heating. At the end of the reaction, the mixture was quenched with several volumes of water, made strongly basic with 10% caustic, and extracted with several volumes of ether. Evaporation of the solvent provided 33.2 g of the desired product (85% yield; b.p. 107–110° at 1.0 mm Hg; $n_D^{22.8}$ 1.5322), which was shown to be free of the starting phenol by analysis on an ethylene glycol succinate g.l.c. column (5% substrate, 10 ft length, $\frac{3}{8}$ inch diameter, 165°*).

2-Allyl-4,6-dimethoxyphenol

The ether (31.0 g) was heated to 215 °C, at which temperature an exothermic reaction ensued that raised the temperature to 270°. The temperature was held at about 260° for an additional 10 min. The rearrangement product thus obtained (n_D^{25} 1.5464) was submitted to methylation without further purification.†

2,3,5-Trimethoxyallylbenzene (Id)

The phenol was methylated directly, in anhydrous ethanol, by treatment with, first, 8.7 g potassium hydroxide dissolved in 75 ml boiling ethanol, and then with 22.4 g methyl iodide. Potassium iodide formed immediately. After 3 h at reflux, the reaction mixture was cooled, quenched with several volumes of water, made strongly basic with 10% caustic, and then extracted with four portions of 100 ml ether. These extracts, after drying and removal of the solvent by evaporation, provided 28 g of an oil. Analysis by g.l.c. showed the presence of about 10% 1,2,4-trimethoxybenzene (from the 2,4-dimethoxyphenol known to be present before methylation) and less than 2% of all other volatile contaminants. The yield of *Id* was thus greater than 80% based on the initial allyl ether. The infrared spectra of the crude reaction product and of the chromatographically isolated specimen were virtually identical; the latter was employed for the refractive index value.

The 2,3,6-trimethoxy isomer obtained similarly from allyl 2,5-dimethoxyphenyl ether was admixed with an almost equal amount of the 2,4,5-isomer. To obtain an adequate amount of the former material both for necessary descriptions and for the subsequent isomerization to the propenyl mixture, it was necessary to repeatedly inject *scores* of 0.15 ml portions into the Wilkins Autoprep machine, utilizing the existing trapping machinery. Trapping efficiency was less than 50%, because of extensive aerosol formation. In this process, a later peak, constituting 12% of the entire crude reaction mixture, was trapped. This trimethoxydiallylbenzene showed a $n_D^{24.5}$ of 1.5228.

Anal. Calcd. for $C_{15}H_{20}O_3$: C, 72.55; H, 8.12. Found: C, 72.11; H, 7.66.

As one might expect the 1,2,4-substitution of the starting ether to be maintained, and as one might assume that the two allyl groups are located either ortho–ortho or ortho–para to the formed hydroxyl group, then these two allyl groups must bear a meta relationship to one another. Thus this material is assigned the structure 1,3-diallyl-2,4,5-trimethoxybenzene.

**It has been found that the thermally unstable allyl ethers can be analyzed if chromatographed on an ethylene glycol succinate column at temperatures below 180°. Under these conditions there is no detectable rearrangement to the allyl phenols. With a silicone column, even at these temperatures, there is extensive continuous rearrangement on the column, providing a complex and misleading picture of the original composition.*

†*The presence of about 10% of 2,4-dimethoxyphenol in this product (a material specifically shown to be absent in the ether precursor) indicates a side reation involving deallylation. The phenol is best removed as its methyl ether (1,2,4-trimethoxybenzene) in the next step.*

For personal use only.

2,3,5-Trimethoxypropenylbenzene (IId and IIId)

A solution of 26 g of the crude trimethoxyallylbenzene in an equal weight of anhydrous ethanol was treated with 52 g finely flaked potassium hydroxide. Heating on the steam bath for 24 h with occasional agitation effected complete isomerization to the propenyl mixture. The reaction mixture was quenched with much water, and extracted with ether. Removal of the solvent provided 24.6 g of the crude mixture, a yield of about 95%. This crude product provided the isomer ratio data incorporated in Table I. Dilution with an equal volume of pentane, intense cooling, and rapid filtration yielded 9.2 g of an amber-colored crystalline solid. This, upon recrystallization from hexane, provided the pure *trans* isomer, m.p. 44–45°. The mother liquors of the original pentane crystallization were stripped of solvent, and then subjected to g.l.c. purification to provide the sample of the *cis* isomer described in this note. The 2,3,4- and 2,4,6-trimethoxyallylbenzenes required twice the time for isomerization.

1. F. W. SEMMLER. Ber. **41**, 1768 (1908); **41**, 1918 (1908); **41**, 2183 (1908).
2. T. KARIYONE and A. MAJIMA. J. Pharm. Soc. Japan, **55**, 41 (1935).
3. E. GUENTHER. The essential oils. Vol. II. D. Van Nostrand Co., Inc., New York. 1949. p. 535.
4. B. S. RAO and K. SUBRANANIAN. J. Chem. Soc. 1338 (1937).
5. M. QUDRAT-I-KHUDA, A. MUKERJEE, and S. K. GHOSH. J. Indian Chem. Soc. **16**, 583 (1939).
6. (*a*) P. HOLMES, D. E. WHITE, and I. H. WILSON. J. Chem. Soc. 2810 (1950). (*b*) V. M. TRIKOJUS and D. E. WHITE. J. Chem. Soc. 436 (1949).
7. A. T. SHULGIN. Nature, **197**, 379 (1963).
8. R. M. BAXTER, M. C. FAN, and S. I. KANDEL. Can. J. Chem. **40**, 154 (1962).
9. E. SPATH, M. PAILER, and G. GERGELEY. Ber. **73B**, 795 (1940).
10. D. D. PRATT and R. ROBINSON. J. Chem. Soc. **125**, 188 (1924).

RECEIVED APRIL 12, 1965.
THE DOW CHEMICAL COMPANY,
WALNUT CREEK, CALIFORNIA.

Can. J. Chem. Downloaded from www.nrcresearchpress.com by 210.87.254.6 on 09/05/12
For personal use only.

DIRECT DISPLACEMENT OF A PRIMARY TOLYL-*p*-SULFONYLOXY GROUP BY THE METHOXIDE ION: A MORE DIRECT ROUTE TO 5-*O*-METHYL-L-ARABINOSE AND 3,5-DI-*O*-METHYL-L-ARABINOSE

S. C. WILLIAMS AND J. K. N. JONES

The direct displacement (S_N2) of a primary tosyloxy group by many other groups has been known for some time. Mitra *et al.* (1) have reported the displacement of a primary mesyloxy (methanesulfonyloxy) group in a hexose derivative by methoxide ion, and we now report the displacement by methoxide of the primary tosyloxy group in a pentose derivative.

Detosylation of 5-*O*-tosyl-L-arabinose derivatives with aqueous methanol and sodium amalgam (2, 3) to give the free hydroxyl on C-5 invariably produced traces of the methylated sugar. It was felt that reaction with sodium methoxide in anhydrous methanol should increase the yield of this methylated sugar by a reaction analogous to that described by Mitra *et al.* (1). Under these conditions 1,2-*O*-isopropylidene-5-*O*-tosyl-L-arabinose (I; R = H, R_1 = tosyl) gave equal amounts of 1,2-*O*-isopropylidene-5-*O*-methyl-L-arabinose (I; R = H, R_1 = CH_3) and 1,2-*O*-isopropylidene-L-arabinose (I; R = R_1 = H), while reaction with 1,2-*O*-isopropylidene-3-*O*-methyl-5-*O*-tosyl-L-arabinose (I; R = CH_3, R_1 = tosyl) gave four times as much 3,5-di-*O*-methyl-L-arabinose derivative (I; R = R_1 = CH_3) as 3-*O*-methyl-L-arabinose derivative (I; R = CH_3, R_1 = H).

The reaction of methyl 3,4-di-*O*-methyl-2-*O*-tosyl-β-L-arabinoside (II; R_2 = tosyl, R_3 = R_4 = CH_3) under the same conditions (sodium methoxide in anhydrous methanol) gave mainly methyl 3,4-di-*O*-methyl-β-L-arabinoside (II; R_2 = H, R_3 = R_4 = CH_3)

2,3,5-Trimethoxypropenylbenzene (IId and IIId)

A solution of 26 g of the crude trimethoxyallylbenzene in an equal weight of anhydrous ethanol was treated with 52 g finely flaked potassium hydroxide. Heating on the steam bath for 24 h with occasional agitation effected complete isomerization to the propenyl mixture. The reaction mixture was quenched with much water, and extracted with ether. Removal of the solvent provided 24.6 g of the crude mixture, a yield of about 95%. This crude product provided the isomer ratio data incorporated in Table I. Dilution with an equal volume of pentane, intense cooling, and rapid filtration yielded 9.2 g of an amber-colored crystalline solid. This, upon recrystallization from hexane, provided the pure *trans* isomer, m.p. 44–45°. The mother liquors of the original pentane crystallization were stripped of solvent, and then subjected to g.l.c. purification to provide the sample of the *cis* isomer described in this note. The 2,3,4- and 2,4,6-trimethoxyallylbenzenes required twice the time for isomerization.

1. F. W. SEMMLER. Ber. **41**, 1768 (1908); **41**, 1918 (1908); **41**, 2183 (1908).
2. T. KARIYONE and A. MAJIMA. J. Pharm. Soc. Japan, **55**, 41 (1935).
3. E. GUENTHER. The essential oils. Vol. II. D. Van Nostrand Co., Inc., New York. 1949. p. 535.
4. B. S. RAO and K. SUBRANANIAN. J. Chem. Soc. 1338 (1937).
5. M. QUDRAT-I-KHUDA, A. MUKERJEE, and S. K. GHOSH. J. Indian Chem. Soc. **16**, 583 (1939).
6. (*a*) P. HOLMES, D. E. WHITE, and I. H. WILSON. J. Chem. Soc. 2810 (1950). (*b*) V. M. TRIKOJUS and D. E. WHITE. J. Chem. Soc. 436 (1949).
7. A. T. SHULGIN. Nature, **197**, 379 (1963).
8. R. M. BAXTER, M. C. FAN, and S. I. KANDEL. Can. J. Chem. **40**, 154 (1962).
9. E. SPATH, M. PAILER, and G. GERGELEY. Ber. **73B**, 795 (1940).
10. D. D. PRATT and R. ROBINSON. J. Chem. Soc. **125**, 188 (1924).

RECEIVED APRIL 12, 1965.
THE DOW CHEMICAL COMPANY,
WALNUT CREEK, CALIFORNIA.

Can. J. Chem. Downloaded from www.nrcresearchpress.com by 210.87.254.40 on 09/05/12
For personal use only.

DIRECT DISPLACEMENT OF A PRIMARY TOLYL-*p*-SULFONYLOXY GROUP BY THE METHOXIDE ION: A MORE DIRECT ROUTE TO 5-*O*-METHYL-L-ARABINOSE AND 3,5-DI-*O*-METHYL-L-ARABINOSE

S. C. WILLIAMS AND J. K. N. JONES

The direct displacement (S_N2) of a primary tosyloxy group by many other groups has been known for some time. Mitra *et al.* (1) have reported the displacement of a primary mesyloxy (methanesulfonyloxy) group in a hexose derivative by methoxide ion, and we now report the displacement by methoxide of the primary tosyloxy group in a pentose derivative.

Detosylation of 5-*O*-tosyl-L-arabinose derivatives with aqueous methanol and sodium amalgam (2, 3) to give the free hydroxyl on C-5 invariably produced traces of the methylated sugar. It was felt that reaction with sodium methoxide in anhydrous methanol should increase the yield of this methylated sugar by a reaction analogous to that described by Mitra *et al.* (1). Under these conditions 1,2-*O*-isopropylidene-5-*O*-tosyl-L-arabinose (I; R = H, R_1 = tosyl) gave equal amounts of 1,2-*O*-isopropylidene-5-*O*-methyl-L-arabinose (I; R = H, R_1 = CH_3) and 1,2-*O*-isopropylidene-L-arabinose (I; R = R_1 = H), while reaction with 1,2-*O*-isopropylidene-3-*O*-methyl-5-*O*-tosyl-L-arabinose (I; R = CH_3, R_1 = tosyl) gave four times as much 3,5-di-*O*-methyl-L-arabinose derivative (I; R = R_1 = CH_3) as 3-*O*-methyl-L-arabinose derivative (I; R = CH_3, R_1 = H).

The reaction of methyl 3,4-di-*O*-methyl-2-*O*-tosyl-β-L-arabinoside (II; R_2 = tosyl, R_3 = R_4 = CH_3) under the same conditions (sodium methoxide in anhydrous methanol) gave mainly methyl 3,4-di-*O*-methyl-β-L-arabinoside (II; R_2 = H, R_3 = R_4 = CH_3)

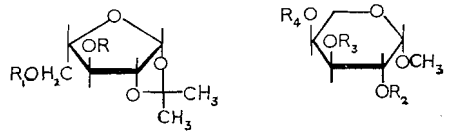

I II

with a small amount of a second material. This material was shown by gas–liquid partition chromatography to be neither methyl 2,3,4-tri-*O*-methyl-β-L-arabinoside (II; $R_2 = R_3 = R_4 = CH_3$) nor methyl 2,3,4-tri-*O*-methyl-β-L-riboside, so that displacement did not occur in this case. This material may possibly contain a double bond between C-1 and C-2 formed by the elimination of *p*-toluenesulfonic acid, as Ball (4) has postulated for a product of a similar type; this is being investigated further.

EXPERIMENTAL

Paper chromatography was carried out in the normal manner with the following solvent systems: (A) butan-1-ol–ethanol–water (3:1:1, v/v/v); (B) butanone saturated with 2% aqueous ammonium hydroxide; (C) butanone–water azeotrope (85:7, v/v). The sugars were located on the paper chromatograms with the following spray reagents: (*i*) alkaline silver nitrate (5); (*ii*) *p*-anisidine hydrochloride (6).

Thin-layer chromatography (t.l.c.) was carried out with silica gel G plates and the following solvent systems: (D) chloroform – 10% methanol; (E) benzene – 1% MeOH. The spots were located by spraying the plate with concentrated sulfuric acid and heating it at 140° for 5–10 min.

Melting points were taken on a Fisher block and are uncorrected. Evaporations were carried out under reduced pressure at 50° or less. Optical rotations were determined at 21° ± 2° on a Hilger standard polarimeter.

1,2-O-Isopropylidene-5-O-methyl-L-arabinose (I; R = H, $R_1 = CH_3$)

A solution of 1,2-*O*-isopropylidene-5-*O*-tosyl-L-arabinose (I; R = H, R_1 = tosyl) (10.0 g) in dry methanol (335 ml) containing sodium methoxide prepared from sodium (11 g) was refluxed under anhydrous conditions until the reaction was complete (26 h) as shown by t.l.c. The solution was cooled and filtered, and the filtrate was concentrated to dryness. The residue was then shaken with a mixture of water (200 ml) and chloroform (100 ml). The water layer was further extracted with chloroform (4 × 50 ml) and these latter extracts were combined, dried over sodium sulfate, and concentrated to a crystalline mass (0.50 g) which, after recrystallization from ether–petrol (100–120°), gave pure 1,2-*O*-isopropylidene-5-*O*-methyl-L-arabinose, m.p. 67–68.5°, $[\alpha]_D$ −9° (*c*, 0.655, in methanol).

Anal. Calcd. for $C_9H_{16}O_5$: C, 52.9; H, 7.9. Found: C, 52.7; H, 7.7.

The water layer yielded 1,2-*O*-isopropylidene-L-arabinose (I; R = R_1 = H) (0.67 g), m.p. 119–120°, $[\alpha]_D$ −28° (*c*, 0.94, in water). Compton and Levene (2) report m.p. 117–118°, $[\alpha]_D$ −29° (*c*, 2, in water). The original chloroform extract was concentrated to a syrup (2.44 g) which crystallized and was a mixture of 1,2-*O*-isopropylidene-5-*O*-methyl-L-arabinose and 1,2-*O*-isopropylidene-L-arabinose. It was separated by partition between chloroform and water. The total yield of pure 1,2-*O*-isopropylidene-5-*O*-methyl-L-arabinose was 1.535 g, i.e. 26%.

5-O-Methyl-L-arabinose

1,2-*O*-Isopropylidene-5-*O*-methyl-L-arabinose (0.49 g) was dissolved in 25% aqueous acetic acid (20 ml) and the solution was refluxed for 3 h. Concentration of the solution then gave syrupy 5-*O*-methyl-L-arabinose (0.39 g) which was chromatographically pure (R_G 0.38 (solvent B) (movement relative to tetramethyl glucose) and R_G 0.39 (solvent C)) and had $[\alpha]_D$ −24° (*c*, 0.86, in water). Siddiqui *et al.* (7) report R_G 0.39 (solvent C) and $[\alpha]_D$ −25° ± 1.5° (*c*, 1, in water). It was further characterized, after oxidation to the lactone, as the crystalline phenylhydrazide, m.p. 176.5–178.5°. The literature gives m.p. 176.5–178° (7).

1,2-O-Isopropylidene-3,5-di-O-methyl-L-arabinose (I; R = $R_1 = CH_3$)

A solution of 1,2-*O*-Isopropylidene-3-*O*-methyl-5-*O*-tosyl-L-arabinose (I; R = CH_3, R_1 = tosyl) (9.3 g) in anhydrous methanol (300 ml) containing sodium methoxide prepared from sodium (9 g) was refluxed, with the exclusion of moisture, for 29 h, at which time t.l.c. showed that no starting material was present. The solution was cooled and filtered, and the filtrate was concentrated to dryness. The product was shaken with water (200 ml) and chloroform (100 ml). The water layer was further extracted with chloroform (3 × 50 ml) and the chloroform extracts were combined, dried, and concentrated to a mobile yellow syrup (5.5 g) which consisted of two components, as shown by t.l.c. (solvents D and E).

Can. J. Chem. Downloaded from www.nrcresearchpress.com by 210.87.254.40 on 09/05/12
For personal use only.

3,5-Di-O-methyl-L-arabinose and 3-O-Methyl-L-arabinose

A solution of the above syrup (5.25 g) in 25% aqueous acetic acid (120 ml) was boiled under reflux for 3½ h. The solution was filtered and concentrated to a syrup (4.4 g). This syrup was dissolved in water (40 ml) and the water layer was continuously extracted with chloroform. The chloroform extract yielded chromatographically pure, syrupy 3,5-di-*O*-methyl-L-arabinose (2.6 g), R_G 0.83 (solvent B), R_G 0.82 (solvent C), $[\alpha]_D$ −41.5° (*c*, 1.08, in water). Percival and Zobrist (8) report $[\alpha]_D$ +47° (*c*, 0.76, in water) for the corresponding D-sugar. It was characterized as its crystalline phenylosazone, m.p. 169–170° (lit. m.p. 170° (9)). The aqueous layer, after the continuous chloroform extraction, yielded chromatographically pure syrupy 3-*O*-methyl-L-arabinose (0.6 g), $[\alpha]_D$ +102° (*c*, 0.77, in water), R_G 0.16 (solvent B), R_G 0.12 (solvent C). Hirst *et al.* (3) report $[\alpha]_D$ +96 and +110° (*c*, 3.6, in water). It was characterized as its crystalline phenylosazone, m.p. 163–165° (lit. m.p. 163° (10)).

Detosylation of Methyl 3,4-Di-O-methyl-2-O-tosyl-β-L-arabinoside (II; R_2 = tosyl, $R_3 = R_4 = CH_3$)

Methyl 3,4-di-*O*-methyl-2-*O*-tosyl-β-L-arabinoside (5.0 g) was dissolved in dry methanol (500 ml) containing sodium methoxide prepared from sodium (10 g), and the solution was refluxed under anhydrous conditions for 24 h. The solution was concentrated to dryness, and the residue was then shaken with a mixture of water (250 ml) and chloroform (125 ml). The water layer was further extracted with chloroform (5 × 125 ml), the combined chloroform extracts were dried over magnesium sulfate and filtered, and the filtrate was concentrated to a syrup (2.3 g). This "glycoside mixture" had $[\alpha]_D$ +203° (*c*, 0.96, in chloroform); Honeyman (11) gives $[\alpha]_D$ +210.6° (chloroform) for methyl 3,4-di-*O*-methyl-β-L-arabinoside.

The above syrup (1.9 g) was refluxed for 4 h in 1 *N* H_2SO_4 (50 ml), the solution was neutralized with barium carbonate and filtered, and the filtrate was concentrated to a syrup (1.3 g). Paper chromatography of the hydrolysate in solvent A revealed a main component (X), which moved at a rate equal to that of a dimethyl sugar (R_F 0.51), and a faster second component (Y) of R_F 0.65. These two components were separated by preparative paper chromatography to give 450 mg of the dimethyl sugar (X) and 93 mg of the faster material (Y). The dimethyl sugar (X) had $[\alpha]_D$ +137° (*c*, 0.84, in water); Whistler and McGilvray (12) give $[\alpha]_D$ +125° (water) for 3,4-di-*O*-methyl-L-arabinose.

Demethylation of Y with boron trichloride gave a mixture of arabinose and ribose. Analysis of the "glycoside mixture" by gas–liquid partition chromatography on a column of Apiezon M, 20% on Celite 545 (30–80 mesh), at 149° with a flow rate of 85 ml argon/min, showed that the glycoside of Y was neither methyl 2,3,4-tri-*O*-methyl-β-L-arabinoside nor methyl 2,3,4-tri-*O*-methyl-β-L-riboside (see Table I).

TABLE I

Separation of glycosides with 20% Apiezon M on Celite 545 (30–80 mesh), 149 °C, 85 ml argon/min

Symbol	Compounds	Retention time (min)
A	Methyl 2,3,4-tri-*O*-methyl-α-D-riboside	5.0
B	Methyl 2,3,4-tri-*O*-methyl-β-D-riboside	6.0
	+ methyl 2,3,4-tri-*O*-methyl-β-L-arabinoside	6.2
C	Unknown glycoside of Y	7.7

ACKNOWLEDGMENTS

The authors thank the National Research Council for a grant (N.R.C. T-19) and Queen's University for a scholarship (to S. C. W.) and a grant.

1. A. K. Mitra, D. H. Ball, and L. Long. J. Org. Chem. **27**, 160 (1962).
2. J. Compton and P. A. Levene. J. Biol. Chem. **116**, 189 (1936).
3. E. L. Hirst, J. K. N. Jones, and E. Williams. J. Chem. Soc. 1062 (1947).
4. D. H. Ball. Personal communication.
5. W. E. Trevelyan, D. P. Procter, and J. S. Harrison. Nature, **166**, 444 (1950).
6. L. Hough, J. K. N. Jones, and W. H. Wadman. J. Chem. Soc. 1702 (1950).
7. I. R. Siddiqui, C. T. Bishop, and G. A. Adams. Can. J. Chem. **39**, 1595 (1961).
8. E. E. Percival and R. Zobrist. J. Chem. Soc. 564 (1953).
9. E. V. White. J. Am. Chem. Soc. **68**, 272 (1946).
10. F. Smith. J. Chem. Soc. 753 (1939).
11. J. Honeyman. J. Chem. Soc. 990 (1946).
12. R. L. Whistler and D. I. McGilvray. J. Am. Chem. Soc. **77**, 1884 (1955).

Received July 19, 1965.
Department of Chemistry
Queen's University,
Kingston, Ontario.

Can. J. Chem. Downloaded from www.nrcresearchpress.com by 210.87.254.40 on 09/05/12
For personal use only.

SUBSTITUTIONS EN SERIE NAPHTALENIQUE
II. DERIVES DU DIMETHOXY-2,7 NAPHTALENE

JEAN-CLAUDE RICHER ET YVON PÉPIN

A la suite des résultats quelque peu surprenant qui ont été obtenus au cours d'un travail précédent (1) sur les réactions de substitution du diméthoxy-1,7 naphtalène, nous avons maintenant porté notre attention vers les réactions de nitration et de bromuration du diméthoxy-2,7 naphtalène (I).

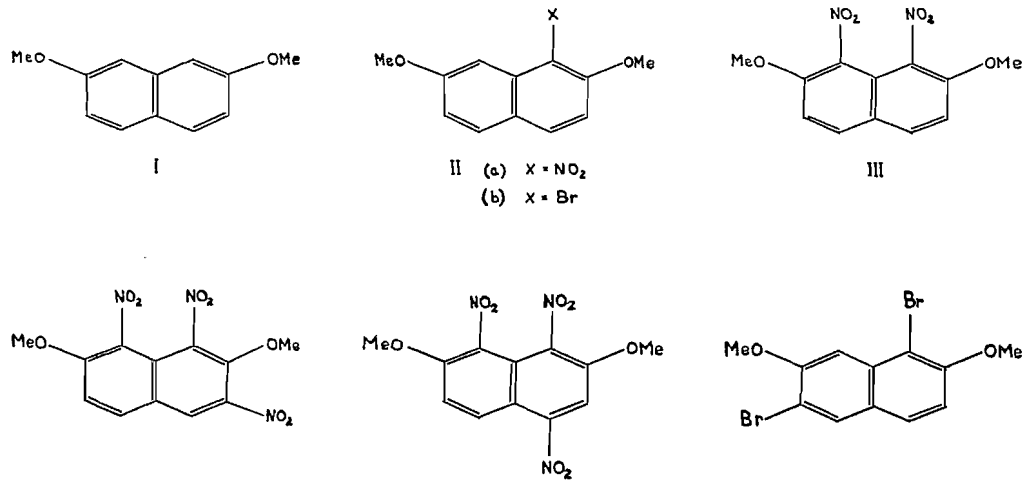

I II (a) X = NO_2 (b) X = Br III

IV V VI

VII VIII

Les réactions de nitration de I ont déjà été étudiées (2, 3). La mononitration conduirait au diméthoxy-2,7 nitro-1 naphtalène (II*a*) alors que la dinitration fournirait le diméthoxy-2,7 dinitro-1,8 naphtalène (III). Les nitrations selon Fisher (2) ont été reprises et les spectres de résonance magnétique nucléaire (r.m.n.) des composés obtenus ont confirmé que les structures II*a* et III doivent être attribuées respectivement au dérivé mononitré, p.f. 142° (litt. (2) 141°), et au dérivé dinitré, p.f. 280° (décomp.) (litt. (2) 286°). Aucune structure n'avait été attribué au trinitro diméthoxy-2,7 naphtalène, p.f. 223° (litt. (2) 216°). En appliquant au dérivé dinitré (II*a*) les paramètres d'additivité proposés par Wells et Alcorn (4) il est possible de prédire que le spectre r.m.n. du trinitro-1,3,8 et du trinitro-1,4,8 auraient les caractéristiques suivantes: trinitro-1,3,8 (IV) doublet à 8.02, doublet à 8.91 et singulet à 9.58 p.p.m.; trinitro-1,4,8 (V) doublet à 8.14, singulet à 8.62 et doublet à 9.02 p.p.m. Considérant que le spectre r.m.n. observé pour le dérivé

Can. J. Chem. Downloaded from www.nrcresearchpress.com by 210.87.254.42 on 09/05/12
For personal use only.

trinitré présente un doublet à 8.24, un doublet à 8.94 et un singulet à 9.48 p.p.m., il en est conclu que la structure IV doit être attribuée au dérivé trinitré.

Les réactions de bromuration de I ont été étudiées par plusieurs auteurs et les structures des produits qui en découlent sont des plus controversées (5–11). Les bromurations ont été reprises selon Wilson (9, 11) et les spectres r.m.n. des dérivés bromés obtenus ont été mesurés; les résultats sont résumés au Tableau I. Ces données sont compatibles avec les

TABLEAU I

Déplacements chimiques des protons aromatiques*

Diméthoxy-2,7 naphtalène	H_3	H_4	H_5	H_6	H_8
Non substitué (I)	7.05	7.83	7.83	7.05	7.34
Nitro-1 (II*a*)	7.64 (9)	8.28 (9.5)	8.12 (9.5)	7.29 (9 et 2.5)	7.02 (2.5)
Dinitro-1,8 (III)	7.89 (9.5)	8.55 (9.5)	8.55 (9.5)	7.89 (9.5)	—
Trinitro-1,3,8 (IV)	—	9.48	8.94 (9)	8.24 (9)	—
Bromo-1 (II*b*)	7.37 (9)	7.96 (9)	7.89 (9)	7.10 (9 et 2.5)	7.50 (2.5)
Dibromo-1,6 (VI)	7.47 (9)	7.87 (9)	8.18	—	7.47
Tribromo-1,3,6 (VII)	—	8.82	8.82	—	7.58

*Les spectres r.m.n. ont été déterminés à l'aide d'un appareil Varian A-60 pour des solutions dans la diméthylacétamide. Les déplacements chimiques ont été mesurés par rapport au tétramethylsilane utilisé comme standard interne et sont rapportés en p.p.m. (échelle δ où tétramethylsilane = 0). Les valeurs entre parenthèses indiquent les constantes de couplage entre protons ortho (H_3 vs. H_4 ou H_5 vs. H_6) ou les protons méta (H_6 vs. H_8).

structures II*b*, VI et VII attribuées respectivement aux dérivés monobromé, p.f. 78° (litt (11) 77.5–78°); dibromé, p.f. 128° (litt (9) 129–130°); tribromé, p.f. 171.5–172.5° (litt (9) 172.5°).

Au point de vue mécanistique, il est prévu que les réactions de nitration et de bromuration du diméthoxy-2,7 naphtalène (I) seront orientées principalement vers les positions 1 ou 8 dû au fait que ce sont des positions "α", adjacentes à des groupes méthoxyles qui les activent par des effets inductifs et mésomériques combinés. Toutefois il est connu (12) que les effets stériques présents dans le di-*t*-butyl-2,7 naphtalène (VIII) orientent la réaction de sulfonation de cet hydrocarbure vers la position 4. Il est alors très intéressant de noter que les effets stériques n'influencent aucunement l'introduction d'un premier substituant dans la molécule de diméthoxy-2,7 naphtalène et que les dérivés II (*a* et *b*) sont obtenus. D'autre part la formation du diméthoxy-2,7 dinitro-1,8 naphtalène (III) par opposition à la formation du dibromo-1,6 diméthoxy-2,7 naphtalène (VI) pourrait indiquer soit que les exigences stériques d'un groupe nitro sont plus faibles que celles d'un atome de brome ou que les effets électroniques d'un atome d'halogène par opposition à ceux d'un groupe nitro ont une influence très différente sur l'orientation de la deuxième substitution. Cette dernière hypothèse peut-être toutefois rejetée à la lumière des résultats de Wilson (13), qui rapporte que la dichloruration du diméthoxy-2,7 naphtalène conduit au dichloro-1,8 diméthoxy-2,7 naphtalène. Il peut donc en être conclu que les exigences stériques d'un atome de brome sont plus grandes que celles d'un groupe nitro. A ce point de vue nous rencontrons les opinions exprimées précédemment par Adams (14) dans ses travaux sur l'activité optique des biphényls.

Quant à l'orientation vers des position β (3 et 6) du troisième groupe nitro (position 3) et des deuxième (position 6) et troisième (position 3) atomes de brome, une seule explication semble nécessaire; ces positions β sont d'une part activées par l'effet inductif du groupe méthoxyle voisin alors que d'autre part l'autre groupe méthoxyle en position *amphi* leur oriente ses électrons par effet mésomérique.

En conclusion on peut donc mentionner que les réactions de substitutions sur le diméthoxy-2,7 naphtalène conduisent à des produits dont la formation peut-être rationalisée

Can. J. Chem. Downloaded from www.nrcresearchpress.com by 210.87.254.42 on 09/05/12
For personal use only.

sans grandes difficultés; il aurait toutefois été difficile de prédire avec certitude le cours que prendraient ces réactions.

REMERCIEMENTS

Les auteurs remercient le Conseil National de Recherches et Bristol Laboratories pour l'aide financière apportée sous forme d'octrois de recherches.

1. J. C. RICHER et C. LAMARRE. Can. J. Chem. **43**, 715 (1965).
2. O. FISHER et W. KERN. J. Prakt. Chem. **94**, 34 (1916).
3. F. BELL et J. R. GARRIE. J. Chem. Soc. 4258 (1961).
4. P. R. WELLS et P. G. E. ALCORN. Australian J. Chem. **16**, 1108 (1963).
5. R. SCHOOLL, C. SEER, R. WEIZENBOCH et A. ERTL. Monatsh. **42**, 407 (1921).
6. I. S. IOAFFE et N. M. FEDOROVA. J. Gen. Chem. USSR Engl. Transl. **6**, 1079 (1936).
7. R. ADAMS, M. W. MILLER, F. C. MCGREW et A. W. ANDERSON. J. Am. Chem. Soc. **64**, 1795 (1942).
8. F. BELL, J. A. GIBSON et R. D. WILSON. J. Chem. Soc. 2335 (1956).
9. R. D. WILSON. Tetrahedron, **3**, 236 (1958).
10. R. G. COOKE, B. L. JOHNSON et W. R. OWEN. Australian J. Chem. **13**, 256 (1960).
11. R. D. WILSON. Tetrahedron, **11**, 263 (1960).
12. M. MENARD, L. MITCHELL, J. KOMLOSSY, A. WRIGLEY et F. L. CHUBB. Can. J. Chem. **39**, 729 (1961).
13. R. D. WILSON. J. Chem. Soc. 3304 (1965).
14. W. M. STANLEY et R. ADAMS. J. Am. Chem. Soc. **52**, 1200 (1930).

REÇU LE 2 JUILLET 1965.
DÉPARTEMENT DE CHIMIE,
UNIVERSITÉ DE MONTRÉAL,
MONTRÉAL, QUÉBEC.

CONFIGURATION AND CONFORMATION OF 2,3-DICHLORO-1,4-DIOXANE, M.P. 52°

ROBERT R. FRASER AND C. REYES-ZAMORA

Considerable confusion has arisen recently concerning the configuration and conformation of the higher melting (52°) isomer, A, of 2,3-dichloro-1,4-dioxane. The compound was originally assigned the *cis* configuration by Summerbell and Lunk (1). This conclusion was arrived at after the compound was found to be less stable than the second isomer, B (m.p. 31°), which was proved to be *trans* by the demonstration that it was capable of kinetic resolution into one enantiomer. Subsequently, Altona and co-workers verified the assignment of the *trans* configuration to isomer B and established the configuration to be diaxial (2) through X-ray analysis, infrared spectra, and dipole moment studies. The dipole moment of isomer A was in agreement with the *cis* configuration. More recently, Caspi *et al.* (3) examined the nuclear magnetic resonance spectrum of isomer A and observed a single peak at 4.3 τ for the tertiary protons, and an A_2B_2 pattern for the hydrogens at the 5 and 6 positions. From the appearance of an A_2B_2 pattern they concluded that the dioxane ring possessed a rigid conformation. The single peak at 4.3 τ then led them to deduce the conformation to be an eclipsed boat, with oxygen occupying the "bowsprit" positions. Such conclusions were entirely unwarranted. A pair of rapidly interconverting chair conformations would also give rise to the observed spectrum. Unfortunately their findings were accepted in part by Chen and Le Fèvre (4), who measured the dipole moments, polarization, and polarizability of the two isomeric 2,3-dichloro- and 2,3-diphenyl-1,4-dioxanes. Because they accepted Caspi's conclusion that isomer A possessed a rigid conformation, they were forced, by elimination, to assign the *trans* diequatorial conformation to it. If assignment of either the *cis* boat conformation or the *trans* diequatorial conformation were correct, then some of the fundamental

Can. J. Chem. Downloaded from www.nrcresearchpress.com by 210.87.254.42 on 09/05/12
For personal use only.

sans grandes difficultés; il aurait toutefois été difficile de prédire avec certitude le cours que prendraient ces réactions.

REMERCIEMENTS

Les auteurs remercient le Conseil National de Recherches et Bristol Laboratories pour l'aide financière apportée sous forme d'octrois de recherches.

1. J. C. Richer et C. Lamarre. Can. J. Chem. **43**, 715 (1965).
2. O. Fisher et W. Kern. J. Prakt. Chem. **94**, 34 (1916).
3. F. Bell et J. R. Garrie. J. Chem. Soc. 4258 (1961).
4. P. R. Wells et P. G. E. Alcorn. Australian J. Chem. **16**, 1108 (1963).
5. R. Schooll, C. Seer, R. Weizenboch et A. Ertl. Monatsh. **42**, 407 (1921).
6. I. S. Ioaffe et N. M. Fedorova. J. Gen. Chem. USSR Engl. Transl. **6**, 1079 (1936).
7. R. Adams, M. W. Miller, F. C. McGrew et A. W. Anderson. J. Am. Chem. Soc. **64**, 1795 (1942).
8. F. Bell, J. A. Gibson et R. D. Wilson. J. Chem. Soc. 2335 (1956).
9. R. D. Wilson. Tetrahedron, **3**, 236 (1958).
10. R. G. Cooke, B. L. Johnson et W. R. Owen. Australian J. Chem. **13**, 256 (1960).
11. R. D. Wilson. Tetrahedron, **11**, 263 (1960).
12. M. Menard, L. Mitchell, J. Komlossy, A. Wrigley et F. L. Chubb. Can. J. Chem. **39**, 729 (1961).
13. R. D. Wilson. J. Chem. Soc. 3304 (1965).
14. W. M. Stanley et R. Adams. J. Am. Chem. Soc. **52**, 1200 (1930).

Reçu le 2 juillet 1965.
Département de Chimie,
Université de Montréal,
Montréal, Québec.

CONFIGURATION AND CONFORMATION OF 2,3-DICHLORO-1,4-DIOXANE, M.P. 52°

Robert R. Fraser and C. Reyes-Zamora

Considerable confusion has arisen recently concerning the configuration and conformation of the higher melting (52°) isomer, A, of 2,3-dichloro-1,4-dioxane. The compound was originally assigned the *cis* configuration by Summerbell and Lunk (1). This conclusion was arrived at after the compound was found to be less stable than the second isomer, B (m.p. 31°), which was proved to be *trans* by the demonstration that it was capable of kinetic resolution into one enantiomer. Subsequently, Altona and co-workers verified the assignment of the *trans* configuration to isomer B and established the configuration to be diaxial (2) through X-ray analysis, infrared spectra, and dipole moment studies. The dipole moment of isomer A was in agreement with the *cis* configuration. More recently, Caspi *et al.* (3) examined the nuclear magnetic resonance spectrum of isomer A and observed a single peak at 4.3 τ for the tertiary protons, and an A_2B_2 pattern for the hydrogens at the 5 and 6 positions. From the appearance of an A_2B_2 pattern they concluded that the dioxane ring possessed a rigid conformation. The single peak at 4.3 τ then led them to deduce the conformation to be an eclipsed boat, with oxygen occupying the "bowsprit" positions. Such conclusions were entirely unwarranted. A pair of rapidly interconverting chair conformations would also give rise to the observed spectrum. Unfortunately their findings were accepted in part by Chen and Le Fèvre (4), who measured the dipole moments, polarization, and polarizability of the two isomeric 2,3-dichloro- and 2,3-diphenyl-1,4-dioxanes. Because they accepted Caspi's conclusion that isomer A possessed a rigid conformation, they were forced, by elimination, to assign the *trans* diequatorial conformation to it. If assignment of either the *cis* boat conformation or the *trans* diequatorial conformation were correct, then some of the fundamental

Can. J. Chem. Downloaded from www.nrcresearchpress.com by 210.87.254.40 on 09/05/12
For personal use only.

energetic concepts in conformational analysis would be invalidated. For this reason we have undertaken a rigorous analysis of the A_2B_2 absorption pattern of isomer A in an attempt to clarify the existing discrepancies.

The nuclear magnetic resonance spectrum of a 15% solution (w/v) of isomer A in chloroform was measured. Figure 1A shows the high-field half of the A_2B_2 absorption.

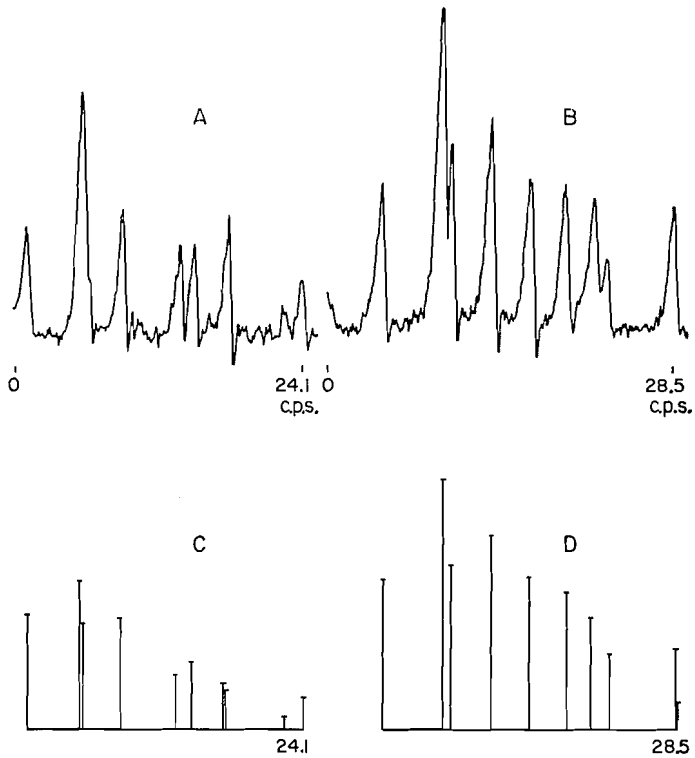

FIG. 1. High-field half of the A_2B_2 absorption of 2,3-dichloro-1,4-dioxane in chloroform (A) and in benzene (B). The spectra calculated from the parameters in the text are shown in C, for chloroform, and in D, for benzene. The points designated 0 refer to the midpoints of the A_2B_2 patterns.

The analysis of this pattern was achieved in the standard manner as recently described by Abraham (5). Assignment of the lines to specific transitions was relatively straightforward, since the spectrum closely resembled that solved by Abraham for 2-methyl-1,3-dioxolane. The parameters K, L, M, N, and δ were adjusted until agreement between calculated and observed line positions was obtained to within 0.15 c.p.s. (Fig. 1C). To check the parameters, we measured the spectrum of a 50% solution (w/v) of isomer A in benzene, and again obtained agreement to within 0.15 c.p.s. between the observed line positions and those calculated from the same values of K, L, M, and N and an adjusted δ. Figure 1 shows the agreement between the observed and calculated spectra in chloroform and in benzene. From the parameters the following coupling constants were found: $J_A = J_B = 3.1$ c.p.s.; $J = -12.25$ c.p.s.; $J' = 6.45$ c.p.s.; $\delta_{CHCl_3} = 22.95$ c.p.s.; $\delta_{benzene} = 31.1$ c.p.s.; where the coupling constants represent the interactions shown below.

$$\begin{array}{l} H_A\text{—}J_A\text{—}H_A \\ \quad | \quad \diagdown \\ \quad J \quad J' \\ \quad | \quad \diagdown \\ H_B\text{—}J_B\text{—}H_B \end{array}$$

Can. J. Chem. Downloaded from www.nrcresearchpress.com by 210.87.254.40 on 09/05/12
For personal use only.

In Fig. 2 all reasonable configurations and conformations for isomer A are shown. If the compound were *cis* and in a rigid chair conformation, we would expect two signals for the protons labelled X and Y in case I. We would also expect an ABCD pattern for the four hydrogens on carbons 5 and 6. Since neither expectation is fulfilled, we can eliminate structure I.

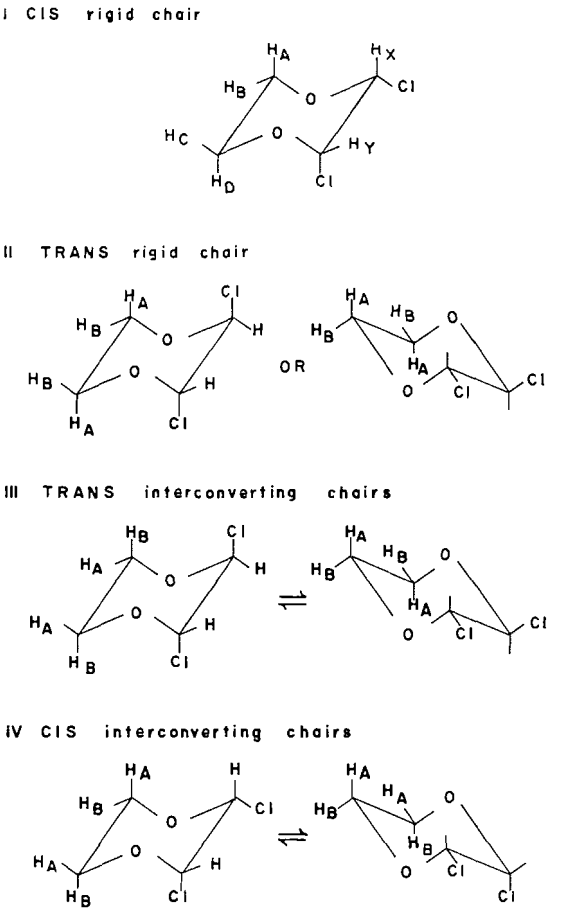

FIG. 2. The four considered representations for 2,3-dichloro-1,4-dioxane, m.p. 52°.

If the compound is *trans* and has its chlorines in either the rigid diaxial or the rigid diequatorial conformation, we would expect an A_2B_2 absorption pattern for the 5 and 6 hydrogens. But in this A_2B_2 system, J_A and J_B should have widely different magnitudes, one typical of diaxial protons and the other typical of diequatorial protons. Since we found $J_A = J_B$, this case is eliminated.

Should the compound possess the *trans* configuration and be rapidly interconverting between the diaxial and diequatorial conformations, there would likely be an unequal population of the two conformations. In this case J_A would not equal J_B, and so this possibility is eliminated. If the two conformations were of equal stability, we would observe coupling constants which are an average of the two contributing structures. This would require $J_A = J_B = (J_{60} + J_{180})/2$ (observed value 3.1 c.p.s.), $J = J_{gem}$, and $J' = J_{60}$ (observed value 6.45 c.p.s.), where the subscripts represent ϕ, the dihedral angle between

Can. J. Chem. Downloaded from www.nrcresearchpress.com by 210.87.254.40 on 09/05/12
For personal use only.

the interacting protons. The experimental results would then require that J_{60} be more than twice as large as $(J_{60} + J_{180})/2$. This completely revokes the Karplus relation between J_{vic} and ϕ. Although the relation is far from quantitative, it is completely reliable in predicting $J_{180} > J_{60}$ (6). Thus III is eliminated.

In case IV the observed parameters compare favorably with those encountered in similar six-membered rings. The best model for comparison is the 1,3-dioxane system (Fig. 3), whose analysis gave the following parameters (7): $J_{60} = J_{AB'} = 3.8$ c.p.s.;

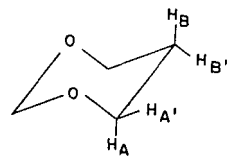

FIG. 3. The chair form of 1,3-dioxane showing the four protons whose coupling constants have been determined (7).

$(J_{60} + J_{180})/2 = (J_{A'B'} + J_{AB})/2 = 6.7$ c.p.s.; $J_{AA'} = -11.0$ c.p.s. (a better model in this case might be $CH_3—\underset{\displaystyle OH}{\underset{|}{CH}}—CH_2OH$, in which $J_{gem} = -11.9$ c.p.s. (8)). In 1,4-dioxane, $J_{60} = 2.7$ c.p.s. and $(J_{60} + J_{180})/2 = 6.1$ c.p.s. (9).

In view of the good agreement between the coupling constants for isomer A and those predicted from the *cis* configuration for interconverting chairs, any consideration of the relatively high energy boat conformations is entirely unwarranted. We therefore conclude that the 52° isomer of 2,3-dichloro-1,4-dioxane has the *cis* configuration and undergoes rapid chair–chair interconversion at room temperature. This is, of course, the original conclusion of Summerbell and Lunk, and is entirely compatible with all other existing physical data.

We are currently examining the isomeric 2,3-diphenyl-1,4-dioxanes, whose original structural assignments have also been questioned by Le Fèvre and Chen.

NOTE ADDED IN PROOF: We have learned of an independent investigation by D. Jung, whose results and conclusions are in complete agreement with our own. Dr. Jung's paper will appear in Chemische Berichte.

EXPERIMENTAL

2,3-Dichloro-1,4-dioxane

This compound was prepared by the procedure of Summerbell and Lunk (1), and after several recrystallizations from pentane–ether melted from 52 to 53 °C.

The nuclear magnetic resonance spectra were recorded on a Varian V-4302 60 Mc spectrometer, and the experimental line positions were obtained from the average of at least six traces, with the standard deviation in all line positions being less than 0.15 c.p.s. Calculations of line positions were carried out on our IBM 1620 computer, using the Frequint IVA program, which was kindly provided by Professor P. C. Lauterbur.

ACKNOWLEDGMENT

This research was supported by a grant from the National Research Council of Canada.

1. R. K. SUMMERBELL and H. E. LUNK. J. Am. Chem. Soc. **79**, 4802 (1957).
2. C. ALTONA, C. ROMERS, and E. HAVINGA. Tetrahedron Letters, **10**, 16 (1959).
3. E. CASPI, T. A. WITTSTRUCK, and D. M. PIATAK. J. Org. Chem. **27**, 3183 (1962).
4. C. Y. CHEN and R. J. LE FÈVRE. J. Chem. Soc. 558 (1965).
5. R. J. ABRAHAM. J. Chem. Soc. 256 (1965).

Can. J. Chem. Downloaded from www.nrcresearchpress.com by 210.87.254.40 on 09/05/12
For personal use only.

6. M. KARPLUS. J. Am. Chem. Soc. **85**, 2870 (1963).
7. C. BARBIER, J. DELMAU, and J. RANFT. Tetrahedron Letters, **45**, 3339 (1964).
8. Varian Nuclear Magnetic Resonance Spectra Catalog. 1962. p. 45.
9. N. SHEPPARD and J. TURNER. Proc. Roy. Soc. London, Ser. A, **252**, 206 (1961).

RECEIVED JULY 22, 1965.
DEPARTMENT OF CHEMISTRY,
UNIVERSITY OF OTTAWA,
OTTAWA, CANADA.

Can. J. Chem. Downloaded from www.nrcresearchpress.com by 210.87.254.40 on 09/05/12
For personal use only.

REACTION OF ARALKYL KETONE PHENYLHYDRAZONES WITH CARBON MONOXIDE; THERMAL INDOLIZATION OF ARALKYL KETONE PHENYLHYDRAZONES

ALEX ROSENTHAL AND M. YALPANI

This note summarizes the principal results obtained when aralkyl ketone phenylhydrazones were caused to react with carbon monoxide using dicobalt octacarbonyl as a catalyst. In earlier work (1, 2) it was shown that aromatic ketone and aldehyde phenylhydrazones containing a C=N group which was conjugated to an aromatic ring cyclized with carbon monoxide to yield N-substituted phthalimidines. Under similar conditions, aralkyl ketone phenylhydrazones might be expected to undergo ring closure to afford heterocyclic substances having six or more members.

Reaction of desoxybenzoin phenylhydrazone with carbon monoxide at 3 500 p.s.i. and a temperature of 235° for 3 h in the presence of preformed dicobalt octacarbonyl afforded mainly 2,3-diphenylindole (I), 3-benzylphthalimidine-N-carboxyanilide (II), 3-benzyl-2-phenylphthalimidine (III), and *sym*-diphenylurea (IV) in 20, 22, 11, and 27% yields,

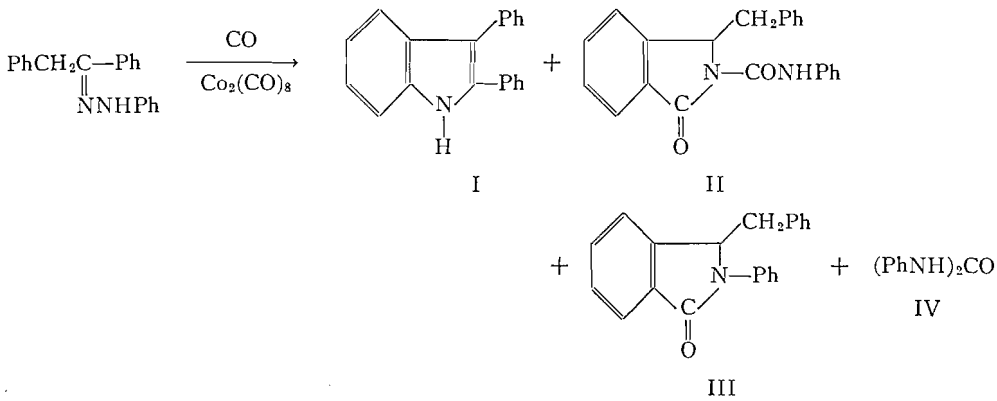

respectively. Separation of these components was achieved by thin-layer chromatography on silica gel G using benzene–methanol (95:5 v:v) as developer or by alumina column chromatography.

Compounds I and IV were identified by direct comparison with authentic samples of 2,3-diphenylindole and *sym*-diphenylurea, respectively. Reaction of 3-benzylphthalimidine with phenylisocyanate afforded an authentic sample of 3-benzylphthalimidine-N-carboxyanilide which was identical (melting point and infrared spectrum) with compound II. Condensation of benzylidene phthalide with aniline afforded 3-benzylidene-2-phenylphthalimidine. Reduction of the latter substance with 1 mole of hydrogen over platinum

6. M. KARPLUS. J. Am. Chem. Soc. **85**, 2870 (1963).
7. C. BARBIER, J. DELMAU, and J. RANFT. Tetrahedron Letters, **45**, 3339 (1964).
8. Varian Nuclear Magnetic Resonance Spectra Catalog. 1962. p. 45.
9. N. SHEPPARD and J. TURNER. Proc. Roy. Soc. London, Ser. A, **252**, 206 (1961).

RECEIVED JULY 22, 1965.
DEPARTMENT OF CHEMISTRY,
UNIVERSITY OF OTTAWA,
OTTAWA, CANADA.

Can. J. Chem. Downloaded from www.nrcresearchpress.com by 210.87.254.40 on 09/05/12
For personal use only.

REACTION OF ARALKYL KETONE PHENYLHYDRAZONES WITH CARBON MONOXIDE; THERMAL INDOLIZATION OF ARALKYL KETONE PHENYLHYDRAZONES

ALEX ROSENTHAL AND M. YALPANI

This note summarizes the principal results obtained when aralkyl ketone phenylhydrazones were caused to react with carbon monoxide using dicobalt octacarbonyl as a catalyst. In earlier work (1, 2) it was shown that aromatic ketone and aldehyde phenylhydrazones containing a C=N group which was conjugated to an aromatic ring cyclized with carbon monoxide to yield N-substituted phthalimidines. Under similar conditions, aralkyl ketone phenylhydrazones might be expected to undergo ring closure to afford heterocyclic substances having six or more members.

Reaction of desoxybenzoin phenylhydrazone with carbon monoxide at 3 500 p.s.i. and a temperature of 235° for 3 h in the presence of preformed dicobalt octacarbonyl afforded mainly 2,3-diphenylindole (I), 3-benzylphthalimidine-N-carboxyanilide (II), 3-benzyl-2-phenylphthalimidine (III), and *sym*-diphenylurea (IV) in 20, 22, 11, and 27% yields,

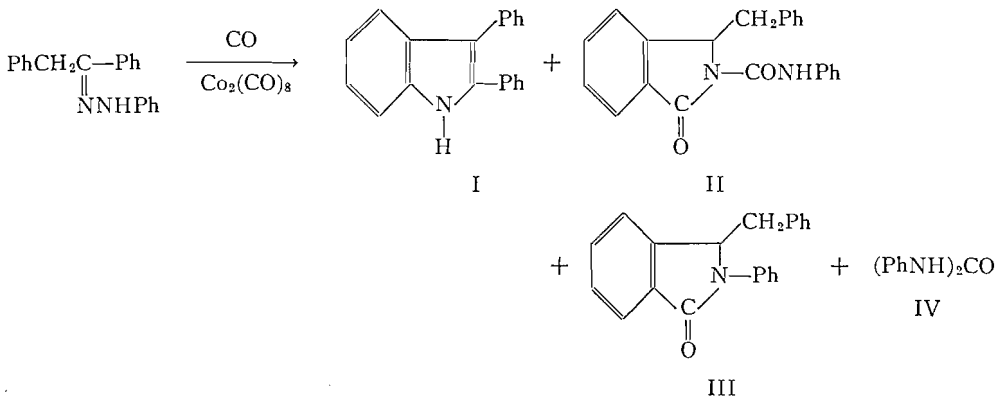

respectively. Separation of these components was achieved by thin-layer chromatography on silica gel G using benzene–methanol (95:5 v:v) as developer or by alumina column chromatography.

Compounds I and IV were identified by direct comparison with authentic samples of 2,3-diphenylindole and *sym*-diphenylurea, respectively. Reaction of 3-benzylphthalimidine with phenylisocyanate afforded an authentic sample of 3-benzylphthalimidine-N-carboxyanilide which was identical (melting point and infrared spectrum) with compound II. Condensation of benzylidene phthalide with aniline afforded 3-benzylidene-2-phenylphthalimidine. Reduction of the latter substance with 1 mole of hydrogen over platinum

oxide as catalyst yielded authentic 3-benzyl-2-phenylphthalimidine having an infrared spectrum which was identical with that of substance III.

Although the high-pressure cyclization reaction of desoxybenzoin phenylhydrazone with carbon monoxide demonstrates the preferential formation of the five-membered ring over the six-membered ring, it did not establish if a six-membered ring could be formed. To ascertain if a six-membered ring could be formed, 1,3-diphenyl-2-propanone phenylhydrazone was treated with carbon monoxide in the presence of dicobalt octacarbonyl. In the latter case no six-membered ring was formed. Interestingly, 2,3-diphenylindole accompanied the product that was obtained from desoxybenzoin phenylhydrazone, and 2-benzyl-3-phenylindole was the major product (65% yield) of the reaction of 1,3-diphenyl-2-propanone phenylhydrazone with carbon monoxide in the presence of dicobalt octacarbonyl.

Because the indoles were formed from the aralkyl ketone phenylhydrazones when the reaction was carried out in the presence of dicobalt octacarbonyl, it was felt that cobalt hydrocarbonyl (which would be formed from the dicobalt octacarbonyl) might be essential for the conversion of the hydrazones into the indoles. This speculation was proved to be incorrect by showing that the same conversion into indoles in higher yield (about 80%) occurred without the presence of the catalyst. A similar thermal indolization of hydrazones has recently been reported by other workers (3).

In the reaction of 2-ethoxy-1-naphthaldehyde phenylhydrazone with carbon monoxide, ring closure to the 8-position was expected, since the 2-position was blocked. However, no cyclization occurred. From these results, as well as those of other workers (4, 5), evidently only five-membered heterocycles can be formed from aromatic compounds containing the C=N group.

EXPERIMENTAL

Melting points are corrected. The alumina used for column chromatography was obtained from British Drug Houses. All molecular weights were determined by mass spectrometry by Mr. F. Bloss of this department on an Atlas CH4 spectrometer. Microanalysis was done in this department.

The high-pressure equipment and general procedure have been described previously (1, 2).

Reaction of Desoxybenzoin Phenylhydrazone with Carbon Monoxide to Yield 2,3-Diphenylindole (I), 3-Benzylphthalimidine-N-carboxyanilide (II), and 3-Benzyl-2-phenylphthalimidine (III)

Desoxybenzoin phenylhydrazone (11 g) was allowed to react with carbon monoxide at 235° and a pressure of 3 500 p.s.i. for 3 h in the presence of dicobalt octacarbonyl (2 g) as described previously (1). After removal of the catalyst, the benzene was evaporated under reduced pressure at 30°. Evaporation of the residual oil under reduced pressure at about 100° afforded aniline (0.5 g, 13%). Crystallization of the residual oil in 50 ml of hot benzene yielded 1.2 g (27%) of *sym*-diphenylurea which was recrystallized from chloroform; m.p. 251–252°; the mixed melting point with an authentic sample of *sym*-diphenylurea was 251–252°.

A 25 ml aliquot of the filtrate was chromatographed on alumina (120 × 71 mm diameter). Benzene (500 ml) eluted 0.23 g of an oil which possessed no carbonyl group.

Substance I (2,3-diphenylindole) was then eluted with 400 ml of benzene; yield 1.1 g (20%). Recrystallization of compound I from cyclohexane gave pure material; m.p. 123–124°; the mixed melting point with an authentic sample of 2,3-diphenylindole (6) was 123–124°. The infrared spectra of both compounds were identical.

Compound II (3-benzylphthalimidine-N-carboxyanilide) was then eluted with 3 000 ml of a 4:1 mixture of benzene–chloroform; yield 1.2 g (22%). Recrystallization of compound II from cyclohexane afforded the pure carboxyanilide; m.p. 146–147°; the mixed melting point with an authentic sample prepared by steps described below was 146–147°. The infrared spectra of both compounds were identical.

Elution of the column with a further 1 500 ml of the benzene–chloroform mixture gave 1.2 g of a mixture of compounds II and III. This mixture was separated by rechromatography on a new alumina column using benzene–ethanol (99.5:0.5) as developer. The yields reported for II and III include the material obtained from the rechromatography of the mixture.

Fraction III (3-benzyl-2-phenylphthalimidine) was then eluted with 1 600 ml of benzene–ethanol (98:2 v:v); yield 1.2 g (11%). Compound III was recrystallized from cyclohexane; m.p. 124–125°; the mixed melting point with a sample prepared by unambiguous steps as described below was 124–125°. The infrared spectra of both compounds were identical.

Can. J. Chem. Downloaded from www.nrcresearchpress.com by 210.87.254.40 on 09/05/12
For personal use only.

Thin-layer chromatography of the original product mixture on silica gel G using benzene–methanol (95:5) as developer showed the presence of trace quantities of at least three additional components.

Thermal Indolization of Desoxybenzoin Phenylhydrazone and of 1,3-Diphenylpropanone Phenylhydrazone

Desoxybenzoin phenylhydrazone dissolved in benzene was heated in an autoclave at 235° for 3 h in the absence of catalyst. 2,3-Diphenylindole was obtained in 80% yield. Similarly, 1,3-diphenylpropanone phenylhydrazone was converted thermally in 75% yield into 2-benzyl-3-phenylindole.

Reaction of 2-Ethoxy-1-naphthaldehyde Phenylhydrazone with Carbon Monoxide

2-Ethoxy-1-naphthaldehyde phenylhydrazone (7 g) was allowed to react with 3 500 p.s.i. of carbon monoxide in the presence of dicobalt octacarbonyl (1 g) in 35 ml of benzene at a temperature of 235° for 3 h. The product (freed of catalyst) was chromatographed on alumina using benzene–chloroform (8:1 v:v) as developer, and was shown to contain no cyclic carbonyl group.

Reaction of 1,3-Diphenyl-2-propanone Phenylhydrazone with Carbon Monoxide

1,3-Diphenyl-2-propanone phenylhydrazone was allowed to react with high purity carbon monoxide in the presence of dicobalt octacarbonyl, and the product worked up as described previously. The main component, 2-benzyl-3-phenylindole, m.p. 100–101°, was obtained in 65% yield. The mixed melting point of the main component and an authentic sample of 2-benzyl-3-phenylindole (7) was 100–101°. In addition, *sym*-diphenylurea was produced in about 20% yield. The remaining product, which consisted of traces of different compounds, contained no cyclic carbonyl group.

Synthesis of Authentic 3-Benzylphthalimidine-N-carboxyanilide

3-Benzylphthalimidine (8) was allowed to react with phenylisocyanate as described previously (1) to afford 3-benzylphthalimidine-N-carboxyanilide; m.p. 146–147°. The infrared spectrum of this substance in a KBr pellet was identical with that of compound II and showed strong carbonyl bands at 1 705 and 1 670 cm^{-1}.

Anal. Calcd. for $C_{22}H_{18}N_2O_2$: N, 8.18; mol. wt. 342. Found: N, 8.44; mol. wt. (by mass spectrum) 342.

Synthesis of 3-Benzyl-2-phenylphthalimidine

(a) 3-Benzylidene-2-phenylphthalimidine

Benzylidene phthalide (3 g) (9), aniline (10 g), and ethyl alcohol (15 ml) were refluxed for 5 h. After the alcohol was evaporated, the remaining oil was dissolved in hot acetic acid. The solid which precipitated from the mixture was recrystallized from ethanol to afford 3-benzylidene-2-phenylphthalimidine; m.p. 200–201°.

Anal. Calcd. for $C_{21}H_{15}NO$: C, 84.25; H, 5.02; N, 4.68. Found: C, 84.10; H, 4.91; N, 4.84.

(b) 3-Benzyl-2-phenylphthalimidine

3-Benzylidene-2-phenylphthalimidine (0.1 g) dissolved in 10 ml of chloroform–ethanol (1:1) was hydrogenated over reduced platinum oxide until 1 mole of hydrogen per mole of substrate was absorbed. After the catalyst was removed by filtration, the solvent was evaporated and the product recrystallized from cyclohexane; m.p. 124–125°. Reduction of 3-benzylidene-2-phenylphthalimidine in chloroform – acetic acid with the same catalyst gave a compound that was contaminated with trace quantities of a material having one aromatic ring which was reduced, as shown by its mass spectrum. The infrared spectrum of 3-benzyl-2-phenylphthalimidine showed a strong carbonyl peak at 1 680 cm^{-1}.

Anal. Calcd. for $C_{21}H_{17}NO$: N, 4.68; mol. wt. 299. Found: N, 4.65; mol. wt. (by mass spectrum) 299.

ACKNOWLEDGMENT

This research was supported by a grant from the Petroleum Research Fund administered by the American Chemical Society. Grateful acknowledgment is hereby made to the donors of this fund.

1. A. Rosenthal and M. R. S. Weir. Can. J. Chem. **40**, 610 (1962).
2. A. Rosenthal and M. R. S. Weir. J. Org. Chem. **28**, 3025 (1963).
3. A. H. Kelly, D. H. McLeod, and J. Parrick. Can. J. Chem. **43**, 296 (1965).
4. A. Rosenthal and M. Yalpani. Can. J. Chem. **43**, 711 (1965).
5. S. Horiie, S. Murahashi, and T. Jō. Bull. Chem. Soc. Japan, **33**, 81 (1960).
6. E. Fischer. Ann. **236**, 135 (1886).
7. V. B. Trenkler. Ann. **248**, 106 (1888).
8. S. Gabriel. Ber. **18**, 1251 (1885).
9. S. Gabriel. Ber. **18**, 2435 (1885).

Received July 7, 1965.
Department of Chemistry,
University of British Columbia,
Vancouver, British Columbia.

Can. J. Chem. Downloaded from www.nrcresearchpress.com by 210.87.254.40 on 09/05/12
For personal use only.

OXIDATION OF SUGARS WITH RUTHENIUM DIOXIDE – SODIUM PERIODATE: A SIMPLE METHOD FOR THE PREPARATION OF SUBSTITUTED KETO SUGARS

V. M. PARIKH AND J. K. N. JONES

The substituted keto sugars have assumed great importance in recent years particularly as intermediates in the synthesis of branched-chain and amino deoxy sugars of antibiotic origin. Beynon *et al.* (1) applied the ruthenium tetroxide oxidation method (2–4) to substituted carbohydrates and reported that the yields by this method were generally better than those obtained when chromium trioxide – pyridine complex (the more usual oxidant) (5–10) is employed. The ruthenium tetroxide oxidation method reported by Beynon *et al.* (1) required two steps, preparation of the oxidant from ruthenium dioxide, and oxidation of the alcohol by at least a molar equivalent of the tetroxide. It has been found that the combination of these two steps has several advantages, some of which are (*a*) nearly quantitative yields of the keto sugars, (*b*) use of only trace quantities of the costly ruthenium dioxide, (*c*) saving of time, and (*d*) destruction of the usual impurities in the starting material, such as unsubstituted or partially substituted sugar derivatives containing vicinal hydroxyl groups.

When this two-step method is used, the carbohydrate derivative is dissolved in carbon tetrachloride or chloroform, trace quantities (20 mg/g of carbohydrate) of ruthenium dioxide* are added, and a 5% aqueous solution of sodium metaperiodate is added dropwise to the mixture, with vigorous stirring, at or below room temperature. The pH of the mixture is meticulously controlled between 6 and 7 (Beckman pH meter Model 72) by the periodic addition of small quantities of dilute sodium bicarbonate solution. Usually about 1.3 molar equivalents of sodium metaperiodate is required, and the end of the reaction, after about 1 to 4 h, is indicated by a change in color from black (ruthenium dioxide) to blackish yellow or yellow (ruthenium tetroxide). The excess of periodate and the ruthenium tetroxide are then destroyed by the addition of *n*-propanol, and ruthenium dioxide is removed by filtration. The carbon tetrachloride is separated from the aqueous layer, washed with water, concentrated, and dried; and this gives the oxidized product in almost quantitative yield.

The oxidations listed in Table I have been achieved with this method.

TABLE I

Oxidation of sugars with ruthenium dioxide – sodium periodate to produce substituted keto sugars

Name of the alcohol	Name of the oxidized product	Yield	Reference
Methyl-2,3-*O*-isopropylidene-α-L-rhamoside	Methyl 6-deoxy-2,3-*O*-isopropylidene-α-L-*glycero*-D-*erythro*-hexos-4-uloside	Quantitative	11
1,3–2,5-Di-*O*-methylene-L-rhamnitol	6-Deoxy-1,3:2,5-Di-*O*-methylene-L-*glycero*-D-*erythro*-4-hexulose	Quantitative	12
1,2–5,6-Di-*O*-isopropylidene-D-glucofuranose	1,2:5,6-Di-*O*-isopropylidene-α-D-*erythro*-D-*glycero*-hexos-3-ribofuranose	85–90%	1
Methyl 3,4-*O*-isopropylidene-β-D-arabinoside	Methyl 3,4-*O*-isopropylidene-β-D-*erythro*-pentos-2-ulopyranose	80%	10
6-*O*-Benzoyl-1,2–4,5-di-*O*-isopropylidene-dulcitol	6-*O*-Benzoyl-1,2:4,5-di-*O*-isopropylidene-*threo*-*glycero*-3-hexulose	Quantitative	6
1,2-*O*-Isopropylidene-L-threose	D-*glycero*-1,2-*O*-Isopropylidene-tetros-3-ulose	70–75%*	New

*The yield is low probably because the product easily sublimes or codistills with the solvent during concentration of the reaction mixture.

**Samples of ruthenium dioxide supplied by a number of manufacturers were tried but only "Ruthenium dioxide 54%" from Engelhard Industries, Inc., 113 Astor Street, Newark 14, New Jersey, was found satisfactory.*

Can. J. Chem. Downloaded from www.nrcresearchpress.com by 210.87.254.105 on 09/05/12
For personal use only.

1. P. J. Beynon, P. M. Collins, and W. G. Overend. Proc. Chem. Soc. 342 (1964).
2. C. Djerassi and R. R. Engle. J. Am. Chem. Soc. **75**, 3838 (1953).
3. L. M. Berkowitz and P. N. Raylander. J. Am. Chem. Soc. **80**, 6682 (1958).
4. H. Nakata. Tetrahedron, **19**, 1959 (1963).
5. J. S. Burton, W. G. Overend, and N. R. Williams. Chem. Ind. London, 175 (1961).
6. G. U. Yuen and J. M. Sugihara. J. Org. Chem. **26**, 1598 (1961).
7. P. M. Collins and W. G. Overend. Chem. Ind. London, 375 (1963).
8. O. Theander. Adv. Carbohydrate Chem. **17**, 223 (1962).
9. A. F. Krosso, E. K. Weiss, and T. Reichstein. Helv. Chim. Acta, **46**, 2538 (1963).
10. J. S. Burton, W. G. Overend, and N. R. Williams. J. Chem. Soc. 3433 (1965).
11. P. M. Collins and W. G. Overend. J. Chem. Soc. 1912 (1965).
12. J. W. Bird and J. K. N. Jones. Can. J. Chem. **41**, 1878 (1963).

Received August 9, 1965.
Department of Chemistry,
Queen's University,
Kingston, Ontario.

THE USE OF DIMETHYLFORMAMIDE AND OF DIMETHYL SULFOXIDE IN THE PREPARATION OF 2,4-DINITROPHENYLHYDRAZONES

J. Parrick and J. W. Rasburn

Although 2,4-dinitrophenylhydrazine is well known as a reagent for the characterization of carbonyl compounds, its application frequently presents difficulties which may largely be ascribed to the low solubility of the weak base in the usual hydroxylic solvents. Techniques that are employed (1) often seek to overcome these solubility limitations by working with hot solutions, by using fairly high concentrations of a strong acid, or by combining both methods. However, such techniques do not always prevent contamination of the resulting derivative with unchanged reagent and may cause undesirable side reactions with sensitive compounds (see below). In recent years attention has been directed to the use of other solvents, such as diglyme (2) (the dimethyl ether of diethylene glycol) and diethyl phosphonate (3) (diethyl phosphite), in which the reagent as the free base is more soluble and which therefore do not require the high acid concentrations used in earlier procedures. We now report the successful application of dimethylformamide and of dimethyl sulfoxide as solvents of this type.

A particularly suitable example to illustrate the advantage of using a solvent and technique of the abovementioned type is the preparation of the 2,4-dinitrophenylhydrazone of the hydroxy ketone (I).

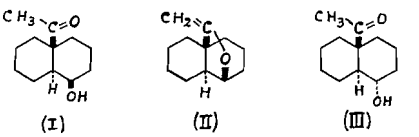

(I) (II) (III)

All attempts by us and, though not reported, by previous workers (4, 5) to prepare this derivative from the hydroxy ketone (I), or directly from its preparative precursor (II) (4), by applying a wide variety of standard techniques using the reagent in alcoholic or aqueous–alcoholic solution containing the usual concentrations of mineral acid, had been completely unsuccessful, notwithstanding the fact that other carbonyl derivatives of (I), such as its oxime, phenylhydrazone, and semicarbazone, had been prepared (5) quite easily. We have now found, however, that the required derivative, m.p. 159–160°, may be obtained in high yield from the hydroxy ketone (I) and 2,4-dinitrophenylhydrazine in

Can. J. Chem. Downloaded from www.nrcresearchpress.com by 210.87.254.105 on 09/05/12
For personal use only.

1. P. J. Beynon, P. M. Collins, and W. G. Overend. Proc. Chem. Soc. 342 (1964).
2. C. Djerassi and R. R. Engle. J. Am. Chem. Soc. **75**, 3838 (1953).
3. L. M. Berkowitz and P. N. Raylander. J. Am. Chem. Soc. **80**, 6682 (1958).
4. H. Nakata. Tetrahedron, **19**, 1959 (1963).
5. J. S. Burton, W. G. Overend, and N. R. Williams. Chem. Ind. London, 175 (1961).
6. G. U. Yuen and J. M. Sugihara. J. Org. Chem. **26**, 1598 (1961).
7. P. M. Collins and W. G. Overend. Chem. Ind. London, 375 (1963).
8. O. Theander. Adv. Carbohydrate Chem. **17**, 223 (1962).
9. A. F. Krosso, E. K. Weiss, and T. Reichstein. Helv. Chim. Acta, **46**, 2538 (1963).
10. J. S. Burton, W. G. Overend, and N. R. Williams. J. Chem. Soc. 3433 (1965).
11. P. M. Collins and W. G. Overend. J. Chem. Soc. 1912 (1965).
12. J. W. Bird and J. K. N. Jones. Can. J. Chem. **41**, 1878 (1963).

Received August 9, 1965.
Department of Chemistry,
Queen's University,
Kingston, Ontario.

THE USE OF DIMETHYLFORMAMIDE AND OF DIMETHYL SULFOXIDE IN THE PREPARATION OF 2,4-DINITROPHENYLHYDRAZONES

J. Parrick and J. W. Rasburn

Although 2,4-dinitrophenylhydrazine is well known as a reagent for the characterization of carbonyl compounds, its application frequently presents difficulties which may largely be ascribed to the low solubility of the weak base in the usual hydroxylic solvents. Techniques that are employed (1) often seek to overcome these solubility limitations by working with hot solutions, by using fairly high concentrations of a strong acid, or by combining both methods. However, such techniques do not always prevent contamination of the resulting derivative with unchanged reagent and may cause undesirable side reactions with sensitive compounds (see below). In recent years attention has been directed to the use of other solvents, such as diglyme (2) (the dimethyl ether of diethylene glycol) and diethyl phosphonate (3) (diethyl phosphite), in which the reagent as the free base is more soluble and which therefore do not require the high acid concentrations used in earlier procedures. We now report the successful application of dimethylformamide and of dimethyl sulfoxide as solvents of this type.

A particularly suitable example to illustrate the advantage of using a solvent and technique of the abovementioned type is the preparation of the 2,4-dinitrophenylhydrazone of the hydroxy ketone (I).

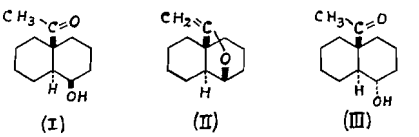

(I) (II) (III)

All attempts by us and, though not reported, by previous workers (4, 5) to prepare this derivative from the hydroxy ketone (I), or directly from its preparative precursor (II) (4), by applying a wide variety of standard techniques using the reagent in alcoholic or aqueous–alcoholic solution containing the usual concentrations of mineral acid, had been completely unsuccessful, notwithstanding the fact that other carbonyl derivatives of (I), such as its oxime, phenylhydrazone, and semicarbazone, had been prepared (5) quite easily. We have now found, however, that the required derivative, m.p. 159–160°, may be obtained in high yield from the hydroxy ketone (I) and 2,4-dinitrophenylhydrazine in

Can. J. Chem. Downloaded from www.nrcresearchpress.com by 210.87.254.5 on 09/05/12
For personal use only.

dimethylformamide containing a trace of concentrated hydrochloric acid as catalyst; after a few hours at room temperature the product was isolated by the addition of dilute hydrochloric acid and was quite pure after one crystallization from ethanol. The use of dimethyl sulfoxide in place of dimethylformamide gave an exactly similar result. The same derivative, i.e. of (I), was obtained also from the vinyl ether (II) by applying this new procedure (using dimethyl sulfoxide), but neither this nor any other procedure has yet afforded any carbonyl derivative from the equatorial hydroxy ketone (III). The low carbonyl reactivity of (III) is as expected from steric considerations, whereas the relatively high reactivity of (I) may be attributed (cf. ref. 5) to the formation of a protonated form of (II) via the intramolecular hemiketal of (I). Under the highly acidic conditions of the older techniques for the preparation of 2,4-dinitrophenylhydrazones it is probable that (I) and (II) undergo not only derivative formation but also other reactions, e.g. the epimerization of (I) to (III) which has already been shown (5) to occur in aqueous acid media. The repeated failure to obtain the derivative, i.e. as a solid, when the older reagents are used may be simply the result of contamination by unreactive by-products, e.g. (III).

The striking success in the above example led us to investigate the possibility of developing a general technique for the preparation of 2,4-dinitrophenylhydrazones with dimethylformamide as solvent. Since the reagent can be dissolved very quickly, and is highly soluble (a 15% solution can be prepared almost instantly by mixing the components at room temperature), there is no need to store a preformed solution, and an excess of the reagent is easily avoided by weighing accurately the required amount and dissolving this immediately before use. All the carbonyl compounds we studied were also readily soluble in the freshly prepared reagent solution but, unlike the hydroxy ketone (I), many of the carbonyl compounds listed below gave derivatives which separated spontaneously usually within 2 h and sometimes within a few seconds. Those derivatives which did not separate spontaneously were isolated by the addition of dilute hydrochloric acid. Satisfactory derivatives were thus obtained from the following: acetophenone, *p*-methyl acetophenone, 2,4-dimethyl acetophenone, 3,4-dimethyl acetophenone, benzil, benzophenone, cyclopentanone, cyclohexanone, 2-methyl cyclohexanone, mesityl oxide, benzaldehyde, vanillin, crotonaldehyde, pyrrol-2-aldehyde, 1,4-naphthoquinone, formaldehyde, acetaldehyde, acetone, *i*-butyl methyl ketone, *n*-hexyl methyl ketone, methyl acetoacetate, ethyl acetoacetate, 4,6-octadien-3-one, and *p*-benzoquinone (those up to, but not including, formaldehyde separated spontaneously within 2 h). The derivatives had melting points in good agreement with literature values; one recrystallization was usually necessary for those derivatives which did not separate spontaneously. A few compounds, including furfural, benzoin, benzal acetophenone, and chloral hydrate, gave products of uncertain purity, but in no case (including those above) was any derivative inferior in quality, as judged by melting point, to that prepared for comparison by using Brady's reagent (1).

The technique does not appear to offer any marked advantage with carbonyl compounds of particularly low reactivity. Thus 2,4,6-trimethyl acetophenone gave only a very small yield of its 2,4-dinitrophenylhydrazone, and even after 1 week the derivative could be isolated only by dilution with hydrochloric acid (2 *N*) and had to be recrystallized several times. The diluted and acidified filtrate gave, after a few more days, a considerable amount of a solid product which was subsequently identified by analysis, and by mixed melting point determination with an authentic sample prepared by orthodox procedures, as the N-formyl derivative, m.p. 182–184°, of 2,4-dinitrophenylhydrazine. Although we obtained no definite evidence that this compound was formed during the reactions with the other carbonyl compounds investigated, its possible presence in very small quantities cannot be

Can. J. Chem. Downloaded from www.nrcresearchpress.com by 210.87.254.5 on 09/05/12
For personal use only.

denied, and it may be partly responsible for the necessity to recrystallize those derivatives which were isolated only by the addition of dilute acid. This possibility discourages the use of prolonged reaction times or of higher reaction temperatures in the case of sluggish reactions.

To avoid any possibility that the 2,4-dinitrophenylhydrazone may be contaminated with this formyl derivative, we investigated the use of dimethyl sulfoxide as an alternative solvent. The reagent base is even more soluble in dimethyl sulfoxide (a 25% solution can be prepared easily at room temperature), and perhaps as a consequence it can be used at a concentration such that some of the more soluble derivatives (e.g. of acetone) separate spontaneously. A preliminary study with about 12 carbonyl compounds of varied types has given excellent results with this solvent, and it is tentatively recommended as being superior to dimethylformamide. Although the reagent appears to be quite stable in dimethyl sulfoxide solution for several weeks if no mineral acid is present, the odor of dimethyl sulfide became apparent in solutions containing a trace of concentrated hydrochloric acid after a few days at room temperature, and more quickly when such solutions were heated.

EXPERIMENTAL

Reagent grade dimethylformamide and dimethyl sulfoxide were used without further purification, since preliminary experiments showed no detectable differences with the results obtained for comparison by using freshly redistilled solvents.

The following procedure was found to be most suitable for the preparation of 2,4-dinitrophenylhydrazones with either of the newer solvents.

The carbonyl compound (0.0025 mole) was added to a solution* of 2,4-dinitrophenylhydrazine (0.5 g) in dimethylformamide (5 ml), or in dimethyl sulfoxide (2.5 ml), and the mixture was swirled gently to obtain a homogeneous solution. Concentrated hydrochloric acid (2 drops) was then added and the mixture was set aside for 2 h unless spontaneous separation of the derivative occurred in a shorter time. The solid product was filtered off, and washed with dilute (2 *N*) hydrochloric acid, then with water, and finally with alcohol or aqueous alcohol depending upon the solubility of the derivative. In those cases in which no solid derivative had separated spontaneously during 2 h† the reaction mixture was diluted with an equal or larger volume of dilute (2 *N*) hydrochloric acid, and the resulting product was collected as soon as possible and washed as described above; scratching with a glass rod was sometimes necessary to induce solidification of an oily initial product. The products were usually dried in a vacuum desiccator. One crystallization from a suitable solvent (generally alcohol, ethyl acetate, or glacial acetic acid) was usually necessary, particularly with those products which did not separate spontaneously, to obtain derivatives with melting points which were in agreement with the literature values. These are listed in most reference works on qualitative organic analysis (see, for example, ref. 1, pp. 138–141); those that are not listed are, with appropriate references, as follows: the 2,4-dinitrophenylhydrazones of 2,4-dimethyl acetophenone (6), 3,4-dimethyl acetophenone (6), 2,4,6-trimethyl acetophenone (7), and 2-formyl pyrrole (8), and the N-formyl derivative of 2,4-dinitrophenylhydrazine (9). Melting points and analytical results are now reported only for the following two derivatives, which have hitherto not been described.

10β-Acetyl-*trans*-decal-1β-ol 2,4-dinitrophenylhydrazone, m.p. 159–160° (ethanol).

Anal. Calcd. for $C_{18}H_{24}N_4O_5$: C, 57.45; H, 6.38; N, 14.90. Found: C, 57.49; H, 6.37; N, 14.82.

4,6-Octadien-3-one 2,4-dinitrophenylhydrazone, m.p. 160–162° (ethanol).

Anal. Calcd. for $C_{14}H_{16}N_4O_4$: C, 55.26; H, 5.26; N, 18.42. Found: C, 55.42; H, 5.44; N, 18.74.

ACKNOWLEDGMENT

The authors thank Mr. R. Hindson for valuable technical assistance during most of this work.

1. F. WILD. Characterisation of organic compounds. 2nd ed. Cambridge University Press, Cambridge, England. 1958. pp. 112–115.
2. H. J. SHINE. J. Org. Chem. **24**, 252 (1959).
3. J. A. MAYNARD. Australian J. Chem. **15**, 867 (1962).

**Solutions prepared immediately before use and those prepared several weeks earlier gave identical results.*

†Longer reaction times were occasionally allowed (see text), but for most carbonyl compounds the reaction appears to be substantially complete after 2 h and the solubility of the derivative probably determines the extent of spontaneous separation.

Can. J. Chem. Downloaded from www.nrcresearchpress.com by 210.87.254.5 on 09/05/12
For personal use only.

4. G. BADDELEY, B. G. HEATON, and J. W. RASBURN. J. Chem. Soc. 4713 (1960).
5. G. BADDELEY, B. G. HEATON, and J. W. RASBURN. J. Chem. Soc. 3828 (1961).
6. J. F. NORRIS and P. ARTHUR, JR. J. Am. Chem. Soc. **62**, 874 (1940).
7. D. E. PEARSON and F. GREER. J. Am. Chem. Soc. **77**, 1294 (1955).
8. H. BREDERECK and E. FRITZSCHE. Ber. **70B**, 802 (1937).
9. J. CEREZO and E. OLAY. Anales Soc. Españ. Fís. y Quím. **32**, 1090 (1934).

RECEIVED APRIL 13, 1965.
DEPARTMENT OF CHEMISTRY,
RUTHERFORD COLLEGE OF TECHNOLOGY,
NEWCASTLE-UPON-TYNE, ENGLAND.

Can. J. Chem. Downloaded from www.nrcresearchpress.com by 210.87.254.5 on 09/05/12
For personal use only.

REACTIONS OF ETHYLDIAZOACETATE WITH CYCLOPENTADIENE SYNTHESIS OF THE EPIMERIC ETHYL BICYCLO[3.1.0]HEX-2-ENE-6-CARBOXYLATES

J. WARKENTIN, ELIZABETH SINGLETON, AND JOAN F. EDGAR

There are numerous reports in the literature to the effect that additions of carbenes to conjugated dienes tend to go exclusively 1,2 rather than 1,4 (1, chaps. 2, 6, 8, and 11, and references therein; 2). Although 1,4-addition of methylene to butadiene was postulated by Franzen (3), it now appears likely that the cyclopentene obtained actually arises by isomerization of an activated 1,2-adduct (1, pp. 32 and 231–233, and references therein).

We thought that one of the more promising substrates for 1,4-addition by a carbene might be cyclopentadiene (I), and we now report the results of experiments in which ethyldiazoacetate (II) was decomposed in the presence of I. Our failure to find substituted bicyclo[2.1.1]hex-2-enes among the reaction products indicates that here, also, 1,4-addition is not favored. The products of 1,2-addition, ethyl bicyclo[3.1.0]hex-2-ene-6-*endo*-carboxylate (III) and ethyl bicyclo[3.1.0]hex-2-ene-6-*exo*-carboxylate (VI), were obtained.* Although separation of the isomers proved difficult, carbene additions should provide a more general synthetic route to C_6-substituted bicyclo[3.1.0]hex-2-enes than the method previously described (6).

The esters III and VI were separated by preparative gas–liquid chromatography (g.l.c.). Yields of 30–50%, based on II, were estimated from the gas chromatograms, which also gave the product ratio VI/III. Photolysis of II in a pentane solution of I gave VI/III = 3, while copper-catalyzed decomposition of II in neat I gave VI/III = 5. Higher *exo/endo* ratios of 8.5 and 16 have been reported for the copper-catalyzed reactions of II with 1,3-cyclohexadiene (2) and with cyclohexene (7), respectively. The photolytic procedure gave, in addition to III and VI, a small amount of yellow material which had $\lambda_{max}^{EtOH} = 293$, expected for a 3-carboethoxy-2-pyrazoline (see, for example, ref. 8). Use of ether solvent in the photolysis led to ethyl ethoxyacetate as the principal product, presumably through a ylide mechanism (1, pp. 107–108 and references therein).

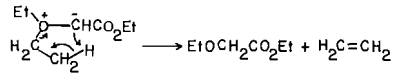

The structures III and VI were established by spectroscopic methods and by chemical conversion into known compounds. *Endo* ester III was saponified to the corresponding acid IV (6) and was also converted into the bromolactone V (6, 9). The *exo* ester was

*Others workers (4, 5) have failed to detect III among the products of the copper-catalyzed reaction of I and II and have wrongly concluded that addition is highly stereospecific.

4. G. BADDELEY, B. G. HEATON, and J. W. RASBURN. J. Chem. Soc. 4713 (1960).
5. G. BADDELEY, B. G. HEATON, and J. W. RASBURN. J. Chem. Soc. 3828 (1961).
6. J. F. NORRIS and P. ARTHUR, JR. J. Am. Chem. Soc. **62**, 874 (1940).
7. D. E. PEARSON and F. GREER. J. Am. Chem. Soc. **77**, 1294 (1955).
8. H. BREDERECK and E. FRITZSCHE. Ber. **70B**, 802 (1937).
9. J. CEREZO and E. OLAY. Anales Soc. Españ. Fís. y Quím. **32**, 1090 (1934).

RECEIVED APRIL 13, 1965.
DEPARTMENT OF CHEMISTRY,
RUTHERFORD COLLEGE OF TECHNOLOGY,
NEWCASTLE-UPON-TYNE, ENGLAND.

Can. J. Chem. Downloaded from www.nrcresearchpress.com by 210.87.254.105 on 09/05/12
For personal use only.

REACTIONS OF ETHYLDIAZOACETATE WITH CYCLOPENTADIENE SYNTHESIS OF THE EPIMERIC ETHYL BICYCLO[3.1.0]HEX-2-ENE-6-CARBOXYLATES

J. WARKENTIN, ELIZABETH SINGLETON, AND JOAN F. EDGAR

There are numerous reports in the literature to the effect that additions of carbenes to conjugated dienes tend to go exclusively 1,2 rather than 1,4 (1, chaps. 2, 6, 8, and 11, and references therein; 2). Although 1,4-addition of methylene to butadiene was postulated by Franzen (3), it now appears likely that the cyclopentene obtained actually arises by isomerization of an activated 1,2-adduct (1, pp. 32 and 231–233, and references therein).

We thought that one of the more promising substrates for 1,4-addition by a carbene might be cyclopentadiene (I), and we now report the results of experiments in which ethyldiazoacetate (II) was decomposed in the presence of I. Our failure to find substituted bicyclo[2.1.1]hex-2-enes among the reaction products indicates that here, also, 1,4-addition is not favored. The products of 1,2-addition, ethyl bicyclo[3.1.0]hex-2-ene-6-*endo*-carboxylate (III) and ethyl bicyclo[3.1.0]hex-2-ene-6-*exo*-carboxylate (VI), were obtained.* Although separation of the isomers proved difficult, carbene additions should provide a more general synthetic route to C_6-substituted bicyclo[3.1.0]hex-2-enes than the method previously described (6).

The esters III and VI were separated by preparative gas–liquid chromatography (g.l.c.). Yields of 30–50%, based on II, were estimated from the gas chromatograms, which also gave the product ratio VI/III. Photolysis of II in a pentane solution of I gave VI/III = 3, while copper-catalyzed decomposition of II in neat I gave VI/III = 5. Higher *exo/endo* ratios of 8.5 and 16 have been reported for the copper-catalyzed reactions of II with 1,3-cyclohexadiene (2) and with cyclohexene (7), respectively. The photolytic procedure gave, in addition to III and VI, a small amount of yellow material which had $\lambda_{max}^{EtOH} = 293$, expected for a 3-carboethoxy-2-pyrazoline (see, for example, ref. 8). Use of ether solvent in the photolysis led to ethyl ethoxyacetate as the principal product, presumably through a ylide mechanism (1, pp. 107–108 and references therein).

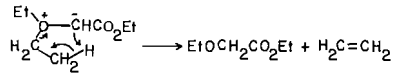

The structures III and VI were established by spectroscopic methods and by chemical conversion into known compounds. *Endo* ester III was saponified to the corresponding acid IV (6) and was also converted into the bromolactone V (6, 9). The *exo* ester was

*Others workers (4, 5) have failed to detect III among the products of the copper-catalyzed reaction of I and II and have wrongly concluded that addition is highly stereospecific.

identified by hydrolysis to the unsaturated acid VII (5) followed by reduction to the saturated acid VIII (6).

Interestingly, III is not readily epimerized by EtO^- in EtOH, a situation which may be fairly general for strained, bicyclic systems (10, 11). Also of interest are some differences in the spectra of the compounds. In the nuclear magnetic resonance (n.m.r.) spectrum of III the vinyl protons give rise to a sharp singlet at 5.64 p.p.m., whereas in the n.m.r. spectrum of VI there are two multiplets centered at 5.52 and 5.92 p.p.m. for those protons. At high field (0.83 p.p.m.) there is a one-proton signal in the spectrum of VI, but not in that of III. This is readily understood in terms of anisotropic shielding of the C_6-*endo* proton of VI by the π-electrons (12). In the ultraviolet spectra, III has an apparent λ_{max}^{EtOH} 286 mμ (ϵ = 160) and end absorption while VI shows only end absorption.

We plan to study the addition of other carbenes to cyclopentadiene and to examine further the effect of geometry and C_6 substituents on the n.m.r. signals of the vinyl protons and on the ultraviolet spectra.

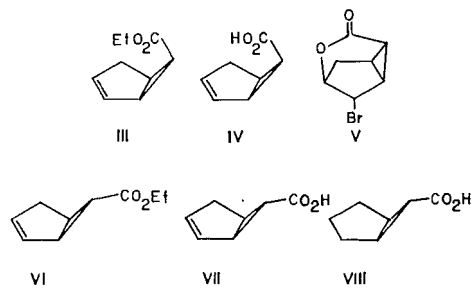

EXPERIMENTAL

Satisfactory elemental analyses were obtained for all new compounds. Melting points and boiling points are uncorrected.

Nuclear magnetic resonance spectra were taken on a Varian A-60 spectrometer with tetramethylsilane as the internal standard. Data are given on the δ-scale, with relative areas in parentheses and with the multiplicity symbols t = triplet, q = quartet, m = multiplet. Ultraviolet spectra were recorded with a Perkin–Elmer Spectrocord model 4000 instrument on ethanol (95%) solutions of rechromatographed samples of the esters. Near infrared spectra were obtained with the same instrument on CCl_4 solutions of the compounds while infrared spectra were done with a Beckman IR5 spectrophotometer. Mass spectra were obtained, through the courtesy of Professor D. B. MacLean, on a Hitachi RMU-6A instrument.

Photolysis Route

A solution of I (13) (238 g, 3.6 moles) and II (Aldrich Chemical Co., Inc., 9.8 g, 0.086 mole) in 400 ml of pure pentane was irradiated for 4 h in a pyrex vessel with the output from the quartz tube of a Westinghouse, 700 W, mercury-arc street lamp. The temperature of the solution was kept at about 30° and an atmosphere of nitrogen was maintained. Cyclopentadiene and pentane were removed by distillation at atmospheric pressure and the dark residue was chromatographed on alumina. Light petroleum eluted most of the dicyclopentadiene and methylene chloride removed the esters, together with a yellow component, from the column. The liquid residue left from distillation of the methylene chloride solution was subjected to preparative g.l.c. in the Aerograph model A-700 gas chromatograph fitted with a 20 ft × $\frac{3}{8}$ in. Argentide* column. At 160° and a helium flow rate of 160 ml min^{-1} the retention times were, in min: dicyclopentadiene, 24; *endo* ester III, 34; *exo* ester VI, 42; pyrazoline, 54.

Copper-Catalyzed Route

To I (13) (171 g, 2.59 moles) and 1.04 g of copper powder in a nitrogen atmosphere was added, dropwise, 30 g (0.26 mole) of II during 1 h. To accelerate the slow evolution of N_2 the flask was gently heated with steam during the addition period and heating was continued for several hours, or overnight. Copper was removed by filtration through Celite before chromatography on alumina and gas chromatography as already described.

**We have coined this name for a packing consisting of deperfumed Tide detergent granules coated with the corresponding silver salt. The packing was prepared by drawing saturated aqueous silver nitrate solution through a bed of the granules.*

Can. J. Chem. Downloaded from www.nrcresearchpress.com by 210.87.254.105 on 09/05/12
For personal use only.

Ethyl Bicyclo[3.1.0]hex-2-ene-6-endo-carboxylate (III)

The following spectra were obtained—infrared (CCl_4): 5.77 μ; near infrared (CCl_4): 1.698 μ (6); n.m.r.: 1.20t (3), 1.54–3.11 (5), 4.01q (2), 5.64s (2); mass spectrum: m/e = 152 (molecular ion), strong signals at 79, 78, 77, 66, and 39.

Bromolactone V

To 71.6 mg of III in 1.25 ml of $CHCl_3$ at 0° was added dropwise, with stirring, a 2.57 M solution of Br_2 in $CHCl_3$ until the bromine color persisted for 20 min (9). Distillation and g.l.c. on the distillate gave ethyl bromide (m/e = 108, 110). Crystallization of the distillation residue from pentane gave mixed bromolactones (6); m.p. 84–91°; infrared (CCl_4) 5.73 μ (δ-lactone) and 5.67 μ (γ-lactone). Further crystallization from pentane gave pure δ-lactone, presumably V; m.p. 89–90.5°; n.m.r. 1.79–2.79 (5), 4.28 (1), 4.62 (1); mass spectrum: highest m/e = 204, 202.

Bicyclo[3.1.0]hex-2-ene-6-endo-carboxylic Acid (IV)

Endo ester III was treated with excess sodium ethoxide in ethanol for 46 h at 60°. The n.m.r. spectrum still showed the sharp vinyl singlet of the *endo* ester and lacked the broader vinyl multiplets of the *exo* ester, indicating no detectable epimerization. Dilution with water followed by reflux for 5 h gave, after acidification, the *endo* acid IV; m.p. 91–91.5°; infrared in good agreement with the published spectrum (6).

Ethyl Bicyclo[3.1.0]hex-2-ene-6-exo-carboxylate (VI)

The ester had b.p. (micro) 201°; infrared (CCl_4) 5.80 μ; near infrared (CCl_4) 1.686 μ (6); n.m.r. 0.83t (1), 1.18t (3), 1.93–2.68 (4), 4.03q (2), 5.52m (1), 5.92m (1); mass spectrum: same as that of III, except for differences in relative intensities.

Bicyclo[3.1.0]hex-2-ene-6-exo-carboxylic Acid (VII)

Ester VI (892 mg) was refluxed overnight with NaOH (718 mg) in a solution of H_2O (15 cc) and ethanol (10 cc). The solution was concentrated and acidified to give VII (5); 360 mg (49%); m.p. 79–79.5° (pentane). The n.m.r. spectrum had the high-field signal of the parent ester as well as the two vinyl multiplets; infrared (CCl_4) 5.92 μ.

Bicyclo[3.1.0]hexane-6-exo-carboxylic Acid (VIII)

This acid, m.p. 60.5–61.5°, was obtained from VII by catalytic hydrogenation on prereduced Adams catalyst. The infrared and near infrared spectra matched those described in the literature (6).

Ethyl Ethoxyacetate

This material was purified by preparative g.l.c. and was identified from its spectra: n.m.r. 1.21t (3) overlapping with 1.25t (3), 3.55q (2), 4.02s (2) over 4.19q (2); infrared (neat) 5.70 μ.

ACKNOWLEDGMENTS

Financial support from the Ontario Research Foundation and from the Petroleum Research Fund (PRF No. 1396-A4) is gratefully acknowledged.

1. W. KIRMSE. Carbene chemistry. Academic Press, Inc., New York. 1964.
2. I. A. D'YAKONOV, T. V. DOMAREVA-MANDEL'SHTAM, and V. V. RAZIN. J. Gen. Chem. USSR Eng. Transl. **33**, 3365 (1963).
3. V. FRANZEN. Chem. Ber. **95**, 571 (1962).
4. P. BESINET, R. FRAISSE, R. JACQUIER, and P. VIALLEFONT. Bull. Soc. Chim. France, 1377 (1960); Chem. Abstr. **55**, 5438 (1961).
5. B. FÖHLISCH. Chem. Ber. **97**, 88 (1964).
6. J. MEINWALD, S. S. LABANA, and M. S. CHADHA. J. Am. Chem. Soc. **85**, 582 (1963).
7. P. S. SKELL and R. M. ETTER. Proc. Chem. Soc. 443 (1961).
8. J. A. MOORE. J. Org. Chem. **20**, 1607 (1955).
9. R. T. ARNOLD, M. DEMOURA CAMPOS, and K. L. LINDSAY. J. Am. Chem. Soc. **75**, 1044 (1953).
10. J. MEINWALD, A. LEWIS, and P. G. GASSMAN. J. Am. Chem. Soc. **84**, 977 (1962).
11. J. MEINWALD and P. G. GASSMAN. J. Am. Chem. Soc. **82**, 5445 (1960).
12. L. M. JACKMAN. Applications of nuclear magnetic resonance spectroscopy in organic chemistry. The Pergamon Press, Ltd., New York. 1959. Chap. 7.
13. L. F. FIESER. Organic experiments. D. C. Heath & Co., Boston. 1964. Chap. 15.

RECEIVED JANUARY 19, 1965.
DEPARTMENT OF CHEMISTRY,
MCMASTER UNIVERSITY,
HAMILTON, ONTARIO.

Can. J. Chem. Downloaded from www.nrcresearchpress.com by 210.87.254.105 on 09/05/12
For personal use only.

THERMAL REARRANGEMENT OF BENZYLDIMETHYLAMINE OXIDE

GARSON P. SHULMAN,[1] PAUL ELLGEN, AND MARGARET CONNOR

The thermal rearrangement of allyl- or benzyl-dimethylamine oxides to O-allyl- or O-benzyl-N,N-dialkylhydroxylamines had been considered as proceeding by intramolecular migration of the benzyl or allyl group with essentially simultaneous C—N bond breaking and C—O bond formation (1). Free carbonium ion intermediates were excluded from consideration because of a failure to detect allyl or benzyl alcohols. A cyclic intramolecular mechanism involving a three-membered ring was proposed for benzyldimethylamine oxide.

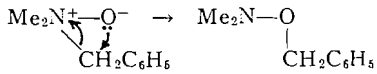

It is now generally accepted that intramolecular electron pair shifts through such small rings are sterically unfavorable. The alternative would be an ion pair mechanism with a transient benzylcarbonium ion.

Recently, a radical mechanism has been suggested (2). The presence of a methylphenylamine oxide radical during the rearrangement of methylphenylbenzylamine oxide was demonstrated by electron spin resonance. Rearrangements of this compound and its allyl analogue occur under milder conditions than those of benzyl- and allyl-dimethylamine oxides (1). Demonstration of a radical intermediate in the one case therefore does not require that a radical intermediate be involved in the other. Kinetic evidence presented by Schöllkopf *et al.* (2) excludes a carbonium ion intermediate, but does not clearly distinguish between radical and anionic mechanisms.

Elimination to olefin and N,N-dialkylhydroxylamine is the principal reaction of aliphatic amine oxides having beta hydrogen atoms. Similarly, alkylbenzyl groups form mainly phenylalkenes. Olefin elimination occurs to a significant extent in benzyldialkylamine oxides having a beta hydrogen. Thus, α-phenethyldimethylamine oxide forms styrene and N,N-dimethylhydroxylamine. Benzyldiethylamine oxide forms 31% of O-benzyl-N,N-diethylhydroxylamine, 34% of N-benzyl-N-ethylhydroxylamine, and 16% of N-ethyl-O,N-dibenzylhydroxylamine, apparently by reaction of the amine oxide with N-benzyl-N-ethylhydroxylamine (3).

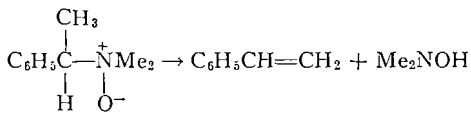

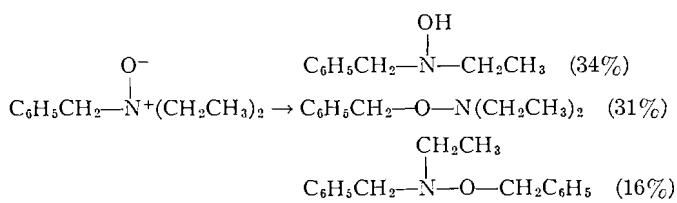

[1]*To whom correspondence should be addressed. Present address: Martin Co., Baltimore, Maryland.*

Can. J. Chem. Downloaded from www.nrcresearchpress.com by 210.87.254.105 on 09/05/12
For personal use only.

Kinetic studies of the pyrolysis to olefin or to amine of a typical aliphatic amine oxide (dimethyllauryl) (4) and of a typical phenethyl type of amine oxide ((3-phenyl-2-butyl) dimethyl) (5) have been reported recently. In beginning a general study of amine oxide pyrolysis, we had hoped that the composition of product mixtures in competitive cases could be predicted from a knowledge of structure and temperature if kinetic data on compounds of typical structures were available. With the observation that a slow dehydration step precedes elimination (4, 5), this approach was abandoned, since the rate of the elimination steps cannot be measured conveniently. Since the rearrangement shows a substituent effect on the rate (2), dehydration must not be rate determining in that reaction. Consideration of the activation parameters which we have determined assists in establishing the proper intermediate for the rearrangement.

EXPERIMENTAL

Preparation of Benzyldimethylamine Oxide

A mixture of 75 ml of isopropyl alcohol and 75 ml (1.1 moles) of 50% hydrogen peroxide was placed in a 50° constant-temperature bath, 135 g (1.0 mole) of benzyldimethylamine[2] was added dropwise, the homogeneous mixture was maintained at 50° for 19 h, and then volatile material was removed under vacuum. Analysis[3] by acidimetric titration (4) indicated a mixture of 12% amine and 79% amine oxide (as hydrate). The mixture was washed 3 times with 100 ml of benzene, then placed in the 50° bath, and stripped of solvent under vacuum. Titration indicated no amine and 96% amine oxide (hydrate). The infrared spectrum was similar to that of benzyldimethylamine except that a strong O—H absorption band was present.

Pyrolysis of Benzyldimethylamine Oxide

An 8.20 g sample of benzyldimethylamine oxide was dropped slowly into a flask which was part of a vacuum micro-distillation apparatus and which had been heated to 150°. The distillate consisted of an aqueous phase (1.63 g) and an organic phase (4.60 g) which was dried over magnesium sulfate. The undistilled "residue" weighed 1.45 g. The dried organic phase contained 96.5% of the principal product and two unidentified lesser components, which were determined to be 2.9% and 0.6% of the total by gas chromatography over 9 ft of ethylene glycol succinate on Chrom P at 150°. The infrared spectrum indicated a trialkylhydroxylamine (presumably O-benzyl-N,N-trimethylhydroxylamine).

Kinetic Studies

A constant-temperature bath was constructed from a 2 l resin kettle fitted with a wooden cover bored to accomodate test tubes and a stirrer, with a thermocouple connected to a Wheelco controller regulating the heating mantle. Weighed samples were placed in the test tubes, left in the silicone oil bath for the required length of time, withdrawn, chilled, and then washed into a beaker with acetic anhydride for titration. Nine to eleven samples were used at each temperature. Runs were carried out to 35–79% of completion. N,N-Diethylhydroxylamine did not interfere with the nonaqueous acidimetric titrations for amine oxides. The results are summarized in Table I. Linear first-order plots (log (percentage of amine oxide) vs. time) and a linear Arrhenius temperature dependence were observed. The energy of activation was calculated from the slope of the Arrhenius plot to be 34.2 ± 1 kcal, and the entropy of activation to be +7.9 ± 2.5 cal deg^{-1}.

TABLE I

Pyrolysis of amine oxides

Amine oxide	Temp. (°C)	Rate constant $\times 10^5$ (s^{-1})
$Me_2NCH_2\phi$	108.2	4.04
$Me_2NCH_2\phi$	119.3	11.1
$Me_2NCH_2\phi$	127.5	31.1
$Me_2NC_{12}H_{25}$	127.5	78*

*Extrapolated from data for reaction to olefin in ref. 4.

Amine Oxide Determination

The nonaqueous potentiometric titration method that was employed has been described in a previous paper (4).

[2]*Miles Chemical Co., Elkhart, Indiana.*

[3]*We thank Miss Catherine Buswell for assistance in the analytical phases of this investigation.*

Can. J. Chem. Downloaded from www.nrcresearchpress.com by 210.87.254.105 on 09/05/12
For personal use only.

Can. J. Chem. Downloaded from www.nrcresearchpress.com by 210.87.254.105 on 09/05/12
For personal use only.

DISCUSSION

The reaction of benzyldimethylamine oxide was reported to give a 61% yield of O-benzyl-N,N-dimethylhydroxylamine (1). This is in good agreement with the 62% yield which we obtained (if one considers only the organic phase). Other products are formed in small-enough quantity that the rate of amine oxide decomposition is a reasonable measurement of the rate of the rearrangement. There is only an approximate relationship between the composition of the product mixture from benzyldiethylamine oxide and that predicted from kinetic data. If one calculates the elimination to rearrangement ratio of benzyldiethylamine oxide (3) to be $(34 + 16)/31 = 1.6$, the result is only of the same order of magnitude as the ratio one would predict for benzyldilaurylamine oxide from rate constants at 127.5° ($2 \times 78/31.1 = 5.0$). This result is of course not entirely unrelated to the rate measurements, since the critical factors are the relative rates of dehydration (and subsequent elimination) and rearrangement. Since dehydration rates of various amine oxides probably do not differ greatly under equivalent conditions, an agreement of such an order of magnitude might be expected.

Schöllkopf *et al.* attempted to distinguish between carbonium ion, carbanion, and free radical pathways on the basis of a substituent effect (2). Clearly, enhancement of the rate by electron-withdrawing substituents on the benzyl group rules out a carbonium ion intermediate. The distinction between the free radical mechanism which they propose and the carbanion mechanism which is rejected is mainly based on the "anticipated" magnitude of the substituent effect for such a reaction. The positive entropy of activation (+7.9 cal deg^{-1}) is not consistent with an anionic mechanism, since reactions of neutral molecules to form ions generally show negative entropies of activation (6). This evidence, combined with that of Schöllkopf *et al.* (2), thus clearly points to a homolytic mechanism for this reaction.

The energy of activation, 34.2 kcal $mole^{-1}$, is much lower than one would expect for such a reaction, since activation energies are generally close to bond energies for thermal homolytic scission. For example, the energy of the carbon–nitrogen single bond is stated as 69.7 kcal (7), while a value of 59 kcal $mole^{-1}$ has been reported for benzylamine dissociation to benzyl and amino radicals (8). This would imply that the carbon–nitrogen bond in amine oxides is relatively weak, which is certainly consistent with the much lower temperature required for this pyrolysis. In this connection, the agreement between the activation energy for rearrangement and that for elimination to olefin (36 kcal $mole^{-1}$) (4) is of interest, since both appear to involve scission of the carbon–nitrogen bond in the transition state, although by different mechanisms.

1. A. C. Cope and P. H. Towle. J. Am. Chem. Soc. **71**, 3423 (1949).
2. H. Schöllkopf, M. Patsch, and H. Schäfer. Tetrahedron Letters, **36**, 2515 (1964).
3. A. C. Cope, T. T. Foster, and P. H. Towle. J. Am. Chem. Soc. **71**, 3929 (1949).
4. G. P. Shulman and W. E. Link. J. Am. Oil Chemists' Soc. **41**, 329 (1964).
5. M. R. V. Sahyun and D. J. Cram. J. Am. Chem. Soc. **85**, 1263 (1963).
6. E. S. Gould. Mechanism and structure in organic chemistry. Henry Holt & Co., New York. 1959. p. 182.
7. L. C. Pauling. Nature of the chemical bond. 3rd ed. Cornell University Press, Ithaca, New York. 1960. p. 85.
8. M. Szwarc. J. Chem. Phys. **17**, 505 (1949).

Received March 30, 1965.
Archer-Daniels-Midland Co.,
Minneapolis, Minnesota.

REACTIONS OF NITRO SUGARS. III.[1] INSTABILITY OF 6-DEOXY-6-NITRO-ALDOHEXOSES AT INTERMEDIATE pH VALUES

HANS H. BAER AND WERNER RANK

A sample of 6-deoxy-6-nitro-L-idose (I) was required for a study concerning the reactivity of nitro sugar glycosides (1). The compound was obtained by sulfuric acid hydrolysis of its crystalline 1,2:3,5-di-*O*-isopropylidene derivative (II), carefully performed according to the directions by Grosheintz and Fischer (2). The specific rotation of the colorless syrup that was obtained, $[\alpha]_D$ −9.9°, agreed well enough with the reported value of −10.4°. However, paper chromatography revealed the presence of, besides I, a considerable amount of 3-deoxy-3-nitro-*muco*-inositol (III) and of traces of the *myo*-1 (IV) and *scyllo* (V) isomers. These by-products, the formation of which in the absence of alkali was unexpected, obviously escaped detection by the earlier authors (2) who, at the time, had not yet available the tool of paper chromatography. We then examined the deacetonation of II employing a sulfonic acid type resin, Rexyn RG-50 (H^+), at reflux temperature in aqueous ethanol. After 30 min the hydrolysate contained the free sugar I and the *muco* inositol III as main components in addition to traces of the other two nitroinositols, and small amounts of starting material and of what was, presumably, the 1,2-monoacetone derivative of I. Hydrolysis for 2 h produced I and the three inositols, all giving similar spot intensities. After 5 h there was noticed a marked decrease in the amount of free sugar relative to the amount of inositols, and among the latter the *myo* and *scyllo* isomers now predominated (Fig. 1).

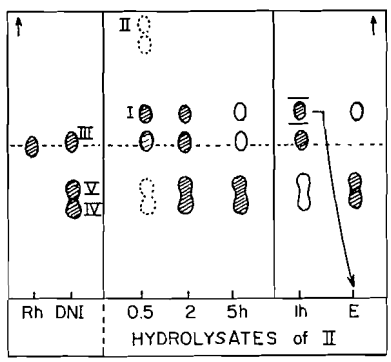

FIG. 1. Paper chromatographic detection of deoxynitroinositols in the hydrolysis of II catalyzed by cation exchange resin. Rh = L-rhamnose; DNI = deoxynitroinositol mixture for comparison; E = zone eluate.

Encouraged by the reasonable differences in the chromatographic mobilities, we then attempted to separate I from the nitroinositols by the zone elution technique. When the zone containing I was cut out and eluted with *distilled water*, the evaporated eluate on rechromatography was found to contain, again, the *myo* and *scyllo* (but no *muco*) inositols, which evidently had arisen during the elution process. This extreme lability of the nitroidose in water was all the more surprising since during the chromatography itself, i.e. in a medium composed of butanol, acetic acid, and water, the compound appeared stable as judged from the absence of trailing on the chromatograms. A chromatographically uniform

[1]*For Part II, see ref. 1.*

Can. J. Chem. Downloaded from www.nrcresearchpress.com by 210.87.254.6 on 09/05/12
For personal use only.

syrup of I free from inositols was indeed obtained when the zone elution was done in the presence of acetic acid.

Thus it became of interest to examine the stability of I over varying periods of time at varying pH values. The loss of reducing power, indicated by the anthrone photometric method, was chosen as a measure of the conversion of I into nitroinositols.[2] The results are depicted in Fig. 2. At pH 1.5 and pH 4, no decrease in reducing power occurred within 24 h. At pH 5 there was a slow decrease over 5 days, amounting to 10% within the first 24 h. At pH 6 a fairly rapid reaction was observed, with 90% of the reducing power disappearing in 24 h. A 90% decrease took place within 4 h at pH 7, and within 2.5 h at pH 9.

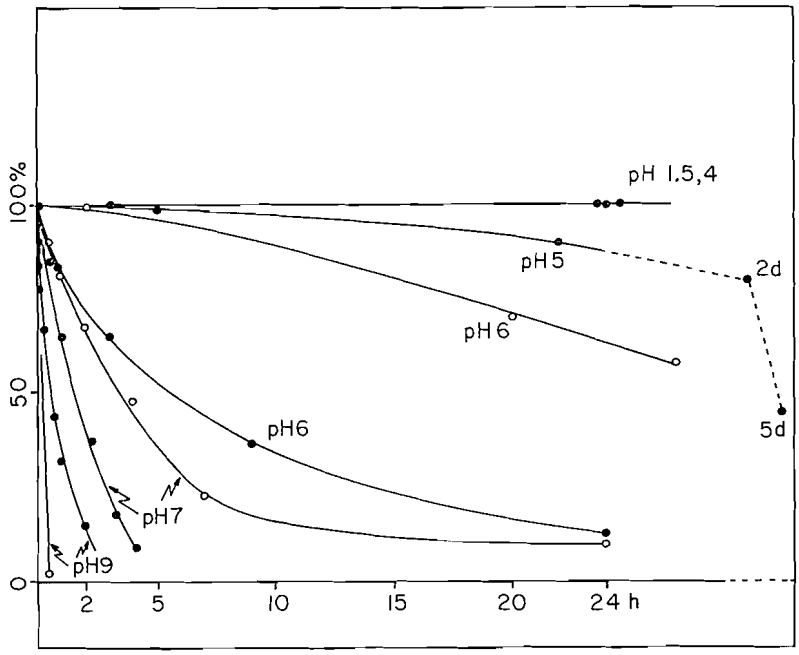

FIG. 2. Decrease in reducing power in 6-deoxy-6-nitro-L-idose (●) and 6-deoxy-6-nitro-D-glucose (○) at various pH values.

6-Deoxy-6-nitro-D-glucose, which differs from I only in the configuration at C-5, exhibited an essentially similar behavior, with gradual differences. It was more stable than in I at pH 6 and 7 but less so at pH 9 (Fig. 2).

Whereas the rapid cyclization of 6-deoxy-6-nitrohexoses in alkaline medium was, of course, known (2), their lability in neutral to slightly acidic media is remarkable. The results indicating stability in more strongly acidic solution were supported when a sample of I was heated in 0.1 *N* sulfuric acid for 1 h at 80° without a loss of reducing power. Therefore, one has to conclude that the nitroinositols were formed, not during the acid hydrolysis of II, but during the subsequent neutralization and work-up procedures despite the care that was exercised to avoid alkalinity. In hydrolyses with cation exchange resin it appears that in the parts of the solution which are not in immediate contact with the resin surface the acidity is insufficient to prevent cyclization effectively. The observed tendency

[2]*We satisfied ourselves that nitrodeoxyinositols do not interfere with the color production. A simpler, polarimetric study was decided against because of the low specific rotation of I and because of unpredictable dependencies of the rotation on the composition of the buffer solutions that were to be used.*

Can. J. Chem. Downloaded from www.nrcresearchpress.com by 210.87.254.6 on 09/05/12
For personal use only.

of the *muco* nitroinositol III to epimerize to thermodynamically more stable isomers (IV and V) is in line with previous findings (3).

The base-catalyzed condensation of nitroalkanes with carbonyl compounds (Henry condensation) normally requires a medium of marked if weak alkalinity. In the 6-deoxy-6-nitro-aldoses the internal Henry condensation appears to be particularly favored, the driving force being the tendency of the molecules to form a stable, six-membered carbocyclic ring. The amount of hydroxyl ion available near neutrality, even on the acid side, is then sufficient for the reaction to be induced although, of course, it proceeds comparatively slowly. The markedly greater reaction speed of the idose derivative as compared to the glucose derivative is reminiscent of the great tendency in idose to form a 1,6-anhydride. The latter fact is attributed to conformational instability by virtue of which the mutual approach of C-6 and C-1 is facilitated. One may perhaps invoke the same conformational factors to explain the faster cyclization of I between pH 5 and 7, but the reversal of the rates at higher pH would remain unexplained.

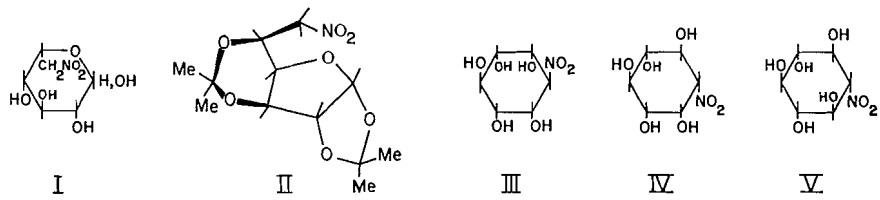

EXPERIMENTAL

Paper Chromatography

Paper chromatography was performed using the descending technique on Whatman No. 1 paper with 1-butanol – acetic acid – water (4:1:5, v/v) as developing system. The running time was 30–40 h and the temperature about 25°. L-Rhamnose served as a reference standard (R_{rh} = 1). The spots were made visible by spraying the chromatogram with ammoniacal silver reagent (0.1 *N* $AgNO_3$, 5 *N* NH_3, 2 *N* NaOH, 1:1:2) and heating it over steam. Lichtenthaler (3), who used the above system for the chromatography of deoxynitroinositols, reported R_{rh} 1.05 for the *muco* isomer (III), 0.57 for the *myo* isomer (IV), and 0.63 for the *scyllo* isomer (V). We prepared mixtures of III, IV, and V according to his directions and found the pattern of the mobilities essentially as reported, although somewhat higher R_{rh} values for IV and V were usually observed, especially at longer running times. Thus, on a 20-h chromatogram the values were 0.61 (IV) and 0.67 (V); on a 30-h chromatogram, 0.64 (IV) and 0.69 (V); and on a 40-h chromatogram, 0.67 (IV) and 0.72 (V). (The isomer III showed R_{rh} 1.04–1.05 in all cases.) These variations were of little concern in the identification of the compounds, which was based on co-chromatography with authentic materials rather than on R_{rh} values alone.

*Hydrolyses of 6-Deoxy-1,2:3,5-di-O-isopropylidene-6-nitro-*L*-idose (II)*

Compound II was prepared according to reference 2; it melted at 148–150° and was shown by paper chromatography to be free from deoxynitroinositols. (Reported, m.p. 150–151°.)

A sample of II was hydrolyzed with sulfuric acid in aqueous ethanol as specified (2). Paper chromatography of the hydrolysate gave spots of R_{rh} 1.20 (6-deoxy-6-nitro-L-idose (I); main product) and R_{rh} 1.04 (III; strong). There were traces of slow-moving material in the R_{rh} 0.6–0.7 region (IV, V) and a faint, unidentified spot of R_{rh} 1.73 which was probably partially deacetonated II.

Three 100-mg samples of II were dissolved in 10 ml of ethanol each. Water (10 ml) and Rexyn RG-50(H^+) (5 ml) were added to the solutions which were refluxed for 30, 120, and 300 min, respectively. The resin was removed and the solutions were decolorized with alkali-free, activated charcoal. Evaporation yielded colorless syrups that were dried *in vacuo* at room temperature to a glassy consistency. The specific rotations were −13.4°, −12.7°, and −9.9°, respectively (*c*, 0.7, 0.7, and 1.1, in water). The paper chromatograms of the products are represented by Fig. 1.

Another sample of II (200 mg) was heated under reflux for 60 min in 40 ml of ethanol–water (1:1) in the presence of 10 ml of the cation exchange resin. The syrup obtained was chromatographed, on a preparative scale, on four sheets (60 × 18 cm) of paper during 30 h. The zones containing I were located by spraying marginal strips; they were then cut out and eluted with warm water. When the eluate was evaporated *in vacuo* it was shown to contain mainly IV and V; there was very little I (R_{rh} 1.20) and no III. A similar experiment using cold water for the zone elution gave the same results (Fig. 1).

When the preceding experiment was repeated with chromatographic solvent mixture instead of water used

Can. J. Chem. Downloaded from www.nrcresearchpress.com by 210.87.254.6 on 09/05/12
For personal use only.

for the elution of the zones of I, I was produced as a syrup that was free from any other products detectable by paper chromatography. 6-Deoxy-6-nitro-L-idose (I) so prepared was employed in the experiments relating to the cyclization at various pH values.

As described elsewhere (1), compound II is converted by *methanolysis* into methyl α,β-glycosides. No deoxynitroinositols were detectable in the product.

A sample of impure I containing much IV and V that originated from cation exchange hydrolysis of II for 5 h, was heated under reflux for 5 h in excess methanol containing 1% of hydrogen chloride. The sugar (R_{rh} 1.20) was thereby converted into methyl glycosides (R_{rh} 1.50 and, mainly, R_{rh} 1.66), while the accompanying inositols seemed unaffected by this treatment.

Estimation of the Changes in Reducing Power of 6-Deoxy-6-nitro-L-idose (I) at Various pH Values

Solutions

Samples of chromatographically pure I (2.0 ± 0.1 mg) were dissolved in 10 ml of solvent. From the solutions, which were stored at room temperature, aliquots (1 ml) were withdrawn from time to time and analyzed for reducing power. The following solvents were used: for pH 1.5, $N/10$ sulfuric acid; for pH 4 and 5, $M/10$ acetate buffer; for pH 6, 7, and 9, potassium dihydrogen phosphate – sodium tetraborate buffer according to Kolthoff. The pH values were checked potentiometrically.

Prccedure

The following modification of the anthrone colorimetric method (4) was worked out. In a small test tube the aliquot (1 ml containing about 200 γ of I) was carefully layered over 2 ml of a freshly prepared, 0.2% solution of anthrone in concentrated sulfuric acid. The two layers were cautiously mixed by stirring them with a thin rod for exactly 1 min, whereby the temperature rose to about 90°. The tube was then immersed for 5 min in a water bath of 80° and thereafter quickly cooled to room temperature with running water. A spectral curve in the visible region was recorded using a Perkin–Elmer spectrophotometer (model 202). The reference cell was charged with an identical mixture of anthrone reagent and blank buffer that had been heated in the same fashion. The absorbance, which had λ_{max} at 634 mμ and was constant over several hours, is plotted in Fig. 2 in relation to the value that was obtained with pure I (at pH 1.5 and zero time), the latter value being equated with 100. Hence the ordinate represents percentages of reducing power. At the sugar concentration chosen (200 γ/ml) the optical density corresponding to the 100% value was about 1.0. D-Glucose under identical test conditions also gave an absorption of 634 mμ but with larger extinction; it produced an optical density of 1.0 at 75 γ/ml.[3] No color was given by the mixture of deoxynitroinositols.

Experiments with 6-Deoxy-6-nitro-D-glucose

This sugar was prepared from its 1,2:3,5-di-*O*-isopropylidene derivative essentially according to given directions (2), although on a smaller scale, which necessitated minor modifications. Diacetone compound (100 mg) in 0.5 ml of $N/10$ sulfuric acid and 1 ml of ethanol was kept at 75–80° for 75 min. Thin-layer chromatography on silica gel with benzene–methanol (4:1) revealed that hydrolysis was incomplete. The heating was therefore continued for a further 2 h, with another 0.5 ml of $N/10$ sulfuric acid being added. The reaction was then complete and the product was worked up as described (2). The recrystallized sugar melted at 153–155°, had R_{rh} 1.03, and showed $[\alpha]_D^{23}$ +43° (10 min; *c*, 0.9 in water). The reported values are m.p. 156–157° and $[\alpha]_D^{23}$ +44.6° (10 min; *c*, 2.9 in water).

No evidence was found for formation of inositols IV and V during this hydrolysis. Inositol III, if formed, would have escaped chromatographic detection, as its mobility is too close to that of the nitro glucose. However, a 2-h hydrolysis with cation exchange resin (which in the case of the *ido* isomer II had resulted in considerable conversion of initially formed III into IV and V; cf. Fig. 1) produced only minute traces of IV and V from the *gluco* isomer. It was therefore unlikely that appreciable quantities of III were formed.

The changes in reducing power in 6-deoxy-6-nitro-D-glucose at pH 6, 7, and 9 were followed as described above for I, and the results are included in Fig. 2.

ACKNOWLEDGMENT

This work was supported by the Ontario Research Foundation.

1. H. H. BAER and W. RANK. Can. J. Chem. This issue.
2. J. M. GROSHEINTZ and H. O. L. FISCHER. J. Am. Chem. Soc. **70**, 1476 (1948).
3. F. W. LICHTENTHALER. Ber. **94**, 3071 (1961).
4. T. A. SCOTT and E. H. MELVIN. Anal. Chem. **25**, 1650 (1953). Z. DISCHE. *In* Methods in carbohydrate chemistry. *Edited by* R. L. Whistler and M. L. Wolfrom. Vol. 1. Academic Press, New York. 1962. p. 490.

RECEIVED JUNE 25, 1965.
DEPARTMENT OF CHEMISTRY,
UNIVERSITY OF OTTAWA,
OTTAWA, CANADA.

[3]*It is noted that hexoses are reported (4) to give* λ_{max} *625 m*μ*; however, the reaction conditions adopted in the present modification are not the same.*

Can. J. Chem. Downloaded from www.nrcresearchpress.com by 210.87.254.6 on 09/05/12
For personal use only.

PREPARATION OF α-FLUORO-γ-AMINOACIDS

R. L. BUCHANAN[1] AND F. L. M. PATTISON

Diethyl fluoromalonate has been shown to be a valuable intermediate in the synthesis of α-fluoroalkanoic acids (1), including γ-fluoroglutamic acid (2). We now wish to report two general procedures, based on diethyl fluoromalonate, for obtaining α-fluoro-γ-aminoacids, $RCH(NH_2)CH_2CHFCOOH$.

Of the compounds prepared, the most interesting from a biological standpoint is "fluoro-GABA" (4-amino-2-fluorobutanoic acid) (I). GABA (γ-aminobutyric acid) is known to have an important physiological action upon brain function as well as upon certain peripheral nervous structures (3). In particular, a depletion of GABA in the brain results in hyperexcitability, leading to convulsive states or epilepsy in man. It was thought possible that the fluorinated analogue of this brain component, as an antimetabolite of GABA, might mimic the symptoms associated with GABA deficiency. Moreover, GABA is thought to be concerned with the regulation or transmission of nerve impulses in central grey matter, thus leading to the suggestion that compound I might prove also to be a useful tool in neurophysiological research. Preliminary examination of I in experiments with mice gave no indication of pharmacological activity. Its value in neurophysiology has yet to be determined.

The first method involves the reaction of an *N*-aroylethyleneimine with diethyl fluoromalonate.

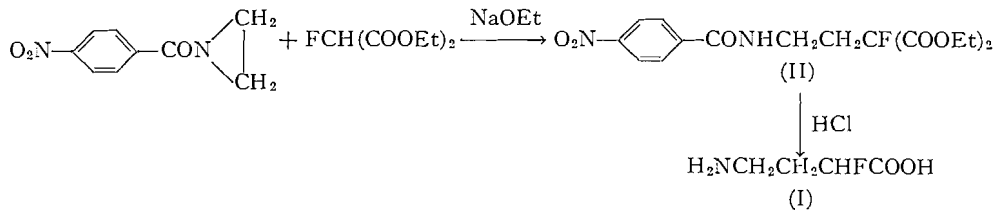

Initial work, with *N*-benzoylethyleneimine and a catalytic quantity of sodium ethoxide, gave an insignificant yield of the product. However, by introducing the electron-withdrawing *p*-nitro substituent onto the benzene ring, the aziridine ring becomes more susceptible to nucleophilic attack; the required intermediate II was thus obtained in 47% yield. Acid hydrolysis then gave I as the monohydrate (65%). It is essential that, in the hydrolysis, the refluxing be continued until the reaction is complete; insufficient heating gives an intractable gum, which is hard to purify. Tolman and Vereš (4) have recently reported an unsuccessful attempt to synthesize I, starting from ethyl α-fluorocrotonate.

The second method involves the Michael addition of diethyl fluoromalonate to 2-nitro-1-alkenes (e.g. 2-nitro-1-butene).

Compound III, obtained in 54.5% yield, on being heated under reflux with iron and hydrochloric acid, gave IV, characterized as its *N*-2,4-dinitrophenyl and *N*-benzyloxycarbonyl derivatives. Attempts to decarboxylate IV to VI resulted in decomposition. Compound III was therefore first hydrolyzed and decarboxylated to give V (in 58% yield) as a viscous, yellow oil, which on reduction as before gave VI; this was characterized as its *N*-2,4-dinitrophenyl derivative. The reaction of diethyl fluoromalonate with nitroethylene, in a proposed alternative synthesis of I, afforded only polymeric products and recovered starting materials.

[1]*Present address: Department of Organic Chemistry, Bristol Laboratories, Syracuse 1, N.Y.*

Can. J. Chem. Downloaded from www.nrcresearchpress.com by 210.87.254.42 on 09/05/12
For personal use only.

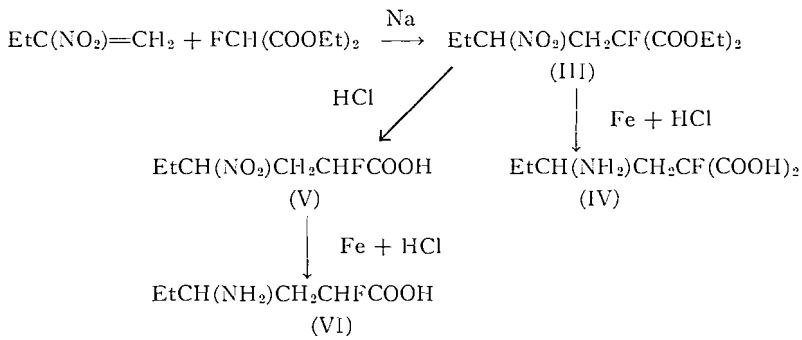

EXPERIMENTAL

4-Amino-2-fluorobutanoic Acid Monohydrate ("Fluoro-GABA") (I)

(a) Diethyl 2-(p-Nitrobenzamido)ethylfluoromalonate (II)

Diethyl fluoromalonate (3.78 g, 21.2 mmoles) and dry dimethylformamide (40 ml) were added to a solution of sodium ethoxide in ethanol, prepared from sodium (50 mg, 2.17 mg-atoms) and dry ethanol (15 ml). The mixture was contained in a 100-ml three-necked flask fitted with a stirrer, a reflux condenser with drying tube, and a gas inlet. The flask was purged with dry nitrogen throughout the reaction. After the mixture had been stirred for 15 min, a solution of *N*-(*p*-nitrobenzoyl)ethyleneimine (3.87 g, 20.1 mmoles) (5) in dry dimethylformamide (15 ml) was added, and this mixture was stirred at 40–45° for 60 h. It was then poured into water, acidified with glacial acetic acid, and extracted twice with ether. The extracts were washed three times with water and dried over anhydrous $MgSO_4$. Removal of the ether gave pale yellow crystals. Benzene was added, followed by an excess of petroleum ether (60–80°), giving II (3.49 g, 47%). Two recrystallizations of a small quantity from benzene – petroleum ether (60–80°) gave the pure product, m.p. 94–95°.

Anal. Calcd. for $C_{16}H_{19}FN_2O_7$: C, 51.89; H, 5.17; N, 7.56. Found: C, 52.07; H, 4.99; N, 7.33.

(b) 4-Amino-2-fluorobutanoic Acid Monohydrate (I)

Compound II (25.0 g, 67.5 mmoles) and concentrated hydrochloric acid (100 ml) were heated under reflux for 75 h. The mixture was allowed to cool and water was added. *p*-Nitrobenzoic acid (10.8 g, 95.5%) was removed by filtration. The filtrate was evaporated to give the syrupy amino acid hydrochloride, which was dissolved in water and stirred with an excess of freshly prepared silver oxide. The mixture was filtered through "Supercel", and the filtrate was treated with excess hydrogen sulfide. The mixture was again filtered through "Supercel". The aqueous filtrate was evaporated, whereupon the product (I) crystallized immediately. After being washed with methanol and dried *in vacuo*, the crystals had m.p. 201–203°. Yield: 5.3 g (65%). Recrystallization from 90% ethanol did not alter the melting point. The infrared spectrum (Nujol mull) had the following bands (cm^{-1}): 1 650($-\overset{+}{N}H_3$ def., m), 1 592 (ionized carboxyl C=O str., s), 1 560 ($-\overset{+}{N}H_3$ def., m), and 1 054 (C—F str., w).

Anal. Calcd. for $C_4H_{10}FNO_3$: C, 34.53; H, 7.25; N, 10.07. Found: C, 34.27; H, 7.11; N, 10.36.

4-Amino-2-fluorohexanoic Acid (VI)

(a) Diethyl (2-Nitrobutyl)fluoromalonate (III)

Diethyl fluoromalonate (10.68 g, 60 mmoles) was added dropwise with stirring to sodium (46 mg, 1.98 mg-atoms) and dry dioxane (8.8 g) in a 50-ml three-necked flask fitted with a stirrer, a reflux condenser with drying tube, and an addition funnel. After all the sodium had reacted, the resultant mixture was cooled in an ice bath, and hydroquinone (10 mg) was added. 2-Nitro-1-butene (4.0 g, 39.6 mmoles) (6) was then added slowly with vigorous stirring over 25 min. Stirring was continued at room temperature for 1 h. The mixture was acidified with glacial acetic acid, poured into water (200 ml), and extracted three times with ether. The ether extract was washed with water and dried over anhydrous $MgSO_4$. The ether was removed and the residue was fractionally distilled through a platinum-plated spinning-band column, giving recovered diethyl fluoromalonate (3.84 g) and the product III (5.84 g, 54.5%), b.p. 90–91.5° at 0.18 mm, n_D^{25} 1.4337, d_4^{20} 1.176, MR_D 61.9 cc/mole (estimated 62.0 cc/mole).

Anal. Calcd. for $C_{11}H_{18}FNO_6$: C, 47.31; H, 6.50; N, 5.02. Found: C, 47.54; H, 6.65; N, 5.23.

(b) (2-Aminobutyl)fluoromalonic Acid (IV)

Diethyl (2-nitrobutyl)fluoromalonate (3.8 g, 13.6 mmoles), powdered iron (5.32 g, 95.2 mg-atoms), concentrated hydrochloric acid (85 ml), water (25 ml), and 95% ethanol (25 ml) were stirred in an atmosphere of nitrogen at room temperature for 20 min. The mixture was then refluxed for 1 h, cooled, made alkaline with 2 *N* sodium hydroxide, and filtered through "Supercel". The filtrate was acidified with concentrated hydrochloric acid and concentrated. The precipitated sodium chloride was filtered off. The silver oxide – hydrogen sulfide treatment (as described above) was carried out. Evaporation and addition of ethanol gave a gummy solid (2.17 g, 83%), which was characterized by the formation of two derivatives.

Can. J. Chem. Downloaded from www.nrcresearchpress.com by 210.87.254.42 on 09/05/12
For personal use only.

(1) *N-2,4-Dinitrophenyl derivative,* prepared by the method of Cheronis and Entrikin (7), was obtained as a yellow oil. Chromatography through silica gel (elution with 4:1 benzene–ether) and recrystallization from benzene gave yellow crystals, m.p. 140–141.5°.

Anal. Calcd. for $C_{13}H_{14}FN_3O_8$: C, 43.46; H, 3.93; N, 11.70. Found: C, 43.68; H, 4.07; N, 11.88.

(2) *N-Benzyloxycarbonyl derivative,* prepared by the method of Neuberger and Tait (8), was recrystallized once from benzene – petroleum ether (60–80°) and twice from ethyl acetate – petroleum ether (60–80°) as white crystals, m.p. 136–139°. The infrared spectra of this and of the previous derivative showed an acid carbonyl band at 1 751 cm^{-1}, indicative of an α-fluoromalonic acid (1).

Anal. Calcd. for $C_{15}H_{18}FNO_6$: C, 55.04; H, 5.54. Found: C, 54.92; H, 5.39.

(c) 4-Amino-2-fluorohexanoic Acid (VI)

Diethyl (2-nitrobutyl)fluoromalonate (1.4 g, 5 mmoles) and 6 *N* hydrochloric acid (40 ml) were heated under reflux at 150° for 4.5 h, by which time evolution of carbon dioxide had ceased. Isolation in the usual manner gave the nitro acid as a yellow oil (0.52 g, 58%). This was then reduced directly to the amino acid. Powdered iron (0.84 g, 15 mg-atoms) was added to concentrated hydrochloric acid (5 ml) in an atmosphere of nitrogen. The crude nitro acid (400 mg, 2.2 mmoles) in 50% aqueous ethanol (10 ml) was added. The mixture was stirred at room temperature for 1 h, at 75° for 6 h, and at 50° for 15 h. Isolation of the crude amino acid (VI) hydrochloride (0.4 g, 98%) was carried out as for IV. It was characterized as its *N-2,4-dinitrophenyl derivative* (7), which on chromatography through silica gel and recrystallization from chloroform – petroleum ether (60–80°) was obtained as yellow needles, m.p. 151–155° (decomp.) The infrared spectrum of this derivative showed an acid carbonyl at 1 730 cm^{-1}, indicative of an α-fluoro monobasic acid (1).

Anal. Calcd. for $C_{12}H_{14}FN_3O_6$: C, 45.72; H, 4.48; N, 13.33. Found: C, 45.68; H, 4.28; N, 13.16.

ACKNOWLEDGMENTS

We express our indebtedness to the National Research Council for financial support and for a studentship (R.L.B.), to Dr. D. A. V. Peters of this department for help in preparing compound I, and to Dr. C. W. Gowdey, Department of Pharmacology, University of Western Ontario, for kindly carrying out the pharmacological examination of I.

1. F. L. M. Pattison, R. L. Buchanan, and F. H. Dean. Can. J. Chem. **43**, 1700 (1965).
2. R. L. Buchanan, F. H. Dean, and F. L. M. Pattison. Can. J. Chem. **40**, 1571 (1962).
3. K. A. C. Elliott and H. H. Jasper. Physiol. Rev. **39**, 383 (1959).
4. V. Tolman and K. Vereš. Tetrahedron Letters, No. 29, 1967 (1964).
5. H. W. Heine, M. E. Fetter, and E. M. Nicholson. J. Am. Chem. Soc. **81**, 2202 (1959).
6. H. B. Hass, A. G. Susie, and R. L. Heider. J. Org. Chem. **15**, 8 (1950).
7. N. D. Cheronis and J. B. Entrikin. Semimicro qualitative organic analysis. 2nd ed. Interscience Publishers, Inc., New York, N.Y. 1957. p. 346.
8. A. Neuberger and G. H. Tait. J. Chem. Soc. 3963 (1962).

Received July 30, 1965.
Department of Chemistry,
University of Western Ontario,
London, Ontario.

THE REACTION OF SOME TITANIUM AND ZIRCONIUM HALIDES WITH CYCLIC ORGANIC LIGANDS CONTAINING OXYGEN AND SULFUR

E. C. Alyea[1] and E. G. Torrible

Recently a number of complexes of titanium and zirconium halides with cyclic ligands $C_4H_8Y_2$ (Y = O or S) have been reported (1–5). The structure of the 1,4-dioxan (D) complexes have been the subject of some debate. Rolsten and Sisler (1) concluded that the complexes were monomeric and the 1,4-dioxan was acting as a bidentate chelating

[1]*Present address: Chemistry Department, Queen Mary College, University of London, England.*

Can. J. Chem. Downloaded from www.nrcresearchpress.com by 210.87.254.42 on 09/05/12
For personal use only.

(1) *N-2,4-Dinitrophenyl derivative,* prepared by the method of Cheronis and Entrikin (7), was obtained as a yellow oil. Chromatography through silica gel (elution with 4:1 benzene–ether) and recrystallization from benzene gave yellow crystals, m.p. 140–141.5°.

Anal. Calcd. for $C_{13}H_{14}FN_3O_8$: C, 43.46; H, 3.93; N, 11.70. Found: C, 43.68; H, 4.07; N, 11.88.

(2) *N-Benzyloxycarbonyl derivative,* prepared by the method of Neuberger and Tait (8), was recrystallized once from benzene – petroleum ether (60–80°) and twice from ethyl acetate – petroleum ether (60–80°) as white crystals, m.p. 136–139°. The infrared spectra of this and of the previous derivative showed an acid carbonyl band at 1 751 cm^{-1}, indicative of an α-fluoromalonic acid (1).

Anal. Calcd. for $C_{15}H_{18}FNO_6$: C, 55.04; H, 5.54. Found: C, 54.92; H, 5.39.

(c) 4-Amino-2-fluorohexanoic Acid (VI)

Diethyl (2-nitrobutyl)fluoromalonate (1.4 g, 5 mmoles) and 6 *N* hydrochloric acid (40 ml) were heated under reflux at 150° for 4.5 h, by which time evolution of carbon dioxide had ceased. Isolation in the usual manner gave the nitro acid as a yellow oil (0.52 g, 58%). This was then reduced directly to the amino acid. Powdered iron (0.84 g, 15 mg-atoms) was added to concentrated hydrochloric acid (5 ml) in an atmosphere of nitrogen. The crude nitro acid (400 mg, 2.2 mmoles) in 50% aqueous ethanol (10 ml) was added. The mixture was stirred at room temperature for 1 h, at 75° for 6 h, and at 50° for 15 h. Isolation of the crude amino acid (VI) hydrochloride (0.4 g, 98%) was carried out as for IV. It was characterized as its *N-2,4-dinitrophenyl derivative* (7), which on chromatography through silica gel and recrystallization from chloroform – petroleum ether (60–80°) was obtained as yellow needles, m.p. 151–155° (decomp.) The infrared spectrum of this derivative showed an acid carbonyl at 1 730 cm^{-1}, indicative of an α-fluoro monobasic acid (1).

Anal. Calcd. for $C_{12}H_{14}FN_3O_6$: C, 45.72; H, 4.48; N, 13.33. Found: C, 45.68; H, 4.28; N, 13.16.

ACKNOWLEDGMENTS

We express our indebtedness to the National Research Council for financial support and for a studentship (R.L.B.), to Dr. D. A. V. Peters of this department for help in preparing compound I, and to Dr. C. W. Gowdey, Department of Pharmacology, University of Western Ontario, for kindly carrying out the pharmacological examination of I.

1. F. L. M. Pattison, R. L. Buchanan, and F. H. Dean. Can. J. Chem. **43**, 1700 (1965).
2. R. L. Buchanan, F. H. Dean, and F. L. M. Pattison. Can. J. Chem. **40**, 1571 (1962).
3. K. A. C. Elliott and H. H. Jasper. Physiol. Rev. **39**, 383 (1959).
4. V. Tolman and K. Vereš. Tetrahedron Letters, No. 29, 1967 (1964).
5. H. W. Heine, M. E. Fetter, and E. M. Nicholson. J. Am. Chem. Soc. **81**, 2202 (1959).
6. H. B. Hass, A. G. Susie, and R. L. Heider. J. Org. Chem. **15**, 8 (1950).
7. N. D. Cheronis and J. B. Entrikin. Semimicro qualitative organic analysis. 2nd ed. Interscience Publishers, Inc., New York, N.Y. 1957. p. 346.
8. A. Neuberger and G. H. Tait. J. Chem. Soc. 3963 (1962).

Received July 30, 1965.
Department of Chemistry,
University of Western Ontario,
London, Ontario.

THE REACTION OF SOME TITANIUM AND ZIRCONIUM HALIDES WITH CYCLIC ORGANIC LIGANDS CONTAINING OXYGEN AND SULFUR

E. C. Alyea[1] and E. G. Torrible

Recently a number of complexes of titanium and zirconium halides with cyclic ligands $C_4H_8Y_2$ (Y = O or S) have been reported (1–5). The structure of the 1,4-dioxan (D) complexes have been the subject of some debate. Rolsten and Sisler (1) concluded that the complexes were monomeric and the 1,4-dioxan was acting as a bidentate chelating

[1]*Present address: Chemistry Department, Queen Mary College, University of London, England.*

agent. Hendra and Powell (6) rejected this structure on the grounds that the chelate structure would require the dioxan ring to be in the boat form. Their infrared data showed that the dioxan was in the same configuration as in free dioxan and in $HgCl_2.D$ where it had been proved to have the chair form (7). They concluded that the $TiX_4.D$ structure would be similar to that of $Al_2Br_6.D$, i.e. the chair configuration of the six-membered ring with one oxygen atom only attached to a metal atom. There are two other possible structures; a polymeric chain structure similar to the proved polymeric structure of $HgCl_2.D$ (7), or an ionic structure $[TiCl_2.2D]^{2+}[TiCl_6]^{2-}$ analogous to $[Ga.2D]^+Cl^-$ (8). Molecular weight determination of the complexes in 1,4-dioxan is of no help in elucidating the structure because all four possibilities could be expected to be "monomeric" in solution. Molecular weight determinations in other non-reacting solvents were not possible because of the very low solubility of the complexes.

Conductance measurements in nitrobenzene and nitromethane (Table II) indicate that the compounds are nonelectrolytes and hence the ionic structure must be rejected.

The infrared spectra of the $TiX_4.D$ complexes are very similar above 500 cm^{-1}, and resemble very closely the spectrum of the polymeric $HgCl_2.D$. The spectra show no bands which can be assigned to uncoordinated —C—O—C— asymmetric and symmetric stretching frequencies (1 121 cm^{-1} and 873 cm^{-1} present in the free ligand). This of course rules out a structure similar to $Al_2Br_6.D$ since evidence of uncoordinated oxygen would be expected and is in fact observed for the aluminium complex (6). The proposed polymeric structure for the titanium(IV) complexes is supported by their very low solubility in non-reacting solvents.

The powder diffraction patterns for $TiCl_4.D$, $TiBr_4.D$, and $ZrCl_4.D$ suggest they have similar structures. The pattern obtained for $TiBr_4.D$ exhibits interplanar spacings and intensities which agree with these recorded by Sisler (1). However, Sisler records an extra line at a *d*-value of 2.62 Å which we did not observe. This line was also absent from partially hydrolyzed samples of the complex.

It was hoped to gain evidence to support the proposed polymeric structures for the 1,4-dioxan complexes by studying the complexes of analogous ring systems containing sulfur and of 1,3-dioxan. With 1,3-dioxan ($D^{1,3}$) only titanium(III) chloride yielded a 1:1 complex. The titanium(IV) halides do not appear to form simple addition complexes but yielded products whose analyses closely agreed with the stoichiometry $TiX_2.D^{1,3}$. All the products were insoluble in common solvents. The infrared spectra of these complexes do not lend themselves to clear interpretation. It is possible that the ring has been opened during the reaction.

Recently Fowles *et al.* (2, 3, 4) reported the preparation and characterization of the 1,4-thioxan (T) complexes $TiX_3.T$, $TiX_3.2T$, and $TiX_4.2T$ (X = Cl, Br). From the infrared spectra Fowles concludes that bonding to the metal occurs through the sulfur and not through the oxygen in the bis-complexes. No molecular weights were reported. We have confirmed their findings and in addition found that the $TiBr_4.2T$ complex is monomeric in nitrobenzene. We also report the preparation and characterization of a series of mono-thioxan complexes of the titanium(IV) and zirconium(IV) halides. The mono-complexes all show very similar spectra in the range 1 500 to 500 cm^{-1}; however, certain differences from the spectra given by the bis-complexes are important. The peaks at 1 105 cm^{-1} and 663 cm^{-1} are negligible indicating bonding through both oxygen and sulfur atoms to the metal. The spectra indicate that the ligand is still in the chair form and hence the mono-complexes are probably polymeric. This conclusion is supported by their low solubility in common organic solvents and their low conductivity (Table II).

TABLE I

Analytical results

Compound	Color and m.p. (°C)	Theoretical					Found				
		M	X	C	H	S	M	X	C	H	S
$TiCl_4$.D	Yellow, 200*	17.2	51.1	17.3	2.88		17.2	50.0	17.2	3.56	
$TiBr_4$.D	Red, 180*	10.5	70.1	10.5	1.76		10.5	69.3	10.8	1.80	
$ZrCl_4$.D†	White	28.4	44.2	14.9	2.49		31.5	38.9	13.5	2.59	
$TiCl_3$.D	Grey, 250*	19.7	43.9	19.8	3.3		20.5	43.1	19.8	3.4	
$TiCl_3$.2D	Blue-green, 164*	14.5	32.2	29.1	4.9		14.8	31.8	26.9	5.04	
$TiCl_4$.T†	Yellow, 188*	16.3	48.3	16.3	2.72		16.5	47.3	16.5	2.96	
$TiCl_4$.2T	Yellow, 150	12.0	35.6	24.1	4.02		12.2	35.2	24.0	4.13	
$TiBr_4$.T†	Red, 160*	10.2	67.8	10.2	1.70		10.9	67.1	—	—	
$TiBr_4$.2T	Orange, 159	8.3	55.5	16.7	2.78		8.4	55.5	—	—	
$ZrCl_4$.T†	White	27.1	42.1	14.22	2.37		26.3	37.2	16.0	2.92	
$TiCl_3$.T	Yellow-green, 178*	18.5	41.2	18.6	3.09		20.1	42.6	18.4	3.25	
$TiCl_4$.Dith	Yellow, 270*	15.4	45.8	15.5	2.58	20.7	15.4	43.8	15.7	2.81	20.6
$TiBr_4$.Dith	Orange, 250*	9.8	65.6	9.9	1.64	13.2	9.9	64.1	10.9	2.02	—
$TiCl_3$.Dith†	Yellow, 230*	17.4	38.9	17.5	2.91	23.3	18.1	40.7	17.5	3.54	23.1
$TiCl_3$.$D^{1,3}$†	Blue, 210*	19.7	43.9	19.8	3.30		21.1	43.5	19.67	3.39	

*Decomposition.
†New compounds.

TABLE II
Molar conductivities

Compound	Solvent	Concentration ($M \times 10^3$)	Molar conductivity (ohm^{-1} cm^2)
$TiBr_4$.D	Nitrobenzene	12.9	1.8
	Nitromethane	4.63	10.6
$TiCl_4$.D	Nitrobenzene	2.0	0.55
	Nitromethane	2.3	3.0
$TiBr_4$.T	Nitrobenzene	2.04	10.1
	Nitromethane	1.72	10.2
$TiBr_4$.2T	Nitrobenzene	1.44	4.0
	Nitromethane	4.35	8.9
1:1 electrolyte	Nitrobenzene	1.0	20–30
	Nitromethane	1.0	~100

There is relatively little data in the literature concerning the complexes of 1,4-dithian (Dith). Recently Fowles and Baker (5) reported the preparation of the titanium(IV) halide 1:1 adducts. The free ligand has been reported to have the chair configuration (9). We have found that the spectra of complexes $TiCl_4$.Dith, $TiBr_4$.Dith, and $TiCl_3$.Dith are similar to that of the free ligand implying a polymeric structure. The complexes were not sufficiently soluble for molecular weights to be determined.

All the ligands reported in this note were reacted with titanium(IV) iodide, but in no instance was a simple product obtained. In most of the reactions iodine was displaced and the infrared spectra indicated possible opening of the rings.

The infrared spectra in the 500–300 cm^{-1} range have been recorded (Table III). The absorptions in this region are mainly due to M—X vibrations. Thus the strong band at 360–385 cm^{-1} in the chloride complexes can be assigned to the Ti—Cl stretching mode (485 cm^{-1} in free $TiCl_4$ (10)). Similarly the strong band at 380 cm^{-1} in free titanium(IV)

TABLE III
Principal absorption bands in the 600–300 cm^{-1} region

Compound		Compound	
1,4-Dioxan (liquid)	608 (s), 270 (m)	$TiBr_4$.T	555 (m), 370 (w), 310 (s), 305 (s)
$TiCl_4$.D	596 (s), 360 (s), 335 (m), 316 (sh)	$TiCl_4$.2T	552 (s), 380 (vs), 363 (sh), 303 (m)
$TiBr_4$.D	595 (s), 332 (vs), 316 (vs)	$TiBr_4$.2T	550 (s), 440 (w), 385 (w), 357 (m), 350 (sh)
$ZrCl_4$.D	605 (s), 470 (m), 345 (vs), 300 (sh)	$ZrCl_4$.T	558 (s), 445 (w), 330 (vs)
$TiCl_3$.D	605 (sh), 372 (vs), 340 (vs), 300 (w)	1,4-Dithian	470 (w), 464 (w)
$TiCl_3$.2D	435 (w), 370 (vs), 340 (vs), 300 (m)	$TiCl_4$.Dith	480 (w), 455 (w), 440 (w), 375 (vs), 310 (m)
1,4-Thioxan (liquid)	550 (s), 385 (m), 335 (w)	$TiBr_4$.Dith	480 (w), 440 (sh), 300 (vs)
$TiCl_3$.T	555 (m), 440 (sh), 380 (vs), 350 (sh)	$TiCl_3$.Dith	480 (w), 430 (w), 375 (vs)
$TiCl_4$.T	560 (m), 380 (vs), 310 (w)		

ABBREVIATIONS: s = strong, m = medium, sh = shoulder, v = very, w = weak.

bromide is lowered to about 300 cm^{-1} in the complexes. The Zr—Cl stretching frequency is lowered from 390 cm^{-1} to 330–345 cm^{-1}, on complex formation. These conclusions are in accord with those recently published by Beattie and Webster (11). For titanium(III) chloride complexes, Fowles *et al.* (12) assigned bands between 400 and 421 cm^{-1} to metal—chlorine stretching modes. We have found that solid titanium(III) chloride shows three absorption bands at 490 cm^{-1} (m), 387 cm^{-1} (s), and 290 cm^{-1} (vs). In the complexes the major absorption bands occur in the range 340–380 cm^{-1} with very little absorption in the 400–420 cm^{-1} region. The spectra recorded by Fowles *et al.* (12) were determined using potassium bromide optics which would not record the absorptions below 400 cm^{-1}.

EXPERIMENTAL

Special precautions were taken to exclude water from the apparatus and chemicals and all reactions were conducted in an atmosphere of dry nitrogen. Reagents and solvents were purified and dried by appropriate methods except 1,4-dithian which was specially prepared by the Aldrich Chemical Co., Inc. and was used as such.

The preparations of the complexes were all done in a similar manner. Either cyclohexane or benzene solutions of the purified reagents were mixed in known molar ratios. Usually a complex was formed on mixing and heat was evolved. However, the reactions involving titanium trichloride required long heating and stirring as the violet trihalide was insoluble in cyclohexane and benzene and reacted only slowly. The products were filtered, washed with suitable solvents to remove the excess of reactants, and dried *in vacuo*.

The infrared spectra were all determined as mulls in Nujol between KRS-5 plates on a Beckman I. R. 10 grating instrument.

Conductivities were measured in a specially adapted cell with a Phillips PR9500 bridge.

Molecular weights were determined cryoscopically using a modified Maier transposed bridge circuit (13). An internal calibration using fluorene was carried out with each determination.

Titanium and halogen were determined by standard gravimetric methods. Carbon, hydrogen, and sulfur were determined commercially.

ACKNOWLEDGMENTS

Grateful acknowledgment is made to the National Research Council of Canada for financial support and to the Government of the Province of Ontario for a Fellowship (to E. C. A.).

1. R. F. Rolsten and H. H. Sisler. J. Am. Chem. Soc. **79**, 1819 (1957).
2. G. W. A. Fowles, R. A. Hoodless, and R. A. Walton. J. Chem. Soc. 5873 (1963).
3. G. W. A. Fowles and R. A. Walton. J. Chem. Soc. 4330 (1964).
4. G. W. A. Fowles and R. A. Walton. J. Chem. Soc. 4953 (1964).
5. K. Baker and G. W. A. Fowles. J. Less-Common Metals, **8**, 47 (1965).
6. P. J. Hendra and D. B. Powell. J. Chem. Soc. 5105 (1960).
7. C. Hassel and J. Hvoslef. Acta Chem. Scand. **8**, 1953 (1954).
8. F. M. Brewer, J. R. Chadwick, and G. Garton. J. Inorg. Nucl. Chem. **23**, 45 (1961).
9. K. Hayasaki. Nippon Kagaku Zasshi, **81**, 1645 (1960).
10. K. Nakamoto. Infra-red spectra of inorganic and coordination compounds. John Wiley, New York. 1963.
11. I. R. Beattie and M. Webster. J. Chem. Soc. 3507 (1964).
12. M. W. Duckworth, G. W. A. Fowles, and R. A. Hoodless. J. Chem. Soc. 5665 (1963).
13. W. F. O'Hara, C. W. Wu, and L. G. Hepler. J. Chem. Educ. **38**, 512 (1961).

Received June 2, 1965.
Chemistry Department,
Queen's University,
Kingston, Ontario.

AN APPROXIMATE DETERMINATION OF THE SECOND-STAGE PROTONATION CONSTANT FOR 2,2′-BIPYRIDYL, 1,10-PHENANTHROLINE, AND DERIVATIVES

W. A. E. McBryde

Although 1,10-phenanthroline has two potentially basic nitrogen atoms per molecule, it is generally regarded as a monoprotic base (1). The related compound 2,2′-bipyridyl, in spite of being a weaker base, shows evidence of the uptake of a second proton (2). The difference in behavior is said to be due to the fused ring system in the former which maintains the two nitrogen atoms at a fixed distance of 2.5 Å; in this circumstance steric or electrostatic factors are thought to preclude the admission of a second proton.

There have been some observations recorded that are consistent with the addition of a second proton to phenanthroline and its analogues. These include a spectral shift in 8 *M*

EXPERIMENTAL

Special precautions were taken to exclude water from the apparatus and chemicals and all reactions were conducted in an atmosphere of dry nitrogen. Reagents and solvents were purified and dried by appropriate methods except 1,4-dithian which was specially prepared by the Aldrich Chemical Co., Inc. and was used as such.

The preparations of the complexes were all done in a similar manner. Either cyclohexane or benzene solutions of the purified reagents were mixed in known molar ratios. Usually a complex was formed on mixing and heat was evolved. However, the reactions involving titanium trichloride required long heating and stirring as the violet trihalide was insoluble in cyclohexane and benzene and reacted only slowly. The products were filtered, washed with suitable solvents to remove the excess of reactants, and dried *in vacuo*.

The infrared spectra were all determined as mulls in Nujol between KRS-5 plates on a Beckman I. R. 10 grating instrument.

Conductivities were measured in a specially adapted cell with a Phillips PR9500 bridge.

Molecular weights were determined cryoscopically using a modified Maier transposed bridge circuit (13). An internal calibration using fluorene was carried out with each determination.

Titanium and halogen were determined by standard gravimetric methods. Carbon, hydrogen, and sulfur were determined commercially.

ACKNOWLEDGMENTS

Grateful acknowledgment is made to the National Research Council of Canada for financial support and to the Government of the Province of Ontario for a Fellowship (to E. C. A.).

1. R. F. Rolsten and H. H. Sisler. J. Am. Chem. Soc. **79**, 1819 (1957).
2. G. W. A. Fowles, R. A. Hoodless, and R. A. Walton. J. Chem. Soc. 5873 (1963).
3. G. W. A. Fowles and R. A. Walton. J. Chem. Soc. 4330 (1964).
4. G. W. A. Fowles and R. A. Walton. J. Chem. Soc. 4953 (1964).
5. K. Baker and G. W. A. Fowles. J. Less-Common Metals, **8**, 47 (1965).
6. P. J. Hendra and D. B. Powell. J. Chem. Soc. 5105 (1960).
7. C. Hassel and J. Hvoslef. Acta Chem. Scand. **8**, 1953 (1954).
8. F. M. Brewer, J. R. Chadwick, and G. Garton. J. Inorg. Nucl. Chem. **23**, 45 (1961).
9. K. Hayasaki. Nippon Kagaku Zasshi, **81**, 1645 (1960).
10. K. Nakamoto. Infra-red spectra of inorganic and coordination compounds. John Wiley, New York. 1963.
11. I. R. Beattie and M. Webster. J. Chem. Soc. 3507 (1964).
12. M. W. Duckworth, G. W. A. Fowles, and R. A. Hoodless. J. Chem. Soc. 5665 (1963).
13. W. F. O'Hara, C. W. Wu, and L. G. Hepler. J. Chem. Educ. **38**, 512 (1961).

Received June 2, 1965.
Chemistry Department,
Queen's University,
Kingston, Ontario.

AN APPROXIMATE DETERMINATION OF THE SECOND-STAGE PROTONATION CONSTANT FOR 2,2′-BIPYRIDYL, 1,10-PHENANTHROLINE, AND DERIVATIVES

W. A. E. McBryde

Although 1,10-phenanthroline has two potentially basic nitrogen atoms per molecule, it is generally regarded as a monoprotic base (1). The related compound 2,2′-bipyridyl, in spite of being a weaker base, shows evidence of the uptake of a second proton (2). The difference in behavior is said to be due to the fused ring system in the former which maintains the two nitrogen atoms at a fixed distance of 2.5 Å; in this circumstance steric or electrostatic factors are thought to preclude the admission of a second proton.

There have been some observations recorded that are consistent with the addition of a second proton to phenanthroline and its analogues. These include a spectral shift in 8 *M*

Can. J. Chem. Downloaded from www.nrcresearchpress.com by 210.87.254.42 on 09/05/12
For personal use only.

hydrochloric acid (3), some dependence of the partition coefficient for 5-methylphenanthroline between chloroform and aqueous solutions on the pH of the latter (4), and some unaccountable discrepancies between formation constants of certain metal–phenanthroline complexes determined by pH-titration methods and by other methods (5, and references therein).

METHOD

Efforts to measure the second stage of protonation by extending titrations of various phenanthrolines into moderately acidic solutions failed to yield conclusive results. The degree of protonation, $\bar{n}_H$, the number of moles of hydrogen bound per mole of base, is given by

$$\bar{n}_H = \frac{[H]_T - [OH]_T - [H]}{[L]_T}$$

where $[H]_T$ is the total concentration of strong acid added, $[OH]_T$ is the total concentration of strong alkali added, $[L]_T$ is the total concentration of phenanthroline, and [H] is the concentration of free hydrogen ion. An empirical relationship between H (= antilog (−pH)) and [H] was established by measurements of pH during titrations of strong acids under conditions of relatively constant ionic strength. Unfortunately the relationship observed was such that at lower values of pH small uncertainties in H corresponded to large uncertainties in [H], so much so that the latter became of the same order of magnitude as $[H]_T - [OH]_T - [H]$.

The spectral shift displayed by 1,10-phenanthroline in moderately acidic solutions (3) is also found in several methyl analogues. If the shift is ascribed to the formation of a doubly protonated species, H_2L^{2+}, one may utilize the spectra at various acidities to estimate a second pK_a by means of the Hammett acidity function. This quantity is defined by sets of indicators whose spectral changes in solutions of varying acidity permit estimation of the concentrations of their acidic and basic forms. It incorporates activity coefficients of the acidic and basic forms of the indicators; and when it is used to determine pK_a of an unknown base the important assumption has to be made that the ratio of these activity coefficients responds to changes in acidity in a fashion comparable to that of the indicators used to define the scale.

The majority of the tabulated values of acidity functions apply to indicators whose basic form is uncharged and whose acidic form is of the type HA^+; these values are designated H_0. For use with solutions of phenanthrolinium compounds the acidity function that applies is H_+, defined by

$$H_+ = -\log (a_H + f_{HA^+}/f_{H_2A^{2+}})$$

where HA^+ is some appropriate indicator. Unfortunately, acidity functions of this type have received scant attention, probably because of the lack of sufficient suitable indicators. One study by Brand and co-workers (6) in concentrated sulfuric acid suggests that in this medium values of H_+ parallel those of H_0 but lie about 0.3 unit more negative.

Notwithstanding this limitation, it was decided to apply acidity functions of the type H_0, as determined in hydrochloric acid by Paul and Long (7) and in perchloric acid by Yates and Wai (8), to data recorded for certain phenanthrolines, and to the functionally similar compound 2,2′-bipyridyl, dissolved in various concentrations of one or both of these acids. The procedure used was to plot

$$\log (\epsilon_1 - \epsilon/\epsilon - \epsilon_2)$$

in which ϵ_1 is a molar extinction coefficient for HL^+, ϵ_2 is a molar extinction coefficient for

Can. J. Chem. Downloaded from www.nrcresearchpress.com by 210.87.254.42 on 09/05/12
For personal use only.

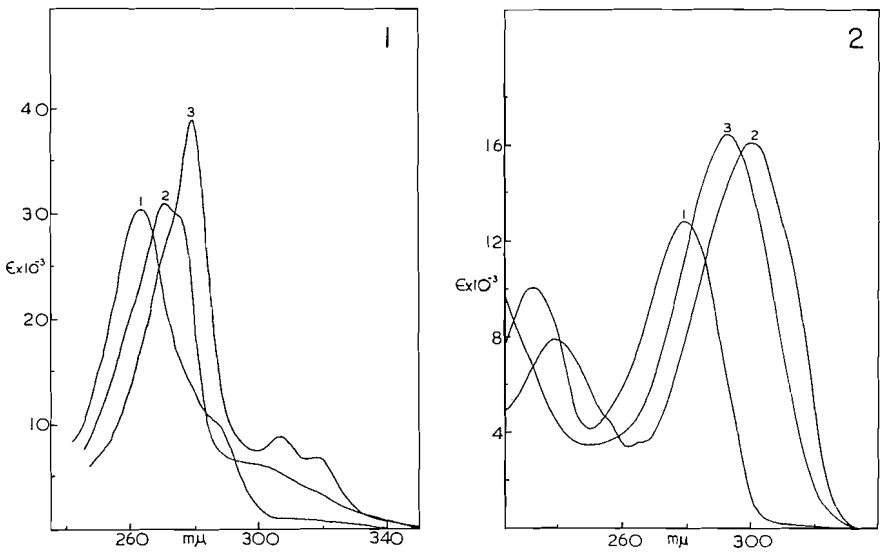

FIG. 1. The spectral shift of 1,10-phenanthroline. (1) L, pH 10.2. (2) HL^+, pH 3.15. (3) H_2L^{2+}, 9.0 *M* HCl.
FIG. 2. The spectral shift of 2,2′-bipyridyl. (1) L, pH 10.2. (2) HL^+, pH 3.0. (3) H_2L^{2+}, 10.0 *M* HCl.

H_2L^{2+}, and ϵ is a molar extinction coefficient for any acidic solution (all values of ϵ applying at the same wavelength) against values of H_0 appropriate to the acid and its concentration in which the base is dissolved. The spectra attributed to L, HL^+, and H_2L^{2+} in the case of 1,10-phenanthroline and of 2,2′-bipyridyl are shown in Figs. 1 and 2 respectively. All of the phenanthrolines showed a shift to longer wavelength in passing from weakly to strongly acidic solutions in contrast with bipyridyl for which, as Krumholtz has noted (2), the shift is in the other direction.

RESULTS AND DISCUSSION

A common difficulty in applying this procedure is the assignment of proper values of ϵ_1 and ϵ_2. Small progressive shifts of the peaks occurred in solutions of changing total acid concentration, so that values of ϵ_1 and ϵ_2 taken respectively from, say, 10^{-3} *M* and 10 *M* solutions of hydrochloric acid could not be assumed to apply exactly in solutions of intermediate concentration of acid. Small lateral displacements of the spectra (5 to 15 Å) were sufficient to bring the characterizing peaks to a common wavelength, and to produce isobestic points. Given this behavior it was possible to take values of ϵ_1 and ϵ_2 from spectra adjusted to correspond to an acid concentration at which $[HL^+] \sim [H_2L^{2+}]$ (9). This practice was followed in the case of 1,10-phenanthroline and 2,2′-bipyridyl, but it was not continued for the substituted phenanthrolines. The direction and extent of the displacement seemed to be approximately symmetrical about the midpoint where $[HL^+] = [H_2L^{2+}]$, and thus the corrective technique did not make much difference to the estimate of p*K*.

A plot of log $([H_2L^{2+}]/[HL^+])$ against H_0 ought to be rectilinear with unit slope if all assumptions applying to acidity functions also apply to the phenanthrolinium ion. In such an event the value of H_0 where $[H_2L^{2+}] = [HL^+]$ may be identified with p*K* for the proton transfer. The results are displayed in Fig. 3. Each point shown represents an average value for three estimates of log $([H_2L^{2+}]/[HL^+])$ made at three wavelengths. The plots

Can. J. Chem. Downloaded from www.nrcresearchpress.com by 210.87.254.42 on 09/05/12
For personal use only.

are reasonably linear, and the slope is not far from unity in each case. The values of pK taken from these data are regarded as estimates only, bearing in mind the various limitations to the use of H_0 values for the process under study. The true values may lie even more negative than those quoted in Table I in which are also given values of pK for first-stage protonation.

TABLE I

Acidity constants

Compound	pK_{HL}*	pK_{H_2L} (estimated)	Hammett† slope
2,2′-Bipyridyl	4.5	−0.5	0.68
1,10-Phenanthroline	4.98	−1.7 ($HClO_4$)	0.83
		−1.6 (HCl)	0.80
5-Methylphenanthroline	5.26	−1.6	0.80
5,6-Dimethylphenanthroline	5.60	−1.6	0.79
4,7-Dimethylphenanthroline	5.95	−1.0	0.74
2,9-Dimethylphenanthroline	5.85	−0.3	0.98

*Values of pK_{HL} for phenanthrolines from ref. 10, bipyridyl from ref. 5. The former are Bronsted constants applicable in 0.1 M KCl.
†Hammett slope $\Delta H_0/\Delta \log (\epsilon_1 - \epsilon)/(\epsilon - \epsilon_2)$.

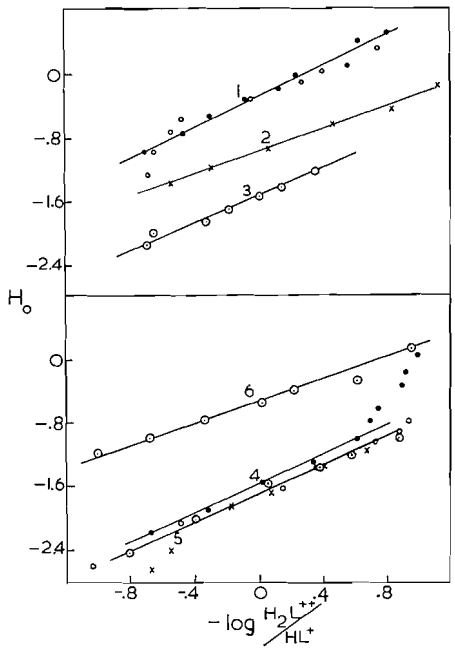

FIG. 3. (1) 2,9-Dimethylphenanthroline (duplicate run). (2) 4,7-Dimethylphenanthroline. (3) 5,6-Dimethylphenanthroline. (4) 5-Methylphenanthroline. (5) 1,10-Phenanthroline: (○) HCl ± 15 Å shift, (×) $HClO_4$, (⊙) HCl. (6) 2,2-Bipyridyl.

It is appropriate to note that these results confirm the greater resistance on the part of phenanthroline toward acceptance of a second proton than shown by 2,2′-bipyridyl. Krumholtz has reported a concentration constant for the latter in 2.2 M (HCl + LiCl) pK_c = −0.18 (2). The species H_2L^{2+} for 5-methylphenanthroline is evidently much too strong an acid to account for the effect of pH on its partition coefficient between chloroform and water mentioned above; this must be due to neglect of activity coefficients.

Can. J. Chem. Downloaded from www.nrcresearchpress.com by 210.87.254.42 on 09/05/12
For personal use only.

Furthermore, all values of pK_{H_2L} lie too negative to admit of any significant amount of H_2L^{2+} being formed during pH titrations suitable for determination of stability constants of metal complexes. Therefore, the existence of protonated metal complexes is possibly indicated, and is being investigated by the author. The correlation between pK_{HL} and pK_{H_2L} is not completely satisfactory, but the two sets of values clearly follow the same trend.

EXPERIMENTAL

The phenanthrolines were purchased from the G. F. Smith Chemical Company, the bipyridyl from British Drug Houses, and were all subjected to purification as follows: First, they were recrystallized from warm benzene, then dissolved in dilute hydrochloric acid, and re-precipitated by the addition of sodium hydroxide. This process was repeated, if necessary, until the product obtained melted sharply and at the melting point published for the appropriate compound. Solutions of these compounds were prepared in hydrochloric or perchloric acid of known molarity prepared by the addition of measured volumes of a concentrated analyzed stock acid to a fixed final volume. The perchlorates of these bases are rather insoluble, so that only 1,10-phenanthroline could be measured over a wide range of perchloric acid concentrations. Absorption spectra were measured with a Cary Model 14 spectrophotometer. In some cases, optical densities at single wavelengths were measured in a Beckman Model DU spectrophotometer.

ACKNOWLEDGMENTS

The author gratefully acknowledges the technical assistance of Miss Janet Rohr, and helpful discussions about acidity functions with Professor Keith Yates, University of Toronto. Thanks are also due to the National Research Council for a supporting research grant.

1. T. S. Lee, I. M. Kolthoff, and D. L. Leussing. J. Am. Chem. Soc. **70**, 2348 (1948).
2. P. Krumholtz. J. Phys. Chem. **60**, 87 (1956).
3. R. Nasanen and E. Uusitalo. Suomen Kemistilehti, B, **29**, 11 (1950).
4. W. A. E. McBryde, D. A. Brisbin, and H. Irving. J. Chem. Soc. 5245 (1962).
5. H. Irving and D. H. Mellor. J. Chem. Soc. 5222 (1962).
6. J. C. D. Brand, W. C. Horning, and M. B. Thornby. J. Chem. Soc. 1374 (1952).
7. M. A. Paul and F. A. Long. Chem. Rev. **57**, 1 (1957).
8. K. Yates and H. Wai. J. Am. Chem. Soc. **86**, 5408 (1964).
9. L. A. Flexser, L. P. Hammett, and A. Dingwall. J. Am. Chem. Soc. **57**, 2103 (1935).
10. D. A. Brisbin and W. A. E. McBryde. Can. J. Chem. **41**, 1135 (1963).

Received July 2, 1965.
Department of Chemistry,
University of Waterloo,
Waterloo, Ontario.

RARE-EARTH ACETATE ION ASSOCIATION

P. G. Manning

Diamond (1) has suggested that the rare-earth acetates are ion pairs that associate according to the "localized hydrolysis" theory of Robinson and Harned (2), in which the acetate ion binds electrostatically to the hydrogen atoms of the cation primary hydration sheath. Each potentially binding acetate has a fixed number of association sites from which to choose, and the magnitudes of the stepwise stability constants will be related statistically. The absolute magnitudes of the stability constant ratios will depend largely on the number of water molecules that comprise the cation hydration sheath, since ligand–ligand interaction should be small (3).

The stepwise stability constant is defined as

$$b_n = [ML_n]/[ML_{n-1}][L],$$

Can. J. Chem. Downloaded from www.nrcresearchpress.com by 210.87.254.42 on 09/05/12
For personal use only.

Furthermore, all values of pK_{H_2L} lie too negative to admit of any significant amount of H_2L^{2+} being formed during pH titrations suitable for determination of stability constants of metal complexes. Therefore, the existence of protonated metal complexes is possibly indicated, and is being investigated by the author. The correlation between pK_{HL} and pK_{H_2L} is not completely satisfactory, but the two sets of values clearly follow the same trend.

EXPERIMENTAL

The phenanthrolines were purchased from the G. F. Smith Chemical Company, the bipyridyl from British Drug Houses, and were all subjected to purification as follows: First, they were recrystallized from warm benzene, then dissolved in dilute hydrochloric acid, and re-precipitated by the addition of sodium hydroxide. This process was repeated, if necessary, until the product obtained melted sharply and at the melting point published for the appropriate compound. Solutions of these compounds were prepared in hydrochloric or perchloric acid of known molarity prepared by the addition of measured volumes of a concentrated analyzed stock acid to a fixed final volume. The perchlorates of these bases are rather insoluble, so that only 1,10-phenanthroline could be measured over a wide range of perchloric acid concentrations. Absorption spectra were measured with a Cary Model 14 spectrophotometer. In some cases, optical densities at single wavelengths were measured in a Beckman Model DU spectrophotometer.

ACKNOWLEDGMENTS

The author gratefully acknowledges the technical assistance of Miss Janet Rohr, and helpful discussions about acidity functions with Professor Keith Yates, University of Toronto. Thanks are also due to the National Research Council for a supporting research grant.

1. T. S. Lee, I. M. Kolthoff, and D. L. Leussing. J. Am. Chem. Soc. **70**, 2348 (1948).
2. P. Krumholtz. J. Phys. Chem. **60**, 87 (1956).
3. R. Nasanen and E. Uusitalo. Suomen Kemistilehti, B, **29**, 11 (1950).
4. W. A. E. McBryde, D. A. Brisbin, and H. Irving. J. Chem. Soc. 5245 (1962).
5. H. Irving and D. H. Mellor. J. Chem. Soc. 5222 (1962).
6. J. C. D. Brand, W. C. Horning, and M. B. Thornby. J. Chem. Soc. 1374 (1952).
7. M. A. Paul and F. A. Long. Chem. Rev. **57**, 1 (1957).
8. K. Yates and H. Wai. J. Am. Chem. Soc. **86**, 5408 (1964).
9. L. A. Flexser, L. P. Hammett, and A. Dingwall. J. Am. Chem. Soc. **57**, 2103 (1935).
10. D. A. Brisbin and W. A. E. McBryde. Can. J. Chem. **41**, 1135 (1963).

Received July 2, 1965.
Department of Chemistry,
University of Waterloo,
Waterloo, Ontario.

RARE-EARTH ACETATE ION ASSOCIATION

P. G. Manning

Diamond (1) has suggested that the rare-earth acetates are ion pairs that associate according to the "localized hydrolysis" theory of Robinson and Harned (2), in which the acetate ion binds electrostatically to the hydrogen atoms of the cation primary hydration sheath. Each potentially binding acetate has a fixed number of association sites from which to choose, and the magnitudes of the stepwise stability constants will be related statistically. The absolute magnitudes of the stability constant ratios will depend largely on the number of water molecules that comprise the cation hydration sheath, since ligand–ligand interaction should be small (3).

The stepwise stability constant is defined as

$$b_n = [ML_n]/[ML_{n-1}][L],$$

Can. J. Chem. Downloaded from www.nrcresearchpress.com by 210.87.254.5 on 09/05/12
For personal use only.

where M and L are metal and acetate ions respectively. Also, let $P = b_1:b_2$. Then P is a measure of the relative ease with which the first and second ligands associate, and its magnitude depends on statistical factors and ligand–ligand interactions upon association (3).

Stability constants for rare-earth acetates in water have been determined independently by Sonesson (4) and Kolat and Powell (5). The data of Kolat and Powell (5) pertain to two stages of ion association, and $b_1:b_2$ values only will be analyzed here. When allowance is made for the difference in experimental conditions employed by these workers, their results are in excellent agreement. Thus, plots of b_1 against Z (the atomic number) show identical trends (Fig. 1). A better indication of this agreement is afforded by a comparison of the P values (Fig. 2). Also included in Fig. 2 are P values for cerium and europium acetates as measured by Fronaeus (6) and Grenthe (7). The rare-earth acetates may be divided into three classes according to the magnitudes of the P values. For the lighter rare earths (La–Eu), $P = 5.3 \pm 0.5$, and for the heavier cations (Dy–Lu), $P = 2.5 \pm 0.1$. The P values for Gd and Tb are intermediate, although it is possible that Tb belongs to the heavier cations.

TABLE I

Mobilities of rare-earth ions (8, 9)

M	La	Ce	Pr	Nd	Sm	Eu	Gd	Tb	Dy	Ho	Er	Tm	Yb	Lu
Λ_0	69.9	69.8	69.5	69.6	68.6	67.8	67.4		67.4	66.3	65.9	65.4	65.4	64.7

There is evidence in the literature that suggests that the rare-earth ions are hydrated to the same extent. The ion size parameters for rare-earth chlorides and perchlorates, as determined from the activity-coefficient data of Spedding and co-workers (8, 9), lie in the range 5.3–6.0 Å and 6.3–7.2 Å respectively. The limiting ionic mobilities presented in Table I confirm the uniformity in size of the hydrated cations (8). As the cation radius decreases, the water molecules become more firmly bound, but it is sterically unlikely that a greater number of water molecules will coexist in the primary hydration sheath. The smaller ionic mobilities of the heavier metals would therefore seem to be unrelated to cation size.

Bjerrum (3) has shown that

$$P = S \times T,$$

where S is a statistical factor readily calculable from a knowledge of the number of cation binding sites and ligand groups, and T is a "ligand effect", the most important contribution to which arises from the electrostatic repulsion between bound ligands and ligands about to bind. The statistical effect may be explained as follows. Let the cation be n-hydrated, and let the anion be a monodentate ligand that displaces one water molecule from the cation hydration sheath. Then, the first ligand to bind has a choice of n possible association sites, but the second ligand has $n - 1$ possible sites. Since the probability of a ligand leaving the ML_2 species is twice that of leaving the ML species, then $S = 2 \times n/(n - 1)$. Clearly, $S > 1$.

The second ligand to bind will be repelled by the ligand already bound to the cation, and since all ligands are negatively charged or possess negative poles $T > 1$. For the chloride complexes of Sn and Hg (radii approximately equal to rare-earth ions), $T = 2.0$ (3). As the cation radius decreases, T will increase, and, provided the number of cation binding sites remains unchanged, P should also increase. The experimental results show that P is smaller for the smaller rare-earth ions and that there is no trend within the two different series of P values. Clearly, electrostatic repulsion is of secondary importance in

Can. J. Chem. Downloaded from www.nrcresearchpress.com by 210.87.254.5 on 09/05/12
For personal use only.

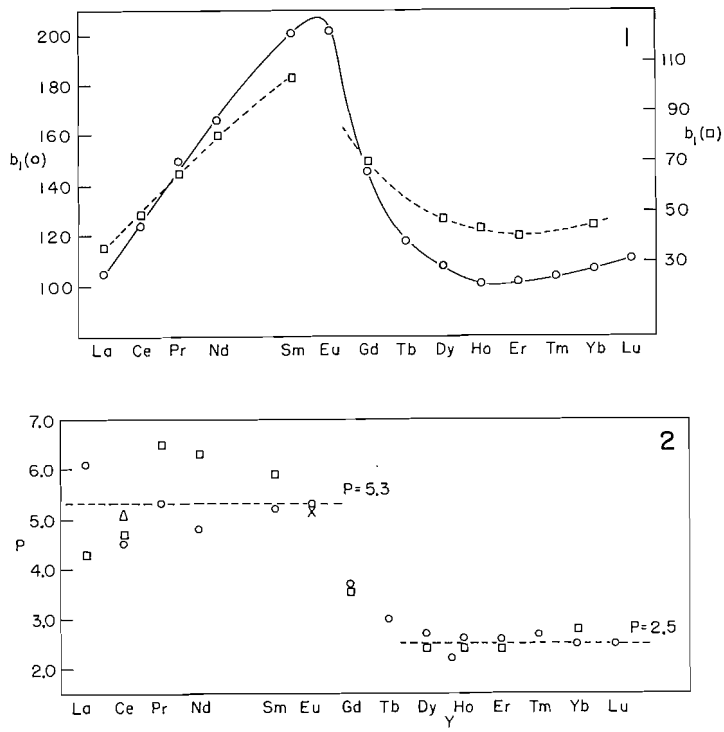

FIG. 1. Plot of b_1 rare-earth acetates against atomic number. ○ Data of Kolat and Powell (16), ionic strength 0.1. □ Data of Sonesson (15), ionic strength 2.0.

FIG. 2. P values as a function of atomic number for rare-earth acetates. ○ Data of Kolat and Powell (16). □ Data of Sonesson (15). △ Data of Fronaeus (7). × Data of Grenthe (8).

this system, which would suggest that the bound acetates are widely separated, i.e. the rare-earth acetates are ion pairs.

Let us suppose that acetate coordinates to the cation with the displacement of water molecules of the primary hydration sheath. Atomic models show that both oxygen atoms of acetate cannot coordinate to the same metal ion, and so acetate is a monodentate ligand. The reaction is

$$M(OH_2)_n + mL = M(OH_2)_{n-m}L_m + mH_2O.$$

If $n = 6$, then $S = 2 \times 6/5 = 2.40$. Hence, T (La–Eu series) = 2.2 and T (Dy–Lu series) = 1.05. The latter figure seems impossibly small when it is considered that $T = 2.0$ for the chloride complexes of Sn and Hg. The T values for the lighter rare earths seem reasonable for metal–acetate coordination, and it is conceivable that the acetate of the lighter metals are complexes, and the acetates of the heavier, ion pairs. This theory is disproved by the almost equal ΔS values for the rare-earth acetates (10), since the displacement of a water molecule from the cation hydration sheath would involve an entropy change of 17 entropy units. The fact that T (La–Eu series) > T (Dy–Lu series) cannot be explained by the metal–acetate coordination theory. These arguments are also true for $n = 8$ or 9.

Let us suppose that the lanthanide acetates are ion pairs. Also, let us assume that cation and water molecule are in contact, and that the hydrogens are directed away from the cation (i.e. ion-dipole configuration). The construction of atomic models, based on cation

Can. J. Chem. Downloaded from www.nrcresearchpress.com by 210.87.254.5 on 09/05/12
For personal use only.

radii = 1.06–0.8 Å and covalent atomic radii for water and acetate, shows that acetate can bind to two hydrogen atoms of neighboring water molecules of the cation primary hydration sheath ($n = 6$), i.e. acetate is a bidentate ligand. Acetate cannot bind to two hydrogens of the same water molecule, as the O—H- - -O hydrogen bonds will not be linear. The C—O- - -H bond angle is expected to be of the order of 110–120° (11). If acetate binds to two hydrogens of water molecules bound at positions ab in Fig. 3, then atomic models show that the two hydrogens are too closely spaced for hydrogen bonding if they lie in the abcd plane. For La, rotation of the water molecules along the M—O axis through an angle of approximately 15° gives optimum hydrogen atom separation for acetate bonding. This angle will be larger for the smaller cations.

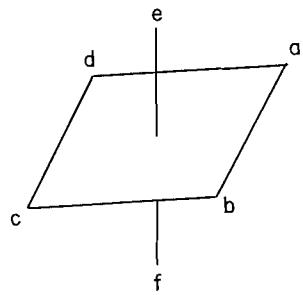

FIG. 3. Octahedral configuration of hexahydrated cation.

Let us further suppose that $n = 6$ and that the first acetate to bind does so at position ab in Fig. 3. Then a second acetate could bind at cd, de, ce, df, and cf, but at cb and ad with reduced probability. If the first two acetates to bind do so at ab and ad, then a 1:4 species would readily be formed, but two independent investigations have failed to detect anionic Gd and Ce species (12, 13). Therefore, for $n = 6$, and assuming two acetates cannot bind at ab and ad, $S = 2 \times 12/5 = 4.8$. Similar calculations in which the water molecules of an eight-hydrated cation are directed towards the corners of a cube and a dodecahedron give $S = 3.4$ and $S = 3.5$ respectively. In Table II are listed P, S, and T values for hexahydrated and octahydrated cations, and for monodentate and bidentate acetates. The dodecahedral arrangement of 8 waters is a more likely structure than the cube. Some of the possible structures may be eliminated on the basis that $T \not< 1.0$. Also, at the comparatively great distances that separate two bound acetates, T should be approximately equal whether acetate is bidentate or monodentate, and $1.0 < T \ll 2.0$. This T factor (= 2.0), being a measure of the work done in bringing an anion from infinity to its equilibrium position in the 1:2 complex, is electrostatic in nature and is independent of the ability of the metal ion to bind (3). This T value (= 2.0) gives a guide as to the T value that might be expected for singly-charged ligands that bind directly to the central metal. The data in Table II suggest that the lighter lanthanides associate with bidentate acetate, and the heavier with monodentate acetate. The hexahydrated cation is favored because the T value for the lighter octahydrated lanthanide – bidentate acetate system is rather large, and, moreover, an octahydrated cation could readily form a 1:4 associate.

The trends in b_1 values for the lanthanide acetates are readily explained. As the central cation radius decreases, the hydrogens of the cation primary hydration sheath become more heavily polarized, and from La–Eu, b_1 increases steadily because of stronger electrostatic attraction. A transition from bidentate acetate to monodentate is paralleled by a

Can. J. Chem. Downloaded from www.nrcresearchpress.com by 210.87.254.5 on 09/05/12
For personal use only.

TABLE II

P, *S*, and *T* values for rare-earth acetates

	Hexahydrated				Octahydrated			
	Light		Heavy		Light		Heavy	
	Monodentate acetate	Bidentate acetate	Monodentate acetate	Bidentate acetate	Monodentate acetate	Bidentate acetate	Monodentate acetate	Bidentate acetate
*P**	5.3	5.3	2.5	2.5	5.3	5.3	2.5	2.5
S†	2.4	4.8	2.4	4.8	2.3‡	3.4‡	2.3‡	3.4‡
T	2.2	1.1	1.1	0.5	2.3‡	1.6‡	1.1‡	0.7‡
S†,§					2.3	3.5	2.3	2.3
T§					2.3	1.5	1.1	0.7

*P values are experimental.
†S values are calculated.
‡Cube structure.
§Dodecahedron structure.

decrease (10) in b_1, and ΔH_1(Dy acetate) $\simeq 2 \times \Delta H_1$(Sm acetate). From Ho to Lu, b_1 values again increase, due presumably to increasing polarization of the hydrogens of the cation hydration sheath. With the smaller Al^{3+} and Fe^{3+}, the repulsion between metal ion and polarized proton is sufficiently great for hydrolysis to occur. Monocarboxylic acids associating with the rare-earth hydration sheath may therefore be characterized by the shape of the b_1 against Z plot and the absolute magnitudes of P values. Plots of b_1 against Z for the rare-earth propionates (14) and isobutyrates (15) are parallel to the acetate curve of Fig. 1 (at an ionic strength of 0.1), but the P values are too inaccurate for statistical analysis.

The transition from bidentate to monodentate acetate could conceivably be due to a change in the structure of the cation primary hydration sheath. This could be brought about by a change in the nature of the metal–water bond, i.e. from ion-dipole to coordinate interaction. Thus, as the degree of polarization of the water molecules increases, the electrons of the oxygen become increasingly available for coordination (16). The orientations of the hydration sheath protons will change, because the oxygen–metal bond, the oxygen–hydrogen bonds, and the oxygen lone pair electrons are directed tetrahedrally (sp^3 hybridization of the oxygen atom). The Gd and Tb cations are presumably equilibrium mixtures of the ion-dipole and coordinate structures. It is hoped to comment further on rare-earth ion – water interaction in a future publication, when the "gadolinium break effect" will be discussed.

For the hexahydrated cation structure (Fig. 3), it was assumed that two bidentate acetates could not bind at position ab and ad. Since there is, theoretically, a 50% probability of acetate binding at ad if ab is occupied, then $S = 2 \times 12/6 = 4.0$, and $T = 1.3$ for the lighter lanthanides. This T value is close to that expected (Table II). If $n = 8$, then $S = 2 \times 12/9 = 2.7$, and $T = 2.0$. This figure is too large both from its absolute magnitude and also in relation to the T value for the heavier rare-earth monodentate – acetate system. The data would still confirm that $n = 6$ for all rare earths, and that the acetates are ion pairs.

Grenthe's (10) measurements of ΔH and ΔS for the rare-earth acetates were interpreted by the worker as indicating that the acetates were complexes and that the ligand was monodentate. Grenthe indicated, however, that the method of interpreting ΔH and ΔS values was qualitative, whereas our approach is semiquantitative. For example, Grenthe's (10) approach shows that, for the rare-earth thioglycolates, the ΔH values favor a monodentate thioglycolate and the ΔS values a bidentate thioglycolate.

Can. J. Chem. Downloaded from www.nrcresearchpress.com by 210.87.254.5 on 09/05/12
For personal use only.

The possibility that Kolat and Powell's (5) b_2 values may contain a significant contribution from b_3 must be considered. As Kolat and Powell pointed out, the low ionic strength employed precludes the use of high acetate concentrations that would aid the formation of higher species. Sonesson (4) used 10 times greater ligand concentrations with an increased probability of forming the third associate. It is not surprising that Kolat and Powell (5) failed to detect the formation of a 1:3 species. A 1:3 species would be more readily formed with the heavier lanthanides (5), and yet the two independent workers produce P values that average at 2.5 ± 0.1. The agreement is sufficiently good so as to exclude the possibility of coincidence. It is reasonable to assume, therefore, that Kolat and Powell's (5) b_2 values are real and that the absolute magnitude of P is independent of ionic strength.

1. R. M. DIAMOND. J. Am. Chem. Soc. **80**, 4808 (1958).
2. R. A. ROBINSON and H. S. HARNED. Chem. Rev. **28**, 419 (1941).
3. J. BJERRUM. Metal ammine formation in aqueous solution. P. Haase and Son, Copenhagen. 1941.
4. A. SONESSON. Acta Chem. Scand. **12**, 165 (1958).
5. R. S. KOLAT and J. E. POWELL. Inorg. Chem. **1**, 293 (1962).
6. S. FRONAEUS. Svensk Kem. Tidskr. **65**, 19 (1953).
7. I. GRENTHE. Acta Chem. Scand. **16**, 1695 (1962).
8. F. H. SPEDDING and J. L. DYE. J. Am. Chem. Soc. **76**, 879 (1954).
9. F. H. SPEDDING and S. JAFFE. J. Am. Chem. Soc. **76**, 884 (1954).
10. I. GRENTHE. Acta Chem. Scand. **18**, 283 (1964).
11. G. C. PIMENTEL and A. L. MCCLELLAN. The hydrogen bond. Freeman, San Francisco. 1960.
12. A. SONESSON. Acta Chem. Scand. **12**, 1937 (1958).
13. S. FRONAEUS. Svensk Kem. Tidskr. **65**, 1 (1953).
14. J. E. POWELL, R. S. KOLAT, and G. S. PAUL. Inorg. Chem. **3**, 518 (1964).
15. W. R. STAGG and J. E. POWELL. Inorg. Chem. **3**, 242 (1964).
16. A. E. MARTELL and M. CALVIN. Metal chelate compounds. Prentice Hall, New York. 1952.

RECEIVED APRIL 30, 1965.
MINES BRANCH,
DEPARTMENT OF MINES AND TECHNICAL SURVEYS,
555 BOOTH STREET,
OTTAWA, ONTARIO.

THE HEAT OF SUBLIMATION AND HEAT OF VAPORIZATION OF TRIMETHYLTHALLIUM

S. J. PRICE AND M. G. JACKO[1]

Trimethylthallium was prepared by the method of Gilman and Jones (1, 2). Final traces of ether were removed from the alkyl by repeated bulb-to-bulb degassing with the cold trap at 0 °C. All operations were carried out in total darkness. A shielded 10 W lamp was used when illumination was required. The final product had a melting point of 38.0 °C. Twenty-one weighed samples were analyzed for thallium and methyl radical content (3). The methyl radical analysis was carried out by measuring the methane, ethane, and ethyl benzene produced when the alkyl was pyrolyzed in the presence of toluene. Thallium was determined by titration with .02 *m* ethylenediaminetetraacetic acid (EDTA) using xylenol orange as indicator. In four runs the total thallium content was determined. It ranged from 99.1% to 99.7% of the expected value. Assuming three methyl radicals per molecule of trimethylthallium, the gas analysis in the 21 runs was always within ±3% of that expected on the basis of the free thallium metal formed by decomposition.

[1]*Recipient of a National Research Council Studentship. Present address: Research Department, Imperial Oil Enterprises Ltd., Sarnia, Ontario.*

Can. J. Chem. Downloaded from www.nrcresearchpress.com by 210.87.254.5 on 09/05/12
For personal use only.

The possibility that Kolat and Powell's (5) b_2 values may contain a significant contribution from b_3 must be considered. As Kolat and Powell pointed out, the low ionic strength employed precludes the use of high acetate concentrations that would aid the formation of higher species. Sonesson (4) used 10 times greater ligand concentrations with an increased probability of forming the third associate. It is not surprising that Kolat and Powell (5) failed to detect the formation of a 1:3 species. A 1:3 species would be more readily formed with the heavier lanthanides (5), and yet the two independent workers produce P values that average at 2.5 ± 0.1. The agreement is sufficiently good so as to exclude the possibility of coincidence. It is reasonable to assume, therefore, that Kolat and Powell's (5) b_2 values are real and that the absolute magnitude of P is independent of ionic strength.

1. R. M. Diamond. J. Am. Chem. Soc. **80**, 4808 (1958).
2. R. A. Robinson and H. S. Harned. Chem. Rev. **28**, 419 (1941).
3. J. Bjerrum. Metal ammine formation in aqueous solution. P. Haase and Son, Copenhagen. 1941.
4. A. Sonesson. Acta Chem. Scand. **12**, 165 (1958).
5. R. S. Kolat and J. E. Powell. Inorg. Chem. **1**, 293 (1962).
6. S. Fronaeus. Svensk Kem. Tidskr. **65**, 19 (1953).
7. I. Grenthe. Acta Chem. Scand. **16**, 1695 (1962).
8. F. H. Spedding and J. L. Dye. J. Am. Chem. Soc. **76**, 879 (1954).
9. F. H. Spedding and S. Jaffe. J. Am. Chem. Soc. **76**, 884 (1954).
10. I. Grenthe. Acta Chem. Scand. **18**, 283 (1964).
11. G. C. Pimentel and A. L. McClellan. The hydrogen bond. Freeman, San Francisco. 1960.
12. A. Sonesson. Acta Chem. Scand. **12**, 1937 (1958).
13. S. Fronaeus. Svensk Kem. Tidskr. **65**, 1 (1953).
14. J. E. Powell, R. S. Kolat, and G. S. Paul. Inorg. Chem. **3**, 518 (1964).
15. W. R. Stagg and J. E. Powell. Inorg. Chem. **3**, 242 (1964).
16. A. E. Martell and M. Calvin. Metal chelate compounds. Prentice Hall, New York. 1952.

Received April 30, 1965.
Mines Branch,
Department of Mines and Technical Surveys,
555 Booth Street,
Ottawa, Ontario.

THE HEAT OF SUBLIMATION AND HEAT OF VAPORIZATION OF TRIMETHYLTHALLIUM

S. J. Price and M. G. Jacko[1]

Trimethylthallium was prepared by the method of Gilman and Jones (1, 2). Final traces of ether were removed from the alkyl by repeated bulb-to-bulb degassing with the cold trap at 0 °C. All operations were carried out in total darkness. A shielded 10 W lamp was used when illumination was required. The final product had a melting point of 38.0 °C. Twenty-one weighed samples were analyzed for thallium and methyl radical content (3). The methyl radical analysis was carried out by measuring the methane, ethane, and ethyl benzene produced when the alkyl was pyrolyzed in the presence of toluene. Thallium was determined by titration with .02 *m* ethylenediaminetetraacetic acid (EDTA) using xylenol orange as indicator. In four runs the total thallium content was determined. It ranged from 99.1% to 99.7% of the expected value. Assuming three methyl radicals per molecule of trimethylthallium, the gas analysis in the 21 runs was always within ±3% of that expected on the basis of the free thallium metal formed by decomposition.

[1]*Recipient of a National Research Council Studentship. Present address: Research Department, Imperial Oil Enterprises Ltd., Sarnia, Ontario.*

Can. J. Chem. Downloaded from www.nrcresearchpress.com by 210.87.254.42 on 09/05/12
For personal use only.

TABLE I

Vapor pressure measurements on trimethylthallium

(*a*) Liquid							
	t (°C)	87.0	83.0	71.0	60.0	48.3	39.7
	P (cm)	12.08	10.47	6.68	4.27	2.40	1.58
(*b*) Solid							
	t (°C)	30.8	21.5	9.8	0.0	−7.0	−15.0
	P (cm)	0.860	0.410	0.154	0.069	0.036	0.015

Vapor pressure measurements were made from −15 °C to 87 °C. Below 40 °C measurements were made in a closed system equipped with an oil manometer. Above 40 °C the oil manometer served as the null arm of an isoteniscope and pressures were read from a mercury manometer. All readings were taken with a Gaertner 1539-A cathetometer. The experimental results are shown in Table I. They may be represented by the following equations:

[i] from −15 °C to 38 °C

$$\log_{10} P \text{ (cm)} = -\frac{3000}{T} + 9.81$$

[ii] from 38 °C to 87 °C

$$\log_{10} P \text{ (cm)} = -\frac{2110}{T} + 6.95.$$

Equation [ii] is in reasonable agreement with that of Gilman and Jones (1) obtained from data covering the temperature range 54.5° to 76 °C:

$$\log_{10} P \text{ (cm)} = -\frac{1980}{T} + 6.603.$$

Liquid trimethylthallium has been shown to be monomolecular (1). Therefore, assuming ideal gas behavior for the vapor the following approximate values may be calculated from the integrated Clapeyron–Clausius equation:

[i] $\Delta H_{vap}^{62\,^\circ C} = 9.7$ kcal/mole, [ii] $\Delta H_{sub}^{12\,^\circ C} = 13.7$ kcal mole.

These values are slightly temperature dependent but since the necessary heat capacity data are not available no correction can be made. If the values at 38 °C are not significantly different from those quoted

$$\Delta H_{fusion}^{38\,^\circ C} = 4.0 \text{ kcal/mole.}$$

ACKNOWLEDGMENTS

This work has been supported by a grant from the National Research Council of Canada.

1. H. Gilman and R. G. Jones. J. Am. Chem. Soc. **68**, 517 (1946).
2. H. Gilman and R. G. Jones. J. Am. Chem. Soc. **72**, 1760 (1950).
3. M. G. Jacko and S. J. W. Price. Can. J. Chem. **43**, 1961 (1965).

Received January 28, 1965.
Chemistry Department,
University of Windsor,
Windsor, Ontario.

Can. J. Chem. Downloaded from www.nrcresearchpress.com by 210.87.254.42 on 09/05/12
For personal use only.

Can. J. Chem. Downloaded from www.nrcresearchpress.com by 210.87.254.42 on 09/05/12
For personal use only.

DESHYDRATATION DES ÉCHANGEURS DE CATIONS

WALTER R. HEUMANN ET FERNANDE D. ROCHON

Plusieurs méthodes de deshydratation des échangeurs sulfoniques de cations (acides forts) ont été proposées. Kunin (1) fait sécher à 115 °C pendant 20 h. Dickel et ses collaborateurs (2) constatent que 4 semaines au dessicateur en présence de P_2O_5 à la température ambiante ne suffit pas pour atteindre le poids constant et qu'il faut après encore 50 h à 80 °C sous 3 Torr de vide pour y arriver. Par contre, Davies et Yoeman (3) trouvent que pour les formes H^+ et K^+ le séchage à 80 °C sous vide pendant 24 h est suffisant. Blasius et Wolf (4, 5) supposent que la forme Li^+ de l'échangeur se deshydrate complètement par lavage dans une colonne avec du dioxane anhydre. Wright et ses collaborateurs (6) soumettent la forme H^+ à la distillation azéotropique avec du toluène et rapportent que l'eau est enlevée quantitativement. Aucun de ces auteurs donne une preuve du caractère quantitatif de sa méthode.

Selon plusieurs auteurs (2, 7, 8, 9) qui ont mesuré les chaleurs d'hydratation des échangeurs anhydres, la chaleur d'absorption du premier équivalent d'eau par équivalent d'échangeur anhydre sous forme d'hydrogène ou de métal alcalin est de -3 à -7 kcal et les chaleurs intégrales pour les trois premiers équivalents d'eau se placent entre -5 et -10 kcal par équivalent d'échangeur. Ces fortes valeurs expliquent facilement l'efficacité de ces échangeurs comme desséchants de liquides organiques selon la méthode de Wymore (10), qui démontre que des liquides peu polaires sont deshydratés ainsi très facilement à une teneur d'eau au-dessous de 5 p.p.m.

A la lumière de ces faits, il paraît peu probable que le dioxane, un liquide peu polaire ayant selon Feodos'ev (11) une chaleur d'hydratation de seulement -0.12 kcal/équivalent, pourrait deshydrater quantitativement un échangeur sulfonique tel que supposé par Blasius et Wolf (4). L'étude présente a été entreprise dans le but d'élucider ces contradictions par comparaison des efficacités quantitatives de ces différentes méthodes.

PARTIE EXPÉRIMENTALE

L'échangeur cationique Dowex 50W-X8 (8% de divinylbenzène) de granulation 20 à 50 mailles/pouce a été utilisé sous forme Li^+ ou Na^+.

Le *dioxane* a été deshydraté et purifié par chauffage à reflux durant 3 h en présence d'hydrure d'aluminium et de lithium, suivi d'une distillation.

Le *toluène* et le *xylène* ont été deshydratés par distillation azéotropique d'environ 10% du volume total.

Le *dosage de l'eau* dans les différents liquides a été effectué électrométriquement par la méthode de Karl Fischer après dilution des échantillons avec du méthanol anhydre.

Les *mélanges de dioxane et toluène* ont été analysés par chromatographie en phase vapeur à l'aide d'une colonne de 1.5 m × 6 mm de squalène à 120 °C, le gaz de support étant hélium et le débit 50 cc/min. On pouvait ainsi détecter facilement moins de 0.1% de dioxane dans le toluène.

RÉSULTATS

Les résultats obtenus *par séchage* par quatre différentes méthodes sont donnés dans le Tableau I. La méthode 1 (120 °C sous vide) semble être la plus efficace, mais elle n'est pas exacte. Une petite perte de poids par décomposition accompagnée d'une coloration foncée permanente peut se produire, surtout lorsque la résine est soumise à ce traitement pour la première fois.

La deshydratation *par le dioxane* fut vérifiée par la méthode de Blasius et Wolf (4),

TABLEAU I

Deshydratation de Dowex 50W-X8 forme Li^+ par séchage

Méthode	Perte de poids en % après 5 h	24 h	48 h	72 h
1. Chauffage à 120 °C, vide de 0.5 à 1 Torr	11.72	11.79	11.78	11.79
2. Chauffage à 120 °C, pression atmosphérique	11.07	11.57	11.75	11.78
3. Chauffage à 70 °C, vide de 10 Torr		10.58	11.09	11.30
4. Dessiccateur, P_2O_5, 25 °C, pression atmosphérique		1.88		3.00

c'est-à-dire par percolation de dioxane anhydre par une colonne d'échangeur sous forme Li^+, jusqu'à ce que l'effluant ne contienne plus d'eau. L'eau trouvée dans l'effluant correspondait à une perte de poids de l'échangeur de 3.63%, tandis qu'un autre échantillon du même échangeur perdait 11.75% par chauffage à 120 °C pendant 48 h. En supposant que cette perte de poids à 120 °C correspondait à la quantité totale d'eau, on peut conclure qu'après le traitement au dioxane l'échangeur contenait encore 8.42% d'eau.

L'échangeur deshydraté ainsi partiellement par le dioxane, fut soumis à une distillation azéotropique subséquente. Le dioxane fut d'abord déplacé de la colonne par du toluène en passant ce dernier solvant jusqu'à ce que la chromatographie ne détecte plus de dioxane dans l'effluant. Ce traitement n'enlevait pas d'eau supplémentaire de l'échangeur. Cependant, par la distillation subséquente une quantité d'eau fut enlevée, qui correspondait à 4.58% du poids initial de l'échangeur ou à une teneur résiduelle de l'échangeur traité de 3.86% d'eau.

Plusieurs échantillons d'échangeur, contenant entre 12 et 28% d'eau (exprimé en perte de poids à 120 °C), furent traités directement par distillation azéotropique avec du toluène ou du xylène. Après 2 à 3 h de distillation assez vive, la vitesse d'entraînement de l'eau par heure avait baissée à environ 0.1% du poids de l'échangeur, qui contenait encore 4 à 6% d'eau après 6 h de distillation. Supposant que la vitesse d'entraînement ne diminuerait pas, il aurait fallu continuer la distillation pendant 40 à 60 h pour atteindre la deshydration complète.

Pour vérifier, si la perte de poids par chauffage à 120 °C était due exclusivement à l'évaporation d'eau et que d'autres produits volatils n'y contribuaient pas, des échantillons furent d'abord séchés à 120 °C, puis de nouveau saturés d'eau, avant d'être soumis au traitement décrit plus haut, c'est-à-dire à la distillation azéotropique d'un aliquot et au séchage à 120 °C d'un autre aliquot. Les résultats obtenus ainsi ne différaient aucunement de ceux obtenus sans chauffage préliminaire. Une perte de poids par décomposition pyrolytique des échangeurs peut être exclue également, puisque Wymore (10) a trouvé, que les échangeurs cationiques sulfonés du type Dowex 50 sous forme métal alcalin, peuvent être chauffés à 195 °C sous pression atmosphérique sans aucun effet chimique détectable. Il semble donc, que parmi les méthodes examinées, le chauffage à 120 °C pendant au moins 48 h est la seule méthode satisfaisante.

REMERCIEMENTS

Les auteurs remercient le Conseil National de Recherches pour l'aide financière apportée sous forme d'un octroi de recherches.

Can. J. Chem. Downloaded from www.nrcresearchpress.com by 210.87.254.42 on 09/05/12
For personal use only.

1. R. KUNIN. Ion exchange resins. 2ième éd. John Wiley and Sons, New York. 1958. p. 340.
2. G. DICKEL *et al.* Z. Physik. Chem. Frankfurt, **20**, 121 (1959).
3. C. W. DAVIES et G. D. YOEMAN. Trans. Faraday Soc. **49**, 968 (1953).
4. E. BLASIUS et F. WOLF. Z. Anal. Chem. **171**, 88 (1959).
5. E. BLASIUS et F. WOLF. Dans. Anomalien bei Ionenaustausch-Vorgängen. K. Issleib, Akademie-Verlag, Berlin. 1962. p. 433.
6. O. L. WRIGHT *et al.* J. Org. Chem. **30**, 1301 (1965).
7. T. MATSUURA. Bull. Chem. Soc. Japan, **27**, 281 (1954).
8. S. LAPANJE et D. DOLAR. Z. Physik. Chem. Frankfurt, **18**, 11 (1958).
9. S. LAPANJE et D. DOLAR. Z. Physik. Chem. Frankfurt, **21**, 376 (1959).
10. C. E. WYMORE. Ind. Eng. Chem. Prod. Res. Develop. **1**, 173 (1962).
11. N. N. FEODOS'EV *et al.* J. Gen. Chem. USSR Eng. Transl. **24**, 1526 (1954).

REÇU LE 23 JUIN 1965.
DÉPARTEMENT DE CHIMIE,
UNIVERSITÉ DE MONTRÉAL,
MONTRÉAL, QUÉBEC.

REACTIVITY OF CH AND NH BONDS IN ETHYLENIMINE

PETER GRAY AND A. JONES

The paper by Klemm (1) on hydrogen abstraction from ethylenimine complements work which we have recently performed. We have studied the position and rate of methyl radical attack on ethylenimine over the temperature range 110–175 °C using the unlabelled imine and ethylenimine-d_1. The photolysis of azomethane was used as the source of methyl radicals. (It was originally chosen (2) to avoid possible difficulties arising from reaction between substrate and acetone.)

When azomethane is photolyzed alone, the following reactions occur.

[1] $$CH_3N_2CH_3 \rightarrow N_2 + 2CH_3$$

[2] $$CH_3 + CH_3N_2CH_3 \rightarrow CH_4 + \cdot CH_2N_2CH_3$$

[3] $$2CH_3 \rightarrow C_2H_6$$

Measurements of the steady rates of production of methane and ethane can furnish a value of k_2 from the relation:

$$R_{CH_4}[2]/R_{C_2H_6}{}^{1/2}[\text{Azo}] = (k_2/k_3{}^{1/2}).$$

The temperature dependence of k_2 can be expressed by the Arrhenius equation:

$$\log_{10} (k_2/\text{mole}^{-1}\,\text{cm}^3\,\text{s}^{-1}) = (10.85 \pm 0.10) - (7830 \pm 200)/2.303RT.$$

This rate expression, and all others quoted here, are based on Shepp's value (3) of $10^{13.34}$ cm^3 mole^{-1} s^{-1} for the recombination of methyl radicals, errors quoted being standard deviations estimated by a least-squares treatment. The values above are in agreement with previously determined values.

Overall Rate of Attack by Methyl Radicals on Ethylenimine

When azomethane is photolyzed in the presence of unlabelled ethylenimine, the following reactions must be added to the reaction scheme for azomethane.

[4] $$CH_3 + CH_2 - \underset{\diagdown\,\diagup}{\overset{}{N}}\overset{}{-}CH_2 \rightarrow CH_4 + \cdot CH - \underset{\diagdown\,\diagup}{\overset{}{N}}\overset{}{-}CH_2$$
$$\qquad\qquad\qquad\quad H \qquad\qquad\qquad\qquad\quad H$$

[5] $$CH_3 + (CH_2)_2NH \rightarrow CH_4 + (CH_2)_2N\cdot$$

Can. J. Chem. Downloaded from www.nrcresearchpress.com by 210.87.254.42 on 09/05/12
For personal use only.

1. R. KUNIN. Ion exchange resins. 2ième éd. John Wiley and Sons, New York. 1958. p. 340.
2. G. DICKEL *et al.* Z. Physik. Chem. Frankfurt, **20**, 121 (1959).
3. C. W. DAVIES et G. D. YOEMAN. Trans. Faraday Soc. **49**, 968 (1953).
4. E. BLASIUS et F. WOLF. Z. Anal. Chem. **171**, 88 (1959).
5. E. BLASIUS et F. WOLF. Dans. Anomalien bei Ionenaustausch-Vorgängen. K. Issleib, Akademie-Verlag, Berlin. 1962. p. 433.
6. O. L. WRIGHT *et al.* J. Org. Chem. **30**, 1301 (1965).
7. T. MATSUURA. Bull. Chem. Soc. Japan, **27**, 281 (1954).
8. S. LAPANJE et D. DOLAR. Z. Physik. Chem. Frankfurt, **18**, 11 (1958).
9. S. LAPANJE et D. DOLAR. Z. Physik. Chem. Frankfurt, **21**, 376 (1959).
10. C. E. WYMORE. Ind. Eng. Chem. Prod. Res. Develop. **1**, 173 (1962).
11. N. N. FEODOS'EV *et al.* J. Gen. Chem. USSR Eng. Transl. **24**, 1526 (1954).

REÇU LE 23 JUIN 1965.
DÉPARTEMENT DE CHIMIE,
UNIVERSITÉ DE MONTRÉAL,
MONTRÉAL, QUÉBEC.

REACTIVITY OF CH AND NH BONDS IN ETHYLENIMINE

PETER GRAY AND A. JONES

The paper by Klemm (1) on hydrogen abstraction from ethylenimine complements work which we have recently performed. We have studied the position and rate of methyl radical attack on ethylenimine over the temperature range 110–175 °C using the unlabelled imine and ethylenimine-d_1. The photolysis of azomethane was used as the source of methyl radicals. (It was originally chosen (2) to avoid possible difficulties arising from reaction between substrate and acetone.)

When azomethane is photolyzed alone, the following reactions occur.

[1] $$CH_3N_2CH_3 \rightarrow N_2 + 2CH_3$$

[2] $$CH_3 + CH_3N_2CH_3 \rightarrow CH_4 + \cdot CH_2N_2CH_3$$

[3] $$2CH_3 \rightarrow C_2H_6$$

Measurements of the steady rates of production of methane and ethane can furnish a value of k_2 from the relation:

$$R_{CH_4}[2]/R_{C_2H_6}{}^{1/2}[\text{Azo}] = (k_2/k_3{}^{1/2}).$$

The temperature dependence of k_2 can be expressed by the Arrhenius equation:

$$\log_{10} (k_2/\text{mole}^{-1}\,\text{cm}^3\,\text{s}^{-1}) = (10.85 \pm 0.10) - (7830 \pm 200)/2.303RT.$$

This rate expression, and all others quoted here, are based on Shepp's value (3) of $10^{13.34}$ cm^3 mole^{-1} s^{-1} for the recombination of methyl radicals, errors quoted being standard deviations estimated by a least-squares treatment. The values above are in agreement with previously determined values.

Overall Rate of Attack by Methyl Radicals on Ethylenimine

When azomethane is photolyzed in the presence of unlabelled ethylenimine, the following reactions must be added to the reaction scheme for azomethane.

[4] $$CH_3 + CH_2 - \underset{\diagdown\,\diagup}{\overset{}{N}}\overset{}{-}CH_2 \rightarrow CH_4 + \cdot CH - \underset{\diagdown\,\diagup}{\overset{}{N}}\overset{}{-}CH_2$$
$$\qquad\qquad\qquad\quad H \qquad\qquad\qquad\qquad\quad H$$

[5] $$CH_3 + (CH_2)_2NH \rightarrow CH_4 + (CH_2)_2N\cdot$$

Can. J. Chem. Downloaded from www.nrcresearchpress.com by 210.87.254.42 on 09/05/12
For personal use only.

The combined effect of reactions [4] and [5] can be represented by the equation

[6] $$CH_3 + (CH_2)_2NH \rightarrow CH_4 + [C_2H_4N].$$

It is this overall velocity constant, k_6, which is obtained by measuring the rates of production of CH_4 and C_2H_6 from the relation:

$$R_{CH_4}[6]/R_{C_2H_6}^{1/2}[\text{imine}] = (k_6/k_3^{1/2}),$$

where [imine] denotes the concentration of ethylenimine. Over the temperature range, 110–175 °C, the results can be fitted by the equation:

$$\log_{10} (k_6/\text{mole}^{-1}\ \text{cm}^3\ \text{s}^{-1}) = (10.29 \pm 0.23) - (4770 \pm 440)/2.303RT.$$

This expression can be compared with Brinton and Volman's (4) values for A and E of $10^{10.5}$ mole^{-1} cm^3 s^{-1} and 4.8 kcal mole^{-1} and those of Klemm (1) of $10^{10.76}$ mole^{-1} cm^3 s^{-1} and 5.28 kcal mole^{-1}, and with the results for the analogous reaction of CD_3 radicals with ethylenimine, for which Klemm obtained $A = 10^{10.94}$ mole^{-1} cm^3 s^{-1} and $E = 5.40$ kcal mole^{-1}.

Rate of Attack on the Imine Group

When methyl radicals are generated in the presence of ethylenimine-d_1, the additional CH_4 comes only from attack on the methylene groups, since attack at the imine position yields CH_3D. By subtracting this rate of formation of methane from the previous rate of formation from the unlabelled imine, a value can be obtained for the velocity constant k_5 for attack on the NH group:

$$\log_{10} (k_5/\text{mole}^{-1}\ \text{cm}^3\ \text{s}^{-1}) = (10.17 \pm 0.05) - (4570 \pm 100)/2.303RT.$$

This expression differs little from that for the overall rate of abstraction [6] confirming Brinton and Volman's original conjecture (4) that attack was principally at the imine group, and to this extent justifying Klemm's implicit identification (1) of k_5 with k_6.

Rate of Attack on the Methylene Groups

When azomethane is photolyzed in the presence of ethylenimine-d_1, most of the methane is produced by attack on (i) the azomethane and (ii) undeuterated impurity (ca. 2%) in the ethylenimine-d_1. The part which comes from attack on the $\cdot CH_2$ groups has thus to be obtained by two subtractions involving quantities of comparable size and is subject to correspondingly larger errors than before. These are especially noticeable in the Arrhenius parameters:

$$\log (k_4/\text{mole}^{-1}\ \text{cm}^3\ \text{s}^{-1}) = (11.44 \pm 1.48) - (10100 \pm 2800)/2.303RT.$$

It is curious to note that although experiments involving four isotopic variations of the methyl radical attack on ethylenimine have now been performed, the reaction which would have yielded the most accurate Arrhenius equation for abstraction of hydrogen from the methylene groups—the attack of CD_3 on $(CH_2)_2ND$—has not been investigated.

Relative Reactivity of the NH and CH_2 Groups in Ethylenimine

It is now possible to compare quantitatively the reactivity of hydrogen atoms attached to carbon and nitrogen in ethylenimine. At 150 °C, hydrogen attached to nitrogen is abstracted nearly 40 times more readily than hydrogen attached to carbon, and on a per-atom basis is thus about 160 times more reactive. This can be compared with previous experiments with deuterated amines, in all of which the hydrogen attached to nitrogen has been found, at 150 °C, to be the more reactive. On a per-atom basis the relative

Can. J. Chem. Downloaded from www.nrcresearchpress.com by 210.87.254.42 on 09/05/12
For personal use only.

reactivity (k_{NH}/k_{CH}) of amine hydrogen in CH_3NH_2, $(CH_3)_2NH$, and CH_3ONH_2 is 3.4, 20, and >75 respectively (refs. 4, 5, 6).

Kinetic Isotope Effects

The velocity constant for deuterium abstraction from ethylenimine-d_1

[7] $$CH_3 + (CH_2)_2ND \rightarrow CH_3D + (CH_2)_2N\cdot$$

obtained from measurements of the rates of formation of CH_3D and C_2H_6 satisfies the Arrhenius expression

$$\log_{10}(k_7/\text{mole}^{-1}\,\text{cm}^3\,\text{s}^{-1}) = (10.17 \pm 0.13) - (6340 \pm 210)/2.303RT.$$

Comparison with the velocity constant k_5 shows that at 150 °C, hydrogen is abstracted nearly eight times as fast from the NH group in ethylenimine as is deuterium from the ND group in ethylenimine-d_1. Since the A-factors are identical, this isotope effect is wholly accounted for by the difference in activation energy, $E_D - E_H = 1.7 \pm 0.5$ kcal mole^{-1}, which can be compared to the loss of zero-point-energy of a single N—H stretching vibration of 1.4 kcal mole^{-1}.

By combining the data of Klemm (1) and that presented here it is possible to obtain an estimate of the kinetic isotope effect for deuterium and hydrogen attached to the carbon atoms in ethylenimine. Thus Klemm quotes, that for abstraction of deuterium and hydrogen from ethylenimine-d_4, $(k_{NH}/k_{CD_2}) > 200$. From our data for abstraction from NH and CH_2 in the unlabelled compound at 150 °C, $(k_{NH}/k_{CH_2}) = 40$. This implies that at 150 °C, the kinetic isotope effect $(k_{CH_2}/k_{CD_2}) > 5$ which is in accord with expectations.

1. R. F. Klemm. Can. J. Chem. **43**, 2633 (1965).
2. P. Gray and J. C. J. Thynne. Trans. Faraday Soc. **59**, 2275 (1963).
3. A. Shepp. J. Chem. Phys. **24**, 939 (1956).
4. R. K. Brinton and D. H. Volman. J. Chem. Phys. **20**, 25 (1952).
5. P. Gray, A. Jones, and J. C. J. Thynne. Trans. Faraday Soc. **61**, 474 (1965).
6. J. C. J. Thynne. Trans. Faraday Soc. **60**, 2207 (1964).

Received June 24, 1965.
School of Chemistry,
The University,
Leeds 2, England.

DEUTERIUM ISOTOPE EFFECT IN VACUUM-ULTRAVIOLET ABSORPTION COEFFICIENTS OF WATER AND METHANE[1]

A. H. Laufer and J. R. McNesby

The effect of isotopic substitution upon the electronic absorption spectra of diatomic molecules is a well-explored subject and has been reviewed by Herzberg (1). As a consequence of the effect of mass on the vibration frequencies, the heavier isotopic species exhibits a general contraction in the electronic band on both sides of the 0–0 vibrational transition. This corresponds to a shift in absorption to the violet on the red end of the band and to the red on the violet end for the heavier species.

Shifts to the violet (on the red end) upon deuteration have also been observed with molecules exhibiting continuous absorption (2–5). These observations are most easily explained by referring to the hypothetical case of a diatomic molecule having a normal

[1]*This work was supported by the U.S. Atomic Energy Commission.*

Can. J. Chem. Downloaded from www.nrcresearchpress.com by 210.87.254.42 on 09/05/12
For personal use only.

reactivity (k_{NH}/k_{CH}) of amine hydrogen in CH_3NH_2, $(CH_3)_2NH$, and CH_3ONH_2 is 3.4, 20, and >75 respectively (refs. 4, 5, 6).

Kinetic Isotope Effects

The velocity constant for deuterium abstraction from ethylenimine-d_1

[7] $$CH_3 + (CH_2)_2ND \rightarrow CH_3D + (CH_2)_2N\cdot$$

obtained from measurements of the rates of formation of CH_3D and C_2H_6 satisfies the Arrhenius expression

$$\log_{10}(k_7/\text{mole}^{-1}\,\text{cm}^3\,\text{s}^{-1}) = (10.17 \pm 0.13) - (6340 \pm 210)/2.303RT.$$

Comparison with the velocity constant k_5 shows that at 150 °C, hydrogen is abstracted nearly eight times as fast from the NH group in ethylenimine as is deuterium from the ND group in ethylenimine-d_1. Since the A-factors are identical, this isotope effect is wholly accounted for by the difference in activation energy, $E_D - E_H = 1.7 \pm 0.5$ kcal mole^{-1}, which can be compared to the loss of zero-point-energy of a single N—H stretching vibration of 1.4 kcal mole^{-1}.

By combining the data of Klemm (1) and that presented here it is possible to obtain an estimate of the kinetic isotope effect for deuterium and hydrogen attached to the carbon atoms in ethylenimine. Thus Klemm quotes, that for abstraction of deuterium and hydrogen from ethylenimine-d_4, $(k_{NH}/k_{CD_2}) > 200$. From our data for abstraction from NH and CH_2 in the unlabelled compound at 150 °C, $(k_{NH}/k_{CH_2}) = 40$. This implies that at 150 °C, the kinetic isotope effect $(k_{CH_2}/k_{CD_2}) > 5$ which is in accord with expectations.

1. R. F. Klemm. Can. J. Chem. **43**, 2633 (1965).
2. P. Gray and J. C. J. Thynne. Trans. Faraday Soc. **59**, 2275 (1963).
3. A. Shepp. J. Chem. Phys. **24**, 939 (1956).
4. R. K. Brinton and D. H. Volman. J. Chem. Phys. **20**, 25 (1952).
5. P. Gray, A. Jones, and J. C. J. Thynne. Trans. Faraday Soc. **61**, 474 (1965).
6. J. C. J. Thynne. Trans. Faraday Soc. **60**, 2207 (1964).

Received June 24, 1965.
School of Chemistry,
The University,
Leeds 2, England.

DEUTERIUM ISOTOPE EFFECT IN VACUUM-ULTRAVIOLET ABSORPTION COEFFICIENTS OF WATER AND METHANE[1]

A. H. Laufer and J. R. McNesby

The effect of isotopic substitution upon the electronic absorption spectra of diatomic molecules is a well-explored subject and has been reviewed by Herzberg (1). As a consequence of the effect of mass on the vibration frequencies, the heavier isotopic species exhibits a general contraction in the electronic band on both sides of the 0–0 vibrational transition. This corresponds to a shift in absorption to the violet on the red end of the band and to the red on the violet end for the heavier species.

Shifts to the violet (on the red end) upon deuteration have also been observed with molecules exhibiting continuous absorption (2–5). These observations are most easily explained by referring to the hypothetical case of a diatomic molecule having a normal

[1]*This work was supported by the U.S. Atomic Energy Commission.*

Can. J. Chem. Downloaded from www.nrcresearchpress.com by 210.87.254.5 on 09/05/12
For personal use only.

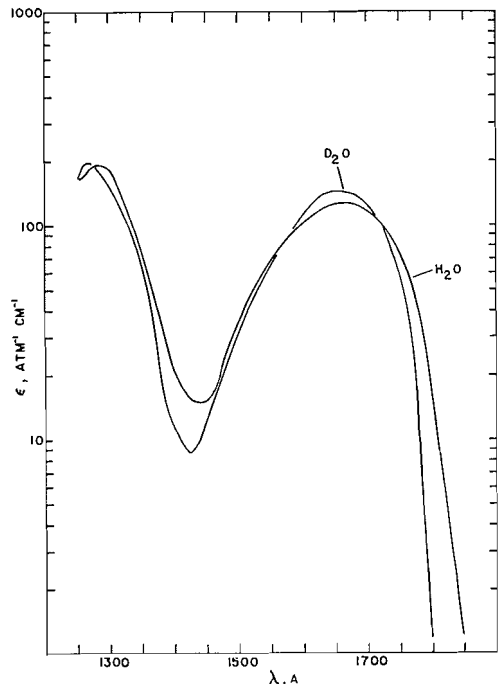

FIG. 1. Deuterium isotope effect on absorption coefficients of water. NOTE ADDED IN PROOF: A series of six maxima between 1 600 and 1 750 Å observed by A. Johannin-Gilles, Compt. Rend. 240, 1523 (1955), were not observed in ref. 6 or in the present work. The explanation for the observation of Johannin-Gilles is not obvious.

potential function for the ground state and a repulsive potential for the non-quantized upper state. The heavier isotopic variation of this molecule has a lower zero point energy in the ground state. For a Franck–Condon vertical transition, the minimum energy needed for the transition to the upper state will be greater for the heavier species by the zero point energy difference and a shift to the violet is the result. While the situation is certainly more complex for polyatomic molecules, a similar principle applies.

In the present work, measurements have been made of the absorption coefficients in the continua of H_2O and D_2O and of CH_4 and CD_4 using a Seya–Namioka type 0.5 m grating vacuum monochromator. An absorption cell with lithium fluoride windows was interposed between the exit slit of the monochromator and the sodium salicylate coated photomultiplier tube. Pressures of methane and water were measured with an oil manometer and the path length was 5.71 cm. In the cases of H_2O and D_2O, pressures were measured after adsorption equilibrium had been established. Measurements on D_2O were made after exposing the apparatus to D_2O vapor for 24 h, removing it, and refilling the absorption cell with pure D_2O. The light source was a hydrogen discharge. Incident intensities were determined before and after an absorption scan to insure constancy of the lamp and to obviate radiation damage to the windows. The entrance and exit slits were 200 μ and the reciprocal linear dispersion was 33 Å/mm corresponding to a band width of 6.6 Å. Absorption coefficients were measured assuming the validity of Beer's law. This assumption was found to be valid in the methane and water continua since the absorption coefficients, ϵ, were found to be independent of pressure. The absorption coefficient is defined by

$$I/I_0 = \exp(-\epsilon Pd)$$

Can. J. Chem. Downloaded from www.nrcresearchpress.com by 210.87.254.5 on 09/05/12
For personal use only.

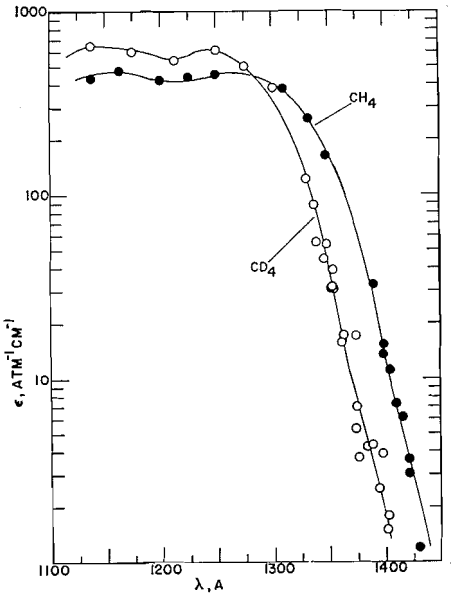

FIG. 2. Deuterium isotope effect on absorption coefficients of methane.

where the units of ϵ are cm^{-1} atm^{-1}. The results are shown in Figs. 1 and 2. The absorption coefficients for H_2O and CH_4 are in good agreement with those reported in the literature (6, 7).

In the 1 450 to 1 250 Å region of the spectrum of H_2O, 12 diffuse bands superimposed on a continuum have been observed (6). It has recently been shown that D_2O also exhibits somewhat irregular diffuse bands in this region although values for ϵ were not included (8). Lack of resolution of our instrument precluded the observation of the banded structure but the values obtained for the absorption coefficients agree well with the literature (6).

The expected shifts to the violet on deuteration are observed for both water and methane on the red ends of the continua. The appearance of a second overlapping continuum in the case of water complicates the picture somewhat but a shift toward the violet is evident in this continuum also. Because of the sharp structure in the water spectrum below

TABLE I

Isotope effect on absorption coefficients of paraffin hydrocarbons at 1 470 Å

	ϵ (atm^{-1} cm^{-1})*	Reference
C_2H_6	38.0±1.5	(2)
C_2D_6	19.0±1.0	(2)
C_3H_8	145.0±10	(2)
C_3D_8	108.0±5	(2)
n-C_4H_{10}	600.0	(3)
n-C_4D_{10}	380.0	(3)
i-C_4H_{10}	510.0±20	(4)
i-C_4D_{10}	425.0±15	(4)
c-C_3H_6	260.0±15	(5)
c-C_3D_6	206.0±20	(5)
CH_4	15.0†	Present work
CD_4	2.0†	Present work

*$I/I_0 = \exp(-\epsilon Px)$.
†1 400 Å.

Can. J. Chem. Downloaded from www.nrcresearchpress.com by 210.87.254.5 on 09/05/12
For personal use only.

1 250 Å (9), the absorption coefficient measurements are not very meaningful and they have, therefore, been omitted from Fig. 1. The absorption coefficient at the photochemically interesting wavelength of 1 235.8 Å was measured using a krypton resonance lamp as the light source. According to the spectra of Johns (9), the D_2O absorption is essentially continuous for at least 1 Å on each side of 1 235.8 Å and this is probably also the case for H_2O. Since the krypton line emitted from our lamp falls entirely within this continuum, the absorption coefficients at 1 235.8 Å are probably correct. The results are $\epsilon_{H_2O} = 171$; $\epsilon_{D_2O} = 270$. Beer's law was found to be obeyed in the range 0.3–1 Torr for the krypton line at 1 235.8 Å.

As shown in Figs. 1 and 2, the violet shift is characterized by a lowering of the absorption coefficient for the heaver isotopic species. A number of absorption coefficients have been measured at 1 470 Å and Table I shows that the violet shift is quite general for saturated hydrocarbons.

1. G. Herzberg. Molecular spectra and molecular structure. 2nd ed. D. Van Nostrand, New York, 1950. p. 163.
2. H. Okabe and J. R. McNesby. J. Chem. Phys. **37**, 1340 (1962).
3. M. C. Sauer and L. M. Dorfman. J. Chem. Phys. **35**, 497 (1961).
4. H. Okabe and D. A. Becker. J. Am. Chem. Soc. **84**, 4004 (1962).
5. C. L. Currie, H. Okabe, and J. R. McNesby. J. Phys. Chem. **67**, 1494 (1963).
6. K. Watanabe and M. Zelikoff. J. Opt. Soc. Am. **43**, 753 (1953).
7. A. J. Harrison, B. J. Cederholm, and M. A. Terwilliger. J. Chem. Phys. **30**, 355 (1959).
8. S. Bell. J. Mol. Spectry. **16**, 205 (1965).
9. J. W. C. Johns. Can. J. Phys. **41**, 209 (1963).

Received July 14, 1965.
National Bureau of Standards,
Washington, D.C.

MEAN LIFETIME OF FREE RADICAL CHAINS IN ^{60}Co γ-IRRADIATED CHLORAL HYDRATE AND BROMAL HYDRATE SOLUTIONS

R. G. McIntosh, R. L. Eager, and J. W. T. Spinks

Previous publications by us have described work on the radiation chemistry of aqueous solutions of chloral hydrate and of bromal hydrate. The first of these (1) reported on the use of a flow system to obtain intermittent irradiation. In a later paper (2) the results obtained by steady irradiation of the samples were reported. In addition to the above work experiments were also done in which a rotating sector was used to obtain intermittent irradiation. This note reports the results of these latter studies.

EXPERIMENTAL

The ^{60}Co radiation facility was the same as that used in the other studies and has been described previously (3). During irradiation the samples were contained in an electrical conductivity cell and the change of conductivity with time of irradiation was noted. The conductivity cell was of the Arrhenius–Ostwald type and has been previously described (2). The Fricke ferrous sulfate dosimeter was used. The purification of the reagents and of the water used in making up the solutions has already been described (2). The sample temperature was that of the cave, between 20 and 25 °C. The reaction rates were corrected to 25.0 °C (2).

The rotating sector was constructed of General Electric Company Heavy Alloy which contains 90% of tungsten alloyed with nickel and copper. The alloy has a specific gravity of 16.3–17.0. The sector was 2 in thick and $7\frac{1}{4}$ in in diameter. A 3/8 in thick steel band encircled the sector. Two inches of the alloy stops approximately 90% of a ^{60}Co γ-ray beam. Two opposed sector openings of 60° each were present, giving a value for r, the ratio of the "dark" to the "light" periods, of 2. Sector speeds of 0.5 to 500 r.p.m. were used.

Can. J. Chem. Downloaded from www.nrcresearchpress.com by 210.87.254.5 on 09/05/12
For personal use only.

1 250 Å (9), the absorption coefficient measurements are not very meaningful and they have, therefore, been omitted from Fig. 1. The absorption coefficient at the photochemically interesting wavelength of 1 235.8 Å was measured using a krypton resonance lamp as the light source. According to the spectra of Johns (9), the D_2O absorption is essentially continuous for at least 1 Å on each side of 1 235.8 Å and this is probably also the case for H_2O. Since the krypton line emitted from our lamp falls entirely within this continuum, the absorption coefficients at 1 235.8 Å are probably correct. The results are $\epsilon_{H_2O} = 171$; $\epsilon_{D_2O} = 270$. Beer's law was found to be obeyed in the range 0.3–1 Torr for the krypton line at 1 235.8 Å.

As shown in Figs. 1 and 2, the violet shift is characterized by a lowering of the absorption coefficient for the heaver isotopic species. A number of absorption coefficients have been measured at 1 470 Å and Table I shows that the violet shift is quite general for saturated hydrocarbons.

1. G. Herzberg. Molecular spectra and molecular structure. 2nd ed. D. Van Nostrand, New York, 1950. p. 163.
2. H. Okabe and J. R. McNesby. J. Chem. Phys. **37**, 1340 (1962).
3. M. C. Sauer and L. M. Dorfman. J. Chem. Phys. **35**, 497 (1961).
4. H. Okabe and D. A. Becker. J. Am. Chem. Soc. **84**, 4004 (1962).
5. C. L. Currie, H. Okabe, and J. R. McNesby. J. Phys. Chem. **67**, 1494 (1963).
6. K. Watanabe and M. Zelikoff. J. Opt. Soc. Am. **43**, 753 (1953).
7. A. J. Harrison, B. J. Cederholm, and M. A. Terwilliger. J. Chem. Phys. **30**, 355 (1959).
8. S. Bell. J. Mol. Spectry. **16**, 205 (1965).
9. J. W. C. Johns. Can. J. Phys. **41**, 209 (1963).

Received July 14, 1965.
National Bureau of Standards,
Washington, D.C.

MEAN LIFETIME OF FREE RADICAL CHAINS IN ^{60}Co γ-IRRADIATED CHLORAL HYDRATE AND BROMAL HYDRATE SOLUTIONS

R. G. McIntosh, R. L. Eager, and J. W. T. Spinks

Previous publications by us have described work on the radiation chemistry of aqueous solutions of chloral hydrate and of bromal hydrate. The first of these (1) reported on the use of a flow system to obtain intermittent irradiation. In a later paper (2) the results obtained by steady irradiation of the samples were reported. In addition to the above work experiments were also done in which a rotating sector was used to obtain intermittent irradiation. This note reports the results of these latter studies.

EXPERIMENTAL

The ^{60}Co radiation facility was the same as that used in the other studies and has been described previously (3). During irradiation the samples were contained in an electrical conductivity cell and the change of conductivity with time of irradiation was noted. The conductivity cell was of the Arrhenius–Ostwald type and has been previously described (2). The Fricke ferrous sulfate dosimeter was used. The purification of the reagents and of the water used in making up the solutions has already been described (2). The sample temperature was that of the cave, between 20 and 25 °C. The reaction rates were corrected to 25.0 °C (2).

The rotating sector was constructed of General Electric Company Heavy Alloy which contains 90% of tungsten alloyed with nickel and copper. The alloy has a specific gravity of 16.3–17.0. The sector was 2 in thick and $7\frac{1}{4}$ in in diameter. A 3/8 in thick steel band encircled the sector. Two inches of the alloy stops approximately 90% of a ^{60}Co γ-ray beam. Two opposed sector openings of 60° each were present, giving a value for r, the ratio of the "dark" to the "light" periods, of 2. Sector speeds of 0.5 to 500 r.p.m. were used.

Can. J. Chem. Downloaded from www.nrcresearchpress.com by 210.87.254.40 on 09/05/12
For personal use only.

RESULTS AND DISCUSSION

To obtain an estimate of the accuracy of the experimental work the standard deviation of a single observation was determined. A series of 5 runs were made using a 1.0 M chloral hydrate solution and a light flash of 890 ms duration. This flash time is in the region where the reaction rate is quite sensitive to variations in the flash time. The mean reaction rate was 16.7 μmoles l^{-1} min^{-1} and the standard deviation was found to be 0.3 μmoles l^{-1} min^{-1}.

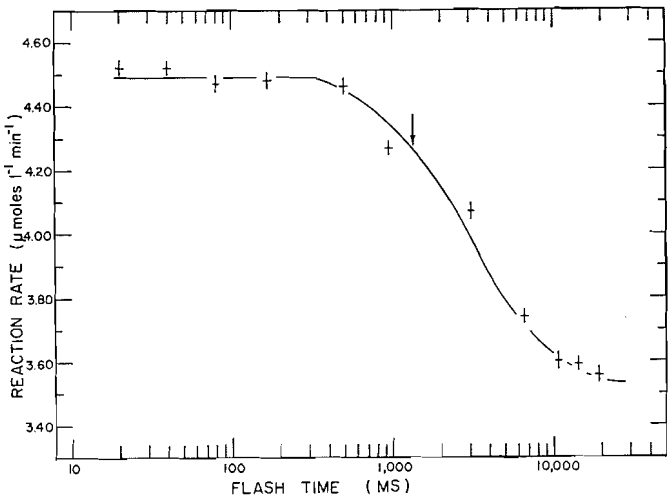

FIG. 1. Mean free radical chain lifetime sector curve: 0.1 M chloral hydrate, 106 rads min^{-1}, pH 5.15.

The mean free radical chain lifetime, τ (see below), was determined for each of a series of solutions of different concentration and pH. For each solution the variation of reaction rate with flash time was measured and the results plotted as shown in Fig. 1, which is a typical example. From these plots the value of τ was obtained using the method given by Melville and Burnett (4). The theory will not be repeated and only the final conclusions used to find values of τ will be given. The theory is based on the following generalized reaction scheme.

[1] $$S \rightsquigarrow \dot{R} \qquad \text{rate} = G_R I^*$$

[2] $$S + \dot{R} \rightarrow \dot{R} + P \qquad \text{rate} = k_p[S][\dot{R}]$$

[3] $$\dot{R} + \dot{R} \rightarrow \text{inactive species} \qquad \text{rate} = k_t[\dot{R}]^2.$$

S is the reactant, $\dot{R}$ is an intermediate free radical, and P is a product of the chain reaction. G_R is the G value for the initiation of radicals $\dot{R}$. I is the dose rate, k_p and k_t are respectively the propagation and termination specific rate constants. In the mathematical analysis of the behavior of the system when exposed to intermittent radiation two parameters arise. One of these is the mean free radical chain lifetime, τ, which is defined as follows:

$$\tau = \frac{\text{number of free radicals per unit volume}}{\text{number of free radicals disappearing per unit volume per unit time}}.$$

The other is a dimensionless parameter, m, which is the number of times that the duration

**In numerical calculations the appropriate conversion factors were used so that the rate of [1] was given in mole l^{-1} s^{-1}.*

Can. J. Chem. Downloaded from www.nrcresearchpress.com by 210.87.254.40 on 09/05/12
For personal use only.

of the light flash, the flash time t, is greater than the lifetime. It follows from this definition that

$$\tau = t/m. \quad [4]$$

A relation between a function which is proportional to the rate of production of product and m is derived. A plot of this function against m is known as the "master curve". The form of this master curve is very similar to the experimentally determined curves, such as that shown in Fig. 1. From [4] it is seen that when m is unity the value of τ is equal to the corresponding flash time. From the master curve it is found that for $m = 1$ the rate of reaction is 0.956 times the maximum rate reached at short flash times. In Fig. 1 an arrow marks the point where the rate of reaction is 0.956 times the maximum rate. Values of τ found in this manner for chloral hydrate and bromal hydrate solutions are given in Table I.

It is important to note that the reaction scheme on which these values of τ are based imply that the reaction rate is proportional to the one-half power of the dose rate and to the first power of the concentration. It has been found (2) that the rate is dependent to the 0.66 power and the 0.58 power of the dose rate for 1.0 M chloral hydrate and 0.1 M bromal hydrate solutions respectively. Similarly it has been found that the rate is dependent to the 0.39 power and the 0.34 power of the concentration for chloral hydrate solutions, at a dose rate of 250 rads min^{-1}, and for bromal hydrate solutions, at a dose rate of 114.5 rads min^{-1}, respectively. This has been taken to mean that there are chain termination processes in addition to a radical–radical reaction. The chain reaction has also been postulated to be more complicated than that in the simple scheme proposed by Melville and Burnett. It is to be expected, therefore, that the values of τ given in Table I will only be approximate values since they were derived on the basis of the simpler mechanism.

By making further assumptions it is possible to estimate values of k_t and k_p. From the definition of τ and eq. [3] we have:

$$\tau = [\dot{R}]/k_t[\dot{R}^2] = 1/k_t[\dot{R}]. \quad [5]$$

From the steady state treatment of [1], [2], and [3] we find:

$$[\dot{R}] = (G_R I/k_t)^{1/2}. \quad [6]$$

I is the average dose rate with the sector rotating. From [5] and [6] we get

$$k_t = (\tau^2 G_R I)^{-1}. \quad [7]$$

The values of τ already found may be used and I is known. The value to be used for G_R is more difficult to assess. If it is assumed that the initiating radicals arise only from the interaction of the incident radiation with water molecules then we are concerned mainly with G values for H, OH, and e_{aq}. Considering that from one to perhaps all of these species may be involved in the initiation of the chain-carrying radical $\dot{R}$ a value of 5 for G_R is probably correct within a factor of 2. In view of the approximate nature of the value of τ found above, this value for G_R appears to be suitable for use in eq. [7]. Values of k_t calculated from [7] are given in Table I.

By substituting [5] and [7] into [2], the expression for the rate of formation of product, and selecting the maximum reaction rate, R_m, we get:

$$R_m = k_p[S]G_R I\tau. \quad [8]$$

Values of k_p were calculated from [8] and are given in Table I. The experimental values of R_m, [S], and I were used. The correct value to use for I is the average dose rate with the sector rotating.

Can. J. Chem. Downloaded from www.nrcresearchpress.com by 210.87.254.40 on 09/05/12
For personal use only.

Can. J. Chem. Downloaded from www.nrcresearchpress.com by 210.87.254.40 on 09/05/12
For personal use only.

TABLE I

Rotating sector experiments, ^{60}Co γ-irradiation

Solute	Conc. (M)	pH	Dose rate sector stationary (rads min^{-1})	τ (s)	$k_t \times 10^{-8}$ (l $mole^{-1}$ s^{-1})	k_p (l $mole^{-1}$ s^{-1})	Ref.
Chloral hydrate	1.0	4.15	106	0.66	8.2	160	Present work
	0.1	5.15	106	1.2	2.5	220	Present work
	1.0	4.15	32.6	1.3	6.9	110	Present work
	1.0	3.50	106	0.62	9.4	180	Present work
	1.0	—	20.5	0.1	—	—	(5)
	1.0	—	50.0*	0.5	—	250	(6)
Bromal hydrate	0.1	4.71	106	1.6	1.4	270	Present work
	0.2	—	17.0†	1.4	—	—	(7)

*^{90}Sr–^{90}Y β-particles.
†Internal ^{32}P β-particles; dose rate with sector rotating.

Also included in Table I are the results of other workers (5, 6, 7). The two values of τ given for chloral hydrate solutions (5, 6) are smaller than those found in the present work. The reason for this discrepancy is not known. The value of τ found for a bromal hydrate solution (7), while for a different concentration, type of radiation, and dose rate, appears to be consistent with the value found in the present work.

The chloral hydrate results obtained in the present work are the only ones where there is a variation in concentration, pH, and dose rate, hence these results will be used in the following discussion. The results for the chloral hydrate solutions presented in Table I indicate that τ, k_t, and k_p are not very pH dependent. This is consistent with the mechanism proposed by the present authors for the irradiation of solutions of chloral hydrate and of bromal hydrate (2). Similarly the variation of τ either with dose rate or with concentration is qualitatively consistent with the proposed reaction scheme (2). It would be expected that if a radical–radical reaction (reaction [e] in ref. 2) was responsible for at least some of the chain termination, a change in any variable which resulted in an increase in the concentration of the radicals would result in a decreased value of τ. This would be the expected result of an increased dose rate or an increased concentration of the solute.

A decrease in the concentration of chloral hydrate is found to cause a marked decrease in k_t and an increase in k_p. A decrease in the dose rate causes a decrease in both k_t and k_p. These results indicate that k_t and k_p are not true specific rate constants but rather that they are composite and may include concentration terms. In the mechanism suggested by the authors (2) it was proposed that the chain termination step is not exclusively a radical–radical reaction, but also the following reaction occurs to a certain extent (reaction [*f*] in ref. 2).

$$[9] \qquad \dot{R} \xrightarrow[M]{k_f} \text{end of chain} \qquad \text{rate} = k_f[\dot{R}][M]$$

As the result of the inclusion of this reaction k_t would include a term $k_f[\dot{R}][M]$. The effect of a decreased concentration of chloral hydrate (if chloral hydrate is M) would be to reduce the rate of removal of $\dot{R}$ from the reaction mixture. The result would be a decrease in the rate of termination, i.e. k_t would be expected to decrease, as is observed. The decreased rate of termination will, however, result in an increase in the rate of the chain reaction (reactions [*b*] to [*d*] in ref. 2), i.e. k_p would be expected to increase, as is observed. The inclusion of reaction [9], and the identification of M with S, implies that chloral hydrate acts as an inhibitor for the reaction. Hence qualitatively it would be expected that the exponent of the concentration term in the rate expression (eq. [8] in ref. 2) would be less than one-half, as it is found to be. This point, which was not made in ref. 2, is further support for the reaction scheme proposed by the present authors (2). The effect of a decreased dose rate would be to lower the concentration of $\dot{R}$. The result would be a decrease in the rate of reaction [9] i.e. k_t would be expected to decrease, as is observed. On the basis of the mechanism proposed in ref. 2 the effect of a decrease in dose rate on k_p is not easy to predict, but the observed decrease in value does not seem to be inconsistent with the proposed mechanism.

ACKNOWLEDGMENTS

Grateful acknowledgment is made to the Atomic Energy Control Board for financial support. One of us (R.G.M.) wishes to thank the National Research Council for a bursary.

1. R. G. McIntosh, R. L. Eager, and J. W. T. Spinks. Science, **131**, 992 (1960).
2. R. G. McIntosh, R. L. Eager, and J. W. T. Spinks. Can. J. Chem. **42**, 2033 (1964).
3. A. L. Riegert and J. W. T. Spinks. Proc. Hot Lab. Equip. Conf. 7th, Cleveland, Ohio. 1959. p. 315.

Can. J. Chem. Downloaded from www.nrcresearchpress.com by 210.87.254.40 on 09/05/12
For personal use only.

4. G. M. BURNETT and H. W. MELVILLE. Technique of organic chemistry. Vol. VIII. Interscience Publishers, Inc., New York. 1953. Chap. 3. Part 4.
5. G. R. FREEMAN, A. B. VAN CLEAVE, and J. W. T. SPINKS. Can. J. Chem. **32**, 322 (1954).
6. R. F. PLATFORD and J. W. T. SPINKS. Can. J. Chem. **37**, 1022 (1959).
7. A. C. BRICKNELL. Ph.D. Thesis, University of Saskatchewan, Saskatoon, Sask. 1959.

RECEIVED JUNE 30, 1965.
DEPARTMENT OF CHEMISTRY AND CHEMICAL ENGINEERING,
UNIVERSITY OF SASKATCHEWAN,
SASKATOON, SASKATCHEWAN.

Can. J. Chem. Downloaded from www.nrcresearchpress.com by 210.87.254.40 on 09/05/12
For personal use only.

SURFACE CHEMISTRY AND CATALYTIC PROPERTIES OF BORON PHOSPHATE. II. A NOTE ON THE FORMATION OF PARAMAGNETIC SPECIES WITH ADSORBED AROMATIC COMPOUNDS

J. B. MOFFAT AND M. A. HALEEM[1]

INTRODUCTION

Earlier work (1) from this laboratory has demonstrated that acidic sites are present on the surface of boron phosphate (BP). It is of interest to attempt to demonstrate whether such acidity is of the Bronsted or Lewis type. Electron spin resonance (e.s.r.) studies of aromatic compounds adsorbed on such solids as silica–alumina have been used by other workers in an attempt to elucidate the nature of the adsorbed species and the type of acidic sites present. The present note reports results of preliminary studies of the species formed by the adsorption of some aromatic compounds on the surface of solid BP. No previous studies of e.s.r. spectra of adsorbed materials on boron phosphate have been reported.

A number of studies of the e.s.r. spectra of aromatic molecules adsorbed on silica–alumina have been reported. Rooney and Pink (2) attributed their e.s.r. signals to radical-ion formation. Recently (3) the presence of paramagnetic species in the adsorption of aromatic molecules on platinum oxide has been reported. However, the observed paramagnetic resonance in this case is attributed to a low lying, thermally populated, triplet state of a charge-transfer complex.

EXPERIMENTAL

Solutions of various aromatic compounds in dried carbon tetrachloride and (or) in dried heptane were added to aliquots of samples of boron phosphate prepared as described previously (1). All reagents were of the best grade available from Eastman Kodak, usually of C.P. grade. No further purification of these chemicals was done. Preliminary treatment of the BP consisted of evacuation at 100 °C for at least 2 days and in some cases, longer. Electron spin resonance scans of the untreated BP showed no signals.

Electron spin resonance spectra were obtained at room temperature with a JEOL model JES-3B spectrometer operating at 9 500 Mc/s and 100 kc/s magnetic field modulation. Samples were held in quartz glass tubes fitted with standard taper joints and stopcocks through graded seals to permit attachment to a high vacuum system.

RESULTS

Perylene (P Y)

When a solution of PY in dried carbon tetrachloride was added to a sample of BP treated as discussed previously, a purple color developed on the catalyst. A strong nine-line e.s.r. spectrum, similar to that obtained by Hodgson and Raley (4) was obtained. The shape of this spectrum for adsorbed PY also agreed with that found by others previously (5). The e.s.r. spectrum yielded a g value of 2.0023 ± 0.0005 and a width measured between centers of extreme peaks of 23 ± 0.5 G.

[1]*Present address: Department of Chemistry, Osmania University, Hyderabad, India.*

4. G. M. BURNETT and H. W. MELVILLE. Technique of organic chemistry. Vol. VIII. Interscience Publishers, Inc., New York. 1953. Chap. 3. Part 4.
5. G. R. FREEMAN, A. B. VAN CLEAVE, and J. W. T. SPINKS. Can. J. Chem. **32**, 322 (1954).
6. R. F. PLATFORD and J. W. T. SPINKS. Can. J. Chem. **37**, 1022 (1959).
7. A. C. BRICKNELL. Ph.D. Thesis, University of Saskatchewan, Saskatoon, Sask. 1959.

RECEIVED JUNE 30, 1965.
DEPARTMENT OF CHEMISTRY AND CHEMICAL ENGINEERING,
UNIVERSITY OF SASKATCHEWAN,
SASKATOON, SASKATCHEWAN.

Can. J. Chem. Downloaded from www.nrcresearchpress.com by 210.87.254.42 on 09/05/12
For personal use only.

SURFACE CHEMISTRY AND CATALYTIC PROPERTIES OF BORON PHOSPHATE. II. A NOTE ON THE FORMATION OF PARAMAGNETIC SPECIES WITH ADSORBED AROMATIC COMPOUNDS

J. B. MOFFAT AND M. A. HALEEM[1]

INTRODUCTION

Earlier work (1) from this laboratory has demonstrated that acidic sites are present on the surface of boron phosphate (BP). It is of interest to attempt to demonstrate whether such acidity is of the Bronsted or Lewis type. Electron spin resonance (e.s.r.) studies of aromatic compounds adsorbed on such solids as silica–alumina have been used by other workers in an attempt to elucidate the nature of the adsorbed species and the type of acidic sites present. The present note reports results of preliminary studies of the species formed by the adsorption of some aromatic compounds on the surface of solid BP. No previous studies of e.s.r. spectra of adsorbed materials on boron phosphate have been reported.

A number of studies of the e.s.r. spectra of aromatic molecules adsorbed on silica–alumina have been reported. Rooney and Pink (2) attributed their e.s.r. signals to radical-ion formation. Recently (3) the presence of paramagnetic species in the adsorption of aromatic molecules on platinum oxide has been reported. However, the observed paramagnetic resonance in this case is attributed to a low lying, thermally populated, triplet state of a charge-transfer complex.

EXPERIMENTAL

Solutions of various aromatic compounds in dried carbon tetrachloride and (or) in dried heptane were added to aliquots of samples of boron phosphate prepared as described previously (1). All reagents were of the best grade available from Eastman Kodak, usually of C.P. grade. No further purification of these chemicals was done. Preliminary treatment of the BP consisted of evacuation at 100 °C for at least 2 days and in some cases, longer. Electron spin resonance scans of the untreated BP showed no signals.

Electron spin resonance spectra were obtained at room temperature with a JEOL model JES-3B spectrometer operating at 9 500 Mc/s and 100 kc/s magnetic field modulation. Samples were held in quartz glass tubes fitted with standard taper joints and stopcocks through graded seals to permit attachment to a high vacuum system.

RESULTS

Perylene (P Y)

When a solution of PY in dried carbon tetrachloride was added to a sample of BP treated as discussed previously, a purple color developed on the catalyst. A strong nine-line e.s.r. spectrum, similar to that obtained by Hodgson and Raley (4) was obtained. The shape of this spectrum for adsorbed PY also agreed with that found by others previously (5). The e.s.r. spectrum yielded a g value of 2.0023 ± 0.0005 and a width measured between centers of extreme peaks of 23 ± 0.5 G.

[1]*Present address: Department of Chemistry, Osmania University, Hyderabad, India.*

Tetraphenylethylene (TPE)

As in the case of Perylene, a dark purple color resulted on addition of a solution of TPE in dried carbon tetrachloride to BP. However, the system with TPE gave an unresolved, relatively weak (compared to perylene) e.s.r. signal, with a g value of 2.0033 ± 0.001 and a width of 15 ± 1 G.

Paramagnetic species have been observed (7) previously with TPE and silica–alumina.

1,1-Diphenylethylene (DPE)

A dark-green color was produced with a DPE–CCl_4 solution and BP. Again an unresolved, relatively weak, e.s.r. signal was obtained, with a g value of 2.0033 ± 0.001 and a width of 11 ± 1 G. Rooney and Hathaway (7) obtained a green color and an e.s.r. signal with DPE on silica–alumina. However, they demonstrated that the green color was apparently due to two species one yellow and one blue, the latter being a carbonium ion rather than a radical-ion. However, they were not able to identify the radical-ion present in their system.

DISCUSSION

In general, the results reported here are not inconsistent with those found by others with PY, TPE, and DPE on silica–alumina. In the present work data are so far insufficient to permit any comment on the nature of the species formed, although one is tempted to believe that the paramagnetic species formed with BP are of the radical-ion type, by analogy with the case of silica–alumina.

It is known (for example, see refs. 2 and 4) that the presence of even small amounts of water often has deleterious effects on the paramagnetic species produced in similar adsorption studies on silica–alumina. In contrast, Leftin and Hobson (8) found that the e.s.r. signal from DPE and silica–alumina was enhanced by the presence of water vapor. There is some evidence (2, 6) at least in the case of perylene, that oxygen alters the shape and size of the e.s.r. signal. In the present work it is presumed, as a result of the drying of the solvent, and the heating and evacuation of the catalyst, that little or no water or oxygen is present.

It is extremely difficult to prove that free phosphoric acid is not present on the surface of the boron phosphate prepared in our laboratory. However, samples of BP which had been heated to 350 °C in air, then evacuated and heated at 100 °C for several days still yielded e.s.r. signals with the aromatic compounds studied. Hence we believe that any phosphorus which was not an intrinsic part of the BP, could presumably not exist as phosphoric acid, but could perhaps be in the form of phosphorus pentoxide. There appears to be little reason to believe that our preparation reactions for BP are not substantially complete, leaving little or no free P_2O_5 remaining. The X-ray diffraction data reported previously (1) appear to support this contention. There is no reason to suspect that any small residual quantities of phosphoric pentoxide would tend to concentrate on the surface as the preparation was being carried out. Of course there is the haunting question of the bulk structure of BP and the suggestion (9) that BP could be thought of as a mixed anhydride of P_2O_5 and B_2O_3. Nevertheless we believe that the catalytic properties of boron phosphate cannot be accounted for on the basis of the properties of P_2O_5 and B_2O_3. Work is underway on this aspect.

It is not possible at this point to say what influence the method of preparation of the BP, the preliminary heating and evacuation, or the presence of gases such as oxygen may have on the paramagnetic species formed. Studies of such variables, together with

Can. J. Chem. Downloaded from www.nrcresearchpress.com by 210.87.254.42 on 09/05/12
For personal use only.

studies of effects of concentrations of the aromatic species and also stability of the paramagnetic and (or) colored species, are in progress, using both resonance and optical spectroscopic methods. These will be reported at a later date.

ACKNOWLEDGMENT

The authors are indebted to the National Research Council for support of this work, and to the University of Waterloo for the provision of a postdoctoral fellowship for one of us (M. A. H.).

1. J. B. MOFFAT and H. L. GOLTZ. Can. J. Chem. **43**, 1680 (1965).
2. J. J. ROONEY and R. C. PINK. Trans. Faraday Soc. **58**, 1632 (1962).
3. L. T. ERNST, J. L. GARNETT, and W. A. SOLLICH-BAUMGARTNER. J. Catalysis, **3**, 568 (1964).
4. R. L. HODGSON and J. H. RALEY. J. Catalysis, **4**, 6 (1965).
5. J. J. ROONEY and R. C. PINK. Proc. Chem. Soc. 70 (1961).
6. H. IMAI, Y. ONO, and T. KEII. J. Phys. Chem. **69**, 1082 (1965).
7. J. J. ROONEY and B. J. HATHAWAY. J. Catalysis, **3**, 447 (1964).
8. H. P. LEFTIN and M. C. HOBSON. Advan. in Catalysis, **14**, 115 (1963).
9. J. R. VAN WAZER. Phosphorus and its compounds. Vol. I. Interscience Publishers, Inc., New York. 1958. p. 551.

RECEIVED MAY 12, 1965.
DEPARTMENT OF CHEMISTRY,
UNIVERSITY OF WATERLOO,
WATERLOO, ONTARIO.

Can. J. Chem. Downloaded from www.nrcresearchpress.com by 210.87.254.42 on 09/05/12
For personal use only.